Review of Particle Physics

To cite this article: K.A. Olive and Particle Data Group 2014 *Chinese Phys. C* **38** 090001

REVIEW OF PARTICLE PHYSICS*

Particle Data Group

Abstract

The *Review* summarizes much of particle physics and cosmology. Using data from previous editions, plus 3,283 new measurements from 899 papers, we list, evaluate, and average measured properties of gauge bosons and the recently discovered Higgs boson, leptons, quarks, mesons, and baryons. We summarize searches for hypothetical particles such as heavy neutrinos, supersymmetric and technicolor particles, axions, dark photons, etc. All the particle properties and search limits are listed in Summary Tables. We also give numerous tables, figures, formulae, and reviews of topics such as Supersymmetry, Extra Dimensions, Particle Detectors, Probability, and Statistics. Among the 112 reviews are many that are new or heavily revised including those on: Dark Energy, Higgs Boson Physics, Electroweak Model, Neutrino Cross Section Measurements, Monte Carlo Neutrino Generators, Top Quark, Dark Matter, Dynamical Electroweak Symmetry Breaking, Accelerator Physics of Colliders, High-Energy Collider Parameters, Big Bang Nucleosynthesis, Astrophysical Constants and Cosmological Parameters.

A booklet is available containing the Summary Tables and abbreviated versions of some of the other sections of this full *Review*. All tables, listings, and reviews (and errata) are also available on the Particle Data Group website: `http://pdg.lbl.gov`.

DOI: 10.1088/1674-1137/38/9/090001

The 2014 edition of *Review of Particle Physics* is published for the Particle Data Group as article 090001 in Volume 38, No. 9 of Chinese Physics C.

This edition should be cited as: K.A. Olive et al. (Particle Data Group), Chin. Phys. C, 2014, **38**(9): 090001

*The publication of the *Review of Particle Physics* is supported by the Director, Office of Science, Office of High Energy Physics of the U.S. Department of Energy under Contract No. DE–AC02–05CH11231; by the U.S. National Science Foundation under Agreement No. PHY-0652989; by the European Laboratory for Particle Physics (CERN); by an implementing arrangement between the governments of Japan (MEXT: Ministry of Education, Culture, Sports, Science and Technology) and the United States (DOE) on cooperative research and development; and by the Italian National Institute of Nuclear Physics (INFN).

Particle Data Group

K.A. Olive,[1] K. Agashe,[2] C. Amsler,[3] M. Antonelli,[4] J.-F. Arguin,[5] D.M. Asner,[6] H. Baer,[7] H.R. Band,[8] R.M. Barnett,[9] T. Basaglia,[10] C.W. Bauer,[9] J.J. Beatty,[11] V.I. Belousov,[12] J. Beringer,[9] G. Bernardi,[13] S. Bethke,[14] H. Bichsel,[15] O. Biebel,[16] E. Blucher,[17] S. Blusk,[18] G. Brooijmans,[19] O. Buchmueller,[20] V. Burkert,[21] M.A. Bychkov,[22] R.N. Cahn,[9] M. Carena,[23,17,24] A. Ceccucci,[10] A. Cerri,[25] D. Chakraborty,[26] M.-C. Chen,[27] R.S. Chivukula,[28] K. Copic,[9] G. Cowan,[29] O. Dahl,[9] G. D'Ambrosio,[30] T. Damour,[31] D. de Florian,[32] A. de Gouvêa,[33] T. DeGrand,[34] P. de Jong,[35] G. Dissertori,[36] B.A. Dobrescu,[23] M. Doser,[10] M. Drees,[37] H.K. Dreiner,[37] D.A. Edwards,[38] S. Eidelman,[39,141] J. Erler,[40,41] V.V. Ezhela,[12] W. Fetscher,[36] B.D. Fields,[42,43‡] B. Foster,[44,38,45] A. Freitas,[46] T.K. Gaisser,[47] H. Gallagher,[48] L. Garren,[23] H.-J. Gerber,[36] G. Gerbier,[49] T. Gershon,[50] T. Gherghetta,[1] S. Golwala,[51] M. Goodman,[52] C. Grab,[36] A.V. Gritsan,[53] C. Grojean,[54] D.E. Groom,[9] M. Grünewald,[55,56] A. Gurtu,[57,10] T. Gutsche,[58] H.E. Haber,[59,9] K. Hagiwara,[60] C. Hanhart,[61] S. Hashimoto,[60] Y. Hayato,[62] K.G. Hayes,[63] M. Heffner,[64] B. Heltsley,[65] J.J. Hernández-Rey,[66] K. Hikasa,[67] A. Höcker,[10] J. Holder,[68,47] A. Holtkamp,[10] J. Huston,[28] J.D. Jackson,[9] K.F. Johnson,[69] T. Junk,[23] M. Kado,[70,10] D. Karlen,[71] U.F. Katz,[72] S.R. Klein,[73] E. Klempt,[74] R.V. Kowalewski,[71] F. Krauss,[75] M. Kreps,[50] B. Krusche,[76] Yu.V. Kuyanov,[12] Y. Kwon,[77] O. Lahav,[78] J. Laiho,[18] P. Langacker,[79] A. Liddle,[80] Z. Ligeti,[9] C.-J. Lin,[9] T.M. Liss,[81] L. Littenberg,[82] K.S. Lugovsky,[12] S.B. Lugovsky,[12] F. Maltoni,[83] T. Mannel,[84] A.V. Manohar,[85] W.J. Marciano,[82] A.D. Martin,[75] A. Masoni,[86] J. Matthews,[87] D. Milstead,[88] P. Molaro,[89] K. Mönig,[90] F. Moortgat,[10] M.J. Mortonson,[91,9] H. Murayama,[92,93,9] K. Nakamura,[92,60] M. Narain,[94] P. Nason,[95] S. Navas,[96] M. Neubert,[97] P. Nevski,[82] Y. Nir,[98] L. Pape,[36] J. Parsons,[19] C. Patrignani,[99] J.A. Peacock,[80] M. Pennington,[21] S.T. Petcov,[100,92,101] A. Piepke,[102] A. Pomarol,[103] A. Quadt,[104] S. Raby,[11] J. Rademacker,[105] G. Raffelt,[106] B.N. Ratcliff,[107] P. Richardson,[75] A. Ringwald,[38] S. Roesler,[10] S. Rolli,[108] A. Romaniouk,[109] L.J. Rosenberg,[15] J.L. Rosner,[17] G. Rybka,[15] C.T. Sachrajda,[110] Y. Sakai,[60] G.P. Salam,[10,111] S. Sarkar,[112,113] F. Sauli,[10] O. Schneider,[114] K. Scholberg,[115] D. Scott,[116] V. Sharma,[85] S.R. Sharpe,[15] M. Silari,[10] T. Sjöstrand,[117] P. Skands,[10,118] J.G. Smith,[34] G.F. Smoot,[119,93,9] S. Spanier,[120] H. Spieler,[9] C. Spiering,[90] A. Stahl,[121] T. Stanev,[47] S.L. Stone,[18] T. Sumiyoshi,[122] M.J. Syphers,[123] F. Takahashi,[67] M. Tanabashi,[124] J. Terning,[125] L. Tiator,[41] M. Titov,[126] N.P. Tkachenko,[12] N.A. Törnqvist,[127] D. Tovey,[128] G. Valencia,[129] G. Venanzoni,[4] M.G. Vincter,[130] P. Vogel,[131] A. Vogt,[132] S.P. Wakely,[17,24] W. Walkowiak,[84] C.W. Walter,[115] D.R. Ward,[133] G. Weiglein,[38] D.H. Weinberg,[134] E.J. Weinberg,[19] M. White,[93,9] L.R. Wiencke,[135] C.G. Wohl,[9] L. Wolfenstein,[136] J. Womersley,[137] C.L. Woody,[82] R.L. Workman,[138] A. Yamamoto,[60] W.-M. Yao,[9] G.P. Zeller,[23] O.V. Zenin,[12,142] J. Zhang,[139] R.-Y. Zhu,[140] F. Zimmermann,[10] P.A. Zyla[9]

Technical Associates: G. Harper,[9] V.S. Lugovsky,[12] P. Schaffner[9]

1. *University of Minnesota, School of Physics and Astronomy, 116 Church St. S.E., Minneapolis, MN 55455, USA*
2. *University of Maryland, Department of Physics, College Park, MD 20742-4111, USA*
3. *Albert Einstein Center for Fundamental Physics, Universität Bern, CH-3012 Bern, Switzerland*
4. *Lab. Nazionali di Frascati dell'INFN, CP 13, via E. Fermi, 40, I-00044 Frascati (Roma), Italy*
5. *Département de physique, Université de Montréal, C.P. 6128, succ. centre-ville, Montréal (Québec) H3C 3J7, Canada*
6. *Pacific Northwest National Laboratory, 902 Battelle Boulevard, Richland, WA 99352, USA*
7. *Department of Physics and Astronomy, University of Oklahoma, Norman, OK 73019, USA*
8. *Department of Physics, University of Wisconsin, Madison, WI 53706, USA*
9. *Physics Division, Lawrence Berkeley National Laboratory, 1 Cyclotron Road, Berkeley, CA 94720, USA*
10. *CERN, European Organization for Nuclear Research, CH-1211 Genève 23, Switzerland*
11. *Department of Physics, The Ohio State University, 191 W. Woodruff Ave., Columbus, OH 43210, USA*
12. *COMPAS Group, Institute for High Energy Physics, RU-142284, Protvino, Russia*
13. *LPNHE, IN2P3-CNRS et Universités de Paris 6 et 7, F-75252 Paris, France*
14. *Max-Planck-Institute of Physics, 80805 Munich, Germany*
15. *Department of Physics, University of Washington, Seattle, WA 98195, USA*
16. *Ludwig-Maximilians-Universität, Fakultät für Physik, Schellingstr. 4, D-80799 München, Germany*
17. *Enrico Fermi Institute and Department of Physics, University of Chicago, Chicago, IL 60637-1433, USA*
18. *Department of Physics, Syracuse University, Syracuse, NY, 13244, USA*
19. *Department of Physics, Columbia University, 538 W. 120th Street, New York, NY, 10027 USA*
20. *High Energy Physics Group, Blackett Laboratory, Imperial College, Prince Consort Road, London SW7 2AZ, UK*
21. *Jefferson Lab, 12000 Jefferson Ave., Newport News, VA 23606, USA*
22. *Department of Physics, University of Virginia, PO Box 400714, Charlottesville, VA 22904, USA*
23. *Fermi National Accelerator Laboratory, P.O. Box 500, Batavia, IL 60510, USA*
24. *Kavli Institute for Cosmological Physics, University of Chicago, Chicago, IL 60637-1433, USA*
25. *Department of Physics and Astronomy, University of Sussex, Falmer, Brighton BN1 9QH, UK*
26. *Department of Physics, Northern Illinois University, DeKalb, IL 60115, USA*
27. *Department of Physics and Astronomy, University of California, Irvine, CA 92697-4575, USA*
28. *Michigan State University, Dept. of Physics and Astronomy, East Lansing, MI 48824-2320, USA*

‡ The work of B.D.F. was supported by the U.S. National Science Foundation Grant PHY-1214082.

29. *Department of Physics, Royal Holloway, University of London, Egham, Surrey TW20 0EX, UK*
30. *INFN - Sezione di Napoli, Complesso Universitario Monte Sant'Angelo, Via Cintia, 80126 Napoli, Italy*
31. *Institut des Hautes Etudes Scientifiques, F-91440 Bures-sur-Yvette, France*
32. *Departamento de Física, FCEyN, Universidad de Buenos Aires, Pab.1, Ciudad Universitaria, (1428) Capital Federal, Argentina*
33. *Department of Physics and Astronomy, Northwestern University, Evanston, IL 60208, USA*
34. *Department of Physics, University of Colorado at Boulder, Boulder, CO 80309, USA*
35. *Nikhef, P.O. Box 41882, 1009 DB Amsterdam, the Netherlands*
36. *Institute for Particle Physics, ETH Zurich, 8093 Zurich, Switzerland*
37. *Universität Bonn, Physikalisches Institut, Nussallee 12, D-53115 Bonn, Germany*
38. *Deutsches Elektronen-Synchrotron DESY, Notkestraße 85, D-22607 Hamburg, Germany*
39. *Budker Institute of Nuclear Physics SB RAS, Novosibirsk 630090, Russia*
40. *Departamento de Física Teórica, Instituto de Física, Universidad Nacional Autónoma de México, México D.F. 04510, México*
41. *Institut für Physik, Johannes-Gutenberg Universität Mainz, D-55099 Mainz, Germany*
42. *Department of Astronomy, University of Illinois, 1002 W. Green St., Urbana, IL 61801, USA*
43. *Department of Physics, University of Illinois, 1110 W. Green St., Urbana, IL 61801, USA*
44. *University of Hamburg, Notkestrasse 85, D-22607 Hamburg, Germany*
45. *Denys Wilkinson Building, Department of Physics, University of Oxford, Oxford, OX1 3RH, UK*
46. *University of Pittsburgh, Department of Physics and Astronomy, 3941 O'Hara St, Pittsburgh, PA 15260, USA*
47. *Bartol Research Institute, University of Delaware, Newark, DE 19716, USA*
48. *Department of Physics and Astronomy, Tufts University, 4 Colby Street, Medford, MA 02155, USA*
49. *CEA/Saclay, DSM/IRFU, BP 2, F-91191 Gif-sur-Yvette, France*
50. *Department of Physics, University of Warwick, Coventry, CV4 7AL, UK*
51. *California Institute of Technology, Division of Physics, Mathematics, and Astronomy, Mail Code 367-17, Pasadena, CA 91125, USA*
52. *Argonne National Laboratory, 9700 S. Cass Ave., Argonne, IL 60439-4815, USA*
53. *Johns Hopkins University, Baltimore, Maryland 21218, USA*
54. *Institució Catalana de Recerca i Estudis Avancats, Institut de Física d'Altes Energies, E-08193 Bellaterra (Barcelona), Spain*
55. *Dept. of Physics and Astronomy, University of Ghent, Proeftuinstraat 86, B-9000 Ghent, Belgium*
56. *School of Physics, University College Dublin, Belfield, Dublin 4, Ireland*
57. *(now retired) TIFR, Homi Bhabha Road, Mumbai, India*
58. *Institut für Theoretische Physik, Universität Tübingen, Auf der Morgenstelle 14, D-72076 Tübingen, Germany*
59. *Santa Cruz Institute for Particle Physics, University of California, Santa Cruz, CA 95064, USA*
60. *KEK, High Energy Accelerator Research Organization, Oho, Tsukuba-shi, Ibaraki-ken 305-0801, Japan*
61. *Institut für Kernphysik and Institute for Advanced Simulation, Forschungszentrum Jülich, Jülich, Germany*
62. *Department of Physics, University of Tokyo, Tokyo 113-0033, Japan*
63. *Department of Physics, Hillsdale College, Hillsdale, MI 49242, USA*
64. *Lawrence Livermore National Laboratory, 7000 East Ave., Livermore, CA 94550, USA*
65. *Laboratory of Elementary-Particle Physics, Cornell University, Ithaca, NY 14853, USA*
66. *IFIC — Instituto de Física Corpuscular, Universitat de València — C.S.I.C., E-46071 València, Spain*
67. *Department of Physics, Tohoku University, Aoba-ku, Sendai 980-8578, Japan*
68. *Department of Physics and Astronomy, University of Delaware, Newark, DE 19716, USA*
69. *Los Alamos National Laboratory, Los Alamos, NM 87545, USA*
70. *LAL, IN2P3-CNRS et Univ. de Paris 11, F-91898 Orsay CEDEX, France*
71. *University of Victoria, Victoria, BC V8W 3P6, Canada*
72. *University of Erlangen-Nuremberg, Erlangen Centre for Astroparticle Physics, Erwin-Rommel-Str. 1, 91058 Erlangen, Germany*
73. *Nuclear Science Division, Lawrence Berkeley National Laboratory, 1 Cyclotron Road, Berkeley, CA 94720, USA*
74. *Helmholtz-Institut für Strahlen- und Kernphysik, Universität Bonn, Bonn, Germany*
75. *Institute for Particle Physics Phenomenology, Department of Physics, University of Durham, Durham DH1 3LE, UK*
76. *Institute of Physics, University of Basel, CH-4056 Basel, Switzerland*
77. *Yonsei University, Department of Physics, 134 Sinchon-dong, Sudaemoon-gu, Seoul 120-749, South Korea*
78. *Department of Physics and Astronomy, University College London, Gower Street, London WC1E 6BT, UK*
79. *School of Natural Science, Institute for Advanced Study, Princeton, NJ 08540, USA*
80. *Institute for Astronomy, University of Edinburgh, Royal Observatory, Blackford Hill, Edinburgh, EH9 3HJ, Scotland, UK*
81. *Division of Science, City College of New York, 160 Convent Avenue, New York, NY 10031*
82. *Physics Department, Brookhaven National Laboratory, Upton, NY 11973, USA*
83. *Centre for Cosmology, Particle Physics and Phenomenology (CP3), Université catholique de Louvain, B-1348 Louvain-la-Neuve, Belgium*
84. *Department für Physik, Universität Siegen, Walter-Flex-Str. 3, 57068 Siegen, Germany*
85. *Department of Physics, University of California at San Diego, La Jolla, CA 92093, USA*

86. *INFN Sezione di Cagliari, Cittadella Universitaria di Monserrato, I-09042 Monserrato (CA), Italy*
87. *Department of Physics and Astronomy, Louisana State University, Baton Rouge, LA 70803, USA*
88. *Fysikum, Stockholms Universitet, AlbaNova University Centre, SE-106 91 Stockholm, Sweden*
89. *INAF-OATS, via G.B. Tiepolo 11, 34143 Trieste, Italy*
90. *DESY, D-15735 Zeuthen, Germany*
91. *The Space Sciences Laboratory (SSL), University of California, 7 Gauss Way, Berkeley, CA 94720, USA*
92. *Kavli IPMU (WPI), Todai Institutes for Advanced Study, University of Tokyo, Kashiwa, Chiba 277-8583, Japan*
93. *Department of Physics, University of California, Berkeley, CA 94720, USA*
94. *Brown University, Department of Physics, 182 Hope Street, Providence, RI 02912, USA*
95. *INFN, Sez. di Milano-Bicocca, Piazza della Scienza, 3, I-20126 Milano, Italy*
96. *Dpto. de Física Teórica y del Cosmos & C.A.F.P.E., Universidad de Granada, 18071 Granada, Spain*
97. *PRISMA Cluster of Excellence and Mainz Institute for Theoretical Physics, Johannes Gutenberg University, D-55099 Mainz, Germany*
98. *Department of Particle Physics and Astrophysics, Weizmann Institute of Science, Rehovot 7610001, Israel*
99. *Dipartimento di Fisica e INFN, Università di Genova, I-16146 Genova, Italy*
100. *SISSA/INFN, via Bonomea, 265, 34136 Trieste TS, Italy*
101. *INRNE, Bulgarian Academy of Sciences, 1784 Sofia, Bulgaria*
102. *Department of Physics and Astronomy, University of Alabama, 206 Gallalee Hall, Tuscaloosa, AL 35487, USA*
103. *Departament de Física, Universitat Autonòma de Barcelona, 08193 Bellaterra, Barcelona, Spain*
104. *Georg-August-Universität Göttingen, II. Physikalisches Institut, Friedrich-Hund-Platz 1, D-37077 Göttingen, Germany*
105. *HH Wills Physics Laboratory, University of Bristol, Tyndall Avenue, Bristol BS8 1TL, UK*
106. *Max-Planck-Institut für Physik (Werner-Heisenberg-Institut), Föhringer Ring 6, D-80805 München, Germany*
107. *SLAC National Accelerator Laboratory, 2575 Sand Hill Road, Menlo Park, CA 94025, USA*
108. *DOE, 1000 Independence Ave, SW, SC-25 Germantown Bldg, Washington, DC 20585, USA*
109. *National Research Nuclear University "MEPhI" (Moscow Engineering Physics Institute), 31, Kashirskoye shosse, 115409 Moscow, Russia*
110. *School of Physics and Astronomy, University of Southampton, Highfield, Southampton S017 1BJ, UK*
111. *(on leave from) LPTHE, UPMC Université de Paris 6, CNRS UMR 7589, 4 place Jussieu, Paris, France*
112. *Rudolf Peierls Centre for Theoretical Physics, University of Oxford, 1 Keble Road, Oxford OX1 3NP, UK*
113. *Niels Bohr Institute, Blegdamsvej 17, 2100 Copenhagen, Denmark*
114. *Ecole Polytechnique Fédérale de Lausanne (EPFL), CH-1015 Lausanne, Switzerland*
115. *Physics Department, Duke University, Durham, NC 27708, USA*
116. *Department of Physics and Astronomy, University of British Columbia, Vancouver, BC V6T 1Z1, Canada*
117. *Department of Astronomy and Theoretical Physics, Lund University, S-223 62 Lund, Sweden*
118. *School of Physics, Monash University, Melbourne, Victoria 3800, Australia*
119. *Paris Centre for Cosmological Physics, APC (CNRS), Université Paris Diderot, Université Sorbonne Paris Cité, Paris 75013 France*
120. *Department of Physics and Astronomy, University of Tennessee, Knoxville, TN 37996, USA*
121. *III. Physikalisches Institut, Physikzentrum, RWTH Aachen University, 52056 Aachen, Germany*
122. *High Energy Physics Laboratory, Tokyo Metropolitan University, Tokyo, 192-0397, Japan*
123. *Michigan State University, National Superconducting Cyclotron Laboratory, East Lansing, MI 48824, USA*
124. *Kobayashi-Maskawa Institute, Nagoya University, Chikusa-ku, Nagoya 464-0028, Japan*
125. *Department of Physics, University of California, Davis, CA 95616, USA*
126. *CEA/Saclay, B.P.2, Orme des Merisiers, F-91191 Gif-sur-Yvette Cedex, France*
127. *Department of Physics, POB 64 FIN-00014 University of Helsinki, Finland*
128. *Department of Physics and Astronomy, University of Sheffield, Sheffield S3 7RH, UK*
129. *Department of Physics, Iowa State University, Ames, IA 50011, USA*
130. *Department of Physics, Carleton University, 1125 Colonel By Drive, Ottawa, ON K1S 5B6, Canada*
131. *California Institute of Technology, Kellogg Radiation Laboratory 106-38, Pasadena, CA 91125, USA*
132. *Division of Theoretical Physics, Department of Mathematical Sciences, The University of Liverpool, Liverpool, L69 3BX, UK*
133. *Cavendish Laboratory, J.J. Thomson Avenue, Cambridge CB3 0HE, UK*
134. *Department of Astronomy and CCAPP, The Ohio State University, 140 W. 18th Ave., Columbus, OH 43210, USA*
135. *Dept. of Physics, Colorado School of Mines, Golden Colorado, 80401 USA*
136. *Department of Physics, Carnegie Mellon University, Pittsburgh, PA 15213, USA*
137. *STFC Rutherford Appleton Laboratory, Didcot, OX11 0QX, UK*
138. *Department of Physics, George Washington University Virginia Campus, Ashburn, VA 20147-2604, USA*
139. *IHEP, Chinese Academy of Sciences, Beijing 100049, P.R. China*
140. *California Institute of Technology, High Energy Physics, MC 256-48, Pasadena, CA 91125, USA*
141. *Novosibirsk State University, Novosibirsk 630090, Russia*
142. *Moscow Institute of Physics and Technology (State University), RU-141700, Dolgoprudny, Moscow region, Russian Federation*

HIGHLIGHTS OF THE 2014 EDITION OF THE REVIEW OF PARTICLE PHYSICS

899 new papers with 3283 new measurements

- Over 330 papers from **LHC** experiments (ATLAS, CMS, and LHCb).
- Extensive **Higgs boson** coverage from 138 papers with 258 measurements.
- **Supersymmetry**: 123 papers with major exclusions, many from LHC experiments.
- **Top quark**: 51 new papers, many from LHC experiments.
- Cosmology reviews updated to include **2013 Planck**.
- Latest from ***B*-meson** physics: 183 papers with 803 measurements, including first observation of $B_s \to \mu^+\mu^-$ from LHCb and CMS.
- Updated and new results in **neutrino mixing** on Δm^2 and mixing angle measurements, including the first Δm^2_{32} result from reactor experiment.
- Final assignment of $\mathbf{1}^{++}$ quantum numbers to the ***X*(3872)** by LHCb.
- Observation of **charmonium-like states** $X(3900)$ and $X(4020)$ (BESIII and BES3).
- Observation of **bottomonium-like states** $X(10620)$ and $X(10650)$ (Belle).
- Heavily revised Atomic-Nuclear Properties website.

112 reviews (most are revised or new)

- **New reviews** on:
  - Higgs Boson Physics
  - Dark Energy
  - Monte Carlo Neutrino Generators
  - Resonances
- **Significant update/revision** to reviews on:
  - The Top Quark
  - Dynamical Electroweak Symmetry Breaking
  - Astrophysical Constants
  - Dark Matter
  - Big-Bang Nucleosynthesis
  - Neutrino Cross Section Measurements
  - Accelerator Physics of Colliders
  - High-Energy Collider Parameters
  - Total Hadronic Cross Sections Plots

See **pdgLive.lbl.gov** for online access to PDG database.

See **pdg.lbl.gov/AtomicNuclearProperties** for Atomic Properties of Materials.

TABLE OF CONTENTS

(Continued on next page.)

PARTICLE LISTINGS*

MAJOR REVIEWS IN THE PARTICLE LISTINGS

*The divider sheets give more detailed indices for each main section of the Particle Listings.

INTRODUCTION

ONLINE PARTICLE PHYSICS INFORMATION

INTRODUCTION

1. Overview

The *Review of Particle Physics* and the abbreviated version, the *Particle Physics Booklet,* are reviews of the field of Particle Physics. This complete *Review* includes a compilation/evaluation of data on particle properties, called the "Particle Listings." These Listings include 3,283 new measurements from 899 papers, in addition to the 32,153 measurements from 8,944 papers that first appeared in previous editions [1].

Both books include Summary Tables with our best values and limits for particle properties such as masses, widths or lifetimes, and branching fractions, as well as an extensive summary of searches for hypothetical particles. In addition, we give a long section of "Reviews, Tables, and Plots" on a wide variety of theoretical and experimental topics, a quick reference for the practicing particle physicist.

The *Review* and the *Booklet* are published in even-numbered years. This edition is an updating through January 2014 (and, in some areas, well into 2014). As described in the section "Online Particle Physics Information" following this introduction, the content of this *Review* is available on the World-Wide Web, and is updated between printed editions (`http://pdg.lbl.gov/`).

The Summary Tables give our best values of the properties of the particles we consider to be well established, a summary of search limits for hypothetical particles, and a summary of experimental tests of conservation laws.

The Particle Listings contain all the data used to get the values given in the Summary Tables. Other measurements considered recent enough or important enough to mention, but which for one reason or another are not used to get the best values, appear separately just beneath the data we do use for the Summary Tables. The Particle Listings also give information on unconfirmed particles and on particle searches, as well as short "reviews" on subjects of particular interest or controversy.

The Particle Listings were once an archive of all published data on particle properties. This is no longer possible because of the large quantity of data. We refer interested readers to earlier editions for data now considered to be obsolete.

We organize the particles into six categories:

Gauge and Higgs bosons
Leptons
Quarks
Mesons
Baryons
Searches for monopoles, supersymmetry, compositeness, extra dimensions, *etc.*

The last category only includes searches for particles that do not belong to the previous groups; searches for heavy charged leptons and massive neutrinos, by contrast, are with the leptons.

In Sec. 2 of this Introduction, we list the main areas of responsibility of the authors, and also list our large number of consultants, without whom we would not have been able to produce this *Review.* In Sec. 4, we mention briefly the naming scheme for hadrons. In Sec. 5, we discuss our procedures for choosing among measurements of particle properties and for obtaining best values of the properties from the measurements.

The accuracy and usefulness of this *Review* depend in large part on interaction between its users and the authors. We appreciate comments, criticisms, and suggestions for improvements of any kind. Please send them to the appropriate author, according to the list of responsibilities in Sec. 2 below, or to the LBNL addresses below.

To order a copy of the *Review* or the *Particle Physics Booklet* from North and South America, Australia, and the Far East, send email to `PDG@LBL.GOV`

or via the web at:
`http://pdg.lbl.gov/pdgmail`

or write to:
Particle Data Group, MS 50R6008
Lawrence Berkeley National Laboratory
Berkeley, CA 94720-8166, USA

From all other areas email `library.desk@cern.ch`

or via the web at:
`http://pdg.lbl.gov/pdgmail`

or write to
CERN Scientific Information Service
CH-1211 Geneva 23, Switzerland

2. Particle Listings responsibilities

* Asterisk indicates the people to contact with questions or comments about Particle Listings sections.

Gauge and Higgs bosons

γ	C. Grab, D.E. Groom*
Gluons	R.M. Barnett,* A.V. Manohar
Graviton	D.E. Groom*
W, Z	A. Gurtu,* M. Grünewald*
Higgs bosons	K. Hikasa, G. Weiglein*
Heavy bosons	H.E. Haber,* M. Tanabashi
Axions	K.A. Olive, F. Takahashi, G. Raffelt*

Leptons

Neutrinos	M. Goodman, C.-J. Lin,* K. Nakamura, K.A. Olive, A. Piepke, P. Vogel
e, μ	C. Grab, C.-J. Lin*
τ	K.G. Hayes, K. Mönig*

Quarks

Quarks	R.M. Barnett,* A.V. Manohar
Top quark	K. Hagiwara, W.-M. Yao*
b', t'	K. Hagiwara, W.-M. Yao*
Free quark	J. Beringer*

Mesons

π, η	J. Beringer,* C. Grab
Unstable mesons	C. Amsler, M. Doser,* S. Eidelman,* T. Gutsche, C. Hanhart, B. Heltsley, J.J. Hernández-Rey, A. Masoni, S. Navas, C. Patrignani, S. Spanier, N.A. Törnqvist, G. Venanzoni
K (stable)	G. D'Ambrosio, C.-J. Lin*
D (stable, no mix.)	J. Rademacker, C.G. Wohl*
D^0 mixing	D.M. Asner, W.-M. Yao*

Baryons

B (stable)	M. Kreps, Y. Kwon, J.G. Smith, W.-M. Yao*
Stable baryons	C. Grab, C.G. Wohl*
Unstable baryons	V. Burkert, E. Klempt, M. Pennington, L. Tiator, R.L. Workman*
Charmed baryons	J. Rademacker, C.G. Wohl*
Bottom baryons	M. Kreps, Y. Kwon, J.G. Smith, W.-M. Yao*

Miscellaneous searches

Monopole	D. Milstead*
Supersymmetry	H.K. Dreiner,* A. de Gouvêa, F. Moortgat, K.A. Olive
Technicolor	K. Agashe,* M. Tanabashi
Compositeness	M. Tanabashi, J. Terning*
Extra Dimensions	T. Gherghetta, H.E. Haber*,
WIMPs and Other	K. Hikasa,*

3. Consultants

The Particle Data Group benefits greatly from the assistance of some 700 physicists who are asked to verify every piece of data entered into this *Review*. Of special value is the advice of the PDG Advisory Committee which meets biennially and thoroughly reviews all aspects of our operation. The members of the 2014 committee are:

D. Harris (FNAL)
T. Carli (CERN)
L. Hall (UC Berkeley)
J. Olson (Princeton)
A. Slosar (BNL)
J. Tanaka (Tokyo)

We have especially relied on the expertise of the following people for advice on particular topics:

- S.I. Alekhin (COMPAS Group, IHEP, Protvino)
- B. Allanach (U. of Cambridge)
- C. Andreopoulos (STFC Rutherford Appleton Lab.)
- H. An (Perimeter Institute)
- F. Anulli (INFN, Rome)
- M. Artuso (Syracuse University)
- R. Barbieri (SNS and INFN, Pisa)
- M. Bardeen (FNAL)
- W. Barletta (MIT)
- J. Bernabeu (University of Valencia)
- F. Bernlochner (University of Victoria)
- W. Bertl (PSI)
- C. Bozzi(INFN, Ferrara)
- T. Browder (University of Hawaii)
- O. Bruening (CERN)
- G. Castelo-Branco (Techn. U. of Lisboa)
- F. Cavanna (Yale University)
- S. Centro (INFN, Padua)
- F. Cerutti (LBNL)
- G. Colangelo (University of Bern)
- J. Conway (UC Davis)
- K. Cranmer (NYU)
- C. Csaki (Cornell U.)
- D. Denisov (FNAL)
- D. d'Enterria (CERN)
- M. Dine (UCSC)
- J. Dingfelder (Bonn, Germany)
- M. D'Onofrio (U. of Liverpool)
- S. Dytman (University of Pittsburgh)
- G. Edda (University of Geneva)
- A. Falkowski (U. of Warsaw)
- W. Fischer (BNL)
- P. Gambino (Univ. degli Studi di Torino)
- I. Garcia Irastorza (U. of Zaragoza)
- R. Garisto (PRL)
- M. Gersabeck (Univ. of Manchester)
- C. Giunti (INFN Turin)
- S. Givannella (INFN, Frascati)
- C. Glasman (Madrid)
- B. Golob (Ljubljana, Slovenia)
- E. Goudzovski (U. of Birmingham)
- J. Guy (UPMC, Paris)
- F. Halzen (U. of Wisconsin)
- F. Harris (University of Hawaii)
- S. Heinemeyer (Karlsruhe Inst. of Techn.)
- W. Hollik (Karlsruhe Inst. of Techn.)
- G. Isidori (INFN, Frascati)
- M. Jose Costa (IFIC Valencia)
- J. Jowett (CERN)
- S.G. Karshenboim (MPQ, Pulkovo Obs., Russia)
- E. Kearns T (Boston University)
- M. Klein (University of Liverpool)
- T. Kobayashi (KEK)
- P. Koppenburg (CERN)
- A. Korytov (U. of Florida)
- T. Koseki (University of Tokyo)
- W. Kozanecki (Saclay)
- A. Kronfeld (FNAL)
- O. Leroy (CPPM, Marseille)
- E.B. Levichev (BINP, Novosibirsk)
- E. Linder (LBNL)
- D. London (University of Montreal)
- P. Lukens (FNAL)
- L. Malgeri (CERN)
- S. Martin (Northern Illinois U.)
- C. Milardi (INFN, Frascati)
- P.J. Mohr (NIST)
- S. Monteil (LPC Clermont)
- U. Mosel (University of Giessen)
- M. Mulders (CERN)
- B. Murray (U. of Warwick)
- T. Nakadaira (KEK)
- H. O'Connell (FNAL)
- Y. Ohnishi (KEK, Japan)
- K. Oide (KEK)
- J. Paul Chou (Rutgers U.)
- A. Pich (Valencia)
- A. Pierce (U. of Michigan)
- L. Pillonen (Virginia Tech)
- R.K. Plunkett (FNAL)
- M. Redi (Stony Brook U.)
- B.L. Roberts (Boston University)
- M. Ross (FNAL)
- M. Rotondo (Padova, INFN)
- B. Sadoulet (UC Berkeley)
- N. Saito (KEK)

- J.E. Sansonetti (NIST)
- C. Schwanda (HEPHY, Vienna)
- A.J. Schwartz (University of Cincinnati)
- J.T. Seeman (SLAC)
- K.K. Seth (Northwestern U.)
- V. Sharyy (CEA)
- Yu.M. Shatunov (BINP, Novosibirsk)
- P. Sikivie (U. of Florida)
- J. Sobczyk (Wroclaw University)
- M. Spira (PSI, Villigen)
- S. Stapnes (CERN)
- S.I. Striganov (FNAL)
- R. Tanaka (LAL, Orsay)
- A. Tapper (Imperial College London)
- X. Tata (U. of Hawaii)
- R. Tesarek (FNAL)
- D. Torigo (Padova and INFN)
- K. Trabelsi (KEK)
- C. van Eldik (U. Erlangen-Nürnberg, MPI)
- R. Van Kooten (Indiana University)
- J. van Tilburg (Nikhef)
- G. Velev (FNAL)
- K. Vellidis (FNAL)
- M. Whalley (Durham U.)
- S. Willocq (U. of Massachusetts, Amherst)
- C.Z. Yuan (IHEP, Beijing)
- D. Zerwas (LAL, Orsay)
- R. Zwaska (FNAL)

4. Naming scheme for hadrons

We introduced in the 1986 edition [2] a new naming scheme for the hadrons. Changes from older terminology affected mainly the heavier mesons made of u, d, and s quarks. Otherwise, the only important change to known hadrons was that the $F^{\pm}$ became the $D_s^{\pm}$. None of the lightest pseudoscalar or vector mesons changed names, nor did the $c\overline{c}$ or $b\overline{b}$ mesons (we do, however, now use χ_c for the $c\overline{c}$ χ states), nor did any of the established baryons. The Summary Tables give both the new and old names whenever a change has occurred.

The scheme is described in "Naming Scheme for Hadrons" (p. 120) of this *Review*.

We give here our conventions on type-setting style. Particle symbols are italic (or slanted) characters: e^-, p, Λ, π^0, K_L, D_s^+, b. Charge is indicated by a superscript: B^-, Δ^{++}. Charge is not normally indicated for p, n, or the quarks, and is optional for neutral isosinglets: η or η^0. Antiparticles and particles are distinguished by charge for charged leptons and mesons: τ^+, K^-. Otherwise, distinct antiparticles are indicated by a bar (overline): $\overline{\nu}_\mu$, $\overline{t}$, $\overline{p}$, $\overline{K}^0$, and $\overline{\Sigma}^+$ (the antiparticle of the Σ^-).

5. Procedures

5.1. ***Selection and treatment of data*** : The Particle Listings contain all relevant data known to us that are published in journals. With very few exceptions, we do not include results from preprints or conference reports. Nor do we include data that are of historical importance only (the Listings are not an archival record). We search every volume of 20 journals through our cutoff date for relevant data. We also include later published papers that are sent to us by the authors (or others).

In the Particle Listings, we clearly separate measurements that are used to calculate or estimate values given in the Summary Tables from measurements that are not used. We give explanatory comments in many such cases. Among the reasons a measurement might be excluded are the following:

- It is superseded by or included in later results.
- No error is given.
- It involves assumptions we question.
- It has a poor signal-to-noise ratio, low statistical significance, or is otherwise of poorer quality than other data available.
- It is clearly inconsistent with other results that appear to be more reliable. Usually we then state the criterion, which sometimes is quite subjective, for selecting "more reliable" data for averaging. See Sec. 5.4.
- It is not independent of other results.
- It is not the best limit (see below).
- It is quoted from a preprint or a conference report.

In some cases, *none* of the measurements is entirely reliable and no average is calculated. For example, the masses of many of the baryon resonances, obtained from partial-wave analyses, are quoted as estimated ranges thought to probably include the true values, rather than as averages with errors. This is discussed in the Baryon Particle Listings.

For upper limits, we normally quote in the Summary Tables the strongest limit. We do not average or combine upper limits except in a very few cases where they may be re-expressed as measured numbers with Gaussian errors.

As is customary, we assume that particle and antiparticle share the same spin, mass, and mean life. The Tests of Conservation Laws table, following the Summary Tables, lists tests of CPT as well as other conservation laws.

We use the following indicators in the Particle Listings to tell how we get values from the tabulated measurements:

- OUR AVERAGE—From a weighted average of selected data.
- OUR FIT—From a constrained or overdetermined multi-parameter fit of selected data.
- OUR EVALUATION—Not from a direct measurement, but evaluated from measurements of related quantities.
- OUR ESTIMATE—Based on the observed range of the data. Not from a formal statistical procedure.
- OUR LIMIT—For special cases where the limit is evaluated by us from measured ratios or other data. Not from a direct measurement.

An experimentalist who sees indications of a particle will of course want to know what has been seen in that region in the past. Hence we include in the Particle Listings all

reported states that, in our opinion, have sufficient statistical merit and that have not been disproved by more reliable data. However, we promote to the Summary Tables only those states that we feel are well established. This judgment is, of course, somewhat subjective and no precise criteria can be given. For more detailed discussions, see the minireviews in the Particle Listings.

5.2. ***Averages and fits*** : We divide this discussion on obtaining averages and errors into three sections: (1) treatment of errors; (2) unconstrained averaging; (3) constrained fits.

5.2.1. *Treatment of errors:* In what follows, the "error" δx means that the range $x \pm \delta x$ is intended to be a 68.3% confidence interval about the central value x. We treat this error as if it were Gaussian. Thus when the error *is* Gaussian, δx is the usual one standard deviation (1σ). Many experimenters now give statistical and systematic errors separately, in which case we usually quote both errors, with the statistical error first. For averages and fits, we then add the the two errors in quadrature and use this combined error for δx.

When experimenters quote asymmetric errors $(\delta x)^+$ and $(\delta x)^-$ for a measurement x, the error that we use for that measurement in making an average or a fit with other measurements is a continuous function of these three quantities. When the resultant average or fit $\overline{x}$ is less than $x-(\delta x)^-$, we use $(\delta x)^-$; when it is greater than $x+(\delta x)^+$, we use $(\delta x)^+$. In between, the error we use is a linear function of x. Since the errors we use are functions of the result, we iterate to get the final result. Asymmetric output errors are determined from the input errors assuming a linear relation between the input and output quantities.

In fitting or averaging, we usually do not include correlations between different measurements, but we try to select data in such a way as to reduce correlations. Correlated errors are, however, treated explicitly when there are a number of results of the form $A_i \pm \sigma_i \pm \Delta$ that have identical systematic errors Δ. In this case, one can first average the $A_i \pm \sigma_i$ and then combine the resulting statistical error with Δ. One obtains, however, the same result by averaging $A_i \pm (\sigma_i^2 + \Delta_i^2)^{1/2}$, where $\Delta_i = \sigma_i \Delta [\sum (1/\sigma_j^2)]^{1/2}$. This procedure has the advantage that, with the modified systematic errors Δ_i, each measurement may be treated as independent and averaged in the usual way with other data. Therefore, when appropriate, we adopt this procedure. We tabulate Δ and invoke an automated procedure that computes Δ_i before averaging and we include a note saying that there are common systematic errors.

Another common case of correlated errors occurs when experimenters measure two quantities and then quote the two and their difference, *e.g.*, m_1, m_2, and $\Delta = m_2 - m_1$. We cannot enter all of m_1, m_2 and Δ into a constrained fit because they are not independent. In some cases, it is a good approximation to ignore the quantity with the largest error and put the other two into the fit. However, in some cases correlations are such that the errors on m_1, m_2 and Δ are comparable and none of the three values can be ignored. In this case, we put all three values into the fit and invoke an automated procedure to increase the errors prior to fitting such that the three quantities can be treated as independent measurements in the constrained fit. We include a note saying that this has been done.

5.2.2. *Unconstrained averaging:* To average data, we use a standard weighted least-squares procedure and in some cases, discussed below, increase the errors with a "scale factor." We begin by assuming that measurements of a given quantity are uncorrelated, and calculate a weighted average and error as

$$\overline{x} \pm \delta\overline{x} = \frac{\sum_i w_i\, x_i}{\sum_i w_i} \pm \left(\sum_i w_i\right)^{-1/2} , \qquad (1)$$

where

$$w_i = 1/(\delta x_i)^2 .$$

Here x_i and δx_i are the value and error reported by the ith experiment, and the sums run over the N experiments. We then calculate $\chi^2 = \sum w_i(\overline{x} - x_i)^2$ and compare it with $N-1$, which is the expectation value of χ^2 if the measurements are from a Gaussian distribution.

If $\chi^2/(N-1)$ is less than or equal to 1, and there are no known problems with the data, we accept the results.

If $\chi^2/(N-1)$ is very large, we may choose not to use the average at all. Alternatively, we may quote the calculated average, but then make an educated guess of the error, a conservative estimate designed to take into account known problems with the data.

Finally, if $\chi^2/(N-1)$ is greater than 1, but not greatly so, we still average the data, but then also do the following:

(a) We increase our quoted error, $\delta\overline{x}$ in Eq. (1), by a scale factor S defined as

$$S = \left[\chi^2/(N-1)\right]^{1/2} . \qquad (2)$$

Our reasoning is as follows. The large value of the χ^2 is likely to be due to underestimation of errors in at least one of the experiments. Not knowing which of the errors are underestimated, we assume they are all underestimated by the same factor S. If we scale up all the input errors by this factor, the χ^2 becomes $N-1$, and of course the output error $\delta\overline{x}$ scales up by the same factor. See Ref. 3.

When combining data with widely varying errors, we modify this procedure slightly. We evaluate S using only the experiments with smaller errors. Our cutoff or ceiling on δx_i is arbitrarily chosen to be

$$\delta_0 = 3N^{1/2}\, \delta\overline{x} ,$$

where $\delta\overline{x}$ is the unscaled error of the mean of all the experiments. Our reasoning is that although the low-precision experiments have little influence on the values $\overline{x}$ and $\delta\overline{x}$, they can make significant contributions to the χ^2, and the contribution of the high-precision experiments thus tends to be obscured. Note that if each experiment has the same error δx_i, then $\delta\overline{x}$ is $\delta x_i/N^{1/2}$, so each δx_i is well below the cutoff. (More often, however, we simply exclude measurements with relatively large errors from averages and fits: new, precise data chase out old, imprecise data.)

Our scaling procedure has the property that if there are two values with comparable errors separated by much more than their stated errors (with or without a number of other values of lower accuracy), the scaled-up error $\delta\,\overline{x}$ is approximately half the interval between the two discrepant values.

We emphasize that our scaling procedure for *errors* in no way affects central values. And if you wish to recover the unscaled error $\delta\overline{x}$, simply divide the quoted error by S.

(b) If the number M of experiments with an error smaller than δ_0 is at least three, and if $\chi^2/(M-1)$ is greater than 1.25, we show in the Particle Listings an ideogram of the data. Figure 1 is an example. Sometimes one or two data points lie apart from the main body; other times the data split into two or more groups. We extract no numbers from these ideograms; they are simply visual aids, which the reader may use as he or she sees fit.

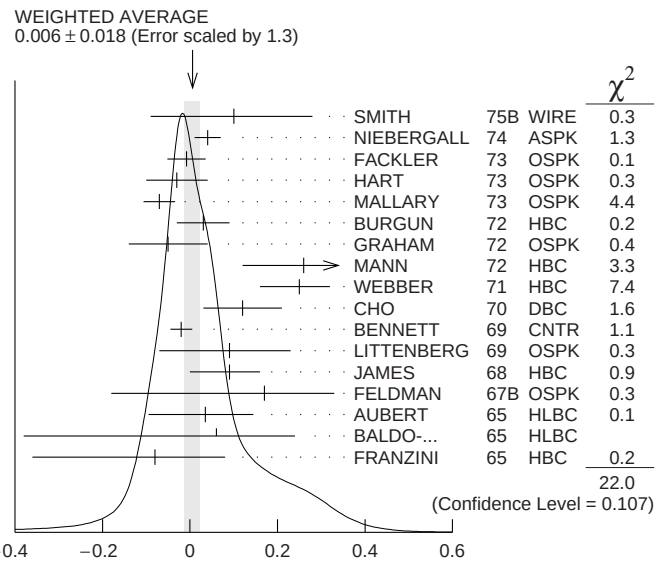

Figure 1: A typical ideogram. The arrow at the top shows the position of the weighted average, while the width of the shaded pattern shows the error in the average after scaling by the factor S. The column on the right gives the χ^2 contribution of each of the experiments. Note that the next-to-last experiment, denoted by the incomplete error flag ($\perp$), is not used in the calculation of S (see the text).

Each measurement in an ideogram is represented by a Gaussian with a central value x_i, error δx_i, and area proportional to $1/\delta x_i$. The choice of $1/\delta x_i$ for the area is somewhat arbitrary. With this choice, the center of gravity of the ideogram corresponds to an average that uses weights $1/\delta x_i$ rather than the $(1/\delta x_i)^2$ actually used in the averages. This may be appropriate when some of the experiments have seriously underestimated systematic errors. However, since for this choice of area the height of the Gaussian for each measurement is proportional to $(1/\delta\, x_i)^2$, the peak position of the ideogram will often favor the high-precision measurements at least as much as does the least-squares average. See our 1986 edition [2] for a detailed discussion of the use of ideograms.

5.2.3. *Constrained fits:* In some cases, such as branching ratios or masses and mass differences, a constrained fit may be needed to obtain the best values of a set of parameters. For example, most branching ratios and rate measurements are analyzed by making a simultaneous least-squares fit to all the data and extracting the partial decay fractions P_i, the partial widths Γ_i, the full width Γ (or mean life), and the associated error matrix.

Assume, for example, that a state has m partial decay fractions P_i, where $\sum P_i = 1$. These have been measured in N_r different ratios R_r, where, e.g., $R_1 = P_1/P_2$, $R_2 = P_1/P_3$, *etc.* [We can handle any ratio R of the form $\sum \alpha_i P_i / \sum \beta_i P_i$, where α_i and β_i are constants, usually 1 or 0. The forms $R = P_i P_j$ and $R = (P_i P_j)^{1/2}$ are also allowed.] Further assume that *each* ratio R has been measured by N_k experiments (we designate each experiment with a subscript k, e.g., R_{1k}). We then find the best values of the fractions P_i by minimizing the χ^2 as a function of the $m-1$ independent parameters:

$$\chi^2 = \sum_{r=1}^{N_r} \sum_{k=1}^{N_k} \left(\frac{R_{rk} - R_r}{\delta R_{rk}} \right)^2 , \qquad (3)$$

where the R_{rk} are the measured values and R_r are the fitted values of the branching ratios.

In addition to the fitted values $\overline{P}_i$, we calculate an error matrix $\langle \delta\overline{P}_i \ \delta\overline{P}_j \rangle$. We tabulate the diagonal elements of $\delta\,\overline{P}_i = \langle \delta\,\overline{P}_i \ \delta\,\overline{P}_i \rangle^{1/2}$ (except that some errors are scaled as discussed below). In the Particle Listings, we give the complete correlation matrix; we also calculate the fitted value of each ratio, for comparison with the input data, and list it above the relevant input, along with a simple unconstrained average of the same input.

Three comments on the example above:

(1) There was no connection assumed between measurements of the full width and the branching ratios. But often we also have information on partial widths Γ_i as well as the total width Γ. In this case we must introduce Γ as a parameter in the fit, along with the P_i, and we give correlation matrices for the widths in the Particle Listings.

(2) We try to pick those ratios and widths that are as independent and as close to the original data as possible. When one experiment measures all the branching fractions and constrains their sum to be one, we leave one of them (usually the least well-determined one) out of the fit to make the set of input data more nearly independent. We now do allow for correlations between input data.

(3) We calculate scale factors for both the R_r and P_i when the measurements for any R give a larger-than-expected contribution to the χ^2. According to Eq. (3), the double sum for χ^2 is first summed over experiments $k = 1$ to N_k, leaving a single sum over ratios $\chi^2 = \sum \chi^2_r$. One is tempted to define a scale factor for the ratio r as $S_r^2 = \chi^2_r / \langle \chi^2_r \rangle$. However, since $\langle \chi^2_r \rangle$ is not a fixed quantity (it is somewhere between N_k and N_{k-1}), we do not know how to evaluate this expression. Instead we define

$$S_r^2 = \frac{1}{N_k} \sum_{k=1}^{N_k} \frac{\left(R_{rk} - \overline{R}_r\right)^2}{\langle (R_{rk} - \overline{R}_r)^2 \rangle}. \qquad (4)$$

With this definition the expected value of S_r^2 is one. We can show that

$$\langle (R_{rk} - \overline{R}_r)^2 \rangle = \langle (\delta R_{rk})^2 \rangle - (\delta \overline{R}_r)^2 , \qquad (5)$$

where $\delta\overline{R}_r$ is the fitted error for ratio r.

The fit is redone using errors for the branching ratios that are scaled by the larger of S_r and unity, from which new and often larger errors $\delta\overline{P}_i{}'$ are obtained. The scale factors we finally list in such cases are defined by $S_i = \delta\overline{P}_i{}'/\delta\overline{P}_i$. However, in line with our policy of not letting S affect the central values, we give the values of $\overline{P}_i$ obtained from the original (unscaled) fit.

There is one special case in which the errors that are obtained by the preceding procedure may be changed. When a fitted branching ratio (or rate) $\overline{P}_i$ turns out to be less than three standard deviations ($\delta\overline{P}_i'$) from zero, a new smaller error $(\delta\overline{P}_i'')^-$ is calculated on the low side by requiring the area under the Gaussian between $\overline{P}_i - (\delta\overline{P}_i'')^-$ and $\overline{P}_i$ to be 68.3% of the area between zero and $\overline{P}_i$. A similar correction is made for branching fractions that are within three standard deviations of one. This keeps the quoted errors from overlapping the boundary of the physical region.

5.3. ***Rounding*** : While the results shown in the Particle Listings are usually exactly those published by the experiments, the numbers that appear in the Summary Tables (means, averages and limits) are subject to a set of rounding rules.

The basic rule states that if the three highest order digits of the error lie between 100 and 354, we round to two significant digits. If they lie between 355 and 949, we round to one significant digit. Finally, if they lie between 950 and 999, we round up to 1000 and keep two significant digits. In all cases, the central value is given with a precision that matches that of the error. So, for example, the result (coming from an average) 0.827 ± 0.119 would appear as 0.83 ± 0.12, while 0.827 ± 0.367 would turn into 0.8 ± 0.4.

Rounding is not performed if a result in a Summary Table comes from a single measurement, without any averaging. In that case, the number of digits published in the original paper is kept, unless we feel it inappropriate. Note that, even for a single measurement, when we combine statistical and systematic errors in quadrature, rounding rules apply to the result of the combination. It should be noted also that most of the limits in the Summary Tables come from a single source (the best limit) and, therefore, are not subject to rounding.

Finally, we should point out that in several instances, when a group of results come from a single fit to a set of data, we have chosen to keep two significant digits for all the results. This happens, for instance, for several properties of the W and Z bosons and the τ lepton.

5.4. ***Discussion*** : The problem of averaging data containing discrepant values is nicely discussed by Taylor in Ref. 4. He considers a number of algorithms that attempt to incorporate inconsistent data into a meaningful average. However, it is difficult to develop a procedure that handles simultaneously in a reasonable way two basic types of situations: (a) data that lie apart from the main body of the data are incorrect (contain unreported errors); and (b) the opposite—it is the main body of data that is incorrect. Unfortunately, as Taylor shows, case (b) is not infrequent. He concludes that the choice of procedure is less significant than the initial choice of data to include or exclude.

We place much emphasis on this choice of data. Often we solicit the help of outside experts (consultants). Sometimes, however, it is simply impossible to determine which of a set of discrepant measurements are correct. Our scale-factor technique is an attempt to address this ignorance by increasing the error. In effect, we are saying that present experiments do not allow a precise determination of this quantity because of unresolvable discrepancies, and one must await further measurements. The reader is warned of this situation by the size of the scale factor, and if he or she desires can go back to the literature (via the Particle Listings) and redo the average with a different choice of data.

Our situation is less severe than most of the cases Taylor considers, such as estimates of the fundamental constants like $\hbar$, *etc.* Most of the errors in his case are dominated by systematic effects. For our data, statistical errors are often at least as large as systematic errors, and statistical errors are usually easier to estimate. A notable exception occurs in partial-wave analyses, where different techniques applied to the same data yield different results. In this case, as stated earlier, we often do not make an average but just quote a range of values.

A brief history of early Particle Data Group averages is given in Ref. 3. Figure 2 shows some histories of our values of a few particle properties. Sometimes large changes occur. These usually reflect the introduction of significant new data or the discarding of older data. Older data are discarded in favor of newer data when it is felt that the newer data have smaller systematic errors, or have more checks on systematic errors, or have made corrections unknown at the time of the older experiments, or simply have much smaller errors. Sometimes, the scale factor becomes large near the time at which a large jump takes place, reflecting the uncertainty introduced by the new and inconsistent data. By and large, however, a full scan of our history plots shows a dull progression toward greater precision at central values quite consistent with the first data points shown.

We conclude that the reliability of the combination of experimental data and our averaging procedures is usually good, but it is important to be aware that fluctuations outside of the quoted errors can and do occur.

ACKNOWLEDGMENTS

The publication of the *Review of Particle Physics* is supported by the Director, Office of Science, Office of High Energy Physics of the U.S. Department of Energy under Contract No. DE–AC02–05CH11231; by the U.S. National Science Foundation under Agreement No. PHY-0652989; by the European Laboratory for Particle Physics (CERN); by an implementing arrangement between the governments of Japan (MEXT: Ministry of Education, Culture, Sports, Science and Technology) and the United States (DOE) on cooperative research and development; and by the Italian National Institute of Nuclear Physics (INFN).

We thank all those who have assisted in the many phases of preparing this *Review*. We particularly thank the many who have responded to our requests for verification of data entered in the Listings, and those who have made suggestions or pointed out errors.

REFERENCES

1. The previous edition was Particle Data Group: J. Beringer *et al.*, Phys. Rev. **D86**, 010001 (2012).
2. Particle Data Group: M. Aguilar-Benitez *et al.*, Phys. Lett. **170B** (1986).
3. A.H. Rosenfeld, Ann. Rev. Nucl. Sci. **25**, 555 (1975).
4. B.N. Taylor, "Numerical Comparisons of Several Algorithms for Treating Inconsistent Data in a Least-Squares Adjustment of the Fundamental Constants," U.S. National Bureau of Standards NBSIR 81-2426 (1982).

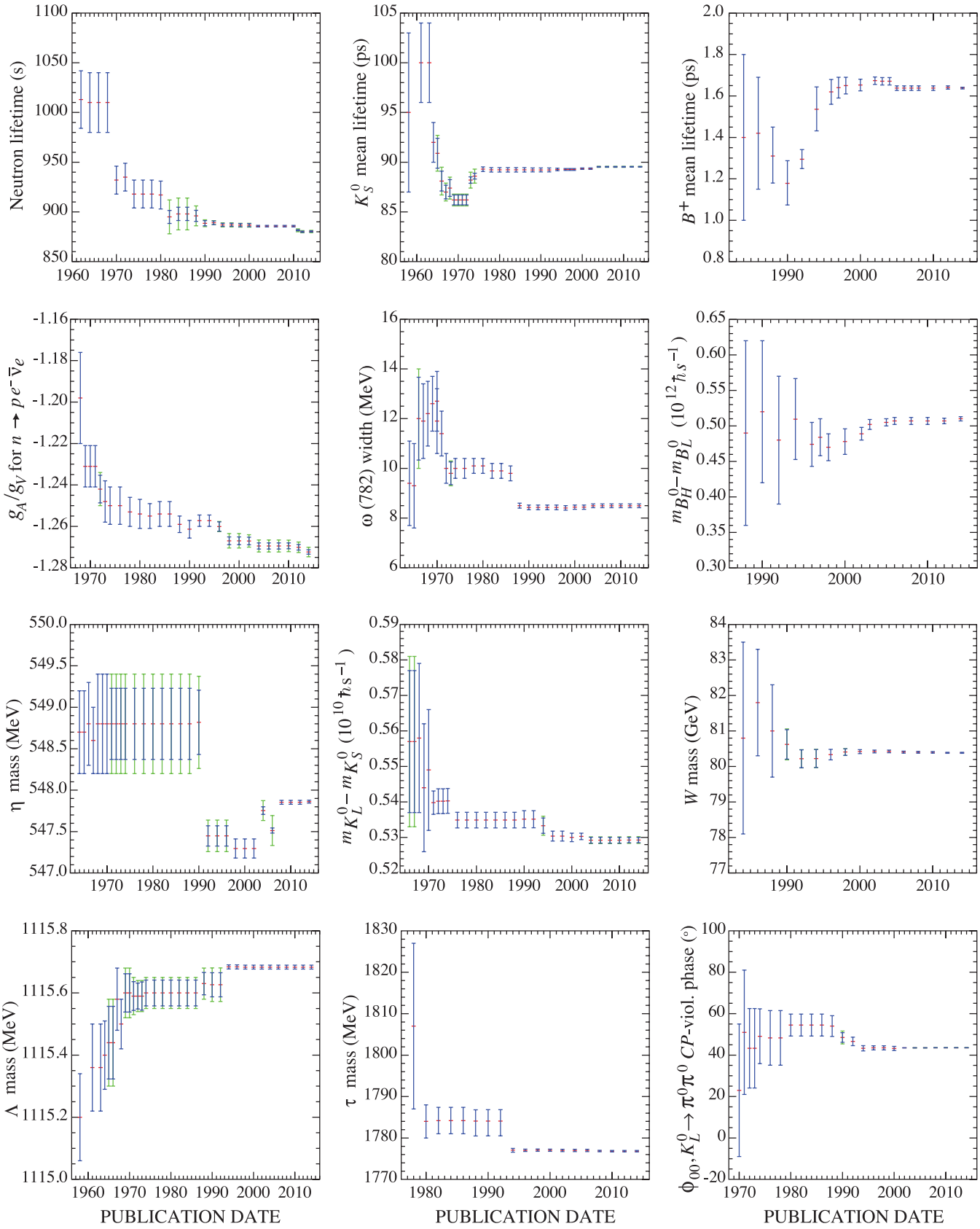

Figure 2: A historical perspective of values of a few particle properties tabulated in this *Review* as a function of date of publication of the *Review*. A full error bar indicates the quoted error; a thick-lined portion indicates the same but without the "scale factor."

ONLINE PARTICLE PHYSICS INFORMATION

Updated Nov. 2013 by T. Basaglia (CERN), A. Holtkamp (CERN).†

1. Introduction

The collection of online information resources in particle physics and related areas presented in this chapter is of necessity incomplete. An expanded and regularly updated online version can be found at:

`http://library.web.cern.ch/particle_physics_information`

Suggestions for additions and updates are very welcome.†

2. Particle Data Group (PDG) resources

- **Review of Particle Physics (RPP)** A comprehensive report on the fields of particle physics and related areas of cosmology and astrophysics, including both review articles and a compilation/evaluation of data on particle properties. The review section includes articles, tables and plots on a wide variety of theoretical and experimental topics of interest to particle physicists and astrophysicists. The particle properties section provides tables of published measurements as well as the Particle Data Groups best values and limits for particle properties such as masses, widths, lifetimes, and branching fractions, and an extensive summary of searches for hypothetical particles. RPP is published as a 1500-page book every two years, with partial updates made available once each year on the web.

  All the contents of the book version of RPP are available online:

  `http://pdg.lbl.gov`

  The printed book can be ordered:

  `http://pdg.lbl.gov/2013/html/receive_our_products.html`

  Of historical interest is the complete RPP collection which can be found online:

  `http://library.web.cern.ch/PDG_publications/review_particle_physics`

- **Particle Physics booklet:** An abridged version of the Review of Particle Physics available as a pocket-sized 300-page booklet. Although produced in print and available online only as a PDF file, the booklet is included in this guide because it is one of the most useful summaries of physics data. The booklet contains an abbreviated set of reviews and the summary tables from the most recent edition of the Review of Particle Physics.

  The PDF file of the booklet can be downloaded:

  `http://pdg.lbl.gov/current/booklet.pdf`

  The printed booklet can be ordered:

  `http://pdg.lbl.gov/2013/html/receive_our_products.html`

- **PDGLive:** A web application for browsing the contents of the PDG database that contains the information published in the Review of Particle Physics. It allows one to navigate to a particle of interest, see a summary of the information available, and then proceed to the detailed information published in the Review of Particle Physics. Data entries are directly linked to the corresponding bibliographic information in INSPIRE.

  `http://pdglive.lbl.gov`

- **Computer-readable files:** Data files that can be downloaded from PDG include tables of particle masses and widths, PDG Monte Carlo particle numbers, and cross-section data. The files are updated with each new edition of the Review of Particle Physics.

  `http://pdg.lbl.gov/current/html/computer_read.html`

3. Particle Physics Information Platforms

- **INSPIRE:** The time-honored SPIRES database suite has in November 2011 been replaced by INSPIRE, which combines the most successful aspects of SPIRES - like comprehensive content and high-quality metadata - with the modern technology of Invenio, the CERN open-source digital-library software, offering major improvements like increased speed and Google-like free-text search syntax. INSPIRE serves as one-stop information platform for the particle physics community, comprising 7 interlinked databases on literature, conferences, institutions, journals, researchers, experiments, jobs. INSPIRE is jointly developed and maintained by CERN, DESY, Fermilab and SLAC. Close interaction with the user community and with arXiv, ADS, HepData, PDG and publishers is the backbone of INSPIRE's evolution.

  `http://inspirehep.net/`

  More information on this project at:

  `http://inspirehep.net/info/general/project/index`

  `blog: http://blog.inspirehep.net/`

  `twitter: @inspirehep`

4. Literature Databases

- **ADS:** The SAO/NASA Astrophysics Data System is a Digital Library portal for researchers in Astronomy and Physics, operated by the Smithsonian Astrophysical Observatory (SAO) under a NASA grant. The ADS maintains three bibliographic databases containing more than 9.3 million records: Astronomy and Astrophysics, Physics, and arXiv e-prints. The main body of data in the ADS consists of bibliographic records, which are searchable through highly customizable query forms, and full-text scans of much of the astronomical literature which can be browsed or searched via a full-text search interface. Integrated in its databases, the ADS provides access and pointers to a wealth of external resources, including electronic articles, data catalogs and archives. In addition, ADS provides the myADS Update Service, a free custom notification service promoting current awareness of the recent literature in astronomy and physics based on each individual subscriber's queries.

  `http://adswww.harvard.edu/`

- **arXiv.org:** A repository of full text papers in physics, mathematics, computer science, statistics, nonlinear sciences, quantitative finance and quantitative biology interlinked with ADS and INSPIRE. Papers are usually sent by their authors to arXiv in advance of submission to a journal for publication. Primarily covers 1991 to the present but authors are encouraged to post older papers retroactively. Permits searching by author, title, and words in

† Please send comments and corrections to `Annette.Holtkamp@cern.ch`.

abstract and experimentally also in the fulltext. Allows limiting by subfield archive or by date.

`http://arXiv.org`

- **CDS:** The CERN Document Server contains records of more than 1,000,000 CERN and non-CERN articles, preprints, theses. It includes records for internal and technical notes, official CERN committee documents, and multimedia objects. CDS is going to focus on its role as institutional repository covering all CERN material from the early 50s and reflecting the holdings of the CERN library. Non-CERN particle and accelerator physics content is in the process of being exported to INSPIRE.

  `http://cds.cern.ch`

- **INSPIRE HEP:** The HEP collection, the flagship of the INSPIRE suite, serves more than 1 million bibliographic records with a growing number of fulltexts attached and metadata including author affiliations, abstracts, references, keywords as well as links to arXiv, ADS, PDG, HepData and publisher platforms. It provides fast metadata and fulltext searches, plots extracted from fulltext, author disambiguation, author profile pages and citation analysis and is expanding its content to, e.g., experimental notes.

  `http://inspirehep.net`

- **JACoW:** The Joint Accelerator Conference Website publishes the proceedings of APAC, EPAC, PAC, IPAC, ABDW, BIW, COOL, CYCLOTRONS, DIPAC, ECRIS, FEL, HIAT, ICALEPCS, IBIC, ICAP, LINAC, North American PAC, PCaPAC, RuPAC, SRF. A custom interface allows searching on keywords, titles, authors, and in the fulltext.

  `http://www.jacow.org/`

- **KISS (KEK Information Service System) for preprints:** The KEK Library preprint and technical report database contains bibliographic records of preprints and technical reports held in the KEK library with links to the full text images of more than 100,000 papers scanned from their worldwide collection of preprints. Particularly useful for older scanned preprints. KISS links are included in INSPIRE HEP.

  `http://www-lib.kek.jp/kiss/kiss_prepri.html`

- **MathSciNet:** This database of over 2.8 million items provides reviews, abstracts and bibliographic information for much of the mathematical sciences literature. Over 100,000 new items are added each year, most of them classified according to the Mathematics Subject Classification. Authors are uniquely identified, enabling a search for publications by individual author. Over 80,000 reviews on the current published literature are added each year. Citation data allows to track the history and influence of research publications.

  `http://www.ams.org/mathscinet`

- **OSTI SciTech Connect:** A portal to free, publicly available DOE-sponsored R&D results including technical reports, bibliographic citations, journal articles, conference papers, books, multimedia anid data information. SciTech Connect is a consolidation of two core DOE search engines, the Information Bridge and the Energy Citations Database. SciTech Connect incorporates all of the R&D information from these two products into one search interface. It includes over 2.5 million citations, including citations to 1.4 million journal articles, 364,000 of which have digital object identifiers (DOIs) linking to full-text articles on publishers' websites. SciTech Connect also has over 313,000 full-text DOE sponsored STI reports; most of these are post-1991, but close to 85,000 of the reports were published prior to 1990.

  `http://www.osti.gov/scitech/`

5. Particle Physics Journals and Conference Proceedings Series

- **CERN Journals List:** This list of journals and conference series publishing particle physics content provides information on Open Access, copyright policies and terms of use.

  `http://library.web.cern.ch/oa/where_publish`

- **INSPIRE Journals:** The database covers more than 3,300 journals publishing HEP-related articles.

  `http://inspirehep.net/collection/journals`

6. Conference Databases

- **INSPIRE Conferences:** The database of more than 19,500 past, present and future conferences, schools, and meetings of interest to high-energy physics and related fields is searchable by title, acronym, series, date, location. Included are information about published proceedings, links to conference contributions in the INSPIRE HEP database, and links to the conference Web site when available. New conferences can be submitted from the entry page.

  `http://inspirehep.net/conferences`

7. Research Institutions

- **INSPIRE Institutions:** The database of more than 10,500 institutes, laboratories, and university departments in which research on particle physics and astrophysics is performed covers six continents and over a hundred countries. Included are address and Web links where available as well as links to the papers from each institution in the HEP database, to scientists listed in HEPNames affiliated to this institution in the past or present and to experiments performed at this institution. Searches can be performed by name, acronym, location, etc. The site offers an alphabetical list by country as well as a list of the top 500 HEP and astrophysics institutions sorted by country.

  `http://inspirehep.net/institutions`

8. People

- **INSPIRE HEPNames:** Searchable worldwide database of over 100,000 people associated with particle physics and related fields. The affiliation history of these researchers, their e-mail addresses, web pages, experiments they participated in, PhD advisor, information on their graduate students and links to their papers in the INSPIRE HEP, arXiv and ADS databases are provided as well as a user interface to update these informations.

  `http://inspirehep.net/hepnames`

9. Experiments

- **INSPIRE Experiments:** Contains more than 2,500 past, present, and future experiments in particle physics. Lists both accelerator and non-accelerator experiments. Includes official experiment name and number, location, and collaboration lists. Simple searches by participant, title, experiment number, institution, date approved, accelerator, or detector, return a description of the experiment, including a complete list of authors, title, overview of the experiment's goals and methods, and a link to the experiment's web page if available. Publication lists distinguish articles in refereed journals, theses, technical or instrumentation papers and those which rank among Topcite at 50 or more citations.

  `http://inspirehep.net/Experiments`

- **Cosmic ray/Gamma ray/Neutrino and similar experiments:** This extensive collection of experimental Web sites is organized by focus of study and also by location. Additional sections link to educational materials, organizations, related Web sites, etc. The site is maintained at the Max Planck Institute for Nuclear Physics, Heidelberg.

  `http://www.mpi-hd.mpg.de/hfm/CosmicRay/CosmicRaySites.html`

10. Jobs

- **AAS Job Register:** The American Astronomical Society publishes once a month graduate, postgraduate, faculty and other positions mainly in astronomy and astrophysics.
  `http://jobregister.aas.org/`
- **APS Careers:** A gateway for physicists, students, and physics enthusiasts to information about physics jobs and careers. Physics job listings, career advice, upcoming workshops and meetings, and career and job related resources provided by the American Physical Society.
  `http://www.aps.org/jobs/`
- **brightrecruits.com:** A recruitment service run by IOP Publishing that connects employers from different industry sectors with jobseekers who have a background in physics and engineering.
  `http://brightrecruits.com/`
- **IOP Careers:** Careers information and resources primarily aimed at university students are provided by the UK Institute of Physics.
  `http://www.iop.org/careers/`
- **INSPIRE HEPJobs:** Lists academic and research jobs in high energy physics, nuclear physics, accelerator physics and astrophysics with the option to post a job or to receive email notices of new job listings. More than 900 jobs are currently listed.
  `http://inspirehep.net/jobs`
- **Physics Today Jobs:** Online recruitment advertising website for Physics Today magazine, published by the American Institute of Physics. Physics Today Jobs is the managing partner of the AIP Career Network, an online job board network for the physical science, engineering, and computing disciplines. 8,000 resumes are currently available, and more than 2,500 jobs were posted in 2012.
  `http://www.physicstoday.org/jobs`

11. Software Repositories

Particle Physics

- **CERNLib:** The CERN Program Library contains a large collection of general purpose libraries and modules offered in both source code and object code forms. It provides programs applicable to a wide range of physics research problems such as general mathematics, data analysis, detectors simulation, data-handling, etc. It also includes links to commercial, free, and other software. Development of this site has been discontinued.
  `http://wwwasd.web.cern.ch/wwwasd/index.html`
- **FastJet:** FastJet is a software package for jet finding in pp and e+e- collisions. It includes fast native implementations of many sequential recombination clustering algorithms, plugins for access to a range of cone jet finders and tools for advanced jet manipulation.
  `http://fastjet.fr/`
- **FermiTools:** Fermilab's software tools program provides a repository of Fermilab- developed software packages of value to the HEP community. Permits searching for packages by title or subject category.
  `http://www.fnal.gov/fermitools/`
- **FreeHEP:** A collection of software and information about software useful in high- energy physics and adjacent disciplines, focusing on open-source software for data analysis and visualization. Searching can be done by title, subject, date acquired, date updated, or by browsing an alphabetical list of all packages.
  `http://www.freehep.org/`
- **GenSer:** The Generator Services project collaborates with Monte Carlo (MC) generators authors and with LHC experiments in order to prepare validated LCG compliant code for both the theoretical and experimental communities at the LHC, sharing the user support duties, providing assistance for the development of the new object-oriented generators and guaranteeing the maintenance of the older packages on the LCG supported platforms. The project consists of the generators repository, validation, HepMC record and MCDB event databases.
  `http://sftweb.cern.ch/generators/`
- **Hepforge:** A development environment for high-energy physics software development projects, in particular housing many event-generator related projects, that offers a ready-made, easy-to-use set of Web based tools, including shell account with up to date development tools, web page hosting, subversion and CVS code management systems, mailing lists, bug tracker and wiki system.
  `http://www.hepforge.org/`
- **QUDA:** Library for performing calculations in lattice QCD on GPUs using NVIDIA's "C for CUDA" API. The current release includes optimized solvers for Wilson, Clover-improved Wilson,Twisted mass, Improved staggered (asqtad or HISQ) and Domain wall fermion actions.
  `http://lattice.github.com/quda/`
- **ROOT:** This framework for data processing in high-energy physics, born at CERN, offers applications to store, access, process, analyze and represent data or perform simulations.
  `http://root.cern.ch/drupal`
- **tmLQCD:** This freely available software suite provides a set of tools to be used in lattice QCD simulations, mainly a (P)HMC implementation for Wilson and Wilson twisted mass fermions and inverter for different versions of the Dirac operator.
  `https://github.com/etmc/tmLQCD`
- **USQCD:** The software suite enables lattice QCD computations to be performed with high performance across a variety of architectures. The page contains links to the project web pages of the individual software modules, as well as to complete lattice QCD application packages which use them.
  `http://usqcd.jlab.org/usqcd-software/`

Astrophysics

- **IRAF:** The Image Reduction and Analysis Facility is a general purpose software system for the reduction and analysis of astronomical data. IRAF is written and supported by the IRAF programming group at the National Optical Astronomy Observatories (NOAO) in Tucson, Arizona.
  `http://iraf.noao.edu/`
- **Starlink:** Starlink was a UK Project supporting astronomical data processing. It was shut down in 2005 but its open-source software continues to be developed at the Joint Astronomy Centre. The software products are a collection of applications and libraries, usually focused on a specific aspect of data reduction or analysis.
  `http://starlink.jach.hawaii.edu/starlink`
- Links to a large number of astronomy software archives are listed at:
  `http://heasarc.nasa.gov/docs/heasarc/astro-update/`

Apps

- **arXiv mobile:** Android app for browsing and searching arXiv.org, and for reading, saving and sharing articles.
  `https://play.google.com/store/apps/details?id=com.commonsware.android.arXiv`
- **arXiv scanner:** Scans downloads folder for pdf files from arXiv. Adds title, authors and summary and makes all this information easily searchable from inside the application.
  `https://play.google.com/store/apps/details?id=com.agio.arxiv.scaner`
- **aNarXiv:** arXiv viewer.
  `https://play.google.com/store/apps/details?id=`

com.nephoapp.anarxiv

- **Scholarley:** Android client for Mendeley. The helper arXiv feeder intercepts pdf downloads from arXiv and sends the pdf link and all metadata to Scholarley.

  https://play.google.com/store/apps/details?id=info.matthewwardrop.scholarley

  https://play.google.com/store/apps/details?id=info.matthewwardrop.scholarley.feeder.arxiv

- **Collider:** This mobile app allows to see data from the ATLAS experiment at the LHC.

  http://collider.physics.ox.ac.uk/

- **LHSee:** This smartphone app allows to see collisions from the Large Hadron Collider.

  http://www2.physics.ox.ac.uk/about-us/outreach/public/lhsee

- **The Particles:** App for Apple iPad, Windows 8 and Microsoft Surface. Allows to browse a wealth of real event images and videos, read popular biographies of each of the particles and explore the A-Z of particle physics with its details and definitions of key concepts, laboratories and physicists. Developed by Science Photo Library in partnership with Prof. Frank Close.

  http://www.sciencephoto.com/apps/particles.html

12. Data repositories

Particle Physics

- **HepData:** The HepData Project, funded by the STFC(UK) and based at the IPPP at Durham University, has for more than 30 years compiled a Reaction Data database, comprising total and differential cross sections, structure functions, fragmentation functions, distributions of jet measures, polarisations, etc from a wide range of particle physics scattering experiments worldwide. It is regularly updated to include the latest data including that from the LHC. HepData and the data therein can also be accessed through Inspire. HepData also provides a series of on-line data reviews on a wide variety of topics with links to the data in the Reaction Database. In addition, HepData hosts a Parton Distribution Function server with an on-line PDF calculator and plotter.

  http://hepdata.cedar.ac.uk/

- **ILDG:** The International Lattice Data Grid is an international organization which provides standards, services, methods and tools that facilitates the sharing and interchange of lattice QCD gauge configurations among scientific collaborations, by uniting their regional data grids. It offers semantic access with local tools to worldwide distributed data.

  http://www.usqcd.org/ildg/

- **MCDB - Monte Carlo Database:** This central database of MC events aims to facilitate communication between Monte-Carlo experts and users of event samples in LHC collaborations. Having these events stored in a public place along with the corresponding documentation allows for direct cross checks of the performances on reference samples.

  http://mcdb.cern.ch/

- **MCPLOTS:** mcplots is a repository of Monte Carlo plots comparing High Energy Physics event generators to a wide variety of available experimental data. The site is supported by the LHC Physics Centre at CERN.

  http://mcplots.cern.ch/

Astrophysics

- **NASA's HEASARC:** The High Energy Astrophysics Science Archive Research Center (HEASARC) is the primary archive for NASA's (and other space agencies') missions dealing with electromagnetic radiation from extremely energetic phenomena ranging from black holes to the Big Bang.

  http://heasarc.gsfc.nasa.gov/

- **LAMBDA @ HEASARC:** This data center for Cosmic Microwave Background research, a merger of the High Energy Astrophysics Science Archive Research Center (HEASARC) and the Legacy Archive for Microwave Background Data Analysis (LAMBDA), provides archive data from NASA missions, software tools, and links to other sites of interest.

  http://lambda.gsfc.nasa.gov/

- The NASA archives provide access to raw and processed datasets from numerous NASA missions.

  Hubble telescope, other missions (UV, optical):

  http://archive.stsci.edu/

  Spitzer telescope, other missions (Infrared):

  http://irsa.ipac.caltech.edu/

  Chandra, Fermi telescopes, other missions:

  http://heasarc.gsfc.nasa.gov/

- **NASA/IPAC Extragalactic Database (NED):** An astronomical database that collates and cross-correlates information on extragalactic objects. It contains their positions, basic data, and names as well as bibliographic references to published papers, and notes from catalogs and other publications. NED supports searches for objects and references, and offers browsing capabilities for abstracts of articles of extragalactic interest.

  http://ned.ipac.caltech.edu/

- **SIMBAD:** The SIMBAD astronomical database provides basic data, cross-identifications, bibliography and measurements for astronomical objects outside the solar system. It can be queried by object name, coordinates and various criteria. Lists of objects and scripts can be submitted.

  http://simbad.u-strasbg.fr/simbad/

- **Virtual Observatory:** The Virtual Observatory provides a suite of resources to query for original data from a large number of archives. Two main tools are provided. One runs queries across multiple databases (such as the SDSS database) and combines the results. The other queries hundreds of archives for all datasets that fall on a particular piece of sky.

  http://www.us-vo.org/

General Physics

- **NIST Physical Measurement Laboratory:** The National Institute of Standards and Technology provides access to physical reference data (physical constants, atomic spectroscopy data, x-ray and gamma-ray data, radiation dosimetry data, nuclear physics data and more) and measurements and calibrations data (dimensional measurements, electromagnetic measurements). The site points to a general interest page, linking to exhibits of the Physical Measurement Laboratory in the NIST Virtual Museum.

  http://physics.nist.gov/

- **Springer Materials - The Landolt-Börnstein Database:** Landolt-Börnstein is a high-quality data collection in all areas of physical sciences and engineering, among others particle physics, electronic structure and transport, magnetism, superconductivity. International experts scan the primary literature in more than 8,000 peer-reviewed journals and evaluate and select the most valid information to be included in the database. It includes more than 100,000 online documents, 1,2 million references, and covers 250,000 chemical substances. The search functionality is freely accessible and the search results are displayed in their context, whereas the full text is secured to subscribers.

  http://www.springermaterials.com/

13. Data preservation

Particle Physics

- **DPHEP:** The efforts to define and coordinate Data Preservation and Long Term Analysis in HEP are coordinated by a study group formed to investigate the issues associated with these activities. The group, DPHEP, was initiated during 2008-2009 and includes all HEP major experiments and labs.

  Details of the organizational structure, the objectives, workshops and publications can be found on the website.

  The group is endorsed by the International Committee for Future Accelerators (ICFA).

  The experiments at colliders: BaBar, Belle, BES-III, Cleo, CDF, D0, H1 and ZEUS and the associated computing centres at SLAC (USA), KEK (Japan), IHEP (China), Jlab (USA), BNL (USA), Fermilab (USA), DESY (Germany), and CERN are all represented in the group. The LHC collabaorations have also joined the initiative in 2011. The participating experiments are in various stages of studying, preparing, or operating long-term data preservation and analysis systems. Technological methods, such as virtualization, and information management tools such as INSPIRE are also helpful in this area of research. Data access policies and outreach in HEP using real data are among the investigative areas of the DPHEP Study Group.

  `http://dphep.org`

Astrophysics

More formal and advanced data preservation activity is ongoing in the field of Experimental Astrophysics, including:

- SDSS

  `http://sdss.org`
- Fermi

  `http://fermi.gsfc.nasa.gov/ssc/data`
- IVOA

  `http://www.ivoa.net/`

14. Particle Physics Education and Outreach Sites

Science Educators' Networks:

- **IPPOG:** The International Particle Physics Outreach Group is a network of particle physicists, researchers, informal science educators and science explainers aiming to raise awareness, understanding and standards of global outreach efforts in particle physics and general science by providing discussion forums and regular information exchange for science institutions, proposing and implementing strategies to share lessons learned and best practices and promoting current outreach efforts of network members.

  `http://ippog.web.cern.ch/ippog/`

- **Interactions.org:** Designed to serve as a central resource for communicators of particle physics. The daily updated site provides links to current particle physics news from the world's press, high-resolution photos and graphics from the particle physics laboratories of the world; links to education and outreach programs; information about science policy and funding; links to universities; a glossary; a conference calendar; and links to many educational sites.

  `http://www.interactions.org`

- **I2U2:** Interactions in Understanding the Universe is an educational virtual organization strengthening the education and outreach activities of scientific experiments at US universities and laboratories by providing an infrastructure for hands-on laboratory courses.

  `http://www.i2u2.org`

Master Classes

- **CMS physics masterclass:** Lectures from active scientists give insight into methods of basic research, enabling the students to perform measurements on real data from the CMS experiment at the LHC. Like in an international research collaboration, the participants then discuss their results and compare with expectations.

  `http://cms.web.cern.ch/content/cms-physics-masterclass`

- **International Masterclasses:** Each year about 6000 high school students in 28 countries come to one of about 130 nearby universities or research centres for one day in order to unravel the mysteries of particle physics. Lectures from active scientists give insight in topics and methods of basic research at the fundaments of matter and forces, enabling the students to perform measurements on real data from particle physics experiments themselves. At the end of each day, like in an international research collaboration, the participants join in a video conference for discussion and combination of their results.

  `http://physicsmasterclasses.org/`

- **MINERVA:** MINERVA (Masterclass INvolving Event recognition visualised with Atlantis) is a masterclass tool for students to learn more about the ATLAS experiment at CERN, based on a simplified setup of the ATLAS event display, Atlantis.

  `http://atlas-minerva.web.cern.ch/atlas-minerva/`

General Sites

- **Contemporary Physics Education Project (CPEP):** Provides charts, brochures, Web links, and classroom activities. Online interactive courses include: Fundamental Particles and Interactions; Plasma Physics and Fusion; History and Fate of the Universe; and Nuclear Science.

  `http://www.cpepweb.org/`

Particle Physics Lessons & Activities

- **Angels and Demons:** With the aim of looking at the myth versus the reality of science at CERN this site offers teacher resources, slide shows and videos of talks given to teachers visiting CERN.

  `http://angelsanddemons.web.cern.ch/`

- **Big Bang:** An exhibition of the UK Science Museum with an interactive game about the hunt for the Higgs.

  `http://www.sciencemuseum.org.uk/antenna/bigbang/`

- **Big Bang Science: Exploring the origins of matter:** This Web site, produced by the Particle Physics and Astronomy Research Council of the UK (PPARC), explains what physicists are looking for with their giant instruments. Big Bang Science focuses on CERN particle detectors and on United Kingdom scientists' contribution to the search for the fundamental building blocks of matter.

  `http://hepwww.rl.ac.uk/pub/bigbang/part1.html`

- **CAMELIA:** CAMELIA (Cross-platform Atlas Multimedia Educational Lab for Interactive Analysis) is a discovery tool for the general public, based on computer gaming technology.

  `http://www.atlas.ch/camelia.html`

- **CERNland:** With a range of games, multimedia applications and films CERNland is the virtual theme park developed to bring the excitement of CERN's research to a young audience aged between 7 and 12. CERNland is designed to show children what is being done at CERN and inspire them with some physics at the same time.

  `http://www.cernland.net/`

- **CollidingParticles:** A series of films following a team of physicists involved in research at the LHC.

  `http://www.collidingparticles.com/`

- **Hands-On Universe:** This educational program enables students to investigate the Universe while applying tools and cocncepts from science, math and technology.

  `http://handsonuniverse.org/`

- **HYPATIA:** HYPATIA (Hybrid Pupil's Analysis Tool for Interactions in Atlas) is a tool for high school students to inspect the

graphic visualizaton of products of particle collisions in the ATLAS detector at CERN.

`http://hypatia.phys.uoa.gr/`

- **Lancaster Particle Physics:** This site, suitable for 16+ students, offers a number of simulations and explanations of particle physics, including a section on the LHC.

  `http://www.lppp.lancs.ac.uk/`

- **LHC @ home:** Platform for volunteers to help physicists develop and exploit particle accelerators like CERN's Large Hadron Collider, and to compare theory with experiment in the search for new fundamental particles.

  `http://lhcathome.web.cern.ch/LHCathome/`

  The LHC @ home 2.0 project Test4Theory allows users to participate in running simulations of high-energy particle physics using their home computers. The results are submitted to a database which is used as a common resource by both experimental and theoretical scientists working on the Large Hadron Collider at CERN.

  `http://boinc01.cern.ch/about-test4theory`

  SIXTRACK is a LHC @ home research project that allows users with Internet-connected computers to participate in advancing Accelerator Physics.

  `http://lhcathomeclassic.cern.ch/sixtrack/`

- **Particle Adventure:** One of the most popular Web sites for learning the fundamentals of matter and force. An award-winning interactive tour of quarks, neutrinos, antimatter, extra dimensions, dark matter, accelerators and particle detectors from the Particle Data Group of Lawrence Berkeley National Laboratory. Simple elegant graphics and translations into 15 languages.

  `http://particleadventure.org/`

- **Particle Detectives:** This website, maintained by the Science and Technology Facilities Council (STFC), is for inquisitive 14-19 year olds, their teachers and for researchers who want to find out and talk about the world's biggest scientific adventure, the Large Hadron Collider, featuring e.g. an LHC experiment simulator.

  `http://www.lhc.ac.uk/The+Particle+Detectives/15273.aspx`

- **Quarked! - Adventures in the Subatomic Universe:** This project, targeted to kids aged 7-12 (and their families), brings subatomic physics to life through a multimedia project including an interactive website, a facilitated program for museums and schools, and an educational outreach program.

  `http://www.quarked.org/`

- **QuarkNet:** Brings the excitement of particle physics research to high school teachers and their students. Teachers join research groups at about 50 universities and labs across the country. These research groups are part of particle physics experiments at CERN or Fermilab. About 100,000 students from 500+ US high schools learn fundamental physics as they participate in inquiry-oriented investigations and analyze real data online. QuarkNet is supported in part by the National Science Foundation and the U.S. Department of Energy.

  `https://quarknet.i2u2.org/`

- **Rewarding Learning videos about CERN:** The three videos based on interviews with scientists and engineers at CERN introduce pupils to CERN and the type of research and work undertaken there and are accompanied by teachers' notes.

  `http://www.nicurriculum.org.uk/STEMWorks/resources/cern/index.asp`

Lab Education Offices

- **Brookhaven National Laboratory (BNL) Educational Programs:** The Office of Educational Programs mission is to design, develop, implement, and facilitate workforce development and education initiatives that support the scientific mission at Brookhaven National Laboratory and the Department of Energy.

  `http://www.bnl.gov/education/`

- **CERN:** The CERN education website offers informations about teacher programmes and educational resources for schools.

  `http://education.web.cern.ch/education/`

- **DESY:** Offers courses for pupils and teachers as well as information for the general public, mostly in German.

  `http://www.desy.de/information_services/education/`

- **FermiLab Education Office:** Provides education resources and information about activities for educators, physicists, students and visitors to the Lab. In addition to information on 25 programs, the site provides online data-based investigations for high school students, online versions of exhibits in the Lederman Science Center, links to particle physics discovery resources, web-based instructional resources, what works for education and outreach, and links to the Lederman Science Center and the Teacher Resource Center.

  `http://ed.fnal.gov/`

- **LBL Education:** Berkeley Lab's Center for Science & Engineering Education (CSEE) carries out the Department of Energys education mission to train the next generation of scientists, as well as helping them to gain an understanding of the relationships among frontier science, technology, and society.

  `http://www.lbl.gov/education/`

- **Exploring SLAC Science:** This Stanford Linear Accelerator Center Web site explains physics concepts related to experiments conducted at SLAC.

  `http://www6.slac.stanford.edu/ExploringSLACScience.aspx`

Educational Programs of Experiments

- **ATLAS Discovery Quest:** One of several access points to ATLAS education and outreach pages. This page gives access to explanations of physical concepts, blogs, ATLAS facts, news, and information for students and teachers.

  `http://www.atlas.ch/physics.html`

- **ATLAS eTours:** Give a description of the Large Hadron Collider, explain how the ATLAS detector at the LHC works and give an overview over the experiments and their physics goals.

  `http://www.atlas.ch/etours.html`

- **CMS Education:** Provides access to educational resources (Story of the Universe, The Size of Things, What is a Particle), and to multimedia material, such as interviews, movies and photos.

  `http://cms.web.cern.ch/tags/education`

- **Education and Outreach @ IceCube:** Educational pages of the IceCube (South Pole Neutrino Detector).

  `http://icecube.wisc.edu/outreach`

- **LIGO Science Education Center:** The LIGO (Laser Interferometer Gravitational-wave Observatory) Science Education Center has over 40 interactive, hands-on exhibits that relate to the science of LIGO. The site hosts field trips for students, teacher training programs, and tours for the general public. Visitors can explore science concepts such as light, gravity, waves, and interference; learn about LIGO's search for gravitational waves; and interact with scientists and engineers.

  `http://www.ligo-la.caltech.edu/SEC.html`

- **Pierre Auger Observatory's Educational Pages:** The site offers information about cosmic rays and their detection, and provides material for students and teachers.

  `http://www.auger.org/cosmic_rays/`

News

- **asimmetrie:** bimonthly magazine about particle physics published by INFN, the Istituto Nazionale di Fisica Nucleare

  `http://www.asimmetrie.it/`

- **CERN Courier:**
  http://cerncourier.com/cws/latest/cern
- **DESY inForm:**
  http://www.desy.de/aktuelles/desy_inform
- **Fermilab Today:**
  http://www.fnal.gov/pub/today/
- **LC Newsline:**
  http://newsline.linearcollider.org/
  twitter: @ILCnewsline
- **IOP News:**
  http://www.iop.org/news/
- **JINR News:**
  http://www1.jinr.ru/News/Jinrnews_index.html
- **News at Interactions.org:** The InterActions site provides news and press releases on particle physics.
  http://www.interactions.org/cms/?pid=1000680
  twitter: @particlenews
- **physics.org news:** This IOP news site presents physics stories from around the world wide web.
  http://www.physics.org/news.asp
- **SLAC Signals:** This email newsletter reports about cutting-edge science, major SLAC milestones and other lab information. It has replaced SLAC Today in November 2013. Its signup page can be found at
  http://eepurl.com/IqPl1
- **symmetry:** This magazine about particle physics and its connections to other aspects of life and science, from interdisciplinary collaborations to policy to culture is published 6 times per year by Fermilab and SLAC.
  http://www.symmetrymagazine.org/
  twitter: @symmetrymag

Art in Physics

- **Arts@CERN:** A 3-year artists residency programme in Digital Arts and Dance/ Performance.
  http://arts.web.cern.ch/collide/
- **Superposition:** This artist-in-residence programme from the Institute of Physics invites visual artists and physicists to collaboratively explore and contribute to contemporary art.
  http://www.physics.org/superposition

Blogs

This is a very incomplete collection of particle physics related blogs:

- **ATLAS blog:**
  http://www.atlas.ch/blog
- **Physics arXiv blog:** Technology Review blog on new ideas at arXiv.org.
  http://www.technologyreview.com/blog/arxiv/
- **Life and Physics:** Jon Butterworth's blog in the Guardian.
  http://www.guardian.co.uk/science/life-and-physics
- **Not Even Wrong:** Peter Woit's blog on topics in physics and mathematics.
  http://www.math.columbia.edu/∼woit/wordpress/
- **Of Particular Significance:** Conversations about science, with a current focus on particle physics, with theoretical physicist Matt Strassler.
  http://profmattstrassler.com/
- **Preposterous Universe:** Theoretical physicist Sean Carroll's blog.
  http://www.preposterousuniverse.com/
- **Quantum diaries:** Thoughts on work and life from particle physicists from around the world.
  http://www.quantumdiaries.org/
  The US LHC blog gives a vivid account of the daily activity of US LHC researchers.
  http://www.quantumdiaries.org/lab-81/
- **Science blogs:** Launched in January 2006, ScienceBlogs features bloggers from a wide array of scientific disciplines, including physics.
  http://scienceblogs.com/channel/physical-science/

More extensive lists of active blogs and tweets can be found on INSPIRE:

- **Scientist blogs:**
  http://tinyurl.com/nmku27s
- **Scientists with twitter accounts:**
  http://tinyurl.com/nrg5k63
- **Experiments with twitter accounts:**
  http://tinyurl.com/q86kma8
- **Institutions with twitter accounts:**
  http://tinyurl.com/mzcm3nw

SUMMARY TABLES OF PARTICLE PHYSICS

* There are also search limits in the Summary Tables for the Gauge and Higgs Bosons, the Leptons, the Quarks, and the Mesons.

SUMMARY TABLES OF PARTICLE PROPERTIES

Extracted from the Particle Listings of the
Review of Particle Physics
K. Olive *et al.* (PDG), Chin. Phys. **C38**, 090001 (2014)
Available at `http://pdg.lbl.gov`

Particle Data Group

K.A. Olive, K. Agashe, C. Amsler, M. Antonelli, J.-F. Arguin, D.M. Asner, H. Baer, H.R. Band, R.M. Barnett, T. Basaglia, C.W. Bauer, J.J. Beatty, V.I. Belousov, J. Beringer, G. Bernardi, S. Bethke, H. Bichsel, O. Biebel, E. Blucher, S. Blusk, G. Brooijmans, O. Buchmueller, V. Burkert, M.A. Bychkov, R.N. Cahn, M. Carena, A. Ceccucci, A. Cerri, D. Chakraborty, M.-C. Chen, R.S. Chivukula, K. Copic, G. Cowan, O. Dahl, G. D'Ambrosio, T. Damour, D. de Florian, A. de Gouvêa, T. DeGrand, P. de Jong, G. Dissertori, B.A. Dobrescu, M. Doser, M. Drees, H.K. Dreiner, D.A. Edwards, S. Eidelman, J. Erler, V.V. Ezhela, W. Fetscher, B.D. Fields, B. Foster, A. Freitas, T.K. Gaisser, H. Gallagher, L. Garren, H.-J. Gerber, G. Gerbier, T. Gershon, T. Gherghetta, S. Golwala, M. Goodman, C. Grab, A.V. Gritsan, C. Grojean, D.E. Groom, M. Grünewald, A. Gurtu, T. Gutsche, H.E. Haber, K. Hagiwara, C. Hanhart, S. Hashimoto, Y. Hayato, K.G. Hayes, M. Heffner, B. Heltsley, J.J. Hernández-Rey, K. Hikasa, A. Höcker, J. Holder, A. Holtkamp, J. Huston, J.D. Jackson, K.F. Johnson, T. Junk, M. Kado, D. Karlen, U.F. Katz, S.R. Klein, E. Klempt, R.V. Kowalewski, F. Krauss, M. Kreps, B. Krusche, Yu.V. Kuyanov, Y. Kwon, O. Lahav, J. Laiho, P. Langacker, A. Liddle, Z. Ligeti, C.-J. Lin, T.M. Liss, L. Littenberg, K.S. Lugovsky, S.B. Lugovsky, F. Maltoni, T. Mannel, A.V. Manohar, W.J. Marciano, A.D. Martin, A. Masoni, J. Matthews, D. Milstead, P. Molaro, K. Mönig, F. Moortgat, M.J. Mortonson, H. Murayama, K. Nakamura, M. Narain, P. Nason, S. Navas, M. Neubert, P. Nevski, Y. Nir, L. Pape, J. Parsons, C. Patrignani, J.A. Peacock, M. Pennington, S.T. Petcov, A. Piepke, A. Pomarol, A. Quadt, S. Raby, J. Rademacker, G. Raffelt, B.N. Ratcliff, P. Richardson, A. Ringwald, S. Roesler, S. Rolli, A. Romaniouk, L.J. Rosenberg, J.L. Rosner, G. Rybka, C.T. Sachrajda, Y. Sakai, G.P. Salam, S. Sarkar, F. Sauli, O. Schneider, K. Scholberg, D. Scott, V. Sharma, S.R. Sharpe, M. Silari, T. Sjöstrand, P. Skands, J.G. Smith, G.F. Smoot, S. Spanier, H. Spieler, C. Spiering, A. Stahl, T. Stanev, S.L. Stone, T. Sumiyoshi, M.J. Syphers, F. Takahashi, M. Tanabashi, J. Terning, L. Tiator, M. Titov, N.P. Tkachenko, N.A. Törnqvist, D. Tovey, G. Valencia, G. Venanzoni, M.G. Vincter, P. Vogel, A. Vogt, S.P. Wakely, W. Walkowiak, C.W. Walter, D.R. Ward, G. Weiglein, D.H. Weinberg, E.J. Weinberg, M. White, L.R. Wiencke, C.G. Wohl, L. Wolfenstein, J. Womersley, C.L. Woody, R.L. Workman, A. Yamamoto, W.-M. Yao, G.P. Zeller, O.V. Zenin, J. Zhang, R.-Y. Zhu, F. Zimmermann, P.A. Zyla

Technical Associates:

G. Harper, V.S. Lugovsky, P. Schaffner

(Approximate closing date for data: January 15, 2014)

GAUGE AND HIGGS BOSONS

γ

$I(J^{PC}) = 0,1(1^{--})$

Mass $m < 1 \times 10^{-18}$ eV
Charge $q < 1 \times 10^{-35}$ e
Mean life τ = Stable

g or gluon

$I(J^{P}) = 0(1^{-})$

Mass $m = 0$ [a]
SU(3) color octet

graviton

$J = 2$

Mass $m < 6 \times 10^{-32}$ eV

W

$J = 1$

Charge = ± 1 e
Mass $m = 80.385 \pm 0.015$ GeV
$m_Z - m_W = 10.4 \pm 1.6$ GeV
$m_{W^+} - m_{W^-} = -0.2 \pm 0.6$ GeV
Full width $\Gamma = 2.085 \pm 0.042$ GeV
$\langle N_{\pi^\pm} \rangle = 15.70 \pm 0.35$
$\langle N_{K^\pm} \rangle = 2.20 \pm 0.19$
$\langle N_p \rangle = 0.92 \pm 0.14$
$\langle N_{\text{charged}} \rangle = 19.39 \pm 0.08$

W^- modes are charge conjugates of the modes below.

W^+ DECAY MODES		Fraction (Γ_i/Γ)	Confidence level	p (MeV/c)
$\ell^+ \nu$	[b]	(10.86± 0.09) %		–
$e^+ \nu$		(10.71± 0.16) %		40192
$\mu^+ \nu$		(10.63± 0.15) %		40192
$\tau^+ \nu$		(11.38± 0.21) %		40173
hadrons		(67.41± 0.27) %		–
$\pi^+ \gamma$		$< 7 \times 10^{-5}$	95%	40192
$D_s^+ \gamma$		$< 1.3 \times 10^{-3}$	95%	40168
cX		(33.3 ± 2.6) %		–
$c\overline{s}$		(31 $^{+13}_{-11}$) %		–
invisible	[c]	(1.4 ± 2.9) %		–

Z

$J = 1$

Charge = 0
Mass $m = 91.1876 \pm 0.0021$ GeV [d]
Full width $\Gamma = 2.4952 \pm 0.0023$ GeV
$\Gamma(\ell^+\ell^-) = 83.984 \pm 0.086$ MeV [b]
$\Gamma(\text{invisible}) = 499.0 \pm 1.5$ MeV [e]
$\Gamma(\text{hadrons}) = 1744.4 \pm 2.0$ MeV
$\Gamma(\mu^+\mu^-)/\Gamma(e^+e^-) = 1.0009 \pm 0.0028$
$\Gamma(\tau^+\tau^-)/\Gamma(e^+e^-) = 1.0019 \pm 0.0032$ [f]

Average charged multiplicity

$\langle N_{charged} \rangle = 20.76 \pm 0.16$ (S = 2.1)

Couplings to quarks and leptons

$g_V^\ell = -0.03783 \pm 0.00041$
$g_V^u = 0.25^{+0.07}_{-0.06}$
$g_V^d = -0.33^{+0.05}_{-0.06}$
$g_A^\ell = -0.50123 \pm 0.00026$
$g_A^u = 0.50^{+0.04}_{-0.06}$
$g_A^d = -0.523^{+0.050}_{-0.029}$
$g^{\nu_\ell} = 0.5008 \pm 0.0008$
$g^{\nu_e} = 0.53 \pm 0.09$
$g^{\nu_\mu} = 0.502 \pm 0.017$

Asymmetry parameters [g]

$A_e = 0.1515 \pm 0.0019$
$A_\mu = 0.142 \pm 0.015$
$A_\tau = 0.143 \pm 0.004$
$A_s = 0.90 \pm 0.09$
$A_c = 0.670 \pm 0.027$
$A_b = 0.923 \pm 0.020$

Charge asymmetry (%) at Z pole

$A_{FB}^{(0\ell)} = 1.71 \pm 0.10$
$A_{FB}^{(0u)} = 4 \pm 7$
$A_{FB}^{(0s)} = 9.8 \pm 1.1$
$A_{FB}^{(0c)} = 7.07 \pm 0.35$
$A_{FB}^{(0b)} = 9.92 \pm 0.16$

Gauge & Higgs Boson Summary Table

Z DECAY MODES		Fraction (Γ_i/Γ)	Scale factor/ Confidence level	p (MeV/c)
e^+e^-		(3.363 ±0.004) %		45594
$\mu^+\mu^-$		(3.366 ±0.007) %		45594
$\tau^+\tau^-$		(3.370 ±0.008) %		45559
$\ell^+\ell^-$	[b]	(3.3658±0.0023) %		–
$\ell^+\ell^-\ell^+\ell^-$	[h]	(4.2 $^{+0.9}_{-0.8}$) $\times 10^{-6}$		45594
invisible		(20.00 ±0.06) %		–
hadrons		(69.91 ±0.06) %		–
$(u\overline{u}+c\overline{c})/2$		(11.6 ±0.6) %		–
$(d\overline{d}+s\overline{s}+b\overline{b})/3$		(15.6 ±0.4) %		–
$c\overline{c}$		(12.03 ±0.21) %		–
$b\overline{b}$		(15.12 ±0.05) %		–
$b\overline{b}b\overline{b}$		(3.6 ±1.3) $\times 10^{-4}$		–
ggg		< 1.1 %	CL=95%	–
$\pi^0\gamma$		< 5.2 $\times 10^{-5}$	CL=95%	45594
$\eta\gamma$		< 5.1 $\times 10^{-5}$	CL=95%	45592
$\omega\gamma$		< 6.5 $\times 10^{-4}$	CL=95%	45590
$\eta'(958)\gamma$		< 4.2 $\times 10^{-5}$	CL=95%	45589
$\gamma\gamma$		< 5.2 $\times 10^{-5}$	CL=95%	45594
$\gamma\gamma\gamma$		< 1.0 $\times 10^{-5}$	CL=95%	45594
$\pi^\pm W^\mp$	[i]	< 7 $\times 10^{-5}$	CL=95%	10162
$\rho^\pm W^\mp$	[i]	< 8.3 $\times 10^{-5}$	CL=95%	10136
$J/\psi(1S)X$		(3.51 $^{+0.23}_{-0.25}$) $\times 10^{-3}$	S=1.1	–
$\psi(2S)X$		(1.60 ±0.29) $\times 10^{-3}$		–
$\chi_{c1}(1P)X$		(2.9 ±0.7) $\times 10^{-3}$		–
$\chi_{c2}(1P)X$		< 3.2 $\times 10^{-3}$	CL=90%	–
$\Upsilon(1S)X + \Upsilon(2S)X + \Upsilon(3S)X$		(1.0 ±0.5) $\times 10^{-4}$		–
$\Upsilon(1S)X$		< 4.4 $\times 10^{-5}$	CL=95%	–
$\Upsilon(2S)X$		< 1.39 $\times 10^{-4}$	CL=95%	–
$\Upsilon(3S)X$		< 9.4 $\times 10^{-5}$	CL=95%	–
$(D^0/\overline{D}^0)X$		(20.7 ±2.0) %		–
$D^\pm X$		(12.2 ±1.7) %		–
$D^*(2010)^\pm X$	[i]	(11.4 ±1.3) %		–
$D_{s1}(2536)^\pm X$		(3.6 ±0.8) $\times 10^{-3}$		–
$D_{sJ}(2573)^\pm X$		(5.8 ±2.2) $\times 10^{-3}$		–
$D^{*\prime}(2629)^\pm X$		searched for		–
B^+X	[j]	(6.08 ±0.13) %		–
$B^0_s X$	[j]	(1.59 ±0.13) %		–
$B^+_c X$		searched for		–
$\Lambda^+_c X$		(1.54 ±0.33) %		–
$\Xi^0_c X$		seen		–
$\Xi_b X$		seen		–
b-baryon X	[j]	(1.38 ±0.22) %		–
anomalous γ+ hadrons	[k]	< 3.2 $\times 10^{-3}$	CL=95%	–
$e^+e^-\gamma$	[k]	< 5.2 $\times 10^{-4}$	CL=95%	45594
$\mu^+\mu^-\gamma$	[k]	< 5.6 $\times 10^{-4}$	CL=95%	45594
$\tau^+\tau^-\gamma$	[k]	< 7.3 $\times 10^{-4}$	CL=95%	45559
$\ell^+\ell^-\gamma\gamma$	[l]	< 6.8 $\times 10^{-6}$	CL=95%	–
$q\overline{q}\gamma\gamma$	[l]	< 5.5 $\times 10^{-6}$	CL=95%	–
$\nu\overline{\nu}\gamma\gamma$	[l]	< 3.1 $\times 10^{-6}$	CL=95%	45594
$e^\pm\mu^\mp$ LF	[i]	< 1.7 $\times 10^{-6}$	CL=95%	45594
$e^\pm\tau^\mp$ LF	[i]	< 9.8 $\times 10^{-6}$	CL=95%	45576
$\mu^\pm\tau^\mp$ LF	[i]	< 1.2 $\times 10^{-5}$	CL=95%	45576
pe L,B		< 1.8 $\times 10^{-6}$	CL=95%	45589
$p\mu$ L,B		< 1.8 $\times 10^{-6}$	CL=95%	45589

H^0

$J = 0$

Mass $m = 125.7 \pm 0.4$ GeV

H^0 Signal Strengths in Different Channels

Combined Final States = 1.17 ± 0.17 (S = 1.2)

$WW^* = 0.87^{+0.24}_{-0.22}$

$ZZ^* = 1.11^{+0.34}_{-0.28}$ (S = 1.3)

$\gamma\gamma = 1.58^{+0.27}_{-0.23}$

$b\overline{b} = 1.1 \pm 0.5$

$\tau^+\tau^- = 0.4 \pm 0.6$

$Z\gamma <$ 9.5, CL = 95%

Neutral Higgs Bosons, Searches for

Searches for a Higgs Boson with Standard Model Couplings

Mass $m >$ 122 and none 128–710 GeV, CL = 95%

The limits for H^0_1 and A^0 in supersymmetric models refer to the $m_h^{\max}$ benchmark scenario for the supersymmetric parameters.

H^0_1 in Supersymmetric Models ($m_{H^0_1} < m_{H^0_2}$)

Mass $m >$ 92.8 GeV, CL = 95%

A^0 Pseudoscalar Higgs Boson in Supersymmetric Models [n]

Mass $m >$ 93.4 GeV, CL = 95% $\tan\beta > 0.4$

Charged Higgs Bosons ($H^\pm$ and $H^{\pm\pm}$), Searches for

$H^\pm$ Mass $m >$ 80 GeV, CL = 95%

New Heavy Bosons (W', Z', leptoquarks, etc.), Searches for

Additional W Bosons

W' with standard couplings

Mass $m >$ 2.900×10^3 GeV, CL = 95% ($p\overline{p}$ direct search)

W_R (Right-handed W Boson)

Mass $m >$ 715 GeV, CL = 90% (electroweak fit)

Additional Z Bosons

$Z'_{\rm SM}$ with standard couplings

Mass $m >$ 2.590×10^3 GeV, CL = 95% ($p\overline{p}$ direct search)

Mass $m >$ 1.500×10^3 GeV, CL = 95% (electroweak fit)

Z_{LR} of $SU(2)_L \times SU(2)_R \times U(1)$ (with $g_L = g_R$)

Mass $m >$ 630 GeV, CL = 95% ($p\overline{p}$ direct search)

Mass $m >$ 1162 GeV, CL = 95% (electroweak fit)

Z_χ of $SO(10) \rightarrow SU(5) \times U(1)_\chi$ (with $g_\chi = e/\cos\theta_W$)

Mass $m >$ 1.970×10^3 GeV, CL = 95% ($p\overline{p}$ direct search)

Mass $m >$ 1.141×10^3 GeV, CL = 95% (electroweak fit)

Z_ψ of $E_6 \rightarrow SO(10) \times U(1)_\psi$ (with $g_\psi = e/\cos\theta_W$)

Mass $m >$ 2.260×10^3 GeV, CL = 95% ($p\overline{p}$ direct search)

Mass $m >$ 476 GeV, CL = 95% (electroweak fit)

Z_η of $E_6 \rightarrow SU(3) \times SU(2) \times U(1) \times U(1)_\eta$ (with $g_\eta = e/\cos\theta_W$)

Mass $m >$ 1.870×10^3 GeV, CL = 95% ($p\overline{p}$ direct search)

Mass $m >$ 619 GeV, CL = 95% (electroweak fit)

Scalar Leptoquarks

Mass $m >$ 830 GeV, CL = 95% (1st generation, pair prod.)

Mass $m >$ 304 GeV, CL = 95% (1st gener., single prod.)

Mass $m >$ 840 GeV, CL = 95% (2nd gener., pair prod.)

Mass $m >$ 73 GeV, CL = 95% (2nd gener., single prod.)

Mass $m >$ 525 GeV, CL = 95% (3rd gener., pair prod.)

(See the Particle Listings for assumptions on leptoquark quantum numbers and branching fractions.)

Diquarks

Mass $m >$ 3.750×10^3 GeV, CL = 95%

Axigluon

Mass $m >$ 3.360×10^3 GeV, CL = 95%

Axions (A^0) and Other Very Light Bosons, Searches for

The standard Peccei-Quinn axion is ruled out. Variants with reduced couplings or much smaller masses are constrained by various data. The Particle Listings in the full *Review* contain a Note discussing axion searches.

The best limit for the half-life of neutrinoless double beta decay with Majoron emission is $> 7.2 \times 10^{24}$ years (CL = 90%).

NOTES

In this Summary Table:

When a quantity has "(S = ...)" to its right, the error on the quantity has been enlarged by the "scale factor" S, defined as $S = \sqrt{\chi^2/(N-1)}$, where N is the number of measurements used in calculating the quantity. We do this when $S > 1$, which often indicates that the measurements are inconsistent. When $S > 1.25$, we also show in the Particle Listings an ideogram of the measurements. For more about S, see the Introduction.

A decay momentum p is given for each decay mode. For a 2-body decay, p is the momentum of each decay product in the rest frame of the decaying particle. For a 3-or-more-body decay, p is the largest momentum any of the products can have in this frame.

[a] Theoretical value. A mass as large as a few MeV may not be precluded.

[b] ℓ indicates each type of lepton (e, μ, and τ), not sum over them.

[c] This represents the width for the decay of the W boson into a charged particle with momentum below detectability, p< 200 MeV.

[d] The Z-boson mass listed here corresponds to a Breit-Wigner resonance parameter. It lies approximately 34 MeV above the real part of the position of the pole (in the energy-squared plane) in the Z-boson propagator.

[e] This partial width takes into account Z decays into $\nu\overline{\nu}$ and any other possible undetected modes.

[f] This ratio has not been corrected for the τ mass.

[g] Here $A \equiv 2g_V g_A/(g_V^2+g_A^2)$.

[h] Here ℓ indicates e or μ.

[i] The value is for the sum of the charge states or particle/antiparticle states indicated.

[j] This value is updated using the product of (i) the $Z \to b\overline{b}$ fraction from this listing and (ii) the b-hadron fraction in an unbiased sample of weakly decaying b-hadrons produced in Z-decays provided by the Heavy Flavor Averaging Group (HFAG, http://www.slac.stanford.edu/xorg/hfag/osc/PDG_2009/#FRACZ).

[k] See the Z Particle Listings for the γ energy range used in this measurement.

[l] For $m_{\gamma\gamma} = (60 \pm 5)$ GeV.

[n] The limits assume no invisible decays.

Lepton Summary Table

LEPTONS

e

$J = \frac{1}{2}$

Mass $m = (548.57990946 \pm 0.00000022) \times 10^{-6}$ u
Mass $m = 0.510998928 \pm 0.000000011$ MeV
$|m_{e^+} - m_{e^-}|/m < 8 \times 10^{-9}$, CL = 90%
$|q_{e^+} + q_{e^-}|/e < 4 \times 10^{-8}$
Magnetic moment anomaly
$(g-2)/2 = (1159.65218076 \pm 0.00000027) \times 10^{-6}$
$(g_{e^+} - g_{e^-}) / g_{\text{average}} = (-0.5 \pm 2.1) \times 10^{-12}$
Electric dipole moment $d < 10.5 \times 10^{-28}$ $e$cm, CL = 90%
Mean life $\tau > 4.6 \times 10^{26}$ yr, CL = 90% [a]

μ

$J = \frac{1}{2}$

Mass $m = 0.1134289267 \pm 0.0000000029$ u
Mass $m = 105.6583715 \pm 0.0000035$ MeV
Mean life $\tau = (2.1969811 \pm 0.0000022) \times 10^{-6}$ s
$\tau_{\mu^+}/\tau_{\mu^-} = 1.00002 \pm 0.00008$
$c\tau = 658.6384$ m
Magnetic moment anomaly $(g-2)/2 = (11659209 \pm 6) \times 10^{-10}$
$(g_{\mu^+} - g_{\mu^-}) / g_{\text{average}} = (-0.11 \pm 0.12) \times 10^{-8}$
Electric dipole moment $d = (-0.1 \pm 0.9) \times 10^{-19}$ $e$cm

Decay parameters [b]

$\rho = 0.74979 \pm 0.00026$
$\eta = 0.057 \pm 0.034$
$\delta = 0.75047 \pm 0.00034$
$\xi P_\mu = 1.0009^{+0.0016}_{-0.0007}$ [c]
$\xi P_\mu \delta/\rho = 1.0018^{+0.0016}_{-0.0007}$ [c]
$\xi' = 1.00 \pm 0.04$
$\xi'' = 0.7 \pm 0.4$
$\alpha/A = (0 \pm 4) \times 10^{-3}$
$\alpha'/A = (-10 \pm 20) \times 10^{-3}$
$\beta/A = (4 \pm 6) \times 10^{-3}$
$\beta'/A = (2 \pm 7) \times 10^{-3}$
$\overline{\eta} = 0.02 \pm 0.08$

μ^+ modes are charge conjugates of the modes below.

μ^- DECAY MODES		Fraction (Γ_i/Γ)	Confidence level	p (MeV/c)
$e^-\overline{\nu}_e\nu_\mu$		$\approx 100\%$		53
$e^-\overline{\nu}_e\nu_\mu\gamma$	[d]	(1.4 ± 0.4) %		53
$e^-\overline{\nu}_e\nu_\mu e^+e^-$	[e]	$(3.4 \pm 0.4) \times 10^{-5}$		53
Lepton Family number (LF) violating modes				
$e^-\nu_e\overline{\nu}_\mu$	LF	[f] < 1.2 %	90%	53
$e^-\gamma$	LF	$< 5.7 \times 10^{-13}$	90%	53
$e^-e^+e^-$	LF	$< 1.0 \times 10^{-12}$	90%	53
$e^-2\gamma$	LF	$< 7.2 \times 10^{-11}$	90%	53

τ

$J = \frac{1}{2}$

Mass $m = 1776.82 \pm 0.16$ MeV
$(m_{\tau^+} - m_{\tau^-})/m_{\text{average}} < 2.8 \times 10^{-4}$, CL = 90%
Mean life $\tau = (290.3 \pm 0.5) \times 10^{-15}$ s
$c\tau = 87.03$ μm
Magnetic moment anomaly > -0.052 and < 0.013, CL = 95%
$\text{Re}(d_\tau) = -0.220$ to 0.45×10^{-16} $e$cm, CL = 95%
$\text{Im}(d_\tau) = -0.250$ to 0.0080×10^{-16} $e$cm, CL = 95%

Weak dipole moment

$\text{Re}(d_\tau^w) < 0.50 \times 10^{-17}$ $e$cm, CL = 95%
$\text{Im}(d_\tau^w) < 1.1 \times 10^{-17}$ $e$cm, CL = 95%

Weak anomalous magnetic dipole moment

$\text{Re}(\alpha_\tau^w) < 1.1 \times 10^{-3}$, CL = 95%
$\text{Im}(\alpha_\tau^w) < 2.7 \times 10^{-3}$, CL = 95%
$\tau^\pm \to \pi^\pm K_S^0 \nu_\tau$ (RATE DIFFERENCE) / (RATE SUM) = (-0.36 ± 0.25)%

Decay parameters

See the τ Particle Listings for a note concerning τ-decay parameters.

$\rho(e \text{ or } \mu) = 0.745 \pm 0.008$
$\rho(e) = 0.747 \pm 0.010$
$\rho(\mu) = 0.763 \pm 0.020$
$\xi(e \text{ or } \mu) = 0.985 \pm 0.030$
$\xi(e) = 0.994 \pm 0.040$
$\xi(\mu) = 1.030 \pm 0.059$
$\eta(e \text{ or } \mu) = 0.013 \pm 0.020$
$\eta(\mu) = 0.094 \pm 0.073$
$(\delta\xi)(e \text{ or } \mu) = 0.746 \pm 0.021$
$(\delta\xi)(e) = 0.734 \pm 0.028$
$(\delta\xi)(\mu) = 0.778 \pm 0.037$
$\xi(\pi) = 0.993 \pm 0.022$
$\xi(\rho) = 0.994 \pm 0.008$
$\xi(a_1) = 1.001 \pm 0.027$
$\xi(\text{all hadronic modes}) = 0.995 \pm 0.007$

τ^+ modes are charge conjugates of the modes below. "$h^\pm$" stands for $\pi^\pm$ or $K^\pm$. "ℓ" stands for e or μ. "Neutrals" stands for γ's and/or π^0's.

τ^- DECAY MODES		Fraction (Γ_i/Γ)	Scale factor/ Confidence level	p (MeV/c)
Modes with one charged particle				
particle$^- \geq 0$ neutrals $\geq 0K^0\nu_\tau$ ("1-prong")		(85.35 ±0.07) %	S=1.3	–
particle$^- \geq 0$ neutrals $\geq 0K_L^0\nu_\tau$		(84.71 ±0.08) %	S=1.3	–
$\mu^-\overline{\nu}_\mu\nu_\tau$	[g]	(17.41 ±0.04) %	S=1.1	885
$\mu^-\overline{\nu}_\mu\nu_\tau\gamma$	[e]	(3.6 ±0.4) $\times 10^{-3}$		885
$e^-\overline{\nu}_e\nu_\tau$	[g]	(17.83 ±0.04) %		888
$e^-\overline{\nu}_e\nu_\tau\gamma$	[e]	(1.75 ±0.18) %		888
$h^- \geq 0K_L^0\nu_\tau$		(12.06 ±0.06) %	S=1.2	883
$h^-\nu_\tau$		(11.53 ±0.06) %	S=1.2	883
$\pi^-\nu_\tau$	[g]	(10.83 ±0.06) %	S=1.2	883
$K^-\nu_\tau$	[g]	(7.00 ±0.10) $\times 10^{-3}$	S=1.1	820
$h^- \geq 1$ neutrals ν_τ		(37.10 ±0.10) %	S=1.2	–
$h^- \geq 1\pi^0\nu_\tau$ (ex.K^0)		(36.58 ±0.10) %	S=1.2	–
$h^-\pi^0\nu_\tau$		(25.95 ±0.09) %	S=1.1	878
$\pi^-\pi^0\nu_\tau$	[g]	(25.52 ±0.09) %	S=1.1	878
$\pi^-\pi^0$ non-$\rho(770)\nu_\tau$		(3.0 ±3.2) $\times 10^{-3}$		878
$K^-\pi^0\nu_\tau$	[g]	(4.29 ±0.15) $\times 10^{-3}$		814
$h^- \geq 2\pi^0\nu_\tau$		(10.87 ±0.11) %	S=1.2	–
$h^-2\pi^0\nu_\tau$		(9.52 ±0.11) %	S=1.1	862
$h^-2\pi^0\nu_\tau$ (ex.K^0)		(9.36 ±0.11) %	S=1.2	862
$\pi^-2\pi^0\nu_\tau$ (ex.K^0)	[g]	(9.30 ±0.11) %	S=1.2	862
$\pi^-2\pi^0\nu_\tau$ (ex.K^0), scalar		< 9 $\times 10^{-3}$	CL=95%	862
$\pi^-2\pi^0\nu_\tau$ (ex.K^0), vector		< 7 $\times 10^{-3}$	CL=95%	862
$K^-2\pi^0\nu_\tau$ (ex.K^0)	[g]	(6.5 ±2.3) $\times 10^{-4}$		796
$h^- \geq 3\pi^0\nu_\tau$		(1.35 ±0.07) %	S=1.1	–
$h^- \geq 3\pi^0\nu_\tau$ (ex. K^0)		(1.26 ±0.07) %	S=1.1	–
$h^-3\pi^0\nu_\tau$		(1.19 ±0.07) %		836
$\pi^-3\pi^0\nu_\tau$ (ex.K^0)	[g]	(1.05 ±0.07) %		836
$K^-3\pi^0\nu_\tau$ (ex.K^0, η)	[g]	(4.8 ±2.2) $\times 10^{-4}$		765
$h^-4\pi^0\nu_\tau$ (ex.K^0)		(1.6 ±0.4) $\times 10^{-3}$		800
$h^-4\pi^0\nu_\tau$ (ex.K^0,η)	[g]	(1.1 ±0.4) $\times 10^{-3}$		800
$K^- \geq 0\pi^0 \geq 0K^0 \geq 0\gamma\ \nu_\tau$		(1.572±0.033) %	S=1.1	820
$K^- \geq 1$ (π^0 or K^0 or γ) ν_τ		(8.72 ±0.32) $\times 10^{-3}$	S=1.1	–
Modes with K^0's				
K_S^0(particles)$^-\nu_\tau$		(9.2 ±0.4) $\times 10^{-3}$	S=1.5	–
$h^-\overline{K}^0\nu_\tau$		(1.00 ±0.05) %	S=1.8	812
$\pi^-\overline{K}^0\nu_\tau$	[g]	(8.4 ±0.4) $\times 10^{-3}$	S=2.1	812
$\pi^-\overline{K}^0$ (non-$K^*(892)^-$)ν_τ		(5.4 ±2.1) $\times 10^{-4}$		812
$K^-K^0\nu_\tau$	[g]	(1.59 ±0.16) $\times 10^{-3}$		737
$K^-K^0 \geq 0\pi^0\nu_\tau$		(3.18 ±0.23) $\times 10^{-3}$		737
$h^-\overline{K}^0\pi^0\nu_\tau$		(5.6 ±0.4) $\times 10^{-3}$		794
$\pi^-\overline{K}^0\pi^0\nu_\tau$	[g]	(4.0 ±0.4) $\times 10^{-3}$		794
$\overline{K}^0\rho^-\nu_\tau$		(2.2 ±0.5) $\times 10^{-3}$		612
$K^-K^0\pi^0\nu_\tau$	[g]	(1.59 ±0.20) $\times 10^{-3}$		685
$\pi^-\overline{K}^0 \geq 1\pi^0\nu_\tau$		(3.2 ±1.0) $\times 10^{-3}$		–

$\pi^- \overline{K}^0 \pi^0 \pi^0 \nu_\tau$		(2.6 ±2.4) × 10^{-4}			763
$K^- K^0 \pi^0 \pi^0 \nu_\tau$		< 1.6	× 10^{-4}	CL=95%	619
$\pi^- K^0 \overline{K}^0 \nu_\tau$		(1.7 ±0.4) × 10^{-3}		S=1.8	682
$\pi^- K^0_S K^0_S \nu_\tau$	[g]	(2.31 ±0.17) × 10^{-4}		S=1.9	682
$\pi^- K^0_S K^0_L \nu_\tau$	[g]	(1.2 ±0.4) × 10^{-3}		S=1.8	682
$\pi^- K^0 \overline{K}^0 \pi^0 \nu_\tau$		(3.1 ±2.3) × 10^{-4}			614
$\pi^- K^0_S K^0_S \pi^0 \nu_\tau$		(1.60 ±0.30) × 10^{-4}			614
$\pi^- K^0_S K^0_L \pi^0 \nu_\tau$		(3.1 ±1.2) × 10^{-4}			614
$K^- K^0_S K^0_S \nu_\tau$		< 6.3	× 10^{-7}	CL=90%	466
$K^- K^0_S K^0_S \pi^0 \nu_\tau$		< 4.0	× 10^{-7}	CL=90%	337
$K^0 h^+ h^- h^- \geq 0$ neutrals ν_τ		< 1.7	× 10^{-3}	CL=95%	760
$K^0 h^+ h^- h^- \nu_\tau$		(2.3 ±2.0) × 10^{-4}			760

Modes with three charged particles

$h^- h^- h^+ \geq 0$ neutrals $\geq 0 K^0_L \nu_\tau$		(15.20 ±0.08) %		S=1.3	861
$h^- h^- h^+ \geq 0$ neutrals ν_τ (ex. $K^0_S \to \pi^+ \pi^-$) ("3-prong")		(14.57 ±0.07) %		S=1.3	861
$h^- h^- h^+ \nu_\tau$		(9.80 ±0.07) %		S=1.2	861
$h^- h^- h^+ \nu_\tau$(ex.K^0)		(9.46 ±0.06) %		S=1.2	861
$h^- h^- h^+ \nu_\tau$(ex.K^0,ω)		(9.42 ±0.06) %		S=1.2	861
$\pi^- \pi^+ \pi^- \nu_\tau$		(9.31 ±0.06) %		S=1.2	861
$\pi^- \pi^+ \pi^- \nu_\tau$(ex.$K^0$)		(9.02 ±0.06) %		S=1.1	861
$\pi^- \pi^+ \pi^- \nu_\tau$(ex.$K^0$), non-axial vector		< 2.4	%	CL=95%	861
$\pi^- \pi^+ \pi^- \nu_\tau$(ex.$K^0$,$\omega$)	[g]	(8.99 ±0.06) %		S=1.1	861
$h^- h^- h^+ \geq 1$ neutrals ν_τ		(5.39 ±0.07) %		S=1.2	–
$h^- h^- h^+ \geq 1 \pi^0 \nu_\tau$(ex. K^0)		(5.09 ±0.06) %		S=1.2	–
$h^- h^- h^+ \pi^0 \nu_\tau$		(4.76 ±0.06) %		S=1.2	834
$h^- h^- h^+ \pi^0 \nu_\tau$(ex.$K^0$)		(4.57 ±0.06) %		S=1.2	834
$h^- h^- h^+ \pi^0 \nu_\tau$(ex. K^0, ω)		(2.79 ±0.08) %		S=1.2	834
$\pi^- \pi^+ \pi^- \pi^0 \nu_\tau$		(4.62 ±0.06) %		S=1.2	834
$\pi^- \pi^+ \pi^- \pi^0 \nu_\tau$(ex.$K^0$)		(4.48 ±0.06) %		S=1.2	834
$\pi^- \pi^+ \pi^- \pi^0 \nu_\tau$(ex.$K^0$,$\omega$)	[g]	(2.70 ±0.08) %		S=1.2	834
$h^- h^- h^+ \geq 2\pi^0 \nu_\tau$(ex. K^0)		(5.21 ±0.32) × 10^{-3}			–
$h^- h^- h^+ 2\pi^0 \nu_\tau$		(5.08 ±0.32) × 10^{-3}			797
$h^- h^- h^+ 2\pi^0 \nu_\tau$(ex.$K^0$)		(4.98 ±0.32) × 10^{-3}			797
$h^- h^- h^+ 2\pi^0 \nu_\tau$(ex.$K^0$,$\omega$,$\eta$)	[g]	(1.0 ±0.4) × 10^{-3}			797
$h^- h^- h^+ 3\pi^0 \nu_\tau$	[g]	(2.3 ±0.6) × 10^{-4}		S=1.2	749
$2\pi^- \pi^+ 3\pi^0 \nu_\tau$(ex.$K^0$)		(2.1 ±0.4) × 10^{-4}			749
$2\pi^- \pi^+ 3\pi^0 \nu_\tau$(ex.$K^0$, η, $f_1(1285)$)		(1.7 ±0.4) × 10^{-4}			–
$2\pi^- \pi^+ 3\pi^0 \nu_\tau$(ex.$K^0$, η, ω, $f_1(1285)$)		< 5.8	× 10^{-5}	CL=90%	–
$K^- h^+ h^- \geq 0$ neutrals ν_τ		(6.35 ±0.24) × 10^{-3}		S=1.5	794
$K^- h^+ \pi^- \nu_\tau$(ex.K^0)		(4.38 ±0.19) × 10^{-3}		S=2.7	794
$K^- h^+ \pi^- \pi^0 \nu_\tau$(ex.$K^0$)		(8.7 ±1.2) × 10^{-4}		S=1.1	763
$K^- \pi^+ \pi^- \geq 0$ neutrals ν_τ		(4.85 ±0.21) × 10^{-3}		S=1.4	794
$K^- \pi^+ \pi^- \geq 0 \pi^0 \nu_\tau$(ex.$K^0$)		(3.75 ±0.19) × 10^{-3}		S=1.5	794
$K^- \pi^+ \pi^- \nu_\tau$		(3.49 ±0.16) × 10^{-3}		S=1.9	794
$K^- \pi^+ \pi^- \nu_\tau$(ex.K^0)	[g]	(2.94 ±0.15) × 10^{-3}		S=2.2	794
$K^- \rho^0 \nu_\tau \to K^- \pi^+ \pi^- \nu_\tau$		(1.4 ±0.5) × 10^{-3}			–
$K^- \pi^+ \pi^- \pi^0 \nu_\tau$		(1.35 ±0.14) × 10^{-3}			763
$K^- \pi^+ \pi^- \pi^0 \nu_\tau$(ex.$K^0$)		(8.1 ±1.2) × 10^{-4}			763
$K^- \pi^+ \pi^- \pi^0 \nu_\tau$(ex.$K^0$,$\eta$)	[g]	(7.8 ±1.2) × 10^{-4}			763
$K^- \pi^+ \pi^- \pi^0 \nu_\tau$(ex.$K^0$,$\omega$)		(3.7 ±0.9) × 10^{-4}			763
$K^- \pi^+ K^- \geq 0$ neut. ν_τ		< 9	× 10^{-4}	CL=95%	685
$K^- K^+ \pi^- \geq 0$ neut. ν_τ		(1.50 ±0.06) × 10^{-3}		S=1.8	685
$K^- K^+ \pi^- \nu_\tau$	[g]	(1.44 ±0.05) × 10^{-3}		S=1.9	685
$K^- K^+ \pi^- \pi^0 \nu_\tau$	[g]	(6.1 ±2.5) × 10^{-5}		S=1.4	618
$K^- K^+ K^- \nu_\tau$		(2.1 ±0.8) × 10^{-5}		S=5.4	471
$K^- K^+ K^- \nu_\tau$(ex. ϕ)		< 2.5	× 10^{-6}	CL=90%	–
$K^- K^+ K^- \pi^0 \nu_\tau$		< 4.8	× 10^{-6}	CL=90%	345
$\pi^- K^+ \pi^- \geq 0$ neut. ν_τ		< 2.5	× 10^{-3}	CL=95%	794
$e^- e^- e^+ \overline{\nu}_e \nu_\tau$		(2.8 ±1.5) × 10^{-5}			888
$\mu^- e^- e^+ \overline{\nu}_\mu \nu_\tau$		< 3.6	× 10^{-5}	CL=90%	885

Modes with five charged particles

$3h^- 2h^+ \geq 0$ neutrals ν_τ (ex. $K^0_S \to \pi^- \pi^+$) ("5-prong")		(1.02 ±0.04) × 10^{-3}		S=1.1	794
$3h^- 2h^+ \nu_\tau$(ex.K^0)	[g]	(8.39 ±0.35) × 10^{-4}		S=1.1	794
$3\pi^- 2\pi^+ \nu_\tau$(ex.K^0, ω)		(8.3 ±0.4) × 10^{-4}			794
$3\pi^- 2\pi^+ \nu_\tau$(ex.K^0, ω, $f_1(1285)$)		(7.7 ±0.4) × 10^{-4}			–
$K^- 2\pi^- 2\pi^+ \nu_\tau$		< 2.4	× 10^{-6}	CL=90%	715
$K^+ 3\pi^- \pi^+ \nu_\tau$		< 5.0	× 10^{-6}	CL=90%	715
$K^+ K^- 2\pi^- \pi^+ \nu_\tau$		< 4.5	× 10^{-7}	CL=90%	528
$3h^- 2h^+ \pi^0 \nu_\tau$(ex.K^0)	[g]	(1.78 ±0.27) × 10^{-4}			746
$3\pi^- 2\pi^+ \pi^0 \nu_\tau$(ex.$K^0$)		(1.65 ±0.10) × 10^{-4}			746
$3\pi^- 2\pi^+ \pi^0 \nu_\tau$(ex.$K^0$, η, $f_1(1285)$)		(1.11 ±0.10) × 10^{-4}			–
$3\pi^- 2\pi^+ \pi^0 \nu_\tau$(ex.$K^0$, η, ω, $f_1(1285)$)		(3.6 ±0.9) × 10^{-5}			–
$K^- 2\pi^- 2\pi^+ \pi^0 \nu_\tau$		< 1.9	× 10^{-6}	CL=90%	657
$K^+ 3\pi^- \pi^+ \pi^0 \nu_\tau$		< 8	× 10^{-7}	CL=90%	657
$3h^- 2h^+ 2\pi^0 \nu_\tau$		< 3.4	× 10^{-6}	CL=90%	687

Miscellaneous other allowed modes

$(5\pi)^- \nu_\tau$		(7.6 ±0.5) × 10^{-3}			800
$4h^- 3h^+ \geq 0$ neutrals ν_τ ("7-prong")		< 3.0	× 10^{-7}	CL=90%	682
$4h^- 3h^+ \nu_\tau$		< 4.3	× 10^{-7}	CL=90%	682
$4h^- 3h^+ \pi^0 \nu_\tau$		< 2.5	× 10^{-7}	CL=90%	612
$X^-(S{=}-1) \nu_\tau$		(2.87 ±0.07) %		S=1.3	–
$K^*(892)^- \geq 0$ neutrals $\geq 0 K^0_L \nu_\tau$		(1.42 ±0.18) %		S=1.4	665
$K^*(892)^- \nu_\tau$		(1.20 ±0.07) %		S=1.8	665
$K^*(892)^- \nu_\tau \to \pi^- \overline{K}^0 \nu_\tau$		(7.9 ±0.5) × 10^{-3}			–
$K^*(892)^0 K^- \geq 0$ neutrals ν_τ		(3.2 ±1.4) × 10^{-3}			542
$K^*(892)^0 K^- \nu_\tau$		(2.1 ±0.4) × 10^{-3}			542
$\overline{K}^*(892)^0 \pi^- \geq 0$ neutrals ν_τ		(3.8 ±1.7) × 10^{-3}			655
$\overline{K}^*(892)^0 \pi^- \nu_\tau$		(2.2 ±0.5) × 10^{-3}			655
$(\overline{K}^*(892)\pi)^- \nu_\tau \to \pi^- \overline{K}^0 \pi^0 \nu_\tau$		(1.0 ±0.4) × 10^{-3}			–
$K_1(1270)^- \nu_\tau$		(4.7 ±1.1) × 10^{-3}			433
$K_1(1400)^- \nu_\tau$		(1.7 ±2.6) × 10^{-3}		S=1.7	335
$K^*(1410)^- \nu_\tau$		(1.5 $^{+1.4}_{-1.0}$) × 10^{-3}			326
$K^*_0(1430)^- \nu_\tau$		< 5	× 10^{-4}	CL=95%	317
$K^*_2(1430)^- \nu_\tau$		< 3	× 10^{-3}	CL=95%	316
$\eta \pi^- \nu_\tau$		< 9.9	× 10^{-5}	CL=95%	797
$\eta \pi^- \pi^0 \nu_\tau$	[g]	(1.39 ±0.10) × 10^{-3}		S=1.4	778
$\eta \pi^- \pi^0 \pi^0 \nu_\tau$		(1.81 ±0.31) × 10^{-4}			746
$\eta K^- \nu_\tau$	[g]	(1.52 ±0.08) × 10^{-4}			719
$\eta K^*(892)^- \nu_\tau$		(1.38 ±0.15) × 10^{-4}			511
$\eta K^- \pi^0 \nu_\tau$		(4.8 ±1.2) × 10^{-5}			665
$\eta K^- \pi^0$ (non-$K^*(892)$) ν_τ		< 3.5	× 10^{-5}	CL=90%	–
$\eta \overline{K}^0 \pi^- \nu_\tau$		(9.3 ±1.5) × 10^{-5}			661
$\eta \overline{K}^0 \pi^- \pi^0 \nu_\tau$		< 5.0	× 10^{-5}	CL=90%	590
$\eta K^- K^0 \nu_\tau$		< 9.0	× 10^{-6}	CL=90%	430
$\eta \pi^+ \pi^- \pi^- \geq 0$ neutrals ν_τ		< 3	× 10^{-3}	CL=90%	743
$\eta \pi^- \pi^+ \pi^- \nu_\tau$(ex.$K^0$)		(2.25 ±0.13) × 10^{-4}			743
$\eta \pi^- \pi^+ \pi^- \nu_\tau$(ex.$K^0$,$f_1(1285)$)		(9.9 ±1.6) × 10^{-5}			–
$\eta a_1(1260)^- \nu_\tau \to \eta \pi^- \rho^0 \nu_\tau$		< 3.9	× 10^{-4}	CL=90%	–
$\eta \eta \pi^- \nu_\tau$		< 7.4	× 10^{-6}	CL=90%	637
$\eta \eta \pi^- \pi^0 \nu_\tau$		< 2.0	× 10^{-4}	CL=95%	559
$\eta \eta K^- \nu_\tau$		< 3.0	× 10^{-6}	CL=90%	382
$\eta'(958) \pi^- \nu_\tau$		< 4.0	× 10^{-6}	CL=90%	620
$\eta'(958) \pi^- \pi^0 \nu_\tau$		< 1.2	× 10^{-5}	CL=90%	591
$\eta'(958) K^- \nu_\tau$		< 2.4	× 10^{-6}	CL=90%	495
$\phi \pi^- \nu_\tau$		(3.4 ±0.6) × 10^{-5}			585
$\phi K^- \nu_\tau$		(3.70 ±0.33) × 10^{-5}		S=1.3	445
$f_1(1285) \pi^- \nu_\tau$		(3.9 ±0.5) × 10^{-4}		S=1.9	408
$f_1(1285) \pi^- \nu_\tau \to \eta \pi^- \pi^+ \pi^- \nu_\tau$		(1.18 ±0.07) × 10^{-4}		S=1.3	–
$f_1(1285) \pi^- \nu_\tau \to 3\pi^- 2\pi^+ \nu_\tau$		(5.2 ±0.5) × 10^{-5}			–
$\pi(1300)^- \nu_\tau \to (\rho\pi)^- \nu_\tau \to (3\pi)^- \nu_\tau$		< 1.0	× 10^{-4}	CL=90%	–
$\pi(1300)^- \nu_\tau \to ((\pi\pi)_{S-\text{wave}}\ \pi)^- \nu_\tau \to (3\pi)^- \nu_\tau$		< 1.9	× 10^{-4}	CL=90%	–
$h^- \omega \geq 0$ neutrals ν_τ		(2.41 ±0.09) %		S=1.2	708
$h^- \omega \nu_\tau$	[g]	(2.00 ±0.08) %		S=1.3	708
$K^- \omega \nu_\tau$		(4.1 ±0.9) × 10^{-4}			610
$h^- \omega \pi^0 \nu_\tau$	[g]	(4.1 ±0.4) × 10^{-3}			684
$h^- \omega 2\pi^0 \nu_\tau$		(1.4 ±0.5) × 10^{-4}			644
$\pi^- \omega 2\pi^0 \nu_\tau$		(7.3 ±1.7) × 10^{-5}			644
$h^- 2\omega \nu_\tau$		< 5.4	× 10^{-7}	CL=90%	249
$2h^- h^+ \omega \nu_\tau$		(1.20 ±0.22) × 10^{-4}			641
$2\pi^- \pi^+ \omega \nu_\tau$		(8.4 ±0.7) × 10^{-5}			641

Lepton Summary Table

Lepton Family number (LF), Lepton number (L), or Baryon number (B) violating modes

L means lepton number violation (*e.g.* $\tau^- \to e^+\pi^-\pi^-$). Following common usage, LF means lepton family violation *and not* lepton number violation (*e.g.* $\tau^- \to e^-\pi^+\pi^-$). B means baryon number violation.

$e^-\gamma$	LF	$<$	3.3	$\times 10^{-8}$	CL=90%	888
$\mu^-\gamma$	LF	$<$	4.4	$\times 10^{-8}$	CL=90%	885
$e^-\pi^0$	LF	$<$	8.0	$\times 10^{-8}$	CL=90%	883
$\mu^-\pi^0$	LF	$<$	1.1	$\times 10^{-7}$	CL=90%	880
$e^-K^0_S$	LF	$<$	2.6	$\times 10^{-8}$	CL=90%	819
$\mu^-K^0_S$	LF	$<$	2.3	$\times 10^{-8}$	CL=90%	815
$e^-\eta$	LF	$<$	9.2	$\times 10^{-8}$	CL=90%	804
$\mu^-\eta$	LF	$<$	6.5	$\times 10^{-8}$	CL=90%	800
$e^-\rho^0$	LF	$<$	1.8	$\times 10^{-8}$	CL=90%	719
$\mu^-\rho^0$	LF	$<$	1.2	$\times 10^{-8}$	CL=90%	715
$e^-\omega$	LF	$<$	4.8	$\times 10^{-8}$	CL=90%	716
$\mu^-\omega$	LF	$<$	4.7	$\times 10^{-8}$	CL=90%	711
$e^-K^*(892)^0$	LF	$<$	3.2	$\times 10^{-8}$	CL=90%	665
$\mu^-K^*(892)^0$	LF	$<$	5.9	$\times 10^{-8}$	CL=90%	659
$e^-\overline{K}^*(892)^0$	LF	$<$	3.4	$\times 10^{-8}$	CL=90%	665
$\mu^-\overline{K}^*(892)^0$	LF	$<$	7.0	$\times 10^{-8}$	CL=90%	659
$e^-\eta'(958)$	LF	$<$	1.6	$\times 10^{-7}$	CL=90%	630
$\mu^-\eta'(958)$	LF	$<$	1.3	$\times 10^{-7}$	CL=90%	625
$e^-f_0(980) \to e^-\pi^+\pi^-$	LF	$<$	3.2	$\times 10^{-8}$	CL=90%	–
$\mu^-f_0(980) \to \mu^-\pi^+\pi^-$	LF	$<$	3.4	$\times 10^{-8}$	CL=90%	–
$e^-\phi$	LF	$<$	3.1	$\times 10^{-8}$	CL=90%	596
$\mu^-\phi$	LF	$<$	8.4	$\times 10^{-8}$	CL=90%	590
$e^-e^+e^-$	LF	$<$	2.7	$\times 10^{-8}$	CL=90%	888
$e^-\mu^+\mu^-$	LF	$<$	2.7	$\times 10^{-8}$	CL=90%	882
$e^+\mu^-\mu^-$	LF	$<$	1.7	$\times 10^{-8}$	CL=90%	882
$\mu^-e^+e^-$	LF	$<$	1.8	$\times 10^{-8}$	CL=90%	885
$\mu^+e^-e^-$	LF	$<$	1.5	$\times 10^{-8}$	CL=90%	885
$\mu^-\mu^+\mu^-$	LF	$<$	2.1	$\times 10^{-8}$	CL=90%	873
$e^-\pi^+\pi^-$	LF	$<$	2.3	$\times 10^{-8}$	CL=90%	877
$e^+\pi^-\pi^-$	L	$<$	2.0	$\times 10^{-8}$	CL=90%	877
$\mu^-\pi^+\pi^-$	LF	$<$	2.1	$\times 10^{-8}$	CL=90%	866
$\mu^+\pi^-\pi^-$	L	$<$	3.9	$\times 10^{-8}$	CL=90%	866
$e^-\pi^+K^-$	LF	$<$	3.7	$\times 10^{-8}$	CL=90%	813
$e^-\pi^-K^+$	LF	$<$	3.1	$\times 10^{-8}$	CL=90%	813
$e^+\pi^-K^-$	L	$<$	3.2	$\times 10^{-8}$	CL=90%	813
$e^-K^0_S K^0_S$	LF	$<$	7.1	$\times 10^{-8}$	CL=90%	736
$e^-K^+K^-$	LF	$<$	3.4	$\times 10^{-8}$	CL=90%	738
$e^+K^-K^-$	L	$<$	3.3	$\times 10^{-8}$	CL=90%	738
$\mu^-\pi^+K^-$	LF	$<$	8.6	$\times 10^{-8}$	CL=90%	800
$\mu^-\pi^-K^+$	LF	$<$	4.5	$\times 10^{-8}$	CL=90%	800
$\mu^+\pi^-K^-$	L	$<$	4.8	$\times 10^{-8}$	CL=90%	800
$\mu^-K^0_S K^0_S$	LF	$<$	8.0	$\times 10^{-8}$	CL=90%	696
$\mu^-K^+K^-$	LF	$<$	4.4	$\times 10^{-8}$	CL=90%	699
$\mu^+K^-K^-$	L	$<$	4.7	$\times 10^{-8}$	CL=90%	699
$e^-\pi^0\pi^0$	LF	$<$	6.5	$\times 10^{-6}$	CL=90%	878
$\mu^-\pi^0\pi^0$	LF	$<$	1.4	$\times 10^{-5}$	CL=90%	867
$e^-\eta\eta$	LF	$<$	3.5	$\times 10^{-5}$	CL=90%	699
$\mu^-\eta\eta$	LF	$<$	6.0	$\times 10^{-5}$	CL=90%	653
$e^-\pi^0\eta$	LF	$<$	2.4	$\times 10^{-5}$	CL=90%	798
$\mu^-\pi^0\eta$	LF	$<$	2.2	$\times 10^{-5}$	CL=90%	784
$p\mu^-\mu^-$	L,B	$<$	4.4	$\times 10^{-7}$	CL=90%	618
$\overline{p}\mu^+\mu^-$	L,B	$<$	3.3	$\times 10^{-7}$	CL=90%	618
$\overline{p}\gamma$	L,B	$<$	3.5	$\times 10^{-6}$	CL=90%	641
$\overline{p}\pi^0$	L,B	$<$	1.5	$\times 10^{-5}$	CL=90%	632
$\overline{p}2\pi^0$	L,B	$<$	3.3	$\times 10^{-5}$	CL=90%	604
$\overline{p}\eta$	L,B	$<$	8.9	$\times 10^{-6}$	CL=90%	475
$\overline{p}\pi^0\eta$	L,B	$<$	2.7	$\times 10^{-5}$	CL=90%	360
$\Lambda\pi^-$	L,B	$<$	7.2	$\times 10^{-8}$	CL=90%	525
$\overline{\Lambda}\pi^-$	L,B	$<$	1.4	$\times 10^{-7}$	CL=90%	525
e^- light boson	LF	$<$	2.7	$\times 10^{-3}$	CL=95%	–
μ^- light boson	LF	$<$	5	$\times 10^{-3}$	CL=95%	–

Heavy Charged Lepton Searches

$L^\pm$ – charged lepton

Mass $m >$ 100.8 GeV, CL = 95% [h] Decay to νW.

$L^\pm$ – stable charged heavy lepton

Mass $m >$ 102.6 GeV, CL = 95%

Neutrino Properties

See the note on "Neutrino properties listings" in the Particle Listings.

Mass $m <$ 2 eV (tritium decay)
Mean life/mass, $\tau/m >$ 300 s/eV, CL = 90% (reactor)
Mean life/mass, $\tau/m > 7\times10^9$ s/eV (solar)
Mean life/mass, $\tau/m >$ 15.4 s/eV, CL = 90% (accelerator)
Magnetic moment $\mu < 0.29\times10^{-10}\ \mu_B$, CL = 90% (reactor)

Number of Neutrino Types

Number $N = 2.984 \pm 0.008$ (Standard Model fits to LEP data)
Number $N = 2.92 \pm 0.05$ (S = 1.2) (Direct measurement of invisible Z width)

Neutrino Mixing

The following values are obtained through data analyses based on the 3-neutrino mixing scheme described in the review "Neutrino Mass, Mixing, and Oscillations" by K. Nakamura and S.T. Petcov in this *Review*.

$\sin^2(2\theta_{12}) = 0.846 \pm 0.021$
$\Delta m^2_{21} = (7.53 \pm 0.18)\times10^{-5}$ eV^2
$\sin^2(2\theta_{23}) = 0.999^{+0.001}_{-0.018}$ (normal mass hierarchy)
$\sin^2(2\theta_{23}) = 1.000^{+0.000}_{-0.017}$ (inverted mass hierarchy)
$\Delta m^2_{32} = (2.44 \pm 0.06)\times10^{-3}$ eV^2 [i] (normal mass hierarchy)
$\Delta m^2_{32} = (2.52 \pm 0.07)\times10^{-3}$ eV^2 [i] (inverted mass hierarchy)
$\sin^2(2\theta_{13}) = (9.3 \pm 0.8)\times10^{-2}$

Stable Neutral Heavy Lepton Mass Limits

Mass $m >$ 45.0 GeV, CL = 95% (Dirac)
Mass $m >$ 39.5 GeV, CL = 95% (Majorana)

Neutral Heavy Lepton Mass Limits

Mass $m >$ 90.3 GeV, CL = 95%
(Dirac ν_L coupling to e, μ, τ; conservative case(τ))
Mass $m >$ 80.5 GeV, CL = 95%
(Majorana ν_L coupling to e, μ, τ; conservative case(τ))

NOTES

In this Summary Table:

When a quantity has "(S = ...)" to its right, the error on the quantity has been enlarged by the "scale factor" S, defined as $S = \sqrt{\chi^2/(N-1)}$, where N is the number of measurements used in calculating the quantity. We do this when S > 1, which often indicates that the measurements are inconsistent. When S > 1.25, we also show in the Particle Listings an ideogram of the measurements. For more about S, see the Introduction.

A decay momentum p is given for each decay mode. For a 2-body decay, p is the momentum of each decay product in the rest frame of the decaying particle. For a 3-or-more-body decay, p is the largest momentum any of the products can have in this frame.

[a] This is the best limit for the mode $e^- \to \nu\gamma$. The best limit for "electron disappearance" is 6.4×10^{24} yr.

[b] See the "Note on Muon Decay Parameters" in the μ Particle Listings for definitions and details.

[c] P_μ is the longitudinal polarization of the muon from pion decay. In standard $V-A$ theory, $P_\mu = 1$ and $\rho = \delta = 3/4$.

[d] This only includes events with the γ energy > 10 MeV. Since the $e^-\overline{\nu}_e\nu_\mu$ and $e^-\overline{\nu}_e\nu_\mu\gamma$ modes cannot be clearly separated, we regard the latter mode as a subset of the former.

[e] See the relevant Particle Listings for the energy limits used in this measurement.

[f] A test of additive vs. multiplicative lepton family number conservation.

[g] Basis mode for the τ.

[h] $L^\pm$ mass limit depends on decay assumptions; see the Full Listings.

[i] The sign of Δm^2_{32} is not known at this time. The range quoted is for the absolute value.

QUARKS

The u-, d-, and s-quark masses are estimates of so-called "current-quark masses," in a mass-independent subtraction scheme such as $\overline{\text{MS}}$ at a scale $\mu \approx 2$ GeV. The c- and b-quark masses are the "running" masses in the $\overline{\text{MS}}$ scheme. For the b-quark we also quote the 1S mass. These can be different from the heavy quark masses obtained in potential models.

u

$I(J^P) = \frac{1}{2}(\frac{1}{2}^+)$

$m_u = 2.3^{+0.7}_{-0.5}$ MeV Charge $= \frac{2}{3}\,e$ $I_z = +\frac{1}{2}$
$m_u/m_d = 0.38$–0.58

d

$I(J^P) = \frac{1}{2}(\frac{1}{2}^+)$

$m_d = 4.8^{+0.5}_{-0.3}$ MeV Charge $= -\frac{1}{3}\,e$ $I_z = -\frac{1}{2}$
$m_s/m_d = 17$–22
$\overline{m} = (m_u + m_d)/2 = 3.5^{+0.7}_{-0.2}$ MeV

s

$I(J^P) = 0(\frac{1}{2}^+)$

$m_s = 95 \pm 5$ MeV Charge $= -\frac{1}{3}\,e$ Strangeness $= -1$
$m_s\ /\ ((m_u + m_d)/2) = 27.5 \pm 1.0$

c

$I(J^P) = 0(\frac{1}{2}^+)$

$m_c = 1.275 \pm 0.025$ GeV Charge $= \frac{2}{3}\,e$ Charm $= +1$

b

$I(J^P) = 0(\frac{1}{2}^+)$

Charge $= -\frac{1}{3}\,e$ Bottom $= -1$

$m_b(\overline{\text{MS}}) = 4.18 \pm 0.03$ GeV
$m_b(1\text{S}) = 4.66 \pm 0.03$ GeV

t

$I(J^P) = 0(\frac{1}{2}^+)$

Charge $= \frac{2}{3}\,e$ Top $= +1$

Mass (direct measurements) $m = 173.21 \pm 0.51 \pm 0.71$ GeV [a,b]
Mass ($\overline{\text{MS}}$ from cross-section measurements) $m = 160^{+5}_{-4}$ GeV [a]
Mass (Pole from cross-section measurements) $m = 176.7^{+4.0}_{-3.4}$ GeV
$m_t - m_{\overline{t}} = -0.2 \pm 0.5$ GeV (S = 1.1)
Full width $\Gamma = 2.0 \pm 0.5$ GeV
$\Gamma(Wb)/\Gamma(Wq(q = b, s, d)) = 0.91 \pm 0.04$

t-quark EW Couplings

$F_0 = 0.690 \pm 0.030$
$F_- = 0.314 \pm 0.025$
$F_+ = 0.008 \pm 0.016$
$F_{V+A} < 0.29$, CL = 95%

t DECAY MODES		Fraction (Γ_i/Γ)	Confidence level	p (MeV/c)
$Wq(q = b, s, d)$				–
Wb				–
$\ell\nu_\ell$anything		[c,d] (9.4±2.4) %		–
$\gamma q(q{=}u,c)$		[e] $< 5.9 \times 10^{-3}$	95%	–
$\Delta T = 1$ weak neutral current ($T1$) modes				
$Zq(q{=}u,c)$	$T1$	[f] $< 2.1 \times 10^{-3}$	95%	–

b′ (4th Generation) Quark, Searches for

Mass $m >$ 190 GeV, CL = 95% ($p\overline{p}$, quasi-stable b')
Mass $m >$ 400 GeV, CL = 95% (pp, neutral-current decays)
Mass $m >$ 675 GeV, CL = 95% (pp, charged-current decays)
Mass $m >$ 46.0 GeV, CL = 95% (e^+e^-, all decays)

t′ (4th Generation) Quark, Searches for

Mass $m >$ 782 GeV, CL = 95% (pp, neutral-current decays)
Mass $m >$ 700 GeV, CL = 95% (pp, charged-current decays)

Free Quark Searches

All searches since 1977 have had negative results.

NOTES

[a] A discussion of the definition of the top quark mass in these measurements can be found in the review "The Top Quark."
[b] Based on published top mass measurements using data from Tevatron Run-I and Run-II and LHC at $\sqrt{s} = 7$ TeV. Including the most recent unpublished results from Tevatron Run-II, the Tevatron Electroweak Working Group reports a top mass of 173.2 ± 0.9 GeV. See the note "The Top Quark' in the Quark Particle Listings of this *Review*.
[c] ℓ means e or μ decay mode, not the sum over them.
[d] Assumes lepton universality and W-decay acceptance.
[e] This limit is for $\Gamma(t \to \gamma q)/\Gamma(t \to Wb)$.
[f] This limit is for $\Gamma(t \to Zq)/\Gamma(t \to Wb)$.

Meson Summary Table

LIGHT UNFLAVORED MESONS ($S = C = B = 0$)

For $I = 1$ (π, b, ρ, a): $u\overline{d}$, $(u\overline{u}-d\overline{d})/\sqrt{2}$, $d\overline{u}$;
for $I = 0$ (η, η', h, h', ω, ϕ, f, f'): $c_1(u\overline{u} + d\overline{d}) + c_2(s\overline{s})$

$\pi^\pm$

$I^G(J^P) = 1^-(0^-)$

Mass $m = 139.57018 \pm 0.00035$ MeV (S = 1.2)
Mean life $\tau = (2.6033 \pm 0.0005) \times 10^{-8}$ s (S = 1.2)
$c\tau = 7.8045$ m

$\pi^\pm \to \ell^\pm \nu\gamma$ form factors [a]

$F_V = 0.0254 \pm 0.0017$
$F_A = 0.0119 \pm 0.0001$
F_V slope parameter $a = 0.10 \pm 0.06$
$R = 0.059^{+0.009}_{-0.008}$

π^- modes are charge conjugates of the modes below.

For decay limits to particles which are not established, see the section on Searches for Axions and Other Very Light Bosons.

π^+ DECAY MODES		Fraction (Γ_i/Γ)	Confidence level	p (MeV/c)
$\mu^+\nu_\mu$		[b] (99.98770±0.00004) %		30
$\mu^+\nu_\mu\gamma$		[c] (2.00 ±0.25) $\times 10^{-4}$		30
$e^+\nu_e$		[b] (1.230 ±0.004) $\times 10^{-4}$		70
$e^+\nu_e\gamma$		[c] (7.39 ±0.05) $\times 10^{-7}$		70
$e^+\nu_e\pi^0$		(1.036 ±0.006) $\times 10^{-8}$		4
$e^+\nu_e e^+ e^-$		(3.2 ±0.5) $\times 10^{-9}$		70
$e^+\nu_e\nu\overline{\nu}$		< 5 $\times 10^{-6}$	90%	70
Lepton Family number (LF) or Lepton number (L) violating modes				
$\mu^+\overline{\nu}_e$	L	[d] < 1.5 $\times 10^{-3}$	90%	30
$\mu^+\nu_e$	LF	[d] < 8.0 $\times 10^{-3}$	90%	30
$\mu^- e^+ e^+\nu$	LF	< 1.6 $\times 10^{-6}$	90%	30

π^0

$I^G(J^{PC}) = 1^-(0^{-+})$

Mass $m = 134.9766 \pm 0.0006$ MeV (S = 1.1)
$m_{\pi^\pm} - m_{\pi^0} = 4.5936 \pm 0.0005$ MeV
Mean life $\tau = (8.52 \pm 0.18) \times 10^{-17}$ s (S = 1.2)
$c\tau = 25.5$ nm

For decay limits to particles which are not established, see the appropriate Search sections (A^0 (axion) and Other Light Boson (X^0) Searches, etc.).

π^0 DECAY MODES		Fraction (Γ_i/Γ)	Scale factor/ Confidence level	p (MeV/c)
2γ		(98.823±0.034) %	S=1.5	67
$e^+e^-\gamma$		(1.174±0.035) %	S=1.5	67
γpositronium		(1.82 ±0.29) $\times 10^{-9}$		67
$e^+e^+e^-e^-$		(3.34 ±0.16) $\times 10^{-5}$		67
e^+e^-		(6.46 ±0.33) $\times 10^{-8}$		67
4γ		< 2 $\times 10^{-8}$	CL=90%	67
$\nu\overline{\nu}$		[e] < 2.7 $\times 10^{-7}$	CL=90%	67
$\nu_e\overline{\nu}_e$		< 1.7 $\times 10^{-6}$	CL=90%	67
$\nu_\mu\overline{\nu}_\mu$		< 1.6 $\times 10^{-6}$	CL=90%	67
$\nu_\tau\overline{\nu}_\tau$		< 2.1 $\times 10^{-6}$	CL=90%	67
$\gamma\nu\overline{\nu}$		< 6 $\times 10^{-4}$	CL=90%	67
Charge conjugation (C) or Lepton Family number (LF) violating modes				
3γ	C	< 3.1 $\times 10^{-8}$	CL=90%	67
$\mu^+ e^-$	LF	< 3.8 $\times 10^{-10}$	CL=90%	26
$\mu^- e^+$	LF	< 3.4 $\times 10^{-9}$	CL=90%	26
$\mu^+ e^- + \mu^- e^+$	LF	< 3.6 $\times 10^{-10}$	CL=90%	26

η

$I^G(J^{PC}) = 0^+(0^{-+})$

Mass $m = 547.862 \pm 0.018$ MeV
Full width $\Gamma = 1.31 \pm 0.05$ keV

C-nonconserving decay parameters

$\pi^+\pi^-\pi^0$ left-right asymmetry = $(0.09^{+0.11}_{-0.12}) \times 10^{-2}$
$\pi^+\pi^-\pi^0$ sextant asymmetry = $(0.12^{+0.10}_{-0.11}) \times 10^{-2}$
$\pi^+\pi^-\pi^0$ quadrant asymmetry = $(-0.09 \pm 0.09) \times 10^{-2}$
$\pi^+\pi^-\gamma$ left-right asymmetry = $(0.9 \pm 0.4) \times 10^{-2}$
$\pi^+\pi^-\gamma$ β (D-wave) = -0.02 ± 0.07 (S = 1.3)

CP-nonconserving decay parameters

$\pi^+\pi^- e^+ e^-$ decay-plane asymmetry $A_\phi = (-0.6 \pm 3.1) \times 10^{-2}$

Dalitz plot parameter

$\pi^0\pi^0\pi^0$ $\alpha = -0.0315 \pm 0.0015$

η DECAY MODES		Fraction (Γ_i/Γ)	Scale factor/ Confidence level	p (MeV/c)
Neutral modes				
neutral modes		(72.12±0.34) %	S=1.2	–
2γ		(39.41±0.20) %	S=1.1	274
$3\pi^0$		(32.68±0.23) %	S=1.1	179
$\pi^0 2\gamma$		(2.7 ±0.5) $\times 10^{-4}$	S=1.1	257
$2\pi^0 2\gamma$		< 1.2 $\times 10^{-3}$	CL=90%	238
4γ		< 2.8 $\times 10^{-4}$	CL=90%	274
invisible		< 1.0 $\times 10^{-4}$	CL=90%	–
Charged modes				
charged modes		(28.10±0.34) %	S=1.2	–
$\pi^+\pi^-\pi^0$		(22.92±0.28) %	S=1.2	174
$\pi^+\pi^-\gamma$		(4.22±0.08) %	S=1.1	236
$e^+e^-\gamma$		(6.9 ±0.4) $\times 10^{-3}$	S=1.3	274
$\mu^+\mu^-\gamma$		(3.1 ±0.4) $\times 10^{-4}$		253
e^+e^-		< 5.6 $\times 10^{-6}$	CL=90%	274
$\mu^+\mu^-$		(5.8 ±0.8) $\times 10^{-6}$		253
$2e^+2e^-$		(2.40±0.22) $\times 10^{-5}$		274
$\pi^+\pi^- e^+ e^-(\gamma)$		(2.68±0.11) $\times 10^{-4}$		235
$e^+e^-\mu^+\mu^-$		< 1.6 $\times 10^{-4}$	CL=90%	253
$2\mu^+2\mu^-$		< 3.6 $\times 10^{-4}$	CL=90%	161
$\mu^+\mu^-\pi^+\pi^-$		< 3.6 $\times 10^{-4}$	CL=90%	113
$\pi^+ e^-\overline{\nu}_e$ + c.c.		< 1.7 $\times 10^{-4}$	CL=90%	256
$\pi^+\pi^- 2\gamma$		< 2.1 $\times 10^{-3}$		236
$\pi^+\pi^-\pi^0\gamma$		< 5 $\times 10^{-4}$	CL=90%	174
$\pi^0\mu^+\mu^-\gamma$		< 3 $\times 10^{-6}$	CL=90%	210
Charge conjugation (C), Parity (P), Charge conjugation × Parity (CP), or Lepton Family number (LF) violating modes				
$\pi^0\gamma$	C	< 9 $\times 10^{-5}$	CL=90%	257
$\pi^+\pi^-$	P,CP	< 1.3 $\times 10^{-5}$	CL=90%	236
$2\pi^0$	P,CP	< 3.5 $\times 10^{-4}$	CL=90%	238
$2\pi^0\gamma$	C	< 5 $\times 10^{-4}$	CL=90%	238
$3\pi^0\gamma$	C	< 6 $\times 10^{-5}$	CL=90%	179
3γ	C	< 1.6 $\times 10^{-5}$	CL=90%	274
$4\pi^0$	P,CP	< 6.9 $\times 10^{-7}$	CL=90%	40
$\pi^0 e^+ e^-$	C	[f] < 4 $\times 10^{-5}$	CL=90%	257
$\pi^0\mu^+\mu^-$	C	[f] < 5 $\times 10^{-6}$	CL=90%	210
$\mu^+ e^- + \mu^- e^+$	LF	< 6 $\times 10^{-6}$	CL=90%	264

$f_0(500)$ or σ [g] was $f_0(600)$

$I^G(J^{PC}) = 0^+(0^{++})$

Mass m = (400–550) MeV
Full width Γ = (400–700) MeV

$f_0(500)$ DECAY MODES	Fraction (Γ_i/Γ)	p (MeV/c)
$\pi\pi$	dominant	–
$\gamma\gamma$	seen	–

$\rho(770)$ [h]

$I^G(J^{PC}) = 1^+(1^{--})$

Mass $m = 775.26 \pm 0.25$ MeV
Full width $\Gamma = 149.1 \pm 0.8$ MeV
$\Gamma_{ee} = 7.04 \pm 0.06$ keV

$\rho(770)$ DECAY MODES	Fraction (Γ_i/Γ)		Scale factor/ Confidence level	p (MeV/c)
$\pi\pi$	~ 100	%		363
$\rho(770)^\pm$ decays				
$\pi^\pm\gamma$	$(4.5 \pm 0.5) \times 10^{-4}$		S=2.2	375
$\pi^\pm\eta$	$< 6 \times 10^{-3}$		CL=84%	152
$\pi^\pm\pi^+\pi^-\pi^0$	$< 2.0 \times 10^{-3}$		CL=84%	254
$\rho(770)^0$ decays				
$\pi^+\pi^-\gamma$	$(9.9 \pm 1.6) \times 10^{-3}$			362
$\pi^0\gamma$	$(6.0 \pm 0.8) \times 10^{-4}$			376
$\eta\gamma$	$(3.00 \pm 0.20) \times 10^{-4}$			194
$\pi^0\pi^0\gamma$	$(4.5 \pm 0.8) \times 10^{-5}$			363
$\mu^+\mu^-$	[i] $(4.55 \pm 0.28) \times 10^{-5}$			373
e^+e^-	[i] $(4.72 \pm 0.05) \times 10^{-5}$			388
$\pi^+\pi^-\pi^0$	$(1.01^{+0.54}_{-0.36} \pm 0.34) \times 10^{-4}$			323
$\pi^+\pi^-\pi^+\pi^-$	$(1.8 \pm 0.9) \times 10^{-5}$			251
$\pi^+\pi^-\pi^0\pi^0$	$(1.6 \pm 0.8) \times 10^{-5}$			257
$\pi^0 e^+ e^-$	$< 1.2 \times 10^{-5}$		CL=90%	376

$\omega(782)$

$I^G(J^{PC}) = 0^-(1^{--})$

Mass $m = 782.65 \pm 0.12$ MeV (S = 1.9)
Full width $\Gamma = 8.49 \pm 0.08$ MeV
$\Gamma_{ee} = 0.60 \pm 0.02$ keV

$\omega(782)$ DECAY MODES	Fraction (Γ_i/Γ)		Scale factor/ Confidence level	p (MeV/c)
$\pi^+\pi^-\pi^0$	(89.2 ± 0.7) %			327
$\pi^0\gamma$	(8.28 ± 0.28) %		S=2.1	380
$\pi^+\pi^-$	$(1.53^{+0.11}_{-0.13})$ %		S=1.2	366
neutrals (excluding $\pi^0\gamma$)	$(8^{+8}_{-5}) \times 10^{-3}$		S=1.1	–
$\eta\gamma$	$(4.6 \pm 0.4) \times 10^{-4}$		S=1.1	200
$\pi^0 e^+ e^-$	$(7.7 \pm 0.6) \times 10^{-4}$			380
$\pi^0\mu^+\mu^-$	$(1.3 \pm 0.4) \times 10^{-4}$		S=2.1	349
e^+e^-	$(7.28 \pm 0.14) \times 10^{-5}$		S=1.3	391
$\pi^+\pi^-\pi^0\pi^0$	$< 2 \times 10^{-4}$		CL=90%	262
$\pi^+\pi^-\gamma$	$< 3.6 \times 10^{-3}$		CL=95%	366
$\pi^+\pi^-\pi^+\pi^-$	$< 1 \times 10^{-3}$		CL=90%	256
$\pi^0\pi^0\gamma$	$(6.6 \pm 1.1) \times 10^{-5}$			367
$\eta\pi^0\gamma$	$< 3.3 \times 10^{-5}$		CL=90%	162
$\mu^+\mu^-$	$(9.0 \pm 3.1) \times 10^{-5}$			377
3γ	$< 1.9 \times 10^{-4}$		CL=95%	391
Charge conjugation (C) violating modes				
$\eta\pi^0$	C $< 2.1 \times 10^{-4}$		CL=90%	162
$2\pi^0$	C $< 2.1 \times 10^{-4}$		CL=90%	367
$3\pi^0$	C $< 2.3 \times 10^{-4}$		CL=90%	330

$\eta'(958)$

$I^G(J^{PC}) = 0^+(0^{-+})$

Mass $m = 957.78 \pm 0.06$ MeV
Full width $\Gamma = 0.198 \pm 0.009$ MeV

$\eta'(958)$ DECAY MODES	Fraction (Γ_i/Γ)	Confidence level	p (MeV/c)
$\pi^+\pi^-\eta$	(42.9 ± 0.7) %		232
$\rho^0\gamma$ (including non-resonant $\pi^+\pi^-\gamma$)	(29.1 ± 0.5) %		165
$\pi^0\pi^0\eta$	(22.2 ± 0.8) %		239
$\omega\gamma$	(2.75 ± 0.23) %		159
$\gamma\gamma$	(2.20 ± 0.08) %		479
$3\pi^0$	$(2.14 \pm 0.20) \times 10^{-3}$		430
$\mu^+\mu^-\gamma$	$(1.08 \pm 0.27) \times 10^{-4}$		467
$\pi^+\pi^-\mu^+\mu^-$	$< 2.9 \times 10^{-5}$	90%	401
$\pi^+\pi^-\pi^0$	$(3.8 \pm 0.4) \times 10^{-3}$		428
$\pi^0\rho^0$	< 4 %	90%	111
$2(\pi^+\pi^-)$	$< 2.4 \times 10^{-4}$	90%	372
$\pi^+\pi^-2\pi^0$	$< 2.5 \times 10^{-3}$	90%	376
$2(\pi^+\pi^-)$ neutrals	< 1 %	95%	–
$2(\pi^+\pi^-)\pi^0$	$< 1.9 \times 10^{-3}$	90%	298
$2(\pi^+\pi^-)2\pi^0$	< 1 %	95%	197
$3(\pi^+\pi^-)$	$< 3.1 \times 10^{-5}$	90%	189
$\pi^+\pi^-e^+e^-$	$(2.4^{+1.3}_{-1.0}) \times 10^{-3}$		458
$\pi^+e^-\nu_e$ + c.c.	$< 2.1 \times 10^{-4}$	90%	469
$\gamma e^+ e^-$	$< 9 \times 10^{-4}$	90%	479
$\pi^0\gamma\gamma$	$< 8 \times 10^{-4}$	90%	469
$4\pi^0$	$< 5 \times 10^{-4}$	90%	380
e^+e^-	$< 2.1 \times 10^{-7}$	90%	479
invisible	$< 5 \times 10^{-4}$	90%	–
Charge conjugation (C), Parity (P), Lepton family number (LF) violating modes			
$\pi^+\pi^-$	P,CP $< 6 \times 10^{-5}$	90%	458
$\pi^0\pi^0$	P,CP $< 4 \times 10^{-4}$	90%	459
$\pi^0 e^+ e^-$	C [f] $< 1.4 \times 10^{-3}$	90%	469
$\eta e^+ e^-$	C [f] $< 2.4 \times 10^{-3}$	90%	322
3γ	C $< 1.0 \times 10^{-4}$	90%	479
$\mu^+\mu^-\pi^0$	C [f] $< 6.0 \times 10^{-5}$	90%	445
$\mu^+\mu^-\eta$	C [f] $< 1.5 \times 10^{-5}$	90%	273
$e\mu$	LF $< 4.7 \times 10^{-4}$	90%	473

$f_0(980)$ [j]

$I^G(J^{PC}) = 0^+(0^{++})$

Mass $m = 990 \pm 20$ MeV
Full width $\Gamma = 40$ to 100 MeV

$f_0(980)$ DECAY MODES	Fraction (Γ_i/Γ)	p (MeV/c)
$\pi\pi$	dominant	476
$K\overline{K}$	seen	36
$\gamma\gamma$	seen	495

$a_0(980)$ [j]

$I^G(J^{PC}) = 1^-(0^{++})$

Mass $m = 980 \pm 20$ MeV
Full width $\Gamma = 50$ to 100 MeV

$a_0(980)$ DECAY MODES	Fraction (Γ_i/Γ)	p (MeV/c)
$\eta\pi$	dominant	319
$K\overline{K}$	seen	†
$\gamma\gamma$	seen	490

$\phi(1020)$

$I^G(J^{PC}) = 0^-(1^{--})$

Mass $m = 1019.461 \pm 0.019$ MeV (S = 1.1)
Full width $\Gamma = 4.266 \pm 0.031$ MeV (S = 1.2)

$\phi(1020)$ DECAY MODES	Fraction (Γ_i/Γ)	Scale factor/ Confidence level	p (MeV/c)
K^+K^-	(48.9 ± 0.5) %	S=1.1	127
$K^0_L K^0_S$	(34.2 ± 0.4) %	S=1.1	110
$\rho\pi$ + $\pi^+\pi^-\pi^0$	(15.32 ± 0.32) %	S=1.1	–
$\eta\gamma$	(1.309 ± 0.024) %	S=1.2	363
$\pi^0\gamma$	$(1.27 \pm 0.06) \times 10^{-3}$		501
$\ell^+\ell^-$	—		510
e^+e^-	$(2.954 \pm 0.030) \times 10^{-4}$	S=1.1	510
$\mu^+\mu^-$	$(2.87 \pm 0.19) \times 10^{-4}$		499
$\eta e^+ e^-$	$(1.15 \pm 0.10) \times 10^{-4}$		363
$\pi^+\pi^-$	$(7.4 \pm 1.3) \times 10^{-5}$		490
$\omega\pi^0$	$(4.7 \pm 0.5) \times 10^{-5}$		172
$\omega\gamma$	< 5 %	CL=84%	209
$\rho\gamma$	$< 1.2 \times 10^{-5}$	CL=90%	215
$\pi^+\pi^-\gamma$	$(4.1 \pm 1.3) \times 10^{-5}$		490
$f_0(980)\gamma$	$(3.22 \pm 0.19) \times 10^{-4}$	S=1.1	29
$\pi^0\pi^0\gamma$	$(1.13 \pm 0.06) \times 10^{-4}$		492
$\pi^+\pi^-\pi^+\pi^-$	$(4.0^{+2.8}_{-2.2}) \times 10^{-6}$		410
$\pi^+\pi^+\pi^-\pi^-\pi^0$	$< 4.6 \times 10^{-6}$	CL=90%	342
$\pi^0 e^+ e^-$	$(1.12 \pm 0.28) \times 10^{-5}$		501
$\pi^0\eta\gamma$	$(7.27 \pm 0.30) \times 10^{-5}$	S=1.5	346

Meson Summary Table

$a_0(980)\gamma$	$(7.6 \pm 0.6) \times 10^{-5}$		39
$K^0\overline{K}^0\gamma$	$< 1.9 \times 10^{-8}$	CL=90%	110
$\eta'(958)\gamma$	$(6.25 \pm 0.21) \times 10^{-5}$		60
$\eta\pi^0\pi^0\gamma$	$< 2 \times 10^{-5}$	CL=90%	293
$\mu^+\mu^-\gamma$	$(1.4 \pm 0.5) \times 10^{-5}$		499
$\rho\gamma\gamma$	$< 1.2 \times 10^{-4}$	CL=90%	215
$\eta\pi^+\pi^-$	$< 1.8 \times 10^{-5}$	CL=90%	288
$\eta\mu^+\mu^-$	$< 9.4 \times 10^{-6}$	CL=90%	321
$\eta U \to \eta e^+ e^-$	$< 1 \times 10^{-6}$	CL=90%	–
Lepton Faminly number (LF) violating modes			
$e^\pm\mu^\mp$ LF	$< 2 \times 10^{-6}$	CL=90%	504

$h_1(1170)$

$I^G(J^{PC}) = 0^-(1^{+-})$

Mass $m = 1170 \pm 20$ MeV
Full width $\Gamma = 360 \pm 40$ MeV

$h_1(1170)$ DECAY MODES	Fraction (Γ_i/Γ)	p (MeV/c)
$\rho\pi$	seen	308

$b_1(1235)$

$I^G(J^{PC}) = 1^+(1^{+-})$

Mass $m = 1229.5 \pm 3.2$ MeV (S = 1.6)
Full width $\Gamma = 142 \pm 9$ MeV (S = 1.2)

$b_1(1235)$ DECAY MODES	Fraction (Γ_i/Γ)	Confidence level	p (MeV/c)
$\omega\pi$	dominant		348
[D/S amplitude ratio $= 0.277 \pm 0.027$]			
$\pi^\pm\gamma$	$(1.6 \pm 0.4) \times 10^{-3}$		607
$\eta\rho$	seen		†
$\pi^+\pi^+\pi^-\pi^0$	< 50 %	84%	535
$K^*(892)^\pm K^\mp$	seen		†
$(K\overline{K})^\pm\pi^0$	< 8 %	90%	248
$K^0_S K^0_L \pi^\pm$	< 6 %	90%	235
$K^0_S K^0_S \pi^\pm$	< 2 %	90%	235
$\phi\pi$	< 1.5 %	84%	147

$a_1(1260)$ [k]

$I^G(J^{PC}) = 1^-(1^{++})$

Mass $m = 1230 \pm 40$ MeV [l]
Full width $\Gamma = 250$ to 600 MeV

$a_1(1260)$ DECAY MODES	Fraction (Γ_i/Γ)	p (MeV/c)
$(\rho\pi)_{S-\text{wave}}$	seen	353
$(\rho\pi)_{D-\text{wave}}$	seen	353
$(\rho(1450)\pi)_{S-\text{wave}}$	seen	†
$(\rho(1450)\pi)_{D-\text{wave}}$	seen	†
$\sigma\pi$	seen	–
$f_0(980)\pi$	not seen	179
$f_0(1370)\pi$	seen	†
$f_2(1270)\pi$	seen	†
$K\overline{K}^*(892) +$ c.c.	seen	†
$\pi\gamma$	seen	608

$f_2(1270)$

$I^G(J^{PC}) = 0^+(2^{++})$

Mass $m = 1275.1 \pm 1.2$ MeV (S = 1.1)
Full width $\Gamma = 185.1^{+2.9}_{-2.4}$ MeV (S = 1.5)

$f_2(1270)$ DECAY MODES	Fraction (Γ_i/Γ)	Scale factor/ Confidence level	p (MeV/c)
$\pi\pi$	$(84.8\ ^{+2.4}_{-1.2})$ %	S=1.2	623
$\pi^+\pi^-2\pi^0$	$(7.1\ ^{+1.4}_{-2.7})$ %	S=1.3	562
$K\overline{K}$	(4.6 ± 0.4) %	S=2.8	403
$2\pi^+2\pi^-$	(2.8 ± 0.4) %	S=1.2	559
$\eta\eta$	$(4.0 \pm 0.8) \times 10^{-3}$	S=2.1	326
$4\pi^0$	$(3.0 \pm 1.0) \times 10^{-3}$		564
$\gamma\gamma$	$(1.64 \pm 0.19) \times 10^{-5}$	S=1.9	638
$\eta\pi\pi$	$< 8 \times 10^{-3}$	CL=95%	477
$K^0K^-\pi^+ +$ c.c.	$< 3.4 \times 10^{-3}$	CL=95%	293
e^+e^-	$< 6 \times 10^{-10}$	CL=90%	638

$f_1(1285)$

$I^G(J^{PC}) = 0^+(1^{++})$

Mass $m = 1281.9 \pm 0.5$ MeV (S = 1.8)
Full width $\Gamma = 24.2 \pm 1.1$ MeV (S = 1.3)

$f_1(1285)$ DECAY MODES	Fraction (Γ_i/Γ)	Scale factor/ Confidence level	p (MeV/c)
4π	$(33.1^{+\ 2.1}_{-\ 1.8})$ %	S=1.3	568
$\pi^0\pi^0\pi^+\pi^-$	$(22.0^{+\ 1.4}_{-\ 1.2})$ %	S=1.3	566
$2\pi^+2\pi^-$	$(11.0^{+\ 0.7}_{-\ 0.6})$ %	S=1.3	563
$\rho^0\pi^+\pi^-$	$(11.0^{+\ 0.7}_{-\ 0.6})$ %	S=1.3	336
$\rho^0\rho^0$	seen		†
$4\pi^0$	$< 7 \times 10^{-4}$	CL=90%	568
$\eta\pi^+\pi^-$	(35 ± 15) %		479
$\eta\pi\pi$	$(52.4^{+\ 1.9}_{-\ 2.2})$ %	S=1.2	482
$a_0(980)\pi$ [ignoring $a_0(980) \to K\overline{K}$]	(36 ± 7) %		238
$\eta\pi\pi$ [excluding $a_0(980)\pi$]	(16 ± 7) %		482
$K\overline{K}\pi$	(9.0 ± 0.4) %	S=1.1	308
$K\overline{K}^*(892)$	not seen		†
$\pi^+\pi^-\pi^0$	$(3.0 \pm 0.9) \times 10^{-3}$		603
$\rho^\pm\pi^\mp$	$< 3.1 \times 10^{-3}$	CL=95%	390
$\gamma\rho^0$	(5.5 ± 1.3) %	S=2.8	407
$\phi\gamma$	$(7.4 \pm 2.6) \times 10^{-4}$		236

$\eta(1295)$

$I^G(J^{PC}) = 0^+(0^{-+})$

Mass $m = 1294 \pm 4$ MeV (S = 1.6)
Full width $\Gamma = 55 \pm 5$ MeV

$\eta(1295)$ DECAY MODES	Fraction (Γ_i/Γ)	p (MeV/c)
$\eta\pi^+\pi^-$	seen	487
$a_0(980)\pi$	seen	248
$\eta\pi^0\pi^0$	seen	490
$\eta(\pi\pi)_{S\text{-wave}}$	seen	–

$\pi(1300)$

$I^G(J^{PC}) = 1^-(0^{-+})$

Mass $m = 1300 \pm 100$ MeV [l]
Full width $\Gamma = 200$ to 600 MeV

$\pi(1300)$ DECAY MODES	Fraction (Γ_i/Γ)	p (MeV/c)
$\rho\pi$	seen	404
$\pi(\pi\pi)_{S\text{-wave}}$	seen	–

$a_2(1320)$

$I^G(J^{PC}) = 1^-(2^{++})$

Mass $m = 1318.3^{+0.5}_{-0.6}$ MeV (S = 1.2)
Full width $\Gamma = 107 \pm 5$ MeV [l]

$a_2(1320)$ DECAY MODES	Fraction (Γ_i/Γ)	Scale factor/ Confidence level	p (MeV/c)
3π	(70.1 ± 2.7) %	S=1.2	624
$\eta\pi$	(14.5 ± 1.2) %		535
$\omega\pi\pi$	(10.6 ± 3.2) %	S=1.3	366
$K\overline{K}$	(4.9 ± 0.8) %		437
$\eta'(958)\pi$	$(5.3 \pm 0.9) \times 10^{-3}$		288
$\pi^\pm\gamma$	$(2.68 \pm 0.31) \times 10^{-3}$		652
$\gamma\gamma$	$(9.4 \pm 0.7) \times 10^{-6}$		659
e^+e^-	$< 5 \times 10^{-9}$	CL=90%	659

$f_0(1370)$ [j]

$I^G(J^{PC}) = 0^+(0^{++})$

Mass $m = 1200$ to 1500 MeV
Full width $\Gamma = 200$ to 500 MeV

$f_0(1370)$ DECAY MODES	Fraction (Γ_i/Γ)	p (MeV/c)
$\pi\pi$	seen	672
4π	seen	617
$4\pi^0$	seen	617
$2\pi^+2\pi^-$	seen	612
$\pi^+\pi^-2\pi^0$	seen	615
$\rho\rho$	dominant	†
$2(\pi\pi)_{S\text{-wave}}$	seen	–
$\pi(1300)\pi$	seen	†
$a_1(1260)\pi$	seen	35
$\eta\eta$	seen	411
$K\overline{K}$	seen	475
$K\overline{K}n\pi$	not seen	†
6π	not seen	508
$\omega\omega$	not seen	†
$\gamma\gamma$	seen	685
e^+e^-	not seen	685

$\pi_1(1400)$ [n]

$I^G(J^{PC}) = 1^-(1^{-+})$

Mass $m = 1354 \pm 25$ MeV (S = 1.8)
Full width $\Gamma = 330 \pm 35$ MeV

$\pi_1(1400)$ DECAY MODES	Fraction (Γ_i/Γ)	p (MeV/c)
$\eta\pi^0$	seen	557
$\eta\pi^-$	seen	556

$\eta(1405)$ [o]

$I^G(J^{PC}) = 0^+(0^{-+})$

Mass $m = 1408.8 \pm 1.8$ MeV [l] (S = 2.1)
Full width $\Gamma = 51.0 \pm 2.9$ MeV [l] (S = 1.8)

$\eta(1405)$ DECAY MODES	Fraction (Γ_i/Γ)	Confidence level	p (MeV/c)
$K\overline{K}\pi$	seen		424
$\eta\pi\pi$	seen		562
$a_0(980)\pi$	seen		345
$\eta(\pi\pi)_{S\text{-wave}}$	seen		–
$f_0(980)\eta$	seen		†
4π	seen		639
$\rho\rho$	<58 %	99.85%	†
$\rho^0\gamma$	seen		491
$K^*(892)K$	seen		123

$f_1(1420)$ [p]

$I^G(J^{PC}) = 0^+(1^{++})$

Mass $m = 1426.4 \pm 0.9$ MeV (S = 1.1)
Full width $\Gamma = 54.9 \pm 2.6$ MeV

$f_1(1420)$ DECAY MODES	Fraction (Γ_i/Γ)	p (MeV/c)
$K\overline{K}\pi$	dominant	438
$K\overline{K}^*(892)+$ c.c.	dominant	163
$\eta\pi\pi$	possibly seen	573
$\phi\gamma$	seen	349

$\omega(1420)$ [q]

$I^G(J^{PC}) = 0^-(1^{--})$

Mass m (1400–1450) MeV
Full width Γ (180–250) MeV

$\omega(1420)$ DECAY MODES	Fraction (Γ_i/Γ)	p (MeV/c)
$\rho\pi$	dominant	486
$\omega\pi\pi$	seen	444
$b_1(1235)\pi$	seen	125
e^+e^-	seen	710

$a_0(1450)$ [j]

$I^G(J^{PC}) = 1^-(0^{++})$

Mass $m = 1474 \pm 19$ MeV
Full width $\Gamma = 265 \pm 13$ MeV

$a_0(1450)$ DECAY MODES	Fraction (Γ_i/Γ)	p (MeV/c)
$\pi\eta$	seen	627
$\pi\eta'(958)$	seen	410
$K\overline{K}$	seen	547
$\omega\pi\pi$	seen	484
$a_0(980)\pi\pi$	seen	342
$\gamma\gamma$	seen	737

$\rho(1450)$ [r]

$I^G(J^{PC}) = 1^+(1^{--})$

Mass $m = 1465 \pm 25$ MeV [l]
Full width $\Gamma = 400 \pm 60$ MeV [l]

$\rho(1450)$ DECAY MODES	Fraction (Γ_i/Γ)	p (MeV/c)
$\pi\pi$	seen	720
4π	seen	669
e^+e^-	seen	732
$\eta\rho$	possibly seen	311
$a_2(1320)\pi$	not seen	54
$K\overline{K}$	not seen	541
$K\overline{K}^*(892)+$ c.c.	possibly seen	229
$\eta\gamma$	possibly seen	630
$f_0(500)\gamma$	not seen	–
$f_0(980)\gamma$	not seen	398
$f_0(1370)\gamma$	not seen	92
$f_2(1270)\gamma$	not seen	178

$\eta(1475)$ [o]

$I^G(J^{PC}) = 0^+(0^{-+})$

Mass $m = 1476 \pm 4$ MeV (S = 1.3)
Full width $\Gamma = 85 \pm 9$ MeV (S = 1.5)

$\eta(1475)$ DECAY MODES	Fraction (Γ_i/Γ)	p (MeV/c)
$K\overline{K}\pi$	dominant	477
$K\overline{K}^*(892)+$ c.c.	seen	245
$a_0(980)\pi$	seen	396
$\gamma\gamma$	seen	738

$f_0(1500)$ [n]

$I^G(J^{PC}) = 0^+(0^{++})$

Mass $m = 1505 \pm 6$ MeV (S = 1.3)
Full width $\Gamma = 109 \pm 7$ MeV

$f_0(1500)$ DECAY MODES	Fraction (Γ_i/Γ)	Scale factor	p (MeV/c)
$\pi\pi$	(34.9±2.3) %	1.2	741
$\pi^+\pi^-$	seen		740
$2\pi^0$	seen		741
4π	(49.5±3.3) %	1.2	691
$4\pi^0$	seen		691
$2\pi^+2\pi^-$	seen		687
$2(\pi\pi)_{S\text{-wave}}$	seen		–
$\rho\rho$	seen		†
$\pi(1300)\pi$	seen		144
$a_1(1260)\pi$	seen		218
$\eta\eta$	(5.1±0.9) %	1.4	516
$\eta\eta'(958)$	(1.9±0.8) %	1.7	†
$K\overline{K}$	(8.6±1.0) %	1.1	568
$\gamma\gamma$	not seen		753

Meson Summary Table

$f_2'(1525)$

$I^G(J^{PC}) = 0^+(2^{++})$

Mass $m = 1525 \pm 5$ MeV [l]
Full width $\Gamma = 73^{+6}_{-5}$ MeV [l]

$f_2'(1525)$ DECAY MODES	Fraction (Γ_i/Γ)	p (MeV/c)
$K\overline{K}$	(88.7 ±2.2) %	581
$\eta\eta$	(10.4 ±2.2) %	530
$\pi\pi$	(8.2 ±1.5) $\times 10^{-3}$	750
$\gamma\gamma$	(1.10±0.14) $\times 10^{-6}$	763

$\pi_1(1600)$ [n]

$I^G(J^{PC}) = 1^-(1^{-+})$

Mass $m = 1662^{+8}_{-9}$ MeV
Full width $\Gamma = 241 \pm 40$ MeV (S = 1.4)

$\pi_1(1600)$ DECAY MODES	Fraction (Γ_i/Γ)	p (MeV/c)
$\pi\pi\pi$	not seen	803
$\rho^0\pi^-$	not seen	641
$f_2(1270)\pi^-$	not seen	318
$b_1(1235)\pi$	seen	357
$\eta'(958)\pi^-$	seen	543
$f_1(1285)\pi$	seen	314

$\eta_2(1645)$

$I^G(J^{PC}) = 0^+(2^{-+})$

Mass $m = 1617 \pm 5$ MeV
Full width $\Gamma = 181 \pm 11$ MeV

$\eta_2(1645)$ DECAY MODES	Fraction (Γ_i/Γ)	p (MeV/c)
$a_2(1320)\pi$	seen	242
$K\overline{K}\pi$	seen	580
$K^*\overline{K}$	seen	404
$\eta\pi^+\pi^-$	seen	685
$a_0(980)\pi$	seen	499
$f_2(1270)\eta$	not seen	†

$\omega(1650)$ [s]

$I^G(J^{PC}) = 0^-(1^{--})$

Mass $m = 1670 \pm 30$ MeV
Full width $\Gamma = 315 \pm 35$ MeV

$\omega(1650)$ DECAY MODES	Fraction (Γ_i/Γ)	p (MeV/c)
$\rho\pi$	seen	647
$\omega\pi\pi$	seen	617
$\omega\eta$	seen	500
e^+e^-	seen	835

$\omega_3(1670)$

$I^G(J^{PC}) = 0^-(3^{--})$

Mass $m = 1667 \pm 4$ MeV
Full width $\Gamma = 168 \pm 10$ MeV [l]

$\omega_3(1670)$ DECAY MODES	Fraction (Γ_i/Γ)	p (MeV/c)
$\rho\pi$	seen	645
$\omega\pi\pi$	seen	615
$b_1(1235)\pi$	possibly seen	361

$\pi_2(1670)$

$I^G(J^{PC}) = 1^-(2^{-+})$

Mass $m = 1672.2 \pm 3.0$ MeV [l] (S = 1.4)
Full width $\Gamma = 260 \pm 9$ MeV [l] (S = 1.2)

$\pi_2(1670)$ DECAY MODES	Fraction (Γ_i/Γ)	Confidence level	p (MeV/c)
3π	(95.8±1.4) %		809
$f_2(1270)\pi$	(56.3±3.2) %		329
$\rho\pi$	(31 ±4) %		648
$\sigma\pi$	(10.9±3.4) %		–
$(\pi\pi)_{S\text{-wave}}$	(8.7±3.4) %		–
$K\overline{K}^*(892)+$ c.c.	(4.2±1.4) %		455
$\omega\rho$	(2.7±1.1) %		304
$\gamma\gamma$	< 2.8 $\times 10^{-7}$	90%	836
$\rho(1450)\pi$	< 3.6 $\times 10^{-3}$	97.7%	147
$b_1(1235)\pi$	< 1.9 $\times 10^{-3}$	97.7%	365
$f_1(1285)\pi$	possibly seen		323
$a_2(1320)\pi$	not seen		292

$\phi(1680)$

$I^G(J^{PC}) = 0^-(1^{--})$

Mass $m = 1680 \pm 20$ MeV [l]
Full width $\Gamma = 150 \pm 50$ MeV [l]

$\phi(1680)$ DECAY MODES	Fraction (Γ_i/Γ)	p (MeV/c)
$K\overline{K}^*(892)+$ c.c.	dominant	462
$K^0_S K\pi$	seen	621
$K\overline{K}$	seen	680
e^+e^-	seen	840
$\omega\pi\pi$	not seen	623
$K^+K^-\pi^+\pi^-$	seen	544

$\rho_3(1690)$

$I^G(J^{PC}) = 1^+(3^{--})$

Mass $m = 1688.8 \pm 2.1$ MeV [l]
Full width $\Gamma = 161 \pm 10$ MeV [l] (S = 1.5)

$\rho_3(1690)$ DECAY MODES	Fraction (Γ_i/Γ)	Scale factor	p (MeV/c)
4π	(71.1 ± 1.9) %		790
$\pi^\pm\pi^+\pi^-\pi^0$	(67 ±22) %		787
$\omega\pi$	(16 ± 6) %		655
$\pi\pi$	(23.6 ± 1.3) %		834
$K\overline{K}\pi$	(3.8 ± 1.2) %		629
$K\overline{K}$	(1.58± 0.26) %	1.2	685
$\eta\pi^+\pi^-$	seen		727
$\rho(770)\eta$	seen		520
$\pi\pi\rho$	seen		633
Excluding 2ρ and $a_2(1320)\pi$.			
$a_2(1320)\pi$	seen		307
$\rho\rho$	seen		335

$\rho(1700)$ [r]

$I^G(J^{PC}) = 1^+(1^{--})$

Mass $m = 1720 \pm 20$ MeV [l] ($\eta\rho^0$ and $\pi^+\pi^-$ modes)
Full width $\Gamma = 250 \pm 100$ MeV [l] ($\eta\rho^0$ and $\pi^+\pi^-$ modes)

$\rho(1700)$ DECAY MODES	Fraction (Γ_i/Γ)	p (MeV/c)
$2(\pi^+\pi^-)$	large	803
$\rho\pi\pi$	dominant	653
$\rho^0\pi^+\pi^-$	large	651
$\rho^\pm\pi^\mp\pi^0$	large	652
$a_1(1260)\pi$	seen	404
$h_1(1170)\pi$	seen	447
$\pi(1300)\pi$	seen	349
$\rho\rho$	seen	372
$\pi^+\pi^-$	seen	849
$\pi\pi$	seen	849
$K\overline{K}^*(892)+$ c.c.	seen	496
$\eta\rho$	seen	545
$a_2(1320)\pi$	not seen	334
$K\overline{K}$	seen	704
e^+e^-	seen	860
$\pi^0\omega$	seen	674

$f_0(1710)$ [t]

$I^G(J^{PC}) = 0^+(0^{++})$

Mass $m = 1722^{+6}_{-5}$ MeV (S = 1.6)
Full width $\Gamma = 135 \pm 7$ MeV (S = 1.1)

$f_0(1710)$ DECAY MODES	Fraction (Γ_i/Γ)	p (MeV/c)
$K\overline{K}$	seen	705
$\eta\eta$	seen	664
$\pi\pi$	seen	850
$\omega\omega$	seen	358

$\pi(1800)$

$I^G(J^{PC}) = 1^-(0^{-+})$

Mass $m = 1812 \pm 12$ MeV (S = 2.3)
Full width $\Gamma = 208 \pm 12$ MeV

$\pi(1800)$ DECAY MODES	Fraction (Γ_i/Γ)	p (MeV/c)
$\pi^+\pi^-\pi^-$	seen	879
$f_0(500)\pi^-$	seen	–
$f_0(980)\pi^-$	seen	625
$f_0(1370)\pi^-$	seen	368
$f_0(1500)\pi^-$	not seen	250
$\rho\pi^-$	not seen	732
$\eta\eta\pi^-$	seen	661
$a_0(980)\eta$	seen	473
$a_2(1320)\eta$	not seen	†
$f_2(1270)\pi$	not seen	442
$f_0(1370)\pi^-$	not seen	368
$f_0(1500)\pi^-$	seen	250
$\eta\eta'(958)\pi^-$	seen	375
$K_0^*(1430)K^-$	seen	†
$K^*(892)K^-$	not seen	570

$\phi_3(1850)$

$I^G(J^{PC}) = 0^-(3^{--})$

Mass $m = 1854 \pm 7$ MeV
Full width $\Gamma = 87^{+28}_{-23}$ MeV (S = 1.2)

$\phi_3(1850)$ DECAY MODES	Fraction (Γ_i/Γ)	p (MeV/c)
$K\overline{K}$	seen	785
$K\overline{K}^*(892)+$ c.c.	seen	602

$\pi_2(1880)$

$I^G(J^{PC}) = 1^-(2^{-+})$

Mass $m = 1895 \pm 16$ MeV
Full width $\Gamma = 235 \pm 34$ MeV

$f_2(1950)$

$I^G(J^{PC}) = 0^+(2^{++})$

Mass $m = 1944 \pm 12$ MeV (S = 1.5)
Full width $\Gamma = 472 \pm 18$ MeV

$f_2(1950)$ DECAY MODES	Fraction (Γ_i/Γ)	p (MeV/c)
$K^*(892)\overline{K}^*(892)$	seen	387
$\pi^+\pi^-$	seen	962
$\pi^0\pi^0$	seen	963
4π	seen	925
$\eta\eta$	seen	803
$K\overline{K}$	seen	837
$\gamma\gamma$	seen	972
$p\overline{p}$	seen	254

$f_2(2010)$

$I^G(J^{PC}) = 0^+(2^{++})$

Mass $m = 2011^{+60}_{-80}$ MeV
Full width $\Gamma = 202 \pm 60$ MeV

$f_2(2010)$ DECAY MODES	Fraction (Γ_i/Γ)	p (MeV/c)
$\phi\phi$	seen	†
$K\overline{K}$	seen	876

$a_4(2040)$

$I^G(J^{PC}) = 1^-(4^{++})$

Mass $m = 1996^{+10}_{-9}$ MeV (S = 1.1)
Full width $\Gamma = 255^{+28}_{-24}$ MeV (S = 1.3)

$a_4(2040)$ DECAY MODES	Fraction (Γ_i/Γ)	p (MeV/c)
$K\overline{K}$	seen	868
$\pi^+\pi^-\pi^0$	seen	974
$\rho\pi$	seen	841
$f_2(1270)\pi$	seen	580
$\omega\pi^-\pi^0$	seen	819
$\omega\rho$	seen	624
$\eta\pi^0$	seen	918
$\eta'(958)\pi$	seen	761

$f_4(2050)$

$I^G(J^{PC}) = 0^+(4^{++})$

Mass $m = 2018 \pm 11$ MeV (S = 2.1)
Full width $\Gamma = 237 \pm 18$ MeV (S = 1.9)

$f_4(2050)$ DECAY MODES	Fraction (Γ_i/Γ)	p (MeV/c)
$\omega\omega$	seen	637
$\pi\pi$	(17.0 ± 1.5) %	1000
$K\overline{K}$	$(6.8^{+3.4}_{-1.8}) \times 10^{-3}$	880
$\eta\eta$	$(2.1 \pm 0.8) \times 10^{-3}$	848
$4\pi^0$	< 1.2 %	964
$a_2(1320)\pi$	seen	567

$\phi(2170)$

$I^G(J^{PC}) = 0^-(1^{--})$

Mass $m = 2175 \pm 15$ MeV (S = 1.6)
Full width $\Gamma = 61 \pm 18$ MeV

$\phi(2170)$ DECAY MODES	Fraction (Γ_i/Γ)	p (MeV/c)
e^+e^-	seen	1087
$\phi f_0(980)$	seen	416
$K^+K^-f_0(980) \rightarrow K^+K^-\pi^+\pi^-$	seen	–
$K^+K^-f_0(980) \rightarrow K^+K^-\pi^0\pi^0$	seen	–
$K^{*0}K^\pm\pi^\mp$	not seen	770
$K^*(892)^0\overline{K}^*(892)^0$	not seen	622

$f_2(2300)$

$I^G(J^{PC}) = 0^+(2^{++})$

Mass $m = 2297 \pm 28$ MeV
Full width $\Gamma = 149 \pm 40$ MeV

$f_2(2300)$ DECAY MODES	Fraction (Γ_i/Γ)	p (MeV/c)
$\phi\phi$	seen	529
$K\overline{K}$	seen	1037
$\gamma\gamma$	seen	1149

$f_2(2340)$

$I^G(J^{PC}) = 0^+(2^{++})$

Mass $m = 2339 \pm 60$ MeV
Full width $\Gamma = 319^{+80}_{-70}$ MeV

$f_2(2340)$ DECAY MODES	Fraction (Γ_i/Γ)	p (MeV/c)
$\phi\phi$	seen	573
$\eta\eta$	seen	1033

Meson Summary Table

STRANGE MESONS ($S = \pm 1, C = B = 0$)

$K^+ = u\bar{s}$, $K^0 = d\bar{s}$, $\overline{K}^0 = \bar{d}s$, $K^- = \bar{u}s$, similarly for K^*'s

$K^\pm$

$I(J^P) = \frac{1}{2}(0^-)$

Mass $m = 493.677 \pm 0.016$ MeV [u] (S = 2.8)
Mean life $\tau = (1.2380 \pm 0.0021) \times 10^{-8}$ s (S = 1.9)
$c\tau = 3.712$ m

Slope parameter g [v]

(See Particle Listings for quadratic coefficients and alternative parametrization related to $\pi\pi$ scattering)

$K^\pm \to \pi^\pm\pi^+\pi^-$ $g = -0.21134 \pm 0.00017$
$(g_+ - g_-)\ /\ (g_+ + g_-) = (-1.5 \pm 2.2) \times 10^{-4}$
$K^\pm \to \pi^\pm\pi^0\pi^0$ $g = 0.626 \pm 0.007$
$(g_+ - g_-)\ /\ (g_+ + g_-) = (1.8 \pm 1.8) \times 10^{-4}$

$K^\pm$ decay form factors [a,x]

Assuming μ-e universality
$\lambda_+(K^+_{\mu 3}) = \lambda_+(K^+_{e3}) = (2.97 \pm 0.05) \times 10^{-2}$
$\lambda_0(K^+_{\mu 3}) = (1.95 \pm 0.12) \times 10^{-2}$

Not assuming μ-e universality
$\lambda_+(K^+_{e3}) = (2.98 \pm 0.05) \times 10^{-2}$
$\lambda_+(K^+_{\mu 3}) = (2.96 \pm 0.17) \times 10^{-2}$
$\lambda_0(K^+_{\mu 3}) = (1.96 \pm 0.13) \times 10^{-2}$

K_{e3} form factor quadratic fit
$\lambda'_+(K^\pm_{e3})$ linear coeff. $= (2.49 \pm 0.17) \times 10^{-2}$
$\lambda''_+(K^\pm_{e3})$ quadratic coeff. $= (0.19 \pm 0.09) \times 10^{-2}$

K^+_{e3} $|f_S/f_+| = (-0.3^{+0.8}_{-0.7}) \times 10^{-2}$
K^+_{e3} $|f_T/f_+| = (-1.2 \pm 2.3) \times 10^{-2}$
$K^+_{\mu 3}$ $|f_S/f_+| = (0.2 \pm 0.6) \times 10^{-2}$
$K^+_{\mu 3}$ $|f_T/f_+| = (-0.1 \pm 0.7) \times 10^{-2}$
$K^+ \to e^+\nu_e\gamma$ $|F_A + F_V| = 0.133 \pm 0.008$ (S = 1.3)
$K^+ \to \mu^+\nu_\mu\gamma$ $|F_A + F_V| = 0.165 \pm 0.013$
$K^+ \to e^+\nu_e\gamma$ $|F_A - F_V| < 0.49$
$K^+ \to \mu^+\nu_\mu\gamma$ $|F_A - F_V| = -0.24$ to 0.04, CL = 90%

Charge Radius

$\langle r \rangle = 0.560 \pm 0.031$ fm

***CP* violation parameters**

$\Delta(K^\pm_{\pi ee}) = (-2.2 \pm 1.6) \times 10^{-2}$
$\Delta(K^\pm_{\pi\mu\mu}) = 0.010 \pm 0.023$
$\Delta(K^\pm_{\pi\pi\gamma}) = (0.0 \pm 1.2) \times 10^{-3}$
$A_{FB}(K^\pm_{\pi\mu\mu}) = \frac{\Gamma(\cos(\theta_{K\mu})>0) - \Gamma(\cos(\theta_{K\mu})<0)}{\Gamma(\cos(\theta_{K\mu})>0) + \Gamma(\cos(\theta_{K\mu})<0)} < 2.3 \times 10^{-2}$, CL = 90%

***T* violation parameters**

$K^+ \to \pi^0\mu^+\nu_\mu$ $P_T = (-1.7 \pm 2.5) \times 10^{-3}$
$K^+ \to \mu^+\nu_\mu\gamma$ $P_T = (-0.6 \pm 1.9) \times 10^{-2}$
$K^+ \to \pi^0\mu^+\nu_\mu$ $\mathrm{Im}(\xi) = -0.006 \pm 0.008$

K^- modes are charge conjugates of the modes below.

K^+ DECAY MODES	Fraction (Γ_i/Γ)	Scale factor/ Confidence level	p (MeV/c)
Leptonic and semileptonic modes			
$e^+\nu_e$	$(1.581 \pm 0.007) \times 10^{-5}$		247
$\mu^+\nu_\mu$	(63.55 ±0.11) %	S=1.2	236
$\pi^0 e^+\nu_e$	(5.07 ±0.04) %	S=2.1	228
Called K^+_{e3}.			
$\pi^0\mu^+\nu_\mu$	(3.353 ±0.034) %	S=1.8	215
Called $K^+_{\mu 3}$.			
$\pi^0\pi^0 e^+\nu_e$	$(2.2 \pm 0.4) \times 10^{-5}$		206
$\pi^+\pi^- e^+\nu_e$	$(4.254 \pm 0.032) \times 10^{-5}$		203
$\pi^+\pi^-\mu^+\nu_\mu$	$(1.4 \pm 0.9) \times 10^{-5}$		151
$\pi^0\pi^0\pi^0 e^+\nu_e$	$< 3.5 \times 10^{-6}$	CL=90%	135
Hadronic modes			
$\pi^+\pi^0$	(20.66 ±0.08) %	S=1.2	205
$\pi^+\pi^0\pi^0$	(1.761±0.022) %	S=1.1	133
$\pi^+\pi^+\pi^-$	(5.59 ±0.04) %	S=1.3	125
Leptonic and semileptonic modes with photons			
$\mu^+\nu_\mu\gamma$	[y,z] $(6.2 \pm 0.8) \times 10^{-3}$		236
$\mu^+\nu_\mu\gamma(\mathrm{SD}^+)$	[a,aa] $(1.33 \pm 0.22) \times 10^{-5}$		–
$\mu^+\nu_\mu\gamma(\mathrm{SD}^+\mathrm{INT})$	[a,aa] $< 2.7 \times 10^{-5}$	CL=90%	–
$\mu^+\nu_\mu\gamma(\mathrm{SD}^- + \mathrm{SD}^-\mathrm{INT})$	[a,aa] $< 2.6 \times 10^{-4}$	CL=90%	–
$e^+\nu_e\gamma$	$(9.4 \pm 0.4) \times 10^{-6}$		247
$\pi^0 e^+\nu_e\gamma$	[y,z] $(2.56 \pm 0.16) \times 10^{-4}$		228
$\pi^0 e^+\nu_e\gamma(\mathrm{SD})$	[a,aa] $< 5.3 \times 10^{-5}$	CL=90%	228
$\pi^0\mu^+\nu_\mu\gamma$	[y,z] $(1.25 \pm 0.25) \times 10^{-5}$		215
$\pi^0\pi^0 e^+\nu_e\gamma$	$< 5 \times 10^{-6}$	CL=90%	206
Hadronic modes with photons or $\ell\bar{\ell}$ pairs			
$\pi^+\pi^0\gamma(\mathrm{INT})$	$(-4.2 \pm 0.9) \times 10^{-6}$		–
$\pi^+\pi^0\gamma(\mathrm{DE})$	[y,bb] $(6.0 \pm 0.4) \times 10^{-6}$		205
$\pi^+\pi^0\pi^0\gamma$	[y,z] $(7.6\ ^{+6.0}_{-3.0}) \times 10^{-6}$		133
$\pi^+\pi^+\pi^-\gamma$	[y,z] $(1.04 \pm 0.31) \times 10^{-4}$		125
$\pi^+\gamma\gamma$	[y] $(9.2 \pm 0.7) \times 10^{-7}$		227
$\pi^+ 3\gamma$	[y] $< 1.0 \times 10^{-4}$	CL=90%	227
$\pi^+ e^+ e^-\gamma$	$(1.19 \pm 0.13) \times 10^{-8}$		227
Leptonic modes with $\ell\bar{\ell}$ pairs			
$e^+\nu_e\nu\overline{\nu}$	$< 6 \times 10^{-5}$	CL=90%	247
$\mu^+\nu_\mu\nu\overline{\nu}$	$< 6.0 \times 10^{-6}$	CL=90%	236
$e^+\nu_e e^+ e^-$	$(2.48 \pm 0.20) \times 10^{-8}$		247
$\mu^+\nu_\mu e^+ e^-$	$(7.06 \pm 0.31) \times 10^{-8}$		236
$e^+\nu_e\mu^+\mu^-$	$(1.7 \pm 0.5) \times 10^{-8}$		223
$\mu^+\nu_\mu\mu^+\mu^-$	$< 4.1 \times 10^{-7}$	CL=90%	185
Lepton Family number (LF), Lepton number (L), $\Delta S = \Delta Q$ (SQ) violating modes, or $\Delta S = 1$ weak neutral current ($S1$) modes			
$\pi^+\pi^- e^-\overline{\nu}_e$	SQ $< 1.3 \times 10^{-8}$	CL=90%	203
$\pi^+\pi^-\mu^-\overline{\nu}_\mu$	SQ $< 3.0 \times 10^{-6}$	CL=95%	151
$\pi^+ e^+ e^-$	$S1$ $(3.00 \pm 0.09) \times 10^{-7}$		227
$\pi^+\mu^+\mu^-$	$S1$ $(9.4 \pm 0.6) \times 10^{-8}$	S=2.6	172
$\pi^+\nu\overline{\nu}$	$S1$ $(1.7 \pm 1.1) \times 10^{-10}$		227
$\pi^+\pi^0\nu\overline{\nu}$	$S1$ $< 4.3 \times 10^{-5}$	CL=90%	205
$\mu^-\nu e^+ e^+$	LF $< 2.1 \times 10^{-8}$	CL=90%	236
$\mu^+\nu_e$	LF [d] $< 4 \times 10^{-3}$	CL=90%	236
$\pi^+\mu^+ e^-$	LF $< 1.3 \times 10^{-11}$	CL=90%	214
$\pi^+\mu^- e^+$	LF $< 5.2 \times 10^{-10}$	CL=90%	214
$\pi^-\mu^+ e^+$	L $< 5.0 \times 10^{-10}$	CL=90%	214
$\pi^- e^+ e^+$	L $< 6.4 \times 10^{-10}$	CL=90%	227
$\pi^-\mu^+\mu^+$	L [d] $< 1.1 \times 10^{-9}$	CL=90%	172
$\mu^+\overline{\nu}_e$	L [d] $< 3.3 \times 10^{-3}$	CL=90%	236
$\pi^0 e^+\overline{\nu}_e$	L $< 3 \times 10^{-3}$	CL=90%	228
$\pi^+\gamma$	[cc] $< 2.3 \times 10^{-9}$	CL=90%	227

K^0

$I(J^P) = \frac{1}{2}(0^-)$

50% K_S, 50% K_L
Mass $m = 497.614 \pm 0.024$ MeV (S = 1.6)
$m_{K^0} - m_{K^\pm} = 3.937 \pm 0.028$ MeV (S = 1.8)

Mean Square Charge Radius

$\langle r^2 \rangle = -0.077 \pm 0.010$ fm^2

***T*-violation parameters in K^0-$\overline{K}^0$ mixing** [x]

Asymmetry A_T in K^0-$\overline{K}^0$ mixing $= (6.6 \pm 1.6) \times 10^{-3}$

***CPT*-violation parameters** [x]

Re $\delta = (2.5 \pm 2.3) \times 10^{-4}$
Im $\delta = (-1.5 \pm 1.6) \times 10^{-5}$
Re(y), K_{e3} parameter $= (0.4 \pm 2.5) \times 10^{-3}$
Re(x$_-$), K_{e3} parameter $= (-2.9 \pm 2.0) \times 10^{-3}$
$|m_{K^0} - m_{\overline{K}^0}|\ /\ m_{\mathrm{average}} < 6 \times 10^{-19}$, CL = 90% [dd]
$(\Gamma_{K^0} - \Gamma_{\overline{K}^0})/m_{\mathrm{average}} = (8 \pm 8) \times 10^{-18}$

Tests of $\Delta S = \Delta Q$

Re(x$_+$), K_{e3} parameter $= (-0.9 \pm 3.0) \times 10^{-3}$

K^0_S

$I(J^P) = \frac{1}{2}(0^-)$

Mean life $\tau = (0.8954 \pm 0.0004) \times 10^{-10}$ s (S = 1.1) Assuming *CPT*

Mean life $\tau = (0.89564 \pm 0.00033) \times 10^{-10}$ s Not assuming *CPT*

$c\tau = 2.6844$ cm Assuming *CPT*

CP-violation parameters [ee]

$\mathrm{Im}(\eta_{+-0}) = -0.002 \pm 0.009$

$\mathrm{Im}(\eta_{000}) = (-0.1 \pm 1.6) \times 10^{-2}$

$|\eta_{000}| = |A(K^0_S \to 3\pi^0)/A(K^0_L \to 3\pi^0)| < 0.0088$, CL = 90%

CP asymmetry A in $\pi^+\pi^- e^+ e^- = (-0.4 \pm 0.8)\%$

K^0_S DECAY MODES		Fraction (Γ_i/Γ)	Scale factor/ Confidence level	p (MeV/c)
Hadronic modes				
$\pi^0\pi^0$		(30.69 ± 0.05) %		209
$\pi^+\pi^-$		(69.20 ± 0.05) %		206
$\pi^+\pi^-\pi^0$		$(3.5 \ ^{+1.1}_{-0.9}) \times 10^{-7}$		133
Modes with photons or $\ell\bar{\ell}$ pairs				
$\pi^+\pi^-\gamma$	[z,ff]	$(1.79 \pm 0.05) \times 10^{-3}$		206
$\pi^+\pi^- e^+ e^-$		$(4.79 \pm 0.15) \times 10^{-5}$		206
$\pi^0\gamma\gamma$	[ff]	$(4.9 \pm 1.8) \times 10^{-8}$		231
$\gamma\gamma$		$(2.63 \pm 0.17) \times 10^{-6}$	S=3.0	249
Semileptonic modes				
$\pi^\pm e^\mp \nu_e$	[gg]	$(7.04 \pm 0.08) \times 10^{-4}$		229
***CP* violating (*CP*) and $\Delta S = 1$ weak neutral current (*S1*) modes**				
$3\pi^0$	*CP*	$< 2.6 \times 10^{-8}$	CL=90%	139
$\mu^+\mu^-$	*S1*	$< 9 \times 10^{-9}$	CL=90%	225
$e^+ e^-$	*S1*	$< 9 \times 10^{-9}$	CL=90%	249
$\pi^0 e^+ e^-$	*S1* [ff]	$(3.0 \ ^{+1.5}_{-1.2}) \times 10^{-9}$		230
$\pi^0\mu^+\mu^-$	*S1*	$(2.9 \ ^{+1.5}_{-1.2}) \times 10^{-9}$		177

K^0_L

$I(J^P) = \frac{1}{2}(0^-)$

$m_{K_L} - m_{K_S}$

$= (0.5293 \pm 0.0009) \times 10^{10}\ \hbar\ \mathrm{s}^{-1}$ (S = 1.3) Assuming *CPT*

$= (3.484 \pm 0.006) \times 10^{-12}$ MeV Assuming *CPT*

$= (0.5289 \pm 0.0010) \times 10^{10}\ \hbar\ \mathrm{s}^{-1}$ Not assuming *CPT*

Mean life $\tau = (5.116 \pm 0.021) \times 10^{-8}$ s (S = 1.1)

$c\tau = 15.34$ m

Slope parameter *g* [v]

(See Particle Listings for other linear and quadratic coefficients)

$K^0_L \to \pi^+\pi^-\pi^0$: $g = 0.678 \pm 0.008$ (S = 1.5)

$K^0_L \to \pi^0\pi^0\pi^0$: $h = (+0.59 \pm 0.20 \pm 1.16) \times 10^{-3}$

K_L decay form factors [x]

Linear parametrization assuming μ-e universality

$\lambda_+(K^0_{\mu 3}) = \lambda_+(K^0_{e3}) = (2.82 \pm 0.04) \times 10^{-2}$ (S = 1.1)

$\lambda_0(K^0_{\mu 3}) = (1.38 \pm 0.18) \times 10^{-2}$ (S = 2.2)

Quadratic parametrization assuming μ-e universality

$\lambda'_+(K^0_{\mu 3}) = \lambda'_+(K^0_{e3}) = (2.40 \pm 0.12) \times 10^{-2}$ (S = 1.2)

$\lambda''_+(K^0_{\mu 3}) = \lambda''_+(K^0_{e3}) = (0.20 \pm 0.05) \times 10^{-2}$ (S = 1.2)

$\lambda_0(K^0_{\mu 3}) = (1.16 \pm 0.09) \times 10^{-2}$ (S = 1.2)

Pole parametrization assuming μ-e universality

$M^\mu_V\ (K^0_{\mu 3}) = M^e_V\ (K^0_{e3}) = 878 \pm 6$ MeV (S = 1.1)

$M^\mu_S\ (K^0_{\mu 3}) = 1252 \pm 90$ MeV (S = 2.6)

Dispersive parametrization assuming μ-e universality

$\Lambda_+ = (0.251 \pm 0.006) \times 10^{-1}$ (S = 1.5)

$\ln(C) = (1.75 \pm 0.18) \times 10^{-1}$ (S = 2.0)

K^0_{e3} $|f_S/f_+| = (1.5^{+1.4}_{-1.6}) \times 10^{-2}$

K^0_{e3} $|f_T/f_+| = (5^{+4}_{-5}) \times 10^{-2}$

$K^0_{\mu 3}$ $|f_T/f_+| = (12 \pm 12) \times 10^{-2}$

$K_L \to \ell^+\ell^-\gamma$, $K_L \to \ell^+\ell^-\ell'^+\ell'^-$: $\alpha_{K^*} = -0.205 \pm 0.022$ (S = 1.8)

$K^0_L \to \ell^+\ell^-\gamma$, $K^0_L \to \ell^+\ell^-\ell'^+\ell'^-$: $\alpha_{DIP} = -1.69 \pm 0.08$ (S = 1.7)

$K_L \to \pi^+\pi^- e^+ e^-$: $a_1/a_2 = -0.737 \pm 0.014$ GeV^2

$K_L \to \pi^0 2\gamma$: $a_V = -0.43 \pm 0.06$ (S = 1.5)

CP-violation parameters [ee]

$A_L = (0.332 \pm 0.006)\%$

$|\eta_{00}| = (2.220 \pm 0.011) \times 10^{-3}$ (S = 1.8)

$|\eta_{+-}| = (2.232 \pm 0.011) \times 10^{-3}$ (S = 1.8)

$|\epsilon| = (2.228 \pm 0.011) \times 10^{-3}$ (S = 1.8)

$|\eta_{00}/\eta_{+-}| = 0.9950 \pm 0.0007$ [hh] (S = 1.6)

$\mathrm{Re}(\epsilon'/\epsilon) = (1.66 \pm 0.23) \times 10^{-3}$ [hh] (S = 1.6)

Assuming *CPT*

$\phi_{+-} = (43.51 \pm 0.05)^\circ$ (S = 1.2)

$\phi_{00} = (43.52 \pm 0.05)^\circ$ (S = 1.3)

$\phi_\epsilon = \phi_{SW} = (43.52 \pm 0.05)^\circ$ (S = 1.2)

$\mathrm{Im}(\epsilon'/\epsilon) = -(\phi_{00} - \phi_{+-})/3 = (-0.002 \pm 0.005)^\circ$ (S = 1.7)

Not assuming *CPT*

$\phi_{+-} = (43.4 \pm 0.5)^\circ$ (S = 1.2)

$\phi_{00} = (43.7 \pm 0.6)^\circ$ (S = 1.2)

$\phi_\epsilon = (43.5 \pm 0.5)^\circ$ (S = 1.3)

CP asymmetry A in $K^0_L \to \pi^+\pi^- e^+ e^- = (13.7 \pm 1.5)\%$

β_{CP} from $K^0_L \to e^+ e^- e^+ e^- = -0.19 \pm 0.07$

γ_{CP} from $K^0_L \to e^+ e^- e^+ e^- = 0.01 \pm 0.11$ (S = 1.6)

j for $K^0_L \to \pi^+\pi^-\pi^0 = 0.0012 \pm 0.0008$

f for $K^0_L \to \pi^+\pi^-\pi^0 = 0.004 \pm 0.006$

$|\eta_{+-\gamma}| = (2.35 \pm 0.07) \times 10^{-3}$

$\phi_{+-\gamma} = (44 \pm 4)^\circ$

$|\epsilon'_{+-\gamma}|/\epsilon < 0.3$, CL = 90%

$|g_{E1}|$ for $K^0_L \to \pi^+\pi^-\gamma < 0.21$, CL = 90%

T-violation parameters

$\mathrm{Im}(\xi)$ in $K^0_{\mu 3} = -0.007 \pm 0.026$

CPT invariance tests

$\phi_{00} - \phi_{+-} = (0.34 \pm 0.32)^\circ$

$\mathrm{Re}(\frac{2}{3}\eta_{+-} + \frac{1}{3}\eta_{00}) - \frac{A_L}{2} = (-3 \pm 35) \times 10^{-6}$

$\Delta S = -\Delta Q$ in $K^0_{\ell 3}$ decay

Re $x = -0.002 \pm 0.006$

Im $x = 0.0012 \pm 0.0021$

K^0_L DECAY MODES		Fraction (Γ_i/Γ)	Scale factor/ Confidence level	p (MeV/c)
Semileptonic modes				
$\pi^\pm e^\mp \nu_e$ Called K^0_{e3}.	[gg]	(40.55 ± 0.11) %	S=1.7	229
$\pi^\pm \mu^\mp \nu_\mu$ Called $K^0_{\mu 3}$.	[gg]	(27.04 ± 0.07) %	S=1.1	216
$(\pi\mu\mathrm{atom})\nu$		$(1.05 \pm 0.11) \times 10^{-7}$		188
$\pi^0\pi^\pm e^\mp \nu$	[gg]	$(5.20 \pm 0.11) \times 10^{-5}$		207
$\pi^\pm e^\mp \nu\, e^+ e^-$	[gg]	$(1.26 \pm 0.04) \times 10^{-5}$		229
Hadronic modes, including Charge conjugation×Parity Violating (*CPV*) modes				
$3\pi^0$		(19.52 ± 0.12) %	S=1.6	139
$\pi^+\pi^-\pi^0$		(12.54 ± 0.05) %		133
$\pi^+\pi^-$	*CPV* [ii]	$(1.967 \pm 0.010) \times 10^{-3}$	S=1.5	206
$\pi^0\pi^0$	*CPV*	$(8.64 \pm 0.06) \times 10^{-4}$	S=1.8	209
Semileptonic modes with photons				
$\pi^\pm e^\mp \nu_e \gamma$	[z,gg,jj]	$(3.79 \pm 0.06) \times 10^{-3}$		229
$\pi^\pm \mu^\mp \nu_\mu \gamma$		$(5.65 \pm 0.23) \times 10^{-4}$		216

Meson Summary Table

Hadronic modes with photons or $\ell\bar{\ell}$ pairs

$\pi^0\pi^0\gamma$		$<$ 2.43	$\times 10^{-7}$	CL=90%	209
$\pi^+\pi^-\gamma$	[z,jj]	(4.15 $\pm$0.15) $\times 10^{-5}$		S=2.8	206
$\pi^+\pi^-\gamma$(DE)		(2.84 $\pm$0.11) $\times 10^{-5}$		S=2.0	206
$\pi^0 2\gamma$	[jj]	(1.273$\pm$0.033) $\times 10^{-6}$			231
$\pi^0\gamma e^+e^-$		(1.62 $\pm$0.17) $\times 10^{-8}$			230

Other modes with photons or $\ell\bar{\ell}$ pairs

2γ		(5.47 $\pm$0.04) $\times 10^{-4}$		S=1.1	249
3γ		$<$ 7.4	$\times 10^{-8}$	CL=90%	249
$e^+e^-\gamma$		(9.4 $\pm$0.4) $\times 10^{-6}$		S=2.0	249
$\mu^+\mu^-\gamma$		(3.59 $\pm$0.11) $\times 10^{-7}$		S=1.3	225
$e^+e^-\gamma\gamma$	[jj]	(5.95 $\pm$0.33) $\times 10^{-7}$			249
$\mu^+\mu^-\gamma\gamma$	[jj]	(1.0 $^{+0.8}_{-0.6}$) $\times 10^{-8}$			225

Charge conjugation $\times$ Parity (CP) or Lepton Family number (LF) violating modes, or $\Delta S = 1$ weak neutral current ($S1$) modes

$\mu^+\mu^-$	S1		(6.84 $\pm$0.11) $\times 10^{-9}$			225
e^+e^-	S1		(9 $^{+6}_{-4}$) $\times 10^{-12}$			249
$\pi^+\pi^-e^+e^-$	S1	[jj]	(3.11 $\pm$0.19) $\times 10^{-7}$			206
$\pi^0\pi^0e^+e^-$	S1		$<$ 6.6	$\times 10^{-9}$	CL=90%	209
$\pi^0\pi^0\mu^+\mu^-$	S1		$<$ 9.2	$\times 10^{-11}$	CL=90%	57
$\mu^+\mu^-e^+e^-$	S1		(2.69 $\pm$0.27) $\times 10^{-9}$			225
$e^+e^-e^+e^-$	S1		(3.56 $\pm$0.21) $\times 10^{-8}$			249
$\pi^0\mu^+\mu^-$	CP,S1	[kk]	$<$ 3.8	$\times 10^{-10}$	CL=90%	177
$\pi^0e^+e^-$	CP,S1	[kk]	$<$ 2.8	$\times 10^{-10}$	CL=90%	230
$\pi^0\nu\overline{\nu}$	CP,S1	[ll]	$<$ 2.6	$\times 10^{-8}$	CL=90%	231
$\pi^0\pi^0\nu\overline{\nu}$	S1		$<$ 8.1	$\times 10^{-7}$	CL=90%	209
$e^\pm\mu^\mp$	LF	[gg]	$<$ 4.7	$\times 10^{-12}$	CL=90%	238
$e^\pm e^\pm\mu^\mp\mu^\mp$	LF	[gg]	$<$ 4.12	$\times 10^{-11}$	CL=90%	225
$\pi^0\mu^\pm e^\mp$	LF	[gg]	$<$ 7.6	$\times 10^{-11}$	CL=90%	217
$\pi^0\pi^0\mu^\pm e^\mp$	LF		$<$ 1.7	$\times 10^{-10}$	CL=90%	159

$K^*(892)$

$I(J^P) = \frac{1}{2}(1^-)$

$K^*(892)^\pm$ hadroproduced mass $m = 891.66 \pm 0.26$ MeV
$K^*(892)^\pm$ in τ decays mass $m = 895.5 \pm 0.8$ MeV
$K^*(892)^0$ mass $m = 895.81 \pm 0.19$ MeV (S = 1.4)
$K^*(892)^\pm$ hadroproduced full width $\Gamma = 50.8 \pm 0.9$ MeV
$K^*(892)^\pm$ in τ decays full width $\Gamma = 46.2 \pm 1.3$ MeV
$K^*(892)^0$ full width $\Gamma = 47.4 \pm 0.6$ MeV (S = 2.2)

$K^*(892)$ DECAY MODES	Fraction (Γ_i/Γ)	Confidence level	p (MeV/c)
$K\pi$	$\sim$ 100 %		289
$K^0\gamma$	(2.46$\pm$0.21) $\times 10^{-3}$		307
$K^\pm\gamma$	(9.9 $\pm$0.9) $\times 10^{-4}$		309
$K\pi\pi$	$<$ 7 $\times 10^{-4}$	95%	223

$K_1(1270)$

$I(J^P) = \frac{1}{2}(1^+)$

Mass $m = 1272 \pm 7$ MeV [l]
Full width $\Gamma = 90 \pm 20$ MeV [l]

$K_1(1270)$ DECAY MODES	Fraction (Γ_i/Γ)	p (MeV/c)
$K\rho$	(42 $\pm$6) %	46
$K_0^*(1430)\pi$	(28 $\pm$4) %	†
$K^*(892)\pi$	(16 $\pm$5) %	302
$K\omega$	(11.0$\pm$2.0) %	†
$Kf_0(1370)$	(3.0$\pm$2.0) %	†
γK^0	seen	539

$K_1(1400)$

$I(J^P) = \frac{1}{2}(1^+)$

Mass $m = 1403 \pm 7$ MeV
Full width $\Gamma = 174 \pm 13$ MeV (S = 1.6)

$K_1(1400)$ DECAY MODES	Fraction (Γ_i/Γ)	p (MeV/c)
$K^*(892)\pi$	(94 $\pm$6) %	402
$K\rho$	(3.0$\pm$3.0) %	293
$Kf_0(1370)$	(2.0$\pm$2.0) %	†
$K\omega$	(1.0$\pm$1.0) %	284
$K_0^*(1430)\pi$	not seen	†
γK^0	seen	613

$K^*(1410)$

$I(J^P) = \frac{1}{2}(1^-)$

Mass $m = 1414 \pm 15$ MeV (S = 1.3)
Full width $\Gamma = 232 \pm 21$ MeV (S = 1.1)

$K^*(1410)$ DECAY MODES	Fraction (Γ_i/Γ)	Confidence level	p (MeV/c)
$K^*(892)\pi$	$>$ 40 %	95%	410
$K\pi$	(6.6$\pm$1.3) %		612
$K\rho$	$<$ 7 %	95%	305
γK^0	seen		619

$K_0^*(1430)$ [nn]

$I(J^P) = \frac{1}{2}(0^+)$

Mass $m = 1425 \pm 50$ MeV
Full width $\Gamma = 270 \pm 80$ MeV

$K_0^*(1430)$ DECAY MODES	Fraction (Γ_i/Γ)	p (MeV/c)
$K\pi$	(93$\pm$10) %	619

$K_2^*(1430)$

$I(J^P) = \frac{1}{2}(2^+)$

$K_2^*(1430)^\pm$ mass $m = 1425.6 \pm 1.5$ MeV (S = 1.1)
$K_2^*(1430)^0$ mass $m = 1432.4 \pm 1.3$ MeV
$K_2^*(1430)^\pm$ full width $\Gamma = 98.5 \pm 2.7$ MeV (S = 1.1)
$K_2^*(1430)^0$ full width $\Gamma = 109 \pm 5$ MeV (S = 1.9)

$K_2^*(1430)$ DECAY MODES	Fraction (Γ_i/Γ)	Scale factor/ Confidence level	p (MeV/c)
$K\pi$	(49.9$\pm$1.2) %		619
$K^*(892)\pi$	(24.7$\pm$1.5) %		419
$K^*(892)\pi\pi$	(13.4$\pm$2.2) %		372
$K\rho$	(8.7$\pm$0.8) %	S=1.2	318
$K\omega$	(2.9$\pm$0.8) %		311
$K^+\gamma$	(2.4$\pm$0.5) $\times 10^{-3}$	S=1.1	627
$K\eta$	(1.5 $^{+3.4}_{-1.0}$) $\times 10^{-3}$	S=1.3	486
$K\omega\pi$	$<$ 7.2 $\times 10^{-4}$	CL=95%	100
$K^0\gamma$	$<$ 9 $\times 10^{-4}$	CL=90%	626

$K^*(1680)$

$I(J^P) = \frac{1}{2}(1^-)$

Mass $m = 1717 \pm 27$ MeV (S = 1.4)
Full width $\Gamma = 322 \pm 110$ MeV (S = 4.2)

$K^*(1680)$ DECAY MODES	Fraction (Γ_i/Γ)	p (MeV/c)
$K\pi$	(38.7$\pm$2.5) %	781
$K\rho$	(31.4 $^{+5.0}_{-2.1}$) %	571
$K^*(892)\pi$	(29.9 $^{+2.2}_{-5.0}$) %	618

$K_2(1770)$ [oo]

$I(J^P) = \frac{1}{2}(2^-)$

Mass $m = 1773 \pm 8$ MeV
Full width $\Gamma = 186 \pm 14$ MeV

$K_2(1770)$ DECAY MODES	Fraction (Γ_i/Γ)	p (MeV/c)
$K\pi\pi$		794
$K_2^*(1430)\pi$	dominant	288
$K^*(892)\pi$	seen	654
$Kf_2(1270)$	seen	55
$K\phi$	seen	441
$K\omega$	seen	607

$K_3^*(1780)$

$I(J^P) = \frac{1}{2}(3^-)$

Mass $m = 1776 \pm 7$ MeV (S = 1.1)
Full width $\Gamma = 159 \pm 21$ MeV (S = 1.3)

$K_3^*(1780)$ DECAY MODES	Fraction (Γ_i/Γ)	Confidence level	p (MeV/c)
$K\rho$	(31 ± 9) %		613
$K^*(892)\pi$	(20 ± 5) %		656
$K\pi$	(18.8± 1.0) %		813
$K\eta$	(30 ±13) %		719
$K_2^*(1430)\pi$	< 16 %	95%	291

$K_2(1820)$ [pp]

$I(J^P) = \frac{1}{2}(2^-)$

Mass $m = 1816 \pm 13$ MeV
Full width $\Gamma = 276 \pm 35$ MeV

$K_2(1820)$ DECAY MODES	Fraction (Γ_i/Γ)	p (MeV/c)
$K_2^*(1430)\pi$	seen	327
$K^*(892)\pi$	seen	681
$Kf_2(1270)$	seen	186
$K\omega$	seen	638

$K_4^*(2045)$

$I(J^P) = \frac{1}{2}(4^+)$

Mass $m = 2045 \pm 9$ MeV (S = 1.1)
Full width $\Gamma = 198 \pm 30$ MeV

$K_4^*(2045)$ DECAY MODES	Fraction (Γ_i/Γ)	p (MeV/c)
$K\pi$	(9.9±1.2) %	958
$K^*(892)\pi\pi$	(9 ±5) %	802
$K^*(892)\pi\pi\pi$	(7 ±5) %	768
$\rho K\pi$	(5.7±3.2) %	741
$\omega K\pi$	(5.0±3.0) %	738
$\phi K\pi$	(2.8±1.4) %	594
$\phi K^*(892)$	(1.4±0.7) %	363

CHARMED MESONS ($C = \pm 1$)

$D^+ = c\overline{d}$, $D^0 = c\overline{u}$, $\overline{D}^0 = \overline{c}u$, $D^- = \overline{c}d$, similarly for D^*'s

$D^\pm$

$I(J^P) = \frac{1}{2}(0^-)$

Mass $m = 1869.61 \pm 0.10$ MeV (S = 1.1)
Mean life $\tau = (1040 \pm 7) \times 10^{-15}$ s
$c\tau = 311.8\ \mu$m

c-quark decays

$\Gamma(c \to \ell^+ \text{anything})/\Gamma(c \to \text{anything}) = 0.096 \pm 0.004$ [qq]
$\Gamma(c \to D^*(2010)^+ \text{anything})/\Gamma(c \to \text{anything}) = 0.255 \pm 0.017$

CP-violation decay-rate asymmetries

$A_{CP}(\mu^\pm\nu) = (8 \pm 8)\%$
$A_{CP}(K_S^0\pi^\pm) = (-0.41 \pm 0.09)\%$
$A_{CP}(K^\mp 2\pi^\pm) = (-0.1 \pm 1.0)\%$
$A_{CP}(K^\mp\pi^\pm\pi^\pm\pi^0) = (1.0 \pm 1.3)\%$
$A_{CP}(K_S^0\pi^\pm\pi^0) = (0.3 \pm 0.9)\%$
$A_{CP}(K_S^0\pi^\pm\pi^+\pi^-) = (0.1 \pm 1.3)\%$
$A_{CP}(\pi^\pm\pi^0) = (2.9 \pm 2.9)\%$
$A_{CP}(\pi^\pm\eta) = (1.0 \pm 1.5)\%$ (S = 1.4)
$A_{CP}(\pi^\pm\eta'(958)) = (-0.5 \pm 1.2)\%$ (S = 1.1)
$A_{CP}(K_S^0 K^\pm) = (-0.11 \pm 0.25)\%$
$A_{CP}(K^+K^-\pi^\pm) = (0.36 \pm 0.29)\%$
$A_{CP}(K^\pm K^{*0}) = (-0.3 \pm 0.4)\%$
$A_{CP}(\phi\pi^\pm) = (0.09 \pm 0.19)\%$ (S = 1.2)
$A_{CP}(K^\pm K_0^*(1430)^0) = (8^{+7}_{-6})\%$
$A_{CP}(K^\pm K_2^*(1430)^0) = (43^{+20}_{-26})\%$
$A_{CP}(K^\pm K_0^*(800)) = (-12^{+18}_{-13})\%$
$A_{CP}(a_0(1450)^0\pi^\pm) = (-19^{+14}_{-16})\%$
$A_{CP}(\phi(1680)\pi^\pm) = (-9 \pm 26)\%$
$A_{CP}(\pi^+\pi^-\pi^\pm) = (-2 \pm 4)\%$
$A_{CP}(K_S^0 K^\pm\pi^+\pi^-) = (-4 \pm 7)\%$
$A_{CP}(K^\pm\pi^0) = (-4 \pm 11)\%$

T-violation decay-rate asymmetry

$A_T(K_S^0 K^\pm\pi^+\pi^-) = (-12 \pm 11) \times 10^{-3}$ [rr]

D^+ form factors

$f_+(0)|V_{cs}|$ in $\overline{K}^0\ell^+\nu_\ell = 0.707 \pm 0.013$
$r_1 \equiv a_1/a_0$ in $\overline{K}^0\ell^+\nu_\ell = -1.7 \pm 0.5$
$r_2 \equiv a_2/a_0$ in $\overline{K}^0\ell^+\nu_\ell = -14 \pm 11$
$f_+(0)|V_{cd}|$ in $\pi^0\ell^+\nu_\ell = 0.146 \pm 0.007$
$r_1 \equiv a_1/a_0$ in $\pi^0\ell^+\nu_\ell = -1.4 \pm 0.9$
$r_2 \equiv a_2/a_0$ in $\pi^0\ell^+\nu_\ell = -4 \pm 5$
$f_+(0)|V_{cd}|$ in $D^+ \to \eta e^+\nu_e = 0.086 \pm 0.006$
$r_1 \equiv a_1/a_0$ in $D^+ \to \eta e^+\nu_e = -1.8 \pm 2.2$
$r_V \equiv V(0)/A_1(0)$ in $D^+, D^0 \to \rho e^+\nu_e = 1.48 \pm 0.16$
$r_2 \equiv A_2(0)/A_1(0)$ in $D^+, D^0 \to \rho e^+\nu_e = 0.83 \pm 0.12$
$r_V \equiv V(0)/A_1(0)$ in $\overline{K}^*(892)^0\ell^+\nu_\ell = 1.51 \pm 0.07$ (S = 2.2)
$r_2 \equiv A_2(0)/A_1(0)$ in $\overline{K}^*(892)^0\ell^+\nu_\ell = 0.807 \pm 0.025$
$r_3 \equiv A_3(0)/A_1(0)$ in $\overline{K}^*(892)^0\ell^+\nu_\ell = 0.0 \pm 0.4$
Γ_L/Γ_T in $\overline{K}^*(892)^0\ell^+\nu_\ell = 1.13 \pm 0.08$
Γ_+/Γ_- in $\overline{K}^*(892)^0\ell^+\nu_\ell = 0.22 \pm 0.06$ (S = 1.6)

Most decay modes (other than the semileptonic modes) that involve a neutral K meson are now given as K_S^0 modes, not as $\overline{K}^0$ modes. Nearly always it is a K_S^0 that is measured, and interference between Cabibbo-allowed and doubly Cabibbo-suppressed modes can invalidate the assumption that $2\,\Gamma(K_S^0) = \Gamma(\overline{K}^0)$.

D^+ DECAY MODES	Fraction (Γ_i/Γ)	Scale factor/ Confidence level	p (MeV/c)
Inclusive modes			
e^+ semileptonic	(16.07±0.30) %		–
μ^+ anything	(17.6 ±3.2) %		–
K^- anything	(25.7 ±1.4) %		–
$\overline{K}^0$ anything + K^0 anything	(61 ±5) %		–
K^+ anything	(5.9 ±0.8) %		–
$K^*(892)^-$ anything	(6 ±5) %		–
$\overline{K}^*(892)^0$ anything	(23 ±5) %		–
$K^*(892)^0$ anything	< 6.6 %	CL=90%	–
η anything	(6.3 ±0.7) %		–
η' anything	(1.04±0.18) %		–
ϕ anything	(1.03±0.12) %		–
Leptonic and semileptonic modes			
$e^+\nu_e$	< 8.8 $\times 10^{-6}$	CL=90%	935
$\mu^+\nu_\mu$	(3.82±0.33) $\times 10^{-4}$		932
$\tau^+\nu_\tau$	< 1.2 $\times 10^{-3}$	CL=90%	90
$\overline{K}^0 e^+\nu_e$	(8.83±0.22) %		869
$\overline{K}^0\mu^+\nu_\mu$	(9.2 ±0.6) %		865
$K^-\pi^+ e^+\nu_e$	(4.00±0.10) %		864
$\overline{K}^*(892)^0 e^+\nu_e$, $\overline{K}^*(892)^0 \to K^-\pi^+$	(3.68±0.10) %		722
$(K^-\pi^+)_{S-wave}\, e^+\nu_e$	(2.32±0.10) $\times 10^{-3}$		–
$\overline{K}^*(1410)^0 e^+\nu_e$, $\overline{K}^*(1410)^0 \to K^-\pi^+$	< 6 $\times 10^{-3}$	CL=90%	–
$\overline{K}_2^*(1430)^0 e^+\nu_e$, $\overline{K}_2^*(1430)^0 \to K^-\pi^+$	< 5 $\times 10^{-4}$	CL=90%	–
$K^-\pi^+ e^+\nu_e$ nonresonant	< 7 $\times 10^{-3}$	CL=90%	864
$K^-\pi^+\mu^+\nu_\mu$	(3.8 ±0.4) %		851
$\overline{K}^*(892)^0\mu^+\nu_\mu$, $\overline{K}^*(892)^0 \to K^-\pi^+$	(3.52±0.10) %		717
$K^-\pi^+\mu^+\nu_\mu$ nonresonant	(2.0 ±0.5) $\times 10^{-3}$		851
$K^-\pi^+\pi^0\mu^+\nu_\mu$	< 1.6 $\times 10^{-3}$	CL=90%	825
$\pi^0 e^+\nu_e$	(4.05±0.18) $\times 10^{-3}$		930
$\eta e^+\nu_e$	(1.14±0.10) $\times 10^{-3}$		855
$\rho^0 e^+\nu_e$	($2.18^{+0.17}_{-0.25}$) $\times 10^{-3}$		774
$\rho^0\mu^+\nu_\mu$	(2.4 ±0.4) $\times 10^{-3}$		770
$\omega e^+\nu_e$	(1.82±0.19) $\times 10^{-3}$		771
$\eta'(958)\, e^+\nu_e$	(2.2 ±0.5) $\times 10^{-4}$		689
$\phi e^+\nu_e$	< 9 $\times 10^{-5}$	CL=90%	657

Fractions of some of the following modes with resonances have already appeared above as submodes of particular charged-particle modes.

$\overline{K}^*(892)^0 e^+\nu_e$	(5.52±0.15) %		722
$\overline{K}^*(892)^0\mu^+\nu_\mu$	(5.28±0.15) %		717
$\overline{K}_0^*(1430)^0\mu^+\nu_\mu$	< 2.4 $\times 10^{-4}$	CL=90%	380
$\overline{K}^*(1680)^0\mu^+\nu_\mu$	< 1.5 $\times 10^{-3}$	CL=90%	105

Meson Summary Table

Hadronic modes with a $\overline{K}$ or $\overline{K}K\overline{K}$

$K^0_S\pi^+$		(1.47±0.07) %	S=2.0	863
$K^0_L\pi^+$		(1.46±0.05) %		863
$K^-2\pi^+$	[ss]	(9.13±0.19) %		846
$(K^-\pi^+)_{S-\text{wave}}\pi^+$		(7.32±0.19) %		846
$\overline{K}^*_0(1430)^0\pi^+$, $\overline{K}^*_0(1430)^0 \to K^-\pi^+$	[tt]	(1.21±0.06) %		382
$\overline{K}^*(892)^0\pi^+$, $\overline{K}^*(892)^0 \to K^-\pi^+$		(1.01±0.11) %		714
$\overline{K}^*(1410)^0\pi^+$, $\overline{K}^{*0} \to K^-\pi^+$		not seen		381
$\overline{K}^*_2(1430)^0\pi^+$, $\overline{K}^*_2(1430)^0 \to K^-\pi^+$	[tt]	(2.2 ±0.7)×10^{-4}		371
$\overline{K}^*(1680)^0\pi^+$, $\overline{K}^*(1680)^0 \to K^-\pi^+$	[tt]	(2.1 ±1.1)×10^{-4}		58
$K^-(2\pi^+)_{I=2}$		(1.41±0.26) %		–
$K^0_S\pi^+\pi^0$	[ss]	(6.99±0.27) %		845
$K^0_S\rho^+$		(4.8 ±1.0) %		677
$\overline{K}^*(892)^0\pi^+$, $\overline{K}^*(892)^0 \to K^0_S\pi^0$		(1.3 ±0.6) %		714
$K^0_S\pi^+\pi^0$ nonresonant		(9 ±7)×10^{-3}		845
$K^-2\pi^+\pi^0$	[uu]	(5.99±0.18) %		816
$K^0_S2\pi^+\pi^-$	[uu]	(3.12±0.11) %		814
$K^-3\pi^+\pi^-$	[ss]	(5.6 ±0.5)×10^{-3}	S=1.1	772
$\overline{K}^*(892)^02\pi^+\pi^-$, $\overline{K}^*(892)^0 \to K^-\pi^+$		(1.2 ±0.4)×10^{-3}		645
$\overline{K}^*(892)^0\rho^0\pi^+$, $\overline{K}^*(892)^0 \to K^-\pi^+$		(2.2 ±0.4)×10^{-3}		239
$\overline{K}^*(892)^0a_1(1260)^+$	[vv]	(9.0 ±1.8)×10^{-3}		†
$K^-\rho^02\pi^+$		(1.68±0.27)×10^{-3}		524
$K^-3\pi^+\pi^-$ nonresonant		(3.9 ±2.9)×10^{-4}		772
$K^+2K^0_S$		(4.5 ±2.0)×10^{-3}		545
$K^+K^-K^0_S\pi^+$		(2.4 ±0.6)×10^{-4}		436

Pionic modes

$\pi^+\pi^0$		(1.19±0.06)×10^{-3}		925
$2\pi^+\pi^-$		(3.18±0.18)×10^{-3}		909
$\rho^0\pi^+$		(8.1 ±1.5)×10^{-4}		767
$\pi^+(\pi^+\pi^-)_{S-\text{wave}}$		(1.78±0.16)×10^{-3}		909
$\sigma\pi^+$, $\sigma \to \pi^+\pi^-$		(1.34±0.12)×10^{-3}		–
$f_0(980)\pi^+$, $f_0(980) \to \pi^+\pi^-$		(1.52±0.33)×10^{-4}		669
$f_0(1370)\pi^+$, $f_0(1370) \to \pi^+\pi^-$		(8 ±4)×10^{-5}		–
$f_2(1270)\pi^+$, $f_2(1270) \to \pi^+\pi^-$		(4.9 ±0.9)×10^{-4}		485
$\rho(1450)^0\pi^+$, $\rho(1450)^0 \to \pi^+\pi^-$		< 8 ×10^{-5}	CL=95%	338
$f_0(1500)\pi^+$, $f_0(1500) \to \pi^+\pi^-$		(1.1 ±0.4)×10^{-4}		–
$f_0(1710)\pi^+$, $f_0(1710) \to \pi^+\pi^-$		< 5 ×10^{-5}	CL=95%	–
$f_0(1790)\pi^+$, $f_0(1790) \to \pi^+\pi^-$		< 6 ×10^{-5}	CL=95%	–
$(\pi^+\pi^+)_{S-\text{wave}}\pi^-$		< 1.2 ×10^{-4}	CL=95%	909
$2\pi^+\pi^-$ nonresonant		< 1.1 ×10^{-4}	CL=95%	909
$\pi^+2\pi^0$		(4.6 ±0.4)×10^{-3}		910
$2\pi^+\pi^-\pi^0$		(1.13±0.08) %		883
$\eta\pi^+$, $\eta \to \pi^+\pi^-\pi^0$		(8.0 ±0.5)×10^{-4}		848
$\omega\pi^+$, $\omega \to \pi^+\pi^-\pi^0$		< 3 ×10^{-4}	CL=90%	763
$3\pi^+2\pi^-$		(1.61±0.16)×10^{-3}		845

Fractions of some of the following modes with resonances have already appeared above as submodes of particular charged-particle modes.

$\eta\pi^+$		(3.53±0.21)×10^{-3}		848
$\eta\pi^+\pi^0$		(1.38±0.35)×10^{-3}		830
$\omega\pi^+$		< 3.4 ×10^{-4}	CL=90%	764
$\eta'(958)\pi^+$		(4.67±0.29)×10^{-3}		681
$\eta'(958)\pi^+\pi^0$		(1.6 ±0.5)×10^{-3}		654

Hadronic modes with a $K\overline{K}$ pair

$K^+K^0_S$		(2.83±0.16)×10^{-3}	S=2.2	793
$K^+K^-\pi^+$	[ss]	(9.54±0.26)×10^{-3}	S=1.1	744
$\phi\pi^+$, $\phi \to K^+K^-$		(2.65$^{+0.08}_{-0.09}$)×10^{-3}		647
$K^+\overline{K}^*(892)^0$, $\overline{K}^*(892)^0 \to K^-\pi^+$		(2.45$^{+0.09}_{-0.14}$)×10^{-3}		613
$K^+\overline{K}^*_0(1430)^0$, $\overline{K}^*_0(1430)^0 \to K^-\pi^+$		(1.79±0.34)×10^{-3}		–
$K^+\overline{K}^*_2(1430)^0$, $\overline{K}^*_2 \to K^-\pi^+$		(1.6 $^{+1.2}_{-0.8}$)×10^{-4}		–
$K^+\overline{K}^*_0(800)$, $\overline{K}^*_0 \to K^-\pi^+$		(6.7 $^{+3.4}_{-2.1}$)×10^{-4}		–
$a_0(1450)^0\pi^+$, $a^0_0 \to K^+K^-$		(4.4 $^{+7.0}_{-1.8}$)×10^{-4}		–
$\phi(1680)\pi^+$, $\phi \to K^+K^-$		(4.9 $^{+4.0}_{-1.9}$)×10^{-5}		–
$K^+K^-\pi^+$ nonresonant		not seen		744
$K^+K^0_S\pi^+\pi^-$		(1.75±0.18)×10^{-3}		678
$K^0_SK^-2\pi^+$		(2.40±0.18)×10^{-3}		678
$K^+K^-2\pi^+\pi^-$		(2.2 ±1.2)×10^{-4}		600

A few poorly measured branching fractions:

$\phi\pi^+\pi^0$		(2.3 ±1.0) %		619
$\phi\rho^+$		< 1.5 %	CL=90%	260
$K^+K^-\pi^+\pi^0$ non-ϕ		(1.5 $^{+0.7}_{-0.6}$) %		682
$K^*(892)^+K^0_S$		(1.6 ±0.7) %		612

Doubly Cabibbo-suppressed modes

$K^+\pi^0$		(1.83±0.26)×10^{-4}	S=1.4	864
$K^+\eta$		(1.08±0.17)×10^{-4}		776
$K^+\eta'(958)$		(1.76±0.22)×10^{-4}		571
$K^+\pi^+\pi^-$		(5.27±0.23)×10^{-4}		846
$K^+\rho^0$		(2.0 ±0.5)×10^{-4}		679
$K^*(892)^0\pi^+$, $K^*(892)^0 \to K^+\pi^-$		(2.5 ±0.4)×10^{-4}		714
$K^+f_0(980)$, $f_0(980) \to \pi^+\pi^-$		(4.7 ±2.8)×10^{-5}		–
$K^*_2(1430)^0\pi^+$, $K^*_2(1430)^0 \to K^+\pi^-$		(4.2 ±2.9)×10^{-5}		–
$K^+\pi^+\pi^-$ nonresonant		not seen		846
$2K^+K^-$		(8.7 ±2.0)×10^{-5}		550

$\Delta C = 1$ weak neutral current ($C1$) modes, or Lepton Family number (LF) or Lepton number (L) violating modes

$\pi^+e^+e^-$	$C1$		< 1.1 ×10^{-6}	CL=90%	930
$\pi^+\phi$, $\phi \to e^+e^-$	[xx]		(1.7 $^{+1.4}_{-0.9}$)×10^{-6}		–
$\pi^+\mu^+\mu^-$	$C1$		< 7.3 ×10^{-8}	CL=90%	918
$\pi^+\phi$, $\phi \to \mu^+\mu^-$	[xx]		(1.8 ±0.8)×10^{-6}		–
$\rho^+\mu^+\mu^-$	$C1$		< 5.6 ×10^{-4}	CL=90%	757
$K^+e^+e^-$	[yy]		< 1.0 ×10^{-6}	CL=90%	870
$K^+\mu^+\mu^-$	[yy]		< 4.3 ×10^{-6}	CL=90%	856
$\pi^+e^+\mu^-$	LF		< 2.9 ×10^{-6}	CL=90%	927
$\pi^+e^-\mu^+$	LF		< 3.6 ×10^{-6}	CL=90%	927
$K^+e^+\mu^-$	LF		< 1.2 ×10^{-6}	CL=90%	866
$K^+e^-\mu^+$	LF		< 2.8 ×10^{-6}	CL=90%	866
π^-2e^+	L		< 1.1 ×10^{-6}	CL=90%	930
$\pi^-2\mu^+$	L		< 2.2 ×10^{-8}	CL=90%	918
$\pi^-e^+\mu^+$	L		< 2.0 ×10^{-6}	CL=90%	927
$\rho^-2\mu^+$	L		< 5.6 ×10^{-4}	CL=90%	757
K^-2e^+	L		< 9 ×10^{-7}	CL=90%	870
$K^-2\mu^+$	L		< 1.0 ×10^{-5}	CL=90%	856
$K^-e^+\mu^+$	L		< 1.9 ×10^{-6}	CL=90%	866
$K^*(892)^-2\mu^+$	L		< 8.5 ×10^{-4}	CL=90%	703

D^0

$I(J^P) = \frac{1}{2}(0^-)$

Mass $m = 1864.84 \pm 0.07$ MeV (S = 1.1)
$m_{D^\pm} - m_{D^0} = 4.77 \pm 0.08$ MeV
Mean life $\tau = (410.1 \pm 1.5) \times 10^{-15}$ s
$c\tau = 122.9\ \mu$m
$|m_{D^0_1} - m_{D^0_2}| = (0.95^{+0.41}_{-0.44}) \times 10^{10}\ \hbar\ \text{s}^{-1}$
$(\Gamma_{D^0_1} - \Gamma_{D^0_2})/\Gamma = 2y = (1.29^{+0.14}_{-0.18}) \times 10^{-2}$
$|q/p| = 0.92^{+0.12}_{-0.09}$
$A_\Gamma = (-0.125 \pm 0.526) \times 10^{-3}$
$K^+\pi^-$ relative strong phase: $\cos\delta = 0.81^{+0.23}_{-0.19}$
$K^-\pi^+\pi^0$ coherence factor $R_{K\pi\pi^0} = 0.78^{+0.11}_{-0.25}$
$K^-\pi^+\pi^0$ average relative strong phase $\delta^{K\pi\pi^0} = (239^{+32}_{-28})^\circ$
$K^-\pi^-2\pi^+$ coherence factor $R_{K3\pi} = 0.36^{+0.24}_{-0.30}$
$K^-\pi^-2\pi^+$ average relative strong phase $\delta^{K3\pi} = (118^{+60}_{-50})^\circ$
$K^0_SK^+\pi^-$ coherence factor $R_{K^0_SK\pi} = 0.73 \pm 0.08$

$K^0_S K^+\pi^-$ average relative strong phase $\delta^{K^0_S K\pi} = (8 \pm 15)^\circ$
$K^* K$ coherence factor $R_{K^* K} = 1.00 \pm 0.16$
$K^* K$ average relative strong phase $\delta^{K^* K} = (26 \pm 16)^\circ$

CP-violation decay-rate asymmetries (labeled by the D^0 decay)

$A_{CP}(K^+K^-) = (-0.21 \pm 0.17)\%$
$A_{CP}(2K^0_S) = (-23 \pm 19)\%$
$A_{CP}(\pi^+\pi^-) = (0.22 \pm 0.21)\%$
$A_{CP}(2\pi^0) = (0 \pm 5)\%$
$A_{CP}(\pi^+\pi^-\pi^0) = (0.3 \pm 0.4)\%$
$A_{CP}(\rho(770)^+\pi^- \to \pi^+\pi^-\pi^0) = (1.2 \pm 0.9)\%$ [zz]
$A_{CP}(\rho(770)^0\pi^0 \to \pi^+\pi^-\pi^0) = (-3.1 \pm 3.0)\%$ [zz]
$A_{CP}(\rho(770)^-\pi^+ \to \pi^+\pi^-\pi^0) = (-1.0 \pm 1.7)\%$ [zz]
$A_{CP}(\rho(1450)^+\pi^- \to \pi^+\pi^-\pi^0) = (0 \pm 70)\%$ [zz]
$A_{CP}(\rho(1450)^0\pi^0 \to \pi^+\pi^-\pi^0) = (-20 \pm 40)\%$ [zz]
$A_{CP}(\rho(1450)^-\pi^+ \to \pi^+\pi^-\pi^0) = (6 \pm 9)\%$ [zz]
$A_{CP}(\rho(1700)^+\pi^- \to \pi^+\pi^-\pi^0) = (-5 \pm 14)\%$ [zz]
$A_{CP}(\rho(1700)^0\pi^0 \to \pi^+\pi^-\pi^0) = (13 \pm 9)\%$ [zz]
$A_{CP}(\rho(1700)^-\pi^+ \to \pi^+\pi^-\pi^0) = (8 \pm 11)\%$ [zz]
$A_{CP}(f_0(980)\pi^0 \to \pi^+\pi^-\pi^0) = (0 \pm 35)\%$ [zz]
$A_{CP}(f_0(1370)\pi^0 \to \pi^+\pi^-\pi^0) = (25 \pm 18)\%$ [zz]
$A_{CP}(f_0(1500)\pi^0 \to \pi^+\pi^-\pi^0) = (0 \pm 18)\%$ [zz]
$A_{CP}(f_0(1710)\pi^0 \to \pi^+\pi^-\pi^0) = (0 \pm 24)\%$ [zz]
$A_{CP}(f_2(1270)\pi^0 \to \pi^+\pi^-\pi^0) = (-4 \pm 6)\%$ [zz]
$A_{CP}(\sigma(400)\pi^0 \to \pi^+\pi^-\pi^0) = (6 \pm 8)\%$ [zz]
$A_{CP}(\text{nonresonant } \pi^+\pi^-\pi^0) = (-13 \pm 23)\%$ [zz]
$A_{CP}(2\pi^+2\pi^-)$
$A_{CP}(K^+K^-\pi^0) = (-1.0 \pm 1.7)\%$
$A_{CP}(K^*(892)^+K^- \to K^+K^-\pi^0) = (-0.9 \pm 1.3)\%$ [zz]
$A_{CP}(K^*(1410)^+K^- \to K^+K^-\pi^0) = (-21 \pm 24)\%$ [zz]
$A_{CP}((K^+\pi^0)_{S-wave}K^- \to K^+K^-\pi^0) = (7 \pm 15)\%$ [zz]
$A_{CP}(\phi(1020)\pi^0 \to K^+K^-\pi^0) = (1.1 \pm 2.2)\%$ [zz]
$A_{CP}(f_0(980)\pi^0 \to K^+K^-\pi^0) = (-3 \pm 19)\%$ [zz]
$A_{CP}(a_0(980)^0\pi^0 \to K^+K^-\pi^0) = (-5 \pm 16)\%$ [zz]
$A_{CP}(f_2'(1525)\pi^0 \to K^+K^-\pi^0) = (0 \pm 160)\%$ [zz]
$A_{CP}(K^*(892)^-K^+ \to K^+K^-\pi^0) = (-5 \pm 4)\%$ [zz]
$A_{CP}(K^*(1410)^-K^+ \to K^+K^-\pi^0) = (-17 \pm 29)\%$ [zz]
$A_{CP}((K^-\pi^0)_{S-wave}K^+ \to K^+K^-\pi^0) = (-10 \pm 40)\%$ [zz]
$A_{CP}(K^0_S\pi^0) = (-0.27 \pm 0.21)\%$
$A_{CP}(K^0_S\eta) = (0.5 \pm 0.5)\%$
$A_{CP}(K^0_S\eta') = (1.0 \pm 0.7)\%$
$A_{CP}(K^0_S\phi) = (-3 \pm 9)\%$
$A_{CP}(K^-\pi^+) = (0.1 \pm 0.7)\%$
$A_{CP}(K^+\pi^-) = (0.0 \pm 1.6)\%$
$A_{CP}(K^-\pi^+\pi^0) = (0.2 \pm 0.9)\%$
$A_{CP}(K^+\pi^-\pi^0) = (0 \pm 5)\%$
$A_{CP}(K^0_S\pi^+\pi^-) = (-0.1 \pm 0.8)\%$
$A_{CP}(K^*(892)^-\pi^+ \to K^0_S\pi^+\pi^-) = (0.4 \pm 0.5)\%$
$A_{CP}(K^*(892)^+\pi^- \to K^0_S\pi^+\pi^-) = (1 \pm 6)\%$
$A_{CP}(\overline{K}^0\rho^0 \to K^0_S\pi^+\pi^-) = (-0.1 \pm 0.5)\%$
$A_{CP}(\overline{K}^0\omega \to K^0_S\pi^+\pi^-) = (-13 \pm 7)\%$
$A_{CP}(\overline{K}^0 f_0(980) \to K^0_S\pi^+\pi^-) = (-0.4 \pm 2.7)\%$
$A_{CP}(\overline{K}^0 f_2(1270) \to K^0_S\pi^+\pi^-) = (-4 \pm 5)\%$
$A_{CP}(\overline{K}^0 f_0(1370) \to K^0_S\pi^+\pi^-) = (-1 \pm 9)\%$
$A_{CP}(\overline{K}^0\rho^0(1450) \to K^0_S\pi^+\pi^-) = (-4 \pm 10)\%$
$A_{CP}(\overline{K}^0 f_0(600) \to K^0_S\pi^+\pi^-) = (-3 \pm 5)\%$
$A_{CP}(K^*(1410)^-\pi^+ \to K^0_S\pi^+\pi^-) = (-2 \pm 9)\%$
$A_{CP}(K^*_0(1430)^-\pi^+ \to K^0_S\pi^+\pi^-) = (4 \pm 4)\%$
$A_{CP}(K^*_0(1430)^+\pi^- \to K^0_S\pi^+\pi^-) = (12 \pm 15)\%$
$A_{CP}(K^*_2(1430)^-\pi^+ \to K^0_S\pi^+\pi^-) = (3 \pm 6)\%$
$A_{CP}(K^*_2(1430)^+\pi^- \to K^0_S\pi^+\pi^-) = (-10 \pm 32)\%$
$A_{CP}(K^*(1680)^-\pi^+ \to K^0_S\pi^+\pi^-)$
$A_{CP}(K^-\pi^+\pi^+\pi^-) = (0.7 \pm 1.0)\%$
$A_{CP}(K^+\pi^-\pi^+\pi^-) = (-2 \pm 4)\%$
$A_{CP}(K^+K^-\pi^+\pi^-) = (-8 \pm 7)\%$
$A_{CP}(K^*_1(1270)^+K^- \to K^{*0}\pi^+K^-) = (-1 \pm 10)\%$
$A_{CP}(K^*_1(1270)^-K^+ \to \overline{K}^{*0}\pi^-K^+) = (-10 \pm 32)\%$
$A_{CP}(K^*_1(1270)^+K^- \to \rho^0K^+K^-) = (-7 \pm 17)\%$
$A_{CP}(K^*_1(1270)^-K^+ \to \rho^0K^-K^+) = (10 \pm 13)\%$
$A_{CP}(K^*(1410)^+K^- \to K^{*0}\pi^+K^-) = (-20 \pm 17)\%$
$A_{CP}(K^*(1410)^-K^+ \to \overline{K}^{*0}\pi^-K^+) = (-1 \pm 14)\%$
$A_{CP}(K^{*0}\overline{K}^{*0}$ S-wave$) = (10 \pm 14)\%$
$A_{CP}(\phi\rho^0$ S-wave$) = (-3 \pm 5)\%$
$A_{CP}(\phi\rho^0$ D-wave$) = (-37 \pm 19)\%$
$A_{CP}(\phi(\pi^+\pi^-)_{S-wave}) = (-9 \pm 10)\%$
$A_{CP}((K^-\pi^+)_{P-wave}\,(K^+\pi^-)_{S-wave}) = (3 \pm 11)\%$

CP-violation asymmetry difference

$\Delta A_{CP} = A_{CP}(K^+K^-) - A_{CP}(\pi^+\pi^-) = (-0.46 \pm 0.25)\%$ (S = 1.8)

T-violation decay-rate asymmetry

$A_T(K^+K^-\pi^+\pi^-) = (1 \pm 7) \times 10^{-3}$ [rr]

CPT-violation decay-rate asymmetry

$A_{CPT}(K^\mp\pi^\pm) = 0.008 \pm 0.008$

Form factors

$r_V \equiv V(0)/A_1(0)$ in $D^0 \to K^*(892)^-\ell^+\nu_\ell = 1.7 \pm 0.8$
$r_2 \equiv A_2(0)/A_1(0)$ in $D^0 \to K^*(892)^-\ell^+\nu_\ell = 0.9 \pm 0.4$
$f_+(0)$ in $D^0 \to K^-\ell^+\nu_\ell = 0.727 \pm 0.011$
$f_+(0)|V_{cs}|$ in $D^0 \to K^-\ell^+\nu_\ell = 0.726 \pm 0.009$
$r_1 \equiv a_1/a_0$ in $D^0 \to K^-\ell^+\nu_\ell = -2.65 \pm 0.35$
$r_2 \equiv a_1/a_0$ in $D^0 \to K^-\ell^+\nu_\ell = 13 \pm 9$
$f_+(0)|V_{cd}|$ in $D^0 \to \pi^-\ell^+\nu_\ell = 0.152 \pm 0.005$
$r_1 \equiv a_1/a_0$ in $D^0 \to \pi^-\ell^+\nu_\ell = -2.8 \pm 0.5$
$r_2 \equiv a_1/a_0$ in $D^0 \to \pi^-\ell^+\nu_\ell = 6 \pm 3.0$

Most decay modes (other than the semileptonic modes) that involve a neutral K meson are now given as K^0_S modes, not as $\overline{K}^0$ modes. Nearly always it is a K^0_S that is measured, and interference between Cabibbo-allowed and doubly Cabibbo-suppressed modes can invalidate the assumption that $2\,\Gamma(K^0_S) = \Gamma(\overline{K}^0)$.

D^0 DECAY MODES		Fraction (Γ_j/Γ)		Scale factor/ Confidence level	p (MeV/c)
Topological modes					
0-prongs	[aaa]	(15 ± 6) %			–
2-prongs		(70 ± 6) %			–
4-prongs	[bbb]	(14.5 ± 0.5) %			–
6-prongs	[ccc]	(6.4 ± 1.3) $\times 10^{-4}$			–
Inclusive modes					
e^+ anything	[ddd]	(6.49 ± 0.11) %			–
μ^+ anything		(6.7 ± 0.6) %			–
K^- anything		(54.7 ± 2.8) %		S=1.3	–
$\overline{K}^0$ anything + K^0 anything		(47 ± 4) %			–
K^+ anything		(3.4 ± 0.4) %			–
$\overline{K}^*(892)^-$ anything		(15 ± 9) %			–
$\overline{K}^*(892)^0$ anything		(9 ± 4) %			–
$K^*(892)^+$ anything		< 3.6	%	CL=90%	–
$K^*(892)^0$ anything		(2.8 ± 1.3) %			–
η anything		(9.5 ± 0.9) %			–
η' anything		(2.48 ± 0.27) %			–
ϕ anything		(1.05 ± 0.11) %			–
Semileptonic modes					
$K^- e^+ \nu_e$		(3.55 ± 0.05) %		S=1.2	867
$K^- \mu^+ \nu_\mu$		(3.31 ± 0.13) %			864
$K^*(892)^- e^+ \nu_e$		(2.16 ± 0.16) %			719
$K^*(892)^- \mu^+ \nu_\mu$		(1.91 ± 0.24) %			714
$K^- \pi^0 e^+ \nu_e$		(1.6 $^{+\ 1.3}_{-\ 0.5}$) %			861
$\overline{K}^0 \pi^- e^+ \nu_e$		(2.7 $^{+\ 0.9}_{-\ 0.7}$) %			860
$K^- \pi^+ \pi^- e^+ \nu_e$		(2.8 $^{+\ 1.4}_{-\ 1.1}$) $\times 10^{-4}$			843
$K_1(1270)^- e^+ \nu_e$		(7.6 $^{+\ 4.0}_{-\ 3.1}$) $\times 10^{-4}$			498
$K^- \pi^+ \pi^- \mu^+ \nu_\mu$		< 1.2	$\times 10^{-3}$	CL=90%	821
$(\overline{K}^*(892)\pi)^- \mu^+ \nu_\mu$		< 1.4	$\times 10^{-3}$	CL=90%	692
$\pi^- e^+ \nu_e$		(2.89 ± 0.08) $\times 10^{-3}$		S=1.1	927
$\pi^- \mu^+ \nu_\mu$		(2.37 ± 0.24) $\times 10^{-3}$			924
$\rho^- e^+ \nu_e$		(1.77 ± 0.16) $\times 10^{-3}$			771
Hadronic modes with one $\overline{K}$					
$K^- \pi^+$		(3.88 ± 0.05) %		S=1.1	861
$K^+ \pi^-$		(1.380 ± 0.028) $\times 10^{-4}$			861
$K^0_S \pi^0$		(1.19 ± 0.04) %			860
$K^0_L \pi^0$		(10.0 ± 0.7) $\times 10^{-3}$			860
$K^0_S \pi^+ \pi^-$	[ss]	(2.83 ± 0.20) %		S=1.1	842
$K^0_S \rho^0$		(6.3 $^{+\ 0.7}_{-\ 0.8}$) $\times 10^{-3}$			674
$K^0_S \omega, \omega \to \pi^+\pi^-$		(2.1 ± 0.6) $\times 10^{-4}$			670
$K^0_S (\pi^+\pi^-)_{S-\text{wave}}$		(3.4 ± 0.8) $\times 10^{-3}$			842
$K^0_S f_0(980)$, $f_0(980) \to \pi^+\pi^-$		(1.22 $^{+\ 0.40}_{-\ 0.24}$) $\times 10^{-3}$			549

Meson Summary Table

$K^0_S f_0(1370)$, $f_0(1370) \to \pi^+\pi^-$		$(\ 2.8\ ^{+\ 0.9}_{-\ 1.3}\ )\times10^{-3}$			†
$K^0_S f_2(1270)$, $f_2(1270) \to \pi^+\pi^-$		$(\ 9\ ^{+10}_{-\ 6}\ )\times10^{-5}$			262
$K^*(892)^-\pi^+$, $K^*(892)^- \to K^0_S\pi^-$		$(\ 1.66\ ^{+\ 0.15}_{-\ 0.17}\ )$ %			711
$K^*_0(1430)^-\pi^+$, $K^*_0(1430)^- \to K^0_S\pi^-$		$(\ 2.70\ ^{+\ 0.40}_{-\ 0.34}\ )\times10^{-3}$			378
$K^*_2(1430)^-\pi^+$, $K^*_2(1430)^- \to K^0_S\pi^-$		$(\ 3.4\ ^{+\ 1.9}_{-\ 1.0}\ )\times10^{-4}$			367
$K^*(1680)^-\pi^+$, $K^*(1680)^- \to K^0_S\pi^-$		$(\ 4\ \pm\ 4\ )\times10^{-4}$			46
$K^*(892)^+\pi^-$, $K^*(892)^+ \to K^0_S\pi^+$	[*eee*]	$(\ 1.14\ ^{+\ 0.60}_{-\ 0.34}\ )\times10^{-4}$			711
$K^*_0(1430)^+\pi^-$, $K^*_0(1430)^+ \to K^0_S\pi^+$	[*eee*]	$<\ 1.4\ \times10^{-5}$		CL=95%	–
$K^*_2(1430)^+\pi^-$, $K^*_2(1430)^+ \to K^0_S\pi^+$	[*eee*]	$<\ 3.4\ \times10^{-5}$		CL=95%	–
$K^0_S\pi^+\pi^-$ nonresonant		$(\ 2.5\ ^{+\ 6.0}_{-\ 1.6}\ )\times10^{-4}$			842
$K^-\pi^+\pi^0$	[*ss*]	$(13.9\ \pm\ 0.5\ )$ %		S=1.7	844
$K^-\rho^+$		$(10.8\ \pm\ 0.7\ )$ %			675
$K^-\rho(1700)^+$, $\rho(1700)^+ \to \pi^+\pi^0$		$(\ 7.9\ \pm\ 1.7\ )\times10^{-3}$			†
$K^*(892)^-\pi^+$, $K^*(892)^- \to K^-\pi^0$		$(\ 2.22\ ^{+\ 0.40}_{-\ 0.19}\ )$ %			711
$\overline{K}^*(892)^0\pi^0$, $\overline{K}^*(892)^0 \to K^-\pi^+$		$(\ 1.88\ \pm\ 0.23\ )$ %			711
$K^*_0(1430)^-\pi^+$, $K^*_0(1430)^- \to K^-\pi^0$		$(\ 4.6\ \pm\ 2.1\ )\times10^{-3}$			378
$\overline{K}^*_0(1430)^0\pi^0$, $\overline{K}^*_0(1430)^0 \to K^-\pi^+$		$(\ 5.7\ ^{+\ 5.0}_{-\ 1.5}\ )\times10^{-3}$			379
$K^*(1680)^-\pi^+$, $K^*(1680)^- \to K^-\pi^0$		$(\ 1.8\ \pm\ 0.7\ )\times10^{-3}$			46
$K^-\pi^+\pi^0$ nonresonant		$(\ 1.11\ ^{+\ 0.50}_{-\ 0.19}\ )$ %			844
$K^0_S 2\pi^0$		$(\ 9.1\ \pm\ 1.1\ )\times10^{-3}$		S=2.2	843
$K^0_S(2\pi^0)$-*S*-wave		$(\ 2.6\ \pm\ 0.7\ )\times10^{-3}$			–
$\overline{K}^*(892)^0\pi^0$, $\overline{K}^*(892)^0 \to K^0_S\pi^0$		$(\ 7.8\ \pm\ 0.7\ )\times10^{-3}$			711
$\overline{K}^*(1430)^0\pi^0$, $\overline{K}^{*0} \to K^0_S\pi^0$		$(\ 4\ \pm23\ )\times10^{-5}$			–
$\overline{K}^*(1680)^0\pi^0$, $\overline{K}^{*0} \to K^0_S\pi^0$		$(\ 1.0\ \pm\ 0.4\ )\times10^{-3}$			–
$K^0_S f_2(1270)$, $f_2 \to 2\pi^0$		$(\ 2.3\ \pm\ 1.1\ )\times10^{-4}$			–
$2K^0_S$, one $K^0_S \to 2\pi^0$		$(\ 3.2\ \pm\ 1.1\ )\times10^{-4}$			–
$K^-2\pi^+\pi^-$	[*ss*]	$(\ 8.08\ ^{+\ 0.21}_{-\ 0.19}\ )$ %		S=1.3	813
$K^-\pi^+\rho^0$ total		$(\ 6.75\ \pm\ 0.33\ )$ %			609
$K^-\pi^+\rho^0$ 3-body		$(\ 5.1\ \pm\ 2.3\ )\times10^{-3}$			609
$\overline{K}^*(892)^0\rho^0$, $\overline{K}^*(892)^0 \to K^-\pi^+$		$(\ 1.05\ \pm\ 0.23\ )$ %			416
$K^-a_1(1260)^+$, $a_1(1260)^+ \to 2\pi^+\pi^-$		$(\ 3.6\ \pm\ 0.6\ )$ %			327
$\overline{K}^*(892)^0\pi^+\pi^-$ total, $\overline{K}^*(892)^0 \to K^-\pi^+$		$(\ 1.6\ \pm\ 0.4\ )$ %			685
$\overline{K}^*(892)^0\pi^+\pi^-$ 3-body, $\overline{K}^*(892)^0 \to K^-\pi^+$		$(\ 9.9\ \pm\ 2.3\ )\times10^{-3}$			685
$K_1(1270)^-\pi^+$, $K_1(1270)^- \to K^-\pi^+\pi^-$	[*fff*]	$(\ 2.9\ \pm\ 0.3\ )\times10^{-3}$			484
$K^-2\pi^+\pi^-$ nonresonant		$(\ 1.88\ \pm\ 0.26\ )$ %			813
$K^0_S\pi^+\pi^-\pi^0$	[*ggg*]	$(\ 5.2\ \pm\ 0.6\ )$ %			813
$K^0_S\eta$, $\eta \to \pi^+\pi^-\pi^0$		$(\ 1.02\ \pm\ 0.09\ )\times10^{-3}$			772
$K^0_S\omega$, $\omega \to \pi^+\pi^-\pi^0$		$(\ 9.9\ \pm\ 0.5\ )\times10^{-3}$			670
$K^-2\pi^+\pi^-\pi^0$		$(\ 4.2\ \pm\ 0.4\ )$ %			771
$\overline{K}^*(892)^0\pi^+\pi^-\pi^0$, $\overline{K}^*(892)^0 \to K^-\pi^+$		$(\ 1.3\ \pm\ 0.6\ )$ %			643
$K^-\pi^+\omega$, $\omega \to \pi^+\pi^-\pi^0$		$(\ 2.7\ \pm\ 0.5\ )$ %			605
$\overline{K}^*(892)^0\omega$, $\overline{K}^*(892)^0 \to K^-\pi^+$, $\omega \to \pi^+\pi^-\pi^0$		$(\ 6.5\ \pm\ 3.0\ )\times10^{-3}$			410
$K^0_S\eta\pi^0$		$(\ 5.5\ \pm\ 1.1\ )\times10^{-3}$			721
$K^0_S a_0(980)$, $a_0(980) \to \eta\pi^0$		$(\ 6.5\ \pm\ 2.0\ )\times10^{-3}$			–
$\overline{K}^*(892)^0\eta$, $\overline{K}^*(892)^0 \to K^0_S\pi$		$(\ 1.6\ \pm\ 0.5\ )\times10^{-3}$			–
$K^0_S 2\pi^+2\pi^-$		$(\ 2.69\ \pm\ 0.31\ )\times10^{-3}$			768
$K^0_S\rho^0\pi^+\pi^-$, no $K^*(892)^-$		$(\ 1.1\ \pm\ 0.7\ )\times10^{-3}$			–
$K^*(892)^-2\pi^+\pi^-$, $K^*(892)^- \to K^0_S\pi^-$, no ρ^0		$(\ 5\ \pm\ 8\ )\times10^{-4}$			642
$K^*(892)^-\rho^0\pi^+$, $K^*(892)^- \to K^0_S\pi^-$		$(\ 1.6\ \pm\ 0.6\ )\times10^{-3}$			230
$K^0_S 2\pi^+2\pi^-$ nonresonant		$<\ 1.2\ \times10^{-3}$		CL=90%	768
$K^-3\pi^+2\pi^-$		$(\ 2.2\ \pm\ 0.6\ )\times10^{-4}$			713

Fractions of many of the following modes with resonances have already appeared above as submodes of particular charged-particle modes. (Modes for which there are only upper limits and $\overline{K}^*(892)\rho$ submodes only appear below.)

$K^0_S\eta$		$(\ 4.79\ \pm\ 0.30\ )\times10^{-3}$			772
$K^0_S\omega$		$(\ 1.11\ \pm\ 0.06\ )$ %			670
$K^0_S\eta'(958)$		$(\ 9.4\ \pm\ 0.5\ )\times10^{-3}$			565
$K^-a_1(1260)^+$		$(\ 7.8\ \pm\ 1.1\ )$ %			327
$K^-a_2(1320)^+$		$<\ 2\ \times10^{-3}$		CL=90%	198
$\overline{K}^*(892)^0\pi^+\pi^-$ total		$(\ 2.4\ \pm\ 0.5\ )$ %			685
$\overline{K}^*(892)^0\pi^+\pi^-$ 3-body		$(\ 1.48\ \pm\ 0.34\ )$ %			685
$\overline{K}^*(892)^0\rho^0$		$(\ 1.58\ \pm\ 0.34\ )$ %			417
$\overline{K}^*(892)^0\rho^0$ transverse		$(\ 1.7\ \pm\ 0.6\ )$ %			417
$\overline{K}^*(892)^0\rho^0$ *S*-wave		$(\ 3.0\ \pm\ 0.6\ )$ %			417
$\overline{K}^*(892)^0\rho^0$ *S*-wave long.		$<\ 3\ \times10^{-3}$		CL=90%	417
$\overline{K}^*(892)^0\rho^0$ *P*-wave		$<\ 3\ \times10^{-3}$		CL=90%	417
$\overline{K}^*(892)^0\rho^0$ *D*-wave		$(\ 2.1\ \pm\ 0.6\ )$ %			417
$K_1(1270)^-\pi^+$	[*fff*]	$(\ 1.6\ \pm\ 0.8\ )$ %			484
$K_1(1400)^-\pi^+$		$<\ 1.2\ $ %		CL=90%	386
$\overline{K}^*(892)^0\pi^+\pi^-\pi^0$		$(\ 1.9\ \pm\ 0.9\ )$ %			643
$K^-\pi^+\omega$		$(\ 3.0\ \pm\ 0.6\ )$ %			605
$\overline{K}^*(892)^0\omega$		$(\ 1.1\ \pm\ 0.5\ )$ %			410
$K^-\pi^+\eta'(958)$		$(\ 7.5\ \pm\ 1.9\ )\times10^{-3}$			479
$\overline{K}^*(892)^0\eta'(958)$		$<\ 1.1\ \times10^{-3}$		CL=90%	119

Hadronic modes with three *K*'s

$K^0_S K^+K^-$		$(\ 4.47\ \pm\ 0.34\ )\times10^{-3}$			544
$K^0_S a_0(980)^0$, $a^0_0 \to K^+K^-$		$(\ 3.0\ \pm\ 0.4\ )\times10^{-3}$			–
$K^-a_0(980)^+$, $a^+_0 \to K^+K^0_S$		$(\ 6.0\ \pm\ 1.8\ )\times10^{-4}$			–
$K^+a_0(980)^-$, $a^-_0 \to K^-K^0_S$		$<\ 1.1\ \times10^{-4}$		CL=95%	–
$K^0_S f_0(980)$, $f_0 \to K^+K^-$		$<\ 9\ \times10^{-5}$		CL=95%	–
$K^0_S\phi$, $\phi \to K^+K^-$		$(\ 2.05\ \pm\ 0.16\ )\times10^{-3}$			520
$K^0_S f_0(1370)$, $f_0 \to K^+K^-$		$(\ 1.7\ \pm\ 1.1\ )\times10^{-4}$			–
$3K^0_S$		$(\ 9.1\ \pm\ 1.3\ )\times10^{-4}$			539
$K^+2K^-\pi^+$		$(\ 2.21\ \pm\ 0.31\ )\times10^{-4}$			434
$K^+K^-\overline{K}^*(892)^0$, $\overline{K}^*(892)^0 \to K^-\pi^+$		$(\ 4.4\ \pm\ 1.7\ )\times10^{-5}$			†
$K^-\pi^+\phi$, $\phi \to K^+K^-$		$(\ 4.0\ \pm\ 1.7\ )\times10^{-5}$			422
$\phi\overline{K}^*(892)^0$, $\phi \to K^+K^-$, $\overline{K}^*(892)^0 \to K^-\pi^+$		$(\ 1.06\ \pm\ 0.20\ )\times10^{-4}$			†
$K^+2K^-\pi^+$ nonresonant		$(\ 3.3\ \pm\ 1.5\ )\times10^{-5}$			434
$2K^0_S K^\pm\pi^\mp$		$(\ 6.0\ \pm\ 1.3\ )\times10^{-4}$			427

Pionic modes

$\pi^+\pi^-$	$(\ 1.402\pm\ 0.026)\times10^{-3}$		S=1.1	922
$2\pi^0$	$(\ 8.20\ \pm\ 0.35\ )\times10^{-4}$			923
$\pi^+\pi^-\pi^0$	$(\ 1.43\ \pm\ 0.06\ )$ %		S=1.9	907
$\rho^+\pi^-$	$(\ 9.8\ \pm\ 0.4\ )\times10^{-3}$			764
$\rho^0\pi^0$	$(\ 3.72\ \pm\ 0.22\ )\times10^{-3}$			764
$\rho^-\pi^+$	$(\ 4.96\ \pm\ 0.24\ )\times10^{-3}$			764
$\rho(1450)^+\pi^-$, $\rho(1450)^+ \to \pi^+\pi^0$	$(\ 1.6\ \pm\ 2.0\ )\times10^{-5}$			–
$\rho(1450)^0\pi^0$, $\rho(1450)^0 \to \pi^+\pi^-$	$(\ 4.3\ \pm\ 1.9\ )\times10^{-5}$			–
$\rho(1450)^-\pi^+$, $\rho(1450)^- \to \pi^-\pi^0$	$(\ 2.6\ \pm\ 0.4\ )\times10^{-4}$			–
$\rho(1700)^+\pi^-$, $\rho(1700)^+ \to \pi^+\pi^0$	$(\ 5.9\ \pm\ 1.4\ )\times10^{-4}$			–
$\rho(1700)^0\pi^0$, $\rho(1700)^0 \to \pi^+\pi^-$	$(\ 7.2\ \pm\ 1.7\ )\times10^{-4}$			–
$\rho(1700)^-\pi^+$, $\rho(1700)^- \to \pi^-\pi^0$	$(\ 4.6\ \pm\ 1.1\ )\times10^{-4}$			–
$f_0(980)\pi^0$, $f_0(980) \to \pi^+\pi^-$	$(\ 3.6\ \pm\ 0.8\ )\times10^{-5}$			–
$f_0(500)\pi^0$, $f_0(500) \to \pi^+\pi^-$	$(\ 1.18\ \pm\ 0.21\ )\times10^{-4}$			–

$f_0(1370)\pi^0$, $f_0(1370) \to \pi^+\pi^-$		$(5.3 \pm 2.1) \times 10^{-5}$		–
$f_0(1500)\pi^0$, $f_0(1500) \to \pi^+\pi^-$		$(5.6 \pm 1.5) \times 10^{-5}$		–
$f_0(1710)\pi^0$, $f_0(1710) \to \pi^+\pi^-$		$(4.4 \pm 1.5) \times 10^{-5}$		–
$f_2(1270)\pi^0$, $f_2(1270) \to \pi^+\pi^-$		$(1.89 \pm 0.20) \times 10^{-4}$		–
$\pi^+\pi^-\pi^0$ nonresonant		$(1.20 \pm 0.35) \times 10^{-4}$		907
$3\pi^0$		$< 3.5 \times 10^{-4}$	CL=90%	908
$2\pi^+2\pi^-$		$(7.42 \pm 0.21) \times 10^{-3}$	S=1.1	880
$a_1(1260)^+\pi^-$, $a_1^+ \to 2\pi^+\pi^-$ total		$(4.45 \pm 0.31) \times 10^{-3}$		–
$a_1(1260)^+\pi^-$, $a_1^+ \to \rho^0\pi^+$ S-wave		$(3.21 \pm 0.25) \times 10^{-3}$		–
$a_1(1260)^+\pi^-$, $a_1^+ \to \rho^0\pi^+$ D-wave		$(1.9 \pm 0.5) \times 10^{-4}$		–
$a_1(1260)^+\pi^-$, $a_1^+ \to \sigma\pi^+$		$(6.2 \pm 0.7) \times 10^{-4}$		–
$2\rho^0$ total		$(1.82 \pm 0.13) \times 10^{-3}$		518
$2\rho^0$, parallel helicities		$(8.2 \pm 3.2) \times 10^{-5}$		–
$2\rho^0$, perpendicular helicities		$(4.8 \pm 0.6) \times 10^{-4}$		–
$2\rho^0$, longitudinal helicities		$(1.25 \pm 0.10) \times 10^{-3}$		–
Resonant $(\pi^+\pi^-)\pi^+\pi^-$ 3-body total		$(1.48 \pm 0.12) \times 10^{-3}$		–
$\sigma\pi^+\pi^-$		$(6.1 \pm 0.9) \times 10^{-4}$		–
$f_0(980)\pi^+\pi^-$, $f_0 \to \pi^+\pi^-$		$(1.8 \pm 0.5) \times 10^{-4}$		–
$f_2(1270)\pi^+\pi^-$, $f_2 \to \pi^+\pi^-$		$(3.6 \pm 0.6) \times 10^{-4}$		–
$\pi^+\pi^-2\pi^0$		(1.00 ± 0.09) %		882
$\eta\pi^0$	[hhh]	$(6.8 \pm 0.7) \times 10^{-4}$		846
$\omega\pi^0$	[hhh]	$< 2.6 \times 10^{-4}$	CL=90%	761
$2\pi^+2\pi^-\pi^0$		$(4.1 \pm 0.5) \times 10^{-3}$		844
$\eta\pi^+\pi^-$	[hhh]	$(1.09 \pm 0.16) \times 10^{-3}$		827
$\omega\pi^+\pi^-$	[hhh]	$(1.6 \pm 0.5) \times 10^{-3}$		738
$3\pi^+3\pi^-$		$(4.2 \pm 1.2) \times 10^{-4}$		795
$\eta'(958)\pi^0$		$(9.0 \pm 1.4) \times 10^{-4}$		678
$\eta'(958)\pi^+\pi^-$		$(4.5 \pm 1.7) \times 10^{-4}$		650
2η		$(1.67 \pm 0.20) \times 10^{-3}$		754
$\eta\eta'(958)$		$(1.05 \pm 0.26) \times 10^{-3}$		537

Hadronic modes with a $K\overline{K}$ pair

K^+K^-		$(3.96 \pm 0.08) \times 10^{-3}$	S=1.4	791
$2K_S^0$		$(1.7 \pm 0.4) \times 10^{-4}$	S=2.5	789
$K_S^0K^-\pi^+$		$(3.5 \pm 0.5) \times 10^{-3}$	S=1.2	739
$\overline{K}^*(892)^0K_S^0$, $\overline{K}^{*0} \to K^-\pi^+$		$< 5 \times 10^{-4}$	CL=90%	608
$K_S^0K^+\pi^-$		$(2.1 \pm 0.4) \times 10^{-3}$	S=1.3	739
$K^*(892)^0K_S^0$, $K^{*0} \to K^+\pi^-$		$< 1.8 \times 10^{-4}$	CL=90%	608
$K^+K^-\pi^0$		$(3.29 \pm 0.14) \times 10^{-3}$		743
$K^*(892)^+K^-$, $K^*(892)^+ \to K^+\pi^0$		$(1.46 \pm 0.07) \times 10^{-3}$		–
$K^*(892)^-K^+$, $K^*(892)^- \to K^-\pi^0$		$(5.2 \pm 0.4) \times 10^{-4}$		–
$(K^+\pi^0)_{S-wave}K^-$		$(2.34 \pm 0.17) \times 10^{-3}$		743
$(K^-\pi^0)_{S-wave}K^+$		$(1.3 \pm 0.4) \times 10^{-4}$		743
$f_0(980)\pi^0$, $f_0 \to K^+K^-$		$(3.5 \pm 0.6) \times 10^{-4}$		–
$\phi\pi^0$, $\phi \to K^+K^-$		$(6.4 \pm 0.4) \times 10^{-4}$		–
$2K_S^0\pi^0$		$< 5.9 \times 10^{-4}$		740
$K^+K^-\pi^+\pi^-$		$(2.43 \pm 0.12) \times 10^{-3}$		677
$\phi(\pi^+\pi^-)_{S-wave}$, $\phi \to K^+K^-$		$(2.50 \pm 0.33) \times 10^{-4}$		614
$(\phi\rho^0)_{S-wave}$, $\phi \to K^+K^-$		$(9.3 \pm 1.2) \times 10^{-4}$		250
$(\phi\rho^0)_{D-wave}$, $\phi \to K^+K^-$		$(8.3 \pm 2.3) \times 10^{-5}$		–
$(K^{*0}\overline{K}^{*0})_{S-wave}$, $K^{*0} \to K^\pm\pi^\mp$		$(1.48 \pm 0.30) \times 10^{-4}$		–
$(K^-\pi^+)_{P-wave}$, $(K^+\pi^-)_{S-wave}$,		$(2.6 \pm 0.5) \times 10^{-4}$		–
$K_1(1270)^+K^-$, $K_1(1270)^+ \to K^{*0}\pi^+$		$(1.8 \pm 0.5) \times 10^{-4}$		–
$K_1(1270)^+K^-$, $K_1(1270)^+ \to \rho^0K^+$		$(1.14 \pm 0.26) \times 10^{-4}$		–
$K_1(1270)^-K^+$, $K_1(1270)^- \to \overline{K}^{*0}\pi^-$		$(2.2 \pm 1.2) \times 10^{-5}$		–
$K_1(1270)^-K^+$, $K_1(1270)^- \to \rho^0K^-$		$(1.46 \pm 0.25) \times 10^{-4}$		–
$K^*(1410)^+K^-$, $K^*(1410)^+ \to K^{*0}\pi^+$		$(1.02 \pm 0.26) \times 10^{-4}$		–
$K^*(1410)^-K^+$, $K^*(1410)^- \to \overline{K}^{*0}\pi^-$		$(1.14 \pm 0.25) \times 10^{-4}$		–
$2K_S^0\pi^+\pi^-$		$(1.23 \pm 0.24) \times 10^{-3}$		673
$K_S^0K^-2\pi^+\pi^-$		$< 1.5 \times 10^{-4}$	CL=90%	595
$K^+K^-\pi^+\pi^-\pi^0$		$(3.1 \pm 2.0) \times 10^{-3}$		600

Other $K\overline{K}X$ modes. They include all decay modes of the ϕ, η, and ω.

$\phi\eta$		$(1.4 \pm 0.5) \times 10^{-4}$		489
$\phi\omega$		$< 2.1 \times 10^{-3}$	CL=90%	238

Radiative modes

$\rho^0\gamma$		$< 2.4 \times 10^{-4}$	CL=90%	771
$\omega\gamma$		$< 2.4 \times 10^{-4}$	CL=90%	768
$\phi\gamma$		$(2.70 \pm 0.35) \times 10^{-5}$		654
$\overline{K}^*(892)^0\gamma$		$(3.27 \pm 0.34) \times 10^{-4}$		719

Doubly Cabibbo suppressed (DC) modes or $\Delta C = 2$ forbidden via mixing ($C2M$) modes

$K^+\ell^-\overline{\nu}_\ell$ via $\overline{D}^0$		$< 2.2 \times 10^{-5}$	CL=90%	–	
K^+ or $K^*(892)^+e^-\overline{\nu}_e$ via $\overline{D}^0$		$< 6 \times 10^{-5}$	CL=90%	–	
$K^+\pi^-$	DC	$(1.47 \pm 0.07) \times 10^{-4}$	S=2.8	861	
$K^+\pi^-$ via DCS		$(1.31 \pm 0.08) \times 10^{-4}$		–	
$K^+\pi^-$ via $\overline{D}^0$		$< 1.6 \times 10^{-5}$	CL=95%	861	
$K_S^0\pi^+\pi^-$ in $D^0 \to \overline{D}^0$		$< 1.8 \times 10^{-4}$	CL=95%	–	
$K^*(892)^+\pi^-$, $K^*(892)^+ \to K_S^0\pi^+$	DC	$(1.14 \pm {}^{0.60}_{0.34}) \times 10^{-4}$		711	
$K_0^*(1430)^+\pi^-$, $K_0^*(1430)^+ \to K_S^0\pi^+$	DC	$< 1.4 \times 10^{-5}$		–	
$K_2^*(1430)^+\pi^-$, $K_2^*(1430)^+ \to K_S^0\pi^+$	DC	$< 3.4 \times 10^{-5}$		–	
$K^+\pi^-\pi^0$	DC	$(3.04 \pm 0.17) \times 10^{-4}$		844	
$K^+\pi^-\pi^0$ via $\overline{D}^0$		$(7.3 \pm 0.5) \times 10^{-4}$		–	
$K^+\pi^+2\pi^-$	DC	$(2.62 \pm 0.11) \times 10^{-4}$		813	
$K^+\pi^+2\pi^-$ via $\overline{D}^0$		$< 4 \times 10^{-4}$	CL=90%	812	
μ^- anything via $\overline{D}^0$		$< 4 \times 10^{-4}$	CL=90%	–	

$\Delta C = 1$ weak neutral current ($C1$) modes, Lepton Family number (LF) violating modes, Lepton (L) or Baryon (B) number violating modes

$\gamma\gamma$	$C1$	$< 2.2 \times 10^{-6}$	CL=90%	932	
e^+e^-	$C1$	$< 7.9 \times 10^{-8}$	CL=90%	932	
$\mu^+\mu^-$	$C1$	$< 6.2 \times 10^{-9}$	CL=90%	926	
$\pi^0e^+e^-$	$C1$	$< 4.5 \times 10^{-5}$	CL=90%	928	
$\pi^0\mu^+\mu^-$	$C1$	$< 1.8 \times 10^{-4}$	CL=90%	915	
ηe^+e^-	$C1$	$< 1.1 \times 10^{-4}$	CL=90%	852	
$\eta\mu^+\mu^-$	$C1$	$< 5.3 \times 10^{-4}$	CL=90%	838	
$\pi^+\pi^-e^+e^-$	$C1$	$< 3.73 \times 10^{-4}$	CL=90%	922	
$\rho^0e^+e^-$	$C1$	$< 1.0 \times 10^{-4}$	CL=90%	771	
$\pi^+\pi^-\mu^+\mu^-$	$C1$	$< 5.5 \times 10^{-7}$	CL=90%	894	
$\rho^0\mu^+\mu^-$	$C1$	$< 2.2 \times 10^{-5}$	CL=90%	754	
ωe^+e^-	$C1$	$< 1.8 \times 10^{-4}$	CL=90%	768	
$\omega\mu^+\mu^-$	$C1$	$< 8.3 \times 10^{-4}$	CL=90%	751	
$K^-K^+e^+e^-$	$C1$	$< 3.15 \times 10^{-4}$	CL=90%	791	
ϕe^+e^-	$C1$	$< 5.2 \times 10^{-5}$	CL=90%	654	
$K^-K^+\mu^+\mu^-$	$C1$	$< 3.3 \times 10^{-5}$	CL=90%	710	
$\phi\mu^+\mu^-$	$C1$	$< 3.1 \times 10^{-5}$	CL=90%	631	
$\overline{K}^0e^+e^-$	[yy]	$< 1.1 \times 10^{-4}$	CL=90%	866	
$\overline{K}^0\mu^+\mu^-$	[yy]	$< 2.6 \times 10^{-4}$	CL=90%	852	
$K^-\pi^+e^+e^-$	$C1$	$< 3.85 \times 10^{-4}$	CL=90%	861	
$\overline{K}^*(892)^0e^+e^-$	[yy]	$< 4.7 \times 10^{-5}$	CL=90%	719	
$K^-\pi^+\mu^+\mu^-$	$C1$	$< 3.59 \times 10^{-4}$	CL=90%	829	
$\overline{K}^*(892)^0\mu^+\mu^-$	[yy]	$< 2.4 \times 10^{-5}$	CL=90%	700	
$\pi^+\pi^-\pi^0\mu^+\mu^-$	$C1$	$< 8.1 \times 10^{-4}$	CL=90%	863	
$\mu^\pm e^\mp$	LF	[gg] $< 2.6 \times 10^{-7}$	CL=90%	929	
$\pi^0e^\pm\mu^\mp$	LF	[gg] $< 8.6 \times 10^{-5}$	CL=90%	924	
$\eta e^\pm\mu^\mp$	LF	[gg] $< 1.0 \times 10^{-4}$	CL=90%	848	
$\pi^+\pi^-e^\pm\mu^\mp$	LF	[gg] $< 1.5 \times 10^{-5}$	CL=90%	911	
$\rho^0e^\pm\mu^\mp$	LF	[gg] $< 4.9 \times 10^{-5}$	CL=90%	767	
$\omega e^\pm\mu^\mp$	LF	[gg] $< 1.2 \times 10^{-4}$	CL=90%	764	
$K^-K^+e^\pm\mu^\mp$	LF	[gg] $< 1.8 \times 10^{-4}$	CL=90%	754	
$\phi e^\pm\mu^\mp$	LF	[gg] $< 3.4 \times 10^{-5}$	CL=90%	648	
$\overline{K}^0e^\pm\mu^\mp$	LF	[gg] $< 1.0 \times 10^{-4}$	CL=90%	863	
$K^-\pi^+e^\pm\mu^\mp$	LF	[gg] $< 5.53 \times 10^{-4}$	CL=90%	848	
$\overline{K}^*(892)^0e^\pm\mu^\mp$	LF	[gg] $< 8.3 \times 10^{-5}$	CL=90%	714	

$2\pi^- 2e^+$ + c.c.	L		< 1.12	$\times 10^{-4}$	CL=90%	922
$2\pi^- 2\mu^+$ + c.c.	L		< 2.9	$\times 10^{-5}$	CL=90%	894
$K^-\pi^- 2e^+$ + c.c.	L		< 2.06	$\times 10^{-4}$	CL=90%	861
$K^-\pi^- 2\mu^+$ + c.c.	L		< 3.9	$\times 10^{-4}$	CL=90%	829
$2K^- 2e^+$ + c.c.	L		< 1.52	$\times 10^{-4}$	CL=90%	791
$2K^- 2\mu^+$ + c.c.	L		< 9.4	$\times 10^{-5}$	CL=90%	710
$\pi^-\pi^- e^+\mu^+$ + c.c.	L		< 7.9	$\times 10^{-5}$	CL=90%	911
$K^-\pi^- e^+\mu^+$ + c.c.	L		< 2.18	$\times 10^{-4}$	CL=90%	848
$2K^- e^+\mu^+$ + c.c.	L		< 5.7	$\times 10^{-5}$	CL=90%	754
pe^-	L,B	[iii]	< 1.0	$\times 10^{-5}$	CL=90%	696
$\overline{p}e^+$	L,B	[jjj]	< 1.1	$\times 10^{-5}$	CL=90%	696

$D^*(2007)^0$

$I(J^P) = \frac{1}{2}(1^-)$
I, J, P need confirmation.

Mass $m = 2006.96 \pm 0.10$ MeV
$m_{D^{*0}} - m_{D^0} = 142.12 \pm 0.07$ MeV
Full width $\Gamma < 2.1$ MeV, CL = 90%

$\overline{D}^*(2007)^0$ modes are charge conjugates of modes below.

$D^*(2007)^0$ DECAY MODES	Fraction (Γ_i/Γ)	p (MeV/c)
$D^0\pi^0$	(61.9±2.9) %	43
$D^0\gamma$	(38.1±2.9) %	137

$D^*(2010)^\pm$

$I(J^P) = \frac{1}{2}(1^-)$
I, J, P need confirmation.

Mass $m = 2010.26 \pm 0.07$ MeV (S = 1.1)
$m_{D^*(2010)^+} - m_{D^+} = 140.66 \pm 0.08$ MeV
$m_{D^*(2010)^+} - m_{D^0} = 145.4257 \pm 0.0017$ MeV
Full width $\Gamma = 83.4 \pm 1.8$ keV

$D^*(2010)^-$ modes are charge conjugates of the modes below.

$D^*(2010)^\pm$ DECAY MODES	Fraction (Γ_i/Γ)	p (MeV/c)
$D^0\pi^+$	(67.7±0.5) %	39
$D^+\pi^0$	(30.7±0.5) %	38
$D^+\gamma$	(1.6±0.4) %	136

$D_0^*(2400)^0$

$I(J^P) = \frac{1}{2}(0^+)$

Mass $m = 2318 \pm 29$ MeV (S = 1.7)
Full width $\Gamma = 267 \pm 40$ MeV

$D_0^*(2400)^0$ DECAY MODES	Fraction (Γ_i/Γ)	p (MeV/c)
$D^+\pi^-$	seen	385

$D_1(2420)^0$

$I(J^P) = \frac{1}{2}(1^+)$
I needs confirmation.

Mass $m = 2421.4 \pm 0.6$ MeV (S = 1.2)
$m_{D_1^0} - m_{D^{*+}} = 411.1 \pm 0.6$ (S = 1.2)
Full width $\Gamma = 27.4 \pm 2.5$ MeV (S = 2.3)

$\overline{D}_1(2420)^0$ modes are charge conjugates of modes below.

$D_1(2420)^0$ DECAY MODES	Fraction (Γ_i/Γ)	p (MeV/c)
$D^*(2010)^+\pi^-$	seen	354
$D^0\pi^+\pi^-$	seen	425
$D^+\pi^-$	not seen	473
$D^{*0}\pi^+\pi^-$	not seen	280

$D_2^*(2460)^0$

$I(J^P) = \frac{1}{2}(2^+)$

$J^P = 2^+$ assignment strongly favored.

Mass $m = 2462.6 \pm 0.6$ MeV (S = 1.2)
$m_{D_2^{*0}} - m_{D^+} = 593.0 \pm 0.6$ MeV (S = 1.2)
$m_{D_2^{*0}} - m_{D^{*+}} = 452.3 \pm 0.6$ MeV (S = 1.2)
Full width $\Gamma = 49.0 \pm 1.3$ MeV (S = 1.5)

$\overline{D}_2^*(2460)^0$ modes are charge conjugates of modes below.

$D_2^*(2460)^0$ DECAY MODES	Fraction (Γ_i/Γ)	p (MeV/c)
$D^+\pi^-$	seen	507
$D^*(2010)^+\pi^-$	seen	391
$D^0\pi^+\pi^-$	not seen	463
$D^{*0}\pi^+\pi^-$	not seen	326

$D_2^*(2460)^\pm$

$I(J^P) = \frac{1}{2}(2^+)$

$J^P = 2^+$ assignment strongly favored.

Mass $m = 2464.3 \pm 1.6$ MeV (S = 1.7)
$m_{D_2^*(2460)^\pm} - m_{D_2^*(2460)^0} = 2.4 \pm 1.7$ MeV
Full width $\Gamma = 37 \pm 6$ MeV (S = 1.4)

$D_2^*(2460)^-$ modes are charge conjugates of modes below.

$D_2^*(2460)^\pm$ DECAY MODES	Fraction (Γ_i/Γ)	p (MeV/c)
$D^0\pi^+$	seen	512
$D^{*0}\pi^+$	seen	395
$D^+\pi^+\pi^-$	not seen	461
$D^{*+}\pi^+\pi^-$	not seen	324

CHARMED, STRANGE MESONS ($C = S = \pm 1$)

$D_s^+ = c\overline{s}$, $D_s^- = \overline{c}s$, similarly for D_s^*'s

$D_s^\pm$

$I(J^P) = 0(0^-)$

Mass $m = 1968.30 \pm 0.11$ MeV (S = 1.1)
$m_{D_s^\pm} - m_{D^\pm} = 98.69 \pm 0.05$ MeV
Mean life $\tau = (500 \pm 7) \times 10^{-15}$ s (S = 1.3)
$c\tau = 149.9$ μm

CP-violating decay-rate asymmetries

$A_{CP}(\mu^\pm\nu) = (5 \pm 6)\%$
$A_{CP}(K^\pm K_S^0) = (0.08 \pm 0.26)\%$
$A_{CP}(K^+K^-\pi^\pm) = (-0.5 \pm 0.9)\%$
$A_{CP}(K^\pm K_S^0\pi^0) = (-2 \pm 6)\%$
$A_{CP}(2K_S^0\pi^\pm) = (3 \pm 5)\%$
$A_{CP}(K^+K^-\pi^\pm\pi^0) = (0.0 \pm 3.0)\%$
$A_{CP}(K^\pm K_S^0\pi^+\pi^-) = (-6 \pm 5)\%$
$A_{CP}(K_S^0 K^\mp 2\pi^\pm) = (4.1 \pm 2.8)\%$
$A_{CP}(\pi^+\pi^-\pi^\pm) = (-0.7 \pm 3.1)\%$
$A_{CP}(\pi^\pm\eta) = (1.1 \pm 3.1)\%$
$A_{CP}(\pi^\pm\eta') = (-2.2 \pm 2.3)\%$
$A_{CP}(\eta\pi^\pm\pi^0) = (-1 \pm 4)\%$
$A_{CP}(\eta'\pi^\pm\pi^0) = (0 \pm 8)\%$
$A_{CP}(K^\pm\pi^0) = (-27 \pm 24)\%$
$A_{CP}(K_S^0\pi^\pm) = (1.2 \pm 1.0)\%$ (S = 1.3)
$A_{CP}(K^\pm\pi^+\pi^-) = (4 \pm 5)\%$
$A_{CP}(K^\pm\eta) = (9 \pm 15)\%$
$A_{CP}(K^\pm\eta'(958)) = (6 \pm 19)\%$

T-violating decay-rate asymmetry

$A_T(K_S^0 K^\pm\pi^+\pi^-) = (-14 \pm 8) \times 10^{-3}$ [rr]

$D_s^+ \to \phi\ell^+\nu_\ell$ form factors

$r_2 = 0.84 \pm 0.11$ (S = 2.4)
$r_v = 1.80 \pm 0.08$
$\Gamma_L/\Gamma_T = 0.72 \pm 0.18$

Unless otherwise noted, the branching fractions for modes with a resonance in the final state include all the decay modes of the resonance. D_s^- modes are charge conjugates of the modes below.

D_s^+ DECAY MODES		Fraction (Γ_i/Γ)	Scale factor / Confidence level	p (MeV/c)
Inclusive modes				
e^+ semileptonic	[kkk]	(6.5 ±0.4) %		–
π^+ anything		(119.3 ±1.4) %		–
π^- anything		(43.2 ±0.9) %		–
π^0 anything		(123 ±7) %		–
K^- anything		(18.7 ±0.5) %		–
K^+ anything		(28.9 ±0.7) %		–
K_S^0 anything		(19.0 ±1.1) %		–
η anything	[lll]	(29.9 ±2.8) %		–
ω anything		(6.1 ±1.4) %		–
η' anything	[nnn]	(11.7 ±1.8) %		–
$f_0(980)$ anything, $f_0 \to \pi^+\pi^-$		< 1.3 %	CL=90%	–
ϕ anything		(15.7 ±1.0) %		–
K^+K^- anything		(15.8 ±0.7) %		–
$K_S^0 K^+$ anything		(5.8 ±0.5) %		–
$K_S^0 K^-$ anything		(1.9 ±0.4) %		–
$2K_S^0$ anything		(1.70±0.32) %		–
$2K^+$ anything		< 2.6 $\times 10^{-3}$	CL=90%	–
$2K^-$ anything		< 6 $\times 10^{-4}$	CL=90%	–
Leptonic and semileptonic modes				
$e^+\nu_e$		< 8.3 $\times 10^{-5}$	CL=90%	984
$\mu^+\nu_\mu$		(5.56±0.25) $\times 10^{-3}$		981
$\tau^+\nu_\tau$		(5.54±0.24) %		182
$K^+K^-e^+\nu_e$		—		851
$\phi e^+\nu_e$	[ooo]	(2.49±0.14) %		720
$\eta e^+\nu_e + \eta'(958) e^+\nu_e$	[ooo]	(3.66±0.37) %		–
$\eta e^+\nu_e$	[ooo]	(2.67±0.29) %	S=1.1	908
$\eta'(958) e^+\nu_e$	[ooo]	(9.9 ±2.3) $\times 10^{-3}$		751
$\omega e^+\nu_e$	[ppp]	< 2.0 $\times 10^{-3}$	CL=90%	829
$K^0 e^+\nu_e$		(3.7 ±1.0) $\times 10^{-3}$		921
$K^*(892)^0 e^+\nu_e$	[ooo]	(1.8 ±0.7) $\times 10^{-3}$		782
$f_0(980) e^+\nu_e$, $f_0 \to \pi^+\pi^-$		(2.00±0.32) $\times 10^{-3}$		–
Hadronic modes with a $K\overline{K}$ pair				
$K^+K_S^0$		(1.49±0.06) %		850
$K^+\overline{K}^0$		(2.95±0.14) %		850
$K^+K^-\pi^+$	[ss]	(5.39±0.21) %	S=1.4	805
$\phi\pi^+$	[ooo,qqq]	(4.5 ±0.4) %		712
$\phi\pi^+$, $\phi \to K^+K^-$	[qqq]	(2.24±0.10) %		712
$K^+\overline{K}^*(892)^0$, $\overline{K}^{*0} \to K^-\pi^+$		(2.58±0.11) %		416
$f_0(980)\pi^+$, $f_0 \to K^+K^-$		(1.14±0.31) %		732
$f_0(1370)\pi^+$, $f_0 \to K^+K^-$		(7 ±5) $\times 10^{-4}$		–
$f_0(1710)\pi^+$, $f_0 \to K^+K^-$		(6.6 ±2.9) $\times 10^{-4}$		198
$K^+\overline{K}_0^*(1430)^0$, $\overline{K}_0^* \to K^-\pi^+$		(1.8 ±0.4) $\times 10^{-3}$		218
$K^+K_S^0\pi^0$		(1.52±0.22) %		805
$2K_S^0\pi^+$		(7.7 ±0.6) $\times 10^{-3}$		802
$K^0\overline{K}^0\pi^+$		—		802
$K^*(892)^+\overline{K}^0$	[ooo]	(5.4 ±1.2) %		683
$K^+K^-\pi^+\pi^0$		(6.3 ±0.7) %	S=1.1	748
$\phi\rho^+$	[ooo]	(8.4 $^{+1.9}_{-2.3}$) %		401
$K_S^0 K^-2\pi^+$		(1.66±0.11) %		744
$K^*(892)^+\overline{K}^*(892)^0$	[ooo]	(7.2 ±2.6) %		417
$K^+K_S^0\pi^+\pi^-$		(1.03±0.10) %		744
$K^+K^-2\pi^+\pi^-$		(8.6 ±1.5) $\times 10^{-3}$		673
$\phi 2\pi^+\pi^-$	[ooo]	(1.21±0.16) %		640
$K^+K^-\rho^0\pi^+$ non-ϕ		< 2.6 $\times 10^{-4}$	CL=90%	249
$\phi\rho^0\pi^+$, $\phi \to K^+K^-$		(6.5 ±1.3) $\times 10^{-3}$		181
$\phi a_1(1260)^+$, $\phi \to K^+K^-$, $a_1^+ \to \rho^0\pi^+$		(7.4 ±1.2) $\times 10^{-3}$		†
$K^+K^-2\pi^+\pi^-$ nonresonant		(9 ±7) $\times 10^{-4}$		673
$2K_S^0 2\pi^+\pi^-$		(8 ±4) $\times 10^{-4}$		669
Hadronic modes without K's				
$\pi^+\pi^0$		< 3.4 $\times 10^{-4}$	CL=90%	975
$2\pi^+\pi^-$		(1.09±0.05) %	S=1.2	959
$\rho^0\pi^+$		(2.0 ±1.2) $\times 10^{-4}$		825
$\pi^+(\pi^+\pi^-)_{S-\text{wave}}$	[rrr]	(9.0 ±0.5) $\times 10^{-3}$		959
$f_2(1270)\pi^+$, $f_2 \to \pi^+\pi^-$		(1.09±0.20) $\times 10^{-3}$		559
$\rho(1450)^0\pi^+$, $\rho^0 \to \pi^+\pi^-$		(3.0 ±1.9) $\times 10^{-4}$		421
$\pi^+ 2\pi^0$		(6.5 ±1.3) $\times 10^{-3}$		960
$2\pi^+\pi^-\pi^0$		—		935
$\eta\pi^+$	[ooo]	(1.69±0.10) %	S=1.2	902
$\omega\pi^+$	[ooo]	(2.4 ±0.6) $\times 10^{-3}$		822
$3\pi^+ 2\pi^-$		(7.9 ±0.8) $\times 10^{-3}$		899
$2\pi^+\pi^- 2\pi^0$		—		902
$\eta\rho^+$	[ooo]	(8.9 ±0.8) %		724
$\eta\pi^+\pi^0$		(9.2 ±1.2) %		885
$\omega\pi^+\pi^0$	[ooo]	(2.8 ±0.7) %		802
$3\pi^+ 2\pi^-\pi^0$		(4.9 ±3.2) %		856
$\omega 2\pi^+\pi^-$	[ooo]	(1.6 ±0.5) %		766
$\eta'(958)\pi^+$	[nnn,ooo]	(3.94±0.25) %		743
$3\pi^+ 2\pi^-2\pi^0$		—		803
$\omega\eta\pi^+$	[ooo]	< 2.13 %	CL=90%	654
$\eta'(958)\rho^+$	[nnn,ooo]	(12.5 ±2.2) %		465
$\eta'(958)\pi^+\pi^0$		(5.6 ±0.8) %		720
Modes with one or three K's				
$K^+\pi^0$		(6.3 ±2.1) $\times 10^{-4}$		917
$K_S^0\pi^+$		(1.21±0.06) $\times 10^{-3}$		916
$K^+\eta$	[ooo]	(1.76±0.35) $\times 10^{-3}$		835
$K^+\omega$	[ooo]	< 2.4 $\times 10^{-3}$	CL=90%	741
$K^+\eta'(958)$	[ooo]	(1.8 ±0.6) $\times 10^{-3}$		646
$K^+\pi^+\pi^-$		(6.5 ±0.4) $\times 10^{-3}$		900
$K^+\rho^0$		(2.5 ±0.4) $\times 10^{-3}$		745
$K^+\rho(1450)^0$, $\rho^0 \to \pi^+\pi^-$		(6.9 ±2.4) $\times 10^{-4}$		–
$K^*(892)^0\pi^+$, $K^{*0} \to K^+\pi^-$		(1.41±0.24) $\times 10^{-3}$		775
$K^*(1410)^0\pi^+$, $K^{*0} \to K^+\pi^-$		(1.23±0.28) $\times 10^{-3}$		–
$K^*(1430)^0\pi^+$, $K^{*0} \to K^+\pi^-$		(5.0 ±3.5) $\times 10^{-4}$		–
$K^+\pi^+\pi^-$ nonresonant		(1.04±0.34) $\times 10^{-3}$		900
$K^0\pi^+\pi^0$		(1.00±0.18) %		899
$K_S^0 2\pi^+\pi^-$		(3.0 ±1.1) $\times 10^{-3}$		870
$K^+\omega\pi^0$	[ooo]	< 8.2 $\times 10^{-3}$	CL=90%	684
$K^+\omega\pi^+\pi^-$	[ooo]	< 5.4 $\times 10^{-3}$	CL=90%	603
$K^+\omega\eta$	[ooo]	< 7.9 $\times 10^{-3}$	CL=90%	366
$2K^+K^-$		(2.16±0.21) $\times 10^{-4}$		627
ϕK^+, $\phi \to K^+K^-$		(8.8 ±2.0) $\times 10^{-5}$		–
Doubly Cabibbo-suppressed modes				
$2K^+\pi^-$		(1.26±0.13) $\times 10^{-4}$		805
$K^+K^*(892)^0$, $K^{*0} \to K^+\pi^-$		(5.9 ±3.4) $\times 10^{-5}$		–
Baryon-antibaryon mode				
$p\overline{n}$		(1.3 ±0.4) $\times 10^{-3}$		295
$\Delta C = 1$ weak neutral current ($C1$) modes, Lepton family number (LF), or Lepton number (L) violating modes				
$\pi^+ e^+ e^-$	[yy]	< 1.3 $\times 10^{-5}$	CL=90%	979
$\pi^+\phi$, $\phi \to e^+e^-$	[xx]	(6 $^{+8}_{-4}$) $\times 10^{-6}$		–
$\pi^+\mu^+\mu^-$	[yy]	< 4.1 $\times 10^{-7}$	CL=90%	968
$K^+e^+e^-$	$C1$	< 3.7 $\times 10^{-6}$	CL=90%	922
$K^+\mu^+\mu^-$	$C1$	< 2.1 $\times 10^{-5}$	CL=90%	909
$K^*(892)^+\mu^+\mu^-$	$C1$	< 1.4 $\times 10^{-3}$	CL=90%	765
$\pi^+e^+\mu^-$	LF	< 1.2 $\times 10^{-5}$	CL=90%	976
$\pi^+e^-\mu^+$	LF	< 2.0 $\times 10^{-5}$	CL=90%	976
$K^+e^+\mu^-$	LF	< 1.4 $\times 10^{-5}$	CL=90%	919
$K^+e^-\mu^+$	LF	< 9.7 $\times 10^{-6}$	CL=90%	919
π^-2e^+	L	< 4.1 $\times 10^{-6}$	CL=90%	979
$\pi^-2\mu^+$	L	< 1.2 $\times 10^{-7}$	CL=90%	968
$\pi^-e^+\mu^+$	L	< 8.4 $\times 10^{-6}$	CL=90%	976
K^-2e^+	L	< 5.2 $\times 10^{-6}$	CL=90%	922
$K^-2\mu^+$	L	< 1.3 $\times 10^{-5}$	CL=90%	909
$K^-e^+\mu^+$	L	< 6.1 $\times 10^{-6}$	CL=90%	919
$K^*(892)^-2\mu^+$	L	< 1.4 $\times 10^{-3}$	CL=90%	765

$D_s^{*\pm}$

$I(J^P) = 0(?^?)$

J^P is natural, width and decay modes consistent with 1^-.

Mass $m = 2112.1 \pm 0.4$ MeV

$m_{D_s^{*\pm}} - m_{D_s^\pm} = 143.8 \pm 0.4$ MeV

Full width $\Gamma < 1.9$ MeV, CL = 90%

D_s^{*-} modes are charge conjugates of the modes below.

D_s^{*+} DECAY MODES	Fraction (Γ_i/Γ)	p (MeV/c)
$D_s^+\gamma$	(94.2±0.7) %	139
$D_s^+\pi^0$	(5.8±0.7) %	48

$D_{s0}^*(2317)^\pm$

$I(J^P) = 0(0^+)$
J, P need confirmation.

J^P is natural, low mass consistent with 0^+.

Mass $m = 2317.7 \pm 0.6$ MeV (S = 1.1)
$m_{D_{s0}^*(2317)^\pm} - m_{D_s^\pm} = 349.4 \pm 0.6$ MeV (S = 1.1)
Full width $\Gamma < 3.8$ MeV, CL = 95%

$D_{s0}^*(2317)^-$ modes are charge conjugates of modes below.

$D_{s0}^*(2317)^\pm$ DECAY MODES	Fraction (Γ_i/Γ)	p (MeV/c)
$D_s^+\pi^0$	seen	298
$D_s^+\pi^0\pi^0$	not seen	205

$D_{s1}(2460)^\pm$

$I(J^P) = 0(1^+)$

Mass $m = 2459.5 \pm 0.6$ MeV (S = 1.1)
$m_{D_{s1}(2460)^\pm} - m_{D_s^{*\pm}} = 347.3 \pm 0.7$ MeV (S = 1.2)
$m_{D_{s1}(2460)^\pm} - m_{D_s^\pm} = 491.2 \pm 0.6$ MeV (S = 1.1)
Full width $\Gamma < 3.5$ MeV, CL = 95%

$D_{s1}(2460)^-$ modes are charge conjugates of the modes below.

$D_{s1}(2460)^+$ DECAY MODES	Fraction (Γ_i/Γ)	Scale factor/ Confidence level	p (MeV/c)
$D_s^{*+}\pi^0$	(48 ±11) %		297
$D_s^+\gamma$	(18 ± 4) %		442
$D_s^+\pi^+\pi^-$	(4.3± 1.3) %	S=1.1	363
$D_s^{*+}\gamma$	< 8 %	CL=90%	323
$D_{s0}^*(2317)^+\gamma$	($3.7^{+\ 5.0}_{-\ 2.4}$) %		138

$D_{s1}(2536)^\pm$

$I(J^P) = 0(1^+)$
J, P need confirmation.

Mass $m = 2535.10 \pm 0.08$ MeV (S = 1.1)
Full width $\Gamma = 0.92 \pm 0.05$ MeV

$D_{s1}(2536)^-$ modes are charge conjugates of the modes below.

$D_{s1}(2536)^+$ DECAY MODES	Fraction (Γ_i/Γ)	Confidence level	p (MeV/c)
$D^*(2010)^+K^0$	0.85 ±0.12		149
$(D^*(2010)^+K^0)_{S-wave}$	0.61 ±0.09		149
$D^+\pi^-K^+$	0.028±0.005		176
$D^*(2007)^0K^+$	**DEFINED AS 1**		167
D^+K^0	<0.34	90%	381
D^0K^+	<0.12	90%	391
$D_s^{*+}\gamma$	possibly seen		388
$D_s^+\pi^+\pi^-$	seen		437

$D_{s2}^*(2573)$

$I(J^P) = 0(?^?)$

J^P is natural, width and decay modes consistent with 2^+.

Mass $m = 2571.9 \pm 0.8$ MeV
Full width $\Gamma = 17 \pm 4$ MeV (S = 1.3)

$D_{s2}^*(2573)^-$ modes are charge conjugates of the modes below.

$D_{s2}^*(2573)^+$ DECAY MODES	Fraction (Γ_i/Γ)	p (MeV/c)
D^0K^+	seen	434
$D^*(2007)^0K^+$	not seen	243

$D_{s1}^*(2700)^\pm$

$I(J^P) = 0(1^-)$

Mass $m = 2709 \pm 4$ MeV
Full width $\Gamma = 117 \pm 13$ MeV

BOTTOM MESONS ($B = \pm 1$)

$B^+ = u\overline{b}$, $B^0 = d\overline{b}$, $\overline{B}^0 = \overline{d}b$, $B^- = \overline{u}b$, similarly for B^*'s

B-particle organization

Many measurements of B decays involve admixtures of B hadrons. Previously we arbitrarily included such admixtures in the $B^\pm$ section, but because of their importance we have created two new sections: "$B^\pm/B^0$ Admixture" for $\Upsilon(4S)$ results and "$B^\pm/B^0/B_s^0/b$-baryon Admixture" for results at higher energies. Most inclusive decay branching fractions and χ_b at high energy are found in the Admixture sections. B^0-$\overline{B}^0$ mixing data are found in the B^0 section, while B_s^0-$\overline{B}_s^0$ mixing data and B-$\overline{B}$ mixing data for a B^0/B_s^0 admixture are found in the B_s^0 section. CP-violation data are found in the $B^\pm$, B^0, and $B^\pm$ B^0 Admixture sections. b-baryons are found near the end of the Baryon section.

The organization of the B sections is now as follows, where bullets indicate particle sections and brackets indicate reviews.

- $B^\pm$
  mass, mean life, CP violation, branching fractions
- B^0
  mass, mean life, B^0-$\overline{B}^0$ mixing, CP violation, branching fractions
- $B^\pm$ B^0 Admixtures
  CP violation, branching fractions
- $B^\pm/B^0/B_s^0/b$-baryon Admixtures
  mean life, production fractions, branching fractions
- B^*
  mass
- $B_1(5721)^0$
  mass
- $B_2^*(5747)^0$
  mass
- B_s^0
  mass, mean life, B_s^0-$\overline{B}_s^0$ mixing, CP violation, branching fractions
- B_s^*
  mass
- $B_{s1}(5830)^0$
  mass
- $B_{s2}^*(5840)^0$
  mass
- $B_c^\pm$
  mass, mean life, branching fractions

At the end of Baryon Listings:

- Λ_b
  mass, mean life, branching fractions
- $\Lambda_b(5912)^0$
  mass, mean life
- $\Lambda_b(5920)^0$
  mass, mean life
- Σ_b
  mass
- Σ_b^*
  mass
- Ξ_b^0, Ξ_b^-
  mass, mean life, branching fractions
- $\Xi_b(5945)^0$

mass, mean life

- Ω_b^-

mass, branching fractions

- b-baryon Admixture

mean life, branching fractions

$B^\pm$ $I(J^P) = \frac{1}{2}(0^-)$

I, J, P need confirmation. Quantum numbers shown are quark-model predictions.

Mass $m_{B^\pm} = 5279.26 \pm 0.17$ MeV
Mean life $\tau_{B^\pm} = (1.638 \pm 0.004) \times 10^{-12}$ s
$c\tau = 491.1\ \mu$m

CP violation

$A_{CP}(B^+ \to J/\psi(1S)K^+) = 0.003 \pm 0.006$ (S = 1.8)
$A_{CP}(B^+ \to J/\psi(1S)\pi^+) = (0.1 \pm 2.8) \times 10^{-2}$ (S = 1.2)
$A_{CP}(B^+ \to J/\psi\rho^+) = -0.11 \pm 0.14$
$A_{CP}(B^+ \to J/\psi K^*(892)^+) = -0.048 \pm 0.033$
$A_{CP}(B^+ \to \eta_c K^+) = -0.02 \pm 0.10$ (S = 2.0)
$A_{CP}(B^+ \to \psi(2S)\pi^+) = 0.03 \pm 0.06$
$A_{CP}(B^+ \to \psi(2S)K^+) = -0.024 \pm 0.023$
$A_{CP}(B^+ \to \psi(2S)K^*(892)^+) = 0.08 \pm 0.21$
$A_{CP}(B^+ \to \chi_{c1}(1P)\pi^+) = 0.07 \pm 0.18$
$A_{CP}(B^+ \to \chi_{c0}K^+) = -0.20 \pm 0.18$ (S = 1.5)
$A_{CP}(B^+ \to \chi_{c1}K^+) = -0.009 \pm 0.033$
$A_{CP}(B^+ \to \chi_{c1}K^*(892)^+) = 0.5 \pm 0.5$
$A_{CP}(B^+ \to \overline{D}^0\pi^+) = -0.007 \pm 0.007$
$A_{CP}(B^+ \to D_{CP(+1)}\pi^+) = 0.035 \pm 0.024$
$A_{CP}(B^+ \to D_{CP(-1)}\pi^+) = 0.017 \pm 0.026$
$A_{CP}([K^\mp\pi^\pm\pi^+\pi^-]_D\pi^+) = 0.13 \pm 0.10$
$A_{CP}(B^+ \to \overline{D}^0K^+) = 0.01 \pm 0.05$ (S = 2.1)
$A_{CP}([K^\mp\pi^\pm\pi^+\pi^-]_DK^+) = -0.42 \pm 0.22$
$r_B(B^+ \to D^0K^+) = 0.096 \pm 0.008$
$\delta_B(B^+ \to D^0K^+) = (115 \pm 13)^\circ$
$r_B(B^+ \to \overline{D}^0K^{*+}) = 0.17 \pm 0.11$ (S = 2.3)
$\delta_B(B^+ \to D^0K^{*+}) = (155 \pm 70)^\circ$ (S = 2.0)
$A_{CP}(B^+ \to [K^-\pi^+]_DK^+) = -0.58 \pm 0.21$
$A_{CP}(B^+ \to [K^-\pi^+\pi^0]_DK^+) = 0.41 \pm 0.30$
$A_{CP}(B^+ \to [K^-\pi^+]_{\overline{D}}K^*(892)^+) = -0.3 \pm 0.5$
$A_{CP}(B^+ \to [K^-\pi^+]_D\pi^+) = 0.00 \pm 0.09$
$A_{CP}(B^+ \to [K^-\pi^+\pi^0]_D\pi^+) = 0.16 \pm 0.27$
$A_{CP}(B^+ \to [K^-\pi^+]_{(D\pi)}\pi^+) = -0.09 \pm 0.27$
$A_{CP}(B^+ \to [K^-\pi^+]_{(D\gamma)}\pi^+) = -0.7 \pm 0.6$
$A_{CP}(B^+ \to [K^-\pi^+]_{(D\pi)}K^+) = 0.8 \pm 0.4$
$A_{CP}(B^+ \to [K^-\pi^+]_{(D\gamma)}K^+) = 0.4 \pm 1.0$
$A_{CP}(B^+ \to [\pi^+\pi^-\pi^0]_DK^+) = -0.02 \pm 0.15$
$A_{CP}(B^+ \to D_{CP(+1)}K^+) = 0.170 \pm 0.033$ (S = 1.2)
$A_{ADS}(B^+ \to DK^+) = -0.52 \pm 0.15$
$A_{ADS}(B^+ \to D\pi^+) = 0.14 \pm 0.06$
$A_{CP}(B^+ \to D_{CP(-1)}K^+) = -0.10 \pm 0.07$
$A_{CP}(B^+ \to \overline{D}^{*0}\pi^+) = -0.014 \pm 0.015$
$A_{CP}(B^+ \to (D^*_{CP(+1)})^0\pi^+) = -0.02 \pm 0.05$
$A_{CP}(B^+ \to (D^*_{CP(-1)})^0\pi^+) = -0.09 \pm 0.05$
$A_{CP}(B^+ \to D^{*0}K^+) = -0.07 \pm 0.04$
$r_B^*(B^+ \to D^{*0}K^+) = 0.114^{+0.023}_{-0.040}$ (S = 1.2)
$\delta_B^*(B^+ \to D^{*0}K^+) = (310^{+22}_{-28})^\circ$ (S = 1.3)
$A_{CP}(B^+ \to D^{*0}_{CP(+1)}K^+) = -0.12 \pm 0.08$
$A_{CP}(B^+ \to D^*_{CP(-1)}K^+) = 0.07 \pm 0.10$
$A_{CP}(B^+ \to D_{CP(+1)}K^*(892)^+) = 0.09 \pm 0.14$
$A_{CP}(B^+ \to D_{CP(-1)}K^*(892)^+) = -0.23 \pm 0.22$
$A_{CP}(B^+ \to D_s^+\phi) = 0.0 \pm 0.4$
$A_{CP}(B^+ \to D^{*+}\overline{D}^{*0}) = -0.15 \pm 0.11$
$A_{CP}(B^+ \to D^{*+}\overline{D}^0) = -0.06 \pm 0.13$
$A_{CP}(B^+ \to D^+\overline{D}^{*0}) = 0.13 \pm 0.18$
$A_{CP}(B^+ \to D^+\overline{D}^0) = -0.03 \pm 0.07$
$A_{CP}(B^+ \to K^0_S\pi^+) = -0.017 \pm 0.016$
$A_{CP}(B^+ \to K^+\pi^0) = 0.037 \pm 0.021$
$A_{CP}(B^+ \to \eta' K^+) = 0.013 \pm 0.017$
$A_{CP}(B^+ \to \eta' K^*(892)^+) = -0.26 \pm 0.27$
$A_{CP}(B^+ \to \eta' K_0^*(1430)^+) = 0.06 \pm 0.20$
$A_{CP}(B^+ \to \eta' K_2^*(1430)^+) = 0.15 \pm 0.13$
$A_{CP}(B^+ \to \eta K^+) = -0.37 \pm 0.08$
$A_{CP}(B^+ \to \eta K^*(892)^+) = 0.02 \pm 0.06$
$A_{CP}(B^+ \to \eta K_0^*(1430)^+) = 0.05 \pm 0.13$
$A_{CP}(B^+ \to \eta K_2^*(1430)^+) = -0.45 \pm 0.30$
$A_{CP}(B^+ \to \omega K^+) = 0.02 \pm 0.05$
$A_{CP}(B^+ \to \omega K^{*+}) = 0.29 \pm 0.35$
$A_{CP}(B^+ \to \omega(K\pi)_0^{*+}) = -0.10 \pm 0.09$
$A_{CP}(B^+ \to \omega K_2^*(1430)^+) = 0.14 \pm 0.15$
$A_{CP}(B^+ \to K^{*0}\pi^+) = -0.04 \pm 0.09$ (S = 2.1)
$A_{CP}(B^+ \to K^*(892)^+\pi^0) = -0.06 \pm 0.24$
$A_{CP}(B^+ \to K^+\pi^-\pi^+) = 0.033 \pm 0.010$
$A_{CP}(B^+ \to K^+K^-K^+$ nonresonant$) = 0.06 \pm 0.05$
$A_{CP}(B^+ \to f(980)^0K^+) = -0.08 \pm 0.09$
$A_{CP}(B^+ \to f_2(1270)K^+) = -0.68^{+0.19}_{-0.17}$
$A_{CP}(B^+ \to f_0(1500)K^+) = 0.28 \pm 0.30$
$A_{CP}(B^+ \to f_2'(1525)^0K^+) = -0.08^{+0.05}_{-0.04}$
$A_{CP}(B^+ \to \rho^0K^+) = 0.37 \pm 0.10$
$A_{CP}(B^+ \to K_0^*(1430)^0\pi^+) = 0.055 \pm 0.033$
$A_{CP}(B^+ \to K_2^*(1430)^0\pi^+) = 0.05^{+0.29}_{-0.24}$
$A_{CP}(B^+ \to K^+\pi^0\pi^0) = -0.06 \pm 0.07$
$A_{CP}(B^+ \to K^0\rho^+) = -0.12 \pm 0.17$
$A_{CP}(B^+ \to K^{*+}\pi^+\pi^-) = 0.07 \pm 0.08$
$A_{CP}(B^+ \to \rho^0K^*(892)^+) = 0.31 \pm 0.13$
$A_{CP}(B^+ \to K^*(892)^+f_0(980)) = -0.15 \pm 0.12$
$A_{CP}(B^+ \to a_1^+K^0) = 0.12 \pm 0.11$
$A_{CP}(B^+ \to b_1^+K^0) = -0.03 \pm 0.15$
$A_{CP}(B^+ \to K^*(892)^0\rho^+) = -0.01 \pm 0.16$
$A_{CP}(B^+ \to b_1^0K^+) = -0.46 \pm 0.20$
$A_{CP}(B^+ \to K^0K^+) = 0.04 \pm 0.14$
$A_{CP}(B^+ \to K^0_SK^+) = -0.21 \pm 0.14$
$A_{CP}(B^+ \to K^+K^0_SK^0_S) = 0.04^{+0.04}_{-0.05}$
$A_{CP}(B^+ \to K^+K^-\pi^+) = -0.12 \pm 0.05$ (S = 1.2)
$A_{CP}(B^+ \to K^+K^-K^+) = -0.036 \pm 0.012$ (S = 1.1)
$A_{CP}(B^+ \to \phi K^+) = 0.04 \pm 0.04$ (S = 2.1)
$A_{CP}(B^+ \to X_0(1550)K^+) = -0.04 \pm 0.07$
$A_{CP}(B^+ \to K^{*+}K^+K^-) = 0.11 \pm 0.09$
$A_{CP}(B^+ \to \phi K^*(892)^+) = -0.01 \pm 0.08$
$A_{CP}(B^+ \to \phi(K\pi)_0^{*+}) = 0.04 \pm 0.16$
$A_{CP}(B^+ \to \phi K_1(1270)^+) = 0.15 \pm 0.20$
$A_{CP}(B^+ \to \phi K_2^*(1430)^+) = -0.23 \pm 0.20$
$A_{CP}(B^+ \to K^+\phi\phi) = -0.10 \pm 0.08$
$A_{CP}(B^+ \to K^+[\phi\phi]_{\eta_c}) = 0.09 \pm 0.10$
$A_{CP}(B^+ \to K^*(892)^+\gamma) = 0.018 \pm 0.029$
$A_{CP}(B^+ \to \eta K^+\gamma) = -0.12 \pm 0.07$
$A_{CP}(B^+ \to \phi K^+\gamma) = -0.13 \pm 0.11$ (S = 1.1)
$A_{CP}(B^+ \to \rho^+\gamma) = -0.11 \pm 0.33$
$A_{CP}(B^+ \to \pi^+\pi^0) = 0.03 \pm 0.04$
$A_{CP}(B^+ \to \pi^+\pi^-\pi^+) = 0.105 \pm 0.029$ (S = 1.3)
$A_{CP}(B^+ \to \rho^0\pi^+) = 0.18^{+0.09}_{-0.17}$
$A_{CP}(B^+ \to f_2(1270)\pi^+) = 0.41 \pm 0.30$
$A_{CP}(B^+ \to \rho^0(1450)\pi^+) = -0.1^{+0.4}_{-0.5}$
$A_{CP}(B^+ \to f_0(1370)\pi^+) = 0.72 \pm 0.22$
$A_{CP}(B^+ \to \pi^+\pi^-\pi^+$ nonresonant$) = -0.14^{+0.23}_{-0.16}$
$A_{CP}(B^+ \to \rho^+\pi^0) = 0.02 \pm 0.11$
$A_{CP}(B^+ \to \rho^+\rho^0) = -0.05 \pm 0.05$
$A_{CP}(B^+ \to \omega\pi^+) = -0.04 \pm 0.06$
$A_{CP}(B^+ \to \omega\rho^+) = -0.20 \pm 0.09$
$A_{CP}(B^+ \to \eta\pi^+) = -0.14 \pm 0.07$ (S = 1.4)
$A_{CP}(B^+ \to \eta\rho^+) = 0.11 \pm 0.11$
$A_{CP}(B^+ \to \eta'\pi^+) = 0.06 \pm 0.16$
$A_{CP}(B^+ \to \eta'\rho^+) = 0.26 \pm 0.17$
$A_{CP}(B^+ \to b_1^0\pi^+) = 0.05 \pm 0.16$
$A_{CP}(B^+ \to p\overline{p}\pi^+) = 0.00 \pm 0.04$
$A_{CP}(B^+ \to p\overline{p}K^+) = -0.08 \pm 0.04$ (S = 1.1)
$A_{CP}(B^+ \to p\overline{p}K^*(892)^+) = 0.21 \pm 0.16$ (S = 1.4)
$A_{CP}(B^+ \to p\overline{\Lambda}\gamma) = 0.17 \pm 0.17$
$A_{CP}(B^+ \to p\overline{\Lambda}\pi^0) = 0.01 \pm 0.17$
$A_{CP}(B^+ \to K^+\ell^+\ell^-) = -0.02 \pm 0.08$
$A_{CP}(B^+ \to K^+e^+e^-) = 0.14 \pm 0.14$
$A_{CP}(B^+ \to K^+\mu^+\mu^-) = -0.003 \pm 0.033$
$A_{CP}(B^+ \to K^{*+}\ell^+\ell^-) = -0.09 \pm 0.14$
$A_{CP}(B^+ \to K^*e^+e^-) = -0.14 \pm 0.23$
$A_{CP}(B^+ \to K^*\mu^+\mu^-) = -0.12 \pm 0.24$
$\gamma(B^+ \to D^{(*)0}K^{(*)+}) = (73^{+7}_{-9})^\circ$

Meson Summary Table

B^- modes are charge conjugates of the modes below. Modes which do not identify the charge state of the B are listed in the $B^\pm/B^0$ ADMIXTURE section.

The branching fractions listed below assume 50% $B^0\overline{B}{}^0$ and 50% B^+B^- production at the $\Upsilon(4S)$. We have attempted to bring older measurements up to date by rescaling their assumed $\Upsilon(4S)$ production ratio to 50:50 and their assumed D, D_s, D^*, and ψ branching ratios to current values whenever this would affect our averages and best limits significantly.

Indentation is used to indicate a subchannel of a previous reaction. All resonant subchannels have been corrected for resonance branching fractions to the final state so the sum of the subchannel branching fractions can exceed that of the final state.

For inclusive branching fractions, *e.g.*, $B \to D^\pm$ anything, the values usually are multiplicities, not branching fractions. They can be greater than one.

B^+ DECAY MODES		Fraction (Γ_i/Γ)	Scale factor/ Confidence level	p (MeV/c)
Semileptonic and leptonic modes				
$\ell^+\nu_\ell$ anything	[sss]	(10.99 ±0.28) %		–
$e^+\nu_e X_c$		(10.8 ±0.4) %		–
$D\ell^+\nu_\ell$ anything		(9.8 ±0.7) %		–
$\overline{D}{}^0\ell^+\nu_\ell$	[sss]	(2.27 ±0.11) %		2310
$\overline{D}{}^0\tau^+\nu_\tau$		(7.7 ±2.5) $\times 10^{-3}$		1911
$\overline{D}{}^*(2007)^0\ell^+\nu_\ell$	[sss]	(5.69 ±0.19) %		2258
$\overline{D}{}^*(2007)^0\tau^+\nu_\tau$		(1.88 ±0.20) %		1839
$D^-\pi^+\ell^+\nu_\ell$		(4.2 ±0.5) $\times 10^{-3}$		2306
$\overline{D}{}_0^*(2420)^0\ell^+\nu_\ell$, $\overline{D}{}_0^{*0}\to D^-\pi^+$		(2.5 ±0.5) $\times 10^{-3}$		–
$\overline{D}{}_2^*(2460)^0\ell^+\nu_\ell$, $\overline{D}{}_2^{*0}\to D^-\pi^+$		(1.53 ±0.16) $\times 10^{-3}$		2065
$D^{(*)}\,n\pi\ell^+\nu_\ell(n\geq 1)$		(1.87 ±0.26) %		–
$D^{*-}\pi^+\ell^+\nu_\ell$		(6.1 ±0.6) $\times 10^{-3}$		2254
$\overline{D}_1(2420)^0\ell^+\nu_\ell$, $\overline{D}{}_1^0\to D^{*-}\pi^+$		(3.03 ±0.20) $\times 10^{-3}$		2084
$\overline{D}{}_1'(2430)^0\ell^+\nu_\ell$, $\overline{D}{}_1'^0\to D^{*-}\pi^+$		(2.7 ±0.6) $\times 10^{-3}$		–
$\overline{D}{}_2^*(2460)^0\ell^+\nu_\ell$, $\overline{D}{}_2^{*0}\to D^{*-}\pi^+$		(1.01 ±0.24) $\times 10^{-3}$	S=2.0	2065
$D_s^{(*)-}K^+\ell^+\nu_\ell$		(6.1 ±1.0) $\times 10^{-4}$		–
$D_s^-K^+\ell^+\nu_\ell$		(3.0 $^{+1.4}_{-1.2}$) $\times 10^{-4}$		2242
$D_s^{*-}K^+\ell^+\nu_\ell$		(2.9 ±1.9) $\times 10^{-4}$		2185
$\pi^0\ell^+\nu_\ell$		(7.80 ±0.27) $\times 10^{-5}$		2638
$\eta\ell^+\nu_\ell$		(3.8 ±0.6) $\times 10^{-5}$		2611
$\eta'\ell^+\nu_\ell$		(2.3 ±0.8) $\times 10^{-5}$		2553
$\omega\ell^+\nu_\ell$	[sss]	(1.19 ±0.09) $\times 10^{-4}$		2582
$\rho^0\ell^+\nu_\ell$	[sss]	(1.58 ±0.11) $\times 10^{-4}$		2583
$p\overline{p}\ell^+\nu_\ell$		(5.8 $^{+2.6}_{-2.3}$) $\times 10^{-6}$		2467
$p\overline{p}\mu^+\nu_\mu$		< 8.5 $\times 10^{-6}$	CL=90%	2446
$p\overline{p}e^+\nu_e$		(8.2 $^{+4.0}_{-3.3}$) $\times 10^{-6}$		2467
$e^+\nu_e$		< 9.8 $\times 10^{-7}$	CL=90%	2640
$\mu^+\nu_\mu$		< 1.0 $\times 10^{-6}$	CL=90%	2639
$\tau^+\nu_\tau$		(1.14 ±0.27) $\times 10^{-4}$	S=1.3	2341
$\ell^+\nu_\ell\gamma$		< 1.56 $\times 10^{-5}$	CL=90%	2640
$e^+\nu_e\gamma$		< 1.7 $\times 10^{-5}$	CL=90%	2640
$\mu^+\nu_\mu\gamma$		< 2.4 $\times 10^{-5}$	CL=90%	2639
Inclusive modes				
D^0X		(8.6 ±0.7) %		–
$\overline{D}{}^0X$		(79 ±4) %		–
D^+X		(2.5 ±0.5) %		–
D^-X		(9.9 ±1.2) %		–
D_s^+X		(7.9 $^{+1.4}_{-1.3}$) %		–
D_s^-X		(1.10 $^{+0.40}_{-0.32}$) %		–
Λ_c^+X		(2.1 $^{+0.9}_{-0.6}$) %		–
$\overline{\Lambda}_c^-X$		(2.8 $^{+1.1}_{-0.9}$) %		–
$\overline{c}X$		(97 ±4) %		–
cX		(23.4 $^{+2.2}_{-1.8}$) %		–
$c/\overline{c}X$		(120 ±6) %		–

D, D^*, or D_s modes				
$\overline{D}{}^0\pi^+$		(4.81 ±0.15) $\times 10^{-3}$		2308
$D_{CP(+1)}\pi^+$	[ttt]	(2.20 ±0.24) $\times 10^{-3}$		–
$D_{CP(-1)}\pi^+$	[ttt]	(2.1 ±0.4) $\times 10^{-3}$		–
$\overline{D}{}^0\rho^+$		(1.34 ±0.18) %		2237
$\overline{D}{}^0K^+$		(3.70 ±0.17) $\times 10^{-4}$		2281
$D_{CP(+1)}K^+$	[ttt]	(1.92 ±0.14) $\times 10^{-4}$		–
$D_{CP(-1)}K^+$	[ttt]	(2.00 ±0.19) $\times 10^{-4}$		–
$[K^-\pi^+]_D K^+$	[uuu]	< 2.8 $\times 10^{-7}$	CL=90%	–
$[K^+\pi^-]_D K^+$	[uuu]	< 1.8 $\times 10^{-5}$	CL=90%	–
$[K^-\pi^+]_D\pi^+$	[uuu]	(6.3 ±1.1) $\times 10^{-7}$		–
$[K^+\pi^-]_D\pi^+$		(1.68 ±0.31) $\times 10^{-4}$		–
$[\pi^+\pi^-\pi^0]_D K^-$		(4.6 ±0.9) $\times 10^{-6}$		–
$\overline{D}{}^0K^*(892)^+$		(5.3 ±0.4) $\times 10^{-4}$		2213
$D_{CP(-1)}K^*(892)^+$	[ttt]	(2.7 ±0.8) $\times 10^{-4}$		–
$D_{CP(+1)}K^*(892)^+$	[ttt]	(5.8 ±1.1) $\times 10^{-4}$		–
$\overline{D}{}^0K^+\pi^+\pi^-$		(5.4 ±2.2) $\times 10^{-4}$		2237
$\overline{D}{}^0K^+\overline{K}{}^0$		(5.5 ±1.6) $\times 10^{-4}$		2189
$\overline{D}{}^0K^+\overline{K}{}^*(892)^0$		(7.5 ±1.7) $\times 10^{-4}$		2071
$\overline{D}{}^0\pi^+\pi^+\pi^-$		(5.7 ±2.2) $\times 10^{-3}$	S=3.6	2289
$\overline{D}{}^0\pi^+\pi^+\pi^-$ nonresonant		(5 ±4) $\times 10^{-3}$		2289
$\overline{D}{}^0\pi^+\rho^0$		(4.2 ±3.0) $\times 10^{-3}$		2207
$\overline{D}{}^0a_1(1260)^+$		(4 ±4) $\times 10^{-3}$		2123
$\overline{D}{}^0\omega\pi^+$		(4.1 ±0.9) $\times 10^{-3}$		2206
$D^*(2010)^-\pi^+\pi^+$		(1.35 ±0.22) $\times 10^{-3}$		2247
$\overline{D}_1(2420)^0\pi^+$, $\overline{D}{}_1^0\to D^*(2010)^-\pi^+$		(5.3 ±2.3) $\times 10^{-4}$		2081
$D^-\pi^+\pi^+$		(1.07 ±0.05) $\times 10^{-3}$		2299
D^+K^0		< 2.9 $\times 10^{-6}$	CL=90%	2278
D^+K^{*0}		< 1.8 $\times 10^{-6}$	CL=90%	2211
$D^+\overline{K}{}^{*0}$		< 1.4 $\times 10^{-6}$	CL=90%	2211
$\overline{D}{}^*(2007)^0\pi^+$		(5.18 ±0.26) $\times 10^{-3}$		2256
$\overline{D}{}^{*0}_{CP(+1)}\pi^+$	[vvv]	(2.9 ±0.7) $\times 10^{-3}$		–
$D^{*0}_{CP(-1)}\pi^+$	[vvv]	(2.6 ±1.0) $\times 10^{-3}$		–
$\overline{D}{}^*(2007)^0\omega\pi^+$		(4.5 ±1.2) $\times 10^{-3}$		2149
$\overline{D}{}^*(2007)^0\rho^+$		(9.8 ±1.7) $\times 10^{-3}$		2181
$\overline{D}{}^*(2007)^0K^+$		(4.20 ±0.34) $\times 10^{-4}$		2227
$\overline{D}{}^{*0}_{CP(+1)}K^+$	[vvv]	(2.8 ±0.4) $\times 10^{-4}$		–
$\overline{D}{}^{*0}_{CP(-1)}K^+$	[vvv]	(2.31 ±0.33) $\times 10^{-4}$		–
$\overline{D}{}^*(2007)^0K^*(892)^+$		(8.1 ±1.4) $\times 10^{-4}$		2156
$\overline{D}{}^*(2007)^0K^+\overline{K}{}^0$		< 1.06 $\times 10^{-3}$	CL=90%	2132
$\overline{D}{}^*(2007)^0K^+K^*(892)^0$		(1.5 ±0.4) $\times 10^{-3}$		2008
$\overline{D}{}^*(2007)^0\pi^+\pi^+\pi^-$		(1.03 ±0.12) %		2236
$\overline{D}{}^*(2007)^0a_1(1260)^+$		(1.9 ±0.5) %		2063
$\overline{D}{}^*(2007)^0\pi^-\pi^+\pi^+\pi^0$		(1.8 ±0.4) %		2219
$\overline{D}{}^{*0}3\pi^+2\pi^-$		(5.7 ±1.2) $\times 10^{-3}$		2196
$D^*(2010)^+\pi^0$		< 3.6 $\times 10^{-6}$		2255
$D^*(2010)^+K^0$		< 9.0 $\times 10^{-6}$	CL=90%	2225
$D^*(2010)^-\pi^+\pi^+\pi^0$		(1.5 ±0.7) %		2235
$D^*(2010)^-\pi^+\pi^+\pi^+\pi^-$		(2.6 ±0.4) $\times 10^{-3}$		2217
$\overline{D}{}^{**0}\pi^+$	[xxx]	(5.9 ±1.3) $\times 10^{-3}$		–
$\overline{D}{}_1^*(2420)^0\pi^+$		(1.5 ±0.6) $\times 10^{-3}$	S=1.3	2081
$\overline{D}_1(2420)^0\pi^+\times$ B($\overline{D}{}_1^0\to\overline{D}{}^0\pi^+\pi^-$)		(2.5 $^{+1.7}_{-1.4}$) $\times 10^{-4}$	S=4.0	2081
$\overline{D}_1(2420)^0\pi^+\times$ B($\overline{D}{}_1^0\to\overline{D}{}^0\pi^+\pi^-$ (nonresonant))		(2.3 ±1.0) $\times 10^{-4}$		2081
$\overline{D}{}_2^*(2462)^0\pi^+\times$ B($\overline{D}{}_2^*(2462)^0\to D^-\pi^+$)		(3.5 ±0.4) $\times 10^{-4}$		–
$\overline{D}{}_2^*(2462)^0\pi^+\times$B($\overline{D}{}_2^{*0}\to\overline{D}{}^0\pi^-\pi^+$)		(2.3 ±1.1) $\times 10^{-4}$		–
$\overline{D}{}_2^*(2462)^0\pi^+\times$B($\overline{D}{}_2^{*0}\to\overline{D}{}^0\pi^-\pi^+$ (nonresonant))		< 1.7 $\times 10^{-4}$	CL=90%	–
$\overline{D}{}_2^*(2462)^0\pi^+\times$B($\overline{D}{}_2^{*0}\to D^*(2010)^-\pi^+$)		(2.2 ±1.1) $\times 10^{-4}$		–
$\overline{D}{}_0^*(2400)^0\pi^+\times$ B($\overline{D}{}_0^*(2400)^0\to D^-\pi^+$)		(6.4 ±1.4) $\times 10^{-4}$		2128
$\overline{D}_1(2421)^0\pi^+\times$ B($\overline{D}_1(2421)^0\to D^{*-}\pi^+$)		(6.8 ±1.5) $\times 10^{-4}$		–
$\overline{D}{}_2^*(2462)^0\pi^+\times$ B($\overline{D}{}_2^*(2462)^0\to D^{*-}\pi^+$)		(1.8 ±0.5) $\times 10^{-4}$		–
$\overline{D}{}_1'(2427)^0\pi^+\times$ B($\overline{D}{}_1'(2427)^0\to D^{*-}\pi^+$)		(5.0 ±1.2) $\times 10^{-4}$		–

$\overline{D}_1(2420)^0\pi^+\times$B($\overline{D}_1^0\to\overline{D}^{*0}\pi^+\pi^-$)	<	6		$\times10^{-6}$	CL=90%	2081
$\overline{D}_1^*(2420)^0\rho^+$	<	1.4		$\times10^{-3}$	CL=90%	1996
$\overline{D}_2^*(2460)^0\pi^+$	<	1.3		$\times10^{-3}$	CL=90%	2062
$\overline{D}_2^*(2460)^0\pi^+\times$B($\overline{D}_2^{*0}\to\overline{D}^{*0}\pi^+\pi^-$)	<	2.2		$\times10^{-5}$	CL=90%	2062
$\overline{D}_2^*(2460)^0\rho^+$	<	4.7		$\times10^{-3}$	CL=90%	1976
$\overline{D}^0D_s^+$	(	9.0	±0.9)	$\times10^{-3}$		1815
$D_{s0}(2317)^+\overline{D}^0\times$B($D_{s0}(2317)^+\to D_s^+\pi^0$)	(	7.3	$^{+2.2}_{-1.7}$)	$\times10^{-4}$		1605
$D_{s0}(2317)^+\overline{D}^0\times$B($D_{s0}(2317)^+\to D_s^{*+}\gamma$)	<	7.6		$\times10^{-4}$	CL=90%	1605
$D_{s0}(2317)^+\overline{D}^*(2007)^0\times$B($D_{s0}(2317)^+\to D_s^+\pi^0$)	(	9	±7)	$\times10^{-4}$		1511
$D_{sJ}(2457)^+\overline{D}^0$	(	3.1	$^{+1.0}_{-0.9}$)	$\times10^{-3}$		–
$D_{sJ}(2457)^+\overline{D}^0\times$B($D_{sJ}(2457)^+\to D_s^+\gamma$)	(	4.6	$^{+1.3}_{-1.1}$)	$\times10^{-4}$		–
$D_{sJ}(2457)^+\overline{D}^0\times$B($D_{sJ}(2457)^+\to D_s^+\pi^+\pi^-$)	<	2.2		$\times10^{-4}$	CL=90%	–
$D_{sJ}(2457)^+\overline{D}^0\times$B($D_{sJ}(2457)^+\to D_s^+\pi^0$)	<	2.7		$\times10^{-4}$	CL=90%	–
$D_{sJ}(2457)^+\overline{D}^0\times$B($D_{sJ}(2457)^+\to D_s^{*+}\gamma$)	<	9.8		$\times10^{-4}$	CL=90%	–
$D_{sJ}(2457)^+\overline{D}^*(2007)^0$	(	1.20	±0.30) %			–
$D_{sJ}(2457)^+\overline{D}^*(2007)^0\times$B($D_{sJ}(2457)^+\to D_s^+\gamma$)	(	1.4	$^{+0.7}_{-0.6}$)	$\times10^{-3}$		–
$\overline{D}^0D_{s1}(2536)^+\times$B($D_{s1}(2536)^+\to D^*(2007)^0K^+ + D^*(2010)^+K^0$)	(	4.0	±1.0)	$\times10^{-4}$		1447
$\overline{D}^0D_{s1}(2536)^+\times$B($D_{s1}(2536)^+\to D^*(2007)^0K^+$)	(	2.2	±0.7)	$\times10^{-4}$		1447
$\overline{D}^*(2007)^0D_{s1}(2536)^+\times$B($D_{s1}(2536)^+\to D^*(2007)^0K^+$)	(	5.5	±1.6)	$\times10^{-4}$		1339
$\overline{D}^0D_{s1}(2536)^+\times$B($D_{s1}(2536)^+\to D^{*+}K^0$)	(	2.3	±1.1)	$\times10^{-4}$		1447
$\overline{D}^0D_{sJ}(2700)^+\times$B($D_{sJ}(2700)^+\to D^0K^+$)	(	1.13	$^{+0.26}_{-0.40}$)	$\times10^{-3}$		–
$\overline{D}^{*0}D_{s1}(2536)^+\times$B($D_{s1}(2536)^+\to D^{*+}K^0$)	(	3.9	±2.6)	$\times10^{-4}$		1339
$\overline{D}^{*0}D_{sJ}(2573)^+\times$B($D_{sJ}(2573)^+\to D^0K^+$)	<	2		$\times10^{-4}$	CL=90%	1306
$\overline{D}^*(2007)^0D_{sJ}(2573)^+\times$B($D_{sJ}(2573)^+\to D^0K^+$)	<	5		$\times10^{-4}$	CL=90%	1306
$\overline{D}^0D_s^{*+}$	(	7.6	±1.6)	$\times10^{-3}$		1734
$\overline{D}^*(2007)^0D_s^+$	(	8.2	±1.7)	$\times10^{-3}$		1737
$\overline{D}^*(2007)^0D_s^{*+}$	(	1.71	±0.24) %			1651
$D_s^{(*)+}\overline{D}^{**0}$	(	2.7	±1.2) %			–
$\overline{D}^*(2007)^0D^*(2010)^+$	(	8.1	±1.7)	$\times10^{-4}$		1713
$\overline{D}^0D^*(2010)^+ + \overline{D}^*(2007)^0D^+$	<	1.30		%	CL=90%	1792
$\overline{D}^0D^*(2010)^+$	(	3.9	±0.5)	$\times10^{-4}$		1792
$\overline{D}^0D^+$	(	3.8	±0.4)	$\times10^{-4}$		1866
$\overline{D}^0D^+K^0$	(	1.55	±0.21)	$\times10^{-3}$		1571
$D^+\overline{D}^*(2007)^0$	(	6.3	±1.7)	$\times10^{-4}$		1791
$\overline{D}^*(2007)^0D^+K^0$	(	2.1	±0.5)	$\times10^{-3}$		1474
$\overline{D}^0\overline{D}^*(2010)^+K^0$	(	3.8	±0.4)	$\times10^{-3}$		1476
$\overline{D}^*(2007)^0D^*(2010)^+K^0$	(	9.2	±1.2)	$\times10^{-3}$		1362
$\overline{D}^0D^0K^+$	(	1.45	±0.33)	$\times10^{-3}$	S=2.6	1577
$\overline{D}^*(2007)^0D^0K^+$	(	2.26	±0.23)	$\times10^{-3}$		1481
$\overline{D}^0D^*(2007)^0K^+$	(	6.3	±0.5)	$\times10^{-3}$		1481
$\overline{D}^*(2007)^0D^*(2007)^0K^+$	(	1.12	±0.13) %			1368
$D^-D^+K^+$	(	2.2	±0.7)	$\times10^{-4}$		1571
$D^-D^*(2010)^+K^+$	(	6.3	±1.1)	$\times10^{-4}$		1475
$D^*(2010)^-D^+K^+$	(	6.0	±1.3)	$\times10^{-4}$		1475
$D^*(2010)^-D^*(2010)^+K^+$	(	1.32	±0.18)	$\times10^{-3}$		1363
$(\overline{D}+\overline{D}^*)(D+D^*)K$	(	4.05	±0.30) %			–
$D_s^+\pi^0$	(	1.6	±0.5)	$\times10^{-5}$		2270
$D_s^{*+}\pi^0$	<	2.6		$\times10^{-4}$	CL=90%	2215
$D_s^+\eta$	<	4		$\times10^{-4}$	CL=90%	2235
$D_s^{*+}\eta$	<	6		$\times10^{-4}$	CL=90%	2178
$D_s^+\rho^0$	<	3.0		$\times10^{-4}$	CL=90%	2197
$D_s^{*+}\rho^0$	<	4		$\times10^{-4}$	CL=90%	2138
$D_s^+\omega$	<	4		$\times10^{-4}$	CL=90%	2195
$D_s^{*+}\omega$	<	6		$\times10^{-4}$	CL=90%	2136
$D_s^+a_1(1260)^0$	<	1.8		$\times10^{-3}$	CL=90%	2079
$D_s^{*+}a_1(1260)^0$	<	1.3		$\times10^{-3}$	CL=90%	2015
$D_s^+\phi$	(	1.7	$^{+1.2}_{-0.7}$)	$\times10^{-6}$		2141
$D_s^{*+}\phi$	<	1.2		$\times10^{-5}$	CL=90%	2079
$D_s^+\overline{K}^0$	<	8		$\times10^{-4}$	CL=90%	2242
$D_s^{*+}\overline{K}^0$	<	9		$\times10^{-4}$	CL=90%	2185
$D_s^+\overline{K}^*(892)^0$	<	4.4		$\times10^{-6}$	CL=90%	2172
$D_s^+K^{*0}$	<	3.5		$\times10^{-6}$	CL=90%	2172
$D_s^{*+}\overline{K}^*(892)^0$	<	3.5		$\times10^{-4}$	CL=90%	2112
$D_s^-\pi^+K^+$	(	1.80	±0.22)	$\times10^{-4}$		2222
$D_s^{*-}\pi^+K^+$	(	1.45	±0.24)	$\times10^{-4}$		2164
$D_s^-\pi^+K^*(892)^+$	<	5		$\times10^{-3}$	CL=90%	2138
$D_s^{*-}\pi^+K^*(892)^+$	<	7		$\times10^{-3}$	CL=90%	2076
$D_s^-K^+K^+$	(	1.1	±0.4)	$\times10^{-5}$		2149
$D_s^{*-}K^+K^+$	<	1.5		$\times10^{-5}$	CL=90%	2088

Charmonium modes

η_cK^+	(	9.6	±1.1)	$\times10^{-4}$		1751
$\eta_cK^+,\ \eta_c\to K_S^0K^\mp\pi^\pm$	(	2.7	±0.6)	$\times10^{-5}$		–
$\eta_cK^*(892)^+$	(	1.0	$^{+0.5}_{-0.4}$)	$\times10^{-3}$		1646
$\eta_c(2S)K^+$	(	3.4	±1.8)	$\times10^{-4}$		1319
$\eta_c(2S)K^+,\ \eta_c\to p\overline{p}$	<	1.06		$\times10^{-7}$	CL=95%	–
$\eta_c(2S)K^+,\ \eta_c\to K_S^0K^\mp\pi^\pm$	(	3.4	$^{+2.3}_{-1.6}$)	$\times10^{-6}$		–
$h_c(1P)K^+,\ h_c\to J/\psi\pi^+\pi^-$	<	3.4		$\times10^{-6}$	CL=90%	1401
$X(3872)K^+$	<	3.2		$\times10^{-4}$	CL=90%	1141
$X(3872)K^+,\ X\to p\overline{p}$	<	1.7		$\times10^{-8}$	CL=95%	–
$X(3872)K^+,\ X\to J/\psi\pi^+\pi^-$	(	8.6	±0.8)	$\times10^{-6}$		1141
$X(3872)K^+,\ X\to J/\psi\gamma$	(	2.1	±0.4)	$\times10^{-6}$	S=1.1	1141
$X(3872)K^+,\ X\to\psi(2S)\gamma$	(	4	±4)	$\times10^{-6}$	S=2.5	1141
$X(3872)K^+,\ X\to J/\psi(1S)\eta$	<	7.7		$\times10^{-6}$	CL=90%	1141
$X(3872)K^+,\ X\to D^0\overline{D}^0$	<	6.0		$\times10^{-5}$	CL=90%	1141
$X(3872)K^+,\ X\to D^+D^-$	<	4.0		$\times10^{-5}$	CL=90%	1141
$X(3872)K^+,\ X\to D^0\overline{D}^0\pi^0$	(	1.0	±0.4)	$\times10^{-4}$		1141
$X(3872)K^+,\ X\to\overline{D}^{*0}D^0$	(	8.5	±2.6)	$\times10^{-5}$	S=1.4	1141
$X(3872)K^*(892)^+,\ X\to J/\psi\gamma$	<	4.8		$\times10^{-6}$	CL=90%	939
$X(3872)K^*(892)^+,\ X\to\psi(2S)\gamma$	<	2.8		$\times10^{-5}$	CL=90%	939
$X(3872)^+K^0,\ X^+\to J/\psi(1S)\pi^+\pi^0$ [yyy]	<	6.1		$\times10^{-6}$	CL=90%	–
$X(4430)^+K^0,\ X^+\to J/\psi\pi^+$	<	1.5		$\times10^{-5}$	CL=95%	–
$X(4430)^+K^0,\ X^+\to\psi(2S)\pi^+$	<	4.7		$\times10^{-5}$	CL=95%	–
$X(4260)^0K^+,\ X^0\to J/\psi\pi^+\pi^-$	<	2.9		$\times10^{-5}$	CL=95%	–
$\chi_{c0}(2P)K^+,\ X^0\to J/\psi\gamma$	<	1.4		$\times10^{-5}$	CL=90%	–
$X(3930)^0K^+,\ X^0\to J/\psi\gamma$	<	2.5		$\times10^{-6}$	CL=90%	–
$J/\psi(1S)K^+$	(	1.027	±0.031)	$\times10^{-3}$		1683
$J/\psi(1S)K^+\pi^+\pi^-$	(	8.1	±1.3)	$\times10^{-4}$	S=2.5	1612
$\chi_{c0}(2P)K^+,\ \chi_{c0}\to p\overline{p}$	<	7.1		$\times10^{-8}$	CL=95%	–
$J/\psi(1S)K^*(892)^+$	(	1.44	±0.08)	$\times10^{-3}$		1571
$J/\psi(1S)K(1270)^+$	(	1.8	±0.5)	$\times10^{-3}$		1390
$J/\psi(1S)K(1400)^+$	<	5		$\times10^{-4}$	CL=90%	1308
$J/\psi(1S)\eta K^+$	(	1.08	±0.33)	$\times10^{-4}$		1510
$J/\psi(1S)\eta'K^+$	<	8.8		$\times10^{-5}$	CL=90%	1273
$J/\psi(1S)\phi K^+$	(	5.2	±1.7)	$\times10^{-5}$	S=1.2	1227
$X(4140)K^+,\ X\to J/\psi(1S)\phi$	(	10	±5)	$\times10^{-6}$		–
$X(4274)K^+,\ X\to J/\psi(1S)\phi$	<	4		$\times10^{-6}$	CL=90%	–
$J/\psi(1S)\omega K^+$	(	3.20	$^{+0.60}_{-0.32}$)	$\times10^{-4}$		1388
$X(3872)K^+,\ X\to J/\psi\omega$	(	6.0	±2.2)	$\times10^{-6}$		1141
$\chi_{c0}(2P)K^+,\ \chi_{c0}\to J/\psi\omega$	(	3.0	$^{+0.9}_{-0.7}$)	$\times10^{-5}$		1103

Meson Summary Table

$J/\psi(1S)\pi^+$	(4.1	±0.4)	$\times10^{-5}$	S=2.6	1727
$J/\psi(1S)\rho^+$	(5.0	±0.8)	$\times10^{-5}$		1611
$J/\psi(1S)\pi^+\pi^0$ nonresonant	< 7.3		$\times10^{-6}$	CL=90%	1717
$J/\psi(1S)a_1(1260)^+$	< 1.2		$\times10^{-3}$	CL=90%	1415
$J/\psi p\overline{p}\pi^+$	< 5.0		$\times10^{-7}$	CL=90%	643
Charmonium modes					
$J/\psi(1S)p\overline{\Lambda}$	(1.18	±0.31)	$\times10^{-5}$		567
$J/\psi(1S)\overline{\Sigma}^0 p$	< 1.1		$\times10^{-5}$	CL=90%	–
$J/\psi(1S)D^+$	< 1.2		$\times10^{-4}$	CL=90%	870
$J/\psi(1S)\overline{D}^0\pi^+$	< 2.5		$\times10^{-5}$	CL=90%	665
$\psi(2S)\pi^+$	(2.44	±0.30)	$\times10^{-5}$		1347
$\psi(2S)K^+$	(6.27	±0.24)	$\times10^{-4}$		1284
$\psi(2S)K^*(892)^+$	(6.7	±1.4)	$\times10^{-4}$	S=1.3	1115
$\psi(2S)K^+\pi^+\pi^-$	(4.3	±0.5)	$\times10^{-4}$		1179
$\psi(3770)K^+$	(4.9	±1.3)	$\times10^{-4}$		1218
$\psi(3770)K+,\psi\to D^0\overline{D}^0$	(1.6	±0.4)	$\times10^{-4}$	S=1.1	1218
$\psi(3770)K+,\psi\to D^+D^-$	(9.4	±3.5)	$\times10^{-5}$		1218
$\chi_{c0}\pi^+,\ \chi_{c0}\to\pi^+\pi^-$	< 1		$\times10^{-7}$	CL=90%	1531
$\chi_{c0}(1P)K^+$	(1.50	$^{+0.15}_{-0.14}$)	$\times10^{-4}$		1478
$\chi_{c0}K^*(892)^+$	< 2.1		$\times10^{-4}$	CL=90%	1341
$\chi_{c2}\pi^+,\ \chi_{c2}\to\pi^+\pi^-$	< 1		$\times10^{-7}$	CL=90%	1437
$\chi_{c2}K^+$	(1.1	±0.4)	$\times10^{-5}$		1379
$\chi_{c2}K^*(892)^+$	< 1.2		$\times10^{-4}$	CL=90%	1227
$\chi_{c1}(1P)\pi^+$	(2.2	±0.5)	$\times10^{-5}$		1468
$\chi_{c1}(1P)K^+$	(4.79	±0.23)	$\times10^{-4}$		1412
$\chi_{c1}(1P)K^*(892)^+$	(3.0	±0.6)	$\times10^{-4}$	S=1.1	1265
$h_c(1P)K^+$	< 3.8		$\times10^{-5}$		1401
$h_c(1P)K^+,\ h_c\to p\overline{p}$	< 6.4		$\times10^{-8}$	CL=95%	–
K* or *K* **modes**					
$K^0\pi^+$	(2.37	±0.08)	$\times10^{-5}$		2614
$K^+\pi^0$	(1.29	±0.05)	$\times10^{-5}$		2615
$\eta' K^+$	(7.06	±0.25)	$\times10^{-5}$		2528
$\eta' K^*(892)^+$	(4.8	$^{+1.8}_{-1.6}$)	$\times10^{-6}$		2472
$\eta' K_0^*(1430)^+$	(5.2	±2.1)	$\times10^{-6}$		–
$\eta' K_2^*(1430)^+$	(2.8	±0.5)	$\times10^{-5}$		2346
ηK^+	(2.4	±0.4)	$\times10^{-6}$	S=1.7	2588
$\eta K^*(892)^+$	(1.93	±0.16)	$\times10^{-5}$		2534
$\eta K_0^*(1430)^+$	(1.8	±0.4)	$\times10^{-5}$		–
$\eta K_2^*(1430)^+$	(9.1	±3.0)	$\times10^{-6}$		2414
$\eta(1295)K^+\times$ B($\eta(1295)\to\eta\pi\pi$)	(2.9	$^{+0.8}_{-0.7}$)	$\times10^{-6}$		2455
$\eta(1405)K^+\times$ B($\eta(1405)\to\eta\pi\pi$)	< 1.3		$\times10^{-6}$	CL=90%	2425
$\eta(1405)K^+\times$ B($\eta(1405)\to K^*K$)	< 1.2		$\times10^{-6}$	CL=90%	2425
$\eta(1475)K^+\times$ B($\eta(1475)\to K^*K$)	(1.38	$^{+0.21}_{-0.18}$)	$\times10^{-5}$		2406
$f_1(1285)K^+$	< 2.0		$\times10^{-6}$	CL=90%	2458
$f_1(1420)K^+\times$ B($f_1(1420)\to\eta\pi\pi$)	< 2.9		$\times10^{-6}$	CL=90%	2420
$f_1(1420)K^+\times$ B($f_1(1420)\to K^*K$)	< 4.1		$\times10^{-6}$	CL=90%	2420
$\phi(1680)K^+\times$ B($\phi(1680)\to K^*K$)	< 3.4		$\times10^{-6}$	CL=90%	2344
$f_0(1500)K^+$	(3.7	±2.2)	$\times10^{-6}$		2398
ωK^+	(6.7	±0.8)	$\times10^{-6}$	S=1.8	2557
$\omega K^*(892)^+$	< 7.4		$\times10^{-6}$	CL=90%	2503
$\omega(K\pi)_0^{*+}$	(2.8	±0.4)	$\times10^{-5}$		–
$\omega K_0^*(1430)^+$	(2.4	±0.5)	$\times10^{-5}$		–
$\omega K_2^*(1430)^+$	(2.1	±0.4)	$\times10^{-5}$		2380
$a_0(980)^+K^0\times$B($a_0(980)^+\to\eta\pi^+$)	< 3.9		$\times10^{-6}$	CL=90%	–
$a_0(980)^0K^+\times$B($a_0(980)^0\to\eta\pi^0$)	< 2.5		$\times10^{-6}$	CL=90%	–
$K^*(892)^0\pi^+$	(1.01	±0.09)	$\times10^{-5}$		2562
$K^*(892)^+\pi^0$	(8.2	±1.9)	$\times10^{-6}$		2563
$K^+\pi^-\pi^+$	(5.10	±0.29)	$\times10^{-5}$		2609
$K^+\pi^-\pi^+$ nonresonant	(1.63	$^{+0.21}_{-0.15}$)	$\times10^{-5}$		2609
$\omega(782)K^+$	(6	±9)	$\times10^{-6}$		2557
$K^+f_0(980)\times$ B($f_0(980)\to\pi^+\pi^-$)	(9.4	$^{+1.0}_{-1.2}$)	$\times10^{-6}$		2522
$f_2(1270)^0K^+$	(1.07	±0.27)	$\times10^{-6}$		–
$f_0(1370)^0K^+\times$ B($f_0(1370)^0\to\pi^+\pi^-$)	< 1.07		$\times10^{-5}$	CL=90%	–
$\rho^0(1450)K^+\times$ B($\rho^0(1450)\to\pi^+\pi^-$)	< 1.17		$\times10^{-5}$	CL=90%	–
$f_2'(1525)K^+\times$ B($f_2'(1525)\to\pi^+\pi^-$)	< 3.4		$\times10^{-6}$	CL=90%	2392
$K^+\rho^0$	(3.7	±0.5)	$\times10^{-6}$		2559
$K_0^*(1430)^0\pi^+$	(4.5	$^{+0.9}_{-0.7}$)	$\times10^{-5}$	S=1.5	2445
$K_2^*(1430)^0\pi^+$	(5.6	$^{+2.2}_{-1.5}$)	$\times10^{-6}$		2445
$K^*(1410)^0\pi^+$	< 4.5		$\times10^{-5}$	CL=90%	2448
$K^*(1680)^0\pi^+$	< 1.2		$\times10^{-5}$	CL=90%	2358
$K^+\pi^0\pi^0$	(1.62	±0.19)	$\times10^{-5}$		2610
$f_0(980)K^+\times$ B($f_0\to\pi^0\pi^0$)	(2.8	±0.8)	$\times10^{-6}$		2522
$K^-\pi^+\pi^+$	< 9.5		$\times10^{-7}$	CL=90%	2609
$K^-\pi^+\pi^+$ nonresonant	< 5.6		$\times10^{-5}$	CL=90%	2609
$K_1(1270)^0\pi^+$	< 4.0		$\times10^{-5}$	CL=90%	2484
$K_1(1400)^0\pi^+$	< 3.9		$\times10^{-5}$	CL=90%	2451
$K^0\pi^+\pi^0$	< 6.6		$\times10^{-5}$	CL=90%	2609
$K^0\rho^+$	(8.0	±1.5)	$\times10^{-6}$		2558
$K^*(892)^+\pi^+\pi^-$	(7.5	±1.0)	$\times10^{-5}$		2557
$K^*(892)^+\rho^0$	(4.6	±1.1)	$\times10^{-6}$		2504
$K^*(892)^+f_0(980)$	(4.2	±0.7)	$\times10^{-6}$		2466
$a_1^+K^0$	(3.5	±0.7)	$\times10^{-5}$		–
$b_1^+K^0\times$ B($b_1^+\to\omega\pi^+$)	(9.6	±1.9)	$\times10^{-6}$		–
$K^*(892)^0\rho^+$	(9.2	±1.5)	$\times10^{-6}$		2504
$K_1(1400)^+\rho^0$	< 7.8		$\times10^{-4}$	CL=90%	2388
$K_2^*(1430)^+\rho^0$	< 1.5		$\times10^{-3}$	CL=90%	2381
$b_1^0K^+\times$ B($b_1^0\to\omega\pi^0$)	(9.1	±2.0)	$\times10^{-6}$		–
$b_1^+K^{*0}\times$ B($b_1^+\to\omega\pi^+$)	< 5.9		$\times10^{-6}$	CL=90%	–
$b_1^0K^{*+}\times$ B($b_1^0\to\omega\pi^0$)	< 6.7		$\times10^{-6}$	CL=90%	–
$K^+\overline{K}^0$	(1.31	±0.17)	$\times10^{-6}$	S=1.2	2593
$\overline{K}^0K^+\pi^0$	< 2.4		$\times10^{-5}$	CL=90%	2578
$K^+K_S^0K_S^0$	(1.08	±0.06)	$\times10^{-5}$		2521
$f_0(980)K^+,\ f_0\to K_S^0K_S^0$	(1.47	±0.33)	$\times10^{-5}$		–
$f_0(1710)K^+,\ f_0\to K_S^0K_S^0$	(4.8	$^{+4.0}_{-2.6}$)	$\times10^{-7}$		–
$K^+K_S^0K_S^0$ nonresonant	(2.0	±0.4)	$\times10^{-5}$		2521
$K_S^0K_S^0\pi^+$	< 5.1		$\times10^{-7}$	CL=90%	2577
$K^+K^-\pi^+$	(5.0	±0.7)	$\times10^{-6}$		2578
$K^+K^-\pi^+$ nonresonant	< 7.5		$\times10^{-5}$	CL=90%	2578
$K^+\overline{K}^*(892)^0$	< 1.1		$\times10^{-6}$	CL=90%	2540
$K^+\overline{K}_0^*(1430)^0$	< 2.2		$\times10^{-6}$	CL=90%	2421
$K^+K^+\pi^-$	< 1.6		$\times10^{-7}$	CL=90%	2578
$K^+K^+\pi^-$ nonresonant	< 8.79		$\times10^{-5}$	CL=90%	2578
$f_2'(1525)K^+$	(1.8	±0.5)	$\times10^{-6}$	S=1.1	2392
$K^{*+}\pi^+K^-$	< 1.18		$\times10^{-5}$	CL=90%	2524
$K^*(892)^+K^*(892)^0$	(1.2	±0.5)	$\times10^{-6}$		2484
$K^{*+}K^+\pi^-$	< 6.1		$\times10^{-6}$	CL=90%	2524
$K^+K^-K^+$	(3.40	±0.14)	$\times10^{-5}$	S=1.4	2523
$K^+\phi$	(8.8	$^{+0.7}_{-0.6}$)	$\times10^{-6}$	S=1.1	2516
$f_0(980)K^+\times$ B($f_0(980)\to K^+K^-$)	(9.4	±3.2)	$\times10^{-6}$		2522
$a_2(1320)K^+\times$ B($a_2(1320)\to K^+K^-$)	< 1.1		$\times10^{-6}$	CL=90%	2449
$X_0(1550)K^+\times$ B($X_0(1550)\to K^+K^-$)	(4.3	±0.7)	$\times10^{-6}$		–
$\phi(1680)K^+\times$ B($\phi(1680)\to K^+K^-$)	< 8		$\times10^{-7}$	CL=90%	2344
$f_0(1710)K^+\times$ B($f_0(1710)\to K^+K^-$)	(1.1	±0.6)	$\times10^{-6}$		2330
$K^+K^-K^+$ nonresonant	(2.38	$^{+0.28}_{-0.50}$)	$\times10^{-5}$		2523
$K^*(892)^+K^+K^-$	(3.6	±0.5)	$\times10^{-5}$		2466
$K^*(892)^+\phi$	(10.0	±2.0)	$\times10^{-6}$	S=1.7	2460
$\phi(K\pi)_0^{*+}$	(8.3	±1.6)	$\times10^{-6}$		–
$\phi K_1(1270)^+$	(6.1	±1.9)	$\times10^{-6}$		2375
$\phi K_1(1400)^+$	< 3.2		$\times10^{-6}$	CL=90%	2339
$\phi K^*(1410)^+$	< 4.3		$\times10^{-6}$	CL=90%	–
$\phi K_0^*(1430)^+$	(7.0	±1.6)	$\times10^{-6}$		–
$\phi K_2^*(1430)^+$	(8.4	±2.1)	$\times10^{-6}$		2333
$\phi K_2^*(1770)^+$	< 1.50		$\times10^{-5}$	CL=90%	–
$\phi K_2^*(1820)^+$	< 1.63		$\times10^{-5}$	CL=90%	–
$a_1^+K^{*0}$	< 3.6		$\times10^{-6}$	CL=90%	–
$K^+\phi\phi$	(5.0	±1.2)	$\times10^{-6}$	S=2.3	2306

$\eta'\eta' K^+$	$<$	2.5		$\times 10^{-5}$	CL=90%	2338
$\omega\phi K^+$	$<$	1.9		$\times 10^{-6}$	CL=90%	2374
$X(1812)K^+ \times$ B($X \to \omega\phi$)	$<$	3.2		$\times 10^{-7}$	CL=90%	–
$K^*(892)^+\gamma$	(	4.21	± 0.18)	$\times 10^{-5}$		2564
$K_1(1270)^+\gamma$	(	4.3	± 1.3)	$\times 10^{-5}$		2486
$\eta K^+\gamma$	(	7.9	± 0.9)	$\times 10^{-6}$		2588
$\eta' K^+\gamma$	(	2.9	$^{+1.0}_{-0.9}$)	$\times 10^{-6}$		2528
$\phi K^+\gamma$	(	2.7	± 0.4)	$\times 10^{-6}$	S=1.2	2516
$K^+\pi^-\pi^+\gamma$	(	2.76	± 0.22)	$\times 10^{-5}$	S=1.2	2609
$K^*(892)^0\pi^+\gamma$	(	2.0	$^{+0.7}_{-0.6}$)	$\times 10^{-5}$		2562
$K^+\rho^0\gamma$	$<$	2.0		$\times 10^{-5}$	CL=90%	2559
$K^+\pi^-\pi^+\gamma$ nonresonant	$<$	9.2		$\times 10^{-6}$	CL=90%	2609
$K^0\pi^+\pi^0\gamma$	(	4.6	± 0.5)	$\times 10^{-5}$		2609
$K_1(1400)^+\gamma$	$<$	1.5		$\times 10^{-5}$	CL=90%	2453
$K_2^*(1430)^+\gamma$	(	1.4	± 0.4)	$\times 10^{-5}$		2447
$K^*(1680)^+\gamma$	$<$	1.9		$\times 10^{-3}$	CL=90%	2360
$K_3^*(1780)^+\gamma$	$<$	3.9		$\times 10^{-5}$	CL=90%	2341
$K_4^*(2045)^+\gamma$	$<$	9.9		$\times 10^{-3}$	CL=90%	2244

Light unflavored meson modes

$\rho^+\gamma$	(	9.8	± 2.5)	$\times 10^{-7}$		2583
$\pi^+\pi^0$	(	5.5	± 0.4)	$\times 10^{-6}$	S=1.2	2636
$\pi^+\pi^+\pi^-$	(	1.52	± 0.14)	$\times 10^{-5}$		2630
$\rho^0\pi^+$	(	8.3	± 1.2)	$\times 10^{-6}$		2581
$\pi^+ f_0(980)$, $f_0 \to \pi^+\pi^-$	$<$	1.5		$\times 10^{-6}$	CL=90%	2545
$\pi^+ f_2(1270)$	(	1.6	$^{+0.7}_{-0.4}$)	$\times 10^{-6}$		2484
$\rho(1450)^0 pi+, \rho^0 \to \pi^+\pi^-$	(	1.4	$^{+0.6}_{-0.9}$)	$\times 10^{-6}$		2434
$f_0(1370)\pi^+$, $f_0 \to \pi^+\pi^-$	$<$	4.0		$\times 10^{-6}$	CL=90%	2460
$f_0(500)\pi^+$, $f_0 \to \pi^+\pi^-$	$<$	4.1		$\times 10^{-6}$	CL=90%	–
$\pi^+\pi^-\pi^+$ nonresonant	(	5.3	$^{+1.5}_{-1.1}$)	$\times 10^{-6}$		2630
$\pi^+\pi^0\pi^0$	$<$	8.9		$\times 10^{-4}$	CL=90%	2631
$\rho^+\pi^0$	(	1.09	± 0.14)	$\times 10^{-5}$		2581
$\pi^+\pi^-\pi^+\pi^0$	$<$	4.0		$\times 10^{-3}$	CL=90%	2622
$\rho^+\rho^0$	(	2.40	± 0.19)	$\times 10^{-5}$		2523
$\rho^+ f_0(980)$, $f_0 \to \pi^+\pi^-$	$<$	2.0		$\times 10^{-6}$	CL=90%	2486
$a_1(1260)^+\pi^0$	(	2.6	± 0.7)	$\times 10^{-5}$		2494
$a_1(1260)^0\pi^+$	(	2.0	± 0.6)	$\times 10^{-5}$		2494
$\omega\pi^+$	(	6.9	± 0.5)	$\times 10^{-6}$		2580
$\omega\rho^+$	(	1.59	± 0.21)	$\times 10^{-5}$		2522
$\eta\pi^+$	(	4.02	± 0.27)	$\times 10^{-6}$		2609
$\eta\rho^+$	(	7.0	± 2.9)	$\times 10^{-6}$	S=2.8	2553
$\eta'\pi^+$	(	2.7	± 0.9)	$\times 10^{-6}$	S=1.9	2551
$\eta'\rho^+$	(	9.7	± 2.2)	$\times 10^{-6}$		2492
$\phi\pi^+$	$<$	1.5		$\times 10^{-7}$	CL=90%	2539
$\phi\rho^+$	$<$	3.0		$\times 10^{-6}$	CL=90%	2480
$a_0(980)^0\pi^+$, $a_0^0 \to \eta\pi^0$	$<$	5.8		$\times 10^{-6}$	CL=90%	–
$a_0(980)^+\pi^0$, $a_0^+ \to \eta\pi^+$	$<$	1.4		$\times 10^{-6}$	CL=90%	–
$\pi^+\pi^+\pi^+\pi^-\pi^-$	$<$	8.6		$\times 10^{-4}$	CL=90%	2608
$\rho^0 a_1(1260)^+$	$<$	6.2		$\times 10^{-4}$	CL=90%	2433
$\rho^0 a_2(1320)^+$	$<$	7.2		$\times 10^{-4}$	CL=90%	2410
$b_1^0\pi^+$, $b_1^0 \to \omega\pi^0$	(	6.7	± 2.0)	$\times 10^{-6}$		–
$b_1^+\pi^0$, $b_1^+ \to \omega\pi^+$	$<$	3.3		$\times 10^{-6}$	CL=90%	–
$\pi^+\pi^+\pi^+\pi^-\pi^-\pi^0$	$<$	6.3		$\times 10^{-3}$	CL=90%	2592
$b_1^+\rho^0$, $b_1^+ \to \omega\pi^+$	$<$	5.2		$\times 10^{-6}$	CL=90%	–
$a_1(1260)^+ a_1(1260)^0$	$<$	1.3		%	CL=90%	2336
$b_1^0\rho^+$, $b_1^0 \to \omega\pi^0$	$<$	3.3		$\times 10^{-6}$	CL=90%	–

Charged particle ($h^\pm$) modes

$h^\pm = K^\pm$ or $\pi^\pm$

$h^+\pi^0$	(	1.6	$^{+0.7}_{-0.6}$)	$\times 10^{-5}$		2636
ωh^+	(	1.38	$^{+0.27}_{-0.24}$)	$\times 10^{-5}$		2580
$h^+ X^0$ (Familon)	$<$	4.9		$\times 10^{-5}$	CL=90%	–

Baryon modes

$p\overline{p}\pi^+$	(	1.62	± 0.20)	$\times 10^{-6}$		2439
$p\overline{p}\pi^+$ nonresonant	$<$	5.3		$\times 10^{-5}$	CL=90%	2439
$p\overline{p}K^+$	(	5.9	± 0.5)	$\times 10^{-6}$	S=1.5	2348
$\Theta(1710)^{++}\overline{p}$, $\Theta^{++} \to pK^+$	[zzz] $<$	9.1		$\times 10^{-8}$	CL=90%	–
$f_J(2220)K^+$, $f_J \to p\overline{p}$	[zzz] $<$	4.1		$\times 10^{-7}$	CL=90%	2135
$p\overline{\Lambda}(1520)$	(	3.9	± 1.0)	$\times 10^{-7}$		2322
$p\overline{p}K^+$ nonresonant	$<$	8.9		$\times 10^{-5}$	CL=90%	2348
$p\overline{p}K^*(892)^+$	(	3.6	$^{+0.8}_{-0.7}$)	$\times 10^{-6}$		2215
$f_J(2220)K^{*+}$, $f_J \to p\overline{p}$	$<$	7.7		$\times 10^{-7}$	CL=90%	2059
$p\overline{\Lambda}$	$<$	3.2		$\times 10^{-7}$	CL=90%	2430
$p\overline{\Lambda}\gamma$	(	2.4	$^{+0.5}_{-0.4}$)	$\times 10^{-6}$		2430
$p\overline{\Lambda}\pi^0$	(	3.0	$^{+0.7}_{-0.6}$)	$\times 10^{-6}$		2402
$p\overline{\Sigma}(1385)^0$	$<$	4.7		$\times 10^{-7}$	CL=90%	2362
$\Delta^+\overline{\Lambda}$	$<$	8.2		$\times 10^{-7}$	CL=90%	–
$p\overline{\Sigma}\gamma$	$<$	4.6		$\times 10^{-6}$	CL=90%	2413
$p\overline{\Lambda}\pi^+\pi^-$	(	5.9	± 1.1)	$\times 10^{-6}$		2367
$p\overline{\Lambda}\rho^0$	(	4.8	± 0.9)	$\times 10^{-6}$		2214
$p\overline{\Lambda}f_2(1270)$	(	2.0	± 0.8)	$\times 10^{-6}$		2026
$\Lambda\overline{\Lambda}\pi^+$	$<$	9.4		$\times 10^{-7}$	CL=90%	2358
$\Lambda\overline{\Lambda}K^+$	(	3.4	± 0.6)	$\times 10^{-6}$		2251
$\Lambda\overline{\Lambda}K^{*+}$	(	2.2	$^{+1.2}_{-0.9}$)	$\times 10^{-6}$		2098
$\overline{\Delta}^0 p$	$<$	1.38		$\times 10^{-6}$	CL=90%	2403
$\Delta^{++}\overline{p}$	$<$	1.4		$\times 10^{-7}$	CL=90%	2403
$D^+ p\overline{p}$	$<$	1.5		$\times 10^{-5}$	CL=90%	1860
$D^*(2010)^+ p\overline{p}$	$<$	1.5		$\times 10^{-5}$	CL=90%	1786
$\overline{D}^0 p\overline{p}\pi^+$	(	3.72	± 0.27)	$\times 10^{-4}$		1789
$\overline{D}^{*0} p\overline{p}\pi^+$	(	3.73	± 0.32)	$\times 10^{-4}$		1709
$D^- p\overline{p}\pi^+\pi^-$	(	1.66	± 0.30)	$\times 10^{-4}$		1705
$D^{*-} p\overline{p}\pi^+\pi^-$	(	1.86	± 0.25)	$\times 10^{-4}$		1621
$p\overline{\Lambda}^0\overline{D}^0$	(	1.43	± 0.32)	$\times 10^{-5}$		–
$p\overline{\Lambda}^0\overline{D}^*(2007)^0$	$<$	5		$\times 10^{-5}$	CL=90%	–
$\overline{\Lambda}_c^- p\pi^+$	(	2.8	± 0.8)	$\times 10^{-4}$		1980
$\overline{\Lambda}_c^- \Delta(1232)^{++}$	$<$	1.9		$\times 10^{-5}$	CL=90%	1928
$\overline{\Lambda}_c^- \Delta_X(1600)^{++}$	(	5.9	± 1.9)	$\times 10^{-5}$		–
$\overline{\Lambda}_c^- \Delta_X(2420)^{++}$	(	4.7	± 1.6)	$\times 10^{-5}$		–
$(\overline{\Lambda}_c^- p)_s\pi^+$	[aaaa] (	3.9	± 1.3)	$\times 10^{-5}$		–
$\overline{\Sigma}_c(2520)^0 p$	$<$	3		$\times 10^{-6}$	CL=90%	1904
$\overline{\Sigma}_c(2800)^0 p$	(	3.3	± 1.3)	$\times 10^{-5}$		–
$\overline{\Lambda}_c^- p\pi^+\pi^0$	(	1.8	± 0.6)	$\times 10^{-3}$		1935
$\overline{\Lambda}_c^- p\pi^+\pi^+\pi^-$	(	2.2	± 0.7)	$\times 10^{-3}$		1880
$\overline{\Lambda}_c^- p\pi^+\pi^+\pi^-\pi^0$	$<$	1.34		%	CL=90%	1823
$\Lambda_c^+\Lambda_c^- K^+$	(	8.7	± 3.5)	$\times 10^{-4}$		–
$\overline{\Sigma}_c(2455)^0 p$	(	3.7	± 1.3)	$\times 10^{-5}$		1938
$\overline{\Sigma}_c(2455)^0 p\pi^0$	(	4.4	± 1.8)	$\times 10^{-4}$		1896
$\overline{\Sigma}_c(2455)^0 p\pi^-\pi^+$	(	4.4	± 1.7)	$\times 10^{-4}$		1845
$\overline{\Sigma}_c(2455)^{--} p\pi^+\pi^+$	(	3.0	± 0.8)	$\times 10^{-4}$		1845
$\overline{\Lambda}_c(2593)^-/\overline{\Lambda}_c(2625)^- p\pi^+$	$<$	1.9		$\times 10^{-4}$	CL=90%	–
$\overline{\Xi}_c^0\Lambda_c^+$, $\overline{\Xi}_c^0 \to \overline{\Xi}^+\pi^-$	(	3.0	± 1.1)	$\times 10^{-5}$		1144
$\overline{\Xi}_c^0\Lambda_c^+$, $\overline{\Xi}_c^0 \to \Lambda K^+\pi^-$	(	2.6	± 1.1)	$\times 10^{-5}$	S=1.1	1144

Lepton Family number (LF) or Lepton number (L) or Baryon number (B) violating modes, or/and $\Delta B = 1$ weak neutral current ($B1$) modes

$\pi^+\ell^+\ell^-$	$B1$	$<$	4.9		$\times 10^{-8}$	CL=90%	2638
$\pi^+ e^+ e^-$	$B1$	$<$	8.0		$\times 10^{-8}$	CL=90%	2638
$\pi^+\mu^+\mu^-$	$B1$	$<$	5.5		$\times 10^{-8}$	CL=90%	2634
$\pi^+\nu\overline{\nu}$	$B1$	$<$	9.8		$\times 10^{-5}$	CL=90%	2638
$K^+\ell^+\ell^-$	$B1$	[sss] (	4.51	± 0.23)	$\times 10^{-7}$	S=1.1	2617
$K^+ e^+ e^-$	$B1$	(	5.5	± 0.7)	$\times 10^{-7}$		2617
$K^+\mu^+\mu^-$	$B1$	(	4.49	± 0.23)	$\times 10^{-7}$	S=1.1	2612
$\psi(4040)K^+$		$<$	1.3		$\times 10^{-4}$	CL=90%	1003
$\psi(4160)K^+$		(	5.1	± 2.7)	$\times 10^{-4}$		868
$K^+\overline{\nu}\nu$	$B1$	$<$	1.6		$\times 10^{-5}$	CL=90%	2617
$\rho^+\nu\overline{\nu}$	$B1$	$<$	2.13		$\times 10^{-4}$	CL=90%	2583
$K^*(892)^+\ell^+\ell^-$	$B1$	[sss] (	1.29	± 0.21)	$\times 10^{-6}$		2564
$K^*(892)^+ e^+ e^-$	$B1$	(	1.55	$^{+0.40}_{-0.31}$)	$\times 10^{-6}$		2564
$K^*(892)^+\mu^+\mu^-$	$B1$	(	1.12	± 0.15)	$\times 10^{-6}$		2560
$K^*(892)^+\nu\overline{\nu}$	$B1$	$<$	4.0		$\times 10^{-5}$	CL=90%	2564
$\pi^+ e^+\mu^-$	LF	$<$	6.4		$\times 10^{-3}$	CL=90%	2637
$\pi^+ e^-\mu^+$	LF	$<$	6.4		$\times 10^{-3}$	CL=90%	2637
$\pi^+ e^\pm\mu^\mp$	LF	$<$	1.7		$\times 10^{-7}$	CL=90%	2637
$\pi^+ e^+\tau^-$	LF	$<$	7.4		$\times 10^{-5}$	CL=90%	2338
$\pi^+ e^-\tau^+$	LF	$<$	2.0		$\times 10^{-5}$	CL=90%	2338
$\pi^+ e^\pm\tau^\mp$	LF	$<$	7.5		$\times 10^{-5}$	CL=90%	2338
$\pi^+\mu^+\tau^-$	LF	$<$	6.2		$\times 10^{-5}$	CL=90%	2333
$\pi^+\mu^-\tau^+$	LF	$<$	4.5		$\times 10^{-5}$	CL=90%	2333
$\pi^+\mu^\pm\tau^\mp$	LF	$<$	7.2		$\times 10^{-5}$	CL=90%	2333
$K^+ e^+\mu^-$	LF	$<$	9.1		$\times 10^{-8}$	CL=90%	2615
$K^+ e^-\mu^+$	LF	$<$	1.3		$\times 10^{-7}$	CL=90%	2615
$K^+ e^\pm\mu^\mp$	LF	$<$	9.1		$\times 10^{-8}$	CL=90%	2615
$K^+ e^+\tau^-$	LF	$<$	4.3		$\times 10^{-5}$	CL=90%	2312
$K^+ e^-\tau^+$	LF	$<$	1.5		$\times 10^{-5}$	CL=90%	2312
$K^+ e^\pm\tau^\mp$	LF	$<$	3.0		$\times 10^{-5}$	CL=90%	2312

Meson Summary Table

$K^+ \mu^+ \tau^-$	LF	<	4.5	$\times 10^{-5}$	CL=90%	2298
$K^+ \mu^- \tau^+$	LF	<	2.8	$\times 10^{-5}$	CL=90%	2298
$K^+ \mu^\pm \tau^\mp$	LF	<	4.8	$\times 10^{-5}$	CL=90%	2298
$K^*(892)^+ e^+ \mu^-$	LF	<	1.3	$\times 10^{-6}$	CL=90%	2563
$K^*(892)^+ e^- \mu^+$	LF	<	9.9	$\times 10^{-7}$	CL=90%	2563
$K^*(892)^+ e^\pm \mu^\mp$	LF	<	1.4	$\times 10^{-6}$	CL=90%	2563
$\pi^- e^+ e^+$	L	<	2.3	$\times 10^{-8}$	CL=90%	2638
$\pi^- \mu^+ \mu^+$	L	<	1.3	$\times 10^{-8}$	CL=95%	2634
$\pi^- e^+ \mu^+$	L	<	1.5	$\times 10^{-7}$	CL=90%	2637
$\rho^- e^+ e^+$	L	<	1.7	$\times 10^{-7}$	CL=90%	2583
$\rho^- \mu^+ \mu^+$	L	<	4.2	$\times 10^{-7}$	CL=90%	2578
$\rho^- e^+ \mu^+$	L	<	4.7	$\times 10^{-7}$	CL=90%	2582
$K^- e^+ e^+$	L	<	3.0	$\times 10^{-8}$	CL=90%	2617
$K^- \mu^+ \mu^+$	L	<	4.1	$\times 10^{-8}$	CL=90%	2612
$K^- e^+ \mu^+$	L	<	1.6	$\times 10^{-7}$	CL=90%	2615
$K^*(892)^- e^+ e^+$	L	<	4.0	$\times 10^{-7}$	CL=90%	2564
$K^*(892)^- \mu^+ \mu^+$	L	<	5.9	$\times 10^{-7}$	CL=90%	2560
$K^*(892)^- e^+ \mu^+$	L	<	3.0	$\times 10^{-7}$	CL=90%	2563
$D^- e^+ e^+$	L	<	2.6	$\times 10^{-6}$	CL=90%	2309
$D^- e^+ \mu^+$	L	<	1.8	$\times 10^{-6}$	CL=90%	2307
$D^- \mu^+ \mu^+$	L	<	6.9	$\times 10^{-7}$	CL=95%	2303
$D^{*-} \mu^+ \mu^+$	L	<	2.4	$\times 10^{-6}$	CL=95%	2251
$D_s^- \mu^+ \mu^+$	L	<	5.8	$\times 10^{-7}$	CL=95%	2267
$\overline{D}{}^0 \pi^- \mu^+ \mu^+$	L	<	1.5	$\times 10^{-6}$	CL=95%	2295
$\Lambda^0 \mu^+$	L,B	<	6	$\times 10^{-8}$	CL=90%	–
$\Lambda^0 e^+$	L,B	<	3.2	$\times 10^{-8}$	CL=90%	–
$\overline{\Lambda}{}^0 \mu^+$	L,B	<	6	$\times 10^{-8}$	CL=90%	–
$\overline{\Lambda}{}^0 e^+$	L,B	<	8	$\times 10^{-8}$	CL=90%	–

B^0

$I(J^P) = \frac{1}{2}(0^-)$

I, *J*, *P* need confirmation. Quantum numbers shown are quark-model predictions.

Mass $m_{B^0} = 5279.58 \pm 0.17$ MeV

$m_{B^0} - m_{B^\pm} = 0.32 \pm 0.06$ MeV

Mean life $\tau_{B^0} = (1.519 \pm 0.005) \times 10^{-12}$ s

$c\tau = 455.4\ \mu$m

$\tau_{B^+}/\tau_{B^0} = 1.076 \pm 0.004$ (direct measurements)

B^0-$\overline{B}{}^0$ mixing parameters

$\chi_d = 0.1874 \pm 0.0018$

$\Delta m_{B^0} = m_{B^0_H} - m_{B^0_L} = (0.510 \pm 0.003) \times 10^{12}\ \hbar\ \mathrm{s}^{-1}$

$= (3.337 \pm 0.033) \times 10^{-10}$ MeV

$x_d = \Delta m_{B^0}/\Gamma_{B^0} = 0.774 \pm 0.006$

Re(λ_{CP} / $|\lambda_{CP}|$) Re(z) $= 0.01 \pm 0.05$

$\Delta\Gamma$ Re(z) $= -0.007 \pm 0.004$

Re(z) $= (2 \pm 5) \times 10^{-2}$

Im(z) $= (-0.8 \pm 0.4) \times 10^{-2}$

CP violation parameters

Re(ϵ_{B^0})/(1+$|\epsilon_{B^0}|^2$) $= (0.1 \pm 0.8) \times 10^{-3}$

$A_{T/CP} = 0.005 \pm 0.018$

$A_{CP}(B^0 \to D^*(2010)^+ D^-) = 0.037 \pm 0.034$

$A_{CP}(B^0 \to [K^+K^-]_D K^*(892)^0) = -0.45 \pm 0.23$

$A_{CP}(B^0 \to [K^+\pi^-]_D K^*(892)^0) = -0.08 \pm 0.08$

$A_{CP}(B^0 \to K^+\pi^-) = -0.082 \pm 0.006$

$A_{CP}(B^0 \to \eta' K^*(892)^0) = 0.02 \pm 0.23$

$A_{CP}(B^0 \to \eta' K_0^*(1430)^0) = -0.19 \pm 0.17$

$A_{CP}(B^0 \to \eta' K_2^*(1430)^0) = 0.14 \pm 0.18$

$A_{CP}(B^0 \to \eta K^*(892)^0) = 0.19 \pm 0.05$

$A_{CP}(B^0 \to \eta K_0^*(1430)^0) = 0.06 \pm 0.13$

$A_{CP}(B^0 \to \eta K_2^*(1430)^0) = -0.07 \pm 0.19$

$A_{CP}(B^0 \to b_1 K^+) = -0.07 \pm 0.12$

$A_{CP}(B^0 \to \omega K^{*0}) = 0.45 \pm 0.25$

$A_{CP}(B^0 \to \omega (K\pi)_0^{*0}) = -0.07 \pm 0.09$

$A_{CP}(B^0 \to \omega K_2^*(1430)^0) = -0.37 \pm 0.17$

$A_{CP}(B^0 \to K^+\pi^-\pi^0) = (0 \pm 6) \times 10^{-2}$

$A_{CP}(B^0 \to \rho^- K^+) = 0.20 \pm 0.11$

$A_{CP}(B^0 \to \rho(1450)^- K^+) = -0.10 \pm 0.33$

$A_{CP}(B^0 \to \rho(1700)^- K^+) = -0.4 \pm 0.6$

$A_{CP}(B^0 \to K^+\pi^-\pi^0 \text{ nonresonant}) = 0.10 \pm 0.18$

$A_{CP}(B^0 \to K^0\pi^+\pi^-) = -0.01 \pm 0.05$

$A_{CP}(B^0 \to K^*(892)^+\pi^-) = -0.22 \pm 0.06$

$A_{CP}(B^0 \to (K\pi)_0^{*+}\pi^-) = 0.09 \pm 0.07$

$A_{CP}(B^0 \to (K\pi)_0^{*0}\pi^0) = -0.15 \pm 0.11$

$A_{CP}(B^0 \to K^{*0}\pi^0) = -0.15 \pm 0.13$

$A_{CP}(B^0 \to K^*(892)^0\pi^+\pi^-) = 0.07 \pm 0.05$

$A_{CP}(B^0 \to K^*(892)^0\rho^0) = -0.06 \pm 0.09$

$A_{CP}(B^0 \to K^{*0} f_0(980)) = 0.07 \pm 0.10$

$A_{CP}(B^0 \to K^{*+}\rho^-) = 0.21 \pm 0.15$

$A_{CP}(B^0 \to K^*(892)^0 K^+K^-) = 0.01 \pm 0.05$

$A_{CP}(B^0 \to a_1^- K^+) = -0.16 \pm 0.12$

$A_{CP}(B^0 \to K^0 K^0) = -0.6 \pm 0.7$

$A_{CP}(B^0 \to K^*(892)^0\phi) = (0 \pm 4) \times 10^{-2}$

$A_{CP}(B^0 \to K^*(892)^0 K^-\pi^+) = 0.2 \pm 0.4$

$A_{CP}(B^0 \to \phi(K\pi)_0^{*0}) = 0.12 \pm 0.08$

$A_{CP}(B^0 \to \phi K_2^*(1430)^0) = -0.11 \pm 0.10$

$A_{CP}(B^0 \to K^*(892)^0\gamma) = -0.002 \pm 0.015$

$A_{CP}(B^0 \to K_2^*(1430)^0\gamma) = -0.08 \pm 0.15$

$A_{CP}(B^0 \to \rho^+\pi^-) = 0.13 \pm 0.06$ (S = 1.1)

$A_{CP}(B^0 \to \rho^-\pi^+) = -0.08 \pm 0.08$

$A_{CP}(B^0 \to a_1(1260)^\pm\pi^\mp) = -0.07 \pm 0.06$

$A_{CP}(B^0 \to b_1^-\pi^+) = -0.05 \pm 0.10$

$A_{CP}(B^0 \to p\overline{p}K^*(892)^0) = 0.05 \pm 0.12$

$A_{CP}(B^0 \to p\overline{\Lambda}\pi^-) = 0.04 \pm 0.07$

$A_{CP}(B^0 \to K^{*0}\ell^+\ell^-) = -0.05 \pm 0.10$

$A_{CP}(B^0 \to K^{*0}e^+e^-) = -0.21 \pm 0.19$

$A_{CP}(B^0 \to K^{*0}\mu^+\mu^-) = -0.07 \pm 0.04$

$C_{D^{*-}D^+}(B^0 \to D^*(2010)^- D^+) = -0.01 \pm 0.11$

$S_{D^{*-}D^+}(B^0 \to D^*(2010)^- D^+) = -0.72 \pm 0.15$

$C_{D^{*+}D^-}(B^0 \to D^*(2010)^+ D^-) = 0.00 \pm 0.13$ (S = 1.3)

$S_{D^{*+}D^-}(B^0 \to D^*(2010)^+ D^-) = -0.73 \pm 0.14$

$C_{D^{*+}D^{*-}}(B^0 \to D^{*+}D^{*-}) = 0.01 \pm 0.09$ (S = 1.6)

$S_{D^{*+}D^{*-}}(B^0 \to D^{*+}D^{*-}) = -0.59 \pm 0.14$ (S = 1.8)

$C_+(B^0 \to D^{*+}D^{*-}) = 0.00 \pm 0.10$ (S = 1.6)

$S_+(B^0 \to D^{*+}D^{*-}) = -0.73 \pm 0.09$

$C_-(B^0 \to D^{*+}D^{*-}) = 0.19 \pm 0.31$

$S_-(B^0 \to D^{*+}D^{*-}) = 0.1 \pm 1.6$ (S = 3.5)

$C(B^0 \to D^*(2010)^+ D^*(2010)^- K_S^0) = 0.01 \pm 0.29$

$S(B^0 \to D^*(2010)^+ D^*(2010)^- K_S^0) = 0.1 \pm 0.4$

$C_{D^+D^-}(B^0 \to D^+D^-) = -0.46 \pm 0.21$ (S = 1.8)

$S_{D^+D^-}(B^0 \to D^+D^-) = -0.99^{+0.17}_{-0.14}$

$C_{J/\psi(1S)\pi^0}(B^0 \to J/\psi(1S)\pi^0) = -0.13 \pm 0.13$

$S_{J/\psi(1S)\pi^0}(B^0 \to J/\psi(1S)\pi^0) = -0.94 \pm 0.29$ (S = 1.9)

$C_{D_{CP}^{(*)}h^0}(B^0 \to D_{CP}^{(*)}h^0) = -0.23 \pm 0.16$

$S_{D_{CP}^{(*)}h^0}(B^0 \to D_{CP}^{(*)}h^0) = -0.56 \pm 0.24$

$C_{K^0\pi^0}(B^0 \to K^0\pi^0) = 0.00 \pm 0.13$ (S = 1.4)

$S_{K^0\pi^0}(B^0 \to K^0\pi^0) = 0.58 \pm 0.17$

$C_{\eta'(958)K_S^0}(B^0 \to \eta'(958)K_S^0) = -0.04 \pm 0.20$ (S = 2.5)

$S_{\eta'(958)K_S^0}(B^0 \to \eta'(958)K_S^0) = 0.43 \pm 0.17$ (S = 1.5)

$C_{\eta' K^0}(B^0 \to \eta' K^0) = -0.05 \pm 0.05$

$S_{\eta' K^0}(B^0 \to \eta' K^0) = 0.60 \pm 0.07$

$C_{\omega K_S^0}(B^0 \to \omega K_S^0) = -0.30 \pm 0.28$ (S = 1.6)

$S_{\omega K_S^0}(B^0 \to \omega K_S^0) = 0.43 \pm 0.24$

$C(B^0 \to K_S^0\pi^0\pi^0) = 0.2 \pm 0.5$

$S(B^0 \to K_S^0\pi^0\pi^0) = 0.7 \pm 0.7$

$C_{\rho^0 K_S^0}(B^0 \to \rho^0 K_S^0) = -0.04 \pm 0.20$

$S_{\rho^0 K_S^0}(B^0 \to \rho^0 K_S^0) = 0.50^{+0.17}_{-0.21}$

$C_{f_0 K_S^0}(B^0 \to f_0(980)K_S^0) = 0.29 \pm 0.20$

$S_{f_0 K_S^0}(B^0 \to f_0(980)K_S^0) = -0.50 \pm 0.16$

$S_{f_2 K_S^0}(B^0 \to f_2(1270)K_S^0) = -0.5 \pm 0.5$

$C_{f_2 K_S^0}(B^0 \to f_2(1270)K_S^0) = 0.3 \pm 0.4$

$S_{f_x K_S^0}(B^0 \to f_x(1300)K_S^0) = -0.2 \pm 0.5$

$C_{f_x K_S^0}(B^0 \to f_x(1300)K_S^0) = 0.13 \pm 0.35$

$S_{K^0\pi^+\pi^-}(B^0 \to K^0\pi^+\pi^- \text{ nonresonant}) = -0.01 \pm 0.33$

$C_{K^0\pi^+\pi^-}(B^0 \to K^0\pi^+\pi^- \text{ nonresonant}) = 0.01 \pm 0.26$

$C_{K_S^0K_S^0}(B^0 \to K_S^0K_S^0) = 0.0 \pm 0.4$ (S = 1.4)

$S_{K_S^0K_S^0}(B^0 \to K_S^0K_S^0) = -0.8 \pm 0.5$

$C_{K^+K^-K_S^0}(B^0 \to K^+K^-K_S^0 \text{ nonresonant}) = 0.06 \pm 0.08$

$S_{K^+K^-K^0_S}$ **($B^0 \to K^+K^-K^0_S$ nonresonant)** $= -0.66 \pm 0.11$
$C_{K^+K^-K^0_S}$ ($B^0 \to K^+K^-K^0_S$ inclusive) $= 0.01 \pm 0.09$
$S_{K^+K^-K^0_S}$ **($B^0 \to K^+K^-K^0_S$ inclusive)** $= -0.65 \pm 0.12$
$C_{\phi K^0_S}$ ($B^0 \to \phi K^0_S$) $= 0.01 \pm 0.14$
$S_{\phi K^0_S}$ **($B^0 \to \phi K^0_S$)** $= 0.59 \pm 0.14$
$C_{K_SK_SK_S}(B^0 \to K_SK_SK_S) = -0.23 \pm 0.14$
$S_{K_SK_SK_S}(B^0 \to K_SK_SK_S) = -0.5 \pm 0.6$ (S = 3.0)
$C_{K^0_S\pi^0\gamma}(B^0 \to K^0_S\pi^0\gamma) = 0.36 \pm 0.33$
$S_{K^0_S\pi^0\gamma}(B^0 \to K^0_S\pi^0\gamma) = -0.8 \pm 0.6$
$C_{K^{*0}\gamma}$ ($B^0 \to K^*(892)^0\gamma$) $= -0.04 \pm 0.16$ (S = 1.2)
$S_{K^{*0}\gamma}$ ($B^0 \to K^*(892)^0\gamma$) $= -0.15 \pm 0.22$
$C_{\eta K^0\gamma}$ ($B^0 \to \eta K^0\gamma$) $= -0.3 \pm 0.4$
$S_{\eta K^0\gamma}$ ($B^0 \to \eta K^0\gamma$) $= -0.2 \pm 0.5$
$C_{K^0\phi\gamma}$ ($B^0 \to K^0\phi\gamma$) $= -0.3 \pm 0.6$
$S_{K^0\phi\gamma}$ ($B^0 \to K^0\phi\gamma$) $= 0.7^{+0.7}_{-1.1}$
$C(B^0 \to K^0_S\rho^0\gamma) = -0.05 \pm 0.19$
$S(B^0 \to K^0_S\rho^0\gamma) = 0.11 \pm 0.34$
C ($B^0 \to \rho^0\gamma$) $= 0.4 \pm 0.5$
S ($B^0 \to \rho^0\gamma$) $= -0.8 \pm 0.7$
$C_{\pi\pi}$ **($B^0 \to \pi^+\pi^-$)** $= -0.31 \pm 0.05$
$S_{\pi\pi}$ **($B^0 \to \pi^+\pi^-$)** $= -0.67 \pm 0.06$
$C_{\pi^0\pi^0}(B^0 \to \pi^0\pi^0) = -0.43 \pm 0.24$
$C_{\rho\pi}$ ($B^0 \to \rho^+\pi^-$) $= -0.03 \pm 0.07$ (S = 1.2)
$S_{\rho\pi}$ ($B^0 \to \rho^+\pi^-$) $= 0.05 \pm 0.07$
$\Delta C_{\rho\pi}$ **($B^0 \to \rho^+\pi^-$)** $= 0.27 \pm 0.06$
$\Delta S_{\rho\pi}$ ($B^0 \to \rho^+\pi^-$) $= 0.01 \pm 0.08$
$C_{\rho^0\pi^0}$ ($B^0 \to \rho^0\pi^0$) $= 0.27 \pm 0.24$
$S_{\rho^0\pi^0}$ ($B^0 \to \rho^0\pi^0$) $= -0.23 \pm 0.34$
$C_{a_1\pi}$ ($B^0 \to a_1(1260)^+\pi^-$) $= -0.05 \pm 0.11$
$S_{a_1\pi}$ ($B^0 \to a_1(1260)^+\pi^-$) $= -0.2 \pm 0.4$ (S = 3.2)
$\Delta C_{a_1\pi}$ **($B^0 \to a_1(1260)^+\pi^-$)** $= 0.43 \pm 0.14$ (S = 1.3)
$\Delta S_{a_1\pi}$ ($B^0 \to a_1(1260)^+\pi^-$) $= -0.11 \pm 0.12$
C ($B^0 \to b_1^- K^+$) $= -0.22 \pm 0.24$
ΔC **($B^0 \to b_1^-\pi^+$)** $= -1.04 \pm 0.24$
$C_{\rho^0\rho^0}$ ($B^0 \to \rho^0\rho^0$) $= 0.2 \pm 0.9$
$S_{\rho^0\rho^0}$ ($B^0 \to \rho^0\rho^0$) $= 0.3 \pm 0.7$
$C_{\rho\rho}$ ($B^0 \to \rho^+\rho^-$) $= -0.05 \pm 0.13$
$S_{\rho\rho}$ ($B^0 \to \rho^+\rho^-$) $= -0.06 \pm 0.17$
$|\lambda|$ ($B^0 \to J/\psi K^*(892)^0$) < 0.25, CL = 95%
cos 2β ($B^0 \to J/\psi K^*(892)^0$) $= 1.7^{+0.7}_{-0.9}$ (S = 1.6)
cos 2β ($B^0 \to [K^0_S\pi^+\pi^-]_{D^{(*)}}h^0$) $= 1.0^{+0.6}_{-0.7}$ (S = 1.8)
$(S_+ + S_-)/2$ ($B^0 \to D^{*-}\pi^+$) $= -0.039 \pm 0.011$
$(S_- - S_+)/2$ ($B^0 \to D^{*-}\pi^+$) $= -0.009 \pm 0.015$
$(S_+ + S_-)/2$ ($B^0 \to D^-\pi^+$) $= -0.046 \pm 0.023$
$(S_- - S_+)/2$ ($B^0 \to D^-\pi^+$) $= -0.022 \pm 0.021$
$(S_+ + S_-)/2$ ($B^0 \to D^-\rho^+$) $= -0.024 \pm 0.032$
$(S_- - S_+)/2$ ($B^0 \to D^-\rho^+$) $= -0.10 \pm 0.06$
$C_{\eta_c K^0_S}$ ($B^0 \to \eta_c K^0_S$) $= 0.08 \pm 0.13$
$S_{\eta_c K^0_S}$ **($B^0 \to \eta_c K^0_S$)** $= 0.93 \pm 0.17$
$C_{c\overline{c}K^{(*)0}}$ ($B^0 \to c\overline{c}K^{(*)0}$) $= (0.5 \pm 1.7) \times 10^{-2}$
sin(2β) $= 0.682 \pm 0.019$
$C_{J/\psi(\mathrm{nS})K^0}$ ($B^0 \to J/\psi(\mathrm{nS})K^0$) $= (0.5 \pm 2.0) \times 10^{-2}$
$S_{J/\psi(\mathrm{nS})K^0}$ **($B^0 \to J/\psi(\mathrm{nS})K^0$)** $= 0.676 \pm 0.021$
$C_{J/\psi K^{*0}}$ ($B^0 \to J/\psi K^{*0}$) $= 0.03 \pm 0.10$
$S_{J/\psi K^{*0}}$ ($B^0 \to J/\psi K^{*0}$) $= 0.60 \pm 0.25$
$C_{\chi_{c0}K^0_S}$ ($B^0 \to \chi_{c0}K^0_S$) $= -0.3^{+0.5}_{-0.4}$
$S_{\chi_{c0}K^0_S}$ ($B^0 \to \chi_{c0}K^0_S$) $= -0.7 \pm 0.5$
$C_{\chi_{c1}K^0_S}$ ($B^0 \to \chi_{c1}K^0_S$) $= 0.06 \pm 0.07$
$S_{\chi_{c1}K^0_S}$ **($B^0 \to \chi_{c1}K^0_S$)** $= 0.63 \pm 0.10$
sin(2β_{eff})($B^0 \to \phi K^0$) $= 0.22 \pm 0.30$
sin(2β_{eff})($B^0 \to \phi K^*_0(1430)^0$) $= 0.97^{+0.03}_{-0.52}$
sin(2β_{eff})($B^0 \to K^+K^-K^0_S$) $= 0.77^{+0.13}_{-0.12}$
sin(2β_{eff})($B^0 \to [K^0_S\pi^+\pi^-]_{D^{(*)}}h^0$) $= 0.45 \pm 0.28$
$|\lambda|$ ($B^0 \to [K^0_S\pi^+\pi^-]_{D^{(*)}}h^0$) $= 1.01 \pm 0.08$
$|\sin(2\beta+\gamma)| > 0.40$, CL = 90%
$2\beta + \gamma = (83 \pm 60)^\circ$
$\gamma(B^0 \to D^0K^{*0}) = (162 \pm 60)^\circ$
$\alpha = (90 \pm 5)^\circ$

$\overline{B}^0$ modes are charge conjugates of the modes below. Reactions indicate the weak decay vertex and do not include mixing. Modes which do not identify the charge state of the B are listed in the $B^\pm/B^0$ ADMIXTURE section.

The branching fractions listed below assume 50% $B^0\overline{B}^0$ and 50% B^+B^- production at the $\Upsilon(4S)$. We have attempted to bring older measurements up to date by rescaling their assumed $\Upsilon(4S)$ production ratio to 50:50 and their assumed D, D_s, D^*, and ψ branching ratios to current values whenever this would affect our averages and best limits significantly.

Indentation is used to indicate a subchannel of a previous reaction. All resonant subchannels have been corrected for resonance branching fractions to the final state so the sum of the subchannel branching fractions can exceed that of the final state.

For inclusive branching fractions, *e.g.*, $B \to D^\pm$ anything, the values usually are multiplicities, not branching fractions. They can be greater than one.

B^0 DECAY MODES		Fraction (Γ_i/Γ)	Scale factor/ Confidence level	p (MeV/c)
$\ell^+\nu_\ell$ anything	[sss]	(10.33± 0.28) %		–
$e^+\nu_e X_c$		(10.1 ± 0.4) %		–
$D\ell^+\nu_\ell$ anything		(9.2 ± 0.8) %		–
$D^-\ell^+\nu_\ell$	[sss]	(2.19± 0.12) %		2309
$D^-\tau^+\nu_\tau$		(1.03± 0.22) %		1909
$D^*(2010)^-\ell^+\nu_\ell$	[sss]	(4.93± 0.11) %		2257
$D^*(2010)^-\tau^+\nu_\tau$		(1.84± 0.22) %		1837
$\overline{D}^0\pi^-\ell^+\nu_\ell$		(4.3 ± 0.6) $\times 10^{-3}$		2308
$D_0^*(2400)^-\ell^+\nu_\ell$, $D_0^{*-} \to \overline{D}^0\pi^-$		(3.0 ± 1.2) $\times 10^{-3}$	S=1.8	–
$D_2^*(2460)^-\ell^+\nu_\ell$, $D_2^{*-} \to \overline{D}^0\pi^-$		(1.21± 0.33) $\times 10^{-3}$	S=1.8	2065
$\overline{D}^{(*)}n\pi\ell^+\nu_\ell(n \geq 1)$		(2.3 ± 0.5) %		–
$\overline{D}^{*0}\pi^-\ell^+\nu_\ell$		(4.9 ± 0.8) $\times 10^{-3}$		2256
$D_1(2420)^-\ell^+\nu_\ell$, $D_1^- \to \overline{D}^{*0}\pi^-$		(2.80± 0.28) $\times 10^{-3}$		–
$D_1'(2430)^-\ell^+\nu_\ell$, $D_1'^- \to \overline{D}^{*0}\pi^-$		(3.1 ± 0.9) $\times 10^{-3}$		–
$D_2^*(2460)^-\ell^+\nu_\ell$, $D_2^{*-} \to \overline{D}^{*0}\pi^-$		(6.8 ± 1.2) $\times 10^{-4}$		2065
$\rho^-\ell^+\nu_\ell$	[sss]	(2.94± 0.21) $\times 10^{-4}$		2583
$\pi^-\ell^+\nu_\ell$	[sss]	(1.45± 0.05) $\times 10^{-4}$		2638
Inclusive modes				
$K^\pm$ anything		(78 ± 8) %		–
$\overline{D}^0X$		(8.1 ± 1.5) %		–
D^0X		(47.4 ± 2.8) %		–
D^+X		< 3.9 %	CL=90%	–
D^-X		(36.9 ± 3.3) %		–
D_s^+X		(10.3 $^{+\ 2.1}_{-\ 1.8}$) %		–
D_s^-X		< 2.6 %	CL=90%	–
Λ_c^+X		< 3.1 %	CL=90%	–
$\overline{\Lambda}_c^-X$		(5.0 $^{+\ 2.1}_{-\ 1.5}$) %		–
$\overline{c}X$		(95 ± 5) %		–
cX		(24.6 ± 3.1) %		–
$\overline{c}cX$		(119 ± 6) %		–
***D*, *D**, or D_s modes**				
$D^-\pi^+$		(2.68± 0.13) $\times 10^{-3}$		2306
$D^-\rho^+$		(7.8 ± 1.3) $\times 10^{-3}$		2235
$D^-K^0\pi^+$		(4.9 ± 0.9) $\times 10^{-4}$		2259
$D^-K^*(892)^+$		(4.5 ± 0.7) $\times 10^{-4}$		2211
$D^-\omega\pi^+$		(2.8 ± 0.6) $\times 10^{-3}$		2204
D^-K^+		(1.97± 0.21) $\times 10^{-4}$		2279
$D^-K^+\pi^+\pi^-$		(3.8 ± 0.9) $\times 10^{-4}$		2236
$D^-K^+\overline{K}^0$		< 3.1 $\times 10^{-4}$	CL=90%	2188
$D^-K^+\overline{K}^*(892)^0$		(8.8 ± 1.9) $\times 10^{-4}$		2070
$\overline{D}^0\pi^+\pi^-$		(8.4 ± 0.9) $\times 10^{-4}$		2301
$D^*(2010)^-\pi^+$		(2.76± 0.13) $\times 10^{-3}$		2255
$\overline{D}^0K^+K^-$		(4.7 ± 1.2) $\times 10^{-5}$		2191
$D^-\pi^+\pi^+\pi^-$		(6.4 ± 0.7) $\times 10^{-3}$		2287
($D^-\pi^+\pi^+\pi^-$) nonresonant		(3.9 ± 1.9) $\times 10^{-3}$		2287
$D^-\pi^+\rho^0$		(1.1 ± 1.0) $\times 10^{-3}$		2206
$D^-a_1(1260)^+$		(6.0 ± 3.3) $\times 10^{-3}$		2121
$D^*(2010)^-\pi^+\pi^0$		(1.5 ± 0.5) %		2248
$D^*(2010)^-\rho^+$		(6.8 ± 0.9) $\times 10^{-3}$		2180
$D^*(2010)^-K^+$		(2.14± 0.16) $\times 10^{-4}$		2226
$D^*(2010)^-K^0\pi^+$		(3.0 ± 0.8) $\times 10^{-4}$		2205

Meson Summary Table

$D^*(2010)^- K^*(892)^+$		(3.3 ± 0.6) × 10^{-4}			2155
$D^*(2010)^- K^+ \overline{K}^0$		< 4.7	× 10^{-4}	CL=90%	2131
$D^*(2010)^- K^+ \overline{K}^*(892)^0$		(1.29 ± 0.33) × 10^{-3}			2007
$D^*(2010)^- \pi^+ \pi^+ \pi^-$		(7.0 ± 0.8) × 10^{-3}		S=1.3	2235
($D^*(2010)^- \pi^+ \pi^+ \pi^-$) non-resonant		(0.0 ± 2.5) × 10^{-3}			2235
$D^*(2010)^- \pi^+ \rho^0$		(5.7 ± 3.2) × 10^{-3}			2150
$D^*(2010)^- a_1(1260)^+$		(1.30 ± 0.27) %			2061
$\overline{D}_1(2420)^0 \pi^- \pi^+$, $\overline{D}_1^0 \to D^{*-} \pi^+$		(1.4 ± 0.4) × 10^{-4}			–
$D^*(2010)^- K^+ \pi^- \pi^+$		(4.5 ± 0.7) × 10^{-4}			2181
$D^*(2010)^- \pi^+ \pi^+ \pi^- \pi^0$		(1.76 ± 0.27) %			2218
$D^{*-} 3\pi^+ 2\pi^-$		(4.7 ± 0.9) × 10^{-3}			2195
$\overline{D}^*(2010)^- \omega \pi^+$		(2.89 ± 0.30) × 10^{-3}			2148
$D_1(2430)^0 \omega \times$ B($D_1(2430)^0 \to D^{*-} \pi^+$)		(4.1 ± 1.6) × 10^{-4}			1992
$\overline{D}^{**-} \pi^+$	[xxx]	(2.1 ± 1.0) × 10^{-3}			–
$D_1(2420)^- \pi^+ \times$ B($D_1^- \to D^- \pi^+ \pi^-$)		(1.00 $^{+0.21}_{-0.25}$) × 10^{-4}			–
$D_1(2420)^- \pi^+ \times$ B($D_1^- \to D^{*-} \pi^+ \pi^-$)		< 3.3	× 10^{-5}	CL=90%	–
$\overline{D}_2^*(2460)^- \pi^+ \times$ B($D_2^*(2460)^- \to D^0 \pi^-$)		(2.15 ± 0.35) × 10^{-4}			2062
$\overline{D}_0^*(2400)^- \pi^+ \times$ B($D_0^*(2400)^- \to D^0 \pi^-$)		(6.0 ± 3.0) × 10^{-5}			2090
$D_2^*(2460)^- \pi^+ \times$ B($(D_2^*)^- \to D^{*-} \pi^+ \pi^-$)		< 2.4	× 10^{-5}	CL=90%	–
$\overline{D}_2^*(2460)^- \rho^+$		< 4.9	× 10^{-3}	CL=90%	1975
$D^0 \overline{D}^0$		(1.4 ± 0.7) × 10^{-5}			1868
$D^{*0} \overline{D}^0$		< 2.9	× 10^{-4}	CL=90%	1794
$D^- D^+$		(2.11 ± 0.18) × 10^{-4}			1864
$D^\pm D^{*\mp}$ (*CP*-averaged)		(6.1 ± 0.6) × 10^{-4}			–
$D^- D_s^+$		(7.2 ± 0.8) × 10^{-3}			1812
$D^*(2010)^- D_s^+$		(8.0 ± 1.1) × 10^{-3}			1735
$D^- D_s^{*+}$		(7.4 ± 1.6) × 10^{-3}			1732
$D^*(2010)^- D_s^{*+}$		(1.77 ± 0.14) %			1649
$D_{s0}(2317)^- K^+ \times$ B($D_{s0}(2317)^- \to D_s^- \pi^0$)		(4.2 ± 1.4) × 10^{-5}			2097
$D_{s0}(2317)^- \pi^+ \times$ B($D_{s0}(2317)^- \to D_s^- \pi^0$)		< 2.5	× 10^{-5}	CL=90%	2128
$D_{sJ}(2457)^- K^+ \times$ B($D_{sJ}(2457)^- \to D_s^- \pi^0$)		< 9.4	× 10^{-6}	CL=90%	–
$D_{sJ}(2457)^- \pi^+ \times$ B($D_{sJ}(2457)^- \to D_s^- \pi^0$)		< 4.0	× 10^{-6}	CL=90%	–
$D_s^- D_s^+$		< 3.6	× 10^{-5}	CL=90%	1759
$D_s^{*-} D_s^+$		< 1.3	× 10^{-4}	CL=90%	1674
$D_s^{*-} D_s^{*+}$		< 2.4	× 10^{-4}	CL=90%	1583
$D_{s0}(2317)^+ D^- \times$ B($D_{s0}(2317)^+ \to D_s^+ \pi^0$)		(9.7 $^{+4.0}_{-3.3}$) × 10^{-4}		S=1.5	1602
$D_{s0}(2317)^+ D^- \times$ B($D_{s0}(2317)^+ \to D_s^{*+} \gamma$)		< 9.5	× 10^{-4}	CL=90%	–
$D_{s0}(2317)^+ D^*(2010)^- \times$ B($D_{s0}(2317)^+ \to D_s^+ \pi^0$)		(1.5 ± 0.6) × 10^{-3}			1509
$D_{sJ}(2457)^+ D^-$		(3.5 ± 1.1) × 10^{-3}			–
$D_{sJ}(2457)^+ D^- \times$ B($D_{sJ}(2457)^+ \to D_s^+ \gamma$)		(6.5 $^{+1.7}_{-1.4}$) × 10^{-4}			–
$D_{sJ}(2457)^+ D^- \times$ B($D_{sJ}(2457)^+ \to D_s^{*+} \gamma$)		< 6.0	× 10^{-4}	CL=90%	–
$D_{sJ}(2457)^+ D^- \times$ B($D_{sJ}(2457)^+ \to D_s^+ \pi^+ \pi^-$)		< 2.0	× 10^{-4}	CL=90%	–
$D_{sJ}(2457)^+ D^- \times$ B($D_{sJ}(2457)^+ \to D_s^+ \pi^0$)		< 3.6	× 10^{-4}	CL=90%	–
$D^*(2010)^- D_{sJ}(2457)^+$		(9.3 ± 2.2) × 10^{-3}			–
$D_{sJ}(2457)^+ D^*(2010) \times$ B($D_{sJ}(2457)^+ \to D_s^+ \gamma$)		(2.3 $^{+0.9}_{-0.7}$) × 10^{-3}			–
$D^- D_{s1}(2536)^+ \times$ B($D_{s1}(2536)^+ \to D^{*0} K^+ + D^{*+} K^0$)		(2.8 ± 0.7) × 10^{-4}			1444
$D^- D_{s1}(2536)^+ \times$ B($D_{s1}(2536)^+ \to D^{*0} K^+$)		(1.7 ± 0.6) × 10^{-4}			1444
$D^- D_{s1}(2536)^+ \times$ B($D_{s1}(2536)^+ \to D^{*+} K^0$)		(2.6 ± 1.1) × 10^{-4}			1444
$D^*(2010)^- D_{s1}(2536)^+ \times$ B($D_{s1}(2536)^+ \to D^{*0} K^+ + D^{*+} K^0$)		(5.0 ± 1.4) × 10^{-4}			1336
$D^*(2010)^- D_{s1}(2536)^+ \times$ B($D_{s1}(2536)^+ \to D^{*0} K^+$)		(3.3 ± 1.1) × 10^{-4}			1336
$D^{*-} D_{s1}(2536)^+ \times$ B($D_{s1}(2536)^+ \to D^{*+} K^0$)		(5.0 ± 1.7) × 10^{-4}			1336
$D^- D_{sJ}(2573)^+ \times$ B($D_{sJ}(2573)^+ \to D^0 K^+$)		< 1	× 10^{-4}	CL=90%	1414
$D^*(2010)^- D_{sJ}(2573)^+ \times$ B($D_{sJ}(2573)^+ \to D^0 K^+$)		< 2	× 10^{-4}	CL=90%	1304
$D^+ \pi^-$		(7.8 ± 1.4) × 10^{-7}			2306
$D_s^+ \pi^-$		(2.16 ± 0.26) × 10^{-5}			2270
$D_s^{*+} \pi^-$		(2.1 ± 0.4) × 10^{-5}		S=1.4	2215
$D_s^+ \rho^-$		< 2.4	× 10^{-5}	CL=90%	2197
$D_s^{*+} \rho^-$		(4.1 ± 1.3) × 10^{-5}			2138
$D_s^+ a_0^-$		< 1.9	× 10^{-5}	CL=90%	–
$D_s^{*+} a_0^-$		< 3.6	× 10^{-5}	CL=90%	–
$D_s^+ a_1(1260)^-$		< 2.1	× 10^{-3}	CL=90%	2080
$D_s^{*+} a_1(1260)^-$		< 1.7	× 10^{-3}	CL=90%	2015
$D_s^+ a_2^-$		< 1.9	× 10^{-4}	CL=90%	–
$D_s^{*+} a_2^-$		< 2.0	× 10^{-4}	CL=90%	–
$D_s^- K^+$		(2.2 ± 0.5) × 10^{-5}		S=1.8	2242
$D_s^{*-} K^+$		(2.19 ± 0.30) × 10^{-5}			2185
$D_s^- K^*(892)^+$		(3.5 ± 1.0) × 10^{-5}			2172
$D_s^{*-} K^*(892)^+$		(3.2 $^{+1.5}_{-1.3}$) × 10^{-5}			2112
$D_s^- \pi^+ K^0$		(1.10 ± 0.33) × 10^{-4}			2222
$D_s^{*-} \pi^+ K^0$		< 1.10	× 10^{-4}	CL=90%	2164
$D_s^- K^+ \pi^+ \pi^-$		(1.8 ± 0.5) × 10^{-4}			2198
$D_s^- \pi^+ K^*(892)^0$		< 3.0	× 10^{-3}	CL=90%	2138
$D_s^{*-} \pi^+ K^*(892)^0$		< 1.6	× 10^{-3}	CL=90%	2076
$\overline{D}^0 K^0$		(5.2 ± 0.7) × 10^{-5}			2280
$\overline{D}^0 K^+ \pi^-$		(8.8 ± 1.7) × 10^{-5}			2261
$\overline{D}^0 K^*(892)^0$		(4.2 ± 0.6) × 10^{-5}			2213
$D_2^*(2460)^- K^+ \times$ B($D_2^*(2460)^- \to \overline{D}^0 \pi^-$)		(1.8 ± 0.5) × 10^{-5}			2029
$\overline{D}^0 K^+ \pi^-$ non-resonant		< 3.7	× 10^{-5}	CL=90%	–
$[K^+ K^-]_D K^*(892)^0$		(5.8 $^{+1.8}_{-1.6}$) × 10^{-5}			–
$\overline{D}^0 \pi^0$		(2.63 ± 0.14) × 10^{-4}			2308
$\overline{D}^0 \rho^0$		(3.2 ± 0.5) × 10^{-4}			2237
$\overline{D}^0 f_2$		(1.2 ± 0.4) × 10^{-4}			–
$\overline{D}^0 \eta$		(2.36 ± 0.32) × 10^{-4}		S=2.5	2274
$\overline{D}^0 \eta'$		(1.38 ± 0.16) × 10^{-4}		S=1.3	2198
$\overline{D}^0 \omega$		(2.53 ± 0.16) × 10^{-4}			2235
$D^0 \phi$		< 1.16	× 10^{-5}	CL=90%	2183
$D^0 K^+ \pi^-$		(5.3 ± 3.2) × 10^{-6}			2261
$D^0 K^*(892)^0$		< 1.1	× 10^{-5}	CL=90%	2213
$\overline{D}^{*0} \gamma$		< 2.5	× 10^{-5}	CL=90%	2258
$\overline{D}^*(2007)^0 \pi^0$		(2.2 ± 0.6) × 10^{-4}		S=2.6	2256
$\overline{D}^*(2007)^0 \rho^0$		< 5.1	× 10^{-4}	CL=90%	2182
$\overline{D}^*(2007)^0 \eta$		(2.3 ± 0.6) × 10^{-4}		S=2.8	2220
$\overline{D}^*(2007)^0 \eta'$		(1.40 ± 0.22) × 10^{-4}			2141
$\overline{D}^*(2007)^0 \pi^+ \pi^-$		(6.2 ± 2.2) × 10^{-4}			2248
$\overline{D}^*(2007)^0 K^0$		(3.6 ± 1.2) × 10^{-5}			2227
$\overline{D}^*(2007)^0 K^*(892)^0$		< 6.9	× 10^{-5}	CL=90%	2157
$D^*(2007)^0 K^*(892)^0$		< 4.0	× 10^{-5}	CL=90%	2157
$D^*(2007)^0 \pi^+ \pi^+ \pi^- \pi^-$		(2.7 ± 0.5) × 10^{-3}			2219
$D^*(2010)^+ D^*(2010)^-$		(8.0 ± 0.6) × 10^{-4}			1711
$\overline{D}^*(2007)^0 \omega$		(3.6 ± 1.1) × 10^{-4}		S=3.1	2180
$D^*(2010)^+ D^-$		(6.1 ± 1.5) × 10^{-4}		S=1.6	1790
$D^*(2007)^0 \overline{D}^*(2007)^0$		< 9	× 10^{-5}	CL=90%	1715
$D^- D^0 K^+$		(1.07 ± 0.11) × 10^{-3}			1574
$D^- D^*(2007)^0 K^+$		(3.5 ± 0.4) × 10^{-3}			1478
$D^*(2010)^- D^0 K^+$		(2.47 ± 0.21) × 10^{-3}			1479
$D^*(2010)^- D^*(2007)^0 K^+$		(1.06 ± 0.09) %			1366
$D^- D^+ K^0$		(7.5 ± 1.7) × 10^{-4}			1568

$D^*(2010)^- D^+ K^0 +$ $D^- D^*(2010)^+ K^0$		$(6.4 \pm 0.5) \times 10^{-3}$		1473
$D^*(2010)^- D^*(2010)^+ K^0$		$(8.1 \pm 0.7) \times 10^{-3}$		1360
$D^{*-} D_{s1}(2536)^+ \times$ B($D_{s1}(2536)^+ \to$ $D^{*+} K^0$)		$(8.0 \pm 2.4) \times 10^{-4}$		1336
$\overline{D}{}^0 D^0 K^0$		$(2.7 \pm 1.1) \times 10^{-4}$		1574
$\overline{D}{}^0 D^*(2007)^0 K^0 +$ $\overline{D}{}^*(2007)^0 D^0 K^0$		$(1.1 \pm 0.5) \times 10^{-3}$		1478
$\overline{D}{}^*(2007)^0 D^*(2007)^0 K^0$		$(2.4 \pm 0.9) \times 10^{-3}$		1365
$(\overline{D}+\overline{D}^*)(D+D^*) K$		(3.68 ± 0.26) %		–
Charmonium modes				
$\eta_c K^0$		$(7.9 \pm 1.2) \times 10^{-4}$		1751
$\eta_c K^*(892)^0$		$(6.3 \pm 0.9) \times 10^{-4}$		1646
$\eta_c(2S) K^{*0}$		$< 3.9 \times 10^{-4}$	CL=90%	1157
$h_c(1P) K^{*0}$		$< 4 \times 10^{-4}$	CL=90%	1253
$J/\psi(1S) K^0$		$(8.73 \pm 0.32) \times 10^{-4}$		1683
$J/\psi(1S) K^+ \pi^-$		$(1.2 \pm 0.6) \times 10^{-3}$		1652
$J/\psi(1S) K^*(892)^0$		$(1.32 \pm 0.06) \times 10^{-3}$		1571
$J/\psi(1S) \eta K^0_S$		$(8 \pm 4) \times 10^{-5}$		1508
$J/\psi(1S) \eta' K^0_S$		$< 2.5 \times 10^{-5}$	CL=90%	1271
$J/\psi(1S) \phi K^0$		$(9.4 \pm 2.6) \times 10^{-5}$		1224
$J/\psi(1S) \omega K^0$		$(2.3 \pm 0.4) \times 10^{-4}$		1386
$X(3872) K^0 \times$ B($X \to$ $J/\psi\omega$)		$(6.0 \pm 3.2) \times 10^{-6}$		1140
$\chi_{c0}(2P)$, $\chi_{c0} \to J/\psi\omega$		$(2.1 \pm 0.9) \times 10^{-5}$		1102
$J/\psi(1S) K(1270)^0$		$(1.3 \pm 0.5) \times 10^{-3}$		1390
$J/\psi(1S) \pi^0$		$(1.76 \pm 0.16) \times 10^{-5}$	S=1.1	1728
$J/\psi(1S) \eta$		$(1.23 \pm 0.19) \times 10^{-5}$		1672
$J/\psi(1S) \pi^+ \pi^-$		$(4.03 \pm 0.18) \times 10^{-5}$		1716
$J/\psi(1S) \pi^+ \pi^-$ nonresonant		$< 1.2 \times 10^{-5}$	CL=90%	1716
$J/\psi(1S) f_0(500)$, $f_0 \to \pi\pi$		$(6.5 \pm {}^{2.6}_{1.1}) \times 10^{-6}$		–
$J/\psi(1S) f_2$		$(4.2 \pm 0.7) \times 10^{-6}$		–
$J/\psi(1S) \rho^0$		$(2.58 \pm 0.21) \times 10^{-5}$		1612
$J/\psi(1S) f_0(980)$, $f_0 \to$ $\pi^+ \pi^-$		$< 1.1 \times 10^{-6}$	CL=90%	–
$J/\psi(1S) \rho(1450)^0$, $\rho^0 \to$ $\pi\pi$		$(2.1 \pm {}^{2.5}_{0.7}) \times 10^{-6}$		–
$J/\psi(1S) \omega$		$(2.3 \pm 0.6) \times 10^{-5}$		1609
$J/\psi(1S) K^+ K^-$		$(2.6 \pm 0.4) \times 10^{-6}$		1533
$J/\psi(1S) a_0(980)$, $a_0 \to$ $K^+ K^-$		$(4.7 \pm 3.4) \times 10^{-7}$		–
$J/\psi(1S) \phi$		$< 1.9 \times 10^{-7}$	CL=90%	1520
$J/\psi(1S) \eta'(958)$		$< 7.4 \times 10^{-6}$	CL=90%	1546
$J/\psi(1S) K^0 \pi^+ \pi^-$		$(1.0 \pm 0.4) \times 10^{-3}$		1611
$J/\psi(1S) K^0 \rho^0$		$(5.4 \pm 3.0) \times 10^{-4}$		1390
$J/\psi(1S) K^*(892)^+ \pi^-$		$(8 \pm 4) \times 10^{-4}$		1514
$J/\psi(1S) K^*(892)^0 \pi^+ \pi^-$		$(6.6 \pm 2.2) \times 10^{-4}$		1447
$X(3872)^- K^+$		$< 5 \times 10^{-4}$	CL=90%	–
$X(3872)^- K^+ \times$ B($X(3872)^- \to$ $J/\psi(1S) \pi^- \pi^0$)	[yyy]	$< 4.2 \times 10^{-6}$	CL=90%	–
$X(3872) K^0 \times$ B($X \to$ $J/\psi \pi^+ \pi^-$)		$(4.3 \pm 1.3) \times 10^{-6}$		1140
$X(3872) K^0 \times$ B($X \to J/\psi\gamma$)		$< 2.4 \times 10^{-6}$	CL=90%	1140
$X(3872) K^*(892)^0 \times$ B($X \to$ $J/\psi\gamma$)		$< 2.8 \times 10^{-6}$	CL=90%	940
$X(3872) K^0 \times$ B($X \to$ $\psi(2S)\gamma$)		$< 6.62 \times 10^{-6}$	CL=90%	1140
$X(3872) K^*(892)^0 \times$ B($X \to$ $\psi(2S)\gamma$)		$< 4.4 \times 10^{-6}$	CL=90%	940
$X(3872) K^0 \times$ B($X \to$ $D^0 \overline{D}{}^0 \pi^0$)		$(1.7 \pm 0.8) \times 10^{-4}$		1140
$X(3872) K^0 \times$ B($X \to \overline{D}{}^{*0} D^0$)		$(1.2 \pm 0.4) \times 10^{-4}$		1140
$X(4430)^\pm K^\mp \times$ B($X^\pm \to$ $\psi(2S) \pi^\pm$)		$(6.0 \pm {}^{3.0}_{2.4}) \times 10^{-5}$		575
$X(4430)^\pm K^\mp \times$ B($X^\pm \to$ $J/\psi \pi^\pm$)		$< 4 \times 10^{-6}$	CL=95%	575
$J/\psi(1S) p\overline{p}$		$< 5.2 \times 10^{-7}$	CL=90%	862
$J/\psi(1S) \gamma$		$< 1.6 \times 10^{-6}$	CL=90%	1731
$J/\psi(1S) \overline{D}{}^0$		$< 1.3 \times 10^{-5}$	CL=90%	877
$\psi(2S) K^0$		$(6.2 \pm 0.5) \times 10^{-4}$		1283
$\psi(3770) K^0 \times$ B($\psi \to \overline{D}{}^0 D^0$)		$< 1.23 \times 10^{-4}$	CL=90%	1217
$\psi(3770) K^0 \times$ B($\psi \to D^- D^+$)		$< 1.88 \times 10^{-4}$	CL=90%	1217
$\psi(2S) \pi^+ \pi^-$		$(2.3 \pm 0.4) \times 10^{-5}$		1331
$\psi(2S) K^+ \pi^-$		$(5.8 \pm 0.4) \times 10^{-4}$		1238
$\psi(2S) K^*(892)^0$		$(6.0 \pm 0.4) \times 10^{-4}$	S=1.1	1116
$\chi_{c0} K^0$		$(1.47 \pm 0.27) \times 10^{-4}$		1477
$\chi_{c0} K^*(892)^0$		$(1.7 \pm 0.4) \times 10^{-4}$		1341
$\chi_{c2} K^0$		$< 1.5 \times 10^{-5}$	CL=90%	1378
$\chi_{c2} K^*(892)^0$		$(5.0 \pm 1.2) \times 10^{-5}$	S=1.1	1228
$\chi_{c1} \pi^0$		$(1.12 \pm 0.28) \times 10^{-5}$		1468
$\chi_{c1} K^0$		$(3.93 \pm 0.27) \times 10^{-4}$		1411
$\chi_{c1} K^- \pi^+$		$(3.8 \pm 0.4) \times 10^{-4}$		1371
$\chi_{c1} K^*(892)^0$		$(2.42 \pm 0.21) \times 10^{-4}$	S=1.3	1265
$X(4051)^+ K^- \times$ B($X^+ \to$ $\chi_{c1} \pi^+$)		$(3.0 \pm {}^{4.0}_{1.8}) \times 10^{-5}$		–
$X(4248)^+ K^- \times$ B($X^+ \to$ $\chi_{c1} \pi^+$)		$(4.0 \pm {}^{20.0}_{1.0}) \times 10^{-5}$		–
K* or *K* **modes**				
$K^+ \pi^-$		$(1.96 \pm 0.05) \times 10^{-5}$		2615
$K^0 \pi^0$		$(9.9 \pm 0.5) \times 10^{-6}$		2615
$\eta' K^0$		$(6.6 \pm 0.4) \times 10^{-5}$	S=1.4	2528
$\eta' K^*(892)^0$		$(3.1 \pm 0.9) \times 10^{-6}$		2472
$\eta' K_0^*(1430)^0$		$(6.3 \pm 1.6) \times 10^{-6}$		2346
$\eta' K_2^*(1430)^0$		$(1.37 \pm 0.32) \times 10^{-5}$		2346
ηK^0		$(1.23 \pm {}^{0.27}_{0.24}) \times 10^{-6}$		2587
$\eta K^*(892)^0$		$(1.59 \pm 0.10) \times 10^{-5}$		2534
$\eta K_0^*(1430)^0$		$(1.10 \pm 0.22) \times 10^{-5}$		2415
$\eta K_2^*(1430)^0$		$(9.6 \pm 2.1) \times 10^{-6}$		2414
ωK^0		$(5.0 \pm 0.6) \times 10^{-6}$		2557
$a_0(980)^0 K^0 \times$ B($a_0(980)^0 \to$ $\eta\pi^0$)		$< 7.8 \times 10^{-6}$	CL=90%	–
$b_1^0 K^0 \times$ B($b_1^0 \to \omega\pi^0$)		$< 7.8 \times 10^{-6}$	CL=90%	–
$a_0(980)^\pm K^\mp \times$ B($a_0(980)^\pm \to$ $\eta\pi^\pm$)		$< 1.9 \times 10^{-6}$	CL=90%	–
$b_1^- K^+ \times$ B($b_1^- \to \omega\pi^-$)		$(7.4 \pm 1.4) \times 10^{-6}$		–
$b_1^0 K^{*0} \times$ B($b_1^0 \to \omega\pi^0$)		$< 8.0 \times 10^{-6}$	CL=90%	–
$b_1^- K^{*+} \times$ B($b_1^- \to \omega\pi^-$)		$< 5.0 \times 10^{-6}$	CL=90%	–
$a_0(1450)^\pm K^\mp \times$ B($a_0(1450)^\pm \to \eta\pi^\pm$)		$< 3.1 \times 10^{-6}$	CL=90%	–
$K^0_S X^0$ (Familon)		$< 5.3 \times 10^{-5}$	CL=90%	–
$\omega K^*(892)^0$		$(2.0 \pm 0.5) \times 10^{-6}$		2503
$\omega (K\pi)^{*0}_0$		$(1.84 \pm 0.25) \times 10^{-5}$		–
$\omega K_0^*(1430)^0$		$(1.60 \pm 0.34) \times 10^{-5}$		2380
$\omega K_2^*(1430)^0$		$(1.01 \pm 0.23) \times 10^{-5}$		2380
$\omega K^+ \pi^-$ nonresonant		$(5.1 \pm 1.0) \times 10^{-6}$		2542
$K^+ \pi^- \pi^0$		$(3.78 \pm 0.32) \times 10^{-5}$		2609
$K^+ \rho^-$		$(7.0 \pm 0.9) \times 10^{-6}$		2559
$K^+ \rho(1450)^-$		$(2.4 \pm 1.2) \times 10^{-6}$		–
$K^+ \rho(1700)^-$		$(6 \pm 7) \times 10^{-7}$		–
$(K^+ \pi^- \pi^0)$ non-resonant		$(2.8 \pm 0.6) \times 10^{-6}$		–
$(K\pi)^{*+}_0 \pi^- \times$ B($(K\pi)^{*+}_0 \to$ $K^+ \pi^0$)		$(3.4 \pm 0.5) \times 10^{-5}$		–
$(K\pi)^{*0}_0 \pi^0 \times$B($(K\pi)^{*0}_0 \to$ $K^+ \pi^-$)		$(8.6 \pm 1.7) \times 10^{-6}$		–
$K_2^*(1430)^0 \pi^0$		$< 4.0 \times 10^{-6}$	CL=90%	2445
$K^*(1680)^0 \pi^0$		$< 7.5 \times 10^{-6}$	CL=90%	2358
$K_x^{*0} \pi^0$	[bbaa]	$(6.1 \pm 1.6) \times 10^{-6}$		–
$K^0 \pi^+ \pi^-$		$(6.5 \pm 0.8) \times 10^{-5}$	S=1.2	2609
$K^0 \pi^+ \pi^-$ non-resonant		$(1.47 \pm {}^{0.40}_{0.26}) \times 10^{-5}$	S=2.1	–
$K^0 \rho^0$		$(4.7 \pm 0.6) \times 10^{-6}$		2558
$K^*(892)^+ \pi^-$		$(8.4 \pm 0.8) \times 10^{-6}$		2563
$K_0^*(1430)^+ \pi^-$		$(3.3 \pm 0.7) \times 10^{-5}$	S=2.0	–
$K_x^{*+} \pi^-$	[bbaa]	$(5.1 \pm 1.6) \times 10^{-6}$		–
$K^*(1410)^+ \pi^- \times$ B($K^*(1410)^+ \to K^0 \pi^+$)		$< 3.8 \times 10^{-6}$	CL=90%	–
$f_0(980) K^0 \times$ B($f_0(980) \to$ $\pi^+ \pi^-$)		$(7.0 \pm 0.9) \times 10^{-6}$		2522
$f_2(1270) K^0$		$(2.7 \pm {}^{1.3}_{1.2}) \times 10^{-6}$		2459
$f_x(1300) K^0 \times$ B($f_x \to$ $\pi^+ \pi^-$)		$(1.8 \pm 0.7) \times 10^{-6}$		–
$K^*(892)^0 \pi^0$		$(3.3 \pm 0.6) \times 10^{-6}$		2563
$K_2^*(1430)^+ \pi^-$		$< 6 \times 10^{-6}$	CL=90%	2445
$K^*(1680)^+ \pi^-$		$< 1.0 \times 10^{-5}$	CL=90%	2358
$K^+ \pi^- \pi^+ \pi^-$	[ccaa]	$< 2.3 \times 10^{-4}$	CL=90%	2600
$\rho^0 K^+ \pi^-$		$(2.8 \pm 0.7) \times 10^{-6}$		2543
$f_0(980) K^+ \pi^-$, $f_0 \to \pi\pi$		$(1.4 \pm {}^{0.5}_{0.6}) \times 10^{-6}$		2506

Meson Summary Table

$K^+\pi^-\pi^+\pi^-$ nonresonant		< 2.1	$\times 10^{-6}$	CL=90%	2600
$K^*(892)^0\pi^+\pi^-$		(5.5 ± 0.5) $\times 10^{-5}$			2557
$K^*(892)^0\rho^0$		(3.9 ± 1.3) $\times 10^{-6}$		S=1.9	2504
$K^*(892)^0 f_0(980)$, $f_0 \to \pi\pi$		($3.9 \pm {}^{2.1}_{1.8}$) $\times 10^{-6}$		S=3.9	2466
$K_1(1270)^+\pi^-$		< 3.0	$\times 10^{-5}$	CL=90%	2484
$K_1(1400)^+\pi^-$		< 2.7	$\times 10^{-5}$	CL=90%	2451
$a_1(1260)^- K^+$	[ccaa]	(1.6 ± 0.4) $\times 10^{-5}$			2471
$K^*(892)^+\rho^-$		(1.03± 0.26) $\times 10^{-5}$			2504
$K_0^*(1430)^+\rho^-$		(2.8 ± 1.2) $\times 10^{-5}$			–
$K_1(1400)^0\rho^0$		< 3.0	$\times 10^{-3}$	CL=90%	2388
$K_0^*(1430)^0\rho^0$		(2.7 ± 0.6) $\times 10^{-5}$			2381
$K_0^*(1430)^0 f_0(980)$, $f_0 \to \pi\pi$		(2.7 ± 0.9) $\times 10^{-6}$			–
$K_2^*(1430)^0 f_0(980)$, $f_0 \to \pi\pi$		(8.6 ± 2.0) $\times 10^{-6}$			–
K^+K^-		(1.3 ± 0.5) $\times 10^{-7}$			2593
$K^0\overline{K}^0$		(1.21± 0.16) $\times 10^{-6}$			2592
$K^0 K^-\pi^+$		(7.3 ± 1.1) $\times 10^{-6}$		S=1.2	2578
$\overline{K}^{*0}K^0 + K^{*0}\overline{K}^0$		< 1.9	$\times 10^{-6}$		–
$K^+K^-\pi^0$		(2.2 ± 0.6) $\times 10^{-6}$			2579
$K_S^0 K_S^0\pi^0$		< 9	$\times 10^{-7}$	CL=90%	2578
$K_S^0 K_S^0\eta$		< 1.0	$\times 10^{-6}$	CL=90%	2515
$K_S^0 K_S^0\eta'$		< 2.0	$\times 10^{-6}$	CL=90%	2452
$K^0 K^+K^-$		(2.63± 0.15) $\times 10^{-5}$		S=1.3	2522
$K^0\phi$		(7.3 ± 0.7) $\times 10^{-6}$			2516
$f_0(980)K^0$, $f_0 \to K^+K^-$		($7.0 \pm {}^{3.5}_{3.0}$) $\times 10^{-6}$			–
$f_0(1500)K^0$		($1.3 \pm {}^{0.7}_{0.5}$) $\times 10^{-5}$			2398
$f_2'(1525)^0 K^0$		($3 \pm {}^{5}_{4}$) $\times 10^{-7}$			–
$f_0(1710)K^0$, $f_0 \to K^+K^-$		(4.4 ± 0.9) $\times 10^{-6}$			–
$K^0K^+K^-$ nonresonant		(3.3 ± 1.0) $\times 10^{-5}$			2522
$K_S^0 K_S^0 K_S^0$		(6.0 ± 0.5) $\times 10^{-6}$		S=1.1	2521
$f_0(980)K^0$, $f_0 \to K_S^0 K_S^0$		(2.7 ± 1.8) $\times 10^{-6}$			–
$f_0(1710)K^0$, $f_0 \to K_S^0 K_S^0$		($5.0 \pm {}^{5.0}_{2.6}$) $\times 10^{-7}$			–
$f_0(2010)K^0$, $f_0 \to K_S^0 K_S^0$		(5 ± 6) $\times 10^{-7}$			–
$K_S^0 K_S^0 K_S^0$ nonresonant		(1.33± 0.31) $\times 10^{-5}$			2521
$K_S^0 K_S^0 K_L^0$		< 1.6	$\times 10^{-5}$	CL=90%	2521
$K^*(892)^0 K^+K^-$		(2.75± 0.26) $\times 10^{-5}$			2467
$K^*(892)^0\phi$		(1.00± 0.05) $\times 10^{-5}$			2460
$K^+K^-\pi^+\pi^-$ nonresonant		< 7.17	$\times 10^{-5}$	CL=90%	2559
$K^*(892)^0 K^-\pi^+$		(4.5 ± 1.3) $\times 10^{-6}$			2524
$K^*(892)^0\overline{K}^*(892)^0$		(8 ± 5) $\times 10^{-7}$		S=2.2	2485
$K^+K^+\pi^-\pi^-$ nonresonant		< 6.0	$\times 10^{-6}$	CL=90%	2559
$K^*(892)^0 K^+\pi^-$		< 2.2	$\times 10^{-6}$	CL=90%	2524
$K^*(892)^0 K^*(892)^0$		< 2	$\times 10^{-7}$	CL=90%	2485
$K^*(892)^+ K^*(892)^-$		< 2.0	$\times 10^{-6}$	CL=90%	2485
$K_1(1400)^0\phi$		< 5.0	$\times 10^{-3}$	CL=90%	2339
$\phi(K\pi)_0^{*0}$		(4.3 ± 0.4) $\times 10^{-6}$			–
$\phi(K\pi)_0^{*0}$ $(1.60 < m_{K\pi} < 2.15)$	[ddaa]	< 1.7	$\times 10^{-6}$	CL=90%	–
$K_0^*(1430)^0 K^-\pi^+$		< 3.18	$\times 10^{-5}$	CL=90%	2403
$K_0^*(1430)^0\overline{K}^*(892)^0$		< 3.3	$\times 10^{-6}$	CL=90%	2360
$K_0^*(1430)^0\overline{K}_0^*(1430)^0$		< 8.4	$\times 10^{-6}$	CL=90%	2222
$K_0^*(1430)^0\phi$		(3.9 ± 0.8) $\times 10^{-6}$			2333
$K_0^*(1430)^0 K^*(892)^0$		< 1.7	$\times 10^{-6}$	CL=90%	2360
$K_0^*(1430)^0 K_0^*(1430)^0$		< 4.7	$\times 10^{-6}$	CL=90%	2222
$K^*(1680)^0\phi$		< 3.5	$\times 10^{-6}$	CL=90%	2238
$K^*(1780)^0\phi$		< 2.7	$\times 10^{-6}$	CL=90%	–
$K^*(2045)^0\phi$		< 1.53	$\times 10^{-5}$	CL=90%	–
$K_2^*(1430)^0\rho^0$		< 1.1	$\times 10^{-3}$	CL=90%	2381
$K_2^*(1430)^0\phi$		(6.8 ± 0.9) $\times 10^{-6}$		S=1.2	2333
$K^0\phi\phi$		(4.5 ± 0.9) $\times 10^{-6}$			2305
$\eta'\eta' K^0$		< 3.1	$\times 10^{-5}$	CL=90%	2337
$\eta K^0\gamma$		(7.6 ± 1.8) $\times 10^{-6}$			2587
$\eta' K^0\gamma$		< 6.4	$\times 10^{-6}$	CL=90%	2528
$K^0\phi\gamma$		(2.7 ± 0.7) $\times 10^{-6}$			2516
$K^+\pi^-\gamma$		(4.6 ± 1.4) $\times 10^{-6}$			2615
$K^*(892)^0\gamma$		(4.33± 0.15) $\times 10^{-5}$			2564
$K^*(1410)\gamma$		< 1.3	$\times 10^{-4}$	CL=90%	2451
$K^+\pi^-\gamma$ nonresonant		< 2.6	$\times 10^{-6}$	CL=90%	2615
$K^*(892)^0 X(214) \times$ B($X \to \mu^+\mu^-$)	[eeaa]	< 2.26	$\times 10^{-8}$	CL=90%	–
$K^0\pi^+\pi^-\gamma$		(1.95± 0.22) $\times 10^{-5}$			2609
$K^+\pi^-\pi^0\gamma$		(4.1 ± 0.4) $\times 10^{-5}$			2609
$K_1(1270)^0\gamma$		< 5.8	$\times 10^{-5}$	CL=90%	2486
$K_1(1400)^0\gamma$		< 1.2	$\times 10^{-5}$	CL=90%	2453
$K_2^*(1430)^0\gamma$		(1.24± 0.24) $\times 10^{-5}$			2447
$K^*(1680)^0\gamma$		< 2.0	$\times 10^{-3}$	CL=90%	2361
$K_3^*(1780)^0\gamma$		< 8.3	$\times 10^{-5}$	CL=90%	2341
$K_4^*(2045)^0\gamma$		< 4.3	$\times 10^{-3}$	CL=90%	2244

Light unflavored meson modes

$\rho^0\gamma$		(8.6 ± 1.5) $\times 10^{-7}$			2583
$\rho^0 X(214) \times$ B($X \to \mu^+\mu^-$)	[eeaa]	< 1.73	$\times 10^{-8}$	CL=90%	–
$\omega\gamma$		($4.4 \pm {}^{1.8}_{1.6}$) $\times 10^{-7}$			2582
$\phi\gamma$		< 8.5	$\times 10^{-7}$	CL=90%	2541
$\pi^+\pi^-$		(5.12± 0.19) $\times 10^{-6}$			2636
$\pi^0\pi^0$		(1.91± 0.22) $\times 10^{-6}$			2636
$\eta\pi^0$		< 1.5	$\times 10^{-6}$	CL=90%	2610
$\eta\eta$		< 1.0	$\times 10^{-6}$	CL=90%	2582
$\eta'\pi^0$		(1.2 ± 0.6) $\times 10^{-6}$		S=1.7	2551
$\eta'\eta'$		< 1.7	$\times 10^{-6}$	CL=90%	2460
$\eta'\eta$		< 1.2	$\times 10^{-6}$	CL=90%	2523
$\eta'\rho^0$		< 1.3	$\times 10^{-6}$	CL=90%	2492
$\eta' f_0(980) \times$ B($f_0(980) \to \pi^+\pi^-$)		< 9	$\times 10^{-7}$	CL=90%	2454
$\eta\rho^0$		< 1.5	$\times 10^{-6}$	CL=90%	2553
$\eta f_0(980) \times$ B($f_0(980) \to \pi^+\pi^-$)		< 4	$\times 10^{-7}$	CL=90%	2516
$\omega\eta$		($9.4 \pm {}^{4.0}_{3.1}$) $\times 10^{-7}$			2552
$\omega\eta'$		($1.0 \pm {}^{0.5}_{0.4}$) $\times 10^{-6}$			2491
$\omega\rho^0$		< 1.6	$\times 10^{-6}$	CL=90%	2522
$\omega f_0(980) \times$ B($f_0(980) \to \pi^+\pi^-$)		< 1.5	$\times 10^{-6}$	CL=90%	2485
$\omega\omega$		(1.2 ± 0.4) $\times 10^{-6}$			2521
$\phi\pi^0$		< 1.5	$\times 10^{-7}$	CL=90%	2540
$\phi\eta$		< 5	$\times 10^{-7}$	CL=90%	2511
$\phi\eta'$		< 5	$\times 10^{-7}$	CL=90%	2448
$\phi\rho^0$		< 3.3	$\times 10^{-7}$	CL=90%	2480
$\phi f_0(980) \times$ B($f_0 \to \pi^+\pi^-$)		< 3.8	$\times 10^{-7}$	CL=90%	2441
$\phi\omega$		< 7	$\times 10^{-7}$	CL=90%	2479
$\phi\phi$		< 2	$\times 10^{-7}$	CL=90%	2435
$a_0(980)^\pm\pi^\mp \times$ B($a_0(980)^\pm \to \eta\pi^\pm$)		< 3.1	$\times 10^{-6}$	CL=90%	–
$a_0(1450)^\pm\pi^\mp \times$ B($a_0(1450)^\pm \to \eta\pi^\pm$)		< 2.3	$\times 10^{-6}$	CL=90%	–
$\pi^+\pi^-\pi^0$		< 7.2	$\times 10^{-4}$	CL=90%	2631
$\rho^0\pi^0$		(2.0 ± 0.5) $\times 10^{-6}$			2581
$\rho^\mp\pi^\pm$	[gg]	(2.30± 0.23) $\times 10^{-5}$			2581
$\pi^+\pi^-\pi^+\pi^-$		< 1.93	$\times 10^{-5}$	CL=90%	2621
$\rho^0\pi^+\pi^-$		< 8.8	$\times 10^{-6}$	CL=90%	2575
$\rho^0\rho^0$		(7.3 ± 2.8) $\times 10^{-7}$			2523
$f_0(980)\pi^+\pi^-$		< 3.8	$\times 10^{-6}$	CL=90%	2539
$\rho^0 f_0(980) \times$ B($f_0(980) \to \pi^+\pi^-$)		< 3	$\times 10^{-7}$	CL=90%	2486
$f_0(980) f_0(980) \times$ B$^2(f_0(980) \to \pi^+\pi^-)$		< 1	$\times 10^{-7}$	CL=90%	2447
$f_0(980) f_0(980) \times$ B($f_0 \to \pi^+\pi^-$) $\times$ B($f_0 \to K^+K^-$)		< 2.3	$\times 10^{-7}$	CL=90%	2447
$a_1(1260)^\mp\pi^\pm$	[gg]	(2.6 ± 0.5) $\times 10^{-5}$		S=1.9	2494
$a_2(1320)^\mp\pi^\pm$	[gg]	< 6.3	$\times 10^{-6}$	CL=90%	2473
$\pi^+\pi^-\pi^0\pi^0$		< 3.1	$\times 10^{-3}$	CL=90%	2622
$\rho^+\rho^-$		(2.42± 0.31) $\times 10^{-5}$			2523
$a_1(1260)^0\pi^0$		< 1.1	$\times 10^{-3}$	CL=90%	2495
$\omega\pi^0$		< 5	$\times 10^{-7}$	CL=90%	2580
$\pi^+\pi^+\pi^-\pi^-\pi^0$		< 9.0	$\times 10^{-3}$	CL=90%	2609
$a_1(1260)^+\rho^-$		< 6.1	$\times 10^{-5}$	CL=90%	2433
$a_1(1260)^0\rho^0$		< 2.4	$\times 10^{-3}$	CL=90%	2433
$b_1^\mp\pi^\pm \times$ B($b_1^\mp \to \omega\pi^\mp$)		(1.09± 0.15) $\times 10^{-5}$			–
$b_1^0\pi^0 \times$ B($b_1^0 \to \omega\pi^0$)		< 1.9	$\times 10^{-6}$	CL=90%	–
$b_1^-\rho^+ \times$ B($b_1^- \to \omega\pi^-$)		< 1.4	$\times 10^{-6}$	CL=90%	–
$b_1^0\rho^0 \times$ B($b_1^0 \to \omega\pi^0$)		< 3.4	$\times 10^{-6}$	CL=90%	–
$\pi^+\pi^+\pi^+\pi^-\pi^-\pi^-$		< 3.0	$\times 10^{-3}$	CL=90%	2592
$a_1(1260)^+ a_1(1260)^- \times$ B$^2(a_1^+ \to 2\pi^+\pi^-)$		(1.18± 0.31) $\times 10^{-5}$			2336
$\pi^+\pi^+\pi^+\pi^-\pi^-\pi^-\pi^0$		< 1.1	%	CL=90%	2572

Baryon modes

$p\overline{p}$		($1.5 \pm {}^{0.7}_{0.5}$) $\times 10^{-8}$			2467
$p\overline{p}\pi^+\pi^-$		< 2.5	$\times 10^{-4}$	CL=90%	2406
$p\overline{p}K^0$		(2.66± 0.32) $\times 10^{-6}$			2347
$\Theta(1540)^+\overline{p}$, $\Theta^+ \to pK_S^0$	[ffaa]	< 5	$\times 10^{-8}$	CL=90%	2318

$f_J(2220)K^0$, $f_J \to p\overline{p}$	$<$	4.5	$\times 10^{-7}$	CL=90%	2135
$p\overline{p}K^*(892)^0$	(	$1.24^{+0.28}_{-0.25}$)	$\times 10^{-6}$		2216
$f_J(2220)K_0^*$, $f_J \to p\overline{p}$	$<$	1.5	$\times 10^{-7}$	CL=90%	–
$p\overline{\Lambda}\pi^-$	(	3.14 ± 0.29)	$\times 10^{-6}$		2401
$p\overline{\Sigma}(1385)^-$	$<$	2.6	$\times 10^{-7}$	CL=90%	2363
$\Delta^0\overline{\Lambda}$	$<$	9.3	$\times 10^{-7}$	CL=90%	2364
$p\overline{\Lambda}K^-$	$<$	8.2	$\times 10^{-7}$	CL=90%	2308
$p\overline{\Sigma}^0\pi^-$	$<$	3.8	$\times 10^{-6}$	CL=90%	2383
$\overline{\Lambda}\Lambda$	$<$	3.2	$\times 10^{-7}$	CL=90%	2392
$\overline{\Lambda}\Lambda K^0$	(	$4.8^{+1.0}_{-0.9}$)	$\times 10^{-6}$		2250
$\overline{\Lambda}\Lambda K^{*0}$	(	$2.5^{+0.9}_{-0.8}$)	$\times 10^{-6}$		2098
$\overline{\Lambda}\Lambda D^0$	(	$1.1^{+0.6}_{-0.5}$)	$\times 10^{-5}$		1661
$\Delta^0\overline{\Delta}^0$	$<$	1.5	$\times 10^{-3}$	CL=90%	2335
$\Delta^{++}\overline{\Delta}^{--}$	$<$	1.1	$\times 10^{-4}$	CL=90%	2335
$\overline{D}^0 p\overline{p}$	(	1.04 ± 0.07)	$\times 10^{-4}$		1863
$D_s^-\overline{\Lambda}p$	(	2.8 ± 0.9)	$\times 10^{-5}$		1710
$\overline{D}^*(2007)^0 p\overline{p}$	(	9.9 ± 1.1)	$\times 10^{-5}$		1788
$D^*(2010)^- p\overline{n}$	(	1.4 ± 0.4)	$\times 10^{-3}$		1785
$D^- p\overline{p}\pi^+$	(	3.32 ± 0.31)	$\times 10^{-4}$		1786
$D^*(2010)^- p\overline{p}\pi^+$	(	4.7 ± 0.5)	$\times 10^{-4}$	S=1.2	1707
$\overline{D}^0 p\overline{p}\pi^+\pi^-$	(	3.0 ± 0.5)	$\times 10^{-4}$		1708
$\overline{D}^{*0} p\overline{p}\pi^+\pi^-$	(	1.9 ± 0.5)	$\times 10^{-4}$		1623
$\Theta_c\overline{p}\pi^+$, $\Theta_c \to D^- p$	$<$	9	$\times 10^{-6}$	CL=90%	–
$\Theta_c\overline{p}\pi^+$, $\Theta_c \to D^{*-} p$	$<$	1.4	$\times 10^{-5}$	CL=90%	–
$\overline{\Sigma}_c^{--}\Delta^{++}$	$<$	1.0	$\times 10^{-3}$	CL=90%	1839
$\overline{\Lambda}_c^- p\pi^+\pi^-$	(	1.3 ± 0.4)	$\times 10^{-3}$		1934
$\overline{\Lambda}_c^- p$	(	2.0 ± 0.4)	$\times 10^{-5}$		2021
$\overline{\Lambda}_c^- p\pi^0$	(	1.9 ± 0.5)	$\times 10^{-4}$		1982
$\Sigma_c(2455)^- p$	$<$	3.0	$\times 10^{-5}$		–
$\overline{\Lambda}_c^- p\pi^+\pi^-\pi^0$	$<$	5.07	$\times 10^{-3}$	CL=90%	1882
$\overline{\Lambda}_c^- p\pi^+\pi^-\pi^+\pi^-$	$<$	2.74	$\times 10^{-3}$	CL=90%	1821
$\overline{\Lambda}_c^- p\pi^+\pi^-$	(	1.17 ± 0.23)	$\times 10^{-3}$		1934
$\overline{\Lambda}_c^- p\pi^+\pi^-$ (nonresonant)	(	7.1 ± 1.4)	$\times 10^{-4}$		1934
$\overline{\Sigma}_c(2520)^{--} p\pi^+$	(	1.17 ± 0.25)	$\times 10^{-4}$		1860
$\overline{\Sigma}_c(2520)^0 p\pi^-$	$<$	3.1	$\times 10^{-5}$	CL=90%	1860
$\overline{\Sigma}_c(2455)^0 p\pi^-$	(	1.04 ± 0.22)	$\times 10^{-4}$		1895
$\overline{\Sigma}_c(2455)^0 N^0$, $N^0 \to p\pi^-$	(	8.0 ± 2.9)	$\times 10^{-5}$		–
$\overline{\Sigma}_c(2455)^{--} p\pi^+$	(	2.2 ± 0.4)	$\times 10^{-4}$		1895
$\Lambda_c^- p K^+\pi^-$	(	4.3 ± 1.4)	$\times 10^{-5}$		–
$\overline{\Sigma}_c(2455)^{--} p K^+$, $\overline{\Sigma}_c^{--} \to \overline{\Lambda}_c^-\pi^-$	(	1.1 ± 0.4)	$\times 10^{-5}$		1754
$\Lambda_c^- p K^*(892)^0$	$<$	2.42	$\times 10^{-5}$	CL=90%	–
$\overline{\Lambda}_c^- \Lambda K^+$	(	3.8 ± 1.3)	$\times 10^{-5}$		1767
$\overline{\Lambda}_c^- \Lambda_c^+$	$<$	6.2	$\times 10^{-5}$	CL=90%	1319
$\overline{\Lambda}_c(2593)^-$ / $\overline{\Lambda}_c(2625)^- p$	$<$	1.1	$\times 10^{-4}$	CL=90%	–
$\overline{\Xi}_c^- \Lambda_c^+$, $\overline{\Xi}_c^- \to \overline{\Xi}^+\pi^-\pi^-$	(	2.2 ± 2.3)	$\times 10^{-5}$	S=1.9	1147
$\Lambda_c^+\Lambda_c^- K^0$	(	5.4 ± 3.2)	$\times 10^{-4}$		–

Lepton Family number (LF) or Lepton number (L) or Baryon number (B) violating modes, or/and $\Delta B = 1$ weak neutral current ($B1$) modes

$\gamma\gamma$	$B1$	$<$	3.2	$\times 10^{-7}$	CL=90%	2640
$e^+ e^-$	$B1$	$<$	8.3	$\times 10^{-8}$	CL=90%	2640
$e^+ e^-\gamma$	$B1$	$<$	1.2	$\times 10^{-7}$	CL=90%	2640
$\mu^+\mu^-$	$B1$	$<$	6.3	$\times 10^{-10}$	CL=90%	2638
$\mu^+\mu^-\gamma$	$B1$	$<$	1.6	$\times 10^{-7}$	CL=90%	2638
$\mu^+\mu^-\mu^+\mu^-$		$<$	5.3	$\times 10^{-9}$	CL=90%	2629
SP, $S \to \mu^+\mu^-$, $P \to \mu^+\mu^-$	[$ggaa$]	$<$	5.1	$\times 10^{-9}$	CL=90%	–
$\tau^+\tau^-$	$B1$	$<$	4.1	$\times 10^{-3}$	CL=90%	1952
$\pi^0\ell^+\ell^-$	$B1$	$<$	5.3	$\times 10^{-8}$	CL=90%	2638
$\pi^0 e^+ e^-$	$B1$	$<$	8.4	$\times 10^{-8}$	CL=90%	2638
$\pi^0\mu^+\mu^-$	$B1$	$<$	6.9	$\times 10^{-8}$	CL=90%	2634
$\eta\ell^+\ell^-$		$<$	6.4	$\times 10^{-8}$	CL=90%	2611
$\eta e^+ e^-$		$<$	1.08	$\times 10^{-7}$	CL=90%	2611
$\eta\mu^+\mu^-$		$<$	1.12	$\times 10^{-7}$	CL=90%	2607
$\pi^0\nu\overline{\nu}$	$B1$	$<$	6.9	$\times 10^{-5}$	CL=90%	2638
$K^0\ell^+\ell^-$	$B1$	[sss]	($3.1^{+0.8}_{-0.7}$)	$\times 10^{-7}$		2616
$K^0 e^+ e^-$	$B1$		($1.6^{+1.0}_{-0.8}$)	$\times 10^{-7}$		2616
$K^0\mu^+\mu^-$	$B1$		(3.4 ± 0.5)	$\times 10^{-7}$		2612
$K^0\nu\overline{\nu}$	$B1$	$<$	4.9	$\times 10^{-5}$	CL=90%	2616
$\rho^0\nu\overline{\nu}$	$B1$	$<$	2.08	$\times 10^{-4}$	CL=90%	2583
$K^*(892)^0\ell^+\ell^-$	$B1$	[sss]	($9.9^{+1.2}_{-1.1}$)	$\times 10^{-7}$		2564
$K^*(892)^0 e^+ e^-$	$B1$		($1.03^{+0.19}_{-0.17}$)	$\times 10^{-6}$		2564
$K^*(892)^0\mu^+\mu^-$	$B1$		(1.05 ± 0.10)	$\times 10^{-6}$		2560
$K^*(892)^0\nu\overline{\nu}$	$B1$	$<$	5.5	$\times 10^{-5}$	CL=90%	2564
$\phi\nu\overline{\nu}$	$B1$	$<$	1.27	$\times 10^{-4}$	CL=90%	2541
$e^\pm\mu^\mp$	LF	[gg] $<$	2.8	$\times 10^{-9}$	CL=90%	2639
$\pi^0 e^\pm\mu^\mp$	LF	$<$	1.4	$\times 10^{-7}$	CL=90%	2637
$K^0 e^\pm\mu^\mp$	LF	$<$	2.7	$\times 10^{-7}$	CL=90%	2615
$K^*(892)^0 e^+\mu^-$	LF	$<$	5.3	$\times 10^{-7}$	CL=90%	2563
$K^*(892)^0 e^-\mu^+$	LF	$<$	3.4	$\times 10^{-7}$	CL=90%	2563
$K^*(892)^0 e^\pm\mu^\mp$	LF	$<$	5.8	$\times 10^{-7}$	CL=90%	2563
$e^\pm\tau^\mp$	LF	[gg] $<$	2.8	$\times 10^{-5}$	CL=90%	2341
$\mu^\pm\tau^\mp$	LF	[gg] $<$	2.2	$\times 10^{-5}$	CL=90%	2339
invisible	$B1$	$<$	2.4	$\times 10^{-5}$	CL=90%	–
$\nu\overline{\nu}\gamma$	$B1$	$<$	1.7	$\times 10^{-5}$	CL=90%	2640
$\Lambda_c^+\mu^-$	L,B	$<$	1.8	$\times 10^{-6}$	CL=90%	2143
$\Lambda_c^+ e^-$	L,B	$<$	5	$\times 10^{-6}$	CL=90%	2145

$B^\pm/B^0$ ADMIXTURE

CP violation

$A_{CP}(B \to K^*(892)\gamma) = -0.003 \pm 0.017$
$A_{CP}(b \to s\gamma) = -0.008 \pm 0.029$
$A_{CP}(b \to (s+d)\gamma) = -0.01 \pm 0.05$
$A_{CP}(B \to X_s\ell^+\ell^-) = -0.22 \pm 0.26$
$A_{CP}(B \to K^* e^+ e^-) = -0.18 \pm 0.15$
$A_{CP}(B \to K^*\mu^+\mu^-) = -0.03 \pm 0.13$
$A_{CP}(B \to K^*\ell^+\ell^-) = -0.04 \pm 0.07$
$A_{CP}(B \to \eta\text{anything}) = -0.13^{+0.04}_{-0.05}$

The branching fraction measurements are for an admixture of B mesons at the $\Upsilon(4S)$. The values quoted assume that $B(\Upsilon(4S) \to B\overline{B}) = 100\%$.

For inclusive branching fractions, *e.g.*, $B \to D^\pm$ *anything*, the treatment of multiple D's in the final state must be defined. One possibility would be to count the number of events with one-or-more D's and divide by the total number of B's. Another possibility would be to count the total number of D's and divide by the total number of B's, which is the definition of average multiplicity. The two definitions are identical if only one D is allowed in the final state. Even though the "one-or-more" definition seems sensible, for practical reasons inclusive branching fractions are almost always measured using the multiplicity definition. For heavy final state particles, authors call their results inclusive branching fractions while for light particles some authors call their results multiplicities. In the B sections, we list all results as inclusive branching fractions, adopting a multiplicity definition. This means that inclusive branching fractions can exceed 100% and that inclusive partial widths can exceed total widths, just as inclusive cross sections can exceed total cross section.

$\overline{B}$ modes are charge conjugates of the modes below. Reactions indicate the weak decay vertex and do not include mixing.

B DECAY MODES	Fraction (Γ_i/Γ)			Scale factor/ Confidence level	p (MeV/c)
Semileptonic and leptonic modes					
$e^+\nu_e$ anything	[$hhaa$]	(10.86 ± 0.16)	%		–
$\overline{p}e^+\nu_e$ anything		$<$ 5.9	$\times 10^{-4}$	CL=90%	–
$\mu^+\nu_\mu$ anything	[$hhaa$]	(10.86 ± 0.16)	%		–
$\ell^+\nu_\ell$ anything	[sss,$hhaa$]	(10.86 ± 0.16)	%		–
$D^-\ell^+\nu_\ell$ anything	[sss]	(2.8 ± 0.9)	%		–
$\overline{D}^0\ell^+\nu_\ell$ anything	[sss]	(7.3 ± 1.5)	%		–
$\overline{D}\ell^+\nu_\ell$		(2.42 ± 0.12)	%		2310
$\overline{D}\tau^+\nu_\tau$		(1.07 ± 0.18)	%		1911
$D^{*-}\ell^+\nu_\ell$ anything	[$iiaa$]	(6.7 ± 1.3)	$\times 10^{-3}$		–
$D^*\ell^+\nu_\ell$	[$jjaa$]	(4.95 ± 0.11)	%		2257
$D^*\tau^+\nu_\tau$		(1.64 ± 0.15)	%		1837
$\overline{D}^{**}\ell^+\nu_\ell$	[sss,$kkaa$]	(2.7 ± 0.7)	%		–
$\overline{D}_1(2420)\ell^+\nu_\ell$ anything		(3.8 ± 1.3)	$\times 10^{-3}$	S=2.4	–
$D\pi\ell^+\nu_\ell$ anything + $D^*\pi\ell^+\nu_\ell$ anything		(2.6 ± 0.5)	%	S=1.5	–
$D\pi\ell^+\nu_\ell$ anything		(1.5 ± 0.6)	%		–
$D^*\pi\ell^+\nu_\ell$ anything		(1.9 ± 0.4)	%		–
$\overline{D}_2^*(2460)\ell^+\nu_\ell$ anything		(4.4 ± 1.6)	$\times 10^{-3}$		–
$D^{*-}\pi^+\ell^+\nu_\ell$ anything		(1.00 ± 0.34)	%		–
$D_s^-\ell^+\nu_\ell$ anything	[sss]	$<$ 7	$\times 10^{-3}$	CL=90%	–
$D_s^-\ell^+\nu_\ell K^+$ anything	[sss]	$<$ 5	$\times 10^{-3}$	CL=90%	–
$D_s^-\ell^+\nu_\ell K^0$ anything	[sss]	$<$ 7	$\times 10^{-3}$	CL=90%	–

Meson Summary Table

$X_c \ell^+ \nu_\ell$		(10.65 ± 0.16) %				–
$X_u \ell^+ \nu_\ell$		(2.14 ± 0.31) $\times 10^{-3}$				–
$K^+ \ell^+ \nu_\ell$ anything	[sss]	(6.3 ± 0.6) %				–
$K^- \ell^+ \nu_\ell$ anything	[sss]	(10 ± 4) $\times 10^{-3}$				–
$K^0/\overline{K}^0 \ell^+ \nu_\ell$ anything	[sss]	(4.6 ± 0.5) %				–

D, D^*, or D_s modes

$D^\pm$ anything		(23.7 ± 1.3) %				–
$D^0/\overline{D}^0$ anything		(62.7 ± 2.9) %			S=1.3	–
$D^*(2010)^\pm$ anything		(22.5 ± 1.5) %				–
$D^*(2007)^0$ anything		(26.0 ± 2.7) %				–
$D_s^\pm$ anything	[gg]	(8.3 ± 0.8) %				–
$D_s^{*\pm}$ anything		(6.3 ± 1.0) %				–
$D_s^{*\pm}\overline{D}^{(*)}$		(3.4 ± 0.6) %				–
$D^{(*)}\overline{D}^{(*)}K^0 + D^{(*)}\overline{D}^{(*)}K^\pm$	[gg,llaa]	(7.1 $^{+\ 2.7}_{-\ 1.7}$) %				–
$b \to c\overline{c}s$		(22 ± 4) %				–
$D_s^{(*)}\overline{D}^{(*)}$	[gg,llaa]	(3.9 ± 0.4) %				–
$D^* D^*(2010)^\pm$	[gg]	< 5.9		$\times 10^{-3}$	CL=90%	1711
$D D^*(2010)^\pm + D^* D^\pm$	[gg]	< 5.5		$\times 10^{-3}$	CL=90%	–
$D D^\pm$	[gg]	< 3.1		$\times 10^{-3}$	CL=90%	1866
$D_s^{(*)\pm}\overline{D}^{(*)}X(n\pi^\pm)$	[gg,llaa]	(9 $^{+\ 5}_{-\ 4}$) %				–
$D^*(2010)\gamma$		< 1.1		$\times 10^{-3}$	CL=90%	2257
$D_s^+\pi^-$, $D_s^{*+}\pi^-$, $D_s^+\rho^-$, $D_s^{*+}\rho^-$, $D_s^+\pi^0$, $D_s^{*+}\pi^0$, $D_s^+\eta$, $D_s^{*+}\eta$, $D_s^+\rho^0$, $D_s^{*+}\rho^0$, $D_s^+\omega$, $D_s^{*+}\omega$	[gg]	< 4		$\times 10^{-4}$	CL=90%	–
$D_{s1}(2536)^+$ anything		< 9.5		$\times 10^{-3}$	CL=90%	–

Charmonium modes

$J/\psi(1S)$ anything		(1.094 ± 0.032) %			S=1.1	–
$J/\psi(1S)$ (direct) anything		(7.8 ± 0.4) $\times 10^{-3}$			S=1.1	–
$\psi(2S)$ anything		(3.07 ± 0.21) $\times 10^{-3}$				–
$\chi_{c1}(1P)$ anything		(3.86 ± 0.27) $\times 10^{-3}$				–
$\chi_{c1}(1P)$ (direct) anything		(3.24 ± 0.25) $\times 10^{-3}$				–
$\chi_{c2}(1P)$ anything		(1.4 ± 0.4) $\times 10^{-3}$			S=1.9	–
$\chi_{c2}(1P)$ (direct) anything		(1.65 ± 0.31) $\times 10^{-3}$				–
$\eta_c(1S)$ anything		< 9		$\times 10^{-3}$	CL=90%	–
$KX(3872) \times$ B($X \to D^0\overline{D}^0\pi^0$)		(1.2 ± 0.4) $\times 10^{-4}$				1141
$KX(3872) \times$ B($X \to D^{*0}D^0$)		(8.0 ± 2.2) $\times 10^{-5}$				1141
$KX(3940) \times$ B($X \to D^{*0}D^0$)		< 6.7		$\times 10^{-5}$	CL=90%	1084
$K\chi_{c0}(2P)$, $\chi_{c0} \to \omega J/\psi$	[nnaa]	(7.1 ± 3.4) $\times 10^{-5}$				1103

K or K^* modes

$K^\pm$ anything	[gg]	(78.9 ± 2.5) %				–
K^+ anything		(66 ± 5) %				–
K^- anything		(13 ± 4) %				–
$K^0/\overline{K}^0$ anything	[gg]	(64 ± 4) %				–
$K^*(892)^\pm$ anything		(18 ± 6) %				–
$K^*(892)^0/\overline{K}^*(892)^0$ anything	[gg]	(14.6 ± 2.6) %				–
$K^*(892)\gamma$		(4.2 ± 0.6) $\times 10^{-5}$				2564
$\eta K\gamma$		(8.5 $^{+\ 1.8}_{-\ 1.6}$) $\times 10^{-6}$				2588
$K_1(1400)\gamma$		< 1.27		$\times 10^{-4}$	CL=90%	2453
$K_2^*(1430)\gamma$		(1.7 $^{+\ 0.6}_{-\ 0.5}$) $\times 10^{-5}$				2447
$K_2(1770)\gamma$		< 1.2		$\times 10^{-3}$	CL=90%	2342
$K_3^*(1780)\gamma$		< 3.7		$\times 10^{-5}$	CL=90%	2341
$K_4^*(2045)\gamma$		< 1.0		$\times 10^{-3}$	CL=90%	2244
$K\eta'(958)$		(8.3 ± 1.1) $\times 10^{-5}$				2528
$K^*(892)\eta'(958)$		(4.1 ± 1.1) $\times 10^{-6}$				2472
$K\eta$		< 5.2		$\times 10^{-6}$	CL=90%	2588
$K^*(892)\eta$		(1.8 ± 0.5) $\times 10^{-5}$				2534
$K\phi\phi$		(2.3 ± 0.9) $\times 10^{-6}$				2306
$\overline{b} \to \overline{s}\gamma$		(3.40 ± 0.21) $\times 10^{-4}$				–
$\overline{b} \to \overline{d}\gamma$		(9.2 ± 3.0) $\times 10^{-6}$				–
$\overline{b} \to \overline{s}$gluon		< 6.8		%	CL=90%	–
η anything		(2.6 $^{+\ 0.5}_{-\ 0.8}$) $\times 10^{-4}$				–
η' anything		(4.2 ± 0.9) $\times 10^{-4}$				–
K^+gluon (charmless)		< 1.87		$\times 10^{-4}$	CL=90%	–
K^0gluon (charmless)		(1.9 ± 0.7) $\times 10^{-4}$				–

Light unflavored meson modes

$\rho\gamma$		(1.39 ± 0.25) $\times 10^{-6}$			S=1.2	2583
$\rho/\omega\gamma$		(1.30 ± 0.23) $\times 10^{-6}$			S=1.2	–
$\pi^\pm$ anything	[gg,ooaa]	(358 ± 7) %				–
π^0 anything		(235 ±11) %				–
η anything		(17.6 ± 1.6) %				–
ρ^0 anything		(21 ± 5) %				–
ω anything		< 81		%	CL=90%	–
ϕ anything		(3.43 ± 0.12) %				–
$\phi K^*(892)$		< 2.2		$\times 10^{-5}$	CL=90%	2460
π^+ gluon (charmless)		(3.7 ± 0.8) $\times 10^{-4}$				–

Baryon modes

Λ_c^+ / $\overline{\Lambda}_c^-$ anything		(4.5 ± 1.2) %				–
Λ_c^+ anything		< 1.7		%	CL=90%	–
$\overline{\Lambda}_c^-$ anything		< 9		%	CL=90%	–
$\overline{\Lambda}_c^- \ell^+$ anything		< 1.1		$\times 10^{-3}$	CL=90%	–
$\overline{\Lambda}_c^- e^+$ anything		< 2.3		$\times 10^{-3}$	CL=90%	–
$\overline{\Lambda}_c^- \mu^+$ anything		< − 1.8		$\times 10^{-3}$	CL=90%	–
$\overline{\Lambda}_c^- p$ anything		(2.6 ± 0.8) %				–
$\overline{\Lambda}_c^- p e^+ \nu_e$		< 1.0		$\times 10^{-3}$	CL=90%	2021
$\overline{\Sigma}_c^{--}$ anything		(4.2 ± 2.4) $\times 10^{-3}$				–
$\overline{\Sigma}_c^-$ anything		< 9.6		$\times 10^{-3}$	CL=90%	–
$\overline{\Sigma}_c^0$ anything		(4.6 ± 2.4) $\times 10^{-3}$				–
$\overline{\Sigma}_c^0 N(N = p$ or $n)$		< 1.5		$\times 10^{-3}$	CL=90%	1938
Ξ_c^0 anything $\times$ B($\Xi_c^0 \to \Xi^-\pi^+$)		(1.93 ± 0.30) $\times 10^{-4}$			S=1.1	–
Ξ_c^+ anything $\times$ B($\Xi_c^+ \to \Xi^-\pi^+\pi^+$)		(4.5 $^{+\ 1.3}_{-\ 1.2}$) $\times 10^{-4}$				–
$p/\overline{p}$ anything	[gg]	(8.0 ± 0.4) %				–
$p/\overline{p}$ (direct) anything	[gg]	(5.5 ± 0.5) %				–
$\Lambda/\overline{\Lambda}$ anything	[gg]	(4.0 ± 0.5) %				–
$\Xi^-/\overline{\Xi}^+$ anything	[gg]	(2.7 ± 0.6) $\times 10^{-3}$				–
baryons anything		(6.8 ± 0.6) %				–
$p\overline{p}$ anything		(2.47 ± 0.23) %				–
$\Lambda\overline{p}/\overline{\Lambda}p$ anything	[gg]	(2.5 ± 0.4) %				–
$\Lambda\overline{\Lambda}$ anything		< 5		$\times 10^{-3}$	CL=90%	–

Lepton Family number (LF) violating modes or $\Delta B = 1$ weak neutral current ($B1$) modes

$s e^+ e^-$	$B1$	(4.7 ± 1.3) $\times 10^{-6}$				–
$s\mu^+\mu^-$	$B1$	(4.3 ± 1.2) $\times 10^{-6}$				–
$s\ell^+\ell^-$	$B1$	[sss] (4.5 ± 1.0) $\times 10^{-6}$				–
$\pi\ell^+\ell^-$	$B1$	< 5.9		$\times 10^{-8}$	CL=90%	2638
$\pi e^+ e^-$		< 1.10		$\times 10^{-7}$	CL=90%	2638
$\pi\mu^+\mu^-$		< 5.0		$\times 10^{-8}$	CL=90%	2634
$K e^+ e^-$	$B1$	(4.4 ± 0.6) $\times 10^{-7}$				2617
$K^*(892) e^+ e^-$	$B1$	(1.19 ± 0.20) $\times 10^{-6}$			S=1.2	2564
$K\mu^+\mu^-$	$B1$	(4.4 ± 0.4) $\times 10^{-7}$				2612
$K^*(892)\mu^+\mu^-$	$B1$	(1.06 ± 0.09) $\times 10^{-6}$				2560
$K\ell^+\ell^-$	$B1$	(4.8 ± 0.4) $\times 10^{-7}$				2617
$K^*(892)\ell^+\ell^-$	$B1$	(1.05 ± 0.10) $\times 10^{-6}$				2564
$K\nu\overline{\nu}$	$B1$	< 1.7		$\times 10^{-5}$	CL=90%	2617
$K^*\nu\overline{\nu}$	$B1$	< 7.6		$\times 10^{-5}$	CL=90%	–
$s e^\pm \mu^\mp$	LF	[gg] < 2.2		$\times 10^{-5}$	CL=90%	–
$\pi e^\pm \mu^\mp$	LF	< 9.2		$\times 10^{-8}$	CL=90%	2637
$\rho e^\pm \mu^\mp$	LF	< 3.2		$\times 10^{-6}$	CL=90%	2582
$K e^\pm \mu^\mp$	LF	< 3.8		$\times 10^{-8}$	CL=90%	2616
$K^*(892) e^\pm \mu^\mp$	LF	< 5.1		$\times 10^{-7}$	CL=90%	2563

$B^\pm/B^0/B_s^0/b$-baryon ADMIXTURE

These measurements are for an admixture of bottom particles at high energy (LHC, LEP, Tevatron, S$p\overline{p}$S).

Mean life $\tau = (1.568 \pm 0.009) \times 10^{-12}$ s

Mean life $\tau = (1.72 \pm 0.10) \times 10^{-12}$ s Charged b-hadron admixture

Mean life $\tau = (1.58 \pm 0.14) \times 10^{-12}$ s Neutral b-hadron admixture

$\tau_{\text{charged } b\text{-hadron}}/\tau_{\text{neutral } b\text{-hadron}} = 1.09 \pm 0.13$

$|\Delta\tau_b|/\tau_{b,\overline{b}} = -0.001 \pm 0.014$

$\text{Re}(\epsilon_b)\ /\ (1 + |\epsilon_b|^2) = (1.2 \pm 0.4) \times 10^{-3}$

The branching fraction measurements are for an admixture of B mesons and baryons at energies above the $\Upsilon(4S)$. Only the highest energy results (LHC, LEP, Tevatron, S$p\overline{p}$S) are used in the branching fraction averages. In the following, we assume that the production fractions are the same at the LHC, LEP, and at the Tevatron.

For inclusive branching fractions, *e.g.*, $B \to D^{\pm}$anything, the values usually are multiplicities, not branching fractions. They can be greater than one.

The modes below are listed for a $\overline{b}$ initial state. b modes are their charge conjugates. Reactions indicate the weak decay vertex and do not include mixing.

$\overline{b}$ DECAY MODES	Fraction (Γ_i/Γ)	Scale factor/ Confidence level	p (MeV/c)

PRODUCTION FRACTIONS

The production fractions for weakly decaying b-hadrons at high energy have been calculated from the best values of mean lives, mixing parameters, and branching fractions in this edition by the Heavy Flavor Averaging Group (HFAG) as described in the note "B^0-$\overline{B}^0$ Mixing" in the B^0 Particle Listings. The production fractions in b-hadronic Z decay or $p\overline{p}$ collisions at the Tevatron are also listed at the end of the section. Values assume

$$\mathrm{B}(\overline{b} \to B^+) = \mathrm{B}(\overline{b} \to B^0)$$
$$\mathrm{B}(\overline{b} \to B^+) + \mathrm{B}(\overline{b} \to B^0) + \mathrm{B}(\overline{b} \to B_s^0) + \mathrm{B}(b \to b\text{-baryon}) = 100\ \%.$$

The correlation coefficients between production fractions are also reported:

$cor(B_s^0, b\text{-baryon}) = -0.291$
$cor(B_s^0, B^{\pm}{=}B^0) = -0.083$
$cor(b\text{-baryon}, B^{\pm}{=}B^0) = -0.929.$

The notation for production fractions varies in the literature (f_d, d_{B^0}, $f(b \to \overline{B}^0)$, Br($b \to \overline{B}^0$)). We use our own branching fraction notation here, B($\overline{b} \to B^0$).

Note these production fractions are b-hadronization fractions, not the conventional branching fractions of b-quark to a B-hadron, which may have considerable dependence on the initial and final state kinematic and production environment.

B^+	(40.2 ± 0.7) %		–
B^0	(40.2 ± 0.7) %		–
B_s^0	(10.5 ± 0.6) %		–
b-baryon	(9.2 ± 1.5) %		–

DECAY MODES

Semileptonic and leptonic modes

νanything		(23.1 ± 1.5) %		–
$\ell^+ \nu_\ell$anything	[sss]	(10.69± 0.22) %		–
$e^+ \nu_e$anything		(10.86± 0.35) %		–
$\mu^+ \nu_\mu$anything		($10.95^{+0.29}_{-0.25}$) %		–
$D^- \ell^+ \nu_\ell$anything	[sss]	(2.27± 0.35) %	S=1.7	–
$D^- \pi^+ \ell^+ \nu_\ell$anything		(4.9 ± 1.9) × 10^{-3}		–
$D^- \pi^- \ell^+ \nu_\ell$anything		(2.6 ± 1.6) × 10^{-3}		–
$\overline{D}^0 \ell^+ \nu_\ell$anything	[sss]	(6.84± 0.35) %		–
$\overline{D}^0 \pi^- \ell^+ \nu_\ell$anything		(1.07± 0.27) %		–
$\overline{D}^0 \pi^+ \ell^+ \nu_\ell$anything		(2.3 ± 1.6) × 10^{-3}		–
$D^{*-} \ell^+ \nu_\ell$anything	[sss]	(2.75± 0.19) %		–
$D^{*-} \pi^- \ell^+ \nu_\ell$anything		(6 ± 7) × 10^{-4}		–
$D^{*-} \pi^+ \ell^+ \nu_\ell$anything		(4.8 ± 1.0) × 10^{-3}		–
$\overline{D}_j^0 \ell^+ \nu_\ell$anything × B($\overline{D}_j^0 \to D^{*+}\pi^-$)	[sss,ppaa]	(2.6 ± 0.9) × 10^{-3}		–
$D_j^- \ell^+ \nu_\ell$anything × B($D_j^- \to D^0\pi^-$)	[sss,ppaa]	(7.0 ± 2.3) × 10^{-3}		–
$\overline{D}_2^*(2460)^0 \ell^+ \nu_\ell$anything × B($\overline{D}_2^*(2460)^0 \to D^{*-}\pi^+$)		< 1.4 × 10^{-3}	CL=90%	–
$D_2^*(2460)^- \ell^+ \nu_\ell$anything × B($D_2^*(2460)^- \to D^0\pi^-$)		($4.2^{+1.5}_{-1.8}$) × 10^{-3}		–
$\overline{D}_2^*(2460)^0 \ell^+ \nu_\ell$anything × B($\overline{D}_2^*(2460)^0 \to D^-\pi^+$)		(1.6 ± 0.8) × 10^{-3}		–
charmless $\ell\overline{\nu}_\ell$	[sss]	(1.7 ± 0.5) × 10^{-3}		–
$\tau^+ \nu_\tau$anything		(2.41± 0.23) %		–
$D^{*-} \tau \nu_\tau$anything		(9 ± 4) × 10^{-3}		–
$\overline{c} \to \ell^- \overline{\nu}_\ell$anything	[sss]	(8.02± 0.19) %		–
$c \to \ell^+ \nu$anything		($1.6^{+0.4}_{-0.5}$) %		–

Charmed meson and baryon modes

$\overline{D}^0$anything		(59.8 ± 2.9) %		–
$D^0 D_s^{\pm}$anything	[gg]	($9.1^{+4.0}_{-2.8}$) %		–
$D^{\mp} D_s^{\pm}$anything	[gg]	($4.0^{+2.3}_{-1.8}$) %		–
$\overline{D}^0 D^0$anything	[gg]	($5.1^{+2.0}_{-1.8}$) %		–
$D^0 D^{\pm}$anything	[gg]	($2.7^{+1.8}_{-1.6}$) %		–
$D^{\pm} D^{\mp}$anything	[gg]	< 9 × 10^{-3}	CL=90%	–
D^-anything		(23.3 ± 1.7) %		–
$D^*(2010)^+$anything		(17.3 ± 2.0) %		–
$D_1(2420)^0$anything		(5.0 ± 1.5) %		–
$D^*(2010)^{\mp} D_s^{\pm}$anything	[gg]	($3.3^{+1.6}_{-1.3}$) %		–
$D^0 D^*(2010)^{\pm}$anything	[gg]	($3.0^{+1.1}_{-0.9}$) %		–
$D^*(2010)^{\pm} D^{\mp}$anything	[gg]	($2.5^{+1.2}_{-1.0}$) %		–
$D^*(2010)^{\pm} D^*(2010)^{\mp}$anything	[gg]	(1.2 ± 0.4) %		–
$\overline{D}D$anything		(10^{+11}_{-10}) %		–
$D_2^*(2460)^0$anything		(4.7 ± 2.7) %		–
D_s^-anything		(14.7 ± 2.1) %		–
D_s^+anything		(10.1 ± 3.1) %		–
Λ_c^+anything		(9.7 ± 2.9) %		–
$\overline{c}/c$ anything	[ooaa]	(116.2 ± 3.2) %		–

Charmonium modes

$J/\psi(1S)$anything		(1.16± 0.10) %		–
$\psi(2S)$anything		(2.83± 0.29) × 10^{-3}		–
$\chi_{c1}(1P)$anything		(1.4 ± 0.4) %		–

K or K^* modes

$\overline{s}\gamma$		(3.1 ± 1.1) × 10^{-4}		–
$\overline{s}\overline{\nu}\nu$	B1	< 6.4 × 10^{-4}	CL=90%	–
$K^{\pm}$anything		(74 ± 6) %		–
K_S^0anything		(29.0 ± 2.9) %		–

Pion modes

$\pi^{\pm}$anything		(397 ±21) %		–
π^0anything	[ooaa]	(278 ±60) %		–
ϕanything		(2.82± 0.23) %		–

Baryon modes

$p/\overline{p}$anything		(13.1 ± 1.1) %		–
$\Lambda/\overline{\Lambda}$anything		(5.9 ± 0.6) %		–
b-baryon anything		(10.2 ± 2.8) %		–

Other modes

charged anything	[ooaa]	(497 ± 7) %		–
hadron$^+$ hadron$^-$		($1.7^{+1.0}_{-0.7}$) × 10^{-5}		–
charmless		(7 ±21) × 10^{-3}		–

$\Delta B = 1$ weak neutral current ($B1$) modes

$\mu^+ \mu^-$anything	B1	< 3.2 × 10^{-4}	CL=90%	–

B^*

$I(J^P) = \frac{1}{2}(1^-)$

I, J, P need confirmation. Quantum numbers shown are quark-model predictions.

Mass $m_{B^*} = 5325.2 \pm 0.4$ MeV
$m_{B^*} - m_B = 45.78 \pm 0.35$ MeV
$m_{B^{*+}} - m_{B^+} = 45.0 \pm 0.4$ MeV

B^* DECAY MODES	Fraction (Γ_i/Γ)	p (MeV/c)
$B\gamma$	dominant	45

$B_1(5721)^0$

$I(J^P) = \frac{1}{2}(1^+)$
I, J, P need confirmation.

$B_1(5721)^0$ MASS = 5723.5 ± 2.0 MeV (S = 1.1)
$m_{B_1^0} - m_{B^+} = 444.3 \pm 2.0$ MeV (S = 1.1)

$B_1(5721)^0$ DECAY MODES	Fraction (Γ_i/Γ)	p (MeV/c)
$B^{*+}\pi^-$	dominant	–

Meson Summary Table

$B_2^*(5747)^0$

$I(J^P) = \frac{1}{2}(2^+)$
I, J, P need confirmation.

$B_2^*(5747)^0$ MASS = 5743 ± 5 MeV (S = 2.9)
Full width $\Gamma = 23^{+5}_{-11}$ MeV
$m_{B_2^{*0}} - m_{B_1^0} = 19 \pm 6$ MeV (S = 3.0)

$B_2^*(5747)^0$ DECAY MODES	Fraction (Γ_i/Γ)	p (MeV/c)
$B^+\pi^-$	dominant	424
$B^{*+}\pi^-$	dominant	–

BOTTOM, STRANGE MESONS ($B = \pm 1, S = \mp 1$)

$B_s^0 = s\overline{b}$, $\overline{B}_s^0 = \overline{s}b$, similarly for B_s^*'s

B_s^0

$I(J^P) = 0(0^-)$

I, J, P need confirmation. Quantum numbers shown are quark-model predictions.

Mass $m_{B_s^0} = 5366.77 \pm 0.24$ MeV
$m_{B_s^0} - m_B = 87.35 \pm 0.23$ MeV
Mean life $\tau = (1.512 \pm 0.007) \times 10^{-12}$ s
$c\tau = 453.3\ \mu$m
$\Delta\Gamma_{B_s^0} = \Gamma_{B_{sL}^0} - \Gamma_{B_{sH}^0} = (0.091 \pm 0.008) \times 10^{12}\ s^{-1}$

B_s^0-$\overline{B}_s^0$ mixing parameters

$\Delta m_{B_s^0} = m_{B_{sH}^0} - m_{B_{sL}^0} = (17.761 \pm 0.022) \times 10^{12}\ \hbar\ s^{-1}$
$= (1.1691 \pm 0.0014) \times 10^{-8}$ MeV
$x_s = \Delta m_{B_s^0}/\Gamma_{B_s^0} = 26.85 \pm 0.13$
$\chi_s = 0.499311 \pm 0.000007$

CP violation parameters in B_s^0

$\mathrm{Re}(\epsilon_{B_s^0}) / (1 + |\epsilon_{B_s^0}|^2) = (-1.9 \pm 1.0) \times 10^{-3}$
$C_{KK}(B_s^0 \to K^+K^-) = 0.14 \pm 0.11$
$S_{KK}(B_s^0 \to K^+K^-) = 0.30 \pm 0.13$
CP Violation phase $\beta_s = (0.0 \pm 3.5) \times 10^{-2}$
$A_{CP}(B_s \to \pi^+K^-) = 0.28 \pm 0.04$
$A_{CP}(B_s^0 \to [K^+K^-]_D \overline{K}^*(892)^0) = 0.04 \pm 0.16$

These branching fractions all scale with $B(\overline{b} \to B_s^0)$.

The branching fraction $B(B_s^0 \to D_s^-\ell^+\nu_\ell \text{anything})$ is not a pure measurement since the measured product branching fraction $B(\overline{b} \to B_s^0) \times B(B_s^0 \to D_s^-\ell^+\nu_\ell \text{anything})$ was used to determine $B(\overline{b} \to B_s^0)$, as described in the note on "B^0-$\overline{B}^0$ Mixing"

For inclusive branching fractions, *e.g.*, $B \to D^\pm$ anything, the values usually are multiplicities, not branching fractions. They can be greater than one.

B_s^0 DECAY MODES		Fraction (Γ_i/Γ)	Scale factor/ Confidence level	p (MeV/c)
D_s^- anything		(93 ±25) %		–
$\ell\nu_\ell X$		(10.5 ± 0.8) %		–
$D_s^-\ell^+\nu_\ell$ anything	[qqaa]	(7.9 ± 2.4) %		–
$D_{s1}(2536)^-\mu^+\nu_\mu$, $D_{s1}^- \to D^{*-}K_S^0$		(2.5 ± 0.7) × 10^{-3}		–
$D_{s1}(2536)^- X\mu^+\nu$, $D_{s1}^- \to \overline{D}^0K^+$		(4.3 ± 1.7) × 10^{-3}		–
$D_{s2}(2573)^- X\mu^+\nu$, $D_{s2}^- \to \overline{D}^0K^+$		(2.6 ± 1.2) × 10^{-3}		–
$D_s^-\pi^+$		(3.04± 0.23) × 10^{-3}		2320
$D_s^-\rho^+$		(7.0 ± 1.5) × 10^{-3}		2249
$D_s^-\pi^+\pi^+\pi^-$		(6.3 ± 1.1) × 10^{-3}		2301
$D_{s1}(2536)^-\pi^+$, $D_{s1}^- \to D_s^-\pi^+\pi^-$		(2.5 ± 0.8) × 10^{-5}		–
$D_s^\mp K^\pm$		(2.03± 0.28) × 10^{-4}	S=1.3	2293
$D_s^-K^+\pi^+\pi^-$		(3.3 ± 0.7) × 10^{-4}		2249
$D_s^+D_s^-$		(4.4 ± 0.5) × 10^{-3}		1824
$D_s^-D^+$		(3.6 ± 0.8) × 10^{-4}		1875
D^+D^-		(2.2 ± 0.6) × 10^{-4}		1925
$D^0\overline{D}^0$		(1.9 ± 0.5) × 10^{-4}		1929
$D_s^{*-}\pi^+$		(2.0 ± 0.5) × 10^{-3}		2265
$D_s^{*-}\rho^+$		(9.7 ± 2.2) × 10^{-3}		2191
$D_s^{*+}D_s^- + D_s^{*-}D_s^+$		(1.28± 0.23) %	S=1.2	1742
$D_s^{*+}D_s^{*-}$		(1.85± 0.30) %		1655
$D_s^{(*)+}D_s^{(*)-}$		(4.5 ± 1.4) %		–
$\overline{D}^0K^-\pi^+$		(9.9 ± 1.5) × 10^{-4}		2312
$\overline{D}^0\overline{K}^*(892)^0$		(3.5 ± 0.6) × 10^{-4}		2264
$\overline{D}^0K^+K^-$		(4.2 ± 1.9) × 10^{-5}		2242
$\overline{D}^0\phi$		(2.4 ± 0.7) × 10^{-5}		2235
$D^{*\mp}\pi^\pm$		< 6.1 × 10^{-6}	CL=90%	–
$J/\psi(1S)\phi$		(1.07± 0.09) × 10^{-3}		1588
$J/\psi(1S)\pi^0$		< 1.2 × 10^{-3}	CL=90%	1786
$J/\psi(1S)\eta$		(4.0 ± 0.7) × 10^{-4}	S=1.3	1733
$J/\psi(1S)K_S^0$		(1.87± 0.17) × 10^{-5}		1743
$J/\psi(1S)K^*(892)^0$		(4.4 ± 0.9) × 10^{-5}		1637
$J/\psi(1S)\eta'$		(3.4 ± 0.5) × 10^{-4}		1612
$J/\psi(1S)\pi^+\pi^-$		(2.12± 0.19) × 10^{-4}		1775
$J/\psi(1S)f_0(980)$, $f_0 \to \pi^+\pi^-$		(1.39± 0.14) × 10^{-4}		–
$J/\psi(1S)f_0(1370)$, $f_0 \to \pi^+\pi^-$		(3.9 $^{+0.8}_{-1.8}$) × 10^{-5}		–
$J/\psi(1S)f_2(1270)$, $f_2 \to \pi^+\pi^-$		(1.1 ± 0.4) × 10^{-6}		–
$J/\psi(1S)\pi^+\pi^-$ (nonresonant)		(1.8 $^{+1.1}_{-0.4}$) × 10^{-5}		1775
$J/\psi(1S)K^+K^-$		(7.9 ± 0.7) × 10^{-4}		1601
$J/\psi(1S)f_2'(1525)$		(2.6 ± 0.6) × 10^{-4}		1304
$J/\psi(1S)p\overline{p}$		< 4.8 × 10^{-6}	CL=90%	982
$\psi(2S)\eta$		(3.3 ± 0.9) × 10^{-4}		1338
$\psi(2S)\pi^+\pi^-$		(7.2 ± 1.2) × 10^{-5}		1397
$\psi(2S)\phi$		(5.4 ± 0.6) × 10^{-4}		1120
$\chi_{c1}\phi$		(2.02± 0.30) × 10^{-4}		1274
$\pi^+\pi^-$		(7.6 ± 1.9) × 10^{-7}	S=1.4	2680
$\pi^0\pi^0$		< 2.1 × 10^{-4}	CL=90%	2680
$\eta\pi^0$		< 1.0 × 10^{-3}	CL=90%	2654
$\eta\eta$		< 1.5 × 10^{-3}	CL=90%	2627
$\rho^0\rho^0$		< 3.20 × 10^{-4}	CL=90%	2569
$\phi\rho^0$		< 6.17 × 10^{-4}	CL=90%	2526
$\phi\phi$		(1.91± 0.31) × 10^{-5}		2482
π^+K^-		(5.5 ± 0.6) × 10^{-6}		2659
K^+K^-		(2.49± 0.17) × 10^{-5}		2638
$K^0\overline{K}^0$		< 6.6 × 10^{-5}	CL=90%	2637
$K^0\pi^+\pi^-$		(1.9 ± 0.5) × 10^{-5}		2653
$K^0K^\pm\pi^\mp$		(9.7 ± 1.7) × 10^{-5}		2622
$K^0K^+K^-$		< 4 × 10^{-6}	CL=90%	2568
$\overline{K}^*(892)^0\rho^0$		< 7.67 × 10^{-4}	CL=90%	2550
$\overline{K}^*(892)^0K^*(892)^0$		(2.8 ± 0.7) × 10^{-5}		2531
$\phi K^*(892)^0$		(1.13± 0.30) × 10^{-6}		2507
$p\overline{p}$		(2.8 $^{+2.2}_{-1.7}$) × 10^{-8}		2514
$\Lambda_c^-\Lambda\pi^+$		(3.6 ± 1.6) × 10^{-4}		–
$\gamma\gamma$	B1	< 8.7 × 10^{-6}	CL=90%	2683
$\phi\gamma$		(3.6 ± 0.4) × 10^{-5}		2587

Lepton Family number (LF) violating modes or $\Delta B = 1$ weak neutral current ($B1$) modes

$\mu^+\mu^-$	B1		(3.1 ± 0.7) × 10^{-9}		2681
e^+e^-	B1		< 2.8 × 10^{-7}	CL=90%	2683
$e^\pm\mu^\mp$	LF	[gg]	< 1.1 × 10^{-8}	CL=90%	2682
$\mu^+\mu^-\mu^+\mu^-$			< 1.2 × 10^{-8}	CL=90%	2673
SP, $S \to \mu^+\mu^-$, $P \to \mu^+\mu^-$		[ggaa]	< 1.2 × 10^{-8}	CL=90%	–
$\phi(1020)\mu^+\mu^-$	B1		(7.6 ± 1.5) × 10^{-7}		2582
$\phi\nu\overline{\nu}$	B1		< 5.4 × 10^{-3}	CL=90%	2587

B_s^*

$I(J^P) = 0(1^-)$

I, J, P need confirmation. Quantum numbers shown are quark-model predictions.

Mass $m = 5415.4^{+2.4}_{-2.1}$ MeV (S = 3.0)
$m_{B_s^*} - m_{B_s} = 48.7^{+2.3}_{-2.1}$ MeV (S = 2.8)

B_s^* DECAY MODES	Fraction (Γ_i/Γ)	p (MeV/c)
$B_s\gamma$	dominant	–

$B_{s1}(5830)^0$

$I(J^P) = 0(1^+)$
I, J, P need confirmation.

Mass $m = 5828.7 \pm 0.4$ MeV (S = 1.2)
$m_{B^0_{s1}} - m_{B^{*+}} = 504.41 \pm 0.25$ MeV

$B_{s1}(5830)^0$ DECAY MODES	Fraction (Γ_i/Γ)	p (MeV/c)
$B^{*+}K^-$	dominant	–

$B^*_{s2}(5840)^0$

$I(J^P) = 0(2^+)$
I, J, P need confirmation.

Mass $m = 5839.96 \pm 0.20$ MeV
$m_{B^{*0}_{s2}} - m_{B^0_{s1}} = 10.5 \pm 0.6$ MeV
Full width $\Gamma = 1.6 \pm 0.5$ MeV

$B^*_{s2}(5840)^0$ DECAY MODES	Fraction (Γ_i/Γ)	p (MeV/c)
B^+K^-	dominant	253

BOTTOM, CHARMED MESONS ($B = C = \pm 1$)

$B_c^+ = c\overline{b}$, $B_c^- = \overline{c}b$, similarly for B_c^*'s

$B_c^\pm$

$I(J^P) = 0(0^-)$
I, J, P need confirmation.

Quantum numbers shown are quark-model predicitions.

Mass $m = 6.2756 \pm 0.0011$ GeV
Mean life $\tau = (0.452 \pm 0.033) \times 10^{-12}$ s

B_c^- modes are charge conjugates of the modes below.

B_c^+ DECAY MODES × B($\overline{b} \to B_c$)	Fraction (Γ_i/Γ)	Confidence level	p (MeV/c)
The following quantities are not pure branching ratios; rather the fraction $\Gamma_i/\Gamma \times$ B($\overline{b} \to B_c$).			
$J/\psi(1S)\ell^+\nu_\ell$ anything	$(5.2\ ^{+2.4}_{-2.1}) \times 10^{-5}$		–
$J/\psi(1S)\pi^+$	seen		2371
$J/\psi(1S)K^+$	seen		2342
$J/\psi(1S)\pi^+\pi^+\pi^-$	seen		2351
$J/\psi(1S)a_1(1260)$	$< 1.2 \times 10^{-3}$	90%	2170
$J/\psi(1S)K^+K^-\pi^+$	seen		2203
$\psi(2S)\pi^+$	seen		2052
$J/\psi(1S)D_s^+$	seen		1822
$J/\psi(1S)D_s^{*+}$	seen		1728
$D^*(2010)^+\overline{D}^0$	$< 6.2 \times 10^{-3}$	90%	2467
D^+K^{*0}	$< 0.20 \times 10^{-6}$	90%	2783
$D^+\overline{K}^{*0}$	$< 0.16 \times 10^{-6}$	90%	2783
$D_s^+K^{*0}$	$< 0.28 \times 10^{-6}$	90%	2752
$D_s^+\overline{K}^{*0}$	$< 0.4 \times 10^{-6}$	90%	2752
$D_s^+\phi$	$< 0.32 \times 10^{-6}$	90%	2728
K^+K^0	$< 4.6 \times 10^{-7}$	90%	3098
$B_s^0\pi^+$ / B($\overline{b} \to B_s$)	$(2.37^{+0.37}_{-0.35}) \times 10^{-3}$		–

$c\overline{c}$ MESONS

$\eta_c(1S)$

$I^G(J^{PC}) = 0^+(0^{-+})$

Mass $m = 2983.6 \pm 0.7$ MeV (S = 1.3)
Full width $\Gamma = 32.2 \pm 0.9$ MeV

$\eta_c(1S)$ DECAY MODES	Fraction (Γ_i/Γ)	Confidence level	p (MeV/c)
Decays involving hadronic resonances			
$\eta'(958)\pi\pi$	(4.1 ±1.7) %		1323
$\rho\rho$	(1.8 ±0.5) %		1275
$K^*(892)^0K^-\pi^+$ + c.c.	(2.0 ±0.7) %		1277
$K^*(892)\overline{K}^*(892)$	(7.0 ±1.3) $\times 10^{-3}$		1196
$K^{*0}\overline{K}^{*0}\pi^+\pi^-$	(1.1 ±0.5) %		1073
ϕK^+K^-	(2.9 ±1.4) $\times 10^{-3}$		1104
$\phi\phi$	(1.76±0.20) $\times 10^{-3}$		1089
$\phi 2(\pi^+\pi^-)$	$< 4 \times 10^{-3}$	90%	1251
$a_0(980)\pi$	< 2 %	90%	1327
$a_2(1320)\pi$	< 2 %	90%	1196
$K^*(892)\overline{K}$ + c.c.	< 1.28 %	90%	1309
$f_2(1270)\eta$	< 1.1 %	90%	1145
$\omega\omega$	$< 3.1 \times 10^{-3}$	90%	1270
$\omega\phi$	$< 1.7 \times 10^{-3}$	90%	1185
$f_2(1270)f_2(1270)$	(9.8 ±2.5) $\times 10^{-3}$		774
$f_2(1270)f_2'(1525)$	(9.7 ±3.2) $\times 10^{-3}$		513
Decays into stable hadrons			
$K\overline{K}\pi$	(7.3 ±0.5) %		1381
$\eta\pi^+\pi^-$	(1.7 ±0.5) %		1428
$\eta 2(\pi^+\pi^-)$	(4.4 ±1.3) %		1385
$K^+K^-\pi^+\pi^-$	(6.9 ±1.1) $\times 10^{-3}$		1345
$K^+K^-\pi^+\pi^-\pi^0$	(3.5 ±0.6) %		1304
$K^0K^-\pi^+\pi^-\pi^+$ + c.c.	(5.6 ±1.5) %		–
$K^+K^-2(\pi^+\pi^-)$	(7.5 ±2.4) $\times 10^{-3}$		1253
$2(K^+K^-)$	(1.47±0.31) $\times 10^{-3}$		1055
$\pi^+\pi^-\pi^0\pi^0$	(4.7 ±1.0) %		1460
$2(\pi^+\pi^-)$	(9.7 ±1.2) $\times 10^{-3}$		1459
$2(\pi^+\pi^-\pi^0)$	(17.4 ±3.3) %		1409
$3(\pi^+\pi^-)$	(1.8 ±0.4) %		1407
$p\overline{p}$	(1.52±0.16) $\times 10^{-3}$		1160
$p\overline{p}\pi^0$	(3.6 ±1.3) $\times 10^{-3}$		1101
$\Lambda\overline{\Lambda}$	(1.09±0.24) $\times 10^{-3}$		990
$\Sigma^+\overline{\Sigma}^-$	(2.1 ±0.6) $\times 10^{-3}$		901
$\Xi^-\overline{\Xi}^+$	(8.9 ±2.7) $\times 10^{-4}$		692
$K\overline{K}\eta$	(10 ±5) $\times 10^{-3}$		1265
$\pi^+\pi^-p\overline{p}$	(5.3 ±1.8) $\times 10^{-3}$		1027
Radiative decays			
$\gamma\gamma$	(1.57±0.12) $\times 10^{-4}$		1492
Charge conjugation (C), Parity (P), Lepton family number (LF) violating modes			
$\pi^+\pi^-$	P,CP $< 1.1 \times 10^{-4}$	90%	1485
$\pi^0\pi^0$	P,CP $< 3.5 \times 10^{-5}$	90%	1486
K^+K^-	P,CP $< 6 \times 10^{-4}$	90%	1408
$K^0_SK^0_S$	P,CP $< 3.1 \times 10^{-4}$	90%	1406

$J/\psi(1S)$

$I^G(J^{PC}) = 0^-(1^{--})$

Mass $m = 3096.916 \pm 0.011$ MeV
Full width $\Gamma = 92.9 \pm 2.8$ keV (S = 1.1)
$\Gamma_{ee} = 5.55 \pm 0.14 \pm 0.02$ keV

$J/\psi(1S)$ DECAY MODES	Fraction (Γ_i/Γ)	Scale factor/ Confidence level	p (MeV/c)
hadrons	(87.7 ±0.5) %		–
virtual $\gamma \to$ hadrons	(13.50 ±0.30) %		–
ggg	(64.1 ±1.0) %		–
γgg	(8.8 ±1.1) %		–
e^+e^-	(5.971±0.032) %		1548
$e^+e^-\gamma$ [rraa]	(8.8 ±1.4) $\times 10^{-3}$		1548
$\mu^+\mu^-$	(5.961±0.033) %		1545
Decays involving hadronic resonances			
$\rho\pi$	(1.69 ±0.15) %	S=2.4	1448
$\rho^0\pi^0$	(5.6 ±0.7) $\times 10^{-3}$		1448
$a_2(1320)\rho$	(1.09 ±0.22) %		1123
$\omega\pi^+\pi^+\pi^-\pi^-$	(8.5 ±3.4) $\times 10^{-3}$		1392
$\omega\pi^+\pi^-\pi^0$	(4.0 ±0.7) $\times 10^{-3}$		1418
$\omega\pi^+\pi^-$	(8.6 ±0.7) $\times 10^{-3}$	S=1.1	1435
$\omega f_2(1270)$	(4.3 ±0.6) $\times 10^{-3}$		1142
$K^*(892)^0\overline{K}^*(892)^0$	(2.3 ±0.7) $\times 10^{-4}$		1266
$K^*(892)^\pm K^*(892)^\mp$	(1.00 $^{+0.22}_{-0.40}$) $\times 10^{-3}$		1266

Meson Summary Table

$K^*(892)^\pm K^*(800)^\mp$		$(1.1 \ {}^{+1.0}_{-0.6}) \times 10^{-3}$		–
$\eta K^*(892)^0 \overline{K}^*(892)^0$		$(1.15 \pm 0.26) \times 10^{-3}$		1003
$K^*(892)^0 \overline{K}_2^*(1430)^0 +$ c.c.		$(6.0 \pm 0.6) \times 10^{-3}$		1012
$K^*(892)^0 \overline{K}_2(1770)^0 +$ c.c. $\rightarrow$ $K^*(892)^0 K^- \pi^+ +$ c.c.		$(6.9 \pm 0.9) \times 10^{-4}$		–
$\omega K^*(892) \overline{K} +$ c.c.		$(6.1 \pm 0.9) \times 10^{-3}$		1097
$K^+ K^*(892)^- +$ c.c.		$(5.12 \pm 0.30) \times 10^{-3}$		1373
$K^+ K^*(892)^- +$ c.c. $\rightarrow$ $K^+ K^- \pi^0$		$(1.97 \pm 0.20) \times 10^{-3}$		–
$K^+ K^*(892)^- +$ c.c. $\rightarrow$ $K^0 K^\pm \pi^\mp +$ c.c.		$(3.0 \pm 0.4) \times 10^{-3}$		–
$K^0 \overline{K}^*(892)^0 +$ c.c.		$(4.39 \pm 0.31) \times 10^{-3}$		1373
$K^0 \overline{K}^*(892)^0 +$ c.c. $\rightarrow$ $K^0 K^\pm \pi^\mp +$ c.c.		$(3.2 \pm 0.4) \times 10^{-3}$		–
$K_1(1400)^\pm K^\mp$		$(3.8 \pm 1.4) \times 10^{-3}$		1170
$\overline{K}^*(892)^0 K^+ \pi^- +$ c.c.		seen		1343
$\omega \pi^0 \pi^0$		$(3.4 \pm 0.8) \times 10^{-3}$		1436
$b_1(1235)^\pm \pi^\mp$	[gg]	$(3.0 \pm 0.5) \times 10^{-3}$		1300
$\omega K^\pm K_S^0 \pi^\mp$	[gg]	$(3.4 \pm 0.5) \times 10^{-3}$		1210
$b_1(1235)^0 \pi^0$		$(2.3 \pm 0.6) \times 10^{-3}$		1300
$\eta K^\pm K_S^0 \pi^\mp$	[gg]	$(2.2 \pm 0.4) \times 10^{-3}$		1278
$\phi K^*(892) \overline{K} +$ c.c.		$(2.18 \pm 0.23) \times 10^{-3}$		969
$\omega K \overline{K}$		$(1.70 \pm 0.32) \times 10^{-3}$		1268
$\omega f_0(1710) \rightarrow \omega K \overline{K}$		$(4.8 \pm 1.1) \times 10^{-4}$		878
$\phi 2(\pi^+ \pi^-)$		$(1.66 \pm 0.23) \times 10^{-3}$		1318
$\Delta(1232)^{++} \overline{p} \pi^-$		$(1.6 \pm 0.5) \times 10^{-3}$		1030
$\omega \eta$		$(1.74 \pm 0.20) \times 10^{-3}$	S=1.6	1394
$\phi K \overline{K}$		$(1.83 \pm 0.24) \times 10^{-3}$	S=1.5	1179
$\phi f_0(1710) \rightarrow \phi K \overline{K}$		$(3.6 \pm 0.6) \times 10^{-4}$		875
$\phi f_2(1270)$		$(7.2 \pm 1.3) \times 10^{-4}$		1036
$\Delta(1232)^{++} \overline{\Delta}(1232)^{--}$		$(1.10 \pm 0.29) \times 10^{-3}$		938
$\Sigma(1385)^- \overline{\Sigma}(1385)^+$ (or c.c.)	[gg]	$(1.10 \pm 0.12) \times 10^{-3}$		697
$\phi f_2'(1525)$		$(8 \pm 4) \times 10^{-4}$	S=2.7	871
$\phi \pi^+ \pi^-$		$(9.4 \pm 0.9) \times 10^{-4}$	S=1.2	1365
$\phi \pi^0 \pi^0$		$(5.6 \pm 1.6) \times 10^{-4}$		1366
$\phi K^\pm K_S^0 \pi^\mp$	[gg]	$(7.2 \pm 0.8) \times 10^{-4}$		1114
$\omega f_1(1420)$		$(6.8 \pm 2.4) \times 10^{-4}$		1062
$\phi \eta$		$(7.5 \pm 0.8) \times 10^{-4}$	S=1.5	1320
$\Xi^0 \overline{\Xi}^0$		$(1.20 \pm 0.24) \times 10^{-3}$		818
$\Xi(1530)^- \overline{\Xi}^+$		$(5.9 \pm 1.5) \times 10^{-4}$		600
$p K^- \overline{\Sigma}(1385)^0$		$(5.1 \pm 3.2) \times 10^{-4}$		646
$\omega \pi^0$		$(4.5 \pm 0.5) \times 10^{-4}$	S=1.4	1446
$\phi \eta'(958)$		$(4.0 \pm 0.7) \times 10^{-4}$	S=2.1	1192
$\phi f_0(980)$		$(3.2 \pm 0.9) \times 10^{-4}$	S=1.9	1178
$\phi f_0(980) \rightarrow \phi \pi^+ \pi^-$		$(1.8 \pm 0.4) \times 10^{-4}$		–
$\phi f_0(980) \rightarrow \phi \pi^0 \pi^0$		$(1.7 \pm 0.7) \times 10^{-4}$		–
$\eta \phi f_0(980) \rightarrow \eta \phi \pi^+ \pi^-$		$(3.2 \pm 1.0) \times 10^{-4}$		–
$\phi a_0(980)^0 \rightarrow \phi \eta \pi^0$		$(5 \pm 4) \times 10^{-6}$		–
$\Xi(1530)^0 \overline{\Xi}^0$		$(3.2 \pm 1.4) \times 10^{-4}$		608
$\Sigma(1385)^- \overline{\Sigma}^+$ (or c.c.)	[gg]	$(3.1 \pm 0.5) \times 10^{-4}$		855
$\phi f_1(1285)$		$(2.6 \pm 0.5) \times 10^{-4}$	S=1.1	1032
$\eta \pi^+ \pi^-$		$(4.0 \pm 1.7) \times 10^{-4}$		1487
$\rho \eta$		$(1.93 \pm 0.23) \times 10^{-4}$		1396
$\omega \eta'(958)$		$(1.82 \pm 0.21) \times 10^{-4}$		1279
$\omega f_0(980)$		$(1.4 \pm 0.5) \times 10^{-4}$		1267
$\rho \eta'(958)$		$(1.05 \pm 0.18) \times 10^{-4}$		1281
$a_2(1320)^\pm \pi^\mp$	[gg]	$< 4.3 \times 10^{-3}$	CL=90%	1263
$K \overline{K}_2^*(1430) +$ c.c.		$< 4.0 \times 10^{-3}$	CL=90%	1159
$K_1(1270)^\pm K^\mp$		$< 3.0 \times 10^{-3}$	CL=90%	1231
$K_2^*(1430)^0 \overline{K}_2^*(1430)^0$		$< 2.9 \times 10^{-3}$	CL=90%	604
$\phi \pi^0$		$< 6.4 \times 10^{-6}$	CL=90%	1377
$\phi \eta(1405) \rightarrow \phi \eta \pi \pi$		$< 2.5 \times 10^{-4}$	CL=90%	946
$\omega f_2'(1525)$		$< 2.2 \times 10^{-4}$	CL=90%	1003
$\omega X(1835) \rightarrow \omega p \overline{p}$		$< 3.9 \times 10^{-6}$	CL=95%	–
$\eta \phi(2170) \rightarrow \eta K^*(892)^0 \overline{K}^*(892)^0$		$< 2.52 \times 10^{-4}$	CL=90%	–
$\Sigma(1385)^0 \overline{\Lambda} +$ c.c.		$< 8.2 \times 10^{-6}$	CL=90%	912
$\Delta(1232)^+ \overline{p}$		$< 1 \times 10^{-4}$	CL=90%	1100
$\Lambda(1520) \overline{\Lambda} +$ c.c. $\rightarrow \gamma \Lambda \overline{\Lambda}$		$< 4.1 \times 10^{-6}$	CL=90%	–
$\Theta(1540) \overline{\Theta}(1540) \rightarrow K_S^0 p K^- \overline{n} +$ c.c.		$< 1.1 \times 10^{-5}$	CL=90%	–
$\Theta(1540) K^- \overline{n} \rightarrow K_S^0 p K^- \overline{n}$		$< 2.1 \times 10^{-5}$	CL=90%	–
$\Theta(1540) K_S^0 \overline{p} \rightarrow K_S^0 \overline{p} K^+ n$		$< 1.6 \times 10^{-5}$	CL=90%	–
$\overline{\Theta}(1540) K^+ n \rightarrow K_S^0 \overline{p} K^+ n$		$< 5.6 \times 10^{-5}$	CL=90%	–
$\overline{\Theta}(1540) K_S^0 p \rightarrow K_S^0 p K^- \overline{n}$		$< 1.1 \times 10^{-5}$	CL=90%	–
$\Sigma^0 \overline{\Lambda}$		$< 9 \times 10^{-5}$	CL=90%	1032

Decays into stable hadrons

$2(\pi^+ \pi^-) \pi^0$		$(4.1 \pm 0.5) \%$	S=2.4	1496
$3(\pi^+ \pi^-) \pi^0$		$(2.9 \pm 0.6) \%$		1433
$\pi^+ \pi^- \pi^0$		$(2.11 \pm 0.07) \%$	S=1.5	1533
$\pi^+ \pi^- \pi^0 K^+ K^-$		$(1.79 \pm 0.29) \%$	S=2.2	1368
$4(\pi^+ \pi^-) \pi^0$		$(9.0 \pm 3.0) \times 10^{-3}$		1345
$\pi^+ \pi^- K^+ K^-$		$(6.6 \pm 0.5) \times 10^{-3}$		1407
$\pi^+ \pi^- K^+ K^- \eta$		$(1.84 \pm 0.28) \times 10^{-3}$		1221
$\pi^0 \pi^0 K^+ K^-$		$(2.45 \pm 0.31) \times 10^{-3}$		1410
$K \overline{K} \pi$		$(6.1 \pm 1.0) \times 10^{-3}$		1442
$2(\pi^+ \pi^-)$		$(3.57 \pm 0.30) \times 10^{-3}$		1517
$3(\pi^+ \pi^-)$		$(4.3 \pm 0.4) \times 10^{-3}$		1466
$2(\pi^+ \pi^- \pi^0)$		$(1.62 \pm 0.21) \%$		1468
$2(\pi^+ \pi^-) \eta$		$(2.29 \pm 0.24) \times 10^{-3}$		1446
$3(\pi^+ \pi^-) \eta$		$(7.2 \pm 1.5) \times 10^{-4}$		1379
$p \overline{p}$		$(2.120 \pm 0.029) \times 10^{-3}$		1232
$p \overline{p} \pi^0$		$(1.19 \pm 0.08) \times 10^{-3}$	S=1.1	1176
$p \overline{p} \pi^+ \pi^-$		$(6.0 \pm 0.5) \times 10^{-3}$	S=1.3	1107
$p \overline{p} \pi^+ \pi^- \pi^0$	[ssaa]	$(2.3 \pm 0.9) \times 10^{-3}$	S=1.9	1033
$p \overline{p} \eta$		$(2.00 \pm 0.12) \times 10^{-3}$		948
$p \overline{p} \rho$		$< 3.1 \times 10^{-4}$	CL=90%	774
$p \overline{p} \omega$		$(9.8 \pm 1.0) \times 10^{-4}$	S=1.3	768
$p \overline{p} \eta'(958)$		$(2.1 \pm 0.4) \times 10^{-4}$		596
$p \overline{p} \phi$		$(4.5 \pm 1.5) \times 10^{-5}$		527
$n \overline{n}$		$(2.09 \pm 0.16) \times 10^{-3}$		1231
$n \overline{n} \pi^+ \pi^-$		$(4 \pm 4) \times 10^{-3}$		1106
$\Sigma^+ \overline{\Sigma}^-$		$(1.50 \pm 0.24) \times 10^{-3}$		992
$\Sigma^0 \overline{\Sigma}^0$		$(1.29 \pm 0.09) \times 10^{-3}$		988
$2(\pi^+ \pi^-) K^+ K^-$		$(4.7 \pm 0.7) \times 10^{-3}$	S=1.3	1320
$p \overline{n} \pi^-$		$(2.12 \pm 0.09) \times 10^{-3}$		1174
$n N(1440)$		seen		984
$n N(1520)$		seen		928
$n N(1535)$		seen		914
$\Xi^- \overline{\Xi}^+$		$(8.6 \pm 1.1) \times 10^{-4}$	S=1.2	807
$\Lambda \overline{\Lambda}$		$(1.61 \pm 0.15) \times 10^{-3}$	S=1.9	1074
$\Lambda \overline{\Sigma}^- \pi^+$ (or c.c.)	[gg]	$(8.3 \pm 0.7) \times 10^{-4}$	S=1.2	950
$p K^- \overline{\Lambda}$		$(8.9 \pm 1.6) \times 10^{-4}$		876
$2(K^+ K^-)$		$(7.6 \pm 0.9) \times 10^{-4}$		1131
$p K^- \overline{\Sigma}^0$		$(2.9 \pm 0.8) \times 10^{-4}$		819
$K^+ K^-$		$(2.70 \pm 0.17) \times 10^{-4}$		1468
$K_S^0 K_L^0$		$(2.1 \pm 0.4) \times 10^{-4}$	S=3.2	1466
$\Lambda \overline{\Lambda} \pi^+ \pi^-$		$(4.3 \pm 1.0) \times 10^{-3}$		903
$\Lambda \overline{\Lambda} \eta$		$(1.62 \pm 0.17) \times 10^{-4}$		672
$\Lambda \overline{\Lambda} \pi^0$		$(3.8 \pm 0.4) \times 10^{-5}$		998
$\overline{\Lambda} n K_S^0 +$ c.c.		$(6.5 \pm 1.1) \times 10^{-4}$		872
$\pi^+ \pi^-$		$(1.47 \pm 0.14) \times 10^{-4}$		1542
$\Lambda \overline{\Sigma} +$ c.c.		$(2.83 \pm 0.23) \times 10^{-5}$		1034
$K_S^0 K_S^0$		$< 1 \times 10^{-6}$	CL=95%	1466

Radiative decays

3γ		$(1.16 \pm 0.22) \times 10^{-5}$		1548
4γ		$< 9 \times 10^{-6}$	CL=90%	1548
5γ		$< 1.5 \times 10^{-5}$	CL=90%	1548
$\gamma \eta_c(1S)$		$(1.7 \pm 0.4) \%$	S=1.6	111
$\gamma \eta_c(1S) \rightarrow 3\gamma$		$(3.8 \ {}^{+1.3}_{-1.0}) \times 10^{-6}$	S=1.1	–
$\gamma \pi^+ \pi^- 2\pi^0$		$(8.3 \pm 3.1) \times 10^{-3}$		1518
$\gamma \eta \pi \pi$		$(6.1 \pm 1.0) \times 10^{-3}$		1487
$\gamma \eta_2(1870) \rightarrow \gamma \eta \pi^+ \pi^-$		$(6.2 \pm 2.4) \times 10^{-4}$		–
$\gamma \eta(1405/1475) \rightarrow \gamma K \overline{K} \pi$	[o]	$(2.8 \pm 0.6) \times 10^{-3}$	S=1.6	1223
$\gamma \eta(1405/1475) \rightarrow \gamma \gamma \rho^0$		$(7.8 \pm 2.0) \times 10^{-5}$	S=1.8	1223
$\gamma \eta(1405/1475) \rightarrow \gamma \eta \pi^+ \pi^-$		$(3.0 \pm 0.5) \times 10^{-4}$		–
$\gamma \eta(1405/1475) \rightarrow \gamma \gamma \phi$		$< 8.2 \times 10^{-5}$	CL=95%	–
$\gamma \rho \rho$		$(4.5 \pm 0.8) \times 10^{-3}$		1340
$\gamma \rho \omega$		$< 5.4 \times 10^{-4}$	CL=90%	1338
$\gamma \rho \phi$		$< 8.8 \times 10^{-5}$	CL=90%	1258
$\gamma \eta'(958)$		$(5.15 \pm 0.16) \times 10^{-3}$	S=1.2	1400
$\gamma 2\pi^+ 2\pi^-$		$(2.8 \pm 0.5) \times 10^{-3}$	S=1.9	1517
$\gamma f_2(1270) f_2(1270)$		$(9.5 \pm 1.7) \times 10^{-4}$		879
$\gamma f_2(1270) f_2(1270)$ (non resonant)		$(8.2 \pm 1.9) \times 10^{-4}$		–
$\gamma K^+ K^- \pi^+ \pi^-$		$(2.1 \pm 0.6) \times 10^{-3}$		1407
$\gamma f_4(2050)$		$(2.7 \pm 0.7) \times 10^{-3}$		891
$\gamma \omega \omega$		$(1.61 \pm 0.33) \times 10^{-3}$		1336
$\gamma \eta(1405/1475) \rightarrow \gamma \rho^0 \rho^0$		$(1.7 \pm 0.4) \times 10^{-3}$	S=1.3	1223
$\gamma f_2(1270)$		$(1.43 \pm 0.11) \times 10^{-3}$		1286
$\gamma f_0(1710) \rightarrow \gamma K \overline{K}$		$(8.5 \ {}^{+1.2}_{-0.9}) \times 10^{-4}$	S=1.2	1075
$\gamma f_0(1710) \rightarrow \gamma \pi \pi$		$(4.0 \pm 1.0) \times 10^{-4}$		–

$\gamma f_0(1710) \to \gamma\omega\omega$	$(3.1 \pm 1.0) \times 10^{-4}$			–
$\gamma\eta$	$(1.104 \pm 0.034) \times 10^{-3}$			1500
$\gamma f_1(1420) \to \gamma K\overline{K}\pi$	$(7.9 \pm 1.3) \times 10^{-4}$			1220
$\gamma f_1(1285)$	$(6.1 \pm 0.8) \times 10^{-4}$			1283
$\gamma f_1(1510) \to \gamma\eta\pi^+\pi^-$	$(4.5 \pm 1.2) \times 10^{-4}$			–
$\gamma f_2'(1525)$	$(4.5\ ^{+0.7}_{-0.4}) \times 10^{-4}$			1173
$\gamma f_2(1640) \to \gamma\omega\omega$	$(2.8 \pm 1.8) \times 10^{-4}$			–
$\gamma f_2(1910) \to \gamma\omega\omega$	$(2.0 \pm 1.4) \times 10^{-4}$			–
$\gamma f_0(1800) \to \gamma\omega\phi$	$(2.5 \pm 0.6) \times 10^{-4}$			–
$\gamma f_2(1950) \to \gamma K^*(892)\overline{K}^*(892)$	$(7.0 \pm 2.2) \times 10^{-4}$			–
$\gamma K^*(892)\overline{K}^*(892)$	$(4.0 \pm 1.3) \times 10^{-3}$			1266
$\gamma\phi\phi$	$(4.0 \pm 1.2) \times 10^{-4}$		S=2.1	1166
$\gamma p\overline{p}$	$(3.8 \pm 1.0) \times 10^{-4}$			1232
$\gamma\eta(2225)$	$(3.3 \pm 0.5) \times 10^{-4}$			749
$\gamma\eta(1760) \to \gamma\rho^0\rho^0$	$(1.3 \pm 0.9) \times 10^{-4}$			1048
$\gamma\eta(1760) \to \gamma\omega\omega$	$(1.98 \pm 0.33) \times 10^{-3}$			–
$\gamma X(1835) \to \gamma\pi^+\pi^-\eta'$	$(2.6 \pm 0.4) \times 10^{-4}$			1006
$\gamma X(1835) \to \gamma p\overline{p}$	$(7.7\ ^{+1.5}_{-0.9}) \times 10^{-5}$			–
$\gamma X(1840) \to \gamma 3(\pi^+\pi^-)$	$(2.4\ ^{+0.7}_{-0.8}) \times 10^{-5}$			–
$\gamma(K\overline{K}\pi)\ [J^{PC} = 0^{-+}]$	$(7 \pm 4) \times 10^{-4}$		S=2.1	1442
$\gamma\pi^0$	$(3.49\ ^{+0.33}_{-0.30}) \times 10^{-5}$			1546
$\gamma p\overline{p}\pi^+\pi^-$	< 7.9	$\times 10^{-4}$	CL=90%	1107
$\gamma\Lambda\overline{\Lambda}$	< 1.3	$\times 10^{-4}$	CL=90%	1074
$\gamma f_J(2220)$	> 2.50	$\times 10^{-3}$	CL=99.9%	745
$\gamma f_J(2220) \to \gamma\pi\pi$	$(8 \pm 4) \times 10^{-5}$			–
$\gamma f_J(2220) \to \gamma K\overline{K}$	< 3.6	$\times 10^{-5}$		–
$\gamma f_J(2220) \to \gamma p\overline{p}$	$(1.5 \pm 0.8) \times 10^{-5}$			–
$\gamma f_0(1500)$	$(1.01 \pm 0.32) \times 10^{-4}$			1183
$\gamma A \to \gamma$ invisible	[ttaa] < 6.3	$\times 10^{-6}$	CL=90%	–
$\gamma A^0 \to \gamma\mu^+\mu^-$	[uuaa] < 2.1	$\times 10^{-5}$	CL=90%	–

Weak decays

$\overline{D}^- e^+\nu_e +$ c.c.	< 1.2	$\times 10^{-5}$	CL=90%	984
$\overline{D}^0 e^+ e^- +$ c.c.	< 1.1	$\times 10^{-5}$	CL=90%	987
$D_s^- e^+\nu_e +$ c.c.	< 3.6	$\times 10^{-5}$	CL=90%	923
$\overline{D}^- \pi^+ +$ c.c.	< 7.5	$\times 10^{-5}$	CL=90%	977
$\overline{D}^0 K^0 +$ c.c.	< 1.7	$\times 10^{-4}$	CL=90%	898
$D_s^- \pi^+ +$ c.c.	< 1.3	$\times 10^{-4}$	CL=90%	916

Charge conjugation (C), Parity (P), Lepton Family number (LF) violating modes

$\gamma\gamma$	C	< 5	$\times 10^{-6}$	CL=90%	1548
$e^\pm\mu^\mp$	LF	< 1.6	$\times 10^{-7}$	CL=90%	1547
$e^\pm\tau^\mp$	LF	< 8.3	$\times 10^{-6}$	CL=90%	1039
$\mu^\pm\tau^\mp$	LF	< 2.0	$\times 10^{-6}$	CL=90%	1035

Other decays

invisible	< 7	$\times 10^{-4}$	CL=90%	–

$\chi_{c0}(1P)$

$I^G(J^{PC}) = 0^+(0^{++})$

Mass $m = 3414.75 \pm 0.31$ MeV
Full width $\Gamma = 10.5 \pm 0.6$ MeV

$\chi_{c0}(1P)$ DECAY MODES	Fraction (Γ_i/Γ)	Scale factor / Confidence level	p (MeV/c)
Hadronic decays			
$2(\pi^+\pi^-)$	(2.24 ± 0.18) %		1679
$\rho^0\pi^+\pi^-$	$(8.7 \pm 2.8) \times 10^{-3}$		1607
$f_0(980) f_0(980)$	$(6.5 \pm 2.1) \times 10^{-4}$		1391
$\pi^+\pi^-\pi^0\pi^0$	(3.3 ± 0.4) %		1680
$\rho^+\pi^-\pi^0 +$ c.c.	(2.8 ± 0.4) %		1607
$4\pi^0$	$(3.2 \pm 0.4) \times 10^{-3}$		1681
$\pi^+\pi^- K^+ K^-$	(1.75 ± 0.14) %		1580
$K_0^*(1430)^0 \overline{K}_0^*(1430)^0 \to \pi^+\pi^- K^+ K^-$	$(9.6\ ^{+3.5}_{-2.8}) \times 10^{-4}$		–
$K_0^*(1430)^0 \overline{K}_2^*(1430)^0 +$ c.c. $\to \pi^+\pi^- K^+ K^-$	$(7.8\ ^{+1.9}_{-2.4}) \times 10^{-4}$		–
$K_1(1270)^+ K^- +$ c.c. $\to \pi^+\pi^- K^+ K^-$	$(6.1 \pm 1.9) \times 10^{-3}$		–
$K_1(1400)^+ K^- +$ c.c. $\to \pi^+\pi^- K^+ K^-$	$< 2.6 \times 10^{-3}$	CL=90%	–
$f_0(980) f_0(980)$	$(1.6\ ^{+1.0}_{-0.9}) \times 10^{-4}$		1391
$f_0(980) f_0(2200)$	$(7.8\ ^{+2.0}_{-2.5}) \times 10^{-4}$		584
$f_0(1370) f_0(1370)$	$< 2.7 \times 10^{-4}$	CL=90%	1019
$f_0(1370) f_0(1500)$	$< 1.7 \times 10^{-4}$	CL=90%	920
$f_0(1370) f_0(1710)$	$(6.6\ ^{+3.5}_{-2.3}) \times 10^{-4}$		721
$f_0(1500) f_0(1370)$	$< 1.3 \times 10^{-4}$	CL=90%	920
$f_0(1500) f_0(1500)$	$< 5 \times 10^{-5}$	CL=90%	805
$f_0(1500) f_0(1710)$	$< 7 \times 10^{-5}$	CL=90%	557
$K^+ K^- \pi^+\pi^-\pi^0$	(1.11 ± 0.26) %		1545
$K^+ K^-\pi^0\pi^0$	$(5.4 \pm 0.9) \times 10^{-3}$		1582
$K^+\pi^-\overline{K}^0\pi^0 +$ c.c.	(2.44 ± 0.33) %		1581
$\rho^+ K^- K^0 +$ c.c.	(1.18 ± 0.21) %		1458
$K^*(892)^- K^+\pi^0 \to K^+\pi^-\overline{K}^0\pi^0 +$ c.c.	$(4.5 \pm 1.1) \times 10^{-3}$		–
$K_S^0 K_S^0\pi^+\pi^-$	$(5.6 \pm 1.0) \times 10^{-3}$		1579
$K^+ K^-\eta\pi^0$	$(3.0 \pm 0.7) \times 10^{-3}$		1468
$3(\pi^+\pi^-)$	(1.20 ± 0.18) %		1633
$K^+\overline{K}^*(892)^0\pi^- +$ c.c.	$(7.2 \pm 1.6) \times 10^{-3}$		1523
$K^*(892)^0\overline{K}^*(892)^0$	$(1.7 \pm 0.6) \times 10^{-3}$		1456
$\pi\pi$	$(8.33 \pm 0.35) \times 10^{-3}$		1702
$\pi^0\eta$	$< 1.8 \times 10^{-4}$		1661
$\pi^0\eta'$	$< 1.1 \times 10^{-3}$		1570
$\eta\eta$	$(2.95 \pm 0.19) \times 10^{-3}$		1617
$\eta\eta'$	$< 2.3 \times 10^{-4}$	CL=90%	1521
$\eta'\eta'$	$(1.96 \pm 0.21) \times 10^{-3}$		1413
$\omega\omega$	$(9.5 \pm 1.1) \times 10^{-4}$		1517
$\omega\phi$	$(1.16 \pm 0.21) \times 10^{-4}$		1447
$K^+ K^-$	$(5.91 \pm 0.32) \times 10^{-3}$		1634
$K_S^0 K_S^0$	$(3.10 \pm 0.18) \times 10^{-3}$		1633
$\pi^+\pi^-\eta$	$< 1.9 \times 10^{-4}$	CL=90%	1651
$\pi^+\pi^-\eta'$	$< 3.5 \times 10^{-4}$	CL=90%	1560
$\overline{K}^0 K^+\pi^- +$ c.c.	$< 9 \times 10^{-5}$	CL=90%	1610
$K^+ K^-\pi^0$	$< 6 \times 10^{-5}$	CL=90%	1611
$K^+ K^-\eta$	$< 2.2 \times 10^{-4}$	CL=90%	1512
$K^+ K^- K_S^0 K_S^0$	$(1.4 \pm 0.5) \times 10^{-3}$		1331
$K^+ K^- K^+ K^-$	$(2.75 \pm 0.28) \times 10^{-3}$		1333
$K^+ K^-\phi$	$(9.5 \pm 2.4) \times 10^{-4}$		1381
$\phi\phi$	$(7.7 \pm 0.7) \times 10^{-4}$		1370
$p\overline{p}$	$(2.25 \pm 0.09) \times 10^{-4}$		1426
$p\overline{p}\pi^0$	$(6.8 \pm 0.7) \times 10^{-4}$	S=1.3	1379
$p\overline{p}\eta$	$(3.5 \pm 0.4) \times 10^{-4}$		1187
$p\overline{p}\omega$	$(5.1 \pm 0.6) \times 10^{-4}$		1043
$p\overline{p}\phi$	$(5.9 \pm 1.4) \times 10^{-5}$		876
$p\overline{p}\pi^+\pi^-$	$(2.1 \pm 0.7) \times 10^{-3}$	S=1.4	1320
$p\overline{p}\pi^0\pi^0$	$(1.02 \pm 0.27) \times 10^{-3}$		1324
$p\overline{p}K^+ K^-$ (non-resonant)	$(1.19 \pm 0.26) \times 10^{-4}$		890
$p\overline{p}K_S^0 K_S^0$	$< 8.8 \times 10^{-4}$	CL=90%	884
$p\overline{n}\pi^-$	$(1.24 \pm 0.11) \times 10^{-3}$		1376
$\overline{p}n\pi^+$	$(1.34 \pm 0.12) \times 10^{-3}$		1376
$p\overline{n}\pi^-\pi^0$	$(2.29 \pm 0.21) \times 10^{-3}$		1321
$\overline{p}n\pi^+\pi^0$	$(2.16 \pm 0.18) \times 10^{-3}$		1321
$\Lambda\overline{\Lambda}$	$(3.21 \pm 0.25) \times 10^{-4}$		1292
$\Lambda\overline{\Lambda}\pi^+\pi^-$	$(1.15 \pm 0.13) \times 10^{-3}$		1153
$\Lambda\overline{\Lambda}\pi^+\pi^-$ (non-resonant)	$< 5 \times 10^{-4}$	CL=90%	1153
$\Sigma(1385)^+\overline{\Lambda}\pi^- +$ c.c.	$< 5 \times 10^{-4}$	CL=90%	1083
$\Sigma(1385)^-\overline{\Lambda}\pi^+ +$ c.c.	$< 5 \times 10^{-4}$	CL=90%	1083
$K^+\overline{p}\Lambda +$ c.c.	$(1.22 \pm 0.12) \times 10^{-3}$	S=1.3	1132
$K^+\overline{p}\Lambda(1520) +$ c.c.	$(2.9 \pm 0.7) \times 10^{-4}$		858
$\Lambda(1520)\overline{\Lambda}(1520)$	$(3.1 \pm 1.2) \times 10^{-4}$		779
$\Sigma^0\overline{\Sigma}^0$	$(4.4 \pm 0.4) \times 10^{-4}$		1222
$\Sigma^+\overline{\Sigma}^-$	$(3.9 \pm 0.7) \times 10^{-4}$	S=1.7	1225
$\Sigma(1385)^+\overline{\Sigma}(1385)^-$	$(1.6 \pm 0.6) \times 10^{-4}$		1001
$\Sigma(1385)^-\overline{\Sigma}(1385)^+$	$(2.3 \pm 0.6) \times 10^{-4}$		1001
$\Xi^0\overline{\Xi}^0$	$(3.1 \pm 0.8) \times 10^{-4}$		1089
$\Xi^-\overline{\Xi}^+$	$(4.7 \pm 0.7) \times 10^{-4}$		1081
Radiative decays			
$\gamma J/\psi(1S)$	(1.27 ± 0.06) %		303
$\gamma\rho^0$	$< 9 \times 10^{-6}$	CL=90%	1619
$\gamma\omega$	$< 8 \times 10^{-6}$	CL=90%	1618
$\gamma\phi$	$< 6 \times 10^{-6}$	CL=90%	1555
$\gamma\gamma$	$(2.23 \pm 0.13) \times 10^{-4}$		1707

$\chi_{c1}(1P)$

$I^G(J^{PC}) = 0^+(1^{++})$

Mass $m = 3510.66 \pm 0.07$ MeV (S = 1.5)
Full width $\Gamma = 0.84 \pm 0.04$ MeV

Meson Summary Table

$\chi_{c1}(1P)$ DECAY MODES	Fraction (Γ_i/Γ)	Scale factor/ Confidence level	p (MeV/c)
Hadronic decays			
$3(\pi^+\pi^-)$	$(5.8 \pm 1.4) \times 10^{-3}$	S=1.2	1683
$2(\pi^+\pi^-)$	$(7.6 \pm 2.6) \times 10^{-3}$		1728
$\pi^+\pi^-\pi^0\pi^0$	(1.22 ± 0.16) %		1729
$\rho^+\pi^-\pi^0$ + c.c.	(1.48 ± 0.25) %		1658
$\rho^0\pi^+\pi^-$	$(3.9 \pm 3.5) \times 10^{-3}$		1657
$4\pi^0$	$(5.5 \pm 0.8) \times 10^{-4}$		1729
$\pi^+\pi^- K^+K^-$	$(4.5 \pm 1.0) \times 10^{-3}$		1632
$K^+K^-\pi^0\pi^0$	$(1.14 \pm 0.28) \times 10^{-3}$		1634
$K^+\pi^-\overline{K}^0\pi^0$ + c.c.	$(8.7 \pm 1.4) \times 10^{-3}$		1632
$\rho^- K^+\overline{K}^0$ + c.c.	$(5.1 \pm 1.2) \times 10^{-3}$		1514
$K^*(892)^0\overline{K}^0\pi^0 \to K^+\pi^-\overline{K}^0\pi^0$ + c.c.	$(2.4 \pm 0.7) \times 10^{-3}$		–
$K^+K^-\eta\pi^0$	$(1.14 \pm 0.35) \times 10^{-3}$		1523
$\pi^+\pi^- K^0_S K^0_S$	$(7.0 \pm 3.0) \times 10^{-4}$		1630
$K^+K^-\eta$	$(3.2 \pm 1.0) \times 10^{-4}$		1566
$\overline{K}^0 K^+\pi^-$ + c.c.	$(7.1 \pm 0.6) \times 10^{-3}$		1661
$K^*(892)^0\overline{K}^0$ + c.c.	$(1.0 \pm 0.4) \times 10^{-3}$		1602
$K^*(892)^+K^-$ + c.c.	$(1.5 \pm 0.7) \times 10^{-3}$		1602
$K^*_J(1430)^0\overline{K}^0$ + c.c. $\to K^0_S K^+\pi^-$ + c.c.	$< 8 \times 10^{-4}$	CL=90%	–
$K^*_J(1430)^+K^-$ + c.c. $\to K^0_S K^+\pi^-$ + c.c.	$< 2.2 \times 10^{-3}$	CL=90%	–
$K^+K^-\pi^0$	$(1.85 \pm 0.25) \times 10^{-3}$		1662
$\eta\pi^+\pi^-$	$(4.9 \pm 0.5) \times 10^{-3}$		1701
$a_0(980)^+\pi^-$ + c.c. $\to \eta\pi^+\pi^-$	$(1.8 \pm 0.6) \times 10^{-3}$		–
$f_2(1270)\eta$	$(2.7 \pm 0.8) \times 10^{-3}$		1468
$\pi^+\pi^-\eta'$	$(2.3 \pm 0.5) \times 10^{-3}$		1612
$\pi^0 f_0(980) \to \pi^0\pi^+\pi^-$	$< 6 \times 10^{-6}$	CL=90%	–
$K^+\overline{K}^*(892)^0\pi^-$ + c.c.	$(3.2 \pm 2.1) \times 10^{-3}$		1577
$K^*(892)^0\overline{K}^*(892)^0$	$(1.5 \pm 0.4) \times 10^{-3}$		1512
$K^+K^- K^0_S K^0_S$	$< 4 \times 10^{-4}$	CL=90%	1390
$K^+K^- K^+K^-$	$(5.5 \pm 1.1) \times 10^{-4}$		1393
$K^+K^-\phi$	$(4.2 \pm 1.6) \times 10^{-4}$		1440
$\omega\omega$	$(5.8 \pm 0.7) \times 10^{-4}$		1571
$\omega\phi$	$(2.1 \pm 0.6) \times 10^{-5}$		1503
$\phi\phi$	$(4.2 \pm 0.5) \times 10^{-4}$		1429
$p\overline{p}$	$(7.72 \pm 0.35) \times 10^{-5}$		1484
$p\overline{p}\pi^0$	$(1.59 \pm 0.19) \times 10^{-4}$		1438
$p\overline{p}\eta$	$(1.48 \pm 0.25) \times 10^{-4}$		1254
$p\overline{p}\omega$	$(2.16 \pm 0.31) \times 10^{-4}$		1117
$p\overline{p}\phi$	$< 1.8 \times 10^{-5}$	CL=90%	962
$p\overline{p}\pi^+\pi^-$	$(5.0 \pm 1.9) \times 10^{-4}$		1381
$p\overline{p}K^+K^-$ (non-resonant)	$(1.30 \pm 0.23) \times 10^{-4}$		974
$p\overline{p}K^0_S K^0_S$	$< 4.5 \times 10^{-4}$	CL=90%	968
$p\overline{n}\pi^-$	$(3.9 \pm 0.5) \times 10^{-4}$		1435
$\overline{p}n\pi^+$	$(4.0 \pm 0.5) \times 10^{-4}$		1435
$p\overline{n}\pi^-\pi^0$	$(1.05 \pm 0.12) \times 10^{-3}$		1383
$\overline{p}n\pi^+\pi^0$	$(1.03 \pm 0.12) \times 10^{-3}$		1383
$\Lambda\overline{\Lambda}$	$(1.16 \pm 0.12) \times 10^{-4}$		1355
$\Lambda\overline{\Lambda}\pi^+\pi^-$	$(3.0 \pm 0.5) \times 10^{-4}$		1223
$\Lambda\overline{\Lambda}\pi^+\pi^-$ (non-resonant)	$(2.5 \pm 0.6) \times 10^{-4}$		1223
$\Sigma(1385)^+\overline{\Lambda}\pi^-$ + c.c.	$< 1.3 \times 10^{-4}$	CL=90%	1157
$\Sigma(1385)^-\overline{\Lambda}\pi^+$ + c.c.	$< 1.3 \times 10^{-4}$	CL=90%	1157
$K^+\overline{p}\Lambda$	$(4.2 \pm 0.4) \times 10^{-4}$	S=1.1	1203
$K^+\overline{p}\Lambda(1520)$ + c.c.	$(1.7 \pm 0.5) \times 10^{-4}$		950
$\Lambda(1520)\overline{\Lambda}(1520)$	$< 1.0 \times 10^{-4}$	CL=90%	879
$\Sigma^0\overline{\Sigma}^0$	$< 4 \times 10^{-5}$	CL=90%	1288
$\Sigma^+\overline{\Sigma}^-$	$< 6 \times 10^{-5}$	CL=90%	1291
$\Sigma(1385)^+\overline{\Sigma}(1385)^-$	$< 1.0 \times 10^{-4}$	CL=90%	1081
$\Sigma(1385)^-\overline{\Sigma}(1385)^+$	$< 5 \times 10^{-5}$	CL=90%	1081
$\Xi^0\overline{\Xi}^0$	$< 6 \times 10^{-5}$	CL=90%	1163
$\Xi^-\overline{\Xi}^+$	$(8.2 \pm 2.2) \times 10^{-5}$		1155
$\pi^+\pi^- + K^+K^-$	$< 2.1 \times 10^{-3}$		–
$K^0_S K^0_S$	$< 6 \times 10^{-5}$	CL=90%	1683
Radiative decays			
$\gamma J/\psi(1S)$	(33.9 ± 1.2) %		389
$\gamma\rho^0$	$(2.20 \pm 0.18) \times 10^{-4}$		1670
$\gamma\omega$	$(6.9 \pm 0.8) \times 10^{-5}$		1668
$\gamma\phi$	$(2.5 \pm 0.5) \times 10^{-5}$		1607

$h_c(1P)$ $I^G(J^{PC}) = ?^?(1^{+-})$

Mass $m = 3525.38 \pm 0.11$ MeV
Full width $\Gamma = 0.7 \pm 0.4$ MeV

$h_c(1P)$ DECAY MODES	Fraction (Γ_i/Γ)	Confidence level	p (MeV/c)
$J/\psi(1S)\pi\pi$	not seen		312
$p\overline{p}$	$< 1.5 \times 10^{-4}$	90%	1492
$\eta_c(1S)\gamma$	(51 ± 6) %		500
$\pi^+\pi^-\pi^0$	$< 2.2 \times 10^{-3}$		1749
$2\pi^+2\pi^-\pi^0$	$(2.2^{+0.8}_{-0.7})$ %		1716
$3\pi^+3\pi^-\pi^0$	< 2.9 %		1661

$\chi_{c2}(1P)$ $I^G(J^{PC}) = 0^+(2^{++})$

Mass $m = 3556.20 \pm 0.09$ MeV
Full width $\Gamma = 1.93 \pm 0.11$ MeV

$\chi_{c2}(1P)$ DECAY MODES	Fraction (Γ_i/Γ)	Confidence level	p (MeV/c)
Hadronic decays			
$2(\pi^+\pi^-)$	(1.07 ± 0.10) %		1751
$\pi^+\pi^-\pi^0\pi^0$	(1.92 ± 0.25) %		1752
$\rho^+\pi^-\pi^0$ + c.c.	(2.3 ± 0.4) %		1682
$4\pi^0$	$(1.16 \pm 0.16) \times 10^{-3}$		1752
$K^+K^-\pi^0\pi^0$	$(2.2 \pm 0.4) \times 10^{-3}$		1658
$K^+\pi^-\overline{K}^0\pi^0$ + c.c.	(1.44 ± 0.21) %		1657
$\rho^- K^+\overline{K}^0$ + c.c.	$(4.3 \pm 1.3) \times 10^{-3}$		1540
$K^*(892)^0 K^-\pi^+ \to K^-\pi^+ K^0\pi^0$ + c.c.	$(3.1 \pm 0.8) \times 10^{-3}$		–
$K^*(892)^0\overline{K}^0\pi^0 \to K^+\pi^-\overline{K}^0\pi^0$ + c.c.	$(4.0 \pm 0.9) \times 10^{-3}$		–
$K^*(892)^- K^+\pi^0 \to K^+\pi^-\overline{K}^0\pi^0$ + c.c.	$(3.9 \pm 0.9) \times 10^{-3}$		–
$K^*(892)^+\overline{K}^0\pi^- \to K^+\pi^-\overline{K}^0\pi^0$ + c.c.	$(3.1 \pm 0.8) \times 10^{-3}$		–
$K^+K^-\eta\pi^0$	$(1.3 \pm 0.5) \times 10^{-3}$		1549
$K^+K^-\pi^+\pi^-$	$(8.8 \pm 1.0) \times 10^{-3}$		1656
$K^+K^-\pi^+\pi^-\pi^0$	(1.23 ± 0.34) %		1623
$K^+\overline{K}^*(892)^0\pi^-$ + c.c.	$(2.2 \pm 1.1) \times 10^{-3}$		1602
$K^*(892)^0\overline{K}^*(892)^0$	$(2.4 \pm 0.5) \times 10^{-3}$		1538
$3(\pi^+\pi^-)$	$(8.6 \pm 1.8) \times 10^{-3}$		1707
$\phi\phi$	$(1.12 \pm 0.10) \times 10^{-3}$		1457
$\omega\omega$	$(8.8 \pm 1.1) \times 10^{-4}$		1597
$\pi\pi$	$(2.33 \pm 0.12) \times 10^{-3}$		1773
$\rho^0\pi^+\pi^-$	$(3.8 \pm 1.6) \times 10^{-3}$		1682
$\pi^+\pi^-\eta$	$(5.0 \pm 1.3) \times 10^{-4}$		1724
$\pi^+\pi^-\eta'$	$(5.2 \pm 1.9) \times 10^{-4}$		1636
$\eta\eta$	$(5.7 \pm 0.5) \times 10^{-4}$		1692
K^+K^-	$(1.05 \pm 0.07) \times 10^{-3}$		1708
$K^0_S K^0_S$	$(5.5 \pm 0.4) \times 10^{-4}$		1707
$\overline{K}^0 K^+\pi^-$ + c.c.	$(1.34 \pm 0.19) \times 10^{-3}$		1685
$K^+K^-\pi^0$	$(3.2 \pm 0.8) \times 10^{-4}$		1686
$K^+K^-\eta$	$< 3.4 \times 10^{-4}$	90%	1592
$\eta\eta'$	$< 6 \times 10^{-5}$	90%	1600
$\eta'\eta'$	$< 1.0 \times 10^{-4}$	90%	1498
$\pi^+\pi^- K^0_S K^0_S$	$(2.3 \pm 0.6) \times 10^{-3}$		1655
$K^+K^- K^0_S K^0_S$	$< 4 \times 10^{-4}$	90%	1418
$K^+K^- K^+K^-$	$(1.73 \pm 0.21) \times 10^{-3}$		1421
$K^+K^-\phi$	$(1.48 \pm 0.31) \times 10^{-3}$		1468
$p\overline{p}$	$(7.5 \pm 0.4) \times 10^{-5}$		1510
$p\overline{p}\pi^0$	$(4.9 \pm 0.4) \times 10^{-4}$		1465
$p\overline{p}\eta$	$(1.82 \pm 0.26) \times 10^{-4}$		1285
$p\overline{p}\omega$	$(3.8 \pm 0.5) \times 10^{-4}$		1152
$p\overline{p}\phi$	$(2.9 \pm 0.9) \times 10^{-5}$		1002
$p\overline{p}\pi^+\pi^-$	$(1.32 \pm 0.34) \times 10^{-3}$		1410
$p\overline{p}\pi^0\pi^0$	$(8.2 \pm 2.5) \times 10^{-4}$		1414
$p\overline{p}K^+K^-$ (non-resonant)	$(2.00 \pm 0.34) \times 10^{-4}$		1013
$p\overline{p}K^0_S K^0_S$	$< 7.9 \times 10^{-4}$	90%	1007
$p\overline{n}\pi^-$	$(8.9 \pm 1.0) \times 10^{-4}$		1463
$\overline{p}n\pi^+$	$(9.3 \pm 0.9) \times 10^{-4}$		1463
$p\overline{n}\pi^-\pi^0$	$(2.27 \pm 0.19) \times 10^{-3}$		1411
$\overline{p}n\pi^+\pi^0$	$(2.21 \pm 0.20) \times 10^{-3}$		1411
$\Lambda\overline{\Lambda}$	$(1.92 \pm 0.16) \times 10^{-4}$		1385
$\Lambda\overline{\Lambda}\pi^+\pi^-$	$(1.31 \pm 0.17) \times 10^{-3}$		1255

$\Lambda\overline{\Lambda}\pi^+\pi^-$ (non-resonant)	$(6.9 \pm 1.6) \times 10^{-4}$			1255
$\Sigma(1385)^+\overline{\Lambda}\pi^-$ + c.c.	$< 4 \times 10^{-4}$		90%	1192
$\Sigma(1385)^-\overline{\Lambda}\pi^+$ + c.c.	$< 6 \times 10^{-4}$		90%	1192
$K^+\overline{p}\Lambda$ + c.c.	$(8.1 \pm 0.6) \times 10^{-4}$			1236
$K^+\overline{p}\Lambda(1520)$ + c.c.	$(2.9 \pm 0.7) \times 10^{-4}$			992
$\Lambda(1520)\overline{\Lambda}(1520)$	$(4.8 \pm 1.5) \times 10^{-4}$			923
$\Sigma^0\overline{\Sigma}^0$	$< 6 \times 10^{-5}$		90%	1319
$\Sigma^+\overline{\Sigma}^-$	$< 7 \times 10^{-5}$		90%	1322
$\Sigma(1385)^+\overline{\Sigma}(1385)^-$	$< 1.6 \times 10^{-4}$		90%	1118
$\Sigma(1385)^-\overline{\Sigma}(1385)^+$	$< 8 \times 10^{-5}$		90%	1118
$\Xi^0\overline{\Xi}^0$	$< 1.1 \times 10^{-4}$		90%	1197
$\Xi^-\overline{\Xi}^+$	$(1.48 \pm 0.33) \times 10^{-4}$			1189
$J/\psi(1S)\pi^+\pi^-\pi^0$	< 1.5	%	90%	185
$\eta_c(1S)\pi^+\pi^-$	< 2.2	%	90%	459

Radiative decays

$\gamma J/\psi(1S)$	(19.2 ± 0.7)	%		430
$\gamma\rho^0$	$< 2.0 \times 10^{-5}$		90%	1694
$\gamma\omega$	$< 6 \times 10^{-6}$		90%	1692
$\gamma\phi$	$< 8 \times 10^{-6}$		90%	1632
$\gamma\gamma$	$(2.74 \pm 0.14) \times 10^{-4}$			1778

$\eta_c(2S)$

$I^G(J^{PC}) = 0^+(0^{-+})$

Quantum numbers are quark model predictions.

Mass $m = 3639.4 \pm 1.3$ MeV (S = 1.2)
Full width $\Gamma = 11.3^{+3.2}_{-2.9}$ MeV

$\eta_c(2S)$ DECAY MODES	Fraction (Γ_i/Γ)	Confidence level	p (MeV/c)
hadrons	not seen		–
$K\overline{K}\pi$	(1.9 ± 1.2) %		1730
$2\pi^+2\pi^-$	not seen		1793
$\rho^0\rho^0$	not seen		1646
$3\pi^+3\pi^-$	not seen		1750
$K^+K^-\pi^+\pi^-$	not seen		1701
$K^{*0}\overline{K}^{*0}$	not seen		1586
$K^+K^-\pi^+\pi^-\pi^0$	(1.4 ± 1.0) %		1668
$K^+K^-2\pi^+2\pi^-$	not seen		1628
$K^0_S K^-2\pi^+\pi^-$ + c.c.	seen		1667
$2K^+2K^-$	not seen		1471
$\phi\phi$	not seen		1507
$p\overline{p}$	$< 2.0 \times 10^{-3}$	90%	1559
$\gamma\gamma$	$(1.9 \pm 1.3) \times 10^{-4}$		1820
$\pi^+\pi^-\eta$	not seen		1767
$\pi^+\pi^-\eta'$	not seen		1681
$K^+K^-\eta$	not seen		1638
$\pi^+\pi^-\eta_c(1S)$	< 25 %	90%	539

$\psi(2S)$

$I^G(J^{PC}) = 0^-(1^{--})$

Mass $m = 3686.109^{+0.012}_{-0.014}$ MeV
Full width $\Gamma = 299 \pm 8$ keV
$\Gamma_{ee} = 2.36 \pm 0.04$ keV

$\psi(2S)$ DECAY MODES	Fraction (Γ_i/Γ)	Scale factor/ Confidence level	p (MeV/c)
hadrons	(97.85 ± 0.13) %		–
virtual $\gamma \rightarrow$ hadrons	(1.73 ± 0.14) %	S=1.5	–
ggg	(10.6 ± 1.6) %		–
γgg	(1.03 ± 0.29) %		–
light hadrons	(15.4 ± 1.5) %		–
e^+e^-	$(7.89 \pm 0.17) \times 10^{-3}$		1843
$\mu^+\mu^-$	$(7.9 \pm 0.9) \times 10^{-3}$		1840
$\tau^+\tau^-$	$(3.1 \pm 0.4) \times 10^{-3}$		490

Decays into $J/\psi(1S)$ and anything

$J/\psi(1S)$ anything	(60.9 ± 0.6) %		–
$J/\psi(1S)$ neutrals	(25.10 ± 0.33) %		–
$J/\psi(1S)\pi^+\pi^-$	(34.45 ± 0.30) %		477
$J/\psi(1S)\pi^0\pi^0$	(18.13 ± 0.31) %		481
$J/\psi(1S)\eta$	(3.36 ± 0.05) %		199
$J/\psi(1S)\pi^0$	$(1.268 \pm 0.032) \times 10^{-3}$		528

Hadronic decays

$\pi^0 h_c(1P)$	$(8.6 \pm 1.3) \times 10^{-4}$			85
$3(\pi^+\pi^-)\pi^0$	$(3.5 \pm 1.6) \times 10^{-3}$			1746
$2(\pi^+\pi^-)\pi^0$	$(2.9 \pm 1.0) \times 10^{-3}$	S=4.7		1799
$\rho a_2(1320)$	$(2.6 \pm 0.9) \times 10^{-4}$			1500
$p\overline{p}$	$(2.80 \pm 0.11) \times 10^{-4}$			1586
$\Delta^{++}\overline{\Delta}^{--}$	$(1.28 \pm 0.35) \times 10^{-4}$			1371
$\Lambda\overline{\Lambda}\pi^0$	$< 2.9 \times 10^{-6}$	CL=90%		1412
$\Lambda\overline{\Lambda}\eta$	$(2.5 \pm 0.4) \times 10^{-5}$			1197
$\Lambda\overline{p}K^+$	$(1.00 \pm 0.14) \times 10^{-4}$			1327
$\Lambda\overline{p}K^+\pi^+\pi^-$	$(1.8 \pm 0.4) \times 10^{-4}$			1167
$\Lambda\overline{\Lambda}\pi^+\pi^-$	$(2.8 \pm 0.6) \times 10^{-4}$			1346
$\Lambda\overline{\Lambda}$	$(2.8 \pm 0.5) \times 10^{-4}$	S=2.6		1467
$\Lambda\overline{\Sigma}^+\pi^-$ + c.c.	$(1.40 \pm 0.13) \times 10^{-4}$			1376
$\Lambda\overline{\Sigma}^-\pi^+$ + c.c.	$(1.54 \pm 0.14) \times 10^{-4}$			1379
$\Sigma^0\overline{p}K^+$ + c.c.	$(1.67 \pm 0.18) \times 10^{-5}$			1291
$\Sigma^+\overline{\Sigma}^-$	$(2.6 \pm 0.8) \times 10^{-4}$			1408
$\Sigma^0\overline{\Sigma}^0$	$(2.2 \pm 0.4) \times 10^{-4}$	S=1.5		1405
$\Sigma(1385)^+\overline{\Sigma}(1385)^-$	$(1.1 \pm 0.4) \times 10^{-4}$			1218
$\Xi^-\overline{\Xi}^+$	$(1.8 \pm 0.6) \times 10^{-4}$	S=2.8		1284
$\Xi^0\overline{\Xi}^0$	$(2.8 \pm 0.9) \times 10^{-4}$			1292
$\Xi(1530)^0\overline{\Xi}(1530)^0$	$(5.2 \, ^{+3.2}_{-1.2}) \times 10^{-5}$			1025
$\Omega^-\overline{\Omega}^+$	$< 7.3 \times 10^{-5}$	CL=90%		774
$\pi^0 p\overline{p}$	$(1.53 \pm 0.07) \times 10^{-4}$			1543
$N(940)\overline{p}$ + c.c. $\rightarrow \pi^0 p\overline{p}$	$(6.4 \, ^{+1.8}_{-1.3}) \times 10^{-5}$			–
$N(1440)\overline{p}$ + c.c. $\rightarrow \pi^0 p\overline{p}$	$(7.3 \, ^{+1.7}_{-1.5}) \times 10^{-5}$	S=2.5		–
$N(1520)\overline{p}$ + c.c. $\rightarrow \pi^0 p\overline{p}$	$(6.4 \, ^{+2.3}_{-1.8}) \times 10^{-6}$			–
$N(1535)\overline{p}$ + c.c. $\rightarrow \pi^0 p\overline{p}$	$(2.5 \pm 1.0) \times 10^{-5}$			–
$N(1650)\overline{p}$ + c.c. $\rightarrow \pi^0 p\overline{p}$	$(3.8 \, ^{+1.4}_{-1.7}) \times 10^{-5}$			–
$N(1720)\overline{p}$ + c.c. $\rightarrow \pi^0 p\overline{p}$	$(1.79 \, ^{+0.26}_{-0.70}) \times 10^{-5}$			–
$N(2300)\overline{p}$ + c.c. $\rightarrow \pi^0 p\overline{p}$	$(2.6 \, ^{+1.2}_{-0.7}) \times 10^{-5}$			–
$N(2570)\overline{p}$ + c.c. $\rightarrow \pi^0 p\overline{p}$	$(2.13 \, ^{+0.40}_{-0.31}) \times 10^{-5}$			–
$\pi^0 f_0(2100) \rightarrow \pi^0 p\overline{p}$	$(1.1 \pm 0.4) \times 10^{-5}$			–
$\eta p\overline{p}$	$(6.0 \pm 0.4) \times 10^{-5}$			1373
$\eta f_0(2100) \rightarrow \eta p\overline{p}$	$(1.2 \pm 0.4) \times 10^{-5}$			–
$N(1535)\overline{p} \rightarrow \eta p\overline{p}$	$(4.4 \pm 0.7) \times 10^{-5}$			–
$\omega p\overline{p}$	$(6.9 \pm 2.1) \times 10^{-5}$			1247
$\phi p\overline{p}$	$< 2.4 \times 10^{-5}$	CL=90%		1109
$\pi^+\pi^- p\overline{p}$	$(6.0 \pm 0.4) \times 10^{-4}$			1491
$p\overline{n}\pi^-$ or c.c.	$(2.48 \pm 0.17) \times 10^{-4}$			–
$p\overline{n}\pi^-\pi^0$	$(3.2 \pm 0.7) \times 10^{-4}$			1492
$2(\pi^+\pi^-\pi^0)$	$(4.7 \pm 1.5) \times 10^{-3}$			1776
$\eta\pi^+\pi^-$	$< 1.6 \times 10^{-4}$	CL=90%		1791
$\eta\pi^+\pi^-\pi^0$	$(9.5 \pm 1.7) \times 10^{-4}$			1778
$2(\pi^+\pi^-)\eta$	$(1.2 \pm 0.6) \times 10^{-3}$			1758
$\eta'\pi^+\pi^-\pi^0$	$(4.5 \pm 2.1) \times 10^{-4}$			1692
$\omega\pi^+\pi^-$	$(7.3 \pm 1.2) \times 10^{-4}$	S=2.1		1748
$b_1^\pm\pi^\mp$	$(4.0 \pm 0.6) \times 10^{-4}$	S=1.1		1635
$b_1^0\pi^0$	$(2.4 \pm 0.6) \times 10^{-4}$			–
$\omega f_2(1270)$	$(2.2 \pm 0.4) \times 10^{-4}$			1515
$\pi^+\pi^-K^+K^-$	$(7.5 \pm 0.9) \times 10^{-4}$	S=1.9		1726
$\rho^0 K^+K^-$	$(2.2 \pm 0.4) \times 10^{-4}$			1616
$K^*(892)^0\overline{K}^*_2(1430)^0$	$(1.9 \pm 0.5) \times 10^{-4}$			1418
$K^+K^-\pi^+\pi^-\eta$	$(1.3 \pm 0.7) \times 10^{-3}$			1574
$K^+K^-2(\pi^+\pi^-)\pi^0$	$(1.00 \pm 0.31) \times 10^{-3}$			1611
$K^+K^-2(\pi^+\pi^-)$	$(1.9 \pm 0.9) \times 10^{-3}$			1654
$K_1(1270)^\pm K^\mp$	$(1.00 \pm 0.28) \times 10^{-3}$			1581
$K^0_S K^0_S \pi^+\pi^-$	$(2.2 \pm 0.4) \times 10^{-4}$			1724
$\rho^0 p\overline{p}$	$(5.0 \pm 2.2) \times 10^{-5}$			1252
$K^+\overline{K}^*(892)^0\pi^-$ + c.c.	$(6.7 \pm 2.5) \times 10^{-4}$			1674
$2(\pi^+\pi^-)$	$(2.4 \pm 0.6) \times 10^{-4}$	S=2.2		1817
$\rho^0\pi^+\pi^-$	$(2.2 \pm 0.6) \times 10^{-4}$	S=1.4		1750
$K^+K^-\pi^+\pi^-\pi^0$	$(1.26 \pm 0.09) \times 10^{-3}$			1694
$\omega f_0(1710) \rightarrow \omega K^+K^-$	$(5.9 \pm 2.2) \times 10^{-5}$			–
$K^*(892)^0 K^-\pi^+\pi^0$ + c.c.	$(8.6 \pm 2.2) \times 10^{-4}$			–
$K^*(892)^+ K^-\pi^+\pi^-$ + c.c.	$(9.6 \pm 2.8) \times 10^{-4}$			–
$K^*(892)^+ K^-\rho^0$ + c.c.	$(7.3 \pm 2.6) \times 10^{-4}$			–
$K^*(892)^0 K^-\rho^+$ + c.c.	$(6.1 \pm 1.8) \times 10^{-4}$			–
ηK^+K^-, no $\eta\phi$	$(3.1 \pm 0.4) \times 10^{-5}$			1664
ωK^+K^-	$(1.85 \pm 0.25) \times 10^{-4}$	S=1.1		1614
$\omega K^*(892)^+ K^-$ + c.c.	$(2.07 \pm 0.26) \times 10^{-4}$			1482
$\omega K^*_2(1430)^+ K^-$ + c.c.	$(6.1 \pm 1.2) \times 10^{-5}$			1253

Meson Summary Table

$\omega\overline{K}^*(892)^0K^0$	(1.68 ±0.30) × 10^{-4}			1481
$\omega\overline{K}_2^*(1430)^0K^0$	(5.8 ±2.2) × 10^{-5}			1251
$\omega X(1440) \to \omega K_S^0 K^-\pi^+$ + c.c.	(1.6 ±0.4) × 10^{-5}			–
$\omega X(1440) \to \omega K^+K^-\pi^0$	(1.09 ±0.26) × 10^{-5}			–
$\omega f_1(1285) \to \omega K_S^0 K^-\pi^+$ + c.c.	(3.0 ±1.0) × 10^{-6}			–
$\omega f_1(1285) \to \omega K^+K^-\pi^0$	(1.2 ±0.7) × 10^{-6}			–
$3(\pi^+\pi^-)$	(3.5 ±2.0) × 10^{-4}		S=2.8	1774
$p\overline{p}\pi^+\pi^-\pi^0$	(7.3 ±0.7) × 10^{-4}			1435
K^+K^-	(7.1 ±0.5) × 10^{-5}		S=1.5	1776
$K_S^0K_L^0$	(5.34 ±0.33) × 10^{-5}			1775
$\pi^+\pi^-\pi^0$	(2.01 ±0.17) × 10^{-4}		S=1.7	1830
$\rho(2150)\pi \to \pi^+\pi^-\pi^0$	(1.9 $^{+1.2}_{-0.4}$) × 10^{-4}			–
$\rho(770)\pi \to \pi^+\pi^-\pi^0$	(3.2 ±1.2) × 10^{-5}		S=1.8	–
$\pi^+\pi^-$	(7.8 ±2.6) × 10^{-6}			1838
$K_1(1400)^\pm K^\mp$	< 3.1	× 10^{-4}	CL=90%	1532
$K_2^*(1430)^\pm K^\mp$	(7.1 $^{+1.3}_{-0.9}$) × 10^{-5}			–
$K^+K^-\pi^0$	(4.07 ±0.31) × 10^{-5}			1754
$K^+K^*(892)^-$ + c.c.	(2.9 ±0.4) × 10^{-5}		S=1.2	1698
$K^*(892)^0\overline{K}^0$ + c.c.	(1.09 ±0.20) × 10^{-4}			1697
$\phi\pi^+\pi^-$	(1.17 ±0.29) × 10^{-4}		S=1.7	1690
$\phi f_0(980) \to \pi^+\pi^-$	(6.8 ±2.4) × 10^{-5}		S=1.1	–
$2(K^+K^-)$	(6.0 ±1.4) × 10^{-5}			1499
ϕK^+K^-	(7.0 ±1.6) × 10^{-5}			1546
$2(K^+K^-)\pi^0$	(1.10 ±0.28) × 10^{-4}			1440
$\phi\eta$	(3.10 ±0.31) × 10^{-5}			1654
$\phi\eta'$	(3.1 ±1.6) × 10^{-5}			1555
$\omega\eta'$	(3.2 $^{+2.5}_{-2.1}$) × 10^{-5}			1623
$\omega\pi^0$	(2.1 ±0.6) × 10^{-5}			1757
$\rho\eta'$	(1.9 $^{+1.7}_{-1.2}$) × 10^{-5}			1625
$\rho\eta$	(2.2 ±0.6) × 10^{-5}		S=1.1	1717
$\omega\eta$	< 1.1	× 10^{-5}	CL=90%	1715
$\phi\pi^0$	< 4	× 10^{-7}	CL=90%	1699
$\eta_c\pi^+\pi^-\pi^0$	< 1.0	× 10^{-3}	CL=90%	–
$p\overline{p}K^+K^-$	(2.7 ±0.7) × 10^{-5}			1118
$\overline{\Lambda}nK_S^0$ + c.c.	(8.1 ±1.8) × 10^{-5}			1324
$\phi f_2'(1525)$	(4.4 ±1.6) × 10^{-5}			1321
$\Theta(1540)\overline{\Theta}(1540) \to K_S^0 pK^-\overline{n}$ + c.c.	< 8.8	× 10^{-6}	CL=90%	–
$\Theta(1540)K^-\overline{n} \to K_S^0 pK^-\overline{n}$	< 1.0	× 10^{-5}	CL=90%	–
$\Theta(1540)K_S^0\overline{p} \to K_S^0\overline{p}K^+n$	< 7.0	× 10^{-6}	CL=90%	–
$\overline{\Theta}(1540)K^+n \to K_S^0\overline{p}K^+n$	< 2.6	× 10^{-5}	CL=90%	–
$\overline{\Theta}(1540)K_S^0p \to K_S^0pK^-\overline{n}$	< 6.0	× 10^{-6}	CL=90%	–
$K_S^0K_S^0$	< 4.6	× 10^{-6}		1775

Radiative decays

$\gamma\chi_{c0}(1P)$	(9.99 ±0.27) %			261
$\gamma\chi_{c1}(1P)$	(9.55 ±0.31) %			171
$\gamma\chi_{c2}(1P)$	(9.11 ±0.31) %			128
$\gamma\eta_c(1S)$	(3.4 ±0.5) × 10^{-3}		S=1.3	636
$\gamma\eta_c(2S)$	(7 ±5) × 10^{-4}			46
$\gamma\pi^0$	(1.6 ±0.4) × 10^{-6}			1841
$\gamma\eta'(958)$	(1.23 ±0.06) × 10^{-4}			1719
$\gamma f_2(1270)$	(2.1 ±0.4) × 10^{-4}			1623
$\gamma f_0(1710) \to \gamma\pi\pi$	(3.0 ±1.3) × 10^{-5}			–
$\gamma f_0(1710) \to \gamma K\overline{K}$	(6.0 ±1.6) × 10^{-5}			–
$\gamma\gamma$	< 1.4	× 10^{-4}	CL=90%	1843
$\gamma\eta$	(1.4 ±0.5) × 10^{-6}			1802
$\gamma\eta\pi^+\pi^-$	(8.7 ±2.1) × 10^{-4}			1791
$\gamma\eta(1405) \to \gamma K\overline{K}\pi$	< 9	× 10^{-5}	CL=90%	1569
$\gamma\eta(1405) \to \eta\pi^+\pi^-$	(3.6 ±2.5) × 10^{-5}			–
$\gamma\eta(1475) \to K\overline{K}\pi$	< 1.4	× 10^{-4}	CL=90%	–
$\gamma\eta(1475) \to \eta\pi^+\pi^-$	< 8.8	× 10^{-5}	CL=90%	–
$\gamma 2(\pi^+\pi^-)$	(4.0 ±0.6) × 10^{-4}			1817
$\gamma K^{*0}K^+\pi^-$ + c.c.	(3.7 ±0.9) × 10^{-4}			1674
$\gamma K^{*0}\overline{K}^{*0}$	(2.4 ±0.7) × 10^{-4}			1613
$\gamma K_S^0K^+\pi^-$ + c.c.	(2.6 ±0.5) × 10^{-4}			1753
$\gamma K^+K^-\pi^+\pi^-$	(1.9 ±0.5) × 10^{-4}			1726
$\gamma p\overline{p}$	(3.9 ±0.5) × 10^{-5}		S=2.0	1586
$\gamma f_2(1950) \to \gamma p\overline{p}$	(1.20 ±0.22) × 10^{-5}			–
$\gamma f_2(2150) \to \gamma p\overline{p}$	(7.2 ±1.8) × 10^{-6}			–
$\gamma X(1835) \to \gamma p\overline{p}$	(4.6 $^{+1.8}_{-4.0}$) × 10^{-6}			–
$\gamma X \to \gamma p\overline{p}$	[vvaa] < 2	× 10^{-6}	CL=90%	–
$\gamma\pi^+\pi^-p\overline{p}$	(2.8 ±1.4) × 10^{-5}			1491
$\gamma 2(\pi^+\pi^-)K^+K^-$	< 2.2	× 10^{-4}	CL=90%	1654
$\gamma 3(\pi^+\pi^-)$	< 1.7	× 10^{-4}	CL=90%	1774
$\gamma K^+K^-K^+K^-$	< 4	× 10^{-5}	CL=90%	1499
$\gamma\gamma J/\psi$	(3.1 $^{+1.0}_{-1.2}$) × 10^{-4}			542

Other decays

invisible	< 1.6	%	CL=90%	–

$\psi(3770)$

$I^G(J^{PC}) = 0^-(1^{--})$

Mass m = 3773.15 ± 0.33 MeV
Full width Γ = 27.2 ± 1.0 MeV
Γ_{ee} = 0.262 ± 0.018 keV (S = 1.4)

In addition to the dominant decay mode to $D\overline{D}$, $\psi(3770)$ was found to decay into the final states containing the J/ψ (BAI 05, ADAM 06). ADAMS 06 and HUANG 06A searched for various decay modes with light hadrons and found a statistically significant signal for the decay to $\phi\eta$ only (ADAMS 06).

$\psi(3770)$ DECAY MODES	Fraction (Γ_i/Γ)	Scale factor/ Confidence level	p (MeV/c)
$D\overline{D}$	(93 $^{+8}_{-9}$) %	S=2.0	286
$D^0\overline{D}^0$	(52 ±5) %	S=2.0	286
D^+D^-	(41 ±4) %	S=2.0	252
$J/\psi\pi^+\pi^-$	(1.93±0.28) × 10^{-3}		560
$J/\psi\pi^0\pi^0$	(8.0 ±3.0) × 10^{-4}		564
$J/\psi\eta$	(9 ±4) × 10^{-4}		360
$J/\psi\pi^0$	< 2.8 × 10^{-4}	CL=90%	603
e^+e^-	(9.6 ±0.7) × 10^{-6}	S=1.3	1887

Decays to light hadrons

$b_1(1235)\pi$	< 1.4	× 10^{-5}	CL=90%	1683
$\phi\eta'$	< 7	× 10^{-4}	CL=90%	1607
$\omega\eta'$	< 4	× 10^{-4}	CL=90%	1672
$\rho^0\eta'$	< 6	× 10^{-4}	CL=90%	1674
$\phi\eta$	(3.1 ±0.7) × 10^{-4}			1703
$\omega\eta$	< 1.4	× 10^{-5}	CL=90%	1762
$\rho^0\eta$	< 5	× 10^{-4}	CL=90%	1764
$\phi\pi^0$	< 3	× 10^{-5}	CL=90%	1746
$\omega\pi^0$	< 6	× 10^{-4}	CL=90%	1803
$\pi^+\pi^-\pi^0$	< 5	× 10^{-6}	CL=90%	1874
$\rho\pi$	< 5	× 10^{-6}	CL=90%	1804
$K^*(892)^+K^-$ + c.c.	< 1.4	× 10^{-5}	CL=90%	1745
$K^*(892)^0\overline{K}^0$ + c.c.	< 1.2	× 10^{-3}	CL=90%	1744
$K_S^0K_L^0$	< 1.2	× 10^{-5}	CL=90%	1820
$2(\pi^+\pi^-)$	< 1.12	× 10^{-3}	CL=90%	1861
$2(\pi^+\pi^-)\pi^0$	< 1.06	× 10^{-3}	CL=90%	1843
$2(\pi^+\pi^-\pi^0)$	< 5.85	%	CL=90%	1821
$\omega\pi^+\pi^-$	< 6.0	× 10^{-4}	CL=90%	1794
$3(\pi^+\pi^-)$	< 9.1	× 10^{-3}		1819
$3(\pi^+\pi^-)\pi^0$	< 1.37	%		1792
$3(\pi^+\pi^-)2\pi^0$	< 11.74	%	CL=90%	1760
$\eta\pi^+\pi^-$	< 1.24	× 10^{-3}	CL=90%	1836
$\pi^+\pi^-2\pi^0$	< 8.9	× 10^{-3}	CL=90%	1862
$\rho^0\pi^+\pi^-$	< 6.9	× 10^{-3}	CL=90%	1796
$\eta 3\pi$	< 1.34	× 10^{-3}	CL=90%	1824
$\eta 2(\pi^+\pi^-)$	< 2.43	%		1804
$\eta\rho^0\pi^+\pi^-$	< 1.45	%	CL=90%	1708
$\eta' 3\pi$	< 2.44	× 10^{-3}	CL=90%	1740
$K^+K^-\pi^+\pi^-$	< 9.0	× 10^{-4}	CL=90%	1772
$\phi\pi^+\pi^-$	< 4.1	× 10^{-4}	CL=90%	1737
$K^+K^-2\pi^0$	< 4.2	× 10^{-3}	CL=90%	1774
$4(\pi^+\pi^-)$	< 1.67	%	CL=90%	1757
$4(\pi^+\pi^-)\pi^0$	< 3.06	%	CL=90%	1720
$\phi f_0(980)$	< 4.5	× 10^{-4}	CL=90%	1597
$K^+K^-\pi^+\pi^-\pi^0$	< 2.36	× 10^{-3}	CL=90%	1741
$K^+K^-\rho^0\pi^0$	< 8	× 10^{-4}	CL=90%	1624
$K^+K^-\rho^+\pi^-$	< 1.46	%	CL=90%	1622
ωK^+K^-	< 3.4	× 10^{-4}	CL=90%	1664
$\phi\pi^+\pi^-\pi^0$	< 3.8	× 10^{-3}	CL=90%	1722
$K^{*0}K^-\pi^+\pi^0$ + c.c.	< 1.62	%	CL=90%	1693
$K^{*+}K^-\pi^+\pi^-$ + c.c.	< 3.23	%	CL=90%	1692
$K^+K^-\pi^+\pi^-2\pi^0$	< 2.67	%	CL=90%	1705
$K^+K^-2(\pi^+\pi^-)$	< 1.03	%	CL=90%	1702
$K^+K^-2(\pi^+\pi^-)\pi^0$	< 3.60	%	CL=90%	1660
ηK^+K^-	< 4.1	× 10^{-4}	CL=90%	1712

$\eta K^+ K^- \pi^+ \pi^-$	$<$	1.24	%	CL=90%	1624
$\rho^0 K^+ K^-$	$<$	5.0	$\times 10^{-3}$	CL=90%	1665
$2(K^+ K^-)$	$<$	6.0	$\times 10^{-4}$	CL=90%	1552
$\phi K^+ K^-$	$<$	7.5	$\times 10^{-4}$	CL=90%	1598
$2(K^+ K^-)\pi^0$	$<$	2.9	$\times 10^{-4}$	CL=90%	1493
$2(K^+ K^-)\pi^+ \pi^-$	$<$	3.2	$\times 10^{-3}$	CL=90%	1425
$K^0_S K^- \pi^+$	$<$	3.2	$\times 10^{-3}$	CL=90%	1799
$K^0_S K^- \pi^+ \pi^0$	$<$	1.33	%	CL=90%	1773
$K^0_S K^- \rho^+$	$<$	6.6	$\times 10^{-3}$	CL=90%	1664
$K^0_S K^- 2\pi^+ \pi^-$	$<$	8.7	$\times 10^{-3}$	CL=90%	1739
$K^0_S K^- \pi^+ \rho^0$	$<$	1.6	%	CL=90%	1621
$K^0_S K^- \pi^+ \eta$	$<$	1.3	%	CL=90%	1669
$K^0_S K^- 2\pi^+ \pi^- \pi^0$	$<$	4.18	%	CL=90%	1703
$K^0_S K^- 2\pi^+ \pi^- \eta$	$<$	4.8	%	CL=90%	1570
$K^0_S K^- \pi^+ 2(\pi^+ \pi^-)$	$<$	1.22	%	CL=90%	1658
$K^0_S K^- \pi^+ 2\pi^0$	$<$	2.65	%	CL=90%	1742
$K^0_S K^- K^+ K^- \pi^+$	$<$	4.9	$\times 10^{-3}$	CL=90%	1490
$K^0_S K^- K^+ K^- \pi^+ \pi^0$	$<$	3.0	%	CL=90%	1427
$K^0_S K^- K^+ K^- \pi^+ \eta$	$<$	2.2	%	CL=90%	1214
$K^{*0} K^- \pi^+ +$ c.c.	$<$	9.7	$\times 10^{-3}$	CL=90%	1722
$p\overline{p}\pi^0$	$<$	1.2	$\times 10^{-3}$		1595
$p\overline{p}\pi^+ \pi^-$	$<$	5.8	$\times 10^{-4}$	CL=90%	1544
$\Lambda\overline{\Lambda}$	$<$	1.2	$\times 10^{-4}$	CL=90%	1521
$p\overline{p}\pi^+ \pi^- \pi^0$	$<$	1.85	$\times 10^{-3}$	CL=90%	1490
$\omega p\overline{p}$	$<$	2.9	$\times 10^{-4}$	CL=90%	1309
$\Lambda\overline{\Lambda}\pi^0$	$<$	7	$\times 10^{-5}$	CL=90%	1469
$p\overline{p}2(\pi^+ \pi^-)$	$<$	2.6	$\times 10^{-3}$	CL=90%	1425
$\eta p\overline{p}$	$<$	5.4	$\times 10^{-4}$	CL=90%	1430
$\eta p\overline{p}\pi^+ \pi^-$	$<$	3.3	$\times 10^{-3}$	CL=90%	1284
$\rho^0 p\overline{p}$	$<$	1.7	$\times 10^{-3}$	CL=90%	1313
$p\overline{p}K^+ K^-$	$<$	3.2	$\times 10^{-4}$	CL=90%	1185
$\eta p\overline{p}K^+ K^-$	$<$	6.9	$\times 10^{-3}$	CL=90%	736
$\pi^0 p\overline{p}K^+ K^-$	$<$	1.2	$\times 10^{-3}$	CL=90%	1093
$\phi p\overline{p}$	$<$	1.3	$\times 10^{-4}$	CL=90%	1178
$\Lambda\overline{\Lambda}\pi^+ \pi^-$	$<$	2.5	$\times 10^{-4}$	CL=90%	1405
$\Lambda\overline{p}K^+$	$<$	2.8	$\times 10^{-4}$	CL=90%	1387
$\Lambda\overline{p}K^+ \pi^+ \pi^-$	$<$	6.3	$\times 10^{-4}$	CL=90%	1234
$\Lambda\overline{\Lambda}\eta$	$<$	1.9	$\times 10^{-4}$	CL=90%	1262
$\Sigma^+\overline{\Sigma}^-$	$<$	1.0	$\times 10^{-4}$	CL=90%	1464
$\Sigma^0\overline{\Sigma}^0$	$<$	4	$\times 10^{-5}$	CL=90%	1462
$\Xi^+\overline{\Xi}^-$	$<$	1.5	$\times 10^{-4}$	CL=90%	–
$\Xi^0\overline{\Xi}^0$	$<$	1.4	$\times 10^{-4}$	CL=90%	1353

Radiative decays

$\gamma\chi_{c2}$	$<$	9	$\times 10^{-4}$	CL=90%	211
$\gamma\chi_{c1}$	(	2.9 $\pm$0.6)	$\times 10^{-3}$		253
$\gamma\chi_{c0}$	(	7.3 $\pm$0.9)	$\times 10^{-3}$		341
$\gamma\eta'$	$<$	1.8	$\times 10^{-4}$	CL=90%	1765
$\gamma\eta$	$<$	1.5	$\times 10^{-4}$	CL=90%	1847
$\gamma\pi^0$	$<$	2	$\times 10^{-4}$	CL=90%	1884

X(3872)

$I^G(J^{PC}) = 0^+(1^{++})$

Mass $m = 3871.69 \pm 0.17$ MeV
$m_{X(3872)} - m_{J/\psi} = 775 \pm 4$ MeV
$m_{X(3872)} - m_{\psi(2S)}$
Full width $\Gamma < 1.2$ MeV, CL = 90%

X(3872) DECAY MODES	Fraction (Γ_i/Γ)		p (MeV/c)
$\pi^+ \pi^- J/\psi(1S)$	> 2.6 %		650
$\omega J/\psi(1S)$	> 1.9 %		†
$D^0\overline{D}^0\pi^0$	>32 %		117
$\overline{D}^{*0} D^0$	>24 %		†
$\gamma J/\psi$	> 6	$\times 10^{-3}$	697
$\gamma\psi(2S)$ [xxaa]	> 3.0 %		181
$\pi^+ \pi^- \eta_c(1S)$	not seen		746
$p\overline{p}$	not seen		1693

X(3900)±

$I(J^P) = ?(1^+)$

Mass $m = 3888.7 \pm 3.4$ MeV (S = 1.3)
Full width $\Gamma = 35 \pm 7$ MeV

X(3900)± DECAY MODES	Fraction (Γ_i/Γ)	p (MeV/c)
$J/\psi\pi^\pm$	seen	700
$h_c\pi^\pm$	not seen	–
$(D\overline{D}^*)^\pm$	seen	–

$\chi_{c0}(2P)$ was X(3915)

$I^G(J^{PC}) = 0^+(0^{++})$

Mass $m = 3918.4 \pm 1.9$ MeV
Full width $\Gamma = 20 \pm 5$ MeV (S = 1.1)

$\chi_{c0}(2P)$ DECAY MODES	Fraction (Γ_i/Γ)	p (MeV/c)
$\omega J/\psi$	seen	222
$\pi^+ \pi^- \eta_c(1S)$	not seen	785
$K\overline{K}$	not seen	–
$\gamma\gamma$	seen	1959

$\chi_{c2}(2P)$

$I^G(J^{PC}) = 0^+(2^{++})$

Mass $m = 3927.2 \pm 2.6$ MeV
Full width $\Gamma = 24 \pm 6$ MeV

$\chi_{c2}(2P)$ DECAY MODES	Fraction (Γ_i/Γ)	p (MeV/c)
$\gamma\gamma$	seen	1964
$D\overline{D}$	seen	615
$D^+ D^-$	seen	600
$D^0\overline{D}^0$	seen	615
$\pi^+ \pi^- \eta_c(1S)$	not seen	792
$K\overline{K}$	not seen	1901

$\psi(4040)$ [yyaa]

$I^G(J^{PC}) = 0^-(1^{--})$

Mass $m = 4039 \pm 1$ MeV
Full width $\Gamma = 80 \pm 10$ MeV
$\Gamma_{ee} = 0.86 \pm 0.07$ keV

Due to the complexity of the $c\overline{c}$ threshold region, in this listing, "seen" ("not seen") means that a cross section for the mode in question has been measured at effective $\sqrt{s}$ near this particle's central mass value, more (less) than 2σ above zero, without regard to any peaking behavior in $\sqrt{s}$ or absence thereof. See mode listing(s) for details and references.

$\psi(4040)$ DECAY MODES	Fraction (Γ_i/Γ)		Confidence level	p (MeV/c)
$e^+ e^-$	$(1.07 \pm 0.16) \times 10^{-5}$			2019
$D\overline{D}$	seen			775
$D^0\overline{D}^0$	seen			775
$D^+ D^-$	seen			764
$D^*\overline{D}+$ c.c.	seen			569
$D^*(2007)^0\overline{D}^0+$ c.c.	seen			575
$D^*(2010)^+ D^-+$ c.c.	seen			561
$D^*\overline{D}^*$	seen			193
$D^*(2007)^0\overline{D}^*(2007)^0$	seen			225
$D^*(2010)^+ D^*(2010)^-$	seen			193
$D^0 D^-\pi^+$+c.c. (excl. $D^*(2007)^0\overline{D}^0$ +c.c., $D^*(2010)^+ D^-$ +c.c.)	not seen			–
$D\overline{D}^*\pi$(excl. $D^*\overline{D}^*$)	not seen			–
$D^0\overline{D}^{*-}\pi^+$+c.c. (excl. $D^*(2010)^+ D^*(2010)^-$)	seen			–
$D_s^+ D_s^-$	seen			452
$J/\psi\pi^+ \pi^-$	< 4	$\times 10^{-3}$	90%	794
$J/\psi\pi^0 \pi^0$	< 2	$\times 10^{-3}$	90%	797
$J/\psi\eta$	(5.2 $\pm$0.7)	$\times 10^{-3}$		675
$J/\psi\pi^0$	< 2.8	$\times 10^{-4}$	90%	823
$J/\psi\pi^+ \pi^- \pi^0$	< 2	$\times 10^{-3}$	90%	746
$\chi_{c1}\gamma$	< 1.1	%	90%	494
$\chi_{c2}\gamma$	< 1.7	%	90%	454
$\chi_{c1}\pi^+ \pi^- \pi^0$	< 1.1	%	90%	306
$\chi_{c2}\pi^+ \pi^- \pi^0$	< 3.2	%	90%	233
$h_c(1P)\pi^+ \pi^-$	< 3	$\times 10^{-3}$	90%	403
$\phi\pi^+ \pi^-$	< 3	$\times 10^{-3}$	90%	1880
$\Lambda\overline{\Lambda}\pi^+ \pi^-$	< 2.9	$\times 10^{-4}$	90%	1578

Meson Summary Table

$\Lambda\overline{\Lambda}\pi^0$	< 9	$\times 10^{-5}$	90%	1636
$\Lambda\overline{\Lambda}\eta$	< 3.0	$\times 10^{-4}$	90%	1452
$\Sigma^+\overline{\Sigma}^-$	< 1.3	$\times 10^{-4}$	90%	1632
$\Sigma^0\overline{\Sigma}^0$	< 7	$\times 10^{-5}$	90%	1630
$\Xi^+\overline{\Xi}^-$	< 1.6	$\times 10^{-4}$	90%	–
$\Xi^0\overline{\Xi}^0$	< 1.8	$\times 10^{-4}$	90%	1533

$\psi(4160)$ [yyaa]

$I^G(J^{PC}) = 0^-(1^{--})$

Mass $m = 4191 \pm 5$ MeV
Full width $\Gamma = 70 \pm 10$ MeV
$\Gamma_{ee} = 0.48 \pm 0.22$ keV

Due to the complexity of the $c\overline{c}$ threshold region, in this listing, "seen" ("not seen") means that a cross section for the mode in question has been measured at effective $\sqrt{s}$ near this particle's central mass value, more (less) than 2σ above zero, without regard to any peaking behavior in $\sqrt{s}$ or absence thereof. See mode listing(s) for details and references.

$\psi(4160)$ DECAY MODES	Fraction (Γ_i/Γ)	Confidence level	p (MeV/c)
e^+e^-	$(6.9\pm3.3)\times10^{-6}$		2096
$\mu^+\mu^-$	seen		2093
$D\overline{D}$	seen		956
$D^0\overline{D}^0$	seen		956
D^+D^-	seen		947
$D^*\overline{D}$ + c.c.	seen		798
$D^*(2007)^0\overline{D}^0$ + c.c.	seen		802
$D^*(2010)^+D^-$ + c.c.	seen		792
$D^*\overline{D}^*$	seen		592
$D^*(2007)^0\overline{D}^*(2007)^0$	seen		603
$D^*(2010)^+D^*(2010)^-$	seen		592
$D^0D^-\pi^+$+c.c. (excl. $D^*(2007)^0\overline{D}^0$ +c.c., $D^*(2010)^+D^-$ +c.c.)	not seen		–
$D\overline{D}^*\pi$+c.c. (excl. $D^*\overline{D}^*$)	seen		–
$D^0D^{*-}\pi^+$+c.c. (excl. $D^*(2010)^+D^*(2010)^-$)	not seen		–
$D_s^+D_s^-$	not seen		720
$D_s^{*+}D_s^-$+c.c.	seen		385
$J/\psi\pi^+\pi^-$	< 3	$\times 10^{-3}$ 90%	919
$J/\psi\pi^0\pi^0$	< 3	$\times 10^{-3}$ 90%	922
$J/\psi K^+K^-$	< 2	$\times 10^{-3}$ 90%	407
$J/\psi\eta$	< 8	$\times 10^{-3}$ 90%	821
$J/\psi\pi^0$	< 1	$\times 10^{-3}$ 90%	944
$J/\psi\eta'$	< 5	$\times 10^{-3}$ 90%	457
$J/\psi\pi^+\pi^-\pi^0$	< 1	$\times 10^{-3}$ 90%	879
$\psi(2S)\pi^+\pi^-$	< 4	$\times 10^{-3}$ 90%	396
$\chi_{c1}\gamma$	< 7	$\times 10^{-3}$ 90%	625
$\chi_{c2}\gamma$	< 1.3	% 90%	587
$\chi_{c1}\pi^+\pi^-\pi^0$	< 2	$\times 10^{-3}$ 90%	496
$\chi_{c2}\pi^+\pi^-\pi^0$	< 8	$\times 10^{-3}$ 90%	445
$h_c(1P)\pi^+\pi^-$	< 5	$\times 10^{-3}$ 90%	556
$h_c(1P)\pi^0\pi^0$	< 2	$\times 10^{-3}$ 90%	560
$h_c(1P)\eta$	< 2	$\times 10^{-3}$ 90%	348
$h_c(1P)\pi^0$	< 4	$\times 10^{-4}$ 90%	600
$\phi\pi^+\pi^-$	< 2	$\times 10^{-3}$ 90%	1961
$\chi_{c0}\omega$	not seen		265
$\chi_{c1}\gamma$	not seen		676
$\chi_{c2}\gamma$	not seen		638
$\chi_{c1}\pi^+\pi^-\pi^0$	not seen		560
$\chi_{c2}\pi^+\pi^-\pi^0$	not seen		512
$h_c(1P)\pi^+\pi^-$	not seen		613
$\phi\pi^+\pi^-$	not seen		1993
$\phi f_0(980) \rightarrow \phi\pi^+\pi^-$	not seen		–
$D\overline{D}$	not seen		1020
$D^0\overline{D}^0$	not seen		1020
D^+D^-	not seen		1011
$D^*\overline{D}$+c.c.	not seen		887
$D^*(2007)^0\overline{D}^0$+c.c.	not seen		–
$D^*(2010)^+D^-$+c.c.	not seen		–
$D^*\overline{D}^*$	not seen		691
$D^*(2007)^0\overline{D}^*(2007)^0$	not seen		700
$D^*(2010)^+D^*(2010)^-$	not seen		691
$D^0D^-\pi^+$+c.c. (excl. $D^*(2007)^0\overline{D}^{*0}$ +c.c., $D^*(2010)^+D^-$ +c.c.)	not seen		–
$D\overline{D}^*\pi$+c.c. (excl. $D^*\overline{D}^*$)	not seen		723
$D^0D^{*-}\pi^+$+c.c. (excl. $D^*(2010)^+D^*(2010)^-$)	not seen		–
$D^0D^*(2010)^-\pi^+$+c.c.	not seen		716
$D^*\overline{D}^*\pi$	not seen		449
$D_s^+D_s^-$	not seen		803
$D_s^{*+}D_s^-$+c.c.	not seen		615
$D_s^{*+}D_s^{*-}$	not seen		239
$p\overline{p}$	not seen		1907
$K_S^0K^\pm\pi^\mp$	not seen		2048
$K^+K^-\pi^0$	not seen		2049

$X(4260)$

$I^G(J^{PC}) = ?^?(1^{--})$

Mass $m = 4251 \pm 9$ MeV (S = 1.6)
Full width $\Gamma = 120 \pm 12$ MeV (S = 1.1)

$X(4260)$ DECAY MODES	Fraction (Γ_i/Γ)	p (MeV/c)
$J/\psi\pi^+\pi^-$	seen	967
$J/\psi f_0(980)$, $f_0(980) \rightarrow \pi^+\pi^-$	seen	–
$X(3900)^\pm\pi^\mp$, $X^\pm \rightarrow J/\psi\pi^\pm$	seen	–
$J/\psi\pi^0\pi^0$	seen	969
$J/\psi K^+K^-$	seen	512
$X(3872)\gamma$	seen	363
$J/\psi\eta$	not seen	876
$J/\psi\pi^0$	not seen	991
$J/\psi\eta'$	not seen	552
$J/\psi\pi^+\pi^-\pi^0$	not seen	930
$J/\psi\eta\eta$	not seen	311
$\psi(2S)\pi^+\pi^-$	not seen	459
$\psi(2S)\eta$	not seen	129

$X(4360)$

$I^G(J^{PC}) = ?^?(1^{--})$

$X(4360)$ MASS $= 4361 \pm 13$ MeV
$X(4360)$ WIDTH $= 74 \pm 18$ MeV

$X(4360)$ DECAY MODES	Fraction (Γ_i/Γ)	p (MeV/c)
$\psi(2S)\pi^+\pi^-$	seen	567

$\psi(4415)$ [yyaa]

$I^G(J^{PC}) = 0^-(1^{--})$

Mass $m = 4421 \pm 4$ MeV
Full width $\Gamma = 62 \pm 20$ MeV
$\Gamma_{ee} = 0.58 \pm 0.07$ keV

Due to the complexity of the $c\overline{c}$ threshold region, in this listing, "seen" ("not seen") means that a cross section for the mode in question has been measured at effective $\sqrt{s}$ near this particle's central mass value, more (less) than 2σ above zero, without regard to any peaking behavior in $\sqrt{s}$ or absence thereof. See mode listing(s) for details and references.

$\psi(4415)$ DECAY MODES	Fraction (Γ_i/Γ)	Confidence level	p (MeV/c)
$D\overline{D}$	not seen		1187
$D^0\overline{D}^0$	seen		1187
D^+D^-	seen		1179
$D^*\overline{D}$ + c.c.	not seen		1063
$D^*(2007)^0\overline{D}^0$ + c.c.	seen		1066
$D^*(2010)^+D^-$ + c.c.	seen		1059
$D^*\overline{D}^*$	not seen		919
$D^*(2007)^0\overline{D}^*(2007)^0$ + c.c.	seen		927
$D^*(2010)^+D^*(2010)^-$ + c.c.	seen		919
$D^0D^-\pi^+$(excl. $D^*(2007)^0\overline{D}^0$ +c.c., $D^*(2010)^+D^-$ +c.c.	< 2.3 %	90%	–
$D\overline{D}_2^*(2460) \rightarrow D^0D^-\pi^+$+c.c.	(10 ± 4) %		–
$D^0D^{*-}\pi^+$+c.c.	< 11 %	90%	926
$D_s^+D_s^-$	not seen		1006
$D_s^{*+}D_s^-$+c.c.	seen		–
$D_s^{*+}D_s^{*-}$	not seen		652
$J/\psi\eta$	< 6 $\times 10^{-3}$	90%	1022
e^+e^-	$(9.4\pm3.2)\times10^{-6}$		2210

$X(4660)$

$I^G(J^{PC}) = ?^?(1^{--})$

$X(4660)$ MASS = 4664 ± 12 MeV
$X(4660)$ WIDTH = 48 ± 15 MeV

$X(4660)$ DECAY MODES	Fraction (Γ_i/Γ)	p (MeV/c)
$\psi(2S)\pi^+\pi^-$	seen	838

$b\overline{b}$ MESONS

$\Upsilon(1S)$

$I^G(J^{PC}) = 0^-(1^{--})$

Mass m = 9460.30 ± 0.26 MeV (S = 3.3)
Full width Γ = 54.02 ± 1.25 keV
Γ_{ee} = 1.340 ± 0.018 keV

$\Upsilon(1S)$ DECAY MODES	Fraction (Γ_i/Γ)	Confidence level	p (MeV/c)
$\tau^+\tau^-$	(2.60 ±0.10) %		4384
e^+e^-	(2.38 ±0.11) %		4730
$\mu^+\mu^-$	(2.48 ±0.05) %		4729
Hadronic decays			
ggg	(81.7 ±0.7) %		–
γgg	(2.2 ±0.6) %		–
$\eta'(958)$ anything	(2.94 ±0.24) %		–
$J/\psi(1S)$ anything	(6.5 ±0.7) $\times 10^{-4}$		4223
χ_{c0} anything	< 5 $\times 10^{-3}$	90%	–
χ_{c1} anything	(2.3 ±0.7) $\times 10^{-4}$		–
χ_{c2} anything	(3.4 ±1.0) $\times 10^{-4}$		–
$\psi(2S)$ anything	(2.7 ±0.9) $\times 10^{-4}$		–
$\rho\pi$	< 3.68 $\times 10^{-6}$	90%	4697
$\omega\pi^0$	< 3.90 $\times 10^{-6}$	90%	4697
$\pi^+\pi^-$	< 5 $\times 10^{-4}$	90%	4728
K^+K^-	< 5 $\times 10^{-4}$	90%	4704
$p\overline{p}$	< 5 $\times 10^{-4}$	90%	4636
$\pi^+\pi^-\pi^0$	(2.1 ±0.8) $\times 10^{-6}$		4725
ϕK^+K^-	(2.4 ±0.5) $\times 10^{-6}$		4622
$\omega\pi^+\pi^-$	(4.5 ±1.0) $\times 10^{-6}$		4694
$K^*(892)^0K^-\pi^+$ + c.c.	(4.4 ±0.8) $\times 10^{-6}$		4667
$\phi f_2'(1525)$	< 1.63 $\times 10^{-6}$	90%	4549
$\omega f_2(1270)$	< 1.79 $\times 10^{-6}$	90%	4611
$\rho(770)a_2(1320)$	< 2.24 $\times 10^{-6}$	90%	4605
$K^*(892)^0\overline{K}_2^*(1430)^0$ + c.c.	(3.0 ±0.8) $\times 10^{-6}$		4579
$K_1(1270)^\pm K^\mp$	< 2.41 $\times 10^{-6}$	90%	4631
$K_1(1400)^\pm K^\mp$	(1.0 ±0.4) $\times 10^{-6}$		4613
$b_1(1235)^\pm\pi^\mp$	< 1.25 $\times 10^{-6}$	90%	4649
$\pi^+\pi^-\pi^0\pi^0$	(1.28 ±0.30) $\times 10^{-5}$		4720
$K_S^0K^+\pi^-$ + c.c.	(1.6 ±0.4) $\times 10^{-6}$		4696
$K^*(892)^0\overline{K}^0$ + c.c.	(2.9 ±0.9) $\times 10^{-6}$		4675
$K^*(892)^-K^+$ + c.c.	< 1.11 $\times 10^{-6}$	90%	4675
$D^*(2010)^\pm$ anything	(2.52 ±0.20) %		–
$\overline{d}$ anything	(2.86 ±0.28) $\times 10^{-5}$		–
Sum of 100 exclusive modes	(1.200±0.017) %		–
Radiative decays			
$\gamma\pi^+\pi^-$	(6.3 ±1.8) $\times 10^{-5}$		4728
$\gamma\pi^0\pi^0$	(1.7 ±0.7) $\times 10^{-5}$		4728
$\gamma\pi^0\eta$	< 2.4 $\times 10^{-6}$	90%	4713
γK^+K^- [zzaa]	(1.14 ±0.13) $\times 10^{-5}$		4704
$\gamma p\overline{p}$ [aabb]	< 6 $\times 10^{-6}$	90%	4636
$\gamma 2h^+2h^-$	(7.0 ±1.5) $\times 10^{-4}$		4720
$\gamma 3h^+3h^-$	(5.4 ±2.0) $\times 10^{-4}$		4703
$\gamma 4h^+4h^-$	(7.4 ±3.5) $\times 10^{-4}$		4679
$\gamma\pi^+\pi^-K^+K^-$	(2.9 ±0.9) $\times 10^{-4}$		4686
$\gamma 2\pi^+2\pi^-$	(2.5 ±0.9) $\times 10^{-4}$		4720
$\gamma 3\pi^+3\pi^-$	(2.5 ±1.2) $\times 10^{-4}$		4703
$\gamma 2\pi^+2\pi^-K^+K^-$	(2.4 ±1.2) $\times 10^{-4}$		4658
$\gamma\pi^+\pi^-p\overline{p}$	(1.5 ±0.6) $\times 10^{-4}$		4604
$\gamma 2\pi^+2\pi^-p\overline{p}$	(4 ±6) $\times 10^{-5}$		4563
$\gamma 2K^+2K^-$	(2.0 ±2.0) $\times 10^{-5}$		4601
$\gamma\eta'(958)$	< 1.9 $\times 10^{-6}$	90%	4682
$\gamma\eta$	< 1.0 $\times 10^{-6}$	90%	4714
$\gamma f_0(980)$	< 3 $\times 10^{-5}$	90%	4678
$\gamma f_2'(1525)$	(3.8 ±0.9) $\times 10^{-5}$		4607
$\gamma f_2(1270)$	(1.01 ±0.09) $\times 10^{-4}$		4644
$\gamma\eta(1405)$	< 8.2 $\times 10^{-5}$	90%	4625
$\gamma f_0(1500)$	< 1.5 $\times 10^{-5}$	90%	4610
$\gamma f_0(1710)$	< 2.6 $\times 10^{-4}$	90%	4573
$\gamma f_0(1710) \to \gamma K^+K^-$	< 7 $\times 10^{-6}$	90%	–
$\gamma f_0(1710) \to \gamma\pi^0\pi^0$	< 1.4 $\times 10^{-6}$	90%	–
$\gamma f_0(1710) \to \gamma\eta\eta$	< 1.8 $\times 10^{-6}$	90%	–
$\gamma f_4(2050)$	< 5.3 $\times 10^{-5}$	90%	4515
$\gamma f_0(2200) \to \gamma K^+K^-$	< 2 $\times 10^{-4}$	90%	4475
$\gamma f_J(2220) \to \gamma K^+K^-$	< 8 $\times 10^{-7}$	90%	4469
$\gamma f_J(2220) \to \gamma\pi^+\pi^-$	< 6 $\times 10^{-7}$	90%	–
$\gamma f_J(2220) \to \gamma p\overline{p}$	< 1.1 $\times 10^{-6}$	90%	–
$\gamma\eta(2225) \to \gamma\phi\phi$	< 3 $\times 10^{-3}$	90%	4469
$\gamma\eta_c(1S)$	< 5.7 $\times 10^{-5}$	90%	4260
$\gamma\chi_{c0}$	< 6.5 $\times 10^{-4}$	90%	4114
$\gamma\chi_{c1}$	< 2.3 $\times 10^{-5}$	90%	4079
$\gamma\chi_{c2}$	< 7.6 $\times 10^{-6}$	90%	4062
$\gamma X(3872) \to \pi^+\pi^-J/\psi$	< 1.6 $\times 10^{-6}$	90%	–
$\gamma X(3872) \to \pi^+\pi^-\pi^0J/\psi$	< 2.8 $\times 10^{-6}$	90%	–
$\gamma\chi_{c0}(2P) \to \omega J/\psi$	< 3.0 $\times 10^{-6}$	90%	–
$\gamma X(4140) \to \phi J/\psi$	< 2.2 $\times 10^{-6}$	90%	–
γX [bbbb]	< 4.5 $\times 10^{-6}$	90%	–
$\gamma X\overline{X}(m_X < 3.1$ GeV) [ccbb]	< 1 $\times 10^{-3}$	90%	–
$\gamma X\overline{X}(m_X < 4.5$ GeV) [ddbb]	< 2.4 $\times 10^{-4}$	90%	–
$\gamma X \to \gamma +\geq 4$ prongs [eebb]	< 1.78 $\times 10^{-4}$	95%	–
$\gamma a_1^0 \to \gamma\mu^+\mu^-$ [ffbb]	< 9 $\times 10^{-6}$	90%	–
$\gamma a_1^0 \to \gamma\tau^+\tau^-$ [zzaa]	< 1.30 $\times 10^{-4}$	90%	–
$\gamma a_1^0 \to \gamma gg$ [ggbb]	< 1 %	90%	–
$\gamma a_1^0 \to \gamma s\overline{s}$ [ggbb]	< 1 $\times 10^{-3}$	90%	–
Lepton Family number (LF) violating modes			
$\mu^\pm\tau^\mp$ LF	< 6.0 $\times 10^{-6}$	95%	4563
Other decays			
invisible	< 3.0 $\times 10^{-4}$	90%	–

$\chi_{b0}(1P)$ [hhbb]

$I^G(J^{PC}) = 0^+(0^{++})$
J needs confirmation.

Mass m = 9859.44 ± 0.42 ± 0.31 MeV

$\chi_{b0}(1P)$ DECAY MODES	Fraction (Γ_i/Γ)	Confidence level	p (MeV/c)
$\gamma\Upsilon(1S)$	(1.76±0.35) %		391
D^0X	< 10.4 %	90%	–
$\pi^+\pi^-K^+K^-\pi^0$	< 1.6 $\times 10^{-4}$	90%	4875
$2\pi^+\pi^-K^+K_S^0$	< 5 $\times 10^{-5}$	90%	4875
$2\pi^+\pi^-K^+K_S^02\pi^0$	< 5 $\times 10^{-4}$	90%	4846
$2\pi^+2\pi^-2\pi^0$	< 2.1 $\times 10^{-4}$	90%	4905
$2\pi^+2\pi^-K^+K^-$	(1.1 ±0.6) $\times 10^{-4}$		4861
$2\pi^+2\pi^-K^+K^-\pi^0$	< 2.7 $\times 10^{-4}$	90%	4846
$2\pi^+2\pi^-K^+K^-2\pi^0$	< 5 $\times 10^{-4}$	90%	4828
$3\pi^+2\pi^-K^-K_S^0\pi^0$	< 1.6 $\times 10^{-4}$	90%	4827
$3\pi^+3\pi^-$	< 8 $\times 10^{-5}$	90%	4904
$3\pi^+3\pi^-2\pi^0$	< 6 $\times 10^{-4}$	90%	4881
$3\pi^+3\pi^-K^+K^-$	(2.4 ±1.2) $\times 10^{-4}$		4827
$3\pi^+3\pi^-K^+K^-\pi^0$	< 1.0 $\times 10^{-3}$	90%	4808
$4\pi^+4\pi^-$	< 8 $\times 10^{-5}$	90%	4880
$4\pi^+4\pi^-2\pi^0$	< 2.1 $\times 10^{-3}$	90%	4850
$J/\psi J/\psi$	< 7 $\times 10^{-5}$	90%	3836
$J/\psi\psi(2S)$	< 1.2 $\times 10^{-4}$	90%	3571
$\psi(2S)\psi(2S)$	< 3.1 $\times 10^{-5}$	90%	3273

$\chi_{b1}(1P)$ [hhbb]

$I^G(J^{PC}) = 0^+(1^{++})$
J needs confirmation.

Mass m = 9892.78 ± 0.26 ± 0.31 MeV

$\chi_{b1}(1P)$ DECAY MODES	Fraction (Γ_i/Γ)	Confidence level	p (MeV/c)
$\gamma\Upsilon(1S)$	(33.9±2.2) %		423
D^0X	(12.6±2.2) %		–
$\pi^+\pi^-K^+K^-\pi^0$	(2.0±0.6) $\times 10^{-4}$		4892
$2\pi^+\pi^-K^+K_S^0$	(1.3±0.5) $\times 10^{-4}$		4892
$2\pi^+\pi^-K^+K_S^02\pi^0$	< 6 $\times 10^{-4}$	90%	4863
$2\pi^+2\pi^-2\pi^0$	(8.0±2.5) $\times 10^{-4}$		4921
$2\pi^+2\pi^-K^+K^-$	(1.5±0.5) $\times 10^{-4}$		4878
$2\pi^+2\pi^-K^+K^-\pi^0$	(3.5±1.2) $\times 10^{-4}$		4863
$2\pi^+2\pi^-K^+K^-2\pi^0$	(8.6±3.2) $\times 10^{-4}$		4845

Meson Summary Table

$3\pi^+ 2\pi^- K^- K^0_S \pi^0$	$(\ 9.3\pm3.3) \times 10^{-4}$			4844
$3\pi^+ 3\pi^-$	$(\ 1.9\pm0.6) \times 10^{-4}$			4921
$3\pi^+ 3\pi^- 2\pi^0$	$(\ 1.7\pm0.5) \times 10^{-3}$			4898
$3\pi^+ 3\pi^- K^+ K^-$	$(\ 2.6\pm0.8) \times 10^{-4}$			4844
$3\pi^+ 3\pi^- K^+ K^- \pi^0$	$(\ 7.5\pm2.6) \times 10^{-4}$			4825
$4\pi^+ 4\pi^-$	$(\ 2.6\pm0.9) \times 10^{-4}$			4897
$4\pi^+ 4\pi^- 2\pi^0$	$(\ 1.4\pm0.6) \times 10^{-3}$			4867
$J/\psi\, J/\psi$	$< 2.7 \times 10^{-5}$		90%	3857
$J/\psi\psi(2S)$	$< 1.7 \times 10^{-5}$		90%	3594
$\psi(2S)\,\psi(2S)$	$< 6 \times 10^{-5}$		90%	3298

$h_b(1P)$

$I^G(J^{PC}) = ?^?(1^{+-})$

Mass $m = 9899.3 \pm 1.0$ MeV

$h_b(1P)$ DECAY MODES	Fraction (Γ_i/Γ)	p (MeV/c)
$\eta_b(1S)\,\gamma$	(49^{+8}_{-7}) %	489

$\chi_{b2}(1P)$ [hhbb]

$I^G(J^{PC}) = 0^+(2^{++})$
J needs confirmation.

Mass $m = 9912.21 \pm 0.26 \pm 0.31$ MeV

$\chi_{b2}(1P)$ DECAY MODES	Fraction (Γ_i/Γ)	Confidence level	p (MeV/c)
$\gamma\,\Upsilon(1S)$	(19.1±1.2) %		442
$D^0 X$	< 7.9 %	90%	–
$\pi^+\pi^- K^+ K^- \pi^0$	$(\ 8\ \pm5\ ) \times 10^{-5}$		4902
$2\pi^+\pi^- K^- K^0_S$	$< 1.0 \times 10^{-4}$	90%	4901
$2\pi^+\pi^- K^- K^0_S\, 2\pi^0$	$(\ 5.3\pm2.4) \times 10^{-4}$		4873
$2\pi^+ 2\pi^- 2\pi^0$	$(\ 3.5\pm1.4) \times 10^{-4}$		4931
$2\pi^+ 2\pi^- K^+ K^-$	$(\ 1.1\pm0.4) \times 10^{-4}$		4888
$2\pi^+ 2\pi^- K^+ K^- \pi^0$	$(\ 2.1\pm0.9) \times 10^{-4}$		4872
$2\pi^+ 2\pi^- K^+ K^- 2\pi^0$	$(\ 3.9\pm1.8) \times 10^{-4}$		4855
$3\pi^+ 2\pi^- K^- K^0_S \pi^0$	$< 5 \times 10^{-4}$	90%	4854
$3\pi^+ 3\pi^-$	$(\ 7.0\pm3.1) \times 10^{-5}$		4931
$3\pi^+ 3\pi^- 2\pi^0$	$(\ 1.0\pm0.4) \times 10^{-3}$		4908
$3\pi^+ 3\pi^- K^+ K^-$	$< 8 \times 10^{-5}$	90%	4854
$3\pi^+ 3\pi^- K^+ K^- \pi^0$	$(\ 3.6\pm1.5) \times 10^{-4}$		4835
$4\pi^+ 4\pi^-$	$(\ 8\ \pm4\ ) \times 10^{-5}$		4907
$4\pi^+ 4\pi^- 2\pi^0$	$(\ 1.8\pm0.7) \times 10^{-3}$		4877
$J/\psi\, J/\psi$	$< 4 \times 10^{-5}$	90%	3869
$J/\psi\psi(2S)$	$< 5 \times 10^{-5}$	90%	3608
$\psi(2S)\,\psi(2S)$	$< 1.6 \times 10^{-5}$	90%	3313

$\Upsilon(2S)$

$I^G(J^{PC}) = 0^-(1^{--})$

Mass $m = 10023.26 \pm 0.31$ MeV
$m_{\Upsilon(3S)} - m_{\Upsilon(2S)} = 331.50 \pm 0.13$ MeV
Full width $\Gamma = 31.98 \pm 2.63$ keV
$\Gamma_{ee} = 0.612 \pm 0.011$ keV

$\Upsilon(2S)$ DECAY MODES	Fraction (Γ_i/Γ)	Scale factor/ Confidence level	p (MeV/c)
$\Upsilon(1S)\,\pi^+\pi^-$	(17.85 ± 0.26) %		475
$\Upsilon(1S)\,\pi^0\pi^0$	(8.6 ± 0.4) %		480
$\tau^+\tau^-$	(2.00 ± 0.21) %		4686
$\mu^+\mu^-$	(1.93 ± 0.17) %	S=2.2	5011
$e^+ e^-$	(1.91 ± 0.16) %		5012
$\Upsilon(1S)\,\pi^0$	$< 4 \times 10^{-5}$	CL=90%	531
$\Upsilon(1S)\,\eta$	$(\ 2.9\ \pm 0.4\ ) \times 10^{-4}$	S=2.0	126
$J/\psi(1S)$ anything	$< 6 \times 10^{-3}$	CL=90%	4533
$\overline{d}$ anything	$(\ 3.4\ \pm 0.6\ ) \times 10^{-5}$		–
hadrons	(94 ±11) %		–
ggg	(58.8 ± 1.2) %		–
γgg	(8.8 ± 1.1) %		–
$\phi K^+ K^-$	$(\ 1.6\ \pm 0.4\ ) \times 10^{-6}$		4910
$\omega\pi^+\pi^-$	$< 2.58 \times 10^{-6}$	CL=90%	4977
$K^*(892)^0 K^-\pi^+ +$ c.c.	$(\ 2.3\ \pm 0.7\ ) \times 10^{-6}$		4952
$\phi f_2'(1525)$	$< 1.33 \times 10^{-6}$	CL=90%	4841
$\omega f_2(1270)$	$< 5.7 \times 10^{-7}$	CL=90%	4899
$\rho(770)\, a_2(1320)$	$< 8.8 \times 10^{-7}$	CL=90%	4894
$K^*(892)^0 \overline{K}{}^*_2(1430)^0 +$ c.c.	$(\ 1.5\ \pm 0.6\ ) \times 10^{-6}$		4869
$K_1(1270)^\pm K^\mp$	$< 3.22 \times 10^{-6}$	CL=90%	4918
$K_1(1400)^\pm K^\mp$	$< 8.3 \times 10^{-7}$	CL=90%	4901
$b_1(1235)^\pm \pi^\mp$	$< 4.0 \times 10^{-7}$	CL=90%	4935
$\rho\pi$	$< 1.16 \times 10^{-6}$	CL=90%	4981
$\pi^+\pi^-\pi^0$	$< 8.0 \times 10^{-7}$	CL=90%	5007
$\omega\pi^0$	$< 1.63 \times 10^{-6}$	CL=90%	4980
$\pi^+\pi^-\pi^0\pi^0$	$(\ 1.30\pm\ 0.28) \times 10^{-5}$		5002
$K^0_S K^+\pi^- +$ c.c.	$(\ 1.14\pm\ 0.33) \times 10^{-6}$		4979
$K^*(892)^0 \overline{K}{}^0 +$ c.c.	$< 4.22 \times 10^{-6}$	CL=90%	4959
$K^*(892)^- K^+ +$ c.c.	$< 1.45 \times 10^{-6}$	CL=90%	4960
Sum of 100 exclusive modes	$(\ 2.90\pm\ 0.30) \times 10^{-3}$		–
Radiative decays			
$\gamma\chi_{b1}(1P)$	(6.9 ± 0.4) %		130
$\gamma\chi_{b2}(1P)$	(7.15 ± 0.35) %		110
$\gamma\chi_{b0}(1P)$	(3.8 ± 0.4) %		162
$\gamma f_0(1710)$	$< 5.9 \times 10^{-4}$	CL=90%	4864
$\gamma f_2'(1525)$	$< 5.3 \times 10^{-4}$	CL=90%	4896
$\gamma f_2(1270)$	$< 2.41 \times 10^{-4}$	CL=90%	4931
$\gamma\eta_c(1S)$	$< 2.7 \times 10^{-5}$	CL=90%	4568
$\gamma\chi_{c0}$	$< 1.0 \times 10^{-4}$	CL=90%	4430
$\gamma\chi_{c1}$	$< 3.6 \times 10^{-6}$	CL=90%	4397
$\gamma\chi_{c2}$	$< 1.5 \times 10^{-5}$	CL=90%	4381
$\gamma X(3872) \to \pi^+\pi^- J/\psi$	$< 8 \times 10^{-7}$	CL=90%	–
$\gamma X(3872) \to \pi^+\pi^-\pi^0 J/\psi$	$< 2.4 \times 10^{-6}$	CL=90%	–
$\gamma X(3872) \to \omega J/\psi$	$< 2.8 \times 10^{-6}$	CL=90%	–
$\gamma X(4140) \to \phi J/\psi$	$< 1.2 \times 10^{-6}$	CL=90%	–
$\gamma X(4350) \to \phi J/\psi$	$< 1.3 \times 10^{-6}$	CL=90%	–
$\gamma\eta_b(1S)$	$(\ 3.9\ \pm 1.5\ ) \times 10^{-4}$		606
$\gamma\eta_b(1S) \to \gamma$Sum of 26 exclusive modes	$< 3.7 \times 10^{-6}$	CL=90%	–
$\gamma X_{b\overline{b}} \to \gamma$Sum of 26 exclusive modes	$< 4.9 \times 10^{-6}$	CL=90%	–
$\gamma X \to \gamma + \geq 4$ prongs [iibb]	$< 1.95 \times 10^{-4}$	CL=95%	–
$\gamma A^0 \to \gamma$hadrons	$< 8 \times 10^{-5}$	CL=90%	–
$\gamma a_1^0 \to \gamma\mu^+\mu^-$	$< 8.3 \times 10^{-6}$	CL=90%	–
Lepton Family number (LF) violating modes			
$e^\pm\tau^\mp$ LF	$< 3.2 \times 10^{-6}$	CL=90%	4854
$\mu^\pm\tau^\mp$ LF	$< 3.3 \times 10^{-6}$	CL=90%	4854

$\Upsilon(1D)$

$I^G(J^{PC}) = 0^-(2^{--})$

Mass $m = 10163.7 \pm 1.4$ MeV (S = 1.7)

$\Upsilon(1D)$ DECAY MODES	Fraction (Γ_i/Γ)	p (MeV/c)
$\gamma\gamma\,\Upsilon(1S)$	seen	679
$\gamma\chi_{bJ}(1P)$	seen	300
$\eta\,\Upsilon(1S)$	not seen	426
$\pi^+\pi^-\,\Upsilon(1S)$	$(6.6\pm1.6) \times 10^{-3}$	623

$\chi_{b0}(2P)$ [hhbb]

$I^G(J^{PC}) = 0^+(0^{++})$
J needs confirmation.

Mass $m = 10232.5 \pm 0.4 \pm 0.5$ MeV

$\chi_{b0}(2P)$ DECAY MODES	Fraction (Γ_i/Γ)	Confidence level	p (MeV/c)
$\gamma\,\Upsilon(2S)$	(4.6±2.1) %		207
$\gamma\,\Upsilon(1S)$	$(9\ \pm6\ ) \times 10^{-3}$		743
$D^0 X$	< 8.2 %	90%	–
$\pi^+\pi^- K^+ K^- \pi^0$	$< 3.4 \times 10^{-5}$	90%	5064
$2\pi^+\pi^- K^- K^0_S$	$< 5 \times 10^{-5}$	90%	5063
$2\pi^+\pi^- K^- K^0_S\, 2\pi^0$	$< 2.2 \times 10^{-4}$	90%	5036
$2\pi^+ 2\pi^- 2\pi^0$	$< 2.4 \times 10^{-4}$	90%	5092
$2\pi^+ 2\pi^- K^+ K^-$	$< 1.5 \times 10^{-4}$	90%	5050
$2\pi^+ 2\pi^- K^+ K^- \pi^0$	$< 2.2 \times 10^{-4}$	90%	5035
$2\pi^+ 2\pi^- K^+ K^- 2\pi^0$	$< 1.1 \times 10^{-3}$	90%	5019
$3\pi^+ 2\pi^- K^- K^0_S \pi^0$	$< 7 \times 10^{-4}$	90%	5018
$3\pi^+ 3\pi^-$	$< 7 \times 10^{-5}$	90%	5091
$3\pi^+ 3\pi^- 2\pi^0$	$< 1.2 \times 10^{-3}$	90%	5070
$3\pi^+ 3\pi^- K^+ K^-$	$< 1.5 \times 10^{-4}$	90%	5017
$3\pi^+ 3\pi^- K^+ K^- \pi^0$	$< 7 \times 10^{-4}$	90%	4999
$4\pi^+ 4\pi^-$	$< 1.7 \times 10^{-4}$	90%	5069
$4\pi^+ 4\pi^- 2\pi^0$	$< 6 \times 10^{-4}$	90%	5039

$\chi_{b1}(2P)$ [hhbb]

$I^G(J^{PC}) = 0^+(1^{++})$
J needs confirmation.

Mass $m = 10255.46 \pm 0.22 \pm 0.50$ MeV
$m_{\chi_{b1}(2P)} - m_{\chi_{b0}(2P)} = 23.5 \pm 1.0$ MeV

$\chi_{b1}(2P)$ DECAY MODES	Fraction (Γ_i/Γ)	Scale factor	p (MeV/c)
$\omega\,\Upsilon(1S)$	$(1.63^{+0.40}_{-0.34})$ %		135
$\gamma\,\Upsilon(2S)$	(19.9 ±1.9) %		230
$\gamma\,\Upsilon(1S)$	(9.2 ±0.8) %	1.1	764
$\pi\pi\chi_{b1}(1P)$	(9.1 ±1.3) $\times 10^{-3}$		238
$D^0 X$	(8.8 ±1.7) %		–
$\pi^+\pi^- K^+ K^- \pi^0$	(3.1 ±1.0) $\times 10^{-4}$		5075
$2\pi^+\pi^- K^- K^0_S$	(1.1 ±0.5) $\times 10^{-4}$		5075
$2\pi^+\pi^- K^- K^0_S 2\pi^0$	(7.7 ±3.2) $\times 10^{-4}$		5047
$2\pi^+ 2\pi^- 2\pi^0$	(5.9 ±2.0) $\times 10^{-4}$		5104
$2\pi^+ 2\pi^- K^+ K^-$	(10 ±4) $\times 10^{-5}$		5062
$2\pi^+ 2\pi^- K^+ K^- \pi^0$	(5.5 ±1.8) $\times 10^{-4}$		5047
$2\pi^+ 2\pi^- K^+ K^- 2\pi^0$	(10 ±4) $\times 10^{-4}$		5030
$3\pi^+ 2\pi^- K^- K^0_S \pi^0$	(6.7 ±2.6) $\times 10^{-4}$		5029
$3\pi^+ 3\pi^-$	(1.2 ±0.4) $\times 10^{-4}$		5103
$3\pi^+ 3\pi^- 2\pi^0$	(1.2 ±0.4) $\times 10^{-3}$		5081
$3\pi^+ 3\pi^- K^+ K^-$	(2.0 ±0.8) $\times 10^{-4}$		5029
$3\pi^+ 3\pi^- K^+ K^- \pi^0$	(6.1 ±2.2) $\times 10^{-4}$		5011
$4\pi^+ 4\pi^-$	(1.7 ±0.6) $\times 10^{-4}$		5080
$4\pi^+ 4\pi^- 2\pi^0$	(1.9 ±0.7) $\times 10^{-3}$		5051

$\chi_{b2}(2P)$ [hhbb]

$I^G(J^{PC}) = 0^+(2^{++})$
J needs confirmation.

Mass $m = 10268.65 \pm 0.22 \pm 0.50$ MeV
$m_{\chi_{b2}(2P)} - m_{\chi_{b1}(2P)} = 13.5 \pm 0.6$ MeV

$\chi_{b2}(2P)$ DECAY MODES	Fraction (Γ_i/Γ)	Scale factor/ Confidence level	p (MeV/c)
$\omega\,\Upsilon(1S)$	$(1.10^{+0.34}_{-0.30})$ %		194
$\gamma\,\Upsilon(2S)$	(10.6 ±2.6) %	S=2.0	242
$\gamma\,\Upsilon(1S)$	(7.0 ±0.7) %		777
$\pi\pi\chi_{b2}(1P)$	(5.1 ±0.9) $\times 10^{-3}$		229
$D^0 X$	< 2.4 %	CL=90%	–
$\pi^+\pi^- K^+ K^- \pi^0$	< 1.1 $\times 10^{-4}$	CL=90%	5082
$2\pi^+\pi^- K^- K^0_S$	< 9 $\times 10^{-5}$	CL=90%	5082
$2\pi^+\pi^- K^- K^0_S 2\pi^0$	< 7 $\times 10^{-4}$	CL=90%	5054
$2\pi^+ 2\pi^- 2\pi^0$	(3.9 ±1.6) $\times 10^{-4}$		5110
$2\pi^+ 2\pi^- K^+ K^-$	(9 ±4) $\times 10^{-5}$		5068
$2\pi^+ 2\pi^- K^+ K^- \pi^0$	(2.4 ±1.1) $\times 10^{-4}$		5054
$2\pi^+ 2\pi^- K^+ K^- 2\pi^0$	(4.7 ±2.3) $\times 10^{-4}$		5037
$3\pi^+ 2\pi^- K^- K^0_S \pi^0$	< 4 $\times 10^{-4}$	CL=90%	5036
$3\pi^+ 3\pi^-$	(9 ±4) $\times 10^{-5}$		5110
$3\pi^+ 3\pi^- 2\pi^0$	(1.2 ±0.4) $\times 10^{-3}$		5088
$3\pi^+ 3\pi^- K^+ K^-$	(1.4 ±0.7) $\times 10^{-4}$		5036
$3\pi^+ 3\pi^- K^+ K^- \pi^0$	(4.2 ±1.7) $\times 10^{-4}$		5017
$4\pi^+ 4\pi^-$	(9 ±5) $\times 10^{-5}$		5087
$4\pi^+ 4\pi^- 2\pi^0$	(1.3 ±0.5) $\times 10^{-3}$		5058

$\Upsilon(3S)$

$I^G(J^{PC}) = 0^-(1^{--})$

Mass $m = 10355.2 \pm 0.5$ MeV
$m_{\Upsilon(3S)} - m_{\Upsilon(2S)} = 331.50 \pm 0.13$ MeV
Full width $\Gamma = 20.32 \pm 1.85$ keV
$\Gamma_{ee} = 0.443 \pm 0.008$ keV

$\Upsilon(3S)$ DECAY MODES	Fraction (Γ_i/Γ)	Scale factor/ Confidence level	p (MeV/c)
$\Upsilon(2S)$ anything	(10.6 ±0.8) %		296
$\Upsilon(2S)\pi^+\pi^-$	(2.82±0.18) %	S=1.6	177
$\Upsilon(2S)\pi^0\pi^0$	(1.85±0.14) %		190
$\Upsilon(2S)\gamma\gamma$	(5.0 ±0.7) %		327
$\Upsilon(2S)\pi^0$	< 5.1 $\times 10^{-4}$	CL=90%	298
$\Upsilon(1S)\pi^+\pi^-$	(4.37±0.08) %		813
$\Upsilon(1S)\pi^0\pi^0$	(2.20±0.13) %		816
$\Upsilon(1S)\eta$	< 1 $\times 10^{-4}$	CL=90%	677
$\Upsilon(1S)\pi^0$	< 7 $\times 10^{-5}$	CL=90%	846
$h_b(1P)\pi^0$	< 1.2 $\times 10^{-3}$	CL=90%	426
$h_b(1P)\pi^0 \to \gamma\eta_b(1S)\pi^0$	(4.3 ±1.4) $\times 10^{-4}$		–
$h_b(1P)\pi^+\pi^-$	< 1.2 $\times 10^{-4}$	CL=90%	353
$\tau^+\tau^-$	(2.29±0.30) %		4863
$\mu^+\mu^-$	(2.18±0.21) %	S=2.1	5177
e^+e^-	seen		5178
ggg	(35.7 ±2.6) %		–
γgg	(9.7 ±1.8) $\times 10^{-3}$		–
Radiative decays			
$\gamma\chi_{b2}(2P)$	(13.1 ±1.6) %	S=3.4	86
$\gamma\chi_{b1}(2P)$	(12.6 ±1.2) %	S=2.4	99
$\gamma\chi_{b0}(2P)$	(5.9 ±0.6) %	S=1.4	122
$\gamma\chi_{b2}(1P)$	(9.9 ±1.3) $\times 10^{-3}$	S=2.0	434
$\gamma A^0 \to \gamma$ hadrons	< 8 $\times 10^{-5}$	CL=90%	–
$\gamma\chi_{b1}(1P)$	(9 ±5) $\times 10^{-4}$	S=1.9	452
$\gamma\chi_{b0}(1P)$	(2.7 ±0.4) $\times 10^{-3}$		484
$\gamma\eta_b(2S)$	< 6.2 $\times 10^{-4}$	CL=90%	350
$\gamma\eta_b(1S)$	(5.1 ±0.7) $\times 10^{-4}$		913
$\gamma X \to \gamma +\geq 4$ prongs	[jjbb] < 2.2 $\times 10^{-4}$	CL=95%	–
$\gamma a_1^0 \to \gamma\mu^+\mu^-$	< 5.5 $\times 10^{-6}$	CL=90%	–
$\gamma a_1^0 \to \gamma\tau^+\tau^-$	[kkbb] < 1.6 $\times 10^{-4}$	CL=90%	–
Lepton Family number (LF) violating modes			
$e^\pm\tau^\mp$	LF < 4.2 $\times 10^{-6}$	CL=90%	5025
$\mu^\pm\tau^\mp$	LF < 3.1 $\times 10^{-6}$	CL=90%	5025

$\chi_b(3P)$

$I^G(J^{PC}) = ?^?(?^{?+})$

Mass $m = 10534 \pm 9$ MeV

$\chi_b(3P)$ DECAY MODES	Fraction (Γ_i/Γ)	p (MeV/c)
$\Upsilon(1S)\gamma$	seen	1019
$\Upsilon(2S)\gamma$	seen	498

$\Upsilon(4S)$ or $\Upsilon(10580)$

$I^G(J^{PC}) = 0^-(1^{--})$

Mass $m = 10579.4 \pm 1.2$ MeV
Full width $\Gamma = 20.5 \pm 2.5$ MeV
$\Gamma_{ee} = 0.272 \pm 0.029$ keV (S = 1.5)

$\Upsilon(4S)$ DECAY MODES	Fraction (Γ_i/Γ)	Confidence level	p (MeV/c)
$B\overline{B}$	> 96 %	95%	327
B^+B^-	(51.4 ±0.6) %		332
D_s^+ anything + c.c.	(17.8 ±2.6) %		–
$B^0\overline{B}^0$	(48.6 ±0.6) %		327
$J/\psi K^0_S(J/\psi,\ \eta_c)K^0_S$	< 4 $\times 10^{-7}$	90%	–
non-$B\overline{B}$	< 4 %	95%	–
e^+e^-	(1.57±0.08) $\times 10^{-5}$		5290
$\rho^+\rho^-$	< 5.7 $\times 10^{-6}$	90%	5233
$K^*(892)^0\overline{K}^0$	< 2.0 $\times 10^{-6}$	90%	5240
$J/\psi(1S)$ anything	< 1.9 $\times 10^{-4}$	95%	–
D^{*+} anything + c.c.	< 7.4 %	90%	5099
ϕ anything	(7.1 ±0.6) %		5240
$\phi\eta$	< 1.8 $\times 10^{-6}$	90%	5226
$\phi\eta'$	< 4.3 $\times 10^{-6}$	90%	5196
$\rho\eta$	< 1.3 $\times 10^{-6}$	90%	5247
$\rho\eta'$	< 2.5 $\times 10^{-6}$	90%	5217
$\Upsilon(1S)$ anything	< 4 $\times 10^{-3}$	90%	1053
$\Upsilon(1S)\pi^+\pi^-$	(8.1 ±0.6) $\times 10^{-5}$		1026
$\Upsilon(1S)\eta$	(1.96±0.28) $\times 10^{-4}$		924
$\Upsilon(2S)\pi^+\pi^-$	(8.6 ±1.3) $\times 10^{-5}$		468
$h_b(1P)\pi^+\pi^-$	not seen		600
$\overline{d}$ anything	< 1.3 $\times 10^{-5}$	90%	–

$\Upsilon(10860)$

$I^G(J^{PC}) = 0^-(1^{--})$

Mass $m = 10876 \pm 11$ MeV
Full width $\Gamma = 55 \pm 28$ MeV
$\Gamma_{ee} = 0.31 \pm 0.07$ keV (S = 1.3)

Meson Summary Table

$\Upsilon(10860)$ DECAY MODES	Fraction (Γ_i/Γ)	Confidence level	p (MeV/c)
$B\overline{B}X$	(76.2 $^{+2.7}_{-4.0}$) %		–
$B\overline{B}$	(5.5 ±1.0) %		1303
$B\overline{B}^*$ + c.c.	(13.7 ±1.6) %		–
$B^*\overline{B}^*$	(38.1 ±3.4) %		1102
$B\overline{B}^{(*)}\pi$	< 19.7 %	90%	990
$B\overline{B}\pi$	(0.0 ±1.2) %		990
$B^*\overline{B}\pi$ + $B\overline{B}^*\pi$	(7.3 ±2.3) %		–
$B^*\overline{B}^*\pi$	(1.0 ±1.4) %		701
$B\overline{B}\pi\pi$	< 8.9 %	90%	504
$B_s^{(*)}\overline{B}_s^{(*)}$	(20.1 ±3.1) %		877
$B_s\overline{B}_s$	(5 ±5) $\times10^{-3}$		877
$B_s\overline{B}_s^*$ + c.c.	(1.35 ±0.32) %		–
$B_s^*\overline{B}_s^*$	(17.6 ±2.7) %		495
no open-bottom	(3.8 $^{+5.0}_{-0.5}$) %		–
e^+e^-	(5.6 ±3.1) $\times10^{-6}$		5438
$K^*(892)^0\overline{K}^0$	< 1.0 $\times10^{-5}$	90%	5390
$\Upsilon(1S)\pi^+\pi^-$	(5.3 ±0.6) $\times10^{-3}$		1297
$\Upsilon(2S)\pi^+\pi^-$	(7.8 ±1.3) $\times10^{-3}$		774
$\Upsilon(3S)\pi^+\pi^-$	(4.8 $^{+1.9}_{-1.7}$) $\times10^{-3}$		429
$\Upsilon(1S)K^+K^-$	(6.1 ±1.8) $\times10^{-4}$		947
$h_b(1P)\pi^+\pi^-$	(3.5 $^{+1.0}_{-1.3}$) $\times10^{-3}$		894
$h_b(2P)\pi^+\pi^-$	(6.0 $^{+2.1}_{-1.8}$) $\times10^{-3}$		534

Inclusive Decays.

These decay modes are submodes of one or more of the decay modes above.

ϕ anything	(13.8 $^{+2.4}_{-1.7}$) %	–
D^0 anything + c.c.	(108 ±8) %	–
D_s anything + c.c.	(46 ±6) %	–
J/ψ anything	(2.06 ±0.21) %	–
B^0 anything + c.c.	(77 ±8) %	–
B^+ anything + c.c.	(72 ±6) %	–

$\Upsilon(11020)$

$I^G(J^{PC}) = 0^-(1^{--})$

Mass $m = 11019 \pm 8$ MeV
Full width $\Gamma = 79 \pm 16$ MeV
$\Gamma_{ee} = 0.130 \pm 0.030$ keV

$\Upsilon(11020)$ DECAY MODES	Fraction (Γ_i/Γ)	p (MeV/c)
e^+e^-	$(1.6\pm0.5)\times10^{-6}$	5510

NOTES

In this Summary Table:

When a quantity has "(S = ...)" to its right, the error on the quantity has been enlarged by the "scale factor" S, defined as S = $\sqrt{\chi^2/(N-1)}$, where N is the number of measurements used in calculating the quantity. We do this when S > 1, which often indicates that the measurements are inconsistent. When S > 1.25, we also show in the Particle Listings an ideogram of the measurements. For more about S, see the Introduction.

A decay momentum p is given for each decay mode. For a 2-body decay, p is the momentum of each decay product in the rest frame of the decaying particle. For a 3-or-more-body decay, p is the largest momentum any of the products can have in this frame.

[a] See the "Note on $\pi^\pm \to \ell^\pm\nu\gamma$ and $K^\pm \to \ell^\pm\nu\gamma$ Form Factors" in the $\pi^\pm$ Particle Listings for definitions and details.

[b] Measurements of $\Gamma(e^+\nu_e)/\Gamma(\mu^+\nu_\mu)$ always include decays with γ's, and measurements of $\Gamma(e^+\nu_e\gamma)$ and $\Gamma(\mu^+\nu_\mu\gamma)$ never include low-energy γ's. Therefore, since no clean separation is possible, we consider the modes with γ's to be subreactions of the modes without them, and let $[\Gamma(e^+\nu_e) + \Gamma(\mu^+\nu_\mu)]/\Gamma_{\rm total} = 100\%$.

[c] See the $\pi^\pm$ Particle Listings for the energy limits used in this measurement; low-energy γ's are not included.

[d] Derived from an analysis of neutrino-oscillation experiments.

[e] Astrophysical and cosmological arguments give limits of order 10^{-13}; see the π^0 Particle Listings.

[f] C parity forbids this to occur as a single-photon process.

[g] See the "Note on scalar mesons" in the $f_0(500)$ Particle Listings . The interpretation of this entry as a particle is controversial.

[h] See the "Note on $\rho(770)$" in the $\rho(770)$ Particle Listings .

[i] The $\omega\rho$ interference is then due to $\omega\rho$ mixing only, and is expected to be small. If $e\mu$ universality holds, $\Gamma(\rho^0 \to \mu^+\mu^-) = \Gamma(\rho^0 \to e^+e^-) \times 0.99785$.

[j] See the "Note on scalar mesons" in the $f_0(500)$ Particle Listings .

[k] See the "Note on $a_1(1260)$" in the $a_1(1260)$ Particle Listings in PDG 06, Journal of Physics (generic for all A,B,E,G) **G33** 1 (2006).

[l] This is only an educated guess; the error given is larger than the error on the average of the published values. See the Particle Listings for details.

[n] See the "Note on non-$q\overline{q}$ mesons" in the Particle Listings in PDG 06, Journal of Physics (generic for all A,B,E,G) **G33** 1 (2006).

[o] See the "Note on the $\eta(1405)$" in the $\eta(1405)$ Particle Listings.

[p] See the "Note on the $f_1(1420)$" in the $\eta(1405)$ Particle Listings.

[q] See also the $\omega(1650)$ Particle Listings.

[r] See the "Note on the $\rho(1450)$ and the $\rho(1700)$" in the $\rho(1700)$ Particle Listings.

[s] See also the $\omega(1420)$ Particle Listings.

[t] See the "Note on $f_0(1710)$" in the $f_0(1710)$ Particle Listings in 2004 edition of *Review of Particle Physics*.

[u] See the note in the $K^\pm$ Particle Listings.

[v] The definition of the slope parameter g of the $K \to 3\pi$ Dalitz plot is as follows (see also "Note on Dalitz Plot Parameters for $K \to 3\pi$ Decays" in the $K^\pm$ Particle Listings):

$$|M|^2 = 1 + g(s_3 - s_0)/m^2_{\pi^+} + \cdots .$$

[x] For more details and definitions of parameters see the Particle Listings.

[y] See the $K^\pm$ Particle Listings for the energy limits used in this measurement.

[z] Most of this radiative mode, the low-momentum γ part, is also included in the parent mode listed without γ's.

[aa] Structure-dependent part.

[bb] Direct-emission branching fraction.

[cc] Violates angular-momentum conservation.

[dd] Derived from measured values of ϕ_{+-}, ϕ_{00}, $|\eta|$, $|m_{K^0_L} - m_{K^0_S}|$, and $\tau_{K^0_S}$, as described in the introduction to "Tests of Conservation Laws."

[ee] The CP-violation parameters are defined as follows (see also "Note on CP Violation in $K_S \to 3\pi$" and "Note on CP Violation in K^0_L Decay" in the Particle Listings):

$$\eta_{+-} = |\eta_{+-}|e^{i\phi_{+-}} = \frac{A(K^0_L \to \pi^+\pi^-)}{A(K^0_S \to \pi^+\pi^-)} = \epsilon + \epsilon'$$

$$\eta_{00} = |\eta_{00}|e^{i\phi_{00}} = \frac{A(K^0_L \to \pi^0\pi^0)}{A(K^0_S \to \pi^0\pi^0)} = \epsilon - 2\epsilon'$$

$$\delta = \frac{\Gamma(K^0_L \to \pi^-\ell^+\nu) - \Gamma(K^0_L \to \pi^+\ell^-\nu)}{\Gamma(K^0_L \to \pi^-\ell^+\nu) + \Gamma(K^0_L \to \pi^+\ell^-\nu)} ,$$

$$\mathrm{Im}(\eta_{+-0})^2 = \frac{\Gamma(K^0_S \to \pi^+\pi^-\pi^0)^{CP\ \mathrm{viol.}}}{\Gamma(K^0_L \to \pi^+\pi^-\pi^0)} ,$$

$$\mathrm{Im}(\eta_{000})^2 = \frac{\Gamma(K^0_S \to \pi^0\pi^0\pi^0)}{\Gamma(K^0_L \to \pi^0\pi^0\pi^0)} .$$

where for the last two relations CPT is assumed valid, *i.e.*, $\mathrm{Re}(\eta_{+-0}) \simeq 0$ and $\mathrm{Re}(\eta_{000}) \simeq 0$.

[ff] See the K^0_S Particle Listings for the energy limits used in this measurement.

[gg] The value is for the sum of the charge states or particle/antiparticle states indicated.

[hh] $\mathrm{Re}(\epsilon'/\epsilon) = \epsilon'/\epsilon$ to a very good approximation provided the phases satisfy CPT invariance.

[ii] This mode includes gammas from inner bremsstrahlung but not the direct emission mode $K^0_L \to \pi^+\pi^-\gamma$(DE).

[jj] See the K^0_L Particle Listings for the energy limits used in this measurement.

[*kk*] Allowed by higher-order electroweak interactions.

[*ll*] Violates *CP* in leading order. Test of direct *CP* violation since the indirect *CP*-violating and *CP*-conserving contributions are expected to be suppressed.

[*nn*] See the "Note on $f_0(1370)$" in the $f_0(1370)$ Particle Listings and in the 1994 edition.

[*oo*] See the note in the $L(1770)$ Particle Listings in Reviews of Modern Physics **56** S1 (1984), p. S200. See also the "Note on $K_2(1770)$ and the $K_2(1820)$" in the $K_2(1770)$ Particle Listings .

[*pp*] See the "Note on $K_2(1770)$ and the $K_2(1820)$" in the $K_2(1770)$ Particle Listings .

[*qq*] This result applies to $Z^0 \to c\overline{c}$ decays only. Here ℓ^+ is an average (not a sum) of e^+ and μ^+ decays.

[*rr*] See the Particle Listings for the (complicated) definition of this quantity.

[*ss*] The branching fraction for this mode may differ from the sum of the submodes that contribute to it, due to interference effects. See the relevant papers in the Particle Listings.

[*tt*] These subfractions of the $K^-2\pi^+$ mode are uncertain: see the Particle Listings.

[*uu*] Submodes of the $D^+ \to K^-2\pi^+\pi^0$ and $K^0_S\,2\pi^+\pi^-$ modes were studied by ANJOS 92C and COFFMAN 92B, but with at most 142 events for the first mode and 229 for the second – not enough for precise results. With nothing new for 18 years, we refer to our 2008 edition, Physics Letters **B667** 1 (2008), for those results.

[*vv*] The unseen decay modes of the resonances are included.

[*xx*] This is *not* a test for the ΔC=1 weak neutral current, but leads to the $\pi^+\ell^+\ell^-$ final state.

[*yy*] This mode is not a useful test for a ΔC=1 weak neutral current because both quarks must change flavor in this decay.

[*zz*] In the 2010 *Review*, the values for these quantities were given using a measure of the asymmetry that was inconsistent with the usual definition.

[*aaa*] This value is obtained by subtracting the branching fractions for 2-, 4- and 6-prongs from unity.

[*bbb*] This is the sum of our $K^-2\pi^+\pi^-$, $K^-2\pi^+\pi^-\pi^0$, $\overline{K}^0 2\pi^+2\pi^-$, $K^+2K^-\pi^+$, $2\pi^+2\pi^-$, $2\pi^+2\pi^-\pi^0$, $K^+K^-\pi^+\pi^-$, and $K^+K^-\pi^+\pi^-\pi^0$, branching fractions.

[*ccc*] This is the sum of our $K^-3\pi^+2\pi^-$ and $3\pi^+3\pi^-$ branching fractions.

[*ddd*] The branching fractions for the $K^-e^+\nu_e$, $K^*(892)^-e^+\nu_e$, $\pi^-e^+\nu_e$, and $\rho^-e^+\nu_e$ modes add up to 6.19 ± 0.17 %.

[*eee*] This is a doubly Cabibbo-suppressed mode.

[*fff*] The two experiments measuring this fraction are in serious disagreement. See the Particle Listings.

[*ggg*] Submodes of the $D^0 \to K^0_S\pi^+\pi^-\pi^0$ mode with a K^* and/or ρ were studied by COFFMAN 92B, but with only 140 events. With nothing new for 18 years, we refer to our 2008 edition, Physics Letters **B667** 1 (2008), for those results.

[*hhh*] This branching fraction includes all the decay modes of the resonance in the final state.

[*iii*] This limit is for either D^0 or $\overline{D}^0$ to pe^-.

[*jjj*] This limit is for either D^0 or $\overline{D}^0$ to $\overline{p}e^+$.

[*kkk*] This is the purely e^+ semileptonic branching fraction: the e^+ fraction from τ^+ decays has been subtracted off. The sum of our (non-τ) e^+ exclusive fractions — an $e^+\nu_e$ with an η, η', ϕ, K^0, K^{*0}, or $f_0(980)$ — is 7.0 ± 0.4 %

[*lll*] This fraction includes η from η' decays.

[*nnn*] Two times (to include μ decays) the $\eta' e^+\nu_e$ branching fraction, plus the $\eta'\pi^+$, $\eta'\rho^+$, and $\eta' K^+$ fractions, is (18.6 ± 2.3)%, which considerably exceeds the inclusive η' fraction of (11.7 ± 1.8)%. Our best guess is that the $\eta'\rho^+$ fraction, (12.5 ± 2.2)%, is too large.

[*ooo*] This branching fraction includes all the decay modes of the final-state resonance.

[*ppp*] A test for $u\overline{u}$ or $d\overline{d}$ content in the D_s^+. Neither Cabibbo-favored nor Cabibbo-suppressed decays can contribute, and ω–ϕ mixing is an unlikely explanation for any fraction above about 2×10^{-4}.

[*qqq*] We decouple the $D_s^+ \to \phi\pi^+$ branching fraction obtained from mass projections (and used to get some of the other branching fractions) from the $D_s^+ \to \phi\pi^+$, $\phi \to K^+K^-$ branching fraction obtained from the Dalitz-plot analysis of $D_s^+ \to K^+K^-\pi^+$. That is, the ratio of these two branching fractions is not exactly the $\phi \to K^+K^-$ branching fraction 0.491.

[*rrr*] This is the average of a model-independent and a K-matrix parametrization of the $\pi^+\pi^-$ S-wave and is a sum over several f_0 mesons.

[*sss*] An ℓ indicates an e or a μ mode, not a sum over these modes.

[*ttt*] An $CP(\pm1)$ indicates the CP=+1 and CP=−1 eigenstates of the D^0-$\overline{D}^0$ system.

[*uuu*] D denotes D^0 or $\overline{D}^0$.

[*vvv*] $D^{*0}_{CP_+}$ decays into $D^0\pi^0$ with the D^0 reconstructed in CP-even eigenstates K^+K^- and $\pi^+\pi^-$.

[*xxx*] $\overline{D}^{**}$ represents an excited state with mass $2.2 < M < 2.8$ GeV/c^2.

[*yyy*] $X(3872)^+$ is a hypothetical charged partner of the $X(3872)$.

[*zzz*] $\Theta(1710)^{++}$ is a possible narrow pentaquark state and $G(2220)$ is a possible glueball resonance.

[*aaaa*] $(\overline{\Lambda}_c^- p)_s$ denotes a low-mass enhancement near 3.35 GeV/c^2.

[*bbaa*] Stands for the possible candidates of $K^*(1410)$, $K^*_0(1430)$ and $K^*_2(1430)$.

[*ccaa*] B^0 and B^0_s contributions not separated. Limit is on weighted average of the two decay rates.

[*ddaa*] This decay refers to the coherent sum of resonant and nonresonant $J^P = 0^+$ $K\pi$ components with $1.60 < m_{K\pi} < 2.15$ GeV/c^2.

[*eeaa*] $X(214)$ is a hypothetical particle of mass 214 MeV/c^2 reported by the HyperCP experiment, Physical Review Letters **94** 021801 (2005)

[*ffaa*] $\Theta(1540)^+$ denotes a possible narrow pentaquark state.

[*ggaa*] Here S and P are the hypothetical scalar and pseudoscalar particles with masses of 2.5 GeV/c^2 and 214.3 MeV/c^2, respectively.

[*hhaa*] These values are model dependent.

[*iiaa*] Here "anything" means at least one particle observed.

[*jjaa*] This is a B($B^0 \to D^{*-}\ell^+\nu_\ell$) value.

[*kkaa*] D^{**} stands for the sum of the $D(1\,^1P_1)$, $D(1\,^3P_0)$, $D(1\,^3P_1)$, $D(1\,^3P_2)$, $D(2\,^1S_0)$, and $D(2\,^1S_1)$ resonances.

[*llaa*] $D^{(*)}\overline{D}^{(*)}$ stands for the sum of $D^*\overline{D}^*$, $D^*\overline{D}$, $D\overline{D}^*$, and $D\overline{D}$.

[*nnaa*] $X(3915)$ denotes a near-threshold enhancement in the $\omega J/\psi$ mass spectrum.

[*ooaa*] Inclusive branching fractions have a multiplicity definition and can be greater than 100%.

[*ppaa*] D_j represents an unresolved mixture of pseudoscalar and tensor D^{**} (P-wave) states.

[*qqaa*] Not a pure measurement. See note at head of B^0_s Decay Modes.

[*rraa*] For $E_\gamma > 100$ MeV.

[*ssaa*] Includes $p\overline{p}\pi^+\pi^-\gamma$ and excludes $p\overline{p}\eta$, $p\overline{p}\omega$, $p\overline{p}\eta'$.

[*ttaa*] For a narrow state A with mass less than 960 MeV.

[*uuaa*] For a narrow scalar or pseudoscalar A^0 with mass 0.21–3.0 GeV.

[*vvaa*] For a narrow resonance in the range $2.2 < M(X) < 2.8$ GeV.

[*xxaa*] BHARDWAJ 11 does not observe this decay and presents a stronger 90% CL limit than this value. See measurements listings for details.

[*yyaa*] J^{PC} known by production in e^+e^- via single photon annihilation. I^G is not known; interpretation of this state as a single resonance is unclear because of the expectation of substantial threshold effects in this energy region.

[*zzaa*] $2m_\tau < M(\tau^+\tau^-) < 9.2$ GeV

[*aabb*] 2 GeV $< m_{K^+K^-} <$ 3 GeV

[*bbbb*] X = scalar with $m < 8.0$ GeV

[*ccbb*] $X\overline{X}$ = vectors with $m < 3.1$ GeV

[*ddbb*] X and $\overline{X}$ = zero spin with $m < 4.5$ GeV

[*eebb*] 1.5 GeV $< m_X <$ 5.0 GeV

[*ffbb*] 201 MeV $< M(\mu^+\mu^-) <$ 3565 MeV

[*ggbb*] 0.5 GeV $< m_X <$ 9.0 GeV, where m_X is the invariant mass of the hadronic final state.

[*hhbb*] Spectroscopic labeling for these states is theoretical, pending experimental information.

[*iibb*] 1.5 GeV $< m_X <$ 5.0 GeV

[*jjbb*] 1.5 GeV $< m_X <$ 5.0 GeV

[*kkbb*] For $m_{\tau^+\tau^-}$ in the ranges 4.03–9.52 and 9.61–10.10 GeV.

Meson Summary Table

See also the table of suggested $q\overline{q}$ quark-model assignments in the Quark Model section.

• Indicates particles that appear in the preceding Meson Summary Table. We do not regard the other entries as being established.

LIGHT UNFLAVORED ($S = C = B = 0$)

	$I^G(J^{PC})$
• $\pi^{\pm}$	$1^-(0^-)$
• π^0	$1^-(0^{-+})$
• η	$0^+(0^{-+})$
• $f_0(500)$	$0^+(0^{++})$
• $\rho(770)$	$1^+(1^{--})$
• $\omega(782)$	$0^-(1^{--})$
• $\eta'(958)$	$0^+(0^{-+})$
• $f_0(980)$	$0^+(0^{++})$
• $a_0(980)$	$1^-(0^{++})$
• $\phi(1020)$	$0^-(1^{--})$
• $h_1(1170)$	$0^-(1^{+-})$
• $b_1(1235)$	$1^+(1^{+-})$
• $a_1(1260)$	$1^-(1^{++})$
• $f_2(1270)$	$0^+(2^{++})$
• $f_1(1285)$	$0^+(1^{++})$
• $\eta(1295)$	$0^+(0^{-+})$
• $\pi(1300)$	$1^-(0^{-+})$
• $a_2(1320)$	$1^-(2^{++})$
• $f_0(1370)$	$0^+(0^{++})$
$h_1(1380)$	$?^-(1^{+-})$
• $\pi_1(1400)$	$1^-(1^{-+})$
• $\eta(1405)$	$0^+(0^{-+})$
• $f_1(1420)$	$0^+(1^{++})$
• $\omega(1420)$	$0^-(1^{--})$
$f_2(1430)$	$0^+(2^{++})$
• $a_0(1450)$	$1^-(0^{++})$
• $\rho(1450)$	$1^+(1^{--})$
• $\eta(1475)$	$0^+(0^{-+})$
• $f_0(1500)$	$0^+(0^{++})$
$f_1(1510)$	$0^+(1^{++})$
• $f_2'(1525)$	$0^+(2^{++})$
$f_2(1565)$	$0^+(2^{++})$
$\rho(1570)$	$1^+(1^{--})$
$h_1(1595)$	$0^-(1^{+-})$
• $\pi_1(1600)$	$1^-(1^{-+})$
$a_1(1640)$	$1^-(1^{++})$
$f_2(1640)$	$0^+(2^{++})$
• $\eta_2(1645)$	$0^+(2^{-+})$
• $\omega(1650)$	$0^-(1^{--})$
• $\omega_3(1670)$	$0^-(3^{--})$
• $\pi_2(1670)$	$1^-(2^{-+})$

	$I^G(J^{PC})$
• $\phi(1680)$	$0^-(1^{--})$
• $\rho_3(1690)$	$1^+(3^{--})$
• $\rho(1700)$	$1^+(1^{--})$
$a_2(1700)$	$1^-(2^{++})$
• $f_0(1710)$	$0^+(0^{++})$
$\eta(1760)$	$0^+(0^{-+})$
• $\pi(1800)$	$1^-(0^{-+})$
$f_2(1810)$	$0^+(2^{++})$
$X(1835)$	$?^?(?^{-+})$
$X(1840)$	$?^?(?^{??})$
• $\phi_3(1850)$	$0^-(3^{--})$
$\eta_2(1870)$	$0^+(2^{-+})$
• $\pi_2(1880)$	$1^-(2^{-+})$
$\rho(1900)$	$1^+(1^{--})$
$f_2(1910)$	$0^+(2^{++})$
• $f_2(1950)$	$0^+(2^{++})$
$\rho_3(1990)$	$1^+(3^{--})$
• $f_2(2010)$	$0^+(2^{++})$
$f_0(2020)$	$0^+(0^{++})$
• $a_4(2040)$	$1^-(4^{++})$
• $f_4(2050)$	$0^+(4^{++})$
$\pi_2(2100)$	$1^-(2^{-+})$
$f_0(2100)$	$0^+(0^{++})$
$f_2(2150)$	$0^+(2^{++})$
$\rho(2150)$	$1^+(1^{--})$
• $\phi(2170)$	$0^-(1^{--})$
$f_0(2200)$	$0^+(0^{++})$
$f_J(2220)$	$0^+(2^{++}$ or $4^{++})$
$\eta(2225)$	$0^+(0^{-+})$
$\rho_3(2250)$	$1^+(3^{--})$
• $f_2(2300)$	$0^+(2^{++})$
$f_4(2300)$	$0^+(4^{++})$
$f_0(2330)$	$0^+(0^{++})$
• $f_2(2340)$	$0^+(2^{++})$
$\rho_5(2350)$	$1^+(5^{--})$
$a_6(2450)$	$1^-(6^{++})$
$f_6(2510)$	$0^+(6^{++})$

OTHER LIGHT

Further States

STRANGE ($S = \pm 1$, $C = B = 0$)

	$I(J^P)$
• $K^{\pm}$	$1/2(0^-)$
• K^0	$1/2(0^-)$
• K_S^0	$1/2(0^-)$
• K_L^0	$1/2(0^-)$
$K_0^*(800)$	$1/2(0^+)$
• $K^*(892)$	$1/2(1^-)$
• $K_1(1270)$	$1/2(1^+)$
• $K_1(1400)$	$1/2(1^+)$
• $K^*(1410)$	$1/2(1^-)$
• $K_0^*(1430)$	$1/2(0^+)$
• $K_2^*(1430)$	$1/2(2^+)$
$K(1460)$	$1/2(0^-)$
$K_2(1580)$	$1/2(2^-)$
$K(1630)$	$1/2(?^?)$
$K_1(1650)$	$1/2(1^+)$
• $K^*(1680)$	$1/2(1^-)$
• $K_2(1770)$	$1/2(2^-)$
• $K_3^*(1780)$	$1/2(3^-)$
• $K_2(1820)$	$1/2(2^-)$
$K(1830)$	$1/2(0^-)$
$K_0^*(1950)$	$1/2(0^+)$
$K_2^*(1980)$	$1/2(2^+)$
• $K_4^*(2045)$	$1/2(4^+)$
$K_2(2250)$	$1/2(2^-)$
$K_3(2320)$	$1/2(3^+)$
$K_5^*(2380)$	$1/2(5^-)$
$K_4(2500)$	$1/2(4^-)$
$K(3100)$	$?^?(?^{??})$

CHARMED ($C = \pm 1$)

	$I(J^P)$
• $D^{\pm}$	$1/2(0^-)$
• D^0	$1/2(0^-)$
• $D^*(2007)^0$	$1/2(1^-)$
• $D^*(2010)^{\pm}$	$1/2(1^-)$
• $D_0^*(2400)^0$	$1/2(0^+)$
$D_0^*(2400)^{\pm}$	$1/2(0^+)$
• $D_1(2420)^0$	$1/2(1^+)$
$D_1(2420)^{\pm}$	$1/2(?^?)$
$D_1(2430)^0$	$1/2(1^+)$
• $D_2^*(2460)^0$	$1/2(2^+)$
• $D_2^*(2460)^{\pm}$	$1/2(2^+)$
$D(2550)^0$	$1/2(0^-)$
$D(2600)$	$1/2(?^?)$
$D^*(2640)^{\pm}$	$1/2(?^?)$
$D(2750)$	$1/2(?^?)$

CHARMED, STRANGE ($C = S = \pm 1$)

	$I(J^P)$
• $D_s^{\pm}$	$0(0^-)$
• $D_s^{*\pm}$	$0(?^?)$
• $D_{s0}^*(2317)^{\pm}$	$0(0^+)$
• $D_{s1}(2460)^{\pm}$	$0(1^+)$
• $D_{s1}(2536)^{\pm}$	$0(1^+)$
• $D_{s2}(2573)$	$0(?^?)$
• $D_{s1}^*(2700)^{\pm}$	$0(1^-)$
$D_{sJ}^*(2860)^{\pm}$	$0(?^?)$
$D_{sJ}(3040)^{\pm}$	$0(?^?)$

BOTTOM ($B = \pm 1$)

	$I(J^P)$
• $B^{\pm}$	$1/2(0^-)$
• B^0	$1/2(0^-)$
• $B^{\pm}/B^0$ ADMIXTURE	
• $B^{\pm}/B^0/B_s^0/b$-baryon ADMIXTURE	
V_{cb} and V_{ub} CKM Matrix Elements	
• B^*	$1/2(1^-)$
$B_J^*(5732)$	$?(?^?)$
• $B_1(5721)^0$	$1/2(1^+)$
• $B_2^*(5747)^0$	$1/2(2^+)$

BOTTOM, STRANGE ($B = \pm 1$, $S = \mp 1$)

	$I(J^P)$
• B_s^0	$0(0^-)$
• B_s^*	$0(1^-)$
• $B_{s1}(5830)^0$	$0(1^+)$
• $B_{s2}^*(5840)^0$	$0(2^+)$
$B_{sJ}^*(5850)$	$?(?^?)$

BOTTOM, CHARMED ($B = C = \pm 1$)

	$I(J^P)$
• $B_c^{\pm}$	$0(0^-)$

$c\overline{c}$

	$I^G(J^{PC})$
• $\eta_c(1S)$	$0^+(0^{-+})$
• $J/\psi(1S)$	$0^-(1^{--})$
• $\chi_{c0}(1P)$	$0^+(0^{++})$
• $\chi_{c1}(1P)$	$0^+(1^{++})$
• $h_c(1P)$	$?^?(1^{+-})$
• $\chi_{c2}(1P)$	$0^+(2^{++})$
• $\eta_c(2S)$	$0^+(0^{-+})$
• $\psi(2S)$	$0^-(1^{--})$
• $\psi(3770)$	$0^-(1^{--})$
$X(3823)$	$?^?(?^{?-})$
• $X(3872)$	$0^+(1^{++})$
• $X(3900)^{\pm}$	$?(1^+)$
$X(3900)^0$	$?(?^?)$
• $\chi_{c0}(2P)$	$0^+(0^{++})$
• $\chi_{c2}(2P)$	$0^+(2^{++})$
$X(3940)$	$?^?(?^{??})$
$X(4020)^{\pm}$	$?(?^?)$
• $\psi(4040)$	$0^-(1^{--})$
$X(4050)^{\pm}$	$?(?^?)$
$X(4140)$	$0^+(?^{?+})$
• $\psi(4160)$	$0^-(1^{--})$
$X(4160)$	$?^?(?^{??})$
$X(4250)^{\pm}$	$?(?^?)$
• $X(4260)$	$?^?(1^{--})$
$X(4350)$	$0^+(?^{?+})$
• $X(4360)$	$?^?(1^{--})$
• $\psi(4415)$	$0^-(1^{--})$
$X(4430)^{\pm}$	$?(1^+)$
• $X(4660)$	$?^?(1^{--})$

$b\overline{b}$

	$I^G(J^{PC})$
$\eta_b(1S)$	$0^+(0^{-+})$
• $\Upsilon(1S)$	$0^-(1^{--})$
• $\chi_{b0}(1P)$	$0^+(0^{++})$
• $\chi_{b1}(1P)$	$0^+(1^{++})$
• $h_b(1P)$	$?^?(1^{+-})$
• $\chi_{b2}(1P)$	$0^+(2^{++})$
$\eta_b(2S)$	$0^+(0^{-+})$
• $\Upsilon(2S)$	$0^-(1^{--})$
• $\Upsilon(1D)$	$0^-(2^{--})$
• $\chi_{b0}(2P)$	$0^+(0^{++})$
• $\chi_{b1}(2P)$	$0^+(1^{++})$
$h_b(2P)$	$?^?(1^{+-})$
• $\chi_{b2}(2P)$	$0^+(2^{++})$
• $\Upsilon(3S)$	$0^-(1^{--})$
• $\chi_b(3P)$	$?^?(?^{?+})$
• $\Upsilon(4S)$	$0^-(1^{--})$
$X(10610)^{\pm}$	$1^+(1^+)$
$X(10610)^0$	$1^+(1^+)$
$X(10650)^{\pm}$	$?^+(1^+)$
• $\Upsilon(10860)$	$0^-(1^{--})$
• $\Upsilon(11020)$	$0^-(1^{--})$

Baryon Summary Table

This short table gives the name, the quantum numbers (where known), and the status of baryons in the Review. Only the baryons with 3- or 4-star status are included in the Baryon Summary Table. Due to insufficient data or uncertain interpretation, the other entries in the table are not established baryons. The names with masses are of baryons that decay strongly. The spin-parity J^P (when known) is given with each particle. For the strongly decaying particles, the J^P values are considered to be part of the names.

p	$1/2^+$	****	$\Delta(1232)$	$3/2^+$	****	Σ^+	$1/2^+$	****	Ξ^0	$1/2^+$	****	Λ_c^+	$1/2^+$	****
n	$1/2^+$	****	$\Delta(1600)$	$3/2^+$	***	Σ^0	$1/2^+$	****	Ξ^-	$1/2^+$	****	$\Lambda_c(2595)^+$	$1/2^-$	***
$N(1440)$	$1/2^+$	****	$\Delta(1620)$	$1/2^-$	****	Σ^-	$1/2^+$	****	$\Xi(1530)$	$3/2^+$	****	$\Lambda_c(2625)^+$	$3/2^-$	***
$N(1520)$	$3/2^-$	****	$\Delta(1700)$	$3/2^-$	****	$\Sigma(1385)$	$3/2^+$	****	$\Xi(1620)$		*	$\Lambda_c(2765)^+$		*
$N(1535)$	$1/2^-$	****	$\Delta(1750)$	$1/2^+$	*	$\Sigma(1480)$		*	$\Xi(1690)$		***	$\Lambda_c(2880)^+$	$5/2^+$	***
$N(1650)$	$1/2^-$	****	$\Delta(1900)$	$1/2^-$	**	$\Sigma(1560)$		**	$\Xi(1820)$	$3/2^-$	***	$\Lambda_c(2940)^+$		***
$N(1675)$	$5/2^-$	****	$\Delta(1905)$	$5/2^+$	****	$\Sigma(1580)$	$3/2^-$	*	$\Xi(1950)$		***	$\Sigma_c(2455)$	$1/2^+$	****
$N(1680)$	$5/2^+$	****	$\Delta(1910)$	$1/2^+$	****	$\Sigma(1620)$	$1/2^-$	*	$\Xi(2030)$	$\geq \frac{5}{2}$?	***	$\Sigma_c(2520)$	$3/2^+$	***
$N(1685)$		*	$\Delta(1920)$	$3/2^+$	***	$\Sigma(1660)$	$1/2^+$	***	$\Xi(2120)$		*	$\Sigma_c(2800)$		***
$N(1700)$	$3/2^-$	***	$\Delta(1930)$	$5/2^-$	***	$\Sigma(1670)$	$3/2^-$	****	$\Xi(2250)$		**	Ξ_c^+	$1/2^+$	***
$N(1710)$	$1/2^+$	***	$\Delta(1940)$	$3/2^-$	**	$\Sigma(1690)$		**	$\Xi(2370)$		**	Ξ_c^0	$1/2^+$	***
$N(1720)$	$3/2^+$	****	$\Delta(1950)$	$7/2^+$	****	$\Sigma(1730)$	$3/2^+$	*	$\Xi(2500)$		*	$\Xi_c'^+$	$1/2^+$	***
$N(1860)$	$5/2^+$	**	$\Delta(2000)$	$5/2^+$	**	$\Sigma(1750)$	$1/2^-$	***				$\Xi_c'^0$	$1/2^+$	***
$N(1875)$	$3/2^-$	***	$\Delta(2150)$	$1/2^-$	*	$\Sigma(1770)$	$1/2^+$	*	Ω^-	$3/2^+$	****	$\Xi_c(2645)$	$3/2^+$	***
$N(1880)$	$1/2^+$	**	$\Delta(2200)$	$7/2^-$	*	$\Sigma(1775)$	$5/2^-$	****	$\Omega(2250)^-$		***	$\Xi_c(2790)$	$1/2^-$	***
$N(1895)$	$1/2^-$	**	$\Delta(2300)$	$9/2^+$	**	$\Sigma(1840)$	$3/2^+$	*	$\Omega(2380)^-$		**	$\Xi_c(2815)$	$3/2^-$	***
$N(1900)$	$3/2^+$	***	$\Delta(2350)$	$5/2^-$	*	$\Sigma(1880)$	$1/2^+$	**	$\Omega(2470)^-$		**	$\Xi_c(2930)$		*
$N(1990)$	$7/2^+$	**	$\Delta(2390)$	$7/2^+$	*	$\Sigma(1900)$	$1/2^-$	*				$\Xi_c(2980)$		***
$N(2000)$	$5/2^+$	**	$\Delta(2400)$	$9/2^-$	**	$\Sigma(1915)$	$5/2^+$	****				$\Xi_c(3055)$		**
$N(2040)$	$3/2^+$	*	$\Delta(2420)$	$11/2^+$	****	$\Sigma(1940)$	$3/2^+$	*				$\Xi_c(3080)$		***
$N(2060)$	$5/2^-$	**	$\Delta(2750)$	$13/2^-$	**	$\Sigma(1940)$	$3/2^-$	***				$\Xi_c(3123)$		*
$N(2100)$	$1/2^+$	*	$\Delta(2950)$	$15/2^+$	**	$\Sigma(2000)$	$1/2^-$	*				Ω_c^0	$1/2^+$	***
$N(2120)$	$3/2^-$	**				$\Sigma(2030)$	$7/2^+$	****				$\Omega_c(2770)^0$	$3/2^+$	***
$N(2190)$	$7/2^-$	****	Λ	$1/2^+$	****	$\Sigma(2070)$	$5/2^+$	*						
$N(2220)$	$9/2^+$	****	$\Lambda(1405)$	$1/2^-$	****	$\Sigma(2080)$	$3/2^+$	**				Ξ_{cc}^+		*
$N(2250)$	$9/2^-$	****	$\Lambda(1520)$	$3/2^-$	****	$\Sigma(2100)$	$7/2^-$	*						
$N(2300)$	$1/2^+$	**	$\Lambda(1600)$	$1/2^+$	***	$\Sigma(2250)$		***				Λ_b^0	$1/2^+$	***
$N(2570)$	$5/2^-$	**	$\Lambda(1670)$	$1/2^-$	****	$\Sigma(2455)$		**				$\Lambda_b(5912)^0$	$1/2^-$	***
$N(2600)$	$11/2^-$	***	$\Lambda(1690)$	$3/2^-$	****	$\Sigma(2620)$		**				$\Lambda_b(5920)^0$	$3/2^-$	***
$N(2700)$	$13/2^+$	**	$\Lambda(1710)$	$1/2^+$	*	$\Sigma(3000)$		*				Σ_b	$1/2^+$	***
			$\Lambda(1800)$	$1/2^-$	***	$\Sigma(3170)$		*				Σ_b^*	$3/2^+$	***
			$\Lambda(1810)$	$1/2^+$	***							Ξ_b^0, Ξ_b^-	$1/2^+$	***
			$\Lambda(1820)$	$5/2^+$	****							$\Xi_b(5945)^0$	$3/2^+$	***
			$\Lambda(1830)$	$5/2^-$	****							Ω_b^-	$1/2^+$	***
			$\Lambda(1890)$	$3/2^+$	****									
			$\Lambda(2000)$		*									
			$\Lambda(2020)$	$7/2^+$	*									
			$\Lambda(2050)$	$3/2^-$	*									
			$\Lambda(2100)$	$7/2^-$	****									
			$\Lambda(2110)$	$5/2^+$	***									
			$\Lambda(2325)$	$3/2^-$	*									
			$\Lambda(2350)$	$9/2^+$	***									
			$\Lambda(2585)$		**									

**** Existence is certain, and properties are at least fairly well explored.

*** Existence ranges from very likely to certain, but further confirmation is desirable and/or quantum numbers, branching fractions, etc. are not well determined.

** Evidence of existence is only fair.

* Evidence of existence is poor.

Baryon Summary Table

N BARYONS ($S = 0$, $I = 1/2$)

p, $N^+ = uud$; n, $N^0 = udd$

p

$I(J^P) = \frac{1}{2}(\frac{1}{2}^+)$

Mass $m = 1.00727646681 \pm 0.00000000009$ u
Mass $m = 938.272046 \pm 0.000021$ MeV [a]
$|m_p - m_{\overline{p}}|/m_p < 7 \times 10^{-10}$, CL = 90% [b]
$|\frac{q_{\overline{p}}}{m_{\overline{p}}}|/(\frac{q_p}{m_p}) = 0.99999999991 \pm 0.00000000009$
$|q_p + q_{\overline{p}}|/e < 7 \times 10^{-10}$, CL = 90% [b]
$|q_p + q_e|/e < 1 \times 10^{-21}$ [c]
Magnetic moment $\mu = 2.792847356 \pm 0.000000023\ \mu_N$
$(\mu_p + \mu_{\overline{p}}) / \mu_p = (0 \pm 5) \times 10^{-6}$
Electric dipole moment $d < 0.54 \times 10^{-23}$ $e$cm
Electric polarizability $\alpha = (11.2 \pm 0.4) \times 10^{-4}$ fm^3
Magnetic polarizability $\beta = (2.5 \pm 0.4) \times 10^{-4}$ fm^3 (S = 1.2)
Charge radius, μp Lamb shift = 0.84087 ± 0.00039 fm [d]
Charge radius, ep CODATA value = 0.8775 ± 0.0051 fm [d]
Magnetic radius = 0.777 ± 0.016 fm
Mean life $\tau > 2.1 \times 10^{29}$ years, CL = 90% [e] ($p \to$ invisible mode)
Mean life $\tau > 10^{31}$ to 10^{33} years [e] (mode dependent)

See the "Note on Nucleon Decay" in our 1994 edition (Phys. Rev. **D50**, 1173) for a short review.

The "partial mean life" limits tabulated here are the limits on τ/B_i, where τ is the total mean life and B_i is the branching fraction for the mode in question. For N decays, p and n indicate proton and neutron partial lifetimes.

p DECAY MODES	Partial mean life (10^{30} years)	Confidence level	p (MeV/c)
Antilepton + meson			
$N \to e^+\pi$	> 2000 (n), > 8200 (p)	90%	459
$N \to \mu^+\pi$	> 1000 (n), > 6600 (p)	90%	453
$N \to \nu\pi$	> 112 (n), > 16 (p)	90%	459
$p \to e^+\eta$	> 4200	90%	309
$p \to \mu^+\eta$	> 1300	90%	297
$n \to \nu\eta$	> 158	90%	310
$N \to e^+\rho$	> 217 (n), > 710 (p)	90%	149
$N \to \mu^+\rho$	> 228 (n), > 160 (p)	90%	113
$N \to \nu\rho$	> 19 (n), > 162 (p)	90%	149
$p \to e^+\omega$	> 320	90%	143
$p \to \mu^+\omega$	> 780	90%	105
$n \to \nu\omega$	> 108	90%	144
$N \to e^+K$	> 17 (n), > 1000 (p)	90%	339
$N \to \mu^+K$	> 26 (n), > 1600 (p)	90%	329
$N \to \nu K$	> 86 (n), > 2300 (p)	90%	339
$n \to \nu K^0_S$	> 260	90%	338
$p \to e^+K^*(892)^0$	> 84	90%	45
$N \to \nu K^*(892)$	> 78 (n), > 51 (p)	90%	45
Antilepton + mesons			
$p \to e^+\pi^+\pi^-$	> 82	90%	448
$p \to e^+\pi^0\pi^0$	> 147	90%	449
$n \to e^+\pi^-\pi^0$	> 52	90%	449
$p \to \mu^+\pi^+\pi^-$	> 133	90%	425
$p \to \mu^+\pi^0\pi^0$	> 101	90%	427
$n \to \mu^+\pi^-\pi^0$	> 74	90%	427
$n \to e^+K^0\pi^-$	> 18	90%	319
Lepton + meson			
$n \to e^-\pi^+$	> 65	90%	459
$n \to \mu^-\pi^+$	> 49	90%	453
$n \to e^-\rho^+$	> 62	90%	150
$n \to \mu^-\rho^+$	> 7	90%	115
$n \to e^-K^+$	> 32	90%	340
$n \to \mu^-K^+$	> 57	90%	330
Lepton + mesons			
$p \to e^-\pi^+\pi^+$	> 30	90%	448
$n \to e^-\pi^+\pi^0$	> 29	90%	449
$p \to \mu^-\pi^+\pi^+$	> 17	90%	425
$n \to \mu^-\pi^+\pi^0$	> 34	90%	427
$p \to e^-\pi^+K^+$	> 75	90%	320
$p \to \mu^-\pi^+K^+$	> 245	90%	279
Antilepton + photon(s)			
$p \to e^+\gamma$	> 670	90%	469
$p \to \mu^+\gamma$	> 478	90%	463
$n \to \nu\gamma$	> 28	90%	470
$p \to e^+\gamma\gamma$	> 100	90%	469
$n \to \nu\gamma\gamma$	> 219	90%	470
Three (or more) leptons			
$p \to e^+e^+e^-$	> 793	90%	469
$p \to e^+\mu^+\mu^-$	> 359	90%	457
$p \to e^+\nu\nu$	> 17	90%	469
$n \to e^+e^-\nu$	> 257	90%	470
$n \to \mu^+e^-\nu$	> 83	90%	464
$n \to \mu^+\mu^-\nu$	> 79	90%	458
$p \to \mu^+e^+e^-$	> 529	90%	463
$p \to \mu^+\mu^+\mu^-$	> 675	90%	439
$p \to \mu^+\nu\nu$	> 21	90%	463
$p \to e^-\mu^+\mu^+$	> 6	90%	457
$n \to 3\nu$	> 0.0005	90%	470
Inclusive modes			
$N \to e^+$ anything	> 0.6 (n, p)	90%	–
$N \to \mu^+$ anything	> 12 (n, p)	90%	–
$N \to e^+\pi^0$ anything	> 0.6 (n, p)	90%	–
$\Delta B = 2$ dinucleon modes			
The following are lifetime limits per iron nucleus.			
$pp \to \pi^+\pi^+$	> 0.7	90%	–
$pn \to \pi^+\pi^0$	> 2	90%	–
$nn \to \pi^+\pi^-$	> 0.7	90%	–
$nn \to \pi^0\pi^0$	> 3.4	90%	–
$pp \to e^+e^+$	> 5.8	90%	–
$pp \to e^+\mu^+$	> 3.6	90%	–
$pp \to \mu^+\mu^+$	> 1.7	90%	–
$pn \to e^+\overline{\nu}$	> 2.8	90%	–
$pn \to \mu^+\overline{\nu}$	> 1.6	90%	–
$nn \to \nu_e\overline{\nu}_e$	> 1.4	90%	–
$nn \to \nu_\mu\overline{\nu}_\mu$	> 1.4	90%	–
$pn \to$ invisible	> 0.000021	90%	–
$pp \to$ invisible	> 0.00005	90%	–

$\overline{p}$ DECAY MODES

$\overline{p}$ DECAY MODES	Partial mean life (years)	Confidence level	p (MeV/c)
$\overline{p} \to e^-\gamma$	$> 7 \times 10^5$	90%	469
$\overline{p} \to \mu^-\gamma$	$> 5 \times 10^4$	90%	463
$\overline{p} \to e^-\pi^0$	$> 4 \times 10^5$	90%	459
$\overline{p} \to \mu^-\pi^0$	$> 5 \times 10^4$	90%	453
$\overline{p} \to e^-\eta$	$> 2 \times 10^4$	90%	309
$\overline{p} \to \mu^-\eta$	$> 8 \times 10^3$	90%	297
$\overline{p} \to e^-K^0_S$	> 900	90%	337
$\overline{p} \to \mu^-K^0_S$	$> 4 \times 10^3$	90%	326
$\overline{p} \to e^-K^0_L$	$> 9 \times 10^3$	90%	337
$\overline{p} \to \mu^-K^0_L$	$> 7 \times 10^3$	90%	326
$\overline{p} \to e^-\gamma\gamma$	$> 2 \times 10^4$	90%	469
$\overline{p} \to \mu^-\gamma\gamma$	$> 2 \times 10^4$	90%	463
$\overline{p} \to e^-\omega$	> 200	90%	143

n

$I(J^P) = \frac{1}{2}(\frac{1}{2}^+)$

Mass $m = 1.0086649160 \pm 0.0000000004$ u
Mass $m = 939.565379 \pm 0.000021$ MeV [a]
$(m_n - m_{\overline{n}})/\ m_n = (9 \pm 6) \times 10^{-5}$
$m_n - m_p = 1.2933322 \pm 0.0000004$ MeV
$= 0.00138844919(45)$ u
Mean life $\tau = 880.3 \pm 1.1$ s (S = 1.9)
$c\tau = 2.6391 \times 10^8$ km
Magnetic moment $\mu = -1.9130427 \pm 0.0000005\ \mu_N$
Electric dipole moment $d < 0.29 \times 10^{-25}$ $e$cm, CL = 90%
Mean-square charge radius $\langle r_n^2 \rangle = -0.1161 \pm 0.0022$ fm^2 (S = 1.3)
Magnetic radius $\sqrt{\langle r_M^2 \rangle} = 0.862^{+0.009}_{-0.008}$ fm
Electric polarizability $\alpha = (11.6 \pm 1.5) \times 10^{-4}$ fm^3
Magnetic polarizability $\beta = (3.7 \pm 2.0) \times 10^{-4}$ fm^3
Charge $q = (-0.2 \pm 0.8) \times 10^{-21}$ e
Mean $n\overline{n}$-oscillation time $> 8.6 \times 10^7$ s, CL = 90% (free n)
Mean $n\overline{n}$-oscillation time $> 1.3 \times 10^8$ s, CL = 90% [f] (bound n)
Mean nn'-oscillation time > 414 s, CL = 90% [g]

$p e^- \nu_e$ decay parameters [h]

$\lambda \equiv g_A / g_V = -1.2723 \pm 0.0023$ (S = 2.2)
$A = -0.1184 \pm 0.0010$ (S = 2.4)
$B = 0.9807 \pm 0.0030$
$C = -0.2377 \pm 0.0026$
$a = -0.103 \pm 0.004$
$\phi_{AV} = (180.017 \pm 0.026)^\circ$ [i]
$D = (-1.2 \pm 2.0) \times 10^{-4}$ [j]
$R = 0.004 \pm 0.013$ [j]

n DECAY MODES	Fraction (Γ_i/Γ)	Confidence level	p (MeV/c)
$p e^- \overline{\nu}_e$	100 %		1
$p e^- \overline{\nu}_e \gamma$	[k] (3.09 ± 0.32) $\times 10^{-3}$		1
Charge conservation (Q) violating mode			
$p \nu_e \overline{\nu}_e$	Q < 8 $\times 10^{-27}$	68%	1

$N(1440)\ 1/2^+$

$I(J^P) = \frac{1}{2}(\frac{1}{2}^+)$

Breit-Wigner mass = 1410 to 1450 (≈ 1430) MeV
Breit-Wigner full width = 250 to 450 (≈ 350) MeV
p_{beam} = 0.59 GeV/c $4\pi\lambda^2$ = 32.2 mb
Re(pole position) = 1350 to 1380 (≈ 1365) MeV
−2Im(pole position) = 160 to 220 (≈ 190) MeV

$N(1440)$ DECAY MODES	Fraction (Γ_i/Γ)	p (MeV/c)
$N\pi$	55–75 %	391
$N\eta$	(0.0±1.0) %	†
$N\pi\pi$	30–40 %	338
$\Delta\pi$	20–30 %	135
$\Delta(1232)\pi$, P-wave	15–30 %	135
$N\rho$	<8 %	†
$N\rho$, S=1/2, P-wave	(0.0±1.0) %	†
$N(\pi\pi)^{I=0}_{S\text{-wave}}$	10–20 %	–
$p\gamma$	0.035–0.048 %	407
$p\gamma$, helicity=1/2	0.035–0.048 %	407
$n\gamma$	0.02–0.04 %	406
$n\gamma$, helicity=1/2	0.02–0.04 %	406

$N(1520)\ 3/2^-$

$I(J^P) = \frac{1}{2}(\frac{3}{2}^-)$

Breit-Wigner mass = 1510 to 1520 (≈ 1515) MeV
Breit-Wigner full width = 100 to 125 (≈ 115) MeV
p_{beam} = 0.73 GeV/c $4\pi\lambda^2$ = 23.9 mb
Re(pole position) = 1505 to 1515 (≈ 1510) MeV
−2Im(pole position) = 105 to 120 (≈ 110) MeV

$N(1520)$ DECAY MODES	Fraction (Γ_i/Γ)	p (MeV/c)
$N\pi$	55–65 %	453
$N\eta$	$(2.3 \pm 0.4) \times 10^{-3}$	142
$N\pi\pi$	20–30 %	410
$\Delta\pi$	15–25 %	225
$\Delta(1232)\pi$, S-wave	10–20 %	225
$\Delta(1232)\pi$, D-wave	10–15 %	225
$N\rho$	15–25 %	†
$N\rho$, S=3/2, S-wave	(9.0±1.0) %	†
$N(\pi\pi)^{I=0}_{S\text{-wave}}$	<8 %	–
$p\gamma$	0.31–0.52 %	467
$p\gamma$, helicity=1/2	0.01–0.02 %	467
$p\gamma$, helicity=3/2	0.30–0.50 %	467
$n\gamma$	0.30–0.53 %	466
$n\gamma$, helicity=1/2	0.04–0.10 %	466
$n\gamma$, helicity=3/2	0.25–0.45 %	466

$N(1535)\ 1/2^-$

$I(J^P) = \frac{1}{2}(\frac{1}{2}^-)$

Breit-Wigner mass = 1525 to 1545 (≈ 1535) MeV
Breit-Wigner full width = 125 to 175 (≈ 150) MeV
p_{beam} = 0.76 GeV/c $4\pi\lambda^2$ = 22.5 mb
Re(pole position) = 1490 to 1530 (≈ 1510) MeV
−2Im(pole position) = 90 to 250 (≈ 170) MeV

$N(1535)$ DECAY MODES	Fraction (Γ_i/Γ)	p (MeV/c)
$N\pi$	35–55 %	468
$N\eta$	(42 ±10) %	186
$N\pi\pi$	1–10 %	426
$\Delta\pi$	<1 %	244
$\Delta(1232)\pi$, D-wave	0–4 %	244
$N\rho$	<4 %	†
$N\rho$, S=1/2, S-wave	(2.0± 1.0) %	†
$N\rho$, S=3/2, D-wave	(0.0± 1.0) %	†
$N(\pi\pi)^{I=0}_{S\text{-wave}}$	(2 ± 1) %	–
$N(1440)\pi$	(8 ± 3) %	†
$p\gamma$	0.15–0.30 %	481
$p\gamma$, helicity=1/2	0.15–0.30 %	481
$n\gamma$	0.01–0.25 %	480
$n\gamma$, helicity=1/2	0.01–0.25 %	480

$N(1650)\ 1/2^-$

$I(J^P) = \frac{1}{2}(\frac{1}{2}^-)$

Breit-Wigner mass = 1645 to 1670 (≈ 1655) MeV
Breit-Wigner full width = 110 to 170 (≈ 140) MeV
p_{beam} = 0.97 GeV/c $4\pi\lambda^2$ = 16.2 mb
Re(pole position) = 1640 to 1670 (≈ 1655) MeV
−2Im(pole position) = 100 to 170 (≈ 135) MeV

$N(1650)$ DECAY MODES	Fraction (Γ_i/Γ)	p (MeV/c)
$N\pi$	50–90 %	551
$N\eta$	5–15 %	354
ΛK	3–11 %	179
$N\pi\pi$	10–20 %	517
$\Delta\pi$	0–25 %	349
$\Delta(1232)\pi$, D-wave	0–25 %	349
$N\rho$	4–12 %	†
$N\rho$, S=1/2, S-wave	(1.0±1.0) %	†
$N\rho$, S=3/2, D-wave	(13.0±3.0) %	†
$N(\pi\pi)^{I=0}_{S\text{-wave}}$	<4 %	–
$N(1440)\pi$	<5 %	168
$p\gamma$	0.04–0.20 %	562
$p\gamma$, helicity=1/2	0.04–0.20 %	562
$n\gamma$	0.003–0.17 %	561
$n\gamma$, helicity=1/2	0.003–0.17 %	561

$N(1675)\ 5/2^-$

$I(J^P) = \frac{1}{2}(\frac{5}{2}^-)$

Breit-Wigner mass = 1670 to 1680 (≈ 1675) MeV
Breit-Wigner full width = 130 to 165 (≈ 150) MeV
Re(pole position) = 1655 to 1665 (≈ 1660) MeV
−2Im(pole position) = 125 to 150 (≈ 135) MeV
p_{beam} = 1.01 GeV/c $4\pi\lambda^2$ = 15.4 mb

$N(1675)$ DECAY MODES	Fraction (Γ_i/Γ)	p (MeV/c)
$N\pi$	35–45 %	564
$N\eta$	(0 ± 7) $\times 10^{-3}$	376
ΛK	<1 %	216
$N\pi\pi$	50–60 %	532
$\Delta\pi$	50–60 %	366
$\Delta(1232)\pi$, D-wave	(50 ±15) %	366
$N\rho$	< 1–3 %	†
$N\rho$, S=1/2, D-wave	(0.0± 1.0) %	†
$N\rho$, S=3/2, D-wave	(1.0± 1.0) %	†
$N(\pi\pi)^{I=0}_{S\text{-wave}}$	(7.0± 3.0) %	–
$p\gamma$	0–0.02 %	575
$p\gamma$, helicity=1/2	0–0.01 %	575
$p\gamma$, helicity=3/2	0–0.01 %	575
$n\gamma$	0–0.15 %	574
$n\gamma$, helicity=1/2	0–0.05 %	574
$n\gamma$, helicity=3/2	0–0.10 %	574

$N(1680)\ 5/2^+$

$I(J^P) = \frac{1}{2}(\frac{5}{2}^+)$

Breit-Wigner mass = 1680 to 1690 (≈ 1685) MeV
Breit-Wigner full width = 120 to 140 (≈ 130) MeV
Re(pole position) = 1665 to 1680 (≈ 1675) MeV
−2Im(pole position) = 110 to 135 (≈ 120) MeV
p_{beam} = 1.02 GeV/c $4\pi\lambda^2$ = 15.0 mb

Baryon Summary Table

N(1680) DECAY MODES	Fraction (Γ_i/Γ)	p (MeV/c)
$N\pi$	65–70 %	571
$N\eta$	$(0\pm7)\times10^{-3}$	386
$N\pi\pi$	30–40 %	539
$\Delta\pi$	5–15 %	374
$\Delta(1232)\pi$, P-wave	(10±5) %	374
$\Delta(1232)\pi$, F-wave	0–12 %	374
$N\rho$	3–15 %	†
$N\rho$, S=3/2, P-wave	<12;%	†
$N\rho$, S=3/2, F-wave	1–5 %	†
$N(\pi\pi)^{I=0}_{S\text{-wave}}$	(11±5) %	–
$p\gamma$	0.21–0.32 %	581
$p\gamma$, helicity=1/2	0.001–0.011 %	581
$p\gamma$, helicity=3/2	0.20–0.32 %	581
$n\gamma$	0.021–0.046 %	581
$n\gamma$, helicity=1/2	0.004–0.029 %	581
$n\gamma$, helicity=3/2	0.01–0.024 %	581

N(1700) 3/2⁻

$I(J^P) = \frac{1}{2}(\frac{3}{2}^-)$

Breit-Wigner mass = 1650 to 1750 (≈ 1700) MeV
Breit-Wigner full width = 100 to 250 (≈ 150) MeV
p_{beam} = 1.05 GeV/c $4\pi\lambda^2$ = 14.5 mb
Re(pole position) = 1650 to 1750 (≈ 1700) MeV
−2Im(pole position) = 100 to 300 MeV

N(1700) DECAY MODES	Fraction (Γ_i/Γ)	p (MeV/c)
$N\pi$	(12 ±5) %	581
$N\eta$	(0.0±1.0) %	402
ΛK	< 3 %	255
$N\pi\pi$	85–95 %	550
$\Delta(1232)\pi$, S-wave	10–90 %	386
$\Delta(1232)\pi$, D-wave	< 20 %	386
$N\rho$	< 35 %	†
$N\rho$, S=3/2, S-wave	(7.0±1.0) %	†
$p\gamma$	0.01–0.05 %	591
$p\gamma$, helicity=1/2	0.0–0.024 %	591
$p\gamma$, helicity=3/2	0.002–0.026 %	591
$n\gamma$	0.01–0.13 %	590
$n\gamma$, helicity=1/2	0.0–0.09 %	590
$n\gamma$, helicity=3/2	0.01–0.05 %	590

N(1710) 1/2⁺

$I(J^P) = \frac{1}{2}(\frac{1}{2}^+)$

Breit-Wigner mass = 1680 to 1740 (≈ 1710) MeV
Breit-Wigner full width = 50 to 250 (≈ 100) MeV
p_{beam} = 1.07 GeV/c $4\pi\lambda^2$ = 14.2 mb
Re(pole position) = 1670 to 1770 (≈ 1720) MeV
−2Im(pole position) = 80 to 380 (≈ 230) MeV

N(1710) DECAY MODES	Fraction (Γ_i/Γ)	Scale factor	p (MeV/c)
$N\pi$	5–20 %		588
$N\eta$	10–30 %		412
$N\omega$	(8±5) %	3.5	†
ΛK	5–25 %		269
$N\pi\pi$	40–90 %		557
$\Delta\pi$	15–40 %		394
$N\rho$	5–25 %		†
$N(\pi\pi)^{I=0}_{S\text{-wave}}$	10–40 %		–
$p\gamma$	0.002–0.08 %		598
$p\gamma$, helicity=1/2	0.002–0.08 %		598
$n\gamma$	0.0–0.02%		597
$n\gamma$, helicity=1/2	0.0–0.02%		597

N(1720) 3/2⁺

$I(J^P) = \frac{1}{2}(\frac{3}{2}^+)$

Breit-Wigner mass = 1700 to 1750 (≈ 1720) MeV
Breit-Wigner full width = 150 to 400 (≈ 250) MeV
p_{beam} = 1.09 GeV/c $4\pi\lambda^2$ = 13.9 mb
Re(pole position) = 1660 to 1690 (≈ 1675) MeV
−2Im(pole position) = 150 to 400 (≈ 250) MeV

N(1720) DECAY MODES	Fraction (Γ_i/Γ)	p (MeV/c)
$N\pi$	(11± 3) %	594
$N\eta$	(4± 1) %	422
ΛK	1–15 %	283
$N\pi\pi$	>70 %	564
$\Delta(1232)\pi$, P-wave	(75±15) %	402
$N\rho$	70–85 %	74
$N\rho$, S=1/2, P-wave	large	74
$p\gamma$	0.05–0.25 %	604
$p\gamma$, helicity=1/2	0.05–0.15 %	604
$p\gamma$, helicity=3/2	0.002–0.16 %	604
$n\gamma$	0.0–0.016 %	603
$n\gamma$, helicity=1/2	0.0–0.01 %	603
$n\gamma$, helicity=3/2	0.0–0.015 %	603

N(1875) 3/2⁻

$I(J^P) = \frac{1}{2}(\frac{3}{2}^-)$

Breit-Wigner mass = 1820 to 1920 (≈ 1875) MeV
Breit-Wigner full width
Re(pole position) = 1800 to 1950 MeV
−2Im(pole position) = 150 to 250 MeV

N(1875) DECAY MODES	Fraction (Γ_i/Γ)	Scale factor	p (MeV/c)
$N\pi$	(7 ± 6) %		695
$N\eta$	(1.2± 1.8) %	2.3	559
$N\omega$	(20 ± 4) %		371
ΣK	$(7\pm4)\times10^{-3}$		384
$\Delta(1232)\pi$, S-wave	(40 ±10) %		520
$\Delta(1232)\pi$, D-wave	(17 ±10) %		520
$N\rho$, S=3/2, S-wave	(6 ± 6) %		379
$N(\pi\pi)^{I=0}_{S\text{-wave}}$	(24 ±24) %		–
$p\gamma$	0.008–0.016 %		703
$p\gamma$, helicity=1/2	0.006–0.010 %		703
$p\gamma$, helicity=3/2	0.002–0.006 %		703

N(1900) 3/2⁺

$I(J^P) = \frac{1}{2}(\frac{3}{2}^+)$

Breit-Wigner mass ≈ 1900 MeV
Breit-Wigner full width ∼ 250 MeV
Re(pole position) = 1900 ± 30 MeV
−2Im(pole position) = 200^{+100}_{-60} MeV

N(1900) DECAY MODES	Fraction (Γ_i/Γ)	Scale factor	p (MeV/c)
$N\pi$	∼ 5 %		710
$N\eta$	∼ 12 %		579
$N\omega$	(13 ±9) %	3.1	401
ΛK	0–10 %		477
ΣK	(5.0±2.0) %		410

N(2190) 7/2⁻

$I(J^P) = \frac{1}{2}(\frac{7}{2}^-)$

Breit-Wigner mass = 2100 to 2200 (≈ 2190) MeV
Breit-Wigner full width = 300 to 700 (≈ 500) MeV
p_{beam} = 2.07 GeV/c $4\pi\lambda^2$ = 6.21 mb
Re(pole position) = 2050 to 2100 (≈ 2075) MeV
−2Im(pole position) = 400 to 520 (≈ 450) MeV

N(2190) DECAY MODES	Fraction (Γ_i/Γ)	p (MeV/c)
$N\pi$	10–20 %	888
$N\eta$	(0.0±1.0) %	791
$N\omega$	seen	676
ΛK	seen	712
$N\pi\pi$	seen	870
$N\rho$	seen	680
$p\gamma$	0.02–0.06 %	894
$p\gamma$, helicity=1/2	0.02–0.04 %	894
$p\gamma$, helicity=3/2	0.002–0.02 %	894

$N(2220)\ 9/2^+$

$I(J^P) = \frac{1}{2}(\frac{9}{2}^+)$

Breit-Wigner mass = 2200 to 2300 (≈ 2250) MeV
Breit-Wigner full width = 350 to 500 (≈ 400) MeV
p_{beam} = 2.21 GeV/c $4\pi\lambda^2$ = 5.74 mb
Re(pole position) = 2130 to 2200 (≈ 2170) MeV
−2Im(pole position) = 400 to 560 (≈ 480) MeV

$N(2220)$ DECAY MODES	Fraction (Γ_i/Γ)	p (MeV/c)
$N\pi$	15–25 %	924

$N(2250)\ 9/2^-$

$I(J^P) = \frac{1}{2}(\frac{9}{2}^-)$

Breit-Wigner mass = 2200 to 2350 (≈ 2275) MeV
Breit-Wigner full width = 230 to 800 (≈ 500) MeV
p_{beam} = 2.27 GeV/c $4\pi\lambda^2$ = 5.56 mb
Re(pole position) = 2150 to 2250 (≈ 2200) MeV
−2Im(pole position) = 350 to 550 (≈ 450) MeV

$N(2250)$ DECAY MODES	Fraction (Γ_i/Γ)	p (MeV/c)
$N\pi$	5–15 %	938

$N(2600)\ 11/2^-$

$I(J^P) = \frac{1}{2}(\frac{11}{2}^-)$

Breit-Wigner mass = 2550 to 2750 (≈ 2600) MeV
Breit-Wigner full width = 500 to 800 (≈ 650) MeV
p_{beam} = 3.12 GeV/c $4\pi\lambda^2$ = 3.86 mb

$N(2600)$ DECAY MODES	Fraction (Γ_i/Γ)	p (MeV/c)
$N\pi$	5–10 %	1126

Δ BARYONS ($S=0, I=3/2$)

$\Delta^{++} = uuu$, $\Delta^{+} = uud$, $\Delta^{0} = udd$, $\Delta^{-} = ddd$

$\Delta(1232)\ 3/2^+$

$I(J^P) = \frac{3}{2}(\frac{3}{2}^+)$

Breit-Wigner mass (mixed charges) = 1230 to 1234 (≈ 1232) MeV
Breit-Wigner full width (mixed charges) = 114 to 120 (≈ 117) MeV
p_{beam} = 0.30 GeV/c $4\pi\lambda^2$ = 94.8 mb
Re(pole position) = 1209 to 1211 (≈ 1210) MeV
−2Im(pole position) = 98 to 102 (≈ 100) MeV

$\Delta(1232)$ DECAY MODES	Fraction (Γ_i/Γ)	p (MeV/c)
$N\pi$	100 %	229
$N\gamma$	0.55–0.65 %	259
$N\gamma$, helicity=1/2	0.11–0.13 %	259
$N\gamma$, helicity=3/2	0.44–0.52 %	259

$\Delta(1600)\ 3/2^+$

$I(J^P) = \frac{3}{2}(\frac{3}{2}^+)$

Breit-Wigner mass = 1500 to 1700 (≈ 1600) MeV
Breit-Wigner full width = 220 to 420 (≈ 320) MeV
p_{beam} = 0.87 GeV/c $4\pi\lambda^2$ = 18.6 mb
Re(pole position) = 1460 to 1560 (≈ 1510) MeV
−2Im(pole position) = 200 to 350 (≈ 275) MeV

$\Delta(1600)$ DECAY MODES	Fraction (Γ_i/Γ)	p (MeV/c)
$N\pi$	10–25 %	513
$N\pi\pi$	75–90 %	477
$\Delta\pi$	40–70 %	303
$N\rho$	<25 %	†
$N(1440)\pi$	10–35 %	98
$N\gamma$	0.001–0.035 %	525
$N\gamma$, helicity=1/2	0.0–0.02 %	525
$N\gamma$, helicity=3/2	0.001–0.015 %	525

$\Delta(1620)\ 1/2^-$

$I(J^P) = \frac{3}{2}(\frac{1}{2}^-)$

Breit-Wigner mass = 1600 to 1660 (≈ 1630) MeV
Breit-Wigner full width = 130 to 150 (≈ 140) MeV
p_{beam} = 0.93 GeV/c $4\pi\lambda^2$ = 17.2 mb
Re(pole position) = 1590 to 1610 (≈ 1600) MeV
−2Im(pole position) = 120 to 140 (≈ 130) MeV

$\Delta(1620)$ DECAY MODES	Fraction (Γ_i/Γ)	p (MeV/c)
$N\pi$	20–30 %	534
$N\pi\pi$	70–80 %	499
$\Delta\pi$	30–60 %	328
$N\rho$	7–25 %	†
$N\gamma$	0.03–0.10 %	545
$N\gamma$, helicity=1/2	0.03–0.10 %	545

$\Delta(1700)\ 3/2^-$

$I(J^P) = \frac{3}{2}(\frac{3}{2}^-)$

Breit-Wigner mass = 1670 to 1750 (≈ 1700) MeV
Breit-Wigner full width = 200 to 400 (≈ 300) MeV
p_{beam} = 1.05 GeV/c $4\pi\lambda^2$ = 14.5 mb
Re(pole position) = 1620 to 1680 (≈ 1650) MeV
−2Im(pole position) = 160 to 300 (≈ 230) MeV

$\Delta(1700)$ DECAY MODES	Fraction (Γ_i/Γ)	p (MeV/c)
$N\pi$	10–20 %	581
$N\pi\pi$	80–90 %	550
$\Delta\pi$	30–60 %	386
$\Delta(1232)\pi$, S-wave	25–50 %	386
$\Delta(1232)\pi$, D-wave	5–15 %	386
$N\rho$	30–55 %	†
$N\rho$, S=3/2, S-wave	5–20 %	†
$\Delta(1232)\eta$	(5.0±2.0) %	†
$N\gamma$	0.22–0.60 %	591
$N\gamma$, helicity=1/2	0.12–0.30 %	591
$N\gamma$, helicity=3/2	0.10–0.30 %	591

$\Delta(1905)\ 5/2^+$

$I(J^P) = \frac{3}{2}(\frac{5}{2}^+)$

Breit-Wigner mass = 1855 to 1910 (≈ 1880) MeV
Breit-Wigner full width = 270 to 400 (≈ 330) MeV
p_{beam} = 1.40 GeV/c $4\pi\lambda^2$ = 10.1 mb
Re(pole position) = 1805 to 1835 (≈ 1820) MeV
−2Im(pole position) = 265 to 300 (≈ 280) MeV

$\Delta(1905)$ DECAY MODES	Fraction (Γ_i/Γ)	p (MeV/c)
$N\pi$	9–15 %	698
$N\pi\pi$	85–95 %	673
$\Delta\pi$	<25 %	524
$N\rho$	>60 %	385
$N\gamma$	0.012–0.036 %	706
$N\gamma$, helicity=1/2	0.002–0.006 %	706
$N\gamma$, helicity=3/2	0.01–0.03 %	706

$\Delta(1910)\ 1/2^+$

$I(J^P) = \frac{3}{2}(\frac{1}{2}^+)$

Breit-Wigner mass = 1860 to 1910 (≈ 1890) MeV
Breit-Wigner full width = 220 to 340 (≈ 280) MeV
p_{beam} = 1.42 GeV/c $4\pi\lambda^2$ = 9.89 mb
Re(pole position) = 1830 to 1880 (≈ 1855) MeV
−2Im(pole position) = 200 to 500 (≈ 350) MeV

$\Delta(1910)$ DECAY MODES	Fraction (Γ_i/Γ)	p (MeV/c)
$N\pi$	15–30 %	704
ΣK	(9± 5) %	400
$\Delta\pi$	(60±28) %	531
$N\gamma$	0.0–0.02 %	712
$N\gamma$, helicity=1/2	0.0–0.02 %	712

Baryon Summary Table

$\Delta(1920)\ 3/2^+$ $\quad I(J^P) = \frac{3}{2}(\frac{3}{2}^+)$

Breit-Wigner mass = 1900 to 1970 ($\approx$ 1920) MeV
Breit-Wigner full width = 180 to 300 ($\approx$ 260) MeV
p_{beam} = 1.48 GeV/c $\quad 4\pi\lambda^2$ = 9.37 mb
Re(pole position) = 1850 to 1950 ($\approx$ 1900) MeV
-2Im(pole position) = 200 to 400 ($\approx$ 300) MeV

$\Delta(1920)$ DECAY MODES	Fraction (Γ_i/Γ)	p (MeV/c)
$N\pi$	5–20 %	723
ΣK	(2.14±0.30) %	431
$\Delta(1232)\eta$	(15 ±8) %	336
$N\gamma$	0.0–0.4 %	731
$N\gamma$, helicity=1/2	0.0–0.2 %	731
$N\gamma$, helicity=3/2	0.0–0.2 %	731

$\Delta(1930)\ 5/2^-$ $\quad I(J^P) = \frac{3}{2}(\frac{5}{2}^-)$

Breit-Wigner mass = 1900 to 2000 ($\approx$ 1950) MeV
Breit-Wigner full width = 220 to 500 ($\approx$ 360) MeV
p_{beam} = 1.54 GeV/c $\quad 4\pi\lambda^2$ = 8.91 mb
Re(pole position) = 1840 to 1960 ($\approx$ 1900) MeV
-2Im(pole position) = 175 to 360 ($\approx$ 270) MeV

$\Delta(1930)$ DECAY MODES	Fraction (Γ_i/Γ)	p (MeV/c)
$N\pi$	5–15 %	742
$N\gamma$	0.0–0.02 %	749
$N\gamma$, helicity=1/2	0.0–0.01 %	749
$N\gamma$, helicity=3/2	0.0–0.01 %	749

$\Delta(1950)\ 7/2^+$ $\quad I(J^P) = \frac{3}{2}(\frac{7}{2}^+)$

Breit-Wigner mass = 1915 to 1950 ($\approx$ 1930) MeV
Breit-Wigner full width = 235 to 335 ($\approx$ 285) MeV
p_{beam} = 1.50 GeV/c $\quad 4\pi\lambda^2$ = 9.21 mb
Re(pole position) = 1870 to 1890 ($\approx$ 1880) MeV
-2Im(pole position) = 220 to 260 ($\approx$ 240) MeV

$\Delta(1950)$ DECAY MODES	Fraction (Γ_i/Γ)	p (MeV/c)
$N\pi$	35–45 %	729
$N\pi\pi$		706
$\Delta\pi$	20–30 %	560
$N\rho$	<10 %	442
$N\gamma$	0.08–0.13 %	737
$N\gamma$, helicity=1/2	0.03–0.055 %	737
$N\gamma$, helicity=3/2	0.05–0.075 %	737

$\Delta(2420)\ 11/2^+$ $\quad I(J^P) = \frac{3}{2}(\frac{11}{2}^+)$

Breit-Wigner mass = 2300 to 2500 ($\approx$ 2420) MeV
Breit-Wigner full width = 300 to 500 ($\approx$ 400) MeV
p_{beam} = 2.64 GeV/c $\quad 4\pi\lambda^2$ = 4.68 mb
Re(pole position) = 2260 to 2400 ($\approx$ 2330) MeV
-2Im(pole position) = 350 to 750 ($\approx$ 550) MeV

$\Delta(2420)$ DECAY MODES	Fraction (Γ_i/Γ)	p (MeV/c)
$N\pi$	5–15 %	1023

Λ BARYONS ($S = -1$, $I = 0$)

$\Lambda^0 = uds$

Λ $\quad I(J^P) = 0(\frac{1}{2}^+)$

Mass m = 1115.683 ± 0.006 MeV
$(m_\Lambda - m_{\overline{\Lambda}}) / m_\Lambda = (-0.1 \pm 1.1) \times 10^{-5}$ (S = 1.6)
Mean life $\tau = (2.632 \pm 0.020) \times 10^{-10}$ s (S = 1.6)
$(\tau_\Lambda - \tau_{\overline{\Lambda}}) / \tau_\Lambda = -0.001 \pm 0.009$
$c\tau$ = 7.89 cm
Magnetic moment $\mu = -0.613 \pm 0.004\ \mu_N$
Electric dipole moment $d < 1.5 \times 10^{-16}$ $e$cm, CL = 95%

Decay parameters

$p\pi^-$	$\alpha_- = 0.642 \pm 0.013$
$\overline{p}\pi^+$	$\alpha_+ = -0.71 \pm 0.08$
$p\pi^-$	$\phi_- = (-6.5 \pm 3.5)^\circ$
"	$\gamma_- = 0.76$ [l]
"	$\Delta_- = (8 \pm 4)^\circ$ [l]
$n\pi^0$	$\alpha_0 = 0.65 \pm 0.04$
$pe^-\overline{\nu}_e$	$g_A/g_V = -0.718 \pm 0.015$ [h]

Λ DECAY MODES	Fraction (Γ_i/Γ)	p (MeV/c)
$p\pi^-$	(63.9 ±0.5) %	101
$n\pi^0$	(35.8 ±0.5) %	104
$n\gamma$	(1.75±0.15) $\times 10^{-3}$	162
$p\pi^-\gamma$	[n] (8.4 ±1.4) $\times 10^{-4}$	101
$pe^-\overline{\nu}_e$	(8.32±0.14) $\times 10^{-4}$	163
$p\mu^-\overline{\nu}_\mu$	(1.57±0.35) $\times 10^{-4}$	131

$\Lambda(1405)\ 1/2^-$ $\quad I(J^P) = 0(\frac{1}{2}^-)$

Mass $m = 1405.1^{+1.3}_{-1.0}$ MeV
Full width Γ = 50.5 ± 2.0 MeV
Below $\overline{K}N$ threshold

$\Lambda(1405)$ DECAY MODES	Fraction (Γ_i/Γ)	p (MeV/c)
$\Sigma\pi$	100 %	155

$\Lambda(1520)\ 3/2^-$ $\quad I(J^P) = 0(\frac{3}{2}^-)$

Mass m = 1519.5 ± 1.0 MeV [o]
Full width Γ = 15.6 ± 1.0 MeV [o]
p_{beam} = 0.39 GeV/c $\quad 4\pi\lambda^2$ = 82.8 mb

$\Lambda(1520)$ DECAY MODES	Fraction (Γ_i/Γ)	p (MeV/c)
$N\overline{K}$	45 ± 1%	243
$\Sigma\pi$	42 ± 1%	268
$\Lambda\pi\pi$	10 ± 1%	259
$\Sigma\pi\pi$	0.9 ± 0.1%	169
$\Lambda\gamma$	0.85 ± 0.15%	350

$\Lambda(1600)\ 1/2^+$ $\quad I(J^P) = 0(\frac{1}{2}^+)$

Mass m = 1560 to 1700 ($\approx$ 1600) MeV
Full width Γ = 50 to 250 ($\approx$ 150) MeV
p_{beam} = 0.58 GeV/c $\quad 4\pi\lambda^2$ = 41.6 mb

$\Lambda(1600)$ DECAY MODES	Fraction (Γ_i/Γ)	p (MeV/c)
$N\overline{K}$	15–30 %	343
$\Sigma\pi$	10–60 %	338

$\Lambda(1670)\ 1/2^-$ $\quad I(J^P) = 0(\frac{1}{2}^-)$

Mass m = 1660 to 1680 ($\approx$ 1670) MeV
Full width Γ = 25 to 50 ($\approx$ 35) MeV
p_{beam} = 0.74 GeV/c $\quad 4\pi\lambda^2$ = 28.5 mb

$\Lambda(1670)$ DECAY MODES	Fraction (Γ_i/Γ)	p (MeV/c)
$N\overline{K}$	20–30 %	414
$\Sigma\pi$	25–55 %	394
$\Lambda\eta$	10–25 %	69
$N\overline{K}^*(892)$, S=3/2, D-wave	(5±4) %	†

$\Lambda(1690)\ 3/2^-$ $\quad I(J^P) = 0(\frac{3}{2}^-)$

Mass m = 1685 to 1695 ($\approx$ 1690) MeV
Full width Γ = 50 to 70 ($\approx$ 60) MeV
p_{beam} = 0.78 GeV/c $\quad 4\pi\lambda^2$ = 26.1 mb

Λ(1690) DECAY MODES	Fraction (Γ_i/Γ)	p (MeV/c)
$N\overline{K}$	20–30 %	433
$\Sigma\pi$	20–40 %	410
$\Lambda\pi\pi$	~ 25 %	419
$\Sigma\pi\pi$	~ 20 %	358

Λ(1800) 1/2⁻

$I(J^P) = 0(\frac{1}{2}^-)$

Mass m = 1720 to 1850 (≈ 1800) MeV
Full width Γ = 200 to 400 (≈ 300) MeV
p_{beam} = 1.01 GeV/c $4\pi\lambda^2$ = 17.5 mb

Λ(1800) DECAY MODES	Fraction (Γ_i/Γ)	p (MeV/c)
$N\overline{K}$	25–40 %	528
$\Sigma\pi$	seen	494
$\Sigma(1385)\pi$	seen	349
$\Lambda\eta$	(6±5) %	326
$N\overline{K}^*(892)$	seen	†

Λ(1810) 1/2⁺

$I(J^P) = 0(\frac{1}{2}^+)$

Mass m = 1750 to 1850 (≈ 1810) MeV
Full width Γ = 50 to 250 (≈ 150) MeV
p_{beam} = 1.04 GeV/c $4\pi\lambda^2$ = 17.0 mb

Λ(1810) DECAY MODES	Fraction (Γ_i/Γ)	p (MeV/c)
$N\overline{K}$	20–50 %	537
$\Sigma\pi$	10–40 %	501
$\Sigma(1385)\pi$	seen	357
$N\overline{K}^*(892)$	30–60 %	†

Λ(1820) 5/2⁺

$I(J^P) = 0(\frac{5}{2}^+)$

Mass m = 1815 to 1825 (≈ 1820) MeV
Full width Γ = 70 to 90 (≈ 80) MeV
p_{beam} = 1.06 GeV/c $4\pi\lambda^2$ = 16.5 mb

Λ(1820) DECAY MODES	Fraction (Γ_i/Γ)	p (MeV/c)
$N\overline{K}$	55–65 %	545
$\Sigma\pi$	8–14 %	509
$\Sigma(1385)\pi$	5–10 %	366
$N\overline{K}^*(892)$, S=3/2, P-wave	(3.0±1.0) %	†

Λ(1830) 5/2⁻

$I(J^P) = 0(\frac{5}{2}^-)$

Mass m = 1810 to 1830 (≈ 1830) MeV
Full width Γ = 60 to 110 (≈ 95) MeV
p_{beam} = 1.08 GeV/c $4\pi\lambda^2$ = 16.0 mb

Λ(1830) DECAY MODES	Fraction (Γ_i/Γ)	p (MeV/c)
$N\overline{K}$	3–10 %	553
$\Sigma\pi$	35–75 %	516
$\Sigma(1385)\pi$	>15 %	374
$\Sigma(1385)\pi$, D-wave	(52±6) %	374

Λ(1890) 3/2⁺

$I(J^P) = 0(\frac{3}{2}^+)$

Mass m = 1850 to 1910 (≈ 1890) MeV
Full width Γ = 60 to 200 (≈ 100) MeV
p_{beam} = 1.21 GeV/c $4\pi\lambda^2$ = 13.6 mb

Λ(1890) DECAY MODES	Fraction (Γ_i/Γ)	p (MeV/c)
$N\overline{K}$	20–35 %	599
$\Sigma\pi$	3–10 %	560
$\Sigma(1385)\pi$	seen	423
$N\overline{K}^*(892)$	seen	236

Λ(2100) 7/2⁻

$I(J^P) = 0(\frac{7}{2}^-)$

Mass m = 2090 to 2110 (≈ 2100) MeV
Full width Γ = 100 to 250 (≈ 200) MeV
p_{beam} = 1.68 GeV/c $4\pi\lambda^2$ = 8.68 mb

Λ(2100) DECAY MODES	Fraction (Γ_i/Γ)	p (MeV/c)
$N\overline{K}$	25–35 %	751
$\Sigma\pi$	~ 5 %	705
$\Lambda\eta$	<3 %	617
ΞK	<3 %	491
$\Lambda\omega$	<8 %	443
$N\overline{K}^*(892)$	10–20 %	515

Λ(2110) 5/2⁺

$I(J^P) = 0(\frac{5}{2}^+)$

Mass m = 2090 to 2140 (≈ 2110) MeV
Full width Γ = 150 to 250 (≈ 200) MeV
p_{beam} = 1.70 GeV/c $4\pi\lambda^2$ = 8.53 mb

Λ(2110) DECAY MODES	Fraction (Γ_i/Γ)	p (MeV/c)
$N\overline{K}$	5–25 %	757
$\Sigma\pi$	10–40 %	711
$\Lambda\omega$	seen	455
$\Sigma(1385)\pi$	seen	591
$N\overline{K}^*(892)$	10–60 %	525

Λ(2350) 9/2⁺

$I(J^P) = 0(\frac{9}{2}^+)$

Mass m = 2340 to 2370 (≈ 2350) MeV
Full width Γ = 100 to 250 (≈ 150) MeV
p_{beam} = 2.29 GeV/c $4\pi\lambda^2$ = 5.85 mb

Λ(2350) DECAY MODES	Fraction (Γ_i/Γ)	p (MeV/c)
$N\overline{K}$	~ 12 %	915
$\Sigma\pi$	~ 10 %	867

Σ BARYONS
($S = -1, I = 1$)

$\Sigma^+ = uus$, $\Sigma^0 = uds$, $\Sigma^- = dds$

Σ⁺

$I(J^P) = 1(\frac{1}{2}^+)$

Mass m = 1189.37 ± 0.07 MeV (S = 2.2)
Mean life $\tau = (0.8018 \pm 0.0026) \times 10^{-10}$ s
$c\tau$ = 2.404 cm
$(\tau_{\Sigma^+} - \tau_{\overline{\Sigma}^-}) / \tau_{\Sigma^+} = (-0.6 \pm 1.2) \times 10^{-3}$
Magnetic moment μ = 2.458 ± 0.010 μ_N (S = 2.1)
$(\mu_{\Sigma^+} + \mu_{\overline{\Sigma}^-}) / \mu_{\Sigma^+} = 0.014 \pm 0.015$
$\Gamma(\Sigma^+ \to n\ell^+\nu)/\Gamma(\Sigma^- \to n\ell^-\overline{\nu}) < 0.043$

Decay parameters

$p\pi^0$	α_0	$= -0.980^{+0.017}_{-0.015}$
"	ϕ_0	$= (36 \pm 34)^\circ$
"	γ_0	$= 0.16$ [I]
"	Δ_0	$= (187 \pm 6)^\circ$ [I]
$n\pi^+$	α_+	$= 0.068 \pm 0.013$
"	ϕ_+	$= (167 \pm 20)^\circ$ (S = 1.1)
"	γ_+	$= -0.97$ [I]
"	Δ_+	$= (-73^{+133}_{-10})^\circ$ [I]
$p\gamma$	α_γ	$= -0.76 \pm 0.08$

Baryon Summary Table

Σ^+ DECAY MODES	Fraction (Γ_i/Γ)	Confidence level	p (MeV/c)
$p\pi^0$	(51.57 ± 0.30) %		189
$n\pi^+$	(48.31 ± 0.30) %		185
$p\gamma$	(1.23 ± 0.05) × 10^{-3}		225
$n\pi^+\gamma$	[n] (4.5 ± 0.5) × 10^{-4}		185
$\Lambda e^+\nu_e$	(2.0 ± 0.5) × 10^{-5}		71
$\Delta S = \Delta Q$ (SQ) violating modes or $\Delta S = 1$ weak neutral current ($S1$) modes			
$ne^+\nu_e$	SQ < 5 × 10^{-6}	90%	224
$n\mu^+\nu_\mu$	SQ < 3.0 × 10^{-5}	90%	202
pe^+e^-	$S1$ < 7 × 10^{-6}		225
$p\mu^+\mu^-$	$S1$ (9 $^{+9}_{-8}$) × 10^{-8}		121

Σ^0

$I(J^P) = 1(\frac{1}{2}^+)$

Mass $m = 1192.642 \pm 0.024$ MeV
$m_{\Sigma^-} - m_{\Sigma^0} = 4.807 \pm 0.035$ MeV (S = 1.1)
$m_{\Sigma^0} - m_\Lambda = 76.959 \pm 0.023$ MeV
Mean life $\tau = (7.4 \pm 0.7) \times 10^{-20}$ s
$c\tau = 2.22 \times 10^{-11}$ m
Transition magnetic moment $|\mu_{\Sigma\Lambda}| = 1.61 \pm 0.08\ \mu_N$

Σ^0 DECAY MODES	Fraction (Γ_i/Γ)	Confidence level	p (MeV/c)
$\Lambda\gamma$	100 %		74
$\Lambda\gamma\gamma$	< 3 %	90%	74
Λe^+e^-	[p] 5×10^{-3}		74

Σ^-

$I(J^P) = 1(\frac{1}{2}^+)$

Mass $m = 1197.449 \pm 0.030$ MeV (S = 1.2)
$m_{\Sigma^-} - m_{\Sigma^+} = 8.08 \pm 0.08$ MeV (S = 1.9)
$m_{\Sigma^-} - m_\Lambda = 81.766 \pm 0.030$ MeV (S = 1.2)
Mean life $\tau = (1.479 \pm 0.011) \times 10^{-10}$ s (S = 1.3)
$c\tau = 4.434$ cm
Magnetic moment $\mu = -1.160 \pm 0.025\ \mu_N$ (S = 1.7)
Σ^- charge radius = 0.78 ± 0.10 fm

Decay parameters

$n\pi^-$	$\alpha_- = -0.068 \pm 0.008$
"	$\phi_- = (10 \pm 15)^\circ$
"	$\gamma_- = 0.98$ [l]
"	$\Delta_- = (249^{+12}_{-120})^\circ$ [l]
$ne^-\overline{\nu}_e$	$g_A/g_V = 0.340 \pm 0.017$ [h]
"	$f_2(0)/f_1(0) = 0.97 \pm 0.14$
"	$D = 0.11 \pm 0.10$
$\Lambda e^-\overline{\nu}_e$	$g_V/g_A = 0.01 \pm 0.10$ [h] (S = 1.5)
"	$g_{WM}/g_A = 2.4 \pm 1.7$ [h]

Σ^- DECAY MODES	Fraction (Γ_i/Γ)	p (MeV/c)
$n\pi^-$	(99.848 ± 0.005) %	193
$n\pi^-\gamma$	[n] (4.6 ± 0.6) × 10^{-4}	193
$ne^-\overline{\nu}_e$	(1.017 ± 0.034) × 10^{-3}	230
$n\mu^-\overline{\nu}_\mu$	(4.5 ± 0.4) × 10^{-4}	210
$\Lambda e^-\overline{\nu}_e$	(5.73 ± 0.27) × 10^{-5}	79

$\Sigma(1385)\ 3/2^+$

$I(J^P) = 1(\frac{3}{2}^+)$

$\Sigma(1385)^+$ mass $m = 1382.80 \pm 0.35$ MeV (S = 1.9)
$\Sigma(1385)^0$ mass $m = 1383.7 \pm 1.0$ MeV (S = 1.4)
$\Sigma(1385)^-$ mass $m = 1387.2 \pm 0.5$ MeV (S = 2.2)
$\Sigma(1385)^+$ full width $\Gamma = 36.0 \pm 0.7$ MeV
$\Sigma(1385)^0$ full width $\Gamma = 36 \pm 5$ MeV
$\Sigma(1385)^-$ full width $\Gamma = 39.4 \pm 2.1$ MeV (S = 1.7)
Below $\overline{K}N$ threshold

$\Sigma(1385)$ DECAY MODES	Fraction (Γ_i/Γ)	Confidence level	p (MeV/c)
$\Lambda\pi$	(87.0 ±1.5) %		208
$\Sigma\pi$	(11.7 ±1.5) %		129
$\Lambda\gamma$	(1.25 $^{+0.13}_{-0.12}$) %		241
$\Sigma^+\gamma$	(7.0 ±1.7) × 10^{-3}		180
$\Sigma^-\gamma$	< 2.4 × 10^{-4}	90%	173

$\Sigma(1660)\ 1/2^+$

$I(J^P) = 1(\frac{1}{2}^+)$

Mass $m = 1630$ to 1690 (≈ 1660) MeV
Full width $\Gamma = 40$ to 200 (≈ 100) MeV
$p_{\text{beam}} = 0.72$ GeV/c $4\pi\lambda^2 = 29.9$ mb

$\Sigma(1660)$ DECAY MODES	Fraction (Γ_i/Γ)	p (MeV/c)
$N\overline{K}$	10–30 %	405
$\Lambda\pi$	seen	440
$\Sigma\pi$	seen	387

$\Sigma(1670)\ 3/2^-$

$I(J^P) = 1(\frac{3}{2}^-)$

Mass $m = 1665$ to 1685 (≈ 1670) MeV
Full width $\Gamma = 40$ to 80 (≈ 60) MeV
$p_{\text{beam}} = 0.74$ GeV/c $4\pi\lambda^2 = 28.5$ mb

$\Sigma(1670)$ DECAY MODES	Fraction (Γ_i/Γ)	p (MeV/c)
$N\overline{K}$	7–13 %	414
$\Lambda\pi$	5–15 %	448
$\Sigma\pi$	30–60 %	394

$\Sigma(1750)\ 1/2^-$

$I(J^P) = 1(\frac{1}{2}^-)$

Mass $m = 1730$ to 1800 (≈ 1750) MeV
Full width $\Gamma = 60$ to 160 (≈ 90) MeV
$p_{\text{beam}} = 0.91$ GeV/c $4\pi\lambda^2 = 20.7$ mb

$\Sigma(1750)$ DECAY MODES	Fraction (Γ_i/Γ)	p (MeV/c)
$N\overline{K}$	10–40 %	486
$\Lambda\pi$	seen	507
$\Sigma\pi$	<8 %	456
$\Sigma\eta$	15–55 %	98
$N\overline{K}^*(892)$, S=1/2	(8±4) %	†

$\Sigma(1775)\ 5/2^-$

$I(J^P) = 1(\frac{5}{2}^-)$

Mass $m = 1770$ to 1780 (≈ 1775) MeV
Full width $\Gamma = 105$ to 135 (≈ 120) MeV
$p_{\text{beam}} = 0.96$ GeV/c $4\pi\lambda^2 = 19.0$ mb

$\Sigma(1775)$ DECAY MODES	Fraction (Γ_i/Γ)	p (MeV/c)
$N\overline{K}$	37–43%	508
$\Lambda\pi$	14–20%	525
$\Sigma\pi$	2–5%	475
$\Sigma(1385)\pi$	8–12%	327
$\Lambda(1520)\pi$, P-wave	17–23%	201

$\Sigma(1915)\ 5/2^+$

$I(J^P) = 1(\frac{5}{2}^+)$

Mass $m = 1900$ to 1935 (≈ 1915) MeV
Full width $\Gamma = 80$ to 160 (≈ 120) MeV
$p_{\text{beam}} = 1.26$ GeV/c $4\pi\lambda^2 = 12.8$ mb

$\Sigma(1915)$ DECAY MODES	Fraction (Γ_i/Γ)	p (MeV/c)
$N\overline{K}$	5–15 %	618
$\Lambda\pi$	seen	623
$\Sigma\pi$	seen	577
$\Sigma(1385)\pi$	<5 %	443

$\Sigma(1940)\ 3/2^-$

$I(J^P) = 1(\frac{3}{2}^-)$

Mass m = 1900 to 1950 ($\approx$ 1940) MeV
Full width Γ = 150 to 300 ($\approx$ 220) MeV
$p_{\rm beam}$ = 1.32 GeV/c $\quad 4\pi\lambda^2$ = 12.1 mb

$\Sigma(1940)$ DECAY MODES	Fraction (Γ_i/Γ)	p (MeV/c)
$N\overline{K}$	<20 %	637
$\Lambda\pi$	seen	640
$\Sigma\pi$	seen	595
$\Sigma(1385)\pi$	seen	463
$\Lambda(1520)\pi$	seen	355
$\Delta(1232)\overline{K}$	seen	410
$N\overline{K}^*(892)$	seen	322

$\Sigma(2030)\ 7/2^+$

$I(J^P) = 1(\frac{7}{2}^+)$

Mass m = 2025 to 2040 ($\approx$ 2030) MeV
Full width Γ = 150 to 200 ($\approx$ 180) MeV
$p_{\rm beam}$ = 1.52 GeV/c $\quad 4\pi\lambda^2$ = 9.93 mb

$\Sigma(2030)$ DECAY MODES	Fraction (Γ_i/Γ)	p (MeV/c)
$N\overline{K}$	17–23 %	702
$\Lambda\pi$	17–23 %	700
$\Sigma\pi$	5–10 %	657
ΞK	<2 %	422
$\Sigma(1385)\pi$	5–15 %	532
$\Lambda(1520)\pi$	10–20 %	430
$\Delta(1232)\overline{K}$	10–20 %	498
$N\overline{K}^*(892)$	<5 %	439

$\Sigma(2250)$

$I(J^P) = 1(?^?)$

Mass m = 2210 to 2280 ($\approx$ 2250) MeV
Full width Γ = 60 to 150 ($\approx$ 100) MeV
$p_{\rm beam}$ = 2.04 GeV/c $\quad 4\pi\lambda^2$ = 6.76 mb

$\Sigma(2250)$ DECAY MODES	Fraction (Γ_i/Γ)	p (MeV/c)
$N\overline{K}$	<10 %	851
$\Lambda\pi$	seen	842
$\Sigma\pi$	seen	803

Ξ BARYONS
$(S = -2, I = 1/2)$

$\Xi^0 = uss, \quad \Xi^- = dss$

Ξ^0

$I(J^P) = \frac{1}{2}(\frac{1}{2}^+)$

P is not yet measured; + is the quark model prediction.

Mass m = 1314.86 ± 0.20 MeV
$m_{\Xi^-} - m_{\Xi^0}$ = 6.85 ± 0.21 MeV
Mean life $\tau = (2.90 \pm 0.09) \times 10^{-10}$ s
$c\tau$ = 8.71 cm
Magnetic moment $\mu = -1.250 \pm 0.014\ \mu_N$

Decay parameters

$\Lambda\pi^0$	$\alpha = -0.406 \pm 0.013$
"	$\phi = (21 \pm 12)^\circ$
"	$\gamma = 0.85$ [l]
"	$\Delta = (218^{+12}_{-19})^\circ$ [l]
$\Lambda\gamma$	$\alpha = -0.70 \pm 0.07$
$\Lambda e^+ e^-$	$\alpha = -0.8 \pm 0.2$
$\Sigma^0\gamma$	$\alpha = -0.69 \pm 0.06$
$\Sigma^+ e^- \overline{\nu}_e$	$g_1(0)/f_1(0) = 1.22 \pm 0.05$
$\Sigma^+ e^- \overline{\nu}_e$	$f_2(0)/f_1(0) = 2.0 \pm 0.9$

Ξ^0 DECAY MODES	Fraction (Γ_i/Γ)	Confidence level	p (MeV/c)
$\Lambda\pi^0$	(99.524±0.012) %		135
$\Lambda\gamma$	(1.17 ±0.07) × 10^{-3}		184
$\Lambda e^+ e^-$	(7.6 ±0.6) × 10^{-6}		184
$\Sigma^0\gamma$	(3.33 ±0.10) × 10^{-3}		117
$\Sigma^+ e^- \overline{\nu}_e$	(2.52 ±0.08) × 10^{-4}		120
$\Sigma^+ \mu^- \overline{\nu}_\mu$	(2.33 ±0.35) × 10^{-6}		64
$\Delta S = \Delta Q$ (SQ) violating modes or $\Delta S = 2$ forbidden ($S2$) modes			
$\Sigma^- e^+ \nu_e$	SQ < 9 × 10^{-4}	90%	112
$\Sigma^- \mu^+ \nu_\mu$	SQ < 9 × 10^{-4}	90%	49
$p\pi^-$	$S2$ < 8 × 10^{-6}	90%	299
$p e^- \overline{\nu}_e$	$S2$ < 1.3 × 10^{-3}		323
$p\mu^- \overline{\nu}_\mu$	$S2$ < 1.3 × 10^{-3}		309

Ξ^-

$I(J^P) = \frac{1}{2}(\frac{1}{2}^+)$

P is not yet measured; + is the quark model prediction.

Mass m = 1321.71 ± 0.07 MeV
$(m_{\Xi^-} - m_{\overline{\Xi}^+}) / m_{\Xi^-} = (-3 \pm 9) \times 10^{-5}$
Mean life $\tau = (1.639 \pm 0.015) \times 10^{-10}$ s
$c\tau$ = 4.91 cm
$(\tau_{\Xi^-} - \tau_{\overline{\Xi}^+}) / \tau_{\Xi^-} = -0.01 \pm 0.07$
Magnetic moment $\mu = -0.6507 \pm 0.0025\ \mu_N$
$(\mu_{\Xi^-} + \mu_{\overline{\Xi}^+}) / |\mu_{\Xi^-}| = +0.01 \pm 0.05$

Decay parameters

$\Lambda\pi^-$	$\alpha = -0.458 \pm 0.012$ (S = 1.8)
	$[\alpha(\Xi^-)\alpha_-(\Lambda) - \alpha(\overline{\Xi}^+)\alpha_+(\overline{\Lambda})]$ / [sum] = $(0 \pm 7) \times 10^{-4}$
"	$\phi = (-2.1 \pm 0.8)^\circ$
"	$\gamma = 0.89$ [l]
"	$\Delta = (175.9 \pm 1.5)^\circ$ [l]
$\Lambda e^- \overline{\nu}_e$	$g_A/g_V = -0.25 \pm 0.05$ [h]

Ξ^- DECAY MODES	Fraction (Γ_i/Γ)	Confidence level	p (MeV/c)
$\Lambda\pi^-$	(99.887±0.035) %		140
$\Sigma^-\gamma$	(1.27 ±0.23) × 10^{-4}		118
$\Lambda e^- \overline{\nu}_e$	(5.63 ±0.31) × 10^{-4}		190
$\Lambda\mu^- \overline{\nu}_\mu$	(3.5 $^{+3.5}_{-2.2}$) × 10^{-4}		163
$\Sigma^0 e^- \overline{\nu}_e$	(8.7 ±1.7) × 10^{-5}		123
$\Sigma^0 \mu^- \overline{\nu}_\mu$	< 8 × 10^{-4}	90%	70
$\Xi^0 e^- \overline{\nu}_e$	< 2.3 × 10^{-3}	90%	7
$\Delta S = 2$ forbidden ($S2$) modes			
$n\pi^-$	$S2$ < 1.9 × 10^{-5}	90%	304
$n e^- \overline{\nu}_e$	$S2$ < 3.2 × 10^{-3}	90%	327
$n\mu^- \overline{\nu}_\mu$	$S2$ < 1.5 %	90%	314
$p\pi^-\pi^-$	$S2$ < 4 × 10^{-4}	90%	223
$p\pi^- e^- \overline{\nu}_e$	$S2$ < 4 × 10^{-4}	90%	305
$p\pi^-\mu^- \overline{\nu}_\mu$	$S2$ < 4 × 10^{-4}	90%	251
$p\mu^-\mu^-$	L < 4 × 10^{-8}	90%	272

$\Xi(1530)\ 3/2^+$

$I(J^P) = \frac{1}{2}(\frac{3}{2}^+)$

$\Xi(1530)^0$ mass m = 1531.80 ± 0.32 MeV (S = 1.3)
$\Xi(1530)^-$ mass m = 1535.0 ± 0.6 MeV
$\Xi(1530)^0$ full width Γ = 9.1 ± 0.5 MeV
$\Xi(1530)^-$ full width $\Gamma = 9.9^{+1.7}_{-1.9}$ MeV

Baryon Summary Table

Ξ(1530) DECAY MODES	Fraction (Γ_i/Γ)	Confidence level	p (MeV/c)
$\Xi\pi$	100 %		158
$\Xi\gamma$	<4 %	90%	202

Ξ(1690)

$I(J^P) = \frac{1}{2}(?^?)$

Mass $m = 1690 \pm 10$ MeV [o]
Full width $\Gamma < 30$ MeV

Ξ(1690) DECAY MODES	Fraction (Γ_i/Γ)	p (MeV/c)
$\Lambda\overline{K}$	seen	240
$\Sigma\overline{K}$	seen	70
$\Xi\pi$	seen	311
$\Xi^-\pi^+\pi^-$	possibly seen	213

Ξ(1820) 3/2⁻

$I(J^P) = \frac{1}{2}(\frac{3}{2}^-)$

Mass $m = 1823 \pm 5$ MeV [o]
Full width $\Gamma = 24^{+15}_{-10}$ MeV [o]

Ξ(1820) DECAY MODES	Fraction (Γ_i/Γ)	p (MeV/c)
$\Lambda\overline{K}$	large	402
$\Sigma\overline{K}$	small	324
$\Xi\pi$	small	421
$\Xi(1530)\pi$	small	237

Ξ(1950)

$I(J^P) = \frac{1}{2}(?^?)$

Mass $m = 1950 \pm 15$ MeV [o]
Full width $\Gamma = 60 \pm 20$ MeV [o]

Ξ(1950) DECAY MODES	Fraction (Γ_i/Γ)	p (MeV/c)
$\Lambda\overline{K}$	seen	522
$\Sigma\overline{K}$	possibly seen	460
$\Xi\pi$	seen	519

Ξ(2030)

$I(J^P) = \frac{1}{2}(\geq \frac{5}{2}^?)$

Mass $m = 2025 \pm 5$ MeV [o]
Full width $\Gamma = 20^{+15}_{-5}$ MeV [o]

Ξ(2030) DECAY MODES	Fraction (Γ_i/Γ)	p (MeV/c)
$\Lambda\overline{K}$	~ 20 %	585
$\Sigma\overline{K}$	~ 80 %	529
$\Xi\pi$	small	574
$\Xi(1530)\pi$	small	416
$\Lambda\overline{K}\pi$	small	499
$\Sigma\overline{K}\pi$	small	428

Ω BARYONS ($S=-3, I=0$)

$\Omega^- = sss$

Ω⁻

$I(J^P) = 0(\frac{3}{2}^+)$

$J^P = \frac{3}{2}^+$ is the quark-model prediction; and $J = 3/2$ is fairly well established.

Mass $m = 1672.45 \pm 0.29$ MeV
$(m_{\Omega^-} - m_{\overline{\Omega}^+}) / m_{\Omega^-} = (-1 \pm 8) \times 10^{-5}$
Mean life $\tau = (0.821 \pm 0.011) \times 10^{-10}$ s
$c\tau = 2.461$ cm
$(\tau_{\Omega^-} - \tau_{\overline{\Omega}^+}) / \tau_{\Omega^-} = 0.00 \pm 0.05$
Magnetic moment $\mu = -2.02 \pm 0.05\ \mu_N$

Decay parameters

ΛK^-	$\alpha = 0.0180 \pm 0.0024$
$\Lambda K^-, \overline{\Lambda} K^+$	$(\alpha + \overline{\alpha})/(\alpha - \overline{\alpha}) = -0.02 \pm 0.13$
$\Xi^0\pi^-$	$\alpha = 0.09 \pm 0.14$
$\Xi^-\pi^0$	$\alpha = 0.05 \pm 0.21$

Ω⁻ DECAY MODES	Fraction (Γ_i/Γ)	Confidence level	p (MeV/c)
ΛK^-	(67.8±0.7) %		211
$\Xi^0\pi^-$	(23.6±0.7) %		294
$\Xi^-\pi^0$	(8.6±0.4) %		289
$\Xi^-\pi^+\pi^-$	$(\ 3.7^{+0.7}_{-0.6}) \times 10^{-4}$		189
$\Xi(1530)^0\pi^-$	$< 7 \times 10^{-5}$	90%	17
$\Xi^0 e^- \overline{\nu}_e$	$(\ 5.6\pm2.8) \times 10^{-3}$		319
$\Xi^-\gamma$	$< 4.6 \times 10^{-4}$	90%	314
$\Delta S = 2$ forbidden ($S2$) modes			
$\Lambda\pi^-$ $S2$	$< 2.9 \times 10^{-6}$	90%	449

Ω(2250)⁻

$I(J^P) = 0(?^?)$

Mass $m = 2252 \pm 9$ MeV
Full width $\Gamma = 55 \pm 18$ MeV

Ω(2250)⁻ DECAY MODES	Fraction (Γ_i/Γ)	p (MeV/c)
$\Xi^-\pi^+K^-$	seen	532
$\Xi(1530)^0K^-$	seen	437

CHARMED BARYONS ($C=+1$)

$\Lambda_c^+ = udc$, $\Sigma_c^{++} = uuc$, $\Sigma_c^+ = udc$, $\Sigma_c^0 = ddc$,
$\Xi_c^+ = usc$, $\Xi_c^0 = dsc$, $\Omega_c^0 = ssc$

Λ_c^+

$I(J^P) = 0(\frac{1}{2}^+)$

J is not well measured; $\frac{1}{2}$ is the quark-model prediction.

Mass $m = 2286.46 \pm 0.14$ MeV
Mean life $\tau = (200 \pm 6) \times 10^{-15}$ s (S = 1.6)
$c\tau = 59.9\ \mu$m

Decay asymmetry parameters

$\Lambda\pi^+$	$\alpha = -0.91 \pm 0.15$
$\Sigma^+\pi^0$	$\alpha = -0.45 \pm 0.32$
$\Lambda\ell^+\nu_\ell$	$\alpha = -0.86 \pm 0.04$
$(\alpha + \overline{\alpha})/(\alpha - \overline{\alpha})$ in $\Lambda_c^+ \to \Lambda\pi^+$, $\overline{\Lambda}_c^- \to \overline{\Lambda}\pi^-$	$= -0.07 \pm 0.31$
$(\alpha + \overline{\alpha})/(\alpha - \overline{\alpha})$ in $\Lambda_c^+ \to \Lambda e^+\nu_e$, $\overline{\Lambda}_c^- \to \overline{\Lambda} e^-\overline{\nu}_e$	$= 0.00 \pm 0.04$

Nearly all branching fractions of the Λ_c^+ are measured relative to the $pK^-\pi^+$ mode, but there are no model-independent measurements of this branching fraction. We explain how we arrive at our value of $B(\Lambda_c^+ \to pK^-\pi^+)$ in a Note at the beginning of the branching-ratio measurements in the Listings. When this branching fraction is eventually well determined, all the other branching fractions will slide up or down proportionally as the true value differs from the value we use here.

Λ_c^+ DECAY MODES		Fraction (Γ_i/Γ)	Scale factor/ Confidence level	p (MeV/c)
Hadronic modes with a p: $S = -1$ final states				
$p\overline{K}^0$		(2.3 ± 0.6) %		873
$pK^-\pi^+$	[q]	(5.0 ± 1.3) %		823
$p\overline{K}^*(892)^0$	[r]	(1.6 ± 0.5) %		685
$\Delta(1232)^{++}K^-$		(8.6 ± 3.0)	$\times 10^{-3}$	710
$\Lambda(1520)\pi^+$	[r]	(1.8 ± 0.6) %		627
$pK^-\pi^+$ nonresonant		(2.8 ± 0.8) %		823
$p\overline{K}^0\pi^0$		(3.3 ± 1.0) %		823
$p\overline{K}^0\eta$		(1.2 ± 0.4) %		568
$p\overline{K}^0\pi^+\pi^-$		(2.6 ± 0.7) %		754
$pK^-\pi^+\pi^0$		(3.4 ± 1.0) %		759
$pK^*(892)^-\pi^+$	[r]	(1.1 ± 0.5) %		580
$p(K^-\pi^+)_{\text{nonresonant}}\pi^0$		(3.6 ± 1.2) %		759
$\Delta(1232)\overline{K}^*(892)$		seen		419
$pK^-\pi^+\pi^+\pi^-$		(1.1 ± 0.8)	$\times 10^{-3}$	671
$pK^-\pi^+\pi^0\pi^0$		(8 ± 4)	$\times 10^{-3}$	678

Hadronic modes with a p: $S = 0$ final states

$p\pi^+\pi^-$		(3.5 ± 2.0) $\times 10^{-3}$			927
$p f_0(980)$	[r]	(2.8 ± 1.9) $\times 10^{-3}$			614
$p\pi^+\pi^+\pi^-\pi^-$		(1.8 ± 1.2) $\times 10^{-3}$			852
pK^+K^-		(7.7 ± 3.5) $\times 10^{-4}$			616
$p\phi$	[r]	(8.2 ± 2.7) $\times 10^{-4}$			590
pK^+K^- non-ϕ		(3.5 ± 1.7) $\times 10^{-4}$			616

Hadronic modes with a hyperon: $S = -1$ final states

$\Lambda\pi^+$		(1.07 ± 0.28) %			864
$\Lambda\pi^+\pi^0$		(3.6 ± 1.3) %			844
$\Lambda\rho^+$		< 5	%	CL=95%	636
$\Lambda\pi^+\pi^+\pi^-$		(2.6 ± 0.7) %			807
$\Sigma(1385)^+\pi^+\pi^-$, $\Sigma^{*+} \to \Lambda\pi^+$		(7 ± 4) $\times 10^{-3}$			688
$\Sigma(1385)^-\pi^+\pi^+$, $\Sigma^{*-} \to \Lambda\pi^-$		(5.5 ± 1.7) $\times 10^{-3}$			688
$\Lambda\pi^+\rho^0$		(1.1 ± 0.5) %			524
$\Sigma(1385)^+\rho^0$, $\Sigma^{*+} \to \Lambda\pi^+$		(3.7 ± 3.1) $\times 10^{-3}$			363
$\Lambda\pi^+\pi^+\pi^-$ nonresonant		< 8	$\times 10^{-3}$	CL=90%	807
$\Lambda\pi^+\pi^+\pi^-\pi^0$ total		(1.8 ± 0.8) %			757
$\Lambda\pi^+\eta$	[r]	(1.8 ± 0.6) %			691
$\Sigma(1385)^+\eta$	[r]	(8.5 ± 3.3) $\times 10^{-3}$			570
$\Lambda\pi^+\omega$	[r]	(1.2 ± 0.5) %			517
$\Lambda\pi^+\pi^+\pi^-\pi^0$, no η or ω		< 7	$\times 10^{-3}$	CL=90%	757
$\Lambda K^+\overline{K}^0$		(4.7 ± 1.5) $\times 10^{-3}$		S=1.2	443
$\Xi(1690)^0K^+$, $\Xi^{*0} \to \Lambda\overline{K}^0$		(1.3 ± 0.5) $\times 10^{-3}$			286
$\Sigma^0\pi^+$		(1.05 ± 0.28) %			825
$\Sigma^+\pi^0$		(1.00 ± 0.34) %			827
$\Sigma^+\eta$		(5.5 ± 2.3) $\times 10^{-3}$			713
$\Sigma^+\pi^+\pi^-$		(3.6 ± 1.0) %			804
$\Sigma^+\rho^0$		< 1.4	%	CL=95%	575
$\Sigma^-\pi^+\pi^+$		(1.7 ± 0.5) %			799
$\Sigma^0\pi^+\pi^0$		(1.8 ± 0.8) %			803
$\Sigma^0\pi^+\pi^+\pi^-$		(8.3 ± 3.1) $\times 10^{-3}$			763
$\Sigma^+\pi^+\pi^-\pi^0$		—			767
$\Sigma^+\omega$	[r]	(2.7 ± 1.0) %			569
$\Sigma^+K^+K^-$		(2.8 ± 0.8) $\times 10^{-3}$			349
$\Sigma^+\phi$	[r]	(3.1 ± 0.9) $\times 10^{-3}$			295
$\Xi(1690)^0K^+$, $\Xi^{*0} \to \Sigma^+K^-$		(8.1 ± 3.0) $\times 10^{-4}$			286
$\Sigma^+K^+K^-$ nonresonant		< 6	$\times 10^{-4}$	CL=90%	349
Ξ^0K^+		(3.9 ± 1.4) $\times 10^{-3}$			653
$\Xi^-K^+\pi^+$		(5.1 ± 1.4) $\times 10^{-3}$			565
$\Xi(1530)^0K^+$	[r]	(2.6 ± 1.0) $\times 10^{-3}$			473

Hadronic modes with a hyperon: $S = 0$ final states

ΛK^+		(5.0 ± 1.6) $\times 10^{-4}$			781
$\Lambda K^+\pi^+\pi^-$		< 4	$\times 10^{-4}$	CL=90%	637
Σ^0K^+		(4.2 ± 1.3) $\times 10^{-4}$			735
$\Sigma^0K^+\pi^+\pi^-$		< 2.1	$\times 10^{-4}$	CL=90%	574
$\Sigma^+K^+\pi^-$		(1.7 ± 0.7) $\times 10^{-3}$			670
$\Sigma^+K^*(892)^0$	[r]	(2.8 ± 1.1) $\times 10^{-3}$			470
$\Sigma^-K^+\pi^+$		< 1.0	$\times 10^{-3}$	CL=90%	664

Doubly Cabibbo-suppressed modes

$pK^+\pi^-$		< 2.3	$\times 10^{-4}$	CL=90%	823

Semileptonic modes

$\Lambda\ell^+\nu_\ell$	[s]	(2.0 ± 0.6) %			871
$\Lambda e^+\nu_e$		(2.1 ± 0.6) %			871
$\Lambda\mu^+\nu_\mu$		(2.0 ± 0.7) %			867

Inclusive modes

e^+ anything		(4.5 ± 1.7) %			–
pe^+ anything		(1.8 ± 0.9) %			–
p anything		(50 ±16) %			–
p anything (no Λ)		(12 ±19) %			–
n anything		(50 ±16) %			–
n anything (no Λ)		(29 ±17) %			–
Λ anything		(35 ±11) %		S=1.4	–
$\Sigma^\pm$ anything	[t]	(10 ± 5) %			–
3prongs		(24 ± 8) %			–

$\Delta C = 1$ weak neutral current ($C1$) modes, or Lepton Family number (LF), or Lepton number (L), or Baryon number (B) violating modes

pe^+e^-	$C1$	< 5.5	$\times 10^{-6}$	CL=90%	951
$p\mu^+\mu^-$	$C1$	< 4.4	$\times 10^{-5}$	CL=90%	937
$pe^+\mu^-$	LF	< 9.9	$\times 10^{-6}$	CL=90%	947
$pe^-\mu^+$	LF	< 1.9	$\times 10^{-5}$	CL=90%	947
$\overline{p}2e^+$	L,B	< 2.7	$\times 10^{-6}$	CL=90%	951
$\overline{p}2\mu^+$	L,B	< 9.4	$\times 10^{-6}$	CL=90%	937
$\overline{p}e^+\mu^+$	L,B	< 1.6	$\times 10^{-5}$	CL=90%	947
$\Sigma^-\mu^+\mu^+$	L	< 7.0	$\times 10^{-4}$	CL=90%	812

$\Lambda_c(2595)^+$ $I(J^P) = 0(\frac{1}{2}^-)$

The spin-parity follows from the fact that $\Sigma_c(2455)\pi$ decays, with little available phase space, are dominant. This assumes that $J^P = 1/2^+$ for the $\Sigma_c(2455)$.

Mass $m = 2592.25 \pm 0.28$ MeV
$m - m_{\Lambda_c^+} = 305.79 \pm 0.24$ MeV
Full width $\Gamma = 2.6 \pm 0.6$ MeV

$\Lambda_c^+\pi\pi$ and its submode $\Sigma_c(2455)\pi$ — the latter just barely — are the only strong decays allowed to an excited Λ_c^+ having this mass; and the submode seems to dominate.

$\Lambda_c(2595)^+$ DECAY MODES	Fraction (Γ_i/Γ)	p (MeV/c)
$\Lambda_c^+\pi^+\pi^-$	[u] ≈ 67 %	117
$\Sigma_c(2455)^{++}\pi^-$	24 ± 7 %	†
$\Sigma_c(2455)^0\pi^+$	24 ± 7 %	†
$\Lambda_c^+\pi^+\pi^-$ 3-body	18 ± 10 %	117
$\Lambda_c^+\pi^0$	[v] not seen	258
$\Lambda_c^+\gamma$	not seen	288

$\Lambda_c(2625)^+$ $I(J^P) = 0(\frac{3}{2}^-)$

J^P has not been measured; $\frac{3}{2}^-$ is the quark-model prediction.

Mass $m = 2628.11 \pm 0.19$ MeV (S = 1.1)
$m - m_{\Lambda_c^+} = 341.65 \pm 0.13$ MeV (S = 1.1)
Full width $\Gamma < 0.97$ MeV, CL = 90%

$\Lambda_c^+\pi\pi$ and its submode $\Sigma(2455)\pi$ are the only strong decays allowed to an excited Λ_c^+ having this mass.

$\Lambda_c(2625)^+$ DECAY MODES	Fraction (Γ_i/Γ)	Confidence level	p (MeV/c)
$\Lambda_c^+\pi^+\pi^-$	[u] ≈ 67%		184
$\Sigma_c(2455)^{++}\pi^-$	<5	90%	102
$\Sigma_c(2455)^0\pi^+$	<5	90%	102
$\Lambda_c^+\pi^+\pi^-$ 3-body	large		184
$\Lambda_c^+\pi^0$	[v] not seen		293
$\Lambda_c^+\gamma$	not seen		319

$\Lambda_c(2880)^+$ $I(J^P) = 0(\frac{5}{2}^+)$

There is some good evidence that indeed $J^P = 5/2^+$

Mass $m = 2881.53 \pm 0.35$ MeV
$m - m_{\Lambda_c^+} = 595.1 \pm 0.4$ MeV
Full width $\Gamma = 5.8 \pm 1.1$ MeV

$\Lambda_c(2880)^+$ DECAY MODES	Fraction (Γ_i/Γ)	p (MeV/c)
$\Lambda_c^+\pi^+\pi^-$	seen	471
$\Sigma_c(2455)^{0,++}\pi^\pm$	seen	376
$\Sigma_c(2520)^{0,++}\pi^\pm$	seen	317
pD^0	seen	316

$\Lambda_c(2940)^+$ $I(J^P) = 0(?^?)$

Mass $m = 2939.3^{+1.4}_{-1.5}$ MeV
Full width $\Gamma = 17^{+8}_{-6}$ MeV

$\Lambda_c(2940)^+$ DECAY MODES	Fraction (Γ_i/Γ)	p (MeV/c)
pD^0	seen	420
$\Sigma_c(2455)^{0,++}\pi^\pm$	seen	–

Baryon Summary Table

$\Sigma_c(2455)$

$I(J^P) = 1(\frac{1}{2}^+)$

$\Sigma_c(2455)^{++}$ mass $m = 2453.98 \pm 0.16$ MeV
$\Sigma_c(2455)^{+}$ mass $m = 2452.9 \pm 0.4$ MeV
$\Sigma_c(2455)^{0}$ mass $m = 2453.74 \pm 0.16$ MeV
$m_{\Sigma_c^{++}} - m_{\Lambda_c^+} = 167.52 \pm 0.08$ MeV
$m_{\Sigma_c^{+}} - m_{\Lambda_c^+} = 166.4 \pm 0.4$ MeV
$m_{\Sigma_c^{0}} - m_{\Lambda_c^+} = 167.27 \pm 0.08$ MeV
$m_{\Sigma_c^{++}} - m_{\Sigma_c^0} = 0.24 \pm 0.09$ MeV (S = 1.1)
$m_{\Sigma_c^{+}} - m_{\Sigma_c^0} = -0.9 \pm 0.4$ MeV
$\Sigma_c(2455)^{++}$ full width $\Gamma = 2.26 \pm 0.25$ MeV
$\Sigma_c(2455)^{+}$ full width $\Gamma < 4.6$ MeV, CL = 90%
$\Sigma_c(2455)^{0}$ full width $\Gamma = 2.16 \pm 0.26$ MeV (S = 1.1)

$\Lambda_c^+\pi$ is the only strong decay allowed to a Σ_c having this mass.

$\Sigma_c(2455)$ DECAY MODES	Fraction (Γ_i/Γ)	p (MeV/c)
$\Lambda_c^+\pi$	≈ 100 %	94

$\Sigma_c(2520)$

$I(J^P) = 1(\frac{3}{2}^+)$

J^P has not been measured; $\frac{3}{2}^+$ is the quark-model prediction.

$\Sigma_c(2520)^{++}$ mass $m = 2517.9 \pm 0.6$ MeV (S = 1.6)
$\Sigma_c(2520)^{+}$ mass $m = 2517.5 \pm 2.3$ MeV
$\Sigma_c(2520)^{0}$ mass $m = 2518.8 \pm 0.6$ MeV (S = 1.5)
$m_{\Sigma_c(2520)^{++}} - m_{\Lambda_c^+} = 231.4 \pm 0.6$ MeV (S = 1.6)
$m_{\Sigma_c(2520)^{+}} - m_{\Lambda_c^+} = 231.0 \pm 2.3$ MeV
$m_{\Sigma_c(2520)^{0}} - m_{\Lambda_c^+} = 232.3 \pm 0.5$ MeV (S = 1.6)
$m_{\Sigma_c(2520)^{++}} - m_{\Sigma_c(2520)^0}$
$\Sigma_c(2520)^{++}$ full width $\Gamma = 14.9 \pm 1.5$ MeV
$\Sigma_c(2520)^{+}$ full width $\Gamma < 17$ MeV, CL = 90%
$\Sigma_c(2520)^{0}$ full width $\Gamma = 14.5 \pm 1.5$ MeV

$\Lambda_c^+\pi$ is the only strong decay allowed to a Σ_c having this mass.

$\Sigma_c(2520)$ DECAY MODES	Fraction (Γ_i/Γ)	p (MeV/c)
$\Lambda_c^+\pi$	≈ 100 %	179

$\Sigma_c(2800)$

$I(J^P) = 1(?^?)$

$\Sigma_c(2800)^{++}$ mass $m = 2801^{+4}_{-6}$ MeV
$\Sigma_c(2800)^{+}$ mass $m = 2792^{+14}_{-5}$ MeV
$\Sigma_c(2800)^{0}$ mass $m = 2806^{+5}_{-7}$ MeV (S = 1.3)
$m_{\Sigma_c(2800)^{++}} - m_{\Lambda_c^+} = 514^{+4}_{-6}$ MeV
$m_{\Sigma_c(2800)^{+}} - m_{\Lambda_c^+} = 505^{+14}_{-5}$ MeV
$m_{\Sigma_c(2800)^{0}} - m_{\Lambda_c^+} = 519^{+5}_{-7}$ MeV (S = 1.3)
$\Sigma_c(2800)^{++}$ full width $\Gamma = 75^{+22}_{-17}$ MeV
$\Sigma_c(2800)^{+}$ full width $\Gamma = 62^{+60}_{-40}$ MeV
$\Sigma_c(2800)^{0}$ full width $\Gamma = 72^{+22}_{-15}$ MeV

$\Sigma_c(2800)$ DECAY MODES	Fraction (Γ_i/Γ)	p (MeV/c)
$\Lambda_c^+\pi$	seen	443

Ξ_c^+

$I(J^P) = \frac{1}{2}(\frac{1}{2}^+)$

J^P has not been measured; $\frac{1}{2}^+$ is the quark-model prediction.

Mass $m = 2467.8^{+0.4}_{-0.6}$ MeV
Mean life $\tau = (442 \pm 26) \times 10^{-15}$ s (S = 1.3)
$c\tau = 132\ \mu$m

Ξ_c^+ DECAY MODES	Fraction (Γ_i/Γ)	Confidence level	p (MeV/c)
No absolute branching fractions have been measured. The following are branching *ratios* relative to $\Xi^-2\pi^+$.			
Cabibbo-favored ($S = -2$) decays — relative to $\Xi^-2\pi^+$			
pK^0_S	0.087 ± 0.021		767
$\Lambda\overline{K}^0\pi^+$	—		852
$\Sigma(1385)^+\overline{K}^0$	[r] 1.0 ± 0.5		746
$\Lambda K^-2\pi^+$	0.323 ± 0.033		787
$\Lambda\overline{K}^*(892)^0\pi^+$	[r] <0.16	90%	608
$\Sigma(1385)^+K^-\pi^+$	[r] <0.23	90%	678
$\Sigma^+K^-\pi^+$	0.94 ± 0.10		810
$\Sigma^+\overline{K}^*(892)^0$	[r] 0.81 ± 0.15		658
$\Sigma^0K^-2\pi^+$	0.27 ± 0.12		735
$\Xi^0\pi^+$	0.55 ± 0.16		877
$\Xi^-2\pi^+$	**DEFINED AS 1**		851
$\Xi(1530)^0\pi^+$	[r] <0.10	90%	750
$\Xi^0\pi^+\pi^0$	2.3 ± 0.7		856
$\Xi^0\pi^-2\pi^+$	1.7 ± 0.5		818
$\Xi^0e^+\nu_e$	$2.3\ ^{+0.7}_{-0.8}$		884
$\Omega^-K^+\pi^+$	0.07 ± 0.04		399
Cabibbo-suppressed decays — relative to $\Xi^-2\pi^+$			
$pK^-\pi^+$	0.21 ± 0.04		944
$p\overline{K}^*(892)^0$	[r] 0.116 ± 0.030		828
$\Sigma^+\pi^+\pi^-$	0.48 ± 0.20		922
$\Sigma^-2\pi^+$	0.18 ± 0.09		918
$\Sigma^+K^+K^-$	0.15 ± 0.06		579
$\Sigma^+\phi$	[r] <0.11	90%	549
$\Xi(1690)^0K^+$, $\Xi(1690)^0 \to \Sigma^+K^-$	<0.05	90%	501

Ξ_c^0

$I(J^P) = \frac{1}{2}(\frac{1}{2}^+)$

J^P has not been measured; $\frac{1}{2}^+$ is the quark-model prediction.

Mass $m = 2470.88^{+0.34}_{-0.80}$ MeV (S = 1.1)
$m_{\Xi_c^0} - m_{\Xi_c^+} = 3.1^{+0.4}_{-0.5}$ MeV
Mean life $\tau = (112^{+13}_{-10}) \times 10^{-15}$ s
$c\tau = 33.6\ \mu$m

Decay asymmetry parameters

$\Xi^-\pi^+$ $\alpha = -0.6 \pm 0.4$

No absolute branching fractions have been measured. Several measurements of ratios of fractions may be found in the Listings that follow.

Ξ_c^0 DECAY MODES	Fraction (Γ_i/Γ)	p (MeV/c)
No absolute branching fractions have been measured. The following are branching *ratios* relative to $\Xi^-\pi^+$.		
Cabibbo-favored (S = −2) decays — relative to $\Xi^-\pi^+$		
$pK^-K^-\pi^+$	0.34 ± 0.04	676
$pK^-\overline{K}^*(892)^0$	0.21 ± 0.05	413
$pK^-K^-\pi^+$ (no $\overline{K}^{*0}$)	0.21 ± 0.04	676
ΛK^0_S	0.210 ± 0.028	906
$\Lambda K^-\pi^+$	1.07 ± 0.14	856
$\Lambda\overline{K}^0\pi^+\pi^-$	seen	787
$\Lambda K^-\pi^+\pi^+\pi^-$	seen	703
$\Xi^-\pi^+$	**DEFINED AS 1**	875
$\Xi^-\pi^+\pi^+\pi^-$	3.3 ± 1.4	816
Ω^-K^+	0.297 ± 0.024	522
$\Xi^-e^+\nu_e$	3.1 ± 1.1	882
$\Xi^-\ell^+$ anything	1.0 ± 0.5	–
Cabibbo-suppressed decays — relative to $\Xi^-\pi^+$		
Ξ^-K^+	0.028 ± 0.006	790
ΛK^+K^- (no ϕ)	0.029 ± 0.007	648
$\Lambda\phi$	0.034 ± 0.007	621

$\Xi_c'^+$

$I(J^P) = \frac{1}{2}(\frac{1}{2}^+)$

J^P has not been measured; $\frac{1}{2}^+$ is the quark-model prediction.

Mass $m = 2575.6 \pm 3.1$ MeV
$m_{\Xi_c'^+} - m_{\Xi_c^+} = 107.8 \pm 3.0$ MeV

The $\Xi_c'^+$–Ξ_c^+ mass difference is too small for any strong decay to occur.

$\Xi_c'^+$ DECAY MODES	Fraction (Γ_i/Γ)	p (MeV/c)
$\Xi_c^+\gamma$	seen	106

$\Xi_c'^0$

$I(J^P) = \frac{1}{2}(\frac{1}{2}^+)$

J^P has not been measured; $\frac{1}{2}^+$ is the quark-model prediction.

Mass $m = 2577.9 \pm 2.9$ MeV
$m_{\Xi_c'^0} - m_{\Xi_c^0} = 107.0 \pm 2.9$ MeV

The $\Xi_c'^0 - \Xi_c^0$ mass difference is too small for any strong decay to occur.

$\Xi_c'^0$ DECAY MODES	Fraction (Γ_i/Γ)	p (MeV/c)
$\Xi_c^0\gamma$	seen	105

$\Xi_c(2645)$

$I(J^P) = \frac{1}{2}(\frac{3}{2}^+)$

J^P has not been measured; $\frac{3}{2}^+$ is the quark-model prediction.

$\Xi_c(2645)^+$ mass $m = 2645.9^{+0.5}_{-0.6}$ MeV (S = 1.1)
$\Xi_c(2645)^0$ mass $m = 2645.9 \pm 0.5$ MeV
$m_{\Xi_c(2645)^+} - m_{\Xi_c^0} = 175.0^{+0.8}_{-0.6}$ MeV (S = 1.2)
$m_{\Xi_c(2645)^0} - m_{\Xi_c^+} = 178.1 \pm 0.6$ MeV
$m_{\Xi_c(2645)^+} - m_{\Xi_c(2645)^0} = 0.0 \pm 0.5$ MeV
$\Xi_c(2645)^+$ full width $\Gamma < 3.1$ MeV, CL = 90%
$\Xi_c(2645)^0$ full width $\Gamma < 5.5$ MeV, CL = 90%

$\Xi_c\pi$ is the only strong decay allowed to a Ξ_c resonance having this mass.

$\Xi_c(2645)$ DECAY MODES	Fraction (Γ_i/Γ)	p (MeV/c)
$\Xi_c^0\pi^+$	seen	102
$\Xi_c^+\pi^-$	seen	107

$\Xi_c(2790)$

$I(J^P) = \frac{1}{2}(\frac{1}{2}^-)$

J^P has not been measured; $\frac{1}{2}^-$ is the quark-model prediction.

$\Xi_c(2790)^+$ mass = 2789.1 ± 3.2 MeV
$\Xi_c(2790)^0$ mass = 2791.8 ± 3.3 MeV
$m_{\Xi_c(2790)^+} - m_{\Xi_c^0} = 318.2 \pm 3.2$ MeV
$m_{\Xi_c(2790)^0} - m_{\Xi_c^+} = 324.0 \pm 3.3$ MeV
$\Xi_c(2790)^+$ width < 15 MeV, CL = 90%
$\Xi_c(2790)^0$ width < 12 MeV, CL = 90%

$\Xi_c(2790)$ DECAY MODES	Fraction (Γ_i/Γ)	p (MeV/c)
$\Xi_c'\pi$	seen	159

$\Xi_c(2815)$

$I(J^P) = \frac{1}{2}(\frac{3}{2}^-)$

J^P has not been measured; $\frac{3}{2}^-$ is the quark-model prediction.

$\Xi_c(2815)^+$ mass $m = 2816.6 \pm 0.9$ MeV
$\Xi_c(2815)^0$ mass $m = 2819.6 \pm 1.2$ MeV
$m_{\Xi_c(2815)^+} - m_{\Xi_c^+} = 348.8 \pm 0.9$ MeV
$m_{\Xi_c(2815)^0} - m_{\Xi_c^0} = 348.7 \pm 1.2$ MeV
$m_{\Xi_c(2815)^+} - m_{\Xi_c(2815)^0} = -3.1 \pm 1.3$ MeV
$\Xi_c(2815)^+$ full width $\Gamma < 3.5$ MeV, CL = 90%
$\Xi_c(2815)^0$ full width $\Gamma < 6.5$ MeV, CL = 90%

The $\Xi_c\pi\pi$ modes are consistent with being entirely via $\Xi_c(2645)\pi$.

$\Xi_c(2815)$ DECAY MODES	Fraction (Γ_i/Γ)	p (MeV/c)
$\Xi_c^+\pi^+\pi^-$	seen	196
$\Xi_c^0\pi^+\pi^-$	seen	191

$\Xi_c(2980)$

$I(J^P) = \frac{1}{2}(?^?)$

$\Xi_c(2980)^+$ $m = 2971.4 \pm 3.3$ MeV (S = 2.1)
$\Xi_c(2980)^0$ $m = 2968.0 \pm 2.6$ MeV (S = 1.2)
$\Xi_c(2980)^+$ width $\Gamma = 26 \pm 7$ MeV (S = 1.5)
$\Xi_c(2980)^0$ width $\Gamma = 20 \pm 7$ MeV (S = 1.3)

$\Xi_c(2980)$ DECAY MODES	Fraction (Γ_i/Γ)	p (MeV/c)
$\Lambda_c^+\overline{K}\pi$	seen	231
$\Sigma_c(2455)\overline{K}$	seen	134
$\Lambda_c^+\overline{K}$	not seen	414
$\Xi_c 2\pi$	seen	–
$\Xi_c(2645)\pi$	seen	277

$\Xi_c(3080)$

$I(J^P) = \frac{1}{2}(?^?)$

$\Xi_c(3080)^+$ $m = 3077.0 \pm 0.4$ MeV
$\Xi_c(3080)^0$ $m = 3079.9 \pm 1.4$ MeV (S = 1.3)
$\Xi_c(3080)^+$ width $\Gamma = 5.8 \pm 1.0$ MeV
$\Xi_c(3080)^0$ width $\Gamma = 5.6 \pm 2.2$ MeV

$\Xi_c(3080)$ DECAY MODES	Fraction (Γ_i/Γ)	p (MeV/c)
$\Lambda_c^+\overline{K}\pi$	seen	415
$\Sigma_c(2455)\overline{K}$	seen	342
$\Sigma_c(2455)\overline{K} + \Sigma_c(2520)\overline{K}$	seen	–
$\Lambda_c^+\overline{K}$	not seen	536
$\Lambda_c^+\overline{K}\pi^+\pi^-$	not seen	143

Ω_c^0

$I(J^P) = 0(\frac{1}{2}^+)$

J^P has not been measured; $\frac{1}{2}^+$ is the quark-model prediction.

Mass $m = 2695.2 \pm 1.7$ MeV (S = 1.3)
Mean life $\tau = (69 \pm 12) \times 10^{-15}$ s
$c\tau = 21\ \mu$m

No absolute branching fractions have been measured.

Ω_c^0 DECAY MODES	Fraction (Γ_i/Γ)	p (MeV/c)
$\Sigma^+K^-K^-\pi^+$	seen	689
$\Xi^0K^-\pi^+$	seen	901
$\Xi^-K^-\pi^+\pi^+$	seen	830
$\Omega^-e^+\nu_e$	seen	829
$\Omega^-\pi^+$	seen	821
$\Omega^-\pi^+\pi^0$	seen	797
$\Omega^-\pi^-\pi^+\pi^+$	seen	753

$\Omega_c(2770)^0$

$I(J^P) = 0(\frac{3}{2}^+)$

J^P has not been measured; $\frac{3}{2}^+$ is the quark-model prediction.

Mass $m = 2765.9 \pm 2.0$ MeV (S = 1.2)
$m_{\Omega_c(2770)^0} - m_{\Omega_c^0} = 70.7^{+0.8}_{-0.9}$ MeV

The $\Omega_c(2770)^0$–Ω_c^0 mass difference is too small for any strong decay to occur.

$\Omega_c(2770)^0$ DECAY MODES	Fraction (Γ_i/Γ)	p (MeV/c)
$\Omega_c^0\gamma$	presumably 100%	70

BOTTOM BARYONS ($B = -1$)

$\Lambda_b^0 = udb$, $\Xi_b^0 = usb$, $\Xi_b^- = dsb$, $\Omega_b^- = ssb$

Λ_b^0

$I(J^P) = 0(\frac{1}{2}^+)$

$I(J^P)$ not yet measured; $0(\frac{1}{2}^+)$ is the quark model prediction.
Mass $m = 5619.5 \pm 0.4$ MeV
$m_{\Lambda_b^0} - m_{B^0} = 339.2 \pm 1.4$ MeV
$m_{\Lambda_b^0} - m_{B^+} = 339.7 \pm 0.7$ MeV
Mean life $\tau = (1.451 \pm 0.013) \times 10^{-12}$ s
$c\tau = 435\ \mu$m
$A_{CP}(\Lambda_b \to p\pi^-) = 0.03 \pm 0.18$
$A_{CP}(\Lambda_b \to pK^-) = 0.37 \pm 0.17$
α decay parameter for $\Lambda_b \to J/\psi\Lambda = 0.05 \pm 0.18$

The branching fractions B(b-baryon $\to \Lambda\ell^-\overline{\nu}_\ell$anything) and B($\Lambda_b^0 \to \Lambda_c^+\ell^-\overline{\nu}_\ell$anything) are not pure measurements because the underlying measured products of these with B($b \to b$-baryon) were used to determine B($b \to b$-baryon), as described in the note "Production and Decay of b-Flavored Hadrons."

For inclusive branching fractions, *e.g.*, $\Lambda_b \to \overline{\Lambda}_c$anything, the values usually are multiplicities, not branching fractions. They can be greater than one.

Λ_b^0 DECAY MODES	Fraction (Γ_i/Γ)	Scale factor/ Confidence level	p (MeV/c)
$J/\psi(1S)\Lambda \times$ B($b \to \Lambda_b^0$)	$(5.8 \pm 0.8) \times 10^{-5}$		1740
$pD^0\pi^-$	$(5.9\ ^{+4.0}_{-3.2}) \times 10^{-4}$		2370
pD^0K^-	$(4.3\ ^{+3.0}_{-2.4}) \times 10^{-5}$		2269
$\Lambda_c^+\pi^-$	$(5.7\ ^{+4.0}_{-2.6}) \times 10^{-3}$	S=1.6	2342
$\Lambda_c^+K^-$	$(4.2\ ^{+2.6}_{-1.9}) \times 10^{-4}$		2314
$\Lambda_c^+ a_1(1260)^-$	seen		2153
$\Lambda_c^+\pi^+\pi^-\pi^-$	$(8\ ^{+5}_{-4}) \times 10^{-3}$	S=1.6	2323
$\Lambda_c(2595)^+\pi^-$, $\Lambda_c(2595)^+ \to \Lambda_c^+\pi^+\pi^-$	$(3.7\ ^{+2.8}_{-2.3}) \times 10^{-4}$		2210
$\Lambda_c(2625)^+\pi^-$, $\Lambda_c(2625)^+ \to \Lambda_c^+\pi^+\pi^-$	$(3.6\ ^{+2.7}_{-2.1}) \times 10^{-4}$		2193
$\Sigma_c(2455)^0\pi^+\pi^-$, $\Sigma_c^0 \to \Lambda_c^+\pi^-$	$(6\ ^{+5}_{-4}) \times 10^{-4}$		2265
$\Sigma_c(2455)^{++}\pi^-\pi^-$, $\Sigma_c^{++} \to \Lambda_c^+\pi^+$	$(3.5\ ^{+2.8}_{-2.3}) \times 10^{-4}$		2265
$\Lambda_c^+\ell^-\overline{\nu}_\ell$anything [x]	(9.9 ± 2.2) %		–
$\Lambda_c^+\ell^-\overline{\nu}_\ell$	$(6.5\ ^{+3.2}_{-2.5})$ %	S=1.8	2345
$\Lambda_c^+\pi^+\pi^-\ell^-\overline{\nu}_\ell$	(5.6 ± 3.1) %		2335
$\Lambda_c(2595)^+\ell^-\overline{\nu}_\ell$	$(8 \pm 5) \times 10^{-3}$		2212
$\Lambda_c(2625)^+\ell^-\overline{\nu}_\ell$	$(1.4\ ^{+0.9}_{-0.7})$ %		2195
ph^- [y]	$< 2.3 \times 10^{-5}$	CL=90%	2730
$p\pi^-$	$(4.1 \pm 0.8) \times 10^{-6}$		2730
pK^-	$(4.9 \pm 0.9) \times 10^{-6}$		2708
$\Lambda\mu^+\mu^-$	$(1.08 \pm 0.28) \times 10^{-6}$		2695
$\Lambda\gamma$	$< 1.3 \times 10^{-3}$	CL=90%	2699

$\Lambda_b(5912)^0$

$J^P = \frac{1}{2}^-$

Mass $m = 5912.1 \pm 0.4$ MeV
Full width $\Gamma < 0.66$ MeV, CL = 90%

$\Lambda_b(5912)^0$ DECAY MODES	Fraction (Γ_i/Γ)	p (MeV/c)
$\Lambda_b^0\pi^+\pi^-$	seen	86

$\Lambda_b(5920)^0$

$J^P = \frac{3}{2}^-$

Mass $m = 5919.73 \pm 0.32$ MeV
Full width $\Gamma < 0.63$ MeV, CL = 90%

$\Lambda_b(5920)^0$ DECAY MODES	Fraction (Γ_i/Γ)	p (MeV/c)
$\Lambda_b^0\pi^+\pi^-$	seen	108

Σ_b

$I(J^P) = 1(\frac{1}{2}^+)$
I, J, P need confirmation.

Mass $m(\Sigma_b^+) = 5811.3 \pm 1.9$ MeV
Mass $m(\Sigma_b^-) = 5815.5 \pm 1.8$ MeV
$m_{\Sigma_b^+} - m_{\Sigma_b^-} = -4.2 \pm 1.1$ MeV
$\Gamma(\Sigma_b^+) = 9.7^{+4.0}_{-3.0}$ MeV
$\Gamma(\Sigma_b^-) = 4.9^{+3.3}_{-2.4}$ MeV

Σ_b DECAY MODES	Fraction (Γ_i/Γ)	p (MeV/c)
$\Lambda_b^0\pi$	dominant	134

Σ_b^*

$I(J^P) = 1(\frac{3}{2}^+)$
I, J, P need confirmation.

Mass $m(\Sigma_b^{*+}) = 5832.1 \pm 1.9$ MeV
Mass $m(\Sigma_b^{*-}) = 5835.1 \pm 1.9$ MeV
$m_{\Sigma_b^{*+}} - m_{\Sigma_b^{*-}} = -3.0^{+1.0}_{-0.9}$ MeV
$\Gamma(\Sigma_b^{*+}) = 11.5 \pm 2.8$ MeV
$\Gamma(\Sigma_b^{*-}) = 7.5 \pm 2.3$ MeV
$m_{\Sigma_b^*} - m_{\Sigma_b} = 21.2 \pm 2.0$ MeV

Σ_b^* DECAY MODES	Fraction (Γ_i/Γ)	p (MeV/c)
$\Lambda_b^0\pi$	dominant	161

Ξ_b^0, Ξ_b^-

$I(J^P) = \frac{1}{2}(\frac{1}{2}^+)$
I, J, P need confirmation.

$m(\Xi_b^-) = 5794.9 \pm 0.9$ MeV (S = 1.1)
$m(\Xi_b^0) = 5793.1 \pm 2.5$ MeV (S = 1.1)
$m_{\Xi_b^-} - m_{\Lambda_b^0} = 176.2 \pm 0.9$ MeV
$m_{\Xi_b^0} - m_{\Lambda_b^0} = 174.8 \pm 2.5$ MeV
$m_{\Xi_b^-} - m_{\Xi_b^0} = 3 \pm 6$ MeV
Mean life $\tau_{\Xi_b^-} = (1.56^{+0.27}_{-0.25}) \times 10^{-12}$ s
Mean life $\tau_{\Xi_b} = (1.49^{+0.19}_{-0.18}) \times 10^{-12}$ s

Ξ_b DECAY MODES	Fraction (Γ_i/Γ)	Scale factor	p (MeV/c)
$\Xi_b \to \Xi^-\ell^-\overline{\nu}_\ell X \times$ B($\overline{b} \to \Xi_b$)	$(3.9 \pm 1.2) \times 10^{-4}$	1.4	–
$\Xi_b^- \to J/\psi\Xi^- \times$ B($b \to \Xi_b^-$)	$(1.02^{+0.26}_{-0.21}) \times 10^{-5}$		1783
$\Xi_b^0 \to pD^0K^- \times$ B($\overline{b} \to \Xi_b$)	$(1.8\ ^{+1.3}_{-1.1}) \times 10^{-6}$		–
$\Xi_b^0 \to \Lambda_c^+K^- \times$ B($\overline{b} \to \Xi_b$)	$(8 \pm 7) \times 10^{-7}$		–

$\Xi_b(5945)^0$

$J^P = \frac{3}{2}^+$

Mass $m = 5949.4 \pm 1.4$ MeV
Full width $\Gamma = 2.1 \pm 1.7$ MeV

$\Xi_b(5945)^0$ DECAY MODES	Fraction (Γ_i/Γ)	p (MeV/c)
$\Xi_b^-\pi^+$	seen	80

Ω_b^-

$I(J^P) = 0(\frac{1}{2}^+)$
I, J, P need confirmation.

Mass $m = 6048.8 \pm 3.2$ MeV (S = 1.5)
$m_{\Omega_b^-} - m_{\Lambda_b^0} = 426.4 \pm 2.2$ MeV
Mean life $\tau = (1.1^{+0.5}_{-0.4}) \times 10^{-12}$ s

Ω_b^- DECAY MODES	Fraction (Γ_i/Γ)	p (MeV/c)
$J/\psi\Omega^- \times$B($b \to \Omega_b$)	$(2.9^{+1.1}_{-0.8}) \times 10^{-6}$	1808

b-baryon ADMIXTURE (Λ_b, Ξ_b, Σ_b, Ω_b)

Mean life $\tau = (1.449 \pm 0.015) \times 10^{-12}$ s

These branching fractions are actually an average over weakly decaying b-baryons weighted by their production rates at the LHC, LEP, and Tevatron, branching ratios, and detection efficiencies. They scale with the b-baryon production fraction B($b \rightarrow$ b-baryon).

The branching fractions B(b-baryon $\rightarrow$ $\Lambda \ell^- \overline{\nu}_\ell$ anything) and B($\Lambda_b^0 \rightarrow$ $\Lambda_c^+ \ell^- \overline{\nu}_\ell$ anything) are not pure measurements because the underlying measured products of these with B($b \rightarrow$ b-baryon) were used to determine B($b \rightarrow$ b-baryon), as described in the note "Production and Decay of b-Flavored Hadrons."

For inclusive branching fractions, *e.g.*, $B \rightarrow D^{\pm}$ anything, the values usually are multiplicities, not branching fractions. They can be greater than one.

b-baryon ADMIXTURE DECAY MODES (Λ_b,Ξ_b,Σ_b,Ω_b)

	Fraction (Γ_i/Γ)	p (MeV/c)
$p\mu^-\overline{\nu}$ anything	($5.3^{+\ 2.2}_{-\ 1.9}$) %	–
$p\ell\overline{\nu}_\ell$ anything	(5.1 ± 1.2) %	–
p anything	(64 ±21) %	–
$\Lambda\ell^-\overline{\nu}_\ell$ anything	(3.5 ± 0.6) %	–
$\Lambda/\overline{\Lambda}$ anything	(36 ± 7) %	–
$\Xi^-\ell^-\overline{\nu}_\ell$ anything	(6.0 ± 1.6) $\times 10^{-3}$	–

NOTES

This Summary Table only includes established baryons. The Particle Listings include evidence for other baryons. The masses, widths, and branching fractions for the resonances in this Table are Breit-Wigner parameters, but pole positions are also given for most of the N and Δ resonances.

For most of the resonances, the parameters come from various partial-wave analyses of more or less the same sets of data, and it is not appropriate to treat the results of the analyses as independent or to average them together. Furthermore, the systematic errors on the results are not well understood. Thus, we usually only give ranges for the parameters. We then also give a best guess for the mass (as part of the name of the resonance) and for the width. The *Note on N and Δ Resonances* and the *Note on Λ and Σ Resonances* in the Particle Listings review the partial-wave analyses.

When a quantity has "(S = ...)" to its right, the error on the quantity has been enlarged by the "scale factor" S, defined as $S = \sqrt{\chi^2/(N-1)}$, where N is the number of measurements used in calculating the quantity. We do this when $S > 1$, which often indicates that the measurements are inconsistent. When $S > 1.25$, we also show in the Particle Listings an ideogram of the measurements. For more about S, see the Introduction.

A decay momentum p is given for each decay mode. For a 2-body decay, p is the momentum of each decay product in the rest frame of the decaying particle. For a 3-or-more-body decay, p is the largest momentum any of the products can have in this frame. For any resonance, the *nominal* mass is used in calculating p. A dagger ("†") in this column indicates that the mode is forbidden when the nominal masses of resonances are used, but is in fact allowed due to the nonzero widths of the resonances.

[a] The masses of the p and n are most precisely known in u (unified atomic mass units). The conversion factor to MeV, 1 u = 931.494061(21) MeV, is less well known than are the masses in u.

[b] The $|m_p - m_{\overline{p}}|/m_p$ and $|q_p + q_{\overline{p}}|/e$ are not independent, and both use the more precise measurement of $|q_{\overline{p}}/m_{\overline{p}}|/(q_p/m_p)$.

[c] The limit is from neutrality-of-matter experiments; it assumes $q_n = q_p + q_e$. See also the charge of the neutron.

[d] The μp and ep values for the charge radius are much too different to average them. The disagreement is not yet understood.

[e] The first limit is for $p \rightarrow$ anything or "disappearance" modes of a bound proton. The second entry, a rough range of limits, assumes the dominant decay modes are among those investigated. For antiprotons the best limit, inferred from the observation of cosmic ray $\overline{p}$'s is $\tau_{\overline{p}} > 10^7$ yr, the cosmic-ray storage time, but this limit depends on a number of assumptions. The best direct observation of stored antiprotons gives $\tau_{\overline{p}}/\mathrm{B}(\overline{p} \rightarrow e^-\gamma) > 7 \times 10^5$ yr.

[f] There is some controversy about whether nuclear physics and model dependence complicate the analysis for bound neutrons (from which the best limit comes). The first limit here is from reactor experiments with free neutrons.

[g] Lee and Yang in 1956 proposed the existence of a mirror world in an attempt to restore global parity symmetry—thus a search for oscillations between the two worlds. Oscillations between the worlds would be maximal when the magnetic fields B and B' were equal. The limit for any B' in the range 0 to 12.5 μT is >12 s (95% CL).

[h] The parameters g_A, g_V, and g_{WM} for semileptonic modes are defined by $\overline{B}_f[\gamma_\lambda(g_V + g_A\gamma_5) + i(g_{WM}/m_{B_i})\ \sigma_{\lambda\nu}\ q^\nu]B_i$, and ϕ_{AV} is defined by $g_A/g_V = |g_A/g_V|e^{i\phi_{AV}}$. See the "Note on Baryon Decay Parameters" in the neutron Particle Listings.

[i] Time-reversal invariance requires this to be 0° or 180°.

[j] This coefficient is zero if time invariance is not violated.

[k] This limit is for γ energies between 15 and 340 keV.

[l] The decay parameters γ and Δ are calculated from α and ϕ using

$$\gamma = \sqrt{1-\alpha^2}\,\cos\phi\,, \qquad \tan\Delta = -\frac{1}{\alpha}\,\sqrt{1-\alpha^2}\,\sin\phi\,.$$

See the "Note on Baryon Decay Parameters" in the neutron Particle Listings.

[n] See the Listings for the pion momentum range used in this measurement.

[o] The error given here is only an educated guess. It is larger than the error on the weighted average of the published values.

[p] A theoretical value using QED.

[q] See the note on "Λ_c^+ Branching Fractions" in the Λ_c^+ Particle Listings.

[r] This branching fraction includes all the decay modes of the final-state resonance.

[s] An ℓ indicates an e or a μ mode, not a sum over these modes.

[t] The value is for the sum of the charge states or particle/antiparticle states indicated.

[u] Assuming isospin conservation, so that the other third is $\Lambda_c^+\pi^0\pi^0$.

[v] A test that the isospin is indeed 0, so that the particle is indeed a Λ_c^+.

[x] Not a pure measurement. See note at head of Λ_b^0 Decay Modes.

[y] Here h^- means π^- or K^-.

Searches Summary Table

SEARCHES FOR MONOPOLES, SUPERSYMMETRY, TECHNICOLOR, COMPOSITENESS, EXTRA DIMENSIONS, etc.

Magnetic Monopole Searches

Isolated supermassive monopole candidate events have not been confirmed. The most sensitive experiments obtain negative results.

Best cosmic-ray supermassive monopole flux limit:

$< 1.4 \times 10^{-16}$ cm^{-2}sr^{-1}s^{-1} for $1.1 \times 10^{-4} < \beta < 1$

Supersymmetric Particle Searches

Limits are based on the Minimal Supersymmetric Standard Model (MSSM) with additional assumptions as follows:

1) $\widetilde{\chi}^0_1$ (or $\widetilde{\gamma}$) is lightest supersymmetric particle; 2) R-parity is conserved; 3) With the exception of $\widetilde{t}$ and $\widetilde{b}$, all scalar quarks are assumed to be degenerate in mass and $m_{\widetilde{q}_R} = m_{\widetilde{q}_L}$. 4) Limits for charged sleptons refer to the $\widetilde{\ell}_R$ states. 5) Unless otherwise stated, gaugino mass unification at the GUT scale is assumed. For squarks and gluinos, the Constrained MSSM (CMSSM) limits and simplified model limits are presented.

See the Particle Listings for a Note giving details of supersymmetry.

$\widetilde{\chi}^0_i$ — neutralinos (mixtures of $\widetilde{\gamma}$, $\widetilde{Z}^0$, and $\widetilde{H}^0_i$)

Mass $m_{\widetilde{\chi}^0_1} > 46$ GeV, CL = 95%
[all tanβ, all m_0, all $m_{\widetilde{\chi}^0_2} - m_{\widetilde{\chi}^0_1}$]

Mass $m_{\widetilde{\chi}^0_2} > 62.4$ GeV, CL = 95%
[1<tanβ <40, all m_0, all $m_{\widetilde{\chi}^0_2} - m_{\widetilde{\chi}^0_1}$]

Mass $m_{\widetilde{\chi}^0_3} > 99.9$ GeV, CL = 95%
[1<tanβ <40, all m_0, all $m_{\widetilde{\chi}^0_3} - m_{\widetilde{\chi}^0_1}$]

Mass $m_{\widetilde{\chi}^0_4} > 116$ GeV, CL = 95%
[1<tanβ <40, all m_0, all $m_{\widetilde{\chi}^0_2} - m_{\widetilde{\chi}^0_1}$]

$\widetilde{\chi}^\pm_i$ — charginos (mixtures of $\widetilde{W}^\pm$ and $\widetilde{H}^\pm_i$)

Mass $m_{\widetilde{\chi}^\pm_1} > 94$ GeV, CL = 95%
[tan$\beta < 40$, $m_{\widetilde{\chi}^\pm_1} - m_{\widetilde{\chi}^0_1} > 3$ GeV, all m_0]

$\widetilde{\nu}$ — sneutrino

Mass $m > 94$ GeV, CL = 95%
[$1 \le$ tan$\beta \le 40$, $m_{\widetilde{e}_R} - m_{\widetilde{\chi}^0_1} > 10$ GeV]

$\widetilde{e}$ — scalar electron (selectron)

Mass $m > 107$ GeV, CL = 95% [all $m_{\widetilde{e}_R} - m_{\widetilde{\chi}^0_1}$]

$\widetilde{\mu}$ — scalar muon (smuon)

Mass $m > 94$ GeV, CL = 95%
[$1 \le$ tan$\beta \le 40$, $m_{\widetilde{\mu}_R} - m_{\widetilde{\chi}^0_1} > 10$ GeV]

$\widetilde{\tau}$ — scalar tau (stau)

Mass $m > 81.9$ GeV, CL = 95%
[$m_{\widetilde{\tau}_R} - m_{\widetilde{\chi}^0_1} > 15$ GeV, all θ_τ]

$\widetilde{q}$ – scalar quark partners (squarks) of the first two quark generations

The first of these limits is within CMSSM with cascade decays, evaluated assuming a fixed value of the parameters μ and tanβ. Limits assume two-generations of mass degenerate squarks ($\widetilde{q}_L$ and $\widetilde{q}_R$) and gaugino mass parameters that are constrained by the unification condition at the grand unification scale. The second limit assumes a simplified model with a 100% branching ratio for the prompt decay $\widetilde{q} \to q\widetilde{\chi}^0_1$.

Mass $m > 1110$ GeV, CL = 95% [tanβ=10, $\mu > 0$, A_0=0]
Mass $m > 750$ GeV, CL = 95%
[jets + $\not{E}_T$, $\widetilde{q} \to q\widetilde{\chi}^0_1$ simplified model, $m_{\widetilde{\chi}^0_1}$= 0 GeV]

$\widetilde{b}$ — scalar bottom (sbottom)

Mass $m > 89$ GeV, CL = 95%
[$\widetilde{b} \to b\widetilde{\chi}^0_1$, $m_{\widetilde{b}_1} - m_{\widetilde{\chi}^0_1} > 8$ GeV, all θ_b]
Mass $m > 600$ GeV, CL = 95%
[jets + $\not{E}_T$, $\widetilde{b} \to b\widetilde{\chi}^0_1$ simplified model, $m_{\widetilde{\chi}^0_1}$= 0 GeV]

$\widetilde{t}$ — scalar top (stop)

Mass $m > 95.7$ GeV, CL = 95%
[$\widetilde{t} \to c\widetilde{\chi}^0_1$, $m_{\widetilde{t}} - m_{\widetilde{\chi}^0_1} > 10$ GeV, all θ_t]
Mass $m > 650$ GeV, CL = 95%
[1 $\ell^\pm$ + jets + $\not{E}_T$, $\widetilde{t} \to t\widetilde{\chi}^0_1$ simplified model, $m_{\widetilde{\chi}^0_1}$=0 GeV]

$\widetilde{g}$ — gluino

The first of these limits is within the CMSSM for ($m_{\widetilde{g}} \gtrsim$ 5 GeV), and includes the effects of cascade decays, evaluated assuming a fixed value of the parameters μ and tanβ. Limit assumes GUT relations between gaugino masses and the gauge couplings. The second limit assumes a simplified model with a 100% branching ratio for the prompt 3 body decay $\widetilde{g} \to q\overline{q}\widetilde{\chi}^0_1$, independent of the squark mass.

Mass $m > 800$ GeV, CL = 95% [any $m_{\widetilde{q}}$]
Mass $m > 950$ GeV, CL = 95%
[jets + $\not{E}_T$, $\widetilde{g} \to q\overline{q}\widetilde{\chi}^0_1$ simplified model, $m_{\widetilde{\chi}^0_1} = 0$ GeV]

Technicolor

The limits for technicolor (and top-color) particles are quite varied depending on assumptions. See the Technicolor section of the full *Review* (the data listings).

Quark and Lepton Compositeness, Searches for

Scale Limits Λ for Contact Interactions
(the lowest dimensional interactions with four fermions)

If the Lagrangian has the form

$$\pm \frac{g^2}{2\Lambda^2}\, \overline{\psi}_L \gamma_\mu \psi_L\, \overline{\psi}_L \gamma^\mu \psi_L$$

(with $g^2/4\pi$ set equal to 1), then we define $\Lambda \equiv \Lambda^\pm_{LL}$. For the full definitions and for other forms, see the Note in the Listings on Searches for Quark and Lepton Compositeness in the full *Review* and the original literature.

$\Lambda^+_{LL}(eeee)$	>	8.3 TeV, CL = 95%
$\Lambda^-_{LL}(eeee)$	>	10.3 TeV, CL = 95%
$\Lambda^+_{LL}(ee\mu\mu)$	>	8.5 TeV, CL = 95%
$\Lambda^-_{LL}(ee\mu\mu)$	>	9.5 TeV, CL = 95%
$\Lambda^+_{LL}(ee\tau\tau)$	>	7.9 TeV, CL = 95%
$\Lambda^-_{LL}(ee\tau\tau)$	>	7.2 TeV, CL = 95%
$\Lambda^+_{LL}(\ell\ell\ell\ell)$	>	9.1 TeV, CL = 95%
$\Lambda^-_{LL}(\ell\ell\ell\ell)$	>	10.3 TeV, CL = 95%
$\Lambda^+_{LL}(eeuu)$	>	23.3 TeV, CL = 95%
$\Lambda^-_{LL}(eeuu)$	>	12.5 TeV, CL = 95%
$\Lambda^+_{LL}(eedd)$	>	11.1 TeV, CL = 95%
$\Lambda^-_{LL}(eedd)$	>	26.4 TeV, CL = 95%
$\Lambda^+_{LL}(eecc)$	>	9.4 TeV, CL = 95%
$\Lambda^-_{LL}(eecc)$	>	5.6 TeV, CL = 95%
$\Lambda^+_{LL}(eebb)$	>	9.4 TeV, CL = 95%
$\Lambda^-_{LL}(eebb)$	>	10.2 TeV, CL = 95%
$\Lambda^+_{LL}(\mu\mu qq)$	>	9.6 TeV, CL = 95%
$\Lambda^-_{LL}(\mu\mu qq)$	>	13.1 TeV, CL = 95%
$\Lambda(\ell\nu\ell\nu)$	>	3.10 TeV, CL = 90%
$\Lambda(e\nu qq)$	>	2.81 TeV, CL = 95%
$\Lambda^+_{LL}(qqqq)$	>	7.6 TeV, CL = 95%
$\Lambda^-_{LL}(qqqq)$	>	7.6 TeV, CL = 95%
$\Lambda^+_{LL}(\nu\nu qq)$	>	5.0 TeV, CL = 95%
$\Lambda^-_{LL}(\nu\nu qq)$	>	5.4 TeV, CL = 95%

Excited Leptons

The limits from $\ell^{*+}\ell^{*-}$ do not depend on λ (where λ is the $\ell\ell^*$ transition coupling). The λ-dependent limits assume chiral coupling.

$e^{*\pm}$ — excited electron

Mass $m >$ 103.2 GeV, CL = 95% (from $e^* e^*$)
Mass $m >$ 2.200×10^3 GeV, CL = 95% (from $e e^*$)
Mass $m >$ 356 GeV, CL = 95% (if $\lambda_\gamma = 1$)

$\mu^{*\pm}$ — excited muon

Mass $m >$ 103.2 GeV, CL = 95% (from $\mu^* \mu^*$)
Mass $m >$ 2.200×10^3 GeV, CL = 95% (from $\mu \mu^*$)

$\tau^{*\pm}$ — excited tau

Mass $m >$ 103.2 GeV, CL = 95% (from $\tau^* \tau^*$)
Mass $m >$ 185 GeV, CL = 95% (from $\tau \tau^*$)

ν^* — excited neutrino

Mass $m >$ 102.6 GeV, CL = 95% (from $\nu^* \nu^*$)
Mass $m >$ 213 GeV, CL = 95% (from $\nu \nu^*$)

q^* — excited quark

Mass $m >$ 338 GeV, CL = 95% (from $q^* q^*$)
Mass $m >$ 3.500×10^3 GeV, CL = 95% (from q^*X)

Color Sextet and Octet Particles

Color Sextet Quarks (q_6)

Mass $m >$ 84 GeV, CL = 95% (Stable q_6)

Color Octet Charged Leptons (ℓ_8)

Mass $m >$ 86 GeV, CL = 95% (Stable ℓ_8)

Color Octet Neutrinos (ν_8)

Mass $m >$ 110 GeV, CL = 90% ($\nu_8 \rightarrow \nu g$)

Extra Dimensions

Please refer to the Extra Dimensions section of the full *Review* for a discussion of the model-dependence of these bounds, and further constraints.

Constraints on the fundamental gravity scale

$M_{TT} >$ 3.2 TeV, CL = 95% ($pp \rightarrow e^+ e^-,\ \mu^+ \mu^-,\ \gamma\gamma$)
$M_C >$ 4.16 TeV, CL = 95% ($pp \rightarrow \ell\bar{\ell}$)
$M_D >$ 2.16 TeV, CL = 95% ($pp \rightarrow G \rightarrow \ell\bar{\ell}$)

Constraints on the radius of the extra dimensions, for the case of two-flat dimensions of equal radii

$R <$ 30 μm, CL = 95% (direct tests of Newton's law)
$R <$ 23 μm, CL = 95% ($pp \rightarrow j G$)
$R <$ 0.16–916 nm (astrophysics; limits depend on technique and assumptions)

TESTS OF CONSERVATION LAWS

Updated May 2014 by L. Wolfenstein (Carnegie-Mellon University) and C.-J. Lin (LBNL).

In keeping with the current interest in tests of conservation laws, we collect together a Table of experimental limits on all weak and electromagnetic decays, mass differences, and moments, and on a few reactions, whose observation would violate conservation laws. The Table is given only in the full *Review of Particle Physics*, not in the Particle Physics Booklet. For the benefit of Booklet readers, we include the best limits from the Table in the following text. Limits in this text are for CL=90% unless otherwise specified. The Table is in two parts: "Discrete Space-Time Symmetries," *i.e.*, C, P, T, CP, and CPT; and "Number Conservation Laws," *i.e.*, lepton, baryon, hadronic flavor, and charge conservation. The references for these data can be found in the the Particle Listings in the *Review*. A discussion of these tests follows.

CPT INVARIANCE

General principles of relativistic field theory require invariance under the combined transformation CPT. The simplest tests of CPT invariance are the equality of the masses and lifetimes of a particle and its antiparticle. The best test comes from the limit on the mass difference between K^0 and $\overline{K}^0$. Any such difference contributes to the CP-violating parameter ϵ. Assuming CPT invariance, ϕ_ϵ, the phase of ϵ should be very close to 44°. (See the review "CP Violation in K_L decay" in this edition.) In contrast, if the entire source of CP violation in K^0 decays were a $K^0 - \overline{K}^0$ mass difference, ϕ_ϵ would be $44° + 90°$.

Assuming that there is no other source of CPT violation than this mass difference, it is possible to deduce that[1]

$$m_{\overline{K}^0} - m_{K^0} \approx \frac{2(m_{K_L^0} - m_{K_S^0})\,|\eta|\,(\frac{2}{3}\phi_{+-} + \frac{1}{3}\phi_{00} - \phi_{\rm SW})}{\sin\phi_{\rm SW}}\ ,$$

where $\phi_{\rm SW} = (43.51 \pm 0.05)°$, the superweak angle. Using our best values of the CP-violation parameters, we get $|(m_{\overline{K}^0} - m_{K^0})/m_{K^0}| \leq 0.6 \times 10^{-18}$ at CL=90%. Limits can also be placed on specific CPT-violating decay amplitudes. Given the small value of $(1 - |\eta_{00}/\eta_{+-}|)$, the value of $\phi_{00} - \phi_{+-}$ provides a measure of CPT violation in $K_L^0 \to 2\pi$ decay. Results from CERN [1] and Fermilab [2] indicate no CPT-violating effect.

CP AND T INVARIANCE

Given CPT invariance, CP violation and T violation are equivalent. The original evidence for CP violation came from the measurement of $|\eta_{+-}| = |A(K_L^0 \to \pi^+\pi^-)/A(K_S^0 \to \pi^+\pi^-)| = (2.232 \pm 0.011) \times 10^{-3}$. This could be explained in terms of K^0–$\overline{K}^0$ mixing, which also leads to the asymmetry $[\Gamma(K_L^0 \to \pi^- e^+ \nu) - \Gamma(K_L^0 \to \pi^+ e^- \overline{\nu})]/[\text{sum}] = (0.334 \pm 0.007)\%$. Evidence for CP violation in the kaon decay amplitude comes from the measurement of $(1 - |\eta_{00}/\eta_{+-}|)/3 = Re(\epsilon'/\epsilon) = (1.66 \pm 0.23) \times 10^{-3}$. In the Standard Model much larger CP-violating effects are expected. The first of these, which is associated with B–$\overline{B}$ mixing, is the parameter $sin(2\beta)$ now measured quite accurately to be 0.682 ± 0.019. A number of other CP-violating observables are being measured in B decays; direct evidence for CP violation in the B decay amplitude comes from the asymmetry $[\Gamma(\overline{B}^0 \to K^-\pi^+) - \Gamma(B^0 \to K^+\pi^-)]/[\text{sum}] = -0.082 \pm 0.006$. Direct tests of T violation are much more difficult; a measurement by CPLEAR of the difference between the oscillation probabilities of K^0 to $\overline{K^0}$ and $\overline{K^0}$ to K^0 is related to T violation [3]. A nonzero value of the electric dipole moment of the neutron and electron requires both P and T violation. The current experimental results are $< 2.9 \times 10^{-26}$ e cm (neutron), and $< (10.5 \pm 0.07) \times 10^{-28}$ e cm (electron). The BABAR experiment has reported the first direct observation of T violation in the B system. The measured T-violating parameters in the time evolution of the neutral B mesons are $\Delta S_T^+ = -1.37 \pm 0.15$ and $\Delta S_T^- = 1.17 \pm 0.21$, with a significance of 14σ [4]. This observation of T violation, with exchange of initial and final states of the neutral B, was made possible in a B-factory using the Einstein-Podolsky-Rosen Entanglement of the two B's produced in the decay of the $\Upsilon(4S)$ and the two time-ordered decays of the B's as filtering measurements of the meson state [5].

CONSERVATION OF LEPTON NUMBERS

Present experimental evidence and the standard electroweak theory are consistent with the absolute conservation of three separate lepton numbers: electron number L_e, muon number L_μ, and tau number L_τ, except for the effect of neutrino mixing associated with neutrino masses. Searches for violations are of the following types:

a) $\Delta L = 2$ for one type of charged lepton. The best limit comes from the search for neutrinoless double beta decay $(Z, A) \to (Z + 2, A) + e^- + e^-$. The best laboratory limit is $t_{1/2} > 2.1 \times 10^{25}$ yr (CL=90%) for ^{76}Ge.

b) Conversion of one charged-lepton type to another. For purely leptonic processes, the best limits are on $\mu \to e\gamma$ and $\mu \to 3e$, measured as $\Gamma(\mu \to e\gamma)/\Gamma(\mu \to \text{all}) < 5.7 \times 10^{-13}$ and $\Gamma(\mu \to 3e)/\Gamma(\mu \to \text{all}) < 1.0 \times 10^{-12}$. For semileptonic processes, the best limit comes from the coherent conversion process in a muonic atom, $\mu^- + (Z, A) \to e^- + (Z, A)$, measured as $\Gamma(\mu^-\text{Ti} \to e^-\text{Ti})/\Gamma(\mu^-\text{Ti} \to \text{all}) < 4.3 \times 10^{-12}$. Of special interest is the case in which the hadronic flavor also changes, as in $K_L \to e\mu$ and $K^+ \to \pi^+ e^- \mu^+$, measured as $\Gamma(K_L \to e\mu)/\Gamma(K_L \to \text{all}) < 4.7 \times 10^{-12}$ and $\Gamma(K^+ \to \pi^+ e^- \mu^+)/\Gamma(K^+ \to \text{all}) < 1.3 \times 10^{-11}$. Limits on the conversion of τ into e or μ are found in τ decay and are much less stringent than those for $\mu \to e$ conversion, *e.g.*, $\Gamma(\tau \to \mu\gamma)/\Gamma(\tau \to \text{all}) < 4.4 \times 10^{-8}$ and $\Gamma(\tau \to e\gamma)/\Gamma(\tau \to \text{all}) < 3.3 \times 10^{-8}$.

c) Conversion of one type of charged lepton into another type of charged antilepton. The case most studied is $\mu^- + (Z, A) \to e^+ + (Z - 2, A)$, the strongest limit being $\Gamma(\mu^-\text{Ti} \to e^+\text{Ca})/\Gamma(\mu^-\text{Ti} \to \text{all}) < 3.6 \times 10^{-11}$.

d) Neutrino oscillations. It is expected even in the standard electroweak theory that the lepton numbers are not separately conserved, as a consequence of lepton mixing analogous

to Cabibbo-Kobayashi-Maskawa quark mixing. However, if the only source of lepton-number violation is the mixing of low-mass neutrinos then processes such as $\mu \to e\gamma$ are expected to have extremely small unobservable probabilities. For small neutrino masses, the lepton-number violation would be observed first in neutrino oscillations, which have been the subject of extensive experimental studies. Compelling evidence for neutrino mixing has come from atmospheric, solar, accelerator, and reactor neutrinos. Recently, the reactor neutrino experiments have measured the last neutrino mixing angle θ_{13} and found it to be relatively large. For a comprehensive review on neutrino mixing, including the latest results on θ_{13}, see the review *"Neutrino Mass, Mixing, and Oscillations"* by K. Nakamura and S.T. Petcov in this edition of RPP.

CONSERVATION OF HADRONIC FLAVORS

In strong and electromagnetic interactions, hadronic flavor is conserved, *i.e.* the conversion of a quark of one flavor (d, u, s, c, b, t) into a quark of another flavor is forbidden. In the Standard Model, the weak interactions violate these conservation laws in a manner described by the Cabibbo-Kobayashi-Maskawa mixing (see the section "Cabibbo-Kobayashi-Maskawa Mixing Matrix"). The way in which these conservation laws are violated is tested as follows:

(a) $\Delta S = \Delta Q$ rule. In the strangeness-changing semileptonic decay of strange particles, the strangeness change equals the change in charge of the hadrons. Tests come from limits on decay rates such as $\Gamma(\Sigma^+ \to ne^+\nu)/\Gamma(\Sigma^+ \to \text{all}) < 5 \times 10^{-6}$, and from a detailed analysis of $K_L \to \pi e\nu$, which yields the parameter x, measured to be $(\mathrm{Re}\, x,\ \mathrm{Im}\, x) = (-0.002 \pm 0.006,\ 0.0012 \pm 0.0021)$. Corresponding rules are $\Delta C = \Delta Q$ and $\Delta B = \Delta Q$.

(b) Change of flavor by two units. In the Standard Model this occurs only in second-order weak interactions. The classic example is $\Delta S = 2$ via $K^0 - \overline{K}^0$ mixing, which is directly measured by $m(K_L) - m(K_S) = (0.5293 \pm 0.0009) \times 10^{10}\ \hbar s^{-1}$. The $\Delta B = 2$ transitions in the B^0 and B_s^0 systems via mixing are also well established. The measured mass differences between the eigenstates are $(m_{B^0_{\rm H}} - m_{B^0_{\rm L}}) = (0.510 \pm 0.003) \times 10^{12}\ \hbar s^{-1}$ and $(m_{B^0_{\rm sH}} - m_{B^0_{\rm sL}}) = (17.761 \pm 0.022) \times 10^{12}\ \hbar s^{-1}$. There is now strong evidence of $\Delta C = 2$ transition in the charm sector with the mass difference $m_{D^0_H} - m_{D^0_L} = (0.95^{+0.41}_{-0.44}) \times 10^{10}\ \hbar s^{-1}$. All results are consistent with the second-order calculations in the Standard Model.

(c) Flavor-changing neutral currents. In the Standard Model the neutral-current interactions do not change flavor. The low rate $\Gamma(K_L \to \mu^+\mu^-)/\Gamma(K_L \to \text{all}) = (6.84 \pm 0.11) \times 10^{-9}$ puts limits on such interactions; the nonzero value for this rate is attributed to a combination of the weak and electromagnetic interactions. The best test should come from $K^+ \to \pi^+\nu\overline{\nu}$, which occurs in the Standard Model only as a second-order weak process with a branching fraction of (0.4 to 1.2)$\times 10^{-10}$. Combining results from BNL-E787 and BNL-E949 experiments yield $\Gamma(K^+ \to \pi^+\nu\overline{\nu})/\Gamma(K^+ \to \text{all}) = (1.7 \pm 1.1) \times 10^{-10}$[6]. Limits for charm-changing or bottom-changing neutral currents are less stringent: $\Gamma(D^0 \to \mu^+\mu^-)/\Gamma(D^0 \to \text{all}) < 6.2 \times 10^{-9}$ and $\Gamma(B^0 \to \mu^+\mu^-)/\Gamma(B^0 \to \text{all}) < 6.3 \times 10^{-10}$. One cannot isolate flavor-changing neutral current (FCNC) effects in non leptonic decays. For example, the FCNC transition $s \to d + (\overline{u} + u)$ is equivalent to the charged-current transition $s \to u + (\overline{u} + d)$. Tests for FCNC are therefore limited to hadron decays into lepton pairs. Such decays are expected only in second-order in the electroweak coupling in the Standard Model. The LHCb and CMS experiments have recently observed the FCNC decay of $B_s^0 \to \mu^+\mu^-$. The current world average value is $\Gamma(B_s^0 \to \mu^+\mu^-)/\Gamma(B_s^0 \to \text{all}) = (3.1 \pm 0.7) \times 10^{-9}$, which is consistent with the Standard Model expectation.

Unless otherwise stated, limits are given at the 90% confidence level, while errors are given as ±1 standard deviation.

References

1. R. Carosi *et al.*, Phys. Lett. **B237**, 303 (1990).
2. E. Abouzaid *et al.*, Phys. Rev. **D83**, 092001 (2011); B. Schwingenheuer *et al.*, Phys. Rev. Lett. **74**, 4376 (1995).
3. A. Angelopoulos *et al.*, Phys. Lett. **B444**, 43 (1998); L. Wolfenstein, Phys. Rev. Lett. **83**, 911 (1999).
4. J.P. Lees *et al.*, Phys. Rev. Lett. **109**, 211801 (2012).
5. M.C. Banuls and J. Bernabeu, Phys. Lett. **B464**, 117 (1999); Nucl. Phys. **B590**, 19 (2000).
6. A.V. Artamonov *et al.*, Phys. Rev. Lett. **101**, 191802 (2008).

TESTS OF DISCRETE SPACE-TIME SYMMETRIES

CHARGE CONJUGATION (C) INVARIANCE

$\Gamma(\pi^0 \to 3\gamma)/\Gamma_{\rm total}$		$<3.1 \times 10^{-8}$, CL = 90%
η C-nonconserving decay parameters		
$\pi^+\pi^-\pi^0$ left-right asymmetry		$(0.09^{+0.11}_{-0.12}) \times 10^{-2}$
$\pi^+\pi^-\pi^0$ sextant asymmetry		$(0.12^{+0.10}_{-0.11}) \times 10^{-2}$
$\pi^+\pi^-\pi^0$ quadrant asymmetry		$(-0.09 \pm 0.09) \times 10^{-2}$
$\pi^+\pi^-\gamma$ left-right asymmetry		$(0.9 \pm 0.4) \times 10^{-2}$
$\pi^+\pi^-\gamma$ parameter β (D-wave)		-0.02 ± 0.07 (S = 1.3)
$\Gamma(\eta \to \pi^0\gamma)/\Gamma_{\rm total}$		$<9 \times 10^{-5}$, CL = 90%
$\Gamma(\eta \to 2\pi^0\gamma)/\Gamma_{\rm total}$		$<5 \times 10^{-4}$, CL = 90%
$\Gamma(\eta \to 3\pi^0\gamma)/\Gamma_{\rm total}$		$<6 \times 10^{-5}$, CL = 90%
$\Gamma(\eta \to 3\gamma)/\Gamma_{\rm total}$		$<1.6 \times 10^{-5}$, CL = 90%
$\Gamma(\eta \to \pi^0 e^+ e^-)/\Gamma_{\rm total}$	[a]	$<4 \times 10^{-5}$, CL = 90%
$\Gamma(\eta \to \pi^0 \mu^+ \mu^-)/\Gamma_{\rm total}$	[a]	$<5 \times 10^{-6}$, CL = 90%
$\Gamma(\omega(782) \to \eta\pi^0)/\Gamma_{\rm total}$		$<2.1 \times 10^{-4}$, CL = 90%
$\Gamma(\omega(782) \to 2\pi^0)/\Gamma_{\rm total}$		$<2.1 \times 10^{-4}$, CL = 90%
$\Gamma(\omega(782) \to 3\pi^0)/\Gamma_{\rm total}$		$<2.3 \times 10^{-4}$, CL = 90%
asymmetry parameter for $\eta'(958) \to \pi^+\pi^-\gamma$ decay		-0.03 ± 0.04
$\Gamma(\eta'(958) \to \pi^0 e^+ e^-)/\Gamma_{\rm total}$	[a]	$<1.4 \times 10^{-3}$, CL = 90%
$\Gamma(\eta'(958) \to \eta e^+ e^-)/\Gamma_{\rm total}$	[a]	$<2.4 \times 10^{-3}$, CL = 90%
$\Gamma(\eta'(958) \to 3\gamma)/\Gamma_{\rm total}$		$<1.0 \times 10^{-4}$, CL = 90%
$\Gamma(\eta'(958) \to \mu^+\mu^-\pi^0)/\Gamma_{\rm total}$	[a]	$<6.0 \times 10^{-5}$, CL = 90%
$\Gamma(\eta'(958) \to \mu^+\mu^-\eta)/\Gamma_{\rm total}$	[a]	$<1.5 \times 10^{-5}$, CL = 90%
$\Gamma(J/\psi(1S) \to \gamma\gamma)/\Gamma_{\rm total}$		$<5 \times 10^{-6}$, CL = 90%

Tests of Conservation Laws

PARITY (P) INVARIANCE

e electric dipole moment		$<10.5 \times 10^{-28}$ e cm, CL = 90%
μ electric dipole moment		$(-0.1 \pm 0.9) \times 10^{-19}$ e cm
Re(d_τ = τ electric dipole moment)		-0.220 to 0.45×10^{-16} e cm, CL = 95%
$\Gamma(\eta \to \pi^+\pi^-)/\Gamma_{\rm total}$		$<1.3 \times 10^{-5}$, CL = 90%
$\Gamma(\eta \to 2\pi^0)/\Gamma_{\rm total}$		$<3.5 \times 10^{-4}$, CL = 90%
$\Gamma(\eta \to 4\pi^0)/\Gamma_{\rm total}$		$<6.9 \times 10^{-7}$, CL = 90%
$\Gamma(\eta'(958) \to \pi^+\pi^-)/\Gamma_{\rm total}$		$<6 \times 10^{-5}$, CL = 90%
$\Gamma(\eta'(958) \to \pi^0\pi^0)/\Gamma_{\rm total}$		$<4 \times 10^{-4}$, CL = 90%
$\Gamma(\eta_c(1S) \to \pi^+\pi^-)/\Gamma_{\rm total}$		$<1.1 \times 10^{-4}$, CL = 90%
$\Gamma(\eta_c(1S) \to \pi^0\pi^0)/\Gamma_{\rm total}$		$<3.5 \times 10^{-5}$, CL = 90%
$\Gamma(\eta_c(1S) \to K^+K^-)/\Gamma_{\rm total}$		$<6 \times 10^{-4}$, CL = 90%
$\Gamma(\eta_c(1S) \to K^0_S K^0_S)/\Gamma_{\rm total}$		$<3.1 \times 10^{-4}$, CL = 90%
p electric dipole moment		$<0.54 \times 10^{-23}$ e cm
n electric dipole moment		$<0.29 \times 10^{-25}$ e cm, CL = 90%
Λ electric dipole moment		$<1.5 \times 10^{-16}$ e cm, CL = 95%

TIME REVERSAL (T) INVARIANCE

e electric dipole moment		$<10.5 \times 10^{-28}$ e cm, CL = 90%
μ electric dipole moment		$(-0.1 \pm 0.9) \times 10^{-19}$ e cm
μ decay parameters		
transverse e^+ polarization normal to plane of μ spin, e^+ momentum		$(-2 \pm 8) \times 10^{-3}$
α'/A		$(-10 \pm 20) \times 10^{-3}$
β'/A		$(2 \pm 7) \times 10^{-3}$
Re(d_τ = τ electric dipole moment)		-0.220 to 0.45×10^{-16} e cm, CL = 95%
P_T in $K^+ \to \pi^0\mu^+\nu_\mu$		$(-1.7 \pm 2.5) \times 10^{-3}$
P_T in $K^+ \to \mu^+\nu_\mu\gamma$		$(-0.6 \pm 1.9) \times 10^{-2}$
Im(ξ) in $K^+ \to \pi^0\mu^+\nu_\mu$ decay (from transverse μ pol.)		-0.006 ± 0.008
asymmetry A_T in K^0-$\overline{K}^0$ mixing		$(6.6 \pm 1.6) \times 10^{-3}$
Im(ξ) in $K^0_{\mu 3}$ decay (from transverse μ pol.)		-0.007 ± 0.026
$A_T(D^\pm \to K^0_S K^\pm\pi^+\pi^-)$	[b]	$(-12 \pm 11) \times 10^{-3}$
$A_T(D^0 \to K^+K^-\pi^+\pi^-)$	[b]	$(1 \pm 7) \times 10^{-3}$
$A_T(D^\pm_s \to K^0_S K^\pm\pi^+\pi^-)$	[b]	$(-14 \pm 8) \times 10^{-3}$
ΔS^+_T ($S^-_{\ell^-,K^0_S} - S^+_{\ell^+,K^0_S}$)		-1.37 ± 0.15
ΔS^-_T ($S^+_{\ell^-,K^0_S} - S^-_{\ell^+,K^0_S}$)		1.17 ± 0.21
ΔC^+_T ($C^-_{\ell^-,K^0_S} - C^+_{\ell^+,K^0_S}$)		0.10 ± 0.16
ΔC^-_T ($C^+_{\ell^-,K^0_S} - C^-_{\ell^+,K^0_S}$)		0.04 ± 0.16
p electric dipole moment		$<0.54 \times 10^{-23}$ e cm
n electric dipole moment		$<0.29 \times 10^{-25}$ e cm, CL = 90%
$n \to pe^-\overline{\nu}_e$ decay parameters		
ϕ_{AV}, phase of g_A relative to g_V	[c]	$(180.017 \pm 0.026)^\circ$
triple correlation coefficient D	[d]	$(-1.2 \pm 2.0) \times 10^{-4}$
triple correlation coefficient R	[d]	0.004 ± 0.013
Λ electric dipole moment		$<1.5 \times 10^{-16}$ e cm, CL = 95%
triple correlation coefficient D for $\Sigma^- \to ne^-\overline{\nu}_e$		0.11 ± 0.10

CP INVARIANCE

Re(d^W_τ)		$<0.50 \times 10^{-17}$ e cm, CL = 95%
Im(d^W_τ)		$<1.1 \times 10^{-17}$ e cm, CL = 95%
$\eta \to \pi^+\pi^- e^+e^-$ decay-plane asymmetry		$(-0.6 \pm 3.1) \times 10^{-2}$
$\Gamma(\eta \to \pi^+\pi^-)/\Gamma_{\rm total}$		$<1.3 \times 10^{-5}$, CL = 90%
$\Gamma(\eta \to 2\pi^0)/\Gamma_{\rm total}$		$<3.5 \times 10^{-4}$, CL = 90%
$\Gamma(\eta \to 4\pi^0)/\Gamma_{\rm total}$		$<6.9 \times 10^{-7}$, CL = 90%
$\Gamma(\eta'(958) \to \pi^+\pi^-)/\Gamma_{\rm total}$		$<6 \times 10^{-5}$, CL = 90%
$\Gamma(\eta'(958) \to \pi^0\pi^0)/\Gamma_{\rm total}$		$<4 \times 10^{-4}$, CL = 90%
$K^\pm \to \pi^\pm\pi^+\pi^-$ rate difference/average		(0.08 ± 0.12)%
$K^\pm \to \pi^\pm\pi^0\pi^0$ rate difference/average		(0.0 ± 0.6)%
$K^\pm \to \pi^\pm\pi^0\gamma$ rate difference/average		(0.9 ± 3.3)%
$K^\pm \to \pi^\pm\pi^+\pi^-$ $(g_+ - g_-)$ / $(g_+ + g_-)$		$(-1.5 \pm 2.2) \times 10^{-4}$
$K^\pm \to \pi^\pm\pi^0\pi^0$ $(g_+ - g_-)$ / $(g_+ + g_-)$		$(1.8 \pm 1.8) \times 10^{-4}$
$\Delta(K^\pm_{\pi ee}) = \frac{\Gamma(K^+_{\pi ee})-\Gamma(K^-_{\pi ee})}{\Gamma(K^+_{\pi ee})+\Gamma(K^-_{\pi ee})}$		$(-2.2 \pm 1.6) \times 10^{-2}$
$\Delta(K^\pm_{\pi\mu\mu}) = \frac{\Gamma(K^+_{\pi\mu\mu})-\Gamma(K^-_{\pi\mu\mu})}{\Gamma(K^+_{\pi\mu\mu})+\Gamma(K^-_{\pi\mu\mu})}$		0.010 ± 0.023
$\Delta(K^\pm_{\pi\pi\gamma}) = \frac{\Gamma(K^+_{\pi\pi\gamma})-\Gamma(K^-_{\pi\pi\gamma})}{\Gamma(K^+_{\pi\pi\gamma})+\Gamma(K^-_{\pi\pi\gamma})}$		$(0.0 \pm 1.2) \times 10^{-3}$
A_S = [$\Gamma(K^0_S \to \pi^- e^+\nu_e)$ - $\Gamma(K^0_S \to \pi^+ e^-\overline{\nu}_e)$] / SUM		$(2 \pm 10) \times 10^{-3}$
Im(η_{+-0}) = Im(A($K^0_S \to \pi^+\pi^-\pi^0$, CP-violating) / A($K^0_L \to \pi^+\pi^-\pi^0$))		-0.002 ± 0.009
Im(η_{000}) = Im($A(K^0_S \to \pi^0\pi^0\pi^0)/A(K^0_L \to \pi^0\pi^0\pi^0)$)		$(-0.1 \pm 1.6) \times 10^{-2}$
$\lvert\eta_{000}\rvert = \lvert A(K^0_S \to 3\pi^0)/A(K^0_L \to 3\pi^0)\rvert$		<0.0088, CL = 90%
CP asymmetry A in $K^0_S \to \pi^+\pi^- e^+e^-$		(-0.4 ± 0.8)%
$\Gamma(K^0_S \to 3\pi^0)/\Gamma_{\rm total}$		$<2.6 \times 10^{-8}$, CL = 90%
linear coefficient j for $K^0_L \to \pi^+\pi^-\pi^0$		0.0012 ± 0.0008
quadratic coefficient f for $K^0_L \to \pi^+\pi^-\pi^0$		0.004 ± 0.006
$\lvert\epsilon'_{+-\gamma}\rvert/\epsilon$ for $K^0_L \to \pi^+\pi^-\gamma$		<0.3, CL = 90%
$\lvert g_{E1}\rvert$ for $K^0_L \to \pi^+\pi^-\gamma$		<0.21, CL = 90%
$\Gamma(K^0_L \to \pi^0\mu^+\mu^-)/\Gamma_{\rm total}$	[e]	$<3.8 \times 10^{-10}$, CL = 90%
$\Gamma(K^0_L \to \pi^0 e^+e^-)/\Gamma_{\rm total}$	[e]	$<2.8 \times 10^{-10}$, CL = 90%
$\Gamma(K^0_L \to \pi^0\nu\overline{\nu})/\Gamma_{\rm total}$	[f]	$<2.6 \times 10^{-8}$, CL = 90%
$A_{CP}(D^\pm \to \mu^\pm\nu)$		(8 ± 8)%
$A_{CP}(D^\pm \to K^0_S\pi^\pm)$		(-0.41 ± 0.09)%
$A_{CP}(D^\pm \to K^\mp 2\pi^\pm)$		(-0.1 ± 1.0)%
$A_{CP}(D^\pm \to K^\mp\pi^\pm\pi^\pm\pi^0)$		(1.0 ± 1.3)%
$A_{CP}(D^\pm \to K^0_S\pi^\pm\pi^0)$		(0.3 ± 0.9)%
$A_{CP}(D^\pm \to K^0_S\pi^\pm\pi^+\pi^-)$		(0.1 ± 1.3)%
$A_{CP}(D^\pm \to \pi^\pm\pi^0)$		(2.9 ± 2.9)%
$A_{CP}(D^\pm \to \pi^\pm\eta)$		(1.0 ± 1.5)% (S = 1.4)
$A_{CP}(D^\pm \to \pi^\pm\eta'(958))$		(-0.5 ± 1.2)% (S = 1.1)
$A_{CP}(D^\pm \to K^0_S K^\pm)$		(-0.11 ± 0.25)%
$A_{CP}(D^\pm \to K^+K^-\pi^\pm)$		(0.36 ± 0.29)%
$A_{CP}(D^\pm \to K^\pm K^{*0})$		(-0.3 ± 0.4)%
$A_{CP}(D^\pm \to \phi\pi^\pm)$		(0.09 ± 0.19)% (S = 1.2)
$A_{CP}(D^\pm \to K^\pm K^*_0(1430)^0)$		(8^{+7}_{-6})%
$A_{CP}(D^\pm \to K^\pm K^*_2(1430)^0)$		(43^{+20}_{-26})%
$A_{CP}(D^\pm \to K^\pm K^*_0(800))$		(-12^{+18}_{-13})%
$A_{CP}(D^\pm \to a_0(1450)^0\pi^\pm)$		(-19^{+14}_{-16})%
$A_{CP}(D^\pm \to \phi(1680)\pi^\pm)$		(-9 ± 26)%
$A_{CP}(D^\pm \to \pi^+\pi^-\pi^\pm)$		(-2 ± 4)%
$A_{CP}(D^\pm \to K^0_S K^\pm\pi^+\pi^-)$		(-4 ± 7)%
$A_{CP}(D^\pm \to K^\pm\pi^0)$		(-4 ± 11)%
$\lvert q/p\rvert$ of D^0-$\overline{D}^0$ mixing		$0.92^{+0.12}_{-0.09}$
A_Γ of D^0-$\overline{D}^0$ mixing		$(-0.125 \pm 0.526) \times 10^{-3}$
Where there is ambiguity, the CP test is labelled by the D^0 decay mode.		
$A_{CP}(D^0 \to K^+K^-)$		(-0.21 ± 0.17)%
$A_{CP}(D^0 \to K^0_S K^0_S)$		(-23 ± 19)%
$A_{CP}(D^0 \to \pi^+\pi^-)$		(0.22 ± 0.21)%
$A_{CP}(D^0 \to \pi^0\pi^0)$		(0 ± 5)%
$A_{CP}(D^0 \to \pi^+\pi^-\pi^0)$		(0.3 ± 0.4)%
$A_{CP}(D^0 \to \rho(770)^+\pi^- \to \pi^+\pi^-\pi^0)$	[g]	(1.2 ± 0.9)%
$A_{CP}(D^0 \to \rho(770)^0\pi^0 \to \pi^+\pi^-\pi^0)$	[g]	(-3.1 ± 3.0)%
$A_{CP}(D^0 \to \rho(770)^-\pi^+ \to \pi^+\pi^-\pi^0)$	[g]	(-1.0 ± 1.7)%
$A_{CP}(D^0 \to \rho(1450)^+\pi^- \to \pi^+\pi^-\pi^0)$	[g]	(0 ± 70)%
$A_{CP}(D^0 \to \rho(1450)^0\pi^0 \to \pi^+\pi^-\pi^0)$	[g]	(-20 ± 40)%
$A_{CP}(D^0 \to \rho(1450)^-\pi^+ \to \pi^+\pi^-\pi^0)$	[g]	(6 ± 9)%
$A_{CP}(D^0 \to \rho(1700)^+\pi^- \to \pi^+\pi^-\pi^0)$	[g]	(-5 ± 14)%
$A_{CP}(D^0 \to \rho(1700)^0\pi^0 \to \pi^+\pi^-\pi^0)$	[g]	(13 ± 9)%
$A_{CP}(D^0 \to \rho(1700)^-\pi^+ \to \pi^+\pi^-\pi^0)$	[g]	(8 ± 11)%
$A_{CP}(D^0 \to f_0(980)\pi^0 \to \pi^+\pi^-\pi^0)$	[g]	(0 ± 35)%
$A_{CP}(D^0 \to f_0(1370)\pi^0 \to \pi^+\pi^-\pi^0)$	[g]	(25 ± 18)%
$A_{CP}(D^0 \to f_0(1500)\pi^0 \to \pi^+\pi^-\pi^0)$	[g]	(0 ± 18)%
$A_{CP}(D^0 \to f_0(1710)\pi^0 \to \pi^+\pi^-\pi^0)$	[g]	(0 ± 24)%
$A_{CP}(D^0 \to f_2(1270)\pi^0 \to \pi^+\pi^-\pi^0)$	[g]	(-4 ± 6)%
$A_{CP}(D^0 \to \sigma(400)\pi^0 \to \pi^+\pi^-\pi^0)$	[g]	(6 ± 8)%
A_{CP}(nonresonant $D^0 \to \pi^+\pi^-\pi^0$)	[g]	(-13 ± 23)%
$A_{CP}(D^0 \to K^+K^-\pi^0)$		(-1.0 ± 1.7)%

Unless otherwise stated, limits are given at the 90% confidence level, while errors are given as ± 1 standard deviation.

$A_{CP}(D^0 \to K^*(892)^+ K^- \to K^+ K^- \pi^0)$	[g]	$(-0.9 \pm 1.3)\%$
$A_{CP}(D^0 \to K^*(1410)^+ K^- \to K^+ K^- \pi^0)$	[g]	$(-21 \pm 24)\%$
$A_{CP}(D^0 \to (K^+ \pi^0)_S K^- \to K^+ K^- \pi^0)$	[g]	$(7 \pm 15)\%$
$A_{CP}(D^0 \to \phi(1020)\pi^0 \to K^+ K^- \pi^0)$	[g]	$(1.1 \pm 2.2)\%$
$A_{CP}(D^0 \to f_0(980)\pi^0 \to K^+ K^- \pi^0)$	[g]	$(-3 \pm 19)\%$
$A_{CP}(D^0 \to a_0(980)^0 \pi^0 \to K^+ K^- \pi^0)$	[g]	$(-5 \pm 16)\%$
$A_{CP}(D^0 \to f_2'(1525)\pi^0 \to K^+ K^- \pi^0)$	[g]	$(0 \pm 160)\%$
$A_{CP}(D^0 \to K^*(892)^- K^+ \to K^+ K^- \pi^0)$	[g]	$(-5 \pm 4)\%$
$A_{CP}(D^0 \to K^*(1410)^- K^+ \to K^+ K^- \pi^0)$	[g]	$(-17 \pm 29)\%$
$A_{CP}(D^0 \to (K^- \pi^0)_{S-wave} K^+ \to K^+ K^- \pi^0)$	[g]	$(-10 \pm 40)\%$
$A_{CP}(D^0 \to K^0_S \pi^0)$		$(-0.27 \pm 0.21)\%$
$A_{CP}(D^0 \to K^0_S \eta)$		$(0.5 \pm 0.5)\%$
$A_{CP}(D^0 \to K^0_S \eta')$		$(1.0 \pm 0.7)\%$
$A_{CP}(D^0 \to K^0_S \phi)$		$(-3 \pm 9)\%$
$A_{CP}(D^0 \to K^- \pi^+)$		$(0.1 \pm 0.7)\%$
$A_{CP}(D^0 \to K^+ \pi^-)$		$(0.0 \pm 1.6)\%$
$A_{CP}(D^0 \to K^- \pi^+ \pi^0)$		$(0.2 \pm 0.9)\%$
$A_{CP}(D^0 \to K^+ \pi^- \pi^0)$		$(0 \pm 5)\%$
$A_{CP}(D^0 \to K^0_S \pi^+ \pi^-)$		$(-0.1 \pm 0.8)\%$
$A_{CP}(D^0 \to K^*(892)^- \pi^+ \to K^0_S \pi^+ \pi^-)$		$(0.4 \pm 0.5)\%$
$A_{CP}(D^0 \to K^*(892)^+ \pi^- \to K^0_S \pi^+ \pi^-)$		$(1 \pm 6)\%$
$A_{CP}(D^0 \to K^0_S \rho^0 \to K^0_S \pi^+ \pi^-)$		$(-0.1 \pm 0.5)\%$
$A_{CP}(D^0 \to K^0_S \omega \to K^0_S \pi^+ \pi^-)$		$(-13 \pm 7)\%$
$A_{CP}(D^0 \to K^0_S f_0(980) \to K^0_S \pi^+ \pi^-)$		$(-0.4 \pm 2.7)\%$
$A_{CP}(D^0 \to K^0_S f_2(1270) \to K^0_S \pi^+ \pi^-)$		$(-4 \pm 5)\%$
$A_{CP}(D^0 \to K^0_S f_0(1370) \to K^0_S \pi^+ \pi^-)$		$(-1 \pm 9)\%$
$A_{CP}(D^0 \to \overline{K}^0 \rho^0(1450) \to K^0_S \pi^+ \pi^-)$		$(-4 \pm 10)\%$
$A_{CP}(D^0 \to \overline{K}^0 f_0(600) \to K^0_S \pi^+ \pi^-)$		$(-3 \pm 5)\%$
$A_{CP}(D^0 \to K^*(1410)^- \pi^+ \to K^0_S \pi^+ \pi^-)$		$(-2 \pm 9)\%$
$A_{CP}(D^0 \to K^*_0(1430)^- \pi^+ \to K^0_S \pi^+ \pi^-)$		$(4 \pm 4)\%$
$A_{CP}(D^0 \to K^*_0(1430)^- \pi^+ \to K^0_S \pi^+ \pi^-)$		$(12 \pm 15)\%$
$A_{CP}(D^0 \to K^*_2(1430)^- \pi^+ \to K^0_S \pi^+ \pi^-)$		$(3 \pm 6)\%$
$A_{CP}(D^0 \to K^*_2(1430)^+ \pi^- \to K^0_S \pi^+ \pi^-)$		$(-10 \pm 32)\%$
$A_{CP}(D^0 \to K^*(1680)^- \pi^+ \to K^0_S \pi^+ \pi^-)$		—
$A_{CP}(D^0 \to K^- \pi^+ \pi^+ \pi^-)$		$(0.7 \pm 1.0)\%$
$A_{CP}(D^0 \to K^+ \pi^- \pi^+ \pi^-)$		$(-2 \pm 4)\%$
$A_{CP}(D^0 \to K^+ K^- \pi^+ \pi^-)$		$(-8 \pm 7)\%$
$A_{CP}(D^0 \to K^*_1(1270)^+ K^- \to K^{*0} \pi^+ K^-)$		$(-1 \pm 10)\%$
$A_{CP}(D^0 \to K^*_1(1270)^- K^+ \to \overline{K}^{*0} \pi^- K^+)$		$(-10 \pm 32)\%$
$A_{CP}(D^0 \to K^*_1(1270)^+ K^- \to \rho^0 K^+ K^-)$		$(-7 \pm 17)\%$
$A_{CP}(D^0 \to K^*_1(1270)^- K^+ \to \rho^0 K^- K^+)$		$(10 \pm 13)\%$
$A_{CP}(D^0 \to K^*(1410)^+ K^- \to K^{*0} \pi^+ K^-)$		$(-20 \pm 17)\%$
$A_{CP}(D^0 \to K^*(1410)^- K^+ \to \overline{K}^{*0} \pi^- K^+)$		$(-1 \pm 14)\%$
$A_{CP}(D^0 \to K^{*0} \overline{K}^{*0}$ S-wave)		$(10 \pm 14)\%$
$A_{CP}(D^0 \to \phi \rho^0$ S-wave)		$(-3 \pm 5)\%$
$A_{CP}(D^0 \to \phi \rho^0$ D-wave)		$(-37 \pm 19)\%$
$A_{CP}(D^0 \to \phi(\pi^+ \pi^-)_{S-wave})$		$(-9 \pm 10)\%$
$\Delta A^{D^0}_{CP} = A_{CP}(K^+ K^-) - A_{CP}(\pi^+ \pi^-)$		$(-0.46 \pm 0.25)\%$ (S = 1.8)
$A_{CP}(D^\pm_s \to \mu^\pm \nu)$		$(5 \pm 6)\%$
$A_{CP}(D^\pm_s \to K^\pm K^0_S)$		$(0.08 \pm 0.26)\%$
$A_{CP}(D^\pm_s \to K^+ K^- \pi^\pm)$		$(-0.5 \pm 0.9)\%$
$A_{CP}(D^\pm_s \to K^+ K^- \pi^\pm \pi^0)$		$(0.0 \pm 3.0)\%$
$A_{CP}(D^\pm_s \to K^0_S K^\mp 2\pi^\pm)$		$(4.1 \pm 2.8)\%$
$A_{CP}(D^\pm_s \to \pi^+ \pi^- \pi^\pm)$		$(-0.7 \pm 3.1)\%$
$A_{CP}(D^\pm_s \to \pi^\pm \eta)$		$(1.1 \pm 3.1)\%$
$A_{CP}(D^\pm_s \to \pi^\pm \eta')$		$(-2.2 \pm 2.3)\%$
$A_{CP}(D^\pm_s \to K^\pm \pi^0)$		$(-27 \pm 24)\%$
$A_{CP}(D^\pm_s \to K^0_S \pi^\pm)$		$(1.2 \pm 1.0)\%$ (S = 1.3)
$A_{CP}(D^\pm_s \to K^\pm \pi^+ \pi^-)$		$(4 \pm 5)\%$
$A_{CP}(D^\pm_s \to K^\pm \eta)$		$(9 \pm 15)\%$
$A_{CP}(D^\pm_s \to K^\pm \eta'(958))$		$(6 \pm 19)\%$
$A_{CP}(B^+ \to J/\psi(1S) K^+)$		0.003 ± 0.006 (S = 1.8)
$A_{CP}(B^+ \to J/\psi(1S) \pi^+)$		$(0.1 \pm 2.8) \times 10^{-2}$ (S = 1.2)
$A_{CP}(B^+ \to J/\psi \rho^+)$		-0.11 ± 0.14
$A_{CP}(B^+ \to J/\psi K^*(892)^+)$		-0.048 ± 0.033
$A_{CP}(B^+ \to \eta_c K^+)$		-0.02 ± 0.10 (S = 2.0)
$A_{CP}(B^+ \to \psi(2S) \pi^+)$		0.03 ± 0.06
$A_{CP}(B^+ \to \psi(2S) K^+)$		-0.024 ± 0.023
$A_{CP}(B^+ \to \psi(2S) K^*(892)^+)$		0.08 ± 0.21
$A_{CP}(B^+ \to \chi_{c1}(1P) \pi^+)$		0.07 ± 0.18
$A_{CP}(B^+ \to \chi_{c0} K^+)$		-0.20 ± 0.18 (S = 1.5)
$A_{CP}(B^+ \to \chi_{c1} K^+)$		-0.009 ± 0.033
$A_{CP}(B^+ \to \chi_{c1} K^*(892)^+)$		0.5 ± 0.5
$A_{CP}(B^+ \to \overline{D}^0 \pi^+)$		-0.007 ± 0.007
$A_{CP}(B^+ \to D_{CP(+1)} \pi^+)$		0.035 ± 0.024
$A_{CP}(B^+ \to D_{CP(-1)} \pi^+)$		0.017 ± 0.026
$A_{CP}(B^+ \to \overline{D}^0 K^+)$		0.01 ± 0.05 (S = 2.1)
$r_B(B^+ \to D^0 K^+)$		0.096 ± 0.008
$\delta_B(B^+ \to D^0 K^+)$		$(115 \pm 13)^\circ$
$r_B(B^+ \to \overline{D}^0 K^{*+})$		0.17 ± 0.11 (S = 2.3)
$\delta_B(B^+ \to D^0 K^{*+})$		$(155 \pm 70)^\circ$ (S = 2.0)
$A_{CP}(B^+ \to [K^- \pi^+]_D K^+)$		-0.58 ± 0.21
$A_{CP}(B^+ \to [K^- \pi^+]_{\overline{D}} K^*(892)^+)$		-0.3 ± 0.5
$A_{CP}(B^+ \to [K^- \pi^+]_D \pi^+)$		0.00 ± 0.09
$A_{CP}(B^+ \to [K^- \pi^+]_{(D\pi)} \pi^+)$		-0.09 ± 0.27
$A_{CP}(B^+ \to [K^- \pi^+]_{(D\gamma)} \pi^+)$		-0.7 ± 0.6
$A_{CP}(B^+ \to [K^- \pi^+]_{(D\pi)} K^+)$		0.8 ± 0.4
$A_{CP}(B^+ \to [K^- \pi^+]_{(D\gamma)} K^+)$		0.4 ± 1.0
$A_{CP}(B^+ \to [\pi^+ \pi^- \pi^0]_D K^+)$		-0.02 ± 0.15
$A_{ADS}(B^+ \to D \pi^+)$		0.14 ± 0.06
$A_{CP}(B^+ \to D_{CP(-1)} K^+)$		-0.10 ± 0.07
$A_{CP}(B^+ \to \overline{D}^{*0} \pi^+)$		-0.014 ± 0.015
$A_{CP}(B^+ \to (D^*_{CP(+1)})^0 \pi^+)$		-0.02 ± 0.05
$A_{CP}(B^+ \to (D^*_{CP(-1)})^0 \pi^+)$		-0.09 ± 0.05
$A_{CP}(B^+ \to D^{*0} K^+)$		-0.07 ± 0.04
$r^*_B(B^+ \to D^{*0} K^+)$		$0.114^{+0.023}_{-0.040}$ (S = 1.2)
$\delta^*_B(B^+ \to D^{*0} K^+)$		$(310^{+22}_{-28})^\circ$ (S = 1.3)
$A_{CP}(B^+ \to D^{*0}_{CP(+1)} K^+)$		-0.12 ± 0.08
$A_{CP}(B^+ \to D^*_{CP(-1)} K^+)$		0.07 ± 0.10
$A_{CP}(B^+ \to D_{CP(+1)} K^*(892)^+)$		0.09 ± 0.14
$A_{CP}(B^+ \to D_{CP(-1)} K^*(892)^+)$		-0.23 ± 0.22
$A_{CP}(B^+ \to D^+_s \phi)$		0.0 ± 0.4
$A_{CP}(B^+ \to D^{*+} \overline{D}^{*0})$		-0.15 ± 0.11
$A_{CP}(B^+ \to D^{*+} \overline{D}^0)$		-0.06 ± 0.13
$A_{CP}(B^+ \to D^+ \overline{D}^{*0})$		0.13 ± 0.18
$A_{CP}(B^+ \to D^+ \overline{D}^0)$		-0.03 ± 0.07
$A_{CP}(B^+ \to K^0_S \pi^+)$		-0.017 ± 0.016
$A_{CP}(B^+ \to K^+ \pi^0)$		0.037 ± 0.021
$A_{CP}(B^+ \to \eta' K^+)$		0.013 ± 0.017
$A_{CP}(B^+ \to \eta' K^*(892)^+)$		-0.26 ± 0.27
$A_{CP}(B^+ \to \eta' K^*_0(1430)^+)$		0.06 ± 0.20
$A_{CP}(B^+ \to \eta' K^*_2(1430)^+)$		0.15 ± 0.13
$A_{CP}(B^+ \to \eta K^*(892)^+)$		0.02 ± 0.06
$A_{CP}(B^+ \to \eta K^*_0(1430)^+)$		0.05 ± 0.13
$A_{CP}(B^+ \to \eta K^*_2(1430)^+)$		-0.45 ± 0.30
$A_{CP}(B^+ \to \omega K^+)$		0.02 ± 0.05
$A_{CP}(B^+ \to \omega K^{*+})$		0.29 ± 0.35
$A_{CP}(B^+ \to \omega(K\pi)^{*+}_0)$		-0.10 ± 0.09

Unless otherwise stated, limits are given at the 90% confidence level, while errors are given as ± 1 standard deviation.

Tests of Conservation Laws

$A_{CP}(B^+ \to \omega K_2^*(1430)^+)$	0.14 ± 0.15
$A_{CP}(B^+ \to K^{*0}\pi^+)$	-0.04 ± 0.09 (S = 2.1)
$A_{CP}(B^+ \to K^*(892)^+\pi^0)$	-0.06 ± 0.24
$A_{CP}(B^+ \to K^+\pi^-\pi^+)$	0.033 ± 0.010
$A_{CP}(B^+ \to K^+K^-K^+$ nonresonant)	0.06 ± 0.05
$A_{CP}(B^+ \to f(980)^0 K^+)$	-0.08 ± 0.09
$A_{CP}(B^+ \to f_0(1500)\,K^+)$	0.28 ± 0.30
$A_{CP}(B^+ \to f_2'(1525)^0 K^+)$	$-0.08^{+0.05}_{-0.04}$
$A_{CP}(B^+ \to K_0^*(1430)^0\pi^+)$	0.055 ± 0.033
$A_{CP}(B^+ \to K_2^*(1430)^0\pi^+)$	$0.05^{+0.29}_{-0.24}$
$A_{CP}(B^+ \to K^+\pi^0\pi^0)$	-0.06 ± 0.07
$A_{CP}(B^+ \to K^0\rho^+)$	-0.12 ± 0.17
$A_{CP}(B^+ \to K^{*+}\pi^+\pi^-)$	0.07 ± 0.08
$A_{CP}(B^+ \to \rho^0 K^*(892)^+)$	0.31 ± 0.13
$A_{CP}(B^+ \to K^*(892)^+ f_0(980))$	-0.15 ± 0.12
$A_{CP}(B^+ \to a_1^+ K^0)$	0.12 ± 0.11
$A_{CP}(B^+ \to b_1^+ K^0)$	-0.03 ± 0.15
$A_{CP}(B^+ \to K^*(892)^0\rho^+)$	-0.01 ± 0.16
$A_{CP}(B^+ \to b_1^0 K^+)$	-0.46 ± 0.20
$A_{CP}(B^+ \to K^0K^+)$	0.04 ± 0.14
$A_{CP}(B^+ \to K^+K_S^0K_S^0)$	$0.04^{+0.04}_{-0.05}$
$A_{CP}(B^+ \to K^+K^-\pi^+)$	-0.12 ± 0.05 (S = 1.2)
$A_{CP}(B^+ \to K^+K^-K^+)$	-0.036 ± 0.012 (S = 1.1)
$A_{CP}(B^+ \to \phi K^+)$	0.04 ± 0.04 (S = 2.1)
$A_{CP}(B^+ \to X_0(1550)\,K^+)$	-0.04 ± 0.07
$A_{CP}(B^+ \to K^{*+}K^+K^-)$	0.11 ± 0.09
$A_{CP}(B^+ \to \phi K^*(892)^+)$	-0.01 ± 0.08
$A_{CP}(B^+ \to \phi(K\pi)_0^{*+})$	0.04 ± 0.16
$A_{CP}(B^+ \to \phi K_1(1270)^+)$	0.15 ± 0.20
$A_{CP}(B^+ \to \phi K_2^*(1430)^+)$	-0.23 ± 0.20
$A_{CP}(B^+ \to K^+\phi\phi)$	-0.10 ± 0.08
$A_{CP}(B^+ \to K^+[\phi\phi]_{\eta_c})$	0.09 ± 0.10
$A_{CP}(B^+ \to K^*(892)^+\gamma)$	0.018 ± 0.029
$A_{CP}(B^+ \to \eta K^+\gamma)$	-0.12 ± 0.07
$A_{CP}(B^+ \to \phi K^+\gamma)$	-0.13 ± 0.11 (S = 1.1)
$A_{CP}(B^+ \to \rho^+\gamma)$	-0.11 ± 0.33
$A_{CP}(B^+ \to \pi^+\pi^0)$	0.03 ± 0.04
$A_{CP}(B^+ \to \pi^+\pi^-\pi^+)$	0.105 ± 0.029 (S = 1.3)
$A_{CP}(B^+ \to \rho^0\pi^+)$	$0.18^{+0.09}_{-0.17}$
$A_{CP}(B^+ \to f_2(1270)\,\pi^+)$	0.41 ± 0.30
$A_{CP}(B^+ \to \rho^0(1450)\,\pi^+)$	$-0.1^{+0.4}_{-0.5}$
$A_{CP}(B^+ \to \pi^+\pi^-\pi^+$ nonresonant)	$-0.14^{+0.23}_{-0.16}$
$A_{CP}(B^+ \to \rho^+\pi^0)$	0.02 ± 0.11
$A_{CP}(B^+ \to \rho^+\rho^0)$	-0.05 ± 0.05
$A_{CP}(B^+ \to \omega\pi^+)$	-0.04 ± 0.06
$A_{CP}(B^+ \to \omega\rho^+)$	-0.20 ± 0.09
$A_{CP}(B^+ \to \eta\pi^+)$	-0.14 ± 0.07 (S = 1.4)
$A_{CP}(B^+ \to \eta\rho^+)$	0.11 ± 0.11
$A_{CP}(B^+ \to \eta'\pi^+)$	0.06 ± 0.16
$A_{CP}(B^+ \to \eta'\rho^+)$	0.26 ± 0.17
$A_{CP}(B^+ \to b_1^0\pi^+)$	0.05 ± 0.16
$A_{CP}(B^+ \to p\overline{p}\pi^+)$	0.00 ± 0.04
$A_{CP}(B^+ \to p\overline{p}K^+)$	-0.08 ± 0.04 (S = 1.1)
$A_{CP}(B^+ \to p\overline{p}K^*(892)^+)$	0.21 ± 0.16 (S = 1.4)
$A_{CP}(B^+ \to p\overline{\Lambda}\gamma)$	0.17 ± 0.17
$A_{CP}(B^+ \to p\overline{\Lambda}\pi^0)$	0.01 ± 0.17
$A_{CP}(B^+ \to K^+\ell^+\ell^-)$	-0.02 ± 0.08
$A_{CP}(B^+ \to K^+e^+e^-)$	0.14 ± 0.14
$A_{CP}(B^+ \to K^+\mu^+\mu^-)$	-0.003 ± 0.033
$A_{CP}(B^+ \to K^{*+}\ell^+\ell^-)$	-0.09 ± 0.14
$A_{CP}(B^+ \to K^*e^+e^-)$	-0.14 ± 0.23
$A_{CP}(B^+ \to K^*\mu^+\mu^-)$	-0.12 ± 0.24
$\mathrm{Re}(\epsilon_{B^0})/(1+\lvert\epsilon_{B^0}\rvert^2)$	$(0.1 \pm 0.8) \times 10^{-3}$
$A_{T/CP}$	0.005 ± 0.018
$A_{CP}(B^0 \to D^*(2010)^+D^-)$	0.037 ± 0.034
$A_{CP}(B^0 \to [K^+K^-]_D K^*(892)^0)$	-0.45 ± 0.23
$A_{CP}(B^0 \to [K^+\pi^-]_D K^*(892)^0)$	-0.08 ± 0.08
$A_{CP}(B^0 \to \eta' K^*(892)^0)$	0.02 ± 0.23
$A_{CP}(B^0 \to \eta' K_0^*(1430)^0)$	-0.19 ± 0.17
$A_{CP}(B^0 \to \eta' K_2^*(1430)^0)$	0.14 ± 0.18
$A_{CP}(B^0 \to \eta K_0^*(1430)^0)$	0.06 ± 0.13
$A_{CP}(B^0 \to \eta K_2^*(1430)^0)$	-0.07 ± 0.19
$A_{CP}(B^0 \to b_1 K^+)$	-0.07 ± 0.12
$A_{CP}(B^0 \to \omega K^{*0})$	0.45 ± 0.25
$A_{CP}(B^0 \to \omega(K\pi)_0^{*0})$	-0.07 ± 0.09
$A_{CP}(B^0 \to \omega K_2^*(1430)^0)$	-0.37 ± 0.17
$A_{CP}(B^0 \to K^+\pi^-\pi^0)$	$(0 \pm 6) \times 10^{-2}$
$A_{CP}(B^0 \to \rho^- K^+)$	0.20 ± 0.11
$A_{CP}(B^0 \to \rho(1450)^- K^+)$	-0.10 ± 0.33
$A_{CP}(B^0 \to \rho(1700)^- K^+)$	-0.4 ± 0.6
$A_{CP}(B^0 \to K^+\pi^-\pi^0$ nonresonant)	0.10 ± 0.18
$A_{CP}(B^0 \to K^0\pi^+\pi^-)$	-0.01 ± 0.05
$A_{CP}(B^0 \to K^*(892)^+\pi^-)$	-0.22 ± 0.06
$A_{CP}(B^0 \to (K\pi)_0^{*+}\pi^-)$	0.09 ± 0.07
$A_{CP}(B^0 \to (K\pi)_0^{*0}\pi^0)$	-0.15 ± 0.11
$A_{CP}(B^0 \to K^{*0}\pi^0)$	-0.15 ± 0.13
$A_{CP}(B^0 \to K^*(892)^0\pi^+\pi^-)$	0.07 ± 0.05
$A_{CP}(B^0 \to K^*(892)^0\rho^0)$	-0.06 ± 0.09
$A_{CP}(B^0 \to K^{*0} f_0(980))$	0.07 ± 0.10
$A_{CP}(B^0 \to K^{*+}\rho^-)$	0.21 ± 0.15
$A_{CP}(B^0 \to K^*(892)^0 K^+K^-)$	0.01 ± 0.05
$A_{CP}(B^0 \to a_1^- K^+)$	-0.16 ± 0.12
$A_{CP}(B^0 \to K^0K^0)$	-0.6 ± 0.7
$A_{CP}(B^0 \to K^*(892)^0\phi)$	$(0 \pm 4) \times 10^{-2}$
$A_{CP}(B^0 \to K^*(892)^0K^-\pi^+)$	0.2 ± 0.4
$A_{CP}(B^0 \to \phi(K\pi)_0^{*0})$	0.12 ± 0.08
$A_{CP}(B^0 \to \phi K_2^*(1430)^0)$	-0.11 ± 0.10
$A_{CP}(B^0 \to K^*(892)^0\gamma)$	-0.002 ± 0.015
$A_{CP}(B^0 \to K_2^*(1430)^0\gamma)$	-0.08 ± 0.15
$A_{CP}(B^0 \to \rho^+\pi^-)$	0.13 ± 0.06 (S = 1.1)
$A_{CP}(B^0 \to \rho^-\pi^+)$	-0.08 ± 0.08
$A_{CP}(B^0 \to a_1(1260)^\pm\pi^\mp)$	-0.07 ± 0.06
$A_{CP}(B^0 \to b_1^-\pi^+)$	-0.05 ± 0.10
$A_{CP}(B^0 \to p\overline{p}K^*(892)^0)$	0.05 ± 0.12
$A_{CP}(B^0 \to p\overline{\Lambda}\pi^-)$	0.04 ± 0.07
$A_{CP}(B^0 \to K^{*0}\ell^+\ell^-)$	-0.05 ± 0.10
$A_{CP}(B^0 \to K^{*0}e^+e^-)$	-0.21 ± 0.19
$A_{CP}(B^0 \to K^{*0}\mu^+\mu^-)$	-0.07 ± 0.04
$C_{D^*(2010)^-D^+}$ $(B^0 \to D^*(2010)^-D^+)$	-0.01 ± 0.11
$C_{D^*(2010)^+D^-}$ $(B^0 \to D^*(2010)^+D^-)$	0.00 ± 0.13 (S = 1.3)
$C_{D^{*+}D^{*-}}$ $(B^0 \to D^{*+}D^{*-})$	0.01 ± 0.09 (S = 1.6)
C_+ $(B^0 \to D^{*+}D^{*-})$	0.00 ± 0.10 (S = 1.6)
C_- $(B^0 \to D^{*+}D^{*-})$	0.19 ± 0.31
S_- $(B^0 \to D^{*+}D^{*-})$	0.1 ± 1.6 (S = 3.5)
C $(B^0 \to D^*(2010)^+D^*(2010)^-K_S^0)$	0.01 ± 0.29
S $(B^0 \to D^*(2010)^+D^*(2010)^-K_S^0)$	0.1 ± 0.4
$C_{D^+D^-}$ $(B^0 \to D^+D^-)$	-0.46 ± 0.21 (S = 1.8)
$C_{J/\psi(1S)\pi^0}$ $(B^0 \to J/\psi(1S)\pi^0)$	-0.13 ± 0.13
$C_{D_{CP}^{(*)}h^0}$ $(B^0 \to D_{CP}^{(*)}h^0)$	-0.23 ± 0.16
$S_{D_{CP}^{(*)}h^0}$ $(B^0 \to D_{CP}^{(*)}h^0)$	-0.56 ± 0.24
$C_{K^0\pi^0}$ $(B^0 \to K^0\pi^0)$	0.00 ± 0.13 (S = 1.4)
$C_{\eta'(958)K_S^0}$ $(B^0 \to \eta'(958)K_S^0)$	-0.04 ± 0.20 (S = 2.5)
$S_{\eta'(958)K_S^0}$ $(B^0 \to \eta'(958)K_S^0)$	0.43 ± 0.17 (S = 1.5)
$C_{\eta' K^0}$ $(B^0 \to \eta' K^0)$	-0.05 ± 0.05
$C_{\omega K_S^0}$ $(B^0 \to \omega K_S^0)$	-0.30 ± 0.28 (S = 1.6)
$S_{\omega K_S^0}$ $(B^0 \to \omega K_S^0)$	0.43 ± 0.24
C $(B^0 \to K_S^0\pi^0\pi^0)$	0.2 ± 0.5
S $(B^0 \to K_S^0\pi^0\pi^0)$	0.7 ± 0.7
$C_{\rho^0K_S^0}$ $(B^0 \to \rho^0K_S^0)$	-0.04 ± 0.20
$S_{\rho^0K_S^0}$ $(B^0 \to \rho^0K_S^0)$	$0.50^{+0.17}_{-0.21}$
$C_{f_0(980)K_S^0}$ $(B^0 \to f_0(980)K_S^0)$	0.29 ± 0.20
$S_{f_0(980)K_S^0}$ $(B^0 \to f_0(980)K_S^0)$	-0.50 ± 0.16

Unless otherwise stated, limits are given at the 90% confidence level, while errors are given as ± 1 standard deviation.

$S_{f_2(1270)K^0_S}$ ($B^0 \to f_2(1270)K^0_S$)	-0.5 ± 0.5
$C_{f_2(1270)K^0_S}$ ($B^0 \to f_2(1270)K^0_S$)	0.3 ± 0.4
$S_{f_x(1300)K^0_S}$ ($B^0 \to f_x(1300)K^0_S$)	-0.2 ± 0.5
$C_{f_x(1300)K^0_S}$ ($B^0 \to f_x(1300)K^0_S$)	0.13 ± 0.35
$S_{K^0\pi^+\pi^-}$ ($B^0 \to K^0\pi^+\pi^-$ nonresonant)	-0.01 ± 0.33
$C_{K^0\pi^+\pi^-}$ ($B^0 \to K^0\pi^+\pi^-$ nonresonant)	0.01 ± 0.26
$C_{K^0_S K^0_S}$ ($B^0 \to K^0_S K^0_S$)	0.0 ± 0.4 (S = 1.4)
$S_{K^0_S K^0_S}$ ($B^0 \to K^0_S K^0_S$)	-0.8 ± 0.5
$C_{K^+K^-K^0_S}$ ($B^0 \to K^+K^-K^0_S$ nonresonant)	0.06 ± 0.08
$C_{K^+K^-K^0_S}$ ($B^0 \to K^+K^-K^0_S$ inclusive)	0.01 ± 0.09
$C_{\phi K^0_S}$ ($B^0 \to \phi K^0_S$)	0.01 ± 0.14
$S_{\phi K^0_S}$ ($B^0 \to \phi K^0_S$)	0.59 ± 0.14
$C_{K_S K_S K_S}$($B^0 \to K_S K_S K_S$)	-0.23 ± 0.14
$S_{K_S K_S K_S}$($B^0 \to K_S K_S K_S$)	-0.5 ± 0.6 (S = 3.0)
$C_{K^0_S\pi^0\gamma}$($B^0 \to K^0_S\pi^0\gamma$)	0.36 ± 0.33
$S_{K^0_S\pi^0\gamma}$($B^0 \to K^0_S\pi^0\gamma$)	-0.8 ± 0.6
$C_{K^*(892)^0\gamma}$ ($B^0 \to K^*(892)^0\gamma$)	-0.04 ± 0.16 (S = 1.2)
$S_{K^*(892)^0\gamma}$ ($B^0 \to K^*(892)^0\gamma$)	-0.15 ± 0.22
$C_{\eta K^0\gamma}$ ($B^0 \to \eta K^0\gamma$)	-0.3 ± 0.4
$S_{\eta K^0\gamma}$ ($B^0 \to \eta K^0\gamma$)	-0.2 ± 0.5
$C_{K^0\phi\gamma}$ ($B^0 \to K^0\phi\gamma$)	-0.3 ± 0.6
$S_{K^0\phi\gamma}$ ($B^0 \to K^0\phi\gamma$)	$0.7^{+0.7}_{-1.1}$
$C(B^0 \to K^0_S\rho^0\gamma)$	-0.05 ± 0.19
$S(B^0 \to K^0_S\rho^0\gamma)$	0.11 ± 0.34
C ($B^0 \to \rho^0\gamma$)	0.4 ± 0.5
S ($B^0 \to \rho^0\gamma$)	-0.8 ± 0.7
$C_{\pi\pi}$ ($B^0 \to \pi^+\pi^-$)	-0.31 ± 0.05
$C_{\pi^0\pi^0}$($B^0 \to \pi^0\pi^0$)	-0.43 ± 0.24
$C_{\rho\pi}$ ($B^0 \to \rho^+\pi^-$)	-0.03 ± 0.07 (S = 1.2)
$S_{\rho\pi}$ ($B^0 \to \rho^+\pi^-$)	0.05 ± 0.07
$\Delta S_{\rho\pi}$ ($B^0 \to \rho^+\pi^-$)	0.01 ± 0.08
$C_{\rho^0\pi^0}$ ($B^0 \to \rho^0\pi^0$)	0.27 ± 0.24
$S_{\rho^0\pi^0}$ ($B^0 \to \rho^0\pi^0$)	-0.23 ± 0.34
$C_{a_1\pi}$ ($B^0 \to a_1(1260)^+\pi^-$)	-0.05 ± 0.11
$S_{a_1\pi}$ ($B^0 \to a_1(1260)^+\pi^-$)	-0.2 ± 0.4 (S = 3.2)
$\Delta C_{a_1\pi}$ ($B^0 \to a_1(1260)^+\pi^-$)	0.43 ± 0.14 (S = 1.3)
$\Delta S_{a_1\pi}$ ($B^0 \to a_1(1260)^+\pi^-$)	-0.11 ± 0.12
C ($B^0 \to b_1^- K^+$)	-0.22 ± 0.24
ΔC ($B^0 \to b_1^-\pi^+$)	-1.04 ± 0.24
$C_{\rho^0\rho^0}$ ($B^0 \to \rho^0\rho^0$)	0.2 ± 0.9
$S_{\rho^0\rho^0}$ ($B^0 \to \rho^0\rho^0$)	0.3 ± 0.7
$C_{\rho\rho}$ ($B^0 \to \rho^+\rho^-$)	-0.05 ± 0.13
$S_{\rho\rho}$ ($B^0 \to \rho^+\rho^-$)	-0.06 ± 0.17
$\lvert\lambda\rvert$ ($B^0 \to J/\psi K^*(892)^0$)	<0.25, CL = 95%
cos 2β ($B^0 \to J/\psi K^*(892)^0$)	$1.7^{+0.7}_{-0.9}$ (S = 1.6)
cos 2β ($B^0 \to [K^0_S\pi^+\pi^-]_{D^{(*)}} h^0$)	$1.0^{+0.6}_{-0.7}$ (S = 1.8)
$(S_+ + S_-)/2$ ($B^0 \to D^{*-}\pi^+$)	-0.039 ± 0.011
$(S_- - S_+)/2$ ($B^0 \to D^{*-}\pi^+$)	-0.009 ± 0.015
$(S_+ + S_-)/2$ ($B^0 \to D^-\pi^+$)	-0.046 ± 0.023
$(S_- - S_+)/2$ ($B^0 \to D^-\pi^+$)	-0.022 ± 0.021
$(S_+ + S_-)/2$ ($B^0 \to D^-\rho^+$)	-0.024 ± 0.032
$(S_- - S_+)/2$ ($B^0 \to D^-\rho^+$)	-0.10 ± 0.06
$C_{\eta_c K^0_S}$ ($B^0 \to \eta_c K^0_S$)	0.08 ± 0.13
$C_{c\overline{c}K^{(*)0}}$ ($B^0 \to c\overline{c}K^{(*)0}$)	$(0.5 \pm 1.7) \times 10^{-2}$
$C_{J/\psi(\mathrm{nS})K^0}$ ($B^0 \to J/\psi(\mathrm{nS})K^0$)	$(0.5 \pm 2.0) \times 10^{-2}$
$C_{J/\psi K^{*0}}$ ($B^0 \to J/\psi K^{*0}$)	0.03 ± 0.10
$S_{J/\psi K^{*0}}$ ($B^0 \to J/\psi K^{*0}$)	0.60 ± 0.25
$C_{\chi_{c0}K^0_S}$ ($B^0 \to \chi_{c0}K^0_S$)	$-0.3^{+0.5}_{-0.4}$
$S_{\chi_{c0}K^0_S}$ ($B^0 \to \chi_{c0}K^0_S$)	-0.7 ± 0.5
$C_{\chi_{c1}K^0_S}$ ($B^0 \to \chi_{c1}K^0_S$)	0.06 ± 0.07
$\sin(2\beta_{\mathrm{eff}})$($B^0 \to \phi K^0$)	0.22 ± 0.30
$\sin(2\beta_{\mathrm{eff}})$($B^0 \to \phi K^*_0(1430)^0$)	$0.97^{+0.03}_{-0.52}$
$\sin(2\beta_{\mathrm{eff}})$($B^0 \to [K^0_S\pi^+\pi^-]_{D^{(*)}} h^0$)	0.45 ± 0.28
$\lvert\lambda\rvert$ ($B^0 \to [K^0_S\pi^+\pi^-]_{D^{(*)}} h^0$)	1.01 ± 0.08
$\lvert\sin(2\beta+\gamma)\rvert$	>0.40, CL = 90%
$2\beta+\gamma$	$(83 \pm 60)^\circ$
$\gamma(B^0 \to D^0K^{*0})$	$(162 \pm 60)^\circ$
$A_{CP}(B \to K^*(892)\gamma)$	-0.003 ± 0.017
$A_{CP}(b \to s\gamma)$	-0.008 ± 0.029
$A_{CP}(b \to (s+d)\gamma)$	-0.01 ± 0.05
$A_{CP}(B \to X_s\ell^+\ell^-)$	-0.22 ± 0.26
$A_{CP}(B \to K^*e^+e^-)$	-0.18 ± 0.15
$A_{CP}(B \to K^*\mu^+\mu^-)$	-0.03 ± 0.13
$A_{CP}(B \to K^*\ell^+\ell^-)$	-0.04 ± 0.07
$A_{CP}(B \to \eta$ anything)	$-0.13^{+0.04}_{-0.05}$
$\mathrm{Re}(\epsilon_{B^0_s})$ / $(1+\lvert\epsilon_{B^0_s}\rvert^2)$	$(-1.9 \pm 1.0) \times 10^{-3}$
CP Violation phase β_s	$(0.0 \pm 3.5) \times 10^{-2}$
$A_{CP}(B_s \to \pi^+K^-)$	0.28 ± 0.04
$A_{CP}(B^0_s \to [K^+K^-]_D\overline{K}^*(892)^0)$	0.04 ± 0.16
$\Gamma(\eta_c(1S) \to \pi^+\pi^-)/\Gamma_{\mathrm{total}}$	$<1.1 \times 10^{-4}$, CL = 90%
$\Gamma(\eta_c(1S) \to \pi^0\pi^0)/\Gamma_{\mathrm{total}}$	$<3.5 \times 10^{-5}$, CL = 90%
$\Gamma(\eta_c(1S) \to K^+K^-)/\Gamma_{\mathrm{total}}$	$<6 \times 10^{-4}$, CL = 90%
$\Gamma(\eta_c(1S) \to K^0_S K^0_S)/\Gamma_{\mathrm{total}}$	$<3.1 \times 10^{-4}$, CL = 90%
$(\alpha+\overline{\alpha})/(\alpha-\overline{\alpha})$ in $\Lambda \to p\pi^-$, $\overline{\Lambda} \to \overline{p}\pi^+$	0.006 ± 0.021
$\frac{[\alpha(\Xi^-)\alpha_-(\Lambda)-\alpha(\overline{\Xi}^+)\alpha_+(\overline{\Lambda})]}{[\alpha(\Xi^-)\alpha_-(\Lambda)+\alpha(\overline{\Xi}^+)\alpha_+(\overline{\Lambda})]}$	$(0 \pm 7) \times 10^{-4}$
$(\alpha+\overline{\alpha})/(\alpha-\overline{\alpha})$ in $\Omega^- \to \Lambda K^-$, $\overline{\Omega}^+ \to \overline{\Lambda}K^+$	-0.02 ± 0.13
$(\alpha+\overline{\alpha})/(\alpha-\overline{\alpha})$ in $\Lambda_c^+ \to \Lambda\pi^+$, $\overline{\Lambda}_c^- \to \overline{\Lambda}\pi^-$	-0.07 ± 0.31
$(\alpha+\overline{\alpha})/(\alpha-\overline{\alpha})$ in $\Lambda_c^+ \to \Lambda e^+\nu_e$, $\overline{\Lambda}_c^- \to \overline{\Lambda}e^-\overline{\nu}_e$	0.00 ± 0.04
$A_{CP}(\Lambda_b \to p\pi^-)$	0.03 ± 0.18
$A_{CP}(\Lambda_b \to pK^-)$	0.37 ± 0.17

CP VIOLATION OBSERVED

$\mathrm{Re}(\epsilon)$	$(1.596 \pm 0.013) \times 10^{-3}$
charge asymmetry in $K^0_{\ell 3}$ decays	
A_L = weighted average of $A_L(\mu)$ and $A_L(e)$	$(0.332 \pm 0.006)\%$
$A_L(\mu) = [\Gamma(\pi^-\mu^+\nu_\mu) - \Gamma(\pi^+\mu^-\overline{\nu}_\mu)]/\mathrm{sum}$	$(0.304 \pm 0.025)\%$
$A_L(e) = [\Gamma(\pi^-e^+\nu_e) - \Gamma(\pi^+e^-\overline{\nu}_e)]/\mathrm{sum}$	$(0.334 \pm 0.007)\%$
parameters for $K^0_L \to 2\pi$ decay	
$\lvert\eta_{00}\rvert = \lvert A(K^0_L \to 2\pi^0)/A(K^0_S \to 2\pi^0)\rvert$	$(2.220 \pm 0.011) \times 10^{-3}$ (S = 1.8)
$\lvert\eta_{+-}\rvert = \lvert A(K^0_L \to \pi^+\pi^-)/A(K^0_S \to \pi^+\pi^-)\rvert$	$(2.232 \pm 0.011) \times 10^{-3}$ (S = 1.8)
$\lvert\epsilon\rvert = (2\lvert\eta_{+-}\rvert + \lvert\eta_{00}\rvert)/3$	$(2.228 \pm 0.011) \times 10^{-3}$ (S = 1.8)
$\lvert\eta_{00}/\eta_{+-}\rvert$ [h]	0.9950 ± 0.0007 (S = 1.6)
$\mathrm{Re}(\epsilon'/\epsilon) = (1-\lvert\eta_{00}/\eta_{+-}\rvert)/3$ [h]	$(1.66 \pm 0.23) \times 10^{-3}$ (S = 1.6)
Assuming CPT	
ϕ_{+-}, phase of η_{+-}	$(43.51 \pm 0.05)^\circ$ (S = 1.2)
ϕ_{00}, phase of η_{00}	$(43.52 \pm 0.05)^\circ$ (S = 1.3)
$\phi_\epsilon = (2\phi_{+-}+\phi_{00})/3$	$(43.52 \pm 0.05)^\circ$ (S = 1.2)
Not assuming CPT	
ϕ_{+-}, phase of η_{+-}	$(43.4 \pm 0.5)^\circ$ (S = 1.2)
ϕ_{00}, phase of η_{00}	$(43.7 \pm 0.6)^\circ$ (S = 1.2)
$\phi_\epsilon = (2\phi_{+-}+\phi_{00})/3$	$(43.5 \pm 0.5)^\circ$ (S = 1.3)
CP asymmetry A in $K^0_L \to \pi^+\pi^-e^+e^-$	$(13.7 \pm 1.5)\%$
β_{CP} from $K^0_L \to e^+e^-e^+e^-$	-0.19 ± 0.07
γ_{CP} from $K^0_L \to e^+e^-e^+e^-$	0.01 ± 0.11 (S = 1.6)
parameters for $K^0_L \to \pi^+\pi^-\gamma$ decay	
$\lvert\eta_{+-\gamma}\rvert = \lvert A(K^0_L \to \pi^+\pi^-\gamma, CP$ violating$)/A(K^0_S \to \pi^+\pi^-\gamma)\rvert$	$(2.35 \pm 0.07) \times 10^{-3}$

Unless otherwise stated, limits are given at the 90% confidence level, while errors are given as ± 1 standard deviation.

Tests of Conservation Laws

$\phi_{+-\gamma}$ = phase of $\eta_{+-\gamma}$		$(44 \pm 4)^\circ$
$\Gamma(K_L^0 \to \pi^+\pi^-)/\Gamma_{\text{total}}$	[i]	$(1.967 \pm 0.010) \times 10^{-3}$ (S = 1.5)
$\Gamma(K_L^0 \to \pi^0\pi^0)/\Gamma_{\text{total}}$		$(8.64 \pm 0.06) \times 10^{-4}$ (S = 1.8)
$A_{CP}(B^+ \to D_{CP(+1)}K^+)$		0.170 ± 0.033 (S = 1.2)
$A_{ADS}(B^+ \to DK^+)$		-0.52 ± 0.15
$A_{CP}(B^+ \to \eta K^+)$		-0.37 ± 0.08
$A_{CP}(B^+ \to f_2(1270)K^+)$		$-0.68^{+0.19}_{-0.17}$
$A_{CP}(B^+ \to \rho^0 K^+)$		0.37 ± 0.10
$A_{CP}(B^+ \to f_0(1370)\pi^+)$		0.72 ± 0.22
$\gamma(B^+ \to D^{(*)0}K^{(*)+})$		$(73^{+7}_{-9})^\circ$
$A_{CP}(B^0 \to K^+\pi^-)$		-0.082 ± 0.006
$A_{CP}(B^0 \to \eta K^*(892)^0)$		0.19 ± 0.05
$S_{D^*(2010)^-D^+}(B^0 \to D^*(2010)^-D^+)$		-0.72 ± 0.15
$S_{D^*(2010)^+D^-}(B^0 \to D^*(2010)^+D^-)$		-0.73 ± 0.14
$S_{D^{*+}D^{*-}}(B^0 \to D^{*+}D^{*-})$		-0.59 ± 0.14 (S = 1.8)
$S_+(B^0 \to D^{*+}D^{*-})$		-0.73 ± 0.09
$S_{D^+D^-}(B^0 \to D^+D^-)$		$-0.99^{+0.17}_{-0.14}$
$S_{J/\psi(1S)\pi^0}(B^0 \to J/\psi(1S)\pi^0)$		-0.94 ± 0.29 (S = 1.9)
$S_{K^0\pi^0}(B^0 \to K^0\pi^0)$		0.58 ± 0.17
$S_{\eta' K^0}(B^0 \to \eta' K^0)$		0.60 ± 0.07
$S_{K^+K^-K_S^0}(B^0 \to K^+K^-K_S^0$ nonresonant)		-0.66 ± 0.11
$S_{K^+K^-K_S^0}(B^0 \to K^+K^-K_S^0$ inclusive)		-0.65 ± 0.12
$S_{\pi\pi}(B^0 \to \pi^+\pi^-)$		-0.67 ± 0.06
$\Delta C_{\rho\pi}(B^0 \to \rho^+\pi^-)$		0.27 ± 0.06
$S_{\eta_c K_S^0}(B^0 \to \eta_c K_S^0)$		0.93 ± 0.17
$\sin(2\beta)(B^0 \to J/\psi K_S^0)$		0.682 ± 0.019
$S_{J/\psi(nS)K^0}(B^0 \to J/\psi(nS)K^0)$		0.676 ± 0.021
$S_{\chi_{c1}K_S^0}(B^0 \to \chi_{c1}K_S^0)$		0.63 ± 0.10
$\sin(2\beta_{\text{eff}})(B^0 \to K^+K^-K_S^0)$		$0.77^{+0.13}_{-0.12}$
α		$(90 \pm 5)^\circ$
$\text{Re}(\epsilon_b)/(1+\lvert\epsilon_b\rvert^2)$		$(1.2 \pm 0.4) \times 10^{-3}$

CPT INVARIANCE

$(m_{W^+} - m_{W^-})/m_{\text{average}}$		-0.002 ± 0.007
$(m_{e^+} - m_{e^-})/m_{\text{average}}$		$<8 \times 10^{-9}$, CL = 90%
$\lvert q_{e^+} + q_{e^-}\rvert/e$		$<4 \times 10^{-8}$
$(g_{e^+} - g_{e^-})/g_{\text{average}}$		$(-0.5 \pm 2.1) \times 10^{-12}$
$(\tau_{\mu^+} - \tau_{\mu^-})/\tau_{\text{average}}$		$(2 \pm 8) \times 10^{-5}$
$(g_{\mu^+} - g_{\mu^-})/g_{\text{average}}$		$(-0.11 \pm 0.12) \times 10^{-8}$
$(m_{\tau^+} - m_{\tau^-})/m_{\text{average}}$		$<2.8 \times 10^{-4}$, CL = 90%
$m_t - m_{\overline{t}}$		-0.2 ± 0.5 GeV (S = 1.1)
$(m_{\pi^+} - m_{\pi^-})/m_{\text{average}}$		$(2 \pm 5) \times 10^{-4}$
$(\tau_{\pi^+} - \tau_{\pi^-})/\tau_{\text{average}}$		$(6 \pm 7) \times 10^{-4}$
$(m_{K^+} - m_{K^-})/m_{\text{average}}$		$(-0.6 \pm 1.8) \times 10^{-4}$
$(\tau_{K^+} - \tau_{K^-})/\tau_{\text{average}}$		$(0.10 \pm 0.09)\%$ (S = 1.2)
$K^\pm \to \mu^\pm\nu_\mu$ rate difference/average		$(-0.5 \pm 0.4)\%$
$K^\pm \to \pi^\pm\pi^0$ rate difference/average	[j]	$(0.8 \pm 1.2)\%$
δ in $K^0 - \overline{K}^0$ mixing		
real part of δ		$(2.5 \pm 2.3) \times 10^{-4}$
imaginary part of δ		$(-1.5 \pm 1.6) \times 10^{-5}$
Re(y), K_{e3} parameter		$(0.4 \pm 2.5) \times 10^{-3}$
Re(x$_-$), K_{e3} parameter		$(-2.9 \pm 2.0) \times 10^{-3}$
$\lvert m_{K^0} - m_{\overline{K}^0}\rvert/m_{\text{average}}$	[k]	$<6 \times 10^{-19}$, CL = 90%
$(\Gamma_{K^0} - \Gamma_{\overline{K}^0})/m_{\text{average}}$		$(8 \pm 8) \times 10^{-18}$
phase difference $\phi_{00} - \phi_{+-}$		$(0.34 \pm 0.32)^\circ$
$\text{Re}(\frac{2}{3}\eta_{+-} + \frac{1}{3}\eta_{00}) - \frac{A_f}{2}$		$(-3 \pm 35) \times 10^{-6}$
$A_{CPT}(D^0 \to K^-\pi^+)$		0.008 ± 0.008
$\Delta S^+_{CPT}(S^-_{\ell^+,K_S^0} - S^+_{\ell^+,K_S^0})$		0.16 ± 0.23
$\Delta S^-_{CPT}(S^+_{\ell^+,K_S^0} - S^-_{\ell^+,K_S^0})$		-0.03 ± 0.14
$\Delta C^+_{CPT}(C^-_{\ell^+,K_S^0} - C^+_{\ell^+,K_S^0})$		0.14 ± 0.17
$\Delta C^-_{CPT}(C^+_{\ell^+,K_S^0} - C^-_{\ell^+,K_S^0})$		0.03 ± 0.14
$\lvert m_p - m_{\overline{p}}\rvert/m_p$	[l]	$<7 \times 10^{-10}$, CL = 90%
$(\lvert\frac{q_{\overline{p}}}{m_{\overline{p}}}\rvert - \lvert\frac{q_p}{m_p}\rvert)/\lvert\frac{q_p}{m_p}\rvert$		$(-9 \pm 9) \times 10^{-11}$
$\lvert q_p + q_{\overline{p}}\rvert/e$	[l]	$<7 \times 10^{-10}$, CL = 90%
$(\mu_p + \mu_{\overline{p}})/\mu_p$		$(0 \pm 5) \times 10^{-6}$
$(m_n - m_{\overline{n}})/m_n$		$(9 \pm 6) \times 10^{-5}$
$(m_\Lambda - m_{\overline{\Lambda}})/m_\Lambda$		$(-0.1 \pm 1.1) \times 10^{-5}$ (S = 1.6)
$(\tau_\Lambda - \tau_{\overline{\Lambda}})/\tau_\Lambda$		-0.001 ± 0.009
$(\tau_{\Sigma^+} - \tau_{\overline{\Sigma}^-})/\tau_{\Sigma^+}$		$(-0.6 \pm 1.2) \times 10^{-3}$
$(\mu_{\Sigma^+} + \mu_{\overline{\Sigma}^-})/\mu_{\Sigma^+}$		0.014 ± 0.015
$(m_{\Xi^-} - m_{\overline{\Xi}^+})/m_{\Xi^-}$		$(-3 \pm 9) \times 10^{-5}$
$(\tau_{\Xi^-} - \tau_{\overline{\Xi}^+})/\tau_{\Xi^-}$		-0.01 ± 0.07
$(\mu_{\Xi^-} + \mu_{\overline{\Xi}^+})/\lvert\mu_{\Xi^-}\rvert$		$+0.01 \pm 0.05$
$(m_{\Omega^-} - m_{\overline{\Omega}^+})/m_{\Omega^-}$		$(-1 \pm 8) \times 10^{-5}$
$(\tau_{\Omega^-} - \tau_{\overline{\Omega}^+})/\tau_{\Omega^-}$		0.00 ± 0.05

TESTS OF NUMBER CONSERVATION LAWS

LEPTON FAMILY NUMBER

Lepton family number conservation means separate conservation of each of L_e, L_μ, L_τ.

$\Gamma(Z \to e^\pm\mu^\mp)/\Gamma_{\text{total}}$	[n]	$<1.7 \times 10^{-6}$, CL = 95%
$\Gamma(Z \to e^\pm\tau^\mp)/\Gamma_{\text{total}}$	[n]	$<9.8 \times 10^{-6}$, CL = 95%
$\Gamma(Z \to \mu^\pm\tau^\mp)/\Gamma_{\text{total}}$	[n]	$<1.2 \times 10^{-5}$, CL = 95%
$\sigma(e^+e^- \to e^\pm\tau^\mp)/\sigma(e^+e^- \to \mu^+\mu^-)$		$<8.9 \times 10^{-6}$, CL = 95%
$\sigma(e^+e^- \to \mu^\pm\tau^\mp)/\sigma(e^+e^- \to \mu^+\mu^-)$		$<4.0 \times 10^{-6}$, CL = 95%
limit on $\mu^- \to e^-$ conversion		
$\sigma(\mu^- {}^{32}\text{S} \to e^- {}^{32}\text{S})/\sigma(\mu^- {}^{32}\text{S} \to \nu_\mu {}^{32}\text{P}^*)$		$<7 \times 10^{-11}$, CL = 90%
$\sigma(\mu^- \text{Ti} \to e^- \text{Ti})/\sigma(\mu^- \text{Ti} \to \text{capture})$		$<4.3 \times 10^{-12}$, CL = 90%
$\sigma(\mu^- \text{Pb} \to e^- \text{Pb})/\sigma(\mu^- \text{Pb} \to \text{capture})$		$<4.6 \times 10^{-11}$, CL = 90%
limit on muonium $\to$ antimuonium conversion $R_g = G_C/G_F$		<0.0030, CL = 90%
$\Gamma(\mu^- \to e^-\nu_e\overline{\nu}_\mu)/\Gamma_{\text{total}}$	[o]	$<1.2 \times 10^{-2}$, CL = 90%
$\Gamma(\mu^- \to e^-\gamma)/\Gamma_{\text{total}}$		$<5.7 \times 10^{-13}$, CL = 90%
$\Gamma(\mu^- \to e^-e^+e^-)/\Gamma_{\text{total}}$		$<1.0 \times 10^{-12}$, CL = 90%
$\Gamma(\mu^- \to e^-2\gamma)/\Gamma_{\text{total}}$		$<7.2 \times 10^{-11}$, CL = 90%
$\Gamma(\tau^- \to e^-\gamma)/\Gamma_{\text{total}}$		$<3.3 \times 10^{-8}$, CL = 90%
$\Gamma(\tau^- \to \mu^-\gamma)/\Gamma_{\text{total}}$		$<4.4 \times 10^{-8}$, CL = 90%
$\Gamma(\tau^- \to e^-\pi^0)/\Gamma_{\text{total}}$		$<8.0 \times 10^{-8}$, CL = 90%
$\Gamma(\tau^- \to \mu^-\pi^0)/\Gamma_{\text{total}}$		$<1.1 \times 10^{-7}$, CL = 90%
$\Gamma(\tau^- \to e^-K_S^0)/\Gamma_{\text{total}}$		$<2.6 \times 10^{-8}$, CL = 90%
$\Gamma(\tau^- \to \mu^-K_S^0)/\Gamma_{\text{total}}$		$<2.3 \times 10^{-8}$, CL = 90%
$\Gamma(\tau^- \to e^-\eta)/\Gamma_{\text{total}}$		$<9.2 \times 10^{-8}$, CL = 90%
$\Gamma(\tau^- \to \mu^-\eta)/\Gamma_{\text{total}}$		$<6.5 \times 10^{-8}$, CL = 90%
$\Gamma(\tau^- \to e^-\rho^0)/\Gamma_{\text{total}}$		$<1.8 \times 10^{-8}$, CL = 90%
$\Gamma(\tau^- \to \mu^-\rho^0)/\Gamma_{\text{total}}$		$<1.2 \times 10^{-8}$, CL = 90%
$\Gamma(\tau^- \to e^-\omega)/\Gamma_{\text{total}}$		$<4.8 \times 10^{-8}$, CL = 90%
$\Gamma(\tau^- \to \mu^-\omega)/\Gamma_{\text{total}}$		$<4.7 \times 10^{-8}$, CL = 90%
$\Gamma(\tau^- \to e^-K^*(892)^0)/\Gamma_{\text{total}}$		$<3.2 \times 10^{-8}$, CL = 90%
$\Gamma(\tau^- \to \mu^-K^*(892)^0)/\Gamma_{\text{total}}$		$<5.9 \times 10^{-8}$, CL = 90%
$\Gamma(\tau^- \to e^-\overline{K}^*(892)^0)/\Gamma_{\text{total}}$		$<3.4 \times 10^{-8}$, CL = 90%
$\Gamma(\tau^- \to \mu^-\overline{K}^*(892)^0)/\Gamma_{\text{total}}$		$<7.0 \times 10^{-8}$, CL = 90%
$\Gamma(\tau^- \to e^-\eta'(958))/\Gamma_{\text{total}}$		$<1.6 \times 10^{-7}$, CL = 90%
$\Gamma(\tau^- \to \mu^-\eta'(958))/\Gamma_{\text{total}}$		$<1.3 \times 10^{-7}$, CL = 90%
$\Gamma(\tau^- \to e^-f_0(980) \to e^-\pi^+\pi^-)/\Gamma_{\text{total}}$		$<3.2 \times 10^{-8}$, CL = 90%
$\Gamma(\tau^- \to \mu^-f_0(980) \to \mu^-\pi^+\pi^-)/\Gamma_{\text{total}}$		$<3.4 \times 10^{-8}$, CL = 90%
$\Gamma(\tau^- \to e^-\phi)/\Gamma_{\text{total}}$		$<3.1 \times 10^{-8}$, CL = 90%
$\Gamma(\tau^- \to \mu^-\phi)/\Gamma_{\text{total}}$		$<8.4 \times 10^{-8}$, CL = 90%
$\Gamma(\tau^- \to e^-e^+e^-)/\Gamma_{\text{total}}$		$<2.7 \times 10^{-8}$, CL = 90%
$\Gamma(\tau^- \to e^-\mu^+\mu^-)/\Gamma_{\text{total}}$		$<2.7 \times 10^{-8}$, CL = 90%

Unless otherwise stated, limits are given at the 90% confidence level, while errors are given as ± 1 standard deviation.

$\Gamma(\tau^- \to e^+\mu^-\mu^-)/\Gamma_{\text{total}}$		$<1.7\times10^{-8}$, CL = 90%
$\Gamma(\tau^- \to \mu^-e^+e^-)/\Gamma_{\text{total}}$		$<1.8\times10^{-8}$, CL = 90%
$\Gamma(\tau^- \to \mu^+e^-e^-)/\Gamma_{\text{total}}$		$<1.5\times10^{-8}$, CL = 90%
$\Gamma(\tau^- \to \mu^-\mu^+\mu^-)/\Gamma_{\text{total}}$		$<2.1\times10^{-8}$, CL = 90%
$\Gamma(\tau^- \to e^-\pi^+\pi^-)/\Gamma_{\text{total}}$		$<2.3\times10^{-8}$, CL = 90%
$\Gamma(\tau^- \to \mu^-\pi^+\pi^-)/\Gamma_{\text{total}}$		$<2.1\times10^{-8}$, CL = 90%
$\Gamma(\tau^- \to e^-\pi^+K^-)/\Gamma_{\text{total}}$		$<3.7\times10^{-8}$, CL = 90%
$\Gamma(\tau^- \to e^-\pi^-K^+)/\Gamma_{\text{total}}$		$<3.1\times10^{-8}$, CL = 90%
$\Gamma(\tau^- \to e^-K^0_S K^0_S)/\Gamma_{\text{total}}$		$<7.1\times10^{-8}$, CL = 90%
$\Gamma(\tau^- \to e^-K^+K^-)/\Gamma_{\text{total}}$		$<3.4\times10^{-8}$, CL = 90%
$\Gamma(\tau^- \to \mu^-\pi^+K^-)/\Gamma_{\text{total}}$		$<8.6\times10^{-8}$, CL = 90%
$\Gamma(\tau^- \to \mu^-\pi^-K^+)/\Gamma_{\text{total}}$		$<4.5\times10^{-8}$, CL = 90%
$\Gamma(\tau^- \to \mu^-K^0_S K^0_S)/\Gamma_{\text{total}}$		$<8.0\times10^{-8}$, CL = 90%
$\Gamma(\tau^- \to \mu^-K^+K^-)/\Gamma_{\text{total}}$		$<4.4\times10^{-8}$, CL = 90%
$\Gamma(\tau^- \to e^-\pi^0\pi^0)/\Gamma_{\text{total}}$		$<6.5\times10^{-6}$, CL = 90%
$\Gamma(\tau^- \to \mu^-\pi^0\pi^0)/\Gamma_{\text{total}}$		$<1.4\times10^{-5}$, CL = 90%
$\Gamma(\tau^- \to e^-\eta\eta)/\Gamma_{\text{total}}$		$<3.5\times10^{-5}$, CL = 90%
$\Gamma(\tau^- \to \mu^-\eta\eta)/\Gamma_{\text{total}}$		$<6.0\times10^{-5}$, CL = 90%
$\Gamma(\tau^- \to e^-\pi^0\eta)/\Gamma_{\text{total}}$		$<2.4\times10^{-5}$, CL = 90%
$\Gamma(\tau^- \to \mu^-\pi^0\eta)/\Gamma_{\text{total}}$		$<2.2\times10^{-5}$, CL = 90%
$\Gamma(\tau^- \to e^-\text{light boson})/\Gamma_{\text{total}}$		$<2.7\times10^{-3}$, CL = 95%
$\Gamma(\tau^- \to \mu^-\text{light boson})/\Gamma_{\text{total}}$		$<5\times10^{-3}$, CL = 95%
LEPTON FAMILY NUMBER VIOLATION IN NEUTRINOS		
$\sin^2(2\theta_{12})$		0.846 ± 0.021
Δm^2_{21}		$(7.53 \pm 0.18)\times10^{-5}$ eV^2
$\sin^2(2\theta_{23})$ (normal mass hierarchy)		$0.999^{+0.001}_{-0.018}$
$\sin^2(2\theta_{23})$ (inverted mass hierarchy)		$1.000^{+0.000}_{-0.017}$
Δm^2_{32} (normal mass hierarchy)	[p]	$(2.44 \pm 0.06)\times10^{-3}$ eV^2
Δm^2_{32} (inverted mass hierarchy)	[p]	$(2.52 \pm 0.07)\times10^{-3}$ eV^2
$\sin^2(2\theta_{13})$		$(9.3 \pm 0.8)\times10^{-2}$
$\Gamma(\pi^+ \to \mu^+\nu_e)/\Gamma_{\text{total}}$	[q]	$<8.0\times10^{-3}$, CL = 90%
$\Gamma(\pi^+ \to \mu^-e^+e^+\nu)/\Gamma_{\text{total}}$		$<1.6\times10^{-6}$, CL = 90%
$\Gamma(\pi^0 \to \mu^+e^-)/\Gamma_{\text{total}}$		$<3.8\times10^{-10}$, CL = 90%
$\Gamma(\pi^0 \to \mu^-e^+)/\Gamma_{\text{total}}$		$<3.4\times10^{-9}$, CL = 90%
$\Gamma(\pi^0 \to \mu^+e^- + \mu^-e^+)/\Gamma_{\text{total}}$		$<3.6\times10^{-10}$, CL = 90%
$\Gamma(\eta \to \mu^+e^- + \mu^-e^+)/\Gamma_{\text{total}}$		$<6\times10^{-6}$, CL = 90%
$\Gamma(\eta'(958) \to e\mu)/\Gamma_{\text{total}}$		$<4.7\times10^{-4}$, CL = 90%
$\Gamma(\phi(1020) \to e^\pm\mu^\mp)/\Gamma_{\text{total}}$		$<2\times10^{-6}$, CL = 90%
$\Gamma(K^+ \to \mu^-\nu e^+e^+)/\Gamma_{\text{total}}$		$<2.1\times10^{-8}$, CL = 90%
$\Gamma(K^+ \to \mu^+\nu_e)/\Gamma_{\text{total}}$	[q]	$<4\times10^{-3}$, CL = 90%
$\Gamma(K^+ \to \pi^+\mu^+e^-)/\Gamma_{\text{total}}$		$<1.3\times10^{-11}$, CL = 90%
$\Gamma(K^+ \to \pi^+\mu^-e^+)/\Gamma_{\text{total}}$		$<5.2\times10^{-10}$, CL = 90%
$\Gamma(K^0_L \to e^\pm\mu^\mp)/\Gamma_{\text{total}}$	[n]	$<4.7\times10^{-12}$, CL = 90%
$\Gamma(K^0_L \to e^\pm e^\pm\mu^\mp\mu^\mp)/\Gamma_{\text{total}}$	[n]	$<4.12\times10^{-11}$, CL = 90%
$\Gamma(K^0_L \to \pi^0\mu^\pm e^\mp)/\Gamma_{\text{total}}$	[n]	$<7.6\times10^{-11}$, CL = 90%
$\Gamma(K^0_L \to \pi^0\pi^0\mu^\pm e^\mp)/\Gamma_{\text{total}}$		$<1.7\times10^{-10}$, CL = 90%
$\Gamma(D^+ \to \pi^+e^+\mu^-)/\Gamma_{\text{total}}$		$<2.9\times10^{-6}$, CL = 90%
$\Gamma(D^+ \to \pi^+e^-\mu^+)/\Gamma_{\text{total}}$		$<3.6\times10^{-6}$, CL = 90%
$\Gamma(D^+ \to K^+e^+\mu^-)/\Gamma_{\text{total}}$		$<1.2\times10^{-6}$, CL = 90%
$\Gamma(D^+ \to K^+e^-\mu^+)/\Gamma_{\text{total}}$		$<2.8\times10^{-6}$, CL = 90%
$\Gamma(D^0 \to \mu^\pm e^\mp)/\Gamma_{\text{total}}$	[n]	$<2.6\times10^{-7}$, CL = 90%
$\Gamma(D^0 \to \pi^0 e^\pm\mu^\mp)/\Gamma_{\text{total}}$	[n]	$<8.6\times10^{-5}$, CL = 90%
$\Gamma(D^0 \to \eta e^\pm\mu^\mp)/\Gamma_{\text{total}}$	[n]	$<1.0\times10^{-4}$, CL = 90%
$\Gamma(D^0 \to \pi^+\pi^-e^\pm\mu^\mp)/\Gamma_{\text{total}}$	[n]	$<1.5\times10^{-5}$, CL = 90%
$\Gamma(D^0 \to \rho^0 e^\pm\mu^\mp)/\Gamma_{\text{total}}$	[n]	$<4.9\times10^{-5}$, CL = 90%
$\Gamma(D^0 \to \omega e^\pm\mu^\mp)/\Gamma_{\text{total}}$	[n]	$<1.2\times10^{-4}$, CL = 90%
$\Gamma(D^0 \to K^-K^+e^\pm\mu^\mp)/\Gamma_{\text{total}}$	[n]	$<1.8\times10^{-4}$, CL = 90%
$\Gamma(D^0 \to \phi e^\pm\mu^\mp)/\Gamma_{\text{total}}$	[n]	$<3.4\times10^{-5}$, CL = 90%
$\Gamma(D^0 \to \overline{K}^0 e^\pm\mu^\mp)/\Gamma_{\text{total}}$	[n]	$<1.0\times10^{-4}$, CL = 90%
$\Gamma(D^0 \to K^-\pi^+e^\pm\mu^\mp)/\Gamma_{\text{total}}$	[n]	$<5.53\times10^{-4}$, CL = 90%
$\Gamma(D^0 \to \overline{K}^*(892)^0 e^\pm\mu^\mp)/\Gamma_{\text{total}}$	[n]	$<8.3\times10^{-5}$, CL = 90%
$\Gamma(D^+_s \to \pi^+e^+\mu^-)/\Gamma_{\text{total}}$		$<1.2\times10^{-5}$, CL = 90%
$\Gamma(D^+_s \to \pi^+e^-\mu^+)/\Gamma_{\text{total}}$		$<2.0\times10^{-5}$, CL = 90%
$\Gamma(D^+_s \to K^+e^+\mu^-)/\Gamma_{\text{total}}$		$<1.4\times10^{-5}$, CL = 90%
$\Gamma(D^+_s \to K^+e^-\mu^+)/\Gamma_{\text{total}}$		$<9.7\times10^{-6}$, CL = 90%
$\Gamma(B^+ \to \pi^+e^+\mu^-)/\Gamma_{\text{total}}$		$<6.4\times10^{-3}$, CL = 90%
$\Gamma(B^+ \to \pi^+e^-\mu^+)/\Gamma_{\text{total}}$		$<6.4\times10^{-3}$, CL = 90%
$\Gamma(B^+ \to \pi^+e^\pm\mu^\mp)/\Gamma_{\text{total}}$		$<1.7\times10^{-7}$, CL = 90%
$\Gamma(B^+ \to \pi^+e^+\tau^-)/\Gamma_{\text{total}}$		$<7.4\times10^{-5}$, CL = 90%
$\Gamma(B^+ \to \pi^+e^-\tau^+)/\Gamma_{\text{total}}$		$<2.0\times10^{-5}$, CL = 90%
$\Gamma(B^+ \to \pi^+e^\pm\tau^\mp)/\Gamma_{\text{total}}$		$<7.5\times10^{-5}$, CL = 90%
$\Gamma(B^+ \to \pi^+\mu^+\tau^-)/\Gamma_{\text{total}}$		$<6.2\times10^{-5}$, CL = 90%
$\Gamma(B^+ \to \pi^+\mu^-\tau^+)/\Gamma_{\text{total}}$		$<4.5\times10^{-5}$, CL = 90%
$\Gamma(B^+ \to \pi^+\mu^\pm\tau^\mp)/\Gamma_{\text{total}}$		$<7.2\times10^{-5}$, CL = 90%
$\Gamma(B^+ \to K^+e^+\mu^-)/\Gamma_{\text{total}}$		$<9.1\times10^{-8}$, CL = 90%
$\Gamma(B^+ \to K^+e^-\mu^+)/\Gamma_{\text{total}}$		$<1.3\times10^{-7}$, CL = 90%
$\Gamma(B^+ \to K^+e^\pm\mu^\mp)/\Gamma_{\text{total}}$		$<9.1\times10^{-8}$, CL = 90%
$\Gamma(B^+ \to K^+e^+\tau^-)/\Gamma_{\text{total}}$		$<4.3\times10^{-5}$, CL = 90%
$\Gamma(B^+ \to K^+e^-\tau^+)/\Gamma_{\text{total}}$		$<1.5\times10^{-5}$, CL = 90%
$\Gamma(B^+ \to K^+e^\pm\tau^\mp)/\Gamma_{\text{total}}$		$<3.0\times10^{-5}$, CL = 90%
$\Gamma(B^+ \to K^+\mu^+\tau^-)/\Gamma_{\text{total}}$		$<4.5\times10^{-5}$, CL = 90%
$\Gamma(B^+ \to K^+\mu^-\tau^+)/\Gamma_{\text{total}}$		$<2.8\times10^{-5}$, CL = 90%
$\Gamma(B^+ \to K^+\mu^\pm\tau^\mp)/\Gamma_{\text{total}}$		$<4.8\times10^{-5}$, CL = 90%
$\Gamma(B^+ \to K^*(892)^+e^+\mu^-)/\Gamma_{\text{total}}$		$<1.3\times10^{-6}$, CL = 90%
$\Gamma(B^+ \to K^*(892)^+e^-\mu^+)/\Gamma_{\text{total}}$		$<9.9\times10^{-7}$, CL = 90%
$\Gamma(B^+ \to K^*(892)^+e^\pm\mu^\mp)/\Gamma_{\text{total}}$		$<1.4\times10^{-6}$, CL = 90%
$\Gamma(B^0 \to e^\pm\mu^\mp)/\Gamma_{\text{total}}$	[n]	$<2.8\times10^{-9}$, CL = 90%
$\Gamma(B^0 \to \pi^0e^\pm\mu^\mp)/\Gamma_{\text{total}}$		$<1.4\times10^{-7}$, CL = 90%
$\Gamma(B^0 \to K^0e^\pm\mu^\mp)/\Gamma_{\text{total}}$		$<2.7\times10^{-7}$, CL = 90%
$\Gamma(B^0 \to K^*(892)^0e^+\mu^-)/\Gamma_{\text{total}}$		$<5.3\times10^{-7}$, CL = 90%
$\Gamma(B^0 \to K^*(892)^0e^-\mu^+)/\Gamma_{\text{total}}$		$<3.4\times10^{-7}$, CL = 90%
$\Gamma(B^0 \to K^*(892)^0e^\pm\mu^\mp)/\Gamma_{\text{total}}$		$<5.8\times10^{-7}$, CL = 90%
$\Gamma(B^0 \to e^\pm\tau^\mp)/\Gamma_{\text{total}}$	[n]	$<2.8\times10^{-5}$, CL = 90%
$\Gamma(B^0 \to \mu^\pm\tau^\mp)/\Gamma_{\text{total}}$	[n]	$<2.2\times10^{-5}$, CL = 90%
$\Gamma(B \to se^\pm\mu^\mp)/\Gamma_{\text{total}}$	[n]	$<2.2\times10^{-5}$, CL = 90%
$\Gamma(B \to \pi e^\pm\mu^\mp)/\Gamma_{\text{total}}$		$<9.2\times10^{-8}$, CL = 90%
$\Gamma(B \to \rho e^\pm\mu^\mp)/\Gamma_{\text{total}}$		$<3.2\times10^{-6}$, CL = 90%
$\Gamma(B \to Ke^\pm\mu^\mp)/\Gamma_{\text{total}}$		$<3.8\times10^{-8}$, CL = 90%
$\Gamma(B \to K^*(892)e^\pm\mu^\mp)/\Gamma_{\text{total}}$		$<5.1\times10^{-7}$, CL = 90%
$\Gamma(B^0_s \to e^\pm\mu^\mp)/\Gamma_{\text{total}}$	[n]	$<1.1\times10^{-8}$, CL = 90%
$\Gamma(J/\psi(1S) \to e^\pm\mu^\mp)/\Gamma_{\text{total}}$		$<1.6\times10^{-7}$, CL = 90%
$\Gamma(J/\psi(1S) \to e^\pm\tau^\mp)/\Gamma_{\text{total}}$		$<8.3\times10^{-6}$, CL = 90%
$\Gamma(J/\psi(1S) \to \mu^\pm\tau^\mp)/\Gamma_{\text{total}}$		$<2.0\times10^{-6}$, CL = 90%
$\Gamma(\Upsilon(1S) \to \mu^\pm\tau^\mp)/\Gamma_{\text{total}}$		$<6.0\times10^{-6}$, CL = 95%
$\Gamma(\Upsilon(2S) \to e^\pm\tau^\mp)/\Gamma_{\text{total}}$		$<3.2\times10^{-6}$, CL = 90%
$\Gamma(\Upsilon(2S) \to \mu^\pm\tau^\mp)/\Gamma_{\text{total}}$		$<3.3\times10^{-6}$, CL = 90%
$\Gamma(\Upsilon(3S) \to e^\pm\tau^\mp)/\Gamma_{\text{total}}$		$<4.2\times10^{-6}$, CL = 90%
$\Gamma(\Upsilon(3S) \to \mu^\pm\tau^\mp)/\Gamma_{\text{total}}$		$<3.1\times10^{-6}$, CL = 90%
$\Gamma(\Lambda_c^+ \to pe^+\mu^-)/\Gamma_{\text{total}}$		$<9.9\times10^{-6}$, CL = 90%
$\Gamma(\Lambda_c^+ \to pe^-\mu^+)/\Gamma_{\text{total}}$		$<1.9\times10^{-5}$, CL = 90%

TOTAL LEPTON NUMBER

Violation of total lepton number conservation also implies violation of lepton family number conservation.

$\Gamma(Z \to pe)/\Gamma_{\text{total}}$		$<1.8\times10^{-6}$, CL = 95%
$\Gamma(Z \to p\mu)/\Gamma_{\text{total}}$		$<1.8\times10^{-6}$, CL = 95%
limit on $\mu^- \to e^+$ conversion		
$\sigma(\mu^-{}^{32}\text{S} \to e^+{}^{32}\text{Si}^*)$ / $\sigma(\mu^-{}^{32}\text{S} \to \nu_\mu{}^{32}\text{P}^*)$		$<9\times10^{-10}$, CL = 90%
$\sigma(\mu^-{}^{127}\text{I} \to e^+{}^{127}\text{Sb}^*)$ / $\sigma(\mu^-{}^{127}\text{I} \to \text{anything})$		$<3\times10^{-10}$, CL = 90%
$\sigma(\mu^-\text{Ti} \to e^+\text{Ca})$ / $\sigma(\mu^-\text{Ti} \to \text{capture})$		$<3.6\times10^{-11}$, CL = 90%
$\Gamma(\tau^- \to e^+\pi^-\pi^-)/\Gamma_{\text{total}}$		$<2.0\times10^{-8}$, CL = 90%
$\Gamma(\tau^- \to \mu^+\pi^-\pi^-)/\Gamma_{\text{total}}$		$<3.9\times10^{-8}$, CL = 90%
$\Gamma(\tau^- \to e^+\pi^-K^-)/\Gamma_{\text{total}}$		$<3.2\times10^{-8}$, CL = 90%
$\Gamma(\tau^- \to e^+K^-K^-)/\Gamma_{\text{total}}$		$<3.3\times10^{-8}$, CL = 90%
$\Gamma(\tau^- \to \mu^+\pi^-K^-)/\Gamma_{\text{total}}$		$<4.8\times10^{-8}$, CL = 90%
$\Gamma(\tau^- \to \mu^+K^-K^-)/\Gamma_{\text{total}}$		$<4.7\times10^{-8}$, CL = 90%
$\Gamma(\tau^- \to p\mu^-\mu^-)/\Gamma_{\text{total}}$		$<4.4\times10^{-7}$, CL = 90%
$\Gamma(\tau^- \to \overline{p}\mu^+\mu^-)/\Gamma_{\text{total}}$		$<3.3\times10^{-7}$, CL = 90%
$\Gamma(\tau^- \to \overline{p}\gamma)/\Gamma_{\text{total}}$		$<3.5\times10^{-6}$, CL = 90%
$\Gamma(\tau^- \to \overline{p}\pi^0)/\Gamma_{\text{total}}$		$<1.5\times10^{-5}$, CL = 90%
$\Gamma(\tau^- \to \overline{p}2\pi^0)/\Gamma_{\text{total}}$		$<3.3\times10^{-5}$, CL = 90%
$\Gamma(\tau^- \to \overline{p}\eta)/\Gamma_{\text{total}}$		$<8.9\times10^{-6}$, CL = 90%
$\Gamma(\tau^- \to \overline{p}\pi^0\eta)/\Gamma_{\text{total}}$		$<2.7\times10^{-5}$, CL = 90%
$\Gamma(\tau^- \to \Lambda\pi^-)/\Gamma_{\text{total}}$		$<7.2\times10^{-8}$, CL = 90%
$\Gamma(\tau^- \to \overline{\Lambda}\pi^-)/\Gamma_{\text{total}}$		$<1.4\times10^{-7}$, CL = 90%
$t_{1/2}(\,{}^{76}\text{Ge} \to {}^{76}\text{Se} + 2\,e^-\,)$		$>1.9\times10^{25}$ yr, CL = 90%

Unless otherwise stated, limits are given at the 90% confidence level, while errors are given as ±1 standard deviation.

Tests of Conservation Laws

$\Gamma(\pi^+ \to \mu^+ \overline{\nu}_e)/\Gamma_{\text{total}}$	[q]	$<1.5 \times 10^{-3}$, CL = 90%
$\Gamma(K^+ \to \pi^- \mu^+ e^+)/\Gamma_{\text{total}}$		$<5.0 \times 10^{-10}$, CL = 90%
$\Gamma(K^+ \to \pi^- e^+ e^+)/\Gamma_{\text{total}}$		$<6.4 \times 10^{-10}$, CL = 90%
$\Gamma(K^+ \to \pi^- \mu^+ \mu^+)/\Gamma_{\text{total}}$	[q]	$<1.1 \times 10^{-9}$, CL = 90%
$\Gamma(K^+ \to \mu^+ \overline{\nu}_e)/\Gamma_{\text{total}}$	[q]	$<3.3 \times 10^{-3}$, CL = 90%
$\Gamma(K^+ \to \pi^0 e^+ \overline{\nu}_e)/\Gamma_{\text{total}}$		$<3 \times 10^{-3}$, CL = 90%
$\Gamma(D^+ \to \pi^- 2e^+)/\Gamma_{\text{total}}$		$<1.1 \times 10^{-6}$, CL = 90%
$\Gamma(D^+ \to \pi^- 2\mu^+)/\Gamma_{\text{total}}$		$<2.2 \times 10^{-8}$, CL = 90%
$\Gamma(D^+ \to \pi^- e^+ \mu^+)/\Gamma_{\text{total}}$		$<2.0 \times 10^{-6}$, CL = 90%
$\Gamma(D^+ \to \rho^- 2\mu^+)/\Gamma_{\text{total}}$		$<5.6 \times 10^{-4}$, CL = 90%
$\Gamma(D^+ \to K^- 2e^+)/\Gamma_{\text{total}}$		$<9 \times 10^{-7}$, CL = 90%
$\Gamma(D^+ \to K^- 2\mu^+)/\Gamma_{\text{total}}$		$<1.0 \times 10^{-5}$, CL = 90%
$\Gamma(D^+ \to K^- e^+ \mu^+)/\Gamma_{\text{total}}$		$<1.9 \times 10^{-6}$, CL = 90%
$\Gamma(D^+ \to K^*(892)^- 2\mu^+)/\Gamma_{\text{total}}$		$<8.5 \times 10^{-4}$, CL = 90%
$\Gamma(D^0 \to 2\pi^- 2e^+ + \text{c.c.})/\Gamma_{\text{total}}$		$<1.12 \times 10^{-4}$, CL = 90%
$\Gamma(D^0 \to 2\pi^- 2\mu^+ + \text{c.c.})/\Gamma_{\text{total}}$		$<2.9 \times 10^{-5}$, CL = 90%
$\Gamma(D^0 \to K^- \pi^- 2e^+ + \text{c.c.})/\Gamma_{\text{total}}$		$<2.06 \times 10^{-4}$, CL = 90%
$\Gamma(D^0 \to K^- \pi^- 2\mu^+ + \text{c.c.})/\Gamma_{\text{total}}$		$<3.9 \times 10^{-4}$, CL = 90%
$\Gamma(D^0 \to 2K^- 2e^+ + \text{c.c.})/\Gamma_{\text{total}}$		$<1.52 \times 10^{-4}$, CL = 90%
$\Gamma(D^0 \to 2K^- 2\mu^+ + \text{c.c.})/\Gamma_{\text{total}}$		$<9.4 \times 10^{-5}$, CL = 90%
$\Gamma(D^0 \to \pi^- \pi^- e^+ \mu^+ + \text{c.c.})/\Gamma_{\text{total}}$		$<7.9 \times 10^{-5}$, CL = 90%
$\Gamma(D^0 \to K^- \pi^- e^+ \mu^+ + \text{c.c.})/\Gamma_{\text{total}}$		$<2.18 \times 10^{-4}$, CL = 90%
$\Gamma(D^0 \to 2K^- e^+ \mu^+ + \text{c.c.})/\Gamma_{\text{total}}$		$<5.7 \times 10^{-5}$, CL = 90%
$\Gamma(D^0 \to p e^-)/\Gamma_{\text{total}}$	[r]	$<1.0 \times 10^{-5}$, CL = 90%
$\Gamma(D^0 \to \overline{p} e^+)/\Gamma_{\text{total}}$	[s]	$<1.1 \times 10^{-5}$, CL = 90%
$\Gamma(D_s^+ \to \pi^- 2e^+)/\Gamma_{\text{total}}$		$<4.1 \times 10^{-6}$, CL = 90%
$\Gamma(D_s^+ \to \pi^- 2\mu^+)/\Gamma_{\text{total}}$		$<1.2 \times 10^{-7}$, CL = 90%
$\Gamma(D_s^+ \to \pi^- e^+ \mu^+)/\Gamma_{\text{total}}$		$<8.4 \times 10^{-6}$, CL = 90%
$\Gamma(D_s^+ \to K^- 2e^+)/\Gamma_{\text{total}}$		$<5.2 \times 10^{-6}$, CL = 90%
$\Gamma(D_s^+ \to K^- 2\mu^+)/\Gamma_{\text{total}}$		$<1.3 \times 10^{-5}$, CL = 90%
$\Gamma(D_s^+ \to K^- e^+ \mu^+)/\Gamma_{\text{total}}$		$<6.1 \times 10^{-6}$, CL = 90%
$\Gamma(D_s^+ \to K^*(892)^- 2\mu^+)/\Gamma_{\text{total}}$		$<1.4 \times 10^{-3}$, CL = 90%
$\Gamma(B^+ \to \pi^- e^+ e^+)/\Gamma_{\text{total}}$		$<2.3 \times 10^{-8}$, CL = 90%
$\Gamma(B^+ \to \pi^- \mu^+ \mu^+)/\Gamma_{\text{total}}$		$<1.3 \times 10^{-8}$, CL = 95%
$\Gamma(B^+ \to \pi^- e^+ \mu^+)/\Gamma_{\text{total}}$		$<1.5 \times 10^{-7}$, CL = 90%
$\Gamma(B^+ \to \rho^- e^+ e^+)/\Gamma_{\text{total}}$		$<1.7 \times 10^{-7}$, CL = 90%
$\Gamma(B^+ \to \rho^- \mu^+ \mu^+)/\Gamma_{\text{total}}$		$<4.2 \times 10^{-7}$, CL = 90%
$\Gamma(B^+ \to \rho^- e^+ \mu^+)/\Gamma_{\text{total}}$		$<4.7 \times 10^{-7}$, CL = 90%
$\Gamma(B^+ \to K^- e^+ e^+)/\Gamma_{\text{total}}$		$<3.0 \times 10^{-8}$, CL = 90%
$\Gamma(B^+ \to K^- \mu^+ \mu^+)/\Gamma_{\text{total}}$		$<4.1 \times 10^{-8}$, CL = 90%
$\Gamma(B^+ \to K^- e^+ \mu^+)/\Gamma_{\text{total}}$		$<1.6 \times 10^{-7}$, CL = 90%
$\Gamma(B^+ \to K^*(892)^- e^+ e^+)/\Gamma_{\text{total}}$		$<4.0 \times 10^{-7}$, CL = 90%
$\Gamma(B^+ \to K^*(892)^- \mu^+ \mu^+)/\Gamma_{\text{total}}$		$<5.9 \times 10^{-7}$, CL = 90%
$\Gamma(B^+ \to K^*(892)^- e^+ \mu^+)/\Gamma_{\text{total}}$		$<3.0 \times 10^{-7}$, CL = 90%
$\Gamma(B^+ \to D^- e^+ e^+)/\Gamma_{\text{total}}$		$<2.6 \times 10^{-6}$, CL = 90%
$\Gamma(B^+ \to D^- e^+ \mu^+)/\Gamma_{\text{total}}$		$<1.8 \times 10^{-6}$, CL = 90%
$\Gamma(B^+ \to D^- \mu^+ \mu^+)/\Gamma_{\text{total}}$		$<6.9 \times 10^{-7}$, CL = 95%
$\Gamma(B^+ \to D^{*-} \mu^+ \mu^+)/\Gamma_{\text{total}}$		$<2.4 \times 10^{-6}$, CL = 95%
$\Gamma(B^+ \to D_s^- \mu^+ \mu^+)/\Gamma_{\text{total}}$		$<5.8 \times 10^{-7}$, CL = 95%
$\Gamma(B^+ \to \overline{D}^0 \pi^- \mu^+ \mu^+)/\Gamma_{\text{total}}$		$<1.5 \times 10^{-6}$, CL = 95%
$\Gamma(B^+ \to \Lambda^0 \mu^+)/\Gamma_{\text{total}}$		$<6 \times 10^{-8}$, CL = 90%
$\Gamma(B^+ \to \Lambda^0 e^+)/\Gamma_{\text{total}}$		$<3.2 \times 10^{-8}$, CL = 90%
$\Gamma(B^+ \to \overline{\Lambda}^0 \mu^+)/\Gamma_{\text{total}}$		$<6 \times 10^{-8}$, CL = 90%
$\Gamma(B^+ \to \overline{\Lambda}^0 e^+)/\Gamma_{\text{total}}$		$<8 \times 10^{-8}$, CL = 90%
$\Gamma(B^0 \to \Lambda_c^+ \mu^-)/\Gamma_{\text{total}}$		$<1.8 \times 10^{-6}$, CL = 90%
$\Gamma(B^0 \to \Lambda_c^+ e^-)/\Gamma_{\text{total}}$		$<5 \times 10^{-6}$, CL = 90%
$\Gamma(\Xi^- \to p \mu^- \mu^-)/\Gamma_{\text{total}}$		$<4 \times 10^{-8}$, CL = 90%
$\Gamma(\Lambda_c^+ \to \overline{p} 2e^+)/\Gamma_{\text{total}}$		$<2.7 \times 10^{-6}$, CL = 90%
$\Gamma(\Lambda_c^+ \to \overline{p} 2\mu^+)/\Gamma_{\text{total}}$		$<9.4 \times 10^{-6}$, CL = 90%
$\Gamma(\Lambda_c^+ \to \overline{p} e^+ \mu^+)/\Gamma_{\text{total}}$		$<1.6 \times 10^{-5}$, CL = 90%
$\Gamma(\Lambda_c^+ \to \Sigma^- \mu^+ \mu^+)/\Gamma_{\text{total}}$		$<7.0 \times 10^{-4}$, CL = 90%

BARYON NUMBER

$\Gamma(Z \to p e)/\Gamma_{\text{total}}$		$<1.8 \times 10^{-6}$, CL = 95%
$\Gamma(Z \to p \mu)/\Gamma_{\text{total}}$		$<1.8 \times 10^{-6}$, CL = 95%
$\Gamma(\tau^- \to p \mu^- \mu^-)/\Gamma_{\text{total}}$		$<4.4 \times 10^{-7}$, CL = 90%
$\Gamma(\tau^- \to \overline{p} \mu^+ \mu^-)/\Gamma_{\text{total}}$		$<3.3 \times 10^{-7}$, CL = 90%
$\Gamma(\tau^- \to \overline{p} \gamma)/\Gamma_{\text{total}}$		$<3.5 \times 10^{-6}$, CL = 90%
$\Gamma(\tau^- \to \overline{p} \pi^0)/\Gamma_{\text{total}}$		$<1.5 \times 10^{-5}$, CL = 90%
$\Gamma(\tau^- \to \overline{p} 2\pi^0)/\Gamma_{\text{total}}$		$<3.3 \times 10^{-5}$, CL = 90%
$\Gamma(\tau^- \to \overline{p} \eta)/\Gamma_{\text{total}}$		$<8.9 \times 10^{-6}$, CL = 90%
$\Gamma(\tau^- \to \overline{p} \pi^0 \eta)/\Gamma_{\text{total}}$		$<2.7 \times 10^{-5}$, CL = 90%
$\Gamma(\tau^- \to \Lambda \pi^-)/\Gamma_{\text{total}}$		$<7.2 \times 10^{-8}$, CL = 90%
$\Gamma(\tau^- \to \overline{\Lambda} \pi^-)/\Gamma_{\text{total}}$		$<1.4 \times 10^{-7}$, CL = 90%
$\Gamma(D^0 \to p e^-)/\Gamma_{\text{total}}$	[r]	$<1.0 \times 10^{-5}$, CL = 90%
$\Gamma(D^0 \to \overline{p} e^+)/\Gamma_{\text{total}}$	[s]	$<1.1 \times 10^{-5}$, CL = 90%
$\Gamma(B^+ \to \Lambda^0 \mu^+)/\Gamma_{\text{total}}$		$<6 \times 10^{-8}$, CL = 90%
$\Gamma(B^+ \to \Lambda^0 e^+)/\Gamma_{\text{total}}$		$<3.2 \times 10^{-8}$, CL = 90%
$\Gamma(B^+ \to \overline{\Lambda}^0 \mu^+)/\Gamma_{\text{total}}$		$<6 \times 10^{-8}$, CL = 90%
$\Gamma(B^+ \to \overline{\Lambda}^0 e^+)/\Gamma_{\text{total}}$		$<8 \times 10^{-8}$, CL = 90%
$\Gamma(B^0 \to \Lambda_c^+ \mu^-)/\Gamma_{\text{total}}$		$<1.8 \times 10^{-6}$, CL = 90%
$\Gamma(B^0 \to \Lambda_c^+ e^-)/\Gamma_{\text{total}}$		$<5 \times 10^{-6}$, CL = 90%
p mean life	[t]	$>2.1 \times 10^{29}$ years, CL = 90%

A few examples of proton or bound neutron decay follow. For limits on many other nucleon decay channels, see the Baryon Summary Table.

$\tau(N \to e^+ \pi)$	$> 2000\ (n), > 8200\ (p) \times 10^{30}$ years, CL = 90%
$\tau(N \to \mu^+ \pi)$	$> 1000\ (n), > 6600\ (p) \times 10^{30}$ years, CL = 90%
$\tau(N \to e^+ K)$	$> 17\ (n), > 1000\ (p) \times 10^{30}$ years, CL = 90%
$\tau(N \to \mu^+ K)$	$> 26\ (n), > 1600\ (p) \times 10^{30}$ years, CL = 90%
limit on $n\overline{n}$ oscillations (free n)	$>0.86 \times 10^8$ s, CL = 90%
limit on $n\overline{n}$ oscillations (bound n) [u]	$>1.3 \times 10^8$ s, CL = 90%
$\Gamma(\Lambda_c^+ \to \overline{p} 2e^+)/\Gamma_{\text{total}}$	$<2.7 \times 10^{-6}$, CL = 90%
$\Gamma(\Lambda_c^+ \to \overline{p} 2\mu^+)/\Gamma_{\text{total}}$	$<9.4 \times 10^{-6}$, CL = 90%
$\Gamma(\Lambda_c^+ \to \overline{p} e^+ \mu^+)/\Gamma_{\text{total}}$	$<1.6 \times 10^{-5}$, CL = 90%

ELECTRIC CHARGE (Q)

$e \to \nu_e \gamma$ and astrophysical limits	[v]	$>4.6 \times 10^{26}$ yr, CL = 90%
$\Gamma(n \to p \nu_e \overline{\nu}_e)/\Gamma_{\text{total}}$		$<8 \times 10^{-27}$, CL = 68%

$\Delta S = \Delta Q$ RULE

Violations allowed in second-order weak interactions.

$\Gamma(K^+ \to \pi^+ \pi^+ e^- \overline{\nu}_e)/\Gamma_{\text{total}}$	$<1.3 \times 10^{-8}$, CL = 90%
$\Gamma(K^+ \to \pi^+ \pi^+ \mu^- \overline{\nu}_\mu)/\Gamma_{\text{total}}$	$<3.0 \times 10^{-6}$, CL = 95%
$\text{Re}(x_+)$, K_{e3} parameter	$(-0.9 \pm 3.0) \times 10^{-3}$
$x = \text{A}(\overline{K}^0 \to \pi^- \ell^+ \nu)/\text{A}(K^0 \to \pi^- \ell^+ \nu) = \text{A}(\Delta S{=}-\Delta Q)/\text{A}(\Delta S{=}\Delta Q)$	
real part of x	-0.002 ± 0.006
imaginary part of x	0.0012 ± 0.0021
$\Gamma(\Sigma^+ \to n \ell^+ \nu)/\Gamma(\Sigma^- \to n \ell^- \overline{\nu})$	<0.043
$\Gamma(\Sigma^+ \to n e^+ \nu_e)/\Gamma_{\text{total}}$	$<5 \times 10^{-6}$, CL = 90%
$\Gamma(\Sigma^+ \to n \mu^+ \nu_\mu)/\Gamma_{\text{total}}$	$<3.0 \times 10^{-5}$, CL = 90%
$\Gamma(\Xi^0 \to \Sigma^- e^+ \nu_e)/\Gamma_{\text{total}}$	$<9 \times 10^{-4}$, CL = 90%
$\Gamma(\Xi^0 \to \Sigma^- \mu^+ \nu_\mu)/\Gamma_{\text{total}}$	$<9 \times 10^{-4}$, CL = 90%

Unless otherwise stated, limits are given at the 90% confidence level, while errors are given as ± 1 standard deviation.

$\Delta S = 2$ FORBIDDEN

Allowed in second-order weak interactions.

$\Gamma(\Xi^0 \to p\pi^-)/\Gamma_{\text{total}}$	$<8 \times 10^{-6}$, CL = 90%
$\Gamma(\Xi^0 \to pe^-\overline{\nu}_e)/\Gamma_{\text{total}}$	$<1.3 \times 10^{-3}$
$\Gamma(\Xi^0 \to p\mu^-\overline{\nu}_\mu)/\Gamma_{\text{total}}$	$<1.3 \times 10^{-3}$
$\Gamma(\Xi^- \to n\pi^-)/\Gamma_{\text{total}}$	$<1.9 \times 10^{-5}$, CL = 90%
$\Gamma(\Xi^- \to ne^-\overline{\nu}_e)/\Gamma_{\text{total}}$	$<3.2 \times 10^{-3}$, CL = 90%
$\Gamma(\Xi^- \to n\mu^-\overline{\nu}_\mu)/\Gamma_{\text{total}}$	$<1.5 \times 10^{-2}$, CL = 90%
$\Gamma(\Xi^- \to p\pi^-\pi^-)/\Gamma_{\text{total}}$	$<4 \times 10^{-4}$, CL = 90%
$\Gamma(\Xi^- \to p\pi^- e^-\overline{\nu}_e)/\Gamma_{\text{total}}$	$<4 \times 10^{-4}$, CL = 90%
$\Gamma(\Xi^- \to p\pi^-\mu^-\overline{\nu}_\mu)/\Gamma_{\text{total}}$	$<4 \times 10^{-4}$, CL = 90%
$\Gamma(\Omega^- \to \Lambda\pi^-)/\Gamma_{\text{total}}$	$<2.9 \times 10^{-6}$, CL = 90%

$\Delta S = 2$ VIA MIXING

Allowed in second-order weak interactions, e.g. mixing.

$m_{K_L^0} - m_{K_S^0}$	$(0.5293 \pm 0.0009) \times 10^{10}\ \hbar\ \text{s}^{-1}$ (S = 1.3)
$m_{K_L^0} - m_{K_S^0}$	$(3.484 \pm 0.006) \times 10^{-12}$ MeV

$\Delta C = 2$ VIA MIXING

Allowed in second-order weak interactions, e.g. mixing.

$\lvert m_{D_1^0} - m_{D_2^0}\rvert = x\Gamma$	$(0.95^{+0.41}_{-0.44}) \times 10^{10}\ \hbar\ \text{s}^{-1}$
$(\Gamma_{D_1^0} - \Gamma_{D_2^0})/\Gamma = 2y$	$(0.65^{+0.07}_{-0.09}) \times 10^{-2}$

$\Delta B = 2$ VIA MIXING

Allowed in second-order weak interactions, e.g. mixing.

χ_d	0.1874 ± 0.0018
$\Delta m_{B^0} = m_{B_H^0} - m_{B_L^0}$	$(0.510 \pm 0.003) \times 10^{12}\ \hbar\ \text{s}^{-1}$
$x_d = \Delta m_{B^0}/\Gamma_{B^0}$	0.774 ± 0.006
$\Delta m_{B_s^0} = m_{B_{sH}^0} - m_{B_{sL}^0}$	$(17.761 \pm 0.022) \times 10^{12}\ \hbar\ \text{s}^{-1}$
$x_s = \Delta m_{B_s^0}/\Gamma_{B_s^0}$	26.85 ± 0.13
χ_s	0.499311 ± 0.000007

$\Delta S = 1$ WEAK NEUTRAL CURRENT FORBIDDEN

Allowed by higher-order electroweak interactions.

$\Gamma(K^+ \to \pi^+ e^+ e^-)/\Gamma_{\text{total}}$		$(3.00 \pm 0.09) \times 10^{-7}$
$\Gamma(K^+ \to \pi^+ \mu^+ \mu^-)/\Gamma_{\text{total}}$		$(9.4 \pm 0.6) \times 10^{-8}$ (S = 2.6)
$\Gamma(K^+ \to \pi^+ \nu\overline{\nu})/\Gamma_{\text{total}}$		$(1.7 \pm 1.1) \times 10^{-10}$
$\Gamma(K^+ \to \pi^+ \pi^0 \nu\overline{\nu})/\Gamma_{\text{total}}$		$<4.3 \times 10^{-5}$, CL = 90%
$\Gamma(K_S^0 \to \mu^+ \mu^-)/\Gamma_{\text{total}}$		$<9 \times 10^{-9}$, CL = 90%
$\Gamma(K_S^0 \to e^+ e^-)/\Gamma_{\text{total}}$		$<9 \times 10^{-9}$, CL = 90%
$\Gamma(K_S^0 \to \pi^0 e^+ e^-)/\Gamma_{\text{total}}$	[x]	$(3.0^{+1.5}_{-1.2}) \times 10^{-9}$
$\Gamma(K_S^0 \to \pi^0 \mu^+ \mu^-)/\Gamma_{\text{total}}$		$(2.9^{+1.5}_{-1.2}) \times 10^{-9}$
$\Gamma(K_L^0 \to \mu^+ \mu^-)/\Gamma_{\text{total}}$		$(6.84 \pm 0.11) \times 10^{-9}$
$\Gamma(K_L^0 \to e^+ e^-)/\Gamma_{\text{total}}$		$(9^{+6}_{-4}) \times 10^{-12}$
$\Gamma(K_L^0 \to \pi^+ \pi^- e^+ e^-)/\Gamma_{\text{total}}$	[y]	$(3.11 \pm 0.19) \times 10^{-7}$
$\Gamma(K_L^0 \to \pi^0 \pi^0 e^+ e^-)/\Gamma_{\text{total}}$		$<6.6 \times 10^{-9}$, CL = 90%
$\Gamma(K_L^0 \to \pi^0 \pi^0 \mu^+ \mu^-)/\Gamma_{\text{total}}$		$<9.2 \times 10^{-11}$, CL = 90%
$\Gamma(K_L^0 \to \mu^+ \mu^- e^+ e^-)/\Gamma_{\text{total}}$		$(2.69 \pm 0.27) \times 10^{-9}$
$\Gamma(K_L^0 \to e^+ e^- e^+ e^-)/\Gamma_{\text{total}}$		$(3.56 \pm 0.21) \times 10^{-8}$
$\Gamma(K_L^0 \to \pi^0 \mu^+ \mu^-)/\Gamma_{\text{total}}$		$<3.8 \times 10^{-10}$, CL = 90%
$\Gamma(K_L^0 \to \pi^0 e^+ e^-)/\Gamma_{\text{total}}$		$<2.8 \times 10^{-10}$, CL = 90%
$\Gamma(K_L^0 \to \pi^0 \nu\overline{\nu})/\Gamma_{\text{total}}$		$<2.6 \times 10^{-8}$, CL = 90%
$\Gamma(K_L^0 \to \pi^0 \pi^0 \nu\overline{\nu})/\Gamma_{\text{total}}$		$<8.1 \times 10^{-7}$, CL = 90%
$\Gamma(\Sigma^+ \to pe^+ e^-)/\Gamma_{\text{total}}$		$<7 \times 10^{-6}$
$\Gamma(\Sigma^+ \to p\mu^+ \mu^-)/\Gamma_{\text{total}}$		$(9^{+9}_{-8}) \times 10^{-8}$

Unless otherwise stated, limits are given at the 90% confidence level, while errors are given as ± 1 standard deviation.

$\Delta C = 1$ WEAK NEUTRAL CURRENT FORBIDDEN

Allowed by higher-order electroweak interactions.

$\Gamma(D^+ \to \pi^+ e^+ e^-)/\Gamma_{\text{total}}$	$<1.1 \times 10^{-6}$, CL = 90%
$\Gamma(D^+ \to \pi^+ \mu^+ \mu^-)/\Gamma_{\text{total}}$	$<7.3 \times 10^{-8}$, CL = 90%
$\Gamma(D^+ \to \rho^+ \mu^+ \mu^-)/\Gamma_{\text{total}}$	$<5.6 \times 10^{-4}$, CL = 90%
$\Gamma(D^0 \to \gamma\gamma)/\Gamma_{\text{total}}$	$<2.2 \times 10^{-6}$, CL = 90%
$\Gamma(D^0 \to e^+ e^-)/\Gamma_{\text{total}}$	$<7.9 \times 10^{-8}$, CL = 90%
$\Gamma(D^0 \to \mu^+ \mu^-)/\Gamma_{\text{total}}$	$<6.2 \times 10^{-9}$, CL = 90%
$\Gamma(D^0 \to \pi^0 e^+ e^-)/\Gamma_{\text{total}}$	$<4.5 \times 10^{-5}$, CL = 90%
$\Gamma(D^0 \to \pi^0 \mu^+ \mu^-)/\Gamma_{\text{total}}$	$<1.8 \times 10^{-4}$, CL = 90%
$\Gamma(D^0 \to \eta e^+ e^-)/\Gamma_{\text{total}}$	$<1.1 \times 10^{-4}$, CL = 90%
$\Gamma(D^0 \to \eta \mu^+ \mu^-)/\Gamma_{\text{total}}$	$<5.3 \times 10^{-4}$, CL = 90%
$\Gamma(D^0 \to \pi^+ \pi^- e^+ e^-)/\Gamma_{\text{total}}$	$<3.73 \times 10^{-4}$, CL = 90%
$\Gamma(D^0 \to \rho^0 e^+ e^-)/\Gamma_{\text{total}}$	$<1.0 \times 10^{-4}$, CL = 90%
$\Gamma(D^0 \to \pi^+ \pi^- \mu^+ \mu^-)/\Gamma_{\text{total}}$	$<5.5 \times 10^{-7}$, CL = 90%
$\Gamma(D^0 \to \rho^0 \mu^+ \mu^-)/\Gamma_{\text{total}}$	$<2.2 \times 10^{-5}$, CL = 90%
$\Gamma(D^0 \to \omega e^+ e^-)/\Gamma_{\text{total}}$	$<1.8 \times 10^{-4}$, CL = 90%
$\Gamma(D^0 \to \omega \mu^+ \mu^-)/\Gamma_{\text{total}}$	$<8.3 \times 10^{-4}$, CL = 90%
$\Gamma(D^0 \to K^- K^+ e^+ e^-)/\Gamma_{\text{total}}$	$<3.15 \times 10^{-4}$, CL = 90%
$\Gamma(D^0 \to \phi e^+ e^-)/\Gamma_{\text{total}}$	$<5.2 \times 10^{-5}$, CL = 90%
$\Gamma(D^0 \to K^- K^+ \mu^+ \mu^-)/\Gamma_{\text{total}}$	$<3.3 \times 10^{-5}$, CL = 90%
$\Gamma(D^0 \to \phi \mu^+ \mu^-)/\Gamma_{\text{total}}$	$<3.1 \times 10^{-5}$, CL = 90%
$\Gamma(D^0 \to K^- \pi^+ e^+ e^-)/\Gamma_{\text{total}}$	$<3.85 \times 10^{-4}$, CL = 90%
$\Gamma(D^0 \to K^- \pi^+ \mu^+ \mu^-)/\Gamma_{\text{total}}$	$<3.59 \times 10^{-4}$, CL = 90%
$\Gamma(D^0 \to \pi^+ \pi^- \pi^0 \mu^+ \mu^-)/\Gamma_{\text{total}}$	$<8.1 \times 10^{-4}$, CL = 90%
$\Gamma(D_s^+ \to K^+ e^+ e^-)/\Gamma_{\text{total}}$	$<3.7 \times 10^{-6}$, CL = 90%
$\Gamma(D_s^+ \to K^+ \mu^+ \mu^-)/\Gamma_{\text{total}}$	$<2.1 \times 10^{-5}$, CL = 90%
$\Gamma(D_s^+ \to K^*(892)^+ \mu^+ \mu^-)/\Gamma_{\text{total}}$	$<1.4 \times 10^{-3}$, CL = 90%
$\Gamma(\Lambda_c^+ \to pe^+ e^-)/\Gamma_{\text{total}}$	$<5.5 \times 10^{-6}$, CL = 90%
$\Gamma(\Lambda_c^+ \to p\mu^+ \mu^-)/\Gamma_{\text{total}}$	$<4.4 \times 10^{-5}$, CL = 90%

$\Delta B = 1$ WEAK NEUTRAL CURRENT FORBIDDEN

Allowed by higher-order electroweak interactions.

$\Gamma(B^+ \to \pi^+ \ell^+ \ell^-)/\Gamma_{\text{total}}$		$<4.9 \times 10^{-8}$, CL = 90%
$\Gamma(B^+ \to \pi^+ e^+ e^-)/\Gamma_{\text{total}}$		$<8.0 \times 10^{-8}$, CL = 90%
$\Gamma(B^+ \to \pi^+ \mu^+ \mu^-)/\Gamma_{\text{total}}$		$<5.5 \times 10^{-8}$, CL = 90%
$\Gamma(B^+ \to \pi^+ \nu\overline{\nu})/\Gamma_{\text{total}}$		$<9.8 \times 10^{-5}$, CL = 90%
$\Gamma(B^+ \to K^+ \ell^+ \ell^-)/\Gamma_{\text{total}}$	[z]	$(4.51 \pm 0.23) \times 10^{-7}$ (S = 1.1)
$\Gamma(B^+ \to K^+ e^+ e^-)/\Gamma_{\text{total}}$		$(5.5 \pm 0.7) \times 10^{-7}$
$\Gamma(B^+ \to K^+ \mu^+ \mu^-)/\Gamma_{\text{total}}$		$(4.49 \pm 0.23) \times 10^{-7}$ (S = 1.1)
$\Gamma(B^+ \to K^+ \nu\overline{\nu})/\Gamma_{\text{total}}$		$<1.6 \times 10^{-5}$, CL = 90%
$\Gamma(B^+ \to \rho^+ \nu\overline{\nu})/\Gamma_{\text{total}}$		$<2.13 \times 10^{-4}$, CL = 90%
$\Gamma(B^+ \to K^*(892)^+ \ell^+ \ell^-)/\Gamma_{\text{total}}$	[z]	$(1.29 \pm 0.21) \times 10^{-6}$
$\Gamma(B^+ \to K^*(892)^+ e^+ e^-)/\Gamma_{\text{total}}$		$(1.55^{+0.40}_{-0.31}) \times 10^{-6}$
$\Gamma(B^+ \to K^*(892)^+ \mu^+ \mu^-)/\Gamma_{\text{total}}$		$(1.12 \pm 0.15) \times 10^{-6}$
$\Gamma(B^+ \to K^*(892)^+ \nu\overline{\nu})/\Gamma_{\text{total}}$		$<4.0 \times 10^{-5}$, CL = 90%
$\Gamma(B^0 \to \gamma\gamma)/\Gamma_{\text{total}}$		$<3.2 \times 10^{-7}$, CL = 90%
$\Gamma(B^0 \to e^+ e^-)/\Gamma_{\text{total}}$		$<8.3 \times 10^{-8}$, CL = 90%
$\Gamma(B^0 \to e^+ e^- \gamma)/\Gamma_{\text{total}}$		$<1.2 \times 10^{-7}$, CL = 90%
$\Gamma(B^0 \to \mu^+ \mu^-)/\Gamma_{\text{total}}$		$<6.3 \times 10^{-10}$, CL = 90%
$\Gamma(B^0 \to \mu^+ \mu^- \gamma)/\Gamma_{\text{total}}$		$<1.6 \times 10^{-7}$, CL = 90%
$\Gamma(B^0 \to \tau^+ \tau^-)/\Gamma_{\text{total}}$		$<4.1 \times 10^{-3}$, CL = 90%
$\Gamma(B^0 \to \pi^0 \ell^+ \ell^-)/\Gamma_{\text{total}}$		$<5.3 \times 10^{-8}$, CL = 90%
$\Gamma(B^0 \to \pi^0 e^+ e^-)/\Gamma_{\text{total}}$		$<8.4 \times 10^{-8}$, CL = 90%
$\Gamma(B^0 \to \pi^0 \mu^+ \mu^-)/\Gamma_{\text{total}}$		$<6.9 \times 10^{-8}$, CL = 90%
$\Gamma(B^0 \to \pi^0 \nu\overline{\nu})/\Gamma_{\text{total}}$		$<6.9 \times 10^{-5}$, CL = 90%
$\Gamma(B^0 \to K^0 \ell^+ \ell^-)/\Gamma_{\text{total}}$	[z]	$(3.1^{+0.8}_{-0.7}) \times 10^{-7}$
$\Gamma(B^0 \to K^0 e^+ e^-)/\Gamma_{\text{total}}$		$(1.6^{+1.0}_{-0.8}) \times 10^{-7}$
$\Gamma(B^0 \to K^0 \mu^+ \mu^-)/\Gamma_{\text{total}}$		$(3.4 \pm 0.5) \times 10^{-7}$
$\Gamma(B^0 \to K^0 \nu\overline{\nu})/\Gamma_{\text{total}}$		$<4.9 \times 10^{-5}$, CL = 90%
$\Gamma(B^0 \to \rho^0 \nu\overline{\nu})/\Gamma_{\text{total}}$		$<2.08 \times 10^{-4}$, CL = 90%
$\Gamma(B^0 \to K^*(892)^0 \ell^+ \ell^-)/\Gamma_{\text{total}}$	[z]	$(9.9^{+1.2}_{-1.1}) \times 10^{-7}$
$\Gamma(B^0 \to K^*(892)^0 e^+ e^-)/\Gamma_{\text{total}}$		$(1.03^{+0.19}_{-0.17}) \times 10^{-6}$
$\Gamma(B^0 \to K^*(892)^0 \mu^+ \mu^-)/\Gamma_{\text{total}}$		$(1.05 \pm 0.10) \times 10^{-6}$
$\Gamma(B^0 \to K^*(892)^0 \nu\overline{\nu})/\Gamma_{\text{total}}$		$<5.5 \times 10^{-5}$, CL = 90%
$\Gamma(B^0 \to \phi\nu\overline{\nu})/\Gamma_{\text{total}}$		$<1.27 \times 10^{-4}$, CL = 90%

Tests of Conservation Laws

$\Gamma(B^0 \to \text{ invisible})/\Gamma_{\text{total}}$		$<2.4 \times 10^{-5}$, CL = 90%
$\Gamma(B^0 \to \nu\overline{\nu}\gamma)/\Gamma_{\text{total}}$		$<1.7 \times 10^{-5}$, CL = 90%
$\Gamma(B \to s e^+ e^-)/\Gamma_{\text{total}}$		$(4.7 \pm 1.3) \times 10^{-6}$
$\Gamma(B \to s \mu^+ \mu^-)/\Gamma_{\text{total}}$		$(4.3 \pm 1.2) \times 10^{-6}$
$\Gamma(B \to s \ell^+ \ell^-)/\Gamma_{\text{total}}$	[z]	$(4.5 \pm 1.0) \times 10^{-6}$
$\Gamma(B \to \pi \ell^+ \ell^-)/\Gamma_{\text{total}}$		$<5.9 \times 10^{-8}$, CL = 90%
$\Gamma(B \to K e^+ e^-)/\Gamma_{\text{total}}$		$(4.4 \pm 0.6) \times 10^{-7}$
$\Gamma(B \to K^*(892) e^+ e^-)/\Gamma_{\text{total}}$		$(1.19 \pm 0.20) \times 10^{-6}$ (S = 1.2)
$\Gamma(B \to K \mu^+ \mu^-)/\Gamma_{\text{total}}$		$(4.4 \pm 0.4) \times 10^{-7}$
$\Gamma(B \to K^*(892) \mu^+ \mu^-)/\Gamma_{\text{total}}$		$(1.06 \pm 0.09) \times 10^{-6}$
$\Gamma(B \to K \ell^+ \ell^-)/\Gamma_{\text{total}}$		$(4.8 \pm 0.4) \times 10^{-7}$
$\Gamma(B \to K^*(892) \ell^+ \ell^-)/\Gamma_{\text{total}}$		$(1.05 \pm 0.10) \times 10^{-6}$
$\Gamma(B \to K \nu\overline{\nu})/\Gamma_{\text{total}}$		$<1.7 \times 10^{-5}$, CL = 90%
$\Gamma(B \to K^* \nu\overline{\nu})/\Gamma_{\text{total}}$		$<7.6 \times 10^{-5}$, CL = 90%
$\Gamma(\overline{b} \to \overline{s}\overline{\nu}\nu)/\Gamma_{\text{total}}$		$<6.4 \times 10^{-4}$, CL = 90%
$\Gamma(\overline{b} \to e^+ e^- \text{ anything})/\Gamma_{\text{total}}$		—
$\Gamma(\overline{b} \to \mu^+ \mu^- \text{ anything})/\Gamma_{\text{total}}$		$<3.2 \times 10^{-4}$, CL = 90%
$\Gamma(\overline{b} \to \nu\overline{\nu} \text{ anything})/\Gamma_{\text{total}}$		—
$\Gamma(B_s^0 \to \gamma\gamma)/\Gamma_{\text{total}}$		$<8.7 \times 10^{-6}$, CL = 90%
$\Gamma(B_s^0 \to \mu^+ \mu^-)/\Gamma_{\text{total}}$		$(3.1 \pm 0.7) \times 10^{-9}$
$\Gamma(B_s^0 \to e^+ e^-)/\Gamma_{\text{total}}$		$<2.8 \times 10^{-7}$, CL = 90%
$\Gamma(B_s^0 \to \phi(1020) \mu^+ \mu^-)/\Gamma_{\text{total}}$		$(7.6 \pm 1.5) \times 10^{-7}$
$\Gamma(B_s^0 \to \phi\nu\overline{\nu})/\Gamma_{\text{total}}$		$<5.4 \times 10^{-3}$, CL = 90%

$\Delta T = 1$ WEAK NEUTRAL CURRENT FORBIDDEN

Allowed by higher-order electroweak interactions.

$\Gamma(t \to Z q(q{=}u,c))/\Gamma_{\text{total}}$	[aa]	$<2.1 \times 10^{-3}$, CL = 95%

NOTES

In this Summary Table:

When a quantity has "(S = ...)" to its right, the error on the quantity has been enlarged by the "scale factor" S, defined as $S = \sqrt{\chi^2/(N-1)}$, where N is the number of measurements used in calculating the quantity. We do this when $S > 1$, which often indicates that the measurements are inconsistent. When $S > 1.25$, we also show in the Particle Listings an ideogram of the measurements. For more about S, see the Introduction.

[a] C parity forbids this to occur as a single-photon process.

[b] See the Particle Listings for the (complicated) definition of this quantity.

[c] Time-reversal invariance requires this to be 0° or 180°.

[d] This coefficient is zero if time invariance is not violated.

[e] Allowed by higher-order electroweak interactions.

[f] Violates CP in leading order. Test of direct CP violation since the indirect CP-violating and CP-conserving contributions are expected to be suppressed.

[g] In the 2010 *Review*, the values for these quantities were given using a measure of the asymmetry that was inconsistent with the usual definition.

[h] $\text{Re}(\epsilon'/\epsilon) = \epsilon'/\epsilon$ to a very good approximation provided the phases satisfy CPT invariance.

[i] This mode includes gammas from inner bremsstrahlung but not the direct emission mode $K_L^0 \to \pi^+\pi^-\gamma(\text{DE})$.

[j] Neglecting photon channels. See, *e.g.*, A. Pais and S.B. Treiman, Phys. Rev. **D12**, 2744 (1975).

[k] Derived from measured values of ϕ_{+-}, ϕ_{00}, $|\eta|$, $|m_{K_L^0} - m_{K_S^0}|$, and $\tau_{K_S^0}$, as described in the introduction to "Tests of Conservation Laws."

[l] The $|m_p - m_{\overline{p}}|/m_p$ and $|q_p + q_{\overline{p}}|/e$ are not independent, and both use the more precise measurement of $|q_{\overline{p}}/m_{\overline{p}}|/(q_p/m_p)$.

[n] The value is for the sum of the charge states or particle/antiparticle states indicated.

[o] A test of additive vs. multiplicative lepton family number conservation.

[p] The sign of Δm^2_{32} is not known at this time. The range quoted is for the absolute value.

[q] Derived from an analysis of neutrino-oscillation experiments.

[r] This limit is for either D^0 or $\overline{D}^0$ to $p e^-$.

[s] This limit is for either D^0 or $\overline{D}^0$ to $\overline{p} e^+$.

[t] The first limit is for $p \to$ anything or "disappearance" modes of a bound proton. The second entry, a rough range of limits, assumes the dominant decay modes are among those investigated. For antiprotons the best limit, inferred from the observation of cosmic ray $\overline{p}$'s is $\tau_{\overline{p}} > 10^7$ yr, the cosmic-ray storage time, but this limit depends on a number of assumptions. The best direct observation of stored antiprotons gives $\tau_{\overline{p}}/\text{B}(\overline{p} \to e^-\gamma) > 7 \times 10^5$ yr.

[u] There is some controversy about whether nuclear physics and model dependence complicate the analysis for bound neutrons (from which the best limit comes). The first limit here is from reactor experiments with free neutrons.

[v] This is the best limit for the mode $e^- \to \nu\gamma$. The best limit for "electron disappearance" is 6.4×10^{24} yr.

[x] See the K_S^0 Particle Listings for the energy limits used in this measurement.

[y] See the K_L^0 Particle Listings for the energy limits used in this measurement.

[z] An ℓ indicates an e or a μ mode, not a sum over these modes.

[aa] This limit is for $\Gamma(t \to Z q)/\Gamma(t \to W b)$.

Unless otherwise stated, limits are given at the 90% confidence level, while errors are given as ±1 standard deviation.

REVIEWS, TABLES, AND PLOTS

MAJOR REVIEWS IN THE PARTICLE LISTINGS

Additional Reviews and Notes related to specific particles are located in the Particle Listings.

1. PHYSICAL CONSTANTS

Table 1.1. Reviewed 2013 by P.J. Mohr (NIST). Mainly from the "CODATA Recommended Values of the Fundamental Physical Constants: 2010" by P.J. Mohr, B.N. Taylor, and D.B. Newell in Rev. Mod. Phys. **84**, 1527 (2012). The last group of constants (beginning with the Fermi coupling constant) comes from the Particle Data Group. The figures in parentheses after the values give the 1-standard-deviation uncertainties in the last digits; the corresponding fractional uncertainties in parts per 10^9 (ppb) are given in the last column. This set of constants (aside from the last group) is recommended for international use by CODATA (the Committee on Data for Science and Technology). The full 2010 CODATA set of constants may be found at `http://physics.nist.gov/constants`. See also P.J. Mohr and D.B. Newell, "Resource Letter FC-1: The Physics of Fundamental Constants," Am. J. Phys. **78**, 338 (2010).

Quantity	Symbol, equation	Value	Uncertainty (ppb)
speed of light in vacuum	c	299 792 458 m s^{-1}	exact*
Planck constant	h	$6.626\ 069\ 57(29)\times10^{-34}$ J s	44
Planck constant, reduced	$\hbar \equiv h/2\pi$	$1.054\ 571\ 726(47)\times10^{-34}$ J s	44
		$= 6.582\ 119\ 28(15)\times10^{-22}$ MeV s	22
electron charge magnitude	e	$1.602\ 176\ 565(35)\times10^{-19}$ C $= 4.803\ 204\ 50(11)\times10^{-10}$ esu	22, 22
conversion constant	$\hbar c$	197.326 9718(44) MeV fm	22
conversion constant	$(\hbar c)^2$	0.389 379 338(17) GeV^2 mbarn	44
electron mass	m_e	$0.510\ 998\ 928(11)$ MeV$/c^2 = 9.109\ 382\ 91(40)\times10^{-31}$ kg	22, 44
proton mass	m_p	$938.272\ 046(21)$ MeV$/c^2 = 1.672\ 621\ 777(74)\times10^{-27}$ kg	22, 44
		$= 1.007\ 276\ 466\ 812(90)$ u $= 1836.152\ 672\ 45(75)\ m_e$	0.089, 0.41
deuteron mass	m_d	1875.612 859(41) MeV$/c^2$	22
unified atomic mass unit (u)	(mass ^{12}C atom)/12 = (1 g)/(N_A mol)	$931.494\ 061(21)$ MeV$/c^2 = 1.660\ 538\ 921(73)\times10^{-27}$ kg	22, 44
permittivity of free space	$\epsilon_0 = 1/\mu_0 c^2$	$8.854\ 187\ 817\ \ldots\ \times10^{-12}$ F m^{-1}	exact
permeability of free space	μ_0	$4\pi \times 10^{-7}$ N $A^{-2} = 12.566\ 370\ 614\ \ldots\ \times10^{-7}$ N A^{-2}	exact
fine-structure constant	$\alpha = e^2/4\pi\epsilon_0\hbar c$	$7.297\ 352\ 5698(24)\times10^{-3} = 1/137.035\ 999\ 074(44)^\dagger$	0.32, 0.32
classical electron radius	$r_e = e^2/4\pi\epsilon_0 m_e c^2$	$2.817\ 940\ 3267(27)\times10^{-15}$ m	0.97
(e^- Compton wavelength)/2π	$\lambda\!\!\!^{-}_e = \hbar/m_e c = r_e\alpha^{-1}$	$3.861\ 592\ 6800(25)\times10^{-13}$ m	0.65
Bohr radius ($m_{\rm nucleus} = \infty$)	$a_\infty = 4\pi\epsilon_0\hbar^2/m_e e^2 = r_e\alpha^{-2}$	$0.529\ 177\ 210\ 92(17)\times10^{-10}$ m	0.32
wavelength of 1 eV/c particle	hc/(1 eV)	$1.239\ 841\ 930(27)\times10^{-6}$ m	22
Rydberg energy	$hcR_\infty = m_e e^4/2(4\pi\epsilon_0)^2\hbar^2 = m_e c^2\alpha^2/2$	13.605 692 53(30) eV	22
Thomson cross section	$\sigma_T = 8\pi r_e^2/3$	0.665 245 8734(13) barn	1.9
Bohr magneton	$\mu_B = e\hbar/2m_e$	$5.788\ 381\ 8066(38)\times10^{-11}$ MeV T^{-1}	0.65
nuclear magneton	$\mu_N = e\hbar/2m_p$	$3.152\ 451\ 2605(22)\times10^{-14}$ MeV T^{-1}	0.71
electron cyclotron freq./field	$\omega^e_{\rm cycl}/B = e/m_e$	$1.758\ 820\ 088(39)\times10^{11}$ rad s^{-1} T^{-1}	22
proton cyclotron freq./field	$\omega^p_{\rm cycl}/B = e/m_p$	$9.578\ 833\ 58(21)\times10^{7}$ rad s^{-1} T^{-1}	22
gravitational constant‡	G_N	$6.673\ 84(80)\times10^{-11}$ m^3 kg^{-1} s^{-2}	1.2×10^5
		$= 6.708\ 37(80)\times10^{-39}\ \hbar c$ $(\mathrm{GeV}/c^2)^{-2}$	1.2×10^5
standard gravitational accel.	g_N	9.806 65 m s^{-2}	exact
Avogadro constant	N_A	$6.022\ 141\ 29(27)\times10^{23}$ mol^{-1}	44
Boltzmann constant	k	$1.380\ 6488(13)\times10^{-23}$ J K^{-1}	910
		$= 8.617\ 3324(78)\times10^{-5}$ eV K^{-1}	910
molar volume, ideal gas at STP	$N_A k$(273.15 K)/(101 325 Pa)	$22.413\ 968(20)\times10^{-3}$ m^3 mol^{-1}	910
Wien displacement law constant	$b = \lambda_{\rm max}T$	$2.897\ 7721(26)\times10^{-3}$ m K	910
Stefan-Boltzmann constant	$\sigma = \pi^2k^4/60\hbar^3c^2$	$5.670\ 373(21)\times10^{-8}$ W m^{-2} K^{-4}	3600
Fermi coupling constant**	$G_F/(\hbar c)^3$	$1.166\ 378\ 7(6)\times10^{-5}$ GeV^{-2}	500
weak-mixing angle	$\sin^2\widehat{\theta}(M_Z)$ ($\overline{\rm MS}$)	0.231 26(5)††	2.2×10^5
$W^\pm$ boson mass	m_W	80.385(15) GeV$/c^2$	1.9×10^5
Z^0 boson mass	m_Z	91.1876(21) GeV$/c^2$	2.3×10^4
strong coupling constant	$\alpha_s(m_Z)$	0.1185(6)	5.1×10^6

$\pi = 3.141\ 592\ 653\ 589\ 793\ 238$ e $= 2.718\ 281\ 828\ 459\ 045\ 235$ $\gamma = 0.577\ 215\ 664\ 901\ 532\ 861$

1 in $\equiv 0.0254$ m 1 G $\equiv 10^{-4}$ T 1 eV $= 1.602\ 176\ 565(35)\times10^{-19}$ J kT at 300 K $= [38.681\ 731(35)]^{-1}$ eV

1 Å $\equiv 0.1$ nm 1 dyne $\equiv 10^{-5}$ N 1 eV$/c^2 = 1.782\ 661\ 845(39)\times10^{-36}$ kg 0 °C $\equiv 273.15$ K

1 barn $\equiv 10^{-28}$ m^2 1 erg $\equiv 10^{-7}$ J $2.997\ 924\ 58\times10^9$ esu $= 1$ C 1 atmosphere $\equiv 760$ Torr $\equiv 101\ 325$ Pa

* The meter is the length of the path traveled by light in vacuum during a time interval of 1/299 792 458 of a second.
† At $Q^2 = 0$. At $Q^2 \approx m_W^2$ the value is $\sim 1/128$.
‡ Absolute lab measurements of G_N have been made only on scales of about 1 cm to 1 m.
** See the discussion in Sec. 10, "Electroweak model and constraints on new physics."
†† The corresponding $\sin^2\theta$ for the effective angle is 0.23155(5).

2. ASTROPHYSICAL CONSTANTS AND PARAMETERS

Table 2.1. Revised November 2013 by D.E. Groom (LBNL). The figures in parentheses after some values give the 1-σ uncertainties in the last digit(s). Physical constants are from Ref. 1. While every effort has been made to obtain the most accurate current values of the listed quantities, the table does not represent a critical review or adjustment of the constants, and is not intended as a primary reference.

The values and uncertainties for the cosmological parameters depend on the exact data sets, priors, and basis parameters used in the fit. Many of the derived parameters reported in this table have non-Gaussian likelihoods. Parameters may be highly correlated, so care must be taken in propagating errors. (But in multiplications by h^{-2} *etc.* in the table below, independent errors were assumed.) Unless otherwise specified, cosmological parameters are from six-parameter fits to a flat ΛCDM cosmology using CMB data alone: *Planck* temperature + WMAP polarization data + high-resolution data from ACT and SPT [2]. For more information see Ref. 3 and the original papers.

Quantity	Symbol, equation	Value	Reference, footnote
speed of light	c	$299\,792\,458$ m s^{-1}	exact[4]
Newtonian gravitational constant	G_N	$6.673\,8(8) \times 10^{-11}$ m^3 kg^{-1} s^{-2}	[1,5]
Planck mass	$\sqrt{\hbar c/G_N}$	$1.220\,93(7) \times 10^{19}$ GeV/c^2	[1]
		$= 2.176\,51(13) \times 10^{-8}$ kg	
Planck length	$\sqrt{\hbar G_N/c^3}$	$1.616\,20(10) \times 10^{-35}$ m	[1]
standard gravitational acceleration	g_N	9.806 65 m s	exact[1]
jansky (flux density)	Jy	10^{-26} W m^{-2} Hz^{-1}	definition
tropical year (equinox to equinox) (2011)	yr	$31\,556\,925.2$ s $\approx \pi \times 10^7$ s	[6]
sidereal year (fixed star to fixed star) (2011)		$31\,558\,149.8$ s $\approx \pi \times 10^7$ s	[6]
mean sidereal day (2011) (time between vernal equinox transits)		$23^{\rm h}\,56^{\rm m}\,04^{\rm s}.090\,53$	[6]
astronomical unit	au	$149\,597\,870\,700$ m	exact [7]
parsec (1 au/1 arc sec)	pc	$3.085\,677\,581\,49 \times 10^{16}$ m = 3.262 . . . ly	exact [8]
light year (deprecated unit)	ly	$0.306\,6\ldots$ pc $= 0.946\,053\ldots \times 10^{16}$ m	
Schwarzschild radius of the Sun	$2G_N M_\odot/c^2$	$2.953\,250\,077(2)$ km	[9]
Solar mass	$M_\odot$	$1.988\,5(2) \times 10^{30}$ kg	[10]
Solar equatorial radius	$R_\odot$	$6.9551(4) \times 10^8$ m	[11]
Solar luminosity	$L_\odot$	3.828×10^{26} W	[12]
Schwarzschild radius of the Earth	$2G_N M_\oplus/c^2$	$8.870\,055\,94(2)$ mm	[13]
Earth mass	$M_\oplus$	$5.972\,6(7) \times 10^{24}$ kg	[14]
Earth mean equatorial radius	$R_\oplus$	$6.378\,137 \times 10^6$ m	[6]
luminosity conversion (deprecated)	L	$3.02 \times 10^{28} \times 10^{-0.4\ M_{\rm bol}}$ W	[15]
		($M_{\rm bol}$ = absolute bolometric magnitude = bolometric magnitude at 10 pc)	
flux conversion (deprecated)	$\mathscr{F}$	$2.52 \times 10^{-8} \times 10^{-0.4\ m_{\rm bol}}$ W m^{-2}	from above
		($m_{\rm bol}$ = apparent bolometric magnitude)	
ABsolute monochromatic magnitude	AB	$-2.5\ \log_{10} f_\nu - 56.10$ (for f_ν in W m^{-2} Hz^{-1})	[16]
		$= -2.5\ \log_{10} f_\nu + 8.90$ (for f_ν in Jy)	
Solar angular velocity around the Galactic center	Θ_0/R_0	30.3 ± 0.9 km s^{-1} kpc^{-1}	[17]
Solar distance from Galactic center	R_0	8.4(6) kpc	[17,18]
circular velocity at R_0	v_0 or Θ_0	254(16) km s^{-1}	[17]
local disk density	$\rho_{\rm\,disk}$	3–12 $\times 10^{-24}$ g cm^{-3} $\approx$ 2–7 GeV/c^2 cm^{-3}	[19]
local dark matter density	ρ_χ	canonical value 0.3 GeV/c^2 cm^{-3} within factor 2–3	[20]
escape velocity from Galaxy	$v_{\rm\,esc}$	498 km/s $< v_{\rm\,esc} <$ 608 km/s	[21]
present day CMB temperature	T_0	2.7255(6) K	[22,23]
present day CMB dipole amplitude		3.355(8) mK	[22,24]
Solar velocity with respect to CMB		369(1) km/s towards $(\ell, b) = (263.99(14)^\circ, 48.26(3)^\circ)$	[22,24]
Local Group velocity with respect to CMB	$v_{\rm LG}$	627(22) km/s towards $(\ell, b) = (276(3)^\circ, 30(3)^\circ)$	[22,24]
entropy density/Boltzmann constant	s/k	$2\,891.2\ (T/2.7255)^3$ cm^{-3}	[25]
number density of CMB photons	n_γ	$410.7(T/2.7255)^3$ cm^{-3}	[25]
baryon-to-photon ratio	$\eta = n_{\rm b}/n_\gamma$	$6.05(7) \times 10^{-10}$ (CMB)	[26]
		$5.7 \times 10^{-10} \le \eta \le 6.7 \times 10^{-10}$ (95% CL)	[26]
present day Hubble expansion rate	H_0	$100\,h$ km s^{-1} Mpc^{-1} $= h \times (9.777\,752$ Gyr$)^{-1}$	[29]
scale factor for Hubble expansion rate	h	0.673(12)	[2,3]
Hubble length	c/H_0	$0.925\,0629 \times 10^{26}\,h^{-1}$ m $= 1.37(2) \times 10^{26}$ m	
scale factor for cosmological constant	$c^2/3H_0^2$	$2.85247 \times 10^{51}\,h^{-2}$ m^2 $= 6.3(2) \times 10^{51}$ m^2	
critical density of the Universe	$\rho_{\rm crit} = 3H_0^2/8\pi G_N$	$2.775\,366\,27 \times 10^{11}\,h^2\ M_\odot$Mpc^{-3}	
		$= 1.878\,47(23) \times 10^{-29}\,h^2$ g cm^{-3}	
		$= 1.053\,75(13) \times 10^{-5}\,h^2$ (GeV/c^2) cm^{-3}	
number density of baryons	$n_{\rm b}$	$2.482(32) \times 10^{-7}$ cm^{-3}	[2,3,27,28]
		$(2.1 \times 10^{-7} < n_{\rm b} < 2.7 \times 10^{-7})$ cm^{-3} (95% CL)	$\eta \times n_\gamma$
baryon density of the Universe	$\Omega_{\rm b} = \rho_{\rm b}/\rho_{\rm crit}$	$^\ddagger\,0.02207(27)\,h^{-2}$ $= {}^\dagger\,0.0499(22)$	[2,3]
cold dark matter density of the universe	$\Omega_{\rm cdm} = \rho_{\rm cdm}/\rho_{\rm crit}$	$^\ddagger\,0.1198(26)\,h^{-2}$ $= {}^\dagger\,0.265(11)$	[2,3]
100 × approx to $r_*/D_{\rm A}$	$100 \times \theta_{\rm MC}$	$^\ddagger\,1.0413(6)$	[2,3]
reionization optical depth	τ	$^\ddagger\,0.091^{+0.013}_{-0.014}$	[2,3]
scalar spectral index	$n_{\rm s}$	$^\ddagger\,0.958(7)$	[2,3]
ln pwr primordial curvature pert. (k_0=0.05 Mpc^{-1})	$\ln(10^{10}\Delta^2_{\mathcal{R}})$	$^\ddagger\,3.090(25)$	[2,3]

Quantity	Symbol, equation	Value	Reference, footnote
dark energy density of the ΛCDM Universe	Ω_Λ	$0.685^{+0.017}_{-0.016}$	[2,3]
pressureless matter density of the Universe	$\Omega_{\rm m} = \Omega_{\rm cdm} + \Omega_{\rm b}$	$0.315^{+0.016}_{-0.017}$ (From Ω_Λ and flatness constraint)	[2,3]
dark energy equation of state parameter	w	♯ $-1.10^{+0.08}_{-0.07}$ (*Planck*+WMAP+BAO+SN)	[32]
CMB radiation density of the Universe	$\Omega_\gamma = \rho_\gamma/\rho_{\rm c}$	$2.473 \times 10^{-5}(T/2.7255)^4\, h^{-2} = 5.46(19) \times 10^{-5}$	[25]
effective number of neutrinos	$N_{\rm eff}$	† 3.36 ± 0.34	[2]
sum of neutrino masses	$\sum m_\nu$	< 0.23 eV (95% CL; CMB+BAO) $\Rightarrow \Omega_\nu h^2 < 0.0025$	[2,30,31]
neutrino density of the Universe	Ω_ν	$< 0.0025\, h^{-2} \Rightarrow < 0.0055$ (95% CL; CMB+BAO)	[2,30,31]
curvature	$\Omega_{\rm tot} = \Omega_{\rm m} + \ldots + \Omega_\Lambda$	♯ $0.96^{+0.4}_{-0.5}$ (95%CL)	[2]
		♯ 1.000(7) (95% CL; CMB+BAO)	[2]
fluctuation amplitude at $8\,h^{-1}$ Mpc scale	σ_8	† 0.828 ± 0.012	[2,3]
running spectral index slope, $k_0 = 0.002$ Mpc^{-1}	$dn_{\rm s}/d\ln k$	♯ $-0.015(9)$	[2]
tensor-to-scalar field perturbations ratio, k_0=0.002 Mpc^{-1}	$r = T/S$	♯ < 0.11 at 95% CL; no running	[2,3]
redshift at decoupling	$z_{\rm dec}$	† 1090.2 ± 0.7	[2]
age at decoupling	t_*	† 3.72×10^5 yr	
sound horizon at decoupling	$r_s(z_*)$	† 147.5 ± 0.6 Mpc (*Planck* CMB)	[32]
redshift of matter-radiation equality	$z_{\rm eq}$	† 3360 ± 70	[2]
redshift at half reionization	$z_{\rm reion}$	† 11.1 ± 1.1	[2]
age at half reionization	$t_{\rm reion}$	† 462 Myr	
age of the Universe	t_0	† 13.81 ± 0.05 Gyr	[2]

‡ Parameter in six-parameter ΛCDM fit [2].
† Derived parameter in six-parameter ΛCDM fit [2].
♯ Extended model parameter [2].

References:

1. P.J. Mohr, B.N. Taylor, and D.B. Newell, J. Phys. Chem. Ref. Data 41, 043109, (2012); `physics.nist.gov/constants`.
2. P.A.R. Ade, *et al.*, (Planck Collab. 2013 XVI), `arXiv: 1303.5076v1`.
3. O. Lahav and A.R. Liddle, "The Cosmological Parameters," in this *Review*.
4. B.W. Petley, Nature **303**, 373 (1983).
5. T. Quinn *et al.*, Phys. Rev. Lett. **111**, 101102 (2013). See especially Fig. 3.
6. *The Astronomical Almanac for the year 2011*, U.S. Government Printing Office, Washington, and The U.K. Hydrographic Office (2010).
7. Astronomical_Constants_2014.pdf, downloaded from `asa.usno.navy.mil/SecK/Constants.html`; also see `www.iau.org/static/resolutions/IAU2012_English.pdf`. The Gaussian gravitational constant k is now deleted from the system of astronomical constants .
8. The distance at which 1 au subtends 1 arc sec: 1 au divided by $\pi/648\,000$.
9. Product of $2/c^2$ and the observationally determined Solar mass parameter $G_N M_\odot$ [7](TDB time scale).
10. $G_N M_\odot$ [7] $\div$ G_N [1].
11. T. M. Brown and J. Christensen-Dalsgaard, Astrophys. J. **500**, L195 (1998) Many values for the Solar radius have been published, most of which are consistent with this result.
12. $4\pi\,(1\text{ au})^2 \times (1361\text{ W m}^{-2})$, assuming isotropic irradiance; G. Kopp and J.L. Lean, Geophys. Res. Lett. **38**, L01706 (2011) give $1360.8 \pm 0.6\text{W m}^{-2}$, but given the scatter in the data we use the rounded value without quoting an error.
13. Product of $2/c^2$ and the geocentric gravitational constant $G_N M_\oplus$ [7](TDB time scale).
14. $G_N M_\oplus$ [7] $\div$ G_N [1].
15. E.W. Kolb and M.S. Turner, *The Early Universe*, Addison-Wesley (1990); The IAU (Commission 36) has recommended 3.055×10^{28} W for the zero point. Based on newer Solar measurements, the value and significance given in the table seems more appropriate.
16. J. B. Oke and J. E. Gunn, Astrophys. J. **266**, 713 (1983). Note that in the definition of AB the sign of the constant is wrong.
17. M.J. Reid, *et al.*, Astrophys. J. **700**, 137 (2009) Note that Θ_0/R_0 is better determined than either Θ_0 or R_0.
18. Z.M. Malkin, Astron. Rep. **57**, 128 (2013). 56 determinations of R_0 are given. The weighted mean of these unevaluated results is 8.0(4), with $\chi^2/dof = 1.2$.
19. G. Gilmore, R.F.G. Wyse, and K. Kuijken, Ann. Rev. Astron. Astrophys. **27**, 555 (1989).
20. Sampling of many references: M. Mori *et al.*, Phys. Lett. **B289**, 463 (1992); E.I. Gates *et al.*, Astrophys. J. **449**, L133 (1995); M. Kamionkowski and A.Kinkhabwala, Phys. Rev. **D57**, 325 (1998); M. Weber and W. de Boer, Astron. & Astrophys. **509**, A25 (2010); P. Salucci *et al.*, Astron. & Astrophys. **523**, A83 (2010); R. Catena and P. Ullio, JCAP **1008**, 004 (2010) conclude $\rho_{\rm DM}^{\rm local} = 0.39 \pm 0.03\,\text{GeV cm}^{-3}$.
21. M. C. Smith *et al.*, Mon. Not. R. Astr. Soc. **379**, 755 (2007) (`astro-ph/0611671`).
22. D. Scott and G.F. Smoot, "Cosmic Microwave Background," in this *Review*.
23. D. Fixsen, Astrophys. J. **707**, 916 (2009).
24. G. Hinshaw *et al.*, Astrophys. J. Suppl. in press, `arXiv:1212.5226`; D.J. Fixsen *et al.*, Astrophys. J. **473**, 576 (1996); A. Kogut *et al.*, Astrophys. J. **419**, 1 (1993).
25. $n_\gamma = \frac{2\zeta(3)}{\pi^2}\left(\frac{kT}{\hbar c}\right)^3$; $\rho_\gamma = \frac{\pi^2 kT}{15\,c^2}\left(\frac{kT}{\hbar c}\right)^3$; $s/k = \frac{2\cdot 43\cdot\pi^2}{11\cdot 45}\left(\frac{kT}{\hbar c}\right)^3$; $kT_0/\hbar c = 11.902(4)/\text{cm}$.
26. B.D. Fields, P. Molarto, and S. Sarkar, "Big-Bang Nucleosynthesis," in this *Review*.
27. $n_{\rm b}$ depends only upon the measured $\Omega_{\rm b}h^2$, the average baryon mass at the present epoch [28], and G_N: $n_{\rm b} = (\Omega_{\rm b}h^2)h^{-2}\rho_{\rm crit}/(0.93711\,\text{GeV}/c^2\text{ per baryon})$.
28. G. Steigman, JCAP **0610**, 016, (2006).
29. Conversion using length of sidereal year.
30. $\Omega_\nu h^2 = \sum m_{\nu_j}/93.04\,\text{eV}$, where the sum is over all neutrino mass eigenstates. The lower limit follows from neutrino mixing results reported in this *Review* combined with the assumptions that there are three light neutrinos ($m_\nu < 45$ GeV/c^2) and that the lightest neutrino is substantially less massive than the others: $\Delta m^2_{32} = (2.32^{+0.12}_{-0.08}) \times 10^{-3}$ eV^2, so $\sum m_{\nu_j} \geq m_{\nu_3} \approx \sqrt{\Delta m^2_{32}} = 0.05$ eV. (This becomes 0.10 eV if the mass hierarchy is inverted, with $m_{\nu_1} \approx m_{\nu_2} \gg m_{\nu_3}$.) Alternatively, if the limit obtained from tritium decay experiments ($m_\nu < 2\,\text{eV}$) is used for the upper limit, then $\Omega_\nu < 0.04$.
31. Astrophysical determinations of $\sum m_{\nu_j}$, reported in the Full Listings of this *Review* under "Sum of the neutrino masses," range from $< 0.17\,\text{eV}$ to $< 2.3\,\text{eV}$ in papers published since 2003.
32. M.J. Mortonson, D.H. Weinberg, and M. White, "Dark Energy," in this *Review*.

3. INTERNATIONAL SYSTEM OF UNITS (SI)

See "The International System of Units (SI)," NIST Special Publication **330**, B.N. Taylor, ed. (USGPO, Washington, DC, 1991); and "Guide for the Use of the International System of Units (SI)," NIST Special Publication **811**, 1995 edition, B.N. Taylor (USGPO, Washington, DC, 1995).

Physical quantity	Name of unit	Symbol
Base units		
length	meter	m
mass	kilogram	kg
time	second	s
electric current	ampere	A
thermodynamic temperature	kelvin	K
amount of substance	mole	mol
luminous intensity	candela	cd
Derived units with special names		
plane angle	radian	rad
solid angle	steradian	sr
frequency	hertz	Hz
energy	joule	J
force	newton	N
pressure	pascal	Pa
power	watt	W
electric charge	coulomb	C
electric potential	volt	V
electric resistance	ohm	Ω
electric conductance	siemens	S
electric capacitance	farad	F
magnetic flux	weber	Wb
inductance	henry	H
magnetic flux density	tesla	T
luminous flux	lumen	lm
illuminance	lux	lx
celsius temperature	degree celsius	°C
activity (of a radioactive source)*	becquerel	Bq
absorbed dose (of ionizing radiation)*	gray	Gy
dose equivalent*	sievert	Sv

*See our section 35, on "Radioactivity and radiation protection," p. 458.

SI prefixes

10^{24}	yotta	(Y)
10^{21}	zetta	(Z)
10^{18}	exa	(E)
10^{15}	peta	(P)
10^{12}	tera	(T)
10^{9}	giga	(G)
10^{6}	mega	(M)
10^{3}	kilo	(k)
10^{2}	hecto	(h)
10	deca	(da)
10^{-1}	deci	(d)
10^{-2}	centi	(c)
10^{-3}	milli	(m)
10^{-6}	micro	(μ)
10^{-9}	nano	(n)
10^{-12}	pico	(p)
10^{-15}	femto	(f)
10^{-18}	atto	(a)
10^{-21}	zepto	(z)
10^{-24}	yocto	(y)

Table 4.1. Revised 2011 by D.E. Groom (LBNL), and E. Bergren. Atomic weights of stable elements are adapted from the Commission on Isotopic Abundances and Atomic Weights, "Atomic Weights of the Elements 2007," `http://www.chem.qmul.ac.uk/iupac/AtWt/`. The atomic number (top left) is the number of protons in the nucleus. The atomic mass (bottom) of a stable elements is weighted by isotopic abundances in the Earth's surface. If the element has no stable isotope, the atomic mass (in parentheses) of the most stable isotope currently known is given. In this case the mass is from `http://www.nndc.bnl.gov/amdc/masstables/Ame2003/mass.mas03` and the longest-lived isotope is from `www.nndc.bnl.gov/ensdf/za_form.jsp`. The exceptions are Th, Pa, and U, which do have characteristic terrestrial compositions. Atomic masses are relative to the mass of ^{12}C, defined to be exactly 12 unified atomic mass units (u) (approx. g/mole). Relative isotopic abundances often vary considerably, both in natural and commercial samples; this is reflected in the number of significant figures given for the atomic mass. IUPAC does not accept the claims for elements 113, 115, 117, and 118 as conclusive at this time.

PERIODIC TABLE OF THE ELEMENTS

1 IA												13 IIIA	14 IVA	15 VA	16 VIA	17 VIIA	18 VIIIA
1 H Hydrogen 1.00794	2 IIA																2 He Helium 4.002602
3 Li Lithium 6.941	4 Be Beryllium 9.012182											5 B Boron 10.811	6 C Carbon 12.0107	7 N Nitrogen 14.0067	8 O Oxygen 15.9994	9 F Fluorine 18.9984032	10 Ne Neon 20.1797
11 Na Sodium 22.98976928	12 Mg Magnesium 24.3050	3 IIIB	4 IVB	5 VB	6 VIB	7 VIIB	8	9 VIII	10	11 IB	12 IIB	13 Al Aluminum 26.9815386	14 Si Silicon 28.0855	15 P Phosph. 30.973762	16 S Sulfur 32.065	17 Cl Chlorine 35.453	18 Ar Argon 39.948
19 K Potassium 39.0983	20 Ca Calcium 40.078	21 Sc Scandium 44.955912	22 Ti Titanium 47.867	23 V Vanadium 50.9415	24 Cr Chromium 51.9961	25 Mn Manganese 54.938045	26 Fe Iron 55.845	27 Co Cobalt 58.933195	28 Ni Nickel 58.6934	29 Cu Copper 63.546	30 Zn Zinc 65.38	31 Ga Gallium 69.723	32 Ge German. 72.64	33 As Arsenic 74.92160	34 Se Selenium 78.96	35 Br Bromine 79.904	36 Kr Krypton 83.798
37 Rb Rubidium 85.4678	38 Sr Strontium 87.62	39 Y Yttrium 88.90585	40 Zr Zirconium 91.224	41 Nb Niobium 92.90638	42 Mo Molybd. 95.96	43 Tc Technet. (97.90722)	44 Ru Ruthen. 101.07	45 Rh Rhodium 102.90550	46 Pd Palladium 106.42	47 Ag Silver 107.8682	48 Cd Cadmium 112.411	49 In Indium 114.818	50 Sn Tin 118.710	51 Sb Antimony 121.760	52 Te Tellurium 127.60	53 I Iodine 126.90447	54 Xe Xenon 131.293
55 Cs Cesium 132.9054519	56 Ba Barium 137.327	57–71 Lantha-nides	72 Hf Hafnium 178.49	73 Ta Tantalum 180.94788	74 W Tungsten 183.84	75 Re Rhenium 186.207	76 Os Osmium 190.23	77 Ir Iridium 192.217	78 Pt Platinum 195.084	79 Au Gold 196.966569	80 Hg Mercury 200.59	81 Tl Thallium 204.3833	82 Pb Lead 207.2	83 Bi Bismuth 208.98040	84 Po Polonium (208.98243)	85 At Astatine (209.98715)	86 Rn Radon (222.01758)
87 Fr Francium (223.01974)	88 Ra Radium (226.02541)	89–103 Actinides	104 Rf Rutherford. (267.122)	105 Db Dubnium (268.125)	106 Sg Seaborg. (271.133)	107 Bh Bohrium (270.134)	108 Hs Hassium (269.134)	109 Mt Meitner. (276.151)	110 Ds Darmstadt. (281.162)	111 Rg Roentgen. (280.164)	112 Cn Copernicium (277)		114 Fl Flerovium (289)		116 Lv Livermorium (288)		

Lanthanide series	57 La Lanthan. 138.90547	58 Ce Cerium 140.116	59 Pr Praseodym. 140.90765	60 Nd Neodym. 144.242	61 Pm Prometh. (144.91275)	62 Sm Samarium 150.36	63 Eu Europium 151.964	64 Gd Gadolin. 157.25	65 Tb Terbium 158.92535	66 Dy Dyspros. 162.500	67 Ho Holmium 164.93032	68 Er Erbium 167.259	69 Tm Thulium 168.93421	70 Yb Ytterbium 173.054	71 Lu Lutetium 174.9668
Actinide series	89 Ac Actinium (227.02775)	90 Th Thorium 232.03806	91 Pa Protactin. 231.03588	92 U Uranium 238.02891	93 Np Neptunium (237.04817)	94 Pu Plutonium (244.06420)	95 Am Americ. (243.06138)	96 Cm Curium (247.07035)	97 Bk Berkelium (247.07031)	98 Cf Californ. (251.07959)	99 Es Einstein. (252.0830)	100 Fm Fermium (257.09510)	101 Md Mendelev. (258.09843)	102 No Nobelium (259.1010)	103 Lr Lawrenc. (262.110)

5. ELECTRONIC STRUCTURE OF THE ELEMENTS

Table 5.1. Reviewed 2011 by J.E. Sansonetti (NIST). The electronic configurations and the ionization energies are from the NIST database, "Ground Levels and Ionization Energies for the Neutral Atoms," W.C. Martin, A. Musgrove, S. Kotochigova, and J.E. Sansonetti, `http://www.nist.gov/pml/data/ion_energy.cfm`. The electron configuration for, say, iron indicates an argon electronic core (see argon) plus six $3d$ electrons and two $4s$ electrons.

	Element		Electron configuration ($3d^5$ = five $3d$ electrons, *etc.*)						Ground state $^{2S+1}L_J$	Ionization energy (eV)
1	H	Hydrogen	$1s$						$^2S_{1/2}$	13.5984
2	He	Helium	$1s^2$						$^1S_0$	24.5874
3	Li	Lithium	(He) $2s$						$^2S_{1/2}$	5.3917
4	Be	Beryllium	(He) $2s^2$						$^1S_0$	9.3227
5	B	Boron	(He) $2s^2$	$2p$					$^2P_{1/2}$	8.2980
6	C	Carbon	(He) $2s^2$	$2p^2$					$^3P_0$	11.2603
7	N	Nitrogen	(He) $2s^2$	$2p^3$					$^4S_{3/2}$	14.5341
8	O	Oxygen	(He) $2s^2$	$2p^4$					$^3P_2$	13.6181
9	F	Fluorine	(He) $2s^2$	$2p^5$					$^2P_{3/2}$	17.4228
10	Ne	Neon	(He) $2s^2$	$2p^6$					$^1S_0$	21.5645
11	Na	Sodium	(Ne) $3s$						$^2S_{1/2}$	5.1391
12	Mg	Magnesium	(Ne) $3s^2$						$^1S_0$	7.6462
13	Al	Aluminum	(Ne) $3s^2$	$3p$					$^2P_{1/2}$	5.9858
14	Si	Silicon	(Ne) $3s^2$	$3p^2$					$^3P_0$	8.1517
15	P	Phosphorus	(Ne) $3s^2$	$3p^3$					$^4S_{3/2}$	10.4867
16	S	Sulfur	(Ne) $3s^2$	$3p^4$					$^3P_2$	10.3600
17	Cl	Chlorine	(Ne) $3s^2$	$3p^5$					$^2P_{3/2}$	12.9676
18	Ar	Argon	(Ne) $3s^2$	$3p^6$					$^1S_0$	15.7596
19	K	Potassium	(Ar)	$4s$					$^2S_{1/2}$	4.3407
20	Ca	Calcium	(Ar)	$4s^2$					$^1S_0$	6.1132
21	Sc	Scandium	(Ar) $3d$	$4s^2$					$^2D_{3/2}$	6.5615
22	Ti	Titanium	(Ar) $3d^2$	$4s^2$					$^3F_2$	6.8281
23	V	Vanadium	(Ar) $3d^3$	$4s^2$					$^4F_{3/2}$	6.7462
24	Cr	Chromium	(Ar) $3d^5$	$4s$					$^7S_3$	6.7665
25	Mn	Manganese	(Ar) $3d^5$	$4s^2$					$^6S_{5/2}$	7.4340
26	Fe	Iron	(Ar) $3d^6$	$4s^2$					$^5D_4$	7.9024
27	Co	Cobalt	(Ar) $3d^7$	$4s^2$					$^4F_{9/2}$	7.8810
28	Ni	Nickel	(Ar) $3d^8$	$4s^2$					$^3F_4$	7.6399
29	Cu	Copper	(Ar) $3d^{10}$	$4s$					$^2S_{1/2}$	7.7264
30	Zn	Zinc	(Ar) $3d^{10}$	$4s^2$					$^1S_0$	9.3942
31	Ga	Gallium	(Ar) $3d^{10}$	$4s^2$	$4p$				$^2P_{1/2}$	5.9993
32	Ge	Germanium	(Ar) $3d^{10}$	$4s^2$	$4p^2$				$^3P_0$	7.8994
33	As	Arsenic	(Ar) $3d^{10}$	$4s^2$	$4p^3$				$^4S_{3/2}$	9.7886
34	Se	Selenium	(Ar) $3d^{10}$	$4s^2$	$4p^4$				$^3P_2$	9.7524
35	Br	Bromine	(Ar) $3d^{10}$	$4s^2$	$4p^5$				$^2P_{3/2}$	11.8138
36	Kr	Krypton	(Ar) $3d^{10}$	$4s^2$	$4p^6$				$^1S_0$	13.9996
37	Rb	Rubidium	(Kr)	$5s$					$^2S_{1/2}$	4.1771
38	Sr	Strontium	(Kr)	$5s^2$					$^1S_0$	5.6949
39	Y	Yttrium	(Kr) $4d$	$5s^2$					$^2D_{3/2}$	6.2173
40	Zr	Zirconium	(Kr) $4d^2$	$5s^2$					$^3F_2$	6.6339
41	Nb	Niobium	(Kr) $4d^4$	$5s$					$^6D_{1/2}$	6.7589
42	Mo	Molybdenum	(Kr) $4d^5$	$5s$					$^7S_3$	7.0924
43	Tc	Technetium	(Kr) $4d^5$	$5s^2$					$^6S_{5/2}$	7.28
44	Ru	Ruthenium	(Kr) $4d^7$	$5s$					$^5F_5$	7.3605
45	Rh	Rhodium	(Kr) $4d^8$	$5s$					$^4F_{9/2}$	7.4589
46	Pd	Palladium	(Kr) $4d^{10}$						$^1S_0$	8.3369
47	Ag	Silver	(Kr) $4d^{10}$	$5s$					$^2S_{1/2}$	7.5762
48	Cd	Cadmium	(Kr) $4d^{10}$	$5s^2$					$^1S_0$	8.9938

Transition elements

49	In	Indium	(Kr) $4d^{10}5s^2$	$5p$				$^2P_{1/2}$	5.7864
50	Sn	Tin	(Kr) $4d^{10}5s^2$	$5p^2$				$^3P_0$	7.3439
51	Sb	Antimony	(Kr) $4d^{10}5s^2$	$5p^3$				$^4S_{3/2}$	8.6084
52	Te	Tellurium	(Kr) $4d^{10}5s^2$	$5p^4$				$^3P_2$	9.0096
53	I	Iodine	(Kr) $4d^{10}5s^2$	$5p^5$				$^2P_{3/2}$	10.4513
54	Xe	Xenon	(Kr) $4d^{10}5s^2$	$5p^6$				$^1S_0$	12.1298
55	Cs	Cesium	(Xe)	$6s$				$^2S_{1/2}$	3.8939
56	Ba	Barium	(Xe)	$6s^2$				$^1S_0$	5.2117
57	La	Lanthanum	(Xe) $5d$	$6s^2$				$^2D_{3/2}$	5.5769
58	Ce	Cerium	(Xe) $4f$ $5d$	$6s^2$				$^1G_4$	5.5387
59	Pr	Praseodymium	(Xe) $4f^3$	$6s^2$				$^4I_{9/2}$	5.473
60	Nd	Neodymium	(Xe) $4f^4$	$6s^2$				$^5I_4$	5.5250
61	Pm	Promethium	(Xe) $4f^5$	$6s^2$				$^6H_{5/2}$	5.582
62	Sm	Samarium	(Xe) $4f^6$	$6s^2$				$^7F_0$	5.6437
63	Eu	Europium	(Xe) $4f^7$	$6s^2$				$^8S_{7/2}$	5.6704
64	Gd	Gadolinium	(Xe) $4f^7$ $5d$	$6s^2$				$^9D_2$	6.1498
65	Tb	Terbium	(Xe) $4f^9$	$6s^2$				$^6H_{15/2}$	5.8638
66	Dy	Dysprosium	(Xe) $4f^{10}$	$6s^2$				$^5I_8$	5.9389
67	Ho	Holmium	(Xe) $4f^{11}$	$6s^2$				$^4I_{15/2}$	6.0215
68	Er	Erbium	(Xe) $4f^{12}$	$6s^2$				$^3H_6$	6.1077
69	Tm	Thulium	(Xe) $4f^{13}$	$6s^2$				$^2F_{7/2}$	6.1843
70	Yb	Ytterbium	(Xe) $4f^{14}$	$6s^2$				$^1S_0$	6.2542
71	Lu	Lutetium	(Xe) $4f^{14}5d$	$6s^2$				$^2D_{3/2}$	5.4259
72	Hf	Hafnium	(Xe) $4f^{14}5d^2$	$6s^2$				$^3F_2$	6.8251
73	Ta	Tantalum	(Xe) $4f^{14}5d^3$	$6s^2$				$^4F_{3/2}$	7.5496
74	W	Tungsten	(Xe) $4f^{14}5d^4$	$6s^2$				$^5D_0$	7.8640
75	Re	Rhenium	(Xe) $4f^{14}5d^5$	$6s^2$				$^6S_{5/2}$	7.8335
76	Os	Osmium	(Xe) $4f^{14}5d^6$	$6s^2$				$^5D_4$	8.4382
77	Ir	Iridium	(Xe) $4f^{14}5d^7$	$6s^2$				$^4F_{9/2}$	8.9670
78	Pt	Platinum	(Xe) $4f^{14}5d^9$	$6s$				$^3D_3$	8.9588
79	Au	Gold	(Xe) $4f^{14}5d^{10}6s$					$^2S_{1/2}$	9.2255
80	Hg	Mercury	(Xe) $4f^{14}5d^{10}6s^2$					$^1S_0$	10.4375
81	Tl	Thallium	(Xe) $4f^{14}5d^{10}6s^2$	$6p$				$^2P_{1/2}$	6.1082
82	Pb	Lead	(Xe) $4f^{14}5d^{10}6s^2$	$6p^2$				$^3P_0$	7.4167
83	Bi	Bismuth	(Xe) $4f^{14}5d^{10}6s^2$	$6p^3$				$^4S_{3/2}$	7.2855
84	Po	Polonium	(Xe) $4f^{14}5d^{10}6s^2$	$6p^4$				$^3P_2$	8.414
85	At	Astatine	(Xe) $4f^{14}5d^{10}6s^2$	$6p^5$				$^2P_{3/2}$	
86	Rn	Radon	(Xe) $4f^{14}5d^{10}6s^2$	$6p^6$				$^1S_0$	10.7485
87	Fr	Francium	(Rn)	$7s$				$^2S_{1/2}$	4.0727
88	Ra	Radium	(Rn)	$7s^2$				$^1S_0$	5.2784
89	Ac	Actinium	(Rn) $6d$	$7s^2$				$^2D_{3/2}$	5.3807
90	Th	Thorium	(Rn) $6d^2$	$7s^2$				$^3F_2$	6.3067
91	Pa	Protactinium	(Rn)$5f^2$ $6d$	$7s^2$				$^4K_{11/2}$*	5.89
92	U	Uranium	(Rn)$5f^3$ $6d$	$7s^2$				$^5L_6$*	6.1939
93	Np	Neptunium	(Rn)$5f^4$ $6d$	$7s^2$				$^6L_{11/2}$*	6.2657
94	Pu	Plutonium	(Rn)$5f^6$	$7s^2$				$^7F_0$	6.0260
95	Am	Americium	(Rn)$5f^7$	$7s^2$				$^8S_{7/2}$	5.9738
96	Cm	Curium	(Rn)$5f^7$ $6d$	$7s^2$				$^9D_2$	5.9914
97	Bk	Berkelium	(Rn)$5f^9$	$7s^2$				$^6H_{15/2}$	6.1979
98	Cf	Californium	(Rn)$5f^{10}$	$7s^2$				$^5I_8$	6.2817
99	Es	Einsteinium	(Rn)$5f^{11}$	$7s^2$				$^4I_{15/2}$	6.3676
100	Fm	Fermium	(Rn)$5f^{12}$	$7s^2$				$^3H_6$	6.50
101	Md	Mendelevium	(Rn)$5f^{13}$	$7s^2$				$^2F_{7/2}$	6.58
102	No	Nobelium	(Rn)$5f^{14}$	$7s^2$				$^1S_0$	6.65
103	Lr	Lawrencium	(Rn)$5f^{14}$	$7s^2$	$7p$?			$^2P_{1/2}$?	4.9?
104	Rf	Rutherfordium	(Rn)$5f^{14}6d^2$	$7s^2$?				$^3F_2$?	6.0?

Lanthanides

Transition elements

Actinides

* The usual LS coupling scheme does not apply for these three elements. See the introductory note to the NIST table from which this table is taken.

6. ATOMIC AND NUCLEAR PROPERTIES OF MATERIALS

Table 6.1 Abridged from `pdg.lbl.gov/AtomicNuclearProperties` by D. E. Groom (2007). See web pages for more detail about entries in this table including chemical formulae, and for several hundred other entries. Quantities in parentheses are for gases at 20° C and 1 atm, and square brackets indicate evaluation at 0° C and 1 atm. Boiling points are at 1 atm. Refractive indices n are evaluated at the sodium D line blend (589.2 nm); values $\gg 1$ in brackets are for $(n-1)\times 10^6$ (gases).

Material	Z	A	$\langle Z/A\rangle$	Nucl.coll. length λ_T {g cm^{-2}}	Nucl.inter. length λ_I {g cm^{-2}}	Rad.len. X_0 {g cm^{-2}}	$dE/dx\|_{\rm min}$ { MeV g^{-1}cm^2}	Density {g cm^{-3}} ({gℓ^{-1}})	Melting point (K)	Boiling point (K)	Refract. index (@ Na D)
H_2	1	1.00794(7)	0.99212	42.8	52.0	63.04	(4.103)	0.071(0.084)	13.81	20.28	1.11[132.]
D_2	1	2.01410177803(8)	0.49650	51.3	71.8	125.97	(2.053)	0.169(0.168)	18.7	23.65	1.11[138.]
He	2	4.002602(2)	0.49967	51.8	71.0	94.32	(1.937)	0.125(0.166)		4.220	1.02[35.0]
Li	3	6.941(2)	0.43221	52.2	71.3	82.78	1.639	0.534	453.6	1615.	
Be	4	9.012182(3)	0.44384	55.3	77.8	65.19	1.595	1.848	1560.	2744.	
C diamond	6	12.0107(8)	0.49955	59.2	85.8	42.70	1.725	3.520			2.42
C graphite	6	12.0107(8)	0.49955	59.2	85.8	42.70	1.742	2.210			
N_2	7	14.0067(2)	0.49976	61.1	89.7	37.99	(1.825)	0.807(1.165)	63.15	77.29	1.20[298.]
O_2	8	15.9994(3)	0.50002	61.3	90.2	34.24	(1.801)	1.141(1.332)	54.36	90.20	1.22[271.]
F_2	9	18.9984032(5)	0.47372	65.0	97.4	32.93	(1.676)	1.507(1.580)	53.53	85.03	[195.]
Ne	10	20.1797(6)	0.49555	65.7	99.0	28.93	(1.724)	1.204(0.839)	24.56	27.07	1.09[67.1]
Al	13	26.9815386(8)	0.48181	69.7	107.2	24.01	1.615	2.699	933.5	2792.	
Si	14	28.0855(3)	0.49848	70.2	108.4	21.82	1.664	2.329	1687.	3538.	3.95
Cl_2	17	35.453(2)	0.47951	73.8	115.7	19.28	(1.630)	1.574(2.980)	171.6	239.1	[773.]
Ar	18	39.948(1)	0.45059	75.7	119.7	19.55	(1.519)	1.396(1.662)	83.81	87.26	1.23[281.]
Ti	22	47.867(1)	0.45961	78.8	126.2	16.16	1.477	4.540	1941.	3560.	
Fe	26	55.845(2)	0.46557	81.7	132.1	13.84	1.451	7.874	1811.	3134.	
Cu	29	63.546(3)	0.45636	84.2	137.3	12.86	1.403	8.960	1358.	2835.	
Ge	32	72.64(1)	0.44053	86.9	143.0	12.25	1.370	5.323	1211.	3106.	
Sn	50	118.710(7)	0.42119	98.2	166.7	8.82	1.263	7.310	505.1	2875.	
Xe	54	131.293(6)	0.41129	100.8	172.1	8.48	(1.255)	2.953(5.483)	161.4	165.1	1.39[701.]
W	74	183.84(1)	0.40252	110.4	191.9	6.76	1.145	19.300	3695.	5828.	
Pt	78	195.084(9)	0.39983	112.2	195.7	6.54	1.128	21.450	2042.	4098.	
Au	79	196.966569(4)	0.40108	112.5	196.3	6.46	1.134	19.320	1337.	3129.	
Pb	82	207.2(1)	0.39575	114.1	199.6	6.37	1.122	11.350	600.6	2022.	
U	92	[238.02891(3)]	0.38651	118.6	209.0	6.00	1.081	18.950	1408.	4404.	
Air (dry, 1 atm)			0.49919	61.3	90.1	36.62	(1.815)	(1.205)		78.80	[289]
Shielding concrete			0.50274	65.1	97.5	26.57	1.711	2.300			
Borosilicate glass (Pyrex)			0.49707	64.6	96.5	28.17	1.696	2.230			
Lead glass			0.42101	95.9	158.0	7.87	1.255	6.220			
Standard rock			0.50000	66.8	101.3	26.54	1.688	2.650			
Methane (CH_4)			0.62334	54.0	73.8	46.47	(2.417)	(0.667)	90.68	111.7	[444.]
Ethane (C_2H_6)			0.59861	55.0	75.9	45.66	(2.304)	(1.263)	90.36	184.5	
Propane (C_3H_8)			0.58962	55.3	76.7	45.37	(2.262)	0.493(1.868)	85.52	231.0	
Butane (C_4H_{10})			0.59497	55.5	77.1	45.23	(2.278)	(2.489)	134.9	272.6	
Octane (C_8H_{18})			0.57778	55.8	77.8	45.00	2.123	0.703	214.4	398.8	
Paraffin ($CH_3(CH_2)_{n\approx 23}CH_3$)			0.57275	56.0	78.3	44.85	2.088	0.930			
Nylon (type 6, 6/6)			0.54790	57.5	81.6	41.92	1.973	1.18			
Polycarbonate (Lexan)			0.52697	58.3	83.6	41.50	1.886	1.20			
Polyethylene ($[CH_2CH_2]_n$)			0.57034	56.1	78.5	44.77	2.079	0.89			
Polyethylene terephthalate (Mylar)			0.52037	58.9	84.9	39.95	1.848	1.40			
Polyimide film (Kapton)			0.51264	59.2	85.5	40.58	1.820	1.42			
Polymethylmethacrylate (acrylic)			0.53937	58.1	82.8	40.55	1.929	1.19			1.49
Polypropylene			0.55998	56.1	78.5	44.77	2.041	0.90			
Polystyrene ($[C_6H_5CHCH_2]_n$)			0.53768	57.5	81.7	43.79	1.936	1.06			1.59
Polytetrafluoroethylene (Teflon)			0.47992	63.5	94.4	34.84	1.671	2.20			
Polyvinyltoluene			0.54141	57.3	81.3	43.90	1.956	1.03			1.58
Aluminum oxide (sapphire)			0.49038	65.5	98.4	27.94	1.647	3.970	2327.	3273.	1.77
Barium flouride (BaF_2)			0.42207	90.8	149.0	9.91	1.303	4.893	1641.	2533.	1.47
Bismuth germanate (BGO)			0.42065	96.2	159.1	7.97	1.251	7.130	1317.		2.15
Carbon dioxide gas (CO_2)			0.49989	60.7	88.9	36.20	1.819	(1.842)			[449.]
Solid carbon dioxide (dry ice)			0.49989	60.7	88.9	36.20	1.787	1.563	Sublimes at 194.7 K		
Cesium iodide (CsI)			0.41569	100.6	171.5	8.39	1.243	4.510	894.2	1553.	1.79
Lithium fluoride (LiF)			0.46262	61.0	88.7	39.26	1.614	2.635	1121.	1946.	1.39
Lithium hydride (LiH)			0.50321	50.8	68.1	79.62	1.897	0.820	965.		
Lead tungstate ($PbWO_4$)			0.41315	100.6	168.3	7.39	1.229	8.300	1403.		2.20
Silicon dioxide (SiO_2, fused quartz)			0.49930	65.2	97.8	27.05	1.699	2.200	1986.	3223.	1.46
Sodium chloride (NaCl)			0.55509	71.2	110.1	21.91	1.847	2.170	1075.	1738.	1.54
Sodium iodide (NaI)			0.42697	93.1	154.6	9.49	1.305	3.667	933.2	1577.	1.77
Water (H_2O)			0.55509	58.5	83.3	36.08	1.992	1.000	273.1	373.1	1.33
Silica aerogel			0.50093	65.0	97.3	27.25	1.740	0.200	(0.03 H_2O, 0.97 SiO_2)		

Material	Dielectric constant ($\kappa = \epsilon/\epsilon_0$) () is ($\kappa$–1)×$10^6$ for gas	Young's modulus [10^6 psi]	Coeff. of thermal expansion [10^{-6}cm/cm-°C]	Specific heat [cal/g-°C]	Electrical resistivity [$\mu\Omega$cm(@°C)]	Thermal conductivity [cal/cm-°C-sec]
H_2	(253.9)	—	—	—	—	—
He	(64)	—	—	—	—	—
Li	—	—	56	0.86	8.55(0°)	0.17
Be	—	37	12.4	0.436	5.885(0°)	0.38
C	—	0.7	0.6–4.3	0.165	1375(0°)	0.057
N_2	(548.5)	—	—	—	—	—
O_2	(495)	—	—	—	—	—
Ne	(127)	—	—	—	—	—
Al	—	10	23.9	0.215	2.65(20°)	0.53
Si	11.9	16	2.8–7.3	0.162	—	0.20
Ar	(517)	—	—	—	—	—
Ti	—	16.8	8.5	0.126	50(0°)	—
Fe	—	28.5	11.7	0.11	9.71(20°)	0.18
Cu	—	16	16.5	0.092	1.67(20°)	0.94
Ge	16.0	—	5.75	0.073	—	0.14
Sn	—	6	20	0.052	11.5(20°)	0.16
Xe	—	—	—	—	—	—
W	—	50	4.4	0.032	5.5(20°)	0.48
Pt	—	21	8.9	0.032	9.83(0°)	0.17
Pb	—	2.6	29.3	0.038	20.65(20°)	0.083
U	—	—	36.1	0.028	29(20°)	0.064

7. ELECTROMAGNETIC RELATIONS

Revised September 2005 by H.G. Spieler (LBNL).

Quantity	Gaussian CGS	SI
Conversion factors:		
Charge:	$2.997\,924\,58 \times 10^9$ esu	$= 1$ C $= 1$ A s
Potential:	$(1/299.792\,458)$ statvolt (ergs/esu)	$= 1$ V $= 1$ J C^{-1}
Magnetic field:	10^4 gauss $= 10^4$ dyne/esu	$= 1$ T $= 1$ N A^{-1}m^{-1}
	$\mathbf{F} = q\,(\mathbf{E} + \frac{\mathbf{v}}{c} \times \mathbf{B})$	$\mathbf{F} = q\,(\mathbf{E} + \mathbf{v} \times \mathbf{B})$
	$\boldsymbol{\nabla} \cdot \mathbf{D} = 4\pi\rho$ $\boldsymbol{\nabla} \times \mathbf{H} - \frac{1}{c}\frac{\partial \mathbf{D}}{\partial t} = \frac{4\pi}{c}\mathbf{J}$ $\boldsymbol{\nabla} \cdot \mathbf{B} = 0$ $\boldsymbol{\nabla} \times \mathbf{E} + \frac{1}{c}\frac{\partial \mathbf{B}}{\partial t} = 0$	$\boldsymbol{\nabla} \cdot \mathbf{D} = \rho$ $\boldsymbol{\nabla} \times \mathbf{H} - \frac{\partial \mathbf{D}}{\partial t} = \mathbf{J}$ $\boldsymbol{\nabla} \cdot \mathbf{B} = 0$ $\boldsymbol{\nabla} \times \mathbf{E} + \frac{\partial \mathbf{B}}{\partial t} = 0$
Constitutive relations:	$\mathbf{D} = \mathbf{E} + 4\pi\mathbf{P}, \quad \mathbf{H} = \mathbf{B} - 4\pi\mathbf{M}$	$\mathbf{D} = \epsilon_0\mathbf{E} + \mathbf{P}, \quad \mathbf{H} = \mathbf{B}/\mu_0 - \mathbf{M}$
Linear media:	$\mathbf{D} = \epsilon\mathbf{E}, \quad \mathbf{H} = \mathbf{B}/\mu$ 1 1	$\mathbf{D} = \epsilon\mathbf{E}, \quad \mathbf{H} = \mathbf{B}/\mu$ $\epsilon_0 = 8.854\,187\ldots \times 10^{-12}$ F m^{-1} $\mu_0 = 4\pi \times 10^{-7}$ N A^{-2}
	$\mathbf{E} = -\boldsymbol{\nabla} V - \frac{1}{c}\frac{\partial \mathbf{A}}{\partial t}$ $\mathbf{B} = \boldsymbol{\nabla} \times \mathbf{A}$	$\mathbf{E} = -\boldsymbol{\nabla} V - \frac{\partial \mathbf{A}}{\partial t}$ $\mathbf{B} = \boldsymbol{\nabla} \times \mathbf{A}$
	$V = \sum_{\text{charges}} \frac{q_i}{r_i} = \int \frac{\rho\,(\mathbf{r}')}{\lvert\mathbf{r} - \mathbf{r}'\rvert}\, d^3x'$ $\mathbf{A} = \frac{1}{c}\oint \frac{I\,d\boldsymbol{\ell}}{\lvert\mathbf{r} - \mathbf{r}'\rvert} = \frac{1}{c}\int \frac{\mathbf{J}(\mathbf{r}')}{\lvert\mathbf{r} - \mathbf{r}'\rvert}\, d^3x'$	$V = \frac{1}{4\pi\epsilon_0}\sum_{\text{charges}} \frac{q_i}{r_i} = \frac{1}{4\pi\epsilon_0}\int \frac{\rho\,(\mathbf{r}')}{\lvert\mathbf{r} - \mathbf{r}'\rvert}\, d^3x'$ $\mathbf{A} = \frac{\mu_0}{4\pi}\oint \frac{I\,d\boldsymbol{\ell}}{\lvert\mathbf{r} - \mathbf{r}'\rvert} = \frac{\mu_0}{4\pi}\int \frac{\mathbf{J}(\mathbf{r}')}{\lvert\mathbf{r} - \mathbf{r}'\rvert}\, d^3x'$
	$\mathbf{E}'_\parallel = \mathbf{E}_\parallel$ $\mathbf{E}'_\perp = \gamma(\mathbf{E}_\perp + \frac{1}{c}\mathbf{v} \times \mathbf{B})$ $\mathbf{B}'_\parallel = \mathbf{B}_\parallel$ $\mathbf{B}'_\perp = \gamma(\mathbf{B}_\perp - \frac{1}{c}\mathbf{v} \times \mathbf{E})$	$\mathbf{E}'_\parallel = \mathbf{E}_\parallel$ $\mathbf{E}'_\perp = \gamma(\mathbf{E}_\perp + \mathbf{v} \times \mathbf{B})$ $\mathbf{B}'_\parallel = \mathbf{B}_\parallel$ $\mathbf{B}'_\perp = \gamma(\mathbf{B}_\perp - \frac{1}{c^2}\mathbf{v} \times \mathbf{E})$
$\frac{1}{4\pi\epsilon_0} = c^2 \times 10^{-7}$ N A^{-2} $= 8.987\,55\ldots \times 10^9$ m F^{-1} ; $\frac{\mu_0}{4\pi} = 10^{-7}$ N A^{-2} ; $c = \frac{1}{\sqrt{\mu_0\epsilon_0}} = 2.997\,924\;\,58 \times 10^8$ m s^{-1}		

7.1. Impedances (SI units)

ρ = resistivity at room temperature in $10^{-8}\,\Omega$ m:

~ 1.7 for Cu	~ 5.5 for W
~ 2.4 for Au	~ 73 for SS 304
~ 2.8 for Al	~ 100 for Nichrome

(Al alloys may have double the Al value.)

For alternating currents, instantaneous current I, voltage V, angular frequency ω:

$$V = V_0\, e^{j\omega t} = ZI\ . \tag{7.1}$$

Impedance of self-inductance L: $Z = j\omega L$.

Impedance of capacitance C: $Z = 1/j\omega C$.

Impedance of free space: $Z = \sqrt{\mu_0/\epsilon_0} = 376.7\ \Omega$.

High-frequency surface impedance of a good conductor:

$$Z = \frac{(1+j)\,\rho}{\delta}\ , \quad \text{where } \delta = \text{skin depth}\ ; \tag{7.2}$$

$$\delta = \sqrt{\frac{\rho}{\pi\nu\mu}} \approx \frac{6.6\text{ cm}}{\sqrt{\nu\,(\text{Hz})}} \quad \text{for Cu}\ . \tag{7.3}$$

7.2. Capacitors, inductors, and transmission Lines

The capacitance between two parallel plates of area A spaced by the distance d and enclosing a medium with the dielectric constant ε is

$$C = K\varepsilon A/d\,, \tag{7.4}$$

where the correction factor K depends on the extent of the fringing field. If the dielectric fills the capacitor volume without extending beyond the electrodes. the correction factor $K \approx 0.8$ for capacitors of typical geometry.

The inductance at high frequencies of a straight wire whose length ℓ is much greater than the wire diameter d is

$$L \approx 2.0\left[\frac{\text{nH}}{\text{cm}}\right]\cdot\ell\left(\ln\left(\frac{4\ell}{d}\right)-1\right)\ . \tag{7.5}$$

For very short wires, representative of vias in a printed circuit board, the inductance is

$$L(\text{in nH}) \approx \ell/d\,. \tag{7.6}$$

A transmission line is a pair of conductors with inductance L and capacitance C. The characteristic impedance $Z = \sqrt{L/C}$ and the phase velocity $v_p = 1/\sqrt{LC} = 1/\sqrt{\mu\varepsilon}$, which decreases with the inverse square root of the dielectric constant of the medium. Typical coaxial and ribbon cables have a propagation delay of about 5 ns/cm.

The impedance of a coaxial cable with outer diameter D and inner diameter d is

$$Z = 60\,\Omega\cdot\frac{1}{\sqrt{\varepsilon_r}}\ln\frac{D}{d}\,, \tag{7.7}$$

where the relative dielectric constant $\varepsilon_r = \varepsilon/\varepsilon_0$. A pair of parallel wires of diameter d and spacing $a > 2.5\,d$ has the impedance

$$Z = 120\,\Omega\cdot\frac{1}{\sqrt{\varepsilon_r}}\ln\frac{2a}{d}\,. \tag{7.8}$$

This yields the impedance of a wire at a spacing h above a ground plane,

$$Z = 60\,\Omega\cdot\frac{1}{\sqrt{\varepsilon_r}}\ln\frac{4h}{d}\,. \tag{7.9}$$

A common configuration utilizes a thin rectangular conductor above a ground plane with an intermediate dielectric (microstrip). Detailed calculations for this and other transmission line configurations are given by Gunston.*

* M.A.R. Gunston. Microwave Transmission Line Data, Noble Publishing Corp., Atlanta (1997) ISBN 1-884932-57-6, TK6565.T73G85.

7.3. Synchrotron radiation (CGS units)

For a particle of charge e, velocity $v = \beta c$, and energy $E = \gamma mc^2$, traveling in a circular orbit of radius R, the classical energy loss per revolution δE is

$$\delta E = \frac{4\pi}{3}\,\frac{e^2}{R}\,\beta^3\,\gamma^4\ . \tag{7.10}$$

For high-energy electrons or positrons ($\beta \approx 1$), this becomes

$$\delta E\ (\text{in MeV}) \approx 0.0885\ [E(\text{in GeV})]^4/R(\text{in m})\ . \tag{7.11}$$

For $\gamma \gg 1$, the energy radiated per revolution into the photon energy interval $d(\hbar\omega)$ is

$$dI = \frac{8\pi}{9}\alpha\,\gamma\,F(\omega/\omega_c)\,d(\hbar\omega)\ , \tag{7.12}$$

where $\alpha = e^2/\hbar c$ is the fine-structure constant and

$$\omega_c = \frac{3\gamma^3 c}{2R} \tag{7.13}$$

is the critical frequency. The normalized function $F(y)$ is

$$F(y) = \frac{9}{8\pi}\sqrt{3}\,y\int_y^\infty K_{5/3}\,(x)\ dx\ , \tag{7.14}$$

where $K_{5/3}\,(x)$ is a modified Bessel function of the third kind. For electrons or positrons,

$$\hbar\omega_c\,(\text{in keV}) \approx 2.22\ [E(\text{in GeV})]^3/R(\text{in m})\ . \tag{7.15}$$

Fig. 7.1 shows $F(y)$ over the important range of y.

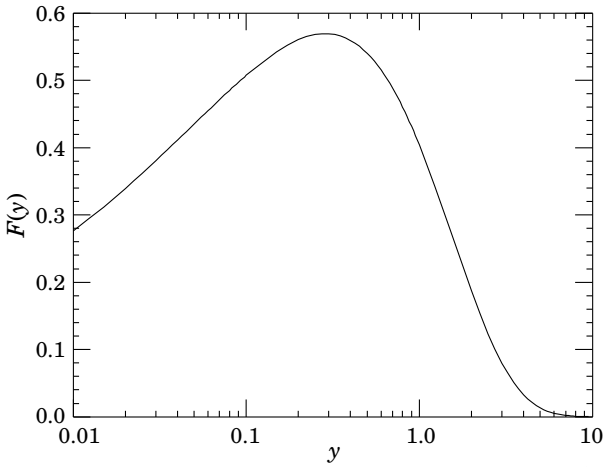

Figure 7.1: The normalized synchrotron radiation spectrum $F(y)$.

For $\gamma \gg 1$ and $\omega \ll \omega_c$,

$$\frac{dI}{d(\hbar\omega)} \approx 3.3\alpha\,(\omega R/c)^{1/3}\ , \tag{7.16}$$

whereas for

$$\gamma \gg 1 \text{ and } \omega \gtrsim 3\omega_c\ ,$$

$$\frac{dI}{d(\hbar\omega)} \approx \sqrt{\frac{3\pi}{2}}\,\alpha\,\gamma\left(\frac{\omega}{\omega_c}\right)^{1/2} e^{-\omega/\omega_c}\left[1+\frac{55}{72}\frac{\omega_c}{\omega}+\ldots\right]\ . \tag{7.17}$$

The radiation is confined to angles $\lesssim 1/\gamma$ relative to the instantaneous direction of motion. For $\gamma \gg 1$, where Eq. (7.12) applies, the mean number of photons emitted per revolution is

$$N_\gamma = \frac{5\pi}{\sqrt{3}}\alpha\gamma\ , \tag{7.18}$$

and the mean energy per photon is

$$\langle\hbar\omega\rangle = \frac{8}{15\sqrt{3}}\hbar\omega_c\ . \tag{7.19}$$

When $\langle\hbar\omega\rangle \gtrsim \mathrm{O}(E)$, quantum corrections are important.

See J.D. Jackson, *Classical Electrodynamics*, 3rd edition (John Wiley & Sons, New York, 1998) for more formulae and details. (Note that earlier editions had ω_c twice as large as Eq. (7.13).

8. NAMING SCHEME FOR HADRONS

Revised 2004 by M. Roos (University of Finland) and C.G. Wohl (LBNL).

8.1. Introduction

We introduced in the 1986 edition [1] a new naming scheme for the hadrons. Changes from older terminology affected mainly the heavier mesons made of the light (u, d, and s) quarks. Old and new names were listed alongside until 1994. Names also change from edition to edition because some characteristic like mass or spin changes. The Summary Tables give both the new and old names whenever a change occurred.

8.2. "Neutral-flavor" mesons ($S=C=B=T=0$)

Table 8.1 shows the names for mesons having the strangeness and all heavy-flavor quantum numbers equal to zero. The scheme is designed for all ordinary non-exotic mesons, but it will work for many exotic types too, if needed.

Table 8.1: Symbols for mesons with the strangeness and all heavy-flavor quantum numbers equal to zero.

	$J^{PC} =$	0^{-+}	1^{+-}	1^{--}	0^{++}
		2^{-+}	3^{+-}	2^{--}	1^{++}
		$\vdots$	$\vdots$	$\vdots$	$\vdots$
$q\overline{q}$ content	$^{2S+1}L_J =$	$^1(L\,\text{even})_J$	$^1(L\,\text{odd})_J$	$^3(L\,\text{even})_J$	$^3(L\,\text{odd})_J$
$u\overline{d}, u\overline{u}-d\overline{d}, d\overline{u}$	$(I=1)$	π	b	ρ	a
$d\overline{d}+u\overline{u}$ and/or $s\overline{s}$	$(I=0)$	η, η'	h, h'	ω, ϕ	f, f'
$c\overline{c}$		η_c	h_c	$\psi^\dagger$	χ_c
$b\overline{b}$		η_b	h_b	Υ	χ_b
$t\overline{t}$		η_t	h_t	θ	χ_t

†The J/ψ remains the J/ψ.

First, we assign names to those states with quantum numbers compatible with being $q\overline{q}$ states. The rows of the Table give the possible $q\overline{q}$ content. The columns give the possible parity/charge-conjugation states,

$$PC = -+,\ +-,\ --, \text{ and } ++\ ;$$

these combinations correspond one-to-one with the angular-momentum state $^{2S+1}L_J$ of the $q\overline{q}$ system being

$$^1(L\text{ even})_J,\ ^1(L\text{ odd})_J,\ ^3(L\text{ even})_J, \text{ or } ^3(L\text{ odd})_J\ .$$

Here S, L, and J are the spin, orbital, and total angular momenta of the $q\overline{q}$ system. The quantum numbers are related by $P=(-1)^{L+1}$, $C=(-1)^{L+S}$, and G parity $=(-1)^{L+S+I}$, where of course the C quantum number is only relevant to neutral mesons.

The entries in the Table give the meson names. The spin J is added as a subscript except for pseudoscalar and vector mesons, and the mass is added in parentheses for mesons that decay strongly. However, for the lightest meson resonances, we omit the mass.

Measurements of the mass, quark content (where relevant), and quantum numbers I, J, P, and C (or G) of a meson thus fix its symbol. Conversely, these properties may be inferred unambiguously from the symbol.

If the main symbol cannot be assigned because the quantum numbers are unknown, X is used. Sometimes it is not known whether a meson is mainly the isospin-0 mix of $u\overline{u}$ and $d\overline{d}$ or is mainly $s\overline{s}$. A prime (or pair ω, ϕ) may be used to distinguish two such mixing states.

We follow custom and use spectroscopic names such as $\Upsilon(1S)$ as the primary name for most of those ψ, Υ, and χ states whose spectroscopic identity is known. We use the form $\Upsilon(9460)$ as an alternative, and as the primary name when the spectroscopic identity is not known.

Names are assigned for $t\overline{t}$ mesons, although the top quark is evidently so heavy that it is expected to decay too rapidly for bound states to form.

Gluonium states or other mesons that are not $q\overline{q}$ states are, if the quantum numbers are *not* exotic, to be named just as are the $q\overline{q}$ mesons. Such states will probably be difficult to distinguish from $q\overline{q}$ states and will likely mix with them, and we make no attempt to distinguish those "mostly gluonium" from those "mostly $q\overline{q}$."

An "exotic" meson with J^{PC} quantum numbers that a $q\overline{q}$ system cannot have, namely $J^{PC}=0^{--}, 0^{+-}, 1^{-+}, 2^{+-}, 3^{-+}, \cdots$, would use the same symbol as does an ordinary meson with all the same quantum numbers as the exotic meson except for the C parity. But then the J subscript may still distinguish it; for example, an isospin-0 1^{-+} meson could be denoted ω_1.

8.3. Mesons with nonzero S, C, B, and/or T

Since the strangeness or a heavy flavor of these mesons is nonzero, none of them are eigenstates of charge conjugation, and in each of them one of the quarks is heavier than the other. The rules are:

1. The main symbol is an upper-case italic letter indicating the heavier quark as follows:
$$s \to \overline{K} \qquad c \to D \qquad b \to \overline{B} \qquad t \to T\ .$$
We use the convention that *the flavor and the charge of a quark have the same sign.* Thus the strangeness of the s quark is negative, the charm of the c quark is positive, and the bottom of the b quark is negative. In addition, I_3 of the u and d quarks are positive and negative, respectively. The effect of this convention is as follows: *Any flavor carried by a charged meson has the same sign as its charge.* Thus the K^+, D^+, and B^+ have positive strangeness, charm, and bottom, respectively, and all have positive I_3. The D_s^+ has positive charm *and* strangeness. Furthermore, the $\Delta(\text{flavor}) = \Delta Q$ rule, best known for the kaons, applies to every flavor.
2. If the lighter quark is not a u or a d quark, its identity is given by a subscript. The D_s^+ is an example.
3. If the spin-parity is in the "normal" series, $J^P = 0^+, 1^-, 2^+, \cdots$, a superscript "*" is added.
4. The spin is added as a subscript except for pseudoscalar or vector mesons.

8.4. Ordinary (3-quark) baryons

The symbols N, Δ, Λ, Σ, Ξ, and Ω used for more than 30 years for the baryons made of light quarks (u, d, and s quarks) tell the isospin and quark content, and the same information is conveyed by the symbols used for the baryons containing one or more heavy quarks (c and b quarks). The rules are:

1. Baryons with *three* u and/or d quarks are N's (isospin 1/2) or Δ's (isospin 3/2).
2. Baryons with *two* u and/or d quarks are Λ's (isospin 0) or Σ's (isospin 1). If the third quark is a c, b, or t quark, its identity is given by a subscript.
3. Baryons with *one* u or d quark are Ξ's (isospin 1/2). One or two subscripts are used if one or both of the remaining quarks are heavy: thus Ξ_c, Ξ_{cc}, Ξ_b, *etc.**
4. Baryons with *no* u or d quarks are Ω's (isospin 0), and subscripts indicate any heavy-quark content.
5. A baryon that decays strongly has its mass as part of its name. Thus p, Σ^-, Ω^-, Λ_c^+, *etc.*, but $\Delta(1232)^0$, $\Sigma(1385)^-$, $\Xi_c(2645)^+$, *etc.*

In short, the number of u plus d quarks together with the isospin determine the main symbol, and subscripts indicate any content of heavy quarks. A Σ always has isospin 1, an Ω always has isospin 0, *etc.*

8.5. Exotic baryons

In 2003, several experiments reported finding a strangeness $S = +1$, charge $Q = +1$ baryon, and one experiment reported finding an $S = -2$, $Q = -2$ baryon. Baryons with such quantum numbers cannot be made from three quarks, and thus they are exotic. The $S = +1$ baryon, which once would have been called a Z, was quickly dubbed the $\Theta(1540)^+$, and we proposed to name the $S = -2$ baryon the $\Phi(1860)$. However, these "discoveries" were then completely ruled out by many experiments with far larger statistics: See our 2008 *Review* [2].

Footnote and Reference:

* Sometimes a prime is necessary to distinguish two Ξ_c's in the same SU(n) multiplet. See the "Note on Charmed Baryons" in the Charmed Baryon Listings.

1. Particle Data Group: M. Aguilar-Benitez *et al.,* Phys. Lett. **170B** (1986).
2. Particle Data Group: C. Amsler *et al.*, Phys. Lett. **B667**, 1 (2008).

9. QUANTUM CHROMODYNAMICS

Revised October 2013 by S. Bethke (Max-Planck-Institute of Physics, Munich), G. Dissertori (ETH Zurich), and G.P. Salam (CERN and LPTHE, Paris).

9.1. Basics

Quantum Chromodynamics (QCD), the gauge field theory that describes the strong interactions of colored quarks and gluons, is the SU(3) component of the SU(3)×SU(2)×U(1) Standard Model of Particle Physics.

The Lagrangian of QCD is given by

$$\mathcal{L} = \sum_q \bar{\psi}_{q,a}(i\gamma^\mu \partial_\mu \delta_{ab} - g_s \gamma^\mu t^C_{ab} \mathcal{A}^C_\mu - m_q \delta_{ab})\psi_{q,b} - \frac{1}{4} F^A_{\mu\nu} F^{A\,\mu\nu} \,, \quad (9.1)$$

where repeated indices are summed over. The γ^μ are the Dirac γ-matrices. The $\psi_{q,a}$ are quark-field spinors for a quark of flavor q and mass m_q, with a color-index a that runs from $a = 1$ to $N_c = 3$, *i.e.* quarks come in three "colors." Quarks are said to be in the fundamental representation of the SU(3) color group.

The $\mathcal{A}^C_\mu$ correspond to the gluon fields, with C running from 1 to $N_c^2 - 1 = 8$, *i.e.* there are eight kinds of gluon. Gluons transform under the adjoint representation of the SU(3) color group. The t^C_{ab} correspond to eight 3×3 matrices and are the generators of the SU(3) group (cf. the section on "SU(3) isoscalar factors and representation matrices" in this *Review* with $t^C_{ab} \equiv \lambda^C_{ab}/2$). They encode the fact that a gluon's interaction with a quark rotates the quark's color in SU(3) space. The quantity g_s is the QCD coupling constant. Finally, the field tensor $F^A_{\mu\nu}$ is given by

$$F^A_{\mu\nu} = \partial_\mu \mathcal{A}^A_\nu - \partial_\nu \mathcal{A}^A_\mu - g_s\, f_{ABC} \mathcal{A}^B_\mu \mathcal{A}^C_\nu \qquad [t^A, t^B] = i f_{ABC} t^C \,, \quad (9.2)$$

where the f_{ABC} are the structure constants of the SU(3) group.

Neither quarks nor gluons are observed as free particles. Hadrons are color-singlet (*i.e.* color-neutral) combinations of quarks, anti-quarks, and gluons.

Ab-initio predictive methods for QCD include lattice gauge theory and perturbative expansions in the coupling. The Feynman rules of QCD involve a quark-antiquark-gluon ($q\bar{q}g$) vertex, a 3-gluon vertex (both proportional to g_s), and a 4-gluon vertex (proportional to g_s^2). A full set of Feynman rules is to be found for example in Ref. 1.

Useful color-algebra relations include: $t^A_{ab} t^A_{bc} = C_F \delta_{ac}$, where $C_F \equiv (N_c^2 - 1)/(2N_c) = 4/3$ is the color-factor ("Casimir") associated with gluon emission from a quark; $f_{ACD} f_{BCD} = C_A \delta_{AB}$ where $C_A \equiv N_c = 3$ is the color-factor associated with gluon emission from a gluon; $t^A_{ab} t^B_{ab} = T_R \delta_{AB}$, where $T_R = 1/2$ is the color-factor for a gluon to split to a $q\bar{q}$ pair.

The fundamental parameters of QCD are the coupling g_s (or $\alpha_s = \frac{g_s^2}{4\pi}$) and the quark masses m_q.

There is freedom for an additional CP-violating term to be present in the QCD Lagrangian, $\theta \frac{\alpha_s}{8\pi} F^A_{\mu\nu} \tilde{F}^{A\,\mu\nu}$, where $\tilde{F}^{A\,\mu\nu}$ is the dual of the gluon field tensor, $\frac{1}{2}\epsilon_{\mu\nu\sigma\rho} F^{A\,\sigma\rho}$. Experimental limits on the neutron electric dipole moment [2] constrain the coefficient of this contribution to satisfy $|\theta| \lesssim 10^{-10}$. Further discussion is to be found in Ref. 3 and in the Axions section in the Listings of this *Review*.

This section will concentrate mainly on perturbative aspects of QCD as they relate to collider physics. Related textbooks and reviews include Refs. 1,4–6. Aspects specific to Monte Carlo event generators are reviewed in a dedicated section Chap. 40. Lattice QCD is also reviewed in a section of its own Chap. 18, with additional discussion of non-perturbative aspects to be found in the sections on "Quark Masses", "The CKM quark-mixing matrix", "Structure Functions", "Fragmentation Functions" and "Event Generators" in this *Review*. For an overview of some of the QCD issues and recent results in heavy-ion physics, see for example Refs. [7–9].

9.1.1. *Running coupling* :

In the framework of perturbative QCD (pQCD), predictions for observables are expressed in terms of the renormalized coupling $\alpha_s(\mu_R^2)$, a function of an (unphysical) renormalization scale μ_R. When one takes μ_R close to the scale of the momentum transfer Q in a given process, then $\alpha_s(\mu_R^2 \simeq Q^2)$ is indicative of the effective strength of the strong interaction in that process.

The coupling satisfies the following renormalization group equation (RGE):

$$\mu_R^2 \frac{d\alpha_s}{d\mu_R^2} = \beta(\alpha_s) = -(b_0 \alpha_s^2 + b_1 \alpha_s^3 + b_2 \alpha_s^4 + \cdots) \quad (9.3)$$

where $b_0 = (11C_A - 4n_f T_R)/(12\pi) = (33 - 2n_f)/(12\pi)$ is referred to as the 1-loop beta-function coefficient, the 2-loop coefficient is $b_1 = (17C_A^2 - n_f T_R(10C_A + 6C_F))/(24\pi^2) = (153 - 19n_f)/(24\pi^2)$, and the 3-loop coefficient is $b_2 = (2857 - \frac{5033}{9} n_f + \frac{325}{27} n_f^2)/(128\pi^3)$ for the SU(3) values of C_A and C_F. The 4-loop coefficient, b_3, is to be found in Refs. 10, 11[†]. The minus sign in Eq. (9.3) is the origin of Asymptotic Freedom, *i.e.* the fact that the strong coupling becomes weak for processes involving large momentum transfers ("hard processes"), $\alpha_s \sim 0.1$ for momentum transfers in the 100 GeV – TeV range.

The β-function coefficients, the b_i, are given for the coupling of an *effective theory* in which n_f of the quark flavors are considered light ($m_q \ll \mu_R$), and in which the remaining heavier quark flavors decouple from the theory. One may relate the coupling for the theory with $n_f + 1$ light flavors to that with n_f flavors through an equation of the form

$$\alpha_s^{(n_f+1)}(\mu_R^2) = \alpha_s^{(n_f)}(\mu_R^2) \left(1 + \sum_{n=1}^{\infty} \sum_{\ell=0}^{n} c_{n\ell} \, [\alpha_s^{(n_f)}(\mu_R^2)]^n \ln^\ell \frac{\mu_R^2}{m_h^2} \right) , \quad (9.4)$$

where m_h is the mass of the $(n_f+1)^{\text{th}}$ flavor, and the first few $c_{n\ell}$ coefficients are $c_{11} = \frac{1}{6\pi}$, $c_{10} = 0$, $c_{22} = c_{11}^2$, $c_{21} = \frac{19}{24\pi^2}$, and $c_{20} = -\frac{11}{72\pi^2}$ when m_h is the $\overline{\text{MS}}$ mass at scale m_h ($c_{20} = \frac{7}{24\pi^2}$ when m_h is the pole mass — mass definitions are discussed below and in the review on "Quark Masses"). Terms up to $c_{4\ell}$ are to be found in Refs. 12, 13. Numerically, when one chooses $\mu_R = m_h$, the matching is a modest effect, owing to the zero value for the c_{10} coefficient. Relations between n_f and (n_f+2) flavors where the two heavy flavors are close in mass are given to three loops in Ref. 14.

Working in an energy range where the number of flavors is taken constant, a simple exact analytic solution exists for Eq. (9.3) only if one neglects all but the b_0 term, giving $\alpha_s(\mu_R^2) = (b_0 \ln(\mu_R^2/\Lambda^2))^{-1}$. Here Λ is a constant of integration, which corresponds to the scale where the perturbatively-defined coupling would diverge, *i.e.* it is the non-perturbative scale of QCD. A convenient approximate analytic solution to the RGE that includes also the b_1, b_2, and b_3 terms is given by (see for example Ref. 15),

$$\alpha_s(\mu_R^2) \simeq \frac{1}{b_0 t} \left(1 - \frac{b_1}{b_0^2} \frac{\ln t}{t} + \frac{b_1^2(\ln^2 t - \ln t - 1) + b_0 b_2}{b_0^4 t^2} - \frac{b_1^3(\ln^3 t - \frac{5}{2}\ln^2 t - 2\ln t + \frac{1}{2}) + 3 b_0 b_1 b_2 \ln t - \frac{1}{2} b_0^2 b_3}{b_0^6 t^3} \right) ,$$

$$t \equiv \ln \frac{\mu_R^2}{\Lambda^2} \,, \quad (9.5)$$

again parametrized in terms of a constant Λ. Note that Eq. (9.5) is one of several possible approximate 4-loop solutions for $\alpha_s(\mu_R^2)$, and that a value for Λ only defines $\alpha_s(\mu_R^2)$ once one knows which particular approximation is being used. An alternative to the use of formulas such as Eq. (9.5) is to solve the RGE exactly, numerically (including

[†] One should be aware that the b_2 and b_3 coefficients are renormalization-scheme-dependent, and given here in the $\overline{\text{MS}}$ scheme, as discussed below.

the discontinuities, Eq. (9.4), at flavor thresholds). In such cases the quantity Λ is not defined at all. For these reasons, in determinations of the coupling, it has become standard practice to quote the value of α_s at a given scale (typically the mass of the Z boson, M_Z) rather than to quote a value for Λ.

The value of the coupling, as well as the exact forms of the b_2, c_{10} (and higher-order) coefficients, depend on the renormalization scheme in which the coupling is defined, *i.e.* the convention used to subtract infinities in the context of renormalization. The coefficients given above hold for a coupling defined in the modified minimal subtraction ($\overline{\rm MS}$) scheme [16], by far the most widely used scheme.

A discussion of determinations of the coupling and a graph illustrating its scale dependence ("running") are to be found in Section 9.3.4. The RunDec package [17,18] is often used to calculate the evolution of the coupling.

9.1.2. ***Quark masses*** :

Free quarks have never been observed, which is understood as a result of a long-distance, confining property of the strong QCD force. Up, down, strange, charm, and bottom quarks all *hadronize*, *i.e.* become part of a meson or baryon, on a timescale $\sim 1/\Lambda$; the top quark instead decays before it has time to hadronize. This means that the question of what one means by the quark mass is a complex one, which requires that one adopts a specific prescription. A perturbatively defined prescription is the pole mass, m_q, which corresponds to the position of the divergence of the propagator. This is close to one's physical picture of mass. However, when relating it to observable quantities, it suffers from substantial non-perturbative ambiguities (see *e.g.* Ref. 19). An alternative is the $\overline{\rm MS}$ mass, $\overline{m}_q(\mu_R^2)$, which depends on the renormalization scale μ_R.

Results for the masses of heavier quarks are often quoted either as the pole mass or as the $\overline{\rm MS}$ mass evaluated at a scale equal to the mass, $\overline{m}_q(\overline{m}_q^2)$; light quark masses are often quoted in the $\overline{\rm MS}$ scheme at a scale $\mu_R \sim 2$ GeV . The pole and $\overline{\rm MS}$ masses are related by a slowly converging series that starts $m_q = \overline{m}_q(\overline{m}_q^2)(1 + \dfrac{4\alpha_s(\overline{m}_q^2)}{3\pi} + \mathcal{O}(\alpha_s^2))$, while the scale-dependence of $\overline{\rm MS}$ masses is given by

$$\mu_R^2 \frac{d\overline{m}_q(\mu_R^2)}{d\mu_R^2} = \left[-\frac{\alpha_s(\mu_R^2)}{\pi} + \mathcal{O}(\alpha_s^2)\right]\overline{m}_q(\mu_R^2)\,. \qquad (9.6)$$

More detailed discussion is to be found in a dedicated section of the *Review*, "Quark Masses."

9.2. Structure of QCD predictions

9.2.1. ***Fully inclusive cross sections*** :

The simplest observables in QCD are those that do not involve initial-state hadrons and that are fully inclusive with respect to details of the final state. One example is the total cross section for $e^+e^- \to$ hadrons at center-of-mass energy Q, for which one can write

$$\frac{\sigma(e^+e^- \to \text{hadrons}, Q)}{\sigma(e^+e^- \to \mu^+\mu^-, Q)} \equiv R(Q) = R_{\rm EW}(Q)(1 + \delta_{\rm QCD}(Q))\,, \qquad (9.7)$$

where $R_{\rm EW}(Q)$ is the purely electroweak prediction for the ratio and $\delta_{\rm QCD}(Q)$ is the correction due to QCD effects. To keep the discussion simple, we can restrict our attention to energies $Q \ll M_Z$, where the process is dominated by photon exchange ($R_{\rm EW} = 3\sum_q e_q^2$, neglecting finite-quark-mass corrections, where the e_q are the electric charges of the quarks),

$$\delta_{\rm QCD}(Q) = \sum_{n=1}^{\infty} c_n \cdot \left(\frac{\alpha_s(Q^2)}{\pi}\right)^n + \mathcal{O}\left(\frac{\Lambda^4}{Q^4}\right)\,. \qquad (9.8)$$

The first four terms in the α_s series expansion are then to be found in Ref. 20

$$c_1 = 1\,, \qquad c_2 = 1.9857 - 0.1152 n_f\,, \qquad (9.9a)$$

$$c_3 = -6.63694 - 1.20013 n_f - 0.00518 n_f^2 - 1.240\eta \qquad (9.9b)$$

$$c_4 = -156.61 + 18.775 n_f - 0.7974 n_f^2 + 0.0215 n_f^3 + (17.828 - 0.575 n_f)\eta, \qquad (9.9c)$$

with $\eta = (\sum e_q)^2/(3\sum e_q^2)$. For corresponding expressions including also Z exchange and finite-quark-mass effects, see Refs. [21–23].

A related series holds also for the QCD corrections to the hadronic decay width of the τ lepton, which essentially involves an integral of $R(Q)$ over the allowed range of invariant masses of the hadronic part of the τ decay (see e.g. Ref. 24). The series expansions for QCD corrections to Higgs-boson (partial) decay widths are summarized in Refs. 25, 26.

One characteristic feature of Eqs. (9.8) and (9.9) is that the coefficients of α_s^n increase rapidly order by order: calculations in perturbative QCD tend to converge more slowly than would be expected based just on the size of α_s[††]. Another feature is the existence of an extra "power-correction" term $\mathcal{O}(\Lambda^4/Q^4)$ in Eq. (9.8), which accounts for contributions that are fundamentally non-perturbative. All high-energy QCD predictions involve such corrections, though the exact power of Λ/Q depends on the observable.

Scale dependence. In Eq. (9.8) the renormalization scale for α_s has been chosen equal to Q. The result can also be expressed in terms of the coupling at an arbitrary renormalization scale μ_R,

$$\delta_{\rm QCD}(Q) = \sum_{n=1}^{\infty} \overline{c}_n\left(\frac{\mu_R^2}{Q^2}\right) \cdot \left(\frac{\alpha_s(\mu_R^2)}{\pi}\right)^n + \mathcal{O}\left(\frac{\Lambda^4}{Q^4}\right)\,, \qquad (9.10)$$

where $\overline{c}_1(\mu_R^2/Q^2) \equiv c_1$, $\overline{c}_2(\mu_R^2/Q^2) = c_2 + \pi b_0 c_1 \ln(\mu_R^2/Q^2)$, $\overline{c}_3(\mu_R^2/Q^2) = c_3 + (2b_0c_2\pi + b_1c_1\pi^2)\ln(\mu_R^2/Q^2) + b_0^2c_1\pi^2\ln^2(\mu_R^2/Q^2)$, *etc.* Given an infinite number of terms in the α_s expansion, the μ_R dependence of the $\overline{c}_n(\mu_R^2/Q^2)$ coefficients will exactly cancel that of $\alpha_s(\mu_R^2)$, and the final result will be independent of the choice of μ_R: physical observables do not depend on unphysical scales.

With just terms up to $n = N$, a residual μ_R dependence will remain, which implies an uncertainty on the prediction of $R(Q)$ due to the arbitrariness of the scale choice. This uncertainty will be $\mathcal{O}(\alpha_s^{N+1})$, *i.e.* of the same order as the neglected terms. For this reason it is standard to use QCD predictions' scale dependence as an estimate of the uncertainties due to neglected terms. One usually takes a central value for $\mu_R \sim Q$, in order to avoid the poor convergence of the perturbative series that results from the large $\ln^{n-1}(\mu_R^2/Q^2)$ terms in the $\overline{c}_n$ coefficients when $\mu_R \ll Q$ or $\mu_R \gg Q$.

9.2.1.1. *Processes with initial-state hadrons:*

Deep Inelastic Scattering. To illustrate the key features of QCD cross sections in processes with initial-state hadrons, let us consider deep-inelastic scattering (DIS), $ep \to e + X$, where an electron e with four-momentum k emits a highly off-shell photon (momentum q) that interacts with the proton (momentum p). For photon virtualities $Q^2 \equiv -q^2$ far above the squared proton mass (but far below the Z mass), the differential cross section in terms of the kinematic variables Q^2, $x = Q^2/(2p\cdot q)$ and $y = (q\cdot p)/(k\cdot p)$ is

$$\frac{d^2\sigma}{dxdQ^2} = \frac{4\pi\alpha}{2xQ^4}\left[(1 + (1-y)^2)F_2(x,Q^2) - y^2F_L(x,Q^2)\right]\,, \qquad (9.11)$$

where α is the electromagnetic coupling and $F_2(x,Q^2)$ and $F_L(x,Q^2)$ are proton structure functions, which encode the interaction between the photon (in given polarization states) and the proton. In the presence of parity-violating interactions (e.g. νp scattering) an additional F_3 structure function is present. For an extended review, including equations for the full electroweak and polarized cases, see Sec. 19 of this *Review*.

Structure functions are not calculable in perturbative QCD, nor is any other cross section that involves initial-state hadrons. To zeroth order in α_s, the structure functions are given directly in terms of non-perturbative parton (quark or gluon) distribution functions (PDFs),

$$F_2(x,Q^2) = x\sum_q e_q^2 f_{q/p}(x)\,, \qquad F_L(x,Q^2) = 0\,, \qquad (9.12)$$

[††] The situation is significantly worse near thresholds, e.g. the $t\bar{t}$ production threshold. An overview of some of the methods used in such cases is to be found for example in Ref. 27.

where $f_{q/p}(x)$ is the PDF for quarks of type q inside the proton, *i.e.* the number density of quarks of type q inside a fast-moving proton that carry a fraction x of its longitudinal momentum (the quark flavor index q, here, is not to be confused with the photon momentum q in the lines preceding Eq. (9.11)). Since PDFs are non-perturbative, and difficult to calculate accurately in lattice QCD [28], they must be extracted from data.

The above result, with PDFs $f_{q/p}(x)$ that are independent of the scale Q, corresponds to the "quark-parton model" picture in which the photon interacts with point-like free quarks, or equivalently, one has incoherent elastic scattering between the electron and individual constituents of the proton. As a consequence, in this picture also F_2 and F_L are independent of Q. When including higher orders in pQCD, Eq. (9.12) becomes

$$F_2(x,Q^2) = x\sum_{n=0}^{\infty}\frac{\alpha_s^n(\mu_R^2)}{(2\pi)^n}\sum_{i=q,g}\int_x^1\frac{dz}{z}C_{2,i}^{(n)}(z,Q^2,\mu_R^2,\mu_F^2)\,f_{i/p}\Big(\frac{x}{z},\mu_F^2\Big) + \mathcal{O}\Big(\frac{\Lambda^2}{Q^2}\Big)\,. \quad (9.13)$$

Just as in Eq. (9.10), we have a series in powers of $\alpha_s(\mu_R^2)$, each term involving a coefficient $C_{2,i}^{(n)}$ that can be calculated using Feynman graphs. An important difference relative to Eq. (9.10) stems from the fact that the quark's momentum, when it interacts with the photon, can differ from its momentum when it was extracted from the proton, because it may have radiated gluons in between. As a result, the $C_{2,i}^{(n)}$ coefficients are functions that depend on the ratio, z, of these two momenta, and one must integrate over z. For the electromagnetic component of DIS with light quarks and gluons, the zeroth order coefficient functions are $C_{2,q}^{(0)} = e_q^2\delta(1-z)$ and $C_{2,g}^{(0)} = 0$, and corrections are known up to $\mathcal{O}(\alpha_s^3)$ (N^{3}LO) [29]. For weak currents they are known fully to α_s^2 (NNLO) [30] with substantial results known also at N^{3}LO [31]. For heavy quark production they are known to $\mathcal{O}(\alpha_s^2)$ [32] (NLO insofar as the series starts at $\mathcal{O}(\alpha_s)$), with work ongoing towards NNLO [33,34,35].

The majority of the emissions that modify a parton's momentum are collinear (parallel) to that parton, and don't depend on the fact that the parton is destined to interact with a photon. It is natural to view these emissions as modifying the proton's structure rather than being part of the coefficient function for the parton's interaction with the photon. Technically, one uses a procedure known as *collinear factorization* to give a well-defined meaning to this distinction, most commonly through the $\overline{\rm MS}$ factorization scheme, defined in the context of dimensional regularization. The $\overline{\rm MS}$ factorization scheme involves an arbitrary choice of *factorization scale*, μ_F, whose meaning can be understood roughly as follows: emissions with transverse momenta above μ_F are included in the $C_{2,q}^{(n)}(z,Q^2,\mu_R^2,\mu_F^2)$; emissions with transverse momenta below μ_F are accounted for within the PDFs, $f_{i/p}(x,\mu_F^2)$. While collinear factorization is generally believed to be valid for suitable (sufficiently inclusive) observables in processes with hard scales, Ref. 36, which reviews the factorization proofs in detail, is cautious in the statements it makes about their exhaustivity, notably for the hadron-collider processes that we shall discuss below. Further discussion is to be found in Refs. 37,38.

The PDFs' resulting dependence on μ_F is described by the Dokshitzer-Gribov-Lipatov-Altarelli-Parisi (DGLAP) equations [39], which to leading order (LO) read

$$\mu_F^2\frac{\partial f_{i/p}(x,\mu_F^2)}{\partial\mu_F^2} = \sum_j\frac{\alpha_s(\mu_F^2)}{2\pi}\int_x^1\frac{dz}{z}P_{i\leftarrow j}^{(1)}(z)f_{j/p}\left(\frac{x}{z},\mu_F^2\right), \quad (9.14)$$

with, for example, $P_{q\leftarrow g}^{(1)}(z) = T_R(z^2+(1-z)^2)$. The other LO* splitting functions are listed in Chap. 19 of this *Review*, while results up to next-to-leading order (NLO), α_s^2, and next-to-next-to-leading order (NNLO), α_s^3, are given in Refs. 40 and 41 respectively. Beyond LO, the coefficient functions are also μ_F dependent, for example $C_{2,i}^{(1)}(x,Q^2,\mu_R^2,\mu_F^2) = C_{2,i}^{(1)}(x,Q^2,\mu_R^2,Q^2) - \ln\left(\frac{\mu_F^2}{Q^2}\right)\sum_j\int_x^1\frac{dz}{z}C_{2,j}^{(0)}(\frac{x}{z})P_{j\leftarrow i}^{(1)}(z)$.

As with the renormalization scale, the choice of factorization scale is arbitrary, but if one has an infinite number of terms in the perturbative series, the μ_F-dependences of the coefficient functions and PDFs will compensate each other fully. Given only N terms of the series, a residual $\mathcal{O}(\alpha_s^{N+1})$ uncertainty is associated with the ambiguity in the choice of μ_F. As with μ_R, varying μ_F provides an input in estimating uncertainties on predictions. In inclusive DIS predictions, the default choice for the scales is usually $\mu_R = \mu_F = Q$.

Hadron-hadron collisions. The extension to processes with two initial-state hadrons can be illustrated with the example of the total (inclusive) cross section for W boson production in collisions of hadrons h_1 and h_2, which can be written as

$$\sigma(h_1h_2\to W+X) = \sum_{n=0}^{\infty}\alpha_s^n(\mu_R^2)\sum_{i,j}\int dx_1dx_2\,f_{i/h_1}\Big(x_1,\mu_F^2\Big)f_{j/h_2}\Big(x_2,\mu_F^2\Big) \times\hat{\sigma}_{ij\to W+X}^{(n)}\Big(x_1x_2s,\mu_R^2,\mu_F^2\Big)\times\left(1+\mathcal{O}\left(\frac{\Lambda^2}{Q^2}\right)\right), \quad (9.15)$$

where s is the squared center-of-mass energy of the collision. At LO, $n=0$, the hard (partonic) cross section $\hat{\sigma}_{ij\to W+X}^{(0)}(x_1x_2s,\mu_R^2,\mu_F^2)$ is simply proportional to $\delta(x_1x_2s - M_W^2)$, in the narrow W-boson width approximation (see Sec. 48 of this *Review* for detailed expressions for this and other hard scattering cross sections). It is non-zero only for choices of i,j that can directly give a W, such as $i=u$, $j=\bar{d}$. At higher orders, $n\geq 1$, new partonic channels contribute, such as gq, and there is no restriction $x_1x_2s = M_W^2$.

Equation 9.15 involves a collinear factorization between hard cross section and PDFs, just like Eq. (9.13). As long as the same factorization scheme is used in DIS and pp or $p\bar{p}$ (usually the $\overline{\rm MS}$ scheme), then PDFs extracted in DIS can be directly used in pp and $p\bar{p}$ predictions [42,36] (with the anti-quark distributions in an anti-proton being the same as the quark distributions in a proton).

Fully inclusive hard cross sections are known to NNLO, i.e. corrections up to relative order α_s^2, for Drell-Yan (DY) lepton-pair and vector-boson production [43,44], Higgs-boson production via gluon fusion [44–46], Higgs-boson production in association with a vector boson [47], Higgs-boson production via vector-boson fusion [48] (in an approximation that factorizes the production of the two vector bosons), Higgs-pair production [49], and top-antitop production [50]. A review of fully inclusive Higgs-related results is to be found in Ref. 51.

Photoproduction. γp (and $\gamma\gamma$) collisions are similar to pp collisions, with the subtlety that the photon can behave in two ways: there is "direct" photoproduction, in which the photon behaves as a point-like particle and takes part directly in the hard collision, with hard subprocesses such as $\gamma g\to q\bar{q}$; there is also resolved photoproduction, in which the photon behaves like a hadron, with non-perturbative partonic substructure and a corresponding PDF for its quark and gluon content, $f_{i/\gamma}(x,Q^2)$.

While useful to understand the general structure of γp collisions, the distinction between direct and resolved photoproduction is not well defined beyond leading order, as discussed for example in Ref. 52.

The high-energy limit. In situations in which the total center-of-mass energy $\sqrt{s}$ is much larger than other scales in the problem (*e.g.*

* LO is generally taken to mean the lowest order at which a quantity is non-zero. This definition is nearly always unambiguous, the one major exception being for the case of the hadronic branching ratio of virtual photons, Z, τ, etc., for which two conventions exist: LO can either mean the lowest order that contributes to the hadronic branching fraction, *i.e.* the term "1" in Eq. (9.7); or it can mean the lowest order at which the hadronic branching ratio becomes sensitive to the coupling, $n=1$ in Eq. (9.8), as is relevant when extracting the value of the coupling from a measurement of the branching ratio. Because of this ambiguity, we avoided use of the term "LO" in that context.

Q in DIS, m_b for $b\bar{b}$ production in pp collisions, *etc.*), each power of α_s beyond LO can be accompanied by a power of $\ln(s/Q^2)$ (or $\ln(s/m_b^2)$, *etc.*). This is known as the high-energy or Balitsky-Fadin-Kuraev-Lipatov (BFKL) limit [53–55]. Currently it is possible to account for the dominant and first subdominant [56,57] power of $\ln s$ at each order of α_s, and also to estimate further subdominant contributions that are numerically large (see Refs. 58–60 and references therein).

Physically, the summation of all orders in α_s can be understood as leading to a growth with s of the gluon density in the proton. At sufficiently high energies this implies non-linear effects, whose treatment has been the subject of intense study (see for example Refs. 61, 62 and references thereto). Note that it is not straightforward to relate these results to the genuinely non-perturbative total, elastic and diffractive cross sections for hadron-hadron scattering (experimental results for which are summarized in section Chap. 50 of this *Review*).

9.2.2. ***Non fully inclusive cross-sections*** :

QCD final states always consist of hadrons, while perturbative QCD calculations deal with partons. Physically, an energetic parton fragments ("showers") into many further partons, which then, on later timescales, undergo a transition to hadrons ("hadronization"). Fixed-order perturbation theory captures only a small part of these dynamics.

This does not matter for the fully inclusive cross sections discussed above: the showering and hadronization stages are unitary, *i.e.* they do not change the overall probability of hard scattering, because they occur long after it has taken place.

Less inclusive measurements, in contrast, may be affected by the extra dynamics. For those sensitive just to the main directions of energy flow (jet rates, event shapes, cf. Sec. 9.3.1) fixed order perturbation theory is often still adequate, because showering and hadronization don't substantially change the overall energy flow. This means that one can make a prediction using just a small number of partons, which should correspond well to a measurement of the same observable carried out on hadrons. For observables that instead depend on distributions of individual hadrons (which, e.g., are the inputs to detector simulations), it is mandatory to account for showering and hadronization. The range of predictive techniques available for QCD final states reflects this diversity of needs of different measurements.

While illustrating the different methods, we shall for simplicity mainly use expressions that hold for e^+e^- scattering. The extension to cases with initial-state partons will be mostly straightforward (space constraints unfortunately prevent us from addressing diffraction and exclusive hadron-production processes; extensive discussion is to be found in Refs. 63, 64).

9.2.2.1. *Preliminaries: Soft and collinear limits:*

Before examining specific predictive methods, it is useful to be aware of a general property of QCD matrix elements in the soft and collinear limits. Consider a squared tree-level matrix element $|M_n^2(p_1,\ldots,p_n)|$ for the process $e^+e^- \to n$ partons with momenta $p_1,\ldots,p_n$, and a corresponding phase-space integration measure $d\Phi_n$. If particle n is a gluon, and additionally it becomes collinear (parallel) to another particle i and its momentum tends to zero (it becomes "soft"), the matrix element simplifies as follows,

$$\lim_{\theta_{in}\to 0,\, E_n\to 0} d\Phi_n |M_n^2(p_1,\ldots,p_n)| = d\Phi_{n-1}|M_{n-1}^2(p_1,\ldots,p_{n-1})| \frac{\alpha_s C_i}{\pi}\frac{d\theta_{in}^2}{\theta_{in}^2}\frac{dE_n}{E_n}\,, \qquad (9.16)$$

where $C_i = C_F$ (C_A) if i is a quark (gluon). This formula has non-integrable divergences both for the inter-parton angle $\theta_{in} \to 0$ and for the gluon energy $E_n \to 0$, which are mirrored also in the structure of divergences in loop diagrams. These divergences are important for at least two reasons: firstly, they govern the typical structure of events (inducing many emissions either with low energy or at small angle with respect to hard partons); secondly, they will determine which observables can be calculated within perturbative QCD.

9.2.2.2. *Fixed-order predictions:*

Let us consider an observable $\mathcal{O}$ that is a function $\mathcal{O}_n(p_1,\ldots,p_n)$ of the four-momenta of the n final-state particles in an event (whether partons or hadrons). In what follows, we shall consider the cross section for events weighted with the value of the observable, $\sigma_{\mathcal{O}}$. As examples, if $\mathcal{O}_n \equiv 1$ for all n, then $\sigma_{\mathcal{O}}$ is just the total cross section; if $\mathcal{O}_n \equiv \hat{\tau}(p_1,\ldots,p_n)$ where $\hat{\tau}$ is the value of the Thrust for that event (see Sec. 9.3.1.2), then the average value of the Thrust is $\langle\tau\rangle = \sigma_{\mathcal{O}}/\sigma_{\rm tot}$; if $\mathcal{O}_n \equiv \delta(\tau - \hat{\tau}(p_1,\ldots,p_n))$ then one gets the differential cross section as a function of the Thrust, $\sigma_{\mathcal{O}} \equiv d\sigma/d\tau$.

In the expressions below, we shall omit to write the non-perturbative power correction term, which for most common observables is proportional to a single power of Λ/Q.

LO. If the observable $\mathcal{O}$ is non-zero only for events with at least n final-state particles, then the LO QCD prediction for the weighted cross section in e^+e^- annihilation is

$$\sigma_{\mathcal{O},LO} = \alpha_s^{n-2}(\mu_R^2)\int d\Phi_n |M_n^2(p_1,\ldots,p_n)|\,\mathcal{O}_n(p_1,\ldots,p_n)\,, \qquad (9.17)$$

where the squared tree-level matrix element, $|M_n^2(p_1,\ldots,p_n)|$, includes relevant symmetry factors, has been summed over all subprocesses (e.g. $e^+e^- \to q\bar{q}q\bar{q}$, $e^+e^- \to q\bar{q}gg$) and has had all factors of α_s extracted in front. In processes other than e^+e^- collisions, the center-of-mass energy of the LO process is generally not fixed, and so the powers of the coupling are often brought inside the integrals, with the scale μ_R chosen event by event, as a function of the event kinematics.

Other than in the simplest cases (see the review on Cross Sections in this *Review*), the matrix elements in Eq. (9.17) are usually calculated automatically with programs such as CompHEP [65], MadGraph [66], Alpgen [67], Comix/Sherpa [68], and Helac/Phegas [69]. Some of these (CompHEP, MadGraph) use formulas obtained from direct evaluations of Feynman diagrams. Others (Alpgen, Helac/Phegas and Comix/Sherpa) use methods designed to be particularly efficient at high multiplicities, such as Berends-Giele recursion [70], which builds up amplitudes for complex processes from simpler ones (see also the reviews and discussion in Refs. [71–73]).

The phase-space integration is usually carried out by Monte Carlo sampling, in order to deal with the sometimes complicated cuts that are used in corresponding experimental measurements. Because of the divergences in the matrix element, Eq. (9.16), the integral converges only if the observable vanishes for kinematic configurations in which one of the n particles is arbitrarily soft or it is collinear to another particle. As an example, the cross section for producing any configuration of n partons will lead to an infinite integral, whereas a finite result will be obtained for the cross section for producing n deposits of energy (or jets, see Sec. 9.3.1.1), each above some energy threshold and well separated from each other in angle.

LO calculations can be carried out for $2 \to n$ processes with $n \lesssim 6-10$. The exact upper limit depends on the process, the method used to evaluate the matrix elements (recursive methods are more efficient), and the extent to which the phase-space integration can be optimized to work around the large variations in the values of the matrix elements.

NLO. Given an observable that is non-zero starting from n final-state particles, its prediction at NLO involves supplementing the LO result, Eq. (9.17), with the $2 \to (n+1)$-particle squared tree-level matrix element ($|M_{n+1}^2|$), and the interference of an $2 \to n$ tree-level and $2 \to n$ 1-loop amplitude ($2\mathrm{Re}(M_n M_{n,1-\mathrm{loop}}^*)$),

$$\sigma_{\mathcal{O}}^{NLO} = \sigma_{\mathcal{O}}^{LO} + \alpha_s^{n-1}(\mu_R^2)\int d\Phi_{n+1} |M_{n+1}^2(p_1,\ldots,p_{n+1})|\,\mathcal{O}_{n+1}(p_1,\ldots,p_{n+1}) + \alpha_s^{n-1}(\mu_R^2)\int d\Phi_n\, 2\mathrm{Re}\,[\, M_n(p_1,\ldots,p_n) M_{n,1-\mathrm{loop}}^*(p_1,\ldots,p_n)\,]\,\mathcal{O}_n(p_1,\ldots,p_n)\,. \qquad (9.18)$$

Relative to LO calculations, two important issues appear in the NLO calculations. Firstly, the extra complexity of loop-calculations

relative to tree-level calculations means that their automation is at a comparatively early stage (see below). Secondly, loop amplitudes are infinite in 4 dimensions, while tree-level amplitudes are finite, but their *integrals* are infinite, due to the divergences of Eq. (9.16). These two sources of infinities have the same soft and collinear origins and cancel after the integration only if the observable $\mathcal{O}$ satisfies the property of infrared and collinear safety,

$$\begin{aligned} \mathcal{O}_{n+1}(p_1,\ldots,p_s,\ldots,p_n) &\to \mathcal{O}_n(p_1,\ldots,p_n) \qquad \text{if } p_s \to 0 \\ \mathcal{O}_{n+1}(p_1,\ldots,p_a,p_b,\ldots,p_n) &\to \mathcal{O}_n(p_1,\ldots,p_a+p_b,\ldots,p_n) \\ &\qquad \text{if } p_a \,||\, p_b\,. \end{aligned} \tag{9.19}$$

Examples of infrared-safe quantities include event-shape distributions and jet cross sections (with appropriate jet algorithms, see below). Unsafe quantities include the distribution of the momentum of the hardest QCD particle (which is not conserved under collinear splitting), observables that require the complete absence of radiation in some region of phase-space (e.g. rapidity gaps or 100% isolation cuts, which are affected by soft emissions), or the particle multiplicity (affected by both soft and collinear emissions). The non-cancellation of divergences at NLO due to infrared or collinear unsafety compromises the usefulness not only of the NLO calculation, but also that of a LO calculation, since LO is only an acceptable approximation if one can prove that higher-order terms are smaller. Infrared and collinear unsafety usually also imply large non-perturbative effects.

As with LO calculations, the phase-space integrals in Eq. (9.18) are usually carried out by Monte Carlo integration, so as to facilitate the study of arbitrary observables. Various methods exist to obtain numerically efficient cancellation among the different infinities. These include notably dipole [74], FKS [75] and antenna [76] subtraction.

NLO calculations exist for a wide range of processes. Many calculations have been performed process by process and are available in dedicated packages, among them NLOJet++ [77] for e^+e^-, DIS, and hadron-hadron processes involving just light partons in the final state, MCFM [78] for hadron-hadron processes with vector bosons and/or heavy quarks in the final state, VBFNLO for vector-boson fusion, di- and tri-boson processes [79], and the Phox family [80] for processes with photons in the final state. Recent years have seen a move towards automated NLO calculations, with publicly available programs such as GoSam [81], Helac-NLO [82], the aMC@NLO framework [83] and NJet [84], as well as other codes such as BlackHat [85], Open Loops [86], Recola [87] and Rocket [88] that have also been used for a range of predictions. These tools rely in part on a wide array of developments reviewed in Refs. 72,89, as well as on external codes for the subtraction of divergences such as Helac-Dipoles [90], MadFKS [91] and Sherpa [92]. The most complex processes for which NLO QCD corrections have been obtained so far are $e^+e^- \to 7$ jets [93], $pp \to W + 5$ jets [94] and $pp \to 5$ jets [95].

NNLO. Conceptually, NNLO and NLO calculations are similar, except that one must add a further order in α_s, consisting of: the squared $(n+2)$-parton tree-level amplitude, the interference of the $(n+1)$-parton tree-level and 1-loop amplitudes, the interference of the n-parton tree-level and 2-loop amplitudes, and the squared n-parton 1-loop amplitude.

Each of these elements involves large numbers of soft and collinear divergences, satisfying relations analogous to Eq. (9.16) that now involve multiple collinear or soft particles and higher loop orders (see e.g. Refs. 96,97,98). Arranging for the cancellation of the divergences after numerical Monte Carlo integration is one of the significant challenges of NNLO calculations, as is the determination of the relevant 2-loop amplitudes. At the time of writing, the processes for which fully exclusive NNLO calculations exist include the 3-jet cross section in e^+e^- collisions [99,100] (for which NNLO means α_s^3), as well as vector-boson [101,102], Higgs-boson [103,104], WH [105], Higgs-pair [49] and di-photon [106] production in pp and $p\bar{p}$ collisions. Progress has also been reported recently on dijet [107] and Higgs+jet [108] production in pp collisions, while the methods used for the total $pp \to t\bar{t}$ cross section [50] lend themselves also to future more differential results.

9.2.2.3. *Resummation:*

Many experimental measurements place tight constraints on emissions in the final state. For example, in e^+e^- events, that one minus the Thrust should be less than some value $\tau \ll 1$, or in $pp \to Z$ events that the Z-boson transverse momentum should be much smaller than its mass, $p_{t,Z} \ll M_Z$. A further example is the production of heavy particles or jets near threshold (so that little energy is left over for real emissions) in DIS and pp collisions.

In such cases, the constraint vetoes a significant part of the integral over the soft and collinear divergence of Eq. (9.16). As a result, there is only a partial cancellation between real emission terms (subject to the constraint) and loop (virtual) contributions (not subject to the constraint), causing each order of α_s to be accompanied by a large coefficient $\sim L^2$, where *e.g.* $L = \ln\tau$ or $L = \ln(M_Z/p_{t,Z})$. One ends up with a perturbative series whose terms go as $\sim (\alpha_s L^2)^n$. It is not uncommon that $\alpha_s L^2 \gg 1$, so that the perturbative series converges very poorly if at all.** In such cases one may carry out a "resummation," which accounts for the dominant logarithmically enhanced terms to all orders in α_s, by making use of known properties of matrix elements for multiple soft and collinear emissions, and of the all-orders properties of the divergent parts of virtual corrections, following original works such as Refs. 109–118 and also through soft-collinear effective theory [119,120] (cf. also the review in Ref. 121).

For cases with double logarithmic enhancements (two powers of logarithm per power of α_s), there are two classification schemes for resummation accuracy. Writing the cross section including the constraint as $\sigma(L)$ and the unconstrained (total) cross section as $\sigma_{\rm tot}$, the series expansion takes the form

$$\sigma(L) \simeq \sigma_{\rm tot} \sum_{n=0}^{\infty} \sum_{k=0}^{2n} R_{nk} \alpha_s^n(\mu_R^2) L^k, \qquad L \gg 1 \tag{9.20}$$

and leading log (LL) resummation means that one accounts for all terms with $k = 2n$, next-to-leading-log (NLL) includes additionally all terms with $k = 2n-1$, *etc.* Often $\sigma(L)$ (or its Fourier or Mellin transform) *exponentiates* ‡,

$$\sigma(L) \simeq \sigma_{\rm tot} \exp\left[\sum_{n=1}^{\infty} \sum_{k=0}^{n+1} G_{nk} \alpha_s^n(\mu_R^2) L^k\right], \qquad L \gg 1\,, \tag{9.21}$$

where one notes the different upper limit on k ($\leq n+1$) compared to Eq. (9.20). This is a more powerful form of resummation: the G_{12} term alone reproduces the full LL series in Eq. (9.20). With the form Eq. (9.21) one still uses the nomenclature LL, but this now means that all terms with $k = n+1$ are included, and NLL implies all terms with $k = n$, *etc.*

For a large number of observables, NLL resummations are available in the sense of Eq. (9.21) (see Refs. 125–127 and references therein). NNLL has been achieved for the DY and Higgs-boson p_t distributions [128–131](also available in the CuTe [132], HRes [133] and ResBos [134] families of programs) and related variables [135], the back-to-back energy-energy correlation in e^+e^- [136], the jet broadening in e^+e^- collisions [137], the jet-veto survival probability in Higgs and Z production in pp collisions [138], an event-shape type observable known as the beam Thrust [139], hadron-collider jet masses in specific limits [140] (see also Ref. 141), the production of

** To be precise one should distinguish two causes of the divergence of perturbative series. That which interests us here is associated with the presence of a new large parameter (*e.g.* ratio of scales). Nearly all perturbative series also suffer from "renormalon" divergences $\alpha_s^n n!$ (reviewed in Ref. 19), which however have an impact only at very high perturbative orders and have a deep connection with non-perturbative contributions.

‡ Whether or not this happens depends on the quantity being resummed. A classic example involves jet rates in e^+e^- collisions as a function of a jet-resolution parameter $y_{\rm cut}$. The logarithms of $1/y_{\rm cut}$ exponentiate for the k_t (Durham) jet algorithm [122], but not [123] for the JADE algorithm [124] (both are discussed below in Sec. 9.3.1.1).

top anti-top pairs near threshold [142–144] (and references therein), and high-p_t W and Z production [145]. Finally, the parts believed to be dominant in the N^{3}LL resummation are available for the Thrust variable and heavy-jet mass in e^+e^- annihilations [146,147] (confirmed for Thrust at NNLL in Ref. 148), and for Higgs- and vector-boson production near threshold [149,150] in hadron collisions (NNLL in Refs. 151,152). The inputs and methods involved in these various calculations are somewhat too diverse to discuss in detail here, so we recommend that the interested reader consult the original references for further details.

9.2.2.4. *Fragmentation functions:*

Since the parton-hadron transition is non-perturbative, it is not possible to perturbatively calculate quantities such as the energy-spectra of specific hadrons in high-energy collisions. However, one can factorize perturbative and non-perturbative contributions via the concept of fragmentation functions. These are the final-state analogue of the parton distribution functions that are used for initial-state hadrons.

It should be added that if one ignores the non-perturbative difficulties and just calculates the energy and angular spectrum of partons in perturbative QCD with some low cutoff scale $\sim \Lambda$ (using resummation to sum large logarithms of $\sqrt{s}/\Lambda$), then this reproduces many features of the corresponding hadron spectra. This is often taken to suggest that hadronization is "local" in momentum space.

Section 20 of this *Review* provides further information (and references) on these topics, including also the question of heavy-quark fragmentation.

9.2.2.5. *Parton-shower Monte Carlo generators:*

Parton-shower Monte Carlo (MC) event generators like PYTHIA [153–155], HERWIG [156–158], SHERPA [92], and ARIADNE [159] provide fully exclusive simulations of QCD events. Because they provide access to "hadron-level" events they are a crucial tool for all applications that involve simulating the response of detectors to QCD events. Here we give only a brief outline of how they work and refer the reader to Chap. 40 and Ref. 160 for a full overview.

The MC generation of an event involves several stages. It starts with the random generation of the kinematics and partonic channels of whatever *hard scattering process* the user has requested at some high scale Q_0 (for complex processes, this may be carried out by an external program). This is followed by a *parton shower*, usually based on the successive random generation of gluon emissions (or $g \to q\bar{q}$ splittings). Each is generated at a scale lower than the previous emission, following a (soft and collinear resummed) perturbative QCD distribution that depends on the momenta of all previous emissions. Common choices of scale for the ordering of emissions are virtuality, transverse momentum or angle. Parton showering stops at a scale of order 1 GeV, at which point a *hadronization model* is used to convert the resulting partons into hadrons. One widely-used model involves stretching a color "string" across quarks and gluons, and breaking it up into hadrons [161,162]. Another breaks each gluon into a $q\bar{q}$ pair and then groups quarks and anti-quarks into colorless "clusters", which then give the hadrons [156]. For pp and γp processes, modeling is also needed to treat the collision between the two hadron remnants, which generates an *underlying event* (UE), usually implemented via additional $2 \to 2$ scatterings ("multiple parton interactions") at a scale of a few GeV, following Ref. 163.

A deficiency of the soft and collinear approximations that underlie parton showers is that they may fail to reproduce the full pattern of hard wide-angle emissions, important, for example, in many new physics searches. It is therefore common to use LO multi-parton matrix elements to generate hard high-multiplicity partonic configurations as additional starting points for the showering, supplemented with some prescription (CKKW [164], MLM [165]) for consistently merging samples with different initial multiplicities.

MCs, as described above, generate cross sections for the requested hard process that are correct at LO. A wide variety of processes are available in MC implementations that are correct to NLO, using the MC@NLO [166] or POWHEG [167] prescriptions, notably through the aMC@NLO [83] and POWHEGBox programs [168]. Techniques have also been developed recently to combine NLO plus shower accuracy for different multiplicities of final-state jets [169]. Building on some of that work, a first example of NNLO plus shower accuracy has been described in Ref. 170 for Higgs production.

9.2.3. ***Accuracy of predictions*** :

Estimating the accuracy of perturbative QCD predictions is not an exact science. It is often said that LO calculations are accurate to within a factor of two. This is based on experience with NLO corrections in the cases where these are available. In processes involving new partonic scattering channels at NLO and/or large ratios of scales (such as jet observables in processes with vector bosons, or the production of high-p_t jets containing B-hadrons), the NLO to LO K-factors can be substantially larger than 2.

For calculations beyond LO, a conservative approach to estimate the perturbative uncertainty is to take it to be the last known perturbative order; a more widely used method is to estimate it from the change in the prediction when varying the renormalization and factorization scales around a central value Q that is taken close to the physical scale of the process. A conventional range of variation is $Q/2 < \mu_R, \mu_F < 2Q$. This should not be assumed to always estimate the full uncertainty from missing higher orders, but it does indicate the size of one important known source of higher-order ambiguity.[‡‡]

There does not seem to be a broad consensus on whether μ_R and μ_F should be kept identical or varied independently. One common option is to vary them independently with the restriction $\frac{1}{2}\mu_R < \mu_F < 2\mu_R$ [177]. This limits the risk of misleadingly small uncertainties due to fortuitous cancellations between the μ_F and μ_R dependence when both are varied together, while avoiding the appearance of large logarithms of μ_R^2/μ_F^2 when both are varied completely independently.

Calculations that involve resummations usually have an additional source of uncertainty associated with the choice of argument of the logarithms being resummed, *e.g.* $\ln(2\frac{p_{t,Z}}{M_Z})$ as opposed to $\ln(\frac{1}{2}\frac{p_{t,Z}}{M_Z})$. In addition to varying renormalization and factorization scales, it is therefore also advisable to vary the argument of the logarithm by a factor of two in either direction with respect to the "natural" argument.

The accuracy of QCD predictions is limited also by non-perturbative corrections, which typically scale as a power of Λ/Q. For measurements that are directly sensitive to the structure of the hadronic final state the corrections are usually linear in Λ/Q. The non-perturbative corrections are further enhanced in processes with a significant underlying event (*i.e.* in pp and $p\bar{p}$ collisions) and in cases where the perturbative cross sections fall steeply as a function of p_t or some other kinematic variable.

Non-perturbative corrections are commonly estimated from the difference between Monte Carlo events at the parton level and after hadronization. An issue to be aware of with this procedure is that "parton level" is not a uniquely defined concept. For example, in an event generator it depends on a (somewhat arbitrary and tunable) internal cutoff scale that separates the parton showering from the hadronization. In contrast no such cutoff scale exists in a NLO or NNLO partonic calculation. For this reason there are widespread reservations as to the appropriateness of deriving hadronization corrections from a Monte Carlo program and then applying them to NLO or NNLO predictions. There exist alternative methods for estimating hadronization corrections, which attempt to analytically deduce non-perturbative effects in one observable based on measurements of other observables (see the reviews [19,178]). While they directly address the problem of different possible definitions of parton level, it should also be said that they are far less flexible than Monte Carlo programs and not always able to provide equally good descriptions of the data.

[‡‡] A number of prescriptions also exist for setting the scale automatically, e.g. Refs. 171–174, eliminating uncertainties from scale variation, though not from the truncation of the perturbative series itself. Recently, there have also been studies of how to estimate uncertainties from missing higher orders that go beyond scale variations [175,176].

9.3. Experimental QCD

Since we are not able to directly measure partons (quarks or gluons), but only hadrons and their decay products, a central issue for every experimental test of perturbative QCD is establishing a correspondence between observables obtained at the partonic and the hadronic level. The only theoretically sound correspondence is achieved by means of *infrared and collinear safe* quantities, which allow one to obtain finite predictions at any order of perturbative QCD.

As stated above, the simplest case of infrared- and collinear-safe observables are total cross sections. More generally, when measuring fully inclusive observables, the final state is not analyzed at all regarding its (topological, kinematical) structure or its composition. Basically the relevant information consists in the rate of a process ending up in a partonic or hadronic final state. In e^+e^- annihilation, widely used examples are the ratios of partial widths or branching ratios for the electroweak decay of particles into hadrons or leptons, such as Z or τ decays, (cf. Sec. 9.2.1). Such ratios are often favored over absolute cross sections or partial widths because of large cancellations of experimental and theoretical systematic uncertainties. The strong suppression of non-perturbative effects, $\mathcal{O}(\Lambda^4/Q^4)$, is one of the attractive features of such observables, however, at the same time the sensitivity to radiative QCD corrections is small, which for example affects the statistical uncertainty when using them for the determination of the strong coupling constant. In the case of τ decays not only the hadronic branching ratio is of interest, but also moments of the spectral functions of hadronic tau decays, which sample different parts of the decay spectrum and thus provide additional information. Other examples of fully inclusive observables are structure functions (and related sum rules) in DIS. These are extensively discussed in Sec. 19 of this *Review*.

On the other hand, often the structure or composition of the final state are analyzed and cross sections differential in one or more variables characterizing this structure are of interest. Examples are jet rates, jet substructure, event shapes or transverse momentum distributions of jets or vector bosons in hadron collisions. The case of fragmentation functions, *i.e.* the measurement of hadron production as a function of the hadron momentum relative to some hard scattering scale, is discussed in Sec. 20 of this *Review*.

It is worth mentioning that, besides the correspondence between the parton and hadron level, also a correspondence between the hadron level and the actually measured quantities in the detector has to be established. The simplest examples are corrections for finite experimental acceptance and efficiencies. Whereas acceptance corrections essentially are of theoretical nature, since they involve extrapolations from the measurable (partial) to the full phase space, other corrections such as for efficiency, resolution and response, are of experimental nature. For example, measurements of differential cross sections such as jet rates require corrections in order to relate, *e.g.* the energy deposits in a calorimeter to the jets at the hadron level. Typically detector simulations and/or data-driven methods are used in order to obtain these corrections. Care should be taken here in order to have a clear separation between the parton-to-hadron level and hadron-to-detector level corrections. Finally, for the sake of an easy comparison to the results of other experiments and/or theoretical calculations, it is suggested to provide, whenever possible, measurements corrected for detector effects and/or all necessary information related to the detector response (*e.g.* the detector response matrix).

9.3.1. *Hadronic final-state observables* :

9.3.1.1. *Jets:*

In hard interactions, final-state partons and hadrons appear predominantly in collimated bunches, which are generically called *jets*. To a first approximation, a jet can be thought of as a hard parton that has undergone soft and collinear showering and then hadronization. Jets are used both for testing our understanding and predictions of high-energy QCD processes, and also for identifying the hard partonic structure of decays of massive particles like top quarks.

In order to map observed hadrons onto a set of jets, one uses a *jet definition*. The mapping involves explicit choices: for example when a gluon is radiated from a quark, for what range of kinematics should the gluon be part of the quark jet, or instead form a separate jet? Good jet definitions are infrared and collinear safe, simple to use in theoretical and experimental contexts, applicable to any type of inputs (parton or hadron momenta, charged particle tracks, and/or energy deposits in the detectors) and lead to jets that are not too sensitive to non-perturbative effects. An extensive treatment of the topic of jet definitions is given in Ref. 179 (for e^+e^- collisions) and Refs. 180, 181 (for pp or $p\bar{p}$ collisions). Here we briefly review the two main classes: cone algorithms, extensively used at older hadron colliders, and sequential recombination algorithms, more widespread in e^+e^- and ep colliders and at the LHC.

Very generically, most (iterative) cone algorithms start with some seed particle i, sum the momenta of all particles j within a cone of opening-angle R, typically defined in terms of (pseudo-)rapidity and azimuthal angle. They then take the direction of this sum as a new seed and repeat until the cone is stable, and call the contents of the resulting stable cone a jet if its transverse momentum is above some threshold $p_{t,\min}$. The parameters R and $p_{t,\min}$ should be chosen according to the needs of a given analysis.

There are many variants of cone algorithm, and they differ in the set of seeds they use and the manner in which they ensure a one-to-one mapping of particles to jets, given that two stable cones may share particles ("overlap"). The use of seed particles is a problem w.r.t. infrared and collinear safety, and seeded algorithms are generally not compatible with higher-order (or sometimes even leading-order) QCD calculations, especially in multi-jet contexts, as well as potentially subject to large non-perturbative corrections and instabilities. Seeded algorithms (JetCLU, MidPoint, and various other experiment-specific iterative cone algorithms) are therefore to be deprecated. A modern alternative is to use a seedless variant, SISCone [182].

Sequential recombination algorithms at hadron colliders (and in DIS) are characterized by a distance $d_{ij} = \min(k_{t,i}^{2p}, k_{t,j}^{2p})\Delta_{ij}^2/R^2$ between all pairs of particles i, j, where Δ_{ij} is their distance in the rapidity-azimuthal plane, $k_{t,i}$ is the transverse momentum w.r.t. the incoming beams, and R is a free parameter. They also involve a "beam" distance $d_{iB} = k_{t,i}^{2p}$. One identifies the smallest of all the d_{ij} and d_{iB}, and if it is a d_{ij}, then i and j are merged into a new pseudo-particle (with some prescription, a recombination scheme, for the definition of the merged four-momentum). If the smallest distance is a d_{iB}, then i is removed from the list of particles and called a jet. As with cone algorithms, one usually considers only jets above some transverse-momentum threshold $p_{t,\min}$. The parameter p determines the kind of algorithm: $p = 1$ corresponds to the (*inclusive-*)k_t algorithm [122,183,184], $p = 0$ defines the *Cambridge-Aachen* algorithm [185,186], while for $p = -1$ we have the *anti-*k_t algorithm [187]. All these variants are infrared and collinear safe to all orders of perturbation theory. Whereas the former two lead to irregularly shaped jet boundaries, the latter results in cone-like boundaries. The *anti-*k_t algorithm has become the de-facto standard for the LHC experiments.

In e^+e^- annihilations the k_t algorithm [122] uses $y_{ij} = 2\min(E_i^2, E_j^2)(1-\cos\theta_{ij})/Q^2$ as distance measure and repeatedly merges the pair with smallest y_{ij}, until all y_{ij} distances are above some threshold $y_{\rm cut}$, the jet resolution parameter. The (pseudo)-particles that remain at this point are called the jets. Here it is $y_{\rm cut}$ (rather than R and $p_{t,\min}$) that should be chosen according to the needs of the analysis. As mentioned above, the k_t algorithm has the property that logarithms $\ln(1/y_{\rm cut})$ exponentiate in resummation calculations. This is one reason why it is preferred over the earlier JADE algorithm [124], which uses the distance measure $y_{ij} = 2\,E_i\,E_j\,(1-\cos\theta_{ij})/Q^2$.

Efficient implementations of the above algorithms are available through the *FastJet* package [188], which is also packaged within *SpartyJet* [189].

9.3.1.2. *Event Shapes:*

Event-shape variables are functions of the four momenta in the hadronic final state that characterize the topology of an event's energy flow. They are sensitive to QCD radiation (and correspondingly to the strong coupling) insofar as gluon emission changes the shape of the energy flow.

The classic example of an event shape is the *Thrust* [190,191] in e^+e^- annihilations, defined as

$$\hat{\tau} = \max_{\vec{n}_\tau} \frac{\sum_i |\vec{p}_i \cdot \vec{n}_\tau|}{\sum_i |\vec{p}_i|} \,, \tag{9.22}$$

where $\vec{p}_i$ are the momenta of the particles or the jets in the final-state and the maximum is obtained for the Thrust axis $\vec{n}_\tau$. In the Born limit of the production of a perfect back-to-back $q\bar{q}$ pair the limit $\hat{\tau} \to 1$ is obtained, whereas a perfectly symmetric many-particle configuration leads to $\hat{\tau} \to 1/2$. Further event shapes of similar nature have been defined and extensively measured at LEP and at HERA, and for their definitions and reviews we refer to Refs. 1,4,178,192,193. Phenomenological discussions of event shapes at hadron colliders can be found in Refs. 194–196. Measurements of hadronic event-shape distributions have been published by CDF [197], ATLAS [198,199] and CMS [200,201].

Event shapes are used for many purposes. These include measuring the strong coupling, tuning the parameters of Monte Carlo programs, investigating analytical models of hadronization and distinguishing QCD events from events that might involve decays of new particles (giving event-shape values closer to the spherical limit).

9.3.1.3. *Jet substructure, quark vs. gluon jets:*

Jet substructure, which can be resolved by finding subjets or by measuring jet shapes, is sensitive to the details of QCD radiation in the shower development inside a jet and has been extensively used to study differences in the properties of quark and gluon induced jets, strongly related to their different color charges. In general there is clear experimental evidence that gluon jets have a softer particle spectrum and are "broader" than (light-) quark jets, when looking at observables such as the jet shape $\Psi(r/R)$. This is the fractional transverse momentum contained within a sub-cone of cone-size r for jets of cone-size R. It is sensitive to the relative fractions of quark and gluon jets in an inclusive jet sample and receives contributions from soft-gluon initial-state radiation and beam remnant-remnant interactions. Therefore, it has been widely employed for validation and tuning of Monte Carlo models. CDF has measured the jet shape $\Psi(r/R)$ for an inclusive jet sample [202] as well as for b-jets [203]. Similar measurements in photo-production and DIS at HERA have been reported in Refs. 204–206. At the LHC, jet shape measurements have been presented in Refs. 207,208 for inclusive jet samples, as well as for top pair events [209]. Further discussions, references and recent summaries can be found in Refs. 193, 210 and Sec. 4 of Ref. 211.

The use of jet substructure has also been suggested in order to distinguish QCD jets from jets that originate from hadronic decays of boosted massive particles (high-p_t electroweak bosons, top quarks and hypothesized new particles). Recently, a number of experimental studies have been carried out with Tevatron and LHC data, in order to investigate on the performance of the proposed algorithms for resolving jet substructure in various event classes, such as inclusive jet [212], dijet and W/Z+jet production [213], as well as in events with high transverse momentum jets (boosted configurations) [214,215]. For reviews and detailed references, see Ref. 211, sec. 5.3 of Ref. 180 and Ref. 216.

9.3.2. ***State of the art QCD measurements at colliders*** :

There exists a wealth of data on QCD-related measurements in e^+e^-, ep, pp, and $p\bar{p}$ collisions, to which a short overview like this would not be able to do any justice. Extensive reviews of the subject have been published in Refs. 192, 193 for e^+e^- colliders and in Ref. 217 for ep scattering, whereas for hadron colliders comprehensive overviews are given in, e.g., Refs. 181, [218–220].

Below we concentrate our discussion on measurements that are most sensitive to hard QCD processes, in particular jet production.

9.3.2.1. e^+e^- *colliders:* Analyses of jet production in e^+e^- collisions are mostly based on JADE data at center-of-mass energies between 14 and 44 GeV, as well as on LEP data at the Z resonance and up to 209 GeV. They cover the measurements of (differential or exclusive) jet rates (with multiplicities typically up to 4, 5 or 6 jets), the study of 3-jet events and particle production between the jets as a tool for testing hadronization models, as well as 4-jet production and angular correlations in 4-jet events. The latter are useful for measurements of the strong coupling constant and putting constraints on the QCD color factors, thus probing the non-abelian nature of QCD. There have also been extensive measurements of event shapes. The tuning of parton shower MC models, typically matched to matrix elements for 3-jet production, has led to good descriptions of the available, highly precise data. Especially for the large LEP data sample at the Z peak, the statistical uncertainties are mostly negligible and the experimental systematic uncertainties are at the per-cent level or even below. These are usually dominated by the uncertainties related to the MC model dependence of the efficiency and acceptance corrections (often referred to as "detector corrections").

9.3.2.2. *DIS and photoproduction:* Multi-jet production in ep collisions at HERA, both in the DIS and photoproduction regime, allows for tests of QCD factorization (one initial-state proton and its associated PDF versus the hard scattering which leads to high-p_t jets) and NLO calculations which exist for 2- and 3-jet final states. Sensitivity is also obtained to the product of the coupling constant and the gluon PDF. Experimental uncertainties of the order of $5-10\%$ have been achieved, mostly dominated by jet energy scale, whereas statistical uncertainties are negligible to a large extent. For comparison to theoretical predictions, at large jet p_t the PDF uncertainty dominates the theoretical uncertainty (typically of order 5 - 10%, in some regions of phase-space up to 20%), therefore jet observables become useful inputs for PDF fits. In general, the data are well described by NLO matrix-element calculations, combined with DGLAP evolution equations, in particular at large Q^2 and central values of jet pseudo-rapidity. At low values of Q^2 and x, in particular for large jet pseudo-rapidities, there are indications for the need of BFKL-type evolution, though the predictions for such schemes are still limited. In the case of photoproduction, a wealth of measurements with low p_t jets were performed in order to constrain the photon PDFs. The uncertainties related to these photon PDFs play a minor role at high jet p_t, which has allowed for precise tests of pQCD calculations.

A few examples of recent measurements can be found in Refs. 221–228 for DIS and in Refs. 229–233 for photoproduction.

9.3.2.3. *Hadron colliders:* Jet measurements at the Tevatron and the LHC have been performed with data samples from a wide range of luminosities and center-of-mass energies. In particular, LHC results have been published for luminosities up to $5\,\mathrm{fb}^{-1}$ and center-of-mass energies of 2.76 and 7 TeV, with preliminary results also available from 8 TeV collisions. Among the most important cross sections measured is the inclusive jet production as a function of the jet transverse energy (E_t) or the jet transverse momentum (p_t), for several rapidity regions and for p_t up to 700 GeV at the Tevatron and ~ 2 TeV at the LHC. The Tevatron measurements are based on the infrared- and collinear-safe k_t algorithm in addition to the more widely used Midpoint and JetCLU algorithms of the past, whereas the LHC experiments focus on the *anti-k_t* algorithm. Results by the CDF and D0 collaborations can be found in Refs. 234–236, whereas measurements by ALICE, ATLAS and CMS have been published in Refs. 237–243. In general we observe a good description of the data by the NLO QCD predictions, over about 9 orders of magnitude in cross section. The experimental systematic uncertainties are dominated by the jet energy scale uncertainty, quoted to be in the range of 1 to 2%, leading to uncertainties of $\sim 5-30\%$ on the cross section, increasing with p_t and rapidity. The PDF uncertainties dominate the theoretical uncertainty at large p_t and rapidity. In fact, inclusive jet data are important inputs to global PDF fits, in particular for constraining the high-x gluon PDF. Constraints on the PDFs can also be obtained from ratios of inclusive cross sections at different center-of-mass energies, as for example shown in Ref. [240].

A rather comprehensive summary, comparing NLO QCD predictions to data for inclusive jet production in DIS, pp, and $p\bar{p}$ collisions, is given in Ref. 244 and reproduced here in Fig. 9.1.

Dijet events are analyzed in terms of their invariant mass and angular distributions, which allows for tests of NLO QCD predictions (see e.g. Refs. [239,242] for recent LHC results), as well as to put stringent limits on deviations from the Standard Model, such as quark compositeness (some examples can be found in Refs. 245–248). Furthermore, dijet azimuthal correlations between the two leading jets, normalized to the total dijet cross cross section, are an extremely valuable tool for studying the spectrum of gluon radiation in the event. For example, results from the Tevatron [249,250] and the LHC [251,252] show that the LO (non-trivial) prediction for this observable, with at most three partons in the final state, is not able to describe the data for an azimuthal separation below $2\pi/3$, where NLO contributions (with 4 partons) restore the agreement with data. In addition, this observable can be employed to tune Monte Carlo predictions of soft gluon radiation. Beyond dijet final states, measurements of the production of three or more jets, including cross section ratios, have been performed [253–259], as a means of testing perturbative QCD predictions, tuning MC models, constraining PDFs or determining the strong coupling constant.

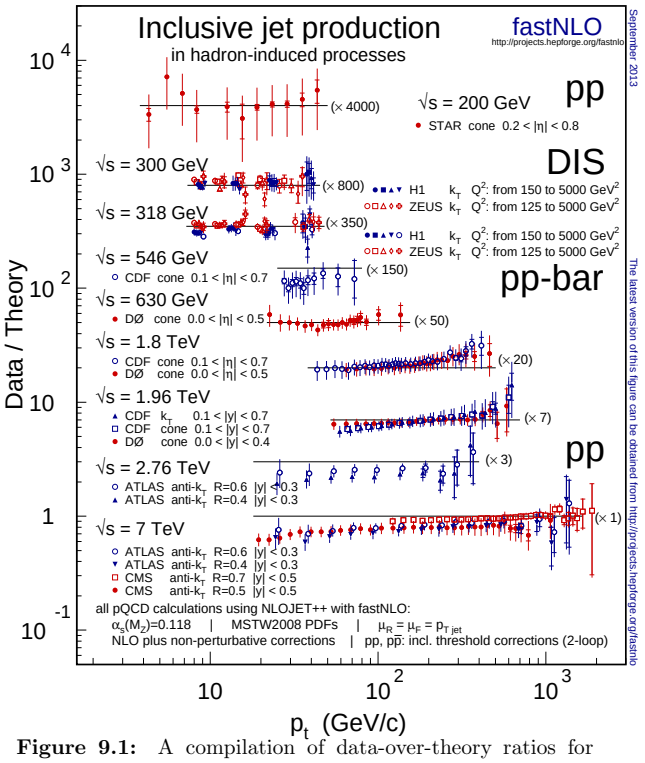

Figure 9.1: A compilation of data-over-theory ratios for inclusive jet cross sections as a function of jet transverse momentum (p_t), measured in different hadron-induced processes at different center-of-mass energies; from Ref. 244. The various ratios are scaled by arbitrary numbers (indicated between parentheses) for better readability of the plot. The theoretical predictions have been obtained at NLO accuracy, for parameter choices (coupling constant, PDFs, renormalization, and factorization scales) as indicated at the bottom of the figure.

Similarly important tests of QCD arise from measurements of vector boson (photon, W, Z) production together with jets, where the presence of the vector boson introduces an additional hard scale in the process. By now, many results have been obtained both at the Tevatron [260–268] and the LHC [201,269–275]. The measurements cover a large phase space, e.g. with jet transverse momenta between 30 GeV and $\sim$ 500 GeV and jet rapidities up to $|y| < 4.4$. Jet multiplicities as high as seven jets accompanying the vector boson have already been probed at the LHC, together with a substantial number of other kinematical observables. A general observation is that MC models, which implement a matching of matrix-element calculations with parton showers, provide a remarkably good description of the data. Also NLO calculations for up to four jets in addition to the vector boson are in good agreement with the data over that phase space, where such calculations are applicable. Altogether, this represents an impressive success of QCD at high jet multiplicities.

Instead of measuring the jets recoiling against the vector boson, where the precision is limited by the jet energy scale uncertainty, the vector boson's p_t distribution can also be directly probed [262,276–278]. For example, the Z p_t distribution, reconstructed using the Z decay to leptons, is sensitive to QCD radiation both at high and low scales and thus probes perturbative as well as non-perturbative effects. Similarly, photon production in special phase-space regions, such as di-photon production with small azimuthal separation between the two photons, allows for sensitive tests of QCD radiation without the need of direct jet reconstruction [279–282].

A substantial fraction of the jets produced at hadron colliders contain heavy quarks (b, c), whose mass introduces an additional scale in the event. Therefore, measurements of heavy quark production, either inclusive or in association with vector bosons, represent very important tests of multi-scale calculations in perturbative QCD. Results for b-jet production at the LHC [283,284] indicate that NLO and/or NLO plus parton shower QCD calculations describe the data well over most of the phase space. However, the observed discrepancies for small angular separation of the heavy quarks suggest that a better understanding of the $g \to b\bar{b}$ vertex may well be required [285]. Tevatron [286–297] and LHC [298–300] measurements for heavy quark production in association with a vector boson have been compared to NLO QCD and MC predictions. Typically, the experimental and theoretical uncertainties are still rather large. Nevertheless, it is worth noting that there are discrepancies between data and QCD predictions, in particular for γ plus (c, b)-jet, Z plus c-jet and W plus b-jet production.

Finally, top-quark production at the LHC starts to become an important tool for probing higher-order QCD calculations. Besides the precise determination of the inclusive cross section, used by CMS to measure the strong coupling constant for the first time at NNLO accuracy from hadron collider data [301], also measurements of differential cross sections and of jet production in association with top quarks start to probe QCD in this regime [302–304].

9.3.3. *Tests of the non-abelian nature of QCD* :

QCD is a gauge theory with SU(3) as underlying gauge group. For a general gauge theory with a simple Lie group, the couplings of the fermion fields to the gauge fields and the self-interactions in the non-abelian case are determined by the coupling constant and Casimir operators of the gauge group, as introduced in Sec. 9.1. Measuring the eigenvalues of these operators, called color factors, probes the underlying structure of the theory in a gauge invariant way and provides evidence of the gluon self-interactions. Typically, cross sections can be expressed as functions of the color factors, for example $\sigma = f(\alpha_s C_F, C_A/C_F, n_f T_R/C_F)$. Sensitivity at leading order in perturbation theory can be achieved by measuring angular correlations in 4-jet events in e^+e^- annihilation or 3-jet events in DIS. Some sensitivity, although only at NLO, is also obtained from event-shape distributions. Scaling violations of fragmentation functions and the different subjet structure in quark and gluon induced jets also give access to these color factors. In order to extract absolute values, *e.g.* for C_F and C_A, certain assumptions have to be made for other parameters, such as T_R, n_f or α_s, since typically only combinations (ratios, products) of all the relevant parameters appear in the perturbative predictions. A compilation of results [193] quotes world average values of $C_A = 2.89 \pm 0.03(\text{stat}) \pm 0.21(\text{syst})$ and $C_F = 1.30 \pm 0.01(\text{stat}) \pm 0.09(\text{syst})$, with a correlation coefficient of 82%. These results are in perfect agreement with the expectations from SU(3) of $C_A = 3$ and $C_F = 4/3$. An overview of the history and the current status of tests of Asymptotic Freedom, closely related to the non-abelian nature of QCD, can be found in Ref. 305.

9.3.4. ***Determinations of the strong coupling constant*** :

Beside the quark masses, the only free parameter in the QCD Lagrangian is the strong coupling constant α_s. The coupling constant in itself is not a physical observable, but rather a quantity defined in the context of perturbation theory, which enters predictions for experimentally measurable observables, such as R in Eq. (9.7).

Many experimental observables are used to determine α_s. Considerations in such determinations include:

- The observable's sensitivity to α_s as compared to the experimental precision. For example, for the e^+e^- cross section to hadrons (cf. R in Sec. 9.2.1), QCD effects are only a small correction, since the perturbative series starts at order α_s^0; 3-jet production or event shapes in e^+e^- annihilations are directly sensitive to α_s since they start at order α_s; the hadronic decay width of heavy quarkonia, $\Gamma(\Upsilon \to \text{hadrons})$, is very sensitive to α_s since its leading order term is $\propto \alpha_s^3$.
- The accuracy of the perturbative prediction, or equivalently of the relation between α_s and the value of the observable. The minimal requirement is generally considered to be an NLO prediction. Some observables are predicted to NNLO (many inclusive observables, 3-jet rates and event shapes in e^+e^- collisions) or even N^{3}LO (e^+e^- hadronic cross section and τ branching fraction to hadrons). In certain cases, fixed-order predictions are supplemented with resummation. The precise magnitude of theory uncertainties is usually estimated as discussed in Sec. 9.2.3.
- The size of uncontrolled non-perturbative effects. Sufficiently inclusive quantities, like the e^+e^- cross section to hadrons, have small non-perturbative uncertainties $\sim \Lambda^4/Q^4$. Others, such as event-shape distributions, have uncertainties $\sim \Lambda/Q$.
- The scale at which the measurement is performed. An uncertainty δ on a measurement of $\alpha_s(Q^2)$, at a scale Q, translates to an uncertainty $\delta' = (\alpha_s^2(M_Z^2)/\alpha_s^2(Q^2)) \cdot \delta$ on $\alpha_s(M_Z^2)$. For example, this enhances the already important impact of precise low-Q measurements, such as from τ decays, in combinations performed at the M_Z scale.

In this review, we update the measurements of α_s summarized in the 2012 edition, and we extract a new world average value of $\alpha_s(M_Z^2)$ from the most significant and complete results available today[♯].

We follow the same selection strategy and summary procedure as applied in the 2012 review, i.e. we restrict the selection of results from which to calculate the world average value of $\alpha_s(M_Z^2)$ to those which are

- published in a peer-reviewed journal
- based on the most complete perturbative QCD predictions, i.e. to those using NNLO or higher-order expansions.

While this excludes e.g. results from jet production in DIS at HERA and at hadron colliders, as well as those from heavy quarkonia decays for which calculations are available at NLO only, they will nevertheless be listed and cited in this review as they are important ingredients for the experimental evidence of the energy dependence of α_s, i.e. for Asymptotic Freedom, one of the key features of QCD.

In detail, we apply an intermediate step of pre-averaging results within certain sub-fields like e^+e^- annihilation, DIS and hadronic τ-decays, and calculate the overall world average from those pre-averages rather than from individual measurements. This is done because in a number of sub-fields one observes that different determinations of the strong coupling from substantially similar datasets lead to values of α_s that are only marginally compatible with each other, or with the final world average value, which presumably is a reflection of the challenges of evaluating systematic uncertainties. In such cases, a pre-average value will be determined, with a symmetric, overall uncertainty that encompasses the central values of all individual determinations ('*range averaging*').

Alternatively, in cases when results within a sub-field are largely independent of each other, we use the method of 'χ^2 *averaging*', as proposed, *e.g.*, in Ref. 308, in order to treat cases of possible (unknown) correlations as well as possibly underestimated systematic uncertainties in a meaningful and well defined manner: the central value is determined as the weighted average of the different input values. An initial uncertainty of the central value is determined treating the uncertainties of all individual measurements as being uncorrelated and being of Gaussian nature, and the overall χ^2 to the central value is determined. If this initial χ^2 is larger than the number of degrees of freedom, then all individual uncertainties are enlarged by a common factor such that χ^2/d.o.f. equals unity. If the initial value of χ^2 is smaller than the number of degrees of freedom, an overall, a-priori unknown correlation coefficient is introduced and determined by requiring that the total χ^2/d.o.f. of the combination equals unity. In both cases, the resulting overall uncertainty of α_s in this sub-field is larger than the initial estimate of the uncertainty.

9.3.5. ***Hadronic τ decays*** :

Several re-analyses of the hadronic τ decay width [24,309–314], based on N^{3}LO predictions [24], have been performed. They are based on different approaches to treat perturbative (fixed-order or contour-improved perturbative expansions) and non-perturbative contributions, the impact of which is a matter of intense discussions, see e.g. [315] and [316]. We also include the result from τ decay and lifetime measurements, obtained in Sec. *Electroweak Model and constraints on New Physics* of this *Review*, which amounts, if converted to the τ-mass scale, to $\alpha_s(M_\tau) = 0.327^{+0.019}_{-0.016}$. This result and the one from Baikov et al. [24] include both fixed-order and contour-improved perturbation theory, while the others adhere to either one or the other of the two. All these results are quoted for $n_f = 3$ quark flavors; they are summarized in Fig. 9.2(a).

We determine the pre-average result from τ-decays, to be used for calculating the final world average of $\alpha_s(M_Z^2)$, using the *range averaging* method defined above, as $\alpha_s(M_\tau^2) = 0.330 \pm 0.014$, unchanged from its value in the 2012 review[**]. This value of $\alpha_s(M_\tau^2)$ corresponds, when evolved to the scale of the Z-boson, using the QCD 4-loop beta-function plus 3-loop matching at the charm- and the bottom-quark masses (see Sec. *Quark Masses* in this *Review*), to $\alpha_s(M_Z^2) = 0.1197 \pm 0.0016$.

9.3.6. ***Lattice QCD*** :

There are several recent results on α_s from lattice QCD, see also Sec. *Lattice QCD* in this *Review*. The HPQCD collaboration [317] computes Wilson loops and similar short-distance quantities with lattice QCD and analyzes them with NNLO perturbative QCD. This yields a value for α_s, but the lattice scale must be related to a physical energy/momentum scale. This is achieved with the Υ'-Υ mass difference, however, many other quantities could be used as well [318]. HPQCD obtains $\alpha_s(M_Z^2) = 0.1184 \pm 0.0006$, where the uncertainty includes effects from truncating perturbation theory, finite lattice spacing and extrapolation of lattice data. An independent perturbative analysis of a subset of the same lattice-QCD data yields $\alpha_s(M_Z^2) = 0.1192 \pm 0.0011$ [319]. Using another, independent methodology, the current-current correlator method, HPQCD obtains $\alpha_s(M_Z^2) = 0.1183 \pm 0.0007$ [317]. The analysis of Ref. 320, which avoids the staggered fermion treatment of Ref. 317, finds $\alpha_s(M_Z^2) = 0.1205 \pm 0.0008 \pm 0.0005\,^{+0.0000}_{-0.0017}$, where the first uncertainty is statistical and the others are from systematics. Since this approach uses a different discretization of lattice fermions and a different general methodology, it provides an independent cross check of other lattice extractions of α_s. The JLQCD collaboration, in an analysis of Adler functions, obtains $\alpha_s(M_Z^2) = 0.1181 \pm 0.0003\,^{+0.0014}_{-0.0012}$ [321]. A study of the ETM collaboration [322] used lattice data with u, d, s and c quarks in the sea, obtaining results which are compatible with those quoted above. Finally, a determination of α_s from the QCD static energy [323] results in $\alpha_s(M_Z) = 0.1156^{+0.0021}_{-0.0022}$.

The published lattice results are summarized in Fig. 9.2(b). In contrast to the results from τ-decays, which were all based on the same (sub-)sets of data, the lattice evaluations are, at least in part, independent from each other, and so we use the χ^2 *averaging* method

[♯] The time evolution of α_s combinations can be followed by consulting Refs. [305–307] as well as earlier editions of this *Review*.

[**] The result from Boito *et al.* [314] is not regarded to extend the range due to its rather large - mainly statistical - uncertainty.

to determine $\alpha_s(M_Z^2) = 0.1185 \pm 0.0005$ which we take as result from the sub-field of lattice determinations†.

9.3.7. ***Deep inelastic lepton-nucleon scattering (DIS)*** :
Studies of DIS final states have led to a number of precise determinations of α_s: a combination [324] of precision measurements at HERA, based on NLO fits to inclusive jet cross sections in neutral current DIS at high Q^2, quotes a combined result of $\alpha_s(M_Z^2) = 0.1198 \pm 0.0032$, which includes a theoretical uncertainty of ± 0.0026. A combined analysis of non-singlet structure functions from DIS [325], based on QCD predictions up to N^{3}LO in some of its parts, gave $\alpha_s(M_Z^2) = 0.1142 \pm 0.0023$, including a theoretical uncertainty of ± 0.0008 (BBG). Further studies of singlet and non-singlet structure functions, based on NNLO predictions, resulted in $\alpha_s(M_Z^2) = 0.1134 \pm 0.0011$ [326] (ABM; only experimental uncertainties are included here) and in $\alpha_s(M_Z^2) = 0.1158 \pm 0.0035$ [327] (JR). The MSTW group [328], also including data on jet production at the Tevatron, obtains, at NNLO[♯♯], $\alpha_s(M_Z^2) = 0.1171 \pm 0.0024$. The NNPDF group [329] presented a result, $\alpha_s(M_Z^2) = 0.1173 \pm 0.0011$, which is in line with the one from the MSTW group.

Summarizing these results from world data on structure functions, applying the *range averaging* method as defined and motivated above, leads to a pre-average value of $\alpha_s(M_Z^2) = 0.1154 \pm 0.0020$ (see Fig. 9.2(c)).

We note that criticism has been expressed on some of the above extractions. Among the issues raised, we mention the neglect of singlet contributions at $x \geq 0.3$ in pure non-singlet fits [330], the impact and detailed treatment of particular classes of data in the fits [330,331], possible biases due to insufficiently flexible parametrizations of the PDFs [332] and the use of a fixed-flavor number scheme [333,334].

9.3.8. ***Heavy quarkonia decays*** :
The most recent extraction of the strong coupling constant from an analysis of radiative Υ decays [335] resulted in $\alpha_s(M_Z) = 0.119^{+0.006}_{-0.005}$. This determination is based on QCD at NLO only, so it will not be considered for the final extraction of the world average value of α_s; it is, however, an important ingredient for the demonstration of Asymptotic Freedom as given in Fig. 9.4.

9.3.9. ***Hadronic final states of e^+e^- annihilations*** :
Re-analyses of event shapes in e^+e^- annihilation, measured at the Z peak and LEP2 energies up to 209 GeV, using NNLO predictions matched to NLL resummation and Monte Carlo models to correct for hadronisation effects, resulted in $\alpha_s(M_Z^2) = 0.1224 \pm 0.0039$ (ALEPH) [336], with a dominant theoretical uncertainty of 0.0035, and in $\alpha_s(M_Z^2) = 0.1189 \pm 0.0043$ (OPAL) [337]. Similarly, an analysis of JADE data [338] at center-of-mass energies between 14 and 46 GeV gives $\alpha_s(M_Z^2) = 0.1172 \pm 0.0051$, with contributions from hadronization model and from perturbative QCD uncertainties of 0.0035 and 0.0030, respectively (JADE). A precise determination of α_s from 3-jet production alone, in NNLO, resulted in $\alpha_s(M_Z^2) = 0.1175 \pm 0.0025$ [339] from ALEPH data and in $\alpha_s(M_Z^2) = 0.1199 \pm 0.0059$ [340] from JADE. These results are summarized in the upper half of Fig. 9.2(d).

Computation of the NLO corrections to 5-jet production and comparison to the measured 5-jet rates at LEP [341] gave $\alpha_s(M_Z^2) = 0.1156^{+0.0041}_{-0.0034}$. A new computation of non-perturbative and perturbative QCD contributions to the scale evolution of quark and gluon jet multiplicities, including resummation and - in part - contributions beyond NLO, is reported [342] to result in $\alpha_s(M_Z^2) = 0.1199 \pm 0.0026$.

Another class of α_s determinations is based on analytic calculations of non-perturbative and hadronisation effects, rather than on Monte Carlo models [146,343–345], using methods like power corrections, factorisation of soft-collinear effective field theory, dispersive models and low scale QCD effective couplings. In these studies, the world data on Thrust distributions are analysed and fitted to perturbative QCD predictions in NNLO matched with resummation of leading logs up to N^{3}LL accuracy. The results range from $\alpha_s(M_Z^2) = 0.1131^{+0.0028}_{-0.0022}$ [345] to 0.1172 ± 0.0021 [146]; they are displayed in the lower half of Fig. 9.2(d).

We note that there is criticism on both classes of α_s extractions just described: those based on corrections of non-perturbative hadronisation effects using QCD-inspired Monte Carlo generators (since the parton level of a Monte Carlo is not defined in a manner equivalent to that of a fixed-order calculation), as well as the studies based on non-perturbative analytic calculations, as their systematics have not yet been verified e.g. by using observables other than Thrust.

Combining the results from e^+e^- annihilation data, using the *range averaging* method as many analyses are either based on similar datasets and/or are only marginally compatible with each other, results in $\alpha_s(M_Z^2) = 0.1177 \pm 0.0046$.

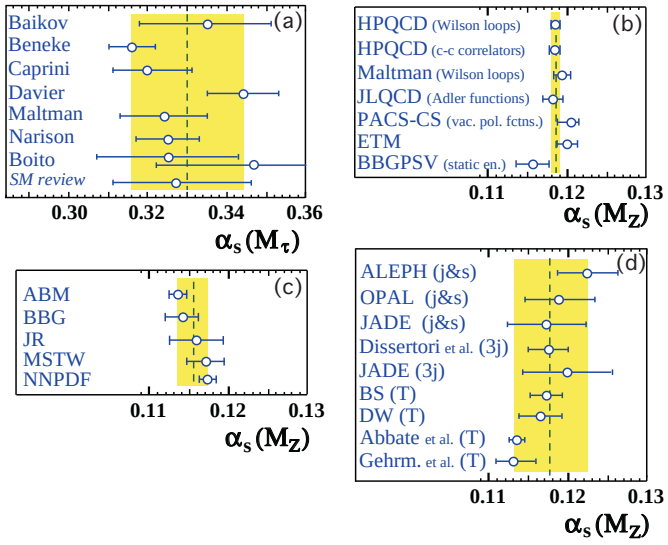

Figure 9.2: Summary of determinations of α_s from hadronic τ-decays (a), from lattice calculations (b), from DIS structure functions (c) and from e^+e^- annihilation (d). The shaded bands indicate the pre-average values explained in the text, to be included in the determination of the final world average of α_s.

9.3.10. ***Hadron collider jets*** :
Significant determinations of α_s from data at hadron colliders, i.e. the Tevatron and the LHC, are obtained, however mostly still limited to QCD at NLO. At $\sqrt{s} = 1.96$ TeV, $\alpha_s(M_Z^2) = 0.1161^{+0.0041}_{-0.0048}$ and $\alpha_s(M_Z^2) = 0.1191^{+0.0048}_{-0.0071}$ result from studies of inclusive jet cross sections [346] and from jet angular correlations [347], respectively. More recently, ATLAS data on inclusive jet production at $\sqrt{s} = 7$ TeV [239] became available, extending the verification of the running of α_s up to jet p_t of 600 GeV, and leading to $\alpha_s(M_Z^2) = 0.1151^{+0.0093}_{-0.0087}$ [348]. Here, experimental systematics, the choice of jet scale and the use of different PDFs dominate the large overall uncertainties. Preliminary determinations of α_s from CMS data on the ratio of inclusive 3-jet to 2-jet cross sections [259], at NLO, and from the top-quark cross section [301], in NNLO, quote values of $\alpha_s(M_Z^2) = 0.1148 \pm 0.0014(\text{exp.}) \pm 0.0018(\text{PDF})^{+0.0050}_{-0.0000}(\text{scale})$ and $\alpha_s(M_Z^2) = 0.1151^{+0.0033}_{-0.0032}$, respectively, indicating many new results to be expected for inclusion in upcoming reviews.

† The initial χ^2/d.o.f. was 4.7/6, requiring an overall correlation factor of 0.21 to bring χ^2/d.o.f. to unity, thereby increasing the initial overall uncertainty from 0.0004 to 0.0005.

♯♯ Note that for jet production at a hadron collider, only NLO predictions are available, while for the structure functions full NNLO was utilized.

9.3.11. ***Electroweak precision fits*** :
The N^{3}LO calculation of the hadronic Z decay width was used in a revision of the global fit to electroweak precision data [349], resulting in $\alpha_s(M_Z^2) = 0.1193 \pm 0.0028$, claiming a negligible theoretical uncertainty. For this *Review* the value obtained in Sec. *Electroweak model and constraints on new physics* from data at the Z-pole, $\alpha_s(M_Z^2) = 0.1197 \pm 0.0028$ will be used instead, as it is based on a more constrained data set where QCD corrections directly enter through the hadronic decay width of the Z. We note that all these results from electroweak precision data, however, strongly depend on the strict validity of Standard Model predictions and the existence of the minimal Higgs mechanism to implement electroweak symmetry breaking. Any - even small - deviation of nature from this model could strongly influence this extraction of α_s.

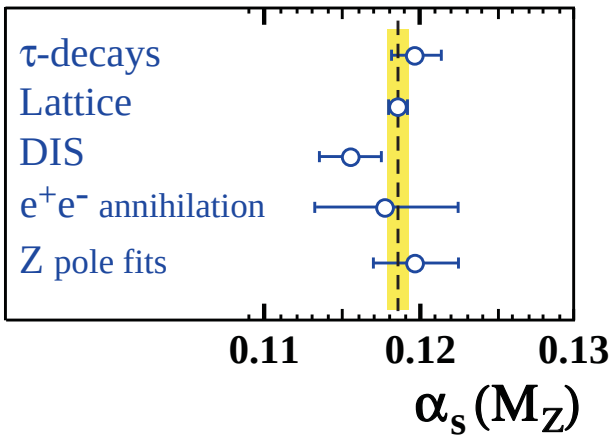

Figure 9.3: Summary of values of $\alpha_s(M_Z^2)$ obtained for various sub-classes of measurements (see Fig. 9.2 (a) to (d)). The new world average value of $\alpha_s(M_Z^2) = 0.1185 \pm 0.0006$ is indicated by the dashed line and the shaded band.

9.3.12. ***Determination of the world average value of $\alpha_s(M_Z^2)$*** :
Obtaining a world average value for $\alpha_s(M_Z^2)$ is a non-trivial exercise. A certain arbitrariness and subjective component is inevitable because of the choice of measurements to be included in the average, the treatment of (non-Gaussian) systematic uncertainties of mostly theoretical nature, as well as the treatment of correlations among the various inputs, of theoretical as well as experimental origin.

We have chosen to determine pre-averages for classes of measurements which are considered to exhibit a maximum of independence between each other, considering experimental as well as theoretical issues. These pre-averages are then combined to the final world average value of $\alpha_s(M_Z^2)$, using the χ^2 *averaging method* and error treatment as described above. The five pre-averages are summarized in Fig. 9.3; we recall that these are exclusively obtained from extractions which are based on (at least) full NNLO QCD predictions, and are published in peer-reviewed journals at the time of completing this *Review*.[◇◇] From these, we determine the new world average value of

$$\alpha_s(M_Z^2) = 0.1185 \pm 0.0006 \ , \tag{9.23}$$

with an uncertainty of well below 1 %.[***] This world average value is in excellent agreement with that from the 2009 [306] and the 2012 version of this review, although several new contributions have entered this determination. For convenience, we also provide corresponding values for $\Lambda_{\overline{MS}}$:

$$\Lambda_{\overline{MS}}^{(6)} = (90.6 \pm 3.4) \ \text{MeV} \ , \tag{9.24a}$$

$$\Lambda_{\overline{MS}}^{(5)} = (214 \pm 7) \ \text{MeV} \ , \tag{9.24b}$$

$$\Lambda_{\overline{MS}}^{(4)} = (297 \pm 8) \ \text{MeV} \ , \tag{9.24c}$$

$$\Lambda_{\overline{MS}}^{(3)} = (340 \pm 8) \ \text{MeV} \ , \tag{9.24d}$$

for $n_f = 6$, 5, 4 and 3 quark flavors, which are calculated using the 4-loop expression for the running of α_s according to Eq. (9.5) and 3-loop matching at the charm-, bottom- and top-quark pole masses of 1.5, 4.7 and 173 GeV/c^2, respectively.

In order to further test and verify the sensitivity of the new average value of $\alpha_s(M_Z^2)$ to the different pre-averages and classes of α_s determinations, we give each of the averages obtained when leaving out one of the five input values, as well as the respective, initial value of χ^2 :

$$\alpha_s(M_Z^2) = 0.1184 \pm 0.0006 \ \ (\text{w/o } \tau \text{ results; } \chi_0^2/\text{d.o.f.} = 2.3/3), \tag{9.25a}$$

$$\alpha_s(M_Z^2) = 0.1183 \pm 0.0012 \ \ (\text{w/o lattice results; } \chi_0^2/\text{d.o.f.} = 2.9/3), \tag{9.25b}$$

$$\alpha_s(M_Z^2) = 0.1187 \pm 0.0007 \ \ (\text{w/o DIS results; } \chi_0^2/\text{d.o.f.} = 0.6/3), \tag{9.25c}$$

$$\alpha_s(M_Z^2) = 0.1185 \pm 0.0005 \ \ (\text{w/o } e^+e^- \text{ results; } \chi_0^2/\text{d.o.f.} = 2.9/3), \text{ and} \tag{9.25d}$$

$$\alpha_s(M_Z^2) = 0.1185 \pm 0.0005 \ \ (\text{w/o e.w. precision fit; } \chi_0^2/\text{d.o.f.} = 2.7/3). \tag{9.25e}$$

They are well within the uncertainty of the overall world average quoted above. The lattice result, which has the smallest assigned uncertainty, agrees well - within 0.2 standard deviations - with the exclusive average of the other results. However, it largely determines the size of the overall uncertainty, which is a factor of 2 larger when disregarding lattice results at all.

Alternative procedures to calculate the world average using different methods of determining pre-average values and their uncertainties, were applied in order to estimate the impact on arbitrariness and subjective components mentioned above. For instance, when applying the *range averaging* throughout, for all pre-averages, then the world average emerges as $\alpha_s(M_Z^2) = 0.1182 \pm 0.0013$, probably constituting a rather conservative choice of error treatment. Using linear averages of α_s and its uncertainty for each of the pre-averages results in a world average of $\alpha_s(M_Z^2) = 0.1185 \pm 0.0011$, while applying the χ^2 averaging method throughout, for all pre-averages, gives $\alpha_s(M_Z^2) = 0.1179 \pm 0.0008$ as final result. The latter case, however, appears difficult to justify as it requires a rather large overall scaling factor for all input uncertainties, due to a very large, initial χ^2 value of 19.7 for 4 degrees of freedom, indicating a gross underestimate of the uncertainties of all pre-averages in this case.

There are apparent systematic differences between the various structure function results, and also between some of the results from Thrust and the other determinations in e^+e^- annihilation. Also, the size of uncertainties assigned for individual determinations largely differs within classes of results, such as from lattice calculations, but also from e^+e^- annihilations and from structure functions. We note that such and other differences have been extensively discussed at a specific workshop on measurements of α_s, however none of the explanations proposed so far have obtained enough of a consensus to definitely resolve the tensions between different extractions [351]. If the degree of consistency does not increase in the coming years, the method of averaging may have to be modified in the future, in order to de-emphasize the impact of results claiming overly optimistic (small) uncertainties.

◇◇ In addition to those mentioned above, one further result that was available only in unpublished form while this review was being prepared was Ref. 350, which quotes $\alpha_S(m_Z) = 0.1174^{+.0010}_{-.0005} \pm .001 \pm .0005_{\text{evol}}$, using an extraction from the pion decay constant. We leave its detailed consideration to future updates.

*** The weighted average, treating all inputs as uncorrelated measurements with Gaussian uncertainties, results in $\alpha_s(M_Z^2) = 0.11851 \pm 0.00048$ with $\chi^2/\text{d.o.f.} = 2.9/4$. Requiring $\chi^2/\text{d.o.f.}$ to reach unity calls for an overall correlation factor of 0.28, which increases the overall uncertainty to 0.00059.

The wealth of available results provides a rather precise and stable world average value of $\alpha_s(M_Z^2)$, as well as a clear signature and proof of the energy dependence of α_s, in full agreement with the QCD prediction of Asymptotic Freedom. This is demonstrated in Fig. 9.4, where results of $\alpha_s(Q^2)$ obtained at discrete energy scales Q, now also including those based just on NLO QCD, are summarized. Thanks to the results from the Tevatron [346,347] and from the LHC [259], the energy scales at which α_s is determined now extend to several hundred GeV up to 1 TeV$^\diamondsuit$.

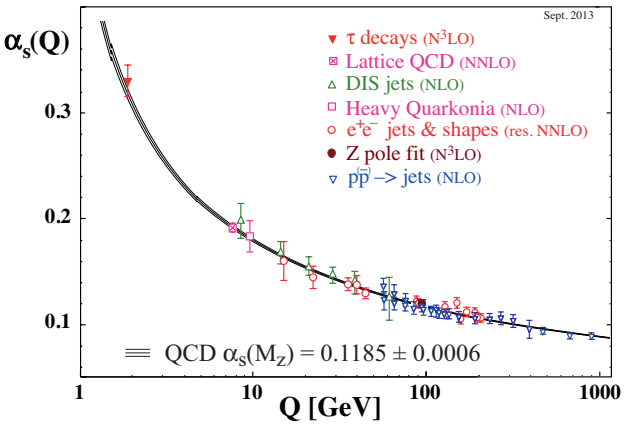

Figure 9.4: Summary of measurements of α_s as a function of the energy scale Q. The respective degree of QCD perturbation theory used in the extraction of α_s is indicated in brackets (NLO: next-to-leading order; NNLO: next-to-next-to leading order; res. NNLO: NNLO matched with resummed next-to-leading logs; N^{3}LO: next-to-NNLO).

9.4. Acknowledgments

We are grateful to J.-F. Arguin, G. Altarelli, J. Butterworth, M. Cacciari, L. del Debbio, D. d'Enterria, P. Gambino, C. Glasman Kuguel, N. Glover, M. Grazzini, A. Kronfeld, K. Kousouris, M. Lüscher, M. d'Onofrio, S. Sharpe, G. Sterman, D. Treille, N. Varelas, M. Wobisch, W.M. Yao, C.P. Yuan, and G. Zanderighi for discussions, suggestions and comments on this and earlier versions of this review.

References:

1. R.K. Ellis, W.J. Stirling, and B.R. Webber, *"QCD and collider physics,"* Camb. Monogr. Part. Phys. Nucl. Phys. Cosmol. **81** (1996).
2. C. A. Baker *et al.*, Phys. Rev. Lett. **97**, 131801 (2006).
3. H. -Y. Cheng, Phys. Reports **158**, 1 (1988).
4. G. Dissertori, I.G. Knowles, and M. Schmelling, *"High energy experiments and theory,"* Oxford, UK: Clarendon (2003).
5. R. Brock *et al.*, [CTEQ Collab.], Rev. Mod. Phys. **67**, 157 (1995), see also `http://www.phys.psu.edu/~cteq/handbook/v1.1/handbook.pdf`.
6. A. S. Kronfeld and C. Quigg, Am. J. Phys. **78**, 1081 (2010).
7. R. Stock (Ed.), Relativistic Heavy Ion Physics, Springer-Verlag Berlin, Heidelberg, 2010.
8. *Proceedings of the XXIII International Conference on Ultrarelativistic Nucleus–Nucleus Collisions, Quark Matter 2012*, Nucl. Phys. A, volumes 904–905.
9. Special Issue: Physics of Hot and Dense QCD in High-Energy Nuclear Collisions, Ed. C. Salgado. Int. J. Mod. Phys. A, volume 28, number 11. `[http://www.worldscientific.com/toc/ijmpa/28/11]`.
10. T. van Ritbergen, J.A.M. Vermaseren, and S.A. Larin, Phys. Lett. **B400**, 379 (1997).
11. M. Czakon, Nucl. Phys. **B710**, 485 (2005).
12. Y. Schroder and M. Steinhauser, JHEP **0601**, 051 (2006).
13. K.G. Chetyrkin, J.H. Kuhn, and C. Sturm, Nucl. Phys. **B744**, 121 (2006).
14. A. G. Grozin *et al.*, JHEP **1109**, 066 (2011).
15. K.G. Chetyrkin, B.A. Kniehl, and M. Steinhauser, Nucl. Phys. **B510**, 61 (1998).
16. See for example section 11.4 of M.E. Peskin and D.V. Schroeder, *"An Introduction To Quantum Field Theory,"* Reading, USA: Addison-Wesley (1995).
17. K. G. Chetyrkin, J. H. Kuhn, and M. Steinhauser, Comp. Phys. Comm. **133**, 43 (2000).
18. B. Schmidt and M. Steinhauser, Comp. Phys. Comm. **183**, 1845 (2012) `http://www.ttp.kit.edu/Progdata/ttp12/ttp12-02/`.
19. M. Beneke, Phys. Reports **317**, 1 (1999).
20. P. A. Baikov *et al.*, Phys. Lett. **B714**, 62 (2012).
21. K.G. Chetyrkin, J.H. Kuhn, and A. Kwiatkowski, Phys. Reports **277**, 189 (1996).
22. Y. Kiyo *et al.*, Nucl. Phys. **B823**, 269 (2009).
23. P. A. Baikov *et al.*, Phys. Rev. Lett. **108**, 222003 (2012).
24. P.A. Baikov, K.G. Chetyrkin, and J.H. Kuhn, Phys. Rev. Lett. **101**, 012002 (2008).
25. A. Djouadi, Phys. Reports **457**, 1 (2008).
26. P.A. Baikov, K.G. Chetyrkin, and J.H. Kuhn, Phys. Rev. Lett. **96**, 012003 (2006).
27. D. Asner *et al.*, `arXiv:1307.8265 [hep-ex]`.
28. C. Alexandrou *et al.*`arXiv:1303.6818 [hep-lat]`.
29. J.A.M. Vermaseren, A. Vogt, and S. Moch, Nucl. Phys. **B724**, 3 (2005).
30. E.B. Zijlstra and W.L. van Neerven, Phys. Lett. **B297**, 377 (1992).
31. S. Moch, J.A.M. Vermaseren, and A. Vogt, Nucl. Phys. **B813**, 220 (2009).
32. E. Laenen *et al.*, Nucl. Phys. **B392**, 162 (1993);
S. Riemersma, J. Smith, and W.L. van Neerven, Phys. Lett. **B347**, 143 (1995).
33. J. Ablinger *et al.*, Nucl. Phys. **B844**, 26 (2011).
34. J. Blümlein *et al.*, `arXiv:1307.7548 [hep-ph]`.
35. H. Kawamura *et al.*, Nucl. Phys. **B864**, 399 (2012).
36. J.C. Collins, D.E. Soper, and G.F. Sterman, Adv. Ser. Direct. High Energy Phys. **5**, 1 (1988).
37. J. C. Collins, *Foundations of Perturbative QCD*, Cambridge University Press, 2011.
38. G. C. Nayak, J. -W. Qiu, and G. F. Sterman, Phys. Rev. **D72**, 114012 (2005).
39. V.N. Gribov and L.N. Lipatov, Sov. J. Nucl. Phys. **15**, 438 (1972);
G. Altarelli and G. Parisi, Nucl. Phys. **B126**, 298 (1977);
Yu.L. Dokshitzer, Sov. Phys. JETP **46**, 641 (1977).
40. G. Curci, W. Furmanski, and R. Petronzio, Nucl. Phys. **B175**, 27 (1980);
W. Furmanski and R. Petronzio, Phys. Lett. **B97**, 437 (1980).
41. A. Vogt, S. Moch, and J.A.M. Vermaseren, Nucl. Phys. **B691**, 129 (2004);
S. Moch, J.A.M. Vermaseren, and A. Vogt, Nucl. Phys. **B688**, 101 (2004).
42. J.C. Collins, D.E. Soper, and G. Sterman, Nucl. Phys. **B261**, 104 (1985).
43. R. Hamberg, W.L. van Neerven, and T. Matsuura, Nucl. Phys. **B359**, 343 (1991); Erratum *ibid.*, B **644** 403, (2002).
44. R.V. Harlander and W.B. Kilgore, Phys. Rev. Lett. **88**, 201801 (2002).
45. C. Anastasiou and K. Melnikov, Nucl. Phys. **B646**, 220 (2002).
46. V. Ravindran, J. Smith, and W.L. van Neerven, Nucl. Phys. **B665**, 325 (2003).

$^\diamondsuit$ We note, however, that in many such studies, like those based on exclusive states of jet multiplicities, the relevant energy scale of the measurement is not uniquely defined. For instance, in studies of the ratio of 3- to 2-jet cross sections at the LHC, the relevant scale was taken to be the average of the transverse momenta of the two leading jets [259], but could alternatively have been chosen to be the transverse momentum of the 3^{rd} jet.

47. O. Brein, A. Djouadi, and R. Harlander, Phys. Lett. **B579**, 149 (2004).
48. P. Bolzoni *et al.*, Phys. Rev. Lett. **105**, 011801 (2010).
49. D. de Florian and J. Mazzitelli, arXiv:1309.6594 [hep-ph].
50. M. Czakon, P. Fiedler and A. Mitov, Phys. Rev. Lett. **110**, 252004 (2013).
51. S. Dittmaier *et al.* [LHC Higgs Cross Section Working Group Collab.], arXiv:1101.0593 [hep-ph].
52. M. Greco and A. Vicini, Nucl. Phys. **B415**, 386 (1994).
53. L.N. Lipatov, Sov. J. Nucl. Phys. **23**, 338 (1976) [Yad. Fiz. **23**, 642 (1976)].
54. E.A. Kuraev, L.N. Lipatov, and V.S. Fadin, Sov. Phys. JETP **45**, 199 (1977) [Zh. Eksp. Teor. Fiz. **72**, 377 (1977)].
55. I.I. Balitsky and L.N. Lipatov, Sov. J. Nucl. Phys. **28**, 822 (1978) [Yad. Fiz. **28**, 1597 (1978)].
56. V.S. Fadin and L.N. Lipatov, Phys. Lett. **B429**, 127 (1998).
57. M. Ciafaloni and G. Camici, Phys. Lett. **B430**, 329 (1998).
58. G. Altarelli, R. D. Ball, and S. Forte, Nucl. Phys. **B799**, 199 (2008).
59. M. Ciafaloni *et al.*, JHEP **0708**, 046 (2007).
60. C.D. White and R.S. Thorne, Phys. Rev. **D75**, 034005 (2007).
61. I. Balitsky, Nucl. Phys. **B463**, 99 (1996).
62. Y.V. Kovchegov, Phys. Rev. **D60**, 034008 (1999).
63. A. Hebecker, Phys. Reports **331**, 1 (2000).
64. A.V. Belitsky and A.V. Radyushkin, Phys. Reports **418**, 1 (2005).
65. E. Boos *et al.*, [CompHEP Collab.], Nucl. Instrum. Methods **A534**, 250 (2004) http://comphep.sinp.msu.ru/.
66. J. Alwall *et al.*, JHEP **1106**, 128 (2011), http://madgraph.hep.uiuc.edu/.
67. M.L. Mangano *et al.*, JHEP **0307**, 001 (2003), http://cern.ch/mlm/alpgen/.
68. T. Gleisberg and S. Hoche, JHEP **0812**, 039 (2008).
69. A. Cafarella, C.G. Papadopoulos, and M. Worek, Comp. Phys. Comm. **180**, 1941 (2009), http://cern.ch/helac-phegas/.
70. F.A. Berends and W.T. Giele, Nucl. Phys. **B306**, 759 (1988).
71. L.J. Dixon, arXiv:hep-ph/9601359.
72. Z. Bern, L. J. Dixon, and D. A. Kosower, Ann. Phys. **322**, 1587 (2007).
73. S. Badger *et al.*, Phys. Rev. **D87**, 3 (2013).
74. S. Catani and M.H. Seymour, Nucl. Phys. **B485**, 291 (1997) [Erratum-ibid. B **510**,503 (1998)].
75. S. Frixione, Z. Kunszt, and A. Signer, Nucl. Phys. **B467**, 399 (1996).
76. D.A. Kosower, Phys. Rev. **D57**, 5410 (1998);
J.M. Campbell, M.A. Cullen, and E.W.N. Glover, Eur. Phys. J. **C9**, 245 (1999);
D.A. Kosower, Phys. Rev. **D71**, 045016 (2005).
77. Z. Nagy, Phys. Rev. **D68**, 094002 (2003), http://www.desy.de/~znagy/Site/NLOJet++.html.
78. J.M. Campbell and R.K. Ellis, Phys. Rev. **D62**, 114012 (2000).
79. K. Arnold *et al.*, arXiv:1107.4038 [hep-ph]; http://www-itp.particle.uni-karlsruhe.de/~vbfnloweb/.
80. T. Binoth *et al.*, Eur. Phys. J. **C16**, 311 (2000), http://lapth.in2p3.fr/PHOX_FAMILY/.
81. G. Cullen *et al.*Eur. Phys. J. **C72**, 1889 (2012).
82. G. Bevilacqua *et al.*, Comp. Phys. Comm. **184**, 986 (2013).
83. V. Hirschi *et al.*, JHEP **1105**, 044 (2011).
84. S. Badger *et al.*, Comp. Phys. Comm. **184**, 1981 (2013).
85. Z. Bern *et al.*, PoS LL **2012**,018 (2012).
86. F. Cascioli, P. Maierhofer, and S. Pozzorini, Phys. Rev. Lett. **108**, 111601 (2012).
87. S. Actis *et al.*, JHEP **1304**, 037 (2013).
88. W. T. Giele and G. Zanderighi, JHEP **0806**, 038 (2008).
89. R. K. Ellis *et al.*, Phys. Reports **518**, 141 (2012).
90. M. Czakon, C. G. Papadopoulos, and M. Worek, JHEP **0908**, 085 (2009).
91. R. Frederix *et al.*, JHEP **0910**, 003 (2009).
92. T. Gleisberg *et al.*, JHEP **0902**, 007 (2009), http://projects.hepforge.org/sherpa/.
93. S. Becker *et al.*, Phys. Rev. Lett. **108**, 032005 (2012).
94. Z. Bern *et al.*, Phys. Rev. **D88**, 014025 (2013).
95. S. Badger *et al.*, arXiv:1309.6585 [hep-ph].
96. Z. Bern *et al.*, Nucl. Phys. **B425**, 217 (1994).
97. J. M. Campbell and E. W. N. Glover, Nucl. Phys. **B527**, 264 (1998).
98. S. Catani and M. Grazzini, Phys. Lett. **B446**, 143 (1999).
99. A. Gehrmann-De Ridder *et al.*, Phys. Rev. Lett. **99**, 132002 (2007);
JHEP **0712**, 094 (2007);
Phys. Rev. Lett. **100**, 172001 (2008).
100. S. Weinzierl, Phys. Rev. Lett. **101**, 162001 (2008);
JHEP **0906**, 041 (2009).
101. K. Melnikov and F. Petriello, Phys. Rev. **D74**, 114017 (2006), http://gate.hep.anl.gov/fpetriello/FEWZ.html.
102. S. Catani *et al.*, Phys. Rev. Lett. **103**, 082001 (2009), http://theory.fi.infn.it/grazzini/dy.html.
103. C. Anastasiou, K. Melnikov, and F. Petriello, Nucl. Phys. **B724**, 197 (2005), http://www.phys.ethz.ch/~pheno/fehipro/.
104. S. Catani and M. Grazzini, Phys. Rev. Lett. **98**, 222002 (2007), http://theory.fi.infn.it/grazzini/codes.html.
105. G. Ferrera, M. Grazzini, and F. Tramontano, Phys. Rev. Lett. **107**, 152003 (2011).
106. S. Catani *et al.*, Phys. Rev. Lett. **108**, 072001 (2012).
107. A. Gehrmann-de Ridder *et al.*, Phys. Rev. Lett. **110**, 162003 (2013).
108. R. Boughezal *et al.*, JHEP **1306**, 072 (2013).
109. Y.L. Dokshitzer, D.Diakonov, and S.I. Troian, Phys. Reports **58**, 269 (1980).
110. G. Parisi and R. Petronzio, Nucl. Phys. **B154**, 427 (1979).
111. G. Curci, M. Greco, and Y. Srivastava, Nucl. Phys. **B159**, 451 (1979).
112. A. Bassetto, M. Ciafaloni, and G. Marchesini, Nucl. Phys. **B163**, 477 (1980).
113. J.C. Collins and D.E. Soper, Nucl. Phys. **B193**, 381 (1981) [Erratum-*ibid.* **B213**, 545 (1983)].
114. J.C. Collins and D.E. Soper, Nucl. Phys. **B197**, 446 (1982).
115. J. Kodaira and L. Trentadue, Phys. Lett. **B112**, 66 (1982).
116. J. Kodaira and L. Trentadue, Phys. Lett. **B123**, 335 (1983).
117. J.C. Collins, D.E. Soper, and G. Sterman, Nucl. Phys. **B250**, 199 (1985).
118. S. Catani, *et al.*, Nucl. Phys. **B407**, 3 (1993).
119. C. W. Bauer *et al.*, Phys. Rev. **D63**, 114020 (2001).
120. C. W. Bauer, D. Pirjol, and I. W. Stewart, Phys. Rev. **D65**, 054022 (2002).
121. S. Fleming, PoS **EFT09**, 002 (2009).
122. S. Catani, *et al.*, Phys. Lett. **B269**, 432 (1991).
123. N. Brown and W.J. Stirling, Phys. Lett. **B252**, 657 (1990).
124. W. Bartel, *et al.*, [JADE Collab.], Z. Phys. **C33**, 23 (1986).
125. N. Kidonakis, G. Oderda, and G. Sterman, Nucl. Phys. **B531**, 365 (1998).
126. R. Bonciani *et al.*, Phys. Lett. **B575**, 268 (2003).
127. A. Banfi, G.P. Salam, and G. Zanderighi, JHEP **0503**, 073 (2005).
128. D. de Florian and M. Grazzini, Phys. Rev. Lett. **85**, 4678 (2000).
129. G. Bozzi *et al.*, Nucl. Phys. **B737**, 73 (2006), http://theory.fi.infn.it/grazzini/codes.html.
130. G. Bozzi *et al.*, Phys. Lett. **B696**, 207 (2011).
131. T. Becher and M. Neubert, Eur. Phys. J. **C71**, 1665 (2011).
132. T. Becher, M. Neubert, and D. Wilhelm, http://cute.hepforge.org/.
133. D. de Florian *et al.*, JHEP **1206**, 132 (2012), http://theory.fi.infn.it/grazzini/codes.html.
134. C. Balazs and C.P. Yuan, Phys. Rev. **D56**, 5558 (1997).

135. A. Banfi *et al.*, Phys. Lett. **B715**, 152 (2012).
136. D. de Florian and M. Grazzini, Nucl. Phys. **B704**, 387 (2005).
137. T. Becher and G. Bell, JHEP **1211**, 126 (2012).
138. A. Banfi *et al.*, Phys. Rev. Lett. **109**, 202001 (2012); T. Becher, M. Neubert, and L. Rothen, arXiv:1307.0025 [hep-ph]; I. W. Stewart *et al.*, arXiv:1307.1808 [hep-ph].
139. I. W. Stewart, F. J. Tackmann, and W. J. Waalewijn, Phys. Rev. Lett. **106**, 032001 (2011).
140. Y. -T. Chien *et al.*, Phys. Rev. **D87**, 014010 (2013); T. T. Jouttenus *et al.*, Phys. Rev. **D88**, 054031 (2013).
141. M. Dasgupta *et al.*, JHEP **1210**, 126 (2012).
142. V. Ahrens *et al.*, JHEP **1009**, 097 (2010).
143. M. Aliev *et al.*, Comp. Phys. Comm. **182**, 1034 (2011).
144. N. Kidonakis, Phys. Rev. **D82**, 114030 (2010).
145. T. Becher, C. Lorentzen, M. D. Schwartz, Phys. Rev. Lett. **108**, 012001 (2012).
146. T. Becher and M.D. Schwartz, JHEP **0807**, 034 (2008).
147. Y. -T. Chien and M. D. Schwartz, JHEP **1008**, 058 (2010).
148. P. F. Monni, T. Gehrmann, and G. Luisoni, JHEP **1108**, 010 (2011).
149. S. Moch and A. Vogt, Phys. Lett. **B631**, 48 (2005).
150. E. Laenen and L. Magnea, Phys. Lett. **B632**, 270 (2006).
151. A. Vogt, Phys. Lett. **B497**, 228 (2001).
152. S. Catani, D. de Florian, M. Grazzini, P. Nason, JHEP **0307**, 028 (2003).
153. T. Sjostrand *et al.*, Comput. Phys. Commun. **135** 238, (2001).
154. T. Sjostrand, S. Mrenna, and P. Skands, JHEP **0605**, 026 (2006), http://projects. hepforge.org/pythia6/.
155. T. Sjostrand, S. Mrenna, and P. Skands, Comput. Phys. Commun. **178** 852, (2008), http://home.thep.lu.se/~torbjorn/Pythia.html.
156. B.R. Webber, Nucl. Phys. **B238**, 492 (1984).
157. G. Corcella *et al.*, JHEP **0101**, 010 (2001), http://www.hep.phy.cam.ac.uk/theory/webber/Herwig/.
158. M. Bahr *et al.*, Eur. Phys. J. **C58**, 639 (2008), http://projects.hepforge.org/herwig/.
159. L. Lonnblad, Comput. Phys. Commun. **71** 15, (1992).
160. A. Buckley *et al.*, Phys. Rept. **504**, 145-233 (2011).
161. B. Andersson *et al.*, Phys. Reports **97**, 31 (1983).
162. T. Sjostrand, Nucl. Phys. **B248**, 469 (1984).
163. T. Sjostrand and M. van Zijl, Phys. Rev. **D36**, 2019 (1987).
164. S. Catani *et al.*, JHEP **0111**, 063 (2001).
165. J. Alwall *et al.*, Eur. Phys. J. **C53**, 473 (2008).
166. S. Frixione and B.R. Webber, JHEP **0206**, 029 (2002).
167. P. Nason, JHEP **0411**, 040 (2004).
168. S. Alioli *et al.*, JHEP **1006**, 043 (2010), http://powhegbox.mib.infn.it/.
169. S. Hoeche *et al.*, JHEP **1304**, 027 (2013); R. Frederix and S. Frixione, JHEP **1212**, 061 (2012); S. Plätzer, JHEP **1308**, 114 (2013); L. Lannblad and S. Prestel, JHEP **1303**, 166 (2013); K. Hamilton *et al.*, JHEP **1305**, 082 (2013).
170. K. Hamilton *et al.*, arXiv:1309.0017 [hep-ph].
171. P. M. Stevenson, Phys. Lett. **B100**, 61 (1981).
172. P. M. Stevenson, Phys. Rev. **D23**, 2916 (1981).
173. G. Grunberg, Phys. Rev. **D29**, 2315 (1984).
174. S. J. Brodsky, G. P. Lepage, and P. B. Mackenzie, Phys. Rev. **D28**, 228 (1983).
175. M. Cacciari and N. Houdeau, JHEP **1109**, 039 (2011).
176. A. David and G. Passarino, Phys. Lett. **B726**, 266 (2013).
177. M. Cacciari *et al.*, JHEP **0404**, 068 (2004).
178. M. Dasgupta and G.P. Salam, J. Phys. **G30**, R143 (2004).
179. S. Moretti, L. Lonnblad, and T. Sjostrand, JHEP **9808**, 001 (1998).
180. G.P. Salam, Eur. Phys. J. **C67**, 637 (2010).
181. S.D. Ellis *et al.*, Prog. in Part. Nucl. Phys. **60**, 484 (2008).
182. G.P. Salam and G. Soyez, JHEP **0705**, 086 (2007).
183. S. Catani *et al.*, Nucl. Phys. **B406**, 187 (1993).
184. S.D. Ellis and D.E. Soper, Phys. Rev. **D48**, 3160 (1993).
185. Y.L. Dokshitzer *et al.*, JHEP **9708**, 001 (1997).
186. M. Wobisch and T. Wengler, arXiv:hep-ph/9907280.
187. M. Cacciari, G.P. Salam, and G. Soyez, JHEP **0804**, 063 (2008).
188. M. Cacciari and G.P. Salam, Phys. Lett. **B641**, 57 (2006); M. Cacciari, G.P. Salam, and G. Soyez, Eur. Phys. J. **C72**, 1896 (2012) http://fastjet.fr/.
189. P.A. Delsart *et al.*, arXiv:1201.3617 [hep-ex]; http://projects.hepforge.org/spartyjet/.
190. S. Brandt *et al.*, Phys. Lett. **12**, 57 (1964).
191. E. Farhi, Phys. Rev. Lett. **39**, 1587 (1977).
192. O. Biebel, Phys. Reports **340**, 165 (2001).
193. S. Kluth, Rept. on Prog. in Phys. **69**, 1771 (2006).
194. A. Banfi, G.P. Salam, and G. Zanderighi, JHEP **0408**, 062 (2004).
195. A. Banfi, G.P. Salam, and G. Zanderighi, JHEP **1006**, 038 (2010).
196. I. W. Stewart, F. J. Tackmann, and W. J. Waalewijn, Phys. Rev. Lett. **105**, 092002 (2010).
197. T. Aaltonen *et al.*, [CDF Collab.], Phys. Rev. **D83**, 112007 (2011).
198. G. Aad *et al.*, [ATLAS Collab.], Eur. Phys. J. **C72**, 2211 (2012).
199. G. Aad *et al.*, [ATLAS Collab.], Phys. Rev. **D88**, 032004 (2013).
200. V. Khachatryan *et al.*, [CMS Collab.], Phys. Lett. **B699**, 48 (2011).
201. S. Chatrchyan *et al.*, [CMS Collab.], Phys. Lett. **B722**, 238 (2013).
202. D.E. Acosta *et al.*, [CDF Collab.], Phys. Rev. **D71**, 112002 (2005).
203. T. Aaltonen *et al.*, [CDF Collab.], Phys. Rev. **D78**, 072005 (2008).
204. J. Breitweg *et al.*, [ZEUS Collab.], Eur. Phys. J. **C2**, 61 (1998).
205. C. Adloff *et al.*, [H1 Collab.], Nucl. Phys. **B545**, 3 (1999).
206. S. Chekanov *et al.*, [ZEUS Collab.], Nucl. Phys. **B700**, 3 (2004).
207. G. Aad *et al.*, [ATLAS Collab.], Phys. Rev. **D83**, 052003 (2011).
208. S. Chatrchyan *et al.*, [CMS Collab.], JHEP **1206**, 160 (2012).
209. G. Aad *et al.*, [ATLAS Collab.], arXiv:1307.5749 [hep-ex].
210. C. Glasman [H1 Collab. and ZEUS Collab.], Nucl. Phys. (Proc. Supp.) **191**, 121 (2009).
211. A. Abdesselam *et al.*, Eur. Phys. J. **C71**, 1661 (2011).
212. G. Aad *et al.*, [ATLAS Collab.], JHEP **1205**, 128 (2012).
213. S. Chatrchyan *et al.*, [CMS Collab.], JHEP **1305**, 090 (2013).
214. T. Aaltonen *et al.*, [CDF Collab.], Phys. Rev. **D85**, 091101 (2012).
215. G. Aad *et al.*, [ATLAS Collab.], Phys. Rev. **D86**, 072006 (2012).
216. A. Altheimer *et al.*, J. Phys. **G39**, 063001 (2012).
217. T. Schorner-Sadenius, Eur. Phys. J. **C72**, 2060 (2012).
218. J.M. Campbell, J.W. Huston, and W.J. Stirling, Rept. on Prog. in Phys. **70**, 89 (2007).
219. M.L. Mangano, Phys. Usp. **53**, 109 (2010).
220. J.M. Butterworth, G. Dissertori, and G.P. Salam, Ann. Rev. Nucl. and Part. Sci. **62**, 387 (2012).
221. F.D. Aaron *et al.*, [H1 Collab.], Eur. Phys. J. **C65**, 363 (2010).
222. F.D. Aaron *et al.*, [H1 Collab.], Eur. Phys. J. **C54**, 389 (2008).
223. S. Chekanov *et al.*, [ZEUS Collab.], Eur. Phys. J. **C52**, 515 (2007).
224. S. Chekanov *et al.*, [ZEUS Collab.], Phys. Rev. **D78**, 032004 (2008).
225. H. Abramowicz *et al.*, [ZEUS Collab.], Eur. Phys. J. **C70**, 965 (2010).
226. H. Abramowicz *et al.*, [ZEUS Collab.], Phys. Lett. **B691**, 127 (2010).
227. S. Chekanov *et al.*, [ZEUS Collab.], Phys. Rev. **D85**, 052008 (2012).
228. F.D. Aaron *et al.*, [H1 Collab.], Eur. Phys. J. **C67**, 1 (2010).
229. S. Chekanov *et al.*, [ZEUS Collab.], Nucl. Phys. **B792**, 1 (2008).

230. S. Chekanov *et al.*, [ZEUS Collab.], Phys. Rev. **D76**, 072011 (2007).
231. A. Aktas *et al.*, [H1 Collab.], Phys. Lett. **B639**, 21 (2006).
232. H. Abramowicz *et al.*, [ZEUS Collab.], Eur. Phys. J. **C71**, 1659 (2011).
233. H. Abramowicz *et al.*, [ZEUS Collab.], Nucl. Phys. **B864**, 1 (2012).
234. A. Abulencia *et al.*, [CDF - Run II Collab.], Phys. Rev. **D75**, 092006 (2007) [Erratum-ibid. 119901].
235. V.M. Abazov *et al.*, [D0 Collab.], Phys. Rev. Lett. **101**, 062001 (2008).
236. V.M. Abazov *et al.*, [D0 Collab.], Phys. Rev. **D85**, 052006 (2012).
237. B. Abelev *et al.*, [ALICE Collab.], Phys. Lett. **B722**, 262 (2013).
238. G. Aad *et al.*, [ATLAS Collab.], Eur. Phys. J. **C71**, 1512 (2011).
239. G. Aad *et al.*, [ATLAS Collab.], Phys. Rev. **D86**, 014022 (2012).
240. G. Aad *et al.*, [ATLAS Collab.], Eur. Phys. J. **C73**, 2509 (2013).
241. S. Chatrchyan *et al.*, [CMS Collab.], Phys. Rev. Lett. **107**, 132001 (2011).
242. S. Chatrchyan *et al.*, [CMS Collab.], Phys. Rev. **D87**, 112002 (2013).
243. S. Chatrchyan *et al.*, [CMS Collab.], JHEP **1206**, 036 (2012).
244. `http://fastnlo.hepforge.org`;
M. Wobisch *et al.*, [fastNLO Collab.], `arXiv:1109.1310 [hep-ph]`;
D. Britzger *et al.*, [fastNLO Collab.], `arXiv:1208.3641 [hep-ph]`.
245. T. Aaltonen *et al.*, [CDF Collab.], Phys. Rev. **D79**, 112002 (2009).
246. V.M. Abazov *et al.*, [D0 Collab.], Phys. Rev. Lett. **103**, 191803 (2009).
247. S. Chatrchyan *et al.*, [CMS Collab.], JHEP **1205**, 055 (2012).
248. G. Aad *et al.*, [ATLAS Collab.], JHEP **1301**, 029 (2013).
249. V.M. Abazov *et al.*, [D0 Collab.], Phys. Rev. Lett. **94**, 221801 (2005).
250. V.M. Abazov *et al.*, [D0 Collab.], Phys. Lett. **B721**, 212 (2013).
251. G. Aad *et al.*, [ATLAS Collab.], Phys. Rev. Lett. **106**, 172002 (2011).
252. V. Khachatryan *et al.*, [CMS Collab.], Phys. Rev. Lett. **106**, 122003 (2011).
253. V. M. Abazov *et al.*, [D0 Collab.], Phys. Lett. **B704**, 434 (2011).
254. V.M. Abazov *et al.*, [D0 Collab.], Phys. Lett. **B720**, 6 (2013).
255. G. Aad *et al.*, [ATLAS Collab.], Eur. Phys. J. **C71**, 1763 (2011).
256. G. Aad *et al.*, [ATLAS Collab.], JHEP **1109**, 053 (2011).
257. S. Chatrchyan *et al.*, [CMS Collab.], Eur. Phys. J. **C72**, 2216 (2012).
258. S. Chatrchyan *et al.*, [CMS Collab.], Phys. Lett. **B702**, 336 (2011).
259. S. Chatrchyan *et al.*, [CMS Collab.], `arXiv:1304.7498 [hep-ex]`.
260. T. Aaltonen *et al.*, [CDF Collab.], Phys. Rev. Lett. **100**, 102001 (2008).
261. T. Aaltonen *et al.*, [CDF Collab.], Phys. Rev. **D77**, 011108 (2008).
262. V.M. Abazov *et al.*, [D0 Collab.], Phys. Lett. **B669**, 278 (2008).
263. V.M. Abazov *et al.*, [D0 Collab.], Phys. Rev. Lett. **678**, 45 (2009).
264. V.M. Abazov *et al.*, [D0 Collab.], Phys. Lett. **B682**, 370 (2010).
265. V.M. Abazov *et al.*, [D0 Collab.], Phys. Rev. Lett. **106**, 122001 (2011).
266. V.M. Abazov *et al.*, [D0 Collab.], Phys. Lett. **B705**, 200 (2011).
267. V.M. Abazov *et al.*, [D0 Collab.], `arXiv:1302.6508 [hep-ex]`.
268. V.M. Abazov *et al.*, [D0 Collab.], `arXiv:1308.2708 [hep-ex]`.
269. G. Aad *et al.*, [ATLAS Collab.], Phys. Lett. **B698**, 325 (2011).
270. G. Aad *et al.*, [ATLAS Collab.], Phys. Lett. **B708**, 221 (2012).
271. S. Chatrchyan *et al.*, [CMS Collab.], JHEP **1201**, 010 (2012).
272. G. Aad *et al.*, [ATLAS Collab.], Phys. Rev. **D85**, 092002 (2012).
273. G. Aad *et al.*, [ATLAS Collab.], Phys. Rev. **D85**, 092014 (2012).
274. G. Aad *et al.*, [ATLAS Collab.], JHEP **1307**, 032 (2013).
275. G. Aad *et al.*, [ATLAS Collab.], Nucl. Phys. **B875**, 483 (2013).
276. G. Aad *et al.*, [ATLAS Collab.], Phys. Lett. **B705**, 415 (2011).
277. G. Aad *et al.*, [ATLAS Collab.], Phys. Rev. **D85**, 012005 (2012).
278. S. Chatrchyan *et al.*, [CMS Collab.], Phys. Rev. **D85**, 032002 (2012).
279. T. Aaltonen *et al.*, [CDF Collab.], Phys. Rev. Lett. **110**, 101801 (2013).
280. V.M. Abazov *et al.*, [D0 Collab.], Phys. Lett. **B725**, 6 (2013).
281. G. Aad *et al.*, [ATLAS Collab.], JHEP **1301**, 086 (2013).
282. S. Chatrchyan *et al.*, [CMS Collab.], JHEP **1201**, 133 (2012).
283. G. Aad *et al.*, [ATLAS Collab.], Eur. Phys. J. **C71**, 1846 (2011).
284. S. Chatrchyan *et al.*, [CMS Collab.], JHEP **1204**, 084 (2012).
285. V. Khachatryan *et al.*, [CMS Collab.], JHEP **1103**, 136 (2011).
286. V.M. Abazov *et al.*, [D0 Collab.], Phys. Rev. Lett. **102**, 192002 (2009).
287. T. Aaltonen *et al.*, [CDF Collab.], Phys. Rev. **D81**, 052006 (2010).
288. V.M. Abazov *et al.*, [D0 Collab.], Phys. Lett. **B714**, 32 (2012).
289. V.M. Abazov *et al.*, [D0 Collab.], Phys. Lett. **B719**, 354 (2013).
290. V.M. Abazov *et al.*, [D0 Collab.], Phys. Lett. **B666**, 23 (2008).
291. T. Aaltonen *et al.*, [CDF Collab.], Phys. Rev. Lett. **110**, 071801 (2013).
292. T. Aaltonen *et al.*, [CDF Collab.], Phys. Rev. **D79**, 052008 (2009).
293. T. Aaltonen *et al.*, [CDF Collab.], Phys. Rev. Lett. **104**, 131801 (2010).
294. V. M. Abazov *et al.*, [D0 Collab.], Phys. Rev. **D83**, 031105 (2011).
295. V. M. Abazov *et al.*, [D0 Collab.], Phys. Lett. **B718**, 1314 (2013).
296. V. M. Abazov *et al.*, [D0 Collab.], Phys. Rev. **D87**, 092010 (2013).
297. V. M. Abazov *et al.*, [D0 Collab.], `arXiv:1308.4384 [hep-ex]`.
298. G. Aad *et al.*, [ATLAS Collab.], Phys. Lett. **B706**, 295 (2012).
299. S. Chatrchyan *et al.*, [CMS Collab.], JHEP **1206**, 126 (2012).
300. G. Aad *et al.*, [ATLAS Collab.], JHEP **1306**, 084 (2013).
301. S. Chatrchyan *et al.*, [CMS Collab.], `arXiv:1307.1907 [hep-ex]`.
302. G. Aad *et al.*, [ATLAS Collab.], Eur. Phys. J. **C72**, 2043 (2012).
303. G. Aad *et al.*, [ATLAS Collab.], Eur. Phys. J. **C73**, 2261 (2013).
304. S. Chatrchyan *et al.*, [CMS Collab.], Eur. Phys. J. **C73**, 2339 (2013).
305. S. Bethke, Prog. in Part. Nucl. Phys. **58**, 351 (2007).
306. S. Bethke, Eur. Phys. J. **C64**, 689 (2009).
307. S. Bethke, J. Phys. **G26**, R27 (2000).
308. M. Schmelling, Phys. Scripta **51**, 676 (1995).
309. M. Beneke and M. Jamin, JHEP **0809**, 044 (2008).
310. M. Davier *et al.*, Eur. Phys. J. **C56**, 305 (2008).
311. K. Maltman and T. Yavin, Phys. Rev. **D78**, 094020 (2008).
312. S. Narison, Phys. Lett. **B673**, 30 (2009).
313. I. Caprini and J. Fischer, Eur. Phys. J. **C64**, 35 (2009).
314. D. Boito *et al.*, Phys. Rev. D 85,093015(2012).
315. A. Pich, PoS ConfinementX (2012) 022.
316. G. Altarelli, PoS Corfu **2012** (2013) 002.
317. C. McNeile *et al.*, [HPQCD Collab.], Phys. Rev. **D82**, 034512 (2010).
318. C.T.H. Davies *et al.*, [HPQCD Collab., UKQCD Collab., and MILC Collab.], Phys. Rev. Lett. **92**, 022001 (2004).
319. K. Maltman, *et al.*, Phys. Rev. **D78**, 114504 (2008).
320. S. Aoki *et al.*, [PACS-CS Collab.], JHEP **0910**, 053 (2009).

321. E. Shintani *et al.*, [JLQCD Collab.], Phys. Rev. **D82**, 074505 (2010).
322. B. Blossier *et al.*, [ETM Collab.], Phys. Rev. Lett. **108**, 262002 (2012).
323. A. Bazavov *et al.*, [BBGPSV collaboration], Phys. Rev. **D86**, 114031 (2012).
324. C. Glasman [H1 Collab. and ZEUS Collab.], J. Phys. Conf. Ser. **110** 022013 (2008).
325. J. Blumlein, H. Bottcher, and A. Guffanti, Nucl. Phys. **B774**, 182 (2007).
326. S. Alekhin, J. Blumlein, and S. Moch, Phys. Rev. D 86, 054009 (2012).
327. P. Jimenez-Delgado and E. Reya, Phys. Rev. **D79**, 074023 (2009).
328. A. D. Martin *et al.*, Eur. Phys. J. **C64**, 653 (2009).
329. R.D. Ball *et al.*, Phys. Lett. **B707**, 66 (2012).
330. R.S. Thorne and G. Watt, JHEP **1108**, 100 (2011).
331. S. Alekhin, J. Blumlein, and S.Moch, Eur. Phys. J. **C71**, 1723 (2011).
332. R.D. Ball *et al.*, Phys. Lett. **B704**, 36 (2011).
333. R.D. Ball *et al.*, Phys. Lett. **B723**, 330 (2013).
334. R.S. Thorne *et al.*, arXiv:1306.3907 [hep-ph].
335. N. Brambilla *et al.*, Phys. Rev. **D75**, 074014 (2007).
336. G. Dissertori *et al.*, JHEP **0908**, 036 (2009).
337. G. Abbiendi *et al.*, Eur. Phys. J. **C71**, 1733 (2011).
338. S. Bethke *et al.*, [JADE Collab.], Eur. Phys. J. **C64**, 351 (2009).
339. G. Dissertori *et al.*, Phys. Rev. Lett. **104**, 072002 (2010).
340. J. Schieck *et al.*, Eur. Phys. J. **C73**, 2332 (2013).
341. R. Frederix *et al.*, JHEP **1011**, 050 (2010).
342. P. Bolzoni, B.A. Kniehl, and A.V. Kotikov, Nucl. Phys. **B875**, 18 (2013).
343. R.A. Davison and B.R. Webber, Eur. Phys. J. **C59**, 13 (2009).
344. R. Abbate *et al.*, Phys. Rev. **D83**, 074021 (2011).
345. T. Gehrmann *et al.*, Eur. Phys. J. **C73**, 2265 (2013).
346. M. Abazov *et al.*, [D0 Collab.], Phys. Rev. **D80**, 111107 (2009).
347. M. Abazov *et al.*, [D0 Collab.], Phys. Lett. **B718**, 56 (2012).
348. B. Malaescu and P. Starovoitov, Eur. Phys. J. **C72**, 2041 (2012).
349. H. Flacher *et al.*, Eur. Phys. J. **C60**, 543 (2009).
350. J.-L. Kneur and A. Neveu, Phys. Rev. D 88, **074025** (2013).
351. S. Bethke *et al.*, *Workshop on precision measurements of* α_s, Munich, Feb. 9-11, 2011 arXiv:1110.0016 [hep-ph].

10. ELECTROWEAK MODEL AND CONSTRAINTS ON NEW PHYSICS

Revised November 2013 by J. Erler (U. Mexico) and A. Freitas (Pittsburgh U.).

10.1. Introduction

The standard model of the electroweak interactions (SM) [1] is based on the gauge group SU(2) × U(1), with gauge bosons W^i_μ, $i = 1, 2, 3$, and B_μ for the SU(2) and U(1) factors, respectively, and the corresponding gauge coupling constants g and g'. The left-handed fermion fields of the $i^{\rm th}$ fermion family transform as doublets $\Psi_i = \begin{pmatrix} \nu_i \\ \ell_i^- \end{pmatrix}$ and $\begin{pmatrix} u_i \\ d'_i \end{pmatrix}$ under SU(2), where $d'_i \equiv \sum_j V_{ij}\, d_j$, and V is the Cabibbo-Kobayashi-Maskawa mixing matrix. [Constraints on V and tests of universality are discussed in Ref. 2 and in the Section on "The CKM Quark-Mixing Matrix". The extension of the formalism to allow an analogous leptonic mixing matrix is discussed in the Section on "Neutrino Mass, Mixing, and Oscillations".] The right-handed fields are SU(2) singlets. In the minimal model there are three fermion families.

A complex scalar Higgs doublet, $\phi \equiv \begin{pmatrix} \phi^+ \\ \phi^0 \end{pmatrix}$, is added to the model for mass generation through spontaneous symmetry breaking with potential* given by,

$$V(\phi) = \mu^2 \phi^\dagger \phi + \frac{\lambda^2}{2} (\phi^\dagger \phi)^2. \tag{10.1}$$

For μ^2 negative, ϕ develops a vacuum expectation value, $v/\sqrt{2} = \mu/\lambda$, where $v \approx 246$ GeV, breaking part of the electroweak (EW) gauge symmetry, after which only one neutral Higgs scalar, H, remains in the physical particle spectrum. In non-minimal models there are additional charged and neutral scalar Higgs particles [3].

After the symmetry breaking the Lagrangian for the fermion fields, ψ_i, is

$$\begin{aligned} \mathscr{L}_F = & \sum_i \overline{\psi}_i \left(i\,\partial\!\!\!/ - m_i - \frac{m_i H}{v} \right) \psi_i \\ & - \frac{g}{2\sqrt{2}} \sum_i \overline{\Psi}_i\, \gamma^\mu\, (1-\gamma^5)(T^+\, W^+_\mu + T^-\, W^-_\mu)\, \Psi_i \\ & - e \sum_i Q_i\, \overline{\psi}_i\, \gamma^\mu\, \psi_i\, A_\mu \\ & - \frac{g}{2\cos\theta_W} \sum_i \overline{\psi}_i\, \gamma^\mu (g^i_V - g^i_A \gamma^5)\, \psi_i\, Z_\mu\ . \end{aligned} \tag{10.2}$$

Here $\theta_W \equiv \tan^{-1}(g'/g)$ is the weak angle; $e = g \sin\theta_W$ is the positron electric charge; and $A \equiv B\cos\theta_W + W^3 \sin\theta_W$ is the photon field (γ). $W^\pm \equiv (W^1 \mp i W^2)/\sqrt{2}$ and $Z \equiv -B \sin\theta_W + W^3 \cos\theta_W$ are the charged and neutral weak boson fields, respectively. The Yukawa coupling of H to ψ_i in the first term in $\mathscr{L}_F$, which is flavor diagonal in the minimal model, is $g m_i/2M_W$. The boson masses in the EW sector are given (at tree level, *i.e.*, to lowest order in perturbation theory) by,

$$M_H = \lambda\, v, \tag{10.3a}$$

$$M_W = \frac{1}{2}\, g\, v = \frac{e\, v}{2 \sin\theta_W}, \tag{10.3b}$$

$$M_Z = \frac{1}{2} \sqrt{g^2 + g'^2}\, v = \frac{e\, v}{2 \sin\theta_W \cos\theta_W} = \frac{M_W}{\cos\theta_W}, \tag{10.3c}$$

$$M_\gamma = 0. \tag{10.3d}$$

* There is no generally accepted convention to write the quartic term. Our numerical coefficient simplifies Eq. (10.3*a*) below and the squared coupling preserves the relation between the number of external legs and the power counting of couplings at a given loop order. This structure also naturally emerges from physics beyond the SM, such as supersymmetry.

The second term in $\mathscr{L}_F$ represents the charged-current weak interaction [4–7], where T^+ and T^- are the weak isospin raising and lowering operators. For example, the coupling of a W to an electron and a neutrino is

$$-\frac{e}{2\sqrt{2}\sin\theta_W} \left[W^-_\mu\, \overline{e}\, \gamma^\mu (1-\gamma^5) \nu + W^+_\mu\, \overline{\nu}\, \gamma^\mu\, (1-\gamma^5) e \right]. \tag{10.4}$$

For momenta small compared to M_W, this term gives rise to the effective four-fermion interaction with the Fermi constant given by $G_F/\sqrt{2} = 1/2v^2 = g^2/8M_W^2$. CP violation is incorporated into the EW model by a single observable phase in V_{ij}.

The third term in $\mathscr{L}_F$ describes electromagnetic interactions (QED) [8–10], and the last is the weak neutral-current interaction [5–7]. The vector and axial-vector couplings are

$$g^i_V \equiv t_{3L}(i) - 2 Q_i \sin^2\theta_W, \tag{10.5a}$$

$$g^i_A \equiv t_{3L}(i), \tag{10.5b}$$

where $t_{3L}(i)$ is the weak isospin of fermion i ($+1/2$ for u_i and ν_i; $-1/2$ for d_i and e_i) and Q_i is the charge of ψ_i in units of e.

The first term in Eq. (10.2) also gives rise to fermion masses, and in the presence of right-handed neutrinos to Dirac neutrino masses. The possibility of Majorana masses is discussed in the Section on "Neutrino Mass, Mixing, and Oscillations".

10.2. Renormalization and radiative corrections

In addition to the Higgs boson mass, M_H, the fermion masses and mixings, and the strong coupling constant, α_s, the SM has three parameters. The set with the smallest experimental errors contains the Z mass**, the Fermi constant, and the fine structure constant, which will be discussed in turn (if not stated otherwise, the numerical values quoted in Sec. 10.2–10.5 correspond to the main fit result in Table 10.6):

The Z boson mass, $M_Z = 91.1876 \pm 0.0021$ GeV, has been determined from the Z lineshape scan at LEP 1 [11].

The Fermi constant, $G_F = 1.1663787(6) \times 10^{-5}$ GeV^{-2}, is derived from the muon lifetime formula***,

$$\frac{\hbar}{\tau_\mu} = \frac{G_F^2 m_\mu^5}{192\pi^3}\, F(\rho) \left[1 + H_1(\rho) \frac{\widehat{\alpha}(m_\mu)}{\pi} + H_2(\rho) \frac{\widehat{\alpha}^2(m_\mu)}{\pi^2} \right], \tag{10.6}$$

where $\rho = m_e^2/m_\mu^2$, and where

$$F(\rho) = 1 - 8\rho + 8\rho^3 - \rho^4 - 12\rho^2 \ln\rho = 0.99981295, \tag{10.7a}$$

$$\begin{aligned} H_1(\rho) = & \frac{25}{8} - \frac{\pi^2}{2} - \left(9 + 4\pi^2 + 12 \ln\rho \right) \rho \\ & + 16\pi^2 \rho^{3/2} + \mathcal{O}(\rho^2) = -1.80793, \end{aligned} \tag{10.7b}$$

$$\begin{aligned} H_2(\rho) = & \frac{156815}{5184} - \frac{518}{81}\pi^2 - \frac{895}{36}\zeta(3) + \frac{67}{720}\pi^4 + \frac{53}{6}\pi^2 \ln 2 \\ & - (0.042 \pm 0.002)_{\rm had} - \frac{5}{4}\pi^2 \sqrt{\rho} + \mathcal{O}(\rho) = 6.64, \end{aligned} \tag{10.7c}$$

$$\widehat{\alpha}(m_\mu)^{-1} = \alpha^{-1} + \frac{1}{3\pi} \ln\rho + \mathcal{O}(\alpha) = 135.901 \tag{10.7d}$$

H_1 and H_2 capture the QED corrections within the Fermi model. The results for $\rho = 0$ have been obtained in Refs. 13 and 14, respectively, where the term in parentheses is from the hadronic

** We emphasize that in the fits described in Sec. 10.6 and Sec. 10.7 the values of the SM parameters are affected by all observables that depend on them. This is of no practical consequence for α and G_F, however, since they are very precisely known.

*** In the spirit of the Fermi theory, we incorporated the small propagator correction, $3/5\ m_\mu^2/M_W^2$, into Δr (see below). This is also the convention adopted by the MuLan collaboration [12]. While this breaks with historical consistency, the numerical difference was negligible in the past.

vacuum polarization [14]. The mass corrections to H_1 have been known for some time [15], while those to H_2 are more recent [16]. Notice the term linear in m_e whose appearance was unforeseen and can be traced to the use of the muon pole mass in the prefactor [16]. The remaining uncertainty in G_F is experimental and has recently been reduced by an order of magnitude by the MuLan collaboration [12] at the PSI.

The experimental determination of the fine structure constant, $\alpha = 1/137.035999074(44)$, is currently dominated by the $e^\pm$ anomalous magnetic moment [10]. In most EW renormalization schemes, it is convenient to define a running α dependent on the energy scale of the process, with $\alpha^{-1} \sim 137$ appropriate at very low energy, *i.e.* close to the Thomson limit. (The running has also been observed [17] directly.) For scales above a few hundred MeV this introduces an uncertainty due to the low energy hadronic contribution to vacuum polarization. In the modified minimal subtraction ($\overline{\rm MS}$) scheme [18] (used for this *Review*), and with $\alpha_s(M_Z) = 0.1193 \pm 0.0016$ we have $\widehat{\alpha}(m_\tau)^{-1} = 133.465 \pm 0.013$ and $\widehat{\alpha}(M_Z)^{-1} = 127.940 \pm 0.014$. (In this Section we denote quantities defined in the modified minimal subtraction ($\overline{\rm MS}$) scheme by a caret; the exception is the strong coupling constant, α_s, which will always correspond to the $\overline{\rm MS}$ definition and where the caret will be dropped.) The latter corresponds to a quark sector contribution (without the top) to the conventional (on-shell) QED coupling, $\alpha(M_Z) = \dfrac{\alpha}{1 - \Delta\alpha(M_Z)}$, of $\Delta\alpha^{(5)}_{\rm had}(M_Z) = 0.02771 \pm 0.00011$. These values are updated from Ref. 19 with $\Delta\alpha^{(5)}_{\rm had}(M_Z)$ moved downwards and its uncertainty halved (partly due to a more precise charm quark mass). Its correlation with the $\mu^\pm$ anomalous magnetic moment (see Sec. 10.5), as well as the non-linear α_s dependence of $\widehat{\alpha}(M_Z)$ and the resulting correlation with the input variable α_s, are fully taken into account in the fits. This is done by using as actual input (fit constraint) instead of $\Delta\alpha^{(5)}_{\rm had}(M_Z)$ the analogous low energy contribution by the three light quarks, $\Delta\alpha^{(3)}_{\rm had}(1.8\ {\rm GeV}) = (55.50 \pm 0.78) \times 10^{-4}$ [20], and by calculating the perturbative and heavy quark contributions to $\widehat{\alpha}(M_Z)$ in each call of the fits according to Ref. 19. Part of the uncertainty ($\pm 0.49 \times 10^{-4}$) is from e^+e^- annihilation data below 1.8 GeV and τ decay data (including uncertainties from isospin breaking effects), but uncalculated higher order perturbative ($\pm 0.41 \times 10^{-4}$) and non-perturbative ($\pm 0.44 \times 10^{-4}$) QCD corrections and the $\overline{\rm MS}$ quark mass values (see below) also contribute. Various evaluations of $\Delta\alpha^{(5)}_{\rm had}$ are summarized in Table 10.1 where the relation† between the $\overline{\rm MS}$ and on-shell definitions is given by [22]

$$\Delta\widehat{\alpha}(M_Z) - \Delta\alpha(M_Z) = \frac{\alpha}{\pi}\Big[\Big(\frac{100}{27} - \frac{1}{6} - \frac{7}{4}\ln\frac{M_Z^2}{M_W^2}\Big) + \frac{\alpha_s(M_Z)}{\pi}\Big(\frac{605}{108} - \frac{44}{9}\zeta(3)\Big) + \frac{\alpha_s^2(M_Z)}{\pi^2}\left(\frac{976481}{23328} - \frac{781}{18}\zeta(3) + \frac{275}{27}\zeta(5)\right)\Big] = 0.007165, \quad (10.8)$$

and where the first entry of the lowest order term is from fermions and the other two are from $W^\pm$ loops, which are usually excluded from the on-shell definition. The most recent results typically assume the validity of perturbative QCD (PQCD) at scales of 1.8 GeV and above, and are in reasonable agreement with each other. There is, however, some discrepancy between analyses based on $e^+e^- \to$ hadrons cross-section data and those based on τ decay spectral functions [20]. The latter utilize data from OPAL [34], CLEO [35], ALEPH [36], and Belle [37] and imply lower central values for the extracted M_H from a global fit to the indirect precision data of about 6%. This discrepancy is smaller than in the past and at least some of it appears to be experimental. The dominant $e^+e^- \to \pi^+\pi^-$ cross-section was measured with the CMD-2 [38] and SND [39] detectors at the VEPP-2M e^+e^- collider at Novosibirsk and the results are (after an initial discrepancy due to a flaw in the Monte Carlo event generator used by SND) in good agreement with each other. As an alternative to cross-section scans, one can use the high statistics radiative return events at e^+e^- accelerators operating at resonances such as the Φ or the $\Upsilon(4S)$. The method [40] is systematics limited but dominates over the Novosibirsk data throughout. The BaBar collaboration [41] studied multi-hadron events radiatively returned from the $\Upsilon(4S)$, reconstructing the radiated photon and normalizing to $\mu^\pm\gamma$ final states. Their result is higher compared to VEPP-2M and in fact agrees quite well with the τ analysis including the energy dependence (shape). In contrast, the shape and smaller overall cross-section from the $\pi^+\pi^-$ radiative return results from the Φ obtained by the KLOE collaboration [42] differs significantly from what is observed by BaBar. The discrepancy originates from the kinematic region $\sqrt{s} \gtrsim 0.6$ GeV, and is most pronounced for $\sqrt{s} \gtrsim 0.85$ GeV. All measurements including older data [43] and multi-hadron final states (there are also discrepancies in the $e^+e^- \to 2\pi^+2\pi^-$ channel [20]) are accounted for and corrections have been applied for missing channels [20]. Further improvement of this dominant theoretical uncertainty in the interpretation of precision data will require better measurements of the cross-section for $e^+e^- \to$ hadrons below the charmonium resonances including multi-pion and other final states. To improve the precisions in $\widehat{m}_c(\widehat{m}_c)$ and $\widehat{m}_b(\widehat{m}_b)$ it would help to remeasure the threshold regions of the heavy quarks as well as the electronic decay widths of the narrow $c\bar{c}$ and $b\bar{b}$ resonances.

Table 10.1: Evaluations of the on-shell $\Delta\alpha^{(5)}_{\rm had}(M_Z)$ by different groups (for a more complete list of evaluations see the 2012 edition of this *Review*). For better comparison we adjusted central values and errors to correspond to a common and fixed value of $\alpha_s(M_Z) = 0.120$. References quoting results without the top quark decoupled are converted to the five flavor definition. Ref. [28] uses $\Lambda_{\rm QCD} = 380 \pm 60$ MeV; for the conversion we assumed $\alpha_s(M_Z) = 0.118 \pm 0.003$.

Reference	Result	Comment
Geshkenbein, Morgunov [24]	0.02780 ± 0.00006	$\mathcal{O}(\alpha_s)$ resonance model
Swartz [25]	0.02754 ± 0.00046	use of fitting function
Krasnikov, Rodenberg [26]	0.02737 ± 0.00039	PQCD for $\sqrt{s} > 2.3$ GeV
Kühn & Steinhauser [27]	0.02778 ± 0.00016	full $\mathcal{O}(\alpha_s^2)$ for $\sqrt{s} > 1.8$ GeV
Erler [19]	0.02779 ± 0.00020	conv. from $\overline{\rm MS}$ scheme
Groote *et al.* [28]	0.02787 ± 0.00032	use of QCD sum rules
Martin *et al.* [29]	0.02741 ± 0.00019	incl. new BES data
de Troconiz, Yndurain [30]	0.02754 ± 0.00010	PQCD for $s > 2$ GeV^2
Jegerlehner [31]	0.02755 ± 0.00013	Adler function approach
Davier *et al.* [20]	0.02750 ± 0.00010	incl. new e^+e^- data, PQCD for $\sqrt{s} > 1.8$ GeV
Davier *et al.* [20]	0.02762 ± 0.00011	incl. τ decay data
Burkhardt, Pietrzyk [32]	0.02750 ± 0.00033	incl. BES/BABAR data, PQCD for $\sqrt{s} > 12$ GeV
Hagiwara *et al.* [33]	0.02764 ± 0.00014	incl. new e^+e^- data, PQCD for $\sqrt{s} = 2.6$–$3.7, >11.1$ GeV

Further free parameters entering into Eq. (10.2) are the quark and lepton masses, where m_i is the mass of the $i^{\rm th}$ fermion ψ_i. For the light quarks, as described in the note on "Quark Masses" in the Quark Listings, $\widehat{m}_u = 2.3^{+0.7}_{-0.5}$ MeV, $\widehat{m}_d = 4.8^{+0.5}_{-0.3}$ MeV, and $\widehat{m}_s = 95 \pm 5$ MeV. These are running $\overline{\rm MS}$ masses evaluated at the scale $\mu = 2$ GeV. For the heavier quarks we use QCD sum rule [44] constraints [45] and recalculate their masses in each call of our fits to account for their direct α_s dependence. We find¶,

† In practice, $\alpha(M_Z)$ is directly evaluated in the $\overline{\rm MS}$ scheme using the FORTRAN package GAPP [21], including the QED contributions of both leptons and quarks. The leptonic three-loop contribution in the on-shell scheme has been obtained in Ref. 23.

¶ Other authors [46] advocate to evaluate and quote $\widehat{m}_c(\mu = 3\ {\rm GeV})$ instead. We use $\widehat{m}_c(\mu = \widehat{m}_c)$ because in the global analysis it is conve-

$\widehat{m}_c(\mu=\widehat{m}_c) = 1.274^{+0.030}_{-0.035}$ GeV and $\widehat{m}_b(\mu=\widehat{m}_b) = 4.199 \pm 0.024$ GeV, with a correlation of 33%.

The top quark "pole" mass (the quotation marks are a reminder that quarks do not form asymptotic states), $m_t = 173.24 \pm 0.81$ GeV, is an average based on the combination, $m_t = 173.20 \pm 0.51_{\,\rm stat.} \pm 0.71_{\,\rm syst.}$ GeV, of published and preliminary CDF and DØ results from the Tevatron [48], with the combination, $m_t = 173.29 \pm 0.23_{\,\rm stat.} \pm 0.92_{\,\rm syst.}$ GeV, obtained by the LHC Top Working Group [49]. Our average[$] differs slightly from the value, $m_t = 173.07 \pm 0.52_{\,\rm stat.} \pm 0.72_{\,\rm syst.}$ GeV, which appears in the top quark Listings in this *Review* and which is based exclusively on published Tevatron results. We are working, however, with $\overline{\rm MS}$ masses in all expressions to minimize theoretical uncertainties. Such a short distance mass definition (unlike the pole mass) is free from non-perturbative and renormalon [50] uncertainties. We therefore convert to the top quark $\overline{\rm MS}$ mass,

$$\widehat{m}_t(\mu=\widehat{m}_t) = m_t[1 - \frac{4}{3}\frac{\alpha_s}{\pi} + \mathcal{O}(\alpha_s^2)], \tag{10.9}$$

using the three-loop formula [51]. This introduces an additional uncertainty which we estimate to 0.5 GeV (the size of the three-loop term) and add in quadrature to the experimental pole mass error. This is convenient because we use the pole mass as an external constraint while fitting to the $\overline{\rm MS}$ mass. We are assuming that the kinematic mass extracted from the collider events corresponds within this uncertainty to the pole mass. In summary, we will use the fit constraint, $m_t = 173.24 \pm 0.81_{\,\rm exp.} \pm 0.5_{\,\rm QCD}$ GeV $= 173.24 \pm 0.95$ GeV.

$\sin^2\theta_W$ and M_W can be calculated from M_Z, $\widehat{\alpha}(M_Z)$, and G_F, when values for m_t and M_H are given, or conversely, M_H can be constrained by $\sin^2\theta_W$ and M_W. The value of $\sin^2\theta_W$ is extracted from neutral-current processes (see Sec. 10.3) and Z pole observables (see Sec. 10.4) and depends on the renormalization prescription. There are a number of popular schemes [52–58] leading to values which differ by small factors depending on m_t and M_H. The notation for these schemes is shown in Table 10.2.

Table 10.2: Notations used to indicate the various schemes discussed in the text. Each definition of $\sin^2\theta_W$ leads to values that differ by small factors depending on m_t and M_H. Numerical values are also given for illustration.

Scheme	Notation	Value
On-shell	s^2_W	0.22333
$\overline{\rm MS}$	$\widehat{s}^2_Z$	0.23126
$\overline{\rm MS}$ ND	$\widehat{s}^2_{\rm ND}$	0.23144
$\overline{\rm MS}$	$\widehat{s}^2_0$	0.23864
Effective angle	$\overline{s}^2_\ell$	0.23155

(*i*) The on-shell scheme [52] promotes the tree-level formula $\sin^2\theta_W = 1 - M^2_W/M^2_Z$ to a definition of the renormalized $\sin^2\theta_W$ to all orders in perturbation theory, *i.e.*, $\sin^2\theta_W \to s^2_W \equiv 1 - M^2_W/M^2_Z$:

$$M_W = \frac{A_0}{s_W(1-\Delta r)^{1/2}}\,, \qquad M_Z = \frac{M_W}{c_W}\,, \tag{10.10}$$

where $c_W \equiv \cos\theta_W$, $A_0 = (\pi\alpha/\sqrt{2}G_F)^{1/2} = 37.28039(1)$ GeV, and Δr includes the radiative corrections relating α, $\alpha(M_Z)$, G_F, M_W, and M_Z. One finds $\Delta r \sim \Delta r_0 - \rho_t/\tan^2\theta_W$, where $\Delta r_0 = 1 - \alpha/\widehat{\alpha}(M_Z) = 0.06637(11)$ is due to the running of α, and $\rho_t = 3G_F m_t^2/8\sqrt{2}\pi^2 = 0.00940\,(m_t/173.24\ {\rm GeV})^2$ represents the dominant (quadratic) m_t dependence. There are additional contributions to Δr from bosonic loops, including those which depend logarithmically on M_H and higher-order corrections[$$]. One has $\Delta r = 0.03639 \mp 0.00036 \pm 0.00011$, where the first uncertainty is from m_t and the second is from $\alpha(M_Z)$. Thus the value of s^2_W extracted from M_Z includes an uncertainty (∓ 0.00012) from the currently allowed range of m_t. This scheme is simple conceptually. However, the relatively large ($\sim 3\%$) correction from ρ_t causes large spurious contributions in higher orders.

s^2_W depends not only on the gauge couplings but also on the spontaneous-symmetry breaking, and it is awkward in the presence of any extension of the SM which perturbs the value of M_Z (or M_W). Other definitions are motivated by the tree-level coupling constant definition $\theta_W = \tan^{-1}(g'/g)$:

(*ii*) In particular, the modified minimal subtraction ($\overline{\rm MS}$) scheme introduces the quantity $\sin^2\widehat{\theta}_W(\mu) \equiv \widehat{g}'^2(\mu)/\big[\widehat{g}^{\,2}(\mu) + \widehat{g}'^2(\mu)\big]$, where the couplings $\widehat{g}$ and $\widehat{g}'$ are defined by modified minimal subtraction and the scale μ is conveniently chosen to be M_Z for many EW processes. The value of $\widehat{s}^2_Z = \sin^2\widehat{\theta}_W(M_Z)$ extracted from M_Z is less sensitive than s^2_W to m_t (by a factor of $\tan^2\theta_W$), and is less sensitive to most types of new physics. It is also very useful for comparing with the predictions of grand unification. There are actually several variant definitions of $\sin^2\widehat{\theta}_W(M_Z)$, differing according to whether or how finite $\alpha\ln(m_t/M_Z)$ terms are decoupled (subtracted from the couplings). One cannot entirely decouple the $\alpha\ln(m_t/M_Z)$ terms from all EW quantities because $m_t \gg m_b$ breaks SU(2) symmetry. The scheme that will be adopted here decouples the $\alpha\ln(m_t/M_Z)$ terms from the γ–Z mixing [18,53], essentially eliminating any $\ln(m_t/M_Z)$ dependence in the formulae for asymmetries at the Z pole when written in terms of $\widehat{s}^2_Z$. (A similar definition is used for $\widehat{\alpha}$.) The on-shell and $\overline{\rm MS}$ definitions are related by

$$\widehat{s}^2_Z = c\,(m_t, M_H)s^2_W = (1.0355 \pm 0.0004)s^2_W\,. \tag{10.11}$$

The quadratic m_t dependence is given by $c \sim 1 + \rho_t/\tan^2\theta_W$. The expressions for M_W and M_Z in the $\overline{\rm MS}$ scheme are

$$M_W = \frac{A_0}{\widehat{s}_Z(1-\Delta\widehat{r}_W)^{1/2}}\,, \qquad M_Z = \frac{M_W}{\widehat{\rho}^{\,1/2}\,\widehat{c}_Z}\,, \tag{10.12}$$

and one predicts $\Delta\widehat{r}_W = 0.06943 \pm 0.00011$. $\Delta\widehat{r}_W$ has no quadratic m_t dependence, because shifts in M_W are absorbed into the observed G_F, so that the error in $\Delta\widehat{r}_W$ is almost entirely due to $\Delta r_0 = 1 - \alpha/\widehat{\alpha}(M_Z)$. The quadratic m_t dependence has been shifted into $\widehat{\rho} \sim 1 + \rho_t$, where including bosonic loops, $\widehat{\rho} = 1.01031 \pm 0.00011$.

(*iii*) A variant $\overline{\rm MS}$ quantity $\widehat{s}^2_{\rm ND}$ (used in the 1992 edition of this *Review*) does not decouple the $\alpha\ln(m_t/M_Z)$ terms [54]. It is related to $\widehat{s}^2_Z$ by

$$\widehat{s}^2_Z = \widehat{s}^2_{\rm ND}/\Big(1 + \frac{\widehat{\alpha}}{\pi}d\Big), \tag{10.13a}$$

$$d = \frac{1}{3}\left(\frac{1}{\widehat{s}^2} - \frac{8}{3}\right)\left[(1+\frac{\alpha_s}{\pi})\,\ln\frac{m_t}{M_Z} - \frac{15\alpha_s}{8\pi}\right], \tag{10.13b}$$

Thus, $\widehat{s}^2_Z - \widehat{s}^2_{\rm ND} \approx -0.0002$.

nient to nullify any explicitly m_c dependent logarithms. Note also that our uncertainty for m_c (and to a lesser degree for m_b) is larger than in Refs. 46 and 47, for example. The reason is that we determine the continuum contribution for charm pair production using only resonance data and theoretical consistency across various sum rule moments, and then use any difference to the experimental continuum data as an additional uncertainty. We also include an uncertainty for the condensate terms which grows rapidly for higher moments in the sum rule analysis.

[$] At the time of writing this review, the efforts to establish a top quark averaging group involving both the Tevatron and the LHC were still in progress. Therefore we perform a simplified average ourselves, conservatively assuming that the entire Tevatron systematics is common to both colliders (ignoring correlations yields the same central value).

[$$] All explicit numbers quoted here and below include the two- and three-loop corrections described near the end of Sec. 10.2.

(*iv*) Some of the low-energy experiments discussed in the next section are sensitive to the weak mixing angle at almost vanishing momentum transfer (for a review, see Ref. 55). Thus, Table 10.2 also includes $\widehat{s}_0^2 \equiv \sin^2\widehat{\theta}_W(0)$.

(*v*) Yet another definition, the effective angle [56–58] $\overline{s}_f^2 = \sin\theta^f_{\rm eff}$ for the Z vector coupling to fermion f, is based on Z pole observables and described in Sec. 10.4.

Experiments are at such level of precision that complete one-loop, dominant two-loop, and partial three-loop radiative corrections must be applied. For neutral-current and Z pole processes, these corrections are conveniently divided into two classes:

1. QED diagrams involving the emission of real photons or the exchange of virtual photons in loops, but not including vacuum polarization diagrams. These graphs often yield finite and gauge-invariant contributions to observable processes. However, they are dependent on energies, experimental cuts, *etc.*, and must be calculated individually for each experiment.
2. EW corrections, including $\gamma\gamma$, γZ, ZZ, and WW vacuum polarization diagrams, as well as vertex corrections, box graphs, *etc.*, involving virtual W and Z bosons. The one-loop corrections are included for all processes, and many two-loop corrections are also important. In particular, two-loop corrections involving the top quark modify ρ_t in $\widehat{\rho}$, Δr, and elsewhere by

$$\rho_t \to \rho_t[1 + R(M_H, m_t)\rho_t/3]. \tag{10.14}$$

$R(M_H, m_t)$ can be described as an expansion in M_Z^2/m_t^2, for which the leading m_t^4/M_Z^4 [59] and next-to-leading m_t^2/M_Z^2 [60] terms are known. The complete two-loop calculation of Δr (without further approximation) has been performed in Refs. 61 and 62 for fermionic and purely bosonic diagrams, respectively. Similarly, the EW two-loop calculation for the relation between $\overline{s}_\ell^2$ and s_W^2 is complete [63,64].

Mixed QCD-EW contributions to gauge boson self-energies of order $\alpha\alpha_s m_t^2$ [65], $\alpha\alpha_s^2 m_t^2$ [66], and $\alpha\alpha_s^3 m_t^2$ [67] increase the predicted value of m_t by 6%. This is, however, almost entirely an artifact of using the pole mass definition for m_t. The equivalent corrections when using the $\overline{\rm MS}$ definition $\widehat{m}_t(\widehat{m}_t)$ increase m_t by less than 0.5%. The subleading $\alpha\alpha_s$ corrections [68] are also included. Further three-loop corrections of order $\alpha\alpha_s^2$ [69,70], $\alpha^3 m_t^6$, and $\alpha^2\alpha_s m_t^4$ [71], are rather small. The same is true for $\alpha^3 M_H^4$ [72] corrections unless M_H approaches 1 TeV.

The theoretical uncertainty from unknown higher-order corrections is estimated to amount to 4 MeV for the prediction of M_W [73] and 4.5×10^{-5} for $\overline{s}_\ell^2$ [74].

Throughout this *Review* we utilize EW radiative corrections from the program GAPP [21], which works entirely in the $\overline{\rm MS}$ scheme, and which is independent of the package ZFITTER [58]. Another resource is the recently developed modular fitting toolkit Gfitter [75].

10.3. Low energy electroweak observables

In the following we discuss EW precision observables obtained at low momentum transfers [6], *i.e.* $Q^2 \ll M_Z^2$. It is convenient to write the four-fermion interactions relevant to ν-hadron, ν-e, as well as parity violating e-hadron and e-e neutral-current processes in a form that is valid in an arbitrary gauge theory (assuming massless left-handed neutrinos). One has★

$$-\mathscr{L}^{\nu e} = \frac{G_F}{\sqrt{2}}\,\overline{\nu}\gamma_\mu(1-\gamma^5)\nu\;\overline{e}\,\gamma^\mu(g_{LV}^{\nu e} - g_{LA}^{\nu e}\,\gamma^5)e, \tag{10.15}$$

$$-\mathscr{L}^{\nu h} = \frac{G_F}{\sqrt{2}}\,\overline{\nu}\,\gamma_\mu(1-\gamma^5)\nu\sum_q[g_{LL}^{\nu q}\,\overline{q}\,\gamma^\mu(1-\gamma^5)q + g_{LR}^{\nu q}\,\overline{q}\,\gamma^\mu(1+\gamma^5)q], \tag{10.16}$$

$$-\mathscr{L}^{ee} = -\frac{G_F}{\sqrt{2}}\,g_{AV}^{ee}\,\overline{e}\,\gamma_\mu\gamma^5 e\,\overline{e}\,\gamma^\mu e, \tag{10.17}$$

$$-\mathscr{L}^{eh} = -\frac{G_F}{\sqrt{2}}\sum_q\left[g_{AV}^{eq}\,\overline{e}\,\gamma_\mu\gamma^5 e\,\overline{q}\,\gamma^\mu q + g_{VA}^{eq}\,\overline{e}\,\gamma_\mu e\,\overline{q}\;\gamma^\mu\gamma^5 q\right], \tag{10.18}$$

where one must include the charged-current contribution for ν_e-e and $\overline{\nu}_e$-e and the parity-conserving QED contribution for electron scattering.

Table 10.3: SM tree level expressions for the neutral-current parameters for ν-hadron, ν-e, and e^--scattering processes. To obtain the SM values in the last column, the tree level expressions have to be multiplied by the low-energy neutral-current ρ parameter, $\rho_{\rm NC} = 1.00066$, and further vertex and box corrections need to be added as detailed in Ref. 76. The dominant m_t dependence is again given by $\rho_{\rm NC} \sim 1 + \rho_t$.

Quantity	SM tree level	SM value
$g_{LV}^{\nu_\mu e}$	$-\frac{1}{2} + 2\,\widehat{s}_0^2$	-0.0396
$g_{LA}^{\nu_\mu e}$	$-\frac{1}{2}$	-0.5064
$g_{LL}^{\nu_\mu u}$	$\frac{1}{2} - \frac{2}{3}\,\widehat{s}_0^2$	0.3457
$g_{LL}^{\nu_\mu d}$	$-\frac{1}{2} + \frac{1}{3}\,\widehat{s}_0^2$	-0.4288
$g_{LR}^{\nu_\mu u}$	$-\frac{2}{3}\,\widehat{s}_0^2$	-0.1553
$g_{LR}^{\nu_\mu d}$	$\frac{1}{3}\,\widehat{s}_0^2$	0.0777
g_{AV}^{ee}	$\frac{1}{2} - 2\,\widehat{s}_0^2$	0.0225
g_{AV}^{eu}	$-\frac{1}{2} + \frac{4}{3}\,\widehat{s}_0^2$	-0.1887
g_{AV}^{ed}	$\frac{1}{2} - \frac{2}{3}\,\widehat{s}_0^2$	0.3419
g_{VA}^{eu}	$-\frac{1}{2} + 2\,\widehat{s}_0^2$	-0.0351
g_{VA}^{ed}	$\frac{1}{2} - 2\,\widehat{s}_0^2$	0.0248

The SM tree level expressions for the four-Fermi couplings are given in Table 10.3. Note that they differ from the respective products of the gauge couplings in Eq. (10.5) in the radiative corrections and in the presence of possible physics beyond the SM.

10.3.1. ***Neutrino scattering*** : For a general review on ν-scattering we refer to Ref. 77 (nonstandard neutrino scattering interactions are surveyed in Ref. 78).

The cross-section in the laboratory system for $\nu_\mu e \to \nu_\mu e$ or $\overline{\nu}_\mu e \to \overline{\nu}_\mu e$ elastic scattering [79] is (in this subsection we drop the redundant index L in the effective neutrino couplings)

$$\frac{d\sigma_{\nu,\bar\nu}}{dy} = \frac{G_F^2 m_e E_\nu}{2\pi}\left[(g_V^{\nu e}\pm g_A^{\nu e})^2 + (g_V^{\nu e}\mp g_A^{\nu e})^2(1-y)^2 - (g_V^{\nu e 2} - g_A^{\nu e 2})\frac{y\,m_e}{E_\nu}\right], \tag{10.19}$$

where the upper (lower) sign refers to $\nu_\mu(\overline{\nu}_\mu)$, and $y \equiv T_e/E_\nu$ (which runs from 0 to $(1 + m_e/2E_\nu)^{-1}$) is the ratio of the kinetic energy of the recoil electron to the incident ν or $\overline{\nu}$ energy. For $E_\nu \gg m_e$ this yields a total cross-section

$$\sigma = \frac{G_F^2 m_e E_\nu}{2\pi}\left[(g_V^{\nu e} \pm g_A^{\nu e})^2 + \frac{1}{3}(g_V^{\nu e} \mp g_A^{\nu e})^2\right]. \tag{10.20}$$

The most accurate measurements [79–84] of $\sin^2\theta_W$ from ν-lepton scattering (see Sec. 10.6) are from the ratio $R \equiv \sigma_{\nu_\mu e}/\sigma_{\bar\nu_\mu e}$, in which many of the systematic uncertainties cancel. Radiative corrections

★ We use here slightly different definitions (and to avoid confusion also a different notation) for the coefficients of these four-Fermi operators than we did in previous editions of this *Review*. The new couplings [76] are defined in the static limit, $Q^2 \to 0$, with specific radiative corrections included, while others (more experiment specific ones) are assumed to be removed by the experimentalist. They are convenient in that their determinations from very different types of processes can be straightforwardly combined.

(other than m_t effects) are small compared to the precision of present experiments and have negligible effect on the extracted $\sin^2\theta_W$. The most precise experiment (CHARM II) [82] determined not only $\sin^2\theta_W$ but $g_{V,A}^{\nu e}$ as well, which are shown in Fig. 10.1. The cross-sections for ν_e-e and $\overline{\nu}_e$-e may be obtained from Eq. (10.19) by replacing $g_{V,A}^{\nu e}$ by $g_{V,A}^{\nu e}+1$, where the 1 is due to the charged-current contribution.

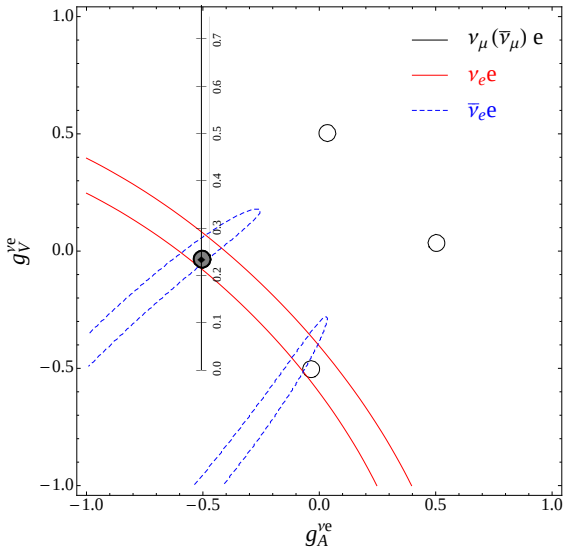

Figure 10.1: Allowed contours in $g_A^{\nu e}$ *vs.* $g_V^{\nu e}$ from neutrino-electron scattering and the SM prediction as a function of $\widehat{s}^2_Z$. (The SM best fit value $\widehat{s}^2_Z = 0.23126$ is also indicated.) The $\nu_e e$ [83] and $\bar{\nu}_e e$ [84] constraints are at 1 σ, while each of the four equivalent $\nu_\mu(\bar{\nu}_\mu)e$ [79–82] solutions ($g_{V,A} \to -g_{V,A}$ and $g_{V,A} \to g_{A,V}$) are at the 90% C.L. The global best fit region (shaded) almost exactly coincides with the corresponding $\nu_\mu(\bar{\nu}_\mu)e$ region. The solution near $g_A = 0, g_V = -0.5$ is eliminated by $e^+e^- \to \ell^+\ell^-$ data under the weak additional assumption that the neutral current is dominated by the exchange of a single Z boson.

A precise determination of the on-shell s^2_W, which depends only very weakly on m_t and M_H, is obtained from deep inelastic scattering (DIS) of neutrinos from (approximately) isoscalar targets [85]. The ratio $R_\nu \equiv \sigma^{NC}_{\nu N}/\sigma^{CC}_{\nu N}$ of neutral-to-charged-current cross-sections has been measured to 1% accuracy by CDHS [86] and CHARM [87] at CERN. CCFR [88] at Fermilab has obtained an even more precise result, so it is important to obtain theoretical expressions for R_ν and $R_{\bar{\nu}} \equiv \sigma^{NC}_{\bar{\nu}N}/\sigma^{CC}_{\bar{\nu}N}$ to comparable accuracy. Fortunately, many of the uncertainties from the strong interactions and neutrino spectra cancel in the ratio. A large theoretical uncertainty is associated with the c-threshold, which mainly affects σ^{CC}. Using the slow rescaling prescription [89] the central value of $\sin^2\theta_W$ from CCFR varies as $0.0111(m_c/\mathrm{GeV} - 1.31)$, where m_c is the effective mass which is numerically close to the $\overline{\rm MS}$ mass $\widehat{m}_c(\widehat{m}_c)$, but their exact relation is unknown at higher orders. For $m_c = 1.31 \pm 0.24$ GeV (determined from ν-induced dimuon production [90]) this contributes ± 0.003 to the total uncertainty $\Delta \sin^2\theta_W \sim \pm 0.004$. (The experimental uncertainty is also ± 0.003.) This uncertainty largely cancels, however, in the Paschos-Wolfenstein ratio [91],

$$R^- = \frac{\sigma^{NC}_{\nu N} - \sigma^{NC}_{\bar{\nu}N}}{\sigma^{CC}_{\nu N} - \sigma^{CC}_{\bar{\nu}N}} \,. \qquad (10.21)$$

It was measured by Fermilab's NuTeV collaboration [92] for the first time, and required a high-intensity and high-energy anti-neutrino beam.

A simple zero$^{\rm th}$-order approximation is

$$R_\nu = g_L^2 + g_R^2 r, \quad R_{\bar{\nu}} = g_L^2 + \frac{g_R^2}{r}, \quad R^- = g_L^2 - g_R^2, \quad (10.22)$$

where

$$g_L^2 \equiv (g_{LL}^{\nu_\mu u})^2 + (g_{LL}^{\nu_\mu d})^2 \approx \frac{1}{2} - \sin^2\theta_W + \frac{5}{9}\sin^4\theta_W, \quad (10.23a)$$

$$g_R^2 \equiv (g_{LR}^{\nu_\mu u})^2 + (g_{LR}^{\nu_\mu d})^2 \approx \frac{5}{9}\sin^4\theta_W, \qquad (10.23b)$$

and $r \equiv \sigma^{CC}_{\bar{\nu}N}/\sigma^{CC}_{\nu N}$ is the ratio of $\overline{\nu}$ to ν charged-current cross-sections, which can be measured directly. [In the simple parton model, ignoring hadron energy cuts, $r \approx (\frac{1}{3}+\epsilon)/(1+\frac{1}{3}\epsilon)$, where $\epsilon \sim 0.125$ is the ratio of the fraction of the nucleon's momentum carried by anti-quarks to that carried by quarks.] In practice, Eq. (10.22) must be corrected for quark mixing, quark sea effects, c-quark threshold effects, non-isoscalarity, W–Z propagator differences, the finite muon mass, QED and EW radiative corrections. Details of the neutrino spectra, experimental cuts, x and Q^2 dependence of structure functions, and longitudinal structure functions enter only at the level of these corrections and therefore lead to very small uncertainties. CCFR quotes $s^2_W = 0.2236 \pm 0.0041$ for $(m_t, M_H) = (175, 150)$ GeV with very little sensitivity to (m_t, M_H).

The NuTeV collaboration found $s^2_W = 0.2277 \pm 0.0016$ (for the same reference values), which was 3.0 σ higher than the SM prediction [92]. The deviation was in g_L^2 (initially 2.7 σ low) while g_R^2 was consistent with the SM. Since then a number of experimental and theoretical developments changed the interpretation of the measured cross section ratios, affecting the extracted $g^2_{L,R}$ (and thus s^2_W) including their uncertainties and correlation. In the following paragraph we give a semi-quantitative and preliminary discussion of these effects, but we stress that the precise impact of them needs to be evaluated carefully by the collaboration with a new and self-consistent set of PDFs, including new radiative corrections, while simultaneously allowing isospin breaking and asymmetric strange seas. This is an effort which is currently on its way and until it is completed we do not include the νDIS constraints in our default set of fits.

(i) In the original analysis NuTeV worked with a symmetric strange quark sea but subsequently measured [93] the difference between the strange and antistrange momentum distributions, $S^- \equiv \int_0^1 dx\, x[s(x) - \bar{s}(x)] = 0.00196 \pm 0.00143$, from dimuon events utilizing the first complete next-to-leading order QCD description [94] and parton distribution functions (PDFs) according to Ref. 95. The global PDF fits in Ref. 96 give somewhat smaller values, $S^- = 0.0013(9)$ [$S^- = 0.0010(13)$], where the semi-leptonic charmed-hadron branching ratio, $B_\mu = 8.8 \pm 0.5\%$, has [not] been used as an external constraint. The resulting S^- also depends on the PDF model used and on whether theoretical arguments (see Ref. 97 and references therein) are invoked favoring a zero crossing of $x[s(x) - \bar{s}(x)]$ at values much larger than seen by NuTeV and suggesting an effect of much smaller and perhaps negligible size. (ii) The measured branching ratio for K_{e3} decays enters crucially in the determination of the $\nu_e(\bar{\nu}_e)$ contamination of the $\nu_\mu(\bar{\nu}_\mu)$ beam. This branching ratio has moved from $4.82 \pm 0.06\%$ at the time of the original publication [92] to the current value of $5.07 \pm 0.04\%$, *i.e.* a change by more than $4\,\sigma$. This moves s^2_W about one standard deviation further away from the SM prediction while reducing the $\nu_e(\bar{\nu}_e)$ uncertainty. (iii) PDFs seem to violate isospin symmetry at levels much stronger than generally expected [98]. A minimum χ^2 set of PDFs [99] allowing charge symmetry violation for both valence quarks $[d_V^p(x) \neq u_V^n(x)]$ and sea quarks $[\bar{d}^p(x) \neq \bar{u}^n(x)]$ shows a reduction in the NuTeV discrepancy by about $1\,\sigma$. But isospin symmetry violating PDFs are currently not well constrained phenomenologically and within uncertainties the NuTeV anomaly could be accounted for in full or conversely made larger [99]. Still, the leading contribution from quark mass differences turns out to be largely model-independent [100] (at least in sign) and a shift, $\delta s^2_W = -0.0015 \pm 0.0003$ [97], has been estimated. (iv) QED splitting effects also violate isospin symmetry with an effect on s^2_W whose sign (reducing the discrepancy) is model-independent. The corresponding shift of $\delta s^2_W = -0.0011$ has been calculated in Ref. 101 but has a large uncertainty. (v) Nuclear shadowing effects [102] are likely to affect the interpretation of the NuTeV result at some level, but the NuTeV collaboration argues that their data are dominated by values of Q^2 at which nuclear shadowing is expected to be relatively

small. However, another nuclear effect, known as the isovector EMC effect [103], is much larger (because it affects all neutrons in the nucleus, not just the excess ones) and model-independently works to reduce the discrepancy. It is estimated to lead to a shift of $\delta s^2_W = -0.0019 \pm 0.0006$ [97]. It would be important to verify and quantify this kind of effect experimentally, *e.g.*, in polarized electron scattering. (vi) The extracted s^2_W may also shift at the level of the quoted uncertainty when analyzed using the most recent QED and EW radiative corrections [104,105], as well as QCD corrections to the structure functions [106]. However, these are scheme-dependent and in order to judge whether they are significant they need to be adapted to the experimental conditions and kinematics of NuTeV, and have to be obtained in terms of observable variables and for the differential cross-sections. In addition, there is the danger of double counting some of the QED splitting effects. (vii) New physics could also affect $g^2_{L,R}$ [107] but it is difficult to convincingly explain the entire effect that way.

10.3.2. *Parity violation* :

The SLAC polarized electron-deuteron DIS (eDIS) experiment [108] measured the right-left asymmetry,

$$A = \frac{\sigma_R - \sigma_L}{\sigma_R + \sigma_L} \,, \tag{10.24}$$

where $\sigma_{R,L}$ is the cross-section for the deep-inelastic scattering of a right- or left-handed electron: $e_{R,L}N \to e\mathrm{X}$. In the quark parton model,

$$\frac{A}{Q^2} = a_1 + a_2 \frac{1-(1-y)^2}{1+(1-y)^2} \,, \tag{10.25}$$

where $Q^2 > 0$ is the momentum transfer and y is the fractional energy transfer from the electron to the hadrons. For the deuteron or other isoscalar targets, one has, neglecting the s-quark and anti-quarks,

$$a_1 = \frac{3G_F}{5\sqrt{2}\pi\alpha}\left(g^{eu}_{AV} - \frac{1}{2}g^{ed}_{AV}\right) \approx \frac{3G_F}{5\sqrt{2}\pi\alpha}\left(-\frac{3}{4} + \frac{5}{3}\widehat{s}^2_0\right) \tag{10.26a}$$

$$a_2 = \frac{3G_F}{5\sqrt{2}\pi\alpha}\left(g^{eu}_{VA} - \frac{1}{2}g^{ed}_{VA}\right) \approx \frac{9G_F}{5\sqrt{2}\pi\alpha}\left(\widehat{s}^2_0 - \frac{1}{4}\right). \tag{10.26b}$$

The Jefferson Lab Hall A Collaboration [109] improved on the SLAC result by determining A at $Q^2 = 1.085$ GeV and 1.901 GeV, and determined the weak mixing angle to 2% precision. In another polarized-electron scattering experiment on deuterons, but in the quasi-elastic kinematic regime, the SAMPLE experiment [110] at MIT-Bates extracted the combination $g^{eu}_{VA} - g^{ed}_{VA}$ at Q^2 values of 0.1 GeV^2 and 0.038 GeV^2. What was actually determined were nucleon form factors from which the quoted results were obtained by the removal of a multi-quark radiative correction [111]. Other linear combinations of the effective couplings have been determined in polarized-lepton scattering at CERN in μ-C DIS, at Mainz in e-Be (quasi-elastic), and at Bates in e-C (elastic). See the review articles in Refs. 112 and 113 for more details. Recent polarized electron asymmetry experiments, *i.e.*, SAMPLE, the PVA4 experiment at Mainz, and the HAPPEX and G0 experiments at Jefferson Lab, have focussed on the strange quark content of the nucleon. These are reviewed in Refs. 114 and 115.

The parity violating asymmetry, A_{PV}, in fixed target polarized Møller scattering, $e^-e^- \to e^-e^-$, is defined as in Eq. (10.24) and reads [116],

$$\frac{A_{PV}}{Q^2} = -2\, g^{ee}_{AV} \frac{G_F}{\sqrt{2}\pi\alpha} \frac{1-y}{1+y^4+(1-y)^4} \,, \tag{10.27}$$

where y is again the energy transfer. It has been measured at low $Q^2 = 0.026$ GeV^2 in the SLAC E158 experiment [117], with the result $A_{PV} = (-1.31 \pm 0.14_{\,\mathrm{stat.}} \pm 0.10_{\,\mathrm{syst.}}) \times 10^{-7}$. Expressed in terms of the weak mixing angle in the $\overline{\mathrm{MS}}$ scheme, this yields $\widehat{s}^2(Q^2) = 0.2403 \pm 0.0013$, and established the scale dependence of the weak mixing angle (see $Q_W(e)$ in Fig. 10.2) at the level of 6.4 σ. One can also extract the model-independent effective coupling, $g^{ee}_{AV} = 0.0190 \pm 0.0027$ [76] (the implications are discussed in Ref. 119).

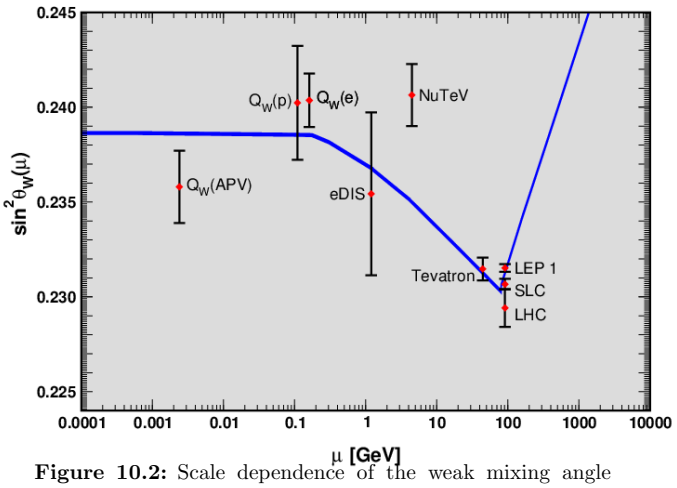

Figure 10.2: Scale dependence of the weak mixing angle defined in the $\overline{\mathrm{MS}}$ scheme [118] (for the scale dependence of the weak mixing angle defined in a mass-dependent renormalization scheme, see Ref. 119). The minimum of the curve corresponds to $\mu = M_W$, below which we switch to an effective theory with the $W^\pm$ bosons integrated out, and where the β-function for the weak mixing angle changes sign. At the location of the W boson mass and each fermion mass there are also discontinuities arising from scheme dependent matching terms which are necessary to ensure that the various effective field theories within a given loop order describe the same physics. However, in the $\overline{\mathrm{MS}}$ scheme these are very small numerically and barely visible in the figure provided one decouples quarks at $\mu = \widehat{m}_q(\widehat{m}_q)$. The width of the curve reflects the theory uncertainty from strong interaction effects which at low energies is at the level of $\pm 7 \times 10^{-5}$ [118]. Following the estimate [121] of the typical momentum transfer for parity violation experiments in Cs, the location of the APV data point is given by $\mu = 2.4$ MeV. For NuTeV we display the updated value from Ref. 120 and chose $\mu = \sqrt{20}$ GeV which is about half-way between the averages of $\sqrt{Q^2}$ for ν and $\overline{\nu}$ interactions at NuTeV. The Tevatron and LHC measurements are strongly dominated by invariant masses of the final state dilepton pair of $\mathcal{O}(M_Z)$ and can thus be considered as additional Z pole data points. For clarity we displayed the Tevatron point horizontally to the left.

In a similar experiment and at about the same $Q^2 = 0.025$ GeV^2, Qweak at Jefferson Lab [122] will be able to measure the weak charge of the proton (which is proportional to $2g^{eu}_{AV} + g^{ed}_{AV}$) and $\sin^2\theta_W$ in polarized ep scattering with relative precisions of 4% and 0.3%, respectively. The result based on the collaborations commissioning run [123] and about 4% of the data corresponds to the constraint $2g^{eu}_{AV} + g^{ed}_{AV} = 0.064 \pm 0.012$.

There are precise experiments measuring atomic parity violation (APV) [124] in cesium [125,126] (at the 0.4% level [125]), thallium [127], lead [128], and bismuth [129]. The EW physics is contained in the nuclear weak charges $Q^{Z,N}_W$, where Z and N are the numbers of protons and neutrons in the nucleus. In terms of the nucleon vector couplings,

$$g^{ep}_{AV} \equiv 2g^{eu}_{AV} + g^{ed}_{AV} \approx -\frac{1}{2} + 2\widehat{s}^2_0, \tag{10.28}$$

$$g^{en}_{AV} \equiv g^{eu}_{AV} + 2g^{ed}_{AV} \approx \frac{1}{2}, \tag{10.29}$$

one has,

$$Q^{Z,N}_W \equiv -2\left[Z(g^{ep}_{AV} + 0.00005) + N(g^{en}_{AV} + 0.00006)\right]\left(1 - \frac{\alpha}{2\pi}\right), \tag{10.30}$$

where the numerically small adjustments are discussed in Ref. 76 and include the result of the γZ-box correction from Ref. 130. *E.g.*, $Q_W(^{133}\mathrm{Cs})$ is extracted by measuring experimentally the ratio of the parity violating amplitude, E_{PNC}, to the Stark vector transition

polarizability, β, and by calculating theoretically $E_{\rm PNC}$ in terms of Q_W. One can then write,

$$Q_W = N \left(\frac{\mathrm{Im}\, E_{\rm PNC}}{\beta}\right)_{\rm exp.} \left(\frac{|e|\, a_B}{\mathrm{Im}\, E_{\rm PNC}} \frac{Q_W}{N}\right)_{\rm th.} \left(\frac{\beta}{a_B^3}\right)_{\rm exp.+th.} \left(\frac{a_B^2}{|e|}\right),$$

where a_B is the Bohr radius. The uncertainties associated with atomic wave functions are quite small for cesium [131]. The semi-empirical value of β used in early analyses added another source of theoretical uncertainty [132]. However, the ratio of the off-diagonal hyperfine amplitude to the polarizability was subsequently measured directly by the Boulder group [133]. Combined with the precisely known hyperfine amplitude [134] one finds $\beta = (26.991 \pm 0.046)\, a_B^3$, in excellent agreement with the earlier results, reducing the overall theory uncertainty (while slightly increasing the experimental error). Utilizing the state-of-the-art many-body calculation in Ref. 135 yields $\mathrm{Im}\, E_{\rm PNC} = (0.8906 \pm 0.0026) \times 10^{-11} |e|\, a_B\, Q_W/N$, while the two measurements [125,126] combine to give $\mathrm{Im}\, E_{\rm PNC}/\beta = -1.5924 \pm 0.0055$ mV/cm, and we would obtain $Q_W(^{133}_{78}\mathrm{Cs}) = -73.20 \pm 0.35$, or equivalently $55 g_{AV}^{ep} + 78 g_{AV}^{en} = 36.64 \pm 0.18$ which is in excellent agreement with the SM prediction of 36.66. However, a very recent atomic structure calculation [136] found significant corrections to two non-dominating terms, changing the result to $\mathrm{Im}\, E_{\rm PNC} = (0.8977 \pm 0.0040) \times 10^{-11} |e|\, a_B\, Q_W/N$, and yielding the constraint, $55 g_{AV}^{ep} + 78 g_{AV}^{en} = 36.35 \pm 0.21$ [$Q_W(^{133}_{78}\mathrm{Cs}) = -72.62 \pm 0.43$], *i.e.* a 1.5 σ SM deviation. Thus, the various theoretical efforts in [135–137] together with an update of the SM calculation [138] reduced an earlier 2.3 σ discrepancy from the SM (see the year 2000 edition of this *Review*), but there still appears to remain a small deviation. The theoretical uncertainties are 3% for thallium [139] but larger for the other atoms. The Boulder experiment in cesium also observed the parity-violating weak corrections to the nuclear electromagnetic vertex (the anapole moment [140]) .

In the future it could be possible to further reduce the theoretical wave function uncertainties by taking the ratios of parity violation in different isotopes [124,141]. There would still be some residual uncertainties from differences in the neutron charge radii, however [142]. Experiments in hydrogen and deuterium are another possibility for reducing the atomic theory uncertainties [143], while measurements of single trapped radium ions are promising [144] because of the much larger parity violating effect.

10.4. Physics of the massive electroweak bosons

If the CM energy $\sqrt{s}$ is large compared to the fermion mass m_f, the unpolarized Born cross-section for $e^+e^- \to f\bar{f}$ can be written as

$$\frac{d\sigma}{d\cos\theta} = \frac{\pi\alpha^2(s)}{2s}\left[F_1(1+\cos^2\theta) + 2F_2\cos\theta\right] + B, \qquad (10.31a)$$

where

$$F_1 = Q_e^2 Q_f^2 - 2\chi\, Q_e Q_f \overline{g}_V^e \overline{g}_V^f \cos\delta_R + \chi^2 (\overline{g}_V^{e2} + \overline{g}_A^{e2})(\overline{g}_V^{f2} + \overline{g}_A^{f2}) \qquad (10.31b)$$

$$F_2 = -2\chi\, Q_e Q_f \overline{g}_A^e \overline{g}_A^f \cos\delta_R + 4\chi^2 \overline{g}_V^e \overline{g}_A^e \overline{g}_V^f \overline{g}_A^f \qquad (10.31c)$$

$$\tan\delta_R = \frac{M_Z\Gamma_Z}{M_Z^2 - s}\ ,\ \chi = \frac{G_F}{2\sqrt{2}\pi\alpha(s)} \frac{sM_Z^2}{\left[(M_Z^2 - s)^2 + M_Z^2\Gamma_Z^2\right]^{1/2}}\ , \qquad (10.32)$$

and B accounts for box graphs involving virtual Z and W bosons, and $\overline{g}_{V,A}^f$ are defined in Eq. (10.33) below. The differential cross-section receives important corrections from QED effects in the initial and final state, and interference between the two, see *e.g.* Ref. 145. For $q\bar{q}$ production, there are additional final-state QCD corrections, which are relatively large. Note also that the equations above are written in the CM frame of the incident e^+e^- system, which may be boosted due to the initial-state QED radiation.

Some of the leading virtual EW corrections are captured by the running QED coupling $\alpha(s)$ and the Fermi constant G_F. The remaining corrections to the $Zf\bar{f}$ interaction are absorbed by replacing the tree-level couplings Eq. (10.5) with the s-dependent *effective couplings* [146]

$$\overline{g}_V^f = \sqrt{\rho_f}\,(t_{3L}^{(f)} - 2Q_f\kappa_f \sin^2\theta_W), \qquad \overline{g}_A^f = \sqrt{\rho_f}\, t_{3L}^{(f)}. \qquad (10.33)$$

In these equations, the effective couplings are to be taken at the scale $\sqrt{s}$, but for notational simplicity we do not show this explicitly. At tree-level $\rho_f = \kappa_f = 1$, but inclusion of EW radiative corrections leads to non-zero $\rho_f - 1$ and $\kappa_f - 1$, which depend on the fermion f and on the renormalization scheme. In the on-shell scheme, the quadratic m_t dependence is given by $\rho_f \sim 1 + \rho_t$, $\kappa_f \sim 1 + \rho_t/\tan^2\theta_W$, while in $\overline{\rm MS}$, $\widehat{\rho}_f \sim \widehat{\kappa}_f \sim 1$, for $f \neq b$ ($\widehat{\rho}_b \sim 1 - \frac{4}{3}\rho_t$, $\widehat{\kappa}_b \sim 1 + \frac{2}{3}\rho_t$). In the $\overline{\rm MS}$ scheme the normalization is changed according to $G_F M_Z^2/2\sqrt{2}\pi \to \widehat{\alpha}/4\widehat{s}_Z^2\widehat{c}_Z^2$ in Eq. (10.32).

For the high-precision Z-pole observables discussed below, additional bosonic and fermionic loops, vertex corrections, and higher order contributions, *etc.*, must be included [60,63,64,147,148]. For example, in the $\overline{\rm MS}$ scheme one has $\widehat{\rho}_\ell = 0.9982$, $\widehat{\kappa}_\ell = 1.0013$, $\widehat{\rho}_b = 0.9870$, and $\widehat{\kappa}_b = 1.0068$.

To connect to measured quantities, it is convenient to define an effective angle $\overline{s}_f^2 \equiv \sin^2\overline{\theta}_{Wf} \equiv \widehat{\kappa}_f \widehat{s}_Z^2 = \kappa_f s_W^2$, in terms of which $\overline{g}_V^f$ and $\overline{g}_A^f$ are given by $\sqrt{\rho_f}$ times their tree-level formulae. One finds that the $\widehat{\kappa}_f$ ($f \neq b$) are almost independent of (m_t, M_H), and thus one can write

$$\overline{s}_\ell^2 = \widehat{s}_Z^2 + 0.00029, \qquad (10.34)$$

while the κ's for the other schemes are m_t dependent.

10.4.1. e^+e^- *scattering below the Z pole* :

Experiments at PEP, PETRA and TRISTAN have measured the unpolarized forward-backward asymmetry, A_{FB}, and the total cross-section relative to pure QED, R, for $e^+e^- \to \ell^+\ell^-$, $\ell = \mu$ or τ at CM energies $\sqrt{s} < M_Z$. They are defined as

$$A_{FB} \equiv \frac{\sigma_F - \sigma_B}{\sigma_F + \sigma_B}\ , \qquad R = \frac{\sigma}{\mathcal{R}_{\rm ini} 4\pi\alpha^2/3s}\ , \qquad (10.35)$$

where σ_F (σ_B) is the cross-section for ℓ^- to travel forward (backward) with respect to the e^- direction. Neglecting box graph contribution, they are given by

$$A_{FB} = \frac{3}{4}\frac{F_2}{F_1}\ , \qquad R = F_1\ . \qquad (10.36)$$

For the available data, it is sufficient to approximate the EW corrections through the leading running $\alpha(s)$ and quadratic m_t contributions [149,150] as described above. Reviews and formulae for $e^+e^- \to$ hadrons may be found in Ref. 151.

10.4.2. *Z pole physics* :

High-precision measurements of various Z pole ($\sqrt{s} \approx M_Z$) observables have been performed at LEP 1 and SLC [11,152–157], as summarized in Table 10.5. These include the Z mass and total width, Γ_Z, and partial widths $\Gamma(f\overline{f})$ for $Z \to f\overline{f}$, where $f = e$, μ, τ, light hadrons, b, or c. It is convenient to use the variables M_Z, Γ_Z, $R_\ell \equiv \Gamma(\mathrm{had})/\Gamma(\ell^+\ell^-)$ ($\ell = e, \mu, \tau$), $\sigma_{\rm had} \equiv 12\pi\,\Gamma(e^+e^-)\,\Gamma(\mathrm{had})/M_Z^2\,\Gamma_Z^2$[††], $R_b \equiv \Gamma(b\overline{b})/\Gamma(\mathrm{had})$, and $R_c \equiv \Gamma(c\overline{c})/\Gamma(\mathrm{had})$, most of which are weakly correlated experimentally. ($\Gamma(\mathrm{had})$ is the partial width into hadrons.) The three values for R_ℓ are consistent with lepton universality (although R_τ is somewhat low compared to R_e and R_μ), but we use the general analysis in which the three observables are treated as independent. Similar remarks apply to $A_{FB}^{0,\ell}$ defined through Eq. (10.39) with $P_e = 0$. ($A_{FB}^{0,\tau}$ is somewhat high). $\mathcal{O}(\alpha^3)$ QED corrections introduce a large anti-correlation (-30%) between Γ_Z and $\sigma_{\rm had}$. The anti-correlation between R_b and R_c is -18% [11]. The R_ℓ are insensitive to m_t except for the $Z \to b\overline{b}$ vertex and final state corrections and the implicit dependence through $\sin^2\theta_W$. Thus, they

[††] Note that in general $\sigma_{\rm had}$ receives additional EW corrections that are not captured in the partial widths [158], but they only become relevant in a full two-loop calculation.

are especially useful for constraining α_s. The invisible decay width [11], $\Gamma(\text{inv}) = \Gamma_Z - 3\,\Gamma(\ell^+\ell^-) - \Gamma(\text{had}) = 499.0 \pm 1.5$ MeV, can be used to determine the number of neutrino flavors, $N_\nu = \Gamma(\text{inv})/\Gamma^{\text{theory}}(\nu\overline{\nu})$, much lighter than $M_Z/2$. In practice, we determine N_ν by allowing it as an additional fit parameter and obtain,

$$N_\nu = 2.990 \pm 0.007\ . \tag{10.37}$$

Additional constraints follow from measurements of various Z-pole asymmetries. These include the forward-backward asymmetry A_{FB} and the polarization or left-right asymmetry,

$$A_{LR} \equiv \frac{\sigma_L - \sigma_R}{\sigma_L + \sigma_R}\ , \tag{10.38}$$

where $\sigma_L(\sigma_R)$ is the cross-section for a left-(right-)handed incident electron. A_{LR} was measured precisely by the SLD collaboration at the SLC [154], and has the advantages of being very sensitive to $\sin^2\theta_W$ and that systematic uncertainties largely cancel. After removing initial state QED corrections and contributions from photon exchange, γ–Z interference and EW boxes, see Eq. (10.31), one can use the effective tree-level expressions

$$A_{LR} = A_e P_e\ , \qquad A_{FB} = \frac{3}{4} A_f\, \frac{A_e + P_e}{1 + P_e A_e}\ , \tag{10.39}$$

where

$$A_f \equiv \frac{2\overline{g}_V^f\, \overline{g}_A^f}{\overline{g}_V^{f\,2} + \overline{g}_A^{f\,2}} = \frac{1 - 4|Q_f|\bar{s}_f^2}{1 - 4|Q_f|\bar{s}_f^2 + 8(|Q_f|\bar{s}_f^2)^2}\ . \tag{10.40}$$

P_e is the initial e^- polarization, so that the second equality in Eq. (10.41) is reproduced for $P_e = 1$, and the Z pole forward-backward asymmetries at LEP 1 ($P_e = 0$) are given by $A_{FB}^{(0,f)} = \frac{3}{4} A_e A_f$ where $f = e,\ \mu,\ \tau,\ b,\ c,\ s$ [11], and q, and where $A_{FB}^{(0,q)}$ refers to the hadronic charge asymmetry. Corrections for t-channel exchange and s/t-channel interference cause $A_{FB}^{(0,e)}$ to be strongly anti-correlated with R_e (-37%). The correlation between $A_{FB}^{(0,b)}$ and $A_{FB}^{(0,c)}$ amounts to 15%.

In addition, SLD extracted the final-state couplings A_b, A_c [11], A_s [155], A_τ, and A_μ [156], from left-right forward-backward asymmetries, using

$$A_{LR}^{FB}(f) = \frac{\sigma_{LF}^f - \sigma_{LB}^f - \sigma_{RF}^f + \sigma_{RB}^f}{\sigma_{LF}^f + \sigma_{LB}^f + \sigma_{RF}^f + \sigma_{RB}^f} = \frac{3}{4} A_f\ , \tag{10.41}$$

where, for example, σ_{LF}^f is the cross-section for a left-handed incident electron to produce a fermion f traveling in the forward hemisphere. Similarly, A_τ and A_e were measured at LEP 1 [11] through the negative total τ polarization, $\mathcal{P}_\tau$, as a function of the scattering angle θ, which can be writte as

$$\mathcal{P}_\tau = -\frac{A_\tau(1 + \cos^2\theta) + 2A_e\cos\theta}{(1 + \cos^2\theta) + 2A_\tau A_e\cos\theta} \tag{10.42}$$

The average polarization, $\langle\mathcal{P}_\tau\rangle$, obtained by integrating over $\cos\theta$ in the numerator and denominator of Eq. (10.42), yields $\langle\mathcal{P}_\tau\rangle = -A_\tau$, while A_e can be extracted from the angular distribution of $\mathcal{P}_\tau$.

The initial state coupling, A_e, was also determined through the left-right charge asymmetry [157] and in polarized Bhabba scattering [156] at SLC. Because $\overline{g}_V^\ell$ is very small, not only $A_{LR}^0 = A_e$, $A_{FB}^{(0,\ell)}$, and $\mathcal{P}_\tau$, but also $A_{FB}^{(0,b)}$, $A_{FB}^{(0,c)}$, $A_{FB}^{(0,s)}$, and the hadronic asymmetries are mainly sensitive to $\overline{s}_\ell^2$.

As mentioned in Sec. 10.2, radiative corrections to $\bar{s}_\ell^2$ have been computed with full two-loop and partial higher-order corrections. Moreover, fermionic two-loop EW corrections to $\bar{s}_q^2$ ($q = b,\ c,\ s$) have been obtained [74,148], but the purely bosonic contributions of this order are still missing. For the partial widths, $\Gamma(f\overline{f})$, and the hadronic peak cross-section, σ_{had}, currently only approximate EW two-loop corrections based on a large-m_t expansion [59,60,159,160] are known. Non-factorizable $\mathcal{O}(\alpha\alpha_s)$ corrections for the $Z \to q\bar{q}$ vertex are also available [147]. They add coherently, resulting in a sizable effect and shift $\alpha_s(M_Z)$ when extracted from Z lineshape observables by $\approx +0.0007$. Very recently, complete fermionic two-loop EW contributions to R_b [161] and to Γ_Z [162] have been calculated, but their numerical impact is relatively small, and they have not been included in the fits in this *Review*.

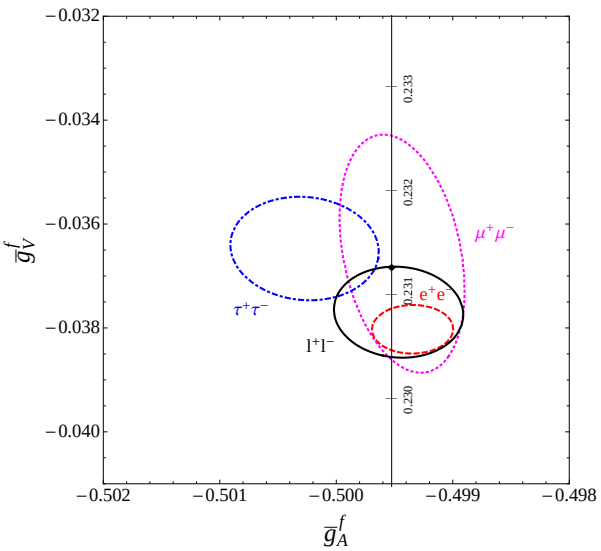

Figure 10.3: 1 σ (39.35% C.L.) contours for the Z-pole observables $\bar{g}_A^f$ and $\bar{g}_V^f$, $f = e, \mu, \tau$ obtained at LEP and SLC [11], compared to the SM expectation as a function of $\widehat{s}_Z^{\,2}$. (The SM best fit value $\widehat{s}_Z^{\,2} = 0.23126$ is also indicated.) Also shown is the 90% CL allowed region in $\bar{g}_{A,V}^\ell$ obtained assuming lepton universality.

As an example of the precision of the Z-pole observables, the values of $\bar{g}_A^f$ and $\bar{g}_V^f$, $f = e, \mu, \tau, \ell$, extracted from the LEP and SLC lineshape and asymmetry data, are shown in Fig. 10.3, which should be compared with Fig. 10.1. (The two sets of parameters coincide in the SM at tree-level.)

As for hadron colliders, the forward-backward asymmetry, A_{FB}, for e^+e^- and $\mu^+\mu^-$ final states (with invariant masses restricted to or dominated by values around M_Z) in $p\bar{p}$ collisions has been measured by the DØ [163] (only e^+e^-) and CDF [164,165] collaborations, and values for $\overline{s}_\ell^2$ were extracted. Assuming lepton universality and that the smallest systematic uncertainty (± 0.0003 from the e^+e^- analysis at CDF [164]) is common to both final states and experiments, these measurements combine to $\overline{s}_\ell^2 = 0.23176 \pm 0.00060$. By varying the invariant mass and the scattering angle (and assuming the electron couplings), information on the effective Z couplings to light quarks, $\overline{g}_{V,A}^{u,d}$, could also be obtained [163,166], but with large uncertainties and mutual correlations and not independently of $\overline{s}_\ell^2$ above. Similar analyses have also been reported by the H1 and ZEUS collaborations at HERA [167] and by the LEP collaborations [11]. This kind of measurement is harder in the pp environment due to the difficulty to assign the initial quark and antiquark in the underlying Drell-Yan process to the protons. Nevertheless, measurements of A_{FB} have been reported by the CMS [168] (only $\mu^+\mu^-$) and ATLAS [169] collaborations. Again assuming lepton universality and that the ± 0.0007 PDF uncertainty from ATLAS [169] is common to both experiments, these measurements combine to give the value, $\overline{s}_\ell^2 = 0.2297 \pm 0.0010$, which is driven by the more precise ATLAS results.

10.4.3. *LEP 2* :

LEP 2 [170,171] ran at several energies above the Z pole up to ~ 209 GeV. Measurements were made of a number of observables, including the cross-sections for $e^+e^- \to f\bar{f}$ for $f = q, \mu, \tau$; the differential cross-sections for $f = e, \mu, \tau$; R_q for $q = b, c$; $A_{FB}(f)$ for $f = \mu, \tau, b, c$; W branching ratios; and $\gamma\gamma$, WW, $WW\gamma$, ZZ, single W, and single Z cross-sections. They are in good agreement with the SM predictions, with the exceptions of R_b (2.1 σ low), $A_{FB}(b)$ (1.6 σ low), and the $W \to \tau\nu_\tau$ branching fraction (2.6 σ high).

The Z boson properties are extracted assuming the SM expressions for the γ–Z interference terms. These have also been tested experimentally by performing more general fits [170,172] to the

LEP 1 and LEP 2 data. Assuming family universality this approach introduces three additional parameters relative to the standard fit [11], describing the γ–Z interference contribution to the total hadronic and leptonic cross-sections, $j^{\rm tot}_{\rm had}$ and $j^{\rm tot}_{\ell}$, and to the leptonic forward-backward asymmetry, $j^{\rm fb}_{\ell}$. *E.g.*,

$$j^{\rm tot}_{\rm had} \sim g^{\ell}_V g^{\rm had}_V = 0.277 \pm 0.065, \tag{10.43}$$

which is in agreement with the SM expectation [11] of 0.21 ± 0.01. These are valuable tests of the SM; but it should be cautioned that new physics is not expected to be described by this set of parameters, since (i) they do not account for extra interactions beyond the standard weak neutral current, and (ii) the photonic amplitude remains fixed to its SM value.

Strong constraints on anomalous triple and quartic gauge couplings have been obtained at LEP 2 and the Tevatron as described in the Gauge & Higgs Bosons Particle Listings.

10.4.4. *W and Z decays* :

The partial decay widths for gauge bosons to decay into massless fermions $f_1\overline{f}_2$ (the numerical values include the small EW radiative corrections and final state mass effects) are given by

$$\Gamma(W^+ \to e^+\nu_e) = \frac{G_F M_W^3}{6\sqrt{2}\pi} \approx 226.32 \pm 0.05 \text{ MeV} , \tag{10.44a}$$

$$\Gamma(W^+ \to u_i\overline{d}_j) = \frac{\mathcal{R}^q_V G_F M_W^3}{6\sqrt{2}\pi} |V_{ij}|^2 \approx 705.5 \pm 0.4 \text{ MeV } |V_{ij}|^2, \tag{10.44b}$$

$$\Gamma(Z \to f\bar{f}) = \frac{G_F M_Z^3}{6\sqrt{2}\pi} \left[\mathcal{R}^f_V \bar{g}^{f2}_V + \mathcal{R}^f_A \bar{g}^{f2}_A\right] \approx \begin{cases} 167.22 \pm 0.02 \text{ MeV } (\nu\overline{\nu}), \\ 84.00 \pm 0.01 \text{ MeV } (e^+e^-), \\ 300.15 \pm 0.20 \text{ MeV } (u\overline{u}), \\ 382.96 \pm 0.14 \text{ MeV } (d\overline{d}), \\ 375.87 \mp 0.17 \text{ MeV } (b\overline{b}). \end{cases} \tag{10.44c}$$

Final-state QED and QCD corrections to the vector and axial-vector form factors are given by

$$\mathcal{R}^f_{V,A} = N_C[1 + \frac{3}{4}(Q_f^2 \frac{\alpha(s)}{\pi} + \frac{N_C^2 - 1}{2N_C}\frac{\alpha_s(s)}{\pi}) + \cdots], \tag{10.45}$$

where $N_C = 3$ (1) is the color factor for quarks (leptons) and the dots indicate finite fermion mass effects proportional to m_f^2/s which are different for $\mathcal{R}^f_V$ and $\mathcal{R}^f_A$, as well as higher-order QCD corrections, which are known to $\mathcal{O}(\alpha_s^4)$ [173–175]. These include singlet contributions starting from two-loop order which are large, strongly top quark mass dependent, family universal, and flavor non-universal [176]. Also the $\mathcal{O}(\alpha^2)$ self-energy corrections from Ref. 177 are taken into account.

For the W decay into quarks, Eq. (10.44*b*), only the universal massless part (non-singlet and $m_q = 0$) of the final-state QCD radiator function in $\mathcal{R}_V$ from Eq. (10.45) is used, and the QED corrections are modified. Expressing the widths in terms of $G_F M^3_{W,Z}$ incorporates the largest radiative corrections from the running QED coupling [52,178]. EW corrections to the Z widths are then taken into account through the effective couplings $\overline{g}^{i2}_{V,A}$. Hence, in the on-shell scheme the Z widths are proportional to $\rho_i \sim 1 + \rho_t$. There is additional (negative) quadratic m_t dependence in the $Z \to b\overline{b}$ vertex corrections [179] which causes $\Gamma(b\overline{b})$ to decrease with m_t. The dominant effect is to multiply $\Gamma(b\overline{b})$ by the vertex correction $1 + \delta\rho_{b\bar{b}}$, where $\delta\rho_{b\bar{b}} \sim 10^{-2}(-\frac{1}{2}m_t^2/M_Z^2 + \frac{1}{5})$. In practice, the corrections are included in ρ_b and κ_b, as discussed in Sec. 10.4.

For three fermion families the total widths are predicted to be

$$\Gamma_Z \approx 2.4955 \pm 0.0009 \text{ GeV} , \qquad \Gamma_W \approx 2.0897 \pm 0.0008 \text{ GeV} . \tag{10.46}$$

The uncertainties in these predictions are almost entirely induced from the fit error in $\alpha_s(M_Z) = 0.1193 \pm 0.0016$. These predictions are to be compared with the experimental results, $\Gamma_Z = 2.4952 \pm 0.0023$ GeV [11] and $\Gamma_W = 2.085 \pm 0.042$ GeV (see the Gauge & Higgs Boson Particle Listings for more details).

10.4.5. *H decays* :

The ATLAS and CMS collaborations at LHC observed a Higgs boson [180] with properties appearing well consistent with the SM Higgs (see the note on "The Higgs Boson H^0" in the Gauge & Higgs Boson Particle Listings). The kinematically reconstructed masses from ATLAS and CMS of the Higgs boson [181,182] average to

$$M_H = 125.6 \pm 0.4 \text{ GeV}. \tag{10.47}$$

In analogy to the W and Z decays discussed in the previous subsection, we can include some of the Higgs decay properties into the global analysis of Sec. 10.6. However, the total Higgs decay width, which in the SM amounts to

$$\Gamma_H = 4.20 \pm 0.08 \text{ MeV}, \tag{10.48}$$

is too small to be resolved at the LHC. Furthermore, it is difficult (and has not been attempted yet by the experimental collaborations) to form branching ratios when the Higgs production mechanisms differ strongly for different final states. On the other hand, Higgs decay rates into WW^* and ZZ^* (with at least one gauge boson off-shell), as well as $\gamma\gamma$ have been deduced predominantly from gluon-gluon fusion (ggF), so that theoretical production uncertainties mostly cancel in ratios of branching fractions. Thus, we can employ the results on the signal strength parameters, μ_{XX}, quantifying the yields of Higgs production and decay into XX, normalized to the SM expectation, to define

$$\rho_{XY} \equiv \ln \frac{\mu_{XX}}{\mu_{YY}} . \tag{10.49}$$

These quantities are constructed to have a SM expectation of zero (for $M_H = 125.5$ GeV for ATLAS and $M_H = 125.7$ GeV for CMS), and their physical range is over all real numbers, which allows one to straightforwardly use Gaussian error propagation (in view of the fairly large errors). Moreover, possible effects of new physics on Higgs production rates would also cancel and one may focus on the decay side of the processes. Presently, one often combines Higgs production in association with $t\bar{t}$-pairs (ttH) into one category with ggF since they are subject to similar theory uncertainties. Higgs production through vector boson fusion (VBF) and Higgs-strahlung (VH) are important for decays into $f\bar{f}$, but at the moment there is clear evidence for VH production only for the $b\bar{b}$ final state [182,183], while the measurement of $\tau\tau$ receives contributions from both ggF and VBF [184]. As a result, one cannot form a meaningful ratio where the dependence on the production mechanism drops out.

For each of the two LHC experiments, we consider the ratios with the smallest mutual correlations. Assuming that theory errors cancel in the ρ_{XY} while experimental systematics does not, we find for ATLAS [185],

$$\rho_{\gamma W} = 0.45 \pm 0.31 , \qquad \rho_{\gamma Z} = 0.08 \pm 0.28 ,$$

with a correlation of 25% (induced by the 15% uncertainty in the common $\mu_{\gamma\gamma}$), while for CMS [182] (using the same relative theory errors as ATLAS) we obtain,

$$\rho_{\gamma W} = 0.12 \pm 0.43 , \qquad \rho_{ZW} = 0.30 \pm 0.39 ,$$

with a correlation of 43% (due to the 27% uncertainty in μ_{WW}). We evaluate the decay rates with the package HDECAY [186].

10.5. Precision flavor physics

In addition to cross-sections, asymmetries, parity violation, W and Z decays, there is a large number of experiments and observables testing the flavor structure of the SM. These are addressed elsewhere in this *Review*, and are generally not included in this Section. However, we identify three precision observables with sensitivity to similar types of new physics as the other processes discussed here. The branching fraction of the flavor changing transition $b \to s\gamma$ is of comparatively low precision, but since it is a loop-level process (in the SM) its sensitivity to new physics (and SM parameters, such as heavy quark masses) is enhanced. A discussion can be found in the 2010

edition of this *Review*. The τ-lepton lifetime and leptonic branching ratios are primarily sensitive to α_s and not affected significantly by many types of new physics. However, having an independent and reliable low energy measurement of α_s in a global analysis allows the comparison with the Z lineshape determination of α_s which shifts easily in the presence of new physics contributions. By far the most precise observable discussed here is the anomalous magnetic moment of the muon (the electron magnetic moment is measured to even greater precision and can be used to determine α, but its new physics sensitivity is suppressed by an additional factor of m_e^2/m_μ^2, unless there is a new light degree of freedom such as a dark Z [187] boson). Its combined experimental and theoretical uncertainty is comparable to typical new physics contributions.

The extraction of α_s from the τ lifetime [188] is standing out from other determinations because of a variety of independent reasons: (i) the τ-scale is low, so that upon extrapolation to the Z scale (where it can be compared to the theoretically clean Z lineshape determinations) the α_s error shrinks by about an order of magnitude; (ii) yet, this scale is high enough that perturbation theory and the operator product expansion (OPE) can be applied; (iii) these observables are fully inclusive and thus free of fragmentation and hadronization effects that would have to be modeled or measured; (iv) duality violation (DV) effects are most problematic near the branch cut but there they are suppressed by a double zero at $s = m_\tau^2$; (v) there are data [34] to constrain non-perturbative effects both within ($\delta_{D=6,8}$) and breaking (δ_{DV}) the OPE; (vi) a complete four-loop order QCD calculation is available [175]; (vii) large effects associated with the QCD β-function can be re-summed [189] in what has become known as contour improved perturbation theory (CIPT). However, while there is no doubt that CIPT shows faster convergence in the lower (calculable) orders, doubts have been cast on the method by the observation that at least in a specific model [190], which includes the exactly known coefficients and theoretical constraints on the large-order behavior, ordinary fixed order perturbation theory (FOPT) may nevertheless give a better approximation to the full result. We therefore use the expressions [45,174,175,191],

$$\tau_\tau = \hbar \frac{1-\mathcal{B}_\tau^s}{\Gamma_\tau^e + \Gamma_\tau^\mu + \Gamma_\tau^{ud}} = 291.13 \pm 0.43 \text{ fs}, \qquad (10.50)$$

$$\Gamma_\tau^{ud} = \frac{G_F^2 m_\tau^5 |V_{ud}|^2}{64\pi^3} S(m_\tau, M_Z) \left(1 + \frac{3}{5}\frac{m_\tau^2 - m_\mu^2}{M_W^2}\right) \times$$
$$\left[1 + \frac{\alpha_s(m_\tau)}{\pi} + 5.202\,\frac{\alpha_s^2}{\pi^2} + 26.37\,\frac{\alpha_s^3}{\pi^3} + \right.$$
$$\left. 127.1\,\frac{\alpha_s^4}{\pi^4} + \frac{\widehat{\alpha}}{\pi}\left(\frac{85}{24} - \frac{\pi^2}{2}\right) + \delta_q\right], \qquad (10.51)$$

and Γ_τ^e and Γ_τ^μ can be taken from Eq. (10.6) with obvious replacements. The relative fraction of decays with $\Delta S = -1$, $\mathcal{B}_\tau^s = 0.0286 \pm 0.0007$, is based on experimental data since the value for the strange quark mass, $\widehat{m}_s(m_\tau)$, is not well known and the QCD expansion proportional to $\widehat{m}_s^2$ converges poorly and cannot be trusted. $S(m_\tau, M_Z) = 1.01907 \pm 0.0003$ is a logarithmically enhanced EW correction factor with higher orders re-summed [192]. δ_q contains the dimension six and eight terms in the OPE, as well as DV effects, $\delta_{D=6,8} + \delta_{DV} = -0.004 \pm 0.012$ [193]. Depending on how $\delta_{D=6}$, $\delta_{D=8}$, and δ_{DV} are extracted, there are strong correlations not only between them, but also with the gluon condensate ($D = 4$) and possibly $D > 8$ terms. These latter are suppressed in Eq. (10.51) by additional factors of α_s, but not so for more general weight functions. A simultaneous fit to all non-perturbative terms [193] (as is necessary if one wants to avoid *ad hoc* assumptions) indicates that the α_s errors may have been underestimated in the past. Higher statistics τ decay data [36] and spectral functions from e^+e^- annihilation (providing a larger fit window and thus more discriminatory power and smaller correlations) are likely to reduce the δ_q error in the future. Also included in δ_q are quark mass effects and the $D = 4$ condensate contributions. An uncertainty of similar size arises from the truncation of the FOPT series and is conservatively taken as the α_s^4 term (this is re-calculated in each call of the fits, leading to an α_s-dependent and thus asymmetric error) until a better understanding of the numerical differences between FOPT and CIPT has been gained. Our perturbative error covers almost the entire range from using CIPT to assuming that the nearly geometric series in Eq. (10.51) continues to higher orders. The experimental uncertainty in Eq. (10.50), is from the combination of the two leptonic branching ratios with the direct τ_τ. Included are also various smaller uncertainties (± 0.5 fs) from other sources which are dominated by the evolution from the Z scale. In total we obtain a $\sim 2\%$ determination of $\alpha_s(M_Z) = 0.1193^{+0.0022}_{-0.0020}$, which corresponds to $\alpha_s(m_\tau) = 0.327^{+0.019}_{-0.016}$, and updates the result of Refs. 45 and 194. For more details, see Refs. 193 and 195 where the τ spectral functions are used as additional input.

The world average of the muon anomalous magnetic moment[‡],

$$a_\mu^{\text{exp}} = \frac{g_\mu - 2}{2} = (1165920.80 \pm 0.63) \times 10^{-9}, \qquad (10.52)$$

is dominated by the final result of the E821 collaboration at BNL [196]. The QED contribution has been calculated to five loops [197] (fully analytic to three loops [198,199]). The estimated SM EW contribution [200–202], $a_\mu^{\text{EW}} = (1.52 \pm 0.03) \times 10^{-9}$, which includes leading two-loop [201] and three-loop [202] corrections, is at the level of twice the current uncertainty.

The limiting factor in the interpretation of the result are the uncertainties from the two- and three-loop hadronic contribution [203]. *E.g.,* Ref. 20 obtained the value $a_\mu^{\text{had}} = (69.23 \pm 0.42) \times 10^{-9}$ which combines CMD-2 [38] and SND [39] $e^+e^- \to$ hadrons cross-section data with radiative return results from BaBar [41] and KLOE [42]. This value suggests a 3.6 σ discrepancy between Eq. (10.52) and the SM prediction. An alternative analysis [20] using τ decay data and isospin symmetry (CVC) yields $a_\mu^{\text{had}} = (70.15 \pm 0.47) \times 10^{-9}$. This result implies a smaller conflict (2.4 σ) with Eq. (10.52). Thus, there is also a discrepancy between the spectral functions obtained from the two methods. For example, the channel that is relevant for the determination of a_μ^{had} from τ data, $\tau^- \to \nu_\tau \pi^- \pi^0$, has been measured to have a branching ratio of 25.51 ± 0.09 (global average), while if one uses the e^+e^- data and CVC to predict the branching ratio [20] we obtain an average of $\mathcal{B}_{\text{CVC}} = 24.93 \pm 0.13 \pm 0.22\,_{\text{CVC}}$, which is 2.3 σ lower. It is important to understand the origin of this difference, but two observations point to the conclusion that at least some of it is experimental: (i) There is also a direct discrepancy of 1.9 σ between $\mathcal{B}_{\text{CVC}}$ derived from BaBar (which is not inconsistent with τ decays) and KLOE. (ii) Isospin violating corrections have been studied in detail in Ref. 204 and found to be largely under control. The largest effect is due to higher-order EW corrections [205] but introduces a negligible uncertainty [192]. Nevertheless, a_μ^{had} is often evaluated excluding the τ decay data arguing [206] that CVC breaking effects (*e.g.*, through a relatively large mass difference between the $\rho^\pm$ and ρ^0 vector mesons) may be larger than expected. (This may also be relevant [206] in the context of the NuTeV result discussed above.) Experimentally [36], this mass difference is indeed larger than expected, but then one would also expect a significant width difference which is contrary to observation [36] [#]. Fortunately, due to the suppression at large s (from where the conflicts originate) these problems are less pronounced as far as a_μ^{had} is concerned. In the

[‡] In what follows, we summarize the most important aspects of $g_\mu - 2$, and give some details on the evaluation in our fits. For more details see the dedicated contribution on "The Muon Anomalous Magnetic Moment" in this *Review*. There are some small numerical differences (at the level of 0.1 standard deviations), which are well understood and mostly arise because internal consistency of the fits requires the calculation of all observables from analytical expressions and common inputs and fit parameters, so that an independent evaluation is necessary for this Section. Note, that in the spirit of a global analysis based on all available information we have chosen here to average in the τ decay data, as well.

[#] In the model of Ref. 207 an additional isospin correction due to γ–ρ mixing leads to a $\rho^\pm$–ρ^0 mass splitting that is large enough to reconcile the discrepancy between τ and e^+e^- data, but there is some debate about the magnitude of this effect [208].

following we view all differences in spectral functions as (systematic) fluctuations and average the results.

An additional uncertainty is induced by the hadronic three-loop light-by-light scattering contribution. Several recent independent model calculations yield compatible results: $a_\mu^{\rm LBLS} = (+1.36 \pm 0.25) \times 10^{-9}$ [209], $a_\mu^{\rm LBLS} = +1.37^{+0.15}_{-0.27} \times 10^{-9}$ [210], $a_\mu^{\rm LBLS} = (+1.16 \pm 0.40) \times 10^{-9}$ [211], and $a_\mu^{\rm LBLS} = (+1.05 \pm 0.26) \times 10^{-9}$ [212]. The sign of this effect is opposite [213] to the one quoted in the 2002 edition of this *Review*, and its magnitude is larger than previous evaluations [213,214]. There is also an upper bound $a_\mu^{\rm LBLS} < 1.59 \times 10^{-9}$ [210] but this requires an *ad hoc* assumption, too. Very recently, first results from lattice simulations have been obtained, finding agreement with the model calculations, although with large errors [215]. For the fits, we take the result from Ref. 212, shifted by 2×10^{-11} to account for the more accurate charm quark treatment of Ref. 210, and with increased error to cover all recent evaluations, resulting in $a_\mu^{\rm LBLS} = (+1.07 \pm 0.32) \times 10^{-9}$.

Other hadronic effects at three-loop order contribute [216] $a_\mu^{\rm had}(\alpha^3) = (-1.00 \pm 0.06) \times 10^{-9}$. Correlations with the two-loop hadronic contribution and with $\Delta\alpha(M_Z)$ (see Sec. 10.2) were considered in Ref. 199 which also contains analytic results for the perturbative QCD contribution.

Altogether, the SM prediction is

$$a_\mu^{\rm theory} = (1165918.41 \pm 0.48) \times 10^{-9} \,, \qquad (10.53)$$

where the error is from the hadronic uncertainties excluding parametric ones such as from α_s and the heavy quark masses. Using a correlation of about 84% from the data input to the vacuum polarization integrals [20], we estimate the correlation of the total (experimental plus theoretical) uncertainty in a_μ with $\Delta\alpha(M_Z)$ as 24%. The overall 3.0 σ discrepancy between the experimental and theoretical a_μ values could be due to fluctuations (the E821 result is statistics dominated) or underestimates of the theoretical uncertainties. On the other hand, the deviation could also arise from physics beyond the SM, such as supersymmetric models with large $\tan\beta$ and moderately light superparticle masses [217], or a dark Z boson [187].

10.6. Global fit results

In this section we present the results of global fits to the experimental data discussed in Sec. 10.3–Sec. 10.5. For earlier analyses see Refs. [11,113,218]

The values for m_t [48,49], M_W [170,219], Γ_W [170,220], M_H [181,182] and the ratios of Higgs branching fractions discussed in Sec. 10.4.5, ν-lepton scattering [79–84], the weak charges of the electron [117], the proton [122], cesium [125,126] and thallium [127], the weak mixing angle extracted from eDIS [109], the muon anomalous magnetic moment [196], and the τ lifetime are listed in Table 10.4. Likewise, the principal Z pole observables can be found in Table 10.5 where the LEP 1 averages of the ALEPH, DELPHI, L3, and OPAL results include common systematic errors and correlations [11]. The heavy flavor results of LEP 1 and SLD are based on common inputs and correlated, as well [11].

Note that the values of $\Gamma(\ell^+\ell^-)$, Γ(had), and Γ(inv) are not independent of Γ_Z, the R_ℓ, and $\sigma_{\rm had}$ and that the SM errors in those latter are largely dominated by the uncertainty in α_s. Also shown in both Tables are the SM predictions for the values of M_Z, M_H, $\alpha_s(M_Z)$, $\Delta\alpha^{(3)}_{\rm had}$ and the heavy quark masses shown in Table 10.6. The predictions result from a global least-square (χ^2) fit to all data using the minimization package MINUIT [221] and the EW library GAPP [21]. In most cases, we treat all input errors (the uncertainties of the values) as Gaussian. The reason is not that we assume that theoretical and systematic errors are intrinsically bell-shaped (which they are not) but because in most cases the input errors are either dominated by the statistical components or they are combinations of many different (including statistical) error sources, which should yield approximately Gaussian *combined* errors by the large number theorem. An exception is the theory dominated error on the τ lifetime, which we recalculate in each χ^2-function call since it depends itself on α_s. Sizes and shapes of the output errors (the uncertainties of the predictions and the SM fit parameters) are fully determined by the fit, and 1 σ errors are defined to correspond to $\Delta\chi^2 = \chi^2 - \chi^2_{\rm min} = 1$, and do not necessarily correspond to the 68.3% probability range or the 39.3% probability contour (for 2 parameters).

Table 10.4: Principal non-Z pole observables, compared with the SM best fit predictions. The first M_W and Γ_W values are from the Tevatron [219,220] and the second ones from LEP 2 [170]. The value of m_t differs from the one in the Particle Listings since it includes recent preliminary results. The world averages for $g^{\nu e}_{V,A}$ are dominated by the CHARM II [82] results, $g_V^{\nu e} = -0.035 \pm 0.017$ and $g_A^{\nu e} = -0.503 \pm 0.017$. The errors are the total (experimental plus theoretical) uncertainties. The τ_τ value is the τ lifetime world average computed by combining the direct measurements with values derived from the leptonic branching ratios [45]; in this case, the theory uncertainty is included in the SM prediction. In all other SM predictions, the uncertainty is from M_Z, M_H, m_t, m_b, m_c, $\widehat{\alpha}(M_Z)$, and α_s, and their correlations have been accounted for. The column denoted Pull gives the standard deviations.

Quantity	Value	Standard Model	Pull
m_t [GeV]	173.24 ± 0.95	173.87 ± 0.87	-0.7
M_W [GeV]	80.387 ± 0.016	80.363 ± 0.006	1.5
	80.376 ± 0.033		0.4
Γ_W [GeV]	2.046 ± 0.049	2.090 ± 0.001	-0.9
	2.196 ± 0.083		1.3
M_H [GeV]	125.6 ± 0.4	125.5 ± 0.4	0.1
$\rho_{\gamma W}$	0.45 ± 0.31	0.01 ± 0.03	1.4
	0.12 ± 0.43	0.00 ± 0.03	0.3
$\rho_{\gamma Z}$	0.08 ± 0.28	0.01 ± 0.04	0.2
ρ_{ZW}	0.30 ± 0.39	0.00 ± 0.01	0.8
$g_V^{\nu e}$	-0.040 ± 0.015	-0.0397 ± 0.0001	0.0
$g_A^{\nu e}$	-0.507 ± 0.014	-0.5064	0.0
$Q_W(e)$	-0.0403 ± 0.0053	-0.0473 ± 0.0003	1.3
$Q_W(p)$	0.064 ± 0.012	0.0708 ± 0.0003	-0.6
Q_W(Cs)	-72.62 ± 0.43	-73.25 ± 0.01	1.5
Q_W(Tl)	-116.4 ± 3.6	-116.90 ± 0.02	0.1
$\widehat{s}^2_Z$(eDIS)	0.2299 ± 0.0043	0.23126 ± 0.00005	-0.3
τ_τ [fs]	291.13 ± 0.43	291.19 ± 2.41	0.0
$\frac{1}{2}(g_\mu - 2 - \frac{\alpha}{\pi})$	$(4511.07 \pm 0.79) \times 10^{-9}$	$(4508.68 \pm 0.08) \times 10^{-9}$	3.0

The agreement is generally very good. Despite the few discrepancies discussed in the following, the fit describes the data well, with a χ^2/d.o.f. = 48.3/44. The probability of a larger χ^2 is 30%. Only the final result for $g_\mu - 2$ from BNL is currently showing a large (3.0 σ) deviation. In addition, $A_{FB}^{(0,b)}$ from LEP 1 and A^0_{LR} (SLD) from hadronic final states differ by more than 2 σ. g_L^2 from NuTeV is nominally in conflict with the SM, as well, but the precise status is under investigation (see Sec. 10.3).

A_b can be extracted from $A_{FB}^{(0,b)}$ when $A_e = 0.1501 \pm 0.0016$ is taken from a fit to leptonic asymmetries (using lepton universality). The result, $A_b = 0.881 \pm 0.017$, is 3.2 σ below the SM prediction[§] and also 1.6 σ below $A_b = 0.923 \pm 0.020$ obtained from $A_{LR}^{FB}(b)$ at SLD. Thus, it appears that at least some of the problem in A_b is due to a statistical fluctuation or other experimental effect in one of the asymmetries. Note, however, that the uncertainty in $A_{FB}^{(0,b)}$ is strongly statistics dominated. The combined value, $A_b = 0.899 \pm 0.013$ deviates by 2.8 σ. It would be difficult to account for this 4.0% deviation by new physics that enters only at the level of radiative corrections

[§] Alternatively, one can use $A_\ell = 0.1481 \pm 0.0027$, which is from LEP 1 alone and in excellent agreement with the SM, and obtain $A_b = 0.893 \pm 0.022$ which is 1.9 σ low. This illustrates that some of the discrepancy is related to the one in A_{LR}.

Table 10.5: Principal Z pole observables and their SM predictions (*cf.* Table 10.4). The first $\bar{s}^2_\ell$ is the effective weak mixing angle extracted from the hadronic charge asymmetry, the second is the combined value from the Tevatron [163,164,165], and the third from the LHC [168,169]. The values of A_e are (i) from A_{LR} for hadronic final states [154]; (ii) from A_{LR} for leptonic final states and from polarized Bhabba scattering [156]; and (iii) from the angular distribution of the τ polarization at LEP 1. The A_τ values are from SLD and the total τ polarization, respectively.

Quantity	Value	Standard Model	Pull
M_Z [GeV]	91.1876 ± 0.0021	91.1880 ± 0.0020	-0.2
Γ_Z [GeV]	2.4952 ± 0.0023	2.4955 ± 0.0009	-0.1
Γ(had) [GeV]	1.7444 ± 0.0020	1.7420 ± 0.0008	—
Γ(inv) [MeV]	499.0 ± 1.5	501.66 ± 0.05	—
$\Gamma(\ell^+\ell^-)$ [MeV]	83.984 ± 0.086	83.995 ± 0.010	—
$\sigma_{\rm had}$[nb]	41.541 ± 0.037	41.479 ± 0.008	1.7
R_e	20.804 ± 0.050	20.740 ± 0.010	1.3
R_μ	20.785 ± 0.033	20.740 ± 0.010	1.4
R_τ	20.764 ± 0.045	20.785 ± 0.010	-0.5
R_b	0.21629 ± 0.00066	0.21576 ± 0.00003	0.8
R_c	0.1721 ± 0.0030	0.17226 ± 0.00003	-0.1
$A_{FB}^{(0,e)}$	0.0145 ± 0.0025	0.01616 ± 0.00008	-0.7
$A_{FB}^{(0,\mu)}$	0.0169 ± 0.0013		0.6
$A_{FB}^{(0,\tau)}$	0.0188 ± 0.0017		1.6
$A_{FB}^{(0,b)}$	0.0992 ± 0.0016	0.1029 ± 0.0003	-2.3
$A_{FB}^{(0,c)}$	0.0707 ± 0.0035	0.0735 ± 0.0002	-0.8
$A_{FB}^{(0,s)}$	0.0976 ± 0.0114	0.1030 ± 0.0003	-0.5
$\bar{s}^2_\ell$	0.2324 ± 0.0012	0.23155 ± 0.00005	0.7
	0.23176 ± 0.00060		0.3
	0.2297 ± 0.0010		-1.9
A_e	0.15138 ± 0.00216	0.1468 ± 0.0004	2.1
	0.1544 ± 0.0060		1.3
	0.1498 ± 0.0049		0.6
A_μ	0.142 ± 0.015		-0.3
A_τ	0.136 ± 0.015		-0.7
	0.1439 ± 0.0043		-0.7
A_b	0.923 ± 0.020	0.9347	-0.6
A_c	0.670 ± 0.027	0.6676 ± 0.0002	0.1
A_s	0.895 ± 0.091	0.9356	-0.4

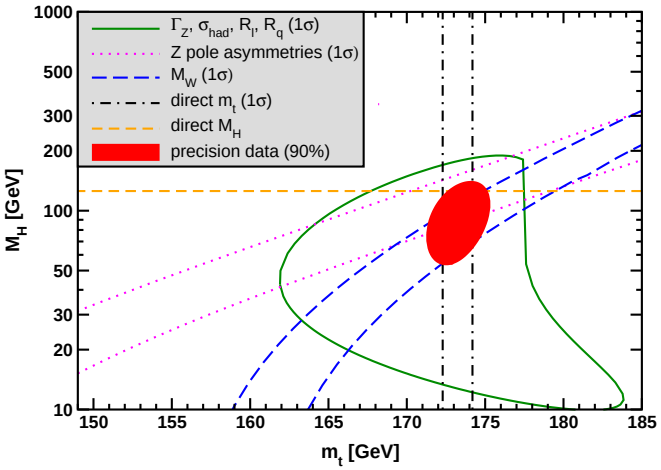

Figure 10.4: Fit result and one-standard-deviation (39.35% for the closed contours and 68% for the others) uncertainties in M_H as a function of m_t for various inputs, and the 90% CL region ($\Delta\chi^2 = 4.605$) allowed by all data. $\alpha_s(M_Z) = 0.1185$ is assumed except for the fits including the Z lineshape. The width of the horizontal dashed (yellow) band is not visible on the scale of the plot.

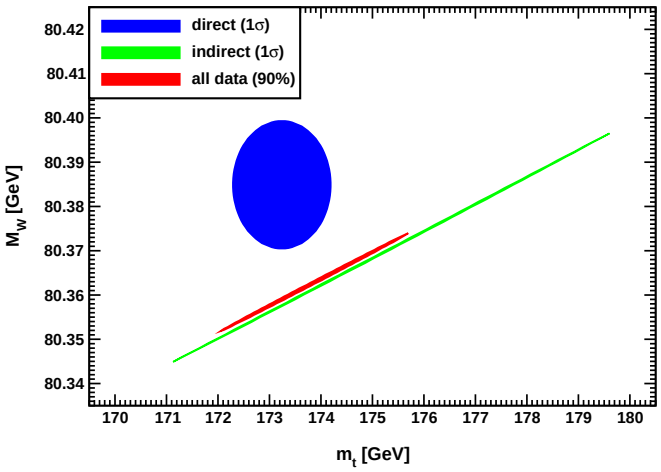

Figure 10.5: One-standard-deviation (39.35%) region in M_W as a function of m_t for the direct and indirect data, and the 90% CL region ($\Delta\chi^2 = 4.605$) allowed by all data.

since about a 20% correction to $\widehat{\kappa}_b$ would be necessary to account for the central value of A_b [222]. If this deviation is due to new physics, it is most likely of tree-level type affecting preferentially the third generation. Examples include the decay of a scalar neutrino resonance [223], mixing of the b quark with heavy exotics [224], and a heavy Z' with family non-universal couplings [225,226]. It is difficult, however, to simultaneously account for R_b, which has been measured on the Z peak and off-peak [227] at LEP 1. An average of R_b measurements at LEP 2 at energies between 133 and 207 GeV is 2.1 σ below the SM prediction, while $A_{FB}^{(b)}$ (LEP 2) is 1.6 σ low [171].

The left-right asymmetry, $A^0_{LR} = 0.15138 \pm 0.00216$ [154], based on all hadronic data from 1992–1998 differs 2.1 σ from the SM expectation of 0.1468 ± 0.0004. The combined value of $A_\ell = 0.1513 \pm 0.0021$ from SLD (using lepton-family universality and including correlations) is also 2.1 σ above the SM prediction; but there is experimental agreement between this SLD value and the LEP 1 value, $A_\ell = 0.1481 \pm 0.0027$, obtained from a fit to $A_{FB}^{(0,\ell)}$, $A_e(\mathcal{P}_\tau)$, and $A_\tau(\mathcal{P}_\tau)$, again assuming universality.

The observables in Table 10.4 and Table 10.5, as well as some other less precise observables, are used in the global fits described below. In all fits, the errors include full statistical, systematic, and theoretical uncertainties. The correlations on the LEP 1 lineshape and τ polarization, the LEP/SLD heavy flavor observables, the SLD lepton asymmetries, and the ν-e scattering observables, are included. The theoretical correlations between $\Delta\alpha^{(5)}_{\rm had}$ and $g_\mu - 2$, and between the charm and bottom quark masses, are also accounted for.

The data allow a simultaneous determination of M_Z, M_H, m_t, and the strong coupling $\alpha_s(M_Z)$. ($\widehat{m}_c$, $\widehat{m}_b$, and $\Delta\alpha^{(3)}_{\rm had}$ are also allowed to float in the fits, subject to the theoretical constraints [19,45] described in Sec. 10.2. These are correlated with α_s.) α_s is determined mainly from R_ℓ, Γ_Z, $\sigma_{\rm had}$, and τ_τ. The global fit to all data, including the hadron collider average $m_t = 173.24 \pm 0.95$ GeV, yields the result in Table 10.6 (the $\overline{\rm MS}$ top quark mass given there corresponds to $m_t = 173.87 \pm 0.87$ GeV). The weak mixing angle, see Table 10.2, is determined to

$$\widehat{s}^2_Z = 0.23126 \pm 0.00005, \qquad s^2_W = 0.22333 \pm 0.00011,$$

while the corresponding effective angle is $\bar{s}^2_\ell = 0.23155 \pm 0.00005$.

One can also perform a fit without the direct mass constraint, $M_H = 125.6 \pm 0.4$ GeV, in Eq. (10.47). In this case we obtain a 2% indirect mass determination,

$$M_H = 123.7 \pm 2.3 \text{ GeV}\,, \qquad (10.54)$$

Table 10.6: Principal SM fit result including mutual correlations (all masses in GeV). Note that $\widehat{m}_c(\widehat{m}_c)$ induces a significant uncertainty in the running of α beyond $\Delta\alpha^{(3)}_{\rm had}(1.8\ {\rm GeV})$ resulting in a relatively large correlation with M_H. Since this effect is proportional to the quark's electric charge squared it is much smaller for $\widehat{m}_b(\widehat{m}_b)$.

M_Z	91.1880 ± 0.0020	1.00	−0.08	0.01	−0.01	0.02	0.04	0.01
$\widehat{m}_t(\widehat{m}_t)$	164.09 ± 0.83	−0.08	1.00	0.00	−0.06	−0.16	0.08	0.06
$\widehat{m}_b(\widehat{m}_b)$	4.199 ± 0.024	0.01	0.00	1.00	0.26	−0.02	0.05	0.02
$\widehat{m}_c(\widehat{m}_c)$	$1.274^{+0.030}_{-0.035}$	−0.01	−0.06	0.26	1.00	0.15	0.08	0.01
$\alpha_s(M_Z)$	0.1193 ± 0.0016	0.02	−0.16	−0.02	0.15	1.00	−0.05	−0.03
$\Delta\alpha^{(3)}_{\rm had}(1.8\ {\rm GeV})$	0.00559 ± 0.00008	0.04	0.08	0.05	0.08	−0.05	1.00	0.05
M_H	125.5 ± 0.4	0.01	0.06	0.02	0.01	−0.03	0.05	1.00

Table 10.7: Values of $\widehat{s}^2_Z$, s^2_W, α_s, m_t and M_H [both in GeV] for various data sets. The M_H constraint refers collectively to the kinematical and decay information from Sec. 10.4.5. In the fit to the LHC (Tevatron) data the α_s constraint is from the $t\bar{t}$ production [228] (inclusive jet [229]) cross section.

Data	$\widehat{s}^2_Z$	s^2_W	$\alpha_s(M_Z)$	m_t	M_H
All data	0.23126(5)	0.22333(11)	0.1193(16)	173.9 ± 0.9	125.5 ± 0.4
All data except M_H	0.23112(10)	0.22304(22)	0.1195(17)	173.3 ± 0.9	$89^{+\ 22}_{-\ 18}$
All data except M_Z	0.23119(7)	0.22330(11)	0.1192(16)	173.4 ± 0.9	125.6 ± 0.4
All data except M_W	0.23129(5)	0.22341(12)	0.1196(17)	173.3 ± 0.9	125.6 ± 0.4
All data except m_t	0.23118(7)	0.22298(25)	0.1196(17)	177.0 ± 2.1	125.6 ± 0.4
M_H, M_Z, Γ_Z, m_t	0.23126(9)	0.22339(17)	0.1190(45)	173.2 ± 0.9	125.6 ± 0.4
LHC	0.2294(10)	0.2215(10)	0.1151(46)	173.3 ± 1.1	125.6 ± 0.4
Tevatron + M_Z	0.23106(15)	0.22295(32)	0.1160(44)	173.2 ± 1.0	$90^{+\ 32}_{-\ 26}$
LEP	0.23143(18)	0.22348(46)	0.1214(31)	$180 \quad \pm 11$	240^{+333}_{-134}
SLD + M_Z, Γ_Z, m_t	0.23067(28)	0.22220(55)	0.1162(46)	173.2 ± 0.9	$40^{+\ 31}_{-\ 22}$
$A^{(b,c)}_{FB}$, M_Z, Γ_Z, m_t	0.23193(29)	0.22497(70)	0.1261(50)	173.2 ± 0.9	363^{+206}_{-132}
$M_{W,Z}$, $\Gamma_{W,Z}$, m_t	0.23105(14)	0.22292(29)	0.1173(43)	173.2 ± 0.9	$86^{+\ 27}_{-\ 23}$
low energy + $M_{H,Z}$	0.2327(14)	0.2289(54)	0.1195(21)	$123 \quad \pm 44$	125.6 ± 0.4

arising predominantly from the quantities in Eq. (10.49), since the branching ratio for $H \to ZZ^*$ varies very rapidly as a function of M_H for Higgs masses near 125 GeV. It is interesting to note that this value is closer to the ATLAS Higgs mass measurement in the ZZ^* channel, $M_H = 124.3^{+0.6}_{-0.5}({\rm stat.})^{+0.5}_{-0.3}({\rm syst.})$ GeV, which differs by more than 2 σ from their $\gamma\gamma$ result, $M_H = 126.8 \pm 0.2\,{\rm stat.} \pm 0.7\,{\rm syst.}$ GeV. Removing also the branching ratio constraints gives the loop-level determination from the precision data alone,

$$M_H = 89^{+22}_{-18}\ {\rm GeV}\ , \tag{10.55}$$

which is 1.5 σ below the kinematical constraint. This is mostly a reflection of the Tevatron determination of M_W, which is 1.5 σ higher than the SM best fit value in Table 10.4. Another consequence is that the 90% central confidence range determined from the precision data,

$$60\ {\rm GeV} < M_H < 127\ {\rm GeV}\ , \tag{10.56}$$

is only marginally consistent with Eq. (10.47). This is illustrated in Fig. 10.4 where one sees that the precision data together with M_H from the LHC prefer that m_t is closer to the upper end of its 1σ allowed range. Conversely, one can remove the direct M_W and Γ_W constraints from the fits and use Eq. (10.47) to obtain $M_W = 80.358 \pm 0.007$ GeV. This is 1.7 σ below the Tevatron/LEP 2 average, $M_W = 80.385 \pm 0.015$ GeV. Finally, one can carry out a fit without including the constraint, $m_t = 173.24 \pm 0.95$ GeV, from the hadron colliders. (The indirect prediction is for the $\overline{\rm MS}$ mass, $\widehat{m}_t(\widehat{m}_t) = 167.1 \pm 2.0$ GeV, which is in the end converted to the pole mass.) One obtains $m_t = 177.0 \pm 2.1$ GeV, which is 1.6 σ higher than the direct Tevatron/LHC average. The situation is summarized in Fig. 10.5 showing the 1 σ contours in the M_W-m_t plane from the direct and indirect determinations, as well as the combined 90% CL region.

As described in Sec. 10.2 and the paragraph following Eq. (10.52) in Sec. 10.5, there is considerable stress in the experimental e^+e^- spectral functions and also conflict when these are compared with τ decay spectral functions. These are below or above the 2σ level (depending on what is actually compared) but not larger than the deviations of some other quantities entering our analyses. The number and size or these deviations are not inconsistent with what one

would expect to happen as a result of random fluctuations. It is nevertheless instructive to study the effect of doubling the uncertainty in $\Delta\alpha^{(3)}_{\rm had}(1.8\ {\rm GeV}) = (55.50 \pm 0.78) \times 10^{-4}$ (see Sec. 10.2) on the loop-level determination. The result, $M_H = 86^{+22}_{-18}$ GeV, deviates even slightly *more* (1.6 σ) than Eq. (10.55), and demonstrates that the uncertainty in $\Delta\alpha_{\rm had}$ is currently of only secondary importance. Note also that a shift of $\pm 10^{-4}$ in $\Delta\alpha^{(3)}_{\rm had}(1.8\ {\rm GeV})$ corresponds to a shift of ∓ 4.3 GeV in M_H. The hadronic contribution to $\alpha(M_Z)$ is correlated with $g_\mu - 2$ (see Sec. 10.5). The measurement of the latter is higher than the SM prediction, and its inclusion in the fit favors a larger $\alpha(M_Z)$ and a lower M_H from the precision data (currently by 3.4 GeV).

The weak mixing angle can be determined from Z pole observables, M_W, and from a variety of neutral-current processes spanning a very wide Q^2 range. The results (for the older low energy neutral-current data see Refs. 113 and 218, as well as earlier editions of this *Review*) shown in Table 10.7 are in reasonable agreement with each other, indicating the quantitative success of the SM. The largest discrepancy is the value $\widehat{s}^2_Z = 0.23193 \pm 0.00029$ from the forward-backward asymmetries into bottom and charm quarks, which is 2.3 σ above the value 0.23126 ± 0.00005 from the global fit to all data, see Table 10.5. Similarly, $\widehat{s}^2_Z = 0.23067 \pm 0.00028$ from the SLD asymmetries (in both cases when combined with M_Z) is 2.1 σ low. The SLD result has the additional difficulty (within the SM) of implying very low and excluded [230] Higgs masses. This is also true for $\widehat{s}^2_Z = 0.23105 \pm 0.00014$ from M_W and M_Z and, as a consequence, for the global fit.

Table 10.8: Values of the model-independent neutral-current parameters, compared with the SM predictions. There is a second $g^{\nu e}_{LV,LA}$ solution, given approximately by $g^{\nu e}_{LV} \leftrightarrow g^{\nu e}_{LA}$, which is eliminated by e^+e^- data under the assumption that the neutral current is dominated by the exchange of a single Z boson. The $g^{\nu q}_{LL}$, as well as the $g^{\nu q}_{LR}$, are strongly correlated and non-Gaussian, so that for implementations we recommend the parametrization using g_i^2 and $\tan\theta_i = g^{\nu u}_{Li}/g^{\nu d}_{Li}$ where $i = L, R$. In the SM predictions, the parametric uncertainties from M_Z, M_H, m_t, m_b, m_c, $\widehat{\alpha}(M_Z)$, and α_s are negligible.

Quantity	Experimental Value	Standard Model	Correlation
$g^{\nu u}_{LL}$	0.328 ± 0.016	0.3457	
$g^{\nu d}_{LL}$	-0.440 ± 0.011	-0.4288	non-
$g^{\nu u}_{LR}$	-0.179 ± 0.013	-0.1553	Gaussian
$g^{\nu d}_{LR}$	$-0.027\ ^{+0.077}_{-0.048}$	0.0777	
g^2_L	0.3005 ± 0.0028	0.3034	
g^2_R	0.0329 ± 0.0030	0.0301	small
$\tan\theta_L$	$2.50 \quad \pm 0.035$	2.4630	
$\tan\theta_R$	$4.56 \quad ^{+0.42}_{-0.27}$	5.1765	
$g^{\nu e}_{LV}$	-0.040 ± 0.015	-0.0396	-0.05
$g^{\nu e}_{LA}$	-0.507 ± 0.014	-0.5064	
$g^{eu}_{AV} + 2\,g^{ed}_{AV}$	0.489 ± 0.005	0.4951	$-0.94 \quad 0.42$
$2\,g^{eu}_{AV} - g^{ed}_{AV}$	-0.708 ± 0.016	-0.7192	-0.45
$2\,g^{eu}_{VA} - g^{ed}_{VA}$	-0.144 ± 0.068	-0.0950	
g^{ee}_{VA}	0.0190 ± 0.0027	0.0225	

The extracted Z pole value of $\alpha_s(M_Z)$ is based on a formula with negligible theoretical uncertainty if one assumes the exact validity of the SM. One should keep in mind, however, that this value, $\alpha_s(M_Z) = 0.1197 \pm 0.0027$, is very sensitive to certain types of new physics such as non-universal vertex corrections. In contrast, the value derived from τ decays, $\alpha_s(M_Z) = 0.1193^{+0.0022}_{-0.0020}$, is theory dominated but less sensitive to new physics. The two values are in remarkable agreement with each other. They are also in perfect agreement with the averages from jet-event shapes in e^+e^- annihilation (0.1177 ± 0.0046) and lattice simulations (0.1185 ± 0.0005), whereas the DIS average (0.1154 ± 0.0020) is somewhat lower. For more details, other determinations, and references, see Section 9 on "Quantum Chromodynamics" in this *Review*.

Using $\alpha(M_Z)$ and $\widehat{s}^2_Z$ as inputs, one can predict $\alpha_s(M_Z)$ assuming grand unification. One finds [231] $\alpha_s(M_Z) = 0.130 \pm 0.001 \pm 0.01$ for the simplest theories based on the minimal supersymmetric extension of the SM, where the first (second) uncertainty is from the inputs (thresholds). This is slightly larger, but consistent with $\alpha_s(M_Z) = 0.1193 \pm 0.0016$ from our fit, as well as with most other determinations. Non-supersymmetric unified theories predict the low value $\alpha_s(M_Z) = 0.073 \pm 0.001 \pm 0.001$. See also the note on "Supersymmetry" in the Searches Particle Listings.

Most of the parameters relevant to ν-hadron, ν-e, e-hadron, and $e^-e^\pm$ processes are determined uniquely and precisely from the data in "model-independent" fits (*i.e.*, fits which allow for an arbitrary EW gauge theory). The values for the parameters defined in Eqs. (10.16)–(10.17) are given in Table 10.8 along with the predictions of the SM. The agreement is very good. (The ν-hadron results including the original NuTeV data can be found in the 2006 edition of this *Review*, and fits with modified NuTeV constraints in the 2008 and 2010 editions.) The off Z pole e^+e^- results are difficult to present in a model-independent way because Z propagator effects are non-negligible at TRISTAN, PETRA, PEP, and LEP 2 energies. However, assuming e-μ-τ universality, the low energy lepton asymmetries imply [151] $4\,(g^e_A)^2 = 0.99 \pm 0.05$, in good agreement with the SM prediction $\simeq 1$.

10.7. Constraints on new physics

The masses and decay properties of the electroweak bosons and low energy data can be used to search for and set limits on deviations from the SM. We will mainly discuss the effects of exotic particles (with heavy masses $M_{\rm new} \gg M_Z$ in an expansion in $M_Z/M_{\rm new}$) on the gauge boson self-energies. (Brief remarks are made on new physics which is not of this type.) Most of the effects on precision measurements can be described by three gauge self-energy parameters S, T, and U. We will define these, as well as the related parameters ρ_0, ϵ_i, and $\widehat{\epsilon}_i$, to arise from new physics only. In other words, they are equal to zero ($\rho_0 = 1$) exactly in the SM, and do not include any (loop induced) contributions that depend on m_t or M_H, which are treated separately. Our treatment differs from most of the original papers.

The dominant effect of many extensions of the SM can be described by the ρ_0 parameter,

$$\rho_0 \equiv \frac{M_W^2}{M_Z^2\,\widehat{c}^2_Z\,\widehat{\rho}}\ , \tag{10.57}$$

which describes new sources of SU(2) breaking that cannot be accounted for by the SM Higgs doublet or m_t effects. $\widehat{\rho}$ is calculated as in Eq. (10.12) assuming the validity of the SM. In the presence of $\rho_0 \neq 1$, Eq. (10.57) generalizes the second Eq. (10.12) while the first remains unchanged. Provided that the new physics which yields $\rho_0 \neq 1$ is a small perturbation which does not significantly affect other radiative corrections, ρ_0 can be regarded as a phenomenological parameter which multiplies G_F in Eqs. (10.16)–(10.17), (10.32), and Γ_Z in Eq. (10.44*c*). There are enough data to determine ρ_0, M_H, m_t, and α_s, simultaneously. From the global fit,

$$\rho_0 = 1.00040 \pm 0.00024\ , \tag{10.58}$$

$$\alpha_s(M_Z) = 0.1194 \pm 0.0017, \tag{10.59}$$

and M_H and m_t are as given in Table 10.6 and Table 10.5. The result in Eq. (10.58) is 1.7 σ above the SM expectation, $\rho_0 = 1$. It can be used to constrain higher-dimensional Higgs representations to have vacuum expectation values of less than a few percent of those of the doublets. Indeed, the relation between M_W and M_Z is modified if there are Higgs multiplets with weak isospin $> 1/2$ with significant vacuum expectation values. For a general (charge-conserving) Higgs structure,

$$\rho_0 = \frac{\sum_i [t(i)(t(i)+1) - t_3(i)^2]|v_i|^2}{2\sum_i t_3(i)^2|v_i|^2}, \tag{10.60}$$

where v_i is the expectation value of the neutral component of a Higgs multiplet with weak isospin $t(i)$ and third component $t_3(i)$. In order to calculate to higher orders in such theories one must define a set of four fundamental renormalized parameters which one may conveniently choose to be α, G_F, M_Z, and M_W, since M_W and M_Z are directly measurable. Then $\widehat{s}^2_Z$ and ρ_0 can be considered dependent parameters.

Eq. (10.58) can also be used to constrain other types of new physics. For example, non-degenerate multiplets of heavy fermions or scalars break the vector part of weak SU(2) and lead to a decrease in the value of M_Z/M_W. Each non-degenerate SU(2) doublet $\binom{f_1}{f_2}$ yields a positive contribution to ρ_0 [232] of

$$\frac{C\,G_F}{8\sqrt{2}\pi^2}\Delta m^2, \tag{10.61}$$

where

$$\Delta m^2 \equiv m_1^2 + m_2^2 - \frac{4m_1^2 m_2^2}{m_1^2 - m_2^2}\ln\frac{m_1}{m_2} \geq (m_1 - m_2)^2, \tag{10.62}$$

and $C = 1$ (3) for color singlets (triplets). Eq. (10.58) taken together with Eq. (10.61) implies the following constraint on the mass splitting at the 95% CL,

$$\sum_i \frac{C_i}{3}\,\Delta m_i^2 \leq (50\ \text{GeV})^2. \tag{10.63}$$

where the sum runs over all new-physics doublets, for example fourth-family quarks or leptons, $\binom{t'}{b'}$ or $\binom{\nu'}{\ell'-}$, vector-like fermion doublets (which contribute to the sum in Eq. (10.63) with an extra factor of 2), and scalar doublets such as $\binom{\tilde{t}}{\tilde{b}}$ in Supersymmetry (in the absence of L–R mixing).

Non-degenerate multiplets usually imply $\rho_0 > 1$. Similarly, heavy Z' bosons decrease the prediction for M_Z due to mixing and generally lead to $\rho_0 > 1$ [233]. On the other hand, additional Higgs doublets which participate in spontaneous symmetry breaking [234] or heavy lepton doublets involving Majorana neutrinos [235], both of which have more complicated expressions, as well as the vacuum expectation values of Higgs triplets or higher-dimensional representations can contribute to ρ_0 with either sign. Allowing for the presence of heavy degenerate chiral multiplets (the S parameter, to be discussed below) affects the determination of ρ_0 from the data, at present leading to a slightly larger value.

A number of authors [236–241] have considered the general effects on neutral-current and Z and W boson observables of various types of heavy (*i.e.*, $M_{\rm new} \gg M_Z$) physics which contribute to the W and Z self-energies but which do not have any direct coupling to the ordinary fermions. In addition to non-degenerate multiplets, which break the vector part of weak SU(2), these include heavy degenerate multiplets of chiral fermions which break the axial generators.

Such effects can be described by just three parameters, S, T, and U, at the (EW) one-loop level. (Three additional parameters are needed if the new physics scale is comparable to M_Z [242]. Further generalizations, including effects relevant to LEP 2, are described in Ref. 243.) T is proportional to the difference between the W and Z self-energies at $Q^2 = 0$ (*i.e.*, vector SU(2)-breaking), while S ($S+U$) is associated with the difference between the Z (W) self-energy at $Q^2 = M^2_{Z,W}$ and $Q^2 = 0$ (axial SU(2)-breaking). Denoting the contributions of new physics to the various self-energies by $\Pi^{\rm new}_{ij}$, we have

$$\widehat{\alpha}(M_Z)T \equiv \frac{\Pi^{\rm new}_{WW}(0)}{M_W^2} - \frac{\Pi^{\rm new}_{ZZ}(0)}{M_Z^2}\ , \tag{10.64a}$$

$$\frac{\widehat{\alpha}(M_Z)}{4\,\widehat{s}^2_Z\widehat{c}^2_Z}S \equiv \frac{\Pi^{\rm new}_{ZZ}(M_Z^2) - \Pi^{\rm new}_{ZZ}(0)}{M_Z^2} - \frac{\widehat{c}^2_Z - \widehat{s}^2_Z}{\widehat{c}_Z\widehat{s}_Z}\,\frac{\Pi^{\rm new}_{Z\gamma}(M_Z^2)}{M_Z^2} - \frac{\Pi^{\rm new}_{\gamma\gamma}(M_Z^2)}{M_Z^2}\ , \tag{10.64b}$$

$$\frac{\widehat{\alpha}(M_Z)}{4\,\widehat{s}^2_Z}(S+U) \equiv \frac{\Pi^{\rm new}_{WW}(M_W^2) - \Pi^{\rm new}_{WW}(0)}{M_W^2} - \frac{\widehat{c}_Z}{\widehat{s}_Z}\,\frac{\Pi^{\rm new}_{Z\gamma}(M_Z^2)}{M_Z^2} - \frac{\Pi^{\rm new}_{\gamma\gamma}(M_Z^2)}{M_Z^2}\ . \tag{10.64c}$$

S, T, and U are defined with a factor proportional to $\widehat{\alpha}$ removed, so that they are expected to be of order unity in the presence of new physics. In the $\overline{\rm MS}$ scheme as defined in Ref. 53, the last two terms in Eqs. (10.64*b*) and (10.64*c*) can be omitted (as was done in some earlier editions of this *Review*). These three parameters are related to other parameters (S_i, h_i, $\widehat{\epsilon}_i$) defined in Refs. [53,237,238] by

$$\begin{aligned} T &= h_V = \widehat{\epsilon}_1/\widehat{\alpha}(M_Z), \\ S &= h_{AZ} = S_Z = 4\,\widehat{s}^2_Z\,\widehat{\epsilon}_3/\widehat{\alpha}(M_Z), \\ U &= h_{AW} - h_{AZ} = S_W - S_Z \\ &= -4\,\widehat{s}^2_Z\,\widehat{\epsilon}_2/\widehat{\alpha}(M_Z). \end{aligned} \tag{10.65}$$

A heavy non-degenerate multiplet of fermions or scalars contributes positively to T as

$$\rho_0 - 1 = \frac{1}{1 - \widehat{\alpha}(M_Z)T} - 1 \simeq \widehat{\alpha}(M_Z)T, \tag{10.66}$$

where $\rho_0 - 1$ is given in Eq. (10.61). The effects of non-standard Higgs representations cannot be separated from heavy non-degenerate multiplets unless the new physics has other consequences, such as vertex corrections. Most of the original papers defined T to include the effects of loops only. However, we will redefine T to include all new sources of SU(2) breaking, including non-standard Higgs, so that T and ρ_0 are equivalent by Eq. (10.66).

A multiplet of heavy degenerate chiral fermions yields

$$S = \frac{C}{3\pi}\sum_i \Big(t_{3L}(i) - t_{3R}(i)\Big)^2, \tag{10.67}$$

where $t_{3L,R}(i)$ is the third component of weak isospin of the left- (right-)handed component of fermion i and C is the number of colors. For example, a heavy degenerate ordinary or mirror family would contribute $2/3\pi$ to S. In models with warped extra dimensions, sizeable correction to the S parameter are generated by mixing effects between the SM gauge bosons and their Kaluza-Klein (KK) excitations. One finds $S \approx 30v^2/M^2_{KK}$, where M_{KK} is the mass of the KK gauge bosons [244]. Large positive values $S > 0$ can also be generated in Technicolor models with QCD-like dynamics, where one expects [236] $S \sim 0.45$ for an iso-doublet of techni-fermions, assuming $N_{TC} = 4$ techni-colors, while $S \sim 1.62$ for a full techni-generation with $N_{TC} = 4$. However, the QCD-like models are excluded on other grounds (flavor changing neutral currents, too-light quarks and pseudo-Goldstone bosons [245], and absence of a Higgs-like scalar).

On the other hand, negative values $S < 0$ are possible, for example, for models of walking Technicolor [246] or loops involving scalars or Majorana particles [247]. The simplest origin of $S < 0$ would probably be an additional heavy Z' boson [233]. Supersymmetric extensions of the SM generally give very small effects. See Refs. 248 and 249 and the note on "Supersymmetry" in the Searches Particle Listings for a complete set of references.

Most simple types of new physics yield $U = 0$, although there are counter-examples, such as the effects of anomalous triple gauge vertices [238].

The SM expressions for observables are replaced by

$$\begin{aligned} M_Z^2 &= M_{Z0}^2\,\frac{1 - \widehat{\alpha}(M_Z)T}{1 - G_F M_{Z0}^2 S/2\sqrt{2}\pi}\ , \\ M_W^2 &= M_{W0}^2\,\frac{1}{1 - G_F M_{W0}^2(S+U)/2\sqrt{2}\pi}\ , \end{aligned} \tag{10.68}$$

where M_{Z0} and M_{W0} are the SM expressions (as functions of m_t and M_H) in the $\overline{\rm MS}$ scheme. Furthermore,

$$\Gamma_Z = \frac{M_Z^3\beta_Z}{1 - \widehat{\alpha}(M_Z)T}, \Gamma_W = M_W^3\beta_W, A_i = \frac{A_{i0}}{1 - \widehat{\alpha}(M_Z)T}\ , \tag{10.69}$$

where β_Z and β_W are the SM expressions for the reduced widths Γ_{Z0}/M^3_{Z0} and Γ_{W0}/M^3_{W0}, M_Z and M_W are the physical masses, and A_i (A_{i0}) is a neutral-current amplitude (in the SM).

The data allow a simultaneous determination of $\widehat{s}^2_Z$ (from the Z pole asymmetries), S (from M_Z), U (from M_W), T (mainly from Γ_Z), α_s (from R_ℓ, $\sigma_{\rm had}$, and τ_τ), M_H and m_t (from the hadron colliders), with little correlation among the SM parameters:

$$\begin{aligned} S &= -0.03 \pm 0.10, \\ T &= 0.01 \pm 0.12, \\ U &= 0.05 \pm 0.10, \end{aligned} \tag{10.70}$$

$\widehat{s}^2_Z = 0.23119 \pm 0.00016$, and $\alpha_s(M_Z) = 0.1196 \pm 0.0017$, where the uncertainties are from the inputs. The parameters in Eqs. (10.70), which by definition are due to new physics only, are in excellent agreement with the SM values of zero. Fixing $U = 0$ (as is also done in Fig. 10.6) moves S and T slightly upwards,

$$\begin{aligned} S &= 0.00 \pm 0.08, \\ T &= 0.05 \pm 0.07. \end{aligned} \tag{10.71}$$

Again, good agreement with the SM is observed. If only any one of the three parameters is allowed, then this parameter would deviate at the 1.5 to 1.7 σ level, reflecting the deviation in M_W. Using Eq. (10.66), the value of ρ_0 corresponding to T in Eq. (10.70) is 1.0000 ± 0.0009, while the one corresponding to Eq. (10.71) is 1.0004 ± 0.0005.

There is a strong correlation (90%) between the S and T parameters. The U parameter is -59% (-81%) anti-correlated with S (T). The allowed regions in S–T are shown in Fig. 10.6. From Eqs. (10.70) one obtains $S \leq 0.14$ and $T \leq 0.20$ at 95% CL, where the former puts the constraint $M_{KK} \gtrsim 3.5$ TeV on the masses of KK gauge bosons in warped extra dimensions.

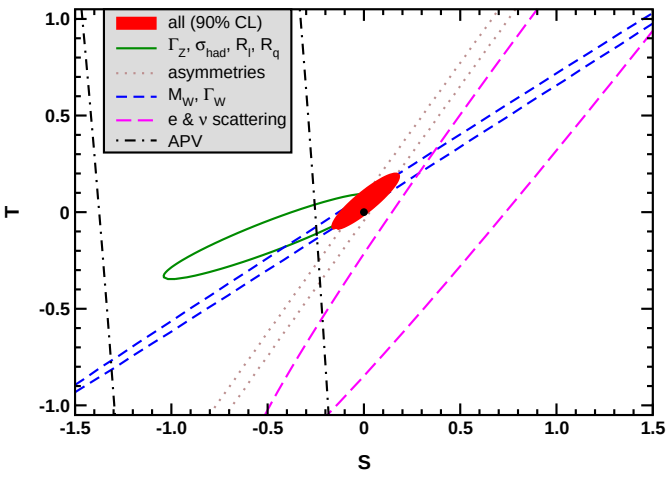

Figure 10.6: 1 σ constraints (39.35%) on S and T (for $U = 0$) from various inputs combined with M_Z. S and T represent the contributions of new physics only. Data sets not involving M_W or Γ_W are insensitive to U. With the exception of the fit to all data, we fix $\alpha_s = 0.1185$. The black dot indicates the Standard Model values $S = T = 0$.

The S parameter can also be used to constrain the number of fermion families, *under the assumption* that there are no new contributions to T or U and therefore that any new families are degenerate; then an extra generation of SM fermions is excluded at the 7 σ level corresponding to $N_F = 2.75 \pm 0.17$. This can be compared to the fit to the number of light neutrinos given in Eq. (10.37), $N_\nu = 2.990 \pm 0.007$. However, the S parameter fits are valid even for a very heavy fourth family neutrino. Allowing T to vary as well, the constraint on a fourth family is weaker [250]. However, a heavy fourth family would increase the Higgs production cross section through gluon fusion by a factor ~ 9, which is in considerable tension with the observed Higgs signal at LHC. Combining the limits from electroweak precision data with the measured Higgs production rate and limits from direct searches for heavy quarks [251], a fourth family of chiral fermions is now excluded by more than five standard deviations [252]. Similar remarks apply to a heavy mirror family [253] involving right-handed SU(2) doublets and left-handed singlets. In contrast, new doublets that receive most of their mass from a different source than the Higgs vacuum expectation value, such as vector-like fermion doublets or scalar doublets in Supersymmetry, give small or no contribution to S, T, U and the Higgs production cross section and thus are still allowed. Partial or complete vector-like fermion families are predicted in many grand unified theories [254].

There is no simple parametrization to describe the effects of every type of new physics on every possible observable. The S, T, and U formalism describes many types of heavy physics which affect only the gauge self-energies, and it can be applied to all precision observables. However, new physics which couples directly to ordinary fermions, such as heavy Z' bosons [233], mixing with exotic fermions [255], or leptoquark exchange [170,256] cannot be fully parametrized in the S, T, and U framework. It is convenient to treat these types of new physics by parameterizations that are specialized to that particular class of theories (*e.g.*, extra Z' bosons), or to consider specific models (which might contain, *e.g.,* Z' bosons and exotic fermions with correlated parameters). Fits to Supersymmetric models are described in Ref. 249. Models involving strong dynamics (such as (extended) Technicolor) for EW breaking are considered in Ref. 257. The effects of compactified extra spatial dimensions at the TeV scale are reviewed in Ref. 258, and constraints on Little Higgs models in Ref. 259. The implications of non-standard Higgs sectors, e.g., involving Higgs singlets or triplets, are discussed in Ref. 260, while additional Higgs doublets are considered in Refs. 234 and 261. Limits on new four-Fermi operators and on leptoquarks using LEP 2 and lower energy data are given in Refs. 170 and 262. Constraints on various types of new physics are reviewed in Refs. [7,75,113,138,153,263,264], and implications for the LHC in Ref. 265.

An alternate formalism [266] defines parameters, ϵ_1, ϵ_2, ϵ_3, and ϵ_b in terms of the specific observables M_W/M_Z, $\Gamma_{\ell\ell}$, $A_{FB}^{(0,\ell)}$, and R_b. The definitions coincide with those for $\widehat{\epsilon}_i$ in Eqs. (10.64) and (10.65) for physics which affects gauge self-energies only, but the ϵ's now parametrize arbitrary types of new physics. However, the ϵ's are not related to other observables unless additional model-dependent assumptions are made. Another approach [267] parametrizes new physics in terms of gauge-invariant sets of operators. It is especially powerful in studying the effects of new physics on non-Abelian gauge vertices. The most general approach introduces deviation vectors [263]. Each type of new physics defines a deviation vector, the components of which are the deviations of each observable from its SM prediction, normalized to the experimental uncertainty. The length (direction) of the vector represents the strength (type) of new physics.

One well explored type of physics beyond the SM are extra Z' bosons [268]. They do not spoil the observed approximate gauge coupling unification, and appear in many Grand Unified Theories (GUTs), models with extra dimensions [258], as well as in dynamical symmetry breaking [257] and Little Higgs models [259]. For example, the SO(10) GUT contains an extra U(1) as can be seen from its maximal subgroup, $\mathrm{SU}(5) \times \mathrm{U}(1)_\chi$. Similarly, the E_6 GUT contains the subgroup $\mathrm{SO}(10) \times \mathrm{U}(1)_\psi$. The Z_ψ possesses only axial-vector couplings to the ordinary fermions, and its mass is generally less constrained. The Z_η boson is the linear combination $\sqrt{3/8}\,Z_\chi - \sqrt{5/8}\,Z_\psi$. The Z_{LR} boson occurs in left-right models with gauge group $\mathrm{SU}(3)_C \times \mathrm{SU}(2)_L \times \mathrm{SU}(2)_R \times \mathrm{U}(1)_{B-L} \subset \mathrm{SO}(10)$, and the secluded Z_S emerges in a supersymmetric bottom-up scenario [269]. The sequential Z_{SM} boson is defined to have the same couplings to fermions as the SM Z boson. Such a boson is not expected in the context of gauge theories unless it has different couplings to exotic fermions than the ordinary Z boson. However, it serves as a useful reference case when comparing constraints from various sources. The physical Z' boson is in general a superposition of the SM Z and the new boson associated with the extra U(1). The mixing angle θ

Table 10.9: 95% CL lower mass limits (in GeV) on various extra Z' gauge bosons, appearing in models of unification. More general parametrizations are described in Refs. 268 and 271. The EW results [272] from low energy and W and Z boson data are for Higgs sectors consisting of doublets and singlets only ($\rho_0 = 1$) with unspecified $U(1)'$ charges. The next two columns show the limits from ATLAS [273] and CMS [274] from the combination of both lepton channels. The CDF [275] and DØ [276] bounds from searches in $\bar{p}p \to \mu^+\mu^-$ and e^+e^-, respectively, are listed in the next two columns, followed by the LEP 2 $e^+e^- \to f\bar{f}$ bounds [170] (assuming $\theta = 0$). The hadron collider bounds would be moderately weakened if there are open exotic decay channels [277]. The last column shows the 1 σ ranges for M_H when it is left unconstrained in the EW fits.

Z'	EW	ATLAS	CMS	CDF	DØ	LEP 2	M_H
Z_χ	1,141	2,540	–	930	903	785	$171^{+493}_{-\ 89}$
Z_ψ	147	2,380	2,600	917	891	500	$97^{+\ 31}_{-\ 25}$
Z_η	427	2,440	–	938	923	500	423^{+577}_{-350}
Z_{LR}	998	–	–	–	–	825	$804^{+174}_{-\ 35}$
Z_S	1,257	2,470	–	858	822	–	$149^{+353}_{-\ 68}$
Z_{SM}	1,403	2,860	2,960	1,071	1,023	1,760	331^{+669}_{-246}

satisfies,

$$\tan^2\theta = \frac{M^2_{Z^0_1} - M^2_Z}{M^2_{Z'} - M^2_{Z^0_1}} \ ,$$

where $M_{Z^0_1}$ is the SM value for M_Z in the absence of mixing. Note that $M_Z < M_{Z^0_1}$, and that the SM Z couplings are changed by the mixing. The couplings of the heavier Z' may also be modified by kinetic mixing [268,270]. If the Higgs U(1)$'$ quantum numbers are known, there will be an extra constraint,

$$\theta = C\,\frac{g_2}{g_1}\frac{M^2_Z}{M^2_{Z'}} \ ,$$

where $g_{1,2}$ are the U(1) and U(1)$'$ gauge couplings with $g_2 = \sqrt{\frac{5}{3}}\sin\theta_W\sqrt{\lambda}\,g_1$ and $g_1 = \sqrt{g^2 + g'^2}$. We assume that $\lambda \sim 1$, which happens if the GUT group breaks directly to SU(3) × SU(2) × U(1) × U(1)$'$. C is a function of vacuum expectation values. For minimal Higgs sectors it can be found in Ref. 233. Table 10.9 shows the 95% CL lower mass limits [272] for $\rho_0 = 1$ and 114.4 GeV $\leq M_H \leq$ 1 TeV. The last column shows the 1 σ ranges for M_H when it is left unconstrained. In cases of specific minimal Higgs sectors where C is known, the Z' mass limits from the EW precision data are generally pushed into the TeV region. The limits on $|\theta|$ are typically smaller than a few $\times 10^{-3}$. The mass bounds from direct searches at the LHC [273,274], however, exceed the EW precison constraints by a factor two or more for the models considered here. While the latter can be slightly improved by fixing M_H to the value measured at LHC, this general conclusion will not change. Also listed in Table 10.9 are the direct lower limits on Z' production from the Tevatron [275,276], as well as the LEP 2 bounds [170]. For more details see [268,272,278,279] and the note on "The Z' Searches" in the Gauge & Higgs Boson Particle Listings.

Acknowledgments:

We are indebted to M. Davier, B. Malaescu, and K. Maltman for providing us with additional information about their work in a form suitable to be included in our fits. We also thank R. H. Bernstein, K. S. McFarland, H. Schellman, and G. P. Zeller for discussions on the NuTeV analysis, and M. Spira for details about HDECAY. J.E. was supported by PAPIIT (DGAPA–UNAM) project IN106913 and CONACyT (México) project 151234, and grateful acknowledges the hospitality and support by the Mainz Institute for Theoretical Physics (MITP) where part of this work was completed. A.F. is supported in part by the National Science Foundation under grant no. PHY-1212635.

References:

1. S. L. Glashow, Nucl. Phys. **22**, 579 (1961); S. Weinberg, Phys. Rev. Lett. **19**, 1264 (1967); A. Salam, p. 367 of *Elementary Particle Theory*, ed. N. Svartholm (Almquist and Wiksells, Stockholm, 1969); S.L. Glashow, J. Iliopoulos, and L. Maiani, Phys. Rev. **D2**, 1285 (1970).
2. CKMfitter Group: J. Charles *et al.*, Eur. Phys. J. **C41**, 1 (2005); updated results and plots are available at `http://ckmfitter.in2p3.fr`.
3. For reviews, see the Section on "Higgs Bosons: Theory and Searches" in this *Review*; J. Gunion *et al.*, *The Higgs Hunter's Guide*, (Addison-Wesley, Redwood City, 1990); M. Carena and H.E. Haber, Prog. in Part. Nucl. Phys. **50**, 63 (2003); A. Djouadi, Phys. Reports **457**, 1 (2008).
4. For reviews, see E.D. Commins and P.H. Bucksbaum, *Weak Interactions of Leptons and Quarks*, (Cambridge Univ. Press, 1983); G. Barbiellini and C. Santoni, Riv. Nuovo Cimento **9(2)**, 1 (1986); N. Severijns, M. Beck, and O. Naviliat-Cuncic, Rev. Mod. Phys. **78**, 991 (2006); W. Fetscher and H.J. Gerber, p. 657 of Ref. 5; J. Deutsch and P. Quin, p. 706 of Ref. 5; P. Herczeg, p. 786 of Ref. 5; P. Herczeg, Prog. in Part. Nucl. Phys. **46**, 413 (2001).
5. *Precision Tests of the Standard Electroweak Model*, ed. P. Langacker (World Scientific, Singapore, 1995).
6. J. Erler and M.J. Ramsey-Musolf, Prog. in Part. Nucl. Phys. **54**, 351 (2005).
7. P. Langacker, *The Standard Model and Beyond*, (CRC Press, New York, 2009).
8. T. Kinoshita, *Quantum Electrodynamics*, (World Scientific, Singapore, 1990).
9. S. G. Karshenboim, Phys. Reports **422**, 1 (2005).
10. P.J. Mohr, B.N. Taylor, and D.B. Newell, Rev. Mod. Phys. **80**, 633 (2008); for updates see `http://physics.nist.gov/cuu/Constants/`.
11. ALEPH, DELPHI, L3, OPAL, SLD, LEP Electroweak Working Group, SLD Electroweak and Heavy Flavour Groups: S. Schael *et al.*, Phys. Reports **427**, 257 (2006); for updates see `http://lepewwg.web.cern.ch/LEPEWWG/`.
12. MuLan: D. M. Webber *et al.*, Phys. Rev. Lett. **106**, 041803 (2011).
13. T. Kinoshita and A. Sirlin, Phys. Rev. **113**, 1652 (1959).
14. T. van Ritbergen and R.G. Stuart, Nucl. Phys. **B564**, 343 (2000); M. Steinhauser and T. Seidensticker, Phys. Lett. **B467**, 271 (1999).
15. Y. Nir, Phys. Lett. **B221**, 184 (1989).
16. A. Pak and A. Czarnecki, Phys. Rev. Lett. **100**, 241807 (2008).
17. For a review, see S. Mele, `arXiv:hep-ex/0610037`.
18. S. Fanchiotti, B. Kniehl, and A. Sirlin, Phys. Rev. **D48**, 307 (1993) and references therein.
19. J. Erler, Phys. Rev. **D59**, 054008 (1999).
20. M. Davier *et al.*, Eur. Phys. J. **C71**, 1515 (2011); the quoted value uses additional information thankfully provided to us by the authors in a private communication.
21. J. Erler, `hep-ph/0005084`.
22. P. A. Baikov *et al.*, JHEP **1207**, 017 (2012).
23. M. Steinhauser, Phys. Lett. **B429**, 158 (1998).
24. B.V. Geshkenbein and V.L. Morgunov, Phys. Lett. **B352**, 456 (1995).
25. M.L. Swartz, Phys. Rev. **D53**, 5268 (1996).
26. N.V. Krasnikov and R. Rodenberg, Nuovo Cimento **111A**, 217 (1998).
27. J.H. Kühn and M. Steinhauser, Phys. Lett. **B437**, 425 (1998).
28. S. Groote *et al.*, Phys. Lett. **B440**, 375 (1998).

29. A.D. Martin, J. Outhwaite, and M.G. Ryskin, Phys. Lett. **B492**, 69 (2000).
30. J.F. de Troconiz and F.J. Yndurain, Phys. Rev. **D65**, 093002 (2002).
31. F. Jegerlehner, Nucl. Phys. Proc. Suppl. **181**, 135 (2008).
32. H. Burkhardt and B. Pietrzyk, Phys. Rev. **D84**, 037502 (2011).
33. K. Hagiwara *et al.*, J. Phys. **G38**, 085003 (2011).
34. OPAL: K. Ackerstaff *et al.*, Eur. Phys. J. **C7**, 571 (1999).
35. CLEO: S. Anderson *et al.*, Phys. Rev. **D61**, 112002 (2000).
36. ALEPH: S. Schael *et al.*, Phys. Reports **421**, 191 (2005).
37. Belle: M. Fujikawa *et al.*: Phys. Rev. **D78**, 072006 (2008).
38. CMD-2: R.R. Akhmetshin *et al.*, Phys. Lett. **B578**, 285 (2004);
CMD-2: V.M. Aulchenko *et al.*, JETP Lett. **82**, 743 (2005);
CMD-2: R.R. Akhmetshin *et al.*, JETP Lett. **84**, 413 (2006);
CMD-2: R.R. Akhmetshin *et al.*, Phys. Lett. **B648**, 28 (2007).
39. SND: M.N. Achasov *et al.*, Sov. Phys. JETP **103**, 380 (2006).
40. A.B. Arbuzov *et al.*, JHEP **9812**, 009 (1998);
S. Binner, J.H. Kühn, and K. Melnikov, Phys. Lett. **B459**, 279 (1999).
41. BaBar: B. Aubert *et al.*, Phys. Rev. **D70**, 072004 (2004);
BaBar: B. Aubert *et al.*, Phys. Rev. **D71**, 052001 (2005);
BaBar: B. Aubert *et al.*, Phys. Rev. **D73**, 052003 (2006);
BaBar: B. Aubert *et al.*, Phys. Rev. **D76**, 092005 (2007);
BaBar: B. Aubert *et al.*, Phys. Rev. Lett. **103**, 231801 (2009).
42. KLOE: F. Ambrosino *et al.*, Phys. Lett. **B670**, 285 (2009);
KLOE: F. Ambrosino *et al.*, Phys. Lett. **B700**, 102 (2011).
43. See *e.g.*, CMD and OLYA: L.M. Barkov *et al.*, Nucl. Phys. **B256**, 365 (1985).
44. V.A. Novikov *et al.*, Phys. Reports **41**, 1 (1978).
45. J. Erler and M. Luo, Phys. Lett. **B558**, 125 (2003).
46. K. G. Chetyrkin *et al.*, Theor. Math. Phys. **170**, 217 (2012).
47. B. Dehnadi *et al.*, JHEP **1309**, 103 (2013).
48. Tevatron Electroweak Working Group, CDF and DØ: `arXiv:1305.3929 [hep-ex]`.
49. ATLAS and CMS: `cds.cern.ch/record/1601811/files/ATLAS-CONF-2013-102.pdf`.
50. M. Beneke, Phys. Reports **317**, 1 (1999).
51. K. G. Chetyrkin and M. Steinhauser, Nucl. Phys. **B573**, 617 (2000);
K. Melnikov and T. van Ritbergen, Phys. Lett. **B482**, 99 (2000).
52. A. Sirlin, Phys. Rev. **D22**, 971 (1980);
D.C. Kennedy *et al.*, Nucl. Phys. **B321**, 83 (1989);
D.Yu. Bardin *et al.*, Z. Phys. **C44**, 493 (1989);
W. Hollik, Fortsch. Phys. **38**, 165 (1990);
for reviews, see W. Hollik, pp. 37 and 117, and W. Marciano, p. 170 of Ref. 5.
53. W.J. Marciano and J.L. Rosner, Phys. Rev. Lett. **65**, 2963 (1990).
54. G. Degrassi, S. Fanchiotti, and A. Sirlin, Nucl. Phys. **B351**, 49 (1991).
55. K.S. Kumar *et al.*, Ann. Rev. Nucl. and Part. Sci. **63**, 237 (2013).
56. G. Degrassi and A. Sirlin, Nucl. Phys. **B352**, 342 (1991).
57. P. Gambino and A. Sirlin, Phys. Rev. **D49**, 1160 (1994).
58. ZFITTER: A.B. Arbuzov *et al.*, Comput. Phys. Commun. **174**, 728 (2006) and references therein.
59. R. Barbieri *et al.*, Nucl. Phys. **B409**, 105 (1993);
J. Fleischer, O.V. Tarasov, and F. Jegerlehner, Phys. Lett. **B319**, 249 (1993).
60. G. Degrassi, P. Gambino, and A. Vicini, Phys. Lett. **B383**, 219 (1996);
G. Degrassi, P. Gambino, and A. Sirlin, Phys. Lett. **B394**, 188 (1997).
61. A. Freitas *et al.*, Phys. Lett. **B495**, 338 (2000) and *ibid.* **570**, 260(E) (2003);
M. Awramik and M. Czakon, Phys. Lett. **B568**, 48 (2003).
62. A. Freitas *et al.*, Nucl. Phys. **B632**, 189 (2002) and *ibid.* **666**, 305(E) (2003);
M. Awramik and M. Czakon, Phys. Rev. Lett. **89**, 241801 (2002);
A. Onishchenko and O. Veretin, Phys. Lett. **B551**, 111 (2003).
63. M. Awramik *et al.*, Phys. Rev. Lett. **93**, 201805 (2004);
W. Hollik, U. Meier, and S. Uccirati, Nucl. Phys. **B731**, 213 (2005).
64. M. Awramik, M. Czakon, and A. Freitas, Phys. Lett. **B642**, 563 (2006);
W. Hollik, U. Meier, and S. Uccirati, Nucl. Phys. **B765**, 154 (2007).
65. A. Djouadi and C. Verzegnassi, Phys. Lett. **B195**, 265 (1987);
A. Djouadi, Nuovo Cimento **100A**, 357 (1988).
66. K.G. Chetyrkin, J.H. Kühn, and M. Steinhauser, Phys. Lett. **B351**, 331 (1995).
67. Y. Schröder and M. Steinhauser, Phys. Lett. **B622**, 124 (2005);
K.G. Chetyrkin *et al.*, Phys. Rev. Lett. **97**, 102003 (2006);
R. Boughezal and M. Czakon, Nucl. Phys. **B755**, 221 (2006);
L. Avdeev *et al.*, Phys. Lett. **B336**, 560 (1994) and *ibid.* **B349**, 597(E) (1995).
68. B.A. Kniehl, J.H. Kühn, and R.G. Stuart, Phys. Lett. **B214**, 621 (1988);
B.A. Kniehl, Nucl. Phys. **B347**, 86 (1990);
F. Halzen and B.A. Kniehl, Nucl. Phys. **B353**, 567 (1991);
A. Djouadi and P. Gambino, Phys. Rev. **D49**, 3499 (1994) and *ibid.* **53**, 4111(E) (1996).
69. A. Anselm, N. Dombey, and E. Leader, Phys. Lett. **B312**, 232 (1993).
70. K.G. Chetyrkin, J.H. Kühn, and M. Steinhauser, Phys. Rev. Lett. **75**, 3394 (1995).
71. J.J. van der Bij *et al.*, Phys. Lett. **B498**, 156 (2001);
M. Faisst *et al.*, Nucl. Phys. **B665**, 649 (2003).
72. R. Boughezal, J.B. Tausk, and J.J. van der Bij, Nucl. Phys. **B725**, 3 (2005).
73. M. Awramik *et al.*, Phys. Rev. **D69**, 053006 (2004).
74. M. Awramik, M. Czakon, and A. Freitas, JHEP **0611**, 048 (2006).
75. M. Baak *et al.*, Eur. Phys. J. **C72**, 2003 (2012).
76. J. Erler and S. Su, Prog. in Part. Nucl. Phys. **71**, 119 (2013).
77. J.M. Conrad, M.H. Shaevitz, and T. Bolton, Rev. Mod. Phys. **70**, 1341 (1998).
78. Z. Berezhiani and A. Rossi, Phys. Lett. **B535**, 207 (2002);
S. Davidson *et al.*, JHEP **0303**, 011 (2003);
A. Friedland, C. Lunardini and C. Pena-Garay, Phys. Lett. **B594**, 347 (2004).
79. J. Panman, p. 504 of Ref. 5.
80. CHARM: J. Dorenbosch *et al.*, Z. Phys. **C41**, 567 (1989).
81. CALO: L.A. Ahrens *et al.*, Phys. Rev. **D41**, 3297 (1990).
82. CHARM II: P. Vilain *et al.*, Phys. Lett. **B335**, 246 (1994).
83. ILM: R.C. Allen *et al.*, Phys. Rev. **D47**, 11 (1993);
LSND: L.B. Auerbach *et al.*, Phys. Rev. **D63**, 112001 (2001).
84. TEXONO: M. Deniz *et al.*, Phys. Rev. **D81**, 072001 (2010).
85. For reviews, see G.L. Fogli and D. Haidt, Z. Phys. **C40**, 379 (1988);
F. Perrier, p. 385 of Ref. 5.
86. CDHS: A. Blondel *et al.*, Z. Phys. **C45**, 361 (1990).
87. CHARM: J.V. Allaby *et al.*, Z. Phys. **C36**, 611 (1987).
88. CCFR: K.S. McFarland *et al.*, Eur. Phys. J. **C1**, 509 (1998).
89. R.M. Barnett, Phys. Rev. **D14**, 70 (1976);
H. Georgi and H.D. Politzer, Phys. Rev. **D14**, 1829 (1976).
90. LAB-E: S.A. Rabinowitz *et al.*, Phys. Rev. Lett. **70**, 134 (1993).
91. E.A. Paschos and L. Wolfenstein, Phys. Rev. **D7**, 91 (1973).
92. NuTeV: G.P. Zeller *et al.*, Phys. Rev. Lett. **88**, 091802 (2002).
93. D. Mason *et al.*, Phys. Rev. Lett. **99**, 192001 (2007).
94. S. Kretzer, D. Mason, and F. Olness, Phys. Rev. **D65**, 074010 (2002).
95. J. Pumplin *et al.*, JHEP **0207**, 012 (2002);
S. Kretzer *et al.*, Phys. Rev. Lett. **93**, 041802 (2004).
96. S. Alekhin, S.A. Kulagin, and R. Petti, Phys. Lett. **B675**, 433 (2009).
97. W. Bentz *et al.*, Phys. Lett. **B693**, 462 (2010).

98. E. Sather, Phys. Lett. **B274**, 433 (1992);
E.N. Rodionov, A.W. Thomas, and J.T. Londergan, Mod. Phys. Lett. **A9**, 1799 (1994).
99. A.D. Martin *et al.*, Eur. Phys. J. **C35**, 325 (2004).
100. J.T. Londergan and A.W. Thomas, Phys. Rev. **D67**, 111901 (2003).
101. M. Glück, P. Jimenez-Delgado, and E. Reya, Phys. Rev. Lett. **95**, 022002 (2005).
102. S. Kumano, Phys. Rev. **D66**, 111301 (2002);
S.A. Kulagin, Phys. Rev. **D67**, 091301 (2003);
S.J. Brodsky, I. Schmidt, and J.J. Yang, Phys. Rev. **D70**, 116003 (2004);
M. Hirai, S. Kumano, and T. H. Nagai, Phys. Rev. **D71**, 113007 (2005);
G.A. Miller and A.W. Thomas, Int. J. Mod. Phys. A **20**, 95 (2005).
103. I.C. Cloet, W. Bentz, and A.W. Thomas, Phys. Rev. Lett. **102**, 252301 (2009).
104. K.P.O. Diener, S. Dittmaier, and W. Hollik, Phys. Rev. **D69**, 073005 (2004);
A.B. Arbuzov, D.Y. Bardin, and L.V. Kalinovskaya, JHEP **0506**, 078 (2005);
K. Park, U. Baur, and D. Wackeroth, `arXiv:0910.5013 [hep-ph]`.
105. K.P.O. Diener, S. Dittmaier, and W. Hollik, Phys. Rev. **D72**, 093002 (2005).
106. B.A. Dobrescu and R.K. Ellis, Phys. Rev. **D69**, 114014 (2004).
107. For a review, see S. Davidson *et al.*, JHEP **0202**, 037 (2002).
108. SSF: C.Y. Prescott *et al.*, Phys. Lett. **B84**, 524 (1979).
109. JLab Hall A: X. Zheng *et al.*, to be published.
110. E.J. Beise, M.L. Pitt, and D.T. Spayde, Prog. in Part. Nucl. Phys. **54**, 289 (2005).
111. S.L. Zhu *et al.*, Phys. Rev. **D62**, 033008 (2000).
112. P. Souder, p. 599 of Ref. 5.
113. P. Langacker, p. 883 of Ref. 5.
114. R.D. Young *et al.*, Phys. Rev. Lett. **99**, 122003 (2007).
115. D.S. Armstrong and R.D. McKeown, Ann. Rev. Nucl. and Part. Sci. **62**, 337 (2012).
116. E. Derman and W.J. Marciano, Annals Phys. **121**, 147 (1979).
117. E158: P.L. Anthony *et al.*, Phys. Rev. Lett. **95**, 081601 (2005).
118. J. Erler and M.J. Ramsey-Musolf, Phys. Rev. **D72**, 073003 (2005).
119. A. Czarnecki and W.J. Marciano, Int. J. Mod. Phys. A **15**, 2365 (2000).
120. K.S. McFarland, in the *Proceedings of DIS* 2008.
121. C. Bouchiat and C.A. Piketty, Phys. Lett. **B128**, 73 (1983).
122. Qweak: M.T. Gericke *et al.*, AIP Conf. Proc. **1149**, 237 (2009).
123. Qweak: D. Androic *et al.*, Phys. Rev. Lett. **111**, 141803 (2013); the implications are discussed in Ref. 138.
124. For reviews and references to earlier work, see M.A. Bouchiat and L. Pottier, Science **234**, 1203 (1986);
B.P. Masterson and C.E. Wieman, p. 545 of Ref. 5.
125. Cesium (Boulder): C.S. Wood *et al.*, Science **275**, 1759 (1997).
126. Cesium (Paris): J. Guéna, M. Lintz, and M.A. Bouchiat, Phys. Rev. **A71**, 042108 (2005).
127. Thallium (Oxford): N.H. Edwards *et al.*, Phys. Rev. Lett. **74**, 2654 (1995);
Thallium (Seattle): P.A. Vetter *et al.*, Phys. Rev. Lett. **74**, 2658 (1995).
128. Lead (Seattle): D.M. Meekhof *et al.*, Phys. Rev. Lett. **71**, 3442 (1993).
129. Bismuth (Oxford): M.J.D. MacPherson *et al.*, Phys. Rev. Lett. **67**, 2784 (1991).
130. P.G. Blunden, W. Melnitchouk and A.W. Thomas, Phys. Rev. Lett. **109**, 262301 (2012).
131. V.A. Dzuba, V.V. Flambaum, and O.P. Sushkov, Phys. Lett. **141A**, 147 (1989);
S.A. Blundell, J. Sapirstein, and W.R. Johnson, Phys. Rev. **D45**, 1602 (1992);
For reviews, see S.A. Blundell, W.R. Johnson, and J. Sapirstein, p. 577 of Ref. 5;
J.S.M. Ginges and V.V. Flambaum, Phys. Reports **397**, 63 (2004);
J. Guéna, M. Lintz, and M. A. Bouchiat, Mod. Phys. Lett. **A20**, 375 (2005);
A. Derevianko and S.G. Porsev, Eur. Phys. J. A **32**, 517 (2007).
132. V.A. Dzuba, V.V. Flambaum, and O.P. Sushkov, Phys. Rev. **A56**, R4357 (1997).
133. S.C. Bennett and C.E. Wieman, Phys. Rev. Lett. **82**, 2484 (1999).
134. M.A. Bouchiat and J. Guéna, J. Phys. (France) **49**, 2037 (1988).
135. S. G. Porsev, K. Beloy, and A. Derevianko, Phys. Rev. Lett. **102**, 181601 (2009).
136. V.A. Dzuba *et al.*, Phys. Rev. Lett. **109**, 203003 (2012).
137. A. Derevianko, Phys. Rev. Lett. **85**, 1618 (2000);
V.A. Dzuba, C. Harabati, and W.R. Johnson, Phys. Rev. **A63**, 044103 (2001);
M.G. Kozlov, S.G. Porsev, and I.I. Tupitsyn, Phys. Rev. Lett. **86**, 3260 (2001);
W.R. Johnson, I. Bednyakov, and G. Soff, Phys. Rev. Lett. **87**, 233001 (2001);
A.I. Milstein and O.P. Sushkov, Phys. Rev. **A66**, 022108 (2002);
V.A. Dzuba, V.V. Flambaum, and J.S. Ginges, Phys. Rev. **D66**, 076013 (2002);
M.Y. Kuchiev and V.V. Flambaum, Phys. Rev. Lett. **89**, 283002 (2002);
A.I. Milstein, O.P. Sushkov, and I.S. Terekhov, Phys. Rev. Lett. **89**, 283003 (2002);
V.V. Flambaum and J.S.M. Ginges, Phys. Rev. **A72**, 052115 (2005).
138. J. Erler, A. Kurylov, and M.J. Ramsey-Musolf, Phys. Rev. **D68**, 016006 (2003).
139. V.A. Dzuba *et al.*, J. Phys. **B20**, 3297 (1987).
140. Ya.B. Zel'dovich, Sov. Phys. JETP **6**, 1184 (1958);
V.V. Flambaum and D.W. Murray, Phys. Rev. **C56**, 1641 (1997);
W.C. Haxton and C.E. Wieman, Ann. Rev. Nucl. Part. Sci. **51**, 261 (2001).
141. J.L. Rosner, Phys. Rev. **D53**, 2724 (1996).
142. S.J. Pollock, E.N. Fortson, and L. Wilets, Phys. Rev. **C46**, 2587 (1992);
B.Q. Chen and P. Vogel, Phys. Rev. **C48**, 1392 (1993).
143. R.W. Dunford and R.J. Holt, J. Phys. **G34**, 2099 (2007).
144. O.O. Versolato *et al.*, Hyperfine Interact. **199**, 9 (2011).
145. W. Hollik and G. Duckeck, *Electroweak Precision Tests at LEP*, Springer Tracts Mod. Phys. **162**, 1 (2000).
146. D.Yu. Bardin *et al.*, *Electroweak Working Group Report*, `hep-ph/9709229`.
147. A. Czarnecki and J.H. Kühn, Phys. Rev. Lett. **77**, 3955 (1996);
R. Harlander, T. Seidensticker, and M. Steinhauser, Phys. Lett. **B426**, 125 (1998);
J. Fleischer *et al.*, Phys. Lett. **B459**, 625 (1999).
148. M. Awramik *et al.*, Nucl. Phys. **B813**, 174 (2009).
149. B.W. Lynn and R.G. Stuart, Nucl. Phys. **B253**, 216 (1985).
150. *Physics at LEP*, ed. J. Ellis and R. Peccei, CERN 86–02, Vol. 1.
151. PETRA: S.L. Wu, Phys. Reports **107**, 59 (1984);
C. Kiesling, *Tests of the Standard Theory of Electroweak Interactions*, (Springer-Verlag, New York, 1988);
R. Marshall, Z. Phys. **C43**, 607 (1989);
Y. Mori *et al.*, Phys. Lett. **B218**, 499 (1989);
D. Haidt, p. 203 of Ref. 5.
152. For reviews, see D. Schaile, p. 215, and A. Blondel, p. 277 of Ref. 5; P. Langacker [7]; and S. Riemann [153].
153. S. Riemann, Rept. on Prog. in Phys. **73**, 126201 (2010).
154. SLD: K. Abe *et al.*, Phys. Rev. Lett. **84**, 5945 (2000).
155. SLD: K. Abe *et al.*, Phys. Rev. Lett. **85**, 5059 (2000).
156. SLD: K. Abe *et al.*, Phys. Rev. Lett. **86**, 1162 (2001).
157. SLD: K. Abe *et al.*, Phys. Rev. Lett. **78**, 17 (1997).
158. P.A. Grassi, B.A. Kniehl, and A. Sirlin, Phys. Rev. Lett. **86**, 389 (2001).
159. G. Degrassi and P. Gambino, Nucl. Phys. **B567**, 3 (2000).

160. J. Fleischer *et al.*, Phys. Lett. **B293**, 437 (1992); K.G. Chetyrkin, A. Kwiatkowski, and M. Steinhauser, Mod. Phys. Lett. **A8**, 2785 (1993).
161. A. Freitas and Y.-C. Huang, JHEP **1208**, 050 (2012) and *ibid.* **1310**, 044(E) (2013).
162. A. Freitas, Phys. Lett. **B730**, 50 (2014); A. Freitas, arXiv:1401.2447 [hep-ph].
163. DØ: V.M. Abazov *et al.*, Phys. Rev. **D84**, 012007 (2011).
164. CDF: T. Aaltonen *et al.*, Phys. Rev. **D88**, 072002 (2013).
165. CDF: www-cdf.fnal.gov/physics/ewk/2013/zAfb9mm/.
166. CDF: D. Acosta *et al.*, Phys. Rev. **D71**, 052002 (2005).
167. H1: A. Aktas *et al.*, Phys. Lett. **B632**, 35 (2006); H1 and ZEUS: Z. Zhang, Nucl. Phys. Proc. Suppl. **191**, 271 (2009).
168. CMS: S. Chatrchyan *et al.*, Phys. Rev. **D84**, 112002 (2011).
169. ATLAS: cds.cern.ch/record/1544035/files/ATLAS-CONF-2013-043.pdf.
170. ALEPH, DELPHI, L3, OPAL, and LEP Electroweak Working Group: S. Schael *et al.*, Phys. Reports **532**, 119 (2013).
171. ALEPH, DELPHI, L3, OPAL, and LEP Electroweak Working Group: J. Alcaraz *et al.*, hep-ex/0612034.
172. A. Leike, T. Riemann, and J. Rose, Phys. Lett. **B273**, 513 (1991); T. Riemann, Phys. Lett. **B293**, 451 (1992).
173. A comprehensive report and further references can be found in K.G. Chetyrkin, J.H. Kühn, and A. Kwiatkowski, Phys. Reports **277**, 189 (1996).
174. J. Schwinger, *Particles, Sources, and Fields*, Vol. II, (Addison-Wesley, New York, 1973); K.G. Chetyrkin, A.L. Kataev, and F.V. Tkachev, Phys. Lett. **B85**, 277 (1979); M. Dine and J. Sapirstein, Phys. Rev. Lett. **43**, 668 (1979); W. Celmaster and R.J. Gonsalves, Phys. Rev. Lett. **44**, 560 (1980); S.G. Gorishnii, A.L. Kataev, and S.A. Larin, Phys. Lett. **B259**, 144 (1991); L.R. Surguladze, M.A. Samuel, Phys. Rev. Lett. **66**, 560 (1991) and *ibid.* 2416(E).
175. P.A. Baikov, K.G. Chetyrkin, and J.H. Kühn, Phys. Rev. Lett. **101**, 012002 (2008).
176. B.A. Kniehl and J.H. Kühn, Nucl. Phys. **B329**, 547 (1990); K.G. Chetyrkin and A. Kwiatkowski, Phys. Lett. **B319**, 307 (1993); S.A. Larin, T. van Ritbergen, and J.A.M. Vermaseren, Phys. Lett. **B320**, 159 (1994); K.G. Chetyrkin and O.V. Tarasov, Phys. Lett. **B327**, 114 (1994).
177. A.L. Kataev, Phys. Lett. **B287**, 209 (1992).
178. D. Albert *et al.*, Nucl. Phys. **B166**, 460 (1980); F. Jegerlehner, Z. Phys. **C32**, 425 (1986); A. Djouadi, J.H. Kühn, and P.M. Zerwas, Z. Phys. **C46**, 411 (1990); A. Borrelli *et al.*, Nucl. Phys. **B333**, 357 (1990).
179. A.A. Akhundov, D.Yu. Bardin, and T. Riemann, Nucl. Phys. **B276**, 1 (1986); W. Beenakker and W. Hollik, Z. Phys. **C40**, 141 (1988); B.W. Lynn and R.G. Stuart, Phys. Lett. **B352**, 676 (1990); J. Bernabeu, A. Pich, and A. Santamaria, Phys. Lett. **B200**, 569 (1988) and Nucl. Phys. **B363**, 326 (1991).
180. ATLAS: G. Aad *et al.*, Phys. Lett. **B716**, 1 (2012); CMS: S. Chatrchyan *et al.*, Phys. Lett. **B716**, 30 (2012); CMS: S. Chatrchyan *et al.*, JHEP **1306**, 081 (2013).
181. ATLAS: G. Aad *et al.*, Phys. Lett. **B726**, 88 (2013).
182. CMS: cds.cern.ch/record/1542387/files/HIG-13-005-pas.pdf.
183. CDF and DØ: T. Aaltonen *et al.*, Phys. Rev. **D88**, 052014 (2013).
184. ATLAS: cds.cern.ch/record/1632191/files/ATLAS-CONF-2013-108.pdf; CMS: S. Chatrchyan *et al.*, arXiv:1401.5041.
185. ATLAS: G. Aad *et al.*, Phys. Lett. **B726**, 88 (2013).
186. A. Djouadi, J. Kalinowski, and M. Spira, Comp. Phys. Comm. **108**, 56 (1998).
187. H. Davoudiasl, H.-S. Lee, and W.J. Marciano, Phys. Rev. **D86**, 095009 (2012).
188. E. Braaten, S. Narison, and A. Pich, Nucl. Phys. **B373**, 581 (1992).
189. F. Le Diberder and A. Pich, Phys. Lett. **B286**, 147 (1992).
190. M. Beneke and M. Jamin, JHEP **0809**, 044 (2008).
191. E. Braaten and C.S. Li, Phys. Rev. **D42**, 3888 (1990).
192. J. Erler, Rev. Mex. Fis. **50**, 200 (2004).
193. D. Boito *et al.*, Phys. Rev. **D85**, 093015 (2012).
194. J. Erler, arXiv:1102.5520 [hep-ph].
195. M. Davier *et al.*, Eur. Phys. J. **C56**, 305 (2008); K. Maltman and T. Yavin, Phys. Rev. **D78**, 094020 (2008).
196. E821: G.W. Bennett *et al.*, Phys. Rev. Lett. **92**, 161802 (2004).
197. T. Aoyama *et al.*, Phys. Rev. Lett. **109**, 111808 (2012); T. Aoyama *et al.*, PTEP **2012**, 01A107 (2012); P. Baikov, A. Maier and P. Marquard, Nucl. Phys. **B877**, 647 (2013).
198. G. Li, R. Mendel, and M.A. Samuel, Phys. Rev. **D47**, 1723 (1993); S. Laporta and E. Remiddi, Phys. Lett. **B301**, 440 (1993); S. Laporta and E. Remiddi, Phys. Lett. **B379**, 283 (1996); A. Czarnecki and M. Skrzypek, Phys. Lett. **B449**, 354 (1999).
199. J. Erler and M. Luo, Phys. Rev. Lett. **87**, 071804 (2001).
200. S.J. Brodsky and J.D. Sullivan, Phys. Rev. **D156**, 1644 (1967); T. Burnett and M.J. Levine, Phys. Lett. **B24**, 467 (1967); R. Jackiw and S. Weinberg, Phys. Rev. **D5**, 2473 (1972); I. Bars and M. Yoshimura, Phys. Rev. **D6**, 374 (1972); K. Fujikawa, B.W. Lee, and A.I. Sanda, Phys. Rev. **D6**, 2923 (1972); G. Altarelli, N. Cabibbo, and L. Maiani, Phys. Lett. **B40**, 415 (1972); W.A. Bardeen, R. Gastmans, and B.E. Laurup, Nucl. Phys. **B46**, 315 (1972).
201. T.V. Kukhto *et al.*, Nucl. Phys. **B371**, 567 (1992); S. Peris, M. Perrottet, and E. de Rafael, Phys. Lett. **B355**, 523 (1995); A. Czarnecki, B. Krause, and W.J. Marciano, Phys. Rev. **D52**, 2619 (1995); A. Czarnecki, B. Krause, and W.J. Marciano, Phys. Rev. Lett. **76**, 3267 (1996).
202. G. Degrassi and G. Giudice, Phys. Rev. **D58**, 053007 (1998); A. Czarnecki, W.J. Marciano and A. Vainshtein, Phys. Rev. **D67**, 073006 (2003) and *ibid.*, **D73**, 119901(E) (2006).
203. For reviews, see M. Davier and W.J. Marciano, Ann. Rev. Nucl. Part. Sci. **54**, 115 (2004); J.P. Miller, E. de Rafael, and B.L. Roberts, Rept. Prog. Phys. **70**, 795 (2007); F. Jegerlehner and A. Nyffeler, Phys. Reports **477**, 1 (2009).
204. V. Cirigliano, G. Ecker, and H. Neufeld, JHEP **0208**, 002 (2002); K. Maltman and C.E. Wolfe, Phys. Rev. **D73**, 013004 (2006); M. Davier *et al.*, Eur. Phys. J. **C66**, 127 (2010).
205. W.J. Marciano and A. Sirlin, Phys. Rev. Lett. **61**, 1815 (1988).
206. S. Ghozzi and F. Jegerlehner, Phys. Lett. **B583**, 222 (2004).
207. F. Jegerlehner and R. Szafron, Eur. Phys. J. **C71**, 1632 (2011).
208. M. Davier and B. Malaescu, Eur. Phys. J. **C73**, 2597 (2013).
209. K. Melnikov and A. Vainshtein, Phys. Rev. **D70**, 113006 (2004).
210. J. Erler and G. Toledo Sánchez, Phys. Rev. Lett. **97**, 161801 (2006).
211. A. Nyffeler, Phys. Rev. **D79**, 073012 (2009).
212. J. Prades, E. de Rafael, and A. Vainshtein, arXiv:0901.0306 [hep-ph].
213. M. Knecht and A. Nyffeler, Phys. Rev. **D65**, 073034 (2002).
214. M. Hayakawa and T. Kinoshita, hep-ph/0112102; J. Bijnens, E. Pallante, and J. Prades, Nucl. Phys. **B626**, 410 (2002); A recent discussion is in J. Bijnens and J. Prades, Mod. Phys. Lett. **A22**, 767 (2007).

215. T. Blum, M. Hayakawa and T. Izubuchi, PoS LATTICE **2012**, 022 (2012).
216. B. Krause, Phys. Lett. **B390**, 392 (1997).
217. J.L. Lopez, D.V. Nanopoulos, and X. Wang, Phys. Rev. **D49**, 366 (1994);
for recent reviews, see Ref. 203.
218. U. Amaldi *et al.*, Phys. Rev. **D36**, 1385 (1987);
G. Costa *et al.*, Nucl. Phys. **B297**, 244 (1988);
P. Langacker and M. Luo, Phys. Rev. **D44**, 817 (1991);
J. Erler and P. Langacker, Phys. Rev. **D52**, 441 (1995).
219. CDF and DØ: T. Aaltonen *et al.*, Phys. Rev. **D88**, 052018 (2013).
220. Tevatron Electroweak Working Group, CDF and DØ: `arXiv:1003.2826 [hep-ex]`.
221. F. James and M. Roos, Comput. Phys. Commun. **10**, 343 (1975).
222. For a more recent study, see J. Cao and J.M. Yang, JHEP **0812**, 006 (2008).
223. J. Erler, J.L. Feng, and N. Polonsky, Phys. Rev. Lett. **78**, 3063 (1997).
224. D. Choudhury, T.M.P. Tait, and C.E.M. Wagner, Phys. Rev. **D65**, 053002 (2002).
225. J. Erler and P. Langacker, Phys. Rev. Lett. **84**, 212 (2000).
226. P. Langacker and M. Plümacher, Phys. Rev. **D62**, 013006 (2000).
227. DELPHI: P. Abreu *et al.*, Eur. Phys. J. **C10**, 415 (1999).
228. CMS: S. Chatrchyan *et al.*, Phys. Lett. **B728**, 496 (2014).
229. DØ: V.M. Abazov *et al.*, Phys. Rev. **D80**, 111107 (2009).
230. ALEPH, DELPHI, L3, OPAL, and the LEP Working Group for Higgs Boson Searches: D. Abbaneo *et al.*, Phys. Lett. **B565**, 61 (2003).
231. P. Langacker and N. Polonsky, Phys. Rev. **D52**, 3081 (1995);
J. Bagger, K.T. Matchev, and D. Pierce, Phys. Lett. **B348**, 443 (1995).
232. M. Veltman, Nucl. Phys. **B123**, 89 (1977);
M. Chanowitz, M.A. Furman, and I. Hinchliffe, Phys. Lett. **B78**, 285 (1978);
The two-loop correction has been obtained by J.J. van der Bij and F. Hoogeveen, Nucl. Phys. **B283**, 477 (1987).
233. P. Langacker and M. Luo, Phys. Rev. **D45**, 278 (1992) and refs. therein.
234. A. Denner, R.J. Guth, and J.H. Kühn, Phys. Lett. **B240**, 438 (1990);
W. Grimus *et al.*, J. Phys. G **35**, 075001 (2008);
H. E. Haber and D. O'Neil, Phys. Rev. **D83**, 055017 (2011).
235. S. Bertolini and A. Sirlin, Phys. Lett. **B257**, 179 (1991).
236. M. Peskin and T. Takeuchi, Phys. Rev. Lett. **65**, 964 (1990);
M. Peskin and T. Takeuchi, Phys. Rev. **D46**, 381 (1992);
M. Golden and L. Randall, Nucl. Phys. **B361**, 3 (1991).
237. D. Kennedy and P. Langacker, Phys. Rev. **D44**, 1591 (1991).
238. G. Altarelli and R. Barbieri, Phys. Lett. **B253**, 161 (1991).
239. B. Holdom and J. Terning, Phys. Lett. **B247**, 88 (1990).
240. B.W. Lynn, M.E. Peskin, and R.G. Stuart, p. 90 of Ref. 150.
241. An alternative formulation is given by K. Hagiwara *et al.*, Z. Phys. **C64**, 559 (1994), and *ibid.* **68**, 352(E) (1995);
K. Hagiwara, D. Haidt, and S. Matsumoto, Eur. Phys. J. **C2**, 95 (1998).
242. I. Maksymyk, C.P. Burgess, and D. London, Phys. Rev. **D50**, 529 (1994);
C.P. Burgess *et al.*, Phys. Lett. **B326**, 276 (1994);
R. Barbieri, M. Frigeni, and F. Caravaglios, Phys. Lett. **B279**, 169 (1992).
243. R. Barbieri *et al.*, Nucl. Phys. **B703**, 127 (2004).
244. M.S. Carena *et al.*, Nucl. Phys. **B759**, 202 (2006).
245. K. Lane, `hep-ph/0202255`.
246. E. Gates and J. Terning, Phys. Rev. Lett. **67**, 1840 (1991);
R. Sundrum and S.D.H. Hsu, Nucl. Phys. **B391**, 127 (1993);
R. Sundrum, Nucl. Phys. **B395**, 60 (1993);
M. Luty and R. Sundrum, Phys. Rev. Lett. **70**, 529 (1993);
T. Appelquist and J. Terning, Phys. Lett. **B315**, 139 (1993);
D.D. Dietrich, F. Sannino, and K. Tuominen, Phys. Rev. **D72**, 055001 (2005);
N.D. Christensen and R. Shrock, Phys. Lett. **B632**, 92 (2006);
M. Harada, M. Kurachi, and K. Yamawaki, Prog. Theor. Phys. **115**, 765 (2006).
247. H. Georgi, Nucl. Phys. **B363**, 301 (1991);
M.J. Dugan and L. Randall, Phys. Lett. **B264**, 154 (1991).
248. R. Barbieri *et al.*, Nucl. Phys. **B341**, 309 (1990).
249. J. Erler and D.M. Pierce, Nucl. Phys. **B526**, 53 (1998);
G.C. Cho and K. Hagiwara, Nucl. Phys. **B574**, 623 (2000);
G. Altarelli *et al.*, JHEP **0106**, 018 (2001);
S. Heinemeyer, W. Hollik, and G. Weiglein, Phys. Reports **425**, 265 (2006);
S.P. Martin, K. Tobe, and J.D. Wells, Phys. Rev. **D71**, 073014 (2005);
G. Marandella, C. Schappacher, and A. Strumia, Nucl. Phys. **B715**, 173 (2005);
M.J. Ramsey-Musolf and S. Su, Phys. Reports **456**, 1 (2008);
A. Djouadi, Phys. Reports **459**, 1 (2008);
S. Heinemeyer *et al.*, JHEP **0804**, 039 (2008);
O. Buchmueller *et al.*, Eur. Phys. J. **C72**, 2020 (2012).
250. J. Erler and P. Langacker, Phys. Rev. Lett. **105**, 031801 (2010).
251. CMS: S. Chatrchyan *et al.*, Phys. Rev. **D86**, 112003 (2012).
252. O. Eberhardt *et al.*, Phys. Rev. Lett. **109**, 241802 (2012);
A. Djouadi and A. Lenz, Phys. Lett. **B715**, 310 (2012).
253. J. Maalampi and M. Roos, Phys. Reports **186**, 53 (1990).
254. For reviews, see the Section on "Grand Unified Theories" in this *Review*;
P. Langacker, Phys. Reports **72**, 185 (1981);
J.L. Hewett and T.G. Rizzo, Phys. Reports **183**, 193 (1989);
J. Kang, P. Langacker and B.D. Nelson, Phys. Rev. **D77**, 035003 (2008);
S.P. Martin, Phys. Rev. **D81**, 035004 (2010);
P.W. Graham *et al.*, Phys. Rev. **D81**, 055016 (2010).
255. P. Langacker and D. London, Phys. Rev. **D38**, 886 (1988);
D. London, p. 951 of Ref. 5;
a recent analysis is F. del Aguila, J. de Blas and M. Perez-Victoria, Phys. Rev. **D78**, 013010 (2008).
256. M. Chemtob, Prog. in Part. Nucl. Phys. **54**, 71 (2005);
R. Barbier *et al.*, Phys. Reports **420**, 1 (2005).
257. R.S. Chivukula and E.H. Simmons, Phys. Rev. **D66**, 015006 (2002);
C.T. Hill and E.H. Simmons, Phys. Reports **381**, 235 (2003);
R.S. Chivukula *et al.*, Phys. Rev. **D70**, 075008 (2004).
258. K. Agashe *et al.*, JHEP **0308**, 050 (2003);
M. Carena *et al.*, Phys. Rev. **D68**, 035010 (2003);
I. Gogoladze and C. Macesanu, Phys. Rev. **D74**, 093012 (2006);
I. Antoniadis, `hep-th/0102202` see also the note on "Extra Dimensions" in the Searches Particle Listings.
259. T. Han, H.E. Logan, and L.T. Wang, JHEP **0601**, 099 (2006);
M. Perelstein, Prog. in Part. Nucl. Phys. **58**, 247 (2007).
260. E. Accomando *et al.*, `arXiv:hep-ph/0608079`;
V. Barger *et al.*, Phys. Rev. **D77**, 035005 (2008);
W. Grimus *et al.*, Nucl. Phys. **B801**, 81 (2008);
M. Maniatis, Int. J. Mod. Phys. **A25**, 3505 (2010);
U. Ellwanger, C. Hugonie, and A.M. Teixeira, Phys. Reports **496**, 1 (2010);
M.C. Chen, S. Dawson, and C.B. Jackson, Phys. Rev. **D78**, 093001 (2008).
261. A. Barroso *et al.*, `arXiv:1304.5225 [hep-ph]`;
B. Grinstein and P. Uttayarat, JHEP **1306**, 094 (2013) and *ibid.* **1309**, 110(E) (2013);
O. Eberhardt, U. Nierste and M. Wiebusch, JHEP **1307**, 118 (2013).
262. G.C. Cho, K. Hagiwara, and S. Matsumoto, Eur. Phys. J. **C5**, 155 (1998);
K. Cheung, Phys. Lett. **B517**, 167 (2001);
Z. Han and W. Skiba, Phys. Rev. **D71**, 075009 (2005).
263. P. Langacker, M. Luo, and A.K. Mann, Rev. Mod. Phys. **64**, 87 (1992);
M. Luo, p. 977 of Ref. 5.

264. F.S. Merritt *et al.*, p. 19 of *Particle Physics: Perspectives and Opportunities: Report of the DPF Committee on Long Term Planning*, ed. R. Peccei *et al.* (World Scientific, Singapore, 1995).
265. D.E. Morrissey, T. Plehn, and T.M.P. Tait, Phys. Reports **515**, 1 (2012).
266. G. Altarelli, R. Barbieri, and S. Jadach, Nucl. Phys. **B369**, 3 (1992) and *ibid.* **B376**, 444(E) (1992).
267. A. De Rújula *et al.*, Nucl. Phys. **B384**, 3 (1992);
K. Hagiwara *et al.*, Phys. Rev. **D48**, 2182 (1993);
C.P. Burgess *et al.*, Phys. Rev. **D49**, 6115 (1994);
Z. Han and W. Skiba, Phys. Rev. **D71**, 075009 (2005);
G. Cacciapaglia *et al.*, Phys. Rev. **D74**, 033011 (2006);
V. Bernard *et al.*, JHEP **0801**, 015 (2008);
Z. Han, Int. J. Mod. Phys. A **23**, 2653 (2008).
268. For reviews, see A. Leike, Phys. Reports **317**, 143 (1999);
P. Langacker, Rev. Mod. Phys. **81**, 1199 (2009).
269. J. Erler, P. Langacker, and T. Li, Phys. Rev. **D66**, 015002 (2002);
G. Cleaver *et al.*, Phys. Rev. **D59**, 055005 (1999).
270. B. Holdom, Phys. Lett. **B166**, 196 (1986).
271. M. Carena *et al.*, Phys. Rev. **D70**, 093009 (2004).
272. J. Erler, P. Langacker, S. Munir and E. Rojas, JHEP **0908**, 017 (2009).
273. ATLAS: `cds.cern.ch/record/1525524/files/ATLAS-CONF-2013-017.pdf`.
274. CMS: `cds.cern.ch/record/1519132/files/EXO-12-061-pas.pdf`.
275. CDF: T. Aaltonen *et al.*, Phys. Rev. Lett. **106**, 121801 (2011).
276. DØ: V.M. Abazov *et al.*, Phys. Lett. **B695**, 88 (2011).
277. J. Kang and P. Langacker, Phys. Rev. **D71**, 035014 (2005);
C.-F. Chang, K. Cheung, and T.-C. Yuan, JHEP **1109**, 058 (2011).
278. F. del Aguila, J. de Blas, and M. Perez-Victoria, JHEP **1009**, 033 (2010).
279. T. Appelquist, B.A. Dobrescu, and A.R. Hopper, Phys. Rev. **D68**, 035012 (2003);
R.S. Chivukula *et al.*, Phys. Rev. **D69**, 015009 (2004).

11. STATUS OF HIGGS BOSON PHYSICS

Written November 2013 by M. Carena (Fermi National Accelerator Laboratory and the University of Chicago), C. Grojean (ICREA at IFAE, Universitat Autònoma de Barcelona), M. Kado (Laboratoire de l'Accélérateur Linéaire, LAL and CERN), and V. Sharma (University of California San Diego).

I. Introduction

The observation by ATLAS [1] and CMS [2] of a new boson with a mass of approximately 125 GeV decaying into $\gamma\gamma$, WW and ZZ bosons and the subsequent studies of the properties of this particle is a milestone in the understanding of the mechanism that breaks electroweak symmetry and generates the masses of the known elementary particles[1], one of the most fundamental problems in particle physics.

In the Standard Model, the mechanism of electroweak symmetry breaking (EWSB) [3] provides a general framework to keep untouched the structure of the gauge interactions at high energy and still generate the observed masses of the W and Z gauge bosons by means of charged and neutral Goldstone bosons that manifest themselves as the longitudinal components of the gauge bosons. The discovery of ATLAS and CMS now strongly suggests that these three Goldstone bosons combine with an extra (elementary) scalar boson to form a weak doublet.

This picture matches very well with the Standard Model (SM) [4] which describes the electroweak interactions by a gauge field theory invariant under the $\mathrm{SU}(2)_L \times \mathrm{U}(1)_Y$ symmetry group. In the SM, the EWSB mechanism posits a self-interacting complex doublet of scalar fields, and the renormalizable interactions are arranged such

[1] In the case of neutrinos, it is possible that the EWSB mechanism plays only a partial role in generating the observed neutrino masses, with additional contributions at a higher scale via the so called see-saw mechanism.

that the neutral component of the scalar doublet acquires a vacuum expectation value (VEV) $v \approx 246\,\text{GeV}$, which sets the scale of electroweak symmetry breaking.

Three massless Goldstone bosons are generated, which are absorbed to give masses to the W and Z gauge bosons. The remaining component of the complex doublet becomes the Higgs boson – a new fundamental scalar particle. The masses of all fermions are also a consequence of EWSB since the Higgs doublet is postulated to couple to the fermions through Yukawa interactions. However, the true structure behind the newly discovered boson, including the exact dynamics that triggers the Higgs VEV, and the corresponding ultraviolet completion is still unsolved.

Even if the discovered boson has weak couplings to all known SM degrees of freedom, it is not impossible that it is part of an extended symmetry structure or that it emerges from a light resonance of a strongly coupled sector. It needs to be established whether the Higgs boson is solitary or whether other states populate the EWSB sector.

Without the Higgs boson, the calculability of the SM would have been spoiled. In particular, perturbative unitarity [5,6] would be lost at high energies as the longitudinal W/Z boson scattering amplitude would grow as the centre-of-mass energy increases. Moreover, the radiative corrections to the self-energies of the gauge boson pertaining their longitudinal components would exhibit dangerous logarithmic divergences. With the discovery of the Higgs boson, it has been experimentally established that the SM is based on a gauge theory that could a priori be consistently extrapolated to the Planck scale. The Higgs boson must have couplings to W/Z gauge bosons and fermions precisely as those in the SM to maintain the consistency of the theory at high energies, hence, formally there is no need for new physics at the EW scale. However, the SM Higgs boson is a scalar particle, therefore without a symmetry to protect its mass, at the quantum level it has sensitivity to the physics in the ultraviolet. Quite generally, the Higgs mass parameter may be affected by the presence of heavy particles. Specifically, apart from terms proportional to m^2 itself, which are corrected by the Higgs field anomalous dimension, if there are fermion and boson particles with squared masses $m^2_{F,B} + \lambda^2_{F,B}\phi^2/2$,

$$m^2(Q) = m^2(\mu) + \delta m^2, \tag{11.1}$$

$$\delta m^2 = \sum_{B,F} g_{B,F}(-1)^{2S}\frac{\lambda^2_{B,F} m^2_{B,F}}{32\pi^2}\log(\frac{Q^2}{\mu^2}), \tag{11.2}$$

where $g_{B,F}$ and S correspond to the number of degrees of freedom and the spin of the boson and fermion particles, respectively. Therefore, particles that couple to the Higgs and have a large mass parameter $m^2_{B,F}$ would induce very large corrections to the Higgs mass parameter, demanding a large fine tuning to explain why m^2 remains small. Hence, in general, light scalars like the Higgs boson cannot naturally survive in the presence of heavy states at the grand-unification, string or Planck scales. This is known as the hierarchy or naturalness problem [7]. In the Standard Model where there are no other explicit mass parameter than the Higgs one, all corrections are proportional to the Higgs mass parameter itself.

There are two possible preferred solutions to the naturalness problem: one is based on a new fermion-boson symmetry in nature called supersymmetry (SUSY) [8–10]. This is a weakly coupled approach to EWSB, and in this case, the Higgs boson remains elementary and the corrections to its mass are cut at the scale at which SUSY is broken and remain insensitive to the details of the physics at higher scales. These theories predict at least one charged and three neutral Higgs particles[2] [12], and one of the neutral Higgs bosons, most often the lightest *CP*-even Higgs, has properties that resemble those of the SM Higgs boson. It will be referred to as a SM-like Higgs boson, meaning that its VEV is predominantly responsible for EWSB, and hence has SM-like couplings to the W and Z gauge bosons.

The other approach invokes the existence of strong interactions at a scale of the order of a TeV or above and induces strong breaking of the electroweak symmetry [13]. In the original incarnation of this second approach, dubbed technicolor, the strong interactions themselves trigger EWSB without the need of a Higgs boson. Another possibility, more compatible with the ATLAS and CMS discovery, is that the strong interactions produce 4 light resonances identified with the Higgs doublet and EWSB proceeds through vacuum misalignment [14].

Both approaches can have important effects on the phenomenology of the Higgs boson associated with EWSB. Also, in each case the Higgs role in unitarization is shared by other particles: additional Higgs bosons in supersymmetry, or new particles in the strong sector.

A third option has also been considered in the literature. It is also a variation of technicolor or Higgsless models [13,15]. In light of the Higgs boson discovery these models are ruled out. However, there still exists the possibility that the Higgs discovered at the LHC is in fact the Goldstone boson of the spontaneous breaking of scale invariance at a scale f [16,17]. Given the good agreement of the coupling measurements with the SM predictions, this scenario now requires rather involved model-building engineering.

The naturalness problem has been the prime argument for new physics at the TeV scale. But the absence of any direct signal of new dynamics and the apparent agreement of the Higgs couplings with the SM predictions, together with the strong bounds inherited from precision electroweak and flavor data leaves open the possibility that the Higgs boson may very well be elementary, weakly coupled and solitary till the Planck scale. Such a scenario, would force physicists to rethink the basic concepts of high energy physics.

In this review, some of the most interesting models proposed in the above two categories will be discussed in detail. Extensions of the SM Higgs sector without low-energy supersymmetry will also be discussed. These type of models do not address the naturalness problem in a specific manner, but provide grounds to explore new Higgs boson signals in a more model-independent way, with different types of coupling structure to fermions and gauge bosons. Extended Higgs sectors are usually quite restricted by experimental constraints from precision electroweak measurements as well as constraints from flavor changing neutral and charged current effects.

Section II is a review of the Higgs boson of the Standard Model, discussing its properties and the production mechanisms and decay rates. In Section III, the SM Higgs boson analysis channels are described. In Section IV, a general theoretical framework to describe the deviations of the Higgs couplings from the SM predictions is introduced and the experimental measurements of these Higgs couplings is reviewed together with the analysis establishing the spin and *CP*-properties of the Higgs boson. Section V presents, in detail, some of the most interesting models proposed for Higgs extensions of the SM and considers their experimental signatures. Section VI provides a brief outlook.

II. The Standard Model and the Mechanism of Electroweak Symmetry Breaking

As mentioned above, in the SM [4], the mechanism of electroweak symmetry breaking [3] is responsible for generating mass for the W and Z gauge bosons rendering the weak interactions short range. The SM scalar potential reads:

$$V(\Phi) = m^2\Phi^\dagger\Phi + \lambda(\Phi^\dagger\Phi)^2 \tag{11.3}$$

with the Higgs field Φ being a self-interacting SU(2) complex doublet (four real degrees of freedom) with weak hypercharge Y=1 (the hypercharge is normalized such that $Q = T_{3L} + Y/2$):

$$\Phi = \frac{1}{\sqrt{2}}\begin{pmatrix}\sqrt{2}\phi^+\\ \phi^0 + ia^0\end{pmatrix}. \tag{11.4}$$

$V(\Phi)$ is the most general renormalizable scalar potential and if the quadratic term is negative the neutral component of the scalar doublet

[2] Except in exotic SUSY scenarios where the Higgs boson is identified as a sneutrino, the scalar partner of a neutrino [11], in which case the gauge anomalies cancel without the need for a second Higgs doublet

acquires a non-zero vacuum expectation value (VEV)

$$\langle\Phi\rangle = \frac{1}{\sqrt{2}}\begin{pmatrix}0\\ v\end{pmatrix}, \tag{11.5}$$

defining $\phi^0 = H + v$, inducing the spontaneous breaking of the SM gauge symmetry $\mathrm{SU(3)}_C \times \mathrm{SU(2)}_L \times \mathrm{U(1)}_Y$ into $\mathrm{SU(3)}_C \times \mathrm{U(1)}_{\rm em}$. The global minimum of the theory defines the ground state, and spontaneous symmetry breaking implies that there is a symmetry of the system (Lagrangian) that is not respected by the ground state. The Higgs field permeates the entire universe and through its self-interactions can cause spontaneous electroweak symmetry-breaking (EWSB) in the vacuum. From the 4 generators of the $\mathrm{SU(2)}_L \times \mathrm{U(1)}_Y$ gauge group, three are spontaneously broken, implying that they lead to non-trivial transformations of the ground state and indicate the existence of three massless Goldstone bosons identified with three of the four Higgs field degrees of freedom. The Higgs field couples to the W_μ and B_μ gauge fields associated with the $\mathrm{SU(2)}_L \times \mathrm{U(1)}_Y$ local symmetry, respectively, through the covariant derivative, $D_\mu\Phi = (\partial_\mu + ig\sigma^a W^a_\mu/2 + ig'YB_\mu/2)\Phi$ (g and g' are the SU(2) and U(1) gauge couplings and $\sigma^a, a = 1, 2, 3$ are the usual Pauli matrices) appearing in the kinetic term of the Higgs Lagrangian

$$\mathcal{L}_{\rm Higgs} = (D_\mu\Phi)^\dagger(D^\mu\Phi) - V(\Phi)\,. \tag{11.6}$$

As a result, the neutral and the two charged massless Goldstone degrees of freedom mix with the gauge fields corresponding to the broken generators of $\mathrm{SU(2)}_L \times \mathrm{U(1)}_Y$ and become the longitudinal components of the Z and W physical gauge bosons, respectively. The fourth generator remains unbroken since it is the one associated to the conserved $\mathrm{U(1)}_{\rm em}$ gauge symmetry, and its corresponding gauge field, the photon, remains massless. Similarly the eight color gauge bosons, the gluons, corresponding to the conserved $\mathrm{SU(3)}_C$ gauge symmetry with 8 unbroken generators, also remain massless. Hence, from the initial four degrees of freedom of the Higgs field, two are absorbed by the $W^\pm$ gauge bosons and one by the Z gauge boson that become massive:

$$M_W^2 = \frac{g^2v^2}{4} \quad M_Z^2 = \frac{(g'^2+g^2)v^2}{4}. \tag{11.7}$$

There is one remaining degree of freedom, H, that is the physical Higgs boson — a new scalar particle. The Higgs boson is neutral under the electromagnetic interactions and transforms as a singlet under $\mathrm{SU(3)}_C$ and hence does not couple at tree level to the massless photons and gluons.

The fermions of the SM acquire mass through a new type of renormalizable interactions between the Higgs field and the fermions: the Yukawa interactions,

$$\mathcal{L}_{\rm Yukawa} = -\hat{h}_{d_{ij}}\bar{q}_{L_i}\Phi\, d_{R_j} - \hat{h}_{u_{ij}}\bar{q}_{L_i}\tilde{\Phi}u_{R_j} - \hat{h}_{l_{ij}}\bar{l}_{L_i}\Phi\, e_{R_j} + h.c., \tag{11.8}$$

that respect the symmetries of the SM but generate fermion masses once EWSB occurs. In the above, $\tilde{\Phi} = i\sigma_2\Phi^*$ and q_L (l_L) and u_R, d_R (e_R) are the quark (lepton) $\mathrm{SU(2)}_L$ doublets and singlets, respectively, while each term is parametrized by a 3×3 matrix in family space. The mass term for neutrinos is omitted, but could be added in an analogous manner to the up type quarks when right-handed neutrinos are supplementing the SM particle content. Once the Higgs acquires a VEV, and after rotation to the fermion mass eigenstate basis that also diagonalize the Higgs-fermion interactions, $\hat{h}_{f_{ij}} \to h_f \mathbf{1_{3\times3}}$, all fermions acquire a mass given by $m_f = h_f v/\sqrt{2}$. It should be noted that the EWSB mechanism provides no additional insight on possible underlying reasons for the large variety of masses of the fermions, often referred to as the flavor hierarchy. The fermion masses, accounting for a large number of the free parameters of the SM are simply translated in terms of Yukawa couplings h_f.

II.1. The SM Higgs boson mass, couplings and quantum numbers

The SM Higgs boson is a *CP*-even scalar of spin 0. Its mass is given by $m_H = \sqrt{2\lambda}\,v$, where λ is the Higgs self-coupling parameter in $V(\Phi)$. The expectation value of the Higgs field, $v = (\sqrt{2}G_F)^{-1/2} \approx 246\,\mathrm{GeV}$, is fixed by the Fermi coupling G_F, which is determined with a precision of 0.6 ppm from muon decay measurements [18]. The quartic coupling λ, instead, is a free parameter in the SM, and hence there is, a priori, no prediction for the Higgs mass. Moreover the sign of the mass parameter $m^2 = -\lambda v^2$ is crucial for the EW symmetry breaking to take place, but it is not specified in the SM. Therefore, if the newly discovered particle is indeed the SM Higgs boson with $m_H \simeq 125\,\mathrm{GeV}$, it implies that $\lambda \simeq 0.13$ and $|m| \simeq 88.8\,\mathrm{GeV}$. It is interesting to observe that in the SM one needs to assume that the mass term in the potential is negative in order to trigger EWSB. In other theories beyond the SM (BSM), such as supersymmetry, the analogue of the Higgs mass parameter can be made negative dynamically.

The Higgs boson couplings to the fundamental particles are set by their masses. This is a new type of interaction, very weak for ordinary particles, such as up and down quarks, and electrons, but strong for heavy particles such as the W and Z bosons and the top quark. More precisely, the SM Higgs couplings to fundamental fermions are linearly proportional to the fermion masses, whereas the couplings to bosons are proportional to the square of the boson masses. The SM Higgs boson couplings to gauge bosons, Higgs bosons and fermions are summarized in the following Lagrangian:

$$\begin{aligned}\mathcal{L} = &- g_{Hff}\bar{f}fH + \frac{g_{HHH}}{6}H^3 + \frac{g_{HHHH}}{24}H^4 \\ &+ \delta_V V_\mu V^\mu\left(g_{HVV}H + \frac{g_{HHVV}}{2}H^2\right)\end{aligned} \tag{11.9}$$

with

$$g_{Hf\bar{f}} = \frac{m_f}{v}, \quad g_{HVV} = \frac{2m_V^2}{v}, \quad g_{HHVV} = \frac{2m_V^2}{v^2} \tag{11.10}$$

$$g_{HHH} = \frac{3m_H^2}{v}, \quad g_{HHHH} = \frac{3m_H^2}{v^2} \tag{11.11}$$

where $V = \mathrm{W}^\pm$ or Z and $\delta_W = 1, \delta_Z = 1/2$. As a result, the dominant mechanisms for Higgs boson production and decay involve the coupling of H to W, Z and/or the third generation quarks and leptons. The Higgs boson coupling to gluons [19,20], is induced at leading order by a one-loop graph in which H couples to a virtual $t\bar{t}$ pair. Likewise, the Higgs boson coupling to photons is also generated via loops, although in this case the one-loop graph with a virtual W^+W^- pair provides the dominant contribution [12] and the one involving a virtual $t\bar{t}$ pair is subdominant.

II.2. The SM custodial symmetry

The SM Higgs Lagrangian, $\mathcal{L}_{\rm Higgs}$ of Eq. (11.6), is, by construction, $\mathrm{SU(2)}_L \times \mathrm{U(1)}_Y$ gauge invariant, but it also has an approximate global symmetry. In the limit $g' \to 0$ and $h_f \to 0$, the Higgs sector has a global $\mathrm{SU(2)}_R$ symmetry, and hence in such limit it is invariant under a global $\mathrm{SU(2)}_L \times \mathrm{SU(2)}_R$ symmetry, with $\mathrm{SU(2)}_L$ just being the global variant of the SM chiral gauge symmetry. This symmetry is preserved for non-vanishing Yukawa couplings, provided $h_u = h_d$. Once the Higgs acquires a VEV, both the $\mathrm{SU(2)}_L$ and $\mathrm{SU(2)}_R$ symmetry groups are broken but the subgroup $\mathrm{SU(2)}_{L+R}$ remains unbroken and is the subgroup that defines the custodial symmetry of the SM [21].

In the limit $g' \to 0$ ($\sin^2\theta_W \to 0$), the W and Z gauge bosons have equal mass and form a triplet of the $\mathrm{SU(2)}_{L+R}$ unbroken global symmetry. The ρ parameter characterizes the breaking of the custodial symmetry, which manifest itself in the equality of the three tree-level SU(2)-gauge boson masses, even when $g' \neq 0$. Using the expressions for the W and Z gauge boson masses in term of the gauge couplings, one obtains

$$\frac{M_W^2}{M_Z^2} = \frac{g^2}{g'^2+g^2} = \cos^2\theta_W \quad \text{or} \quad \rho = \frac{M_W^2}{M_Z^2\cos^2\theta_W} = 1 \tag{11.12}$$

at tree level. The custodial symmetry protects the above relation between the W and Z masses under radiative corrections. All corrections to the ρ parameter are therefore proportional to terms that break the custodial symmetry. For instance, radiative corrections

involving the Higgs are proportional to g'^2. Since $m_t \neq m_b$, there are also relevant radiative corrections generated by massive fermions. They are proportional to $m_t^2 + m_b^2 - 2(m_t^2 m_b^2)\,\log(m_t^2/m_b^2)/(m_t^2 - m_b^2)$ [22].

One can conceive BSM theories in which the Higgs is a pseudo Nambu–Goldstone boson of a strongly interacting sector [23], and/or where there are additional degrees of freedom that may contribute to the W and Z mass via virtual loops, but in as much as the electroweak sector has a manifest custodial symmetry, the theory is protected from large radiative corrections. Precision measurement of the electroweak observables are powerful in constraining such large radiative corrections. The custodial isospin symmetry is a powerful probe of BSM physics. For a pedagogical discussion, see Ref. [24].

II.3. Stability of the Higgs potential

The discovery of a scalar particle with mass $m_H \approx 125\,\text{GeV}$ has far reaching consequences within the SM framework. Such a low value of the Higgs boson mass is in perfect agreement with the upper bound on the Higgs boson mass from perturbative unitarity constraints [5,6], thereby rendering the SM a consistent, calculable theory. Moreover, the precise value of m_H determines the value of the quartic coupling λ at the electroweak scale and makes it possible to investigate its behavior up to high energy scales. A larger value of m_H would have implied that the Higgs self-coupling would become non-perturbative at some scale Λ that could be well below the Planck scale. From the measured values of the Higgs mass, the top quark mass, the W and Z boson masses, and the strong gauge coupling, all within their experimental uncertainties, it follows that, similar to the SM gauge and Yukawa couplings, the Higgs quartic coupling remains perturbative all the way up to M_{Planck} [25].

The recently measured Higgs mass, however, generates an EW Higgs potential in which the vacuum state is at the edge between being stable and metastable. Indeed, for $m_H = 125.7 \pm 0.3\,\text{GeV}$ and allowing all relevant SM observables to fluctuate within their experimental and theoretical uncertainties, the metastability condition seems to be favored [26]. The high energy evolution of λ shows that it becomes negative at energies $\Lambda = \mathcal{O}(10^{10} - 10^{12})\,\text{GeV}$, with a broader range if a 3σ fluctuation in the top quark mass value is allowed, as shown in Fig. 11.1 [26]. When this occurs, the SM Higgs potential develops an instability and the long term existence of the EW vacuum is challenged. This behavior may call for new physics at an intermediate scale before the instability develops, i.e., below M_{Planck} or, otherwise, the electroweak vacuum remains metastable [27]. Therefore, within the SM framework, the relevant question is related to the lifetime of the EW metastable vacuum that is determined by the rate of quantum tunneling from this vacuum into the true vacuum of the theory. The running of the Higgs self coupling slows down at high energies with a cancellation of its β-function at energies just one to two orders of magnitude below the Planck scale [28,26]. This slow evolution of the quartic coupling is responsible for saving the EW vacuum from premature collapse allowing it to survive much longer times than those relevant from astrophysical considerations. It might help the Higgs boson to play the role of an inflaton [30] (see, however, Ref. [31] and references therein for potential issues with this Higgs-as-inflaton idea).

The peculiar behavior of the quartic coupling does not exclude the possibility that the SM might be all what is there up to the quantum gravity scale [29] or it could be the result of a special dynamics or a new symmetry at high energies, such as supersymmetry with possible flat directions. Still, physics at lower energies is desirable to solve other mysteries of the universe such as dark matter or the matter-antimatter asymmetry. The Higgs boson discovery at the LHC leaves all these options open.

II.4. Higgs production and decay mechanisms

Reviews of the SM Higgs boson's properties and phenomenology, with an emphasis on the impact of loop corrections to the Higgs boson decay rates and cross sections, can be found in Refs. [32–38].

II.4.1. Production mechanisms at hadron colliders

The main production mechanisms at the Tevatron and the LHC are gluon fusion, weak-boson fusion, associated production with a gauge boson and associated production with top quarks. Figure 11.2 depicts representative diagrams for these dominant Higgs production processes.

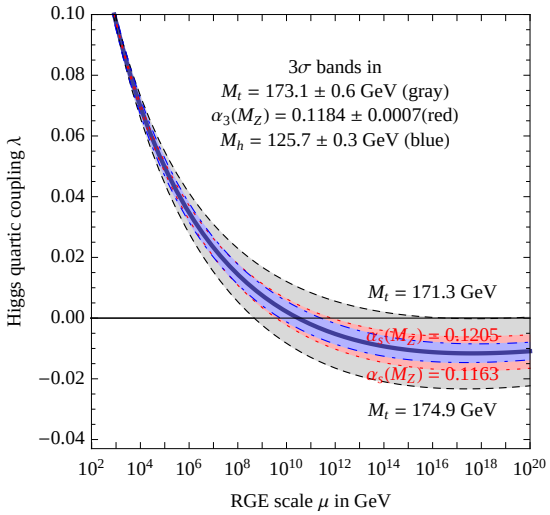

Figure 11.1: Renormalization group evolution of the Higgs self coupling λ, for the central values of $m_H = 125.7\,\text{GeV}$, $m_t = 173.4\,\text{GeV}$ and $\alpha_S(M_Z) = 0.1184$ (solid curve), and variation of these central values by $\pm$ 3 σ for the blue, gray and red, dashed curves, respectively. For negative values of λ, the lifetime of the SM vacuum due to quantum tunneling at zero temperature is longer than the age of the universe. From Ref. [26].

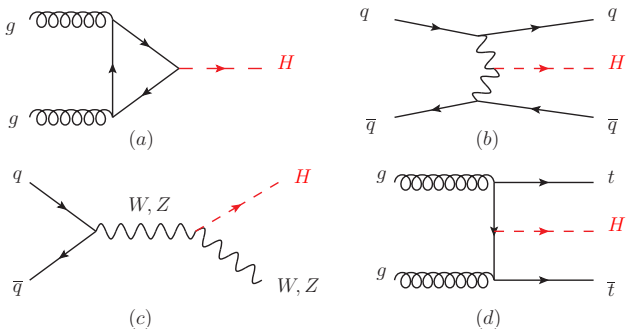

Figure 11.2: Generic Feynman diagrams contributing to the Higgs production in (a) gluon fusion, (b) weak-boson fusion, (c) Higgs-strahlung (or associated production with a gauge boson) and (d) associated production with top quarks.

The cross sections for the production of a SM Higgs boson as a function of $\sqrt{s}$, the center of mass energy, for pp collisions, including bands indicating the theoretical uncertainties, are summarized in Fig. 11.3 [39]. A detailed discussion, including uncertainties in the theoretical calculations due to missing higher order effects and experimental uncertainties on the determination of SM parameters involved in the calculations can be found in Refs. [36–38]. These references also contain state of the art discussions on the impact of PDF's uncertainties, QCD scale uncertainties and uncertainties due to different matching procedures when including higher order corrections matched to parton shower simulations as well as uncertainties due to hadronization and parton-shower events.

Table 11.1, from Refs. [36,38], summarizes the Higgs boson production cross sections and relative uncertainties for a Higgs mass of 125 GeV, for $\sqrt{s} = 7$, 8 and 14 TeV.

Table 11.1: The SM Higgs boson production cross sections or $m_H = 125\,\text{GeV}$ in pp collisions, as a function of the center of mass energy, $\sqrt{s}$. The predictions for the LHC energies are taken from Refs. [36,38], the ones for the Tevatron energy are from Ref. [40].

$\sqrt{s}$ (TeV)	Production cross section (in pb) for $m_H = 125\,\text{GeV}$					
	ggF	VBF	WH	ZH	$t\bar{t}H$	total
1.96	$0.95^{+17\%}_{-17\%}$	$0.065^{+8\%}_{-7\%}$	$0.13^{+8\%}_{-8\%}$	$0.079^{+8\%}_{-8\%}$	$0.004^{+10\%}_{-10\%}$	1.23
7	$15.1^{+15\%}_{-15\%}$	$1.22^{+3\%}_{-2\%}$	$0.58^{+4\%}_{-4\%}$	$0.33^{+6\%}_{-6\%}$	$0.09^{+12\%}_{-18\%}$	17.4
8	$19.3^{+15\%}_{-15\%}$	$1.58^{+3\%}_{-2\%}$	$0.70^{+4\%}_{-5\%}$	$0.41^{+6\%}_{-6\%}$	$0.13^{+12\%}_{-18\%}$	22.1
14	$49.8^{+20\%}_{-15\%}$	$4.18^{+3\%}_{-3\%}$	$1.50^{+4\%}_{-4\%}$	$0.88^{+6\%}_{-5\%}$	$0.61^{+15\%}_{-28\%}$	57.0

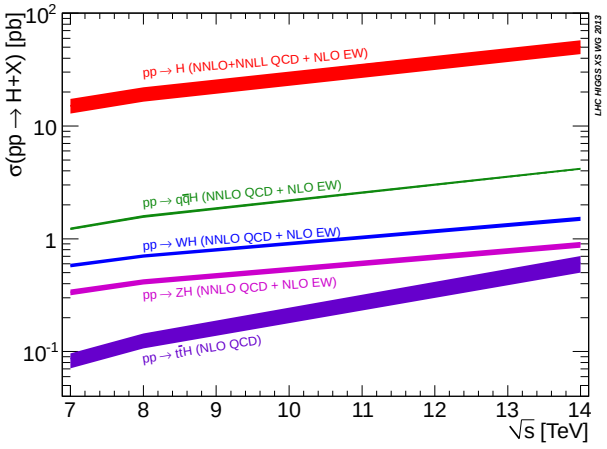

Figure 11.3: The SM Higgs boson production cross sections as a function of the center of mass energy, $\sqrt{s}$, for pp collisions. The theoretical uncertainties [39] are indicated as a band.

(i) Gluon fusion production mechanism

At high-energy hadron colliders, the Higgs boson production mechanism with the largest cross section is the gluon-fusion process, $gg \to H + X$, mediated by the exchange of a virtual, heavy top quark [41]. Contributions from lighter quarks propagating in the loop are suppressed proportional to m_q^2. QCD radiative corrections to the gluon-fusion process are very important and have been studied in detail. Including the full dependence on the quark and Higgs boson masses, the cross section has been calculated at the next-to-leading order (NLO) in α_s [42,43]. To a very good approximation, the leading top-quark contribution can be evaluated in the limit $m_t \to \infty$ by matching the Standard Model to an effective theory. The gluon-fusion amplitude is then evaluated from an effective Lagrangian containing a local $HG^a_{\mu\nu}G^{a\,\mu\nu}$ operator [19,20]. In this approximation the cross section is known at NLO [44] and at next-to-next-to-leading order (NNLO) [45], and a strong effort is under way to extend the calculations to NNNLO. The validity of the large top-quark mass approximation in NNLO calculations has been established at the percent level by means of approximate calculations of the m_t dependence based on asymptotic expansions [46].

The NLO QCD corrections increase the leading-order prediction for the cross section by about 80%, and the NNLO corrections further enhance the cross section by approximately 20% (at $\mu_f = \mu_r = m_H$). The convergence of the perturbation series can be improved by lowering the factorization and renormalization scales. Electroweak radiative corrections have been computed at NLO and increase the cross section by about 5% for $m_H \simeq 125\,\text{GeV}$ [47]. Mixed QCD-electroweak corrections of $O(\alpha\alpha_s)$ have been calculated in Ref. [48].

The NLO and NNLO fixed-order QCD predictions for the gluon-fusion cross section have been improved by resumming the soft-gluon contributions to the cross section at next-to-next-to-leading logarithmic (NNLL) and partial NNNLL accuracy [49]. The convergence of the perturbation series can be improved significantly by systematically resumming a subset of enhanced corrections contained in the time-like gluon form factor, using methods of soft-collinear effective theory [50]. Up-to-date predictions for the gluon-fusion cross section for different Higgs boson masses and LHC energies, and including detailed error budgets, have been obtained by combining the NNLO fixed-order QCD results with soft-gluon resummation at NNLL or NNNLL accuracy and two-loop electroweak corrections, and using the most recent sets of parton distribution functions [48,51].

Besides considering the inclusive Higgs boson production cross section at the LHC, it is important to study differential distributions in order to probe the properties of the Higgs boson in a detailed way. A more exclusive account of Higgs production is also required because experimental analyses often impose cuts on the final states in order to improve the signal-to-background ratio. To this end, it is useful to define benchmark cuts and compare the differential distributions obtained at various levels of theoretical accuracy (i.e., at NLO or NNLO) and with Monte Carlo generators. Many search modes for the Higgs boson are carried out by separating the events according to the number of jets or the transverse momentum and rapidity of the Higgs boson. For $p_T < 30\,\text{GeV}$, predictions for the transverse-momentum distribution can only be trusted after large logarithms of the form $\alpha_s^n \ln^{2n-1}(m_H/p_T)$ have been resummed to all orders in perturbation theory [52]. This has been accomplished with NNLL accuracy [53], and the results have been matched onto the fixed-order prediction at NNLO [54]. Electroweak corrections, and in particular the effect of the non-zero b-quark mass, on the p_T spectrum have been studied in Refs. [55,56]. Recently, there has been much activity in computing Higgs plus jet(s) production processes at NLO (see e.g. Refs. [57] and [58] for associated production with one and two jets, respectively), and even at NNLO [59]. In addition, efforts to improve the calculation of the Higgs production cross section with a jet veto (the "0-jet bin") by resumming large logarithms of the form $\alpha_s^n \ln^{2n-1}(m_H/p_T^{\text{veto}})$ at NNLL order and beyond [60] have been made. Accurate predictions for the jet-veto cross section are required, e.g., to suppress the background in the $H \to WW$ channel.

(ii) Vector boson fusion production mechanism

The SM Higgs production mode with the second-largest cross section at the LHC is the vector boson fusion (VBF). At the Tevatron, VBF also occurs, but for $m_H = 125\,\text{GeV}$ exhibits a smaller cross section than Higgs production in association with a W or Z boson. Higgs production via VBF, $qq \to qqH$, proceeds by the scattering of two (anti-)quarks, mediated by t- or u-channel exchange of a W or Z boson, with the Higgs boson radiated off the weak-boson propagator. The scattered quarks give rise to two hard jets in the forward and backward regions of the detector.[3] Because of the color-singlet nature of the weak-gauge boson exchange, gluon radiation from the central-rapidity regions is strongly suppressed [63]. These characteristic features of VBF processes can be exploited to distinguish them from a priori overwhelming QCD backgrounds, including gluon-fusion induced Higgs + 2 jet production, and from s-channel WH or ZH production with a hadronically decaying weak boson. After the application of specific selection cuts, the VBF channel provides a particularly clean environment not only for Higgs searches but also for the determination of Higgs boson couplings at the LHC [64].

Computations for total cross sections and differential distributions to Higgs production via VBF including NLO QCD and EW corrections have been presented in Refs. [33,65] and are available in the form of flexible parton-level Monte-Carlo generators. Parton-shower effects have been considered in Ref. [66]. Parts of the NNLO QCD corrections have been presented in Refs. [67,68]. The NNLO QCD corrections of Ref. [67] reduce the residual scale uncertainties on the inclusive cross section to approximately 2%. The uncertainties due to parton distributions are estimated to be at the same level.

[3] The production of a Higgs boson with two additional jets has been computed in Refs. [61] and [62].

(iii) WH and ZH associated production mechanism

The next most relevant Higgs boson production mechanisms after gluon fusion and VBF at the LHC, and the most relevant ones after gluon fusion at the Tevatron, are associated production with W and Z gauge bosons. The cross sections for the associated production processes, $pp \to VH + X$, with $V = W^{\pm}, Z$ receive contributions at NLO given by NLO QCD corrections to the Drell–Yan cross section [69,70,71] and from NLO EW corrections. The latter, unlike the QCD corrections, do not respect the factorization into Drell–Yan production since there are irreducible box contributions already at one loop [72]. At NNLO, the Drell-Yan-like corrections to WH production also give the bulk of the corrections to ZH production [73]. For ZH production there are, however, gluon-gluon induced contributions that do not involve a virtual Z gauge boson but are such that the Z gauge boson and H boson couple to gluons via top quark loops [74]. In addition, WH and ZH production receive non Drell–Yan-like corrections in the $q\bar{q}'$ and $q\overline{q}$ initiated channels, respectively, at the NNLO level, where the Higgs is radiated off top quark loops [75]. The full QCD corrections up to NNLO order, the NLO EW corrections and the NLO corrections to the gluon-gluon channel are available in a public program [76].

As neither the Higgs boson nor the weak gauge bosons are stable particles, their decays also have to be taken into account. Providing full kinematical information for the decay products can furthermore help in the suppression of large QCD backgrounds. Differential distributions for the processes $pp \to WH \to \nu_\ell \ell H$ and $pp \to ZH \to \ell^+\ell^- H \to \nu_\ell \bar{\nu}_\ell H$, including NLO QCD and EW corrections, have been presented in Ref. [77]. The NNLO QCD corrections to differential observables for WH production at the LHC, including the leptonic decays of the W boson and the decay of the Higgs boson into a $b\bar{b}$ pair, are presented in Ref. [78]. The WH and ZH production modes, together with Higgs production in association with a top quark pair, provide a relatively clean environment for studying the decay of the Higgs boson into bottom quarks.

(iv) Higgs production in association with $t\bar{t}$

Higgs radiation off top quarks, $pp \to Ht\bar{t}$, can provide important information on the the top-Higgs Yukawa coupling and gives access to the Higgs decay into bottom quarks. The LO cross section for this production process was computed in Ref. [79]. Later, the NLO QCD corrections [80] were evaluated yielding a moderate increase in the total cross section of at most 20%, but reducing significantly the scale dependence of the inclusive cross section. The total theoretical errors, estimated by combining the uncertainties from factorization and renormalization scales, strong gauge coupling, and parton distributions, amount to 10–15% of the corresponding inclusive cross section. Interfaces between NLO QCD calculations for $Ht\bar{t}$ production with parton-shower Monte Carlo programs have been provided in Ref. [81]. These programs provide the most flexible tools to date for the computation of differential distributions, including experimental selection cuts and vetoes on the final-state particles and their decay products.

(v) Subleading Higgs production mechanisms at the LHC

The Higgs boson production in association with bottom quarks is known at NNLO in the case of five quark flavors [82–84]. The coupling of the Higgs boson to a b quark is suppressed in the SM by the bottom quark mass over the Higgs VEV, m_b/v, implying that associated production of a SM Higgs boson with b quarks is very small at the LHC. In a two Higgs doublet model or a supersymmetric model, which will be discussed in Section V, this coupling is proportional to the ratio of neutral Higgs boson vacuum expectation values, $\tan\beta$, and can be significantly enhanced for large values of this ratio.

II.4.2. Production mechanisms at e^+e^- colliders

The main Higgs boson production cross sections at an e^+e^- collider are the Higgs-strahlung process $e^+e^- \to ZH$ [6,19,85], and the WW fusion process [86] $e^+e^- \to \bar{\nu}_e\nu_e W^*W^* \to \bar{\nu}_e\nu_e H$. As the center-of-mass energy $\sqrt{s}$ is increased, the cross-section for the Higgs-strahlung process decreases as s^{-1} and is dominant at low energies, while the cross-section for the WW fusion process grows as $\ln(s/m_H^2)$ and dominates at high energies [87–89]. The ZZ fusion mechanism, $e^+e^- \to e^+e^- Z^*Z^* \to e^+e^- H$, also contributes to Higgs boson production, with a cross-section suppressed by an order of magnitude with respect to that of WW fusion. The process $e^+e^- \to t\bar{t}H$ [90,91] becomes relevant for large $\sqrt{s} \geq 500\,\text{GeV}$. For a more detailed discussion of Higgs production properties at lepton colliders see for example Refs. [34,35,92,93] and references therein.

II.4.3. SM Higgs branching ratios and total width

For the understanding and interpretation of the experimental results, the computation of all relevant Higgs decay widths is essential, including an estimate of their uncertainties and, when appropriate, the effects of Higgs decays into off-shell particles with successive decays into lighter SM ones. A Higgs mass of about 125 GeV provides an excellent opportunity to explore the Higgs couplings to many SM particles. In particular the dominant decay modes are $H \to b\bar{b}$ and $H \to WW^*$, followed by $H \to gg$, $H \to \tau^+\tau^-$, $H \to c\bar{c}$ and $H \to ZZ^*$. With much smaller rates follow the Higgs decays into $H \to \gamma\gamma$, $H \to \gamma Z$ and $H \to \mu^+\mu^-$. Since the decays into gluons, diphotons and $Z\gamma$ are loop induced, they provide indirect information on the Higgs to WW, ZZ and $t\bar{t}$ couplings in different combinations. The Higgs decays into WW^* and ZZ^* effectively need to be studied considering the decays of the gauge bosons into four fermions, i.e., the leptonic, semi-leptonic and full hadronic final states. The uncertainties in the branching ratios include the missing higher order corrections in the theoretical calculations as well as the errors in the SM input parameters, in particular fermions masses and gauge couplings, involved in the calculations. In the following the state of the art of the theoretical calculations will be discussed and the reader is referred to Refs. [36,37,94] for further details.

The evaluation of radiative corrections of fermionic decays of the SM Higgs at different levels of accuracy are implemented in HDECAY [95]. The decays $H \to b\bar{b}$ and $H \to c\bar{c}$ are computed including the complete massless QCD corrections up to and including NNNNLO, with a corresponding scale dependence of about 0.1% [96]. Both the electroweak corrections to $H \to b\bar{b}$, $c\bar{c}$ as well as $H \to \tau^+\tau^-$ are known at NLO [97] providing predictions with an overall accuracy of about 1-2% for $m_H \simeq 125\,\text{GeV}$.

The loop induced decays of the SM Higgs are known at NLO and partially beyond that approximation. For $H \to gg$, the QCD corrections are known up to NNNLO in the limit of heavy top quarks [98,43] and the uncertainty from the scale dependence is about 3%. For the $H \to \gamma\gamma$, the full NLO QCD corrections are available [43,99]. The NLO electroweak corrections to $H \to gg$ and $H \to \gamma\gamma$ have been computed in Ref. [100]. Missing higher orders corrections are estimated to be below 1%. All these corrections are implemented in HDECAY. In addition the contribution of the $H \to \gamma e^+e^-$ decay via virtual photon conversion has been computed in Ref. [101]. The partial decay width $H \to Z\gamma$ is only implemented at LO in HDECAY, including the virtual W, top, bottom, and τ loop contributions. The QCD corrections have been calculated and are at the percent level [102], The theoretical uncertainty due to unknown electroweak corrections is estimated to be less than 5%, an accuracy that will be hard to achieve in measurements at the LHC.

The decays $H \to WW/ZZ \to 4f$ can be simulated with the Monte-Carlo generator of Ref. [103] that includes complete NLO QCD and EW corrections for Higgs decays into any possible four-fermion final state. All calculations are consistently performed with off-shell gauge bosons, without any on-shell approximation. For the SM Higgs boson the missing higher-order corrections are estimated to roughly 0.5%. Such uncertainties will have to be combined with the parametric uncertainties, in particular those associated to the bottom quark mass and the strong gauge coupling, to arrive at the full theory uncertainties. A detailed treatment of the differential distributions for a Higgs decay with four charged leptons in the final state is presented in Refs. [104,38].

The branching ratios for the most relevant decay modes of the SM Higgs boson as functions of m_H, including the most recent theoretical uncertainties, are shown in Fig. 11.4 and listed for $m_H = 125\,\text{GeV}$ in Table 11.2. The total width of a 125 GeV SM Higgs boson is

$\Gamma_H = 4.07 \times 10^{-3}$ GeV, with a relative uncertainty of $^{+4.0\%}_{-3.9\%}$. Further details of these calculations can be found in Refs. [94,105] and in the reviews [33–38].

Table 11.2: The branching ratios and the relative uncertainty [38] for a SM Higgs boson with $m_H = 125$ GeV.

Decay channel	Branching ratio	Rel. uncertainty
$H \to \gamma\gamma$	2.28×10^{-3}	$^{+5.0\%}_{-4.9\%}$
$H \to ZZ$	2.64×10^{-2}	$^{+4.3\%}_{-4.1\%}$
$H \to W^+W^-$	2.15×10^{-1}	$^{+4.3\%}_{-4.2\%}$
$H \to \tau^+\tau^-$	6.32×10^{-2}	$^{+5.7\%}_{-5.7\%}$
$H \to b\bar{b}$	5.77×10^{-1}	$^{+3.2\%}_{-3.3\%}$
$H \to Z\gamma$	1.54×10^{-3}	$^{+9.0\%}_{-8.9\%}$
$H \to \mu^+\mu^-$	2.19×10^{-4}	$^{+6.0\%}_{-5.9\%}$

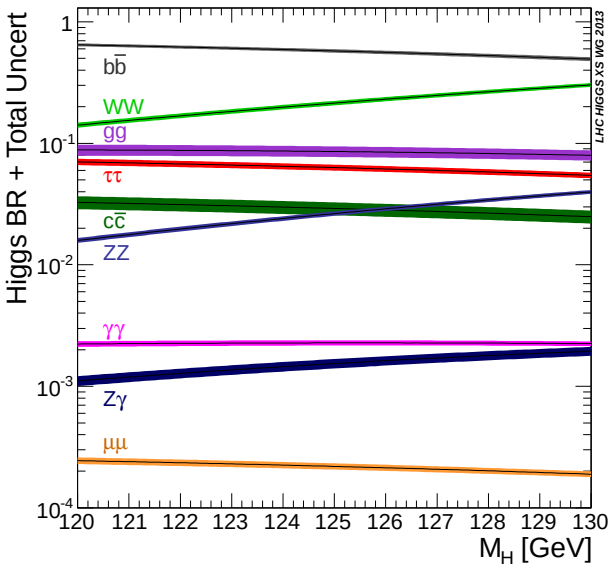

Figure 11.4: The branching ratios for the main decays of the SM Higgs boson near $m_H = 125$ GeV. The theoretical uncertainties [38] are indicated as a band.

III. The discovery of a Higgs boson

Indirect experimental bounds on the SM Higgs boson mass are obtained from a global fit of precision electroweak measurements of electroweak observables, by comparing them with theory predictions which account for M_H effects at higher orders (see the electroweak model and constraints on new physics in this review for more details). This global fit to the precision electroweak data accumulated in the last two decades at LEP, SLC, the Tevatron, and elsewhere, suggests $m_H = 89^{+22}_{-18}$ GeV, or $m_H < 127$ GeV at 90% confidence level [106].

Direct and model-independent searches for the Higgs boson were conducted by the ALEPH, DELPHI, L3, and OPAL experiments at the LEP e^+e^- collider. The combination of LEP data collected near the Z resonance and at centre-of-mass energies of up to 209 GeV yielded a 95% Confidence level (CL) lower bound [107] of 114.4 GeV for the mass of the SM Higgs boson.

Following the shutdown of the LEP collider in 2000, the direct search for the Higgs boson continued at Fermilab's Tevatron $p\overline{p}$ collider. The combined results [108] from approximately 10 fb^{-1} recorded by the CDF and D0 experiments excluded two ranges in m_H: between 90 GeV and 109 GeV, and between 149 GeV and 182 GeV. In addition, a broad excess in data was seen in the mass range 115 GeV $< m_H <$ 140 GeV with a local significance[4] of 3 standard deviations at $m_H = 125$ GeV. The commissioning in 2010 and the high intensity running of the LHC pp collider at CERN at $\sqrt{s}$ =7 TeV in 2011 followed by an energy boost to $\sqrt{s}$ =8 TeV in 2012 opened up a new landscape where the Higgs boson could be searched for, quickly and effectively, in the 110–1000 GeV mass range.

The announcement on July 4, 2012 of the observation [1,2] at the LHC of a narrow resonance with a mass of about 125 GeV has provided an important new direction in the decades-long search for the SM Higgs boson. The analyzed data corresponded to integrated luminosities of up to 4.8 (5.1) fb^{-1} at $\sqrt{s} = 7$ TeV in 2011 and 5.9 (5.3) at $\sqrt{s} = 8$ TeV in 2012 recorded by the ATLAS and CMS experiments, respectively. The observed decay channels indicated that the new particle is a boson. The evidence was strong that the new particle decays to $\gamma\gamma$ and ZZ with rates consistent with those predicted for the Standard Model (SM) Higgs boson. There were indications that the new particle also decays to W^+W^-. Although the experiments searched for decays to $b\bar{b}$ and $\tau^+\tau^-$, no statistically significant signal was found. The significance of these observations are quantified by a p-value [110], the probability for a background only experiment to give a result at least as signal-like as that observed in the data. For example, a p-value of 2.87×10^{-7} corresponds to a five-standard-deviation excess over the background-only prediction. ATLAS observed the largest excess with a local significance of 5.9σ at a mass $m_H = 126.5$ GeV, to be compared with an expected significance of 4.6σ if a SM Higgs boson were present at such a mass. CMS observed an excess with a local significance of 4.9σ at a mass of 125.5 GeV, to be compared with an expected significance of 5.9σ in this dataset.

Even as this discovery was being announced, ATLAS and CMS continued to accumulate pp collision data at $\sqrt{s} = 8$ TeV recording a total of about 20 fb^{-1} each at this energy. Figure 11.5 shows four snapshots of the evolution of the p-value and the signal significance near 125 GeV with increasing datasets analyzed by the two experiments.

In the remainder of this section the focus will be on the recent major results. Unless explicitly mentioned, all measurements are based on the full dataset of about 10 fb^{-1} recorded by the Tevatron experiments and about 25 fb^{-1} recorded by the LHC experiments. An extensive review of the searches for the Higgs boson from LEP to the LHC can be found in Ref [111].

III.1. The discovery channels

For a given m_H the sensitivity of a search channel depends on the production cross section of the Higgs bosons, its decay branching fraction, reconstructed mass resolution, selection efficiency and the level of background in the final state. For a low mass Higgs boson ($110 < m_H < 150$ GeV) where the natural width of the Higgs boson is only a few MeV, the five decay channels that play an important role at the LHC are listed in Table 11.3. In the $H \to \gamma\gamma$ and $H \to ZZ \to 4\ell$ channels, all final state particles can be very precisely measured and the reconstructed m_H resolution is excellent. While the $H \to W^+W^- \to \ell^+\nu_\ell\ell'^-\bar{\nu}_{\ell'}$ channel has relatively large branching fraction, the m_H resolution is poor due to the presence of neutrinos. The $H \to b\bar{b}$ and the $H \to \tau^+\tau^-$ channels suffer from large backgrounds and a poor mass resolution. For $m_H > 150$ GeV, the sensitive channels are $H \to WW$ and $H \to ZZ$ where the W or Z boson decays into a variety of leptonic and hadronic final states.

In order to distinguish between different production modes, the LHC experiments usually split the Higgs boson candidates into several mutually exclusive categories (or tags) based on the topological and/or kinematics features present in the event. These categories

[4] In this review, we use the phrase "local significance" to indicate a calculation of the significance not corrected for the look-elsewhere effect [109].

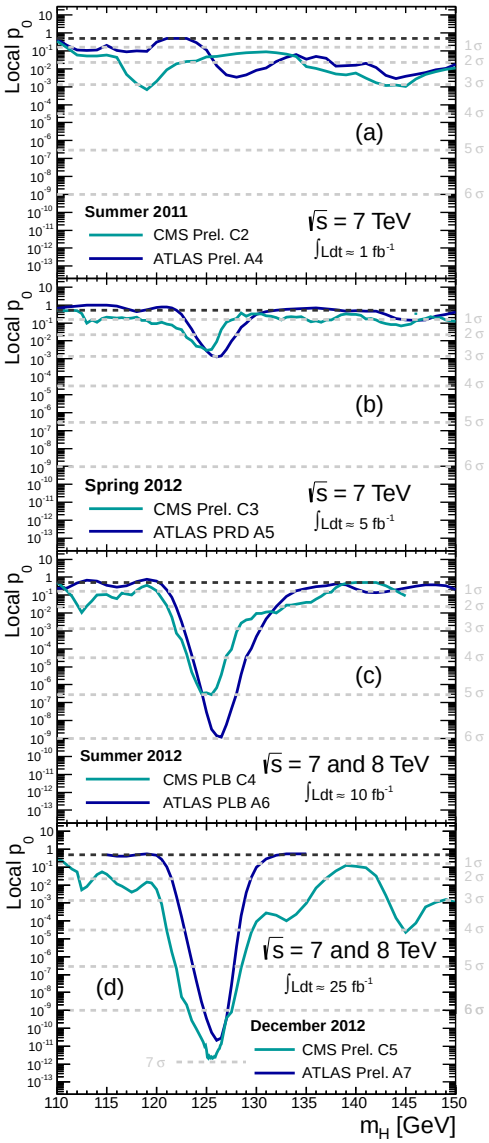

Figure 11.5: Evolution of the p-value and the signal significance observed by the ATLAS and CMS experiments with increasingly larger datasets: (a) Summer 2011 ($\approx 1\,\text{fb}^{-1}$/expt) for ATLAS A4 [112] and CMS C4 [113], (b) Spring 2012 ($\approx 5\,\text{fb}^{-1}$/expt) for ATLAS A5 [114] and CMS C3 [115], (c) Summer 2012 ($\approx 10\,\text{fb}^{-1}$/expt) for ATLAS A6 [1] and CMS C4 [2], and (d) December 2012 ($\approx 25\,\text{fb}^{-1}$/expt) for ATLAS A7 [116] and CMS C4 [117].

Table 11.3: The five sensitive channels for low mass SM Higgs boson searches at the LHC. The numbers reported are for $m_H = 125\,\text{GeV}$.

Decay channel	Mass resolution
$H \to \gamma\gamma$	1-2%
$H \to ZZ \to \ell^+\ell^-\ell'^+\ell'^-$	1-2%
$H \to W^+W^- \to \ell^+\nu_\ell\ell'^-\bar{\nu}_{\ell'}$	20%
$H \to b\bar{b}$	10%
$H \to \tau^+\tau^-$	15%

contain an admixture of various signal production modes. For example, a typical VBF category contains Higgs boson candidates accompanied by two energetic jets ($\geq 30\,\text{GeV}$) with a large dijet mass ($\geq 400\,\text{GeV}$) and separated by a large pseudorapidity ($\Delta\eta_{jj} \geq 3.5$).

While such a category is enriched in Higgs boson produced via VBF, the contamination from the dominant gluon fusion production mechanism can be significant. Hence a measurement of the Higgs boson production cross section in the VBF category does not imply a measurement of VBF production cross-section. Simulations are used to determine the relative contributions of the various Higgs production modes in a particular category.

III.1.1. $H \to \gamma\gamma$

In the $H \to \gamma\gamma$ channel a search is performed for a narrow peak over a smoothly falling background in the invariant mass distribution of two high p_T photons. The background in this channel is high and stems from prompt $\gamma\gamma$, γ+jet and dijet processes. In order to optimize search sensitivity and also to separate the various Higgs production modes, ATLAS and CMS experiments split events into several mutually exclusive categories. Diphoton events containing a high p_T muon, electron, dijets or missing energy (E_T^{miss}) consistent with the decay of a W or Z boson are tagged in the VH production category, those containing energetic dijets with a large mass and pseudorapidity difference are assigned to the VBF production category and the remaining events ($\approx 99\%$ of the total) are considered in the gluon fusion production category. While the VH category is relatively pure, the VBF category has significant contamination from the gluon fusion process. ATLAS uses the diphoton transverse momentum orthogonal to the diphoton thrust axis in the transverse plane (p_{Tt}) [118] to differentiate between Higgs boson produced via gluon fusion and the VBF/VH production modes.

Untagged events are further categorized according to their expected $m_{\gamma\gamma}$ resolution and signal-to-background ratio. Categories with good m_H resolution and larger signal-to-background ratio contribute most to the sensitivity of the search.

In each category, $Z \to e^+e^-$ and $Z \to \mu^+\mu^-\gamma$ events from data are used to construct a parametric signal model. The functional form of the background is determined by a fit to the full $m_{\gamma\gamma}$ distribution in each category. All categories are fitted simultaneously to determine the signal yield at a particular mass. In the full dataset, the $m_{\gamma\gamma}$ distribution after combining all categories are shown for the ATLAS experiment in Fig. 11.6 and for the CMS experiment in Fig. 11.7. ATLAS observes [119] its largest excess over background at $m_H = 126.8\,\text{GeV}$ with a significance of 7.4σ compared with 4.3σ expected for SM Higgs boson at that mass. CMS observes [120] its largest excess at $m_H = 125.4\,\text{GeV}$ with a significance of 3.2σ compared with 4.2σ expected for SM Higgs boson of that mass.

The signal strength $\mu = (\sigma \cdot \mathcal{B})_{\text{obs}}/(\sigma \cdot \mathcal{B})_{\text{SM}}$ which is the observed product of the Higgs boson production cross section (σ) and its branching ratio ($\mathcal{B}$) in units of the corresponding SM values, is $1.65^{+0.34}_{-0.30}$ for ATLAS and 0.78 ± 0.27 for CMS at $m_H = 125.5$ and $125\,\text{GeV}$ respectively.

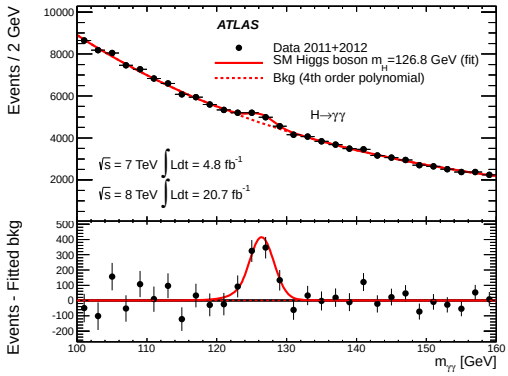

Figure 11.6: The combined invariant mass distribution of diphoton candidates observed by ATLAS [119]. The residuals of the data with respect to the fitted background are displayed in the lower panel.

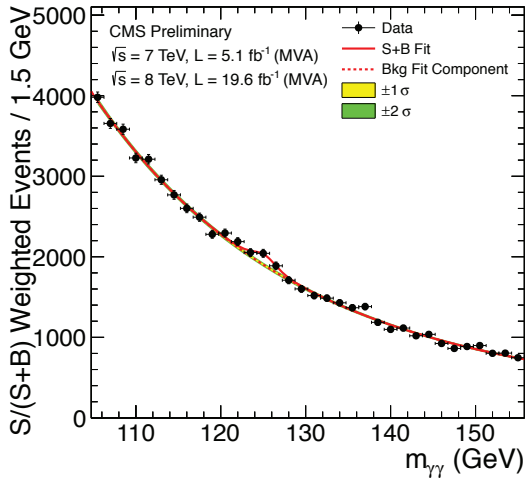

Figure 11.7: The combined CMS $M_{\gamma\gamma}$ distribution with each event weighted by the ratio of signal-to-background in each event category [120].

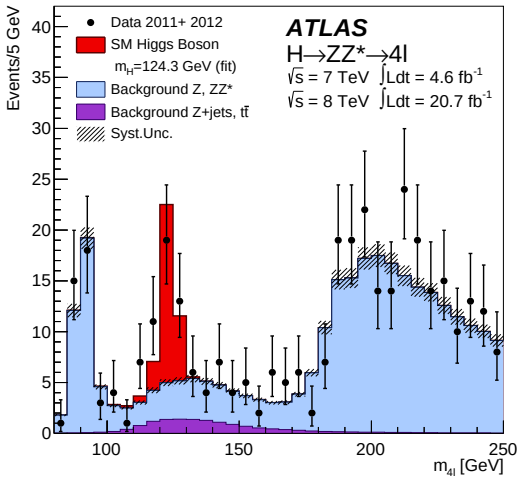

Figure 11.8: The combined $m_{4\ell}$ distribution from ATLAS [119].

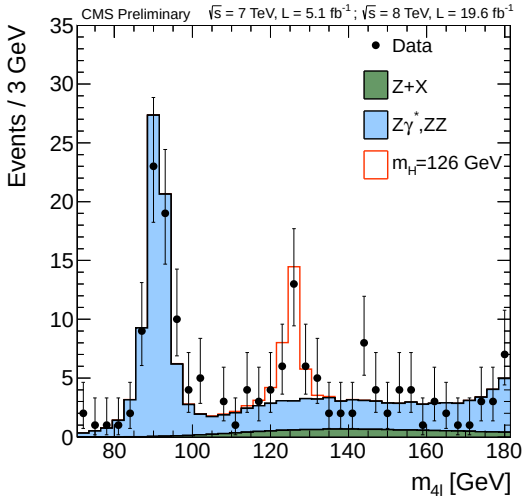

Figure 11.9: The combined $m_{4\ell}$ distribution from CMS [121].

III.1.2. $H \to ZZ^{(*)} \to \ell^+\ell^-\ell'^+\ell'^-$, $(\ell, \ell' = e, \mu)$

In the $H \to ZZ^{(*)} \to \ell^+\ell^-\ell'^+\ell'^-$ channel a search is performed for a narrow mass peak over a small continuous background dominated by non-resonant $ZZ^{(*)}$ production from $q\overline{q}$ annihilation and gg fusion processes. The contribution and the shape of this background is taken from simulated events. The subdominant and reducible backgrounds stem from $Z + b\bar{b}$, $t\bar{t}$ and $Z +$ jets events. Their contribution is suppressed by requirements on lepton isolation and lepton impact parameter and their yield is estimated from control samples in data.

To help distinguish the Higgs signal from the dominant non-resonant $ZZ^{(*)}$ background, CMS uses a matrix element likelihood approach [2] to construct a kinematic discriminant built for each 4ℓ event based on the ratio of complete leading-order matrix elements $|\mathcal{M}_{sig}{}^2/\mathcal{M}_{bkg}{}^2|$ for the signal ($gg \to H \to 4\ell$) and background($q\overline{q} \to ZZ \to 4\ell$) hypotheses. The signal matrix element $\mathcal{M}_{sig}$ is computed assuming $m_H = m_{4\ell}$.

To enhance the sensitivity to VBF and VH production processes, the ATLAS and CMS experiment divide 4ℓ events into mutually exclusive categories. Events containing dijets with a large mass and pseudorapidity difference populate the VBF category. ATLAS requires presence of an additional lepton in the VH category. In events with less than two jets, CMS uses the $p_T^{4\ell}$ to distinguish between production via the gluon fusion and the VH/VBF processes.

Since the $m_{4\ell}$ resolutions and the reducible background levels are different in the 4μ, $4e$ and $2e2\mu$ sub-channels, they are analyzed separately and the results are then combined.

The combined ATLAS $m_{4\ell}$ distribution is shown in Fig. 11.8. The largest deviation from the SM background-only expectation is observed [119] at $m_H = 124.3\,\text{GeV}$ where the significance of the observed peak is 6.7σ in the full 7 and 8 TeV data. The expected significance for the SM Higgs boson at that mass is 4.4σ. As shown in Fig. 11.9, the CMS experiment observes [121] its largest excess at $m_H = 125.8\,\text{GeV}$ with a observed significance of 6.7σ to be compared with an expected significance of 7.2σ at that mass. Both experiments also observe a clear peak at $m_{4\ell} = 91\,\text{GeV}$ from Z/γ^* production at the expected SM rate [122].

The signal strength μ for the inclusive $H \to 4\ell$ production measured by the ATLAS and CMS experiments are $1.43^{+0.40}_{-0.35}$ at $m_H = 125.5\,\text{GeV}$ and $0.91^{+0.30}_{-0.24}$ at $m_H = 125.8\,\text{GeV}$ respectively.

III.2. Mass and width measurements

In order to measure the mass of the observed state, the ATLAS and CMS experiments combine the measurements from the $\gamma\gamma$ and ZZ channels which have excellent mass resolution and where excesses with large significance are observed. For a model-independent mass measurement, the signal strengths in the $\gamma\gamma$ and ZZ channels are assumed to be independent and not constrained to the expected rate ($\mu = 1$) for the SM Higgs boson. The combined mass measured by ATLAS [119] and CMS [124] are $125.5 \pm 0.2(\text{stat.})\,^{+0.5}_{-0.6}(\text{syst.})\,\text{GeV}$ and $125.7 \pm 0.3(\text{stat.}) \pm 0.3(\text{syst.})\,\text{GeV}$ respectively. In both experiments the systematic uncertainty is dominated by the imprecision in the knowledge of the photon energy and the lepton momentum scale. The significance of the difference between the measurements of the masses in the $\gamma\gamma$ and ZZ channels by the ATLAS experiment is 2.4σ [119]. Fig. 11.10 summarizes these measurements and our combination of the ATLAS and CMS results assuming uncorrelated systematic uncertainties between the two experiments.

The natural width of a SM Higgs boson with a mass of 125 GeV is about 4 MeV, much smaller than the instrumental mass resolution in the $\gamma\gamma$ and ZZ channels. CMS has placed 95% CL bound [123] on the natural width of the observed boson of $\Gamma_H < 3.4\,\text{GeV}$.

III.3. $H \to W^+W^- \to \ell^+\nu\ell^-\overline{\nu}$

While the production rate in the $H \to W^+W^- \to \ell^+\nu\ell^-\bar{\nu}$ channel is large, due to the presence of two neutrinos in the decay, the m_H

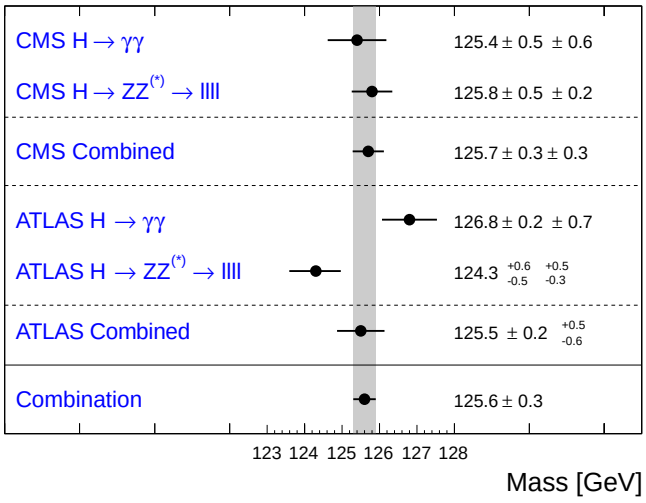

Figure 11.10: A compilation of the CMS and ATLAS mass measurements in the $\gamma\gamma$ and ZZ channels, the combined result from each experiment and our average of the combinations.

resolution is quite poor ($\approx 20\%\ m_H$) so the search is reduced to a counting experiment of the event yield in broad bins in m_H.

Experiments search for an excess of events with two leptons of opposite charge accompanied by missing energy and up to two jets. Events are divided into several categories depending on the lepton flavor combination (e^+e^-, $\mu^+\mu^-$and $e^\pm\mu^\mp$) and the number of accompanying jets ($N_{jet} = 0, 1, \geq 2$). The $N_{jet} \geq 2$ category is optimized for VBF production process by selecting two leading jets with a large pseudorapidity difference and with a large mass ($m_{jj} > 500\,\text{GeV}$). Backgrounds contributing to this channel are numerous and vary by the category of selected events. Reducing them and accurately estimating the remainder is major challenge in this analysis. For events with opposite flavor lepton and no accompanying high p_T jets, the dominant background stems from non-resonant WW production. Events with same-flavor leptons suffer from large Drell–Yan contamination. The $t\bar{t}$, Wt and W + jets (with the jet misidentified as a lepton) events contaminate all categories. Non-resonant WZ, ZZ and $W\gamma$ processes also contribute to the background at a sub-leading level.

A requirement of large missing transverse energy (E_T^{miss}) is used to reduce the Drell–Yan and multi-jet backgrounds. In the e^+e^- and $\mu^+\mu^-$ categories, events with $m_{\ell\ell}$ consistent with the Z mass are vetoed. The $t\bar{t}$ background is suppressed by a veto against identified b-jets or low p_T muons (assumed to be coming from semileptonic b-hadron decays within jets) and tight isolation requirements diminish the W+jets background. The scalarity of the Higgs boson and the $V-A$ nature of the W boson decay implies that the two charged leptons in the final state are emitted at small angles with respect to each other. Therefore the dilepton invariant mass ($m_{\ell\ell}$) and the azimuthal angle difference between the leptons ($\Delta\phi_{\ell\ell}$) are used to discriminate between the signal and non-resonant WW events. The transverse mass constructed from the dilepton p_T ($p_T^{\ell\ell}$) , E_T^{miss} and the azimuthal angle between E_T^{miss} and $p_T^{\ell\ell}$ and defined as $m_T = \sqrt{2p_T^{\ell\ell}E_T^{\text{miss}}(1-\cos\Delta\phi_{E_T^{\text{miss}}\ell\ell})}$ serves as an effective discriminant against backgrounds. The transverse mass variable also tracks the Higgs boson mass but with a poor mass resolution. All residual background rates except for the small contributions from non-resonant WZ, ZZ and $W\gamma$ are evaluated from control samples devised from data.

The m_T distributions of selected events is shown in Fig. 11.11 and Fig. 11.12 for the ATLAS and CMS experiments respectively. The 0-jet category is dominated by non-resonant WW background while $t\bar{t}$ dominates the 1 and 2 jet categories. Both experiments see a clear excess over background expectation in the 0 and 1 jet categories. ATLAS fits the m_T distributions and observes [119,126] the most significant excess for $m_H = 140\,\text{GeV}$. The significance of the observed excess for $m_H = 125.5\,\text{GeV}$ is 3.8σ, the same as expected. The measured inclusive signal strength $\mu = 1.01 \pm 0.31$ at $m_H = 125\,\text{GeV}$. In the VBF category an excess with a significance of 2.5σ corresponding to a signal strength of $\mu = 1.66 \pm 0.67 \pm 0.43$ is observed for $m_H = 125\,\text{GeV}$. The CMS analysis of 0 and 1 jet categories, using all lepton flavor combinations, shows [127] an excess with an observed significance of 4σ consistent with the expected significance of 5.1σ for a 125 GeV Higgs boson. A separate analysis optimized for the VBF production mode reports [128] no significant excess and sets a 95% CL upper limit of $\mu < 1.7$ for $m_H = 125\,\text{GeV}$.

The ATLAS and CMS experiments have also performed dedicated searches for the associated Higgs boson production (VH) in this channel. The signal consists of three (WH) or four (ZH) high p_T isolated leptons with missing transverse energy and low hadronic activity. The major backgrounds stem from triboson and diboson production where each boson decays leptonically. The 95% CL limits on μ of 7.2 [129] and 5.0 [130] have been set by ATLAS and CMS respectively for a $m_H = 125\,\text{GeV}$.

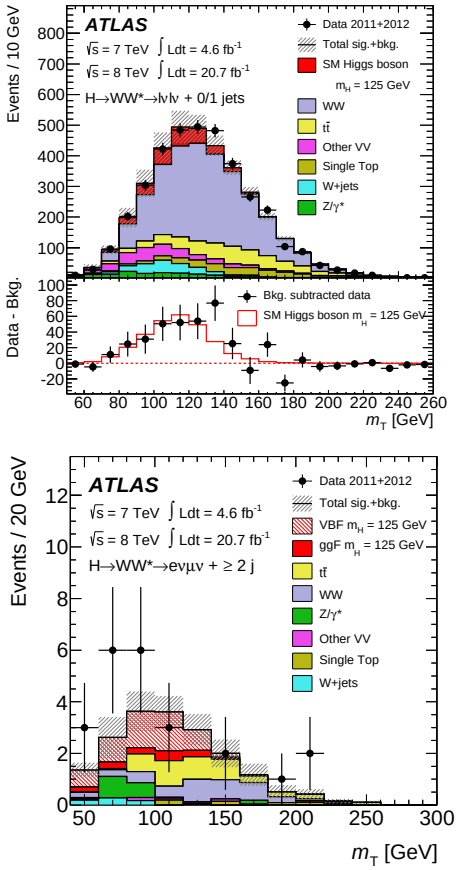

Figure 11.11: (Top) The m_T distribution for selected events summed over all lepton flavors and with ≤ 1 associated jets. The observed excess over the estimated SM background and the expectation from a SM Higgs boson with $m_H = 125\,\text{GeV}$ are shown in the lower panel. (Bottom) The m_T distribution for selected $e^\pm\mu^\mp$ events and with ≥ 2 associated jets [119].

III.4. Decays to fermions

As described in Section III.1, significant signals for the decay of the observed boson in the the $\gamma\gamma$, ZZ and W^+W^- channels have been measured by the ATLAS and CMS experiments. The measured signal strengths in these channels are consistent with this boson playing a role in electroweak symmetry breaking. However the nature of its interaction with fermions and whether this boson serves also

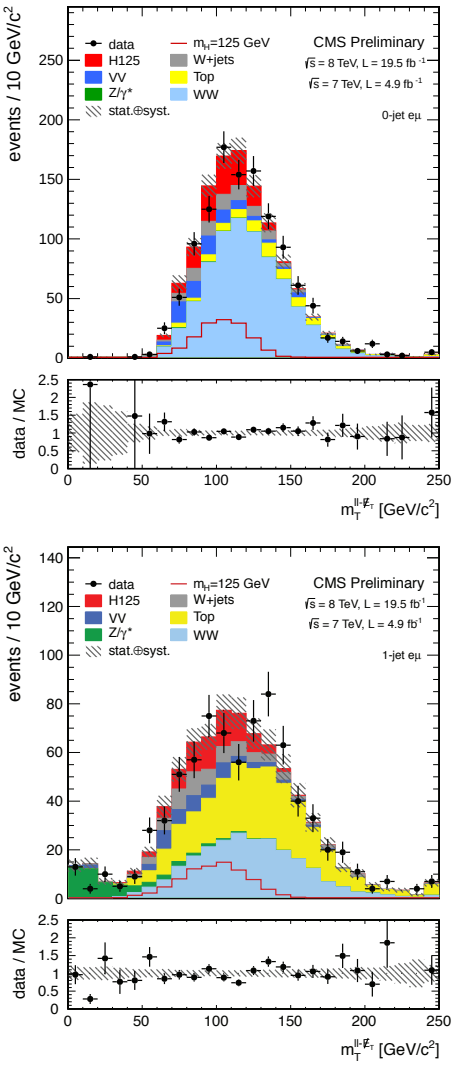

Figure 11.12: The m_T distribution for events, selected with a cut-based analysis, summed over all lepton flavors and with zero accompanying reconstructed jets (Top) and 1-jet (Bottom). The contributions of all SM background sources and a SM Higgs with m_H=125 GeV are stacked together [127].

as a source of mass generation for quarks and leptons via Yukawa interactions is a topic of active investigation[5].

At the hadron colliders, the most promising channel for probing the coupling of the Higgs field to the quarks and leptons are $H \to b\bar{b}$ and $H \to \tau^+\tau^-$ respectively. For a Higgs boson with $m_H \approx 125\,\text{GeV}$, the branching fraction to $b\bar{b}$ is about 57% and to $\tau^+\tau^-$ is about 6%. Nevertheless the presence of very large backgrounds makes the isolation of a Higgs boson signal in these channels quite challenging.

III.4.1. $H \to \tau^+\tau^-$

In the $H \to \tau\tau$ search, τ leptons decaying to electrons (τ_e), muons (τ_μ) and hadrons (τ_{had}) are considered. The $\tau^+\tau^-$ invariant mass ($m_{\tau\tau}$) is reconstructed from a kinematic fit of the visible products from the two τ leptons and the missing energy observed in the event. Due to the presence of missing neutrinos, the $m_{\tau^+\tau^-}$ resolution is poor ($\approx 15\%$). As a result, a broad excess over the expected background in the $m_{\tau\tau}$ distribution is searched for. The major sources of background stem from Drell–Yan $Z \to \tau^+\tau^-$ and $Z \to e^+e^-$, W+jets, $t\bar{t}$ and multijet production. Events in all sub-channels are divided into categories based on the number and kinematic properties of additional energetic jets in the event. The sensitivity of the search is generally higher for categories with one or more additional jets. The VBF category, consisting of a $\tau\tau$ pair with two energetic jets separated by a large pseudorapidity, has the best signal-to-background and search sensitivity followed by the $\tau^+\tau^-$+1 jet category. The signal to background discrimination relies in part on $m_{\tau\tau}$ resolution which improves with the boost of the Higgs boson, the non-VBF categories are further subdivided according to the observed boost of the $\tau^+\tau^-$ system. The 0-jet category which has the poorest signal/background ratio is used to constrain the background yields, the reconstruction efficiencies, and the energy scales. The CMS experiment uses the reconstructed mass as discriminating variable [131,132] while the ATLAS experiment combines various kinematic properties of each event categories with multivariate techniques to build a discriminant [133].

$H \to \tau^+\tau^-$ decays in the VH production mode are searched for in final states where the W or Z boson decays into leptons or into two jets (in [134] but currently not in the latest ATLAS results [133]) . While the decays to tau pairs are the dominant Higgs boson signal contribution, the final states used can additionally be produced by the decay of the Higgs boson into a pair of W bosons that both decay to leptons. The irreducible background in this search arises from non-resonant WZ and ZZ diboson production. The reducible backgrounds originate from W, Z, and $t\bar{t}$ events that contain at least one fake lepton in the final state due to a misidentified jet. The shape and yield of the major backgrounds in each category is estimated from control samples in data. Contributions from non-resonant WZ and ZZ diboson production is estimated from simulations but corrected for reconstruction efficiency using control samples formed from observed data.

Figure 11.13 shows the CMS [131] $m_{\tau\tau}$ distributions combining all non-VH categories, weighing the distributions in each category of each sub-channel by the ratio between the expected signal and background yields for that category. The inset plot shows the difference between the observed data and expected background distributions, together with the expected distribution for a SM Higgs boson signal with $m_H = 125\,\text{GeV}$. The significance of the observed excess at $m_H = 125\,\text{GeV}$ is 2.85 standard deviations and corresponds to a signal strength of $\mu = 1.10 \pm 0.41$. The result in this channel has been updated with an optimized analysis [132] yielding an observed excess of 3.4 standard deviations at $m_H = 125\,\text{GeV}$ corresponding to a signal strength of $\mu = 0.87 \pm 0.29$. It has not yet been included in the combination of all low mass Higgs boson searches.

The ATLAS results [133] are based on the full 8 TeV data sample of $20.3\,\text{fb}^{-1}$. At $m_H = 125\,\text{GeV}$, the observed (expected) deviation from the background-only hypothesis corresponds to a local significance of 4.1 (3.2) standard deviations and the best fit value of the signal strength $\mu = 1.4^{+0.5}_{-0.4}$. This result does not include the aforementioned leptonic VH modes. These results are summarized in Table 11.4.

Both ATLAS and CMS measurements provide substantial evidence of the coupling of the Higgs boson to leptons.

III.4.2. $H \to b\bar{b}$

The dominant production mode $gg \to H$ with $H \to b\bar{b}$ is overwhelmed by the background from the inclusive production of $p\bar{p} \to b\bar{b} + X$ via the strong interaction. The associated production modes WH and ZH (collectively termed VH modes) allow use of the leptonic W and Z decays to purify the signal and reject QCD backgrounds. The W bosons are reconstructed via their leptonic decay $W \to \ell\bar{\nu}_\ell$ where $\ell = e, \mu$ or τ. The Z boson is reconstructed via their decay into $e^+e^-, \mu^+\mu^-$or $\nu\bar{\nu}$. The Higgs boson candidate mass is reconstructed from two b-tagged jets in the event. Backgrounds arise from production of W and Z bosons in association with gluon, light and heavy-flavored jets (V+jets), $t\bar{t}$, non-resonant diboson (ZZ and WZ with $Z \to b\bar{b}$) and QCD multijet processes. Due to the limited $m_{b\bar{b}}$ mass resolution, a SM Higgs boson signal is expected to appear as a broad enhancement in the reconstructed dijet mass distribution. The crucial elements in this search are b-jet tagging

[5] We note here that the Higgs boson production via gluon fusion as observed in the $\gamma\gamma$, ZZ and W^+W^- channels provides indirect measurement of the Higgs boson coupling to the top quark at approximately the expected rate.

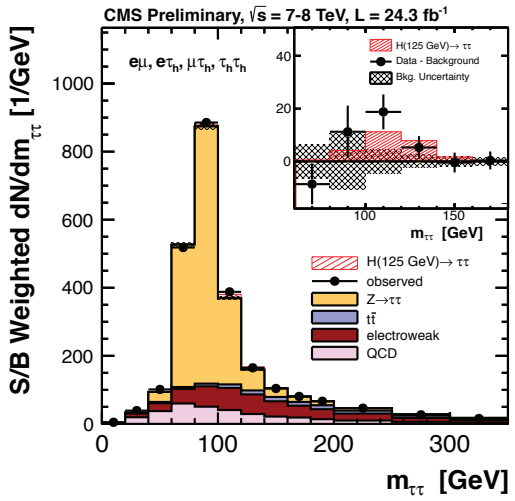

Figure 11.13: CMS results : The combined observed and expected $m_{\tau\tau}$ distributions for all sub-channels combined. The insert shows the difference between the observed data and the expected background distributions, together with the expected signal distribution for a SM Higgs signal at $m_H = 125\,\text{GeV}$ [131].

with high efficiency and low fake rate, accurate estimate of b-jet momentum and estimate of backgrounds from various signal depleted control samples constructed from data.

At the Tevatron, the $H \to b\bar{b}$ channel contributes the majority of the Higgs boson search sensitivity below $m_H = 130\,\text{GeV}$. The CDF and D0 experiments use multivariate analysis (MVA) techniques that combine several discriminating variables into a single final discriminant used to separate signal from background. Each channel is divided into exclusive sub-channels according to various lepton, jet multiplicity, and b-tagging characteristics in order to group events with similar signal-to-background ratio and thus optimize the overall search sensitivity. The combined CDF and D0 data show [135,108] an excess of events with respect to the predicted background in the 115-140 GeV mass range in the most sensitive bins of the discriminant distributions suggesting the presence of a signal. At $m_H = 125\,\text{GeV}$ the local significance of the excess is 3.0 standard deviations. At that mass, the observed signal strength $\mu = 1.59^{+0.69}_{-0.72}$. Figure 11.14 shows the best-fit cross section times branching ratio $(\sigma_{\text{WH}} + \sigma_{\text{ZH}}) \times \text{B}(H \to b\bar{b})$ as well as the SM prediction as a function of m_H.

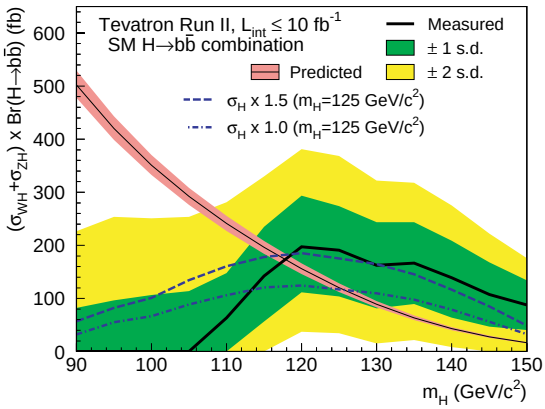

Figure 11.14: The combined CDF and D0 results on the best-fit cross section times branching ratio $(\sigma_{\text{WH}} + \sigma_{\text{ZH}}) \times \text{B}(H \to b\bar{b})$ as well as the SM prediction as a function of m_H [108].

To reduce the dominant V+jets background, following Ref. [136], the LHC experiments select a region in VH production phase space where the vector boson is significantly boosted and recoils from the $H \to b\bar{b}$ candidate with a large azimuthal angle $\Delta\phi_{\text{VH}}$. For each channel, events are categorized into different $p_T(\text{V})$ regions with varying signal/background ratios. Events with higher $p_T(\text{V})$ have smaller backgrounds and better $m_{b\bar{b}}$ resolution. CMS uses [137] MVA classifiers based on kinematic, topological and quality of b-jet tagging and trained on different values of m_H to separate Higgs boson signal in each category from backgrounds. The MVA outputs for all categories are then fit simultaneously. Figure 11.15 (Top) shows the combined MVA output of all channels where events are gathered in bins of similar expected signal-to-background ratios as predicted by the MVA discriminants. The excess of events observed in bins with the largest signal-to-background ratios is consistent with the production of a 125 GeV SM Higgs boson with a significance of 2.1 standard deviations. The observed signal strength at 125 GeV is $\mu = 1.0 \pm 0.5$. Figure 11.15 (Bottom) shows the $m_{b\bar{b}}$ distribution for all categories combined, weighted by the signal-to-background ratio in each category, with all backgrounds except dibosons subtracted. The data show the clear presence of a diboson ($W/Z + \text{Z} \to b\bar{b}$) signal, with a rate consistent with the Standard Model prediction, together with an excess that agrees with that expected from the production of a 125 GeV SM Higgs boson.

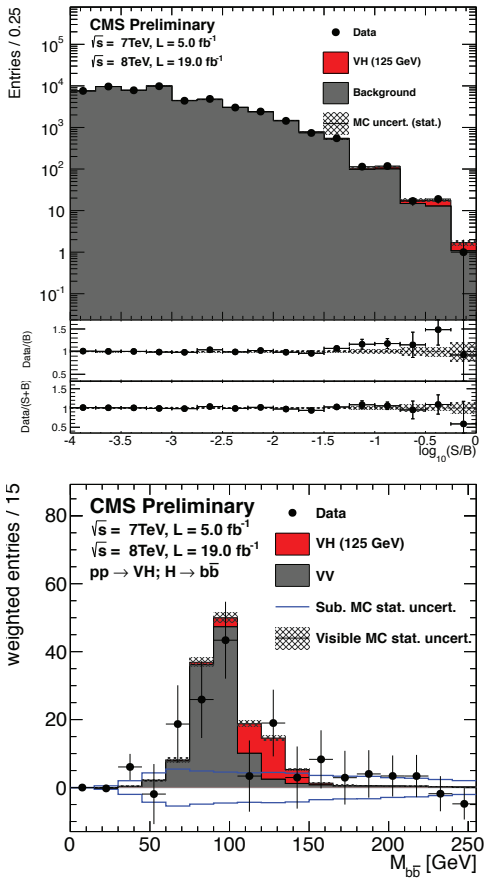

Figure 11.15: CMS results: (Top) The combination of all channels into a single distribution. The two bottom panels show the ratio of the data to the background-only prediction (above) and to the predicted sum of background and SM Higgs boson signal with a mass of 125 GeV (below). (Bottom) The $m_{b\bar{b}}$ distribution with all backgrounds, except dibosons, subtracted. The solid histograms for the backgrounds and the signal are summed cumulatively. The line histogram for signal and for VV backgrounds are also shown superimposed [137].

Table 11.4: Summary of the results in the five low mass Higgs channels measured at the LHC and the Tevatron. It should be noted that the ATLAS combined signal strength measurement only includes the bosonic $\gamma\gamma$, ZZ and WW channels. The latest result of the CMS experiment in the $H \to \tau^+\tau^-$ final state [132] is reported and denoted by (*).

	$\gamma\gamma$	ZZ (4ℓ)	WW ($\ell\nu\ell\nu$)	$\tau\tau$	W/Z(bb)	Combination
ATLAS						
μ (at 125.5 GeV)	$1.55^{+0.33}_{-0.28}$	$1.43^{+0.40}_{-0.35}$	$0.99^{+0.31}_{-0.28}$	$1.4^{+0.5}_{-0.4}$	0.2±0.7	1.3±0.2
Z Exp.	4.1	4.4	3.8	4.1	1.4	–
Z Obs.	7.4	6.6	3.8	3.2	0.3	–
Mass (GeV)	126.8±0.2±0.7	124.3±0.5±0.5	–	–	–	125.5±0.2±0.6
Reference	[119]	[119]	[119]	[133]	[138]	[119]
CMS						
μ (at 125.7 GeV)	0.77±0.27	0.92±0.28	0.68±0.20	1.10±0.41 0.87±0.29*	1.15±0.62	0.80±0.14
Z Exp.	3.9	7.1	5.3	2.6 (3.6*)	2.2	–
Z Obs.	3.2	6.7	3.9	2.8 (3.4*)	2.0	–
Mass (GeV)	125.4±0.5±0.6	125.8±0.5±0.2				125.7±0.3±0.3
Reference	[120]	[121]	[127]	[131,132]	[137]	[124]
Tevatron						
μ (at 125 GeV)	$6.0^{+3.4}_{-3.1}$	–	0.9±0.8	$1.7^{+2.3}_{-1.7}$	1.6±0.7	1.4±0.6
Reference	[108]		[108]	[108]	[108]	[108]

ATLAS performs a cut based analysis [138], with selected events divided into a large number of categories in p_T(V). The discriminating variable used is $m_{b\bar{b}}$, and customized control samples devised from data are used to constrain the contributions of the dominant background processes. No significant excess is observed. The signal strength for $m_H = 125$ GeV is measured to be $\mu = 0.2 \pm 0.5(\text{stat.}) \pm 0.4(\text{syst.})$.

III.5. Observed signal strengths

The μ value obtained by ATLAS [119] and CMS [124] in the five channels and the combined best fit value are displayed in Fig. 11.16. The μ value for each channel and the combination is calculated for the best fit mass of 125.5 and 125.7 GeV by ATLAS and CMS respectively. The ATLAS combination used only the $\gamma\gamma$, WW and ZZ channels for which the full 7 and 8 TeV data were analyzed. Table 11.4 summarizes the measurements from the Tevatron and the LHC. All measurements are consistent with the expectation from the SM Higgs boson with a mass of 125 GeV.

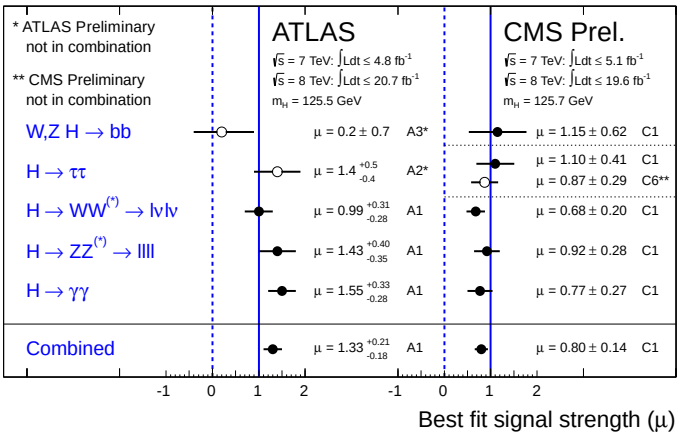

Figure 11.16: The signal strengths μ measured by the ATLAS experiment from Refs. A1 [119], A2 [133] and A3 [138], and CMS experiment from Ref. C1 [124] and C6 [132] in the five principal channels and their combination. It should be noted that the ATLAS combination only includes the bosonic $\gamma\gamma$, ZZ and WW channels.

III.6. Higgs Production in association with top quarks

As discussed in Section II, the coupling of the Higgs particle to top quarks plays a special role in the electroweak breaking mechanism and in its possible extensions. Substantial indirect evidence of this coupling is provided by the compatibility of observed rates of the Higgs boson in the main discovery channels as one of the main production processes, the gluon fusion, is dominated by a top quark loop. Direct evidence of this coupling at the LHC and the future e^+e^- colliders will be mainly available through the $t\bar{t}H$ final state. The analyses channels for such complex final states can be separated in four classes according to the decays of the Higgs boson. In each of these classes, most of the decay final states of the top quarks are considered. The topologies related to the decays of the top quarks are denoted 0L, 1L and 2L, for the fully hadronic, semi-leptonic and dilepton final states of the $t\bar{t}$ pair respectively.

The first in this set is the search for $t\bar{t}H$ production in the $H \to \gamma\gamma$ channel. This analysis relies on the search of a narrow mass peak in the $m_{\gamma\gamma}$ distribution. The background is estimated from the $m_{\gamma\gamma}$ sidebands. The sensitivity in this channel is mostly limited by the available statistics. This search was done in all three 0L and 1L final states by the ATLAS and CMS collaborations with the full 8 TeV datasets [139,140].

The second is the search in the $H \to b\bar{b}$ channel. This search is extremely intricate due to the large backgrounds, both physical and combinatorial in resolving the $b\bar{b}$ system related to the Higgs particle, in events with six jets and four b-tagged jets which are very hard to simulate. With the current dataset, the sensitivity of this analysis is already limited by the systematic uncertainties on the background predictions. The ATLAS search was done in the 1L channel with the 7 TeV dataset only [141]. The CMS collaboration after having published first results with the full 7 TeV dataset [142,143], has complemented this result with a full 8 TeV analysis [144] with the 1L and 2L channels.

The third channel is a specific search for $\tau^+\tau^-$ where the two taus decay to hadrons and in the 1L channel only performed by CMS with the full 8 TeV dataset [144].

Finally, both W^+W^- and $\tau^+\tau^-$ final states are searched for inclusively by CMS in the full 8 TeV dataset in multilepton topologies [145]. The corresponding $t\bar{t}H$ modes can be simply decomposed in terms of the decays of the Higgs boson and those of the top quarks as having four W bosons in the final state (or two W

Table 11.5: Summary of the results of searches for a Higgs boson in association with a top quark pair by the ATLAS and CMS collaborations. The results are given in terms of upper limits at the 95% CL on the signal strength, the expected limits are given in parentheses. For the results of the CMS searches, the measured signal strengths in each channel are also given. The ATLAS results indicated by ‡ are with the 7 TeV dataset only, and the results indicate by * are combining the full 7 TeV and 8 TeV datasets. The unmarked results are with the full 8 TeV dataset.

	ATLAS limits	CMS limits	CMS signal strengths
$t\bar{t}(H \to \gamma\gamma)$	<5.3 (6.4)	<5.4 (5.5)	$\mu = -0.2^{+2.4}_{-1.9}$
$t\bar{t}(H \to b\bar{b})$	<13.1 (10.5)‡	<4.5 (3.7)*	$\mu = 1.0^{+1.9}_{-2.0}$
$t\bar{t}(H \to 4\ell)$	–	<6.8 (8.8)	$\mu = -4.8^{+5.0}_{-1.2}$
$t\bar{t}(H \to 3\ell)$	–	<6.7 (3.8)	$\mu = 2.7^{+2.2}_{-1.8}$
$t\bar{t}(H \to SS2\ell)$	–	<9.1 (3.4)	$\mu = 5.3^{+2.2}_{-1.8}$
$t\bar{t}(H \to \tau^+\tau^-)$	–	<12.9 (14.2)	$\mu = -1.4^{+6.3}_{-5.5}$
Combination	–	<4.3 (1.8)	$\mu = 2.5\ ^{+1.1}_{-1.0}$

and two taus) and two b-quarks. Three resulting distinctive topologies with leptonic decays of the W bosons or the taus have been investigate by CMS [145] with the full 8 TeV dataset: (i) the same sign dileptons, (ii) the trileptons and (iii) the four leptons.

The results of all aforementioned analyses are reported in Table 11.5. CMS has performed a combination of all their channels [146] yielding an upper limit on the signal strength at the 95% CL of 4.3, while having an expected sensitivity of 1.8. This difference is due to an excess of events observed in various sensitive channels. The measured combined signal strength is $\mu = 2.5^{+1.1}_{-1.0}$, yielding first hints of the presence of a signal in this channel.

III.7. Searches for rare decays of the Higgs boson

III.7.1. $H \to Z\gamma$

The search for $H \to Z\gamma$ is performed in the final states where the Z boson decays into opposite sign and same flavor leptons ($\ell^+\ell^-$), ℓ here refers to e or μ. While the branching fraction for $H \to Z\gamma$ is comparable to $H \to \gamma\gamma$ (about 10^{-3}) at $m_H = 125\,\text{GeV}$, the observable signal yield is brought down by the small branching ratio of $Z \to (e^+e^- + \mu^+\mu^-) = 6.7 \times 10^{-2}$. In these channels, the $m_{\ell\ell\gamma}$ mass resolution is excellent (1-3%) so the analyses search for a narrow mass peak over a continuous background. The major backgrounds arise from the $Z + \gamma$, final state radiation in Drell–Yan decays and $Z +$ jets process where a jet is misidentified as a photon.

Events are divided into mutually exclusive categories on basis of the expected $m_{Z\gamma}$ resolution and the signal-to-background ratio. A VBF category is formed for $H \to Z\gamma$ candidates which are accompanied by two energetic jets separated by a large pseudorapidity. While this category contains only about 2% of the total event count, the signal-to-noise is about an order of magnitude higher. The search for a Higgs boson is conducted independently in each category and the results from all categories are then combined.

No excess of events is observed. The expected and observed 95% CL upper limits [147] on the signal strength μ are 10 and 9.5 respectively for $m_H = 125\,\text{GeV}$. The ATLAS expected and observed upper limits [148] on μ are 13.5 and 18.2 respectively at that mass.

III.7.2. $H \to \mu^+\mu^-$

$H \to \mu^+\mu^-$ is the only channel where the Higgs coupling to second generation fermions can be measured at the LHC. The branching fraction in this channel for a 125 GeV SM Higgs boson is 2.2×10^{-4}, about ten times smaller than that for $H \to \gamma\gamma$. The dominant and irreducible background arises from the $Z/\gamma^* \to \mu^+\mu^-$ process which has a rate several orders of magnitude larger than that from the SM Higgs boson signal. Due to the precise muon momentum measurement achieved by ATLAS and CMS, the $m_{\mu^+\mu^-}$ mass resolution is excellent ($\approx 2-3\%$) but rendered marginally asymmetric due to final state radiation from the muons. A search is performed for a narrow peak over a large but smoothly falling background. For optimal search sensitivity, events are divided into several categories. To take advantage of the superior muon momentum measurement in the central region, the two experiments subdivide events by the pseudorapidity of the muons. To suppress the Drell–Yan background, ATLAS requires $p_T^{\mu^+\mu^-} > 15\,\text{GeV}$ while CMS separates them into two $p_T^{\mu^+\mu^-}$ based categories. CMS further categorizes events by the number and the topology of additional energetic jets in the event.

No excess in the $m_{\mu^+\mu^-}$ spectrum is observed near 125 GeV. From an analysis of $21\,\text{fb}^{-1}$ data at 8 TeV, ATLAS sets [149] a 95% CL upper limit on the signal strength $\mu < 9.8$. The CMS analysis [150] of their 7 and 8 TeV data sets a limit of $\mu < 7.4$.

III.7.3. Rare modes outlook

Rare decays such as those described in the above sections are clearly limited by statistics. They however already deliver a remarkable message. If the coupling of the Higgs boson was as strong in the dimuon channel as it is for the top quark, this mode would have been observed already with large significance. Thus it leads to the conclusion that, contrary to gauge bosons, the observed Higgs boson couples in a non-universal way to the different families of the SM fermions.

These searches play an increasingly important role in the characterization of the couplings of the Higgs particle. New channels such as those related to charm decays [151] and exclusive quarkonia final states such as $J/\Psi\gamma$ [152] are also of great interest.

III.8. Non-standard decay channels

The main decay and production properties of H are consistent with a standard model Higgs boson. It may however have other decay channels beyond those predicted by the Standard Model. Among these and of great interest are those invisible decays into stable particles that do not interact with the detector. The other non-standard decay channels that have been investigated are the decays of the Higgs particle to hidden valley or dark particles.

III.8.1. Invisible Higgs boson decays

The discovery of the Higgs particle has immediately raised the question of its couplings to dark matter and how it could be used to further try to reveal its existence at colliders, using the Higgs boson as a portal to dark matter, see Ref. [153] and references therein. If kinematically accessible and with a sufficiently large coupling to the Higgs boson, dark matter particles, such as, e.g., neutralinos in SUSY models or heavy neutrinos in the context of fourth generation of fermions models, would manifest themselves as invisible decays of the Higgs boson, thus strongly motivating searches for invisible decays of the Higgs boson.

Searches for invisible decays of the Higgs particle have been carried out in the following channels, taking advantage of the VBF and associated production with a vector boson signatures: (i) the search for high transverse momentum mono-vector boson production by the ALTAS collaboration [154] using fat-jet substructure techniques; (ii) the associated production with a vector boson subsequently decaying either to a pair of leptons by the ATLAS [155] and the CMS [156] collaborations or a pair of b-quarks by CMS [157]; (iii) in the VBF production process by the CMS experiment [158]. An independent reinterpretation of the monojet search results by the ATLAS and CMS collaborations was also done in Ref. [153]. The results of these searches are reported in Table 11.6.

A combination of the VH and VBF channels by the CMS collaboration yields an upper limit on the invisible branching fraction of the Higgs boson, assuming SM production cross sections, of 54% at the 95% CL, while the expected sensitivity is 46% at 95% CL [156].

Table 11.6: Summary of the results of searches for invisible decays of the Higgs particle H. Results can be interpreted in terms of 95% CL limit on the invisible branching fraction for a Standard Model production cross section or as the ratio of the product of the ZH production cross section times the Higgs invisible branching fraction its SM expectation. The results in parentheses are the expected exclusions.

	ATLAS	CMS
$W, Z \to$ fatjet, $H \to$ inv.	1.6 (2.2)	–
$Z \to \ell^+\ell^-$, $H \to$ inv.	65% (84%)	75% (91%)
$Z \to b\bar{b}$, $H \to$ inv.	–	1.8 (2.0)
VBF $H \to$ inv.	–	69% (53%)

III.8.2. Exotic Higgs boson decays

The discovered Higgs particle not only serves as a probe for potential dark matter candidates, but also to search for other exotic particles arising from fields associated with a low-mass hidden sector. Such hidden sectors are composed of fields that are singlets under the SM group SU(3) × SU(2) × $U(1)$. These models are referred to as hidden valley models [159,160]. Since a light Higgs boson is a particle with a narrow width, even modest couplings to new states can give rise to a significant modification of Higgs phenomenology through exotic decays. Simple hidden valley models exist in which the Higgs boson decays to an invisible fundamental particle, which has a long lifetime to decay back to SM particles through small mixings with the SM Higgs boson; Ref. [160] describes an example. The Higgs boson may also decay to a pair of hidden valley "v-quarks," which subsequently hadronize in the hidden sector, forming "v-mesons." These mesons often prefer to decay to the heaviest state kinematically available, so that a possible signature is $h \to 4b$. Some of the v-mesons may be stable, implying a mixed missing energy plus heavy flavor final state. In other cases, the v-mesons may decay to leptons, implying the presence of low mass lepton resonances in high H_T events [161]. Other scenarios have been studied [162] in which Higgs bosons decay predominantly into light hidden sector particles, either directly, or through light SUSY states, and with subsequent cascades that increase the multiplicity of hidden sector particles. In such scenarios, the high multiplicity hidden sector particles, after decaying back into the Standard Model, appear in the detector as clusters of collimated leptons known as lepton jets.

A variety of models have been investigated searching for final states involving dark photons and hidden valley scalars. The resulting topologies searched for are prompt electron jets in the WH production process [163], displaced muonic jets [164], the four muons final state where and the search for long lived weakly interacting particles [165]. The latter occur not only in hidden valley scenarios, but also in gauge-mediated extensions of the Minimal Supersymmetric Standard Model (MSSM), the MSSM with R-parity violation, and inelastic dark matter [166]. Finally the CMS collaboration has performed a search for pair production of light bosons [167]. Such a scenario can occur in supersymmetric models with additional hidden (or dark) valleys.

IV. Properties and nature of the new bosonic resonance

As discussed in Section II, within the SM, all the Higgs couplings are fixed unambiguously once all the particle masses are known. Any deviation in the measurement of the couplings of the recently discovered Higgs boson could thus signal the presence of new physics beyond the Standard Model.

Measuring the Higgs couplings without relying on the SM assumption requires a general framework treating deviations from the SM coherently at the quantum level in order to provide theoretical predictions for relevant observables to be confronted with experimental data. The effective Lagrangian approach offers such a coherent framework. It assumes that the new physics degrees of freedom are sufficiently heavy to be integrated out and simply give rise to effective interactions among the light SM particles. By construction these effective Lagrangians cannot account for deviations in Higgs physics induced by light degrees of freedom, unless they are added themselves as extra fields in the effective Lagrangians. In Section V, several examples of models with light degrees of freedom affecting Higgs production and decay rates will be presented.

IV.1. Theoretical framework

IV.1.1. Effective Lagrangian formalism

The most general $\mathrm{SU(3)}_C \times \mathrm{SU(2)}_L \times \mathrm{U(1)}_Y$-invariant Lagrangian for a weak doublet Φ at the level of dimension-6 operators was first classified in a systematic way in Ref. [168]. Subsequent analyses pointed out the presence of redundant operators, and a minimal and complete list of operators was finally provided in Ref. [169]. For a single family of fermions, there are 59 independent ways to deform the SM. With the 3 families of fermions of the SM, a flavor index can be added to these 59 operators. Furthermore, new operator structures, that have been dismissed by means of Fierz transformations in the single family case, have to be considered. Of particular interest are the 18 CP-invariant[6] and the 4 CP-breaking[7] deformation-directions, in addition to 8 dipole operators, that affect, at tree-level, the Higgs production and decay rates [170,171,172].

A convenient basis of these operators relevant for Higgs physics, assuming that the Higgs is a CP-even weak doublet and the baryon and lepton numbers are conserved, is the following:

$$\mathcal{L} = \mathcal{L}_{SM} + \sum_i \bar{c}_i \mathcal{O}_i \,, \tag{11.13}$$

where the operators are listed in Table 11.7, Table 11.8 and Table 11.9. When the operator $\mathcal{O}_i$ is not hermitian, like $\mathcal{O}_{t,b,\tau,Htb}$ and the dipole operators, it is understood that the hermitian-conjugated operator is added to the Lagrangian. The factor multiplying each operator in the effective Lagrangian has been conveniently defined such that the new physics dependence is fully encoded in the dimensionless coefficients $\bar{c}_i$ which will all have to be smaller than 1 to ensure the consistency of the expansion in terms of higher dimensional operators. The SM gauge couplings are denoted by g', g, g_S while $y_{t,b,\tau}$ are the SM Yukawa couplings (in the mass eigenstate basis that diagonalizes the general Yukawa coupling matrices $Y_{u,d,l}$), λ is the SM Higgs quartic coupling and v denotes the weak scale defined through the Fermi constant at tree-level $v \equiv 1/(\sqrt{2}G_F)^{1/2} \approx 246.2\,\mathrm{GeV}$. $i\Phi^\dagger \overleftrightarrow{D}^\mu \Phi$ denotes the Hermitian derivative $i\Phi^\dagger(D^\mu\Phi) - i(D^\mu\Phi)^\dagger\Phi$, and $\sigma^{\mu\nu} \equiv i[\gamma^\mu, \gamma^\nu]/2$ and Φ^c is the Higgs charge-conjugate doublet: $\Phi^c = i\sigma^2\Phi^*$. Each operator $\mathcal{O}_{t,b,\tau}$ is further assumed to be flavor-aligned with the corresponding fermion mass term, as required in order to avoid large Flavor-Changing Neutral Currents (FCNC) mediated by the tree-level exchange of the Higgs boson. This implies one coefficient for the up-type quarks ($\bar{c}_t$), one for down-type quarks ($\bar{c}_b$), and one for the charged leptons ($\bar{c}_\tau$), i.e. the $\bar{c}_{t,b,\tau}$ matrices should be proportional to the identity matrix in flavor space. Requiring that the only source of flavor violation in the new physics sector are proportional to the SM Yukawa interactions, the so-called minimal flavor violation assumption, imposes the presence of the $y_u y_d$ factor in the $\mathcal{O}_{Hud}$ operator,and the Yukawa dependence in the 8 dipole operators, while all the other operators are flavor universal up to corrections like $Y_u Y_u^\dagger$ or $Y_d Y_d^\dagger$.

The choice of the basis of operators is not unique and using the equations of motion, i.e., performing field redefinitions, different dimension-6 operators can be obtained as linear combinations of the operators in the previous tables and of four-fermion operators. In

[6] When the 3 fermion families are considered, there is a nineteenth operator involving different families of leptons, $(\bar{L}^i\gamma^\mu\sigma^a L^i)(\bar{L}^j\gamma^\mu\sigma^a L^j)$, that alters the Fermi constant and hence indirectly affects the predictions of the Higgs rates. The coefficient of this operator is actually constrained by the fit of EW precision data and thus cannot give any observable deviation in Higgs physics.

[7] In this counting, non-hermitian operators with fermions that could have complex Wilson coefficients and would also break the CP-invariance are not included.

Table 11.7: List of 9 CP-even and 4 CP-odd bosonic operators affecting Higgs production and decay rates. The 4 CP-odd operators involve the dual field strengths defined as $\tilde{F}_{\mu\nu} = 1/2\,\epsilon_{\mu\nu\rho\sigma}F^{\rho\sigma}$ for $F = W, B, G$ (ϵ is the totally antisymmetric tensor normalized to $\epsilon_{0123} = 1$). See text for notations.

Operators involving bosons only
$\mathcal{O}_H = 1/(2v^2)\left(\partial^\mu\left(\Phi^\dagger\Phi\right)\right)^2$
$\mathcal{O}_T = 1/(2v^2)\left(\Phi^\dagger \overleftrightarrow{D}^\mu\Phi\right)^2$
$\mathcal{O}_6 = -\lambda/(v^2)\left(\Phi^\dagger\Phi\right)^3$
$\mathcal{O}_B = (ig')/(2m_W^2)\left(\Phi^\dagger \overleftrightarrow{D}^\mu\Phi\right)(\partial^\nu B_{\mu\nu})$
$\mathcal{O}_W = (ig)/(2m_W^2)\left(\Phi^\dagger\sigma^i \overleftrightarrow{D}^\mu\Phi\right)(D^\nu W_{\mu\nu})^i$
$\mathcal{O}_{HB} = (ig')/m_W^2\,(D^\mu\Phi)^\dagger(D^\nu\Phi)B_{\mu\nu}$
$\mathcal{O}_{HW} = (ig)/m_W^2\,(D^\mu\Phi)^\dagger\sigma^i(D^\nu\Phi)W^i_{\mu\nu}$
$\mathcal{O}_{BB} = g'^2/m_W^2\,\Phi^\dagger\Phi\,B_{\mu\nu}B^{\mu\nu}$
$\mathcal{O}_{GG} = g_S^2/m_W^2\,\Phi^\dagger\Phi\,G^A_{\mu\nu}G^{A\mu\nu}$
$\mathcal{O}_{H\tilde{B}} = (ig')/m_W^2\,(D^\mu\Phi)^\dagger(D^\nu\Phi)\tilde{B}_{\mu\nu}$
$\mathcal{O}_{H\tilde{W}} = (ig)/m_W^2\,(D^\mu\Phi)^\dagger\sigma^i(D^\nu\Phi)\tilde{W}^i_{\mu\nu}$
$\mathcal{O}_{B\tilde{B}} = g'^2/m_W^2\,\Phi^\dagger\Phi\,B_{\mu\nu}\tilde{B}^{\mu\nu}$
$\mathcal{O}_{G\tilde{G}} = g_S^2/m_W^2\,\Phi^\dagger\Phi\,G^A_{\mu\nu}\tilde{G}^{A\mu\nu}$

Table 11.8: List of 9 operators with bosons and fermions affecting Higgs production and decay rates. See text for notations.

Ops. involving bosons and fermions
$\mathcal{O}_t = y_t/v^2\,(\Phi^\dagger\Phi)\,(\bar{q}_L\Phi^c t_R)$
$\mathcal{O}_b = y_b/v^2\,(\Phi^\dagger\Phi)\,(\bar{q}_L\Phi b_R)$
$\mathcal{O}_\tau = y_\tau/v^2\,(\Phi^\dagger\Phi)\,(\bar{L}_L\Phi\tau_R)$
$\mathcal{O}_{Hq} = i/v^2\,(\bar{q}_L\gamma^\mu q_L)\left(\Phi^\dagger\overleftrightarrow{D_\mu}\Phi\right)$
$\mathcal{O}^{(3)}_{Hq} = i/v^2\,(\bar{q}_L\gamma^\mu\sigma^i q_L)\left(\Phi^\dagger\sigma^i\overleftrightarrow{D_\mu}\Phi\right)$
$\mathcal{O}_{Hu} = i/v^2\,(\bar{u}_R\gamma^\mu u_R)\left(\Phi^\dagger\overleftrightarrow{D_\mu}\Phi\right)$
$\mathcal{O}_{Hd} = i/v^2\,(\bar{d}_R\gamma^\mu d_R)\left(\Phi^\dagger\overleftrightarrow{D_\mu}\Phi\right)$
$\mathcal{O}_{Hud} = i\,y_u y_d/v^2\,(\bar{u}_R\gamma^\mu d_R)\left(\Phi^{c\dagger}\overleftrightarrow{D_\mu}\Phi\right)$
$\mathcal{O}_{Hl} = i/v^2\,(\bar{l}_R\gamma^\mu l_R)\left(\Phi^\dagger\overleftrightarrow{D_\mu}\Phi\right)$

Table 11.9: List of 8 dipoles operators. See text for notations.

Ops. involving bosons and fermions
$\mathcal{O}_{uB} = (g'\,y_u)/m_W^2\,(\bar{q}_L\Phi^c\sigma^{\mu\nu}u_R)\,B_{\mu\nu}$
$\mathcal{O}_{uW} = (g\,y_u)/m_W^2\,(\bar{q}_L\sigma^i\Phi^c\sigma^{\mu\nu}u_R)\,W^i_{\mu\nu}$
$\mathcal{O}_{uG} = (g_S\,y_u)/m_W^2\,(\bar{q}_L\Phi^c\sigma^{\mu\nu}t^A u_R)\,G^A_{\mu\nu}R$
$\mathcal{O}_{dB} = (g'\,y_d)/m_W^2\,(\bar{q}_L\Phi\sigma^{\mu\nu}d_R)\,B_{\mu\nu}$
$\mathcal{O}_{dW} = (g\,y_d)/m_W^2\,(\bar{q}_L\sigma^i\Phi\sigma^{\mu\nu}d_R)\,W^i_{\mu\nu}$
$\mathcal{O}_{dG} = (g_S\,y_d)/m_W^2\,(\bar{q}_L\Phi\sigma^{\mu\nu}t^A d_R)\,G^A_{\mu\nu}$
$\mathcal{O}_{lB} = (g'\,y_l)/m_W^2\,(\bar{L}_L\Phi\sigma^{\mu\nu}l_R)\,B_{\mu\nu}$
$\mathcal{O}_{lW} = (g\,y_l)/m_W^2\,(\bar{L}_L\sigma^i\Phi\sigma^{\mu\nu}l_R)\,W^i_{\mu\nu}$

particular, two other standard bases [173,169] involve the two extra bosonic operators

$$\begin{aligned}\mathcal{O}_{WW} &\equiv \frac{g^2}{4m_W^2}\,\Phi^\dagger\Phi\,W^i_{\mu\nu}W^{i\,\mu\nu}\\ &= \mathcal{O}_W - \mathcal{O}_B + \mathcal{O}_{HB} - \mathcal{O}_{HW} + \frac{1}{4}\,\mathcal{O}_{BB} \qquad (11.14)\\ \mathcal{O}_{WB} &\equiv \frac{gg'}{4m_W^2}\,\Phi^\dagger\sigma^i\Phi\,W^i_{\mu\nu}B^{\mu\nu} = \mathcal{O}_B - \mathcal{O}_{HB} - \frac{1}{4}\,\mathcal{O}_{BB}\,.\end{aligned}$$

IV.1.2. Constraints on Higgs physics from other measurements

Among the 30 operators affecting Higgs physics, some of them were already severely constrained before the Higgs discovery and result in deviations of the Higgs couplings that remain below the LHC sensitivity. This is obviously the case of the operators giving rise to some oblique corrections

$$\Delta\epsilon_1 \equiv \Delta\rho \equiv \Delta\hat{T} = \bar{c}_T, \quad \Delta\epsilon_3 \equiv \Delta\hat{S} = \bar{c}_W + \bar{c}_B. \qquad (11.15)$$

Electroweak precision data from LEP-I physics at the Z-pole constrain these oblique parameters and restrict the deviations of the couplings of the Z to e_R, u_L, u_R, d_L and d_R, leaving the following intervals for the values of the Wilson coefficients with 95% probability [171,174]

$$\begin{aligned}-1.5\times10^{-3} < \bar{c}_T < 2.2\times10^{-3}\,,\\ -1.4\times10^{-3} < \bar{c}_W + \bar{c}_B < 1.9\times10^{-3}\,,\\ -5\times10^{-3} < \bar{c}_{Hl} < 0\times10^{-3}\,,\\ -1\times10^{-3} < \bar{c}_{Hq} < 2\times10^{-3}\,,\\ -8\times10^{-3} < \bar{c}_{Hu} < 0\times10^{-3}\,,\\ -53\times10^{-3} < \bar{c}_{Hd} < 1\times10^{-3}\,,\\ -7\times10^{-3} < \bar{c}^{(3)}_{Hq} < 4\times10^{-3}\,.\end{aligned} \qquad (11.16)$$

Two other linear combinations of the operators are constrained by the bounds on the anomalous triple gauge boson self-couplings [174]

$$\begin{aligned}-8.8\times10^{-2} < \bar{c}_W - \bar{c}_B + \bar{c}_{HW} - \bar{c}_{HB} < 13.2\times10^{-2}\,,\\ -2.2\times10^{-2} < \bar{c}_{HW} + \bar{c}_{HB} < 1.9\times10^{-2}\,.\end{aligned} \qquad (11.17)$$

Notice, that there is one linear combination of the four bosonic operators $\mathcal{O}_B, \mathcal{O}_W, \mathcal{O}_{HB}$ and $\mathcal{O}_{HW}$ that remains unconstrained. This direction, $\bar{c}_B = -\bar{c}_W = -\bar{c}_{HB} = \bar{c}_{HW}$, induces a deviation of the $H \to Z\gamma$ decay rate that can thus only be constrained directly from the Higgs data. This free direction is a simple linear combination of $\mathcal{O}_{WW}$ and $\mathcal{O}_{BB}$.

The minimal flavor violation assumption imposes Yukawa dependences in the 8 dipole operators and in the $\mathcal{O}_{Hud}$ operator. For the light generations of fermions, this dependence lowers the induced deviations in the Higgs rates below the experimental sensitivity reachable in any foreseeable future. The corresponding operators in the top sector are not suppressed but they are already constrained by the limit of the top dipole operators imposed by the bounds on the neutron electric dipole moment, on the $b \to s\gamma$ and $b \to s\ell^+\ell^-$ rates and on the $t\bar{t}$ cross section [175,171].

Finally, in the CP-even sector, only 8 operators can potentially induce sizable deviations of the Higgs rates and can only be constrained, at tree-level, by Higgs data. These 8 operators correspond to $\{\mathcal{O}_H, \mathcal{O}_6, \mathcal{O}_{BB}, \mathcal{O}_{GG}, \mathcal{O}_{WW}, \mathcal{O}_t, \mathcal{O}_b, \mathcal{O}_\tau\}$, where by $\mathcal{O}_{WW}$ is the linear combination defined in Eq. (11.14). Section IV.2 illustrates how the Higgs data accumulated at the LHC can (partially) constrain the Wilson coefficients of these 8 directions. Automatic tools [171,176] are being developed to analyze the experimental data within an effective field theory framework.

IV.2. Experimental results

IV.2.1. Introduction

As described in Section II, there are five main production modes of a Standard Model Higgs boson at the LHC. In the current dataset corresponding to an integrated luminosity of approximately 20 fb^{-1} of pp collisions at 8 TeV, and approximately 5 fb^{-1} of collisions at 7 TeV, the predicted numbers of SM Higgs bosons produced per experiment are 0.5 million, 40,000, 20,000 and 3,000 events produced in the gluon fusion, vector boson fusion, the associated WH or ZH, and the associated $t\bar{t}H$ production modes respectively. The typical number of events selected eventually in each decay channel is then much smaller ranging from O(10) to O(100) events per experiment. For

each main decay mode, exclusive categories according to production modes have been designed to maximize the sensitivity of the analyses to the presence of a signal and using known discriminating features of these modes. These categories can also be used to further separate production modes for each decay channel. Similarly at the Tevatron where the CDF and DØ experiments have gathered approximately 10 fb^{-1} of data at 1.96 TeV, the predicted numbers of SM Higgs boson events produced per experiment are approximately 10000 and 2000 events in the gluon fusion and VH associated production, respectively.

At the LHC or the Tevatron, in none of the production modes is the total cross section measurable. As a consequence, neither absolute branching fractions nor the total natural width of the Higgs boson can be directly measured. However a combined measurement of the large variety of categories described in Section III, with different sensitivities to various production and decay modes permits a wide variety of measurements of the production, decay or in general coupling properties. These measurements require in general a limited but nevertheless restrictive number of assumptions.

include the $b\bar{b}$ [178] and $\tau^+\tau^-$ channels [179]. The results of these two individual channels are nonetheless reported in Table 11.10. It should also be noted that the CMS combination includes the search for a Higgs boson in the $b\bar{b}$ decay channel and produced in association to a pair of top quarks [180].

From the categories individual signal strengths, an already quite coherent picture emerges with a good consistency of the observation in each of the channels categories with the expectation for a Standard Model Higgs boson. The errors on the measurements reported in Table 11.10 reflect both statistical and systematic uncertainties.

IV.2.3. Characterization of the main production modes

Coupling properties can be measured via a combined fit of all categories simultaneously with a parametrization of the number of signal events per categories defined as follows.

$$n^c_{signal} = (\sum_i \mu_i \sigma_{i,SM} \times A^c_{if} \times \varepsilon^c_{if}) \times \mu_f \times B_{f,SM} \times \mathcal{L}\,, \qquad (11.19)$$

Table 11.10: Summary of the individual categories signal strengths for the main analysis channels of ATLAS (A) and CMS (C). It should be noted that the expected number of SM signal events in each category is typically composed of various production modes. * denotes those results which are are not in the combination. ‡ denotes the $H \to \tau^+\tau^-$ ATLAS analysis which is the only measurement not based on the full dataset, but the full 2011 7 TeV dataset and a partial 2012 8 TeV set of pp collision events, corresponding to an integrated luminosity of approximately 13 fb^{-1}.

	$\gamma\gamma$	ZZ (4ℓ)	WW ($\ell\nu\ell\nu$)	$\tau^+\tau^-$	$b\bar{b}$
Untagged	0.7 ± 0.3 (C)	$1.6^{+0.5}_{-0.4}$ (A)	—	—	—
Low ptT	$1.6^{+0.5}_{-0.4}$ (A)	—	—	—	—
High ptT	$1.7^{+0.7}_{-0.6}$ (A)	—	—	—	—
0/1-jet tag	—	0.9 ± 0.3 (C)	$0.82^{+0.33}_{-0.32}$ (A)	—	—
	—	—	0.7 ± 0.2 (C)	0.8 ± 0.6 (C)	—
VBF tag	$1.9^{+0.8}_{-0.6}$ (A)	$1.2^{+1.6}_{-0.9}$ (A)	$1.4^{+0.7}_{-0.6}$ (A)	—	
	$1.0^{+0.6}_{-0.5}$ (C)	$1.2^{+0.6}_{-0.9}$ (C)	$0.6^{+0.6}_{-0.5}$ (C)	$1.4^{+0.7}_{-0.6}$ (C)	$1.3^{+0.7}_{-0.6}$ (C)
VH tag	$1.3^{+1.2}_{-1.1}$ (A)	—	—		0.2 ± 0.7 (A*)
	$0.6^{+1.3}_{-1.1}$ (C)	—	$0.5^{+1.3}_{-0.9}$ (C)	$1.0^{+1.7}_{-1.5}$ (C)	$1.4^{+0.7}_{-0.6}$ (C*)
ttH tag	—	—	—	—	$0.1^{+2.8}_{-2.9}$ (C)
Overall	1.5 ± 0.3 (A)	1.4 ± 0.4 (A)	1.0 ± 0.3 (A)	0.7 ± 0.7 (A*)	0.2 ± 0.7 (A*)
	0.8 ± 0.3 (C)	0.9 ± 0.3 (C)	0.7 ± 0.2 (C)	1.1 ± 0.4 (C)	1.1 ± 0.6 (C)

IV.2.2. Measuring the signal in categories

For each category of a given channel the number of signal events yield can be measured and be converted to signal strengths per categories μ_c. These categories signal strengths can be expressed as follows in terms of the number of signal events fitted in a given category c:

$$n^c_{signal} = \mu_c(\sum_i \sigma_{i,SM} \times A^c_{if} \times \varepsilon^c_{if}) \times B_{f,SM} \times \mathcal{L} \qquad (11.18)$$

where A represents the detector acceptance, ε the reconstruction efficiency and $\mathcal{L}$ the integrated luminosity. μ_c can be interpreted as the ratio of the number of signal events n^c_{signal} fitted in category c divided by the expected number of events in that category. The production index $i \in \{ggH, VBF, VH, ttH\}$ and the decay index $f \in \{\gamma\gamma, WW, ZZ, bb, \tau\tau\}$. Typically a given category covers mainly one decay mode, but possibly various production modes. Table 11.10 summarizes the individual categories signal strengths for the main categories considered by the two experiments ATLAS [119] and CMS [177] in their combined measurement of the coupling properties of the H. It should be noted that the ATLAS combination does not

where μ_i and μ_f are the main parameters of interest. It is manifest in the above equation that production mode (μ_i) and decay mode (μ_f) signal strengths cannot be determined simultaneously. However given that in the main channels the decay mode strength parameters factorize, for each decay mode individually, the products of the $\mu_i \times \mu_f$, where f is fixed can be measured simultaneously. The results of such fits in the $H \to \gamma\gamma$, $H \to W^{(*)}W^{(*)} \to \ell\nu\ell\nu$ and $H \to Z^{(*)}Z^{(*)} \to 4\ell$ channels are shown in Fig. 11.17, illustrating a probe of the main production modes, where the small $t\bar{t}H$ mode component is assumed to scale as the gluon fusion mode ($\mu_{ggH+ttH} = \mu_{ggH} = \mu_{ttH}$). Similarly the VBF and VH production modes are scaled simultaneously ($\mu_{VBF+VH} = \mu_{VBF} = \mu_{VH}$). The SM expectation correspond to the (1,1) coordinates. The aspect ratio of the contours of Fig. 11.17 also shows the relative strength of the gluon fusion and the VBF+VH the observations for each individual channel.

IV.2.4. Evidence for VBF production

To cancel the dependence on the branching fractions, a measure of the presence of a VBF or VBF+VH signal is given by the ratio of the productions times decay signal strength parameters.

$$\rho_{VBF+VH,ggH+ttH} = \frac{\mu_{VBF+VH}\mu_f}{\mu_{ggF+ttH}\mu_f} = \frac{\mu_{VBF+VH}}{\mu_{ggF+ttH}} \qquad (11.20)$$

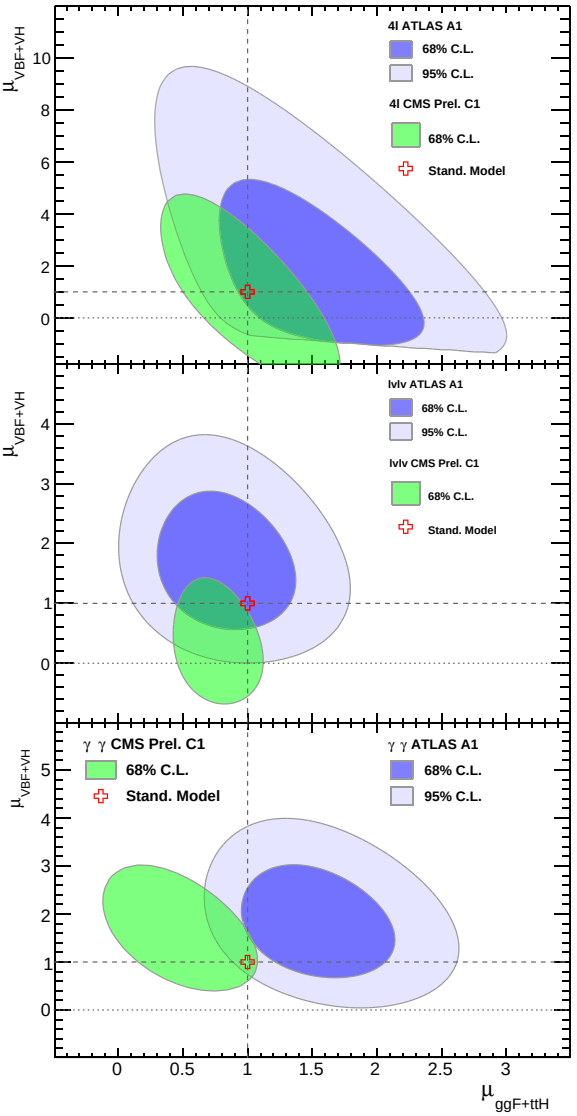

Figure 11.17: Likelihood contours for individual production mode signal strengths ($ggF+ttH$ versus $VBF+VH$) for various decay modes for the ATLAS experiment A1 [119] and the CMS experiment C1 [120] results.

For the VBF-only ratio $\rho_{VBF,ggH+ttH}$, the VH production mode is independently determined from the fit, thus needing at least one exclusive category to be sensitive enough to VH in order to remove the degeneracy with the VBF signal. The measured values of these parameters by the ATLAS (A) and CMS (C) experiments are the following:

$$\begin{aligned} \rho_{VBF,ggH+ttH} &= 1.1^{+0.4}_{-0.3} \ (A) \\ \rho_{VBF+VH,ggH+ttH} &= 1.1^{+0.4}_{-0.3} \ (A) \\ \rho_{VBF+VH,ggH+ttH} &= 1.7^{+0.7}_{-0.5} \ (C) \end{aligned} \tag{11.21}$$

The observation by ATLAS excludes a value of the $\rho_{VBF,ggH+ttH} = 0$ at more than 3σ, thus providing a quantitative evidence for VBF production. The observations by ATLAS and CMS exclude a value of $\rho_{VBF+VH,ggH+ttH} = 0$ at an even greater level of confidence.

IV.2.5. Measurement of the coupling properties of H

(i) From effective Lagrangians to Higgs observables

All 8 operators of the effective Lagrangian Eq. (11.13) that were unconstrained before the Higgs data induce, at tree-level, deviations in the Higgs couplings that respect the Lorentz structure of the SM interactions, or generate simple new interactions of the Higgs boson to the W and Z field strengths, or induce some contact interactions of the Higgs boson to photons (and to a photon and a Z boson) and gluons that take the form of the ones that are generated by integrating out the top quark. In other words, the Higgs couplings are described, in the unitary gauge, by the following effective Lagrangian [181,38]

Table 11.11: Correspondence between the κ's and the Wilson coefficients of the dimension-6 operators of the Higgs EFT Lagrangian constrained only by Higgs physics.

Coupling modifier	Wilson coefficient dependence
κ_3	$1 + \bar{c}_6 - 3\bar{c}_H/2$
κ_V	$1 - \bar{c}_H/2$
κ_f	$1 - \bar{c}_f - \bar{c}_H/2$
κ_γ	$(2\pi/\alpha)\,\sin^2\theta_W\,(4\bar{c}_{BB} + \bar{c}_{WW})$
$\kappa_{Z\gamma}$	$(\pi/\alpha)\,\sin 2\theta_W\,\bar{c}_{WW}$
κ_{VV}	$(\pi/\alpha)\,\bar{c}_{WW}$
κ_g	$(48\pi/\alpha)\,\sin^2\theta_W\,\bar{c}_{GG}$

$$\begin{aligned} \mathcal{L} = {} & \kappa_3 \frac{m_H^2}{2v} H^3 + \kappa_Z \frac{m_Z^2}{v} Z_\mu Z^\mu H + \kappa_W \frac{2m_W^2}{v} W^+_\mu W^{-\mu} H \\ & + \kappa_g \frac{\alpha_s}{12\pi v} G^a_{\mu\nu} G^{a\mu\nu} H + \kappa_\gamma \frac{\alpha}{2\pi v} A_{\mu\nu} A^{\mu\nu} H + \kappa_{Z\gamma} \frac{\alpha}{\pi v} A_{\mu\nu} Z^{\mu\nu} H \\ & + \kappa_{VV} \frac{\alpha}{2\pi v} \left(\cos^2\theta_W Z_{\mu\nu} Z^{\mu\nu} + 2\, W^+_{\mu\nu} W^{-\mu\nu} \right) H \\ & - \left(\kappa_t \sum_{f=u,c,t} \frac{m_f}{v} f\bar{f} + \kappa_b \sum_{f=d,s,b} \frac{m_f}{v} f\bar{f} + \kappa_\tau \sum_{f=e,\mu,\tau} \frac{m_f}{v} f\bar{f} \right) H. \end{aligned} \tag{11.22}$$

The correspondence between the Wilson coefficients of the dimension-6 operators and the κ's is given in Table 11.11. In the SM, the Higgs boson does not couple to massless gauge bosons at tree level, hence $\kappa_g = \kappa_\gamma = \kappa_{Z\gamma} = 0$. Nonetheless, the contact operators are generated radiatively by SM particles loops. In particular, the top quark gives a contribution to the 3 coefficients $\kappa_g, \kappa_\gamma, \kappa_{Z\gamma}$ that does not decouple in the infinite top mass limit. For instance, in that limit $\kappa_\gamma = \kappa_g = 1$ [19,20,182] (the contribution of the top quark to $\kappa_{Z\gamma}$ can be found in Ref. [182]).

The coefficient for the contact interactions of the Higgs boson to the W and Z field strengths is not independent but obeys the relation

$$(1 - \cos^4\theta_W)\kappa_{VV} = \sin 2\theta_W \kappa_{Z\gamma} + \sin^2\theta_W \kappa_{\gamma\gamma}. \tag{11.23}$$

This relation is a general consequence of the custodial symmetry [171]. When the Higgs boson is part of an $SU(2)_L$ doublet, the custodial symmetry could only be broken by the $\mathcal{O}_T$ operator at the level of dimension-6 operators and it is accidentally realized among the interactions with four derivatives, like the contact interactions considered.

The coefficient κ_3 can be accessed only through double Higgs production processes, hence it will remain largely unconstrained at the LHC. The LHC will also have a limited sensitivity on the coefficient κ_τ since the lepton contribution to the Higgs production cross section remains subdominant and the only way to access the Higgs coupling is via the $H \to \tau^+\tau^-$ and possibly $H \to \mu^+\mu^-$ channels. Until the associated production of a Higgs with a pair of top quarks is observed, the Higgs coupling to the top quark is only probed indirectly via the one-loop gluon fusion production or the radiative decay into two photons. However, these two processes are only sensitive to the two combinations $(\kappa_t + \kappa_g)$ and $(\kappa_t + \kappa_\gamma)$ and a deviation in the Higgs coupling to the top quark can in principle always be masked by new contact interactions to photons and gluons.

The operators already bounded by EW precision data and the limits on anomalous gauge couplings modify in general the Lorentz structure of the Higgs couplings and hence induce some modifications of the kinematical differential distributions [183,174]. A promising way to have a direct access to the Wilson coefficients of these operators in Higgs physics is to study the VH associated production with a W or

a Z at large invariant mass [183,184]. It has not been estimated yet whether the sensitivity on the determination of the Wilson coefficients in these measurements can compete with the one derived for the study of anomalous gauge couplings. In any case, these differential distributions could also be a way to directly test the hypothesis that the Higgs boson belongs to a $SU(2)_L$ doublet together with the longitudinal components of the massive electroweak gauge bosons.

(ii) Interpretations of the experimental data

To further interpret the observations in the analysis categories, a global approach can be adopted where the μ_i and μ_f categories signal strength parameters are further interpreted in terms of modifiers of the SM couplings κ_k where $k \in \{Z, W, f, g, \gamma, Z\gamma\}$ as in Eq. (11.22). These coupling modifiers κ are motivated as leading order coupling scale factors defined such that the cross sections σ_j and the partial decay widths Γ_j associated with the SM particle j scale with the factor κ_j^2 when compared to the corresponding SM prediction. The number of signal events per category for the various production modes are typically estimated at higher orders in the analyses but are scaled by these single LO-inspired factors, thus not taking into account possible intricacies and correlations of these parameters through the higher order corrections. This approximation is valid within the level of precision of current results and their compatibility with the SM expectation.

The κ_g, κ_γ and $\kappa_{Z\gamma}$, can be treated effectively as free parameters in the fit or in terms of the know SM field content and as a function of the SM coupling modifiers, in the following way:

$$\begin{aligned}
\kappa_g^2(\kappa_t, \kappa_b) &= 1.06 \cdot \kappa_t^2 - 0.07 \cdot \kappa_t\kappa_b + 0.01 \cdot \kappa_b^2 \\
\kappa_\gamma^2(\kappa_F, \kappa_V) &= 1.59 \cdot \kappa_V^2 - 0.66 \cdot \kappa_V\kappa_F + 0.07 \cdot \kappa_F^2 \\
\kappa_{Z\gamma}^2(\kappa_F, \kappa_V) &= 1.12 \cdot \kappa_V^2 - 0.15 \cdot \kappa_V\kappa_F + 0.03 \cdot \kappa_F^2
\end{aligned} \qquad (11.24)$$

These parametrizations are given for a Higgs boson mass hypothesis of 125 GeV. It can be noted from the expression of κ_γ that the coupling of the Higgs boson to photons is dominated by the loop of W bosons, and it is affected by the top quark loop mostly through its interference with the W loop. The sensitivity of the current measurements to the relative sign of the fermion and vector boson couplings to the Higgs boson is due to this large negative interference term. The κ_g parameter is expressed in terms of the scaling of production cross sections and therefore also depends on the pp collisions centre-of-mass energy. The parametrizations of κ_γ and $\kappa_{Z\gamma}$ are obtained from the scaling of partial widths and are only dependent on the Higgs boson mass hypothesis. Experiments use a more complete parametrization with the contributions from the b-quarks, τ-leptons in the loop [181,38].

The global fit is then performed expressing the μ_i and μ_f parameters in terms of a limited number of κ_k parameters or their ratios, under various assumptions. The parametrization for the production modes are: $\mu_{ggF} = \kappa_g^2$ for the gluon fusion; $\mu_{VBF,VH} = \kappa_V^2$ for the VBF and VH processes when the W and Z couplings are assumed to scale equally, and the following expression for the VBF production mode is used:

$$\kappa_{VBF}^2(\kappa_W, \kappa_Z) = \frac{\kappa_W^2\sigma_{WWH} + \kappa_Z^2\sigma_{ZZH}}{\sigma_{WWH} + \sigma_{ZZH}} \qquad (11.25)$$

when the couplings to the W and Z bosons are varied independently (σ_{WWH} and σ_{ZZH} denote the VBF cross sections via the fusion of a W and a Z boson respectively, the small interference term is neglected); $\mu_{ttH} = \kappa_t^2$ for the $t\bar{t}$H production mode. The decay mode signal strengths are parametrized as $\mu_k = \kappa_k^2/\kappa_H^2$ where $k \in \{Z, W, f, g, \gamma, Z\gamma\}$ denotes the decay mode and κ_H the overall modifier of the total width. Similarly to κ_g, κ_γ, and $\kappa_{Z\gamma}$, κ_H can be treated as an effective parameter or expressed in terms of the coupling modifiers to the SM field content.

Beyond this approximation two further assumptions are implicitly made: (i) the signals observed in the different search channels originate from a single narrow resonance with a mass of 125 GeV. The width of the assumed Higgs boson is neglected, both in the fitted signal model (for both approaches) and in the zero-width approximation (in the second case to allow the decomposition of signal yields); (ii) the tensor structure of the couplings is assumed to be the same as that of a SM Higgs boson. This means in particular that the observed state is assumed to be a CP-even scalar as in the SM.

A global fit to the data is then performed to specifically test three aspects of the coupling properties of the H under different assumptions: (i) the relative couplings of the Higgs boson to fermions and bosons; (ii) the relative couplings of the Higgs boson to the W and the Z, and (iii) the potential impact of the presence of new particles beyond the SM either in the loops or both in the loops and the decay of the H.

(iii) Relative couplings to bosons and fermions

In this benchmark only SM particles are assumed to contribute to the gluon fusion and the diphoton loops, all fermion couplings modifiers are required to scale simultaneously with a unique factor κ_F and all vector boson couplings modifiers must scale simultaneously with a unique factor κ_V. The global fit is then performed under both the assumption that no new particles affect the direct decays or the loops, and without assumptions on the total width.

In the first scenario it is a two parameters fit with κ_V and κ_F as parameters of interest. The contours from the two LHC experiments and the Tevatron combination are shown in Fig. 11.18.

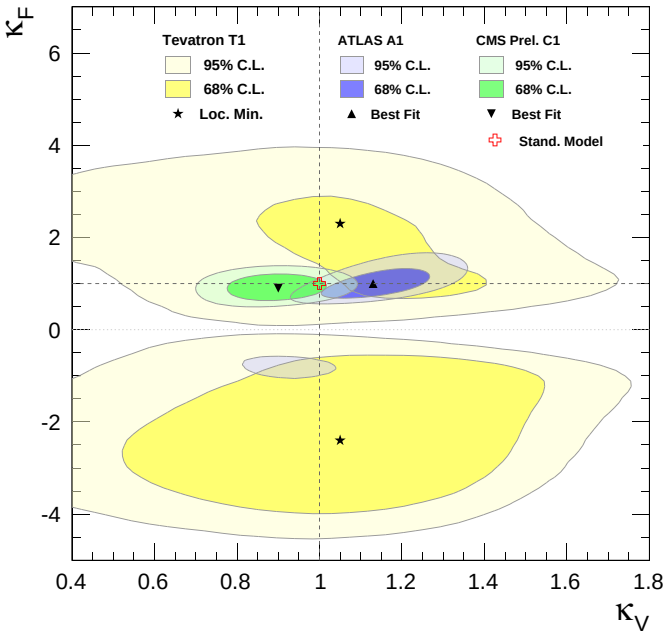

Figure 11.18: Likelihood contours of the global fit in the (κ_F, κ_V) plane for the ATLAS A1 [119], the CMS C1 [120] and the D0 and CDF combined T1 [108] results.

The global fit is only sensitive to the relative sign of κ_V and κ_F. By convention negative values of κ_F are considered. Such values are not excluded a priori, but would imply the existence of new physics at a light scale and would also raise questions about the stability of such a vacuum [185]. Among the five low mass Higgs channels, only the $\gamma\gamma$ is sensitive to the sign of κ_F through the interference of the W and t loops as shown in Eq. (11.24). The current global fit disfavors a negative value of κ_F at more than two standard deviations. A specific analysis for the Higgs boson production in association with a single top quark has been proposed [186,187] in order to more directly probe the sign of κ_F. All available experimental data show a fair agreement of the SM prediction of the couplings of the Higgs boson to fermions and gauge bosons. These results yield an indirect evidence for the coupling of the H to fermions.

In the second scenario the number of signal events per categories are parametrized using the two following parameters $\lambda_{FV} = \kappa_F/\kappa_V$

and $\lambda_{VV} = \kappa_V^2/\kappa_H$ where no assumption is made on the total width. It should be noted that this scenario corresponds to a model where the total width can vary but the field content that might modify the width should not sizably affect the loops.

The results for these two scenarios are reported in Table 11.12.

(iv) Probing the ratio of couplings to the W and Z bosons

The ratio of the couplings of the Higgs boson to W and Z bosons is an important probe of the EWSB mechanism as it is directly related to the tree level prediction $\rho = 1$ and the custodial symmetry. The W to Z couplings are probed in various production processes and decay modes of the Higgs boson. The ratio $\lambda_{WZ} = \kappa_W/\kappa_Z$ can therefore be probed under a large number of conditions.

The first requires that all fermion couplings scale with a single coupling modifier κ_F and the total width is allowed to vary, embedded in a single factor κ_{ZZ}. Both the ATLAS and CMS experiments have performed the a global fit using this model. Similarly to the λ_{FV} ratio, no assumption is made on the total width but the loops assume exclusively a SM content.

In order to be less dependent on loops, which in the case of the diphoton decay channel are dominated by the coupling to the W boson, and to the yet to be fully established coupling to fermions, since the main channels in the direct fermion decay channels rely on production processes dominated by gauge boson couplings (VH and VBF), additional models are used. In the first, performed by CMS only and denoted λ^*_{WZ} in Table 11.12, only the $H \to W^{(*)}W^{(*)} \to \ell\nu\ell\nu$ and $H \to Z^{(*)}Z^{(*)} \to 4\ell$ channels are used in the fit. The second, similar to the latter and performed by the ATLAS collaboration only, consists in a fit of the ratio of categories signal strengths:

$$(\lambda^{\circ}_{WZ})^2 = \frac{\mu_{H\to WW^*}}{\mu_{H\to ZZ^*}} \qquad (11.26)$$

The other parameters of this model are the $\mu_{ggF+ttH} \times \mu_{H\to ZZ^*}$ and the ratio $\mu_{VBF+VH}/\mu_{ggF+ttH}$ which are fitted independently.

In the third, performed by ATLAS, the coupling to photons is taken as effective in the fit, thus decoupling the observation in the diphoton channel. The latter is denoted $\lambda^{\ddagger}_{WZ}$.

The results of all models are reported in Table 11.12. For all models probed the measured ratios λ_{WZ} are compatible with the SM expectation. Although these measurements are not the most precise tests of the custodial symmetry it is of fundamental check of the nature of the electroweak symmetry breaking mechanism to see that the ratio of the couplings of the H to the W and Z bosons are compatible with what is expected from the SM Higgs sector.

(v) Probing new physics in loops and in the decay

In the models described above the assumption is that no new fields sizably distort the loop contributions in the couplings of the H to gluons and photons and its couplings to known SM particles are probed. Assuming that the couplings of the H are equal to their SM expectation, the effective coupling of the H to photons and gluons can be used to probe new physics beyond the SM through the loops. These assumptions can be simply expressed as $\kappa_F = \kappa_V = 1$ and the κ_g and κ_γ couplings modifiers are free in the fit. A first approach is to probe for new physics beyond the SM in the loops and not in the decay. The total width is then defined as a function of the two effective coupling modifiers (for a Higgs boson mass hypothesis of $m_H = 125\,\text{GeV}$) as follows.

$$\kappa_H^2 = 0.085 \cdot \kappa_g^2 + 0.0023 \cdot \kappa_\gamma^2 + 0.91. \qquad (11.27)$$

The results of the combined fits performed by the ATLAS and CMS experiments are given in Table 11.12 and the contours of the combined likelihood in the $(\kappa_\gamma, \kappa_g)$ plane are shown in Fig. 11.19.

In the second approach, new physics is considered also in the decay thus affecting the total width of the H through decays to particles which are either "invisible" in that they escape detection in the experiments, or "undetected" in that they are not distinctive enough to be seen in the current analyses. This contribution is parametrized as an invisible and undetected branching fraction $Br_{inv,und}$ which is fitted in addition to the κ_γ and κ_g parameters. The ATLAS result on $Br_{inv,und}$ is from the preliminary combination including the fermion modes [116]. The results of this fit are also reported in Table 11.12. This indirect approach, can be combined with direct invisible decay searches.

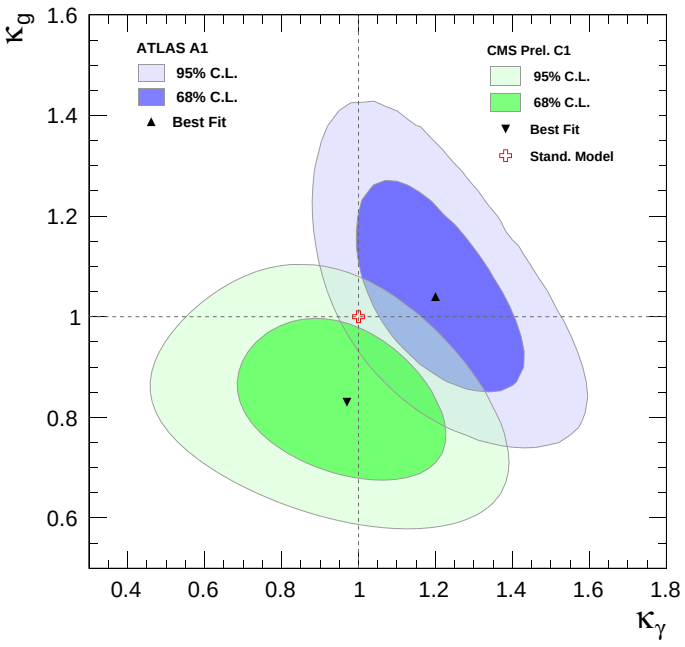

Figure 11.19: Likelihood contours of the global fit in the $(\kappa_g, \kappa_\gamma)$ plane for the ATLAS experiment A1 [119] and the CMS experiment C1 [120] results.

Table 11.12: Summary of the coupling properties measurements in terms of 68% confidence intervals. The ATLAS limit on the invisible or undetected branching fraction denoted by (*) is from the preliminary combination reported in Ref. [116].

	ATLAS	CMS
κ_F	$[0.76, 1.18]$	$[0.71, 1.11]$
κ_V	$[1.05, 1.22]$	$[0.81, 0.97]$
λ_{FV}	$[0.70, 1.01]$	–
λ_{WZ}	$[0.67, 0.97]$	$[0.73, 1.00]$
λ^*_{WZ}	–	$[0.75, 1.13]$
λ°_{WZ}	$[0.66, 0.97]$	–
$\lambda^{\ddagger}_{WZ}$	$[0.61, 1.04]$	–
κ_g	$[0.90, 1.18]$	$[0.73, 0.94]$
κ_γ	$[1.05, 1.35]$	$[0.79, 1.14]$
$\text{BR}_{inv,und}$	$< 60\%^*$ at 95% CL	$< 64\%$ at 95% CL
κ_V	–	$[0.84, 1.23]$
κ_b	–	$[0.61, 1.69]$
κ_τ	–	$[0.82, 1.45]$
κ_t	–	$[0.00, 2.03]$
κ_g	–	$[0.65, 1.15]$
κ_γ	–	$[0.77, 1.27]$

(vi) Generic measurement of the H couplings to fermions and gauge bosons

A more generic model testing the couplings of the H to the W and Z bosons through a single coupling modifier parameter κ_V and the couplings to the third generation fermions are tested separatedly κ_b, κ_τ and κ_t. In this model the effective couplings to photons and gluons take into account possible loop induced contributions in the κ_γ and κ_g modifiers, respectively. The assumption is that no additional contribution affect the total width and that the couplings to the fermions of the first and second generation are equal to those of the third (separating charged leptons, and up and down type quarks).

The results of this global fit are reported in Table 11.12. It illustrates the good agreement of the measured coupling modifiers with the SM Higgs boson couplings, in particular with its dependence in mass as described in Section II.

IV.2.6. Differential cross sections

To further characterize the production and decay properties of H, first measurements of fiducial and differential cross sections have been carried out by the ATLAS collaboration [188], with the 8 TeV dataset of pp collision at LHC, corresponding to an integrated luminosity of 20.3 fb^{-1}, in the diphoton channel. The selection criteria to define the fiducial volume are the following: the two highest transverse momentum (E_T), isolated final state photons, within $|\eta| < 2.37$ and with $105\,\text{GeV} < M_{\gamma\gamma} < 160\,\text{GeV}$ are selected (the transition region between the barrel and endcap calorimeters is not removed); after the pair is selected, the same cut on $E_T/M_{\gamma\gamma}$ as in the event selection *i.e.* in excess of 0.35 (0.25) for the two photons is applied. Several observables have been studied: the transverse momentum rapidity of the diphoton system, the production angle in the Collins–Soper frame, the jet multiplicity, the jet veto fractions for a given jet multiplicity, and the transverse momentum distribution of the leading jet. The following additional observables: the difference in azimuthal angle between the leading and the subleading jets, and the transverse component of the vector sum of the momenta of the Higgs boson and dijet system, have also been measured in two jet events. To minimize the model dependence the differential cross sections are given within a specific fiducial region of the two photons. The observables were chosen to probe the production properties and the spin and parity of the H. The differential cross section in H transverse momentum is given in Fig. 11.20.

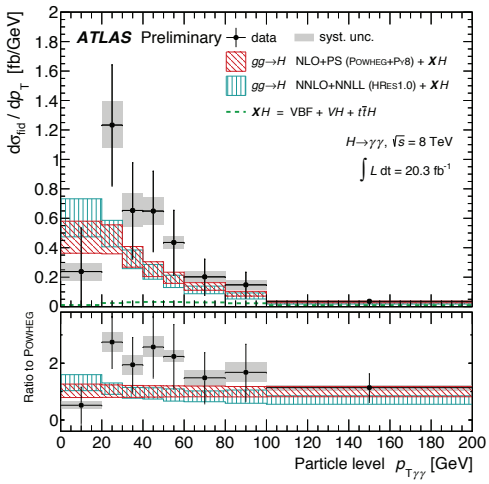

Figure 11.20: Observed differential cross sections in transverse momentum of the H in the diphoton channel, compared to the prediction of the ggH process [188].

IV.3. Main quantum numbers J^{PC}

The measurements of the signal event yields of the observed new state in all the channels discussed above and their compatibility with the Standard Model Higgs boson predictions, gives qualitative, but nonetheless compelling evidence of its nature. This qualitative picture is further complemented by the implications of the observation of the particle in the diphoton channel. According to the Landau–Yang theorem [189], the observation made in the diphoton channel excludes the spin 1 hypothesis and restricts possibilities for the spin of the observed particle to 0 or 2.

However, the Landau–Yang theorem does not apply if the observed state is not decaying to a pair of photons but to a pair of scalars subsequently decaying to two very collimated pairs of photons (as for example in the case of $H \to a_1 a_1 \to 4\gamma$). This possibility has not been rigorously tested but it is not experimentally favored as tight selection criteria are applied on the electromagnetic shower shapes of the reconstructed photons. A more systematic analysis of shower shapes and the fraction of conversions could be performed to further discriminate between the single prompt photon and the two overlapping photons hypotheses. There are also potential theoretical loopholes concerning the applicability of the Landau–Yang theorem, such as off-shell vector boson decays.

For the observed particle not to be of spin 0 and +1 parity would require an improbable conspiracy of effects. It is nevertheless very important that this hypothesis be independently tested.

IV.3.1. Charge conjugation C

The charge conjugation quantum number is multiplicative, therefore given that the Higgs-like particle is observed in the $H \to \gamma\gamma$ channel, and given that photons are C-odd eigenstates, assuming C conservation, the observed neutral particle should be C-even.

IV.3.2. General framework

To further assess the spin and parity quantum numbers of the discovered particle, a systematic analysis of its production and decay processes is performed. These analyses have been designed to be as independent as possible from the event yields measured in each exclusive categories, relying instead on the production and the decay angles, and on the threshold distributions, of the produced particle.

This leads to test hypotheses which are typically disfavored by the analysis of the rates, such as a pseudoscalar particle decaying to a pair of W or Z bosons which requires, decays through loops or to test spin 2 hypotheses for which no renormalizable model exist. The sizable interaction of the observed state with electroweak gauge bosons, if it were pseudoscalar, would imply low scale physics in the loops and therefore would be ruled out by the absence of direct observation of such states.

To define, generate and test the newly observed state without theoretical prejudice, the most general tensor structure is used for the three possible spin hypotheses of spin 0, spin 1 and spin 2. The most general spin-0 interaction amplitude with two gauge bosons can be written as follows [190,191]

$$\begin{aligned} A^{(0)} =& v^{-1}\left(g_1^{(0)} m_V^2 \varepsilon_1^* \varepsilon_2^* + g_2^{(0)} f_{\mu\nu}^{*(1)} f^{*(2),\mu\nu}\right. \\ &\left. + g_3^{(0)} f^{*(1),\mu\nu} f_{\mu\alpha}^{*(2)} \frac{q_\nu q_\alpha}{\Lambda^2} + g_4^{(0)} f_{\mu\nu}^{*(1)} \tilde{f}^{*(2),\mu\nu}\right), \end{aligned} \tag{11.28}$$

where the ε denotes the polarization vector of a spin 1 boson, q the momentum of the a vector boson, $f^{(i),\mu\nu} = \varepsilon_i^\mu q_i^\nu - \varepsilon_i^\nu q_i^\mu$ is the field strength tensor of a gauge boson with momentum q_i and polarization ε_i, and Λ is the new physics mass scale. The $g_j^{(0)}$ are dimensionless and momentum dependent complex form factors.

The first term corresponds to the Standard Model case 0^{++} where

$$\mathcal{L} \supset g_1^{(0)} H Z_\mu Z^\mu \tag{11.29}$$

The second (CP conserving if H^0 is 0^+) and fourth (CP violating) terms correspond to 5 dimensional operator couplings through loops of the type

$$\mathcal{L} \supset g_2^{(0)} H Z_{\mu\nu} Z^{\mu\nu} + g_4^{(0)} H Z_{\mu\nu} \tilde{Z}^{\mu\nu} \tag{11.30}$$

The third term corresponds to a dimension-7 operator involving new physics possibly appearing at a scale Λ.

Table 11.13: Benchmark scenarios for the analysis of the production and decay of the observed state with J^P quantum numbers. The subscripts refer to the specificities of the couplings of the observed state, where m denotes minimal couplings and h denotes couplings with higher dimension operators. For each scenarios only the non vanishing coupling constants are reported in this table. 0_h^+ denotes a scalar with higher orer (HO) couplings.

Scenario	Production	Decay	Scenario
0_m^+	$gg \to X$	$g_1^{(0)} = 2$	SM Higgs bosons
0_h^+	$gg \to X$	$g_2^{(0)} \neq 0$	HO scalar
0^-	$gg \to X$	$g_4^{(0)} \neq 0$	PSeudo scalar
1^+	$qq \to X$	$g_2^{(1)} \neq 0$	Pseudo vector
1^-	$qq \to X$	$g_a^{(1)} \neq 0$	Vector
2_m^+	$g_1^{(2)} \neq 0$	$g_1^{(2)} = g_5^{(2)} \neq 0$	Graviton tensor MC
2_h^+	$g_4^{(2)} \neq 0$	$g_4^{(2)} \neq 0$	Graviton tensor HD op.
2^-	$g_8^{(2)} \neq 0$	$g_8^{(2)} \neq 0$	Pseudo tensor

Analogously the most general spin 1 interaction amplitude with two gauge bosons can be expressed as follows

$$A^{(1)} = g_1^{(1)}\left[(\varepsilon_1^* q)(\varepsilon_2^* \varepsilon_X)\right] + g_2^{(1)} \epsilon_{\alpha\beta\mu\nu} \varepsilon_X^{\alpha} \varepsilon_1^{*,\mu} \varepsilon_2^{*,\nu} \tilde{q}^{\beta} \qquad (11.31)$$

Finally the general spin 2 case can be expressed as follows [190]

$$\begin{aligned} A^{(2)} = \frac{1}{\Lambda}\Bigg[& 2g_1^{(2)} t_{\mu\nu} f^{*1,\mu\alpha} f^{*2,\nu\alpha} + 2g_2^{(2)} t_{\mu\nu} \frac{q_\alpha q_\beta}{\Lambda^2} f^{*1,\mu\alpha} f^{*2,\nu\beta} \\ & + g_3^{(2)} \frac{\tilde{q}^\beta \tilde{q}^\alpha}{\Lambda^2} t_{\beta\nu} (f^{*1,\mu\nu} f^{*2}_{\nu\alpha} + f^{*2,\mu\nu} f^{*1}_{\nu\alpha}) \\ & + g_4^{(2)} \frac{\tilde{q}^\mu \tilde{q}^\nu}{\Lambda^2} t_{\mu\nu} f^{*1,\alpha\beta} f^{*2}_{\alpha\beta} + 2g_5^{(2)} m_V^2 t_{\mu\nu} \varepsilon_1^{*\mu} \varepsilon_2^{*\nu} \\ & + 2g_6^{(2)} m_V^2 \frac{\tilde{q}^\mu \tilde{q}^\nu}{\Lambda^2} t_{\mu\nu} (\varepsilon_1^{*\nu} \varepsilon_2^{*\alpha} - \varepsilon_1^{*\alpha} \varepsilon_2^{*\nu}) + g_7^{(2)} m_V^2 \frac{\tilde{q}^\mu \tilde{q}^\nu}{\Lambda^2} t_{\mu\nu} \varepsilon_1^* \varepsilon_2^* \\ & + g_8^{(2)} \frac{\tilde{q}^\mu \tilde{q}^\nu}{\Lambda^2} t_{\mu\nu} f^{*1,\alpha\beta} \tilde{f}^{*2}_{\alpha\beta} + g_9^{(2)} t_{\mu\alpha} \tilde{q}^\alpha \epsilon_{\mu\nu\rho\sigma} \varepsilon_1^{*\nu} \varepsilon_2^{*\rho} q^\sigma \\ & + g_{10}^{(2)} \frac{t_{\mu\alpha} \tilde{q}^\alpha}{\Lambda^2} \epsilon_{\mu\nu\rho\sigma} q^\rho \tilde{q}^\sigma (\varepsilon_1^{*\nu}(q\varepsilon_2^*) + \varepsilon_2^{*\nu}(q\varepsilon_1^*)) \Bigg] \end{aligned} \qquad (11.32)$$

where $t_{\mu\nu}$ is a symmetric traceless tensor, transverse to the momentum of the spin 2 state $t_{\mu\nu} q^\nu = 0$ [190]. As in the general spin 0 case $g_1^{(1),(2)}$ are dimensionless and momentum dependent complex form factors are effective and dimensionless. Similar amplitudes are derived in the case of fermion couplings, as reported in Ref. [36]. Studies of the spin and CP properties of the discovered state can either use an effective Lagrangian approach or generic scattering amplitudes. The two are equivalent at leading order. However the effective Lagrangian is typically used to generate specific hypotheses and the scattering amplitudes are used in analyses.

The JHU generator [190,192] has been used to define benchmark scenarios for exotic hypotheses of the nature of the observed state according to the general couplings of the observed new particle to gluons and quarks in production and to vector bosons in decay and includes all spin correlations and interferences of all contributing amplitudes. The models which have been investigated by experiments are reported in Table 11.13. It should be noted that while the 0_m^+ has a very detailed simulation at NLO in QCD, the alternative hypotheses do not.

The 2_m^+ scenario is investigated in different production modes according to the fraction of $q\overline{q}$ versus gg initiated processes. Results were derived by experiments for various fractions. These results will be reported for the two extreme cases where the observed state is fully produced in one or the other processes and will be denoted 2_{gg}^+ and 2_{qq}^+.

IV.3.3. Statistical procedure

Discriminant distributions are used to define the likelihood functions for a given J^P hypothesis and the background $\mathcal{L}_{J^P}$. The test statistic used to probe a given model is defined as $q = -2\ln \mathcal{L}_{J^P}/\mathcal{L}_{0^+}$. This test statistic is kept as independent as possible independent of the measured signal strength, which is left as a free parameter. To measure the compatibility of the observation with one or the other hypotheses, distributions of this test statistic are derived under a signal J^P and under the 0_m^+ hypotheses. It is important to note that to generate these distributions the number of signal events used is the number of signal events fitted on the data under the given hypothesis. Consequently the number of signal events generated under a given null hypothesis can be different from that of the alternative hypothesis. For the 0_m^+ hypothesis in some cases the SM signal normalization has been used. The two numbers characterizing the observation are: (i) the compatibility with the 0_m^+ hypothesis and (ii) the level of confidence of the exclusion of the hypothesis J^P. An example of distributions is illustrated in Fig. 11.22.

To quantify the compatibility of an observation with test statistic q_{obs} with the 0_m^+ hypothesis the cumulative probability $P_{0^+} = P(q > q_{obs}|0_m^+)$ is used. A perfect compatibility is obtained for a P_{0^+} value close to 50%. For a given analysis the observed P_{0^+} can change depending on which alternative hypothesis is tested.

To quantify the exclusion of an alternative hypothesis J^P, a probability $P_{J^P} = P(q > q_{obs}|J^P)$ is defined. The level of confidence at which the J^P is excluded is given by the CL_S criterion [193]

$$CL_S = \frac{P_{J^P}}{1 - P_{0^+}} \qquad (11.33)$$

IV.3.4. J^P determination

At the LHC, the determination of the spin and CP properties of the discovered state is done independently from the rates observed, from a global angular helicity analysis, derived from the general scattering amplitude expressed in Section IV.3.2 and when applicable in the threshold effects in the decay. The channels used for this analysis, the $H \to \gamma\gamma$, $H \to W^{(*)}W^{(*)} \to \ell\nu\ell\nu$ and $H \to Z^{(*)}Z^{(*)} \to 4\ell$, are those where a the observation of a signal is established.

At the Tevatron, an analysis using the threshold distribution of the production of the discovered state [194] in the associated production mode VH with subsequent decay to a pair of b-quarks was performed by the D0 collaboration.

(i) The VH production at D0

The mass of the VH system is a very powerful discriminant to distinguish a $J^P = 0_m^+$, with a threshold behavior in $d\sigma/dM^2 \sim \beta$ from 0^- or 2^+ with threshold behaviors respectively in $\sim \beta^3$ and $\sim \beta^5$ (for a graviton like spin 2) [194]. The VH mass observable, is not only strongly discriminating signal hypotheses, but also have an increased separation of the 0^- and 2^+ hypotheses with respect to the backgrounds, thus allowing, with a small and not yet significant signal, to exclude that the observed state is 0^- at 98% CL [195] and 2^+ at the 99.9% CL [196].

(ii) The $\gamma\gamma$ channel at LHC

In the $H \to \gamma\gamma$ channel, the analysis is performed by ATLAS inclusively using the production angle $\cos\theta^*_{CS}$ as discriminant [197]. The definition chosen for the polar angle in the rest frame is the Collins–Soper frame, which is defined as the bisector axis of the momenta of the incoming protons in the diphoton rest frame. The 0_m^+ signal distribution is expected to be uniform with a cutoff due to the lower selection requirements on the photons transverse momentum. The $H \to \gamma\gamma$ channel is mostly sensitive to the gluon-initiated production scenario 2_{gg}^+, which yields a $\cos\theta^*_{CS}$ distribution peaking at values close to 1. It is much less so for the quark-initiated scenarios 2_{qq}^+. The results are derived from a fit of the signal in bins of $\cos\theta^*_{CS}$ and are summarized in Table 11.14. The data shows a good compatibility with the SM 0_m^+ hypothesis. ATLAS excludes the alternative hypotheses 2_{gg}^+ and 2_{qq}^+ at the 99% CL and 95% CL.

(iii) The $H \to W^{(*)}W^{(*)} \to \ell\nu\ell\nu$ channel at LHC

The $H \to W^{(*)}W^{(*)} \to \ell\nu\ell\nu$ the production and decay angles cannot be easily reconstructed due to the neutrinos in the final state, however an important feature is the V-A structure of the decay of the W bosons. A scalar state thus yields a clear spin correlation pattern that implies that the charged leptons e or μ from the decays of the W bosons are produced close to one another in the transverse plane. In the main analysis this feature is used to gain sensitivity, in this case the initial selection need to be reappraised in order not to discriminate specific J^P hypotheses. This feature, which immediately impacts observables such as the azimuthal angle between the two leptons $\Delta\Phi_{\ell\ell}$ or their invariant mass $M_{\ell\ell}$ in addition of the threshold behavior of the decay which is used in kinematic variables such as the transverse mass defined in Section III, can be used to discriminate spin and parity hypotheses. The approach adopted by ATLAS is a multivariate discriminant, whereas CMS uses a 2D-fit of the dilepton mass and the transverse mass. The results of the $H \to W^{(*)}W^{(*)} \to \ell\nu\ell\nu$ analyses are summarized in Table 11.14. The hypotheses tested by this approach are the 1^+ and 1^- by the ATLAS experiment and the 2^+ by ATLAS and CMS. A good compatibility of the observation with the 0^+_m hypothesis is observed in the discrimination of all hypotheses. ATLAS excludes the 1^+ and 1^- hypotheses at the 98% CL and 99% CL respectively. When discriminating the 2^+ hypothesis, the $H \to W^{(*)}W^{(*)} \to \ell\nu\ell\nu$ analysis is more sensitive to the quark-initiated production mode and is therefore complementary to the $H \to \gamma\gamma$ channel. ATLAS [197] and CMS [198] disfavor the 2^+_{gg} and 2^+_{qq} at different levels of confidence. The strongest observed exclusion is obtained by ATLAS excluding the 2^+_{gg} and 2^+_{qq} at the 98% CL and 99% CL respectively.

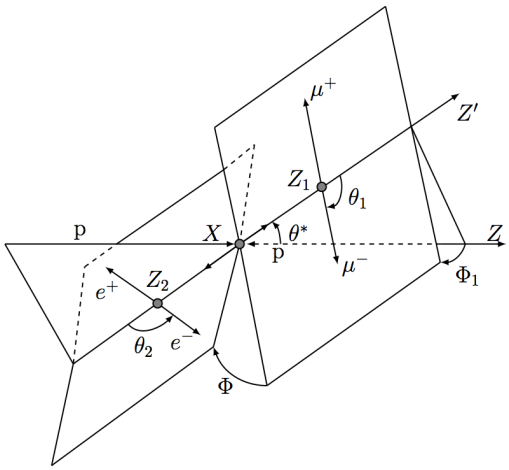

Figure 11.21: Definition of the production and decay angles defined for the $H \to Z^{(*)}Z^{(*)} \to 4\ell$ final state [199].

(iv) The $H \to Z^{(*)}Z^{(*)} \to 4\ell$ channel at LHC

The main $H \to Z^{(*)}Z^{(*)} \to 4\ell$ coupling analysis, as described in Section III, also uses a discriminant based on the 0^+_m nature of the Higgs boson to further discriminate the signal from the background. In this analysis this feature is used to discriminate between signal hypotheses. The observables sensitive to the spin and parity are the masses of the two Z bosons [191](due to the threshold dependence of the mass of the off-shell Z boson), two production angle θ^* and ϕ_1, and three decay angles, ϕ, θ_1 and θ_2. The production and decay angles defined as:

– θ_1 and θ_2, the angles between the negative final state lepton and the direction of flight of Z_1 and Z_2 in the rest frame.

– ϕ, the angle between the decay planes of the four final state leptons expressed in the four lepton rest frame.

– ϕ_1, the angle defined between the decay plane of the leading lepton pair and a plane defined by the vector of the Z_1 in the four lepton rest frame and the positive direction of the proton axis.

– θ^*, the production angle of the Z_1 defined in the four lepton rest frame with respect to the proton axis.

These angles are illustrated in Fig. 11.21. There are two approaches to this analysis. The first, used by CMS, is a matrix element likelihood approach where a kinematic discriminant is defined based on the ratio of the signal and background probabilities. These probabilities are defined using the leading-order matrix elements. A similar approach is also performed by ATLAS as a cross check of their main result. The main approach adopted by ATLAS is the combination of sensitive variables in a boosted decision tree. These analyses are sensitive to various J^P hypotheses and in particular to discriminate the 0^+_m hypothesis from the 0^-. In all scenarios investigated and for both the ATLAS and CMS experiments the data are compatible with the 0^+_m hypothesis. ATLAS [197] and CMS [199] exclude a pseudo scalar nature of the H^0 at CL_S levels of 98% and 99.8%. The distribution of the test statistic q defined in Section IV.3.3 is illustrated in Fig. 11.22 for the 0^+_m and 0^- hypotheses. All benchmark scenarios results are summarized in Table 11.14.

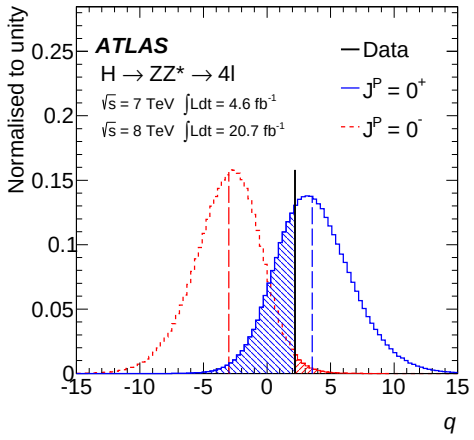

Figure 11.22: Expected distributions of q, for the Standard Model 0^+ (blue/solid line distribution) or 0^- (red/dashed line distribution) signals [197]. The observed value is indicated by the vertical solid line and the expected medians by the dashed lines. The colored areas correspond to the integrals of the expected distributions up to the observed value and are used to compute the p_0-values for the rejection of each hypothesis.

IV.3.5. Probing CP mixing

The most general decay amplitude for spin-0 state decaying to a pair of gauge bosons described in Section IV.3.2 can be expressed in a more compact form [190]

$$A^{(0)} = \frac{\varepsilon_1^{*\mu}\varepsilon_2^{*\nu}}{v}(a_1\, m_H^2\, g_{\mu\nu} + a_2\, q_\mu q_\nu + a_3\, \epsilon_{\mu\nu\alpha\beta}\, q_1^\alpha q_2^\beta) = A_1 + A_2 + A_3\,, \tag{11.34}$$

where q_i and ε_i are the momenta and polarization vectors of the two gauge bosons, and $q = q_1 + q_2$ is the four-momentum of the spin 0 boson.

The SM Higgs boson is dominated by the A_1 amplitude, while a 0^- state is dominated by A_3. The CMS collaboration has performed an analysis of the ratio $f_{a_3} = |A_3|^2/(|A_1|^2 + |A_3|^2)$ in the $H \to Z^{(*)}Z^{(*)} \to 4\ell$ channel [199], where the presence of the A_2 term is neglected. This second term corresponds to higher order couplings of the 0^+ state. The two extreme cases $f_{a_3} = 0, 1$ correspond

Table 11.14: Results in all benchmark scenarios for the analysis of the production and decay of the observed state with J^P quantum numbers, for the ATLAS (A) and CMS (C) experiments. The upper part of the table gives the compatibility of the observation with the SM 0_m^+ hypothesis. The lower part of the table gives the CL_S observed exclusion and in parenthesis the sensitivity of the given alternative model.

J^P	ZZ	WW	$\gamma\gamma$	Combined
0^-	31% A	–	–	–
	31% C	–	–	–
0_h^+	50% C	–	–	–
1^+	55% A	70% A	–	62% A
	4.5% C	–	–	–
1^-	15% A	66% A	–	33% A
	8.1% C	–	–	–
$2^+_{q\overline{q}}$	96% A	54% A	80% A	81% A
	3.6% C	–	–	–
2^+_{gg}	53% A	73% A	59% A	63% A
	82% C	33% C	–	63% C
0^-	2.2% (0.4%) A	–	–	–
	0.2% (0.5%) C	–	–	–
0_h^+	8.1% (4.5%) C	–	–	–
1^+	0.2% (0.2%) A	8.0% (8.0%) A	–	<0.1% (<0.1%) A
	<0.1% (1.1%) C	–	–	–
1^-	6.0% (0.4%) A	1.7% (2.0%) A	–	0.3% (<0.1%) A
	<0.1% (0.3%) C	–	–	–
$2^+_{q\overline{q}}$	2.6% (8.2%) A	<0.1% (<0.1%) A	12.4% A (13.5%)	<0.1% (<0.1%) A
	<0.1% (4.0%) C	–	–	–
2^+_{gg}	16.9% (9.2%) A	4.8% (5.4%) A	0.7% A (0.5%)	<0.1% (<0.1%) A
	1.4% (5.5%) C	14.0% (5.5%) C	–	0.6% (1.1%) C

approximately to the 0^+ and 0^- cases respectively. Other values of f_{a_3} would be an indication of *CP*-violation. The analysis uses a kinematic discriminant defined similarly to the cases discussed in Section IV.3.4 taking the dependence with f_{a_3} into account. Using the full dataset corresponding to an integrated luminosity of approximately 25 pb^{-1} of pp collisions at 7 TeV and 8 TeV, CMS measures $f_{a_3} = 0.00 \pm 0.23$ corresponding to a limit of $f_{a_3} < 0.58$ at 95% CL. It should be noted that an indication of *CP*-violation from f_{a_3} would not yield a measure of the mixing of opposite parity states.

V. New physics models of EWSB in the light of the Higgs boson discovery

A main theoretical motivation to add a Higgs boson to the Standard Model is that, without it, the longitudinal components of the massive EW gauge bosons would form a strongly coupled system as their scattering amplitude would have grown with their energy, destroying all the predictive power of the model above $4\pi v \sim 3$ TeV. The discovery of a light scalar with couplings to gauge bosons and fermions that are apparently consistent with SM predictions and the slow running of the Higgs self-coupling at high energies allows one to consider the SM as a valid perturbative description of nature all the way to the Planck scale. This picture is admittedly very attractive, but it posits that the Higgs boson is an elementary scalar field, which comes with an intrinsic instability of its mass under radiative corrections. This Higgs naturalness problem calls for new physics around the TeV scale. Supersymmetric models are the most elegant solution to maintain the perturbativity of the SM while alleviating the instability issue. Another possibility is that the Higgs boson itself has a finite size and is composite and thus never feels the UV degrees of freedom that would drag its mass to much higher scales. Both classes of models predict specific modifications from the SM Higgs properties. In this section, these possible deviations will be discussed in detail.

The realization of supersymmetry at low energies has many good qualities that render it attractive as a model of new physics. First of all since for every fermion there is a boson of equal mass and effective coupling to the SM-like Higgs, in the case of exact supersymmetry it yields an automatic cancellation of loop corrections to the Higgs mass parameter: (analogous to Eq. (11.2)) $\delta m^2 = 0$ [8,10]. In practice, it is known that SUSY must be broken in nature since no superpartners of the SM particles have been observed so far. Taking into account the fact that the fermion and boson couplings to the Higgs and the number of degrees of freedom of the SM particles and their superpartners are the same, the Higgs mass correction simply writes

$$\delta m^2 = \sum_F g_F \lambda_F^2 \frac{(m_B^2 - m_F^2)}{32\pi^2} \log \frac{Q^2}{\mu^2}, \qquad (11.35)$$

where the sum is over all fermion fields of mass m_F and includes implicitly their superpartners with a squared mass m_B^2. The mass difference between the boson and fermion degrees of freedom is governed by the soft supersymmetry breaking parameters. Therefore, independently of how large m_B^2 and m_F^2 are, all corrections are proportional to M_{SUSY}^2. Hence, provided that $M_{SUSY} \simeq \mathcal{O}(1$–few) TeV, the fine-tuning problem is solved, in the sense that the low energy mass parameters become insensitive to physics at the GUT or Planck scale. Another interesting feature of SUSY theories is related to the dynamical generation of EWSB [201]. In the SM a negative Higgs mass parameter, m^2, needs to be inserted by hand to induce EWSB. In SUSY, instead, even if the relevant Higgs mass parameter is positive in the ultraviolet, it may become negative and induce electroweak symmetry breaking radiatively through the strong effect of the top quark-Higgs coupling in its renormalization group evolution. Moreover, supersymmetry with a supersymmetry breaking scale of order 1 TeV allows for grand unification of the electroweak and strong gauge interactions in a consistent way, strongly supported by the prediction of the electroweak mixing angle at low energy scales, with an accuracy at the percent level [202,203]. In addition, supersymmetry theories can provide a suitable dark matter candidate [204] and even a low energy physics explanation of baryogenesis [205], all of this compatible with existing precision data.

In the following discussion, the Higgs sector will be explored in specific SUSY models. In all of them there is one neutral Higgs boson with properties that resemble those of the SM Higgs boson whereas additional neutral and charged Higgs bosons are also predicted and are intensively being sought for at the LHC (see Section V.9). In the simplest SUSY model the lightest Higgs boson mass, that usually plays the role of the SM-like Higgs, is predicted to be less than 135 GeV for stops in the TeV to few TeV range [206–220], whereas, larger values of the SM-like Higgs boson mass – up to about 250 GeV – can be obtained in non-minimal SUSY extensions of the SM [344,221–227]. In general, accommodating a SM-like Higgs boson with mass of 125 GeV results in constraints on the supersymmetric parameter space of specific SUSY models, as discussed below.

The more and more constraining bounds on the SUSY parameter space do not preclude a solution to the naturalness problem but they require either heavier SUSY partners or some specific engineering to hide any SUSY signal from the optimized searches conducted at the LHC. In their most commonly studied incarnations, SUSY models distinguish themselves from the background by a substantial amount of missing transverse energy (MET) taken away by the stable lightest supersymmetric particle (LSP), and by a large activity associated with the superpartners around the TeV scale. Nonetheless, light SUSY is still allowed by current LHC limits if these two characteristic features of the generic SUSY signals are softened. Compressing the SUSY spectrum [228] reduces the amount of available energy transferred to the visible particles at the end of the cascade decays of the heavy superpartners. Also the LSP's tend to be produced back-to-back, minimizing the amount of missing energy along the transverse direction. A compressed spectrum can be obtained if the gluino happens to be lighter than the other gauginos at the high scale in gravity mediated or gauge mediated SUSY breaking scenarios. Another approach, dubbed as stealth supersymmetry [229], is designed to reduce the SUSY signals by introducing a new light and approximately supersymmetric multiplet that is complementary to the

MSSM matter content. The heavy MSSM particles will chain-decay to the R-odd particle of this new multiplet but the small mass splitting within this multiplet kinematically limits the amount of MET finally taken away by the LSP. Dedicated experimental searches have already been designed to probe such scenarios.

A more radical solution to reduce the amount of MET in the final state is to revoke the R-parity assumption that is usually imposed to save the proton from a fast decay and also to guarantee the existence of a stable particle with a relic abundance compatible with what is expected to form the dark matter component of the Universe. R-parity is however not a necessity. For instance if the 96 new complex parameters of the R-parity violating MSSM [230] are arranged to follow a minimal flavor violation pattern [231], the proton lifetime will exceed the current bounds. Such scenarios predict either multilepton or multijet final states that are already the target of ongoing LHC searches.

While naturalness dictates relatively light stops and gluinos, the first and second generation of squarks and sleptons couple weakly to the Higgs sector and may be heavy. Moreover, small values of the μ parameter and therefore light Higgsinos would be a signature of a natural realization of electroweak symmetry breaking. Such SUSY spectra, consisting of light stops and light Higgsinos, have been under intense scrutiny by the experimental collaborations [232] in order to derive model-independent bounds on the stop masses and to understand if such natural SUSY scenarios endure [233] and can explain why the Higgs boson remains light.

In the context of weakly coupled models of EWSB one can also consider multiple Higgs $\mathrm{SU}(2)_L$ doublets as well as additional Higgs singlets, triplets or even more complicated multiplet structures, with or without low energy supersymmetry. In general for such models one needs to take into account experimental constraints from precision measurements and flavor changing neutral currents. The LHC signatures of such extended Higgs sectors are largely shaped by the role of the exotic scalar fields in EWSB.

The idea that the Higgs boson itself could be a composite bound state emerging from a new strongly-coupled sector has regained some interest. The composite Higgs idea is an interesting incarnation of EWSB via strong dynamics that smoothly interpolates between the standard Technicolor approach and the true SM limit. To avoid the usual conflict with EW data, it is sufficient if not necessary that a mass gap separates the Higgs resonance from the other resonances of the strong sector. Such a mass gap can naturally follow from dynamics if the strongly-interacting sector exhibits a global symmetry, G, broken dynamically to a subgroup H at the scale f, such that, in addition to the three Nambu–Goldstone bosons of SO(4)/SO(3) that describe the longitudinal components of the massive W and Z, the coset G/H contains, a fourth Nambu–Goldstone boson that can be identified with the physical Higgs boson. Simple examples of such a coset are SU(3)/SU(2) or SO(5)/SO(4), the latter being favored since it is invariant under the custodial symmetry (it is also possible to have non-minimal custodial cosets with extra Goldstone bosons, see for instance Ref. [234]). Attempts to construct composite Higgs models in 4D have been made by Georgi and Kaplan (see for instance Ref. [235]) and modern incarnations have been recently investigated in the framework of 5D warped models where, according to the principles of the AdS/CFT correspondence, the holographic composite Higgs boson then originates from a component of a gauge field along the 5th dimension with appropriate boundary conditions.

A last crucial ingredient in the construction of viable composite Higgs models is the concept of partial compositeness [236], i.e., the idea that there are only linear mass mixings between elementary fields and composite states[8]. After diagonalization of the mass matrices, the SM particles, fermions and gauge bosons, are admixtures of elementary and composite states and thus they interact with the strong sector, and in particular with the Higgs boson, through their composite component. This setup has important consequences on the flavor properties, chiefly the suppression of large flavor changing neutral currents involving light fermions. It also plays an important role in dynamically generating a potential for the would-be Goldstone bosons. Partial compositeness also links the properties of the Higgs boson to the spectrum of the fermionic resonances, i.e. the partners of the top quark. As in the MSSM, these top partners are really the agents that trigger the EWSB and also generate the mass of the Higgs boson that otherwise would remain an exact Goldstone boson and hence massless. The bounds from the direct searches for the top partners in addition to the usual constraints from EW precision data force the minimal composite Higgs models into some rather unnatural corners of their parameter spaces [238].

V.1. Higgs bosons in the Minimal Supersymmetric Standard Model (MSSM)

The particle masses and interactions in a supersymmetric theory are uniquely defined as a function of the superpotential and the Kähler potential [200]. A fundamental theory of supersymmetry breaking, however, is unknown at this time. Nevertheless, one can parameterize the low-energy theory in terms of the most general set of soft supersymmetry-breaking operators [239]. The simplest realistic model of low-energy supersymmetry is the Minimal Supersymmetric extension of the Standard Model (MSSM) [10,200], that associates a supersymmetric partner to each gauge boson and chiral fermion of the SM, and provides a realistic model of physics at the weak scale. However, even in this minimal model with the most general set of soft supersymmetry-breaking terms, more than 100 new parameters are introduced [240]. Fortunately, only a subset of these parameters impact the Higgs phenomenology through tree-level and quantum effects. Reviews of the properties and phenomenology of the Higgs bosons of the MSSM can be found for example in Refs. [34,200,241].

The MSSM contains the particle spectrum of a two-Higgs-doublet model (2HDM) extension of the SM and the corresponding supersymmetric partners. Two Higgs doublets,

$$\Phi_1 = \frac{1}{\sqrt{2}} \begin{pmatrix} \phi_1^0 + i a_1^0 \\ \sqrt{2}\phi_1^- \end{pmatrix}, \tag{11.36}$$

$$\Phi_2 = \frac{1}{\sqrt{2}} \begin{pmatrix} \sqrt{2}\phi_2^+ \\ \phi_2^0 + i a_2^0 \end{pmatrix}, \tag{11.37}$$

with $Y = -1$ and $Y = 1$, respectively, are required to ensure an anomaly-free SUSY extension of the SM and to generate mass for both up-type and down-type quarks and charged leptons [12]. In our notation $\Phi_{1(2)}$ gives mass to the down(up) type fermions. The Higgs potential reads

$$\begin{aligned} V = {} & m_1^2 \Phi_1^\dagger \Phi_1 + m_2^2 \Phi_2^\dagger \Phi_2 - m_3^2 (\Phi_1^T i\sigma_2 \Phi_2 + \text{h.c.}) \\ & + \frac{1}{2}\lambda_1 (\Phi_1^\dagger \Phi_1)^2 + \frac{1}{2}\lambda_2 (\Phi_2^\dagger \Phi_2)^2 + \lambda_3 (\Phi_1^\dagger \Phi_1)(\Phi_2^\dagger \Phi_2) \\ & + \lambda_4 |\Phi_1^T i\sigma_2 \Phi_2|^2 + \frac{1}{2}\lambda_5 [(\Phi_1^T i\sigma_2 \Phi_2)^2 + \text{h.c.}] \\ & + [[\lambda_6 (\Phi_1^\dagger \Phi_1) + \lambda_7 (\Phi_2^\dagger \Phi_2)] \Phi_1^T i\sigma_2 \Phi_2 + \text{h.c.}] \end{aligned} \tag{11.38}$$

where $m_i^2 = \mu^2 + m_{H_i}^2$, with μ being the supersymmetric Higgsino mass parameter and m_{H_i} (for $i = 1, 2$) the Higgs doublet soft supersymmetric breaking mass parameters; $m_3^2 \equiv B\mu$ is associated to the B-term soft SUSY breaking parameter; and λ_i, for $i = 1$ to 7, are all the Higgs quartic couplings. After the spontaneous breaking of the electroweak symmetry, five physical Higgs particles are left in the spectrum: one charged Higgs pair, $H^\pm$, one CP-odd scalar, A, and two CP-even states, H and h.

$$\begin{aligned} H^\pm &= \sin\beta \phi_1^\pm + \cos\beta \phi_2^\pm , \\ A &= \sin\beta \, \mathrm{Im}\phi_1^0 + \cos\beta \, \mathrm{Im}\phi_2^0 , \\ H &= \cos\alpha (\mathrm{Re}(\phi_1^0) - v_1) + \sin\alpha (\mathrm{Re}(\phi_2^0) - v_2), \\ h &= -\sin\alpha (\mathrm{Re}(\phi_1^0) - v_1) + \cos\alpha (\mathrm{Re}(\phi_2^0) - v_2), \end{aligned} \tag{11.39}$$

where $\langle \phi_i^0 \rangle = v_i$ for i=1,2 and $v_1^2 + v_2^2 \approx (246\,\mathrm{GeV})^2$. The angle α diagonalizes the CP-even Higgs squared-mass matrix, while β

[8] For a pedagogical introduction to models of partial compositeness, see Ref. [237].

diagonalizes both the *CP*-odd and charged Higgs sectors with $\tan\beta = v_2/v_1$. The h and H denote the lightest and heaviest *CP*-even Higgs bosons, respectively.[9]

V.1.1. The MSSM Higgs boson masses

Quite generally for any two Higgs doublet model, including the MSSM, the phenomenology depends strongly on the size of the mixing angle α and therefore on the quartic couplings,

$$\sin\alpha = \frac{\mathcal{M}_{12}^2}{\sqrt{(\mathcal{M}_{12}^2)^2 + \left(\mathcal{M}_{11}^2 - m_h^2\right)^2}}, \tag{11.40}$$

where

$$\begin{aligned}\mathcal{M}_{12}^2 &= -\left(m_A^2 - (\lambda_3+\lambda_4)v^2\right)\sin\beta\cos\beta + \lambda_7 v^2\sin^2\beta \\ &\quad + \lambda_6 v^2\cos^2\beta, \\ \mathcal{M}_{11}^2 &= \left(m_A^2 + \lambda_5 v^2\right)\sin^2\beta + \lambda_1 v^2\cos^2\beta \\ &\quad + 2\lambda_6 v^2\cos\beta\sin\beta.\end{aligned} \tag{11.41}$$

The spectrum is given by

$$m_{h,H}^2 = \frac{\mathcal{M}_{11}^2 + \mathcal{M}_{22}^2 \mp \sqrt{\left(\mathcal{M}_{11}^2 - \mathcal{M}_{22}^2\right)^2 + 4(\mathcal{M}_{12}^2)^2}}{2}, \tag{11.42}$$

with

$$\mathcal{M}_{22}^2 = \left(m_A^2 + \lambda_5 v^2\right)\cos^2\beta + \lambda_2 v^2\sin^2\beta + 2\lambda_7 v^2\cos\beta\sin\beta\ . \tag{11.43}$$

The charged Higgs boson mass is given by

$$m_{H^\pm}^2 = m_A^2 + (\lambda_5 - \lambda_4)\frac{v^2}{2}. \tag{11.44}$$

The supersymmetric structure of the theory imposes constraints on the Higgs sector of the model. In particular, at tree level, the parameters of the Higgs self-interaction, $\lambda_{1,\ldots,4}$, are defined in terms of the electroweak gauge coupling constants,

$$\lambda_1 = \lambda_2 = g_2^2/4,\ \ \lambda_3 = -(g_1^2 - g_2^2)/4,\ \ \lambda_4 = -g_2^2/2, \tag{11.45}$$

and $\lambda_{5,6,7} = 0$. As a result, the Higgs sector at tree level is determined by only two free parameters: $\tan\beta$ and one Higgs boson mass, conventionally chosen to be the *CP*-odd Higgs boson mass, m_A. The other tree-level Higgs boson masses are then given in terms of these parameters. In the large $m_A \gg M_Z$ limit, also called the decoupling limit [242], $\sin\alpha \to -\cos\beta$, $\cos\alpha \to \sin\beta$, hence, $\cos(\beta-\alpha) \to 0$ and this implies that the lightest *CP*-even Higgs h behaves as the SM Higgs. The condition $\cos(\beta-\alpha) \to 0$ is also obtained if the quartic couplings are such that $\mathcal{M}_{12}^2\sin\beta = -(\mathcal{M}_{11}^2 - m_h^2)\cos\beta$ [243–245], independent of the value of m_A. The limit $\cos(\beta-\alpha) \to 0$ is called the alignment limit. As will be discussed below, in the MSSM the alignment limit can only occur once quantum corrections to the quartic couplings have been included.

The tree level value of m_h is maximized not only for $m_A \gg M_Z$ but also for $\tan\beta \gg 1$. In the large m_A limit, one finds $m_h^2 \simeq (M_Z\cos 2\beta)^2$ and $m_A \simeq m_H \simeq m_{H^\pm}$, up to corrections of $\mathcal{O}({M_Z}^2/m_A)$. Below the scale m_A, the Higgs sector of the effective low-energy theory consists only of h, which behaves as the SM Higgs boson. This scenario would have been excluded already by LEP and would not accommodate the recently discovered Higgs boson. However, radiative corrections have a significant impact on the values of Higgs boson masses and couplings in the MSSM. In particular, m_h can be lifted to agree with present LHC measurements.

[9] Observe that in the SM sections of this review, H denotes the SM Higgs, whereas in the sections about SUSY and more generally extensions of the SM with two Higgs doublets, H is used for the heaviest *CP*-even Higgs boson, since this is the standard notation in the literature.

The dominant radiative effects to the SM-like Higgs mass arise from the incomplete cancellation between top and scalar-top (stop) loops and at large $\tan\beta$ also from sbottom and stau loops. The loop contributions to the tree level quartic couplings depend on the SUSY spectrum, and render $\lambda_{5,6,7}$ non zero. The stop, sbottom and stau masses and mixing angles depend on the supersymmetric Higgsino mass parameter μ and on the soft-supersymmetry-breaking parameters [10,200]: M_Q, M_U, M_D, M_L, M_E, and A_t, A_b A_τ. The first three of these are the left-chiral and the two right-chiral top and bottom scalar quark mass parameters. The next two are the left-chiral stau/sneutrino and the right-chiral stau mass parameters, and the last three are the trilinear parameters that enter in the off-diagonal squark/slepton mixing elements: $X_t \equiv A_t - \mu\cot\beta$ and $X_{b,\tau} \equiv A_{b,\tau} - \mu\tan\beta$. The corrections affecting the Higgs boson masses, production, and decay properties depend on all of these parameters in various ways. At the two-loop level, the masses of the gluino and the electroweak gaugino also enter in the calculations. For simplicity, it is initially assumed that A_t, A_b, A_τ, μ, and the gluino and electroweak gaugino masses are real parameters. The impact of complex phases on MSSM parameters, which will induce *CP*-violation in the Higgs sector, is addressed below.

Radiative corrections to the Higgs boson masses have been computed using a number of techniques, with a variety of approximations; see Refs. [206–219,246]. The radiative corrections to m_h depend quartically on the top quark mass, quadratically and quartically on stop mixing parameter, and there is also a logarithmic dependence on the stop masses. For large $\tan\beta$, the stau/sbottom mixing parameters and masses are also relevant. In the large m_A (decoupling) limit and for $\tan\beta \gg 1$, which maximizes m_h at tree level, the m_h value can be maximized at loop level for $X_t \simeq \sqrt{6}M_{\rm SUSY}$ [10] where $M_{\rm SUSY} \simeq M_Q \simeq M_U \simeq M_D$ is an assumed common value of the soft SUSY-breaking squark mass parameters. This choice of X_t is called the "maximal-mixing scenario". For fixed X_t, the value of m_h can vary by several GeV by varying $M_{\rm SUSY}$ within a few TeV or by varying m_t within its experimental uncertainty, as well as by varying SUSY particle parameters that enter only beyond the one-loop order. Moreover, in the large $\tan\beta$ regime light staus and/or sbottoms with sizable mixing, governed by the μ parameter, yield negative radiative corrections to the mass of the lightest Higgs boson, and can lower it by several GeV [215,247]. Allowing for experimental and theoretical uncertainties, one finds that for $M_{\rm SUSY} \lesssim 2\,\text{TeV}$, large m_A, $\tan\beta \gg 1$ and for $X_t \simeq \sqrt{6}M_{\rm SUSY}$, the maximal value for the lightest Higgs mass is $m_h^{\rm max} = 135\,\text{GeV}$ [220,248–250]. Interestingly, the upper bound on the lightest neutral scalar boson is a prediction for both the *CP*-conserving (*CPC*) and *CP*-violating (*CPV*) MSSM scenarios [251,252].

The newly discovered SM-like Higgs boson, if interpreted as the lightest MSSM Higgs with a mass of about 125 GeV, provides information on the possible MSSM parameter space. In particular a sizable mixing in the stop sector is required ($|X_t/M_{\rm SUSY}| \geq 1.5$) for values of $M_{\rm SUSY} \simeq M_Q \simeq M_U \simeq M_D \simeq 1$ to a few TeV [247–258]. See for example Fig. 11.23 and Fig. 11.24. On the other hand, as shown in Fig. 11.25, considering the third generation soft SUSY breaking parameters as independent inputs, $M_Q \neq M_U \neq M_D$, one observes that $m_h \simeq$125 GeV can be obtained for one stop that is as light as can be experimentally allowed [259]- - i.e. in the few hundred GeV mass range- and the other one with a mass of the order of the stop mixing parameter. It is also possible to consider both stops significantly above a few TeV by varying/lowering the values of X_t and $\tan\beta$, in that case the impact of higher loops in the computation of the Higgs mass becomes relevant [246].

[10] The parameters X_t and $M_{\rm SUSY}$ depend on the renormalization scheme. The radiative corrections to the Higgs masses computed in the Feynman diagrammatic approach have been obtained in the on-shell (OS) renormalization scheme, whereas those based on the Renormalization Group approach have been calculated using the $\overline{MS}$ scheme. A detailed comparison of the results in the two schemes is presented in Refs. [218,214]. In particular, the lightest Higgs mass is maximized for $X_t^{\bar{M}S} \simeq \sqrt{6}M_{\rm SUSY}$ or equivalently $X_t^{OS} \simeq 2M_{\rm SUSY}$.

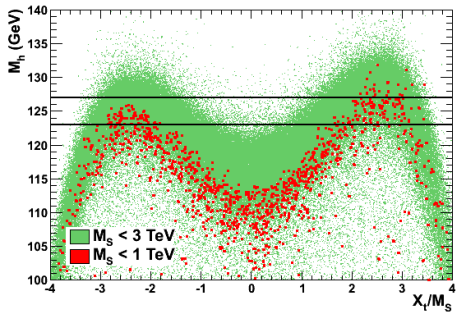

Figure 11.23: The maximal value of m_h as a function of $X_t/M_{\rm SUSY}$ ($M_{\rm SUSY} \equiv M_S$) in the pMSSM when all other soft SUSY-breaking parameters and $\tan\beta$ are scanned as defined in Ref. [253].

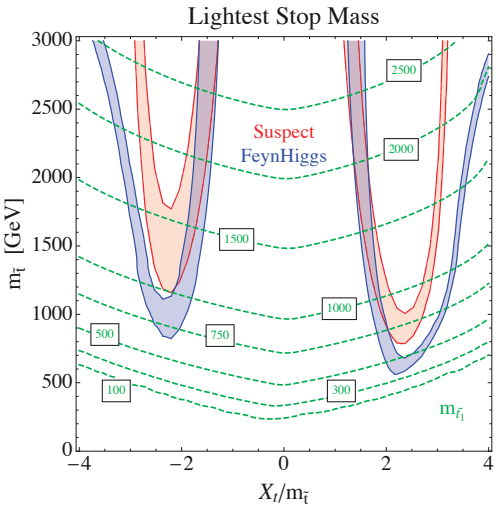

Figure 11.24: Contours of m_h in the MSSM as a function of $m_{\tilde{t}}$, a common stop mass $M_Q = M_U$, and the stop mixing parameter X_t for $\tan\beta = 20$. The red/blue bands show the result from Suspect/FeynHiggs for m_h in the range 124-126 GeV. The contours of constant lightest stop mass are shown in green Ref. [254].

For a given CP-odd Higgs mass m_A, the masses of the other two Higgs bosons, H and $H^\pm$, also receive radiative corrections (for a summary, see for instance Ref. [241]) , but in the absence of additional CP-violating phases, and for m_A larger than $m_h \simeq 125$ GeV, they are all similar, and at most about a few tens of GeV apart. Instead, for smaller values of m_A, the heavy Higgs is the SM one, $m_H \simeq 125$ GeV and $m_h \simeq m_A$, but this scenario is strongly challenged by present data [248]. For a more detailed discussion of the effect of radiative corrections on the heavy Higgs masses see for example Refs. [34] and [241].

V.1.2. MSSM Higgs boson couplings

The phenomenology of the Higgs sector depends on the couplings of the Higgs bosons to gauge bosons and fermions. The couplings of the two CP-even Higgs bosons to W and Z bosons are given in terms of the angles α and β

$$g_{hVV} = g_V m_V \sin(\beta-\alpha), \quad g_{HVV} = g_V m_V \cos(\beta-\alpha), \qquad (11.46)$$

where $g_V \equiv 2m_V/v$, for $V = \mathrm{W}^\pm$ or Z ($g_V m_V$ is the SM hVV coupling). There are no tree-level couplings of A or $H^\pm$ to VV. The couplings of the Z boson to two neutral Higgs bosons, which must have opposite CP-quantum numbers, are given by $g_{\phi AZ}(p_\phi - p_A)$,

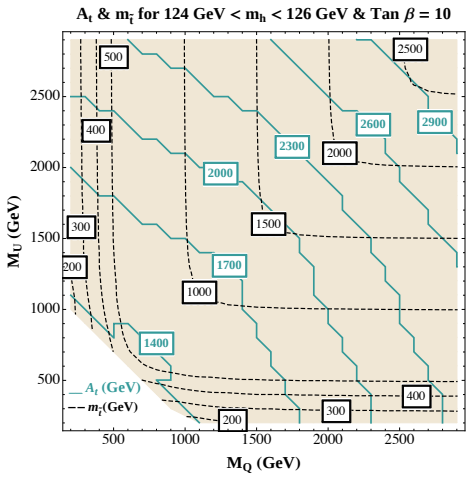

Figure 11.25: Contours of the stop mixing parameter, A_t, necessary for m_h to be in the 124–126 GeV range, given in the plane of the left- and right-handed stop soft supersymmetry-breaking mass parameters, M_Q and M_U, respectively. Other relevant parameters are fixed to be: $\mu = 650$ GeV, $m_A = 1500$ GeV, $A_\tau = 500$ GeV and $\tan\beta = 10$. From Ref. [247].

where $\phi = H$ or h, the momenta p_ϕ and p_A point into the vertex, and

$$g_{hAZ} = g_Z \cos(\beta-\alpha)/2, \quad g_{HAZ} = -g_Z \sin(\beta-\alpha)/2\,. \qquad (11.47)$$

Charged Higgs-W boson couplings to neutral Higgs bosons and four-point couplings of vector bosons and Higgs bosons can be found in Ref. [12].

The tree-level Higgs couplings to fermions obey the following property: the neutral components of one Higgs doublet, Φ_1, couple exclusively to down-type fermion pairs while the neutral components of the other doublet, Φ_2, couple exclusively to up-type fermion pairs [12]. This Higgs-fermion coupling structure defines the Type-II 2HDM [260]. In the MSSM, fermion masses are generated when both neutral Higgs components acquire vacuum expectation values, and the relations between Yukawa couplings and fermion masses are (in third-generation notation)

$$h_b = \sqrt{2}\, m_b/(v\cos\beta), \quad h_t = \sqrt{2}\, m_t/(v\sin\beta)\,. \qquad (11.48)$$

Similarly, one can define the Yukawa coupling of the Higgs boson to τ-leptons (the latter is a down-type fermion).

The couplings of the neutral Higgs bosons to $f\bar{f}$ relative to the SM value, $gm_f/2M_W$, are given by

$$\begin{aligned}
h b\bar{b}&: \; -\sin\alpha/\cos\beta = \sin(\beta-\alpha) - \tan\beta\cos(\beta-\alpha)\,,\\
h t\bar{t}&: \; \cos\alpha/\sin\beta = \sin(\beta-\alpha) + \cot\beta\cos(\beta-\alpha)\,,\\
H b\bar{b}&: \; \cos\alpha/\cos\beta = \cos(\beta-\alpha) + \tan\beta\sin(\beta-\alpha)\,,\\
H t\bar{t}&: \; \sin\alpha/\sin\beta = \cos(\beta-\alpha) - \cot\beta\sin(\beta-\alpha)\,,\\
A b\bar{b}&: \; \gamma_5\tan\beta\,,\\
A t\bar{t}&: \; \gamma_5\cot\beta\,,
\end{aligned} \qquad (11.49)$$

where the γ_5 indicates a pseudoscalar coupling. In each relation above, the factor listed for $b\bar{b}$ also pertains to $\tau^+\tau^-$. The charged Higgs boson couplings to fermion pairs are given by

$$\begin{aligned}
g_{H^- t\bar{b}} &= \frac{g}{\sqrt{2}M_W}\left[m_t\cot\beta\frac{1+\gamma_5}{2} + m_b\tan\beta\frac{1-\gamma_5}{2}\right],\\
g_{H^-\tau^+\nu} &= \frac{g}{\sqrt{2}M_W}\left[m_\tau\tan\beta\frac{1-\gamma_5}{2}\right].
\end{aligned} \qquad (11.50)$$

The non-standard neutral Higgs bosons have significantly enhanced couplings to down-type fermions at sizeable $\tan\beta$. From the above equations it is clear that this occurs near the alignment limit:

$\cos(\beta-\alpha) \ll 1$, where in the mass eigenbasis only one Higgs acquires a VEV [244,245]. In this case the lightest Higgs boson behaves like the SM one and H, A have $\tan\beta$ enhanced couplings to down type fermions, and analogous enhanced couplings are in place for the charged Higgs.

Quite in general, radiative corrections can modify significantly the values of the Higgs boson couplings to fermion pairs and to vector boson pairs. In a first approximation, when radiative corrections to the quartic couplings are computed, the diagonalizing angle α is shifted from its tree-level value, and hence one may compute a "radiatively-corrected" value for $\cos(\beta-\alpha)$. This shift provides an important source of the radiative corrections to the Higgs couplings [217,247]. The radiative corrections to the angle α can enable the alignment without decoupling for sizeable values of the Higgs mass parameter $\mu \geq M_{\rm SUSY}$ and sizeable $\tan\beta$. Additional contributions from the one-loop vertex corrections to tree-level Higgs couplings must also be considered [211,261–268]. These contributions alter significantly the Higgs-fermion Yukawa couplings at large $\tan\beta$, both in the neutral and charged Higgs sector. Moreover, these radiative corrections can modify the basic relationship $g_{h,H,A b\bar{b}}/g_{h,H,A\tau^+\tau^-} \propto m_b/m_\tau$, and change the main features of MSSM Higgs phenomenology.

V.1.3. Decay properties of MSSM Higgs bosons

In the MSSM, one must consider the decay properties of three neutral Higgs bosons and one charged Higgs pair. The mass, *CP* properties, decay and production properties of one of the neutral Higgs bosons should agree with Higgs data. Given that present data allows only for moderate departures from the SM predictions, it implies that some degree of alignment is necessary. In this subsection possible *CP*-violating effects are neglected, and will be commented upon later.

For heavy SUSY particles and sufficiently heavy non-SM-like Higgs bosons, the alignment is triggered by decoupling and departures of the lightest MSSM Higgs boson couplings to gauge bosons and fermions from those predicted in the SM would be minimal. If m_A is below a few hundred GeV, instead, departures from alignment depend on the radiative corrections to the mixing angle α that are proportional to ratios of mass parameters associated to the SUSY particles, and hence do not decouple for heavy SUSY spectra. The main effects occur in departures from the $h \to b\bar{b}$ decay rate, hence also in its total width and, thus, in all branching ratios. As mentioned before, additional effects induced through SUSY-QCD radiative corrections to the $hb\bar{b}$ coupling may also be relevant even in the presence of heavy SUSY particles.

The SM-like branching ratios of h can be modified if decays into supersymmetric particles are kinematically allowed, and, in particular, decays into a pair of the lightest supersymmetric particles - i.e. lightest neutralinos - can become dominant and would be invisible if R-parity is conserved [269–271], Moreover, if light superpartners exist that couple to photons and/or gluons, the h loop-induced coupling to gg and $\gamma\gamma$ could deviate sizeably from the corresponding SM predictions [247,272–275]. Light staus close to 100 GeV with large mixing can enhance the Higgs decay rate into diphotons by up to 40% with respect to the SM, without being in conflict with the stability of the Higgs potential [276]. Light charginos, close to the LEP limit, can also induce up to 10% variations in the Higgs to diphoton decay rate for small values of $\tan\beta \simeq 4$, and hence heavy stops with masses in the 10 TeV range [277]. Given the smallness of the Higgs to diphoton rate, and hence its negligible contribution to the total Higgs decay width, both light staus and charginos have the possibility of altering $BR(h \to \gamma\gamma)$ without altering any other decay rates. Light stops and light sbottoms could contribute to the Higgs-diphoton rate, but in practice they are strongly constrained by the fact that they would at the same time yield a much larger contribution to gluon fusion Higgs production. The Higgs to digluon decay rate and gluon fusion Higgs production can be suppressed due to sbottom effects at large $\tan\beta$ and large μ, but in practice such effects are very small for masses above 500 GeV as presently preferred by LHC searches [278]. Light stops, could give relevant contributions to the Higgs digluon rate and gluon fusion Higgs production, which depending on the value of the stop mixing and the stop masses could yield both suppression or enhancement with respect to the SM. In practice, due to the m_h constrains on the stop sector, light stops can only moderately vary the effective gluon-Higgs coupling and correspondingly the gluon fusion-Higgs production rate [56,38,279].

Given that some degree of alignment is necessary to agree with data, for the heavier Higgs states there are two possibilities to be considered: i) Alignment triggered by decoupling, hence $m_A \geq$ several hundred GeV: The HWW and HZZ couplings are very small. The dominant decay branching ratios strongly depend on $\tan\beta$. After incorporating the leading radiative corrections to Higgs couplings, the following decay features are relevant in the MSSM. The decay modes $H, A \to b\overline{b}$, $\tau^+\tau^-$ dominate when $\tan\beta$ is large (this holds even away from decoupling). For small $\tan\beta$, the $t\overline{t}$ decay mode dominates above its kinematic threshold. In contrast to the lightest SM-like Higgs boson, the vector boson decay modes of H are strongly suppressed due to the suppressed HVV couplings in the decoupling limit. For the charged Higgs boson, $H^+ \to t\bar{b}$ dominates. ii) Alignment without decoupling, hence $m_A \leq$ a few hundred GeV. The main difference with the previous case is that in the low $\tan\beta$ regime ($\tan\beta \leq 5$) additional decay channels may be allowed which involve decays into the lightest SM-like Higgs boson. For A and H, besides the $H, A \to b\overline{b}$, $\tau^+\tau^-$ decay modes, also $A \to Zh$, $H \to hh$ as well as $H \to WW/ZZ$ decay modes are available. For the charged Higgs boson, $H^+ \to \tau^+\nu_\tau$ dominates below the $t\bar{b}$ threshold, and also $H^\pm \to W^\pm h$ may be searched for. Both in i) and ii), the heavier Higgs states, H, A and $H^\pm$, are roughly mass degenerate (with masses $\pm$ 20 GeV or less apart).

In the case of sufficiently light SUSY particles, the heavy Higgs boson decays into charginos, neutralinos and third-generation squarks and sleptons can be important if they are kinematically allowed [269]. An interesting possibility is a significant branching ratio for the decay of a neutral Higgs boson to the invisible mode $\tilde{\chi}_1^0\tilde{\chi}_1^0$ (where the lightest neutralino $\tilde{\chi}_1^0$ is the lightest supersymmetric particle) [270], which poses a challenge at hadron colliders.

V.1.4. Production mechanisms of MSSM Higgs bosons

The production mechanisms for the SM Higgs boson at e^+e^- and hadron colliders can also be relevant for the production of the MSSM neutral Higgs bosons. However, one must take into account the possibility of enhanced or suppressed couplings with respect to those of the Standard Model, as previously discussed. The SUSY-QCD corrections due to the exchange of virtual squarks and gluinos may modify the cross sections depending on the values of these supersymmetric particle masses. At both lepton and hadron colliders there are new mechanisms that produce two neutral Higgs bosons, as well as processes that produce charged Higgs bosons singly or in pairs. In the following discussion, the main processes for MSSM Higgs boson production are summarized. For more detailed discussions see Refs. [34,241], and for the state-of-the-art calculations of higher order corrections as well as estimates of uncertainties at hadron colliders see Refs. [36–38] and references therein.

The main production mechanisms for the neutral MSSM Higgs bosons at e^+e^- colliders are Higgs-strahlung ($e^+e^- \to Zh, ZH$), vector boson fusion ($e^+e^- \to \nu\bar{\nu}h, \nu\bar{\nu}H$) – with W^+W^- fusion about an order of magnitude larger than ZZ fusion – and s-channel Z boson exchange ($e^+e^- \to Ah, AH$) [280]. For the Higgs-strahlung process [281], it is possible to reconstruct the mass and momentum of the Higgs boson recoiling against the particles from the Z boson decay, and hence sensitive searches for Higgs bosons decaying even to invisible final states are possible.

The main charged Higgs boson production process at e^+e^- colliders is via s-channel γ or Z boson exchange ($e^+e^- \to H^+H^-$). Charged Higgs bosons can also be produced in top quark decays via $t \to b + H^+$ if $m_H^\pm < m_t - m_b$ or via the one-loop process $e^+e^- \to W^\pm H^\mp$ [282,283], which allows the production of a charged Higgs boson with $m_H^\pm > \sqrt{s}/2$, even when H^+H^- production is kinematically forbidden. Other single charged Higgs production mechanisms include $t\bar{b}H^-/\bar{t}bH^+$ production [90], $\tau^+\nu H^-/\tau^-\bar{\nu}H^+$ production [284], and a variety of processes in which $H^\pm$ is produced in association with a one or two other gauge and/or Higgs bosons [285].

At hadron colliders, the dominant neutral Higgs production mechanism over the majority of the MSSM parameter space is gluon fusion, mediated by loops containing heavy top and bottom quarks and the corresponding supersymmetric partners [286]. The effect of light stops that may contribute to the gluon fusion production will be partially cancelled by the fact that they need to have sizeable mixing, while light sbottoms that could suppress gluon fusion through mixing effects are disfavored by data. Higgs boson radiation off bottom quarks becomes important for large $\tan\beta$, where at least two of the three neutral Higgs bosons have enhanced couplings to bottom-type fermions [287,288]. In the search for non-standard neutral Higgs bosons, A and H, the production can be via either of the above channels in the final inclusive ditau mode and via radiation off bottom quarks in the 4b's final mode. The total production rates of bottom quarks and τ pairs mediated by the production of a CP-odd Higgs boson in the large $\tan\beta$ regime are approximately given by

$$\begin{aligned}\sigma_{b\bar{b}A} \times \mathrm{BR}(A \to b\bar{b}) &\simeq \sigma^{\mathrm{SM}}_{b\bar{b}A}\ \frac{\tan^2\beta}{(1+\Delta_b)^2}\frac{9}{(1+\Delta_b)^2+9},\\ \sigma_{gg\to A,b\bar{b}A} \times \mathrm{BR}(A \to \tau^+\tau^-) &\simeq \sigma^{\mathrm{SM}}_{gg\to A,b\bar{b}A}\ \frac{\tan^2\beta}{(1+\Delta_b)^2+9},\end{aligned} \tag{11.51}$$

where $\sigma^{\mathrm{SM}}_{b\bar{b}A}$ and $\sigma^{\mathrm{SM}}_{gg\to A,b\bar{b}A}$ denote the values of the corresponding SM Higgs boson cross sections for a SM Higgs boson mass equal to m_A. For high $\tan\beta$, the function Δ_b includes the dominant effects of the SUSY radiative corrections affecting the relation between the bottom quark mass and the bottom Yukawa coupling [211,217,265–267,249], and it depends strongly on $\tan\beta$ and on the SUSY mass parameters. As a result of the Δ_b dependence shown in Eq. (11.51), it follows that the $b\bar{b}A$ channel is more sensitive to the specific SUSY scenario, while the inclusive $\tau^+\tau^-$ channel is rather robust under variations of the SUSY spectra. The production and decay rates of H, for m_A larger m_h^{max}, are governed by formulas similar to the ones presented above, and given that A and H are nearly degenerate in mass, the total signal cross section is increased by roughly a factor of two. Detailed discussions of the impact of radiative corrections in these search modes are presented in Refs. [249,289].

The vector boson fusion and Higgs-strahlung production of the CP-even Higgs bosons as well as the associated production of neutral Higgs bosons with top quark pairs have lower production cross sections by at least an order of magnitude with respect to the dominant ones, depending on the precise region of MSSM parameter space [36]. Higgs pair production of non-standard MSSM Higgs bosons has been studied in Ref. [290].

Charged Higgs bosons can be produced in several different modes at hadron colliders. If $m_{H^\pm} < m_t - m_b$, the charged Higgs boson can be produced in decays of the top quark via the decay $t \to bH^+$, which would compete with the SM process $t \to bW^+$. Relevant radiative corrections to $\mathrm{BR}(t \to H^+b)$ have been computed in Refs. [291–294]. For values of $m_{H^\pm}$ near m_t, width effects are important. In addition, the full $2 \to 3$ processes $pp/p\bar{p} \to H^+\bar{t}b + X$ and $pp/p\bar{p} \to H^-t\bar{b} + X$ must be considered. If $m_{H^\pm} > m_t - m_b$, then charged Higgs boson production occurs mainly through radiation from a third generation quark. Charged Higgs bosons may also be produced singly in association with a top quark via the $2 \to 3$ partonic processes gg, $q\bar{q} \to t\bar{b}H^-$ (and the charge conjugate final states). Charged Higgs bosons can also be produced via associated production with $W^\pm$ bosons through $b\bar{b}$ annihilation and gg-fusion [295]. They can also be produced in pairs via $q\bar{q}$ annihilation [296]. The inclusive H^+H^- cross section is less than the cross section for single charged Higgs associated production [296,297]. For a more extensive discussion of charged Higgs boson production at LHC see Refs. [10,298,36].

V.1.5. Benchmark scenarios in the MSSM for a 125 GeV light Higgs

The experimental uncertainties on the measurements of the production cross sections times branching ratios are at present rather large, and a Higgs sector that differs significantly from the SM case can still fit the data. Hence it is important to explore scenarios where the lightest Higgs agrees with present data but still allows for novel new physics features, and to consider the implications of such scenarios in the search for the remaining MSSM Higgs bosons. The additional Higgs bosons are sought for mainly via the channels

$$\begin{aligned}&pp \to A/H \to \tau^+\tau^- \ \text{(inclusive)},\\ &b\bar{b}A/H, A/H \to \tau^+\tau^- \ \text{(with } b\text{−tag)},\\ &b\bar{b}A/H, A/H \to b\bar{b} \ \text{(with } b\text{−tag)},\\ &pp \to t\bar{t} \to H^\pm W^\mp b\bar{b},\ H^\pm \to \tau\nu_\tau\ ,\\ &gb \to H^-t \quad \text{or} \quad g\bar{b} \to H^+\bar{t},\ H^\pm \to \tau\nu_\tau\ .\end{aligned} \tag{11.52}$$

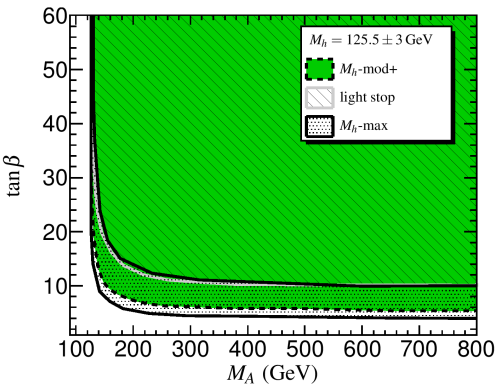

Figure 11.26: Allowed regions in the $(m_A, \tan\beta)$ plane, compatible with the lightest Higgs boson mass, $m_h = 125.5 \pm 3\,\mathrm{GeV}$, for the maximal mixing scenario (hatched black region), the moderate stop mixing benchmark scenario (green shaded region) and the light stop scenario (blue hatched region), as defined in Ref. [248].

The non-observation of any additional state in these production and decay modes puts by now stringent constraints on the MSSM parameter space, in particular on the values of the tree level parameters m_A and $\tan\beta$. Similarly, the non-observation of supersymmetric particles puts constraints on masses of stops and sbottoms as well as gluinos and electroweak gauginos that are relevant for the Higgs sector. Assuming $m_h \simeq 125$ GeV, it is possible to do a scan of the MSSM parameters considering a simplified structure of the Higgs radiative corrections [299], or varying a restricted number of the most relevant parameters [300], and obtain a best fit to the various, measured rates of cross sections and branching ratios. However, due to the large number of free parameters that are relevant for the Higgs sector, a complete scan of the MSSM parameter space is impractical in experimental analyses and phenomenological studies. In the past, for LEP, the Tevatron and the LHC it has been useful to define a set of benchmark scenarios to highlight interesting conditions for MSSM Higgs searches [248,249]. After the Higgs boson discovery, updated MSSM benchmarks scenarios have been defined, that over a wide range of parameter space are compatible with both the mass and the detected production and decay rates of the observed signal [248,38]. They include: i) an updated version of the maximal mixing scenario with a larger value of the gluino mass compatible with LHC bounds. This scenario was originally defined to consider values of the stop mixing to maximize the m_h value and, as a result, only a small region of parameter space is compatible with $m_h \approx 125\,\mathrm{GeV}$; ii) a moderate mixing scenario in which the light CP-even Higgs boson can be interpreted as the newly discovered state within almost the whole parameter space of the $m_A - \tan\beta$ plane that is un-excluded by limits from Higgs searches at LEP and the LHC; iii) a light stop scenario with stop masses in the few to several hundred GeV range that can give contributions to gluon fusion Higgs production; iv) a light stau scenario where the light stau can enhance the SM branching ratio into diphotons for large $\tan\beta$ and v) a tau-phobic scenario that exhibits variations of $BR(h \to b\bar{b})$ and $BR(h \to \tau^+\tau^-)$ with respect to their SM values.

The above benchmarks are just examples that interpret the LHC signal as the lightest *CP*-even MSSM Higgs boson. In Fig. 11.26 the regions in the $(m_A, \tan\beta)$ plane that are compatible with a light *CP* even Higgs mass, $m_h = (125.5 \pm 3)\,\text{GeV}$, are shown for the above benchmarks scenarios. The parameter space allowed by cases ii, iv and v is overlapping, hence only the moderate mixing scenario is shown in the figure. In the light stop and light stau scenarios the lightest Higgs properties would deviate from those of the SM Higgs in all of the allowed parameter space due to loop effects, irrespective of the precise value of m_A. In the maximal mixing and moderate mixing scenarios, h tends to behave as a SM-like Higgs as the theory approaches the decoupling limit. In the tau-phobic scenario, h behaves SM-like due to alignment for specific regions of $\tan\beta$ and large μ, irrespective of the value of m_A. The above benchmarks also have different behavior for the properties of the heavy Higgs bosons. In particular, in the light stau scenario, the decay of $A/H \to \tilde{\tau}_1^+\tilde{\tau}_1^-$ becomes relevant. In the above benchmarks it is also possible to have decays of $H \to hh$ in regions of moderate m_A and moderate $\tan\beta$ as far as one is away from alignment. Also for the previous benchmarks, under the assumption of gaugino mass unification: $M_1 \simeq M_2/2$, and considering the traditional $A/H \to \tau^+\tau^-$ search channel, one would observe variations in the LHC reach depending on the values of μ and M_2. If both parameters are small, as in the maximal and moderate mixing scenarios, then the decays of heavy neutral Higgs bosons into electroweakinos become competitive for small to moderate $\tan\beta$ and m_A. On the contrary, if at least one of the two parameters becomes larger, as in the rest of the benchmark scenarios, then the decay of heavy neutral Higgs bosons into electroweakinos closes up and the reach in $A/H \to \tau^+\tau^-$ is significantly enhanced for the same regions of $\tan\beta$ and m_A. Lastly, varying the parameter μ in both sign and magnitude induces relevant variations in the possible discovery reach through the 4*b*'s channel, and to a lesser extent through the inclusive ditau channel. Future precision measurements of the Higgs boson couplings to fermions and gauge bosons together with information on heavy Higgs searches will provide powerful information on the SUSY parameter space [245,299]. If no other new states beyond the current Higgs candidate are discovered at the LHC, it becomes mandatory to understand what would be the required precision of the Higgs rate measurements to distinguish the MSSM from the SM.

V.2. Indirect constraints on additional states

Interpreting the lightest Higgs as the observed Higgs with a mass of about 125 GeV, improvements in our understanding of *B*-physics observables put indirect constraints on additional Higgs bosons in mass ranges that would be accessible in direct LHC searches. In particular, $\text{BR}(B_s \to \mu^+\mu^-)$, $\text{BR}(b \to s\gamma)$, and $\text{BR}(B_u \to \tau\nu)$ play an important role within minimal flavor-violating (MFV) models [301], in which flavor effects proportional to the CKM matrix elements are induced, as in the SM. For example, see Refs. [302–309]. The supersymmetric contributions to these observables come both at the tree and loop level, and have a different parametric dependence, but share the property that they become significant for large values of $\tan\beta$, which is also the regime in which searches for non-standard MSSM Higgs bosons at hadron colliders are the most powerful.

In the SM, the relevant contributions to the rare decay $B_s \to \mu^+\mu^-$ come through the *Z*-penguin and the *W*-box diagrams [310]. In supersymmetry with large $\tan\beta$, there are also significant contributions from Higgs-mediated neutral currents [311–314], which depend on the SUSY spectra, and grow with the sixth power of $\tan\beta$ and decrease with the fourth power of the *CP*-odd Higgs boson mass m_A. Therefore, measurements at the LHC experiments [315] put strong restrictions on possible flavor-changing neutral currents (FCNC) in the MSSM at large $\tan\beta$ [302,309,316].

Further constraints are obtained from the rare decay $b \to s\gamma$. The SM rate is known up to NNLO corrections [317,318] and is in good agreement with measurements [319]. In the Type-II 2HDM and in the absence of other sources of new physics at the electroweak scale, a bound on $m_{H^\pm} > 380\,\text{GeV}$ can be derived [320]. Although this indirect bound appears much stronger than the results from direct charged Higgs searches, it can be invalidated by new physics contributions, such as those which can be present in the MSSM. In the minimal flavor-violating MSSM, there are new contributions from charged Higgs as well as chargino-stop and gluino-sbottom diagrams. The charged Higgs boson's contribution is enhanced for small values of its mass and can be partially canceled by the chargino and gluino contributions or by higher-order $\tan\beta$-enhanced loop effects.

The branching ratio $B_u \to \tau\nu$, measured by the Belle [321] and BaBar [322] collaborations is in good agreement with the SM prediction [323], but still leaves room for new physics In the MSSM, there is an extra tree-level contribution from the charged Higgs which interferes destructively with the SM contribution, and which increases for small values of the charged Higgs boson mass and large values of $\tan\beta$ [324]. Closely related decay modes that are also sensitive to charged Higgs effects are the $B \to D\tau\nu$ and $B \to D^*\tau\nu$ decays [325]. While predictions of the corresponding branching ratios suffer from large hadronic uncertainties coming from the $B \to D$ and $B \to D^*$ form factors, the ratios $\text{BR}(B \to D\tau\nu)/\text{BR}(B \to D\ell\nu)$ and $\text{BR}(B \to D^*\tau\nu)/\text{BR}(B \to D^*\ell\nu)$, where $\ell = e$ or μ, can be predicted with reasonable accuracy in the SM. Interestingly, recent results from BaBar [326] on these ratios are around 2σ above the SM predictions in both decay modes. Older results from Belle [327] give similar central values but with much larger uncertainties. The tensions in $B \to D\tau\nu$ and $B \to D^*\tau\nu$ cannot be addressed in the context of the MSSM with MFV [309] but would require more radical approaches. These observables constrain in an important way the parameter space for small values of the charged Higgs boson mass and sizeable values of $\tan\beta$ and are only mildly dependent on the SUSY spectra.

Several recent studies [307–309,302] show that, in extended regions of parameter space, the combined *B*-physics measurements impose strong constraints on minimally flavor-violating MSSM models to which Higgs boson searches at the LHC are sensitive. Consequently, the observation of a non-SM Higgs boson at the LHC would point to a rather narrow, well-defined region of MSSM parameter space or to something beyond the minimal flavor violation framework.

Another indirect constraint on the Higgs sector comes from the search for dark matter. Assuming a standard cosmological model, the proper thermal relic density is naturally obtained in particle physics models in which dark matter particles are weakly interacting and with masses of the order of the weak scale. In particular, the lightest supersymmetric particle, typically the lightest neutralino, is an excellent dark matter particle candidate [204]. Within the MSSM, the measured relic density places constraints in the parameter space, which in turn - for specific SUSY low energy spectra- have implications for Higgs searches at colliders, and also for experiments looking for direct evidence of dark matter particles in elastic scattering with atomic nuclei. Large values of $\tan\beta$ and small m_A are relevant for the $b\bar{b}A/H$ and $A/H \to \tau^+\tau^-$ searches at the LHC, and also provide a significant contribution from the *CP*-even Higgs *H* exchange to the spin-independent cross sections for direct detection experiments such as LUX, CDMS or Xenon, for example. Consequently, a signal at colliders would raise prospects for a signal in direct detection experiments and vice-versa, see for example Refs [302,307–309,328–334]. Theoretical uncertainties in the calculation of dark matter scattering cross sections, and in the precise value of the local dark matter density and velocity distributions, may dilute these model-dependent correlations.

V.3. Higgs Bosons in singlet extensions of the MSSM

In the MSSM, the Higgs mass parameter μ is a supersymmetric parameter, and as such, it should naturally be of order M_{GUT} or M_{Planck}. However, in order to enable electroweak symmetry breaking, μ should be of the order of the SUSY breaking scale, that for naturalness we argue should be reasonably close to the electroweak scale. The fact that phenomenologically it is required that μ be at the electroweak/TeV scale is known as the μ problem [335]. Supersymmetric models with additional singlets can provide a solution to the μ problem [335], by promoting the μ parameter to a dynamical singlet superfield *S* that only interacts with the MSSM Higgs doublets through a coupling λ_S at the level of the superpotential. An effective μ is generated when the real scalar component of *S* acquires a vacuum expectation value $\langle S \rangle$

$$\mu_{\mathit{eff}} = \lambda_S \langle S \rangle. \tag{11.53}$$

Table 11.15: Symmetries associated to various models with singlet extensions, the corresponding terms in the superpotential that only involve Higgs and singlet fields, and the number of neutral states in the Higgs sector for the case of CP conservation.

Model	MSSM	NMSSM	nMSSM	UMSSM
Symmetry	-	Z_3	Z_5^R, Z_7^R	$U(1)'$
Superpot.	$\mu\Phi_2\cdot\Phi_1$	$\lambda_S S\Phi_2\cdot\Phi_1+\frac{\kappa}{3}S^3$	$\lambda_S S\Phi_2\cdot\Phi_1+t_F S$	$\lambda_S S\Phi_2\cdot\Phi_1$
H_i^0	2	3	3	3
A_i^0	1	2	2	1

After the minimization of the Higgs potential the vacuum state relates the vacuum expectation values of the three *CP*-even neutral scalars, ϕ_1^0, ϕ_2^0 and S, to their soft supersymmetry breaking masses, hence, one expects that these VEVs should all be of order $M_{\rm SUSY}$ and therefore the μ problem is solved.

The solution of the μ problem through the addition of a singlet superfield to the MSSM comes along with the existence of an extra global U(1) symmetry, known as the Peccei–Quinn (PQ) symmetry [336]. Once the PQ symmetry is spontaneously broken by the Higgs VEVs, a pseudo-Nambu–Goldstone boson, the PQ axion appears in the theory. For values of λ_S of order one the lack of detection of such an axion rules out the theory. Making λ_S very small ($\leq 10^{-6}$) would decouple the axion and render things compatible with experimental results, but then one would be trading the μ problem by a λ_S problem, since there is no explanation to why λ_S should be so small. Promoting the PQ symmetry to a local symmetry involving additional gauge bosons and matter fields could be a viable option that has been explored in the literature. Alternatively there is the possibility to break the PQ symmetry explicitly. For that purpose one can consider a discrete Z_3 symmetry that allows the existence of a PQ odd S^3 term in the superpotential. This model extension has been called the Next-to-Minimal Supersymmetric SM (NMSSM) [337]. It is known however that discrete symmetries may come along with the existence of domain wall structures that imply that our universe would consist of disconnected domains with different ground states, creating unacceptably large anisotropies in the cosmic microwave background [338]. To avoid the problem of domain walls one can consider the existence of non-renormalizable operators that would lead to the preferred vacuum state. However, the same operators in turn may generate quadratically divergent tadpole contributions [339] that could shift the VEV of S to be much larger, order M_{GUT}, and ruin the singlet solution to the μ problem. To cure the problem of destabilizing tadpoles, discrete R-symmetries have been proposed that secure that tadpoles would only appear at very high order loops and be safely suppressed. Depending on the symmetries imposed on the theory, different models with singlet extensions of the MSSM (xMSSM) have been proposed. In Table 11.15 we show the most studied examples: the NMSSM, the Nearly-Minimal Supersymmetric SM (nMSSM) [340], and the U(1)′-extended MSSM (UMSSM) [341], specifying the new parameters appearing in the superpotential and the respective symmetries. A Secluded U(1)′-extended MSSM (sMSSM) [342] contains three singlets in addition to the standard UMSSM Higgs singlet; this model is equivalent to the nMSSM in the limit that the additional singlet VEV's are large, and the trilinear singlet coupling, λ_S, is small [343].

Based on the extended models defined in Table 11.15, we write the most generic supersymmetric and soft supersymmetry breaking scalar potentials for the three scalar fields: Φ_1, Φ_2 and S:

$$\begin{aligned} V_{xMSSM} = &\left|\lambda_S\Phi_2\cdot\Phi_1+t_F+\kappa S^2\right|^2+|\lambda_S S|^2\left(|\Phi_1|^2+|\Phi_2|^2\right)\\ &+\frac{g'^2+g^2}{8}\left(|\Phi_1|^2-|\Phi_2|^2\right)^2\\ &+\frac{g^2}{2}\left(|\Phi_1|^2|\Phi_2|^2-|\Phi_2\cdot\Phi_1|^2\right)\\ &+\frac{g_1'^2}{2}\left(Q_{\Phi_1}|\Phi_1|^2+Q_{\Phi_2}|\Phi_2|^2+Q_S|S|^2\right)^2 \end{aligned} \tag{11.54}$$

$$\begin{aligned} V_{\rm soft} = &\, m_{H_1}^2|\Phi_1|^2+m_{H_2}^2|\Phi_2|^2+m_s^2|S|^2\\ &+\left(A_s\lambda_S S H_u\cdot H_d+\frac{\kappa}{3}A_\kappa S^3+t_S S+h.c.\right). \end{aligned} \tag{11.55}$$

where $\Phi_2\cdot\Phi_1=\epsilon_{ij}\Phi_2^i\Phi_1^j$ and the couplings g', g, and g_1' are associated to the $U(1)_Y$, $SU(2)_L$, and $U(1)'$ gauge symmetries, respectively. t_F and t_S are supersymmetric and SUSY breaking tadpole terms, respectively, m_s is a SUSY breaking mass term for the scalar component of the field S, and A_s and A_κ are the trilinear soft SUSY breaking mass parameters associated with the new terms $\lambda_S S\Phi_2\cdot\Phi_1$ and $\kappa S^3/3$ in the superpotential, with the B-term of the MSSM expressed as $B\mu\equiv A_s\mu_{eff}$. In particular, κ and A_κ are the parameters for the NMSSM model, while t_F and t_S are those of the nMSSM. The UMSSM depends on the new coupling g_1' as well as on the U(1)′ charges of the Higgs fields, Q_{Φ_1}, Q_{Φ_2} and Q_S, that are free parameters with the restriction that they have to add to zero for the superpotential $\lambda_3 S\Phi_2\Phi_1$ to be gauge invariant. In a given U(1)′ construction the charges are specified. The addition of the singlet scalar field(s) imply that additional *CP*-even and *CP*-odd Higgs bosons will appear in the spectra, whereas the charged Higgs sector remains the same as in the MSSM given that the number of Higgs doublets remains unchanged. The mixing with the extra scalar S alters the masses and properties of the physical Higgs bosons, that in general can differ significantly from the SM or the MSSM. A detailed discussion of typical mass spectra and decay properties in these models can be found for example in Refs. [344,343]. Moreover, these models have extra neutralinos and in some cases extra neutral gauge bosons, Z'. The extra gauge boson sector is constrained by experimental data through direct Z' searches as well as the $Z-Z'$ mixing angle $\alpha_{ZZ'}$ constrained to be less that $\mathcal{O}(10^{-3})$ by precision electroweak data .

An interesting feature of models with a singlet extension of the MSSM is that they can easily lead to a strong first order phase transition that enables the possibility of baryogenesis at the electroweak scale [345]. In these models, the strong first order phase transition, necessary to preserve the baryon asymmetry created at the EW scale, is connected to the existence of the cubic soft SUSY breaking term A_S connecting the singlet scalar field with the two Higgs doublets, and does not require a too light SM like Higgs boson mass as it occurs in the MSSM. On the other hand, in SUSY models with extended singlets there is the possibility of additional *CP*-violating phases that may allow to generate the baryon asymmetry and are much less restricted by present electric dipole moments (EDM's) data than those in the MSSM.

V.3.1. The xMSSM Higgs boson masses and phenomenology

In singlet extensions of the MSSM the lightest *CP*-even Higgs mass at tree level, $m_{H_1}^{tree}$ receives a contribution from the singlet scalar that renders it larger than the MSSM value, in particular for small values of $\tan\beta$. The tree level upper bound reads[11]

$$m_{H_1}^{tree}\leq M_Z^2\cos^2 2\beta+\frac{1}{2}\lambda_S^2 v^2\sin^2 2\beta\,. \tag{11.56}$$

At the one-loop level, the top and stop loops (sbottom and stau loops for large $\tan\beta$) are the dominant contributions, that are common to the MSSM and to all the singlet extensions. Gauge couplings in the UMSSM are small compared to the top quark Yukawa coupling, hence the one-loop gauge contributions are negligible. Corrections exclusive to the NMSSM and the nMSSM enter only at the two loop level. Therefore, there are no significant model-dependent contributions at one loop order, and as a result, for large $\tan\beta$ the lightest *CP*-even Higgs mass does not differ in any significant way from the MSSM one. Fig. 11.27 shows the mass ranges for the lightest *CP*-even Higgs boson in the MSSM, NMSSM, nMSSM and UMSSM for a scan over parameters as defined in Ref. [343]. The value of $M_{\rm SUSY}$ is fixed to 1 TeV and the radiative corrections are computed only at one loop level. The upper bounds in Fig. 11.27 are indicative, since two loop corrections, as has been shown for the MSSM, can be rather relevant and have not been included. A value of the lightest SM Higgs mass of about 125 GeV is achievable in all these MSSM extensions, and this remains the case even after higher order corrections are implemented.

[11] Additional gauge interactions contribute to this increase with a term of $\mathcal{O}(g_1'^2v^2(Q_{\phi_2}^2\cos^2\beta+Q_{\phi_1}^2\sin^2\beta))$ in the UMSSM.

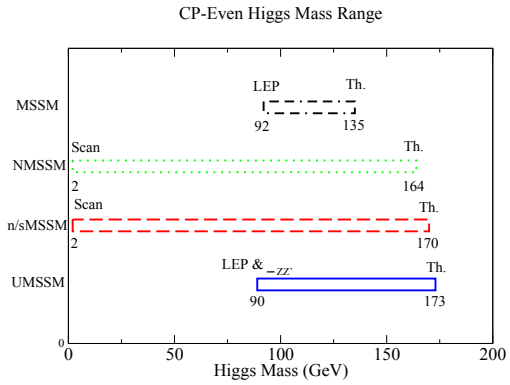

Figure 11.27: Mass ranges for the lightest *CP*-even Higgs boson in each extended MSSM scenario discussed in the text, and in the MSSM, for comparison. The value of $M_{\rm SUSY}$ is fixed to 1 TeV and the rest of parameters are scanned as defined in Ref. [343]. The radiative corrections are computed only at one loop level.

A singlet extended supersymmetric Higgs sector opens new avenues for discovery. Since the singlet pseudoscalar particle may be identified as the pseudo-Goldstone boson of a spontaneously broken Peccei–Quinn symmetry, it may become naturally light [346,347]. Generally, there is mixing of the singlet sector with the MSSM Higgs sector, and with a sufficiently light, singlet dominated scalar or pseudoscalar, H_1^0 or A_1^0, respectively, the SM-like Higgs boson H_2^0 may decay to pairs of H_1^0 or A_1^0. The light scalar and/or pseudoscalar may subsequently decay to $\tau\tau$ or $b\bar{b}$ pairs [348]. Such cascade decays are more difficult to detect than standard searches due to the potentially soft decay products. In addition, the light singlet scenario in the NMSSM or nMSSM is typically associated with a light singlino-dominated neutralino. The recently discovered SM-like Higgs boson can then decay to pairs of this neutralino [349,343], opening an invisible decay mode that is not excluded by present data. In the case of a heavy singlet dominated scalar, its detection would be more challenging than for a SM-like Higgs of similar mass due to the reduced couplings.

An indirect probe of an extended Higgs sector is through precision Higgs production and decay rate measurements of the recently discovered Higgs boson at the LHC. In models with extended singlets, at low $\tan\beta$ it is possible to trade the requirement of a large stop mixing by a sizeable trilinear Higgs-Higgs singlet coupling λ_S, rendering more freedom on the requirements for gluon fusion production. Similar to the MSSM, mixing in the Higgs sector -additionally triggered by the extra new parameter λ_S - can produce variations in the Higgs-$b\bar{b}$ and Higgs-$\tau^-\tau^+$ couplings that can alter the Higgs to ZZ/WW and diphoton rates. Light charginos at low $\tan\beta$ can independently contribute to enhance the di-photon rate, without altering any other of the Higgs decay rates [275,350]

V.4. Supersymmetry with extended gauge sectors

In the MSSM, the tree-level value of the lightest *CP*-even Higgs mass originates from the D-term dependence of the scalar potential that comes from the supersymmetric kinetic terms in the Kähler potential. The D-terms lead to tree-level quartic couplings which are governed by the squares of the gauge couplings of the weak interactions, under which the Higgs has non-trivial charges and hence the lightest Higgs mass is bounded to be smaller than M_Z. If new gauge interactions were present at the TeV scale, and the Higgs bosons would have non-trivial charges under them, there would be new D-term contributions that would lead to an enhancement of the tree-level Higgs mass value. Since the low energy gauge interactions reduce to the known $\mathrm{SU}(3)_c \times \mathrm{SU}(2)_L \times \mathrm{U}(1)_Y$ ones, in order for this mechanism to work, the extended gauge and Higgs sectors should be integrated out in a non-supersymmetric way. This means that there must be supersymmetry breaking terms that are of the order or larger than the new gauge boson masses. The tree-level quartic couplings would then be enhanced through their dependence on the square of the gauge couplings of the extended Higgs sector. This effect will be suppressed when the heavy gauge boson masses are larger than the supersymmetry breaking scale and will acquire its full potential only for large values of this scale.

One of the simplest possibilities is to extend the weak interactions to a $\mathrm{SU}(2)_1 \times \mathrm{SU}(2)_2$ sector, such that the known weak interactions are obtained after the spontaneous breaking of these groups to $\mathrm{SU}(2)_L$ [223]. This may be achieved by introducing a bi-doublet Σ under the two SU(2) gauge groups, which acquires a non-trivial vacuum expectation value u in the diagonal direction. The heavy gauge boson masses are therefore given by $M^2_{W'} = (g_1^2 + g_2^2)u^2/2$, and the weak coupling $g^2 = g_1^2 g_2^2/(g_1^2 + g_2^2)$. To obtain a new tree-level contribution to the Higgs potential, the Higgs bosons must be charged under the new gauge interactions. One possibility is to assume that the third generation quarks and leptons as well as the Higgs doublets have charges under the $\mathrm{SU}(2)_1$ group, while the second and third generations have charges under $\mathrm{SU}(2)_2$. This provides a natural explanation of the largeness of the third generation couplings compared to the first and second generation ones.

Under the above conditions, the D-term contributions to the neutral Higgs effective potential are given by

$$V_D = \frac{g^2\Delta + g'^2}{8}\left(|H_2^0|^2 - |H_1^0|^2\right)^2 \qquad (11.57)$$

with

$$\Delta = \left(1 + \frac{4m_\Sigma^2}{g_2^2 u^2}\right)\left(1 + \frac{4m_\Sigma^2}{(g_1^2 + g_2^2)u^2}\right)^{-1}, \qquad (11.58)$$

where m_Σ is the supersymmetry breaking term associated with the bi-doublet Σ. It is easy to see that while the MSSM D-term is recovered when $m_\Sigma \to 0$, it is replaced by the $\mathrm{SU}(2)_1 \times \mathrm{U}(1)_Y$ D-term when m_Σ becomes much larger than $M_{W'}$. The tree-level mass now reads

$$m_h^2|_{\rm tree} = \frac{g^2\Delta + g'^2}{4} v^2 \cos^2 2\beta, \qquad (11.59)$$

and reduces to the MSSM value, $M_Z^2 \cos^2 2\beta$, for $\Delta = 1$.

Assuming $g_1 \simeq g_2$, values of $g_{1,2}$ of order one are necessary to obtain the proper value of the weak gauge coupling. In addition, if values of m_Σ of order $M_{W'}$ are assumed, enhancements of order 50 percent of the MSSM D-term contribution to the Higgs mass may be obtained. Such enhancements are sufficient to obtain the measured Higgs mass value without the need of very heavy stops or large stop mixing parameters.

The gauge extension described above leads to new, heavy gauge and Higgs bosons, as well as new neutralinos and charginos. Constraints from precision measurements put bounds of the order of a few TeV on the mass of these gauge bosons, which may be probed at the higher energy run of the LHC collider. If the new gaugino supersymmetry breaking masses are smaller than the gauge boson masses, the new electroweakinos will have masses of the order of a few TeV and therefore the weak scale phenomenology reduces to the MSSM one.

Although a particular gauge extension of the MSSM was taken as an example, the results are rather general. Provided that the MSSM Higgs bosons are charged under the extended gauge group and that the supersymmetry breaking parameters associated with the new spontaneously broken gauge sector are large compared to the new gauge boson masses, non-decoupled D-terms for the Higgs fields are generated, leading to a modification of the tree-level Higgs mass prediction. Similar gauge extensions, including also new abelian gauge groups have been considered, for instance, in Ref. [351].

Gauge extensions of the MSSM can also lead to an enhancement of the Higgs mass value by modifying the renormalization group evolution of the Higgs quartic coupling to low energies. In the MSSM, the evolution of the quartic coupling is governed by the top-quark Yukawa interactions and depends on the fourth power of the top-quark Yukawa coupling. The neutralino and chargino contributions, which depend on the fourth power of the weak gauge couplings, are small due to the smallness of these couplings. Depending on the values of the soft supersymmetry breaking parameters in the gaugino and Higgsino

sectors, the $SU(2)_1$ gauginos may become light, with masses of the order of the weak scale. Since the $SU(2)_1$ coupling may be significantly larger than the $SU(2)_L$ one, for small values of the Higgsino mass parameter μ, the associated charginos and neutralinos may modify the evolution of the quartic coupling in a significant way [352]. This may lead to a significant increase of the lightest *CP*-even Higgs mass, even for small values of $\tan\beta \simeq 1$ for which the D-term contributions become small. In addition, under these conditions, light charginos may lead to a significant modification of the Higgs diphoton decay rate, which may be as large as 50% of the SM [352–356].

V.5. Effects of CP violation

In the Standard Model, *CP*-violation (*CPV*) is induced by phases in the Yukawa couplings of the quarks to the Higgs field, which results in one non-trivial phase in the CKM mixing matrix. SUSY scenarios with new *CPV* phases are theoretically appealing, since additional *CPV* beyond that observed in the K, D, and B meson systems is required to explain the observed cosmic matter-antimatter asymmetry [357]. In the MSSM *CP*-violation effects in the Higgs sector appear at the quantum level and are mostly determined by *CP* phases active in the third generation squark soft SUSY breaking trilinear mass parameters as well as in the gaugino/gluino masses. In extensions of the MSSM such as singlet extensions *CP* violation effects can be effective already at tree level and due to the larger number of new parameters there are many more sources of *CP* violation. In general *CP* violation effects in the Higgs sector are importantly constrained from electric dipole moments data [358].

V.5.1. Effects of CP violation on the MSSM Higgs spectrum

In the MSSM, there are additional sources of *CPV* from phases in the various mass parameters. In particular, the gaugino mass parameters ($M_{1,2,3}$), the Higgsino mass parameter, μ, the bilinear Higgs squared-mass parameter, m_{12}^2, and the trilinear couplings of the squark and slepton fields to the Higgs fields, A_f, may carry non-trivial phases. The two parameter combinations $\arg[\mu A_f (m_{12}^2)^*]$ and $\arg[\mu M_i (m_{12}^2)^*]$ are invariant under phase redefinitions of the MSSM fields [359,252]. Therefore, if one of these quantities is non-zero, there would be new sources of *CP*-violation, which affects the MSSM Higgs sector through radiative corrections [251,252,360–364]. The mixing of the neutral *CP*-odd and *CP*-even Higgs boson states is no longer forbidden. Hence, m_A is no longer a physical parameter. However, the charged Higgs boson mass $m_{H^\pm}$ is still physical and can be used as an input for the computation of the neutral Higgs spectrum of the theory.

For large values of $m_{H^\pm}$, corresponding to the decoupling limit, the properties of the lightest neutral Higgs boson state approach those of the SM Higgs boson. That is, for $m_{H^\pm} \gg M_W$, the lightest neutral Higgs boson is approximately a *CP*-even state, with *CPV* couplings that are suppressed by terms of $\mathcal{O}(m_W^2/m_{H^\pm}^2)$. In particular, the upper bound on the lightest neutral Higgs boson mass, takes the same value as in the *CP*-conserving case [252]. Nevertheless, there still can be significant mixing between the two heavier neutral mass eigenstates. For a detailed study of the Higgs boson mass spectrum and parametric dependence of the associated radiative corrections, see Refs. [360,363].

Major variations to the MSSM Higgs phenomenology occur in the presence of explicit *CPV* phases. In the *CPV* case, vector boson pairs couple to all three neutral Higgs boson mass eigenstates, H_i ($i = 1, 2, 3$), with couplings

$$g_{H_i VV} = \cos\beta \mathcal{O}_{1i} + \sin\beta \mathcal{O}_{2i}\,, \tag{11.60}$$

$$\begin{aligned} g_{H_i H_j Z} =& \mathcal{O}_{3i}\left(\cos\beta \mathcal{O}_{2j} - \sin\beta \mathcal{O}_{1j}\right) \\ & - \mathcal{O}_{3j}\left(\cos\beta \mathcal{O}_{2i} - \sin\beta \mathcal{O}_{1i}\right)\,, \end{aligned} \tag{11.61}$$

where the $g_{H_i VV}$ couplings are normalized to the analogous SM coupling and the $g_{H_i H_j Z}$ have been normalized to $g_Z^{\rm SM}/2$. The orthogoanl matrix $\mathcal{O}_{ij}$ is relating the weak eigenstates to the mass eigenstates. It has non-zero off-diagonal entries mixing the *CP*-even and *CP*-odd components of the weak eigenstates. The above couplings obey the relations

$$\sum_{i=1}^{3} g_{H_i ZZ}^2 = 1 \quad \text{and} \quad g_{H_k ZZ} = \varepsilon_{ijk}\, g_{H_i H_j Z}\,, \tag{11.62}$$

where ε_{ijk} is the Levi-Civita symbol.

Another consequence of *CPV* effects in the scalar sector is that all neutral Higgs bosons can couple to both scalar and pseudoscalar fermion bilinear densities. The couplings of the mass eigenstates H_i to fermions depend on the loop-corrected fermion Yukawa couplings (similarly to the *CPC* case), on $\tan\beta$ and on the $\mathcal{O}_{ji}$. The resulting expressions for the scalar and pseudoscalar components of the neutral Higgs boson mass eigenstates to fermions and the charged Higgs boson to fermions are given in Refs. [360,365].

The production processes of neutral MSSM Higgs bosons in the *CPV* scenario are similar to those in the *CPC* scenario, except for the fact that in any process, the *CP* eigenstates h, H, and A can be replaced by any of the three neutral Higgs mass eigenstates H_i. This is the case, since, in the presence of *CP* violation, the H_i's do not have well-defined *CP* quantum numbers. Regarding the decay properties, the lightest mass eigenstate, H_1, predominantly decays to $b\bar{b}$ if kinematically allowed, with a smaller fraction decaying to $\tau^+\tau^-$, similar to the *CPC* case. If kinematically allowed, a SM-like neutral Higgs boson, H_2 or H_3 can decay predominantly to $H_1 H_1$ leading to many new interesting signals both at lepton and hadron colliders; otherwise it will decay preferentially to $b\bar{b}$.

The discovery of a 125 GeV Higgs boson has put strong constraints on the realization of the *CPV* scenario within the MSSM. This is partly due to the fact that the observed Higgs rates are close to the SM values, and a large *CP*-violating component would necessary induce a large variation in the rate of the SM-like Higgs decay into the weak gauge bosons $W^\pm$ and Z. The measured Higgs mass imposes an additional constraint on the realization of this scenario. The *CP*-violating effects are enhanced for values of the modulus of X_t larger than the ones leading to maximal mixing, $|X_t| > \sqrt{6} M_S$. Such large values of $|X_t|$, however, lead to a decrease of the radiative corrections to the Higgs mass, and for sufficiently large $|X_t|$, the SM-like Higgs mass falls below the experimentally allowed range. This effect is increased by the fact that larger mixings in the Higgs sector lead to a reduction of the smaller mass eigenvalue. Once these effects are considered, the lightest Higgs component on the would be *CP*-odd Higgs A tends to be smaller than about 10 percent, and therefore difficult to test at the LHC. The Higgs mass constraints can be alleviated in more general two Higgs doublet models, or in the NMSSM, where the Higgs mass can be fixed in a way independent of the stop mass parameters.

CP-violating effects can still be significant in the heavy Higgs sector. For instance, the Higgs bosons H_2 and H_3 may be admixtures of *CP*-even and *CP*-odd scalars, and therefore both may be able to decay into pairs of weak gauge bosons. Although the observation of this effect would be a clear signal of *CP*-violation, the proximity of the masses of H_2 and H_3 within the MSSM makes the measurement of such effects quite challenging. In generic two Higgs doublet models, the mass splitting between the two heavy mass eigenstates may become larger, which could facilitate the detection of *CP*-violating effects at collider experiments.

V.6. Non-supersymmetric extensions of the Higgs sector

There are many ways to extend the minimal Higgs sector of the Standard Model. In the preceding sections the phenomenology of SUSY Higgs sectors is considered, which at tree level implies a constrained type-II 2HDM (with restrictions on the Higgs boson masses and couplings). In the following discussion, more generic 2HDM's [12,260,243,366] are presented. These models are theoretically less compelling since they do not provide an explanation for the SM Higgs naturalness problem, but can lead to different patterns of Higgs-fermion couplings, hence, to different phenomenology. It is also possible to consider models with a SM Higgs boson and one or more additional scalar SU(2) doublets that acquire no VEV and hence play

no role in the EWSB mechanism. These models are dubbed Inert Higgs Doublet Models (IHD) [367]. Due to the lack of a VEV, the inert Higgs bosons cannot decay into a pair of gauge bosons. And imposing a Z_2 symmetry that prevents them from coupling to the fermions, it follows that, if the lightest inert Higgs boson is neutral, it becomes a good dark matter candidate with interesting associated collider signals. Recent studies of IHD models in the light of a 125 GeV Higgs have been performed [368], showing that there can be non-negligible enhancement or suppression of Higgs to diphotons or Higgs to $Z\gamma$. This may be due to the presence of a light charged Higgs, as light as 100 GeV, that is not in conflict with collider or flavor constraints, because it has no couplings to fermions. It is interesting to study the interplay between collider and direct dark matter detection signals in these models.

Other extensions of the Higgs sector can include [344,369] multiple copies of $\mathrm{SU}(2)_L$ doublets, additional Higgs singlets [370], triplets or more complicated combinations of Higgs multiplets. It is also possible to enlarge the gauge symmetry beyond $\mathrm{SU}(2)_L\times\mathrm{U}(1)_Y$ along with the necessary Higgs structure to generate gauge boson and fermion masses. There are two main experimental constraints on these extensions: *(i)* precision measurements which constrain $\rho = m_W^2/(m_Z^2\cos^2\theta_W)$ to be very close to 1 and *(ii)* flavor changing neutral current (FCNC) effects. In electroweak models based on the SM gauge group, the tree-level value of ρ is determined by the Higgs multiplet structure. By suitable choices for the hypercharges, and in some cases the mass splitting between the charged and neutral Higgs sector or the vacuum expectation values of the Higgs fields, it is possible to obtain a richer combination of singlets, doublets, triplets and higher multiplets compatible with precision measurements [371]. Concerning the constraints coming from FCNC effects, the Glashow–Weinberg (GW) criterion [372] states that, in the presence of multiple Higgs doublets the tree-level FCNC's mediated by neutral Higgs bosons will be absent if all fermions of a given electric charge couple to no more than one Higgs doublet. An alternative way of suppressing FCNC in a two Higgs doublet model has been considered in Ref. [373], where it is shown that it is possible to have tree level FCNC completely fixed by the CKM matrix, as a result of an abelian symmetry.

V.6.1. Two-Higgs-doublet models

Supersymmetry demands the existence of two Higgs doublets such that one doublet couples to up-type quarks and the other to down-type quarks and charged leptons. This Higgs-fermion coupling structure is the one identified as type-II 2HDM [260] and assures that masses for both up and down-type quarks can be generated in a supersymmetric and gauge invariant way. Two Higgs doublet models [243], however, can have a more diverse Higgs-fermion coupling structure and can be viewed as a simple extension of the SM to realize the spontaneous breakdown of $\mathrm{SU}(2)_L\times\mathrm{U}(1)_Y$ to $\mathrm{U}(1)_{\mathrm{em}}$. Quite generally, if the two Higgs doublets contain opposite hypercharges, the scalar potential will contain mixing mass parameters of the kind $m_{12}^2\Phi_1^T i\sigma_2\Phi_2 + h.c.$. In the presence of such terms, both Higgs doublets will acquire vacuum expectation values, $v_1/\sqrt{2}$ and $v_2/\sqrt{2}$, respectively, and the gauge boson masses will keep their SM expressions with the Higgs vacuum expectation value v replaced by $v=\sqrt{v_1^2+v_2^2}$. Apart from the mass terms, the most generic renormalizable and gauge invariant scalar potential contains seven quartic couplings, which are defined in Eq. (11.38).

Considering two doublets with hypercharges, with $Y_{\Phi_1}=-1$ and $Y_{\Phi_2}=1$ as in Eqs. (11.36) and (11.37), and the most general, renormalizable Higgs potential will be given by Eq. (11.38). The same as in the MSSM case, after electroweak symmetry breaking and in the absence of *CP*-violation, the physical spectrum contains a pair of charged Higgs bosons $H^\pm$, a *CP*-odd Higgs boson A and two neutral *CP*-even Higgs bosons, h and H. The angles α and β diagonalize the *CP*-even, and the *CP*-odd and Charged Higgs sectors, respectively

The complete 2HDM is defined only after considering the interactions of the Higgs fields to fermions. Yukawa couplings of the generic from

$$-h_{ij}^a\bar{\Psi}_L^i H_a \Psi_R^j + h.c. \tag{11.63}$$

may be added to the renormalizable Lagrangian of the theory.

Table 11.16: Higgs boson couplings to up, down and charged lepton-type $SU(2)_L$ singlet fermions in the four discrete types of 2HDM models that satisfy the Glashow–Weinberg criterion, from Ref. [374].

Model	2HDM I	2HDM II	2HDM III	2HDM IV
u	Φ_2	Φ_2	Φ_2	Φ_2
d	Φ_2	Φ_1	Φ_2	Φ_1
e	Φ_2	Φ_1	Φ_1	Φ_2

Contrary to the SM, the two Higgs doublet structure does not ensure the alignment of the fermion mass terms $m_{ij}=h_{ij}^a v_a/\sqrt{2}$ with the Yukawa couplings h_{ij}^a. This implies that quite generally, the neutral Higgs boson will mediate flavor changing interactions between the different mass eigenstates of the fermion fields. Such flavor changing interactions should be suppressed in order to describe properly the Kaon, D and B meson phenomenology. Based on the Glashow–Weinberg criterion, it is clear that the simplest way of avoiding such transitions is to assume the existence of a symmetry that ensures the couplings of the fermions of each given quantum number (up-type and down-type quarks, charged and neutral leptons) to only one of the two Higgs doublets. Different models may be defined depending on which of these fermion fields couple to a given Higgs boson, see Table 11.16. Models of type-I [366] are those in which all SM fermions couple to a single Higgs field. In type-II models [260] down-type quarks and charged leptons couple to a common Higgs field, while the up-type quarks and neutral leptons couple to the other. In models of type-III (lepton-specific) quarks couple to one of the Higgs bosons, while leptons couple to the other. Finally, in models of type-IV (flipped), up-type quarks and charged leptons couple to one of the Higgs fields while down-quarks and neutral leptons couple to the other.

The two Higgs doublet model phenomenology depends strongly on the size of the mixing angle α and therefore on the quartic couplings. For large values of m_A, $\sin\alpha\to-\cos\beta$, $\cos\alpha\to\sin\beta$, $\cos(\beta-\alpha)\to 0$, and the lightest *CP*-even Higgs h behaves as the SM Higgs. The same behavior is obtained if the quartic couplings are such that $\mathcal{M}_{12}^2\sin\beta = -(\mathcal{M}_{11}^2 - m_h^2)\cos\beta$. The latter condition represents a situation in which the coupling of h to fermions and weak gauge bosons become the same as in the SM, without decoupling the rest of the non-standard scalars and it is of particular interest due to the fact that the recently discovered Higgs boson has SM-like properties. This situation will be referred to as alignment, as in the MSSM case.

In type-II Higgs doublet models, at large values of $\tan\beta$ and moderate values of m_A, the non-standard Higgs bosons H, A and $H^\pm$ couple strongly to bottom quarks and τ leptons. Hence the decay modes of the non-standard Higgs bosons tend to be dominated by b-quark and tau-lepton modes, including top quarks or neutrinos in the case of the charged Higgs. However, for large and negative values of λ_4, the charged Higgs boson mass may be sufficiently heavy to allow on-shell decays

$$\begin{aligned} &H^\pm\to W^\pm + (H,A),\\ &\qquad g_{H^\pm W^\mp H,A}\simeq\frac{M_W}{v}\sin(\beta-\alpha)(p_{H^+}-p_{H,A})\,, \end{aligned} \tag{11.64}$$

where p_{H^+} and $p_{H,A}$ are the charged and neutral scalar Higgs momenta pointing into the vertex. On the other hand, for large and positive values of λ_5, the above charged Higgs decay into a $W^\pm$ and the *CP*-odd Higgs boson may be allowed, but the heavy Higgs H may be sufficiently heavy to decay into a *CP*-odd Higgs boson and an on-shell Z.

$$H\to Z+A,\quad g_{HZA}\simeq\frac{M_Z}{v}\sin(\beta-\alpha)(p_H-p_A). \tag{11.65}$$

The decay $H^\pm\to W^\pm+H$, on the other hand may be allowed only if $\lambda_4<-\lambda_5$. The couplings controlling all the above decay modes are proportional to $\sin(\beta-\alpha)$ and therefore they are unsuppressed in the alignment limit. Moreover, these could still be the dominant decay modes at moderate values of $\tan\beta$, offering a way to evade the current bounds obtained assuming a dominant decay into bottom quarks or τ leptons.

The quartic couplings are restricted by the condition of stability of the effective potential as well as by the restriction of obtaining the proper value of the lightest *CP*-even Higgs mass. Close to the alignment limit, the lightest *CP*-even Higgs mass becomes, approximately independent of m_A and is given by

$$\begin{aligned} m_h^2 \simeq & v^2(\lambda_1 \cos^4\beta + \lambda_2 \sin^4\beta + 2\tilde{\lambda}_3 v^2 \cos^2\beta \sin^2\beta) \\ & + v^2(4\lambda_6 \cos^3\beta \sin\beta + 4\lambda_7 \sin^3\beta \cos\beta)\,, \end{aligned} \tag{11.66}$$

where $\tilde{\lambda}_3 = \lambda_3 + \lambda_4 + \lambda_5$.

The stability conditions imply the positiveness of all masses, as well as the avoidance of run-away solutions to large negative values of the fields in the scalar potential. These conditions imply

$$\begin{aligned} & \lambda_1 \geq 0, \quad \lambda_2 \geq 0, \quad \lambda_3 + \lambda_4 - |\lambda_5| \geq -\sqrt{\lambda_1 \lambda_2}, \\ & \lambda_3 \geq -\sqrt{\lambda_1 \lambda_2}, \quad 2|\lambda_6 + \lambda_7| < \frac{\lambda_1 + \lambda_2}{2} + \tilde{\lambda}_3, \end{aligned} \tag{11.67}$$

where the first four are necessary and sufficient conditions in the case of $\lambda_6 = \lambda_7 = 0$, while the last one is a necessary condition in the case all couplings are non-zero. Therefore, to obtain the conditions that allow the decays $H^\pm \to W^\pm H, A$ and $H \to ZA$, λ_3 should take large positive values in order to compensate for the effects of λ_4 and λ_5. For recent detailed discussions about 2HDM phenomenology see Refs. [369,375–378,245].

V.6.2. Higgs Triplets

Electroweak triplet scalars are the simplest non-doublet extension of the SM that can participate in the spontaneous breakdown of $\mathrm{SU}(2)_L \times \mathrm{U}(1)_Y$ to $\mathrm{U}(1)_{\rm em}$. Two types of model have been developed in enough detail to make a meaningful comparison to LHC data: the Higgs triplet model (HTM) [379,380] and the Georgi–Machacek model (GM) [381–384].

The Higgs triplet model extends the SM by the addition of a complex $\mathrm{SU}(2)_L$ triplet scalar field Δ with hypercharge $Y = 2$, and a general gauge-invariant renormalizable potential $V(\Phi, \Delta)$ for Δ and the SM Higgs doublet Φ. The components of the triplet field can be parameterized as

$$\Delta = \frac{1}{\sqrt{2}} \begin{pmatrix} \Delta^+ & \sqrt{2}\Delta^{++} \\ v_\Delta + \delta + i\xi & -\Delta^+ \end{pmatrix}. \tag{11.68}$$

where Δ^+ is a singly-charged field, Δ^{++} is a doubly-charged field, δ is a neutral *CP*-even scalar, ξ is a neutral *CP*-odd scalar, and v_Δ is the triplet VEV. The general scalar potential mixes the doublet and triplet components. After electroweak symmetry breaking there are seven physical mass eigenstates, denoted $H^{\pm\pm}$, $H^\pm$, A, H, and h.

A distinguishing feature of the HTM is that it violates the custodial symmetry of the SM; thus the ρ parameter deviates from 1 even at tree level. Letting x denote the ratio of triplet and doublet VEVs, the tree level expression [385] is:

$$\rho = \frac{1 + 2x^2}{1 + 4x^2}\,. \tag{11.69}$$

The measured value of the ρ parameter then limits [386] the triplet VEV to be quite small, $x \lesssim 0.03$, or $v_\Delta < 8\,\mathrm{GeV}$. This constraint severely limits the role of the triplet scalar in the EWSB mechanism.

The small VEV of the Higgs triplet in the HTM is a virtue from the point of view of generating neutrino masses without the necessity for introducing right-handed neutrino fields. The gauge invariant dimension four interaction

$$h_{\nu_{ij}}\, \ell_i^T C^{-1} i\sigma_2\, \Delta\, \ell_j\,, \tag{11.70}$$

where ℓ_i are the lepton doublets, C is the charge conjugation matrix, and $h_{\nu_{ij}}$ is a complex symmetric coupling matrix, generates a Majorana mass matrix for the neutrinos:

$$m_{\nu_{ij}} = \sqrt{2} h_{\nu_{ij}} v_\Delta\,. \tag{11.71}$$

This can be combined with the usual neutrino seesaw to produce what is known as the type-II seesaw [387].

The HTM suggests the exciting possibility of measuring parameters of the neutrino mass matrix at the LHC. If the doubly-charged Higgs is light enough and/or its couplings to W^+W^+ are sufficiently suppressed, then its primary decay is into same-sign lepton pairs: $H^{++} \to \ell_i^+ \ell_j^+$; from Eq. (11.70) and Eq. (11.71) it is apparent that these decays are in general lepton-flavor violating with branchings proportional to elements of the neutrino mass matrix [388].

Precision electroweak data constrain the mass spectrum as well as the triplet VEV of the HTM [389,385,390]. As described in Ref. [390], these constraints favor a spectrum where H^{++} is the lightest of the exotic bosons, and where the mass difference between H^+ and H^{++} is a few hundred GeV. The favored triplet VEV is a few GeV, which also favors H^{++} decays into W^+W^+ over same-sign dileptons.

The Georgi–Machacek model addresses the ρ parameter constraint directly by building in custodial symmetry. Writing the complex doublet scalar of the SM as a $(2,2)$ under $\mathrm{SU}(2)_L \times \mathrm{SU}(2)_R$, it is obvious that the next simplest construction respecting custodial symmetry is a scalar transforming like a $(3,3)$ [391]. These nine real degrees of freedom correspond to a complex electroweak triplet combined with a real triplet, with the scalar potential required to be invariant under $\mathrm{SU}(2)_R$. Under the custodial $\mathrm{SU}(2)_{L+R}$, they transform as $1 \oplus 3 \oplus 5$, with a *CP*-even neutral scalar as the custodial singlet (thus matching the SM Higgs boson), a *CP*-odd neutral scalar in the custodial triplet, and another *CP*-even neutral scalar in the custodial 5-plet.

The scalar components can be decomposed as [392]:

$$\Xi = \begin{pmatrix} \chi_3^* & \xi_1 & \chi_1 \\ -\chi_2^* & \xi_2 & \chi_2 \\ \chi_1^* & -\xi_1^* & \chi_3 \end{pmatrix}, \tag{11.72}$$

where ξ_2 is a real scalar and the others are complex scalars. Linear combinations of these account for the neutral custodial singlet, a neutral and singly-charged field making up the custodial triplet, and neutral, singly-charged, and doubly-charged fields making up the custodial 5-plet.

When combined with the usual SM doublet field Φ, the electroweak scale v is now related to the doublet and triplet VEVs by

$$v^2 = v_\Phi^2 + 8 v_\Xi^2\,. \tag{11.73}$$

Note that the GM triplets by themselves are sufficient to explain electroweak symmetry breaking and the existence of a 125 GeV neutral boson along with a custodial triplet of Goldstone bosons; the complex doublet field in the GM model is required to generate fermion masses via the usual dimension four Yukawa couplings. This raises the question of whether one can rule out the possibility that the 125 GeV boson is the neutral member of a custodial 5-plet rather than a custodial singlet, without invoking decays to fermions. A conclusive answer is given by observing that the ratio of the branching fractions to W versus Z bosons is completely determined by the custodial symmetry properties of the boson. For a custodial 5-plet, the ratio of the signal strength to WW over that to ZZ is predicted to be 1/4 that of a SM Higgs boson [391,393], and thus already ruled out by the experimental results shown in Table 11.12 of Section IV.2.5.

Another interesting general feature of Higgs triplet models is that, after mixing, the SM-like neutral boson can have stronger couplings to WW and ZZ than predicted by the SM [384,394]; this is in contrast to mixing with additional doublets and singlet, which can only reduce the WW and ZZ couplings versus the SM. This has interesting implications for trying to extract the total width of the 125 GeV boson without making theoretical assumptions [181,395].

Because of the built-in custodial symmetry, the triplet VEV in the GM model can be large compared to the doublet VEV. The custodial singlet neutral boson from the triplets mixes with the neutral boson from the doublet. Two interesting special cases are (i) the triplet VEV is small and the 125 GeV boson is SM-like except for small deviations, and (ii) the 125 GeV boson is mostly the custodial singlet

neutral boson from the electroweak triplets. The phenomenology of the doubly-charged and singly-charged bosons is similar to that of the HTM. The constraints on the GM model from precision electroweak data, LEP data, and current LHC data are described in Refs. [392,396–399].

V.7. Composite Higgs models

Within the SM, EWSB is posited but has no dynamical origin. Furthermore, the Higgs boson appears to be unnaturally light. A scenario that remedies these two catches is to consider the Higgs boson as a bound state of new dynamics becoming strong around the weak scale. The Higgs boson can be made significantly lighter than the other resonances of the strong sector if it appears as a pseudo-Nambu–Goldstone boson.

V.7.1. Little Higgs models

The idea behind the Little Higgs models [400,401] is to identify the Higgs doublet as a (pseudo) Nambu–Goldstone boson while keeping some sizable non-derivative interactions. By analogy with QCD where the pions $\pi^{\pm,0}$ appear as Nambu–Goldstone bosons associated to the breaking of the chiral symmetry $\mathrm{SU(2)_L \times SU(2)_R/SU(2)}$, switching on some interactions that break explicitly the global symmetry will generate masses for the would-be massless Nambu–Goldstone bosons of the order of $g\Lambda_{G/H}/(4\pi)$, where g is the coupling of the symmetry breaking interaction and $\Lambda_{G/H} = 4\pi f_{G/H}$ is the dynamical scale of the global symmetry breaking G/H. In the case of the Higgs boson, the top Yukawa interaction or the gauge interactions themselves will certainly break explicitly (part of) the global symmetry since they act non-linearly on the Higgs boson. Therefore, obtaining a Higgs mass around 100 GeV would demand a dynamical scale $\Lambda_{G/H}$ of the order of 1 TeV, which is known to lead to too large oblique corrections. Raising the strong dynamical scale by at least one order of magnitude requires an additional selection rule to ensure that a Higgs mass is generated at the 2-loop level only

$$m_H^2 = \frac{g^2}{16\pi^2}\Lambda_{G/H}^2 \rightarrow m_H^2 = \frac{g_1^2 g_2^2}{(16\pi^2)^2}\Lambda_{G/H}^2 \qquad (11.74)$$

The way to enforce this selection rule is through a "collective breaking" of the global symmetry:

$$\mathcal{L} = \mathcal{L}_{G/H} + g_1\mathcal{L}_1 + g_2\mathcal{L}_2. \qquad (11.75)$$

Each interaction $\mathcal{L}_1$ or $\mathcal{L}_2$ individually preserves a subset of the global symmetry such that the Higgs remains an exact Nambu–Goldstone boson whenever either g_1 or g_2 is vanishing. A mass term for the Higgs boson can be generated only by diagrams involving simultaneously both interactions. At one-loop, there is no such diagram that would be quadratically divergent. Explicitly, the cancellation of the SM quadratic divergences is achieved by a set of new particles around the Fermi scale: gauge bosons, vector-like quarks, and extra massive scalars, which are related, by the original global symmetry, to the SM particles with the same spin. Contrary to supersymmetry, the cancellation of the quadratic divergences is achieved by same-spin particles. These new particles, with definite couplings to SM particles as dictated by the global symmetries of the theory, are perfect goals for the LHC.

The simplest incarnation of the collective breaking idea, the so-called littlest Higgs model, is based on a non-linear σ-model describing the spontaneous breaking SU(5) down to SO(5). A subgroup $\mathrm{SU(2)_1 \times U(1)_1 \times SU(2)_2 \times U(1)_2}$ is weakly gauged. This model contains a weak doublet, that is identified with the Higgs doublet, and a complex weak triplet whose mass is not protected by collective breaking. Other popular little Higgs models are based on different coset spaces: minimal moose $(\mathrm{SU(3)^2/SU(3)})$ [402], the simplest little Higgs $(\mathrm{SU(3)^2/SU(2)^2})$ [403], the bestest little Higgs $(\mathrm{SO(6)^2/SO(6)})$ [404] *etc.* For comprehensive reviews, see Refs. [405,406].

Generically, oblique corrections in Little Higgs models are reduced either by increasing the coupling of one of the gauge groups (in the case of product group models) or by increasing the masses of the W and Z partners, leading ultimately to a fine-tuning of the order of a few percents, i.e., improving only marginally the situation of the MSSM (see for instance Ref. [407] and references therein). The compatibility of Little Higgs models with experimental data is significantly improved when the global symmetry involves a custodial symmetry as well as a T-parity [408] under which, in analogy with R-parity in SUSY models, the SM particles are even and their partners are odd. Such Little Higgs models would therefore appear in colliders as jet(s) with missing transverse energy [409] and the ATLAS and CMS searches for squarks and gluinos [410] can be recast to obtain limits on the masses of the heavy vector-like quarks. The T-even top partner, with an expected mass below 1 TeV to cancel the top loop quadratic divergence without too much fine-tuning, would decay dominantly into a $t + Z$ pair or into a $b + W$ pair or even into $t + H$. The latest CMS and ATLAS direct searches [411] for vector-like top partners put a lower bound around 700 GeV on their mass, excluding the most natural region of the parameter space of these models.

Table 11.17: Global symmetry breaking patterns and the corresponding Goldstone boson contents of the SM, the minimal composite Higgs model, the next to minimal composite Higgs model, and the minimal composite two Higgs doublet model. Note that the SU(3) model does not have a custodial invariance. a denotes a CP-odd scalar while h and H are CP-even scalars.

Model	Symmetry Pattern	Goldstone's
SM	SO(4)/SO(3)	W_L, Z_L
–	SU(3)/SU(2)×U(1)	W_L, Z_L, H
MCHM	SO(5)/SO(4)×U(1)	W_L, Z_L, H
NMCHM	SO(6)/SO(5)×U(1)	W_L, Z_L, H, a
MC2HM	SO(6)/SO(4)×SO(2) ×U(1)	$W_L, Z_L, h, H, H^\pm, a$

The motivation for Little Higgs models is to solve the little hierarchy problem, i.e., to push the need for new physics (responsible for the stability of the weak scale) up to around 10 TeV. Per se, Little Higgs models are effective theories valid up to their cutoff scale $\Lambda_{G/H}$. Their UV completions could either be weakly or strongly coupled.

V.7.2. Models of partial compositeness

The Higgs boson is a special object. Even in composite models, it cannot appear as a regular resonance of the strong sector without endangering the viability of the setup when confronted to data. The way out is that the Higgs appears as a pseudo Nambu–Goldstone boson: the new strongly coupled sector is supposed to be invariant under a global symmetry G spontaneously broken to a subgroup H at the scale f. To avoid conflict with EW precision measurements, it is better to avoid the strong interactions themselves to break the EW symmetry, hence the SM gauge symmetry itself should be contained in H. See Table 11.17 for a few examples of coset spaces.

The SM (light) fermions and gauge bosons cannot be part of the strong sector itself since LEP data have already put stringent bounds on the compositeness scale of these particles far above the TeV scale. The gauge bosons couple to the strong sector by a weak gauging of an SU(2)×U(1) subgroup of the global symmetry G. Inspiration for the construction of such models comes from the AdS/CFT correspondence: the components of a gauge field along extra warped space dimension can be interpreted as the Goldstone boson resulting from the breaking of global symmetry of the strong sector, see Fig. 11.28. The couplings of the SM fermions to the strong sector could a priori take two different forms: (i) a bilinear coupling of two SM fermions to a composite scalar operator, $\mathcal{O}$, of the form $\mathcal{L} = y\,\bar{q}_L u_R \mathcal{O} + \mathrm{hc}$ in simple analogy with the SM Yukawa interactions. This is the way fermion masses were introduced in Technicolor theories and it generically comes with severe flavor problems and calls for extended model building gymnastics [412] to circumvent them; (ii) a linear mass mixing with fermionic vector-like operators: $\mathcal{L} = \lambda_L\,\bar{q}_L \mathcal{Q}_R + \lambda_R \bar{\mathcal{U}}_L u_R$. $\mathcal{Q}$ and $\mathcal{U}$ are two fermionic composite operators of mass M_Q and M_U. Being part of the composite sector, they can have a direct coupling of generic order Y_* to the Higgs boson. In analogy with the photon-rho mixing in QCD, once the linear mixings are diagonalized, the physical states are a linear combination of elementary and composite fields. Effective

Yukawa couplings are generated and read for instance for the up-type quark

$$y = Y_* \sin\theta_L \sin\theta_R \tag{11.76}$$

where $\sin\theta_i = \lambda_i/\sqrt{M_U^2+\lambda_i^2}$, $i = L, R$, measure the amount of compositeness of the SM left- and right-handed up-type quark. If the strong sector is flavor-anarchic, i.e., if the couplings of the Higgs to the composite fermions does not exhibit any particular flavor structure, the relation Eq. (11.76) implies that the light fermions are mostly elementary states ($\sin\theta_i \ll 1$), while the third generation quarks need to have a sizable degree of compositeness. The partial compositeness paradigm offers an appealing dynamical explanation of the hierarchies in the fermion masses. In fact, assuming the strong sector to be almost conformal above the confinement scale, the low-energy values of the mass-mixing parameters $\lambda_{L,R}$ are determined by the (constant) anomalous dimension of the composite operator they mix with. If the UV scale at which the linear mixings are generated is large, then $\mathcal{O}(1)$ differences in the anomalous dimensions can generate naturally large hierarchies in the fermion masses via renormalization group running [413]. While the introduction of partial compositeness greatly ameliorated the flavor problem of the original composite Higgs models, nevertheless it did not solve the issue completely, at least in the case where the strong sector is assumed to be flavor-anarchic [414]. While the partial compositeness set-up naturally emerges in models built in space-times with extra dimensions, no fully realistic microscopic realization of partial compositeness has been proposed in the literature.

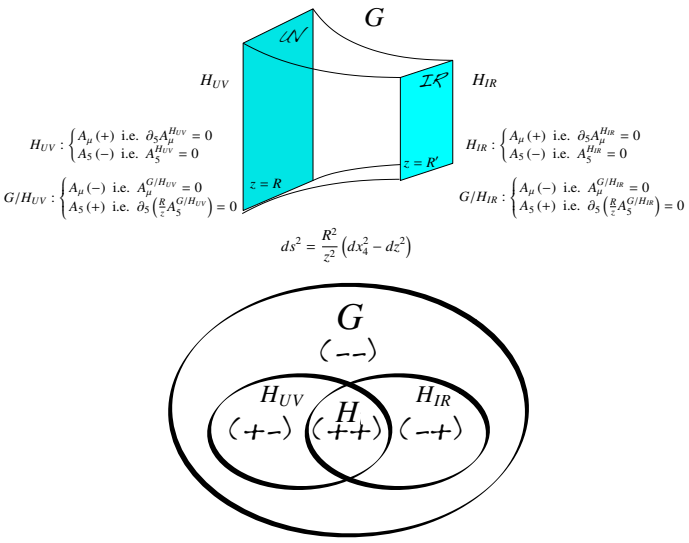

Figure 11.28: Composite models built in five dimensional Anti-de-Sitter space-time and their symmetry breaking pattern interpretation. In 5D, the gauge symmetry in the bulk, G, is broken by suitable boundary conditions to H_{UV} on the UV brane and to H_{IR} on the IR brane. The low energy theory mimics in 4D a strongly interacting sector invariant under a global symmetry G spontaneously broken to H_{IR} at the IR scale with a subgroup H_{UV} which is weakly gauged. The number of Goldstone bosons is equal to $\dim(G/H_{IR})$, $\dim(H_{UV}/H)$ being eaten to give a mass to some gauge bosons ($H = H_{UV} \cap H_{IR}$). The remaining $\dim(G/H_{IR}) - \dim(H_{UV}/H)$ massless Goldstone's are described on the 5D side by the massless modes of the gauge fields along the fifth dimension, A_5^H.

Another nice aspect of the partial compositeness structure is the dynamical generation of the Higgs potential. The Higgs being a pseudo-Nambu–Goldstone boson, its mass does not receive any contribution from the strong sector itself but it is generated at the one-loop level via the couplings of the SM particles to the strong sector since these interactions are breaking the global symmetries under which the Higgs doublet transforms non-linearly. The leading contribution to the potential arises from top loops and it takes the form

$$V(H) = m_\rho^4 \frac{\sin\theta_{tL}\sin\theta_{tR}}{16\pi^2}\left(\alpha\cos(H/f) + \beta\sin^2(H/f) + \gamma\sin^4(H/f)\right), \tag{11.77}$$

where α, β, γ are numbers of order 1 subject to selection rules following the transformation properties of the top quark under the global symmetries of the strong sector[12], and $m_\rho \approx g_\rho f$ is the typical mass scale of the strong sector resonances. The gauge contribution to the potential takes the form (g denotes the SU(2) gauge coupling)

$$m_\rho^4 \frac{g^2/g_\rho^2}{16\pi^2}\sin^2(H/f), \tag{11.78}$$

which is parametrically suppressed with respect to the top contribution by $g^2/(g_\rho y_t)$. The gauge term is always positive, and cannot trigger EWSB by itself. When $\alpha = 0$, the minimization condition of the potential simply reads

$$\sin^2\frac{\langle H\rangle}{f} = -\frac{\beta}{2\gamma}, \tag{11.79}$$

which implies that the natural expectation is that the scale f is generically of the order of the weak scale. Obtaining $v \ll f$, as required phenomenologically, requires some degree of tuning, which scales like $\xi \equiv v^2/f^2$. A mild tuning of the order of 10% ($\xi \approx 0.1$) is typically enough to comply with electroweak precision constraints. This is an important point: in partial compositeness models, the entire Higgs potential is generated at one loop, therefore the separation between v and f can only be obtained at a price of a tuning. This marks a difference with respect to the Little Higgs models, which realize a parametric hierarchy between the quartic and mass terms through the collective symmetry breaking mechanism. In fact in Little Higgs models, the quartic coupling is a tree-level effect, leading to a potential

$$V(H) \approx \frac{g_{\rm SM}^2}{16\pi^2} m_\rho^2 H^2 + g_{\rm SM}^2 H^4, \tag{11.80}$$

where $g_{\rm SM}$ generically denotes the SM couplings. The minimization condition now reads $v^2/f^2 \sim g_\rho^2/(16\pi^2)$, therefore v is formally loop suppressed with respect to f. This is the major achievement of the Little Higgs constructions, which however comes at the price of the presence of sub-TeV vectors carrying EW quantum numbers and therefore giving rise generically to large oblique corrections to the propagators of the W and the Z gauge bosons.

After minimization, the potential Eq. (11.77) leads to an estimate of the Higgs mass as

$$m_H^2 \approx g_\rho^3 y_t 2\pi^2 v^2. \tag{11.81}$$

It follows that the limit $f \to \infty$, i.e. $\xi \to 0$, is a true decoupling limit: all the resonances of the strong sector become heavy but the Higgs whose mass is protected by the symmetries of the coset G/H. When compared to the experimentally measured Higgs mass, this estimate puts an upper bound on the strength of the strong interactions: $1 \lesssim g_\rho \lesssim 2$. In this limit of not so large coupling, the Higgs potential receives additional contributions. In particular, the fermionic resonances in the top sector which follow from the global symmetry structure of the new physics sector can help raising the Higgs mass. For instance in the minimal SO(5)/SO(4) model, using some dispersion relation techniques, one obtains [416]

$$m_H^2 \approx \frac{6}{\pi^2}\frac{m_t^2}{f^2}\frac{m_{Q_4}^2 m_{Q_1}^2}{m_{Q_1}^2 - m_{Q_4}^2}\log\left(\frac{m_{Q_1}}{m_{Q_4}}\right) \tag{11.82}$$

[12] For instance in the SO(5)/SO(4) composite models, when the top quark is embedded into a spinorial representation of SO(5), then $\gamma = 0$ and when it is part of a **5**, **10** or **14** representation, $\alpha = 0$ as it can be inferred by looking at the structure of the H-dependent invariants built out of these representations [415]. The coefficient γ also generically comes with an extra power of the top compositeness fractions.

where Q_4 and Q_1 are fermionic color resonances transforming as a weak bi-doublet of hypercharge $Y = 1/6$ and $Y = 7/6$ and a weak singlet with hypercharge $Y = -1/3$. Therefore a 125 GeV mass is obtained if at least one of the fermionic resonances is lighter than $\sim 1.4\, f$. As in supersymmetric scenarios, the top sector is playing a crucial role in the dynamics of EWSB and can provide the first direct signs of new physics. The direct searches for these top partners, in particular the ones with exotic electric charges 5/3, are already exploring the natural parameter spaces of these models [417,418,411].

The main physics properties of a pseudo Nambu–Goldstone Higgs boson can be captured in a model-independent way by a few number of higher-dimensional operators. Indeed, the strong dynamics at the origin of the composite Higgs singles out a few operators among the complete list presented earlier in Section IV: these are the operators that involve extra powers of the Higgs doublets and they are therefore generically suppressed by a factor $1/f^2$ as opposed to the operators that involve extra derivatives or gauge bosons and are suppressed by a factor $1/(g_\rho^2 f^2)$. The relevant effective Lagrangian describing a strongly interacting light Higgs is:

$$\mathcal{L}_{\rm SILH} = \frac{c_H}{2f^2}\left(\partial_\mu\left(\Phi^\dagger\Phi\right)\right)^2 + \frac{c_T}{2f^2}\left(\Phi^\dagger \overleftrightarrow{D}^\mu \Phi\right)^2 - \frac{c_6\lambda}{f^2}\left(\Phi^\dagger\Phi\right)^3 + \left(\sum_f \frac{c_f\, y_f}{f^2}\Phi^\dagger\Phi\bar{f}_L\Phi f_R + \text{h.c.}\right). \tag{11.83}$$

Typically, these new interactions induce deviations in the Higgs couplings that scale like $\mathcal{O}(v^2/f^2)$, hence the measurements of the Higgs couplings can be translated into some constraints on the compositeness scale, $4\pi f$, of the Higgs boson. The peculiarity of these composite models is that, due to the Goldstone nature of the Higgs boson, the direct couplings to photons and gluons are further suppressed and generically the coupling modifiers defined in Section IV scale like

$$\begin{aligned}\kappa_{W,Z,f} &\sim 1 + \mathcal{O}\left(\frac{v^2}{f^2}\right),\\ \kappa_{Z\gamma} &\sim \mathcal{O}\left(\frac{v^2}{f^2}\right),\\ \kappa_{\gamma,g} &\sim \mathcal{O}\left(\frac{v^2}{f^2}\times\frac{y_t^2}{g_\rho^2}\right),\end{aligned} \tag{11.84}$$

where g_ρ denotes the typical coupling strength among the states of the strongly coupled sector and y_t is the top Yukawa coupling, the largest interaction that breaks the Goldstone symmetry. The $\kappa_{\rm Z\gamma,\gamma,g}$ coupling modifiers are not generated by the strong coupling operators of Eq. (11.83) but some subleading form-factor operator generated by loops of heavy resonances of the strong sector. The coupling modifiers also receive additional contributions from the other resonances of the strong sector, in particular the fermionic resonances of the top sector that are required to be light to generate a 125 GeV Higgs mass. Some indirect information on the resonance spectrum could thus be inferred by a precise measurement of the Higgs coupling deviations. However, it was realized [419] that the task is actually complicated by the fact that, in the minimal models, these top partners give a contribution to both κ_t (resulting from a modification of the top Yukawa coupling) and κ_γ and κ_g (resulting from new heavy particles running into the loops) and the structure of interactions are such that the net effect vanishes for inclusive quantities like $\sigma(gg \to H)$ or $\Gamma(H \to \gamma\gamma)$ as a consequence of the Higgs low energy theorem [19,20,182]. So one would need to rely on differential distribution, like the Higgs p_T distribution [420] (for a recent analysis and further references, see Ref. [421]), to *see* the top partner effects in Higgs data [422].

V.7.3. Minimal composite Higgs models

The minimal composite Higgs models (MCHM) are concrete examples of the partial compositeness paradigm. The Higgs doublet is described by the coset space SO(5)/SO(4) where a subgroup $\mathrm{SU}(2)_L\times\mathrm{U}(1)_Y$ is weakly gauged under which the four Goldstone bosons transform as a doublet of hypercharge 1. There is some freedom on how the global symmetry is acting on the SM fermions: in MCHM4 [415] the quarks and leptons are embedded into spinorial representations of SO(5), while in MHCM5 [423] they are part of fundamental representations (it might also be interesting phenomenologically to consider larger representations like MCHM14 [424] with the SM fermions inside a representation of dimension 14). The non-linearly realized symmetry acting on the Goldstone bosons leads to general predictions of the coupling of the Higgs boson to the EW gauge bosons. For instance, it can be shown that the quadratic terms in the W and Z bosons read

$$m_W^2(H)\left(W_\mu W^\mu + \frac{1}{2\cos^2\theta_W}Z_\mu Z^\mu\right)$$

with $m_W(H) = \dfrac{gf}{2}\sin\dfrac{H}{f}$. Expanding around the EW vacuum, the expression of the weak scale is:

$$v = f\sin(\langle H\rangle/f), \tag{11.85}$$

and the values of the modified Higgs couplings to the W and Z:

$$g_{HVV} = \frac{2m_V^2}{v}\sqrt{1-v^2/f^2}\,, \quad g_{HHVV} = \frac{2m_V^2}{v^2}(1-2v^2/f^2)\,. \tag{11.86}$$

Note that the Higgs couplings to gauge bosons is always suppressed compared to the SM prediction. This is a general result [425] that holds as long as the coset space is compact.

The Higgs couplings to the fermions depend on the representation which the SM fermions are embedded into. For the most commonly used embeddings, they take the following forms

$$\begin{aligned}&\text{MCHM4}: g_{Hff} = \frac{m_f}{v}\sqrt{1-v^2/f^2}\,,\\ &\text{MCHM5}: g_{Hff} = \frac{m_f}{v}\frac{1-2v^2/f^2}{\sqrt{1-v^2/f^2}}\,,\\ &\text{MCHM14}: g_{Hff} = \frac{m_f}{v}\left(1 + A(M_{1,4,9})\frac{v^2}{f^2} + O(v^4/f^4)\right),\\ &\qquad\text{with } A(M_{1,4,9}) = \frac{3M_1M_4 - 11M_1M_9 + 8M_4M_9}{2M_9(M_1-M_4)}\,.\end{aligned} \tag{11.87}$$

While in MHCM4 and MCHM5, the modifications of the couplings depend only on the Higgs compositeness scale, in MCHM14 the leading corrections do depend also on the mass spectrum of the resonances parametrized by M_1, M_4 and M_9 [424]. This is due to the fact that more than one SO(5) invariant give rise to SM fermion masses.

The (κ_V, κ_f) experimental fit of the Higgs couplings can thus be used to derive a lower bound on the Higgs compositeness scale $4\pi f \gtrsim 9$ TeV, which is less stringent than the indirect bound obtained from EW precision data, $4\pi f \gtrsim 15$ TeV [426], which is however subject to various assumptions [427].

V.8. The Higgs boson as a dilaton

The possibility that the new particle H^0 discovered at the LHC is in fact the Goldstone boson associated to the spontaneous breaking of scale invariance at a scale f attracted some attention [16,17] but is now challenged by the fact that all its properties are in good agreement with those predicted for the SM Higgs. And this scenario now requires rather involved model-building engineering. The first issue is the fact that the observed scalar couplings are close to their SM values. In a generic theory of spontaneously broken scale invariance, order one shifts are possible, and indeed expected in most models. Also, the apparent hierarchy between the light scalar and the cutoff of the dilaton effective theory is not reconcilable with the general walking technicolor (or Higgsless) type scenario unless a tuning is imposed.

The general couplings of a wide class of dilaton models are given (at leading order in a low-energy theorem limit for dilatons) by

$$\mathcal{L}_{dilaton} = \frac{\sigma}{f}\left[2M_W^2 W_\mu^\pm W^{\pm\mu} + M_Z^2 Z_\mu Z^\mu + \sum_{ij}\sqrt{m_f^i m_f^j}\Gamma^{ij}\bar{\psi}^i\psi^j\right] + \frac{\sigma}{f}\left[\frac{2}{e}\Delta\beta^{\rm em}F_{\mu\nu}^2 + \frac{2}{g_3}\Delta\beta^{\rm QCD}G_{\mu\nu}^{a\,2}\right] \tag{11.88}$$

where Γ^{ij} is a matrix that depends upon anomalous dimensions of operators in the conformal theory that give rise to fermion masses, and the terms $\Delta\beta$ are the differences in the beta functions of electromagnetism or QCD at scales above and below the scale at which conformal symmetry is spontaneously broken. The SM low energy theorem limit for the standard model Higgs is obtained from this expression by taking

$$f = v, \quad \Gamma^{ij} = I_{3\times 3}, \quad \Delta\beta^{em} = \beta^{em}_{top} + \beta^{em}_{W}, \quad \Delta\beta^{qcd} = \beta^{qcd}_{top}. \quad (11.89)$$

It is unclear why these relations might be approximately realized in a generic conformal field theory, as must be the case to be consistent with current data and allow for a scalar with mass of about 125 GeV . For example, in warped models of electroweak symmetry breaking (AdS/CFT duals to theories with strongly broken conformal invariance), the ratio v/f is a function of the geometry, and is suppressed when the 5D theory is perturbative, contrary to the experimental result that the v/f ratio should be close to 1.

An additional complication is that the mass of the dilaton is expected to appear, along with many other resonances, around the cutoff scale of the strongly interacting theory responsible for breaking the scale invariance spontaneously. Suppression of the dilation mass either requires a tuning of order $v^2/\Lambda^2 \sim$ percent, or a very special conformal dynamics where the beta function of the interaction leading to the scale invariance breaking remains small over a large region of couplings [428].

V.9. Searches for signatures of extended Higgs sectors

The measurements described in Section III and Section IV have established the existence of one state of the electroweak symmetry breaking sector, compatible within with a SM Higgs boson, but not that it is the only one.

Various classes of models beyond the Standard Model discussed above require extended Higgs sectors. These models, and in particular the MSSM and the NMSSM serve as guiding principle of the experimental searches for additional scalar states beyond the Standard Model. However these searches are made as model-independent as possible and can be summarized in the following classes: (i) the search for an additional *CP*-even state mostly in the high mass domain decaying to vector bosons, which would correspond to the heavy *CP*-even state in a generic 2HDM where the light state would be the discovered H or a generic additional singlet; (ii) the search for a state in the high mass domain decaying to pairs of fermions, which would correspond a *CP*-odd A and the heavy *CP*-even state H in a generic 2HDM; (iii) the search for charged Higgs bosons, which also appear in generic 2HDMs; (iv) the search for a *CP*-odd state a in the low mass region which appears in the NMSSM; and (v) doubly charged Higgs which are motivated in extensions of the Higgs sector with triplets.

(i) Searches for an additional CP-even state

(a) Exclusion limits from LEP

The negative result of LEP searches for the SM Higgs boson and the absolute lower limit on its mass of 114 GeV strongly disfavors the existence of a lower mass *CP*-even state, but does not exclude it if its couplings are reduced enough with respect to those of the SM Higgs boson. These searches were also interpreted as 95% CL upper bounds on the ratio of the coupling g_{HZZ} to its SM prediction as a function of the Higgs boson mass [107]. Among the MSSM new benchmarks, the low-m_H is one example which is disfavored by these function of the Higgs boson mass [107] searches, and nearly ruled out by current direct constraints and charged Higgs limits from LHC [429]. Another example is the light *CP*-even Higgs boson of the NMSSM, which is constrained to have a strong function of the Higgs boson mass [107] singlet component. An additional motivation for these scenarios is given by the slight excess observed at LEP [107] at a Higgs boson mass hypothesis of approximately 98 GeV. The light *CP*-even Higgs boson h was also searched for in association with the *CP*-odd A, these searches are described in Section III.

(b) Searches at Tevatron and at the LHC

The searches for the Standard Model Higgs boson before the discovery were covering a wide range of mass hypotheses. Until recently the range of investigation at LHC was from 100 GeV to 600 GeV. It has been extended to masses of up to 1 TeV. At the Tevatron this mass range was limited to up to 200 GeV. Since the discovery, the SM Higgs boson searches are reappraised to search for a heavy *CP*-even state. This state could be the heavy *CP*-even Higgs boson of a 2HDM, or a generic additional singlet. In both cases the natural width of the additional H state can be very different from that of the SM Higgs boson. To preserve unitarity of the longitudinal vector boson scattering and the longitudinal vector boson scattering into fermion pairs, the couplings of the additional *CP*-even Higgs boson to gauge bosons and fermions should not be too large and should constrain the natural width to be smaller than that of a unique Higgs boson at high mass with couplings to fermions and gauge bosons as predicted by the SM (and provided that trilinear and quartic couplings are not too large and that no new state affects the heavy state total width). It is therefore reasonable to consider total widths for the high mass *CP*-even state smaller than the equivalent SM width. For the sake of generality these searches should be done as a function of Higgs boson mass and total width. Until recently only two cases have been investigated: (i) the SM width using the complex pole scheme (CPS), and (ii) the narrow width approximation.

One example of searches for high mass *CP*-even Higgs bosons decaying to a pair of gauge bosons in the narrow width approximation in the $H \to W^{(*)}W^{(*)} \to \ell\nu\ell\nu$ inclusive search channel by the ATLAS collaboration is given in Fig. 11.29. The searches for the Higgs boson in the $H \to \gamma\gamma$ and $H \to W^{(*)}W^{(*)}$ in the $\ell\nu\ell\nu$ and $\ell\nu q\overline{q}$ channels and the $H \to Z^{(*)}Z^{(*)}$ searches in the 4ℓ, $\ell\ell q\overline{q}$ and $\ell\ell\nu\nu$ channels have also been done, but in most cases are simple reinterpretations of the SM Higgs search in the CPS scheme. Recent references are summarized in Table 11.18.

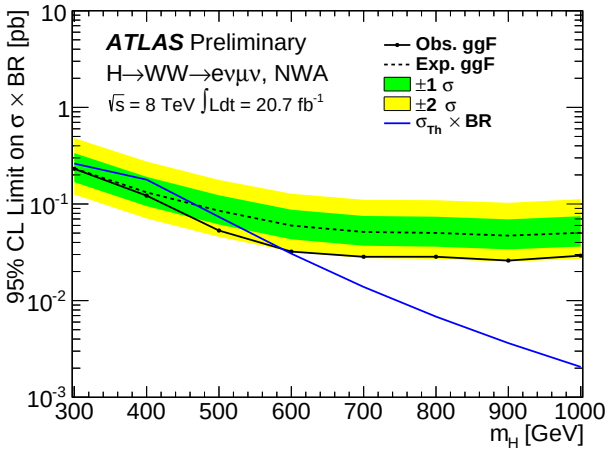

Figure 11.29: The 95% CL upper limits on the Higgs boson production cross section times branching ratio for $H \to W^{(*)}W^{(*)} \to \ell\nu\ell\nu$ for the gluon-fusion process and a Higgs boson with a narrow lineshape (NWA). The green and yellow bands show the 1σ and 2σ uncertainties on the expected limit [478]. The expected cross section times branching ratio for the production of a SM Higgs boson is shown as a blue line.

(c) Searches for an additional state with the presence of H

In the post-discovery era, analyses in general need to take into account the presence of the newly discovered state. For searches with sufficiently high resolution of additional states non degenerate in mass, the strength of the observed state and limits on the signal strength of a

potential additional state can be set independently as discussed in the next section. However in some cases, such as when a channel does not have a sufficiently fine mass resolution or when the states are nearly degenerate in mass, specific analyses need to be designed. There are two examples of such analyses: (i) the search for an additional state in the $H \to W^{(*)}W^{(*)} \to \ell\nu\ell\nu$ channel in ATLAS and (ii) the search for nearly degenerate states in the $H \to \gamma\gamma$ channel with the CMS detector.

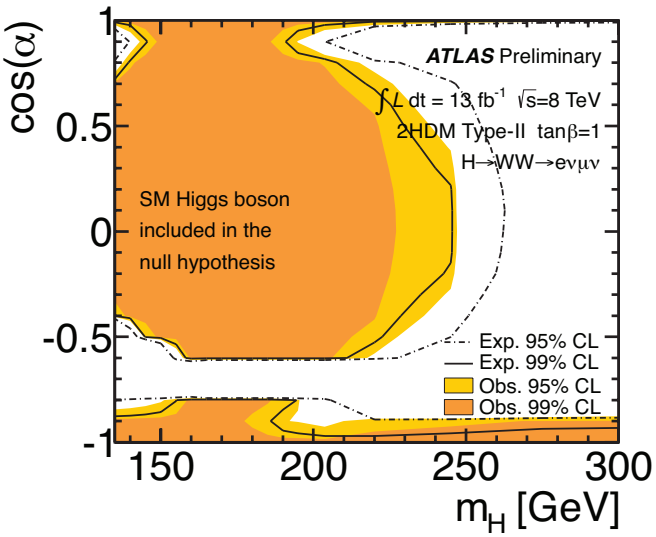

Figure 11.30: The ATLAS 95% CL exclusion contours in the $(\cos\alpha, m_H)$ plane for $\tan\beta = 1$ of the type-II 2HDM [430].

The search, in the $H \to W^{(*)}W^{(*)} \to \ell\nu\ell\nu$ channel, for an additional state is done using boosted decision tree combining several discriminating kinematic characteristics to optimally separate the signal from the background and a high mass signal H from the lower mass state h [430]. A simultaneous fit of the two states h and H is then made to test the presence of an additional state. In this case, the usual null hypothesis of background is generated including the SM signal. The results of this search are shown in Fig. 11.30.

The CMS search for nearly degenerate mass states decaying to a pair of photons [431] is more generic and could for instance apply to *CP*-odd Higgs bosons as well. It consists of a fit to the diphoton mass spectrum using two nearly degenerate mass templates.

(d) Type I 2HDM and Fermiophobia

The measurements of coupling properties of H indirectly excludes that the discovered state is fermiophobic. However, the presence of an additional fermiophobic state, as predicted by Type I 2HDMs, is not excluded. Prior to the discovery, ATLAS and CMS have performed searches for a fermiophobic Higgs boson, *i.e.* produced through couplings with vector bosons only (VBF and VH) and decaying in $h_f \to \gamma\gamma$, optimized for fermiophobic signatures in the diphoton channel [432,433]. CMS has further combined these results with searches for $h_f \to W^+W^-$ and $h_f \to ZZ$ assuming fermiophobic production and decay [434]. CMS excludes a fermiophobic Higgs boson in the range $110\,\text{GeV} < m_H < 188\,\text{GeV}$ at the 95% C.L.

(e) Interpretation benchmarks in the light of the discovered Higgs boson

Two specific benchmark scenarios driven by unitarity relations are proposed in Ref. [38], assuming the existence of an additional state h' with coupling scale factors, i.e, deviations from the couplings predicted for the SM Higgs at the same mass, denoted κ'_V and κ'_F for the couplings of h' to vector bosons and fermions respectively. The gauge boson scattering unitarity then yields the following sum rule

$$\kappa_V^2 + \kappa_V'^2 = 1 \tag{11.90}$$

and the unitarization of the gauge boson scattering to fermions yields

$$\kappa_V \cdot \kappa_F + \kappa'_V \cdot \kappa'_F = 1 \tag{11.91}$$

The two benchmark scenarios are then defined as follows: (i) a single coupling scale factor is assumed for the gauge bosons and the fermions, with an additional parameter to take into account decays to new states; (ii) two parameters are used to describe independently the couplings to fermions and the couplings to vector bosons. A direct application of the latter can be done in the *CP*-even sector of the type-I 2HDM.

(ii) Searches for additional states decaying to fermions

(a) Exclusion limits from LEP

In e^+e^- collisions at LEP centre-of-mass energies, the main production mechanisms of the neutral MSSM Higgs bosons were the Higgs-strahlung processes $e^+e^- \to hZ$, HZ and the pair production processes $e^+e^- \to hA$, HA, while the vector boson fusion processes played a marginal role. Higgs boson decays to $b\bar{b}$ and $\tau^+\tau^-$ were used in these searches.

The searches and limits from the four LEP experiments are described in Refs. [435,436]. The combined LEP data did not contain any excess of events which would imply the production of a Higgs boson, and combined limits were derived [437]. For $m_A \gg M_Z$ the limit on m_h is nearly that of the SM searches, as $\sin^2(\beta-\alpha) \approx 1$. For high values of $\tan\beta$ and low m_A ($m_A \leq m_h^{max}$), the $e^+e^- \to hA$ searches become the most important, and the lightest Higgs h is non SM-like. In this region, the 95% CL mass bounds are $m_h > 92.8\,\text{GeV}$ and $m_A > 93.4\,\text{GeV}$. In the m_h-max. scenario, values of $\tan\beta$ from 0.7 to 2.0 are excluded taking $m_t = 174.3\,\text{GeV}$, while a much larger $\tan\beta$ region is excluded for other benchmark scenarios such as the no-mixing one.

Neutral Higgs bosons may also be produced by Yukawa processes $e^+e^- \to f\bar{f}\phi$, where the Higgs particle $\phi \equiv h$, H, A, is radiated off a massive fermion ($f \equiv b$ or $\tau^\pm$). These processes can be dominant at low masses, and whenever the $e^+e^- \to hZ$ and hA processes are suppressed. The corresponding ratios of the $f\bar{f}h$ and $f\bar{f}A$ couplings to the SM coupling are $\sin\alpha/\cos\beta$ and $\tan\beta$, respectively. The LEP data have been used to search for $b\bar{b}b\bar{b}$, $b\bar{b}\tau^+\tau^-$, and $\tau^+\tau^-\tau^+\tau^-$ final states [438,439]. Regions of low mass and high enhancement factors are excluded by these searches.

A flavor-independent limit for Higgs bosons in the Higgs-strahlung process at LEP has also been set at 112 GeV [440].

In the case where the Higgs boson does not predominantly decay to a pair of b quarks, the searches for the SM Higgs boson have been performed at LEP. All four collaborations conducted dedicated searches for the Higgs boson with reduced model dependence, assuming it is produced via the Higgs-strahlung process, and not addressing its flavor of decay, a lower limit on the Higgs mass of 112.9 GeV is set by combining the data of all four experiments [440]. Using an effective Lagrangian approach and combining several results sensitive to the $h\gamma\gamma$, $hZ\gamma$ and hZZ couplings, an interpretation of several searches for the Higgs boson was made and set a lower limit of 106.7 GeV on the mass of a Higgs boson that can couple anomalously to photons [440].

(b) Searches at the Tevatron and LHC

The best sensitivity is in the regime with low to moderate m_A and with large $\tan\beta$ which enhances the couplings of the Higgs bosons to down-type fermions. The corresponding limits on the Higgs boson production cross section times the branching ratio of the Higgs boson into down-type fermions can be interpreted in MSSM benchmark scenarios [249]. If $\phi = A, H$ for $m_A > m_h^{\max}$, and $\phi = A, h$ for $m_A < m_h^{\max}$, the most promising channels at the Tevatron are the inclusive $p\bar{p} \to \phi \to \tau^+\tau^-$ process, with contributions from both

$gg \to \phi$ and $b\bar{b}\phi$ production, and $b\bar{b}\phi, \phi \to \tau^+\tau^-$ or $\phi \to b\bar{b}$, with $b\tau\tau$ or three tagged b-jets in the final state, respectively. Although Higgs boson production via gluon fusion has a higher cross section in general than via associated production, it cannot be used to study the $\phi \to b\bar{b}$ decay mode since the signal is overwhelmed by the QCD background.

The CDF and D0 collaborations have searched for neutral Higgs bosons produced in association with bottom quarks and which decay into $b\bar{b}$ [441,442], or into $\tau^+\tau^-$ [443,444]. The most recent searches in the $b\bar{b}\phi$ channel with $\phi \to b\bar{b}$ analyze approximately 2.6 fb^{-1} of data (CDF) and 5.2 fb^{-1} (D0), seeking events with at least three b-tagged jets. The cross section is defined such that at least one b quark not from ϕ decay is required to have $p_T > 20$ GeV and $|\eta| < 5$. The decay widths of the Higgs bosons are assumed to be much smaller than the experimental resolution. The invariant mass of the two leading jets as well as b-tagging variables are used to discriminate the signal from the backgrounds. The QCD background rates and shapes are inferred from data control samples, in particular, the sample with two b-tagged jets and a third, untagged jet. Separate-signal hypotheses are tested and limits are placed on $\sigma(p\overline{p} \to b\bar{b}\phi) \times \mathrm{BR}(\phi \to b\bar{b})$. A local excess of approximately 2.5σ significance has been observed in the mass range of 130–160 GeV, but D0's search is more sensitive and sets stronger limits. The D0 result had an $\mathcal{O}(2\sigma)$ local upward fluctuation in the 110 to 125 GeV mass range. These results have been superseded by the LHC searches and the excess seen in the D0 experiment has not been confirmed elsewhere.

ATLAS and CMS also search for $\phi \to \tau^+\tau^-$ in pp collisions at $\sqrt{s} = 7$ TeV. ATLAS seeks tau pairs in 4.7–4.8 fb^{-1} of data [445], and the search by CMS uses the full 4.9 fb^{-1} of 7 TeV data 4.9 fb^{-1} of 8 TeV data [446] and bb [448]. The searches are performed in categories of the decays of the two tau leptons: $e\tau_{\mathrm{had}}$, $\mu\tau_{\mathrm{had}}$, $e\mu$, and $\mu\mu$, where τ_{had} denotes a tau lepton which decays to one or more hadrons plus a tau neutrino, e denotes $\tau \to e\nu\nu$, and μ denotes $\tau \to \mu\nu\nu$. The dominant background comes from $Z \to \tau^+\tau^-$ decays, although $t\bar{t}$, W+jets and Z+jets events contribute as well. Separating events into categories based on the number of b-tagged jets improves the sensitivity in the MSSM. The $b\bar{b}$ annihilation process and radiation of a Higgs boson from a b quark gives rise to events in which the Higgs boson is accompanied by a $b\bar{b}$ pair in the final state. Requiring the presence of one or more b jets reduces the background from Z+jets. Data control samples are used to constrain background rates. The rates for jets to be identified as a hadronically decaying tau lepton are measured in dijet samples, and W+jets samples provide a measurement of the rate of events that, with a fake hadronic tau, can pass the signal selection requirements. Lepton fake rates are measured using samples of unisolated lepton candidates and same-sign lepton candidates. Constraints from the CMS searches for $h \to \tau^+\tau^-$ and $h \to b\bar{b}$ are shown in Fig. 11.31 in the m_h-max benchmark scenario, with $\mu = 200$ GeV and $\mu = -200$ GeV respectively. The neutral Higgs boson searches consider the contributions of both the CP-odd and CP-even neutral Higgs bosons with enhanced couplings to bottom quarks, as they were for the Tevatron results.

A search for $\phi \to \mu^+\mu^-$ has also been performed by the ATLAS collaboration [445]. The exclusion limits obtained are given in terms of cross section times branching fraction and combined with those of $\phi \to \tau^+\tau^-$ [445].

The LHC has the potential to explore a broad range of SUSY parameter space through the search for non-SM-like Higgs bosons. Nevertheless, Fig. 11.31 shows a broad region with intermediate $\tan\beta$ and large values of m_A that is not tested by present neutral or charged Higgs boson searches, and which cannot be covered completely via these searches, even with much larger data sets. In this region of parameter space it is possible that only the SM-like Higgs boson can be within the LHC's reach. If no other state of the EWSB sector than H is discovered, it may be challenging to determine only from the Higgs sector whether there is a supersymmetric extension of the SM in nature.

(iii) Searches for Charged Higgs bosons $H^\pm$

At e^+e^- colliders charged Higgs bosons can pair produced in the s-channel via γ or Z boson exchange. This process is dominant in the LEP centre-of-mass energies range *i.e.* up to 209 GeV. At higher

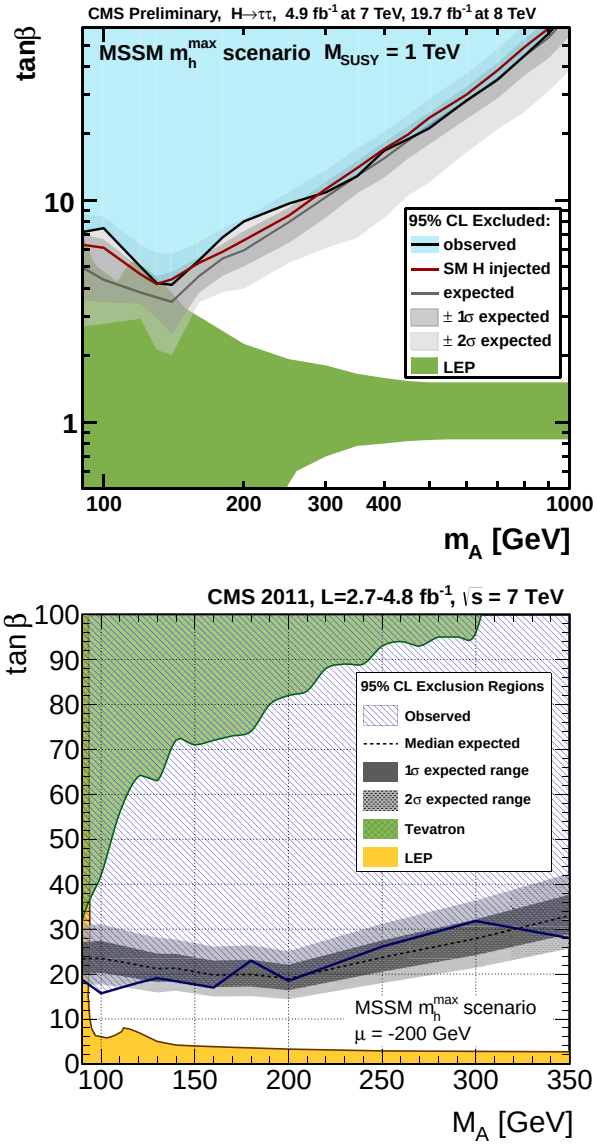

Figure 11.31: The 95% CL exclusion contours in the $(M_A, \tan\beta)$ parameter space for the MSSM mhmax scenario, for the $\tau^+\tau^-$ channel [446] (upper plot) and the $b\bar{b}$ channel [448](lower plot).

centre-of-mass energies, other processes can play an important role such as the production in top quark decays via $t \to b + H^+$ if $m_H^\pm < m_t - m_b$ or via the one-loop process $e^+e^- \to W^\pm H^\mp$ [282,283], which allows the production of a charged Higgs boson with $m_H^\pm > \sqrt{s}/2$, even when H^+H^- production is kinematically forbidden. Other single charged Higgs production mechanisms include $t\bar{b}H^-/\bar{t}bH^+$ production [90], $\tau^+\nu H^-/\tau^-\bar{\nu}H^+$ production [284], and a variety of processes in which $H^\pm$ is produced in association with a one or two other gauge and/or Higgs bosons [285].

At hadron colliders, Charged Higgs bosons can be produced in several different modes. If $m_{H^\pm} < m_t - m_b$, the charged Higgs boson can be produced in decays of the top quark via the decay $t \to bH^\pm$. Relevant QCD and SUSY-QCD corrections to $\mathrm{BR}(t \to H^\pm b)$ have been computed [291–294]. For values of $m_{H^\pm}$ near m_t, width effects are important. In addition, the full $2 \to 3$ processes $pp/p\bar{p} \to H^+\bar{t}b + X$ and $pp/p\bar{p} \to H^-t\bar{b} + X$ must be considered. If $m_{H^\pm} > m_t - m_b$, then charged Higgs boson production occurs mainly through radiation from a third generation quark. Charged Higgs bosons may also be

produced singly in association with a top quark via the $2 \to 3$ partonic processes gg, $q\bar{q} \to t\bar{b}H^-$. For charged Higgs boson production cross section predictions for the Tevatron and the LHC, see Refs. [38,10,37]. Charged Higgs bosons can also be produced via associated production with $W^\pm$ bosons through $b\bar{b}$ annihilation and gg-fusion [295] and in pairs via $q\bar{q}$ annihilation [296].

(a) Exclusion limits from LEP

Charged Higgs bosons have been searched for at LEP, where the combined data of the four experiments, ALEPH, DELPHI, L3, and OPAL, were sensitive to masses of up to about 90 GeV [437] in two decay channels, the $\tau\nu$ and $c\bar{s}$. The exclusion limit independent of the admixture of the two above mentioned branching fractions was 78.6 GeV.

(b) Exclusion limits from Tevatron

Compared to the LEP mass domain of searches, Tevatron covered a complementary range of charged Higgs mass hypotheses. The CDF and D0 collaborations have also searched for charged Higgs bosons in top quark decays with subsequent decays to $\tau\nu$ or to $c\bar{s}$ [449–451]. In the $H^+ \to c\bar{s}$, the limits on BR$(t \to H^+b)$ from CDF and D0 are $\approx 20\%$ in the mass range 90 GeV $< m_{H^+} <$ 160 GeV and assuming a branching fraction of 100% in this specific final state. $H^+ \to \tau^+\nu_\tau$ channel, D0's limits on BR$(t \to H^+b)$ are also $\approx 20\%$ in the same mass range and assuming a branching fraction of 100% in this final state. These limits are valid in general 2HDMs, and they have also been interpreted in terms of the MSSM [449–451].

(c) Exclusion limits from LHC

At the LHC the sensitive mass domain is much larger and the variety of search channels wider. Until recently, only the $\tau\nu$ and $c\bar{s}$ final states have been investigated.

The ATLAS and CMS collaborations have searched for charged Higgs bosons produced in the decay of top quarks in $t\bar{t}$ events. ATLAS has searched for the decay $H^+ \to \tau^+\nu_\tau$ in three final state topologies [452]: (i) lepton+jets: with $t\bar{t} \to \bar{b}WH^+ \to b\bar{b}(q\bar{q}')(\tau_{\rm lep}\nu)$, i.e., the W boson decays hadronically and the tau decays into an electron or a muon, with two neutrinos; (ii) τ +lepton: with $t\bar{t} \to \bar{b}WH^+ \to b\bar{b}(l\nu)(\tau_{\rm had}\nu)$ i.e., the W boson decays leptonically (with $\ell = e,\ \mu$) and the tau decays hadronically; (iii) τ+jets: $t\bar{t} \to \bar{b}WH^+ \to b\bar{b}(q\bar{q}')(\tau_{\rm had}\nu)$, i.e., both the W boson and the τ decay hadronically [453]. The latter channel has been recently updated with the full 8 TeV dataset of pp collisions, corresponding to an integrated luminosity of 19.5 fb^{-1} [453]. Assuming BR$(H^+ \to \tau^+\nu_\tau) = 100\%$, ATLAS sets upper limits on BR$(t \to H^+b)$ between 0.24% and 2.1% for charged Higgs boson masses between 90 GeV to 160 GeV. When interpreted in the context of the $m_h^{\rm max}$ scenario of the MSSM, these bounds exclude a large fraction of the ($m_{H^\pm}$,tan β) plane as illustrated in Fig. 11.32.

The CMS collaboration has searched for the charged Higgs boson in the decay products of top quark pairs: $t\bar{t} \to H^\pm W^\mp b\bar{b}$ and $t\bar{t} \to H^+H^-b\bar{b}$ [454,455] as well. Three types of final states with large missing transverse energy and jets originating from b-quark hadronization have been analyzed: the fully-hadronic channel with a hadronically decaying tau in association with jets, the dilepton channel with a hadronically decaying tau in association with an electron or muon and the dilepton channel with an electron-muon pair. Combining the results of these three analyses and assuming BR$(H^\pm \to \tau\nu)$=1, the upper limits on BR$(t \to H^+b)$ are less than 2% to 3% depending on the charged Higgs boson mass in the interval 80 GeV $< m_{H^+} <$160 GeV.

ATLAS has also searched for charged Higgs bosons in top quark decays assuming BR$(H^+ \to c\bar{s}) = 100\%$ [456], and sets limits of $\approx 20\%$ on BR$(t \to H^+b)$ in the 90 GeV $< m_{H^+} <$ 160 GeV mass range.

At the LHC various other channels can be investigated, in particular the challenging search for a heavy charged Higgs decaying to $t\bar{b}$, searches involving additional neutral scalars in particular in

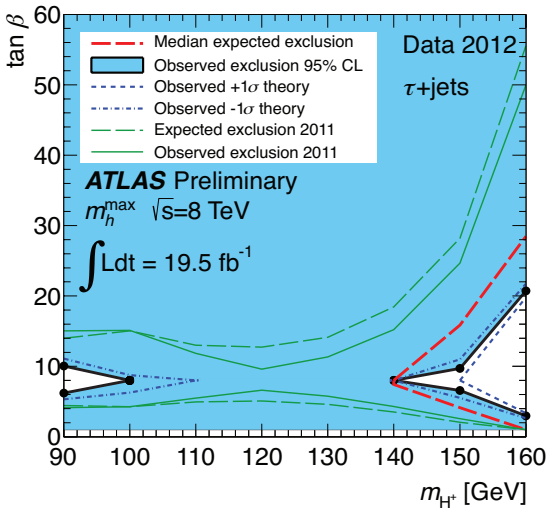

Figure 11.32: ATLAS exclusion limits of the searches of the light $H^\pm$, in the context of the MSSM m_h^{max} scenario with $\mu = 200$ GeV [453]. For comparison, the 2011 limits are also indicated.

WH, WA where A is the pseudo scalar MSSM Higgs boson, and Wa where a is the light CP-odd scalars of the NMSSM.

(iv) Searches for a light CP-odd Higgs boson a

A light pseudoscalar boson a from a two Higgs double model or a model, such as the NMSSM, enhanced with an additional singlet field. The theoretical motivations for singlet extensions of the MSSM are discussed in Section V.2. The main focus of searches for signatures of the NMSSM is on low mass pseudo-scalar boson a for several reasons: (i) in the NMSSM, the light pseudo-scalar a boson can, as a pseudo goldstone boson, be a natural candidate for an axion; (ii) scenarios where $m_a > 2m_b$ and a CP-even state h can decay to a pair of a ($m_h > 2m_a$) are excluded by direct searches at LEP in the $4b$ channel [437,457,458]. for Higgs boson decays to $4b$-quarks have been carried out at LEP; (iii) in the pre-discovery era, LEP limits on a CP-even higgs boson resulted in fine tuning MSSM constraints [459], these could be evaded through non standard decays of the Higgs to aa; (iv) an NMSSM CP-odd a boson with a mass in the range 9.2–12 GeV can also account for the difference observed between the measured anomalous muon magnetic moment and its prediction [460]. A scenario that has drawn particular attention was motivated by a small excess of events 2.3σ in the SM Higgs search at LEP at Higgs boson masse of around 98 GeV. Speculative interpretations of this excess as a signal of a Higgs boson with reduced couplings to b-quarks were given [459]. Complete reviews of the NMSSM phenomenology can be found in Refs. [461,458].

The potential benchmark scenarios have changed in the light of the H discovery. The discovered state could be the lightest or the next-to-lightest of the three CP-even states of the NMSSM. Light pseudoscalar scenarios are still very interesting in particular for the potential axion candidate. There are three main types of direct searches for the light a boson: (i) for masses below the Υ resonance, the search is for radiative decays $\Upsilon \to a\gamma$ at B-factories; (ii) the inclusive search for in high energy pp collisions at the LHC; (iii) the search for decays of a CP-even Higgs h boson to a pair of a bosons.

Radiative decays $\Upsilon \to a\gamma$, have been searched for in various colliders, the most recent results are searches for radiative decays of the $\Upsilon(1s)$ to $a\gamma$ with a subsequent decay of the a boson to a pair of taus at CLEO [462] and the radiative decays of the $\Upsilon(1s, 2s, 3s)$ to $a\gamma$ with subsequent decays to a pair of muons or taus by the Babar collaboration [463,464].

Direct inclusive searches for the light pseudo scalar a boson were performed in the $a \to \mu\mu$ channel at the Tevatron by the D0 experiment [465] and by the ATLAS [466] and CMS [467]

Table 11.18: Summary of references to searches for additional states from extended Higgs sectors, where BBr denotes the BaBar experiment, TeV the Tevatron experiments.

	ATLAS	CMS	Other exps
CP-even H			
$h, H \to \gamma\gamma$	–	[431]	–
$h, H \to ZZ \to 4\ell$	[471]	[472]	–
$h, H \to ZZ \to \ell\ell\nu\nu$	[473]	[474]	–
$h, H \to ZZ \to \ell\ell q\overline{q}$	[475,476]	[477]	–
$h, H \to WW \to \ell\nu\ell\nu$	[478]	[472]	–
$h, H \to WW \to \ell\nu\ell\nu$ (2HDM)	[430]	[472]	–
$h, H \to WW \to \ell\nu q\overline{q'}$	[479]	[480,481]	–
CP-odd A			
$h, H, A \to \tau^+\tau^-$	[445]	[446]	[443,444]-TeV [447]-LHCb
$h, H, A \to \mu^+\mu^-$	[445]	–	–
$h, H, A \to b\overline{b}$	–	[448]	[441,442]-TeV
Charged $H^\pm$			
$H^\pm \to \tau^\pm\nu$	[453]	[455]	–
$H^\pm \to cs$	[482]	–	–
CP-odd NMSSM a			
$a \to \mu^+\mu^-$	[466]	[467]	–
$h \to aa \to 4\mu, 4\tau, 4\gamma$	[468]	[469]	–
$\Upsilon_{1s,3s} \to a\gamma$	–	–	[463,464]-BBr
Doubly Charged $H^\pm$	[483]	[484]	–

collaborations at the LHC.

Finally searches for the decays of a *CP*-even Higgs boson to a pair of a bosons where performed with subsequent decays to four photons by the ATLAS experiment [468], in the four muons final state by the CMS and D0 experiments [469,458], in the two muons and two taus final state by the D0 collaboration [458], and in the four taus final state by the ALEPH collaboration at LEP [470].

No significant excess in the searches for a light *CP*-odd a boson were found and limits on the production times branching fractions of the a boson have been set.

(v) Searches for doubly charged Higgs bosons $H^{\pm\pm}$

As discussed in Section V.6.2 the generation of small neutrino masses via the standard EWSB mechanism described in Section II, requires unnaturally small Yukawa couplings, provided that neutrinos are Dirac-type fermions. A Majorana mass term with a see-saw mechanism for neutrinos, would allow for naturally small masses and yield a framework for the appealing scenario of leptogenesis. However within the SM Majorana mass terms correspond to (non-renomalizable) dimension-5 operators. Such effective interactions can be generated via renormalizable interactions with an electroweak triplet of complex scalar fields (corresponding to a type-II see-saw mechanism). Other models such as the Zee–Babu model, with the introduction of two $SU(2)_L$ singlets, also generate Majorana mass terms. The signature of such models would be the presence of doubly charged Higgs bosons $H^{\pm\pm}$.

The main production mechanisms of $H^{\pm\pm}$ bosons at hadron colliders are the pair production in the s-channel through the exchange of a Z boson or a photon and the associated production with a Charged Higgs boson through the exchange of a W boson.

V.9.1. Standard decays for non-standard processes

The discovery of the H state has also allowed for searches of BSM (beyond the SM) processes involving standard decays of the Higgs boson. One example directly pertaining to the search for additional states of the EWSB sector is the search for Higgs bosons in the cascade decay of a heavy *CP*-even Higgs boson decaying to charged Higgs boson and a W boson, and the charged Higgs boson subsequently decaying to H and another W boson. This search has been performed by the ATLAS collaboration in $b\overline{b}$ decays of the H particle [485].

Another example of searches for non standard processes through the presence of the H particle is the search for large flavor changing neutral current decays of the top quark to H and a charm quark. This search has been performed with the ATLAS experiment in the $H \to \gamma\gamma$ channel [486].

V.9.2. Outlook of searches for additional states

Although the LHC program of searches for additional states covers a large variety of decay channels for additional states, various important topologies are still not covered. In particular when searching for additional states the decays of heavy additional particles such as those of the neutral states decaying to a pair of HH or to ZH are important. Similarly the search for charged Higgs bosons can be extended to include the search for HW and cover the high mass region with $t\overline{b}$ decays. The LHC program for searches of additional scalar states is also rich in other yet to be explored final states such as heavy neutral Higgs bosons decays to a top-quark pair or charged Higgs boson decays to a, AW.

VI. Summary and Outlook

The discovery of the Higgs boson is a milestone in particle physics and an extraordinary success of the LHC machine and the ATLAS and CMS collaborations. The emerging understanding of the nature of this new particle is confirmed by various measurements of its properties, all consistent with the EWSB mechanism and other properties of the Standard Model. The Higgs coupling to gauge bosons has been measured to a precision of nearly 10%. The combination of LHC and Tevatron experiments have accessed couplings to the heavier fermions, although this still needs further confirmation from the LHC experiments. The quantum numbers of the new particle have been probed and show an excellent consistency with $J^{PC} = 0^{++}$. Hints of the direct large Yukawa coupling to the top quark are emerging. Rare decay modes (e.g. $\mu\mu$ and $Z\gamma$) have been searched for, and the experiments will eventually have sensitivity to the expected SM rates. These measurements mark the start of a new era of precision Higgs boson measurements and the use of the Higgs boson as a portal to new physics. Positive or negative, searches for additional states belonging to the EWSB sector will bring invaluable insights on the needed extension(s) of the Standard Model at higher energies.

The Higgs boson couplings are not dictated by gauge symmetries. Thus, in addition to a new particle, the LHC has also discovered a new force, different in nature from the other fundamental interactions since it is non-universal and distinguishes between the three families of quarks and leptons.

Furthermore, the mere existence of the Higgs boson with a mass of approximately 125 GeV, embodies the problem of an unnatural cancellation among the quantum corrections to its mass. The non-observation of additional states which could stabilize the Higgs mass is a challenge for natural scenarios like supersymmetry or models with a new strong interaction in which the Higgs boson is not a fundamental particle. This increasingly pressing paradox starts questioning the principle of naturalness relying on the hypothesis that phenomena at different scales do not influence each others.

The unitarization of the vector boson scattering (VBS) amplitudes, dominated at high energies by their longitudinal polarizations, has been the basis of the *no lose* theorem at the LHC and was one of the main motivations to build the accelerator and the detectors. It motivated the existence of a Higgs boson or the observability of manifestations of strong dynamics at TeV scale. Now that a Higgs boson has been found and that its couplings to gauge bosons follow the SM predictions, perturbative unitarity is preserved to a large amount with the sole exchange of the Higgs boson and without the need for any additional states. It is, however, still an important channel to investigate further in order to better understand the nature of the Higgs sector and the possible completion of the SM at the TeV scale. In association with the double Higgs boson production channel by vector boson fusion, VBS could, for instance, confirm that the Higgs

boson is part of a weak doublet and also establish if it is a composite state and whether or not it emerges as a pseudo-Nambu–Goldstone boson from an underlying broken symmetry.

The search for the Higgs boson has occupied the Particle physics community for the last 50 years. Its discovery is now shaping and sharpening the physics programs of future accelerators.

Acknowledgements

We would like to thank many of our colleagues for proofreading parts of the review, for useful criticism and their input in general: W. Altmannshofer, G. Branco, F. Cerutti, R. Contino, J. Conway, J.B. De Vivie, J.R. Espinosa, A. Falkowski, W. Fischer, M. Grazzini, H. Haber, S. Heinemeyer, J. Hubisz, A. Korytov, B. Jäger, H. Ji, T. Junk, P. Langacker, J. Lykken, F. Maltoni, M. Mühlleitner, B. Murray, M. Neubert, G. Perez, G. Petrucciani, A. Pomarol, E. Pontón, D. Rebuzzi, E. Salvioni, N. Shah, G. Shaughnessy, M. Spira, O. Stål, A. Strumia, R. Tanaka, A. Vartak, C. Wagner, and A. Weiler.

We are also most grateful to the ATLAS, CDF, CMS and D0 collaborations for their help with this review.

M.C. is supported by Fermilab, that is operated by Fermi Research Alliance, LLC under Contract No. DE–AC02–07CH11359 with the United States Department of Energy. C.G. is supported by the Spanish Ministry MICINN under contract FPA2010–17747, the European Commission under the ERC Advanced Grant 22637 MassTeV and the contract PITN–GA–2009–237920 UNILHC. M.K. is supported by the ANR HiggsNet grant. V.S. is supported by the grant DE–SC0009919 of the United States Department of Energy.

References

1. G. Aad *et al.*, [ATLAS Collab.], Phys. Lett. **B716**, 1 (2012).
2. S. Chatrchyan *et al.*, [CMS Collab.], CMS Collab., Phys. Lett. **B716**, 30 (2012).
3. F. Englert and R. Brout, Phys. Rev. Lett. **13**, 321 (1964);
   P.W. Higgs, Phys. Rev. Lett. **13**, 508 (1964) and Phys. Rev. **145**, 1156 (1966);
   G.S. Guralnik, C.R. Hagen, and T.W. Kibble, Phys. Rev. Lett. **13**, 585 (1964).
4. S.L. Glashow, Nucl. Phys. **20**, 579 (1961);
   S. Weinberg, Phys. Rev. Lett. **19**, 1264 (1967);
   A. Salam, *Elementary Particle Theory*, eds.: Svartholm, Almquist and Wiksells, Stockholm, 1968;
   S. Glashow, J. Iliopoulos, and L. Maiani, Phys. Rev. **D2**, 1285 (1970).
5. J.M. Cornwall, D.N. Levin, and G. Tiktopoulos, Phys. Rev. Lett. **30**, 1286 (1973) and Phys. Rev. **D10**, 1145 (1974);
   C.H. Llewellyn Smith, Phys. Lett. **B46**, 233 (1973).
6. B.W. Lee, C. Quigg, and H.B. Thacker, Phys. Rev. **D16**, 1519 (1977).
7. K. Wilson, Phys. Rev. D 3,1818(1971);
   G.t'Hooft, in *Proc. of 1979 Cargèse Institute on Recent Developments in Gauge Theories,* p. 135 Press, New York 1980;
   For a recent review, see G.F. Giudice, `arXiv:1307.7879 [hep-ph]` (2013).
8. J. Wess and B. Zumino, Nucl. Phys. **B70**, 39 (1974) and Phys. Lett. **49B**, 52 (1974);
   H.P. Nilles, Phys. Rev. **C110**, 1 (1984);
   S.P. Martin, `arXiv:hep-ph/9709356` (1997);
   P. Fayet, Phys. Lett. **B69**, 489 (1977) Phys. Lett. **B84**, 421 (1979), Phys. Lett. **B86**, 272 (1979) and Nucl. Phys. **B101**, 81 (2001).
9. E. Witten, Nucl. Phys. **B188**, 513 (1981);
   R.K. Kaul, Phys. Lett. **B109**, 19 (1982) and Pramana **19**, 183 (1982);
   L. Susskind, Phys. Rev. **104**, 181 (1984).
10. H.E. Haber and G.L. Kane, Phys. Rev. **C117**, 75 (1985).
11. P. Fayet, Phys. Lett. **B64**, 159 (1976);
    F. Riva, C. Biggio, and A. Pomarol, JHEP **1302**, 081 (2013).
12. J. F. Gunion *et al.*, *The Higgs Hunter's Guide*, Addison-Wesley (1990).
13. S. Weinberg, Phys. Rev. **D13**, 974 (1979) and Phys. Rev. **D19**, 1277 (1979);
    L. Susskind, Phys. Rev. **D20**, 2619 (1979);
    E. Farhi and L. Susskind, Phys. Rev. **74**, 277 (1981);
    R.K. Kaul, Rev. Mod. Phys. **55**, 449 (1983);
    C. T. Hill and E. H. Simmons, Phys. Reports **381**, 235 (2003) [E: **390**, 553 (2004)].
14. D. B. Kaplan and H. Georgi, Phys. Lett. **B136**, 183 (1984).
15. C. Csaki *et al.*, Phys. Rev. **D69**, 055006 (2004);
    C. Csaki *et al.*, Phys. Rev. Lett. **92**, 101802 (2004);
    C. Csaki, J. Hubisz, and P. Meade, `hep-ph/0510275` (2005).
16. C. Csaki *et al.*, Phys. Rev. **D62**, 045015 (2000);
    C. Csaki, M. L. Graesser, and G. D. Kribs, Phys. Rev. **D63**, 065002 (2001);
    G. F. Giudice, R. Rattazzi, and J. D. Wells, Nucl. Phys. **B595**, 250 (2001);
    M. Chaichian *et al.*, Phys. Lett. **B524**, 161 (2002);
    D. Dominici *et al.*, Acta Phys. Polon. **B 33**, 2507 (2002);
    J. L. Hewett and T. G. Rizzo, JHEP **0308**, 028 (2003);
    B. Grzadkowski and J. F. Gunion, `arXiv:1202.5017 [hep-ph]` (2012);
    C. Csaki, J. Hubisz, and S. J. Lee, Phys. Rev. **D76**, 125015 (2007);
    B. Coleppa, T. Gregoire, and H. Logan, Phys. Rev. **D85**, 055001 (2012).
17. W. D. Goldberger, B. Grinstein, and W. Skiba, Phys. Rev. Lett. **100**, 111802 (2008);
    J. Fan *et al.*, Phys. Rev. **D79**, 035017 (2009);
    B. Bellazzini *et al.*, Eur. Phys. J. **C73**, 2333 (2013);
    Z. Chacko and R. K. Mishra, Phys. Rev. **D87**, 115006 (2013);
    Z. Chacko, R. Franceschini, and R. K. Mishra, JHEP **1304**, 015 (2013).
18. T. van Ritbergen and R. G. Stuart, Phys. Rev. Lett. **82**, 488 (1999) and Nucl. Phys. **B564**, 343 (2000);
    M. Steinhauser and T. Seidensticker, Phys. Lett. **B467**, 271 (1999);
    D. M. Webber *et al.*, [MuLan Collab.], Phys. Rev. Lett. **106**, 041803 (2011).
19. J. Ellis, M.K. Gaillard, and D.V. Nanopoulos, Nucl. Phys. **B106**, 292 (1976).
20. M.A. Shifman *et al.*, Sov. J. Nucl. Phys. **30**, 711 (1979) [Yad. Fiz. **30**, 1368 (1979)].
21. P. Sikivie *et al.*, Nucl. Phys. **B173**, 189 (1980);
    H. Georgi, Ann. Rev. Nucl. and Part. Sci. **43**, 209 (1993).
22. M. J. G. Veltman, Nucl. Phys. **B123**, 89 (1977).
23. R. S. Chivukula *et al.*, Ann. Rev. Nucl. and Part. Sci. **45**, 255 (1995).
24. S. Willenbrock, `arXiv:0410370 [hep-ph]` (2008).
25. I. V. Krive and A. D. Linde, Nucl. Phys. **B117**, 265 (1976);
    P. Q. Hung, Phys. Rev. Lett. **42**, 873 (1979);
    N. Cabibbo *et al.*, Nucl. Phys. **B158**, 295 (1979);
    M. Lindner, Z. Phys. **C31**, 295 (1986);
    M. Luscher and P. Weisz, Nucl. Phys. **B290**, 25 (1987) and Nucl. Phys. **B295**, 65 (1988);
    M. Lindner, M. Sher, and H. W. Zaglauer, Phys. Lett. **B228**, 139 (1989);
    M. Sher, Phys. Reports **179**, 273 (1989);
    G. Altarelli and G. Isidori, Phys. Lett. **B337**, 141 (1994);
    J.A. Casas, J.R. Espinosa, and M. Quiros, Phys. Lett. **B342**, 171 (1995) and Phys. Lett. **B382**, 374 (1996);
    T. Hambye and K. Riesselmann, Phys. Rev. **D55**, 7255 (1997).
26. J. Elias-Miro *et al.*, Phys. Lett. **B709**, 222 (2012);
    G. Degrassi *et al.*, JHEP **1208**, 098 (2012);
    D. Buttazzo *et al.*, `arXiv:1307.3536 [hep-ph]`.
27. J.R. Espinosa and M. Quiros, Phys. Lett. **B353**, 257 (1995);
    G. Isidori, G. Ridolfi, and A. Strumia, Nucl. Phys. **B609**, 387 (2001).
28. C. D. Froggatt and H. B. Nielsen, Phys. Lett. **B368**, 96 (1996);

M. Shaposhnikov and C. Wetterich, Phys. Lett. **B683**, 196 (2010);
M. Holthausen, K. S. Lim, and M. Lindner, JHEP **1202**, 037 (2012).

29. F. Bezrukov *et al.*, JHEP **1210**, 140 (2012).
30. F. L. Bezrukov and M. Shaposhnikov, Phys. Lett. **B659**, 703 (2008);
F. L. Bezrukov, A. Magnin, and M. Shaposhnikov, Phys. Lett. **B675**, 88 (2009).
31. A. Salvio, Phys. Lett. **B727**, 234 (2013).
32. B.A. Kniehl, Phys. Reports **240**, 211 (1994).
33. M. Spira, Fortsch. Phys. **46**, 203 (1998).
34. M. Carena and H.E. Haber, Prog. in Part. Nucl. Phys. **50**, 152 (2003).
35. A. Djouadi, Phys. Reports **457**, 1 (2008).
36. S. Dittmaier *et al.*, [LHC Higgs Cross Section Working Group], arXiv:1101.0593[hep-ph] (2011).
37. S. Dittmaier *et al.*, [LHC Higgs Cross Section Working Group], arXiv:1201.3084 [hep-ph] (2012).
38. S. Heinemeyer *et al.*, [LHC Higgs Cross Section Working Group], arXiv:1307.1347[hep-ph] (2013).
39. LHC Higgs Cross Section Working Group, https://twiki.cern.ch/twiki/bin/view/LHCPhysics/CrossSections.
40. T. Aaltonen *et al.*, [CDF and D0 Collaborations], Phys. Rev. **D88**, 052014 (2013).
41. H.M. Georgi *et al.*, Phys. Rev. Lett. **40**, 692 (1978).
42. D. Graudenz, M. Spira, and P.M. Zerwas, Phys. Rev. Lett. **70**, 1372 (1993).
43. M. Spira *et al.*, Nucl. Phys. **B453**, 17 (1995).
44. S. Dawson, Nucl. Phys. **B359**, 283 (1991);
A. Djouadi, M. Spira, and P.M. Zerwas, Phys. Lett. **B264**, 440 (1991).
45. R.V. Harlander and W.B. Kilgore, Phys. Rev. Lett. **88**, 201801 (2002);
C. Anastasiou and K. Melnikov, Nucl. Phys. **B646**, 220 (2002);
V. Ravindran, J. Smith, and W.L. van Neerven, Nucl. Phys. **B665**, 325 (2003).
46. R.V. Harlander and K.J. Ozeren, JHEP **0911**, 088 (2009);
A. Pak, M. Rogal, and M. Steinhauser, JHEP **1002**, 025 (2010).
47. A. Djouadi and P. Gambino, Phys. Rev. Lett. **73**, 2528 (1994);
S. Actis *et al.*, Phys. Lett. **B670**, 12 (2008);
U. Aglietti *et al.*, Phys. Lett. **B595**, 432 (2004);
G. Degrassi and F. Maltoni, Phys. Lett. **B600**, 255 (2004).
48. C. Anastasiou, R. Boughezal, and F. Petriello, JHEP **0904**, 003 (2009).
49. S. Catani *et al.*, JHEP **0307**, 028 (2003);
S. Moch and A. Vogt, Phys. Lett. **B631**, 48 (2005);
E. Laenen and L. Magnea, Phys. Lett. **B632**, 270 (2006);
A. Idilbi *et al.*, Phys. Rev. **D73**, 077501 (2006);
V. Ravindran, Nucl. Phys. **B752**, 173 (2006);
V. Ahrens *et al.*, Eur. Phys. J. **C62**, 333 (2009).
50. V. Ahrens *et al.*, Phys. Rev. **D79**, 033013 (2009).
51. V. Ahrens *et al.*, Phys. Lett. **B698**, 271 (2011);
D. de Florian and M. Grazzini, Phys. Lett. **B718**, 117 (2012);
C. Anastasiou *et al.*, JHEP **1204**, 004 (2012).
52. J.C. Collins, D.E. Soper, and G.F. Sterman, Nucl. Phys. **B250**, 199 (1985).
53. D. de Florian *et al.*, JHEP **1111**, 064 (2011);
T. Becher and M. Neubert, Eur. Phys. J. **C71**, 1665 (2011);
J.-Y. Chiu *et al.*, JHEP **1205**, 084 (2012);
J. Wang *et al.*, Phys. Rev. **D86**, 094026 (2012);
T. Becher, M. Neubert, and D. Wilhelm, JHEP **1305**, 110 (2013).
54. S. Catani and M. Grazzini, Eur. Phys. J. **C72**, 2013 (2012) [E: **C72**, 2132 (2012)].
55. W.-Y. Keung and F.J. Petriello, Phys. Rev. **D80**, 01007 (2009);
S. Boehler *et al.*, JHEP **1207**, 115 (2012);
M. Grazzini and H. Sargsyan, JHEP **1309**, 129 (2013).
56. R.V. Harlander, S. Liebler, and H. Mantler, Comp. Phys. Comm. **184**, 1605 (2013).
57. D. de Florian, M. Grazzini, and Z. Kunszt, Phys. Rev. Lett. **82**, 5209 (1999);
X. Liu and F. Petriello, Phys. Rev. **D87**, 014018 (2013).
58. J.M. Campbell, R.K. Ellis, and G. Zanderighi, JHEP **0610**, 028 (2006);
J.M. Campbell, R.K. Ellis, and C. Williams, Phys. Rev. **D81**, 074023 (2010).
59. R. Boughezal *et al.*, JHEP **1306**, 072 (2013).
60. C. F. Berger *et al.*, JHEP **1104**, 092 (2011);
A. Banfi, G.P. Salam, and G. Zanderighi, JHEP **1206**, 159 (2012);
T. Becher and M. Neubert, JHEP **1207**, 108 (2012);
A. Banfi *et al.*, Phys. Rev. Lett. **109**, 202001 (2012);
F. J. Tackmann, J. R. Walsh, and S. Zuberi, Phys. Rev. **D86**, 053011 (2012);
T. Becher, M. Neubert, and L. Rothen, JHEP **1310**, 125 (2013).
61. S. Dawson and R. P. Kauffman, Phys. Rev. Lett. **68**, 2273 (1992);
R. P. Kauffman, S. V. Desai, and D. Risal, Phys. Rev. **D55**, 4005 (1997) [E: **D58**, 119901 (1998)];
V. Del Duca *et al.*, Phys. Rev. Lett. **87**, 122001 (2001);
V. Del Duca *et al.*, Nucl. Phys. **B616**, 367 (2001).
62. R. K. Ellis, W. T. Giele, and G. Zanderighi, Phys. Rev. **D72**, 054018 (2005) [Erratum-ibid. **D74**, 079902 (2006)];
L. J. Dixon and Y. Sofianatos, JHEP **0908**, 058 (2009);
S. Badger *et al.*, JHEP **1001**, 036 (2010);
H. van Deurzen *et al.*, Phys. Lett. **B721**, 74 (2013);
G. Cullen *et al.*, Phys. Rev. Lett. **111**, 131801 (2013).
63. V. D. Barger, R. J. N. Phillips, and D. Zeppenfeld, Phys. Lett. **B346**, 106 (1995);
V. Del Duca *et al.*, JHEP **0610**, 016 (2006).
64. M. Duhrssen *et al.*, Phys. Rev. **D70**, 113009 (2004).
65. T. Han, G. Valencia, and S. Willenbrock, Phys. Rev. Lett. **69**, 3274 (1992);
T. Figy, C. Oleari, and D. Zeppenfeld, Phys. Rev. **D68**, 073005 (2003);
T. Figy and D. Zeppenfeld, Phys. Lett. **B591**, 297 (2004);
E.L. Berger and J. Campbell, Phys. Rev. **D70**, 073011 (2004);
M. Ciccolini, A. Denner, and S. Dittmaier, Phys. Rev. Lett. **99**, 161803 (2007);
Ciccolini, A. Denner, and S. Dittmaier, Phys. Rev. **D77**, 103002 (2008);
A. Denner, S. Dittmaier, and A. Muck, HAWK, http://omnibus.uni-freiburg.de/∼sd565/programs/hawk/hawk.html;
K. Arnold *et al.*, VBFNLO, Comp. Phys. Comm. **180**, 1661 (2009);
M. Spira, VV2H, http://people.web.psi.ch/spira/vv2h ;
N. Adam *et al.*, arXiv:0803.1154 [hep-ph] (2008);
T. Figy, S. Palmer, and G. Weiglein, JHEP **1202**, 105 (2012).
66. P. Nason and C. Oleari, JHEP **1002**, 037 (2010);
S. Frixione, P. Torrielli, and M. Zaro, Phys. Lett. **B726**, 273 (2013);
F. Maltoni, K. Mawatari, and M. Zaro, arXiv:1311.1829 [hep-ph] (2013).
67. P. Bolzoni *et al.*, Phys. Rev. Lett. **105**, 011801 (2010).
68. R. V. Harlander, J. Vollinga, and M. M. Weber, Phys. Rev. **D77**, 053010 (2008).
69. S L. Glashow, D.V. Nanopoulos, and A. Yildiz, Phys. Rev. **D18**, 1724 (1978);
T. Han and S. Willenbrock, Phys. Lett. **B273**, 167 (1991);
T. Han, G. Valencia, and S. Willenbrock, Phys. Rev. Lett. **69**, 3274 (1992);
H. Baer, B. Bailey, and J. F. Owens, Phys. Rev. **D47**, 2730

(1993);
J. Ohnemus and W. J. Stirling, Phys. Rev. **D47**, 2722 (1993).
70. A. Stange, W. Marciano, and S. Willenbrock, Phys. Rev. **D49**, 1354 (1994).
71. A. Stange, W. Marciano, and S. Willenbrock, Phys. Rev. **D50**, 4491 (1994).
72. M.L. Ciccolini, S. Dittmaier, and M. Kramer, Phys. Rev. **D68**, 073003 (2003);
A. Denner, S Dittmaier, and S. Kalweit, JHEP **1203**, 075 (2012).
73. R. Hamberg, W. L. van Neerven, and T. Matsuura, Nucl. Phys. **B359**, 343 (1991).
74. O. Brein, A. Djouadi, and R. Harlander, Phys. Lett. **B579**, 149 (2004);
L. Altenkamp *et al.*, JHEP **1302**, 078 (2013).
75. O. Brein *et al.*, Eur. Phys. J. **C72**, 1868 (2012).
76. O. Brein, R. V. Harlander, and T. J. Zirke, Comp. Phys. Comm. **184**, 998 (2013).
77. A. Denner *et al.*, JHEP **1203**, 075 (2012).
78. G. Ferrera, M. Grazzini, and F. Tramontano, Phys. Rev. Lett. **107**, 152003 (2011).
79. R. Raitio and W. W. Wada, Phys. Rev. **D19**, 941 (1979);
J. N. Ng and P. Zakarauskas, Nucl. Phys. **B247**, 339 (1984);
J. F. Gunion, Phys. Lett. **B261**, 510 (1991);
W. J. Marciano and F. E. Paige, Phys. Rev. Lett. **66**, 2433 (1991).
80. W. Beenakker *et al.*, Phys. Rev. Lett. **87**, 201805 (2001);
L. Reina and S. Dawson, Phys. Rev. Lett. **87**, 201804 (2001);
S. Dawson *et al.*, Phys. Rev. **D67**, 071503 (2003);
W. Beenakker *et al.*, Nucl. Phys. **B653**, 151 (2003).
81. R. Frederix *et al.*, Phys. Lett. **B701**, 427 (2011);
M. Garzelli *et al.*, Europhys. Lett. **96**, 11001 (2011).
82. K.A.Assamagan *et al.*, [Higgs Working Group Collab.], `arXiv:hep-ph/0406152`(2004).
83. R.V. Harlander and W.B. Kilgore, Phys. Rev. **D68**, 013001 (2003);
J. M. Campbell *et al.*, Phys. Rev. **D67**, 095002 (2003);
S. Dawson *et al.*, Phys. Rev. Lett. **94**, 031802 (2005);
S. Dittmaier, M. Kramer, and M. Spira, Phys. Rev. **D70**, 074010 (2004);
S. Dawson *et al.*, Phys. Rev. **D69**, 074027 (2004).
84. W.J. Stirling and D.J. Summers, Phys. Lett. **B283**, 411 (1992);
F. Maltoni *et al.*, Phys. Rev. **D64**, 094023 (2001).
85. B.L. Ioffe and V.A. Khoze, Sov. J. Nucl. Phys. **9**, 50 (1978).
86. D.R.T. Jones and S. Petcov, Phys. Lett. **B84**, 440 (1979);
R.N. Cahn and S. Dawson, Phys. Lett. **B136**, 196 (1984);
G.L. Kane, W.W. Repko, and W.B. Rolnick, Phys. Lett. **B148**, 367 (1984);
G. Altarelli, B. Mele, and F. Pitolli, Nucl. Phys. **B287**, 205 (1987);
W. Kilian, M. Kramer, and P.M. Zerwas, Phys. Lett. **B373**, 135 (1996).
87. B.A. Kniehl, Z. Phys. **C55**, 605 (1992).
88. J. Fleischer and F. Jegerlehner, Nucl. Phys. **B216**, 469 (1983);
A. Denner *et al.*, Z. Phys. **C56**, 261 (1992).
89. B.A. Kniehl, Int. J. Mod. Phys. **A17**, 1457 (2002).
90. K.J. Gaemers and G.J. Gounaris, Phys. Lett. **B77**, 379 (1978);
A. Djouadi, J. Kalinowski, and P. M. Zerwas, Z. Phys. **C54**, 255 (1992);
B.A. Kniehl, F. Madricardo, and M. Steinhauser, Phys. Rev. **D66**, 054016 (2002).
91. S. Dittmaier *et al.*, Phys. Lett. **B441**, 383 (1998);
S. Dittmaier *et al.*, Phys. Lett. **B478**, 247 (2000);
S. Dawson and L. Reina, Phys. Rev. **D59**, 054012 (1999).
92. S. Dawson *et al.*, `arXiv:1310.8361 [hep-ex]` (2013).
93. D. M. Asner *et al.*, `arXiv:1310.0763 [hep-ph]` (2013).
94. A. Denner *et al.*, Eur. Phys. J. **C71**, 1753 (2011).
95. A. Djouadi, J. Kalinowski, and M. Spira, Comp. Phys. Comm. **108**, 56 (1998);
A. Djouadi *et al.*, `arXiv:1003.1643 [hep-ph]` (2010).
96. S. Gorishnii *et al.*, Mod. Phys. Lett. **A5**, 2703 (1990);
S. Gorishnii *et al.*, Phys. Rev. **D43**, 1633 (1991);
A. L. Kataev and V. T. Kim, Mod. Phys. Lett. **A9**, 1309 (1994);
L. R. Surguladze, Phys. Lett. **B341**, 60 (1994);
S. Larin, T. van Ritbergen, and J. Vermaseren, Phys. Lett. **B362**, 134 (1995);
K. Chetyrkin and A. Kwiatkowski, Nucl. Phys. **B461**, 3 (1996);
K. Chetyrkin, Phys. Lett. **B390**, 309 (1997);
P. A. Baikov, K. G. Chetyrkin, and J. H. Kuhn, Phys. Rev. Lett. **96**, 012003 (2006).
97. J. Fleischer and F. Jegerlehner, Phys. Rev. **D23**, 2001 (1981);
D. Bardin, B. Vilensky, and P. Khristova, Sov. J. Nucl. Phys. **53**, 152 (1991);
A. Dabelstein and W. Hollik, Z. Phys. **C53**, 507 (1992);
B.A. Kniehl, Nucl. Phys. **B376**, 3 (1992);
A. Djouadi *et al.*, *Proceedings e^+e^- collisions at 500 GeV* (1991).
98. T. Inami, T. Kubota, and Y. Okada, Z. Phys. **C18**, 69 (1983);
K.G. Chetyrkin, B.A. Kniehl, and M. Steinhauser, Phys. Rev. Lett. **79**, 353 (1997);
P.A. Baikov and K.G. Chetyrkin, Phys. Rev. Lett. **97**, 061803 (2006).
99. H.-Q. Zheng and D.-D. Wu, Phys. Rev. **D42**, 3760 (1990);
A. Djouadi *et al.*, Phys. Lett. **B257**, 187 (1991);
S. Dawson and R. Kauffman, Phys. Rev. **D47**, 1264 (1993);
A. Djouadi, M. Spira, and P. Zerwas, Phys. Lett. **B311**, 255 (1993);
K. Melnikov and O. I. Yakovlev, Phys. Lett. **B312**, 179 (1993);
M. Inoue *et al.*, Mod. Phys. Lett. **A9**, 1189 (1994).
100. U. Aglietti *et al.*, Phys. Lett. **B595**, 432 (2004);
G. Degrassi and F. Maltoni, Phys. Lett. **B600**, 255 (2004);
S. Actis *et al.*, Phys. Lett. **B670**, 12 (2008);
U. Aglietti *et al.*, Phys. Lett. **B600**, 57 (2004);
G. Degrassi and F. Maltoni, Nucl. Phys. **B724**, 183 (2005);
U. Aglietti *et al.*, `arXiv:hep-ph/0612172` (2006).
101. A. Abbasabadi *et al.*, Phys. Rev. **D55**, 5647 (1997);
A. Abbasabadi and W. W. Repko, Phys. Rev. **D71**, 017304 (2005);
A. Abbasabadi and W. W. Repko, JHEP **0608**, 048 (2006);
D. A. Dicus and W. W. Repko, Phys. Rev. **D87**, 077301 (2013);
L. -B. Chen, C. -F. Qiao, and R. -L. Zhu, Phys. Lett. **B726**, 306 (2013);
Y. Sun, H. -R. Chang, and D. -N. Gao, JHEP **1305**, 061 (2013);
G. Passarino, `arXiv:1308.0422 [hep-ph]` (2013).
102. M. Spira, A. Djouadi, and P. M. Zerwas, Phys. Lett. **B276**, 350 (1992).
103. A. Bredenstein *et al.*, Phys. Rev. **D74**, 013004 (2006);
A. Bredenstein *et al.*, JHEP **0702**, 080 (2007);
A. Bredenstein *et al.*, Prophecy4f: A Monte Carlo generator for a proper description of the Higgs decay into 4 fermions, `http://omnibus.uni-freiburg.de/~sd565/programs/prophecy4f/prophecy4f.html`.
104. A. Ghinculov, Phys. Lett. **B337**, 137 (1994) [E: **B346**, 426 (1995)];
L. Durand, B. A. Kniehl, and K. Riesselmann, Phys. Rev. **D51**, 5007 (1995);
L. Durand, K. Riesselmann, and B. A. Kniehl, Phys. Rev. Lett. **72**, 2534 (1994) [E: **74**, 1699 (1995)].
105. E. Braaten and J.P. Leveille, Phys. Rev. **D22**, 715 (1980);
L. Durand, K. Riesselmann, and B.A. Kniehl, Phys. Rev. Lett. **72**, 2534 (1994);
E. Gross, G. Wolf, and B. A. Kniehl, Z. Phys. **C63**, 417 (1994); [E: *ibid.*, **C66**, 32 (1995)];
A. Ghinculov, Phys. Lett. **B337**, 137 (1994) and Nucl. Phys. **B455**, 21 (1995);
A. Djouadi, M. Spira, and P. M. Zerwas, Z. Phys. **C70**, 427 (1996);
A. Frink *et al.*, Phys. Rev. **D54**, 4548 (1996);

K.G. Chetyrkin and M. Steinhauser, Phys. Lett. **B408**, 320 (1997);
R. Harlander and M. Steinhauser, Phys. Rev. **D56**, 3980 (1997);
A.L. Kataev, Sov. Phys. JETP Lett. **66**, 327 (1997) [*Pis'ma Zh. Éksp. Teor. Fiz.* **66** (1997) 308];
S. Actis *et al.*, Nucl. Phys. **B811**, 182 (2009).

106. J. Erler and A. Freitas, *Electroweak Model and Constraints on New Physics*, review article in this volume.
107. ALEPH, DELPHI, L3, and OPAL Collaborations, The LEP Working Group for Higgs Boson Searches, Phys. Lett. **B565**, 61 (2003).
108. CDF and D0 Collaborations, Phys. Rev. D 88 ,052014 (2013).
109. L. Lyons, *The Annals of Applied Statistics,* Vol. 2, No. 3, 887 (2008).
110. L. Demortier, "P-Values and Nuisance Parameters", *Proceedings of PHYSTAT 2007,* CERN-2008-001, p. 23 (2008).
111. S. Dittmaier and M. Schumacher, Prog. Part. Nucl. Phys. **70**, 1 (2013).
112. ATLAS Collab., ATLAS-CONF-2011-112 (2011).
113. CMS Collab., CMS-HIG-11-011 (2011).
114. G. Aad *et al.*, [ATLAS Collab.], Phys. Rev. **D86**, 032003 (2012).
115. CMS Collab., CMS-HIG-12-008 (2012).
116. ATLAS Collab., ATLAS-CONF-2013-034 (2013).
117. CMS Collab., CMS-HIG-12-045 (2012).
118. M. Vesterinen and T. R. Wyatt, Nucl. Instrum. Methods **A602**, 88 (2012).
119. G. Aad *et al.*, [ATLAS Collab.], Phys. Lett. **B726**, 88 (2013).
120. CMS Collab., CMS-PAS-HIG-13-001 (2013).
121. CMS Collab., CMS-PAS-HIG-13-002 (2013).
122. S. Chatrchyan *et al.*, [CMS Collab.], JHEP **12**, 034 (2012).
123. S. Chatrchyan *et al.*, [CMS Collab.], arXiv:1312.5353 (2013), Submitted to Phys. Rev. (D).
124. CMS Collab., CMS-PAS-HIG-13-005 (2013).
125. CMS Collab., CMS-PAS-HIG-13-016 (2013).
126. ATLAS Collab., ATLAS-CONF-2013-030 (2013).
127. CMS Collab., CMS-PAS-HIG-13-003 (2013).
128. CMS Collab., CMS-PAS-HIG-13-022 (2013).
129. ATLAS Collab., ATLAS-CONF-2013-075 (2013).
130. CMS Collab., CMS-PAS-HIG-13-017 (2013).
131. CMS Collab., CMS-PAS-HIG-13-004 (2013) and CMS-PAS-HIG-12-053 (2013).
132. CMS Collab., arXiv:1401.5041 (2014), Submitted to JHEP.
133. ATLAS Collab., ATLAS-CONF-2013-108 (2013).
134. ATLAS Collab., ATLAS-CONF-2012-160 (2012).
135. CDF and D0 Collaborations, Phys. Rev. Lett. **109**, 071804 (2012).
136. J. M. Butterworth *et al.*, Phys. Rev. Lett. **100**, 242001 (2008).
137. CMS Collab., CMS-PAS-HIG-13-012 (2013).
138. ATLAS Collab., ATLAS-CONF-2013-079 (2013).
139. ATLAS Collab., ATLAS-CONF-2013-080 (2013).
140. CMS Collab., CMS-PAS-HIG-13-015 (2013).
141. ATLAS Collab., ATLAS-CONF-2012-135 (2012).
142. CMS Collab., CMS-PAS-HIG-12-025 (2012).
143. S. Chatrchyan *et al.*, [CMS Collab.], JHEP **1305**, 145 (2013).
144. CMS Collab., CMS-PAS-HIG-13-019 (2013).
145. CMS Collab., CMS-PAS-HIG-13-020 (2013).
146. CMS Collab., CMS-PAS-HIG-13-015 (2013).
147. S. Chatrchyan *et al.*, [CMS Collab.] Phys. Lett. **B726**, 587 (2013).
148. ATLAS Collab., ATLAS-CONF-2013-009 (2013).
149. ATLAS Collab., ATLAS-CONF-2013-010 (2013).
150. CMS Collab., CMS-PAS-HIG-13-007 (2013).
151. C. Delaunay *et al.*, `arXiv:1310.7029 [hep-ph]` (2013).
152. G. T. Bodwin *et al.*, Phys. Rev. **D88**, 053003 (2013).
153. A. Djouadi *et al.*, Eur. Phys. J. **C73**, 2455 (2013).
154. ATLAS Collab., `arXiv:1309.4017 [hep-ex]` (2013).
155. ATLAS Collab., ATLAS-CONF-2013-011 (2013).
156. CMS Collab., CMS-PAS-HIG-13-018 (2013).
157. CMS Collab., CMS-PAS-HIG-13-028 (2013).
158. CMS Collab., CMS-PAS-HIG-13-013 (2013).
159. M. J. Strassler and K. M. Zurek, Phys. Lett. **B651**, 374 (2007).
160. M. J. Strassler and K. M. Zurek, Phys. Lett. **B661**, 263 (2008).
161. T. Han *et al.*, JHEP **0807**, 008 (2008).
162. A. Falkowski *et al.*, JHEP **1005**, 077 (2010) and Phys. Rev. Lett. **105**, 241801 (2010).
163. G. Aad *et al.*, [ATLAS Collab.], New J. Phys. **15**, 043009 (2013).
164. G. Aad *et al.*, [ATLAS Collab.], Phys. Lett. **B721**, 32 (2013).
165. G. Aad *et al.*, [ATLAS Collab.], Phys. Rev. Lett. **108**, 251801 (2012).
166. D. Tucker-Smith and N. Weiner, Phys. Rev. **D64**, 043502 (2001).
167. S. Chatrchyan *et al.*, [CMS Collab.], Phys. Lett. **B726**, 564 (2013).
168. W. Buchmuller and D. Wyler, Nucl. Phys. **B268**, 621 (1986).
169. B. Grzadkowski *et al.*, JHEP **1010**, 085 (2010).
170. G. F. Giudice *et al.*, JHEP **0706**, 045 (2007).
171. R. Contino *et al.*, JHEP **1307**, 035 (2013).
172. J. Elias-Miro *et al.*, `arXiv:1308.1879 [hep-ph]`.
173. K. Hagiwara *et al.*, Phys. Lett. **B283**, 353 (1992);
K. Hagiwara *et al.*, Phys. Rev. **D48**, 2182 (1993);
K. Hagiwara, R. Szalapski, and D. Zeppenfeld, Phys. Lett. **B318**, 155 (1993).
174. A. Pomarol and F. Riva, `arXiv:1308.2803 [hep-ph]`.
175. C. Degrande *et al.*, JHEP **1207**, 036 (2012) J. F. Kamenik, M. Papucci, and A. Weiler, Phys. Rev. **D85**, 071501 (2012).
176. P. Artoisenet *et al.*, JHEP **1311**, 043 (2013);
A. Alloul, B. Fuks, and V. Sanz, `arXiv:1310.5150 [hep-ph]`.
177. CMS Collab., CMS-PAS-HIG-13-005 (2013).
178. ATLAS Collab., ATLAS-CONF-2013-079 (2013).
179. ATLAS Collab., ATLAS-CONF-2012-160 (2012).
180. S. Chatrchyan *et al.*, [CMS Collab.], JHEP **1305**, 145 (2013).
181. A. David *et al.*, [LHC Higgs Cross Section Working Group Collab.], `arXiv:1209.0040 [hep-ph]` (2012).
182. B. A. Kniehl and M. Spira, Z. Phys. **C69**, 77 (1995).
183. G. Isidori, A. V. Manohar, and M. Trott, `arXiv:1305.0663 [hep-ph]`;
G. Isidori and M. Trott, `arXiv:1307.4051 [hep-ph]`.
184. R. Godbole *et al.*, `arXiv:1306.2573 [hep-ph]`.
185. M. Reece, New J. Phys. **15**, 043003 (2013).
186. S. Biswas, E. Gabrielli, and B. Mele, JHEP **1301**, 088 (2013);
S. Biswas *et al.*, JHEP **07**, 073 (2013).
187. M. Farina *et al.*, JHEP **1305**, 022 (2013).
188. ATLAS Collab., ATLAS-CONF-2013-072 (2013).
189. L. D. Landau, Dokl. Akad. Nauk Ser. Fiz. **60**, 207 (1948);
C. -N. Yang, Phys. Rev. **D77**, 242 (1950).
190. S. Bolognesi *et al.*, Phys. Rev. **D86**, 095031 (2012).
191. A. De Rujula *et al.*, Phys. Rev. **D82**, 013003 (2010).
192. Y. Gao *et al.*, Phys. Rev. **D81**, 075022 (2010).
193. A. L. Read, J. Phys. **G28**, 2693 (2002).
194. J. Ellis *et al.*, JHEP **1211**, 134 (2012).
195. D0 Collab., Note 6387-CONF (2013).
196. D0 Collab., Note 6406-CONF (2013).
197. G. Aad *et al.* [ATLAS Collab.], Phys. Lett. B **726**, 120 (2013).
198. CMS Collab., CMS-PAS-HIG-13-003 (2013).
199. CMS Collab., CMS-PAS-HIG-13-002 (2013).
200. H.E. Haber, *Supersymmetry*, in this volume.
201. L.E. Ibanez and G.G. Ross, Phys. Lett. **B110**, 215 (1982);
L.E. Ibanez, Phys. Lett. **B118**, 73 (1982);
J. Ellis, D.V. Nanopoulos, and K. Tamvakis, Phys. Lett. **B121**, 123 (1983);
L. Alvarez-Gaume, J. Polchinski, and M.B. Wise, Nucl. Phys. **B221**, 495 (1983).
202. L.E. Ibanez and G.G. Ross, Phys. Lett. **B105**, 439 (1981);
S. Dimopoulos, S. Raby, and F. Wilczek, Phys. Rev. **D24**, 1681 (1981);
M.B. Einhorn and D.R.T. Jones, Nucl. Phys. **B196**, 475 (1982);
W.J. Marciano and G. Senjanovic, Phys. Rev. **D25**, 3092 (1982).

203. J. Ellis, S. Kelley, and D.V. Nanopoulos, Phys. Lett. **B249**, 441 (1990);
P. Langacker and M. Luo, Phys. Rev. **D44**, 817 (1991);
U. Amaldi, W. de Boer, and H.Furstenau, Phys. Lett. **B260**, 447 (1991);
P. Langacker and N. Polonsky, Phys. Rev. **D52**, 3081 (1995);
S. Pokorski, Act. Phys. Pol. **B30**, 1759 (1999);
For a recent review, see R.N. Mohapatra, in *Proceedings of the ICTP Summer School in Particle Physics,* Trieste, Italy, 21 June–9 July, 1999, edited by G. Senjanovic and A.Yu. Smirnov. (World Scientific, Singapore, 2000) pp. 336–394.
204. N. Cabibbo, G.R. Farrar, and L. Maiani, Phys. Lett. **B105**, 155 (1981);
H. Goldberg, Phys. Rev. Lett. **50**, 1419 (1983);
J. R. Ellis *et al.*, Nucl. Phys. **B238**, 453 (1984);
G. Bertone, D. Hooper, and J. Silk, Phys. Reports **405**, 279 (2005).
205. A. G. Cohen, D. B. Kaplan, and A. E. Nelson, Ann. Rev. Nucl. and Part. Sci. **43**, 27 (1993);
M. Quiros, Helv. Phys. Acta **67**, 451 (1994);
V. A. Rubakov and M. E. Shaposhnikov, Usp. Fiz. Nauk **166**, 493 (1996) [Phys. Usp. **39**, 461 (1996)];
M. Quiros, `hep-ph/9901312`;
A. Riotto and M. Trodden, Ann. Rev. Nucl. and Part. Sci. **49**, 35 (1999).
206. Y. Okada, M. Yamaguchi, and T. Yanagida, Prog. Theor. Phys. **85**, 1 (1991);
J. Ellis, G. Ridolfi, and F. Zwirner, Phys. Lett. **B257**, 83 (1991).
207. H.E. Haber and R. Hempfling, Phys. Rev. Lett. **66**, 1815 (1991).
208. S.P. Li and M. Sher, Phys. Lett. **B140**, 339 (1984);
R. Barbieri and M. Frigeni, Phys. Lett. **B258**, 395 (1991);
M. Drees and M.M. Nojiri, Phys. Rev. **D45**, 2482 (1992);
J. A. Casas *et al.*, Nucl. Phys. **B436**, 3 (1995) [E: **B439** (1995) 466];
J. Ellis, G. Ridolfi, and F. Zwirner, Phys. Lett. **B262**, 477 (1991);
A. Brignole *et al.*, Phys. Lett. **B271**, 123 (1991) [E: **B273** (1991) 550].
209. R.-J. Zhang, Phys. Lett. **B447**, 89 (1999);
J.R. Espinosa and R.-J. Zhang, JHEP **0003**, 026 (2000);
J.R. Espinosa and R.-J. Zhang, Nucl. Phys. **B586**, 3 (2000);
A. Dedes, G. Degrassi, and P. Slavich, Nucl. Phys. **B672**, 144 (2003).
210. J.F. Gunion and A. Turski, Phys. Rev. **D39**, 2701 (1989), Phys. Rev. **D40**, 2333 (1989);
M.S. Berger, Phys. Rev. **D41**, 225 (1990);
A. Brignole, Phys. Lett. **B277**, 313 (1992), Phys. Lett. **B281**, 284 (1992);
M.A. Diaz and H.E. Haber, Phys. Rev. **D45**, 4246 (1992);
P.H. Chankowski, S. Pokorski, and J. Rosiek, Phys. Lett. **B274**, 191 (1992), Nucl. Phys. **B423**, 437 (1994);
A. Yamada, Phys. Lett. **B263**, 233 (1991), Z. Phys. **C61**, 247 (1994);
A. Dabelstein, Z. Phys. **C67**, 496 (1995);
R. Hempfling and A.H. Hoang, Phys. Lett. **B331**, 99 (1994);
S. Heinemeyer, W. Hollik, and G. Weiglein, Phys. Rev. **D58**, 091701 (1998), Phys. Lett. **B440**, 296 (1998), Eur. Phys. J. **C9**, 343 (1999).
211. D. M. Pierce *et al.*, Nucl. Phys. **B491**, 3 (1997).
212. R. Barbieri, M. Frigeni, and F. Caravaglios, Phys. Lett. **B258**, 167 (1991);
Y. Okada, M. Yamaguchi, and T. Yanagida, Phys. Lett. **B262**, 45 (1991);
J.R. Espinosa and M. Quiros, Phys. Lett. **B266**, 389 (1991);
D.M. Pierce, A. Papadopoulos, and S. Johnson, Phys. Rev. Lett. **68**, 3678 (1992);
R. Hempfling, in *Phenomenological Aspects of Supersymmetry*, edited by W. Hollik, R. Rückl and J. Wess (Springer-Verlag, Berlin, 1992) pp. 260–279;
J. Kodaira, Y. Yasui, and K. Sasaki, Phys. Rev. **D50**, 7035 (1994);
H.E. Haber and R. Hempfling, Phys. Rev. **D48**, 4280 (1993);
M. Carena *et al.*, Phys. Lett. **B355**, 209 (1995).
213. H.E. Haber, R. Hempfling, and A.H. Hoang,Z. Phys. **C75**, 539 (1997).
214. M. Carena *et al.*, Nucl. Phys. **B580**, 29 (2000).
215. M. Carena, M. Quiros, and C.E.M. Wagner, Nucl. Phys. **B461**, 407 (1996).
216. S. Martin, Phys. Rev. **D67**, 095012 (2003);
S. Martin Phys. Rev. **D71**, 016012 (2005);
S. Martin Phys. Rev. **D75**, 055005 (2007).
217. M. Carena, S. Mrenna, and C.E.M. Wagner, Phys. Rev. **D60**, 075010 (1999);
ibid., Phys. Rev. **D62**, 055008 (2000).
218. S. Heinemeyer, W. Hollik, and G. Weiglein, Phys. Lett. **B455**, 179 (1999).
219. J.R. Espinosa and I. Navarro, Nucl. Phys. **B615**, 82 (2001);
G. Degrassi, P. Slavich, and F. Zwirner, Nucl. Phys. **B611**, 403 (2001);
A. Brignole *et al.*, Nucl. Phys. **B631**, 195 (2002);
A. Brignole *et al.*, Nucl. Phys. **B643**, 79 (2002);
S. Heinemeyer *et al.*,.
220. G. Degrassi *et al.*, Eur. Phys. J. **C28**, 133 (2003).
221. U. Ellwanger and C. Hugonie, Mod. Phys. Lett. **A22**, 1581 (2007).
222. J.R. Espinosa and M. Quiros, Phys. Rev. Lett. **81**, 516 (1998).
223. P. Batra *et al.*, JHEP **0402**, 043 (2004).
224. M. Dine, N. Seiberg, and S. Thomas, Phys. Rev. **D76**, 095004 (2007) and references therein.
225. K. Blum, C. Delaunay, and Y. Hochberg, Phys. Rev. **D80**, 075004 (2009).
226. M. Carena *et al.*, Phys. Rev. **D81**, 015001 (2010);
W. Altmannshofer *et al.*, Phys. Rev. **D84**, 095027 (2011).
227. I. Antoniadis *et al.*, Nucl. Phys. **B831**, 133 (2010).
228. T. J. LeCompte and S. P. Martin, Phys. Rev. **D84**, 015004 (2011) and Phys. Rev. **D85**, 035023 (2012).
229. J. Fan, M. Reece, and J. T. Ruderman, JHEP **1111**, 012 (2011) and JHEP **1207**, 196 (2012).
230. R. Barbier *et al.*, `hep-ph/9810232` (1998); R. Barbier *et al.*, Phys. Reports **420**, 1 (2005).
231. C. Smith, `arXiv:0809.3152 [hep-ph]` (2008);
C. Csaki, Y. Grossman, and B. Heidenreich, Phys. Rev. **D85**, 095009 (2012).
232. S. Chatrchyan *et al.*, [CMS Collab.], `arXiv:1301.2175 [hep-ex]` 2013.
233. M. Papucci, J. T. Ruderman, and A. Weiler, JHEP **1209**, 035 (2012);
R. Essig *et al.*, JHEP **1201**, 074 (2012);
Y. Kats *et al.*, JHEP **1202**, 115 (2012);
C. Brust *et al.*, JHEP **1203**, 103 (2012).
234. J. Mrazek, A. Pomarol, R. Rattazzi, M. Redi, J. Serra and A. Wulzer, Nucl. Phys. **B853**, 1 (2011).
235. H. Georgi and D. B. Kaplan, Phys. Lett. **B145**, 216 (1984).
236. D. B. Kaplan, Nucl. Phys. **B365**, 259 (1991).
237. E. Savioni, PhD thesis, 2013
`http://www.infn.it/thesis/thesis_dettaglio.php?tid=8079`.
238. G. Panico *et al.*, JHEP **1303**, 051 (2013).
239. S. Dimopoulos and H. Georgi, Nucl. Phys. **B193**, 150 (1981);
K. Harada and N. Sakai, Prog. Theor. Phys. **67**, 1877 (1982);
K. Inoue *et al.*, Prog. Theor. Phys. **67**, 1889 (1982);
L. Girardello and M.T. Grisaru, Nucl. Phys. **B194**, 65 (1982);
L.J. Hall and L. Randall, Phys. Rev. Lett. **65**, 2939 (1990);
I. Jack and D.R.T. Jones, Phys. Lett. **B457**, 101 (1999).
240. S. Dimopoulos and D.W. Sutter, Nucl. Phys. **B452**, 496 (1995);
D.W. Sutter, Stanford Ph. D. thesis, `hep-ph/9704390` (1997);
H.E. Haber, Nucl. Phys. (Proc. Supp.) **B62A-C**, 469 (1998).
241. A. Djouadi, Phys. Reports **459**, 1 (2008).
242. H.E. Haber and Y. Nir, Nucl. Phys. **B335**, 363 (1990);
A. Dabelstein, Nucl. Phys. **B456**, 25 (1995);
S. Heinemeyer, W. Hollik, and G. Weiglein, Eur. Phys. J. **C16**,

139 (2000);
A. Dobado, M. J. Herrero, and S. Penaranda, Eur. Phys. J. **C17**, 487 (2000);
J.F. Gunion and H.E. Haber, Phys. Rev. **D67**, 075019 (2003).
243. J. F. Gunion and H. E. Haber, Phys. Rev. **D67**, 075019 (2003);
G. C. Branco *et al.*, Phys. Reports **516**, 1 (2012).
244. N. Craig, J. Galloway, and S. Thomas, `arXiv:1305.2424 [hep-ph]` (2013);
D. Asner *et al.*, `arXiv:1310.0763 [hep-ph]` (2013).
245. M. Carena *et al.*, `arXiv:1310.2248 [hep-ph]` (2013).
246. S. P. Martin, Phys. Rev. **D75**, 055005 (2007);
P. Kant *et al.*, JHEP **1008**, 104 (2010);
J. L. Feng *et al.*, Phys. Rev. Lett. **111**, 131802 (2013).
247. M. Carena *et al.*, JHEP **1203**, 014 (2012);
M. Carena *et al.*, JHEP **1207**, 175 (2012).
248. M. Carena *et al.*, Eur. Phys. J. **C26**, 601 (2003);
M. Carena *et al.*, Eur. Phys. J. **C73**, 2552 (2013).
249. M. Carena *et al.*, Eur. Phys. J. **C45**, 797 (2006).
250. S. Heinemeyer *et al.*, JHEP **0808**, 087 (2008).
251. S. Y. Choi, M. Drees, and J. S. Lee, Phys. Lett. **B481**, 57 (2000);
M. Carena *et al.*, Nucl. Phys. **B625**, 345 (2002).
252. A. Pilaftsis and C.E.M. Wagner, Nucl. Phys. **B553**, 3 (1999).
253. A. Arbey *et al.*, Phys. Lett. **B708**, 162 (2012);
A. Arbey *et al.*, JHEP **1209**, 107 (2012).
254. L.J. Hall, D. Pinner, and J.T. Ruderman, JHEP **1204**, 131 (2012).
255. H. Baer, V. Barger, and A. Mustafayev, Phys. Rev. **D85**, 075010 (2012).
256. P. Draper *et al.*, Phys. Rev. **D85**, 095007 (2012).
257. S. Heinemeyer, O. Stal, and G. Weiglein, Phys. Lett. **B710**, 201 (2012).
258. M. Kadastik *et al.*, JHEP **1205**, 061 (2012).
259. ATLAS Collab., `https://twiki.cern.ch/twiki/bin/view/AtlasPublic/Publications`;
CMS Collab., `https://twiki.cern.ch/twiki/bin/view/AtlasPublic/CombinedSummaryPlots#Susy DirectStopSummary`.
260. T.D. Lee, Phys. Rev. **D8**, 1226 (1973);
P. Fayet, Nucl. Phys. **B78**, 14 (1974);
R.D. Peccei and H.R. Quinn, Phys. Rev. Lett. **38**, 1440 (1977);
P. Fayet and S. Ferrara, Phys. Reports **32**, 249 (1977);
L.J. Hall and M.B. Wise, Nucl. Phys. **B187**, 397 (1981);
V.D. Barger, J.L. Hewett, and R.J.N. Phillips, Phys. Rev. **D41**, 3421 (1990).
261. A. Dabelstein, Nucl. Phys. **B456**, 25 (1995);
F. Borzumati *et al.*, Nucl. Phys. **B555**, 53 (1999);
H. Eberl *et al.*, Phys. Rev. **D62**, 055006 (2000).
262. J.A. Coarasa, R.A. Jimenez, and J. Sola, Phys. Lett. **B389**, 312 (1996);
R.A. Jimenez and J. Sola, Phys. Lett. **B389**, 53 (1996);
A. Bartl *et al.*, Phys. Lett. **B378**, 167 (1996).
263. S. Heinemeyer, W. Hollik, and G. Weiglein, Eur. Phys. J. **C16**, 139 (2000).
264. H. E. Haber *et al.*, Phys. Rev. **D63**, 055004 (2001).
265. L. Hall, R. Rattazzi, and U. Sarid, Phys. Rev. **D50**, 7048 (1994);
R. Hempfling, Phys. Rev. **D49**, 6168 (1994).
266. M. S. Carena *et al.*, Nucl. Phys. **B426**, 269 (1994).
267. J. Guasch, P. Hafliger, and M. Spira, Phys. Rev. **D68**, 115001 (2003);
D. Noth and M. Spira, Phys. Rev. Lett. **101**, 181801 (2008);
D. Noth and M. Spira, JHEP **1106**, 084 (2011);
L. Mihaila and C. Reisser, JHEP **1008**, 021 (2010).
268. M. S. Carena *et al.*, Phys. Lett. **B499**, 141 (2001).
269. A. Djouadi, J. Kalinowski, and P.M. Zerwas, Z. Phys. **C57**, 569 (1993);
H. Baer *et al.*, Phys. Rev. **D47**, 1062 (1993);
A. Djouadi *et al.*, Phys. Lett. **B376**, 220 (1996);
A. Djouadi *et al.*, Z. Phys. **C74**, 93 (1997);
S. Heinemeyer and W. Hollik, Nucl. Phys. **B474**, 32 (1996).
270. J.F. Gunion, Phys. Rev. Lett. **72**, 199 (1994);
D. Choudhury and D.P. Roy, Phys. Lett. **B322**, 368 (1994);
O.J. Eboli and D. Zeppenfeld, Phys. Lett. **B495**, 147 (2000);
B.P. Kersevan, M. Malawski, and E. Richter-Was, Eur. Phys. J. **C29**, 541 (2003).
271. E. L. Berger *et al.*, Phys. Rev. **D66**, 095001 (2002).
272. A. Brignole *et al.*, Nucl. Phys. **B643**, 79 (2002);
R. Dermisek and I. Low, Phys. Rev. **D77**, 035012 (2008).
273. A. Djouadi, Phys. Lett. **B435**, 101 (1998).
274. M. R. Buckley and D. Hooper, Phys. Rev. **D86**, 075008 (2012);
M. W. Cahill-Rowley *et al.*, Phys. Rev. **D86**, 075015 (2012);
A. Fowlie *et al.*, Phys. Rev. **D86**, 075010 (2012);
F. Brummer, S. Kraml, and S. Kulkarni, JHEP **1208**, 089 (2012);
N. D. Christensen, T. Han, and S. Su, Phys. Rev. **D85**, 115018 (2012);
H. Baer, V. Barger, and A. Mustafayev, JHEP **1205**, 091 (2012);
L. Aparicio, D. G. Cerdeno, and L. E. Ibanez, JHEP **1204**, 126 (2012);
J. Cao *et al.*, Phys. Lett. **B710**, 665 (2012);
M. Kadastik *et al.*, JHEP **1205**, 061 (2012);
H. Baer, V. Barger, and A. Mustafayev, Phys. Rev. **D85**, 075010 (2012).
275. J. -J. Cao *et al.*, JHEP **1203**, 086 (2012);
R. Benbrik *et al.*, Eur. Phys. J. **C72**, 2171 (2012);
Z. Kang, J. Li, and T. Li, JHEP **1211**, 024 (2012);
S. F. King, M. Muhlleitner, and R. Nevzorov, Nucl. Phys. **B860**, 207 (2012);
J. F. Gunion, Y. Jiang, and S. Kraml, Phys. Lett. **B710**, 454 (2012);
U. Ellwanger, JHEP **1203**, 044 (2012).
276. T. Kitahara, JHEP **1211**, 021 (2012);
M. Carena *et al.*, JHEP **1302**, 114 (2013).
277. B. Batell, S. Jung, and C. E. M. Wagner, `arXiv:1309.2297 [hep-ph]` (2013).
278. ATLAS Collab., `https://twiki.cern.ch/twiki/bin/view/AtlasPublic/Publications`;
CMS Collab., `https://twiki.cern.ch/twiki/bin/view/CMSPublic/Snowmass2013SUSY`.
279. M. Carena *et al.*, JHEP **1308**, 087 (2013).
280. J. F. Gunion *et al.*, Phys. Rev. **D38**, 3444 (1988).
281. S. Heinemeyer *et al.*, Eur. Phys. J. **C19**, 535 (2001).
282. S.H. Zhu, `hep-ph/9901221` (1999);
S. Kanemura, Eur. Phys. J. **C17**, 473 (2000);
A. Arhrib *et al.*, Nucl. Phys. **B581**, 34 (2000).
283. H.E. Logan and S. Su, Phys. Rev. **D66**, 035001 (2002).
284. A. Gutierrez-Rodriguez and O.A. Sampayo, Phys. Rev. **D62**, 055004 (2000);
A. Gutierrez-Rodriguez, M.A. Hernandez-Ruiz, and O.A. Sampayo, J. Phys. Soc. Jap. **70**, 2300 (2001);
S. Moretti, EPJdirect **C15**, 1 (2002).
285. S. Kanemura, S. Moretti, and K. Odagiri, JHEP **0102**, 011 (2001).
286. R. Raitio and W. W. Wada, Phys. Rev. **D19**, 941 (1979);
J. N. Ng and P. Zakarauskas, Phys. Rev. **D29**, 876 (1984);
Z. Kunszt, Nucl. Phys. **B247**, 339 (1984);
J. F. Gunion and H.E. Haber, Nucl. Phys. **B278**, 449 (1986) [E: **B402**, 567 (1993)];
D. A. Dicus and S. Willenbrock, Phys. Rev. **D39**, 751 (1989);
J. F. Gunion, Phys. Lett. **B261**, 510 (1991);
W. J. Marciano and F. E. Paige, Phys. Rev. Lett. **66**, 2433 (1991);
M. Spira *et al.*, Phys. Lett. **B318**, 347 (1993);
S. Dawson, A. Djouadi, and M. Spira, Phys. Rev. Lett. **77**, 16 (1996);
D. Dicus *et al.*, Phys. Rev. **D59**, 094016 (1999);

C. Balazs, H. -J. He, and C. P. Yuan, Phys. Rev. **D60**, 114001 (1999);
A. Djouadi and M. Spira, Phys. Rev. **D62**, 014004 (2000);
R.V. Harlander and W.B. Kilgore, JHEP **0210**, 017 (2002) and Phys. Rev. **D68**, 013001 (2003);
C. Anastasiou and K. Melnikov, Phys. Rev. **D67**, 037501 (2003);
J. Guasch, P. Hafliger, and M. Spira, Phys. Rev. **D68**, 115001 (2003);
S. Dittmaier, M. Kramer, and M. Spira, Phys. Rev. **D70**, 074010 (2004);
S. Dawson *et al.*, Phys. Rev. **D69**, 074027 (2004);
R.V. Harlander and M. Steinhauser, JHEP **0409**, 066 (2004);
S. Dawson *et al.*, Mod. Phys. Lett. **A21**, 89 (2006);
T. Hahn *et al.*, arXiv:hep-ph/0607308 (2006);
M. Muhlleitner and M. Spira, Nucl. Phys. **B790**, 1 (2008).

287. D. Dicus *et al.*, Phys. Rev. **D59**, 094016 (1999).
288. C. Balazs, H.-J. He, and C.P. Yuan, Phys. Rev. **D60**, 114001 (1999).
289. E. Boos *et al.*, Phys. Rev. **D66**, 055004 (2002);
E. Boos, A. Djouadi, and A. Nikitenko, Phys. Lett. **B578**, 384 (2004);
E. Boos *et al.*, Phys. Lett. **B622**, 311 (2005);
M. Carena *et al.*, JHEP **1207**, 091 (2012).
290. A. A. Barrientos Bendezu and B. A. Kniehl, Phys. Rev. **D64**, 035006 (2001).
291. J. A. Coarasa Perez *et al.*, Eur. Phys. J. **C2**, 373 (1998);
J. A. Coarasa Perez *et al.*, Phys. Lett. **B425**, 329 (1998).
292. C.S. Li and T.C. Yuan, Phys. Rev. **D42**, 3088 (1990) [E: **D47**, 2156 (1993)];
A. Czarnecki and S. Davidson, Phys. Rev. **D47**, 3063 (1993);
C.S. Li, Y.-S. Wei, and J.-M. Yang, Phys. Lett. **B285**, 137 (1992).
293. J. Guasch, R.A. Jimenez, and J. Sola, Phys. Lett. **B360**, 47 (1995).
294. M. S. Carena *et al.*,Nucl. Phys. **B577**, 88 (2000).
295. A.A. Barrientos Bendezu and B.A. Kniehl, Phys. Rev. **D59**, 015009 (1999), Phys. Rev. **D61**, 015009 (2000) and Phys. Rev. **D63**, 015009 (2001).
296. A.A. Barrientos Bendezu and B.A. Kniehl, Nucl. Phys. **B568**, 305 (2000).
297. A. Krause *et al.*, Nucl. Phys. **B519**, 85 (1998);
O. Brein and W. Hollik, Eur. Phys. J. **C13**, 175 (2000).
298. R.M. Barnett, H.E. Haber, and D.E. Soper, Nucl. Phys. **B306**, 697 (1988);
F. Olness and W.-K. Tung, Nucl. Phys. **B308**, 813 (1988);
F. Borzumati, J.-L. Kneur, and N. Polonsky, Phys. Rev. **D60**, 115011 (1999);
L. G. Jin *et al.*, Eur. Phys. J. **C14**, 91 (2000) and Phys. Rev. **D62**, 053008 (2000);
S. -h. Zhu, Phys. Rev. **D67**, 075006 (2003);
A. Belyaev *et al.*, JHEP **0206**, 059 (2002);
G. -p. Gao *et al.*, Phys. Rev. **D66**, 015007 (2002);
M. Guchait and S. Moretti, JHEP **0201**, 001 (2002);
H. Baer *et al.*, Phys. Rev. **D65**, 031701 (2002);
G. Gao *et al.*, Phys. Rev. **D66**, 015007 (2002);
T. Plehn, Phys. Rev. **D67**, 014018 (2003);
S.-H. Zhu, Phys. Rev. **D67**, 075006 (2005);
E. L. Berger *et al.*, Phys. Rev. **D71**, 115012 (2005);
S. Dittmaier *et al.*, Phys. Rev. **D83**, 055005 (2011).
299. K. Blum, R. T. D'Agnolo, and J. Fan, JHEP **1301**, 057 (2013);
A. Azatov *et al.*, Phys. Rev. **D86**, 075033 (2012);
J. R. Espinosa *et al.*, JHEP **1212**, 077 (2012);
R. S. Gupta, M. Montull, and F. Riva, JHEP **1304**, 132 (2013);
R. T. D'Agnolo, PhD thesis, Scuola Normale Superiore, Pisa, 2013.
300. C. F. Berger *et al.*, JHEP **0902**, 023 (2009);
S. S. AbdusSalam *et al.*, Phys. Rev. **D81**, 095012 (2010);
P. Bechtle *et al.*, Eur. Phys. J. **C73**, 2354 (2013);
P. Bechtle *et al.*, arXiv:1305.1933 [hep-ph] (2013).
301. G. D'Ambrosio *et al.*, Nucl. Phys. **B645**, 155 (2002);
R. S. Chivukula and H. Georgi, Phys. Lett. **B188**, 99 (1987);
L. J. Hall and L. Randall, Phys. Rev. Lett. **65**, 2939 (1990);
A. J. Buras *et al.*, Phys. Lett. **B500**, 161 (2001).
302. A Arbey, M Battaglia, and F. Mahmoudi, Phys. Rev. **D88**, 015007 (2013).
303. S. Bertolini *et al.*, Nucl. Phys. **B353**, 591 (1991);
T. Goto, Y. Okada, and Y. Shimizu, Phys. Rev. **D58**, 094006 (1998);
G. Isidori and P. Paradisi, Phys. Lett. **B639**, 499 (2006);
W. Altmannshofer, A. J. Buras, and D. Guadagnoli, JHEP **0711**, 065 (2007);
F. Domingo and U. Ellwanger, JHEP **0712**, 090 (2007);
W. Altmannshofer and D. M. Straub, JHEP **1009**, 078 (2010).
304. M. S. Carena *et al.*, Phys. Rev. **D74**, 015009 (2006).
305. J. R. Ellis *et al.*, JHEP **0708**, 083 (2007).
306. E. Lunghi, W. Porod, and O. Vives, Phys. Rev. **D74**, 075003 (2006).
307. A. Arbey *et al.*, JHEP **1209**, 107 (2012).
308. U. Haisch and F. Mahmoudi JHEP **1301**, 061 (2013);
J. Cao *et al.*, JHEP **1210**, 079 (2012).
309. W. Altmannshofer *et al.*, JHEP **1301**, 160 (2013).
310. G. Buchalla, A.J. Buras, and M.E. Lautenbacher, Rev. Mod. Phys. **68**, 1125 (1996).
311. A. Dedes and A. Pilaftsis, Phys. Rev. **D67**, 015012 (2003).
312. A. J. Buras *et al.*, Phys. Lett. **B546**, 96 (2002).
313. A. J. Buras *et al.*, Nucl. Phys. **B659**, 2 (2003).
314. S. R. Choudhury and N. Gaur, Phys. Lett. B **451**, 86 (1999);
G. Isidori and A. Retico, JHEP **0111**, 001 (2001);
K.S. Babu and C.F. Kolda, Phys. Rev. Lett. **84**, 228 (2000).
315. R. Aaij *et al.*, [LHCb Collab.], Phys. Rev. Lett. **111**, 101805 (2013);
CMS Collab., Phys. Rev. Lett. **111**, 101804 (2013).
316. A. G. Akeroyd, F. Mahmoudi, and D. Martinez Santos, JHEP **1112**, 088 (2011);
A. Arbey, M. Battaglia, and F. Mahmoudi, Eur. Phys. J. **C72**, 1906 (2012);
A. Arbey *et al.*, Phys. Lett. **B720**, 153 (2013).
317. M. Misiak *et al.*, Phys. Rev. Lett. **98**, 022002 (2007) and references therein.
318. T. Becher and M. Neubert, Phys. Rev. Lett. **98**, 022003 (2007);
M. Benzke *et al.*, JHEP **1008**, 099 (2010).
319. Heavy Flavor Averaging Group (HFAG), arXiv:1207.1158 [hep-ex] (2012).
320. T. Hermann, M. Misiak, and M. Steinhauser, JHEP **1211**, 036 (2012).
321. I. Adachi *et al.*, [Belle Collab.], Phys. Rev. Lett. **110**, 131801 (2013);
K. Hara *et al.*, [Belle Collab.], Phys. Rev. **D82**, 071101 (2010).
322. J. P. Lees *et al.*, [BaBar Collab.], Phys. Rev. **D88**, 031102 (2013);
B. Aubert *et al.*, [BaBar Collab.], Phys. Rev. **D81**, 051101 (2010).
323. M. Bona *et al.*, [UTfit Collab.], Phys. Lett. B **687**, 61 (2010).
324. G. Isidori and P. Paradisi, Phys. Lett. **B639**, 499 (2006).
325. M. Tanaka, Z. Phys. **C67**, 321 (1995);
U. Nierste, S. Trine, and S. Westhoff, Phys. Rev. **D78**, 015006 (2008);
J. F. Kamenik and F. Mescia, Phys. Rev. **D78**, 014003 (2008);
S. Fajfer, J. F. Kamenik, and I. Nisandzic, Phys. Rev. **D85**, 094025 (2012);
D. Becirevic, N. Kosnik, and A. Tayduganov, Phys. Lett. **B716**, 208 (2012);
J. A. Bailey *et al.*, Phys. Rev. Lett. **109**, 071802 (2012).
326. J. P. Lees *et al.*, [BaBar Collab.], Phys. Rev. Lett. **109**, 101802 (2012).
327. A. Bozek *et al.*, [Belle Collab.], Phys. Rev. **D82**, 072005 (2010).

328. M. Carena, A. Menon, and C.E.M. Wagner, Phys. Rev. **D79**, 075025 (2009).
329. J. R. Ellis *et al.*, Phys. Lett. **B653**, 292 (2007).
330. A. Djouadi and Y. Mambrini, JHEP **0612**, 001 (2006).
331. M. Carena, D. Hooper, and A. Vallinotto, Phys. Rev. **D75**, 055010 (2007).
332. J. R. Ellis, K.A. Olive, and Y. Santoso, Phys. Rev. **D71**, 095007 (2005).
333. C. Boehm *et al.*, JHEP **1306**, 113 (2013).
334. T. Han, Z. Liu, and A. Natarajan, JHEP **1311**, 008 (2013).
335. L. J. Hall, J. Lykken, and S. Weinberg, Phys. Rev. **D27**, 2359 (1983);
J. E. Kim and H. P. Nilles, Phys. Lett. **B138**, 150 (1984);
G. F. Giudice and A. Masiero, Phys. Lett. **B206**, 480 (1988);
E. J. Chun, J. E. Kim, and H. P. Nilles, Nucl. Phys. **B370**, 105 (1992);
I. Antoniadis *et al.*, Nucl. Phys. **B432**, 187 (1994).
336. R. D. Peccei and H. R. Quinn, Phys. Rev. Lett. **38**, 1440 (1977).
337. P. Fayet, Phys. Lett. **B90**, 104 (1975);
H.-P. Nilles, M. Srednicki, and D. Wyler, Phys. Lett. **B120**, 346 (1983);
J.-M. Frere, D.R.T. Jones, and S. Raby, Nucl. Phys. **B222**, 11 (1983);
J.-P. Derendinger and C.A. Savoy, Nucl. Phys. **B237**, 307 (1984);
B.R. Greene and P.J. Miron, Phys. Lett. **B168**, 226 (1986);
J. R. Ellis *et al.*, Phys. Lett. **B176**, 403 (1986);
L. Durand and J.L. Lopez, Phys. Lett. **B217**, 463 (1989);
M. Drees, Int. J. Mod. Phys. **A4**, 3635 (1989);
U. Ellwanger, Phys. Lett. **B303**, 271 (1993);
U. Ellwanger, M. Rausch de Taubenberg, and C.A. Savoy, Phys. Lett. **B315**, 331 (1993), Z. Phys. **C67**, 665 (1995) and Phys. Lett. **B492**, 21 (1997);
P.N. Pandita, Phys. Lett. **B318**, 338 (1993) and Z. Phys. **C59**, 575 (1993);
T. Elliott, S.F. King, and P.L.White, Phys. Lett. **B305**, 71 (1993), Phys. Lett. **B314**, 56 (1993), Phys. Rev. **D49**, 2435 (1994) and Phys. Lett. **B351**, 213 (1995);
K.S. Babu and S.M. Barr, Phys. Rev. **D49**, R2156 (1994);
S.F. King and P.L. White, Phys. Rev. **D52**, 4183 (1995);
N. Haba, M. Matsuda, and M. Tanimoto, Phys. Rev. **D54**, 6928 (1996);
F. Franke and H. Fraas, Int. J. Mod. Phys. **A12**, 479 (1997);
S.W. Ham, S.K. Oh, and H.S. Song, Phys. Rev. **D61**, 055010 (2000);
D.A. Demir, E. Ma, and U. Sarkar, J. Phys. **G26**, L117 (2000);
R. B. Nevzorov and M. A. Trusov, Phys. Atom. Nucl. **64**, 1299 (2001);
U. Ellwanger and C. Hugonie, Eur. Phys. J. **C25**, 297 (2002);
U. Ellwanger *et al.*, `arXiv:hep-ph/0305109` (2003);
D.J. Miller and S. Moretti, `arXiv:hep-ph/0403137` (2004).
338. Y. B. Zeldovich, I. Y. Kobzarev, and L. B. Okun, Zh. Eksp. Teor. Fiz. **67**, 3 (1974);
A. Vilenkin, Phys. Reports **121**, 263 (1985).
339. H. P. Nilles, M. Srednicki, and D. Wyler, Phys. Lett. **B124**, 337 (1983);
A. B. Lahanas, Phys. Lett. **B124**, 341 (1983);
U. Ellwanger, Phys. Lett. **B133**, 187 (1983);
J. Bagger and E. Poppitz, Phys. Rev. Lett. **71**, 2380 (1993);
J. Bagger, E. Poppitz, and L. Randall, Nucl. Phys. **B426**, 3 (1994);
V. Jain, Phys. Lett. **B351**, 481 (1995);
S. A. Abel, Nucl. Phys. **B480**, 55 (1996);
C. F. Kolda, S. Pokorski, and N. Polonsky, Phys. Rev. Lett. **80**, 5263 (1998).
340. C. Panagiotakopoulos and K. Tamvakis, Phys. Lett. **B469**, 145 (1999);
A. Dedes *et al.*, Phys. Rev. **D63**, 055009 (2001);
A. Menon, D. Morrissey, and C.E.M. Wagner, Phys. Rev. **D70**, 035005, (2004).
341. M. Cvetic *et al.*, Phys. Rev. **D56**, 2861 (1997) [E: **D58**, 119905 (1998)];
P. Langacker and J. Wang, Phys. Rev. **D58**, 115010 (1998) and references therein.
342. J. Erler, P. Langacker, and T. j. Li, Phys. Rev. **D66**, 015002 (2002);
T. Han, P. Langacker and B. McElrath, Phys. Rev. **D70**, 115006 (2004);
V. Barger *et al.*, Phys. Rev. **D73**, 115010 (2006).
343. V. Barger *et al.*, Phys. Rev. **D73**, 115010 (2006);
V. Barger, P. Langacker, and G. Shaughnessy, Phys. Rev. **D75**, 055013 (2007).
344. E. Accomando, *et al.*, hep-ph/0608079 (2006).
345. M. Pietroni, Nucl. Phys. **B402**, 27 (1993);
A. T. Davies, C. D. Froggatt, and R. G. Moorhouse, Phys. Lett. **B372**, 88 (1996);
S. J. Huber *et al.*, Nucl. Phys. **A785**, 206 (2007);
S. J. Huber *et al.*, Nucl. Phys. **B757**, 172 (2006);
A. Menon, D. E. Morrissey, and C. E. M. Wagner, Phys. Rev. **D70**, 035005 (2004).
346. B. A. Dobrescu, G. L. Landsberg, and K. T. Matchev, Phys. Rev. **D63**, 075003 (2001).
347. R. Dermisek and J. F. Gunion, Phys. Rev. Lett. **95**, 041801 (2005).
348. M. Carena *et al.*, JHEP **0804**, 092 (2008).
349. O. J. P. Eboli and D. Zeppenfeld, Phys. Lett. **B495**, 147 (2000);
H. Davoudiasl, T. Han, and H. E. Logan, Phys. Rev. **D71**, 115007 (2005).
350. L. Wang and X. -F. Han, Phys. Rev. **D87**, 015015 (2013);
K. Schmidt-Hoberg and F. Staub, JHEP **1210**, 195 (2012);
H. An, T. Liu, and L. -T. Wang, Phys. Rev. **D86**, 075030 (2012);
D. A. Vasquez *et al.*, Phys. Rev. **D86**, 035023 (2012);
S. F. King, M. Muhlleitner, and R. Nevzorov, Nucl. Phys. **B860**, 207 (2012).
351. P. Batra *et al.*, JHEP **0406**, 032 (2004);
A. Maloney, A. Pierce, and J. G. Wacker, JHEP **0606**, 034 (2006);
Y. Zhang *et al.*, Phys. Rev. **D78**, 011302 (2008);
C. W. Chiang *et al.*, Phys. Rev. **D81**, 015006 (2010);
A. D. Medina, N. R. Shah, and C. E. M. Wagner, Phys. Rev. **D80**, 015001 (2009);
M. Endo *et al.*, Phys. Rev. **D85**, 095006 (2012);
C. Cheung and H. L. Roberts, `arXiv:1207.0234 [hep-ph]` (2012).
352. R. Huo *et al.*, Phys. Rev. **D87**, 055011 (2013).
353. R. T. D'Agnolo, E. Kuflik, and M. Zanetti, JHEP **1303**, 043 (2013).
354. A. Azatov and J. Galloway, Int. J. Mod. Phys. **A28**, 1330004 (2013).
355. N. Craig and A. Katz, JHEP **1305**, 015 (2013).
356. T. -F. Feng *et al.*, Nucl. Phys. **B871**, 223 (2013).
357. A. D. Sakharov, Sov. Phys. JETP Lett. **5**, 24 (1967);
M. B. Gavela *et al.*, Nucl. Phys. **B430**, 382 (1994).
358. J. R. Ellis, J. S. Lee, and A. Pilaftsis, JHEP **0810**, 049 (2008);
Y. Li, S. Profumo, and M. Ramsey-Musolf, JHEP **1008**, 062 (2010);
M. Pospelov and A. Ritz, Ann. Phys. **318**, 119 (2005).
359. S. Dimopoulos and S. Thomas, Nucl. Phys. **B465**, 23, (1996);
S. Thomas, Int. J. Mod. Phys. **A13**, 2307 (1998).
360. M. S. Carena *et al.*, Nucl. Phys. **B586**, 92 (2000).
361. A. Pilaftsis, Phys. Rev. **D58**, 096010 (1998) and Phys. Lett. **B435**, 88 (1998);
K. S. Babu *et al.*, Phys. Rev. **D59**, 016004 (1999).
362. G.L. Kane and L.-T. Wang, Phys. Lett. **B488**, 383 (2000);
S.Y. Choi, M. Drees, and J.S. Lee, Phys. Lett. **B481**, 57 (2000);
S.Y. Choi and J.S. Lee, Phys. Rev. **D61**, 015003 (2000);
S.Y. Choi, K. Hagiwara, and J.S. Lee, Phys. Rev. **D64**, 032004

(2001) and Phys. Lett. **B529**, 212 (2002);
T. Ibrahim and P. Nath, Phys. Rev. **D63**, 035009 (2001);
T. Ibrahim, Phys. Rev. **D64**, 035009 (2001);
S. Heinemeyer, Eur. Phys. J. **C22**, 521 (2001);
S. W. Ham *et al.*, Phys. Rev. **D68**, 055003 (2003).
363. M. Frank *et al.*, JHEP **0702**, 047 (2007);
S. Heinemeyer *et al.*, Phys. Lett. **B652**, 300 (2007);
T. Hahn *et al.*, arXiv:0710.4891 (2007).
364. D.A. Demir, Phys. Rev. **D60**, 055006 (1999);
S. Y. Choi, M. Drees, and J. S. Lee, Phys. Lett. **B481**, 57 (2000);
K. E. Williams, H. Rzehak, and G. Weiglein, Eur. Phys. J. **C71**, 1669 (2011).
365. E. Christova *et al.*, Nucl. Phys. **B639**, 263 (2002) [E: Nucl. Phys. **B647**, 359 (2002)].
366. S.L. Glashow and S. Weinberg, Phys. Rev. **D15**, 1958 (1977);
E.A. Paschos, Phys. Rev. **D15**, 1966 (1977);
H. Georgi, Hadronic J. **1,** 1227 (1978);
H. Haber, G Kane, and T Sterling, Nucl. Phys. **B161**, 493 (1979);
A. G. Akeroyd, Phys. Lett. **B368**, 89 (1996);
A.G. Akeroyd, Nucl. Phys. **B544**, 557 (1999);
A. G. Akeroyd, A. Arhrib, and E. Naimi, Eur. Phys. J. **C20**, 51 (2001).
367. N.G. Deshpande and E. Ma Phys. Rev. **D18**, 2574 (1978);
R. Barbieri, L.J. Hall, and V. Rychkov Phys. Rev. **D74**, 015007 (2006);
L. Lopez Honorez *et al.*, JCAP **0702**, 028 (2007);
E. Lundstrom, M. Gustafsson, and J. Edsjo, Phys. Rev. D **79**, 035013 (2009);
E. Dolle *et al.*, Phys. Rev. **D8**, 035003 (2010);
X. Miao, S. Su, and B. Thomas, Phys. Rev. **D82**, 035009 (2010);
L. Lopez-Honorez and C.Yaguna, JCAP **1101**, 002 (2011).
368. A. Arhrib, R. Benbrik, and N. Gaur, Phys. Rev. D **85**, 095021 (2012);
B. Swiezewska and M. Krawczyk, Phys. Rev. D **88**, 035019 (2013);
A. Goudelis, B. Herrmann, and O. Stoel, JHEP **1309**, 106 (2013).
369. V. Barger, H. E. Logan, and G. Shaughnessy, Phys. Rev. **D79**, 115018 (2009).
370. D. O'Connell, M. J. Ramsey-Musolf, and M. B. Wise, Phys. Rev. **D75**, 037701 (2007);
V. Barger *et al.*, Phys. Rev. **D77**, 035005 (2008);
V. Barger *et al.*, Phys. Rev. **D79**, 015018 (2009).
371. H.E. Haber, *Proceedings of the 1990 Theoretical Advanced Study Institute in Elementary Particle Physics,* edited by M. Cvetič and Paul Langacker (World Scientific, Singapore, 1991) pp. 340–475 and references therein.
372. S. Glashow and S. Weinberg, Phys. Rev. **D15**, 1958 (1977).
373. G. C. Branco, W. Grimus, and L. Lavoura, Phys. Lett. **B380**, 119 (1996);
F. J. Botella, G. C. Branco, M. N. Rebelo Phys. Lett. **B687**, 194 (2010).
374. N. Craig and S. Thomas, JHEP **1211**, 083 (2012).
375. G. C. Branco *et al.*, Phys. Reports **516**, 1 (2012).
376. C. -Y. Chen, S. Dawson, and M. Sher, Phys. Rev. **D88**, 015018 (2013).
377. B. Swiezewska and M. Krawczyk, Phys. Rev. **D88**, 035019 (2013).
378. N. Craig, J. Galloway, and S. Thomas, arXiv:1305.2424 [hep-ph] (2013).
379. J. Schechter and J. W. F. Valle, Phys. Rev. **D22**, 2227 (1980).
380. T. P. Cheng and L. -F. Li, Phys. Rev. **D22**, 2860 (1980).
381. H. Georgi and M. Machacek, Nucl. Phys. **B262**, 463 (1985).
382. M. S. Chanowitz and M. Golden, Phys. Lett. **B165**, 105 (1985).
383. J. F. Gunion, R. Vega, and J. Wudka, Phys. Rev. **D42**, 1673 (1990).
384. H. E. Logan and M. -A. Roy, Phys. Rev. **D82**, 115011 (2010).
385. H. E. Haber and H. E. Logan, Phys. Rev. **D62**, 015011 (2000).
386. A. G. Akeroyd, M. Aoki, and H. Sugiyama, Phys. Rev. **D77**, 075010 (2008).
387. P. Nath *et al.*, Nucl. Phys. (Proc. Supp.) **B200**, 185 (2010).
388. J. Garayoa and T. Schwetz, JHEP **0803**, 009 (2008).
389. J. F. Gunion, R. Vega, and J. Wudka, Phys. Rev. **D43**, 2322 (1991).
390. S. Kanemura and K. Yagyu, Phys. Rev. **D85**, 115009 (2012).
391. I. Low and J. Lykken, JHEP **1010**, 053 (2010).
392. C. Englert, E. Re, and M. Spannowsky, Phys. Rev. **D87**, 095014 (2013).
393. I. Low, J. Lykken, and G. Shaughnessy, Phys. Rev. **D86**, 093012 (2012).
394. A. Falkowski, S. Rychkov, and A. Urbano, JHEP **1204**, 073 (2012).
395. B. A. Dobrescu and J. D. Lykken, JHEP **1302**, 073 (2013).
396. D. Carmi *et al.*, JHEP **1210**, 196 (2012).
397. C. -W. Chiang and K. Yagyu, JHEP **1301**, 026 (2013).
398. G. Belanger *et al.*, Phys. Rev. **D88**, 075008 (2013).
399. C. Englert, E. Re, and M. Spannowsky, Phys. Rev. **D88**, 035024 (2013).
400. N. Arkani-Hamed *et al.*, JHEP **0207**, 034 (2002).
401. N. Arkani-Hamed, A. G. Cohen, and H. Georgi, Phys. Lett. **B513**, 232 (2001).
402. N. Arkani-Hamed *et al.*, JHEP **0208**, 021 (2002).
403. M. Schmaltz, JHEP **0408**, 056 (2004).
404. M. Schmaltz, D. Stolarski, and J. Thaler, JHEP **1009**, 018 (2010).
405. M. Perelstein, Prog. in Part. Nucl. Phys. **58**, 247 (2007).
406. M. Schmaltz and D. Tucker-Smith, Ann. Rev. Nucl. and Part. Sci. **55**, 229 (2005).
407. J. A. Casas, J. R. Espinosa, and I. Hidalgo, JHEP **0503**, 038 (2005).
408. H. -C. Cheng and I. Low, JHEP **0309**, 051 (2003).
409. M. S. Carena *et al.*, Phys. Rev. **D75**, 091701 (2007).
410. ATLAS Collab., ATLAS-CONF-2012-147, ATLAS-CONF-2012-109 and ATLAS-CONF-2013-024;
CMS Collab., CMS-PAS-EXO-12-048 and CMS-SUS-12-028.
411. CMS Collab., CMS-PAS-B2G-12-015;
ATLAS Collab., ATLAS-CONF-2013-060.
412. R. S. Chivukula, M. Narain, and J. Womersley, *Dynamical Electroweak Symmetry Breaking*, in this volume.
413. H. Georgi, A. E. Nelson, and A. Manohar, Phys. Lett. **B126**, 169 (1983);
A. E. Nelson and M. J. Strassler, JHEP **0009**, 030 (2000);
S. Davidson, G. Isidori, and S. Uhlig, Phys. Lett. **B663**, 73 (2008).
414. C. Csaki, A. Falkowski, and A. Weiler, JHEP **0809**, 008 (2008);
B. Keren-Zur *et al.*, Nucl. Phys. **B867**, 429 (2013).
415. K. Agashe, R. Contino, and A. Pomarol, Nucl. Phys. **B719**, 165 (2005).
416. O. Matsedonskyi, G. Panico, and A. Wulzer, JHEP **1301**, 164 (2013);
M. Redi and A. Tesi, JHEP **1210**, 166 (2012);
D. Marzocca, M. Serone, and J. Shu, JHEP **1208**, 013 (2012);
A. Pomarol and F. Riva, JHEP **1208**, 135 (2012).
417. R. Contino and G. Servant, JHEP **0806**, 026 (2008);
J. Mrazek and A. Wulzer, Phys. Rev. **D81**, 075006 (2010).
418. A. De Simone *et al.*, JHEP **1304**, 004 (2013) A. Azatov *et al.*, arXiv:1308.6601 [hep-ph] (2013).
419. A. Falkowski, Phys. Rev. **D77**, 055018 (2008);
I. Low and A. Vichi, Phys. Rev. **D84**, 045019 (2011);
A. Azatov and J. Galloway, Phys. Rev. **D85**, 055013 (2012);
C. Delaunay, C. Grojean, and G. Perez, JHEP **1309**, 090 (2013).
420. R.K. Ellis *et al.*, Nucl. Phys. **B297**, 221 (1988);
U. Baur and E.W.N. Glover, Nucl. Phys. **B339**, 38 (1990);
O. Brein and W. Hollik, Phys. Rev. **D68**, 095006 (2003);
U. Langenegger *et al.*, JHEP **0606**, 035 (2006).
421. M. Grazzini and H. Sargsyan, JHEP **1309**, 129 (2013).

422. A. Banfi, A. Martin, and V. Sanz, arXiv:1308.4771 [hep-ph] (2013);
A. Azatov and A. Paul, arXiv:1309.5273 [hep-ph] (2013);
C. Grojean *et al.*, arXiv:1312.3317 [hep-ph] (2013).
423. R. Contino, L. Da Rold, and A. Pomarol, Phys. Rev. **D75**, 055014 (2007).
424. D. Pappadopulo, A. Thamm, and R. Torre, JHEP **1307**, 058 (2013);
M. Montull *et al.*, arXiv:1308.0559 [hep-ph] (2013).
425. I. Low, R. Rattazzi, and A. Vichi, JHEP **1004**, 126 (2010).
426. M. Ciuchini *et al.*, JHEP **1308**, 106 (2013).
427. C. Grojean, O. Matsedonskyi, and G. Panico, arXiv:1306.4655 [hep-ph] (2013).
428. B. Bellazzini *et al.*, arXiv:1305.3919 [hep-th] (2013);
F. Coradeschi *et al.*, JHEP **1311**, 057 (2013).
429. M. Carena, S. Heinemeyer, G. Weiglein, and C. Wagner, private communication.
430. ATLAS Collab., ATLAS-CONF-2013-027 (2013).
431. CMS Collab., CMS-PAS-HIG-13-016 (2013).
432. ATLAS Collab., ATLAS-CONF-2012-013 (2012).
433. CMS Collab., CMS-PAS-HIG-12-002 (2012).
434. CMS Collab., CMS-HIG-12-013 (2013), CERN-PH-EP/2013-011.
435. ALEPH Collab., Phys. Lett. **B526**, 191 (2002).
436. L3 Collab., Phys. Lett. **B545**, 30 (2002).
437. S. Schael *et al.*, [ALEPH, DELPHI, L3 and OPAL Collaborationsand LEP Working Group for Higgs Boson Searches], Eur. Phys. J. **C47**, 547 (2006).
438. OPAL Collab., Eur. Phys. J. **C23**, 397 (2002).
439. DELPHI Collab., Eur. Phys. J. **C38**, 1 (2004).
440. M. M. Kado and C. G. Tully, Ann. Rev. Nucl. and Part. Sci. **52**, 65 (2002).
441. V.M. Abazov *et al.*, [D0 Collab.], Phys. Lett. **B698**, 97 (2011).
442. T. Aaltonen *et al.*, [CDF Collab.], Phys. Rev. **D85**, 032005 (2012).
443. V.M. Abazov *et al.*, [D0 Collab.], Phys. Rev. Lett. **104**, 151801 (2010).
444. D0 Collab., D0 Note 5974-CONF (2011).
445. ATLAS Collab., ATLAS-CONF-2012-094 (2012).
446. CMS Collab., CMS-PAS-HIG-13-021 (2013).
447. RAaij *et al.*, [LHCb Collab.], JHEP **1305**, 132 (2013).
448. S. Chatrchyan *et al.*, [CMS Collab.], Phys. Lett. **B722**, 207 (2013).
449. B. Abbott *et al.*, [D0 Collab.], Phys. Rev. Lett. **82**, 4975 (1999).
450. A. Abulencia *et al.*, [CDF Collab.], Phys. Rev. Lett. **96**, 042003 (2006).
451. V.M. Abazov *et al.*, [D0 Collab.], Phys. Lett. **B682**, 278 (2009).
452. ATLAS Collab., JHEP **1206**, 039 (2012).
453. ATLAS Collab., ATLAS-CONF-2012-090 (2013).
454. CMS Collab., CMS-PAS-HIG-11-019.
455. S. Chatrchyan *et al.*, [CMS Collab.], JHEP **1207**, 143 (2012).
456. ATLAS Collab., ATLAS-CONF-2011-094 (2011).
457. J. Abdallah *et al.*, [DELPHI Collab.], Eur. Phys. J. **C54**, 1 (2008) [E: **C56**, 165 (2008)].
458. V. M. Abazov *et al.*, [D0 Collab.], Phys. Rev. Lett. **103**, 061801 (2009).
459. R. Dermisek, Mod. Phys. Lett. **A24**, 1631 (2009).
460. J. F. Gunion, JHEP **0908**, 032 (2009).
461. U. Ellwanger, Eur. Phys. J. **C71**, 1782 (2011).
462. W. Love *et al.*, [CLEO Collab.], Phys. Rev. Lett. **101**, 151802 (2008).
463. B. Aubert *et al.*, [BaBar Collab.], Phys. Rev. Lett. **103**, 081803 (2009).
464. B. Aubert *et al.*, [BaBar Collab.], Phys. Rev. Lett. **103**, 181801 (2009).
465. V. M. Abazov *et al.*, [D0 Collab.], Phys. Rev. Lett. **103**, 061801 (2009).
466. ATLAS Collab., ATLAS-CONF-2011-020 (2011).
467. S. Chatrchyan *et al.*, [CMS Collab.], Phys. Rev. Lett. **109**, 121801 (2012).
468. ATLAS Collab., ATLAS-CONF-2011-020 (2011).
469. CMS Collab., CMS-PAS-HIG-13-010 (2013).
470. S. Schael *et al.*, [ALEPH Collab.], JHEP **1005**, 049 (2010).
471. ATLAS Collab., ATLAS-CONF-2013-013 (2013).
472. S. Chatrchyan *et al.*, [CMS Collab.], Eur. Phys. J. **C73**, 2469 (2013).
473. ATLAS Collab., ATLAS-CONF-2012-016 (2012).
474. CMS Collab., CMS-PAS-HIG-13-014 (2013).
475. ATLAS Collab., ATLAS-CONF-2012-017 (2012).
476. ATLAS Collab., ATLAS-CONF-2012-163 (2012).
477. CMS Collab., CMS-PAS-HIG-12-024 (2012).
478. ATLAS Collab., ATLAS-CONF-2013-067 (2013).
479. ATLAS Collab., ATLAS-CONF-2012-018 (2012).
480. CMS Collab., CMS-PAS-HIG-13-008 (2013).
481. CMS Collab., CMS-PAS-HIG-12-046 (2012).
482. ATLAS Collab., ATLAS-CONF-2012-010 (2012).
483. G. Aad *et al.*, [ATLAS Collab.], Eur. Phys. J. **C72**, 2244 (2012).
484. S. Chatrchyan *et al.*, [CMS Collab.], Eur. Phys. J. **C72**, 2189 (2012).
485. ATLAS Collab., CERN-PH-EP-2013-172 (2013).
486. ATLAS Collab., ATLAS-CONF-2013-081 (2013).

12. THE CKM QUARK-MIXING MATRIX

Revised February 2014 by A. Ceccucci (CERN), Z. Ligeti (LBNL), and Y. Sakai (KEK).

12.1. Introduction

The masses and mixings of quarks have a common origin in the Standard Model (SM). They arise from the Yukawa interactions with the Higgs condensate,

$$\mathcal{L}_Y = -Y^d_{ij}\,\overline{Q^I_{Li}}\,\phi\,d^I_{Rj} - Y^u_{ij}\,\overline{Q^I_{Li}}\,\epsilon\,\phi^* u^I_{Rj} + \text{h.c.}, \tag{12.1}$$

where $Y^{u,d}$ are 3×3 complex matrices, ϕ is the Higgs field, i,j are generation labels, and ϵ is the 2×2 antisymmetric tensor. Q^I_L are left-handed quark doublets, and d^I_R and u^I_R are right-handed down- and up-type quark singlets, respectively, in the weak-eigenstate basis. When ϕ acquires a vacuum expectation value, $\langle\phi\rangle = (0, v/\sqrt{2})$, Eq. (12.1) yields mass terms for the quarks. The physical states are obtained by diagonalizing $Y^{u,d}$ by four unitary matrices, $V^{u,d}_{L,R}$, as $M^f_{\rm diag} = V^f_L\,Y^f\,V^{f\dagger}_R(v/\sqrt{2})$, $f = u, d$. As a result, the charged-current $W^\pm$ interactions couple to the physical u_{Lj} and d_{Lk} quarks with couplings given by

$$\frac{-g}{\sqrt{2}}(\overline{u_L},\,\overline{c_L},\,\overline{t_L})\gamma^\mu\,W^+_\mu\,V_{\rm CKM}\begin{pmatrix} d_L \\ s_L \\ b_L\end{pmatrix} + \text{h.c.},$$

$$V_{\rm CKM} \equiv V^u_L V^{d\dagger}_L = \begin{pmatrix} V_{ud} & V_{us} & V_{ub} \\ V_{cd} & V_{cs} & V_{cb} \\ V_{td} & V_{ts} & V_{tb}\end{pmatrix}. \tag{12.2}$$

This Cabibbo-Kobayashi-Maskawa (CKM) matrix [1,2] is a 3×3 unitary matrix. It can be parameterized by three mixing angles and the CP-violating KM phase [2]. Of the many possible conventions, a standard choice has become [3]

$$V_{\rm CKM} = \begin{pmatrix} c_{12}c_{13} & s_{12}c_{13} & s_{13}e^{-i\delta} \\ -s_{12}c_{23}-c_{12}s_{23}s_{13}e^{i\delta} & c_{12}c_{23}-s_{12}s_{23}s_{13}e^{i\delta} & s_{23}c_{13} \\ s_{12}s_{23}-c_{12}c_{23}s_{13}e^{i\delta} & -c_{12}s_{23}-s_{12}c_{23}s_{13}e^{i\delta} & c_{23}c_{13}\end{pmatrix}, \tag{12.3}$$

where $s_{ij} = \sin\theta_{ij}$, $c_{ij} = \cos\theta_{ij}$, and δ is the phase responsible for all CP-violating phenomena in flavor-changing processes in the SM. The angles θ_{ij} can be chosen to lie in the first quadrant, so $s_{ij}, c_{ij} \geq 0$.

It is known experimentally that $s_{13} \ll s_{23} \ll s_{12} \ll 1$, and it is convenient to exhibit this hierarchy using the Wolfenstein parameterization. We define [4–6]

$$s_{12} = \lambda = \frac{|V_{us}|}{\sqrt{|V_{ud}|^2 + |V_{us}|^2}}\,, \qquad s_{23} = A\lambda^2 = \lambda\left|\frac{V_{cb}}{V_{us}}\right|,$$
$$s_{13}e^{i\delta} = V^*_{ub} = A\lambda^3(\rho + i\eta) = \frac{A\lambda^3(\bar\rho + i\bar\eta)\sqrt{1-A^2\lambda^4}}{\sqrt{1-\lambda^2}[1 - A^2\lambda^4(\bar\rho + i\bar\eta)]}\,, \tag{12.4}$$

These relations ensure that $\bar\rho + i\bar\eta = -(V_{ud}V^*_{ub})/(V_{cd}V^*_{cb})$ is phase-convention-independent, and the CKM matrix written in terms of λ, A, $\bar\rho$, and $\bar\eta$ is unitary to all orders in λ. The definitions of $\bar\rho, \bar\eta$ reproduce all approximate results in the literature. For example, $\bar\rho = \rho(1-\lambda^2/2+\ldots)$ and we can write $V_{\rm CKM}$ to $\mathcal{O}(\lambda^4)$ either in terms of $\bar\rho, \bar\eta$ or, traditionally,

$$V_{\rm CKM} = \begin{pmatrix} 1-\lambda^2/2 & \lambda & A\lambda^3(\rho - i\eta) \\ -\lambda & 1-\lambda^2/2 & A\lambda^2 \\ A\lambda^3(1-\rho-i\eta) & -A\lambda^2 & 1\end{pmatrix} + \mathcal{O}(\lambda^4)\,. \tag{12.5}$$

The CKM matrix elements are fundamental parameters of the SM, so their precise determination is important. The unitarity of the CKM matrix imposes $\sum_i V_{ij}V^*_{ik} = \delta_{jk}$ and $\sum_j V_{ij}V^*_{kj} = \delta_{ik}$. The six vanishing combinations can be represented as triangles in a complex plane, of which the ones obtained by taking scalar products of neighboring rows or columns are nearly degenerate. The areas of all triangles are the same, half of the Jarlskog invariant, J [7], which is a phase-convention-independent measure of CP violation, defined by $\text{Im}\big[V_{ij}V_{kl}V^*_{il}V^*_{kj}\big] = J\sum_{m,n}\varepsilon_{ikm}\varepsilon_{jln}$.

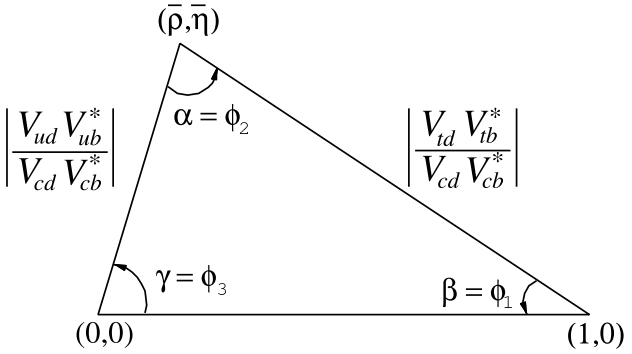

Figure 12.1: Sketch of the unitarity triangle.

The most commonly used unitarity triangle arises from

$$V_{ud}\,V^*_{ub} + V_{cd}\,V^*_{cb} + V_{td}\,V^*_{tb} = 0\,, \tag{12.6}$$

by dividing each side by the best-known one, $V_{cd}V^*_{cb}$ (see Fig. 1). Its vertices are exactly $(0,0)$, $(1,0)$, and, due to the definition in Eq. (12.4), $(\bar\rho, \bar\eta)$. An important goal of flavor physics is to overconstrain the CKM elements, and many measurements can be conveniently displayed and compared in the $\bar\rho, \bar\eta$ plane.

Processes dominated by loop contributions in the SM are sensitive to new physics, and can be used to extract CKM elements only if the SM is assumed. We describe such measurements assuming the SM in Sec. 12.2 and 12.3, give the global fit results for the CKM elements in Sec. 12.4, and discuss implications for new physics in Sec. 12.5.

12.2. Magnitudes of CKM elements

12.2.1. $|V_{ud}|$:

The most precise determination of $|V_{ud}|$ comes from the study of superallowed $0^+ \to 0^+$ nuclear beta decays, which are pure vector transitions. Taking the average of the twenty most precise determinations [8] yields

$$|V_{ud}| = 0.97425 \pm 0.00022. \tag{12.7}$$

The error is dominated by theoretical uncertainties stemming from nuclear Coulomb distortions and radiative corrections. A precise determination of $|V_{ud}|$ is also obtained from the measurement of the neutron lifetime. The theoretical uncertainties are very small, but the determination is limited by the knowledge of the ratio of the axial-vector and vector couplings, $g_A = G_A/G_V$ [9]. The PIBETA experiment [10] has improved the measurement of the $\pi^+ \to \pi^0 e^+\nu$ branching ratio to 0.6%, and quote $|V_{ud}| = 0.9728 \pm 0.0030$, in agreement with the more precise result listed above. The interest in this measurement is that the determination of $|V_{ud}|$ is very clean theoretically, because it is a pure vector transition and is free from nuclear-structure uncertainties.

12.2.2. $|V_{us}|$:

The product of $|V_{us}|$ and the form factor at $q^2 = 0$, $|V_{us}|\,f_+(0)$, has been extracted traditionally from $K^0_L \to \pi e\nu$ decays in order to avoid isospin-breaking corrections ($\pi^0 - \eta$ mixing) that affect $K^\pm$ semileptonic decay, and the complications induced by a second (scalar) form factor present in the muonic decays. The last round of measurements has lead to enough experimental constraints to justify the comparison between different decay modes. Systematic errors related to the experimental quantities, *e.g.*, the lifetime of neutral or charged kaons, and the form factor determinations for electron and muonic decays, differ among decay modes, and the consistency between different determinations enhances the confidence in the final result. For this reason, we follow the prescription [11] to average $K^0_L \to \pi e\nu$, $K^0_L \to \pi\mu\nu$, $K^\pm \to \pi^0 e^\pm\nu$, $K^\pm \to \pi^0\mu^\pm\nu$ and $K^0_S \to \pi e\nu$. The average of these five decay modes yields $|V_{us}|\,f_+(0) = 0.2163 \pm 0.0005$. Results obtained from each decay mode, and exhaustive references to

the experimental data, are listed for instance in Ref. [9]. The form factor value $f_+(0) = 0.960^{+0.005}_{-0.006}$ [12] from a three-flavor unquenched lattice QCD calculation gives [9] $|V_{us}| = 0.2253 \pm 0.0014$.[1] The broadly used classic calculation of $f_+(0)$ [15] is in good agreement with this value, while other calculations [16] differ by as much as 2%.

The calculation of the ratio of the kaon and pion decay constants enables one to extract $|V_{us}/V_{ud}|$ from $K \to \mu\nu(\gamma)$ and $\pi \to \mu\nu(\gamma)$, where (γ) indicates that radiative decays are included [17]. The KLOE measurement of the $K^+ \to \mu^+\nu(\gamma)$ branching ratio [18], combined with the lattice QCD calculation, $f_K/f_\pi = 1.1947 \pm 0.0045$ [19], leads to $|V_{us}| = 0.2253 \pm 0.0010$, where the accuracy is limited by the knowledge of the ratio of the decay constants. The average of these two determinations is quoted by Ref. 9 as

$$|V_{us}| = 0.2253 \pm 0.0008. \tag{12.8}$$

The latest determination from hyperon decays can be found in Ref. 21. The authors focus on the analysis of the vector form factor, protected from first order $SU(3)$ breaking effects by the Ademollo-Gatto theorem [22], and treat the ratio between the axial and vector form factors g_1/f_1 as experimental input, thus avoiding first order $SU(3)$ breaking effects in the axial-vector contribution. They find $|V_{us}| = 0.2250 \pm 0.0027$, although this does not include an estimate of the theoretical uncertainty due to second-order $SU(3)$ breaking, contrary to Eq. (12.8). Concerning hadronic τ decays to strange particles, the latest determinations based on LEP, *BABAR*, and Belle data yield $|V_{us}| = 0.2202 \pm 0.0015$ [23]. A measurement of the ratio of branching fractions $\mathcal{B}(\tau \to K\nu)/\mathcal{B}(\tau \to \pi\nu)$ by *BABAR* [24] combined with the above f_K/f_π value gives $|V_{us}| = 0.2244 \pm 0.0024$.

12.2.3. $|V_{cd}|$:

The magnitude of V_{cd} can be extracted from semileptonic charm decays, using theoretical knowledge of the form factors. In semileptonic D decays, unquenched lattice QCD calculations have predicted the normalization of the $D \to \pi\ell\nu$ and $D \to K\ell\nu$ form factors [13]. The dependence on the invariant mass of the lepton pair, q^2, is determined from lattice QCD and theoretical constraints from analyticity [14]. Using three-flavor unquenched lattice QCD calculations for $D \to \pi\ell\nu$, $f_+^{D\pi}(0) = 0.666 \pm 0.029$ [13], and the average of recent CLEO-c [25] and Belle [26] measurements of $D \to \pi\ell\nu$ decays, one obtains $|V_{cd}| = 0.220 \pm 0.006 \pm 0.010$, where the first uncertainty is experimental, and the second is from the theoretical uncertainty of the form factor.

Earlier determinations of $|V_{cd}|$ came from neutrino scattering data. The difference of the ratio of double-muon to single-muon production by neutrino and antineutrino beams is proportional to the charm cross section off valence d quarks, and therefore to $|V_{cd}|^2$ times the average semileptonic branching ratio of charm mesons, $\mathcal{B}_\mu$. The method was used first by CDHS [27] and then by CCFR [28,29] and CHARM II [30]. Averaging these results is complicated, because it requires assumptions about the scale of the QCD corrections, and because $\mathcal{B}_\mu$ is an effective quantity, which depends on the specific neutrino beam characteristics. Given that no recent experimental input is available, we quote the average from a past review, $\mathcal{B}_\mu |V_{cd}|^2 = (0.463 \pm 0.034) \times 10^{-2}$ [31]. Analysis cuts make these experiments insensitive to neutrino energies smaller than 30 GeV. Thus, $\mathcal{B}_\mu$ should be computed using only neutrino interactions with visible energy larger than 30 GeV. An appraisal [32] based on charm-production fractions measured in neutrino interactions [33,34] gives $\mathcal{B}_\mu = 0.088 \pm 0.006$. Data from the CHORUS experiment [35] are sufficiently precise to extract $\mathcal{B}_\mu$ directly, by comparing the number of charm decays with a muon to the total number of charmed hadrons found in the nuclear emulsions. Requiring the visible energy to be larger than 30 GeV, CHORUS finds $\mathcal{B}_\mu = 0.085 \pm 0.009 \pm 0.006$. We use the average of these two determinations, $\mathcal{B}_\mu = 0.087 \pm 0.005$, and obtain $|V_{cd}| = 0.230 \pm 0.011$. Averaging the two determinations above, we find

$$|V_{cd}| = 0.225 \pm 0.008. \tag{12.9}$$

[1] For lattice QCD inputs, we use the averages from Ref. 13 whenever possible, unless the minireviews [9,14] choose other values. Hereafter, the first error is statistical and the second is systematic, unless mentioned otherwise.

12.2.4. $|V_{cs}|$:

The direct determination of $|V_{cs}|$ is possible from semileptonic D or leptonic D_s decays, using unquenched lattice QCD calculations of the semileptonic D form factor or the D_s decay constant. For muonic decays, the average of Belle [36], CLEO-c [37] and *BABAR* [38] is $\mathcal{B}(D_s^+ \to \mu^+\nu) = (5.56 \pm 0.24) \times 10^{-3}$ [39]. For decays to τ leptons, the average of CLEO-c [37,40,41], *BABAR* [38] and Belle [36] gives $\mathcal{B}(D_s^+ \to \tau^+\nu) = (5.56 \pm 0.22) \times 10^{-2}$ [39]. From each of these values, determinations of $|V_{cs}|$ can be obtained using the PDG values for the mass and lifetime of the D_s, the masses of the leptons, and $f_{D_s} = (248.6 \pm 2.7)$ MeV [13]. The average of these determinations gives $|V_{cs}| = 1.008 \pm 0.021$, where the error is dominated by the lattice QCD determination of f_{D_s}. In semileptonic D decays, unquenched lattice QCD calculations of the $D \to K\ell\nu$ form factor is available [13]. Using $f_+^{DK}(0) = 0.747 \pm 0.019$ and the average of recent CLEO-c [25], Belle [26] and *BABAR* [42] measurements of $B \to K\ell\nu$ decays, one obtains $|V_{cs}| = 0.953 \pm 0.008 \pm 0.024$, where the first error is experimental and the second, which is dominant, is from the theoretical uncertainty of the form factor. Averaging the determinations from leptonic and semileptonic decays, we find

$$|V_{cs}| = 0.986 \pm 0.016. \tag{12.10}$$

Measurements of on-shell $W^\pm$ decays sensitive to $|V_{cs}|$ were made by LEP-2. The W branching ratios depend on the six CKM elements involving quarks lighter than m_W. The W branching ratio to each lepton flavor is $1/\mathcal{B}(W \to \ell\bar{\nu}_\ell) = 3\big[1 + \sum_{u,c,d,s,b} |V_{ij}|^2 \,(1 + \alpha_s(m_W)/\pi) + \ldots\big]$. Assuming lepton universality, the measurement $\mathcal{B}(W \to \ell\bar{\nu}_\ell) = (10.83 \pm 0.07 \pm 0.07)\,\%$ [43] implies $\sum_{u,c,d,s,b} |V_{ij}|^2 = 2.002 \pm 0.027$. This is a precise test of unitarity; however, only flavor-tagged W-decays determine $|V_{cs}|$ directly, such as DELPHI's tagged $W^+ \to c\bar{s}$ analysis, yielding $|V_{cs}| = 0.94^{+0.32}_{-0.26} \pm 0.13$ [44].

12.2.5. $|V_{cb}|$:

This matrix element can be determined from exclusive and inclusive semileptonic decays of B mesons to charm. The inclusive determinations use the semileptonic decay rate measurement, together with the leptonic energy and the hadronic invariant-mass spectra. The theoretical foundation of the calculation is the operator product expansion [45,46]. It expresses the total rate and moments of differential energy and invariant-mass spectra as expansions in α_s, and inverse powers of the heavy quark mass. The dependence on m_b, m_c, and the parameters that occur at subleading order is different for different moments, and a large number of measured moments overconstrains all the parameters, and tests the consistency of the determination. The precise extraction of $|V_{cb}|$ requires using a "threshold" quark mass definition [47,48]. Inclusive measurements have been performed using B mesons from Z^0 decays at LEP, and at e^+e^- machines operated at the $\Upsilon(4S)$. At LEP, the large boost of B mesons from the Z^0 allows the determination of the moments throughout phase space, which is not possible otherwise, but the large statistics available at the B factories lead to more precise determinations. An average of the measurements and a compilation of the references are provided by Ref. [14]: $|V_{cb}| = (42.2 \pm 0.7) \times 10^{-3}$.

Exclusive determinations are based on semileptonic B decays to D and D^*. In the $m_{b,c} \gg \Lambda_{\rm QCD}$ limit, all form factors are given by a single Isgur-Wise function [49], which depends on the product of the four-velocities of the B and $D^{(*)}$ mesons, $w = v \cdot v'$. Heavy quark symmetry determines the normalization of the rate at $w = 1$, the maximum momentum transfer to the leptons, and $|V_{cb}|$ is obtained from an extrapolation to $w = 1$. The exclusive determination, $|V_{cb}| = (39.5 \pm 0.8) \times 10^{-3}$ [14], has a comparable precision to the inclusive one, and the main theoretical uncertainty in the form factor and the experimental uncertainty in the rate near $w = 1$ are to a large extent independent of the inclusive determination. The V_{cb} and V_{ub} minireview [14] quotes a combination with a scaled error as

$$|V_{cb}| = (41.1 \pm 1.3) \times 10^{-3}. \tag{12.11}$$

Determinations of $|V_{cb}|$ with larger uncertainties, not included in this average, can be obtained from $\mathcal{B}(B \to D^{(*)}\tau\bar{\nu})$. The most precise

measurements involving the τ modes are those of the $|V_{cb}|$-independent ratios $\mathcal{B}(B \to D^{(*)}\tau\bar{\nu})/\mathcal{B}(B \to D^{(*)}\ell\bar{\nu})$ [50], which are 2–3 σ above the SM predictions.

12.2.6. $|V_{ub}|$:

The determination of $|V_{ub}|$ from inclusive $B \to X_u\ell\bar{\nu}$ decay is complicated due to large $B \to X_c\ell\bar{\nu}$ backgrounds. In most regions of phase space where the charm background is kinematically forbidden, the hadronic physics enters via unknown nonperturbative functions, so-called shape functions. (In contrast, the nonperturbative physics for $|V_{cb}|$ is encoded in a few parameters.) At leading order in $\Lambda_{\rm QCD}/m_b$, there is only one shape function, which can be extracted from the photon energy spectrum in $B \to X_s\gamma$ [51,52], and applied to several spectra in $B \to X_u\ell\bar{\nu}$. The subleading shape functions are modeled in the current determinations. Phase space cuts for which the rate has only subleading dependence on the shape function are also possible [53]. The measurements of both the hadronic and the leptonic systems are important for an optimal choice of phase space. A different approach is to make the measurements more inclusive by extending them deeper into the $B \to X_c\ell\bar{\nu}$ region, and thus reduce the theoretical uncertainties. Analyses of the electron-energy endpoint from CLEO [54], *BABAR* [55], and Belle [56] quote $B \to X_u e\bar{\nu}$ partial rates for $|\vec{p}_e| \geq 2.0\,\text{GeV}$ and 1.9 GeV, which are well below the charm endpoint. The large and pure $B\overline{B}$ samples at the B factories permit the selection of $B \to X_u\ell\bar{\nu}$ decays in events where the other B is fully reconstructed [57]. With this full-reconstruction tag method, the four-momenta of both the leptonic and the hadronic systems can be measured. It also gives access to a wider kinematic region because of improved signal purity. Ref. 14 quotes an inclusive average as $|V_{ub}| = (4.41 \pm 0.15\ ^{+0.15}_{-0.19}) \times 10^{-3}$.

To extract $|V_{ub}|$ from an exclusive channel, the form factors have to be known. Experimentally, better signal-to-background ratios are offset by smaller yields. The $B \to \pi\ell\bar{\nu}$ branching ratio is now known to 5%. Unquenched lattice QCD calculations of the $B \to \pi\ell\bar{\nu}$ form factor are available [58,59] for the high q^2 region ($q^2 > 16$ or $18\,\text{GeV}^2$). A fit to the experimental partial rates and lattice results versus q^2 yields $|V_{ub}| = (3.23 \pm 0.31) \times 10^{-3}$ [59]. Light-cone QCD sum rules are supposed to be applicable for $q^2 < 12\,\text{GeV}^2$ [60]. The minireview quotes a combination, $|V_{ub}| = (3.28 \pm 0.29) \times 10^{-3}$.

The uncertainties in extracting $|V_{ub}|$ from inclusive and exclusive decays are different to a large extent. A combination of the determinations is quoted by Ref. [14] as

$$|V_{ub}| = (4.13 \pm 0.49) \times 10^{-3}. \tag{12.12}$$

A determination of $|V_{ub}|$ not included in this average can be obtained from $\mathcal{B}(B \to \tau\bar{\nu}) = (1.14 \pm 0.22) \times 10^{-4}$ [65]. Using $f_B = (190.5 \pm 4.2)\,\text{MeV}$ [13] and $\tau_{B^\pm} = (1.641 \pm 0.008)\,\text{ps}$ [66], we find $|V_{ub}| = (4.22 \pm 0.42) \times 10^{-3}$. This decay is sensitive, for example, to tree-level charged Higgs contributions, and the measured rate is somewhat higher than the SM fit value.

12.2.7. $|V_{td}|$ *and* $|V_{ts}|$:

The CKM elements $|V_{td}|$ and $|V_{ts}|$ are not likely to be precisely measurable in tree-level processes involving top quarks, so one has to rely on determinations from B–$\overline{B}$ oscillations mediated by box diagrams with top quarks, or loop-mediated rare K and B decays. Theoretical uncertainties in hadronic effects limit the accuracy of the current determinations. These can be reduced by taking ratios of processes that are equal in the flavor $SU(3)$ limit to determine $|V_{td}/V_{ts}|$.

The mixing of the two B^0 mesons was discovered by ARGUS [61], and the mass difference is precisely measured by now, $\Delta m_d = (0.510 \pm 0.003)\,\text{ps}^{-1}$ [62]. In the B_s^0 system, Δm_s was first measured significantly by CDF [63] and the world average, dominated by a recent LHCb measurement [64], is $\Delta m_s = (17.761 \pm 0.022)\,\text{ps}^{-1}$ [62]. Assuming $|V_{tb}| = 1$, and using the unquenched lattice QCD calculations $f_{B_d}\sqrt{\widehat{B}_{B_d}} = (216 \pm 15)\,\text{MeV}$ and $f_{B_s}\sqrt{\widehat{B}_{B_s}} = (266 \pm 18)\,\text{MeV}$ [13],

$$|V_{td}| = (8.4 \pm 0.6) \times 10^{-3}, \qquad |V_{ts}| = (40.0 \pm 2.7) \times 10^{-3}. \tag{12.13}$$

The uncertainties are dominated by lattice QCD. Several uncertainties are reduced in the calculation of the ratio $\xi = (f_{B_s}\sqrt{\widehat{B}_{B_s}})/(f_{B_d}\sqrt{\widehat{B}_{B_d}}) = 1.268 \pm 0.063$ [13] and therefore the constraint on $|V_{td}/V_{ts}|$ from $\Delta m_d/\Delta m_s$ is more reliable theoretically. These provide a theoretically clean and significantly improved constraint

$$\left|V_{td}/V_{ts}\right| = 0.216 \pm 0.001 \pm 0.011. \tag{12.14}$$

The inclusive branching ratio $\mathcal{B}(B \to X_s\gamma) = (3.43 \pm 0.22) \times 10^{-4}$ extrapolated to $E_\gamma > E_0 = 1.6\,\text{GeV}$ [67] is also sensitive to $|V_{tb}V_{ts}|$. In addition to t-quark penguins, a large part of the sensitivity comes from charm contributions proportional to $V_{cb}V_{cs}^*$ via the application of 3×3 CKM unitarity (which is used here). With the NNLO calculation of $\mathcal{B}(B \to X_s\gamma)_{E_\gamma > E_0}/\mathcal{B}(B \to X_c e\bar{\nu})$ [68], we obtain $|V_{ts}/V_{cb}| = 1.02 \pm 0.05$. The $B_s \to \mu^+\mu^-$ rate [69] is also proportional to $|V_{tb}V_{ts}|^2$ in the SM, and the observed signal $\mathcal{B}(B_s \to \mu^+\mu^-) = (2.9 \pm 0.7) \times 10^{-9}$ is consistent with the SM, with sizable uncertainties.

A complementary determination of $|V_{td}/V_{ts}|$ is possible from the ratio of $B \to \rho\gamma$ and $K^*\gamma$ rates. The ratio of the neutral modes is theoretically cleaner than that of the charged ones, because the poorly known spectator-interaction contribution is expected to be smaller (W-exchange vs. weak annihilation). For now, because of low statistics we average the charged and neutral rates assuming the isospin symmetry and heavy quark limit motivated relation, $|V_{td}/V_{ts}|^2/\xi_\gamma^2 = [\Gamma(B^+ \to \rho^+\gamma) + 2\Gamma(B^0 \to \rho^0\gamma)]/[\Gamma(B^+ \to K^{*+}\gamma) + \Gamma(B^0 \to K^{*0}\gamma)] = (3.19 \pm 0.46)\%$ [67]. Here ξ_γ contains the poorly known hadronic physics. Using $\xi_\gamma = 1.2 \pm 0.2$ [70], and combining the experimental and theoretical errors in quadrature, gives $|V_{td}/V_{ts}| = 0.21 \pm 0.04$.

A theoretically clean determination of $|V_{td}V_{ts}^*|$ is possible from $K^+ \to \pi^+\nu\bar{\nu}$ decay [71]. Experimentally, only seven events have been observed [72] and the rate is consistent with the SM with large uncertainties. Much more data are needed for a precision measurement.

12.2.8. $|V_{tb}|$:

The determination of $|V_{tb}|$ from top decays uses the ratio of branching fractions $R = \mathcal{B}(t \to Wb)/\mathcal{B}(t \to Wq) = |V_{tb}|^2/(\sum_q |V_{tq}|^2) = |V_{tb}|^2$, where $q = b, s, d$. The CDF and DØ measurements performed on data collected during Run II of the Tevatron give $|V_{tb}| > 0.78$ [73] and $0.99 > |V_{tb}| > 0.90$ [74], respectively, at 95% CL. CMS recently measured the same quantity at 7 TeV and gives $|V_{tb}| > 0.92$ [75] at 95% CL.

The direct determination of $|V_{tb}|$, without assuming unitarity, is possible from the single top-quark-production cross section. The $(3.51^{+0.40}_{-0.37})$ pb average cross section measured by DØ [76] and CDF [77] implies $|V_{tb}| = 1.03 \pm 0.06$. The average t-channel single-top cross section at CMS [78] and ATLAS [79] at 7 TeV, $(68.5 \pm 5.8)\,\text{pb}$, implies $|V_{tb}| = 1.03 \pm 0.05$; the average cross section at 8 TeV from a subset of the data, $(85 \pm 12)\,\text{pb}$ [80], implies $|V_{tb}| = 0.99 \pm 0.07$. The average of these gives

$$|V_{tb}| = 1.021 \pm 0.032\,. \tag{12.15}$$

This does not include correlations between the 7 and 8 TeV measurements. The experimental uncertainties dominate, and a dedicated combination would be welcome.

A weak constraint on $|V_{tb}|$ can be obtained from precision electroweak data, where top quarks enter in loops. The sensitivity is best in $\Gamma(Z \to b\bar{b})$ and yields $|V_{tb}| = 0.77^{+0.18}_{-0.24}$ [81].

12.3. Phases of CKM elements

As can be seen from Fig. 12.1, the angles of the unitarity triangle are

$$\beta = \phi_1 = \arg\left(-\frac{V_{cd}V_{cb}^*}{V_{td}V_{tb}^*}\right),$$
$$\alpha = \phi_2 = \arg\left(-\frac{V_{td}V_{tb}^*}{V_{ud}V_{ub}^*}\right),$$
$$\gamma = \phi_3 = \arg\left(-\frac{V_{ud}V_{ub}^*}{V_{cd}V_{cb}^*}\right). \tag{12.16}$$

Since CP violation involves phases of CKM elements, many measurements of CP-violating observables can be used to constrain these angles and the $\bar{\rho}, \bar{\eta}$ parameters.

12.3.1. ϵ and ϵ' :

The measurement of CP violation in K^0–$\overline{K}^0$ mixing, $|\epsilon| = (2.233 \pm 0.015) \times 10^{-3}$ [82], provides important information about the CKM matrix. In the SM, in the basis where $V_{ud}V_{us}^*$ is real [83]

$$|\epsilon| = \frac{G_F^2 f_K^2 m_K m_W^2}{12\sqrt{2}\,\pi^2 \Delta m_K} \widehat{B}_K \Big\{ \eta_1 S(x_c)\, \mathrm{Im}[(V_{cs}V_{cd}^*)^2] + \eta_2 S(x_t)\, \mathrm{Im}[(V_{ts}V_{td}^*)^2] + 2\eta_3 S(x_c, x_t)\, \mathrm{Im}(V_{cs}V_{cd}^* V_{ts}V_{td}^*) \Big\}, \quad (12.17)$$

where S is an Inami-Lim function [84], $x_q = m_q^2/m_W^2$, and η_i are perturbative QCD corrections. The constraint from ϵ in the $\bar{\rho}, \bar{\eta}$ plane is bounded by approximate hyperbolas. The dominant uncertainties are due to the bag parameter, for which we use $\widehat{B}_K = 0.766 \pm 0.010$ from lattice QCD [13], and the parametric uncertainty proportional to $\sigma(A^4)$ from $(V_{ts}V_{td}^*)^2$, which is approximately $\sigma(|V_{cb}|^4)$.

The measurement of $6\,\mathrm{Re}(\epsilon'/\epsilon) = 1 - |\eta_{00}/\eta_{+-}|^2$, where η_{00} and η_{+-} are the CP-violating amplitude ratios of K_S^0 and K_L^0 decays to two pions, provides a qualitative test of the CKM mechanism. Its nonzero experimental average, $\mathrm{Re}(\epsilon'/\epsilon) = (1.67 \pm 0.23) \times 10^{-3}$ [82], demonstrates the existence of direct CP violation, a prediction of the KM ansatz. While $\mathrm{Re}(\epsilon'/\epsilon) \propto \mathrm{Im}(V_{td}V_{ts}^*)$, this quantity cannot easily be used to extract CKM parameters, because the electromagnetic penguin contributions tend to cancel the gluonic penguins for large m_t [85], thereby significantly increasing the hadronic uncertainties. Most estimates [86–89] agree with the observed value, indicating that $\bar{\eta}$ is positive. Progress in lattice QCD, in particular finite-volume calculations [90,91], may eventually provide a determination of the $K \to \pi\pi$ matrix elements.

12.3.2. β / ϕ_1 :

12.3.2.1. *Charmonium modes:*

CP-violation measurements in B-meson decays provide direct information on the angles of the unitarity triangle, shown in Fig. 12.1. These overconstraining measurements serve to improve the determination of the CKM elements, or to reveal effects beyond the SM.

The time-dependent CP asymmetry of neutral B decays to a final state f common to B^0 and $\overline{B}^0$ is given by [92,93]

$$\mathcal{A}_f = \frac{\Gamma(\overline{B}^0(t) \to f) - \Gamma(B^0(t) \to f)}{\Gamma(\overline{B}^0(t) \to f) + \Gamma(B^0(t) \to f)} = S_f \sin(\Delta m_d\, t) - C_f \cos(\Delta m_d\, t), \quad (12.18)$$

where

$$S_f = \frac{2\,\mathrm{Im}\lambda_f}{1 + |\lambda_f|^2}, \qquad C_f = \frac{1 - |\lambda_f|^2}{1 + |\lambda_f|^2}, \qquad \lambda_f = \frac{q}{p}\frac{\bar{A}_f}{A_f}. \quad (12.19)$$

Here, q/p describes B^0–$\overline{B}^0$ mixing and, to a good approximation in the SM, $q/p = V_{tb}^* V_{td}/V_{tb}V_{td}^* = e^{-2i\beta + \mathcal{O}(\lambda^4)}$ in the usual phase convention. A_f ($\bar{A}_f$) is the amplitude of the $B^0 \to f$ ($\overline{B}^0 \to f$) decay. If f is a CP eigenstate, and amplitudes with one CKM phase dominate the decay, then $|A_f| = |\bar{A}_f|$, $C_f = 0$, and $S_f = \sin(\arg\lambda_f) = \eta_f \sin 2\phi$, where η_f is the CP eigenvalue of f and 2ϕ is the phase difference between the $B^0 \to f$ and $B^0 \to \overline{B}^0 \to f$ decay paths. A contribution of another amplitude to the decay with a different CKM phase makes the value of S_f sensitive to relative strong interaction phases between the decay amplitudes (it also makes $C_f \neq 0$ possible).

The $b \to c\bar{c}s$ decays to CP eigenstates ($B^0 \to$ charmonium $K_{S,L}^0$) are the theoretically cleanest examples, measuring $S_f = -\eta_f \sin 2\beta$. The $b \to sq\bar{q}$ penguin amplitudes have dominantly the same weak phase as the $b \to c\bar{c}s$ tree amplitude. Since only λ^2-suppressed penguin amplitudes introduce a new CP-violating phase, amplitudes with a single weak phase dominate, and we expect $\big||\bar{A}_{\psi K}/A_{\psi K}| - 1\big| < 0.01$. The e^+e^- asymmetric-energy B-factory experiments, *BABAR* [95] and Belle [96], provide precise measurements. The world average including LHCb [97] and other measurements is [98]

$$\sin 2\beta = 0.682 \pm 0.019\,. \quad (12.20)$$

This measurement has a four-fold ambiguity in β, which can be resolved by a global fit as mentioned in Sec. 12.4. Experimentally, the two-fold ambiguity $\beta \to \pi/2 - \beta$ (but not $\beta \to \pi + \beta$) can be resolved by a time-dependent angular analysis of $B^0 \to J/\psi K^{*0}$ [99,100], or a time-dependent Dalitz plot analysis of $B^0 \to \overline{D}^0 h^0$ ($h^0 = \pi^0, \eta, \omega$) with $\overline{D}^0 \to K_S^0\pi^+\pi^-$ [101,102]. These results indicate that negative $\cos 2\beta$ solutions are very unlikely, in agreement with the global CKM fit result.

The $b \to c\bar{c}d$ mediated transitions, such as $B^0 \to J/\psi\pi^0$ and $B^0 \to D^{(*)+}D^{(*)-}$, also measure approximately $\sin 2\beta$. However, the dominant component of the $b \to d$ penguin amplitude has a different CKM phase ($V_{tb}^*V_{td}$) than the tree amplitude ($V_{cb}^*V_{cd}$), and its magnitudes are of the same order in λ. Therefore, the effect of penguins could be large, resulting in $S_f \neq -\eta_f \sin 2\beta$ and $C_f \neq 0$. These decay modes have also been measured by *BABAR* and Belle. The world averages [98], $S_{J/\psi\pi^0} = -0.93 \pm 0.15$, $S_{D^+D^-} = -0.98 \pm 0.17$, and $S_{D^{*+}D^{*-}} = -0.71 \pm 0.09$ ($\eta_f = +1$ for these modes), are consistent with $\sin 2\beta$ obtained from $B^0 \to$ charmonium K^0 decays, and the C_f's are consistent with zero, although the uncertainties are sizable.

The $b \to c\bar{u}d$ decays, $B^0 \to \overline{D}^0 h^0$ with $\overline{D}^0 \to CP$ eigenstates, have no penguin contributions and provide theoretically clean $\sin 2\beta$ measurements. *BABAR* measured $S_{D^{(*)}h^0} = -0.56 \pm 0.25$ [94].

12.3.2.2. *Penguin-dominated modes:*

The $b \to s\bar{q}q$ penguin-dominated decays have the same CKM phase as the $b \to c\bar{c}s$ tree level decays, up to corrections suppressed by λ^2, since $V_{tb}^*V_{ts} = -V_{cb}^*V_{cs}[1 + \mathcal{O}(\lambda^2)]$. Therefore, decays such as $B^0 \to \phi K^0$ and $\eta' K^0$ provide $\sin 2\beta$ measurements in the SM. Any new physics contribution to the amplitude with a different weak phase would give rise to $S_f \neq -\eta_f \sin 2\beta$, and possibly $C_f \neq 0$. Therefore, the main interest in these modes is not simply to measure $\sin 2\beta$, but to search for new physics. Measurements of many other decay modes in this category, such as $B \to \pi^0 K_S^0$, $K_S^0 K_S^0 K_S^0$, *etc.*, have also been performed by *BABAR* and Belle. The results and their uncertainties are summarized in Fig. 12.3 and Table 12.1 of Ref. 93.

12.3.3. α / ϕ_2 :

Since α is the phase between $V_{tb}^*V_{td}$ and $V_{ub}^*V_{ud}$, only time-dependent CP asymmetries in $b \to u\bar{u}d$ decay dominated modes can directly measure $\sin 2\alpha$, in contrast to $\sin 2\beta$, where several different transitions can be used. Since $b \to d$ penguin amplitudes have a different CKM phase than $b \to u\bar{u}d$ tree amplitudes, and their magnitudes are of the same order in λ, the penguin contribution can be sizable, which makes the determination of α complicated. To date, α has been measured in $B \to \pi\pi$, $\rho\pi$ and $\rho\rho$ decay modes.

12.3.3.1. $B \to \pi\pi$*:*

It is now experimentally well established that there is a sizable contribution of $b \to d$ penguin amplitudes in $B \to \pi\pi$ decays. Thus, $S_{\pi^+\pi^-}$ in the time-dependent $B^0 \to \pi^+\pi^-$ analysis does not measure $\sin 2\alpha$, but

$$S_{\pi^+\pi^-} = \sqrt{1 - C_{\pi^+\pi^-}^2}\, \sin(2\alpha + 2\Delta\alpha), \quad (12.21)$$

where $2\Delta\alpha$ is the phase difference between $e^{2i\gamma}\bar{A}_{\pi^+\pi^-}$ and $A_{\pi^+\pi^-}$. The value of $\Delta\alpha$, hence α, can be extracted using the isospin relation among the amplitudes of $B^0 \to \pi^+\pi^-$, $B^0 \to \pi^0\pi^0$, and $B^+ \to \pi^+\pi^0$ decays [103],

$$\frac{1}{\sqrt{2}}\, A_{\pi^+\pi^-} + A_{\pi^0\pi^0} - A_{\pi^+\pi^0} = 0\,, \quad (12.22)$$

and a similar expression for the $\bar{A}_{\pi\pi}$'s. This method utilizes the fact that a pair of pions from $B \to \pi\pi$ decay must be in a zero angular momentum state, and, because of Bose statistics, they must have even isospin. Consequently, $\pi^0\pi^\pm$ is in a pure isospin-2 state, while the penguin amplitudes only contribute to the isospin-0 final state. The

latter does not hold for the electroweak penguin amplitudes, but their effect is expected to be small. The isospin analysis uses the world averages [98,104] $S_{\pi^+\pi^-} = -0.66 \pm 0.06$, $C_{\pi^+\pi^-} = -0.31 \pm 0.05$, the branching fractions of all three modes, and the direct CP asymmetry $C_{\pi^0\pi^0} = -0.43^{+0.25}_{-0.24}$. This analysis leads to 16 mirror solutions for $0 \le \alpha < 2\pi$. Because of this, and the sizable experimental error of the $B^0 \to \pi^0\pi^0$ rate and CP asymmetry, only a loose constraint on α can be obtained at present [105], $0° < \alpha < 10.1°$, $80.0° < \alpha < 104.0°$, $119.0° < \alpha < 151.0°$, and $165.2° < \alpha < 180°$ at 68% CL.

12.3.3.2. $B \to \rho\rho$:

The decay $B^0 \to \rho^+\rho^-$ contains two vector mesons in the final state, which in general is a mixture of CP-even and CP-odd components. Therefore, it was thought that extracting α from this mode would be complicated.

However, the longitudinal polarization fractions (f_L) in $B^+ \to \rho^+\rho^0$ and $B^0 \to \rho^+\rho^-$ decays were measured to be close to unity [106], which implies that the final states are almost purely CP-even. Furthermore, $\mathcal{B}(B^0 \to \rho^0\rho^0) = (0.97 \pm 0.24) \times 10^{-6}$ is much smaller than $\mathcal{B}(B^0 \to \rho^+\rho^-) = (24.2^{+3.1}_{-3.2}) \times 10^{-6}$ and $\mathcal{B}(B^+ \to \rho^+\rho^0) = (24.0^{+1.9}_{-2.0}) \times 10^{-6}$ [65], which implies that the effect of the penguin diagrams is small. The isospin analysis using the world averages, $S_{\rho^+\rho^-} = -0.05 \pm 0.17$ and $C_{\rho^+\rho^-} = -0.06 \pm 0.13$ [65], together with the time-dependent CP asymmetry, $S_{\rho^0\rho^0} = -0.3 \pm 0.7$ and $C_{\rho^0\rho^0} = -0.2 \pm 0.9$ [107], and the above-mentioned branching fractions, gives $0° < \alpha < 5.4°$, $84.6° < \alpha < 95.3°$ and $174.8° < \alpha < 180°$ at 68% CL [105], with mirror solutions at $3\pi/2 - \alpha$. A possible small violation of Eq. (12.22) due to the finite width of the ρ [108] is neglected.

12.3.3.3. $B \to \rho\pi$:

The final state in $B^0 \to \rho^+\pi^-$ decay is not a CP eigenstate, but this decay proceeds via the same quark-level diagrams as $B^0 \to \pi^+\pi^-$, and both B^0 and $\overline{B}{}^0$ can decay to $\rho^+\pi^-$. Consequently, mixing-induced CP violations can occur in four decay amplitudes, $B^0 \to \rho^\pm\pi^\mp$ and $\overline{B}{}^0 \to \rho^\pm\pi^\mp$. The time-dependent Dalitz plot analysis of $B^0 \to \pi^+\pi^-\pi^0$ decays permits the extraction of α with a single discrete ambiguity, $\alpha \to \alpha + \pi$, since one knows the variation of the strong phases in the interference regions of the $\rho^+\pi^-$, $\rho^-\pi^+$, and $\rho^0\pi^0$ amplitudes in the Dalitz plot [109]. The combination of Belle [110] and *BABAR* [111] measurements gives $\alpha = (54.1^{+7.7}_{-10.3})°$ and $(141.8^{+4.7}_{-5.4})°$ [105]. This constraint is still moderate.

Combining the $B \to \pi\pi$, $\rho\pi$, and $\rho\rho$ decay modes [105], α is constrained as

$$\alpha = (85.4^{+3.9}_{-3.8})°. \tag{12.23}$$

A different statistical approach [112] gives similar constraint from the combination of these measurements.

12.3.4. γ / ϕ_3 :

By virtue of Eq. (12.16), γ does not depend on CKM elements involving the top quark, so it can be measured in tree-level B decays. This is an important distinction from the measurements of α and β, and implies that the measurements of γ are unlikely to be affected by physics beyond the SM.

12.3.4.1. $B^\pm \to DK^\pm$:

The interference of $B^- \to D^0K^-$ ($b \to c\bar{u}s$) and $B^- \to \overline{D}{}^0K^-$ ($b \to u\bar{c}s$) transitions can be studied in final states accessible in both D^0 and $\overline{D}{}^0$ decays [92]. In principle, it is possible to extract the B and D decay amplitudes, the relative strong phases, and the weak phase γ from the data.

A practical complication is that the precision depends sensitively on the ratio of the interfering amplitudes

$$r_B = \left| A(B^- \to \overline{D}{}^0K^-)/A(B^- \to D^0K^-) \right|, \tag{12.24}$$

which is around 0.1−0.2. The original GLW method [113,114] considers D decays to CP eigenstates, such as $B^\pm \to D^{(*)}_{CP}(\to \pi^+\pi^-)K^{\pm(*)}$. To alleviate the smallness of r_B and make the interfering amplitudes (which are products of the B and D decay amplitudes) comparable in magnitude, the ADS method [115] considers final states where Cabibbo-allowed $\overline{D}{}^0$ and doubly-Cabibbo-suppressed D^0 decays interfere. Extensive measurements have been made by the B factories [116,117], CDF [118] and LHCb [119] using both methods.

It was realized that both D^0 and $\overline{D}{}^0$ have large branching fractions to certain three-body final states, such as $K_S\pi^+\pi^-$, and the analysis can be optimized by studying the Dalitz plot dependence of the interferences [120,121]. The best present determination of γ comes from this method. Belle [122] and *BABAR* [123] obtained $\gamma = (78^{+11}_{-12} \pm 4 \pm 9)°$ and $\gamma = (68 \pm 14 \pm 4 \pm 3)°$, respectively, where the last uncertainty is due to the D-decay modeling. (LHCb also measured $\gamma = (44^{+43}_{-38})°$ with the same method [124].) The error is sensitive to the central value of the amplitude ratio r_B (and r_B^* for the D^*K mode), for which Belle found somewhat larger central values than *BABAR*. The same values of $r_B^{(*)}$ enter the ADS analyses, and the data can be combined to fit for $r_B^{(*)}$ and γ. The D^0–$\overline{D}{}^0$ mixing has been neglected in all measurements, but its effect on γ is far below the present experimental accuracy [125], unless D^0–$\overline{D}{}^0$ mixing is due to CP-violating new physics, in which case it can be included in the analysis [126].

Combining the GLW, ADS, and Dalitz analyses [105], γ is constrained as

$$\gamma = (68.0^{+8.0}_{-8.5})°. \tag{12.25}$$

Similar results are found in Ref. [112].

12.3.4.2. $B^0 \to D^{(*)\pm}\pi^\mp$:

The interference of $b \to u$ and $b \to c$ transitions can be studied in $\overline{B}{}^0 \to D^{(*)+}\pi^-$ ($b \to c\bar{u}d$) and $\overline{B}{}^0 \to B^0 \to D^{(*)+}\pi^-$ ($\bar{b} \to \bar{u}c\bar{d}$) decays and their CP conjugates, since both B^0 and $\overline{B}{}^0$ decay to $D^{(*)\pm}\pi^\mp$ (or $D^\pm\rho^\mp$, *etc.*). Since there are only tree and no penguin contributions to these decays, in principle, it is possible to extract from the four time-dependent rates the magnitudes of the two hadronic amplitudes, their relative strong phase, and the weak phase between the two decay paths, which is $2\beta + \gamma$.

A complication is that the ratio of the interfering amplitudes is very small, $r_{D\pi} = A(B^0 \to D^+\pi^-)/A(\overline{B}{}^0 \to D^+\pi^-) = \mathcal{O}(0.01)$ (and similarly for $r_{D^*\pi}$ and $r_{D\rho}$), and therefore it has not been possible to measure it. To obtain $2\beta + \gamma$, $SU(3)$ flavor symmetry and dynamical assumptions have been used to relate $A(\overline{B}{}^0 \to D^-\pi^+)$ to $A(\overline{B}{}^0 \to D_s^-\pi^+)$, so this measurement is not model-independent at present. Combining the $D^\pm\pi^\mp$, $D^{*\pm}\pi^\mp$ and $D^\pm\rho^\mp$ measurements [127] gives $\sin(2\beta + \gamma) > 0.68$ at 68% CL [105], consistent with the previously discussed results for β and γ. The amplitude ratio is much larger in the analogous $B_s^0 \to D_s^\pm K^\mp$ decays, which will allow a model-independently extraction of $\gamma - 2\beta_s$ [128] at LHCb [129] (here $\beta_s = \arg(-V_{ts}V_{tb}^*/V_{cs}V_{cb}^*)$ is related to the phase of B_s mixing).

12.4. Global fit in the Standard Model

Using the independently measured CKM elements mentioned in the previous sections, the unitarity of the CKM matrix can be checked. We obtain $|V_{ud}|^2 + |V_{us}|^2 + |V_{ub}|^2 = 0.9999 \pm 0.0006$ (1st row), $|V_{cd}|^2 + |V_{cs}|^2 + |V_{cb}|^2 = 1.024 \pm 0.032$ (2nd row), $|V_{ud}|^2 + |V_{cd}|^2 + |V_{td}|^2 = 1.000 \pm 0.004$ (1st column), and $|V_{us}|^2 + |V_{cs}|^2 + |V_{ts}|^2 = 1.025 \pm 0.032$ (2nd column), respectively. The uncertainties in the second row and column are dominated by that of $|V_{cs}|$. For the second row, a slightly better check is obtained from the measurement of $\sum_{u,c,d,s,b} |V_{ij}|^2$ in Sec. 12.2.4 minus the sum in the first row above: $|V_{cd}|^2 + |V_{cs}|^2 + |V_{cb}|^2 = 1.002 \pm 0.027$. These provide strong tests of the unitarity of the CKM matrix. With the significantly improved direct determination of $|V_{tb}|$, the unitarity checks for the third row and column have also become fairly precise, leaving decreasing room for mixing with other states. The sum of the three angles of the unitarity triangle, $\alpha + \beta + \gamma = (175 \pm 9)°$, is also consistent with the SM expectation.

The CKM matrix elements can be most precisely determined using a global fit to all available measurements and imposing the SM constraints (*i.e.*, three generation unitarity). The fit must also use theory predictions for hadronic matrix elements, which

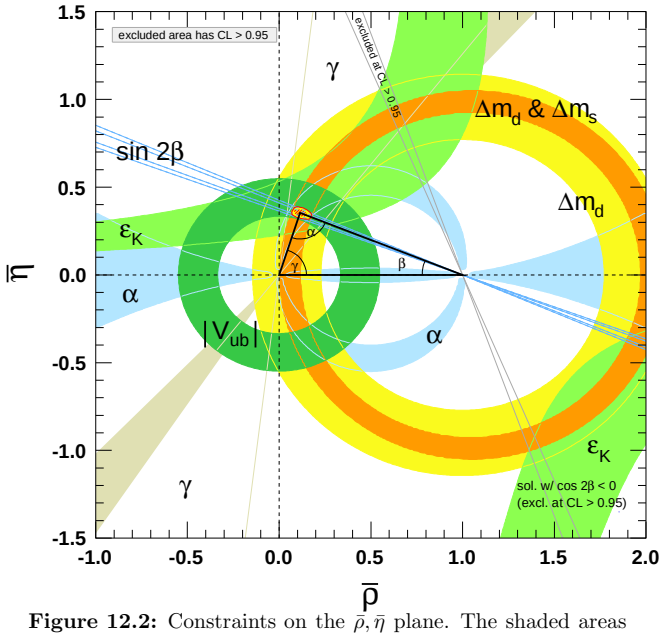

Figure 12.2: Constraints on the $\bar{\rho}, \bar{\eta}$ plane. The shaded areas have 95% CL.

sometimes have significant uncertainties. There are several approaches to combining the experimental data. CKMfitter [6,105] and Ref. 130 (which develops [131,132] further) use frequentist statistics, while UTfit [112,133] uses a Bayesian approach. These approaches provide similar results.

The constraints implied by the unitarity of the three generation CKM matrix significantly reduce the allowed range of some of the CKM elements. The fit for the Wolfenstein parameters defined in Eq. (12.4) gives

$$\lambda = 0.22537 \pm 0.00061\,, \qquad A = 0.814^{+0.023}_{-0.024}\,,$$
$$\bar{\rho} = 0.117 \pm 0.021\,, \qquad \bar{\eta} = 0.353 \pm 0.013\,. \qquad (12.26)$$

These values are obtained using the method of Refs. [6,105]. Using the prescription of Refs. [112,133] gives $\lambda = 0.2255 \pm 0.0006$, $A = 0.818 \pm 0.015$, $\bar{\rho} = 0.124 \pm 0.024$, $\bar{\eta} = 0.354 \pm 0.015$ [134]. The fit results for the magnitudes of all nine CKM elements are

$$V_{\rm CKM} = \begin{pmatrix} 0.97427 \pm 0.00014 & 0.22536 \pm 0.00061 & 0.00355 \pm 0.00015 \\ 0.22522 \pm 0.00061 & 0.97343 \pm 0.00015 & 0.0414 \pm 0.0012 \\ 0.00886^{+0.00033}_{-0.00032} & 0.0405^{+0.0011}_{-0.0012} & 0.99914 \pm 0.00005 \end{pmatrix}, \qquad (12.27)$$

and the Jarlskog invariant is $J = (3.06^{+0.21}_{-0.20}) \times 10^{-5}$.

Figure 12.2 illustrates the constraints on the $\bar{\rho}, \bar{\eta}$ plane from various measurements and the global fit result. The shaded 95% CL regions all overlap consistently around the global fit region.

12.5. Implications beyond the SM

The effects in B, B_s, K, and D decays and mixings due to high-scale physics (W, Z, t, H in the SM, and unknown heavier particles) can be parameterized by operators composed of SM fields, obeying the $SU(3) \times SU(2) \times U(1)$ gauge symmetry. Flavor-changing neutral currents, suppressed in the SM, are especially sensitive to beyond SM (BSM) contributions. Processes studied in great detail, both experimentally and theoretically, include neutral meson mixings, $B_{(s)} \to X\gamma$, $X\ell^+\ell^-$, $\ell^+\ell^-$, $K \to \pi\nu\bar{\nu}$, etc. The BSM contributions to these operators are suppressed by powers of the scale of new physics. Already at lowest order, there are many dimension-6 operators, and the observable effects of BSM interactions are encoded in their coefficients. In the SM, these coefficients are determined by just the four CKM parameters, and the W, Z, and quark masses. For example, Δm_d, $\Gamma(B \to \rho\gamma)$, $\Gamma(B \to \pi\ell^+\ell^-)$, and $\Gamma(B \to \ell^+\ell^-)$ are all proportional to $|V_{td}V_{tb}|^2$ in the SM, however, they may receive unrelated contributions from new physics. The new physics contributions may or may not obey the SM relations. (For example, the flavor sector of the MSSM contains 69 CP-conserving parameters and 41 CP-violating phases, *i.e.*, 40 new ones [135]). Thus, similar to the measurements of $\sin 2\beta$ in tree- and loop-dominated decay modes, overconstraining measurements of the magnitudes and phases of flavor-changing neutral-current amplitudes give good sensitivity to new physics.

To illustrate the level of suppression required for BSM contributions, consider a class of models in which the unitarity of the CKM matrix is maintained, and the dominant effect of new physics is to modify the neutral meson mixing amplitudes [136] by $(z_{ij}/\Lambda^2)(\overline{q}_i\gamma^\mu P_L q_j)^2$ (for recent reviews, see [137,138]). It is only known since the measurements of γ and α that the SM gives the leading contribution to $B^0 - \overline{B}^0$ mixing [6,139]. Nevertheless, new physics with a generic weak phase may still contribute to neutral meson mixings at a significant fraction of the SM [140,141,133]. The existing data imply that $\Lambda/|z_{ij}|^{1/2}$ has to exceed about 10^4 TeV for $K^0 - \overline{K}^0$ mixing, 10^3 TeV for $D^0 - \overline{D}^0$ mixing, 500 TeV for $B^0 - \overline{B}^0$ mixing, and 100 TeV for $B_s^0 - \overline{B}_s^0$ mixing [133,138]. (Some other operators are even better constrained [133].) The constraints are the strongest in the kaon sector, because the CKM suppression is the most severe. Thus, if there is new physics at the TeV scale, $|z_{ij}| \ll 1$ is required. Even if $|z_{ij}|$ are suppressed by a loop factor and $|V_{ti}^* V_{tj}|^2$ (in the down quark sector), similar to the SM, one expects percent-level effects, which may be observable in forthcoming flavor physics experiments. To constrain such extensions of the SM, many measurements irrelevant for the SM-CKM fit, such as the CP asymmetry in semileptonic $B_{d,s}^0$ decays, $A_{\rm SL}^{d,s}$, are important [142]. A DØ measurement sensitive to certain linear combinations of $A_{\rm SL}^d$ and $A_{\rm SL}^s$ shows a 3.6σ hint of a deviation from the SM [143].

Many key measurements which are sensitive to BSM flavor physics are not useful to think about in terms of constraining the unitarity triangle in Fig. 12.1. For example, besides the angles in Eq. (12.16), a key quantity in the B_s system is $\beta_s = \arg(-V_{ts}V_{tb}^*/V_{cs}V_{cb}^*)$, which is the small, λ^2-suppressed, angle of a "squashed" unitarity triangle, obtained by taking the scalar product of the second and third columns. This angle can be measured via time-dependent CP violation in $B_s^0 \to J/\psi\,\phi$, similar to β in $B^0 \to J/\psi K^0$. Since the $J/\psi\,\phi$ final state is not a CP eigenstate, an angular analysis of the decay products is needed to separate the CP-even and CP-odd components, which give opposite asymmetries. In the SM, the asymmetry for the CP-even part is $2\beta_s$ (sometimes the notation $\phi_s = -2\beta_s$ plus a possible BSM contribution to the B_s mixing phase is used). Testing if the data agree with the SM prediction, $2\beta_s = 0.0363 \pm 0.0018$ [105], is another sensitive test of the SM. After the first Tevatron CP-asymmetry measurements of $B_s^0 \to J/\psi\phi$ hinted at a possible tension with the SM, the current world average, dominated by LHCb [145] and including $B_s \to J/\psi\,K^+K^-$ and $J/\psi\,\pi^+\pi^-$ measurements, is $2\beta_s = 0.00 \pm 0.07$ [65]. This uncertainty is about 40 times the SM uncertainty; thus a lot will be learned from higher precision measurements in the future.

In the kaon sector, the two measured CP-violating observables ϵ and ϵ' are tiny, so models in which all sources of CP violation are small were viable before the B-factory measurements. Since the measurement of $\sin 2\beta$, we know that CP violation can be an $\mathcal{O}(1)$ effect, and only flavor mixing is suppressed between the three quark generations. Thus, many models with spontaneous CP violation are excluded. In the kaon sector, a very clean test of the SM will come from measurements of $K^+ \to \pi^+\nu\bar{\nu}$ and $K_L^0 \to \pi^0\nu\bar{\nu}$. These loop-induced rare decays are sensitive to new physics, and will allow a determination of β, independent of its value measured in B decays [146].

The CKM elements are fundamental parameters, so they should be measured as precisely as possible. The overconstraining measurements of CP asymmetries, mixing, semileptonic, and rare decays severely constrain the magnitudes and phases of possible new physics contributions to flavor-changing interactions. If new particles are observed at the LHC, it will be important to explore their flavor parameters as precisely as possible to understand the underlying physics.

References:

1. N. Cabibbo, Phys. Rev. Lett. **10**, 531 (1963).
2. M. Kobayashi and T. Maskawa, Prog. Theor. Phys. **49**, 652 (1973).
3. L.L. Chau and W.Y. Keung, Phys. Rev. Lett. **53**, 1802 (1984).
4. L. Wolfenstein, Phys. Rev. Lett. **51**, 1945 (1983).
5. A.J. Buras *et al.*, Phys. Rev. **D50**, 3433 (1994) [hep-ph/9403384].
6. J. Charles *et al.* [CKMfitter Group], Eur. Phys. J. **C41**, 1 (2005) [hep-ph/0406184].
7. C. Jarlskog, Phys. Rev. Lett. **55**, 1039 (1985).
8. J.C. Hardy and I. S. Towner, Phys. Rev. **C70**, 055502 (2009) [arXiv:0812.1202].
9. E. Blucher and W.J. Marciano, "V_{ud}, V_{us}, the Cabibbo Angle and CKM Unitarity," in this *Review*.
10. D. Pocanic *et al.*, Phys. Rev. Lett. **93**, 181803 (2004) [hep-ex/0312030].
11. M. Antonelli *et al.* [The FlaviaNet Kaon Working Group], arXiv:0801.1817; see also http://www.lnf.infn.it/wg/vus.
12. P.A. Boyle *et al.* Eur. Phys. J. **C69**, 159 (2010) [arXiv:1004.0886 [hep-lat]]; P.A. Boyle *et al.* Phys. Rev. Lett. **100**, 141601 (2008).
13. S. Aoki *et al.*, "Review of lattice results concerning low energy particle physics," arXiv:1310.8555, http://itpwiki.unibe.ch/flag.
14. R. Kowalewski and T. Mannel, "Determination of V_{cb} and V_{ub}," in this *Review*.
15. H. Leutwyler and M. Roos, Z. Phys. **C25**, 91 (1984).
16. J. Bijnens and P. Talavera, Nucl. Phys. **B669**, 341 (2003) [hep-ph/0303103];
    M. Jamin *et al.*, JHEP **402**, 047 (2004) [hep-ph/0401080];
    V. Cirigliano *et al.*, JHEP **504**, 6 (2005) [hep-ph/0503108];
    C. Dawson *et al.*, PoS **LAT2005**, 337 (2005) [hep-lat/0510018];
    N. Tsutsui *et al.* [JLQCD Collab.], PoS **LAT2005**, 357 (2005) [hep-lat/0510068];
    M. Okamoto [Fermilab Lattice Collab.], hep-lat/0412044.
17. W.J. Marciano, Phys. Rev. Lett. **93**, 231803 (2004) [hep-ph/0402299].
18. F. Ambrosino *et al.* [KLOE Collab.], Phys. Lett. **B632**, 76 (2006) [hep-ex/0509045].
19. A. Bazavov *et al.* [MILC Collab.], Phys. Rev. Lett. **110**, 172003 (2013) [arXiv:1301.5855].
20. C. Bernard *et al.* [MILC Collab.], PoS **LAT2007**, 090 (2006) [arXiv:0710.1118].
21. N. Cabibbo *et al.*, Ann. Rev. Nucl. and Part. Sci. **53**, 39 (2003) [hep-ph/0307298];
    Phys. Rev. Lett. **92**, 251803 (2004) [hep-ph/0307214].
22. M. Ademollo and R. Gatto, Phys. Rev. Lett. **13**, 264 (1964).
23. I.M. Nugent, arXiv:1301.0637.
24. B. Aubert *et al.* [*BABAR* Collab.], Phys. Rev. Lett. **105**, 051602 (2010) [arXiv:0912.0242].
25. D. Besson *et al.* [CLEO Collab.], Phys. Rev. **D80**, 032005 (2009) [arXiv:0906.2983].
26. L. Widhalm *et al.* [Belle Collab.], Phys. Rev. Lett. **97**, 061804 (2006) [hep-ex/0604049].
27. H. Abramowicz *et al.* [CHDS Collab.], Z. Phys. **C15**, 19 (1982).
28. S.A. Rabinowitz *et al.* [CCFR Collab.], Phys. Rev. Lett. **70**, 134 (1993).
29. A.O. Bazarko *et al.* [CCFR Collab.], Z. Phys. **C65**, 189 (1995) [hep-ex/9406007].
30. P. Vilain *et al.* [CHARM II Collab.], Eur. Phys. J. **C11**, 19 (1999).
31. F.J. Gilman *et al.*, Phys. Lett. **B592**, 793 (2004).
32. G.D. Lellis *et al.*, Phys. Rept. **399**, 227 (2004) [Erratum *ibid.* **411**, 323 (2005)].
33. N. Ushida *et al.* [Fermilab E531 Collab.], Phys. Lett. **B206**, 380 (1988).
34. T. Bolton, hep-ex/9708014.
35. A. Kayis-Topaksu *et al.* [CHORUS Collab.], Phys. Lett. **B626**, 24 (2005).
36. A. Zupanc *et al.* [Belle Collab.], JHEP **1309**, 139 (2013) [arXiv:1307.6240].
37. J.P. Alexander *et al.* [CLEO Collab.], Phys. Rev. **D79**, 052001 (2009) [arXiv:0901.1216].
38. P. del Amo Sanchez *et al.* [*BABAR* Collab.], Phys. Rev. **D82**, 091103 (2010) [arXiv:1008.4080].
39. J. Rosner and S. Stone, "Leptonic Decays of Charged Pseudoscalar Leptons," in this *Review*.
40. P.U.E. Onyisi *et al.* [CLEO Collab.], Phys. Rev. **D79**, 052002 (2009) [arXiv:0901.1147].
41. P. Naik *et al.* [CLEO Collab.], Phys. Rev. **D80**, 112004 (2009) [arXiv:0910.3602].
42. B. Aubert *et al.* [*BABAR* Collab.], Phys. Rev. **D76**, 052005 (2007) [arXiv:0704.0020].
43. LEP W branching fraction results for this Review of Particle Physics, LEPEWWG/ XSEC/2005-01, http://lepewwg.web.cern.ch/LEPEWWG/lepww/4f/Winter05/.
44. P. Abreu *et al.* [DELPHI Collab.], Phys. Lett. **B439**, 209 (1998).
45. I.I.Y. Bigi *et al.*, Phys. Rev. Lett. **71**, 496 (1993) [hep-ph/9304225].
46. A.V. Manohar and M.B. Wise, Phys. Rev. **D49**, 1310 (1994) [hep-ph/9308246].
47. I.I.Y. Bigi *et al.*, Phys. Rev. **D56**, 4017 (1997) [hep-ph/9704245].
48. A.H. Hoang *et al.*, Phys. Rev. **D59**, 074017 (1999) [hep-ph/9811239]; Phys. Rev. Lett. **82**, 277 (1999) [hep-ph/9809423];
    A.H. Hoang and T. Teubner, Phys. Rev. **D60**, 114027 (1999) [hep-ph/9904468].
49. N. Isgur and M.B. Wise, Phys. Lett. **B237**, 527 (1990);
    N. Isgur and M.B. Wise, Phys. Lett. **B232**, 113 (1989).
50. J.P. Lees *et al.* [*BABAR* Collab.], Phys. Rev. Lett. **109**, 101802 (2012) [arXiv:1205.5442].
51. M. Neubert, Phys. Rev. **D49**, 3392 (1994) [hep-ph/9311325]; Phys. Rev. **D49**, 4623 (1994) [hep-ph/9312311].
52. I.I.Y. Bigi *et al.*, Int. J. Mod. Phys. **A9**, 2467 (1994) [hep-ph/9312359].
53. C.W. Bauer *et al.*, Phys. Lett. **B479**, 395 (2000) [hep-ph/0002161];
    Phys. Rev. **D64**, 113004 (2001) [hep-ph/0107074].
54. A. Bornheim *et al.* [CLEO Collab.], Phys. Rev. Lett. **88**, 231803 (2002) [hep-ex/0202019].
55. B. Aubert *et al.* [*BABAR* Collab.], Phys. Rev. **D73**, 012006 (2006) [hep-ex/0509040].
56. A. Limosani *et al.* [Belle Collab.], Phys. Lett. **B621**, 28 (2005) [hep-ex/0504046].
57. P. Urquijo *et al.* [Belle Collab.], Phys. Rev. Lett. **104**, 021801 (2010) [arXiv:0907.0379];
    B. Aubert *et al.* [*BABAR* Collab.], Phys. Rev. Lett. **100**, 171802 (2008) [arXiv:0708.3702].
58. E. Dalgic *et al.*, Phys. Rev. **D73**, 074502 (2006) [Erratum *ibid.* **D75**, 119906 (2007)] [hep-lat/0601021].
59. J.A. Bailey *et al.* [Fermilab Lattice and MILC Collabs.], Phys. Rev. **D79**, 054507 (2009) [arXiv:0811.3640].
60. P. Ball and R. Zwicky, Phys. Rev. **D71**, 014015 (2005) [hep-ph/0406232]; A. Khodjamirian *et al.*, Phys. Rev. **D83**, 094031 (2011) [arXiv:1103.2655].
61. H. Albrecht *et al.* [ARGUS Collab.], Phys. Lett. **B192**, 245 (1987).
62. O. Schneider, "B^0–$\overline{B}^0$ mixing," in this *Review*.
63. A. Abulencia *et al.* [CDF Collab.], Phys. Rev. Lett. **97**, 242003 (2006) [hep-ex/0609040].
64. R. Aaij *et al.* [LHCb Collab.], New J. Phys. 15, 053021 (2013) [arXiv:1304.4741].
65. Y. Amhis *et al.*, Heavy Flavor Averaging Group, arXiv:1207.1158, and updates at http://www.slac.stanford.edu/xorg/hfag/.
66. "$B^{\pm}$ meson" particle listing, in this *Review*.
67. Heavy Flavor Averaging Group [65], and updates for Rare Decays at http://www.slac.stanford.edu/xorg/hfag/rare/index.html.

68. M. Misiak *et al.*, Phys. Rev. Lett. **98**, 022002 (2007) [hep-ph/0609232].
69. R. Aaij *et al.* [LHCb Collab.], Phys. Rev. Lett. **111**, 101805 (2013) [arXiv:1307.5024]; S. Chatrchyan *et al.* [CMS Collab.], Phys. Rev. Lett. **111**, 101804 (2013) [arXiv:1307.5025]; CMS and LHCb Collabs., CMS-PAS-BPH-13-007, LHCb-CONF-2013-012.
70. B. Grinstein and D. Pirjol, Phys. Rev. **D62**, 093002 (2000) [hep-ph/0002216];
A. Ali *et al.*, Phys. Lett. **B595**, 323 (2004) [hep-ph/0405075];
M. Beneke *et al.*, Nucl. Phys. **B612**, 25 (2001) [hep-ph/0106067];
S.W. Bosch and G. Buchalla, Nucl. Phys. **B621**, 459 (2002) [hep-ph/0106081];
Z. Ligeti and M. B. Wise, Phys. Rev. **D60**, 117506 (1999) [hep-ph/9905277];
D. Becirevic *et al.*, JHEP **305**, 7 (2003) [hep-lat/0301020];
P. Ball *et al.*, Phys. Rev. **D75**, 054004 (2007) [hep-ph/0612081];
W. Wang *et al.*, arXiv:0711.0432;
C.D. Lu *et al.*, Phys. Rev. **D76**, 014013 (2007) [hep-ph/0701265].
71. A. J. Buras *et al.*, Phys. Rev. Lett. **95**, 261805 (2005) [hep-ph/0508165].
72. A.V. Artamonov *et al.* [E949 Collab.], Phys. Rev. Lett. **101**, 191802 (2008) [arXiv:0808.2459]; Phys. Rev. **D79**, 092004 (2009) [arXiv:0903.0030].
73. D. Acosta *et al.* [CDF Collab.], Phys. Rev. Lett. **95**, 102002 (2005) [hep-ex/0505091].
74. V.M. Abazov *et al.* [DØ Collab.], Phys. Rev. Lett. **107**, 121802 (2011) [arXiv:1106.5436].
75. CMS-PAS-TOP-11-029 (2011) [CMS Collab.].
76. V.M. Abazov *et al.* [DØ Collab.], Phys. Lett. **B726**, 656 (2013) [arXiv:1307.0731].
77. T. Aaltonen *et al.* [CDF Collab.], CDF Note 10979 (2013); CDF Note 10793 (2012).
78. S. Chatrchyan *et al.* [CMS Collab.], JHEP **1212**, 035 (2012) [arXiv:1209.4533].
79. G. Aad *et al.* [ATLAS Collab.], Phys. Lett. **B717**, 330 (2012) [arXiv:1205.3130].
80. "Combination of single top-quark cross-sectrions measurements in the t-channel at $\sqrt{s} = 8$ TeV with the ATLAS and CMS experiments", CMS PAS TOP-12-002, ATLAS-CONF-2013-098.
81. J. Swain and L. Taylor, Phys. Rev. **D58**, 093006 (1998) [hep-ph/9712420].
82. "K^0_L meson" particle listing, in this *Review*.
83. G. Buchalla *et al.*, Rev. Mod. Phys. **68**, 1125 (1996) [hep-ph/9512380].
84. T. Inami and C.S. Lim, Prog. Theor. Phys. **65**, 297 (1981) [Erratum *ibid.* **65**, 1772 (1981)].
85. J.M. Flynn and L. Randall, Phys. Lett. **B224**, 221 (1989);
G. Buchalla, A. J. Buras, and M. K. Harlander, Nucl. Phys. **B337**, 313 (1990).
86. M. Ciuchini *et al.*, Phys. Lett. **B301**, 263 (1993) [hep-ph/9212203];
A.J. Buras, M. Jamin, and M.E. Lautenbacher, Nucl. Phys. **B408**, 209 (1993) [hep-ph/9303284].
87. T. Hambye *et al.*, Nucl. Phys. **B564**, 391 (2000) [hep-ph/9906434].
88. S. Bertolini *et al.*, Phys. Rev. **D63**, 056009 (2001) [hep-ph/0002234].
89. A. Pich, hep-ph/0410215.
90. L. Lellouch and M. Luscher, Comm. Math. Phys. **219**, 31 (2001) [hep-lat/0003023].
91. C.h. Kim *et al.*, Nucl. Phys. **B727**, 218 (2005) [hep-lat/0507006].
92. A.B. Carter and A.I. Sanda, Phys. Rev. Lett. **45**, 952 (1980); Phys. Rev. **D23**, 1567 (1981).
93. A more detailed discussion and references can be found in: D. Kirkby and Y. Nir, "CP violation in meson decays," in this *Review*.
94. B. Aubert *et al.* [BABAR Collab.], Phys. Rev. Lett. **99**, 081801 (2007) [hep-ex/0703019].
95. B. Aubert *et al.* [*BABAR* Collab.], Phys. Rev. **D79**, 072009 (2009) [arXiv:0902.1708].
96. I. Adachi *et al.* [Belle Collab.], Phys. Rev. Lett. **108**, 171802 (2012) [arXiv:1201.4643].
97. R. Aaij *et al.* [LHCb Collab.], Phys. Lett. **B721**, 24 (2013) [arXiv:1211.6093].
98. Heavy Flavor Averaging Group [65], Winter 2014 updates for Unitarity Triangle Parameters:http://www.slac.stanford.edu/xorg/hfag/triangle/winter2014/.
99. B. Aubert *et al.* [*BABAR* Collab.], Phys. Rev. **D71**, 032005 (2005) [hep-ex/0411016].
100. R. Itoh *et al.* [Belle Collab.], Phys. Rev. Lett. **95**, 091601 (2005) [hep-ex/0504030].
101. P. Krokovny *et al.* [Belle Collab.], Phys. Rev. Lett. **97**, 081801 (2006) [hep-ex/0507065].
102. B. Aubert *et al.* [*BABAR* Collab.], Phys. Rev. Lett. **99**, 231802 (2007) [arXiv:0708.1544].
103. M. Gronau and D. London, Phys. Rev. Lett. **65**, 3381 (1990).
104. Averages of $S_{\pi\pi}$ and $C_{\pi\pi}$ include the LHCb result, R. Aaij *et al.*, JHEP 1310, 183 (2013) [arXiv:1308.1428].
105. A. Höcker *et al.*, Eur. Phys. J. **C21**, 225 (2001) [hep-ph/0104062]; see also Ref. [6] and updates at http://ckmfitter.in2p3.fr/.
106. J. Zhang *et al.* [Belle Collab.], Phys. Rev. Lett. **91**, 221801 (2003) [hep-ex/0306007];
A. Somov *et al.* [Belle Collab.], Phys. Rev. Lett. **96**, 171801 (2006) [hep-ex/0601024];
B. Aubert *et al.* [*BABAR* Collab.], Phys. Rev. Lett. **97**, 261801 (2006) [hep-ex/0607092]; Phys. Rev. **D76**, 052007 (2007) [arXiv:0705.2157].
107. B. Aubert *et al.* [*BABAR* Collab.], Phys. Rev. **D78**, 071104 (2008) [arXiv:0807.4977].
108. A.F. Falk *et al.*, Phys. Rev. **D69**, 011502 (2004) [hep-ph/0310242].
109. H.R. Quinn and A.E. Snyder, Phys. Rev. **D48**, 2139 (1993).
110. A. Kusaka *et al.* [Belle Collab.], Phys. Rev. Lett. **98**, 221602 (2007) [hep-ex/0701015].
111. B. Aubert *et al.* [*BABAR* Collab.], Phys. Rev. **D88**, 121003 (2013) [arXiv:1304.3503].
112. M. Bona *et al.* [UTfit Collab.], JHEP **507**, 28 (2005) [hep-ph/0501199], and updates at http://www.utfit.org/.
113. M. Gronau and D. London, Phys. Lett. **B253**, 483 (1991).
114. M. Gronau and D. Wyler, Phys. Lett. **B265**, 172 (1991).
115. D. Atwood *et al.*, Phys. Rev. Lett. **78**, 3257 (1997) [hep-ph/9612433]; Phys. Rev. **D63**, 036005 (2001) [hep-ph/0008090].
116. P. del Amo Sanchez *et al.* [*BABAR* Collab.], Phys. Rev. **D82**, 072004 (2010) [arXiv:1007.0504]; B. Aubert *et al.* [*BABAR* Collab.], Phys. Rev. **D78**, 092002 (2008) [arXiv:0807.2408]; Phys. Rev. **D80**, 092001 (2009) [arXiv:0909.3981]; P. del Amo Sanchez *et al.* Phys. Rev. **D82**, 072006 (2010) [arXiv:1006.4241]; J.P. Lees *et al.* Phys. Rev. **D84**, 012002 (2011) [arXiv:1104.4472].
117. K. Abe *et al.* [Belle Collab.], Phys. Rev. **D73**, 051106 (2006) [hep-ex/0601032]; Y. Horii *et al.*, Phys. Rev. Lett. **106**, 231803 (2011) [arXiv:1103.5951].
118. T. Aaltonen *et al.* [CDF Collab.], Phys. Rev. **D81**, 031105 (2010) [arXiv:0911.0425].
119. R. Aaij *et al.* [LHCb Collab.], Phys. Lett. **B712**, 203 (2012) [Erratum *ibid.* **713**, 351 (2012)] [arXiv:1203.3662]; Phys. Lett. **B723**, 44 (2013) [arXiv:1303.4646].
120. A. Bondar, talk at the Belle analysis workshop, Novosibirsk, September 2002;
A. Poluektov *et al.* [Belle Collab.], Phys. Rev. **D70**, 072003 (2004) [hep-ex/0406067].
121. A. Giri *et al.*, Phys. Rev. **D68**, 054018 (2003) [hep-ph/0303187].
122. A. Poluektov *et al.* [Belle Collab.], Phys. Rev. **D81**, 112002 (2010) [arXiv:1003.3360].
123. B. Aubert *et al.* [*BABAR* Collab.], Phys. Rev. Lett. **105**, 121801 (2010) [arXiv:1005.1096].

124. R. Aaij *et al.*, Phys. Lett. **B718**, 43 (2012) [arXiv:1209.5869].
125. Y. Grossman *et al.*, Phys. Rev. **D72**, 031501 (2005) [hep-ph/0505270].
126. A. Amorim *et al.*, Phys. Rev. **D59**, 056001 (1999) [hep-ph/9807364].
127. B. Aubert *et al.* [*BABAR* Collab.], Phys. Rev. **D71**, 112003 (2005) [hep-ex/0504035]; Phys. Rev. **D73**, 111101 (2006) [hep-ex/0602049]; F.J. Ronga *et al.* [Belle Collab.], Phys. Rev. **D73**, 092003 (2006) [hep-ex/0604013]; S. Bahinipati *et al.* [Belle Collab.], Phys. Rev. **D84**, 021101 (2011) [arXiv:1102.0888].
128. R. Aleksan *et al.*, Z. Phys. **C54**, 653 (1992).
129. LHCb Collab., LHCb-CONF-2012-029.
130. G.P. Dubois-Felsmann *et al.*, hep-ph/0308262.
131. "The *BABAR* physics book: Physics at an asymmetric B factory," (P.F. Harrison and H.R. Quinn, eds.), SLAC-R-0504, 1998.
132. S. Plaszczynski and M.H. Schune, hep-ph/9911280.
133. M. Bona *et al.* [UTfit Collab.], JHEP **0803**, 049 (2008) [arXiv:0707.0636].
134. We thank the CKMfitter and UTfit groups for performing fits and preparing plots using input values from this *Review*.
135. H.E. Haber, Nucl. Phys. Proc. Supp. **62**, 469 (1998) [hep-ph/9709450];
Y. Nir, hep-ph/0109090.
136. J.M. Soares and L. Wolfenstein, Phys. Rev. **D47**, 1021 (1993);
T. Goto *et al.*, Phys. Rev. **D53**, 6662 (1996) [hep-ph/9506311];
J.P. Silva and L. Wolfenstein, Phys. Rev. **D55**, 5331 (1997) [hep-ph/9610208].
137. Y. Grossman, Z. Ligeti, and Y. Nir, Prog. Theor. Phys. **122**, 125 (2009) [arXiv:0904.4262].
138. G. Isidori, Y. Nir, and G. Perez, Ann. Rev. Nucl. and Part. Sci. **60**, 355 (2010) [arXiv:1002.0900].
139. Z. Ligeti, Int. J. Mod. Phys. **A20**, 5105 (2005) [hep-ph/0408267].
140. J. Charles *et al.*, arXiv:1309.2293.
141. K. Agashe *et al.*, hep-ph/0509117.
142. S. Laplace *et al.*, Phys. Rev. **D65**, 094040 (2002) [hep-ph/0202010].
143. V.M. Abazov *et al.* [DØ Collab.], Phys. Rev. **D89**, 012002 (2014) [arXiv:1310.0447].
144. V.M. Abazov *et al.* [DØ Collab.], Phys. Rev. **D85**, 032006 (2012) [arXiv:1109.3166];
T. Aaltonen *et al.* [CDF Collab.], CDF note 10778 (2012).
145. R. Aaij *et al.* [LHCb Collab.], Phys. Rev. **D87**, 112010 (2013) [arXiv:1304.2600].
146. G. Buchalla and A.J. Buras, Phys. Lett. **B333**, 221 (1994) [hep-ph/9405259].

13. *CP* VIOLATION IN THE QUARK SECTOR

Revised February 2014 by T. Gershon (University of Warwick) and Y. Nir (Weizmann Institute).

The CP transformation combines charge conjugation C with parity P. Under C, particles and antiparticles are interchanged, by conjugating all internal quantum numbers, *e.g.*, $Q \to -Q$ for electromagnetic charge. Under P, the handedness of space is reversed, $\vec{x} \to -\vec{x}$. Thus, for example, a left-handed electron e^-_L is transformed under CP into a right-handed positron, e^+_R.

If CP were an exact symmetry, the laws of Nature would be the same for matter and for antimatter. We observe that most phenomena are C- and P-symmetric, and therefore, also CP-symmetric. In particular, these symmetries are respected by the gravitational, electromagnetic, and strong interactions. The weak interactions, on the other hand, violate C and P in the strongest possible way. For example, the charged W bosons couple to left-handed electrons, e^-_L, and to their CP-conjugate right-handed positrons, e^+_R, but to neither their C-conjugate left-handed positrons, e^+_L, nor their P-conjugate right-handed electrons, e^-_R. While weak interactions violate C and P separately, CP is still preserved in most weak interaction processes. The CP symmetry is, however, violated in certain rare processes, as discovered in neutral K decays in 1964 [1], and observed in recent years in B decays. A K_L meson decays more often to $\pi^- e^+ \nu_e$ than to $\pi^+ e^- \overline{\nu}_e$, thus allowing electrons and positrons to be unambiguously distinguished, but the decay-rate asymmetry is only at the 0.003 level. The CP-violating effects observed in the B system are larger: the parameter describing the CP asymmetry in the decay time distribution of $B^0/\overline{B}^0$ meson transitions to CP eigenstates like $J/\psi K_S$ is about 0.7 [2,3]. These effects are related to $K^0 - \overline{K}^0$ and $B^0 - \overline{B}^0$ mixing, but CP violation arising solely from decay amplitudes has also been observed, first in $K \to \pi\pi$ decays [4–6], and more recently in B^0 [7,8], B^+ [9–11], and B^0_s [12] decays. CP violation is not yet experimentally established in the D system. Moreover, CP violation has not yet been observed in the decay of any baryon, nor in processes involving the top quark, nor in flavor-conserving processes such as electric dipole moments, nor in the lepton sector.

In addition to parity and to continuous Lorentz transformations, there is one other spacetime operation that could be a symmetry of the interactions: time reversal T, $t \to -t$. Violations of T symmetry have been observed in neutral K decays [13]. More recently, exploiting the fact that for neutral B mesons both flavor tagging and CP tagging can be used [14], T violation has been observed between states that are not CP-conjugate [15]. Moreover, T violation is expected as a corollary of CP violation if the combined CPT transformation is a fundamental symmetry of Nature [16]. All observations indicate that CPT is indeed a symmetry of Nature. Furthermore, one cannot build a locally Lorentz-invariant quantum field theory with a Hermitian Hamiltonian that violates CPT. (At several points in our discussion, we avoid assumptions about CPT, in order to identify cases where evidence for CP violation relies on assumptions about CPT.)

Within the Standard Model, CP symmetry is broken by complex phases in the Yukawa couplings (that is, the couplings of the Higgs scalar to quarks). When all manipulations to remove unphysical phases in this model are exhausted, one finds that there is a single CP-violating parameter [17]. In the basis of mass eigenstates, this single phase appears in the 3×3 unitary matrix that gives the W-boson couplings to an up-type antiquark and a down-type quark. (If the Standard Model is supplemented with Majorana mass terms for the neutrinos, the analogous mixing matrix for leptons has three CP-violating phases.) The beautifully consistent and economical Standard-Model description of CP violation in terms of Yukawa couplings, known as the Kobayashi-Maskawa (KM) mechanism [17], agrees with all measurements to date. (Some measurements are in tension with the predictions, and are discussed in more detail below. Pending verification, the results are not considered to change the overall picture of agreement with the Standard Model.) Furthermore, one can fit the data allowing new physics contributions to loop processes to compete with, or even dominate over, the Standard Model amplitudes [18,19]. Such an analysis provides model-independent proof that the KM phase is different from zero, and that the matrix of three-generation quark mixing is the dominant source of CP violation in meson decays.

The current level of experimental accuracy and the theoretical uncertainties involved in the interpretation of the various observations leave room, however, for additional subdominant sources of CP violation from new physics. Indeed, almost all extensions of the Standard Model imply that there are such additional sources. Moreover, CP violation is a necessary condition for baryogenesis, the process of dynamically generating the matter-antimatter asymmetry of the Universe [20]. Despite the phenomenological success of the KM mechanism, it fails (by several orders of magnitude) to accommodate the observed asymmetry [21]. This discrepancy strongly suggests that Nature provides additional sources of CP violation beyond the KM mechanism. (The evidence for neutrino masses implies that CP can be violated also in the lepton sector. This situation makes leptogenesis [22], a scenario where CP-violating phases in the Yukawa couplings of the neutrinos play a crucial role in the generation of the baryon asymmetry, a very attractive possibility.) The expectation of new sources motivates the large ongoing experimental effort to find deviations from the predictions of the KM mechanism.

CP violation can be experimentally searched for in a variety of processes, such as hadron decays, electric dipole moments of neutrons, electrons and nuclei, and neutrino oscillations. Hadron decays via the weak interaction probe flavor-changing CP violation. The search for electric dipole moments may find (or constrain) sources of CP violation that, unlike the KM phase, are not related to flavor-changing couplings. Following the discovery of the Higgs boson [23,24], searches for CP violation in the Higgs sector are becoming feasible. Future searches for CP violation in neutrino oscillations might provide further input on leptogenesis.

The present measurements of CP asymmetries provide some of the strongest constraints on the weak couplings of quarks. Future measurements of CP violation in K, D, B, and B^0_s meson decays will provide additional constraints on the flavor parameters of the Standard Model, and can probe new physics. In this review, we give the formalism and basic physics that are relevant to present and near future measurements of CP violation in the quark sector.

Before going into details, we list here the observables where CP violation has been observed at a level above 5σ [25–27]:

- Indirect CP violation in $K \to \pi\pi$ and $K \to \pi\ell\nu$ decays, and in the $K_L \to \pi^+\pi^- e^+ e^-$ decay, is given by

$$|\epsilon| = (2.228 \pm 0.011) \times 10^{-3}\,. \tag{13.1}$$

- Direct CP violation in $K \to \pi\pi$ decays is given by

$$\mathcal{R}e(\epsilon'/\epsilon) = (1.65 \pm 0.26) \times 10^{-3}\,. \tag{13.2}$$

- CP violation in the interference of mixing and decay in the tree-dominated $b \to c\bar{c}s$ transitions, such as $B^0 \to \psi K^0$, is given by (we use K^0 throughout to denote results that combine K_S and K_L modes, but use the sign appropriate to K_S):

$$S_{\psi K^0} = +0.682 \pm 0.019\,. \tag{13.3}$$

- CP violation in the interference of mixing and decay in various modes related to $b \to q\bar{q}s$ (penguin) transitions is given by

$$S_{\eta' K^0} = +0.63 \pm 0.06\,, \tag{13.4}$$

$$S_{\phi K^0} = +0.74\,^{+0.11}_{-0.13}\,, \tag{13.5}$$

$$S_{f_0 K^0} = +0.69\,^{+0.10}_{-0.12}\,, \tag{13.6}$$

$$S_{K^+K^-K_S} = +0.68\,^{+0.09}_{-0.10}\,, \tag{13.7}$$

- CP violation in the interference of mixing and decay in the $B^0 \to \pi^+\pi^-$ mode is given by

$$S_{\pi^+\pi^-} = -0.66 \pm 0.06\,. \tag{13.8}$$

- Direct CP violation in the $B^0 \to \pi^+\pi^-$ mode is given by

$$C_{\pi^+\pi^-} = -0.31 \pm 0.05\,. \tag{13.9}$$

- CP violation in the interference of mixing and decay in various modes related to $b \to c\bar{c}d$ transitions is given by

$$S_{\psi\pi^0} = -0.93 \pm 0.15\,, \tag{13.10}$$

$$S_{D^+D^-} = -0.98 \pm 0.17\,. \tag{13.11}$$

$$S_{D^{*+}D^{*-}} = -0.71 \pm 0.09\,. \tag{13.12}$$

- Direct CP violation in the $\overline{B}^0 \to K^-\pi^+$ mode is given by

$$\mathcal{A}_{\overline{B}^0 \to K^-\pi^+} = -0.082 \pm 0.006\,. \tag{13.13}$$

- Direct CP violation in $B^\pm \to D_+K^\pm$ decays (D_+ is the CP-even neutral D state) is given by

$$\mathcal{A}_{B^+ \to D_+K^+} = +0.19 \pm 0.03\,. \tag{13.14}$$

- Direct CP violation in the $\overline{B}{}^0_s \to K^+\pi^-$ mode is given by

$$\mathcal{A}_{\overline{B}{}^0_s \to K^+\pi^-} = +0.26 \pm 0.04\,. \tag{13.15}$$

In addition, large CP violation effects have recently been observed in certain regions of the phase space of $B^\pm \to K^+K^-K^\pm$, $\pi^+\pi^-K^\pm$, $\pi^+\pi^-\pi^\pm$ and $K^+K^-\pi^\pm$ decays [28,29].

13.1. Formalism

The phenomenology of CP violation for neutral flavored mesons is particularly interesting, since many of the observables can be cleanly interpreted. Although the phenomenology is superficially different for K^0, D^0, B^0, and B^0_s decays, this is primarily because each of these systems is governed by a different balance between decay rates, oscillations, and lifetime splitting. However, the general considerations presented in this section are identical for all flavored neutral pseudoscalar mesons. The phenomenology of CP violation for neutral mesons that do not carry flavor quantum numbers (such as the $\eta^{(\prime)}$ state) is quite different: such states are their own antiparticles and have definite CP eigenvalues, so the signature of CP violation is simply the decay to a final state with the opposite CP. Such decays are mediated by the electromagnetic or (OZI-suppressed) strong interaction, where CP violation is not expected and has not yet been observed. In the remainder of this review, we restrict ourselves to considerations of weakly decaying hadrons.

In this section, we present a general formalism for, and classification of, CP violation in the decay of a weakly decaying hadron, denoted M. We pay particular attention to the case that M is a K^0, D^0, B^0, or B^0_s meson. Subsequent sections describe the CP-violating phenomenology, approximations, and alternative formalisms that are specific to each system.

13.1.1. ***Charged- and neutral-hadron decays*** : We define decay amplitudes of M (which could be charged or neutral) and its CP conjugate $\overline{M}$ to a multi-particle final state f and its CP conjugate $\overline{f}$ as

$$A_f = \langle f\,|\mathcal{H}|\,M\rangle\,, \quad \overline{A}_f = \langle f\,|\mathcal{H}|\,\overline{M}\rangle\,,$$
$$A_{\overline{f}} = \langle \overline{f}\,|\mathcal{H}|\,M\rangle\,, \quad \overline{A}_{\overline{f}} = \langle \overline{f}\,|\mathcal{H}|\,\overline{M}\rangle\,, \tag{13.16}$$

where $\mathcal{H}$ is the Hamiltonian governing weak interactions. The action of CP on these states introduces phases ξ_M and ξ_f that depend on their flavor content, according to

$$CP|M\rangle = e^{+i\xi_M}\,|\overline{M}\rangle\,, \quad CP|f\rangle = e^{+i\xi_f}\,|\overline{f}\rangle\,, \tag{13.17}$$

with

$$CP|\overline{M}\rangle = e^{-i\xi_M}\,|M\rangle\,, \quad CP|\overline{f}\rangle = e^{-i\xi_f}\,|f\rangle \tag{13.18}$$

so that $(CP)^2 = 1$. The phases ξ_M and ξ_f are arbitrary and unobservable because of the flavor symmetry of the strong interaction. If CP is conserved by the dynamics, $[CP, \mathcal{H}] = 0$, then A_f and $\overline{A}_{\overline{f}}$ have the same magnitude and an arbitrary unphysical relative phase

$$\overline{A}_{\overline{f}} = e^{i(\xi_f - \xi_M)}\,A_f\,. \tag{13.19}$$

13.1.2. ***Neutral-meson mixing*** : A state that is initially a superposition of M^0 and $\overline{M}^0$, say

$$|\psi(0)\rangle = a(0)|M^0\rangle + b(0)|\overline{M}^0\rangle\,, \tag{13.20}$$

will evolve in time acquiring components that describe all possible decay final states $\{f_1, f_2, \ldots\}$, that is,

$$|\psi(t)\rangle = a(t)|M^0\rangle + b(t)|\overline{M}^0\rangle + c_1(t)|f_1\rangle + c_2(t)|f_2\rangle + \cdots\,. \tag{13.21}$$

If we are interested in computing only the values of $a(t)$ and $b(t)$ (and not the values of all $c_i(t)$), and if the times t in which we are interested are much larger than the typical strong interaction scale, then we can use a much simplified formalism [30]. The simplified time evolution is determined by a 2×2 effective Hamiltonian $\mathbf{H}$ that is not Hermitian, since otherwise the mesons would only oscillate and not decay. Any complex matrix, such as $\mathbf{H}$, can be written in terms of Hermitian matrices $\mathbf{M}$ and $\mathbf{\Gamma}$ as

$$\mathbf{H} = \mathbf{M} - \frac{i}{2}\mathbf{\Gamma}\,. \tag{13.22}$$

$\mathbf{M}$ and $\mathbf{\Gamma}$ are associated with $(M^0, \overline{M}^0) \leftrightarrow (M^0, \overline{M}^0)$ transitions via off-shell (dispersive), and on-shell (absorptive) intermediate states, respectively. Diagonal elements of $\mathbf{M}$ and $\mathbf{\Gamma}$ are associated with the flavor-conserving transitions $M^0 \to M^0$ and $\overline{M}^0 \to \overline{M}^0$, while off-diagonal elements are associated with flavor-changing transitions $M^0 \leftrightarrow \overline{M}^0$.

The eigenvectors of $\mathbf{H}$ have well-defined masses and decay widths. To specify the components of the strong interaction eigenstates, M^0 and $\overline{M}^0$, in the light (M_L) and heavy (M_H) mass eigenstates, we introduce three complex parameters: p, q, and, for the case that both CP and CPT are violated in mixing, z:

$$|M_L\rangle \propto p\sqrt{1-z}\,|M^0\rangle + q\sqrt{1+z}\,|\overline{M}^0\rangle$$
$$|M_H\rangle \propto p\sqrt{1+z}\,|M^0\rangle - q\sqrt{1-z}\,|\overline{M}^0\rangle\,, \tag{13.23}$$

with the normalization $|q|^2 + |p|^2 = 1$ when $z = 0$. (Another possible choice, which is in standard usage for K mesons, defines the mass eigenstates according to their lifetimes: K_S for the short-lived and K_L for the long-lived state. The K_L is experimentally found to be the heavier state. Yet another choice is often used for the D mesons: the eigenstates are labelled according to their dominant CP content [31].)

The real and imaginary parts of the eigenvalues $\omega_{L,H}$ corresponding to $|M_{L,H}\rangle$ represent their masses and decay widths, respectively. The mass and width splittings are

$$\Delta m \equiv m_H - m_L = \mathcal{R}e(\omega_H - \omega_L)\,,$$
$$\Delta\Gamma \equiv \Gamma_H - \Gamma_L = -2\,\mathcal{I}m(\omega_H - \omega_L)\,. \tag{13.24}$$

Note that here Δm is positive by definition, while the sign of $\Delta\Gamma$ is to be experimentally determined. The sign of $\Delta\Gamma$ has not yet been established for B^0 mesons, while $\Delta\Gamma < 0$ is established for K and B^0_s mesons. The Standard Model predicts $\Delta\Gamma < 0$ also for $B^0_{(s)}$ mesons (for this reason, $\Delta\Gamma = \Gamma_L - \Gamma_H$, which is still a signed quantity, is often used in the B^0 and B^0_s literature and is the convention used in the PDG experimental summaries).

Solving the eigenvalue problem for $\mathbf{H}$ yields

$$\left(\frac{q}{p}\right)^2 = \frac{\mathbf{M}^*_{12} - (i/2)\mathbf{\Gamma}^*_{12}}{\mathbf{M}_{12} - (i/2)\mathbf{\Gamma}_{12}} \tag{13.25}$$

and

$$z \equiv \frac{\delta m - (i/2)\delta\Gamma}{\Delta m - (i/2)\Delta\Gamma}\,, \tag{13.26}$$

where

$$\delta m \equiv \mathbf{M}_{11} - \mathbf{M}_{22}\,, \quad \delta\Gamma \equiv \mathbf{\Gamma}_{11} - \mathbf{\Gamma}_{22} \tag{13.27}$$

are the differences in effective mass and decay-rate expectation values for the strong interaction states M^0 and $\overline{M}^0$.

If either CP or CPT is a symmetry of $\mathbf{H}$ (independently of whether T is conserved or violated), then the values of δm and $\delta\Gamma$ are both zero, and hence $z = 0$. We also find that

$$\omega_H - \omega_L = 2\sqrt{\left(\mathbf{M}_{12} - \frac{i}{2}\mathbf{\Gamma}_{12}\right)\left(\mathbf{M}^*_{12} - \frac{i}{2}\mathbf{\Gamma}^*_{12}\right)}\,. \tag{13.28}$$

If either CP or T is a symmetry of $\mathbf{H}$ (independently of whether CPT is conserved or violated), then $\mathbf{\Gamma}_{12}/\mathbf{M}_{12}$ is real, leading to

$$\left(\frac{q}{p}\right)^2 = e^{2i\xi_M} \quad \Rightarrow \quad \left|\frac{q}{p}\right| = 1\,, \tag{13.29}$$

where ξ_M is the arbitrary unphysical phase introduced in Eq. (13.18). If, and only if, CP is a symmetry of $\mathbf{H}$ (independently of CPT and T), then both of the above conditions hold, with the result that the mass eigenstates are orthogonal

$$\langle M_H | M_L \rangle = |p|^2 - |q|^2 = 0\,. \tag{13.30}$$

13.1.3. ***CP-violating observables*** : All CP-violating observables in M and $\overline{M}$ decays to final states f and $\overline{f}$ can be expressed in terms of phase-convention-independent combinations of A_f, $\overline{A}_f$, $A_{\overline{f}}$, and $\overline{A}_{\overline{f}}$, together with, for neutral meson decays only, q/p. CP violation in charged meson and all baryon decays depends only on the combination $|\overline{A}_{\overline{f}}/A_f|$, while CP violation in flavored neutral meson decays is complicated by $M^0 \leftrightarrow \overline{M}^0$ oscillations, and depends, additionally, on $|q/p|$ and on $\lambda_f \equiv (q/p)(\overline{A}_f/A_f)$.

The decay rates of the two neutral kaon mass eigenstates, K_S and K_L, are different enough ($\Gamma_S/\Gamma_L \sim 500$) that one can, in most cases, actually study their decays independently. For D^0, B^0, and B^0_s mesons, however, values of $\Delta\Gamma/\Gamma$ (where $\Gamma \equiv (\Gamma_H + \Gamma_L)/2$) are relatively small, and so both mass eigenstates must be considered in their evolution. We denote the state of an initially pure $|M^0\rangle$ or $|\overline{M}^0\rangle$ after an elapsed proper time t as $|M^0_{\rm phys}(t)\rangle$ or $|\overline{M}^0_{\rm phys}(t)\rangle$, respectively. Using the effective Hamiltonian approximation, but not assuming CPT is a good symmetry, we obtain

$$\begin{aligned}
|M^0_{\rm phys}(t)\rangle &= \left(g_+(t) + z\,g_-(t)\right)|M^0\rangle - \sqrt{1-z^2}\,\frac{q}{p}\,g_-(t)|\overline{M}^0\rangle\,,\\
|\overline{M}^0_{\rm phys}(t)\rangle &= \left(g_+(t) - z\,g_-(t)\right)|\overline{M}^0\rangle - \sqrt{1-z^2}\,\frac{p}{q}\,g_-(t)|M^0\rangle\,,
\end{aligned} \tag{13.31}$$

where

$$g_\pm(t) \equiv \frac{1}{2}\left(e^{-im_H t - \frac{1}{2}\Gamma_H t} \pm e^{-im_L t - \frac{1}{2}\Gamma_L t}\right) \tag{13.32}$$

and $z = 0$ if either CPT or CP is conserved.

Defining $x \equiv \Delta m/\Gamma$ and $y \equiv \Delta\Gamma/(2\Gamma)$, and assuming $z = 0$, one obtains the following time-dependent decay rates:

$$\begin{aligned}
&\frac{d\Gamma\left[M^0_{\rm phys}(t) \to f\right]/dt}{e^{-\Gamma t}\mathcal{N}_f} =\\
&\quad\left(|A_f|^2 + |(q/p)\overline{A}_f|^2\right)\cosh(y\Gamma t) + \left(|A_f|^2 - |(q/p)\overline{A}_f|^2\right)\cos(x\Gamma t)\\
&\quad + 2\,\mathcal{R}e((q/p)A^*_f\overline{A}_f)\sinh(y\Gamma t) - 2\,\mathcal{I}m((q/p)A^*_f\overline{A}_f)\sin(x\Gamma t)\,,
\end{aligned} \tag{13.33}$$

$$\begin{aligned}
&\frac{d\Gamma\left[\overline{M}^0_{\rm phys}(t) \to f\right]/dt}{e^{-\Gamma t}\mathcal{N}_f} =\\
&\quad\left(|(p/q)A_f|^2 + |\overline{A}_f|^2\right)\cosh(y\Gamma t) - \left(|(p/q)A_f|^2 - |\overline{A}_f|^2\right)\cos(x\Gamma t)\\
&\quad + 2\,\mathcal{R}e((p/q)A_f\overline{A}^*_f)\sinh(y\Gamma t) - 2\,\mathcal{I}m((p/q)A_f\overline{A}^*_f)\sin(x\Gamma t)\,,
\end{aligned} \tag{13.34}$$

where $\mathcal{N}_f$ is a common, time-independent, normalization factor that can be determined bearing in mind that the range of t is $0 < t < \infty$. Decay rates to the CP-conjugate final state $\overline{f}$ are obtained analogously, with $\mathcal{N}_f = \mathcal{N}_{\overline{f}}$ and the substitutions $A_f \to A_{\overline{f}}$ and $\overline{A}_f \to \overline{A}_{\overline{f}}$ in Eqs. (13.33, 13.34). Terms proportional to $|A_f|^2$ or $|\overline{A}_f|^2$ are associated with decays that occur without any net $M^0 \leftrightarrow \overline{M}^0$ oscillation, while terms proportional to $|(q/p)\overline{A}_f|^2$ or $|(p/q)A_f|^2$ are associated with decays following a net oscillation. The $\sinh(y\Gamma t)$ and $\sin(x\Gamma t)$ terms of Eqs. (13.33, 13.34) are associated with the interference between these two cases. Note that, in multi-body decays, amplitudes are functions of phase-space variables. Interference may be present in some regions but not others, and is strongly influenced by resonant substructure.

When neutral pseudoscalar mesons are produced coherently in pairs from the decay of a vector resonance, $V \to M^0\overline{M}^0$ (for example, $\Upsilon(4S) \to B^0\overline{B}^0$ or $\phi \to K^0\overline{K}^0$), the time-dependence of their subsequent decays to final states f_1 and f_2 has a similar form to Eqs. (13.33, 13.34):

$$\begin{aligned}
&\frac{d\Gamma\left[V_{\rm phys}(t_1,t_2) \to f_1 f_2\right]/d(\Delta t)}{e^{-\Gamma|\Delta t|}\mathcal{N}_{f_1 f_2}} =\\
&\quad\left(|a_+|^2 + |a_-|^2\right)\cosh(y\Gamma\Delta t) + \left(|a_+|^2 - |a_-|^2\right)\cos(x\Gamma\Delta t)\\
&\quad - 2\,\mathcal{R}e(a^*_+ a_-)\sinh(y\Gamma\Delta t) + 2\,\mathcal{I}m(a^*_+ a_-)\sin(x\Gamma\Delta t)\,,
\end{aligned} \tag{13.35}$$

where $\Delta t \equiv t_2 - t_1$ is the difference in the production times, t_1 and t_2, of f_1 and f_2, respectively, and the dependence on the average decay time and on decay angles has been integrated out. The normalisation factor $\mathcal{N}_{f_1 f_2}$ can be evaluated, noting that the range of Δt is $-\infty < \Delta t < \infty$. The coefficients in Eq. (13.35) are determined by the amplitudes for no net oscillation from $t_1 \to t_2$, $\overline{A}_{f_1}A_{f_2}$, and $A_{f_1}\overline{A}_{f_2}$, and for a net oscillation, $(q/p)\overline{A}_{f_1}\overline{A}_{f_2}$ and $(p/q)A_{f_1}A_{f_2}$, via

$$a_+ \equiv \overline{A}_{f_1}A_{f_2} - A_{f_1}\overline{A}_{f_2}\,, \tag{13.36}$$

$$a_- \equiv -\sqrt{1-z^2}\left(\frac{q}{p}\overline{A}_{f_1}\overline{A}_{f_2} - \frac{p}{q}A_{f_1}A_{f_2}\right) + z\left(\overline{A}_{f_1}A_{f_2} + A_{f_1}\overline{A}_{f_2}\right)\,.$$

Assuming CPT conservation, $z = 0$, and identifying $\Delta t \to t$ and $f_2 \to f$, we find that Eqs. (13.35, 13.36) reduce essentially to Eq. (13.33) with $A_{f_1} = 0$, $\overline{A}_{f_1} = 1$, or to Eq. (13.34) with $\overline{A}_{f_1} = 0$, $A_{f_1} = 1$. Indeed, such a situation plays an important role in experiments that exploit the coherence of $V \to M^0\overline{M}^0$ (for example $\psi(3770) \to D^0\overline{D}^0$ or $\Upsilon(4S) \to B^0\overline{B}^0$) production. Final states f_1 with $A_{f_1} = 0$ or $\overline{A}_{f_1} = 0$ are called tagging states, because they identify the decaying pseudoscalar meson as, respectively, $\overline{M}^0$ or M^0. Before one of M^0 or $\overline{M}^0$ decays, they evolve in phase, so that there is always one M^0 and one $\overline{M}^0$ present. A tagging decay of one meson sets the clock for the time evolution of the other: it starts at t_1 as purely M^0 or $\overline{M}^0$, with time evolution that depends only on $t_2 - t_1$.

When f_1 is a state that both M^0 and $\overline{M}^0$ can decay into, then Eq. (13.35) contains interference terms proportional to $A_{f_1}\overline{A}_{f_1} \neq 0$ that are not present in Eqs. (13.33, 13.34). Even when f_1 is dominantly produced by M^0 decays rather than $\overline{M}^0$ decays, or vice versa, $A_{f_1}\overline{A}_{f_1}$ can be non-zero owing to doubly-CKM-suppressed decays (with amplitudes suppressed by at least two powers of λ relative to the dominant amplitude, in the language of Section 13.3), and these terms should be considered for precision studies of CP violation in coherent $V \to M^0\overline{M}^0$ decays [32]. The correlations in $V \to M^0\overline{M}^0$ decays can also be exploited to determine strong phase differences between favored and suppressed decay amplitudes [33,34].

13.1.4. ***Classification of CP-violating effects*** : We distinguish three types of CP-violating effects that can occur in the quark sector:

I. CP violation in decay is defined by

$$|\overline{A}_{\overline{f}}/A_f| \neq 1\,. \tag{13.37}$$

In charged meson (and all baryon) decays, where mixing effects are absent, this is the only possible source of CP

asymmetries:

$$\mathcal{A}_{f^\pm} \equiv \frac{\Gamma(M^- \to f^-) - \Gamma(M^+ \to f^+)}{\Gamma(M^- \to f^-) + \Gamma(M^+ \to f^+)} = \frac{|\overline{A}_{f^-}/A_{f^+}|^2 - 1}{|\overline{A}_{f^-}/A_{f^+}|^2 + 1} \,. \quad (13.38)$$

Note that the usual sign convention for CP asymmetries of hadrons is for the difference between the rate involving the particle that contains a heavy quark and that which contains an antiquark. Hence Eq. (13.38) corresponds to the definition for $B^\pm$ mesons, but the opposite sign is used for $D^\pm_{(s)}$ decays.

II. CP (and T) violation in mixing is defined by

$$|q/p| \neq 1 \,. \quad (13.39)$$

In charged-current semileptonic neutral meson decays $M, \overline{M} \to \ell^\pm X$ (taking $|A_{\ell^+X}| = |\overline{A}_{\ell^-X}|$ and $A_{\ell^-X} = \overline{A}_{\ell^+X} = 0$, as is the case in the Standard Model, to lowest order in G_F, and in most of its reasonable extensions), this is the only source of CP violation, and can be measured via the asymmetry of "wrong-sign" decays induced by oscillations:

$$\mathcal{A}_{\rm SL}(t) \equiv \frac{d\Gamma/dt\big[\overline{M}^0_{\rm phys}(t) \to \ell^+ X\big] - d\Gamma/dt\big[M^0_{\rm phys}(t) \to \ell^- X\big]}{d\Gamma/dt\big[\overline{M}^0_{\rm phys}(t) \to \ell^+ X\big] + d\Gamma/dt\big[M^0_{\rm phys}(t) \to \ell^- X\big]}$$
$$= \frac{1 - |q/p|^4}{1 + |q/p|^4}. \quad (13.40)$$

Note that this asymmetry of time-dependent decay rates is actually time-independent.

III. CP violation in interference between a decay without mixing, $M^0 \to f$, and a decay with mixing, $M^0 \to \overline{M}^0 \to f$ (such an effect occurs only in decays to final states that are common to M^0 and $\overline{M}^0$, including all CP eigenstates), is defined by

$$\mathcal{I}m(\lambda_f) \neq 0 \,, \quad (13.41)$$

with

$$\lambda_f \equiv \frac{q}{p}\frac{\overline{A}_f}{A_f} \,. \quad (13.42)$$

This form of CP violation can be observed, for example, using the asymmetry of neutral meson decays into final CP eigenstates f_{CP}

$$\mathcal{A}_{f_{CP}}(t) \equiv \frac{d\Gamma/dt\big[\overline{M}^0_{\rm phys}(t) \to f_{CP}\big] - d\Gamma/dt\big[M^0_{\rm phys}(t) \to f_{CP}\big]}{d\Gamma/dt\big[\overline{M}^0_{\rm phys}(t) \to f_{CP}\big] + d\Gamma/dt\big[M^0_{\rm phys}(t) \to f_{CP}\big]} \,. \quad (13.43)$$

If $\Delta\Gamma = 0$, as expected to a good approximation for B^0 mesons, but not for K^0 and B^0_s mesons, and $|q/p| = 1$, then $\mathcal{A}_{f_{CP}}$ has a particularly simple form (see Eq. (13.88), below). If, in addition, the decay amplitudes fulfill $|\overline{A}_{f_{CP}}| = |A_{f_{CP}}|$, the interference between decays with and without mixing is the only source of the asymmetry and $\mathcal{A}_{f_{CP}}(t) = \mathcal{I}m(\lambda_{f_{CP}})\sin(x\Gamma t)$.

Examples of these three types of CP violation will be given in Sections 13.4, 13.5, and 13.6.

13.2. Theoretical Interpretation: General Considerations

Consider the $M \to f$ decay amplitude A_f, and the CP conjugate process, $\overline{M} \to \overline{f}$, with decay amplitude $\overline{A}_{\overline{f}}$. There are two types of phases that may appear in these decay amplitudes. Complex parameters in any Lagrangian term that contributes to the amplitude will appear in complex conjugate form in the CP-conjugate amplitude. Thus, their phases appear in A_f and $\overline{A}_{\overline{f}}$ with opposite signs. In the Standard Model, these phases occur only in the couplings of the $W^\pm$ bosons, and hence, are often called "weak phases." The weak phase of any single term is convention-dependent. However, the difference between the weak phases in two different terms in A_f is convention-independent. A second type of phase can appear in scattering or decay amplitudes, even when the Lagrangian is real. This phase originates from the possible contribution from intermediate on-shell states in the decay process. Since these phases are generated by CP-invariant interactions, they are the same in A_f and $\overline{A}_{\overline{f}}$. Usually the dominant rescattering is due to strong interactions; hence the designation "strong phases" for the phase shifts so induced. Again, only the relative strong phases between different terms in the amplitude are physically meaningful.

The "weak" and "strong" phases discussed here appear in addition to the spurious CP-transformation phases of Eq. (13.19). Those spurious phases are due to an arbitrary choice of phase convention, and do not originate from any dynamics or induce any CP violation. For simplicity, we set them to zero from here on.

It is useful to write each contribution a_i to A_f in three parts: its magnitude $|a_i|$, its weak phase ϕ_i, and its strong phase δ_i. If, for example, there are two such contributions, $A_f = a_1 + a_2$, we have

$$A_f = |a_1|e^{i(\delta_1+\phi_1)} + |a_2|e^{i(\delta_2+\phi_2)},$$
$$\overline{A}_{\overline{f}} = |a_1|e^{i(\delta_1-\phi_1)} + |a_2|e^{i(\delta_2-\phi_2)}. \quad (13.44)$$

Similarly, for neutral mesons, it is useful to write

$$\mathbf{M}_{12} = |\mathbf{M}_{12}|e^{i\phi_M} \,, \quad \mathbf{\Gamma}_{12} = |\mathbf{\Gamma}_{12}|e^{i\phi_\Gamma} \,. \quad (13.45)$$

Each of the phases appearing in Eqs. (13.44, 13.45) is convention-dependent, but combinations such as $\delta_1 - \delta_2$, $\phi_1 - \phi_2$, $\phi_M - \phi_\Gamma$, and $\phi_M + \phi_1 - \overline{\phi}_1$ (where $\overline{\phi}_1$ is a weak phase contributing to $\overline{A}_f$) are physical.

It is now straightforward to evaluate the various asymmetries in terms of the theoretical parameters introduced here. We will do so with approximations that are often relevant to the most interesting measured asymmetries.

1. The CP asymmetry in charged meson and all baryon decays [Eq. (13.38)] is given by

$$\mathcal{A}_f = -\frac{2|a_1a_2|\sin(\delta_2-\delta_1)\sin(\phi_2-\phi_1)}{|a_1|^2 + |a_2|^2 + 2|a_1a_2|\cos(\delta_2-\delta_1)\cos(\phi_2-\phi_1)} \,. \quad (13.46)$$

The quantity of most interest to theory is the weak phase difference $\phi_2 - \phi_1$. Its extraction from the asymmetry requires, however, that the amplitude ratio $|a_2/a_1|$ and the strong phase difference $\delta_2 - \delta_1$ are known. Both quantities depend on non-perturbative hadronic parameters that are difficult to calculate, but in some cases can be obtained from experiment.

2. In the approximation that $|\mathbf{\Gamma}_{12}/\mathbf{M}_{12}| \ll 1$ (valid for B^0 and B^0_s mesons), the CP asymmetry in semileptonic neutral-meson decays [Eq. (13.40)] is given by

$$\mathcal{A}_{\rm SL} = -\left|\frac{\mathbf{\Gamma}_{12}}{\mathbf{M}_{12}}\right|\sin(\phi_M - \phi_\Gamma) \,. \quad (13.47)$$

The quantity of most interest to theory is the weak phase $\phi_M - \phi_\Gamma$. Its extraction from the asymmetry requires, however, that $|\mathbf{\Gamma}_{12}/\mathbf{M}_{12}|$ is known. This quantity depends on long-distance physics that is difficult to calculate.

3. In the approximations that only a single weak phase contributes to decay, $A_f = |a_f|e^{i(\delta_f+\phi_f)}$, and that $|\mathbf{\Gamma}_{12}/\mathbf{M}_{12}| = 0$, we obtain $|\lambda_f| = 1$, and the CP asymmetries in decays to a final CP eigenstate f [Eq. (13.43)] with eigenvalue $\eta_f = \pm 1$ are given by

$$\mathcal{A}_{f_{CP}}(t) = \mathcal{I}m(\lambda_f)\ \sin(\Delta m t)\ \text{ with }\ \mathcal{I}m(\lambda_f) = \eta_f \sin(\phi_M + 2\phi_f) \,. \quad (13.48)$$

Note that the phase so measured is purely a weak phase, and no hadronic parameters are involved in the extraction of its value from $\mathcal{I}m(\lambda_f)$.

The discussion above allows us to introduce another classification of CP-violating effects:

1. *Indirect CP violation* is consistent with taking $\phi_M \neq 0$ and setting all other CP violating phases to zero. CP violation in mixing (type II) belongs to this class.
2. *Direct CP violation* cannot be accounted for by just $\phi_M \neq 0$. CP violation in decay (type I) belongs to this class.

The historical significance of this classification is related to theory. In superweak models [35], CP violation appears only in diagrams that contribute to $\mathbf{M}_{12}$, hence they predict that there is no direct CP violation. In most models and, in particular, in the Standard Model, CP violation is both direct and indirect. As concerns type III CP violation, observing $\eta_{f_1}\mathcal{I}m(\lambda_{f_1}) \neq \eta_{f_2}\mathcal{I}m(\lambda_{f_2})$ (for the same decaying meson and two different final CP eigenstates f_1 and f_2) would establish direct CP violation. The experimental observation of $\epsilon' \neq 0$, which was achieved by establishing that $\mathcal{I}m(\lambda_{\pi^+\pi^-}) \neq \mathcal{I}m(\lambda_{\pi^0\pi^0})$ (see Section 13.4), excluded the superweak scenario.

13.3. Theoretical Interpretation: The KM Mechanism

Of all the Standard Model quark parameters, only the Kobayashi-Maskawa (KM) phase is CP-violating. Having a single source of CP violation, the Standard Model is very predictive for CP asymmetries: some vanish, and those that do not are correlated.

To be precise, CP could be violated also by strong interactions. The experimental upper bound on the electric-dipole moment of the neutron implies, however, that $\theta_{\rm QCD}$, the non-perturbative parameter that determines the strength of this type of CP violation, is tiny, if not zero. (The smallness of $\theta_{\rm QCD}$ constitutes a theoretical puzzle, known as "the strong CP problem.") In particular, it is irrelevant to our discussion of hadron decays.

The charged current interactions (that is, the $W^\pm$ interactions) for quarks are given by

$$-\mathcal{L}_{W^\pm} = \frac{g}{\sqrt{2}}\,\overline{u_{Li}}\,\gamma^\mu\,(V_{\rm CKM})_{ij}\,d_{Lj}\,W^+_\mu + \text{h.c.} \qquad (13.49)$$

Here $i,j = 1,2,3$ are generation numbers. The Cabibbo-Kobayashi-Maskawa (CKM) mixing matrix for quarks is a 3×3 unitary matrix [36]. Ordering the quarks by their masses, *i.e.*, $(u_1,u_2,u_3) \to (u,c,t)$ and $(d_1,d_2,d_3) \to (d,s,b)$, the elements of $V_{\rm CKM}$ are written as follows:

$$V_{\rm CKM} = \begin{pmatrix} V_{ud} & V_{us} & V_{ub} \\ V_{cd} & V_{cs} & V_{cb} \\ V_{td} & V_{ts} & V_{tb} \end{pmatrix} . \qquad (13.50)$$

While a general 3×3 unitary matrix depends on three real angles and six phases, the freedom to redefine the phases of the quark mass eigenstates can be used to remove five of the phases, leaving a single physical phase, the Kobayashi-Maskawa phase, that is responsible for all CP violation in the Standard Model.

The fact that one can parametrize $V_{\rm CKM}$ by three real and only one imaginary physical parameters can be made manifest by choosing an explicit parametrization. The Wolfenstein parametrization [37,38] is particularly useful:

$$V_{\rm CKM} = \begin{pmatrix} 1-\frac{1}{2}\lambda^2-\frac{1}{8}\lambda^4 & \lambda & A\lambda^3(\rho-i\eta) \\ -\lambda+\frac{1}{2}A^2\lambda^5[1-2(\rho+i\eta)] & 1-\frac{1}{2}\lambda^2-\frac{1}{8}\lambda^4(1+4A^2) & A\lambda^2 \\ A\lambda^3[1-(1-\frac{1}{2}\lambda^2)(\rho+i\eta)] & -A\lambda^2+\frac{1}{2}A\lambda^4[1-2(\rho+i\eta)] & 1-\frac{1}{2}A^2\lambda^4 \end{pmatrix} . \qquad (13.51)$$

Here $\lambda \approx 0.23$ (not to be confused with λ_f), the sine of the Cabibbo angle, plays the role of an expansion parameter, and η represents the CP-violating phase. Terms of $\mathcal{O}(\lambda^6)$ have been neglected.

The unitarity of the CKM matrix, $(VV^\dagger)_{ij} = (V^\dagger V)_{ij} = \delta_{ij}$, leads to twelve distinct complex relations among the matrix elements. The six relations with $i \neq j$ can be represented geometrically as triangles in the complex plane. Two of these,

$$V_{ud}V^*_{ub} + V_{cd}V^*_{cb} + V_{td}V^*_{tb} = 0$$
$$V_{td}V^*_{ud} + V_{ts}V^*_{us} + V_{tb}V^*_{ub} = 0\,,$$

have terms of equal order, $\mathcal{O}(A\lambda^3)$, and so have corresponding triangles whose interior angles are all $\mathcal{O}(1)$ physical quantities that can be independently measured. The angles of the first triangle (see Fig. 13.1) are given by

$$\alpha \equiv \varphi_2 \equiv \arg\left(-\frac{V_{td}V^*_{tb}}{V_{ud}V^*_{ub}}\right) \simeq \arg\left(-\frac{1-\rho-i\eta}{\rho+i\eta}\right),$$
$$\beta \equiv \varphi_1 \equiv \arg\left(-\frac{V_{cd}V^*_{cb}}{V_{td}V^*_{tb}}\right) \simeq \arg\left(\frac{1}{1-\rho-i\eta}\right),$$
$$\gamma \equiv \varphi_3 \equiv \arg\left(-\frac{V_{ud}V^*_{ub}}{V_{cd}V^*_{cb}}\right) \simeq \arg\left(\rho+i\eta\right). \qquad (13.52)$$

The angles of the second triangle are equal to (α,β,γ) up to corrections of $\mathcal{O}(\lambda^2)$. The notations (α,β,γ) and $(\varphi_1,\varphi_2,\varphi_3)$ are both in common usage but, for convenience, we only use the first convention in the following.

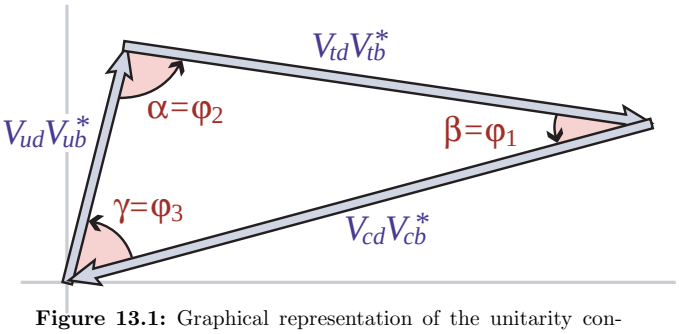

Figure 13.1: Graphical representation of the unitarity constraint $V_{ud}V^*_{ub} + V_{cd}V^*_{cb} + V_{td}V^*_{tb} = 0$ as a triangle in the complex plane.

Another relation that can be represented as a triangle,

$$V_{us}V^*_{ub} + V_{cs}V^*_{cb} + V_{ts}V^*_{tb} = 0\,, \qquad (13.53)$$

and, in particular, its small angle, of $\mathcal{O}(\lambda^2)$,

$$\beta_s \equiv \arg\left(-\frac{V_{ts}V^*_{tb}}{V_{cs}V^*_{cb}}\right), \qquad (13.54)$$

is convenient for analyzing CP violation in the B^0_s sector.

All unitarity triangles have the same area, commonly denoted by $J/2$ [39]. If CP is violated, J is different from zero and can be taken as the single CP-violating parameter. In the Wolfenstein parametrization of Eq. (13.51), $J \simeq \lambda^6 A^2 \eta$.

13.4. Kaons

CP violation was discovered in $K \to \pi\pi$ decays in 1964 [1]. The same mode provided the first observation of direct CP violation [4–6].

The decay amplitudes actually measured in neutral K decays refer to the mass eigenstates K_L and K_S, rather than to the K and $\overline{K}$ states referred to in Eq. (13.16). The final $\pi^+\pi^-$ and $\pi^0\pi^0$ states are CP-even. In the CP conservation limit, K_S (K_L) would be CP-even (odd), and therefore would (would not) decay to two pions. We define CP-violating amplitude ratios for two-pion final states,

$$\eta_{00} \equiv \frac{\langle\pi^0\pi^0|\mathcal{H}|K_L\rangle}{\langle\pi^0\pi^0|\mathcal{H}|K_S\rangle}\,, \quad \eta_{+-} \equiv \frac{\langle\pi^+\pi^-|\mathcal{H}|K_L\rangle}{\langle\pi^+\pi^-|\mathcal{H}|K_S\rangle}\,. \qquad (13.55)$$

Another important observable is the asymmetry of time-integrated semileptonic decay rates:

$$\delta_L \equiv \frac{\Gamma(K_L \to \ell^+\nu_\ell\pi^-) - \Gamma(K_L \to \ell^-\overline{\nu}_\ell\pi^+)}{\Gamma(K_L \to \ell^+\nu_\ell\pi^-) + \Gamma(K_L \to \ell^-\overline{\nu}_\ell\pi^+)}\,. \qquad (13.56)$$

CP violation has been observed as an appearance of K_L decays to two-pion final states [25],

$$|\eta_{00}| = (2.221 \pm 0.011)\times10^{-3} \qquad |\eta_{+-}| = (2.232 \pm 0.011)\times10^{-3} \qquad (13.57)$$

$$|\eta_{00}/\eta_{+-}| = 0.9951 \pm 0.0008\,, \tag{13.58}$$

where the phase ϕ_{ij} of the amplitude ratio η_{ij} has been determined both assuming CPT invariance:

$$\phi_{00} = (43.52 \pm 0.06)^\circ\,, \qquad \phi_{+-} = (43.51 \pm 0.05)^\circ\,, \tag{13.59}$$

and without assuming CPT invariance:

$$\phi_{00} = (43.7 \pm 0.8)^\circ\,, \qquad \phi_{+-} = (43.4 \pm 0.7)^\circ\,. \tag{13.60}$$

CP violation has also been observed in semileptonic K_L decays [25]

$$\delta_L = (3.32 \pm 0.06) \times 10^{-3}\,, \tag{13.61}$$

where δ_L is a weighted average of muon and electron measurements, as well as in K_L decays to $\pi^+\pi^-\gamma$ and $\pi^+\pi^-e^+e^-$ [25]. CP violation in $K \to 3\pi$ decays has not yet been observed [25,40].

Historically, CP violation in neutral K decays has been described in terms of the complex parameters ϵ and ϵ'. The observables η_{00}, η_{+-}, and δ_L are related to these parameters, and to those of Section 13.1, by

$$\begin{aligned}
\eta_{00} &= \frac{1-\lambda_{\pi^0\pi^0}}{1+\lambda_{\pi^0\pi^0}} &&= \epsilon - 2\epsilon'\,,\\
\eta_{+-} &= \frac{1-\lambda_{\pi^+\pi^-}}{1+\lambda_{\pi^+\pi^-}} &&= \epsilon + \epsilon'\,,\\
\delta_L &= \frac{1-|q/p|^2}{1+|q/p|^2} &&= \frac{2\mathcal{R}e(\epsilon)}{1+|\epsilon|^2}\,,
\end{aligned} \tag{13.62}$$

where, in the last line, we have assumed that $\left|A_{\ell^+\nu_\ell\pi^-}\right| = \left|\overline{A}_{\ell^-\overline{\nu}_\ell\pi^+}\right|$ and $\left|A_{\ell^-\overline{\nu}_\ell\pi^+}\right| = \left|\overline{A}_{\ell^+\nu_\ell\pi^-}\right| = 0$. (The convention-dependent parameter $\tilde{\epsilon} \equiv (1-q/p)/(1+q/p)$, sometimes used in the literature, is, in general, different from ϵ but yields a similar expression, $\delta_L = 2\mathcal{R}e(\tilde{\epsilon})/(1+|\tilde{\epsilon}|^2)$.) A fit to the $K \to \pi\pi$ data yields [25]

$$\begin{aligned}
|\epsilon| &= (2.228 \pm 0.011) \times 10^{-3}\,,\\
\mathcal{R}e(\epsilon'/\epsilon) &= (1.65 \pm 0.26) \times 10^{-3}\,.
\end{aligned} \tag{13.63}$$

In discussing two-pion final states, it is useful to express the amplitudes $A_{\pi^0\pi^0}$ and $A_{\pi^+\pi^-}$ in terms of their isospin components via

$$\begin{aligned}
A_{\pi^0\pi^0} &= \sqrt{\frac{1}{3}}\,|A_0|\,e^{i(\delta_0+\phi_0)} - \sqrt{\frac{2}{3}}\,|A_2|\,e^{i(\delta_2+\phi_2)},\\
A_{\pi^+\pi^-} &= \sqrt{\frac{2}{3}}\,|A_0|\,e^{i(\delta_0+\phi_0)} + \sqrt{\frac{1}{3}}\,|A_2|\,e^{i(\delta_2+\phi_2)}\,,
\end{aligned} \tag{13.64}$$

where we parameterize the amplitude $A_I(\overline{A}_I)$ for $K^0(\overline{K}^0)$ decay into two pions with total isospin $I = 0$ or 2 as

$$\begin{aligned}
A_I &\equiv \langle(\pi\pi)_I\,|\mathcal{H}|\,K^0\rangle = |A_I|\,e^{i(\delta_I+\phi_I)}\,,\\
\overline{A}_I &\equiv \langle(\pi\pi)_I\,|\mathcal{H}|\,\overline{K}^0\rangle = |A_I|\,e^{i(\delta_I-\phi_I)}\,.
\end{aligned} \tag{13.65}$$

The smallness of $|\eta_{00}|$ and $|\eta_{+-}|$ allows us to approximate

$$\epsilon \simeq \frac{1}{2}(1-\lambda_{(\pi\pi)_{I=0}})\,, \qquad \epsilon' \simeq \frac{1}{6}\left(\lambda_{\pi^0\pi^0} - \lambda_{\pi^+\pi^-}\right)\,. \tag{13.66}$$

The parameter ϵ represents indirect CP violation, while ϵ' parameterizes direct CP violation: $\mathcal{R}e(\epsilon')$ measures CP violation in decay (type I), $\mathcal{R}e(\epsilon)$ measures CP violation in mixing (type II), and $\mathcal{I}m(\epsilon)$ and $\mathcal{I}m(\epsilon')$ measure the interference between decays with and without mixing (type III).

The following expressions for ϵ and ϵ' are useful for theoretical evaluations:

$$\epsilon \simeq \frac{e^{i\pi/4}}{\sqrt{2}}\frac{\mathcal{I}m(\mathbf{M}_{12})}{\Delta m}\,, \qquad \epsilon' = \frac{i}{\sqrt{2}}\left|\frac{A_2}{A_0}\right| e^{i(\delta_2-\delta_0)}\sin(\phi_2-\phi_0)\,. \tag{13.67}$$

The expression for ϵ is only valid in a phase convention where $\phi_2 = 0$, corresponding to a real $V_{ud}V_{us}^*$, and in the approximation that also $\phi_0 = 0$. The phase of ϵ, $\arg(\epsilon) \approx \arctan(-2\Delta m/\Delta\Gamma)$, is independent of the electroweak model and is experimentally determined to be about $\pi/4$. The calculation of ϵ benefits from the fact that $\mathcal{I}m(\mathbf{M}_{12})$ is dominated by short distance physics. Consequently, the main sources of uncertainty in theoretical interpretations of ϵ are the values of matrix elements, such as $\langle K^0\,|(\overline{s}d)_{V-A}(\overline{s}d)_{V-A}|\,\overline{K}^0\rangle$. The expression for ϵ' is valid to first order in $|A_2/A_0| \sim 1/20$. The phase of ϵ' is experimentally determined, $\pi/2 + \delta_2 - \delta_0 \approx \pi/4$, and is independent of the electroweak model. Note that, accidentally, ϵ'/ϵ is real to a good approximation.

A future measurement of much interest is that of CP violation in the rare $K \to \pi\nu\overline{\nu}$ decays. The signal for CP violation is simply observing the $K_L \to \pi^0\nu\overline{\nu}$ decay. The effect here is that of interference between decays with and without mixing (type III) [41]:

$$\frac{\Gamma(K_L \to \pi^0\nu\overline{\nu})}{\Gamma(K^+ \to \pi^+\nu\overline{\nu})} = \frac{1}{2}\left[1 + |\lambda_{\pi\nu\overline{\nu}}|^2 - 2\,\mathcal{R}e(\lambda_{\pi\nu\overline{\nu}})\right] \simeq 1 - \mathcal{R}e(\lambda_{\pi\nu\overline{\nu}}), \tag{13.68}$$

where in the last equation we neglect CP violation in decay and in mixing (expected, model-independently, to be of order 10^{-5} and 10^{-3}, respectively). Such a measurement is experimentally very challenging but would be theoretically very rewarding [42]. Similar to the CP asymmetry in $B^0 \to J/\psi K_S$, the CP violation in $K \to \pi\nu\overline{\nu}$ decay is predicted to be large (that is, the ratio in Eq. (13.68) is neither CKM- nor loop-suppressed) and can be very cleanly interpreted.

Within the Standard Model, the $K_L \to \pi^0\nu\overline{\nu}$ decay is dominated by an intermediate top quark contribution and, consequently, can be interpreted in terms of CKM parameters [43]. (For the charged mode, $K^+ \to \pi^+\nu\overline{\nu}$, the contribution from an intermediate charm quark is not negligible, and constitutes a source of hadronic uncertainty.) In particular, $\mathcal{B}(K_L \to \pi^0\nu\overline{\nu})$ provides a theoretically clean way to determine the Wolfenstein parameter η [44]:

$$\mathcal{B}(K_L \to \pi^0\nu\overline{\nu}) = \kappa_L[X(m_t^2/m_W^2)]^2A^4\eta^2\,, \tag{13.69}$$

where the hadronic parameter $\kappa_L \sim 2 \times 10^{-10}$ incorporates the value of the four-fermion matrix element which is deduced, using isospin relations, from $\mathcal{B}(K^+ \to \pi^0e^+\nu_e)$, and $X(m_t^2/m_W^2)$ is a known function of the top mass. An explicit calculation gives $\mathcal{B}(K_L \to \pi^0\nu\overline{\nu}) = (2.4 \pm 0.4) \times 10^{-11}$ [45]. The currently tightest experimental limit is $\mathcal{B}(K_L \to \pi^0\nu\overline{\nu}) < 2.6 \times 10^{-8}$ [46], which does not yet reach the bound $\mathcal{B}(K_L \to \pi^0\nu\overline{\nu}) < 4.4 \times \mathcal{B}(K^+ \to \pi^+\nu\overline{\nu})$ [41]. Significant further progress is anticipated from experiments searching for $K \to \pi\nu\overline{\nu}$ decays in the next few years.

13.5. Charm

The existence of D^0–$\overline{D}^0$ mixing has been established in recent years [48–51]. The experimental constraints read [27,52] $x \equiv \Delta m/\Gamma = (0.48 \pm 0.18) \times 10^{-2}$ and $y \equiv \Delta\Gamma/(2\Gamma) = (0.66 \pm 0.09) \times 10^{-2}$. Thus, the data clearly show that $y \neq 0$, but improved measurements are needed to be sure of the size of x. Long-distance contributions make it difficult to calculate Standard Model predictions for the D^0–$\overline{D}^0$ mixing parameters. Therefore, the goal of the search for D^0–$\overline{D}^0$ mixing is not to constrain the CKM parameters, but rather to probe new physics. Here CP violation plays an important role. Within the Standard Model, the CP-violating effects are predicted to be small, since the mixing and the relevant decays are described, to an excellent approximation, by the physics of the first two generations only. The expectation is that the Standard Model size of CP violation in D decays is $\mathcal{O}(10^{-3})$ or less, but theoretical work is ongoing to understand whether QCD effects can significantly enhance it. At present, the most sensitive searches involve the $D^0 \to K^+K^-$, $D^0 \to \pi^+\pi^-$ and $D^0 \to K^\pm\pi^\mp$ modes.

The neutral D mesons decay via a singly-Cabibbo-suppressed transition to the CP eigenstates K^+K^- and $\pi^+\pi^-$. These decays are dominated by Standard-Model tree diagrams. Thus, we can write, for $f = K^+K^-$ or $\pi^+\pi^-$,

$$\begin{aligned}
A_f &= A_f^T e^{+i\phi_f^T}\left[1 + r_f e^{i(\delta_f+\phi_f)}\right]\,,\\
\bar{A}_f &= A_f^T e^{-i\phi_f^T}\left[1 + r_f e^{i(\delta_f-\phi_f)}\right]\,,
\end{aligned} \tag{13.70}$$

where $A_f^T e^{\pm i\phi_f^T}$ is the Standard Model tree-level contribution, ϕ_f^T and ϕ_f are weak, CP violating phases, δ_f is a strong phase difference, and r_f is the ratio between a subleading ($r_f \ll 1$) contribution with a weak phase different from ϕ_f^T and the Standard Model tree-level contribution. Neglecting r_f, λ_f is universal, and we can define an observable phase ϕ_D via

$$\lambda_f \equiv -|q/p|e^{i\phi_D} \,. \tag{13.71}$$

(In the limit of CP conservation, choosing $\phi_D = 0$ is equivalent to defining the mass eigenstates by their CP eigenvalue: $|D_\mp\rangle = p|D^0\rangle \pm q|\overline{D}^0\rangle$, with $D_-(D_+)$ being the CP-odd (CP-even) state; that is, the state that does not (does) decay into K^+K^-.)

We define the time integrated CP asymmetry for a final CP eigenstate f as follows:

$$a_f \equiv \frac{\int_0^\infty \Gamma(D^0_{\rm phys}(t) \to f)dt - \int_0^\infty \Gamma(\overline{D}^0_{\rm phys}(t) \to f)dt}{\int_0^\infty \Gamma(D^0_{\rm phys}(t) \to f)dt + \int_0^\infty \Gamma(\overline{D}^0_{\rm phys}(t) \to f)dt} \,. \tag{13.72}$$

(This expression corresponds to the D meson being tagged at production, hence the integration goes from 0 to $+\infty$; measurements are also possible with $\psi(3770) \to D^0\overline{D}^0$, in which case the integration goes from $-\infty$ to $+\infty$ giving slightly different results.) We take $x, y, r_f \ll 1$ and expand to leading order in these parameters. We can then separate the contribution to a_f into three parts [53],

$$a_f = a_f^d + a_f^m + a_f^i \,, \tag{13.73}$$

with the following underlying mechanisms:

1. a_f^d signals CP violation in decay (similar to Eq. (13.38)):

$$a_f^d = 2r_f \sin\phi_f \sin\delta_f \,. \tag{13.74}$$

2. a_f^m signals CP violation in mixing (similar to Eq. (13.47)). With our approximations, it is universal:

$$a^m = -\frac{y}{2}\left(\left|\frac{q}{p}\right| - \left|\frac{p}{q}\right|\right)\cos\phi_D \,. \tag{13.75}$$

3. a_f^i signals CP violation in the interference of mixing and decay (similar to Eq. (13.48)). With our approximations, it is universal:

$$a^i = \frac{x}{2}\left(\left|\frac{q}{p}\right| + \left|\frac{p}{q}\right|\right)\sin\phi_D \,. \tag{13.76}$$

One can isolate the effects of direct CP violation by taking the difference between the CP asymmetries in the K^+K^- and $\pi^+\pi^-$ modes:

$$\Delta a_{CP} \equiv a_{K^+K^-} - a_{\pi^+\pi^-} = a^d_{K^+K^-} - a^d_{\pi^+\pi^-} \,, \tag{13.77}$$

where we neglected a residual, experiment-dependent, contribution from indirect CP violation due to the fact that there may be a decay time dependent acceptance function that can be different for the K^+K^- and $\pi^+\pi^-$ channels. Recent evidence for such direct CP violation [54] has become less significant when including more data, with the current average giving [27]:

$$a^d_{K^+K^-} - a^d_{\pi^+\pi^-} = (-3.3 \pm 1.2) \times 10^{-3} \,. \tag{13.78}$$

One can also isolate the effects of indirect CP violation in the following way. Consider the time dependent decay rates in Eq. (13.33) and Eq. (13.34). The mixing processes modify the time dependence from a pure exponential. However, given the small values of x and y, the time dependences can be recast, to a good approximation, into purely exponential form, but with modified decay-rate parameters [55,56](given here for the K^+K^- final state):

$$\begin{aligned} \Gamma_{D^0\to K^+K^-} &= \Gamma \times [1 + |q/p|\,(y\cos\phi_D - x\sin\phi_D)] \;, \\ \Gamma_{\overline{D}^0\to K^+K^-} &= \Gamma \times [1 + |p/q|\,(y\cos\phi_D + x\sin\phi_D)] \;. \end{aligned} \tag{13.79}$$

One can define CP-conserving and CP-violating combinations of these two observables (normalized to the true width Γ):

$$\begin{aligned} y_{CP} &\equiv \frac{\Gamma_{\overline{D}^0\to K^+K^-} + \Gamma_{D^0\to K^+K^-}}{2\Gamma} - 1 \\ &= (y/2)\,(|q/p| + |p/q|)\cos\phi_D - (x/2)\,(|q/p| - |p/q|)\sin\phi_D \;, \\ A_\Gamma &\equiv \frac{\Gamma_{D^0\to K^+K^-} - \Gamma_{\overline{D}^0\to K^+K^-}}{2\Gamma} \\ &= -(a^m + a^i) \;. \end{aligned} \tag{13.80}$$

In the limit of CP conservation (and, in particular, within the Standard Model), $y_{CP} = (\Gamma_+ - \Gamma_-)/2\Gamma = y$ (where $\Gamma_+(\Gamma_-)$ is the decay width of the CP-even (-odd) mass eigenstate) and $A_\Gamma = 0$. Indeed, present measurements imply that CP violation is small [27],

$$\begin{aligned} y_{CP} &= (+0.87 \pm 0.16) \times 10^{-2} \;, \\ A_\Gamma &= (-0.01 \pm 0.05) \times 10^{-2} \;. \end{aligned}$$

The $K^\pm\pi^\mp$ states are not CP eigenstates, but they are still common final states for D^0 and $\overline{D}^0$ decays. Since $D^0(\overline{D}^0) \to K^-\pi^+$ is a Cabibbo-favored (doubly-Cabibbo-suppressed) process, these processes are particularly sensitive to x and/or $y = \mathcal{O}(\lambda^2)$. Taking into account that $\left|\lambda_{K^-\pi^+}\right|, \left|\lambda^{-1}_{K^+\pi^-}\right| \ll 1$ and $x, y \ll 1$, assuming that there is no direct CP violation (these are Standard Model tree-level decays dominated by a single weak phase, and there is no contribution from penguin-like and chromomagnetic operators), and expanding the time-dependent rates for $xt, yt \lesssim \Gamma^{-1}$, one obtains

$$\begin{aligned} \Gamma[D^0_{\rm phys}(t) \to K^+\pi^-] = \;& e^{-\Gamma t}|\overline{A}_{K^-\pi^+}|^2 \\ &\times \left[r_d^2 + r_d\left|\frac{q}{p}\right|(y'\cos\phi_D - x'\sin\phi_D)\Gamma t + \left|\frac{q}{p}\right|^2 \frac{y^2+x^2}{4}(\Gamma t)^2\right] \;, \\ \Gamma[\overline{D}^0_{\rm phys}(t) \to K^-\pi^+] = \;& e^{-\Gamma t}|\overline{A}_{K^-\pi^+}|^2 \\ &\times \left[r_d^2 + r_d\left|\frac{p}{q}\right|(y'\cos\phi_D + x'\sin\phi_D)\Gamma t + \left|\frac{p}{q}\right|^2 \frac{y^2+x^2}{4}(\Gamma t)^2\right] \;, \end{aligned} \tag{13.81}$$

where

$$\begin{aligned} y' &\equiv y\cos\delta - x\sin\delta \;, \\ x' &\equiv x\cos\delta + y\sin\delta \;. \end{aligned} \tag{13.82}$$

The weak phase ϕ_D is the same as that of Eq. (13.71) (a consequence of neglecting direct CP violation) and $r_d = \mathcal{O}(\tan^2\theta_c)$ is the amplitude ratio, $r_d = \left|\overline{A}_{K^-\pi^+}/A_{K^-\pi^+}\right| = \left|A_{K^+\pi^-}/\overline{A}_{K^+\pi^-}\right|$, that is, $\lambda_{K^-\pi^+} = r_d|q/p|e^{-i(\delta-\phi_D)}$ and $\lambda^{-1}_{K^+\pi^-} = r_d|p/q|e^{-i(\delta+\phi_D)}$. The parameter δ is a strong-phase difference for these processes, that can be obtained from measurements of quantum correlated $\psi(3770) \to D^0\overline{D}^0$ decays [34]. By fitting to the six coefficients of the various time-dependences, one can determine r_d, $|q/p|$, (x^2+y^2), $y'\cos\phi_D$, and $x'\sin\phi_D$. In particular, finding CP violation ($|q/p| \neq 1$ and/or $\sin\phi_D \neq 0$) at a level much higher than 10^{-3} would constitute evidence for new physics. The most stringent constraints to date on CP violation in charm mixing have been obtained with this method [57].

A fit to all data [27], including also results from time dependent analyses of $D^0 \to K_S\pi^+\pi^-$ decays, from which x, y, $|q/p|$ and ϕ_D can be determined directly, yields no evidence for indirect CP violation:

$$\begin{aligned} 1 - |q/p| &= +0.09\,^{+0.09}_{-0.11} \;, \\ \phi_D &= \left(-11\,^{+11}_{-12}\right)^\circ \;. \end{aligned}$$

More details on various theoretical and experimental aspects of $D^0 - \overline{D}^0$ mixing can be found in Ref. [31].

Searches for CP violation in charged $D_{(s)}$ decays have been performed in many modes. Searches in decays to Cabibbo-suppressed final states are particularly interesting, since in other channels effects are likely to be too small to be observable in current experiments.

Examples of relevant two-body modes are $D^+ \to \pi^+\pi^0$, $K_S K^+$, $\phi\pi^+$ and $D_s^+ \to K^+\pi^0$, $K_S\pi^+$, ϕK^+. The most precise results are $\mathcal{A}_{D^+\to K_S K^+} = -0.0011 \pm 0.0025$ and $\mathcal{A}_{D_s^+\to K_S\pi^+} = +0.031 \pm 0.015$ [27]. The precision of experiments is now sufficient that the effect from CP violation in the neutral kaon system can be seen in $D^+ \to K_S\pi^+$ decays [58,59].

Three-body final states provide additional possibilities to search for CP violation, since effects may vary over the phase-space. A number of methods have been proposed to exploit this feature and search for CP violation in ways that do not require modelling of the decay distribution [60–62]. Such methods are useful for analysis of charm decays since they are less sensitive to biases from production asymmetries, and are well suited to address the issue of whether or not CP violation effects are present. The results of all searches to date have been null – no significant CP violation effect has yet been observed in $D^+_{(s)}$ decays.

13.6. Beauty

13.6.1. ***CP violation in mixing of B^0 and B_s^0 mesons*** : The upper bound on the CP asymmetry in semileptonic B decays [26] implies that CP violation in $B^0 - \overline{B}^0$ mixing is a small effect (we use $\mathcal{A}_{\rm SL}/2 \approx 1 - |q/p|$, see Eq. (13.40)):

$$\mathcal{A}^d_{\rm SL} = (+0.7 \pm 2.7) \times 10^{-3} \implies |q/p| = 0.9997 \pm 0.0013 \,. \quad (13.83)$$

The Standard Model prediction is

$$\mathcal{A}^d_{\rm SL} = \mathcal{O}\left[(m_c^2/m_t^2)\sin\beta\right] \lesssim 0.001 \,. \quad (13.84)$$

An explicit calculation gives $(-4.1 \pm 0.6) \times 10^{-4}$ [63].

The experimental constraint on CP violation in $B_s^0 - \overline{B}_s^0$ mixing is somewhat weaker than that in the $B^0 - \overline{B}^0$ system [26]

$$\mathcal{A}^s_{\rm SL} = (-17.1 \pm 5.5) \times 10^{-3} \implies |q/p| = 1.0086 \pm 0.0028 \,. \quad (13.85)$$

The Standard Model prediction is $\mathcal{A}^s_{\rm SL} = \mathcal{O}\left[(m_c^2/m_t^2)\sin\beta_s\right] \lesssim 10^{-4}$, with an explicit calculation giving $(1.9 \pm 0.3) \times 10^{-5}$ [63]. The tension between the measurement and the prediction originates from a result from D0 for the inclusive same-sign dimuon asymmetry that deviates from the Standard Model prediction by 3.6σ [64]. As yet, this has not been confirmed by independent studies.

In models where $\mathbf{\Gamma}_{12}/\mathbf{M}_{12}$ is approximately real, such as the Standard Model, an upper bound on $\Delta\Gamma/\Delta m \approx \mathcal{R}e(\mathbf{\Gamma}_{12}/\mathbf{M}_{12})$ provides yet another upper bound on the deviation of $|q/p|$ from one. This constraint does not hold if $\mathbf{\Gamma}_{12}/\mathbf{M}_{12}$ is approximately imaginary. (An alternative parameterization uses $q/p = (1-\tilde{\epsilon}_B)/(1+\tilde{\epsilon}_B)$, leading to $\mathcal{A}_{\rm SL} \simeq 4\mathcal{R}e(\tilde{\epsilon}_B)$.)

13.6.2. ***CP violation in interference of B^0 decays with and without mixing*** : The small deviation (less than one percent) of $|q/p|$ from 1 implies that, at the present level of experimental precision, CP violation in B^0 mixing is a negligible effect. Thus, for the purpose of analyzing CP asymmetries in hadronic B^0 decays, we can use

$$\lambda_f = e^{-i\phi_{M(B^0)}}(\overline{A}_f/A_f) \,, \quad (13.86)$$

where $\phi_{M(B^0)}$ refers to the phase of $\mathbf{M}_{12}$ appearing in Eq. (13.45) that is appropriate for $B^0 - \overline{B}^0$ oscillations. Within the Standard Model, the corresponding phase factor is given by

$$e^{-i\phi_{M(B^0)}} = (V_{tb}^* V_{td})/(V_{tb} V_{td}^*) \,. \quad (13.87)$$

The class of CP violation effects in interference between mixing and decay is studied with final states that are common to B^0 and $\overline{B}^0$ decays [65,66]. It is convenient to rewrite Eq. (13.43) for B^0 decays as [67–69]

$$\mathcal{A}_f(t) = S_f \sin(\Delta m t) - C_f \cos(\Delta m t) \,,$$

$$S_f \equiv \frac{2\,\mathcal{I}m(\lambda_f)}{1+|\lambda_f|^2} \,, \quad C_f \equiv \frac{1-|\lambda_f|^2}{1+|\lambda_f|^2} \,, \quad (13.88)$$

where we assume that $\Delta\Gamma = 0$ and $|q/p| = 1$. An alternative notation in use is $A_f \equiv -C_f$ – this A_f should not be confused with the A_f of Eq. (13.16), but in the limit that $|q/p| = 1$ is equivalent with the $\mathcal{A}_f$ of Eq. (13.38).

A large class of interesting processes proceed via quark transitions of the form $\overline{b} \to \overline{q}q\overline{q}'$ with $q' = s$ or d. For $q = c$ or u, there are contributions from both tree (t) and penguin (p^{q_u}, where $q_u = u, c, t$ is the quark in the loop) diagrams (see Fig. 13.2) which carry different weak phases:

$$A_f = \left(V_{qb}^* V_{qq'}\right) t_f + \sum_{q_u=u,c,t} \left(V_{q_u b}^* V_{q_u q'}\right) p_f^{q_u} \,. \quad (13.89)$$

(The distinction between tree and penguin contributions is a heuristic one; the separation by the operator that enters is more precise. For a detailed discussion of the more complete operator product approach, which also includes higher order QCD corrections, see, for example, Ref. [70].) Using CKM unitarity, these decay amplitudes can always be written in terms of just two CKM combinations. For example, for $f = \pi\pi$, which proceeds via a $\overline{b} \to \overline{u}u\overline{d}$ transition, we can write

$$A_{\pi\pi} = (V_{ub}^* V_{ud})\, T_{\pi\pi} + (V_{tb}^* V_{td})\, P^t_{\pi\pi} \,, \quad (13.90)$$

where $T_{\pi\pi} = t_{\pi\pi} + p^u_{\pi\pi} - p^c_{\pi\pi}$ and $P^t_{\pi\pi} = p^t_{\pi\pi} - p^c_{\pi\pi}$. CP-violating phases in Eq. (13.90) appear only in the CKM elements, so that

$$\frac{\overline{A}_{\pi\pi}}{A_{\pi\pi}} = \frac{(V_{ub}V_{ud}^*)\, T_{\pi\pi} + (V_{tb}V_{td}^*)\, P^t_{\pi\pi}}{(V_{ub}^* V_{ud})\, T_{\pi\pi} + (V_{tb}^* V_{td})\, P^t_{\pi\pi}} \,. \quad (13.91)$$

For $f = J/\psi K$, which proceeds via a $\overline{b} \to \overline{c}c\overline{s}$ transition, we can write

$$A_{\psi K} = (V_{cb}^* V_{cs})\, T_{\psi K} + (V_{ub}^* V_{us})\, P^u_{\psi K} \,, \quad (13.92)$$

where $T_{\psi K} = t_{\psi K} + p^c_{\psi K} - p^t_{\psi K}$ and $P^u_{\psi K} = p^u_{\psi K} - p^t_{\psi K}$. A subtlety arises in this decay that is related to the fact that B^0 decays into a final $J/\psi K^0$ state while $\overline{B}^0$ decays into a final $J/\psi\overline{K}^0$ state. A common final state, *e.g.*, $J/\psi K_S$, is reached only via $K^0 - \overline{K}^0$ mixing. Consequently, the phase factor (defined in Eq. (13.45)) corresponding to neutral K mixing, $e^{-i\phi_{M(K)}} = (V_{cd}^* V_{cs})/(V_{cd} V_{cs}^*)$, plays a role:

$$\frac{\overline{A}_{\psi K_S}}{A_{\psi K_S}} = -\frac{(V_{cb}V_{cs}^*)\, T_{\psi K} + (V_{ub}V_{us}^*)\, P^u_{\psi K}}{(V_{cb}^* V_{cs})\, T_{\psi K} + (V_{ub}^* V_{us})\, P^u_{\psi K}} \times \frac{V_{cd}^* V_{cs}}{V_{cd} V_{cs}^*} \,. \quad (13.93)$$

For $q = s$ or d, there are only penguin contributions to A_f, that is, $t_f = 0$ in Eq. (13.89). (The tree $\overline{b} \to \overline{u}u\overline{q}'$ transition followed by $\overline{u}u \to \overline{q}q$ rescattering is included below in the P^u terms.) Again, CKM unitarity allows us to write A_f in terms of two CKM combinations. For example, for $f = \phi K_S$, which proceeds via a $\overline{b} \to \overline{s}s\overline{s}$ transition, we can write

$$\frac{\overline{A}_{\phi K_S}}{A_{\phi K_S}} = -\frac{(V_{cb}V_{cs}^*)\, P^c_{\phi K} + (V_{ub}V_{us}^*)\, P^u_{\phi K}}{(V_{cb}^* V_{cs})\, P^c_{\phi K} + (V_{ub}^* V_{us})\, P^u_{\phi K}} \times \frac{V_{cd}^* V_{cs}}{V_{cd} V_{cs}^*} \,, \quad (13.94)$$

where $P^c_{\phi K} = p^c_{\phi K} - p^t_{\phi K}$ and $P^u_{\phi K} = p^u_{\phi K} - p^t_{\phi K}$.

Since in general the amplitude A_f involves two different weak phases, the corresponding decays can exhibit both CP violation in the interference of decays with and without mixing, $S_f \neq 0$, and CP violation in decays, $C_f \neq 0$. (At the present level of experimental precision, the contribution to C_f from CP violation in mixing is negligible, see Eq. (13.83).) If the contribution from a second weak phase is suppressed, then the interpretation of S_f in terms of Lagrangian CP-violating parameters is clean, while C_f is small. If such a second contribution is not suppressed, S_f depends on hadronic parameters and, if the relevant strong phase difference is large, C_f is large.

A summary of $\overline{b} \to \overline{q}\overline{q}q'$ modes with $q' = s$ or d is given in Table 13.1. The $\overline{b} \to \overline{d}d\overline{q}$ transitions lead to final states that are similar to those from $\overline{b} \to \overline{u}u\overline{q}$ transitions and have similar phase dependence. Final states that consist of two vector mesons ($\psi\phi$ and $\phi\phi$) are not CP eigenstates, and angular analysis is needed to separate the CP-even from the CP-odd contributions.

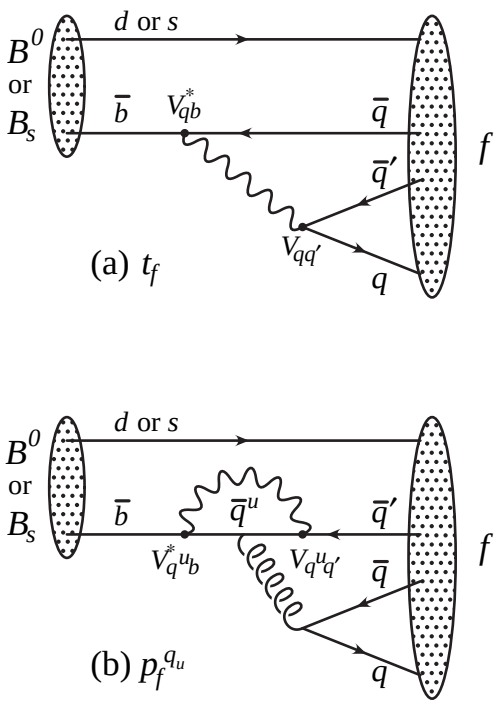

Figure 13.2: Feynman diagrams for (a) tree and (b) penguin amplitudes contributing to $B^0 \to f$ or $B_s^0 \to f$ via a $\overline{b} \to \overline{q}q\overline{q}'$ quark-level process.

Table 13.1: Summary of $\overline{b} \to \overline{q}q\overline{q}'$ modes with $q' = s$ or d. The second and third columns give examples of final hadronic states (usually those which are experimentally most convenient to study). The fourth column gives the CKM dependence of the amplitude A_f, using the notation of Eqs. (13.90, 13.92, 13.94), with the dominant term first and the subdominant second. The suppression factor of the second term compared to the first is given in the last column. "Loop" refers to a penguin versus tree-suppression factor (it is mode-dependent and roughly $\mathcal{O}(0.2-0.3)$) and $\lambda \simeq 0.23$ is the expansion parameter of Eq. (13.51).

$\overline{b} \to \overline{q}q\overline{q}'$	$B^0 \to f$	$B_s^0 \to f$	CKM dependence of A_f	Suppression
$\bar{b} \to \bar{c}c\bar{s}$	ψK_S	$\psi\phi$	$(V_{cb}^* V_{cs})T + (V_{ub}^* V_{us})P^u$	loop $\times\, \lambda^2$
$\bar{b} \to \bar{s}s\bar{s}$	ϕK_S	$\phi\phi$	$(V_{cb}^* V_{cs})P^c + (V_{ub}^* V_{us})P^u$	λ^2
$\bar{b} \to \bar{u}u\bar{s}$	$\pi^0 K_S$	K^+K^-	$(V_{cb}^* V_{cs})P^c + (V_{ub}^* V_{us})T$	λ^2/loop
$\bar{b} \to \bar{c}c\bar{d}$	D^+D^-	ψK_S	$(V_{cb}^* V_{cd})T + (V_{tb}^* V_{td})P^t$	loop
$\bar{b} \to \bar{s}s\bar{d}$	$K_S K_S$	ϕK_S	$(V_{tb}^* V_{td})P^t + (V_{cb}^* V_{cd})P^c$	$\lesssim 1$
$\bar{b} \to \bar{u}u\bar{d}$	$\pi^+\pi^-$	$\rho^0 K_S$	$(V_{ub}^* V_{ud})T + (V_{tb}^* V_{td})P^t$	loop
$\bar{b} \to \bar{c}u\bar{d}$	$D_{CP}\pi^0$	$D_{CP}K_S$	$(V_{cb}^* V_{ud})T + (V_{ub}^* V_{cd})T'$	λ^2
$\bar{b} \to \bar{c}u\bar{s}$	$D_{CP}K_S$	$D_{CP}\phi$	$(V_{cb}^* V_{us})T + (V_{ub}^* V_{cs})T'$	$\lesssim 1$

The cleanliness of the theoretical interpretation of S_f can be assessed from the information in the last column of Table 13.1. In case of small uncertainties, the expression for S_f in terms of CKM phases can be deduced from the fourth column of Table 13.1 in combination with Eq. (13.87) (and, for $b \to q\overline{q}s$ decays, the example in Eq. (13.93)). Here we consider several interesting examples.

For $B^0 \to J/\psi K_S$ and other $\overline{b} \to \overline{c}c\overline{s}$ processes, we can neglect the P^u contribution to A_f, in the Standard Model, to an approximation that is better than one percent, giving:

$$\lambda_{\psi K_S} = -e^{-2i\beta} \;\Rightarrow\; S_{\psi K_S} = \sin 2\beta\,, \quad C_{\psi K_S} = 0\,. \tag{13.95}$$

It is important to verify experimentally the level of suppression of the penguin contribution. Methods based on flavor symmetries [71–74] allow limits to be obtained. All are currently consistent with the P^u term being negligible.

In the presence of new physics, A_f is still likely to be dominated by the T term, but the mixing amplitude might be modified. We learn that, model-independently, $C_f \approx 0$ while S_f cleanly determines the mixing phase $(\phi_M - 2\arg(V_{cb}V_{cd}^*))$. The experimental measurement [27], $S_{\psi K} = +0.682 \pm 0.019$, gave the first precision test of the Kobayashi-Maskawa mechanism, and its consistency with the predictions for $\sin 2\beta$ makes it very likely that this mechanism is indeed the dominant source of CP violation in the quark sector.

For $B^0 \to \phi K_S$ and other $\overline{b} \to \overline{s}s\overline{s}$ processes (as well as some $\overline{b} \to \overline{u}u\overline{s}$ processes), we can neglect the subdominant contributions, in the Standard Model, to an approximation that is good to the order of a few percent:

$$\lambda_{\phi K_S} = -e^{-2i\beta} \;\Rightarrow\; S_{\phi K_S} = \sin 2\beta\,, \quad C_{\phi K_S} = 0\,. \tag{13.96}$$

A review of explicit calculations of the effects of subleading amplitudes can be found in Ref. [75]. In the presence of new physics, both A_f and $\mathbf{M}_{12}$ can have contributions that are comparable in size to those of the Standard Model and carry new weak phases. Such a situation gives several interesting consequences for penguin-dominated $b \to q\overline{q}s$ decays ($q = u, d, s$) to a final state f:

1. The value of $-\eta_f S_f$ may be different from $S_{\psi K_S}$ by more than a few percent, where η_f is the CP eigenvalue of the final state.
2. The values of $\eta_f S_f$ for different final states f may be different from each other by more than a few percent (for example, $S_{\phi K_S} \neq S_{\eta' K_S}$).
3. The value of C_f may be different from zero by more than a few percent.

While a clear interpretation of such signals in terms of Lagrangian parameters will be difficult because, under these circumstances, hadronic parameters play a role, any of the above three options will clearly signal new physics. Fig. 13.3 summarizes the present experimental results: none of the possible signatures listed above is unambiguously established, but there is definitely still room for new physics.

For the $\overline{b} \to \overline{u}u\overline{d}$ process $B \to \pi\pi$ and other related channels, the penguin-to-tree ratio can be estimated using SU(3) relations and experimental data on related $B \to K\pi$ decays. The result (for $\pi\pi$) is that the suppression is at the level of $0.2 - 0.3$ and so cannot be neglected. The expressions for $S_{\pi\pi}$ and $C_{\pi\pi}$ to leading order in $R_{PT} \equiv (|V_{tb}V_{td}|\, P_{\pi\pi}^t)/(|V_{ub}V_{ud}|\, T_{\pi\pi})$ are:

$$\lambda_{\pi\pi} = e^{2i\alpha}\left[(1 - R_{PT}e^{-i\alpha})/(1 - R_{PT}e^{+i\alpha})\right] \;\Rightarrow$$

$$S_{\pi\pi} \approx \sin 2\alpha + 2\,\mathcal{R}e(R_{PT})\cos 2\alpha \sin\alpha\,, \quad C_{\pi\pi} \approx 2\,\mathcal{I}m(R_{PT})\sin\alpha\,. \tag{13.97}$$

Note that R_{PT} is mode-dependent and, in particular, could be different for $\pi^+\pi^-$ and $\pi^0\pi^0$. If strong phases can be neglected, then R_{PT} is real, resulting in $C_{\pi\pi} = 0$. The size of $C_{\pi\pi}$ is an indicator of how large the strong phase is. The present experimental average is $C_{\pi^+\pi^-} = -0.31 \pm 0.05$ [27]. As concerns $S_{\pi\pi}$, it is clear from Eq. (13.97) that the relative size or strong phase of the penguin contribution must be known to extract α. This is the problem of penguin pollution.

The cleanest solution involves isospin relations among the $B \to \pi\pi$ amplitudes [76]:

$$\frac{1}{\sqrt{2}}A_{\pi^+\pi^-} + A_{\pi^0\pi^0} = A_{\pi^+\pi^0}\,. \tag{13.98}$$

The method exploits the fact that the penguin contribution to $P_{\pi\pi}^t$ is pure $\Delta I = 1/2$ (this is not true for the electroweak penguins which,

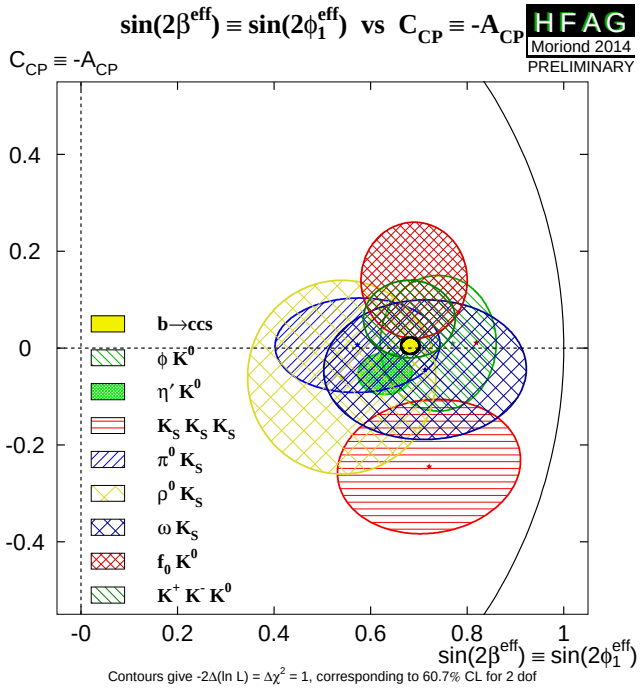

Figure 13.3: Summary of the results [27] of time-dependent analyses of $b \to q\overline{q}s$ decays, which are potentially sensitive to new physics.

however, are expected to be small), while the tree contribution to $T_{\pi\pi}$ contains pieces that are both $\Delta I = 1/2$ and $\Delta I = 3/2$. A simple geometric construction then allows one to find R_{PT} and extract α cleanly from $S_{\pi^+\pi^-}$. The key experimental difficulty is that one must measure accurately the separate rates for $B^0, \overline{B}^0 \to \pi^0\pi^0$.

CP asymmetries in $B \to \rho\pi$ and $B \to \rho\rho$ can also be used to determine α. In particular, the $B \to \rho\rho$ measurements are presently very significant in constraining α. The extraction proceeds via isospin analysis similar to that of $B \to \pi\pi$. There are, however, several important differences. First, due to the finite width of the ρ mesons, a final $(\rho\rho)_{I=1}$ state is possible [77]. The effect is, however, small, of the order of $(\Gamma_\rho/m_\rho)^2 \sim 0.04$. Second, due to the presence of three helicity states for the two vector mesons, angular analysis is needed to separate the CP-even and CP-odd components. The theoretical expectation is that the CP-odd component is small, which is supported by experiments which find that the $\rho^+\rho^-$ and $\rho^\pm\rho^0$ modes are dominantly longitudinally polarized. Third, an important advantage of the $\rho\rho$ modes is that the penguin contribution is expected to be small due to different hadronic dynamics. This expectation is confirmed by the smallness of $\mathcal{B}(B^0 \to \rho^0\rho^0) = (0.97 \pm 0.24) \times 10^{-6}$ [78,79] compared to $\mathcal{B}(B^0 \to \rho^+\rho^-) = (24.2 \pm 3.1) \times 10^{-6}$ [27]. Thus, $S_{\rho^+\rho^-}$ is not far from $\sin 2\alpha$. Finally, both $S_{\rho^0\rho^0}$ and $C_{\rho^0\rho^0}$ are experimentally accessible, which may allow a precision determination of α. However, a full isospin analysis should allow that the fractions of longitudinal polarisation in B and $\overline{B}$ decays may differ, which has not yet been done by the experiments. The consistency between the range of α determined by the $B \to \pi\pi, \rho\pi, \rho\rho$ measurements and the range allowed by CKM fits (excluding these direct determinations) provides further support to the Kobayashi-Maskawa mechanism.

All modes discussed in this Section so far have possible contributions from penguin amplitudes. As shown in Table 13.1, CP violation can also be studied with final states, typically containing charmed mesons, where no such contribution is possible. The neutral charmed meson must be reconstructed in a final state, such as a CP eigenstate, common to D^0 and $\overline{D}^0$ so that the amplitudes for the B and $\overline{B}$ meson decays interfere. Although there is a second tree amplitude with a different weak phase, the contributions of the different diagrams can in many cases be separated experimentally (for example by exploiting different decays of the $\overline{D}^0$ mesons) making these channels very clean theoretically. Moreover, the interference between the two tree diagrams gives sensitivity to γ, as will be discussed in Section 13.6.4.

13.6.3. ***CP violation in interference of B_s^0 decays with and without mixing*** : As discussed in Section 13.6.1, the world average for $|q/p|$ in the B_s^0 system currently deviates from the Standard Model expectation due to an anomalous value of the dimuon asymmetry. Attributing the dimuon asymmetry result to a fluctuation, we again neglect the deviation of $|q/p|$ from 1, and use

$$\lambda_f = e^{-i\phi_M(B_s^0)}(\overline{A}_f/A_f) \,. \tag{13.99}$$

Within the Standard Model,

$$e^{-i\phi_{M(B_s^0)}} = (V_{tb}^* V_{ts})/(V_{tb} V_{ts}^*) \,. \tag{13.100}$$

Note that $\Delta\Gamma/\Gamma = 0.116 \pm 0.020$ [27] and therefore y should not be put to zero in Eqs. (13.33, 13.34). However, $|q/p| = 1$ is expected to hold to an even better approximation than for B^0 mesons. One therefore obtains

$$\mathcal{A}_f(t) = \frac{S_f \sin(\Delta m t) - C_f \cos(\Delta m t)}{\cosh(\Delta\Gamma t/2) - A_f^{\Delta\Gamma} \sinh(\Delta\Gamma t/2)} \,,$$

$$A_f^{\Delta\Gamma} \equiv \frac{-2\,\mathcal{R}e(\lambda_f)}{1 + |\lambda_f|^2} \,. \tag{13.101}$$

The presence of the $A_f^{\Delta\Gamma}$ term implies that information on λ_f can be obtained from analyses that do not use tagging of the initial flavor, through so-called effective lifetime measurements [80].

The $B_s^0 \to J/\psi\phi$ decay proceeds via the $\overline{b} \to \overline{c}c\overline{s}$ transition. The CP asymmetry in this mode thus determines (with angular analysis to disentangle the CP-even and CP-odd components of the final state) $\sin 2\beta_s$, where β_s is defined in Eq. (13.54) [81]. The $B_s^0 \to J/\psi\pi^+\pi^-$ decay, which has a large contributions from $J/\psi f_0(980)$ and is assumed to also proceed dominantly via the $\overline{b} \to \overline{c}c\overline{s}$ transition, has also been used to determine β_s. In this case no angular analysis is necessary, since the final state has been shown to be dominated by the CP-even component [82]. The combination of ATLAS, CDF, D0 and LHCb measurements yields [27]

$$-2\beta_s = +0.04\,^{+0.10}_{-0.13}, \tag{13.102}$$

consistent with the Standard Model prediction, $\beta_s = 0.018 \pm 0.001$ [18].

The experimental investigation of CP violation in the B_s^0 sector is still at a relatively early stage, and far fewer modes have been studied than in the B^0 system. First results on the $\overline{b} \to \overline{q}q\overline{s}$ decays $B_s^0 \to \phi\phi$ [83] and K^+K^- [84] have been reported recently. More channels are expected to be studied in the near future.

13.6.4. ***Direct CP violation in the B system*** :

An interesting class of decay modes is that of the tree-level decays $B^\pm \to D^{(*)}K^\pm$. These decays provide golden methods for a clean determination of the angle γ [86–90]. The method uses the decays $B^+ \to D^0K^+$, which proceeds via the quark transition $\overline{b} \to \overline{u}c\overline{s}$, and $B^+ \to \overline{D}^0K^+$, which proceeds via the quark transition $\overline{b} \to \overline{c}u\overline{s}$, with the D^0 and $\overline{D}^0$ decaying into a common final state. The decays into common final states, such $(\pi^0K_S)_DK^+$, involve interference effects between the two amplitudes, with sensitivity to the relative phase, $\delta + \gamma$ (δ is the relevant strong phase). The CP-conjugate processes are sensitive to $\delta - \gamma$. Measurements of branching ratios and CP asymmetries allow the determination of γ and δ from amplitude triangle relations. The method suffers from discrete ambiguities but, since all hadronic parameters can be determined from the data, has negligible theoretical uncertainty [85].

Unfortunately, the smallness of the CKM-suppressed $b \to u$ transitions makes it difficult at present to use the simplest methods [86–88] to determine γ. These difficulties are overcome (and the discrete ambiguities are removed) by performing a Dalitz plot analysis for multi-body D decays [89,90]. The consistency between the range of γ determined by the $B \to DK$ measurements and the range allowed by CKM fits (excluding these direct determinations) provides

further support to the Kobayashi-Maskawa mechanism. As more data becomes available, determinations of γ from $B_s^0 \to D_s^{\mp} K^{\pm}$ [91,92] and $B^0 \to DK^{*0}$ [93–96] are expected to also give competitive measurements.

Decays to the final state $K^{\mp}\pi^{\pm}$ provided the first observations of direct CP violation in both B^0 and B_s^0 systems. The asymmetry arises due to interference between tree and penguin diagrams [97], similar to the effect discussed in Section 13.6.2. In principle, measurements of $\mathcal{A}_{\overline{B}^0 \to K^-\pi^+}$ and $\mathcal{A}_{\overline{B}_s^0 \to K^+\pi^-}$ could be used to determine the weak phase difference γ, but lack of knowledge of the relative magnitude and strong phase of the contributing amplitudes limits the achievable precision. The uncertainties on these hadronic parameters can be reduced by exploiting flavor symmetries, which predict a number of relations between asymmetries in different modes. One such relation is that the partial rate differences for B^0 and B_s^0 decays to $K^{\mp}\pi^{\pm}$ are expected to be approximately equal and opposite [98], which is consistent with current data. It is also expected that the partial rate asymmetries for $\overline{B}^0 \to K^-\pi^+$ and $B^- \to K^-\pi^0$ should be approximately equal; however, the experimental results currently show a significant discrepancy [27]:

$$\mathcal{A}_{\overline{B}^0 \to K^-\pi^+} = -0.082 \pm 0.006 \ , \qquad \mathcal{A}_{B^- \to K^-\pi^0} = 0.040 \pm 0.021 \ .$$

It is therefore of great interest to understand whether this originates from Standard Model QCD corrections, or whether it is a signature of new dynamics. Improved tests of a more precise relation between the partial rate differences of all four $K\pi$ final states [99–102], currently limited by knowledge of the CP asymmetry in $\overline{B}^0 \to K_S\pi^0$ decays, may help to resolve the situation.

13.7. Summary and Outlook

CP violation has been experimentally established in K and B meson decays. A full list of CP asymmetries that have been measured at a level higher than 5σ is given in the introduction to this review. In Section 13.1.4 we introduced three types of CP-violating effects. Examples of these three types include the following:

1. All three types of CP violation have been observed in $K \to \pi\pi$ decays:

$$\begin{aligned}
\mathcal{R}e(\epsilon') &= \frac{1}{6}\left(\left|\frac{\overline{A}_{\pi^0\pi^0}}{A_{\pi^0\pi^0}}\right| - \left|\frac{\overline{A}_{\pi^+\pi^-}}{A_{\pi^+\pi^-}}\right|\right) = (2.5 \pm 0.4) \times 10^{-6} \quad \text{(I)} \\
\mathcal{R}e(\epsilon) &= \frac{1}{2}\left(1 - \left|\frac{q}{p}\right|\right) = (1.66 \pm 0.02) \times 10^{-3} \quad \text{(II)} \\
\mathcal{I}m(\epsilon) &= -\frac{1}{2}\mathcal{I}m(\lambda_{(\pi\pi)_{I=0}}) = (1.57 \pm 0.02) \times 10^{-3} \ . \quad \text{(III)}
\end{aligned} \tag{13.103}$$

2. Direct CP violation has been observed in, for example, the $B^0 \to K^+\pi^-$ decays, while CP violation in interference of decays with and without mixing has been observed in, for example, the $B^0 \to J/\psi K_S$ decay:

$$\begin{aligned}
\mathcal{A}_{K^+\pi^-} &= \frac{|\overline{A}_{K^-\pi^+}/A_{K^+\pi^-}|^2 - 1}{|\overline{A}_{K^-\pi^+}/A_{K^+\pi^-}|^2 + 1} = -0.082 \pm 0.006 \quad \text{(I)} \\
S_{\psi K} &= \mathcal{I}m(\lambda_{\psi K}) = +0.682 \pm 0.019 \ . \quad \text{(III)}
\end{aligned} \tag{13.104}$$

Based on Standard Model predictions, further observations of CP violation in B^0, B^+ and B_s^0 decays seem likely in the near future, at both LHCb and its upgrade [103,104] as well as the Belle II experiment [105]. The first observation of CP violation in b baryons is also likely to be within reach of LHCb. The same experiments have great potential to improve the sensitivity to CP violation effects in the charm sector, though uncertainty in the Standard Model predictions makes it difficult to forecast whether or not discoveries will be forthcoming. A number of upcoming experiments have potential to make significant progress on rare kaon decays. Observables that are subject to clean theoretical interpretation, such as β from $S_{\psi K_S}$, β_s from $B_s^0 \to J/\psi\phi$, $\mathcal{B}(K_L \to \pi^0\nu\overline{\nu})$ and γ from CP violation in $B \to DK$ decays, are of particular value for constraining the values of the CKM parameters and probing the flavor sector of extensions to the Standard Model. Progress in lattice QCD calculations is also needed to complement the anticipated experimental results. Other probes of CP violation now being pursued experimentally include the electric dipole moments of the neutron and electron, and the decays of tau leptons. Additional processes that are likely to play an important role in future CP studies include top-quark production and decay, Higgs boson decays and neutrino oscillations.

All measurements of CP violation to date are consistent with the predictions of the Kobayashi-Maskawa mechanism of the Standard Model. In fact, it is now established that the KM mechanism plays a major role in the CP violation measured in the quark sector. However, a dynamically-generated matter-antimatter asymmetry of the universe requires additional sources of CP violation, and such sources are naturally generated by extensions to the Standard Model. New sources might eventually reveal themselves as small deviations from the predictions of the KM mechanism, or else might not be observable in the quark sector at all, but observable with future probes such as neutrino oscillations or electric dipole moments. We cannot guarantee that new sources of CP violation will ever be found experimentally, but the fundamental nature of CP violation demands a vigorous effort.

A number of excellent reviews of CP violation are available [106–112], where the interested reader may find a detailed discussion of the various topics that are briefly reviewed here.

We thank David Kirkby for significant contributions to earlier version of this review.

References:

1. J.H. Christenson *et al.*, Phys. Rev. Lett. **13**, 138 (1964).
2. B. Aubert *et al.*, [BABAR Collab.], Phys. Rev. Lett. **87**, 091801 (2001).
3. K. Abe *et al.*, [Belle Collab.], Phys. Rev. Lett. **87**, 091802 (2001).
4. H. Burkhardt *et al.*, [NA31 Collab.], Phys. Lett. **B206**, 169 (1988).
5. V. Fanti *et al.*, [NA48 Collab.], Phys. Lett. **B465**, 335 (1999).
6. A. Alavi-Harati *et al.*, [KTeV Collab.], Phys. Rev. Lett. **83**, 22 (1999).
7. B. Aubert *et al.*, [BABAR Collab.], Phys. Rev. Lett. **93**, 131801 (2004).
8. Y. Chao *et al.*, [Belle Collab.], Phys. Rev. Lett. **93**, 191802 (2004).
9. A. Poluektov *et al.*, [Belle Collab.], Phys. Rev. **D81**, 112002 (2010).
10. P. del Amo Sanchez *et al.*, [BABAR Collab.], Phys. Rev. **D82**, 072004 (2010).
11. R. Aaij *et al.*, [LHCb Collab.], Phys. Lett. **B712**, 203 (2012).
12. R. Aaij *et al.*, [LHCb Collab.], Phys. Rev. Lett. **110**, 221601 (2013).
13. See results on the "Time reversal invariance," within the review on "Tests of Conservation Laws," in this *Review*.
14. J. Bernabeu, F. Martinez-Vidal, and P. Villanueva-Perez, JHEP **1208**, 064 (2012).
15. J. P. Lees *et al.*, [BABAR Collab.], Phys. Rev. Lett. **109**, 211801 (2012).
16. See, for example, R. F. Streater and A. S. Wightman, *CPT, Spin and Statistics, and All That,* reprinted by Addison-Wesley, New York (1989).
17. M. Kobayashi and T. Maskawa, Prog. Theor. Phys. **49**, 652 (1973).
18. J. Charles *et al.*, [CKMfitter Group], Eur. Phys. J. **C41**, 1 (2005), updated results and plots available at: `http://ckmfitter.in2p3.fr`.
19. M. Bona *et al.*, [UTfit Collab.], JHEP **0603**, 080 (2006), updated results and plots available at: `http://www.utfit.org/UTfit/` .
20. A.D. Sakharov, Pisma Zh. Eksp. Teor. Fiz. **5**, 32 (1967) [Sov. Phys. JETP Lett. **5**, 24 (1967)].

21. For a review, see *e.g.*, A. Riotto, "Theories of baryogenesis," arXiv:hep-ph/9807454.
22. M. Fukugita and T. Yanagida, Phys. Lett. **B174**, 45 (1986).
23. G. Aad *et al.*, [ATLAS Collab.], Phys. Lett. **B716**, 1 (2012).
24. S. Chatrchyan *et al.*, [CMS Collab.], Phys. Lett. **B716**, 30 (2012).
25. See the K-meson Listings in this *Review*.
26. See the B-meson Listings in this *Review*.
27. Y. Amhis *et al.*, [HFAG Collab.], arXiv:1207.1158 [hep-ex], and online update at http://www.slac.stanford.edu/xorg/hfag.
28. R. Aaij *et al.*, [LHCb Collab.], Phys. Rev. Lett. **111**, 101801 (2013).
29. R. Aaij *et al.*, [LHCb Collab.], Phys. Rev. Lett. **112**, 011801 (2014).
30. V. Weisskopf and E. P. Wigner, Z. Phys. **63**, 54 (1930); Z. Phys. **65**, 18 (1930). [See also Appendix A of P.K. Kabir, *The CP Puzzle: Strange Decays of the Neutral Kaon,* Academic Press (1968)].
31. See the review on "$D^0 - \overline{D}^0$ Mixing" in this *Review*.
32. O. Long *et al.*, Phys. Rev. **D68**, 034010 (2003).
33. M. Gronau, Y. Grossman, and J. L. Rosner, Phys. Lett. **B508**, 37 (2001).
34. D. M. Asner *et al.*, [CLEO Collab.], Phys. Rev. **D78**, 012001 (2008).
35. L. Wolfenstein, Phys. Rev. Lett. **13**, 562 (1964).
36. See the review on "Cabibbo-Kobayashi-Maskawa Mixing Matrix," in this *Review*.
37. L. Wolfenstein, Phys. Rev. Lett. **51**, 1945 (1983).
38. A.J. Buras, M.E. Lautenbacher, and G. Ostermaier, Phys. Rev. **D50**, 3433 (1994).
39. C. Jarlskog, Phys. Rev. Lett. **55**, 1039 (1985).
40. See the review on "CP violation in $K_S \to 3\pi$," in this *Review*.
41. Y. Grossman and Y. Nir, Phys. Lett. **B398**, 163 (1997).
42. L.S. Littenberg, Phys. Rev. **D39**, 3322 (1989).
43. A.J. Buras, Phys. Lett. **B333**, 476 (1994).
44. G. Buchalla and A.J. Buras, Nucl. Phys. **B400**, 225 (1993).
45. J. Brod, M. Gorbahn, and E. Stamou, Phys. Rev. **D83**, 034030 (2011).
46. J. K. Ahn *et al.*, [E391a Collab.], Phys. Rev. **D81**, 072004 (2010).
47. T. Holmstrom *et al.*, [HyperCP Collab.], Phys. Rev. Lett. **93**, 262001 (2004).
48. B. Aubert *et al.*, [BABAR Collab.], Phys. Rev. Lett. **98**, 211802 (2007).
49. M. Staric *et al.*, [Belle Collab.], Phys. Rev. Lett. **98**, 211803 (2007).
50. T. Aaltonen *et al.*, [CDF Collab.], Phys. Rev. Lett. **100**, 121802 (2008).
51. R. Aaij *et al.*, [LHCb Collab.], Phys. Rev. Lett. **110**, 101802 (2013).
52. See the D-meson Listings in this *Review*.
53. Y. Grossman, A. L. Kagan, and Y. Nir, Phys. Rev. **D75**, 036008 (2007).
54. R. Aaij *et al.*, [LHCb Collab.], Phys. Rev. Lett. **108**, 111602 (2012).
55. S. Bergmann *et al.*, Phys. Lett. **B486**, 418 (2000).
56. M. Gersabeck *et al.*, J. Phys. **G39**, 045005 (2012).
57. R. Aaij *et al.*, [LHCb Collab.], Phys. Rev. Lett. **111**, 251801 (2013).
58. Y. Grossman and Y. Nir, JHEP **1204**, 002 (2012).
59. B. R. Ko *et al.*, [Belle Collab.], Phys. Rev. Lett. **109**, 021601 (2012). Erratum-ibid. **109**, 119903 (2012).
60. B. Aubert *et al.*, [BABAR Collab.], Phys. Rev. **D78**, 051102 (2008).
61. I. Bediaga *et al.*, Phys. Rev. **D80**, 096006 (2009); Phys. Rev. **D86**, 036005 (2012).
62. M. Williams, Phys. Rev. **D84**, 054015 (2011).
63. A. Lenz and U. Nierste, arXiv:1102.4274 [hep-ph].
64. V. M. Abazov *et al.*, [D0 Collab.], Phys. Rev. **D82**, 032001 (2010); Phys. Rev. **D84**, 052007 (2011); Phys. Rev. **D89**, 012002 (2014).
65. A.B. Carter and A.I. Sanda, Phys. Rev. Lett. **45**, 952 (1980); Phys. Rev. **D23**, 1567 (1981).
66. I.I. Bigi and A.I. Sanda, Nucl. Phys. **B193**, 85 (1981).
67. I. Dunietz and J.L. Rosner, Phys. Rev. **D34**, 1404 (1986).
68. Ya.I. Azimov, N.G. Uraltsev, and V.A. Khoze, Sov. J. Nucl. Phys. **45**, 878 (1987) [Yad. Fiz. **45**, 1412 (1987)].
69. I.I. Bigi and A.I. Sanda, Nucl. Phys. **B281**, 41 (1987).
70. G. Buchalla, A.J. Buras, and M.E. Lautenbacher, Rev. Mod. Phys. **68**, 1125 (1996).
71. R. Fleischer, Eur. Phys. J. **C10**, 299 (1999).
72. M. Ciuchini, M. Pierini, and L. Silvestrini, Phys. Rev. Lett. **95**, 221804 (2005).
73. S. Faller *et al.*, Phys. Rev. **D79**, 014030 (2009).
74. M. Jung, Phys. Rev. **D86**, 053008 (2012).
75. L. Silvestrini, Ann. Rev. Nucl. Part. Sci. **57**, 405 (2007).
76. M. Gronau and D. London, Phys. Rev. Lett. **65**, 3381 (1990).
77. A. F. Falk *et al.*, Phys. Rev. **D69**, 011502 (2004).
78. B. Aubert *et al.*, [BABAR Collab.], Phys. Rev. **D78**, 071104 (2008).
79. I. Adachi *et al.*, [Belle Collab.], arXiv:1212.4015 [hep-ex].
80. R. Fleischer and R. Knegjens, Eur. Phys. J. **C71**, 1789 (2011).
81. A. S. Dighe, I. Dunietz, and R. Fleischer, Eur. Phys. J. **C6**, 647 (1999).
82. R. Aaij *et al.*, [LHCb Collab.], Phys. Rev. **D86**, 052006 (2012).
83. R. Aaij *et al.*, [LHCb Collab.], Phys. Rev. Lett. **110**, 241802 (2013).
84. R. Aaij *et al.*, [LHCb Collab.], JHEP **1310**, 183 (2013).
85. J. Brod and J. Zupan, JHEP **1401**, 051 (2014).
86. M. Gronau and D. London, Phys. Lett. **B253**, 483 (1991).
87. M. Gronau and D. Wyler, Phys. Lett. **B265**, 172 (1991).
88. D. Atwood, I. Dunietz, and A. Soni, Phys. Rev. Lett. **78**, 3257 (1997).
89. D. Atwood, I. Dunietz, and A. Soni, Phys. Rev. **D63**, 036005 (2001).
90. A. Giri *et al.*, Phys. Rev. **D68**, 054018 (2003).
91. R. Aleksan, I. Dunietz, and B. Kayser, Z. Phys. **C54**, 653 (1992).
92. R. Fleischer, Nucl. Phys. **B671**, 459 (2003).
93. I. Dunietz, Phys. Lett. **B270**, 75 (1991).
94. M. Gronau, Phys. Lett. **B557**, 198 (2003).
95. T. Gershon, Phys. Rev. **D79**, 051301 (2009).
96. T. Gershon and M. Williams, Phys. Rev. **D80**, 092002 (2009).
97. M. Bander, D. Silverman, and A. Soni, Phys. Rev. Lett. **43**, 242 (1979).
98. X. -G. He, Eur. Phys. J. **C9**, 443 (1999).
99. D. Atwood and A. Soni, Phys. Rev. **D58**, 036005 (1998).
100. M. Gronau and J. L. Rosner, Phys. Rev. **D59**, 113002 (1999).
101. H. J. Lipkin, Phys. Lett. **B445**, 403 (1999).
102. M. Gronau, Phys. Lett. **B627**, 82 (2005).
103. A.A. Alves *et al.*, [LHCb Collab.], JINST **3** S08005 (2008).
104. I. Bediaga *et al.*, [LHCb Collab.], CERN-LHCC-2012-007, LHCb-TDR-12.
105. T. Aushev *et al.*, arXiv:1002.5012 [hep-ex] , KEK Report 2009-12.
106. G.C. Branco, L. Lavoura, and J.P. Silva, *CP Violation,* Oxford University Press, Oxford (1999).
107. I.I. Y. Bigi and A.I. Sanda, *CP Violation,* Cambridge Monogr., Part. Phys. Nucl. Phys. Cosmol. **9**, 1 (2000).
108. P.F. Harrison and H.R. Quinn, editors [BABAR Collab.], *The BABAR physics book: Physics at an asymmetric B factory,* SLAC-R-0504.
109. H.R. Quinn and Y. Nir, "The Mystery of the Missing Antimatter," Princeton University Press, Princeton (2008).
110. T.E. Browder *et al.*, Rev. Mod. Phys. **81**, 1887 (2009).
111. M. Ciuchini and A. Stocchi, Ann. Rev. Nucl. Part. Sci. **61**, 491 (2011).
112. R. Aaij *et al.*, [LHCb Collab.] and A. Bharucha *et al.*, Eur. Phys. J. **C73**, 2373 (2013).

14. NEUTRINO MASS, MIXING, AND OSCILLATIONS

Updated May 2014 by K. Nakamura (Kavli IPMU (WPI), U. Tokyo, KEK), and S.T. Petcov (SISSA/INFN Trieste, Kavli IPMU (WPI), U. Tokyo, Bulgarian Academy of Sciences).

The experiments with solar, atmospheric, reactor and accelerator neutrinos have provided compelling evidences for oscillations of neutrinos caused by nonzero neutrino masses and neutrino mixing. The data imply the existence of 3-neutrino mixing in vacuum. We review the theory of neutrino oscillations, the phenomenology of neutrino mixing, the problem of the nature - Dirac or Majorana, of massive neutrinos, the issue of CP violation in the lepton sector, and the current data on the neutrino masses and mixing parameters. The open questions and the main goals of future research in the field of neutrino mixing and oscillations are outlined.

14.1. Introduction: Massive neutrinos and neutrino mixing

It is a well-established experimental fact that the neutrinos and antineutrinos which take part in the standard charged current (CC) and neutral current (NC) weak interaction are of three varieties (types) or flavours: electron, ν_e and $\bar{\nu}_e$, muon, ν_μ and $\bar{\nu}_\mu$, and tauon, ν_τ and $\bar{\nu}_\tau$. The notion of neutrino type or flavour is dynamical: ν_e is the neutrino which is produced with e^+, or produces an e^- in CC weak interaction processes; ν_μ is the neutrino which is produced with μ^+, or produces μ^-, *etc.* The flavour of a given neutrino is Lorentz invariant. Among the three different flavour neutrinos and antineutrinos, no two are identical. Correspondingly, the states which describe different flavour neutrinos must be orthogonal (within the precision of the current data): $\langle\nu_{l'}|\nu_l\rangle = \delta_{l'l}$, $\langle\bar{\nu}_{l'}|\bar{\nu}_l\rangle = \delta_{l'l}$, $\langle\bar{\nu}_{l'}|\nu_l\rangle = 0$.

It is also well-known from the existing data (all neutrino experiments were done so far with relativistic neutrinos or antineutrinos), that the flavour neutrinos ν_l (antineutrinos $\bar{\nu}_l$), are always produced in weak interaction processes in a state that is predominantly left-handed (LH) (right-handed (RH)). To account for this fact, ν_l and $\bar{\nu}_l$ are described in the Standard Model (SM) by a chiral LH flavour neutrino field $\nu_{lL}(x)$, $l = e, \mu, \tau$. For massless ν_l, the state of ν_l ($\bar{\nu}_l$) which the field $\nu_{lL}(x)$ annihilates (creates) is with helicity (-1/2) (helicity +1/2). If ν_l has a non-zero mass $m(\nu_l)$, the state of ν_l ($\bar{\nu}_l$) is a linear superposition of the helicity (-1/2) and (+1/2) states, but the helicity +1/2 state (helicity (-1/2) state) enters into the superposition with a coefficient $\propto m(\nu_l)/E$, E being the neutrino energy, and thus is strongly suppressed. Together with the LH charged lepton field $l_L(x)$, $\nu_{lL}(x)$ forms an $SU(2)_L$ doublet. In the absence of neutrino mixing and zero neutrino masses, $\nu_{lL}(x)$ and $l_L(x)$ can be assigned one unit of the additive lepton charge L_l and the three charges L_l, $l = e, \mu, \tau$, are conserved by the weak interaction.

At present there is no compelling evidence for the existence of states of relativistic neutrinos (antineutrinos), which are predominantly right-handed, ν_R (left-handed, $\bar{\nu}_L$). If RH neutrinos and LH antineutrinos exist, their interaction with matter should be much weaker than the weak interaction of the flavour LH neutrinos ν_l and RH antineutrinos $\bar{\nu}_l$, *i.e.*, ν_R ($\bar{\nu}_L$) should be "sterile" or "inert" neutrinos (antineutrinos) [1]. In the formalism of the Standard Model, the sterile ν_R and $\bar{\nu}_L$ can be described by $SU(2)_L$ singlet RH neutrino fields $\nu_R(x)$. In this case, ν_R and $\bar{\nu}_L$ will have no gauge interactions, *i.e.*, will not couple to the weak $W^\pm$ and Z^0 bosons. If present in an extension of the Standard Model, the RH neutrinos can play a crucial role i) in the generation of neutrino masses and mixing, ii) in understanding the remarkable disparity between the magnitudes of neutrino masses and the masses of the charged leptons and quarks, and iii) in the generation of the observed matter-antimatter asymmetry of the Universe (via the leptogenesis mechanism [2]) . In this scenario which is based on the see-saw theory [3], there is a link between the generation of neutrino masses and the generation of the baryon asymmetry of the Universe. The simplest hypothesis (based on symmetry considerations) is that to each LH flavour neutrino field $\nu_{lL}(x)$ there corresponds a RH neutrino field $\nu_{lR}(x)$, $l = e, \mu, \tau$, although schemes with less (more) than three RH neutrinos are also being considered.

The experiments with solar, atmospheric, reactor and accelerator neutrinos have provided compelling evidences for the existence of neutrino oscillations [4,5], transitions in flight between the different flavour neutrinos ν_e, ν_μ, ν_τ (antineutrinos $\bar{\nu}_e$, $\bar{\nu}_\mu$, $\bar{\nu}_\tau$), caused by nonzero neutrino masses and neutrino mixing.

The existence of flavour neutrino oscillations implies that if a neutrino of a given flavour, say ν_μ, with energy E is produced in some weak interaction process, at a sufficiently large distance L from the ν_μ source the probability to find a neutrino of a different flavour, say ν_τ, $P(\nu_\mu \to \nu_\tau; E, L)$, is different from zero. $P(\nu_\mu \to \nu_\tau; E, L)$ is called the $\nu_\mu \to \nu_\tau$ oscillation or transition probability. If $P(\nu_\mu \to \nu_\tau; E, L) \neq 0$, the probability that ν_μ will not change into a neutrino of a different flavour, *i.e.*, the "ν_μ survival probability" $P(\nu_\mu \to \nu_\mu; E, L)$, will be smaller than one. If only muon neutrinos ν_μ are detected in a given experiment and they take part in oscillations, one would observe a "disappearance" of muon neutrinos on the way from the ν_μ source to the detector. Disappearance of the solar ν_e, reactor $\bar{\nu}_e$ and of atmospheric ν_μ and $\bar{\nu}_\mu$ due to the oscillations have been observed respectively, in the solar neutrino [6–14], KamLAND [15,16] and Super-Kamokande [17,18] experiments. Strong evidences for ν_μ disappearance due to oscillations were obtained also in the long-baseline accelerator neutrino experiments K2K [19]. Subsequently, the MINOS [20,21] and T2K [22,23] long baseline experiments reported compelling evidence for ν_μ disappearance due to oscillations, while evidences for ν_τ appearance due to $\nu_\mu \to \nu_\tau$ oscillations were published by the Super-Kamiokande [24] and OPERA [25] collaborations. As a consequence of the results of the experiments quoted above the existence of oscillations or transitions of the solar ν_e, atmospheric ν_μ and $\bar{\nu}_\mu$, accelerator ν_μ (at $L \sim 250$ km, $L \sim 295$ km and $L \sim 730$ km) and reactor $\bar{\nu}_e$ (at $L \sim 180$ km), driven by nonzero neutrino masses and neutrino mixing, was firmly established. There are strong indications that the solar ν_e transitions are affected by the solar matter [26,27].

Further important developments took place more recently in the period starting from June 2011. First, the T2K Collaboration reported [28] indications for $\nu_\mu \to \nu_e$ oscillations, *i.e.*, of "appearance" of ν_e in a beam of ν_μ, which had a statistical significance of 2.5σ. The MINOS [29] Collaboration also obtained data consistent with $\nu_\mu \to \nu_e$ oscillations. Subsequently, the Double Chooz Collaboration reported [30] indications for disappearance of reactor $\bar{\nu}_e$ at $L \sim 1.1$ km. Strong evidences for reactor $\bar{\nu}_e$ disappearance at $L \sim 1.65$ km and $L \sim 1.38$ km and (with statistical significance of 5.2σ and 4.9σ) were obtained respectively in the Daya Bay [31] and RENO [32] experiments. Further evidences for reactor $\bar{\nu}_e$ disappearance (at 2.9σ) and for $\nu_\mu \to \nu_e$ oscillations (at 3.1σ) were reported by the Double Chooz [33] and T2K [34] experiments, while the Daya Bay and RENO Collaborations presented updated, more precise results on reactor $\bar{\nu}_e$ disappearance [35,36,37](for the latest results of the Daya Bay, RENO, Double Chooz, MINOS and T2K experiments, see Section 14.6).

Oscillations of neutrinos are a consequence of the presence of flavour neutrino mixing, or lepton mixing, in vacuum. In the formalism of local quantum field theory, used to construct the Standard Model, this means that the LH flavour neutrino fields $\nu_{lL}(x)$, which enter into the expression for the lepton current in the CC weak interaction Lagrangian, are linear combinations of the fields of three (or more) neutrinos ν_j, having masses $m_j \neq 0$:

$$\nu_{lL}(x) = \sum_j U_{lj}\, \nu_{jL}(x), \quad l = e, \mu, \tau, \tag{14.1}$$

where $\nu_{jL}(x)$ is the LH component of the field of ν_j possessing a mass m_j and U is a unitary matrix - the neutrino mixing matrix [1,4,5]. The matrix U is often called the Pontecorvo-Maki-Nakagawa-Sakata (PMNS) or Maki-Nakagawa-Sakata (MNS) mixing matrix. Obviously, Eq. (14.1) implies that the individual lepton charges L_l, $l = e, \mu, \tau$, are not conserved.

All compelling neutrino oscillation data can be described assuming 3-flavour neutrino mixing in vacuum. The data on the invisible decay width of the Z-boson is compatible with only 3 light flavour neutrinos coupled to Z [38]. The number of massive neutrinos ν_j, n, can,

in general, be bigger than 3, $n > 3$, if, for instance, there exist sterile neutrinos and they mix with the flavour neutrinos. It is firmly established on the basis of the current data that at least 3 of the neutrinos ν_j, say ν_1, ν_2, ν_3, must be light, $m_{1,2,3} \lesssim 1$ eV (Section 14.6), and must have different masses, $m_1 \neq m_2 \neq m_3$. At present there are several experimental hints for existence of one or two light sterile neutrinos at the eV scale, which mix with the flavour neutrinos, implying the presence in the neutrino mixing of additional one or two neutrinos, ν_4 or $\nu_{4,5}$, with masses m_4 ($m_{4,5}$) ~ 1 eV. These hints will be briefly discusssed in Section 14.7 of the present review.

Being electrically neutral, the neutrinos with definite mass ν_j can be Dirac fermions or Majorana particles [39,40]. The first possibility is realised when there exists a lepton charge carried by the neutrinos ν_j, which is conserved by the particle interactions. This could be, *e.g.*, the total lepton charge $L = L_e + L_\mu + L_\tau$: $L(\nu_j) = 1$, $j = 1, 2, 3$. In this case the neutrino ν_j has a distinctive antiparticle $\bar{\nu}_j$: $\bar{\nu}_j$ differs from ν_j by the value of the lepton charge L it carries, $L(\bar{\nu}_j) = -1$. The massive neutrinos ν_j can be Majorana particles if no lepton charge is conserved (see, *e.g.*, Refs. [41,42]) . A massive Majorana particle χ_j is identical with its antiparticle $\bar{\chi}_j$: $\chi_j \equiv \bar{\chi}_j$. On the basis of the existing neutrino data it is impossible to determine whether the massive neutrinos are Dirac or Majorana fermions.

In the case of n neutrino flavours and n massive neutrinos, the $n \times n$ unitary neutrino mixing matrix U can be parametrised by $n(n-1)/2$ Euler angles and $n(n+1)/2$ phases. If the massive neutrinos ν_j are Dirac particles, only $(n-1)(n-2)/2$ phases are physical and can be responsible for CP violation in the lepton sector. In this respect the neutrino (lepton) mixing with Dirac massive neutrinos is similar to the quark mixing. For $n = 3$ there is just one CP violating phase in U, which is usually called "the Dirac CP violating phase." CP invariance holds if (in a certain standard convention) U is real, $U^* = U$.

If, however, the massive neutrinos are Majorana fermions, $\nu_j \equiv \chi_j$, the neutrino mixing matrix U contains $n(n-1)/2$ CP violation phases [43,44], *i.e.*, by $(n-1)$ phases more than in the Dirac neutrino case: in contrast to Dirac fields, the massive Majorana neutrino fields cannot "absorb" phases. In this case U can be cast in the form [43]

$$U = V\,P \tag{14.2}$$

where the matrix V contains the $(n-1)(n-2)/2$ Dirac CP violation phases, while P is a diagonal matrix with the additional $(n-1)$ Majorana CP violation phases α_{21}, α_{31},..., α_{n1},

$$P = diag\left(1, e^{i\frac{\alpha_{21}}{2}}, e^{i\frac{\alpha_{31}}{2}}, ..., e^{i\frac{\alpha_{n1}}{2}}\right) . \tag{14.3}$$

The Majorana phases will conserve CP if [45] $\alpha_{j1} = \pi q_j$, $q_j = 0, 1, 2$, $j = 2, 3, ..., n$. In this case $\exp[i(\alpha_{j1} - \alpha_{k1})] = \pm 1$ has a simple physical interpretation: this is the relative CP-parity of Majorana neutrinos χ_j and χ_k. The condition of CP invariance of the leptonic CC weak interaction in the case of mixing and massive Majorana neutrinos reads [41]:

$$U^*_{lj} = U_{lj}\,\rho_j\,, \quad \rho_j = \frac{1}{i}\eta_{CP}(\chi_j) = \pm 1\,, \tag{14.4}$$

where $\eta_{CP}(\chi_j) = i\rho_j = \pm i$ is the CP parity of the Majorana neutrino χ_j [45]. Thus, if CP invariance holds, the elements of U are either real or purely imaginary.

In the case of $n = 3$ there are altogether 3 CP violation phases - one Dirac and two Majorana. Even in the mixing involving only 2 massive Majorana neutrinos there is one physical CP violation Majorana phase. In contrast, the CC weak interaction is automatically CP-invariant in the case of mixing of two massive Dirac neutrinos or of two quarks.

14.2. Neutrino oscillations in vacuum

Neutrino oscillations are a quantum mechanical consequence of the existence of nonzero neutrino masses and neutrino (lepton) mixing, Eq. (14.1), and of the relatively small splitting between the neutrino masses. The neutrino mixing and oscillation phenomena are analogous to the $K^0 - \bar{K}^0$ and $B^0 - \bar{B}^0$ mixing and oscillations.

In what follows we will present a simplified version of the derivation of the expressions for the neutrino and antineutrino oscillation probabilities. The complete derivation would require the use of the wave packet formalism for the evolution of the massive neutrino states, or, alternatively, of the field-theoretical approach, in which one takes into account the processes of production, propagation and detection of neutrinos [46].

Suppose the flavour neutrino ν_l is produced in a CC weak interaction process and after a time T it is observed by a neutrino detector, located at a distance L from the neutrino source and capable of detecting also neutrinos $\nu_{l'}$, $l' \neq l$. We will consider the evolution of the neutrino state $|\nu_l\rangle$ in the frame in which the detector is at rest (laboratory frame). The oscillation probability, as we will see, is a Lorentz invariant quantity. If lepton mixing, Eq. (14.1), takes place and the masses m_j of all neutrinos ν_j are sufficiently small, the state of the neutrino ν_l, $|\nu_l\rangle$, will be a coherent superposition of the states $|\nu_j\rangle$ of neutrinos ν_j:

$$|\nu_l\rangle = \sum_j U^*_{lj}\,|\nu_j; \tilde{p}_j\rangle, \quad l = e, \mu, \tau\,, \tag{14.5}$$

where U is the neutrino mixing matrix and $\tilde{p}_j$ is the 4-momentum of ν_j [47].

We will consider the case of relativistic neutrinos ν_j, which corresponds to the conditions in both past and currently planned future neutrino oscillation experiments [49]. In this case the state $|\nu_j; \tilde{p}_j\rangle$ practically coincides with the helicity (-1) state $|\nu_j, L; \tilde{p}_j\rangle$ of the neutrino ν_j, the admixture of the helicity (+1) state $|\nu_j, R; \tilde{p}_j\rangle$ in $|\nu_j; \tilde{p}_j\rangle$ being suppressed due to the factor $\sim m_j/E_j$, where E_j is the energy of ν_j. If ν_j are Majorana particles, $\nu_j \equiv \chi_j$, due to the presence of the helicity (+1) state $|\chi_j, R; \tilde{p}_j\rangle$ in $|\chi_j; \tilde{p}_j\rangle$, the neutrino ν_l can produce an l^+ (instead of l^-) when it interacts, e.g., with nucleons. The cross section of such a $|\Delta L_l| = 2$ process is suppressed by the factor $(m_j/E_j)^2$, which renders the process unobservable at present.

If the number n of massive neutrinos ν_j is bigger than 3 due to a mixing between the active flavour and sterile neutrinos, one will have additional relations similar to that in Eq. (14.5) for the state vectors of the (predominantly LH) sterile antineutrinos. In the case of just one RH sterile neutrino field $\nu_{sR}(x)$, for instance, we will have in addition to Eq. (14.5):

$$|\bar{\nu}_{sL}\rangle = \sum_{j=1}^{4} U^*_{sj}\,|\nu_j; \tilde{p}_j\rangle \cong \sum_{j=1}^{4} U^*_{sj}\,|\nu_j, L; \tilde{p}_j\rangle\,, \tag{14.6}$$

where the neutrino mixing matrix U is now a 4×4 unitary matrix.

For the state vector of RH flavour antineutrino $\bar{\nu}_l$, produced in a CC weak interaction process we similarly get:

$$|\bar{\nu}_l\rangle = \sum_j U_{lj}\,|\bar{\nu}_j; \tilde{p}_j\rangle \cong \sum_{j=1} U_{lj}\,|\bar{\nu}_j, R; \tilde{p}_j\rangle, \quad l = e, \mu, \tau\,, \tag{14.7}$$

where $|\bar{\nu}_j, R; \tilde{p}_j\rangle$ is the helicity (+1) state of the antineutrino $\bar{\nu}_j$ if ν_j are Dirac fermions, or the helicity (+1) state of the neutrino $\nu_j \equiv \bar{\nu}_j \equiv \chi_j$ if the massive neutrinos are Majorana particles. Thus, in the latter case we have in Eq. (14.7): $|\bar{\nu}_j; \tilde{p}_j\rangle \cong |\nu_j, R; \tilde{p}_j\rangle \equiv |\chi_j, R; \tilde{p}_j\rangle$. The presence of the matrix U in Eq. (14.7) (and not of U^*) follows directly from Eq. (14.1).

We will assume in what follows that the spectrum of masses of neutrinos is not degenerate: $m_j \neq m_k$, $j \neq k$. Then the states $|\nu_j; \tilde{p}_j\rangle$ in the linear superposition in the r.h.s. of Eq. (14.5) will have, in general, different energies and different momenta, independently of whether they are produced in a decay or interaction process: $\tilde{p}_j \neq \tilde{p}_k$,

or $E_j \neq E_k$, $\mathbf{p}_j \neq \mathbf{p}_k$, $j \neq k$, where $E_j = \sqrt{p_j^2 + m_j^2}$, $p_j \equiv |\mathbf{p}_j|$. The deviations of E_j and p_j from the values for a massless neutrino E and $p = E$ are proportional to m_j^2/E_0, E_0 being a characteristic energy of the process, and are extremely small. In the case of $\pi^+ \to \mu^+ + \nu_\mu$ decay at rest, for instance, we have: $E_j = E + m_j^2/(2m_\pi)$, $p_j = E - \xi m_j^2/(2E)$, where $E = (m_\pi/2)(1 - m_\mu^2/m_\pi^2) \cong 30$ MeV, $\xi = (1 + m_\mu^2/m_\pi^2)/2 \cong 0.8$, and m_μ and m_π are the μ^+ and π^+ masses. Taking $m_j = 1$ eV we find: $E_j \cong E\,(1 + 1.2 \times 10^{-16})$ and $p_j \cong E\,(1 - 4.4 \times 10^{-16})$.

Suppose that the neutrinos are observed via a CC weak interaction process and that in the detector's rest frame they are detected after time T after emission, after traveling a distance L. Then the amplitude of the probability that neutrino $\nu_{l'}$ will be observed if neutrino ν_l was produced by the neutrino source can be written as [46,48,50]:

$$A(\nu_l \to \nu_{l'}) = \sum_j U_{l'j}\, D_j\, U_{jl}^\dagger, \qquad l, l' = e, \mu, \tau\,, \tag{14.8}$$

where $D_j = D_j(p_j; L, T)$ describes the propagation of ν_j between the source and the detector, $U_{jl}^\dagger$ and $U_{l'j}$ are the amplitudes to find ν_j in the initial and in the final flavour neutrino state, respectively. It follows from relativistic Quantum Mechanics considerations that [46,48]

$$D_j \equiv D_j(\tilde{p}_j; L, T) = e^{-i\tilde{p}_j\,(x_f - x_0)} = e^{-i(E_j T - p_j L)}\,, \qquad p_j \equiv |\mathbf{p}_j|\,, \tag{14.9}$$

where [51] x_0 and x_f are the space-time coordinates of the points of neutrino production and detection, $T = (t_f - t_0)$ and $L = \mathbf{k}(\mathbf{x}_f - \mathbf{x}_0)$, $\mathbf{k}$ being the unit vector in the direction of neutrino momentum, $\mathbf{p}_j = \mathbf{k}\mathrm{p_j}$. What is relevant for the calculation of the probability $P(\nu_l \to \nu_{l'}) = |A(\nu_l \to \nu_{l'})|^2$ is the interference factor $D_j D_k^*$ which depends on the phase

$$\delta\varphi_{jk} = (E_j - E_k)T - (p_j - p_k)L = (E_j - E_k)\left[T - \frac{E_j + E_k}{p_j + p_k}\,L\right] + \frac{m_j^2 - m_k^2}{p_j + p_k}\,L\,. \tag{14.10}$$

Some authors [52] have suggested that the distance traveled by the neutrinos L and the time interval T are related by $T = (E_j + E_k)\,L/(p_j + p_k) = L/\bar{v}$, $\bar{v} = (E_j/(E_j + E_k))v_j + (E_k/(E_j + E_k))v_k$ being the "average" velocity of ν_j and ν_k, where $v_{j,k} = p_{j,k}/E_{j,k}$. In this case the first term in the r.h.s. of Eq. (14.10) vanishes. The indicated relation has not emerged so far from any dynamical wave packet calculations. We arrive at the same conclusion concerning the term under discussion in Eq. (14.10) if one assumes [53] that $E_j = E_k = E_0$. Finally, it was proposed in Ref. 50 and Ref. 54 that the states of ν_j and $\bar{\nu}_j$ in Eq. (14.5) and Eq. (14.7) have the same 3-momentum, $p_j = p_k = p$. Under this condition the first term in the r.h.s. of Eq. (14.10) is negligible, being suppressed by the additional factor $(m_j^2 + m_k^2)/p^2$ since for relativistic neutrinos $L = T$ up to terms $\sim m_{j,k}^2/p^2$. We arrive at the same conclusion if $E_j \neq E_k$, $p_j \neq p_k$, $j \neq k$, and we take into account that neutrinos are relativistic and therefore, up to corrections $\sim m_{j,k}^2/E_{j,k}^2$, we have $L \cong T$ (see, *e.g.*, C. Giunti quoted in Ref. 46).

Although the cases considered above are physically quite different, they lead to the same result for the phase difference $\delta\varphi_{jk}$. Thus, we have:

$$\delta\varphi_{jk} \cong \frac{m_j^2 - m_k^2}{2p}\,L = 2\pi\,\frac{L}{L_{jk}^v}\,\mathrm{sgn}(m_j^2 - m_k^2)\,, \tag{14.11}$$

where $p = (p_j + p_k)/2$ and

$$L_{jk}^v = 4\pi\frac{p}{|\Delta m_{jk}^2|} \cong 2.48\ \mathrm{m}\ \frac{p[MeV]}{|\Delta m_{jk}^2|[eV^2]} \tag{14.12}$$

is the neutrino oscillation length associated with Δm_{jk}^2. We can safely neglect the dependence of p_j and p_k on the masses m_j and m_k and consider p to be the zero neutrino mass momentum, $p = E$. The phase difference $\delta\varphi_{jk}$, Eq. (14.11), is Lorentz-invariant.

Eq. (14.9) corresponds to a plane-wave description of the propagation of neutrinos ν_j. It accounts only for the movement of the center of the wave packet describing ν_j. In the wave packet treatment of the problem, the interference between the states of ν_j and ν_k is subject to a number of conditions [46], the localisation condition and the condition of overlapping of the wave packets of ν_j and ν_k at the detection point being the most important. For relativistic neutrinos, the localisation condition in space, for instance, reads: $\sigma_{xP}, \sigma_{xD} < L_{jk}^v/(2\pi)$, $\sigma_{xP(D)}$ being the spatial width of the production (detection) wave packet. Thus, the interference will not be suppressed if the spatial width of the neutrino wave packets determined by the neutrino production and detection processes is smaller than the corresponding oscillation length in vacuum. In order for the interference to be nonzero, the wave packets describing ν_j and ν_k should also overlap in the point of neutrino detection. This requires that the spatial separation between the two wave packets at the point of neutrinos detection, caused by the two wave packets having different group velocities $v_j \neq v_k$, satisfies $|(v_j - v_k)T| \ll \max(\sigma_{xP}, \sigma_{xD})$. If the interval of time T is not measured, T in the preceding condition must be replaced by the distance L between the neutrino source and the detector (for further discussion see, *e.g.*, Refs. [46,48,50]) .

For the $\nu_l \to \nu_{l'}$ and $\bar{\nu}_l \to \bar{\nu}_{l'}$ oscillation probabilities we get from Eq. (14.8), Eq. (14.9), and Eq. (14.11):

$$P(\nu_l \to \nu_{l'}) = \sum_j |U_{l'j}|^2\,|U_{lj}|^2 + 2\sum_{j>k} |U_{l'j}\,U_{lj}^*\,U_{lk}\,U_{l'k}^*| \cos(\frac{\Delta m_{jk}^2}{2p}\,L - \phi_{l'l;jk})\,, \tag{14.13}$$

$$P(\bar{\nu}_l \to \bar{\nu}_{l'}) = \sum_j |U_{l'j}|^2\,|U_{lj}|^2 + 2\sum_{j>k} |U_{l'j}\,U_{lj}^*\,U_{lk}\,U_{l'k}^*| \cos(\frac{\Delta m_{jk}^2}{2p}\,L + \phi_{l'l;jk})\,, \tag{14.14}$$

where $l, l' = e, \mu, \tau$ and $\phi_{l'l;jk} = \arg\left(U_{l'j}\,U_{lj}^*\,U_{lk}\,U_{l'k}^*\right)$. It follows from Eq. (14.8) - Eq. (14.10) that in order for neutrino oscillations to occur, at least two neutrinos ν_j should not be degenerate in mass and lepton mixing should take place, $U \neq \mathbf{1}$. The neutrino oscillations effects can be large if we have

$$\frac{|\Delta m_{jk}^2|}{2p}\,L = 2\pi\,\frac{L}{L_{jk}^v} \gtrsim 1\,,\ \ j \neq k\,. \tag{14.15}$$

at least for one Δm_{jk}^2. This condition has a simple physical interpretation: the neutrino oscillation length L_{jk}^v should be of the order of, or smaller, than source-detector distance L, otherwise the oscillations will not have time to develop before neutrinos reach the detector.

We see from Eq. (14.13) and Eq. (14.14) that $P(\nu_l \to \nu_{l'}) = P(\bar{\nu}_{l'} \to \bar{\nu}_l)$, $l, l' = e, \mu, \tau$. This is a consequence of CPT invariance. The conditions of CP and T invariance read [43,55,56]: $P(\nu_l \to \nu_{l'}) = P(\bar{\nu}_l \to \bar{\nu}_{l'})$, $l, l' = e, \mu, \tau$ (CP), $P(\nu_l \to \nu_{l'}) = P(\nu_{l'} \to \nu_l)$, $P(\bar{\nu}_l \to \bar{\nu}_{l'}) = P(\bar{\nu}_{l'} \to \bar{\nu}_l)$, $l, l' = e, \mu, \tau$ (T). In the case of CPT invariance, which we will assume to hold throughout this article, we get for the survival probabilities: $P(\nu_l \to \nu_l) = P(\bar{\nu}_l \to \bar{\nu}_l)$, $l, l' = e, \mu, \tau$. Thus, the study of the "disappearance" of ν_l and $\bar{\nu}_l$, caused by oscillations in vacuum, cannot be used to test whether CP invariance holds in the lepton sector. It follows from Eq. (14.13) and Eq. (14.14) that we can have CP violation effects in neutrino oscillations only if $\phi_{l'l;jk} \neq \pi q$, $q = 0, 1, 2$, *i.e.*, if $U_{l'j}\,U_{lj}^*\,U_{lk}\,U_{l'k}^*$, and therefore U itself, is not real. As a measure of CP and T violation in neutrino oscillations we can consider the asymmetries:

$$A_{\mathrm{CP}}^{(l'l)} \equiv P(\nu_l \to \nu_{l'}) - P(\bar{\nu}_l \to \bar{\nu}_{l'})\,, \quad A_{\mathrm{T}}^{(l'l)} \equiv P(\nu_l \to \nu_{l'}) - P(\nu_{l'} \to \nu_l)\,. \tag{14.16}$$

CPT invariance implies: $A_{\rm CP}^{(l'l)} = -A_{\rm CP}^{(ll')}$, $A_{\rm T}^{(l'l)} = P(\bar\nu_{l'} \to \bar\nu_l) - P(\bar\nu_l \to \bar\nu_{l'}) = A_{\rm CP}^{(l'l)}$. It follows further directly from Eq. (14.13) and Eq. (14.14) that

$$A_{\rm CP}^{(l'l)} = 4 \sum_{j>k} {\rm Im}\left(U_{l'j}\, U_{lj}^*\, U_{lk}\, U_{l'k}^*\right) \sin\frac{\Delta m^2_{jk}}{2p}\, L\,,\ \ l, l' = e, \mu, \tau\,. \tag{14.17}$$

Eq. (14.2) and Eq. (14.13) - Eq. (14.14) imply that $P(\nu_l \to \nu_{l'})$ and $P(\bar\nu_l \to \bar\nu_{l'})$ do not depend on the Majorana CP violation phases in the neutrino mixing matrix U [43]. Thus, the experiments investigating the $\nu_l \to \nu_{l'}$ and $\bar\nu_l \to \bar\nu_{l'}$ oscillations, $l, l' = e, \mu, \tau$, cannot provide information on the nature - Dirac or Majorana, of massive neutrinos. The same conclusions hold also when the $\nu_l \to \nu_{l'}$ and $\bar\nu_l \to \bar\nu_{l'}$ oscillations take place in matter [57]. In the case of $\nu_l \leftrightarrow \nu_{l'}$ and $\bar\nu_l \leftrightarrow \bar\nu_{l'}$ oscillations in vacuum, only the Dirac phase(s) in U can cause CP violating effects leading to $P(\nu_l \to \nu_{l'}) \neq P(\bar\nu_l \to \bar\nu_{l'})$, $l \neq l'$.

In the case of 3-neutrino mixing all different ${\rm Im}(U_{l'j} U_{lj}^* U_{lk} U_{l'k}^*) \neq 0$, $l' \neq l = e, \mu, \tau$, $j \neq k = 1, 2, 3$, coincide up to a sign as a consequence of the unitarity of U. Therefore one has [58]:

$$A_{\rm CP}^{(\mu e)} = -\,A_{\rm CP}^{(\tau e)} = A_{\rm CP}^{(\tau\mu)} = 4\, J_{\rm CP}\, \left(\sin\frac{\Delta m^2_{32}}{2p}\, L + \sin\frac{\Delta m^2_{21}}{2p}\, L + \sin\frac{\Delta m^2_{13}}{2p}\, L\right) \tag{14.18}$$

where

$$J_{\rm CP} = {\rm Im}\left(U_{\mu 3}\, U_{e3}^*\, U_{e2}\, U_{\mu 2}^*\right)\,, \tag{14.19}$$

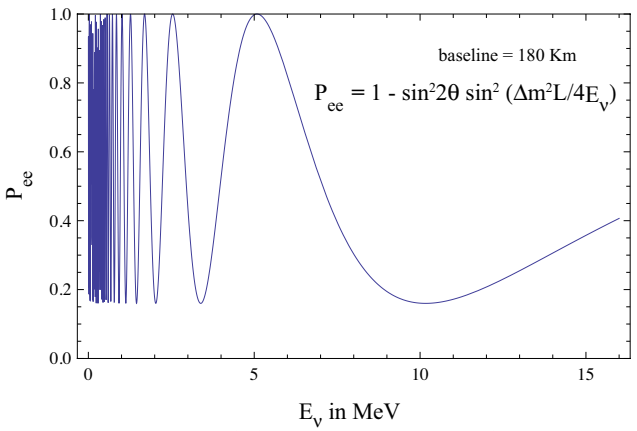

Figure 14.1: The ν_e ($\bar\nu_e$) survival probability $P(\nu_e \to \nu_e) = P(\bar\nu_e \to \bar\nu_e)$, Eq. (14.30), as a function of the neutrino energy for $L = 180$ km, $\Delta m^2 = 7.0 \times 10^{-5}$ eV^2 and $\sin^2 2\theta = 0.84$ (from Ref. 64).

is the "rephasing invariant" associated with the Dirac CP violation phase in U. It is analogous to the rephasing invariant associated with the Dirac CP violating phase in the CKM quark mixing matrix [59]. It is clear from Eq. (14.18) that $J_{\rm CP}$ controls the magnitude of CP violation effects in neutrino oscillations in the case of 3-neutrino mixing. If $\sin(\Delta m^2_{ij}/(2p)L) \cong 0$ for $(ij) = (32)$, or (21), or (13), we get $A_{\rm CP}^{(l'l)} \cong 0$. Thus, if as a consequence of the production, propagation and/or detection of neutrinos, effectively oscillations due only to one non-zero neutrino mass squared difference take place, the CP violating effects will be strongly suppressed. In particular, we get $A_{\rm CP}^{(l'l)} = 0$, unless all three $\Delta m^2_{ij} \neq 0$, $(ij) = (32), (21), (13)$.

If the number of massive neutrinos n is equal to the number of neutrino flavours, $n = 3$, one has as a consequence of the unitarity of the neutrino mixing matrix: $\sum_{l'=e,\mu,\tau} P(\nu_l \to \nu_{l'}) = 1$, $l = e, \mu, \tau$, $\sum_{l=e,\mu,\tau} P(\nu_l \to \nu_{l'}) = 1$, $l' = e, \mu, \tau$. Similar "probability conservation" equations hold for $P(\bar\nu_l \to \bar\nu_{l'})$. If, however, the number of light massive neutrinos is bigger than the number of flavour neutrinos as a consequence, *e.g.*, of a flavour neutrino - sterile neutrino mixing, we would have $\sum_{l'=e,\mu,\tau} P(\nu_l \to \nu_{l'}) = 1 - P(\nu_l \to \bar\nu_{sL})$, $l = e, \mu, \tau$, where we have assumed the existence of just one sterile neutrino. Obviously, in this case $\sum_{l'=e,\mu,\tau} P(\nu_l \to \nu_{l'}) < 1$ if $P(\nu_l \to \bar\nu_{sL}) \neq 0$. The former inequality is used in the searches for oscillations between active and sterile neutrinos.

Consider next neutrino oscillations in the case of one neutrino mass squared difference "dominance": suppose that $|\Delta m^2_{j1}| \ll |\Delta m^2_{n1}|$, $j = 2, ..., (n-1)$, $|\Delta m^2_{n1}|\, L/(2p) \gtrsim 1$ and $|\Delta m^2_{j1}|\, L/(2p) \ll 1$, so that $\exp[i(\Delta m^2_{j1}\, L/(2p)] \cong 1$, $j = 2, ..., (n-1)$. Under these conditions we obtain from Eq. (14.13) and Eq. (14.14), keeping only the oscillating terms involving Δm^2_{n1}:

$$P(\nu_{l(l')} \to \nu_{l'(l)}) \cong P(\bar\nu_{l(l')} \to \bar\nu_{l'(l)}) \cong \delta_{ll'} - 2|U_{ln}|^2 \left[\delta_{ll'} - |U_{l'n}|^2\right] (1 - \cos\frac{\Delta m^2_{n1}}{2p}\, L)\,. \tag{14.20}$$

It follows from the neutrino oscillation data (Sections 14.4 and 14.5) that in the case of 3-neutrino mixing, one of the two independent neutrino mass squared differences, say Δm^2_{21}, is much smaller in absolute value than the second one, Δm^2_{31}: $|\Delta m^2_{21}| \ll |\Delta m^2_{31}|$. The data imply:

$$\begin{aligned} |\Delta m^2_{21}| &\cong 7.5 \times 10^{-5}\ {\rm eV}^2\,, \\ |\Delta m^2_{31}| &\cong 2.5 \times 10^{-3}\ {\rm eV}^2\,, \\ |\Delta m^2_{21}|/|\Delta m^2_{31}| &\cong 0.03\,. \end{aligned} \tag{14.21}$$

Neglecting the effects due to Δm^2_{21} we get from Eq. (14.20) by setting $n = 3$ and choosing, *e.g.*, i) $l = l' = e$ and ii) $l = e(\mu)$, $l' = \mu(e)$ [60]:

$$P(\nu_e \to \nu_e) = P(\bar\nu_e \to \bar\nu_e) \cong 1 - 2|U_{e3}|^2 \left(1 - |U_{e3}|^2\right) \left(1 - \cos\frac{\Delta m^2_{31}}{2p}\, L\right)\,, \tag{14.22}$$

$$P(\nu_{\mu(e)} \to \nu_{e(\mu)}) \cong 2\,|U_{\mu 3}|^2\,|U_{e3}|^2 \left(1 - \cos\frac{\Delta m^2_{31}}{2p}\, L\right) = \frac{|U_{\mu 3}|^2}{1 - |U_{e3}|^2}\, P^{2\nu}\left(|U_{e3}|^2, m^2_{31}\right)\,, \tag{14.23}$$

Table 14.1: Sensitivity of different oscillation experiments.

Source	Type of ν	$\overline{E}$[MeV]	L[km]	min(Δm^2)[eV^2]
Reactor	$\overline{\nu}_e$	~ 1	1	$\sim 10^{-3}$
Reactor	$\overline{\nu}_e$	~ 1	100	$\sim 10^{-5}$
Accelerator	$\nu_\mu, \overline{\nu}_\mu$	$\sim 10^3$	1	~ 1
Accelerator	$\nu_\mu, \overline{\nu}_\mu$	$\sim 10^3$	1000	$\sim 10^{-3}$
Atmospheric ν's	$\nu_{\mu,e}, \overline{\nu}_{\mu,e}$	$\sim 10^3$	10^4	$\sim 10^{-4}$
Sun	ν_e	~ 1	1.5×10^8	$\sim 10^{-11}$

and $P(\bar\nu_{\mu(e)} \to \bar\nu_{e(\mu)}) = P(\nu_{\mu(e)} \to \nu_{e(\mu)})$. Here $P^{2\nu}\left(|U_{e3}|^2, m^2_{31}\right)$ is the probability of the 2-neutrino transition $\nu_e \to (s_{23}\nu_\mu + c_{23}\nu_\tau)$ due to Δm^2_{31} and a mixing with angle θ_{13}, where

$$\sin^2\theta_{13} = |U_{e3}|^2,\ \ s^2_{23} \equiv \sin^2\theta_{23} = \frac{|U_{\mu 3}|^2}{1 - |U_{e3}|^2},$$
$$c^2_{23} \equiv \cos^2\theta_{23} = \frac{|U_{\tau 3}|^2}{1 - |U_{e3}|^2}. \tag{14.24}$$

Eq. (14.22) describes with a relatively high precision the oscillations of reactor $\bar\nu_e$ on a distance $L \sim 1$ km in the case of 3-neutrino mixing. It was used in the analysis of the data of the Chooz [61], Double Chooz [30], Daya Bay [31] and RENO [32] experiments. Eq. (14.20) with $n = 3$ and $l = l' = \mu$ describes with a relatively good precision the effects of "disappearance" due to oscillations of the accelerator ν_μ,

seen in the K2K [19] MINOS [20,21] and T2K [22,23] experiments. The $\nu_\mu \to \nu_\tau$ transitions due to the oscillations, which the OPERA experiment [62,63] is observing, can be described by Eq. (14.20) with $n = 3$ and $l = \mu$, $l' = \tau$. Finally, the probability Eq. (14.23) describes with a good precision the $\nu_\mu \to \nu_e$ and $\bar\nu_\mu \to \bar\nu_e$ oscillations under the conditions of the K2K experiment.

In certain cases the dimensions of the neutrino source, ΔL, are not negligible in comparison with the oscillation length. Similarly, when analyzing neutrino oscillation data one has to include the energy resolution of the detector, ΔE, *etc.* in the analysis. As can be shown [41], if $2\pi\Delta L/L^v_{jk} \gg 1$, and/or $2\pi(L/L^v_{jk})(\Delta E/E) \gg 1$, the oscillating terms in the neutrino oscillation probabilities will be strongly suppressed. In this case (as well as in the case of sufficiently large separation of the ν_j and ν_k wave packets at the detection point) the interference terms in $P(\nu_l \to \nu_{l'})$ and $P(\bar\nu_{l'} \to \bar\nu_l)$ will be negligibly small and the neutrino flavour conversion will be determined by the average probabilities:

$$\bar P(\nu_l \to \nu_{l'}) = \bar P(\bar\nu_l \to \bar\nu_{l'}) \cong \sum_j |U_{l'j}|^2\, |U_{lj}|^2\,. \tag{14.25}$$

Suppose next that in the case of 3-neutrino mixing, $|\Delta m^2_{21}|\, L/(2p) \sim 1$, while at the same time $|\Delta m^2_{31(32)}|\, L/(2p) \gg 1$, and the oscillations due to Δm^2_{31} and Δm^2_{32} are strongly suppressed (averaged out) due to integration over the region of neutrino production, the energy resolution function, *etc.* In this case we get for the ν_e and $\bar\nu_e$ survival probabilities:

$$P(\nu_e \to \nu_e) = P(\bar\nu_e \to \bar\nu_e) \cong |U_{e3}|^4 + \left(1 - |U_{e3}|^2\right)^2\, P^{2\nu}(\nu_e \to \nu_e)\,, \tag{14.26}$$

$$\begin{aligned} P^{2\nu}(\nu_e \to \nu_e) &= P^{2\nu}(\bar\nu_e \to \bar\nu_e) \equiv P^{2\nu}_{ee}(\theta_{12}, \Delta m^2_{21}) \\ &= 1 - \frac{1}{2}\,\sin^2 2\theta_{12}\,\left(1 - \cos\frac{\Delta m^2_{21}}{2p}\,L\right) \\ &= 1 - \sin^2 2\theta_{12}\,\sin^2\left(\frac{\Delta m^2_{21}}{4E}\,L\right) \end{aligned} \tag{14.27}$$

being the ν_e and $\bar\nu_e$ survival probability in the case of 2-neutrino oscillations "driven" by the angle θ_{12} and Δm^2_{21}, with θ_{12} determined by

$$\cos^2\theta_{12} = \frac{|U_{e1}|^2}{1 - |U_{e3}|^2}\,, \quad \sin^2\theta_{12} = \frac{|U_{e2}|^2}{1 - |U_{e3}|^2}\,. \tag{14.28}$$

Eq. (14.26) with $P^{2\nu}(\bar\nu_e \to \bar\nu_e)$ given by Eq. (14.27) describes the effects of neutrino oscillations of reactor $\bar\nu_e$ observed by the KamLAND experiment.

In the case of 3-neutrino mixing with $0 < \Delta m^2_{21} < |\Delta m^2_{31(32)}|$ and $|U_{e3}|^2 = |\sin\theta_{13}|^2 \ll 1$ (see Section 14.8), one can identify Δm^2_{21} and θ_{12} as the neutrino mass squared difference and mixing angle responsible for the solar ν_e oscillations, and Δm^2_{31} and θ_{23} as those associated with the dominant atmospheric ν_μ and $\bar\nu_\mu$ oscillations. Thus, θ_{12} and θ_{23} are often called "solar" and "atmospheric" neutrino mixing angles and denoted as $\theta_{12} = \theta_\odot$ and $\theta_{23} = \theta_{\rm A}$ (or $\theta_{\rm atm}$), while Δm^2_{21} and Δm^2_{31} are often referred to as the "solar" and "atmospheric" neutrino mass squared differences and denoted as $\Delta m^2_{21} \equiv \Delta m^2_\odot$ and $\Delta m^2_{31} \equiv \Delta m^2_{\rm A}$ (or $\Delta m^2_{\rm atm}$).

The data of ν-oscillations experiments is often analyzed assuming 2-neutrino mixing:

$$|\nu_l\rangle \;= |\nu_1\rangle\cos\theta + |\nu_2\rangle\sin\theta\,, \quad |\nu_x\rangle \;= -|\nu_1\rangle\sin\theta + |\nu_2\rangle\cos\theta\;, \tag{14.29}$$

where θ is the neutrino mixing angle in vacuum and ν_x is another flavour neutrino or sterile (anti-) neutrino, $x = l' \neq l$ or $\nu_x \equiv \bar\nu_{sL}$. In this case we have [54]:

$$\begin{aligned} P^{2\nu}(\nu_l \to \nu_l) &= 1 - \frac{1}{2}\sin^2 2\theta\left(1 - \cos 2\pi\frac{L}{L^v}\right) = 1 - \sin^2 2\theta\left(\sin^2\frac{\Delta m^2}{4E}L\right), \\ P^{2\nu}(\nu_l \to \nu_x) &= 1 - P^{2\nu}(\nu_l \to \nu_l)\,, \end{aligned} \tag{14.30}$$

where $L^v = 4\pi\, E/\Delta m^2$ ($p = E$), $\Delta m^2 = m^2_2 - m^2_1 > 0$. Combining the CPT invariance constraints with the probability conservation one obtains: $P(\nu_l \to \nu_x) = P(\bar\nu_l \to \bar\nu_x) = P(\nu_x \to \nu_l) = P(\bar\nu_x \to \bar\nu_l)$. These equalities and Eq. (14.30) with $l = \mu$ and $x = \tau$ were used, for instance, in the analysis of the Super-K atmospheric neutrino data [17], in which the first compelling evidence for oscillations of neutrinos was obtained. The probability $P^{2\nu}(\nu_l \to \nu_x)$, Eq. (14.30), depends on two factors: on $(1 - \cos 2\pi L/L^v)$, which exhibits oscillatory dependence on the distance L and on the neutrino energy $p = E$ (hence the name "neutrino oscillations"), and on $\sin^2 2\theta$, which determines the amplitude of the oscillations. In order to have $P^{2\nu}(\nu_l \to \nu_x) \cong 1$, two conditions have to be fulfilled: one should have $\sin^2 2\theta \cong 1$ and $L^v \lesssim 2\pi L$ with $\cos 2\pi L/L^v \cong -1$. If $L^v \gg 2\pi L$, the oscillations do not have enough time to develop on the way to the neutrino detector and $P(\nu_l \to \nu_x) \cong 0$, while $P(\nu_l \to \nu_l) \cong 1$. The preceding comments are illustrated in Fig. 14.1 showing the dependence of the probability $P^{2\nu}(\nu_e \to \nu_e) = P^{2\nu}(\bar\nu_e \to \bar\nu_e)$ on the neutrino energy.

A given experiment searching for neutrino oscillations is specified, in particular, by the average energy of the neutrinos being studied, $\bar E$, and by the source-detector distance L. The requirement $L^v_{jk} \lesssim 2\pi L$ determines the minimal value of a generic neutrino mass squared difference $\Delta m^2 > 0$, to which the experiment is sensitive (figure of merit of the experiment): $\min(\Delta m^2) \sim 2\bar E/L$. Because of the interference nature of neutrino oscillations, experiments can probe, in general, rather small values of Δm^2 (see, *e.g.*, Ref. 50). Values of $\min(\Delta m^2)$, characterizing qualitatively the sensitivity of different experiments are given in Table 14.1. They correspond to the reactor experiments Chooz, Daya Bay, RENO, Double Chooz ($L \sim 1$ km) and KamLAND ($L \sim 100$ km), to accelerator experiments - past ($L \sim 1$ km), recent, current and future (K2K, MINOS, OPERA, T2K, NOνA [65]) , $L \sim (300 \div 1000)$ km), to the Super-Kamiokande experiment studying atmospheric neutrino oscillations, and to the solar neutrino experiments.

14.3. Matter effects in neutrino oscillations

The presence of matter can change drastically the pattern of neutrino oscillations: neutrinos can interact with the particles forming the matter. Accordingly, the Hamiltonian of the neutrino system in matter H_m, differs from the Hamiltonian in vacuum H_0, $H_m = H_0 + H_{int}$, where H_{int} describes the interaction of neutrinos with the particles of matter. When, for instance, ν_e and ν_μ propagate in matter, they can scatter (due to H_{int}) on the electrons ($\rm e^-$), protons (p) and neutrons (n) present in matter. The incoherent elastic and the quasi-elastic scattering, in which the states of the initial particles change in the process (destroying the coherence between the neutrino states), are not of interest - they have a negligible effect on the solar neutrino propagation in the Sun and on the solar, atmospheric and reactor neutrino propagation in the Earth [66]: even in the center of the Sun, where the matter density is relatively high (~ 150 g/cm^3), a ν_e with energy of 1 MeV has a mean free path with respect to the indicated scattering processes $\sim 10^{10}$ km. We recall that the solar radius is much smaller: $\rm R_\odot = 6.96 \times 10^5$ km. The oscillating ν_e and ν_μ can scatter also elastically in the forward direction on the $\rm e^-$, p and n, with the momenta and the spin states of the particles remaining unchanged. In such a process the coherence of the neutrino states is preserved.

The ν_e and ν_μ coherent elastic scattering on the particles of matter generates nontrivial indices of refraction of the ν_e and ν_μ in matter [26]: $\kappa(\nu_e) \neq 1$, $\kappa(\nu_\mu) \neq 1$. Most importantly, we have $\kappa(\nu_e) \neq \kappa(\nu_\mu)$. The difference $\kappa(\nu_e) - \kappa(\nu_\mu)$ is determined essentially by the difference of the real parts of the forward $\nu_e - e^-$ and $\nu_\mu - e^-$ elastic scattering amplitudes [26] Re $[\rm F_{\nu_e - e^-}(0)]$ − Re $[\rm F_{\nu_\mu - e^-}(0)]$: due to the flavour symmetry of the neutrino – quark (neutrino – nucleon) neutral current interaction, the forward $\nu_e - p, n$ and $\nu_\mu - p, n$ elastic scattering amplitudes are equal and therefore do not contribute to the difference of interest [67]. The imaginary parts of the forward scattering amplitudes (responsible, in particular, for decoherence effects) are proportional to the corresponding total scattering cross-sections and in the case of interest are negligible in comparison with the real parts. The real parts of the amplitudes

$\mathrm{F}_{\nu_e-e^-}(0)$ and $\mathrm{F}_{\nu_\mu-e^-}(0)$ can be calculated in the Standard Model. To leading order in the Fermi constant G_F, only the term in $\mathrm{F}_{\nu_e-e^-}(0)$ due to the diagram with exchange of a virtual $W^{\pm}$-boson contributes to $\mathrm{F}_{\nu_e-e^-}(0) - \mathrm{F}_{\nu_\mu-e^-}(0)$. One finds the following result for $\kappa(\nu_e) - \kappa(\nu_\mu)$ in the rest frame of the scatters [26,69,70]:

$$\kappa(\nu_e) - \kappa(\nu_\mu) = \frac{2\pi}{p^2}\ \left(\mathrm{Re}\ [\mathrm{F}_{\nu_e-e^-}(0)] - \mathrm{Re}\ [\mathrm{F}_{\nu_\mu-e^-}(0)]\right) = -\ \frac{1}{p}\sqrt{2}G_F N_e\ , \tag{14.31}$$

where N_e is the electron number density in matter. Given $\kappa(\nu_e) - \kappa(\nu_\mu)$, the system of evolution equations describing the $\nu_e \leftrightarrow \nu_\mu$ oscillations in matter reads [26]:

$$i\frac{d}{dt}\begin{pmatrix} A_e(t,t_0) \\ A_\mu(t,t_0)\end{pmatrix} = \begin{pmatrix} -\epsilon(t) & \epsilon' \\ \epsilon' & \epsilon(t)\end{pmatrix}\begin{pmatrix} A_e(t,t_0) \\ A_\mu(t,t_0)\end{pmatrix} \tag{14.32}$$

where $A_e(t,t_0)$ ($A_\mu(t,t_0)$) is the amplitude of the probability to find ν_e (ν_μ) at time t of the evolution of the system if at time $t_0 \leq t$ the neutrino ν_e or ν_μ has been produced and

$$\epsilon(t) = \frac{1}{2}\ [\frac{\Delta m^2}{2E}\cos 2\theta - \sqrt{2}G_F N_e(t)],\ \ \epsilon' = \frac{\Delta m^2}{4E}\sin 2\theta. \tag{14.33}$$

The term $\sqrt{2}G_F N_e(t)$ in $\epsilon(t)$ accounts for the effects of matter on neutrino oscillations. The system of evolution equations describing the oscillations of antineutrinos $\bar\nu_e \leftrightarrow \bar\nu_\mu$ in matter has exactly the same form except for the matter term in $\epsilon(t)$ which changes sign. The effect of matter in neutrino oscillations is usually called the Mikheyev, Smirnov, Wolfenstein (or MSW) effect.

Consider first the case of $\nu_e \leftrightarrow \nu_\mu$ oscillations in matter with constant density: $N_e(t) = N_e = const.$ Due to the interaction term H_{int} in H_m, the eigenstates of the Hamiltonian of the neutrino system in vacuum, $|\nu_{1,2}\rangle$ are not eigenstates of H_m. For the eigenstates $|\nu^m_{1,2}\rangle$ of H_m, which diagonalize the evolution matrix in the r.h.s. of the system Eq. (14.32) we have:

$$|\nu_e\rangle = |\nu^m_1\rangle\cos\theta_m + |\nu^m_2\rangle\sin\theta_m\,, \qquad |\nu_\mu\rangle = -|\nu^m_1\rangle\sin\theta_m\ + |\nu^m_2\rangle\cos\theta_m\ . \tag{14.34}$$

Here θ_m is the neutrino mixing angle in matter [26],

$$\sin 2\theta_m = \frac{\tan 2\theta}{\sqrt{(1-\frac{N_e}{N_e^{res}})^2 + \tan^2 2\theta}},\ \cos 2\theta_m = \frac{1 - N_e/N_e^{res}}{\sqrt{(1-\frac{N_e}{N_e^{res}})^2 + \tan^2 2\theta}}, \tag{14.35}$$

where the quantity

$$N_e^{res} = \frac{\Delta m^2\cos 2\theta}{2E\sqrt{2}G_F} \cong 6.56\times 10^6\ \frac{\Delta m^2[\mathrm{eV}^2]}{E[\mathrm{MeV}]}\cos 2\theta\,\mathrm{cm}^{-3}\ \mathrm{N_A}\,, \tag{14.36}$$

is called (for $\Delta m^2\cos 2\theta > 0$) "resonance density" [27,69], $\mathrm{N_A}$ being Avogadro's number. The "adiabatic" states $|\nu^m_{1,2}\rangle$ have energies $E^m_{1,2}$ whose difference is given by

$$E^m_2 - E^m_1 = \frac{\Delta m^2}{2E}\ \left((1-\frac{N_e}{N_e^{res}})^2\cos^2 2\theta + \sin^2 2\theta\right)^{\frac{1}{2}} \equiv \frac{\Delta M^2}{2E}\,. \tag{14.37}$$

The probability of $\nu_e \to \nu_\mu$ transition in matter with $N_e = const.$ has the form [26,69]

$$P^{2\nu}_m(\nu_e \to \nu_\mu) = |A_\mu(t)|^2 = \frac{1}{2}\sin^2 2\theta_m\ [1 - \cos 2\pi\frac{L}{L_m}\ ] \qquad L_m = 2\pi/(E^m_2 - E^m_1)\,, \tag{14.38}$$

where L_m is the oscillation length in matter. As Eq. (14.35) indicates, the dependence of $\sin^2 2\theta_m$ on N_e has a resonance character [27]. Indeed, if $\Delta m^2\cos 2\theta > 0$, for any $\sin^2 2\theta \neq 0$ there exists a value of N_e given by N_e^{res}, such that when $N_e = N_e^{res}$ we have $\sin^2 2\theta_m = 1$ independently of the value of $\sin^2 2\theta < 1$. This implies that the presence of matter can lead to a strong enhancement of the oscillation probability $P^{2\nu}_m(\nu_e \to \nu_\mu)$ even when the $\nu_e \leftrightarrow \nu_\mu$ oscillations in vacuum are suppressed due to a small value of $\sin^2 2\theta$. For obvious reasons

$$N_e = N_e^{res} \equiv \frac{\Delta m^2\cos 2\theta}{2E\sqrt{2}G_F}\,, \tag{14.39}$$

is called the "resonance condition" [27,69], while the energy at which Eq. (14.39) holds for given N_e and $\Delta m^2\cos 2\theta$, is referred to as the "resonance energy", E^{res}. The oscillation length at resonance is given by [27] $L^{res}_m = L^v/\sin 2\theta$, while the width in N_e of the resonance at half height reads $\Delta N_e^{res} = 2N_e^{res}\tan 2\theta$. Thus, if the mixing angle in vacuum is small, the resonance is narrow, $\Delta N_e^{res} \ll N_e^{res}$, and $L^{res}_m \gg L^v$. The energy difference $E^m_2 - E^m_1$ has a minimum at the resonance: $(E^m_2 - E^m_1)^{res} = \min\ (E^m_2 - E^m_1) = (\Delta m^2/(2E))\sin 2\theta$.

It is instructive to consider two limiting cases. If $N_e \ll N_e^{res}$, we have from Eq. (14.35) and Eq. (14.37), $\theta_m \cong \theta$, $\mathrm{L_m} \cong \mathrm{L^v}$ and neutrinos oscillate practically as in vacuum. In the limit $N_e \gg N_e^{res}$, $N_e^{res}\tan^2 2\theta$, one finds $\theta_m \cong \pi/2$ ($\cos 2\theta_m \cong -1$) and the presence of matter suppresses the $\nu_e \leftrightarrow \nu_\mu$ oscillations. In this case $|\nu_e\rangle \cong |\nu^m_2\rangle$, $|\nu_\mu\rangle = -|\nu^m_1\rangle$, *i.e.*, ν_e practically coincides with the heavier matter-eigenstate, while ν_μ coincides with the lighter one.

Since the neutral current weak interaction of neutrinos in the Standard Model is flavour symmetric, the formulae and results we have obtained are valid for the case of $\nu_e - \nu_\tau$ mixing and $\nu_e \leftrightarrow \nu_\tau$ oscillations in matter as well. The case of $\nu_\mu - \nu_\tau$ mixing, however, is different: to a relatively good precision we have [71] $\kappa(\nu_\mu) \cong \kappa(\nu_\tau)$ and the $\nu_\mu \leftrightarrow \nu_\tau$ oscillations in the matter of the Earth and the Sun proceed practically as in vacuum [72].

The analogs of Eq. (14.35) to Eq. (14.38) for oscillations of antineutrinos, $\bar\nu_e \leftrightarrow \bar\nu_\mu$, in matter can formally be obtained by replacing N_e with $(-N_e)$ in the indicated equations. It should be clear that depending on the sign of $\Delta m^2\cos 2\theta$, the presence of matter can lead to resonance enhancement either of the $\nu_e \leftrightarrow \nu_\mu$ or of the $\bar\nu_e \leftrightarrow \bar\nu_\mu$ oscillations, but not of both types of oscillations [69]. For $\Delta m^2\cos 2\theta < 0$, for instance, the matter can only suppress the $\nu_e \to \nu_\mu$ oscillations, while it can enhance the $\bar\nu_e \to \bar\nu_\mu$ transitions. This disparity between the behavior of neutrinos and that of antineutrinos is a consequence of the fact that the matter in the Sun or in the Earth we are interested in is not charge-symmetric (it contains e^-, p and n, but does not contain their antiparticles) and therefore the oscillations in matter are neither CP- nor CPT- invariant [57]. Thus, even in the case of 2-neutrino mixing and oscillations we have, *e.g.*, $P^{2\nu}_m(\nu_e \to \nu_{\mu(\tau)}) \neq P^{2\nu}_m(\bar\nu_e \to \bar\nu_{\mu(\tau)})$.

The matter effects in the $\nu_e \leftrightarrow \nu_{\mu(\tau)}$ ($\bar\nu_e \leftrightarrow \bar\nu_{\mu(\tau)}$) oscillations will be invariant with respect to the operation of time reversal if the N_e distribution along the neutrino path is symmetric with respect to this operation [58,73]. The latter condition is fulfilled (to a good approximation) for the N_e distribution along a path of a neutrino crossing the Earth [74].

14.3.1. *Effects of Earth matter on oscillations of neutrinos* :

The formalism we have developed can be applied, *e.g.*, to the study of matter effects in the $\nu_e \leftrightarrow \nu_{\mu(\tau)}$ ($\nu_{\mu(\tau)} \leftrightarrow \nu_e$) and $\bar\nu_e \leftrightarrow \bar\nu_{\mu(\tau)}$ ($\bar\nu_{\mu(\tau)} \leftrightarrow \bar\nu_e$) oscillations of neutrinos which traverse the Earth [75]. Indeed, the Earth density distribution in the existing Earth models [74] is assumed to be spherically symmetric and there are two major density structures - the core and the mantle, and a certain number of substructures (shells or layers). The Earth radius is $R_\oplus = 6371$ km; the Earth core has a radius of $R_c = 3486$ km, so the Earth mantle depth is 2885 km. For a spherically symmetric Earth density distribution, the neutrino trajectory in the Earth is specified by the value of the nadir angle θ_n of the trajectory. For $\theta_n \leq 33.17^o$, or path lengths $L \geq 10660$ km, neutrinos cross the Earth core. The path length for neutrinos which cross only the Earth mantle is given by $L = 2R_\oplus\cos\theta_n$. If neutrinos cross the Earth core, the lengths of the paths in the mantle, $2L^{\mathrm{man}}$, and in the core, L^{core}, are determined by: $L^{\mathrm{man}} = R_\oplus\cos\theta_n - (R_c^2 - R_\oplus^2\sin^2\theta_n)^{\frac{1}{2}}$, $L^{\mathrm{core}} = 2(R_c^2 - R_\oplus^2\sin^2\theta_n)^{\frac{1}{2}}$. The mean electron number densities in the mantle and in the core according to the PREM model read [74]: $\bar N_e^{man} \cong 2.2$ cm^{-3} $\mathrm{N_A}$, $\bar N_e^c \cong 5.4$ cm^{-3} $\mathrm{N_A}$. Thus, we have $\bar N_e^c \cong 2.5\ \bar N_e^{man}$. The change of N_e from the mantle to the core can well be approximated by a step function [74]. The electron number density N_e changes

relatively little around the indicated mean values along the trajectories of neutrinos which cross a substantial part of the Earth mantle, or the mantle and the core, and the two-layer constant density approximation, $N_e^{man} = const. = \bar{N}_e^{man}$, $N_e^c = const. = \bar{N}_e^c$, $\bar{N}_e^{man}$ and $\bar{N}_e^c$ being the mean densities along the given neutrino path in the Earth, was shown to be sufficiently accurate in what concerns the calculation of neutrino oscillation probabilities [58,77,78] (and references quoted in [77,78]) in a large number of specific cases. This is related to the fact that the relatively small changes of density along the path of the neutrinos in the mantle (or in the core) take place over path lengths which are typically considerably smaller than the corresponding oscillation length in matter.

In the case of 3-neutrino mixing and for neutrino energies of $E \gtrsim 2$ GeV, the effects due to Δm^2_{21} ($|\Delta m^2_{21}| \ll |\Delta m^2_{31}|$, see Eq. (14.21)) in the neutrino oscillation probabilities are sub-dominant and to leading order can be neglected: the corresponding resonance density $|N^{res}_{e21}| \lesssim 0.25\ cm^{-3}\ N_A \ll \bar{N}_e^{man,c}$ and the Earth matter strongly suppresses the oscillations due to Δm^2_{21}. For oscillations in vacuum this approximation is valid as long as the leading order contribution due to Δm^2_{31} in the relevant probabilities is bigger than approximately 10^{-3}. In this case the 3-neutrino $\nu_e \to \nu_{\mu(\tau)}$ ($\bar{\nu}_e \to \bar{\nu}_{\mu(\tau)}$) and $\nu_{\mu(\tau)} \to \nu_e$ ($\bar{\nu}_{\mu(\tau)} \to \bar{\nu}_e$) transition probabilities for neutrinos traversing the Earth, reduce effectively to a 2-neutrino transition probability (see, *e.g.*, Refs. [78–80]) , with Δm^2_{31} and θ_{13} playing the role of the relevant 2-neutrino vacuum oscillation parameters. As will be discussed in Sections 14.6 and 14.8, the value of $\sin^2 2\theta_{13}$ has been determined with a rather high precision in the Daya Bay [31] and RENO [32] experiments. The best fit values found in the two experiments read, respectively, $\sin^2 2\theta_{13} = 0.090$ [36] and 0.100 [37]. The 3-neutrino oscillation probabilities of the atmospheric and accelerator $\nu_{e,\mu}$ having energy E and crossing the Earth along a trajectory characterized by a nadir angle θ_n, for instance, have the following form:

$$P^{3\nu}_m(\nu_e \to \nu_e) \cong 1 - P^{2\nu}_m, \tag{14.40}$$

$$P^{3\nu}_m(\nu_e \to \nu_\mu) \cong P^{3\nu}_m(\nu_\mu \to \nu_e) \cong s^2_{23}\ P^{2\nu}_m, \qquad P^{3\nu}_m(\nu_e \to \nu_\tau) \cong c^2_{23}\ P^{2\nu}_m, \tag{14.41}$$

$$P^{3\nu}_m(\nu_\mu \to \nu_\mu) \cong 1 - s^4_{23}\ P^{2\nu}_m - 2c^2_{23}s^2_{23}\ \left[1 - Re\ (e^{-i\kappa} A^{2\nu}_m(\nu' \to \nu'))\right], \tag{14.42}$$

$$P^{3\nu}_m(\nu_\mu \to \nu_\tau) = 1 - P^{3\nu}_m(\nu_\mu \to \nu_\mu) - P^{3\nu}_m(\nu_\mu \to \nu_e). \tag{14.43}$$

Here $P^{2\nu}_m \equiv P^{2\nu}_m(\Delta m^2_{31}, \theta_{13}; E, \theta_n)$ is the probability of the 2-neutrino $\nu_e \to \nu' \equiv (s_{23}\nu_\mu + c_{23}\nu_\tau)$ oscillations in the Earth, and κ and $A^{2\nu}_m(\nu' \to \nu') \equiv A^{2\nu}_m$ are known phase and 2-neutrino transition probability amplitude (see, *e.g.*, Refs. [78,79]). We note that Eq. (14.40) to Eq. (14.42) are based only on the assumptions that $|N^{res}_{e21}|$ is much smaller than the densities in the Earth mantle and core and that $|\Delta m^2_{21}| \ll |\Delta m^2_{31}|$, and does not rely on the constant density approximation. Similar results are valid for the corresponding antineutrino oscillation probabilities: one has just to replace $P^{2\nu}_m$, κ and $A^{2\nu}_m$ in the expressions given above with the corresponding quantities for antineutrinos (the latter are obtained from those for neutrinos by changing the sign in front of N_e). Obviously, we have: $P(\nu_{e(\mu)} \to \nu_{\mu(e)}), P(\bar{\nu}_{e(\mu)} \to \bar{\nu}_{\mu(e)}) \leq \sin^2\theta_{23}$, and $P(\nu_e \to \nu_\tau), P(\bar{\nu}_e \to \bar{\nu}_\tau) \leq \cos^2\theta_{23}$. The one Δm^2 dominance approximation and correspondingly Eq. (14.40) to Eq. (14.43) were used by the Super-Kamiokande Collaboration in their 2006 neutrino oscillation analysis of the multi-GeV atmospheric neutrino data [81].

In the case of neutrinos crossing only the Earth mantle and in the constant density approximation, $P^{2\nu}_m$ is given by the r.h.s. of Eq. (14.38) with θ and Δm^2 replaced by θ_{13} and Δm^2_{31}, while for κ and $A^{2\nu}_m$ we have (see, *e.g.*, Ref. 78):

$$\kappa \cong \frac{1}{2}[\frac{\Delta m^2_{31}}{2E}\ L + \sqrt{2}G_F \bar{N}_e^{man} L - \frac{\Delta M^2 L}{2E}],$$
$$A^{2\nu}_m = 1 + (e^{-i\frac{\Delta M^2 L}{2E}} - 1)\cos^2\theta'_m\ , \tag{14.44}$$

where ΔM^2 is defined in Eq. (14.37) (with $\theta = \theta_{13}$ and $\Delta m^2 = \Delta m^2_{31}$), θ'_m is the mixing angle in the mantle which coincides in vacuum with θ_{13} (Eq. (14.35) with $N_e = \bar{N}_e^{man}$ and $\theta = \theta_{13}$), and $L = 2R_\oplus \cos\theta_n$ is the distance the neutrino travels in the mantle.

It follows from Eq. (14.40) and Eq. (14.41) that for $\Delta m^2_{31}\cos 2\theta_{13} > 0$, the oscillation effects of interest, *e.g.*, in the $\nu_{e(\mu)} \to \nu_{\mu(e)}$ and $\nu_e \to \nu_\tau$ transitions will be maximal if $P^{2\nu}_m \cong 1$, *i.e.*, if Eq. (14.39) leading to $\sin^2 2\theta_m \cong 1$ is fulfilled, and ii) $\cos(\Delta M^2 L/(2E)) \cong -1$. Given the value of $\bar{N}_e^{man}$, the first condition determines the neutrino's energy, while the second determines the path length L, for which one can have $P^{2\nu}_m \cong 1$. For $\Delta m^2_{31} \cong 2.5 \times 10^{-3}$ eV^2, $\sin^2 2\theta_{13} \cong 0.090$ and $\bar{\mathrm{N}}_\mathrm{e}^{\mathrm{man}} \cong 2.2\ \mathrm{N_A cm^{-3}}$, one finds that $E_{res} \cong 7.1$ GeV and $L \cong 3522/\sin 2\theta_{13}$ km $\cong 11739$ km. Since for neutrinos crossing only the mantle $L \lesssim 10660$ km, the second condition can be satisfied only if $\sin^2 2\theta_{13} \gtrsim 0.11$, which falls in the 3σ range of the experimentally allowed values of $\sin^2 2\theta_{13}$. We still get a significant amplification of the probability $P^{2\nu}_m$, and therefore of $P(\nu_{e(\mu)} \to \nu_{\mu(e)})$ and $P(\nu_e \to \nu_\tau)$, even when $\cos(\Delta M^2 L/(2E)) = -0.5(-0.2)$: in this case $P^{2\nu}_m \cong 0.75$ (0.60). For $\sin^2 2\theta_{13} \cong 0.090$ we have $\cos(\Delta M^2 L/(2E)) = -0.5(-0.2)$ if $L \cong 7826$ (6622) km. Thus, for $\Delta m^2_{31} > 0$, the Earth matter effects can amplify $P^{2\nu}_m$, and therefore $P(\nu_{e(\mu)} \to \nu_{\mu(e)})$ and $P(\nu_e \to \nu_\tau)$, significantly when the neutrinos cross only the mantle, for $E \sim 7$ GeV and sufficiently large path lengths L. If $\Delta m^2_{31} < 0$ the same considerations apply for the corresponding antineutrino oscillation probabilities $\bar{P}^{2\nu}_m = \bar{P}^{2\nu}_m(\bar{\nu}_e \to (s_{23}\bar{\nu}_\mu + c_{23}\bar{\nu}_\tau))$ and correspondingly for $P(\bar{\nu}_{e(\mu)} \to \bar{\nu}_{\mu(e)})$ and $P(\bar{\nu}_e \to \bar{\nu}_\tau)$. For $\Delta m^2_{31} > 0$, the $\bar{\nu}_{e(\mu)} \to \bar{\nu}_{\mu(e)}$ and $\bar{\nu}_e \to \bar{\nu}_\tau$ oscillations are suppressed by the Earth matter, while if $\Delta m^2_{31} < 0$, the same conclusion holds for the $\nu_{e(\mu)} \to \nu_{\mu(e)}$ and $\nu_e \to \nu_\tau$, oscillations.

In the case of neutrinos crossing the Earth core, new resonance-like effects become possible in the $\nu_\mu \to \nu_e$ and $\nu_e \to \nu_{\mu(\tau)}$ (or $\bar{\nu}_\mu \to \bar{\nu}_e$ and $\bar{\nu}_e \to \bar{\nu}_{\mu(\tau)}$) transitions [77–79,82–84]. For $\Delta m^2_{31} > 0$ and certain values of $\sin^2\theta_{13} \lesssim 0.05$ we can have [83] $P^{2\nu}_m(\Delta m^2_{31}, \theta_{13}) \cong 1$, and correspondingly maximal $P^{3\nu}_m(\nu_e \to \nu_\mu) = P^{3\nu}_m(\nu_\mu \to \nu_e) \cong s^2_{23}$, only due to the effect of maximal constructive interference between the amplitudes of the $\nu_e \to \nu'$ transitions in the Earth mantle and in the Earth core. The effect differs from the MSW one and the enhancement happens in the case of interest at a value of the energy between the MSW resonance energies corresponding to the density in the mantle and that of the core, or at a value of the resonance density N^{res}_e which lies between the values of N_e in the mantle and in the core [77]. In Refs. [77,78] the enhancement was called "neutrino oscillation length resonance", while in Refs. [79,82] the term "parametric resonance" for the same effect was used [85]. The *mantle-core enhancement effect* is caused by the existence (for a given neutrino trajectory through the Earth core) of points of resonance-like maximal neutrino conversion, $P^{2\nu}_m(\Delta m^2_{31}, \theta_{13}) = 1$, in the corresponding space of neutrino oscillation parameters [83]. For $\Delta m^2_{31} < 0$ the mantle-core enhancement can take place for the antineutrino transitions, $\bar{\nu}_\mu \to \bar{\nu}_e$ and $\bar{\nu}_e \to \bar{\nu}_{\mu(\tau)}$.

A rather complete set of values of $\Delta m^2_{31}/E > 0$ and $\sin^2 2\theta_{13}$ for which $P^{2\nu}_m(\Delta m^2_{31}, \theta_{13}) = 1$ was found in Ref. 83. The location of these points in the $\Delta m^2_{31}/E - \sin^2 2\theta_{13}$ plane determines the regions in the plane where $P^{2\nu}_m(\Delta m^2_{31}, \theta_{13})$ is large, $P^{2\nu}_m(\Delta m^2_{31}, \theta_{13}) \gtrsim 0.5$. These regions vary slowly with the nadir angle, being remarkably wide in the nadir angle and rather wide in the neutrino energy [83], so that the transitions of interest can produce noticeable effects in the measured observables. For $\sin^2\theta_{13} \lesssim 0.05$, there are two sets of values of $(\Delta m^2_{31}/E, \sin^2\theta_{13})$ for which $P^{2\nu}_m(\Delta m^2_{31}, \theta_{13}) = 1$, and thus two regions in $\Delta m^2_{31}/E - \sin^2 2\theta_{13}$ plane where $P^{2\nu}_m(\Delta m^2_{31}, \theta_{13}) \gtrsim 0.5$. For $\Delta m^2_{31} = 2.5 \times 10^{-3}$ eV^2 and nadir angle, *e.g.*, θ_n=0 (Earth center crossing neutrinos), we have $P^{2\nu}_m(\Delta m^2_{31}, \theta_{13}) = 1$ at $(E, \sin^2 2\theta_{13})$ =(3.4 GeV,0.034) and (5.2 GeV,0.15). At the same time for E =3.4 GeV (5.2 Gev), the probability $P^{2\nu}_m(\Delta m^2_{31}, \theta_{13}) \gtrsim 0.5$ for the values of $\sin^2 2\theta_{13}$ from the interval $0.02 \lesssim \sin^2 2\theta_{13} \lesssim 0.10$ ($0.04 \lesssim \sin^2 2\theta_{13} \lesssim 0.26$). Similar results hold for neutrinos crossing the Earth core along the trajectories with $\theta_n \neq 0$ (for further details see the last article in Ref. 83; see also the last article in Ref. 84).

The mantle-core enhancement of $P^{2\nu}_m$ (or $\bar{P}^{2\nu}_m$) is relevant, in particular, for the searches of sub-dominant $\nu_{e(\mu)} \to \nu_{\mu(e)}$ (or $\bar{\nu}_{e(\mu)} \to \bar{\nu}_{\mu(e)}$) oscillations of atmospheric neutrinos having energies $E \gtrsim 2$ GeV and crossing the Earth core on the way to the detector (see Ref. 77 to Ref. 84 and the references quoted therein). The effects

of Earth matter on the oscillations of atmospheric and accelerator neutrinos have not been observed so far. At present there are no compelling evidences for oscillations of the atmospheric ν_e and/or $\bar{\nu}_e$.

The expression for the probability of the $\nu_\mu \to \nu_e$ oscillations taking place in the Earth mantle in the case of 3-neutrino mixing, in which both neutrino mass squared differences Δm^2_{21} and Δm^2_{31} contribute and the CP violation effects due to the Dirac phase in the neutrino mixing matrix are taken into account, has the following form in the constant density approximation and keeping terms up to second order in the two small parameters $|\alpha| \equiv |\Delta m^2_{21}|/|\Delta m^2_{31}| \ll 1$ and $\sin^2\theta_{13} \ll 1$ [86]:

$$P^{3\nu\ man}_m(\nu_\mu \to \nu_e) \cong P_0 + P_{\sin\delta} + P_{\cos\delta} + P_3\,. \tag{14.45}$$

Here

$$P_0 = \sin^2\theta_{23}\,\frac{\sin^2 2\theta_{13}}{(A-1)^2}\,\sin^2[(A-1)\Delta]$$

$$P_3 = \alpha^2\,\cos^2\theta_{23}\,\frac{\sin^2 2\theta_{12}}{A^2}\,\sin^2(A\Delta)\,, \tag{14.46}$$

$$P_{\sin\delta} = -\,\alpha\,\frac{8\,J_{CP}}{A(1-A)}\,(\sin\Delta)\,(\sin A\Delta)\,(\sin[(1-A)\Delta])\,, \tag{14.47}$$

$$P_{\cos\delta} = \alpha\,\frac{8\,J_{CP}\,\cot\delta}{A(1-A)}\,(\cos\Delta)\,(\sin A\Delta)\,(\sin[(1-A)\Delta])\,, \tag{14.48}$$

where

$$\alpha = \frac{\Delta m^2_{21}}{\Delta m^2_{31}}\,,\ \Delta = \frac{\Delta m^2_{31}\,L}{4E}\,,\ A = \sqrt{2}G_{\rm F}N_e^{man}\frac{2E}{\Delta m^2_{31}}\,, \tag{14.49}$$

and $\cot\delta = J^{-1}_{CP}{\rm Re}(U_{\mu 3}U^*_{e3}U_{e2}U^*_{\mu 2})$, $J_{CP} = {\rm Im}(U_{\mu 3}U^*_{e3}U_{e2}U^*_{\mu 2})$. The analytic expression for $P^{3\nu\ man}_m(\nu_\mu \to \nu_e)$ given above is valid for [86] neutrino path lengths in the mantle ($L \leq 10660$ km) satisfying $L \lesssim 10560$ km $E[{\rm GeV}]\,(7.6\times10^{-5}\ {\rm eV}^2/\Delta m^2_{21})$, and energies $E \gtrsim 0.34$ GeV$(\Delta m^2_{21}/7.6\times10^{-5}\ {\rm eV}^2)\,(1.4\ {\rm cm}^{-3}N_A/N_e^{man})$. The expression for the $\bar{\nu}_\mu \to \bar{\nu}_e$ oscillation probability can be obtained formally from that for $P^{3\nu\ man}_m(\nu_\mu \to \nu_e)$ by making the changes $A \to -A$ and $J_{CP} \to -J_{CP}$, with $J_{CP}\cot\delta \equiv {\rm Re}(U_{\mu 3}U^*_{e3}U_{e2}U^*_{\mu 2})$ remaining unchanged. The term $P_{\sin\delta}$ in $P^{3\nu\ man}_m(\nu_\mu \to \nu_e)$ would be equal to zero if the Dirac phase in the neutrino mixing matrix U possesses a CP-conserving value. Even in this case, however, we have $A^{(e\mu)\ man}_{CP} \equiv (P^{3\nu\ man}_m(\nu_\mu \to \nu_e) - P^{3\nu\ man}_m(\bar{\nu}_\mu \to \bar{\nu}_e)) \neq 0$ due to the effects of the Earth matter. It will be important to experimentally disentangle the effects of the Earth matter and of J_{CP} in $A^{(e\mu)\ man}_{CP}$: this will allow to get information about the Dirac CP violation phase in U. This can be done, in principle, by studying the energy dependence of $P^{3\nu\ man}_m(\nu_\mu \to \nu_e)$ and $P^{3\nu\ man}_m(\bar{\nu}_\mu \to \bar{\nu}_e)$. Since the sign of $\Delta m^2_{31(32)}$ determines for given L whether the probability $P^{3\nu\ man}_m(\nu_\mu \to \nu_e)$ or $P^{3\nu\ man}_m(\bar{\nu}_\mu \to \bar{\nu}_e)$, as a function of energy, can be resonantly enhanced or suppressed by the matter effects, the study of the energy dependence of $P^{3\nu\ man}_m(\nu_\mu \to \nu_e)$ and/or of $P^{3\nu\ man}_m(\bar{\nu}_\mu \to \bar{\nu}_e)$ can provide also information on ${\rm sgn}(\Delta m^2_{31(32)})$. In the vacuum limit of $N_e^{man} = 0$ ($A = 0$) we have $A^{(e\mu)\ man}_{CP} = A^{(e\mu)}_{CP}$ (see Eq. (14.18)) and only the term $P_{\sin\delta}$ contributes to the asymmetry $A^{(e\mu)}_{CP}$.

The preceding remarks apply also to the probabilities $P^{3\nu\ man}_m(\nu_e \to \nu_\mu)$ and $P^{3\nu\ man}_m(\bar{\nu}_e \to \bar{\nu}_\mu)$). The probability $P^{3\nu\ man}_m(\nu_e \to \nu_\mu)$, for example, can formally be obtained from the expression for the probability $P^{3\nu\ man}_m(\nu_\mu \to \nu_e)$ by changing the sign of the term $P_{\sin\delta}$.

14.3.2. *Oscillations of solar neutrinos* :

Consider next the oscillations of solar ν_e while they propagate from the central part of the Sun, where they are produced, to the surface of the Sun [27,76](see also Ref. 26 and, *e.g.*, Ref. 87) Details concerning the production, spectrum, magnitude and particularities of the solar neutrino flux, the methods of detection of solar neutrinos, description of solar neutrino experiments and of the data they provided will be discussed in the next section (see also Ref. 88). The electron number density N_e changes considerably along the neutrino path in the Sun: it decreases monotonically from the value of ~ 100 cm^{-3} N_A in the center of the Sun to 0 at the surface of the Sun. According to the contemporary solar models (see, *e.g.*, Ref. [88,89]), N_e decreases approximately exponentially in the radial direction towards the surface of the Sun:

$$N_e(t) = N_e(t_0)\exp\left\{-\frac{t-t_0}{r_0}\right\}\,, \tag{14.50}$$

where $(t - t_0) \cong d$ is the distance traveled by the neutrino in the Sun, $N_e(t_0)$ is the electron number density at the point of ν_e production in the Sun, r_0 is the scale-height of the change of $N_e(t)$ and one has [88,89] $r_0 \sim 0.1R_\odot$.

Consider the case of 2-neutrino mixing, Eq. (14.34). Obviously, if N_e changes with t (or equivalently with the distance) along the neutrino trajectory, the matter-eigenstates, their energies, the mixing angle and the oscillation length in matter, become, through their dependence on N_e, also functions of t: $|\nu^m_{1,2}\rangle = |\nu^m_{1,2}(t)\rangle$, $E^m_{1,2} = E^m_{1,2}(t)$, $\theta_m = \theta_m(t)$ and $L_m = L_m(t)$. It is not difficult to understand qualitatively the possible behavior of the neutrino system when solar neutrinos propagate from the center to the surface of the Sun if one realizes that one is dealing effectively with a two-level system whose Hamiltonian depends on time and admits "jumps" from one level to the other (see Eq. (14.32)). Consider the case of $\Delta m^2\cos 2\theta > 0$. Let us assume first for simplicity that the electron number density at the point of a solar ν_e production in the Sun is much bigger than the resonance density, $N_e(t_0) \gg N_e^{res}$. Actually, this is one of the cases relevant to the solar neutrinos. In this case we have $\theta_m(t_0) \cong \pi/2$ and the state of the electron neutrino in the initial moment of the evolution of the system practically coincides with the heavier of the two matter-eigenstates:

$$|\nu_e\rangle \ \cong\ |\nu^m_2(t_0)\rangle\,. \tag{14.51}$$

Thus, at t_0 the neutrino system is in a state corresponding to the "level" with energy $E^m_2(t_0)$. When neutrinos propagate to the surface of the Sun they cross a layer of matter in which $N_e = N_e^{res}$: in this layer the difference between the energies of the two "levels" $(E^m_2(t) - E^m_1(t))$ has a minimal value on the neutrino trajectory (Eq. (14.37) and Eq. (14.39)). Correspondingly, the evolution of the neutrino system can proceed basically in two ways. First, the system can stay on the "level" with energy $E^m_2(t)$, *i.e.*, can continue to be in the state $|\nu^m_2(t)\rangle$ up to the final moment t_s, when the neutrino reaches the surface of the Sun. At the surface of the Sun $N_e(t_s) = 0$ and therefore $\theta_m(t_s) = \theta$, $|\nu^m_{1,2}(t_s)\rangle \equiv |\nu_{1,2}\rangle$ and $E^m_{1,2}(t_s) = E_{1,2}$. Thus, in this case the state describing the neutrino system at t_0 will evolve continuously into the state $|\nu_2\rangle$ at the surface of the Sun. Using Eq. (14.29) with $l = e$ and $x = \mu$, it is easy to obtain the probabilities to find ν_e and ν_μ at the surface of the Sun:

$$P(\nu_e \to \nu_e; t_s, t_0) \cong |\langle\nu_e|\nu_2\rangle|^2 = \sin^2\theta$$
$$P(\nu_e \to \nu_\mu; t_s, t_0) \cong |\langle\nu_\mu|\nu_2\rangle|^2 = \cos^2\theta\,. \tag{14.52}$$

It is clear that under the assumption made and if $\sin^2\theta \ll 1$, practically a total $\nu_e \to \nu_\mu$ conversion is possible. This type of evolution of the neutrino system and the $\nu_e \to \nu_\mu$ transitions taking place during the evolution, are called [27] "adiabatic." They are characterized by the fact that the probability of the "jump" from the upper "level" (having energy $E^m_2(t)$) to the lower "level" (with energy $E^m_1(t)$), P', or equivalently the probability of the $\nu^m_2(t_0) \to \nu^m_1(t_s)$ transition, $P' \equiv P'(\nu^m_2(t_0) \to \nu^m_1(t_s))$, on the whole neutrino trajectory is negligible:

$$P' \equiv P'(\nu^m_2(t_0) \to \nu^m_1(t_s)) \cong 0\ :\ \textit{adiabatic transitions}\,. \tag{14.53}$$

The second possibility is realized if in the resonance region, where the two "levels" approach each other closest the system "jumps" from the upper "level" to the lower "level" and after that continues to be in the state $|\nu^m_1(t)\rangle$ until the neutrino reaches the surface of the Sun. Evidently, now we have $P' \equiv P'(\nu^m_2(t_0) \to \nu^m_1(t_s)) \sim 1$. In this case

the neutrino system ends up in the state $|\nu_1^m(t_s)\rangle \equiv |\nu_1\rangle$ at the surface of the Sun and

$$P(\nu_e \to \nu_e; t_s, t_0) \cong |\langle \nu_e | \nu_1 \rangle|^2 = \cos^2\theta$$
$$P(\nu_e \to \nu_\mu; t_s, t_0) \cong |\langle \nu_\mu | \nu_1 \rangle|^2 = \sin^2\theta\,. \qquad (14.54)$$

Obviously, if $\sin^2\theta \ll 1$, practically no transitions of the solar ν_e into ν_μ will occur. The considered regime of evolution of the neutrino system and the corresponding $\nu_e \to \nu_\mu$ transitions are usually referred to as "extremely nonadiabatic."

Clearly, the value of the "jump" probability P' plays a crucial role in the the $\nu_e \to \nu_\mu$ transitions: it fixes the type of the transition and determines to a large extent the $\nu_e \to \nu_\mu$ transition probability [76,90,91]. We have considered above two limiting cases. Obviously, there exists a whole spectrum of possibilities since P' can have any value from 0 to $\cos^2\theta$ [92,93]. In general, the transitions are called "nonadiabatic" if P' is non-negligible.

Numerical studies have shown [27] that solar neutrinos can undergo both adiabatic and nonadiabatic $\nu_e \to \nu_\mu$ transitions in the Sun and the matter effects can be substantial in the solar neutrino oscillations for 10^{-8} eV$^2 \lesssim \Delta m^2 \lesssim 10^{-4}$ eV^2, $10^{-4} \lesssim \sin^2 2\theta < 1.0$.

The condition of adiabaticity of the solar ν_e transitions in Sun can be written as [76,90]

$$\gamma(t) \equiv \sqrt{2} G_F \frac{(N_e^{res})^2}{|\dot{N}_e(t)|} \tan^2 2\theta \left(1 + \tan^{-2} 2\theta_m(t)\right)^{\frac{3}{2}} \gg 1$$
$$\text{adiabatic transitions}\,, \qquad (14.55)$$

while if $\gamma(t) \lesssim 1$ the transitions are nonadiabatic (see also Ref. 93), where $\dot{N}_e(t) \equiv \frac{d}{dt} N_e(t)$. Condition in Eq. (14.55) implies that the $\nu_e \to \nu_{\mu(\tau)}$ transitions in the Sun will be adiabatic if $N_e(t)$ changes sufficiently slowly along the neutrino path. In order for the transitions to be adiabatic, condition in Eq. (14.55) has to be fulfilled at any point of the neutrino's path in the Sun.

Actually, the system of evolution equations Eq. (14.32) can be solved exactly for N_e changing exponentially, Eq. (14.50), along the neutrino path in the Sun [92,94]. More specifically, the system in Eq. (14.32) is equivalent to one second order differential equation (with appropriate initial conditions). The latter can be shown [95] to coincide in form, in the case of N_e given by Eq. (14.50), with the Schroedinger equation for the radial part of the nonrelativistic wave function of the Hydrogen atom [96]. On the basis of the exact solution, which is expressed in terms of confluent hypergeometric functions, it was possible to derive a complete, simple and very accurate analytic description of the matter-enhanced transitions of solar neutrinos in the Sun for any values of Δm^2 and θ [26,92,93,97,98] (see also Refs. [27,76,91,99,100]) .

The probability that a ν_e, produced at time t_0 in the central part of the Sun, will not transform into $\nu_{\mu(\tau)}$ on its way to the surface of the Sun (reached at time t_s) is given by

$$P_\odot^{2\nu}(\nu_e \to \nu_e; t_s, t_0) = \bar{P}_\odot^{2\nu}(\nu_e \to \nu_e; t_s, t_0) + \ \textit{Oscillating terms}. \qquad (14.56)$$

Here

$$\bar{P}_\odot^{2\nu}(\nu_e \to \nu_e; t_s, t_0) \equiv \bar{P}_\odot = \frac{1}{2} + \left(\frac{1}{2} - \mathrm{P}'\right) \cos 2\theta_m(t_0) \cos 2\theta\ , \qquad (14.57)$$

is the average survival probability for ν_e having energy $\mathrm{E} \cong \mathrm{p}$ [91], where

$$P' = \frac{\exp\left[-2\pi \mathrm{r}_0 \frac{\Delta m^2}{2E} \sin^2\theta\right] - \exp\left[-2\pi \mathrm{r}_0 \frac{\Delta m^2}{2E}\right]}{1 - \exp\left[-2\pi \mathrm{r}_0 \frac{\Delta m^2}{2E}\right]}\,, \qquad (14.58)$$

is [92] the "jump" probability for exponentially varying N_e, and $\theta_m(t_0)$ is the mixing angle in matter at the point of ν_e production [99]. The expression for $\bar{P}_\odot^{2\nu}(\nu_e \to \nu_e; t_s, t_0)$ with P' given by Eq. (14.58) is valid for $\Delta m^2 > 0$, but for both signs of $\cos 2\theta \neq 0$ [92,100]; it is valid for any given value of the distance along the neutrino trajectory and does not take into account the finite dimensions of the region of ν_e production in the Sun. This can be done by integrating over the different neutrino paths, *i.e.*, over the region of ν_e production.

The oscillating terms in the probability $P_\odot^{2\nu}(\nu_e \to \nu_e; t_s, t_0)$ [97,95] were shown [98] to be strongly suppressed for $\Delta m^2 \gtrsim 10^{-7}$ eV^2 by the various averagings one has to perform when analyzing the solar neutrino data. The current solar neutrino and KamLAND data suggest that $\Delta m^2 \cong 7.6 \times 10^{-5}$ eV^2. For $\Delta m^2 \gtrsim 10^{-7}$ eV^2, the averaging over the region of neutrino production in the Sun *etc.* renders negligible all interference terms which appear in the probability of ν_e survival due to the $\nu_e \leftrightarrow \nu_{\mu(\tau)}$ oscillations in vacuum taking place on the way of the neutrinos from the surface of the Sun to the surface of the Earth. Thus, the probability that ν_e will remain ν_e while it travels from the central part of the Sun to the surface of the Earth is effectively equal to the probability of survival of the ν_e while it propagates from the central part to the surface of the Sun and is given by the average probability $\bar{P}_\odot(\nu_e \to \nu_e; t_s, t_0)$ (determined by Eq. (14.57) and Eq. (14.58)).

If the solar ν_e transitions are adiabatic ($P' \cong 0$) and $\cos 2\theta_m(t_0) \cong -1$ (*i.e.*, $N_e(t_0)/|N_e^{res}| \gg 1, |\tan 2\theta|$, the ν_e are born "above" (in N_e) the resonance region), one has [27]

$$\bar{P}^{2\nu}(\nu_e \to \nu_e; t_s, t_0) \cong \frac{1}{2} - \frac{1}{2}\cos 2\theta. \qquad (14.59)$$

The regime under discussion is realised for $\sin^2 2\theta \cong 0.8$ (suggested by the data, Section 14.4), if $E/\Delta m^2$ lies approximately in the range $(2 \times 10^4 - 3 \times 10^7)$ MeV/eV^2 (see Ref. 93). This result is relevant for the interpretation of the Super-Kamiokande and SNO solar neutrino data. We see that depending on the sign of $\cos 2\theta \neq 0$, $\bar{P}^{2\nu}(\nu_e \to \nu_e)$ is either bigger or smaller than 1/2. It follows from the solar neutrino data that in the range of validity (in $E/\Delta m^2$) of Eq. (14.59) we have $\bar{P}^{2\nu}(\nu_e \to \nu_e) \cong 0.3$. Thus, the possibility of $\cos 2\theta \leq 0$ is ruled out by the data. Given the choice $\Delta m^2 > 0$ we made, the data imply that $\Delta m^2 \cos 2\theta > 0$.

If $E/\Delta m^2$ is sufficiently small so that $N_e(t_0)/|N_e^{res}| \ll 1$, we have $P' \cong 0$, $\theta_m(t_0) \cong \theta$ and the oscillations take place in the Sun as in vacuum [27]:

$$\bar{P}^{2\nu}(\nu_e \to \nu_e; t_s, t_0) \cong 1 - \frac{1}{2}\sin^2 2\theta\,, \qquad (14.60)$$

which is the average two-neutrino vacuum oscillation probability. This expression describes with good precision the transitions of the solar *pp* neutrinos (Section 14.4). The extremely nonadiabatic ν_e transitions in the Sun, characterised by $\gamma(t) \ll 1$, are also described by the average vacuum oscillation probability (Eq. (14.60)) (for $\Delta m^2 \cos 2\theta > 0$ in this case we have (see *e.g.*, Refs. [92,93]) $\cos 2\theta_m(t_0) \cong -1$ and $P' \cong \cos^2\theta$).

The probability of ν_e survival in the case 3-neutrino mixing takes a simple form for $|\Delta m^2_{31}| \cong 2.4 \times 10^{-3}$ eV$^2 \gg |\Delta m^2_{21}|$. Indeed, for the energies of solar neutrinos $E \lesssim 10$ MeV, N^{res} corresponding to $|\Delta m^2_{31}|$ satisfies $N^{res}_{e31} \gtrsim 10^3$ cm^{-3} $\mathrm{N_A}$ and is by a factor of 10 bigger than N_e in the center of the Sun. As a consequence, the oscillations due to Δm^2_{31} proceed as in vacuum. The oscillation length associated with $|\Delta m^2_{31}|$ satisfies $L^v_{31} \lesssim 10$ km $\ll \Delta R$, ΔR being the dimension of the region of ν_e production in the Sun. We have for the different components of the solar ν_e flux [88] $\Delta R \cong (0.04 - 0.20) R_\odot$. Therefore the averaging over ΔR strongly suppresses the oscillations due to Δm^2_{31} and we get [80,101]:

$$P_\odot^{3\nu} \cong \sin^4\theta_{13} + \cos^4\theta_{13}\ P_\odot^{2\nu}(\Delta m^2_{21}, \theta_{12}; N_e \cos^2\theta_{13})\,, \qquad (14.61)$$

where $P_\odot^{2\nu}(\Delta m^2_{21}, \theta_{12}; N_e \cos^2\theta_{13})$ is given by Eq. (14.56) to Eq. (14.58) in which $\Delta m^2 = \Delta m^2_{21}$, $\theta = \theta_{12}$ and the solar e^- number density N_e is replaced by $N_e \cos^2\theta_{13}$. Thus, the solar ν_e transitions observed by the Super-Kamiokande and SNO experiments are described approximately by:

$$P_\odot^{3\nu} \cong \sin^4\theta_{13} + \cos^4\theta_{13}\ \sin^2\theta_{12}\,. \qquad (14.62)$$

The data show that $P_{\odot}^{3\nu} \cong 0.3$, which is a strong evidence for matter effects in the solar ν_e transitions [102] since in the case of oscillations in vacuum $P_{\odot}^{3\nu} \cong \sin^4\theta_{13} + (1 - 0.5\sin^2 2\theta_{12})\cos^4\theta_{13} \gtrsim 0.51$, where we have used $\sin^2\theta_{13} \lesssim 0.0315$ and where we have used $\sin^2\theta_{13} \lesssim 0.0297$ and $\sin^2 2\theta_{12} \lesssim 0.92$ (see Section 14.8).

14.4. Measurements of $\Delta m^2_{\odot}$ and $\theta_{\odot}$

14.4.1. *Solar neutrino observations* :

Observation of solar neutrinos directly addresses the theory of stellar structure and evolution, which is the basis of the standard solar model (SSM). The Sun as a well-defined neutrino source also provides extremely important opportunities to investigate nontrivial neutrino properties such as nonzero mass and mixing, because of the wide range of matter density and the great distance from the Sun to the Earth.

The solar neutrinos are produced by some of the fusion reactions in the pp chain or CNO cycle. The combined effect of these reactions is written as

$$4p \rightarrow {}^4\mathrm{He} + 2e^+ + 2\nu_e. \qquad (14.63)$$

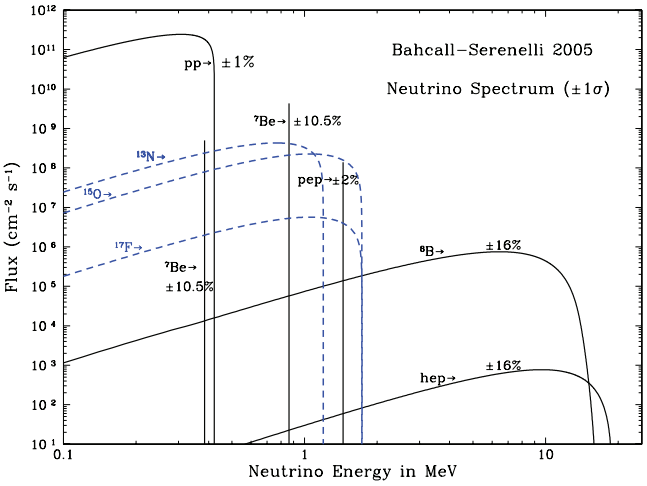

Figure 14.2: The solar neutrino spectrum predicted by the BS05(OP) standard solar model [103]. The neutrino fluxes are given in units of $\mathrm{cm}^{-2}\mathrm{s}^{-1}\mathrm{MeV}^{-1}$ for continuous spectra and $\mathrm{cm}^{-2}\mathrm{s}^{-1}$ for line spectra. The numbers associated with the neutrino sources show theoretical errors of the fluxes. This figure is taken from the late John Bahcall's web site, `http://www.sns.ias.edu/~jnb/`.

Positrons annihilate with electrons. Therefore, when considering the solar thermal energy generation, a relevant expression is

$$4p + 2e^- \rightarrow {}^4\mathrm{He} + 2\nu_e + 26.73\ \mathrm{MeV} - E_\nu\ , \qquad (14.64)$$

where E_ν represents the energy taken away by neutrinos, with an average value being $\langle E_\nu \rangle \sim 0.6$ MeV. There have been efforts to calculate solar neutrino fluxes from these reactions on the basis of SSM. A variety of input information is needed in the evolutionary calculations. The most elaborate SSM calculations have been developed by Bahcall and his collaborators, who define their SSM as the solar model which is constructed with the best available physics and input data. Therefore, their SSM calculations have been rather frequently updated. SSM's labelled as BS05(OP) [103], BSB06(GS) and BSB06(AGS) [89], and BPS08(GS) and BPS08(AGS) [104] represent some of recent model calculations. Here, "OP" means that newly calculated radiative opacities from the "Opacity Project" are used. The later models are also calculated with OP opacities. "GS" and "AGS" refer to old and new determinations of solar abundances of heavy elements. There are significant differences between the old, higher heavy element abundances (GS) and the new, lower heavy element abundances (AGS). The models with GS are consistent with helioseismological data, but the models with AGS are not.

The prediction of the BPS08(GS) model for the fluxes from neutrino-producing reactions is given in Table 14.2. Fig. 14.2 shows the solar-neutrino spectra calculated with the BS05(OP) model which is similar to the BPS08(GS) model. Here we note that in Ref. 105 the authors point out that electron capture on ^{13}N, ^{15}O, and ^{17}F produces line spectra of neutrinos, which have not been considered in the SSM calculations quoted above.

In 2011, a new SSM calculations [106] have been presented by A.M. Serenelli, W.C. Haxton, and C. Peña-Garay, by adopting the newly analyzed nuclear fusion cross sections. Their high metalicity SSM is labelled as SHP11(GS). For the same solar abundances as used in Ref. 103 and Ref. 89, the most significant change is a decrease of ^{8}B flux by $\sim 5\%$.

Table 14.2: Neutrino-producing reactions in the Sun (first column) and their abbreviations (second column). The neutrino fluxes predicted by the BPS08(GS) model [104] are listed in the third column.

Reaction	Abbr.	Flux ($\mathrm{cm}^{-2}\ \mathrm{s}^{-1}$)
$pp \rightarrow d\,e^+\,\nu$	pp	$5.97(1 \pm 0.006) \times 10^{10}$
$pe^-p \rightarrow d\,\nu$	pep	$1.41(1 \pm 0.011) \times 10^{8}$
$^3\mathrm{He}\ p \rightarrow {}^4\mathrm{He}\ e^+\nu$	hep	$7.90(1 \pm 0.15) \times 10^{3}$
$^7\mathrm{Be}\ e^- \rightarrow {}^7\mathrm{Li}\ \nu + (\gamma)$	^{7}Be	$5.07(1 \pm 0.06) \times 10^{9}$
$^8\mathrm{B} \rightarrow {}^8\mathrm{Be}^*\ e^+\nu$	^{8}B	$5.94(1 \pm 0.11) \times 10^{6}$
$^{13}\mathrm{N} \rightarrow {}^{13}\mathrm{C}\ e^+\nu$	^{13}N	$2.88(1 \pm 0.15) \times 10^{8}$
$^{15}\mathrm{O} \rightarrow {}^{15}\mathrm{N}\ e^+\nu$	^{15}O	$2.15(1^{+0.17}_{-0.16}) \times 10^{8}$
$^{17}\mathrm{F} \rightarrow {}^{17}\mathrm{O}\ e^+\nu$	^{17}F	$5.82(1^{+0.19}_{-0.17}) \times 10^{6}$

So far, solar neutrinos have been observed by chlorine (Homestake) and gallium (SAGE, GALLEX, and GNO) radiochemical detectors and water Cherenkov detectors using light water (Kamiokande and Super-Kamiokande) and heavy water (SNO). Recently, a liquid scintillation detector (Borexino) successfully observed low energy solar neutrinos.

A pioneering solar neutrino experiment by Davis and collaborators at Homestake using the ^{37}Cl - ^{37}Ar method proposed by Pontecorvo [107] started in the late 1960's. This experiment exploited ν_e absorption on ^{37}Cl nuclei followed by the produced ^{37}Ar decay through orbital e^- capture,

$$\nu_e + {}^{37}\mathrm{Cl} \rightarrow {}^{37}\mathrm{Ar} + e^- \ \ (\text{threshold } 814 \text{ keV}). \qquad (14.65)$$

The ^{37}Ar atoms produced are radioactive, with a half life ($\tau_{1/2}$) of 34.8 days. After an exposure of the detector for two to three times $\tau_{1/2}$, the reaction products were chemically extracted and introduced into a low-background proportional counter, where they were counted for a sufficiently long period to determine the exponentially decaying signal and a constant background. Solar-model calculations predict that the dominant contribution in the chlorine experiment came from ^{8}B neutrinos, but ^{7}Be, *pep*, ^{13}N, and ^{15}O neutrinos also contributed (for notations, refer to Table 14.2).

From the very beginning of the solar-neutrino observation [108], it was recognized that the observed flux was significantly smaller than the SSM prediction, provided nothing happens to the electron neutrinos after they are created in the solar interior. This deficit has been called "the solar-neutrino problem."

Gallium experiments (GALLEX and GNO at Gran Sasso in Italy and SAGE at Baksan in Russia) utilize the reaction

$$\nu_e + {}^{71}\mathrm{Ga} \rightarrow {}^{71}\mathrm{Ge} + e^- \ \ (\text{threshold } 233 \text{ keV}). \qquad (14.66)$$

They are sensitive to the most abundant *pp* solar neutrinos. The solar-model calculations predict that more than 80% of the capture rate in gallium is due to low energy *pp* and ^{7}Be solar neutrinos with

Table 14.3: Results from radiochemical solar-neutrino experiments. The predictions of a recent standard solar model BPS08(GS) are also shown. The first and the second errors in the experimental results are the statistical and systematic errors, respectively. SNU (Solar Neutrino Unit) is defined as 10^{-36} neutrino captures per atom per second.

	^{37}Cl→^{37}Ar (SNU)	^{71}Ga→^{71}Ge (SNU)
Homestake [6]	$2.56 \pm 0.16 \pm 0.16$	–
GALLEX [10]	–	$77.5 \pm 6.2^{+4.3}_{-4.7}$
GALLEX-Reanalysis [109]	–	$73.4^{+6.1+3.7}_{-6.0-4.1}$
GNO [11]	–	$62.9^{+5.5}_{-5.3} \pm 2.5$
GNO+GALLEX [11]	–	$69.3 \pm 4.1 \pm 3.6$
GNO+GALLEX-Reanalysis [109]	–	$67.6^{+4.0+3.2}_{-4.0-3.2}$
SAGE [8]	–	$65.4^{+3.1+2.6}_{-3.0-2.8}$
SSM [BPS08(GS)] [104]	$8.46^{+0.87}_{-0.88}$	$127.9^{+8.1}_{-8.2}$

the *pp* rate being about twice the ^{7}Be rate. SAGE reported the first results in 1991 [110]. They observed the capture rate to be $20^{+15}_{-20} \pm 32$ SNU, or a 90% confidence-level upper limit of 79 SNU. In 1992, GALLEX reported the observed capture rate of $83 \pm 19 \pm 8$ SNU [9]. It was the first evidence for low-energy solar-neutrino observation. Later, SAGE observed similar flux [111] to GALLEX. The latest SAGE results are published in Ref. 8. The GALLEX Collaboration finished observations in early 1997 [10,109]. Since April, 1998, a newly defined collaboration, GNO (Gallium Neutrino Observatory) continued the observations until April 2003. The GNO results are published in Ref. 11. The GNO + GALLEX joint analysis results are also presented in Ref. 11 and Ref. 109. The results from radiochemical solar neutrino experiments are shown in Table 14.3.

In 1987, the Kamiokande experiment in Japan succeeded in real-time solar neutrino observation, utilizing νe scattering,

$$\nu_x + e^- \to \nu_x + e^- \,, \tag{14.67}$$

in a large water-Cherenkov detector. This experiment takes advantage of the directional correlation between the incoming neutrino and the recoil electron. This feature greatly helps the clear separation of the solar-neutrino signal from the background. The Kamiokande result gave the first direct evidence that neutrinos come from the direction of the Sun [112]. Later, the high-statistics Super-Kamiokande experiment [113–116] with a 50-kton water Cherenkov detector replaced the Kamiokande experiment. Due to the high thresholds (recoil-electron total energy of 7 MeV in Kamiokande and 5 MeV at present in Super-Kamiokande) the experiments observe pure ^{8}B solar neutrinos. It should be noted that the reaction (Eq. (14.67)) is sensitive to all active neutrinos, $x = e$, μ, and τ. However, the sensitivity to ν_μ and ν_τ is much smaller than the sensitivity to ν_e, $\sigma(\nu_{\mu,\tau} e) \approx 0.16\, \sigma(\nu_e e)$.

Recently, the Super-Kamiokande experiment has reported [117] a $2.7\,\sigma$ indication of non-zero day-night asymmetry of ^{8}B solar neutrinos, $A_{DN} = 2(R_D - R_N)/(R_D + R_N) = -0.032 \pm 0.011 \pm 0.005$, where R_D and R_N are the average day and average night νe elastic-scattering rates of ^{8}B solar neutrinos. A non-zero day-night asymmetry implies the Earth matter effects on flavour oscillations of solar neutrinos (see, Subsections 14.4.2 and 14.4.3).

In 1999, a new real time solar-neutrino experiment, SNO (Sudbury Neutrino Observatory), in Canada started observation. This experiment used 1000 tons of ultra-pure heavy water (D_2O) contained in a spherical acrylic vessel, surrounded by an ultra-pure H_2O shield. SNO measured ^{8}B solar neutrinos via the charged-current (CC) and neutral-current (NC) reactions

$$\nu_e + d \to e^- + p + p \qquad \text{(CC)}\,, \tag{14.68}$$

and

$$\nu_x + d \to \nu_x + p + n \qquad \text{(NC)}\,, \tag{14.69}$$

as well as νe scattering, (Eq. (14.67)). The CC reaction, (Eq. (14.68)), is sensitive only to ν_e, while the NC reaction, (Eq. (14.69)), is sensitive to all active neutrinos. This is a key feature to solve the solar neutrino problem. If it is caused by flavour transitions such as neutrino oscillations, the solar neutrino fluxes measured by CC and NC reactions would show a significant difference.

The Q-value of the CC reaction is -1.4 MeV and the e^- energy is strongly correlated with the ν_e energy. Thus, the CC reaction provides an accurate measure of the shape of the ^{8}B neutrino spectrum. The contributions from the CC reaction and νe scattering can be distinguished by using different $\cos\,\theta$ distributions, where θ is the angle of the e^- momentum with respect to the Sun-Earth axis. While the νe scattering events have a strong forward peak, CC events have an approximate angular distribution of $1 - 1/3\,\cos\theta$.

The neutrino energy threshold of the NC reaction is 2.2 MeV. In the pure D_2O [13,14], the signal of the NC reaction was neutron capture in deuterium, producing a 6.25-MeV γ-ray. In this case, the capture efficiency was low and the deposited energy was close to the detection threshold of 5 MeV. In order to enhance both the capture efficiency and the total γ-ray energy (8.6 MeV), 2 tons of NaCl were added to the heavy water in the second phase of the experiment [118]. Subsequently NaCl was removed and an array of ^{3}He neutron counters were installed for the third phase measurement [119]. These neutron counters provided independent NC measurement with different systematics from that of the second phase, and thus strengthened the reliability of the NC measurement. After completion of data acquisition in 2006, the SNO group presented the results of Phase I and Phase II joint analysis [120] as well as the results of a combined analysis of all three phases [121].

Table 14.4 shows the ^{8}B solar neutrino results from real time experiments. The standard solar model predictions are also shown. Table 14.4 includes the results from the SNO group's joint analysis of the SNO Phase I and Phase II data with the analysis threshold as low as 3.5 MeV (effective electron kinetic energy) and significantly improved systematic uncertainties [120]. Also, the recent result from a combined analysis of all three phases [121] is included. It is seen from these tables that the results from all the solar-neutrino experiments, except SNO's NC result, indicate significantly less flux than expected from the solar-model predictions.

Another real time solar neutrino experiment, Borexino at Gran Sasso in Italy, started solar neutrino observation in 2007. This experiment measures solar neutrinos via νe scattering in 300 tons of ultra-pure liquid scintillator. With a detection threshold as low as 250 keV, the flux of monochromatic 0.862 MeV ^{7}Be solar neutrinos has been directly observed for the first time (see Table 14.5). The observed energy spectrum shows the characteristic Compton-edge over the background [122,123]. Borexino also reported an observation of null day-night asymmetry of the ^{7}Be neutrino flux, $A_{DN} = 2(R_D - R_N)/(R_D + R_N) = -0.001 \pm 0.012 \pm 0.007$ [124], where R_D and R_N are the day and night count rates of ^{7}Be neutrinos.

Further, Borexino measured the flux of monochromatic 1.44 MeV *pep* solar neutrinos [125]. The absence of the *pep* solar neutrino signal is disfavored at 98% CL. The *pep* solar neutrino flux measured *via* νe scattering (calculated from the measured interaction rate and the expected one with the assumption of no neutrino oscillations and the SHP11(GS) SSM [106], both given in [125]) is shown in Table 14.6 and compared with the SSM predictions. Also, an upper limit of the "unoscillated" CNO solar neutrino flux is determined [125] as $< 7.7 \times 10^8$ cm^{-2}s^{-1} (95% CL) by assuming the MSW large mixing angle solution with $\Delta m^2_\odot = (7.6 \pm 0.2) \times 10^{-5}$ eV^2 and $\tan^2\theta_\odot = 0.47^{+0.05}_{-0.04}$ and the SHP11(GS) SSM prediction [106] for the *pep* ν flux.

Borexino also measured ^{8}B solar neutrinos with an energy threshold of 3 MeV [126]. Measurements of low energy solar neutrinos are important not only to test the SSM further, but also to study the MSW effect over the energy region spanning from sub-MeV to 10 MeV.

Table 14.4: ^{8}B solar neutrino results from real time experiments. The predictions of BPS08(GS) and SHP11(GS) standard solar models are also shown. The first and the second errors in the experimental results are the statistical and systematic errors, respectively.

	Reaction	^{8}B ν flux (10^6cm^{-2}s^{-1})
Kamiokande [7]	νe	$2.80 \pm 0.19 \pm 0.33$
Super-K I [114,116]	νe	$2.38 \pm 0.02 \pm 0.08$
Super-K II [115,116]	νe	$2.41 \pm 0.05^{+0.16}_{-0.15}$
Super-K III [116]	νe	$2.32 \pm 0.04 \pm 0.05$
SNO Phase I [14]	CC	$1.76^{+0.06}_{-0.05} \pm 0.09$
(pure D_20)	νe	$2.39^{+0.24}_{-0.23} \pm 0.12$
	NC	$5.09^{+0.44+0.46}_{-0.43-0.43}$
SNO Phase II [118]	CC	$1.68 \pm 0.06^{+0.08}_{-0.09}$
(NaCl in D_2O)	νe	$2.35 \pm 0.22 \pm 0.15$
	NC	$4.94 \pm 0.21^{+0.38}_{-0.34}$
SNO Phase III [119]	CC	$1.67^{+0.05+0.07}_{-0.04-0.08}$
(^{3}He counters)	νe	$1.77^{+0.24+0.09}_{-0.21-0.10}$
	NC	$5.54^{+0.33+0.36}_{-0.31-0.34}$
SNO Phase I+II [120]	NC	$5.140^{+0.160+0.132}_{-0.158-0.117}$
	Φ_B from fit to all reactions	$5.046^{+0.159+0.107}_{-0.152-0.123}$
SNO Phase I+II+III [121]	Φ_B from fit to all reactions	$5.25 \pm 0.16^{+0.11}_{-0.13}$
Borexino [126]	νe	$2.4 \pm 0.4 \pm 0.1$
SSM [BPS08(GS)] [104]	–	$5.94(1 \pm 0.11)$
SSM [SHP11(GS)] [106]	–	$5.58(1 \pm 0.14)$

Table 14.5: ^{7}Be solar neutrino result from Borexino [123]. The predictions of BPS08(GS) and SHP11(GS) standard solar models are also shown.

	Reaction	^{7}Be ν flux (10^9cm^{-2}s^{-1})
Borexino [123]	νe	3.10 ± 0.15
SSM [BPS08(GS)] [104]	–	$5.07(1 \pm 0.06)$
SSM [SHP11(GS)] [106]	–	$5.00(1 \pm 0.07)$

Table 14.6: *pep* solar neutrino result from Borexino [125]. The predictions of BPS08(GS) and SHP11(GS) standard solar models are also shown.

	Reaction	*pep* ν flux (10^8cm^{-2}s^{-1})
Borexino [125]	νe	1.0 ± 0.2
SSM [BPS08(GS)] [104]	–	$1.41(1 \pm 0.011)$
SSM [SHP11(GS)] [106]	–	$1.44(1 \pm 0.012)$

14.4.2. *Evidence for solar neutrino flavour conversion* :

Solar neutrino experiments achieved remarkable progress in the past ten years, and the solar-neutrino problem, which had remained unsolved for more than 30 years, has been understood as due to neutrino flavour conversion. In 2001, the initial SNO CC result combined with the Super-Kamiokande's high-statistics νe elastic scattering result [127] provided direct evidence for flavour conversion of solar neutrinos [13]. Later, SNO's NC measurements further strengthened this conclusion [14,118,119]. From the salt-phase measurement [118], the fluxes measured with CC, ES, and NC events were obtained as

$$\phi^{CC}_{SNO} = (1.68 \pm 0.06^{+0.08}_{-0.09}) \times 10^6 \text{cm}^{-2}\text{s}^{-1} , \quad (14.70)$$

$$\phi^{ES}_{SNO} = (2.35 \pm 0.22 \pm 0.15) \times 10^6 \text{cm}^{-2}\text{s}^{-1} , \quad (14.71)$$

$$\phi^{NC}_{SNO} = (4.94 \pm 0.21^{+0.38}_{-0.34}) \times 10^6 \text{cm}^{-2}\text{s}^{-1} , \quad (14.72)$$

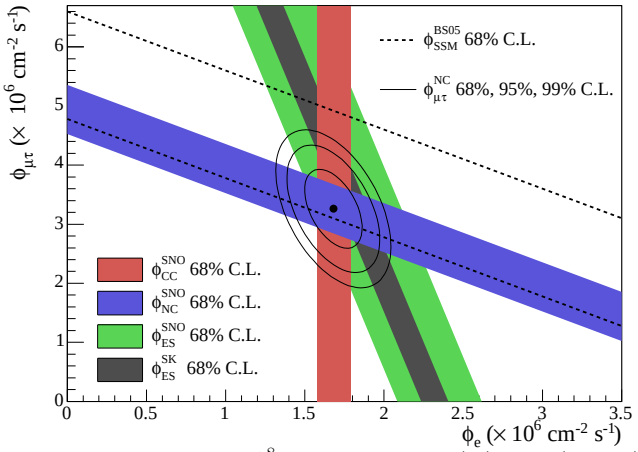

Figure 14.3: Fluxes of ^{8}B solar neutrinos, $\phi(\nu_e)$, and $\phi(\nu_{\mu \text{ or } \tau})$, deduced from the SNO's CC, ES, and NC results of the salt phase measurement [118]. The Super-Kamiokande ES flux is from Ref. 128. The BS05(OP) standard solar model prediction [103] is also shown. The bands represent the 1σ error. The contours show the 68%, 95%, and 99% joint probability for $\phi(\nu_e)$ and $\phi(\nu_{\mu \text{ or } \tau})$. The figure is from Ref. 118.

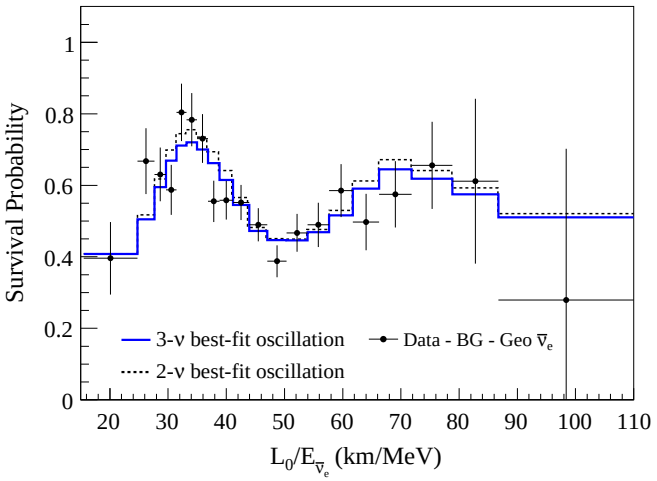

Figure 14.4: The ratio of the background and geoneutrino-subtracted $\bar{\nu}_e$ spectrum, observed in the KamLAND experiment, to the predicted one without oscillations (survival probability) as a function of L_0/E, where L_0=180 km. The histograms show the expected distributions based on the best-fit parameter values from the two- and three-flavor neutrino oscillation analyses. The figure is from Ref. 131.

where the first errors are statistical and the second errors are systematic. In the case of $\nu_e \to \nu_{\mu,\tau}$ transitions, Eq. (14.72) is a mixing-independent result and therefore tests solar models. It shows

good agreement with the ^{8}B solar-neutrino flux predicted by the solar model [103]. Fig. 14.3 shows the salt phase result of $\phi(\nu_\mu \text{ or } \tau)$ versus the flux of electron neutrinos $\phi(\nu_e)$ with the 68%, 95%, and 99% joint probability contours. The flux of non-ν_e active neutrinos, $\phi(\nu_\mu \text{ or } \tau)$, can be deduced from these results. It is

$$\phi(\nu_\mu \text{ or } \tau) = \left(3.26 \pm 0.25^{+0.40}_{-0.35}\right) \times 10^6 \text{cm}^{-2}\text{s}^{-1}. \quad (14.73)$$

The non-zero $\phi(\nu_\mu \text{ or } \tau)$ is strong evidence for neutrino flavor conversion. These results are consistent with those expected from the LMA (large mixing angle) solution of solar neutrino oscillation in matter [26,27] with $\Delta m^2_\odot \sim 7.5 \times 10^{-5}$ eV^2 and $\tan^2\theta_\odot \sim 0.45$. However, with the SNO data alone, the possibility of other solutions cannot be excluded with sufficient statistical significance.

14.4.3. *KamLAND experiment* :

KamLAND is a 1-kton ultra-pure liquid scintillator detector located at the old Kamiokande's site in Japan. The primary goal of the KamLAND experiment was a long-baseline (flux-weighted average distance of $\sim$ 180 km) neutrino oscillation studies using $\bar{\nu}_e$'s emitted from nuclear power reactors. The reaction $\bar{\nu}_e + p \to e^+ + n$ is used to detect reactor $\bar{\nu}_e$'s and a delayed coincidence of the positron with a 2.2 MeV γ-ray from neutron capture on a proton is used to reduce the backgrounds. With the reactor $\bar{\nu}_e$'s energy spectrum (< 8 MeV) and a prompt-energy analysis threshold of 2.6 MeV, this experiment has a sensitive Δm^2 range down to $\sim 10^{-5}$ eV^2. Therefore, if the LMA solution is the real solution of the solar neutrino problem, KamLAND should observe reactor $\bar{\nu}_e$ disappearance, assuming CPT invariance.

The first KamLAND results [15] with 162 ton·yr exposure were reported in December 2002. The ratio of observed to expected (assuming no $\bar{\nu}_e$ oscillations) number of events was

$$\frac{N_{\text{obs}} - N_{\text{BG}}}{N_{\text{NoOsc}}} = 0.611 \pm 0.085 \pm 0.041 \quad (14.74)$$

with obvious notation. This result showed clear evidence of an event deficit expected from neutrino oscillations. The 95% CL allowed regions are obtained from the oscillation analysis with the observed event rates and positron spectrum shape. A combined global solar + KamLAND analysis showed that the LMA is a unique solution to the solar neutrino problem with $> 5\sigma$ CL [129]. With increased statistics [16,130,131], KamLAND observed not only the distortion of the $\bar{\nu}_e$ spectrum, but also for the first time the periodic feature of the $\bar{\nu}_e$ survival probability expected from neutrino oscillations (see Fig. 14.4).

In the latest neutrino oscillation analysis in Ref. 132, parameters are better determined because of the reduction of uncertainties in the geo $\bar{\nu}_e$ flux and other backgrounds, resulted from the recent long-term shutdown of nuclear reactors in Japan. Including the data on θ_{13} from accelerator and short-baseline reactor experiments (see Section 14.6), a combined 3-neutrino oscillation analysis of solar and KamLAND data gives $\tan^2\theta_{12} = 0.436^{+0.029}_{-0.025}$, $\Delta m^2_{21} = (7.53 \pm 0.18) \times 10^{-5}$ eV^2, and $\sin^2\theta_{13} = 0.023 \pm 0.002$.

14.5. Measurements of $|\Delta m^2_{\text{A}}|$ and θ_{A}

14.5.1. *Atmospheric neutrino results* :

The interactions in massive underground detectors of atmospheric neutrinos provide a means of studying neutrino oscillations, because of the large range of distances traveled by these neutrinos ($\sim$10 to 1.3$\times$10^4 km) to reach a detector on Earth and relatively well-understood fluxes which are up-down symmetric (except for geomagnetic effects). Atmospheric neutrinos are produced by the decay of π and K mesons produced in the nuclear interactions of the primary component of cosmic rays in the atmosphere. Since pions are dominant and they decay according to $\pi^\pm \to \mu^\pm + \nu_\mu\,(\bar{\nu}_\mu)$, $\mu^\pm \to e^\pm + \nu_e\,(\bar{\nu}_e) + \bar{\nu}_\mu\,(\nu_\mu)$, we have for the ratio of the fluxes of $(\nu_\mu + \bar{\nu}_\mu)$ and $(\nu_e + \bar{\nu}_e)$ at low energies ($\lesssim$ 1 GeV) approximately $\Phi(\nu_\mu + \bar{\nu}_\mu) : \Phi(\nu_e + \bar{\nu}_e) \approx 2 : 1$. More elaborate calculations of the atmospheric neutrino fluxes are found in Refs. [133,134] (Honda *et al.*), [135] (Bartol), and [136] (FLUKA) with a typical uncertainty of 10 $\sim$ 20%.

The first compelling evidence for the neutrino oscillation was presented by the Super-Kamiokande Collaboration (SK-I) in 1998 [17] from the observation of atmospheric neutrinos. The zenith-angle distributions of the μ-like events which are mostly muon-neutrino and muon antineutrino initiated charged-current interactions, showed a clear deficit compared to the no-oscillation expectation. Note that a water Cherenkov detector cannot measure the charge of the final-state leptons, and therefore neutrino and antineutrino induced events cannot be discriminated. Neutrino events having their vertex in the 22.5 kton fiducial volume in Super-Kamiokande are classified into fully contained (FC) events and partially contained (PC) events. The FC events are required to have no activity in the anti-counter. Single-ring events have only one charged lepton which radiates Cherenkov light in the final state, and particle identification is particularly clean for single-ring FC events. A ring produced by an e-like ($e^\pm$, γ) particle exhibits a more diffuse pattern than that produced by a μ-like ($\mu^\pm$, $\pi^\pm$) particle, since an e-like particle produces an electromagnetic shower and low-energy electrons suffer considerable multiple Coulomb scattering in water. All the PC events were assumed to be μ-like since the PC events comprise a 98% pure charged-current ν_μ sample.

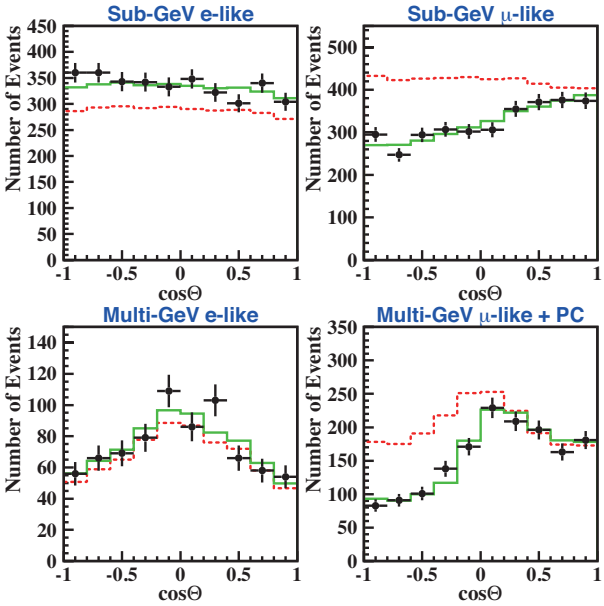

Figure 14.5: The zenith angle distributions for fully contained 1-ring e-like and μ-like events with visible energy < 1.33 GeV (sub-GeV) and > 1.33 GeV (multi-GeV). For multi-GeV μ-like events, a combined distribution with partially contained (PC) events is shown. The dotted histograms show the non-oscillated Monte Carlo events, and the solid histograms show the best-fit expectations for $\nu_\mu \leftrightarrow \nu_\tau$ oscillations. (This figure is provided by the Super-Kamiokande Collab.)

Fig. 14.5 shows the zenith-angle distributions of e-like and μ-like events from the SK-I measurement [137]. $\cos\theta = 1$ corresponds to the downward direction, while $\cos\theta = -1$ corresponds to the upward direction. Events included in these plots are single-ring FC events subdivided into sub-GeV (visible energy < 1.33 GeV) events and multi-GeV (visible energy > 1.33 GeV) events. The zenith-angle distribution of the multi-GeV μ-like events is shown combined with that of the PC events. The final-state leptons in these events have good directional correlation with the parent neutrinos. The dotted histograms show the Monte Carlo expectation for neutrino events. If the produced flux of atmospheric neutrinos of a given flavour remains unchanged at the detector, the data should have similar distributions to the expectation. However, the zenith-angle distribution of the μ-like events shows a strong deviation from the expectation. On the other hand, the zenith-angle distribution of the e-like events is consistent with the expectation. This characteristic feature may be interpreted that muon neutrinos coming from the opposite side of the

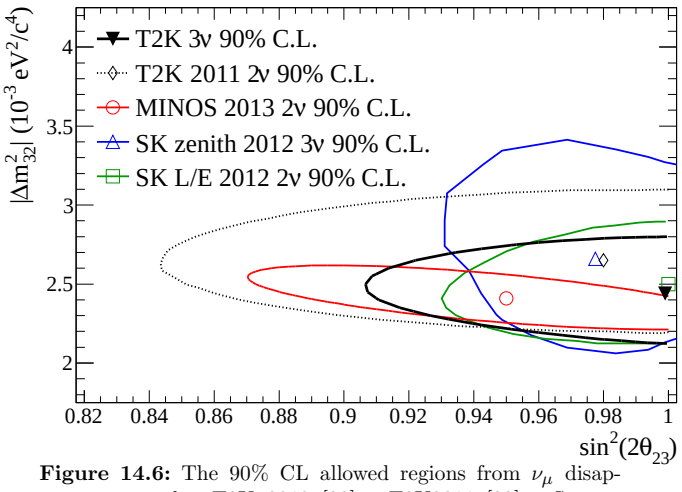

Figure 14.6: The 90% CL allowed regions from ν_μ disappearance results: T2K 2013 [23], T2K2011 [22], Super-Kamiokande [138], and MINOS [143]. The MINOS contour was obtained by assuming identical neutrino and antineutrino oscillation parameters. This figure is taken from Ref. 23.

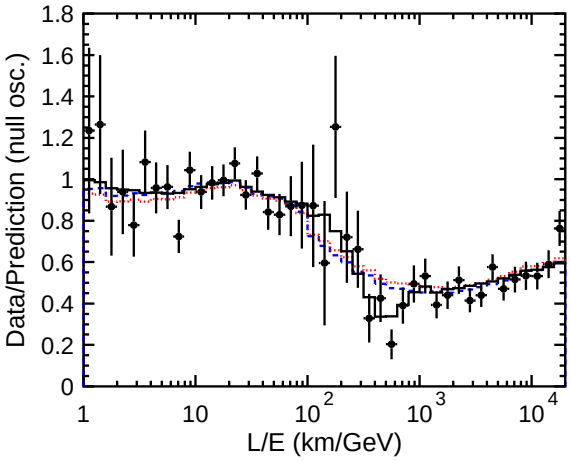

Figure 14.7: Results of the L/E analysis of SK-I atmospheric neutrino data. The points show the ratio of the data to the Monte Carlo prediction without oscillations, as a function of the reconstructed L/E. The error bars are statistical only. The solid line shows the best fit with 2-flavour $\nu_\mu \leftrightarrow \nu_\tau$ oscillations. The dashed and dotted lines show the best fit expectations for neutrino decay and neutrino decoherence hypotheses, respectively. (From Ref. 18.)

Earth's atmosphere, having travelled $\sim 10,000$ km, oscillate into other neutrinos and disappeared, while oscillations still do not take place for muon neutrinos coming from above the detector, having travelled from a few to a few tens km. Disappeared muon neutrinos may have oscillated into tau neutrinos because there is no indication of electron neutrino appearance. The atmospheric neutrinos corresponding to the events shown in Fig. 14.5 have $E = 1 \sim 10$ GeV. With $L = 10000$ km, the hypothesis of neutrino oscillations suggests $\Delta m^2 \sim 10^{-3} - 10^{-4}$ eV^2. The solid histograms show the best-fit results of a two-neutrino oscillation analysis with the hypothesis of $\nu_\mu \leftrightarrow \nu_\tau$. For the allowed parameter region from the recent results [138], see Fig. 14.6.

Although the SK-I atmospheric neutrino observations gave compelling evidence for muon neutrino disappearance which is consistent with two-neutrino oscillation $\nu_\mu \leftrightarrow \nu_\tau$ [139], the question may be asked whether the observed muon neutrino disappearance is really due to neutrino oscillations. First, other exotic explanations such as neutrino decay [140] and quantum decoherence [141] cannot be completely ruled out from the zenith-angle distributions alone. To confirm neutrino oscillation, characteristic sinusoidal behavior of the conversion probability as a function of neutrino energy E for a fixed distance L in the case of long-baseline neutrino oscillation experiments, or as a function of L/E in the case of atmospheric neutrino experiments, should be observed. By selecting events with high L/E resolution, evidence for the dip in the L/E distribution was observed at the right place expected from the interpretation of the SK-I data in terms of $\nu_\mu \leftrightarrow \nu_\tau$ oscillations [18], see Fig. 14.7. This dip cannot be explained by alternative hypotheses of neutrino decay and neutrino decoherence, and they are excluded at more than 3σ in comparison with the neutrino oscillation interpretation. For the constraints obtained from the L/E analysis, see Fig. 14.6.

Second, a search for ν_τ appearance signal was performed by using the SK-I, -II, -III, and -IV atmospheric neutrino data. Though the Super-Kamiokande detector cannot identify a CC ν_τ interaction on event by event basis, the Super-Kamiokande Collaboration demonstrated ν_τ appearance at the 3.8σ level through a neural network analysis on the zenith-angle distribution of multi-GeV contained events [24].

A more direct search for ν_τ appearance with identified CC ν_τ interaction has been performed by an accelerator long baseline experiment OPERA; see the next subsection.

14.5.2. *Results from accelerator experiments* :

The $\Delta m^2 \geq 2 \times 10^{-3}$ eV^2 region can be explored by accelerator-based long-baseline experiments with typically $E \sim 1$ GeV and $L \sim$ several hundred km. With a fixed baseline distance and a narrower, well understood neutrino spectrum, the value of $|\Delta m^2_{\rm A}|$ and, with higher statistics, also the mixing angle, are potentially better constrained in accelerator experiments than from atmospheric neutrino observations.

The K2K (KEK-to-Kamioka) long-baseline neutrino oscillation experiment [19] is the first accelerator-based experiment with a neutrino path length extending hundreds of kilometers. K2K aimed at confirmation of the neutrino oscillation in ν_μ disappearance in the $|\Delta m^2_{\rm A}| \geq 2 \times 10^{-3}$ eV^2 region. A horn-focused wide-band muon neutrino beam having an average $L/E_\nu \sim 200$ ($L = 250$ km, $\langle E_\nu \rangle \sim 1.3$ GeV), was produced by 12-GeV protons from the KEK-PS and directed to the Super-Kamiokande detector. The spectrum and profile of the neutrino beam were measured by a near neutrino detector system located 300 m downstream from the production target.

The construction of the K2K neutrino beam line and the near detector began before Super-Kamiokande's discovery of atmospheric neutrino oscillations. K2K experiment started data-taking in 1999 and was completed in 2004. The total number of protons on target (POT) for physics analysis amounted to 0.92×10^{20}. The observed number of beam-originated FC events in the 22.5 kton fiducial volume of Super-Kamiokande was 112, compared with an expectation of $158.1^{+9.2}_{-8.6}$ events without oscillation. For 58 1-ring μ-like subset of the data, the neutrino energy was reconstructed from measured muon momentum and angle, assuming CC quasi-elastic kinematics. The measured energy spectrum showed the distortion expected from neutrino oscillations. The probability that the observations are due to a statistical fluctuation instead of neutrino oscillation is 0.0015% or 4.3 σ [19].

MINOS is the second long-baseline neutrino oscillation experiment with near and far detectors. Neutrinos are produced by the NuMI (Neutrinos at the Main Injector) facility using 120 GeV protons from the Fermilab Main Injector. The far detector is a 5.4 kton (total mass) iron-scintillator tracking calorimeter with toroidal magnetic field, located underground in the Soudan mine. The baseline distance is 735 km. The near detector is also an iron-scintillator tracking calorimeter with toroidal magnetic field, with a total mass of 0.98 kton. The neutrino beam is a horn-focused wide-band beam. Its energy spectrum can be varied by moving the target position relative to the first horn and changing the horn current.

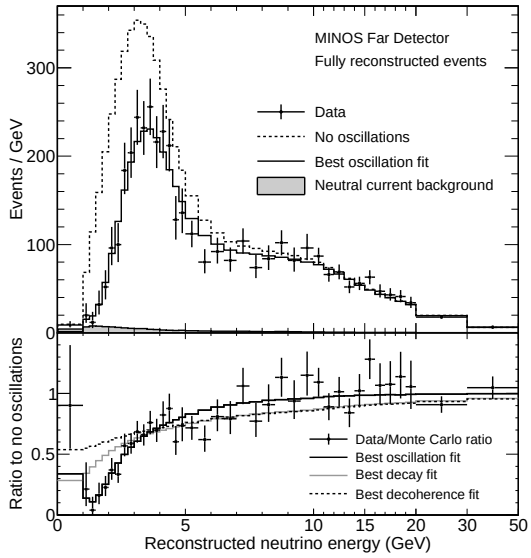

Figure 14.8: The top panel shows the energy spectra of fully reconstructed events in the MINOS far detector classified as CC interactions. The bottom panel shows the background subtracted ratios of data to the no-oscillation hypothesis. The best fit with the hypothesis of $\nu_\mu \to \nu_\tau$ oscillations as well as the best fit to alternative models (neutrino decay and decoherence) is also shown. This figure is taken from Ref. 21.

MINOS started the neutrino-beam run in 2005. Earlier ν_μ disappearance results were reported in Refs. [20,21]. Most of the data were taken with a "low-energy" option for the spectrum of the neutrino beam (the flux was enhanced in the 1-5 GeV energy range, peaking at 3 GeV). Fig. 14.8 shows the ratio of observed energy spectra and the expected spectra with no oscillation [21]. The MINOS data clearly favor the ν_μ disappearance. The alternative models to explain the ν_μ disappearance, neutrino decay and quantum decoherence of neutrinos, are disfavored at the 7σ and 9σ, respectively, by these MINOS data (see Fig. 14.8).

In addition to ν_μ disappearance, MINOS first observed muon antineutrino disappearance [142] with the NUMI beam line optimized for $\bar{\nu}_\mu$ production. Actually, MINOS produced a "ν_μ-dominated" or "$\bar{\nu}_\mu$-enhanced" beam by selectively focusing positive or negative pions and kaons. MINOS recently reported [143] the results of the neutrino oscillation analysis based on the data obtained with 10.71×10^{20} POT of the ν_μ-dominated beam and 3.36×10^{20} POT of the $\bar{\nu}_\mu$-enhanced beam. In addition, they used the atmospheric neutrino data based on the MINOS far detector exposure of 37.88 kt·yr [144]. Because the MINOS detector has a capability to separate neutrinos and antineutrinos on the event-by-event basis, it can use both ν_μ and $\bar{\nu}_\mu$ contained events from the ν_μ-dominated beam. From the $\bar{\nu}_\mu$-enhanced beam, $\bar{\nu}_\mu$ contained events are used. For the complete data sets used, refer to Ref. 143. Assuming the identical oscillation parameters for neutrinos and antineutrinos, the results of the fit within the two-neutrino oscillation framework using the full MINOS data sample yielded $|\Delta m^2_{\rm A}| = (2.41^{+0.09}_{-0.10}) \times 10^{-3}$ eV^2 and $\sin^2 2\theta_{\rm A} = 0.950^{+0.035}_{-0.036}$, or $\sin^2 2\theta_{\rm A} > 0.890$ at 90% CL. This result disfavors maximal mixing at the 86% CL. The 90% CL allowed region obtained from this analysis is shown in Fig. 14.6. Allowing independent oscillations for neutrinos and antineutrinos, characterised respectively by $|\Delta m^2_{\rm A}|$, $\theta_{\rm A}$ and $|\Delta \bar{m}^2_{\rm A}|$, $\bar{\theta}_{\rm A}$, the results of the fit are $|\Delta \bar{m}^2_{\rm A}| = (2.50^{+0.23}_{-0.25}) \times 10^{-3}$ eV^2 and $\sin^2 2\bar{\theta}_{\rm A} = 0.97^{+0.03}_{-0.08}$, or $\sin^2 2\theta_{\rm A} > 0.83$ at 90% CL, and $|\Delta m^2_{\rm A}|$ - $|\Delta \bar{m}^2_{\rm A}| = (0.12^{+0.24}_{-0.26}) \times 10^{-3}$ eV^2.

The T2K experiment is the first off-axis long-baseline neutrino oscillation experiment. The baseline distance is 295 km between the J-PARC in Tokai, Japan and Super-Kamiokande. A narrow-band ν_μ beam with a peak energy of 0.6 GeV, produced by 30 GeV protons from the J-PARC Main Ring, is directed 2.5° off-axis to SK. With this configuration, the ν_μ beam is tuned to the first oscillation maximum. T2K started the first physics run in 2010. The first ν_μ disappearance results with an off-axis beam were published in Ref. 22. In the recently updated ν_μ disappearance results [23] with 3.01×10^{20} POT, 58 1-ring μ-like events are observed, while 205 ± 17 events are expected for no neutrino oscillation. From three-neutrino oscillation analysis assuming $\Delta m^2_{32} > 0$ (normal mass ordering/hierarchy; see Section 14.8) and using $\sin^2 2\theta_{13} = 0.098$, $\Delta m^2_{21} = 7.5 \times 10^{-5}$ eV^2, $\sin^2 2\theta_{12} = 0.857$, and $\delta = 0$, the best-fit values of $\sin^2 \theta_{23} = 0.514 \pm 0.082$ and $|\Delta m^2_{32}| = 2.44^{+0.17}_{-0.15} \times 10^{-3}$ eV^2 are obtained. At the best-fit point, $\sin^2 2\theta_{23} = 0.999$. The T2K result is, therefore, consistent with maximal mixing. Fig. 14.6 shows the 90% CL allowed region of $\sin^2 2\theta_{23}$ and $|\Delta m^2_{32}|$, which is compared with the 90% CL allowed regions from the SK atmospheric neutrino observations [138], the MINOS experiment [143], and the earlier T2K result [22].

As of May 2014, both the T2K [145] and the MINOS [146] experiments have published more precise measurements of $\sin^2 \theta_{23}$ and $|\Delta m^2_{32}|$, using the three-neutrino oscillation formalism. Based on the data corresponding to 6.57×10^{20} POT, T2K [145] has estimated these parameters by fitting the reconstructed neutrino energy spectrum of 120 1-ring μ-like events. The 1D 68% CL intervals obtained are $\sin^2 \theta_{23} = 0.514^{+0.055}_{-0.056}$ and $\Delta m^2_{32} = (2.51 \pm 0.10) \times 10^{-3}$ eV^2 for normal mass ordering/hierarchy and $\sin^2 \theta_{23} = 0.511 \pm 0.055$ and $\Delta m^2_{13} = (2.48 \pm 0.10) \times 10^{-3}$ eV^2 for inverted mass ordering/hierarchy. The T2K results for $\sin^2 \theta_{23}$ is consistent with maximal mixing, $\theta_{23} = \pi/4$. MINOS [146] has made a combined analysis of the ν_μ disappearance [143] and $\nu_\mu \to \nu_e$ appearance [147] data using the complete set of accelerator and atmospheric neutrino data. The results obtained are $|\Delta m^2_{32}| = (2.28 - 2.46) \times 10^{-3}$ eV^2 (68% CL) and $\sin^2 \theta_{23} = 0.35 - 0.65$ (90% CL) for normal mass ordering/hierarchy and $|\Delta m^2_{32}| = (2.32 - 2.53) \times 10^{-3}$ eV^2 (68% CL) and $\sin^2 \theta_{23} = 0.34 - 0.67$ (90% CL) for inverted mass ordering/hierarchy. From this analysis, the best-fit value of $\sin^2 \theta_{23} < 0.5$ ($\theta_{23} < \pi/4$) is obtained for inverted hierarchy.

The regions of neutrino parameter space favored or excluded by various neutrino oscillation experiments are shown in Fig. 14.9.

Although the atmospheric neutrino oscillations and accelerator long-baseline ν_μ disappearance data are fully consistent with $\nu_\mu \to \nu_\tau$ oscillations, detection of identified CC ν_τ interaction on event-by-event basis remained to be demonstrated. For this purpose, a promising method is an accelerator long-baseline experiment using emulsion technique to identify short-lived τ leptons event-by-event. The only experiment of this kind is OPERA with a target mass of 1290 tons, a neutrino source at CERN and a detector at Gran Sasso with the baseline distance of 730 km. The detector is a combination of the "Emulsion Cloud Chamber" and magnetized spectrometer. The CNGS (CERN Neutrinos to Gran Sasso) neutrino beam with $\langle E_\nu \rangle = 17$ GeV is produced by high-energy protons from the CERN SPS, and the data were collected during 2008 and 2012, corresponding to a live exposure of 17.97×10^{19} POT in total. OPERA reported observation of the first ν_τ candidate in the hadronic decay channel of τ, $\tau \to 1h$ [62], in 2008 and 2009 data, and the second ν_τ candidate satisfying the criteria for the $\tau \to 3h$ decay kinematics [63] in a sub-sample of 2010 and 2011 data. As of July 2013, OPERA found the third ν_τ candidate in the $\tau \to \mu$ channel. With a simple counting method (likelihood approach), the observation of these three ν_τ candidates correspond to 3.2σ (3.5σ) significance of non-null observation [25]. OPERA's analysis is still on-going.

14.6. Measurements of θ_{13}

Reactor $\bar{\nu}_e$ disappearance experiments with $L \sim 1$ km, $\langle E \rangle \sim 3$ MeV are sensitive to $\sim E/L \sim 3 \times 10^{-3}$ eV^2 $\sim |\Delta m^2_{\rm A}|$. At this baseline distance, the reactor $\bar{\nu}_e$ oscillations driven by $\Delta m^2_\odot$ are negligible. Therefore, as can be seen from Eq. (14.22) and Eq. (14.24), θ_{13} can be directly measured. A reactor neutrino oscillation experiment at the Chooz nuclear power station in France [61] was the first experiment of this kind. The detector was located in an underground laboratory with 300 mwe (meter water equivalent) rock overburden, at about 1 km from the neutrino source. It consisted of a central 5-ton target filled with 0.09% gadolinium loaded liquid scintillator, surrounded by an intermediate 17-ton and outer 90-ton regions filled

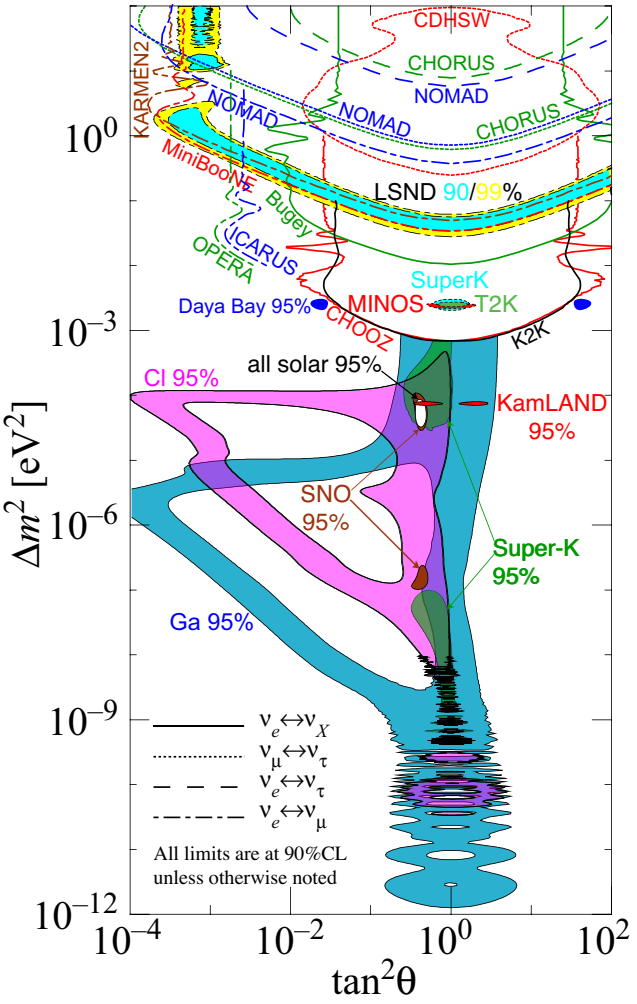

Figure 14.9: The regions of squared-mass splitting and mixing angle favored or excluded by various experiments based on two-flavor neutrino oscillation analyses. The figure was contributed by H. Murayama (University of California, Berkeley, and IPMU, University of Tokyo). References to the data used in the figure can be found at `http://hitoshi.berkeley.edu/neutrino`.

with undoped liquid scintillator. Reactor $\bar{\nu}_e$'s were detected via the reaction $\bar{\nu}_e + p \to e^+ + n$. Gd-doping was chosen to maximize the neutron capture efficiency. The Chooz experiment [61] found no evidence for $\bar{\nu}_e$ disappearance.

In 2012, the three reactor neutrino experiments Double Chooz [30], Daya Bay [31], and RENO [32] reported their first results on reactor $\bar{\nu}_e$ disappearance. Daya Bay and RENO measured reactor $\bar{\nu}_e$s with near and far detectors, and they obtained evidence for non-zero θ_{13} with a significance around 5σ. These three experiments have been accumulating statistics and improved results have been frequently reported (see below).

The $\bar{\nu}_e$ detectors of all the three experiments have similar structures; an antineutrino detector consisting of three layers and an optically independent outer veto detector. The innermost layer of the antineutrino detector is filled with Gd-doped liquid scintillator (LS), which is surrounded by a "γ-catcher" layer filled with Gd-free LS, and outside the γ-catcher is a buffer layer filled with mineral oil. An outer veto detector is filled with purified water (Daya Bay and RENO) or LS (Double Chooz). Double Chooz is planning to have a near detector in 2014.

The Daya Bay experiment [31,35] measured $\bar{\nu}_e$s from the Daya Bay nuclear power complex (six 2.9 GW_{th} reactors) in China with six functionally identical detectors deployed in two near (470 m and 576 m of flux-weighted baselines) and one far (1648 m) underground halls. Initially, Daya Bay reported [31] 5.2σ evidence for non-zero θ_{13} with live time of 55 days. More recent Daya Bay results [35] with live time of 139 days showed that the ratio of the observed to expected number of $\bar{\nu}_e$s at the far hall is $R = 0.944 \pm 0.007 \pm 0.003$ and the rate-only analysis in a three neutrino framework yielded $\sin^2 2\theta_{13} = 0.089 \pm 0.010 \pm 0.005$. This result excludes the no-oscillation hypothesis with a significance of 7.7σ [35]. In Ref. 36 the Day Bay collaboration reported their latest results based on live time of 217 days. In particular, from the rate+spectra oscillation analysis, $\sin^2 2\theta_{13} = 0.090^{+0.008}_{-0.009}$ is obtained.

The RENO experiment [32] measured $\bar{\nu}_e$s from six 2.8 GW_{th} reactors at Yonggwang Nuclear Power Plant in Korea with two identical detectors located at 294 m and 1383 m from the reactor array center. Initially with 229 days of running time, RENO reported [32] the ratio of the observed to expected number of $\bar{\nu}_e$s in the far detector of $R = 0.920 \pm 0.009 \pm 0.014$, and $\sin^2 2\theta_{13} = 0.113 \pm 0.013 \pm 0.019$ obtained from a rate-only analysis. This result excluded the no-oscillation hypothesis at the 4.9σ level. In September, 2013, RENO reported [37] a new result of $\sin^2 2\theta_{13} = 0.100 \pm 0.010 \pm 0.012$ from 403 live days of data, based on improved data analysis.

The Double Chooz experiment [30,33] measured $\bar{\nu}_e$s from two 4.25 GW_{th} reactors with a far detector at 1050 m from the two reactor cores. Double Chooz initially reported [30] $\sin^2 2\theta_{13} = 0.086 \pm 0.041 \pm 0.030$ with 101 days of data, and more recently [33] $\sin^2 2\theta_{13} = 0.109 \pm 0.030 \pm 0.025$ with 227.93 live days of running, by analyzing the rate and energy spectrum of prompt positrons using the reactor $\bar{\nu}_e$ spectrum of Ref. 160 and Ref. 156 and the Bugey4 rate measurement [148]. The latter data exclude the no-oscillation hypothesis at 2.9σ. Double Chooz also measured θ_{13} using inverse β-decay interactions with neutron capture on hydrogen (H-capture) [149], or from combined fit of Gd-capture and H-capture rate+spectrum, etc. [150], and consistent results are obtained. A near detector at 415 m from the cores will be operational in 2014.

In the accelerator neutrino oscillation experiments with conventional neutrino beams, θ_{13} can be measured using $\nu_\mu \to \nu_e$ appearance. By examining the expression for the probability of $\nu_\mu \to \nu_e$ oscillations in matter (given by Eq. (14.45)) it is understood that subleading terms could have rather large effects and the unknown CP-violating phase δ causes uncertainties in determining the value of θ_{13}. Actually, from the measurement of $\nu_\mu \to \nu_e$ appearance, θ_{13} is given as a function of δ for a given sign and value of Δm^2_{31}, and values of θ_{23}, Δm^2_{21} and θ_{12}. Therefore, a single experiment with a neutrino beam cannot determine the value of θ_{13}, although it is possible to establish a non-zero θ_{13}.

In 2011, experimental indications of $\nu_\mu \to \nu_e$ oscillations and a non-zero θ_{13} have been reported by the T2K [28] experiment. The T2K [28] Collaboration observed, with 1.43×10^{20} POT, six ν_e candidate events having all characteristics of being due to $\nu_\mu \to \nu_e$ oscillations, while the expectation for $\theta_{13} = 0$ is 1.5 ± 0.3 events. This result implies a non-zero θ_{13} with statistical significance of 2.5σ. In [34] T2K reported updated results. With 3.01×10^{20} POT, 11 ν_e candidates were observed, while the number of expected events for $\theta_{13} = 0$ is 3.3 ± 0.4, implying a non-zero θ_{13} with a significance of 3.1σ. For $\delta = 0$, $\sin^2 2\theta_{23} = 1$ and $\Delta m^2_A = 2.4 \times 10^{-3}$ eV^2, this result gives $\sin^2 2\theta_{13} = 0.088^{+0.049}_{-0.039}$. Recently, T2K announced [151] the observation of 28 ν_e appearance events with 4.92 ± 0.55 predicted background events. For $\sin^2 2\theta_{23} = 1$ and $\delta = 0$, this result means that $\theta_{13} = 0$ is excluded with a significance of 7.3σ. The probability relevant for the interpretation of this result of the T2K experiment is given in Eq. (14.45). For $\delta = 0$, $\sin^2 \theta_{23} = 0.5$ and $|\Delta m^2_{31(32)}| = 2.4 \times 10^{-3}$eV^2, the T2K collaborations finds in the case of $\Delta m^2_{31(32)} > 0$ ($\Delta m^2_{31(32)} < 0$): $\sin^2 2\theta_{13} = 0.140^{+0.038}_{-0.032}$ ($0.170^{+0.045}_{-0.037}$). Thus, the best fit value of $\sin^2 2\theta_{13}$ thus found in the T2K experiment is approximately by a factor of 1.6 (1.9) bigger than that found in the Daya Bay experiment [36]. This implies that the compatibility of the results of the two experiments on $\sin^2 2\theta_{13}$ requires, in particular, that $\delta \neq 0$ and/or $\sin^2 \theta_{23} \neq 0.5$. As we will see in Section 14.8, the indicated results will lead to a certain indication about the possible value of δ in the global analyses of the neutrino oscillation data.

The MINOS Collaboration [29] also searched for the $\nu_\mu \to \nu_e$

appearance signal. Though dependent on the definition of the signal, typically 62 candidate events are observed with an exposure of 8.2×10^{20} POT, while the expectation for $\theta_{13} = 0$ is $49.6 \pm 7.0 \pm 2.7$ events. The MINOS data disfavored the $\theta_{13} = 0$ hypothesis at the 89% CL [29]. Recently, MINOS has extended the analysis using 10.6×10^{20} POT ν-beam mode and 3.3×10^{20} POT $\bar{\nu}$-beam mode data [147]. Assuming $\Delta m^2_{\rm A} > 0$ ($\Delta m^2_{\rm A} < 0$), $\delta = 0$, and $\theta_{23} < \pi/4$, the results of this analysis imply that $0.01\ (0.03) < 2\ \sin^2\theta_{23}\ \sin^2 2\theta_{13} < 0.12\ (0.18)$ at the 90% CL, with the best fit value $2\ \sin^2\theta_{23}\ \sin^2 2\theta_{13} = 0.051^{+0.038}_{-0.030}\ (0.093^{+0.054}_{-0.049})$.

14.7. Search for Oscillations Involving Light Sterile Neutrinos

Although the mixing of the 3 flavour neutrino states has been experimentally well established, implying the existence of 3 light neutrinos ν_j having masses m_j not exceeding approximately 1 eV, there have been possible hints for the presence in the mixing of one or more additional neutrino states with masses at the eV scale. If these states exist, they must be related to the existence of one or more sterile neutrinos (sterile neutrino fields) which mix with the active flavour neutrinos (active flavour neutrino fields). The hints under discussion have been obtained: i) in the LSND $\bar{\nu}_\mu \to \bar{\nu}_e$ appearance experiment [152], in which a significant excess of events over the background is claimed to have been observed, ii) from the analysis of the $\bar{\nu}_\mu \to \bar{\nu}_e$ and $\nu_\mu \to \nu_e$ appearance data of the MiniBooNE experiment [153,154], iii) from the re-analyses of the short baseline (SBL) reactor neutrino oscillation data using newly calculated fluxes of reactor $\bar{\nu}_e$ [155,156], which show a possible "disappearance" of the reactor $\bar{\nu}_e$ ("reactor neutrino anomaly"), and iv) from the data of the radioactive source calibrations of the GALLEX [157] and SAGE [158] solar neutrino experiments.

The short baseline neutrino oscillation experiment MiniBooNE at Fermilab investigated ν_e and $\bar{\nu}_e$ appearance in ν_μ and $\bar{\nu}_\mu$ beams, respectively, with a detector containing 800 tons of mineral oil and located 541 m downstream of the production target. With the antineutrino running mode [153,154], a 2.8σ excess of events over the background was observed in the energy range of $200 < E_\nu < 1250$ MeV in the charged-current quasielastic data. Excess events were observed, in particular, in the interval of energies $200 < E_\nu < 475$ MeV, which corresponds to L/E range outside of that probed in the LSND experiment. The origin of this excess is not understood. Employing a simple 2-neutrino oscillation hypothesis and using the data from the entire neutrino energy interval $200 < E_\nu < 1250$ MeV used in the data analysis, this result, interpreted in terms of $\nu_\mu \to \nu_e$ oscillations, corresponds to an allowed region in the $\sin^2 2\theta - \Delta m^2$ plane, which overlaps with the allowed region obtained from the interpretation of the LSND data in terms of $\bar{\nu}_\mu \to \bar{\nu}_e$ oscillations. The overlap region at the 90% CL extends over $\Delta m^2 \sim$ a few $\times 10^{-2}$ eV^2 at $\sin^2 2\theta = 1$ to 1 eV^2 at $\sin^2 2\theta =$ a few $\times 10^{-3}$. The MiniBooNE Collaboration studied also the CP conjugate oscillation channel [154], $\nu_\mu \to \nu_e$, and observed a 3.4 σ excess of events in the same energy range. Most of the excess events lie in the interval $200 < E_\nu < 475$ MeV and are incompatible with the $\bar{\nu}_\mu \to \bar{\nu}_e$ oscillation interpretation of the LSND data. The energy spectra of the excess events observed in the ν_μ and $\bar{\nu}_\mu$ runs are only marginally compatible with each other and thus with the simple 2-neutrino oscillation hypothesis.

The reactor neutrino anomaly [155] is related to the results of a new and very detailed calculation of the reactor $\bar{\nu}_e$ fluxes [156] which were found to be by approximately 3.5% larger than the fluxes calculated in Ref. 159 and widely used in the past in the interpretation of the data of the SBL reactor $\bar{\nu}_e$ oscillation experiments. These data show indications for reactor $\bar{\nu}_e$ "disappearance" when analysed using the fluxes from [156]. It should be added that there are a number of uncertainties in the calculation of the fluxes under discussion (associated, *e.g.*, with the weak magnetism term contribution to the corresponding β-decay rates [160], the contribution of a relatively large number of "forbidden" β-decays [161], etc.) which can be of the order of the difference between the "old" and "new" fluxes.

Radioactive source calibrations of the GALLEX [157] and SAGE [158] experiments also showed a deficit of the measured fluxes compared to the expected fluxes ("Gallium anomaly"), and therefore might be interpreted as hints for ν_e disappearance.

Significant constraints on the parameters characterising the oscillations involving sterile neutrinos follow from the negative results of the searches for $\nu_\mu \to \nu_e$ and/or $\bar{\nu}_\mu \to \bar{\nu}_e$ oscillations in the KARMEN [162], NOMAD [163], ICARUS [164], and OPERA [165] experiments, and from the nonobservation of effects of oscillations into sterile neutrinos in the solar neutrino experiments and in the studies of ν_μ and/or $\bar{\nu}_\mu$ disappearance in the CDHSW [166], MINOS and SuperKamiokande experiments.

Two possible "minimal" phenomenological models (or schemes) with light sterile neutrinos are widely used in order to explain the data discussed in this section in terms of neutrino oscillations: the so-called "3 + 1" and "3 + 2" models. They contain respectively one and two sterile neutrinos (right-handed sterile neutrino fields). Thus, the "3 + 1" and "3 + 2" models have altogether 4 and 5 light massive neutrinos ν_j, which in the minimal versions of these models are Majorana particles. The additional neutrinos ν_4 and ν_4, ν_5 should have masses m_4 and m_4, m_5 at the eV scale (see below). It follows from the data that if ν_4 or ν_4, ν_5 exist, they couple to the electron and muon in the weak charged lepton current with couplings U_{ek} and $U_{\mu k}$, $k = 4;\ 4, 5$, which are approximately $|U_{ek}| \sim 0.1$ and $|U_{\mu k}| \sim 0.1$.

Global analysis of all the data (positive evidences and negative results) relevant for the test of the sterile neutrino hypothesis were performed recently in Ref. 167 and in Ref. 168. Analysing the data within the 3 + 1 scheme, the authors of Ref. 167 find for the best fit values of the parameters $|U_{e4}|^2$, $|U_{\mu 4}|^2$ and $\Delta m^2_{\rm SBL} \equiv m^2_4 - m^2_{min}$, where $m_{min} = \min(m_j)$, $j = 1, 2, 3$, characterising the active-sterile neutrino (antineutrino) oscillations:

$$|U_{e4}|^2 = 0.0225\,, \quad |U_{\mu 4}|^2 = 0.0289\,, \quad \Delta m^2_{\rm SBL} = 0.93\ {\rm eV}^2\,. \quad (14.75)$$

In contrast to Ref. 167, the authors of Ref. 168 reported also results within the 3 + 1 scheme without including in the data set used in their global analysis the MiniBooNE data at $E_\nu \leq 0.475$ GeV. As we have already mentioned, these data show an excess of events over the estimated background [154,169] whose nature is presently not well understood. For the best fit values of $|U_{e4}|^2$, $|U_{\mu 4}|^2$ and $\Delta m^2_{\rm SBL}$ in this case the authors of Ref. 168 find:

$$|U_{e4}|^2 = 0.03\,, \quad |U_{\mu 4}|^2 = 0.013\,, \quad \Delta m^2_{\rm SBL} = 1.60\ {\rm eV}^2\,. \quad (14.76)$$

The existence of light sterile neutrinos has cosmological implications the discussion of which lies outside the scope of the present article (for a discussion of the cosmological constraints on light sterile neutrinos see, e.g., [170,171]) .

The hypothesis of existence of light sterile neutrinos with eV scale masses and charged current couplings to the electron and muon quoted above will be tested in a number of experiments with reactor and accelerator neutrinos, and neutrinos from artificial sources, some of which are under preparation and planned to start taking data already this year (see, e.g., [172,173] for a detailed list and discussion of the planned experiments).

14.8. The three neutrino mixing

All existing compelling data on neutrino oscillations can be described assuming 3-flavour neutrino mixing in vacuum. This is the minimal neutrino mixing scheme which can account for the currently available data on the oscillations of the solar (ν_e), atmospheric (ν_μ and $\bar{\nu}_\mu$), reactor ($\bar{\nu}_e$) and accelerator (ν_μ) neutrinos. The (left-handed) fields of the flavour neutrinos ν_e, ν_μ and ν_τ in the expression for the weak charged lepton current in the CC weak interaction Lagrangian, are linear combinations of the LH components of the fields of three massive neutrinos ν_j:

$$\mathcal{L}_{\rm CC} = -\ \frac{g}{\sqrt{2}} \sum_{l=e,\mu,\tau} \overline{l_L}(x)\, \gamma_\alpha\, \nu_{lL}(x)\, W^{\alpha\dagger}(x) + h.c.\,,$$

$$\nu_{l\rm L}(x) = \sum_{j=1}^{3} U_{lj}\, \nu_{j\rm L}(x), \quad (14.77)$$

where U is the 3×3 unitary neutrino mixing matrix [4,5]. The mixing matrix U can be parameterized by 3 angles, and, depending on whether the massive neutrinos ν_j are Dirac or Majorana particles, by 1 or 3 CP violation phases [43,44]:

$$U = \begin{bmatrix} c_{12}c_{13} & s_{12}c_{13} & s_{13}e^{-i\delta} \\ -s_{12}c_{23} - c_{12}s_{23}s_{13}e^{i\delta} & c_{12}c_{23} - s_{12}s_{23}s_{13}e^{i\delta} & s_{23}c_{13} \\ s_{12}s_{23} - c_{12}c_{23}s_{13}e^{i\delta} & -c_{12}s_{23} - s_{12}c_{23}s_{13}e^{i\delta} & c_{23}c_{13} \end{bmatrix} \times \mathrm{diag}(1,\ e^{i\frac{\alpha_{21}}{2}},\ e^{i\frac{\alpha_{31}}{2}}) \ . \quad (14.78)$$

where $c_{ij} = \cos\theta_{ij}$, $s_{ij} = \sin\theta_{ij}$, the angles $\theta_{ij} = [0, \pi/2]$, $\delta = [0, 2\pi]$ is the Dirac CP violation phase and α_{21}, α_{31} are two Majorana CP violation phases. Thus, in the case of massive Dirac neutrinos, the neutrino mixing matrix U is similar, in what concerns the number of mixing angles and CP violation phases, to the CKM quark mixing matrix. The presence of two additional physical CP violation phases in U if ν_j are Majorana particles is a consequence of the special properties of the latter (see, *e.g.*, Refs. [41,43]) .

As we see, the fundamental parameters characterizing the 3-neutrino mixing are: i) the 3 angles θ_{12}, θ_{23}, θ_{13}, ii) depending on the nature of massive neutrinos ν_j - 1 Dirac (δ), or 1 Dirac + 2 Majorana ($\delta, \alpha_{21}, \alpha_{31}$), CP violation phases, and iii) the 3 neutrino masses, m_1, m_2, m_3. Thus, depending on whether the massive neutrinos are Dirac or Majorana particles, this makes 7 or 9 additional parameters in the minimally extended Standard Model of particle interactions with massive neutrinos.

The neutrino oscillation probabilities depend (Section 14.2), in general, on the neutrino energy, E, the source-detector distance L, on the elements of U and, for relativistic neutrinos used in all neutrino experiments performed so far, on $\Delta m^2_{ij} \equiv (m^2_i - m^2_j)$, $i \neq j$. In the case of 3-neutrino mixing there are only two independent neutrino mass squared differences, say $\Delta m^2_{21} \neq 0$ and $\Delta m^2_{31} \neq 0$. The numbering of massive neutrinos ν_j is arbitrary. It proves convenient from the point of view of relating the mixing angles θ_{12}, θ_{23} and θ_{13} to observables, to identify $|\Delta m^2_{21}|$ with the smaller of the two neutrino mass squared differences, which, as it follows from the data, is responsible for the solar ν_e and, the observed by KamLAND, reactor $\bar{\nu}_e$ oscillations. We will number (just for convenience) the massive neutrinos in such a way that $m_1 < m_2$, so that $\Delta m^2_{21} > 0$. With these choices made, there are two possibilities: either $m_1 < m_2 < m_3$, or $m_3 < m_1 < m_2$. Then the larger neutrino mass square difference $|\Delta m^2_{31}|$ or $|\Delta m^2_{32}|$, can be associated with the experimentally observed oscillations of the atmospheric ν_μ and $\bar{\nu}_\mu$ and accelerator ν_μ. The effects of Δm^2_{31} or Δm^2_{32} in the oscillations of solar ν_e, and of Δm^2_{21} in the oscillations of atmospheric ν_μ and $\bar{\nu}_\mu$ and of accelerator ν_μ, are relatively small and subdominant as a consequence of the facts that i) L, E and L/E in the experiments with solar ν_e and with atmospheric ν_μ and $\bar{\nu}_\mu$ or accelerator ν_μ, are very different, ii) the conditions of production and propagation (on the way to the detector) of the solar ν_e and of the atmospheric ν_μ and $\bar{\nu}_\mu$ or accelerator ν_μ, are very different, and iii) $|\Delta m^2_{21}|$ and $|\Delta m^2_{31}|$ ($|\Delta m^2_{32}|$) in the case of $m_1 < m_2 < m_3$ ($m_3 < m_1 < m_2$), as it follows from the data, differ by approximately a factor of 30, $|\Delta m^2_{21}| \ll |\Delta m^2_{31(32)}|$, $|\Delta m^2_{21}|/|\Delta m^2_{31(32)}| \cong 0.03$. This implies that in both cases of $m_1 < m_2 < m_3$ and $m_3 < m_1 < m_2$ we have $\Delta m^2_{32} \cong \Delta m^2_{31}$ with $|\Delta m^2_{31} - \Delta m^2_{32}| = |\Delta m^2_{21}| \ll |\Delta m^2_{31,32}|$. Obviously, in the case of $m_1 < m_2 < m_3$ ($m_3 < m_1 < m_2$) we have $\Delta m^2_{31(32)} > 0$ ($\Delta m^2_{31(32)} < 0$).

It follows from the results of the CHOOZ experiment with reactor $\bar{\nu}_e$ [61] and from the more recent data of the Daya Bay, RENO, Double Chooz and T2K experiments, discussed in the preceding subsection, that, in the convention we use, in which $0 < \Delta m^2_{21} < |\Delta m^2_{31(32)}|$, the element $|U_{e3}| = \sin\theta_{13}$ of the neutrino mixing matrix U is relatively small. This makes it possible to identify the angles θ_{12} and θ_{23} as the neutrino mixing angles associated with the solar ν_e and the dominant atmospheric ν_μ (and $\bar{\nu}_\mu$) oscillations, respectively. The angles θ_{12} and θ_{23} are often called "solar" and "atmospheric" neutrino mixing angles, and are often denoted as $\theta_{12} = \theta_\odot$ and $\theta_{23} = \theta_{\rm A}$ (or $\theta_{\rm atm}$) while Δm^2_{21} and Δm^2_{31} are often referred to as the "solar" and "atmospheric" neutrino mass squared differences and are often denoted as $\Delta m^2_{21} \equiv \Delta m^2_\odot$, $\Delta m^2_{31} \equiv \Delta m^2_{\rm A}$ (or $\Delta m^2_{\rm atm}$).

The solar neutrino data tell us that $\Delta m^2_{21} \cos 2\theta_{12} > 0$. In the convention employed by us we have $\Delta m^2_{21} > 0$. Correspondingly, in this convention one must have $\cos 2\theta_{12} > 0$.

Global analyses of the neutrino oscillation data [174,175] available by the second half of 2013 and including, in particular, the latest Daya Bay [36], RENO [37] and T2K [151,23] and MINOS [143,147] data, allowed us to determine the 3-neutrino oscillation parameters Δm^2_{21}, θ_{12}, $|\Delta m^2_{31}|$ ($|\Delta m^2_{32}|$), θ_{23} and θ_{13} with a relatively high precision. We present in Table 14.7 the best fit values and the 99.73% CL allowed ranges of these parameters found in Ref. 174. The results obtained in Ref. 174 show, in particular, that in the case of $\Delta m^2_{31(32)} > 0$ (i.e., $m_1 < m_2 < m_3$), the best fit value of $\sin^2\theta_{23} = 0.425$ increased somewhat with respect to that found in the analyses of the 2012 data. At 2σ we now have: $0.376 \lesssim \sin^2\theta_{23} \lesssim 0.506$, i.e., the 2σ indication from 2012 data that θ_{23} lies in the first quadrant [176] is not confirmed by including the 2013 data. In both analyses [174,175] the authors find that the best fit value of $\delta \cong 3\pi/2$. The CP conserving values $\delta = 0$ (2π) and π ($\delta = 0$ (2π)) are disfavored at 1.6σ to 2.0σ (at 2.0σ) for $\Delta m^2_{31(32)} > 0$ ($\Delta m^2_{31(32)} < 0$). In the case of $\Delta m^2_{31(32)} < 0$, the value $\delta = \pi$ is statistically 1σ away from the best fit value $\delta \cong 3\pi/2$.

Table 14.7: The best-fit values and 3σ allowed ranges of the 3-neutrino oscillation parameters, derived from a global fit of the current neutrino oscillation data (from [174]) . The values (values in brackets) correspond to $m_1 < m_2 < m_3$ ($m_3 < m_1 < m_2$). The definition of Δm^2 used is: $\Delta m^2 = m^2_3 - (m^2_2 + m^2_1)/2$. Thus, $\Delta m^2 = \Delta m^2_{31} - \Delta m^2_{21}/2 > 0$, if $m_1 < m_2 < m_3$, and $\Delta m^2 = \Delta m^2_{32} + \Delta m^2_{21}/2 < 0$ for $m_3 < m_1 < m_2$.

Parameter	best-fit ($\pm 1\sigma$)	3σ
Δm^2_{21} [10^{-5} eV ^{2}]	$7.54^{+0.26}_{-0.22}$	$6.99 - 8.18$
$\lvert\Delta m^2\rvert$ [10^{-3} eV ^{2}]	2.43 ± 0.06 (2.38 ± 0.06)	$2.23 - 2.61$ ($2.19 - 2.56$)
$\sin^2\theta_{12}$	0.308 ± 0.017	$0.259 - 0.359$
$\sin^2\theta_{23}$, $\Delta m^2 > 0$	$0.437^{+0.033}_{-0.023}$	$0.374 - 0.628$
$\sin^2\theta_{23}$, $\Delta m^2 < 0$	$0.455^{+0.039}_{-0.031}$,	$0.380 - 0.641$
$\sin^2\theta_{13}$, $\Delta m^2 > 0$	$0.0234^{+0.0020}_{-0.0019}$	$0.0176 - 0.0295$
$\sin^2\theta_{13}$, $\Delta m^2 < 0$	$0.0240^{+0.0019}_{-0.0022}$	$0.0178 - 0.0298$
δ/π (2σ range quoted)	$1.39^{+0.38}_{-0.27}$ ($1.31^{+0.29}_{-0.33}$)	$(0.00 - 0.16) \oplus (0.86 - 2.00)$ $((0.00 - 0.02) \oplus (0.70 - 2.00))$

It follows from the results given in Table 14.7 that θ_{23} is close to, but can be different from, $\pi/4$, $\theta_{12} \cong \pi/5.4$ and that $\theta_{13} \cong \pi/20$. Correspondingly, the pattern of neutrino mixing is drastically different from the pattern of quark mixing.

Note also that Δm^2_{21}, $\sin^2\theta_{12}$, $|\Delta m^2_{31(32)}|$, $\sin^2\theta_{23}$ and $\sin^2\theta_{13}$ are determined from the data with a 1σ uncertainty (= 1/6 of the 3σ range) of approximately 2.6%, 5.4%, 2.6%, 9.6% and 8.5%,respectively.

The existing SK atmospheric neutrino, K2K and MINOS data do not allow to determine the sign of $\Delta m^2_{31(32)}$. Maximal solar neutrino mixing, *i.e.*, $\theta_{12} = \pi/4$, is ruled out at more than 6σ by the data. Correspondingly, one has $\cos 2\theta_{12} \geq 0.28$ (at 99.73% CL).

At present no experimental information on the Dirac and Majorana CP violation phases in the neutrino mixing matrix is available. Thus, the status of CP symmetry in the lepton sector is unknown. With $\theta_{13} \neq 0$, the Dirac phase δ can generate CP violation effects in neutrino oscillations [43,55,56]. The magnitude of CP violation in $\nu_l \to \nu_{l'}$ and $\bar{\nu}_l \to \bar{\nu}_{l'}$ oscillations, $l \neq l' = e, \mu, \tau$, is determined, as we have seen, by the rephasing invariant J_{CP} (see Eq. (14.19)), which in the "standard" parametrisation of the neutrino mixing matrix (Eq. (14.78)) has the form:

$$J_{CP} \equiv \mathrm{Im}\,(U_{\mu 3}\, U^*_{e3}\, U_{e2}\, U^*_{\mu 2}) = \frac{1}{8}\, \cos\theta_{13} \sin 2\theta_{12}\ \sin 2\theta_{23}\ \sin 2\theta_{13}\ \sin\delta \,. \quad (14.79)$$

Thus, given the fact that $\sin 2\theta_{12}$, $\sin 2\theta_{23}$ and $\sin 2\theta_{13}$ have been determined experimentally with a relatively good precision, the size of CP violation effects in neutrino oscillations depends essentially only on the magnitude of the currently not well determined value of the Dirac phase δ. The current data implies $|J_{CP}| \lesssim 0.040\,|\sin\delta|$, where we have used the 3σ ranges of $\sin^2\theta_{12}$, $\sin^2\theta_{23}$ and $\sin^2\theta_{13}$ given in Table 14.7. For the best fit values of $\sin^2\theta_{12}$, $\sin^2\theta_{23}$ and $\sin^2\theta_{13}$ and δ we find in the case of $\Delta m^2_{31(2)} > 0$ ($\Delta m^2_{31(2)} < 0$): $J_{CP} \cong -0.032$ (-0.029). Thus, if the indication that $\delta \cong 3\pi/2$ is confirmed by future more precise data, the CP violation effects in neutrino oscillations would be relatively large.

As we have indicated, the existing data do not allow one to determine the sign of $\Delta m^2_{\rm A} = \Delta m^2_{31(2)}$. In the case of 3-neutrino mixing, the two possible signs of $\Delta m^2_{31(2)}$ correspond to two types of neutrino mass spectrum. In the widely used conventions of numbering the neutrinos with definite mass in the two cases, the two spectra read:

– *i) spectrum with normal ordering (NO)*:

$$m_1 < m_2 < m_3,\ \Delta m^2_{\rm A} = \Delta m^2_{31} > 0,$$
$$\Delta m^2_{\odot} \equiv \Delta m^2_{21} > 0,\ m_{2(3)} = (m_1^2 + \Delta m^2_{21(31)})^{\frac{1}{2}};$$

– *ii) spectrum with inverted ordering (IO)*:

$$m_3 < m_1 < m_2,\ \Delta m^2_{\rm A} = \Delta m^2_{32} < 0,\ \Delta m^2_{\odot} \equiv \Delta m^2_{21} > 0,$$
$$m_2 = (m_3^2 + \Delta m^2_{23})^{\frac{1}{2}},\ m_1 = (m_3^2 + \Delta m^2_{23} - \Delta m^2_{21})^{\frac{1}{2}}.$$

Depending on the values of the lightest neutrino mass [177], $\min(m_j)$, the neutrino mass spectrum can also be:

– *Normal Hierarchical (NH)*:

$$m_1 \ll m_2 < m_3,\ m_2 \cong (\Delta m^2_{\odot})^{\frac{1}{2}} \cong 0.0087\ \text{eV},$$
$$m_3 \cong |\Delta m^2_{31}|^{\frac{1}{2}} \cong 0.050\ \text{eV};\ \text{or}$$

– *Inverted Hierarchical (IH)*:

$$m_3 \ll m_1 < m_2,\ \text{with}\ m_{1,2} \cong |\Delta m^2_{32}|^{\frac{1}{2}} \cong 0.049\ \text{eV};\ \text{or}$$

– *Quasi-Degenerate (QD)*:

$$m_1 \cong m_2 \cong m_3 \cong m_0,\ m_j^2 \gg |\Delta m^2_{\rm A}|,\ m_0 \gtrsim 0.10\ \text{eV}.$$

Sometimes the determination of the neutrino mass spectrum is referred to in the literature on the subject as determination of "neutrino mass hierarchy".

All three types of spectrum are compatible with the existing constraints on the absolute scale of neutrino masses m_j. Information about the latter can be obtained, *e.g.*, by measuring the spectrum of electrons near the end point in ^{3}H β-decay experiments [179–183] and from cosmological and astrophysical data. The most stringent upper bounds on the $\bar\nu_e$ mass were obtained in the Troitzk [183,180] experiment:

$$m_{\bar\nu_e} < 2.05\ \text{eV} \quad \text{at}\ 95\%\ \text{CL}. \tag{14.80}$$

Similar result was obtained in the Mainz experiment [181]: $m_{\bar\nu_e} < 2.3$ eV at 95% CL. We have $m_{\bar\nu_e} \cong m_{1,2,3}$ in the case of QD spectrum. The KATRIN experiment [182] is planned to reach sensitivity of $m_{\bar\nu_e} \sim 0.20$ eV, *i.e.*, it will probe the region of the QD spectrum.

The Cosmic Microwave Background (CMB) data of the WMAP experiment, combined with supernovae data and data on galaxy clustering can be used to obtain an upper limit on the sum of neutrinos masses (see review on Cosmological Parameters [171] and, *e.g.*, Ref. 184). Depending on the model complexity and the input data used one obtains [184]: $\sum_j m_j \lesssim (0.3 - 1.3)$ eV, 95% CL.

In March of 2013 the Planck Collaboration published their first constraints on $\sum_j m_j$ [185]. Assuming the existence of three massive neutrinos and the validity of the Λ CDM (Cold Dark Matter) model, and combining their data on the CMB temperature power spectrum with the WMAP polarisation low-multiple ($\ell \leq 23$) and ACT high-multiple ($\ell \geq 2500$) CMB data [186,187], the Planck Collaboration reported the following upper limit on the sum of the neutrino masses [185]:

$$\sum_j m_j < 0.66\ eV, \quad 95\%\ \text{CL}.$$

Adding the data on the Baryon Acoustic Oscillations (BAO) lowers significantly the limit [185]: $\sum_j m_j < (0.23$ eV), 95% CL. It follows from these data that neutrino masses are much smaller than the masses of charged leptons and quarks. If we take as an indicative upper limit $m_j \lesssim 0.5$ eV, we have $m_j/m_{l,q} \lesssim 10^{-6}$, $l = e, \mu, \tau$, $q = d, s, b, u, c, t$. It is natural to suppose that the remarkable smallness of neutrino masses is related to the existence of a new fundamental mass scale in particle physics, and thus to new physics beyond that predicted by the Standard Model.

14.8.1. *The see-saw mechanism and the baryon asymmetry of the Universe* :

A natural explanation of the smallness of neutrino masses is provided by the (type I) see-saw mechanism of neutrino mass generation [3]. An integral part of this rather simple mechanism [188] are the RH neutrinos ν_{lR} (RH neutrino fields $\nu_{lR}(x)$). The latter are assumed to possess a Majorana mass term as well as Yukawa type coupling $\mathcal{L}_{\rm Y}(x)$ with the Standard Model lepton and Higgs doublets, $\psi_{lL}(x)$ and $\Phi(x)$, respectively, $(\psi_{lL}(x))^T = (\nu^T_{lL}(x) \quad l^T_L(x))$, $l = e, \mu, \tau$, $(\Phi(x))^T = (\Phi^{(0)}(x) \ \ \Phi^{(-)}(x))$. In the basis in which the Majorana mass matrix of RH neutrinos is diagonal, we have:

$$\mathcal{L}_{\rm Y,M}(x) = \left(\lambda_{il}\,\overline{N_{iR}}(x)\,\Phi^\dagger(x)\,\psi_{lL}(x) + \text{h.c.}\right) - \frac{1}{2}\,M_i\,\overline{N_i}(x)\,N_i(x)\,, \tag{14.81}$$

where λ_{il} is the matrix of neutrino Yukawa couplings and N_i ($N_i(x)$) is the heavy RH Majorana neutrino (field) possessing a mass $M_i > 0$. When the electroweak symmetry is broken spontaneously, the neutrino Yukawa coupling generates a Dirac mass term: $m^D_{il}\,\overline{N_{iR}}(x)\,\nu_{lL}(x) + \text{h.c.}$, with $m^D = v\lambda$, $v = 174$ GeV being the Higgs doublet v.e.v. In the case when the elements of m^D are much smaller than M_k, $|m^D_{il}| \ll M_k$, $i, k = 1, 2, 3$, $l = e, \mu, \tau$, the interplay between the Dirac mass term and the mass term of the heavy (RH) Majorana neutrinos N_i generates an effective Majorana mass (term) for the LH flavour neutrinos [3]: $m^{LL}_{l'l} \cong -(m^D)^T_{l'j} M_j^{-1} m^D_{jl}$. In grand unified theories, m^D is typically of the order of the charged fermion masses. In $SO(10)$ theories, for instance, m^D coincides with the up-quark mass matrix. Taking indicatively $m^{LL} \sim 0.1$ eV, $m^D \sim 100$ GeV, one finds $M \sim 10^{14}$ GeV, which is close to the scale of unification of the electroweak and strong interactions, $M_{GUT} \cong 2 \times 10^{16}$ GeV. In GUT theories with RH neutrinos one finds that indeed the heavy Majorana neutrinos N_j naturally obtain masses which are by few to several orders of magnitude smaller than M_{GUT}. Thus, the enormous disparity between the neutrino and charged fermion masses is explained in this approach by the huge difference between effectively the electroweak symmetry breaking scale and M_{GUT}.

An additional attractive feature of the see-saw scenario is that the generation and smallness of neutrino masses is related via the leptogenesis mechanism [2] to the generation of the baryon asymmetry of the Universe. The Yukawa coupling in Eq. (14.81), in general, is not CP conserving. Due to this CP-nonconserving coupling the heavy Majorana neutrinos undergo, *e.g.*, the decays $N_j \to l^+ + \Phi^{(-)}$, $N_j \to l^- + \Phi^{(+)}$, which have different rates: $\Gamma(N_j \to l^+ + \Phi^{(-)}) \neq \Gamma(N_j \to l^- + \Phi^{(+)})$. When these decays occur in the Early Universe at temperatures somewhat below the mass of, say, N_1, so that the latter are out of equilibrium with the rest of the particles present at that epoch, CP violating asymmetries in the individual lepton charges L_l, and in the total lepton charge L, of the Universe are generated. These lepton asymmetries are converted into a baryon asymmetry by $(B - L)$ conserving, but $(B + L)$ violating, sphaleron processes, which exist in the Standard Model and are effective at temperatures $T \sim (100 - 10^{12})$ GeV. If the heavy neutrinos N_j have hierarchical spectrum, $M_1 \ll M_2 \ll M_3$, the observed baryon asymmetry can be reproduced provided the mass of the lightest one satisfies $M_1 \gtrsim 10^9$ GeV [189]. Thus, in this scenario, the neutrino masses and mixing and the baryon asymmetry have the same origin - the neutrino Yukawa couplings and the existence of (at least two) heavy Majorana neutrinos. Moreover, quantitative studies based on recent advances in leptogenesis theory [190] have shown that the Dirac and/or Majorana phases in the neutrino mixing matrix U can provide the CP violation, necessary in leptogenesis for the generation of the

observed baryon asymmetry of the Universe [191]. This implies, in particular, that if the CP symmetry is established not to hold in the lepton sector due to U, at least some fraction (if not all) of the observed baryon asymmetry might be due to the Dirac and/or Majorana CP violation present in the neutrino mixing.

14.8.2. ***The nature of massive neutrinos*** :

The experiments studying flavour neutrino oscillations cannot provide information on the nature - Dirac or Majorana, of massive neutrinos [43,57]. Establishing whether the neutrinos with definite mass ν_j are Dirac fermions possessing distinct antiparticles, or Majorana fermions, i.e. spin 1/2 particles that are identical with their antiparticles, is of fundamental importance for understanding the origin of ν-masses and mixing and the underlying symmetries of particle interactions (see *e.g.*, Ref. 68). The neutrinos with definite mass ν_j will be Dirac fermions if the particle interactions conserve some additive lepton number, *e.g.*, the total lepton charge $L = L_e + L_\mu + L_\tau$. If no lepton charge is conserved, ν_j will be Majorana fermions (see *e.g.*, Ref. 41). The massive neutrinos are predicted to be of Majorana nature by the see-saw mechanism of neutrino mass generation [3]. The observed patterns of neutrino mixing and of neutrino mass squared differences can be related to Majorana massive neutrinos and the existence of an approximate flavour symmetry in the lepton sector (see, *e.g.*, Ref. 192). Determining the nature of massive neutrinos ν_j is one of the fundamental and most challenging problems in the future studies of neutrino mixing.

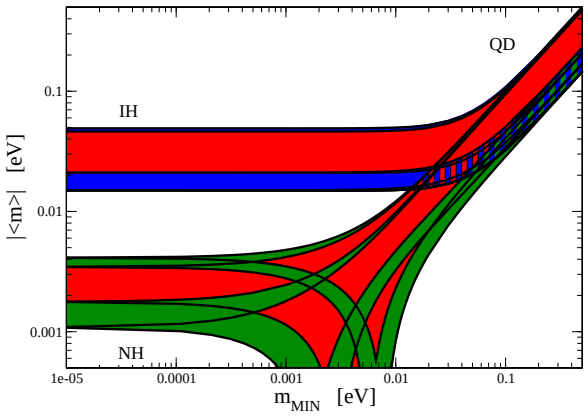

The effective Majorana mass $|<m>|$ (including a 2σ uncertainty), as a function of $\min(m_j)$. The figure is obtained using the best fit values and the 2σ ranges of allowed values of Δm^2_{21}, $\sin^2\theta_{12}$, and $|\Delta m^2_{31}| \cong |\Delta m^2_{32}|$ from Ref. 174. The phases $\alpha_{21,31}$ are varied in the interval $[0,\pi]$. The predictions for the NH, IH and QD spectra are indicated. The red regions correspond to at least one of the phases $\alpha_{21,31}$ and $(\alpha_{31} - \alpha_{21})$ having a CP violating value, while the blue and green areas correspond to $\alpha_{21,31}$ possessing CP conserving values. (Update by S. Pascoli of a figure from the last article quoted in Ref. 196.)

The Majorana nature of massive neutrinos ν_j manifests itself in the existence of processes in which the total lepton charge L changes by two units: $K^+ \to \pi^- + \mu^+ + \mu^+$, $\mu^- + (A,Z) \to \mu^+ + (A, Z-2)$, *etc.* Extensive studies have shown that the only feasible experiments having the potential of establishing that the massive neutrinos are Majorana particles are at present the experiments searching for $(\beta\beta)_{0\nu}$-decay: $(A,Z) \to (A, Z+2) + e^- + e^-$ (see *e.g.*, Ref. 193). The observation of $(\beta\beta)_{0\nu}$-decay and the measurement of the corresponding half-life with sufficient accuracy, would not only be a proof that the total lepton charge is not conserved, but might also provide unique information on the i) type of neutrino mass spectrum (see, *e.g.*, Ref. 194), ii) Majorana phases in U [178,195] and iii) the absolute scale of neutrino masses (for details see Ref. 193 to Ref. 196 and references quoted therein).

Under the assumptions of 3-ν mixing, of massive neutrinos ν_j being Majorana particles, and of $(\beta\beta)_{0\nu}$-decay generated only by the (V-A) charged current weak interaction via the exchange of the three Majorana neutrinos ν_j having masses $m_j \lesssim$ few MeV, the $(\beta\beta)_{0\nu}$-decay amplitude has the form (see, *e.g.*, Ref. 41 and Ref. 193): $A(\beta\beta)_{0\nu} \cong <m>\, M$, where M is the corresponding nuclear matrix element which does not depend on the neutrino mixing parameters, and

$$|<m>| = \left| m_1 U^2_{e1} + m_2 U^2_{e2} + m_3 U^2_{e3} \right| = \left| \left(m_1 c^2_{12} + m_2 s^2_{12} e^{i\alpha_{21}} \right) c^2_{13} + m_3 s^2_{13} e^{i(\alpha_{31} - 2\delta)} \right|, \quad (14.82)$$

is the effective Majorana mass in $(\beta\beta)_{0\nu}$-decay. In the case of CP-invariance one has [45], $\eta_{21} \equiv e^{i\alpha_{21}} = \pm 1$, $\eta_{31} \equiv e^{i\alpha_{31}} = \pm 1$, $e^{-i2\delta} = 1$. The three neutrino masses $m_{1,2,3}$ can be expressed in terms of the two measured Δm^2_{jk} and, *e.g.*, $\min(m_j)$. Thus, given the neutrino oscillation parameters Δm^2_{21}, $\sin^2\theta_{12}$, Δm^2_{31} and $\sin^2\theta_{13}$, $|<m>|$ is a function of the lightest neutrino mass $\min(m_j)$, the Majorana (and Dirac) CP violation phases in U and of the type of neutrino mass spectrum. In the case of NH, IH and QD spectrum we have (see, *e.g.*, Ref. 178 and Ref. 196):

$$|<m>| \cong \left| \sqrt{\Delta m^2_{21}}\, s^2_{12} c^2_{13} + \sqrt{\Delta m^2_{31}}\, s^2_{13} e^{i(\alpha_{31} - \alpha_{21} - 2\delta)} \right|, \quad \text{NH}, \quad (14.83)$$

$$|<m>| \cong \tilde{m} \left(1 - \sin^2 2\theta_{12} \sin^2 \frac{\alpha_{21}}{2} \right)^{\frac{1}{2}}, \quad \text{IH (IO) and QD}, \quad (14.84)$$

where $\tilde{m} \equiv \sqrt{\Delta m^2_{23} + m^2_3}$ and $\tilde{m} \equiv m_0$ for IH (IO) and QD spectrum, respectively. In Eq. (14.84) we have exploited the fact that $\sin^2\theta_{13} \ll \cos 2\theta_{12}$. The CP conserving values of the Majorana phases $(\alpha_{31} - \alpha_{21})$ and α_{21} determine the intervals of possible values of $|<m>|$, corresponding to the different types of neutrino mass spectrum. Using the 3σ ranges of the allowed values of the neutrino oscillation parameters Table 14.7 one finds that: i) 0.58×10^{-3} eV $\lesssim |<m>| \lesssim 4.22 \times 10^{-3}$ eV in the case of NH spectrum; ii) $\sqrt{\Delta m^2_{23}} \cos 2\theta_{12}\, c^2_{13} \lesssim |<m>| \lesssim \sqrt{\Delta m^2_{23}}\, c^2_{13}$, or 1.3×10^{-2} eV $\lesssim |<m>| \lesssim 5.0 \times 10^{-2}$ eV in the case of IH spectrum; iii) $m_0 \cos 2\theta_{12} \lesssim |<m>| \lesssim m_0$, or 2.8×10^{-2} eV $\lesssim |<m>| \lesssim m_0$ eV, $m_0 \gtrsim 0.10$ eV, in the case of QD spectrum. The difference in the ranges of $|<m>|$ in the cases of NH, IH and QD spectrum opens up the possibility to get information about the type of neutrino mass spectrum from a measurement of $|<m>|$ [194]. The predicted $(\beta\beta)_{0\nu}$-decay effective Majorana mass $|<m>|$ as a function of the lightest neutrino mass $\min(m_j)$ is shown in Fig. 14.10.

14.9. Outlook

After the spectacular experimental progress made in the studies of neutrino oscillations, further understanding of the pattern of neutrino masses and neutrino mixing, of their origins and of the status of CP symmetry in the lepton sector requires an extensive and challenging program of research. The main goals of such a research program, outlined in the 2010 PDG edition of the Review of Particle Physics, included:

- Determining the nature - Dirac or Majorana, of massive neutrinos ν_j. This is of fundamental importance for making progress in our understanding of the origin of neutrino masses and mixing and of the symmetries governing the lepton sector of particle interactions.
- Determination of the sign of $\Delta m^2_{\rm A}$ (Δm^2_{31}) and of the type of neutrino mass spectrum.
- Determining or obtaining significant constraints on the absolute scale of neutrino masses.
- Measurement of, or improving by at least a factor of (5 - 10) the existing upper limit on, the small neutrino mixing angle θ_{13}. Together with the Dirac CP-violating phase, the angle θ_{13}

determines the magnitude of CP-violation effects in neutrino oscillations.

- Determining the status of CP symmetry in the lepton sector.
- High precision measurement of Δm^2_{21}, θ_{12}, and $|\Delta m^2_{31}|$, θ_{23}.
- Understanding at a fundamental level the mechanism giving rise to neutrino masses and mixing and to L_l-non-conservation. This includes understanding the origin of the patterns of ν-mixing and ν-masses suggested by the data. Are the observed patterns of ν-mixing and of $\Delta m^2_{21,31}$ related to the existence of a new fundamental symmetry of particle interactions? Is there any relation between quark mixing and neutrino mixing, *e.g.*, does the relation $\theta_{12} + \theta_c = \pi/4$, where θ_c is the Cabibbo angle, hold? What is the physical origin of CP violation phases in the neutrino mixing matrix U? Is there any relation (correlation) between the (values of) CP violation phases and mixing angles in U? Progress in the theory of neutrino mixing might also lead to a better understanding of the mechanism of generation of baryon asymmetry of the Universe.

The successful realization of this research program, which would be a formidable task and would require many years, already began with the high precision measurement of the value of $\sin^2 2\theta_{13}$ in the Daya Bay experiment, and with the subsequent results on θ_{13} obtained by the RENO, Double Chooz and T2K collaborations. It follows from these measurements and from the global neutrino oscillation data that at 99.73% CL one has [174] $0.0177 \lesssim \sin^2\theta_{13} \lesssim 0.0297$ ($0.0171 \lesssim \sin^2\theta_{13} \lesssim 0.0315$) for NO (IO) neutrino mass spectrum. The data provide also a hint that the Dirac phase δ has a CP nonconserving value $\delta \cong 3\pi/2$, the CP conserving values $\delta = 0(2\pi), \pi$ [$0(2\pi)$] being disfavored at 1.6σ to 2σ [at 2σ] in the case of NO [IO] spectrum. For IO spectrum though, the value $\delta = \pi$ is statistically only 1σ away from the best fit value $\delta \cong 3\pi/2$.

The results on θ_{13} have far reaching implications. The measured relatively large value of θ_{13} opens up the possibilities, in particular,

i) for searching for CP violation effects in neutrino oscillation experiments with high intensity accelerator neutrino beams, like T2K, NOνA, etc. NOνA [65], an off-axis ν_e appearance experiment using the NuMI beam, is under construction and expected to be completed in 2014. The sensitivities of T2K and NOνA on CP violation in neutrino oscillations are discussed in, *e.g.*, Refs. [197,173].

ii) for determining the sign of Δm^2_{32}, and thus the type of neutrino mass spectrum in the long baseline neutrino oscillation experiments at accelerators (NOνA, etc.), in the experiments studying the oscillations of atmospheric neutrinos as well as in experiments with reactor antineutrinos [198](for a review see, *e.g.*, Ref. 199).

There are also long term plans extending beyond 2025 for seraches for CP violation and neutrino mass spectrum determination in long baseline neutrino oscillation experiments with accelerator neutrino beams (see, *e.g.*, Refs. [173,200]) .

A value of $|\sin\theta_{13}\sin\delta| \gtrsim 0.09$, and thus $\sin\theta_{13} \gtrsim 0.09$, is a necessary condition for a successful "flavoured" leptogenesis with hierarchical heavy Majorana neutrinos when the CP violation required for the generation of the matter-antimatter asymmetry of the Universe is provided entirely by the Dirac CP violating phase in the neutrino mixing matrix [191]. This condition is comfortably compatible both with the measured value of $\sin^2\theta_{13}$ and with the best fit value of $\delta \cong 3\pi/2$.

With the measurement of θ_{13}, the first steps on the long "road" leading to a comprehensive understanding of the patterns of neutrino masses and mixing, of their origin and implications, were made.

References:

1. B. Pontecorvo, Zh. Eksp. Teor. Fiz. **53**, 1717 (1967) [Sov. Phys. JETP **26**, 984 (1968)].
2. M. Fukugita and T. Yanagida, Phys. Lett. **B174**, 45 (1986); V.A. Kuzmin, V.A. Rubakov, and M.E. Shaposhnikov, Phys. Lett. **B155**, 36 (1985).
3. P. Minkowski, Phys. Lett. **B67**, 421 (1977); see also: M. Gell-Mann, P. Ramond, and R. Slansky in *Supergravity*, p. 315, edited by F. Nieuwenhuizen and D. Friedman, North Holland, Amsterdam, 1979; T. Yanagida, *Proc. of the Workshop on Unified Theories and the Baryon Number of the Universe*, edited by O. Sawada and A. Sugamoto, KEK, Japan 1979; R.N. Mohapatra and G. Senjanović, Phys. Rev. Lett. **44**, 912 (1980).
4. B. Pontecorvo, Zh. Eksp. Teor. Fiz. **33**, 549 (1957) and **34**, 247 (1958).
5. Z. Maki, M. Nakagawa, and S. Sakata, Prog. Theor. Phys. **28**, 870 (1962).
6. B.T. Cleveland *et al.*, Astrophys. J. **496**, 505 (1988).
7. Y. Fukuda *et al.*, [Kamiokande Collab.], Phys. Rev. Lett. **77**, 1683 (1996).
8. J.N. Abdurashitov *et al.*, [SAGE Collab.], Phys. Rev. **C80**, 015807 (2009).
9. P. Anselmann *et al.*, [GALLEX Collab.], Phys. Lett. **B285**, 376 (1992).
10. W. Hampel *et al.*, [GALLEX Collab.], Phys. Lett. **B447**, 127 (1999).
11. M. Altmann *et al.*, [GNO Collab.], Phys. Lett. **B616**, 174 (2005).
12. S. Fukuda *et al.*, [Super-Kamiokande Collab.], Phys. Lett. **B539**, 179 (2002).
13. Q.R. Ahmad *et al.*, [SNO Collab.], Phys. Rev. Lett. **87**, 071301 (2001).
14. Q.R. Ahmad *et al.*, [SNO Collab.], Phys. Rev. Lett. **89**, 011301 (2002).
15. K. Eguchi *et al.*, [KamLAND Collab.], Phys. Rev. Lett. **90**, 021802 (2003).
16. T. Araki *et al.*, [KamLAND Collab.], Phys. Rev. Lett. **94**, 081801 (2005).
17. Y. Fukuda *et al.*, [Super-Kamiokande Collab.], Phys. Rev. Lett. **81**, 1562 (1998).
18. Y. Ashie *et al.*, [Super-Kamiokande Collab.], Phys. Rev. Lett. **93**, 101801 (2004).
19. M.H. Ahn *et al.*, [K2K Collab.], Phys. Rev. **D74**, 072003 (2006).
20. D.G. Michael *et al.*, [MINOS Collab.], Phys. Rev. Lett. **97**, 191801 (2006); P. Adamson *et al.*, [MINOS Collab.], Phys. Rev. Lett. **101**, 131802 (2008).
21. P. Adamson *et al.*, [MINOS Collab.], Phys. Rev. Lett. **106**, 181801 (2011).
22. K. Abe *et al.*, [T2K Collab.], Phys. Rev. **D85**, 031103 (R) (2012).
23. K. Abe *et al.*, [T2K Collab.], Phys. Rev. Lett. **111**, 211803 (2013).
24. K. Abe *et al.*, [Super-Kamiokande Collab.], Phys. Rev. Lett. **110**, 181802 (2013).
25. A. Pastore, talk at the EPS HEP 2013 Conference, July 18-24, 2013, Stockholm.
26. L. Wolfenstein, Phys. Rev. **D17**, 2369 (1978); *Proc. of the 8th International Conference on Neutrino Physics and Astrophysics - "Neutrino'78"* (ed. E.C. Fowler, Purdue University Press, West Lafayette, 1978), p. C3.
27. S.P. Mikheev and A.Y. Smirnov, Sov. J. Nucl. Phys. **42**, 913 (1985); Nuovo Cimento **9C**, 17 (1986).
28. K. Abe *et al.*, [T2K Collab.], Phys. Rev. Lett. **107**, 041801 (2011).
29. P. Adamson *et al.*, [MINOS Collab.], Phys. Rev. Lett. **107**, 181802 (2011).
30. Y. Abe *et al.*, [Double Chooz Collab.], Phys. Rev. Lett. **108**, 131801 (2012).
31. F.P. An *et al.*, [Daya Bay Collab.], Phys. Rev. Lett. **108**, 171803 (2012).

32. J.K. Ahn *et al.*, [RENO Collab.], Phys. Rev. Lett. **108**, 191802 (2012).
33. Y. Abe *et al.*, [Double Chooz Collab.], Phys. Rev. **D86**, 052008 (2012).
34. K. Abe *et al.*, [T2K Collab.], Phys. Rev. **D88**, 032002 (2013).
35. F.P. An *et al.*, [Daya Bay Collab.], Chinese Phys. **C37**, 011001 (2013).
36. F.P. An *et al.*, [Daya Bay Collab.], Phys. Rev. Lett. **112**, 061801 (2014).
37. S.-H. Seo [for the RENO Collab.], talk at the TAUP2013 International Workshop, September 9-13, 2013, Asilomar, California, USA.
38. D. Karlen in RPP2012 [Phys. Rev. **D86**, Part I, 629 (2012)].
39. E. Majorana, Nuovo Cimento **5**, 171 (1937).
40. Majorana particles, in contrast to Dirac fermions, are their own antiparticles. An electrically charged particle (like the electron) cannot coincide with its antiparticle (the positron) which carries the opposite non-zero electric charge.
41. S.M. Bilenky and S.T. Petcov, Rev. Mod. Phys. **59**, 671 (1987).
42. S.T. Petcov, Adv. High Energy Phys. **2013**, 852987 (2013) and arXiv:1303.5819.
43. S.M. Bilenky, J. Hosek, and S.T. Petcov, Phys. Lett. **B94**, 495 (1980).
44. J. Schechter and J.W.F. Valle, Phys. Rev. **D22**, 2227 (1980); M. Doi *et al.*, Phys. Lett. **B102**, 323 (1981).
45. L. Wolfenstein, Phys. Lett. **B107**, 77 (1981); J. Bernabeu and P. Pascual, Nucl. Phys. **B228**, 21 (1983); S.M. Bilenky, N.P. Nedelcheva, and S.T. Petcov, Nucl. Phys. **B247**, 61 (1984); B. Kayser, Phys. Rev. **D30**, 1023 (1984).
46. S. Nussinov, Phys. Lett. **B63**, 201 (1976); B. Kayser, Phys. Rev. **D24**, 110 (1981); J. Rich, Phys. Rev. **D48**, 4318 (1993); H. Lipkin, Phys. Lett. **B348**, 604 (1995); W. Grimus and P. Stockinger, Phys. Rev. **D54**, 3414 (1996); L. Stodolski, Phys. Rev. **D58**, 036006 (1998); W. Grimus, P. Stockinger, and S. Mohanty, Phys. Rev. **D59**, 013011 (1999); L.B. Okun, Surv. High Energy Physics **15**, 75 (2000); J.-M. Levy, hep-ph/0004221 and arXiv:0901.0408; A.D. Dolgov, Phys. Reports **370**, 333 (2002); C. Giunti, Phys. Scripta **67**, 29 (2003) and Phys. Lett. **B17**, 103 (2004); M. Beuthe, Phys. Reports **375**, 105 (2003); H. Lipkin, Phys. Lett. **B642**, 366 (2006); S.M. Bilenky, F. von Feilitzsch, and W. Potzel, J. Phys. **G34**, 987 (2007); C. Giunti and C.W. Kim, *Fundamentals of Neutrino Physics and Astrophysics* (Oxford University Press, Oxford, 2007); E.Kh. Akhmedov, J. Kopp, and M. Lindner, JHEP **0805**, 005 (2008); E.Kh. Akhmedov and A.Yu. Smirnov, Phys. Atom. Nucl. **72**, 1363 (2009).
47. For the subtleties involved in the step leading from Eq. (14.1) to Eq. (14.5) see, *e.g.*, Ref. 48.
48. A.G. Cohen, S.L. Glashow, and Z. Ligeti, Phys. Lett. **B678**, 191 (2009).
49. The neutrino masses do not exceed approximately 1 eV, $m_j \lesssim 1$, while in neutrino oscillation experiments neutrinos with energy $E \gtrsim 100$ keV are detected.
50. S.M. Bilenky and B. Pontecorvo, Phys. Reports **41**, 225 (1978).
51. In Eq. (14.9) we have neglected the possible instability of neutrinos ν_j. In most theoretical models with nonzero neutrino masses and neutrino mixing, the predicted half life-time of neutrinos with mass of 1 eV exceeds the age of the Universe, see, *e.g.*, S.T. Petcov, Yad. Fiz. **25**, 641 (1977), (E) *ibid.*, **25** (1977) 1336 [Sov. J. Nucl. Phys. **25**, 340 (1977), (E) *ibid.*, **25**, (1977), 698], and Phys. Lett. **B115**, 401 (1982); W. Marciano and A.I. Sanda, Phys. Lett. **B67**, 303 (1977); P. Pal and L. Wolfenstein, Phys. Rev. **D25**, 766 (1982).
52. L.B. Okun (2000), J.-M. Levy (2000) and H. Lipkin (2006) quoted in Ref. 46 and Ref. 48.
53. The articles by L. Stodolsky (1998) and H. Lipkin (1995) quoted in Ref. 46.
54. V. Gribov and B. Pontecorvo, Phys. Lett. **B28**, 493 (1969).
55. N. Cabibbo, Phys. Lett. **B72**, 333 (1978).
56. V. Barger *et al.*, Phys. Rev. Lett. **45**, 2084 (1980).
57. P. Langacker *et al.*, Nucl. Phys. **B282**, 589 (1987).
58. P.I. Krastev and S.T. Petcov, Phys. Lett. **B205**, 84 (1988).
59. C. Jarlskog, Z. Phys. **C29**, 491 (1985).
60. A. De Rujula *et al.*, Nucl. Phys. **B168**, 54 (1980).
61. M. Apollonio *et al.*, [Chooz Collab.], Phys. Lett. **B466**, 415 (1999); Eur. Phys. J. **C27**, 331 (2003).
62. N. Agafonova *et al.*, [OPERA Collab.], Phys. Lett. **B691**, 138 (2010); New J. Phys. **14**, 033017 (2012).
63. N. Agafonova *et al.*, [OPERA Collab.], JHEP **1311**, 036 (2013).
64. S. Goswami *et al.*, Nucl. Phys. (Proc. Supp.) **B143**, 121 (2005).
65. R.B. Patterson [for the NOvA Collab.], Nucl. Phys. (Proc. Supp.) **B235-236**, 151 (2013).
66. These processes are important, however, for the supernova neutrinos see, *e.g.*, G. Raffelt, *Proc. International School of Physics "Enrico Fermi", CLII Course "Neutrino Physics"*, 23 July-2 August 2002, Varenna, Italy [hep-ph/0208024]), and articles quoted therein.
67. We standardly assume that the weak interaction of the flavour neutrinos ν_l and antineutrinos $\bar{\nu}_l$ is described by the Standard Model (for alternatives see, *e.g.*, Ref. 26; M.M. Guzzo *et al.*, Phys. Lett. **B260**, 154 (1991); E. Roulet, Phys. Rev. **D44**, R935 (1991) and Ref. 68).
68. R. Mohapatra *et al.*, Rept. on Prog. in Phys. **70**, 1757 (2007); A. Bandyopadhyay *et al.*, Rept. on Prog. in Phys. **72**, 106201 (2009).
69. V. Barger *et al.*, Phys. Rev. **D22**, 2718 (1980).
70. P. Langacker, J.P. Leveille, and J. Sheiman, Phys. Rev. **D27**, 1228 (1983).
71. The difference between the ν_μ and ν_τ indices of refraction arises at one-loop level and can be relevant for the $\nu_\mu - \nu_\tau$ oscillations in very dense media, like the core of supernovae, *etc.*; see F.J. Botella, C.S. Lim, and W.J. Marciano, Phys. Rev. **D35**, 896 (1987).
72. The relevant formulae for the oscillations between the ν_e and a sterile neutrino ν_s, $\nu_e \leftrightarrow \nu_s$, can be obtained from those derived for the case of $\nu_e \leftrightarrow \nu_{\mu(\tau)}$ oscillations by Refs. [57,70] replacing N_e with $(N_e - 1/2N_n)$, N_n being the neutron number density in matter.
73. T.K. Kuo and J. Pantaleone, Phys. Lett. **B198**, 406 (1987).
74. A.D. Dziewonski and D.L. Anderson, Physics of the Earth and Planetary Interiors **25**, 297 (1981).
75. The first studies of the effects of Earth matter on the oscillations of neutrinos were performed numerically in Refs. [69,76] and in E.D. Carlson, Phys. Rev. **D34**, 1454 (1986); A. Dar *et al.*, *ibid.*, **D35**, 3607 (1988); in Ref. 58 and in G. Auriemma *et al.*, *ibid.*, **D37**, 665 (1988).
76. A.Yu. Smirnov and S.P. Mikheev, *Proc. of the VIth Moriond Workshop* (eds. O. Fackler, J. Tran Thanh Van, Frontières, Gif-sur-Yvette, 1986), p. 355.
77. S.T. Petcov, Phys. Lett. **B434**, 321 (1998), (E) *ibid.* **B444**, 584 (1998); see also: Nucl. Phys. (Proc. Supp.) **B77**, 93 (1999) and hep-ph/9811205.
78. M.V. Chizhov, M. Maris, and S.T. Petcov, hep-ph/9810501.
79. E.Kh. Akhmedov *et al.*, Nucl. Phys. **B542**, 3 (1999).
80. S.T. Petcov, Phys. Lett. **B214**, 259 (1988).
81. J. Hosaka *et al.*, [Super-Kamiokande Collab.], Phys. Rev. **D74**, 032002 (2006).
82. E.Kh. Akhmedov, Nucl. Phys. **B538**, 25 (1999).
83. M.V. Chizhov and S.T. Petcov, Phys. Rev. Lett. **83**, 1096 (1999) and Phys. Rev. Lett. **85**, 3979 (2000); Phys. Rev. **D63**, 073003 (2001).
84. J. Bernabéu, S. Palomares-Ruiz, and S.T. Petcov, Nucl. Phys. **B669**, 255 (2003); S.T. Petcov and T. Schwetz, Nucl. Phys. **B740**, 1 (2006); R. Gandhi *et al.*, Phys. Rev. **D76**, 073012 (2007); E.Kh. Akhmedov, M. Maltoni, and A.Yu. Smirnov, JHEP **0705**, 077 (2007).
85. The mantle-core enhancement maxima, *e.g.*, in $P_m^{2\nu}(\nu_\mu \to \nu_\mu)$, appeared in some of the early numerical calculations, but with incorrect interpretation (see, *e.g.*, the articles quoted in Ref. 75).
86. M. Freund, Phys. Rev. **D64**, 053003 (2001).

87. M.C. Gonzalez-Garcia and Y. Nir, Rev. Mod. Phys. **75**, 345 (2003); S.M. Bilenky, W. Grimus, and C. Giunti, Prog. in Part. Nucl. Phys. **43**, 1 (1999).
88. J.N. Bahcall, *Neutrino Astrophysics*, Cambridge University Press, Cambridge, 1989; J.N. Bahcall and M. Pinsonneault, Phys. Rev. Lett. **92**, 121301 (2004).
89. J.N. Bahcall, A.M. Serenelli, and S. Basu, Astrophys. J. Supp. **165**, 400 (2006).
90. A. Messiah, *Proc. of the VIth Moriond Workshop* (eds. O. Fackler, J. Tran Thanh Van, Frontières, Gif-sur-Yvette, 1986), p. 373.
91. S.J. Parke, Phys. Rev. Lett. **57**, 1275 (1986).
92. S.T. Petcov, Phys. Lett. **B200**, 373 (1988).
93. P.I. Krastev and S.T. Petcov, Phys. Lett. **B207**, 64 (1988); M. Bruggen, W.C. Haxton, and Y.-Z. Quian, Phys. Rev. **D51**, 4028 (1995).
94. T. Kaneko, Prog. Theor. Phys. **78**, 532 (1987); S. Toshev, Phys. Lett. **B196**, 170 (1987); M. Ito, T. Kaneko, and M. Nakagawa, Prog. Theor. Phys. **79**, 13 (1988), (E) *ibid.*, **79**, 555 (1988).
95. S.T. Petcov, Phys. Lett. **B406**, 355 (1997).
96. C. Cohen-Tannoudji, B. Diu, and F. Laloe, *Quantum Mechanics*, Vol. 1 (Hermann, Paris, and John Wiley & Sons, New York, 1977).
97. S.T. Petcov, Phys. Lett. **B214**, 139 (1988); E. Lisi *et al.*, Phys. Rev. **D63**, 093002 (2000); A. Friedland, Phys. Rev. **D64**, 013008 (2001).
98. S.T. Petcov and J. Rich, Phys. Lett. **B224**, 401 (1989).
99. An expression for the "jump" probability P' for N_e varying linearly along the neutrino path was derived in W.C. Haxton, Phys. Rev. Lett. **57**, 1271 (1986) and in Ref. 91 on the basis of the old Landau-Zener result: L.D. Landau, Phys. Z. USSR **1**, 426 (1932), C. Zener, Proc. R. Soc. A **137**, 696 (1932). An analytic description of the solar ν_e transitions based on the Landau-Zener jump probability was proposed in Ref. 91 and in W.C. Haxton, Phys. Rev. **D35**, 2352 (1987). The precision limitations of this description, which is less accurate than that based on the exponential density approximation, were discussed in S.T. Petcov, Phys. Lett. **B191**, 299 (1987) and in Ref. 93.
100. A. de Gouvea, A. Friedland, and H. Murayama, JHEP **0103**, 009 (2001).
101. C.-S. Lim, Report BNL 52079, 1987; S.P. Mikheev and A.Y. Smirnov, Phys. Lett. **B200**, 560 (1988).
102. G.L. Fogli *et al.*, Phys. Lett. **B583**, 149 (2004).
103. J.N. Bahcall, A.M. Serenelli, and S. Basu, Astrophys. J. **621**, L85 (2005).
104. C. Peña-Garay and A.M. Serenelli, `arXiv:0811.2424`.
105. L.C. Stonehill, J.A. Formaggio, and R.G.H. Robertson, Phys. Rev. **C69**, 015801 (2004).
106. A.M. Serenelli, W.C. Haxton, and C. Peña-Garay, Astrophys. J. **743**, 24 (2011).
107. B. Pontecorvo, Chalk River Lab. report PD-205, 1946.
108. D. Davis, Jr., D.S. Harmer, and K.C. Hoffman, Phys. Rev. Lett. **20**, 1205 (1968).
109. F. Kaether *et al.*, Phys. Lett. **B685**, 47 (2010). These authors reanalyzed a complete set of the GALLEX data with a method providing a better background reduction than that adopted in Ref. 10.
110. A.I. Abazov *et al.*, [SAGE Collab.], Phys. Rev. Lett. **67**, 3332 (1991).
111. J.N. Abdurashitov *et al.*, [SAGE Collab.], Phys. Lett. **B328**, 234 (1994).
112. K.S. Hirata *et al.*, [Kamiokande Collab.], Phys. Rev. Lett. **63**, 16 (1989).
113. Y. Fukuda *et al.*, [Super-Kamiokande Collab.], Phys. Rev. Lett. **81**, 1158 (1998).
114. J. Hosaka *et al.*, [Super-Kamiokande Collab.], Phys. Rev. **D73**, 112001 (2006).
115. J.P. Cravens *et al.*, [Super-Kamiokande Collab.], Phys. Rev. **D78**, 032002 (2008).
116. K. Abe *et al.*, [Super-Kamiokande Collab.], Phys. Rev. **D83**, 052010 (2011).
117. A. Renshaw *et al.*, [Super-Kamiokande Collab.], Phys. Rev. Lett. **112**, 091805 (2014).
118. B. Aharmim *et al.*, [SNO Collab.], Phys. Rev. **C72**, 055502 (2005).
119. B. Aharmim *et al.*, [SNO Collab.], Phys. Rev. Lett. **101**, 111301 (2008); Phys. Rev. **C87**, 015502 (2013).
120. B. Aharmim *et al.*, [SNO Collab.], Phys. Rev. **C81**, 055504 (2010).
121. B. Aharmim *et al.*, [SNO Collab.], Phys. Rev. **C88**, 025501 (2013).
122. C. Arpesella *et al.*, [Borexino Collab.], Phys. Lett. **B658**, 101 (2008); Phys. Rev. Lett. **101**, 091302 (2008).
123. G. Bellini *et al.*, [Borexino Collab.], Phys. Rev. Lett. **107**, 141302 (2011).
124. G. Bellini *et al.*, [Borexino Collab.], Phys. Lett. **B707**, 22 (2012).
125. G. Bellini *et al.*, [Borexino Collab.], Phys. Rev. Lett. **108**, 051302 (2012).
126. G. Bellini *et al.*, [Borexino Collab.], Phys. Rev. **D82**, 033006 (2010).
127. Y. Fukuda *et al.*, [Super-Kamiokande Collab.], Phys. Rev. Lett. **86**, 5651 (2001).
128. Y. Fukuda *et al.*, [Super-Kamiokande Collab.], Phys. Lett. **B539**, 179 (2002).
129. G. L. Fogli *et al.*, Phys. Rev. **D67**, 073002 (2003); M. Maltoni, T. Schwetz, and J.W. Valle, Phys. Rev. **D67**, 093003 (2003); A. Bandyopadhyay *et al.*, Phys. Lett. **B559**, 121 (2003); J.N. Bahcall, M.C. Gonzalez-Garcia, and C. Peña-Garay, JHEP **0302**, 009 (2003); P.C. de Holanda and A.Y. Smirnov, JCAP **0302**, 001 (2003).
130. S. Abe *et al.*, [KamLAND Collab.], Phys. Rev. Lett. **100**, 221803 (2008).
131. A. Gando *et al.*, [KamLAND Collab.], Phys. Rev. **D83**, 052002 (2011).
132. A. Gando *et al.*, [KamLAND Collab.], Phys. Rev. **D88**, 033001 (2013).
133. M. Honda *et al.*, Phys. Rev. **D70**, 043008 (2004).
134. M. Honda *et al.*, Phys. Rev. **D75**, 043006 (2007).
135. G.D. Barr *et al.*, Phys. Rev. **D70**, 023006 (2004).
136. G. Battistoni *et al.*, Astopart. Phys. **19**, 269 (2003).
137. Y. Ashie *et al.*, [Super-Kamiokande Collab.], Phys. Rev. **D71**, 112005 (2005).
138. Y. Itow, Nucl. Phys. (Proc. Supp.) **B235-236**, 79 (2013).
139. K. Abe *et al.*, [Super-Kamiokande Collab.], Phys. Rev. Lett. **97**, 171801 (2006).
140. V. Barger *et al.*, Phys. Rev. Lett. **82**, 2640 (1999).
141. E. Lisi *et al.*, Phys. Rev. Lett. **85**, 1166 (2000).
142. P. Adamson *et al.*, [MINOS Collab.], Phys. Rev. Lett. **107**, 021801 (2011); Phys. Rev. Lett. **108**, 191801 (2012).
143. P. Adamson *et al.*, [MINOS Collab.], Phys. Rev. Lett. **110**, 251801 (2013).
144. P. Adamson *et al.*, [MINOS Collab.], Phys. Rev. **D86**, 052007 (2012).
145. K. Abe *et al.*, [T2K Collab.], Phys. Rev. Lett. **112**, 181801 (2014).
146. P. Adamson *et al.*, [MINOS Collab.], Phys. Rev. Lett. **112**, 191801 (2014).
147. P. Adamson *et al.*, [MINOS Collab.], Phys. Rev. Lett. **110**, 171801 (2013).
148. Y. Declais *et al.*, Phys. Lett. **B338**, 383 (1994).
149. Y. Abe *et al.*, [Double Chooz Collab.], Phys. Lett. **B723**, 66 (2013).
150. C. Buck, talk at the EPS HEP 2013 Conference, July 18-24, 2013, Stockholm.
151. K. Abe *et al.*, [T2K Collab.], Phys. Rev. Lett. **112**, 061802 (2014).
152. A. Aguilar *et al.*, [LSND Collab.], Phys. Rev. **D64**, 112007 (2001).
153. A.A. Aguilar-Arevalo *et al.*, [MiniBooNE Collab.], Phys. Rev. Lett. **105**, 181801 (2010).

154. A.A. Aguilar-Arevalo *et al.*, [MiniBooNE Collab.], Phys. Rev. Lett. **110**, 161801 (2013).
155. G. Mention *et al.*, Phys. Rev. **D83**, 073006 (2011).
156. T.A. Mueller *et al.*, Phys. Rev. **C83**, 054615 (2011).
157. P. Anselmann *et al.*, [GALLEX Collab.], Phys. Lett. **B342**, 440 (1995); W. Hampel *et al.*, [GALLEX Collab.], Phys. Lett. **B420**, 114 (1998).
158. J.N. Abdurashitov *et al.*, [SAGE Collab], Phys. Rev. Lett. **77**, 4708 (1996); Phys. Rev. **C59**, 2246 (1999).
159. K. Schreckenbach *et al.*, Phys. Lett. **B160**, 325 (1985).
160. P. Huber, Phys. Rev. **C84**, 024617 (2011).
161. A. Hayes *et al.*, arXiv:1309.4146.
162. B. Armbruster *et al.*, [KARMEN Collab.], Phys. Rev. **D65**, 112001 (2002).
163. P. Astier *et al.*, [NOMAD Collab.], Phys. Lett. **B570**, 19 (2003).
164. M. Antonello *et al.*, [ICARUS Collab.], Eur. Phys. J. **C73**, 2345 (2013); Eur. Phys. J. **C73**, 2599 (2013).
165. N. Agafanova *et al.*, [OPERA Collab.], JHEP **1307**, 004 (2013); JHEP **1307**, 085 (2013).
166. F. Dydak *et al.*, [CDHSW Collab.], Phys. Lett. **B134**, 281 (1984).
167. J. Kopp *et al.*, JHEP **1305**, 050 (2013).
168. C. Giunti *et al.*, Phys. Rev. **D88**, 073008 (2013).
169. A.A. Aguilar-Arevalo *et al.*, [MiniBooNE Collab.], Phys. Rev. Lett. **98**, 231801 (2007); Phys. Rev. Lett. **102**, 101802 (2009).
170. M. Archidiacono *et al.*, Phys. Rev. **D86**, 065028 (2012).
171. O. Lahav and A.R. Liddle in RPP2014.
172. An overview of possible future experiments to test the sterile neutrino hypothesis is given by K.N. Abazajian *et al.*, arXiv:1204.5379; see also T. Lasserre, talk given at TAUP2013, September 9-13, 2013, Asilomar, California, USA.
173. A. de Gouvea *et al.*, arXiv:1310.4340.
174. F. Capozzi *et al.*, Phys. Rev. **D89**, 093018 (2014).
175. M.C. Gonzalez-Garcia *et al.*, JHEP **1212**, 123 (2012); the updated results obtained after the TAUP2013 International Conference (held in September of 2013) are posted at the URL www.nu-fit.org/?q=node/45.
176. G.L. Fogli *et al.*, Phys. Rev. **D86**, 013012 (2012).
177. In the convention we use, the neutrino masses are not ordered in magnitude according to their index number: $\Delta m^2_{31} < 0$ corresponds to $m_3 < m_1 < m_2$. We can also number the massive neutrinos in such a way that one always has $m_1 < m_2 < m_3$, see, *e.g.*, Ref. 178.
178. S.M. Bilenky, S. Pascoli, and S.T. Petcov, Phys. Rev. **D64**, 053010 (2001), and *ibid.*, 113003.
179. F. Perrin, Comptes Rendus **197**, 868 (1933); E. Fermi, Nuovo Cim. **11**, 1 (1934).
180. V. Lobashev *et al.*, Nucl. Phys. **A719**, 153c, (2003).
181. Ch. Kraus *et al.*, Eur. Phys. J. **C40**, 447 (2005).
182. K. Eitel *et al.*, Nucl. Phys. (Proc. Supp.) **B143**, 197 (2005).
183. V.N. Aseev *et al.*, Phys. Rev. **D84**, 112003 (2011).
184. K.N. Abazajian *et al.*, Astopart. Phys. **35**, 177 (2011).
185. P.A.R. Ade *et al.*, [Planck Collab.], arXiv:1303.5076, to be published in Astronomy and Astrophys..
186. C. L. Bennett *et al.*, Astrophys. J. Supp. **208**, 20 (2013).
187. J. Dunkley *et al.*, JCAP **1307**, 025 (2013).
188. For alternative mechanisms of neutrino mass generation see, *e.g.*, the first article in Ref. 68 and references quoted therein.
189. S. Davidson and A. Ibarra, Phys. Lett. **B535**, 25 (2002).
190. A. Abada *et al.*, JCAP **0604**, 004 (2006); E. Nardi *et al.*, JHEP **0601**, 164 (2006).
191. S. Pascoli, S.T. Petcov, and A. Riotto, Phys. Rev. **D75**, 083511 (2007) and Nucl. Phys. **B774**, 1 (2007); E. Molinaro and S.T. Petcov, Phys. Lett. **B671**, 60 (2009).
192. S.T. Petcov, Phys. Lett. **B110**, 245 (1982); R. Barbieri *et al.*, JHEP **9812**, 017 (1998); P.H. Frampton, S.T. Petcov, and W. Rodejohann, Nucl. Phys. **B687**, 31 (2004).
193. A. Morales and J. Morales, Nucl. Phys. (Proc. Supp.) **B114**, 141 (2003); C. Aalseth *et al.*, hep-ph/0412300; A. Giuliani and A. Poves, Adv. High Energy Phys. **2012**, 857016 (2012) (http://www.hindawi.com/journals/ahep/si/437630/).
194. S. Pascoli and S.T. Petcov, Phys. Lett. **B544**, 239 (2002); see also: S. Pascoli, S.T. Petcov, and L. Wolfenstein, Phys. Lett. **B524**, 319 (2002).
195. S.M. Bilenky *et al.*, Phys. Rev. **D54**, 4432 (1996).
196. S.M. Bilenky *et al.*, Phys. Lett. **B465**, 193 (1999); F. Vissani, JHEP **9906**, 022 (1999); K. Matsuda *et al.*, Phys. Rev. **D62**, 093001 (2000); K. Czakon *et al.*, hep-ph/0003161; H.V. Klapdor-Kleingrothaus, H. Päs and A.Yu. Smirnov, Phys. Rev. **D63**, 073005 (2001); S. Pascoli, S.T. Petcov and W. Rodejohann, Phys. Lett. **B549**, 177 (2002), and *ibid.* **B558**, 141 (2003); H. Murayama and Peña-Garay, Phys. Rev. **D69**, 031301 (2004); S. Pascoli, S.T. Petcov, and T. Schwetz, Nucl. Phys. **B734**, 24 (2006); M. Lindner, A. Merle, and W. Rodejohann, Phys. Rev. **D73**, 053005 (2006); A. Faessler *et al.*, Phys. Rev. **D79**, 053001 (2009); S. Pascoli and S.T. Petcov, Phys. Rev. **D77**, 113003 (2008); W. Rodejohann, Int. J. Mod. Phys. E **20**, 1833 (2011).
197. J. Bernabeu *et al.*, arXiv:1005.3146.
198. S.T. Petcov and M. Piai, Phys. Lett. **B533**, 94 (2002); S. Choubey, S.T. Petcov and M. Piai, Phys. Rev. **D68**, 113006 (2003); J. Learned *et al.*, Phys. Rev. **D78**, 071302 (2008); L. Zhan *et al.*, Phys. Rev. **D78**, 111103 (2008) and Phys. Rev. **D79**, 073007 (2009); P. Ghoshal and S.T. Petcov, JHEP **1103**, 058 (2011).
199. R.N. Cahn *et al.*, arXiv:1307.5487.
200. S.K. Agarwalla *et al.*, arXiv:1312.6520; C. Adams *et al.*, arXiv:1307.5700.

15. QUARK MODEL

Revised August 2013 by C. Amsler (University of Bern), T. DeGrand (University of Colorado, Boulder), and B. Krusche (University of Basel).

15.1. Quantum numbers of the quarks

Quantum chromodynamics (QCD) is the theory of the strong interactions. QCD is a quantum field theory and its constituents are a set of fermions, the quarks, and gauge bosons, the gluons. Strongly interacting particles, the hadrons, are bound states of quark and gluon fields. As gluons carry no intrinsic quantum numbers beyond color charge, and because color is believed to be permanently confined, most of the quantum numbers of strongly interacting particles are given by the quantum numbers of their constituent quarks and antiquarks. The description of hadronic properties which strongly emphasizes the role of the minimum-quark-content part of the wave function of a hadron is generically called the quark model. It exists on many levels: from the simple, almost dynamics-free picture of strongly interacting particles as bound states of quarks and antiquarks, to more detailed descriptions of dynamics, either through models or directly from QCD itself. The different sections of this review survey the many approaches to the spectroscopy of strongly interacting particles which fall under the umbrella of the quark model.

Table 15.1: Additive quantum numbers of the quarks.

	d	u	s	c	b	t
Q – electric charge	$-\frac{1}{3}$	$+\frac{2}{3}$	$-\frac{1}{3}$	$+\frac{2}{3}$	$-\frac{1}{3}$	$+\frac{2}{3}$
I – isospin	$\frac{1}{2}$	$\frac{1}{2}$	0	0	0	0
I_z – isospin z-component	$-\frac{1}{2}$	$+\frac{1}{2}$	0	0	0	0
S – strangeness	0	0	-1	0	0	0
C – charm	0	0	0	$+1$	0	0
B – bottomness	0	0	0	0	-1	0
T – topness	0	0	0	0	0	$+1$

Quarks are strongly interacting fermions with spin 1/2 and, by convention, positive parity. Antiquarks have negative parity. Quarks have the additive baryon number 1/3, antiquarks -1/3. Table 15.1 gives the other additive quantum numbers (flavors) for the three generations of quarks. They are related to the charge Q (in units of the elementary charge e) through the generalized Gell-Mann-Nishijima formula

$$\mathsf{Q} = \mathsf{I}_z + \frac{\mathcal{B} + \mathsf{S} + \mathsf{C} + \mathsf{B} + \mathsf{T}}{2} \ , \tag{15.1}$$

where $\mathcal{B}$ is the baryon number. The convention is that the *flavor* of a quark (I_z, S, C, B, or T) has the same sign as its *charge* Q. With this convention, any flavor carried by a charged meson has the same sign as its charge, *e.g.*, the strangeness of the K^+ is $+1$, the bottomness of the B^+ is $+1$, and the charm and strangeness of the D_s^- are each -1. Antiquarks have the opposite flavor signs.

The hypercharge is defined as

$$\mathsf{Y} = \mathcal{B} + \mathsf{S} - \frac{\mathsf{C} - \mathsf{B} + \mathsf{T}}{3} \ .$$

Thus Y is equal to $\frac{1}{3}$ for the u and d quarks, $-\frac{2}{3}$ for the s quark, and 0 for all other quarks.

15.2. Mesons

Mesons have baryon number $\mathcal{B} = 0$. In the quark model, they are $q\overline{q}'$ bound states of quarks q and antiquarks $\overline{q}'$ (the flavors of q and q' may be different). If the orbital angular momentum of the $q\overline{q}'$ state is ℓ, then the parity P is $(-1)^{\ell+1}$. The meson spin J is given by the usual relation $|\ell - s| \leq J \leq |\ell + s|$, where s is 0 (antiparallel quark spins) or 1 (parallel quark spins). The charge conjugation, or C-parity $C = (-1)^{\ell+s}$, is defined only for the $q\bar{q}$ states made of quarks and their own antiquarks. The C-parity can be generalized to the G-parity $G = (-1)^{I+\ell+s}$ for mesons made of quarks and their own antiquarks (isospin $\mathsf{I}_z = 0$), and for the charged $u\bar{d}$ and $d\bar{u}$ states (isospin $\mathsf{I} = 1$).

The mesons are classified in J^{PC} multiplets. The $\ell = 0$ states are the pseudoscalars (0^{-+}) and the vectors (1^{--}). The orbital excitations $\ell = 1$ are the scalars (0^{++}), the axial vectors (1^{++}) and (1^{+-}), and the tensors (2^{++}). Assignments for many of the known mesons are given in Tables 15.2 and 15.3. Radial excitations are denoted by the principal quantum number n. The very short lifetime of the t quark makes it likely that bound-state hadrons containing t quarks and/or antiquarks do not exist.

States in the natural spin-parity series $P = (-1)^J$ must, according to the above, have $s = 1$ and hence, $CP = +1$. Thus, mesons with natural spin-parity and $CP = -1$ (0^{+-}, 1^{-+}, 2^{+-}, 3^{-+}, *etc.*) are forbidden in the $q\bar{q}'$ model. The $J^{PC} = 0^{--}$ state is forbidden as well. Mesons with such *exotic* quantum numbers may exist, but would lie outside the $q\bar{q}'$ model (see section below on exotic mesons).

Following SU(3), the nine possible $q\bar{q}'$ combinations containing the light u, d, and s quarks are grouped into an octet and a singlet of light quark mesons:

$$\mathbf{3} \otimes \overline{\mathbf{3}} = \mathbf{8} \oplus \mathbf{1} \ . \tag{15.2}$$

A fourth quark such as charm c can be included by extending SU(3) to SU(4). However, SU(4) is badly broken owing to the much heavier c quark. Nevertheless, in an SU(4) classification, the sixteen mesons are grouped into a 15-plet and a singlet:

$$\mathbf{4} \otimes \overline{\mathbf{4}} = \mathbf{15} \oplus \mathbf{1} \ . \tag{15.3}$$

The *weight diagrams* for the ground-state pseudoscalar (0^{-+}) and vector (1^{--}) mesons are depicted in Fig. 15.1. The light quark mesons are members of nonets building the middle plane in Fig. 15.1(a) and (b).

Isoscalar states with the same J^{PC} will mix, but mixing between the two light quark isoscalar mesons, and the much heavier charmonium or bottomonium states, are generally assumed to be negligible. In the following, we shall use the generic names a for the $\mathsf{I} = 1$, K for the $\mathsf{I} = 1/2$, and f and f' for the $\mathsf{I} = 0$ members of the light quark nonets. Thus, the physical isoscalars are mixtures of the SU(3) wave function ψ_8 and ψ_1:

$$f' = \psi_8 \cos\theta - \psi_1 \sin\theta \ , \tag{15.4}$$

$$f = \psi_8 \sin\theta + \psi_1 \cos\theta \ , \tag{15.5}$$

where θ is the nonet mixing angle and

$$\psi_8 = \frac{1}{\sqrt{6}}(u\bar{u} + d\bar{d} - 2s\bar{s}) \ , \tag{15.6}$$

$$\psi_1 = \frac{1}{\sqrt{3}}(u\bar{u} + d\bar{d} + s\bar{s}) \ . \tag{15.7}$$

Table 15.2: Suggested $q\overline{q}$ quark-model assignments for some of the observed light mesons. Mesons in bold face are included in the Meson Summary Table. The wave functions f and f' are given in the text. The singlet-octet mixing angles from the quadratic and linear mass formulae are also given for the well established nonets. The classification of the 0^{++} mesons is tentative: The light scalars $a_0(980)$, $f_0(980)$, and $f_0(500)$ are often considered as meson-meson resonances or four-quark states, and are omitted from the table. Not shown either is the $f_0(1500)$ which is hard to accommodate in the nonet. The isoscalar 0^{++} mesons are expected to mix. See the "Note on Scalar Mesons" in the Meson Listings for details and alternative schemes.

$n\,^{2s+1}\ell_J$ J^{PC}	I = 1 $u\overline{d}$, $\overline{u}d$, $\frac{1}{\sqrt{2}}(d\overline{d}-u\overline{u})$	I = $\frac{1}{2}$ $u\overline{s}$, $d\overline{s}$; $\overline{d}s$, $-\overline{u}s$	I = 0 f'	I = 0 f	$\theta_{\rm quad}$ [°]	$\theta_{\rm lin}$ [°]
$1\,^1S_0$ 0^{-+}	$\boldsymbol{\pi}$	$\boldsymbol{K}$	$\boldsymbol{\eta}$	$\boldsymbol{\eta'(958)}$	−11.4	−24.5
$1\,^3S_1$ 1^{--}	$\boldsymbol{\rho(770)}$	$\boldsymbol{K^*(892)}$	$\boldsymbol{\phi(1020)}$	$\boldsymbol{\omega(782)}$	39.1	36.4
$1\,^1P_1$ 1^{+-}	$\boldsymbol{b_1(1235)}$	$\boldsymbol{K_{1B}}^\dagger$	$h_1(1380)$	$\boldsymbol{h_1(1170)}$		
$1\,^3P_0$ 0^{++}	$\boldsymbol{a_0(1450)}$	$\boldsymbol{K_0^*(1430)}$	$\boldsymbol{f_0(1710)}$	$\boldsymbol{f_0(1370)}$		
$1\,^3P_1$ 1^{++}	$\boldsymbol{a_1(1260)}$	$\boldsymbol{K_{1A}}^\dagger$	$\boldsymbol{f_1(1420)}$	$\boldsymbol{f_1(1285)}$		
$1\,^3P_2$ 2^{++}	$\boldsymbol{a_2(1320)}$	$\boldsymbol{K_2^*(1430)}$	$\boldsymbol{f_2'(1525)}$	$\boldsymbol{f_2(1270)}$	32.1	30.5
$1\,^1D_2$ 2^{-+}	$\boldsymbol{\pi_2(1670)}$	$\boldsymbol{K_2(1770)}^\dagger$	$\eta_2(1870)$	$\boldsymbol{\eta_2(1645)}$		
$1\,^3D_1$ 1^{--}	$\boldsymbol{\rho(1700)}$	$\boldsymbol{K^*(1680)}$		$\boldsymbol{\omega(1650)}$		
$1\,^3D_2$ 2^{--}		$\boldsymbol{K_2(1820)}$				
$1\,^3D_3$ 3^{--}	$\boldsymbol{\rho_3(1690)}$	$\boldsymbol{K_3^*(1780)}$	$\boldsymbol{\phi_3(1850)}$	$\boldsymbol{\omega_3(1670)}$	31.8	30.8
$1\,^3F_4$ 4^{++}	$\boldsymbol{a_4(2040)}$	$\boldsymbol{K_4^*(2045)}$		$\boldsymbol{f_4(2050)}$		
$1\,^3G_5$ 5^{--}	$\rho_5(2350)$	$K_5^*(2380)$				
$1\,^3H_6$ 6^{++}	$a_6(2450)$			$f_6(2510)$		
$2\,^1S_0$ 0^{-+}	$\boldsymbol{\pi(1300)}$	$K(1460)$	$\boldsymbol{\eta(1475)}$	$\boldsymbol{\eta(1295)}$		
$2\,^3S_1$ 1^{--}	$\boldsymbol{\rho(1450)}$	$\boldsymbol{K^*(1410)}$	$\boldsymbol{\phi(1680)}$	$\boldsymbol{\omega(1420)}$		

† The $1^{+\pm}$ and $2^{-\pm}$ isospin $\frac{1}{2}$ states mix. In particular, the K_{1A} and K_{1B} are nearly equal (45°) mixtures of the $K_1(1270)$ and $K_1(1400)$. The physical vector mesons listed under 1^3D_1 and 2^3S_1 may be mixtures of 1^3D_1 and 2^3S_1, or even have hybrid components.

Table 15.3: $q\overline{q}$ quark-model assignments for the observed heavy mesons with established J^{PC}. Mesons in bold face are included in the Meson Summary Table.

$n\,^{2s+1}\ell_J$ J^{PC}	I = 0 $c\overline{c}$	I = 0 $b\overline{b}$	I = $\frac{1}{2}$ $c\overline{u}$, $c\overline{d}$; $\overline{c}u$, $\overline{c}d$	I = 0 $c\overline{s}$; $\overline{c}s$	I = $\frac{1}{2}$ $b\overline{u}$, $b\overline{d}$; $\overline{b}u$, $\overline{b}d$	I = 0 $b\overline{s}$; $\overline{b}s$	I = 0 $b\overline{c}$; $\overline{b}c$
$1\,^1S_0$ 0^{-+}	$\boldsymbol{\eta_c(1S)}$	$\boldsymbol{\eta_b(1S)}$	$\boldsymbol{D}$	$\boldsymbol{D_s^\pm}$	$\boldsymbol{B}$	$\boldsymbol{B_s^0}$	$\boldsymbol{B_c^\pm}$
$1\,^3S_1$ 1^{--}	$\boldsymbol{J/\psi(1S)}$	$\boldsymbol{\Upsilon(1S)}$	$\boldsymbol{D^*}$	$\boldsymbol{D_s^{*\pm}}$	$\boldsymbol{B^*}$	B_s^*	
$1\,^1P_1$ 1^{+-}	$\boldsymbol{h_c(1P)}$	$\boldsymbol{h_b(1P)}$	$\boldsymbol{D_1(2420)}$	$\boldsymbol{D_{s1}(2536)^\pm}$	$\boldsymbol{B_1(5721)}$	$\boldsymbol{B_{s1}(5830)^0}$	
$1\,^3P_0$ 0^{++}	$\boldsymbol{\chi_{c0}(1P)}$	$\boldsymbol{\chi_{b0}(1P)}$	$\boldsymbol{D_0^*(2400)}$	$\boldsymbol{D_{s0}^*(2317)^{\pm\dagger}}$			
$1\,^3P_1$ 1^{++}	$\boldsymbol{\chi_{c1}(1P)}$	$\boldsymbol{\chi_{b1}(1P)}$	$D_1(2430)$	$\boldsymbol{D_{s1}(2460)^{\pm\dagger}}$			
$1\,^3P_2$ 2^{++}	$\boldsymbol{\chi_{c2}(1P)}$	$\boldsymbol{\chi_{b2}(1P)}$	$\boldsymbol{D_2^*(2460)}$	$\boldsymbol{D_{s2}^*(2573)^\pm}$	$\boldsymbol{B_2^*(5747)}$	$\boldsymbol{B_{s2}^*(5840)^0}$	
$1\,^3D_1$ 1^{--}	$\boldsymbol{\psi(3770)}$			$\boldsymbol{D_{s1}^*(2700)^\pm}$			
$2\,^1S_0$ 0^{-+}	$\boldsymbol{\eta_c(2S)}$		$D(2550)$				
$2\,^3S_1$ 1^{--}	$\boldsymbol{\psi(2S)}$	$\boldsymbol{\Upsilon(2S)}$					
$2\,^1P_1$ 1^{+-}		$h_b(2P)$					
$2\,^3P_{0,1,2}$ $0^{++},1^{++},2^{++}$	$\boldsymbol{\chi_{c2}(2P)}$	$\boldsymbol{\chi_{b0,1,2}(2P)}$					

† The masses of these states are considerably smaller than most theoretical predictions. They have also been considered as four-quark states The open flavor states in the 1^{+-} and 1^{++} rows are mixtures of the $1^{+\pm}$ states.

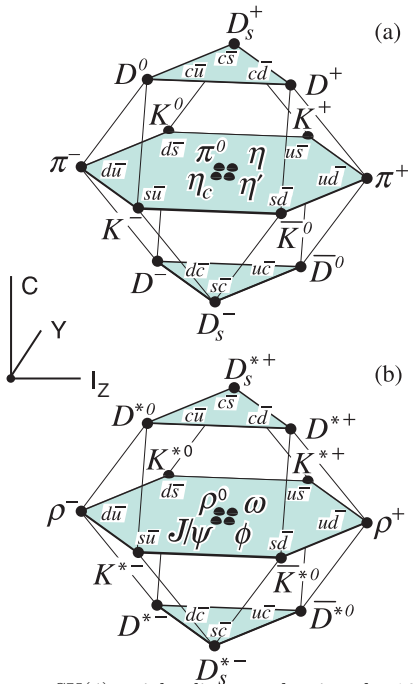

Figure 15.1: SU(4) weight diagram showing the 16-plets for the pseudoscalar (a) and vector mesons (b) made of the u, d, s, and c quarks as a function of isospin I_z, charm C, and hypercharge $\mathsf{Y} = \mathcal{B} + \mathsf{S} - \frac{\mathsf{C}}{3}$. The nonets of light mesons occupy the central planes to which the $c\bar{c}$ states have been added.

These mixing relations are often rewritten to exhibit the $u\bar{u} + d\bar{d}$ and $s\bar{s}$ components which decouple for the "ideal" mixing angle θ_i, such that $\tan\theta_i = 1/\sqrt{2}$ (or $\theta_i = 35.3°$). Defining $\alpha = \theta + 54.7°$, one obtains the physical isoscalar in the flavor basis

$$f' = \frac{1}{\sqrt{2}}(u\bar{u} + d\bar{d})\cos\alpha - s\bar{s}\ \sin\alpha\ , \tag{15.8}$$

and its orthogonal partner f (replace α by α –90°). Thus for ideal mixing ($\alpha_i = 90°$), the f' becomes pure $s\bar{s}$ and the f pure $u\bar{u} + d\bar{d}$. The mixing angle θ can be derived by diagonalizing the mass matrix

$$\begin{pmatrix} m_8 & m_{81} \\ m_{18} & m_1 \end{pmatrix}$$

The mass eigenvalues are $m_{f'}$ and m_f. The mixing angle is given by

$$\tan\theta = \frac{m_8 - m_{f'}}{m_{81}}\ .$$

Calculating m_8 and m_{81} from the wave functions Eq. (15.6) and Eq. (15.7), and expressing the quark masses as a function of the $\mathsf{I} = 1/2$ and $\mathsf{I} = 1$ meson masses, one obtains

$$\tan\theta = \frac{4m_K - m_a - 3m_{f'}}{2\sqrt{2}(m_a - m_K)}\ , \tag{15.9}$$

which also determines the sign of θ. Alternatively, one can express the mixing angle as a function of all nonet masses. The octet mass is given by

$$m_8 = m_{f'}\cos^2\theta + m_f \sin^2\theta$$

whence

$$\tan^2\theta = \frac{4m_K - m_a - 3m_{f'}}{-4m_K + m_a + 3m_f}\ . \tag{15.10}$$

Eliminating θ from Eq. (15.9) and Eq. (15.10) leads to the sum rule [1]

$$(m_f + m_{f'})(4m_K - m_a) - 3m_f m_{f'} = 8m_K^2 - 8m_K m_a + 3m_a^2. \tag{15.11}$$

This relation is verified for the ground-state vector mesons. We identify the $\phi(1020)$ with the f' and the $\omega(783)$ with the f. Thus

$$\phi(1020) = \psi_8\cos\theta_V - \psi_1\sin\theta_V\ , \tag{15.12}$$

$$\omega(782) = \psi_8\sin\theta_V + \psi_1\cos\theta_V\ , \tag{15.13}$$

with the vector mixing angle $\theta_V = 36.4°$ from Eq. (15.10), very close to ideal mixing. Thus $\phi(1020)$ is nearly pure $s\bar{s}$. For ideal mixing, Eq. (15.9) and Eq. (15.10) lead to the relations

$$m_K = \frac{m_f + m_{f'}}{2}\ ,\quad m_a = m_f\ , \tag{15.14}$$

which are satisfied for the vector mesons.

The situation for the pseudoscalar and scalar mesons is not so clear cut, either theoretically or experimentally. For the pseudoscalars, the mixing angle is small. This can be understood qualitatively via gluon-line counting of the mixing process. The size of the mixing process between the nonstrange and strange mass bases scales as α_s^2, not α_s^3, because of two rather than three gluon exchange as it does for the vector mesons. It may also be that the lightest isoscalar pseudoscalars mix more strongly with excited states or with states of substantial non-$\bar{q}q$ content, as will be discussed below.

A variety of analysis methods lead to similar results: First, for these states, Eq. (15.11) is satisfied only approximately. Then Eq. (15.9) and Eq. (15.10) lead to somewhat different values for the mixing angle. Identifying the η with the f' one gets

$$\eta = \psi_8\cos\theta_P - \psi_1\sin\theta_P\ , \tag{15.15}$$

$$\eta' = \psi_8\sin\theta_P + \psi_1\cos\theta_P\ . \tag{15.16}$$

Following chiral perturbation theory, the meson masses in the mass formulae (Eq. (15.9) and Eq. (15.10)) might be replaced by their squares. Table 15.2 lists the mixing angle $\theta_{\rm lin}$ from Eq. (15.10) (using the neutral members of the nonets) and the corresponding $\theta_{\rm quad}$ obtained by replacing the meson masses by their squares throughout.

The pseudoscalar mixing angle θ_P can also be measured by comparing the partial widths for radiative J/ψ decay into a vector and a pseudoscalar [2], radiative $\phi(1020)$ decay into η and η' [3], or $\bar{p}p$ annihilation at rest into a pair of vector and pseudoscalar or into two pseudoscalars [4,5]. One obtains a mixing angle between –10° and –20°. More recently, a lattice QCD simulation, Ref. [6], has successfully reproduced the masses of the η and η', and as a byproduct find a mixing angle $\theta_{lin} = -14.1(2.8)°$. We return to this point in Sec. 15.6.

The nonet mixing angles can be measured in $\gamma\gamma$ collisions, *e.g.*, for the 0^{-+}, 0^{++}, and 2^{++} nonets. In the quark model, the amplitude for the coupling of neutral mesons to two photons is proportional to $\sum_i Q_i^2$, where Q_i is the charge of the i-th quark. The 2γ partial width of an isoscalar meson with mass m is then given in terms of the mixing angle α by

$$\Gamma_{2\gamma} = C(5\cos\alpha - \sqrt{2}\sin\alpha)^2 m^3\ , \tag{15.17}$$

for f' and f ($\alpha \to \alpha$ – 90°). The coupling C may depend on the meson mass. It is often assumed to be a constant in the nonet. For the isovector a, one then finds $\Gamma_{2\gamma} = 9\ C\ m^3$. Thus the members of an ideally mixed nonet couple to 2γ with partial widths in the ratios $f : f' : a = 25 : 2 : 9$. For tensor mesons, one finds from the ratios of the measured 2γ partial widths for the $f_2(1270)$ and $f_2'(1525)$ mesons a mixing angle α_T of $(81\pm 1)°$, or $\theta_T = (27 \pm 1)°$, in accord with the linear mass formula. For the pseudoscalars, one finds from the ratios of partial widths $\Gamma(\eta' \to 2\gamma)/\Gamma(\eta \to 2\gamma)$ a mixing angle $\theta_P = (-18 \pm 2)°$, while the ratio $\Gamma(\eta' \to 2\gamma)/\Gamma(\pi^0 \to 2\gamma)$ leads to $\sim$ –24 °. SU(3) breaking effects for pseudoscalars are discussed in Ref. [7].

The partial width for the decay of a scalar or a tensor meson into a pair of pseudoscalar mesons is model-dependent. Following Ref. [8],

$$\Gamma = C \times \gamma^2 \times |F(q)|^2 \times q\ . \tag{15.18}$$

C is a nonet constant, q the momentum of the decay products, $F(q)$ a form factor, and γ^2 the SU(3) coupling. The model-dependent form factor may be written as

$$|F(q)|^2 = q^{2\ell} \times \exp(-\frac{q^2}{8\beta^2}), \tag{15.19}$$

where ℓ is the relative angular momentum between the decay products. The decay of a $q\bar{q}$ meson into a pair of mesons involves the creation of a $q\bar{q}$ pair from the vacuum, and SU(3) symmetry assumes that the matrix elements for the creation of $s\bar{s}$, $u\bar{u}$, and $d\bar{d}$ pairs are equal. The couplings γ^2 are given in Table 15.4, and their dependence upon the mixing angle α is shown in Fig. 15.2 for isoscalar decays. The generalization to unequal $s\bar{s}$, $u\bar{u}$, and $d\bar{d}$ couplings is given in Ref. [8]. An excellent fit to the tensor meson decay widths is obtained assuming SU(3) symmetry, with $\beta \simeq 0.5$ GeV/c, $\theta_V \simeq 26\,^\circ$ and $\theta_P \simeq -17\,^\circ$ [8].

Table 15.4: SU(3) couplings γ^2 for quarkonium decays as a function of nonet mixing angle α, up to a common multiplicative factor C ($\phi \equiv 54.7^\circ + \theta_P$).

Isospin	Decay channel	γ^2
0	$\pi\pi$	$3\cos^2\alpha$
	$K\overline{K}$	$(\cos\alpha - \sqrt{2}\sin\alpha)^2$
	$\eta\eta$	$(\cos\alpha\cos^2\phi - \sqrt{2}\sin\alpha\sin^2\phi)^2$
	$\eta\eta'$	$\frac{1}{2}\sin^2 2\phi\ (\cos\alpha + \sqrt{2}\sin\alpha)^2$
1	$\eta\pi$	$2\cos^2\phi$
	$\eta'\pi$	$2\sin^2\phi$
	$K\overline{K}$	1
$\frac{1}{2}$	$K\pi$	$\frac{3}{2}$
	$K\eta$	$(\sin\phi - \frac{\cos\phi}{\sqrt{2}})^2$
	$K\eta'$	$(\cos\phi + \frac{\sin\phi}{\sqrt{2}})^2$

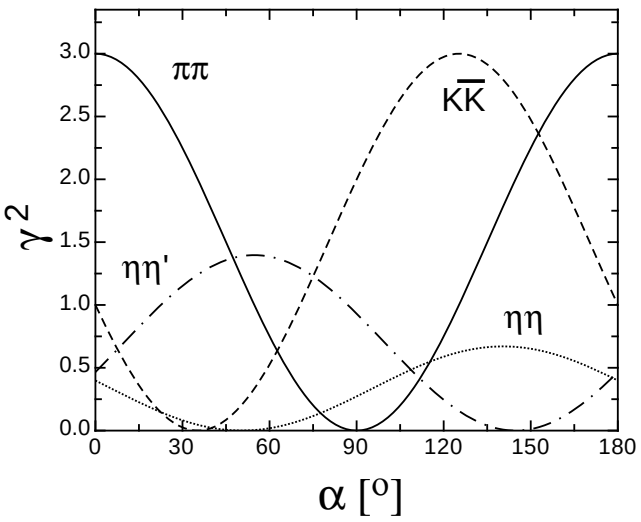

Figure 15.2: SU(3) couplings as a function of mixing angle α for isoscalar decays, up to a common multiplicative factor C and for $\theta_P = -17.3°$.

15.3. Exotic mesons

The existence of a light nonet composed of four quarks with masses below 1 GeV was suggested a long time ago [9]. Coupling two triplets of light quarks u, d, and s, one obtains nine states, of which the six symmetric (uu, dd, ss, $ud+du$, $us+su$, $ds+sd$) form the six dimensional representation **6**, while the three antisymmetric ($ud-du$, $us-su$, $ds-sd$) form the three dimensional representation $\overline{\mathbf{3}}$ of SU(3):

$$\mathbf{3} \otimes \mathbf{3} = \mathbf{6} \oplus \overline{\mathbf{3}}\ . \tag{15.20}$$

Combining with spin and color and requiring antisymmetry, one finds that the most deeply bound diquark (and hence the lightest) is the one in the $\overline{\mathbf{3}}$ and spin singlet state. The combination of the diquark with an antidiquark in the **3** representation then gives a light nonet of four-quark scalar states. Letting the number of strange quarks determine the mass splitting, one obtains a mass inverted spectrum with a light isosinglet ($ud\bar{u}\bar{d}$), a medium heavy isodoublet (*e.g.*, $ud\bar{s}\bar{d}$) and a heavy isotriplet (*e.g.*, $ds\bar{u}\bar{s}$) + isosinglet (*e.g.*, $us\bar{u}\bar{s}$). It is then tempting to identify the lightest state with the $f_0(500)$, and the heaviest states with the $a_0(980)$, and $f_0(980)$. Then the meson with strangeness $\kappa(800)$ would lie in-between.

QCD predicts the existence of extra isoscalar mesons. In the pure gauge theory they contain only gluons, and are called the glueballs. The ground state glueball is predicted by lattice gauge theories to be 0^{++}, the first excited state 2^{++}. Errors on the mass predictions are large. From Ref. 10 one obtains 1750 (50) (80) MeV for the mass of the lightest 0^{++} glueball from quenched QCD. As an example for the glueball mass spectrum, we show in Fig. 15.3 a calculation from Ref. 11. A mass of 1710 MeV is predicted for the ground state, also with an error of about 100 MeV. Earlier work by other groups produced masses at 1650 MeV [12] and 1550 MeV [13] (see also [14]) . The first excited state has a mass of about 2.4 GeV, and the lightest glueball with exotic quantum numbers (2^{+-}) has a mass of about 4 GeV.

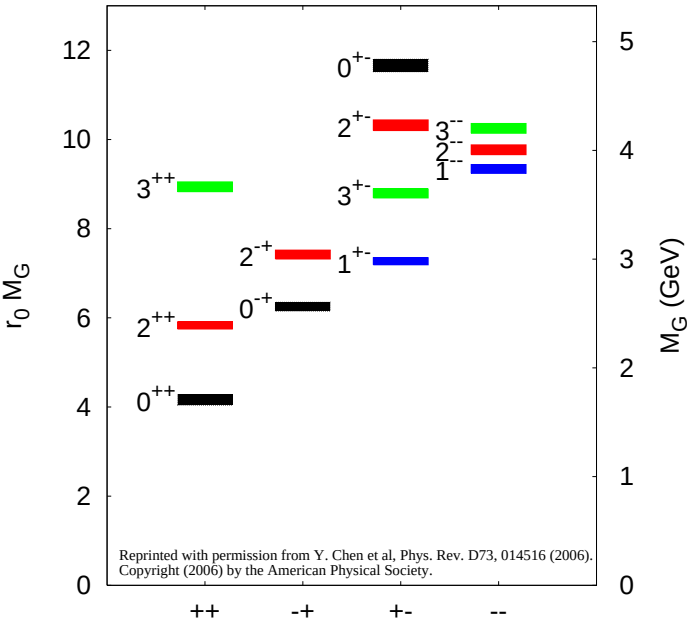

Figure 15.3: Predicted glueball mass spectrum from the lattice in quenched approximation (from Ref. 11)

These calculations are made in the so-called "quenched approximation" which neglects $q\bar{q}$ loops. However, both glue and $q\bar{q}$ states will couple to singlet scalar mesons. Therefore glueballs will mix with nearby $q\bar{q}$ states of the same quantum numbers. For example, the two isoscalar 0^{++} mesons around 1500 MeV will mix with the pure ground state glueball to generate the observed physical states $f_0(1370)$, $f_0(1500)$, and $f_0(1710)$ [8,15]. Lattice calculations are only beginning to include these effects. We return to a discussion of this point in Sec. 15.6.

The existence of three singlet scalar mesons around 1.5 GeV suggests additional degrees of freedom such as glue, since only two mesons are predicted in this mass range. The $f_0(1500)$ [8,15] or, alternatively, the $f_0(1710)$ [12], have been proposed as candidates for the scalar glueball, both states having considerable mixing also with the $f_0(1370)$. Other mixing schemes, in particular with the $f_0(500)$ and the $f_0(980)$, have also been proposed [16]. Details can be found in the "Note on Scalar Mesons" in the Meson Listings and in Ref. 17

Mesons made of $q\bar{q}$ pairs bound by excited gluons g, the hybrid states $q\bar{q}g$, are also predicted. They should lie in the 1.9 GeV mass region, according to gluon flux tube models [18]. Lattice QCD also predicts the lightest hybrid, an exotic 1^{-+}, at a mass of 1.8 to 1.9 GeV [19]. However, the bag model predicts four nonets, among them an exotic 1^{-+} around or above 1.4 GeV [20,21]. There are so far two candidates for exotic states with quantum numbers 1^{-+}, the $\pi_1(1400)$ and $\pi_1(1600)$, which could be hybrids or four-quark states (see the "Note on Non-$q\bar{q}$ Mesons" in the 2006 issue of this *Review* [22] and in Ref. 17)

15.4. Baryons: *qqq* states

Baryons are fermions with baryon number $\mathcal{B} = 1$, *i.e.*, in the most general case, they are composed of three quarks plus any number of quark - antiquark pairs. So far all established baryons are 3-quark (qqq) configurations. The color part of their state functions is an SU(3) singlet, a completely antisymmetric state of the three colors. Since the quarks are fermions, the state function must be antisymmetric under interchange of any two equal-mass quarks (up and down quarks in the limit of isospin symmetry). Thus it can be written as

$$|\,qqq\,\rangle_A = |\,\text{color}\,\rangle_A \times |\,\text{space, spin, flavor}\,\rangle_S\ , \tag{15.21}$$

where the subscripts S and A indicate symmetry or antisymmetry under interchange of any two equal-mass quarks. Note the contrast with the state function for the three nucleons in ^{3}H or ^{3}He:

$$|\,NNN\,\rangle_A = |\,\text{space, spin, isospin}\,\rangle_A\ . \tag{15.22}$$

This difference has major implications for internal structure, magnetic moments, *etc.* (For a nice discussion, see Ref. 23.)

The "ordinary" baryons are made up of u, d, and s quarks. The three flavors imply an approximate flavor SU(3), which requires that baryons made of these quarks belong to the multiplets on the right side of

$$\mathbf{3}\otimes\mathbf{3}\otimes\mathbf{3} = \mathbf{10}_S \oplus \mathbf{8}_M \oplus \mathbf{8}_M \oplus \mathbf{1}_A \tag{15.23}$$

(see Sec. 45, on "SU(n) Multiplets and Young Diagrams"). Here the subscripts indicate symmetric, mixed-symmetry, or antisymmetric states under interchange of any two quarks. The **1** is a uds state (Λ_1), and the octet contains a similar state (Λ_8). If these have the same spin and parity, they can mix. The mechanism is the same as for the mesons (see above). In the ground state multiplet, the SU(3) flavor singlet Λ_1 is forbidden by Fermi statistics. Section 44, on "SU(3) Isoscalar Factors and Representation Matrices," shows how relative decay rates in, say, $\mathbf{10} \to \mathbf{8}\otimes\mathbf{8}$ decays may be calculated.

The addition of the c quark to the light quarks extends the flavor symmetry to SU(4). However, due to the large mass of the c quark, this symmetry is much more strongly broken than the SU(3) of the three light quarks. Figures 15.4(a) and 15.4(b) show the SU(4) baryon multiplets that have as their bottom levels an SU(3) octet, such as the octet that includes the nucleon, or an SU(3) decuplet, such as the decuplet that includes the $\Delta(1232)$. All particles in a given SU(4) multiplet have the same spin and parity. The charmed baryons are discussed in more detail in the "Note on Charmed Baryons" in the Particle Listings. The addition of a b quark extends the flavor symmetry to SU(5); the existence of baryons with t-quarks is very unlikely due to the short lifetime of the t-quark.

For the "ordinary" baryons (no c or b quark), flavor and spin may be combined in an approximate flavor-spin SU(6), in which the six basic states are $d\uparrow$, $d\downarrow$, $\cdots$, $s\downarrow$ ($\uparrow$, $\downarrow$ = spin up, down). Then the baryons belong to the multiplets on the right side of

$$\mathbf{6}\otimes\mathbf{6}\otimes\mathbf{6} = \mathbf{56}_S \oplus \mathbf{70}_M \oplus \mathbf{70}_M \oplus \mathbf{20}_A\ . \tag{15.24}$$

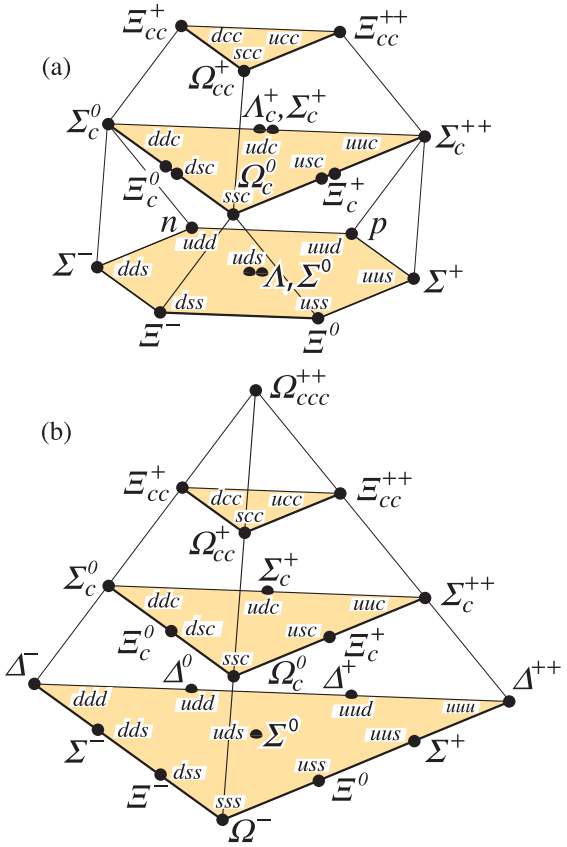

Figure 15.4: SU(4) multiplets of baryons made of u, d, s, and c quarks. (a) The 20-plet with an SU(3) octet. (b) The 20-plet with an SU(3) decuplet.

These SU(6) multiplets decompose into flavor SU(3) multiplets as follows:

$$\mathbf{56} = {}^4\mathbf{10} \oplus {}^2\mathbf{8} \tag{15.25a}$$

$$\mathbf{70} = {}^2\mathbf{10} \oplus {}^4\mathbf{8} \oplus {}^2\mathbf{8} \oplus {}^2\mathbf{1} \tag{15.25b}$$

$$\mathbf{20} = {}^2\mathbf{8} \oplus {}^4\mathbf{1}\ , \tag{15.25c}$$

where the superscript $(2S+1)$ gives the net spin S of the quarks for each particle in the SU(3) multiplet. The $J^P = 1/2^+$ octet containing the nucleon and the $J^P = 3/2^+$ decuplet containing the $\Delta(1232)$ together make up the "ground-state" 56-plet, in which the orbital angular momenta between the quark pairs are zero (so that the spatial part of the state function is trivially symmetric). The **70** and **20** require some excitation of the spatial part of the state function in order to make the overall state function symmetric. States with nonzero orbital angular momenta are classified in SU(6)$\otimes$O(3) supermultiplets.

It is useful to classify the baryons into bands that have the same number N of quanta of excitation. Each band consists of a number of supermultiplets, specified by (D, L_N^P), where D is the dimensionality of the SU(6) representation, L is the total quark orbital angular momentum, and P is the total parity. Supermultiplets contained in bands up to N = 12 are given in Ref. 24. The N = 0 band, which contains the nucleon and $\Delta(1232)$, consists only of the $(56,0_0^+)$ supermultiplet. The N = 1 band consists only of the $(70,1_1^-)$ multiplet and contains the negative-parity baryons with masses below about 1.9 GeV. The N = 2 band contains five supermultiplets: $(56,0_2^+)$, $(70,0_2^+)$, $(56,2_2^+)$, $(70,2_2^+)$, and $(20,1_2^+)$.

The wave functions of the non-strange baryons in the harmonic oscillator basis are often labeled by $|X^{2S+1}L_\pi J^P\rangle$, where S, L, J, P are as above, $X = N$ or Δ, and $\pi = S, M$ or A denotes the symmetry of the spatial wave function. The possible model states for the bands with N=0,1,2 are given in Table 15.5. The assignment of experimentally observed states is only complete and well established

up to the N=1 band. Some more tentative assignments for higher multiplets are suggested in Ref. 25.

In Table 15.6, quark-model assignments are given for many of the established baryons whose SU(6)⊗O(3) compositions are relatively unmixed. One must, however, keep in mind that apart from the mixing of the Λ singlet and octet states, states with same J^P but different L, S combinations can also mix. In the quark model with one-gluon exchange motivated interactions, the size of the mixing is determined by the relative strength of the tensor term with respect to the contact term (see below). The mixing is more important for the decay patterns of the states than for their positions. An example are the lowest lying $(70, 1^-_1)$ states with J^P=1/2$^-$ and 3/2$^-$. The physical states are:

$$|\, N(1535)1/2^-\rangle = \cos(\Theta_S)|N^2P_M1/2^-\rangle - \sin(\Theta_S)|N^4P_M1/2^-\rangle \quad (15.26)$$

$$|\, N(1520)3/2^-\rangle = \cos(\Theta_D)|N^2P_M3/2^-\rangle - \sin(\Theta)_D|N^4P_M3/2^-\rangle \quad (15.27)$$

and the orthogonal combinations for $N(1650)1/2^-$ and $N(1700)3/2^-$. The mixing is large for the J^P=1/2$^-$ states ($\Theta_S \approx$ -32^o), but small for the J^P=3/2$^-$ states ($\Theta_D \approx +6^o$) [26,27].

All baryons of the ground state multiplets are known. Many of their properties, in particular their masses, are in good agreement even with the most basic versions of the quark model, including harmonic (or linear) confinement and a spin-spin interaction, which is responsible for the octet - decuplet mass shifts. A consistent description of the ground-state electroweak properties, however, requires refined relativistic constituent quark models.

The situation for the excited states is much less clear. The assignment of some experimentally observed states with strange quarks to model configurations is only tentative and in many cases candidates are completely missing. Recently, Melde, Plessas and Sengl [28] have calculated baryon properties in relativistic constituent quark models, using one-gluon exchange and Goldstone-boson exchange for the modeling of the hyperfine interactions (see Sec. 15.5 on Dynamics). Both types of models give qualitatively comparable results, and underestimate in general experimentally observed decay widths. Nevertheless, in particular on the basis of the observed decay patterns, the authors have assigned some additional states with strangeness to the SU(3) multiplets and suggest re-assignments for a few others. Among the new assignments are states with weak experimental evidence (two or three star ratings) and partly without firm spin/parity assignments, so that further experimental efforts are necessary before final conclusions can be drawn. We have added their suggestions in Table 15.6.

In the non-strange sector there are two main problems which are illustrated in Fig. 15.5, where the experimentally observed excitation spectrum of the nucleon (N and Δ resonances) is compared to the results of a typical quark model calculation [29]. The lowest states from the N=2 band, the $N(1440)1/2^+$, and the $\Delta(1600)3/2^+$, appear lower than the negative parity states from the N=1 band (see Table 15.5) and much lower than predicted by most models. Also negative parity Δ states from the N=3 band ($\Delta(1900)1/2^-$, $\Delta(1940)3/2^-$, and $\Delta(1930)5/2-$) are too low in energy. Part of the problem could be experimental. Among the negative parity Δ states, only the $\Delta(1930)5/2^-$ has three stars and the uncertainty in the position of the $\Delta(1600)3/2^+$ is large (1550 - 1700 MeV).

Table 15.5: N and Δ states in the N=0,1,2 harmonic oscillator bands. L^P denotes angular momentum and parity, S the three-quark spin and 'sym'=A,S,M the symmetry of the spatial wave function. Only dominant components indicated. Assignments in the N=2 band are partly tentative.

N	sym	L^P	S	$N(I=1/2)$				$\Delta(I=3/2)$			
2	A	1$^+$	1/2	1/2$^+$	3/2$^+$						
2	M	2$^+$	3/2	1/2$^+$	3/2$^+$	5/2$^+$	7/2$^+$				
2	M	2$^+$	1/2		3/2$^+$	5/2$^+$		3/2$^+$	5/2$^+$		
2	M	0$^+$	3/2		3/2$^+$						
2	M	0$^+$	1/2	1/2$^+$				1/2$^+$			
				$N(1710)$				$\Delta(1750)$			
2	S	2$^+$	3/2					1/2$^+$	3/2$^+$	5/2$^+$	7/2$^+$
								$\Delta(1910)$	$\Delta(1920)$	$\Delta(1905)$	$\Delta(1950)$
2	S	2$^+$	1/2		3/2$^+$	5/2$^+$					
					$N(1720)$	$N(1680)$					
2	S	0$^+$	3/2						3/2$^+$		
									$\Delta(1600)$		
2	S	0$^+$	1/2	1/2$^+$							
				$N(1440)$							
1	M	1$^-$	3/2	1/2$^-$	3/2$^-$	5/2$^-$					
				$N(1650)$	$N(1700)$	$N(1675)$					
1	M	1$^-$	1/2	1/2$^-$	3/2$^-$			1/2$^-$	3/2$^-$		
				$N(1535)$	$N(1520)$			$\Delta(1620)$	$\Delta(1700)$		
0	S	0$^+$	3/2						3/2$^+$		
									$\Delta(1232)$		
0	S	0$^+$	1/2	1/2$^+$							
				$N(938)$							

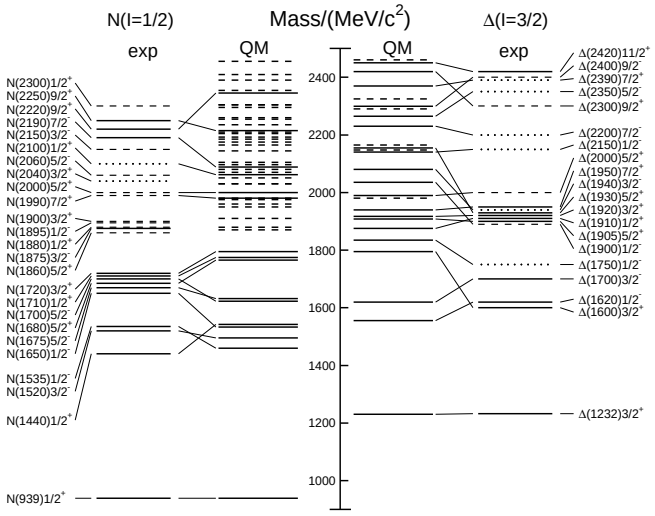

Figure 15.5: Excitation spectrum of the nucleon. Compared are the positions of the excited states identified in experiment, to those predicted by a relativized quark model calculation. Left hand side: isospin $I = 1/2$ N-states, right hand side: isospin $I = 3/2$ Δ-states. Experimental: (columns labeled 'exp'), three- and four-star states are indicated by full lines (two-star dashed lines, one-star dotted lines). At the very left and right of the figure, the spectroscopic notation of these states is given. Quark model [29]: (columns labeled 'QM'), all states for the N=1,2 bands, low-lying states for the N=3,4,5 bands. Full lines: at least tentative assignment to observed states, dashed lines: so far no observed counterparts. Many of the assignments between predicted and observed states are highly tentative.

Furthermore, many more states are predicted than observed. This has been known for a long time as the 'missing resonance' problem [26]. Up to an excitation energy of 2.4 GeV, about 45 N states are predicted, but only 14 are established (four- or three-star; see Note on N and Δ Resonances for the rating of the status of resonances) and 10 are tentative (two- or one-star). Even for the N=2 band, up to now only half of the predicted states have been observed. The most recent partial wave analysis of elastic pion scattering and charge exchange data by Arndt and collaborators [30] has made the situation even worse. They found no evidence for almost half of the states listed in this review (and included in Fig. 15.5). Such analyses are of course biased against resonances which couple only weakly to the $N\pi$ channel. Quark model predictions for the couplings to other hadronic channels and to photons are given in Ref. 29. A large experimental effort is ongoing at several electron accelerators to study the baryon resonance spectrum with real and virtual photon-induced meson production reactions. This includes the search for as-yet-unobserved states, as well as detailed studies of the properties of the low lying states (decay patterns, electromagnetic couplings, magnetic moments, *etc.*) (see Ref. 31 for recent reviews). This experimental effort has currently entered its final phase with the measurement of single and double polarization observables for many different meson production channels, so that a much better understanding of the experimental spectrum can be expected for the near future.

In quark models, the number of excited states is determined by the effective degrees of freedom, while their ordering and decay properties are related to the residual quark - quark interaction. An overview of quark models for baryons is given in Ref. 27, a recent discussion of baryon spectroscopy is given in Ref. 25. The effective degrees of freedom in the standard nonrelativistic quark model are three equivalent valence quarks with one-gluon exchange-motivated, flavor-independent color-magnetic interactions. A different class of models uses interactions which give rise to a quark - diquark clustering of the baryons (for a review see Ref. 32). If there is a tightly bound diquark, only two degrees of freedom are available at low energies, and thus *fewer* states are predicted. Furthermore, selection rules in the

Table 15.6: Quark-model assignments for some of the known baryons in terms of a flavor-spin SU(6) basis. Only the dominant representation is listed. Assignments for several states, especially for the $\Lambda(1810)$, $\Lambda(2350)$, $\Xi(1820)$, and $\Xi(2030)$, are merely educated guesses. † recent suggestions for assignments and re-assignments from Ref. [28]. For assignments of the charmed baryons, see the "Note on Charmed Baryons" in the Particle Listings.

J^P	$(D, L_N^P)\,S$	Octet members			Singlets
$1/2^+$	$(56,0_0^+)\ 1/2$	$N(939)$	$\Lambda(1116)$	$\Sigma(1193)$	$\Xi(1318)$	
$1/2^+$	$(56,0_2^+)\ 1/2$	$N(1440)$	$\Lambda(1600)$	$\Sigma(1660)$	$\Xi(1690)^\dagger$	
$1/2^-$	$(70,1_1^-)\ 1/2$	$N(1535)$	$\Lambda(1670)$	$\Sigma(1620)$	$\Xi(?)$	$\Lambda(1405)$
				$\Sigma(1560)^\dagger$		
$3/2^-$	$(70,1_1^-)\ 1/2$	$N(1520)$	$\Lambda(1690)$	$\Sigma(1670)$	$\Xi(1820)$	$\Lambda(1520)$
$1/2^-$	$(70,1_1^-)\ 3/2$	$N(1650)$	$\Lambda(1800)$	$\Sigma(1750)$	$\Xi(?)$	
				$\Sigma(1620)^\dagger$		
$3/2^-$	$(70,1_1^-)\ 3/2$	$N(1700)$	$\Lambda(?)$	$\Sigma(1940)^\dagger$	$\Xi(?)$	
$5/2^-$	$(70,1_1^-)\ 3/2$	$N(1675)$	$\Lambda(1830)$	$\Sigma(1775)$	$\Xi(1950)^\dagger$	
$1/2^+$	$(70,0_2^+)\ 1/2$	$N(1710)$	$\Lambda(1810)$	$\Sigma(1880)$	$\Xi(?)$	$\Lambda(1810)^\dagger$
$3/2^+$	$(56,2_2^+)\ 1/2$	$N(1720)$	$\Lambda(1890)$	$\Sigma(?)$	$\Xi(?)$	
$5/2^+$	$(56,2_2^+)\ 1/2$	$N(1680)$	$\Lambda(1820)$	$\Sigma(1915)$	$\Xi(2030)$	
$7/2^-$	$(70,3_3^-)\ 1/2$	$N(2190)$	$\Lambda(?)$	$\Sigma(?)$	$\Xi(?)$	$\Lambda(2100)$
$9/2^-$	$(70,3_3^-)\ 3/2$	$N(2250)$	$\Lambda(?)$	$\Sigma(?)$	$\Xi(?)$	
$9/2^+$	$(56,4_4^+)\ 1/2$	$N(2220)$	$\Lambda(2350)$	$\Sigma(?)$	$\Xi(?)$	
		Decuplet members				
$3/2^+$	$(56,0_0^+)\ 3/2$	$\Delta(1232)$	$\Sigma(1385)$	$\Xi(1530)$	$\Omega(1672)$	
$3/2^+$	$(56,0_2^+)\ 3/2$	$\Delta(1600)$	$\Sigma(1690)^\dagger$	$\Xi(?)$	$\Omega(?)$	
$1/2^-$	$(70,1_1^-)\ 1/2$	$\Delta(1620)$	$\Sigma(1750)^\dagger$	$\Xi(?)$	$\Omega(?)$	
$3/2^-$	$(70,1_1^-)\ 1/2$	$\Delta(1700)$	$\Sigma(?)$	$\Xi(?)$	$\Omega(?)$	
$5/2^+$	$(56,2_2^+)\ 3/2$	$\Delta(1905)$	$\Sigma(?)$	$\Xi(?)$	$\Omega(?)$	
$7/2^+$	$(56,2_2^+)\ 3/2$	$\Delta(1950)$	$\Sigma(2030)$	$\Xi(?)$	$\Omega(?)$	
$11/2^+$	$(56,4_4^+)\ 3/2$	$\Delta(2420)$	$\Sigma(?)$	$\Xi(?)$	$\Omega(?)$	

decay pattern may arise from the quantum numbers of the diquark. *More* states are predicted by collective models of the baryon like the algebraic approach in Ref. 33. In this approach, the quantum numbers of the valence quarks are distributed over a Y-shaped string-like configuration, and additional states arise *e.g.*, from vibrations of the strings. *More* states are also predicted in the framework of flux-tube models (see Ref. 34), which are motivated by lattice QCD. In addition to the quark degrees of freedom, flux-tubes responsible for the confinement of the quarks are considered as degrees of freedom. These models include hybrid baryons containing explicit excitations of the gluon fields. However, since all half integral J^P quantum numbers are possible for ordinary baryons, such 'exotics' will be very hard to identify, and probably always mix with ordinary states. So far, the experimentally observed number of states is still far lower even than predicted by the quark–diquark models.

Recently, the influence of chiral symmetry on the excitation spectrum of the nucleon has been hotly debated from a somewhat new perspective. Chiral symmetry, the fundamental symmetry of QCD, is strongly broken for the low lying states, resulting in large mass differences of parity partners like the $J^P{=}1/2^+$ $N(938)1/2^+$ ground state and the $J^P{=}1/2^-$ $N(1535)1/2^-$ excitation. However, at higher excitation energies there is some evidence for parity doublets and even some very tentative suggestions for full chiral multiplets of N^* and Δ resonances. An effective restoration of chiral symmetry at high excitation energies due to a decoupling from the quark condensate of the vacuum has been discussed (see Ref. 35 for recent reviews) as a possible cause. In this case, the mass generating mechanisms

for low and high lying states would be essentially different. As a further consequence, the parity doublets would decouple from pions, so that experimental bias would be worse. However, parity doublets might also arise from the spin-orbital dynamics of the 3-quark system. Presently, the status of data does not allow final conclusions.

The most recent developments on the theory side are the first unquenched lattice calculations for the excitation spectrum discussed in Sec. 15.6. The results are basically consistent with the level counting of SU(6)⊗O(3) in the standard non-relativistic quark model and show no indication for quark-diquark structures or parity doubling. Consequently, there is as yet no indication from lattice that the mis-match between the excitation spectrum predicted by the standard quark model and experimental observations is due to inappropriate degrees of freedom in the quark model.

15.5. Dynamics

Quantum chromodynamics (QCD) is well-established as the theory for the strong interactions. As such, one of the goals of QCD is to predict the spectrum of strongly-interacting particles. To date, the only first-principles calculations of spectroscopy from QCD use lattice methods. These are the subject of Sec. 15.6. These calculations are difficult and unwieldy, and many interesting questions do not have a good lattice-based method of solution. Therefore, it is natural to build models, whose ingredients are abstracted from QCD, or from the low-energy limit of QCD (such as chiral Lagrangians) or from the data itself. The words "quark model" are a shorthand for such phenomenological models. Many specific quark models exist, but most contain a similar basic set of dynamical ingredients. These include:

i) A confining interaction, which is generally spin-independent (*e.g.*, harmonic oscillator or linear confinement);

ii) Different types of spin-dependent interactions:

a) commonly used is a color-magnetic flavor-independent interaction modeled after the effects of gluon exchange in QCD (see *e.g.*, Ref. 36) For example, in the S-wave states, there is a spin-spin hyperfine interaction of the form

$$H_{HF} = -\alpha_S M \sum_{i>j} (\overrightarrow{\sigma}\lambda_a)_i (\overrightarrow{\sigma}\lambda_a)_j \ , \tag{15.28}$$

where M is a constant with units of energy, λ_a $(a = 1, \cdots, 8,)$ is the set of SU(3) unitary spin matrices, defined in Sec. 44, on "SU(3) Isoscalar Factors and Representation Matrices," and the sum runs over constituent quarks or antiquarks. Spin-orbit interactions, although allowed, seem to be small in general, but a tensor term is responsible for the mixing of states with the same J^P but different L, S combinations.

b) other approaches include flavor-dependent short-range quark forces from instanton effects (see *e.g.*, Ref. 37) This interaction acts only on scalar, isoscalar pairs of quarks in a relative S-wave state:

$$\langle q^2; S, L, T|W|q^2; S, L, T\rangle = -4g\delta_{S,0}\delta_{L,0}\delta_{I,0}\mathcal{W} \tag{15.29}$$

where $\mathcal{W}$ is the radial matrix element of the contact interaction.

c) a rather different and controversially discussed approach is based on flavor-dependent spin-spin forces arising from one-boson exchange. The interaction term is of the form:

$$H_{HF} \propto \sum_{i<j} V(\overrightarrow{r}_{ij})\lambda_i^F \cdot \lambda_j^F \overrightarrow{\sigma}_i \cdot \overrightarrow{\sigma}_j \tag{15.30}$$

where the λ_i^F are in flavor space (see *e.g.*, Ref. 38).

iii) A strange quark mass somewhat larger than the up and down quark masses, in order to split the SU(3) multiplets;

iv) In the case of spin-spin interactions (iia,c), a flavor-symmetric interaction for mixing $q\overline{q}$ configurations of different flavors (*e.g.*, $u\overline{u} \leftrightarrow d\overline{d} \leftrightarrow s\overline{s}$), in isoscalar channels, so as to reproduce *e.g.*, the η - η' and ω - ϕ mesons.

These ingredients provide the basic mechanisms that determine the hadron spectrum in the standard quark model.

15.6. Lattice Calculations of Hadronic Spectroscopy

Lattice calculations are a major source of information about QCD masses and matrix elements. The necessary theoretical background is given in Sec. 18 of this *Review*. Here we confine ourselves to some general comments and illustrations of lattice calculations for spectroscopy.

In general, the cleanest lattice results come from computations of processes in which there is only one particle in the simulation volume. These quantities include masses of hadrons, simple decay constants, like pseudoscalar meson decay constants, and semileptonic form factors (such as the ones appropriate to $B \to Dl\nu$, $Kl\nu$, $\pi l\nu$). The cleanest predictions for masses are for states which have narrow decay widths and are far below any thresholds to open channels, since the effects of final state interactions are not yet under complete control on the lattice. As a simple corollary, the lightest state in a channel is easier to study than the heavier ones. "Difficult" states for the quark model (such as exotics) are also difficult for the lattice because of the lack of simple operators which couple well to them.

Good-quality modern lattice calculations will present multi-part error budgets with their predictions. A small part of the uncertainty is statistical, from sample size. Typically, the quoted statistical uncertainty includes uncertainty from a fit: it is rare that a simulation computes one global quantity which is the desired observable. Simulations which include virtual quark-antiquark pairs (also known as "dynamical quarks" or "sea quarks") are often done at up and down quark mass values heavier than the experimental ones, and it is then necessary to extrapolate in these quark masses. Simulations can work at the physical values of the heavier quarks' masses. They are always done at nonzero lattice spacing, and so it is necessary to extrapolate to zero lattice spacing. Some theoretical input is needed to do this. Much of the uncertainty in these extrapolations is systematic, from the choice of fitting function. Other systematics include the effect of finite simulation volume, the number of flavors of dynamical quarks actually simulated, and technical issues with how these dynamical quarks are included. The particular choice of a fiducial mass (to normalize other predictions) is not standardized; there are many possible choices, each with its own set of strengths and weaknesses, and determining it usually requires a second lattice simulation from that used to calculate the quantity under consideration.

A systematic error of major historical interest is the "quenched approximation," in which dynamical quarks are simply left out of the simulation. This was done because the addition of these virtual pairs presented an expensive computational problem. No generally-accepted methodology has ever allowed one to correct for quenching effects, short of redoing all calculations with dynamical quarks. Recent advances in algorithms and computer hardware have rendered it obsolete.

With these brief remarks, we turn to examples. The field of lattice QCD simulations is vast, and so it is not possible to give a comprehensive review of them in a small space. The history of lattice QCD simulations is a story of thirty years of incremental improvements in physical understanding, algorithm development, and ever faster computers, which have combined to bring the field to a present state where it is possible to carry out very high quality calculations. We present a few representative illustrations, to show the current state of the art.

By far, the major part of all lattice spectroscopy is concerned with that of the light hadrons, and so we illustrate results in Fig. 15.6, a comprehensive summary provided by A. Kronfeld [39].

Flavor singlet mesons are at the frontier of lattice QCD calculations, because one must include the effects of "annihilation graphs," for the valence q and $\bar{q}$. Recently, the RBC and UKQCD collaborations, Ref. 6, have reported a calculation of the η and η' mesons, finding masses of 573(6) and 947(142) MeV, respectively. The singlet-octet mixing angle (in the conventions of Table 15.2) is $\theta_{lin} = -14.1(2.8)°$.

The spectroscopy of mesons containing heavy quarks has become a truly high-precision endeavor. These simulations use Non-Relativistic QCD (NRQCD) or Heavy Quark Effective Theory (HQET), systematic

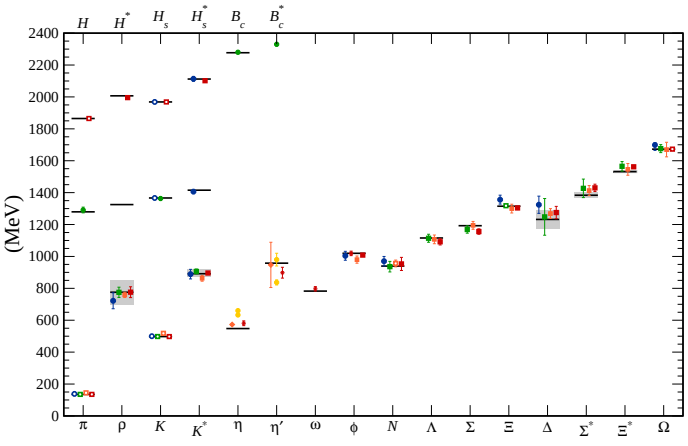

Figure 15.6: Lattice results for spectroscopy. The plot combines data for mesons and baryons from the MILC [40,41], PACS-CS [42], BMW [43] and QCDSF [44] collaborations. The results for the η and η' are from the RBC and UKQCD collaborations [6], the Hadron Spectrum collaboration (they also measured the ω) [45] and UKQCD [46]. Data for heavy-light hadrons comes from the Fermilab-MILC collaboration [47], HPQCD [48], and Mohler and Woloshyn [49]. Circles, squares, and diamonds represent different kinds of lattice discretizations for fermions: staggered, Wilson and chiral sea quarks. Asterisks show lattices with different spatial and temporal lattice spacings. Open symbols show the masses which were used to fix parameters. Red, orange, yellow, green, and blue stand for increasing numbers of ensembles (different lattice spacings and quark masses). Horizontal bands and gray boxes show experimentally measured masses and widths. The b-mesons are offset by about 4 GeV.

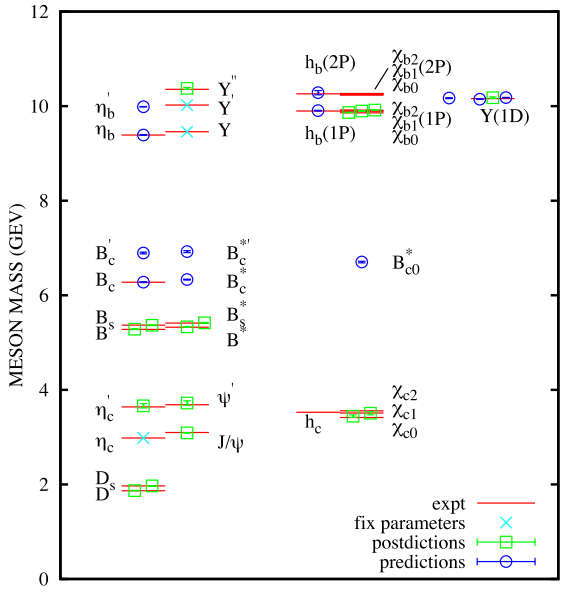

Figure 15.7: Spectroscopy for mesonic systems containing one or more heavy quarks (adapted from Ref. 50) Particles whose masses are used to fix lattice parameters are shown with crosses; the authors distinguish between "predictions" and "postdictions" of their calculation. Lines represent experiment.

expansions of the QCD Lagrangian in powers of the heavy quark velocity, or the heavy quark mass. Terms in the Lagrangian have obvious quark model analogs, but are derived directly from QCD. For example, the heavy quark potential is a derived quantity, extracted from simulations. Fig. 15.7 shows the mass spectrum for mesons containing at least one heavy (b or c) quark from Ref. 50 It also contains results from Refs. [51] and [52]. The calculations uses a discretization of nonrelativistic QCD for bottom quarks with charm and lighter quarks being handled with an improved relativistic action. Four flavors (u, d, s, c) of dynamical quarks are included.

Finally, Fig. 15.8 and Fig. 15.9 show recent lattice calculations of singly and double charmed baryons. These figures were provided by S. Collins and are based on ones in the review Ref. 53. Here we are at the forefront of theory and experiment.

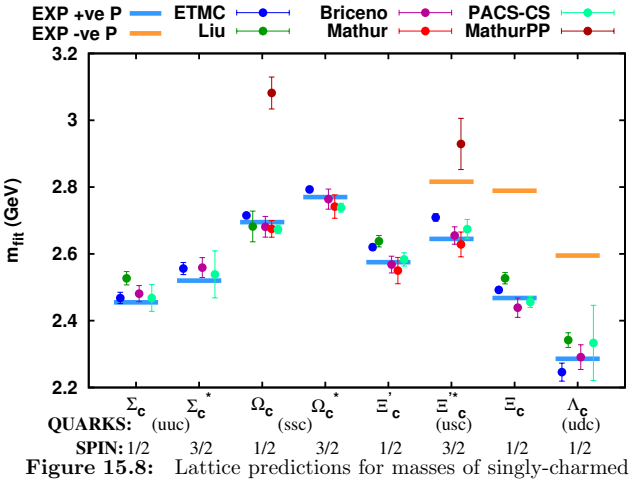

Figure 15.8: Lattice predictions for masses of singly-charmed baryons. Data are labeled ETMC, Ref. 54 Liu, Ref. 55; Briceno, Ref. 56; PACS-CS, Ref. 57; and Mathur and Mathur-PP, Ref. 58. Lines are from experiment (positive and negative parity states).

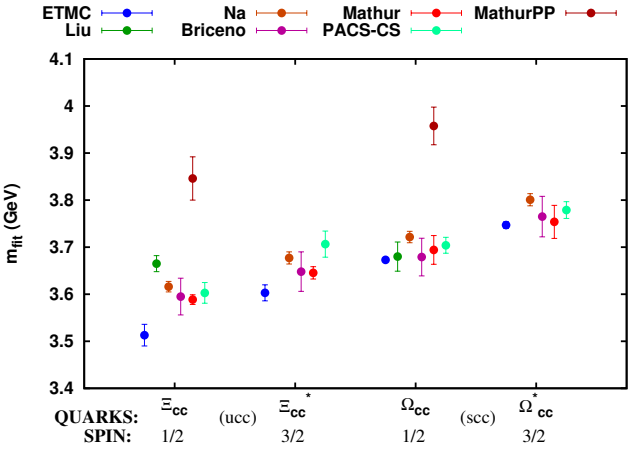

Figure 15.9: Lattice predictions for masses of doubly-charmed baryons. Data are ETMC, Ref. 54; Liu, Ref. 55; Briceno, Ref. 56; PACS-CS, Ref. 57; Mathur and Mathur-PP, Ref. 58. and Na, Ref. 59.

Recall that lattice calculations take operators which are interpolating fields with quantum numbers appropriate to the desired states, compute correlation functions of these operators, and fit the correlation functions to functional forms parametrized by a set of masses and matrix elements. As we move away from hadrons which can be created by the simplest quark model operators (appropriate to the lightest meson and baryon multiplets) we encounter a host of new problems: either no good interpolating fields, or too many possible interpolating fields, and many states with the same quantum numbers. Techniques for dealing with these interrelated problems vary from collaboration to collaboration, but all share common features: typically, correlation functions from many different interpolating fields are used, and the signal is extracted in what amounts to a variational calculation using the chosen operator basis. In addition to mass

spectra, wave function information can be garnered from the form of the best variational wave function. Of course, the same problems which are present in the spectroscopy of the lightest hadrons (the need to extrapolate to infinite volume, physical values of the light quark masses, and zero lattice spacing) are also present. We briefly touch on three different kinds of hadrons: excited states of baryons, glueballs, and hybrid mesons. The quality of the data is not as good as for the ground states, and so the results continue to evolve.

Ref. 60 is a good recent review of excited baryon spectroscopy. The interesting physics questions to be addressed are precisely those enumerated in the last section. An example of a recent calculation, due to Ref. 61 is shown in Fig. 15.10. Notice that the pion is not yet at its physical value. The lightest positive parity state is the nucleon, and the Roper resonance has not yet appeared as a light state.

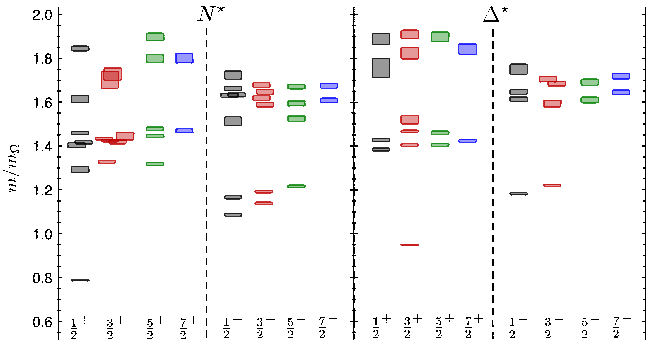

Figure 15.10: Spin-identified spectrum of nucleons and deltas, from lattices where $m_\pi = 396$ MeV, in units of the calculated Ω mass, from Ref. 61. The colors just correspond to the different J assignments: grey for $J = 1/2$, red for $J = 3/2$, green for 5/2, blue for $J = 7/2$.

Exotic mesons share the difficulties of ordinary excited states, and some recent calculations actually include both kinds of states in their combined fits. Ref. 62 provides a good summary of the theoretical and experimental situation regarding mesons with exotic quantum numbers, including a compilation of lattice data. The lightest exotics, the h_0, η_1, and h_2, have long been targets of lattice studies. Recently, the authors of Ref. 45 have presented new results for isoscalar and isovector meson spectroscopy, which observe the three states around 2 GeV. Again, the light quark masses in the simulations are higher than in nature; the pion is at 396 MeV.

In Fig. 15.3 we showed a figure from Ref. 11 showing a lattice prediction for the glueball mass spectrum in quenched approximation. A true QCD prediction of the glueball spectrum requires dynamical light quarks and (because glueball operators are intrinsically noisy) high statistics. Only recently have the first useful such calculations appeared. Fig. 15.11 shows results from Ref. 63, done with dynamical u, d and s quarks at two lattice spacings, 0.123 and 0.092 fm, along with comparisons to the quenched lattice calculation of Ref. 10 and to experimental isosinglet mesons. The dynamical simulation is, of course, not the last word on this subject, but it shows that the effects of quenching seem to be small.

Several other features of hadronic spectroscopy are also being studied on the lattice.

Electromagnetic mass splittings (such as the neutron - proton mass difference) are interesting but difficult. The mass difference has two origins: the first is that the up and down quarks have slightly different masses. The second is that the quarks have (different) charges, so electromagnetic interactions must be included in the simulations. This creates a host of technical issues. An important one is that electromagnetic interactions are long range, but lattice simulations are done in finite volumes. Two recent calculations, Refs. [64] and [65], find reasonable agreement with experiment. The situation is summarized in the review Ref. 66.

Most hadrons are resonances, and their widths are the last target of lattice simulations we will mention. The actual calculation is of the combined mass of two (or more) hadrons in a box of finite size.

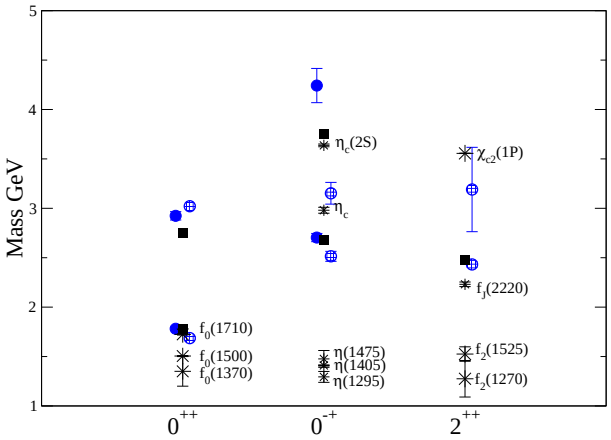

Figure 15.11: Lattice QCD predictions for glueball masses. The open and closed circles are the larger and smaller lattice spacing data of the full QCD calculation of glueball masses of Ref. 63. Squares are the quenched data for glueball masses of Ref. 10. The bursts labeled by particle names are experimental states with the appropriate quantum numbers.

The combined mass is shifted from being the sum of the individual masses because the finite box forces the hadrons to interact with each other. The volume-dependent mass shift yields the phase shift for the continuum scattering amplitude, which in turn can be used to extract the resonance mass and width, with some degree of modeling. So far only two-body resonances, the rho meson and a few others, have been well studied. This is an active research topic, and recent reviews, Ref. 67, summarize the situation.

References:

1. J. Schwinger, Phys. Rev. **135**, B116 (1964).
2. A. Bramon *et al.*, Phys. Lett. **B403**, 339 (1997).
3. A. Aloisio *et al.*, Phys. Lett. **B541**, 45 (2002).
4. C. Amsler *et al.*, Phys. Lett. **B294**, 451 (1992).
5. C. Amsler, Rev. Mod. Phys. **70**, 1293 (1998).
6. N.H. Christ *et al.*, Phys. Rev. Lett. **105**, 241601 (2010).
7. T. Feldmann, Int. J. Mod. Phys. **A915**, 159 (2000).
8. C. Amsler and F.E. Close, Phys. Rev. **D53**, 295 (1996).
9. R.L. Jaffe, Phys. Rev. **D 15** 267, 281 (1977).
10. C. Morningstar and M. Peardon, Phys. Rev. **D60**, 034509 (1999).
11. Y. Chen *et al.*, Phys. Rev. **D73**, 014516 (2006).
12. W.J. Lee and D. Weingarten, Phys. Rev. **D61**, 014015 (2000).
13. G.S. Bali, et. al. Phys. Lett. **B309**, 378 (1993).
14. C. Michael, *AIP Conf. Proc.* **432**, 657 (1998).
15. F.E. Close and A. Kirk, Eur. Phys. J. **C21**, 531 (2001).
16. W. Ochs, J. Phys. G: Nucl. Part. Phys. **40**, 043001 (2013).
17. C. Amsler and N.A. Törnqvist, Phys. Reports **389**, 61 (2004).
18. N. Isgur and J. Paton, Phys. Rev. **D31**, 2910 (1985).
19. P. Lacock *et al.*, Phys. Lett. **B401**, 308 (1997);
    C. Bernard *et al.*, Phys. Rev. **D56**, 7039 (1997);
    C. Bernard *et al.*, Phys. Rev. **D68**, 074505 (2003).
20. M. Chanowitz and S. Sharpe, Nucl. Phys. **B222**, 211 (1983).
21. T. Barnes *et al.*, Nucl. Phys. **B224**, 241 (1983).
22. W.-M Yao *et al.*, J. Phys. **G33**, 1 (2006).
23. F.E. Close, in *Quarks and Nuclear Forces* (Springer-Verlag, 1982), p. 56.
24. R.H. Dalitz and L.J. Reinders, in "Hadron Structure as Known from Electromagnetic and Strong Interactions," *Proceedings of the Hadron '77 Conference* (Veda, 1979), p. 11.
25. E. Klempt and J.M. Richard, Rev. Mod. Phys. **82**, 1095 (2010).
26. N. Isgur and G. Karl, Phys. Rev. **D18**, 4187 (1978); *ibid.*, **D19**, 2653 (1979); *ibid.*, **D20**, 1191 (1979).
27. S. Capstick and W. Roberts, Prog. Part. Nucl. Phys. **45**, 241 (2000).
28. T. Melde, W. Plessas, and B. Sengl, Phys. Rev. **D77**, 114002 (2008).

29. S. Capstick and W. Roberts, Phys. Rev. **D49**, 4570 (1994); *ibid.*, **D57**, 4301 (1998); *ibid.*, **D58**, 074011 (1998); S. Capstick, Phys. Rev. **D46**, 2864 (1992).
30. R.A. Arndt *et al.*, Phys. Rev. **C74**, 045205 (2006).
31. B. Krusche and S. Schadmand, Prog. Part. Nucl. Phys. **51**, 399 (2003); V.D. Burkert and T.-S.H. Lee, Int. J. Mod. Phys. **E13**, 1035 (2004); see also A.J.G. Hey and R.L. Kelly, Phys. Reports **96**, 71 (1983).
32. M. Anselmino *et al.*, Rev. Mod. Phys. **65**, 1199 (1993).
33. R. Bijker *et al.*, Ann. of. Phys. **236** 69 (1994).
34. N. Isgur and J. Paton, Phys. Rev. **D31**, 2910 (1985); S. Capstick and P.R. Page, Phys. Rev. **C66**, 065204 (2002).
35. R.L. Jaffe, D. Pirjol, and A. Scardicchio, Phys. Rept. **435** 157 (2006); L. Ya. Glozman, Phys. Rept. **444**, 1 (2007).
36. A. De Rujula *et al.*, Phys. Rev. **D12**, 147 (1975).
37. W.H. Blask *et al.*, Z. Phys. **A337** 327 (1990); U. Löring *et al.*, Eur. Phys. J. **A10** 309 (2001); U. Löring *et al.*, Eur. Phys. J. **A10** 395 (2001); *ibid.*, **A10** 447 (2001).
38. L.Y. Glozman and D.O. Riska, Phys. Rept. **268**, 263 (1996); L.Y. Glozman *et al.*, Phys. Rev. **D58**, 094030 (1998).
39. A. Kronfeld, private comunication. See also Ann. Rev. Nucl. Part. Sci. **62**, 265 (2012).
40. C. Aubin *et al.* [MILC Collab.], Phys. Rev. **D70**, 094505 (2004).
41. A. Bazavov *et al.*, Rev. Mod. Phys. **82**, 1349 (2010).
42. S. Aoki *et al.* [PACS-CS Collab.], Phys. Rev. D **79**, 034503 (2009).
43. S. Durr *et al.*, Science **322**, 1224 (2008).
44. W. Bietenholz *et al.*, Phys. Rev. D **84**, 054509 (2011).
45. J. J. Dudek *et al.*, Phys. Rev. D **83**, 111502 (2011) *ibid.*, Phys. Rev. D **82**, 034508 (2010); *ibid.*, Phys. Rev. Lett. **103**, 262001 (2009).
46. E. B. Gregory *et al.* [UKQCD Collab.], Phys. Rev. D **86**, 014504 (2012).
47. C. Bernard *et al.* [Fermilab Lattice and MILC Collabs.], Phys. Rev. D **83**, 034503 (2011).
48. E.B. Gregory *et al.*, Phys. Rev. **D83**, 014506 (2011); C.T.H. Davies *et al.*, Phys. Rev. **D82**, 114504 (2010); E.B. Gregory *et al.*, Phys. Rev. Lett. **104**, 022001 (2010).
49. D. Mohler and R. M. Woloshyn, Phys. Rev. D **84** (2011) 054505.
50. R. J. Dowdall *et al.*, Phys. Rev. **D86**, 094510 (2012).
51. J. O. Daldrop *et al.* [HPQCD Collab.], Phys. Rev. Lett. **108**, 102003 (2012).
52. G. C. Donald *et al.*, Phys. Rev. **D86**, 094501 (2012).
53. G. Bali, S. Collins, and P. Perez-Rubio, J. Phys. Conf. Ser. **426**, 012017 (2013).
54. C. Alexandrou *et al.*, Phys. Rev. **D86**, 114501 (2012).
55. L. Liu *et al.*, Phys. Rev. **D81**, 094505 (2010).
56. R. A. Briceno, H. -W. Lin, and D. R. Bolton, Phys. Rev. **D86**, 094504 (2012).
57. Y. Namekawa [PACS-CS Collab.], PoS LATTICE **2012**, 139 (2012).
58. S. Basak *et al.*, PoS LATTICE **2012**, 141 (2012).
59. H. Na and S.A. Gottlieb, PoS **LAT2007**, 124 (2007); PoS **LATTICE2008**, 119 (2008).
60. H.W. Lin, Chin. J. Phys. **49**, 827 (2011).
61. R.G. Edwards *et al.*, Phys. Rev. **D84**, 074508 (2011).
62. C.A. Meyer and Y. Van Haarlem, Phys. Rev. C **82**, 025208 (2010).
63. C.M. Richards *et al.*, [UKQCD Collab.], Phys. Rev. **D82**, 034501 (2010).
64. T. Blum *et al.*, Phys. Rev. **D82**, 094508 (2010).
65. S. Borsanyi *et al.*, *et al.*, `arXiv:1306.2287 [hep-lat]`.
66. A. Portelli, `arXiv:1307.6056 [hep-lat]`.
67. S. Prelovsek *et al.*, `arXiv:1304.2143 [hep-ph]`; D. Mohler, PoS LATTICE **2012**, 003 (2012).

16. GRAND UNIFIED THEORIES

Revised October 2011 by S. Raby (Ohio State University).

16.1. Grand Unification

16.1.1. *Standard Model : An Introduction* :

In spite of all the successes of the Standard Model [SM] it is unlikely to be the final theory. It leaves many unanswered questions. Why the local gauge interactions $SU(3)_C \times SU(2)_L \times U(1)_Y$ and why 3 families of quarks and leptons? Moreover why does one family consist of the states $[Q, u^c, d^c; L, e^c]$ transforming as $[(3,2,1/3), (\bar{3},1,-4/3), (\bar{3},1,2/3); (1,2,-1), (1,1,2)]$, where $Q = (u,d)$ and $L = (\nu, e)$ are $SU(2)_L$ doublets and u^c, d^c, e^c are charge conjugate $SU(2)_L$ singlet fields with the $U(1)_Y$ quantum numbers given? [We use the convention that electric charge $Q_{EM} = T_{3L} + Y/2$ and all fields are left handed Weyl spinors.] Note the SM gauge interactions of quarks and leptons are completely fixed by their gauge charges. Thus if we understood the origin of this charge quantization, we would also understand why there are no fractionally charged hadrons. Finally, what is the origin of quark and lepton masses or the apparent hierarchy of family masses and quark and leptonic mixing angles? Perhaps if we understood this, we would also know the origin of CP violation, the solution to the strong CP problem, the origin of the cosmological matter - antimatter asymmetry. In addition, it lacks an explanation for the observed dark matter and dark energy of the universe.

The SM has 19 arbitrary parameters; their values are chosen to fit the data. Three arbitrary gauge couplings: g_3, g, g' (where g, g' are the $SU(2)_L$, $U(1)_Y$ couplings, respectively) or equivalently $\alpha_s = (g_3^2/4\pi)$, $\alpha_{EM} = (e^2/4\pi)$ $(e = g \sin\theta_W)$ and $\sin^2\theta_W = (g')^2/(g^2 + (g')^2)$. In addition there are 13 parameters associated with the 9 charged fermion masses and the four mixing angles in the CKM matrix. The remaining 3 parameters are v, λ [the Higgs VEV and quartic coupling] (or equivalently M_Z, m_h^0) and the QCD θ parameter. In addition, data from neutrino oscillation experiments provide convincing evidence for neutrino masses. With 3 light Majorana neutrinos there are at least 9 additional parameters in the neutrino sector; 3 masses and 6 mixing angles and phases. In summary, the SM has too many arbitrary parameters and leaves open too many unresolved questions to be considered complete. These are the problems which grand unified theories hope to address.

16.1.2. *Charge Quantization* :

In the Standard Model, quarks and leptons are on an equal footing; both fundamental particles without substructure. It is now clear that they may be two faces of the same coin; unified, for example, by extending QCD (or $SU(3)_C$) to include leptons as the fourth color, $SU(4)_C$ [1]. The complete Pati-Salam gauge group is $SU(4)_C \times SU(2)_L \times SU(2)_R$ with the states of one family $[(Q,L),(Q^c,L^c)]$ transforming as $[(4,2,1), (\bar{4},1,\bar{2})]$ where $Q^c = (d^c, u^c)$, $L^c = (e^c, \nu^c)$ are doublets under $SU(2)_R$. Electric charge is now given by the relation $Q_{EM} = T_{3L} + T_{3R} + 1/2(B-L)$ and $SU(4)_C$ contains the subgroup $SU(3)_C \times (B-L)$ where B (L) is baryon (lepton) number. Note ν^c has no SM quantum numbers and is thus completely "sterile". It is introduced to complete the $SU(2)_R$ lepton doublet. This additional state is desirable when considering neutrino masses.

Although quarks and leptons are unified with the states of one family forming two irreducible representations of the gauge group; there are still 3 independent gauge couplings (two if one also imposes parity, i.e. $L \leftrightarrow R$ symmetry). As a result the three low energy gauge couplings are still independent arbitrary parameters. This difficulty is resolved by embedding the SM gauge group into the simple unified gauge group, Georgi-Glashow $SU(5)$, with one universal gauge coupling α_G defined at the grand unification scale M_G [2]. Quarks and leptons still sit in two irreducible representations, as before, with a $\mathbf{10} = [Q, u^c, e^c]$ and $\bar{\mathbf{5}} = [d^c, L]$. Nevertheless, the three low energy gauge couplings are now determined in terms of two independent parameters : α_G and M_G. Hence there is one prediction.

In order to break the electroweak symmetry at the weak scale and give mass to quarks and leptons, Higgs doublets are needed which can sit in either a $\mathbf{5_H}$ or $\bar{\mathbf{5}}_\mathbf{H}$. The additional 3 states are color triplet Higgs scalars. The couplings of these color triplets violate baryon and lepton number and nucleons decay via the exchange of a single color triplet Higgs scalar. Hence in order not to violently disagree with the non-observation of nucleon decay, their mass must be greater than $\sim 10^{11}$ GeV [3]. Moreover, in supersymmetric GUTs, in order to cancel anomalies as well as give mass to both up and down quarks, both Higgs multiplets $\mathbf{5_H}$, $\bar{\mathbf{5}}_\mathbf{H}$ are required. As we shall discuss later, nucleon decay now constrains the color triplet Higgs states in a SUSY GUT to have mass significantly greater than M_G.

Complete unification is possible with the symmetry group $SO(10)$ with one universal gauge coupling α_G and one family of quarks and leptons sitting in the 16 dimensional spinor representation $\mathbf{16} = [\mathbf{10} + \bar{\mathbf{5}} + \mathbf{1}]$ [4]. The $SU(5)$ singlet $\mathbf{1}$ is identified with ν^c. In Table 1 we present the states of one family of quarks and leptons, as they appear in the **16**. It is an amazing and perhaps even profound fact that all the states of a single family of quarks and leptons can be represented digitally as a set of 5 zeros and/or ones or equivalently as the tensor product of 5 "spin" 1/2 states with $\pm = |\pm\frac{1}{2}>$ and with the condition that we have an even number of $|+>$ spins. The first three "spins" correspond to $SU(3)_C$ color quantum numbers, while the last two are $SU(2)_L$ weak quantum numbers. In fact an $SU(3)_C$ rotation just raises one color index and lowers another, thereby changing colors $\{r,\ b,\ y\}$. Similarly an $SU(2)_L$ rotation raises one weak index and lowers another, thereby flipping the weak isospin from up to down or vice versa. In this representation weak hypercharge Y is given by the simple relation $Y = -2/3(\sum \text{ color spins}) + (\sum \text{ weak spins})$. $SU(5)$ rotations [in particular, the ones NOT in $SU(3)_C \times SU(2)_L \times U(1)_Y$] then raise (or lower) a color index, while at the same time lowering (or raising) a weak index. It is easy to see that such rotations can mix the states $\{Q,\ u^c,\ e^c\}$ and $\{d^c, L\}$ among themselves and ν^c is a singlet. The new $SO(10)$ rotations [not in $SU(5)$] are then given by either raising or lowering any two spins. For example, by raising the two weak indices ν^c rotates into e^c, etc.

Table 16.1: The quantum numbers of the **16** dimensional representation of SO(10).

State	Y	Color	Weak
$\boldsymbol{\nu^c}$	0	$- - -$	$- -$
$\boldsymbol{e^c}$	2	$- - -$	$+ +$
$\boldsymbol{u}_r$	1/3	$+ - -$	$- +$
$\boldsymbol{d}_r$	1/3	$+ - -$	$+ -$
$\boldsymbol{u}_b$	1/3	$- + -$	$- +$
$\boldsymbol{d}_b$	1/3	$- + -$	$+ -$
$\boldsymbol{u}_y$	1/3	$- - +$	$- +$
$\boldsymbol{d}_y$	1/3	$- - +$	$+ -$
$\boldsymbol{u}_r^c$	$-4/3$	$- + +$	$- -$
$\boldsymbol{u}_b^c$	$-4/3$	$+ - +$	$- -$
$\boldsymbol{u}_y^c$	$-4/3$	$+ + -$	$- -$
$\boldsymbol{d}_r^c$	2/3	$- + +$	$+ +$
$\boldsymbol{d}_b^c$	2/3	$+ - +$	$+ +$
$\boldsymbol{d}_y^c$	2/3	$+ + -$	$+ +$
$\boldsymbol{\nu}$	-1	$+ + +$	$- +$
$\boldsymbol{e}$	-1	$+ + +$	$+ -$

$SO(10)$ has two inequivalent maximal breaking patterns. $SO(10) \to SU(5) \times U(1)_X$ and $SO(10) \to SU(4)_C \times SU(2)_L \times SU(2)_R$. In the first case we obtain Georgi-Glashow $SU(5)$ if Q_{EM} is given in terms of $SU(5)$ generators alone or so-called flipped $SU(5)$ [5] if Q_{EM} is partly in $U(1)_X$. In the latter case we have the Pati-Salam symmetry. If $SO(10)$ breaks directly to the SM at M_G, then we retain the prediction for gauge coupling unification. However more possibilities for breaking (hence more breaking scales and more parameters) are available in $SO(10)$. Nevertheless with one breaking pattern $SO(10) \to SU(5) \to$ SM, where the last breaking scale is M_G, the predictions from gauge coupling unification are preserved. The Higgs multiplets in

minimal $SO(10)$ are contained in the fundamental $\mathbf{10_H} = [\mathbf{5_H}, \bar{\mathbf{5}}_\mathbf{H}]$ representation. Note, only in $SO(10)$ does the gauge symmetry distinguish quark and lepton multiplets from Higgs multiplets.

Finally, larger symmetry groups have been considered. For example, $E(6)$ has a fundamental representation **27** which under $SO(10)$ transforms as a $[\mathbf{16} + \mathbf{10} + \mathbf{1}]$. The breaking pattern $E(6) \to SU(3)_C \times SU(3)_L \times SU(3)_R$ is also possible. With the additional permutation symmetry $Z(3)$ interchanging the three $SU(3)$s we obtain so-called "trinification" [6] with a universal gauge coupling. The latter breaking pattern has been used in phenomenological analyses of the heterotic string [7]. However, in larger symmetry groups, such as $E(6)$, $SU(6)$, etc., there are now many more states which have not been observed and must be removed from the effective low energy theory. In particular, three families of **27**s in $E(6)$ contain three Higgs type multiplets transforming as **10**s of $SO(10)$. This makes these larger symmetry groups unattractive starting points for model building.

16.1.3. *String Theory and Orbifold GUTs* :

Orbifold compactification of the heterotic string [8–10], and recent field theoretic constructions known as orbifold GUTs [11], contain grand unified symmetries realized in 5 and 6 dimensions. However, upon compactifying all but four of these extra dimensions, only the MSSM is recovered as a symmetry of the effective four dimensional field theory.[1] These theories can retain many of the nice features of four dimensional SUSY GUTs, such as charge quantization, gauge coupling unification and sometimes even Yukawa unification; while at the same time resolving some of the difficulties of 4d GUTs, in particular problems with unwieldy Higgs sectors necessary for spontaneously breaking the GUT symmetry, and problems with doublet-triplet Higgs splitting or rapid proton decay. We will comment further on the corrections to the four dimensional GUT picture due to orbifold GUTs in the following sections. Finally, recent progress has been made in finding MSSM-like theories in the string landscape. This success is made possible by incorporating SUSY GUTs at an intermediate step in the construction. For a brief discussion, see Sec. 16.1.

16.1.4. *Gauge coupling unification* :

The biggest paradox of grand unification is to understand how it is possible to have a universal gauge coupling g_G in a grand unified theory [GUT] and yet have three unequal gauge couplings at the weak scale with $g_3 > g > g'$. The solution is given in terms of the concept of an effective field theory [EFT] [18]. The GUT symmetry is spontaneously broken at the scale M_G and all particles not in the SM obtain mass of order M_G. When calculating Green's functions with external energies $E \gg M_G$, we can neglect the mass of all particles in the loop and hence all particles contribute to the renormalization group running of the universal gauge coupling. However, for $E \ll M_G$ one can consider an effective field theory

[1] Also, in recent years there has been a great deal of progress in constructing three and four family models in Type IIA string theory with intersecting D6 branes [12]. Although these models can incorporate SU(5) or a Pati-Salam symmetry group in four dimensions, they typically have problems with gauge coupling unification. In the former case this is due to charged exotics which affect the RG running, while in the latter case the $SU(4)\times SU(2)_L \times SU(2)_R$ symmetry never unifies. Local models, however, with D-branes at singularities have had some more success in obtaining gauge coupling unification [13]. Note, heterotic string theory models also exist whose low energy effective 4d field theory is a SUSY GUT [14]. These models have all the virtues and problems of 4d GUTs. Finally, many heterotic string models have been constructed with the standard model gauge symmetry in 4d and no intermediate GUT symmetry in less than 10d. Some minimal 3 family supersymmetric models have been constructed [15,16]. These theories may retain some of the symmetry relations of GUTs, however the unification scale would typically be the string scale, of order 5×10^{17} GeV, which is inconsistent with low energy data. A way out of this problem was discovered in the context of the strongly coupled heterotic string, defined in an effective 11 dimensions [17]. In this case the 4d Planck scale (which controls the value of the string scale) now unifies with the GUT scale.

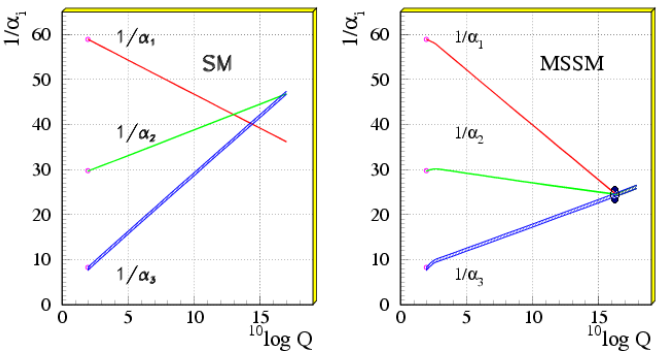

Figure 16.1: Gauge coupling unification in non-SUSY GUTs on the left vs. SUSY GUTs on the right using the LEP data as of 1991. Note, the difference in the running for SUSY is the inclusion of supersymmetric partners of standard model particles at scales of order a TeV (Fig. taken from Ref. 24). Given the present accurate measurements of the three low energy couplings, in particular $\alpha_s(M_Z)$, GUT scale threshold corrections are now needed to precisely fit the low energy data. The dark blob in the plot on the right represents these model dependent corrections.

including only the states with mass $< E \ll M_G$. The gauge symmetry of the EFT is $SU(3)_C \times SU(2)_L \times U(1)_Y$ and the three gauge couplings renormalize independently. The states of the EFT include only those of the SM; 12 gauge bosons, 3 families of quarks and leptons and one or more Higgs doublets. At M_G the two effective theories [the GUT itself is most likely the EFT of a more fundamental theory defined at a higher scale] must give identical results; hence we have the boundary conditions $g_3 = g_2 = g_1 \equiv g_G$ where at any scale $\mu < M_G$ we have $g_2 \equiv g$ and $g_1 = \sqrt{5/3}\, g'$. Then using two low energy couplings, such as $\alpha_s(M_Z)$, $\alpha_{EM}(M_Z)$, the two independent parameters α_G, M_G can be fixed. The third gauge coupling, $\sin^2\theta_W$ in this case, is then predicted. This was the procedure up until about 1991 [19,20]. Subsequently, the uncertainties in $\sin^2\theta_W$ were reduced ten fold. Since then, $\alpha_{EM}(M_Z)$, $\sin^2\theta_W$ have been used as input to predict α_G, M_G and $\alpha_s(M_Z)$ [21].

We emphasize that the above boundary condition is only valid when using one loop renormalization group [RG] running. With precision electroweak data, however, it is necessary to use two loop RG running. Hence one must include one loop threshold corrections to gauge coupling boundary conditions at both the weak and GUT scales. In this case it is always possible to define the GUT scale as the point where $\alpha_1(M_G) = \alpha_2(M_G) \equiv \tilde{\alpha}_G$ and $\alpha_3(M_G) = \tilde{\alpha}_G\,(1+\epsilon_3)$. The threshold correction ϵ_3 is a logarithmic function of all states with mass of order M_G and $\tilde{\alpha}_G = \alpha_G + \Delta$ where α_G is the GUT coupling constant above M_G and Δ is a one loop threshold correction. Note, the popular code "SOFTSUSY" [22] has defined the GUT scale in just this way. The value of ϵ_3 can be read off from the output data. To the extent that gauge coupling unification is perturbative, the GUT threshold corrections are small and calculable. This presumes that the GUT scale is sufficiently below the Planck scale or any other strong coupling extension of the GUT, such as a strongly coupled string theory.

Supersymmetric grand unified theories [SUSY GUTs] are an extension of non-SUSY GUTs [23]. The key difference between SUSY GUTs and non-SUSY GUTs is the low energy effective theory. The low energy effective field theory in a SUSY GUT is assumed to satisfy N=1 supersymmetry down to scales of order the weak scale in addition to the SM gauge symmetry. Hence the spectrum includes all the SM states plus their supersymmetric partners. It also includes one pair (or more) of Higgs doublets; one to give mass to up-type quarks and the other to down-type quarks and charged leptons. Two doublets with opposite hypercharge Y are also needed to cancel fermionic triangle anomalies. Finally, it is important to recognize that a low energy SUSY breaking scale (the scale at which the SUSY partners of SM particles obtain mass) is necessary to solve the gauge hierarchy problem.

Simple non-SUSY $SU(5)$ is ruled out; initially by the increased accuracy in the measurement of $\sin^2\theta_W$ and by early bounds on the proton lifetime (see below) [20]. However, by now LEP data [21] has conclusively shown that SUSY GUTs is the *new standard model*; by which we mean the theory used to guide the search for new physics beyond the present SM (see Fig. Fig. 16.1). SUSY extensions of the SM have the property that their effects decouple as the effective SUSY breaking scale is increased. Any theory beyond the SM must have this property simply because the SM works so well. However, the SUSY breaking scale cannot be increased with impunity, since this would reintroduce a gauge hierarchy problem. Unfortunately there is no clear-cut answer to the question, when is the SUSY breaking scale too high. A conservative bound would suggest that the third generation quarks and leptons must be lighter than about 1 TeV, in order that the one loop corrections to the Higgs mass from Yukawa interactions remains of order the Higgs mass bound itself.

At present gauge coupling unification within SUSY GUTs works extremely well. Exact unification at M_G, with two loop renormalization group running from M_G to M_Z, and one loop threshold corrections at the weak scale, fits to within 3 σ of the present precise low energy data. A small threshold correction at M_G ($\epsilon_3 \sim$ - 3% to - 4%) is sufficient to fit the low energy data precisely [25,26,27]. [2] This may be compared to non-SUSY GUTs where the fit misses by ~ 12 σ and a precise fit requires new weak scale states in incomplete GUT multiplets or multiple GUT breaking scales.[3]

Following the analysis of Ref. 27 let us try to understand the need for the GUT threshold correction and its order of magnitude. The renormalization group equations relate the low energy gauge coupling constants $\alpha_i(M_Z)$, $i = 1, 2, 3$ to the value of the unification scale Λ_U and the GUT coupling α_U by the expression

$$\frac{1}{\alpha_i(M_Z)} = \frac{1}{\alpha_U} + \frac{b_i}{2\pi}\log\left(\frac{\Lambda_U}{M_Z}\right) + \delta_i \qquad (16.1)$$

where Λ_U is the GUT scale evaluated at one loop and the threshold corrections, δ_i, are given by $\delta_i = \delta_i^{(2)} + \delta_i^{(l)} + \delta_i^{(g)}$ with $\delta_i^{(2)}$ representing two loop running effects, $\delta_i^{(l)}$ the light threshold corrections at the SUSY breaking scale and $\delta_i^{(g)} = \delta_i^{(h)} + \delta_i^{(b)}$ representing GUT scale threshold corrections. Note, in this analysis, the two loop RG running is treated on the same footing as weak and GUT scale threshold corrections. One then obtains the prediction

$$(\alpha_3(M_Z) - \alpha_3^{LO}(M_Z))/\alpha_3^{LO}(M_Z) = -\alpha_3^{LO}(M_Z)\ \delta_s \qquad (16.2)$$

where $\alpha_3^{LO}(M_Z)$ is the leading order one loop RG result and $\delta_s = \frac{1}{7}(5\delta_1 - 12\delta_2 + 7\delta_3)$ is the net threshold correction. [A similar formula applies at the GUT scale with the GUT threshold correction, ϵ_3, given by $\epsilon_3 = -\tilde{\alpha}_G\ \delta_s^{(g)}$.] Given the experimental inputs [31,32]:

$$\begin{aligned} \alpha_{em}^{-1}(M_Z) &= 127.916 \pm 0.015 \\ sin^2\theta_W(M_Z) &= 0.23116 \pm 0.00013 \\ \alpha_3(M_Z) &= 0.1184 \pm 0.0007 \end{aligned} \qquad (16.3)$$

and taking into account the light threshold corrections, assuming an ensemble of 10 SUSY spectra [27](corresponding to the Snowmass benchmark points), we have

$$\alpha_3^{LO}(M_Z) \approx 0.118 \qquad (16.4)$$

and

$$\begin{aligned} \delta_s^{(2)} &\approx -0.82 \\ \delta_s^{(l)} &\approx -0.50 + \frac{19}{28\pi}\log\frac{M_{SUSY}}{M_Z}. \end{aligned}$$

For $M_{SUSY} = 1$ TeV, we have $\delta_s^{(2)} + \delta_s^{(l)} \approx -0.80$. Since the one loop result $\alpha_3^{LO}(M_Z)$ is very close to the experimental value, we need $\delta_s \approx 0$ or equivalently, $\delta_s^{(g)} \approx 0.80$. This corresponds, at the GUT scale, to $\epsilon_3 \approx -3\%$. Note, this result depends implicitly on the assumption of universal soft SUSY breaking masses at the GUT scale, which directly affect the spectrum of SUSY particles at the weak scale. For example, if gaugino masses were not unified at M_G and, in particular, gluinos were lighter than winos at the weak scale, then it is possible that, due to weak scale threshold corrections, a much smaller or even slightly positive threshold correction at the GUT scale would be consistent with gauge coupling unification [34].

In four dimensional SUSY GUTs, the threshold correction ϵ_3 receives a positive contribution from Higgs doublets and triplets.[4] Thus a larger, negative contribution must come from the GUT breaking sector of the theory. This is certainly possible in specific SO(10) [35] or SU(5) [36] models, but it is clearly a significant constraint on the 4d GUT sector of the theory. In five or six dimensional orbifold GUTs, on the other hand, the "GUT scale" threshold correction comes from the Kaluza-Klein modes between the compactification scale, M_c, and the effective cutoff scale M_*.[5] Thus, in orbifold GUTs, gauge coupling unification at two loops is only consistent with the low energy data with a fixed value for M_c and M_*.[6] Typically, one finds $M_c < M_G = 3 \times 10^{16}$ GeV, where M_G is the 4d GUT scale. Since the grand unified gauge bosons, responsible for nucleon decay, get mass at the compactification scale, the result $M_c < M_G$ for orbifold GUTs has significant consequences for nucleon decay.

A few final comments are in order. We do not consider the scenario of split supersymmetry [39] in this review. In this scenario squarks and sleptons have mass at a scale $\tilde{m} \gg M_Z$, while gauginos and Higgsinos have mass of order the weak scale. Gauge coupling unification occurs at a scale of order 10^{16} GeV, *provided that the scale $\tilde{m}$ lies in the range* $10^3 - 10^{11}$ *GeV* [40]. A serious complaint concerning the split SUSY scenario is that it does not provide a solution to the gauge hierarchy problem. Moreover, it is only consistent with grand unification if it also postulates an "intermediate" scale, $\tilde{m}$, for scalar masses. In addition, it is in conflict with $b - \tau$ Yukawa unification, unless $\tan\beta$ is fine-tuned to be close to 1 [40]. [7]

[2] This result implicitly assumes universal GUT boundary conditions for soft SUSY breaking parameters at M_G. In the simplest case we have a universal gaugino mass $M_{1/2}$, a universal mass for squarks and sleptons m_{16} and a universal Higgs mass m_{10}, as motivated by $SO(10)$. In some cases, threshold corrections to gauge coupling unification can be exchanged for threshold corrections to soft SUSY parameters. See for example, Ref. 28 and references therein.

[3] Non-SUSY GUTs with a more complicated breaking pattern can still fit the data. For example, non-SUSY $SO(10) \to SU(4)_C \times SU(2)_L \times SU(2)_R \to SM$ with the second breaking scale of order an intermediate scale, determined by light neutrino masses using the see-saw mechanism, can fit the low energy data for gauge couplings [29] and at the same time survive nucleon decay bounds [30], discussed in the following section.

[4] Note, the Higgs contribution is given by $\epsilon_3 = \frac{3\tilde{\alpha}_G}{5\pi}\log|\frac{\tilde{M}_t\,\gamma}{M_G}|$ where $\tilde{M}_t$ is the effective color triplet Higgs mass (setting the scale for dimension 5 baryon and lepton number violating operators) and $\gamma = \lambda_b/\lambda_t$ at M_G. Since $\tilde{M}_t$ is necessarily greater than M_G, the Higgs contribution to ϵ_3 is positive.

[5] In string theory, the cutoff scale is the string scale.

[6] It is interesting to note that a ratio $M_*/M_c \sim 100$, needed for gauge coupling unification to work in orbifold GUTs is typically the maximum value for this ratio consistent with perturbativity [37]. In addition, in orbifold GUTs brane-localized gauge kinetic terms may destroy the successes of gauge coupling unification. However, for values of $M_*/M_c = M_*\pi R \gg 1$ the unified bulk gauge kinetic terms can dominate over the brane-localized terms [38].

[7] $b - \tau$ Yukawa unification only works for $\tilde{m} < 10^4$ for $\tan\beta \geq 1.5$. This is because the effective theory between the gaugino mass scale and $\tilde{m}$ includes only one Higgs doublet, as in the standard model. In this case, the large top quark Yukawa coupling tends to increase the ratio λ_b/λ_τ as one runs down in energy below $\tilde{m}$. This is opposite to what happens in MSSM where the large top quark Yukawa coupling decreases the ratio λ_b/λ_τ [41].

We have also neglected to discuss non-supersymmetric GUTs in four dimensions which still survive once one allows for several scales of GUT symmetry breaking [29]. Finally, it has been shown that non-supersymmetric GUTs in warped 5 dimensional orbifolds can be consistent with gauge coupling unification, assuming that the right-handed top quark and the Higgs doublets are composite-like objects with a compositeness scale of order a TeV [42]. However perturbative unification seems to fail.

16.1.5. ***Nucleon Decay*** :

Baryon number is necessarily violated in any GUT [43]. In $SU(5)$, nucleons decay via the exchange of gauge bosons with GUT scale masses, resulting in dimension 6 baryon number violating operators suppressed by $(1/M_G^2)$. The nucleon lifetime is calculable and given by $\tau_N \propto M_G^4/(\alpha_G^2\, m_p^5)$. The dominant decay mode of the proton (and the baryon violating decay mode of the neutron), via gauge exchange, is $p \to e^+\,\pi^0$ $(n \to e^+\,\pi^-)$. In any simple gauge symmetry, with one universal GUT coupling and scale $(\alpha_G,\ M_G)$, the nucleon lifetime from gauge exchange is calculable. Hence, the GUT scale may be directly observed via the extremely rare decay of the nucleon. Experimental searches for nucleon decay began with the Kolar Gold Mine, Homestake, Soudan, NUSEX, Frejus, HPW, and IMB detectors [19]. The present experimental bounds come from Super-Kamiokande and Soudan II. We discuss these results shortly. Non-SUSY GUTs are also ruled out by the non-observation of nucleon decay [20]. In SUSY GUTs, the GUT scale is of order 3×10^{16} GeV, as compared to the GUT scale in non-SUSY GUTs which is of order 10^{15} GeV. Hence the dimension 6 baryon violating operators are significantly suppressed in SUSY GUTs [23] with $\tau_p \sim 10^{34-38}$ yrs.

However, in SUSY GUTs there are additional sources for baryon number violation – dimension 4 and 5 operators [44]. Although our notation does not change, when discussing SUSY GUTs all fields are implicitly chiral superfields and the operators considered are the so-called F terms which contain two fermionic components and the rest scalars or products of scalars. Within the context of $SU(5)$ the dimension 4 and 5 operators have the form $(\mathbf{10}\ \bar{\mathbf{5}}\ \bar{\mathbf{5}}) \supset (u^c\ d^c\ d^c) + (Q\ L\ d^c) + (e^c\ L\ L)$ and $(\mathbf{10}\ \mathbf{10}\ \mathbf{10}\ \bar{\mathbf{5}}) \supset (Q\ Q\ Q\ L) + (u^c\ u^c\ d^c\ e^c) + B$ and L conserving terms, respectively. The dimension 4 operators are renormalizable with dimensionless couplings; similar to Yukawa couplings. On the other hand, the dimension 5 operators have a dimensionful coupling of order $(1/M_G)$.

The dimension 4 operators violate baryon number or lepton number, respectively, but not both. The nucleon lifetime is extremely short if both types of dimension 4 operators are present in the low energy theory. However both types can be eliminated by requiring R parity. In $SU(5)$ the Higgs doublets reside in a $\mathbf{5_H}$, $\bar{\mathbf{5}}_\mathbf{H}$ and R parity distinguishes the $\bar{\mathbf{5}}$ (quarks and leptons) from $\bar{\mathbf{5}}_\mathbf{H}$ (Higgs). R parity [45](or its cousin, family reflection symmetry (or *matter parity*) (see Dimopoulos and Georgi [23] and DRW [46]) takes $F \to -F$, $H \to H$ with $F = \{\mathbf{10},\ \bar{\mathbf{5}}\}$, $H = \{\bar{\mathbf{5}}_\mathbf{H},\ \mathbf{5_H}\}$. This forbids the dimension 4 operator $(\mathbf{10}\ \bar{\mathbf{5}}\ \bar{\mathbf{5}})$, but allows the Yukawa couplings of the form $(\mathbf{10}\ \bar{\mathbf{5}}\ \bar{\mathbf{5}}_\mathbf{H})$ and $(\mathbf{10}\ \mathbf{10}\ \mathbf{5_H})$. It also forbids the dimension 3, lepton number violating, operator $(\bar{\mathbf{5}}\ \mathbf{5_H}) \supset (L\ H_u)$ with a coefficient with dimensions of mass which, like the μ parameter, could be of order the weak scale and the dimension 5, baryon number violating, operator $(\mathbf{10}\ \mathbf{10}\ \mathbf{10}\ \bar{\mathbf{5}}_\mathbf{H}) \supset (Q\ Q\ Q\ H_d) + \cdots$.

Note, in the MSSM it is possible to retain R parity violating operators at low energy as long as they violate either baryon number or lepton number only but not both. Such schemes are natural if one assumes a low energy symmetry, such as lepton number, baryon number, baryon triality [47] or proton hexality [48]. However these symmetries cannot be embedded in a GUT. Thus, in a SUSY GUT, only R parity can prevent all the dimension three and four baryon and lepton number violating operators. This does not mean to say that R parity is guaranteed to be satisfied in any GUT. For example the authors of Refs. [51,52] use constrained matter content to selectively generate safe effective R parity violating operators in a GUT. For a review on R parity violating interactions, see [53]. In Ref. [52], the authors show how to obtain the effective R parity violating operator $O^{ijk} = (\bar{5}^j \cdot \bar{5}^k)_{\overline{15}} \cdot (10^i \cdot \Sigma)_{15}$ where Σ is an $SU(5)$ adjoint field and the subscripts $\overline{15}, 15$ indicate that the product of fields in parentheses have been projected into these $SU(5)$ directions. As a consequence the operator O^{ijk} is symmetric under interchange of the two $\bar{5}$ states, $O^{ijk} = O^{ikj}$, and out of $\mathbf{10}\ \bar{\mathbf{5}}\ \bar{\mathbf{5}}$ only the lepton number/R parity violating operator $QL\bar{D}$ survives.

Note also, R parity distinguishes Higgs multiplets from ordinary families. In $SU(5)$, Higgs and quark/lepton multiplets have identical quantum numbers; while in $E(6)$, Higgs and families are unified within the fundamental **27** representation. Only in SO(10) are Higgs and ordinary families distinguished by their gauge quantum numbers. Moreover the Z(4) center of SO(10) distinguishes **10**s from **16**s and can be associated with R parity [49].

Dimension 5 baryon number violating operators may be forbidden at tree level by symmetries in $SU(5)$, etc. These symmetries are typically broken however by the VEVs responsible for the color triplet Higgs masses. Consequently these dimension 5 operators are generically generated via color triplet Higgsino exchange. Hence, the color triplet partners of Higgs doublets must necessarily obtain mass of order the GUT scale. [It is also important to note that Planck or string scale physics may independently generate dimension 5 operators, even without a GUT. These contributions must be suppressed by some underlying symmetry; for example, the same flavor symmetry which may be responsible for hierarchical fermion Yukawa matrices.]

The dominant decay modes from dimension 5 operators are $p \to K^+\,\bar{\nu}$ $(n \to K^0\,\bar{\nu})$. This is due to a simple symmetry argument; the operators $(Q_i\ Q_j\ Q_k\ L_l)$, $(u_i^c\ u_j^c\ d_k^c\ e_l^c)$ (where $i,\ j,\ k,\ l = 1, 2, 3$ are family indices and color and weak indices are implicit) must be invariant under $SU(3)_C$ and $SU(2)_L$. As a result their color and weak doublet indices must be anti-symmetrized. However since these operators are given by bosonic superfields, they must be totally symmetric under interchange of all indices. Thus the first operator vanishes for $i = j = k$ and the second vanishes for $i = j$. Hence a second or third generation member must exist in the final state [46].

Recent Super-Kamiokande bounds on the proton lifetime severely constrain these dimension 6 and 5 operators with (172.8 kt-yr) of data they find $\tau_{(p\to e^+\pi^0)} > 1.0 \times 10^{34}$ yrs, $\tau_{(p\to K^+\bar{\nu})} > 3.3 \times 10^{33}$ yrs and $\tau_{(n\to e^+\pi^-)} > 2 \times 10^{33}$ yrs at (90% CL) [54]. These constraints are now sufficient to rule out minimal SUSY $SU(5)$ [55]. [8] Non-minimal Higgs sectors in $SU(5)$ or $SO(10)$ theories still survive [26,36]. The upper bound on the proton lifetime from these theories are approximately a factor of 10 above the experimental bounds. They are also being pushed to their theoretical limits. Hence if SUSY GUTs are correct, then nucleon decay must be seen soon.

Is there a way out of this conclusion? Orbifold GUTs and string theories, see Sec. 16.1, contain grand unified symmetries realized in higher dimensions. In the process of compactification and GUT symmetry breaking, color triplet Higgs states are removed (projected out of the massless sector of the theory). In addition, the same projections typically rearrange the quark and lepton states so that the massless states which survive emanate from different GUT multiplets. In these models, proton decay due to dimension 5 operators can be severely suppressed or eliminated completely. However, proton decay due to dimension 6 operators may be enhanced, since the gauge bosons mediating proton decay obtain mass at the compactification scale, M_c, which is typically less than the 4d GUT scale (see the discussion at the end of Sec. 16.1), or suppressed, if the states of one family come from different irreducible representations. Which effect dominates is a model dependent issue. In some complete 5d orbifold

[8] This conclusion relies on the mild assumption that the three-by-three matrices diagonalizing squark and slepton mass matrices are not so different from their fermionic partners. It has been shown that if this caveat is violated, then dimension five proton decay in minimal SUSY $SU(5)$ may not be ruled out [56]. This is however a very fine-tuned resolution of the problem. Another possible way out is to allow for a more complicated $SU(5)$ breaking Higgs sector in the otherwise minimal model [57]. I have also implicitly assumed a hierarchical structure for Yukawa matrices in this analysis. It is however possible to fine-tune a hierarchical structure for quarks and leptons which baffles the family structure. In this case it is possible to avoid the present constraints on minimal SUSY $SU(5)$, for example see [58].

GUT models [59,27] the lifetime for the decay $\tau(p \to e^+\pi^0)$ can be near the excluded bound of 1×10^{34} years with, however, large model dependent and/or theoretical uncertainties. In other cases, the modes $p \to K^+\bar{\nu}$ and $p \to K^0\mu^+$ may be dominant [27]. To summarize, in either 4d or orbifold string/field theories, nucleon decay remains a premier signature for SUSY GUTs. Moreover, the observation of nucleon decay may distinguish extra-dimensional orbifold GUTs from four dimensional ones.

As a final note, in orbifold GUTs or string theory new discrete symmetries consistent with SUSY GUTs can forbid all dimension 3 and 4 baryon [B] and lepton [L] number violating operators and even forbid the mu term and dimension 5 B and L violating operators to all orders in perturbation theory [50]. The mu term and dimension 5 B and L violating operators may then be generated, albeit sufficiently suppressed, via non-perturbative effects. The simplest example of this is a Z_4^R symmetry which is the unique discrete R symmetry consistent with SO(10) [50]. In this case, proton decay is completely dominated by dimension 6 operators.

Before concluding the topic of baryon number violation, consider the status of $\Delta B = 2$ neutron- anti-neutron oscillations. Generically the leading operator for this process is the dimension 9 six quark operator $G_{(\Delta B=2)}$ $(u^c\ d^c\ d^c\ u^c\ d^c\ d^c)$ with dimensionful coefficient $G_{(\Delta B=2)} \sim 1/M^5$. The present experimental bound $\tau_{n-\bar{n}} \geq 0.86 \times 10^8$ sec. at 90% CL [60] probes only up to the scale $M \leq 10^6$ GeV. For $M \sim M_G$, $n - \bar{n}$ oscillations appear to be unobservable for any GUT (for a recent discussion see [61]) .

16.1.6. *Yukawa coupling unification* :

16.1.6.1. *3rd generation, $b - \tau$ or $t - b - \tau$ unification:*

If quarks and leptons are two sides of the same coin, related by a new grand unified gauge symmetry, then that same symmetry relates the Yukawa couplings (and hence the masses) of quarks and leptons. In $SU(5)$, there are two independent renormalizable Yukawa interactions given by λ_t $(\mathbf{10\ 10\ 5_H}) + \lambda$ $(\mathbf{10\ \bar{5}\ \bar{5}_H})$. These contain the SM interactions λ_t $(\mathbf{Q\ u^c\ H_u}) + \lambda$ $(\mathbf{Q\ d^c\ H_d\ +\ e^c\ L\ H_d})$. Hence, at the GUT scale we have the tree level relation, $\lambda_b = \lambda_\tau \equiv \lambda$ [41]. In $SO(10)$ there is only one independent renormalizable Yukawa interaction given by λ $(\mathbf{16\ 16\ 10_H})$ which gives the tree level relation, $\lambda_t = \lambda_b = \lambda_\tau \equiv \lambda$ [62,63]. Note, in the discussion above we assume the minimal Higgs content with Higgs in $\mathbf{5}$, $\bar{\mathbf{5}}$ for $SU(5)$ and $\mathbf{10}$ for $SO(10)$. With Higgs in higher dimensional representations there are more possible Yukawa couplings [75,76,77].

In order to make contact with the data, one now renormalizes the top, bottom and τ Yukawa couplings, using two loop RG equations, from M_G to M_Z. One then obtains the running quark masses $m_t(M_Z) = \lambda_t(M_Z)\ v_u$, $m_b(M_Z) = \lambda_b(M_Z)\ v_d$ and $m_\tau(M_Z) = \lambda_\tau(M_Z)\ v_d$ where $< H_u^0 > \equiv v_u = \sin\beta\ v/\sqrt{2}$, $< H_d^0 > \equiv v_d = \cos\beta\ v/\sqrt{2}$, $v_u/v_d \equiv \tan\beta$ and $v \sim 246$ GeV is fixed by the Fermi constant, G_μ.

Including one loop threshold corrections at M_Z and additional RG running, one finds the top, bottom and τ pole masses. In SUSY, $b - \tau$ unification has two possible solutions with $\tan\beta \sim 1$ or $40 - 50$. The small $\tan\beta$ solution is now disfavored by the LEP limit, $\tan\beta > 2.4$ [64]. [9] The large $\tan\beta$ limit overlaps the $SO(10)$ symmetry relation.

When $\tan\beta$ is large there are significant weak scale threshold corrections to down quark and charged lepton masses from either gluino and/or chargino loops [66]. Yukawa unification (consistent with low energy data) is only possible in a restricted region of SUSY parameter space with important consequences for SUSY searches [67]. More recent analyses of Yukawa unification can be found in Refs. [68,69,70,71]. There seems to be at least four possible choices of soft SUSY breaking parameters which fit the data, possibly more. Each case then leads to a distinct sparticle spectrum and phenomenology for LHC and dark matter experiments. They correspond to:

- universal squark and slepton masses (m_{16}), universal A parameter (A_0) and gaugino masses ($M_{1/2}$), and non-universal Higgs masses ($m_{H_u},\ m_{H_d}$) with "just-so" splitting [67,68].
- a universal squark and slepton mass term for the first two families ($m_{16_{1,2}}$) which is larger than the universal scalar mass for the third family (m_{16_3}), universal A parameter (A_0) and gaugino masses ($M_{1/2}$) and universal Higgs mass term (m_{10}). However all scalar masses then receive a D-term contribution to their masses given by the $U(1)$ from $SO(10)$ which commutes with $SU(5)$. This is of the form

$$m_Q^2 = m_E^2 = m_U^2 = m_{16}^2 + M_D^2,$$
$$m_D^2 = m_L^2 = m_{16}^2 - 3M_D^2,$$
$$m_\nu^2 = m_{16}^2 + 5M_D^2,$$
$$m_{H_{u,d}}^2 = m_{10}^2 \mp 2M_D^2.$$

  This is the so-called "DR3 splitting" [69]. The R is associated with taking into account the renormalization group [RG] running of the right-handed neutrino from the GUT scale to the nominal value of its mass of order 10^{10-14} GeV, as indicated by light neutrino masses via the See-Saw mechanism. This RG running contributes to an additional splitting of the H_u and H_d masses [67].
- universal squark and slepton masses (m_0), split Higgs masses and non-universal gaugino masses satisfying ($M_1 = \frac{3}{5}M_2 + \frac{2}{5}M_3$), and $\mu, M_2 < 0$ [70], and
- universal squark and slepton mass term (m_{16}), A parameter (A_0), Higgs mass term (m_{10}). All scalar masses then receive a D-term contribution to their masses given by the $U(1)$ from $SO(10)$ which commutes with $SU(5)$, as above. Finally, non-universal gaugino masses satisfying ($M_3 : M_2 : M_1 = 2 : -3 : -1$) with $M_3 > 0$ and $\mu < 0$ [71].

16.1.6.2. *Three families:*

Simple Yukawa unification is not possible for the first two generations of quarks and leptons. Consider the $SU(5)$ GUT scale relation $\lambda_b = \lambda_\tau$. If extended to the first two generations one would have $\lambda_s = \lambda_\mu$, $\lambda_d = \lambda_e$ which gives $\lambda_s/\lambda_d = \lambda_\mu/\lambda_e$. The last relation is a renormalization group invariant and is thus satisfied at any scale. In particular, at the weak scale one obtains $m_s/m_d = m_\mu/m_e$ which is in serious disagreement with the data with $m_s/m_d \sim 20$ and $m_\mu/m_e \sim 200$. An elegant solution to this problem was given by Georgi and Jarlskog [72]. For a recent anaylsis in the context of supersymmetric GUTs, see Ref. [73]. Of course, a three family model must also give the observed CKM mixing in the quark sector. Note, although there are typically many more parameters in the GUT theory above M_G, it is possible to obtain effective low energy theories with many fewer parameters making strong predictions for quark and lepton masses.

Three family models which make significant predictions for low energy experiments have been constructed in the context of supersymmetric GUTs. It is important to note that grand unification alone is not sufficient to obtain predictive theories of fermion masses and mixing angles. Other ingredients are needed. In one approach additional global family symmetries are introduced (non-abelian family symmetries can significantly reduce the number of arbitrary parameters in the Yukawa matrices). These family symmetries constrain the set of effective higher dimensional fermion mass operators. In addition, sequential breaking of the family symmetry is correlated with the hierarchy of fermion masses. Three-family models exist which fit all the data, including neutrino masses and mixing [74]. In a completely separate approach for $SO(10)$ models, the Standard Model Higgs bosons are contained in the higher dimensional Higgs representations including the $\mathbf{10}$, $\overline{\mathbf{126}}$ and/or $\mathbf{120}$. Such theories have been shown to make predictions for neutrino masses and mixing angles [75–77]. A recent paper on this subject argues the necessity of split supersymmetry [78].

[9] However, this bound disappears if one takes $M_{SUSY} = 2$ TeV and $m_t = 180$ GeV [65]. This apparent loop hole is now inconsistent with the observed top quark mass.

16.1.7. ***Neutrino Masses*** :

Atmospheric and solar neutrino oscillations, along with long baseline accelerator and reactor experiments, require neutrino masses. Adding three "sterile" neutrinos ν^c with the Yukawa coupling λ_ν ($\nu^{\mathbf{c}}$ **L** $\mathbf{H_u}$), one easily obtains three massive Dirac neutrinos with mass $m_\nu = \lambda_\nu\ v_u$.[10] However in order to obtain a tau neutrino with mass of order 0.1 eV, one needs $\lambda_{\nu_\tau}/\lambda_\tau \leq 10^{-10}$. The see-saw mechanism, on the other hand, can naturally explain such small neutrino masses [79,80]. Since ν^c has no SM quantum numbers, there is no symmetry (other than global lepton number) which prevents the mass term $\frac{1}{2}\ \nu^c\ M\ \nu^c$. Moreover one might expect $M \sim M_G$. Heavy "sterile" neutrinos can be integrated out of the theory, defining an effective low energy theory with only light active Majorana neutrinos with the effective dimension 5 operator $\frac{1}{2}$ (**L** $\mathbf{H_u}$) $\lambda_\nu^T\ M^{-1}\ \lambda_\nu$ (**L** $\mathbf{H_u}$). This then leads to a 3×3 Majorana neutrino mass matrix $\mathbf{m} = m_\nu^T\ M^{-1}\ m_\nu$.

Atmospheric neutrino oscillations require neutrino masses with $\Delta m_\nu^2 \sim 3 \times 10^{-3}$ eV^2 with maximal mixing, in the simplest two neutrino scenario. With hierarchical neutrino masses $m_{\nu_\tau} = \sqrt{\Delta m_\nu^2} \sim 0.055$ eV. Moreover via the "see-saw" mechanism $m_{\nu_\tau} = m_t(m_t)^2/(3M)$. Hence one finds $M \sim 2 \times 10^{14}$ GeV; remarkably close to the GUT scale. Note we have related the neutrino Yukawa coupling to the top quark Yukawa coupling $\lambda_{\nu_\tau} = \lambda_t$ at M_G as given in $SO(10)$ or $SU(4) \times SU(2)_L \times SU(2)_R$. However at low energies they are no longer equal and we have estimated this RG effect by $\lambda_{\nu_\tau}(M_Z) \approx \lambda_t(M_Z)/\sqrt{3}$.

Neutrinos pose a special problem for SUSY GUTs. The question is why are the quark mixing angles in the CKM matrix small, while there are two large lepton mixing angles in the PMNS matrix. For a recent discussion of neutrino masses and mixing angles, see Refs. [81] and [82]. For SUSY GUT models which fit quark and lepton masses, see Ref. [74]. Finally, for a compilation of the range of SUSY GUT predictions for neutrino mixing, see [83].

16.1.8. ***Selected Topics*** :

16.1.8.1. *Magnetic Monopoles:*

In the broken phase of a GUT there are typically localized classical solutions carrying magnetic charge under an unbroken $U(1)$ symmetry [84]. These magnetic monopoles with mass of order M_G/α_G are produced during the GUT phase transition in the early universe. The flux of magnetic monopoles is experimentally found to be less than $\sim 10^{-16}$ cm^{-2} s^{-1} sr^{-1} [85]. Many more are however predicted, hence the GUT monopole problem. In fact, one of the original motivations for an inflationary universe is to solve the monopole problem by invoking an epoch of rapid inflation after the GUT phase transition [86]. This would have the effect of diluting the monopole density as long as the reheat temperature is sufficiently below M_G. Other possible solutions to the monopole problem include: sweeping them away by domain walls [87], U(1) electromagnetic symmetry breaking at high temperature [88] or GUT symmetry non-restoration [89]. Parenthetically, it was also shown that GUT monopoles can catalyze nucleon decay [90]. A significantly lower bound on the monopole flux can then be obtained by considering X-ray emission from radio pulsars due to monopole capture and the subsequent nucleon decay catalysis [91].

16.1.8.2. *Baryogenesis via Leptogenesis:*

Baryon number violating operators in $SU(5)$ or $SO(10)$ preserve the global symmetry $B - L$. Hence the value of the cosmological $B - L$ density is an initial condition of the theory and is typically assumed to be zero. On the other hand, anomalies of the electroweak symmetry violate $B + L$ while also preserving $B - L$. Hence thermal fluctations in the early universe, via so-called sphaleron processes, can drive $B + L$ to zero, washing out any net baryon number generated in the early universe at GUT temperatures.

One way out of this dilemma is to generate a net $B - L$ dynamically in the early universe. We have just seen that neutrino oscillations suggest a new scale of physics of order 10^{14} GeV. This scale is associated with heavy Majorana neutrinos with mass M. If in the early universe, the decay of the heavy neutrinos is out of equilibrium and violates both lepton number and CP, then a net lepton number may be generated. This lepton number will then be partially converted into baryon number via electroweak processes [92].

16.1.8.3. *GUT symmetry breaking:*

The grand unification symmetry is necessarily broken spontaneously. Scalar potentials (or superpotentials) exist whose vacua spontaneously break $SU(5)$ and $SO(10)$. These potentials are ad hoc (just like the Higgs potential in the SM) and therefore it is hoped that they may be replaced with better motivated sectors. Gauge coupling unification now tests GUT breaking sectors, since it is one of the two dominant corrections to the GUT threshold correction ϵ_3. The other dominant correction comes from the Higgs sector and doublet-triplet splitting. This latter contribution is always positive $\epsilon_3 \propto \ln(M_T/M_G)$ (where M_T is an effective color triplet Higgs mass), while the low energy data typically requires $\epsilon_3 < 0$. Hence the GUT breaking sector must provide a significant (of order -8%) contribution to ϵ_3 to be consistent with the Super-K bound on the proton lifetime [35,26,36,74].

In string theory (and GUTs in extra-dimensions), GUT breaking may occur due to boundary conditions in the compactified dimensions [8,11]. This is still ad hoc. The major benefit is that it does not require complicated GUT breaking sectors.

16.1.8.4. *Doublet-triplet splitting:*

The minimal supersymmetric standard model has a μ problem; why is the coefficient of the bilinear Higgs term in the superpotential μ ($\mathbf{H_u}$ $\mathbf{H_d}$) of order the weak scale when, since it violates no low energy symmetry, it could be as large as M_G. In a SUSY GUT, the μ problem is replaced by the problem of *doublet-triplet* splitting — giving mass of order M_G to the color triplet Higgs and mass μ to the Higgs doublets. Several mechanisms for natural doublet-triplet splitting have been suggested, such as the sliding singlet [93], missing partner or missing VEV [94], and pseudo-Nambu-Goldstone boson mechanisms. Particular examples of the missing partner mechanism for $SU(5)$ [36], the missing VEV mechanism for $SO(10)$ [74,26] and the pseudo-Nambu-Goldstone boson mechanism for $SU(6)$ [95] have been shown to be consistent with gauge coupling unification and proton decay. There are also several mechanisms for explaining why μ is of order the SUSY breaking scale [96]. Finally, for a recent review of the μ problem and some suggested solutions in SUSY GUTs and string theory, see Ref. [97,10,98,50] and references therein.

Once again, in string theory (and orbifold GUTs), the act of breaking the GUT symmetry via orbifolding projects certain states out of the theory. It has been shown that it is possible to remove the color triplet Higgs while retaining the Higgs doublets in this process. Hence the doublet-triplet splitting problem is finessed. As discussed earlier (see Sec. 16.1), this can have the effect of eliminating the contribution of dimension 5 operators to nucleon decay.

16.1.9. ***String theory*** :

String theory has made significant progress in locating the minimal supersymmetric standard model [MSSM] in the string landscape. Random searches for MSSM-like models have found some success, see for example Ref. 99. However, recently a solid leap forward has been made by imposing a supersymmetric GUT locally in the extra dimensions of the string. Many MSSM-like models have been found in $E(8) \times E(8)$ heterotic orbifold constructions [100–103] or more recently on smooth Calabi-Yau three-folds [104]. See also in F theory constructions [105–107]. There appear, however, to be some problems associated with large threshold corrections to gauge coupling unification in the F theory constructions which make use of a non-vanishing hypercharge field strength to break $SU(5)$ to $SU(3)_C \times SU(2)_L \times U(1)_Y$ [108]. Nevertheless, a SUSY GUT guarantees the correct particle content of the Standard Model and also allows for reasonable looking hierarchical Yukawa matrices. For a more detailed discussion, see [109].

[10] Note, these "sterile" neutrinos are quite naturally identified with the right-handed neutrinos necessarily contained in complete families of $SO(10)$ or Pati-Salam.

16.2. Conclusion

Grand unification of the strong and electroweak interactions requires that the three low energy gauge couplings unify (up to small threshold corrections) at a unique scale, M_G. Supersymmetric grand unified theories provide, by far, the most predictive and economical framework allowing for perturbative unification.

The three pillars of SUSY GUTs are:

- gauge coupling unification at $M_G \sim 3 \times 10^{16}$ GeV;
- low-energy supersymmetry [with a large SUSY desert], and
- nucleon decay.

The first prediction has already been verified (see Fig. Fig. 16.1). Perhaps the next two will soon appear. Whether or not Yukawa couplings unify is more model dependent. Nevertheless, the "digital" 16 dimensional representation of quarks and leptons in $SO(10)$ is very compelling and may yet lead to an understanding of fermion masses and mixing angles.

In any event, the experimental verification of the first three pillars of SUSY GUTs would forever change our view of Nature. Moreover, the concomitant evidence for a vast SUSY desert would expose a huge lever arm for discovery. For then it would become clear that experiments probing the TeV scale could reveal physics at the GUT scale and perhaps beyond. Of course, some questions will still remain: Why do we have three families of quarks and leptons? How is the grand unified symmetry and possible family symmetries chosen by Nature? At what scale might stringy physics become relevant? Etc.

References:

1. J. Pati and A. Salam, Phys. Rev. **D8**, 1240 (1973);
   For more discussion on the standard charge assignments in this formalism, see A. Davidson, Phys. Rev. **D20**, 776 (1979); and R.N. Mohapatra and R.E. Marshak, Phys. Lett. **B91**, 222 (1980).
2. H. Georgi and S.L. Glashow, Phys. Rev. Lett. **32**, 438 (1974).
3. E. Golowich, Phys. Rev. **D24**, 2899 (1981).
4. H. Georgi, Particles and Fields, *Proceedings of the APS Div. of Particles and Fields*, ed. C. Carlson, p. 575 (1975);
   H. Fritzsch and P. Minkowski, Ann. Phys. **93**, 193 (1975).
5. S.M. Barr, Phys. Lett. **B112**, 219 (1982).
6. A. de Rujula *et al.*, *5th Workshop on Grand Unification*, ed. K. Kang *et al.*, World Scientific, Singapore (1984), p. 88;
   See also earlier paper by Y. Achiman and B. Stech, p. 303, "New Phenomena in Lepton-Hadron Physics," ed. D.E.C. Fries and J. Wess, Plenum, NY (1979).
7. B.R. Greene *et al.*, Nucl. Phys. **B278**, 667 (1986);
   ibid., Nucl. Phys. **B292**, 606 (1987);
   B.R. Greene *et al.*, Nucl. Phys. **B325**, 101 (1989);
   J.E. Kim, Phys. Lett. **B591**, 119 (2004).
8. P. Candelas *et al.*, Nucl. Phys. **B258**, 46 (1985);
   L.J. Dixon *et al.*, Nucl. Phys. **B261**, 678 (1985);
   ibid., Nucl. Phys. **B274**, 285 (1986);
   L. E. Ibanez *et al.*, Phys. Lett. **B187**, 25 (1987);
   ibid., Phys. Lett. **B191**, 282 (1987);
   J.E. Kim *et al.*, Nucl. Phys. **B712**, 139 (2005).
9. T.Kobayashi *et al.*, Phys. Lett. **B593**, 262 (2004);
   S. Forste *et al.*, Phys. Rev. **D70**, 106008 (2004);
   T. Kobayashi *et al.*, Nucl. Phys. **B704**, 3 (2005);
   W. Buchmuller *et al.*, Nucl. Phys. **B712**, 139 (2005);
   W. Buchmuller *et al.*, Phys. Rev. Lett. **96**, 121602 (2006);
   ibid., Nucl. Phys. **B785**, 149 (2007);
   O. Lebedev, *et al.*, Phys. Lett. **B645**, 88 (2007);
   J. E. Kim, J. H. Kim and B. Kyae, JHEP **0706**, 034 (2007);
   O. Lebedev, *et al.*, Phys. Rev. **D77**, 046013 (2008).
10. E. Witten, [hep-ph/0201018];
    M. Dine *et al.*, Phys. Rev. **D66**, 115001 (2002), [hep-ph/0206268].
11. Y. Kawamura, Prog. Theor. Phys. **103**, 613 (2000);
    ibid., **105**, 999 (2001);
    G. Altarelli *et al.*, Phys. Lett. **B5111**, 257 (2001);
    L.J. Hall *et al.*, Phys. Rev. **D64**, 055003 (2001);
    A. Hebecker and J. March-Russell, Nucl. Phys. **B613**, 3 (2001);
    T. Asaka *et al.*, Phys. Lett. **B523**, 199 (2001);
    L.J. Hall *et al.*, Phys. Rev. **D65**, 035008 (2002);
    R. Dermisek and A. Mafi, Phys. Rev. **D65**, 055002 (2002);
    H.D. Kim and S. Raby, JHEP **0301**, 056 (2003).
12. For a recent review see, R. Blumenhagen *et al.*, "Toward realistic intersecting D-brane models," hep-th/0502005.
13. M.J. Dolan, S. Krippendorf, and F. Quevedo, JHEP **1110**, 024 (2011).
14. G. Aldazabal *et al.*, Nucl. Phys. **B452**, 3 (1995);
    Z. Kakushadze and S.H.H. Tye, Phys. Rev. **D54**, 7520 (1996);
    Z. Kakushadze *et al.*, Int. J. Mod. Phys. **A13**, 2551 (1998).
15. G. B. Cleaver *et al.*, Int. J. Mod. Phys. **A16**, 425 (2001), hep-ph/9904301;
    ibid., Nucl. Phys. **B593**, 471 (2001) hep-ph/9910230.
16. V. Braun *et al.*, Phys. Lett. **B618**, 252 (2005), hep-th/0501070;
    ibid., JHEP **506**, 039 (2005), [hep-th/0502155].
17. E. Witten, Nucl. Phys. **B471**, 135 (1996), [hep-th/9602070].
18. H. Georgi *et al.*, Phys. Rev. Lett. **33**, 451 (1974);
    See also the definition of effective field theories by S. Weinberg, Phys. Lett. **91B**, 51 (1980).
19. See talks on proposed and running nucleon decay experiments, and theoretical talks by P. Langacker, p. 131, and W.J. Marciano and A. Sirlin, p. 151, in *The Second Workshop on Grand Unification*, eds. J.P. Leveille *et al.*, Birkhäuser, Boston (1981).
20. W.J. Marciano, p. 190, *Eighth Workshop on Grand Unification*, ed. K. Wali, World Scientific Publishing Co., Singapore (1987).
21. U. Amaldi *et al.*, Phys. Lett. **B260**, 447 (1991);
    J. Ellis *et al.*, Phys. Lett. **B260**, 131 (1991);
    P. Langacker and M. Luo, Phys. Rev. **D44**, 817 (1991);
    P. Langacker and N. Polonsky, Phys. Rev. **D47**, 4028 (1993);
    M. Carena *et al.*, Nucl. Phys. **B406**, 59 (1993);
    see also the review by S. Dimopoulos *et al.*, Physics Today, p. 25 October (1991).
22. B.C. Allanach, Comput. Phys. Commun. **143**, 305 (2002) [hep-ph/0104145].
23. S. Dimopoulos *et al.*, Phys. Rev. **D24**, 1681 (1981);
    S. Dimopoulos and H. Georgi, Nucl. Phys. **B193**, 150 (1981);
    L. Ibanez and G.G. Ross, Phys. Lett. **105B**, 439 (1981);
    N. Sakai, Z. Phys. **C11**, 153 (1981);
    M.B. Einhorn and D.R.T. Jones, Nucl. Phys. **B196**, 475 (1982);
    W.J. Marciano and G. Senjanovic, Phys. Rev. **D25**, 3092 (1982).
24. D.I. Kazakov, Lectures given at the European School on High Energy Physics, Aug.-Sept. 2000, Caramulo, Portugal [hep-ph/0012288v2].
25. V. Lucas and S. Raby, Phys. Rev. **D54**, 2261 (1996) [hep-ph/9601303];
    T. Blazek *et al.*, Phys. Rev. **D56**, 6919 (1997) [hep-ph/9611217];
    G. Altarelli *et al.*, JHEP **0011**, 040 (2000) [hep-ph/0007254].
26. R. Dermíšek *et al.*, Phys. Rev. **D63**, 035001 (2001);
    K.S. Babu *et al.*, Nucl. Phys. **B566**, 33 (2000).
27. M. L. Alciati *et al.*, JHEP **0503**, 054 (2005) [hep-ph/0501086].
28. G. Anderson *et al.*, eConf **C960625**, SUP107 (1996) [hep-ph/9609457].
29. R.N. Mohapatra and M.K. Parida, Phys. Rev. **D47**, 264 (1993).
30. D.G. Lee *et al.*, Phys. Rev. **D51**, 229 (1995).
31. Eur. Phys. J. **C64**, 689 (2009).
32. K. Nakamura *et al.*, (Particle Data Group), J. Phys. **G37**, 075021 (2010).
33. K. Nakamura *et al.*, (Particle Data Group), J. Phys. **G37**, 075021 (2010).
34. S. Raby *et al.*, Phys. Lett. **B687**, 342 (2010) [arXiv:0911.4249 [hep-ph]].
35. K.S. Babu and S.M. Barr, Phys. Rev. **D48**, 5354 (1993);
    V. Lucas and S. Raby, Phys. Rev. **D54**, 2261 (1996);
    S.M. Barr and S. Raby, Phys. Rev. Lett. **79**, 4748 (1997) and references therein.

36. G. Altarelli *et al.*, JHEP **0011**, 040 (2000) See also earlier papers by A. Masiero *et al.*, Phys. Lett. **B115**, 380 (1982); B. Grinstein, Nucl. Phys. **B206**, 387 (1982).
37. K.R. Dienes *et al.*, Phys. Rev. Lett. **91**, 061601 (2003).
38. L. J. Hall *et al.*, Phys. Rev. **D64**, 055003 (2001).
39. N. Arkani-Hamed and S. Dimopoulos, JHEP **0506**, 073 (2005) [hep-th/0405159].
40. G.F. Giudice and A. Romanino, Nucl. Phys. **B699**, 65 (2004) [Erratum: *ibid.*, Nucl. Phys. **B706**, 65 (2005)] [hep-ph/0406088].
41. M. Chanowitz *et al.*, Nucl. Phys. **B135**, 66 (1978); For the corresponding SUSY analysis, see M. Einhorn and D.R.T. Jones, Nucl. Phys. **B196**, 475 (1982); K. Inoue *et al.*, Prog. Theor. Phys. **67**, 1889 (1982); L. E. Ibanez and C. Lopez, Phys. Lett. **B126**, 54 (1983); *ibid.*, Nucl. Phys. **B233**, 511 (1984).
42. K. Agashe *et al.*, [hep-ph/0502222].
43. M. Gell-Mann *et al.*, in *Supergravity*, eds. P. van Nieuwenhuizen and D.Z. Freedman, North-Holland, Amsterdam, 1979, p. 315.
44. S. Weinberg, Phys. Rev. **D26**, 287 (1982); N. Sakai and T Yanagida, Nucl. Phys. **B197**, 533 (1982).
45. G. Farrar and P. Fayet, Phys. Lett. **B76**, 575 (1978).
46. S. Dimopoulos *et al.*, Phys. Lett. **112B**, 133 (1982); J. Ellis *et al.*, Nucl. Phys. **B202**, 43 (1982).
47. L.E. Ibanez and G.G. Ross, Nucl. Phys. **B368**, 3 (1992).
48. H. K. Dreiner, C. Luhn, and M. Thormeier, Phys. Rev. **D73**, 075007 (2006).
49. For a recent discussion, see C.S. Aulakh *et al.*, Nucl. Phys. **B597**, 89 (2001).
50. H. M. Lee *et al.*, Phys. Lett. **B694**, 491 (2011); R. Kappl *et al.*, Nucl. Phys. **B847**, 325 (2011); H. M. Lee *et al.*, Nucl. Phys. **B850**, 1 (2011).
51. R. Barbieri *et al.*, Phys. Lett. **B407**, 250 (1997).
52. G. F. Giudice and R. Rattazzi, Phys. Lett. **B406**, 321 (1997).
53. R. Barbier *et al.*, Phys. Rev. **420**, 1 (2005).
54. Makoto Miura [Super-Kamiokande Collab.], ICHEP 2010.
55. T. Goto and T. Nihei, Phys. Rev. **D59**, 115009 (1999) [hep-ph/9808255]; H. Murayama and A. Pierce, Phys. Rev. **D65**, 055009 (2002) hep-ph/0108104.
56. B. Bajc *et al.*, Phys. Rev. **D66**, 075005 (2002) [hep-ph/0204311].
57. J.L. Chkareuli and I.G. Gogoladze, Phys. Rev. **D58**, 055011 (1998) [hep-ph/9803335].
58. K.S. Choi, Phys. Lett. **B668**, 392 (2008).
59. L.J. Hall and Y. Nomura, Phys. Rev. **D66**, 075004 (2002); H.D. Kim *et al.*, JHEP **0505**, 036 (2005).
60. M. Baldoceolin et al., Z. Phys. **C63**, 409 (1994).
61. K. S. Babu and R. N. Mohapatra, Phys. Lett. **B518**, 269 (2001) [hep-ph/0108089].
62. H. Georgi and D.V. Nanopoulos, Nucl. Phys. **B159**, 16 (1979); J. Harvey *et al.*, Phys. Lett. **B92**, 309 (1980); *ibid.*, Nucl. Phys. **B199**, 223 (1982).
63. T. Banks, Nucl. Phys. **B303**, 172 (1988); M. Olechowski and S. Pokorski, Phys. Lett. **B214**, 393 (1988); S. Pokorski, Nucl. Phys. (Proc. Supp.) **B13**, 606 (1990); B. Ananthanarayan *et al.*, Phys. Rev. **D44**, 1613 (1991); Q. Shafi and B. Ananthanarayan, ICTP Summer School lectures (1991); S. Dimopoulos *et al.*, Phys. Rev. Lett. **68**, 1984 (1992); *ibid.*, Phys. Rev. **D45**, 4192 (1992); G. Anderson *et al.*, Phys. Rev. **D47**, 3702 (1993); B. Ananthanarayan *et al.*, Phys. Lett. **B300**, 245 (1993); G. Anderson *et al.*, Phys. Rev. **D49**, 3660 (1994); B. Ananthanarayan *et al.*, Phys. Rev. **D50**, 5980 (1994).
64. LEP Higgs Working Group and ALEPH Collab. and DELPHI Collab. and L3 Collab. and OPAL Collab., Preliminary results, [hep-ex/0107030] (2001).
65. M. Carena and H.E. Haber, Prog. in Part. Nucl. Phys. **50**, 63 (2003) [hep-ph/0208209].
66. L.J. Hall *et al.*, Phys. Rev. **D50**, 7048 (1994); M. Carena *et al.*, Nucl. Phys. **B419**, 213 (1994); R. Rattazzi and U. Sarid, Nucl. Phys. **B501**, 297 (1997).
67. Blazek *et al.*, Phys. Rev. Lett. **88**, 111804 (2002) [hep-ph/0107097]; *ibid.*, Phys. Rev. **D65**, 115004 (2002) [hep-ph/0201081]; K. Tobe and J. D. Wells, Nucl. Phys. **B663**, 123 (2003) [hep-ph/0301015]; D. Auto *et al.*, JHEP **0306**, 023 (2003) [hep-ph/0302155]; R. Dermisek *et al.*, JHEP **0304**, 037 (2003); *ibid.*, JHEP **0509**, 029 (2005).
68. W. Altmannshofer *et al.*, Phys. Lett. **B668**, 385 (2008); D. Guadagnoli *et al.*, JHEP **0910**, 059 (2009).
69. H. Baer *et al.*, JHEP **0810**, 079 (2008); H. Baer *et al.*, JHEP **0909**, 005 (2009).
70. I. Gogoladze *et al.*, JHEP **1012**, 055 (2010); S. Dar *et al.*, [arXiv:1105.5122 [hep-ph]]; I. Gogoladze *et al.*, [arXiv:1107.1228 [hep-ph]].
71. M. Badziak, M. Olechowski, and S. Pokorski, JHEP **1108**, 147 (2011).
72. H. Georgi and C. Jarlskog, Phys. Lett. **B86**, 297 (1979).
73. S. Antusch and M. Spinrath, Phys. Rev. **D79**, 095004 (2009).
74. K.S. Babu and R.N. Mohapatra, Phys. Rev. Lett. **74**, 2418 (1995); V. Lucas and S. Raby, Phys. Rev. **D54**, 2261 (1996); T. Blažek *et al.*, Phys. Rev. **D56**, 6919 (1997); R. Barbieri *et al.*, Nucl. Phys. **B493**, 3 (1997); T. Blazek *et al.*, Phys. Rev. **D60**, 113001 (1999); *ibid.*, Phys. Rev. **D62**, 055001 (2000); Q. Shafi and Z. Tavartkiladze, Phys. Lett. **B487**, 145 (2000); C.H. Albright and S.M. Barr, Phys. Rev. Lett. **85**, 244 (2000); K.S. Babu *et al.*, Nucl. Phys. **B566**, 33 (2000); M. -C. Chen and K. T. Mahanthappa, Phys. Rev. **D62**, 113007 (2000); G. Altarelli *et al.*, Ref. 36; Z. Berezhiani and A. Rossi, Nucl. Phys. **B594**, 113 (2001); C. H. Albright and S. M. Barr, Phys. Rev. **D64**, 073010 (2001); M. -C. Chen, K. T. Mahanthappa, Int. J. Mod. Phys. **A18**, 5819 (2003); R. Dermisek and S. Raby, Phys. Lett. **B622**, 327 (2005); R. Dermisek *et al.*, Phys. Rev. **D74**, 035011 (2006); M. Albrecht *et al.*, JHEP **0710**, 055 (2007); K. S. Babu *et al.*, JHEP **1006**, 084 (2010).
75. G. Lazarides *et al.*, Nucl. Phys. **B181**, 287 (1981); T. E. Clark *et al.*, Phys. Lett. **B115**, 26 (1982); K. S. Babu and R. N. Mohapatra, Phys. Rev. Lett. **70**, 2845 (1993).
76. B. Bajc *et al.*, Phys. Rev. Lett. **90**, 051802 (2003).
77. H. S. Goh *et al.*, Phys. Lett. **B570**, 215 (2003) [hep-ph/0303055]; *ibid.*, Phys. Rev. **D68**, 115008 (2003) [hep-ph/0308197]; B. Dutta *et al.*, Phys. Rev. **D69**, 115014 (2004) [hep-ph/0402113]; S. Bertolini and M. Malinsky, [hep-ph/0504241]; K. S. Babu and C. Macesanu, [hep-ph/0505200].
78. B. Bajc *et al.*, JHEP **0811**, 007 (2008).
79. P. Minkowski, Phys. Lett. **B67**, 421 (1977).
80. T. Yanagida, in *Proceedings of the Workshop on the Unified Theory and the Baryon Number of the Universe*, eds. O. Sawada and A. Sugamoto, KEK report No. 79-18, Tsukuba, Japan, 1979; S. Glashow, Quarks and leptons, published in *Proceedings of the Carg'ese Lectures,*M. Levy (ed.), Plenum Press, New York, (1980); M. Gell-Mann *et al.*, in *Supergravity,*ed. P. van Nieuwenhuizen *et al.*, North-Holland, Amsterdam, (1979), p. 315; R.N. Mohapatra and G. Senjanovic, Phys. Rev. Lett. **44**, 912 (1980).
81. G.L. Fogli *et al.*, Phys. Rev. **D84**, 053007 (2011).
82. T. Schwetz, M. Tortola, and J.W.F. Valle, New J. Phys. **13**, 109401 (2011), [arXiv:1108.1376 [hep-ph]].

83. C.H. Albright and M.-C. Chen, Phys. Rev. **D74**, 113006 (2006).
84. G. 't Hooft, Nucl. Phys. **B79**, 276 (1974);
A.M. Polyakov, Pis'ma Zh. Eksp. Teor. Fiz. **20**, 430 (1974) [JETP Lett. **20**, 194 (1974)];
For a pedagogical introduction, see S. Coleman, in *Aspects of Symmetry*, Selected Erice Lectures, Cambridge University Press, Cambridge, (1985), and P. Goddard and D. Olive, Rep. Prog. Phys. **41**, 1357 (1978).
85. I. De Mitri, (MACRO Collab.), Nucl. Phys. (Proc. Suppl.) **B95**, 82 (2001).
86. For a review, see A.D. Linde, *Particle Physics and Inflationary Cosmology*, Harwood Academic, Switzerland (1990).
87. G. R. Dvali *et al.*, Phys. Rev. Lett. **80**, 2281 (1998) [hep-ph/9710301].
88. P. Langacker and S. Y. Pi, Phys. Rev. Lett. **45**, 1 (1980).
89. G. R. Dvali *et al.*, Phys. Rev. Lett. **75**, 4559 (1995) [hep-ph/9507230].
90. V. Rubakov, Nucl. Phys. **B203**, 311 (1982), Institute of Nuclear Research Report No. P-0211, Moscow (1981), unpublished;
C. Callan, Phys. Rev. **D26**, 2058 (1982);
F. Wilczek, Phys. Rev. Lett. **48**, 1146 (1982);
See also, S. Dawson and A.N. Schellekens, Phys. Rev. **D27**, 2119 (1983).
91. K. Freese *et al.*, Phys. Rev. Lett. **51**, 1625 (1983).
92. M. Fukugita and T. Yanagida, Phys. Lett. **B174**, 45 (1986);
See also the recent review by W. Buchmuller *et al.*, hep-ph/0502169 and references therein.
93. E. Witten, Phys. Lett. **105B**, 267 (1981).
94. S. Dimopoulos and F. Wilczek, *Proceedings Erice Summer School*, ed. A. Zichichi (1981);
K.S. Babu and S.M. Barr, Phys. Rev. **D50**, 3529 (1994).
95. R. Barbieri *et al.*, Nucl. Phys. **B391**, 487 (1993);
Z. Berezhiani *et al.*, Nucl. Phys. **B444**, 61 (1995);
Q. Shafi and Z. Tavartkiladze, Phys. Lett. **B522**, 102 (2001).
96. G.F. Giudice and A. Masiero, Phys. Lett. **B206**, 480 (1988);
J.E. Kim and H.P. Nilles, Mod. Phys. Lett. **A9**, 3575 (1994).
97. L. Randall and C. Csaki, hep-ph/9508208.
98. A. Hebecker *et al.*, [arXiv:0801.4101 [hep-ph]];
F. Brümmer *et al.*, JHEP **08**, 011 (2009);
F. Brümmer *et al.*, JHEP **04**, 006 (2010).
99. T. P. T. Dijkstra *et al.*, Phys. Lett. **B609**, 408 (2005).
100. T. Kobayashi *et al.*, Phys. Lett. **B593**, 262 (2004);
ibid., Nucl. Phys. **B704**, 3 (2005).
101. W. Buchmuller *et al.*, Phys. Rev. Lett. **96**, 121602 (2006);
ibid., Nucl. Phys. **B785**, 149 (2007).
102. O. Lebedev *et al.*, Phys. Lett. **B645**, 88 (2007);
ibid., [arXiv:0708.2691[hep-th]];
O. Lebedev *et al.*, Phys. Lett. **B668**, 331 (2008).
103. J. E. Kim *et al.*, JHEP **0706**, 034 (2007);
J. E. Kim and B. Kyae, Phys. Rev. **D77**, 106008 (2008).
104. L. B. Anderson *et al.*, [arXiv:1106.4804 [hep-th]].
105. C. Beasley *et al.*, JHEP **01**, 058 (2009);
R. Donagi and M. Wijnholt, [arXiv:0802.2969 [hep-th]];
C. Beasley *et al.*, JHEP **01**, 059 (2009);
R. Donagi and M. Wijnholt, [arXiv:0808.2223 [hep-th]];
R. Blumenhagen *et al.*, [arXiv:0811.2936 [hep-th]].
106. C. M. Chen and Y. C. Chung, Nucl. Phys. **B824**, 273 (2010).
107. J. Marsano *et al.*, JHEP **0908**, 030 (2009).
108. R. Blumenhagen, Phys. Rev. Lett. **102**, 071601 (2009).
109. S. Raby, Rept. on Prog. in Phys. **74**, 036901 (2011).

17. HEAVY-QUARK AND SOFT-COLLINEAR EFFECTIVE THEORY

Updated September 2013 by C.W. Bauer (LBNL) and M. Neubert (U. Mainz).

17.1. Effective Field Theories

Quantum field theories represent the most precise computational tool for describing physics at the highest energies. One of their characteristic features is that they almost inevitably involve multiple length scales. When trying to determine the value of an observable, quantum field theory demands that all possible virtual states and hence all particles be included in the calculation. Since these particles have widely different masses, the final prediction is sensitive to many scales. This fact represents a formidable challenge from a practical point of view. No realistic quantum field theories can be solved exactly, so that one has to resort to approximation schemes; these, however, are typically most straightforward when only a single scale is involved at a time.

Effective field theories (EFTs) provide a general theoretical framework to deal with the multi-scale problems of realistic quantum field theories. This framework aims to reduce such problems to a combination of separate and simpler single-scale problems; simultaneously, however, it provides an organization scheme whereby the other scales are not omitted but allowed to play their role in a separate step of the computation. The philosophy and basic principles of this approach are very generic, and correspondingly EFTs represent a widely used method in many different areas of high-energy physics, from the low-energy scales of atomic and nuclear physics to the high-energy scales of (partly yet unknown) elementary particle physics. EFTs can play a role both within analytic perturbative computations and in the context of non-perturbative numerical simulations; see [1–3] for some early references. One of the simplest applications of EFTs to particle physics is to describe an underlying theory that is only probed at energy scales $E < \Lambda$. Any particle with mass $m > \Lambda$ cannot be produced as a real state and therefore only leads to short-distance virtual effects. Thus, one can construct an effective theory in which the quantum fluctuations of such heavy particles are "integrated out" from the generating functional integral for Green functions. This results in a simpler theory containing only those degrees of freedom that are relevant to the energy scales under consideration. In fact, the standard model of particle physics itself is widely viewed as an EFT of some yet unknown, more fundamental theory.

The development of any effective theory starts by identifying the degrees of freedom that are relevant to describe the physics at a given energy (or length) scale, and constructing the Lagrangian describing the interactions among these fields. Short-distance quantum fluctuations associated with much smaller length scales are absorbed into the coefficients of the various operators in the effective theory. These coefficients are determined in a matching procedure, by requiring that the EFT reproduces the matrix elements of the full theory up to power corrections. In many cases the effective Lagrangian exhibits enhanced symmetries compared with the fundamental theory, allowing for simple and sometimes striking predictions relating different observables.

17.2. Heavy-Quark Effective Theory

Heavy-quark systems provide prime examples for applications of the EFT technology, because the hierarchy $m_Q \gg \Lambda_{\rm QCD}$ (with $Q = b, c$) provides a natural separation of scales. Physics at the scale m_Q is of a short-distance nature and can be treated perturbatively, while for heavy-quark systems there is always also some hadronic physics governed by the confinement scale $\Lambda_{\rm QCD}$ of the strong interaction. Being able to separate the short-distance and long-distance effects associated with these two scales is crucial for any quantitative description in heavy-quark physics. For instance, if the long-distance hadronic matrix elements are obtained from lattice QCD, then it is necessary to analytically compute the short-distance effects, which come from short-wavelength modes that do not fit on present-day lattices. In many other instances, the long-distance hadronic physics can be encoded in a small number of universal parameters.

17.2.1. ***General idea & derivation of the effective Lagrangian*** : The simplest effective theory for heavy-quark systems is the heavy-quark effective theory (HQET) [4–7] (see [8,9] for detailed discussions). It provides a simplified description of the soft interactions of a single heavy quark interacting with soft, light partons. This includes the interactions that bind the heavy quark with other light partons inside heavy mesons (B, B^*, ...) and baryons (Λ_b, Σ_b, ...).

A softly interacting heavy quark is nearly on-shell. Its momentum may be decomposed as $p_Q = m_Q v + k$, where v is the 4-velocity of the hadron containing the heavy quark. The "residual momentum" k results from the soft interactions of the heavy quark with its environment and satisfies $v \cdot k \sim \Lambda_{\rm QCD}$ and $k^2 \sim \Lambda^2_{\rm QCD}$, which in the rest frame of the heavy hadron reduces to $k^\mu \sim \Lambda_{\rm QCD}$. In the limit $m_Q \gg \Lambda_{\rm QCD}$, the soft interactions do not change the 4-velocity of the heavy quark, which is therefore a conserved quantum number that is often used as a label on the effective heavy-quark fields. A nearly on-shell Dirac spinor has two large and two small components. We define

$$Q(x) = e^{-im_Q v\cdot x}\,[h_v(x) + H_v(x)]\,, \tag{17.1}$$

where

$$h_v(x) = e^{im_Q v\cdot x}\,\frac{1+\not v}{2}\,Q(x)\,, \qquad H_v(x) = e^{im_Q v\cdot x}\,\frac{1-\not v}{2}\,Q(x) \tag{17.2}$$

are the large ("upper") and small ("lower") components of the spinor field, respectively. The extraction of the phase factor in Eq. (17.1) implies that the fields h_v and H_v carry the residual momentum k. These fields obey the projection relations $\not v\, h_v = h_v$ and $\not v\, H_v = -H_v$. Inserting these definitions into the Dirac Lagrangian yields

$$\mathcal{L}_Q = \bar h_v\, iv\cdot D\, h_v + \bar H_v(-iv\cdot D - 2m_Q)H_v + \bar h_v\, i\vec{\not D}\, H_v + \bar H_v\, i\vec{\not D}\, h_v\,, \tag{17.3}$$

where $i\vec D^\mu = iD^\mu - v^\mu\, iv\cdot D$ is the "spatial" covariant derivative (note that $v^\mu = (1,\vec 0)$ in the heavy-hadron rest frame). The interpretation of Eq. (17.3) is that the field h_v describes a massless fermion, while H_v describes a heavy fermion with mass $2m_Q$. Both modes are coupled to each other via the last two terms. Soft interactions cannot excite the heavy fermion, so one can integrate it out from the generating functional of the theory. The light field which remains describes the fluctuations of the heavy quark about its mass shell. Solving the classical equation of motion for the field H_v yields

$$H_v = \frac{1}{2m_Q + iv\cdot D}\, i\vec{\not D}\, h_v = \frac{1}{2m_Q}\sum_{n=0}^{\infty}\left(-\frac{iv\cdot D}{2m_Q}\right)^n i\vec{\not D}\, h_v\,, \tag{17.4}$$

which implies $H_v = O(\Lambda_{\rm QCD}/m_Q)\, h_v$, provided the residual momenta are small. The effective Lagrangian of HQET is obtained by inserting this result into Eq. (17.3). At subleading order in $1/m_Q$ one finds

$$\mathcal{L}_{\rm HQET} = \bar h_v\, iv\cdot D_s\, h_v + \frac{1}{2m_Q}$$

$$\left[\bar h_v (i\vec D_s)^2 h_v + C_{\rm mag}(\mu)\,\frac{g}{2}\,\bar h_v\,\sigma_{\mu\nu}\,G_s^{\mu\nu} h_v\right] + \ldots\,. \tag{17.5}$$

Note that the covariant derivative $iD_s^\mu = i\partial^\mu + gA_s^\mu$ and the field strength $G_s^{\mu\nu}$ contain only the soft gluon field. Hard gluons have been integrated out, and their effects are contained in the Wilson coefficients of the various operators in the effective Lagrangian. From the leading operator one derives the Feynman rules of HQET. The new operators entering at subleading order are referred to as the "kinetic energy" and "chromo-magnetic interaction". The kinetic-energy operator corresponds to the first correction term in the Taylor expansion of the relativistic energy $E = m_Q + \vec p^{\,2}/2m_Q + \ldots$. Lorentz invariance, which is encoded as a reparametrization invariance of the effective Lagrangian [10], ensures that its Wilson coefficient is not renormalized ($C_{\rm kin} \equiv 1$). The coefficient of the chromo-magnetic operator, $C_{\rm mag}(\mu) = 1 + \mathcal{O}(\alpha_s)$, receives corrections starting at one-loop order.

17.2.2. ***Spin-flavor symmetry and applications in spectroscopy*** : The leading term in the HQET Lagrangian exhibits a global spin-flavor symmetry. Its physical meaning is that, in the infinite mass limit, the properties of hadronic systems containing a single heavy quark are insensitive to the spin and flavor of the heavy quark [11,12]. The spin symmetry results from the fact that there appear no Dirac matrices in the leading term of the effective Lagrangian in Eq. (17.5), implying that the interactions of the heavy quark with soft gluons leave its spin unchanged. The flavor symmetry arises since the mass of the heavy quark does not appear at leading order. When there are n_Q heavy quarks moving at the same velocity, one can simply extend Eq. (17.5) by summing over n_Q identical terms for heavy-quark fields h_v^i. The result is invariant under rotations in flavor space. When combined with the spin symmetry, the symmetry group becomes promoted to SU($2n_Q$). The flavor symmetry is broken by the operators arising at order $1/m_Q$ and higher. However, at first order only the chromo-magnetic operator breaks the spin symmetry.

The spin-flavor symmetry leads to many interesting relations between the properties of hadrons containing a heavy quark. The most direct consequences concern the spectroscopy of such states [13]. In the heavy-quark limit, the spin of the heavy quark and the total angular momentum j of the light degrees of freedom are separately conserved by the strong interactions. Because of heavy-quark symmetry, the dynamics is independent of the spin and mass of the heavy quark. Hadronic states can thus be classified by the quantum numbers (flavor, spin, parity, etc.) of the light degrees of freedom. The spin symmetry predicts that, for fixed $j \neq 0$, there is a doublet of degenerate states with total spin $J = j \pm 1/2$. The flavor symmetry relates the properties of states with different heavy-quark flavor. In the case of the ground-state mesons containing a heavy quark, the light degrees of freedom have the quantum numbers of an antiquark, and the degenerate states are the pseudoscalar ($J = 0$) and vector ($J = 1$) mesons. Their masses are split by hyperfine corrections of order $1/m_Q$, such that one expects $m_{B^*} - m_B = O(1/m_b)$ and $m_{D^*} - m_D = O(1/m_c)$. It follows that $m_{B^*}^2 - m_B^2 \simeq m_{D^*}^2 - m_D^2 \simeq$ const. The data are compatible with this result: $m_{B^*}^2 - m_B^2 \simeq 0.49\,\mathrm{GeV}^2$ and $m_{D^*}^2 - m_D^2 \simeq 0.55\,\mathrm{GeV}^2$.

17.2.3. ***Weak decay form factors*** : Of particular interest are the relations between the weak decay form factors of heavy mesons, which parametrize hadronic matrix elements of currents between two meson states containing a heavy quark. These relations have been derived by Isgur and Wise [12], generalizing ideas developed by Nussinov and Wetzel [14] and Voloshin and Shifman [15]. For the purpose of this discussion, it is convenient to work with a mass-independent normalization of meson states and use velocity rather than momentum variables.

Consider the elastic scattering of a pseudoscalar meson, $P(v) \to P(v')$, induced by an external vector current coupled to the heavy quark contained in P, which acts as a color source moving with the meson's velocity v. The action of the current is to replace instantaneously the color source by one moving at velocity v'. Soft gluons need to be exchanged in order to rearrange the light degrees of freedom and build the final state meson moving at velocity v'. This rearrangement leads to a form factor suppression. The important observation is that, in the $m_Q \to \infty$ limit, the form factor can only depend on the Lorentz boost $\gamma = v \cdot v'$ connecting the rest frames of the initial and final-state mesons (as long as $\gamma = \mathcal{O}(1)$). In the effective theory the hadronic matrix element describing the scattering process can be written as

$$\langle P(v')|\,\bar h_{v'}\gamma^\mu h_v\,|P(v)\rangle = \xi(v\cdot v')(v+v')^\mu, \tag{17.6}$$

with a form factor $\xi(v \cdot v')$ that is real and independent of m_Q. By flavor symmetry, the form factor remains identical when one replaces the heavy quark Q in one of the meson states by a heavy quark Q' of a different flavor, thereby turning P into another pseudoscalar meson P'. At the same time, the current becomes a flavor-changing vector current. This universal form factor is called the Isgur-Wise function [12]. For equal velocities the vector current $J^\mu = \bar h_v \gamma^\mu h_v$ is conserved in the effective theory, irrespective of the flavor of the heavy quarks. The corresponding conserved charges are the generators of the flavor symmetry. It follows that the Isgur-Wise function is normalized at the point of equal velocities: $\xi(1) = 1$. Since the recoil energy of the daughter meson P' in the rest frame of the parent meson P is $E_{\rm recoil} = m_{P'}\,(v \cdot v' - 1)$, the point $v \cdot v' = 1$ is referred to as the zero-recoil limit. The heavy-quark spin symmetry leads to additional relations among weak decay form factors. It can be used to relate matrix elements involving vector mesons to those involving pseudoscalar mesons, which once again can be described completely in terms of the universal Isgur-Wise function.

These form factor relations imposed by heavy-quark symmetry describe the semileptonic decay processes $\bar B \to D\,\ell\,\bar\nu$ and $\bar B \to D^*\ell\,\bar\nu$ in the limit of infinite heavy-quark masses. They are model-independent consequences of QCD. The known normalization of the Isgur-Wise function at zero recoil can be used to obtain a model-independent measurement of the element $|V_{cb}|$ of the Cabibbo-Kobayashi-Maskawa (CKM) matrix. The semileptonic decay $\bar B \to D^*\ell\,\bar\nu$ is ideally suited for this purpose [16]. Experimentally, this is a particularly clean mode, since the reconstruction of the D^* meson mass provides a powerful rejection against background. From the theoretical point of view, it is ideal since the decay rate at zero recoil is protected by Luke's theorem against first-order power corrections in $1/m_Q$ [17]. This is described in more detail in Section 12 of the PDG Book.

17.2.4. ***Decoupling transformation*** : At leading order in $1/m_Q$, the couplings of soft gluons to heavy quarks in the effective Lagrangian Eq. (17.5) can be removed by the field redefinition $h_v(x) = Y_v(x)\,h_v^{(0)}(x)$, where $Y_v(x)$ denotes a time-like soft Wilson line along the direction of v, extending from minus infinity to the point x. In terms of the new fields, the HQET Lagrangian becomes

$$\mathcal{L}_{\rm HQET} = \bar h_v^{(0)} iv\cdot\partial\, h_v^{(0)} + O(1/m_Q). \tag{17.7}$$

At leading order in $1/m_Q$, this is a free theory as far as the strong interactions of heavy quarks are concerned. However, the theory is nevertheless non-trivial in the presence of external sources. Consider, e.g., the case of a weak-interaction heavy-quark current

$$\bar h_{v'}\gamma^\mu(1-\gamma_5)h_v = \bar h_{v'}^{(0)}\gamma^\mu(1-\gamma_5)\,Y_{v'}^\dagger Y_v\,h_v^{(0)}, \tag{17.8}$$

where v and v' are the velocities of the heavy mesons containing the heavy quarks. Unless the two velocities are equal, corresponding to the zero-recoil limit discussed above, the object $Y_{v'}^\dagger Y_v$ is non-trivial, and hence the soft gluons do not decouple from the heavy quarks inside the current operator. One may interpret $Y_{v'}^\dagger Y_v$ as a Wilson loop with a cusp at the point x, where the two paths parallel to the different velocity vectors intersect. The presence of the cusp leads to non-trivial ultra-violet behavior (for $v \neq v'$), which is described by a cusp anomalous dimension $\Gamma_c(v \cdot v')$ that was calculated at two-loop order in Ref. 18. It coincides with the velocity-dependent anomalous dimension of heavy-quark currents, which was introduced in the context of HQET in [19]. The interpretation of heavy quarks as Wilson lines is a useful tool, which was put forward in some of the very first papers on the subject, e.g. Ref. 4. This technology will be useful in the study of the interactions of heavy quarks with collinear degrees of freedom discussed later in this review.

17.2.5. ***Heavy-quark expansion for inclusive decays*** : The theoretical description of inclusive decays of hadrons containing a heavy quark exploits two observations [20–24]: bound-state effects related to the initial state can be calculated using the heavy-quark expansion, and the fact that the final state consists of a sum over many hadronic channels eliminates the sensitivity to the properties of individual final-state hadrons. The second feature rests on the hypothesis of quark-hadron duality, i.e. the assumption that decay rates are calculable in QCD after a smearing procedure has been applied [25]. In semileptonic decays, the integration over the lepton spectrum provides a smearing over the invariant hadronic mass of the final state (global duality). For nonleptonic decays, where the total hadronic mass is fixed, the summation over many hadronic final states provides an averaging (local duality). Since global duality is a much weaker assumption, the theoretical control of inclusive semileptonic decays is on much firmer footing.

Using the optical theorem, the inclusive decay width of a hadron H_b containing a b quark can be written in the form

$$\Gamma(H_b) = \frac{1}{M_{H_b}} \,\mathrm{Im}\,\langle H_b|\, i \int \mathrm{d}^4x\, T\,\{\mathcal{H}_{\rm eff}(x), \mathcal{H}_{\rm eff}(0)\}\,|H_b\rangle\,. \qquad (17.9)$$

The effective weak Hamiltonian for b-quark decays consists of dimension-6 four-fermion operators and dipole operators [26]. It follows that the leading contributions to the inclusive decay rate in Eq. (17.9) arise from two-loop diagrams. Because of the large mass of the b quark, the momenta flowing through the internal propagators are large. It is thus possible to construct an operator-product expansion (OPE) for the time-ordered product in Eq. (17.9), in which it is represented as a series of local operators containing two b-quark fields. The operator with the lowest dimension is $\bar{b}b$. The next non-trivial operator has dimension 5 and contains the gluon field. It arises from diagrams in which a soft gluon is emitted from one of the internal lines of the two-loop diagrams. From dimension 6 on, an increasing number of operators contribute. For dimensional reasons, the matrix elements of higher-dimensional operators are suppressed by inverse powers of the b-quark mass. Thus, the total inclusive decay rate of a hadron H_b can be written as [21,22]

$$\Gamma(H_b) = \frac{G_F^2 m_b^5 |V_{cb}|^2}{192\pi^3} \times$$

$$\left\{ c_3\,\langle \bar{b}b\rangle + c_5\,\frac{\langle \bar{b}\, g\sigma_{\mu\nu}G^{\mu\nu} b\rangle}{m_b^2} + \sum_n c_6^{(n)}\,\frac{\langle O_6^{(n)}\rangle}{m_b^3} + \ldots \right\}, \qquad (17.10)$$

where the prefactor arises from the loop integrations, c_i are calculable coefficient functions, and $\langle O_i\rangle$ are the (normalized) forward matrix elements between H_b states. These matrix elements can be systematically expanded in powers of $1/m_b$ using HQET. The result is [21,22]

$$\langle \bar{b}b\rangle = 1 - \frac{\mu_\pi^2(H_b) - \mu_G^2(H_b)}{2m_b^2} + \ldots, \qquad \frac{\langle \bar{b}\, g\sigma_{\mu\nu}G^{\mu\nu} b\rangle}{m_b^2} = \frac{2\mu_G^2(H_b)}{m_b^2} + \ldots, \qquad (17.11)$$

where $\mu_\pi^2(H_b)$ and $\mu_G^2(H_b)$ are the matrix elements of the heavy-quark kinetic energy and chromomagnetic interaction inside the hadron H_b, respectively [27]. For the ground-state heavy mesons and baryons, one has $\mu_G^2(B) = 3(m_{B^*}^2 - m_B^2)/4 \simeq 0.36\,\mathrm{GeV}^2$ and $\mu_G^2(\Lambda_b) = 0$.

From the fully inclusive width Eq. (17.10) one can obtain the lifetime of a heavy hadron via $\tau(H_b) = 1/\Gamma(H_b)$. Due to the universality of the leading term in the heavy-quark expansion, lifetime ratios such as $\tau(B^-)/\tau(\bar{B}^0)$, $\tau(\bar{B}_s^0)/\tau(\bar{B}^0)$, and $\tau(\Lambda_b)/\tau(\bar{B}^0)$ are particularly sensitive to the hadronic parameters determining the power corrections in the expansion. In order to understand these ratios theoretically, it is necessary to include phase-space enhanced power corrections of order $(\Lambda_{\rm QCD}/m_b)^3$ as well as short-distance perturbative effects in the calculation [28,29].

A formula analogous to Eq. (17.10) can be derived for differential distributions in specific inclusive decay processes, assuming that these distributions are integrated over sufficiently large portions of phase space to ensure quark-hadron duality. Important examples are the distributions in lepton energy ($d\Gamma/dE_\ell$) or lepton invariant mass ($d\Gamma/dq^2$), as well as moments of the invariant hadronic mass distribution in the semileptonic processes $\bar{B} \to X_u\,\ell\,\bar{\nu}$ and $\bar{B} \to X_c\,\ell\,\bar{\nu}$, as well as the photon energy spectrum ($d\Gamma/dE_\gamma$) in the radiative process $\bar{B} \to X_s\gamma$. While the latter process is primarily used to test the Standard Model and search for hints of new physics, an analysis of decay distributions in the semileptonic processes can be employed to perform a global fit determining the CKM matrix elements $|V_{ub}|$ and $|V_{cb}|$ along with heavy-quark parameters such as the masses m_b, m_c and the hadronic parameters $\mu_\pi^2(B)$, $\mu_G^2(B)$. These determinations provide some of the most accurate values for these parameters [30].

17.2.6. ***Shape functions and non-local power corrections*** : In certain regions of phase space, in which the hadronic final state in an inclusive heavy-hadron decay is made up of light energetic partons, the local OPE for inclusive decays must be replaced by a more complicated expansion involving hadronic matrix elements of non-local light-ray operators [31,32]. Prominent examples are the radiative decay $\bar{B} \to X_s\gamma$ for large photon energy E_γ near $m_B/2$, and the semileptonic decay $\bar{B} \to X_u\,\ell\,\bar{\nu}$ at large lepton energy or small hadronic invariant mass. In these cases, the differential decay rates at leading order in the heavy-quark expansion can be written in the factorized form $d\Gamma \propto H\,J \otimes S$ [33], where the hard function H and the jet function J are calculable in perturbation theory. The characteristic scales for these functions are set by m_b and $(m_b\Lambda_{\rm QCD})^{1/2}$, respectively. The soft function

$$S(\omega) = \int \frac{dt}{4\pi}\, e^{-i\omega t}\,\langle \bar{B}(v)|\,\bar{h}_v(tn) Y_n(tn) Y_n^\dagger(0) h_v(0)|\bar{B}(v)\rangle \qquad (17.12)$$

is a genuinely non-perturbative object, called the shape function [31,32]. Here Y_n are soft Wilson lines along a light-like direction n aligned with the momentum of the hadronic final-state jet. The jet function and the shape function share a common variable $\omega \sim \Lambda_{\rm QCD}$, and the symbol $\otimes$ denotes a convolution in this variable.

While the hard function is different for the two decays, the jet and soft functions are identical at leading order in $\Lambda_{\rm QCD}/m_Q$. This is particularly important for the soft function. It is this shape function that introduces non-perturbative physics into the theoretical predictions for the cross sections of $\bar{B} \to X_s\gamma$ and $\bar{B} \to X_u\,\ell\bar{\nu}$ in the regions of experimental interest. The fact that both decays depend on the same non-perturbative function makes it possible to determine this non-perturbative information from the measured shape of the photon spectrum in $\bar{B} \to X_s\gamma$, allowing for a better understanding of the process used to determine the CKM element $|V_{ub}|$. In higher orders of the heavy-quark expansion, an increasing number of subleading jet and soft functions is required to describe the decay distributions [34]. These have been analyzed in detail at order $1/m_b$ [35–37]. In the case of $\bar{B} \to X_s\gamma$, some of these non-local effects survive in the total decay rate and give rise to irreducible hadronic uncertainties [38]. The technology for deriving the corresponding factorization theorems relies on SCET, which is discussed below.

17.3. Soft-Collinear Effective Theory

As discussed in the previous section, soft gluons that bind a heavy quark inside a heavy meson cannot change the virtuality of that heavy quark by a significant amount. The ratio of $\Lambda_{\rm QCD}/m_Q$ provided the expansion parameter in HQET, which is a small parameter since $m_Q \gg \Lambda_{\rm QCD}$. This obviously does not work when considering light quarks. However, if the energy Q of the quarks is large, the ratio $\Lambda_{\rm QCD}/Q$ provides a small parameter which can be used to construct an effective theory. One major difference to HQET is that light energetic quarks cannot only emit soft gluons, but they can also emit collinear gluons (an energetic gluon in the same direction as the original quark), without parametrically changing their virtuality. Thus, to fully reproduce the long-distance physics of energetic quarks requires that one includes their interactions with both soft and collinear particles. The resulting effective theory is therefore called soft-collinear effective theory (SCET) [39–41].

A single energetic particle can always be boosted to a frame where all momentum components have similar size, in which case there is no small expansion parameter. Thus the presence of energetic particles must refer to a reference frame defined by external kinematics. SCET has a wide range of applications, with examples being the production of energetic, light states in the decay of a heavy particle in its rest frame, the production of energetic jets in collider environments, and the scattering of energetic particles off a target at rest. In this brief review we will outline the main features of this effective theory and mention a few selected applications.

17.3.1. ***General idea of the expansion*** : Consider a quark with energy Q and virtuality $m \ll Q$, moving along the direction $\vec{n}$. It is convenient to parameterize the momentum p_n of this particle in terms of its light-cone components, defined by $(p_n^-, p_n^+, p_n^\perp) = (\bar{n}\cdot p_n, n\cdot p_n, p_n^\perp)$, where $n^\mu = (1,\vec{n})$ and $\bar{n}^\mu = (1,-\vec{n})$ are light-like 4-vectors, and $n\cdot p_\perp = \bar{n}\cdot p_\perp = 0$. A subscript n has been added to the momentum to identify it as a collinear particle in direction n (more precisely, a particle with energy much larger than its virtuality moving along a direction $\vec{n}$). In terms of these light-cone components, the virtuality satisfies $m^2 = p_n^+ p_n^- + p_n^{\perp 2}$. The individual components of the momentum satisfy

$$(p_n^-, p_n^+, p_n^\perp) \sim (Q, m^2/Q, m) \equiv Q(1,\lambda^2,\lambda), \tag{17.13}$$

where $\lambda = m/Q$ is the expansion parameter of SCET. The virtuality of such an energetic particle remains parametrically unchanged if it interacts with energetic particles in the same direction n, or with soft particles with momentum scaling as

$$(p_s^-, p_s^+, p_s^\perp) \sim Q(\lambda^2,\lambda^2,\lambda^2). \tag{17.14}$$

It is the interactions of collinear and soft degrees of freedom that give rise to the long-distance physics. SCET, which is constructed to reproduce this long-distance dynamics, is therefore an effective theory describing the interactions of collinear and soft particles.

The above power counting treats the soft momentum to be of order m^2/Q, where m denotes the invariant mass of a collinear system. If this mass is of order $\Lambda_{\rm QCD}$, as would be the case for a single energetic hadron, this power counting is no longer applicable, since $\Lambda_{\rm QCD}$ provides a natural cutoff to QCD and the soft momentum cannot be below this scale. To describe such systems requires a modified version of SCET, called $\rm SCET_{II}$, in which the scaling of the soft modes is $Q(\lambda,\lambda,\lambda)$. In this review we will focus mostly on SCET with the scaling discussed before, which is sometimes called $\rm SCET_I$. We will briefly comment on factorization theorems derived in the context of $\rm SCET_{II}$ in Section 17.3.7.

17.3.2. ***Leading-order Lagrangian*** : The derivation of the SCET Lagrangian follows similar steps as the derivation of the HQET Lagrangian in Section 17.2.1, but care needs to be taken to properly account for the interactions of collinear fields with one another. We begin by deriving the Lagrangian for a theory containing only a single collinear sector. We are interested in the interactions of fermion fields $q_n(x)$ with gluon fields $A_n(x)$, which have collinear momentum in the same light-like direction n. Similar to HQET, one can separate the full QCD field into two components, $q_n(x) = \psi_n(x) + \Xi_n(x)$, where (with $n\cdot\bar{n} = 2$)

$$\psi_n(x) = \frac{\not{n}\bar{\not{n}}}{4}\, q_n(x)\,, \qquad \Xi_n(x) = \frac{\bar{\not{n}}\not{n}}{4}\, q_n(x).$$

In terms of these fields, the massless QCD Lagrangian is

$$\begin{aligned}\mathcal{L}_n = {}& \bar\psi_n(x)\frac{\bar{\not{n}}}{2}\, in\cdot D_n\, \psi_n(x) + \bar\Xi_n(x)\frac{\not{n}}{2}\, i\bar{n}\cdot D_n\, \Xi_n(x) \\ & + \bar\psi_n(x) i\not{D}_n^\perp\, \Xi_n(x) + \bar\Xi_n(x) i\not{D}_n^\perp\, \psi_n(x),\end{aligned} \tag{17.15}$$

where we have defined the transverse derivative $D_n^{\perp\mu} = D_n^\mu - \frac{n^\mu}{2}\bar{n}\cdot D_n - \frac{\bar{n}^\mu}{2} n\cdot D_n$. Since $\bar{n}\cdot p_n \gg \Lambda_{\rm QCD}$ the degrees of freedom described by Ξ_n are far off shell. This is similar to the situation with the field H_v in Eq. (17.3). Ξ_n can therefore be eliminated using its equation of motion. Inserting this back into Eq. (17.15), one finds

$$\mathcal{L}_n = \bar\psi_n(x)\left[in\cdot D_n + i\not{D}_n^\perp \frac{1}{i\bar{n}\cdot D_n} i\not{D}_n^\perp\right]\frac{\bar{\not{n}}}{2}\,\psi_n(x). \tag{17.16}$$

While this Lagrangian leads to the correct Feynman rules of SCET, there is one feature that warrants extra discussion. In contrast to the Lagrangian of HQET given in Eq. (17.5), where the derivative scales like the residual momentum k of the heavy quark, the derivatives in Eq. (17.16) pick up both the large momentum components of order Q and $Q\lambda$, as well as the residual momentum of order $Q\lambda^2$. One can separate the large and residual momentum components using a procedure similar to the HQET case. Separating the collinear momentum into a "label" and a residual component, $p^\mu = P^\mu + k^\mu$, and performing a phase redefinition on the collinear fields $\psi_n(x) = e^{iP\cdot x}\,\xi_n(x)$, derivatives acting on the fields $\xi_n(x)$ now only pick out the residual momentum. Since the label momentum in SCET is not conserved as in HQET, one defines a label operator $\mathcal{P}^\mu$ acting as $\mathcal{P}^\mu\xi_n(x) = P^\mu\xi_n(x)$ [40], as well as a corresponding covariant label operator $i\mathcal{D}_n^\mu = \mathcal{P}^\mu + gA_n(x)$.

The final step to complete the Lagrangian of SCET is to include the interactions of collinear fields with soft fields. At leading power, these interactions can be included by adding the soft gluons to the covariant derivatives, while preserving the power counting. This leads to the final SCET Lagrangian [40–42]

$$\mathcal{L}_n = \bar\xi_n(x)\left[in\cdot D_n + gn\cdot A_s + i\not{\mathcal{P}}_n^\perp \frac{1}{i\bar{n}\cdot\mathcal{D}_n} i\not{\mathcal{P}}_n^\perp\right]\frac{\bar{\not{n}}}{2}\,\xi_n(x) + \ldots, \tag{17.17}$$

where the ellipses represent higher-order interactions between soft and collinear particles. The Lagrangian describing collinear fields in different light-like directions is simply given by the sum of the Lagrangians for each direction n separately, i.e. $\mathcal{L} = \sum_n \mathcal{L}_n$. The soft gluons are the same in each individual Lagrangian. An alternative way to understand the separation between large and small momentum components is to derive the Lagrangian of SCET in position space. In this case no label operators are required to describe interactions in SCET, and the dependence on short-distance effects is contained in non-localities at short distances [43]. An important difference between SCET and HQET is that the SCET Lagrangian is not corrected by short distance fluctuations. The physical reason is that in the construction described above no high-momentum modes are integrated out (since no large invariants can be formed out of soft and collinear momenta). Such hard modes arise when different collinear sectors are coupled via some external current (e.g. in jet production at e^+e^- or hadron colliders), or when collinear particles are produced in the rest frame of a decaying heavy object (such as in B decays). Short-distance effects are then incorporated in the Wilson coefficients of the external source operators.

17.3.3. ***Collinear gauge invariance and Wilson lines*** : An important aspect of SCET is the gauge structure of the theory. Because the effective field operators in SCET describe modes with certain momentum scalings, the effective Lagrangian respects only residual gauge symmetries. One of them satisfies the collinear scaling

$$(\bar{n}\cdot\partial_n, n\cdot\partial_n, \partial_n^\perp)\, U_n(x) \sim Q(1,\lambda^2,\lambda)\, U_n(x), \tag{17.18}$$

and one the soft scaling

$$(\bar{n}\cdot\partial_n, n\cdot\partial_n, \partial_n^\perp)\, U_s(x) \sim Q(\lambda^2,\lambda^2,\lambda^2)\, U_s(x). \tag{17.19}$$

The fact that collinear fields in different directions do not transform under the same gauge transformations implies that each collinear sector, containing particles with large momenta along a certain direction, has to be separately gauge invariant. This requires the introduction of collinear Wilson lines [40]

$$W_n(x) = P\exp\left[-ig\int_{-\infty}^0 ds\, \bar{n}\cdot A_n(s\bar{n}+x)\right], \tag{17.20}$$

which transform under collinear gauge transformations according to $W_n \to U_n W_n$. Thus, the combination $\chi_n \equiv W_n^\dagger\,\psi_n$ is gauge invariant. In a similar manner, one can define the gauge-invariant gluon field $B_n^\mu = g^{-1} W_n^\dagger\, iD_n^\mu W_n$ [44]. Operators in SCET are typically constructed from such gauge-invariant collinear fields.

17.3.4. ***Decoupling of soft gluons*** : Soft gluons in SCET couple to collinear quarks only through the term $\bar{\xi}_n\, gn\cdot A_s\, \dfrac{\bar{n}\!\!\!/}{2}\,\xi_n$ in the effective Lagrangian in Eq. (17.17). This coupling is similar to the coupling of soft gluons to heavy quarks in HQET, and soft gluons in SCET can thus be decoupled from collinear fields, in analogy to the discussion in Section 17.2.4. Written in terms of the redefined fields

$$\psi_n(x) = Y_n(x)\psi_n^{(0)}(x)\,, \qquad A_n(x) = Y_n(x)A_n^{(0)}(x)Y_n^\dagger(x), \quad (17.21)$$

the soft gluons decouple from the SCET Lagrangian [41]. This fact greatly facilitates proofs of factorization theorems in SCET.

17.3.5. ***Factorization Theorems*** : One of the important applications of SCET is to understand how to factorize cross sections involving energetic particles in different directions into simpler pieces that can either be calculated perturbatively or determined from data. Factorization theorems have been around for much longer than SCET. For a review on the subject, see [45]. However, the effective theory allows for a conceptually simpler understanding of certain classes of factorization theorems [46], since most simplifications happen already at the level of the Lagrangian. The discussion in this section is valid to leading order in the power counting of the effective theory.

As discussed in the previous section, the Lagrangian of SCET does not involve any couplings between collinear degrees of freedom in different light-like directions, or between soft and collinear degrees of freedom after the field redefinition Eq. (17.21) has been performed. An operator describing the scattering and production of collinear partons at short distances can thus be written as (omitting color indices for simplicity)

$$\langle O(x)\rangle \simeq C_O(\mu)\left\langle \mathcal{C}_{n_a}^{(0)}(x)\mathcal{C}_{n_b}^{(0)}(x)\mathcal{C}_{n_1}^{(0)}(x)\ldots\mathcal{C}_{n_N}^{(0)}(x)\times \right.$$
$$\left. [\mathcal{Y}_{n_a}\mathcal{Y}_{n_b}\mathcal{Y}_{n_1}\ldots\mathcal{Y}_{n_N}](x)\right\rangle_\mu . \quad (17.22)$$

Here $\mathcal{C}_n(x)$ denotes a gauge-invariant combination of collinear fields (either quark or gluon fields) in the direction n, and the matching coefficient accounting for short-distance effects is denoted by C_O. The soft Wilson lines can either be in a color triplet or color octet representation, and are collectively denoted by $\mathcal{Y}_n$. Both the matrix elements and the coefficient C_O depend on the renormalization scale μ.

Having defined the operator mediating a given process, one can calculate the cross section by squaring the operator, taking the forward matrix element and integrating over the phase space of all final-state particles. The absence of interactions between collinear degrees of freedom moving along different directions or soft degrees of freedom implies that the forward matrix element of the operator can be factorized as

$$\begin{aligned}\left\langle \text{in}\left|O(x)O^\dagger(0)\right|\text{in}\right\rangle &= \left\langle \text{in}_a\left|\mathcal{C}_{n_a}(x)\mathcal{C}_{n_a}^\dagger(0)\right|\text{in}_a\right\rangle\left\langle \text{in}_b\left|\mathcal{C}_{n_b}(x)\mathcal{C}_{n_b}^\dagger(0)\right|\text{in}_b\right\rangle \\ &\times\left\langle 0\left|\mathcal{C}_{n_1}(x)\mathcal{C}_{n_1}^\dagger(0)\right|0\right\rangle\cdots\left\langle 0\left|\mathcal{C}_{n_N}(x)\mathcal{C}_{n_N}^\dagger(0)\right|0\right\rangle \\ &\times\left\langle 0\left|[\mathcal{Y}_{n_a}\ldots\mathcal{Y}_{n_N}](x)[\mathcal{Y}_{n_a}\ldots\mathcal{Y}_{n_N}]^\dagger(0)\right|0\right\rangle . \end{aligned} \quad (17.23)$$

Thus, the matrix element required for the differential cross section has factorized into a product of simpler structures, each of which can be evaluated separately.

For many applications the matrix elements of incoming collinear fields are non-perturbative objects given in terms of the well-known parton distribution functions, while the matrix elements of outgoing collinear fields are determined by perturbatively calculable jet functions $J_i(\mu)$. Finally, the vacuum matrix element of the soft Wilson lines defines a so-called soft function, commonly denoted by $S(\mu)$. The shared dependence on x in the above equation implies that in momentum space the various components of the factorization theorem are convoluted with one another. Deriving this convolution requires a careful treatment of the phase-space integration, in particular treating the large and residual components of each momentum appropriately.

Putting all information together, the differential cross section can be written as

$$\mathrm{d}\sigma \sim H(\mu)\otimes\left[f_{p_1/P}(\mu)f_{p_2/P}(\mu)\right]\otimes[J_1(\mu)\ldots J_N(\mu)]\otimes S(\mu). \quad (17.24)$$

The hard coefficient is equal to the square of the matching coefficient, $H(\mu) = |C_O(\mu)|^2$. It should be mentioned that the most difficult part of traditional factorization proofs involves showing that so-called Glauber gluons do not spoil the above factorization theorem [47]. This question has not yet been fully addressed in the context of SCET.

17.3.6. ***Resummation of large logarithms*** : SCET can be used to sum the large logarithmic terms that arise in perturbative calculations to all orders in the strong coupling constant α_s. In general, perturbation theory will generate a logarithmic dependence on any ratio of scales r in a problem, and for processes that involve initial or final states with energy much in excess of their mass, there are two powers of logarithms for every power of α_s. Thus, for widely separated scales these large logarithms can spoil the convergence of fixed-order perturbation theory. One thus needs to reorganize the expansion in such a way that $\alpha_s L = \mathcal{O}(1)$ is kept fixed, with $L = \ln r$. More precisely, a proper resummation requires summing logarithms of the form $\alpha_s^n L^m$ with $m \le n+1$ in the logarithm of a cross section, by writing $\ln\sigma \sim Lg_0(\alpha_s L) + g_1(\alpha_s L) + \alpha_s g_2(\alpha_s L) + \ldots$, with functions $g_n(x)$ that need to be determined.

The important ingredient in achieving this resummation is the fact that SCET factorizes a given cross section into simpler pieces, as discussed in the previous section. Each of the ingredients of the factorization theorem depends on a single physical scale, and the only dependence on that scale can arise through logarithms of its ratio with the renormalization scale μ. Thus, for each of the components in the factorization theorem one can choose a renormalization scale μ for which the large logarithmic terms are absent.

Of course, the factorization formula requires a common renormalization scale μ in all its components, and one therefore has to use the renormalization group (RG) to evolve the various component functions from their preferred scale to the common scale μ. For example, for the hard coefficient $H(\mu)$, the RG equation can be written as

$$\mu\frac{\mathrm{d}}{\mathrm{d}\mu}H(\mu) = \gamma_H(\mu)H(\mu). \quad (17.25)$$

In general, the anomalous dimension is of the form $\gamma_H(\mu) = c_H\,\Gamma_{\text{cusp}}(\alpha_s)\log(Q/\mu) + \gamma(\alpha_s)$, where c_H is a process-dependent coefficient and Γ_{cusp} denotes the so-called cusp anomalous dimension [18,48]. The non-cusp part of the anomalous dimension γ is again process dependent. The presence of a logarithm of the hard scale Q in the anomalous dimension is characteristic of Sudakov problems and arises since the perturbative series contains double logarithms of scale ratios. The anomalous dimension γ_H is known at two-loop order for arbitrary n-parton amplitudes containing massless or massive external partons [49–52]. Solving the RG equation yields

$$H(\mu) = U_H(\mu,\mu_h)H(\mu_h)\,, \quad (17.26)$$

which can be used to write the hard function at a scale $\mu_h \sim Q$, where its perturbative expression does not contain any large logarithms, in terms of the common renormalization scale μ. The RG evolution factor $U_H(\mu,\mu_h)$ sums logarithms of the form μ/μ_h. By calculating the anomalous dimension $\gamma_H(\mu)$ to higher orders in perturbation theory, one can resum more logarithms in the evolution kernel. The RG equations for the jet and soft functions are more complicated, since they involve convolutions over the relevant momentum variables.

17.3.7. ***Factorization and resummation in*** $\mathrm{SCET_{II}}$:

The effective theory $\mathrm{SCET_{II}}$ contains collinear and soft particles with momenta scaling as $(p_n^-, p_n^+, p_n^\perp) \sim Q(1,\lambda^2,\lambda)$ and $(p_s^-, p_s^+, p_s^\perp) \sim Q(\lambda,\lambda,\lambda)$. They have the same small virtuality ($p_n^2 \sim p_s^2 \sim Q^2\lambda^2$) but differ in their rapidities. An important class of observables, for which this scaling is relevant, contains cross sections for processes in which the transverse momenta of particles are contrained by external kinematics. The prime example are the transverse-momentum

distributions of electroweak gauge bosons or Higgs bosons produced at hadron colliders. The parton transverse momenta are constrained by the fact that their vector sum must be equal and opposite to the transverse momentum q_T of the boson. Standard RG evolution in the effective theory controls the logarithms arising from the fact that the virtualities of the collinear and soft modes are much smaller than the hard scale Q in the process (the boson mass). However, additional large logarithms arise since the rapidities of collinear and soft modes are parametrically different, such that $e^{y_c - y_s} \sim 1/\lambda$. These logarithms need to be factorized in the cross section and resummed by other means.

Two equivalent approaches exist for how to deal with the additional rapidity logarithms. In the first approach, they are interpreted as a consequence of a "collinear anomaly" of the effective theory $\mathrm{SCET_{II}}$, resulting from the fact that a classical rescaling symmetry of the effective Lagrangian is broken by quantum effects [53]. The extra large logarithms can be resummed by means of simple differential equations, which typically state that (in an appropriate space) the logarithm of the cross section contains only a single logarithm of $\lambda \sim q_T/Q$, to all orders in perturbation theory. An alternative approach to resum the rapidity logarithms uses the "rapidity renormalization group", in which the relevant differential equations are obtained by considering a new type of scale variation in a parameter ν, which separates the phase space for collinear and soft particles along a hyperbola in the (p_-, p_+) plane [54]. In contrast to the standard RG, there is no physical coupling constant involved in the ν evolution, since the different contributions live at the same virtuality.

$\mathrm{SCET_{II}}$ also plays an important role in the study of factorization for nonleptonic and radiative decays of B mesons such as $\bar{B} \to \pi\pi$ and $\bar{B} \to K^*\gamma$, for which the virtualities of energetic (collinear) finals-state particles are of order $\Lambda_{\rm QCD}$, which is also the scale for the soft light degrees of freedom contained in the initial-state B meson.

17.3.8. ***Applications*** : Most of the applications of SCET are either in flavor physics, where the decay of a heavy B meson can give rise to energetic light partons, or in collider physics, where the presence of jets naturally leads to collimated sets of energetic particles. For several of these applications alternative approaches existed before the invention of SCET, but the effective theory has opened up alternative ways to understand the physics of these processes. There are, however, many examples for which SCET has allowed new insights that were not available or possible without the effective theory. In particular, it has provided a field-theoretic basis for the QCD factorization approach to exclusive, non-leptonic decays of B mesons [55]. Using SCET methods, proofs of factorization were derived for the color-allowed decay $\bar{B}^0 \to D^+\pi^-$ [56], the color-suppressed decay $\bar{B}^0 \to D^0\pi^0$ [57], and the radiative decay $\bar{B} \to K^*\gamma$ [58]. Further examples are factorization theorems and the resummation of endpoint logarithms for quarkonia production [59], factorization theorems for cross sections defined through jet algorithms [60], the resummation of large logarithmic terms for the thrust [61] and jet broadening [62] distributions in e^+e^- annihilation beyond NLL order, the development of new factorizable observables to veto extra jets [63], all-orders factorization theorems for processes containing electroweak Sudakov logarithms [64], as well as the resummation of threshold (soft gluon) logarithms for several important processes at hadron colliders [65–67]. Recently, there has been a lot of activity describing p_T based resummation at hadron colliders. Examples the transverse-momentum distributions of electroweak gauge bosons and Higgs bosons [53] and the resummation of jet-veto cross sections [68–70]. An active research area is the understanding of non-global logarithms arising in hadron collider processes with jets [71,72]. SCET-based fixed-order calculations has helped to shed light on the nature of these logarithms [73,74].

We now describe one of these applications in more detail. Event-shape distributions, in particular the thrust distribution, have been measured to high accuracy at LEP [75]. Comparing these data to precise theoretical predictions allows for a determination of the strong coupling constant α_s. For small values of $\tau \equiv 1 - T$, the distribution can be factorized into the form [76,77]

$$\frac{1}{Q\sigma_0}\frac{\mathrm{d}\sigma}{\mathrm{d}\tau} = H(\mu) \int \mathrm{d}s \int \mathrm{d}k\, J(s,\mu)\, S(Q\tau - s/Q - k, \mu). \qquad (17.27)$$

Here Q denotes the center-of-mass energy of the collision, σ_0 is the total hadronic cross section, and H, J and S are the hard, jet and soft functions in SCET. Large logarithms of the form $(\alpha_s^n \ln^{2n-1}\tau)/\tau$ become important and have to be resummed. Furthermore, for $\tau \sim \Lambda_{\rm QCD}/Q$ non-perturbative effects in the soft function become important. Using SCET the resummation of these large logarithms has been performed to $\mathrm{N^3LL}$ [61], which is two orders beyond what was previously available. The factorization in the effective theory has also allowed one to include the non-perturbative physics through a shape function, in analogy with the B-physics case discussed in Section 17.2.6. The known perturbative effects for large values of τ can be included by matching the SCET result to the known two-loop spectrum [78,79]. Comparing the predicted to the measured thrust distribution allows for a precise determination of the strong coupling constant α_s [80].

17.4. Open issues and perspectives

HQET has successfully passed many experimental tests, and there are not too many open questions that still need to be addressed. One issue that has not been derived from first principles is quark-hadron duality. The validity of global duality (at energies even lower than those relevant in B decays) has been tested experimentally using high-precision data on semileptonic B decays and on hadronic τ decays, and there has been good agreement between theory and data. However, assigning a theoretical uncertainty to possible duality violations is difficult. Another known issue is the that the measured value of the CKM element $|V_{cb}|$ is different depending of whether one uses inclusive or exclusive B decays to derive it (see the relevant section in the Particle Data Book). Both measurements rely on the heavy-quark limit, and the uncertainties quoted include the effects from power corrections arising from the finite b-quark mass.

SCET, on the other hand, is still an active field of research, and there are several open questions that need to be answered. There are still some open issues in how to properly formulate $\mathrm{SCET_{II}}$, which are under active investigation. They include the treatment of endpoint singularities of convolution integrals and double counting between overlapping momentum regions. This is important, for example, to describe exclusive decays of B mesons into light, energetic mesons. Glauber gluons are known to affect factorization theorems, but how to properly include them in SCET is still an open question.

References:

1. E. Witten, Nucl. Phys. B **122**, 109 (1977).
2. S. Weinberg, Phys. Lett. B **91**, 51 (1980).
3. L.J. Hall, Nucl. Phys. B **178**, 75 (1981).
4. E. Eichten and B. Hill, Phys. Lett. B **234**, 511 (1990).
5. H. Georgi, Phys. Lett. B **240**, 447 (1990).
6. B. Grinstein, Nucl. Phys. B **339**, 253 (1990).
7. T. Mannel, W. Roberts, and Z. Ryzak, Nucl. Phys. B **368**, 204 (1992).
8. M. Neubert, Phys. Rept. **245**, 259 (1994) [hep-ph/9306320].
9. A.V. Manohar and M.B. Wise, Camb. Monogr. Part. Phys. Nucl. Phys. Cosmol. **10**, 1 (2000).
10. M.E. Luke and A.V. Manohar, Phys. Lett. B **286**, 348 (1992) [hep-ph/9205228].
11. E.V. Shuryak, Phys. Lett. B**93**, 134 (1980).
12. N. Isgur and M.B. Wise, Phys. Lett. B **232**, 113 (1989); Phys. Lett. B **237**, 527 (1990).
13. N. Isgur and M.B. Wise, Phys. Rev. Lett. **66**, 1130 (1991).
14. S. Nussinov and W. Wetzel, Phys. Rev. D **36**, 130 (1987).
15. M.A. Shifman and M.B. Voloshin, Sov. J. Nucl. Phys. **45**, 292 (1987); Sov. J. Nucl. Phys. **47**, 511 (1988).
16. M. Neubert, Phys. Lett. B **264**, 455 (1991).
17. M.E. Luke, Phys. Lett. B **252**, 447 (1990).
18. G.P. Korchemsky and A.V. Radyushkin, Nucl. Phys. B **283**, 342 (1987).

19. A.F. Falk *et al.*, Nucl. Phys. B **343**, 1 (1990).
20. J. Chay, H. Georgi, and B. Grinstein, Phys. Lett. B **247**, 399 (1990).
21. I.I.Y. Bigi, N.G. Uraltsev, and A.I. Vainshtein, Phys. Lett. B **293**, 430 (1992) [hep-ph/9207214]; I.I.Y. Bigi *et al.*, Phys. Rev. Lett. **71**, 496 (1993) [hep-ph/9304225].
22. A.V. Manohar and M.B. Wise, Phys. Rev. D **49**, 1310 (1994) [hep-ph/9308246].
23. T. Mannel, Nucl. Phys. B **413**, 396 (1994) [hep-ph/9308262].
24. A.F. Falk, M.E. Luke, and M.J. Savage, Phys. Rev. D **49**, 3367 (1994) [hep-ph/9308288].
25. E.C. Poggio, H.R. Quinn, and S. Weinberg, Phys. Rev. D **13**, 1958 (1976).
26. G. Buchalla, A.J. Buras, and M.E. Lautenbacher, Rev. Mod. Phys. **68**, 1125 (1996) [hep-ph/9512380].
27. A.F. Falk and M. Neubert, Phys. Rev. D **47**, 2965 (1993) [hep-ph/9209268].
28. M. Neubert and C.T. Sachrajda, Nucl. Phys. B **483**, 339 (1997) [hep-ph/9603202].
29. M. Beneke, G. Buchalla, and I. Dunietz, Phys. Rev. D **54**, 4419 (1996) [hep-ph/9605259].
30. C.W. Bauer *et al.*, Phys. Rev. D **70**, 094017 (2004) [hep-ph/0408002].
31. M. Neubert, Phys. Rev. D **49**, 4623 (1994) [hep-ph/9312311].
32. I.I.Y. Bigi *et al.*, Int. J. Mod. Phys. A **9**, 2467 (1994) [hep-ph/9312359].
33. G. P. Korchemsky and G.F. Sterman, Phys. Lett. B **340**, 96 (1994) [hep-ph/9407344].
34. C.W. Bauer, M.E. Luke, and T. Mannel, Phys. Rev. D **68**, 094001 (2003) [hep-ph/0102089].
35. K.S.M. Lee and I.W. Stewart, Nucl. Phys. B **721**, 325 (2005) [hep-ph/0409045].
36. S.W. Bosch, M. Neubert, and G. Paz, JHEP **0411**, 073 (2004) [hep-ph/0409115].
37. M. Beneke *et al.*, JHEP **0506**, 071 (2005) [hep-ph/0411395].
38. M. Benzke, S. J. Lee, M. Neubert and G. Paz, JHEP **1008**, 099 (2010) [arXiv:1003.5012 [hep-ph]].
39. C. W. Bauer, S. Fleming, and M.E. Luke, Phys. Rev. D **63**, 014006 (2000) [hep-ph/0005275]; C.W. Bauer *et al.*, Phys. Rev. D **63**, 114020 (2001) [hep-ph/0011336].
40. C.W. Bauer and I.W. Stewart, Phys. Lett. B **516**, 134 (2001) [hep-ph/0107001].
41. C.W. Bauer, D. Pirjol, and I.W. Stewart, Phys. Rev. D **65**, 054022 (2002) [hep-ph/0109045].
42. J. Chay and C. Kim, Phys. Rev. D **65**, 114016 (2002) [hep-ph/0201197].
43. M. Beneke *et al.*, Nucl. Phys. B **643**, 431 (2002) [hep-ph/0206152].
44. R.J. Hill and M. Neubert, Nucl. Phys. B **657**, 229 (2003) [hep-ph/0211018].
45. J. C. Collins, D.E. Soper, and G.F. Sterman, Adv. Ser. Direct. High Energy Phys. **5**, 1 (1988) [hep-ph/0409313].
46. C.W. Bauer *et al.*, Phys. Rev. D **66**, 014017 (2002) [hep-ph/0202088].
47. J. C. Collins, D. E. Soper, and G. Sterman, Nucl. Phys. B **261**, 104 (1985); Nucl. Phys. B **308**, 833 (1988).
48. I.A. Korchemskaya and G.P. Korchemsky, Phys. Lett. B **287**, 169 (1992).
49. T. Becher and M. Neubert, Phys. Rev. Lett. **102**, 162001 (2009) [arXiv:0901.0722 [hep-ph]]; JHEP **0906**, 081 (2009) [arXiv:0903.1126 [hep-ph]].
50. E. Gardi and L. Magnea, JHEP **0903**, 079 (2009) [arXiv:0901.1091 [hep-ph]].
51. A. Mitov, G.F. Sterman, and I. Sung, Phys. Rev. D **79**, 094015 (2009) [arXiv:0903.3241 [hep-ph]].
52. A. Ferroglia *et al.*, Phys. Rev. Lett. **103**, 201601 (2009) [arXiv:0907.4791 [hep-ph]].
53. T. Becher and M. Neubert, Eur. Phys. J. C **71**, 1665 (2011) [arXiv:1007.4005 [hep-ph]].
54. J. -Y. Chiu *et al.*, JHEP **1205**, 084 (2012) [arXiv:1202.0814 [hep-ph]].
55. M. Beneke *et al.*, Phys. Rev. Lett. **83**, 1914 (1999) [hep-ph/9905312]; Nucl. Phys. B **591**, 313 (2000) [hep-ph/0006124].
56. C.W. Bauer, D. Pirjol, and I.W. Stewart, Phys. Rev. Lett. **87**, 201806 (2001) [hep-ph/0107002].
57. S. Mantry, D. Pirjol, and I.W. Stewart, Phys. Rev. D **68**, 114009 (2003) [hep-ph/0306254].
58. T. Becher, R.J. Hill, and M. Neubert, Phys. Rev. D **72**, 094017 (2005) [hep-ph/0503263].
59. S. Fleming, A.K. Leibovich, and T. Mehen, Phys. Rev. D **68**, 094011 (2003) [hep-ph/0306139].
60. C.W. Bauer, A. Hornig, and F.J. Tackmann, Phys. Rev. D **79**, 114013 (2009) [arXiv:0808.2191 [hep-ph]].
61. T. Becher and M.D. Schwartz, JHEP **0807**, 034 (2008) [arXiv:0803.0342 [hep-ph]].
62. T. Becher, G. Bell, and M. Neubert, Phys. Lett. B **704**, 276 (2011) [arXiv:1104.4108 [hep-ph]].
63. I.W. Stewart, F.J. Tackmann, and W.J. Waalewijn, Phys. Rev. D **81**, 094035 (2010) [arXiv:0910.0467 [hep-ph]].
64. J.-y. Chiu, R. Kelley, and A.V. Manohar, Phys. Rev. D **78**, 073006 (2008) [arXiv:0806.1240 [hep-ph]].
65. T. Becher, M. Neubert, and G. Xu, JHEP **0807**, 030 (2008) [arXiv:0710.0680 [hep-ph]].
66. V. Ahrens *et al.*, Eur. Phys. J. C **62**, 333 (2009) [arXiv:0809.4283 [hep-ph]]; V. Ahrens *et al.*, JHEP **1009**, 097 (2010) [arXiv:1003.5827 [hep-ph]].
67. X. Liu, S. Mantry, and F. Petriello, Phys. Rev. D **86**, 074004 (2012) [arXiv:1205.4465 [hep-ph]].
68. T. Becher and M. Neubert, JHEP **1207**, 108 (2012) [arXiv:1205.3806 [hep-ph]].
69. F. J. Tackmann, J. R. Walsh, and S. Zuberi, Phys. Rev. D **86**, 053011 (2012) [arXiv:1206.4312 [hep-ph]].
70. X. Liu and F. Petriello, Phys. Rev. D **87**, 014018 (2013) [arXiv:1210.1906 [hep-ph]].
71. M. Dasgupta and G. P. Salam, Phys. Lett. B **512**, 323 (2001) [hep-ph/0104277]; JHEP **0203**, 017 (2002) [hep-ph/0203009].
72. R. B. Appleby and M. H. Seymour, JHEP **0212**, 063 (2002) [hep-ph/0211426].
73. R. Kelley, M. D. Schwartz, R. M. Schabinger and H. X. Zhu, Phys. Rev. D **84**, 045022 (2011) [arXiv:1105.3676 [hep-ph]].
74. A. Hornig, C. Lee, I. W. Stewart, J. R. Walsh and S. Zuberi, JHEP **1108**, 054 (2011) [arXiv:1105.4628 [hep-ph]].
75. For a review, see: S. Kluth, Rept. Prog. Phys. **69**, 1771 (2006) [hep-ex/0603011].
76. G.P. Korchemsky and G.F. Sterman, Nucl. Phys. B **555**, 335 (1999) [hep-ph/9902341]; G.P. Korchemsky and S. Tafat, JHEP **0010**, 010 (2000) [hep-ph/0007005].
77. C.F. Berger and G.F. Sterman, JHEP **0309**, 058 (2003) [hep-ph/0307394].
78. A. Gehrmann-De Ridder *et al.*, Phys. Rev. Lett. **99**, 132002 (2007) [arXiv:0707.1285 [hep-ph]].
79. S. Weinzierl, Phys. Rev. Lett. **101**, 162001 (2008) [arXiv:0807.3241 [hep-ph]].
80. R. Abbate *et al.*, Phys. Rev. **D83**, 074021 (2011) [arXiv:1006.3080 [hep-ph]].

18. LATTICE QUANTUM CHROMODYNAMICS

Updated September 2013 by S. Hashimoto (KEK), J. Laiho (Syracuse University), and S.R. Sharpe (University of Washington).

18.1. Lattice regularization of QCD

Gauge theories form the building blocks of the Standard Model. While the SU(2) and U(1) parts have weak couplings and can be studied accurately with perturbative methods, the SU(3) component—QCD—is only amenable to a perturbative treatment at high energies. The growth of the coupling constant in the infrared—the flip-side of asymptotic freedom—requires the use of non-perturbative methods to determine the low energy properties of QCD. Lattice gauge theory, proposed by K. Wilson in 1974 [1], provides such a method, for it gives a non-perturbative definition of vector-like gauge field theories like QCD. In lattice regularized QCD—commonly called lattice QCD or LQCD—Euclidean space-time is discretized, usually on a hypercubic lattice with lattice spacing a, with quark fields placed on sites and gauge fields on the links between sites. The lattice spacing plays the role of the ultraviolet regulator, rendering the quantum field theory finite. The continuum theory is recovered by taking the limit of vanishing lattice spacing, which can be reached by tuning the bare coupling constant to zero according to the renormalization group.

Unlike dimensional regularization, which is commonly used in continuum QCD calculations, the definition of LQCD does not rely on the perturbative expansion. Indeed, LQCD allows non-perturbative calculations by numerical evaluation of the path integral that defines the theory.

Practical LQCD calculations are limited by the availability of computational resources and the efficiency of algorithms. Because of this, LQCD results come with both statistical and systematic errors, the former arising from the use of Monte-Carlo integration, the latter, for example, from the use of non-zero values of a. There are also different ways in which the QCD action can be discretized, and all must give consistent results in the continuum limit, $a \to 0$. It is the purpose of this review to provide an outline of the methods of LQCD, with particular focus on applications to particle physics, and an overview of the various sources of error. This should allow the reader to better understand the LQCD results that are presented in other sections for a variety of quantities (quark masses, the hadron spectrum and several electroweak matrix elements). For more extensive explanations the reader should consult the available textbooks or lecture notes, the most up-to-date of which are Refs. [2–4].

18.1.1. *Gauge invariance, gluon fields and the gluon action* :

A key feature of the lattice formulation of QCD is that it preserves gauge invariance. This is in contrast to perturbative calculations, where gauge fixing is an essential step. The preservation of gauge invariance leads to considerable simplifications, e.g. restricting the form of operators that can mix under renormalization.

The gauge transformations of lattice quark fields are just as in the continuum: $q(x) \longrightarrow V(x)q(x)$ and $\bar{q}(x) \longrightarrow \bar{q}(x)V^\dagger(x)$, with $V(x)$ an arbitrary element of SU(3). The only difference is that the Euclidean space-time positions x are restricted to lie on the sites of the lattice, i.e. $x = a(n_1, n_2, n_3, n_4)$ for a hypercubic lattice, with the n_j being integers. Quark bilinears involving different lattice points can be made gauge invariant by introducing the gluon field $U_\mu(x)$. For example, for adjacent points the bilinear is $\bar{q}(x)U_\mu(x)q(x+a\hat{\mu})$, with $\hat{\mu}$ the unit vector in the μ'th direction. (This form is used in the construction of the lattice covariant derivative.) The gluon field (or "gauge link") is an element of the group, SU(3), in contrast to the continuum field A_μ which takes values in the Lie algebra. The bilinear is invariant if U_μ transforms as $U_\mu(x) \to V(x)U_\mu(x)V^\dagger(x+a\hat{\mu})$. The lattice gluon field is naturally associated with the link joining x and $x+a\hat{\mu}$, and corresponds in the continuum to a Wilson line connecting these two points, $P\exp(i\int_x^{x+a\hat{\mu}} dx_\mu A_\mu^{\rm cont}(x))$ (where P indicates a path-ordered integral, and the superscript on A_μ indicates that it is a continuum field). The trace of a product of the $U_\mu(x)$ around any closed loop is easily seen to be gauge invariant and is the lattice version of a Wilson loop.

The simplest possible gauge action, usually called the Wilson gauge action, is given by the product of gauge links around elementary plaquettes:

$$S_g = \beta \sum_{x,\mu,\nu} [1 - \frac{1}{3}{\rm ReTr}[U_\mu(x)U_\nu(x+a\hat{\mu})U_\mu^\dagger(x+a\hat{\nu})U_\nu^\dagger(x)]] \,. \quad (18.1)$$

For small a, assuming that the fields are slowly varying, one can expand the action in powers of a using $U_\mu(x) = \exp(iaA_\mu(x))$. Keeping only the leading non-vanishing term, and replacing the sum with an integral, one finds the continuum form,

$$S_g \longrightarrow \int d^4x \frac{1}{4g_{\rm lat}^2}{\rm Tr}[F_{\mu\nu}^2(x)] \,, \qquad (F_{\mu\nu} = \partial_\mu A_\nu - \partial_\nu A_\mu + i[A_\mu, A_\nu]) \quad (18.2)$$

as long as one chooses $\beta = 6/g_{\rm lat}^2$ for the lattice coupling. In this expression, $g_{\rm lat}$ is the bare coupling constant in the lattice scheme, which can be related (by combining continuum and lattice perturbation theory) to a more conventional coupling constant such as that in the $\overline{\rm MS}$ scheme (see Sec. 18.3.4 below).

In practice, the lattice spacing a is non-zero, leading to discretization errors. In particular, the lattice breaks Euclidean rotational invariance (which is the Euclidean version of Lorentz invariance) down to a discrete hypercubic subgroup. One wants to reduce discretization errors as much as possible. A very useful tool for understanding and then reducing discretization errors is the Symanzik effective action: the interactions of quarks and gluons with momenta low compared to the lattice cutoff ($|p| \ll 1/a$) are described by a continuum action consisting of the standard continuum terms (e.g. the gauge action given in Eq. (18.2)) augmented by higher dimensional operators suppressed by powers of a [5]. For the Wilson lattice gauge action, the leading corrections come in at $\mathcal{O}(a^2)$. They take the form $\sum_j a^2 c_j O_6^{(j)}$, with the sum running over all dimension-six operators $O_6^{(j)}$ allowed by the *lattice* symmetries, and c_j unknown coefficients. Some of these operators violate Euclidean invariance, and all of them lead to discretization errors of the form $a^2\Lambda^2$, where Λ is a typical momentum scale for the quantity being calculated. These errors can, however, be reduced by adding corresponding operators to the lattice action and tuning their coefficients to eliminate the dimension-six operators in the effective action to a given order in perturbation theory or even non-perturbatively. This is the idea of the Symanzik improvement program [5]. In the case of the gauge action, one adds Wilson loops involving six gauge links (as opposed to the four links needed for the original plaquette action, Eq. (18.1)) to define the $\mathcal{O}(a^2)$ improved (or "Symanzik") action [6]. In practical implementations, the improvement is either at tree-level (so that residual errors are proportional to $\alpha_s a^2$, where the coupling is evaluated at a scale $\sim 1/a$), or at one loop order (errors proportional to $\alpha_s^2 a^2$). Another popular choice is motivated by studies of renormalization group (RG) flow. It has the same terms as the $\mathcal{O}(a^2)$ improved action but with different coefficients, and is called the RG-improved or "Iwasaki" action [7].

18.1.2. *Lattice fermions* :

Discretizing the fermion action turns out to involve subtle issues, and the range of actions being used is more extensive than for gauge fields. Recall that the continuum fermion action is $S_f = \int d^4x \bar{q}[iD_\mu\gamma_\mu + m_q]q$, where $D_\mu = \partial_\mu + iA_\mu$ is the gauge-covariant derivative. The simplest discretization replaces the derivative with a symmetric difference:

$$D_\mu q(x) \longrightarrow \frac{1}{2a}[U_\mu(x)q(x+a\hat{\mu}) - U_\mu(x-a\hat{\mu})^\dagger q(x-a\hat{\mu})] \,. \quad (18.3)$$

The factors of U_μ ensure that $D_\mu q(x)$ transforms under gauge transformations in the same way as $q(x)$, so that the discretized version of $\bar{q}(x)D_\mu\gamma_\mu q(x)$ is gauge invariant. The choice in Eq. (18.3) leads to the so-called naive fermion action. This, however, suffers from the fermion doubling problem—in d dimensions it describes 2^d equivalent fermion fields in the continuum limit . The appearance of the extra "doubler" fermions is related to the deeper theoretical problem of formulating chirally symmetric fermions on the lattice. This is encapsulated by the Nielsen-Ninomiya theorem [8]: one cannot define lattice fermions having exact, continuum-like chiral

symmetry without producing doublers. Naive lattice fermions do have chiral symmetry but at the cost of introducing 15 unwanted doublers (for $d = 4$).

There are a number of different strategies for dealing with the doubling problem, each with their own theoretical and computational advantages and disadvantages. Wilson fermions [1] add a term proportional to $a\bar{q}\Delta q$ to the fermion action (the "Wilson term"—in which Δ is a covariant lattice Laplacian). This gives a mass of $\mathcal{O}(1/a)$ to the doublers, so that they decouple in the continuum limit. The Wilson term, however, violates chiral symmetry, and also introduces discretization errors linear in a. A commonly used variant that eliminates the $\mathcal{O}(a)$ discretization error is the $\mathcal{O}(a)$-improved Wilson (or "clover") fermion [9]. In this application of Symanzik improvement, methods have been developed to remove $\mathcal{O}(a)$ terms non-perturbatively using auxiliary simulations to tune parameters [10]. Such "non-perturbative improvement" is of great practical importance as it brings the discretization error from the fermion action down to the same level as that from the gauge action. It is used by essentially all simulations using clover fermions.

The advantages of Wilson fermions are their theoretical simplicity and relatively low computational cost. Their main disadvantage is the lack of chiral symmetry, which makes them difficult to use in cases where mixing with wrong chirality operators can occur, particularly if this involves divergences proportional to powers of $1/a$. A related problem is the presence of potential numerical instabilities due to spurious near-zero modes of the lattice Dirac operator. Ongoing work has, however, been successful at ameliorating these problems and increasing the range of quantities for which Wilson fermions can be used [11,12].

Twisted-mass fermions [13] are a variant of Wilson fermions in which two flavors are treated together with an isospin-breaking mass term (the "twisted mass" term). The main advantage of this approach is that all errors linear in a are automatically removed (without the need for tuning of parameters) by a clever choice of twisted mass and operators [14]. A disadvantage is the presence of isospin breaking effects (such as a splitting between charged and neutral pion masses even when up and down quarks are degenerate), which, however, vanish as $a^2\Lambda^2$ in the continuum limit.

Staggered fermions are a reduced version of naive fermions in which there is only a single fermion Dirac component on each lattice site, with the full Dirac structure built up from neighboring sites [15]. They have the advantages of being somewhat faster to simulate than Wilson-like fermions, of preserving some chiral symmetry, and of having discretization errors of $\mathcal{O}(a^2)$. Their disadvantage is that they retain some of the doublers (3 for $d = 4$). The action thus describes four degenerate fermions in the continuum limit. These are usually called "tastes", to distinguish them from physical flavors, and the corresponding SU(4) symmetry is referred to as the "taste symmetry". The preserved chiral symmetry in this formulation has non-singlet taste. Practical applications usually introduce one staggered fermion for each physical flavor, and remove contributions from the unwanted tastes by taking the fourth-root of the fermion determinant appearing in the path integral. The validity of this "rooting" procedure is not obvious because taste symmetry is violated for non-zero lattice spacing. Theoretical arguments, supported by numerical evidence, suggest that the procedure is valid as long as one takes the continuum limit before approaching the light quark mass region [16]. Additional issues arise for the valence quarks (those appearing in quark propagators, as described in Sec. 18.2 below), where rooting is not possible, and one must remove the extra tastes by hand [17].

Just as for Wilson fermions, the staggered action can be improved, so as to reduce discretization errors. The widely used "asqtad" action [18] removes tree-level $\mathcal{O}(a^2)$ errors, and leads to substantial reduction in the breaking of taste symmetry. More recently, a highly improved staggered quark ("HISQ") action has been introduced [19], which further reduces discretization errors, both those which break taste symmetry and those which do not. It is tuned to reduce discretization errors for both light and heavier quarks, and is being used to directly simulate charm quarks.

There is an important class of lattice fermions, "Ginsparg-Wilsons fermions", that possess a continuum-like chiral symmetry without introducing unwanted doublers. The lattice Dirac operator D for these fermions satisfies the Ginsparg-Wilson relation $D\gamma_5 + \gamma_5 D = aD\gamma_5 D$ [20]. In the continuum, the right-hand-side vanishes due to chiral symmetry. On the lattice, it is non-vanishing, but with a particular form (with two factors of D) that restricts the violations of chiral symmetry in Ward-Takahashi identities to short-distance terms that do not contribute to physical matrix elements [21]. In fact, one can define a modified chiral transformation on the lattice (by including dependence on the gauge fields) such that Ginsparg-Wilson fermions have an exact chiral symmetry for on-shell quantities [22]. The net result is that such fermions essentially have the same properties under chiral transformations as do continuum fermions, including the index theorem [21]. Their leading discretization errors are of $\mathcal{O}(a^2)$.

Two types of Ginsparg-Wilson fermions are currently being used in large-scale numerical simulations. The first are Domain-wall fermions (DWF). These are defined on a five-dimensional space, in which the fifth dimension is fictitious [23]. The action is chosen so that the low-lying modes are chiral, with left- and right-handed modes localized on opposite four-dimensional surfaces. For an infinite fifth dimension, these fermions satisfy the Ginsparg-Wilson relation. In practice, the fifth dimension is kept finite, and there remains a small, controllable violation of chiral symmetry. The second type are Overlap fermions. These appeared from a completely different context and have an explicit form that exactly satisfies the Ginsparg-Wilson relation [24]. Their numerical implementation requires an approximation of the matrix sign function of a Wilson-like fermion operator, and various approaches are being used. In fact, it is possible to rewrite these approximations in terms of a five-dimensional formulation, showing that the DWF and Overlap approaches are essentially equivalent [25]. Numerically, the five-dimensional approach appears to be the most computationally efficient.

As noted above, each fermion formulation has its own advantages and disadvantages. For instance, domain-wall and overlap fermions are theoretically preferred as they have chiral symmetry without doublers, but their computational cost is at least an order of magnitude greater than for other choices. If the physics application of interest and the target precision do not require near-exact chiral symmetry, there is no strong motivation to use these expensive formulations. On the other hand, there is a class of applications (including the calculation of the $\Delta I = 1/2$ amplitude for $K \to \pi\pi$ decays and the S-parameter [26]) where chiral symmetry plays an essential role and for which the use of Ginsparg-Wilson fermions is strongly favored.

18.1.3. *Heavy quarks on the lattice* :

The fermion formulations described in the previous subsection can be used straightforwardly only for quarks whose masses are small compared to the lattice cutoff, $m_q \lesssim 1/a$. This is because there are discretization errors proportional to powers of am_q, and if $am_q \gtrsim 1$ these errors are large and uncontrolled. Present LQCD simulations typically have cutoffs in the range of $1/a = 2 - 4$ GeV (corresponding to $a \approx 0.1 - 0.05$ fm). Thus, while for the up, down and strange quarks one has $am_q \ll 1$, for bottom quarks (with $m_b \approx 4.5$ GeV) one must use alternative approaches. Charm quarks ($m_c \approx 1.5$ GeV) are an intermediate case, allowing simulations using both direct and alternative approaches.

For the charm quark, the straightforward approach is to simultaneously reduce the lattice spacing and to improve the fermion action so as to reduce the size of errors proportional to powers of am_c. This approach has, for example, been followed successfully using the HISQ and twisted-mass actions [19,27,28]. It is important to note, however, that reducing a increases the computational cost because an increased number of lattice points are needed for the same physical volume. One cannot reduce the spatial size below $2 - 3$ fm without introducing finite volume errors. Present lattices have sizes up to $\sim 96^3 \times 192$ (with the long direction being Euclidean time), and thus allow a lattice cutoff up to $1/a \sim 4$ GeV.

Alternative approaches for discretizing heavy quarks are motivated by effective field theories. For a bottom quark in heavy-light hadrons, one can use Heavy Quark Effective Theory (HQET) to expand about the infinite quark-mass limit. In this limit, the bottom quark is a static

color source, and one can straightforwardly write the corresponding lattice action [29]. Corrections, proportional to powers of $1/m_b$, can be introduced as operator insertions, with coefficients that can be determined non-perturbatively using existing techniques [30]. This method allows the continuum limit to be taken controlling all $1/m_b$ corrections.

Another way of introducing the $1/m_b$ corrections is to include the relevant terms in the effective action. This leads to a non-relativistic QCD (NRQCD) action, in which the heavy quark is described by a two-component spinor [31]. This approach has the advantage over HQET that it can also be used for heavy-heavy systems, such as the Upsilon states. A disadvantage is that some of the parameters in this effective theory are determined perturbatively (originally at tree-level, but more recently at one-loop), which limits the precision of the final results. Although discretization effects can be controlled with good numerical precision for a range of lattice spacings, at fine enough lattice spacing the NRQCD effective theory no longer applies since power divergent terms become important, and taking the continuum limit would require fine-tuning a large number of couplings non-perturbatively.

This problem can be avoided if one uses HQET power counting to analyze and reduce discretization effects for heavy quarks while using conventional fermion actions [32]. For instance, one can tune the parameters of an improved Wilson quark action so that the leading HQET corrections to the static quark limit are correctly accounted for. As the lattice spacing becomes finer, the action smoothly goes over to that of a light Wilson quark action, where the continuum limit can be taken as usual. In principle, one can improve the action in the heavy quark regime up to arbitrarily high orders using HQET, but so far large-scale simulations have typically used clover improved Wilson quarks, where tuning the parameters of the action corresponds to including all corrections through next-to-leading order in HQET. Three different methods for tuning the parameters of the clover action are being used: the Fermilab [32], Tsukuba [33] and Columbia [34] approaches. An advantage of this HQET approach is that the c and b quarks can be treated on the same footing. Parameter tuning has typically been done perturbatively, as in NRQCD, but recent work using the Columbia approach has used non-perturbative tuning [35].

18.1.4. *Basic inputs for lattice calculations* :

Since LQCD is nothing but a regularization of QCD, the renormalizability of QCD implies that the number of input parameters in LQCD is the same as for continuum QCD—the strong coupling constant $\alpha_s = g^2/(4\pi)$, the quark masses for each flavor, and the CP violating phase θ. The θ parameter is usually assumed to be zero, while the other parameters must be determined using experimental inputs.

18.1.4.1. *Lattice spacing:* In QCD, the coupling constant is a function of scale. With lattice regularization, this scale is the inverse lattice spacing $1/a$, and choosing the bare coupling constant is equivalent to fixing the lattice spacing.

In principle, a can be determined using any dimensionful quantity measured by experiments. For example, using the mass of hadron H one has $a = (am_H)^{\rm lat}/m_H^{\rm exp}$. (Of course, one must first tune the quark masses to their physical values, as discussed below.) In practice, one chooses quantities that can be calculated accurately on the lattice, and that are only weakly dependent on the light quark masses. The latter property minimizes errors from extrapolating or interpolating to the physical light quark masses or from mistuning of these masses. Commonly used choices are the spin-averaged 1S-1P or 1S-2S splittings in the Upsilon system, the mass of the Ω^- baryon, and the pion decay constant f_π. Ultimately, all choices must give the consistent results for a, and that this is the case provides a highly non-trivial check of both the calculational method and of QCD.

The determination of a using quantities involving light (up and down) quarks—such as f_π—involves particular challenges. Most current lattice simulations are done using light quark masses heavier than those in nature. One thus has to extrapolate the lattice data towards the physical quark masses. This "chiral extrapolation" is non-trivial because the quark mass dependence may involve non-analytic terms due to the loops of nearly massless pions, as predicted by Chiral Perturbation Theory (ChPT) [36].

18.1.4.2. *Light quark masses:* In LQCD simulations, the up, down and strange quarks are usually referred to as the light quarks, in the sense that $m_q < \Lambda_{\rm QCD}$. (The standard definition of $\Lambda_{\rm QCD}$ is given in the "Quantum Chromodynamics" review; in this review we are using it only to indicate the approximate non-perturbative scale of QCD.) This condition is stronger than that used above to distinguish quarks with small discretization errors, $m_q < 1/a$. Loop effects from light quarks must be included in the simulations to accurately represent QCD. At present, most simulations are done in the isospin symmetric limit $m_u = m_d \equiv m_\ell$, and are often referred to as "$N_f = 2+1$" simulations. (If, in addition, one includes the charm quark, this is denoted as an $N_f = 2+1+1$ simulation.) Precision is now reaching the point where isospin breaking effects, as well as those of electromagnetism (EM) must be included. This can be done approximately using ChPT and other theoretical input, but ultimately one needs to simulate directly with $m_u \neq m_d$ and including QED corrections. Such work is now beginning.

To tune m_ℓ and m_s to their physical values, the most commonly used quantities are, respectively, m_π and m_K. If the scale is being set by m_Ω, then one adjusts the lattice light quark masses until the ratios m_π/m_Ω and m_K/m_Ω take their physical values. At leading order in ChPT, one has the Gell-Mann-Oakes-Renner relations $m^2_{\pi^0} \propto (m_u + m_d)$ and $m^2_{K^0} \propto (m_d + m_s)$, which show the sensitivity of these quantities to the quark masses. In practice one uses higher order ChPT (or other fit functions) to extrapolate or interpolate the lattice results so as to match the desired ratios, correcting for the (small) effects of isospin breaking and electromagnetic corrections. Most present calculations need to extrapolate to the physical value of m_ℓ, while simulating directly at or near to the physical value of m_s.

18.1.4.3. *Heavy quark masses:* Heavy quarks (c and b) are usually treated only as valence quarks, with no loop effects included. The errors introduced by this approximation can be estimated to be $\sim \alpha_s(m_c)\Lambda^2_{\rm QCD}/m_c^2$ and are likely to be small. For high precision, however, dynamical charm quarks may be necessary, and simulations are beginning to include them.

The heavy quark masses can be tuned by setting heavy-heavy or heavy-light meson masses to their experimental values. For the charm quark, for example, one could use the J/ψ or the D_s meson. Consistency between these two determinations provides an important check that the determination of parameters in the heavy quark lattice formulations is being done correctly (see, e.g. Ref. 37).

18.1.5. *Sources of systematic error* :

Lattice results have statistical and systematic errors that must be quantified for any calculation in order for the result to be a useful input to phenomenology. The statistical error is due to the use of Monte Carlo importance sampling to evaluate the path integral (a method discussed below). There are, in addition, a number of systematic errors that are always present to some degree in lattice calculations, although the size of any given error depends on the particular quantity under consideration and the parameters of the ensembles being used. The most common lattice errors are reviewed below.

Although not strictly a systematic error, it is important to note that the presence of long autocorrelations in the sequence of lattice configurations generated by the Monte Carlo method can lead to uncertainty in the estimates of statistical errors. It is known that the global topological charge of the gauge fields decorrelates very slowly with certain algorithms [38]. This issue is particularly important for quantities, like the η' mass, which are sensitive to topology. It is an active area of research.

18.1.5.1. *Continuum limit:* Physical results are obtained in the limit that the lattice spacing a goes to zero. The Symanzik effective theory determines the scaling of lattice artefacts with a. Most lattice calculations use improved actions with leading discretizations errors of $\mathcal{O}(a^2\Lambda^2)$, $\mathcal{O}(\alpha_s a^2\Lambda^2)$, or $\mathcal{O}(\alpha_s a\Lambda)$, where Λ is a typical momentum scale in the system. Knowledge of the scaling of the leading discretization errors allows controlled extrapolation to $a = 0$ when multiple lattice spacings are available, as in current state-of-the-art calculations. Residual errors arise from the exclusion of subleading a dependence from the fits.

For many quantities the typical momentum scale in the system is $\sim \Lambda_{\rm QCD} \approx 300$ MeV. Discretization errors are expected to be larger for quantities involving larger scales, for example form factors or decays involving particles with momenta larger than $\Lambda_{\rm QCD}$.

18.1.5.2. *Infinite volume limit:* LQCD calculations are necessarily carried out in finite space-time boxes, leading to departures of physical quantities (masses, decay constants, etc.) from their measured, infinite volume values. These finite-volume shifts are an important systematic that must be estimated and minimized.

Typical lattices are asymmetric, with N_s points in the three spatial directions and N_t in the (Euclidean) temporal direction. The spatial and temporal sizes in physical units are thus $L_s = aN_s$ and $L_t = aN_t$, respectively. (Anisotropic lattice spacings are also sometimes used, as discussed below in Sec. 1.3.1.) Typically, $L_t \geq 2L_s$, a longer temporal direction being used to allow excited-state contributions to correlators to decay. This means that the dominant impact of using finite volume is from the presence of a finite spatial box.

At present, high-precision LQCD calculations are of quantities involving no more than a single particle in initial and final states. For such quantities, once the volume exceeds about 2 fm (so that the particle is not "squeezed"), the dominant finite-volume effect comes from virtual pions wrapping around the lattice in the spatial directions. This effect is exponentially suppressed as the volume becomes large, roughly as $\sim \exp(-m_\pi L_s)$, and has been estimated using ChPT [39] or other methods [40]. The estimates suggest that finite volume shifts are sub-percent effects when $m_\pi L_s \gtrsim 4$, and most large-scale simulations use lattices satisfying this condition. This becomes challenging as one approaches the physical pion mass, for which $L_s \gtrsim 5$ fm is required. At present, this can only be achieved by using relatively coarse lattices, $a \gtrsim 0.07$ fm.

Finite volume errors are usually determined by repeating the simulations on two or more different volumes (with other parameters fixed). If different volumes are not available, the ChPT estimate can be used, often inflated to account for the fact that the ChPT calculation is truncated at some order.

In the future, LQCD calculations involving more than a single hadron will become increasingly precise. Examples include the calculation of resonance parameters and $K \to \pi\pi$ amplitudes. Finite volume effects are much larger in these cases, with power-law terms (e.g. $1/L_s^3$) in addition to exponential dependence. Indeed, as will be discussed in Sec. 1.2.4., one can use the volume dependence to indirectly extract infinite-volume quantities such as scattering lengths. Doing so, however, requires a set of lattice volumes satisfying $m_\pi L_s \gtrsim 4$ and is thus more challenging than for single-particle quantities.

18.1.5.3. *Chiral extrapolation:* An important source of systematic error in most LQCD calculations is the need to extrapolate in m_u and m_d (or, equivalently, in m_π). To do this, one needs a functional form that is, at least approximately, valid for pion masses ranging from the unphysical values used in simulations down to the physical value. A theoretically favored choice is to use the predictions of SU(3) or SU(2) ChPT. This is a valid description of QCD for $m_q \ll \Lambda_{QCD}$ (or $m_\pi \ll m_\rho$), but the extent to which it applies at larger pion masses is not known *a priori*. This concern is exacerbated in practice since one must truncate the ChPT expressions, typically at one-loop or two-loop order. Experience to date suggests that one-loop expressions are not sufficiently accurate if $m_\pi \gtrsim 400$ MeV [41].

Another choice of fit function is based on the observation that one does not need to extrapolate to the chiral limit, but only to the physical, non-zero, value of m_π, and thus an analytic description might suffice. In practice, of course, one must truncate the analytic form at low order, and a concern is whether the curvature from known non-analytic terms is adequately reproduced.

Extrapolation errors are estimated by comparing fits based on ChPT to those using analytic fits, or by varying the fit function in some other way, and/or by varying the number of data points included. We also note that, in many calculations, additional input to the chiral extrapolation is obtained from "partially quenched" results in which the valence and sea-quark masses differ [42].

Recently, simulations with physical light quark masses (except that $m_u = m_d = (m_u^{\rm phys} + m_d^{\rm phys})/2$) have been undertaken [43], and are now becoming increasingly common [44]. This is a major step forward as it removes the need for chiral extrapolation. As noted above, such simulations require large boxes, and thus very large lattices, and to date the results have been used to compute a limited number of observables. In the future, however, such simulations will play an increasingly important role in the determination of physical quantities.

18.1.5.4. *Operator matching:* Many of the quantities that LQCD can precisely calculate involve hadronic matrix elements of operators from the electroweak Hamiltonian. Examples include the pion and kaon decay constants, semileptonic form factors and the kaon mixing parameter B_K (the latter defined in Eq. (18.13)). The operators in the lattice matrix elements are defined in the lattice regularization scheme. To be used in tests of the Standard Model, however, they must be matched to the continuum regularization scheme in which the corresponding Wilson coefficients have been calculated. The only case in which such matching is not needed is if the operator is a conserved or partially conserved current. Similar matching is also needed for the conversion of lattice bare quark masses to those in the continuum $\overline{\rm MS}$ scheme.

Three methods are used to calculate the matching factors: perturbation theory (usually to one- or two-loop order), non-perturbative renormalization (NPR) using Landau-gauge quark and gluon propagators [45], and NPR using gauge-invariant methods based on the Schrödinger functional [46]. The NPR methods replace truncation errors (which can only be approximately estimated) by statistical and systematic errors which can be determined reliably and systematically reduced.

A common issue that arises in many such calculations (e.g. for quark masses and B_K) is that, using NPR, one ends up with operators regularized in a MOM-like (or Schrödinger functional) scheme, rather than the $\overline{\rm MS}$ scheme mostly used for calculating the Wilson coefficients. To make contact with this scheme requires a purely continuum perturbative matching calculation. The resultant truncation error can, however, be minimized by pushing up the momentum scale at which the matching is done using step-scaling techniques as part of the NPR calculation [47]. It should also be noted that this final step in the conversion to the $\overline{\rm MS}$ scheme could be avoided if continuum calculations used a MOM-like scheme.

18.2. Methods and status

Once the lattice action is chosen, it is straightforward to define the quantum theory using the path integral formulation. The Euclidean-space partition function is

$$Z = \int [dU] \prod_f [dq_f][d\bar{q}_f] e^{-S_g[U] - \sum_f \bar{q}_f (D[U] + m_f) q_f} \,, \qquad (18.4)$$

where link variables are integrated over the SU(3) manifold, q_f and $\bar{q}_f$ are Grassmann (anticommuting) quark and antiquark fields of flavor f, and $D[U]$ is the chosen lattice Dirac operator with m_f the quark mass in lattice units. Integrating out the quark and antiquark fields, one arrives at a form suitable for simulation:

$$Z = \int [dU] e^{-S_g[U]} \prod_f \det(D[U] + m_f) \,. \qquad (18.5)$$

The building blocks for calculations are expectation values of multi-local gauge-invariant operators, also known as "correlation functions",

$$\langle \mathcal{O}(U,q,\bar{q})\rangle = (1/Z)\int [dU]\prod_f [dq_f][d\bar{q}_f]\mathcal{O}(U,q,\bar{q})e^{-S_g[U]-\sum_f \bar{q}_f(D[U]+m_f)q_f}\,. \tag{18.6}$$

If the operators depend on the (anti-)quark fields q_f and $\bar{q}_f$, then integrating these fields out leads not only to the fermion determinant but also, through Wick's theorem, to a series of quark "propagators", $(D[U]+m_f)^{-1}$, connecting the positions of the fields.

This set-up allows one to choose, by hand, the masses of the quarks in the determinant (the sea quarks) differently from those in the propagators (valence quarks). This is called "partial quenching", and, as noted above, is used by some calculations as a way of obtaining more data points from which to extrapolate both sea and valence quarks to their physical values.

18.2.1. *Monte-Carlo method* :

Since the number of integration variables U is huge ($N_s^3\times N_t\times 4\times 9$), direct numerical integration is impractical and one has to use Monte-Carlo techniques. In this method, one generates a Markov chain of gauge configurations (a "configuration" being the set of U's on all links) distributed according to the probability measure $[dU]e^{-S_g[U]}\prod_f \det(D[U]+m_f)$. Once the configurations are generated, expectation values $\langle\mathcal{O}(U,q,\bar{q})\rangle$ are calculated by averaging over those configurations. In this way the configurations can be used repeatedly for many different calculations, and there are several large collections of ensembles of configurations (with a range of values of a, lattice sizes and quark masses) that are publicly available through the International Lattice Data Grid (ILDG). As the number of the configurations, N, is increased, the error decreases as $1/\sqrt{N}$.

The most challenging part of the generation of gauge configurations is the need to include the fermion determinant. Direct evaluation of the determinant is not feasible, as it requires $\mathcal{O}((N_s^3\times N_t)^3)$ computations. Instead, one rewrites it in terms of "pseudofermion" fields ϕ (auxiliary fermion fields with bosonic statistics). For example, for two degenerate quarks one has

$$\det(D[U]+m_f)^2 = \int [d\phi]e^{-\phi^\dagger(D[U]+m_f)^{-2}\phi}\,. \tag{18.7}$$

By treating the pseudofermions as additional integration variables in the path integral, one obtains a totally bosonic representation. The price one pays is that the pseudofermion effective action is highly non-local since it includes the inverse Dirac operator $(D[U]+m_f)^{-1}$. Thus, the large sparse matrix $(D[U]+m)$ has to be inverted every time one needs an evaluation of the effective action.

Present simulations generate gauge configurations using the Hybrid Monte Carlo (HMC) algorithm [48], or variants thereof. This algorithm combines molecular dynamics (MD) evolution in a fictitious time (which is also discretized) with a Metropolis "accept-reject" step. It makes a global update of the configuration, and is made exact by the Metropolis step. In its original form it can be used only for two degenerate flavors, but extensions (particularly the rational HMC [49]) are available for single flavors. Considerable speed-up of the algorithms has been achieved over the last two decades using a variety of techniques.

All these algorithms spend the bulk of their computational time on the repeated inversion of $(D[U]+m)$ acting on a source (which is required at every step of the MD evolution). Inversions are done using a variety of iterative algorithms, *e.g.* the conjugate gradient algorithm. In this class of algorithms, computational cost is proportional to the condition number of the matrix, which is the ratio of maximum and minimum eigenvalues. For $(D[U]+m)$ the smallest eigenvalue is $\approx m$, so the condition number and cost are inversely proportional to the quark mass. This is a major reason why simulations at the physical quark mass are challenging. Recent algorithmic studies are making progress in significantly reducing this problem.

A practical concern is the inevitable presence of correlations between configurations in the Markov chain. These are characterized by an autocorrelation length in the fictitious MD time. One aims to use configurations separated in MD time by greater than this autocorrelation length. In practice, it is difficult to measure this length accurately, and this leads to some uncertainty in the resulting statistical errors, as well as the possibility of insufficient equilibration.

For most of the applications of LQCD discussed in this review, the cost of generating gauge configurations is larger than that of performing the "measurements" on those configurations. The computational cost of gauge generation grows with the lattice volume, $V_{\rm lat}=N_s^3N_t$, as $V_{\rm lat}^{1+\delta}$. Here $\delta=1/4$ for the HMC algorithm [50] and can be reduced slightly using modern variants. Such growth with $V_{\rm lat}$ provides a (time-dependent) limit on the largest lattice volumes that can be simulated. At present, the largest lattices being used have $N_s=96$ and $N_t=192$. Typically one aims to create an ensemble of $\sim 10^3$ statistically independent configurations at each choice of parameters (a, m_q and $V_{\rm lat}$). For most physical quantities of interest, this is sufficient to make the resulting statistical errors smaller than or comparable to the systematic errors.

18.2.2. *Two-point functions* :

One can extract properties of stable hadrons using two-point correlation functions, $\langle O_X(x)O_Y^\dagger(0)\rangle$. Here $O_{X,Y}(x)$ are operators that have non-zero overlaps with the hadronic state of interest $|H\rangle$, *i.e.* $\langle 0|O_{X,Y}(x)|H\rangle\neq 0$. One usually Fourier-transforms in the spatial directions and considers correlators as a function of Euclidean time:

$$C_{XY}(t;\vec{p}) = \sum_{\vec{x}}\langle O_X(t,\vec{x})O_Y^\dagger(0)\rangle e^{-i\vec{p}\cdot\vec{x}}. \tag{18.8}$$

(Here and throughout this section all quantities are expressed in dimensionless lattice units, so that, for example, $\vec{p}=a\vec{p}_{\rm phys}$.) By inserting a complete set of states having spatial momentum $\vec{p}$, the two-point function can be written as

$$C_{XY}(t;\vec{p}) = \sum_{i=0}^{\infty}\frac{1}{2E_i(\vec{p})}\langle 0|O_X(0)|H_i(\vec{p})\rangle\langle H_i(\vec{p})|O_Y^\dagger(0)|0\rangle e^{-E_i(\vec{p})t}, \tag{18.9}$$

where the energy of the i-th state $E_i(\vec{p})$ appears as an eigenvalue of the time evolution operator e^{-Ht} in the Euclidean time direction. The factor of $1/[2E_i(\vec{p})]$ is due to the relativistic normalization used for the states. For large enough t, the dominant contribution is that of the lowest energy state $|H_0(\vec{p})\rangle$:

$$C_{XY}(t)\overset{t\to\infty}{\longrightarrow}\frac{1}{2E_0(\vec{p})}\langle 0|O_X(0)|H_0(\vec{p})\rangle\langle H_0(\vec{p})|O_Y^\dagger(0)|0\rangle e^{-E_0(\vec{p})t}\,. \tag{18.10}$$

One can thus obtain the energy $E_0(\vec{p})$, which equals the hadron mass m_H when $\vec{p}=0$, and the product of matrix elements $\langle 0|O_X(0)|H_i(\vec{p})\rangle\langle H_i(\vec{p})|O_Y^\dagger(0)|0\rangle$.

This method can be used to determine the masses of all the stable mesons and baryons by making appropriate choices of operators. For example, if one uses the axial current, $O_X=O_Y=A_\mu=\bar{d}\gamma_\mu\gamma_5 u$, then one can determine m_{π^+} from the rate of exponential fall-off, and in addition the decay constant f_π from the coefficient of the exponential. A complication arises for states with high spins ($j\geq 4$ for bosons) because the spatial rotation group on the lattice is a discrete subgroup of the continuum group SO(3). This implies that lattice operators, even when chosen to lie in irreducible representations of the lattice rotation group, have overlap with states that have a number of values of j in the continuum limit [51]. For example $j=0$ operators can also create mesons with $j=4$. A method to overcome this problem has recently been introduced [52,53].

The expression given above for the correlator $C_{XY}(t;\vec{p})$ shows how, in principle, one can determine the energies of the excited hadron states having the same quantum numbers as the operators $O_{X,Y}$, by fitting the correlation function to a sum of exponentials. In practice, this usually requires using a large basis of operators and adopting the variational approach such as that of Ref. 54. One can also use an anisotropic lattice in which a_t, the lattice spacing in the time direction, is smaller than its spatial counterpart a_s. This allows better separation of the different exponentials. Using a combination of these and other technical improvements extensive excited-state spectra have recently been obtained [53,55,56](for a recent review, see Ref. 57).

18.2.3. ***Three-point functions*** :

Hadronic matrix elements needed to calculate semileptonic form factors and neutral meson mixing amplitudes can be computed from three-point correlation functions. We discuss here, as a representative example, the $D \to K$ amplitude. As in the case of two-point correlation functions one constructs operators O_D and O_K having overlap, respectively, with the D and K mesons. We are interested in calculating the matrix element $\langle K|V_\mu|D\rangle$, with $V_\mu = \bar{c}\gamma_\mu s$ the vector current. To obtain this, we use the three-point correlator

$$C_{KV_\mu D}(t_x, t_y; \vec{p}) = \sum_{\vec{x},\vec{y}} \langle O_K(t_x, \vec{x}) V_\mu(0) O_D^\dagger(t_y, \vec{y})\rangle e^{-i\vec{p}\cdot\vec{x}}\,, \quad (18.11)$$

and focus on the limit $t_x \to \infty$, $t_y \to -\infty$. In this example we set the D-meson at rest while the kaon carries three-momentum $\vec{p}$. Momentum conservation then implies that the weak operator V_μ inserts three-momentum $-\vec{p}$. Inserting a pair of complete sets of states between each pair of operators, we find

$$C_{KV_\mu D}(t_x, t_y; \vec{p}) = \sum_{i,j} \frac{1}{2m_{D_i} 2E_{K_j}(\vec{p})} e^{-m_{D_i} t_x - E_{K_j}(\vec{p})|t_y|} \times$$

$$\times \langle 0|O_K(t_x, \vec{x})|K_i(\vec{p})\rangle \langle K_i(\vec{p})|V_\mu(0)|D_j(\vec{0})\rangle \langle D_j(\vec{0})|O_D^\dagger(0)|0\rangle. \quad (18.12)$$

The matrix element $\langle K_i(\vec{p})|V_\mu(0)|D_j(\vec{0})\rangle$ can then be extracted, since all other quantities in this expression can be obtained from two-point correlation functions. Typically one is interested in the weak matrix elements of ground states, such as the lightest pseudoscalar mesons. In the limit of large separation between the three operators in Euclidean time, the three-point correlation function yields the weak matrix element of the transition between ground states.

18.2.4. ***Scattering amplitudes and resonances*** :

The methods described thus far yield matrix elements involving single, stable particles (where by stable here we mean absolutely stable to strong interaction decays). Most of the particles listed in the Review of Particle Properties are, however, unstable—they are resonances decaying into final states consisting of multiple strongly interacting particles. LQCD simulations cannot directly calculate resonance properties, but methods have been developed to do so indirectly for resonances coupled to two-particle final states in the elastic regime [58].

The difficulty faced by LQCD calculations is that, to obtain resonance properties, or, more generally, scattering phase-shifts, one must calculate multiparticle scattering amplitudes in momentum space and put the external particles on their mass-shells. This requires analytically continuing from Euclidean to Minkowski momenta. Although it is straightforward in LQCD to generalize the methods described above to calculate four- and higher-point correlation functions, one necessarily obtains them at a discrete and finite set of Euclidean momenta. Analytic continuation to $p_E^2 = -m^2$ is then an ill-posed and numerically unstable problem. The same problem arises for single-particle states, but can be largely overcome by picking out the exponential fall-off of the Euclidean correlator, as described above. With a multi-particle state, however, there is no corresponding trick, except for two particles at threshold [59].

What LQCD can calculate are the energies of the eigenstates of the QCD Hamiltonian in a finite box. The energies of states containing two stable particles, e.g. two pions, clearly depend on the interactions between the particles. It is possible to invert this dependence and, with plausible assumptions, determine the scattering phase-shifts at a discrete set of momenta from a calculation of the two-particle energy levels for a variety of spatial volumes [58]. This is a challenging calculation, but it has recently been carried through in several channels with quark masses approaching physical values. Channels studied include $\pi\pi$ (for $I = 2$, 1 and 0), $K\pi$, KD and DD^*. For recent reviews see Ref. 60. Extensions to nucleon interactions are also being actively studied [61]. The generalization of the formalism to the case of three particles is under active consideration [62].

It is also possible to extend the methodology to calculate electroweak decay amplitudes to two particles below the inelastic threshold, e.g. $\Gamma(K \to \pi\pi)$ [63]. Results for the $\Delta I = 3/2$ amplitude with physical quark masses have been obtained [64], and significant progress made toward a calculation of the $\Delta I = 1/2$ amplitude [65]. Partial extensions of the formalism above the elastic threshold have been worked out, in particular for the case of multiple two-particle channels [66]. An extension to decays with many multiparticle channels, e.g. hadronic B decays, has, however, yet to be formulated.

18.2.5. ***Status of LQCD simulations*** :

Until the 1990s, most large-scale lattice simulations were limited to the "quenched" approximation, wherein the fermion determinant is omitted from the path integral. While much of the basic methodology was developed in this era, the results obtained had uncontrolled systematic errors and were not suitable for use in placing precision constraints on the Standard Model. During the 1990s, more extensive simulations including the fermion determinant (also known as simulations with "dynamical" fermions) were begun, but with unphysically high light quark masses ($m_\ell \sim 50 - 100$ MeV), such that the extrapolation to the physical light quark masses was a source of large systematic errors [67]. In the last 5-10 years, advances in both algorithms and computers have allowed simulations to reach much smaller quark masses ($m_\ell \sim 10 - 20$ MeV) and even, as noted above, to work at the physical light quark mass. The net effect is that LQCD calculations of selected quantities now have all sources of error controlled and small, such that they can be used effectively in phenomenological analyses.

On a more qualitative level, analytic and numerical results from LQCD have demonstrated that QCD confines color and spontaneously breaks chiral symmetry. Confinement can be seen as a linearly rising potential between heavy quark and anti-quark in the absence of quark loops. Analytically, this can be shown in the strong coupling limit $g_{\rm lat} \to \infty$ [1]. At weaker couplings there are precise numerical calculations of the potential that clearly show that this behavior persists in the continuum limit [68–70].

Chiral symmetry breaking was also demonstrated in the strong coupling limit on the lattice [15,71], and there have been a number of numerical studies showing that this holds also in the continuum limit. The accumulation of low-lying modes of the Dirac operator, which is the analog of Cooper pair condensation in superconductors, has been observed, yielding a determination of the chiral condensate [72–74] Many relations among physical quantities that can be derived under the assumption of broken chiral symmetry have been confirmed by a number of lattice groups [75].

18.3. Physics applications

In this section we describe the main applications of LQCD that are both computationally mature and relevant for the determination of particle properties.

A general feature to keep in mind is that, since there are many different choices for lattice actions, all of which lead to the same continuum theory, a crucial test is that results for any given quantity are consistent. In many cases, different lattice calculations are completely independent and often have very different systematic errors. Thus final agreement, if found, is a highly non-trivial check, just as it is for different experimental measurements.

The number, variety and precision of the calculations has progressed to the point that an international "Flavour Lattice Averaging Group" (FLAG) has been formed. The main aims of FLAG include collecting all lattice results of relevance for a variety of phenomenologically interesting quantities and providing averages of those results which pass appropriate quality criteria. The averages attempt to account for possible correlations between results (which can arise, for example, if they use common gauge configurations). The quantities considered are those we discuss in this section, with the exception of the hadron spectrum. FLAG has recently completed their review [75], and we have made extensive use of it in preparing the following summary. We stress that the results we quote below are those obtained using the physical complement of light quarks (i.e. $N_f = 2 + 1$ or $2 + 1 + 1$ simulations).

18.3.1. *Spectrum* :

The most basic prediction of LQCD is of the hadron spectrum. Once the input parameters are fixed as described in Sec. 18.1.4, the masses or resonance parameters of all other states can be predicted. This includes hadrons composed of light (u, d and s) quarks, as well as heavy-light and heavy-heavy hadrons. It also includes quark-model exotics (e.g. $J^{PC} = 1^{-+}$ mesons) and glueballs. Thus, in principle, LQCD calculations should be able to reproduce many of the experimental results compiled in the Review of Particle Properties. Doing so would test both that the error budgets of LQCD calculations are accurate and that QCD indeed describes the strong interactions in the low-energy domain. The importance of the latter test can hardly be overstated.

What is the status of this fundamental test? As discussed in Sec. 1.2, LQCD calculations are most straightforward for stable, low-lying hadrons. Resonances which can decay into only two particles are more challenging, though substantial progress has been made. First theoretical work on decays to more than two particles has begun, but the methodology is not yet practical. It is also more technically challenging to calculate masses of flavor singlet states (which can annihilate into purely gluonic intermediate states) than those of flavor non-singlets, although again algorithmic and computational advances have made such calculations accessible in some cases. The present status for light hadrons is that fully controlled results are available for the masses of the octet light baryons, while results with less than complete control are available for the decuplet baryon resonances, the vector meson resonances and the η and η'. There are more extensive results for heavy-light (D and B systems) and heavy-heavy (J/ψ and Υ systems). All present results, which are discussed in the "Quark Model" review, are consistent with experimental values. For a recent extensive review of lattice results see also Ref. 76.

18.3.2. *Decay constants and bag parameters* :

The pseudoscalar decay constants can be determined from two point correlation functions involving the axial-vector current, as discussed in Sec. 18.2.2. The decay constant f_P of a meson P is extracted from the weak matrix element involving the axial-vector current using the relation $\langle 0|A_\mu(x)|P(\vec{p})\rangle = f_P p_\mu \exp(-ip\cdot x)$, where p_μ is the momentum of P and $A_\mu(x)$ is the axial-vector current. For the pion and kaon decay constants, this calculation is by now straightforward. The ratio f_K/f_π is especially important for the extraction of $|V_{us}|/|V_{ud}|$ from experiment, and many of the systematic errors in the lattice calculation cancel or are significantly reduced when forming the ratio [77]. A number of lattice groups have calculated this ratio with precision at the percent level or better; all the results are in good agreement, with sub-percent precision in the world average [78,79,75]. A summary is shown in Fig. 18.1. The most significant advance in the last two years is the addition of a calculation including dynamical charm quarks ("$N_f = 2+1+1$") [44], the result from which is in complete agreement with the average of results with $N_f = 2+1$.

The heavy-light decay constants f_D and f_{D_s} involve a charm valence quark, which can be simulated using various methods, as discussed in Sec. 18.1.3. The most accurate result uses the same HISQ action for the charm quark as for the light quarks, which means that the matching factor for the axial currents of interest are unity. This allows Ref. 83 to quote values for the charm decay constants with 1-1.5% errors. Calculations using alternative quark actions give consistent results, but with larger errors [84,85]. The FLAG averages are $f_D = 209(3)$ MeV, $f_{D_s} = 249(3)$ MeV, $f_{D_s}/f_D = 1.187(12)$.

The bottom meson decay constants f_B and f_{B_s} require a valence b quark. Lattice calculations of these quantities are available using the Fermilab formulation [84], NRQCD [86] or HQET [87] to treat the bottom quark or using an interpolation between results from around m_c to infinite quark mass [88,89]. Results have precisions ranging down to $\sim 2\%$. The FLAG averages are $f_B = 191(4)$ MeV, $f_{B_s} = 228(5)$ MeV, $f_{B_s}/f_B = 1.20(2)$.

The kaon bag parameter B_K is needed to turn the precise measurement of CP-violation in kaon mixing into a constraint on the Standard Model. It is defined by

$$\frac{8}{3} m_K^2 f_K^2 B_K(\mu) = \langle \overline{K}^0 | Q_{\Delta_S=2}(\mu) | K^0 \rangle, \qquad (18.13)$$

where m_K is the kaon mass, f_K is the kaon decay constant, $Q_{\Delta S=2} = \overline{s}\gamma_\mu(1-\gamma_5)d\overline{s}\gamma_\mu(1-\gamma_5)d$ is the four-quark operator of the effective electroweak Hamiltonian and μ is the renormalization scale. The short distance contribution to the electroweak Hamiltonian can be calculated perturbatively, but the hadronic matrix element parameterized by B_K must be computed using non-perturbative methods. In order to be of use to phenomenology, the renormalization factor of the four-quark operator must be matched to a continuum renormalization scheme, e.g. to $\overline{\rm MS}$, as described in Sec. 18.1.5.4. Determinations with percent-level precision using different fermion actions are now available with DWF [82], staggered fermions [90], DWF valence on staggered sea quarks [91], twisted mass fermions [92] and Wilson fermions [12]. The results are all consistent, and the FLAG average is $\hat{B}_K = 0.766(10)$.

The bag parameters for B and B_s meson mixing are defined analogously to that for kaon mixing. The B and B_s mesons contain a valence b-quark so that calculations of these quantities must use one of the methods for heavy quarks described above. Calculations have been done using NRQCD [93], the Fermilab formalism [94], the Columbia formalism [95] and twisted-mass fermions [96]. For $f_B\sqrt{B_B}$ and $f_{B_s}\sqrt{B_{B_s}}$ the averages are dominated by the HPQCD results [93]. The errors ($\sim 7\%$) are dominated by that from operator matching. For the ratio of these two quantities, ξ, the total error ($\sim 5\%$) is somewhat smaller due to cancelations: the dominant errors are due to chiral extrapolation and statistics. The FLAG averages are $f_B\sqrt{B_B} = 216(15)$ MeV, $f_{B_s}\sqrt{B_{B_s}} = 266(18)$ Mev and $\xi = 1.268(63)$.

The results discussed in this section are used in the reviews "The CKM Quark-Mixing Matrix," "V_{ud}, V_{us}, the Cabibbo Angle and CKM Unitarity," and "$B_0 - \bar{B}_0$ Mixing."

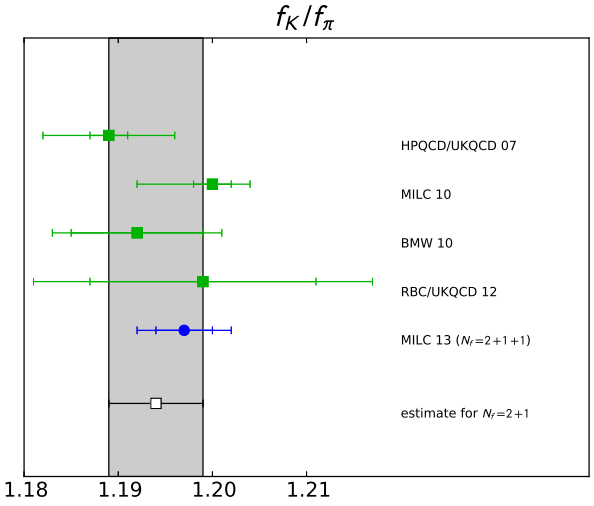

Figure 18.1: Results for f_K/f_π in the isospin limit from simulations with $N_f = 2+1$ and $N_f = 2+1+1$. These are from the HPQCD/UKQCD [37], BMW [80], MILC [81,44], and RBC/UKQCD collaborations [82]. The MILC collaboration results have been shifted upward (by $\sim 0.2\%$, following Ref. 75) since they were originally quoted for $m_u \neq m_d$. The FLAG average of the $N_f = 2+1$ results is 1.194 ± 0.005 [75].

18.3.3. ***Form factors ($K \to \pi\ell\nu$, $D \to K\ell\nu$, $B \to \pi\ell\nu$, $B \to D^{(*)}\ell\nu$)*** :

Semileptonic decay rates can be used to extract CKM matrix elements once the semileptonic form factors are known from lattice calculations. For example, the matrix element of a pseudoscalar meson P undergoing semileptonic decay to another pseudoscalar meson D is mediated by the vector current, and can be written in terms of form factors as

$$\langle D(p_D)|V_\mu|P(p_P)\rangle = f_+(q^2)(p_D + p_P - \Delta)_\mu + f_0(q^2)\Delta_\mu\,, \quad (18.14)$$

where $q = p_D - p_P$, $\Delta_\mu = (m_D^2 - m_P^2)q_\mu/q^2$ and V_μ is the quark vector current. The shape of the form factor is typically well determined by experiment, and the value of $f_+(q^2)$ at some reference value of q^2 is needed from the lattice in order to extract CKM matrix elements. Typically $f_+(q^2)$ dominates the decay rate, since the contribution from $f_0(q^2)$ is suppressed when the final state lepton is light.

The form factor $f_+(0)$ for $K \to \pi\ell\nu$ decays is highly constrained by the Ademollo-Gatto theorem [97] and chiral symmetry. Old estimates using chiral perturbation theory combined with quark models quote sub-percent precision [98], though they suffer from some model dependence. The lattice has now matched this precision while also eliminating the model dependence; good agreement with the old estimate is found [99–102]. The FLAG average is $f_+(0) = 0.967(4)$.

Charm meson semileptonic decays have been calculated by different groups using methods similar to those used for charm decay constants, and results are steadily improving in precision [103,104]. For semileptonic decays involving a bottom quark, one uses HQET or NRQCD to control the discretization errors of the bottom quark. The form factors for the semileptonic decay $B \to \pi\ell\nu$ have been calculated in unquenched lattice QCD by HPQCD [105] and Fermilab/MILC Collaborations [106]. These B semileptonic form factors are difficult to calculate at low q^2, *i.e.* when the mass of the B-meson must be balanced by a large pion momentum, in order to transfer a small momentum to the lepton pair. The low q^2 region has large discretization errors and very large statistical errors, while the high q^2 region is much more accessible to the lattice. For experiment, the opposite is true. To combine lattice and experimental results it has proved helpful to use the z-parameter expansion [107]. This provides a theoretically constrained parameterization of the entire q^2 range, and allows one to obtain $|V_{ub}|$ without model dependence [108,106].

The semileptonic decays $B \to D\ell\nu$ and $B \to D^*\ell\nu$ can be used to extract $|V_{cb}|$ once the corresponding form factors are known. At present only one unquenched calculation exists for the $B \to D^*\ell\nu$ form factor, where the Fermilab formulation of the heavy quark was adopted [109]. This calculation is done at zero-recoil because that is where the lattice systematic errors are smallest. Calculations of the necessary form factors for both processes at non-zero recoil have been done in the quenched approximation [110] using a step-scaling approach for the heavy quarks. Lattice calculations at non-zero recoil are needed in order to decrease the error associated with the extrapolation of the experimental data to the zero-recoil point.

The results discussed in this section are used in the reviews "The CKM Quark-Mixing Matrix," "V_{ud}, V_{us}, the Cabibbo Angle and CKM Unitarity," and "V_{cb} and V_{ub} CKM Matrix Elements."

18.3.4. ***Strong coupling constant*** :

As explained in Sec. 18.1.4.1, for a given lattice action, the choice of bare lattice coupling constant, $g_{\rm lat}$, determines the lattice spacing a. If one then calculates a as described in Sec. 18.1.4.1, one knows the strong coupling constant in the bare lattice scheme at the scale $1/a$, $\alpha_{\rm lat} = g_{\rm lat}^2/(4\pi)$. This is not, however, useful for comparing to results for α_s obtained from other inputs, such as deep inelastic scattering or jet shape variables. This is because the latter results give α_s in the $\overline{\rm MS}$ scheme, which is commonly used in such analyses, and the conversion factor between these two schemes is known to converge extremely poorly in perturbation theory. Instead one must use a method which directly determines α_s on the lattice in a scheme closer to $\overline{\rm MS}$.

Several such methods have been used, all following a similar strategy. One calculates a short-distance quantity K both perturbatively ($K^{\rm PT}$) and non-perturbatively ($K^{\rm NP}$) on the lattice, and requires equality: $K^{\rm NP} = K^{\rm PT} = \sum_{i=0}^{n} c_i \alpha_s^i$. Solving this equation one obtains α_s at a scale related to the quantity being used. Often, α_s thus obtained is not defined in the conventional $\overline{\rm MS}$ scheme, and one has to convert among the different schemes using perturbation theory. Unlike for the bare lattice scheme, the required conversion factors are reasonably convergent. As a final step, one uses the renormalization group to run the resulting coupling to a canonical scale (such as M_Z).

In the work of the HPQCD collaboration [111], the short-distance quantities are Wilson loops of several sizes and their ratios. These quantities are perturbatively calculated to $\mathcal{O}(\alpha_s^3)$ using the V-scheme defined through the heavy quark potential. The coefficients of even higher orders are estimated using the data at various values of a.

Another choice of short-distance quantities is to use current-current correlators. Appropriate moments of these correlators are ultraviolet finite, and by matching lattice results to the *continuum* perturbative predictions, one can directly extract the $\overline{\rm MS}$ coupling. The JLQCD collaboration [112] uses this approach with light overlap fermions, while the HPQCD collaboration uses charm-quark correlators and HISQ fermions [113]. Yet another choice of short-distance quantity is the static-quark potential, where the lattice result for the potential is compared to perturbative calculations; this method was used to compute α_s within 2+1 flavor QCD [114]. The ETM Collaboration obtains α_s by a comparison of lattice data for the ghost-gluon coupling with that of perturbation theory [115], providing the first determination of α_s with 2+1+1 flavors of dynamical quarks.

With a definition of α_s given using the Schrödinger functional, one can non-perturbatively control the evolution of α_s to high-energy scales, such as 100 GeV, where the perturbative expansion converges very well. This method developed by the ALPHA collaboration [47] has been applied to 2+1-flavor QCD by the PACS-CS collaboration [116].

The various lattice methods for calculating α_s have significantly different sources of systematic error. Thus the good agreement between the approaches (which can be seen in the "Quantum Chromodynamics" review) provides a strong check on the final result.

18.3.5. ***Quark masses*** :

Once the quark mass parameters are tuned in the lattice action, the remaining task is to convert them to those of the conventional definition. Since the quarks do not appear as asymptotic states due to confinement, the pole mass of the quark propagator is not a physical quantity. Instead, one defines the quark mass after subtracting the ultra-violet divergences in some particular way. The conventional choice is again the $\overline{\rm MS}$ scheme at a canonical scale such as 2 or 3 GeV.

As discussed in Sec. 18.1.5.4, one must convert the lattice bare quark mass to that in the $\overline{\rm MS}$ scheme. The most common approaches used for doing so are perturbation theory and the NPR method, the latter using an RI/MOM intermediate scheme.

Alternatively, one can use a definition based on the Schrödinger functional, which allows one to evolve the quark mass to a high scale non-perturbatively [117]. In practice, one can reach scales as high as ∼100 GeV, at which matching to the $\overline{\rm MS}$ scheme can be reliably calculated in perturbation theory.

Another approach available for heavy quarks is to match current-current correlators at short distances calculated on the lattice to those obtained in continuum perturbation theory in the $\overline{\rm MS}$ scheme. This has allowed an accurate determination of $m_c(\overline{\rm MS})$ [118].

Results are summarized in the review of "Quark Masses".

18.3.6. ***Other applications*** :

In this review we have concentrated on applications of LQCD that are relevant to the quantities discussed in the Review of Particle Properties. We have not discussed at all several other applications which are being actively pursued by simulations. Here we list the major such applications. The reader can consult the texts [2,3,4] for further details, as well as the proceedings of recent lattice conferences [119].

LQCD can be used, in principle, to simulate QCD at non-zero temperature and density, and in particular to study how confinement and chiral-symmetry breaking are lost as T and μ (the chemical

potential) are increased. This is of relevance to heavy-ion collisions, the early Universe and neutron-star structure. In practice, finite temperature simulations are computationally tractable and relatively mature, while simulations at finite μ suffer from a "sign problem" and are at a rudimentary stage.

Another topic under active investigation is nucleon structure (generalized structure functions) and inter-nucleon interactions.

Finally, we note that there is much recent interest in studying QCD-like theories with more fermions, possibly in other representations of the gauge group. The main interest is to find nearly conformal theories which might be candidates for "walking technicolor" models.

18.4. Outlook

While LQCD calculations have made major strides in the last decade, and are now playing an important role in constraining the Standard Model, there are many calculations that could be done in principle but are not yet mature due to limitations in computational resources. As we move to exascale resources (e.g. 10^{18} floating point operations per second), the list of mature calculations will grow. Examples that we expect to mature in the next few years are results for excited hadrons, including quark-model exotics; $\langle N|\bar{s}s|N\rangle$ and related matrix elements (needed for dark-matter searches); results for moments of structure functions; $K \to \pi\pi$ amplitudes (allowing a prediction of ϵ'/ϵ from the Standard Model); $\bar{K} \leftrightarrow K$ and $\bar{B} \leftrightarrow B$ mixing amplitudes from operators arising in models of new physics (allowing one to constrain these models in a manner complementary to the direct searches at the LHC); hadronic vacuum polarization contributions to muon $g-2$, the running of $\alpha_{\rm EM}$ and α_s; $\pi \to \gamma\gamma$ and related amplitudes; and perhaps the long-distance contribution to $\overline{K} \leftrightarrow K$ mixing and the light-by-light contribution to muon $g-2$. There will also be steady improvement in the precision attained for the mature quantities discussed above. As already noted, this will ultimately require simulations with $m_u \neq m_d$ and including electromagnetic effects.

18.5. Acknowledgments

We are grateful to Jean-Francois Arguin, Christine Davies, Aida El-Khadra, Max Hansen, Tony Kennedy, Andreas Kronfeld, Laurent Lellouch, Vittorio Lubicz, Paul Mackenzie and Hartmut Wittig for comments.

References:

1. K. G. Wilson, Phys. Rev. **D10**, 2445-2459 (1974).
2. T. Degrand and C. DeTar, "Lattice Methods for Quantum Chromodynamics," World Scientific (2006).
3. C. Gattringer and C.B. Lang, "Quantum Chromodynamics on the Lattice: An Introductory Presentation," Springer (2009).
4. "Modern Pespectives in Lattice QCD: quantum field theory and high performance computing" (Lecture notes of the Les Houches Summer School, Vol. 93) eds. L. Lellouch *et al.*, Oxford Univ. Press. (Aug. 2011).
5. W. Zimmermann, in "Lectures on Elementary Particles and Quantum Field Theory", ed. S. Deser *et al.*, MIT Press, Cambridge, MA (1971); K. Symanzik, Nucl. Phys. **B226**, 187 (1983); Nucl. Phys. **B226**, 205 (1983).
6. M. Lüscher and P. Weisz, Commun. Math. Phys. **97**, 59 (1985).
7. Y. Iwasaki, UT-HEP-118.
8. H. B. Nielsen and M. Ninomiya, Phys. Lett. **B105**, 219 (1981).
9. B. Sheikholeslami and R. Wohlert, Nucl. Phys. B **259**, 572 (1985).
10. K. Jansen *et al.*, Phys. Lett. **B372**, 275-282 (1996).
11. M. Lüscher, JHEP **0305**, 052 (2003); Comput. Phys. Commun. 156, 209 (2004) and 165, 199 (2005); M. Hasenbusch, Phys. Lett. **B519**, 177 (2001); C. Urbach *et al.*, Comput. Phys. Commun. 174, 87 (2006).
12. S. Durr *et al.*, Phys. Lett. B **705**, 477 (2011).
13. R. Frezzotti *et al.* [Alpha Collab.], JHEP **0108**, 058 (2001).
14. R. Frezzotti and G. C. Rossi, JHEP **0408**, 007 (2004).
15. L. Susskind, Phys. Rev. D **16**, 3031 (1977).
16. M. Golterman, PoS **CONFINEMENT8**, 014 (2008).
17. C. Bernard, Phys. Rev. D **73**, 114503 (2006); S. R. Sharpe, PoS LAT **2006**, 022 (2006).
18. G. P. Lepage, Phys. Rev. D **59**, 074502 (1999).
19. E. Follana *et al.* [HPQCD and UKQCD Collabs.], Phys. Rev. D **75**, 054502 (2007).
20. P. H. Ginsparg and K. G. Wilson, Phys. Rev. D **25**, 2649 (1982).
21. P. Hasenfratz, V. Laliena, and F. Niedermayer, Phys. Lett. B **427**, 125 (1998).
22. M. Lüscher, Phys. Lett. B **428**, 342 (1998).
23. D. B. Kaplan, Phys. Lett. B **288**, 342 (1992); Y. Shamir, Nucl. Phys. B **406**, 90 (1993); Nucl. Phys. B **417**, 167 (1994).
24. H. Neuberger, Phys. Lett. B **417**, 141 (1998); Phys. Lett. B **427**, 353 (1998).
25. A. Borici, `hep-lat/9912040`; A. D. Kennedy, `hep-lat/0607038`.
26. E. Shintani *et al.* [JLQCD Collab.], Phys. Rev. Lett. **101**, 242001 (2008).
27. A. Bazavov *et al.* [MILC Collab.], Phys. Rev. D **87**, 054505 (2013).
28. R. Baron *et al.* [ETM Collab.], JHEP **1006**, 111 (2010).
29. E. Eichten and B. R. Hill, Phys. Lett. B **234**, 511 (1990).
30. J. Heitger and R. Sommer [ALPHA Collab.], JHEP **0402**, 022 (2004); B. Blossier *et al.* [ALPHA Collab.], JHEP **1012**, 039 (2010).
31. B. A. Thacker and G. P. Lepage, Phys. Rev. D **43**, 196 (1991); G. P. Lepage *et al.*, Phys. Rev. D **46**, 4052 (1992).
32. A. X. El-Khadra *et al.,* Phys. Rev. D **55**, 3933 (1997).
33. S. Aoki *et al.*, Prog. Theor. Phys. **109**, 383 (2003).
34. N. H. Christ *et al.*, Phys. Rev. D **76**, 074505 (2007).
35. Y. Aoki *et al.* [RBC and UKQCD Collabs.], Phys. Rev. D **86**, 116003 (2012).
36. For lecture notes on applications of Chiral Perturbation Theory to lattice QCD, see S. R. Sharpe, `arXiv:hep-lat/0607016`and M. Golterman in Ref. [4].
37. E. Follana *et al.* [HPQCD and UKQCD Collabs.], Phys. Rev. Lett. **100**, 062002 (2008); C. T. H. Davies *et al.* [HPQCD Collab.] Phys. Rev. **D82**, 114504 (2010).
38. M. Lüscher, PoS LATTICE **2010**, 015 (2010); S. Schaefer *et al.* [ALPHA Collab.], Nucl. Phys. B **845**, 93 (2011).
39. G. Colangelo *et al.*, Nucl. Phys. **B721**, 136-174 (2005).
40. M. Lüscher, Commun. Math. Phys. **104**, 177 (1986).
41. J. Noaki *et al.* [JLQCD and TWQCD Collabs.], Phys. Rev. Lett. **101**, 202004 (2008).
42. C. W. Bernard and M. F. L. Golterman, Phys. Rev. **D49**, 486-494 (1994); S. R. Sharpe, Phys. Rev. **D56**, 7052 (1997); S. R. Sharpe and N. Shoresh, Phys. Rev. **D62**, 094503 (2000).
43. S. Aoki *et al.* [PACS-CS Collab.], Phys. Rev. D **81**, 074503 (2010); S. Durr *et al.*, Phys. Lett. B **701**, 265 (2011).
44. A. Bazavov *et al.* [MILC Collab.], Phys. Rev. Lett. **110**, 172003 (2013).
45. G. Martinelli *et al.*, Nucl. Phys. B **445**, 81 (1995).
46. M. Lüscher *et al.*, Nucl. Phys. **B384**, 168 (1992).
47. M. Lüscher *et al.*, Nucl. Phys. B **413**, 481 (1994); M. Della Morte *et al.*, [ALPHA Collab.], Nucl. Phys. B **713**, 378 (2005).
48. S. Duane *et al.*, Phys. Lett. B **195**, 216 (1987).
49. M. A. Clark and A. D. Kennedy, Phys. Rev. Lett. **98**, 051601 (2007).
50. M. Creutz, Phys. Rev. **D38**, 1228 (1988); R. Gupta *et al.*, Phys. Rev. **D38**, 1278 (1988).
51. J. E. Mandula *et al.*, Nucl. Phys. **B228**, 91 (1983); J. E. Mandula and E. Shpiz, Nucl. Phys. **B232**, 180 (1984).
52. H. B. Meyer and M. J. Teper, Nucl. Phys. B658, 113 (2003).
53. J. J. Dudek *et al.*, Phys. Rev. **D82**, 034508 (2010); J. J. Dudek *et al.*, Phys. Rev. **D83**, 111502 (2011); R. G. Edwards *et al.*, Phys. Rev. D **84**, 074508 (2011).
54. M. Lüscher and U. Wolff, Nucl. Phys. **B339**, 222 (1990).
55. G. P. Engel *et al.* [Bern-Graz-Regensburg Collab.], Phys. Rev. **D82**, 034505 (2010).
56. M. S. Mahbub *et al.*, `arXiv:1310.6803 [hep-lat]`.
57. D. Mohler, PoS LATTICE **2012**, 003 (2012).

58. M. Lüscher, Commun. Math. Phys. **105**, 153 (1986); Nucl. Phys. **B354**, 531 (1991) and **B364**, 237 (1991).
59. L. Maiani and M. Testa, Phys. Lett. **B245**, 585 (1990).
60. D. Mohler, PoS LATTICE **2012**, 003 (2012); S. Prelovsek *et al.*, arXiv:1304.2143 [hep-ph].
61. S. R. Beane *et al.*, Int. J. Mod. Phys. **E17**, 1157-1218 (2008); M. J. Savage, Prog. Part. Nucl. Phys. **67**, 140 (2012).
62. K. Polejaeva and A. Rusetsky, Eur. Phys. J. A **48**, 67 (2012); R. A. Briceno and Z. Davoudi, Phys. Rev. D **87**, 094507 (2013).
63. L. Lellouch and M. Lüscher, Commun. Math. Phys. **219**, 31 (2001).
64. T. Blum *et al.*, Phys. Rev. Lett. **108**, 141601 (2012); Phys. Rev. D **86**, 074513 (2012).
65. P. A. Boyle *et al.* [RBC and UKQCD Collabs.], Phys. Rev. Lett. **110**, 152001 (2013).
66. V. Bernard *et al.*, JHEP **1101**, 019 (2011); M. Doring *et al.*, Eur. Phys. J. A **47**, 139 (2011); M. T. Hansen and S. R. Sharpe, Phys. Rev. D **86**, 016007 (2012); R. A. Briceno and Z. Davoudi, arXiv:1204.1110 [hep-lat].
67. C. Bernard *et al.*, Nucl. Phys. Proc. Suppl. **119**, 170 (2003).
68. S. Perantonis and C. Michael, Nucl. Phys. B **347**, 854 (1990).
69. G. S. Bali and K. Schilling, Phys. Rev. D **46**, 2636 (1992).
70. S. Necco and R. Sommer, Nucl. Phys. B **622**, 328 (2002).
71. J. M. Blairon *et al.*, Nucl. Phys. **B180**, 439 (1981).
72. H. Fukaya *et al.* [JLQCD Collab.], Phys. Rev. Lett. **104**, 122002 (2010); H. Fukaya *et al.* [JLQCD and TWQCD Collabs.], Phys. Rev. **D83**, 074501 (2011).
73. L. Giusti and M. Luscher, JHEP **0903**, 013 (2009).
74. K. Cichy, E. Garcia-Ramos, and K. Jansen, JHEP **1310**, 175 (2013) arXiv:1303.1954 [hep-lat].
75. S. Aoki, *et al.*, arXiv:1310.8555 [hep-lat]; itpwiki.unibe.ch/flag/index.php/.
76. Z. Fodor and C. Hoelbling, Rev. Mod. Phys. **84**, 449 (2012).
77. W. Marciano, Phys. Rev. Lett. 93, 231803 (2004).
78. J. Laiho *et al.*, Phys. Rev. **D81**, 034503 (2010).
79. G. Colangelo *et al.*, Eur. Phys. J. **C71**, 1695 (2011).
80. S. Durr *et al.*, Phys. Rev. **D81**, 054507 (2010).
81. A. Bazavov *et al.* [MILC Collab.], PoS **LATTICE2010**, 074 (2010).
82. R. Arthur *et al.* [RBC and UKQCD Collabs.], Phys. Rev. D **87**, 094514 (2013).
83. C. T. H. Davies *et al.* Phys. Rev. D **82**, 114504 (2010); H. Na *et al.*, Phys. Rev. D **86**, 054510 (2012).
84. A. Bazavov *et al.* [FNAL/MILC Collab.], Phys. Rev. D **85**, 114506 (2012).
85. P. Dimopoulos *et al.* [ETM Collab.], JHEP **1201**, 046 (2012).
86. F. Bernardoni *et al.*, PoS LATTICE **2012**, 273 (2012).
87. H. Na *et al.*, Phys. Rev. D **86**, 034506 (2012).
88. C. McNeile *et al.*, Phys. Rev. D **85**, 031503 (2012).
89. N. Carrasco *et al.*, PoS LATTICE **2012**, 104 (2012).
90. T. Bae *et al.* [SWME Collab.], Phys. Rev. Lett. **109**, 041601 (2012).
91. J. Laiho and R. S. Van de Water, PoS LATTICE **2011**, 293 (2011).
92. M. Constantinou *et al.* [ETM Collab.], Phys. Rev. **D83**, 014505 (2011).
93. E. Gamiz *et al.* [HPQCD Collab.], Phys. Rev. **D80**, 014503 (2009).
94. C. M. Bouchard *et al.*, PoS LATTICE **2011**, 274 (2011).
95. C. Albertus *et al.*, Phys. Rev. D **82**, 014505 (2010).
96. N. Carrasco *et al.* [ETM Collab.], PoS LATTICE **2012**, 105 (2012).
97. M. Ademollo and R. Gatto, Phys. Rev. Lett. **13**, 264-265 (1964).
98. H. Leutwyler and M. Roos, Z. Phys. **C25**, 91 (1984).
99. P. A. Boyle *et al.*, Eur. Phys. J. **C69**, 159-167 (2010).
100. V. Lubicz *et al.* [ETM Collab.], Phys. Rev. **D80**, 111502 (2009); PoS LATTICE **2010**, 316 (2010).
101. A. Bazavov *et al.* [FNAL/MILC Collabs.] Phys. Rev. D **87**, 073012 (2013).
102. T. Kaneko *et al.* [JLQCD Collab.], PoS LATTICE **2012**, 111 (2012).
103. H. Na *et al.* [HPQCD Collab.], Phys. Rev. D **84**, 114505 (2011).
104. H. Na *et al.* [HPQCD Collab.], Phys. Rev. **D82**, 114506 (2010).
105. E. Dalgic *et al.* [HPQCD Collab.], Phys. Rev. **D73**, 074502 (2006).
106. J. A. Bailey *et al.*, Phys. Rev. **D79**, 054507 (2009).
107. C. Bourrely *et al.*, Nucl. Phys. **B189**, 157 (1981); C. G. Boyd *et al.*, Phys. Rev. Lett. **74**, 4603 (1995); T. Becher and R. J. Hill, Phys. Lett. **B633**, 61 (2006); C. Bourrely *et al.*, Phys. Rev. **D79**, 013008 (2009).
108. M. C. Arnesen *et al.*, Phys. Rev. Lett. **95**, 071802 (2005).
109. C. Bernard *et al,*, Phys. Rev. **D79**, 014506 (2009); J. A. Bailey *et al.* [Fermilab Lattice and MILC Collabs.], PoS **LATTICE2010**, 311 (2010).
110. G. M. de Divitiis *et al.* Phys. Lett. **B655**, 45 (2007); Nucl. Phys. **B807**, 373 (2009).
111. C. T. H. Davies *et al.* [HPQCD Collab.], Phys. Rev. D **78**, 114507 (2008).
112. E. Shintani *et al.*, Phys. Rev. D **82**, 074505 (2010).
113. C. McNeile *et al.*, [HPQCD Collab.], Phys. Rev. D **82**, 034512 (2010).
114. A. Bazavov *el al.* Phys. Rev. D **86**, 114031 (2012).
115. B. Blossier *et al.* Phys. Rev. D **85**, 034503 (2012); Phys. Rev. Lett. **108**, 262002 (2012).
116. S. Aoki *et al.* [PACS-CS Collab.], JHEP **0910**, 053 (2009).
117. S. Capitani *et al.* [ALPHA Collab.], Nucl. Phys. B **544**, 669 (1999).
118. I. Allison *et al.* [HPQCD Collab.], Phys. Rev. **D78**, 054513 (2008); C. McNeile *et al.* [HPQCD Collab.], Phys. Rev. D **82**, 034512 (2010).
119. D. Leinweber *et al.* (ed.), PoS Lattice **2012** (2012).

19. STRUCTURE FUNCTIONS

Updated September 2013 by B. Foster (University of Hamburg/DESY), A.D. Martin (University of Durham), and M.G. Vincter (Carleton University).

19.1. Deep inelastic scattering

High-energy lepton-nucleon scattering (deep inelastic scattering) plays a key role in determining the partonic structure of the proton. The process $\ell N \to \ell' X$ is illustrated in Fig. 19.1. The filled circle in this figure represents the internal structure of the proton which can be expressed in terms of structure functions.

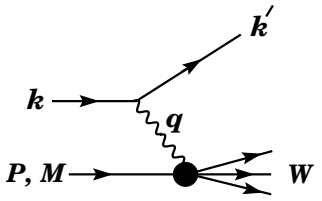

Figure 19.1: Kinematic quantities for the description of deep inelastic scattering. The quantities k and k' are the four-momenta of the incoming and outgoing leptons, P is the four-momentum of a nucleon with mass M, and W is the mass of the recoiling system X. The exchanged particle is a γ, $W^{\pm}$, or Z; it transfers four-momentum $q = k - k'$ to the nucleon.

Invariant quantities:

$\nu = \dfrac{q\cdot P}{M} = E - E'$ is the lepton's energy loss in the nucleon rest frame (in earlier literature sometimes $\nu = q\cdot P$). Here, E and E' are the initial and final lepton energies in the nucleon rest frame.

$Q^2 = -q^2 = 2(EE' - \vec{k}\cdot\vec{k}\,') - m_\ell^2 - m_{\ell'}^2$ where $m_\ell(m_{\ell'})$ is the initial (final) lepton mass. If $EE'\sin^2(\theta/2) \gg m_\ell^2,\, m_{\ell'}^2$, then

$\approx 4EE'\sin^2(\theta/2)$, where θ is the lepton's scattering angle with respect to the lepton beam direction.

$x = \dfrac{Q^2}{2M\nu}$ where, in the parton model, x is the fraction of the nucleon's momentum carried by the struck quark.

$y = \dfrac{q\cdot P}{k\cdot P} = \dfrac{\nu}{E}$ is the fraction of the lepton's energy lost in the nucleon rest frame.

$W^2 = (P+q)^2 = M^2 + 2M\nu - Q^2$ is the mass squared of the system X recoiling against the scattered lepton.

$s = (k+P)^2 = \dfrac{Q^2}{xy} + M^2 + m_\ell^2$ is the center-of-mass energy squared of the lepton-nucleon system.

The process in Fig. 19.1 is called deep ($Q^2 \gg M^2$) inelastic ($W^2 \gg M^2$) scattering (DIS). In what follows, the masses of the initial and scattered leptons, m_ℓ and $m_{\ell'}$, are neglected.

19.1.1. *DIS cross sections* :

The double-differential cross section for deep inelastic scattering can be expressed in terms of kinematic variables in several ways.

$$\frac{d^2\sigma}{dx\,dy} = x\,(s-M^2)\,\frac{d^2\sigma}{dx\,dQ^2} = \frac{2\pi\,M\nu}{E'}\frac{d^2\sigma}{d\Omega_{\rm Nrest}\,dE'}\,. \qquad (19.1)$$

In lowest-order perturbation theory, the cross section for the scattering of polarized leptons on polarized nucleons can be expressed in terms of the products of leptonic and hadronic tensors associated with the coupling of the exchanged bosons at the upper and lower vertices in Fig. 19.1 (see Refs. 1–4)

$$\frac{d^2\sigma}{dxdy} \;=\; \frac{2\pi y\alpha^2}{Q^4}\,\sum_j\,\eta_j\,L_j^{\mu\nu}\,W_{\mu\nu}^j\,. \qquad (19.2)$$

For neutral-current processes, the summation is over $j = \gamma, Z$ and γZ representing photon and Z exchange and the interference between them, whereas for charged-current interactions there is only W exchange, $j = W$. (For transverse nucleon polarization, there is a dependence on the azimuthal angle of the scattered lepton.) The lepton tensor $L_{\mu\nu}$ is associated with the coupling of the exchange boson to the leptons. For incoming leptons of charge $e = \pm 1$ and helicity $\lambda = \pm 1$,

$$\begin{aligned} L_{\mu\nu}^{\gamma} &= 2\left(k_\mu k'_\nu + k'_\mu k_\nu - (k\cdot k' - m_\ell^2)g_{\mu\nu} - i\lambda\varepsilon_{\mu\nu\alpha\beta}k^\alpha k'^\beta\right), \\ L_{\mu\nu}^{\gamma Z} &= (g_V^e + e\lambda g_A^e)\,L_{\mu\nu}^{\gamma}, \qquad L_{\mu\nu}^{Z} = (g_V^e + e\lambda g_A^e)^2\,L_{\mu\nu}^{\gamma}, \\ L_{\mu\nu}^{W} &= (1+e\lambda)^2\,L_{\mu\nu}^{\gamma}, \end{aligned} \qquad (19.3)$$

where $g_V^e = -\frac{1}{2} + 2\sin^2\theta_W, \qquad g_A^e = -\frac{1}{2}$.

Although here the helicity formalism is adopted, an alternative approach is to express the tensors in Eq. (19.3) in terms of the polarization of the lepton.

The factors η_j in Eq. (19.2) denote the ratios of the corresponding propagators and couplings to the photon propagator and coupling squared

$$\begin{aligned} \eta_\gamma \;&=\; 1 \quad ; \quad \eta_{\gamma Z} \;=\; \left(\frac{G_F M_Z^2}{2\sqrt{2}\pi\alpha}\right)\left(\frac{Q^2}{Q^2+M_Z^2}\right); \\ \eta_Z \;&=\; \eta_{\gamma Z}^2 \quad ; \quad \eta_W \;=\; \tfrac{1}{2}\left(\frac{G_F M_W^2}{4\pi\alpha}\,\frac{Q^2}{Q^2+M_W^2}\right)^2. \end{aligned} \qquad (19.4)$$

The hadronic tensor, which describes the interaction of the appropriate electroweak currents with the target nucleon, is given by

$$W_{\mu\nu} \;=\; \frac{1}{4\pi}\int d^4z\; e^{iq\cdot z}\,\left\langle P,S\left|\left[J_\mu^\dagger(z), J_\nu(0)\right]\right|\,P,S\right\rangle, \qquad (19.5)$$

where S denotes the nucleon-spin 4-vector, with $S^2 = -M^2$ and $S\cdot P = 0$.

19.2. Structure functions of the proton

The structure functions are defined in terms of the hadronic tensor (see Refs. 1–3)

$$\begin{aligned} W_{\mu\nu} = &\left(-g_{\mu\nu} + \frac{q_\mu q_\nu}{q^2}\right)\,F_1(x,Q^2) + \frac{\hat{P}_\mu\hat{P}_\nu}{P\cdot q}\,F_2(x,Q^2) \\ &- i\varepsilon_{\mu\nu\alpha\beta}\,\frac{q^\alpha P^\beta}{2P\cdot q}\,F_3(x,Q^2) \\ &+ i\varepsilon_{\mu\nu\alpha\beta}\,\frac{q^\alpha}{P\cdot q}\,\left[S^\beta g_1(x,Q^2) + \left(S^\beta - \frac{S\cdot q}{P\cdot q}\,P^\beta\right)\,g_2(x,Q^2)\right] \\ &+ \frac{1}{P\cdot q}\,\left[\tfrac{1}{2}\left(\hat{P}_\mu\hat{S}_\nu + \hat{S}_\mu\hat{P}_\nu\right) - \frac{S\cdot q}{P\cdot q}\,\hat{P}_\mu\hat{P}_\nu\right]\,g_3(x,Q^2) \\ &+ \frac{S\cdot q}{P\cdot q}\,\left[\frac{\hat{P}_\mu\hat{P}_\nu}{P\cdot q}\,g_4(x,Q^2) + \left(-g_{\mu\nu} + \frac{q_\mu q_\nu}{q^2}\right)\,g_5(x,Q^2)\right] \end{aligned} \qquad (19.6)$$

where

$$\hat{P}_\mu \;=\; P_\mu - \frac{P\cdot q}{q^2}\,q_\mu, \qquad \hat{S}_\mu \;=\; S_\mu - \frac{S\cdot q}{q^2}\,q_\mu\,. \qquad (19.7)$$

In Ref. 2, the definition of $W_{\mu\nu}$ with $\mu \leftrightarrow \nu$ is adopted, which changes the sign of the $\varepsilon_{\mu\nu\alpha\beta}$ terms in Eq. (19.6), although the formulae given below are unchanged. Ref. 1 tabulates the relation between the structure functions defined in Eq. (19.6) and other choices available in the literature.

The cross sections for neutral- and charged-current deep inelastic scattering on unpolarized nucleons can be written in terms of the structure functions in the generic form

$$\begin{aligned} \frac{d^2\sigma^i}{dxdy} \;=\; &\frac{4\pi\alpha^2}{xyQ^2}\,\eta^i\left\{\left(1 - y - \frac{x^2y^2M^2}{Q^2}\right)\,F_2^i\right. \\ &\left. + y^2xF_1^i \mp \left(y - \frac{y^2}{2}\right)\,xF_3^i\right\}, \end{aligned} \qquad (19.8)$$

where i = NC, CC corresponds to neutral-current ($eN \to eX$) or charged-current ($eN \to \nu X$ or $\nu N \to eX$) processes, respectively. For incoming neutrinos, $L^W_{\mu\nu}$ of Eq. (19.3) is still true, but with e, λ corresponding to the outgoing charged lepton. In the last term of Eq. (19.8), the $-$ sign is taken for an incoming e^+ or $\overline{\nu}$ and the $+$ sign for an incoming e^- or ν. The factor $\eta^{\rm NC} = 1$ for unpolarized $e^\pm$ beams, whereas*

$$\eta^{\rm CC} \;=\; (1 \pm \lambda)^2 \eta_W \tag{19.9}$$

with $\pm$ for $\ell^\pm$; and where λ is the helicity of the incoming lepton and η_W is defined in Eq. (19.4); for incoming neutrinos $\eta^{\rm CC} = 4\eta_W$. The CC structure functions, which derive exclusively from W exchange, are

$$F_1^{\rm CC} = F_1^W,\; F_2^{\rm CC} = F_2^W,\; xF_3^{\rm CC} = xF_3^W. \tag{19.10}$$

The NC structure functions $F_2^\gamma, F_2^{\gamma Z}, F_2^Z$ are, for $e^\pm N \to e^\pm X$, given by Ref. 5,

$$F_2^{\rm NC} \;=\; F_2^\gamma \;-\; (g_V^e \pm \lambda g_A^e)\eta_{\gamma Z} F_2^{\gamma Z} \;+\; (g_V^{e\,2} + g_A^{e\,2} \pm 2\lambda g_V^e g_A^e)\;\eta_Z F_2^Z \tag{19.11}$$

and similarly for $F_1^{\rm NC}$, whereas

$$xF_3^{\rm NC} = \; -(g_A^e \pm \lambda g_V^e)\eta_{\gamma Z} xF_3^{\gamma Z} + [2g_V^e g_A^e \pm \lambda(g_V^{e\,2} + g_A^{e\,2})]\eta_Z xF_3^Z \;. \tag{19.12}$$

The polarized cross-section difference

$$\Delta\sigma \;=\; \sigma(\lambda_n = -1, \lambda_\ell) \;-\; \sigma(\lambda_n = 1, \lambda_\ell) \;, \tag{19.13}$$

where λ_ℓ, λ_n are the helicities (± 1) of the incoming lepton and nucleon, respectively, may be expressed in terms of the five structure functions $g_{1,\ldots 5}(x, Q^2)$ of Eq. (19.6). Thus,

$$\begin{aligned}\frac{d^2\Delta\sigma^i}{dxdy} \;=\; & \frac{8\pi\alpha^2}{xyQ^2}\;\eta^i \left\{ -\lambda_\ell y \left(2 - y - 2x^2y^2\frac{M^2}{Q^2}\right)\; xg_1^i + \lambda_\ell 4x^3y^2\;\frac{M^2}{Q^2}\;g_2^i \right. \\ & +\; 2x^2 y \frac{M^2}{Q^2}\left(1 - y - x^2y^2\frac{M^2}{Q^2}\right)\; g_3^i \\ & \left. -\;\left(1 + 2x^2y\frac{M^2}{Q^2}\right)\left[\left(1 - y - x^2y^2\frac{M^2}{Q^2}\right)\; g_4^i + xy^2 g_5^i\right]\right\}\end{aligned} \tag{19.14}$$

with i = NC or CC as before. The Eq. (19.13) corresponds to the difference of antiparallel minus parallel spins of the incoming particles for e^- or ν initiated reactions, but the difference of parallel minus antiparallel for e^+ or $\overline{\nu}$ initiated processes. For longitudinal nucleon polarization, the contributions of g_2 and g_3 are suppressed by powers of M^2/Q^2. These structure functions give an unsuppressed contribution to the cross section for transverse polarization [1], but in this case the cross-section difference vanishes as $M/Q \to 0$.

Because the same tensor structure occurs in the spin-dependent and spin-independent parts of the hadronic tensor of Eq. (19.6) in the $M^2/Q^2 \to 0$ limit, the differential cross-section difference of Eq. (19.14) may be obtained from the differential cross section Eq. (19.8) by replacing

$$F_1 \;\to\; -g_5 \;, \quad F_2 \;\to\; -g_4 \;, \quad F_3 \;\to\; 2g_1 \;, \tag{19.15}$$

and multiplying by two, since the total cross section is the average over the initial-state polarizations. In this limit, Eq. (19.8) and Eq. (19.14) may be written in the form

$$\begin{aligned}\frac{d^2\sigma^i}{dxdy} &= \frac{2\pi\alpha^2}{xyQ^2}\;\eta^i \left[Y_+ F_2^i \mp Y_- xF_3^i - y^2 F_L^i\right], \\ \frac{d^2\Delta\sigma^i}{dxdy} &= \frac{4\pi\alpha^2}{xyQ^2}\;\eta^i \left[-Y_+ g_4^i \mp Y_- 2xg_1^i + y^2 g_L^i\right],\end{aligned} \tag{19.16}$$

with i = NC or CC, where $Y_\pm = 1 \pm (1-y)^2$ and

$$F_L^i \;=\; F_2^i \;-\; 2xF_1^i \;, \qquad g_L^i \;=\; g_4^i \;-\; 2xg_5^i \;. \tag{19.17}$$

In the naive quark-parton model, the analogy with the Callan-Gross relations [6] $F_L^i = 0$, are the Dicus relations [7] $g_L^i = 0$. Therefore, there are only two independent polarized structure functions: g_1 (parity conserving) and g_5 (parity violating), in analogy with the unpolarized structure functions F_1 and F_3.

19.2.1. *Structure functions in the quark-parton model* :

In the quark-parton model [8,9], contributions to the structure functions F^i and g^i can be expressed in terms of the quark distribution functions $q(x, Q^2)$ of the proton, where $q = u, \overline{u}, d, \overline{d}$ etc. The quantity $q(x, Q^2)dx$ is the number of quarks (or antiquarks) of designated flavor that carry a momentum fraction between x and $x + dx$ of the proton's momentum in a frame in which the proton momentum is large.

For the neutral-current processes $ep \to eX$,

$$\begin{aligned}\left[F_2^\gamma,\; F_2^{\gamma Z},\; F_2^Z\right] &= x\sum_q \left[e_q^2,\; 2e_q g_V^q,\; g_V^{q\,2} + g_A^{q\,2}\right]\;\; (q + \overline{q})\;, \\ \left[F_3^\gamma,\; F_3^{\gamma Z},\; F_3^Z\right] &= \sum_q \left[0,\; 2e_q g_A^q,\; 2g_V^q g_A^q\right]\;\; (q - \overline{q})\;, \\ \left[g_1^\gamma,\; g_1^{\gamma Z},\; g_1^Z\right] &= \tfrac{1}{2}\sum_q \left[e_q^2,\; 2e_q g_V^q,\; g_V^{q\,2} + g_A^{q\,2}\right]\;\; (\Delta q + \Delta\overline{q})\;, \\ \left[g_5^\gamma,\; g_5^{\gamma Z},\; g_5^Z\right] &= \sum_q \left[0,\; e_q g_A^q,\; g_V^q g_A^q\right]\;\; (\Delta q - \Delta\overline{q})\;,\end{aligned} \tag{19.18}$$

where $g_V^q = \pm\frac{1}{2} - 2e_q \sin^2\theta_W$ and $g_A^q = \pm\frac{1}{2}$, with $\pm$ according to whether q is a $u-$ or $d-$type quark respectively. The quantity Δq is the difference $q\uparrow - q\downarrow$ of the distributions with the quark spin parallel and antiparallel to the proton spin.

For the charged-current processes $e^- p \to \nu X$ and $\overline{\nu} p \to e^+ X$, the structure functions are:

$$\begin{aligned}F_2^{W^-} &= 2x(u + \overline{d} + \overline{s} + c\ldots)\;, \\ F_3^{W^-} &= 2(u - \overline{d} - \overline{s} + c\ldots)\;, \\ g_1^{W^-} &= (\Delta u + \Delta\overline{d} + \Delta\overline{s} + \Delta c\ldots)\;, \\ g_5^{W^-} &= (-\Delta u + \Delta\overline{d} + \Delta\overline{s} - \Delta c\ldots)\;,\end{aligned} \tag{19.19}$$

where only the active flavors have been kept and where CKM mixing has been neglected. For $e^+ p \to \overline{\nu} X$ and $\nu p \to e^- X$, the structure functions F^{W^+}, g^{W^+} are obtained by the flavor interchanges $d \leftrightarrow u, s \leftrightarrow c$ in the expressions for F^{W^-}, g^{W^-}. The structure functions for scattering on a neutron are obtained from those of the proton by the interchange $u \leftrightarrow d$. For both the neutral- and charged-current processes, the quark-parton model predicts $2xF_1^i = F_2^i$ and $g_4^i = 2xg_5^i$.

Neglecting masses, the structure functions g_2 and g_3 contribute only to scattering from transversely polarized nucleons (for which $S \cdot q = 0$), and have no simple interpretation in terms of the quark-parton model. They arise from off-diagonal matrix elements $\langle P, \lambda' | [J_\mu^\dagger(z), J_\nu(0)] | P, \lambda\rangle$, where the proton helicities satisfy $\lambda' \neq \lambda$. In fact, the leading-twist contributions to both g_2 and g_3 are both twist-2 and twist-3, which contribute at the same order of Q^2. The Wandzura-Wilczek relation [10] expresses the twist-2 part of g_2 in terms of g_1 as

$$g_2^i(x) \;=\; -g_1^i(x) \;+\; \int_x^1 \frac{dy}{y}\; g_1^i(y)\;. \tag{19.20}$$

However, the twist-3 component of g_2 is unknown. Similarly, there is a relation expressing the twist-2 part of g_3 in terms of g_4. A complete set of relations, including M^2/Q^2 effects, can be found in Ref. 11.

19.2.2. *Structure functions and QCD* :

One of the most striking predictions of the quark-parton model is that the structure functions F_i, g_i *scale*, i.e., $F_i(x, Q^2) \to F_i(x)$ in the Bjorken limit that Q^2 and $\nu \to \infty$ with x fixed [12]. This property is related to the assumption that the transverse momentum of the partons in the infinite-momentum frame of the proton is small. In QCD, however, the radiation of hard gluons from the quarks violates this assumption, leading to logarithmic scaling violations, which are particularly large at small x, see Fig. 19.2. The radiation of gluons produces the evolution of the structure functions. As Q^2 increases, more and more gluons are radiated, which in turn split into $q\overline{q}$ pairs. This process leads both to the softening of the initial quark momentum distributions and to the growth of the gluon density and the $q\overline{q}$ sea as x decreases.

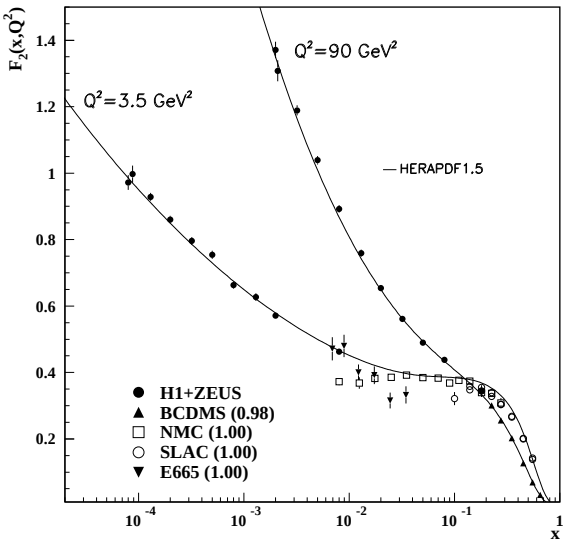

Figure 19.2: The proton structure function F_2^p given at two Q^2 values (3.5 GeV^2 and 90 GeV^2), which exhibit scaling at the 'pivot' point $x \sim 0.14$. See the captions in Fig. 19.8 and Fig. 19.10 for the references of the data. The various data sets have been renormalized by the factors shown in brackets in the key to the plot, which were globally determined in the full HERAPDF analysis [13]. In practice, data for the reduced cross section, $F_2(x,Q^2) - (y^2/Y_+)F_L(x,Q^2)$, are fitted, rather than F_2 and F_L separately.

In QCD, the above process is described in terms of scale-dependent parton distributions $f_a(x,\mu^2)$, where $a = g$ or q and, typically, μ is the scale of the probe Q. For $Q^2 \gg M^2$, the structure functions are of the form

$$F_i = \sum_a C_i^a \otimes f_a, \tag{19.21}$$

where $\otimes$ denotes the convolution integral

$$C \otimes f = \int_x^1 \frac{dy}{y}\, C(y)\, f\left(\frac{x}{y}\right) , \tag{19.22}$$

and where the coefficient functions C_i^a are given as a power series in α_s. The parton distribution f_a corresponds, at a given x, to the density of parton a in the proton integrated over transverse momentum k_t up to μ. Its evolution in μ is described in QCD by a DGLAP equation (see Refs. 14–17) which has the schematic form

$$\frac{\partial f_a}{\partial \ln \mu^2} \sim \frac{\alpha_s(\mu^2)}{2\pi} \sum_b (P_{ab} \otimes f_b) , \tag{19.23}$$

where the P_{ab}, which describe the parton splitting $b \to a$, are also given as a power series in α_s. Although perturbative QCD can predict, via Eq. (19.23), the evolution of the parton distribution functions from a particular scale, μ_0, these DGLAP equations cannot predict them *a priori* at any particular μ_0. Thus they must be measured at a starting point μ_0 before the predictions of QCD can be compared to the data at other scales, μ. In general, all observables involving a hard hadronic interaction (such as structure functions) can be expressed as a convolution of calculable, process-dependent coefficient functions and these universal parton distributions, e.g. Eq. (19.21).

It is often convenient to write the evolution equations in terms of the gluon, non-singlet (q^{NS}) and singlet (q^S) quark distributions, such that

$$q^{NS} = q_i - \overline{q}_i \quad (\text{or } q_i - q_j), \qquad q^S = \sum_i (q_i + \overline{q}_i) . \tag{19.24}$$

The non-singlet distributions have non-zero values of flavor quantum numbers, such as isospin and baryon number. The DGLAP evolution equations then take the form

$$\frac{\partial q^{NS}}{\partial \ln \mu^2} = \frac{\alpha_s(\mu^2)}{2\pi}\, P_{qq} \otimes q^{NS} ,$$

$$\frac{\partial}{\partial \ln \mu^2} \begin{pmatrix} q^S \\ g \end{pmatrix} = \frac{\alpha_s(\mu^2)}{2\pi} \begin{pmatrix} P_{qq} & 2n_f\, P_{qg} \\ P_{gq} & P_{gg} \end{pmatrix} \otimes \begin{pmatrix} q^S \\ g \end{pmatrix}, \tag{19.25}$$

where P are splitting functions that describe the probability of a given parton splitting into two others, and n_f is the number of (active) quark flavors. The leading-order Altarelli-Parisi [16] splitting functions are

$$P_{qq} = \frac{4}{3}\left[\frac{1+x^2}{(1-x)}\right]_+ = \frac{4}{3}\left[\frac{1+x^2}{(1-x)_+}\right] + 2\delta(1-x) , \tag{19.26}$$

$$P_{qg} = \frac{1}{2}\left[x^2 + (1-x)^2\right] , \tag{19.27}$$

$$P_{gq} = \frac{4}{3}\left[\frac{1+(1-x)^2}{x}\right] , \tag{19.28}$$

$$P_{gg} = 6\left[\frac{1-x}{x} + x(1-x) + \frac{x}{(1-x)_+}\right] + \left[\frac{11}{2} - \frac{n_f}{3}\right]\delta(1-x), \tag{19.29}$$

where the notation $[F(x)]_+$ defines a distribution such that for any sufficiently regular test function, $f(x)$,

$$\int_0^1 dx f(x)[F(x)]_+ = \int_0^1 dx\, (f(x) - f(1))F(x) . \tag{19.30}$$

In general, the splitting functions can be expressed as a power series in α_s. The series contains both terms proportional to $\ln \mu^2$ and to $\ln\ 1/x$. The leading-order DGLAP evolution sums up the $(\alpha_s \ln \mu^2)^n$ contributions, while at next-to-leading order (NLO) the sum over the $\alpha_s(\alpha_s \ln \mu^2)^{n-1}$ terms is included [18,19]. In fact, the NNLO contributions to the splitting functions and the DIS coefficient functions are now also all known [20–22].

In the kinematic region of very small x, it is essential to sum leading terms in $\ln\ 1/x$, independent of the value of $\ln \mu^2$. At leading order, LLx, this is done by the BFKL equation for the unintegrated distributions (see Refs. [23,24]). The leading-order $(\alpha_s \ln(1/x))^n$ terms result in a power-like growth, $x^{-\omega}$ with $\omega = (12\alpha_s \ln 2)/\pi$, at asymptotic values of $\ln\ 1/x$. More recently, the next-to-leading $\ln\ 1/x$ (NLLx) contributions have become available [25,26]. They are so large (and negative) that the result appears to be perturbatively unstable. Methods, based on a combination of collinear and small-x resummations, have been developed which reorganize the perturbative series into a more stable hierarchy [27–30]. There are indications that small-x resummations become necessary for sufficient precision for $x \lesssim 10^{-3}$ at low scales. On the other hand, there is no convincing indication for a 'non-linear' regime, for $Q^2 \gtrsim 2$ GeV^2, in which the gluon density would be so high that gluon-gluon recombination effects would become significant.

The precision of the experimental data demands that at least NLO, and preferably NNLO, DGLAP evolution be used in comparisons between QCD theory and experiment. Beyond the leading order, it is necessary to specify, and to use consistently, both a renormalization and a factorization scheme. The renormalization scheme used almost universally is the modified minimal subtraction ($\overline{\rm MS}$) scheme [31,32]. There are two popular choices for factorization scheme, in which the form of the correction for each structure function is different. The most-used factorization scheme is again $\overline{\rm MS}$ [33]. However, sometimes the DIS [34] scheme is adopted, in which there are no higher-order corrections to the F_2 structure function. The two schemes differ in how the non-divergent pieces are assimilated in the parton distribution functions.

The discussion above relates to the Q^2 behavior of leading-twist (twist-2) contributions to the structure functions. Higher-twist terms, which involve their own non-perturbative input, exist. These die off as powers of Q; specifically twist-n terms are damped by $1/Q^{n-2}$. Provided a cut, say $W^2 > 15$ GeV^2 is imposed, the higher-twist terms appear to be numerically unimportant for Q^2 above a few GeV^2, except for x close to 1 [35–37].

Table 19.1: The main processes relevant to global PDF analyses, ordered in three groups: fixed-target experiments, HERA and the $p\bar{p}$ Tevatron / pp LHC. For each process we give an indication of their dominant partonic subprocesses, the primary partons which are probed and the approximate range of x constrained by the data.

Process	Subprocess	Partons	x range
$\ell^\pm\{p,n\} \to \ell^\pm X$	$\gamma^* q \to q$	$q, \bar{q}, g$	$x \gtrsim 0.01$
$\ell^\pm n/p \to \ell^\pm X$	$\gamma^* d/u \to d/u$	d/u	$x \gtrsim 0.01$
$pp \to \mu^+\mu^- X$	$u\bar{u}, d\bar{d} \to \gamma^*$	$\bar{q}$	$0.015 \lesssim x \lesssim 0.35$
$pn/pp \to \mu^+\mu^- X$	$(u\bar{d})/(u\bar{u}) \to \gamma^*$	$\bar{d}/\bar{u}$	$0.015 \lesssim x \lesssim 0.35$
$\nu(\bar{\nu})\, N \to \mu^-(\mu^+)\, X$	$W^* q \to q'$	$q, \bar{q}$	$0.01 \lesssim x \lesssim 0.5$
$\nu\, N \to \mu^-\mu^+\, X$	$W^* s \to c$	s	$0.01 \lesssim x \lesssim 0.2$
$\bar{\nu}\, N \to \mu^+\mu^-\, X$	$W^* \bar{s} \to \bar{c}$	$\bar{s}$	$0.01 \lesssim x \lesssim 0.2$
$e^\pm p \to e^\pm X$	$\gamma^* q \to q$	$g, q, \bar{q}$	$10^{-4} \lesssim x \lesssim 0.1$
$e^+ p \to \bar{\nu}\, X$	$W^+\{d,s\} \to \{u,c\}$	d, s	$x \gtrsim 0.01$
$e^\pm p \to e^\pm c\bar{c}X, e^\pm b\bar{b}X$	$\gamma^* c \to c$, $\gamma^* g \to c\bar{c}$	c, b, g	$10^{-4} \lesssim x \lesssim 0.01$
$e^\pm p \to$ jet$+X$	$\gamma^* g \to q\bar{q}$	g	$0.01 \lesssim x \lesssim 0.1$
$p\bar{p}, pp \to$ jet$+X$	$gg, qg, qq \to 2j$	g, q	$0.005 \lesssim x \lesssim 0.5$
$p\bar{p} \to (W^\pm \to \ell^\pm\nu)\, X$	$ud \to W^+, \bar{u}\bar{d} \to W^-$	$u, d, \bar{u}, \bar{d}$	$x \gtrsim 0.05$
$pp \to (W^\pm \to \ell^\pm\nu)\, X$	$u\bar{d} \to W^+, d\bar{u} \to W^-$	$u, d, \bar{u}, \bar{d}, g$	$x \gtrsim 0.001$
$p\bar{p}(pp) \to (Z \to \ell^+\ell^-)X$	$uu, dd, ..(u\bar{u}, ..) \to Z$	$u, d, ..(g)$	$x \gtrsim 0.001$
$pp \to W^- c$, $W^+\bar{c}$	$gs \to W^- c$	$s, \bar{s}$	$x \sim 0.01$
$pp \to (\gamma^* \to \ell^+\ell^-)X$	$u\bar{u}, d\bar{d}, .. \to \gamma^*$	$\bar{q}, g$	$x \gtrsim 10^{-5}$
$pp \to b\bar{b}\, X$, $t\bar{t}X$	$gg \to b\bar{b}$, $t\bar{t}$	g	$x \gtrsim 10^{-5}, 10^{-2}$
$pp \to$ exclusive J/ψ, Υ	$\gamma^*(gg) \to J/\psi$, Υ	g	$x \gtrsim 10^{-5}, 10^{-4}$
$pp \to \gamma\, X$	$gq \to \gamma q$, $g\bar{q} \to \gamma\bar{q}$	g	$x \gtrsim 0.005$

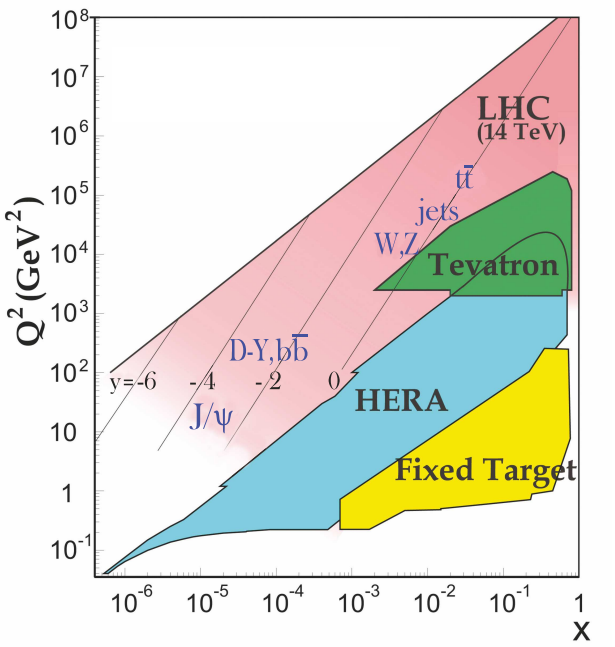

Figure 19.3: Kinematic domains in x and Q^2 probed by fixed-target and collider experiments. Some of the final states accessible at the LHC are indicated in the appropriate regions, where y is the rapidity. The incoming partons have $x_{1,2} = (M/14\ \text{TeV})e^{\pm y}$ with $Q = M$ where M is the mass of the state shown in blue in the figure. For example, exclusive J/ψ production at high $|y|$ at the LHC may probe the gluon PDF down to $x \sim 10^{-5}$.

19.3. Determination of parton distributions

The parton distribution functions (PDFs) can be determined from an analysis of data for deep inelastic lepton-nucleon scattering and for related hard-scattering processes initiated by nucleons; see [38–42] for reviews. Table 19.1 highlights some of the processes, and their primary sensitivity to PDFs. The kinematic reach of fixed-target and collider experiments are complementary (as is shown in Fig. 19.3), which enables the determination of PDFs over a wide range in x and Q^2. As more precise LHC data for J/ψ, $W^\pm$, Z, γ, jet, $b\bar{b}$ and $t\bar{t}$ production become available, tighter constraints on the PDFs are expected in a wider kinematic range.

Recent determinations of the unpolarized PDFs up to NNLO have been made by six groups: MSTW [43,44], NNPDF [45], CT(EQ) [46], HERAPDF [13], ABM [47] and GJR [48,49]. Most groups use input PDFs of the form $xf = x^a(...)(1-x)^b$ with 10-25 free parameters in total. Note, however, that the NNPDF group combines a Monte Carlo representation of the probability measure in the space of PDFs with the use of neural networks to give a set of unbiased input distributions, while GJR generate 'dynamical' PDFs from a valence-like input at a very low starting scale, $Q_0^2 = 0.5$ GeV^2.

In these analyses the u, d and s quarks are taken to be massless, but the treatment of the heavy c and b quark masses, m_Q, differs, and has a long and chequered history, which may be traced from Refs. [50–61]. The MSTW, CT and NNPDF analyses use different variants of the General-Mass Variable-Flavour-Number Scheme (GM-VFNS). This combines fixed-order contributions to the coefficient functions (or partonic cross sections) calculated with the full m_Q dependence, with the all-order resummation of contributions via DGLAP evolution in which the heavy quarks are treated as massless. The ABM analysis uses a FFNS where only the three light (massless) quarks enter the evolution, while the heavy quarks enter the partonic cross sections with their full m_Q dependence; transition matrix elements are computed, following [53], which provide the boundary conditions between n_f and $n_f + 1$ PDFs. The GM-VFNS and FFNS approaches yield different results: in particular $\alpha_s(M_Z^2)$ and a large-x gluon PDF at large Q^2 are both significantly smaller in the FFNS. It has been argued [36,37,60] that the difference is due to the slow convergence of the $\ln^n(Q^2/m_Q^2)$ terms in a FFNS.

The most recent determinations of the groups using GM-VFNS (MSTW, NNPDF and CT(EQ)) have converged, so that now a reasonable agreement has been achieved between the resulting PDFs, the value obtained for $\alpha_s(M_Z^2)$, and their predictions for the LHC. For illustration, we show in Fig. 19.4 the PDFs obtained in the NNLO NNPDF analysis [45] at scales $\mu^2 = 10$ and 10^4 GeV^2. The values of α_s found by MSTW [43,63] may be taken as representative of those resulting from the GM-VFNS analyses

$$\text{NLO} : \alpha_s(M_Z^2) = 0.1202^{+0.0012}_{-0.0015} \pm 0.003,$$

$$\text{NNLO} : \alpha_s(M_Z^2) = 0.1171 \pm 0.0014 \pm 0.002,$$

where the first error (at 68% C.L.) corresponds to the uncertainties resulting from the data fitted and the second is an estimate of the theory error (that is, the uncertainty that might be expected from the neglect of higher orders), see also [64]. The ABM analysis [47], which uses a FFNS, finds $\alpha_s(M_Z^2) = 0.1134 \pm 0.0011$ at NNLO.

Spin-dependent (or polarized) PDFs have been obtained through NLO global analyses which include measurements of the g_1 structure function in inclusive polarized DIS, 'flavour-tagged' semi-inclusive DIS data, and results from polarized pp scattering at RHIC. Recent NLO analyses are given in Refs. [65–68]. Improved parton-to-hadron fragmentation functions, needed to describe the semi-inclusive DIS data, can be found in [69–71]. Fig. 19.5 shows several global analyses at a scale of 2.5 GeV^2 along with the data from semi-inclusive DIS. A recent determination [72], using the NNPDF methodology, concentrates just on the inclusive polarized DIS data, and finds the errors on the polarized gluon PDF have been underestimated in the earlier analyses.

Comprehensive sets of PDFs are available as program-callable functions from the HepData website [78], which includes comparison

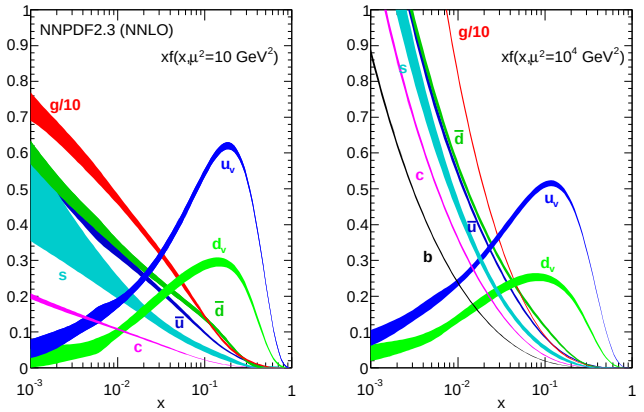

Figure 19.4: The bands are x times the unpolarized parton distributions $f(x)$ (where $f = u_v, d_v, \overline{u}, \overline{d}, s \simeq \bar{s}, c = \bar{c}, b = \bar{b}, g$) obtained in NNLO NNPDF2.3 global analysis [45] at scales $\mu^2 = 10$ GeV^2 and $\mu^2 = 10^4$ GeV^2, with $\alpha_s(M_Z^2) = 0.118$. The analogous results obtained in the NNLO MSTW analysis [43] can be found in Ref. [62].

graphics of PDFs, and from the LHAPDF library [79], which can be linked directly into a user's programme to provide access to recent PDFs in a standard format.

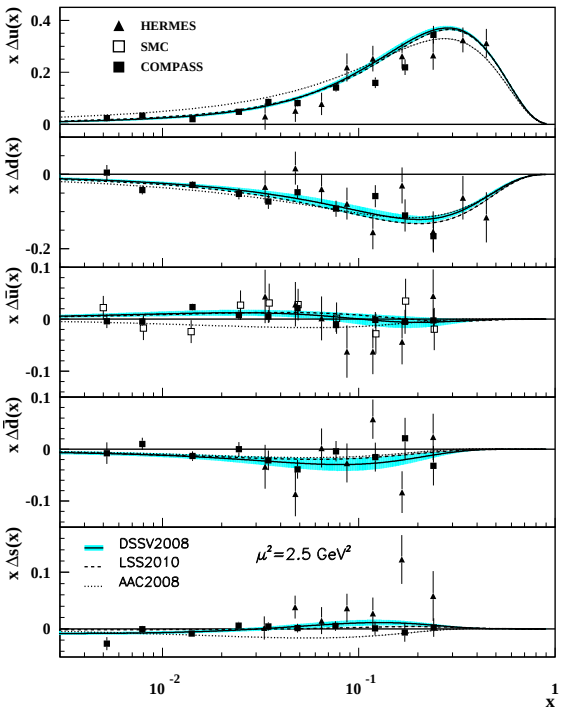

Figure 19.5: Distributions of x times the polarized parton distributions $\Delta q(x)$ (where $q = u, d, \overline{u}, \overline{d}, s$) using the AAC2008 [65], DSSV2008 [66], and LSS2010 [68] parameterizations at a scale $\mu^2 = 2.5$ GeV^2, showing the blue-shaded error corridor of the DSSV2008 set (corresponding to a one-unit increase in χ^2) (see also BB2010 [67]) . The points represent data from semi-inclusive positron (HERMES [73,74]) and muon (SMC [75] and COMPASS [76,77]) deep inelastic scattering given at $Q^2 = 2.5$ GeV^2. The SMC results are extracted under the assumption that $\Delta\overline{u}(x) = \Delta\overline{d}(x)$.

19.4. The hadronic structure of the photon

Besides the *direct* interactions of the photon, it is possible for it to fluctuate into a hadronic state via the process $\gamma \to q\overline{q}$. While in this state, the partonic content of the photon may be *resolved*, for example, through the process $e^+e^- \to e^+e^-\gamma^*\gamma \to e^+e^-X$, where the virtual photon emitted by the DIS lepton probes the hadronic structure of the quasi-real photon emitted by the other lepton. The perturbative LO contributions, $\gamma \to q\overline{q}$ followed by $\gamma^* q \to q$, are subject to QCD corrections due to the coupling of quarks to gluons.

Often the equivalent-photon approximation is used to express the differential cross section for deep inelastic electron–photon scattering in terms of the structure functions of the transverse quasi-real photon times a flux factor N_γ^T (for these incoming quasi-real photons of transverse polarization)

$$\frac{d^2\sigma}{dxdQ^2} = N_\gamma^T \frac{2\pi\alpha^2}{xQ^4}\left[\left(1+(1-y)^2\right)F_2^\gamma(x,Q^2) - y^2 F_L^\gamma(x,Q^2)\right],$$

where we have used $F_2^\gamma = 2xF_T^\gamma + F_L^\gamma$, not to be confused with F_2^γ of Sec. 19.2. Complete formulae are given, for example, in the comprehensive review of Ref. 80.

The hadronic photon structure function, F_2^γ, evolves with increasing Q^2 from the 'hadron-like' behavior, calculable via the vector-meson-dominance model, to the dominating 'point-like' behaviour, calculable in perturbative QCD. Due to the point-like coupling, the logarithmic evolution of F_2^γ with Q^2 has a *positive* slope for all values of x, see Fig. 19.15. The 'loss' of quarks at large x due to gluon radiation is over-compensated by the 'creation' of quarks via the point-like $\gamma \to q\bar{q}$ coupling. The logarithmic evolution was first predicted in the quark–parton model ($\gamma^*\gamma \to q\bar{q}$) [81,82], and then in QCD in the limit of large Q^2 [83]. The evolution is now known to NLO [84–86]. The NLO data analyses to determine the parton densities of the photon can be found in [87–89].

19.5. Diffractive DIS (DDIS)

Some 10% of DIS events are diffractive, $\gamma^* p \to X + p$, in which the slightly deflected proton and the cluster X of outgoing hadrons are well-separated in rapidity. Besides x and Q^2, two extra variables are needed to describe a DDIS event: the fraction $x_{I\!P}$ of the proton's momentum transferred across the rapidity gap and t, the square of the 4-momentum transfer of the proton. The DDIS data [90,91] are usually analyzed using two levels of factorization. First, the diffractive structure function $F_2^{\rm D}$ satisfies *collinear factorization*, and can be expressed as the convolution [92]

$$F_2^{\rm D} = \sum_{a=q,g} C_2^a \otimes f_{a/p}^{\rm D}, \tag{19.31}$$

with the same coefficient functions as in DIS (see Eq. (19.21)), and where the diffractive parton distributions $f_{a/p}^{\rm D}$ ($a = q, g$) satisfy DGLAP evolution. Second, *Regge factorization* is assumed [93],

$$f_{a/p}^{\rm D}(x_{I\!P}, t, z, \mu^2) = f_{I\!P/p}(x_{I\!P}, t)\, f_{a/I\!P}(z, \mu^2), \tag{19.32}$$

where $f_{a/I\!P}$ are the parton densities of the Pomeron, which itself is treated like a hadron, and $z \in [x/x_{I\!P}, 1]$ is the fraction of the Pomeron's momentum carried by the parton entering the hard subprocess. The Pomeron flux factor $f_{I\!P/p}(x_{I\!P}, t)$ is taken from Regge phenomenology. There are also secondary Reggeon contributions to Eq. (19.32). A sample of the t-integrated diffractive parton densities, obtained in this way, is shown in Fig. 19.6.

Although collinear factorization holds as $\mu^2 \to \infty$, there are non-negligible corrections for finite μ^2 and small $x_{I\!P}$. Besides the *resolved* interactions of the Pomeron, the perturbative QCD Pomeron may also interact *directly* with the hard subprocess, giving rise to an inhomogeneous evolution equation for the diffractive parton densities analogous to the photon case. The results of the MRW analysis [96], which includes these contributions, are also shown in Fig. 19.6. Unlike the inclusive case, the diffractive parton densities cannot be directly used to calculate diffractive hadron-hadron cross sections, since account must first be taken of "soft" rescattering effects.

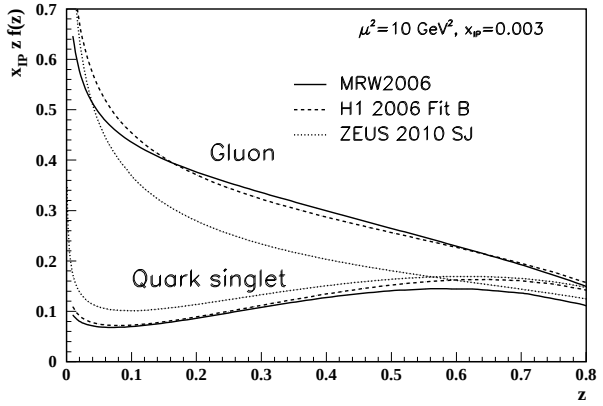

Figure 19.6: Diffractive parton distributions, $x_{I\!P}\, z f^{\rm D}_{a/p}$, obtained from fitting to the ZEUS data with $Q^2 > 5$ GeV^2 [94], H1 data with $Q^2 > 8.5$ GeV^2 assuming Regge factorization [95], and from MRW2006 [96] using a more perturbative QCD approach [96]. Only the Pomeron contributions are shown and not the secondary Reggeon contributions, which are negligible at the value of $x_{I\!P} = 0.003$ chosen here. The H1 2007 Jets distribution [97] is similar to H1 2006 Fit B.

19.6. Generalized parton distributions

The parton distributions of the proton of Sec. 19.3 are given by the diagonal matrix elements $\langle P,\lambda|\hat{O}|P,\lambda\rangle$, where P and λ are the 4-momentum and helicity of the proton, and $\hat{O}$ is a twist-2 quark or gluon operator. However, there is new information in the so-called generalised parton distributions (GPDs) defined in terms of the off-diagonal matrix elements $\langle P',\lambda'|\hat{O}|P,\lambda\rangle$; see [98–102] for reviews. Unlike the diagonal PDFs, the GPDs cannot be regarded as parton densities, but are to be interpreted as probability amplitudes.

The physical significance of GPDs is best seen using light-cone coordinates, $z^\pm = (z^0 \pm z^3)/\sqrt{2}$, and in the light-cone gauge, $A^+ = 0$. It is conventional to define the generalised quark distributions in terms of quark operators at light-like separation

$$F_q(x,\xi,t) \;=\; \frac{1}{2}\int \frac{dz^-}{2\pi}\; e^{ix\bar{P}^+z^-}\;\; \langle P'|\bar{\psi}(-z/2)\gamma^+\psi(z/2)|P\rangle \;\Big|_{z^+=z^1=z^2=0} \tag{19.33}$$

$$= \frac{1}{2\bar{P}^+}\left(H_q(x,\xi,t)\;\; \bar{u}(P')\gamma^+u(P) \;\;+\;\; E_q(x,\xi,t)\;\; \bar{u}(P')\frac{i\sigma^{+\alpha}\Delta_\alpha}{2m}u(P)\right) \tag{19.34}$$

with $\bar{P} = (P+P')/2$ and $\Delta = P' - P$, and where we have suppressed the helicity labels of the protons and spinors. We now have two extra kinematic variables:

$$t = \Delta^2, \qquad \xi = -\Delta^+/(P+P')^+. \tag{19.35}$$

We see that $-1 \le \xi \le 1$. Similarly, we may define GPDs $\tilde{H}_q$ and $\tilde{E}_q$ with an additional γ_5 between the quark operators in Eq. (19.33); and also an analogous set of gluon GPDs, H_g, E_g, $\tilde{H}_g$ and $\tilde{E}_g$. After a Fourier transform with respect to the transverse components of Δ, we are able to describe the spatial distribution of partons in the impact parameter plane in terms of GPDs [103,104].

For $P' = P$, $\lambda' = \lambda$ the matrix elements reduce to the ordinary PDFs of Sec. 19.2.1

$$H_q(x,0,0) = q(x), \qquad H_q(-x,0,0) = -\bar{q}(x), \qquad H_g(x,0,0) = xg(x), \tag{19.36}$$

$$\tilde{H}_q(x,0,0) = \Delta q(x), \qquad \tilde{H}_q(-x,0,0) = \Delta\bar{q}(x), \qquad \tilde{H}_g(x,0,0) = x\Delta g(x), \tag{19.37}$$

where $\Delta q = q\uparrow - q\downarrow$ as in Eq. (19.18). No corresponding relations exist for E, $\tilde{E}$ as they decouple in the forward limit, $\Delta = 0$.

The functions H_g, E_g are even in x, and $\tilde{H}_g, \tilde{E}_g$ are odd functions of x. We can introduce valence and 'singlet' quark distributions which are even and odd functions of x respectively. For example

$$H_q^V(x,\xi,t) \equiv H_q(x,\xi,t) + H_q(-x,\xi,t) = H_q^V(-x,\xi,t), \tag{19.38}$$

$$H_q^S(x,\xi,t) \equiv H_q(x,\xi,t) - H_q(-x,\xi,t) = -H_q^S(-x,\xi,t). \tag{19.39}$$

All the GPDs satisfy relations of the form

$$H(x,-\xi,t) = H(x,\xi,t) \qquad \text{and} \qquad H(x,-\xi,t)^* = H(x,\xi,t), \tag{19.40}$$

and so are real-valued functions. Moreover, the moments of GPDs, that is the x integrals of $x^n H_q$ etc., are *polynomials* in ξ of order $n+1$. Another important property of GPDs are Ji's sum rules [98]

$$\frac{1}{2}\int_{-1}^{1} dx\;\; x\left(H_q(x,\xi,t) + E_q(x,\xi,t)\right) = J_q(t), \tag{19.41}$$

where $J_q(0)$ is the total angular momentum carried by quarks and antiquarks of flavour q, with a similar relation for gluons.

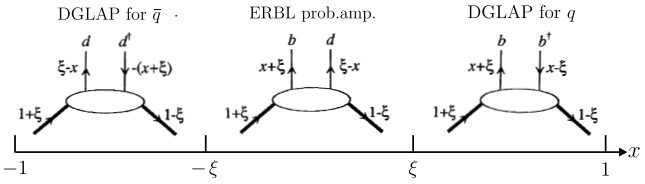

Figure 19.7: Schematic diagrams of the three distinct kinematic regions of the imaginary part of H_q. The proton and quark momentum fractions refer to $\bar{P}^+$, and x covers the interval (-1,1). In the ERBL domain the GPDs are generalisations of distribution amplitudes which occur in processes such as $p\bar{p} \to J/\psi$.

To visualize the physical content of H_q, we Fourier expand ψ and $\bar{\psi}$ in terms of quark, antiquark creation (b,d) and annihilation $(b^\dagger, d^\dagger)$ operators, and sketch the result in Fig. 19.7. There are two types of domain: (i) the time-like or 'annihilation' domain, with $|x| < |\xi|$, where the GPDs describe the wave functions of a t-channel $q\bar{q}$ (or gluon) pair and evolve according to modified ERBL equations [105,106]; (ii) the space-like or 'scattering' domain, with $|x| > |\xi|$, where the GPDs generalise the familiar $\bar{q}$, q (and gluon) PDFs and describe processes such as 'deeply virtual Compton scattering' ($\gamma^* p \to \gamma p$), $\gamma p \to J/\psi p$, etc., and evolve according to modified DGLAP equations. The splitting functions for the evolution of GPDs are known to NLO [107].

GPDs describe new aspects of proton structure and must be determined from experiment. We can parametrise them in terms of 'double distributions' [108,109], which reduce to diagonal PDFs as $\xi \to 0$. With an additional physically reasonable 'Regge' assumption of no extra singularity at $\xi = 0$, GPDs at low ξ are uniquely given in terms of diagonal PDFs to $O(\xi)$, and have been used [110] to describe $\gamma p \to J/\psi p$ data. Alternatively, flexible $SO(3)$-based parametrisations have been used to determine GPDs from DVCS data [111].

* The value of $\eta^{\rm CC}$ deduced from Ref. 1 is found to be a factor of two too small; $\eta^{\rm CC}$ of Eq. (19.9) agrees with Refs. [2,3].

References:

1. J. Blümlein and N. Kochelev, Nucl. Phys. **B498**, 285 (1997).
2. S. Forte *et al.*, Nucl. Phys. **B602**, 585 (2001).
3. M. Anselmino *et al.*, Z. Phys. **C64**, 267 (1994).
4. M. Anselmino *et al.*, Phys. Rep. **261**, 1 (1995).
5. M. Klein and T. Riemann, Z. Phys. **C24**, 151 (1984).
6. C.G. Callan and D.J. Gross, Phys. Rev. Lett. **22**, 156 (1969).
7. D.A. Dicus, Phys. Rev. **D5**, 1367 (1972).
8. J.D. Bjorken and E.A. Paschos, Phys. Rev. **185**, 1975 (1969).

9. R.P. Feynman, Photon Hadron Interactions (Benjamin, New York, 1972).
10. S. Wandzura and F. Wilczek, Phys. Rev. **B72**, 195 (1977).
11. J. Blümlein and A. Tkabladze, Nucl. Phys. **B553**, 427 (1999).
12. J.D. Bjorken, Phys. Rev. **179**, 1547 (1969).
13. V. Radescu for the H1 and ZEUS Collaborations, arXiv:1308.0374.
14. V.N. Gribov and L.N. Lipatov, Sov. J. Nucl. Phys. **15**, 438 (1972).
15. L.N. Lipatov, Sov. J. Nucl. Phys. **20**, 95 (1975).
16. G. Altarelli and G. Parisi, Nucl. Phys. **B126**, 298 (1977).
17. Yu.L. Dokshitzer, Sov. Phys. JETP **46**, 641 (1977).
18. G. Curci *et al.*, Nucl. Phys. **B175**, 27 (1980); W. Furmanski, and R. Petronzio, Phys. Lett. **B97**, 437 (1980).
19. R.K. Ellis *et al.*, QCD and Collider Physics (Cambridge UP, 1996).
20. E.B. Zijlstra and W.L. van Neerven, Phys. Lett. **B272**, 127 (1991); Phys. Lett. **B273**, 476 (1991); Phys. Lett. **B297**, 377 (1992); Nucl. Phys. **B383**, 525 (1992).
21. S. Moch and J.A.M. Vermaseren, Nucl. Phys. **B573**, 853 (2000).
22. S. Moch *et al.*, Nucl. Phys. **B688**, 101 (2004); Nucl. Phys. **B691**, 129 (2004); Phys. Lett. **B606**, 123 (2005); Nucl. Phys. **B724**, 3 (2005).
23. E.A. Kuraev *et al.*, Phys. Lett. **B60**, 50 (1975); Sov. Phys. JETP **44**, 443 (1976); Sov. Phys. JETP **45**, 199 (1977).
24. Ya.Ya. Balitsky and L.N. Lipatov, Sov. J. Nucl. Phys. **28**, 822 (1978).
25. V.S. Fadin, and L.N. Lipatov, Phys. Lett. **B429**, 127 (1998).
26. G. Camici and M. Ciafaloni, Phys. Lett. **B412**, 396 (1997), erratum-Phys. Lett. **B147**, 390 (1997); Phys. Lett. **B430**, 349 (1998).
27. M. Ciafaloni *et al.*, Phys. Rev. **D60**, 114036 (1999); JHEP **0007** 054 (2000).
28. M. Ciafaloni *et al.*, Phys. Lett. **B576**, 143 (2003); Phys. Rev. **D68**, 114003 (2003).
29. G. Altarelli *et al.*, Nucl. Phys. **B742**, 1 (2006); Nucl. Phys. **B799**, 199 (2008).
30. C.D. White and R.S. Thorne, Phys. Rev. **D75**, 034005 (2007).
31. G. 't Hooft and M. Veltman, Nucl. Phys. **B44**, 189 (1972).
32. G. 't Hooft, Nucl. Phys. **B61**, 455 (1973).
33. W.A. Bardeen *et al.*, Phys. Rev. **D18**, 3998 (1978).
34. G. Altarelli *et al.*, Nucl. Phys. **B143**, 521 (1978) and erratum: Nucl. Phys. **B146**, 544 (1978).
35. A.D. Martin *et al.*, Eur. Phys. J. **C35**, 325 (2004).
36. NNPDF, R.D. Ball *et al.*, Phys. Lett. **B723**, 330 (2013).
37. R.S. Thorne arXiv:1306.3907.
38. A. De Roeck and R.S. Thorne, Prog. in Part. Nucl. Phys. **66**, 727 (2011).
39. S. Forte and G. Watt, Ann.Rev.Nucl.Part.Sci. **63**; arXiv:1301.6754.
40. J. Blumlein, Prog. in Part. Nucl. Phys. **69**, 28 (2013).
41. E. Perez and E. Rizvi, Rept. on Prog. in Phys. **76**, 046201 (2013).
42. R.D. Ball *et al.*, JHEP **1304**, 125 (2013).
43. MSTW, A.D. Martin *et al.*, Eur. Phys. J. **C63**, 189 (2009).
44. A.D. Martin *et al.*, Eur. Phys. J. **C73**, 2318 (2013).
45. NNPDF, R.D. Ball *et al.*, Nucl. Phys. **B867**, 244 (2013).
46. CT10, Jun Gao *et al.*, arXiv:1302.6246.
47. S. Alekhin, *et al.*, Phys. Rev. **D86**, 054009 (2012).
48. M. Glück *et al.*, Eur. Phys. J. **C53**, 355 (2008).
49. P. Jimenez-Delgado and E. Reya, Phys. Rev. **D79**, 074023 (2009).
50. J.C. Collins, F. Wilczek, and A. Zee, Phys. Rev. **D18**, 242 (1978).
51. E. Laenen *et al.*, Nucl. Phys. **B392**, 162 (1993).
52. M.A.G. Aivazis *et al.*, Phys. Rev. **D50**, 3102 (1994).
53. M. Buza *et al.*, Eur. Phys. J. **C1**, 301 (1998).
54. A. Chuvakin *et al.*, Phys. Rev. **D61**, 096004 (2000).
55. S. Kretzer *et al.*, Phys. Rev. **D69**, 114005 (2004).
56. R.S. Thorne, Phys. Rev. **D73**, 054019 (2006).
57. R.S. Thorne and W.-K. Tung, Proc. 4th HERA-LHC Workshop, arXiv:0809.0714.
58. S. Alekhin and S. Moch, Phys. Lett. **B699**, 345 (2011).
59. S. Forte *et al.*, Nucl. Phys. **B834**, 116 (2010).
60. R.S. Thorne, Phys. Rev. **D86**, 074017 (2012).
61. E.G. de Oliveira *et al.*, Eur. Phys. J. **C73**, 2616 (2013).
62. J. Beringer *et al.*, (PDG), Phys. Rev. **D86**, 010001 (2012).
63. MSTW, A.D. Martin *et al.*, Eur. Phys. J. **C64**, 653 (2009).
64. NNPDF, R.D. Ball *et al.*, Phys. Lett. **B701**, 346 (2011).
65. M. Hirai *et al.*, Nucl. Phys. **B813**, 106 (2009).
66. D. de Florian *et al.*, Phys. Rev. Lett. **101**, 072001 (2008); Phys. Rev. **D80**, 034030 (2009).
67. J. Blümlein and H. Böttcher, Nucl. Phys. **B841**, 205 (2010).
68. E. Leader *et al.*, Phys. Rev. **D82**, 114018 (2010).
69. D. de Florian *et al.*, Phys. Rev. **D75**, 114010 (2007); Phys. Rev. **D76**, 074033 (2007).
70. S. Albino *et al.*, Nucl. Phys. **B803**, 42 (2008).
71. M. Hirai and S. Kumano, Comp. Phys. Comm. **183**, 1002 (2012).
72. NNPDF, R.D. Ball *et al.*, Nucl. Phys. **B874**, 36 (2013).
73. HERMES, A. Airpetian *et al.*, Phys. Rev. Lett. **92**, 012005 (2004); A. Airpetian *et al.*, Phys. Rev. **D71**, 012003 (2005).
74. HERMES, A. Airpetian *et al.*, Phys. Lett. **B666**, 446 (2008).
75. SMC, B. Adeva *et al.*, Phys. Lett. **B420**, 180 (1998).
76. COMPASS, M. Alekseev *et al.*, Phys. Lett. **B680**, 217 (2009).
77. COMPASS, M. Alekseev *et al.*, Phys. Lett. **B693**, 227 (2010).
78. http://hepdata.cedar.ac.uk/pdfs.
79. http://lhapdf.hepforge.org/.
80. R. Nisius, Phys. Reports **332**, 165 (2000).
81. T.F. Walsh and P.M. Zerwas, Phys. Lett. **B44**, 195 (1973).
82. R.L. Kingsley, Nucl. Phys. **B60**, 45 (1973).
83. E. Witten, Nucl. Phys. **B120**, 189 (1977).
84. W.A. Bardeen and A.J. Buras, Phys. Rev. **D20**, 166 (1979), erratum Phys. Rev. **D21**, 2041 (1980).
85. M. Fontannaz and E. Pilon, Phys. Rev. **D45**, 382 (1992), erratum Phys. Rev. **D46**, 484 (1992).
86. M. Glück *et al.*, Phys. Rev. **D45**, 3986 (1992).
87. F. Cornet *et al.*, Phys. Rev. **D70**, 093004 (2004).
88. P. Aurenche, *et al.*, Eur. Phys. J. **C44**, 395 (2005).
89. W. Slominski *et al.*, Eur. Phys. J. **C45**, 633 (2006).
90. H1+ZEUS, F.D. Aaron *et al.*, Eur. Phys. J. **C72**, 2175 (2012).
91. H1, F.D. Aaron *et al.*, Eur. Phys. J. **C72**, 2074 (2012).
92. J.C. Collins, Phys. Rev. **D57**, 3051 (1998); Erratum Phys. Rev. **D61**, 019902 (2000).
93. G. Ingelman and P. E. Schlein, Phys. Lett. **B152**, 256 (1985).
94. ZEUS, S. Chekanov *et al.*, Nucl. Phys. **B831**, 1 (2010).
95. H1, A. Aktas *et al.*, Eur. Phys. J. **C48**, 715 (2006).
96. A.D. Martin, M.G. Ryskin, and G. Watt, Phys. Lett. **B644**, 131 (2007).
97. H1, A. Aktas *et al.*, JHEP **0710**, 042 (2007).
98. X. Ji, J. Phys. **G24**, 1181 (1998).
99. K. Goeke *et al.*, Prog. in Part. Nucl. Phys. **47**, 401 (2001).
100. M. Diehl, Phys. Rept. **388**, 41 (2003).
101. A.V. Belitsky and A.V. Radyushkin, Phys. Rept. **418**, 1 (2005).
102. S. Boffi and B. Pasquini, Riv. Nuovo Cimento **30**, 387 (2007).
103. M. Burkardt, Int. J. Mod. Phys. **A18**, 173 (2003).
104. M. Diehl, Eur. Phys. J. **C25**, 223 (2002).
105. A.V. Efremov and A.V. Radyushkin, Phys. Lett. **B94**, 245 (1980).
106. G.P. Lepage and S.J. Brodsky, Phys. Rev. **D22**, 2157 (1980).
107. A.V. Belitsky *et al.*, Phys. Lett. **B493**, 341 (2000).
108. A.V. Radyushkin, Phys. Rev. **D59**, 014030 (1999).
109. A.V. Radyushkin, Phys. Lett. **B449**, 81 (1999).
110. A.D. Martin *et al.*, Eur. Phys. J. **C63**, 57 (2009).
111. K. Kumerički and D. Müller, Nucl. Phys. **B841**, 1 (2010).

NOTE: THE FIGURES IN THIS SECTION ARE INTENDED TO SHOW THE REPRESENTATIVE DATA.
THEY ARE NOT MEANT TO BE COMPLETE COMPILATIONS OF ALL THE WORLD'S RELIABLE DATA.

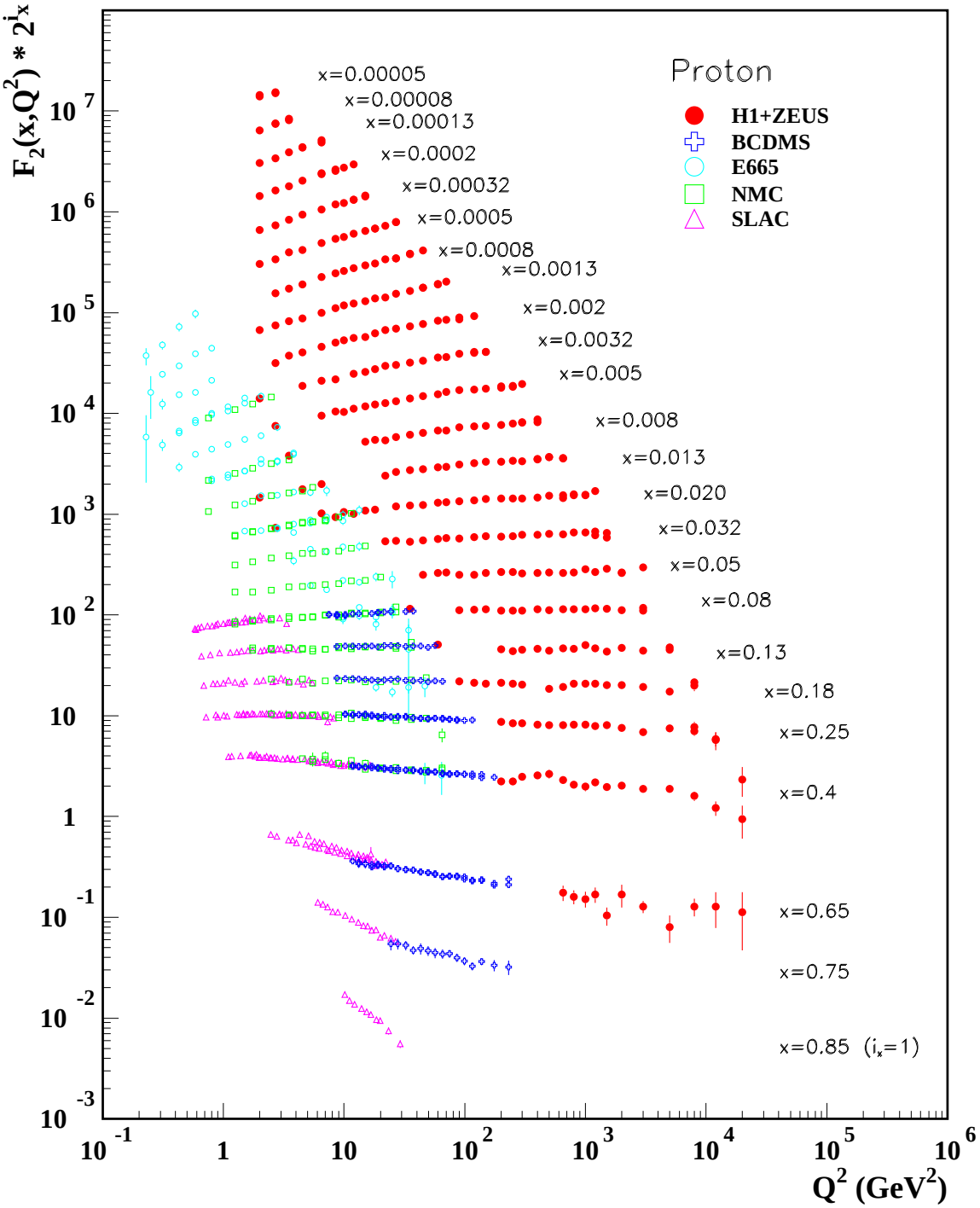

Figure 19.8: The proton structure function F_2^p measured in electromagnetic scattering of electrons and positrons on protons (collider experiments H1 and ZEUS for $Q^2 \geq 2$ GeV^2), in the kinematic domain of the HERA data (see Fig. 19.10 for data at smaller x and Q^2), and for electrons (SLAC) and muons (BCDMS, E665, NMC) on a fixed target. Statistical and systematic errors added in quadrature are shown. The data are plotted as a function of Q^2 in bins of fixed x. Some points have been slightly offset in Q^2 for clarity. The H1+ZEUS combined binning in x is used in this plot; all other data are rebinned to the x values of these data. For the purpose of plotting, F_2^p has been multiplied by 2^{ix}, where i_x is the number of the x bin, ranging from $i_x = 1$ ($x = 0.85$) to $i_x = 24$ ($x = 0.00005$). References: **H1 and ZEUS**—F.D. Aaron *et al.*, JHEP **1001**, 109 (2010); **BCDMS**—A.C. Benvenuti *et al.*, Phys. Lett. **B223**, 485 (1989) (as given in [78]) ; **E665**—M.R. Adams *et al.*, Phys. Rev. **D54**, 3006 (1996); **NMC**—M. Arneodo *et al.*, Nucl. Phys. **B483**, 3 (1997); **SLAC**—L.W. Whitlow *et al.*, Phys. Lett. **B282**, 475 (1992).

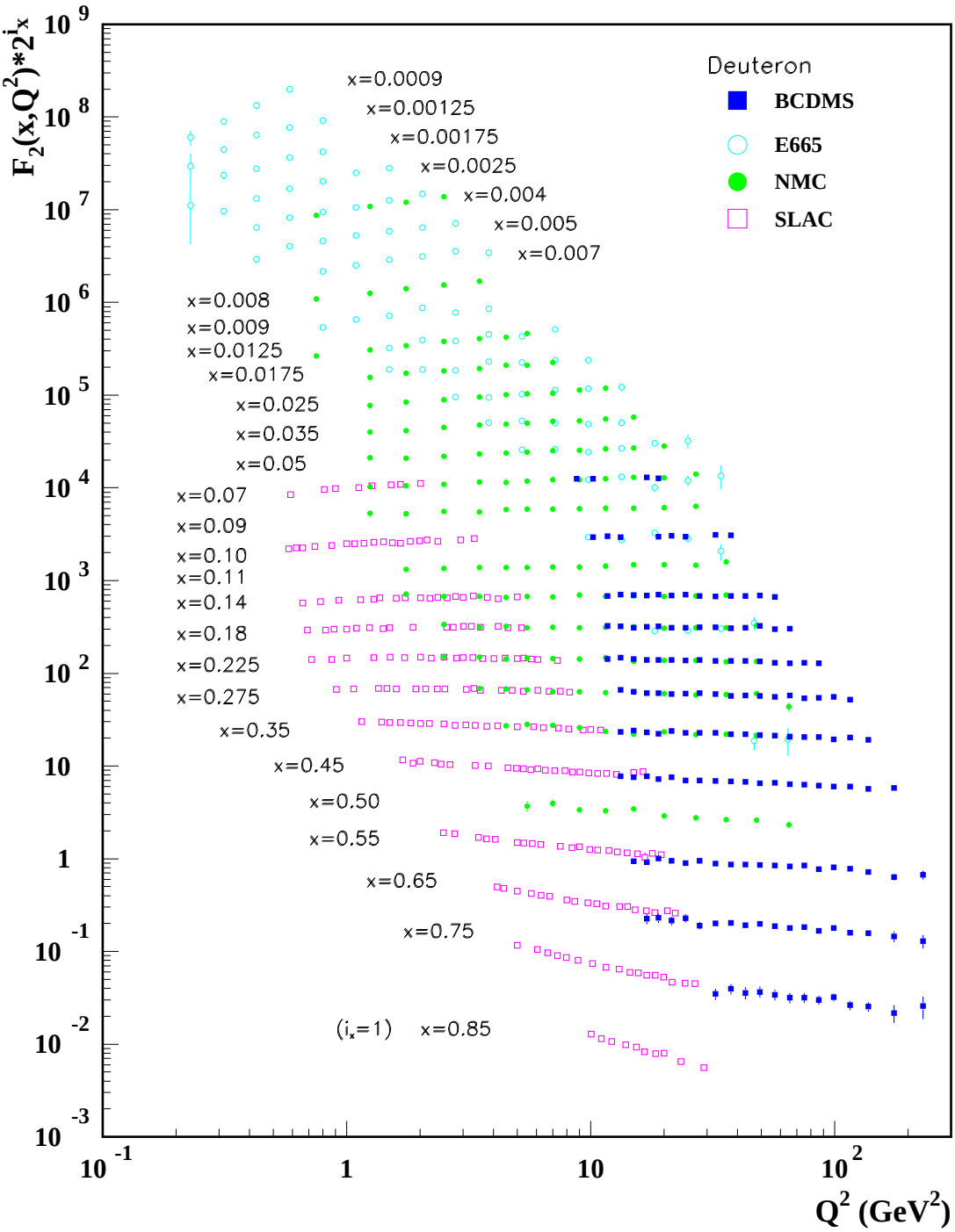

Figure 19.9: The deuteron structure function F_2^d measured in electromagnetic scattering of electrons (SLAC) and muons (BCDMS, E665, NMC) on a fixed target, shown as a function of Q^2 for bins of fixed x. Statistical and systematic errors added in quadrature are shown. For the purpose of plotting, F_2^d has been multiplied by 2^{ix}, where i_x is the number of the x bin, ranging from 1 ($x = 0.85$) to 29 ($x = 0.0009$). References: **BCDMS**—A.C. Benvenuti *et al.*, Phys. Lett. **B237**, 592 (1990). **E665, NMC, SLAC**—same references as Fig. 19.8.

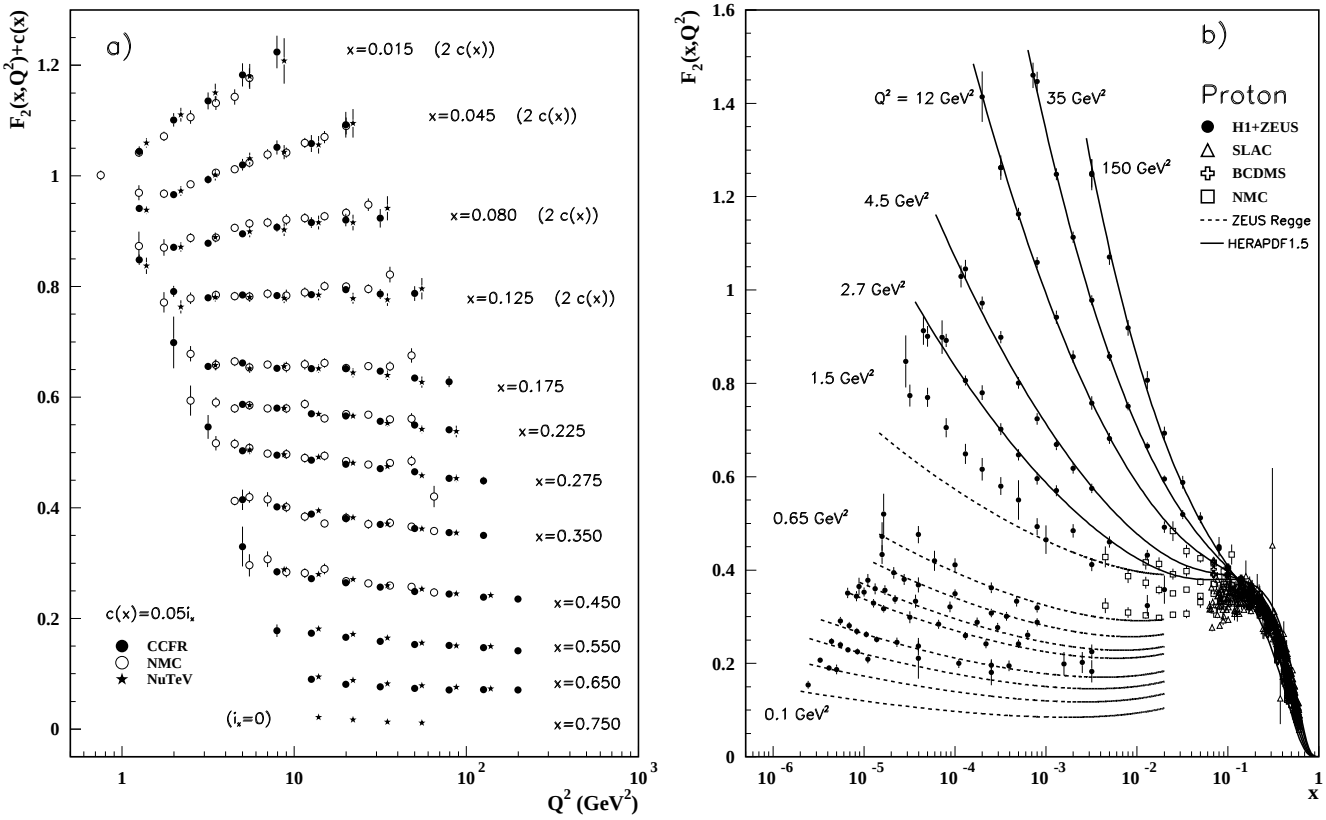

Figure 19.10: a) The deuteron structure function F_2 measured in deep inelastic scattering of muons on a fixed target (NMC) is compared to the structure function F_2 from neutrino-iron scattering (CCFR and NuTeV) using $F_2^{\mu} = (5/18)F_2^{\nu} - x(s+\overline{s})/6$, where heavy-target effects have been taken into account. The data are shown versus Q^2, for bins of fixed x. The NMC data have been rebinned to CCFR and NuTeV x values. For the purpose of plotting, a constant $c(x) = 0.05i_x$ is added to F_2, where i_x is the number of the x bin, ranging from 0 ($x = 0.75$) to 7 ($x = 0.175$). For $i_x = 8$ ($x = 0.125$) to 11 ($x = 0.015$), $2c(x)$ has been added. References: **NMC**—M. Arneodo *et al.*, Nucl. Phys. **B483**, 3 (1997); **CCFR/NuTeV**—U.K. Yang *et al.*, Phys. Rev. Lett. **86**, 2741 (2001); **NuTeV**—M. Tzanov *et al.*, Phys. Rev. **D74**, 012008 (2006).

b) The proton structure function F_2^p mostly at small x and Q^2, measured in electromagnetic scattering of electrons and positrons (H1, ZEUS), electrons (SLAC), and muons (BCDMS, NMC) on protons. Lines are ZEUS Regge and HERAPDF parameterizations for lower and higher Q^2, respectively. The width of the bins can be up to 10% of the stated Q^2. Some points have been slightly offset in x for clarity. References: **H1 and ZEUS**—F.D. Aaron *et al.*, JHEP **1001**, 109 (2010) (data), POS ICHEP 2010, 168 (2010) (HERAPDF parameterization) **ZEUS**—J. Breitweg *et al.*, Phys. Lett. **B487**, 53 (2000) (ZEUS Regge parameterization); **BCDMS, NMC, SLAC**—same references as Fig. 19.8.

Statistical and systematic errors added in quadrature are shown for both plots.

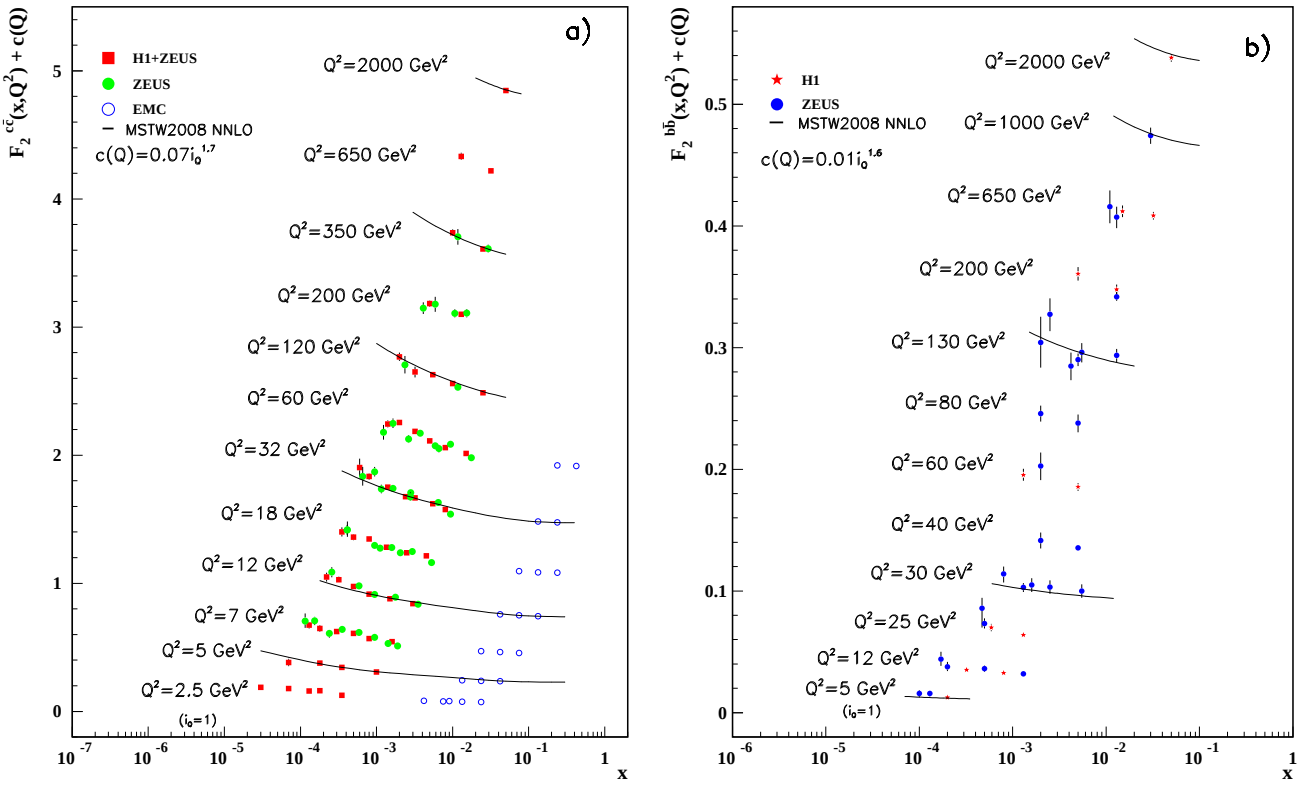

Figure 19.11: a) The charm-quark structure function $F_2^{c\overline{c}}(x)$, i.e. that part of the inclusive structure function F_2^p arising from the production of charm quarks, measured in electromagnetic scattering of positrons on protons (H1, ZEUS) and muons on iron (EMC). For the purpose of plotting, a constant $c(Q) = 0.07 i_Q{}^{1.7}$ is added to $F_2^{c\overline{c}}$ where i_Q is the number of the Q^2 bin, ranging from 1 ($Q^2 = 2.5$ GeV^2) to 12 ($Q^2 = 2000$ GeV^2). References: **H1 and ZEUS run I combination**—H. Abramowicz *et al.*, Eur. Phys. J. **C73**, 2311 (2013); **ZEUS run II**—H. Abramowicz *et al.*, JHEP **05**, 023 (2013); H. Abramowicz *et al.*, JHEP **05**, 097 (2013); **EMC**—J.J. Aubert *et al.*, Nucl. Phys. **B213**, 31 (1983).

b) The bottom-quark structure function $F_2^{b\overline{b}}(x)$. For the purpose of plotting, a constant $c(Q) = 0.01 i_Q^{1.6}$ is added to $F_2^{b\overline{b}}$ where i_Q is the number of the Q^2 bin, ranging from 1 ($Q^2 = 5$ GeV^2) to 12 ($Q^2 = 2000$ GeV^2). References: **ZEUS**—S. Chekanov *et al.*, Eur. Phys. J. **C65**, 65 (2010); H. Abramowicz *et al.*, Eur. Phys. J. **C69**, 347 (2010); H. Abramowicz *et al.*, Eur. Phys. J. **C71**, 1573 (2011); **H1**—F.D. Aaron *et al.*, Eur. Phys. J. **C65**, 89 (2010).

For both plots, statistical and systematic errors added in quadrature are shown. The data are given as a function of x in bins of Q^2. Points may have been slightly offset in x for clarity. Some data have been rebinned to common Q^2 values. Also shown is the MSTW2008 parameterization given at several Q^2 values (A.D. Martin *et al.*, Eur. Phys. J. **C63**, 189 (2009)).

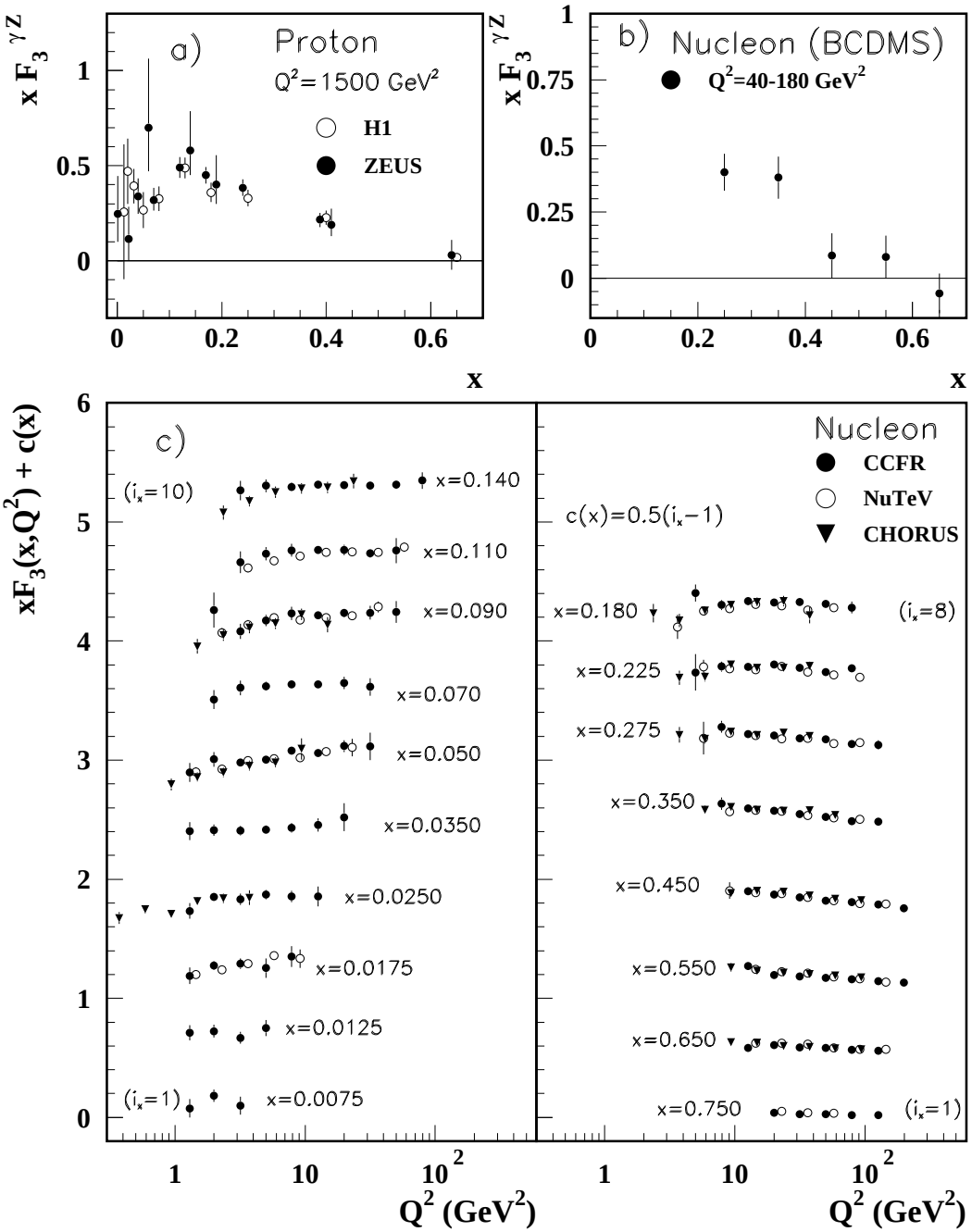

Figure 19.12: The structure function $xF_3^{\gamma Z}$ measured in electroweak scattering of **a)** electrons on protons (H1 and ZEUS) and **b)** muons on carbon (BCDMS). The ZEUS points have been slightly offset in x for clarity. References: **H1**—F.D. Aaron *et al.*, JHEP **1209**, 061 (2012); **ZEUS**—S. Chekanov *et al.*, Eur. Phys. J. **C28**, 175 (2003); H. Abramowicz *et al.*, Phys. Rev. **D87**, 052014 (2013); **BCDMS**—A. Argento *et al.*, Phys. Lett. **B140**, 142 (1984).
c) The structure function xF_3 of the nucleon measured in ν-Fe scattering. The data are plotted as a function of Q^2 in bins of fixed x. For the purpose of plotting, a constant $c(x) = 0.5(i_x - 1)$ is added to xF_3, where i_x is the number of the x bin as shown in the plot. The NuTeV and CHORUS points have been shifted to the nearest corresponding x bin as given in the plot and slightly offset in Q^2 for clarity. References: **CCFR**—W.G. Seligman *et al.*, Phys. Rev. Lett. **79**, 1213 (1997); **NuTeV**—M. Tzanov *et al.*, Phys. Rev. **D74**, 012008 (2006); **CHORUS**—G. Önengüt *et al.*, Phys. Lett. **B632**, 65 (2006).

Statistical and systematic errors added in quadrature are shown for all plots.

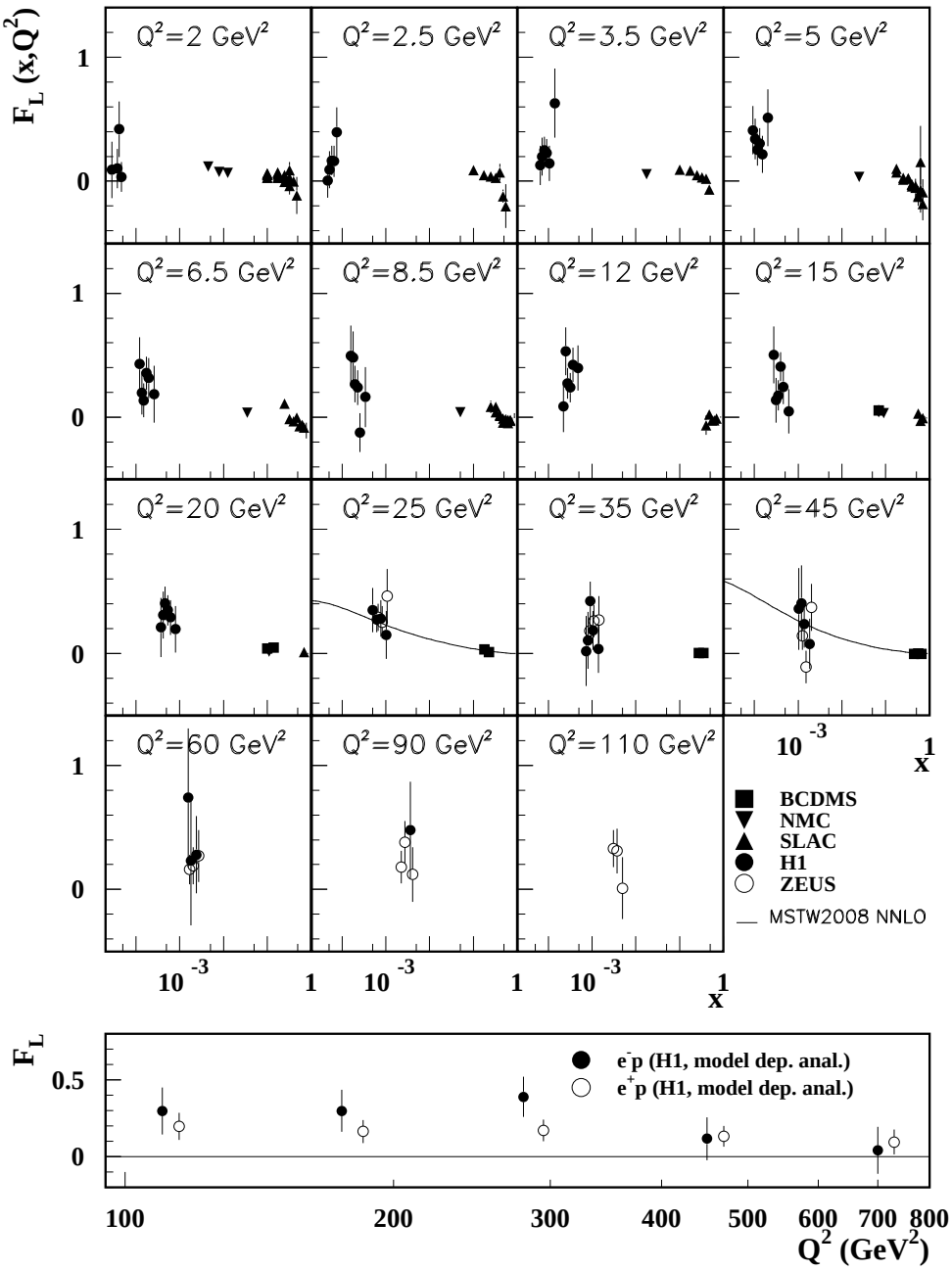

Figure 19.13: Top panel: The longitudinal structure function F_L as a function of x in bins of fixed Q^2 measured on the proton (except for the SLAC data which also contain deuterium data). BCDMS, NMC, and SLAC results are from measurements of R (the ratio of longitudinal to transverse photon absorption cross sections) which are converted to F_L by using the BDCMS parameterization of F_2 (A.C. Benvenuti *et al.*, Phys. Lett. **B223**, 485 (1989)). It is assumed that the Q^2 dependence of the fixed-target data is small within a given Q^2 bin. Some of the other data may have been rebinned to common Q^2 values. Also shown is the MSTW2008 parameterization given at two Q^2 values (A.D. Martin *et al.*, Eur. Phys. J. **C63**, 189 (2009)). References: **H1**—F.D. Aaron *et al.*, Phys. Lett. **B665**, 139 (2008); F.D. Aaron *et al.*, Eur. Phys. J. **C71**, 1579 (2011); **ZEUS**—S. Chekanov *et al.*, Phys. Lett. **B682**, 8 (2009); **BCDMS**—A. Benvenuti *et al.*, Phys. Lett. **B223**, 485 (1989); **NMC**—M. Arneodo *et al.*, Nucl. Phys. **B483**, 3 (1997); **SLAC**— L.W. Whitlow *et al.*, Phys. Lett. **B250**, 193 (1990) and numerical values from the thesis of L.W. Whitlow (SLAC-357).

Bottom panel: Higher Q^2 values of the longitudinal structure function F_L as a function of Q^2 given at the measured x for e^+/e^--proton scattering. Points have been slightly offset in Q^2 for clarity. References: **H1**—C. Adloff *et al.*, Eur. Phys. J. **C30**, 1 (2003).

The H1 results shown in the bottom plot require the assumption of the validity of the QCD form for the F_2 structure function in order to extract F_L. Statistical and systematic errors added in quadrature are shown for both plots.

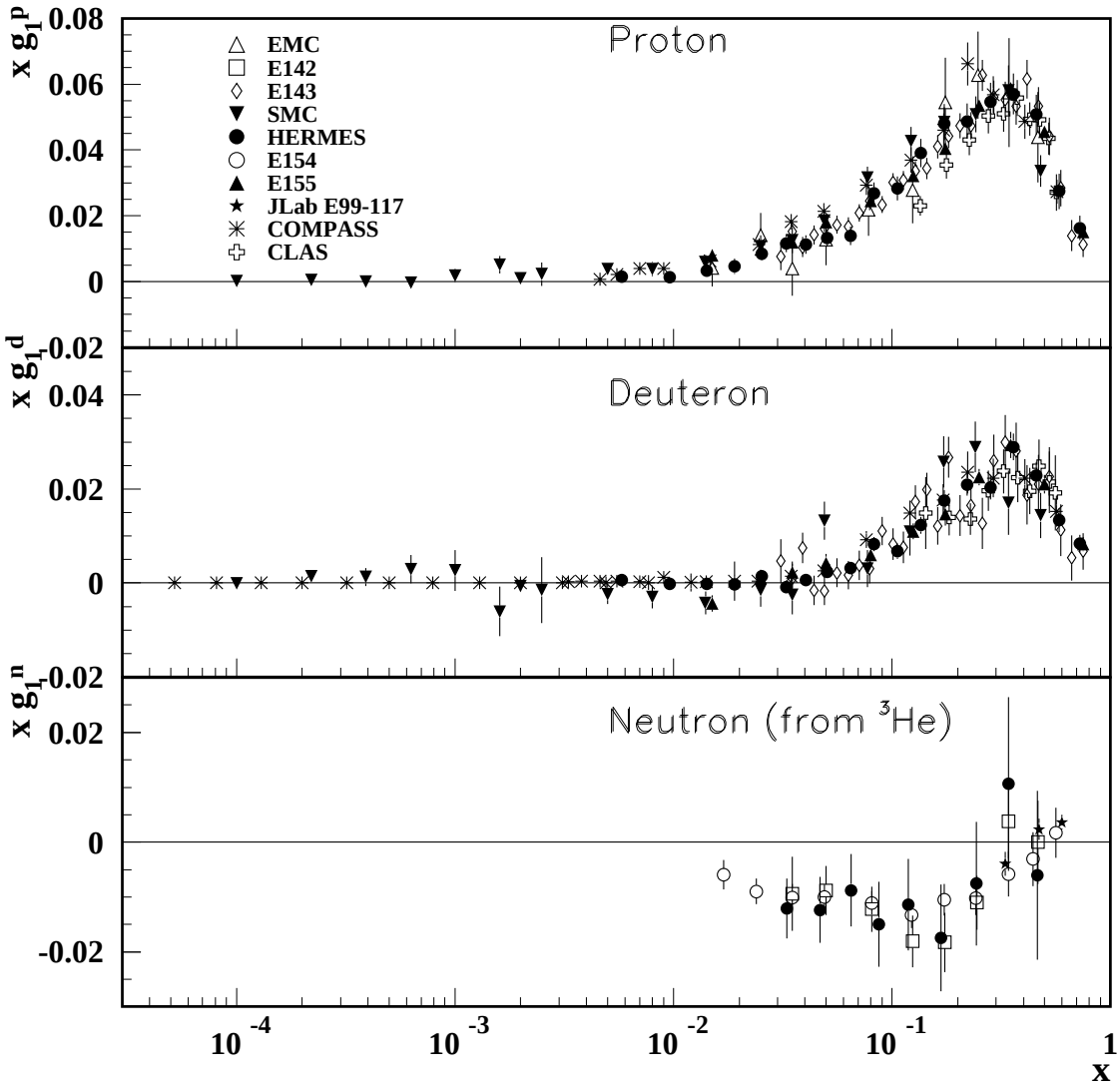

Figure 19.14: The spin-dependent structure function $xg_1(x)$ of the proton, deuteron, and neutron (from ^{3}He target) measured in deep inelastic scattering of polarized electrons/positrons: E142 ($Q^2 \sim 0.3 - 10$ GeV^2), E143 ($Q^2 \sim 0.3 - 10$ GeV^2), E154 ($Q^2 \sim 1 - 17$ GeV^2), E155 ($Q^2 \sim 1 - 40$ GeV^2), JLab E99-117 ($Q^2 \sim 2.71 - 4.83$ GeV^2), HERMES ($Q^2 \sim 0.18 - 20$ GeV^2), CLAS ($Q^2 \sim 1 - 5$ GeV^2) and muons: EMC ($Q^2 \sim 1.5 - 100$ GeV^2), SMC ($Q^2 \sim 0.01 - 100$ GeV^2), COMPASS ($Q^2 \sim 0.001 - 100$ GeV^2), shown at the measured Q^2 (except for EMC data given at $Q^2 = 10.7$ GeV^2 and E155 data given at $Q^2 = 5$ GeV^2). Note that $g_1^n(x)$ may also be extracted by taking the difference between $g_1^d(x)$ and $g_1^p(x)$, but these values have been omitted in the bottom plot for clarity. Statistical and systematic errors added in quadrature are shown. References: **EMC**—J. Ashman *et al.*, Nucl. Phys. **B328**, 1 (1989); **E142**—P.L. Anthony *et al.*, Phys. Rev. **D54**, 6620 (1996); **E143**—K. Abe *et al.*, Phys. Rev. **D58**, 112003 (1998); **SMC**—B. Adeva *et al.*, Phys. Rev. **D58**, 112001 (1998), B. Adeva *et al.*, Phys. Rev. **D60**, 072004 (1999) and Erratum-Phys. Rev. **D62**, 079902 (2000); **HERMES**—A. Airapetian *et al.*, Phys. Rev. **D75**, 012007 (2007) and K. Ackerstaff *et al.*, Phys. Lett. **B404**, 383 (1997); **E154**—K. Abe *et al.*, Phys. Rev. Lett. **79**, 26 (1997); **E155**—P.L. Anthony *et al.*, Phys. Lett. **B463**, 339 (1999) and P.L. Anthony *et al.*, Phys. Lett. **B493**, 19 (2000); **Jlab-E99-117**—X. Zheng *et al.*, Phys. Rev. **C70**, 065207 (2004); **COMPASS**—V.Yu. Alexakhin *et al.*, Phys. Lett. **B647**, 8 (2007), E.S. Ageev *et al.*, Phys. Lett. **B647**, 330 (2007), and M.G. Alekseev *et al.*, Phys. Lett. **B690**, 466 (2010); **CLAS**—K.V. Dharmawardane *et al.*, Phys. Lett. **B641**, 11 (2006) (which also includes resonance region data not shown on this plot).

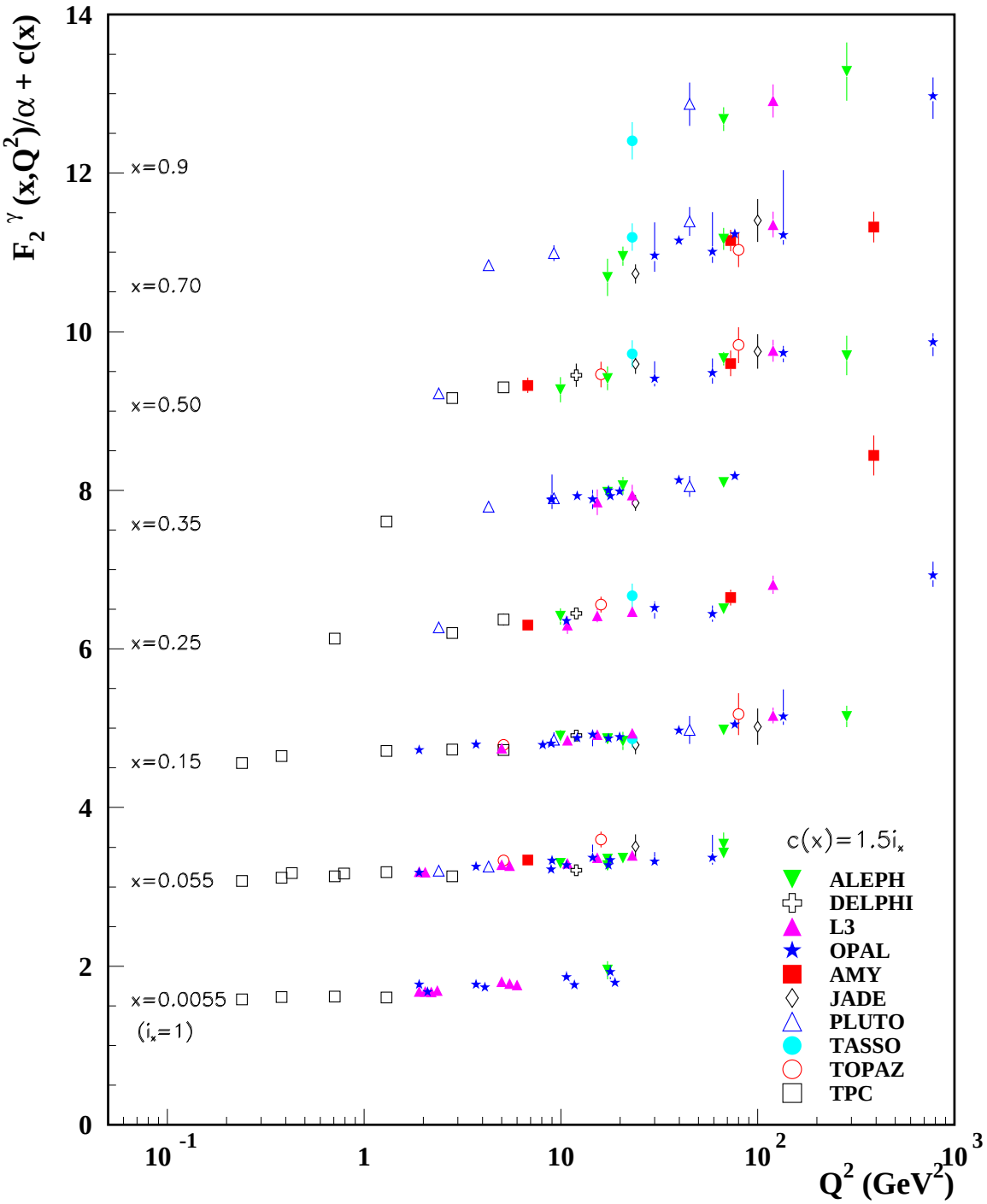

Figure 19.15: The hadronic structure function of the photon F_2^γ divided by the fine structure constant α measured in e^+e^- scattering, shown as a function of Q^2 for bins of x. Data points have been shifted to the nearest corresponding x bin as given in the plot. Some points have been offset in Q^2 for clarity. Statistical and systematic errors added in quadrature are shown. For the purpose of plotting, a constant $c(x) = 1.5i_x$ is added to F_2^γ/α where i_x is the number of the x bin, ranging from 1 ($x = 0.0055$) to 8 ($x = 0.9$). References: **ALEPH**–R. Barate *et al.*, Phys. Lett. **B458**, 152 (1999); A. Heister *et al.*, Eur. Phys. J. **C30**, 145 (2003);**DELPHI**–P. Abreu *et al.*, Z. Phys. **C69**, 223 (1995); **L3**–M. Acciarri *et al.*, Phys. Lett. **B436**, 403 (1998); M. Acciarri *et al.*, Phys. Lett. **B447**, 147 (1999); M. Acciarri *et al.*, Phys. Lett. **B483**, 373 (2000); **OPAL**–A. Ackerstaff *et al.*, Phys. Lett. **B411**, 387 (1997); A. Ackerstaff *et al.*, Z. Phys. **C74**, 33 (1997); G. Abbiendi *et al.*, Eur. Phys. J. **C18**, 15 (2000); G. Abbiendi *et al.*, Phys. Lett. **B533**, 207 (2002) (note that there is overlap of the data samples in these last two papers); **AMY**–S.K. Sahu *et al.*, Phys. Lett. **B346**, 208 (1995); T. Kojima *et al.*, Phys. Lett. **B400**, 395 (1997); **JADE**–W. Bartel *et al.*, Z. Phys. **C24**, 231 (1984); **PLUTO**–C. Berger *et al.*, Phys. Lett. **142B**, 111 (1984); C. Berger *et al.*, Nucl. Phys. **B281**, 365 (1987); **TASSO**–M. Althoff *et al.*, Z. Phys. **C31**, 527 (1986); **TOPAZ**–K. Muramatsu *et al.*, Phys. Lett. **B332**, 477 (1994); **TPC/Two Gamma**–H. Aihara *et al.*, Z. Phys. **C34**, 1 (1987).

20. FRAGMENTATION FUNCTIONS IN e^+e^-, ep AND pp COLLISIONS

Revised August 2013 by O. Biebel (Ludwig-Maximilians-Universität, Munich, Germany), D. de Florian (Dep. de Física, FCEyN-UBA, Buenos Aires, Argentina), D. Milstead (Fysikum, Stockholms Universitet, Sweden), and A. Vogt (Dep. of Mathematical Sciences, University of Liverpool, UK).

20.1. Introduction to fragmentation

The term 'fragmentation functions' is widely used for two conceptually different (albeit related) sets of functions describing final-state single particle energy distributions in hard scattering processes (see Refs. [1,2] for introductory reviews, and Refs. [3,4] for summaries of experimental and theoretical research in this field).

The first are cross-section observables such as the functions $F_{T,L,A}(x,s)$ in semi-inclusive e^+e^- annihilation at center-of-mass (CM) energy $\sqrt{s}$ via an intermediate photon or Z-boson, $e^+e^- \to \gamma/Z \to h + X$, given by

$$\frac{1}{\sigma_0}\frac{d^2\sigma^h}{dx\, d\cos\theta} \;=$$

$$\frac{3}{8}(1+\cos^2\theta)F_T^h(x,s) + \frac{3}{4}\sin^2\theta\, F_L^h(x,s) + \frac{3}{4}\cos\theta\, F_A^h(x,s)\,. \quad (20.1)$$

Here $x = 2E_h/\sqrt{s} \le 1$ is the scaled energy of the hadron h (in practice the approximation $x \simeq x_p = 2p_h/\sqrt{s}$ or $x \simeq p/p_{max}$ is often used), and θ is its angle relative to the electron beam in the CM frame. Eq. (20.1) is the most general form for unpolarized inclusive single-particle production via vector bosons [5]. The transverse and longitudinal fragmentation functions F_T and F_L represent the contributions from γ/Z polarizations transverse or longitudinal with respect to the direction of motion of the hadron. The parity-violating term with the asymmetric fragmentation function F_A arises from the interference between vector and axial-vector contributions. Normalization factors σ_0 used in the literature range from the total cross section $\sigma_{\rm tot}$ for $e^+e^- \to$ hadrons, including all weak and QCD contributions, to $\sigma_0 = 4\pi\alpha^2 N_c/3s$ with $N_c = 3$, the lowest-order QED cross section for $e^+e^- \to \mu^+\mu^-$ times the number of colors N_c. LEP1 measurements of all three fragmentation functions are shown in Fig. 20.1. Integration of Eq. (20.1) over θ yields the total fragmentation function $F^h = F_T^h + F_L^h$,

$$\frac{1}{\sigma_0}\frac{d\sigma^h}{dx} \;=\; F^h(x,s) \;=$$

$$\sum_i \int_x^1 \frac{dz}{z}\, C_i(z,\alpha_{\rm s}(\mu),\frac{s}{\mu^2}) D_i^h(\frac{x}{z},\mu^2) \;+\; \mathcal{O}(\frac{1}{\sqrt{s}}) \quad (20.2)$$

with $i = u,\ \bar{u},\ d,\ \bar{d},\ \ldots,\ g$. Here the second set of functions mentioned in the first paragraph has been introduced, the parton fragmentation functions (or fragmentation densities) D_i^h. These functions are the final-state analogue of the initial-state parton distribution functions (pdf) addressed in Section 19 of this *Review*. Due to the different sign of the squared four-momentum q^2 of the intermediate gauge boson these two sets of fragmentation distributions are also referred to as the timelike (e^+e^- annihilation, $q^2 > 0$) and spacelike (deep-inelastic scattering (DIS), $q^2 < 0$) parton distribution functions. The function $D_i^h(z,\mu^2)$ describes the probability that the parton i fragments into a hadron h carrying a probability that the parton i fragments into a hadron h carrying a fraction z of the parton's momentum. Beyond the leading order (LO) of perturbative QCD these universal functions are factorization-scheme dependent, with 'reasonable' scheme choices retaining certain quark-parton-model (QPM) constraints such as the momentum sum rule

$$\sum_h \int_0^1 dz\, z\, D_i^h(z,\mu^2) \;=\; 1\,. \quad (20.3)$$

The dependence of the functions D_i^h on the factorization scale μ^2 is discussed in Section 20.2. Like in Eq. (20.2) and below, this scale is often taken to be equal to the factorization or renomalization scale, but this equivalence is not required in the theory.

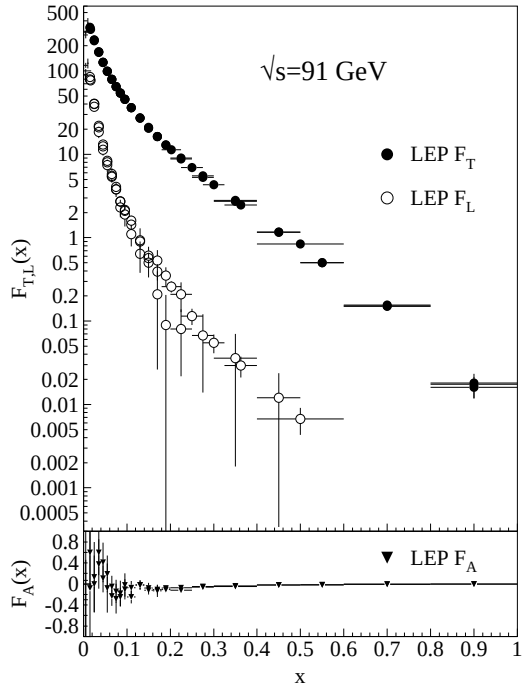

Figure 20.1: LEP1 measurements of total transverse (F_T), longitudinal (F_L), and asymmetric (F_A) fragmentation functions [6–8]. Data points with relative errors greater than 100% are omitted.

The second ingredient in Eq. (20.2), and analogous expressions for the functions $F_{T,L,A}$, are the observable-dependent coefficient functions C_i. At the zeroth order in the strong coupling $\alpha_{\rm s}$ the coefficient functions C_g for gluons are zero, while for (anti-) quarks $C_i = g_i(s)\,\delta(1-z)$ except for F_L, where $g_i(s)$ is the appropriate electroweak coupling. In particular, $g_i(s)$ is proportional to the squared charge of the quark i at $s \ll M_Z^2$, when weak effects can be neglected. The full electroweak prefactors $g_i(s)$ can be found in Ref. 5. The power corrections in Eq. (20.2) arise from quark and hadron mass terms and from non-perturbative effects.

Measurements of fragmentation in lepton-hadron and hadron-hadron scattering are complementary to those in e^+e^- annihilation. The latter provides a clean environment (no initial-state hadron remnant) and stringent constraints on the combinations $D_{q_i}^h + D_{\bar{q}_i}^h$. However e^+e^- annihilation is far less sensitive to D_g^h and insensitive to the charge asymmetries $D_{q_i}^h - D_{\bar{q}_i}^h$. These quantities are best constrained in proton–(anti-)proton and electron-proton scattering, respectively. Especially the latter provides a more complicated environment with which it is possible to study the influence on the fragmentation process from initial state QCD radiation, the partonic and spin structure of the hadron target, and the target remnant system (see Ref. 9 for a comprehensive review of the measurements and models of fragmentation in lepton-hadron scattering).

Moreover, unlike e^+e^- annihilation where $q^2 = s$ is fixed by the collider energy, lepton-hadron scattering has two independent scales, $Q^2 = -q^2$ and the invariant mass W^2 of the hadronic final state, which both can vary by several orders of magnitudes for a given CM energy, thus allowing the study of fragmentation in different environments by a single experiment. E.g., in photoproduction the exchanged photon is quasi-real ($Q^2 \approx 0$) leading to processes akin to hadron-hadron scattering. In DIS ($Q^2 \gg 1$ GeV^2), using the QPM, the hadronic fragments of the struck quark can be directly compared with quark fragmentation in e^+e^- in a suitable frame. Results from lepton-hadron experiments quoted in this report primarily concern

fragmentation in the DIS regime. Studies performed by lepton-hadron experiments of fragmentation with photoproduction data containing high transverse momentum jets or particles are also reported, when these are directly comparable to DIS and e^+e^- results.

Fragmentation studies in lepton-hadron collisions are usually performed in one of two frames in which the target hadron and the exchanged boson are collinear. The hadronic center-of-mass frame (HCMS) is defined as the rest system of the exchanged boson and incoming hadron, with the z^*-axis defined along the direction of the exchanged boson. The positive z^* direction defines the so-called current region. Fragmentation measurements performed in the HCMS often use the Feynman-x variable $x_F = 2p_z^*/W$, where p_z^* is the longitudinal momentum of the particle in this frame. As W is the invariant mass of the hadronic final state, x_F ranges between -1 and 1.

The Breit system [10] is connected to the HCMS by a longitudinal boost such that the time component of q vanishes, i.e, $q = (0, 0, 0, -Q)$. In the QPM, the struck parton then has the longitudinal momentum $Q/2$ which becomes $-Q/2$ after the collision. As compared with the HCMS, the current region of the Breit frame is more closely matched to the partonic scattering process, and is thus appropriate for direct comparisons of fragmentation functions in DIS with those from e^+e^- annihilation. The variable $x_p = 2p^*/Q$ is used at HERA for measurements in the Breit frame, ensuring rather directly comparable DIS and e^+e^- results, where p^* is the particle's momentum in the current region of the Breit frame.

20.2. Scaling violation

The simplest parton-model approach would predict scale-independent x-distributions ('scaling') for both the fragmentation function F^h and the parton fragmentation functions D_i^h. Perturbative QCD corrections lead, after factorization of the final-state collinear singularities for light partons, to logarithmic scaling violations via the evolution equations

$$\frac{\partial}{\partial \ln \mu^2} D_i(x,\mu^2) \;=\; \sum_j \int_x^1 \frac{dz}{z}\, P_{ji}(z, \alpha_{\rm s}(\mu^2)) D_j(\frac{x}{z}, \mu^2)\,, \qquad (20.4)$$

where the splitting functions $P_{ij}(z, \alpha_{\rm s}(\mu^2))$ describe in leading order the probability to find parton i with a longitudinal momentum fraction z in parton j. Usually this system of equations is decomposed into a 2×2 flavour-singlet sector comprising gluon and the sum of all quark and antiquark fragmentation functions, and scalar ('non-singlet') equations for quark-antiquark and flavour differences. The singlet splitting-function matrix is now P_{ji}, rather than P_{ij} as for the initial-state parton distributions, since D_j represents the fragmentation of the final parton.

The splitting functions in Eq. (20.4) have perturbative expansion of the form

$$P_{ji}(z, \alpha_{\rm s}) \;=\; \frac{\alpha_{\rm s}}{2\pi} P_{ji}^{(0)}(z) + \Big(\frac{\alpha_{\rm s}}{2\pi}\Big)^2 P_{ji}^{(1)}(z) + \Big(\frac{\alpha_{\rm s}}{2\pi}\Big)^3 P_{ji}^{(2)}(z) + \ldots \quad (20.5)$$

where the leading-order (LO) functions $P^{(0)}(z)$ [11,12] are the same as those for the initial-state parton distributions. The next-to-leading order (NLO) corrections $P^{(1)}(z)$ have been calculated in Refs. [13–17] (there are well-known misprints in the journal version of Ref. 14). Ref. 17 also includes the spin-dependent case. These functions are different from, but related to their space-like counterparts, see also Ref. 18. These relations have facilitated recent calculations of the next-to-next-to-leading order (NNLO) quantities $P_{qq}^{(2)}(z)$ and $P_{gg}^{(2)}(z)$ in Eq. (20.5) [19,20]. The corresponding off-diagonal quantities $P_{qg}^{(2)}$ and $P_{gq}^{(2)}$ were recently obtained in Ref. 21 by using similar relations supplemented with constrains from the momentum sum rule Eq. (20.3) [20] and the supersymmetric limit. An uncertainty, which does not affect the logarithmic behaviour at small and large momentum fractions, still remains on the $P_{qg}^{(2)}$ kernel. All these results refer to the standard $\overline{\rm MS}$ scheme, with the exception of Ref. 16, with a fixed number n_f of light flavours. The NLO treatment of flavour thresholds in the evolution has been addressed in Ref. 22.

The QCD parts of the coefficient functions for $F_{T,L,A}(x,s)$ in Eq. (20.1) and the total fragmentation function $F_2^h \equiv F^h$ in Eq. (20.2) are given by

$$C_{a,i}(z, \alpha_{\rm s}) \;=\; (1-\delta_{aL})\,\delta_{iq} + \frac{\alpha_{\rm s}}{2\pi}\, c_{a,i}^{(1)}(z) + \Big(\frac{\alpha_{\rm s}}{2\pi}\Big)^2 c_{a,i}^{(2)}(z) + \ldots\,. \quad (20.6)$$

The first-order corrections have been calculated in Ref. 23, and the second-order terms in [24]. The latter results have been verified (and some typos corrected) in Refs. [19,25]. The coefficient functions are known to NNLO except for F_L where the leading contribution is of order $\alpha_{\rm s}$.

The effect of the evolution is similar in the timelike and spacelike cases: as the scale increases, one observes a scaling violation in which the x-distribution is shifted towards lower values. This can be seen from Fig. 20.2 where a large amount of measurements of the total fragmentation function in e^+e^- annihilation are summarized. QCD analyses of these data are discussed in Section 20.5 below.

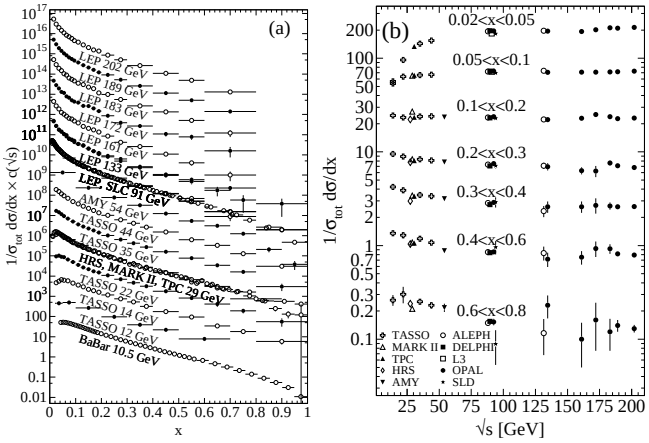

Figure 20.2: The e^+e^- fragmentation function for all charged particles is shown [8,26–43] (a) for different CM energies $\sqrt{s}$ versus x and (b) for various ranges of x versus $\sqrt{s}$. For the purpose of plotting (a), the distributions were scaled by $c(\sqrt{s}) = 10^i$ with i ranging from $i = 0$ ($\sqrt{s} = 12$ GeV) to $i = 13$ ($\sqrt{s} = 202$ GeV).

Unlike the splitting functions in Eq. (20.5), see Refs. [18–20], the coefficient functions for $F_{2,T,A}$ in Eq. (20.6) show a threshold enhancement with terms up to $\alpha_{\rm s}^n (1-z)^{-1} \ln^{2n-1}(1-z)$. Such logarithms can be resummed to all orders in $\alpha_{\rm s}$ using standard soft-gluon techniques [44–46]. Recently this resummation has been extended to the subleading (and for F_L leading) class $\alpha_{\rm s}^n \ln^k(1-z)$ of large-x logarithms [47,48].

In Ref. 23, the NLO coefficient functions have been calculated also for single hadron production in lepton-proton scattering, $ep \to e + h + X$. More recently corresponding results have been obtained for the case that a non-vanishing transverse momentum is required in the HCMS frame [49].

Scaling violations in DIS are shown in Fig. 20.3 for both HCMS and Breit frame. In Fig. 1.3(a) the distribution in terms of $x_F = 2p_z^*/W$ shows a steeper slope in ep data than for the lower-energy μp data for $x_F > 0.15$, indicating the scaling violations. At smaller values of x_F in the current jet region, the multiplicity of particles substantially increases with W owing to the increased phase space available for the fragmentation process. The EMC data access both the current region and the region of the fragmenting target remnant system. At higher values of $|x_F|$, due to the extended nature of the remnant, the multiplicity in the target region far exceeds that in the current region. For acceptance reasons the remnant hemisphere of the HCMS is only accessible by the lower-energy fixed-target experiments.

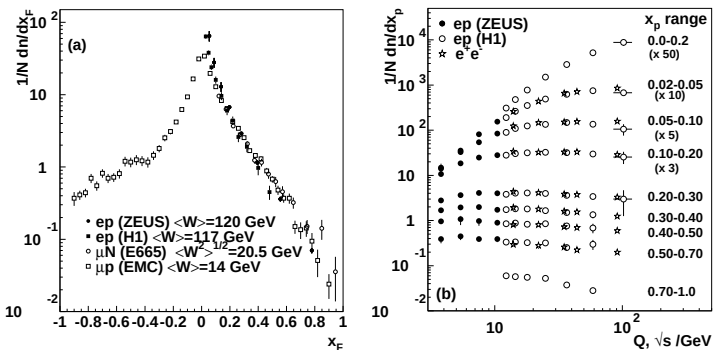

Figure 20.3: (a) The distribution $1/N \cdot dN/dx_F$ for all charged particles in DIS lepton-hadron experiments at different values of W, and measured in the HCMS [50–53]. (b) Scaling violations of the fragmentation function for all charged particles in the current region of the Breit frame of DIS [54,59] and in e^+e^- interactions [41,60]. The data are shown as a function of $\sqrt{s}$ for e^+e^- results, and as a function of Q for the DIS results, each within the same indicated intervals of the scaled momentum x_p. The data for the four lowest intervals of x_p are multiplied by factors 50, 10, 5, and 3, respectively for clarity.

Using hadrons from the current hemisphere in the Breit frame, measurements of fragmentation functions and the production properties of particles in ep scattering have been made by Refs. [54–59]. Fig. 20.3(b) compares results from ep scattering and e^+e^- experiments, the latter results are halved as they cover both event hemispheres. The agreement between the DIS and e^+e^- results is fairly good. However, processes in DIS which are not present in e^+e^- annihilation, such as boson-gluon fusion and initial state QCD radiation, can depopulate the current region. These effects become most prominent at low values of Q and x_p. Hence, when compared with e^+e^- annihilation data at $\sqrt{s} = 5.2$, 6.5 GeV [61] not shown here, the DIS particle rates tend to lie below those from e^+e^- annihilation. A ZEUS study [62] finds that the direct comparability of the ep data to e^+e^- results at low scales is improved if twice the energy in the current hemisphere of the Breit frame, $2E_B^{\rm cr}$, is used instead of Q as the fragmentation scale.

20.3. Fragmentation functions for small particle momenta

The higher-order timelike splitting functions in Eq. (20.5) are very singular at small x. They show a double-logarithmic (LL) enhancement with leading terms of the form $\alpha_{\rm s}^n \ln^{2n-2} x$ corresponding to poles $\alpha_{\rm s}^n\,(N-1)^{1-2n}$ for the Mellin moments

$$P^{(n)}(N) \;=\; \int_0^1 dx\; x^{N-1}\; P^{(n)}(x)\;. \qquad (20.7)$$

Despite large cancellations between leading and non-leading logarithms at non-asymptotic value of x, the resulting small-x rise in the timelike splitting functions dwarfs that of their spacelike counterparts for the evolution of the parton distributions in Section 19 of this *Review*, see Fig. 1 of Ref. 20. Consequently the fixed-order approximation to the evolution breaks down orders of magnitude in x earlier in fragmentation than in DIS.

The pattern of the known coefficients and other considerations suggest that the LL terms sum to all-order expressions without any pole at $N = 1$ such as [63,64]

$$P_{gg}^{\rm LL}(N) \;=\; -\frac{1}{4}(N - 1 - \sqrt{(N-1)^2 \cdot 24\,\alpha_{\rm s}/\pi}\,)\;. \qquad (20.8)$$

Keeping the first three terms in the resulting expansion of Eq. (20.4) around $N = 1$ yields a Gaussian in the variable $\xi = \ln(1/x)$ for the small-x fragmentation functions,

$$xD(x,s) \;\propto\; \exp\left[-\frac{1}{2\sigma^2}(\xi - \xi_p)^2\right]\;, \qquad (20.9)$$

with the peak position and width varying with the energy as [65] (see also Ref. 2)

$$\xi_p \;\simeq\; \frac{1}{4}\ln\left(\frac{s}{\Lambda^2}\right)\;,\quad \sigma \;\propto\; \left[\ln\left(\frac{s}{\Lambda^2}\right)\right]^{3/4}\;. \qquad (20.10)$$

Next-to-leading logarithmic corrections to the above predictions have been calculated [66]. In the method of Ref. 67, see also Refs. [68,69], the corrections are included in an analytical form known as the 'modified leading logarithmic approximation' (MLLA). Alternatively they can be used to compute higher-moment corrections to the shape in Eq. (20.9) [70]. The small-x resummation of the coefficient functions for semi-inclusive e^+e^- annihilation and the timelike spitting functions in the standard $\overline{\rm MS}$ scheme was recently extended in Refs. [71,72] and has reached fully analytic next-to-next-to-leading logarithmic accuracy. First applications of these results to gluon and quark jet multiplicities have been presented in Ref. 73.

Fig. 20.4 shows the ξ distribution for charged particles produced in the current region of the Breit frame in DIS and in e^+e^- annihilation. Consistent with Eq. (20.9) (the 'hump backed plateau') and Eq. (20.10) the distributions have a Gaussian shape with the peak position and area increasing with the CM energy (e^+e^-) and Q^2 (DIS).

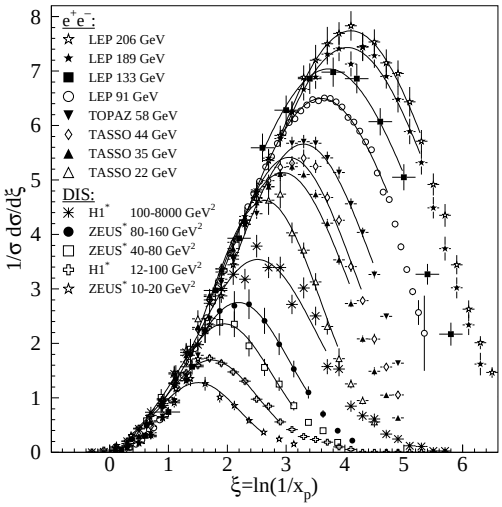

Figure 20.4: Distribution of $\xi = \ln(1/x_p)$ at several CM energies ($\rm e^+e^-$) [26–28,33–36,41,74–77] and intervals of Q^2 (DIS) [57,58]. At each energy only one representative measurement is displayed. For clarity some measurements at intermediate CM energies (e^+e^-) or Q^2 ranges (DIS) are not shown. The DIS measurements ($*$) have been scaled by a factor of 2 for direct comparability with the e^+e^- results. Fits of simple Gaussian functions are overlaid for illustration.

The predicted energy dependence Eq. (20.10) of the peak in the ξ distribution is explained by soft gluon coherence (angular ordering) which correctly predicts the suppression of hadron production at small x. Of course, a decrease at very small x is expected on purely kinematical grounds, but this would occur at particle energies proportional to their masses, *i.e.*, at $x \propto m/\sqrt{s}$ and hence $\xi \sim \frac{1}{2}\ln s$. Thus, if the suppression were purely kinematic, the peak position ξ_p would vary twice as rapidly with the energy, which is ruled out by the data in Fig. 20.5. The $\rm e^+e^-$ and DIS data agree well with each other, demonstrating the universality of hadronization, and the MLLA prediction. Measurements of the higher moments of the ξ distribution in e^+e^- [41,77–79] and DIS [58] have also been performed and show consistency with each other.

The average charged particle multiplicity is another observable sensitive to fragmentation functions for small particle momenta. Perturbative predictions using both NLO [88] and MLLA [89,91] have been obtained from solving Eq. (20.4) yielding

$$\left\langle n_G(Q^2)\right\rangle \propto \alpha_S^b(Q^2)\cdot\exp\left[\frac{c}{4\pi b_0\sqrt{\alpha_S(Q^2)}}\cdot\left(1+6a_2\frac{\alpha_S(Q^2)}{\pi}\right)\right] \qquad (20.11)$$

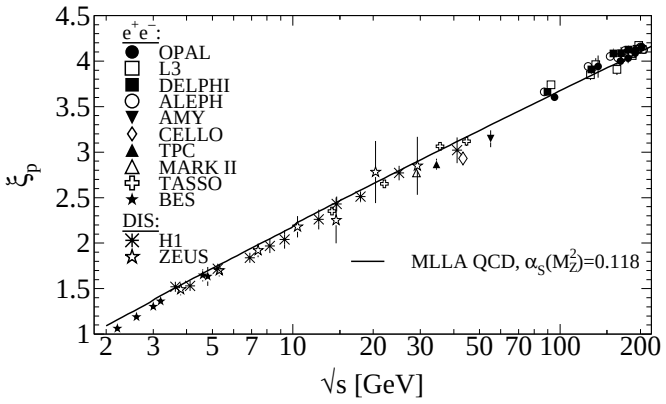

Figure 20.5: Evolution of the peak position, ξ_p, of the ξ distribution with the CM energy $\sqrt{s}$. The MLLA QCD prediction using $\alpha_S(s = M_Z^2) = 0.118$ is superimposed to the data of Refs. [26,28,29,32–34,36,41,56,57,75,76,79–87].

where $b = \frac{1}{4} + \frac{10}{27}\frac{n_f}{4\pi b_0}$, $c = \sqrt{96\pi}$, with $b_0 = (33 - 2n_f)/(12\pi)$, cp. Section 9 of this *Review*, for n_f contributing quark flavours. Higher order corrections to Eq. (20.11) are known up to next-to-next-to-next-to-leading order (3NLO), for details and references see [92]. The term proportional to $a_2 \approx -0.502 + 0.0421\,n_f - 0.00036\,n_f^2$ in Eq. (20.11) is the contribution due to NNLO corrections [93]. The quantity $\langle n_G(Q^2)\rangle$ strictly refers to the average number of gluons, while for quarks a correction factor $r = \langle n_G\rangle/\langle n_q\rangle$ weakly depending on Q^2 is required due to the different colour factors in quark and gluon couplings, respectively. Higher order corrections up to 3NLO on the asymptotic value $r = C_A/C_F = 9/4$ [94] are quoted in [92].

Employing the hypothesis of 'Local Parton-Hadron Duality' (LPHD) [89], Eq. (20.11) can be applied to describe average charged particle multiplicities obtained in e^+e^- annihilation. The equation can also be applied to $e^\pm p$ scattering if the current fragmentation region of the Breit frame is considered for measuring the average charged particle multiplicity. Fig. 20.6 shows corresponding data and fits of Eq. (20.11) where apart from a LPHD normalization factor a constant offset has been allowed for, that is $\langle n_{\rm ch}(Q)\rangle = K_{\rm LHPD}\cdot\langle n_G(Q)\rangle/r + n_0$.

In hadron-hadron collisions beam remnants, e.g. from single-diffractive (SD) scattering, contribute to the measurement of the hadron multiplicity from a hard parton-parton scattering, making interpretation of the data more model dependent. Experimental results are usually given for inelastic processes or for non-single diffractive processes (NSD). Due to the large beam particle momenta at Tevatron and LHC, not all final state particles can be detected within the limited detector acceptance. Therefore, experiments at Tevatron and LHC quote particle multiplicities for limited ranges of pseudo-rapidity $\eta = -\ln\tan(\vartheta/2)$ or at central rapidity, i.e. $\eta = 0$, shown in Fig. 20.6.

An universality of the average particle multiplicities in e^+e^- and $p(\overline{p})$ processes has been reported in Ref. 120 when considering an effective collision energy $Q_{\rm eff} = \sqrt{s}/k$ in $p(\overline{p})$ reduced by a factor of $k \approx 3$ plus a constant offset of $n_0 \approx 2$. A more detailed review is available in Ref. 121. According to investigations presented in Ref. 122 the universality of the energy dependence of average particle multiplicities also applies to hadron-hadron and nucleus-nucleus collisions for both full and central rapidity multiplicities. Evidence for this universality is given by the good agreement for the energy dependence of Eq. (20.11) when fit to the $p(\overline{p})$ data as shown in Fig. 20.6.

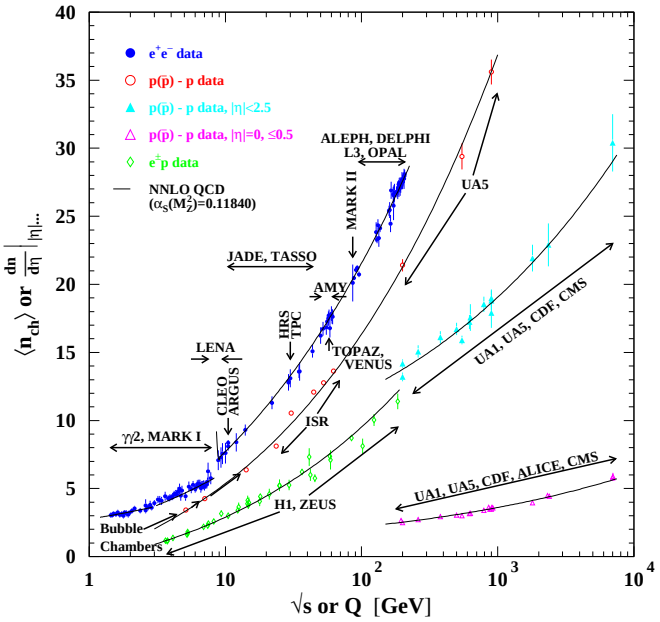

Figure 20.6: Average charged particle multiplicity $\langle n_{\rm ch}\rangle$ as a function of $\sqrt{s}$ or Q for e^+e^- and $p\overline{p}$ annihilations, and pp and ep collisions. The indicated errors are statistical and systematic uncertainties added in quadrature, except when no systematic uncertainties are given. All NNLO QCD curves are Eq. (20.11) with fitted normalization, K_{LHPD}, and offset, n_0, using a fixed $\alpha_S(M_Z^2) = 0.1184$ [90] and for e^+e^- annihilation data $n_f = 3$, 4, or 5 depending on $\sqrt{s}$, else $n_f = 3$. $\mathbf{e^+e^-}$: Contributions from K_S^0 and Λ decays included. Data compiled from Refs. [7,8,26,33,34,37,76,82,95–105]. $\mathbf{e^\pm p}$: Multiplicities have been measured in the current fragmentation region of the Breit frame. Data compiled from Refs. [57,58,62,106,107]. $\mathbf{p(\overline{p})}$: Measured values above 20 GeV refer to non-single diffractive (NSD) processes. Central pseudorapidity multiplicities $(dn/d\eta)|_{|\eta|...}$ refer to either $|\eta| < 2.5$ (CMS: $|\eta| < 2.4$) or $|\eta| = 0$ (UA5, CMS, ALICE: $|\eta| < 0.5$). Data compiled from Refs. [108–119].

20.4. Fragmentation models

Although the scaling violation can be calculated perturbatively, the actual form of the parton fragmentation functions is non-perturbative. Perturbative evolution gives rise to a shower of quarks and gluons (partons). Multi-parton final states from leading and higher order matrix element calculations are linked to these parton showers using factorization prescriptions, also called matching schemes, see Ref. 123 for an overview. Phenomenological schemes are then used to model the carry-over of parton momenta and flavor to the hadrons. Implemented in Monte Carlo event generators (see Section 40 of this *Review*), these schemes have been tuned using e^+e^- data and provide good description of hadron collisions as well, thus providing evidence of the universality of the fragmentation functions.

20.5. Quark and gluon fragmentation functions

The fragmentation functions are solutions to the evolution equations Eq. (20.4), but need to be parametrized at some initial scale μ_0^2 (usually around 1 GeV^2 for light quarks and gluons and m_Q^2 for heavy quarks). A usual parametrization for light hadrons is [132–138]

$$D_i^h(x,\mu_0^2) = Nx^\alpha(1-x)^\beta\left(1+\gamma(1-x)^\delta\right)\ , \qquad (20.12)$$

where the normalization N, and the parameters α, β, γ and δ in general depend on the energy scale μ_0^2, and also on the type of the parton, i, and the hadron, h. Frequently the term involving γ and δ

is left out [134–137]. Heavy flavor fragmentation into heavy mesons is discussed in Sec. 20.9. The parameters of Eq. (20.12) (see [132–137]) are obtained by performing global fits to data on various hadron types for different combinations of partons and hadrons in e^+e^-, lepton-hadron and hadron-hadron collisions.

Sets of fragmentation functions are available for pions, kaons, protons, neutrons, etas, Lambdas and charged hadrons [132–138].

Data from e^+e^- annihilation present the cleanest experimental source for the measurement of fragmentation functions, but can not contribute to disentangle quark from antiquark distributions. Since the bulk of the e^+e^- annihilation data is obtained at the mass of the Z-boson, where the electroweak couplings are roughly the same for the different partons, it provides the most precise determination of the flavor-singlet quark fragmentation. Flavor tagged results [139], distinguishing between the light quark, charm and bottom contributions are of particular value for flavor decomposition, even though those measurements can not be unambiguously interpreted in perturbative QCD.

The most relevant source for quark-antiquark (and also flavor) separation is provided by data from semi-inclusive DIS (SIDIS). Semi-inclusive measurements are usually performed at much lower scales than for e^+e^- annihilation. The inclusion of SIDIS data in global fits allows for a wider coverage in the evolution of the fragmentation functions, resulting at the same time in a stringent test of the universality of these distributions. Charged-hadron production data in hadronic collisions also presents a sensitivity on (anti-)quark fragmentation functions.

The gluon fragmentation function $D_g(x)$ can be extracted, in principle, from the longitudinal fragmentation function F_L in Eq. (20.2), as the coefficient functions $C_{L,i}$ for quarks and gluons are comparable at order α_s. However at NLO, *i.e.*, including the $\mathcal{O}(\alpha_s^2)$ coefficient functions $C_{L,i}^{(2)}$ [24], quark fragmentation is dominant in F_L over a large part of the kinematic range, reducing the sensitivity on D_g. This distribution could be determined also analyzing the evolution of the fragmentation functions. This possibility is limited by the lack of sufficiently precise data at energy scales away from the Z-resonance and the dominance of the quark contributions and at medium and large values of x.

D_g can also be deduced from the fragmentation of three-jet events in which the gluon jet is identified, for example, by tagging the other two jets with heavy quark decays. To leading order, the measured distributions of $x = E_{\rm had}/E_{\rm jet}$ for particles in gluon jets can be identified directly with the gluon fragmentation function $D_g(x)$. At higher orders the theoretical interpretation of this observable is ambiguous.

A comparison of recent fits of NLO fragmentation functions for $\pi^+ + \pi^-$ obtained by DSS07 [132], AKK08 [133] and HKNS07 [137] is shown in Fig. 20.7. Differences between the sets are large especially for the gluon fragmentation function over the full range of x and for the quark distribution at large momentum fractions. The differences are even larger for other species of hadrons like kaons and protons [132,133,137]. Recent analyses [137,140] estimate the uncertainties involved in the extraction of fragmentation functions.

A direct constraint on D_g is provided by $pp, p\bar{p} \to hX$ data. At variance with e^+e^- annihilation and SIDIS, for this process gluon fragmentation starts to contribute at the lowest order in the coupling constant, introducing a strong sensitivity on D_g. At large $x \gtrsim 0.5$, where information from e^+e^- is sparse, data from hadronic colliders facilitate significantly improved extractions of D_g [132,133].

Photonic fragmentation functions play a relevant role in the theoretical understanding of inclusive photon production in (leptonic and hadronic) high energy processes. Since photons have a pointlike coupling to quarks [141], the corresponding fragmentation functions obey inhomogeneous evolution equations and are generally decomposed into a perturbative and a non-perturbative component [136,142,143]. The hadronic part, sometimes approximated by the Vector Meson Dominance Model, can be obtained by performing global analysis to the available prompt photon data [6,29,32,35,39,41,84,144,176].

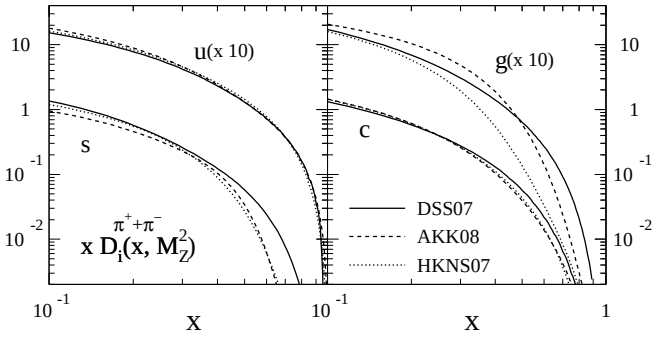

Figure 20.7: Comparison of up, strange, charm and gluon NLO fragmentation functions for $\pi^+ + \pi^-$ at the mass of the Z. The different lines correspond to the result of the most recent analyses performed in Refs. [132,133,137].

20.6. Identified particles in e^+e^- and semi-inclusive DIS

A great wealth of measurements of e^+e^- fragmentation into identified particles exists. A collection of references for data on fragmentation into identified particles is given on Table 50.1 of this *Review*. Representative of this body of data is Fig. 20.8 which shows fragmentation functions as the scaled momentum spectra of charged particles at several CM energies.

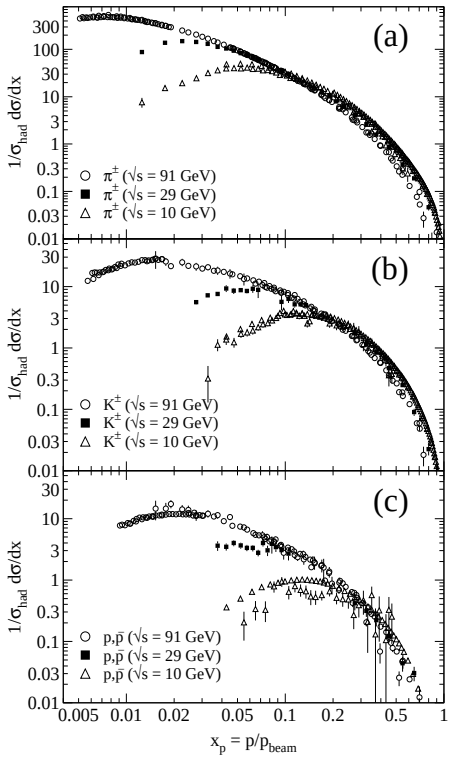

Figure 20.8: Scaled momentum spectra of (a) $\pi^\pm$, (b) $K^\pm$, and (c) $p/\overline{p}$ at $\sqrt{s} = 10$, 29, and 91 GeV [38,42,43,84,144,145].

Quantitative results of studies of scaling violation in e^+e^- fragmentation have been reported in [6,39,146,147]. The values of α_s obtained are consistent with the world average (see review on QCD in Section 9 of this *Review*).

Many studies have been made of identified particles produced in lepton-hadron scattering, although fewer particle species have been measured than in e^+e^- collisions. References [148–155] and [156–162] are representative of the data from fixed target and ep collider experiments, respectively.

QCD calculations performed at NLO provide an overall good description of the HERA data [53,54,58,157,163,164] for both SIDIS [165] and the hadron transverse momentum distribution [49] in the kinematic regions in which the calculations are predictive.

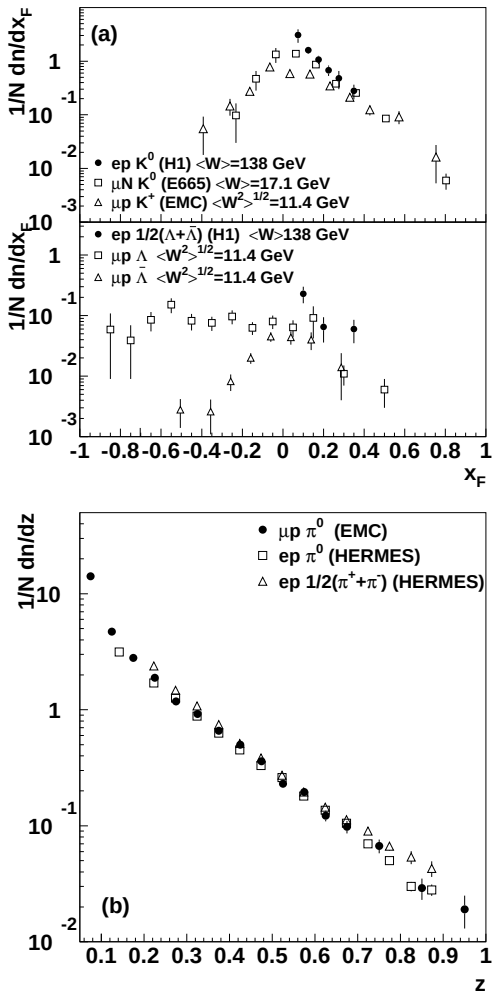

Figure 20.9: (a) $1/N \cdot dn/dx_F$ for identified strange particles in DIS at various values of W [148,151,156]. (b) $1/N \cdot dn/dz$ for measurements of pions from fixed-target DIS experiment [149,152,155].

Fig. 20.9(a) compares lower-energy fixed-target and HERA data on strangeness production, showing that the HERA spectra have substantially increased multiplicities, albeit with insufficient statistical precision to study scaling violations. The fixed-target data show that the Λ rate substantially exceeds the $\overline{\Lambda}$ rate in the remnant region, owing to the conserved baryon number from the baryon target. Fig. 20.9(b) shows neutral and charged pion fragmentation functions $1/N \cdot dn/dz$, where z is defined as the ratio of the pion energy to that of the exchanged boson, both measured in the laboratory frame. Results are shown from HERMES and the EMC experiments, where HERMES data have been evolved with NLO QCD to $\langle Q^2 \rangle = 25$ GeV^2 in order to be consistent with the EMC. Each of the experiments uses various kinematic cuts to ensure that the measured particles lie in the region which is expected to be associated with the struck quark. In the DIS kinematic regime accessed at these experiments, and over the range in z shown in Fig. 20.9, the z and x_F variables have similar values [50]. The precision data on identified particles can be used in the study of the quark flavor content of the proton [166].

Data on identified particle production can aid the investigation of the universality of jet fragmentation in e^+e^- and DIS. The strangeness suppression factor γ_s, as derived principally from tuning the Lund string model [125] within JETSET [126], is typically found to be around 0.3 in e^+e^- experiments [74], although values closer to 0.2 [167] have also been obtained. A number of measurements of so-called V^0-particles (K^0, Λ^0) and the relative rates of V^0's and inclusively produced charged particles have been performed at HERA [156,158,162] and fixed target experiments [148]. These typically favour a stronger suppression ($\gamma_s \approx 0.2$) than usually obtained from e^+e^- data although values close to 0.3 have also been obtained [168,169].

However, when comparing the description of QCD-based models for lepton-hadron interactions and e^+e^- collisions, it is important to note that the overall description by event generators of inclusively produced hadronic final states is more accurate in e^+e^- collisions than lepton-hadron interactions [170]. Predictions of particle rates in lepton-hadron scattering are affected by uncertainties in the modelling of the parton composition of the proton and photon, the extended target remnant, and initial and final state QCD radiation. Furthermore, the tuning of event generators for e^+e^- collisions is typically based on a larger set of parameters and uses more observables [74] than are used when optimizing models for lepton-hadron data [171].

20.7. Fragmentation in hadron-hadron collisions

An extensive set on high-transverse momentum (p_T) single-inclusive hadron data has been collected in $h_1h_2 \to hX$ scattering processes, both at high energy colliders and fixed-target experiments [172–195]. Only the transverse momentum p_T is considered in hadron-hadron collisions because of lack of knowledge of the longitudinal momentum of the hard subprocess. Fig. 20.10 shows a compilation of neutral pion and charged hadron production data for energies in the range $\sqrt{s} \approx 23$ - 800 GeV.

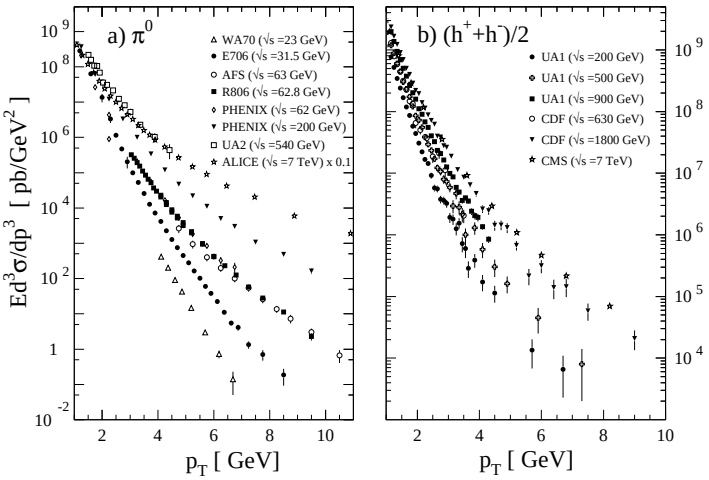

Figure 20.10: Selection of inclusive (a) π^0 and (b) charged-hadron production data from pp [118,180,188,192–195] and $p\bar{p}$ [172,175,178] collisions.

The differential cross-section for high-transverse momentum distributions has been computed to next-to-leading order accuracy in perturbative QCD [196]. NLO calculations yield a good description of the collider data, but significantly under-predict the cross-section for several fixed-target energy data sets [197,198]. Data collected at high energy colliders are either included in global fit analyses or used as a test for the universality of fragmentation functions.

Different strategies have been developed to ameliorate the theoretical description at fixed-target energies. A possible phenomenological approach involves the introduction of a non-perturbative intrinsic partonic transverse momentum [195,199,200]. From the perturbative side, the resummation of the dominant higher order corrections at threshold produces an enhancement of the theoretical calculation that significantly improves the description of the data [201,202].

Measurements of hadron production in longitudinally polarized pp collisions are used mainly in the determination of the polarized gluon distribution in the proton [203,204].

Hadron production provides a critical observable for probing the high energy-density matter produced in heavy-ion collisions. Measurements at colliders show a suppression of inclusive hadron yields at high transverse momentum for AA collisions compared to pp scattering, indicating the formation of a dense medium opaque to quark and gluons, see e.g. [205].

20.8. Spin-dependent fragmentation

Measurements of charged-hadron production in unpolarized lepton-hadron scattering provide a unique tool to perform a flavor-separation determination of polarized parton densities from DIS interactions with longitudinally polarized targets [206–210].

Polarized scattering presents the possibility to measure the spin transfer from the struck quark to the final hadron, and thus develop spin-dependent fragmentation functions [211,212]. Early measurements of the longitudinal spin transfer to Lambda hyperons have been presented in [213,214]. This process is also useful in the study of the quark transversity distribution [215], which describes the probability of finding a transversely polarized quark with its spin aligned or anti-aligned with the spin of a transversely polarized nucleon. The transversity function is chiral-odd, and therefore not accessible through measurements of inclusive lepton-hadron scattering. Semi-inclusive DIS, in which another chiral-odd observable may be involved, provides a valuable tool to probe transversity. The Collins fragmentation function [216] relates the transverse polarization of the quark to that of the final hadron. It is chiral-odd and naive T-odd, leading to a characteristic single spin asymmetry in the azimuthal angular distribution of the produced hadron in the hadron scattering plane. Azimuthal angular distributions in semi-inclusive DIS can also be produced by other processes requiring non-polarized fragmentation functions, like the Sivers mechanism [217].

A number of experiments have measured these asymmetries [218–228]. Collins and Sivers asymmetries have been shown experimentally to be non zero by the HERMES measurements on transversely polarized proton targets [219–221]. Independent information on the Collins function has been provided by the BELLE Collaboration [222–223]. Measurements performed by the COMPASS collaboration on deuteron targets show results compatible with zero for both asymmetries [224–226].

20.9. Heavy quark fragmentation

It was recognized very early [229] that a heavy flavored meson should retain a large fraction of the momentum of the primordial heavy quark, and therefore its fragmentation function should be much harder than that of a light hadron. In the limit of a very heavy quark, one expects the fragmentation function for a heavy quark to go into any heavy hadron to be peaked near $x = 1$.

When the heavy quark is produced at a momentum much larger than its mass, one expects important perturbative effects, enhanced by powers of the logarithm of the transverse momentum over the heavy quark mass, to intervene and modify the shape of the fragmentation function. In leading logarithmic order (*i.e.*, including all powers of $\alpha_s \log m_Q/p_T$), the total (*i.e.*, summed over all hadron types) perturbative fragmentation function is simply obtained by solving the leading evolution equation for fragmentation functions, Eq. (20.4), with the initial condition at a scale $\mu^2 = m_Q^2$ given by $D_Q(z, m_Q^2) = \delta(1-z)$ and $D_i(z, m_Q^2) = 0$ for $i \neq Q$ (here $D_i(z)$, stands for the probability to produce a heavy quark Q from parton i with a fraction z of the parton momentum).

Several extensions of the leading logarithmic result have appeared in the literature. Next-to-leading-log (NLL) order results for the perturbative heavy quark fragmentation function have been obtained in [230]. The resummation of the dominant logarithmic contributions at large z was performed in [44] to next-to-leading-log accuracy. Fixed-order calculations of the fragmentation function at order α_s^2 in e^+e^- annihilation have appeared in [231] while the initial condition for the perturbative heavy quark fragmentation function has been extended to NNLO in [232].

Inclusion of non-perturbative effects in the calculation of the heavy-quark fragmentation function is done by convoluting the perturbative result with a phenomenological non-perturbative form. Among the most popular parametrizations we have the following:

$$\text{Peterson } \textit{et al.}\ [233]: \quad D_{\rm np}(z) \propto \frac{1}{z}\left(1 - \frac{1}{z} - \frac{\epsilon}{1-z}\right)^{-2} \tag{20.13}$$

$$\text{Kartvelishvili } \textit{et al.}\ [234]: \quad D_{\rm np}(z) \propto z^{\alpha}(1-z)\,, \tag{20.14}$$

$$\text{Collins\&Spiller } [235]: \quad D_{\rm np}(z) \propto \left(\frac{1-z}{z} + \frac{(2-z)\epsilon_C}{1-z}\right) \times (1+z^2)\left(1 - \frac{1}{z} - \frac{\epsilon_C}{1-z}\right)^{-2} \tag{20.15}$$

$$\text{Colangelo\&Nason } [236]: \quad D_{\rm np}(z) \propto (1-z)^{\alpha} z^{\beta} \tag{20.16}$$

$$\text{Bowler } [237]: \quad D_{\rm np}(z) \propto z^{-(1+bm_{h,\perp}^2)} (1-z)^{a} \exp\left(-\frac{bm_{h,\perp}^2}{z}\right) \tag{20.17}$$

$$\text{Braaten } \textit{et al.}\ [238]: \quad \text{(see Eq. (31), (32) in [238])} \tag{20.18}$$

where ϵ, ϵ_C, a, $bm_{h,\perp}^2$, α, and β are non-perturbative parameters, depending upon the heavy hadron considered. The parameters entering the non-perturbative forms are fitted together with some model of hard radiation, which can be either a shower Monte Carlo, a leading-log or NLL calculation (which may or may not include Sudakov resummation), or a fixed order calculation. In [231], for example, the Peterson *et al.* [233] ϵ parameter for charm and bottom production is fitted from the measured distributions of refs. [239,252] for charm, and of [257] for bottom. If the leading-logarithmic approximation (LLA) is used for the perturbative part, one finds $\epsilon_c \approx 0.05$ and $\epsilon_b \approx 0.006$; if a second order calculation is used one finds $\epsilon_c \approx 0.035$ and $\epsilon_b \approx 0.0033$; if a NLLO calculation is used instead one finds $\epsilon_c \approx 0.022$ and $\epsilon_b \approx 0.0023$. The larger values found in the LL approximation are consistent with what is obtained in the context of parton shower models [241], as expected. The ϵ parameter for charm and bottom scales roughly with the inverse square of the heavy flavour mass. This behaviour can be justified by several arguments [229,242,243]. It can be used to relate the non-perturbative parts of the fragmentation functions of charm and bottom quarks [231,236,244].

A more conventional approach [245] involves the introduction of a unique set of heavy quark fragmentation functions of non-perturbative nature that obey the usual massless evolution equations in Eq. (20.4). Finite mass terms of the form $(m_Q/p_T)^n$ are kept in the corresponding short distance coefficient function for each scattering process. Within this approach, the initial condition for the perturbative fragmentation function provides the term needed to define the correct subtraction scheme to match the massless limit for the coefficient function (see e.g. [246]) . Such implementation is in line with the variable flavor number scheme introduced for parton distributions functions, as described in Section 19 of this *Review*.

High statistics data for charmed mesons production near the Υ resonance (excluding decay products of B mesons) have been published [247,248]. They include results for D and D^*, D_s (see also [249,250]) and Λ_c. Shown in Fig. 20.11(a) are the CLEO and BELLE inclusive cross-sections times branching ratio $\mathcal{B}$, $s \cdot \mathcal{B}d\sigma/dx_p$, for the production of D^0 and D^{*+}. The variable x_p approximates the light-cone momentum fraction z, but is not identical to it. The two measurements are consistent with each other.

The branching ratio $\mathcal{B}$ represents $D^0 \to K^-\pi^+$ for the D^0 results and for the D^{*+} the product branching fraction: $D^{*+} \to D^0\pi^+$, $D^0 \to K^-\pi^+$. Given the high precision of CLEO's and BELLE's data, a superposition of different parametric forms for the non-perturbative contribution is needed to obtain a good fit [22]. Older studies are reported in Refs. [251–253]. Charmed meson spectra on the Z peak have been published by OPAL and ALEPH [131,254].

Charm quark production has also been extensively studied at HERA by the H1 and ZEUS collaborations. Measurements have been

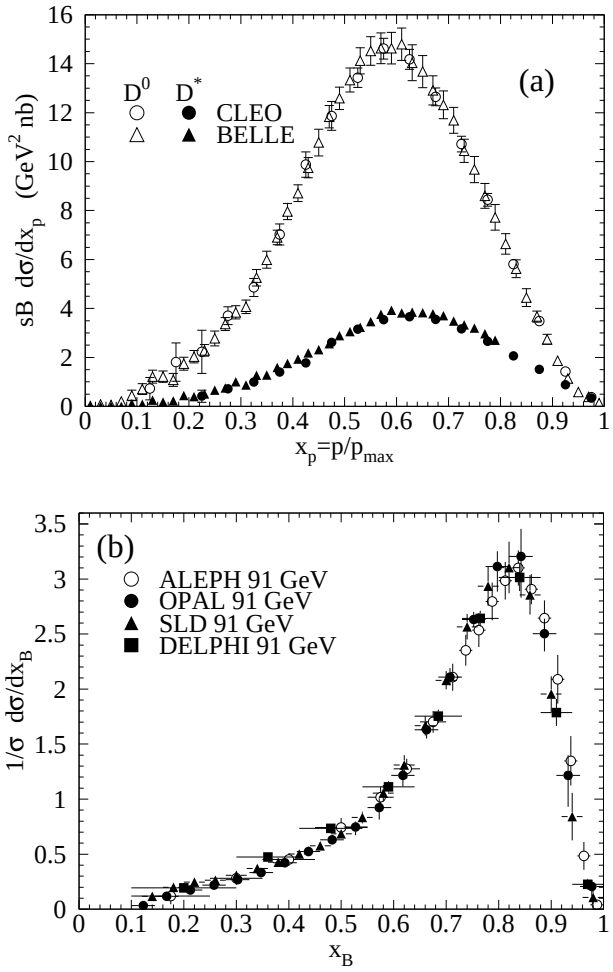

Figure 20.11: (a) Efficiency-corrected inclusive cross-section measurements for the production of D^0 and D^{*+} in e^+e^- measurements at $\sqrt{s} \approx 10.6$ GeV, excluding B decay products [247,248]. (b) Measured e^+e^- fragmentation function of b quarks into B hadrons at $\sqrt{s} \approx 91$ GeV [258].

made of $D^{*\pm}$, $D^{\pm}$, and $D_s^{\pm}$ mesons and the Λ_c baryon. See, for example, Refs. [255,256].

Experimental studies of the fragmentation function for b quarks, shown in Fig. 20.11(b), have been performed at LEP and SLD [257–259]. Commonly used methods identify the B meson through its semileptonic decay or based upon tracks emerging from the B secondary vertex. Heavy flavour contributions from gluon splitting are usually explicitly removed before fitting for the fragmentation functions. The studies in [258] fit the B spectrum using a Monte Carlo shower model supplemented with non-perturbative fragmentation functions yielding consistent results.

The experiments measure primarily the spectrum of B mesons. This defines a fragmentation function which includes the effect of the decay of higher mass excitations, like the B^* and B^{**}. In the literature, there is sometimes ambiguity in what is defined to be the bottom fragmentation function. Instead of using what is directly measured (*i.e.*, the B meson spectrum) corrections are applied to account for B^* or B^{**} production in some cases.

Heavy-flavor production in e^+e^- collisions is the primary source of information for the role of fragmentation effects in heavy-flavor production in hadron-hadron and lepton-hadron collisions. The QCD calculations tend to underestimate the data in certain regions of phase space. Some recent experimental results from LHC summarized in [261] show such deviations e.g. at high transverse jet momentum and also at low di-jet separation angles, see [262] for details, and were already theoretically investigated in [263].

Both bottomed- and charmed-mesons spectra have been measured at the Tevatron with unprecedented accuracy [264]. The measured spectra are in good agreement with QCD calculations (including non-perturbative fragmentation effects inferred from e^+e^- data [265]).

The HERA collaborations have produced a number of measurements of beauty production; see, for example, Refs. [255,266–269]. As for the Tevatron data, the HERA results are described well by QCD-based calculations using fragmentation models optimised with e^+e^- data.

Besides degrading the fragmentation function by gluon radiation, QCD evolution can also generate soft heavy quarks, increasing in the small x region as $\sqrt{s}$ increases. Several theoretical studies are available on the issue of how often $b\bar{b}$ or $c\bar{c}$ pairs are produced indirectly, via a gluon splitting mechanism [270–272]. Experimental results from studies on charm and bottom production via gluon splitting, given in [254,273–277], yield weighted averages of $\overline{n}_{g\to c\bar{c}} = 3.05 \pm 0.45\%$ and $\overline{n}_{g\to b\bar{b}} = 0.277 \pm 0.072\%$, respectively.

References:

1. G. Altarelli, Phys. Reports **81**, 1 (1982).
2. R.K. Ellis *et al.*, *QCD and Collider Physics*, Cambridge University Press (1996).
3. S. Albino *et al.*, `arXiv:0804.2021 [hep-ph]`.
4. F. Arleo, Eur. Phys. J. **C61**, 603 (2009).
5. P. Nason and B.R. Webber, Nucl. Phys. **B421**, 473 (1994); Erratum *ibid.* **B480**, 755 (1996).
6. ALEPH Collab.: D. Barate *et al.*, Phys. Lett. **B357**, 487 (1995); Erratum *ibid.*, **B364**, 247 (1995).
7. OPAL Collab.: R. Akers *et al.*, Z. Phys. **C68**, 203 (1995).
8. DELPHI Collab.: P. Abreu *et al.*, Eur. Phys. J. **C6**, 19 (1999).
9. W. Kittel and E.A. De Wolf, *Soft Multihadron Dynamics*, World Scientific (2005).
10. H.F. Jones, Nuovo Cimento **40A**, 1018 (1965); K.H. Streng *et al.*, Z. Phys. **C2**, 237 (1979).
11. V.N. Gribov and L.N. Lipatov, Sov. J. Nucl. Phys. **15**, 438 (1972); V.N. Gribov and L.N. Lipatov, Sov. J. Nucl. Phys. **15**, 675 (1972); G. Altarelli and G. Parisi, Nucl. Phys. **B126**, 298 (1977); Yu.L. Dokshitzer, Sov. Phys. JETP Lett. **46**, 641 (1977).
12. H. Georgi and H.D. Politzer, Nucl. Phys. **B136**, 445 (1978); J.F. Owens, Phys. Lett. **B76**, 85 (1978); T. Uematsu, Phys. Lett. **B79**, 97 (1978).
13. G. Curci *et al.*, Nucl. Phys. **B175**, 27 (1980).
14. W. Furmanski and R. Petronzio, Phys. Lett. **97B**, 437 (1980).
15. E.G. Floratos *et al.*, Nucl. Phys. **B192**, 417 (1981); T. Munehisa *et al.*, Prog. Theor. Phys. **67**, 609 (1982).
16. J. Kalinowski *et al.*, Nucl. Phys. **B181**, 221 (1981); J. Kalinowski *et al.*, Nucl. Phys. **B181**, 253 (1981).
17. M. Stratmann and W. Vogelsang, Nucl. Phys. **B496**, 41 (1997).
18. Yu.L. Dokshitzer *et al.*, Phys. Lett. **B634**, 504 (2006).
19. A. Mitov *et al.*, Phys. Lett. **B638**, 61 (2006).
20. S. Moch and A. Vogt, Phys. Lett. **B659**, 290 (2008).
21. A. A. Almasy, A. Vogt, and S. Moch, Nucl. Phys. **B854**, 133 (2013).
22. M. Cacciari *et al.*, JHEP **0604**, 006 (2006).
23. G. Altarelli *et al.*, Nucl. Phys. **B160**, 301 (1979); R. Baier and K. Fey, Z. Phys. **C2**, 339 (1979).
24. P.J. Rijken and W.L. van Neerven, Phys. Lett. **B386**, 422 (1996); P.J. Rijken and W.L. van Neerven, Phys. Lett. **B392**, 207 (1997); P.J. Rijken and W.L. van Neerven, Nucl. Phys. **B487**, 233 (1997).
25. A. Mitov and S. Moch, Nucl. Phys. **B751**, 18 (2006).
26. ALEPH Collab.: D. Buskulic *et al.*, Z. Phys. **C73**, 409 (1997).
27. ALEPH Collab.: E. Barate *et al.*, Phys. Reports **294**, 1 (1998).
28. L3 Collab.: B. Adeva *et al.*, Phys. Lett. **B259**, 199 (1991).
29. AMY Collab.: Y.K. Li *et al.*, Phys. Rev. **D41**, 2675 (1990).
30. HRS Collab.: D.Bender *et al.*, Phys. Rev. **D31**, 1 (1984).

31. MARK II Collab.: G.S. Abrams *et al.*, Phys. Rev. Lett. **64**, 1334 (1990).
32. MARK II Collab.: A. Petersen *et al.*, Phys. Rev. **D37**, 1 (1988).
33. OPAL Collab.: R. Akers *et al.*, Z. Phys. **C72**, 191 (1996).
34. OPAL Collab.: K. Ackerstaff *et al.*, Z. Phys. **C75**, 193 (1997).
35. OPAL Collab.: K. Ackerstaff *et al.*, Eur. Phys. J. **C7**, 369 (1998).
36. OPAL Collab.: G. Abbiendi *et al.*, Eur. Phys. J. **C16**, 185 (2000);
    OPAL Collab.: G. Abbiendi *et al.*, Eur. Phys. J. **C27**, 467 (2003).
37. OPAL Collab.: G. Abbiendi *et al.*, Eur. Phys. J. **C37**, 25 (2004).
38. SLD Collab.: K. Abe *et al.*, Phys. Rev. **D69**, 072003 (2004).
39. DELPHI Collab.: P. Abreu *et al.*, Phys. Lett. **B398**, 194 (1997).
40. TASSO Collab.: R. Brandelik *et al.*, Phys. Lett. **B114**, 65 (1982).
41. TASSO Collab.: W. Braunschweig *et al.*, Z. Phys. **C47**, 187 (1990).
42. TPC Collab.: H. Aihara *et al.*, Phys. Rev. Lett. **61**, 1263 (1988).
43. BELLE Collab.: M. Leitgab *et al.*, Phys. Rev. Lett. **111**, 062002 (2013);
    BaBar Collab.: J.P. Lees *et al.*, Phys. Rev. **D88**, 032011 (2013).
44. M. Cacciari and S. Catani, Nucl. Phys. **B617**, 253 (2001).
45. J. Blümlein and V. Ravindran, Phys. Lett. **B640**, 40 (2006).
46. S. Moch and A. Vogt, Phys. Lett. **B680**, 239 (2009).
47. S. Moch and A. Vogt, JHEP **0911**, 099 (2009).
48. A. Vogt, Phys. Lett. **B691**, 77 (2010).
49. P. Aurenche *et al.*, Eur. Phys. J. **C34**, 277 (2004);
    A. Daleo *et al.*, Phys. Rev. **D71**, 034013 (2005);
    B.A. Kniehl *et al.*, Nucl. Phys. **B711**, 345 (2005);
    Erratum *ibid.* **B720**, 231 (2005).
50. E665 Collab.: M.R. Adams *et al.*, Phys. Lett. **B272**, 163 (1991).
51. EMC Collab.: M. Arneodo *et al.*, Z. Phys. **C35**, 417 (1987).
52. H1 Collab.: I. Abt *et al.*, Z. Phys. **C63**, 377 (1994).
53. ZEUS Collab.: M. Derrick *et al.*, Z. Phys. **C70**, 1 (1996).
54. ZEUS Collab.: J. Breitweg *et al.*, Phys. Lett. **B414**, 428 (1997).
55. H1 Collab.: S. Aid *et al.*, Nucl. Phys. **B445**, 3 (1995).
56. ZEUS Collab.: M. Derrick *et al.*, Z. Phys. **C67**, 93 (1995).
57. H1 Collab.: C. Adloff *et al.*, Nucl. Phys. **B504**, 3 (1997).
58. ZEUS Collab.: J. Breitweg *et al.*, Eur. Phys. J. **C11**, 251 (1999).
59. H1 Collab.: F.D. Aaron *et al.*, Phys. Lett. **B654**, 148 (2007).
60. DELPHI Collab.: P. Abreu *et al.*, Phys. Lett. **B311**, 408 (1993).
61. MARK II Collab.: J.F. Patrick *et al.*, Phys. Rev. Lett. **49**, 1232, (1982).
62. ZEUS Collab.: S. Chekanov *et al.*, JHEP **0806**, 061 (2008).
63. A.H. Mueller, Phys. Lett. **B104**, 161 (1981).
64. A. Bassetto *et al.*, Nucl. Phys. **B207**, 189 (1982).
65. Yu.L. Dokshitzer *et al.*, Z. Phys. **C15**, 324 (1982).
66. A.H. Mueller, Nucl. Phys. **B213**, 85 (1983);
    Erratum in *ibid.* **B241**, 141 (196).
67. Yu.L. Dokshitzer *et al.*, Int. J. Mod. Phys. **A7**, 1875 (1992).
68. Yu.L. Dokshitzer *et al.*, *Basics of Perturbative QCD*, Editions Frontières (1991).
69. V.A. Khoze and W. Ochs, Int. J. Mod. Phys. **A12**, 2949 (1997).
70. C.P. Fong and B.R. Webber, Nucl. Phys. **B355**, 54 (1992).
71. S. Albino *et al.*, Nucl. Phys. **B851**, 86 (2011);
    S. Albino *et al.*, Nucl. Phys. **B855**, 801 (2012).
72. A. Vogt, JHEP **1110**, 025 (2011);
    C.-H. Kom, A. Vogt, and K. Yeats, JHEP **1210**, 033 (2012).
73. P. Bolzoni, B.A. Kniehl, and A.V. Kotikov, Phys. Rev. Lett. **109**, 242002 (2012);
    P. Bolzoni, B.A. Kniehl, and A.V. Kotikov, Nucl. Phys. **B875**, 18 (2013).
74. DELPHI Collab.: P. Abreu *et al.*, Z. Phys. **C73**, 11 (1996).
75. DELPHI Collab.: P. Abreu *et al.*, Z. Phys. **C73**, 229 (1997).
76. L3 Collab.: P. Achard *et al.*, Phys. Reports **399**, 71 (2004).
77. TOPAZ Collab.: R. Itoh *et al.*, Phys. Lett. **B345**, 335 (1995).
78. TASSO Collab.: W. Braunschweig *et al.*, Z. Phys. **C22**, 307 (1990).
79. OPAL Collab.: M.Z. Akrawy *et al.*, Phys. Lett. **B247**, 617 (1990).
80. BES Collab.: J.Z. Bai *et al.*, Phys. Rev. **D69**, 072002 (2004).
81. ALEPH Collab.: D. Buskulic *et al.*, Z. Phys. **C55**, 209 (1992).
82. ALEPH Collab.: A. Heister *et al.*, Eur. Phys. J. **C35**, 457 (2004).
83. DELPHI Collab.: P. Abreu *et al.*, Phys. Lett. **B275**, 231 (1992).
84. DELPHI Collab.: P. Abreu *et al.*, Eur. Phys. J. **C5**, 585 (1998).
85. DELPHI Collab.: P. Abreu *et al.*, Phys. Lett. **B459**, 397 (1999).
86. L3 Collab.: M. Acciarri *et al.*, Phys. Lett. **B444**, 569 (1998).
87. TPC/TWO-GAMMA Collab.: H. Aihara *et al.*, LBL 23737.
88. B.R. Webber, Phys. Lett. **B143**, 501 (1984).
89. Ya.I. Azimov *et al.*, Z. Phys. **C27**, 65 (1985).
90. J. Beringer *et al.*(Particle Data Group), Phys. Rev. **D86**, 010001 (2012).
91. Ya.I. Azimov *et al.*, Z. Phys. **C31**, 213 (1986).
92. I.M. Dremin and J.W. Gary, Phys. Reports **349**, 301 (2001).
93. I.M. Dremin and V.A. Nechitailo, Mod. Phys. Lett. **A9**, 1471 (1994).
94. S.J. Brodsky and J.F. Gunion, Phys. Rev. Lett. **37**, 402 (1976).
95. OPAL Collab.: P.D. Acton *et al.*, Z. Phys. **C53**, 539 (1992) and references therein.
96. ALEPH Collab.: D. Buskulic *et al.*, Z. Phys. **C69**, 15 (1996).
97. DELPHI Collab.: P. Abreu *et al.*, Phys. Lett. **B372**, 172 (1996).
98. DELPHI Collab.: P. Abreu *et al.*, Phys. Lett. **B416**, 233 (1998).
99. DELPHI Collab.: P. Abreu *et al.*, Eur. Phys. J. **C18**, 203 (2000).
100. L3 Collab.: M. Acciarri *et al.*, Phys. Lett. **B371**, 137 (1996).
101. L3 Collab.: M. Acciarri *et al.*, Phys. Lett. **B404**, 390 (1997).
102. L3 Collab.: M. Acciarri *et al.*, Phys. Lett. **B444**, 569 (1998).
103. TOPAZ Collab.: K. Nakabayashi *et al.*, Phys. Lett. **B413**, 447 (1997).
104. VENUS Collab.: K. Okabe *et al.*, Phys. Lett. **B423**, 407 (1998).
105. ARGUS Collab.: H. Albrecht *et al.*, Z. Phys. **C54**, 13 (1992).
106. H1 Collab.: F.D. Aaron *et al.*, Phys. Lett. **B654**, 148 (2007).
107. ZEUS Collab.: S. Chekanov *et al.*, Phys. Lett. **B510**, 36 (2001).
108. J. Benecke *et al.*, Nucl. Phys. **B76**, 29 (1976).
109. W.M. Morse *et al.*, Phys. Rev. **D15**, 66 (1977).
110. W. Thomé *et al.*, Nucl. Phys. **B129**, 365 (1977).
111. A. Breakstone *et al.*, Phys. Rev. **D30**, 528 (1984).
112. UA5 Collab.: G.J. Alner *et al.*, Phys. Reports **154**, 247 (1987).
113. UA5 Collab.: R.E. Ansorge *et al.*, Z. Phys. **C43**, 357 (1989).
114. UA1 Collab.: C. Albajar *et al.*, Nucl. Phys. **B335**, 261 (1990).
115. CDF Collab.: F.Abe *et al.*, Phys. Rev. **D41**, 2330 (1990).
116. ALICE Collab.: K. Aamodt *et al.*, Eur. Phys. J. **C68**, 89 (2010).
117. CMS Collab.: V. Khachatryan *et al.*, JHEP **1002**, 041 (2010).
118. CMS Collab.: V. Khachatryan *et al.*, JHEP **1101**, 079 (2011).
119. CMS Collab.: V. Khachatryan *et al.*, Phys. Rev. Lett. **105**, 022002 (2010).
120. P.V. Chliapnikov and V.A. Uvarov, Phys. Lett. **B251**, 192 (1990).
121. J.F. Grosse-Oetringhaus and K. Reygers, J. Phys. **G37**, 083001 (2010).
122. E.K.G. Sarkisyan and A.S. Sakharov, hep-ph/0410324;
    E.K.G. Sarkisyan and A.S. Sakharov, AIP Conf. Proc. **828**, 35 (2005), `hep-ph/0510191`;
    E.K.G. Sarkisyan and A.S. Sakharov, Eur. Phys. J. **C70**, 533 (2010).
123. S. Höche *et al.*, `arXiv:hep-ph/0602031`;
    J. Alwall *et al.*, Eur. Phys. J. **C53**, 473 (2008);
    S. Mrenna and P.Richardson, JHEP **0405**, 040 (2004).
124. X. Artru and G. Mennessier, Nucl. Phys. **B70**, 93 (1974).
125. B. Andersson *et al.*, Phys. Reports **97**, 31 (1983).
126. T. Sjöstrand and M. Bengtsson, Comp. Phys. Comm. **43**, 367 (1987);
    T. Sjöstrand, Comp. Phys. Comm. **82**, 74 (1994).
127. T. Sjöstrand, S. Mrenna, and P. Skands, JHEP **0605**, 026 (2006);

T. Sjöstrand, S. Mrenna, and P. Skands, Comp. Phys. Comm. **178**, 852 (2008).
128. S. Chun and C. Buchanan, Phys. Reports **292**, 239 (1998).
129. G. Marchesini *et al.*, Comp. Phys. Comm. **67**, 465 (1992); G. Corcella *et al.*, JHEP **0101**, 010 (2001); M. Bähr *et al.*, Eur. Phys. J. **C58**, 639 (2008).
130. T. Gleisberg *et al.*, JHEP **0902**, 007 (2009).
131. OPAL Collab.: G. Alexander *et al.*, Z. Phys. **C69**, 543 (1996).
132. D. de Florian *et al.*, Phys. Rev. **D76**, 074033 (2007); D. de Florian *et al.*, Phys. Rev. **D75**, 114010 (2007).
133. S. Albino *et al.*, Nucl. Phys. **B803**, 42 (2008).
134. S. Kretzer *et al.*, Eur. Phys. J. **C22**, 269 (2001).
135. S. Kretzer, Phys. Rev. **D62**, 054001 (2000).
136. L. Bourhis *et al.*, Eur. Phys. J. **C19**, 89 (2001).
137. M. Hirai *et al.*, Phys. Rev. **D75**, 094009 (2007).
138. C. Aidala *et al.*, Phys. Rev. **D83**, 034002 (2011).
139. ALEPH Collab.: R. Barate *et al.*, Eur. Phys. J. **C17**, 1 (2000); OPAL Collab.: R. Akers *et al.*, Z. Phys. **C68**, 179 (1995); OPAL Collab.: G. Abbiendi *et al.*, Eur. Phys. J. **C11**, 217 (1999).
140. M. Epele *et al.*, Phys. Rev. **D86**, 074028 (2012).
141. E. Witten, Nucl. Phys. **210**, 189 (1977).
142. L. Bourhis, M. Fontannaz and J. P. Guillet, Eur. Phys. J. **C2**, 529 (1998).
143. M. Gluck, E. Reya, and A. Vogt, Phys. Rev. **D48**, 116 (1993); Erratum *ibid.* **D51**, 1427 (1995).
144. SLD Collab.: K. Abe *et al.*, Phys. Rev. **D59**, 052001 (1999).
145. ALEPH Collab.: D. Buskulic *et al.*, Z. Phys. **C66**, 355 (1995); ARGUS Collab.: H. Albrecht *et al.*, Z. Phys. **C44**, 547 (1989); OPAL Collab.: R. Akers *et al.*, Z. Phys. **C63**, 181 (1994).
146. DELPHI Collab.: P. Abreu *et al.*, Eur. Phys. J. **C13**, 573 (2000).
147. B.A. Kniehl *et al.*, Phys. Rev. Lett. **85**, 5288 (2000).
148. E665 Collab.: M.R. Adams *et al.*, Z. Phys. **C61**, 539 (1994).
149. EMC Collab.: J.J. Aubert *et al.*, Z. Phys. **C18**, 189 (1983); EMC Collab.: M. Arneodo *et al.*, Phys. Lett. **B150**, 458 (1985).
150. EMC Collab.: M. Arneodo *et al.*, Z. Phys. **C33**, 167 (1986).
151. EMC Collab.: M. Arneodo *et al.*, Z. Phys. **C34**, 283 (1987).
152. HERMES Collab.: A. Airapetian *et al.*, Eur. Phys. J. **C21**, 599 (2001).
153. HERMES Collab.: A. Airapetian *et al.*, Phys. Rev. **D87**, 074029 (2013).
154. COMPASS Collab.: N. Makke, `arXiv:1307.3407 [hep-ex]`.
155. T.P. M$^{\rm c}$Pharlin *et al.*, Phys. Lett. **B90**, 479 (1980).
156. H1 Collab.: S. Aid *et al.*, Nucl. Phys. **B480**, 3 (1996).
157. H1 Collab.: C. Adloff *et al.*, Eur. Phys. J. **C18**, 293 (2000); H1 Collab.: A. Aktas *et al.*, Eur. Phys. J. **C36**, 413 (2004).
158. ZEUS Collab.: M. Derrick *et al.*, Z. Phys. **C68**, 29 (1995); ZEUS Collab.: J. Breitweg *et al.*, Eur. Phys. J. **C2**, 77 (1998).
159. ZEUS Collab.: S. Chekanov *et al.*, Phys. Lett. **B553**, 141 (2003).
160. ZEUS Collab.: S. Chekanov *et al.*, Nucl. Phys. **B786**, 181 (2007).
161. H1 Collab.: F. D. Aaron *et al.*, Eur. Phys. J. **C61**, 185 (2009).
162. H1 Collab.: F. D. Aaron *et al.*, Phys. Lett. **B673**, 119 (2009).
163. P. Dixon *et al.*, J. Phys. **G25**, 1453 (1999).
164. H1 Collab.: C. Adloff *et al.*, Phys. Lett. **B462**, 440 (1999).
165. D. Graudenz, Fortsch. Phys. **45**, 629 (1997).
166. S. Albino *et al.*, Phys. Rev. **D75**, 034018 (2007).
167. OPAL Collab.: P.D. Acton *et al.*, Phys. Lett. **B305**, 407 (1993).
168. E632 Collab.: D. DeProspo *et al.*, Phys. Rev. **D50**, 6691 (1994).
169. ZEUS Collab.: S. Chekanov *et al.*, Eur. Phys. J. **C51**, 1 (2007).
170. G. Grindhammer *et al.*, in: *Proceedings of the Workshop on Monte Carlo Generators for HERA Physics*, Hamburg, Germany, 1998/1999.
171. N. Brook *et al.*, in: *Proceedings of the Workshop for Future HERA Physics at HERA*, Hamburg, Germany, 1996.
172. CDF Collab.: F. Abe *et al.*, Phys. Rev. Lett. **61**, 1819 (1988).
173. CDF Collab.: D. E. Acosta *et al.*, Phys. Rev. **D72**, 052001 (2005).
174. UA1 Collab.: G. Arnison *et al.*, Phys. Lett. **B118**, 167 (1982).
175. UA1 Collab.: C. Albajar *et al.*, Nucl. Phys. **B335**, 261 (1990).
176. UA1 Collab.: G. Bocquet *et al.*, Phys. Lett. **B366**, 434 (1996).
177. UA2 Collab.:M. Banner *et al.*, Phys. Lett. **B122**, 322 (1983).
178. UA2 Collab.:M. Banner *et al.*, Phys. Lett. **B115**, 59 (1982).
179. UA2 Collab.:M. Banner *et al.*, Z. Phys. **C27**, 329 (1985).
180. PHENIX Collab.: S. S. Adler *et al.*, Phys. Rev. Lett. **91**, 241803 (2003).
181. PHENIX Collab.: A. Adare *et al.*, Phys. Rev. **D76**, 051106 (2007).
182. BRAHMS Collab.:, I. Arsene *et al.*, Phys. Rev. Lett. **98**, 252001 (2007).
183. STAR Collab.: J. Adams *et al.*, Phys. Lett. **B637**, 161 (2006).
184. STAR Collab.:, J. Adams *et al.*, Phys. Rev. Lett. **97**, 152302 (2006).
185. STAR Collab.: B. I. Abelev *et al.*, Phys. Rev. **C75**, 064901 (2007).
186. STAR Collab.:, G. Agakishiev *et al.*, Phys. Rev. Lett. **108**, 072302 (2012).
187. STAR Collab.: B. I. Abelev *et al.*, Phys. Rev. **C81**, 064904 (2010).
188. ALICE Collab.: B. Abelev *et al.*, Phys. Lett. **B717**, 162 (2012).
189. ALICE B. Abelev *et al.*, `arXiv:1307.1093 [nucl-ex]`.
190. E706 Collab.: L. Apanasevich *et al.*, Phys. Rev. Lett. **81**, 2642 (1998).
191. UA6 Collab.: G. Ballocchi *et al.*, Phys. Lett. **B436**, 222 (1998).
192. WA70 Collab.: M. Bonesini *et al.*, Z. Phys. **C38**, 371 (1988).
193. AFS Collab.: E. Anassontzis *et al.*, Sov. J. Nucl. Phys. **51**, 836 (1990).
194. R806 Collab.: C. Kourkoumelis *et al.*, Z. Phys. **C5**, 95 (1980).
195. E706 Collab.: L. Apanasevich *et al.*, Phys. Rev. **D68**, 052001 (2003).
196. F. Aversa *et al.*, Nucl. Phys. **B327**, 105 (1989); D. de Florian, Phys. Rev. **D67**, 054004 (2003); B. Jager *et al.*, Phys. Rev. **D67**, 054005 (2003).
197. U. Baur *et al.*, `arXiv:hep-ph/0005226`.
198. P. Aurenche, *et al.*, Eur. Phys. J. **C13**, 347 (2000).
199. L. Apanasevich *et al.*, Phys. Rev. **D59**, 074007 (1999).
200. U. D'Alesio and F. Murgia, Phys. Rev. **D70**, 074009 (2004).
201. D. de Florian and W. Vogelsang, Phys. Rev. **D71**, 114004 (2005).
202. L. G. Almeida *et al.*, Phys. Rev. **D80**, 074016 (2009).
203. PHENIX Collab.: A. Adare *et al.*, Phys. Rev. **D76**, 051106 (2007).
204. PHENIX Collab.: A. Adare *et al.*, Phys. Rev. **D79**, 012003 (2009).
205. PHENIX Collab.: K. Adcox *et al.*, Phys. Rev. Lett. **88**, 022301 (2002); STAR Collab.: C. Adler *et al.*, Phys. Rev. Lett. **90**, 082302 (2003).
206. COMPASS Collab.: M. Alekseev *et al.*, Phys. Lett. **B660**, 458, (2008).
207. HERMES Collab.: A. Airapetian *et al.*, Phys. Rev. **D71**, 012003 (2005).
208. SMC Collab.: B. Adeva *et al.*, Phys. Lett. **B420**, 180 (1998).
209. HERMES Collab.: A. Airapetian *et al.*, Phys. Lett. **B666**, 446 (2008).
210. D. de Florian *et al.*, Phys. Rev. Lett. **101**, 072001 (2008).
211. P.J. Mulders and R.D. Tangerman, Nucl. Phys. **B461**, 197 (1996); Erratum *ibid.*, **B484**, 538 (1997).
212. R. Jacob, Nucl. Phys. **A711**, 35 (2002).
213. COMPASS Collab.: M. Alekseev *et al.*, Eur. Phys. J. **C64**, 171 (2009).
214. HERMES Collab.: A. Airapetian *et al.*, Phys. Rev. **D74**, 072004 (2006).
215. J.P. Ralston and D.E. Soper, Nucl. Phys. **B152**, 109 (1979).
216. J. Collins, Nucl. Phys. **B396**, 161 (1993).
217. D. Sivers, Phys. Rev. **D43**, 261 (1991).
218. CLAS Collab.: H. Avakian *et al.*, Phys. Rev. **D69**, 112004 (2004).

219. HERMES Collab.: A. Airapetian *et al.*, Phys. Rev. Lett. **84**, 4047 (2000).
220. HERMES Collab.: A. Airapetian *et al.*, Phys. Rev. **D64**, 097101 (2001).
221. HERMES Collab.: A. Airapetian *et al.*, Phys. Rev. Lett. **94**, 012002 (2005).
222. BELLE Collab.: K. Abe *et al.*, Phys. Rev. Lett. **96**, 232002 (2006).
223. BELLE Collab.: K. Abe *et al.*, Phys. Rev. **D78**, 032011 (2008).
224. COMPASS Collab.: V.Y Alexakhin *et al.*, Phys. Rev. Lett. **94**, 202002 (2005).
225. COMPASS Collab.: V.Y Alexakhin *et al.*, Nucl. Phys. **B765**, 31 (2007).
226. COMPASS Collab.: M. Alekseev *et al.*, Phys. Lett. **B673**, 127 (2009).
227. COMPASS Collab.: M. Alekseev *et al.*, Phys. Lett. **B692**, 240 (2010).
228. COMPASS Collab.: M. Alekseev *et al.*, Eur. Phys. J. **C70**, 39 (2010).
229. V.A. Khoze *et al.*, *Proceedings, Conference on High-Energy Physics, Tbilisi 1976*;
J.D. Bjorken, Phys. Rev. **D17**, 171 (1978).
230. B. Mele and P. Nason, Phys. Lett. **B245**, 635 (1990);
B. Mele and P. Nason, Nucl. Phys. **B361**, 626 (1991).
231. P. Nason and C. Oleari, Phys. Lett. **B418**, 199 (1998);
P. Nason and C. Oleari, Phys. Lett. **B447**, 327 (1999);
P. Nason and C. Oleari, Nucl. Phys. **B565**, 245 (2000).
232. K. Melnikov and A. Mitov, Phys. Rev. **D70**, 034027 (2004).
233. C. Peterson *et al.*, Phys. Rev. **D27**, 105 (1983).
234. V.G. Kartvelishvili *et al.*, Phys. Lett. **B78**, 615 (1978).
235. P. Collins and T. Spiller, J. Phys. **G11**, 1289 (1985).
236. G. Colangelo and P. Nason, Phys. Lett. **B285**, 167 (1992).
237. M.G. Bowler, Z. Phys. **C11**, 169 (1981).
238. E. Braaten *et al.*, Phys. Rev. **D51**, 4819 (1995).
239. OPAL Collab.: R. Akers *et al.*, Z. Phys. **C67**, 27 (1995).
240. Particle Data Group: C. Amsler *et al.*, Phys. Lett. **B667**, 1 (2008).
241. J. Chrin, Z. Phys. **C36**, 163 (1987).
242. R.L. Jaffe and L. Randall, Nucl. Phys. **B412**, 79 (1994).
243. M. Cacciari and E. Gardi, Nucl. Phys. **B664**, 299 (2003).
244. L. Randall and N. Rius, Nucl. Phys. **B441**, 167 (1995).
245. J. Collins, Phys. Rev. **D58**, 094002 (1998).
246. B.A. Kniehl *et al.*, Eur. Phys. J. **C41**, 199 (2005).
247. CLEO Collab.: M. Artuso *et al.*, Phys. Rev. **D70**, 112001 (2004).
248. BELLE Collab.: R. Seuster *et al.*, Phys. Rev. **D73**, 032002 (2006).
249. CLEO Collab.: R.A. Briere *et al.*, Phys. Rev. **D62**, 112003 (2000).
250. BABAR Collab.: B. Aubert *et al.*, Phys. Rev. **D65**, 091104 (2002).
251. CLEO Collab.: D. Bortoletto *et al.*, Phys. Rev. **D37**, 1719 (1988).
252. ARGUS Collab.: H. Albrecht *et al.*, Z. Phys. **C52**, 353 (1991).
253. ARGUS Collab.: H. Albrecht *et al.*, Z. Phys. **C54**, 1 (1992).
254. ALEPH Collab.: R. Barate *et al.*, Phys. Lett. **B561**, 213 (2003).
255. H1 Collab.: F.D. Aaron *et al.*, Eur. Phys. J. **C65**, 89 (2010).
256. ZEUS Collab.: S. Chekanov *et al.*, JHEP **0707**, 074 (2007);
ZEUS Collab: H. Abramowicz *et al.*, arXiv:1306.4862(2013);
H1 Collab.: A. Aktas *et al.*, Eur. Phys. J. **C51**, 271 (2007);
H1 Collab.: F. D. Aaron *et al.*, Eur. Phys. J. **C59**, 589 (2009).
257. ALEPH Collab.: D. Buskulic *et al.*, Phys. Lett. **B357**, 699 (1995).
258. ALEPH Collab.: A. Heister *et al.*, Phys. Lett. **B512**, 30 (2001);
DELPHI Collab.: J. Abdallah *et al.*, Eur. Phys. J. **C71**, 1557 (2011);
OPAL Collab.: G. Abbiendi *et al.*, Eur. Phys. J. **C29**, 463 (2003);
SLD Collab.: K. Abe *et al.*, Phys. Rev. **D65**, 092006 (2002);
Erratum *ibid.*, **D66**, 079905 (2002).
259. L3 Collab.: B. Adeva *et al.*, Phys. Lett. **B261**, 177 (1991).
260. CDF Collab.: F. Abe *et al.*, Phys. Rev. Lett. **71**, 500 (1993);
CDF Collab.: F. Abe *et al.*, Phys. Rev. Lett. **71**, 2396 (1993);
CDF Collab.: F. Abe *et al.*, Phys. Rev. **D50**, 4252 (1994);
CDF Collab.: F. Abe *et al.*, Phys. Rev. Lett. **75**, 1451 (1995);
CDF Collab.: D. Acosta *et al.*, Phys. Rev. **D66**, 032002 (2002);
CDF Collab.: D. Acosta *et al.*, Phys. Rev. **D65**, 052005 (2002);
D0 Collab.: S. Abachi *et al.*, Phys. Rev. Lett. **74**, 3548 (1995);
UA1 Collab.: C. Albajar *et al.*, Phys. Lett. **B186**, 237 (1987);
UA1 Collab.: C. Albajar *et al.*, Phys. Lett. **B256**, 121 (1991);
Erratum *ibid.*, **B272**, 497 (1991).
261. H. Evans, arXiv:1110.5294 [hep-ex];
E. Aguiló, arXiv:1205.5278 [hep-ex];
F. Simonetto, Journal of Physics: Conference Series **347**, 012014 (2012).
262. CMS Collab.: V. Khachatryan *et al.*, JHEP **1103**, 136 (2011);
ATLAS Collab.: G. Aad *et al.*, Eur. Phys. J. **C71**, 1846 (2011);
CMS Collab.: S. Chatrychyan *et al.*, JHEP **1204**, 084 (2012);
ATLAS Collab.: G. Aad *et al.*, Eur. Phys. J. **C73**, 2301 (2013).
263. H. Jung *et al.*, Phys. Rev. **D85**, 034035 (2012).
264. CDF Collab.: D. Acosta *et al.*, Phys. Rev. Lett. **91**, 241804 (2003);
CDF Collab.: D. Acosta *et al.*, Phys. Rev. **D71**, 032001 (2005).
265. M. Cacciari and P. Nason, JHEP **0309**, 006 (2003);
M. Cacciari *et al.*, JHEP **0407**, 033 (2004);
B.A. Kniehl *et al.*, Phys. Rev. Lett. **96**, 012001 (2006).
266. ZEUS Collab.: H. Abramovicz *et al.*, Eur. Phys. J. **C71**, 1573 (2011).
267. ZEUS Collab.: S. Chekanov *et al.*, Phys. Rev. **D78**, 072001 (2008).
268. ZEUS Collab.: S. Chekanov *et al.*, JHEP **0902**, 032 (2009).
269. H1 Collab.: F.D. Aaron *et al.*, Eur. Phys. J. **C72**, 2148 (2012).
270. A.H. Mueller and P. Nason, Nucl. Phys. **B266**, 265 (1986);
M.L. Mangano and P. Nason, Phys. Lett. **B285**, 160 (1992).
271. M.H. Seymour, Nucl. Phys. **B436**, 163 (1995).
272. D.J. Miller and M.H. Seymour, Phys. Lett. **B435**, 213 (1998).
273. ALEPH Collab.: R. Barate *et al.*, Phys. Lett. **B434**, 437 (1998).
274. DELPHI Collab.: P. Abreu *et al.*, Phys. Lett. **B405**, 202 (1997).
275. L3 Collab.: M. Acciarri *et al.*, Phys. Lett. **B476**, 243 (2000).
276. OPAL Collab.: G. Abbiendi *et al.*, Eur. Phys. J. **C13**, 1 (2000).
277. SLD Collab.: K. Abe *et al.*, SLAC-PUB-8157, hep-ex/9908028.

21. EXPERIMENTAL TESTS OF GRAVITATIONAL THEORY

Revised September 2013 by T. Damour (IHES, Bures-sur-Yvette, France).

Einstein's General Relativity, the current "standard" theory of gravitation, describes gravity as a universal deformation of the Minkowski metric:

$$g_{\mu\nu}(x^\lambda) = \eta_{\mu\nu} + h_{\mu\nu}(x^\lambda) \ , \text{ where } \eta_{\mu\nu} = \mathrm{diag}(-1,+1,+1,+1) \ . \quad (21.1)$$

General Relativity is classically defined by two postulates. One postulate states that the Lagrangian density describing the propagation and self-interaction of the gravitational field is

$$\mathcal{L}_{\rm Ein}[g_{\mu\nu}] = \frac{c^4}{16\pi G_N}\sqrt{g} g^{\mu\nu} R_{\mu\nu}(g) \ , \quad (21.2)$$

$$R_{\mu\nu}(g) = \partial_\alpha \Gamma^\alpha_{\mu\nu} - \partial_\nu \Gamma^\alpha_{\mu\alpha} + \Gamma^\beta_{\alpha\beta}\Gamma^\alpha_{\mu\nu} - \Gamma^\beta_{\alpha\nu}\Gamma^\alpha_{\mu\beta} \ , \quad (21.3)$$

$$\Gamma^\lambda_{\mu\nu} = \tfrac{1}{2} g^{\lambda\sigma}(\partial_\mu g_{\nu\sigma} + \partial_\nu g_{\mu\sigma} - \partial_\sigma g_{\mu\nu}) \ , \quad (21.4)$$

where G_N is Newton's constant, $g = -\det(g_{\mu\nu})$, and $g^{\mu\nu}$ is the matrix inverse of $g_{\mu\nu}$. A second postulate states that $g_{\mu\nu}$ couples universally, and minimally, to all the fields of the Standard Model by replacing everywhere the Minkowski metric $\eta_{\mu\nu}$. Schematically (suppressing matrix indices and labels for the various gauge fields and fermions and for the Higgs doublet),

$$\mathcal{L}_{\rm SM}[\psi, A_\mu, H, g_{\mu\nu}] = -\tfrac{1}{4}\sum \sqrt{g} g^{\mu\alpha} g^{\nu\beta} F^a_{\mu\nu} F^a_{\alpha\beta} - \sum \sqrt{g}\,\overline{\psi}\,\gamma^\mu D_\mu \psi$$
$$-\tfrac{1}{2}\sqrt{g} g^{\mu\nu}\overline{D_\mu H} D_\nu H - \sqrt{g}\,V(H) - \sum \lambda \sqrt{g}\,\overline{\psi}\,H\psi \ , \quad (21.5)$$

where $\gamma^\mu\gamma^\nu + \gamma^\nu\gamma^\mu = 2g^{\mu\nu}$, and where the covariant derivative D_μ contains, besides the usual gauge field terms, a spin-dependent gravitational contribution. From the total action follow Einstein's field equations,

$$R_{\mu\nu} - \tfrac{1}{2} R g_{\mu\nu} = \frac{8\pi G_N}{c^4} T_{\mu\nu} \ . \quad (21.6)$$

Here $R = g^{\mu\nu}R_{\mu\nu}$, $T_{\mu\nu} = g_{\mu\alpha}g_{\nu\beta}T^{\alpha\beta}$, and $T^{\mu\nu} = (2/\sqrt{g})\delta\mathcal{L}_{\rm SM}/\delta g_{\mu\nu}$ is the (symmetric) energy-momentum tensor of the Standard Model matter. The theory is invariant under arbitrary coordinate transformations: $x'^\mu = f^\mu(x^\nu)$. To solve the field equations Eq. (21.6), one needs to fix this coordinate gauge freedom. *E.g.*, the "harmonic gauge" (which is the analogue of the Lorenz gauge, $\partial_\mu A^\mu = 0$, in electromagnetism) corresponds to imposing the condition $\partial_\nu(\sqrt{g}g^{\mu\nu}) = 0$.

In this *Review*, we only consider the classical limit of gravitation (*i.e.* classical matter and classical gravity). Considering quantum matter in a classical gravitational background already poses interesting challenges, notably the possibility that the zero-point fluctuations of the matter fields generate a nonvanishing vacuum energy density $\rho_{\rm vac}$, corresponding to a term $-\sqrt{g}\ \rho_{\rm vac}$ in $\mathcal{L}_{\rm SM}$ [1]. This is equivalent to adding a "cosmological constant" term $+\Lambda\, g_{\mu\nu}$ on the left-hand side of Einstein's equations Eq. (21.6), with $\Lambda = 8\pi G_N\, \rho_{\rm vac}/c^4$. Recent cosmological observations (see the following *Reviews*) suggest a positive value of Λ corresponding to $\rho_{\rm vac} \approx (2.3\times 10^{-3}{\rm eV})^4$. Such a small value has a negligible effect on the (non cosmological) tests discussed below.

21.1. Experimental tests of the coupling between matter and gravity

The universality of the coupling between $g_{\mu\nu}$ and the Standard Model matter postulated in Eq. (21.5) ("Equivalence Principle") has many observable consequences [2]. First, it predicts that the outcome of a local non-gravitational experiment, referred to local standards, does not depend on where, when, and in which locally inertial frame, the experiment is performed. This means, for instance, that local experiments should neither feel the cosmological evolution of the universe (constancy of the "constants"), nor exhibit preferred directions in spacetime (isotropy of space, local Lorentz invariance). These predictions are consistent with many experiments and observations. Stringent limits on a possible time variation of the basic coupling constants have been obtained by analyzing a natural fission reactor phenomenon which took place at Oklo, Gabon, two billion years ago [3,4]. These limits are at the 1×10^{-7} level for the fractional variation of the fine-structure constant $\alpha_{\rm em}$ [4], and at the 4×10^{-9} level for the fractional variation of the ratio m_q/Λ_{QCD} between the light quark masses and Λ_{QCD} [5]. The determination of the lifetime of Rhenium 187 from isotopic measurements of some meteorites dating back to the formation of the solar system (about 4.6 Gyr ago) yields comparably strong limits [6]. Measurements of absorption lines in astronomical spectra also give stringent limits on the variability of both $\alpha_{\rm em}$ (at the 10^{-5} level [7]) , and $\mu = m_p/m_e$, e.g.

$$|\Delta\mu/\mu| < 1.8\times 10^{-6} (95\%\ C.L.) \ , \quad (21.7)$$

at a redshift $z = 0.68466$ [8], and $\Delta\mu/\mu = (0.3 \pm 3.2_{\rm stat} \pm 1.9_{\rm sys})\times 10^{-6}$ at the large redshift $z = 2.811$ [9]. Direct laboratory limits (based on monitoring the frequency ratio of several different atomic clocks) on the present time variation of $\alpha_{\rm em}$, $\mu = m_p/m_e$, and m_q/Λ_{QCD} have reached the levels [10]:

$$d\ln(\alpha_{\rm em})/dt = (-2.5\pm 2.6)\times 10^{-17}{\rm yr}^{-1},$$
$$d\ln(\mu)/dt = (-1.5\pm 3.0)\times 10^{-16}{\rm yr}^{-1},$$
$$d\ln(m_q/\Lambda_{QCD})/dt = (7.1\pm 4.4)\times 10^{-15}{\rm yr}^{-1}. \quad (21.8)$$

There are also experimental limits on a possible dependence of coupling constants on the gravitational potential [10,11]. See Ref. 12 for a review of the issue of "variable constants."

The highest precision tests of the isotropy of space have been performed by looking for possible quadrupolar shifts of nuclear energy levels [13]. The (null) results can be interpreted as testing the fact that the various pieces in the matter Lagrangian Eq. (21.5) are indeed coupled to one and the same external metric $g_{\mu\nu}$ to the 10^{-29} level. For astrophysical constraints on possible Planck-scale violations of Lorentz invariance, see Ref. 14.

The universal coupling to $g_{\mu\nu}$ postulated in Eq. (21.5) implies that two (electrically neutral) test bodies dropped at the same location and with the same velocity in an external gravitational field fall in the same way, independently of their masses and compositions. The universality of the acceleration of free fall has been verified at the 10^{-13} level for laboratory bodies, notably Beryllium-Titanium, and Beryllium-Aluminum test bodies [15,16],

$$(\Delta a/a)_{\rm BeTi} = (0.3\pm 1.8)\times 10^{-13} \ ,$$
$$(\Delta a/a)_{\rm BeAl} = (-0.7\pm 1.3)\times 10^{-13} \ , \quad (21.9)$$

as well as for the gravitational accelerations of the Earth and the Moon toward the Sun [17],

$$(\Delta a/a)_{\rm EarthMoon} = (-0.8\pm 1.3)\times 10^{-13} \ . \quad (21.10)$$

The latter result constrains not only how $g_{\mu\nu}$ couples to matter, but also how it couples to itself [18]("strong equivalence principle"; see Eq. (21.16) below, and the end of the section on binary pulsar tests). See also Ref. 19 for a review of torsion balance experiments.

Finally, Eq. (21.5) also implies that two identically constructed clocks located at two different positions in a static external Newtonian potential $U(\boldsymbol{x}) = \sum G_N m/r$ exhibit, when intercompared by means of electromagnetic signals, the (apparent) difference in clock rate, $\tau_1/\tau_2 = \nu_2/\nu_1 = 1 + [U(\boldsymbol{x}_1) - U(\boldsymbol{x}_2)]/c^2 + O(1/c^4)$, independently of their nature and constitution. This universal gravitational redshift of clock rates has been verified at the 10^{-4} level by comparing a hydrogen-maser clock flying on a rocket up to an altitude $\sim 10,000$ km to a similar clock on the ground [20]. The redshift due to a height change of only 33 cm has been detected by comparing two optical clocks based on $^{27}{\rm Al}^+$ ions [21].

21.2. Tests of the dynamics of the gravitational field in the weak field regime

The effect on matter of one-graviton exchange, *i.e.*, the interaction Lagrangian obtained when solving Einstein's field equations Eq. (21.6) written in, say, the harmonic gauge at first order in $h_{\mu\nu}$,

$$\Box h_{\mu\nu} = -\frac{16\pi G_N}{c^4}(T_{\mu\nu} - \tfrac{1}{2}T\eta_{\mu\nu}) + O(h^2) + O(hT) \ , \qquad (21.11)$$

reads $-(8\pi G_N/c^4)T^{\mu\nu}\Box^{-1}(T_{\mu\nu} - \frac{1}{2}T\eta_{\mu\nu})$. For a system of N moving point masses, with free Lagrangian $L^{(1)} = \sum_{A=1}^{N} - m_A c^2\sqrt{1 - \boldsymbol{v}_A^2/c^2}$, this interaction, expanded to order v^2/c^2, reads (with $r_{AB} \equiv |\boldsymbol{x}_A - \boldsymbol{x}_B|$, $\boldsymbol{n}_{AB} \equiv (\boldsymbol{x}_A - \boldsymbol{x}_B)/r_{AB}$)

$$L^{(2)} = \tfrac{1}{2}\sum_{A\neq B}\frac{G_N\, m_A\, m_B}{r_{AB}}\Big[1 + \frac{3}{2c^2}(\boldsymbol{v}_A^2 + \boldsymbol{v}_B^2) - \frac{7}{2c^2}(\boldsymbol{v}_A\cdot\boldsymbol{v}_B) - \frac{1}{2c^2}(\boldsymbol{n}_{AB}\cdot\boldsymbol{v}_A)(\boldsymbol{n}_{AB}\cdot\boldsymbol{v}_B) + O\left(\frac{1}{c^4}\right)\Big] \ . \qquad (21.12)$$

The two-body interactions, Eq. (21.12), exhibit v^2/c^2 corrections to Newton's $1/r$ potential induced by spin-2 exchange ("gravito-magnetism"). Consistency at the "post-Newtonian" level $v^2/c^2 \sim G_N\, m/rc^2$ requires that one also considers the three-body interactions induced by some of the three-graviton vertices and other nonlinearities (terms $O(h^2)$ and $O(hT)$ in Eq. (21.11)),

$$L^{(3)} = -\frac{1}{2}\sum_{B\neq A\neq C}\frac{G_N^2\, m_A\, m_B\, m_C}{r_{AB}\, r_{AC}\, c^2} + O\left(\frac{1}{c^4}\right) \ . \qquad (21.13)$$

All currently performed gravitational experiments in the solar system, including perihelion advances of planetary orbits, the bending and delay of electromagnetic signals passing near the Sun, and very accurate ranging data to the Moon obtained by laser echoes, are compatible with the post-Newtonian results Eqs. (21.11)–(21.13). The "gravito-magnetic" interactions $\propto v_A v_B$ contained in Eq. (21.12) are involved in many of these experimental tests. They have been particularly tested in lunar laser ranging data [17], in the LAGEOS satellite observations [22,23], and in the dedicated Gravity Probe B mission [24]. The recently launched LARES satellite promises to improve the accuracy of such tests [23].

Similar to what is done in discussions of precision electroweak experiments, it is useful to quantify the significance of precision gravitational experiments by parameterizing plausible deviations from General Relativity. The addition of a mass-term in Einstein's field equations leads to a score of theoretical difficulties which have not yet received any consensual solution. We shall, therefore, not consider here the ill-defined "mass of the graviton" as a possible deviation parameter from General Relativity (see, however, Ref. 25). Deviations from Einstein's pure spin-2 theory are then defined by adding new, bosonic light or massless, macroscopically coupled fields. The possibility of new gravitational-strength couplings leading (on small, and possibly large, scales) to deviations from Einsteinian (and Newtonian) gravity is suggested by String Theory [26], and by Brane World ideas [27]. For reviews of experimental constraints on Yukawa-type additional interactions, see Refs. [19,28,16]. Experiments have set limits on non-Newtonian forces down to 0.056 mm [29].

Here, we shall focus on the parametrization of long-range deviations from relativistic gravity obtained by adding a strictly massless (*i.e.* without self-interaction $V(\varphi) = 0$) scalar field φ coupled to the trace of the energy-momentum tensor $T = g_{\mu\nu}T^{\mu\nu}$ [30]. The most general such theory contains an arbitrary function $a(\varphi)$ of the scalar field, and can be defined by the Lagrangian

$$\mathcal{L}_{\rm tot}[g_{\mu\nu},\varphi,\psi,A_\mu,H] = \frac{c^4}{16\pi G}\sqrt{g}(R(g_{\mu\nu}) - 2g^{\mu\nu}\partial_\mu\varphi\partial_\nu\varphi) + \mathcal{L}_{\rm SM}[\psi, A_\mu, H, \widetilde{g}_{\mu\nu}] \ , \qquad (21.14)$$

where G is a "bare" Newton constant, and where the Standard Model matter is coupled not to the "Einstein" (pure spin-2) metric $g_{\mu\nu}$, but to the conformally related ("Jordan-Fierz") metric $\widetilde{g}_{\mu\nu} = \exp(2a(\varphi))g_{\mu\nu}$. The scalar field equation $\Box_g\varphi = -(4\pi G/c^4)\alpha(\varphi)T$ displays $\alpha(\varphi) \equiv \partial a(\varphi)/\partial\varphi$ as the basic (field-dependent) coupling between φ and matter [31]. The one-parameter (ω) Jordan-Fierz-Brans-Dicke theory [30] is the special case $a(\varphi) = \alpha_0\varphi$ leading to a field-independent coupling $\alpha(\varphi) = \alpha_0$ (with ${\alpha_0}^2 = 1/(2\omega + 3)$). The addition of a self-interaction term $V(\varphi)$ in Eq. (21.14) introduces new phenomenological possibilities; notably the "chameleon mechanism" [32].

In the weak-field slow-motion limit appropriate to describing gravitational experiments in the solar system, the addition of φ modifies Einstein's predictions only through the appearance of two "post-Einstein" dimensionless parameters: $\overline{\gamma} = -2\alpha_0^2/(1+\alpha_0^2)$ and $\overline{\beta} = +\frac{1}{2}\beta_0\alpha_0^2/(1+\alpha_0^2)^2$, where $\alpha_0 \equiv \alpha(\varphi_0)$, $\beta_0 \equiv \partial\alpha(\varphi_0)/\partial\varphi_0$, φ_0 denoting the vacuum expectation value of φ. These parameters show up also naturally (in the form $\gamma_{\rm PPN} = 1+\overline{\gamma}$, $\beta_{\rm PPN} = 1+\overline{\beta}$) in phenomenological discussions of possible deviations from General Relativity [2]. The parameter $\overline{\gamma}$ measures the admixture of spin 0 to Einstein's graviton, and contributes an extra term $+\overline{\gamma}(\boldsymbol{v}_A - \boldsymbol{v}_B)^2/c^2$ in the square brackets of the two-body Lagrangian Eq. (21.12). The parameter $\overline{\beta}$ modifies the three-body interaction Eq. (21.13) by an overall multiplicative factor $1 + 2\overline{\beta}$. Moreover, the combination $\eta \equiv 4\overline{\beta} - \overline{\gamma}$ parameterizes the lowest order effect of the self-gravity of orbiting masses by modifying the Newtonian interaction energy terms in Eq. (21.12) into $G_{AB}m_A m_B/r_{AB}$, with a body-dependent gravitational "constant" $G_{AB} = G_N[1 + \eta(E_A^{\rm grav}/m_A c^2 + E_B^{\rm grav}/m_B c^2) + O(1/c^4)]$, where $G_N = G\exp[2a(\varphi_0)](1+\alpha_0^2)$ and where $E_A^{\rm grav}$ denotes the gravitational binding energy of body A.

The best current limits on the post-Einstein parameters $\overline{\gamma}$ and $\overline{\beta}$ are (at the 68% confidence level):

$$\overline{\gamma} = (2.1 \pm 2.3) \times 10^{-5} \ , \qquad (21.15)$$

deduced from the additional Doppler shift experienced by radio-wave beams connecting the Earth to the Cassini spacecraft when they passed near the Sun [33], and

$$4\overline{\beta} - \overline{\gamma} = (1.8 \pm 2.9) \times 10^{-4} \ , \qquad (21.16)$$

from Lunar Laser Ranging measurements [17] of a possible polarization of the Moon toward the Sun [18]. More stringent limits on $\overline{\gamma}$ are obtained in models (*e.g.*, string-inspired ones [26]) where scalar couplings violate the Equivalence Principle.

21.3. Tests of the dynamics of the gravitational field in the radiative and/or strong field regimes

The discovery of pulsars (*i.e.*, rotating neutron stars emitting a beam of radio noise) in gravitationally bound orbits [34,35] has opened up an entirely new testing ground for relativistic gravity, giving us an experimental handle on the regime of radiative and/or strong gravitational fields. In these systems, the finite velocity of propagation of the gravitational interaction between the pulsar and its companion generates damping-like terms at order $(v/c)^5$ in the equations of motion [36]. These damping forces are the local counterparts of the gravitational radiation emitted at infinity by the system ("gravitational radiation reaction"). They cause the binary orbit to shrink and its orbital period P_b to decrease. The remarkable stability of pulsar clocks has allowed one to measure the corresponding very small orbital period decay $\dot{P}_b \equiv dP_b/dt \sim -(v/c)^5 \sim -10^{-12}$ in several binary systems, thereby giving us a direct experimental confirmation of the propagation properties of the gravitational field, and, in particular, an experimental confirmation that the speed of propagation of gravity is equal to the velocity of light to better than a part in a thousand. In addition, the surface gravitational potential of a neutron star $h_{00}(R) \simeq 2Gm/c^2R \simeq 0.4$ being a factor $\sim 10^8$ higher than the surface potential of the Earth, and a mere factor 2.5 below the black hole limit ($h_{00}(R) = 1$), pulsar data have allowed one to obtain several accurate tests of the strong-gravitational-field regime, as we discuss next.

Binary pulsar timing data record the times of arrival of successive electromagnetic pulses emitted by a pulsar orbiting around the center of mass of a binary system. After correcting for the Earth motion around the Sun and for the dispersion due to propagation in the interstellar plasma, the time of arrival of the Nth pulse t_N can be described by a generic, parameterized "timing formula" [37] whose functional form is common to the whole class of tensor-scalar gravitation theories:

$$t_N - t_0 = F[T_N(\nu_p, \dot\nu_p, \ddot\nu_p)\,;\,\{p^K\}\,;\,\{p^{PK}\}]\ . \tag{21.17}$$

Here, T_N is the pulsar proper time corresponding to the Nth turn given by $N/2\pi = \nu_p T_N + \frac{1}{2}\dot\nu_p T_N^2 + \frac{1}{6}\ddot\nu_p T_N^3$ (with $\nu_p \equiv 1/P_p$ the spin frequency of the pulsar, *etc.*), $\{p^K\} = \{P_b, T_0, e, \omega_0, x\}$ is the set of "Keplerian" parameters (notably, orbital period P_b, eccentricity e, periastron longitude ω_0 and projected semi-major axis $x = a\sin i/c$), and $\{p^{PK}\} = \{k, \gamma_{\rm timing}, \dot P_b, r, s, \delta_\theta, \dot e, \dot x\}$ denotes the set of (separately measurable) "post-Keplerian" parameters. Most important among these are: the fractional periastron advance per orbit $k \equiv \dot\omega P_b/2\pi$, a dimensionful time-dilation parameter $\gamma_{\rm timing}$, the orbital period derivative $\dot P_b$, and the "range" and "shape" parameters of the gravitational time delay caused by the companion, r and s.

Without assuming any specific theory of gravity, one can phenomenologically analyze the data from any binary pulsar by least-squares fitting the observed sequence of pulse arrival times to the timing formula Eq. (21.17). This fit yields the "measured" values of the parameters $\{\nu_p, \dot\nu_p, \ddot\nu_p\}$, $\{p^K\}$, $\{p^{PK}\}$. Now, each specific relativistic theory of gravity predicts that, for instance, k, $\gamma_{\rm timing}$, $\dot P_b$, r and s (to quote parameters that have been successfully measured from some binary pulsar data) are some theory-dependent functions of the Keplerian parameters and of the (unknown) masses m_1, m_2 of the pulsar and its companion. For instance, in General Relativity, one finds (with $M \equiv m_1 + m_2$, $n \equiv 2\pi/P_b$)

$$\begin{aligned}
k^{\rm GR}(m_1,m_2) =& 3(1-e^2)^{-1}(G_N M n/c^3)^{2/3}\ ,\\
\gamma^{\rm GR}_{\rm timing}(m_1,m_2) =& e n^{-1}(G_N M n/c^3)^{2/3} m_2(m_1+2m_2)/M^2\ ,\\
\dot P_b^{\rm GR}(m_1,m_2) =& -(192\pi/5)(1-e^2)^{-7/2}\left(1+\tfrac{73}{24}e^2+\tfrac{37}{96}e^4\right)\\
&\times (G_N M n/c^3)^{5/3} m_1 m_2/M^2\ ,\\
r(m_1,m_2) =& G_N m_2/c^3\ ,\\
s(m_1,m_2) =& n x (G_N M n/c^3)^{-1/3} M/m_2\ .
\end{aligned} \tag{21.18}$$

In tensor-scalar theories, each of the functions $k^{\rm theory}(m_1,m_2)$, $\gamma^{\rm theory}_{\rm timing}(m_1,m_2)$, $\dot P_b^{\rm theory}(m_1,m_2)$, *etc.*, is modified by quasi-static strong field effects (associated with the self-gravities of the pulsar and its companion), while the particular function $\dot P_b^{\rm theory}(m_1,m_2)$ is further modified by radiative effects (associated with the spin 0 propagator) [31,38,39].

Let us give some highlights of the current experimental situation. In the first discovered binary pulsar PSR 1913+16 [34,35], it has been possible to measure with accuracy *three* post-Keplerian parameters: k, $\gamma_{\rm timing}$ and $\dot P_b$. The three equations $k^{\rm measured} = k^{\rm theory}(m_1,m_2)$, $\gamma^{\rm measured}_{\rm timing} = \gamma^{\rm theory}_{\rm timing}(m_1,m_2)$, $\dot P_b^{\rm measured} = \dot P_b^{\rm theory}(m_1,m_2)$ determine, for each given theory, three curves in the two-dimensional mass plane. This yields *one* (combined radiative/strong-field) test of the specified theory, according to whether the three curves meet at one point, as they should. After subtracting a small ($\sim 10^{-14}$ level in $\dot P_b^{\rm obs} = (-2.423 \pm 0.001)\times 10^{-12}$), but significant, "galactic" perturbing effect (linked to galactic accelerations and to the pulsar proper motion) [40], one finds that General Relativity passes this $(k - \gamma_{\rm timing} - \dot P_b)_{1913+16}$ test with complete success at the 10^{-3} level [35,41,42]

$$\left[\frac{\dot P_b^{\rm obs} - \dot P_b^{\rm gal}}{\dot P_b^{\rm GR}[k^{\rm obs}, \gamma^{\rm obs}_{\rm timing}]}\right]_{1913+16} = 0.997 \pm 0.002\ . \tag{21.19}$$

Here $\dot P_b^{\rm GR}[k^{\rm obs}, \gamma^{\rm obs}_{\rm timing}]$ is the result of inserting in $\dot P_b^{\rm GR}(m_1,m_2)$ the values of the masses predicted by the two equations $k^{\rm obs} = k^{\rm GR}(m_1,m_2)$, $\gamma^{\rm obs}_{\rm timing} = \gamma^{\rm GR}_{\rm timing}(m_1,m_2)$. This yields experimental evidence for the reality of gravitational radiation damping forces at the $(-3 \pm 2)\times 10^{-3}$ level.

The discovery of the binary pulsar PSR 1534+12 [43] has allowed one to measure *five* post-Keplerian parameters: k, $\gamma_{\rm timing}$, r, s, and (with less accuracy) $\dot P_b$ [44,45]. This allows one to obtain *three* (five observables minus two masses) tests of relativistic gravity. Two among these tests probe strong field gravity, without mixing of radiative effects [44]. General Relativity passes all these tests within the measurement accuracy. The most precise of the new, pure strong-field tests is the one obtained by combining the measurements of k, γ, and s. Using the most recent data [45], one finds agreement at the 1% level:

$$\left[\frac{s^{\rm obs}}{s^{\rm GR}[k^{\rm obs}, \gamma^{\rm obs}_{\rm timing}]}\right]_{1534+12} = 1.000 \pm 0.007\ . \tag{21.20}$$

The discovery of the binary pulsar PSR J1141−6545 [46](whose companion is probably a white dwarf) has allowed one to measure *four* observable parameters: $k, \gamma_{\rm timing}, \dot P_b$ [47,48], and the parameter s [49,48]. The latter parameter (which is equal to the sine of the inclination angle, $s = \sin i$) was consistently measured in two ways: from a scintillation analysis [49], and from timing measurements [48]. General Relativity passes all the corresponding tests within measurement accuracy. See Fig. 21.1 which uses the (more precise) scintillation measurement of $s = \sin i$.

The discovery of the remarkable *double* binary pulsar PSR J0737−3039 A and B [50,51] has led to the measurement of *seven* independent parameters [52,53]: five of them are the post-Keplerian parameters k, $\gamma_{\rm timing}$, r, s and $\dot P_b$ entering the relativistic timing formula of the fast-spinning pulsar PSR J0737−3039 A, a sixth is the ratio $R = x_B/x_A$ between the projected semi-major axis of the more slowly spinning companion pulsar PSR J0737−3039 B, and that of PSR J0737−3039 A. [The theoretical prediction for the ratio $R = x_B/x_A$, considered as a function of the (inertial) masses $m_1 = m_A$ and $m_2 = m_B$, is $R^{\rm theory} = m_1/m_2 + O((v/c)^4)$ [37], independently of the gravitational theory considered.] Finally, the seventh parameter $\Omega_{\rm SO,B}$ is the angular rate of (spin-orbit) precession of PSR J0737−3039 B around the total angular momentum [53]. These seven measurements give us *five* tests of relativistic gravity [52,54,55]. General Relativity passes all those tests with flying colors (see Fig. 21.1). Let us highlight here two of them (from [55]) .

One test is a new confirmation of the reality of gravitational radiation at the 10^{-3} level

$$\left[\frac{\dot P_b^{\rm obs}}{\dot P_b^{\rm GR}[k^{\rm obs}, R^{\rm obs}]}\right]_{0737-3039} = 1.000 \pm 0.001\ . \tag{21.21}$$

Another one is a new, 5×10^{-4} level, strong-field confirmation of General Relativity:

$$\left[\frac{s^{\rm obs}}{s^{\rm GR}[k^{\rm obs}, R^{\rm obs}]}\right]_{0737-3039} = 1.0000 \pm 0.0005\ . \tag{21.22}$$

Fig. 21.1 illustrates all the tests of strong-field and radiative gravity derived from the above-mentioned binary pulsars: $(3-2=)$ one test from PSR1913+16, $(5-2=)$ 3 tests from PSR1534+12, $(4-2=)$ 2 tests from PSR J1141−6545, and $(7-2=)$ 5 tests from PSR J0737−3039.

Data from several nearly circular binary systems (made of a neutron star and a white dwarf) have also led to strong-field confirmations (at the 4.6×10^{-3} level) of the 'strong equivalence principle,' *i.e.*, the fact that neutron stars and white dwarfs fall with the same acceleration in the gravitational field of the Galaxy [56,57,58]. The measurements of $\dot P_b$ in some pulsar-white dwarf systems lead to strong constraints on the variation of Newton's G_N, and on the existence of gravitational dipole radiation [59,60,61,62]. In addition, arrays of millisecond pulsars are sensitive detectors of ultra low frequency gravitational

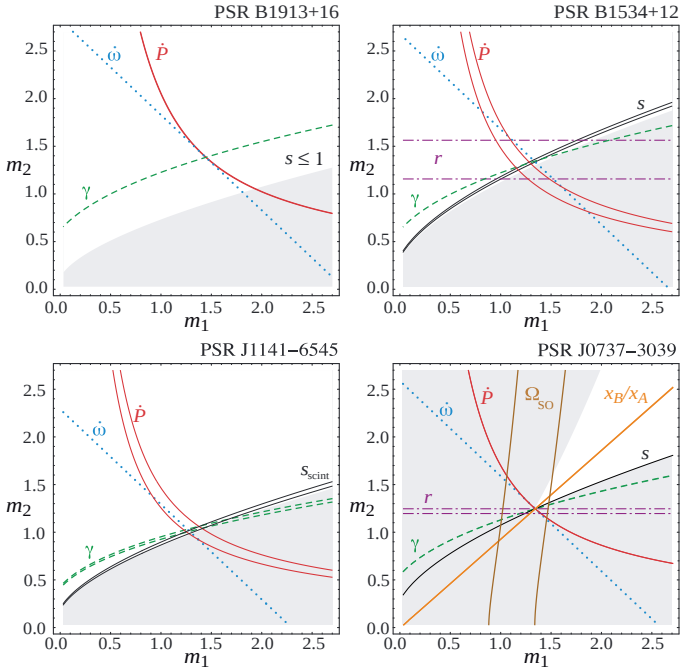

Figure 21.1: Illustration of the *eleven* tests of relativistic gravity obtained in the four different binary pulsar systems PSR1913+16 (one test), PSR1534+12 (3 tests), PSR J1141−6545 (2 tests), and PSR J0737−3039 A,B (5 tests). Each curve (or strip) in the mass plane corresponds to the interpretation, within General Relativity, of some observable parameter among: $\dot{P}_b$, $k \equiv \dot{\omega} P_b/2\pi$, $\gamma_{\rm timing}$, r, $s = \sin i$, $\Omega_{\rm SO,B}$ and R. (Figure updated from [66]; courtesy of G. Esposito-Farèse.)

waves ($f \sim 10^{-9} - 10^{-8}$ Hz) [63,64]. Such waves might be generated by supermassive black-hole binary systems, by cosmic strings and/or during the inflationary era. The sensitivity of pulsar timing arrays is comparable to predicted gravitational wave signal levels [65].

The constraints on tensor-scalar theories provided by the various binary-pulsar "experiments" have been analyzed in [39,66,67,61] and shown to exclude a large portion of the parameter space allowed by solar-system tests. The most stringent tests follow from the measurement of the orbital period decay $\dot{P}_b$ of the low-eccentricity 8.5-hour pulsar-white dwarf system PSR J1738+0333 with [61]

$$\left[\dot{P}_b^{\rm obs} - \dot{P}_b^{\rm gal} - \dot{P}_b^{\rm GR}\right]_{1738+0333} = (2.0 \pm 3.7) \times 10^{-15}. \qquad (21.23)$$

Dissymetric binary systems are strong emitters of dipolar gravitational radiation in tensor-scalar theories, with $\dot{P}_b$ scaling (modulo matter-scalar couplings) like $m_1 m_2/(m_1+m_2)^2 (v/c)^3$ ($\sim 10^{-9}$ for PSR J1738+0333), instead of the smaller quadrupolar radiation $\dot{P}_b \sim (v/c)^5$ [2,31]. Thereby, the result Eq. (21.23) constrains the basic matter-scalar coupling α_0^2 more strongly, over most of the parameter space, than the best current solar-system limits Eq. (21.15), Eq. (21.16) (namely below the 10^{-5} level) [61]. In the particular case of the Jordan-Fierz-Brans-Dicke theory, the pulsar bound on α_0^2 is (when choosing an equation of state of medium stiffness) $\alpha_0^2 < 2 \times 10^{-5}$, wich is within a factor two of the Cassini bound Eq. (21.15) (where $\overline{\gamma} = -2\alpha_0^2/(1+\alpha_0^2)$).

Finally, measurements over several years of the pulse profiles of various pulsars have detected secular profile changes compatible with the prediction [68] that the general relativistic spin-orbit coupling should cause a secular change in the orientation of the pulsar beam with respect to the line of sight ("geodetic precession"). Such confirmations of general-relativistic spin-orbit effects were obtained in PSR 1913+16 [69], PSR B1534+12 [70], PSR J1141−6545 [71], and PSR J0737−3039 [53].

The tests considered above have examined the gravitational interaction on scales between a fraction of a millimeter and a few astronomical units. The general relativistic action on light and matter of an external gravitational field have been verified on much larger scales in many gravitational lensing systems [72]. Some tests on cosmological scales are also available [73].

21.4. Conclusions

All present experimental tests are compatible with the predictions of the current "standard" theory of gravitation: Einstein's General Relativity. The universality of the coupling between matter and gravity (Equivalence Principle) has been verified around the 10^{-13} level. Solar system experiments have tested the weak-field predictions of Einstein's theory at the 10^{-4} level (and down to the 2×10^{-5} level for the post-Einstein parameter $\overline{\gamma}$). The propagation properties of relativistic gravity, as well as several of its strong-field aspects, have been verified at the 10^{-3} level (or better) in several binary pulsar experiments. Recent laboratory experiments have set strong constraints on sub-millimeter modifications of Newtonian gravity. Quantitative confirmations of General Relativity have also been obtained on astrophysical and cosmological scales (assuming dark matter and a cosmological constant).

References:

1. S. Weinberg, Rev. Mod. Phys. **61**, 1 (1989).
2. C.M. Will, *Theory and Experiment in Gravitational Physics* (Cambridge University Press, Cambridge, 1993); *idem,* Living Rev. Rel. **9**, 3 (2006).
3. A.I. Shlyakhter, Nature **264**, 340 (1976).
4. T. Damour and F. Dyson, Nucl. Phys. **B480**, 37 (1996); C.R. Gould, E.I. Sharapov, and S.K. Lamoreaux, Phys. Rev. C **74**, 024607 (2006); Yu. V. Petrov *et al.*, Phys. Rev. C **74**, 064610 (2006).
5. V.V. Flambaum and R.B. Wiringa, Phys. Rev. **C79**, 034302 (2009).
6. K.A. Olive *et al.*, Phys. Rev. **D66**, 045022 (2002); K.A. Olive *et al.*, Phys. Rev. D **69**, 027701 (2004).
7. J.K. Webb *et al.*, Phys. Rev. Lett. **87**, 091301 (2001); M.T. Murphy, J.K. Webb, and V.V. Flambaum, Mon. Not. Roy. Astron. Soc. **384**, 1053 (2008).
8. M.T. Murphy *et al.*, Science **320**, 1611 (2008).
9. J.A. King *et al.*, Mon. Not. Roy. Astron. Soc. **417**, 3010 (2011).
10. T. Rosenband *et al.*, Science, **319**, 1808 (2008); J. Guéna *et al.*, Phys. Rev. Lett. **109**, 080801 (2012).
11. T.M. Fortier *et al.*, Phys. Rev. Lett. **98**, 070801 (2007); S. Blatt *et al.*, Phys. Rev. Lett. **100**, 140801 (2008); T. Dent, Phys. Rev. Lett. **101**, 041102 (2008).
12. J.-P. Uzan, Living Rev. Rel. **14**, 2 (2011).
13. M. Smiciklas *et al.*, Phys. Rev. Lett. **107**, 171604 (2011).
14. T. Jacobson, S. Liberati, and D. Mattingly, Annals Phys. **321**, 150 (2006).
15. S. Schlamminger *et al.*, Phys. Rev. Lett. **100**, 041101 (2008).
16. T.A. Wagner *et al.*, Class. Quantum Grav. **29**, 184002 (2012).
17. J.G. Williams, S.G. Turyshev, and D.H. Boggs, Class. Quantum Grav. **29**, 184004 (2012); J. Müller, F. Hofmann, and L. Biskupek, Class. Quantum Grav. **29**, 184006 (2012).
18. K. Nordtvedt, Phys. Rev. **170**, 1186 (1968).
19. E.G. Adelberger *et al.*, Prog. Part. Nucl. Phys. **62**, 102 (2009).
20. R.F.C. Vessot and M.W. Levine, Gen. Rel. Grav. **10**, 181 (1978); R.F.C. Vessot *et al.*, Phys. Rev. Lett. **45**, 2081 (1980).
21. C.W. Chou *et al.*, Science **329**, 1630 (2010).
22. I. Ciufolini and E. C. Pavlis, Nature **431**,958 (2004).
23. I. Ciufolini *et al.*, [arXiv:1309.1699 [gr-qc]].
24. C.W.F. Everitt *et al.*, Phys. Rev. Lett. **106**, 221101 (2011).
25. A.S. Goldhaber and M.M. Nieto, Rev. Mod. Phys. **82**, 939 (2010).
26. T.R. Taylor and G. Veneziano, Phys. Lett. **B213**, 450 (1988); T. Damour and A.M. Polyakov, Nucl. Phys. **B423**, 532 (1994); S. Dimopoulos and G. Giudice, Phys. Lett. **B379**, 105 (1996); I. Antoniadis, S. Dimopoulos, and G. Dvali, Nucl. Phys. **B516**, 70 (1998); T. Damour and J. F. Donoghue, Phys. Rev. D 82,084033 (2010).

27. V.A. Rubakov, Phys. Usp **44**, 871 (2001);
R. Maartens and K. Koyama, Living Rev. Rel. **13**, 5 (2010).
28. R. D. Newman *et al.*, Space Sci. Rev. **148**, 175 (2009).
29. D. J. Kapner *et al.*, Phys. Rev. Lett. **98**, 021101 (2007).
30. P. Jordan, *Schwerkraft und Weltall* (Vieweg, Braunschweig, 1955);
M. Fierz, Helv. Phys. Acta **29**, 128 (1956);
C. Brans and R.H. Dicke, Phys. Rev. **124**, 925 (1961).
31. T. Damour and G. Esposito-Farèse, Class. Quantum Grav. **9**, 2093 (1992).
32. J. Khoury and A. Weltman, Phys. Rev. Lett. **93**, 171104 (2004).
33. B. Bertotti, L. Iess, and P. Tortora, Nature, **425**, 374 (2003).
34. R.A. Hulse, Rev. Mod. Phys. **66**, 699 (1994).
35. J.H. Taylor, Rev. Mod. Phys. **66**, 711 (1994).
36. T. Damour and N. Deruelle, Phys. Lett. **A87**, 81 (1981);
T. Damour, C.R. Acad. Sci. Paris **294**, 1335 (1982).
37. T.Damour and N. Deruelle, Ann. Inst. H. Poincaré A, **44**, 263 (1986);
Damour and J.H. Taylor, Phys. Rev. **D45**, 1840 (1992).
38. C.M. Will and H.W. Zaglauer, Astrophys. J. **346**, 366 (1989).
39. T. Damour and G. Esposito-Farèse, Phys. Rev. **D54**, 1474 (1996);
idem, Phys. Rev. **D58**, 042001 (1998).
40. T. Damour and J.H. Taylor, Astrophys. J. **366**, 501 (1991).
41. J.M. Weisberg and J.H. Taylor, in *Radio Pulsars, ASP Conference Series* **328**, 25 (2005); `astro-ph/0407149`.
42. J.M. Weisberg, D.J. Nice, and J.H. Taylor, Astrophys. J. **722**, 1030-1034 (2010).
43. A. Wolszczan, Nature **350**, 688 (1991).
44. J.H. Taylor *et al.*, Nature **355**, 132 (1992).
45. I.H. Stairs *et al.*, Astrophys. J. **505**, 352 (1998);
I.H. Stairs *et al.*, Astrophys. J. **581**, 501 (2002).
46. V.M. Kaspi *et al.*, Astrophys. J. **528**, 445 (2000).
47. M. Bailes *et al.*, Astrophys. J. **595**, L49 (2003).
48. N.D.R. Bhat, M. Bailes, and J.P.W. Verbiest, Phys. Rev. **D77**, 124017 (2008).
49. S.M. Ord *et al.*, Astrophys. J. **574**, L75 (2002).
50. M. Burgay *et al.*, Nature **426**, 531 (2003).
51. A.G. Lyne *et al.*, Science **303**, 1153 (2004).
52. M. Kramer *et al.*, Science **314**, 97 (2006).
53. R.P. Breton *et al.*, Science **321**, 104 (2008).
54. M. Kramer and N. Wex, Class. Quant. Grav. **26**, 073001 (2009).
55. M. Kramer, in *Neutron Stars and Pulsars: Challenges and Opportunities after 80 Years; Proceedings of the International Astronomical Union Symposium S291, 2012*, J. van Leeuwen, ed. (Cambridge University Press, 2013), pp 19-26, `[arXiv:1211.2457 [astro-ph.HE]]`.
56. T. Damour and G. Schäfer, Phys. Rev. Lett. **66**, 2549 (1991).
57. M.E. Gonzalez *et al.*, Astrophys. J. 743,102 (2011).
58. P.C.C. Freire, M. Kramer, and N. Wex , Class. Quantum Grav. **29**, 184007 (2012).
59. J.P.W. Verbiest *et al.*, Astrophys. J., **679**, 675 (2008).
60. K. Lazaridis *et al.*, Mon. Not. Roy. Astron. Soc. **400**, 805 (2009).
61. P.C.C. Freire *et al.*, Mon. Not. Roy. Astron. Soc. **423**, 3328 (2012).
62. J. Antoniadis *et al.*, Science **340**, 6131 (2013).
63. A.N. Lommen and D.C. Backer, Bulletin of the American Astronomical Society **33**, 1347 (2001);
idem, Astrophys. J. **562**, 297 (2001).
64. J.P.W. Verbiest *et al.*, Class. Quantum Grav. **27**, 084015 (2010);
G. Hobbs *et al.*, Class. Quantum Grav. **27**, 084013 (2010).
65. F.A. Jenet, J.W. Armstrong and M. Tinto, Phys. Rev. D 83,081301 (2011).
66. G. Esposito-Farèse, in *Proceedings of the 10th Marcel Grossmann Meeting on Recent Developments in Theoretical and Experimental General Relativity*, edited by M. Novello *et al.*, (World Scientific, 2006), part A, pp 647-666.
67. G. Esposito-Farèse, in *Mass and Motion in General Relativity*, eds L. Blanchet *et al.*, series Fundam. Theor. Phys. **162** (Springer, Dordrecht, 2011) 461-489.
68. T. Damour and R. Ruffini, C. R. Acad. Sc. Paris **279**, série A, 971 (1974);
B.M. Barker and R.F. O'Connell, Phys. Rev. **D12**, 329 (1975).
69. M. Kramer, Astrophys. J. **509**, 856 (1998);
J.M. Weisberg and J.H. Taylor, Astrophys. J. **576**, 942 (2002).
70. I.H. Stairs, S.E. Thorsett, and Z. Arzoumanian, Phys. Rev. Lett. **93**, 141101 (2004).
71. A.W. Hotan, M. Bailes, and S.M. Ord, Astrophys. J. **624**, 906 (2005).
72. A.S. Bolton, S. Rappaport, and S. Burles, Phys. Rev. **D74**, 061501 (2006);
J. Schwab, A.S. Bolton, and S.A. Rappaport, Astrophys. J. **708**, 750-757 (2010).
73. J. -P. Uzan, Gen. Rel. Grav. **42**, 2219-2246 (2010);
R. Reyes *et al.*, Nature **464**, 256 (2010);
B. Jain and J. Khoury, Annals Phys. **325**, 1479 (2010);
S. F. Daniel, *et al.*, Phys. Rev. D **81**, 123508 (2010).

22. BIG-BANG COSMOLOGY

Revised September 2013 by K.A. Olive (University of Minnesota) and J.A. Peacock (University of Edinburgh).

22.1. Introduction to Standard Big-Bang Model

The observed expansion of the Universe [1–3] is a natural (almost inevitable) result of any homogeneous and isotropic cosmological model based on general relativity. However, by itself, the Hubble expansion does not provide sufficient evidence for what we generally refer to as the Big-Bang model of cosmology. While general relativity is in principle capable of describing the cosmology of any given distribution of matter, it is extremely fortunate that our Universe appears to be homogeneous and isotropic on large scales. Together, homogeneity and isotropy allow us to extend the Copernican Principle to the Cosmological Principle, stating that all spatial positions in the Universe are essentially equivalent.

The formulation of the Big-Bang model began in the 1940s with the work of George Gamow and his collaborators, Alpher and Herman. In order to account for the possibility that the abundances of the elements had a cosmological origin, they proposed that the early Universe which was once very hot and dense (enough so as to allow for the nucleosynthetic processing of hydrogen), and has expanded and cooled to its present state [4,5]. In 1948, Alpher and Herman predicted that a direct consequence of this model is the presence of a relic background radiation with a temperature of order a few K [6,7]. Of course this radiation was observed 16 years later as the microwave background radiation [8]. Indeed, it was the observation of the 3 K background radiation that singled out the Big-Bang model as the prime candidate to describe our Universe. Subsequent work on Big-Bang nucleosynthesis further confirmed the necessity of our hot and dense past. (See the review on BBN—Sec. 23 of this *Review* for a detailed discussion of BBN.) These relativistic cosmological models face severe problems with their initial conditions, to which the best modern solution is inflationary cosmology, discussed in Sec. 22.3.5. If correct, these ideas would strictly render the term 'Big Bang' redundant, since it was first coined by Hoyle to represent a criticism of the lack of understanding of the initial conditions.

22.1.1. *The Robertson-Walker Universe* :

The observed homogeneity and isotropy enable us to describe the overall geometry and evolution of the Universe in terms of two cosmological parameters accounting for the spatial curvature and the overall expansion (or contraction) of the Universe. These two quantities appear in the most general expression for a space-time metric which has a (3D) maximally symmetric subspace of a 4D space-time, known as the Robertson-Walker metric:

$$ds^2 = dt^2 - R^2(t)\left[\frac{dr^2}{1-kr^2} + r^2\left(d\theta^2 + \sin^2\theta\, d\phi^2\right)\right] \ . \qquad (22.1)$$

Note that we adopt $c = 1$ throughout. By rescaling the radial coordinate, we can choose the curvature constant k to take only the discrete values $+1$, -1, or 0 corresponding to closed, open, or spatially flat geometries. In this case, it is often more convenient to re-express the metric as

$$ds^2 = dt^2 - R^2(t)\left[d\chi^2 + S_k^2(\chi)\left(d\theta^2 + \sin^2\theta\, d\phi^2\right)\right] \ , \qquad (22.2)$$

where the function $S_k(\chi)$ is $(\sin\chi, \chi, \sinh\chi)$ for $k = (+1, 0, -1)$. The coordinate r (in Eq. (22.1)) and the 'angle' χ (in Eq. (22.2)) are both dimensionless; the dimensions are carried by $R(t)$, which is the cosmological scale factor which determines proper distances in terms of the comoving coordinates. A common alternative is to define a dimensionless scale factor, $a(t) = R(t)/R_0$, where $R_0 \equiv R(t_0)$ is R at the present epoch. It is also sometimes convenient to define a dimensionless or conformal time coordinate, η, by $d\eta = dt/R(t)$. Along constant spatial sections, the proper time is defined by the time coordinate, t. Similarly, for $dt = d\theta = d\phi = 0$, the proper distance is given by $R(t)\chi$. For standard texts on cosmological models see *e.g.*, Refs. [9–16].

22.1.2. *The redshift* :

The cosmological redshift is a direct consequence of the Hubble expansion, determined by $R(t)$. A local observer detecting light from a distant emitter sees a redshift in frequency. We can define the redshift as

$$z \equiv \frac{\nu_1 - \nu_2}{\nu_2} \simeq v_{12} \ , \qquad (22.3)$$

where ν_1 is the frequency of the emitted light, ν_2 is the observed frequency and v_{12} is the relative velocity between the emitter and the observer. While the definition, $z = (\nu_1 - \nu_2)/\nu_2$ is valid on all distance scales, relating the redshift to the relative velocity in this simple way is only true on small scales (*i.e.*, less than cosmological scales) such that the expansion velocity is non-relativistic. For light signals, we can use the metric given by Eq. (22.1) and $ds^2 = 0$ to write

$$v_{12} = \dot{R}\,\delta r = \frac{\dot{R}}{R}\,\delta t = \frac{\delta R}{R} = \frac{R_2 - R_1}{R_1} \ , \qquad (22.4)$$

where $\delta r(\delta t)$ is the radial coordinate (temporal) separation between the emitter and observer. Noting that physical distance, D, is $R\delta r$ or δt, Eq. (22.4) gives us Hubble's law, $v = HD$. In addition, we obtain the simple relation between the redshift and the scale factor

$$1 + z = \frac{\nu_1}{\nu_2} = \frac{R_2}{R_1} \ . \qquad (22.5)$$

This result does not depend on the non-relativistic approximation.

22.1.3. *The Friedmann-Lemaître equations of motion* :

The cosmological equations of motion are derived from Einstein's equations

$$\mathcal{R}_{\mu\nu} - \tfrac{1}{2}g_{\mu\nu}\mathcal{R} = 8\pi G_{\rm N} T_{\mu\nu} + \Lambda g_{\mu\nu} \ . \qquad (22.6)$$

Gliner [17] and Zeldovich [18] have pioneered the modern view, in which the Λ term is taken to the rhs and interpreted as an effective energy–momentum tensor $T_{\mu\nu}$ for the vacuum of $\Lambda g_{\mu\nu}/8\pi G_{\rm N}$. It is common to assume that the matter content of the Universe is a perfect fluid, for which

$$T_{\mu\nu} = -p g_{\mu\nu} + (p + \rho)\, u_\mu u_\nu \ , \qquad (22.7)$$

where $g_{\mu\nu}$ is the space-time metric described by Eq. (22.1), p is the isotropic pressure, ρ is the energy density and $u = (1, 0, 0, 0)$ is the velocity vector for the isotropic fluid in co-moving coordinates. With the perfect fluid source, Einstein's equations lead to the Friedmann-Lemaître equations

$$H^2 \equiv \left(\frac{\dot{R}}{R}\right)^2 = \frac{8\pi\, G_{\rm N}\, \rho}{3} - \frac{k}{R^2} + \frac{\Lambda}{3} \ , \qquad (22.8)$$

and

$$\frac{\ddot{R}}{R} = \frac{\Lambda}{3} - \frac{4\pi G_{\rm N}}{3}\ (\rho + 3p) \ , \qquad (22.9)$$

where $H(t)$ is the Hubble parameter and Λ is the cosmological constant. The first of these is sometimes called the Friedmann equation. Energy conservation via $T^{\mu\nu}_{\ \ ;\mu} = 0$, leads to a third useful equation [which can also be derived from Eq. (22.8) and Eq. (22.9)]

$$\dot{\rho} = -3H\,(\rho + p) \ . \qquad (22.10)$$

Eq. (22.10) can also be simply derived as a consequence of the first law of thermodynamics.

Eq. (22.8) has a simple classical mechanical analog if we neglect (for the moment) the cosmological term Λ. By interpreting $-k/R^2$ Newtonianly as a 'total energy', then we see that the evolution of the Universe is governed by a competition between the potential energy, $8\pi G_{\rm N}\rho/3$, and the kinetic term $(\dot{R}/R)^2$. For $\Lambda = 0$, it is clear that the Universe must be expanding or contracting (except at the turning point prior to collapse in a closed Universe). The ultimate fate of the Universe is determined by the curvature constant k. For $k = +1$, the Universe will recollapse in a finite time, whereas for $k = 0, -1$, the Universe will expand indefinitely. These simple conclusions can be altered when $\Lambda \neq 0$ or more generally with some component with $(\rho + 3p) < 0$.

22.1.4. ***Definition of cosmological parameters*** :

In addition to the Hubble parameter, it is useful to define several other measurable cosmological parameters. The Friedmann equation can be used to define a critical density such that $k = 0$ when $\Lambda = 0$,

$$\rho_c \equiv \frac{3H^2}{8\pi G_N} = 1.88 \times 10^{-26}\, h^2 \text{ kg m}^{-3} = 1.05 \times 10^{-5}\, h^2 \text{ GeV cm}^{-3} , \quad (22.11)$$

where the scaled Hubble parameter, h, is defined by

$$H \equiv 100\, h \text{ km s}^{-1} \text{ Mpc}^{-1} \Rightarrow H^{-1} = 9.78\, h^{-1} \text{ Gyr} = 2998\, h^{-1} \text{ Mpc} \rho_c . \quad (22.12)$$

The cosmological density parameter Ω_{tot} is defined as the energy density relative to the critical density,

$$\Omega_{tot} = \rho/\rho_c . \quad (22.13)$$

Note that one can now rewrite the Friedmann equation as

$$k/R^2 = H^2(\Omega_{tot} - 1) . \quad (22.14)$$

From Eq. (22.14), one can see that when $\Omega_{tot} > 1$, $k = +1$ and the Universe is closed, when $\Omega_{tot} < 1$, $k = -1$ and the Universe is open, and when $\Omega_{tot} = 1$, $k = 0$, and the Universe is spatially flat.

It is often necessary to distinguish different contributions to the density. It is therefore convenient to define present-day density parameters for pressureless matter (Ω_m) and relativistic particles (Ω_r), plus the quantity $\Omega_\Lambda = \Lambda/3H^2$. In more general models, we may wish to drop the assumption that the vacuum energy density is constant, and we therefore denote the present-day density parameter of the vacuum by Ω_v. The Friedmann equation then becomes

$$k/R_0^2 = H_0^2(\Omega_m + \Omega_r + \Omega_v - 1) , \quad (22.15)$$

where the subscript 0 indicates present-day values. Thus, it is the sum of the densities in matter, relativistic particles, and vacuum that determines the overall sign of the curvature. Note that the quantity $-k/R_0^2H_0^2$ is sometimes referred to as Ω_k. This usage is unfortunate: it encourages one to think of curvature as a contribution to the energy density of the Universe, which is not correct.

22.1.5. ***Standard Model solutions*** :

Much of the history of the Universe in the standard Big-Bang model can be easily described by assuming that either matter or radiation dominates the total energy density. During inflation and again today the expansion rate for the Universe is accelerating, and domination by a cosmological constant or some other form of dark energy should be considered. In the following, we shall delineate the solutions to the Friedmann equation when a single component dominates the energy density. Each component is distinguished by an equation of state parameter $w = p/\rho$.

22.1.5.1. *Solutions for a general equation of state:*

Let us first assume a general equation of state parameter for a single component, w which is constant. In this case, Eq. (22.10) can be written as $\dot\rho = -3(1+w)\rho\dot R/R$ and is easily integrated to yield

$$\rho \propto R^{-3(1+w)} . \quad (22.16)$$

Note that at early times when R is small, the less singular curvature term k/R^2 in the Friedmann equation can be neglected so long as $w > -1/3$. Curvature domination occurs at rather late times (if a cosmological constant term does not dominate sooner). For $w \neq -1$, one can insert this result into the Friedmann equation Eq. (22.8), and if one neglects the curvature and cosmological constant terms, it is easy to integrate the equation to obtain,

$$R(t) \propto t^{2/[3(1+w)]} . \quad (22.17)$$

22.1.5.2. *A Radiation-dominated Universe:*

In the early hot and dense Universe, it is appropriate to assume an equation of state corresponding to a gas of radiation (or relativistic particles) for which $w = 1/3$. In this case, Eq. (22.16) becomes $\rho \propto R^{-4}$. The 'extra' factor of $1/R$ is due to the cosmological redshift; not only is the number density of particles in the radiation background decreasing as R^{-3} since volume scales as R^3, but in addition, each particle's energy is decreasing as $E \propto \nu \propto R^{-1}$. Similarly, one can substitute $w = 1/3$ into Eq. (22.17) to obtain

$$R(t) \propto t^{1/2} ; \qquad H = 1/2t . \quad (22.18)$$

22.1.5.3. *A Matter-dominated Universe:*

At relatively late times, non-relativistic matter eventually dominates the energy density over radiation (see Sec. 22.3.8). A pressureless gas ($w = 0$) leads to the expected dependence $\rho \propto R^{-3}$ from Eq. (22.16) and, if $k = 0$, we get

$$R(t) \propto t^{2/3} ; \qquad H = 2/3t . \quad (22.19)$$

22.1.5.4. *A Universe dominated by vacuum energy:*

If there is a dominant source of vacuum energy, V_0, it would act as a cosmological constant with $\Lambda = 8\pi G_N V_0$ and equation of state $w = -1$. In this case, the solution to the Friedmann equation is particularly simple and leads to an exponential expansion of the Universe

$$R(t) \propto e^{\sqrt{\Lambda/3}t} . \quad (22.20)$$

A key parameter is the equation of state of the vacuum, $w \equiv p/\rho$: this need not be the $w = -1$ of Λ, and may not even be constant [19–21]. There is now much interest in the more general possibility of a dynamically evolving vacuum energy, for which the name 'dark energy' has become commonly used. A variety of techniques exist whereby the vacuum density as a function of time may be measured, usually expressed as the value of w as a function of epoch [22,23]. The best current measurement for the equation of state (assumed constant, but without assuming zero curvature) is $w = -1.00 \pm 0.06$ [24]. Unless stated otherwise, we will assume that the vacuum energy is a cosmological constant with $w = -1$ exactly.

The presence of vacuum energy can dramatically alter the fate of the Universe. For example, if $\Lambda < 0$, the Universe will eventually recollapse independent of the sign of k. For large values of $\Lambda > 0$ (larger than the Einstein static value needed to halt any cosmological expansion or contraction), even a closed Universe will expand forever. One way to quantify this is the deceleration parameter, q_0, defined as

$$q_0 = -\left.\frac{R\ddot R}{\dot R^2}\right|_0 = \frac{1}{2}\Omega_m + \Omega_r + \frac{(1+3w)}{2}\Omega_v . \quad (22.21)$$

This equation shows us that $w < -1/3$ for the vacuum may lead to an accelerating expansion. To the continuing astonishment of cosmologists, such an effect has been observed; one piece of direct evidence is the Supernova Hubble diagram [25–31] (see Fig. 22.1 below); current data indicate that vacuum energy is indeed the largest contributor to the cosmological density budget, with $\Omega_v = 0.68 \pm 0.02$ and $\Omega_m = 0.32 \pm 0.01$ if $k = 0$ is assumed (Planck) [32].

The existence of this constituent is without doubt the greatest puzzle raised by the current cosmological model; the final section of this review discusses some of the ways in which the vacuum-energy problem is being addressed.

22.2. Introduction to Observational Cosmology

22.2.1. *Fluxes, luminosities, and distances* :

The key quantities for observational cosmology can be deduced quite directly from the metric.

(1) The *proper* transverse size of an object seen by us to subtend an angle $d\psi$ is its comoving size $d\psi\, S_k(\chi)$ times the scale factor at the time of emission:

$$d\ell = d\psi\; R_0 S_k(\chi)/(1+z)\;. \tag{22.22}$$

(2) The apparent flux density of an object is deduced by allowing its photons to flow through a sphere of current radius $R_0 S_k(\chi)$; but photon energies and arrival rates are redshifted, and the bandwidth $d\nu$ is reduced. The observed photons at frequency ν_0 were emitted at frequency $\nu_0(1+z)$, so the flux density is the luminosity at this frequency, divided by the total area, divided by $1+z$:

$$S_\nu(\nu_0) = \frac{L_\nu([1+z]\nu_0)}{4\pi R_0^2 S_k^2(\chi)(1+z)}\;. \tag{22.23}$$

These relations lead to the following common definitions:

$$\begin{aligned} \text{angular-diameter distance:}\quad & D_{\rm A} = (1+z)^{-1} R_0 S_k(\chi) \\ \text{luminosity distance:}\quad & D_{\rm L} = (1+z)\; R_0 S_k(\chi)\;. \end{aligned} \tag{22.24}$$

These distance-redshift relations are expressed in terms of observables by using the equation of a null radial geodesic ($R(t)d\chi = dt$) plus the Friedmann equation:

$$\begin{aligned} R_0 d\chi =& \frac{1}{H(z)}\,dz = \frac{1}{H_0}\,\Big[(1-\Omega_{\rm m}-\Omega_{\rm v}-\Omega_{\rm r})(1+z)^2 \\ &+\;\Omega_{\rm v}(1+z)^{3+3w}\;+\;\Omega_{\rm m}(1+z)^3+\Omega_{\rm r}(1+z)^4\Big]^{-1/2}\,dz\;. \end{aligned} \tag{22.25}$$

The main scale for the distance here is the Hubble length, $1/H_0$.

The flux density is the product of the specific intensity I_ν and the solid angle $d\Omega$ subtended by the source: $S_\nu = I_\nu\, d\Omega$. Combining the angular size and flux-density relations thus gives the relativistic version of surface-brightness conservation:

$$I_\nu(\nu_0) = \frac{B_\nu([1+z]\nu_0)}{(1+z)^3}\;, \tag{22.26}$$

where B_ν is surface brightness (luminosity emitted into unit solid angle per unit area of source). We can integrate over ν_0 to obtain the corresponding total or bolometric formula:

$$I_{\rm tot} = \frac{B_{\rm tot}}{(1+z)^4}\;. \tag{22.27}$$

This cosmology-independent form expresses Liouville's Theorem: photon phase-space density is conserved along rays.

22.2.2. *Distance data and geometrical tests of cosmology* :

In order to confront these theoretical predictions with data, we have to bridge the divide between two extremes. Nearby objects may have their distances measured quite easily, but their radial velocities are dominated by deviations from the ideal Hubble flow, which typically have a magnitude of several hundred $\mathrm{km\,s^{-1}}$. On the other hand, objects at redshifts $z \gtrsim 0.01$ will have observed recessional velocities that differ from their ideal values by $\lesssim 10\%$, but absolute distances are much harder to supply in this case. The traditional solution to this problem is the construction of the distance ladder: an interlocking set of methods for obtaining relative distances between various classes of object, which begins with absolute distances at the 10 to 100 pc level, and terminates with galaxies at significant redshifts. This is reviewed in the review on Cosmological Parameters—Sec. 24 of this *Review*.

By far the most exciting development in this area has been the use of type Ia Supernovae (SNe), which now allow measurement of relative distances with 5% precision. In combination with Cepheid data from the HST and a direct geometrical distance to the maser galaxy NGC4258, SNe results extend the distance ladder to the point where deviations from uniform expansion are negligible, leading to the best existing direct value for H_0: $72.0 \pm 3.0\,\mathrm{km\,s^{-1}Mpc^{-1}}$ [33]. Better still, the analysis of high-z SNe has allowed a simple and direct test of cosmological geometry to be carried out: as shown in Fig. 22.1 and Fig. 22.2, supernova data and measurements of microwave-background anisotropies strongly favor a $k=0$ model dominated by vacuum energy. (See the review on Cosmological Parameters—Sec. 24 of this *Review* for a more comprehensive review of Hubble parameter determinations.)

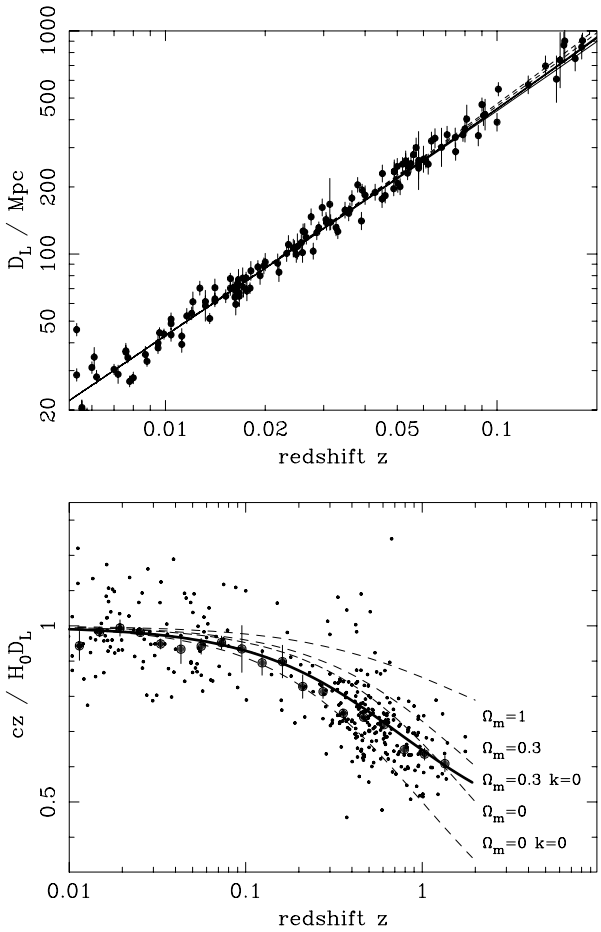

Figure 22.1: The type Ia supernova Hubble diagram [25–29]. The first panel shows that for $z \ll 1$ the large-scale Hubble flow is indeed linear and uniform; the second panel shows an expanded scale, with the linear trend divided out, and with the redshift range extended to show how the Hubble law becomes nonlinear. ($\Omega_{\rm r} = 0$ is assumed.) Larger points with errors show median values in redshift bins. Comparison with the prediction of Friedmann-Lemaître models appears to favor a vacuum-dominated Universe.

22.2.3. *Age of the Universe* :

The most striking conclusion of relativistic cosmology is that the Universe has not existed forever. The dynamical result for the age of the Universe may be written as

$$\begin{aligned} H_0 t_0 &= \int_0^\infty \frac{dz}{(1+z)H(z)} \\ &= \int_0^\infty \frac{dz}{(1+z)\,[(1+z)^2(1+\Omega_{\rm m}z) - z(2+z)\Omega_{\rm v}]^{1/2}}\;, \end{aligned} \tag{22.28}$$

where we have neglected $\Omega_{\rm r}$ and chosen $w=-1$. Over the range of interest ($0.1 \lesssim \Omega_{\rm m} \lesssim 1$, $|\Omega_{\rm v}| \lesssim 1$), this exact answer may be

approximated to a few % accuracy by

$$H_0 t_0 \simeq \tfrac{2}{3}\,(0.7\Omega_{\rm m} + 0.3 - 0.3\Omega_{\rm v})^{-0.3}\ . \qquad (22.29)$$

For the special case that $\Omega_{\rm m} + \Omega_{\rm v} = 1$, the integral in Eq. (22.28) can be expressed analytically as

$$H_0 t_0 = \frac{2}{3\sqrt{\Omega_{\rm v}}}\,\ln\frac{1+\sqrt{\Omega_{\rm v}}}{\sqrt{1-\Omega_{\rm v}}} \quad (\Omega_{\rm m} < 1)\ . \qquad (22.30)$$

The most accurate means of obtaining ages for astronomical objects is based on the natural clocks provided by radioactive decay. The use of these clocks is complicated by a lack of knowledge of the initial conditions of the decay. In the Solar System, chemical fractionation of different elements helps pin down a precise age for the pre-Solar nebula of 4.6 Gyr, but for stars it is necessary to attempt an a priori calculation of the relative abundances of nuclei that result from supernova explosions. In this way, a lower limit for the age of stars in the local part of the Milky Way of about 11 Gyr is obtained [35,36].

The other major means of obtaining cosmological age estimates is based on the theory of stellar evolution. In principle, the main-sequence turnoff point in the color-magnitude diagram of a globular cluster should yield a reliable age. However, these have been controversial owing to theoretical uncertainties in the evolution model, as well as observational uncertainties in the distance, dust extinction, and metallicity of clusters. The present consensus favors ages for the oldest clusters of about 12 Gyr [37,38].

These methods are all consistent with the age deduced from studies of structure formation, using the microwave background and large-scale structure: $t_0 = 13.81 \pm 0.05$ Gyr [32], where the extra accuracy comes at the price of assuming the Cold Dark Matter model to be true.

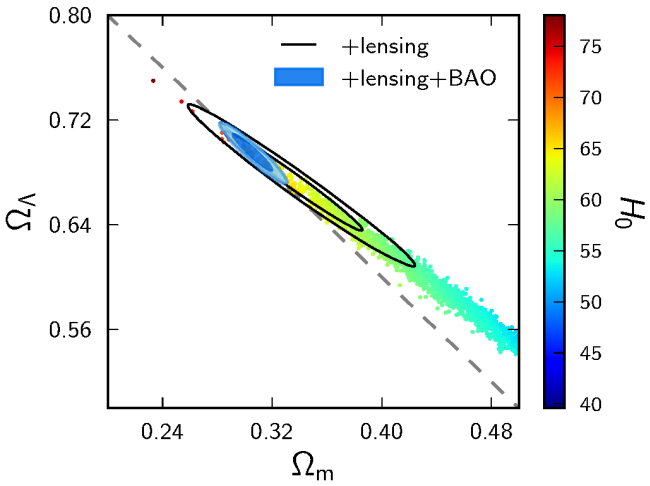

Figure 22.2: Likelihood-based probability densities on the plane Ω_Λ (*i.e.*, $\Omega_{\rm v}$ assuming $w = -1$) vs $\Omega_{\rm m}$. The colored locus derives from Planck [32] and shows that the CMB alone requires a flat universe $\Omega_{\rm v} + \Omega_{\rm m} \simeq 1$ if the Hubble constant is not too high. The SNe Ia results [34] very nearly constrain the orthogonal combination $\Omega_{\rm v} - \Omega_{\rm m}$, and the intersection of these constraints directly favors a flat model with $\Omega_{\rm m} \simeq 0.3$, as does the measurement of the Baryon Acoustic Oscillation lengthscale (for which a joint constraint is shown on this plot). The CMB alone is capable of breaking the degeneracy with H_0 by using the measurements of gravitational lensing that can be made with modern high-resolution CMB data.

22.2.4. *Horizon, isotropy, flatness problems* :

For photons, the radial equation of motion is just $c\,dt = R\,d\chi$. How far can a photon get in a given time? The answer is clearly

$$\Delta\chi = \int_{t_1}^{t_2} \frac{dt}{R(t)} \equiv \Delta\eta\ , \qquad (22.31)$$

i.e., just the interval of conformal time. We can replace dt by $dR/\dot{R}$, which the Friedmann equation says is $\propto dR/\sqrt{\rho R^2}$ at early times. Thus, this integral converges if $\rho R^2 \to \infty$ as $t_1 \to 0$, otherwise it diverges. Provided the equation of state is such that ρ changes faster than R^{-2}, light signals can only propagate a finite distance between the Big Bang and the present; there is then said to be a particle horizon. Such a horizon therefore exists in conventional Big-Bang models, which are dominated by radiation ($\rho \propto R^{-4}$) at early times.

At late times, the integral for the horizon is largely determined by the matter-dominated phase, for which

$$D_{\rm H} = R_0\,\chi_{\rm H} \equiv R_0 \int_0^{t(z)} \frac{dt}{R(t)} \simeq \frac{6000}{\sqrt{\Omega_{\rm m} z}}\ h^{-1}\,{\rm Mpc} \quad (z \gg 1)\ . \qquad (22.32)$$

The horizon at the time of formation of the microwave background ('last scattering:' $z \simeq 1100$) was thus of order 100 Mpc in size, subtending an angle of about 1°. Why then are the large number of causally disconnected regions we see on the microwave sky all at the same temperature? The Universe is very nearly isotropic and homogeneous, even though the initial conditions appear not to permit such a state to be constructed.

A related problem is that the $\Omega = 1$ Universe is unstable:

$$\Omega(a) - 1 = \frac{\Omega - 1}{1 - \Omega + \Omega_{\rm v} a^2 + \Omega_{\rm m} a^{-1} + \Omega_{\rm r} a^{-2}}\ , \qquad (22.33)$$

where Ω with no subscript is the total density parameter, and $a(t) = R(t)/R_0$. This requires $\Omega(t)$ to be unity to arbitrary precision as the initial time tends to zero; a universe of non-zero curvature today requires very finely tuned initial conditions.

22.3. The Hot Thermal Universe

22.3.1. *Thermodynamics of the early Universe* :

As alluded to above, we expect that much of the early Universe can be described by a radiation-dominated equation of state. In addition, through much of the radiation-dominated period, thermal equilibrium is established by the rapid rate of particle interactions relative to the expansion rate of the Universe (see Sec. 22.3.3 below). In equilibrium, it is straightforward to compute the thermodynamic quantities, ρ, p, and the entropy density, s. In general, the energy density for a given particle type i can be written as

$$\rho_i = \int E_i\ dn_{q_i}\ , \qquad (22.34)$$

with the density of states given by

$$dn_{q_i} = \frac{g_i}{2\pi^2}\left(\exp[(E_{q_i} - \mu_i)/T_i] \pm 1\right)^{-1}\ q_i^2\ dq_i\ , \qquad (22.35)$$

where g_i counts the number of degrees of freedom for particle type i, $E_{q_i}^2 = m_i^2 + q_i^2$, μ_i is the chemical potential, and the $\pm$ corresponds to either Fermi or Bose statistics. Similarly, we can define the pressure of a perfect gas as

$$p_i = \frac{1}{3}\int \frac{q_i^2}{E_i}\ dn_{q_i}\ . \qquad (22.36)$$

The number density of species i is simply

$$n_i = \int dn_{q_i}\ , \qquad (22.37)$$

and the entropy density is

$$s_i = \frac{\rho_i + p_i - \mu_i n_i}{T_i}\ . \qquad (22.38)$$

In the Standard Model, a chemical potential is often associated with baryon number, and since the net baryon density relative to the photon density is known to be very small (of order 10^{-10}), we can neglect any such chemical potential when computing total thermodynamic quantities.

For photons, we can compute all of the thermodynamic quantities rather easily. Taking $g_i = 2$ for the 2 photon polarization states, we have (in units where $\hbar = k_B = 1$)

$$\rho_\gamma = \frac{\pi^2}{15}T^4 \; ; \quad p_\gamma = \frac{1}{3}\rho_\gamma \; ; \quad s_\gamma = \frac{4\rho_\gamma}{3T} \; ; \quad n_\gamma = \frac{2\zeta(3)}{\pi^2}T^3 \; , \quad (22.39)$$

with $2\zeta(3)/\pi^2 \simeq 0.2436$. Note that Eq. (22.10) can be converted into an equation for entropy conservation. Recognizing that $\dot{p} = s\dot{T}$, Eq. (22.10) becomes

$$d(sR^3)/dt = 0 \; . \quad (22.40)$$

For radiation, this corresponds to the relationship between expansion and cooling, $T \propto R^{-1}$ in an adiabatically expanding universe. Note also that both s and n_γ scale as T^3.

22.3.2. *Radiation content of the Early Universe* :

At the very high temperatures associated with the early Universe, massive particles are pair produced, and are part of the thermal bath. If for a given particle species i we have $T \gg m_i$, then we can neglect the mass in Eq. (22.34) to Eq. (22.38), and the thermodynamic quantities are easily computed as in Eq. (22.39). In general, we can approximate the energy density (at high temperatures) by including only those particles with $m_i \ll T$. In this case, we have

$$\rho = \left(\sum_B g_B + \frac{7}{8}\sum_F g_F\right)\frac{\pi^2}{30}T^4 \equiv \frac{\pi^2}{30}\,N(T)\,T^4 \; , \quad (22.41)$$

where $g_{B(F)}$ is the number of degrees of freedom of each boson (fermion) and the sum runs over all boson and fermion states with $m \ll T$. The factor of 7/8 is due to the difference between the Fermi and Bose integrals. Eq. (22.41) defines the effective number of degrees of freedom, $N(T)$, by taking into account new particle degrees of freedom as the temperature is raised. This quantity is plotted in Fig. 22.3 [39]. For a more recent examination of $N(T)$ near the QCD transition, see [40].

The value of $N(T)$ at any given temperature depends on the particle physics model. In the standard SU(3) × SU(2) × U(1) model, we can specify $N(T)$ up to temperatures of O(100) GeV. The change in N (ignoring mass effects) can be seen in the table below.

Temperature	New Particles	$4N(T)$
$T < m_e$	γ's + ν's	29
$m_e < T < m_\mu$	$e^\pm$	43
$m_\mu < T < m_\pi$	$\mu^\pm$	57
$m_\pi < T < T_c$ †	π's	69
$T_c < T < m_{\rm strange}$	π's + $u, \bar{u}, d, \bar{d}$ + gluons	205
$m_s < T < m_{\rm charm}$	$s, \bar{s}$	247
$m_c < T < m_\tau$	$c, \bar{c}$	289
$m_\tau < T < m_{\rm bottom}$	$\tau^\pm$	303
$m_b < T < m_{\rm W,Z}$	$b, \bar{b}$	345
$m_{W,Z} < T < m_{\rm Higgs}$	$W^\pm, Z$	381
$m_H < T < m_{\rm top}$	H^0	385
$m_t < T$	$t, \bar{t}$	427

†T_c corresponds to the confinement-deconfinement transition between quarks and hadrons.

At higher temperatures, $N(T)$ will be model-dependent. For example, in the minimal SU(5) model, one needs to add 24 states to $N(T)$ for the X and Y gauge bosons, another 24 from the adjoint Higgs, and another 6 (in addition to the 4 already counted in $W^\pm, Z$, and H) from the $\overline{5}$ of Higgs. Hence for $T > m_X$ in minimal SU(5), $N(T) = 160.75$. In a supersymmetric model this would at least double, with some changes possibly necessary in the table if the lightest supersymmetric particle has a mass below m_t.

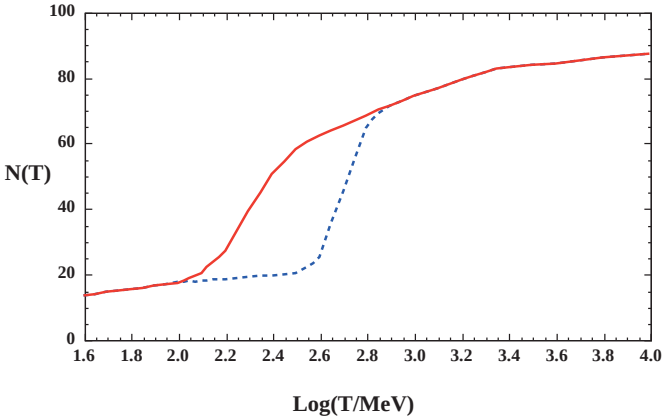

Figure 22.3: The effective numbers of relativistic degrees of freedom as a function of temperature. The sharp drop corresponds to the quark-hadron transition. The solid curve assume a QCD scale of 150 MeV, while the dashed curve assumes 450 MeV.

In the radiation-dominated epoch, Eq. (22.10) can be integrated (neglecting the T-dependence of N) giving us a relationship between the age of the Universe and its temperature

$$t = \left(\frac{90}{32\pi^3 G_{\rm N} N(T)}\right)^{1/2} T^{-2} \; . \quad (22.42)$$

Put into a more convenient form

$$t\,T_{\rm MeV}^2 = 2.4[N(T)]^{-1/2} \; , \quad (22.43)$$

where t is measured in seconds and $T_{\rm MeV}$ in units of MeV.

22.3.3. *Neutrinos and equilibrium* :

Due to the expansion of the Universe, certain rates may be too slow to either establish or maintain equilibrium. Quantitatively, for each particle i, as a minimal condition for equilibrium, we will require that some rate Γ_i involving that type be larger than the expansion rate of the Universe or

$$\Gamma_i > H \; . \quad (22.44)$$

Recalling that the age of the Universe is determined by H^{-1}, this condition is equivalent to requiring that on average, at least one interaction has occurred over the lifetime of the Universe.

A good example for a process which goes in and out of equilibrium is the weak interactions of neutrinos. On dimensional grounds, one can estimate the thermally averaged scattering cross section

$$\langle\sigma v\rangle \sim O(10^{-2})T^2/m_{\rm W}^4 \quad (22.45)$$

for $T \lesssim m_{\rm W}$. Recalling that the number density of leptons is $n \propto T^3$, we can compare the weak interaction rate, $\Gamma_{\rm wk} \sim n\langle\sigma v\rangle$, with the expansion rate,

$$H = \left(\frac{8\pi G_{\rm N}\rho}{3}\right)^{1/2} = \left(\frac{8\pi^3}{90}N(T)\right)^{1/2} T^2/M_{\rm P} \sim 1.66 N(T)^{1/2} T^2/M_{\rm P}, \quad (22.46)$$

where the Planck mass $M_{\rm P} = G_{\rm N}^{-1/2} = 1.22 \times 10^{19}$ GeV.

Neutrinos will be in equilibrium when $\Gamma_{\rm wk} > H$ or

$$T > (500\, m_{\rm W}^4/M_{\rm P})^{1/3} \sim 1 \text{ MeV} \; . \quad (22.47)$$

However, this condition assumes $T \ll m_{\rm W}$; for higher temperatures, we should write $\langle\sigma v\rangle \sim O(10^{-2})/T^2$, so that $\Gamma \sim 10^{-2}T$. Thus, in the very early stages of expansion, at temperatures $T \gtrsim 10^{-2}M_{\rm P}/\sqrt{N}$, equilibrium will not have been established.

Having attained a quasi-equilibrium stage, the Universe then cools further to the point where the interaction and expansion timescales

match once again. The temperature at which these rates are equal is commonly referred to as the neutrino decoupling or freeze-out temperature and is defined by $\Gamma_{\rm wk}(T_d) = H(T_d)$. For $T < T_d$, neutrinos drop out of equilibrium. The Universe becomes transparent to neutrinos and their momenta simply redshift with the cosmic expansion. The effective neutrino temperature will simply fall with $T \sim 1/R$.

Soon after decoupling, $e^{\pm}$ pairs in the thermal background begin to annihilate (when $T \lesssim m_e$). Because the neutrinos are decoupled, the energy released due to annihilation heats up the photon background relative to the neutrinos. The change in the photon temperature can be easily computed from entropy conservation. The neutrino entropy must be conserved separately from the entropy of interacting particles. A straightforward computation yields

$$T_\nu = (4/11)^{1/3}\, T_\gamma \simeq 1.9\ {\rm K}\ . \tag{22.48}$$

Today, the total entropy density is therefore given by

$$s = \frac{4}{3}\frac{\pi^2}{30}\left(2 + \frac{21}{4}(T_\nu/T_\gamma)^3\right) T_\gamma^3 = \frac{4}{3}\frac{\pi^2}{30}\left(2 + \frac{21}{11}\right) T_\gamma^3 = 7.04\, n_\gamma\ . \tag{22.49}$$

Similarly, the total relativistic energy density today is given by

$$\rho_r = \frac{\pi^2}{30}\left[2 + \frac{21}{4}(T_\nu/T_\gamma)^4\right] T_\gamma^4 \simeq 1.68\rho_\gamma\ . \tag{22.50}$$

In practice, a small correction is needed to this, since neutrinos are not totally decoupled at $e^{\pm}$ annihilation: the effective number of massless neutrino species is 3.046, rather than 3 [41].

This expression ignores neutrino rest masses, but current oscillation data require at least one neutrino eigenstate to have a mass exceeding 0.05 eV. In this minimal case, $\Omega_\nu h^2 = 5 \times 10^{-4}$, so the neutrino contribution to the matter budget would be negligibly small (which is our normal assumption). However, a nearly degenerate pattern of mass eigenstates could allow larger densities, since oscillation experiments only measure differences in m^2 values. Note that a 0.05-eV neutrino has $kT_\nu = m_\nu$ at $z \simeq 297$, so the above expression for the total present relativistic density is really only an extrapolation. However, neutrinos are almost certainly relativistic at all epochs where the radiation content of the Universe is dynamically significant.

22.3.4. *Field Theory and Phase transitions* :

It is very likely that the Universe has undergone one or more phase transitions during the course of its evolution [42–45]. Our current vacuum state is described by $\mathrm{SU}(3)_c \times \mathrm{U}(1)_{\rm em}$, which in the Standard Model is a remnant of an unbroken $\mathrm{SU}(3)_c \times \mathrm{SU}(2)_L \times \mathrm{U}(1)_Y$ gauge symmetry. Symmetry breaking occurs when a non-singlet gauge field (the Higgs field in the Standard Model) picks up a non-vanishing vacuum expectation value, determined by a scalar potential. For example, a simple (non-gauged) potential describing symmetry breaking is $V(\phi) = \frac{1}{4}\lambda\phi^4 - \frac{1}{2}\mu^2\phi^2 + V(0)$. The resulting expectation value is simply $\langle\phi\rangle = \mu/\sqrt{\lambda}$.

In the early Universe, finite temperature radiative corrections typically add terms to the potential of the form ϕ^2T^2. Thus, at very high temperatures, the symmetry is restored and $\langle\phi\rangle = 0$. As the Universe cools, depending on the details of the potential, symmetry breaking will occur via a first order phase transition in which the field tunnels through a potential barrier, or via a second order transition in which the field evolves smoothly from one state to another (as would be the case for the above example potential).

The evolution of scalar fields can have a profound impact on the early Universe. The equation of motion for a scalar field ϕ can be derived from the energy-momentum tensor

$$T_{\mu\nu} = \partial_\mu\phi\partial_\nu\phi - \frac{1}{2}g_{\mu\nu}\partial_\rho\phi\partial^\rho\phi - g_{\mu\nu}V(\phi)\ . \tag{22.51}$$

By associating $\rho = T_{00}$ and $p = R^{-2}(t)T_{ii}$ we have

$$\begin{aligned}\rho &= \frac{1}{2}\dot\phi^2 + \frac{1}{2}R^{-2}(t)(\nabla\phi)^2 + V(\phi)\\ p &= \frac{1}{2}\dot\phi^2 - \frac{1}{6}R^{-2}(t)(\nabla\phi)^2 - V(\phi)\ ,\end{aligned} \tag{22.52}$$

and from Eq. (22.10) we can write the equation of motion (by considering a homogeneous region, we can ignore the gradient terms)

$$\ddot\phi + 3H\dot\phi = -\partial V/\partial\phi\ . \tag{22.53}$$

22.3.5. *Inflation* :

In Sec. 22.2.4, we discussed some of the problems associated with the standard Big-Bang model. However, during a phase transition, our assumptions of an adiabatically expanding universe are generally not valid. If, for example, a phase transition occurred in the early Universe such that the field evolved slowly from the symmetric state to the global minimum, the Universe may have been dominated by the vacuum energy density associated with the potential near $\phi \approx 0$. During this period of slow evolution, the energy density due to radiation will fall below the vacuum energy density, $\rho \ll V(0)$. When this happens, the expansion rate will be dominated by the constant V(0), and we obtain the exponentially expanding solution given in Eq. (22.20). When the field evolves towards the global minimum it will begin to oscillate about the minimum, energy will be released during its decay, and a hot thermal universe will be restored. If released fast enough, it will produce radiation at a temperature $NT_R{}^4 \lesssim V(0)$. In this reheating process, entropy has been created and the final value of RT is greater than the initial value of RT. Thus, we see that, during a phase transition, the relation $RT \sim$ constant need not hold true. This is the basis of the inflationary Universe scenario [46–48].

If, during the phase transition, the value of RT changed by a factor of $O(10^{29})$, the cosmological problems discussed above would be solved. The observed isotropy would be generated by the immense expansion; one small causal region could get blown up, and thus our entire visible Universe would have been in thermal contact some time in the past. In addition, the density parameter Ω would have been driven to 1 (with exponential precision). Density perturbations will be stretched by the expansion, $\lambda \sim R(t)$. Thus it will appear that $\lambda \gg H^{-1}$ or that the perturbations have left the horizon, where in fact the size of the causally connected region is now no longer simply H^{-1}. However, not only does inflation offer an explanation for large scale perturbations, it also offers a source for the perturbations themselves through quantum fluctuations.

Early models of inflation were based on a first order phase transition of a Grand Unified Theory [49]. Although these models led to sufficient exponential expansion, completion of the transition through bubble percolation did not occur, and lack of bubble collisions meant that the interior of the bubbles was not reheated. Subsequent models of inflation [50,51] considered second-order transitions within Grand Unified theories, thus successfully ending inflation with reheating from oscillations of the scalar field. But these models predicted too high an amplitude of relic density fluctuations. As a result, current models of inflation postulate second-order transitions in a completely new scalar field: the inflaton, ϕ. The potential of this field, $V(\phi)$, needs to have a very low gradient and curvature in order to match observed metric fluctuations.

In viable inflation models of this type, reheated bubbles again typically do not percolate, so inflation is 'eternal' and continues with exponential expansion in the region outside bubbles. These causally disconnected bubble universes constitute a 'multiverse', where low-energy physics can vary between different bubbles. This has led to a controversial 'anthropic' approach to cosmology [52–54], where observer selection within the multiverse can be introduced as a means of understanding e.g. why the observed level of vacuum energy is so low (because larger values suppress growth of structure).

22.3.6. *Baryogenesis* :

The Universe appears to be populated exclusively with matter rather than antimatter. Indeed antimatter is only detected in accelerators or in cosmic rays. However, the presence of antimatter in the latter is understood to be the result of collisions of primary particles in the interstellar medium. There is in fact strong evidence against primary forms of antimatter in the Universe. Furthermore, the density of baryons compared to the density of photons is extremely small, $\eta \sim 10^{-10}$.

The production of a net baryon asymmetry requires baryon number violating interactions, C and CP violation and a departure from thermal equilibrium [55]. The first two of these ingredients are expected to be contained in grand unified theories as well as in the non-perturbative sector of the Standard Model, the third can be realized in an expanding universe where as we have seen interactions come in and out of equilibrium.

There are several interesting and viable mechanisms for the production of the baryon asymmetry. While, we can not review any of them here in any detail, we mention some of the important scenarios. In all cases, all three ingredients listed above are incorporated. One of the first mechanisms was based on the out of equilibrium decay of a massive particle such as a superheavy GUT gauge of Higgs boson [56,57]. A novel mechanism involving the decay of flat directions in supersymmetric models is known as the Affleck-Dine scenario [58]. There is also the possibility of generating the baryon asymmetry at the electro-weak scale using the non-perturbative interactions of sphalerons [59]. Because these interactions conserve the sum of baryon and lepton number, $B + L$, it is possible to first generate a lepton asymmetry (*e.g.*, by the out-of-equilibrium decay of a superheavy right-handed neutrino), which is converted to a baryon asymmetry at the electro-weak scale [60]. This mechanism is known as lepto-baryogenesis.

22.3.7. *Nucleosynthesis* :

An essential element of the standard cosmological model is Big-Bang nucleosynthesis (BBN), the theory which predicts the abundances of the light element isotopes D, ^{3}He, ^{4}He, and ^{7}Li. Nucleosynthesis takes place at a temperature scale of order 1 MeV. The nuclear processes lead primarily to ^{4}He, with a primordial mass fraction of about 25%. Lesser amounts of the other light elements are produced: about 10^{-5} of D and ^{3}He and about 10^{-10} of ^{7}Li by number relative to H. The abundances of the light elements depend almost solely on one key parameter, the baryon-to-photon ratio, η. The nucleosynthesis predictions can be compared with observational determinations of the abundances of the light elements. Consistency between theory and observations driven primarily by recent D/H measurements [69] leads to a range of

$$5.7 \times 10^{-10} < \eta < 6.7 \times 10^{-10} \; . \tag{22.54}$$

η is related to the fraction of Ω contained in baryons, $\Omega_{\rm b}$

$$\Omega_{\rm b} = 3.66 \times 10^7 \eta \, h^{-2} \; , \tag{22.55}$$

or $10^{10}\eta = 274\Omega_{\rm b}h^2$. The Planck result [32] for $\Omega_{\rm b}h^2$ of 0.0221 ± 0.0003 translates into a value of $\eta = 6.05 \pm 0.07$. This result can be used to 'predict' the light element abundance which can in turn be compared with observation [61]. The resulting D/H abundance is in excellent agreement with that found in quasar absorption systems. It is in reasonable agreement with the helium abundance observed in extra-galactic HII regions (once systematic uncertainties are accounted for), but is in poor agreement with the Li abundance observed in the atmospheres of halo dwarf stars [62]. (See the review on BBN—Sec. 23 of this *Review* for a detailed discussion of BBN or references [63,64].)

22.3.8. *The transition to a matter-dominated Universe* :

In the Standard Model, the temperature (or redshift) at which the Universe undergoes a transition from a radiation dominated to a matter dominated Universe is determined by the amount of dark matter. Assuming three nearly massless neutrinos, the energy density in radiation at temperatures $T \ll 1$ MeV, is given by

$$\rho_{\rm r} = \frac{\pi^2}{30}\left[2 + \frac{21}{4}\left(\frac{4}{11}\right)^{4/3}\right] T^4 \; . \tag{22.56}$$

In the absence of non-baryonic dark matter, the matter density can be written as

$$\rho_{\rm m} = m_{\rm N} \eta \, n_\gamma \; , \tag{22.57}$$

where $m_{\rm N}$ is the nucleon mass. Recalling that $n_\gamma \propto T^3$ [cf. Eq. (22.39)], we can solve for the temperature or redshift at the matter-radiation equality when $\rho_{\rm r} = \rho_{\rm m}$,

$$T_{\rm eq} = 0.22 \, m_{\rm N} \, \eta \qquad \text{or} \qquad (1 + z_{\rm eq}) = 0.22 \, \eta \frac{m_{\rm N}}{T_0} \; , \tag{22.58}$$

where T_0 is the present temperature of the microwave background. For $\eta = 6.1 \times 10^{-10}$, this corresponds to a temperature $T_{\rm eq} \simeq 0.13$ eV or $(1 + z_{\rm eq}) \simeq 550$. A transition this late is very problematic for structure formation (see Sec. 22.4.5).

The redshift of matter domination can be pushed back significantly if non-baryonic dark matter is present. If instead of Eq. (22.57), we write

$$\rho_{\rm m} = \Omega_{\rm m} \rho_{\rm c} \left(\frac{T}{T_0}\right)^3 \; , \tag{22.59}$$

we find that

$$T_{\rm eq} = 0.9 \frac{\Omega_{\rm m} \rho_{\rm c}}{T_0^3} \qquad \text{or} \qquad (1 + z_{\rm eq}) = 2.4 \times 10^4 \Omega_{\rm m} h^2 \; . \tag{22.60}$$

22.4. The Universe at late times

22.4.1. *The CMB* :

One form of the infamous Olbers' paradox says that, in Euclidean space, surface brightness is independent of distance. Every line of sight will terminate on matter that is hot enough to be ionized and so scatter photons: $T \gtrsim 10^3$ K; the sky should therefore shine as brightly as the surface of the Sun. The reason the night sky is dark is entirely due to the expansion, which cools the radiation temperature to 2.73 K. This gives a Planck function peaking at around 1 mm to produce the microwave background (CMB).

The CMB spectrum is a very accurate match to a Planck function [65]. (See the review on CBR–Sec. 27 of this *Review*.) The COBE estimate of the temperature is [66]

$$T = 2.7255 \pm 0.0006 \, {\rm K} \; . \tag{22.61}$$

The lack of any distortion of the Planck spectrum is a strong physical constraint. It is very difficult to account for in any expanding universe other than one that passes through a hot stage. Alternative schemes for generating the radiation, such as thermalization of starlight by dust grains, inevitably generate a superposition of temperatures. What is required in addition to thermal equilibrium is that $T \propto 1/R$, so that radiation from different parts of space appears identical.

Although it is common to speak of the CMB as originating at 'recombination', a more accurate terminology is the era of 'last scattering'. In practice, this takes place at $z \simeq 1100$, almost independently of the main cosmological parameters, at which time the fractional ionization is very small. This occurred when the age of the Universe was a few hundred thousand years. (See the review on CBR–Sec. 27 of this *Review* for a full discussion of the CMB.)

22.4.2. *Matter in the Universe* :

One of the main tasks of cosmology is to measure the density of the Universe, and how this is divided between dark matter and baryons. The baryons consist partly of stars, with $0.002 \lesssim \Omega_* \lesssim 0.003$ [67] but mainly inhabit the intergalactic medium (IGM). One powerful way in which this can be studied is via the absorption of light from distant luminous objects such as quasars. Even very small amounts of neutral hydrogen can absorb rest-frame UV photons (the Gunn-Peterson effect), and should suppress the continuum by a factor $\exp(-\tau)$, where

$$\tau \simeq 10^{4.62} h^{-1} \left[\frac{n_{\rm HI}(z)/{\rm m}^{-3}}{(1+z)\sqrt{1+\Omega_{\rm m} z}}\right] \; , \tag{22.62}$$

and this expression applies while the Universe is matter dominated ($z \gtrsim 1$ in the $\Omega_{\rm m} = 0.3$ $\Omega_{\rm v} = 0.7$ model). It is possible that this general absorption has now been seen at $z = 6.2 - 6.4$ [68]. In any case, the dominant effect on the spectrum is a 'forest' of narrow absorption lines, which produce a mean $\tau = 1$ in the Lyα forest at about $z = 3$, and so we have $\Omega_{\rm HI} \simeq 10^{-6.7} h^{-1}$. This is such a small number that clearly the IGM is very highly ionized at these redshifts.

The Lyα forest is of great importance in pinning down the abundance of deuterium. Because electrons in deuterium differ in reduced mass by about 1 part in 4000 compared to hydrogen, each absorption system in the Lyα forest is accompanied by an offset

deuterium line. By careful selection of systems with an optimal HI column density, a measurement of the D/H ratio can be made. This has now been done with high accuracy in 5 quasars, with consistent results [69]. Combining these determinations with the theory of primordial nucleosynthesis yields a baryon density of $\Omega_{\rm b}h^2 = 0.021 - 0.023$ (95% confidence) in excellent agreement with the Planck result. (See also the review on BBN—Sec. 23 of this *Review*.)

Ionized IGM can also be detected in emission when it is densely clumped, via bremsstrahlung radiation. This generates the spectacular X-ray emission from rich clusters of galaxies. Studies of this phenomenon allow us to achieve an accounting of the total baryonic material in clusters. Within the central $\simeq 1$ Mpc, the masses in stars, X-ray emitting gas and total dark matter can be determined with reasonable accuracy (perhaps 20% rms), and this allows a minimum baryon fraction to be determined [70,71]:

$$\frac{M_{\rm baryons}}{M_{\rm total}} \gtrsim 0.009 + (0.066 \pm 0.003)\, h^{-3/2} \ . \tag{22.63}$$

Because clusters are the largest collapsed structures, it is reasonable to take this as applying to the Universe as a whole. This equation implies a minimum baryon fraction of perhaps 12% (for reasonable h), which is too high for $\Omega_{\rm m} = 1$ if we take $\Omega_{\rm b}h^2 \simeq 0.02$ from nucleosynthesis. This is therefore one of the more robust arguments in favor of $\Omega_{\rm m} \simeq 0.3$. (See the review on Cosmological Parameters—Sec. 24 of this *Review*.) This argument is also consistent with the inference on $\Omega_{\rm m}$ that can be made from Fig. 22.2.

This method is much more robust than the older classical technique for weighing the Universe: '$L \times M/L$.' The overall light density of the Universe is reasonably well determined from redshift surveys of galaxies, so that a good determination of mass M and luminosity L for a single object suffices to determine $\Omega_{\rm m}$ *if* the mass-to-light ratio is universal.

22.4.3. *Gravitational lensing* :

A robust method for determining masses in cosmology is to use gravitational light deflection. Most systems can be treated as a geometrically thin gravitational lens, where the light bending is assumed to take place only at a single distance. Simple geometry then determines a mapping between the coordinates in the intrinsic source plane and the observed image plane:

$$\alpha(D_{\rm L}\theta_{\rm I}) = \frac{D_{\rm S}}{D_{\rm LS}}(\theta_{\rm I} - \theta_{\rm S}) \ , \tag{22.64}$$

where the angles $\theta_{\rm I}, \theta_{\rm S}$ and α are in general two-dimensional vectors on the sky. The distances $D_{\rm LS}$ etc. are given by an extension of the usual distance-redshift formula:

$$D_{\rm LS} = \frac{R_0 S_k(\chi_{\rm S} - \chi_{\rm L})}{1 + z_{\rm S}} \ . \tag{22.65}$$

This is the angular-diameter distance for objects on the source plane as perceived by an observer on the lens.

Solutions of this equation divide into weak lensing, where the mapping between source plane and image plane is one-to-one, and strong lensing, in which multiple imaging is possible. For circularly-symmetric lenses, an on-axis source is multiply imaged into a 'caustic' ring, whose radius is the Einstein radius:

$$\begin{aligned} \theta_{\rm E} &= \left(4GM\,\frac{D_{\rm LS}}{D_{\rm L}D_{\rm S}}\right)^{1/2} \\ &= \left(\frac{M}{10^{11.09}M_\odot}\right)^{1/2} \left(\frac{D_{\rm L}D_{\rm S}/D_{\rm LS}}{\rm Gpc}\right)^{-1/2} \quad \text{arcsec} \ . \end{aligned} \tag{22.66}$$

The observation of 'arcs' (segments of near-perfect Einstein rings) in rich clusters of galaxies has thus given very accurate masses for the central parts of clusters—generally in good agreement with other indicators, such as analysis of X-ray emission from the cluster IGM [72].

Gravitational lensing has also developed into a particularly promising probe of cosmological structure on 10 to 100 Mpc scales. Weak image distortions manifest themselves as an additional ellipticity of galaxy images ('shear'), which can be observed by averaging many images together (the corresponding flux amplification is less readily detected). The result is a 'cosmic shear' field of order 1% ellipticity, coherent over scales of around 30 arcmin, which is directly related to the cosmic mass field, without any astrophysical uncertainties. For this reason, weak lensing is seen as potentially the cleanest probe of matter fluctuations, next to the CMB. Already, impressive results have been obtained in measuring cosmological parameters, based on survey data from only ~ 150 deg^2 [73]. The particular current strength of this technique is the ability to measure the amplitude of mass fluctuations; this can be deduced from the CMB only subject to uncertainty over the optical depth due to Thomson scattering after reionization.

22.4.4. *Density Fluctuations* :

The overall properties of the Universe are very close to being homogeneous; and yet telescopes reveal a wealth of detail on scales varying from single galaxies to large-scale structures of size exceeding 100 Mpc. The existence of these structures must be telling us something important about the initial conditions of the Big Bang, and about the physical processes that have operated subsequently. This motivates the study of the density perturbation field, defined as

$$\delta(\mathbf{x}) \equiv \frac{\rho(\mathbf{x}) - \langle\rho\rangle}{\langle\rho\rangle} \ . \tag{22.67}$$

A critical feature of the δ field is that it inhabits a universe that is isotropic and homogeneous in its large-scale properties. This suggests that the statistical properties of δ should also be statistically homogeneous—*i.e.*, it is a stationary random process.

It is often convenient to describe δ as a Fourier superposition:

$$\delta(\mathbf{x}) = \sum \delta_{\mathbf{k}} e^{-i\mathbf{k}\cdot\mathbf{x}} \ . \tag{22.68}$$

We avoid difficulties with an infinite universe by applying periodic boundary conditions in a cube of some large volume V. The cross-terms vanish when we compute the variance in the field, which is just a sum over modes of the power spectrum

$$\langle\delta^2\rangle = \sum |\delta_{\mathbf{k}}|^2 \equiv \sum P(k) \ . \tag{22.69}$$

Note that the statistical nature of the fluctuations must be isotropic, so we write $P(k)$ rather than $P(\mathbf{k})$. The $\langle\ldots\rangle$ average here is a volume average. Cosmological density fields are an example of an ergodic process, in which the average over a large volume tends to the same answer as the average over a statistical ensemble.

The statistical properties of discrete objects sampled from the density field are often described in terms of N-point correlation functions, which represent the excess probability over random for finding one particle in each of N boxes in a given configuration. For the 2-point case, the correlation function is readily shown to be identical to the autocorrelation function of the δ field: $\xi(r) = \langle\delta(x)\delta(x+r)\rangle$.

The power spectrum and correlation function are Fourier conjugates, and thus are equivalent descriptions of the density field (similarly, k-space equivalents exist for the higher-order correlations). It is convenient to take the limit $V \to \infty$ and use k-space integrals, defining a dimensionless power spectrum, which measures the contribution to the fractional variance in density per unit logarithmic range of scale, as $\Delta^2(k) = d\langle\delta^2\rangle/d\ln k = Vk^3P(k)/2\pi^2$:

$$\xi(r) = \int \Delta^2(k)\,\frac{\sin kr}{kr}\,d\ln k; \quad \Delta^2(k) = \frac{2}{\pi}k^3\int_0^\infty \xi(r)\,\frac{\sin kr}{kr}\,r^2\,dr \ . \tag{22.70}$$

For many years, an adequate approximation to observational data on galaxies was $\xi = (r/r_0)^{-\gamma}$, with $\gamma \simeq 1.8$ and $r_0 \simeq 5\,h^{-1}\,$Mpc. Modern surveys are now able to probe into the large-scale linear regime where unaltered traces of the curved post-recombination spectrum can be detected [74–76].

22.4.5. *Formation of cosmological structure* :

The simplest model for the generation of cosmological structure is gravitational instability acting on some small initial fluctuations (for the origin of which a theory such as inflation is required). If the perturbations are adiabatic (*i.e.*, fractionally perturb number densities of photons and matter equally), the linear growth law for matter perturbations is simple:

$$\delta \propto \begin{cases} a^2(t) & \text{(radiation domination; } \Omega_{\rm r} = 1) \\ a(t) & \text{(matter domination; } \Omega_{\rm m} = 1) \ . \end{cases} \tag{22.71}$$

For low-density universes, the growth is slower:

$$d\ln\delta/d\ln a \simeq \Omega_{\rm m}^{\gamma}(a), \tag{22.72}$$

where the parameter γ is close to 0.55 independent of the vacuum density [77].

The alternative perturbation mode is isocurvature: only the equation of state changes, and the total density is initially unperturbed. These modes perturb the total entropy density, and thus induce additional large-scale CMB anisotropies [78]. Although the character of perturbations in the simplest inflationary theories are purely adiabatic, correlated adiabatic and isocurvature modes are predicted in many models; the simplest example is the curvaton, which is a scalar field that decays to yield a perturbed radiation density. If the matter content already exists at this time, the overall perturbation field will have a significant isocurvature component. Such a prediction is inconsistent with current CMB data [79], and most analyses of CMB and large scale structure (LSS) data assume the adiabatic case to hold exactly.

Linear evolution preserves the shape of the power spectrum. However, a variety of processes mean that growth actually depends on the matter content:

(1) Pressure opposes gravity effectively for wavelengths below the horizon length while the Universe is radiation dominated. The *comoving* horizon size at $z_{\rm eq}$ is therefore an important scale:

$$D_{\rm H}(z_{\rm eq}) = \frac{2(\sqrt{2}-1)}{(\Omega_{\rm m} z_{\rm eq})^{1/2} H_0} = \frac{16.0}{\Omega_{\rm m} h^2}\,{\rm Mpc} \ . \tag{22.73}$$

(2) At early times, dark matter particles will undergo free streaming at the speed of light, and so erase all scales up to the horizon—a process that only ceases when the particles go nonrelativistic. For light massive neutrinos, this happens at $z_{\rm eq}$; all structure up to the horizon-scale power-spectrum break is in fact erased. Hot(cold) dark matter models are thus sometimes dubbed large(small)-scale damping models.

(3) A further important scale arises where photon diffusion can erase perturbations in the matter–radiation fluid; this process is named Silk damping.

The overall effect is encapsulated in the transfer function, which gives the ratio of the late-time amplitude of a mode to its initial value (see Fig. 22.4). The overall power spectrum is thus the primordial scalar-mode power law, times the square of the transfer function:

$$P(k) \propto k^{n_{\rm s}}\, T_k^2 \ . \tag{22.74}$$

The most generic power-law index is $n_{\rm s} = 1$: the 'Zeldovich' or 'scale-invariant' spectrum. Inflationary models tend to predict a small 'tilt:' $|n_{\rm s} - 1| \lesssim 0.03$ [12,13]. On the assumption that the dark matter is cold, the power spectrum then depends on 5 parameters: $n_{\rm s}$, h, $\Omega_{\rm b}$, $\Omega_{\rm c}$ ($\equiv \Omega_{\rm m} - \Omega_{\rm b}$) and an overall amplitude. The latter is often specified as σ_8, the linear-theory fractional rms in density when a spherical filter of radius $8\,h^{-1}\,{\rm Mpc}$ is applied in linear theory. This scale can be probed directly via weak gravitational lensing, and also via its effect on the abundance of rich galaxy clusters. The favored value from the latter is approximately [80]

$$\sigma_8 \simeq [0.813 \pm 0.013\,({\rm stat}) \pm 0.024\,({\rm sys})]\,(\Omega_{\rm m}/0.25)^{-0.47}, \tag{22.75}$$

which is consistent with the Planck values of $(\sigma_8, \Omega_{\rm m}) = (0.828 \pm 0.012, 0.315^{+0.017}_{-0.016})$.

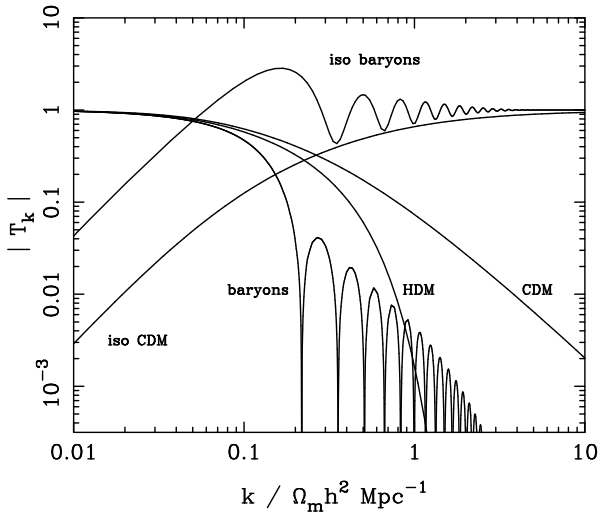

Figure 22.4: A plot of transfer functions for various models. For adiabatic models, $T_k \to 1$ at small k, whereas the opposite is true for isocurvature models. For dark-matter models, the characteristic wavenumber scales proportional to $\Omega_{\rm m}h^2$. The scaling for baryonic models does not obey this exactly; the plotted cases correspond to $\Omega_{\rm m} = 1$, $h = 0.5$.

A direct measure of mass inhomogeneity is valuable, since the galaxies inevitably are biased with respect to the mass. This means that the fractional fluctuations in galaxy number, $\delta n/n$, may differ from the mass fluctuations, $\delta\rho/\rho$. It is commonly assumed that the two fields obey some proportionality on large scales where the fluctuations are small, $\delta n/n = b\delta\rho/\rho$, but even this is not guaranteed [81].

The main shape of the transfer function is a break around the horizon scale at $z_{\rm eq}$, which depends just on $\Omega_{\rm m}h$ when wavenumbers are measured in observable units ($h\,{\rm Mpc}^{-1}$). For reasonable baryon content, weak oscillations in the transfer function are also expected, and these BAOs (Baryon Acoustic Oscillations) have been clearly detected [82,83]. As well as directly measuring the baryon fraction, the scale of the oscillations directly measures the acoustic horizon at decoupling; this can be used as an additional standard ruler for cosmological tests, and the BAO signature has become one of the most important applications of large galaxy surveys. Overall, current power-spectrum data [74–76] favor $\Omega_{\rm m}h \simeq 0.20$ and a baryon fraction of about 0.15 for $n_{\rm s} = 1$ (see Fig. 22.5).

In principle, accurate data over a wide range of k could determine both $\Omega_{\rm m}h$ and n, but in practice there is a strong degeneracy between these. In order to constrain $n_{\rm s}$ itself, it is necessary to examine data on anisotropies in the CMB.

22.4.6. *CMB anisotropies* :

The CMB has a clear dipole anisotropy, of magnitude 1.23×10^{-3}. This is interpreted as being due to the Earth's motion, which is equivalent to a peculiar velocity for the Milky Way of

$$v_{\rm MW} \simeq 600\,{\rm km\,s^{-1}} \quad \text{towards} \quad (\ell, b) \simeq (270^\circ, 30^\circ) \ . \tag{22.76}$$

All higher-order multipole moments of the CMB are however much smaller (of order 10^{-5}), and interpreted as signatures of density fluctuations at last scattering ($\simeq 1100$). To analyze these, the sky is expanded in spherical harmonics as explained in the review on CBR–Sec. 27 of this *Review*. The dimensionless power per ln k or 'bandpower' for the CMB is defined as

$$\mathcal{T}^2(\ell) = \frac{\ell(\ell+1)}{2\pi} C_\ell \ . \tag{22.77}$$

This function encodes information from the three distinct mechanisms that cause CMB anisotropies:

(1) Gravitational (Sachs–Wolfe) perturbations. Photons from high-density regions at last scattering have to climb out of potential wells, and are thus redshifted.

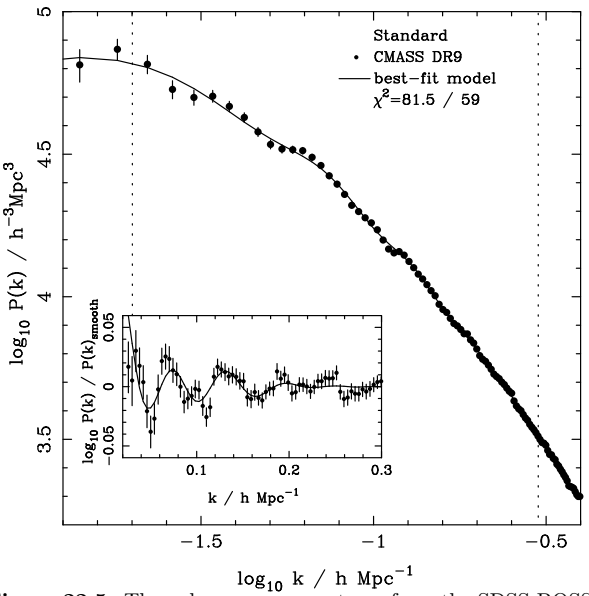

Figure 22.5: The galaxy power spectrum from the SDSS BOSS survey [76]. The solid points with error bars show the power estimate. The solid line shows a standard ΛCDM model with $\Omega_{\rm b}h^2 \simeq 0.02$ and $\Omega_{\rm m}h \simeq 0.2$. The inset amplifies the region where BAO features are visible. The fact that these perturb the power by $\sim 20\%$ rather than order unity is direct evidence that the matter content of the universe is dominated by collisionless dark matter.

(2) Intrinsic (adiabatic) perturbations. In high-density regions, the coupling of matter and radiation can compress the radiation also, giving a higher temperature.

(3) Velocity (Doppler) perturbations. The plasma has a non-zero velocity at recombination, which leads to Doppler shifts in frequency and hence shifts in brightness temperature.

Because the potential fluctuations obey Poisson's equation, $\nabla^2\Phi = 4\pi G\rho\delta$, and the velocity field satisfies the continuity equation $\nabla\cdot\mathbf{u} = -\dot{\delta}$, the resulting different powers of k ensure that the Sachs-Wolfe effect dominates on large scales and adiabatic effects on small scales.

The relation between angle and comoving distance on the last-scattering sphere requires the comoving angular-diameter distance to the last-scattering sphere; because of its high redshift, this is effectively identical to the horizon size at the present epoch, $D_{\rm H}$:

$$\begin{aligned} D_{\rm H} &= \frac{2}{\Omega_{\rm m}H_0} \quad (\Omega_{\rm v}=0) \\ D_{\rm H} &\simeq \frac{2}{\Omega_{\rm m}^{0.4}H_0} \quad (\text{flat}: \Omega_{\rm m}+\Omega_{\rm v}=1)\ . \end{aligned} \tag{22.78}$$

These relations show how the CMB is strongly sensitive to curvature: the horizon length at last scattering is $\propto 1/\sqrt{\Omega_{\rm m}}$, so that this subtends an angle that is virtually independent of $\Omega_{\rm m}$ for a flat model. Observations of a peak in the CMB power spectrum at relatively large scales ($\ell \simeq 225$) are thus strongly inconsistent with zero-Λ models with low density: current CMB + BAO +SN data require $\Omega_{\rm m}+\Omega_{\rm v} = 1.001 \pm 0.003$ [32]. (See *e.g.*, Fig. 22.2).

In addition to curvature, the CMB encodes information about several other key cosmological parameters. Within the compass of simple adiabatic CDM models, there are 9 of these:

$$\omega_{\rm c},\ \omega_{\rm b},\ \Omega_{\rm tot},\ h,\ \tau,\ n_{\rm s},\ n_{\rm t},\ r,\ Q\ . \tag{22.79}$$

The symbol ω denotes the physical density, Ωh^2: the transfer function depends only on the densities of CDM ($\omega_{\rm c}$) and baryons ($\omega_{\rm b}$). Transcribing the power spectrum at last scattering into an angular power spectrum brings in the total density parameter ($\Omega_{\rm tot} \equiv \Omega_{\rm m}+\Omega_{\rm v} = \Omega_{\rm c}+\Omega_{\rm b}+\Omega_{\rm v}$) and h: there is an exact geometrical degeneracy [84] between these that keeps the angular-diameter distance to last scattering invariant, so that models with substantial spatial curvature and large vacuum energy cannot be ruled out without prior knowledge of the Hubble parameter. Alternatively, the CMB alone cannot measure the Hubble parameter.

A further approximate degeneracy involves the tensor contribution to the CMB anisotropies. These are important at large scales (up to the horizon scales); for smaller scales, only scalar fluctuations (density perturbations) are important. Each of these components is characterized by a spectral index, n, and a ratio between the power spectra of tensors and scalars (r). See the review on Cosmological Parameters—Sec. 24 of this *Review* for a technical definition of the r parameter. Finally, the overall amplitude of the spectrum must be specified (Q), together with the optical depth to Compton scattering owing to recent reionization (τ). The tensor degeneracy operates as follows: the main effect of adding a large tensor contribution is to reduce the contrast between low ℓ and the peak at $\ell \simeq 225$ (because the tensor spectrum has no acoustic component). The required height of the peak can be recovered by increasing $n_{\rm s}$ to increase the small-scale power in the scalar component; this in turn over-predicts the power at $\ell \sim 1000$, but this effect can be counteracted by raising the baryon density [85]. This degeneracy is reduced as we increase the range of multipoles sampled.

The reason the tensor component is introduced, and why it is so important, is that it is the only non-generic prediction of inflation. Slow-roll models of inflation involve two dimensionless parameters:

$$\epsilon \equiv \frac{M_{\rm P}^2}{16\pi}\left(\frac{V'}{V}\right)^2 \qquad \eta \equiv \frac{M_{\rm P}^2}{8\pi}\left(\frac{V''}{V}\right)\ , \tag{22.80}$$

where V is the inflaton potential, and dashes denote derivatives with respect to the inflation field. In terms of these, the tensor-to-scalar ratio is $r \simeq 16\epsilon$, and the spectral indices are $n_{\rm s} = 1-6\epsilon+2\eta$ and $n_{\rm t} = -2\epsilon$. The natural expectation of inflation is that the quasi-exponential phase ends once the slow-roll parameters become significantly non-zero, so that both $n_{\rm s} \neq 1$ and a significant tensor component are expected. These prediction can be avoided in some models, but it is undeniable that observation of such features would be a great triumph for inflation. Cosmology therefore stands at a fascinating point given that the most recent CMB data appear to reject the zero-tensor $n_{\rm s} = 1$ model at over 6σ: $n_{\rm s} = 0.958 \pm 0.007$ [32]. This rejection is strong enough that it is also able to break the tensor degeneracy, so that no model with $n_{\rm s} = 1$ is acceptable, whatever the value of r.

The current limit on r is < 0.11 at 95% confidence [86]. In conjunction with the measured value of $n_{\rm s}$, this upper limit sits close to the prediction of a linear potential (i.e. $|\eta| \ll |\epsilon|$). Any further reduction in the limit on r will force η to be negative – i.e. a convex potential at the point where LSS scales were generated (sometimes called a 'hilltop'), in contrast to simple early models such as $V(\phi) = m^2\phi^2$ or $\lambda\phi^4$. Examples of models which are currently in excellent agreement with the Planck results are the Starobinsky model of $\mathcal{R}+\mathcal{R}^2$ gravity [87], or the Higgs-inflation model where the Higgs field is non-minimally coupled [88]. Assuming 55 e-foldings of inflation, these models predict $n_{\rm s} = 0.965$ and $r = 0.0035$. Assuming that no systematic error in the CMB data can be identified, cosmology has passed a critical hurdle in rejecting scale-invariant fluctuations. The years ahead will be devoted to the task of searching for the tensor fluctuations – for which the main tool will be the polarization of the CMB [14].

22.4.6.1. *CMB foregrounds:*

As the quality of CMB data improves, there is a growing interest in effects that arise along the line of sight. The CMB temperature is perturbed by dark-matter structures and by Compton scattering from ionized gas. In the former case, we have the Integrated Sachs-Wolfe effect, which is sensitive to the time derivative of the gravitational potential. In the linear regime, this is damped when the universe becomes Λ-dominated, and this is an independent way of detecting Λ [89]. The potential also causes gravitational lensing of the CMB: structures at $z \sim 1-2$ displace features on the CMB sky by

about 2 arcmin over coherent degree-scale patches. Detection of these distortions allows a map to be made of overdensity projected from $z = 0$ to 1100 [90]. This is a very powerful calibration for direct studies of gravitational lensing using galaxies. Finally, Comptonization affects the CMB in two ways: the thermal Sunyaev-Zeldovich effect measures the blurring of photons energies by hot gas; the kinetic Sunyaev-Zeldovich effect is sensitive to the bulk velocity of the gas. Both these effects start to dominate over the intrinsic CMB fluctuations at multipoles $\ell \gtrsim 2000$ [91].

22.4.7. *Probing dark energy and the nature of gravity* :

The most radical element of our current cosmological model is the dark energy that accelerates the expansion. The energy density of this component is approximately $(2.2\,\mathrm{meV})^4$ (for $w = -1$, $\Omega_v = 0.68$, $h = 0.67$), or roughly $10^{-123} M_{\rm P}^4$, and such an un-naturally small number is hard to understand. Various quantum effects (most simply zero-point energy) should make contributions to the vacuum energy density: these may be truncated by new physics at high energy, but this presumably occurs at $> 1\,\mathrm{TeV}$ scales, not meV; thus the apparent energy scale of the vacuum is at least 10^{15} times smaller than its natural value. This situation is well analysed in [52], which lists extreme escape routes – especially the multiverse viewpoint, according to which low values of Λ are rare, but high values suppress the formation of structure and observers. It is certainly impressive that Weinberg used such reasoning to predict the value of Λ before any data strongly indicated a non-zero value.

But it may be that the phenomenon of dark energy is entirely illusory. The necessity for this constituent arises from using the Friedmann equation to describe the evolution of the cosmic expansion; if this equation is incorrect, it would require the replacement of Einstein's relativistic theory of gravity with some new alternative. A frontier of current cosmological research is to distinguish these possibilities [92,93]. We also note that it has been suggested that dark energy might be an illusion even within general relativity, owing to an incorrect treatment of averaging in an inhomogeneous Universe [94,95]. Many would argue that a standard Newtonian treatment of such issues should be adequate inside the cosmological horizon, but debate on this issue continues.

Dark Energy can differ from a classical cosmological constant in being a dynamical phenomenon [96,97], *e.g.*, a rolling scalar field (sometimes dubbed 'quintessence'). Empirically, this means that it is endowed with two thermodynamic properties that astronomers can try to measure: the bulk equation of state and the sound speed. If the sound speed is close to the speed of light, the effect of this property is confined to very large scales, and mainly manifests itself in the large-angle multipoles of the CMB anisotropies [98]. The equation of state parameter governs the rate of change of the vacuum density: $d\ln\rho_v/d\ln a = -3(1+w)$, so it can be accessed via the evolving expansion rate, $H(a)$. This can be measured most cleanly by using the inbuilt natural ruler of large-scale structure: the Baryon Acoustic Oscillation horizon scale [99]:

$$D_{\rm BAO} \simeq 147\,(\Omega_{\rm m}h^2/0.13)^{-0.25}(\Omega_{\rm b}h^2/0.023)^{-0.08}\ \mathrm{Mpc}\ . \qquad (22.81)$$

$H(a)$ is measured by radial clustering, since $dr/dz = c/H$; clustering in the plane of the sky measures the integral of this. The expansion rate is also measured by the growth of density fluctuations, where the pressure-free growth equation for the density perturbation is $\ddot\delta + 2H(a)\dot\delta = 4\pi G\rho_0\,\delta$. Thus, both the scale and amplitude of density fluctuations are sensitive to $w(a)$ – but only weakly. These observables change by only typically 0.2% for a 1% change in w. Current constraints [32] place a constant w to within 5-10% of -1, depending on the data combination chosen A substantial improvement in this precision will require us to limit systematics in data to a few parts in 1000.

Testing whether theories of gravity require revision can also be done using data on cosmological inhomogeneities. Two separate issues arise, concerning the metric perturbation potentials Ψ and Φ, which affect respectively the time and space parts of the metric. In Einstein gravity, these potentials are both equal to the Newtonian gravitational potential, which satisfies Poisson's equation: $\nabla^2\Phi/a^2 = 4\pi G\bar\rho\delta$. Empirically, modifications of gravity require us to explore a change with scale and with time of the 'slip' (Ψ/Φ) and the effective G on the rhs of the Poisson equation. The former aspect can only be probed via gravitational lensing, whereas the latter can be addressed on 10-100 Mpc scales via the growth of clustering. Various schemes for parameterising modified gravity exist, but a practical approach is to assume that the growth rate can be tied to the density parameter: $d\ln\delta/d\ln a = \Omega_{\rm m}^{\gamma}(a)$ [77]. The parameter γ is close to 0.55 for standard relativistic gravity, but can differ by around 0.1 from this value in many non-standard models. Clearly this parameterization is incomplete, since it explicitly rejects the possibility of early dark energy ($\Omega_{\rm m}(a) \to 1$ as $a \to 0$), but it is a convenient way of capturing the power of various experiments. Current data are consistent with standard ΛCDM [100], and exclude variations in slip or effective G of larger than a few times 10%.

Current planning envisages a set of satellite probes that, a decade hence, will pursue these fundamental tests via gravitational lensing measurements over thousands of square degrees, $> 10^8$ redshifts, and photometry of > 1000 supernovae (WFIRST in the USA, Euclid in Europe) [22,23]. These experiments will measure both w and the perturbation growth rate to an accuracy of around 1%. The outcome will be either a validation of the standard relativistic vacuum-dominated big bang cosmology at a level of precision far beyond anything attempted to date, or the opening of entirely new directions in cosmological models. For a more complete discussion of dark energy and future probes see the review on Dark Energy—Sec. 26

References:

1. V.M. Slipher, Pop. Astr. **23**, 21 (1915).
2. K. Lundmark, MNRAS **84**, 747 (1924).
3. E. Hubble and M.L. Humason, Astrophys. J. **74**, 43 (1931).
4. G. Gamow, Phys. Rev. **70**, 572 (1946).
5. R.A. Alpher *et al.*, Phys. Rev. **73**, 803 (1948).
6. R.A. Alpher and R.C. Herman, Phys. Rev. **74**, 1737 (1948).
7. R.A. Alpher and R.C. Herman, Phys. Rev. **75**, 1089 (1949).
8. A.A. Penzias and R.W. Wilson, Astrophys. J. **142**, 419 (1965).
9. P.J.E. Peebles, *Principles of Physical Cosmology*, Princeton University Press (1993).
10. G. Börner, *The Early Universe: Facts and Fiction*, Springer-Verlag (1988).
11. E.W. Kolb and M.S. Turner, *The Early Universe*, Addison-Wesley (1990).
12. J.A. Peacock, *Cosmological Physics*, Cambridge Univ. Press (1999).
13. A.R. Liddle and D. Lyth, *Cosmological Inflation and Large-Scale Structure*, Cambridge University Press (2000).
14. S. Dodelson, *Modern Cosmology*, Academic Press (2003).
15. V. Mukhanov, *Physical Foundations of Cosmology*, Cambridge University Press (2005).
16. S. Weinberg, *Cosmology*, Oxford Press (2008).
17. E.B. Gliner, Sov. Phys. JETP **22**, 378 (1966).
18. Y.B. Zeldovich, (1967), Sov. Phys. Usp. **11**, 381 (1968).
19. P.M. Garnavich *et al.*, Astrophys. J. **507**, 74 (1998).
20. S. Perlmutter *et al.*, Phys. Rev. Lett. **83**, 670 (1999).
21. I. Maor *et al.*, Phys. Rev. **D65**, 123003 (2002).
22. A. Albrecht *et al.*, `astro-ph/0609591`.
23. J. Peacock *et al.*, `astro-ph/0610906`.
24. E. Komatsu *et al.*, Astrophys. J. Supp. **191**, 18 (2011).
25. A.G. Riess *et al.*, Astrophys. J. **116**, 1009 (1998).
26. S. Perlmutter *et al.*, Astrophys. J. **517**, 565 (1999).
27. A.G. Riess, Pub. Astron. Soc. Pac. **112**, 1284 (2000).
28. A.G. Riess *et al.*, Astrophys. J. **659**, 98 (2007).
29. T.M. Davis *et al.*, Astrophys. J. **666**, 716 (2007).
30. J.L. Tonry *et al.*, Astrophys. J. **594**, 1 (2003).
31. M. Kowalski *et al.*, Astrophys. J. **686**, 749 (2008).
32. P.A.R. Ade *et al.*, `arXiv:1303.5076`.
33. L. Humphreys *et al.*, `arXiv:1307.6031`.
34. P. Astier *et al.*, Astron. & Astrophys. **447**, 31 (2006).
35. J.A. Johnson and M. Bolte, Astrophys. J. **554**, 888 (2001).
36. R. Cayrel *et al.*, Nature **409**, 691 (2001).
37. R. Jimenez and P. Padoan, Astrophys. J. **498**, 704 (1998).

38. E. Carretta *et al.*, Astrophys. J. **533**, 215 (2000).
39. M. Srednicki *et al.*, Nucl. Phys. **B310**, 693 (1988).
40. S. Borsanyi *et al.*, JHEP **1011**, 077 (2010).
41. G. Mangano *et al.*, Phys. Lett. **B534**, 8 (2002).
42. A. Linde, Phys. Rev. **D14**, 3345 (1976).
43. A. Linde, Rept. on Prog. in Phys. **42**, 389 (1979).
44. C.E. Vayonakis, Surv. High Energy Physics **5**, 87 (1986).
45. S.A. Bonometto and A. Masiero, Nuovo Cimento **9N5**, 1 (1986).
46. A. Linde, *Particle Physics And Inflationary Cosmology*, Harwood (1990).
47. K.A. Olive, Phys. Reports **190**, 3345 (1990).
48. D. Lyth and A. Riotto, Phys. Reports **314**, 1 (1999).
49. A.H. Guth, Phys. Rev. **D23**, 347 (1981).
50. A.D. Linde, Phys. Lett. **108B**, 389 (1982).
51. A. Albrecht and P.J. Steinhardt, Phys. Rev. Lett. **48**, 1220 (1982).
52. S. Weinberg, Rev. Mod. Phys. **60**, 1 (1989).
53. L. Susskind, `hep-th/0302219` (2003).
54. B. Carr, *Universe or multiverse?* C.U.P. (2007).
55. A.D. Sakharov, Sov. Phys. JETP Lett. **5**, 24 (1967).
56. S. Weinberg, Phys. Rev. Lett. **42**, 850 (1979).
57. D. Toussaint *et al.*, Phys. Rev. **D19**, 1036 (1979).
58. I. Affleck and M. Dine, Nucl. Phys. **B249**, 361 (1985).
59. V. Kuzmin *et al.*, Phys. Lett. **B155**, 36 (1985).
60. M. Fukugita and T. Yanagida, Phys. Lett. **B174**, 45 (1986).
61. R.H. Cyburt *et al.*, Phys. Lett. **B567**, 227 (2003).
62. R.H. Cyburt *et al.*, JCAP **0811**, 012 (2008).
63. K.A. Olive *et al.*, Phys. Reports **333**, 389 (2000).
64. J. M. O'meara *et al.*, Astrophys. J. **649**, L61 (2006).
65. D.J. Fixsen *et al.*, Astrophys. J. **473**, 576 (1996).
66. J.C. Mather *et al.*, Astrophys. J. **512**, 511 (1999).
67. S.M. Cole *et al.*, MNRAS **326**, 255 (2001).
68. A. Mesinger and Z. Haiman, Astrophys. J. **660**, 923 (2007).
69. R.Y. Cooke, `arXiv:1308.3240`.
70. S.D.M. White *et al.*, Nature **366**, 429 (1993).
71. S.W. Allen *et al.*, MNRAS **334**, L11 (2002).
72. S.W. Allen, MNRAS **296**, 392 (1998).
73. M. Kilbinger *et al.*, `arXiv:1212.3338`.
74. S.M. Cole *et al.*, MNRAS **362**, 505 (2005).
75. W.J. Percival *et al.*, Astrophys. J. **657**, 645 (2007).
76. L. Anderson *et al.*, MNRAS **427**, 3435 (2012).
77. E. Linder, Phys. Rev. **D72**, 43529 (2005).
78. G. Efstathiou and J.R. Bond, MNRAS **218**, 103 (1986).
79. C. Gordon and A. Lewis, Phys. Rev. **D67**, 123513 (2003).
80. A. Vikhlinin *et al.*, Astrophys. J. **692**, 1060 (2009).
81. A. Dekel and O. Lahav, Astrophys. J. **520**, 24 (1999).
82. W.J. Percival *et al.*, MNRAS **381**, 1053 (2007).
83. W.J. Percival *et al.*, MNRAS **401**, 2148 (2010).
84. G. Efstathiou and J.R. Bond, MNRAS **304**, 75 (1999).
85. G.P. Efstathiou *et al.*, MNRAS **330**, L29 (2002).
86. P.A.R. Ade *et al.*, `arXiv:1303.5082`.
87. A. A. Starobinsky, Phys. Lett. **B91**, 99 (1980).
88. F. Bezrukov and M. Shaposhnikov, JHEP **0907**, 089 (2009).
89. P.A.R. Ade *et al.*, `arXiv:1303.5079`.
90. P.A.R. Ade *et al.*, `arXiv:1303.5077`.
91. P.A.R. Ade *et al.*, `arXiv:1303.5081`.
92. W. Hu and I. Sawicki, Phys. Rev. **D76**, 4043 (2007).
93. B. Jain and P. Zhang, Phys. Rev. **D78**, 3503 (2008).
94. D.L. Wiltshire, Phys. Rev. Lett. **99**, 251101 (2007).
95. T. Buchert, Gen. Rel. Grav. **40**, 467 (2008).
96. I. Zlatev *et al.*, Phys. Rev. Lett. **82**, 896 (1999).
97. C. Armendariz-Picon, V. Mukhanov, and P.J. Steinhardt, Phys. Rev. **D63**, 3510 (2001).
98. S. DeDeo, R.R. Caldwell, and P.J. Steinhardt, Phys. Rev. **D67**, 3509 (2003).
99. W. Hu, `arXiv:astro-ph/0407158` (2004).
100. S.F. Daniel *et al.*, Phys. Rev. **D81**, 123508 (2010).

23. BIG-BANG NUCLEOSYNTHESIS

Revised October 2013 by B.D. Fields, (Univ. of Illinois) P. Molaro (Trieste Observatory) and S. Sarkar (Univ. of Oxford & Niels Bohr Institute, Copenhagen).

Big-Bang nucleosynthesis (BBN) offers the deepest reliable probe of the early Universe, being based on well-understood Standard Model physics [1]. Predictions of the abundances of the light elements, D, ^{3}He, ^{4}He, and ^{7}Li, synthesized at the end of the 'first three minutes', are in good overall agreement with the primordial abundances inferred from observational data, thus validating the standard hot Big-Bang cosmology (see [2–4] for reviews). This is particularly impressive given that these abundances span nine orders of magnitude – from $^4\mathrm{He/H} \sim 0.08$ down to $^7\mathrm{Li/H} \sim 10^{-10}$ (ratios by number). Thus BBN provides powerful constraints on possible deviations from the standard cosmology, and on new physics beyond the Standard Model [5–8].

23.1. Theory

The synthesis of the light elements is sensitive to physical conditions in the early radiation-dominated era at a temperature $T \sim 1$ MeV, corresponding to an age $t \sim 1$ s. At higher temperatures, weak interactions were in thermal equilibrium, thus fixing the ratio of the neutron and proton number densities to be $n/p = \mathrm{e}^{-Q/T}$, where $Q = 1.293$ MeV is the neutron-proton mass difference. As the temperature dropped, the neutron-proton inter-conversion rate per nucleon, $\Gamma_{n \leftrightarrow p} \sim G_\mathrm{F}^2 T^5$, fell faster than the Hubble expansion rate, $H \sim \sqrt{g_* G_\mathrm{N}}\, T^2$, where g_* counts the number of relativistic particle species determining the energy density in radiation (see 'Big Bang Cosmology' review). This resulted in departure from chemical equilibrium ('freeze-out') at $T_\mathrm{fr} \sim (g_* G_\mathrm{N}/G_\mathrm{F}^4)^{1/6} \simeq 1$ MeV. The neutron fraction at this time, $n/p = \mathrm{e}^{-Q/T_\mathrm{fr}} \simeq 1/6$, is thus sensitive to every known physical interaction, since Q is determined by both strong and electromagnetic interactions while T_fr depends on the weak as well as gravitational interactions. Moreover, the sensitivity to the Hubble expansion rate affords a probe of, *e.g.,* the number of relativistic neutrino species [9]. After freeze-out, the neutrons were free to β-decay, so the neutron fraction dropped to $n/p \simeq 1/7$ by the time nuclear reactions began. A simplified analytic model of freeze-out yields the n/p ratio to an accuracy of $\sim 1\%$ [10,11].

The rates of these reactions depend on the density of baryons (strictly speaking, nucleons), which is usually expressed normalized to the relic blackbody photon density as $\eta \equiv n_\mathrm{b}/n_\gamma$. As we shall see, all the light-element abundances can be explained with $\eta_{10} \equiv \eta \times 10^{10}$ in the range 5.7–6.7 (95% CL). With n_γ fixed by the present CMB temperature 2.7255 K (see 'Cosmic Microwave Background' review), this can be stated as the allowed range for the baryon mass density today, $\rho_\mathrm{b} = (3.9\text{–}4.6) \times 10^{-31}$ g cm^{-3}, or as the baryonic fraction of the critical density, $\Omega_\mathrm{b} = \rho_\mathrm{b}/\rho_\mathrm{crit} \simeq \eta_{10} h^{-2}/274 = (0.021\text{–}0.025) h^{-2}$, where $h \equiv H_0/100$ km s^{-1} Mpc^{-1} is the present Hubble parameter (see Cosmological Parameters review).

The nucleosynthesis chain begins with the formation of deuterium in the process $p(n,\gamma)$D. However, photo-dissociation by the high number density of photons delays production of deuterium (and other complex nuclei) until well after T drops below the binding energy of deuterium, $\Delta_\mathrm{D} = 2.23$ MeV. The quantity $\eta^{-1}\mathrm{e}^{-\Delta_\mathrm{D}/T}$, *i.e.,* the number of photons per baryon above the deuterium photo-dissociation threshold, falls below unity at $T \simeq 0.1$ MeV; nuclei can then begin to form without being immediately photo-dissociated again. Only 2-body reactions, such as $\mathrm{D}(p,\gamma)^3\mathrm{He}$, $^3\mathrm{He}(\mathrm{D},p)^4\mathrm{He}$, are important because the density by this time has become rather low – comparable to that of air!

Nearly all neutrons end up bound in the most stable light element ^{4}He. Heavier nuclei do not form in any significant quantity both because of the absence of stable nuclei with mass number 5 or 8 (which impedes nucleosynthesis via n^4He, p^4He or ^{4}He^{4}He reactions), and the large Coulomb barriers for reactions such as $^3\mathrm{He}(^4\mathrm{He},\gamma)^7\mathrm{Li}$ and $^3\mathrm{He}(^4\mathrm{He},\gamma)^7\mathrm{Be}$. Hence the primordial mass fraction of ^{4}He, $Y_\mathrm{p} \equiv \rho(^4\mathrm{He})/\rho_\mathrm{b}$, can be estimated by the simple counting argument

$$Y_\mathrm{p} = \frac{2(n/p)}{1 + n/p} \simeq 0.25\ . \qquad (23.1)$$

There is little sensitivity here to the actual nuclear reaction rates, which are, however, important in determining the other 'left-over' abundances: D and ^{3}He at the level of a few times 10^{-5} by number relative to H, and ^{7}Li/H at the level of about 10^{-10} (when η_{10} is in the range 1–10). These values can be understood in terms of approximate analytic arguments [11,12]. The experimental parameter most important in determining Y_p is the neutron lifetime, τ_n, which normalizes (the inverse of) $\Gamma_{n \leftrightarrow p}$. Its value has recently been significantly revised downwards to $\tau_n = 880.0 \pm 0.9$ s (see *N* Baryons Listing).

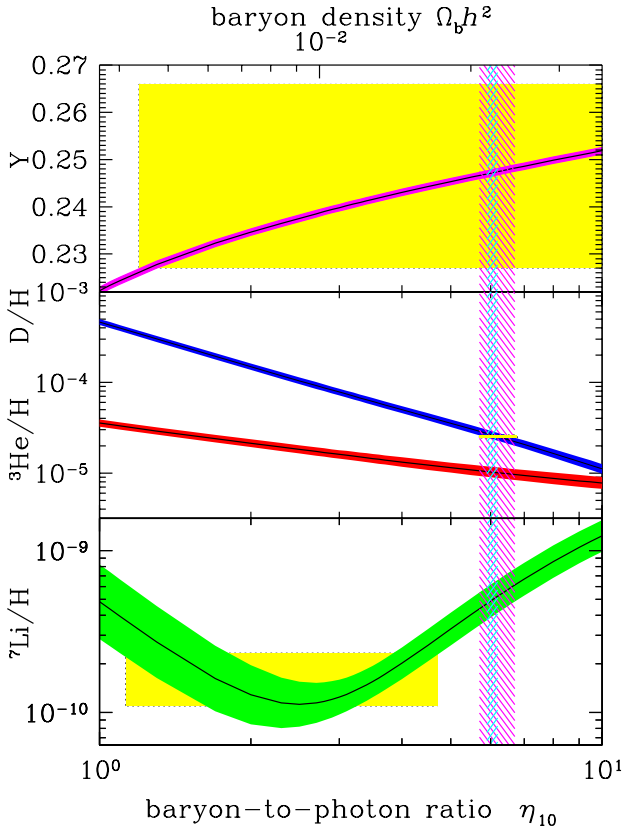

Figure 23.1: The abundances of ^{4}He, D, ^{3}He, and ^{7}Li as predicted by the standard model of Big-Bang nucleosynthesis — the bands show the 95% CL range. Boxes indicate the observed light element abundances. The narrow vertical band indicates the CMB measure of the cosmic baryon density, while the wider band indicates the BBN concordance range (both at 95% CL).

The elemental abundances shown in Fig. 23.1 as a function of η_{10} were calculated [13] using an updated version [14] of the Wagoner code [1]; other versions [15–17] are publicly available. The ^{4}He curve includes small corrections due to radiative processes at zero and finite temperatures [18], non-equilibrium neutrino heating during $e^\pm$ annihilation [19], and finite nucleon mass effects [20]; the range reflects primarily the 2σ uncertainty in the neutron lifetime. The spread in the curves for D, ^{3}He, and ^{7}Li corresponds to the 2σ uncertainties in nuclear cross sections, as estimated by Monte Carlo methods [14,21–23]. The input nuclear data have been carefully reassessed [13, 23–27], leading to improved precision in the abundance predictions. In particular, the uncertainty in ^{7}Li/H at interesting values of η has been reduced recently by a factor ~ 2, a consequence of a similar reduction in the error budget [28] for the dominant mass-7 production channel $^3\mathrm{He}(^4\mathrm{He},\gamma)^7\mathrm{Be}$. Polynomial fits to the predicted abundances and the error correlation matrix have been given [22,29].

The boxes in Fig. 23.1 show the observationally inferred primordial abundances with their associated uncertainties, as discussed below.

The nuclear reaction cross sections important for BBN have all been measured at the relevant energies. We will see, however, that recently there have been substantial advances in the precision of light element observations (e.g., D/H) and in cosmological parameters (e.g., from *Planck*). This motivates corresponding improvement in BBN precision and thus in the key reaction cross sections. For example, it has been suggested [30] that $d(p,\gamma)^3$He measurements may suffer from systematic errors and be inferior to *ab initio* theory; if so, this could alter D/H abundances at a level that is now significant.

23.2. Light Element Abundances

BBN theory predicts the universal abundances of D, ^{3}He, ^{4}He, and ^{7}Li, which are essentially fixed by $t \sim 180$ s. Abundances are, however, observed at much later epochs, after stellar nucleosynthesis has commenced. This produces heavy elements such as C, N, O, and Fe ('metals'), while the ejected remains of this stellar processing alters the light element abundances from their primordial values. Thus, one seeks astrophysical sites with low metal abundances, in order to measure light element abundances that are closer to primordial. For all of the light elements, systematic errors are the dominant limitation to the precision with which primordial abundances can be inferred.

BBN is the only significant source of deuterium, which is entirely destroyed when it is cycled into stars [31]. Thus, any detection provides a lower limit to primordial D/H, and an upper limit on η_{10}; for example, the local interstellar value of $\mathrm{D/H} = (1.56 \pm 0.40) \times 10^{-5}$ [32] requires $\eta_{10} \leq 9$. The best proxy to the primordial value of D is its measure in distant and chemically unprocessed matter where stellar processing (astration) is minimal [31]. This has become possible with the advent of large telescopes, but after two decades of observational efforts we have only about a dozen determinations [33–41]. High-resolution spectra reveal the presence of D in high-redshift, low-metallicity quasar absorption systems via its isotope-shifted Lyman-α absorption features; these are, unfortunately, usually obscured by the Lyman-α forest. The available D measurements are performed in systems with metallicities from 0.1 to 0.001 Solar where no significant astration is expected [34]. In the best-measured systems, D/H shows no hint of correlation with metallicity, redshift or the hydrogen column density $N(\mathrm{H}) (= \int_{\mathrm{los}} n_{\mathrm{H}}\, ds)$ integrated over the line-of-sight through the absorber. This is consistent with the measured D/H being representative of the primordial value.

The first measurements in 'damped' Lyman-α systems (DLAs: $N(\mathrm{H}) > 10^{20}$ cm^{-2}) [33,35] showed that D/H can be measured in this class of absorbers where the Lorentzian damping wings of Lyman-α and Lyman-β (if relatively uncontaminated by Lyman-α clouds) provide a precise H column density. Subsequently DLA systems have been found that also show resolved higher members of the Lyman series. Systems with a particularly simple kinematic structure are desirable to avoid uncertainties with complex, only partially resolved components. Recently a DLA showing 13 resolved D I absorption lines has been analyzed together with 4 other suitable systems. This provides a strikingly improved precision over earlier work, with a weighted mean of $\log(\mathrm{D/H}) = -4.597 \pm 0.006$, corresponding to

$$\mathrm{D/H}|_{\mathrm{p}} = (2.53 \pm 0.04) \times 10^{-5}. \tag{23.2}$$

D/H values in the Galaxy show an unexpected scatter of a factor of ~ 2 [42], with a bimodal distribution as well as an anti-correlation with metal abundances. This suggests that interstellar D not only suffers stellar astration but also partly resides in dust particles that evade gas-phase observations. This is supported by a measurement in the lower halo [43], which indicates that the Galactic D abundance has decreased by a factor of only 1.1 ± 0.13 since its formation. However in the DLA the dust content is apparently quite small; this is implied by the abundances of refractory elements such as Fe, Cr and Si, which are in nearly Solar proportions. Thus, the value derived in Eq. (23.2) appears safe against D depletion into dust grains.

The primordial ^{4}He abundance is best determined through recombination emission lines of He and H in the most metal-poor extragalactic H II (ionized) regions, *viz.* blue compact galaxies. There is now a large body of data on ^{4}He and CNO in these galaxies, with over 1000 such systems in the Sloan Digital Sky Survey alone [44,50]. These data confirm that the small stellar contribution to the helium abundance is positively correlated with metal production, so extrapolation to zero metallicity gives the primordial ^{4}He abundance Y_{p}. However, H II regions are complex systems and several physical parameters enter in the He/H determination, notably the electron density and temperature, as well as reddening. Thus systematic effects dominate the uncertainties in the abundance determination [44,45]. In recent work that has accounted for the underlying ^{4}He stellar absorption, and/or the newly derived values of the HeI-recombination and H-excitation-collisional coefficients, the ^{4}He abundances have significantly increased. Some recent results are: $Y_{\mathrm{p}} = 0.249 \pm 0.009$ [45]; $Y_{\mathrm{p}} = 0.248 \pm 0.003$ [46]; $Y_{\mathrm{p}} = 0.254 \pm 0.003$ or 0.252 ± 0.001 (depending on which set of He I emissivities are used) [47]; $Y_{\mathrm{p}} = 0.2534 \pm 0.0083$ [48]; and $Y_{\mathrm{p}} = 0.2465 \pm 0.0097$ [49]. In the first and last two determinations the quoted error is a conservative estimate of the systematic uncertainties. Ref. [50] used a subsample of 111 H II regions drawn from a sample of 1610 objects, as those providing Y with an accuracy better than 3%; the linear regression in $Y - \mathrm{O/H}$ gives $Y_{\mathrm{p}} = 0.254 \pm 0.0006$ (stat) ± 0.003 (syst). Our recommended ^{4}He abundance is

$$Y_{\mathrm{p}} = 0.2465 \pm 0.0097, \tag{23.3}$$

where we have adopted the result of the recent analysis with the most detailed error budget [49]. Note that it does not find a significant growth of Y_{p} with O/H.

The CMB damping tail is sensitive to the primordial ^{4}He abundance, and is independent from both BBN and local ^{4}He measurements. [51]. Recent measurements yield $Y_{\mathrm{p}} = 0.266 \pm 0.021$ (see Cosmic Microwave Background review) [52], *i.e.*, consistent with the H II region helium abundance determination.

As we will see in more detail below, the primordial abundance of ^{7}Li now plays a central role in BBN, and possibly points to new physics. The systems best suited for Li observations are metal-poor (Pop II) stars in the spheroid of the Galaxy, which have metallicities going down to perhaps 10^{-5} of the solar value [53]. Observations have long shown [54–57] that Li does not vary significantly in Pop II stars with metallicities $\lesssim 1/30$ of Solar — the 'Spite plateau' [54]. However there are systematic uncertainties due to different techniques used to determine the physical parameters (*e.g.*, the temperature) of the stellar atmosphere in which the Li absorption line is formed. Different analyses and in some cases different stars and stellar systems (globular clusters), yield $\mathrm{Li/H}|_{\mathrm{p}} = (1.7 \pm 0.3) \times 10^{-10}$ [57], $\mathrm{Li/H}|_{\mathrm{p}} = (2.19 \pm 0.28) \times 10^{-10}$ [58], and $\mathrm{Li/H}|_{\mathrm{p}} = (1.86 \pm 0.23) \times 10^{-10}$ [59].

Recent observations find a puzzling drop in Li/H in metal-poor stars with $[\mathrm{Fe/H}] \equiv \log_{10}[(\mathrm{Fe/H})/(\mathrm{Fe/H})_{\odot}] < -3.0$ [60,61,62]. In particular Li is not detected in the two metal poor dwarfs with metallicities of $[\mathrm{Fe/H}] \lesssim -5$ (HE 1327−2326 and SDSS J102915+172927 where $\mathrm{Li/H} < 10^{-11}$) suggesting that something is depleting Li at very low metallicity [63]. Since these stars have small masses and are almost fully convective during pre-main sequence evolution, they could have burned some Li [64]. The same effect may produce the melting of the Li plateau at low metallicities [61,62] thus making quite uncertain any primordial Li value obtained by extrapolating to zero metallicity. Hence to estimate $\mathrm{Li/H}|_{\mathrm{p}}$ it is safer to consider stars with $-2.8 < [\mathrm{Fe/H}] < -1.5$ [62] which provides

$$\mathrm{Li/H}|_{\mathrm{p}} = (1.6 \pm 0.3) \times 10^{-10}. \tag{23.4}$$

Moreover, the Li in Pop II stars may have been partially destroyed due to mixing of the outer layers with the hotter interior [65]. Such processes can be constrained by observations of the fragile isotope ^{6}Li [55], and by the absence of significant scatter in Li versus Fe [56]. Li depletion by a factor as large as ~ 1.8 has been suggested [66].

Stellar determination of Li abundances typically sum over both stable isotopes ^{6}Li and ^{7}Li. Recent high-precision measurements are sensitive to the tiny isotopic shift in Li absorption (which manifests

itself in the shape of the blended, thermally broadened line) and indicate $^6\mathrm{Li}/^7\mathrm{Li} \leq 0.05$ [67,68], thus confirming that ^{7}Li is dominant. A claim of a ^{6}Li plateau (analogous to the ^{7}Li plateau) has been made [67], suggesting a significant primordial ^{6}Li abundance. This has, however, been challenged by new observations and analyses [69,70,68], which show that stellar convective motions can generate asymmetries in the line shape that mimic the presence of ^{6}Li. Hence the deduced abundance ratio $^6\mathrm{Li}/^7\mathrm{Li} < 0.05$ in the best studied stars presently provides a robust upper limit on the ^{6}Li abundance [68].

Turning to ^{3}He, the only data available are from the Solar system and (high-metallicity) H II regions in our Galaxy [71]. This makes inferring the primordial abundance difficult, a problem compounded by the fact that stellar nucleosynthesis models for ^{3}He are in conflict with observations [72]. Consequently, it is no longer appropriate to use ^{3}He as a cosmological probe; instead, one might hope to turn the problem around and constrain stellar astrophysics using the predicted primordial ^{3}He abundance [73].

23.3. Concordance, Dark Matter, and the CMB

We now use the observed light element abundances to test the theory. We first consider standard BBN, which is based on Standard Model physics alone, so $N_\nu = 3$ and the only free parameter is the baryon-to-photon ratio η. (The implications of BBN for physics beyond the Standard Model will be considered below, Section 23.5). Thus, any abundance measurement determines η, and additional measurements overconstrain the theory and thereby provide a consistency check.

While the η ranges spanned by the boxes in Fig. 23.1 do not all overlap, they are all within a factor ~ 2 of each other. In particular, the lithium abundance corresponds to η values that are inconsistent with that of the (now very precise) D/H abundance as well as the less-constraining ^{4}He abundance. This discrepancy marks the "lithium problem". The problem could simply reflect difficulty in determining the primordial lithium abundance; or could hint at a more fundamental omission in the theory. The possibility that lithium reveals new physics is addressed in detail in the next section. If however we exclude the lithium constraint because its inferred abundance may suffer from systematic uncertainties, then D/H and ^{4}He are in agreement. The concordant η range is essentially that implied by D/H, namely

$$5.7 \leq \eta_{10} \leq 6.7 \text{ (95\% CL)}. \tag{23.5}$$

Despite the lithium problem, the overall concordance remains remarkable: using only well-established microphysics we can extrapolate back to $t \sim 1$ s to predict light element abundances spanning 9 orders of magnitude, in approximate agreement with observation. This is a major success for the standard cosmology, and inspires confidence in extrapolation back to still earlier times.

This concordance provides a measure of the baryon content:

$$0.021 \leq \Omega_\mathrm{b} h^2 \leq 0.025 \text{ (95\% CL)}, \tag{23.6}$$

a result that plays a key role in our understanding of the matter budget of the Universe. First we note that $\Omega_\mathrm{b} \ll 1$, *i.e.*, baryons cannot close the Universe [74]. Furthermore, the cosmic density of (optically) luminous matter is $\Omega_\mathrm{lum} \simeq 0.0024 h^{-1}$ [75], so that $\Omega_\mathrm{b} \gg \Omega_\mathrm{lum}$: most baryons are optically dark, probably in the form of a diffuse intergalactic medium [76]. Finally, given that $\Omega_\mathrm{m} \sim 0.3$ (see Dark Matter and Cosmological Parameters reviews), we infer that most matter in the Universe is not only dark, but also takes some non-baryonic (more precisely, non-nucleonic) form.

The BBN prediction for the cosmic baryon density can be tested through precision observations of CMB temperature fluctuations (see Cosmic Microwave Background review). One can determine η from the amplitudes of the acoustic peaks in the CMB angular power spectrum [77], making it possible to compare two measures of η using very different physics, at two widely separated epochs. In the standard cosmology, there is no change in η between BBN and CMB decoupling, thus, a comparison of η_BBN and η_CMB is a key test. Agreement would endorse the standard picture, while disagreement could point to new physics during/between the BBN and CMB epochs.

The analysis described in the Cosmic Microwave Background review, based on recent *Planck* data, yields $\Omega_\mathrm{b} h^2 = 0.02207 \pm 0.00027$ or $\eta_{10} = 6.047 \pm 0.074$ [52]. As shown in Fig. 23.1, this CMB estimate of the baryon density (narrow vertical band) is remarkably consistent with the BBN range quoted in Eq. (23.6) and thus in very good agreement with the value inferred from recent high-redshift D/H measurements [36] and ^{4}He determinations; together these observations span diverse environments from redshifts $z = 1000$ to the present [78].

The precision determinations of the baryon density using the CMB motivates the use of this value as an input to BBN calculations. Within the context of the Standard Model, BBN then becomes a zero-parameter theory, and the light element abundances are completely determined to within the uncertainties in η_CMB and the BBN theoretical errors. Comparison with the observed abundances then can be used to test the astrophysics of post-BBN light element evolution [79]. Alternatively, one can consider possible physics beyond the Standard Model (*e.g.*, which might change the expansion rate during BBN) and then use all of the abundances to test such models; this is discussed in Section 23.5.

23.4. The Lithium Problem

As Fig. 23.1 shows, stellar Li/H measurements are inconsistent with the CMB (and D/H), given the error budgets we have quoted. Recent updates in nuclear cross sections and stellar abundance systematics *increase* the discrepancy to over 5σ, depending on the stellar abundance analysis adopted [13].

The question then becomes pressing as to whether this mismatch comes from systematic errors in the observed abundances, and/or uncertainties in stellar astrophysics or nuclear inputs, or whether there might be new physics at work [8]. Nuclear inputs (cross sections) for BBN reactions are constrained by extensive laboratory measurements; to increase ^{7}Be destruction requires enhancement of otherwise subdominant processes that can be attained by missed resonances in a few reactions such as $^7\mathrm{Be}(d,p)2\alpha$ if the compound nuclear state properties are particularly favorable [80]. However, experimental searches have now closed off the most promising of these cases [81], making a "nuclear fix" increasingly unlikely.

Another conventional means to solve the lithium problem is by *in situ* destruction over the long lifetimes of the host halo stars. Stellar depletion mechanisms include diffusion, rotationally induced mixing, or pre-main-sequence depletion. These effects certainly occur, but to reduce lithium to the required levels generally requires some *ad hoc* mechanism and fine tuning of the initial stellar parameters [64,82]. A putative signature of diffusion has been reported for the globular clusters NGC 6397 and NGC 6752, where the 'turnoff' stars exhibit slightly lower (by ~ 0.1 dex) abundances of Fe II, Ti II, Sc II, Ca I and Mg I, than in more evolved stars [66,83]. General features of diffusive models are a dispersion in the Li abundances and a pronounced downturn in the Li abundances at the hot end of the Li plateau. Some extra turbulence needs to be invoked to limit diffusion in the hotter stars and to restore uniform Li abundance along the Spite plateau [82]. In the framework of these models (and also assuming identical initial stellar rotation) depletion by at most a factor ~ 1.8 is conceivable [66,83].

As nuclear and astrophysical solutions to the lithium problem become increasingly constrained (even if difficult to rule out definitively), the possibility of new physics arises. Nucleosynthesis models in which the baryon-to-photon ratio is inhomogeneous can alter abundances for a given η_BBN, but will overproduce ^{7}Li [84]. Entropy generation by some non-standard process could have decreased η between the BBN era and CMB decoupling, however the lack of spectral distortions in the CMB rules out any significant energy injection upto a redshift $z \sim 10^7$ [85]. The most intriguing resolution of the lithium problem thus involves new physics during BBN [6–8].

We summarize the general features of such solutions here, and later consider examples in the context of specific particle physics models. Many proposed solutions introduce perturbations to light-element

formation during BBN; while all element abundances may suffer perturbations, the interplay of ^{7}Li and D is often the most important *i.e.* observations of D often provide the strongest constraints on the allowed perturbations to ^{7}Li. In this connection it is important to note that the new, very precise determination of D/H [36] will significantly constrain the ability of such models to ameliorate or solve the lithium problem.

A well studied class of models invokes the injection of suprathermal hadronic or electromagnetic particles due to decays of dark matter particles. The effects are complex and depend on the nature of the decaying particles and their branchings and spectra. However, the models that most successfully solve the lithium problem generally feature non-thermal nucleons, which dissociate all light elements. Dissociation of even a small fraction of ^{4}He introduces a large abundance of free neutrons, which quickly thermalize. The thermal neutrons drive the ^{7}Be$(n,p)^7$Li conversion of ^{7}Be. The resulting ^{7}Li has a lower Coulomb barrier relative to ^{7}Be and is readily destroyed via ^{7}Li$(p,\alpha)^4$He [86,87]. But ^{4}He dissociation also produces D directly and via nonthermal neutron $n(p,\gamma)d$ reactions; this introduces a tension between Li/H reduction and D/H enhancement.

Another important class of models retains the standard cosmic particle content, but changes their interactions via time variations in the fundamental constants [88]. Here too, the details are model-dependent, but scenarios that solve or alleviate the lithium problem often feature perturbations to the deuteron binding energy. A weaker D binding leads to the D bottleneck being overcome later, so that element formation commences at a lower temperature and lower density. This leads in turn to slower nuclear rates that freeze out earlier. The net result is a *higher* final D/H, due to less efficient processing into ^{4}He, but also *lower* Li, due to suppressed production via ^{3}He$(\alpha,\gamma)^7$Be.

The lithium problem remains an unresolved issue in BBN. Nevertheless, the remarkable concordance between the CMB and the D (as well as ^{4}He) abundance, remains a non-trivial success, and provides constraints on the early Universe and particle physics.

23.5. Beyond the Standard Model

Given the simple physics underlying BBN, it is remarkable that it still provides the most effective test for the cosmological viability of ideas concerning physics beyond the Standard Model. Although baryogenesis and inflation must have occurred at higher temperatures in the early Universe, we do not as yet have 'standard models' for these, so BBN still marks the boundary between the established and the speculative in Big Bang cosmology. It might appear possible to push the boundary back to the quark-hadron transition at $T \sim \Lambda_{\rm QCD}$, or electroweak symmetry breaking at $T \sim 1/\sqrt{G_{\rm F}}$; however, so far no observable relics of these epochs have been identified, either theoretically or observationally. Thus, although the Standard Model provides a precise description of physics up to the Fermi scale, cosmology cannot be traced in detail before the BBN era.

Limits on new physics come mainly from the observational bounds on the ^{4}He abundance. This is proportional to the n/p ratio when the weak-interaction rate falls behind the Hubble expansion rate at $T_{\rm fr} \sim 1$ MeV. The presence of additional neutrino flavors (or of any other relativistic species) at this time increases g_*, hence the expansion rate, leading to a larger value of $T_{\rm fr}$, n/p, and therefore $Y_{\rm p}$ [9,89]. In the Standard Model at $T = 1$ MeV, $g_* = 5.5 + \frac{7}{4}N_\nu$, where N_ν is the *effective* number of (nearly) massless neutrino flavors (see Big Bang Cosmology review). The helium curves in Fig. 23.1 were computed taking $N_\nu = 3$; small corrections for non-equilibrium neutrino heating [19] are included in the thermal evolution and lead to an effective $N_\nu = 3.04$ compared to assuming instantaneous neutrino freezeout (see Big Bang Cosmology review). The computed ^{4}He abundance scales as $\Delta Y_{\rm p} \simeq 0.013\Delta N_\nu$ [10]. Clearly the central value for N_ν from BBN will depend on η, which is independently determined (with weaker sensitivity to N_ν) by the adopted D or ^{7}Li abundance. For example, if the best value for the observed primordial ^{4}He abundance is 0.249, then, for $\eta_{10} \sim 6$, the central value for N_ν is very close to 3. A maximum likelihood analysis on η and N_ν based on the above ^{4}He and D abundances finds the (correlated) 95% CL ranges to be $4.9 < \eta_{10} < 7.1$ and $1.8 < N_\nu < 4.5$ [90]. Identical results are obtained using a simpler method to extract such bounds based on χ^2 statistics, given a set of input abundances [91].

The CMB power spectrum in the damping tail is independently sensitive to N_ν (*e.g.* [92]) . The CMB value $N_\nu^{\rm CMB}$ probes the cosmic radiation content at (re)combination, so a discrepancy would imply new physics or astrophysics. Indeed, observations by the South Pole Telescope implied $N_\nu^{\rm CMB} = 3.85 \pm 0.62$ [93], prompting discussion of "dark radiation" such as sterile neutrinos [94]. However, recent *Planck* results give $N_\nu^{\rm CMB} = 3.36^{+0.34}_{-0.32}$ with a precision now apparently better than BBN, which is quite consistent with the Standard Model [52]. If we *assume* that η did not change between BBN and (re)combination, the constraint can be improved by including the recent D/H measurements, which yields $N_\nu = 3.28 \pm 0.28$ [36].

Just as one can use the measured helium abundance to place limits on g_* [89], any changes in the strong, weak, electromagnetic, or gravitational coupling constants, arising *e.g.*, from the dynamics of new dimensions, can be similarly constrained [95], as can be any speed-up of the expansion rate in, *e.g.*, scalar-tensor theories of gravity [96].

The limits on N_ν can be translated into limits on other types of particles or particle masses that would affect the expansion rate of the Universe during nucleosynthesis. For example, consider 'sterile' neutrinos with only right-handed interactions of strength $G_{\rm R} < G_{\rm F}$. Such particles would decouple at higher temperature than (left-handed) neutrinos, so their number density ($\propto T^3$) relative to neutrinos would be reduced by any subsequent entropy release, *e.g.*, due to annihilations of massive particles that become non-relativistic between the two decoupling temperatures. Thus (relativistic) particles with less than full strength weak interactions contribute less to the energy density than particles that remain in equilibrium up to the time of nucleosynthesis [97]. If we impose $N_\nu < 4$ as an illustrative constraint, then the three right-handed neutrinos must have a temperature $3(T_{\nu_{\rm R}}/T_{\nu_{\rm L}})^4 < 1$. Since the temperature of the decoupled $\nu_{\rm R}$ is determined by entropy conservation (see Big Bang Cosmology review), $T_{\nu_{\rm R}}/T_{\nu_{\rm L}} = [(43/4)/g_*(T_{\rm d})]^{1/3} < 0.76$, where $T_{\rm d}$ is the decoupling temperature of the $\nu_{\rm R}$. This requires $g_*(T_{\rm d}) > 24$, so decoupling must have occurred at $T_{\rm d} > 140$ MeV. The decoupling temperature is related to $G_{\rm R}$ through $(G_{\rm R}/G_{\rm F})^2 \sim (T_{\rm d}/3\,{\rm MeV})^{-3}$, where 3 MeV is the decoupling temperature for $\nu_{\rm L}$s. This yields a limit $G_{\rm R} \lesssim 10^{-2}G_{\rm F}$. The above argument sets lower limits on the masses of new Z' gauge bosons to which right-handed neutrinos would be coupled in models of superstrings [98], or extended technicolor [99]. Similarly a Dirac magnetic moment for neutrinos, which would allow the right-handed states to be produced through scattering and thus increase g_*, can be significantly constrained [100], as can any new interactions for neutrinos that have a similar effect [101]. Right-handed states can be populated directly by helicity-flip scattering if the neutrino mass is large enough, and this property has been used to infer a bound of $m_{\nu_\tau} \lesssim 1$ MeV taking $N_\nu < 4$ [102]. If there is mixing between active and sterile neutrinos then the effect on BBN is more complicated [103].

BBN limits on the cosmic expansion rate constrain supersymmetric scenarios in which the neutralino or gravitino are very light, so that they contribute to g_* [104]. A gravitino in the mass range $\sim 10^{-4} - 10$ eV will affect the expansion rate of the Universe similarly to a light neutralino (which is however now probably ruled out by collider data, especially the decays of the Higgs-like boson). The net contribution to N_ν then ranges between 0.74 and 1.69, depending on the gravitino and slepton masses [105].

The limit on the expansion rate during BBN can also be translated into bounds on the mass/lifetime of non-relativistic particles that decay during BBN. This results in an even faster speed-up rate, and typically also changes the entropy [106]. If the decays include Standard Model particles, the resulting electromagnetic [107–108] and/or hadronic [109] cascades can strongly perturb the light elements, which leads to even stronger constraints. Such arguments had been applied to rule out an MeV mass for ν_τ, which decays during nucleosynthesis [110].

Decaying-particle arguments have proved very effective in probing

supersymmetry. Light-element abundances generally are complementary to accelerator data in constraining SUSY parameter space, with BBN reaching to values kinematically inaccessible to the LHC. Much recent interest has focused on the case in which the next-to-lightest supersymmetric particle is metastable and decays during or after BBN. The constraints on unstable particles discussed above imply stringent bounds on the allowed abundance of such particles [109]; if the metastable particle is charged (*e.g.*, the stau), then it is possible for it to form atom-like electromagnetic bound states with nuclei, and the resulting impact on light elements can be quite complex [111]. Moreover, SUSY decays can destroy ^{7}Li and/or produce ^{6}Li, leading to a possible supersymmetric solution to the lithium problems noted above [112](see [6] for a review).

These arguments impose powerful constraints on supersymmetric inflationary cosmology [108–109], particularly thermal leptogenesis [113]. These can be evaded only if the gravitino is massive enough to decay before BBN, *i.e.*, $m_{3/2} \gtrsim 50$ TeV [114](which would be unnatural), or if it is in fact the lightest supersymmetric particle and thus stable [108,115]. Similar constraints apply to moduli – very weakly coupled fields in string theory that obtain an electroweak-scale mass from supersymmetry breaking [116].

Finally, we mention that BBN places powerful constraints on the possibility that there are new large dimensions in nature, perhaps enabling the scale of quantum gravity to be as low as the electroweak scale [117]. Thus, Standard Model fields may be localized on a 'brane,' while gravity alone propagates in the 'bulk.' It has been further noted that the new dimensions may be non-compact, even infinite [118], and the cosmology of such models has attracted considerable attention. The expansion rate in the early Universe can be significantly modified, so BBN is able to set interesting constraints on such possibilities [119].

References:

1. R.V. Wagoner *et al.*, Astrophys. J. **148**, 3 (1967).
2. D.N. Schramm and M.S. Turner, Rev. Mod. Phys. **70**, 303 (1998).
3. G. Steigman, Ann. Rev. Nucl. and Part. Sci. **57**, 463 (2007).
4. F. Iocco *et al.*, Phys. Reports **472**, 1 (2009).
5. S. Sarkar, Rept. on Prog. in Phys. **59**, 1493 (1996).
6. K. Jedamzik and M. Pospelov, New J. Phys. **11**, 105028 (2009).
7. M. Pospelov and J. Pradler, Ann. Rev. Nucl. and Part. Sci. **60**, 539 (2010).
8. B.D. Fields, Ann. Rev. Nucl. and Part. Sci. **61**, 47 (2011).
9. P.J.E. Peebles, Phys. Rev. Lett. **16**, 411 (1966).
10. J. Bernstein *et al.*, Rev. Mod. Phys. **61**, 25 (1989).
11. S. Mukhanov, Int. J. Theor. Phys. **143**, 669 (2004).
12. R. Esmailzadeh *et al.*, Astrophys. J. **378**, 504 (1991).
13. R.H. Cyburt *et al.*, JCAP **0811**, 012 (2008).
14. R.H. Cyburt *et al.*, New Astron. **6**, 215 (2001).
15. L. Kawano, FERMILAB-PUB-92/04-A.
16. O. Pisanti *et al.*, Comput. Phys. Commun. **178**, 956 (2008).
17. A. Arbey, Comput. Phys. Commun. **183**, 1822 (2012).
18. S. Esposito *et al.*, Nucl. Phys. **B568**, 421 (2000).
19. S. Dodelson and M.S. Turner, Phys. Rev. **D46**, 3372 (1992).
20. D. Seckel, `hep-ph/9305311`;
    R. Lopez and M.S. Turner, Phys. Rev. **D59**, 103502 (1999).
21. M.S. Smith *et al.*, Astrophys. J. Supp. **85**, 219 (1993).
22. G. Fiorentini *et al.*, Phys. Rev. **D58**, 063506 (1998).
23. A. Coc *et al.*, Astrophys. J. **744**, 158 (2012).
24. K.M. Nollett and S. Burles, Phys. Rev. **D61**, 123505 (2000).
25. R.H. Cyburt, Phys. Rev. **D70**, 023505 (2004).
26. P.D. Serpico *et al.*, JCAP **12**, 010 (2004).
27. R.N. Boyd *et al.*, Phys. Rev. **D82**, 105005 (2010).
28. R.H. Cyburt and B. Davids, Phys. Rev. **C78**, 012 (2008).
29. K.M. Nollett *et al.*, Astrophys. J. Lett. **552**, L1 (2001).
30. K.M. Nollett and G.P. Holder, `arXiv:1112.2683`.
31. R.I. Epstein *et al.*, Nature **263**, 198 (1976).
32. B.E. Wood *et al.*, Astrophys. J. **609**, 838 (2004).
33. S. D'Odorico *et al.*, Astron. & Astrophys. **368**, L21 (2001).
34. D. Romano *et al.*, MNRAS **369**, 295 (2006).
35. M. Pettini and D. Bowen, Astrophys. J. **560**, 41 (2001).
36. R. Cooke *et al.*, Astrophys. J. **781**, 31 (2013).
37. S.A. Levshakov *et al.*, Astrophys. J. **565**, 696 (2002).
38. M. Fumagalli *et al.*, Science **334**, 1245 (2011).
39. R. Srianand *et al.*, MNRAS **405**, 1888 (2010).
40. P. Noterdaeme *et al.*, Astron. & Astrophys. **542**, L33 (2012).
41. M. Pettini and R. Cooke, MNRAS **425**, 2477 (2012).
42. J.L. Linsky *et al.*, Astrophys. J. **647**, 1106 (2006).
43. B.D. Savage *et al.*, Astrophys. J. **659**, 1222 (2007).
44. Y.I. Izotov *et al.*, Astrophys. J. **527**, 757 (1999).
45. K.A. Olive and E. Skillman, Astrophys. J. **617**, 29 (2004).
46. M. Peimbert *et al.*, Astrophys. J. **667**, 636 (2007).
47. Y.I. Izotov *et al.*, Astrophys. J. **662**, 15 (2007).
48. E. Aver *et al.*, JCAP **04**, 004 (2012).
49. E. Aver *et al.*, JCAP **11**, 017 (2013).
50. Y.I. Izotov *et al.*, Astron. & Astrophys. **558**, A57 (2013).
51. R. Trotta and S.H. Hansen, Phys. Rev. **D69**, 023509 (2004).
52. P.A.R. Ade *et al.* (Planck Collaboration), `arXiv:1303.5076`.
53. N. Christlieb *et al.*, Nature **419**, 904 (2002).
54. M. Spite and F. Spite, Nature **297**, 483 (1982).
55. E. Vangioni-Flam *et al.*, New Astron. **4**, 245 (1999).
56. S.G. Ryan *et al.*, Astrophys. J. Lett. **530**, L57 (2000).
57. P. Bonifacio and P. Molaro, MNRAS **285**, 847 (1997).
58. P. Bonifacio *et al.*, Astron. & Astrophys. **390**, 91 (2002).
59. J. Melendez *et al.*, Astron. & Astrophys. **515**, L3 (2010).
60. P. Bonifacio *et al.*, Astron. & Astrophys. **462**, 851 (2007).
61. W. Aoki, Astrophys. J. **698**, 1803 (2009);
    A. Hosford *et al.*, Astron. & Astrophys. **493**, 601 (2009).
62. L. Sbordone *et al.*, Astron. & Astrophys. **522**, A26 (2010).
63. E. Caffau *et al.*, Nature **477**, 67 (2011).
64. P. Molaro *et al.*, Memorie della Soc. Astronomica Italiana Supp. **22**, 233 (2012).
65. M.H. Pinsonneault *et al.*, Astrophys. J. **574**, 389 (2002).
66. A.J. Korn *et al.*, Nature **442**, 657 (2006).
67. M. Asplund *et al.*, Astrophys. J. **644**, 229 (2006).
68. K. Lind *et al.*, Astron. & Astrophys. **554**, 96 (2013).
69. R. Cayrel *et al.*, Astron. & Astrophys. **473**, L37 (2007).
70. M. Steffen *et al.*, Memorie della Soc. Astronomica Italiana Supp. **22**, 152 (2012).
71. T.M. Bania *et al.*, Nature **415**, 54 (2002).
72. K.A. Olive *et al.*, Astrophys. J. **479**, 752 (1997).
73. E. Vangioni-Flam *et al.*, Astrophys. J. **585**, 611 (2003).
74. H. Reeves *et al.*, Astrophys. J. **179**, 909 (1973).
75. M. Fukugita and P.J.E. Peebles, Astrophys. J. **616**, 643 (2004).
76. R. Cen and J.P. Ostriker, Astrophys. J. **514**, 1 (1999).
77. G. Jungman *et al.*, Phys. Rev. **D54**, 1332 (1996).
78. A. Coc *et al.*, `arXiv:1307:6955`.
79. R.H. Cyburt *et al.*, Phys. Lett. **B567**, 227 (2003).
80. R.H. Cyburt and M. Pospelov, Int. J. Mod. Phys. E **21**, 1250004 (2012);
    R.N. Boyd *et al.*, Phys. Rev. **D82**, 105005 (2010);
    N. Chakraborty *et al.*, Phys. Rev. **D83**, 063006 (2011);
    C. Broggini *et al.*, JCAP **06**, 030 (2012).
81. P.D. O'Malley *et al.*, Phys. Rev. **C84**, 042801 (2011).
82. O. Richard *et al.*, Astrophys. J. **619**, 538 (2005).
83. P. Gruyters *et al.*, Astron. Astrophys. **555**, 31 (2013).
84. K. Jedamzik and J.B. Rehm, Phys. Rev. **D64**, 023510 (2001).
85. D.J. Fixsen *et al.*, Astrophys. J. **473**, 576 (1996).
86. K. Jedamzik, Phys. Rev. **D70**, 063524 (2004).
87. M. Kawasaki *et al.*, Phys. Rev. **D71**, 083502 (2005).
88. J.D. Barrow, Phys. Rev. **D35**, 1805 (1987);
    B.A. Campbell and K.A. Olive, Phys. Lett. **B345**, 429 (1995);
    L. Bergström, Phys. Rev. **D60**, 045005 (1999);
    V.V. Flambaum and E.V. Shuryak, Phys. Rev. **D65**, 103503 (2002);
    A. Coc *et al.*, Phys. Rev. **D76**, 023511 (2007);
    J.C. Berengut *et al.*, Phys. Rev. **D87**, 085018 (2013).
89. G. Steigman *et al.*, Phys. Lett. **B66**, 202 (1977).
90. R.H. Cyburt *et al.*, Astropart. Phys. **23**, 313 (2005).
91. E. Lisi *et al.*, Phys. Rev. **D59**, 123520 (1999).
92. Z. Hou *et al.*, Phys. Rev. **D87**, 083008 (2013).

93. R. Keisler *et al.*, Astrophys. J. **743**, 28 (2011).
94. J. Hamann *et al.*, Phys. Rev. Lett. **105**, 181301 (2010).
95. E.W. Kolb *et al.*, Phys. Rev. **D33**, 869 (1986); F.S. Accetta *et al.*, Phys. Lett. **B248**, 146 (1990); B.A. Campbell and K.A. Olive, Phys. Lett. **B345**, 429 (1995); K.M. Nollett and R. Lopez, Phys. Rev. **D66**, 063507 (2002); C. Bambi *et al.*, Phys. Rev. **D71**, 123524 (2005).
96. A. Coc *et al.*, Phys. Rev. **D73**, 083525 (2006).
97. K.A. Olive *et al.*, Nucl. Phys. **B180**, 497 (1981).
98. J. Ellis *et al.*, Phys. Lett. **B167**, 457 (1986).
99. L.M. Krauss *et al.*, Phys. Rev. Lett. **71**, 823 (1993).
100. J.A. Morgan, Phys. Lett. **B102**, 247 (1981).
101. E.W. Kolb *et al.*, Phys. Rev. **D34**, 2197 (1986); J.A. Grifols and E. Massó, Mod. Phys. Lett. **A2**, 205 (1987); K.S. Babu *et al.*, Phys. Rev. Lett. **67**, 545 (1991).
102. A.D. Dolgov *et al.*, Nucl. Phys. **B524**, 621 (1998).
103. K. Enqvist *et al.*, Nucl. Phys. **B373**, 498 (1992); A.D. Dolgov, Phys. Reports **370**, 333 (2002).
104. J.A. Grifols *et al.*, Phys. Lett. **B400**, 124 (1997).
105. H. Dreiner *et al.*, Phys. Rev. **D85**, 065027 (2012).
106. K. Sato and M. Kobayashi, Prog. Theor. Phys. **58**, 1775 (1977); D.A. Dicus *et al.*, Phys. Rev. **D17**, 1529 (1978); R.J. Scherrer and M.S. Turner, Astrophys. J. **331**, 19 (1988).
107. D. Lindley, MNRAS **188**, 15 (1979); Astrophys. J. **294**, 1 (1985).
108. J. Ellis *et al.*, Nucl. Phys. **B259**, 175 (1985); J. Ellis *et al.*, Nucl. Phys. **B373**, 399 (1992); R.H. Cyburt *et al.*, Phys. Rev. **D67**, 103521 (2003).
109. M.H. Reno and D. Seckel, Phys. Rev. **D37**, 3441 (1988); S. Dimopoulos *et al.*, Nucl. Phys. **B311**, 699 (1989); K. Kohri *et al.*, Phys. Rev. **D71**, 083502 (2005).
110. S. Sarkar and A.M. Cooper, Phys. Lett. **B148**, 347 (1984).
111. M. Pospelov *et al.*, Phys. Rev. Lett. **98**, 231301 (2007); M. Kawasaki *et al.*, Phys. Lett. **B649**, 436 (2007); R.H. Cyburt *et al.*, JCAP **05**, 014 (2013).
112. K. Jedamzik *et al.*, JCAP **07**, 007 (2006).
113. S. Davidson *et al.*, Phys. Rev. **466**, 105 (2008).
114. S. Weinberg, Phys. Rev. Lett. **48**, 1303 (1979).
115. M. Bolz *et al.*, Nucl. Phys. **B606**, 518 (2001).
116. G. Coughlan *et al.*, Phys. Lett. **B131**, 59 (1983).
117. N. Arkani-Hamed *et al.*, Phys. Rev. **D59**, 086004 (1999).
118. L. Randall and R. Sundrum, Phys. Rev. Lett. **83**, 3370 (1999).
119. J.M. Cline *et al.*, Phys. Rev. Lett. **83**, 4245 (1999); P. Binetruy *et al.*, Phys. Lett. **B477**, 285 (2000).

24. THE COSMOLOGICAL PARAMETERS

Updated November 2013, by O. Lahav (University College London) and A.R. Liddle (University of Edinburgh).

24.1. Parametrizing the Universe

Rapid advances in observational cosmology have led to the establishment of a precision cosmological model, with many of the key cosmological parameters determined to one or two significant figure accuracy. Particularly prominent are measurements of cosmic microwave background (CMB) anisotropies, with the highest precision observations being those of the *Planck* Satellite [1,2] which for temperature anisotropies supersede the iconic *WMAP* results [3,4]. However the most accurate model of the Universe requires consideration of a range of different types of observation, with complementary probes providing consistency checks, lifting parameter degeneracies, and enabling the strongest constraints to be placed.

The term 'cosmological parameters' is forever increasing in its scope, and nowadays often includes the parameterization of some functions, as well as simple numbers describing properties of the Universe. The original usage referred to the parameters describing the global dynamics of the Universe, such as its expansion rate and curvature. Also now of great interest is how the matter budget of the Universe is built up from its constituents: baryons, photons, neutrinos, dark matter, and dark energy. We need to describe the nature of perturbations in the Universe, through global statistical descriptors such as the matter and radiation power spectra. There may also be parameters describing the physical state of the Universe, such as the ionization fraction as a function of time during the era since recombination. Typical comparisons of cosmological models with observational data now feature between five and ten parameters.

24.1.1. *The global description of the Universe* :

Ordinarily, the Universe is taken to be a perturbed Robertson–Walker space-time with dynamics governed by Einstein's equations. This is described in detail by Olive and Peacock in this volume. Using the density parameters Ω_i for the various matter species and Ω_Λ for the cosmological constant, the Friedmann equation can be written

$$\sum_i \Omega_i + \Omega_\Lambda - 1 = \frac{k}{R^2 H^2}\,, \tag{24.1}$$

where the sum is over all the different species of material in the Universe. This equation applies at any epoch, but later in this article we will use the symbols Ω_i and Ω_Λ to refer to the present values.

The complete present state of the homogeneous Universe can be described by giving the current values of all the density parameters and the Hubble constant h (the present-day Hubble parameter being written $H_0 = 100h\,\mathrm{km\,s^{-1}\,Mpc^{-1}}$). A typical collection would be baryons Ω_b, photons Ω_γ, neutrinos Ω_ν, and cold dark matter Ω_c (given charge neutrality, the electron density is guaranteed to be too small to be worth considering separately and is included with the baryons). The spatial curvature can then be determined from the other parameters using Eq. (24.1). The total present matter density $\Omega_\mathrm{m} = \Omega_\mathrm{c} + \Omega_\mathrm{b}$ is sometimes used in place of the cold dark matter density Ω_c.

These parameters also allow us to track the history of the Universe back in time, at least until an epoch where interactions allow interchanges between the densities of the different species, which is believed to have last happened at neutrino decoupling, shortly before Big Bang Nucleosynthesis (BBN). To probe further back into the Universe's history requires assumptions about particle interactions, and perhaps about the nature of physical laws themselves.

The standard neutrino sector has three flavors. For neutrinos of mass in the range $5 \times 10^{-4}\,\mathrm{eV}$ to $1\,\mathrm{MeV}$, the density parameter in neutrinos is predicted to be

$$\Omega_\nu h^2 = \frac{\sum m_\nu}{93\,\mathrm{eV}}\,, \tag{24.2}$$

where the sum is over all families with mass in that range (higher masses need a more sophisticated calculation). We use units with $c = 1$ throughout. Results on atmospheric and Solar neutrino oscillations [5] imply non-zero mass-squared differences between the three neutrino flavors. These oscillation experiments cannot tell us the absolute neutrino masses, but within the simple assumption of a mass hierarchy suggest a lower limit of approximately 0.06 eV on the sum of the neutrino masses.

Even a mass this small has a potentially observable effect on the formation of structure, as neutrino free-streaming damps the growth of perturbations. Analyses commonly now either assume a neutrino mass sum fixed at this lower limit, or allow the neutrino mass sum as a variable parameter. To date there is no decisive evidence of any effects from either neutrino masses or an otherwise non-standard neutrino sector, and observations impose quite stringent limits, which we summarize in Section 24.3.4. However, we note that the inclusion of the neutrino mass sum as a free parameter can affect the derived values of other cosmological parameters.

24.1.2. *Inflation and perturbations* :

A complete model of the Universe should include a description of deviations from homogeneity, at least in a statistical way. Indeed, some of the most powerful probes of the parameters described above come from the evolution of perturbations, so their study is naturally intertwined in the determination of cosmological parameters.

There are many different notations used to describe the perturbations, both in terms of the quantity used to describe the perturbations and the definition of the statistical measure. We use the dimensionless power spectrum Δ^2 as defined in Olive and Peacock (also denoted $\mathcal{P}$ in some of the literature). If the perturbations obey Gaussian statistics, the power spectrum provides a complete description of their properties.

From a theoretical perspective, a useful quantity to describe the perturbations is the curvature perturbation $\mathcal{R}$, which measures the spatial curvature of a comoving slicing of the space-time. A simple case is the Harrison–Zel'dovich spectrum, which corresponds to a constant $\Delta^2_\mathcal{R}$. More generally, one can approximate the spectrum by a power-law, writing

$$\Delta^2_\mathcal{R}(k) = \Delta^2_\mathcal{R}(k_*)\left[\frac{k}{k_*}\right]^{n_\mathrm{s}-1}\,, \tag{24.3}$$

where n_s is known as the spectral index, always defined so that $n_\mathrm{s} = 1$ for the Harrison–Zel'dovich spectrum, and k_* is an arbitrarily chosen scale. The initial spectrum, defined at some early epoch of the Universe's history, is usually taken to have a simple form such as this power-law, and we will see that observations require n_s close to one. Subsequent evolution will modify the spectrum from its initial form.

The simplest mechanism for generating the observed perturbations is the inflationary cosmology, which posits a period of accelerated expansion in the Universe's early stages [6,7]. It is a useful working hypothesis that this is the sole mechanism for generating perturbations, and it may further be assumed to be the simplest class of inflationary model, where the dynamics are equivalent to that of a single scalar field ϕ with canonical kinetic energy slowly rolling on a potential $V(\phi)$. One may seek to verify that this simple picture can match observations and to determine the properties of $V(\phi)$ from the observational data. Alternatively, more complicated models, perhaps motivated by contemporary fundamental physics ideas, may be tested on a model-by-model basis.

Inflation generates perturbations through the amplification of quantum fluctuations, which are stretched to astrophysical scales by the rapid expansion. The simplest models generate two types, density perturbations which come from fluctuations in the scalar field and its corresponding scalar metric perturbation, and gravitational waves which are tensor metric fluctuations. The former experience gravitational instability and lead to structure formation, while the latter can influence the CMB anisotropies. Defining slow-roll parameters, with primes indicating derivatives with respect to the scalar field, as

$$\epsilon = \frac{m_\mathrm{Pl}^2}{16\pi}\left(\frac{V'}{V}\right)^2 \quad ; \quad \eta = \frac{m_\mathrm{Pl}^2}{8\pi}\frac{V''}{V}\,, \tag{24.4}$$

which should satisfy $\epsilon, |\eta| \ll 1$, the spectra can be computed using the slow-roll approximation as

$$\Delta^2_{\mathcal{R}}(k) \simeq \frac{8}{3m_{\rm Pl}^4}\frac{V}{\epsilon}\bigg|_{k=aH} \quad ; \quad \Delta^2_{\rm t}(k) \simeq \frac{128}{3m_{\rm Pl}^4}V\bigg|_{k=aH} . \qquad (24.5)$$

In each case, the expressions on the right-hand side are to be evaluated when the scale k is equal to the Hubble radius during inflation. The symbol '$\simeq$' here indicates use of the slow-roll approximation, which is expected to be accurate to a few percent or better.

From these expressions, we can compute the spectral indices [8]

$$n_{\rm s} \simeq 1 - 6\epsilon + 2\eta \quad ; \quad n_{\rm t} \simeq -2\epsilon\,. \qquad (24.6)$$

Another useful quantity is the ratio of the two spectra, defined by

$$r \equiv \frac{\Delta^2_{\rm t}(k_*)}{\Delta^2_{\mathcal{R}}(k_*)}\,. \qquad (24.7)$$

We have

$$r \simeq 16\epsilon \simeq -8n_{\rm t}\,, \qquad (24.8)$$

which is known as the consistency equation.

One could consider corrections to the power-law approximation, which we discuss later. However, for now we make the working assumption that the spectra can be approximated by power laws. The consistency equation shows that r and $n_{\rm t}$ are not independent parameters, and so the simplest inflation models give initial conditions described by three parameters, usually taken as $\Delta^2_{\mathcal{R}}$, $n_{\rm s}$, and r, all to be evaluated at some scale k_*, usually the 'statistical center' of the range explored by the data. Alternatively, one could use the parametrization V, ϵ, and η, all evaluated at a point on the putative inflationary potential.

After the perturbations are created in the early Universe, they undergo a complex evolution up until the time they are observed in the present Universe. While the perturbations are small, this can be accurately followed using a linear theory numerical code such as CAMB or CLASS [9]. This works right up to the present for the CMB, but for density perturbations on small scales non-linear evolution is important and can be addressed by a variety of semi-analytical and numerical techniques. However the analysis is made, the outcome of the evolution is in principle determined by the cosmological model, and by the parameters describing the initial perturbations, and hence can be used to determine them.

Of particular interest are CMB anisotropies. Both the total intensity and two independent polarization modes are predicted to have anisotropies. These can be described by the radiation angular power spectra C_ℓ as defined in the article of Scott and Smoot in this volume, and again provide a complete description if the density perturbations are Gaussian.

24.1.3. *The standard cosmological model* :

We now have most of the ingredients in place to describe the cosmological model. Beyond those of the previous subsections, we need a measure of the ionization state of the Universe. The Universe is known to be highly ionized at low redshifts (otherwise radiation from distant quasars would be heavily absorbed in the ultra-violet), and the ionized electrons can scatter microwave photons altering the pattern of observed anisotropies. The most convenient parameter to describe this is the optical depth to scattering τ (*i.e.*, the probability that a given photon scatters once); in the approximation of instantaneous and complete reionization, this could equivalently be described by the redshift of reionization $z_{\rm ion}$.

As described in Sec. 24.4, models based on these parameters are able to give a good fit to the complete set of high-quality data available at present, and indeed some simplification is possible. Observations are consistent with spatial flatness, and indeed the inflation models so far described automatically generate negligible spatial curvature, so we can set $k = 0$; the density parameters then must sum to unity, and so one can be eliminated. The neutrino energy density is often not taken as an independent parameter. Provided the neutrino sector has the standard interactions, the neutrino energy density, while relativistic, can be related to the photon density using thermal physics arguments, and a minimal assumption takes the neutrino mass sum to be that of the lowest mass solution to the neutrino oscillation constraints, namely 0.06 eV. In addition, there is no observational evidence for the existence of tensor perturbations (though the upper limits are fairly weak), and so r could be set to zero. This leaves seven parameters, which is the smallest set that can usefully be compared to the present cosmological data set. This model is referred to by various names, including ΛCDM, the concordance cosmology, and the standard cosmological model.

Of these parameters, only $\Omega_{\rm r}$ is accurately measured directly. The radiation density is dominated by the energy in the CMB, and the COBE satellite FIRAS experiment determined its temperature to be $T = 2.7255 \pm 0.0006\,{\rm K}$ [10], ‡ corresponding to $\Omega_{\rm r} = 2.47 \times 10^{-5} h^{-2}$. It typically need not be varied in fitting other data. Hence the minimum number of cosmological parameters varied in fits to data is six, though as described below there may additionally be many 'nuisance' parameters necessary to describe astrophysical processes influencing the data.

In addition to this minimal set, there is a range of other parameters which might prove important in future as the data-sets further improve, but for which there is so far no direct evidence, allowing them to be set to a specific value for now. We discuss various speculative options in the next section. For completeness at this point, we mention one other interesting parameter, the helium fraction, which is a non-zero parameter that can affect the CMB anisotropies at a subtle level. Fields, Molaro and Sarkar in this volume discuss current measures of this parameter. It is usually fixed in microwave anisotropy studies, but the data are approaching a level where allowing its variation may become mandatory.

Most attention to date has been on parameter estimation, where a set of parameters is chosen by hand and the aim is to constrain them. Interest has been growing towards the higher-level inference problem of model selection, which compares different choices of parameter sets. Bayesian inference offers an attractive framework for cosmological model selection, setting a tension between model predictiveness and ability to fit the data.

24.1.4. *Derived parameters* :

The parameter list of the previous subsection is sufficient to give a complete description of cosmological models which agree with observational data. However, it is not a unique parameterization, and one could instead use parameters derived from that basic set. Parameters which can be obtained from the set given above include the age of the Universe, the present horizon distance, the present neutrino background temperature, the epoch of matter–radiation equality, the epochs of recombination and decoupling, the epoch of transition to an accelerating Universe, the baryon-to-photon ratio, and the baryon to dark matter density ratio. In addition, the physical densities of the matter components, $\Omega_i h^2$, are often more useful than the density parameters. The density perturbation amplitude can be specified in many different ways other than the large-scale primordial amplitude, for instance, in terms of its effect on the CMB, or by specifying a short-scale quantity, a common choice being the present linear-theory mass dispersion on a scale of $8\,h^{-1}$Mpc, known as σ_8.

Different types of observation are sensitive to different subsets of the full cosmological parameter set, and some are more naturally interpreted in terms of some of the derived parameters of this subsection than on the original base parameter set. In particular, most types of observation feature degeneracies whereby they are unable to separate the effects of simultaneously varying several of the base parameters.

‡ Unless stated otherwise, all quoted uncertainties in this article are one-sigma/68% confidence and all upper limits are 95% confidence. Cosmological parameters sometimes have significantly non-Gaussian uncertainties. Throughout we have rounded central values, and especially uncertainties, from original sources in cases where they appear to be given to excessive precision.

24.2. Extensions to the standard model

This section discusses some ways in which the standard model could be extended. At present, there is no positive evidence in favor of any of these possibilities, which are becoming increasingly constrained by the data, though there always remains the possibility of trace effects at a level below present observational capability.

24.2.1. *More general perturbations* :

The standard cosmology assumes adiabatic, Gaussian perturbations. Adiabaticity means that all types of material in the Universe share a common perturbation, so that if the space-time is foliated by constant-density hypersurfaces, then all fluids and fields are homogeneous on those slices, with the perturbations completely described by the variation of the spatial curvature of the slices. Gaussianity means that the initial perturbations obey Gaussian statistics, with the amplitudes of waves of different wavenumbers being randomly drawn from a Gaussian distribution of width given by the power spectrum. Note that gravitational instability generates non-Gaussianity; in this context, Gaussianity refers to a property of the initial perturbations, before they evolve.

The simplest inflation models, based on one dynamical field, predict adiabatic perturbations and a level of non-Gaussianity which is too small to be detected by any experiment so far conceived. For present data, the primordial spectra are usually assumed to be power laws.

24.2.1.1. *Non-power-law spectra:*

For typical inflation models, it is an approximation to take the spectra as power laws, albeit usually a good one. As data quality improves, one might expect this approximation to come under pressure, requiring a more accurate description of the initial spectra, particularly for the density perturbations. In general, one can expand $\ln \Delta^2_{\mathcal{R}}$ as

$$\ln \Delta^2_{\mathcal{R}}(k) = \ln \Delta^2_{\mathcal{R}}(k_*) + (n_{\rm s,*} - 1) \ln \frac{k}{k_*} + \frac{1}{2} \left. \frac{dn_{\rm s}}{d \ln k} \right|_* \ln^2 \frac{k}{k_*} + \cdots \,, \quad (24.9)$$

where the coefficients are all evaluated at some scale k_*. The term $dn_{\rm s}/d\ln k|_*$ is often called the running of the spectral index [11]. Once non-power-law spectra are allowed, it is necessary to specify the scale k_* at which the spectral index is defined.

24.2.1.2. *Isocurvature perturbations:*

An isocurvature perturbation is one which leaves the total density unperturbed, while perturbing the relative amounts of different materials. If the Universe contains N fluids, there is one growing adiabatic mode and $N-1$ growing isocurvature modes (for reviews see Ref. 12 and Ref. 7). These can be excited, for example, in inflationary models where there are two or more fields which acquire dynamically-important perturbations. If one field decays to form normal matter, while the second survives to become the dark matter, this will generate a cold dark matter isocurvature perturbation.

In general, there are also correlations between the different modes, and so the full set of perturbations is described by a matrix giving the spectra and their correlations. Constraining such a general construct is challenging, though constraints on individual modes are beginning to become meaningful, with no evidence that any other than the adiabatic mode must be non-zero.

24.2.1.3. *Seeded perturbations:*

An alternative to laying down perturbations at very early epochs is that they are seeded throughout cosmic history, for instance by topological defects such as cosmic strings. It has long been excluded that these are the sole original of structure, but they could contribute part of the perturbation signal, current limits being just a few percent [13]. In particular, cosmic defects formed in a phase transition ending inflation is a plausible scenario for such a contribution.

24.2.1.4. *Non-Gaussianity:*

Multi-field inflation models can also generate primordial non-Gaussianity (reviewed, *e.g.*, in Ref. 7). The extra fields can either be in the same sector of the underlying theory as the inflaton, or completely separate, an interesting example of the latter being the curvaton model [14]. Current upper limits on non-Gaussianity are becoming stringent, but there remains strong motivation to push down those limits and perhaps reveal trace non-Gaussianity in the data. If non-Gaussianity is observed, its nature may favor an inflationary origin, or a different one such as topological defects.

24.2.2. *Dark matter properties* :

Dark matter properties are discussed in the article by Drees and Gerbier in this volume. The simplest assumption concerning the dark matter is that it has no significant interactions with other matter, and that its particles have a negligible velocity as far as structure formation is concerned. Such dark matter is described as 'cold,' and candidates include the lightest supersymmetric particle, the axion, and primordial black holes. As far as astrophysicists are concerned, a complete specification of the relevant cold dark matter properties is given by the density parameter $\Omega_{\rm c}$, though those seeking to directly detect it are as interested in its interaction properties.

Cold dark matter is the standard assumption and gives an excellent fit to observations, except possibly on the shortest scales where there remains some controversy concerning the structure of dwarf galaxies and possible substructure in galaxy halos. It has long been excluded for all the dark matter to have a large velocity dispersion, so-called 'hot' dark matter, as it does not permit galaxies to form; for thermal relics the mass must be above about 1 keV to satisfy this constraint, though relics produced non-thermally, such as the axion, need not obey this limit. However, in future further parameters might need to be introduced to describe dark matter properties relevant to astrophysical observations. Suggestions which have been made include a modest velocity dispersion (warm dark matter) and dark matter self-interactions. There remains the possibility that the dark matter is comprized of two separate components, *e.g.*, a cold one and a hot one, an example being if massive neutrinos have a non-negligible effect.

24.2.3. *Relativistic species* :

The number of relativistic species in the young Universe (omitting photons) is denoted $N_{\rm eff}$. In the standard cosmological model only the three neutrino species contribute, and its baseline value is assumed fixed at 3.046 (the small shift from 3 is because of a slight predicted deviation from a thermal distribution [15]) . However other species could contribute, for example extra neutrino species, possibly of sterile type, or massless Goldstone bosons or other scalars. It is hence interesting to study the effect of allowing this parameter to vary, and indeed although 3.046 is consistent with the data, most analyses currently suggest a somewhat higher value (*e.g.*, Ref. 16).

24.2.4. *Dark energy* :

While the standard cosmological model given above features a cosmological constant, in order to explain observations indicating that the Universe is presently accelerating, further possibilities exist under the general headings of 'dark energy' and 'modified gravity'. These topics are described in detail in the article by Mortonson, Weinberg and White in this volume. This article focuses on the case of the cosmological constant, as this simple case is a good match to existing data. We note that more general treatments of dark energy/modified gravity will lead to weaker constraints on other parameters.

24.2.5. *Complex ionization history* :

The full ionization history of the Universe is given by the ionization fraction as a function of redshift z. The simplest scenario takes the ionization to have the small residual value left after recombination up to some redshift $z_{\rm ion}$, at which point the Universe instantaneously reionizes completely. Then there is a one-to-one correspondence between τ and $z_{\rm ion}$ (that relation, however, also depending on other cosmological parameters). An accurate treatment of this process will track separate histories for hydrogen and helium. While currently rapid ionization appears to be a good approximation, as data improve a more complex ionization history may need to be considered.

24.2.6. *Varying 'constants'* :

Variation of the fundamental constants of Nature over cosmological times is another possible enhancement of the standard cosmology. There is a long history of study of variation of the gravitational constant $G_{\rm N}$, and more recently attention has been drawn to the possibility of small fractional variations in the fine-structure constant. There is presently no observational evidence for the former, which is tightly constrained by a variety of measurements. Evidence for the latter has been claimed from studies of spectral line shifts in quasar spectra at redshift $z \approx 2$ [17], but this is presently controversial and in need of further observational study.

24.2.7. *Cosmic topology* :

The usual hypothesis is that the Universe has the simplest topology consistent with its geometry, for example that a flat Universe extends forever. Observations cannot tell us whether that is true, but they can test the possibility of a non-trivial topology on scales up to roughly the present Hubble scale. Extra parameters would be needed to specify both the type and scale of the topology, for example, a cuboidal topology would need specification of the three principal axis lengths. At present, there is no evidence for non-trivial cosmic topology [18].

24.3. Probes

The goal of the observational cosmologist is to utilize astronomical information to derive cosmological parameters. The transformation from the observables to the parameters usually involves many assumptions about the nature of the objects, as well as of the dark sector. Below we outline the physical processes involved in each probe, and the main recent results. The first two subsections concern probes of the homogeneous Universe, while the remainder consider constraints from perturbations.

In addition to statistical uncertainties we note three sources of systematic uncertainties that will apply to the cosmological parameters of interest: (i) due to the assumptions on the cosmological model and its priors (*i.e.*, the number of assumed cosmological parameters and their allowed range); (ii) due to the uncertainty in the astrophysics of the objects (*e.g.*, light curve fitting for supernovae or the mass–temperature relation of galaxy clusters); and (iii) due to instrumental and observational limitations (*e.g.*, the effect of 'seeing' on weak gravitational lensing measurements, or beam shape on CMB anisotropy measurements).

These systematics, the last two of which appear as 'nuisance parameters', pose a challenging problem to the statistical analysis. We attempt to fit the whole Universe with 6 to 12 parameters, but we might need to include hundreds of nuisance parameters, some of them highly correlated with the cosmological parameters of interest (for example time-dependent galaxy biasing could mimic growth of mass fluctuations). Fortunately, there is some astrophysical prior knowledge on these effects, and a small number of physically-motivated free parameters would ideally be preferred in the cosmological parameter analysis.

24.3.1. *Direct measures of the Hubble constant* :

In 1929, Edwin Hubble discovered the law of expansion of the Universe by measuring distances to nearby galaxies. The slope of the relation between the distance and recession velocity is defined to be the Hubble constant H_0. Astronomers argued for decades on the systematic uncertainties in various methods and derived values over the wide range $40\,{\rm km\,s^{-1}\,Mpc^{-1}} \lesssim H_0 \lesssim 100\,{\rm km\,s^{-1}\,Mpc^{-1}}$.

One of the most reliable results on the Hubble constant comes from the Hubble Space Telescope Key Project [19]. This study used the empirical period–luminosity relations for Cepheid variable stars to obtain distances to 31 galaxies, and calibrated a number of secondary distance indicators—Type Ia Supernovae (SNe Ia), the Tully–Fisher relation, surface-brightness fluctuations, and Type II Supernovae—measured over distances of 400 to 600 Mpc. They estimated $H_0 = 72 \pm 3$ (statistical) $\pm\, 7$ (systematic) $\,{\rm km\,s^{-1}\,Mpc^{-1}}$.

A recent study [20] of over 600 Cepheids in the host galaxies of eight recent SNe Ia, observed with an improved camera on board the Hubble Space Telescope, was used to calibrate the magnitude–redshift relation for 240 SNe Ia. This yielded an even more precise figure, $H_0 = 73.8 \pm 2.4\,{\rm km\,s^{-1}\,Mpc^{-1}}$ (including both statistical and systematic errors). The major sources of uncertainty in this result are due to the heavy element abundance of the Cepheids and the distance to the fiducial nearby galaxy, the Large Magellanic Cloud, relative to which all Cepheid distances are measured.

The indirect determination of H_0 by the *Planck* Collaboration [2] found a lower value, $H_0 = 67.3 \pm 1.2\,{\rm km\,s^{-1}\,Mpc^{-1}}$. As discussed in that paper, there is strong degeneracy of H_0 with other parameters, e.g. $\Omega_{\rm m}$ and the neutrino mass. The tension between the H_0 from *Planck* and the traditional cosmic distance-ladder methods is under investigation.

24.3.2. *Supernovae as cosmological probes* :

Empirically, the peak luminosity of SNe Ia can be used as an efficient distance indicator (*e.g.*, Ref. 21), thus allowing cosmology to be constrained via the distance–redshift relation. The favorite theoretical explanation for SNe Ia is the thermonuclear disruption of carbon–oxygen white dwarfs. Although not perfect 'standard candles', it has been demonstrated that by correcting for a relation between the light curve shape, color, and the luminosity at maximum brightness, the dispersion of the measured luminosities can be greatly reduced. There are several possible systematic effects which may affect the accuracy of the use of SNe Ia as distance indicators, *e.g.*, evolution with redshift and interstellar extinction in the host galaxy and in the Milky Way.

Two major studies, the Supernova Cosmology Project and the High-z Supernova Search Team, found evidence for an accelerating Universe [22], interpreted as due to a cosmological constant or a dark energy component. When combined with the CMB data (which indicates flatness, *i.e.*, $\Omega_{\rm m} + \Omega_\Lambda = 1$), the best-fit values were $\Omega_{\rm m} \approx 0.3$ and $\Omega_\Lambda \approx 0.7$. Most results in the literature are consistent with the $w = -1$ cosmological constant case. Taking $w = -1$, the SNLS3 team found, by combining their SNIa data with baryon acoustic oscillation (BAO) and *WMAP*7 data, $\Omega_{\rm m} = 0.279^{+0.019}_{-0.015}$ and $\Omega_\Lambda = 0.724^{+0.017}_{-0.016}$, including both statistical and systematic errors [23]. This includes a correction for the recently-discovered relationship between host galaxy mass and supernova absolute brightness. This agrees with earlier results [24,25], but note the somewhat higher value for $\Omega_{\rm m}$ from *Planck* (see Table 24.1). Future experiments will aim to set constraints on the cosmic equation of state $w(z)$.

24.3.3. *Cosmic microwave background* :

The physics of the CMB is described in detail by Scott and Smoot in this volume. Before recombination, the baryons and photons are tightly coupled, and the perturbations oscillate in the potential wells generated primarily by the dark matter perturbations. After decoupling, the baryons are free to collapse into those potential wells. The CMB carries a record of conditions at the time of last scattering, often called primary anisotropies. In addition, it is affected by various processes as it propagates towards us, including the effect of a time-varying gravitational potential (the integrated Sachs–Wolfe effect), gravitational lensing, and scattering from ionized gas at low redshift.

The primary anisotropies, the integrated Sachs–Wolfe effect, and scattering from a homogeneous distribution of ionized gas, can all be calculated using linear perturbation theory. Available codes include CAMB and CLASS [9], the former widely used embedded within the analysis package CosmoMC [26]. Gravitational lensing is also calculated in these codes. Secondary effects such as inhomogeneities in the reionization process, and scattering from gravitationally-collapsed gas (the Sunyaev–Zel'dovich (SZ) effect), require more complicated, and more uncertain, calculations.

The upshot is that the detailed pattern of anisotropies depends on all of the cosmological parameters. In a typical cosmology, the anisotropy power spectrum [usually plotted as $\ell(\ell+1)C_\ell$] features a flat plateau at large angular scales (small ℓ), followed by a series of oscillatory features at higher angular scales, the first and most prominent being at around one degree ($\ell \simeq 200$). These features, known as acoustic peaks, represent the oscillations of the photon–baryon fluid around the time of decoupling. Some features can be closely related to specific parameters—for instance, the location of the first peak probes the spatial geometry, while the relative heights

of the peaks probes the baryon density—but many other parameters combine to determine the overall shape.

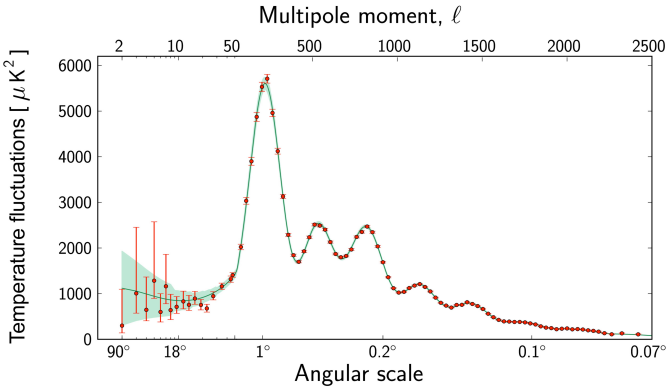

Figure 24.1: The angular power spectrum of the CMB temperature anisotropies from *Planck*, from Ref. 1. Note the x-axis switches from logarithmic to linear at $\ell = 50$. The solid line shows the prediction from the best-fitting ΛCDM model and the band indicates the cosmic variance uncertainty. [Figure courtesy ESA/*Planck* Collaboration.]

The 2013 data release from the *Planck* satellite [1] has provided the most powerful results to date on the spectrum of CMB temperature anisotropies, with a precision determination of the temperature power spectrum to beyond $\ell = 2000$, shown in Fig. 24.1. The Atacama Cosmology Telescope (ACT) and South Pole Telescope (SPT) experiments extend these results to higher angular resolution, though without full-sky coverage. The most comprehensive measurements of CMB polarization come from the *WMAP* satellite final (9-year) data release [3], giving the spectrum of E-polarization anisotropies and the correlation spectrum between temperature and polarization (those spectra having first been detected by DASI [27]) . These are consistent with models based on the parameters we have described, and provide accurate determinations of many of those parameters [2].

The data provide an exquisite measurement of the location of the first acoustic peak, determining the angular-diameter distance of the last-scattering surface. In combination with other data this strongly constrains the spatial geometry, in a manner consistent with spatial flatness and excluding significantly-curved Universes. CMB data also gives a precision measurement of the age of the Universe. It gives a baryon density consistent with, and at higher precision than, that coming from BBN. It affirms the need for both dark matter and dark energy. It shows no evidence for dynamics of the dark energy, being consistent with a pure cosmological constant ($w = -1$). The density perturbations are consistent with a power-law primordial spectrum, and there is no indication yet of tensor perturbations. The current best-fit for the reionization optical depth from CMB data, $\tau = 0.091$, is in line with models of how early structure formation induces reionization.

Planck has also made the first all-sky map of the CMB lensing field, which probes the entire matter distribution in the Universe; this detection corresponds to about 25σ and adds some additional constraining power to the CMB-only data-sets. ACT previously announced the first detection of gravitational lensing of the CMB from the four-point correlation of temperature variations [28]. These measurements agree with the expected effect in the standard cosmology.

24.3.4. *Galaxy clustering* :

The power spectrum of density perturbations depends on the nature of the dark matter. Within the ΛCDM model, the power spectrum shape depends primarily on the primordial power spectrum and on the combination $\Omega_{\rm m}h$ which determines the horizon scale at matter–radiation equality, with a subdominant dependence on the baryon density. The matter distribution is most easily probed by observing the galaxy distribution, but this must be done with care as the galaxies do not perfectly trace the dark matter distribution. Rather, they are a 'biased' tracer of the dark matter. The need to allow for such bias is emphasized by the observation that different types of galaxies show bias with respect to each other. In particular scale-dependent and stochastic biasing may introduce a systematic effect on the determination of cosmological parameters from redshift surveys. Prior knowledge from simulations of galaxy formation or from gravitational lensing data could help to quantify biasing. Furthermore, the observed 3D galaxy distribution is in redshift space, *i.e.*, the observed redshift is the sum of the Hubble expansion and the line-of-sight peculiar velocity, leading to linear and non-linear dynamical effects which also depend on the cosmological parameters. On the largest length scales, the galaxies are expected to trace the location of the dark matter, except for a constant multiplier b to the power spectrum, known as the linear bias parameter. On scales smaller than 20 h^{-1} Mpc or so, the clustering pattern is 'squashed' in the radial direction due to coherent infall, which depends approximately on the parameter $\beta \equiv \Omega_{\rm m}^{0.6}/b$ (on these shorter scales, more complicated forms of biasing are not excluded by the data). On scales of a few h^{-1} Mpc, there is an effect of elongation along the line of sight (colloquially known as the 'finger of God' effect) which depends on the galaxy velocity dispersion.

24.3.4.1. *Baryonic acoustic oscillations:*

The power spectra of the 2-degree Field (2dF) Galaxy Redshift Survey and the Sloan Digital Sky Survey (SDSS) are well fit by a ΛCDM model and both surveys showed evidence for BAOs [29,30]. The Baryon Oscillation Spectroscopic Survey (BOSS) of Luminous Red Galaxies (LRGs) in the SDSS found consistency with the dark energy equation of state $w = -1$ to within ± 0.06 [31]. Similar results for w were obtained by the WiggleZ survey [32]. The BAO data from recent galaxy redshift surveys together with SN Ia data are shown in a Hubble diagram in Fig. 24.2.

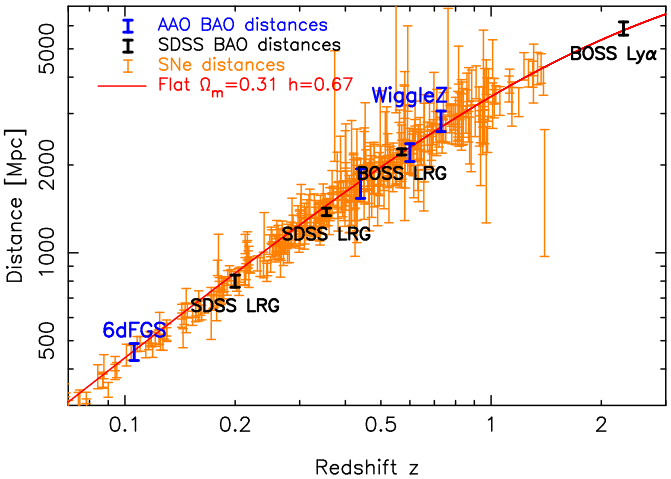

Figure 24.2: The cosmic distance scale with redshift. This modern version of the 'Hubble Diagram' combines data from SN Ia as standard candles and BAO as standard rulers in the LRG SSDS, BOSS, 6dFGRS, and WiggleZ galaxy surveys and from the BOSS Lyman-alpha at high redshift. [Figure courtesy of C. Blake, based on Ref. 33.]

24.3.4.2. *Redshift distortion:*

There is renewed interest in the 'redshift distortion' effect. As the measured redshift of a galaxy is the sum of its redshift due to the Hubble expansion and its peculiar velocity, this distortion depends on cosmological parameters [34] via the perturbation growth rate in linear theory $f(z) = d\ln\delta/d\ln a \approx \Omega^\gamma(z)$, where $\gamma \simeq 0.55$ for the ΛCDM model and is different for modified gravity models. Recent observational results show that by measuring $f(z)$ it is feasible to constrain γ and rule out certain modified gravity models [35,36]. We note the degeneracy of the redshift-distortion pattern and the geometric distortion (the so-called Alcock–Paczynski effect), *e.g.* as illustrated by the WiggleZ survey [37].

24.3.4.3. *Integrated Sachs–Wolfe effect:*

The integrated Sachs–Wolfe (ISW) effect, described in the article by Scott and Smoot, is the change in CMB photon energy when propagating through the changing gravitational potential wells of developing cosmic structures. In linear theory, the ISW signal is expected in universes where there is dark energy, curvature, or modified gravity. Correlating the large-angle CMB anisotropies with very large scale structures, first proposed in Ref. 38, has provided results which vary from no detection of this effect to 4σ detection [39,40].

24.3.4.4. *Limits on neutrino mass from galaxy surveys and other probes:*

Large-scale structure data constraints on Ω_ν due to the neutrino free-streaming effect [41]. Presently there is no clear detection, and upper limits on neutrino mass are commonly estimated by comparing the observed galaxy power spectrum with a four-component model of baryons, cold dark matter, a cosmological constant, and massive neutrinos. Such analyses also assume that the primordial power spectrum is adiabatic, scale-invariant, and Gaussian. Potential systematic effects include biasing of the galaxy distribution and non-linearities of the power spectrum. An upper limit can also be derived from CMB anisotropies alone, while additional cosmological data-sets can improve the results.

Results using a photometric redshift sample of LRGs combined with *WMAP*, BAO, Hubble constant and SNe Ia data gave a 95% confidence upper limit on the total neutrino mass of 0.28eV [42]. Recent spectroscopic redshift surveys, with more accurate redshifts but fewer galaxies, yielded similar upper limits for assumed flat ΛCDM model and additional data-sets: 0.34eV from BOSS [43] and 0.29eV from WiggleZ [44]. *Planck* + *WMAP* polarization + highL CMB [2] give an upper limit of 0.66eV, and with additional BAO data 0.23eV. The effective number of relativistic degrees of freedom is $N_{\rm eff} = 3.30 \pm 0.27$ in good agreement with the standard value $N_{\rm eff} = 3.046$. While the latest cosmological data do not yet constrain the sum of neutrino masses to below 0.2eV, as the lower limit on neutrino mass from terrestrial experiments is 0.06eV, it looks promising that future cosmological surveys will detect the neutrino mass.

24.3.5. ***Clusters of galaxies*** :

A cluster of galaxies is a large collection of galaxies held together by their mutual gravitational attraction. The largest ones are around 10^{15} Solar masses, and are the largest gravitationally-collapsed structures in the Universe. Even at the present epoch they are relatively rare, with only a few percent of galaxies being in clusters. They provide various ways to study the cosmological parameters.

The first objects of a given kind form at the rare high peaks of the density distribution, and if the primordial density perturbations are Gaussian distributed, their number density is exponentially sensitive to the size of the perturbations, and hence can strongly constrain it. Clusters are an ideal application in the present Universe. They are usually used to constrain the amplitude σ_8, as a sphere of radius $8\,h^{-1}\,$Mpc contains about the right amount of material to form a cluster. One of the most useful observations at present are of X-ray emission from hot gas lying within the cluster, whose temperature is typically a few keV, and which can be used to estimate the mass of the cluster. A theoretical prediction for the mass function of clusters can come either from semi-analytic arguments or from numerical simulations. The same approach can be adopted at high redshift (which for clusters means redshifts of order one) to attempt to measure σ_8 at an earlier epoch. The evolution of σ_8 is primarily driven by the value of the matter density $\Omega_{\rm m}$, with a sub-dominant dependence on the dark energy properties.

The *Planck* observations were used to produce a sample of 189 clusters selected by the SZ effect. The cluster mass function was constructed using a relation between the SZ signal Y and cluster mass M. For an assumed flat ΛCDM model, the *Planck* Collaboration found $\sigma_8 = 0.77 \pm 0.02$ and $\Omega_{\rm m} = 0.29 \pm 0.02$ [45]. Somewhat larger values of both parameters are preferred by the *Planck*'s measurements of the primary CMB anisotropies. The discrepancy might be resolved, for example, by using a different Y–M calibration. For comparison with other results in the literature see their Fig. 10.

24.3.6. ***Clustering in the inter-galactic medium*** :

It is commonly assumed, based on hydrodynamic simulations, that the neutral hydrogen in the inter-galactic medium (IGM) can be related to the underlying mass distribution. It is then possible to estimate the matter power spectrum on scales of a few megaparsecs from the absorption observed in quasar spectra, the so-called Lyman-α forest. The usual procedure is to measure the power spectrum of the transmitted flux, and then to infer the mass power spectrum. Photo-ionization heating by the ultraviolet background radiation and adiabatic cooling by the expansion of the Universe combine to give a simple power-law relation between the gas temperature and the baryon density. It also follows that there is a power-law relation between the optical depth τ and $\rho_{\rm b}$. Therefore, the observed flux $F = \exp(-\tau)$ is strongly correlated with $\rho_{\rm b}$, which itself traces the mass density. The matter and flux power spectra can be related by

$$P_{\rm m}(k) = b^2(k) P_{\rm F}(k)\,, \tag{24.10}$$

where $b(k)$ is a bias function which is calibrated from simulations. The BOSS survey has been used to detect and measure the BAO feature in the Lyman-α forest fluctuation at redshift $z = 2.4$, with a result impressively consistent with the standard ΛCDM model [46]. The Lyman-α flux power spectrum has also been used to constrain the nature of dark matter, for example constraining the amount of warm dark matter [47].

24.3.7. ***Gravitational lensing*** :

Images of background galaxies are distorted by the gravitational effect of mass variations along the line of sight. Deep gravitational potential wells such as galaxy clusters generate 'strong lensing', leading to arcs, arclets and multiple images, while more moderate perturbations give rise to 'weak lensing'. Weak lensing is now widely used to measure the mass power spectrum in selected regions of the sky (see Ref. 48 for reviews). As the signal is weak, the image of deformed galaxy shapes (the 'shear map') must be analyzed statistically to measure the power spectrum, higher moments, and cosmological parameters.

The shear measurements are mainly sensitive to a combination of $\Omega_{\rm m}$ and the amplitude σ_8. For example, the weak-lensing signal detected by the CFHTLens Survey (over 154 sq. deg. in 5 optical bands) yields, for a flat ΛCDM model, $\sigma_8(\Omega_{\rm m}/0.27)^{0.6} = 0.79 \pm 0.03$ [49]. Earlier results for comparison are summarized in Ref. 48. There are various systematic effects in the interpretation of weak lensing, *e.g.*, due to atmospheric distortions during observations, the redshift distribution of the background galaxies, the intrinsic correlation of galaxy shapes, and non-linear modeling uncertainties.

24.3.8. ***Peculiar velocities*** :

Deviations from the Hubble flow directly probe the mass perturbations in the Universe, and hence provide a powerful probe of the dark matter [50]. Peculiar velocities are deduced from the difference between the redshift and the distance of a galaxy. The observational difficulty is in accurately measuring distances to galaxies. Even the best distance indicators (*e.g.*, the Tully–Fisher relation) give an uncertainty of 15% per galaxy, hence limiting the application of the method at large distances. Peculiar velocities are mainly sensitive to $\Omega_{\rm m}$, not to Ω_Λ or dark energy. While at present cosmological parameters derived from peculiar velocities are strongly affected by

random and systematic errors, a new generation of surveys may improve their accuracy. Three promising approaches are the 6dF near-infrared survey of 15,000 peculiar velocities, peculiar velocities of SNe Ia, and the kinematic Sunyaev–Zel'dovich effect.

24.4. Bringing observations together

Although it contains two ingredients—dark matter and dark energy—which have not yet been verified by laboratory experiments, the ΛCDM model is almost universally accepted by cosmologists as the best description of the present data. The approximate values of some of the key parameters are $\Omega_{\rm b} \approx 0.05$, $\Omega_{\rm c} \approx 0.25$, $\Omega_\Lambda \approx 0.70$, and a Hubble constant $h \approx 0.70$. The spatial geometry is very close to flat (and usually assumed to be precisely flat), and the initial perturbations Gaussian, adiabatic, and nearly scale-invariant.

The most powerful data source is the CMB, which on its own supports all these main tenets. Values for some parameters, as given in Ade *et al.* [2] and Hinshaw *et al.* [4], are reproduced in Table 24.1. These particular results presume a flat Universe. The constraints are somewhat strengthened by adding additional data-sets such as BAO, as shown in the Table, though most of the constraining power resides in the CMB data. We see that the *Planck* and *WMAP* constraints are similar, though with some shifts within the uncertainties. For these six-parameter fits the parameter uncertainties are also comparable; the additional precision of *Planck* data versus *WMAP* is only really apparent when considering significantly larger parameter sets.

If the assumption of spatial flatness is lifted, it turns out that the CMB on its own only weakly constrains the spatial curvature, due to a parameter degeneracy in the angular-diameter distance. However inclusion of other data readily removes this. For example, inclusion of BAO data, plus the assumption that the dark energy is a cosmological constant, yields a constraint on $\Omega_{\rm tot} \equiv \sum \Omega_i + \Omega_\Lambda$ of $\Omega_{\rm tot} = 1.0005 \pm 0.0033$ [2]. Results of this type are normally taken as justifying the restriction to flat cosmologies.

One parameter which is very robust is the age of the Universe, as there is a useful coincidence that for a flat Universe the position of the first peak is strongly correlated with the age. The CMB data give 13.81 ± 0.05 Gyr (assuming flatness). This is in good agreement with the ages of the oldest globular clusters and radioactive dating.

The baryon density $\Omega_{\rm b}$ is now measured with high accuracy from CMB data alone, and is consistent with the determination from BBN; Fields *et al.* in this volume quote the range $0.021 \leq \Omega_{\rm b} h^2 \leq 0.025$ (95% confidence).

While Ω_Λ is measured to be non-zero with very high confidence, there is no evidence of evolution of the dark energy density. Mortonson *et al.* in this volume quote the constraint $w = -1.13^{+0.13}_{-0.11}$ on a constant equation of state from a compilation of CMB and BAO data, with the cosmological constant case $w = -1$ giving an excellent fit to the data. Allowing more complicated forms of dark energy weakens the limits.

The data provide strong support for the main predictions of the simplest inflation models: spatial flatness and adiabatic, Gaussian, nearly scale-invariant density perturbations. But it is disappointing that there is no sign of primordial gravitational waves, with the CMB data compilation providing an upper limit $r < 0.11$ at 95% confidence [2] (weakening to 0.26 if running is allowed). The spectral index is clearly required to be less than one by this data, though the strength of that conclusion can weaken if additional parameters are included in the model fits.

Tests have been made for various types of non-Gaussianity, a particular example being a parameter $f_{\rm NL}$ which measures a quadratic contribution to the perturbations. Various non-gaussianity shapes are possible (see Ref. 51 for details), and current constraints on the popular 'local', 'equilateral', and 'orthogonal' types are $f_{\rm NL}^{\rm local} = 3 \pm 6$, $f_{\rm NL}^{\rm equil} = -42 \pm 75$, and $f_{\rm NL}^{\rm ortho} = -25 \pm 39$ (these look weak, but prominent non-Gaussianity requires the product $f_{\rm NL}\Delta_{\mathcal{R}}$ to be large, and $\Delta_{\mathcal{R}}$ is of order 10^{-5}). Clearly none of these give any indication of primordial non-gaussianity.

Table 24.1: Parameter constraints reproduced from Ref. 2 (Table 5) and Ref. 4 (Table 4), with some additional rounding. All columns assume the ΛCDM cosmology with a power-law initial spectrum, no tensors, spatial flatness, and a cosmological constant as dark energy. *Planck* take the sum of neutrino masses fixed to 0.06eV, while *WMAP* set it to zero. Above the line are the six parameter combinations actually fit to the data in the *Planck* analysis ($\theta_{\rm MC}$ is a measure of the sound horizon at last scattering); those below the line are derived from these. Two different data combinations including *Planck* are shown to highlight the extent to which additional data improve constraints. The first column is a combination of CMB data only — *Planck* temperature plus *WMAP* polarization data plus high-resolution data from ACT and SPT — while the second column adds BAO data from the SDSS, BOSS, 6dF, and WiggleZ surveys. For comparison the last column shows the final nine-year results from the *WMAP* satellite, combined with the same BAO data and high-resolution CMB data (which they call eCMB). Note *WMAP* use Ω_Λ directly as a fit parameter rather than $\theta_{\rm MC}$. The perturbation amplitude $\Delta^2_{\mathcal{R}}$ is specified at the scale $0.05\,{\rm Mpc}^{-1}$ for *Planck*, but $0.002\,{\rm Mpc}^{-1}$ for *WMAP*, so the spectral index $n_{\rm s}$ needs to be taken into account in comparing them. Uncertainties are shown at 68% confidence.

	Planck+WP +highL	*Planck*+WP +highL+BAO	*WMAP*9+eCMB +BAO
$\Omega_{\rm b}h^2$	0.02207 ± 0.00027	0.02214 ± 0.00024	0.02211 ± 0.00034
$\Omega_{\rm c}h^2$	0.1198 ± 0.0026	0.1187 ± 0.0017	0.1162 ± 0.0020
$100\,\theta_{\rm MC}$	1.0413 ± 0.0006	1.0415 ± 0.0006	–
$n_{\rm s}$	0.958 ± 0.007	0.961 ± 0.005	0.958 ± 0.008
τ	$0.091^{+0.013}_{-0.014}$	0.092 ± 0.013	$0.079^{+0.011}_{-0.012}$
$\ln(10^{10}\Delta^2_{\mathcal{R}})$	3.090 ± 0.025	3.091 ± 0.025	3.212 ± 0.029
h	0.673 ± 0.012	0.678 ± 0.008	0.688 ± 0.008
σ_8	0.828 ± 0.012	0.826 ± 0.012	$0.822^{+0.013}_{-0.014}$
$\Omega_{\rm m}$	$0.315^{+0.016}_{-0.017}$	0.308 ± 0.010	0.293 ± 0.010
Ω_Λ	$0.685^{+0.017}_{-0.016}$	0.692 ± 0.010	0.707 ± 0.010

24.5. Outlook for the future

The concordance model is now well established, and there seems little room left for any dramatic revision of this paradigm. A measure of the strength of that statement is how difficult it has proven to formulate convincing alternatives.

Should there indeed be no major revision of the current paradigm, we can expect future developments to take one of two directions. Either the existing parameter set will continue to prove sufficient to explain the data, with the parameters subject to ever-tightening constraints, or it will become necessary to deploy new parameters. The latter outcome would be very much the more interesting, offering a route towards understanding new physical processes relevant to the cosmological evolution. There are many possibilities on offer for striking discoveries, for example:

- The cosmological effects of a neutrino mass may be unambiguously detected, shedding light on fundamental neutrino properties;
- Detection of primordial non-Gaussianities would indicate that non-linear processes influence the perturbation generation mechanism;
- Detection of variation in the dark-energy density (*i.e.*, $w \neq -1$) would provide much-needed experimental input into the nature of the properties of the dark energy.

These provide more than enough motivation for continued efforts to test the cosmological model and improve its accuracy.

Over the coming years, there are a wide range of new observations which will bring further precision to cosmological studies. Indeed, there are far too many for us to be able to mention them all here, and so we will just highlight a few areas.

The CMB observations will improve in several directions. A current frontier is the study of polarization, first detected in 2002 by DASI and for which power spectrum measurements have now been made by several experiments. *Planck* will announce its first polarization results in 2014. Future measurements may be able to separately detect the two modes of polarization and a number of projects are underway with this goal.

An impressive array of dark energy surveys are already operational, under construction, or proposed, including ground-based imaging surveys the Dark Energy Survey and LSST, spectroscopic surveys such as MS-DESI, and space missions *Euclid* and *WFIRST*.

An exciting area for the future is radio surveys of the redshifted 21-cm line of hydrogen. Because of the intrinsic narrowness of this line, by tuning the bandpass the emission from narrow redshift slices of the Universe will be measured to extremely high redshift, probing the details of the reionization process at redshifts up to perhaps 20. LOFAR is the first instrument able to do this and is beginning its operations. In the longer term, the Square Kilometre Array (SKA) will take these studies to a precision level.

The development of the first precision cosmological model is a major achievement. However, it is important not to lose sight of the motivation for developing such a model, which is to understand the underlying physical processes at work governing the Universe's evolution. On that side, progress has been much less dramatic. For instance, there are many proposals for the nature of the dark matter, but no consensus as to which is correct. The nature of the dark energy remains a mystery. Even the baryon density, now measured to an accuracy of a percent, lacks an underlying theory able to predict it within orders of magnitude. Precision cosmology may have arrived, but at present many key questions remain to motivate and challenge the cosmology community.

References:

1. P.A.R. Ade *et al.* (Planck Collab. 2013 I), arXiv:1303.5062v1.
2. P.A.R. Ade *et al.* (Planck Collab. 2013 XVI), arXiv:1303.5076v1.
3. C. Bennett *et al.*, to appear, Astrophys. J. Supp., arXiv:1212.5225v3.
4. G. Hinshaw *et al.*, to appear, Astrophys. J. Supp., arXiv:1212.5226v3.
5. S. Fukuda *et al.*, Phys. Rev. Lett. **85**, 3999 (2000); Q.R. Ahmad *et al.*, Phys. Rev. Lett. **87**, 071301 (2001).
6. E.W. Kolb and M.S. Turner, *The Early Universe*, Addison–Wesley (Redwood City, 1990).
7. D.H. Lyth and A.R. Liddle, *The Primordial Density Perturbation*, Cambridge University Press (2009).
8. A.R. Liddle and D.H. Lyth, Phys. Lett. **B291**, 391 (1992).
9. A. Lewis, A Challinor, and A. Lasenby, Astrophys. J. **538**, 473 (2000); D. Blas, J. Lesgourgues, and T. Tram, JCAP **1107**, 034 (2011).
10. D. Fixsen, Astrophys. J. **707**, 916 (2009).
11. A. Kosowsky and M.S. Turner, Phys. Rev. **D52**, 1739 (1995).
12. K.A. Malik and D. Wands, Phys. Reports **475**, 1 (2009).
13. P.A.R. Ade *et al.* (Planck Collab. 2013 XXV), arXiv:1303.5085v1.
14. D.H. Lyth and D. Wands, Phys. Lett. **B524**, 5 (2002); K. Enqvist and M.S. Sloth, Nucl. Phys. **B626**, 395 (2002); T. Moroi and T. Takahashi, Phys. Lett. **B522**, 215 (2001).
15. G. Mangano *et al.*, Nucl. Phys. **B729**, 221 (2005).
16. S. Riemer-Sørensen, D. Parkinson, and T.M. Davis, PASA **30**, e029 (2013).
17. J.K. Webb *et al.*, Phys. Rev. Lett. **107**, 191101 (2011); J.A. King *et al.*, MNRAS **422**, 3370 (2012); P. Molaro *et al.*, Astron. & Astrophys. **555**, 68 (2013).
18. P.A.R. Ade *et al.*, (Planck Collab. 2013 XXVI), arXiv:1303.5086v1.
19. W.L. Freedman *et al.*, Astrophys. J. **553**, 47 (2001).
20. A.G. Riess *et al.*, Astrophys. J. **730**, 119 (2011).
21. B. Leibundgut, Ann. Rev. Astron. Astrophys. **39**, 67 (2001).
22. A.G. Riess *et al.*, Astron. J. **116**, 1009 (1998); P. Garnavich *et al.*, Astrophys. J. **509**, 74 (1998); S. Perlmutter *et al.*, Astrophys. J. **517**, 565 (1999).
23. A. Conley *et al.*, Astrophys. J. Supp. **192**, 1 (2011); M. Sullivan *et al.*, Astrophys. J. **737**, 102 (2011).
24. M. Kowalski *et al.*, Astrophys. J. **686**, 749 (2008).
25. R. Kessler *et al.*, Astrophys. J. Supp. **185**, 32 (2009).
26. A. Lewis and S. Bridle, Phys. Rev. **D66**, 103511 (2002).
27. J. Kovac *et al.*, Nature **420**, 772 (2002).
28. S. Das *et al.*, Phys. Rev. Lett. **107**, 021301 (2011).
29. D. Eisenstein *et al.*, Astrophys. J. **633**, 560 (2005).
30. S. Cole *et al.*, MNRAS **362**, 505 (2005).
31. A. Sanchez *et al.*, arXiv:1303.4396.
32. D. Parkinson *et al.*, arXiv:1210.2130.
33. C. Blake *et al.*, MNRAS **418**, 1707 (2011).
34. N. Kaiser, MNRAS **227**, 1 (1987).
35. L. Guzzo *et al.*, Nature **451**, 541 (2008).
36. A. Nusser and M. Davis, Astrophys. J. **736**, 93 (2011).
37. C. Blake *et al.*, arXiv:1204.3674.
38. R.G. Crittenden and N. Turok, Phys. Rev. Lett. **75**, 2642 (1995).
39. T. Giannatonio *et al.*, MNRAS **426**, 258 (2012).
40. P.A.R. Ade *et al.* (Planck Collab. 2013 XIX), arXiv:1303.5076v1.
41. J. Lesgourgues and S. Pastor, Phys. Reports **429**, 307 (2006).
42. S. Thomas, F.B. Abdalla, and O. Lahav, Phys. Rev. Lett. **105**, 031301 (2010).
43. G.-B. Zhao *et al.*, MNRAS, doi:10.1093/mnras/stt1710 (early on-line).
44. S. Riemer-Sørensen *et al.*, Phys. Rev. **D85**, 081101 (2012).
45. P.A.R. Ade *et al.* (Planck Collab. 2013 XX), arXiv:1303.5080v1.
46. A. Slosar *et al.*, arXiv:1301.3459.
47. M. Viel *et al.*, arXiv:1306.2314.
48. A. Refregier, Ann. Rev. Astron. Astrophys. **41**, 645 (2003); R. Massey *et al.*, Nature **445**, 286 (2007); H. Hoekstra and B. Jain, Ann. Rev. Nucl. and Part. Sci. **58**, 99 (2008).
49. M. Kilbinger *et al.*, MNRAS **430**, 2200 (2013); C. Heymans *et al.*, MNRAS **427**, 146 (2012).
50. A. Dekel, Ann. Rev. Astron. Astrophys. **32**, 371 (1994).
51. P.A.R. Ade *et al.* (Planck Collab. 2013 XXIV), arXiv:1303.5084v1.

25. DARK MATTER

Revised September 2013 by M. Drees (Bonn University) and G. Gerbier (Saclay, CEA).

25.1. Theory

25.1.1. *Evidence for Dark Matter* :

The existence of Dark (*i.e.*, non-luminous and non-absorbing) Matter (DM) is by now well established [1,2]. The earliest, and perhaps still most convincing, evidence for DM came from the observation that various luminous objects (stars, gas clouds, globular clusters, or entire galaxies) move faster than one would expect if they only felt the gravitational attraction of other visible objects. An important example is the measurement of galactic rotation curves. The rotational velocity v of an object on a stable Keplerian orbit with radius r around a galaxy scales like $v(r) \propto \sqrt{M(r)/r}$, where $M(r)$ is the mass inside the orbit. If r lies outside the visible part of the galaxy and mass tracks light, one would expect $v(r) \propto 1/\sqrt{r}$. Instead, in most galaxies one finds that v becomes approximately constant out to the largest values of r where the rotation curve can be measured; in our own galaxy, $v \simeq 240$ km/s at the location of our solar system, with little change out to the largest observable radius. This implies the existence of a *dark halo*, with mass density $\rho(r) \propto 1/r^2$, *i.e.*, $M(r) \propto r$; at some point ρ will have to fall off faster (in order to keep the total mass of the galaxy finite), but we do not know at what radius this will happen. This leads to a lower bound on the DM mass density, $\Omega_{\rm DM} \gtrsim 0.1$, where $\Omega_X \equiv \rho_X/\rho_{\rm crit}$, $\rho_{\rm crit}$ being the critical mass density (*i.e.*, $\Omega_{\rm tot} = 1$ corresponds to a flat Universe).

The observation of clusters of galaxies tends to give somewhat larger values, $\Omega_{\rm DM} \simeq 0.2$. These observations include measurements of the peculiar velocities of galaxies in the cluster, which are a measure of their potential energy if the cluster is virialized; measurements of the *X-ray* temperature of hot gas in the cluster, which again correlates with the gravitational potential felt by the gas; and—most directly—studies of (weak) gravitational lensing of background galaxies on the cluster.

A particularly compelling example involves the bullet cluster (1E0657-558) which recently (on cosmological time scales) passed through another cluster. As a result, the hot gas forming most of the clusters' baryonic mass was shocked and decelerated, whereas the galaxies in the clusters proceeded on ballistic trajectories. Gravitational lensing shows that most of the total mass also moved ballistically, indicating that DM self-interactions are indeed weak [1].

The currently most accurate, if somewhat indirect, determination of $\Omega_{\rm DM}$ comes from global fits of cosmological parameters to a variety of observations; see the Section on Cosmological Parameters for details. For example, using measurements of the anisotropy of the cosmic microwave background (CMB) and of the spatial distribution of galaxies, Ref. 3 finds a density of cold, non-baryonic matter

$$\Omega_{\rm nbm} h^2 = 0.1198 \pm 0.0026 \ , \tag{25.1}$$

where h is the Hubble constant in units of 100 km/(s·Mpc). Some part of the baryonic matter density [3],

$$\Omega_{\rm b} h^2 = 0.02207 \pm 0.00027 \ , \tag{25.2}$$

may well contribute to (baryonic) DM, *e.g.*, MACHOs [4] or cold molecular gas clouds [5].

The DM density in the "neighborhood" of our solar system is also of considerable interest. This was first estimated as early as 1922 by J.H. Jeans, who analyzed the motion of nearby stars transverse to the galactic plane [2]. He concluded that in our galactic neighborhood, the average density of DM must be roughly equal to that of luminous matter (stars, gas, dust). Remarkably enough, the most recent estimate finds a quite similar result for the smooth component of the local Dark Matter density [6]:

$$\rho_{\rm DM}^{\rm local} = (0.39 \pm 0.03) \frac{\rm GeV}{\rm cm^3} \ . \tag{25.3}$$

This value may have to be increased by a factor of 1.2 ± 0.2 since the baryons in the galactic disk, in which the solar system is located, also increase the local DM density [7]. Small substructures (minihaloes, streams) are not likely to change the local DM density significantly [1]. Note that Eq. (25.3) has been derived by fitting a complete model of our galaxy to a host of data, including the galactic rotation curve. A "purely local" analysis, only using the motion of nearby stars, gives a consistent result, with an error three times as large [8].

25.1.2. *Candidates for Dark Matter* :

Analyses of structure formation in the Universe indicate that most DM should be "cold" or "cool", *i.e.*, should have been non-relativistic at the onset of galaxy formation (when there was a galactic mass inside the causal horizon) [1]. This agrees well with the upper bound [3] on the contribution of light neutrinos to Eq. (25.1),

$$\Omega_\nu h^2 \leq 0.0062 \quad 95\% \text{ CL} \ . \tag{25.4}$$

Candidates for non-baryonic DM in Eq. (25.1) must satisfy several conditions: they must be stable on cosmological time scales (otherwise they would have decayed by now), they must interact very weakly with electromagnetic radiation (otherwise they wouldn't qualify as *dark* matter), and they must have the right relic density. Candidates include primordial black holes, axions, sterile neutrinos, and weakly interacting massive particles (WIMPs).

Primordial black holes must have formed before the era of Big-Bang nucleosynthesis, since otherwise they would have been counted in Eq. (25.2) rather than Eq. (25.1). Such an early creation of a large number of black holes is possible only in certain somewhat contrived cosmological models [9].

The existence of axions [10] was first postulated to solve the strong *CP* problem of QCD; they also occur naturally in superstring theories. They are pseudo Nambu-Goldstone bosons associated with the (mostly) spontaneous breaking of a new global "Peccei-Quinn" (PQ) U(1) symmetry at scale f_a; see the Section on Axions in this *Review* for further details. Although very light, axions would constitute cold DM, since they were produced non-thermally. At temperatures well above the QCD phase transition, the axion is massless, and the axion field can take any value, parameterized by the "misalignment angle" θ_i. At $T \lesssim 1$ GeV, the axion develops a mass $m_a \sim f_\pi m_\pi / f_a$ due to instanton effects. Unless the axion field happens to find itself at the minimum of its potential ($\theta_i = 0$), it will begin to oscillate once m_a becomes comparable to the Hubble parameter H. These coherent oscillations transform the energy originally stored in the axion field into physical axion quanta. The contribution of this mechanism to the present axion relic density is [1]

$$\Omega_a h^2 = \kappa_a \left(f_a / 10^{12} \text{ GeV} \right)^{1.175} \theta_i^2 \ , \tag{25.5}$$

where the numerical factor κ_a lies roughly between 0.5 and a few. If $\theta_i \sim \mathcal{O}(1)$, Eq. (25.5) will saturate Eq. (25.1) for $f_a \sim 10^{11}$ GeV, comfortably above laboratory and astrophysical constraints [10]; this would correspond to an axion mass around 0.1 meV. However, if the post-inflationary reheat temperature $T_R > f_a$, cosmic strings will form during the PQ phase transition at $T \simeq f_a$. Their decay will give an additional contribution to Ω_a, which is often bigger than that in Eq. (25.5) [1], leading to a smaller preferred value of f_a, *i.e.*, larger m_a. On the other hand, values of f_a near the Planck scale become possible if θ_i is for some reason very small.

"Sterile" $SU(2) \times U(1)_Y$ singlet neutrinos with keV masses [11] could alleviate the "cusp/core problem" [1] of cold DM models. If they were produced non-thermally through mixing with standard neutrinos, they would eventually decay into a standard neutrino and a photon.

Weakly interacting massive particles (WIMPs) χ are particles with mass roughly between 10 GeV and a few TeV, and with cross sections of approximately weak strength. Within standard cosmology, their present relic density can be calculated reliably if the WIMPs were in thermal and chemical equilibrium with the hot "soup" of Standard Model (SM) particles after inflation. In this case, their density would become exponentially (Boltzmann) suppressed at $T < m_\chi$. The WIMPs therefore drop out of thermal equilibrium ("freeze out") once

the rate of reactions that change SM particles into WIMPs or vice versa, which is proportional to the product of the WIMP number density and the WIMP pair annihilation cross section into SM particles σ_A times velocity, becomes smaller than the Hubble expansion rate of the Universe. After freeze out, the co-moving WIMP density remains essentially constant; if the Universe evolved adiabatically after WIMP decoupling, this implies a constant WIMP number to entropy density ratio. Their present relic density is then approximately given by (ignoring logarithmic corrections) [12]

$$\Omega_\chi h^2 \simeq const. \cdot \frac{T_0^3}{M_{\rm Pl}^3 \langle \sigma_A v \rangle} \simeq \frac{0.1 \text{ pb} \cdot c}{\langle \sigma_A v \rangle} \ . \qquad (25.6)$$

Here T_0 is the current CMB temperature, $M_{\rm Pl}$ is the Planck mass, c is the speed of light, σ_A is the total annihilation cross section of a pair of WIMPs into SM particles, v is the relative velocity between the two WIMPs in their cms system, and $\langle \ldots \rangle$ denotes thermal averaging. Freeze out happens at temperature $T_F \simeq m_\chi/20$ almost independently of the properties of the WIMP. This means that WIMPs are already non-relativistic when they decouple from the thermal plasma; it also implies that Eq. (25.6) is applicable if $T_R > T_F$. Notice that the 0.1 pb in Eq. (25.6) contains factors of T_0 and $M_{\rm Pl}$; it is, therefore, quite intriguing that it "happens" to come out near the typical size of weak interaction cross sections.

The seemingly most obvious WIMP candidate is a heavy neutrino. However, an SU(2) doublet neutrino will have too small a relic density if its mass exceeds $M_Z/2$, as required by LEP data. One can suppress the annihilation cross section, and hence increase the relic density, by postulating mixing between a heavy SU(2) doublet and some sterile neutrino. However, one also has to require the neutrino to be stable; it is not obvious why a massive neutrino should not be allowed to decay.

The currently best motivated WIMP candidate is, therefore, the lightest superparticle (LSP) in supersymmetric models [13] with exact R-parity (which guarantees the stability of the LSP). Searches for exotic isotopes [14] imply that a stable LSP has to be neutral. This leaves basically two candidates among the superpartners of ordinary particles, a sneutrino, and a neutralino. The negative outcome of various WIMP searches (see below) rules out "ordinary" sneutrinos as primary component of the DM halo of our galaxy. The most widely studied WIMP is therefore the lightest neutralino. Detailed calculations [1] show that the lightest neutralino will have the desired thermal relic density Eq. (25.1) in at least four distinct regions of parameter space. χ could be (mostly) a bino or photino (the superpartner of the $U(1)_Y$ gauge boson and photon, respectively), if both χ and some sleptons have mass below ~ 150 GeV, or if m_χ is close to the mass of some sfermion (so that its relic density is reduced through co-annihilation with this sfermion), or if $2m_\chi$ is close to the mass of the *CP*-odd Higgs boson present in supersymmetric models. Finally, Eq. (25.1) can also be satisfied if χ has a large higgsino or wino component.

Many non-supersymmetric extensions of the Standard Model also contain viable WIMP candidates [1]. Examples are the lightest $T-$odd particle in "Little Higgs" models with conserved $T-$parity, or "techni-baryons" in scenarios with an additional, strongly interacting ("technicolor" or similar) gauge group.

There also exist models where the DM particles, while interacting only weakly with ordinary matter, have quite strong interactions within an extended "dark sector" of the theory. These were motivated by measurements by the PAMELA, ATIC and FERMI satellites indicating excesses in the cosmic e^+ and/or e^- fluxes at high energies. However, these excesses are relative to background estimates that are clearly too simplistic (*e.g.*, neglecting primary sources of electrons and positrons, and modeling the galaxy as a homogeneous cylinder). Moreover, the excesses, if real, are far too large to be due to usual WIMPs, but can be explained by astrophysical sources. It therefore seems unlikely that they are due to Dark Matter [15]. Similarly, claims of positive signals for direct WIMP detection by the DAMA and, more recently, CoGeNT and CRESST collaborations (see below) led to the development of tailor-made models to alleviate tensions with null experiments. Since we are not convinced that these data indeed signal WIMP detection, and these models (some of which were quickly excluded by improved measurements) lack independent motivation, we will not discuss them any further in this Review.

Although thermally produced WIMPs are attractive DM candidates because their relic density naturally has at least the right order of magnitude, non-thermal production mechanisms have also been suggested, *e.g.*, LSP production from the decay of some moduli fields [16], from the decay of the inflaton [17], or from the decay of "$Q-$balls" (non-topological solitons) formed in the wake of Affleck-Dine baryogenesis [18]. Although LSPs from these sources are typically highly relativistic when produced, they quickly achieve kinetic (but not chemical) equilibrium if T_R exceeds a few MeV [19](but stays below $m_\chi/20$). They therefore also contribute to cold DM. Finally, if the WIMPs aren't their own antiparticles, an asymmetry between WIMPs and antiWIMPs might have been created in the early Universe, possibly by the same (unknown) mechanism that created the baryon antibaryon asymmetry. In such "asymmetric DM" models [20] the WIMP antiWIMP annihilation cross section $\langle \sigma_A v \rangle$ should be significantly larger than $1 \text{ pb} \cdot c$, cf Eq. (25.6).

The absence of signals at the LHC for physics beyond the Standard Model, as well as the discovery of an SM-like Higgs boson with mass near 126 GeV, constrains many well-motivated WIMP models. For example, in constrained versions of the minimal supersymmetrized Standard Model (MSSM) both the absence of supersymmetric signals and the relatively large mass of the Higgs boson favor larger WIMP masses and lower scattering cross sections on nucleons. However, constraints from "new physics" searches apply most directly to strongly interacting particles. Many WIMP models therefore can still accommodate a viable WIMP for a wide range of masses. For example, in supersymmetric models where the bino mass is not related to the other gaugino masses a bino with mass as small as 15 GeV can still have the correct thermal relic density [21]. Even lighter supersymmetric WIMPs can be realized in models with extended Higgs sector [22].

Primary black holes (as MACHOs), axions, sterile neutrinos, and WIMPs are all (in principle) detectable with present or near-future technology (see below). There are also particle physics DM candidates which currently seem almost impossible to detect, unless they decay; the present lower limit on their lifetime is of order 10^{25} to 10^{26} s for 100 GeV particles. These include the gravitino (the spin-3/2 superpartner of the graviton), states from the "hidden sector" thought responsible for supersymmetry breaking, and the axino (the spin-1/2 superpartner of the axion) [1].

25.2. Experimental detection of Dark Matter

25.2.1. *The case of baryonic matter in our galaxy* :

The search for hidden galactic baryonic matter in the form of MAssive Compact Halo Objects (MACHOs) has been initiated following the suggestion that they may represent a large part of the galactic DM and could be detected through the microlensing effect [4]. The MACHO, EROS, and OGLE collaborations have performed a program of observation of such objects by monitoring the luminosity of millions of stars in the Large and Small Magellanic Clouds for several years. EROS concluded that MACHOs cannot contribute more than 8% to the mass of the galactic halo [23], while MACHO observed a signal at 0.4 solar mass and put an upper limit of 40%. Overall, this strengthens the need for non-baryonic DM, also supported by the arguments developed above.

25.2.2. *Axion searches* :

Axions can be detected by looking for $a \to \gamma$ conversion in a strong magnetic field [1]. Such a conversion proceeds through the loop-induced $a\gamma\gamma$ coupling, whose strength $g_{a\gamma\gamma}$ is an important parameter of axion models. There is currently only one experiment searching for axionic DM: the ADMX experiment [30], originally situated at the LLNL in California but now running at the University of Washington, started taking data in the first half of 1996. It employs a high quality cavity, whose "Q factor" enhances the conversion rate on resonance, *i.e.*, for $m_a(c^2 + v_a^2/2) = \hbar\omega_{\rm res}$. One then needs to scan the resonance frequency in order to cover a significant range in m_a or, equivalently, f_a. ADMX now uses SQUIDs as first-stage

amplifiers; their extremely low noise temperature (1.2 K) enhances the conversion signal. Published results [24], combining data taken with conventional amplifiers and SQUIDs, exclude axions with mass between 1.9 and 3.53 μeV, corresponding to $f_a \simeq 4 \cdot 10^{13}$ GeV, for an assumed local DM density of 0.45 GeV/cm^3, if $g_{a\gamma\gamma}$ is near the upper end of the theoretically expected range. About five times better limits on $g_{a\gamma\gamma}$ were achieved [25] for 1.98 μeV $\leq m_a \leq$ 2.18 μeV as well as for 3.3 μeV $\leq m_a \leq$ 3.65 μeV, if a large fraction of the local DM density is due to a single flow of axions with very low velocity dispersion. The ADMX experiment is being upgraded by reducing the cavity and SQUID temperature from the current 1.2 K to about 0.1 K. This should increase the frequency scanning speed for given sensitivity by more than two orders of magnitude, or increase the sensitivity for fixed observation time.

25.2.3. *Searches for keV Neutrinos* :

Relic keV neutrinos ν_s can only be detected if they mix with the ordinary neutrinos. This mixing leads to radiative $\nu_s \to \nu\gamma$ decays, with lifetime $\tau_{\nu_s} \simeq 1.8 \cdot 10^{21}$ s $\cdot (\sin\theta)^{-2} \cdot (1 \text{ keV}/m_{\nu_s})^5$, where θ is the mixing angle [11]. This gives rise to a flux of mono-energetic photons with $E_\gamma = m_{\nu_s}/2$, which might be observable by *X-ray* satellites. In the simplest case the relic ν_s are produced only by oscillations of standard neutrinos. Assuming that all lepton-antilepton asymmetries are well below 10^{-3}, the ν_s relic density can then be computed uniquely in terms of the mixing angle θ and the mass m_{ν_s}. The combination of lower bounds on m_{ν_s} from analyses of structure formation (in particular, the Lyα "forest") and upper bounds on *X-ray* fluxes from various (clusters of) galaxies exclude this scenario if ν_s forms all of DM. This conclusion can be evaded if ν_s forms only part of DM, and/or if there is a lepton asymmetry $\geq 10^{-3}$ (i.e. some 7 orders of magnitude above the observed baryon-antibaryon asymmetry), and/or if there is an additional source of ν_s production in the early Universe, e.g. from the decay of heavier particles [11].

25.2.4. *Basics of direct WIMP search* :

As stated above, WIMPs should be gravitationally trapped inside galaxies and should have the adequate density profile to account for the observed rotational curves. These two constraints determine the main features of experimental detection of WIMPs, which have been detailed in the reviews in [1].

Their mean velocity inside our galaxy relative to its center is expected to be similar to that of stars, *i.e.*, a few hundred kilometers per second at the location of our solar system. For these velocities, WIMPs interact with ordinary matter through elastic scattering on nuclei. With expected WIMP masses in the range 10 GeV to 10 TeV, typical nuclear recoil energies are of order of 1 to 100 keV.

The shape of the nuclear recoil spectrum results from a convolution of the WIMP velocity distribution, usually taken as a Maxwellian distribution in the galactic rest frame, shifted into the Earth rest frame, with the angular scattering distribution, which is isotropic to first approximation but forward-peaked for high nuclear mass (typically higher than Ge mass) due to the nuclear form factor. Overall, this results in a roughly exponential spectrum. The higher the WIMP mass, the higher the mean value of the exponential. This points to the need for low nuclear recoil energy threshold detectors.

On the other hand, expected interaction rates depend on the product of the local WIMP flux and the interaction cross section. The first term is fixed by the local density of dark matter, taken as 0.39 GeV/cm^3 [see Eq. (25.3)], the mean WIMP velocity, typically 220 km/s, the galactic escape velocity, typically 544 km/s [26] and the mass of the WIMP. The expected interaction rate then mainly depends on two unknowns, the mass and cross section of the WIMP (with some uncertainty [6] due to the halo model). This is why the experimental observable, which is basically the scattering rate as a function of energy, is usually expressed as a contour in the WIMP mass–cross section plane.

The cross section depends on the nature of the couplings. For non-relativistic WIMPs, one in general has to distinguish spin-independent and spin-dependent couplings. The former can involve scalar and vector WIMP and nucleon currents (vector currents are absent for Majorana WIMPs, *e.g.*, the neutralino), while the latter involve axial vector currents (and obviously only exist if χ carries spin). Due to coherence effects, the spin-independent cross section scales approximately as the square of the mass of the nucleus, so higher mass nuclei, from Ge to Xe, are preferred for this search. For spin-dependent coupling, the cross section depends on the nuclear spin factor; used target nuclei include ^{19}F, ^{23}Na, ^{73}Ge, ^{127}I, ^{129}Xe, ^{131}Xe, and ^{133}Cs.

Cross sections calculated in MSSM models [27] induce rates of at most 1 evt day^{-1} kg^{-1} of detector, much lower than the usual radioactive backgrounds. This indicates the need for underground laboratories to protect against cosmic ray induced backgrounds, and for the selection of extremely radio-pure materials.

The typical shape of exclusion contours can be anticipated from this discussion: at low WIMP mass, the sensitivity drops because of the detector energy threshold, whereas at high masses, the sensitivity also decreases because, for a fixed mass density, the WIMP flux decreases $\propto 1/m_\chi$. The sensitivity is best for WIMP masses near the mass of the recoiling nucleus.

Two important points are to be kept in mind when comparing exclusion curves from various experiments between them or with positive indications of a signal.

For an experiment with a fixed nuclear recoil energy threshold, the lower is the considered WIMP mass, the lower is the fraction of the spectrum to which the experiment is sensitive. This fraction may be extremely small in some cases. For instance CoGeNT [28], using a Germanium detector with an energy threshold of around 2 keV, is sensitive to about 10 % of the total recoil spectrum of a 7 GeV WIMP, while for XENON100 [29], using a liquid Xenon detector with a threshold of 8.4 keV, this fraction is only 0.05 % (that is the extreme tail of the distribution), for the same WIMP mass. The two experiments are then sensitive to very different parts of the WIMP velocity distribution.

A second important point to consider is the energy resolution of the detector. Again at low WIMP mass, the expected roughly exponential spectrum is very steep and when the characteristic energy of the exponential becomes of the same order as the energy resolution, the energy smearing becomes important. In particular, a significant fraction of the expected spectrum below effective threshold is smeared above threshold, increasing artificially the sensitivity. For instance, a Xenon detector with a threshold of 8 keV and infinitely good resolution is actually insensitive to a 7 GeV mass WIMP, because the expected energy distribution has a cut-off at roughly 5 keV. When folding in the experimental resolution of XENON100 (corresponding to a photostatistics of 0.5 photoelectron per keV), then around 1 % of the signal is smeared above 5 keV and 0.05 % above 8 keV. Setting reliable cross section limits in this mass range thus requires a complete understanding of the response of the detector at energies well below the nominal threshold.

In order to homogenize the reliability of the presented exclusion curves, and save the reader the trouble of performing tedious calculations, we propose to set cross section limits only for WIMP mass above a *"WIMP safe"* minimal mass value defined as the maximum of 1) the mass where the increase of sensitivity from infinite resolution to actual experimental resolution is not more than a factor two, and 2) the mass where the experiment is sensitive to at least 1 % of the total WIMP signal recoil spectrum. These recommendations are irrespective of the content of the experimental data obtained by the experiments.

Two experimental signatures are predicted for WIMP signals. One is a strong daily forward/backward asymmetry of the nuclear recoil direction, due to the alternate sweeping of the WIMP cloud by the rotating Earth. Detection of this effect requires gaseous detectors or anisotropic response scintillators (stilbene). The second is a few percent annual modulation of the recoil rate due to the Earth speed adding to or subtracting from the speed of the Sun. This tiny effect can only be detected with large masses; nuclear recoil identification should also be performed, as the otherwise much larger background may also be subject to seasonal modulation.

25.2.5. ***Status and prospects of direct WIMP searches*** :

Given the intense activity of the field, readers interested in more details than the ones given below may refer to [1], as well as to presentations at recent conferences [30].

The first searches have been performed with ultra-pure semiconductors installed in pure lead and copper shields in underground environments. Combining a priori excellent energy resolutions and very pure detector material, they produced the first limits on WIMP searches (Heidelberg-Moscow, IGEX, COSME-II, HDMS) [1]. Planned experiments using several tens of kg to a ton of Germanium run at liquid nitrogen temperature (designed for double-beta decay search) – GERDA, MAJORANA – are based in addition on passive reduction of the external and internal electromagnetic and neutron background by using Point Contact detectors (discussed below), minimal detector housing, close electronics, pulse shape discrimination and large liquid nitrogen or argon shields. Their sensitivity to WIMP interactions will depend on their ability to lower the energy threshold sufficiently, while keeping the background rate small.

Great progress has recently been made in the development of so called Point Contact Germanium detectors, with a very small capacitance allowing one to reach sub-keV thresholds. The CoGeNT collaboration was first operating a single 440 g Germanium detector with an effective threshold of 400 eV in the Soudan Underground Laboratory for 56 days [28]. After applying a rise time cut on the pulse shapes in order to remove the surface interactions known to suffer from incomplete charge collection, the resulting spectrum below 4 keV is said by the authors to exhibit an irreducible excess of events, with energy spectrum roughly exponential, compatible with a light WIMP with mass in the 7 to 11 GeV range, and cross section around 10^{-4} pb. The most recent published result [31] claims the presence of a signal, compatible with WIMPs in the same mass range but with a lower central cross section of 3×10^{-5} pb.

However, at energies around 1 keV where this signal is claimed to reside, the bulk and surface event populations show overlapping rise time distributions. According to the TEXONO [32] and MALBEK [33] collaborations, this makes an accurate separation of these populations very difficult. Additional confusion has been added by the multiplicity of "regions of interest" published by the CoGeNT collaboration and in other analyses [34].

Results [35] based on data accumulated by CoGeNT during one year led to the claim of a modulated signal. However, the modulation is much stronger than expected from a standard WIMP. Moreover, CDMS has similar sensitivity but sees no modulation [36].

The new CDEX/TEXONO consortium plans to build a 10 kg array of small Ge detectors with a claimed very low (100 eV) threshold, and to operate them in the new Chinese Jinping underground laboratory, the deepest in the world. Such a detector would be sensitive to all recently claimed "signal regions" or "regions of interest" of ~ 10 GeV WIMPs.

In order to make progress in the reliability of any claimed signal, active background rejection and signal identification questions have to be addressed. Active background rejection in detectors relies on the relatively small ionization in nuclear recoils due to their low velocity. This induces a reduction ("quenching") of the ionization/scintillation signal for nuclear recoil signal events relative to e or γ induced backgrounds. Energies calibrated with gamma sources are then called "electron equivalent energies" (keVee unit used below). This effect has been both calculated and measured [1]. It is exploited in cryogenic detectors described later. In scintillation detectors, it induces in addition a difference in decay times of pulses induced by e/γ events vs nuclear recoils. In most cases, due to the limited resolution and discrimination power of this technique at low energies, this effect allows only a statistical background rejection. It has been used in NaI(Tl) (DAMA, LIBRA, NAIAD, Saclay NaI), in CsI(Tl) (KIMS), and Xe (ZEPLIN-I) [1,30]. Pulse shape discrimination is particularly efficient in liquid argon. Using a high energy threshold, it has been used for an event by event discrimination by the WARP experiment, but the high threshold led to a moderate signal sensitivity. No observation of nuclear recoils has been reported by any of these experiments.

The DAMA collaboration has reported results from a total of 6 years exposure with the LIBRA phase involving 250 kg of detectors, plus the earlier 6 years exposure of the original DAMA/NaI experiment with 100 kg of detectors [37], for a cumulated exposure of 1.17 t·y. They observe an annual modulation of the signal in the 2 to 6 keVee bin, with the expected period (1 year) and phase (maximum around June 2), at 8.9 σ level. If interpreted within the standard halo model described above, two possible explanations have been proposed: a WIMP with $m_\chi \simeq 50$ GeV and $\sigma_{\chi p} \simeq 7 \cdot 10^{-6}$ pb (central values) or at low mass, in the 6 to 10 GeV range with $\sigma_{\chi p} \sim 10^{-3}$ pb; the cross section could be somewhat lower if there is a significant channeling effect [1].

Interpreting these observations as positive WIMP signal raises several issues of internal consistency. First, the proposed WIMP solutions would induce a sizeable fraction of nuclear recoils in the total measured rate in the 2 to 6 keVee bin. No pulse shape analysis has been reported by the authors to check whether the unmodulated signal was detectable this way. Secondly, the residual e/γ-induced background, inferred by subtracting the signal predicted by the WIMP interpretation from the data, has an unexpected shape [38], starting near zero at threshold and quickly rising to reach its maximum near 3 to 3.5 keVee; from general arguments one would expect the background (e.g. due to electronic noise) to increase towards the threshold. Finally, the amplitude of the annual modulation shows a somewhat troublesome tendency to decrease with time. The original DAMA data, taken 1995 to 2001, gave an amplitude of the modulation of 20.0 ± 3.2 in units of 10^{-3} counts/(kg·day·keVee), in the 2-6 keVee bin. During the first phase of DAMA/LIBRA, covering data taken between 2003 and 2007, this amplitude became 10.7 ± 1.9, and in the second phase of DAMA/LIBRA, covering data taken between 2007 and 2009, it further decreased to 8.5 ± 2.2. The ratio of amplitudes inferred from the DAMA/LIBRA phase 2 and original DAMA data is 0.43 ± 0.13, differing from the expected value of 1 by more than 4 standard deviations. (The results for the DAMA/LIBRA phase 2 have been calculated by us using published results for the earlier data alone [39] as well as for the latest grand total [37].) Similar conclusions can be drawn from analyses of the 2-4 and 2-5 keVee bins.

Concerning compatibility with other experiments (see below), the high mass solution is clearly excluded by many null observations, while possibly a small parameter space remains available for the low mass solution (according to [38] this possibility is excluded if the energy spectrum measured by DAMA/LIBRA is taken into account). It should be noted that these comparisons have to make assumptions about the WIMP velocity distribution (see above), but varying this within reasonable limits does not resolve the tension [38]. Moreover, one usually assumes that the WIMP scatters elastically, and that the spin-independent cross section for scattering off protons and neutrons is roughly the same. These assumptions are satisfied by all models we know that are either relatively simple (i.e. do not introduce many new particles) or have independent motivation (e.g. attempting to solve the hierarchy problem). As noted earlier, models have been constructed where these assumptions do not hold, but at least some of these are no longer able to make the WIMP interpretation of the DAMA(/LIBRA) observations compatible with all null results from other experiments. Finally, appealing to spin-dependent interactions does not help, either [40], in view of null results from direct searches as well as limits on neutrino fluxes from the Sun (see the subsection on indirect WIMP detection below).

KIMS [41], an experiment operating 12 crystals of CsI(Tl) with a total mass of 104.4 kg in the Yang Yang (renamed CUNP) laboratory in Korea, has given an upper limit on nuclear recoils present in a 24 t·d exposure. This translates into an upper limit on the cross section roughly two orders of magnitude below that required to explain the DAMA signal by a 60 GeV WIMP. It should be noted that these results are directly comparable as they involve the same nucleus (I). Based on a modulation analysis of 2.5 years of continuous operation which failed to find a signal, the KIMS collaboration very recently announced [42] preliminary results which exclude the high mass solution and most of the low mass WIMP explanation of DAMA signal.

ANAIS [30], a 100 kg NaI(Tl) project planned to be run at the Canfranc lab, is in the phase of crystal selection and purification.

DM-ice is a new project with the aim of checking the DAMA/LIBRA modulation signal in the southern hemisphere. It will consist of 250 kg of NaI(Tl) installed in the heart of the IceCube array. The counting rate of crystals from the previous NAIAD array recently measured in situ is currently dominated by internal radioactivity.

At mK temperature, the simultaneous measurement of the phonon and ionization signals in semiconductor detectors permits event by event discrimination between nuclear and electronic recoils down to 5 to 10 keV recoil energy. This feature is being used by the CDMS [30] and EDELWEISS [30] collaborations. Surface interactions, exhibiting incomplete charge collection, are an important residual background, which has been treated so far by two different techniques: CDMS uses the timing information of the phonon pulse, while EDELWEISS uses the ionization pulses in an interleaved electrodes scheme. In 2011 CDMS published [43] results using 19 Germanium cryogenic detectors at the Soudan mine involving a total exposure of around 612 kg·d (around 300 kg·d fiducial); they exclude spin-independent WIMP nucleon cross sections above 3.8×10^{-8} pb, at 90% CL for a 70 GeV WIMP.

The recent announcement [44] of a possible excess of events in data obtained with the CDMS Silicon detectors drew particular attention. They found three events after cuts in a blind analysis of 140 kg·d exposure obtained with eight Silicon detectors run in 2007-2008. While the expected background of 0.7 events lead to a 5 % probability for the three events to be background based on the number of events alone, the phonon rise time and ionization yield values of the three events appear perfectly compatible with nuclear recoils, giving a total probability of 0.19 % that they are due to known background from a profile likelihood ratio test. The best fit yields a cross section $\sim 10^{-7}$ pb and a WIMP mass of 8 GeV. The corresponding 90 % confidence contour has some overlap with the "region of interest" claimed by CoGeNT.

However, the case made by CDMS is weakened by 1) the very close proximity of the strength of the ionization signal of all three events to the cut, 2) the simultaneous publication by the same collaboration of a second paper on an independent set of 56 kg·d Silicon data with no events observed and an estimated background of 1.1 events [45]. One would like to see a combined analysis, and how the population of events surviving a relaxed cut on ionization energy behaves in rise time and ionization yield.

Very recently, CDMS has reported [46] the result of the analysis of a data set named CDMS-Lite obtained by running a single detector in a particular mode allowing an equivalent electron energy threshold of 170 eV. This is obtained by applying a high voltage (69 V) across the ionization measurement electrodes. The phonons then generated by the ionization electrons traveling inside the crystal – so called Neganov Luke effect – largely overcome the normal induced phonon pulse by the initial interaction. This amplifies the ionization pulse, but no discrimination between electron and nuclear recoils is possible in this mode. The sensitivity is then fixed by the counting rate at threshold, and could be anticipated from a downward extrapolation of the background above 1.5 keV. An interesting rejection curve is obtained, quite flat for WIMP masses between 6 to 12 GeV, and rather insensitive to the systematic uncertainty on the quenching factor. It cuts the latest CoGeNT "region of interest" in the middle and lies a factor 1.8 above the central value of the CDMS Si result.

Results of a run using 9 kg of new detectors fitted with interleaved electrodes and operated in Soudan mine since November 2011 are expected by the end of 2013.

The EDELWEISS collaboration [30], which operates Germanium cryogenic detectors in the Laboratoire Souterrain de Modane, has reported a low energy analysis [47], with a similar principle to the CDMS low energy analysis of 2011 [48]. The exclusion curve happens to complement the gap in sensitivity in the CDMS limits for WIMP masses between 8 and 10 GeV, precisely a factor 3 above the central value of the CDMS-Si result (see above).

EDELWEISS is assembling new 800 g detectors featuring a complete coverage of the crystal with annular electrodes, and better rejection of non-recoil events. Around 30 kg of these detectors are expected to be operated inside an improved cryostat starting in 2014.

The combined analysis of CDMS and EDELWEISS data [49] currently gives the second best limit on the SI cross sections for WIMPS masses above 80 GeV.

The cryogenic experiment CRESST [30] in the Gran Sasso laboratory uses the scintillation of $CaWO_4$ as second variable for background discrimination. In their analysis of 730 kg·d exposure they reported [50] the observation of 67 events in the signal region, where about 40 background events were expected. The event excess is said to be compatible with WIMP scattering. A likelihood method provides two solutions, respectively for WIMPs with mass 12 and 25 GeV. The size of the signal (if any) hinges on the reliability of the background model, which has to account for several classes of background whose properties bracket those of the signal. New detectors, with hopefully reduced backgrounds and better coverage of the scintillating layer allowing the identification of α particles, are being operated.

The next stages of solid state detectors, SuperCDMS and EURECA-I (a combination of EDELWEISS and CRESST), will involve typically 150 kg to 200 kg of detectors. Various presentations at conferences indicate that these two collaborations are working on a possible merger to a common project.

Noble gas detectors for dark matter detection are being actively developed by several groups [1]. Dual (liquid and gas) phase detectors allow to measure both the primary scintillation and the ionization electrons drifted through the liquid and amplified in the gas, which is used for background rejection.

The XENON collaboration [30] operates the 161 kg XENON100 setup at Gran Sasso laboratory. It has published a result [29] based on 225 days of operating time. Within a fiducial mass of 34 kg, two events were observed in the signal region, while 1.0 were expected. The obtained minimum cross section for spin-independent interactions is 2.0×10^{-9} pb for a mass of 55 GeV. The reliability of limits set at masses lower than 12 GeV, especially with respect to the relative light efficiency factor, have been discussed in the community. Moreover, as underlined near the end of section 1.2.4, the limits at low mass can be set *only* thanks to the poor energy resolution at threshold – 8.4 keV – due to the low photoelectron yield of 0.5 pe/keV. With infinite energy resolution, a Xe detector *with the same threshold of 8.4 keV* is not sensitive to a WIMP mass of 7 GeV. The *"WIMP safe"* minimal mass for XENON100 is around 12 GeV. This data set provides the best limit for spin dependent WIMPs with pure neutron couplings at all masses [51].

A reanalysis of part of the XENON10 data [52], using the ionization signal only, with an ionization yield of around 3.5 electron/keV at a threshold of 1.4 keV, sets a more stringent limit for WIMP masses below 12 GeV. The *"WIMP safe"* minimal mass for this XENON10 analysis is around 5 GeV. However, a reanalysis of the data [53] showed that the published limit was too strong. The authors acknowledged this error.

XENON1t, the successor of XENON100 again planned to be run at the Gran Sasso lab, is starting construction.

The ZEPLIN III experiment [30], using a dual phase Xenon detector with an active mass of 12 kg, operated in the Boulby laboratory. It published final results with an exposure of 1344 kg·d [54]. This provides the second best limit for SD interactions on neutrons. The limits on SI interactions are comparable to those from CDMS and EDELWEISS. This experiment has ended.

A new liquid Xenon based project, PANDA-X, with pancake geometry, planned to be housed in the new Jinping lab, will start operating soon.

The LUX detector [30], a 370 kg double phase Xenon detector installed in a large water shield, is being operated in the new SURF (previous Homestake) laboratory in US. The LUX collaboration has recently announced [55](results not published at the edition time of this review) results from an 85 days run, with a fiducial mass of 118 kg . Thanks to an extremely low content of ^{85}Kr (5 times lower than in Xenon100) and a very good light collection efficiency of 14 %, they could reach unprecedented sensitivity both at high and low mass WIMP's. After cuts, they observed 160 events inside the fiducial volume, in the nuclear recoil energy window of roughly 4 to 27 keV. A profile likelihood ratio analysis shows that the discrimination

parameter versus scintillation energy scatter plot is compatible with a pure population of electron events, with upper limits on the presence of nuclear recoils ranging from 2.4 to 5.3 events, depending on the WIMP mass. This allowed LUX to set the best lower limit on the cross section for spin-independent interactions at 7.6×10^{-10} pb for a 33 GeV WIMP mass. Limits in the range 7 to 8 GeV are between a factor 100 and 1000 lower than the cross section of the CoGeNT and CDMS-Silicon "regions of interest". It should be kept in mind however that the *"WIMP safe"* minimal mass" for this LUX data set is around 8-10 GeV. The fraction of WIMP signal (and thus WIMP velocities) probed by LUX at around 8 GeV is less than a few 10^{-3} (that is the highest WIMP velocity tail) while it is a few 10^{-2} for the CDMS-Silicon data and few 10^{-1} for CoGeNT data.

XMASS [30] in Japan has taken first data with a single-phase 800 kg Xenon detector (100 kg fiducial mass, allowing a strong self shielding) installed in a large pure water shield at the SuperKamiokande site. Unfortunately a strong radioactive contamination of some aluminum pieces of the detector was found in the first run. The detector is being upgraded with radiopure materials.

The ArDM project [30] is a double phase Argon detector with a total mass of 1,100 kg. It will soon take data at the Canfranc laboratory. MiniCLEAN and DEAP-3600 [30], both measuring only scintillation signals in spherical geometries in single phase mode, are being assembled at SNOLab and will operate respectively 500 kg of Ar/Ne and 3600 kg of Ar [1]. DarkSide [30] is another Argon based, double phase project, beginning with about 50 kg of ^{39}Ar depleted Argon, to be operated from 2014 in the Gran Sasso lab.

The low pressure Time Projection Chamber technique is currently the only convincing way to measure the direction of nuclear recoils and prove the galactic origin of a possible signal [1]. The DRIFT collaboration [30] has operated a 1 m^3 volume detector filled with CS2 in the UK Boulby mine. The target mass is too small to probe WIMP models not already excluded by other experiments. The MIMAC collaboration [30], investigating a low pressure TPC detector, has published numerous papers on expected performances. A 2.5 l 1000 channel prototype has been operated in the Fréjus laboratory, with no new results yet. Other groups developing similar techniques, though with lower sensitivity, are DMTPC in the US and NewAge in Japan.

The following more unconventional detectors based on metastable liquids or gels, with the advantage to be insensitive to electromagnetic interactions and the drawback of being threshold yes/no detectors, were initially using compounds rich in ^{19}F nucleus in order to set limits on the spin dependent coupling of WIMPs, with less than kg mass detectors. However, by varying the sensitive material and increasing the detector mass, they may also compete for SI interactions. The COUPP [30] collaboration using a 4 kg CF3I bubble chamber like detector, run at Fermilab, has published results [56] allowing them to set the best limit for spin dependent proton coupling at 3×10^{-3} pb for a WIMP mass of 30 GeV. Picasso [30], a superheated droplet detector run at SNOLAB, obtained a better limit below 5 GeV on the same type of WIMPs [57]. SIMPLE [30], a similar experiment run at Laboratoire Souterrain de Rustrel, also produced competitive limits in an intermediate mass range [58].

PICO, combining the PICASSO and COUPP collaborations, is planning a dedicated detector, PICO2L, to search for light WIMPs, with mass between 1 and 10 GeV. Given the recent attractiveness of this mass range, several other experiments were proposed in the last couple of years, with the aim to operate less than 1 kg detectors with order of 0.1 keV energy threshold: DAMIC, using CCDs; and NEWS, using a spherical gaseous detector [42].

Figures 25.1 and 25.2 illustrate the limits on and positive claims for WIMP scattering cross sections, normalized to scattering on a single nucleon, for spin independent and spin dependent couplings, respectively, as functions of WIMP mass. Only the two or three currently best limits are presented. Also shown are constraints from indirect observations (see the next section) and typical regions of SUSY models, before and after LHC results. These figures have been made with the `dmtools` web page, thanks to a nice new feature which allows to include new limits uploaded by the user into the plot [59].

Sensitivities down to $\sigma_{\chi p}$ of 10^{-13} pb, as needed to probe nearly

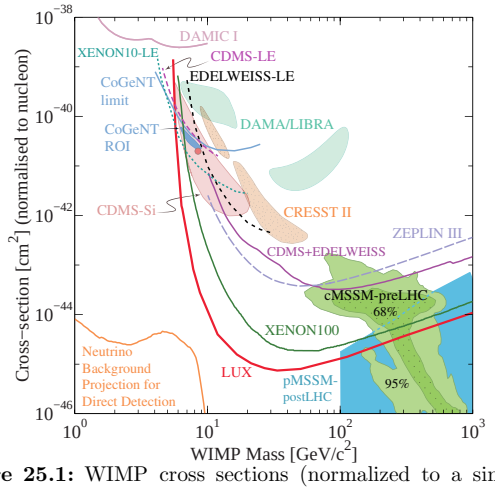

Figure 25.1: WIMP cross sections (normalized to a single nucleon) for spin-independent coupling versus mass. The DAMA/LIBRA [61], CREST II, CDMS-Si, and CoGeNT enclosed areas are regions of interest from possible signal events; the dot is the central value for CDMS-Si ROI. References to the experimental results are given in the text. For context, some supersymmetry implications are given: Green shaded 68% and 95% regions are pre-LHC cMSSM predictions by Ref. 62. Constraints set by XENON100 and the LHC experiments in the framework of the cMSSM [63] give regions in [300-1000 GeV; $1 \times 10^{-9} - 1 \times 10^{-12}$ pb] (but are not shown here). For the blue shaded region, pMSSM, an expansion of cMSSM with 19 parameters instead of 5 [64], also integrates constraints set by LHC experiments.

all of the MSSM parameter space [27] at WIMP masses above 10 GeV and to saturate the limit of the irreducible neutrino-induced background [60], will be reached with detectors of multi ton masses, assuming nearly perfect background discrimination capabilities. Such experiments are envisaged by the US project LZ (6 tons), the European consortium DARWIN, and the MAX project (a liquid Xe and Ar multiton project). For WIMP masses below 10 GeV, this cross section limit is set by the solar neutrinos, inducing an irreducible background at an equivalent cross section around 10^{-9} pb, which in principle is accessible with less massive low threshold detectors [30].

25.2.6. *Status and prospects of indirect WIMP searches* :

WIMPs can annihilate and their annihilation products can be detected; these include neutrinos, gamma rays, positrons, antiprotons, and antinuclei [1]. These methods are complementary to direct detection and might be able to explore higher masses and different coupling scenarios. "Smoking gun" signals for indirect detection are GeV neutrinos coming from the center of the Sun or Earth, and monoenergetic photons from WIMP annihilation in space.

WIMPs can be slowed down, captured, and trapped in celestial objects like the Earth or the Sun, thus enhancing their density and their probability of annihilation. This is a source of muon neutrinos which can interact in the Earth. Upward going muons can then be detected in large neutrino telescopes such as MACRO, BAKSAN, SuperKamiokande, Baikal, AMANDA, ANTARES, NESTOR, and the large sensitive area IceCube [1]. The best upper limit for relatively soft muons comes from SuperKamiokande [30]. For example, the upper bound on the muon flux due to neutrinos from the Sun originating from a 50 GeV WIMP annihilating into $b\bar{b}$ pairs is about 1500 muons/km^2/year [65]. For more energetic muons the best bounds have been derived from a combination of AMANDA and IceCube40 data (i.e. data using 40 strings of the IceCube detector). For example, for a 1 TeV WIMP annihilating into W^+W^- the upper bound on the muon flux is 103 muons/km^2/year [66]. In future data including the DeepCore array, which has become part of the completed IceCube detector, will likely dominate this field, possibly except at the very lowest muon energies. However, published bounds from DeepCore in combination with IceCube79 [67] are still weaker

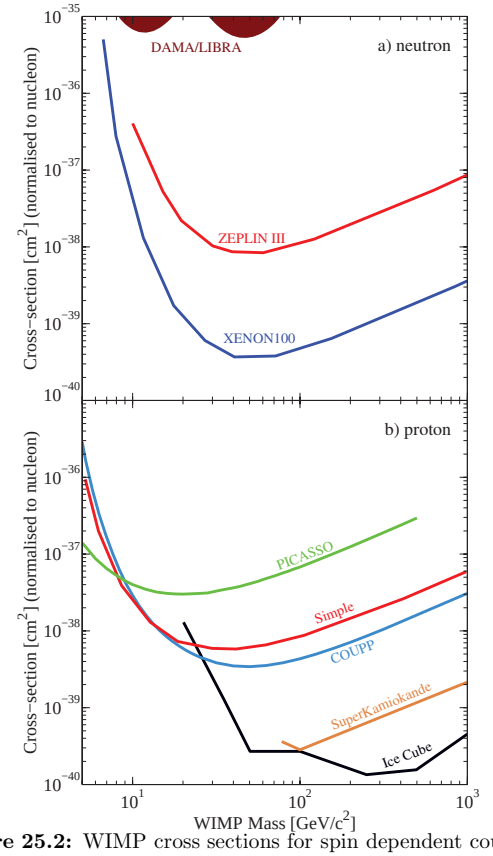

Figure 25.2: WIMP cross sections for spin dependent coupling versus mass. (a) interactions with the neutron; (b) interactions with the proton. References to the experimental results are given in the text. The limits quoted here from SuperKamiokande and IceCube assumes annihilation into W^+W^-. Assuming annihilation into $b\bar{b}$ gives softer neutrino spectrum and hence higher limits on the cross section, the better limit coming from SuperKamiokande at low mass. The limit quoted for COUPP assumes the most favorable bubble nucleation efficiency, The least favorable one gives a limit roughly 2 times higher.

than those from SuperKamiokande for relatively soft muons, and are weaker than the combined AMANDA / IceCube40 bound for very energetic muons. For standard halo velocity profiles, only the limits from the Sun, which mostly probe spin-dependent couplings, are competitive with direct WIMP search limits.

WIMP annihilation in the halo can give a continuous spectrum of gamma rays and (at one-loop level) also monoenergetic photon contributions from the $\gamma\gamma$ and γZ channels. These channels also allow to search for WIMPs for which direct detection experiments have little sensitivity, *e.g.*, almost pure higgsinos. The size of this signal depends strongly on the halo model, but is expected to be most prominent near the galactic center. The central region of our galaxy hosts a strong TeV point source discovered [68] by the H.E.S.S. Cherenkov telescope [30]. Moreover, FERMI/LAT [30] data revealed a new extended source of GeV photons near the galactic center above and below the galactic plane [69]. Both of these sources are very likely of (mostly) astrophysical origin. The presence of these unexpected backgrounds makes it more difficult to discover WIMPs in this channel.

Nevertheless a feature has been found [70] in public FERMI/LAT data using a predetermined search region around the galactic center, where known point sources have been removed. Within the resolution of the detector this feature could be due to monoenergetic photons with energy ~ 130 GeV. The "local" (in energy and search region) significance of this excess has been estimated as 4.6 standard deviations [70]. However, FERMI/LAT themselves, using a slightly larger data sample and an improved algorithm to reconstruct the photons, later estimated the local significance to only 3.3 standard deviations [71]. Since the spectrum contains many independent bins, the global significance is estimated to 1.6 standard deviations in [71]. Ref. [70] cites a global significance of 3.2 standard deviations. This triggered a large amount of speculative work, but is well below the significance required of an unambiguous signal. Note that the cross section required to explain this feature through WIMP annihilation is larger than that predicted by nearly all models that have been suggested before ref. [70] was published.

All other observations by FERMI/LAT as well as by Cherenkov telescopes are in agreement with predictions based on purely astrophysical sources. In particular, a combination [72] of FERMI/LAT limits from dwarf galaxies excludes WIMPs annihilating hadronically with the standard cross section needed for thermal relics, if the WIMP mass is below 25 GeV; the main assumption is annihilation from an $S-$wave initial state. Carefully modeling continuum γ emission from a region near (but excluding) the galactic center leads to similar upper bounds on the WIMP annihilation cross section [73]. These limits exclude many models with enhanced WIMP annihilation cross sections that had been designed to explain the electron and/or positron excess observed by PAMELA, FERMI/LAT and AMS02.

Antiparticles arise as additional WIMP annihilation products in the halo. To date the best measurement of the antiproton flux comes from the PAMELA satellite [30], and covers kinetic energies between 60 MeV and 180 GeV [74]. The result is in good agreement with secondary production and propagation models. These data exclude WIMP models that attempt to explain the $e^{\pm}$ excesses via annihilation into $W^{\pm}$ or Z^0 boson pairs; however, largely due to systematic uncertainties they do not significantly constrain conventional WIMP models.

The best measurements of the positron (and electron) flux at energies of tens to hundreds GeV comes from AMS02 [76] and PAMELA [75], showing a rather marked rise of the positron fraction between 10 and 200 GeV; the AMS02 data are compatible with a flattening of the positron fraction at the highest energies. While the observed positron spectrum falls within the one order of magnitude span (largely due to differences in the propagation model used) of fluxes predicted by secondary production models [77], the increase of the positron fraction is difficult to reconcile with the rather hard electron spectrum measured by PAMELA [78], if all positrons were due to secondary interactions of cosmic ray particles. Measurements of the total electron+positron energy spectrum by ATIC [79], FERMI/LAT [80] and H.E.S.S. [81] between 100 and 1000 GeV also exceed the predicted purely secondary spectrum, but with very large dispersion of the magnitude of these excesses. These observations can in principle be explained through WIMP annihilation. However, this requires cross sections well above that indicated by Eq. (25.6) for a thermal WIMP. This tension can be resolved only in somewhat baroque WIMP models. Most of these models have by now been excluded by the stringent bounds from FERMI/LAT on the flux of high energy photons due to WIMP annihilation. This is true also for models trying to explain the leptonic excesses through the decay of WIMPs with lifetime of the order of 10^{26} s. In contrast, viable astrophysical explanations of these excesses introducing new primary sources of electrons and positrons, e.g. pulsars, have been suggested [15]. On the other hand, the high quality of the AMS02 data on the positron fraction, which does not show any marked features, allows one to impose stringent bounds on WIMPs with mass below 300 GeV annihilating directly into leptons [82].

Last but not least, an antideuteron signal [1], as potentially observable by AMS02 or PAMELA, could constitute a signal for WIMP annihilation in the halo.

An interesting comparison of respective sensitivities to MSSM parameter space of future direct and various indirect searches has been performed with the DARKSUSY tool [83]. A web-based up-to-date collection of results from direct WIMP searches, theoretical predictions, and sensitivities of future experiments can be found in [59]. Also, the web page [84] allows to make predictions for WIMP signals in various experiments, within a variety of SUSY models and to extract limits from simply parametrised data. Integrated analysis of all data from direct and indirect WIMP detection, and also from LHC

experiments should converge to a comprehensive approach, required to fully unravel the mysteries of dark matter.

References:

1. For details, recent reviews and many more references about particle dark matter, see G. Bertone, *Particle Dark Matter* (Cambridge University Press, 2010).
2. For a brief but delightful history of DM, see V. Trimble, in *Proceedings of the First International Symposium on Sources of Dark Matter in the Universe*, Bel Air, California, 1994, published by World Scientific, Singapore (ed. D.B. Cline). See also the recent review G. Bertone, D. Hooper, and J. Silk, Phys. Rep. **405**, 279 (2005).
3. See *Cosmological Parameters* in this *Review*.
4. B. Paczynski, Astrophys. J. **304**, 1 (1986); K. Griest, Astrophys. J. **366**, 412 (1991).
5. F. De Paolis *et al.*, Phys. Rev. Lett. **74**, 14 (1995).
6. R. Catena and P. Ullio, JCAP **1008**, 004 (2010).
7. M. Pato *et al.*, Phys. Rev. **D82**, 023531 (2010).
8. J. Bovy and S. Tremaine, Astrophys. J. **756**, 89 (2012).
9. K. Kohri, D.H. Lyth, and A. Melchiorri, JCAP **0804**, 038 (2008).
10. See *Axions and Other Very Light Bosons* in this *Review*.
11. A. Kusenko, Phys. Reports **481**, 1 (2009).
12. E.W. Kolb and M.E. Turner, *The Early Universe*, Addison-Wesley (1990).
13. For a general introduction to SUSY, see the section devoted in this *Review of Particle Physics*. For a review of SUSY Dark Matter, see G. Jungman, M. Kamionkowski, and K. Griest, Phys. Reports **267**, 195 (1996).
14. See *Searches for WIMPs and Other Particles* in this *Review*.
15. M. Cirelli, Pramana **79**, 1021 (2012); S. Profumo, Central Eur. J. Phys. **10**, 1 (2011).
16. T. Moroi and L. Randall, Nucl. Phys. **B570**, 455 (2000).
17. R. Allahverdi and M. Drees, Phys. Rev. Lett. **89**, 091302 (2002).
18. M. Fujii and T. Yanagida, Phys. Lett. **B542**, 80 (2002).
19. J. Hisano, K. Kohri, and M.M. Nojiri, Phys. Lett. **B505**, 169 (2001).
20. D.E. Kaplan, M.A. Luty, and K.M. Zurek, Phys. Rev. **D79**, 115016 (2009).
21. G. Belanger *et al.*, arXiv:1308.3735.
22. J. Kozaczuk and S. Profumo, arXiv:1308.5705.
23. MACHO Collab., C. Alcock *et al.*, Astrophys. J. **542**, 257 (2000); EROS Collab., AA **469**, 387 (2007); OGLE Collab., arXiv:1106.2925 [astro-ph.GA], (MNRAS, to appear).
24. S.J. Asztalos *et al.*, Phys. Rev. **D69**, 011101 (2004); S.J. Asztalos *et al.*, Phys. Rev. Lett. **104**, 041301 (2010).
25. L.D. Duffy *et al.*, Phys. Rev. **D74**, 012006 (2006); J. Hoskins *et al.*, Phys. Rev. **D84**, 121302 (R) (2011).
26. M.C. Smith *et al.*, Mon. Not. R. Astron. Soc. **379**, 755 (2007).
27. J. Ellis *et al.*, Phys. Rev. **D77**, 065026 (2008).
28. C.E. Aalseth *et al.*, Phys. Rev. Lett. **106**, 131301 (2011).
29. XENON100 Collab., E. Aprile *et al.*, Phys. Rev. Lett. **109**, 181301 (2012).
30. A very useful collection of web links to the homepages of Dark Matter related conferences, and of experiments searching for WIMP Dark Matter, is the "Dark Matter Portal" at http://lpsc.in2p3.fr/mayet/dm.php. See TAUP and IDM conference series sites : http://www.taup-conference.to.infn.it/ and http://kicp-workshops.uchicago.edu/IDM2012/overview.php.
31. C.E. Aalseth et al., Phys. Rev. **D88**, 012002 (2013).
32. TEXONO Collab., H.B. Li et al., Phys. Rev. Lett. **110**, 261301 (2013).
33. https://commons.lbl.gov/display/TAUP2013/TAUP2013+Home.
34. C. Kelso et al., Phys. Rev. **D85**, 043515 (2012).
35. C.E. Aalseth et al., Phys. Rev. Lett. **107**, 141301 (2011).
36. CDMS Collab., Z. Ahmed et al., arXiv:1203.1309.
37. DAMA Collab., R. Bernabei *et al.*, Eur. Phys. J. **C67**, 39 (2010).
38. M. Fairbairn and T. Schwetz, JCAP **0901**, 037 (2009).
39. DAMA Collab., R. Bernabei *et al.*, Eur. Phys. J. **C56**, 333 (2008).
40. C.J. Copi and L.M. Krauss, New Astron. Rev. **49**, 185 (2005).
41. S.C. Kim et al., Phys. Rev. Lett. **108**, 181301 (2012).
42. http://vietnam.in2p3.fr/2013/Inauguration.
43. CDMS Collab., Z. Ahmed *et al.*, Science **327**, 1619 (2010).
44. CDMS Collab., Z. Ahmed *et al.*, to appear in Phys. Rev. Lett., arXiv:1304.4279.
45. CDMS Collab., R. Agnese *et al.*, Phys. Rev. **D88**, 031104 (2013).
46. SuperCDMS Collab., R. Agnese *et al.*, arXiv:1309.3259.
47. EDELWEISS Collab., E. Armengaud *et al.*, Phys. Rev. **D86**, 051701 (2012).
48. CDMS Collab., Z. Ahmed *et al.*, Phys. Rev. Lett. **06**, 131302 (2011).
49. EDELWEISS and CDMS Collab., Z. Ahmed *et al.*, Phys. Rev. **84**, 011102 (2011).
50. CRESST Collab., G. Angloher *et al.*, Eur. Phys. J. **C72**, 197 (2012).
51. XENON100 Collab., E. Aprile *et al.*, Phys. Rev. Lett. **111**, 021301 (2013).
52. XENON10 Collab., J Angle *et al.*, Phys. Rev. Lett. **107**, 051301 (2011).
53. M.T. Frandsen *et al.*, JCAP 1307 (2013) 023.
54. ZEPLIN Collab., D.Yu. Akimov *et al.*, Phys. Lett. **B709**, 14-20 (2012).
55. LUX Collab., D.S. Akerib *et al.*. arXiv:1310.8214.
56. E. Behnke *et al.*, Phys. Rev. Lett. **106**, 021303 (2011).
57. S. Archambault *et al.*, Phys. Lett. **B682**, 185 (2009).
58. M. Felizardo *et al.*., Phys. Rev. Lett. **108**, 201302 (2012).
59. DMTOOLS site : http://dmtools.brown.edu:8080/.
60. J. Billard, L. Strigari, E. Figueroa-Feliciano, arXiv:1307.545.
61. C. Savage *et al.*., JCAP **0904**, 010, 2009.
62. R. Trotta *et al.*., JHEP **0812** 024, 2008.
63. O. Buchmueller *et al.*., Eur. Phys. J. C72, 2243(2012).
64. M. Cahill-Rowley *et al.*., arXiv:1305.6921v2.
65. SuperKamiokande Collab., T. Tanaka et al., Astrophys. J. **742**, 78 (2011).
66. IceCube Collab., R. Abbasi *et al.*, Phys. Rev. **D85**, 042002 (2012).
67. IceCube Collab., M.G. Aartsen et al., Phys. Rev. Lett. **110**, 131302 (2013).
68. H.E.S.S. Collab., F. Aharonian *et al.*, Astron. Astrophys. **503**, 817 (2009); H.E.S.S. Collab., F. Acero *et al.*, MNRAS **402**, 1877 (2010).
69. M. Su, T.R. Slatyer, and D.P. Finkbeiner, Astrophys. J. **724**, 1044 (2010).
70. C. Weniger, JCAP **1208**, 007 (2012).
71. Fermi-LAT Collab., M. Ackermann et al., arXiv:1305.5597.
72. Fermi-LAT Collab., M. Ackermann et al., Phys. Rev. Lett. **107**, 241302 (2011).
73. Fermi-LAT Collab., M. Ackermann *et al.*, Astrophys. J. **761**, 91 (2012).
74. PAMELA Collab, O. Adriani *et al.*, Phys. Rev. Lett. **105**, 121101 (2010).
75. PAMELA Collab., O. Adriani *et al.*, arXiv:1308.0133.
76. AMS02 Collab., M. Aguilar *et al.*, Phys. Rev. Lett. **110**, 141102 (2013).
77. T. Delahaye *et al.*, Astronomy and Astrophysics **501**, 821 (2009).
78. PAMELA Collab., O. Adriani *et al.*, Phys. Rev. Lett. **106**, 201101 (2011).
79. ATIC collab, J. Chang *et al.*, Nature (London) **456**, 362 (2008).
80. FERMI/LAT collab, A.A. Abdo *et al.*, Phys. Rev. Lett. **102**, 181101 (2009).
81. H.E.S.S. collab, F. Aharonian *et al.*, Astron. Astrophys. **508**, 561 (2009).
82. L. Bergstrom *et al.*, arXiv:1306.3983.
83. DARKSUSY site: http://www.physto.se/ edsjo/darksusy/.
84. ILIAS web page: http://pisrv0.pit.physik.uni-tuebingen.de/darkmatter/.

26. DARK ENERGY

Written November 2013 by M. J. Mortonson (UCB, LBL), D. H. Weinberg (OSU), and M. White (UCB, LBL).

26.1. Repulsive Gravity and Cosmic Acceleration

In the first modern cosmological model, Einstein [1] modified his field equation of General Relativity (GR), introducing a "cosmological term" that enabled a solution with time-independent, spatially homogeneous matter density $\rho_{\rm m}$ and constant positive space curvature. Although Einstein did not frame it this way, one can view the "cosmological constant" Λ as representing a constant energy density of the vacuum [2], whose repulsive gravitational effect balances the attractive gravity of matter and thereby allows a static solution. After the development of dynamic cosmological models [3,4] and the discovery of cosmic expansion [5], the cosmological term appeared unnecessary, and Einstein and de Sitter [6] advocated adopting an expanding, homogeneous and isotropic, spatially flat, matter-dominated universe as the default cosmology until observations dictated otherwise. Such a model has matter density equal to the critical density, $\Omega_{\rm m} \equiv \rho_{\rm m}/\rho_{\rm c} = 1$, and negligible contribution from other energy components [7].

By the mid-1990s, Big Bang cosmology was convincingly established, but the Einstein-de Sitter model was showing numerous cracks, under the combined onslaught of data from the cosmic microwave background (CMB), large scale galaxy clustering, and direct estimates of the matter density, the expansion rate (H_0), and the age of the Universe. Introducing a cosmological constant offered a potential resolution of many of these tensions. In the late 1990s, supernova surveys by two independent teams provided direct evidence for accelerating cosmic expansion [8,9], establishing the cosmological constant model (with $\Omega_{\rm m} \approx 0.3$, $\Omega_\Lambda \approx 0.7$) as the preferred alternative to the $\Omega_{\rm m} = 1$ scenario. Shortly thereafter, CMB evidence for a spatially flat universe [10,11], and thus for $\Omega_{\rm tot} \approx 1$, cemented the case for cosmic acceleration by firmly eliminating the free-expansion alternative with $\Omega_{\rm m} \ll 1$ and $\Omega_\Lambda = 0$. Today, the accelerating universe is well established by multiple lines of independent evidence from a tight web of precise cosmological measurements.

As discussed in the Big Bang Cosmology article of this *Review* (Sec. 22), the scale factor $R(t)$ of a homogeneous and isotropic universe governed by GR grows at an accelerating rate if the pressure $p < -\frac{1}{3}\rho$. A cosmological constant has $\rho_\Lambda = $ const. and pressure $p_\Lambda = -\rho_\Lambda$ (see Eq. 22.10), so it will drive acceleration if it dominates the total energy density. However, acceleration could arise from a more general form of "dark energy" that has negative pressure, typically specified in terms of the equation-of-state-parameter $w = p/\rho$ ($= -1$ for a cosmological constant). Furthermore, the conclusion that acceleration requires a new energy component beyond matter and radiation relies on the assumption that GR is the correct description of gravity on cosmological scales. The title of this article follows the common but inexact usage of "dark energy" as a catch-all term for the origin of cosmic acceleration, regardless of whether it arises from a new form of energy or a modification of GR. Our account here draws on the much longer review of cosmic acceleration by Ref. [12], which provides background explanation and extensive literature references for most of the points in this article, but is less up to date in its description of current empirical constraints.

Below we will use the abbreviation ΛCDM to refer to a model with cold dark matter, a cosmological constant, inflationary initial conditions, and standard radiation and neutrino content. We will use "flat ΛCDM" to further specify a flat universe with $\Omega_{\rm tot} = 1$. We will use wCDM to denote a model with the same assumptions (including flatness) but a free, constant value of w.

26.2. Theories of Cosmic Acceleration

26.2.1. *Dark Energy or Modified Gravity?* :

A cosmological constant is the mathematically simplest, and perhaps the physically simplest, theoretical explanation for the accelerating universe. The problem is explaining its unnaturally small magnitude, as discussed in Sec. 22.4.7 of this *Review*. An alternative (which still requires finding a way to make the cosmological constant zero or at least negligibly small) is that the accelerating cosmic expansion is driven by a new form of energy such as a scalar field [13] with potential $V(\phi)$. The energy density and pressure of the field $\phi(\mathbf{x})$ take the same forms as for inflationary scalar fields, given in Eq. (22.52) of the Big Bang Cosmology article. In the limit that $\frac{1}{2}\dot\phi^2 \ll |V(\phi)|$, the scalar field acts like a cosmological constant, with $p_\phi \approx -\rho_\phi$. In this scenario, today's cosmic acceleration is closely akin to the epoch of inflation, but with radically different energy and timescale.

More generally, the value of $w = p_\phi/\rho_\phi$ in scalar field models evolves with time in a way that depends on $V(\phi)$ and on the initial conditions $(\phi_i, \dot\phi_i)$; some forms of $V(\phi)$ have attractor solutions in which the late-time behavior is insensitive to initial values. Many forms of time evolution are possible, including ones where w is approximately constant and broad classes where w "freezes" towards or "thaws" away from $w = -1$, with the transition occurring when the field comes to dominate the total energy budget. If ρ_ϕ is even approximately constant, then it becomes dynamically insignificant at high redshift, because the matter density scales as $\rho_{\rm m} \propto (1+z)^3$. "Early dark energy" models are ones in which ρ_ϕ is a small but not negligible fraction (*e.g.*, a few percent) of the total energy throughout the matter and radiation dominated eras, tracking the dominant component before itself coming to dominate at low redshift.

Instead of introducing a new energy component, one can attempt to modify gravity in a way that leads to accelerated expansion [14]. One option is to replace the Ricci scalar $\mathcal{R}$ with a function $\mathcal{R} + f(\mathcal{R})$ in the gravitational action [15]. Other changes can be more radical, such as introducing extra dimensions and allowing gravitons to "leak" off the brane that represents the observable universe (the "DGP" model [16]) . The DGP example has inspired a more general class of "galileon" and massive gravity models. Constructing viable modified gravity models is challenging, in part because it is easy to introduce theoretical inconsistencies (such as "ghost" fields with negative kinetic energy) but above all because GR is a theory with many high-precision empirical successes on solar system scales [17]. Modified gravity models typically invoke screening mechanisms that force model predictions to approach those of GR in regions of high density or strong gravitational potential. Screening offers potentially distinctive signatures, as the strength of gravity (*i.e.*, the effective value of $G_{\rm N}$) can vary by order unity in environments with different gravitational potentials.

More generally, one can search for signatures of modified gravity by comparing the history of cosmic structure growth to the history of cosmic expansion. Within GR, these two are linked by a consistency relation, as described below (Eq. (26.2)). Modifying gravity can change the predicted rate of structure growth, and it can make the growth rate dependent on scale or environment. In some circumstances, modifying gravity alters the combinations of potentials responsible for gravitational lensing and the dynamics of non-relativistic tracers (such as galaxies or stars) in different ways (see Sec. 22.4.7 in this *Review*), leading to order unity mismatches between the masses of objects inferred from lensing and those inferred from dynamics in unscreened environments.

At present there are no fully realized and empirically viable modified gravity theories that explain the observed level of cosmic acceleration. The constraints on $f(\mathcal{R})$ models now force them so close to GR that they cannot produce acceleration without introducing a separate dark energy component [18]. The DGP model is empirically ruled out by several tests, including the expansion history, the integrated Sachs-Wolfe effect, and redshift-space distortion measurements of the structure growth rate [19]. The elimination of these models should be considered an important success of the program to empirically test theories of cosmic acceleration. However, it is worth recalling that

there was no fully realized gravitational explanation for the precession of Mercury's orbit prior to the completion of GR in 1915, and the fact that no complete and viable modified gravity theory exists today does not mean that one will not arise in the future. In the meantime, we can continue empirical investigations that can tighten restrictions on such theories or perhaps point towards the gravitational sector as the origin of accelerating expansion.

26.2.2. *Expansion History and Growth of Structure* :

The main line of empirical attack on dark energy is to measure the history of cosmic expansion and the history of matter clustering with the greatest achievable precision over a wide range of redshift. Within GR, the expansion rate $H(z)$ is governed by the Friedmann equation (see the articles on Big Bang Cosmology and Cosmological Parameters—Secs. 22 and 24 in this *Review*). For dark energy with an equation of state $w(z)$, the cosmological constant contribution to the expansion, Ω_Λ, is replaced by a redshift-dependent contribution with the evolution of the dark energy density following from Eq. (22.10),

$$\Omega_{\rm DE}\frac{\rho_{\rm DE}(z)}{\rho_{\rm DE}(z=0)} = \Omega_{\rm DE}\exp\left[3\int_0^z [1+w(z')]\frac{dz'}{1+z'}\right] = \Omega_{\rm DE}(1+z)^{3(1+w)}, \tag{26.1}$$

where the second equality holds for constant w. If $\Omega_{\rm m}$, $\Omega_{\rm r}$, and the present value of $\Omega_{\rm tot}$ are known, then measuring $H(z)$ pins down $w(z)$. (Note that $\Omega_{\rm DE}$ is the same quantity denoted $\Omega_{\rm v}$ in Sec. 22, but we have adopted the DE subscript to avoid implying that dark energy is necessarily a vacuum effect.)

While some observations can probe $H(z)$ directly, others measure the distance-redshift relation. The basic relations between angular diameter distance or luminosity distance and $H(z)$ are given in Ch. 22 —and these are generally unaltered in time-dependent dark energy or modified gravity models. For convenience, in later sections, we will sometimes refer to the comoving angular distance, $D_{\rm A,c}(z) = (1+z)D_{\rm A}(z)$.

In GR-based linear perturbation theory, the density contrast $\delta(\mathbf{x},t) \equiv \rho(\mathbf{x},t)/\bar\rho(t) - 1$ of pressureless matter grows in proportion to the linear growth function $G(t)$ (not to be confused with the gravitational constant $G_{\rm N}$), which follows the differential equation

$$\ddot G + 2H(z)\dot G - \frac{3}{2}\Omega_{\rm m}H_0^2(1+z)^3 G = 0\ . \tag{26.2}$$

To a good approximation, the logarithmic derivative of $G(z)$ is

$$f(z) \equiv -\frac{d\ln G}{d\ln(1+z)} \approx \left[\Omega_{\rm m}(1+z)^3\frac{H_0^2}{H^2(z)}\right]^\gamma\ , \tag{26.3}$$

where $\gamma \approx 0.55$ for relevant values of cosmological parameters [20]. In an $\Omega_{\rm m} = 1$ universe, $G(z) \propto (1+z)^{-1}$, but growth slows when $\Omega_{\rm m}$ drops significantly below unity. One can integrate Eq. (26.3) to get an approximate integral relation between $G(z)$ and $H(z)$, but the full (numerical) solution to Eq. (26.2) should be used for precision calculations. Even in the non-linear regime, the amplitude of clustering is determined mainly by $G(z)$, so observations of non-linear structure can be used to infer the linear $G(z)$, provided one has good theoretical modeling to relate the two.

In modified gravity models the growth rate of gravitational clustering may differ from the GR prediction. A general strategy to test modified gravity, therefore, is to measure both the expansion history and the growth history to see whether they yield consistent results for $H(z)$ or $w(z)$.

26.2.3. *Parameters* :

Constraining a general history of $w(z)$ is nearly impossible, because the dark energy density, which affects $H(z)$, is given by an integral over $w(z)$, and distances and the growth factor involve a further integration over functions of $H(z)$. Oscillations in $w(z)$ over a range $\Delta z/(1+z) \ll 1$ are therefore extremely difficult to constrain. It has become conventional to phrase constraints or projected constraints on $w(z)$ in terms of a linear evolution model,

$$w(a) = w_0 + w_a(1-a) = w_{\rm p} + w_a(a_{\rm p} - a), \tag{26.4}$$

where $a \equiv (1+z)^{-1}$, w_0 is the value of w at $z = 0$, and $w_{\rm p}$ is the value of w at a "pivot" redshift $z_{\rm p} \equiv a_{\rm p}^{-1} - 1$, where it is best constrained by a given set of experiments. For typical data combinations, $z_{\rm p} \approx 0.5$. This simple parameterization can provide a good approximation to the predictions of many physically motivated models for observables measured with percent-level precision. A widely used "Figure of Merit" (FoM) for dark energy experiments [21] is the projected combination of errors $[\sigma(w_{\rm p})\sigma(w_a)]^{-1}$. Ambitious future experiments with 0.1–0.3% precision on observables can constrain richer descriptions of $w(z)$, which can be characterized by principal components.

There has been less convergence on a standard parameterization for describing modified gravity theories. Deviations from the GR-predicted growth rate can be described by a deviation $\Delta\gamma$ in the index of Eq. (26.3), together with an overall multiplicative offset relative to the $G(z)$ expected from extrapolating the CMB-measured fluctuation amplitude to low redshift. However, these two parameters may not accurately capture the growth predictions of all physically interesting models. Another important parameter to constrain is the ratio of the gravitational potentials governing space curvature and the acceleration of non-relativistic test particles. The possible phenomenology of modified gravity models is rich, which enables many consistency tests but complicates the task of constructing parameterized descriptions.

The more general set of cosmological parameters is discussed elsewhere in this *Review* (Sec. 24), but here we highlight a few that are particularly important to the dark energy discussion:

- The dimensionless Hubble parameter $h \equiv H_0/100\,{\rm km\,s^{-1}\,Mpc^{-1}}$ determines the present day value of the critical density and the overall scaling of distances inferred from redshifts.
- $\Omega_{\rm m}$ and $\Omega_{\rm tot}$ affect the expansion history and the distance-redshift relation.
- The sound horizon $r_{\rm s} = \int_0^{t_{\rm rec}} c_{\rm s}(t)dt/a(t)$, the comoving distance that pressure waves can propagate between $t = 0$ and recombination, determines the physical scale of the acoustic peaks in the CMB and the baryon acoustic oscillation (BAO) feature in low redshift matter clustering [22].
- The amplitude of matter fluctuations, conventionally represented by the quantity $\sigma_8(z)$, scales the overall amplitude of growth measures such as weak lensing or redshift-space distortions (discussed in the next section).

Specifically, $\sigma_8(z)$ refers to the rms fluctuation of the matter overdensity $\rho/\bar\rho$ in spheres of radius $8\,h^{-1}$Mpc, computed from the linear theory matter power spectrum at redshift z, and σ_8 on its own refers to the value at $z = 0$ (just like our convention for $\Omega_{\rm m}$).

While discussions of dark energy are frequently phrased in terms of values and errors on quantities like $w_{\rm p}$, w_a, $\Delta\gamma$, and $\Omega_{\rm tot}$, parameter precision is the means to an end, not an end in itself. The underlying goal of empirical studies of cosmic acceleration is to address two physically profound questions:

1. Does acceleration arise from a breakdown of GR on cosmological scales or from a new energy component that exerts repulsive gravity within GR?
2. If acceleration is caused by a new energy component, is its energy density constant in space and time, as expected for a fundamental vacuum energy, or does it show variations that indicate a dynamical field?

Substantial progress towards answering these questions, in particular any definitive rejection of the cosmological constant "null hypothesis," would be a major breakthrough in cosmology and fundamental physics.

26.3. Observational Probes

We briefly summarize the observational probes that play the greatest role in current constraints on dark energy. Further discussion and references can be found in other articles of this *Review*, in particular Secs. 24 (Cosmological Parameters) and 27 (The Cosmic Microwave Background), and in Ref. [12].

Cosmic Microwave Background Anisotropies: Although CMB anisotropies provide limited information about dark energy on

their own, CMB constraints on the geometry, matter content, and radiation content of the Universe play a critical role in dark energy studies when combined with low redshift probes. In particular, CMB data supply measurements of $\theta_{\rm s} = r_{\rm s}/D_{\rm A,c}(z_{\rm rec})$, the angular size of the sound horizon at recombination, from the angular location of the acoustic peaks, measurements of $\Omega_{\rm m}h^2$ and $\Omega_{\rm b}h^2$ from the heights of the peaks, and normalization of the amplitude of matter fluctuations at $z_{\rm rec}$ from the amplitude of the CMB fluctuations themselves. Planck data yield a 0.4% determination of r_s, which scales as $(\Omega_{\rm m}h^2)^{-0.25}$ for cosmologies with standard matter and radiation content. The uncertainty in the matter fluctuation amplitude is 3%, dominated by uncertainty in the electron scattering optical depth τ, and it should drop substantially with future analyses of Planck polarization maps. Secondary anisotropies, including the Integrated Sachs-Wolfe effect, the Sunyaev-Zel'dovich (SZ, [23]) effect, and gravitational lensing of primary anisotropies, provide additional information about dark energy by constraining low-redshift structure growth.

Type Ia Supernovae: Type Ia supernovae, produced by the thermonuclear explosions of white dwarfs, exhibit 10-15% scatter in peak luminosity after correction for light curve duration (the time to rise and fall) and color (which is a diagnostic of dust extinction). Since the peak luminosity is not known *a priori*, supernova surveys constrain ratios of luminosity distances at different redshifts. If one is comparing a high redshift sample to a local calibrator sample measured with much higher precision (and distances inferred from Hubble's law), then one essentially measures the luminosity distance in h^{-1}Mpc, constraining the combination $hD_{\rm L}(z)$. With distance uncertainties of 5–8% precision per well observed supernova, a sample of ~ 100 SNe is sufficient to achieve sub-percent statistical precision. The 1–2% systematic uncertainties in current samples are dominated by uncertainties associated with photometric calibration and dust extinction corrections. Another potential systematic is redshift evolution of the supernova population itself, which can be tested by analyzing subsamples grouped by spectral properties or host galaxy properties to confirm that they yield consistent results.

Baryon Acoustic Oscillations (BAO): Pressure waves that propagate in the pre-recombination photo-baryon fluid imprint a characteristic scale in the clustering of matter and galaxies, which appears in the galaxy correlation function as a localized peak at the sound horizon scale $r_{\rm s}$, or in the power spectrum as a series of oscillations. Since observed galaxy coordinates consist of angles and redshifts, measuring this "standard ruler" scale in a galaxy redshift survey determines the angular diameter distance $D_{\rm A}(z)$ and the expansion rate $H(z)$, which convert coordinate separations to comoving distances. Errors on the two quantities are correlated, and in existing galaxy surveys the best determined combination is approximately $D_V(z) = [zD^2_{\rm A,c}(z)/H(z)]^{1/3}$. As an approximate rule of thumb, a survey that fully samples structures at redshift z over a comoving volume V, and is therefore limited by cosmic variance rather than shot noise, measures $D_{A,c}(z)$ with a fractional error of $0.005(V/10\,{\rm Gpc}^3)^{-1/2}$ and $H(z)$ with a fractional error $1.6-1.8$ times higher. BAO can also be measured in the Lyman-α forest of intergalactic hydrogen absorption towards background quasars, where the best measured parameter combination is more heavily weighted towards $H(z)$ because of strong redshift-space distortions that enhance clustering along the line of sight. BAO distance measurements complement SN distance measurements by providing absolute rather than relative distances (with precise calibration of $r_{\rm s}$ from the CMB) and by achieving greater precision at high redshift thanks to the increasing comoving volume available. Theoretical modeling suggests that BAO measurements from even the largest feasible redshift surveys will be limited by statistical rather than systematic uncertainties.

Weak Gravitational Lensing: Gravitational light bending by a clustered distribution of matter shears the shapes of higher redshift background galaxies in a spatially coherent manner, producing a correlated pattern of apparent ellipticities. By studying the weak lensing signal for source galaxies binned by photometric redshift (estimated from broad-band colors), one can probe the history of structure growth. For a specified expansion history, the predicted signal scales approximately as $\sigma_8\Omega_{\rm m}^\alpha$, with $\alpha \approx 0.3$–0.5. The predicted signal also depends on the distance-redshift relation, so weak lensing becomes more powerful in concert with SN or BAO measurements that can pin this relation down independently. The most challenging systematics are shape measurement biases, biases in the distribution of photometric redshifts, and intrinsic alignments of galaxy orientations that could contaminate the lensing-induced signal. Predicting the large-scale weak lensing signal is straightforward in principle, but exploiting small-scale measurements also requires modeling the effects of complex physical processes such as star formation and feedback on the matter power spectrum.

Clusters of Galaxies: Like weak lensing, the abundance of massive dark matter halos probes structure growth by constraining $\sigma_8\Omega_{\rm m}^\alpha$, where $\alpha \approx 0.3$–0.5. These halos can be identified as dense concentrations of galaxies or through the signatures of hot (10^7–10^8 K) gas in X-ray emission or SZ distortion of the CMB. The critical challenge in cluster cosmology is calibrating the relation $P(M_{\rm halo}|O)$ between the halo mass as predicted from theory and the observable O used for cluster identification. Measuring the stacked weak lensing signal from clusters has emerged as a promising approach to achieve percent-level accuracy in calibration of the mean relation, which is required for clusters to remain competitive with other growth probes.

Redshift-Space Distortions (RSD) and the Alcock-Paczynksi (AP) Effect: Redshift-space distortions of galaxy clustering, induced by peculiar motions, probe structure growth by constraining the parameter combination $f(z)\sigma_8(z)$, where $f(z)$ is the growth rate defined by Eq. (26.3) [25,26]. Uncertainties in theoretical modeling of non-linear gravitational evolution and the non-linear bias between the galaxy and matter distributions currently limit application of the method to large scales (comoving separations $r \gtrsim 10\,h^{-1}$Mpc or wavenumbers $k \lesssim 0.2h\,{\rm Mpc}^{-1}$). A second source of anisotropy arises if one adopts the wrong cosmological metric to convert angles and redshifts into comoving separations, a phenomenon known as the Alcock-Paczynksi effect [27]. Demanding isotropy of clustering at redshift z constrains the parameter combination $H(z)D_{\rm A}(z)$. The main challenge for the AP method is correcting for the anisotropy induced by peculiar velocity RSD.

Direct Determination of H_0: The value of H_0 sets the current value of the critical density $\rho_{\rm c} = 3H_0^2/8\pi G_{\rm N}$, and combination with CMB measurements provides a long lever arm for constraining the evolution of dark energy. The challenge in direct H_0 measurements is establishing distances to galaxies that are far enough away that their peculiar velocities are small compared to the expansion velocity $v = H_0 d$. This can be done by building a ladder of distance indicators tied to stellar parallax on its lowest rung, or by using gravitational lens time delays or geometrical measurements of maser data to circumvent this ladder.

26.4. Current Constraints on Expansion, Growth, and Dark Energy

The last decade has seen dramatic progress in measurements of the cosmic expansion history and structure growth, leading to much tighter constraints on the parameters of dark energy models. CMB data from the WMAP and Planck satellites and from higher resolution ground-based experiments have provided an exquisitely detailed picture of structure at the recombination epoch and the first CMB-based measures of low redshift structure through lensing and SZ cluster counts. Cosmological supernova samples have increased in size from tens to many hundreds, with continuous coverage from $z = 0$ to $z \approx 1.4$, alongside major improvements in data quality, analysis methods, and detailed understanding of local populations. BAO measurements have advanced from the first detections to 2% precision at multiple redshifts, with increasingly sophisticated methods for testing systematics, fitting models, and evaluating statistical errors. Constraints on low redshift structure from galaxy clusters have become more robust, with improved X-ray and SZ data and weak lensing mass calibrations, and they have been joined by the first precise structure constraints from cosmic shear weak lensing, galaxy-galaxy lensing, and redshift-space distortions. The precision of direct H_0 measurements has sharpened from the $\sim 10\%$ error of the HST Key Project [28] to 3–4% in some recent analyses.

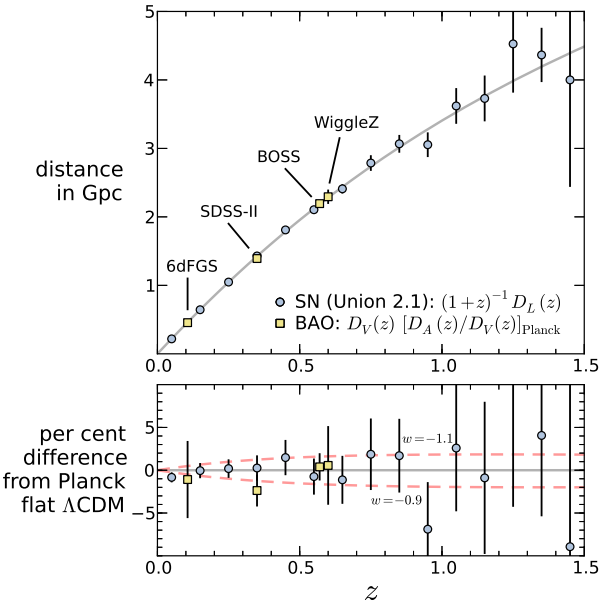

Figure 26.1: The distance-redshift relation measured from Type Ia SNe and BAO compared to the predictions (gray curve) of a flat ΛCDM model with the best-fit parameters inferred from Planck+WP CMB data. Circles show binned luminosity distances from the Union2.1 SN sample, multiplied by $(1+z)^{-1}$ to convert to comoving angular diameter distance. Squares show BAO distance measurements, converted to $D_{\rm A,c}(z)$ for the Planck+WP cosmology and sound horizon, from the references given in the text. The lower panel plots residuals from the Planck+WP ΛCDM prediction, with dashed curves that show the effect of changing w by ±0.1 while all other parameters are held fixed. Note that the SN data points can be shifted up or down by a constant factor to account for freedom in the peak luminosity, while the BAO points are calibrated to 0.4% precision by the sound horizon scale computed from Planck+WP data.

As an illustration of current measurements of the cosmic expansion history, Figure 26.1 compares distance-redshift measurements from SN and BAO data to the predictions for a flat universe with a cosmological constant. SN cosmology relies on compilation analyses that try to bring data from different surveys probing distinct redshift ranges to a common scale. The most influential current compilations are SNLS3 [29], which combines data from the 3-year Supernova Legacy Survey sample and the 1st-year SDSS-II Supernova Survey sample with local calibrators and high-redshift SNe from HST surveys, and Union2.1 [30], which has a broader selection of data, including some but not all of the sources in SNLS3. Here we have used binned distance measurements from Union2.1, but we caution that the different sample selections and analysis methodologies lead to systematic differences comparable to the statistical uncertainties, and it is not obvious which compilation, if either, should be preferred. Because the peak luminosity of a fiducial SN Ia is an unknown free parameter, the SN distance measurements could all be shifted up and down by a constant multiplicative factor; cosmological information resides in the relative distances as a function of redshift. The four BAO data points are taken from analyses of the 6dFGS survey [31], SDSS-II [32], BOSS [33], and WiggleZ [34]. For the BAO measurements we have adopted the sound horizon scale $r_{\rm s} = 147.49$ Mpc from Planck CMB data, whose 0.4% uncertainty is small compared to the current BAO measurement errors [36]. We have converted both SN luminosity distances and BAO D_V distances to an equivalent comoving angular diameter distance.

The plotted cosmological model has $\Omega_{\rm m} = 0.315$ and $h = 0.673$, the best-fit values [37] from Planck+WP CMB data assuming $w = -1$ and $\Omega_{\rm tot} = 1$. Specifically, here and below we use parameter values and MCMC chains from the "Planck + WP" analysis of [38], which combines the Planck temperature power spectrum with low multipole polarization measurements from WMAP [39]. In contrast to the Cosmological Parameters article of this *Review*, we do not use the CMB data set that includes higher resolution ground-based results because the corresponding chains are not available for all of the cases we wish to examine, but differences in cases where they are available are small. The SN, BAO, and CMB data sets, probing a wide range of redshifts with radically different techniques, are mutually consistent with the predictions of a flat ΛCDM cosmology. We have not included the $z = 2.5$ BAO measurement from the BOSS Lyman-α forest [24] on this plot, but it is also consistent with this fiducial model. Other curves in the lower panel of Figure 26.1 show the effect of changing w by ±0.1 with all other parameters held fixed. However, such a single-parameter comparison does not capture the impact of parameter degeneracies or the ability of complementary data sets to break them, and if one instead forces a match to CMB data by changing h and $\Omega_{\rm m}$ when changing w then the predicted BAO distances diverge at $z = 0$ rather than converging there.

Figure 26.2a plots joint constraints on $\Omega_{\rm m}$ and Ω_Λ in a ΛCDM cosmological model, assuming $w = -1$ but not requiring spatial flatness. The SN constraints are computed from the Union2 sample, and the CMB, CMB+BAO, and CMB+BAO+SN constraints are taken from MCMC chains provided by the Planck Collaboration [38]. We do not examine BAO constraints separately from CMB, because the constraining power of BAO relies heavily on the CMB calibration of $r_{\rm s}$. The SN data or CMB data on their own are sufficient to reject an $\Omega_\Lambda = 0$ universe, but individually they allow a wide range of $\Omega_{\rm m}$ and significant non-zero curvature. The CMB+BAO combination zeroes in on a tightly constrained region with $\Omega_{\rm m} = 0.309 \pm 0.011$ and $\Omega_{\rm tot} = 1.000 \pm 0.0033$. Combining SN with CMB would lead to a consistent constraint with around 3–4× larger errors. Adding the SN data to the CMB+BAO combination makes only a small difference to the constraints in this restricted model space.

Figure 26.2b plots constraints in the $\Omega_{\rm m} - w$ space, where we now consider models with constant $w(z)$ and (in contrast to panel a) assume spatial flatness. CMB data alone allow a wide range of w, but combination with BAO narrows the allowed range sharply. The preferred region is consistent with the orthogonal SN constraint, and the combination of the three data sets yields smaller uncertainties. The black curve on the left axis shows the posterior p.d.f. for w after marginalizing (with a flat prior) over $\Omega_{\rm m}$; we find $w = -1.10 \pm 0.08$ at 68.3% CL and -1.10 ± 0.15 at 95.4% CL. The dashed contours and dashed marginal curve show the impact of substituting WMAP9 data for Planck+WP in the CMB+BAO combination. The two constraints are compatible, but the shift from WMAP to Planck+WP has reduced the uncertainty in w and pulled the best-fit value lower.

Figure 26.2c considers a model space with time varying w, evolving according to the linear parameterization $w(a) = w_0 + w_a(1-a)$, again assuming flat space. Instead of w_0 we show constraints on $w(z = 0.5)$, approximately the pivot redshift where w is best determined and covariance with w_a is minimized. This plot shows that even the combination of current CMB, BAO, and SN data places only weak constraints on time evolution of the equation of state, still allowing order unity changes in w between $z = 1$ and $z = 0$ ($\Delta a = 0.5$). The value of $w(z = 0.5)$, on the other hand, is reasonably well constrained, with errors only slightly larger than those for the constant-w model of panel b. Errors on $w_0 = w(z = 0.5) - 0.333 w_a$ are much larger and are strongly correlated with the w_a errors.

While the CMB, BAO, and SN data sets considered here are mutually consistent with a flat ΛCDM model, tensions arise when other cosmological measurements enter the mix. Blue and yellow contours in Figure 26.3a show CMB and CMB+BAO constraints in the $\Omega_{\rm m} - H_0$ plane, assuming $w = -1$ and $\Omega_{\rm tot} = 1$. Red horizontal bars represent the direct estimate $H_0 = 73.8 \pm 2.4\,{\rm km\,s^{-1}\,Mpc^{-1}}$ from Ref. [40], who use SN Ia distances to galaxies in the Hubble flow with the Ia luminosity scale calibrated by HST observations of Cepheids in nearby SN host galaxies. Another recent estimate by Ref. [41], which employs 3.6 μm Cepheid observations to recalibrate the HST Key Project distance ladder and reduce its uncertainties, yields a similar central value and estimated error, $H_0 = 74.3 \pm 2.1\,{\rm km\,s^{-1}\,Mpc^{-1}}$. Figure 26.3a indicates a roughly 2σ tension between these direct

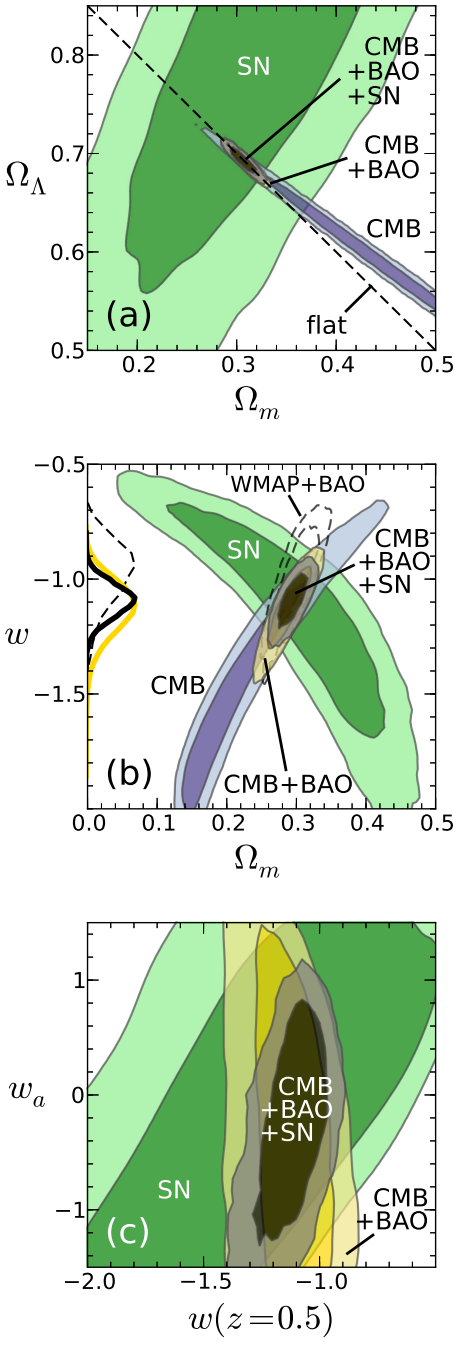

Figure 26.2: Constraints on the present matter fraction Ω_m and dark energy model parameters. Dark and light shaded regions indicate 68.3% and 95.4% confidence levels, respectively. "CMB" is Planck+WP, "BAO" is the combination of SDSS-II, BOSS, and 6dFGS, and "SN" is Union2. (a) The present dark energy fraction Ω_Λ vs. Ω_m, assuming a ΛCDM model. CMB data, especially when combined with BAO constraints, strongly favor a flat universe (diagonal dashed line). (b) The dark energy equation of state w vs. Ω_m, assuming a constant value of w. The dashed contours show the 68.3% and 95.4% CL regions for the combination of WMAP9 and BAO data. Curves on the left vertical axis show the probability distributions for w (normalized arbitrarily), after marginalizing over Ω_m, for the CMB+BAO and CMB+BAO+SN combinations (yellow and black, respectively), using Planck+WP CMB data, and for the WMAP9+BAO combination (dashed black). (c) Constraints on the two parameters of the dark energy model with a time-dependent equation of state given by Eq. (26.4): $w(z = 0.5)$ and $w_a = -dw/da$.

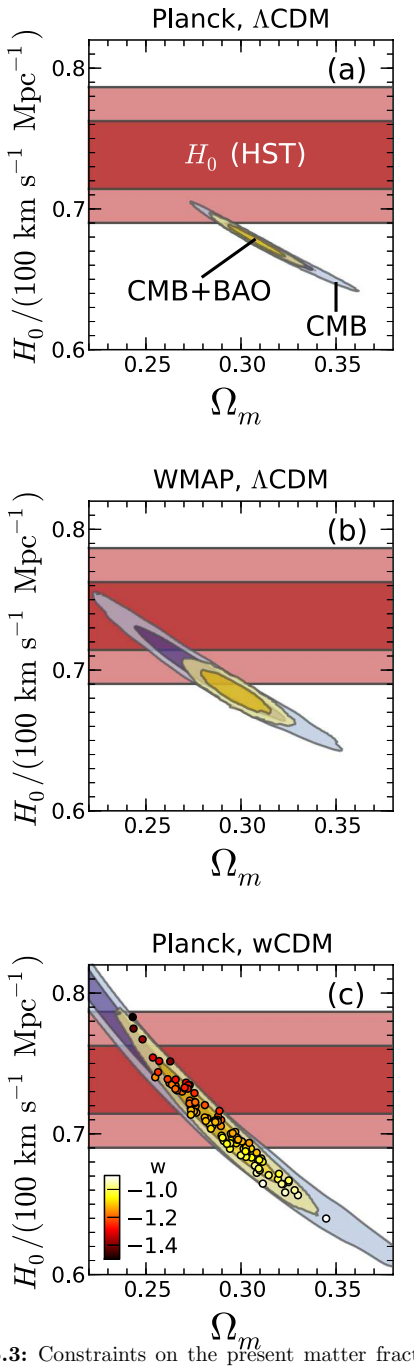

Figure 26.3: Constraints on the present matter fraction Ω_m and the Hubble constant H_0 from various combinations of data, assuming flat ΛCDM (left and middle panels) or a constant dark energy equation of state w (right panel). Dark and light shaded regions indicate 68.3% and 95.4% confidence levels, respectively. The right panel also shows 100 Monte Carlo samples from the CMB+BAO constraints with the value of w indicated by the colors of the dots. "CMB" is Planck+WP in the outer panels and WMAP9 in the middle panel, "BAO" is the combination of SDSS-II, BOSS, and 6dFGS, and "H_0 (HST)" is the HST constraint from [40].

measurements and the CMB+BAO predictions. The tension was already present with WMAP CMB data, as shown in Figure 26.3b, but it has become stiffer with Planck+WP, because of smaller CMB+BAO errors and a shift of central values to slightly higher Ω_m and lower H_0. In models with free, constant w (still assuming $\Omega_\mathrm{tot} = 1$), the tension can be lifted by going to $w < -1$ and lower Ω_m, as illustrated in Figure 26.3c. CMB data determine $\Omega_\mathrm{m}h^2$ with

high precision from the heights of the acoustic peaks, essentially independent of w. Within the flat ΛCDM framework, the well determined distance to the last scattering surface pins down a specific combination of (Ω_m, h), but with free w one can obtain the same distance from other combinations along the $\Omega_m h^2$ degeneracy axis.

One should not immediately conclude from Figure 26.3 that $w \neq -1$, but this comparison highlights the importance of fully understanding (and reducing) systematic uncertainties in direct H_0 measurements. If errors were reduced and the central value remained close to that plotted in Figure 26.3, then the implications would be striking. Other recent H_0 determinations exhibit less tension with CMB+BAO, because of lower central values and/or larger errors [42,43], including the values of $H_0 = 69 \pm 7\,\mathrm{km\,s^{-1}\,Mpc^{-1}}$ and $68 \pm 9\,\mathrm{km\,s^{-1}\,Mpc^{-1}}$ from Refs. [44,45], who circumvent the traditional distance ladder by using maser distances to galaxies in the Hubble flow. Gravitational lens time delays offer another alternative to the traditional distance ladder, and their precision could become competitive over the next few years, with increasing sample sizes and better constrained lens models.

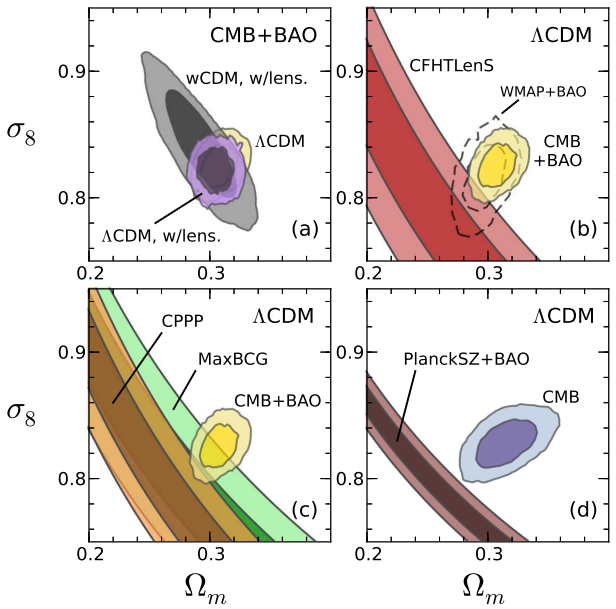

Figure 26.4: Constraints on the present matter fraction Ω_m and the present matter fluctuation amplitude σ_8. Dark and light shaded regions indicate 68.3% and 95.4% confidence levels, respectively. The upper left panel compares CMB+BAO constraints (using the same data sets as in Fig. 26.2) for ΛCDM with and without CMB lensing, and for a constant w model (including CMB lensing). The other three panels compare flat ΛCDM constraints between various dark energy probes, including weak lensing (upper right panel) and clusters (lower panels).

The amplitude of CMB anisotropies is proportional to the amplitude of density fluctuations present at recombination, and by assuming GR and a specified dark energy model one can extrapolate the growth of structure forward to the present day to predict σ_8. As discussed in Sec. 26.3 probes of low redshift structure typically constrain the combination $\sigma_8\Omega_m^\alpha$ with $\alpha \approx 0.3$–0.5. Figure 26.4 displays constraints in the $\sigma_8 - \Omega_m$ plane from CMB+BAO data and from weak lensing and cluster surveys [46]. Planck data themselves reveal a CMB lensing signature that constrains low redshift matter clustering and suggests a fluctuation amplitude somewhat lower than the extrapolated value for flat ΛCDM. However, including the CMB lensing signal only slightly alters the Planck+WP confidence interval for ΛCDM (purple vs. yellow contours in Fig. 26.4a). Allowing free w (gray contours) expands this interval, primarily in the direction of lower Ω_m and higher σ_8 (with $w < -1$).

The red contours in Figure 26.4b plot the constraint $\sigma_8(\Omega_m/0.27)^{0.46} = 0.774^{+0.032}_{-0.041}$ inferred from tomographic cosmic shear measurements in the CFHTLens survey [47]. An independent analysis of galaxy-galaxy lensing and galaxy clustering in the SDSS yields a similar result [48], $\sigma_8(\Omega_m/0.27)^{0.57} = 0.77 \pm 0.05$. Note that σ_8 and Ω_m refer to $z = 0$ values; the weak lensing samples and the cluster samples discussed below are not at zero redshift, but the values of σ_8 are effectively extrapolated to $z = 0$ for a fiducial cosmology. (Within current parameter bounds, the uncertainty in extrapolating growth from $z = 0.5$ to $z = 0$ is 1–2%, small compared to the observational uncertainties.) There is approximately 2σ tension between the $\sigma_8 - \Omega_m$ combination predicted by Planck+WP CMB+BAO for ΛCDM and the lower value implied by the weak lensing measurements. This tension was weaker for WMAP+BAO data (dotted contour) because of the larger error and slightly lower best-fit parameter values.

Additional contours in Figures 26.4c and d show $\sigma_8 - \Omega_m$ constraints inferred from three representative cluster analyses [49]: $\sigma_8(\Omega_m/0.27)^{0.47} = 0.784 \pm 0.027$ (CPPP), $\sigma_8(\Omega_m/0.27)^{0.41} = 0.806 \pm 0.032$ (MaxBCG), and $\sigma_8(\Omega_m/0.27)^{0.32} = 0.782 \pm 0.010$ (PlanckSZ). The basic mass calibration comes from X-ray data in CPPP, from weak lensing data in MaxBCG, and from SZ data in PlanckSZ. Because the PlanckSZ constraint itself incorporates BAO data, we have replaced the CMB+BAO contour with a CMB-only contour in panel d. The $\sigma_8\Omega_m^\alpha$ constraints from recent cluster analyses are not in perfect agreement, and the examples shown here are far from exhaustive. Nonetheless, on balance the cluster analyses, like the weak lensing analyses, favor lower $\sigma_8\Omega_m^\alpha$ than the value extrapolated forward from Planck+WP assuming flat ΛCDM. Redshift-space distortion analyses also tend to favor lower $\sigma_8\Omega_m^\alpha$, though statistical errors are still fairly large. For example, [50] find $f(z)\sigma_8(z) = 0.415 \pm 0.034$ from SDSS-III BOSS galaxies at $z = 0.57$, while the best-fit Planck+WP+BAO flat ΛCDM model predicts $f(z)\sigma_8(z) = 0.478 \pm 0.008$ at this redshift. With somewhat more aggressive modeling assumptions, [51] infer $f(z)\sigma_8(z)$ from the WiggleZ survey at $z = 0.22$, 0.41, 0.60, and 0.78, with $\approx 10\%$ errors in the three highest redshift bins (and 17% at $z = 0.22$), finding excellent agreement with a flat ΛCDM model that has $\Omega_m = 0.27$ and $\sigma_8 = 0.8$, and thus with the structure measurements plotted in Figure 26.4.

Going from ΛCDM to wCDM does not readily resolve this tension, because the CMB degeneracy direction with free w is roughly parallel to the $\sigma_8\Omega_m^\alpha$ tracks from low redshift structure (though the tracks themselves could shift or widen for $w \neq -1$). Each of the low redshift probes has significant systematic uncertainties that may not be fully represented in the quoted observational errors, and the tensions are only about 2σ in the first place, so they may be resolved by larger samples, better data, and better modeling. However, it is notable that all of the discrepancies are in the same direction. On the CMB side, the tensions would be reduced if the value of Ω_m or the optical depth τ (and thus the predicted σ_8) has been systematically overestimated. The most exciting but speculative possibility is that these tensions reflect a deviation from GR-predicted structure growth, pointing towards a gravitational explanation of cosmic acceleration. Other possible physical resolutions could come from dark energy models with significant time evolution, from a massive neutrino component that suppresses low redshift structure growth, or from decaying dark matter that reduces Ω_m at low z.

Table 1.1 summarizes key results from Figures 26.2–26.4, with marginalized constraints on Ω_m, Ω_{tot}, w, h, and $\sigma_8(\Omega_m/0.27)^{0.4}$ for the Planck+WP+BAO, Planck+WP+BAO+SN, and WMAP9+BAO combinations. We list 68.3% errors, and also 95.4% errors for WMAP9+BAO constraints on wCDM; in all other cases, the 95.4% errors are very close to double the 68.3% errors. For ΛCDM the Planck+WP combinations give $\Omega_{tot} = 1.000$ with an error of 0.3% and they predict, approximately, $h = 0.68 \pm 0.01$ and $\sigma_8(\Omega_m/0.27)^{0.4} = 0.87 \pm 0.02$. Note that the Ω_m and h constraints are not identical to those in Table 24.1 of the Cosmological Parameters article of this *Review* because those values assume spatial flatness. For wCDM, where flatness *is* assumed, the Planck+WP+BAO+SN combination yields $w = -1.10^{+0.08}_{-0.07}$, consistent with a cosmological constant at 1.2σ. With free w the best-fit h increases and its error roughly doubles, but the error in $\sigma_8(\Omega_m/0.27)^{0.4}$ grows only slightly,

Table 26.1: Constraints on selected parameters from various combinations of CMB, BAO, and SN data, given as mean values ± 68.3% CL limits (and ± 95.4% CL limits for WMAP9-wCDM). "Planck+WP" combines the Planck temperature power spectrum with WMAP large scale polarization. "BAO" combines the measurements of SDSS-II, BOSS, and 6dFGS. "SN" refers to the Union2.1 compilation. The upper (lower) half of the table assumes a ΛCDM (flat wCDM) cosmological model.

	Data combination		
Parameter	Planck+ WP+BAO	Planck+WP+ BAO+SN	WMAP9+ BAO
ΛCDM			
$\Omega_{\rm m}$	$0.309^{+0.010}_{-0.011}$	$0.307^{+0.011}_{-0.010}$	$0.295^{+0.012}_{-0.012}$
$\Omega_{\rm tot}$	$1.000^{+0.0033}_{-0.0033}$	$1.000^{+0.0032}_{-0.0033}$	$1.003^{+0.004}_{-0.004}$
h	$0.678^{+0.011}_{-0.010}$	$0.679^{+0.010}_{-0.011}$	$0.681^{+0.011}_{-0.011}$
$\sigma_8(\Omega_{\rm m}/0.27)^{0.4}$	$0.871^{+0.020}_{-0.021}$	$0.869^{+0.020}_{-0.021}$	$0.836^{+0.033}_{-0.033}$
wCDM (flat)			
$\Omega_{\rm m}$	$0.287^{+0.021}_{-0.021}$	$0.294^{+0.014}_{-0.014}$	$0.299^{+0.022}_{-0.019}\left(^{+0.045}_{-0.042}\right)$
w	$-1.13^{+0.13}_{-0.11}$	$-1.10^{+0.08}_{-0.07}$	$-0.98^{+0.16}_{-0.12}\left(^{+0.33}_{-0.29}\right)$
h	$0.708^{+0.026}_{-0.030}$	$0.699^{+0.017}_{-0.018}$	$0.681^{+0.025}_{-0.032}\left(^{+0.060}_{-0.066}\right)$
$\sigma_8(\Omega_{\rm m}/0.27)^{0.4}$	$0.888^{+0.025}_{-0.025}$	$0.885^{+0.023}_{-0.023}$	$0.84^{+0.05}_{-0.05}\left(^{+0.09}_{-0.09}\right)$

and its best-fit value moves a bit further away from the lower amplitudes suggested by measurements of low redshift structure.

26.5. Summary and Outlook

The preceding figures and table focus on model parameter constraints, but as a description of the observational situation it is most useful to characterize the precision, redshift range, and systematic uncertainties of the basic expansion and growth measurements. At present, supernova surveys constrain distance ratios at the 1–2% level in redshift bins of width $\Delta z = 0.1$ over the range $0 < z < 0.6$, with larger but still interesting error bars out to $z \approx 1.2$. These measurements are currently limited by systematics tied to photometric calibration, extinction, and reddening, and possible evolution of the SN population. BAO surveys have measured the absolute distance scale (calibrated to the sound horizon $r_{\rm s}$) to 4.5% at $z = 0.11$, 2% at $z = 0.35$ and $z = 0.57$, 6% at $z = 0.73$, and 3% at $z = 2.5$. Multiple studies have used clusters of galaxies or weak lensing cosmic shear or galaxy-galaxy lensing to measure a parameter combination $\sigma_8\Omega_{\rm m}^{\alpha}$ with $\alpha \approx 0.3$–0.5. The estimated errors of these studies, including both statistical contributions and identified systematic uncertainties, are about 5%. RSD measurements constrain the combination $f(z)\sigma_8(z)$, with recent determinations spanning the redshift range $0 < z < 0.9$ with typical estimated errors of about 10%. These errors are dominated by statistics, but shrinking them further will require improvements in modeling non-linear effects on small scales. Direct distance-ladder estimates of H_0 now span a small range (using overlapping data but distinct treatments of key steps), with individual studies quoting uncertainties of 3–5%, with similar statistical and systematic contributions. Planck data and higher resolution ground-based experiments now measure CMB anisotropy with exquisite precision.

A flat ΛCDM model with standard radiation and neutrino content can fit the CMB data and the BAO and SN distance measurements to within their estimated uncertainties. However the Planck+WP+BAO parameters for this model are in approximately 2σ tension with some of the direct H_0 measurements and most of the cluster and weak lensing analyses, disagreeing by about 10% in each case. Similar tensions are present when using WMAP data in place of Planck+WP data, but they are less evident because the WMAP errors are larger and the best-fit $\Omega_{\rm m}$ value is lower. Moving from ΛCDM to wCDM can relieve the tension with H_0, but only by going to $w < -1$ (which would be more physically startling than $w > -1$), and this change on its own does not produce better agreement with the structure growth data. It is not clear whether current tensions should be taken as a sign of new physics or as a sign that at least some of the experiments are underestimating their systematic uncertainties. Factor-of-two reductions in error bars, if convincing, could lead to exciting physical implications, or to a resolution of the existing mild discrepancies. Moving forward, the community will have to balance the requirement of strong evidence for interesting claims (such as $w \neq -1$ or deviations from GR) against the danger of confirmation bias, *i.e.*, discounting observations or error estimates when they do not overlap simple theoretical expectations.

There are many ongoing projects that should lead to improvement in observational constraints in the near-term and over the next two decades [52]. Final analyses of Planck temperature and polarization maps will significantly tighten the CMB constraints, including an important reduction of the uncertainty in the matter fluctuation amplitude that will sharpen tests based on structure growth. Final data from the SDSS-III BOSS survey, finishing in 2014, will reduce BAO errors by a factor of two at $z = 0.3$, 0.6, and 2.5. Its SDSS-IV successor eBOSS will yield the first BAO measurements in the redshift range $1 < z < 2$ and improved precision at lower and higher redshifts. The HETDEX project will measure BAO with Lyman-α emission line galaxies at $z = 2$–3. The same galaxy surveys carried out for BAO also provide data for RSD measurements of structure growth and AP measurements of cosmic geometry, and with improved theoretical modeling there is potential for large precision gains over current constraints from these methods. The Dark Energy Survey (DES), which started operations in August 2013 and will run through 2018, will provide a sample of several thousand Type Ia SNe, enabling smaller statistical errors and division of the sample into subsets for cross-checking evolutionary effects and other systematics. DES imaging will be similar in depth but 50 times larger in area than CFHTLens, providing a much more powerful weak lensing data set and weak lensing mass calibration of enormous samples of galaxy clusters (tens of thousands). Weak lensing surveys from the newly commissioned Hyper Suprime-Cam on the Subaru telescope will be smaller in area but deeper, with a comparable number of lensed galaxies. Reducing weak lensing systematics below the small statistical errors of these samples will be a major challenge, but one with a large payoff in precision measurements of structure growth. Uncertainties in direct determinations of H_0 should be reduced by further observations with HST and, in the longer run, by Cepheid parallaxes from the GAIA mission, by the ability of the James Webb Space Telescope to discover Cepheids in more distant SN Ia calibrator galaxies, and by independent estimates from larger samples of maser galaxies and gravitational lensing time delays.

A still more ambitious period begins late in this decade and continues through the 2020s, with experiments that include the Dark Energy Spectroscopic Instrument (DESI), the Subaru Prime Focus Spectrograph (PFS), the Large Synoptic Survey Telescope (LSST), and the space missions Euclid and WFIRST (Wide Field Infrared Survey Telescope). DESI and PFS both aim for major improvements in the precision of BAO, RSD, and other measurements of galaxy clustering in the redshift range $0.8 < z < 2$, where large comoving volume allows much smaller cosmic variance errors than low redshift surveys like BOSS. LSST will be the ultimate ground-based optical weak lensing experiment, measuring several billion galaxy shapes over 20,000 deg^2 of the southern hemisphere sky, and it will detect and monitor many thousands of SNe per year. Euclid and WFIRST also have weak lensing as a primary science goal, taking advantage of the high angular resolution and extremely stable image quality achievable from space. Both missions plan large spectroscopic galaxy surveys, which will provide better sampling at high redshifts than DESI or PFS because of the lower infrared sky background above the atmosphere. WFIRST is also designed to carry out what should be the ultimate supernova cosmology experiment, with deep, high resolution, near-IR observations and the stable calibration achievable

with a space platform.

Performance forecasts necessarily become more uncertain the further ahead we look, but collectively these experiments are likely to achieve 1–2 order of magnitude improvements over the precision of current expansion and growth measurements, while simultaneously extending their redshift range, improving control of systematics, and enabling much tighter cross-checks of results from entirely independent methods. The critical clue to the origin of cosmic acceleration could also come from a surprising direction, such as laboratory or solar system tests that challenge GR, time variation of fundamental "constants," or anomalous behavior of gravity in some astronomical environments. Experimental advances along these multiple axes could confirm today's relatively simple, but frustratingly incomplete, "standard model" of cosmology, or they could force yet another radical revision in our understanding of energy, or gravity, or the spacetime structure of the Universe.

References:

1. A. Einstein, Sitzungsber. Preuss. Akad. Wiss. Berlin (Math. Phys.), 142 (1917).
2. Y.B. Zeldovich, Soviet Physics Uspekhi **11**, 381 (1968).
3. A. Friedmann, On the curvature of space. Z. Phys. **10**, 377 (1922).
4. G. Lemaître, Annales de la Societe Scietifique de Bruxelles **47**, 49 (1927).
5. E. Hubble, Proc. Nat. Acad. Sci. **15**, 168 (1929).
6. A. Einstein and W. de Sitter, Proc. Nat. Acad. Sci. **18**, 213 (1932).
7. For background and definitions, see Big-Bang Cosmology – Sec. 22 of this *Review*.
8. A.G. Riess *et al.* [Supernova Search Team Collab.], Astron. J. **116**, 1009 (1998).
9. S. Perlmutter *et al.* [Supernova Cosmology Project Collab.], Astrophys. J. **517**, 565 (1999).
10. P. de Bernardis *et al.* [Boomerang Collab.], Nature **404**, 955 (2000).
11. S. Hanany *et al.*, Astrophys. J. **545**, L5 (2000).
12. D.H. Weinberg *et al.*, Phys. Rept. **530**, 87 (2013).
13. B. Ratra and P.J.E. Peebles, Phys. Rev. D **37**, 3406 (1988).
14. An excellent overview of the theory and phenomenology of modified gravity models can be found in the review article of B. Jain and J. Khoury, Annals Phys. **325**, 1479 (2010).
15. S.M. Carroll *et al.*, Phys. Rev. D **70**, 043528 (2004).
16. G.R. Dvali, G. Gabadadze, and M. Porrati, Phys. Lett. B **485**, 208 (2000).
17. C.M. Will, Living Reviews in Relativity, **9**, 3 (2006). See also the review on Experimental Tests of Gravitational Theory — in this *Review*.
18. B. Jain, V. Vikram, and J. Sakstein, `arXiv:1204.6044`; J. Wang, L. Hui, and J. Khoury, Phys. Rev. Lett. **109**, 241301 (2012).
19. Multiple investigations including M. Fairbairn and A. Goobar, Phys. Lett. B **642**, 432 (2006); Y.-S. Song, I. Sawicki, and W. Hu, Phys. Rev. D **75**, 064003 (2007); C. Blake *et al.*, Mon. Not. Roy. Astron. Soc. **415**, 2876 (2011).
20. E.V. Linder, Phys. Rev. D **72**, 043529 (2005).
21. This is essentially the FoM proposed in the Dark Energy Task Force (DETF) report, A. Albrecht *et al.*, `astro-ph/0609591`,though they based their FoM on the area of the 95% confidence ellipse in the $w_0 - w_a$ plane.
22. For high accuracy, the impact of acoustic oscillations must be computed with a full Boltzmann code, but the simple integral for r_s captures the essential physics and the scaling with cosmological parameters.
23. R.A. Sunyaev and Y.B. Zeldovich, Astrophys. Space Sci. **7**, 3 (1970).
24. N.G. Busca *et al.*, Astron. Astrophys. **552**, A96 (2013); A. Slosar *et al.*, J. Cosmol. Astropart. Phys. **1304**, 026 (2013).
25. N. Kaiser, Mon. Not. Roy. Astron. Soc. **227**, 1 (1987).
26. W.J. Percival and M. White, Mon. Not. Roy. Astron. Soc. **393**, 297 (2009).
27. C. Alcock and B. Paczynski, Nature **281**, 358 (1979).
28. W.L. Freedman et al., Astrophys. J. **553**, 47 (2001).
29. M. Sullivan *et al.*, Astrophys. J. **737**, 102 (2011).
30. N. Suzuki *et al.*, Astrophys. J. **746**, 85 (2012).
31. F. Beutler *et al.*, Mon. Not. Roy. Astron. Soc. **416**, 3017 (2011).
32. N. Padmanabhan *et al.*, Mon. Not. Roy. Astron. Soc. **427**, 2132 (2012).
33. L. Anderson *et al.*, Mon. Not. Roy. Astron. Soc. **427**, 3435 (2013).
34. C. Blake *et al.*, Mon. Not. Roy. Astron. Soc. **418**, 1707 (2011).
35. D.J. Eisenstein and W. Hu, Astrophys. J. **496**, 605 (1998).
36. We have multiplied the measured value of D_V from each of the BAO experiments by a factor of 1.0275 to correct from the convention of [35] to the more accurate r_s definition used by [38](see Sec. 5.2 of that paper for full details).
37. More precisely, throughout the paper we quote mean values computed from the posterior p.d.f., which we refer to as "best-fit" for brevity.
38. Planck Collab., `arXiv:1303.5076`, MCMC chains are obtained from the Planck public web site and assume neutrinos with $N_{\rm eff} = 3.046$ and mass approximated as a single eigenstate of 0.06 eV.
39. C.L. Bennett *et al.* [WMAP Collab.], Astrophys. J. Supp. **208**, 20 (2013).
40. A.G. Riess *et al.*, Astrophys. J. **730**, 119 (2011).
41. W.L. Freedman *et al.*, Astrophys. J. **758**, 24 (2012).
42. E.M.L. Humphreys *et al.*, Astrophys. J. **775**, 13 (2013).
43. H.M. Courtois and R.B. Tully, `arXiv:1202.3832`.
44. M.J. Reid *et al.*, Astrophys. J. **767**, 154 (2013).
45. C. Kuo *et al.*, Astrophys. J. **767**, 155 (2013).
46. We have plotted only the best constrained $\sigma_8 - \Omega_m$ combination, but some of these studies also break the degeneracy of the two parameters (*e.g.*, through redshift dependence) and produce closed contours even in the absence of external data.
47. C. Heymans *et al.*, `arXiv:1303.1808`.
48. R. Mandelbaum *et al.*, Mon. Not. Roy. Astron. Soc. **432**, 1544 (2013).
49. We have taken these values from Table 3 of Planck Collab. XX, Astron & Astrophys. in press, `arXiv:1303.5080`. The original sources for CPPP and MaxBCG are, respectively, A. Vikhlinin *et al.*, Astrophys. J. **692**, 1060 (2009); E. Rozo *et al.* [DSDD Collab.], Astrophys. J. **708**, 645 (2010).
50. B.A. Reid *et al.*, Mon. Not. Roy. Astron. Soc. **426**, 2719 (2012).
51. C. Blake *et al.*, Mon. Not. Roy. Astron. Soc. **415**, 2876 (2011).
52. 2-page summaries of many of these projects, plus references to more extensive documentation, can be found in the Snowmass 2013 report on Facilities for Dark Energy Investigations, by D. Weinberg *et al.*, `arXiv:1309.5380`.

27. COSMIC MICROWAVE BACKGROUND

Revised September 2013 by D. Scott (University of British Columbia) and G.F. Smoot (UCB/LBNL). Appendix A, describing the BICEP2 B-mode polarization result, added April 2014.

27.1. Introduction

The energy content in radiation from beyond our Galaxy is dominated by the cosmic microwave background (CMB), discovered in 1965 [1]. The spectrum of the CMB is well described by a blackbody function with $T = 2.7255\,\mathrm{K}$, this spectral form being one of the main pillars of the hot Big Bang model for the early Universe. The lack of any observed deviations from a blackbody spectrum constrains physical processes over cosmic history at redshifts $z \lesssim 10^7$ (see earlier versions of this review). All viable cosmological models predict a very nearly Planckian spectrum inside the current observational limits (although that could change with more sensitive spectral experiments in the future [2]).

Currently the key CMB observable is the angular variation in temperature (or intensity) correlations, and now to some extent polarization [3] . Since the first detection of these anisotropies by the Cosmic Background Explorer (*COBE*) satellite [4] , there has been intense activity to map the sky at increasing levels of sensitivity and angular resolution by ground-based and balloon-borne measurements. These were joined in 2003 by the first results from NASA's Wilkinson Microwave Anisotropy Probe (*WMAP*) [5], which were improved upon by analyses of the 3-year, 5-year, 7-year, and 9-year *WMAP* data [6,7,8,9]. Now the *WMAP* data have been improved upon through the first cosmological results [10] from ESA's *Planck* satellite [11,12] , and extended to smaller angular scales by ground-based experiments, particularly the Atacama Cosmology Telescope (ACT) [13] and the South Pole Telescope (SPT) [14] . Together these observations have led to a stunning confirmation of the 'Standard Model of Cosmology.' In combination with other astrophysical data, the CMB anisotropy measurements place quite precise constraints on a number of cosmological parameters, and have launched us into an era of precision cosmology.

27.2. Description of CMB Anisotropies

Observations show that the CMB contains anisotropies at the 10^{-5} level, over a wide range of angular scales. These anisotropies are usually expressed by using a spherical harmonic expansion of the CMB sky:

$$T(\theta,\phi) = \sum_{\ell m} a_{\ell m} Y_{\ell m}(\theta,\phi).$$

Increasing angular resolution requires that the expansion goes to higher and higher multipoles. The vast majority of the cosmological information is contained in the temperature 2-point function, *i.e.*, the variance as a function only of angular separation, since we notice no preferred direction. Equivalently, the power per unit $\ln \ell$ is $\ell \sum_m |a_{\ell m}|^2 / 4\pi$.

27.2.1. *The Monopole* :

The CMB has a mean temperature of $T_\gamma = 2.7255 \pm 0.0006\,\mathrm{K}$ (1σ) [15], which can be considered as the monopole component of CMB maps, a_{00}. Since all mapping experiments involve difference measurements, they are insensitive to this average level. Monopole measurements can only be made with absolute temperature devices, such as the FIRAS instrument on the *COBE* satellite [16]. Such measurements of the spectrum are consistent with a blackbody distribution over more than three decades in frequency (with some recent suggestions of a possible deviation at low frequencies [17]) . A blackbody of the measured temperature corresponds to $n_\gamma = (2\zeta(3)/\pi^2)\, T_\gamma^3 \simeq 411\,\mathrm{cm}^{-3}$ and $\rho_\gamma = (\pi^2/15)\, T_\gamma^4 \simeq 4.64 \times 10^{-34}\,\mathrm{g\,cm}^{-3} \simeq 0.260\,\mathrm{eV\,cm}^{-3}$.

27.2.2. *The Dipole* :

The largest anisotropy is in the $\ell = 1$ (dipole) first spherical harmonic, with amplitude $3.355 \pm 0.008\,\mathrm{mK}$ [7] . The dipole is interpreted to be the result of the Doppler shift caused by the solar system motion relative to the nearly isotropic blackbody field, as broadly confirmed by measurements of the radial velocities of local galaxies (although with some debate [18]) . The motion of an observer with velocity $\beta \equiv v/c$ relative to an isotropic Planckian radiation field of temperature T_0 produces a Doppler-shifted temperature pattern

$$\begin{aligned} T(\theta) &= T_0(1-\beta^2)^{1/2}/(1-\beta\cos\theta) \\ &\simeq T_0 \left(1 + \beta\cos\theta + \left(\beta^2/2\right)\cos 2\theta + O\left(\beta^3\right)\right). \end{aligned}$$

At every point in the sky, one observes a blackbody spectrum, with temperature $T(\theta)$. The spectrum of the dipole has been confirmed to be the differential of a blackbody spectrum [19]. At higher order there are additional effects arising from aberration and from modulation of the anisotropy pattern, which have also been observed [20].

The implied velocity for the solar system barycenter is $v = 369.0 \pm 0.9\,\mathrm{km\,s}^{-1}$, assuming a value $T_0 = T_\gamma$, towards $(l,b) = (263.99^\circ \pm 0.14^\circ, 48.26^\circ \pm 0.03^\circ)$ [7,21]. Such a solar system motion implies a velocity for the Galaxy and the Local Group of galaxies relative to the CMB. The derived value is $v_{\mathrm{LG}} = 627 \pm 22\,\mathrm{km\,s}^{-1}$ towards $(l,b) = (276^\circ \pm 3^\circ, 30^\circ \pm 3^\circ)$, where most of the error comes from uncertainty in the velocity of the solar system relative to the Local Group.

The dipole is a frame-dependent quantity, and one can thus determine the 'absolute rest frame' as that in which the CMB dipole would be zero. Our velocity relative to the Local Group, as well as the velocity of the Earth around the Sun, and any velocity of the receiver relative to the Earth, is normally removed for the purposes of CMB anisotropy study. The dipole is now routinely used as a primary calibrator for mapping experiments, either via the time-varying orbital dipole of the Earth, or through the cosmological dipole measured by satellite experiments.

27.2.3. *Higher-Order Multipoles* :

The variations in the CMB temperature maps at higher multipoles ($\ell \geq 2$) are interpreted as being mostly the result of perturbations in the density of the early Universe, manifesting themselves at the epoch of the last scattering of the CMB photons. In the hot Big Bang picture, the expansion of the Universe cools the plasma so that by a redshift $z \simeq 1100$ (with little dependence on the details of the model), the hydrogen and helium nuclei can bind electrons into neutral atoms, a process usually referred to as recombination [22]. Before this epoch, the CMB photons were tightly coupled to the baryons, while afterwards they could freely stream towards us. By measuring the $a_{\ell m}$s we are thus learning directly about physical conditions in the early Universe.

A statistically isotropic sky means that all ms are equivalent, *i.e.*, there is no preferred axis, so that the temperature correlation function between two positions on the sky depends only on angular separation and not orientation. Together with the assumption of Gaussian statistics (i.e. no correlations between the modes), the variance of the temperature field (or equivalently the power spectrum in ℓ) then fully characterizes the anisotropies. The power summed over all ms at each ℓ is $(2\ell+1)C_\ell/(4\pi)$, where $C_\ell \equiv \left\langle |a_{\ell m}|^2 \right\rangle$. Thus averages of $a_{\ell m}$s over m can be used as estimators of the C_ℓs to constrain their expectation values, which are the quantities predicted by a theoretical model. For an idealized full-sky observation, the variance of each measured C_ℓ (*i.e.*, the variance of the variance) is $[2/(2\ell+1)]C_\ell^2$. This sampling uncertainty (known as 'cosmic variance') comes about because each C_ℓ is χ^2 distributed with $(2\ell+1)$ degrees of freedom for our observable volume of the Universe. For fractional sky coverage, f_{sky}, this variance is increased by $1/f_{\mathrm{sky}}$ and the modes become partially correlated.

It is important to understand that theories predict the expectation value of the power spectrum, whereas our sky is a single realization. Hence the cosmic variance is an unavoidable source of uncertainty when constraining models; it dominates the scatter at lower ℓs, while the effects of instrumental noise and resolution dominate at higher ℓs [23].

Theoretical models generally predict that the $a_{\ell m}$ modes are Gaussian random fields to high precision, matching the empirical tests, *e.g.*, standard slow-roll inflation's non-Gaussian contribution is expected to be at least an order of magnitude below current observational limits [24]. Although non-Gaussianity of various forms is possible in early Universe models, tests show that Gaussianity is an extremely good simplifying approximation [25]. The only current indications of any non-Gaussianity or statistical anisotropy are some

relatively weak signatures at large scales, seen in both *WMAP* [26] and *Planck* data [27], but not of high enough significance to reject the simplifying assumption. Nevertheless, models which deviate from the inflationary slow-roll conditions can have measurable non-Gaussian signatures. So while the current observational limits make the power spectrum the dominant probe of cosmology, it is worth noting that higher-order correlations are beginning to be a tool for constraining otherwise viable theories.

27.2.4. *Angular Resolution and Binning* :

There is no one-to-one conversion between multipole ℓ and the angle subtended by a particular spatial scale projected onto the sky. However, a single spherical harmonic $Y_{\ell m}$ corresponds to angular variations of $\theta \sim \pi/\ell$. CMB maps contain anisotropy information from the size of the map (or in practice some fraction of that size) down to the beam-size of the instrument, σ (the standard deviation of the beam, in radians). One can think of the effect of a Gaussian beam as rolling off the power spectrum with the function $\mathrm{e}^{-\ell(\ell+1)\sigma^2}$.

For less than full sky coverage, the ℓ modes become correlated. Hence, experimental results are usually quoted as a series of 'band powers,' defined as estimators of $\ell(\ell+1)C_\ell/2\pi$ over different ranges of ℓ. Because of the strong foreground signals in the Galactic Plane, even 'all-sky' surveys, such as *WMAP* and *Planck* involve a cut sky. The amount of binning required to obtain uncorrelated estimates of power also depends on the map size.

27.3. Cosmological Parameters

The current 'Standard Model' of cosmology contains around 10 free parameters (see The Cosmological Parameters—Sec. 24 of this *Review*). The basic framework is the Friedmann-Robertson-Walker (FRW) metric (*i.e.*, a universe that is approximately homogeneous and isotropic on large scales), with density perturbations laid down at early times and evolving into today's structures (see Big-Bang cosmology—Sec. 22 of this *Review*). The most general possible set of density variations is a linear combination of an adiabatic density perturbation and some isocurvature perturbations. Adiabatic means that there is no change to the entropy per particle for each species, *i.e.*, $\delta\rho/\rho$ for matter is $(3/4)\delta\rho/\rho$ for radiation. Isocurvature means that the set of individual density perturbations adds to zero, for example, matter perturbations compensate radiation perturbations so that the total energy density remains unperturbed, *i.e.*, $\delta\rho$ for matter is $-\delta\rho$ for radiation. These different modes give rise to distinct (temporal) phases during growth, with those of the adiabatic scenario looking exactly like the data. Models that generate mainly isocurvature type perturbations (such as most topological defect scenarios) are no longer considered to be viable. However, an admixture of the adiabatic mode with up to about 4% isocurvature contribution (depending on details of the mode) is still allowed [28].

Within the adiabatic family of models, there is, in principle, a free function describing the variation of comoving curvature perturbations, $\mathcal{R}(\mathbf{x}, t)$. The great virtue of $\mathcal{R}$ is that it is constant in time for a purely adiabatic perturbation. There are physical reasons to anticipate that the variance of these perturbations will be described well by a power law in scale, *i.e.*, in Fourier space $\left\langle |\mathcal{R}|_k^2 \right\rangle \propto k^{n_\mathrm{s}-4}$, where k is wavenumber and n_s is the usual definition of spectral index. So-called 'scale-invariant' initial conditions (meaning gravitational potential fluctuations that are independent of k) correspond to $n_\mathrm{s} = 1$. In inflationary models [29], perturbations are generated by quantum fluctuations, which are set by the energy scale of inflation, together with the slope and higher derivatives of the inflationary potential. One generally expects that the Taylor series expansion of $\ln \mathcal{R}_k(\ln k)$ has terms of steadily decreasing size. For the simplest models, there are thus two parameters describing the initial conditions for density perturbations: the amplitude and slope of the power spectrum. These can be explicitly defined, for example, through:

$$\Delta^2_{\mathcal{R}} \equiv (k^3/2\pi^2) \left\langle |\mathcal{R}|_k^2 \right\rangle \simeq A\,(k/k_0)^{n_\mathrm{s}-1}\,,$$

with $A \equiv \Delta^2_{\mathcal{R}}(k_0)$ and $k_0 = 0.05\,\mathrm{Mpc}^{-1}$, say. There are many other equally valid definitions of the amplitude parameter (see also Sec. 22 and Sec. 24 of this *Review*), and we caution that the relationships between some of them can be cosmology-dependent. In 'slow roll' inflationary models, this normalization is proportional to the combination $V^3/(V')^2$, for the inflationary potential $V(\phi)$. The slope n_s also involves V'', and so the combination of A and n_s can constrain potentials.

Inflation generates tensor (gravitational wave) modes, as well as scalar (density perturbation) modes. This fact introduces another parameter, measuring the amplitude of a possible tensor component, or equivalently the ratio of the tensor to scalar contributions. The tensor amplitude is $A_\mathrm{t} \propto V$, and thus one expects a larger gravitational wave contribution in models where inflation happens at higher energies. The tensor power spectrum also has a slope, often denoted n_t, but since this seems unlikely to be measured in the near future, it is sufficient for now to focus only on the amplitude of the gravitational wave component. It is most common to define the tensor contribution through r, the ratio of tensor to scalar perturbation spectra at some small value of k (although sometimes it is defined in terms of the ratio of contributions at $\ell = 2$). Different inflationary potentials will lead to different predictions, *e.g.*, for $\lambda\phi^4$ inflation with 50 e-folds, $r = 0.32$, and for $m^2\phi^2$ inflation $r = 0.16$, while other models can have arbitrarily small values of r. In any case, whatever the specific definition, and whether they come from inflation or something else, the 'initial conditions' give rise to a minimum of three parameters: A, n_s, and r.

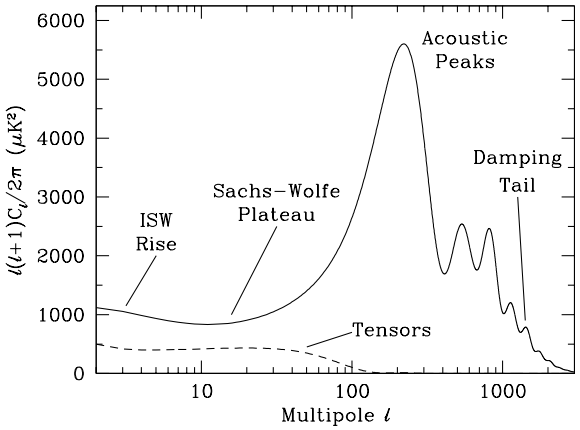

Figure 27.1: Theoretical CMB temperature anisotropy power spectrum, C_ℓ^{TT}, using a standard ΛCDM model from `CAMB`. The x-axis is logarithmic here. The regions, each covering roughly a decade in ℓ, are labeled as in the text: the ISW rise; Sachs-Wolfe plateau; acoustic peaks; and damping tail. Also shown is the shape of the tensor (gravitational wave) contribution, with an arbitrary normalization.

The background cosmology requires an expansion parameter (the Hubble Constant, H_0, often represented through $H_0 = 100\,h\,\mathrm{km\,s^{-1}Mpc^{-1}}$) and several parameters to describe the matter and energy content of the Universe. These are usually given in terms of the critical density, *i.e.*, for species 'x,' $\Omega_\mathrm{x} \equiv \rho_\mathrm{x}/\rho_\mathrm{crit}$, where $\rho_\mathrm{crit} \equiv 3H_0^2/8\pi G$. Since physical densities $\rho_\mathrm{x} \propto \Omega_\mathrm{x} h^2 \equiv \omega_\mathrm{x}$ are what govern the physics of the CMB anisotropies, it is these ωs that are best constrained by CMB data. In particular CMB, observations constrain $\Omega_\mathrm{b}h^2$ for baryons and $\Omega_\mathrm{c}h^2$ for cold dark matter (with $\rho_\mathrm{m} = \rho_\mathrm{c} + \rho_\mathrm{b}$ for the sum).

The contribution of a cosmological constant Λ (or other form of dark energy) is usually included via a parameter that quantifies the curvature, $\Omega_K \equiv 1 - \Omega_\mathrm{tot}$, where $\Omega_\mathrm{tot} = \Omega_\mathrm{m} + \Omega_\Lambda$. The radiation content, while in principle a free parameter, is precisely enough determined by the measurement of T_γ, and makes a $< 10^{-4}$ contribution to Ω_tot today.

Astrophysical processes at relatively low redshift can also affect the C_ℓs, a particularly significant effect coming through reionization. The Universe became reionized at some redshift z_i, long after recombination, affecting the CMB through the integrated Thomson scattering optical depth:

$$\tau = \int_0^{z_\mathrm{i}} \sigma_\mathrm{T} n_\mathrm{e}(z) \frac{dt}{dz} dz,$$

where σ_T is the Thomson cross-section, $n_e(z)$ is the number density of free electrons (which depends on astrophysics), and dt/dz is fixed by the background cosmology. In principle, τ can be determined from the small-scale matter power spectrum, together with the physics of structure formation and radiative feedback processes. However, this is a sufficiently intricate calculation that in practice τ needs to be considered as a free parameter.

Thus, we have eight basic cosmological parameters: A, n_s, r, h, $\Omega_b h^2$, $\Omega_c h^2$, Ω_{tot}, and τ. One can add additional parameters to this list, particularly when using the CMB in combination with other data sets. The next most relevant ones might be: $\Omega_\nu h^2$, the massive neutrino contribution; w ($\equiv p/\rho$), the equation of state parameter for the dark energy; and $dn_s/d\ln k$, measuring deviations from a constant spectral index. To these 11 one could of course add further parameters describing additional physics, such as details of the reionization process, features in the initial power spectrum, a sub-dominant contribution of isocurvature modes, *etc.*

As well as these underlying parameters, there are other (dependent) quantities that can be obtained from them. Such derived parameters include the actual Ωs of the various components (*e.g.*, Ω_m), the variance of density perturbations at particular scales (*e.g.*, σ_8), the angular scale of the sound horizon (θ_*), the age of the Universe today (t_0), the age of the Universe at recombination, reionization, *etc.*

27.4. Physics of Anisotropies

The cosmological parameters affect the anisotropies through the well understood physics of the evolution of linear perturbations within a background FRW cosmology. There are very effective, fast, and publicly available software codes for computing the CMB anisotropy, polarization, and matter power spectra, *e.g.*, `CMBFAST` [30] and `CAMB` [31]. These have been tested over a wide range of cosmological parameters and are considered to be accurate to much better than the 1% level [32], so that numerical errors are less than 10% of the parameter uncertainties for *Planck* [10].

A description of the physics underlying the C_ℓs can be separated into four main regions (the first two combined below), as shown in Fig. 27.1

27.4.1. *The ISW rise,* $\ell \lesssim 10$*, and Sachs-Wolfe plateau,* $10 \lesssim \ell \lesssim 100$:

The horizon scale (or more precisely, the angle subtended by the Hubble radius) at last scattering corresponds to $\ell \simeq 100$. Anisotropies at larger scales have not evolved significantly, and hence directly reflect the 'initial conditions.' Temperature variations are $\delta T/T = -(1/5)\mathcal{R}(\mathbf{x}_{LSS}) \simeq (1/3)\delta\phi/c^2$, where $\delta\phi$ is the perturbation to the gravitational potential, evaluated on the last scattering surface (LSS). This is a result of the combination of gravitational redshift and intrinsic temperature fluctuations, and is usually referred to as the Sachs-Wolfe effect [33].

Assuming that a nearly scale-invariant spectrum of curvature and corresponding density perturbations was laid down at early times (*i.e.*, $n_s \simeq 1$, meaning equal power per decade in k), then $\ell(\ell+1)C_\ell \simeq$ constant at low ℓs. This effect is hard to see unless the multipole axis is plotted logarithmically (as in Fig. 27.1 but not Fig. 27.2).

Time variation of the potentials (*i.e.*, time-dependent metric perturbations) leads to an upturn in the C_ℓs in the lowest several multipoles; any deviation from a total equation of state $w = 0$ has such an effect. So the dominance of the dark energy at low redshift (see Dark Energy—Sec. 26) makes the lowest ℓs rise above the plateau. This is sometimes called the integrated Sachs-Wolfe effect (or ISW rise), since it comes from the line integral of $\dot\phi$; it has been confirmed through correlations between the large-angle anisotropies and large-scale structure [34]. Specific models can also give additional contributions at low ℓ (*e.g.*, perturbations in the dark energy component itself [35]), but typically these are buried in the cosmic variance.

In principle, the mechanism that produces primordial perturbations could generate scalar, vector, and tensor modes. However, the vector (vorticity) modes decay with the expansion of the Universe. The tensors (transverse trace-free perturbations to the metric) generate temperature anisotropies through the integrated effect of the locally anisotropic expansion of space. Since the tensor modes also redshift away after they enter the horizon, they contribute only to angular scales above about 1° (see Fig. 27.1). Hence some fraction of the low-ℓ signal could be due to a gravitational wave contribution, although small amounts of tensors are essentially impossible to discriminate from other effects that might raise the level of the plateau. However, the tensors *can* be distinguished using polarization information (see Sec. 27.6).

27.4.2. *The acoustic peaks,* $100 \lesssim \ell \lesssim 1000$:

On sub-degree scales, the rich structure in the anisotropy spectrum is the consequence of gravity-driven acoustic oscillations occurring before the atoms in the Universe became neutral. Perturbations inside the horizon at last scattering have been able to evolve causally and produce anisotropy at the last scattering epoch, which reflects this evolution. The frozen-in phases of these sound waves imprint a dependence on the cosmological parameters, which gives CMB anisotropies their great constraining power.

The underlying physics can be understood as follows. Before the Universe became neutral, the proton-electron plasma was tightly coupled to the photons, and these components behaved as a single 'photon-baryon fluid.' Perturbations in the gravitational potential, dominated by the dark matter component, were steadily evolving. They drove oscillations in the photon-baryon fluid, with photon pressure providing most of the restoring force and baryons giving some additional inertia. The perturbations were quite small in amplitude, $O(10^{-5})$, and so evolved linearly. That means each Fourier mode developed independently, and hence can be described by a driven harmonic oscillator, with frequency determined by the sound speed in the fluid. Thus the fluid density underwent oscillations, giving time variations in temperature. These combine with a velocity effect, which is $\pi/2$ out of phase and has its amplitude reduced by the sound speed.

After the Universe recombined, the radiation decoupled from the baryons and could travel freely towards us. At that point, the (temporal) phases of the oscillations were frozen-in, and became projected on the sky as a harmonic series of peaks. The main peak is the mode that went through 1/4 of a period, reaching maximal compression. The even peaks are maximal *under*-densities, which are generally of smaller amplitude because the rebound has to fight against the baryon inertia. The troughs, which do not extend to zero power, are partially filled by the Doppler effect because they are at the velocity maxima.

The physical length scale associated with the peaks is the sound horizon at last scattering, which can be straightforwardly calculated. This length is projected onto the sky, leading to an angular scale that depends on the geometry of space, as well as the distance to last scattering. Hence the angular position of the peaks is a sensitive probe of a particular combination of cosmological parameters. In fact, the angular scale, θ_*, is the most precisely measured observable, and hence is often treated as an element of the cosmological parameter set.

One additional effect arises from reionization at redshift z_i. A fraction of photons (τ) will be isotropically scattered at $z < z_i$, partially erasing the anisotropies at angular scales smaller than those subtended by the Hubble radius at z_i. This corresponds typically to ℓs above about a few 10s, depending on the specific reionization model. The acoustic peaks are therefore reduced by a factor $e^{-2\tau}$ relative to the plateau.

These peaks were a clear theoretical prediction going back to about 1970 [36]. One can think of them as a snapshot of stochastic standing waves. Since the physics governing them is simple and their structure rich, then one can see how they encode extractable information about the cosmological parameters. Their empirical existence started to become clear around 1994 [37], and the emergence, over the following decade, of a coherent series of acoustic peaks and troughs is a triumph of modern cosmology. This picture has received further confirmation with the detection in the power spectrum of galaxies (at redshifts close to zero) of the imprint of these same acoustic oscillations in the baryon component [38,39].

27.4.3. *The damping tail, $\ell \gtrsim 1000$* :

The recombination process is not instantaneous, which imparts a thickness to the last scattering surface. This leads to a damping of the anisotropies at the highest ℓs, corresponding to scales smaller than that subtended by this thickness. One can also think of the photon-baryon fluid as having imperfect coupling, so that there is diffusion between the two components, and hence the amplitudes of the oscillations decrease with time. These effects lead to a damping of the C_ℓs, sometimes called Silk damping [40], which cuts off the anisotropies at multipoles above about 2000.

An extra effect at high ℓs comes from gravitational lensing, caused mainly by non-linear structures at low redshift. The C_ℓs are convolved with a smoothing function in a calculable way, partially flattening the peaks, generating a power-law tail at the highest multipoles, and complicating the polarization signal [41]. The effects of lensing on the CMB have now been definitively detected through the 4-point function, which correlates temperature gradients and small-scale anisotropies, enabling a map of the lensing potential to be constructed [42], as well as through the smoothing effect on the shape of the C_ℓs.

Lensing is an example of a 'secondary effect,' *i.e.*, the processing of anisotropies due to relatively nearby structures (see Sec. 27.7.2). Galaxies and clusters of galaxies give several such effects; all are expected to be of low amplitude, but are increasingly important at the highest ℓs. Such effects carry additional cosmological information and are increasing in importance as experiments push to higher sensitivity and angular resolution.

27.5. Current Temperature Anisotropy Data

There has been a steady improvement in the quality of CMB data that has led to the development of the present-day cosmological model. Probably the most robust constraints currently available come from *Planck* satellite [43] data combined with smaller scale results from the ACT [44] and SPT [45] experiments (together with constraints from non-CMB cosmological data-sets). We plot power spectrum estimates from these experiments in Fig. 27.2, along with *WMAP* data to show the consistency (see previous versions of this review for data from earlier experiments). Comparisons among data-sets show very good agreement, both in maps and in derived power spectra (up to systematic uncertainties in the overall calibration for some experiments). This makes it clear that systematic effects are largely under control.

The band-powers shown in Fig. 27.2 are in very good agreement with a 'ΛCDM' model. As described earlier, several (at least eight) of the peaks and troughs are quite apparent. For details of how these estimates were arrived at, the strength of correlations between band-powers and other information required to properly interpret them, the original papers should be consulted.

27.6. CMB Polarization

Since Thomson scattering of an anisotropic radiation field also generates linear polarization, the CMB is predicted to be polarized at the level of roughly 5% of the temperature anisotropies [46]. Polarization is a spin-2 field on the sky, and the algebra of the modes in ℓ-space is strongly analogous to spin-orbit coupling in quantum mechanics [47]. The linear polarization pattern can be decomposed in a number of ways, with two quantities required for each pixel in a map, often given as the Q and U Stokes parameters. However, the most intuitive and physical decomposition is a geometrical one, splitting the polarization pattern into a part that comes from a divergence (often referred to as the 'E-mode') and a part with a curl (called the 'B-mode') [48]. More explicitly, the modes are defined in terms of second derivatives of the polarization amplitude, with the Hessian for the E-modes having principle axes in the same sense as the polarization, while the B-mode pattern can be thought of as a 45° rotation of the E-mode pattern. Globally one sees that the E-modes have $(-1)^\ell$ parity (like the spherical harmonics), while the B-modes have $(-1)^{\ell+1}$ parity.

The existence of this linear polarization allows for six different cross power spectra to be determined from data that measure the full temperature and polarization anisotropy information. Parity considerations make two of these zero, and we are left with four

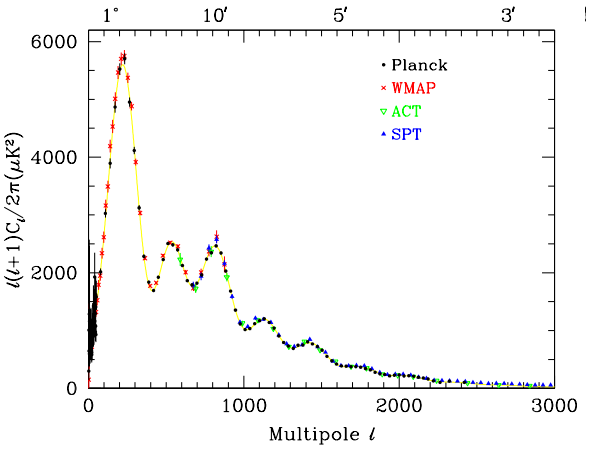

Figure 27.2: Band-power estimates from the *Planck*, *WMAP*, ACT, and SPT experiments. Note that the widths of the ℓ-bands vary between experiments and have not been plotted. This figure represents only a selection of the most recent available experimental results, and some points with large error bars have been omitted. At the higher multipoles these band-powers come from subtraction of particular foreground models, while proper analysis requires simultaneous fitting of CMB and foregrounds over multiple frequencies. The multipole axis here is linear, so the Sachs-Wolfe plateau is hard to see. However, the acoustic peaks and damping region are very clearly observed, with no need for a theoretical curve to guide the eye; the curve plotted is a best-fit model from *Planck* plus other CMB data.

potential observables: $C_\ell^{\rm TT}$, $C_\ell^{\rm TE}$, $C_\ell^{\rm EE}$, and $C_\ell^{\rm BB}$. Because scalar perturbations have no handedness, the B-mode power spectrum can only be sourced by vectors or tensors. Moreover, since inflationary scalar perturbations give only E-modes, while tensors generate roughly equal amounts of E- and B-modes, then the determination of a non-zero B-mode signal is a way to measure the gravitational wave contribution (and thus potentially derive the energy scale of inflation), even if it is rather weak. However, one must first eliminate the foreground contributions and other systematic effects down to very low levels.

The polarization C_ℓs also exhibit a series of acoustic peaks generated by the oscillating photon-baryon fluid. The main 'EE' power spectrum has peaks that are out of phase with those in the 'TT' spectrum, because the polarization anisotropies are sourced by the fluid velocity. The 'TE' part of the polarization and temperature patterns comes from correlations between density and velocity perturbations on the last scattering surface, which can be both positive and negative, and is of larger amplitude than the EE signal. There is no polarization Sachs-Wolfe effect, and hence no large-angle plateau. However, scattering during a recent period of reionization can create a polarization 'bump' at large angular scales.

Because the polarization anisotropies have only a fraction of the amplitude of the temperature anisotropies, they took longer to detect. The first measurement of a polarization signal came in 2002 from the DASI experiment [49], which provided a convincing detection, confirming the general paradigm, but of low enough significance that it lent little constraint to models. As well as the E-mode signal, DASI also made a statistical detection of the TE correlation.

The TE signal has now been mapped out quite accurately through data from *WMAP* [50], together with the BICEP [51], BOOMERANG [52], CBI [53], DASI [54], and QUAD [55] experiments, which are shown in Fig. 27.3 The anti-correlation at $\ell \simeq 150$ and the peak at $\ell \simeq 300$ are now quite distinct. The measured shape of the cross-correlation power spectrum provides supporting evidence for the general cosmological picture, as well as directly constraining the thickness of the last scattering surface. Since the polarization anisotropies are generated in this scattering surface, the existence of correlations at angles above about a degree demonstrates that there were super-Hubble fluctuations at the recombination epoch. The sign of this correlation also confirms the adiabatic paradigm.

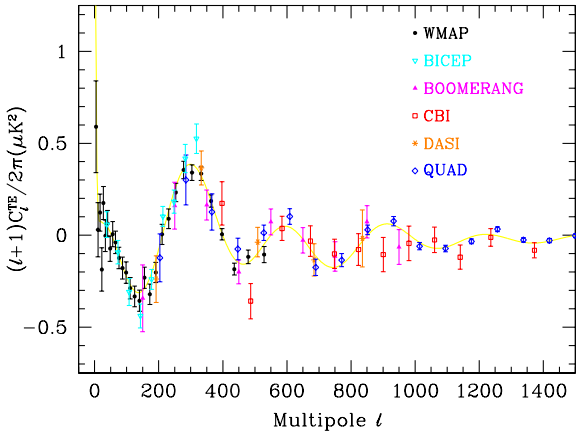

Figure 27.3: Cross power spectrum of the temperature anisotropies and E-mode polarization signal from *WMAP*, together with estimates from BICEP, BOOMERANG, CBI, DASI, and QUAD, several of which extend to higher ℓ. The curve is the prediction from the best fit to the temperature band-powers (with a prior from $\ell \leq 23$ polarization) and is not a fit to these data. Note that the y-axis here is not multiplied by the additional ℓ, which helps to show both the large and small angular scale features.

The overall picture of the source of CMB polarization and its oscillations has been confirmed through tests which average the maps around both temperature hot spots and cold spots [56,12]. One sees precisely the expected patterns of radial and tangential polarization configurations, as well as the phase shift between polarization and temperature. This leaves no doubt that the oscillation picture is the correct one and that the polarization is coming from Thomson scattering at $z \simeq 1100$.

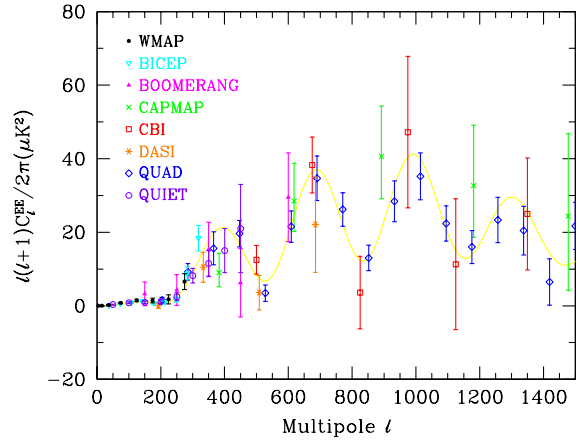

Figure 27.4: Power spectrum of E-mode polarization from several different experiments, plotted along with a theoretical model that fits *Planck* plus other CMB data. Note that the widths of the bands have been suppressed for clarity, but that in some cases they are almost as wide as the features in the power spectrum.

Experimental band-powers for C_ℓ^{EE} from *WMAP*, as well as BICEP [51], BOOMERANG [57], CAPMAP [58], CBI [53], DASI [54], QUAD [55], and QUIET [59], are shown in Fig. 27.4. Without the benefit of correlating with the temperature anisotropies (*i.e.*, measuring C_ℓ^{TE}), the polarization anisotropies are very weak and challenging to measure. Nevertheless, there is a highly significant overall detection, which is consistent with expectation. The data convincingly show the peak at $\ell \simeq 140$ (hard to see on this scale), the next peak at $\ell \simeq 400$ (corresponding to the first trough in C_ℓ^{TT}) and the generally oscillatory structure. Although *Planck* polarization data have not yet been released, a simple power spectrum estimate [10] shows at least four peaks in the EE spectrum.

Several experiments have reported upper limits on C_ℓ^{BB}, but they are currently not very constraining. This situation should change as increasingly ambitious experiments report results. The first indication of the existence of the BB signal has come from the detection of the expected conversion of E-modes to B-modes by gravitational lensing, through a correlation technique using the lensing potential and polarization measurements from SPT [60]. This is seen as a significant step on the road towards a future detection of primordial B-modes. An update to the B-mode situation is given in an Appendix at the end of this Chapter.

The most distinctive result from the polarization measurements is at the largest angular scales ($\ell < 10$) in C_ℓ^{TE}, where there is an excess signal compared to that expected from the temperature power spectrum alone. This is precisely the signal anticipated from an early period of reionization, arising from Doppler shifts during the partial scattering at $z < z_i$. The effect is also confirmed in the *WMAP* C_ℓ^{EE} results at $\ell = 2$–7 [50]. The amplitude of the signal indicates that the first stars, presumably the source of the ionizing radiation, formed around $z \simeq 10$ (although the uncertainty is still quite large). Since this corresponds to scattering optical depth $\tau \simeq 0.1$, then roughly 10% of CMB photons were re-scattered at the reionization epoch, with the other 90% last scattering at $z \simeq 1100$.

27.7. Complications

There are a number of issues that complicate the interpretation of CMB anisotropy data (and are considered to be *signal* by many astrophysicists), some of which we sketch out below.

27.7.1. *Foregrounds* :

The microwave sky contains significant emission from our Galaxy and from extra-galactic sources [61]. Fortunately, the frequency dependence of these various sources is in general substantially different from that of the CMB anisotropy signals. The combination of Galactic synchrotron, bremsstrahlung, and dust emission reaches a minimum at a wavelength of roughly 3 mm (or about 100 GHz). As one moves to greater angular resolution, the minimum moves to slightly higher frequencies, but becomes more sensitive to unresolved (point-like) sources.

At frequencies around 100 GHz, and for portions of the sky away from the Galactic Plane, the foregrounds are typically 1 to 10% of the CMB anisotropies. By making observations at multiple frequencies, it is relatively straightforward to separate the various components and determine the CMB signal to the few per cent level. For greater sensitivity, it is necessary to use the spatial information and statistical properties of the foregrounds to separate them from the CMB. Furthermore, at higher ℓs it is necessary to carefully model extragalactic foregrounds, particularly the clustering of infrared-emitting galaxies, which dominate the measured power spectrum as we move into the damping tail.

The foregrounds for CMB polarization follow a similar pattern, but are less well studied, and are intrinsically more complicated. *WMAP* has shown that the polarized foregrounds dominate at large angular scales, and that they must be well characterized in order to be discriminated [62]. Whether it is possible to achieve sufficient separation to detect primordial B-mode CMB polarization is still an open question. However, for the time being, foreground contamination is not a fundamental limit for CMB experiments.

27.7.2. *Secondary Anisotropies* :

With increasingly precise measurements of the primary anisotropies, there is growing theoretical and experimental interest in 'secondary anisotropies,' pushing experiments to higher angular resolution and sensitivity. These secondary effects arise from the processing of the CMB due to ionization history and the evolution of structure, including gravitational lensing and patchy reionization effects [63]. Additional information can thus be extracted about the Universe at $z \ll 1000$. This tends to be most effectively done through correlating CMB maps with other cosmological probes of structure. Secondary signals are also typically non-Gaussian, unlike the primary CMB anisotropies.

A secondary signal of great current interest is the Sunyaev-Zeldovich (SZ) effect [64], which is Compton scattering ($\gamma e \to \gamma' e'$) of the CMB photons by hot electron gas. This creates spectral distortions by transferring energy from the electrons to the photons. It is particularly important for clusters of galaxies, through which one observes a partially Comptonized spectrum, resulting in a decrement at radio wavelengths and an increment in the submillimeter.

The imprint on the CMB sky is of the form $\Delta T/T = y\, f(x)$, with the y-parameter being the integral of Thomson optical depth times $kT_e/m_e c^2$ through the cluster, and $f(x)$ describing the frequency dependence. This is simply $x\coth(x/2) - 4$ for a non-relativistic gas (the electron temperature in a cluster is typically a few keV), where the dimensionless frequency $x \equiv h\nu/kT_\gamma$. As well as this 'thermal' SZ effect, there is also a smaller 'kinetic' effect due to the bulk motion of the cluster gas, giving $\Delta T/T \sim \tau(v/c)$, with either sign, but having the same spectrum as the primary CMB anisotropies.

A significant advantage in finding galaxy clusters this way is that the SZ effect is largely independent of redshift, so in principle clusters can be found to arbitrarily large distances. The SZ effect can be used to find and study individual clusters, and to obtain estimates of the Hubble constant. There is also the potential to constrain cosmological parameters such as the clustering amplitude σ_8 and the equation of state of the dark energy, through counts of detected clusters as a function of redshift. The promise of the method has been realized through detections of clusters purely through the SZ effect, by SPT [65], ACT [66] and *Planck* [67]. Results from *Planck* clusters [68] suggest a somewhat lower value of σ_8 than inferred from CMB anisotropies, but there are still systematic uncertainties which might encompass the difference. Further analysis of scaling relations among cluster properties should enable more robust cosmological constraints to be placed in future.

27.7.3. *Higher-order Statistics* :

Although most of the CMB anisotropy information is contained in the power spectra, there will also be weak signals present in higher-order statistics. These can measure any primordial non-Gaussianity in the perturbations, as well as non-linear growth of the fluctuations on small scales and other secondary effects (plus residual foreground contamination of course). Although there are an infinite variety of ways in which the CMB could be non-Gaussian [24], there is a generic form to consider for the initial conditions, where a quadratic contribution to the curvature perturbations is parameterized through a dimensionless number $f_{\rm NL}$. This weakly non-linear component can be constrained in several ways, the most popular being through measurements of the bispectrum.

The constraints depend on the shape of the triangles in harmonic space, and it has become common to distinguish the 'local' or 'squeezed' configuration (in which one side is much smaller than the other two) from the 'equilateral' configuration. Other configurations are also relevant for specific theories, such as 'orthogonal' non-Gaussianity, which has positive correlations for $k_1 \simeq 2k_2 \simeq 2k_3$, and negative correlations for the equilateral configuration. The results from the *Planck* team [69] are $f_{\rm NL}^{\rm local} = 3 \pm 6$, $f_{\rm NL}^{\rm equil} = -42 \pm 75$, and $f_{\rm NL}^{\rm ortho} = -25 \pm 39$.

These results are consistent with zero, but are at a level which is now interesting for model predictions. The amplitude of $f_{\rm NL}$ expected is small, so that a detection of $f_{\rm NL} \gg 1$ would rule out all single field, slow-roll inflationary models. It is still possible to improve upon these *Planck* results, and it certainly seems feasible that a measurement of primordial non-Gaussianity may yet be within reach. Non-primordial signatures of non-Gaussianity have certainly been detected from expected signatures. For example, the bispectrum and trispectrum contain evidence of gravitational lensing, the ISW effect, and Doppler boosting. For now the primordial signal is elusive, but should it be detected, then detailed measurements of non-Gaussianity will become a unique probe of inflationary-era physics. Because of that, much effort continues to be devoted to honing predictions and measurement techniques.

27.7.4. *Anomalies* :

Several features seen in the *Planck* data [27,70] confirm those found earlier with *WMAP* [26], showing mild deviations from a simple description of the data, which are often referred to as 'anomalies.' One such feature is the apparent lack of power in the first 30 or so multipoles [10]. The other examples involve the breaking of statistical anisotropy, caused by alignment of the lowest multipoles, or a somewhat excessive cold spot, or a power asymmetry between hemispheres. No such feature is significant at more than the roughly 3σ level, and since these are at large angular scales, where cosmic variance dominates, the results will not increase in significance with more data.

27.8. Constraints on Cosmological Parameters

The most striking outcome of the newer experimental results is that the standard cosmological paradigm is in very good shape. A large amount of high precision data on the power spectrum is adequately fit with fewer than 10 free parameters (and only six need non-trivial values). The framework is that of FRW models, which have nearly flat geometry, containing dark matter and dark energy, and with adiabatic perturbations having close to scale invariant initial conditions.

Within this basic picture, the values of the cosmological parameters can be constrained. Of course, much more stringent bounds can be placed on models which cover a restricted parameter space, *e.g.*, assuming that $\Omega_{\rm tot} = 1$ or $r = 0$. More generally, the constraints depend upon the adopted prior probability distributions, even if they are implicit, for example by restricting the parameter freedom or their ranges (particularly where likelihoods peak near the boundaries), or by using different choices of other data in combination with the CMB. When the data become even more precise, these considerations will be less important, but for now we caution that restrictions on model space and choice of priors need to be kept in mind when adopting specific parameter values and uncertainties.

There are some combinations of parameters that fit the CMB anisotropies almost equivalently. For example, there is a nearly exact geometric degeneracy, where any combination of $\Omega_{\rm m}$ and Ω_Λ that gives the same angular diameter distance to last scattering will give nearly identical C_ℓs. There are also other less exact degeneracies among the parameters. Such degeneracies can be broken when using the CMB results in combination with other cosmological data-sets. Particularly useful are complementary constraints from baryon acoustic oscillations, galaxy clustering, the abundance of galaxy clusters, weak gravitational lensing measurements, and Type Ia supernova distances. For an overview of some of these other cosmological constraints, see The Cosmological Parameters—Sec. 24 of this *Review*.

Within the context of a six parameter family of models (which fixes $\Omega_{\rm tot} = 1$, $dn_{\rm s}/d\ln k = 0$, $r = 0$, and $w = -1$) the *Planck* results, together with a low-ℓ polarization constraint from *WMAP* and high-ℓ data from ACT and SPT, yields [10]: $\ln(10^{10}A) = 3.090 \pm 0.025$; $n_{\rm s} = 0.958 \pm 0.007$; $\Omega_{\rm b}h^2 = 0.02207 \pm 0.00027$; $\Omega_{\rm c}h^2 = 0.1198 \pm 0.0026$; $100\theta_* = 1.0415 \pm 0.0006$; and $\tau = 0.091 \pm 0.014$. Other parameters can be derived from this basic set, including $h = 0.673 \pm 0.012$, $\Omega_\Lambda = 0.685 \pm 0.016$ ($= 1 - \Omega_{\rm m}$) and $\sigma_8 = 0.828 \pm 0.012$. Somewhat different (although consistent) values are obtained using other data combinations, such as including BAO or CMB lensing data (see Sec. 24 of this *Review*). However, the results quoted above are currently the best available from CMB anisotropies alone.

There has been little substantive change compared with earlier results from *WMAP* and other experiments, although the error bars have shrunk substantially. The improved measurement of higher acoustic peaks has dramatically reduced the uncertainty in the θ_* parameter, which is now detected at $> 1700\sigma$. The evidence for non-zero reionization optical depth is convincing, but still not of very high significance. However, the evidence for $n_{\rm s} < 1$ is now above the 5σ level.

Constraints can also be placed on parameters beyond the basic six, particularly when including other astrophysical data-sets. Relaxing the flatness assumption, the constraint on $\Omega_{\rm tot}$ is $1.042^{+0.024}_{-0.022}$. Note that for h, the CMB data alone provide only a very weak constraint if spatial flatness is not assumed. However, with the addition of other data (from a compilation of BAO measurements for example [39,71])

, the constraints on the Hubble constant and curvature improve considerably, leading to $\Omega_{\rm tot} = 1.0010^{+0.0033}_{-0.0031}$ [10].

For $\Omega_{\rm b}h^2$ the CMB-derived value is generally consistent with completely independent constraints from Big Bang nucleosynthesis (see Sec. 23 of this *Review*). Related are constraints on additional neutrino-like relativistic degrees of freedom, which lead to $N_{\rm eff} = 3.36^{+0.34}_{-0.32}$ (68%), *i.e.*, no evidence for extra neutrino species.

The 95% confidence upper limit on r (measured at $k = 0.002\,{\rm Mpc}^{-1}$) is 0.11. This limit depends on how the slope n is restricted and whether $dn_{\rm s}/d\ln k \neq 0$ is allowed. A combination of constraints on n and r allows specific inflationary models to be tested [72]. It is clear that $\lambda\phi^4$ (sometimes called self-coupled) inflation is disfavored by the data, while the $m^2\phi^2$ (sometimes called mass term) inflationary model is still marginally allowed. The current limit on r is the tightest constraint that can be placed using CMB temperature anisotropies alone, and is pulled down somewhat by the fact that the measured power spectrum is a little low at low-ℓ, opposite to what a tensor contribution would produce (see Fig. 27.1). Further improvement will only come from B-mode measurements.

The addition of the dark energy equation of state w adds the partial degeneracy of being able to fit a ridge in (w, h) space, extending to low values of both parameters. This degeneracy is broken when the CMB is used in combination with other data-sets, *e.g.*, adding a compilation of BAO data gives $w = -1.13 \pm 0.12$. However, some H_0 combinations (*e.g.*, Ref. [73]) suggest a roughly 2σ preference for $w < -1$, which is a reflection of the mild tension between *Planck*'s preferred H_0 and those obtained by some local calibration methods.

For the optical depth τ, the best-fit corresponds to a reionization redshift centered on 11 in the best-fit cosmology, and assuming instantaneous reionization. This redshift appears to be higher that that suggested from studies of absorption in high-z quasar spectra [74] , perhaps indicating that the process of reionization was complex. The important constraint provided by CMB polarization, in combination with astrophysical measurements, thus allows us to investigate how the first stars formed and brought about the end of the cosmic dark ages.

27.9. Particle Physics Constraints

CMB data place limits on parameters that are directly relevant for particle physics models. For example, there is a limit on the sum of the masses of the neutrinos, $\sum m_\nu < 0.66\,{\rm eV}$ (95%) [10]. This assumes the usual number density of fermions which decoupled when they were relativistic. Somewhat different constraints are be derived using the CMB in combination with other data-sets.

The current suite of data suggests that $n < 1$, with a best-fitting value about 0.04 below unity. This is already quite constraining for inflationary models. Moreover, it gives a real target for B-mode searches, since the value of r in simple models may be in the range of detectability. There is no current evidence for running of the spectral index, with $dn_{\rm s}/d\ln k = -0.015 \pm 0.009$ (68%) [10], although this is less of a constraint on models. Similarly, primordial non-Gaussianity is being probed to interesting levels, although tests of simple inflationary models will only come with significant reductions in uncertainty.

The large-angle anomalies, such as the hemispheric modulation of power, have the potential to be hints of new physics. Such effects might be expected in a universe that has a large-scale power cut-off, or anisotropy in the initial power spectrum, or is topologically non-trivial. However, cosmic variance and *a posteriori* statistics limit the significance of these anomalies,

It is also possible to put limits on other pieces of physics [76], for example decaying particles, primordial magnetic fields, and time variation of the fine-structure constant [10], as well as parity violation, the neutrino chemical potential, a contribution of warm dark matter, topological defects, or physics beyond general relativity. Further particle physics constraints will follow as the anisotropy measurements increase in precision.

More generally, careful measurement of the CMB power spectra and non-Gaussianity can in principle put constraints on physics at the highest energies, including ideas of string theory, extra dimensions, colliding branes, *etc.* At the moment any calculation of predictions appears to be far from definitive. However, there is a great deal of activity on implications of string theory for the early Universe, and hence a very real chance that there might be observational implications for specific scenarios.

27.10. Fundamental Lessons

More important than the precise values of parameters is what we have learned about the general features that describe our observable Universe. Beyond the basic hot Big Bang picture, the CMB has taught us that:

- The Universe recombined at $z \simeq 1100$ and started to become ionized again at $z \simeq 10$.
- The geometry of the Universe is close to flat.
- Both dark matter and dark energy are required.
- Gravitational instability is sufficient to grow all of the observed large structures in the Universe.
- Topological defects were not important for structure formation.
- There are 'synchronized' super-Hubble modes generated in the early Universe.
- The initial perturbations were predominantly adiabatic in nature.
- The perturbation spectrum has a slightly red tilt.
- The perturbations had close to Gaussian (*i.e.*, maximally random) initial conditions.

These features form the basis of the cosmological standard model, ΛCDM, for which it is tempting to make an analogy with the Standard Model of particle physics (see earlier Sections of this *Review*). The cosmological model is much further from any underlying 'fundamental theory,' which may ultimately provide the values of the parameters from first principles. Nevertheless, any genuinely complete 'theory of everything' must include an explanation for the values of these cosmological parameters as well as the parameters of the Standard Model of particle physics.

27.11. Future Directions

Given the significant progress in measuring the CMB sky, which has been instrumental in tying down the cosmological model, what can we anticipate for the future? There will be a steady improvement in the precision and confidence with which we can determine the appropriate cosmological parameters. Ground-based experiments operating at smaller angular scales will continue to place tighter constraints on the damping tail. New polarization experiments at small scales will probe further into the damping tail, without the limitation of extragalactic foregrounds. And polarization experiments at large angular scales will push down the limits on primordial B-modes.

Planck, the third generation CMB satellite mission, was launched in May 2009, and has produced many papers, including a set of cosmological studies based on the first two full surveys of the sky (accompanied by a public release of data products) in March 2013. In 2014 results are expected from the full mission (eight surveys for the Low Frequency Instrument and five surveys for the High Frequency Instrument), including polarization information.

A set of cosmological parameters is now known to percent level accuracy, and that may seem sufficient for many people. However, we should certainly demand more of measurements that describe *the entire observable Universe!* Hence a lot of activity in the coming years will continue to focus on determining those parameters with increasing precision. This necessarily includes testing for consistency among different predictions of the cosmological Standard Model, and searching for signals that might require additional physics.

A second area of focus will be the smaller scale anisotropies and 'secondary effects.' There is a great deal of information about structure formation at $z \ll 1000$ encoded in the CMB sky. This may involve higher-order statistics as well as spectral signatures, with many experiments targeting the galaxy cluster SZ effect. Such investigations can also provide constraints on the dark energy equation of state, for example. *Planck*, as well as new telescopes aimed at the highest ℓs, should be able to make considerable progress in this arena.

A third direction is increasingly sensitive searches for specific signatures of physics at the highest energies. The most promising of these may be the primordial gravitational wave signals in $C_\ell^{\rm BB}$, which

could be a probe of the $\sim 10^{16}$ GeV energy range. As well as *Planck*, there are several ground- and balloon-based experiments underway that are designed to search for the polarization B-modes. Additionally, non-Gaussianity holds the promise of constraining models beyond single field slow-roll inflation.

Anisotropies in the CMB have proven to be the premier probe of cosmology and the early Universe. Theoretically the CMB involves well understood physics in the linear regime, and is under very good calculational control. A substantial and improving set of observational data now exists. Systematics appear to be under control and not a limiting factor. And so for the next few years we can expect an increasing amount of cosmological information to be gleaned from CMB anisotropies, with the prospect also of some genuine surprises.

Appendix A. New Polarization Results

After this review was completed, further information emerged which led to the addition of this appendix. New experimental results from the BICEP2 experiment [78] suggest a detection of the primordial B-mode signature around the peak expected in $C_\ell^{\rm BB}$ at $\ell \simeq 100$. BICEP2 has mapped a small part of the CMB sky with the lowest noise level yet reached, below 100 nK, allowing an overall detection of B-modes (including some contribution from the lensed signature at higher multipoles) at 7σ. The best-fit primordial tensor amplitude corresponds to $r \simeq 0.2$, with the precise value depending on how foregrounds are treated.

These results are certainly preliminary, and one needs to be cautious about the possibility of foreground contamination, but nevertheless the implications of a detection of this telltale signature of inflation are obviously of enormous importance for high energy physics. Within the slow-roll inflationary picture, the amplitude of the gravitational wave power spectrum is directly proportional to the potential during inflation. For $r = 0.2$ for example, we have $V/m_{\rm Pl}^4 = 1.0 \times 10^{-11}$ (or 6.5×10^{-9} if one uses the reduced Planck mass, $m_{\rm Pl}/\sqrt{8\pi}$).

A tensor-to-scalar ratio of 0.2 is formally inconsistent with results from a 7-parameter fit to data from the *Planck* experiment [10], based purely on the contribution of gravitational waves to the $C_\ell^{\rm TT}$ spectrum (see Fig. 27.1). Although it is clear that the results could be made consistent in more complicated models (with running of $n_{\rm s}$ or a step in the power spectrum of scalars, for example), the need for additional physics will become much clearer if the results are confirmed and clarified. We present the current experimental situation for $C_\ell^{\rm BB}$ in Fig. 27.5. Additional band-power estimates are expected late in 2014 from *Planck*'s first polarization results, as well as from BICEP's successor experiment Keck, and other ground-based experiments, such as POLARBEAR, SPT-Pol and ACT-Pol.

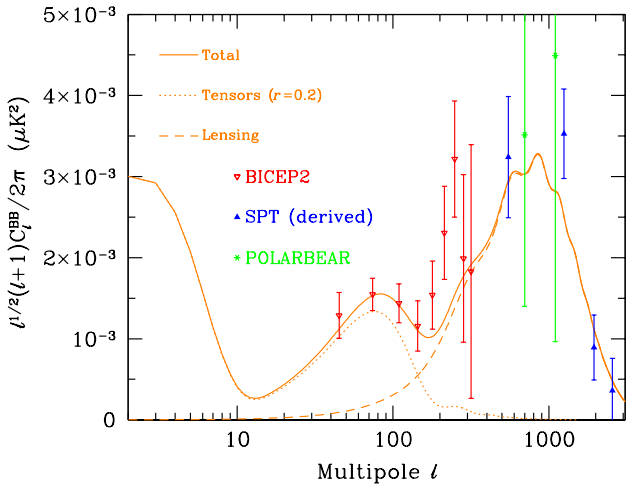

Figure 27.5: Power spectrum of B-mode polarization, including results from the BICEP2 [78], POLARBEAR [79], and SPT (derived from a lensing correlation analysis) [60] experiments. Note that several experiments have previous reported upper limits, which are all off the top of this plot. A logarithmic x-axis is adopted here and the y-axis has been divided by a factor of $\sqrt{\ell}$ in order to show all three theoretically expected contributions: the low-ℓ reionization bump, $\ell \sim 100$ primordial tensor peak, and high-ℓ lensing signature. The dotted line is for a tensor (gravitational wave) fraction $r = 0.2$, simply to guide the eye, with all other cosmological parameters set at the best *Planck*-derived values, for which model the expected lensing B-modes have also been shown with a dashed line.

References:

1. A.A. Penzias and R. Wilson, Astrophys. J. **142**, 419 (1965); R.H. Dicke *et al.*, Astrophys. J. **142**, 414 (1965).
2. R. Khatri and R.A. Sunyaev, J. Cosmol. Astropart. Phys. in press, arXiv:1303.7212.
3. M. White, D. Scott, and J. Silk, Ann. Rev. Astron. & Astrophys. **32**, 329 (1994); W. Hu and S. Dodelson, Ann. Rev. Astron. & Astrophys. **40**, 171 (2002).
4. G.F. Smoot *et al.*, Astrophys. J. **396**, L1 (1992).
5. C.L. Bennett *et al.*, Astrophys. J. Supp. **148**, 1 (2003).
6. N. Jarosik *et al.*, Astrophys. J. Supp. **170**, 263 (2007).
7. G. Hinshaw *et al.*, Astrophys. J. Supp. **180**, 225 (2009).
8. N. Jarosik *et al.*, Astrophys. J. Supp. **192**, 14 (2011).
9. G. Hinshaw *et al.*, Astrophys. J. Suppl. in press arXiv:1212.5226.
10. Planck Collab. XVI, Astron. & Astrophys. in press, arXiv:1303.5076.
11. J.A. Tauber *et al.*, Astron. & Astrophys. **520**, 1 (2010); Planck Collab. I, Astron. & Astrophys. **536**, 1 (2011).
12. Planck Collab. I, Astron. & Astrophys. in press, arXiv:1303.5062.
13. D.S. Swetz *et al.*,Astrophys. J. Supp. **194**, 41 (2011).
14. J.E. Carlstron *et al.*, Publ. Astron. Soc. Pacific **123**, 568 (2011).
15. D.J. Fixsen, Astrophys. J. **707**, 916 (2009).
16. J.C. Mather *et al.*, Astrophys. J. **512**, 511 (1999).
17. D.J. Fixsen *et al.*, Astrophys. J. **734**, 5 (2011).
18. R. Watkins, H.A. Feldman, and M.J. Hudson, MNRAS **392**, 743 (2009).
19. D.J. Fixsen *et al.*, Astrophys. J. **420**, 445 (1994).
20. Planck Collab. XXVII, Astron. & Astrophys. in press, arXiv:1303.5087.
21. D.J. Fixsen *et al.*, Astrophys. J. **473**, 576 (1996); A. Kogut *et al.*, Astrophys. J. **419**, 1 (1993).
22. S. Seager, D.D. Sasselov, and D. Scott, Astrophys. J. Supp. **128**, 407 (2000).
23. L. Knox, Phys. Rev. **D52**, 4307 (1995).
24. N. Bartolo *et al.*, Phys. Rep. **402**, 103 (2004); E. Komatsu, Class. Quant. Grav. **27**,124010(2010); A.P.S. Yadav and B.D. Wandelt, Adv. Astron. **2010**, 565248 (2010).
25. Planck Collab. XXIV, Astron. & Astrophys. in press, arXiv:1303.5084.
26. C.L. Bennett *et al.*, Astrophys. J. Supp. **192**, 17 (2011).
27. Planck Collab. XXIII, Astron. & Astrophys. in press, arXiv:1303.5083.
28. Planck Collab. XXII, Astron. & Astrophys. in press, arXiv:1303.5082.
29. A.R. Liddle and D.H. Lyth, Cosmological Inflation and Large-Scale Structure, Cambridge University Press (2000).
30. U. Seljak and M. Zaldarriaga, Astrophys. J. **469**, 437 (1996).
31. A. Lewis, A. Challinor, and A. Lasenby, Astrophys. J. **538**, 473 (2000).
32. U. Seljak *et al.*, Phys. Rev. **D68**, 083507 (2003); C. Howlett *et al.*, J. Cosmol. Astropart. Phys. **04**, 027 (2012).
33. R.K. Sachs and A.M. Wolfe, Astrophys. J. **147**, 73 (1967).
34. R. Crittenden and N. Turok, Phys. Rev. Lett. **76**, 575 (1996); Planck Collab. XIX, Astron. & Astrophys. in press, arXiv:1303.5079.
35. W. Hu *et al.*, Phys. Rev. **D59**, 023512 (1999).
36. P.J.E. Peebles and J.T. Yu, Astrophys. J. **162**, 815 (1970); R.A. Sunyaev and Ya.B. Zel'dovich, Astrophys. & Space Sci. **7**, 3 (1970).
37. D. Scott, J. Silk, and M. White, Science **268**, 829 (1995).

38. D.J. Eisenstein, New Astron. Rev. **49**, 360 (2005); W.J. Percival *et al.*, MNRAS **381**, 1053 (2007).
39. W.J. Percival *et al.*, MNRAS **401**, 2148 (2010).
40. J. Silk, Astrophys. J. **151**, 459 (1968).
41. M. Zaldarriaga and U. Seljak, Phys. Rev. **D58**, 023003 (1998); A. Lewis and A. Challinor, Phys. Rep. **429**, 1 (2006).
42. Planck Collab. XVII, Astron. & Astrophys. in press, arXiv:1303.5077.
43. Planck Collab. XV, Astron. & Astrophys. in press, arXiv:1303.5075.
44. S. Das *et al.*, Astrophys. J. in press, arXiv:1301.1037.
45. R. Keisler *et al.*, Astrophys. J. **743**, 28 (2011); C.L. Reichardt *et al.*, Astrophys. J. **755**, 70 (2012); K.T. Story *et al.*, Astrophys. J. in press, arXiv:1210.7231.
46. W. Hu and M. White, New Astron. **2**, 323 (1997).
47. W. Hu and M. White, Phys. Rev. **D56**, 596 (1997).
48. M. Zaldarriaga and U. Seljak, Phys. Rev. **D55**, 1830 (1997); M. Kamionkowski, A. Kosowsky, and A. Stebbins, Phys. Rev. **D55**, 7368 (1997).
49. J. Kovac *et al.*, Nature, **420**, 772 (2002).
50. D. Larson *et al.*, Astrophys. J. Supp. **192**, 16 (2011).
51. H.C. Chiang *et al.*, Astrophys. J. **711**, 1123 (2010).
52. F. Piacentini *et al.*, Astrophys. J. **647**, 833 (2006).
53. J.L. Sievers *et al.*, Astrophys. J. **660**, 976 (2007).
54. E.M. Leitch *et al.*, Astrophys. J. **624**, 10 (2005).
55. M.L. Brown *et al.*, Astrophys. J. **705**, 978 (2009).
56. E. Komatsu *et al.*, Astrophys. J. Supp. **192**, 18 (2011).
57. T.E. Montroy *et al.*, Astrophys. J. **647**, 813 (2006).
58. C. Bischoff *et al.*, Astrophys. J. **684**, 771 (2008).
59. QUIET Collab. Astrophys. J. **760**, 145 (2012).
60. D. Hanson *et al.*, Phys. Rev. Lett. **111**, 141301 (2013) arXiv:1307.5830.
61. Planck Collab. XII, Astron. & Astrophys. in press, arXiv:1303.5072.
62. B. Gold *et al.*, Astrophys. J. Supp. **192**, 15 (2011).
63. N. Aghanim, S. Majumdar, and J. Silk, Rept. Prog. Phys., **71**, 066902 (2008); M. Millea *et al.*, Astrophys. J. **746**, 4 (2012).
64. R.A. Sunyaev and Ya.B. Zel'dovich, Ann. Rev. Astron. Astrophys. **18**, 537 (1980); M. Birkinshaw, Phys. Rep. **310**, 98 (1999); J.E. Carlstrom, G.P. Holder, and E.D. Reese, Ann. Rev. Astron. & Astrophys. **40**, 643 (2002).
65. R. Williamson *et al.*, Astrophys. J. **738**, 139 (2011); C.L. Reichardt *et al.*, Astrophys. J. **763**, 127 (2013).
66. T.A. Marriage *et al.*, Astrophys. J. **737**, 61 (2011); M. Hasselfield *et al.*, J. Cosm. & Astropart. Phys. **07**, 008 (2013).
67. Planck Collab. VIII, Astron. & Astrophys. **536**, 8 (2011); Planck Collab. XXIX, Astron. & Astrophys. in press, arXiv:1303.5089.
68. Planck Collab. XX, Astron. & Astrophys. in press, arXiv:1303.5080.
69. Planck Collab. XXIV, Astron. & Astrophys. in press, arXiv:1303.5084.
70. Planck Collab. XXVI, Astron. & Astrophys. in press, arXiv:1303.5086.
71. C. Blake *et al.*, MNRAS **418**, 1707 (2011); F. Beutler *et al.*, MNRAS **416**, 3017 (2011); N. Padmanabhan *et al.*, MNRAS **427**, 2132 (2012).
72. Planck Collab. XXII, Astron. & Astrophys. in press, arXiv:1303.5082.
73. A.G. Riess *et al.*, Astrophys. J. **730**, 119 (2011).
74. X. Fan, C.L. Carilli, and B. Keating, Ann. Rev. Astron. & Astrophys. **44**, 415 (2006).
75. J. Hoftuft *et al.*, Astrophys. J. **699**, 985 (2009); D. Hanson and A. Lewis, Phys. Rev. **D80**, 063004 (2010).
76. M. Kamionkowski and A. Kosowsky, Ann. Rev. Nucl. Part. Sci. **49**, 77 (1999); A. Lasenby, Space Sci. Rev. **148**, 329 (2009).
77. R. Maartens, Living Rev. Rel. **7**, 7 (2004).
78. BICEP2 Collab., Astrophys. J. in press arXiv:1403.3985.
79. POLARBEAR Collab., Astrophys. J. in press arXiv:1403.2369.

28. COSMIC RAYS

Revised October 2013 by J.J. Beatty (Ohio State Univ.), J. Matthews (Louisiana State Univ.), and S.P. Wakely (Univ. of Chicago); revised August 2009 by T.K. Gaisser and T. Stanev (Bartol Research Inst., Univ. of Delaware).

28.1. Primary spectra

The cosmic radiation incident at the top of the terrestrial atmosphere includes all stable charged particles and nuclei with lifetimes of order 10^6 years or longer. Technically, "primary" cosmic rays are those particles accelerated at astrophysical sources and "secondaries" are those particles produced in interaction of the primaries with interstellar gas. Thus electrons, protons and helium, as well as carbon, oxygen, iron, and other nuclei synthesized in stars, are primaries. Nuclei such as lithium, beryllium, and boron (which are not abundant end-products of stellar nucleosynthesis) are secondaries. Antiprotons and positrons are also in large part secondary. Whether a small fraction of these particles may be primary is a question of current interest.

Apart from particles associated with solar flares, the cosmic radiation comes from outside the solar system. The incoming charged particles are "modulated" by the solar wind, the expanding magnetized plasma generated by the Sun, which decelerates and partially excludes the lower energy galactic cosmic rays from the inner solar system. There is a significant anticorrelation between solar activity (which has an alternating eleven-year cycle) and the intensity of the cosmic rays with energies below about 10 GeV. In addition, the lower-energy cosmic rays are affected by the geomagnetic field, which they must penetrate to reach the top of the atmosphere. Thus the intensity of any component of the cosmic radiation in the GeV range depends both on the location and time.

There are four different ways to describe the spectra of the components of the cosmic radiation: (1) By particles per unit rigidity. Propagation (and probably also acceleration) through cosmic magnetic fields depends on gyroradius or *magnetic rigidity,* R, which is gyroradius multiplied by the magnetic field strength:

$$R = \frac{p\,c}{Z\,e} = r_L B\ . \qquad (28.1)$$

(2) By particles per energy-per-nucleon. Fragmentation of nuclei propagating through the interstellar gas depends on energy per nucleon, since that quantity is approximately conserved when a nucleus breaks up on interaction with the gas. (3) By nucleons per energy-per-nucleon. Production of secondary cosmic rays in the atmosphere depends on the intensity of nucleons per energy-per-nucleon, approximately independently of whether the incident nucleons are free protons or bound in nuclei. (4) By particles per energy-per-nucleus. Air shower experiments that use the atmosphere as a calorimeter generally measure a quantity that is related to total energy per particle.

The units of differential intensity I are $[\mathrm{m}^{-2}\,\mathrm{s}^{-1}\mathrm{sr}^{-1}\mathcal{E}^{-1}]$, where $\mathcal{E}$ represents the units of one of the four variables listed above.

The intensity of primary nucleons in the energy range from several GeV to somewhat beyond 100 TeV is given approximately by

$$I_N(E)\ \approx\ 1.8\times10^4\,(E/1\ \mathrm{GeV})^{-\alpha}\ \frac{\text{nucleons}}{\mathrm{m}^2\ \mathrm{s}\ \mathrm{sr}\ \mathrm{GeV}}\ , \qquad (28.2)$$

where E is the energy-per-nucleon (including rest mass energy) and $\alpha\ (\equiv\gamma+1) = 2.7$ is the differential spectral index of the cosmic-ray flux and γ is the integral spectral index. About 79% of the primary nucleons are free protons and about 70% of the rest are nucleons bound in helium nuclei. The fractions of the primary nuclei are nearly constant over this energy range (possibly with small but interesting variations). Fractions of both primary and secondary incident nuclei are listed in Table 28.1. Figure 28.1 shows the major components for energies greater than 2 GeV/nucleon. A useful compendium of experimental data for cosmic-ray nuclei and electrons is described in [1].

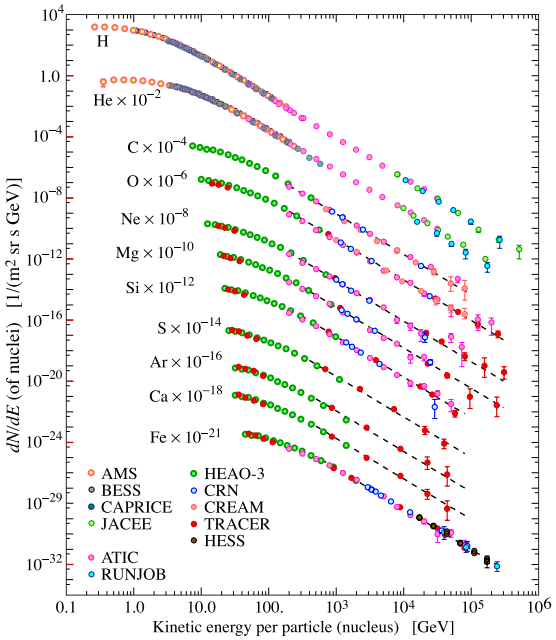

Figure 28.1: Fluxes of nuclei of the primary cosmic radiation in particles per energy-per-nucleus are plotted vs energy-per-nucleus using data from Refs. [2–13]. The figure was created by P. Boyle and D. Muller.

The composition and energy spectra of nuclei are typically interpreted in the context of propagation models, in which the sources of the primary cosmic radiation are located within the Galaxy [14]. The ratio of secondary to primary nuclei is observed to decrease with increasing energy, a fact interpreted to mean that the lifetime of cosmic rays in the galaxy decreases with energy. Measurements of radioactive "clock" isotopes in the low energy cosmic radiation are consistent with a lifetime in the galaxy of about 15 Myr [15].

Table 28.1: Relative abundances F of cosmic-ray nuclei at 10.6 GeV/nucleon normalized to oxygen ($\equiv 1$) [7]. The oxygen flux at kinetic energy of 10.6 GeV/nucleon is 3.29×10^{-2} $(\mathrm{m}^2\ \mathrm{s\ sr\ GeV/nucleon})^{-1}$. Abundances of hydrogen and helium are from Refs. [3,4]. Note that one can not use these values to extend the cosmic-ray flux to high energy because the power law indicies for each element may differ slightly.

Z	Element	F	Z	Element	F
1	H	540	13–14	Al-Si	0.19
2	He	26	15–16	P-S	0.03
3–5	Li-B	0.40	17–18	Cl-Ar	0.01
6–8	C-O	2.20	19–20	K-Ca	0.02
9–10	F-Ne	0.30	21–25	Sc-Mn	0.05
11–12	Na-Mg	0.22	26–28	Fe-Ni	0.12

Cosmic rays are nearly isotropic at most energies due to diffusive propagation in the galactic magnetic field. Milagro [16], IceCube [17], and the Tibet-III air shower array [18] have observed anisotropy at the level of about 10^{-3} for cosmic rays with energy of a few TeV, possibly due to nearby sources.

The spectrum of electrons and positrons incident at the top of the atmosphere is expected to steepen by one power of E at an energy of ∼5 GeV because of strong radiative energy loss effects in the galaxy. The ATIC experiment [19] measured an excess of electrons over propagation model expectations, at energies of ∼300-800 GeV. The *Fermi*/LAT γ-ray observatory measured a not-entirely flat

spectrum [20] without confirming the peak of the ATIC excess at ∼600 GeV. The HESS imaging atmospheric Cherenkov array also measured the electron flux above ∼400 GeV, finding indications of a cutoff above ∼1 TeV [21], but no evidence for a pronounced peak.

The PAMELA [24] and AMS-02 [25] satellite experiments measured the positron to electron ratio to increase above 10 GeV instead of the expected decrease [26] at higher energy, confirming earlier hints seen by the HEAT balloon-borne experiment [28]. The structure in the electron spectrum, as well as the increase in the positron fraction, may be related to contributions from individual nearby sources (supernova remnants or pulsars) emerging above a background suppressed at high energy by synchrotron losses [29]. Other explanations have invoked propagation effects [30] or dark matter decay/annihilation processes (see, e.g., [27]) . The significant disagreement in the ratio below ∼10 GeV is attributable to differences in charge-sign dependent solar modulation effects present near earth at the times of measurement.

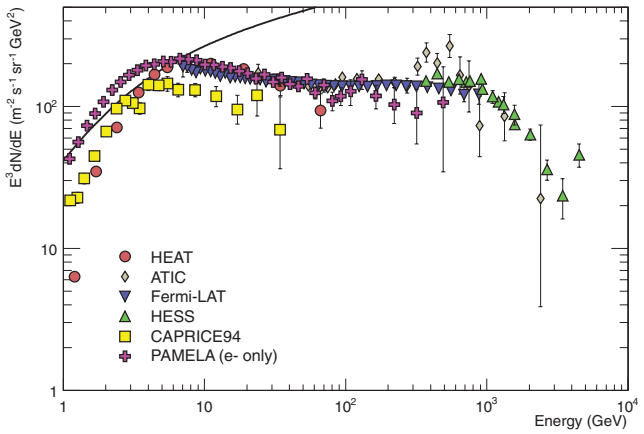

Figure 28.2: Differential spectrum of electrons plus positrons (except PAMELA data, which are electrons only) multiplied by E^3 [19–22,31,32]. The line shows the proton spectrum [23] multiplied by 0.01.

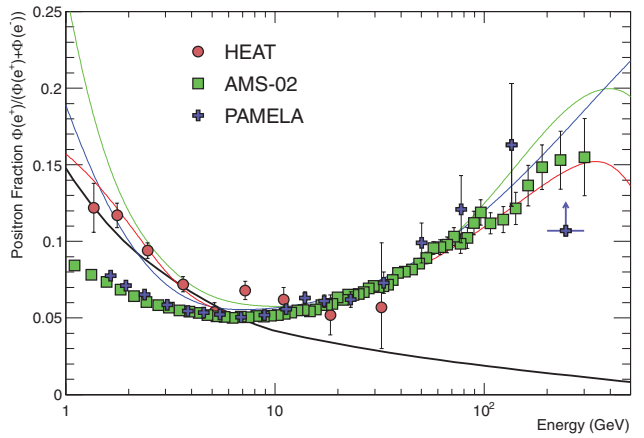

Figure 28.3: The positron fraction (ratio of the flux of e^+ to the total flux of e^+ and e^-) [24,25,28]. The heavy black line is a model of pure secondary production [26] and the three thin lines show three representative attempts to model the positron excess with different phenomena: green: dark matter decay [27]; blue: propagation physics [30]; red: production in pulsars [38]. The ratio below 10 GeV is dependent on the polarity of the solar magnetic field.

The ratio of antiprotons to protons is $\sim 2 \times 10^{-4}$ [33] at around 10–20 GeV, and there is clear evidence [34] for the kinematic suppression at lower energy that is the signature of secondary antiprotons. The $\overline{p}/p$ ratio also shows a strong dependence on the phase and polarity of the solar cycle [35] in the opposite sense to that of the positron fraction. There is at this time no evidence for a significant primary component of antiprotons. No antihelium or antideuteron has been found in the cosmic radiation. The best measured upper limit on the ratio antihelium/helium is currently approximately 1×10^{-7} [36] The upper limit on the flux of antideuterons around 1 GeV/nucleon is approximately $2 \times 10^{-4}\,(\mathrm{m^2\ s\ sr\ GeV/nucleon})^{-1}$ [37].

28.2. Cosmic rays in the atmosphere

Figure 28.4 shows the vertical fluxes of the major cosmic-ray components in the atmosphere in the energy region where the particles are most numerous (except for electrons, which are most numerous near their critical energy, which is about 81 MeV in air). Except for protons and electrons near the top of the atmosphere, all particles are produced in interactions of the primary cosmic rays in the air. Muons and neutrinos are products of the decay chain of charged mesons, while electrons and photons originate in decays of neutral mesons.

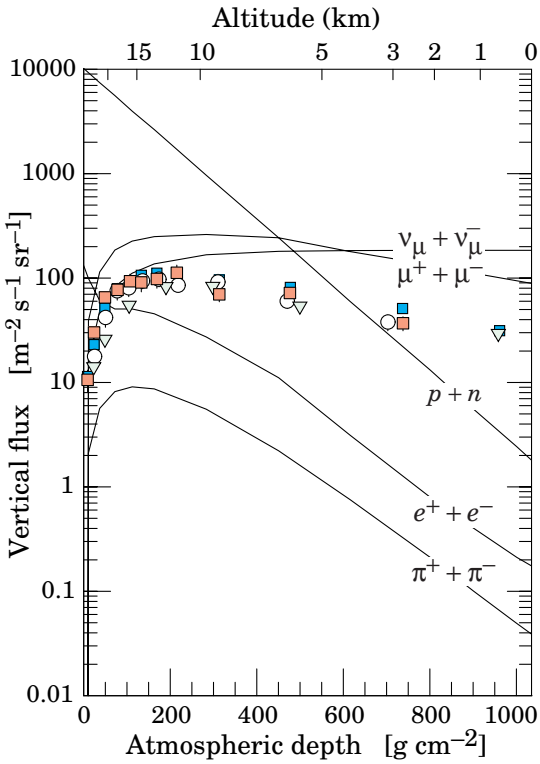

Figure 28.4: Vertical fluxes of cosmic rays in the atmosphere with $E > 1$ GeV estimated from the nucleon flux of Eq. (28.2). The points show measurements of negative muons with $E_\mu > 1$ GeV [39–43].

Most measurements are made at ground level or near the top of the atmosphere, but there are also measurements of muons and electrons from airplanes and balloons. Fig. 28.4 includes recent measurements of negative muons [39–43]. Since $\mu^+(\mu^-)$ are produced in association with $\nu_\mu(\overline{\nu}_\mu)$, the measurement of muons near the maximum of the intensity curve for the parent pions serves to calibrate the atmospheric ν_μ beam [44]. Because muons typically lose almost 2 GeV in passing through the atmosphere, the comparison near the production altitude is important for the sub-GeV range of $\nu_\mu(\overline{\nu}_\mu)$ energies.

The flux of cosmic rays through the atmosphere is described by a set of coupled cascade equations with boundary conditions at the top of the atmosphere to match the primary spectrum. Numerical or Monte Carlo calculations are needed to account accurately for decay and energy-loss processes, and for the energy-dependences of the cross

sections and of the primary spectral index γ. Approximate analytic solutions are, however, useful in limited regions of energy [45,46]. For example, the vertical intensity of charged pions with energy $E_\pi \ll \epsilon_\pi = 115$ GeV is

$$I_\pi(E_\pi, X) \approx \frac{Z_{N\pi}}{\lambda_N} I_N(E_\pi, 0)\, e^{-X/\Lambda} \frac{X\, E_\pi}{\epsilon_\pi} , \qquad (28.3)$$

where Λ is the characteristic length for exponential attenuation of the parent nucleon flux in the atmosphere. This expression has a maximum at $X = \Lambda \approx 121 \pm 4$ g cm^{-2} [47], which corresponds to an altitude of 15 kilometers. The quantity $Z_{N\pi}$ is the spectrum-weighted moment of the inclusive distribution of charged pions in interactions of nucleons with nuclei of the atmosphere. The intensity of low-energy pions is much less than that of nucleons because $Z_{N\pi} \approx 0.079$ is small and because most pions with energy much less than the critical energy ϵ_π decay rather than interact.

28.3. Cosmic rays at the surface

28.3.1. ***Muons*** : Muons are the most numerous charged particles at sea level (see Fig. 28.4). Most muons are produced high in the atmosphere (typically 15 km) and lose about 2 GeV to ionization before reaching the ground. Their energy and angular distribution reflect a convolution of the production spectrum, energy loss in the atmosphere, and decay. For example, 2.4 GeV muons have a decay length of 15 km, which is reduced to 8.7 km by energy loss. The mean energy of muons at the ground is ≈ 4 GeV. The energy spectrum is almost flat below 1 GeV, steepens gradually to reflect the primary spectrum in the 10–100 GeV range, and steepens further at higher energies because pions with $E_\pi > \epsilon_\pi$ tend to interact in the atmosphere before they decay. Asymptotically ($E_\mu \gg 1$ TeV), the energy spectrum of atmospheric muons is one power steeper than the primary spectrum. The integral intensity of vertical muons above 1 GeV/c at sea level is ≈ 70 m^{-2}s^{-1}sr^{-1} [48,49], with recent measurements [50–52] favoring a lower normalization by 10-15%. Experimentalists are familiar with this number in the form $I \approx 1$ cm^{-2} min^{-1} for horizontal detectors. The overall angular distribution of muons at the ground is $\propto \cos^2\theta$, which is characteristic of muons with $E_\mu \sim 3$ GeV. At lower energy the angular distribution becomes increasingly steep, while at higher energy it flattens, approaching a $\sec\theta$ distribution for $E_\mu \gg \epsilon_\pi$ and $\theta < 70°$.

Figure 28.5 shows the muon energy spectrum at sea level for two angles. At large angles low energy muons decay before reaching the surface and high energy pions decay before they interact, thus the average muon energy increases. An approximate extrapolation formula valid when muon decay is negligible ($E_\mu > 100/\cos\theta$ GeV) and the curvature of the Earth can be neglected ($\theta < 70°$) is

$$\frac{dN_\mu}{dE_\mu d\Omega} \approx \frac{0.14\, E_\mu^{-2.7}}{\text{cm}^2 \text{ s sr GeV}} \times \left\{ \frac{1}{1 + \frac{1.1 E_\mu \cos\theta}{115\,\text{GeV}}} + \frac{0.054}{1 + \frac{1.1 E_\mu \cos\theta}{850\,\text{GeV}}} \right\} , \qquad (28.4)$$

where the two terms give the contribution of pions and charged kaons. Eq. (28.4) neglects a small contribution from charm and heavier flavors which is negligible except at very high energy [53].

The muon charge ratio reflects the excess of π^+ over π^- and K^+ over K^- in the forward fragmentation region of proton initiated interactions together with the fact that there are more protons than neutrons in the primary spectrum. The increase with energy of μ^+/μ^- shown in Fig. 28.6 reflects the increasing importance of kaons in the TeV range [58] and indicates a significant contribution of associated production by cosmic-ray protons ($p \to \Lambda + K^+$). The same process is even more important for atmospheric neutrinos at high energy.

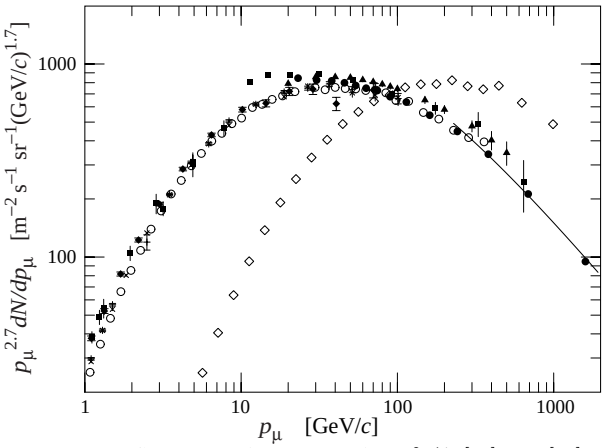

Figure 28.5: Spectrum of muons at $\theta = 0°$ (♦ [48], ■ [54], ▼ [55], ▲ [56], ×, + [50], ○ [51], and ● [52] and $\theta = 75°$ ◊ [57]) . The line plots the result from Eq. (28.4) for vertical showers.

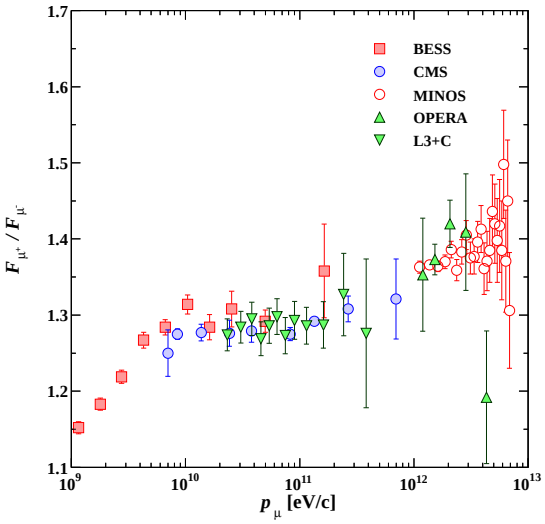

Figure 28.6: Muon charge ratio as a function of the muon momentum from Refs. [51,52,58,63,64].

28.3.2. ***Electromagnetic component*** : At the ground, this component consists of electrons, positrons, and photons primarily from cascades initiated by decay of neutral and charged mesons. Muon decay is the dominant source of low-energy electrons at sea level. Decay of neutral pions is more important at high altitude or when the energy threshold is high. Knock-on electrons also make a small contribution at low energy [59]. The integral vertical intensity of electrons plus positrons is very approximately 30, 6, and 0.2 m^{-2}s^{-1}sr^{-1} above 10, 100, and 1000 MeV respectively [49,60], but the exact numbers depend sensitively on altitude, and the angular dependence is complex because of the different altitude dependence of the different sources of electrons [59–61]. The ratio of photons to electrons plus positrons is approximately 1.3 above 1 GeV and 1.7 below the critical energy [61].

28.3.3. ***Protons*** : Nucleons above 1 GeV/c at ground level are degraded remnants of the primary cosmic radiation. The intensity is approximately $I_N(E, 0) \times \exp(-X/\cos\theta\Lambda)$ for $\theta < 70°$. At sea level, about 1/3 of the nucleons in the vertical direction are neutrons (up from $\approx 10\%$ at the top of the atmosphere as the n/p ratio approaches equilibrium). The integral intensity of vertical protons above 1 GeV/c at sea level is ≈ 0.9 m^{-2}s^{-1}sr^{-1} [49,62].

28.4. Cosmic rays underground

Only muons and neutrinos penetrate to significant depths underground. The muons produce tertiary fluxes of photons, electrons, and hadrons.

28.4.1. ***Muons*** : As discussed in Section 32.6 of this *Review*, muons lose energy by ionization and by radiative processes: bremsstrahlung, direct production of e^+e^- pairs, and photonuclear interactions. The total muon energy loss may be expressed as a function of the amount of matter traversed as

$$-\frac{dE_\mu}{dX} = a + b\,E_\mu \ , \tag{28.5}$$

where a is the ionization loss and b is the fractional energy loss by the three radiation processes. Both are slowly varying functions of energy. The quantity $\epsilon \equiv a/b$ (≈ 500 GeV in standard rock) defines a critical energy below which continuous ionization loss is more important than radiative losses. Table 28.2 shows a and b values for standard rock, and b for ice, as a function of muon energy. The second column of Table 28.2 shows the muon range in standard rock ($A = 22$, $Z = 11$, $\rho = 2.65$ g cm^{-3}). These parameters are quite sensitive to the chemical composition of the rock, which must be evaluated for each location.

Table 28.2: Average muon range R and energy loss parameters a and b calculated for standard rock [65] and the total energy loss parameter b for ice. Range is given in km-water-equivalent, or 10^5 g cm^{-2}.

E_μ	R	a	$b_{\rm brems}$	$b_{\rm pair}$	$b_{\rm nucl}$	$\sum b_i$	$\sum b$(ice)
GeV	km.w.e.	MeV g^{-1} cm^2	—	10^{-6} g^{-1} cm^2	—		
10	0.05	2.17	0.70	0.70	0.50	1.90	1.66
100	0.41	2.44	1.10	1.53	0.41	3.04	2.51
1000	2.45	2.68	1.44	2.07	0.41	3.92	3.17
10000	6.09	2.93	1.62	2.27	0.46	4.35	3.78

The intensity of muons underground can be estimated from the muon intensity in the atmosphere and their rate of energy loss. To the extent that the mild energy dependence of a and b can be neglected, Eq. (28.5) can be integrated to provide the following relation between the energy $E_{\mu,0}$ of a muon at production in the atmosphere and its average energy E_μ after traversing a thickness X of rock (or ice or water):

$$E_{\mu,0} = (E_\mu + \epsilon)\, e^{bX} - \epsilon \ . \tag{28.6}$$

Especially at high energy, however, fluctuations are important and an accurate calculation requires a simulation that accounts for stochastic energy-loss processes [66].

There are two depth regimes for which Eq. (28.6) can be simplified. For $X \ll b^{-1} \approx 2.5$ km water equivalent, $E_{\mu,0} \approx E_\mu(X) + aX$, while for $X \gg b^{-1}$ $E_{\mu,0} \approx (\epsilon + E_\mu(X))\exp(bX)$. Thus at shallow depths the differential muon energy spectrum is approximately constant for $E_\mu < aX$ and steepens to reflect the surface muon spectrum for $E_\mu > aX$, whereas for $X > 2.5$ km.w.e. the differential spectrum underground is again constant for small muon energies but steepens to reflect the surface muon spectrum for $E_\mu > \epsilon \approx 0.5$ TeV. In the deep regime the shape is independent of depth although the intensity decreases exponentially with depth. In general the muon spectrum at slant depth X is

$$\frac{dN_\mu(X)}{dE_\mu} = \frac{dN_\mu}{dE_{\mu,0}}\frac{dE_{\mu,0}}{dE_\mu} = \frac{dN_\mu}{dE_{\mu,0}}\, e^{bX} \ , \tag{28.7}$$

where $E_{\mu,0}$ is the solution of Eq. (28.6) in the approximation neglecting fluctuations.

Fig. 28.7 shows the vertical muon intensity versus depth. In constructing this "depth-intensity curve," each group has taken account of the angular distribution of the muons in the atmosphere, the map of the overburden at each detector, and the properties of the local medium in connecting measurements at various slant depths and zenith angles to the vertical intensity. Use of data from a range of angles allows a fixed detector to cover a wide range of depths. The flat portion of the curve is due to muons produced locally by charged-current interactions of ν_μ. The inset shows the vertical intensity curve for water and ice published in Refs. [68–71]. It is not as steep as the one for rock because of the lower muon energy loss in water.

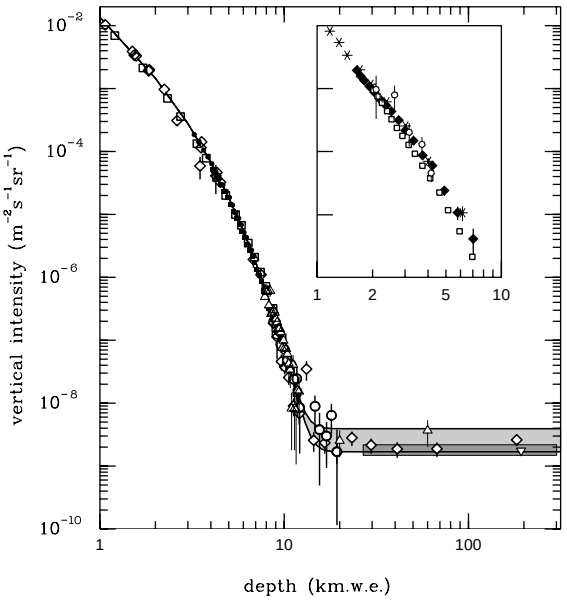

Figure 28.7: Vertical muon intensity vs depth (1 km.w.e. = 10^5 g cm^{-2}of standard rock). The experimental data are from: ◇: the compilations of Crouch [67], □: Baksan [72], ○: LVD [73], ●: MACRO [74], ■: Frejus [75], and △: SNO [76]. The shaded area at large depths represents neutrino-induced muons of energy above 2 GeV. The upper line is for horizontal neutrino-induced muons, the lower one for vertically upward muons. Darker shading shows the muon flux measured by the SuperKamiokande experiment. The inset shows the vertical intensity curve for water and ice published in Refs. [68–71].

28.4.2. ***Neutrinos*** :

Because neutrinos have small interaction cross sections, measurements of atmospheric neutrinos require a deep detector to avoid backgrounds. There are two types of measurements: contained (or semi-contained) events, in which the vertex is determined to originate inside the detector, and neutrino-induced muons. The latter are muons that enter the detector from zenith angles so large (*e.g.*, nearly horizontal or upward) that they cannot be muons produced in the atmosphere. In neither case is the neutrino flux measured directly. What is measured is a convolution of the neutrino flux and cross section with the properties of the detector (which includes the surrounding medium in the case of entering muons).

Contained and semi-contained events reflect neutrinos in the sub-GeV to multi-GeV region where the product of increasing cross section and decreasing flux is maximum. In the GeV region the neutrino flux and its angular distribution depend on the geomagnetic location of the detector and, to a lesser extent, on the phase of the solar cycle. Naively, we expect $\nu_\mu/\nu_e = 2$ from counting neutrinos of the two flavors coming from the chain of pion and muon decay. Contrary to expectation, however, the numbers of the two classes of events are similar rather than different by a factor of two. This is now understood to be a consequence of neutrino flavor oscillations [79]. (See the article on neutrino properties in this *Review*.)

Two well-understood properties of atmospheric cosmic rays provide a standard for comparison of the measurements of atmospheric

Table 28.3: Measured fluxes (10^{-9} m^{-2} s^{-1} sr^{-1}) of neutrino-induced muons as a function of the effective minimum muon energy E_μ.

$E_\mu >$	1 GeV	1 GeV	1 GeV	2 GeV	3 GeV	3 GeV
Ref.	CWI [80]	Baksan [81]	MACRO [82]	IMB [83]	Kam [84]	SuperK [85]
F_μ	2.17±0.21	2.77±0.17	2.29 ± 0.15	2.26±0.11	1.94±0.12	1.74±0.07

neutrinos to expectation. These are the "sec θ effect" and the "east-west effect" [78]. The former refers originally to the enhancement of the flux of > 10 GeV muons (and neutrinos) at large zenith angles because the parent pions propagate more in the low density upper atmosphere where decay is enhanced relative to interaction. For neutrinos from muon decay, the enhancement near the horizontal becomes important for $E_\nu > 1$ GeV and arises mainly from the increased pathlength through the atmosphere for muon decay in flight. Fig. 14.5 from Ref. 77 shows a comparison between measurement and expectation for the zenith angle dependence of multi-GeV electron-like (mostly ν_e) and muon-like (mostly ν_μ) events separately. The ν_e show an enhancement near the horizontal and approximate equality for nearly upward ($\cos\theta \approx -1$) and nearly downward ($\cos\theta \approx 1$) events. There is, however, a very significant deficit of upward ($\cos\theta < 0$) ν_μ events, which have long pathlengths comparable to the radius of the Earth. This feature is the principal signature for atmosperic neutrino oscillations [79].

Muons that enter the detector from outside after production in charged-current interactions of neutrinos naturally reflect a higher energy portion of the neutrino spectrum than contained events because the muon range increases with energy as well as the cross section. The relevant energy range is $\sim 10 < E_\nu < 1000$ GeV, depending somewhat on angle. Neutrinos in this energy range show a $\sec\theta$ effect similar to muons (see Eq. (28.4)). This causes the flux of horizontal neutrino-induced muons to be approximately a factor two higher than the vertically upward flux. The upper and lower edges of the horizontal shaded region in Fig. 28.7 correspond to horizontal and vertical intensities of neutrino-induced muons. Table 28.3 gives the measured fluxes of upward-moving neutrino-induced muons averaged over the lower hemisphere. Generally the definition of minimum muon energy depends on where it passes through the detector. The tabulated effective minimum energy estimates the average over various accepted trajectories.

28.5. Air showers

So far we have discussed inclusive or uncorrelated fluxes of various components of the cosmic radiation. An air shower is caused by a single cosmic ray with energy high enough for its cascade to be detectable at the ground. The shower has a hadronic core, which acts as a collimated source of electromagnetic subshowers, generated mostly from $\pi^0 \to \gamma\,\gamma$ decays. The resulting electrons and positrons are the most numerous charged particles in the shower. The number of muons, produced by decays of charged mesons, is an order of magnitude lower. Air showers spread over a large area on the ground, and arrays of detectors operated for long times are useful for studying cosmic rays with primary energy $E_0 > 100$ TeV, where the low flux makes measurements with small detectors in balloons and satellites difficult.

Greisen [86] gives the following approximate expressions for the numbers and lateral distributions of particles in showers at ground level. The total number of muons N_μ with energies above 1 GeV is

$$N_\mu(> 1\ \mathrm{GeV}) \;\approx\; 0.95 \times 10^5 \left(N_e/10^6\right)^{3/4} \;, \qquad (28.8)$$

where N_e is the total number of charged particles in the shower (not just $e^\pm$). The number of muons per square meter, ρ_μ, as a function of the lateral distance r (in meters) from the center of the shower is

$$\rho_\mu = \frac{1.25\,N_\mu}{2\pi\,\Gamma(1.25)} \left(\frac{1}{320}\right)^{1.25} r^{-0.75} \left(1 + \frac{r}{320}\right)^{-2.5} \;, \qquad (28.9)$$

where Γ is the gamma function. The number density of charged particles is

$$\rho_e = C_1(s,d,C_2)\, x^{(s-2)} (1+x)^{(s-4.5)} (1 + C_2 x^d) \;. \qquad (28.10)$$

Here s, d, and C_2 are parameters in terms of which the overall normalization constant $C_1(s,d,C_2)$ is given by

$$C_1(s,d,C_2) = \frac{N_e}{2\pi r_1^2} \left[\, B(s, 4.5-2s) + C_2\, B(s+d,\, 4.5-d-2s)\right]^{-1} \;, \qquad (28.11)$$

where $B(m,n)$ is the beta function. The values of the parameters depend on shower size (N_e), depth in the atmosphere, identity of the primary nucleus, etc. For showers with $N_e \approx 10^6$ at sea level, Greisen uses $s = 1.25$, $d = 1$, and $C_2 = 0.088$. Finally, x is r/r_1, where r_1 is the Molière radius, which depends on the density of the atmosphere and hence on the altitude at which showers are detected. At sea level $r_1 \approx 78$ m. It increases with altitude as the air density decreases. (See the section on electromagnetic cascades in the article on the passage of particles through matter in this *Review*).

The lateral spread of a shower is determined largely by Coulomb scattering of the many low-energy electrons and is characterized by the Moliere radius. The lateral spread of the muons (ρ_μ) is larger and depends on the transverse momenta of the muons at production as well as multiple scattering.

There are large fluctuations in development from shower to shower, even for showers of the same energy and primary mass—especially for small showers, which are usually well past maximum development when observed at the ground. Thus the shower size N_e and primary energy E_0 are only related in an average sense, and even this relation depends on depth in the atmosphere. One estimate of the relation is [93]

$$E_0 \;\sim\; 3.9 \times 10^6\ \mathrm{GeV}\ (N_e/10^6)^{0.9} \qquad (28.12)$$

for vertical showers with $10^{14} < E < 10^{17}$ eV at 920 g cm^{-2} (965 m above sea level). As E_0 increases the shower maximum (on average) moves down into the atmosphere and the relation between N_e and E_0 changes. Moreover, because of fluctuations, N_e as a function of E_0 is not correctly obtained by inverting Eq. (28.12). At the maximum of shower development, there are approximately 2/3 particles per GeV of primary energy.

There are three common types of air shower detectors: shower arrays that study the shower size N_e and the lateral distribution on the ground, Cherenkov detectors that detect the Cherenkov radiation emitted by the charged particles of the shower, and fluorescence detectors that study the nitrogen fluorescence excited by the charged particles in the shower. The fluorescence light is emitted isotropically so the showers can be observed from the side. Detailed simulations and cross-calibrations between different types of detectors are necessary to establish the primary energy spectrum from air-shower experiments.

Figure 28.8 shows the "all-particle" spectrum. The differential energy spectrum has been multiplied by $E^{2.6}$ in order to display the features of the steep spectrum that are otherwise difficult to discern. The steepening that occurs between 10^{15} and 10^{16} eV is known as the *knee* of the spectrum. The feature around $10^{18.5}$ eV is called the *ankle* of the spectrum.

Measurements of flux with small air shower experiments in the knee region differ by as much as a factor of two, indicative of systematic uncertainties in interpretation of the data. (For a review see Ref. 87.) In establishing the spectrum shown in Fig. 28.8, efforts have been made to minimize the dependence of the analysis on the

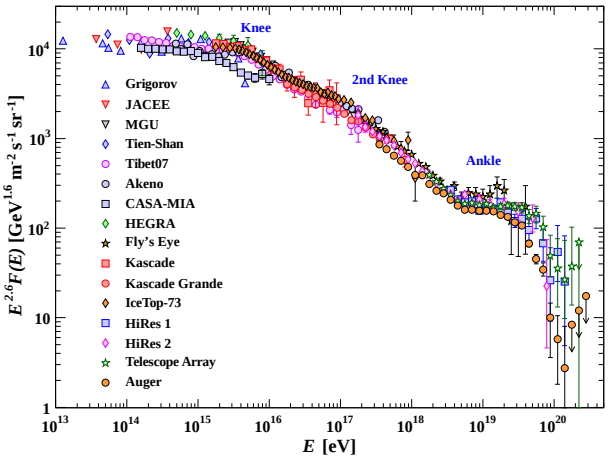

Figure 28.8: The all-particle spectrum as a function of E (energy-per-nucleus) from air shower measurements [88–99,101–104].

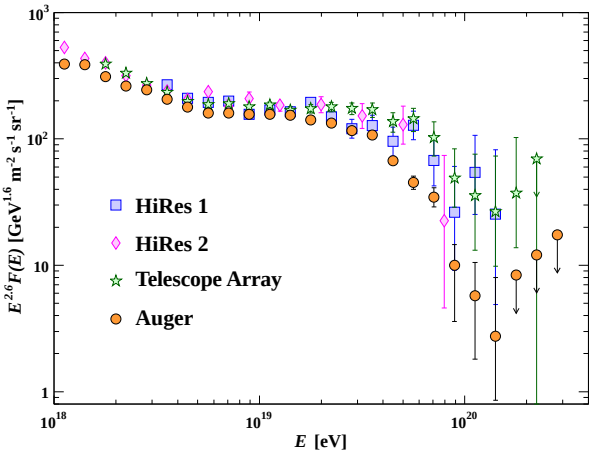

Figure 28.9: Expanded view of the highest energy portion of the cosmic-ray spectrum from data of HiRes 1&2 [101], the Telescope Array [103], and the Auger Observatory [104]. The HiRes stereo spectrum [122] is consistent with the HiRes 1&2 monocular results. The differential cosmic-ray flux is multiplied by $E^{2.6}$. The red arrow indicates the change in the plotted data for a systematic shift in the energy scale of 20%.

primary composition. Ref. 96 uses an unfolding procedure to obtain the spectra of the individual components, giving a result for the all-particle spectrum between 10^{15} and 10^{17} eV that lies toward the upper range of the data shown in Fig. 28.8. In the energy range above 10^{17} eV, the fluorescence technique [100] is particularly useful because it can establish the primary energy in a model-independent way by observing most of the longitudinal development of each shower, from which E_0 is obtained by integrating the energy deposition in the atmosphere. The result, however, depends strongly on the light absorption in the atmosphere and the calculation of the detector's aperture.

Assuming the cosmic-ray spectrum below 10^{18} eV is of galactic origin, the *knee* could reflect the fact that most cosmic accelerators in the galaxy have reached their maximum energy. Some types of expanding supernova remnants, for example, are estimated not to be able to accelerate protons above energies in the range of 10^{15} eV. Effects of propagation and confinement in the galaxy [106] also need to be considered. The Kascade-Grande experiment [98] has reported observation of a second steepening of the spectrum near 8×10^{16} eV, with evidence that this structure is accompanied a transition to heavy primaries.

Concerning the ankle, one possibility is that it is the result of a higher energy population of particles overtaking a lower energy population, for example an extragalactic flux beginning to dominate over the galactic flux (e.g. Ref. 100). Another possibility is that the dip structure in the region of the ankle is due to $\gamma p \to e^+ + e^-$ energy losses of extragalactic protons on the 2.7 K cosmic microwave radiation (CMB) [108]. This dip structure has been cited as a robust signature of both the protonic and extragalactic nature of the highest energy cosmic rays [107]. If this interpretation is correct, then the galactic cosmic rays do not contribute significantly to the flux above 10^{18} eV, consistent with the maximum expected range of acceleration by supernova remnants.

The energy-dependence of the composition from the knee through the ankle is useful in discriminating between these two viewpoints, since a heavy composition above 10^{18} eV is inconsistent with the formation of the ankle by pair production losses on the CMB. The HiRes and Auger experiments, however, present very different interpretations of data on the depth of shower maximum X_{max}, a quantity that correlates strongly with the interaction cross section of the primary particle. If these results are interpreted using standard extrapolations of measured proton and nuclear cross sections, then the HiRes data [109] is consistent with the ultrahigh-energy cosmic-ray (UHECR) composition getting lighter and containing only protons and helium above 10^{19} eV, while Auger [110,111] sees a composition getting lighter up to 2×10^{18} eV and becoming heavier after that, intermediate between protons and iron at 3×10^{19} eV. This may mean that the extragalactic cosmic rays have a mixed composition at acceleration similar to the GeV galactic cosmic rays. It is important to note that the measurements of X_{max} may be interpreted with equal validity in terms of a changing proton-air cross-section and no change in composition.

If the cosmic-ray flux at the highest energies is cosmological in origin, there should be a rapid steepening of the spectrum (called the GZK feature) around 5×10^{19} eV, resulting from the onset of inelastic interactions of UHE cosmic rays with the cosmic microwave background [112,113]. Photo-dissociation of heavy nuclei in the mixed composition model [114] would have a similar effect. UHECR experiments have detected events of energy above 10^{20} eV [100–105]. The AGASA experiment [105], with lower statistics, did not observe the expected GZK feature. The HiRes fluorescence experiment [101,122] has detected evidence of the GZK suppression, and the Auger observatory [102–104] has presented spectra showing this suppression based on surface detector measurements calibrated against fluorescence detectors using events detected in hybrid mode, i.e. with both the surface and the fluorescence detectors. The Telescope Array [103] has also presented a surface detector spectrum showing this suppression.

Figure 28.9 gives an expanded view of the high energy end of the spectrum, showing only the more recent data. This figure shows the differential flux multiplied by $E^{2.6}$. The experiments are consistent in normalization if one takes quoted systematic errors in the energy scales into account.

One half of the energy that UHECR protons lose in photoproduction interactions that cause the GZK effects ends up in neutrinos [115]. Measuring this *cosmogenic* neutrino flux above 10^{18} eV would help resolve the UHECR uncertainties mentioned above. The magnitude of this flux depends strongly on the cosmic-ray spectrum at acceleration, the cosmic-ray composition, and the cosmological evolution of the cosmic-ray sources. In the case that UHECR have mixed composition only the proton fraction would produce cosmogenic neutrinos. Heavy nuclei propagation produces mostly $\bar{\nu}_e$ at lower energy from neutron decay.

The expected rate of cosmogenic neutrinos is lower than current limits obtained by IceCube [116], the Auger observatory [117], RICE [118], and ANITA-2 [119], which are shown in Figure 28.10

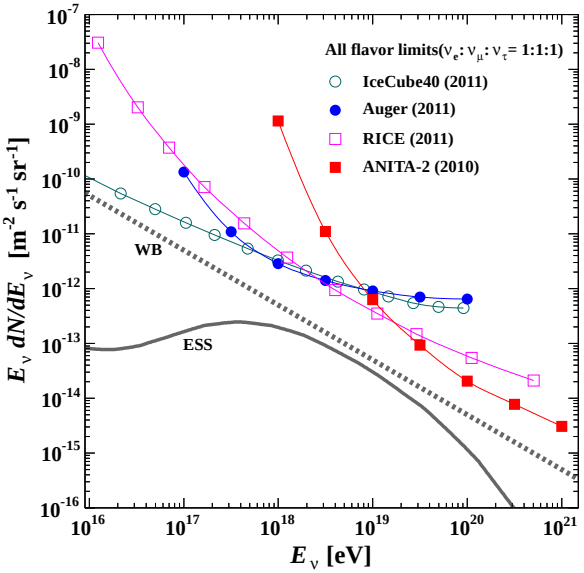

Figure 28.10: Differential limits on the flux of cosmogenic neutrinos set by four neutrino experiments. The curves show the Waxman-Bahcall benchmark flux (WB, [121]) and a representative midrange model for the expected flux of cosmogenic neutrinos (ESS, [120]) . The expected flux is uncertain by over an order of magnitude in either direction.

together with a model for cosmogenic neutrino production [120] and the Waxman-Bahcall benchmark flux of neutrinos produced in cosmic ray sources [121]. At production, the dominant component of neutrinos comes from $\pi^{\pm}$ decays and has flavor content $\nu_e : \nu_\mu : \nu_\tau = 1 : 2 : 0$. After oscillations, the arriving cosmogenic neutrinos are expected to be an equal mixture of all three flavors. The sensitivity of each experiment depends on neutrino flavor. IceCube, RICE, and ANITA are sensitive to all three flavors, and the sensitivity to different flavors is energy dependent. The limit of Auger is only for ν_τ and $\bar{\nu}_\tau$ which should be about 1/3 of the total neutrino flux after oscillations, so this limit is plotted multiplied by a factor of three for comparison with the other limits and with the theoretical estimates.

IceCube has recently reported the observation of two events with deposited energy of about 10^{15} eV [123] as well as a population of events above 30 TeV that exceeds expected atmospheric backgrounds [124].

References:

1. D. Maurin, *et al.*, arXiv:1302.5525.
2. M. Boezio *et al.*, Astropart. Phys. **19**, 583 (2003).
3. AMS Collab., Phys. Lett. **B490**, 27 (2000); Phys. Lett. **B494**, 193 (2000).
4. T. Sanuki *et al.*, Astrophys. J. **545**, 1135 (2000).
5. S. Haino *et al.*, Phys. Lett. **B594**, 35 (2004).
6. H.S. Ahn *et al.*, Astrophys. J. **707**, 593 (2000).
7. J.J. Engelmann *et al.*, Astron. & Astrophys. **233**, 96 (1990).
8. D. Müller *et al.*, Ap J, **374**, 356 (1991).
9. M. Ave *et al.*, Astrophys. J. **678**, 262 (2008).
10. A.D. Panov *et al.*, Bull Russian Acad of Science, Physics, **71**, 494 (2007).
11. V.A. Derbina *et al.*, Astrophys. J. **628**, L41 (2005).
12. K. Asakimori *et al.* (JACEE Collab.), Astrophys. J. **502**, 278 (1998).
13. F. Aharonian *et al.* (HESS Collab.), Phys. Rev. **D75**, 042004 (2007).
14. A.W. Strong *et al.*, Ann. Rev. Nucl. and Part. Sci. **57**, 285 (2007).
15. R.A. Mewaldt *et al.*, Space Science Reviews 99,27(2001).
16. A.A. Abdo *et al.*, Astrophys. J. **698**, 2121 (2009).
17. R. Abbasi *et al.*, Astrophys. J. **718**, L194 (2010).
18. M. Amenomori *et al.*, Astrophys. J. **711**, 119 (2010).
19. J. Chang *et al.* (ATIC Collab.), Nature **456**, 362 (2008).
20. A.A. Abdo *et al.* (Fermi/LAT Collab.), Phys. Rev. Lett. **102**, 181101 (2009); M. Ackermann *et al.*, Phys. Rev. **D82**, 092004 (2010).
21. F. Aharonian *et al.* (HESS Collab.), Phys. Rev. Lett. **101**, 261104 (2008) and Astron. & Astrophys. **508**, 561 (2009).
22. O Adriani *et al.*, Phys. Rev. Lett. **106**, 201101 (2011).
23. Y. Shizake *et al.*, Astroparticle Physics 28, 154 (2007).
24. O. Adriani *et al.* (Pamela Collab.), Nature **458**, 607 (2009); Phys. Rev. Lett. **102**, 051101 (2009).
25. M. Aguilar *et al.*, Phys. Rev. Lett. **110**, 141102 (2013).
26. I.V. Moskalenko and A.W. Strong, Astrophys. J. **493**, 694 (1998).
27. A. Ibarra *et al.*, Int. J. Mod Phys A, in press arXiv1307.6434I.
28. J.J. Beatty *et al.*, Phys. Rev. Lett. **93**, 24112 (2004).
29. J. Nishimura *et al.*, Adv. Space Research **19**, 767 (1997).
30. D. Gaggero *et al.*, Phys. Rev. Lett. **111**, 021102 (2013).
31. M.A. DuVernois *et al.*, Astrophys. J. **559**, 296 (2001).
32. M. Boezio *et al.*, Astrophys. J. **532**, 653 (2000).
33. A.S. Beach *et al.*, Phys. Rev. Lett. **87**, 271101 (2001).
34. A. Yamamoto *et al.*, Adv. Space Research**42**, 443(2008).
35. Y. Asaoka *et al.*, Phys. Rev. Lett. **88**, 51101 (2002).
36. K. Abe *et al.*, Phys. Rev. Lett. **108**, 081102 (2013).
37. H. Fuke *et al.*, Phys. Rev. Lett. **95**, 081101 (2005).
38. P. Yin *et al.*, Phys. Rev. **D88**, 023001 (2013).
39. R. Bellotti *et al.*, Phys. Rev. **D53**, 35 (1996).
40. R. Bellotti *et al.*, Phys. Rev. **D60**, 052002 (1999).
41. M. Boezio *et al.*, Phys. Rev. **D62**, 032007 (2000); M. Boezio *et al.*, Phys. Rev. **D67**, 072003 (2003).
42. S. Coutu *et al.*, Phys. Rev. **D62**, 032001 (2000).
43. S. Haino *et al.*. Phys. Lett. **B594**, 35 (2004).
44. T. Sanuki *et al.*, Phys. Rev. **D75**, 043005 (2007).
45. T.K. Gaisser, *Cosmic Rays and Particle Physics*, Cambridge University Press (1990).
46. P. Lipari, Astropart. Phys. **1**, 195 (1993).
47. E. Mocchiutto *et al.*, in *Proc. 28th Int. Cosmic Ray Conf.*, Tsukuba, 1627 (2003). [http://adsabs.harvard.edu/abs/2003ICRC....3.1627M].
48. M.P. De Pascale *et al.*, J. Geophys. Res. **98**, 3501 (1993).
49. P.K.F. Grieder, *Cosmic Rays at Earth*, Elsevier Science (2001).
50. J. Kremer *et al.*, Phys. Rev. Lett. **83**, 4241 (1999).
51. S. Haino *et al.* (BESS Collab.), Phys. Lett. **B594**, 35 (2004).
52. P. Archard *et al.* (L3+C Collab.), Phys. Lett. **B598**, 15 (2004).
53. C.G.S. Costa, Astropart. Phys. **16**, 193 (2001).
54. O.C. Allkofer, K. Carstensen, and W.D. Dau, Phys. Lett. **B36**, 425 (1971).
55. B.C. Rastin, J. Phys. **G10**, 1609 (1984).
56. C.A. Ayre *et al.*, J. Phys. **G1**, 584 (1975).
57. H. Jokisch *et al.*, Phys. Rev. **D19**, 1368 (1979).
58. P. Adamson *et al.* (MINOS Collab.), Phys. Rev. **D76**, 052003 (2007).
59. S. Hayakawa, *Cosmic Ray Physics*, Wiley, Interscience, New York (1969).
60. R.R. Daniel and S.A. Stephens, Revs. Geophysics & Space Sci. **12**, 233 (1974).
61. K.P. Beuermann and G. Wibberenz, Can. J. Phys. **46**, S1034 (1968).
62. I.S. Diggory *et al.*, J. Phys. **A7**, 741 (1974).
63. V. Khachatryan *et al.*(CMS Collab.) Phys. Lett. **B692**, 83 (2010).
64. N. Agafonova *et al.*(OPERA Collab.) Eur. Phys. J. **C67**, 25 (2010).
65. D.E. Groom, N.V. Mokhov, and S.I. Striganov, *"Muon stopping-power and range tables,"*Atomic Data and Nuclear Data Tables, **78**, 183 (2001).
66. P. Lipari and T. Stanev, Phys. Rev. **D44**, 3543 (1991).
67. M. Crouch, in *Proc. 20th Int. Cosmic Ray Conf.*, Moscow, **6**, 165 (1987) [http://adsabs.harvard.edu/abs/1987ICRC....6..165C].
68. I.A. Belolaptikov *et al.*, Astropart. Phys. **7**, 263 (1997).

69. J. Babson *et al.*, Phys. Rev. **D42**, 3613 (1990).
70. P. Desiati *et al.*, in *Proc. 28th Int. Cosmic Ray Conf.*, Tsukuba, 1373 (2003) [http://adsabs.harvard.edu/abs/2003ICRC....3.1373D].
71. T. Pradier *et al.* (ANTARES Collab.), arXiv:0805.2545 and 31st ICRC, 7-15 July 2009, Łódź, Poland (paper #0340).
72. Yu.M. Andreev, V.I. Gurentzov, and I.M. Kogai, in *Proc. 20th Int. Cosmic Ray Conf.*, Moscow, **6**, 200 (1987), [http://adsabs.harvard.edu/abs/1987ICRC....6..200A].
73. M. Aglietta *et al.* (LVD Collab.), Astropart. Phys. **3**, 311 (1995).
74. M. Ambrosio *et al.* (MACRO Collab.), Phys. Rev. **D52**, 3793 (1995).
75. Ch. Berger *et al.* (Frejus Collab.), Phys. Rev. **D40**, 2163 (1989).
76. C. Waltham *et al.*, in *Proc. 27th Int. Cosmic Ray Conf.*, Hamburg, 991 (2001), [http://adsabs.harvard.edu/abs/2001ICRC....3..991W].
77. Y. Ashie *et al.* (SuperKamiokande Collab.), Phys. Rev. **D71**, 112005 (2005).
78. T. Futagami *et al.*, Phys. Rev. Lett. **82**, 5194 (1999).
79. Y. Fukuda *et al.*, Phys. Rev. Lett. **81**, 1562 (1998).
80. F. Reines *et al.*, Phys. Rev. Lett. **15**, 429 (1965).
81. M.M. Boliev *et al.*, in *Proc. 3rd Int. Workshop on Neutrino Telescopes* (ed. Milla Baldo Ceolin), 235 (1991).
82. M. Ambrosio *et al.*, (MACRO) Phys. Lett. **B434**, 451 (1998). The number quoted for MACRO is the average over 90% of the lower hemisphere, $\cos\theta < -0.1$; see F. Ronga *et al.*, hep-ex/9905025.
83. R. Becker-Szendy *et al.*, Phys. Rev. Lett. **69**, 1010 (1992); *Proc. 25th Int. Conf. High-Energy Physics*, Singapore (eds. K.K. Phua and Y. Yamaguchi, World Scientific), 662 1991.
84. S. Hatakeyama *et al.*, Phys. Rev. Lett. **81**, 2016 (1998).
85. Y. Fukuda *et al.*, Phys. Rev. Lett. **82**, 2644 (1999).
86. K. Greisen, Ann. Rev. Nucl. Sci. **10**, 63 (1960).
87. S.P. Swordy *et al.*, Astropart. Phys. **18**, 129 (2002).
88. N.L. Grigorov *et al.*, *Sov. J. Nucl. Phys.* 11, 588. *Proc. 12th Int. Cosmic Ray Conf.*, Hobart, **1**, 1746 and 1752 (1971).
89. K. Asakimori *et al.*, *Proc. 23rd Int. Cosmic Ray Conf.*, Calgary, **2**, 25 (1993);
Proc. 22nd Int. Cosmic Ray Conf., Dublin, **2**, 57 and 97 (1991) [http://adsabs.harvard.edu/abs/1991ICRC....2...57A] [http://adsabs.harvard.edu/abs/1991ICRC....2...97A].
90. T.V. Danilova *et al.*, *Proc. 15th Int. Cosmic Ray Conf.*, Plovdiv, **8**, 129 (1977) [http://adsabs.harvard.edu/abs/1977ICRC....8..129D].
91. Yu. A. Fomin *et al.*, *Proc. 22nd Int. Cosmic Ray Conf.*, Dublin, **2**, 85 (1991) [http://adsabs.harvard.edu/abs/1991ICRC....2...85F].
92. M. Amenomori *et al.*, Astrophys. J. **461**, 408 (1996).
93. M. Nagano *et al.*, J. Phys. **G10**, 1295 (1984).
94. F. Arqueros *et al.*, Astron. & Astrophys. **359**, 682 (2000).
95. M.A.K. Glasmacher *et al.*, Astropart. Phys. **10**, 291 (1999).
96. T. Antoni *et al.* (Kascade Collab.), Astropart. Phys. **24**, 1 (2005).
97. M. Amenomori *et al.*, Astrophys. J. **268**, 1165 (2008).
98. W.D. Apel *et al.*, Phys. Rev. Lett. **107**, 171104 (2011).
99. M.G. Aartson *et al.*, (IceCube Collab.) arXiv:1307.3795v1(2013).
100. D.J. Bird *et al.*, (Fly's Eye Collab.), Astrophys. J. **424**, 491 (1994).
101. R. Abbasi *et al.*, (HiRes Collab.), Phys. Rev. Lett. **100**, 101101 (2008).
102. J. Abraham *et al.*, (Auger Collab.), Phys. Rev. Lett. **101**, 061101 (2008).
103. T. Abu-Zayad *et al.*, (Telescope Array Collab.), Astrophys. J. 768,L1(2013).
104. A. Aab *et al.*, (Auger Collab.), in *Proc. 33rd Int. Cosmic Ray Conf.,* Rio de Janiero, Brazil (arXiv:1307.5059v1).
105. M. Takeda *et al.*, (The AGASA Collab.), Astropart. Phys. **19**, 447 (2003).
106. V.S. Ptuskin *et al.*, Astron. & Astrophys. **268**, 726 (1993).
107. V.S. Berezinsky and S.I. Grigor'eva, Astron. & Astrophys. **199**, 1 (1988).
108. V. Berezinsky, A. Gazizov, and S. Grigorieva, Phys. Rev. **D74**, 043005 (2006).
109. R.U. Abbasi *et al.*, (The HiRes Collab.), Astrophys. J. **622**, 910 (2005).
110. M. Unger *et al.*, (Auger Collab.), *Proc. 30th Int. Cosmic Ray Conf.,* Merida, Mexico, 2007 (arXiv:0706.1495).
111. J. Abraham *et al.*, (Auger Collab.), *Proc. 31st Int. Cosmic Ray Conf.,* Lodz, Poland, 2009; (arXiv:0906.2319).
112. K. Greisen, Phys. Rev. Lett. **16**, 748 (1966).
113. G.T. Zatsepin and V.A. Kuz'min, Sov. Phys. JETP Lett. **4**, 78 (1966).
114. D. Allard *et al.*, Astron. & Astrophys. **443**, L29 (2005).
115. V.S. Berezinsky and G.T. Zatsepin, Phys. Lett. **B28**, 423 (1969).
116. R. Abbasi *et al.*, (IceCube Collab.) Phys. Rev. **D83**, 092003 (2011).
117. J. Abraham *et al.*, (Auger Collab.), Phys. Rev. Lett. **100**, 211101 (2008);
P Abreu *et al.* (Auger Collab.), in *Proc. 32nd Int. Cosmic Ray Conf.,* Bejing, China (arXiv:1107.4805).
118. I. Kravchenko *et al.*, (RICE Collab.), Phys. Rev. **D73**, 082002 (2006);
I. Kravchenko *et al.*, arXiv:1106.1164 (2011).
119. P. Gorham *et al.*, (ANITA Collab.), Phys. Rev. **D82**, 022004 (2010);
P. Gorham *et al.*, (ANITA Collab.),(arXiv:1011.5004).
120. R. Engel, D. Seckel, and T. Stanev, Phys. Rev. **D64**, 09310 (2001).
121. E. Waxman and J. Bahcall, Phys. Rev. **D59**, 023002 (1999).
122. R.U. Abbasi *et al.*, (HiRes Collab.), Astropart. Phys. **32**, 53 (2009).
123. M. Aartsen *et al.*, (IceCube Collab.) Phys. Rev. Lett. **111**, 021103 (2013).
124. M. Aartsen *et al.*, (IceCube Collab.) Science **342**, 1242856 (2013).

29. ACCELERATOR PHYSICS OF COLLIDERS

Revised August 2013 by M.J. Syphers (MSU) and F. Zimmermann (CERN).

29.1. Luminosity

This article provides background for the High-Energy Collider Parameter Tables that follow. The number of events, N_{exp}, is the product of the cross section of interest, σ_{exp}, and the time integral over the instantaneous *luminosity*, $\mathscr{L}$:

$$N_{exp} = \sigma_{exp} \times \int \mathscr{L}(t)dt. \tag{29.1}$$

Today's colliders all employ bunched beams. If two bunches containing n_1 and n_2 particles collide head-on with frequency $f_{\rm coll}$, a basic expression for the luminosity is

$$\mathscr{L} = f_{\rm coll}\frac{n_1 n_2}{4\pi\sigma_x\sigma_y} \tag{29.2}$$

where σ_x and σ_y characterize the rms transverse beam sizes in the horizontal (bend) and vertical directions. In this form it is assumed that the bunches are identical in transverse profile, that the profiles are Gaussian and independent of position along the bunch, and the particle distributions are not altered during bunch crossing. Nonzero beam crossing angles and long bunches will reduce the luminosity from this value.

Whatever the distribution at the source, by the time the beam reaches high energy, the normal form is a useful approximation as suggested by the σ-notation. In the case of an electron storage ring, synchrotron radiation leads to a Gaussian distribution in equilibrium, but even in the absence of radiation the central limit theorem of probability and the diminished importance of space charge effects produce a similar result.

The luminosity may be obtained directly by measurement of the beam properties in Eq. (29.2). For continuous measurements, an expression similar to Eq. (29.1) with N_{ref} from a known reference cross section, σ_{ref}, may be used to determine σ_{exp} according to $\sigma_{exp} = (N_{exp}/N_{ref})\sigma_{ref}$.

In the Tables, luminosity is stated in units of $\rm cm^{-2}s^{-1}$. Integrated luminosity, on the other hand is usually quoted as the inverse of the standard measures of cross section such as femtobarns and, recently, attobarns. Subsequent sections in this report briefly expand on the dynamics behind collider design, comment on the realization of collider performance in a selection of today's facilities, and end with some remarks on future possibilities.

29.2. Beam Dynamics

The first concern of beam dynamics is stability. While a reference particle proceeds along the design, or reference, trajectory other particles in the bunch are to remain close by. Assume that the reference particle carries a right-handed Cartesian coordinate system, with the z-coordinate pointed in the direction of motion along the reference trajectory. The independent variable is the distance s of the reference particle along this trajectory rather than time, and for simplicity this path is taken to be planar. The transverse coordinates are x and y, where $\{x, z\}$ defines the plane of the reference trajectory.

Several time scales are involved, and the approximations used in writing the equations of motion reflect that circumstance. All of today's high energy colliders are alternating gradient synchrotrons [1,2], and the shortest time scale is that associated with transverse motion, that is described in terms of betatron oscillations, so called because of their analysis for the betatron accelerator species years ago. The linearized equations of motion of a particle displaced from the reference particle are

$$\begin{aligned} x'' + K_x x = 0, \qquad & K_x \equiv \frac{q}{p}\frac{\partial B}{\partial x} + \frac{1}{\rho^2} \\ y'' + K_y y = 0, \qquad & K_y \equiv -\frac{q}{p}\frac{\partial B}{\partial x} \\ z' = -x/\rho & \end{aligned} \tag{29.3}$$

where the magnetic field $B(s)$ along the design trajectory is only in the y direction, contains only dipole and quadrupole terms, and is treated as static here. The radius of curvature due to the field on the reference orbit is ρ; z represents the longitudinal distance from the reference particle; p and q are the particle's momentum and charge, respectively. The prime denotes d/ds. The pair $(x,\ x')$ describes approximately-canonical variables. For more general cases (e.g. acceleration) one should use $(x,\ p_x)$ instead, where p_x denotes the transverse momentum in the x-direction.

The equations for x and y are those of harmonic oscillators but with a restoring force periodic in s; that is, they are instances of Hill's equation. The solution may be written in the form

$$\begin{aligned} x(s) &= A_x\sqrt{\beta_x}\,\cos\psi_x \\ x'(s) &= -\frac{A_x}{\sqrt{\beta_x}}\left[\alpha\cos\psi_x + \sin\psi_x\right] \end{aligned} \tag{29.4}$$

where A_x is a constant of integration, $\alpha \equiv -(1/2)d\beta_x(s)/ds$, and the envelope of the motion is modulated by the *amplitude function*, β_x. A solution of the same form describes the motion in y. The subscripts will be suppressed in the following discussion.

The amplitude function satisfies

$$2\beta\beta'' - \beta'^2 + 4\beta^2 K = 4, \tag{29.5}$$

and in a region free of magnetic field it should be noted that the solution of Eq. (29.5) is a parabola. Expressing A in terms of $x,\ x'$ yields

$$\begin{aligned} A^2 &= \gamma x^2 + 2\alpha x x' + \beta x'^2 \\ &= \frac{1}{\beta}\left[x^2 + (\alpha x + \beta x')^2\right] \end{aligned} \tag{29.6}$$

with $\gamma \equiv (1+\alpha^2)/\beta$. In a single pass system such as a linac, the *Courant-Snyder parameters* α, β, γ may be selected to match the $x,\ x'$ distribution of the input beam; in a recursive system, the parameters are usually defined by the structure rather than by the beam.

The relationships between the parameters and the structure may be seen by treatment of a simple *lattice* consisting of equally-spaced thin-lens quadrupoles whose magnetic-field gradients are equal in magnitude but alternating in sign. For this discussion, the weak focusing effects of the bending magnets may be neglected. The propagation of $X \equiv \{x, x'\}$ through a repetition period may be written $X_2 = MX_1$, with the matrix $M = FODO$ composed of the matrices

$$F = \begin{pmatrix} 1 & 0 \\ -1/f & 1 \end{pmatrix},\ D = \begin{pmatrix} 1 & 0 \\ 1/f & 1 \end{pmatrix},\ O = \begin{pmatrix} 1 & L \\ 0 & 1 \end{pmatrix},$$

where f is the magnitude of the focal length and L the lens spacing. Then

$$M = \begin{pmatrix} 1+\dfrac{L}{f} & 2L+\dfrac{L^2}{f} \\ -\dfrac{L}{f^2} & 1-\dfrac{L}{f}-\dfrac{L^2}{f^2} \end{pmatrix}. \tag{29.7}$$

The matrix for y is identical in form differing only by a change in sign of the terms linear in $1/f$. An eigenvector-eigenvalue analysis of the matrix M shows that the motion is stable provided $f > L/2$. While that criterion is easily met, in practice instability may be caused by many other factors, including the beam-beam interaction itself.

Standard focus-drift-defocus-drift, or *FODO*, cells such as characterized in simple form by Eq. (29.7) occupy most of the layout of a large collider ring and may be used to set the scale of the amplitude function and related phase advance. Conversion of Eq. (29.4) to a matrix form equivalent to Eq. (29.7) (but more generally valid, i.e. for any stable periodic linear motion) gives

$$M = \begin{pmatrix} C+\alpha S & \beta S \\ -\gamma S & C-\alpha S \end{pmatrix} \tag{29.8}$$

where $C \equiv \cos\Delta\psi$, $S \equiv \sin\Delta\psi$, and the relation between structure and amplitude function is specified by setting the values of the

latter to be the same at both ends of the cell. By comparison of Eq. (29.7) and Eq. (29.8) one finds $C = 1 - L^2/(2f^2)$, so that the choice $f = L/\sqrt{2}$ would give a phase advance $\Delta\psi$ of 90 degrees for the standard cell. The amplitude function would have a maximum at the focusing quadrupole of magnitude $\hat{\beta} = 2.7L$, illustrating the relationship of alternating gradient focusing amplitudes to relatively local aspects of the design. Other functionalities such as injection, extraction, and HEP experiments are included by lattice sections matched to the standard cell parameters (β, α) at the insertion points.

The phase advances according to $d\psi/ds = 1/\beta$; that is, β also plays the role of a local $\lambda/2\pi$, and the *tune*, ν, is the number of such oscillations per turn about the closed path. In the neighborhood of an interaction point (IP), the beam optics of the ring is configured so as to produce a narrow focus; the value of the amplitude function at this point is designated β^*.

The motion as it develops with s describes an ellipse in $\{x, x' \equiv dx/ds\}$ phase space, the area of which is πA^2, where A is the constant in Eq. (29.4). If the interior of that ellipse is populated by an ensemble of non-interacting particles, that area, given the name *emittance* and denoted by ε, would change only with energy. More precisely, for a beam with a Gaussian distribution in x, x', the area containing one standard deviation σ_x, divided by π, is used as the definition of emittance in the Tables:

$$\varepsilon_x \equiv \frac{\sigma_x^2}{\beta_x}\,, \tag{29.9}$$

with a corresponding expression in the other transverse direction, y. This definition includes 39% of the beam. For most of the entries in the Tables the standard deviation is used as the beam radius.

To complete the coordinates used to describe the motion, we take as the variable conjugate to z the fractional momentum deviation $\delta p/p$ from that of the reference particle. Radiofrequency electric fields in the s direction provide a means for longitudinal oscillations, and the frequency determines the bunch length. The frequency of this system appears in the Tables as does the rms value of $\delta p/p$ characterized as "energy spread" of the beam.

For HEP bunch length is a significant quantity for a variety of reasons, but in the present context if the bunch length becomes larger than β^* the luminosity is adversely affected. This is because β grows parabolically as one proceeds away from the interaction point and so the beam size increases thus lowering the contribution to the luminosity from such locations. This is often called the "hourglass" effect.

The other major external electromagnetic field interaction in the single particle context is the production of synchrotron radiation due to centripetal acceleration, given by the Larmor formula multiplied by a relativistic magnification factor of γ^4 [3]. In the case of electron rings this process determines the equilibrium emittance through a balance between radiation damping and excitation of oscillations, and further serves as a barrier to future higher energy versions in this variety of collider. A related phenomenon is beamstrahlung, i.e. the synchrotron radiation emitted during the collision in the field of the opposing beam, which is relevant for both linear colliders (where it degrades the luminosity spectrum) and future highest-energy circular colliders (where it limits the beam lifetime). For both types of colliders the beamstrahlung is mitigated by making the colliding beams as flat as possible ($\sigma_x^* \gg \sigma_y^*$).

A more comprehensive discussion of betatron oscillations, longitudinal motion, and synchrotron radiation is available in the 2008 version of the PDG review [4].

29.3. Impediments to High Luminosity

Eq. (29.2) can be recast in terms of emittances and amplitude functions as

$$\mathscr{L} = f\frac{n_1 n_2}{4\pi\sqrt{\epsilon_x\,\beta_x^*\,\epsilon_y\,\beta_y^*}}\ . \tag{29.10}$$

So to achieve high luminosity, all one has to do is make high population bunches of low emittance collide at high frequency at locations where the beam optics provides as low values of the amplitude functions as possible.

Such expressions as Eq. (29.10) of the luminosity are special cases of the more general forms available elsewhere [5], wherein the reduction due to crossing angle and other effects can be found. But while there are no fundamental limits to the process, there are certainly challenges. Here we have space to mention only a few of these. The beam-beam tune shift appears in the Tables. A bunch in beam 1 presents a (nonlinear) lens to a particle in beam 2 resulting in changes to the particle's transverse tune with a range characterized by the parameter [5]

$$\xi_{y,2} = \frac{\mu_0}{8\pi^2}\frac{q_1 q_2 n_1 \beta_{y,2}^*}{m_{A,2}\gamma_2\sigma_{y,1}(\sigma_{x,1}+\sigma_{y,1})} \tag{29.11}$$

where q_1 (q_2) denotes the particle charge of beam 1 (2) in units of the elementary charge, $m_{A,2}$ the mass of beam-2 particles, and μ_0 the vacuum permeability. The transverse oscillations are susceptible to resonant perturbations from a variety of sources such as imperfections in the magnetic guide field, so that certain values of the tune must be avoided. Accordingly, the tune spread arising from ξ is limited, but limited to a value difficult to predict. But a glance at the Tables shows that electrons are more forgiving than protons thanks to the damping effects of synchrotron radiation; the ξ-values for the former are about an order of magnitude larger than those for protons.

A subject of present intense interest is the *electron-cloud effect* [6,7]; actually a variety of related processes come under this heading. They typically involve a buildup of electron density in the vacuum chamber due to emission from the chamber walls stimulated by electrons or photons originating from the beam itself. For instance, there is a process closely resembling the multipacting effects familiar from radiofrequency system commissioning. Low energy electrons are ejected from the walls by photons from positron or proton beam-produced synchrotron radiation. These electrons are accelerated toward a beam bunch, but by the time they reach the center of the vacuum chamber the bunch has gone and so the now-energetic electrons strike the opposite wall to produce more secondaries. These secondaries are now accelerated by a subsequent bunch, and so on. Among the disturbances that this electron accumulation can produce is an enhancement of the tune spread within the bunch; the near-cancellation of bunch-induced electric and magnetic fields is no longer in effect.

If the luminosity of Eq. (29.10) is rewritten in terms of the beam-beam parameter, Eq. (29.11)), the emittance itself disappears. However, the emittance must be sufficiently small to realize a desired magnitude of beam-beam parameter, but once ξ_y reaches this limit, further lowering the emittance does not lead to higher luminosity.

For electron synchrotrons, radiation damping provides an automatic route to achieve a small emittance. In fact, synchrotron radiation is of key importance in the design and optimization of e^+e^- colliders. While vacuum stability and electron clouds can be of concern in the positron rings, synchrotron radiation along with the restoration of longitudinal momentum by the RF system has the positive effect of generating very small transverse beam sizes and small momentum spread. Further reduction of beam size at the interaction points using standard beam optics techniques and successfully contending with high beam currents has led to record luminosities in these rings, even exceeding those of hadron colliders. To maximize integrated luminosity the beam can be "topped off" by injecting new particles without removing existing ones – a feature difficult to imitate in hadron colliders.

For hadrons, particularly antiprotons, two inventions have played a prominent role. Stochastic cooling [8] was employed first to prepare beams for the $S\bar{p}pS$ and subsequently in the Tevatron and in RHIC [9,10]. Electron cooling [11] was also used in the Tevatron complex to great advantage. Further innovations are underway driven by the needs of potential future projects; these are noted in the final section.

29.4. Recent High Energy Colliders

Collider accelerator physics of course goes far beyond the elements of the preceding sections. In this and the following section elaboration is made on various issues associated with some of the recently operating colliders, particularly factors which impact integrated luminosity. The various colliders utilizing hadrons each have unique characteristics and are, therefore, discussed separately. As space is limited, general references are provided where much further information can be obtained. A more complete list of recent colliders and their parameters can be found in the High-Energy Collider Parameters tables.

29.4.1. ***Tevatron*** : [18] The first superconducting synchrotron in history, the Tevatron, was the highest energy collider for 25 years. Operation was terminated in September 2011, after delivering more than 10 fb^{-1} to the p-p collider experiments CDF and D0. The route to high integrated luminosity in the Tevatron was governed by the antiproton production rate, the turn-around time to produce another store, and the resulting optimization of store time. The proton and antiproton beams in the Tevatron circulated in a single vacuum pipe and thus were placed on separated orbits which wrapped around each other in a helical pattern outside of the interaction regions. Hence, long-range encounters played an important role here as well, with the 70 long-range encounters distributed about the synchrotron, and mitigation was limited by the available aperture. The Tevatron ultimately achieved luminosities a factor of 400 over its original design specification.

29.4.2. ***HERA*** : [21] HERA, operated between 1992 and 2007, delivered nearly 1 fb^{-1} of integrated luminosity to the electron-proton collider experiments H1 and ZEUS. HERA was the first high-energy lepton-hadron collider, and also the first facility to employ both applications of superconductivity: magnets and accelerating structures. The proton beams of HERA had a maximum energy of 920 GeV. The lepton beams (positrons or electrons) were provided by the existing DESY complex, and were accelerated to 27.5 GeV using conventional magnets. At collision a 4-times higher frequency RF system, compared with the injection RF, was used to generate shorter bunches, thus helping alleviate the hourglass effect at the collision points. The lepton beam naturally would become transversely polarized (within about 40 minutes) and "spin rotators" were implemented on either side of an IP to produce longitudinal polarization at the experiment.

29.4.3. ***LEP*** : [12] Installed in a tunnel of 27 km circumference, LEP was the largest circular e^+e^- collider built so far. It was operated from 1989 to 2000 with beam energies ranging from 45.6 to 104.5 GeV and a maximum luminosity of 10^{32} $\text{cm}^{-2}\text{s}^{-1}$, at 98 GeV, surpassing all relevant design parameters.

29.5. Present Collider Facilities

29.5.1. ***LHC*** : [13] The superconducting Large Hadron Collider is the world's highest energy collider. In 2012 operation for HEP has been at 4 TeV per proton. The beam energy is expected to reach 6.5 TeV in 2015. The current status is best checked at the Web site referenced in the heading of this subsection. To meet its luminosity goals the LHC will have to contend with a high beam current of 0.5 A, leading to stored energies of several hundred MJ per beam. Component protection, beam collimation, and controlled energy deposition are given very high priorities. Additionally, at energies of 5-7 TeV per particle, synchrotron radiation will move from being a curiosity to a challenge in a hadron accelerator for the first time. At design beam current the cryogenic system must remove roughly 7 kW due to synchrotron radiation, intercepted at a temperature of 4.5-20 K. As the photons are emitted their interactions with the vacuum chamber wall can generate free electrons, with consequent "electron cloud" development. Much care was taken to design a special liner for the chamber to mitigate this issue.

The two proton beams are contained in separate pipes throughout most of the circumference, and are brought together into a single pipe at the interaction points. The large number of bunches, and subsequent short bunch spacing, would lead to approximately 30 head-on collisions through 120 m of common beam pipe at each IP. Thus, a small crossing angle is employed, which reduces the luminosity by about 15%. Still, the bunches moving in one direction will have long-range encounters with the counter-rotating bunches and the resulting perturbations of the particle motion constitute a continued course of study. The luminosity scale is absolutely calibrated by the "van der Meer method" as was invented for the ISR [14], and followed by multiple, redundant luminosity monitors (see for example [15] and references therein). The Tables also show the performance anticipated for Pb-Pb collisions. The ALICE [16] experiment is designed to concentrate on these high energy-density phenomena, which are studied as well by ATLAS and CMS. The LHC can also provide Pb-p collisions as it did in early 2013.

In the coming years, an ambitious upgrade program, HL-LHC [17], has as its target an order-of-magnitude increase in luminosity through the utilization of Nb_3Sn superconducting magnets, superconducting compact "crab" cavities and luminosity leveling as key ingredients.

29.5.2. ***e^+e^- Rings*** : Asymmetric energies of the two beams have allowed for the enhancement of B-physics research and for interesting interaction region designs. As the bunch spacing can be quite short, the lepton beams sometimes pass through each other at an angle and hence have reduced luminosity. Recently, however, the use of high frequency "crab crossing" schemes has produced full restoration of the luminous region. KEK-B attained over 1 fb^{-1} of integrated luminosity in a single day, and its upgrade, SuperKEKB, is aiming for initial luminosities of 8×10^{35} $\text{cm}^{-2}\text{s}^{-1}$ [19]. A different collision approach, called "crab waist", which relies on special sextupoles together with a large crossing angle, has been successfully implemented at DAΦNE [20].

29.5.3. ***RHIC*** : [22] The Relativistic Heavy Ion Collider employs superconducting magnets, and collides combinations of fully-stripped ions such as H-H (p-p), U-U, Au-Au, Cu-Au, Cu-Cu, and d-Au. The high charge per particle (+79 for gold, for instance) makes intra-beam scattering of particles within the bunch a special concern, even for seemingly moderate bunch intensities. In 2012, 3-D stochastic cooling was successfully implemented in RHIC, reducing the transverse emittances of heavy ion beams by a factor of 5 [10]. Another special feature of accelerating heavy ions in RHIC is that the beams experience a "transition energy" during acceleration – a point where the derivative with respect to momentum of the revolution period is zero. This is more typical of low-energy accelerators, where the necessary phase jump required of the RF system is implemented rapidly and little time is spent near this condition. In the case of RHIC with heavy ions, the superconducting magnets do not ramp very quickly and the period of time spent crossing transition is long and must be dealt with carefully. For p-p operation the beams are always above their transition energy and so this condition is completely avoided.

RHIC is also distinctive in its ability to accelerate and collide polarized proton beams. As proton beam polarization must be maintained from its low-energy source, successful acceleration through the myriad of depolarizing resonance conditions in high energy circular accelerators has taken years to accomplish. An energy of 255 GeV per proton with $> 50\%$ final polarization per beam has been realized.

29.6. Future High Energy Colliders and Prospects

Recent accomplishments of particle physics have been obtained through high-energy and high-intensity experiments using hadron-hadron, lepton-lepton, and lepton-proton colliders. Following the discovery of the Higgs particle at the LHC and in view of ongoing searches for "new physics" and rare phenomena, various options are under discussions and development to pursue future particle-physics research at higher energy and with appropriate luminosity. This is the basis for various new projects, ideas, and R&D activities, which can only briefly be summarized here. Specifically, the following projects are noted: two approaches to an electron-positron linear collider, a larger 100-km circular tunnel supporting e^+e^- collisions up to 350 or 500 GeV in the centre of mass along with a 100-TeV proton-proton

Table 29.1: Tentative parameters of selected future high-energy colliders. Parameters of HL-LHC, ILC and CLIC can be found in the High-Energy Collider Parameters tables.

	LHeC	TLEP			VHE-LHC	μ collider	
Species	ep	e^+e^-			pp	$\mu^+\mu^-$	
Beam Energy (TeV)	0.06(e), 7 (p)	0.046	0.12	0.175	50	0.063	1.5
Circumference (km)	9(e), 27 (p)	100			100	0.3	4.5
Interaction regions	1	4			2 or 4	1	2
Estimated integrated luminosity per exp. (ab^{-1}/year)	0.1	6.1	0.5	0.1	0.2	0.001	0.44
Peak luminosity (10^{34} cm^{-2} s^{-1})	1	59	5	1.3	5	0.8	24
Time between collisions (μs)	0.025	0.04	2.0	2.0	0.05	1	15
Energy spread (rms, 10^{-3})	0.03 (e), 0.1(p)	1.3	3.0	2.3	0.1	0.04	1.0
Bunch length (rms, mm)	0.06 (e), 75.5(p)	2.9	2.1	0.8	80	63	5
IP beam size (μm)	4.1 (round)	121(H), 0.25(V)	61(H), 0.12(V)	45(H), 0.12(V)	9.4 (round)	75 (round)	3.0(round)
Injection energy (GeV)	1(e), 450(p)	on energy (topping off)			3000	on energy (topping off)	
Transverse emittance (rms, nm)	0.43(e), 0.34(p)	29(II), 0.06(V)	7.5(II), 0.015(V)	2.0(II), 0.002(V)	0.08 (round)	335	1.8
β^*, amplitude function at interaction point (cm)	4.7(e), 5.0(p)	50(H), 0.1(V)	50(H), 0.1(V)	100(H), 0.1(V)	1.1 (round)	1.7	0.5
Beam-beam tune shift per crossing (10^{-3})	$-$(e), 0.4(p)	68	94	57	5	20	90
RF frequency (MIIz)	800(e), 400(p)	800			400 or 800	805	
Particles per bunch (10^{10})	0.25(e), 22(p)	40	37	8.8	19.6	400	200
Bunches per beam	$-$(e), 2808	7500	167	160	5265	1	1
Average beam current (mA)	16(e), 883(p)	1440	29.8	6.7	495	640	21
Length of standard cell (m)	52.4(e arc), 107(p)	300	100	50	200	N/A	175
Phase advance per cell (deg)	310 (eH), 90(e V), 90 (p)	90			90	N/A	300
Peak magnetic field (T)	0.264(e), 8.33(p)	0.011	0.033	0.049	15	10	10
Polarization (%)	90(e), 0(p)	60	0	0	0	20 (energy calibration)	
SR power loss/beam (MW)	30(e), 0.01(p)	50			2.1	3×10^{-5}	0.006
Novel technology	high-energy ERL	—			high-field magnets	ionization cooling, high-power target	

collider, a muon ring collider, and potential use of plasma acceleration and other advanced schemes. Complementary studies are ongoing of a high-energy lepton-hadron collider bringing into collision a 60-GeV electron beam from an energy-recovery linac with the 7-TeV protons circulating in the LHC (LHeC) [23,24], and of $\gamma\gamma$ collider Higgs factories based on recirculating electron linacs (e.g. SAPPHiRE at CERN [24], HFiTT at FNAL). Tentative parameters of some of the colliders discussed, or mentioned, in this section are summarized in Table 29.1.

29.6.1. ***Electron-Positron Linear Colliders*** : For three decades efforts have been devoted to develop high-gradient technology e^+e^- colliders in order to overcome the synchrotron radiation limitations of circular e^+e^- machines in the TeV energy range.

The primary challenge confronting a high energy, high luminosity single pass collider design is the power requirement, so that measures must be taken to keep the demand within bounds as illustrated in a transformed Eq. (29.2) [25]:

$$\mathscr{L} \approx \frac{137}{8\pi r_e}\,\frac{P_{\rm wall}}{E_{cm}}\,\frac{\eta}{\sigma_y^*}\,N_\gamma\,H_D\,. \qquad (29.12)$$

wall-plug power into beam power $P_b = f_{\rm coll} n E_{cm}$, E_{cm} the cms energy, n ($= n_1 = n_2$) the bunch population, and σ_y^* the vertical rms beam size at the collision point. In formulating Eq. (29.12) the number of beamstrahlung photons emitted per $e^\pm$, was approximated as $N_\gamma \approx 2\alpha r_e n/\sigma_x^*$. The management of $P_{\rm wall}$ leads to an upward push on the bunch population n with an attendant rise in the energy radiated due to the electromagnetic field of one bunch acting on the particles of the other. Keeping a significant fraction of the luminosity close to the nominal energy represents a design goal, which is met if N_γ does not exceed a value of about 1. A consequence is the use of flat beams, where N_γ is managed by the beam width, and luminosity adjusted by the beam height, thus the explicit appearance of the vertical beam size σ_y^*. The final factor in Eq. (29.12), H_D, represents the enhancement of luminosity due to the pinch effect during bunch crossing (the effect of which has been neglected in the expression for N_γ).

Here, $P_{\rm wall}$ is the total wall-plug power of the collider, $\eta \equiv P_b/P_{\rm wall}$ the efficiency of converting The approach designated by the International Linear Collider (ILC) is presented in the Tables, and the contrast with the collision-point parameters of the circular colliders is striking, though reminiscent in direction of those of the SLAC Linear Collider. The ILC *Reference Design Report* [26] has a baseline cms energy of 500 GeV with upgrade provision for 1 TeV, and luminosity comparable to the LHC. The ILC is based on superconducting accelerating structures of the 1.3 GHz TESLA variety.

At CERN, a design effort is underway on the Compact Linear Collider (CLIC), each linac of which is itself a two-beam accelerator, in that a high energy, low current beam is fed by a low energy, high current driver [27]. The CLIC design employs normal conducting 12 GHz accelerating structures at a gradient of 100 MeV/m, some three times the current capability of the superconducting ILC cavities. The design cms energy is 3 TeV.

29.6.2. ***Future Circular Colliders*** : The discovery, in 2012, of the Higgs boson at the LHC has stimulated interest in constructing a large circular tunnel which could host a variety of energy-frontier machines, including high-energy electron-positron, proton-proton, and lepton-hadron colliders. Such projects are under study at CERN (VHE-LHC/TLEP) and in China (CEPC), following earlier proposals for a Very Large Hadron Collider (VLHC) [28] and a Very Large Lepton Collider (VLLC) in the US, which would have been housed in

the same 230-km long tunnel.

The maximum beam energy of a hadron collider is directly proportional to the magnetic field and to the ring circumference. The LHC magnets, based on Nb-Ti superconductor, achieve a maximum operational field of 8.33 T. The HL-LHC project develops the technology of higher field Nb_3Sn magnets as well as cables made from high-temperature superconductor (HTS). Nb_3Sn dipoles could ultimately reach an operational field around 15 T, and HTS inserts, requiring new engineering materials and substantial dedicated R&D, could boost this further. A cost-effective hybrid magnet design incorporating Nb-Ti, two types of Nb_3Sn, and an inner layer of HTS could provide a field of 20 T [29]. If installed in the LHC tunnel, such dipoles would increase the beam energy by a factor 2.5 compared with the LHC. The vacuum system for such a machine has not yet been designed. Warm photon absorbers installed in the magnet interconnections are one of the proposed approaches, requiring experimental tests for design validation.

Further substantial increases in collision energy are possible only with a larger tunnel. The Very High Energy LHC (VHE-LHC) [30] is based on a new tunnel of 80–100 km circumference, which would allow exploring energies up to 100 TeV in the centre of mass with proton-proton collisions, using 15–20 T magnets. This new tunnel could also accommodate a high-luminosity circular e^+e^- Higgs factory (TLEP) as well as a lepton-hadron collider (VHE-LHeC).

In order to serve as a Higgs factory a new circular e^+e^- collider needs to achieve a cms energy of at least 240 GeV. TLEP [31], installed in the 80–100 km tunnel of the VHE-LHC, could reach even higher energies, e.g. 350 GeV cms for $t\bar{t}$ production, or up to 500 GeV for ZHH and $Ht\bar{t}$ physics. At these energies, the luminosity, limited by the synchrotron radiation power, would still be close to 10^{34} $\mathrm{cm}^{-2}\mathrm{s}^{-1}$ at each of four collision points. At lower energies (Z pole and WW threshold) TLEP could deliver up to two orders of magnitude higher luminosities, and also profit from radiative self polarization for precise energy calibration. The short beam lifetime at the high target luminosity, due to radiative Bhabha scattering, requires TLEP to be constructed as a double ring, where the collider ring operating at constant energy is complemented by a second injector ring installed in the same tunnel to "top off" the collider current. Beamstrahlung, i.e. synchrotron radiation emitted during the collision in the field of the opposing beam, introduces an additional beam lifetime limitation depending on momentum acceptance (so that achieving sufficient off-momentum dynamic aperture becomes one of the design challenges), as well as some bunch lengthening.

29.6.3. ***Muon Collider*** : The muon to electron mass ratio of 210 implies less concern about synchrotron radiation by a factor of about 2×10^9 and its 2.2 μs lifetime means that it will last for some $150B$ turns in a ring about half of which is occupied by bend magnets with average field B (Tesla). Design effort became serious in the mid 1990s and a collider outline emerged quickly.

Removal of the synchrotron radiation barrier reduces the scale of a muon collider facility to a level compatible with on-site placement at existing accelerator laboratories. The Higgs production cross section in the s-channel is enhanced by a factor of $(m_\mu/m_e)^2$ compared to that in e^+e^- collisions. And a neutrino factory could potentially be realized in the course of construction [32].

The challenges to luminosity achievement are clear and amenable to immediate study: targeting, collection, and emittance reduction are paramount, as well as the bunch manipulation required to produce $> 10^{12}$ muons per bunch without emittance degradation. The proton source needs to deliver a beam power of several MW, collection would be aided by magnetic fields common on neutron stars (though scaled back for application on earth), and the emittance requirements have inspired fascinating investigations into phase space manipulations that are finding applications in other facilities. The status was summarized in a White Paper submitted to "Snowmass 2013" [33].

29.6.4. ***Plasma Acceleration and Other Advanced Concepts*** : At the 1956 CERN Symposium, a paper by Veksler, in which he suggested acceleration of protons to the TeV scale using a bunch of electrons, anticipated current interest in plasma acceleration [34]. A half-century later this is more than a suggestion, with the demonstration, as a striking example, of electron energy doubling from 42 to 84 GeV over 85 cm at SLAC [35].

Whether plasma acceleration will find application in an HEP facility is not yet clear, given the necessity of staging and phase-locking acceleration in multiple plasma chambers. Maintaining beam quality and beam position as well as the acceleration of high-repetition bunch trains are also primary feasibility issues, addressed by active R&D. For recent discussions of parameters for a laser-plasma based electron positron collider, see, for example, relevant papers in an Advanced Accelerator Concepts Workshop [36].

Additional approaches aiming at accelerating gradients higher, or much higher, than those achievable with conventional metal cavities include the use of dielectric materials and, for the long-term future, crystals. Combining several innovative ideas, even a linear crystal muon collider driven by X-ray lasers has been proposed [37].

References:

1. E. D. Courant and H. S. Snyder, Ann. Phys. **3**, 1 (1958). This is the classic article on the alternating gradient synchrotron.
2. A.W. Chao, K.H. Mess, M. Tigner and F. Zimmermann, *eds.*, *Handbook of Accelerator Physics and Engineering*, World Science Publishing Co. (Singapore, 2nd edition, 2013.), Sec. 2.1, 2.2.
3. H. Wiedemann, *Handbook of Accelerator Physics and Engineering*, *ibid*, Sec. 3.1.
4. C. Amsler *et al.* (Particle Data Group), Physics Letters **B667**, 1 (2008) `http://pdg.lbl.gov/2008/reviews/contents_sports.html`.
5. M. A. Furman and M. S. Zisman, *Handbook of Accelerator Physics and Engineering, ibid*, Sec. 4.1.
6. M.A. Furman, *Handbook of Accelerator Physics and Engineering*, *ibid*, Sec. 2.4.14.
7. `http://ab-abp-rlc.web.cern.ch/ab-abp-rlc-ecloud/`. This site contains many references as well as videos of electron cloud simulations.
8. D. Möhl *et al.*, Phys. Rep. **58**, 73 (1980).
9. M. Blaskiewicz, J.M. Brennan, and K. Mernick, Phys. Rev. Lett. **105**, 094801 (2010).
10. J. M. Brennan, M. Blaskiewicz, K. Mernick, "Stochastic Cooling in RHIC," *Proc. IPAC'12, New Orleans.*
11. G.I. Budker, *Proc. Int. Symp. Electron & Positron Storage Rings*, (1966).
12. R. Assmann *et al.*, Nucl. Phys. B, Proc. Suppl. **9**, 17–31 (2002).
13. Detailed information from the multi-volume design report to present status may be found at `http://lhc.web.cern.ch/lhc/`.
14. S. van der Meer, "Calibration of the Effective Beam Height at the ISR," CERN-ISR-PO/68-31 (1968).
15. ATLAS Collaboration, "Improved Luminosity Determination in pp Collisions at $\sqrt{s} = 7$ TeV using the ATLAS Detector at the LHC," Eur. Phys. J. **C73**, 2518 (2013).
16. `http://aliceinfo.cern.ch/Public/Welcome.html`.
17. `http://hilumilhc.web.cern.ch`.
18. H.T. Edwards, "The Tevatron Energy Doubler: A Superconducting Accelerator," Ann. Rev. Nucl. Part. Sci. **35**, 605 (1985).
19. An overview of electron-positron colliders past and present may be found in ICFA Beam Dynamics Newsletter No. 46, April 2009, `http://www-bd.fnal.gov/icfabd/`. A day-by-day account of the luminosity progress at KEK-B may be found at `http://belle.kek.jp/bdocs/lumi_belle.png`.
20. M. Zobov *et al.*, "Test of 'Crab-Waist' Collisions at the DAΦNE Φ Factory," Phys. Rev. Lett. **104**, 174801 (2010).
21. Brief history at `http://en.wikipedia.org/wiki/Hadron_Elektron_Ring_Anlage`.
22. M. Harrison, T. Ludlam, and S. Ozaki, *eds.*, "Special Issue: The Relativisitic Heavy Ion Collider Project: RHIC and its Detectors," Nucl. Inst. & Meth. A**499** (2003).
23. J. L. Abelleira *et al.*, J. Phys. G **39**, 075001 (2012).

24. J. L. Abelleira *et al.*, http://arxiv.org/pdf/1211.5102v1.pdf (2012).
25. F. Zimmermann, "Tutorial on Linear Colliders," AIP Conf. Proc. **592**, 494 (2001).
26. http://www.linearcollider.org/ILC/Publications/Technical-Design-Report.
27. http://lcd.web.cern.ch/lcd/CDR/CDR.html.
28. http://vlhc.org.
29. L. Rossi, E. Todesco, arXiv:1108:1619, in *Proc. HE-LHC10*, Malta, 14–16 October 2010, *CERN Yellow Report CERN-2011-003*.
30. C.O. Dominguez, F. Zimmermann, "Beam Parameters and Luminosity Time Evolution for an 80-km VHE-LHC," *Proc. IPAC'13 Shanghai*.
31. http://www.cern.ch/tlep.
32. http://en.wikipedia.org/wiki/Neutrino_Factory.
33. J.P. Delahaye *et al.*, http://arxiv.org/pdf/1308.0494v1.pdf (2013).
34. V.I. Veksler, CERN Symposium on High Energy Accelerators and Pion Physics, 11–23 June 1956, p. 80. This paper may be downloaded from http://cdsweb.cern.ch/record/1241563?ln=en.
35. I. Blumenfeld *et al.*, Nature **445**, 741 (2007).
36. Advanced Accelerator Concepts, edited by R. Zgadzaj, E. Gaul and M. Downer, *AIP Conference Proceedings 1507*, Austin TX 10 – 15 June 2012.
37. V. Shiltsev, Phys. Usp. **55**, 965 (2012).

HIGH-ENERGY COLLIDER PARAMETERS: e^+e^- Colliders (I)

Updated in September 2013 with numbers received from representatives of the colliders (contact J. Beringer, LBNL). The table shows parameter values as achieved by July 1, 2013. Quantities are, where appropriate, r.m.s.; unless noted otherwise, energies refer to beam energy; H and V indicate horizontal and vertical directions; s.c. stands for superconducting. Parameters for the defunct SPEAR, DORIS, PETRA, PEP, TRISTAN, and VEPP-2M colliders may be found in our 1996 edition (Phys. Rev. **D54**, 1 July 1996, Part I).

	VEPP-2000 (Novosibirsk)	VEPP-4M (Novosibirsk)	BEPC (China)	BEPC-II (China)	DAΦNE (Frascati)
Physics start date	2010	1994	1989	2008	1999
Physics end date	—	—	2005	—	—
Maximum beam energy (GeV)	1.0	6	2.5	1.89 (2.3 max)	0.510
Delivered integrated luminosity per exp. (fb^{-1})	0.030	0.027	0.11	3.74	$\approx$ 4.7 in 2001-2007 2.7 w/crab-waist
Luminosity (10^{30} $cm^{-2}s^{-1}$)	100	20	12.6 at 1.843 GeV 5 at 1.55 GeV	649	453
Time between collisions (μs)	0.04	0.6	0.8	0.008	0.0027
Full crossing angle (μ rad)	0	0	0	2.2×10^4	5×10^4
Energy spread (units 10^{-3})	0.64	1	0.58 at 2.2 GeV	0.52	0.40
Bunch length (cm)	4	5	$\approx$ 5	$\approx$ 1.5	low current: 1 at 15mA: 2
Beam radius (10^{-6} m)	125 (round)	H: 1000 V: 30	H: 890 V: 37	H: 380 V: 5.7	H: 260 V: 4.8
Free space at interaction point (m)	$\pm$1	$\pm$2	$\pm$2.15	$\pm$0.63	$\pm$0.295
Luminosity lifetime (hr)	continuous	2	7–12	1.5	0.2
Turn-around time (min)	continuous	18	32	26	2 (topping up)
Injection energy (GeV)	0.2–1.0	1.8	1.55	1.89	on energy
Transverse emittance ($10^{-9}\pi$ rad-m)	H: 250 V: 250	H: 200 V: 20	H: 660 V: 28	H: 144 V: 2.2	H: 260 V: 2.6
β^*, amplitude function at interaction point (m)	H: 0.06 – 0.11 V: 0.06 – 0.10	H: 0.75 V: 0.05	H: 1.2 V: 0.05	H: 1.0 V: 0.015	H: 0.26 V: 0.009
Beam-beam tune shift per crossing (units 10^{-4})	H: 750 V: 750	500	350	327	440
RF frequency (MHz)	172	180	199.53	499.8	356
Particles per bunch (units 10^{10})	16	15	20 at 2 GeV 11 at 1.55 GeV	4.1	e^-: 3.2 e^+: 2.1
Bunches per ring per species	1	2	1	88	100 to 105 (120 buckets)
Average beam current per species (mA)	150	80	40 at 2 GeV 22 at 1.55 GeV	725	e^-: 1500 e^+: 1000
Circumference or length (km)	0.024	0.366	0.2404	0.23753	0.098
Interaction regions	2	1	2	1	1
Magnetic length of dipole (m)	1.2	2	1.6	outer ring: 1.6 inner ring: 1.41	outer ring: 1.2 inner ring: 1
Length of standard cell (m)	12	7.2	6.6	outer ring: 6.6 inner ring: 6.2	n/a
Phase advance per cell (deg)	H: 738 V: 378	65	$\approx$ 60	60–90 non-standard cells	—
Dipoles in ring	8	78	40 + 4 weak	84 + 8 weak	8
Quadrupoles in ring	20	150	68	134+2 s.c.	48
Peak magnetic field (T)	2.4	0.6	0.903 at 2.8 GeV	outer ring: 0.677 inner ring: 0.766	1.2

HIGH-ENERGY COLLIDER PARAMETERS: e^+e^- Colliders (II)

Updated in September 2013 with numbers received from representatives of the colliders (contact J. Beringer, LBNL). For existing colliders, the table shows parameter values as achieved by July 1, 2013. For future colliders, design values are quoted. Quantities are, where appropriate, r.m.s.; unless noted otherwise, energies refer to beam energy; H and V indicate horizontal and vertical directions; s.c. stands for superconducting.

	CESR (Cornell)	CESR-C (Cornell)	LEP (CERN)	SLC (SLAC)	ILC (TBD)	CLIC (TBD)
Physics start date	1979	2002	1989	1989	TBD	TBD
Physics end date	2002	2008	2000	1998	—	—
Maximum beam energy (GeV)	6	6	100 - 104.6	50	250 (upgradeable to 500)	1500 (first phase: 175)
Delivered integrated luminosity per experiment (fb^{-1})	41.5	2.0	0.221 at Z peak 0.501 at 65 – 100 GeV 0.275 at >100 GeV	0.022	—	—
Luminosity (10^{30} $cm^{-2}s^{-1}$)	1280 at 5.3 GeV	76 at 2.08 GeV	24 at Z peak 100 at > 90 GeV	2.5	1.5×10^4	6×10^4
Time between collisions (μs)	0.014 to 0.22	0.014 to 0.22	22	8300	0.55†	0.0005‡
Full crossing angle (μ rad)	±2000	±3300	0	0	14000	20000
Energy spread (units 10^{-3})	0.6 at 5.3 GeV	0.82 at 2.08 GeV	0.7→1.5	1.2	1	3.4
Bunch length (cm)	1.8	1.2	1.0	0.1	0.03	0.0044
Beam radius (μm)	H: 460 V: 4	H: 340 V: 6.5	H: 200 → 300 V: 2.5 → 8	H: 1.5 V: 0.5	H: 0.474 V: 0.0059	H: 0.045 * V: 0.0009
Free space at interaction point (m)	±2.2 (±0.6 to REC quads)	±2.2 (±0.3 to PM quads)	±3.5	±2.8	±3.5	±3.5
Luminosity lifetime (hr)	2–3	2–3	20 at Z peak 10 at > 90 GeV	—	n/a	n/a
Turn-around time (min)	5 (topping up)	1.5 (topping up)	50	120 Hz (pulsed)	n/a	n/a
Injection energy (GeV)	1.8–6	1.5–6	22	45.64	n/a	n/a
Transverse emittance ($10^{-9}\pi$ rad-m)	H: 210 V: 1	H: 120 V: 3.5	H: 20–45 V: 0.25 → 1	H: 0.5 V: 0.05	H: 0.02 V: 7×10^{-5}	H: 2.2×10^{-4} V: 6.8×10^{-6}
β^*, amplitude function at interaction point (m)	H: 1.0 V: 0.018	H: 0.94 V: 0.012	H: 1.5 V: 0.05	H: 0.0025 V: 0.0015	H: 0.01 V: 5×10^{-4}	H: 0.0069 V: 6.8×10^{-5}
Beam-beam tune shift per crossing (10^{-4}) or disruption	H: 250 V: 620	e^-: 420 (H), 280 (V) e^+: 410 (H), 270 (V)	830	0.75 (H) 2.0 (V)	n/a	7.7
RF frequency (MHz)	500	500	352.2	2856	1300	11994
Particles per bunch (units 10^{10})	1.15	4.7	45 in collision 60 in single beam	4.0	2	0.37
Bunches per ring per species	9 trains of 5 bunches	8 trains of 3 bunches	4 trains of 1 or 2	1	1312	312 (in train)
Average beam current per species (mA)	340	72	4 at Z peak 4→6 at > 90 GeV	0.0008	6 (in pulse)	1205 (in train)
Beam polarization (%)	—	—	55 at 45 GeV 5 at 61 GeV	e^-: 80	e^-: > 80% e^+: > 60%	e^-: 70% at IP
Circumference or length (km)	0.768	0.768	26.66	1.45 +1.47	31	48
Interaction regions	1	1	4	1	1	1
Magnetic length of dipole (m)	1.6–6.6	1.6–6.6	11.66/pair	2.5	n/a	n/a
Length of standard cell (m)	16	16	79	5.2	n/a	n/a
Phase advance per cell (deg)	45–90 (no standard cell)	45–90 (no standard cell)	102/90	108	n/a	n/a
Dipoles in ring	86	84	3280 + 24 inj. + 64 weak	460+440	n/a	n/a
Quadrupoles in ring	101 + 4 s.c.	101 + 4 s.c.	520 + 288 + 8 s.c.	—	n/a	n/a
Peak magnetic field (T)	0.3 / 0.8 at 8 GeV	0.3 / 0.8 at 8 GeV, 2.1 wigglers at 1.9 GeV	0.135	0.597	n/a	n/a

†Time between bunch trains: 200ms.

‡Time between bunch trains: 20ms.

*Effective beam size including non-linear and chromatic effects.

HIGH-ENERGY COLLIDER PARAMETERS: e^+e^- Colliders (III)

Updated in September 2013 with numbers received from representatives of the colliders (contact J. Beringer, LBNL). For existing colliders, the table shows parameter values as achieved by July 1, 2013. For future colliders, design values are quoted. Quantities are, where appropriate, r.m.s.; unless noted otherwise, energies refer to beam energy; H and V indicate horizontal and vertical directions; s.c. stands for superconducting.

	KEKB (KEK)	PEP-II (SLAC)	SuperKEKB (KEK)
Physics start date	1999	1999	2015
Physics end date	2010	2008	—
Maximum beam energy (GeV)	e^-: 8.33 (8.0 nominal) e^+: 3.64 (3.5 nominal)	e^-: 7–12 (9.0 nominal) e^+: 2.5–4 (3.1 nominal)	e^-: 7 e^+: 4
Delivered integrated luminosity per exp. (fb^{-1})	1040	557	—
Luminosity (10^{30} $cm^{-2}s^{-1}$)	21083	12069 (design: 3000)	8×10^5
Time between collisions (μs)	0.00590 or 0.00786	0.0042	0.004
Full crossing angle (μ rad)	$\pm 11000^\dagger$	0	± 41500
Energy spread (units 10^{-3})	0.7	e^-/e^+: 0.61/0.77	e^-/e^+: 0.64/0.81
Bunch length (cm)	0.65	e^-/e^+: 1.1/1.0	e^-/e^+: 0.5/0.6
Beam radius (μm)	H: 124 (e^-), 117 (e^+) V: 1.9	H: 157 V: 4.7	e^-: 11 (H), 0.062 (V) e^+: 10 (H), 0.048 (V)
Free space at interaction point (m)	+0.75/−0.58 (+300/−500) mrad cone	±0.2, ±300 mrad cone	e^- : +1.20/ − 1.28, e^+ : +0.78/ − 0.73 (+300/−500) mrad cone
Luminosity lifetime (hr)	continuous	continuous	continuous
Turn-around time (min)	continuous	continuous	continuous
Injection energy (GeV)	e^-/e^+ : 8.0/3.5 (nominal)	e^-/e^+ : 9.0/3.1 (nominal)	e^-/e^+ : 7/4
Transverse emittance ($10^{-9}\pi$ rad-m)	e^-: 24 (57*) (H), 0.61 (V) e^+: 18 (55*) (H), 0.56 (V)	e^-: 48 (H), 1.8 (V) e^+: 24 (H), 1.8 (V)	e^-: 4.6 (H), 0.013 (V) e^+: 3.2 (H), 0.0086 (V)
β^*, amplitude function at interaction point (m)	e^-: 1.2 (0.27*) (H), 0.0059 (V) e^+: 1.2 (0.23*) (H), 0.0059 (V)	e^-: 0.50 (H), 0.012 (V) e^+: 0.50 (H), 0.012 (V)	e^-: 0.025 (H), 3×10^{-4} (V) e^+: 0.032 (H), 2.7×10^{-4} (V)
Beam-beam tune shift per crossing (units 10^{-4})	e^-: 1020 (H), 900 (V) e^+: 1270 (H), 1290 (V)	e^-: 703 (H), 498 (V) e^+: 510 (H), 727 (V)	e^-: 12 (H), 807 (V) e^+: 28 (H), 881 (V)
RF frequency (MHz)	508.887	476	508.887
Particles per bunch (units 10^{10})	e^-/e^+: 4.7/6.4	e^-/e^+: 5.2/8.0	e^-/e^+: 6.53/9.04
Bunches per ring per species	1585	1732	2500
Average beam current per species (mA)	e^-/e^+: 1188/1637	e^-/e^+: 1960/3026	e^-/e^+: 2600/3600
Beam polarization (%)	—	—	—
Circumference or length (km)	3.016	2.2	3.016
Interaction regions	1	1	1
Magnetic length of dipole (m)	e^-/e^+ : 5.86/0.915	e^-/e^+: 5.4/0.45	e^-/e^+ : 5.9/4.0
Length of standard cell (m)	e^-/e^+ : 75.7/76.1	15.2	e^-/e^+ : 75.7/76.1
Phase advance per cell (deg)	450	e^-/e^+: 60/90	450
Dipoles in ring	e^-/e^+ : 116/112	e^-/e^+: 192/192	e^-/e^+ : 116/112
Quadrupoles in ring	e^-/e^+ : 452/452	e^-/e^+: 290/326	e^-/e^+ : 466/460
Peak magnetic field (T)	e^-/e^+ : 0.25/0.72	e^-/e^+: 0.18/0.75	e^-/e^+ : 0.22/0.19

†KEKB was operated with crab crossing from 2007 to 2010.

*With dynamic beam-beam effect.

HIGH-ENERGY COLLIDER PARAMETERS: ep, $\overline{p}p$, pp Colliders

Updated in September 2013 with numbers received from representatives of the colliders (contact J. Beringer, LBNL). The table shows parameter values as achieved by July 1, 2013. For LHC, the parameters expected at the ATLAS and CMS experiments for running in 2015 and design values for a high-luminosity upgrade (HL-LHC) are also given. Quantities are, where appropriate, r.m.s.; unless noted otherwise, energies refer to beam energy; H and V indicate horizontal and vertical directions; s.c. stands for superconducting; pk and avg denote peak and average values.

	HERA (DESY)	TEVATRON* (Fermilab)	RHIC (Brookhaven)	LHC (CERN)		
Physics start date	1992	1987	2001	2009	2015 (expected)	2023 (HL-LHC)
Physics end date	2007	2011	—	—		
Particles collided	ep	$p\overline{p}$	pp (polarized)	pp		
Maximum beam energy (TeV)	e: 0.030 p: 0.92	0.980	0.255 57% polarization	4.0	6.5	7.0
Maximum delivered integrated luminosity per exp. (fb^{-1})	0.8	12	0.18 at 100 GeV 0.75 at 250/255 GeV	23.3 at 4.0 TeV 6.1 at 3.5 TeV	40/y to 60/y	250/y
Luminosity (10^{30} $\text{cm}^{-2}\text{s}^{-1}$)	75	431	215 (pk) 132 (avg)	7.7×10^3	$(1-2) \times 10^4$	5.0×10^4 (leveled)
Time between collisions (ns)	96	396	107	49.90	24.95	24.95
Full crossing angle (μ rad)	0	0	0	290	298	590
Energy spread (units 10^{-3})	e: 0.91 p: 0.2	0.14	0.15	0.1445	0.105	0.123
Bunch length (cm)	e: 0.83 p: 8.5	p: 50 $\bar{p}$: 45	60	9.4	9	9
Beam radius (10^{-6} m)	e: $110(H), 30(V)$ p: $111(H), 30(V)$	p: 28 $\bar{p}$: 16	90	18.8	11.1	7.4
Free space at interaction point (m)	± 2	± 6.5	16	38	38	38
Initial luminosity decay time, $-L/(dL/dt)$ (hr)	10	6 (avg)	5.5	≈ 6	≈ 6	≈ 6 (leveled)
Turn-around time (min)	e: 75, p: 135	90	150	180	240	240
Injection energy (TeV)	e: 0.012 p: 0.040	0.15	0.023	0.450	0.450	0.450
Transverse emittance ($10^{-9}\pi$ rad-m)	e: $20(H), 3.5(V)$ p: $5(H), 5(V)$	p: 3 $\bar{p}$: 1	15	0.59	0.28	0.36
β^*, ampl. function at interaction point (m)	e: $0.6(H), 0.26(V)$ p: $2.45(H), 0.18(V)$	0.28	0.65	0.6	0.45	0.15
Beam-beam tune shift per crossing (units 10^{-4})	e: $190(H), 450(V)$ p: $12(H), 9(V)$	p: 120 $\bar{p}$: 120	70	72	79	110
RF frequency (MHz)	e: 499.7 p: 208.2/52.05	53	accel: 9 store: 28	400.8	400.8	400.8
Particles per bunch (units 10^{10})	e: 3 p: 7	p: 26 $\bar{p}$: 9	18.5	16	12	22
Bunches per ring per species	e: 189 p: 180	36	111	1380	2508	2760
Average beam current per species (mA)	e: 40 p: 90	p: 70 $\bar{p}$: 24	257	400	540	1200
Circumference (km)	6.336	6.28	3.834	26.659		
Interaction regions	2 colliding beams 1 fixed target (e beam)	2 high $\mathscr{L}$	6 total, 2 high $\mathscr{L}$	4 total, 2 high $\mathscr{L}$		
Magnetic length of dipole (m)	e: 9.185 p: 8.82	6.12	9.45	14.3		
Length of standard cell (m)	e: 23.5 p: 47	59.5	29.7	106.90		
Phase advance per cell (deg)	e: 60 p: 90	67.8	84	90		
Dipoles in ring	e: 396 p: 416	774	192 per ring + 12 common	1232 main dipoles		
Quadrupoles in ring	e: 580 p: 280	216	246 per ring	482 2-in-1 24 1-in-1		
Magnet type	e: C-shaped p: s.c., collared, cold iron	s.c. $\cos\theta$ warm iron	s.c. $\cos\theta$ cold iron	s.c. 2 in 1 cold iron		
Peak magnetic field (T)	e: 0.274, p: 5	4.4	3.5	8.3		

*Additional TEVATRON parameters: $\overline{p}$ source accum. rate: $25{\times}10^{10}$ hr^{-1}; max. no. of $\overline{p}$ stored: $3.4{\times}10^{12}$ (Accumulator), $6.1{\times}10^{12}$ (Recycler).

HIGH-ENERGY COLLIDER PARAMETERS: Heavy Ion Colliders

Updated in September 2013 with numbers received from representatives of the colliders (contact J. Beringer, LBNL). The table shows parameter values as achieved by July 1, 2013. For LHC, the parameters expected at the ALICE experiment for running in 2015 and design values for a high-luminosity upgrade are also given. Quantities are, where appropriate, r.m.s.; unless noted otherwise, energies refer to beam energy; s.c. stands for superconducting; pk and avg denote peak and average values.

	RHIC (Brookhaven)		LHC (CERN)			
Physics start date	2000	2012 / 2012 / 2004 / 2002	2010	2012	2015 (expected)	$\geq$ 2019 (high lum.)‡
Physics end date	—		—			
Particles collided	Au Au	U U / Cu Au / Cu Cu / d Au	Pb Pb	p Pb	Pb Pb	Pb Pb
Maximum beam energy (TeV/n)	0.1	0.1	1.38	*p*: 4 *Pb*: 1.58	2.76	2.76
$\sqrt{s_{NN}}$ (TeV)	0.2	0.2	2.76	5.0	5.5	5.5
Max. delivered int. nucleon-pair lumin. per exp. (pb^{-1})	568 (at 100 GeV/n)	21 / 167 / 65 / 103 (at 100 GeV/n)	7.4	6.6	$\approx 15/y$	$\approx 56/y$
Luminosity (10^{27} $\text{cm}^{-2}\text{s}^{-1}$)	5.0 (pk) 3.0 (avg)	0.9 / 12 / 20 / 270 (pk) 0.6 / 10 / 0.8 / 140 (avg)	0.5	100 (leveled) 116 (pk ATLAS/CMS)	1 (leveled)	4
Time between collisions (ns)	107	107 / 107 / 321 / 107	199.6	199.6 / 224.6	199.6	49.9
Full crossing angle (μ rad)	0	0	140	120	120	> 160
Energy spread (units 10^{-3})	0.75	0.75	0.11	0.11	0.11	0.11
Bunch length (cm)	30	30	9.7	*p*: 9 *Pb*: 11.5	9.7	7.9
Beam radius (10^{-6} m)	135	50 / 160 / 145 / 145	50	*p*: 19 *Pb*: 27	16	16
Free space at interaction point (m)	16	16	38	38	38	38
Initial luminosity decay time, $-L/(dL/dt)$ (hr)	1.2	-0.35†/ ∞†/ 1.8 / 1.5	5	≈ 6	n/a (leveled)	3.5
Turn-around time (min)	60	60 / 160 / 90 / 90	180	≈ 240	≈ 180	≈ 180
Injection energy (TeV)	0.011 TeV/n	0.011 TeV/n	0.177 TeV/n	*p*: 0.45 TeV/n *Pb*: 0.177 TeV/n	0.177 TeV/n	0.177 TeV/n
Transverse emittance ($10^{-9}\pi$ rad-m)	23	4 / 11 / 23 / 25	1.0	*p*: 0.5 *Pb*: 0.9	0.5	0.5
β^*, ampl. function at interaction point (m)	0.75	0.7 / 0.7 / 0.9 / 0.85	1.0	0.8	0.5	0.5
Beam-beam tune shift per crossing (units 10^{-4})	16	7 / 14 (Cu), 14 (Au) / 30 / 21 (d), 17 (Au)	3	*p*: 9 *Pb*: 10	9	6.7
RF frequency (MHz)	accel: 28 store: 197	accel: 28 store: 197	400.8	400.8	400.8	400.8
Particles per bunch (units 10^{10})	0.13	0.03 / 0.4 (Cu), 0.13 (Au) / 0.45 / 10 (d), 0.1 Au	0.011 (r.m.s.)	*p*: 1.6 *Pb*: 0.014	0.014	0.01
Bunches per ring per species	111	111 / 111 / 37 / 95	356	338	358	≈ 1100
Average beam current per species (mA)	145	38 / 159 (Cu), 138 (Au) / 60 / 119 (d), 94 Au	6.85	*p*: 9.7 *Pb*: 7	7.4	16
Circumference (km)	3.834		26.659			
Interaction regions	6 total, 2 high $\mathscr{L}$		1 dedicated +2	3 high $\mathscr{L}$ +1	1 dedicated +2	1 dedicated +2
Magnetic length of dipole (m)	9.45		14.3			
Length of standard cell (m)	29.7		106.90			
Phase advance per cell (deg)	93	84 / 84 / 84 / 84 (d), 93 (Au)	90			
Dipoles in ring	192 per ring + 12 common		1232 main dipoles			
Quadrupoles in ring	246 per ring		482 2-in-1 24 1-in-1			
Magnet type	s.c. $\cos\theta$ cold iron		s.c. 2 in 1 cold iron			
Peak magnetic field (T)	3.5		8.3			

†Negative or infinite decay time is effect of cooling.

‡High luminosity upgrade expected >= 2019; will extend throughout HL-LHC running. Very preliminary, conservative estimates.

31. NEUTRINO BEAM LINES AT HIGH-ENERGY PROTON SYNCHROTRONS

Revised September 2013 with numbers verified by representatives of the synchrotrons (contact C.-J. Lin, LBNL). For existing (future) neutrino beam lines the latest achieved (design) values are given.

The main source of neutrinos at proton synchrotrons is from the decay of pions and kaons produced by protons striking a nuclear target. There are different schemes to focus the secondary particles to enhance neutrino flux and/or tune the neutrino energy profile. In wide-band beams (WBB), the neutrino parent mesons are focused over a wide momentum range to obtain maximum neutrino intensity. In narrow-band beams (NBB), the secondary particles are first momentum-selected to produce a monochromatic parent beam. Another approach to generate a narrow-band neutrino spectrum is to select neutrinos that are emitted off-axis relative to the momentum of the parent mesons. For a comprehensive review of the topic, including other historical neutrino beam lines, see the article by S. E. Kopp, "Accelerator-based neutrino beams," Phys. Rept. **439**, 101 (2007).

	PS (CERN)				SPS (CERN)				PS (KEK)	Main Ring (JPARC)
Date	1963	1969	1972	1983	1977	1977	1995	2006	1999	2009
Proton Kinetic Energy (GeV)	20.6	20.6	26	19	350	350	450	400	12	30 (50)
Protons per Cycle (10^{12})	0.7	0.6	5	5	10	10	36	48	6	123 (330)
Cycle Time (s)	3	2.3	-	-	-	-	14.4	6	2.2	2.48 (3.5)
Beam Power (kW)	0.8	0.9	-	-	-	-	180	510	5	240 (750)
Target	-	-	-	-	-	-	Be	Graphite	Al	Graphite
Target Length (cm)	-	-	-	-	-	-	290	1000	66	91
Secondary Focussing	1-horn WBB	3-horn WBB	2-horn WBB	bare target	dichromatic NBB	2-horn WBB	2-horn WBB	2-horn WBB	2-horn WBB	3-horn off-axis
Decay Pipe Length (m)	-	-	-	-	-	-	110	130	200	96
$\langle E_\nu \rangle$ (GeV)	1.5	1.5	1.5	1	50,150[†]	20	24.3	17	1.3	0.6
Experiments	HLBC, Spark Ch.	HLBC, Spark Ch.	GGM, Aachen-Padova	CDHS, CHARM	CDHS, CHARM, BEBC	GGM,CDHS, CHARM, BEBC	NOMAD, CHORUS	OPERA, ICARUS	K2K	T2K

	Main Ring (Fermilab)							Booster (Fermilab)	Main Injector (Fermilab)	
Date	1975	1975	1974	1979	1976	1991	1998	2002	2005	2013
Proton Kinetic Energy (GeV)	300,400	300,400	300	400	350	800	800	8	120	120
Protons per Cycle (10^{12})	10	10	10	10	13	10	12	4.5	37	(49)
Cycle Time (s)	-	-	-	-	-	60	60	0.5	2	(1.333)
Beam Power (kW)	-	-	-	-	-	20	25	12	350	(700)
Target	-	-	-	-	-	-	BeO	Be	Graphite	Graphite
Target Length (cm)	-	-	-	-	-	-	31	71	95	120
Secondary Focussing	bare target	quad trip., SSBT	dichromatic NBB	2-horn WBB	1-horn WBB	quad trip.	SSQT WBB	1-horn WBB	2-horn WBB	2-horn off-axis
Decay Pipe Length (m)	350	350	400	400	400	400	400	50	675	675
$\langle E_\nu \rangle$ (GeV)	40	50,180[†]	50,180[†]	25	100	90,260	70,180	1	3-20[‡]	2
Experiments	HPWF	CITF, HPWF	CITF, HPWF, 15' BC	15' BC	HPWF 15' BC	15' BC, CCFRR	NuTeV	MiniBooNE, SciBooNE, MicroBooNE	MINOS, MINERνA	NOνA, MINERνA, MINOS+

[†]Pion and kaon peaks in the momentum-selected channel.

[‡]Tunable WBB energy spectrum.

32. PASSAGE OF PARTICLES THROUGH MATTER

Revised September 2013 by H. Bichsel (University of Washington), D.E. Groom (LBNL), and S.R. Klein (LBNL).

This review covers the interactions of photons and electrically charged particles in matter, concentrating on energies of interest for high-energy physics and astrophysics and processes of interest for particle detectors (ionization, Cherenkov radiation, transition radiation). Much of the focus is on particles heavier than electrons ($\pi^{\pm}$, p, etc.). Although the charge number z of the projectile is included in the equations, only $z = 1$ is discussed in detail. Muon radiative losses are discussed, as are photon/electron interactions at high to ultrahigh energies. Neutrons are not discussed. The notation and important numerical values are shown in Table 32.1.

32.1. Notation

Table 32.1: Summary of variables used in this section. The kinematic variables β and γ have their usual relativistic meanings.

Symbol	Definition	Value or (usual) units
α	fine structure constant $e^2/4\pi\epsilon_0\hbar c$	$1/137.035\,999\,074(44)$
M	incident particle mass	MeV/c^2
E	incident part. energy γMc^2	MeV
T	kinetic energy, $(\gamma-1)Mc^2$	MeV
W	energy transfer to an electron in a single collision	MeV
k	bremsstrahlung photon energy	MeV
m_ec^2	electron mass $\times\, c^2$	$0.510\,998\,928(11)$ MeV
r_e	classical electron radius $e^2/4\pi\epsilon_0 m_ec^2$	$2.817\,940\,3267(27)$ fm
N_A	Avogadro's number	$6.022\,141\,29(27)\times10^{23}$ mol^{-1}
z	charge number of incident particle	
Z	atomic number of absorber	
A	atomic mass of absorber	g mol^{-1}
K	$4\pi N_A r_e^2 m_e c^2$	0.307 075 MeV mol^{-1} cm^2
I	mean excitation energy	eV (*Nota bene!*)
$\delta(\beta\gamma)$	density effect correction to ionization energy loss	
$\hbar\omega_p$	plasma energy $\sqrt{4\pi N_e r_e^3}\; m_ec^2/\alpha$	$\sqrt{\rho\,\langle Z/A\rangle}\times 28.816$ eV, $\hookrightarrow\ \rho$ in g cm^{-3}
N_e	electron density	(units of r_e)$^{-3}$
w_j	weight fraction of the jth element in a compound or mixture	
n_j	$\propto$ number of jth kind of atoms in a compound or mixture	
X_0	radiation length	g cm^{-2}
E_c	critical energy for electrons	MeV
$E_{\mu c}$	critical energy for muons	GeV
E_s	scale energy $\sqrt{4\pi/\alpha}\; m_ec^2$	21.2052 MeV
R_M	Molière radius	g cm^{-2}

32.2. Electronic energy loss by heavy particles [1–33]

32.2.1. ***Moments and cross sections*** :

The electronic interactions of fast charged particles with speed $v = \beta c$ occur in *single collisions with energy losses* W [1], leading to ionization, atomic, or collective excitation. Most frequently the energy losses are small (for 90% of all collisions the energy losses are less than 100 eV). In thin absorbers few collisions will take place and the total energy loss will show a large variance [1]; also see Sec. 32.2.9 below. For particles with charge ze more massive than electrons ("heavy" particles), scattering from free electrons is adequately described by the Rutherford differential cross section [2],

$$\frac{d\sigma_R(W;\beta)}{dW} = \frac{2\pi r_e^2 m_e c^2 z^2}{\beta^2}\,\frac{(1-\beta^2 W/W_{\rm max})}{W^2}\,, \qquad (32.1)$$

where $W_{\rm max}$ is the maximum energy transfer possible in a single collision. But in matter electrons are not free. W must be finite and

depends on atomic and bulk structure. For electrons bound in atoms Bethe [3] used "Born Theorie" to obtain the differential cross section

$$\frac{d\sigma_B(W;\beta)}{dW} = \frac{d\sigma_R(W,\beta)}{dW} B(W) \ . \tag{32.2}$$

Electronic binding is accounted for by the correction factor $B(W)$. Examples of $B(W)$ and $d\sigma_B/dW$ can be seen in Figs. 5 and 6 of Ref. 1.

Bethe's theory extends only to some energy above which atomic effects are not important. The free-electron cross section (Eq. (32.1)) can be used to extend the cross section to $W_{\rm max}$. At high energies σ_B is further modified by polarization of the medium, and this "density effect," discussed in Sec. 32.2.5, must also be included. Less important corrections are discussed below.

The mean number of collisions with energy loss between W and $W + dW$ occurring in a distance δx is $N_e \delta x\, (d\sigma/dW) dW$, where $d\sigma(W;\beta)/dW$ contains all contributions. It is convenient to define the moments

$$M_j(\beta) = N_e\, \delta x \int W^j \frac{d\sigma(W;\beta)}{dW} dW \ , \tag{32.3}$$

so that M_0 is the mean number of collisions in δx, M_1 is the mean energy loss in δx, $(M_2 - M_1)^2$ is the variance, *etc.* The number of collisions is Poisson-distributed with mean M_0. N_e is either measured in electrons/g ($N_e = N_A Z/A$) or electrons/cm^3 ($N_e = N_A \rho Z/A$). The former is used throughout this chapter, since quantities of interest (dE/dx, X_0, *etc.*) vary smoothly with composition when there is no density dependence.

not for large nuclei) corrections to dE/dx are negligible below energies where radiative effects dominate. While the cross section for rare hard collisions is modified, the average stopping power, dominated by many softer collisions, is almost unchanged.

32.2.3. ***Stopping power at intermediate energies*** :

The mean rate of energy loss by moderately relativistic charged heavy particles, $M_1/\delta x$, is well-described by the "Bethe equation,"

$$\left\langle -\frac{dE}{dx} \right\rangle = K z^2 \frac{Z}{A} \frac{1}{\beta^2} \left[\frac{1}{2} \ln \frac{2 m_e c^2 \beta^2 \gamma^2 W_{\rm max}}{I^2} - \beta^2 - \frac{\delta(\beta\gamma)}{2} \right] . \tag{32.5}$$

It describes the mean rate of energy loss in the region $0.1 \lesssim \beta\gamma \lesssim 1000$ for intermediate-Z materials with an accuracy of a few %. With the symbol definitions and values given in Table 32.1, the units are MeV g^{-1}cm^2. $W_{\rm max}$ is defined in Sec. 32.2.2. At the lower limit the projectile velocity becomes comparable to atomic electron "velocities" (Sec. 32.2.6), and at the upper limit radiative effects begin to be important (Sec. 32.6). Both limits are Z dependent. A minor dependence on M at the highest energies is introduced through $W_{\rm max}$, but for all practical purposes $\langle dE/dx \rangle$ in a given material is a function of β alone.

Few concepts in high-energy physics are as misused as $\langle dE/dx \rangle$. The main problem is that the mean is weighted by very rare events with large single-collision energy deposits. Even with samples of hundreds of events a dependable value for the mean energy loss cannot be obtained.

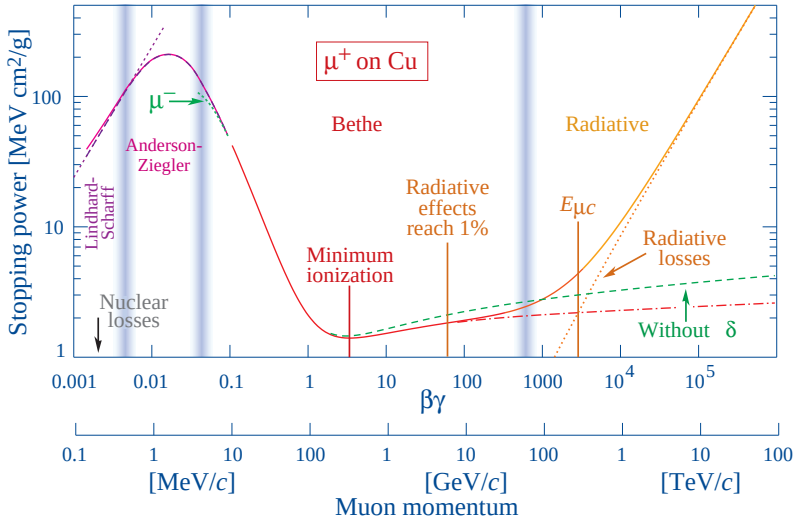

Fig. 32.1: Stopping power ($= \langle -dE/dx \rangle$) for positive muons in copper as a function of $\beta\gamma = p/Mc$ over nine orders of magnitude in momentum (12 orders of magnitude in kinetic energy). Solid curves indicate the total stopping power. Data below the break at $\beta\gamma \approx 0.1$ are taken from ICRU 49 [4], and data at higher energies are from Ref. 5. Vertical bands indicate boundaries between different approximations discussed in the text. The short dotted lines labeled "μ^-" illustrate the "Barkas effect," the dependence of stopping power on projectile charge at very low energies [6]. dE/dx in the radiative region is not simply a function of β.

32.2.2. ***Maximum energy transfer in a single collision*** : For a particle with mass M,

$$W_{\rm max} = \frac{2 m_e c^2 \beta^2 \gamma^2}{1 + 2\gamma m_e/M + (m_e/M)^2} \ . \tag{32.4}$$

In older references [2,8] the "low-energy" approximation $W_{\rm max} = 2 m_e c^2 \beta^2 \gamma^2$, valid for $2\gamma m_e \ll M$, is often implicit. For a pion in copper, the error thus introduced into dE/dx is greater than 6% at 100 GeV. For $2\gamma m_e \gg M$, $W_{\rm max} = Mc^2 \beta^2 \gamma$.

At energies of order 100 GeV, the maximum 4-momentum transfer to the electron can exceed 1 GeV/c, where hadronic structure effects significantly modify the cross sections. This problem has been investigated by J.D. Jackson [9], who concluded that for hadrons (but

Far better and more easily measured is the most probable energy loss, discussed in Sec. 32.2.9. The most probable energy loss in a detector is considerably below the mean given by the Bethe equation.

In a TPC (Sec. 33.6.5), the mean of 50%–70% of the samples with the smallest signals is often used as an estimator.

Although it must be used with cautions and caveats, $\langle dE/dx \rangle$ as described in Eq. (32.5) still forms the basis of much of our understanding of energy loss by charged particles. Extensive tables are available[4,5, `pdg.lbl.gov/AtomicNuclearProperties/`].

For heavy projectiles, like ions, additional terms are required to account for higher-order photon coupling to the target, and to account for the finite size of the target radius. These can change dE/dx by a factor of two or more for the heaviest nuclei in certain kinematic

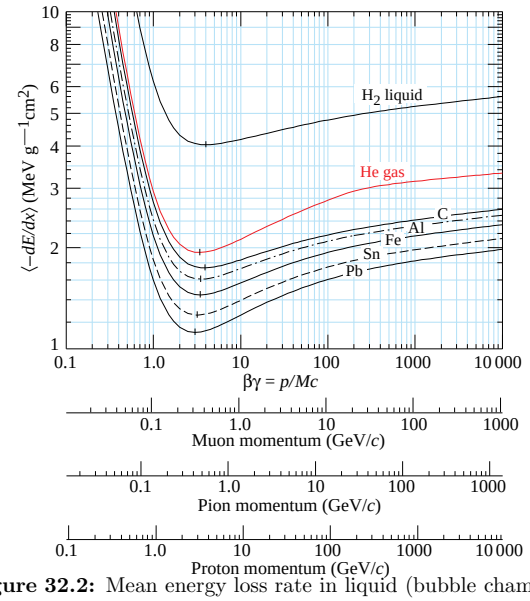

Figure 32.2: Mean energy loss rate in liquid (bubble chamber) hydrogen, gaseous helium, carbon, aluminum, iron, tin, and lead. Radiative effects, relevant for muons and pions, are not included. These become significant for muons in iron for $\beta\gamma \gtrsim 1000$, and at lower momenta for muons in higher-Z absorbers. See Fig. 32.23.

regimes [7].

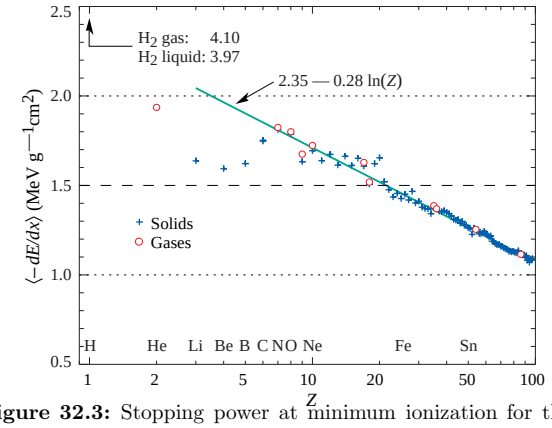

Figure 32.3: Stopping power at minimum ionization for the chemical elements. The straight line is fitted for $Z > 6$. A simple functional dependence on Z is not to be expected, since $\langle -dE/dx \rangle$ also depends on other variables.

The function as computed for muons on copper is shown as the "Bethe" region of Fig. 32.1. Mean energy loss behavior below this region is discussed in Sec. 32.2.6, and the radiative effects at high energy are discussed in Sec. 32.6. Only in the Bethe region is it a function of β alone; the mass dependence is more complicated elsewhere. The stopping power in several other materials is shown in Fig. 32.2. Except in hydrogen, particles with the same velocity have similar rates of energy loss in different materials, although there is a slow decrease in the rate of energy loss with increasing Z. The qualitative behavior difference at high energies between a gas (He in the figure) and the other materials shown in the figure is due to the density-effect correction, $\delta(\beta\gamma)$, discussed in Sec. 32.2.5. The stopping power functions are characterized by broad minima whose position drops from $\beta\gamma = 3.5$ to 3.0 as Z goes from 7 to 100. The values of minimum ionization as a function of atomic number are shown in Fig. 32.3.

In practical cases, most relativistic particles (*e.g.*, cosmic-ray muons) have mean energy loss rates close to the minimum; they are "minimum-ionizing particles," or mip's.

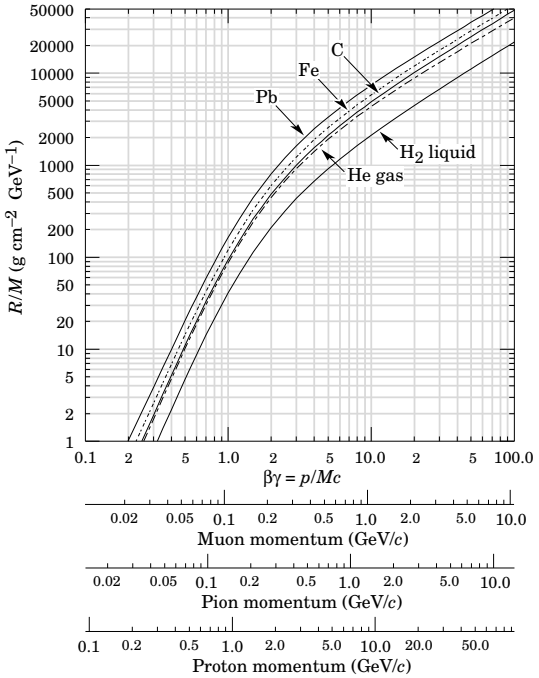

Figure 32.4: Range of heavy charged particles in liquid (bubble chamber) hydrogen, helium gas, carbon, iron, and lead. For example: For a K^+ whose momentum is 700 MeV/c, $\beta\gamma = 1.42$. For lead we read $R/M \approx 396$, and so the range is 195 g cm^{-2} (17 cm).

Eq. (32.5) may be integrated to find the total (or partial) "continuous slowing-down approximation" (CSDA) range R for a particle which loses energy only through ionization and atomic excitation. Since dE/dx depends only on β, R/M is a function of E/M or pc/M. In practice, range is a useful concept only for low-energy hadrons ($R \lesssim \lambda_I$, where λ_I is the nuclear interaction length), and for muons below a few hundred GeV (above which radiative effects dominate). R/M as a function of $\beta\gamma = p/Mc$ is shown for a variety of materials in Fig. 32.4.

The mass scaling of dE/dx and range is valid for the electronic losses described by the Bethe equation, but not for radiative losses, relevant only for muons and pions.

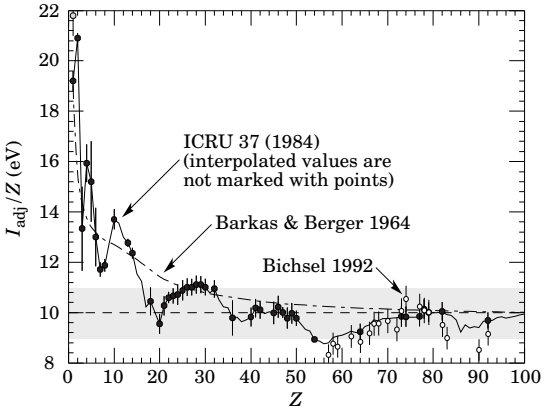

Figure 32.5: Mean excitation energies (divided by Z) as adopted by the ICRU [11]. Those based on experimental measurements are shown by symbols with error flags; the interpolated values are simply joined. The grey point is for liquid H_2; the black point at 19.2 eV is for H_2 gas. The open circles show more recent determinations by Bichsel [13]. The dash-dotted curve is from the approximate formula of Barkas [14] used in early editions of this *Review*.

32.2.4. ***Mean excitation energy*** : *"The determination of the mean excitation energy is the principal non-trivial task in the evaluation of the Bethe stopping-power formula"* [10]. Recommended values have varied substantially with time. Estimates based on experimental stopping-power measurements for protons, deuterons, and alpha particles and on oscillator-strength distributions and dielectric-response functions were given in ICRU 49 [4]. See also ICRU 37 [11]. These values, shown in Fig. 32.5, have since been widely used. Machine-readable versions can also be found [12].

32.2.5. ***Density effect*** : As the particle energy increases, its electric field flattens and extends, so that the distant-collision contribution to Eq. (32.5) increases as $\ln\beta\gamma$. However, real media become polarized, limiting the field extension and effectively truncating this part of the logarithmic rise [2–8,15–16]. At very high energies,

$$\delta/2 \to \ln(\hbar\omega_p/I) + \ln\beta\gamma - 1/2 \ , \tag{32.6}$$

where $\delta(\beta\gamma)/2$ is the density effect correction introduced in Eq. (32.5) and $\hbar\omega_p$ is the plasma energy defined in Table 32.1. A comparison with Eq. (32.5) shows that $|dE/dx|$ then grows as $\ln\beta\gamma$ rather than $\ln\beta^2\gamma^2$, and that the mean excitation energy I is replaced by the plasma energy $\hbar\omega_p$. The ionization stopping power as calculated with and without the density effect correction is shown in Fig. 32.1. Since the plasma frequency scales as the square root of the electron density, the correction is much larger for a liquid or solid than for a gas, as is illustrated by the examples in Fig. 32.2.

The density effect correction is usually computed using Sternheimer's parameterization [15]:

$$\delta(\beta\gamma) = \begin{cases} 2(\ln 10)x - \overline{C} & \text{if } x \geq x_1; \\ 2(\ln 10)x - \overline{C} + a(x_1 - x)^k & \text{if } x_0 \leq x < x_1; \\ 0 & \text{if } x < x_0 \text{ (nonconductors);} \\ \delta_0 10^{2(x-x_0)} & \text{if } x < x_0 \text{ (conductors)} \end{cases} \tag{32.7}$$

Here $x = \log_{10}\eta = \log_{10}(p/Mc)$. $\overline{C}$ (the negative of the C used in Ref. 15) is obtained by equating the high-energy case of Eq. (32.7) with the limit given in Eq. (32.6). The other parameters are adjusted to give a best fit to the results of detailed calculations for momenta below $Mc\exp(x_1)$. Parameters for elements and nearly 200 compounds and mixtures of interest are published in a variety of places, notably in Ref. 16. A recipe for finding the coefficients for nontabulated materials is given by Sternheimer and Peierls [17], and is summarized in Ref. 5.

The remaining relativistic rise comes from the $\beta^2\gamma$ growth of $W_{\max}$, which in turn is due to (rare) large energy transfers to a few electrons. When these events are excluded, the energy deposit in an absorbing layer approaches a constant value, the Fermi plateau (see Sec. 32.2.8 below). At even higher energies (*e.g.*, > 332 GeV for muons in iron, and at a considerably higher energy for protons in iron), radiative effects are more important than ionization losses. These are especially relevant for high-energy muons, as discussed in Sec. 32.6.

32.2.6. ***Energy loss at low energies*** : Shell corrections C/Z must be included in the square brackets of of Eq. (32.5) [4,11,13,14] to correct for atomic binding having been neglected in calculating some of the contributions to Eq. (32.5). The Barkas form [14] was used in generating Fig. 32.1. For copper it contributes about 1% at $\beta\gamma = 0.3$ (kinetic energy 6 MeV for a pion), and the correction decreases very rapidly with increasing energy.

Equation 32.2, and therefore Eq. (32.5), are based on a first-order Born approximation. Higher-order corrections, again important only at lower energies, are normally included by adding the "Bloch correction" $z^2L_2(\beta)$ inside the square brackets (Eq.(2.5) in [4]) .

An additional "Barkas correction" $zL_1(\beta)$ reduces the stopping power for a negative particle below that for a positive particle with the same mass and velocity. In a 1956 paper, Barkas *et al.* noted that negative pions had a longer range than positive pions [6]. The effect has been measured for a number of negative/positive particle pairs, including a detailed study with antiprotons [18].

A detailed discussion of low-energy corrections to the Bethe formula is given in ICRU 49 [4]. When the corrections are properly included, the Bethe treatment is accurate to about 1% down to $\beta \approx 0.05$, or about 1 MeV for protons.

For $0.01 < \beta < 0.05$, there is no satisfactory theory. For protons, one usually relies on the phenomenological fitting formulae developed by Andersen and Ziegler [4,19]. As tabulated in ICRU 49 [4], the nuclear plus electronic proton stopping power in copper is 113 MeV cm^2 g^{-1} at $T = 10$ keV ($\beta\gamma = 0.005$), rises to a maximum of 210 MeV cm^2 g^{-1} at $T \approx 120$ keV ($\beta\gamma = 0.016$), then falls to 118 MeV cm^2 g^{-1} at $T = 1$ MeV ($\beta\gamma = 0.046$). Above 0.5–1.0 MeV the corrected Bethe theory is adequate.

For particles moving more slowly than $\approx 0.01c$ (more or less the velocity of the outer atomic electrons), Lindhard has been quite successful in describing electronic stopping power, which is proportional to β [20]. Finally, we note that at even lower energies, *e.g.*, for protons of less than several hundred eV, non-ionizing nuclear recoil energy loss dominates the total energy loss [4,20,21].

32.2.7. ***Energetic knock-on electrons (δ rays)*** : The distribution of secondary electrons with kinetic energies $T \gg I$ is [2]

$$\frac{d^2N}{dTdx} = \frac{1}{2}Kz^2\frac{Z}{A}\frac{1}{\beta^2}\frac{F(T)}{T^2} \tag{32.8}$$

for $I \ll T \leq W_{\max}$, where $W_{\max}$ is given by Eq. (32.4). Here β is the velocity of the primary particle. The factor F is spin-dependent, but is about unity for $T \ll W_{\max}$. For spin-0 particles $F(T) = (1 - \beta^2 T/W_{\max})$; forms for spins 1/2 and 1 are also given by Rossi [2](Sec. 2.3, Eqns. 7 and 8). Additional formulae are given in Ref. 22. Equation (32.8) is inaccurate for T close to I [23].

δ rays of even modest energy are rare. For a $\beta \approx 1$ particle, for example, on average only one collision with $T_e > 10$ keV will occur along a path length of 90 cm of Ar gas [1].

A δ ray with kinetic energy T_e and corresponding momentum p_e is produced at an angle θ given by

$$\cos\theta = (T_e/p_e)(p_{\max}/W_{\max}) \ , \tag{32.9}$$

where $p_{\max}$ is the momentum of an electron with the maximum possible energy transfer $W_{\max}$.

32.2.8. ***Restricted energy loss rates for relativistic ionizing particles*** : Further insight can be obtained by examining the mean energy deposit by an ionizing particle when energy transfers are restricted to $T \leq W_{\rm cut} \leq W_{\max}$. The restricted energy loss rate is

$$-\left.\frac{dE}{dx}\right|_{T<W_{\rm cut}} = Kz^2\frac{Z}{A}\frac{1}{\beta^2}\left[\frac{1}{2}\ln\frac{2m_ec^2\beta^2\gamma^2W_{\rm cut}}{I^2} - \frac{\beta^2}{2}\left(1 + \frac{W_{\rm cut}}{W_{\max}}\right) - \frac{\delta}{2}\right] . \tag{32.10}$$

This form approaches the normal Bethe function (Eq. (32.5)) as $W_{\rm cut} \to W_{\max}$. It can be verified that the difference between Eq. (32.5) and Eq. (32.10) is equal to $\int_{W_{\rm cut}}^{W_{\max}} T(d^2N/dTdx)dT$, where $d^2N/dTdx$ is given by Eq. (32.8).

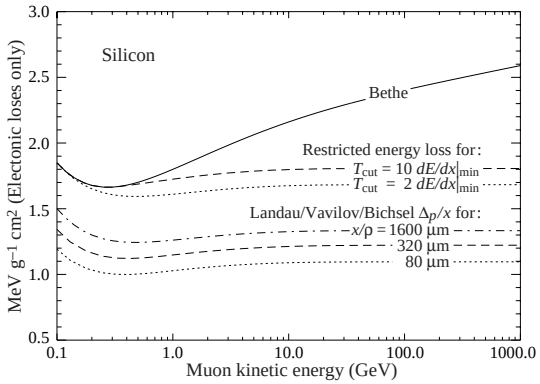

Figure 32.6: Bethe dE/dx, two examples of restricted energy loss, and the Landau most probable energy per unit thickness in silicon. The change of Δ_p/x with thickness x illustrates its $a\ln x + b$ dependence. Minimum ionization ($dE/dx|_{\rm min}$) is 1.664 MeV g^{-1} cm^2. Radiative losses are excluded. The incident particles are muons.

Since $W_{\rm cut}$ replaces $W_{\rm max}$ in the argument of the logarithmic term of Eq. (32.5), the $\beta\gamma$ term producing the relativistic rise in the close-collision part of dE/dx is replaced by a constant, and $|dE/dx|_{T<W_{\rm cut}}$ approaches the constant "Fermi plateau." (The density effect correction δ eliminates the explicit $\beta\gamma$ dependence produced by the distant-collision contribution.) This behavior is illustrated in Fig. 32.6, where restricted loss rates for two examples of $W_{\rm cut}$ are shown in comparison with the full Bethe dE/dx and the Landau-Vavilov most probable energy loss (to be discussed in Sec. 32.2.9 below).

"Restricted energy loss" is cut at the total mean energy, not the single-collision energy above $W_{\rm cut}$ It is of limited use. The most probable energy loss, discussed in the next Section, is far more useful in situations where single-particle energy loss is observed.

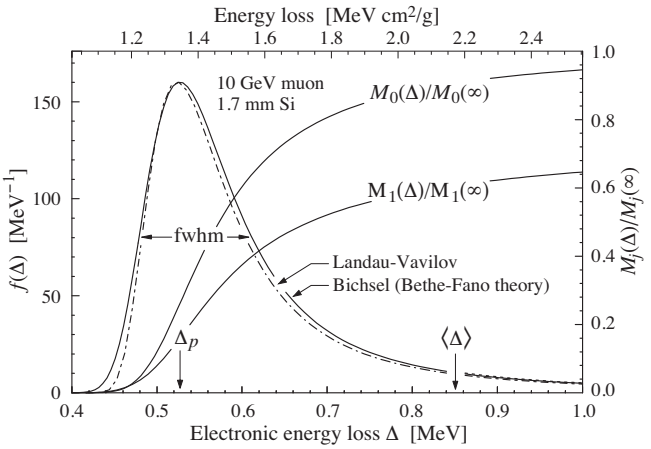

Figure 32.7: Electronic energy deposit distribution for a 10 GeV muon traversing 1.7 mm of silicon, the stopping power equivalent of about 0.3 cm of PVC scintillator [1,13,28]. The Landau-Vavilov function (dot-dashed) uses a Rutherford cross section without atomic binding corrections but with a kinetic energy transfer limit of $W_{\rm max}$. The solid curve was calculated using Bethe-Fano theory. $M_0(\Delta)$ and $M_1(\Delta)$ are the cumulative 0th moment (mean number of collisions) and 1st moment (mean energy loss) in crossing the silicon. (See Sec. 32.2.1. The fwhm of the Landau-Vavilov function is about 4ξ for detectors of moderate thickness. Δ_p is the most probable energy loss, and $\langle\Delta\rangle$ divided by the thickness is the Bethe $\langle dE/dx\rangle$.

32.2.9. ***Fluctuations in energy loss*** : For detectors of moderate thickness x (*e.g.* scintillators or LAr cells),* the energy loss probability distribution $f(\Delta;\beta\gamma,x)$ is adequately described by the highly-skewed Landau (or Landau-Vavilov) distribution [24,25]. The most probable energy loss is [26]†

$$\Delta_p = \xi\left[\ln\frac{2mc^2\beta^2\gamma^2}{I} + \ln\frac{\xi}{I} + j - \beta^2 - \delta(\beta\gamma)\right] , \qquad (32.11)$$

where $\xi = (K/2)\langle Z/A\rangle(x/\beta^2)$ MeV for a detector with a thickness x in g cm^{-2}, and $j = 0.200$ [26]. ‡ While dE/dx is independent of thickness, Δ_p/x scales as $a\ln x + b$. The density correction $\delta(\beta\gamma)$ was not included in Landau's or Vavilov's work, but it was later included by Bichsel [26]. The high-energy behavior of $\delta(\beta\gamma)$ (Eq. (32.6)) is such that

$$\Delta_p \underset{\beta\gamma\gtrsim 100}{\longrightarrow} \xi\left[\ln\frac{2mc^2\xi}{(\hbar\omega_p)^2} + j\right] . \qquad (32.12)$$

Thus the Landau-Vavilov most probable energy loss, like the restricted energy loss, reaches a Fermi plateau. The Bethe dE/dx and Landau-Vavilov-Bichsel Δ_p/x in silicon are shown as a function of muon energy in Fig. 32.6. The energy deposit in the 1600 μm case is roughly the same as in a 3 mm thick plastic scintillator.

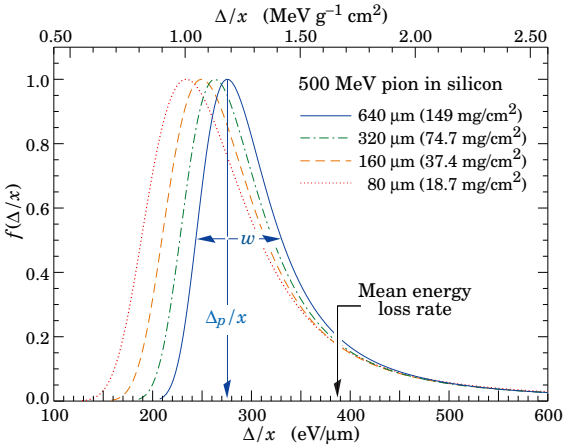

Figure 32.8: Straggling functions in silicon for 500 MeV pions, normalized to unity at the most probable value δ_p/x. The width w is the full width at half maximum.

The distribution function for the energy deposit by a 10 GeV muon going through a detector of about this thickness is shown in Fig. 32.7. In this case the most probable energy loss is 62% of the mean ($M_1(\langle\Delta\rangle)/M_1(\infty)$). Folding in experimental resolution displaces the peak of the distribution, usually toward a higher value. 90% of the collisions ($M_1(\langle\Delta\rangle)/M_1(\infty)$) contribute to energy deposits below the mean. It is the very rare high-energy-transfer collisions, extending to $W_{\rm max}$ at several GeV, that drives the mean into the tail of the distribution. The large weight of these rare events makes the mean of an experimental distribution consisting of a few hundred events subject to large fluctuations and sensitive to cuts. *The mean of the energy loss given by the Bethe equation, Eq. (32.5), is thus ill-defined experimentally and is not useful for describing energy loss by single particles.*♮ It rises as $\ln\gamma$ because $W_{\rm max}$ increases as γ at high energies. *The most probable energy loss should be used.*

A practical example: For muons traversing 0.25 inches of PVT plastic scintillator, the ratio of the most probable E loss rate to the mean loss rate via the Bethe equation is $[0.69, 0.57, 0.49, 0.42, 0.38]$ for $T_\mu = [0.01, 0.1, 1, 10, 100]$ GeV. Radiative losses add less than 0.5% to the total mean energy deposit at 10 GeV, but add 7% at 100 GeV. The most probable E loss rate rises slightly beyond the minimum ionization energy, then is essentially constant.

The Landau distribution fails to describe energy loss in thin absorbers such as gas TPC cells [1] and Si detectors [26], as shown clearly in Fig. 1 of Ref. 1 for an argon-filled TPC cell. Also see Talman [27]. While Δ_p/x may be calculated adequately with Eq. (32.11), the distributions are significantly wider than the Landau width $w = 4\xi$ [Ref. 26, Fig. 15]. Examples for 500 MeV pions incident on thin silicon detectors are shown in Fig. 32.8. For very thick absorbers the distribution is less skewed but never approaches a Gaussian.

The most probable energy loss, scaled to the mean loss at minimum ionization, is shown in Fig. 32.9 for several silicon detector thicknesses.

* $G \lesssim 0.05$–0.1, where G is given by Rossi [Ref. 2, Eq. 2.7(10)]. It is Vavilov's κ [25]. It is proportional to the absorber's thickness, and as such parameterizes the constants describing the Landau distribution. These are fairly insensitive to thickness for $G \lesssim 0.1$, the case for most detectors.

† Practical calculations can be expedited by using the tables of δ and β from the text versions of the muon energy loss tables to be found at `pdg.lbl.gov/AtomicNuclearProperties`.

‡ Rossi [2], Talman [27], and others give somewhat different values for j. The most probable loss is not sensitive to its value.

♮ It does find application in dosimetry, where only bulk deposit is relevant.

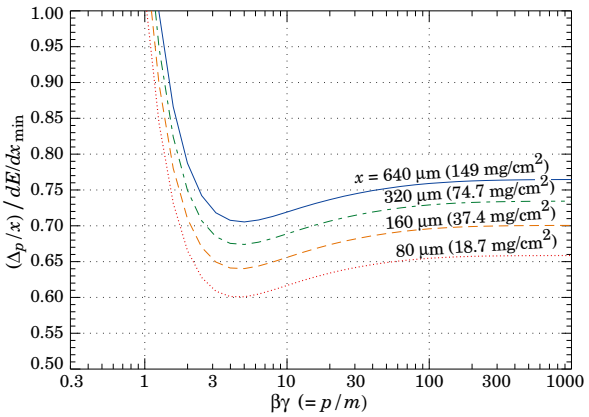

Figure 32.9: Most probable energy loss in silicon, scaled to the mean loss of a minimum ionizing particle, 388 eV/μm (1.66 MeV g^{-1}cm^2).

32.2.10. ***Energy loss in mixtures and compounds*** : A mixture or compound can be thought of as made up of thin layers of pure elements in the right proportion (Bragg additivity). In this case,

$$\left\langle \frac{dE}{dx} \right\rangle = \sum w_j \left\langle \frac{dE}{dx} \right\rangle_j \ , \tag{32.13}$$

where $dE/dx|_j$ is the mean rate of energy loss (in MeV g cm^{-2}) in the jth element. Eq. (32.5) can be inserted into Eq. (32.13) to find expressions for $\langle Z/A\rangle$, $\langle I\rangle$, and $\langle\delta\rangle$; for example, $\langle Z/A\rangle = \sum w_j Z_j/A_j = \sum n_j Z_j / \sum n_j A_j$. However, $\langle I\rangle$ as defined this way is an underestimate, because in a compound electrons are more tightly bound than in the free elements, and $\langle\delta\rangle$ as calculated this way has little relevance, because it is the electron density that matters. If possible, one uses the tables given in Refs. 16 and 29, that include effective excitation energies and interpolation coefficients for calculating the density effect correction for the chemical elements and nearly 200 mixtures and compounds. Otherwise, use the recipe for δ given in Ref. 5 and 17, and calculate $\langle I\rangle$ following the discussion in Ref. 10. (Note the "13%" rule!)

32.2.11. ***Ionization yields*** : Physicists frequently relate total energy loss to the number of ion pairs produced near the particle's track. This relation becomes complicated for relativistic particles due to the wandering of energetic knock-on electrons whose ranges exceed the dimensions of the fiducial volume. For a qualitative appraisal of the nonlocality of energy deposition in various media by such modestly energetic knock-on electrons, see Ref. 30. The mean local energy dissipation per local ion pair produced, W, while essentially constant for relativistic particles, increases at slow particle speeds [31]. For gases, W can be surprisingly sensitive to trace amounts of various contaminants [31]. Furthermore, ionization yields in practical cases may be greatly influenced by such factors as subsequent recombination [32].

32.3. Multiple scattering through small angles

A charged particle traversing a medium is deflected by many small-angle scatters. Most of this deflection is due to Coulomb scattering from nuclei as described by the Rutherford cross section. (However, for hadronic projectiles, the strong interactions also contribute to multiple scattering.) For many small-angle scatters the net scattering and displacement distributions are Gaussian via the central limit theorem. Less frequent "hard" scatters produce non-Gaussian tails. These Coulomb scattering distributions are well-represented by the theory of Molière [34]. Accessible discussions are given by Rossi [2] and Jackson [33], and exhaustive reviews have been published by Scott [35] and Motz *et al.* [36]. Experimental measurements have been published by Bichsel [37](low energy protons) and by Shen *et al.* [38](relativistic pions, kaons, and protons).*

* Shen *et al.*'s measurements show that Bethe's simpler methods of including atomic electron effects agrees better with experiment than does Scott's treatment.

If we define

$$\theta_0 = \theta^{\rm rms}_{\rm plane} = \frac{1}{\sqrt{2}}\,\theta^{\rm rms}_{\rm space} \ , \tag{32.14}$$

then it is sufficient for many applications to use a Gaussian approximation for the central 98% of the projected angular distribution, with an rms width given by [39,40]

$$\theta_0 = \frac{13.6\ {\rm MeV}}{\beta cp}\ z\ \sqrt{x/X_0}\Big[1 + 0.038\ln(x/X_0)\Big] \ . \tag{32.15}$$

Here p, βc, and z are the momentum, velocity, and charge number of the incident particle, and x/X_0 is the thickness of the scattering medium in radiation lengths (defined below). This value of θ_0 is from a fit to Molière distribution for singly charged particles with $\beta = 1$ for all Z, and is accurate to 11% or better for $10^{-3} < x/X_0 < 100$.

Eq. (32.15) describes scattering from a single material, while the usual problem involves the multiple scattering of a particle traversing many different layers and mixtures. Since it is from a fit to a Molière distribution, it is incorrect to add the individual θ_0 contributions in quadrature; the result is systematically too small. It is much more accurate to apply Eq. (32.15) once, after finding x and X_0 for the combined scatterer.

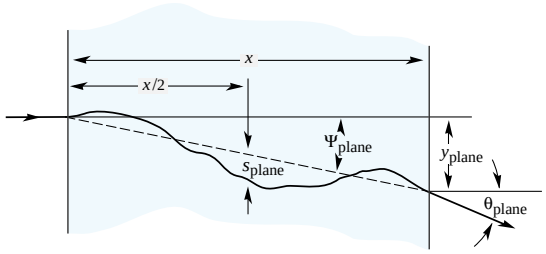

Figure 32.10: Quantities used to describe multiple Coulomb scattering. The particle is incident in the plane of the figure.

The nonprojected (space) and projected (plane) angular distributions are given approximately by [34]

$$\frac{1}{2\pi\,\theta_0^2}\ \exp\left(-\frac{\theta^2_{\rm space}}{2\theta_0^2}\right)\ d\Omega \ , \tag{32.16}$$

$$\frac{1}{\sqrt{2\pi}\,\theta_0}\ \exp\left(-\frac{\theta^2_{\rm plane}}{2\theta_0^2}\right)\ d\theta_{\rm plane} \ , \tag{32.17}$$

where θ is the deflection angle. In this approximation, $\theta^2_{\rm space} \approx (\theta^2_{{\rm plane},x} + \theta^2_{{\rm plane},y})$, where the x and y axes are orthogonal to the direction of motion, and $d\Omega \approx d\theta_{{\rm plane},x}\, d\theta_{{\rm plane},y}$. Deflections into $\theta_{{\rm plane},x}$ and $\theta_{{\rm plane},y}$ are independent and identically distributed.

Fig. 32.10 shows these and other quantities sometimes used to describe multiple Coulomb scattering. They are

$$\psi^{\rm rms}_{\rm plane} = \frac{1}{\sqrt{3}}\,\theta^{\rm rms}_{\rm plane} = \frac{1}{\sqrt{3}}\,\theta_0 \ , \tag{32.18}$$

$$y^{\rm rms}_{\rm plane} = \frac{1}{\sqrt{3}}\,x\,\theta^{\rm rms}_{\rm plane} = \frac{1}{\sqrt{3}}\,x\,\theta_0 \ , \tag{32.19}$$

$$s^{\rm rms}_{\rm plane} = \frac{1}{4\sqrt{3}}\,x\,\theta^{\rm rms}_{\rm plane} = \frac{1}{4\sqrt{3}}\,x\,\theta_0 \ . \tag{32.20}$$

All the quantitative estimates in this section apply only in the limit of small $\theta^{\rm rms}_{\rm plane}$ and in the absence of large-angle scatters. The random variables s, ψ, y, and θ in a given plane are correlated. Obviously, $y \approx x\psi$. In addition, y and θ have the correlation coefficient $\rho_{y\theta} = \sqrt{3}/2 \approx 0.87$. For Monte Carlo generation of a joint $(y_{\rm plane}, \theta_{\rm plane})$ distribution, or for other calculations, it may be most convenient to work with independent Gaussian random variables (z_1, z_2) with mean zero and variance one, and then set

$$y_{\rm plane} = z_1\,x\,\theta_0(1-\rho^2_{y\theta})^{1/2}/\sqrt{3} + z_2\,\rho_{y\theta}x\,\theta_0/\sqrt{3} \tag{32.21}$$

$$= z_1\,x\,\theta_0/\sqrt{12} + z_2\,x\,\theta_0/2 \ ; \tag{32.22}$$

$$\theta_{\rm plane} = z_2\,\theta_0 \ . \tag{32.23}$$

Note that the second term for $y_{\rm plane}$ equals $x\,\theta_{\rm plane}/2$ and represents the displacement that would have occurred had the deflection $\theta_{\rm plane}$ all occurred at the single point $x/2$.

For heavy ions the multiple Coulomb scattering has been measured and compared with various theoretical distributions [41].

32.4. Photon and electron interactions in matter

At low energies electrons and positrons primarily lose energy by ionization, although other processes (Møller scattering, Bhabha scattering, e^+ annihilation) contribute, as shown in Fig. 32.11. While ionization loss rates rise logarithmically with energy, bremsstrahlung losses rise nearly linearly (fractional loss is nearly independent of energy), and dominates above the critical energy (Sec. 32.4.4 below), a few tens of MeV in most materials

32.4.1. ***Collision energy losses by*** $e^{\pm}$: Stopping power differs somewhat for electrons and positrons, and both differ from stopping power for heavy particles because of the kinematics, spin, charge, and the identity of the incident electron with the electrons that it ionizes. Complete discussions and tables can be found in Refs. 10, 11, and 29.

For electrons, large energy transfers to atomic electrons (taken as free) are described by the Møller cross section. From Eq. (32.4), the maximum energy transfer in a single collision should be the entire kinetic energy, $W_{\rm max} = m_e c^2(\gamma - 1)$, but because the particles are identical, the maximum is half this, $W_{\rm max}/2$. (The results are the same if the transferred energy is ϵ or if the transferred energy is $W_{\rm max} - \epsilon$. The stopping power is by convention calculated for the faster of the two emerging electrons.) The first moment of the Møller cross section [22](divided by dx) is the stopping power:

$$\left\langle -\frac{dE}{dx} \right\rangle = \frac{1}{2} K \frac{Z}{A} \frac{1}{\beta^2} \left[\ln \frac{m_e c^2 \beta^2 \gamma^2 \{m_e c^2 (\gamma - 1)/2\}}{I^2} + (1 - \beta^2) - \frac{2\gamma - 1}{\gamma^2} \ln 2 + \frac{1}{8} \left(\frac{\gamma - 1}{\gamma} \right)^2 - \delta \right] \quad (32.24)$$

The logarithmic term can be compared with the logarithmic term in the Bethe equation (Eq. (32.2)) by substituting $W_{\rm max} = m_e c^2(\gamma - 1)/2$. The two forms differ by $\ln 2$.

Electron-positron scattering is described by the fairly complicated Bhabha cross section [22]. There is no identical particle problem, so $W_{\rm max} = m_e c^2(\gamma - 1)$. The first moment of the Bhabha equation yields

$$\left\langle -\frac{dE}{dx} \right\rangle = \frac{1}{2} K \frac{Z}{A} \frac{1}{\beta^2} \left[\ln \frac{m_e c^2 \beta^2 \gamma^2 \{m_e c^2 (\gamma - 1)\}}{2I^2} + 2 \ln 2 - \frac{\beta^2}{12} \left(23 + \frac{14}{\gamma + 1} + \frac{10}{(\gamma + 1)^2} + \frac{4}{(\gamma + 1)^3} \right) - \delta \right] . \quad (32.25)$$

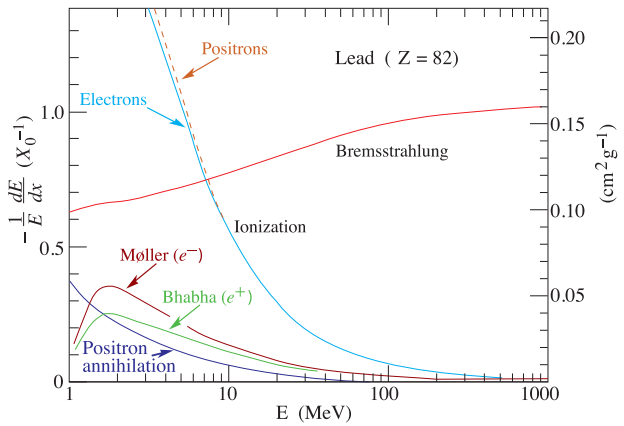

Figure 32.11: Fractional energy loss per radiation length in lead as a function of electron or positron energy. Electron (positron) scattering is considered as ionization when the energy loss per collision is below 0.255 MeV, and as Møller (Bhabha) scattering when it is above. Adapted from Fig. 3.2 from Messel and Crawford, *Electron-Photon Shower Distribution Function Tables for Lead, Copper, and Air Absorbers*, Pergamon Press, 1970. Messel and Crawford use X_0(Pb) = 5.82 g/cm^2, but we have modified the figures to reflect the value given in the Table of Atomic and Nuclear Properties of Materials (X_0(Pb) = 6.37 g/cm^2).

Following ICRU 37 [11], the density effect correction δ has been added to Uehling's equations [22] in both cases.

For heavy particles, shell corrections were developed assuming that the projectile is equivalent to a perturbing potential whose center moves with constant velocity. This assumption has no sound theoretical basis for electrons. The authors of ICRU 37 [11] estimated the possible error in omitting it by assuming the correction was twice as great as for a proton of the same velocity. At $T = 10$ keV, the error was estimated to be ≈2% for water, ≈9% for Cu, and ≈21% for Au.

As shown in Fig. 32.11, stopping powers for e^-, e^+, and heavy particles are not dramatically different. In silicon, the minimum value for electrons is 1.50 MeV cm^2/g (at $\gamma = 3.3$); for positrons, 1.46 MeV cm^2/g (at $\gamma = 3.7$), and for muons, 1.66 MeV cm^2/g (at $\gamma = 3.58$).

32.4.2. ***Radiation length*** : High-energy electrons predominantly lose energy in matter by bremsstrahlung, and high-energy photons by e^+e^- pair production. The characteristic amount of matter traversed for these related interactions is called the radiation length X_0, usually measured in g cm^{-2}. It is both (a) the mean distance over which a high-energy electron loses all but $1/e$ of its energy by bremsstrahlung, and (b) $\frac{7}{9}$ of the mean free path for pair production by a high-energy photon [42]. It is also the appropriate scale length for describing high-energy electromagnetic cascades. X_0 has been calculated and tabulated by Y.S. Tsai [43]:

$$\frac{1}{X_0} = 4\alpha r_e^2 \frac{N_A}{A} \left\{ Z^2 \left[L_{\rm rad} - f(Z) \right] + Z\, L'_{\rm rad} \right\} . \quad (32.26)$$

For $A = 1$ g mol^{-1}, $4\alpha r_e^2 N_A/A = (716.408\ {\rm g\ cm^{-2}})^{-1}$. $L_{\rm rad}$ and $L'_{\rm rad}$ are given in Table 32.2. The function $f(Z)$ is an infinite sum, but for elements up to uranium can be represented to 4-place accuracy by

$$f(Z) = a^2 \left[(1 + a^2)^{-1} + 0.20206 - 0.0369\, a^2 + 0.0083\, a^4 - 0.002\, a^6 \right] , \quad (32.27)$$

where $a = \alpha Z$ [44].

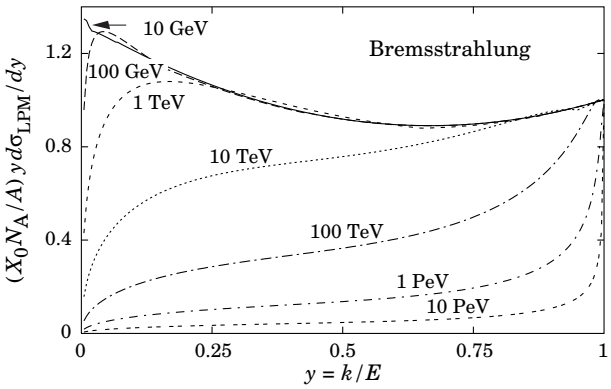

Figure 32.12: The normalized bremsstrahlung cross section $k\, d\sigma_{LPM}/dk$ in lead versus the fractional photon energy $y = k/E$. The vertical axis has units of photons per radiation length.

Table 32.2: Tsai's $L_{\rm rad}$ and $L'_{\rm rad}$, for use in calculating the radiation length in an element using Eq. (32.26).

Element	Z	$L_{\rm rad}$	$L'_{\rm rad}$
H	1	5.31	6.144
He	2	4.79	5.621
Li	3	4.74	5.805
Be	4	4.71	5.924
Others	> 4	$\ln(184.15\, Z^{-1/3})$	$\ln(1194\, Z^{-2/3})$

The radiation length in a mixture or compound may be approximated by

$$1/X_0 = \sum w_j / X_j , \quad (32.28)$$

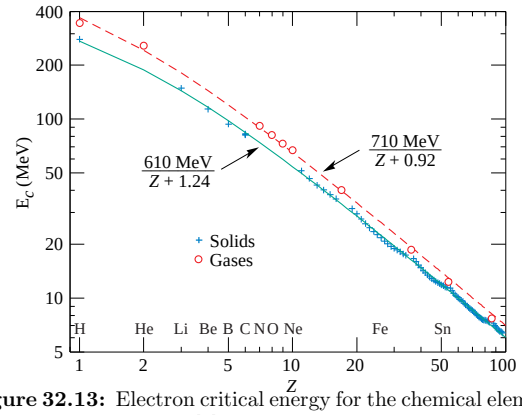

Figure 32.13: Electron critical energy for the chemical elements, using Rossi's definition [2]. The fits shown are for solids and liquids (solid line) and gases (dashed line). The rms deviation is 2.2% for the solids and 4.0% for the gases. (Computed with code supplied by A. Fassó.)

where w_j and X_j are the fraction by weight and the radiation length for the jth element.

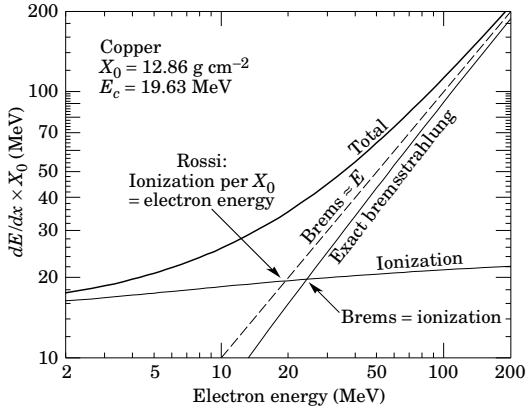

Figure 32.14: Two definitions of the critical energy E_c.

32.4.3. ***Bremsstrahlung energy loss by $e^{\pm}$*** : At very high energies and except at the high-energy tip of the bremsstrahlung spectrum, the cross section can be approximated in the "complete screening case" as [43]

$$d\sigma/dk = (1/k)4\alpha r_e^2\{(\tfrac{4}{3} - \tfrac{4}{3}y + y^2)[Z^2(L_{\rm rad} - f(Z)) + Z\,L'_{\rm rad}] + \tfrac{1}{9}(1-y)(Z^2+Z)\}\ , \tag{32.29}$$

where $y = k/E$ is the fraction of the electron's energy transferred to the radiated photon. At small y (the "infrared limit") the term on the second line ranges from 1.7% (low Z) to 2.5% (high Z) of the total. If it is ignored and the first line simplified with the definition of X_0 given in Eq. (32.26), we have

$$\frac{d\sigma}{dk} = \frac{A}{X_0 N_A k}\left(\tfrac{4}{3} - \tfrac{4}{3}y + y^2\right)\ . \tag{32.30}$$

This cross section (times k) is shown by the top curve in Fig. 32.12.

This formula is accurate except in near $y = 1$, where screening may become incomplete, and near $y = 0$, where the infrared divergence is removed by the interference of bremsstrahlung amplitudes from nearby scattering centers (the LPM effect) [45,46] and dielectric suppression [47,48]. These and other suppression effects in bulk media are discussed in Sec. 32.4.6.

With decreasing energy ($E \lesssim 10$ GeV) the high-y cross section drops and the curves become rounded as $y \to 1$. Curves of this familar shape can be seen in Rossi [2] (Figs. 2.11.2,3); see also the review by Koch & Motz [49].

Except at these extremes, and still in the complete-screening approximation, the number of photons with energies between $k_{\rm min}$ and $k_{\rm max}$ emitted by an electron travelling a distance $d \ll X_0$ is

$$N_\gamma = \frac{d}{X_0}\left[\frac{4}{3}\ln\left(\frac{k_{\rm max}}{k_{\rm min}}\right) - \frac{4(k_{\rm max} - k_{\rm min})}{3E} + \frac{k_{\rm max}^2 - k_{\rm min}^2}{2E^2}\right]\ . \tag{32.31}$$

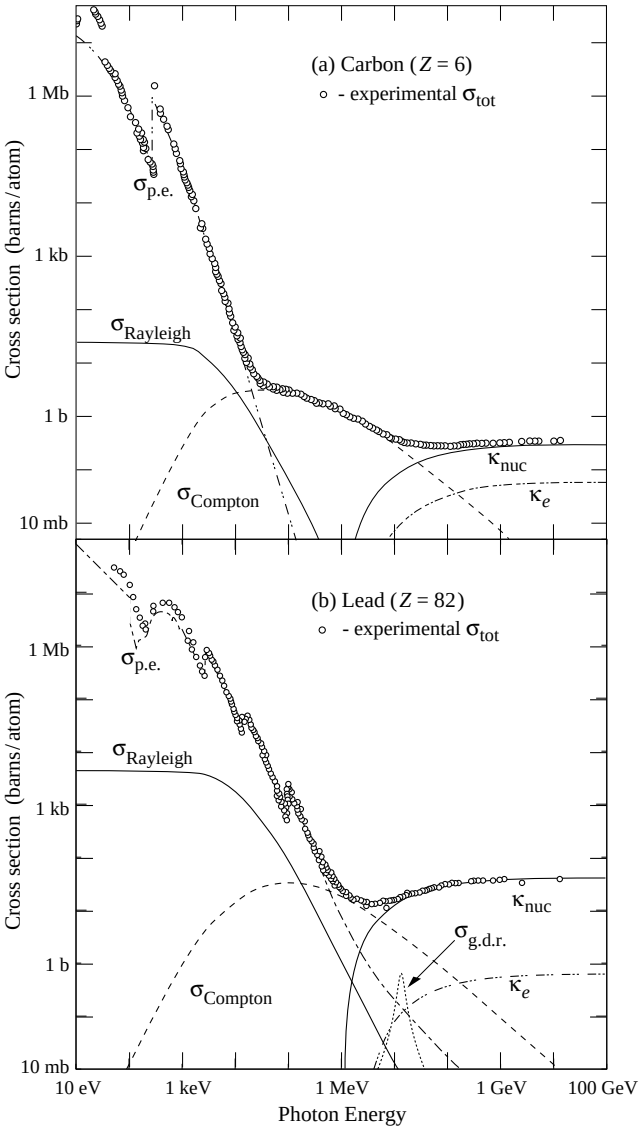

Figure 32.15: Photon total cross sections as a function of energy in carbon and lead, showing the contributions of different processes [51]:

$\sigma_{\rm p.e.}$ = Atomic photoelectric effect (electron ejection, photon absorption)
$\sigma_{\rm Rayleigh}$ = Rayleigh (coherent) scattering–atom neither ionized nor excited
$\sigma_{\rm Compton}$ = Incoherent scattering (Compton scattering off an electron)
$\kappa_{\rm nuc}$ = Pair production, nuclear field
κ_e = Pair production, electron field
$\sigma_{\rm g.d.r.}$ = Photonuclear interactions, most notably the Giant Dipole Resonance [52]. In these interactions, the target nucleus is broken up.

Original figures through the courtesy of John H. Hubbell (NIST).

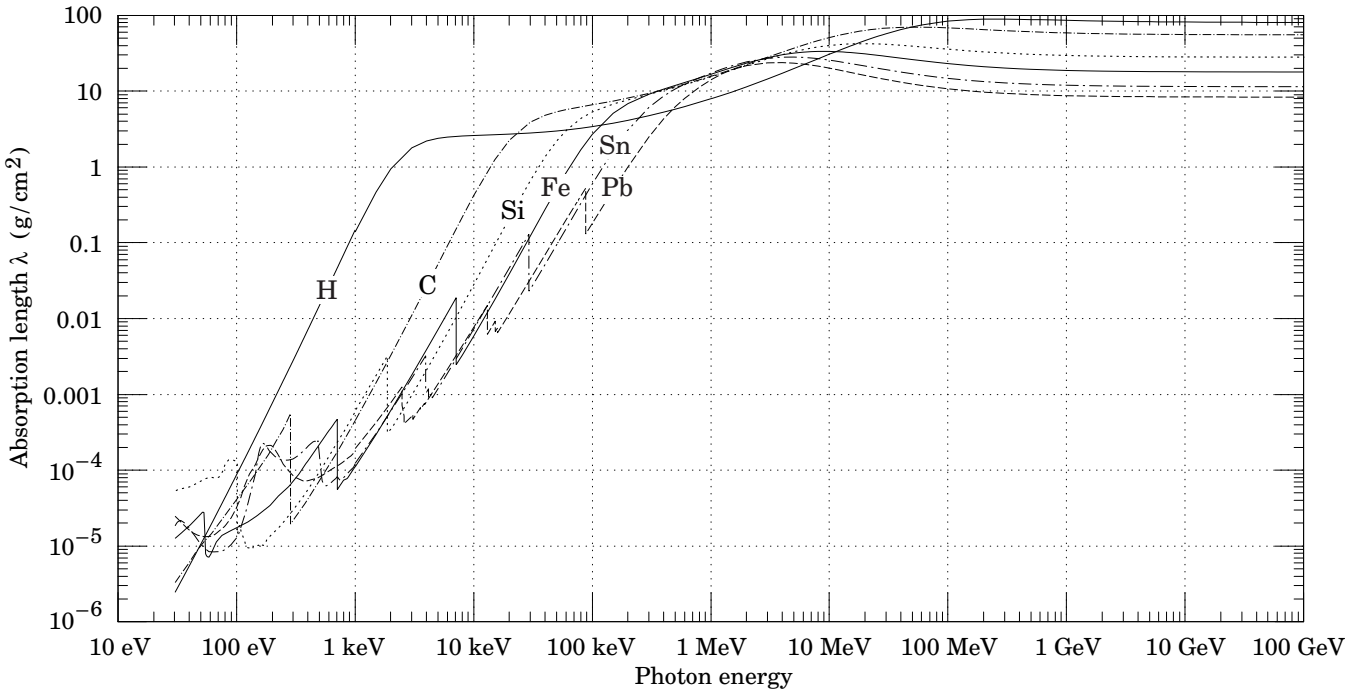

Fig. 32.16: The photon mass attenuation length (or mean free path) $\lambda = 1/(\mu/\rho)$ for various elemental absorbers as a function of photon energy. The mass attenuation coefficient is μ/ρ, where ρ is the density. The intensity I remaining after traversal of thickness t (in mass/unit area) is given by $I = I_0 \exp(-t/\lambda)$. The accuracy is a few percent. For a chemical compound or mixture, $1/\lambda_{\rm eff} \approx \sum_{\rm elements} w_Z/\lambda_Z$, where w_Z is the proportion by weight of the element with atomic number Z. The processes responsible for attenuation are given in Fig. 32.11. Since coherent processes are included, not all these processes result in energy deposition. The data for 30 eV $< E <$ 1 keV are obtained from `http://www-cxro.lbl.gov/optical_constants` (courtesy of Eric M. Gullikson, LBNL). The data for 1 keV $< E <$ 100 GeV are from `http://physics.nist.gov/PhysRefData`, through the courtesy of John H. Hubbell (NIST).

32.4.4. ***Critical energy*** : An electron loses energy by bremsstrahlung at a rate nearly proportional to its energy, while the ionization loss rate varies only logarithmically with the electron energy. The *critical energy* E_c is sometimes defined as the energy at which the two loss rates are equal [50]. Among alternate definitions is that of Rossi [2], who defines the critical energy as the energy at which the ionization loss per radiation length is equal to the electron energy. Equivalently, it is the same as the first definition with the approximation $|dE/dx|_{\rm brems} \approx E/X_0$. This form has been found to describe transverse electromagnetic shower development more accurately (see below). These definitions are illustrated in the case of copper in Fig. 32.14.

The accuracy of approximate forms for E_c has been limited by the failure to distinguish between gases and solid or liquids, where there is a substantial difference in ionization at the relevant energy because of the density effect. We distinguish these two cases in Fig. 32.13. Fits were also made with functions of the form $a/(Z+b)^\alpha$, but α was found to be essentially unity. Since E_c also depends on A, I, and other factors, such forms are at best approximate.

Values of E_c for both electrons and positrons in more than 300 materials can be found at `pdg.lbl.gov/AtomicNuclearProperties`.

32.4.5. ***Energy loss by photons*** : Contributions to the photon cross section in a light element (carbon) and a heavy element (lead) are shown in Fig. 32.15. At low energies it is seen that the photoelectric effect dominates, although Compton scattering, Rayleigh scattering, and photonuclear absorption also contribute. The photoelectric cross section is characterized by discontinuities (absorption edges) as thresholds for photoionization of various atomic levels are reached. Photon attenuation lengths for a variety of elements are shown in Fig. 32.16, and data for 30 eV$< k <$100 GeV for all elements are available from the web pages given in the caption. Here k is the photon energy.

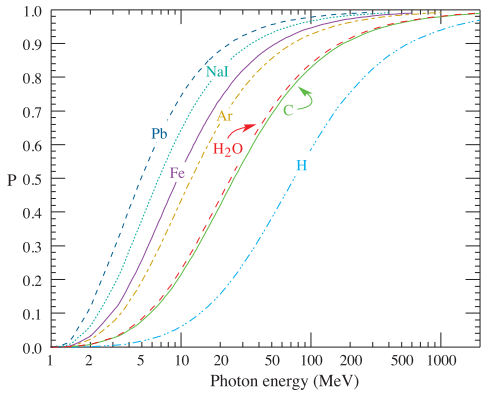

Figure 32.17: Probability P that a photon interaction will result in conversion to an e^+e^- pair. Except for a few-percent contribution from photonuclear absorption around 10 or 20 MeV, essentially all other interactions in this energy range result in Compton scattering off an atomic electron. For a photon attenuation length λ (Fig. 32.16), the probability that a given photon will produce an electron pair (without first Compton scattering) in thickness t of absorber is $P[1 - \exp(-t/\lambda)]$.

The increasing domination of pair production as the energy increases is shown in Fig. 32.17. Using approximations similar to those used to obtain Eq. (32.30), Tsai's formula for the differential cross section [43] reduces to

$$\frac{d\sigma}{dx} = \frac{A}{X_0 N_A}\left[1 - \tfrac{4}{3}x(1-x)\right] \qquad (32.32)$$

in the complete-screening limit valid at high energies. Here $x = E/k$ is the fractional energy transfer to the pair-produced electron (or

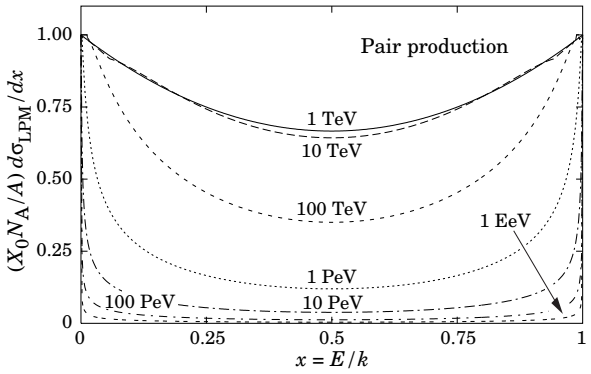

Figure 32.18: The normalized pair production cross section $d\sigma_{LPM}/dy$, versus fractional electron energy $x = E/k$.

positron), and k is the incident photon energy. The cross section is very closely related to that for bremsstrahlung, since the Feynman diagrams are variants of one another. The cross section is of necessity symmetric between x and $1-x$, as can be seen by the solid curve in Fig. 32.18. See the review by Motz, Olsen, & Koch for a more detailed treatment [53].

Eq. (32.32) may be integrated to find the high-energy limit for the total e^+e^- pair-production cross section:

$$\sigma = \tfrac{7}{9}(A/X_0 N_A)\ . \tag{32.33}$$

Equation Eq. (32.33) is accurate to within a few percent down to energies as low as 1 GeV, particularly for high-Z materials.

32.4.6. ***Bremsstrahlung and pair production at very high energies*** : At ultrahigh energies, Eqns. 32.29–32.33 will fail because of quantum mechanical interference between amplitudes from different scattering centers. Since the longitudinal momentum transfer to a given center is small ($\propto k/E(E-k)$, in the case of bremsstrahlung), the interaction is spread over a comparatively long distance called the formation length ($\propto E(E-k)/k$) via the uncertainty principle. In alternate language, the formation length is the distance over which the highly relativistic electron and the photon "split apart." The interference is usually destructive. Calculations of the "Landau-Pomeranchuk-Migdal" (LPM) effect may be made semi-classically based on the average multiple scattering, or more rigorously using a quantum transport approach [45,46].

In amorphous media, bremsstrahlung is suppressed if the photon energy k is less than $E^2/(E + E_{LPM})$ [46], where*

$$E_{LPM} = \frac{(m_e c^2)^2 \alpha X_0}{4\pi\hbar c \rho} = (7.7\ \text{TeV/cm}) \times \frac{X_0}{\rho}\ . \tag{32.34}$$

Since physical distances are involved, X_0/ρ, in cm, appears. The energy-weighted bremsstrahlung spectrum for lead, $k\, d\sigma_{LPM}/dk$, is shown in Fig. 32.12. With appropriate scaling by X_0/ρ, other materials behave similarly.

For photons, pair production is reduced for $E(k-E) > k\, E_{LPM}$. The pair-production cross sections for different photon energies are shown in Fig. 32.18.

If $k \ll E$, several additional mechanisms can also produce suppression. When the formation length is long, even weak factors can perturb the interaction. For example, the emitted photon can coherently forward scatter off of the electrons in the media. Because of this, for $k < \omega_p E/m_e \sim 10^{-4}$, bremsstrahlung is suppressed by a factor $(k m_e/\omega_p E)^2$ [48]. Magnetic fields can also suppress bremsstrahlung.

In crystalline media, the situation is more complicated, with coherent enhancement or suppression possible. The cross section depends on the electron and photon energies and the angles between the particle direction and the crystalline axes [55].

* This definition differs from that of Ref. 54 by a factor of two. E_{LPM} scales as the 4th power of the mass of the incident particle, so that $E_{LPM} = (1.4 \times 10^{10}\ \text{TeV/cm}) \times X_0/\rho$ for a muon.

32.4.7. ***Photonuclear and electronuclear interactions at still higher energies*** : At still higher photon and electron energies, where the bremsstrahlung and pair production cross-sections are heavily suppressed by the LPM effect, photonuclear and electronuclear interactions predominate over electromagnetic interactions.

At photon energies above about 10^{20} eV, for example, photons usually interact hadronically. The exact cross-over energy depends on the model used for the photonuclear interactions. These processes are illustrated in Fig. 32.19. At still higher energies ($\gtrsim 10^{23}$ eV), photonuclear interactions can become coherent, with the photon interaction spread over multiple nuclei. Essentially, the photon coherently converts to a ρ^0, in a process that is somewhat similar to kaon regeneration [56].

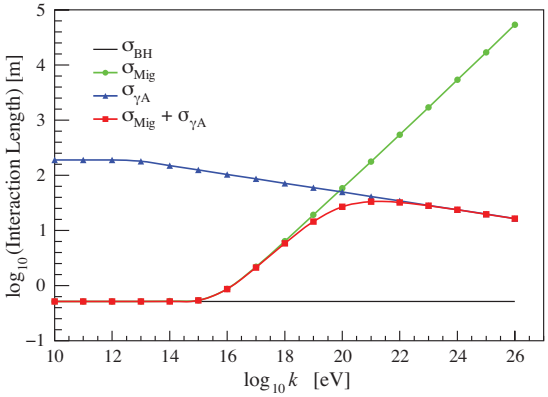

Figure 32.19: Interaction length for a photon in ice as a function of photon energy for the Bethe-Heitler (BH), LPM (Mig) and photonuclear (γA) cross sections [56]. The Bethe-Heitler interaction length is $9X_0/7$, and X_0 is 0.393 m in ice.

Similar processes occur for electrons. As electron energies increase and the LPM effect suppresses bremsstrahlung, electronuclear interactions become more important. At energies above 10^{21}eV, these electronuclear interactions dominate electron energy loss [56].

32.5. Electromagnetic cascades

When a high-energy electron or photon is incident on a thick absorber, it initiates an electromagnetic cascade as pair production and bremsstrahlung generate more electrons and photons with lower energy. The longitudinal development is governed by the high-energy part of the cascade, and therefore scales as the radiation length in the material. Electron energies eventually fall below the critical energy, and then dissipate their energy by ionization and excitation rather than by the generation of more shower particles. In describing shower behavior, it is therefore convenient to introduce the scale variables

$$t = x/X_0\ , \qquad y = E/E_c\ , \tag{32.35}$$

so that distance is measured in units of radiation length and energy in units of critical energy.

Longitudinal profiles from an EGS4 [57] simulation of a 30 GeV electron-induced cascade in iron are shown in Fig. 32.20. The number of particles crossing a plane (very close to Rossi's Π function [2]) is sensitive to the cutoff energy, here chosen as a total energy of 1.5 MeV for both electrons and photons. The electron number falls off more quickly than energy deposition. This is because, with increasing depth, a larger fraction of the cascade energy is carried by photons. Exactly what a calorimeter measures depends on the device, but it is not likely to be exactly any of the profiles shown. In gas counters it may be very close to the electron number, but in glass Cherenkov detectors and other devices with "thick" sensitive regions it is closer to the energy deposition (total track length). In such detectors the signal is proportional to the "detectable" track length T_d, which is in general less than the total track length T. Practical devices are sensitive to electrons with energy above some detection threshold E_d, and $T_d = T\, F(E_d/E_c)$. An analytic form for $F(E_d/E_c)$ obtained by Rossi [2] is given by Fabjan in Ref. 58; see also Amaldi [59].

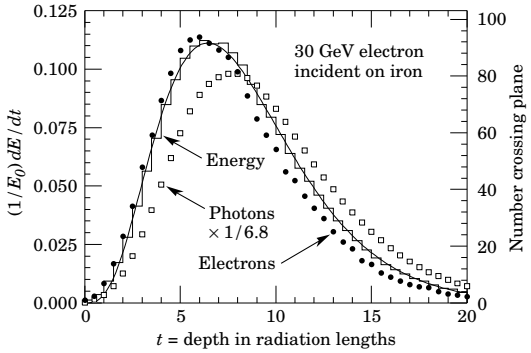

Figure 32.20: An EGS4 simulation of a 30 GeV electron-induced cascade in iron. The histogram shows fractional energy deposition per radiation length, and the curve is a gamma-function fit to the distribution. Circles indicate the number of electrons with total energy greater than 1.5 MeV crossing planes at $X_0/2$ intervals (scale on right) and the squares the number of photons with $E \geq 1.5$ MeV crossing the planes (scaled down to have same area as the electron distribution).

The mean longitudinal profile of the energy deposition in an electromagnetic cascade is reasonably well described by a gamma distribution [60]:

$$\frac{dE}{dt} = E_0\, b\, \frac{(bt)^{a-1} e^{-bt}}{\Gamma(a)} \tag{32.36}$$

The maximum $t_{\max}$ occurs at $(a-1)/b$. We have made fits to shower profiles in elements ranging from carbon to uranium, at energies from 1 GeV to 100 GeV. The energy deposition profiles are well described by Eq. (32.36) with

$$t_{\max} = (a-1)/b = 1.0 \times (\ln y + C_j)\ , \qquad j = e, \gamma\ , \tag{32.37}$$

where $C_e = -0.5$ for electron-induced cascades and $C_\gamma = +0.5$ for photon-induced cascades. To use Eq. (32.36), one finds $(a-1)/b$ from Eq. (32.37) and Eq. (32.35), then finds a either by assuming $b \approx 0.5$ or by finding a more accurate value from Fig. 32.21. The results are very similar for the electron number profiles, but there is some dependence on the atomic number of the medium. A similar form for the electron number maximum was obtained by Rossi in the context of his "Approximation B," [2] (see Fabjan's review in Ref. 58), but with $C_e = -1.0$ and $C_\gamma = -0.5$; we regard this as superseded by the EGS4 result.

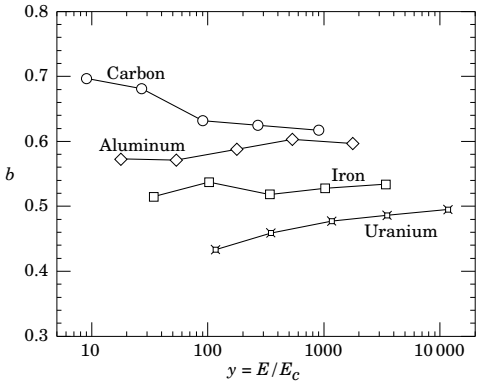

Figure 32.21: Fitted values of the scale factor b for energy deposition profiles obtained with EGS4 for a variety of elements for incident electrons with $1 \leq E_0 \leq 100$ GeV. Values obtained for incident photons are essentially the same.

The "shower length" $X_s = X_0/b$ is less conveniently parameterized, since b depends upon both Z and incident energy, as shown in Fig. 32.21. As a corollary of this Z dependence, the number of electrons crossing a plane near shower maximum is underestimated using Rossi's approximation for carbon and seriously overestimated for uranium. Essentially the same b values are obtained for incident electrons and photons. For many purposes it is sufficient to take $b \approx 0.5$.

The length of showers initiated by ultra-high energy photons and electrons is somewhat greater than at lower energies since the first or first few interaction lengths are increased via the mechanisms discussed above.

The gamma function distribution is very flat near the origin, while the EGS4 cascade (or a real cascade) increases more rapidly. As a result Eq. (32.36) fails badly for about the first two radiation lengths; it was necessary to exclude this region in making fits.

Because fluctuations are important, Eq. (32.36) should be used only in applications where average behavior is adequate. Grindhammer *et al.* have developed fast simulation algorithms in which the variance and correlation of a and b are obtained by fitting Eq. (32.36) to individually simulated cascades, then generating profiles for cascades using a and b chosen from the correlated distributions [61].

The transverse development of electromagnetic showers in different materials scales fairly accurately with the *Molière radius* R_M, given by [62,63]

$$R_M = X_0\, E_s/E_c\ , \tag{32.38}$$

where $E_s \approx 21$ MeV (Table 32.1), and the Rossi definition of E_c is used.

In a material containing a weight fraction w_j of the element with critical energy E_{cj} and radiation length X_j, the Molière radius is given by

$$\frac{1}{R_M} = \frac{1}{E_s} \sum \frac{w_j\, E_{cj}}{X_j}\ . \tag{32.39}$$

Measurements of the lateral distribution in electromagnetic cascades are shown in Refs. 62 and 63. On the average, only 10% of the energy lies outside the cylinder with radius R_M. About 99% is contained inside of $3.5R_M$, but at this radius and beyond composition effects become important and the scaling with R_M fails. The distributions are characterized by a narrow core, and broaden as the shower develops. They are often represented as the sum of two Gaussians, and Grindhammer [61] describes them with the function

$$f(r) = \frac{2r\, R^2}{(r^2 + R^2)^2}\ , \tag{32.40}$$

where R is a phenomenological function of x/X_0 and $\ln E$.

At high enough energies, the LPM effect (Sec. 32.4.6) reduces the cross sections for bremsstrahlung and pair production, and hence can cause significant elongation of electromagnetic cascades [46].

32.6. Muon energy loss at high energy

At sufficiently high energies, radiative processes become more important than ionization for all charged particles. For muons and pions in materials such as iron, this "critical energy" occurs at several hundred GeV. (There is no simple scaling with particle mass, but for protons the "critical energy" is much, much higher.) Radiative effects dominate the energy loss of energetic muons found in cosmic rays or produced at the newest accelerators. These processes are characterized by small cross sections, hard spectra, large energy fluctuations, and the associated generation of electromagnetic and (in the case of photonuclear interactions) hadronic showers [64–72]. As a consequence, at these energies the treatment of energy loss as a uniform and continuous process is for many purposes inadequate.

It is convenient to write the average rate of muon energy loss as [73]

$$-dE/dx = a(E) + b(E)\, E\ . \tag{32.41}$$

Here $a(E)$ is the ionization energy loss given by Eq. (32.5), and $b(E)$ is the sum of e^+e^- pair production, bremsstrahlung, and photonuclear contributions. To the approximation that these slowly-varying functions are constant, the mean range x_0 of a muon with initial energy E_0 is given by

$$x_0 \approx (1/b) \ln(1 + E_0/E_{\mu c})\ , \tag{32.42}$$

where $E_{\mu c} = a/b$. Fig. 32.22 shows contributions to $b(E)$ for iron. Since $a(E) \approx 0.002$ GeV g^{-1} cm^2, $b(E)E$ dominates the energy loss above several hundred GeV, where $b(E)$ is nearly constant. The rates of energy loss for muons in hydrogen, uranium, and iron are shown in Fig. 32.23 [5].

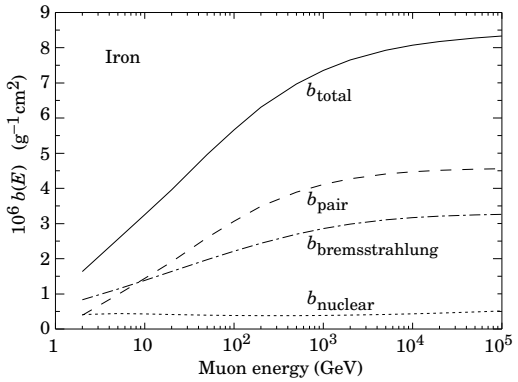

Figure 32.22: Contributions to the fractional energy loss by muons in iron due to e^+e^- pair production, bremsstrahlung, and photonuclear interactions, as obtained from Groom *et al.* [5] except for post-Born corrections to the cross section for direct pair production from atomic electrons.

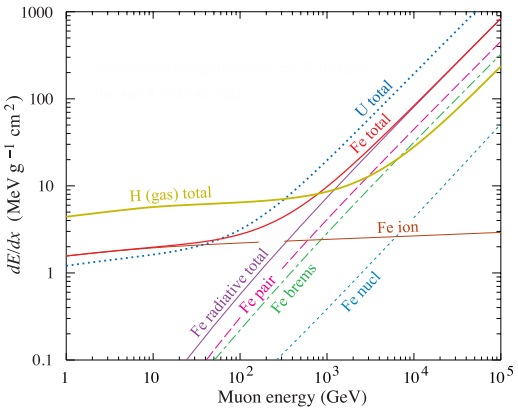

Figure 32.23: The average energy loss of a muon in hydrogen, iron, and uranium as a function of muon energy. Contributions to dE/dx in iron from ionization and the processes shown in Fig. 32.22 are also shown.

The "muon critical energy" $E_{\mu c}$ can be defined more exactly as the energy at which radiative and ionization losses are equal, and can be found by solving $E_{\mu c} = a(E_{\mu c})/b(E_{\mu c})$. This definition corresponds to the solid-line intersection in Fig. 32.14, and is different from the Rossi definition we used for electrons. It serves the same function: below $E_{\mu c}$ ionization losses dominate, and above $E_{\mu c}$ radiative effects dominate. The dependence of $E_{\mu c}$ on atomic number Z is shown in Fig. 32.24.

The radiative cross sections are expressed as functions of the fractional energy loss ν. The bremsstrahlung cross section goes roughly as $1/\nu$ over most of the range, while for the pair production case the distribution goes as ν^{-3} to ν^{-2} [74]. "Hard" losses are therefore more probable in bremsstrahlung, and in fact energy losses due to pair production may very nearly be treated as continuous. The simulated [72] momentum distribution of an incident 1 TeV/c muon beam after it crosses 3 m of iron is shown in Fig. 32.25. The most probable loss is 8 GeV, or 3.4 MeV g^{-1}cm^2. The full width at half maximum is 9 GeV/c, or 0.9%. The radiative tail is almost entirely due to bremsstrahlung, although most of the events in which more than 10% of the incident energy lost experienced relatively hard photonuclear interactions. The latter can exceed detector resolution [75], necessitating the reconstruction of lost energy. Tables in Ref. 5 list the stopping power as 9.82 MeV g^{-1}cm^2 for a 1 TeV muon, so that the mean loss should be 23 GeV ($\approx$ 23 GeV/c), for a final momentum of 977 GeV/c, far below the peak. This agrees with the indicated mean calculated from the simulation. Electromagnetic and hadronic cascades in detector materials can obscure muon tracks in detector planes and reduce tracking efficiency [76].

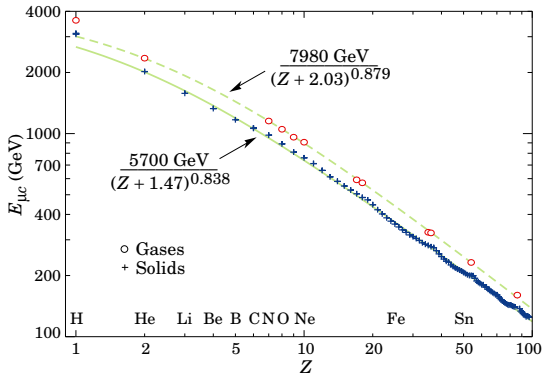

Figure 32.24: Muon critical energy for the chemical elements, defined as the energy at which radiative and ionization energy loss rates are equal [5]. The equality comes at a higher energy for gases than for solids or liquids with the same atomic number because of a smaller density effect reduction of the ionization losses. The fits shown in the figure exclude hydrogen. Alkali metals fall 3–4% above the fitted function, while most other solids are within 2% of the function. Among the gases the worst fit is for radon (2.7% high).

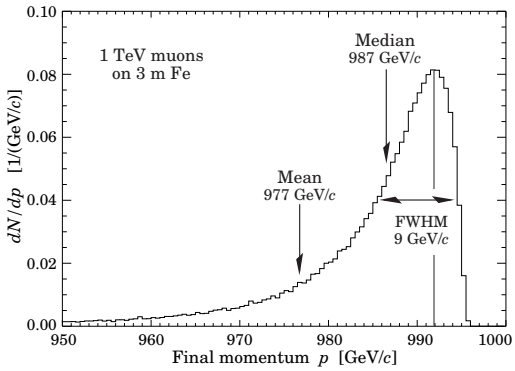

Figure 32.25: The momentum distribution of 1 TeV/c muons after traversing 3 m of iron as calculated with the MARS15 Monte Carlo code [72] by S.I. Striganov [5].

32.7. Cherenkov and transition radiation [33,77,78]

A charged particle radiates if its velocity is greater than the local phase velocity of light (Cherenkov radiation) or if it crosses suddenly from one medium to another with different optical properties (transition radiation). Neither process is important for energy loss, but both are used in high-energy and cosmic-ray physics detectors.

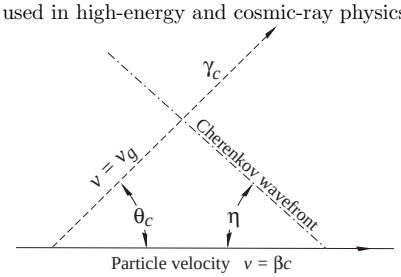

Figure 32.26: Cherenkov light emission and wavefront angles. In a dispersive medium, $\theta_c + \eta \neq 90^0$.

32.7.1. ***Optical Cherenkov radiation*** : The angle θ_c of Cherenkov radiation, relative to the particle's direction, for a particle with velocity βc in a medium with index of refraction n is

$$\cos\theta_c = (1/n\beta)$$

$$\text{or} \quad \tan\theta_c = \sqrt{\beta^2 n^2 - 1}$$

$$\approx \sqrt{2(1 - 1/n\beta)} \quad \text{for small } \theta_c, \textit{e.g.} \text{ in gases.} \quad (32.43)$$

The threshold velocity β_t is $1/n$, and $\gamma_t = 1/(1-\beta_t^2)^{1/2}$. Therefore, $\beta_t\gamma_t = 1/(2\delta+\delta^2)^{1/2}$, where $\delta = n-1$. Values of δ for various commonly used gases are given as a function of pressure and wavelength in Ref. 79. For values at atmospheric pressure, see Table 6.1. Data for other commonly used materials are given in Ref. 80.

Practical Cherenkov radiator materials are dispersive. Let ω be the photon's frequency, and let $k = 2\pi/\lambda$ be its wavenumber. The photons propage at the group velocity $v_g = d\omega/dk = c/[n(\omega)+\omega(dn/d\omega)]$. In a non-dispersive medium, this simplies to $v_g = c/n$.

In his classical paper, Tamm [81] showed that for dispersive media the radiation is concentrated in a thin conical shell whose vertex is at the moving charge, and whose opening half-angle η is given by

$$\cot\eta = \left[\frac{d}{d\omega}(\omega\tan\theta_c)\right]_{\omega_0} = \left[\tan\theta_c + \beta^2\omega\, n(\omega)\frac{dn}{d\omega}\cot\theta_c\right]_{\omega_0} , \qquad (32.44)$$

where ω_0 is the central value of the small frequency range under consideration. (See Fig. 32.26.) This cone has a opening half-angle η, and, unless the medium is non-dispersive ($dn/d\omega = 0$), $\theta_c + \eta \neq 90^0$. The Cherenkov wavefront 'sideslips' along with the particle [82]. This effect has timing implications for ring imaging Cherenkov counters [83], but it is probably unimportant for most applications.

The number of photons produced per unit path length of a particle with charge ze and per unit energy interval of the photons is

$$\frac{d^2N}{dEdx} = \frac{\alpha z^2}{\hbar c}\sin^2\theta_c = \frac{\alpha^2 z^2}{r_e\, m_e c^2}\left(1 - \frac{1}{\beta^2 n^2(E)}\right) \approx 370\,\sin^2\theta_c(E)\ \mathrm{eV}^{-1}\mathrm{cm}^{-1} \qquad (z=1)\ , \qquad (32.45)$$

or, equivalently,

$$\frac{d^2N}{dxd\lambda} = \frac{2\pi\alpha z^2}{\lambda^2}\left(1 - \frac{1}{\beta^2 n^2(\lambda)}\right) . \qquad (32.46)$$

The index of refraction n is a function of photon energy $E = \hbar\omega$, as is the sensitivity of the transducer used to detect the light. For practical use, Eq. (32.45) must be multiplied by the the transducer response function and integrated over the region for which $\beta\, n(\omega) > 1$. Further details are given in the discussion of Cherenkov detectors in the Particle Detectors section (Sec. 33 of this *Review*).

When two particles are close together (lateral separation $\lesssim 1$ wavelength), the electromagnetic fields from the particles may add coherently, affecting the Cherenkov radiation. Because of their opposite charges, the radiation from an e^+e^- pair at close separation is suppressed compared to two independent leptons [84].

32.7.2. ***Coherent radio Cherenkov radiation*** :

Coherent Cherenkov radiation is produced by many charged particles with a non-zero net charge moving through matter on an approximately common "wavefront"—for example, the electrons and positrons in a high-energy electromagnetic cascade. The signals can be visible above backgrounds for shower energies as low as 10^{17} eV; see Sec. 34.3.3 for more details. The phenomenon is called the Askaryan effect [85]. Near the end of a shower, when typical particle energies are below E_c (but still relativistic), a charge imbalance develops. Photons can Compton-scatter atomic electrons, and positrons can annihilate with atomic electrons to contribute even more photons which can in turn Compton scatter. These processes result in a roughly 20% excess of electrons over positrons in a shower. The net negative charge leads to coherent radio Cherenkov emission. The radiation includes a component from the decelerating charges (as in bremsstrahlung). Because the emission is coherent, the electric field strength is proportional to the shower energy, and the signal power increases as its square. The electric field strength also increases linearly with frequency, up to a maximum frequency determined by the lateral spread of the shower. This cutoff occurs at about 1 GHz in ice, and scales inversely with the Moliere radius. At low frequencies, the radiation is roughly isotropic, but, as the frequency rises toward the cutoff frequency, the radiation becomes increasingly peaked around the Cherenkov angle. The radiation is linearly polarized in the plane containing the shower axis and the photon direction. A measurement of the signal polarization can be used to help determine the shower direction. The characteristics of this radiation have been nicely demonstrated in a series of experiments at SLAC [86]. A detailed discussion of the radiation can be found in Ref. 87.

32.7.3. ***Transition radiation*** : The energy radiated when a particle with charge ze crosses the boundary between vacuum and a medium with plasma frequency ω_p is

$$I = \alpha z^2\gamma\hbar\omega_p/3\ , \qquad (32.47)$$

where

$$\hbar\omega_p = \sqrt{4\pi N_e r_e^3}\, m_e c^2/\alpha = \sqrt{\rho\ (\mathrm{in\ g/cm^3})\ \langle Z/A\rangle}\times 28.81\ \mathrm{eV}\ . \qquad (32.48)$$

For styrene and similar materials, $\hbar\omega_p \approx 20$ eV; for air it is 0.7 eV.

The number spectrum $dN_\gamma/d(\hbar\omega$ diverges logarithmically at low energies and decreases rapidly for $\hbar\omega/\gamma\hbar\omega_p > 1$. About half the energy is emitted in the range $0.1 \leq \hbar\omega/\gamma\hbar\omega_p \leq 1$. Inevitable absorption in a practical detector removes the divergence. For a particle with $\gamma = 10^3$, the radiated photons are in the soft x-ray range 2 to 40 keV. The γ dependence of the emitted energy thus comes from the hardening of the spectrum rather than from an increased quantum yield.

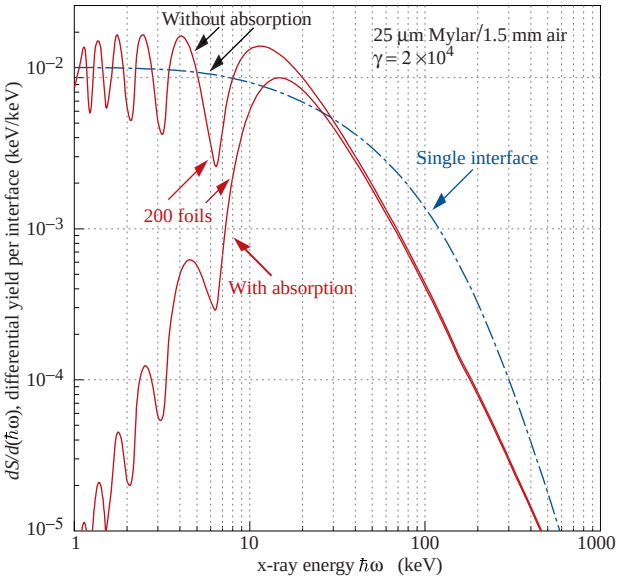

Figure 32.27: X-ray photon energy spectra for a radiator consisting of 200 25 μm thick foils of Mylar with 1.5 mm spacing in air (solid lines) and for a single surface (dashed line). Curves are shown with and without absorption. Adapted from Ref. 88.

The number of photons with energy $\hbar\omega > \hbar\omega_0$ is given by the answer to problem 13.15 in Ref. 33,

$$N_\gamma(\hbar\omega > \hbar\omega_0) = \frac{\alpha z^2}{\pi}\left[\left(\ln\frac{\gamma\hbar\omega_p}{\hbar\omega_0} - 1\right)^2 + \frac{\pi^2}{12}\right] , \qquad (32.49)$$

within corrections of order $(\hbar\omega_0/\gamma\hbar\omega_p)^2$. The number of photons above a fixed energy $\hbar\omega_0 \ll \gamma\hbar\omega_p$ thus grows as $(\ln\gamma)^2$, but the number above a fixed fraction of $\gamma\hbar\omega_p$ (as in the example above) is constant. For example, for $\hbar\omega > \gamma\hbar\omega_p/10$, $N_\gamma = 2.519\,\alpha z^2/\pi = 0.59\% \times z^2$.

The particle stays "in phase" with the x ray over a distance called the formation length, $d(\omega) = (2c/\omega)(1/\gamma^2 + \theta^2 + \omega_p^2/\omega^2)^{-1}$. Most of the radiation is produced in this distance. Here θ is the x-ray emission angle, characteristically $1/\gamma$. For $\theta = 1/\gamma$ the formation length has a maximum at $d(\gamma\omega_p/\sqrt{2}) = \gamma c/\sqrt{2}\,\omega_p$. In practical situations it is tens of μm.

Since the useful x-ray yield from a single interface is low, in practical detectors it is enhanced by using a stack of N foil radiators—foils L thick, where L is typically several formation lengths—separated by gas-filled gaps. The amplitudes at successive interfaces interfere to cause oscillations about the single-interface spectrum. At increasing frequencies above the position of the last interference maximum $(L/d(w) = \pi/2)$, the formation zones, which have opposite phase,

overlap more and more and the spectrum saturates, $dI/d\omega$ approaching zero as $L/d(\omega) \to 0$. This is illustrated in Fig. 32.27 for a realistic detector configuration.

For regular spacing of the layers fairly complicated analytic solutions for the intensity have been obtained [88,89]. Although one might expect the intensity of coherent radiation from the stack of foils to be proportional to N^2, the angular dependence of the formation length conspires to make the intensity $\propto N$.

References:

1. H. Bichsel, Nucl. Instrum. Methods **A562**, 154 (2006).
2. B. Rossi, *High Energy Particles*, Prentice-Hall, Inc., Englewood Cliffs, NJ, 1952.
3. H.A. Bethe, *Zur Theorie des Durchgangs schneller Korpuskularstrahlen durch Materie,* H. Bethe, Ann. Phys. **5**, 325 (1930).
4. "Stopping Powers and Ranges for Protons and Alpha Particles," ICRU Report No. 49 (1993); tables and graphs of these data are available at `http://physics.nist.gov/PhysRefData/`.
5. D.E. Groom, N.V. Mokhov, and S.I. Striganov, "Muon stopping-power and range tables: 10 MeV–100 TeV," Atomic Data and Nuclear Data Tables **78**, 183–356 (2001). Since submission of this paper it has become likely that post-Born corrections to the direct pair production cross section should be made. Code used to make Figs. 32.22–32.24 included these corrections [D.Yu. Ivanov *et al.*, Phys. Lett. **B442**, 453 (1998)]. The effect is negligible except at high Z. (It is less than 1% for iron.); More extensive printable and machine-readable tables are given at `http://pdg.lbl.gov/AtomicNuclearProperties/`.
6. W.H. Barkas, W. Birnbaum, and F.M. Smith, Phys. Rev. **101**, 778 (1956).
7. J. Lindhard and A. H. Sørensen, Phys. Rev. **A53**, 2443 (1996).
8. U. Fano, Ann. Rev. Nucl. Sci. **13**, 1 (1963).
9. J.D. Jackson, Phys. Rev. **D59**, 017301 (1999).
10. S.M. Seltzer and M.J. Berger, Int. J. of Applied Rad. **33**, 1189 (1982).
11. "Stopping Powers for Electrons and Positrons," ICRU Report No. 37 (1984).
12. `http://physics.nist.gov/PhysRefData/XrayMassCoef/tab1.html`.
13. H. Bichsel, Phys. Rev. **A46**, 5761 (1992).
14. W.H. Barkas and M.J. Berger, *Tables of Energy Losses and Ranges of Heavy Charged Particles*, NASA-SP-3013 (1964).
15. R.M. Sternheimer, Phys. Rev. **88**, 851 (1952).
16. R.M. Sternheimer, S.M. Seltzer, and M.J. Berger, "The Density Effect for the Ionization Loss of Charged Particles in Various Substances," Atomic Data and Nuclear Data Tables **30**, 261 (1984). Minor errors are corrected in Ref. 5. Chemical composition for the tabulated materials is given in Ref. 10.
17. R.M. Sternheimer and R.F. Peierls, Phys. Rev. **B3**, 3681 (1971).
18. S.P. Møller *et al.*, Phys. Rev. **A56**, 2930 (1997).
19. H.H. Andersen and J.F. Ziegler, *Hydrogen: Stopping Powers and Ranges in All Elements*. Vol. 3 of *The Stopping and Ranges of Ions in Matter* (Pergamon Press 1977).
20. J. Lindhard, Kgl. Danske Videnskab. Selskab, Mat.-Fys. Medd. **28**, No. 8 (1954); J. Lindhard, M. Scharff, and H.E. Schiøtt, Kgl. Danske Videnskab. Selskab, Mat.-Fys. Medd. **33**, No. 14 (1963).
21. J.F. Ziegler, J.F. Biersac, and U. Littmark, *The Stopping and Range of Ions in Solids*, Pergamon Press 1985.
22. E.A. Uehling, Ann. Rev. Nucl. Sci. **4**, 315 (1954) (For heavy particles with unit charge, but $e^{\pm}$ cross sections and stopping powers are also given).
23. N.F. Mott and H.S.W. Massey, *The Theory of Atomic Collisions*, Oxford Press, London, 1965.
24. L.D. Landau, J. Exp. Phys. (USSR) **8**, 201 (1944).
25. P.V. Vavilov, Sov. Phys. JETP **5**, 749 (1957).
26. H. Bichsel, Rev. Mod. Phys. **60**, 663 (1988).
27. R. Talman, Nucl. Instrum. Methods **159**, 189 (1979).
28. H. Bichsel, Ch. 87 in the Atomic, Molecular and Optical Physics Handbook, G.W.F. Drake, editor (Am. Inst. Phys. Press, Woodbury NY, 1996).
29. S.M. Seltzer and M.J. Berger, Int. J. of Applied Rad. **35**, 665 (1984). This paper corrects and extends the results of Ref. 10.
30. L.V. Spencer "Energy Dissipation by Fast Electrons," Nat'l Bureau of Standards Monograph No. 1 (1959).
31. "Average Energy Required to Produce an Ion Pair," ICRU Report No. 31 (1979).
32. N. Hadley *et al.*, "List of Poisoning Times for Materials," Lawrence Berkeley Lab Report TPC-LBL-79-8 (1981).
33. J.D. Jackson, *Classical Electrodynamics*, 3rd edition, (John Wiley and Sons, New York, 1998).
34. H.A. Bethe, Phys. Rev. **89**, 1256 (1953).
35. W.T. Scott, Rev. Mod. Phys. **35**, 231 (1963).
36. J.W. Motz, H. Olsen, and H.W. Koch, Rev. Mod. Phys. **36**, 881 (1964).
37. H. Bichsel, Phys. Rev. **112**, 182 (1958).
38. G. Shen *et al.*, (Phys. Rev. **D20**, 1584 (1979)).
39. V.L. Highland, Nucl. Instrum. Methods **129**, 497 (1975); Nucl. Instrum. Methods **161**, 171 (1979).
40. G.R. Lynch and O.I Dahl, Nucl. Instrum. Methods **B58**, 6 (1991). Eq. (32.15) is Eq. 12 from this paper.
41. M. Wong *et al.*, Med. Phys. **17**, 163 (1990).
42. E. Segrè, *Nuclei and Particles*, New York, Benjamin (1964) p. 65 ff.
43. Y.S. Tsai, Rev. Mod. Phys. **46**, 815 (1974).
44. H. Davies, H.A. Bethe, and L.C. Maximon, Phys. Rev. **93**, 788 (1954).
45. L.D. Landau and I.J. Pomeranchuk, Dokl. Akad. Nauk. SSSR **92**, 535 (1953); **92**, 735 (1953). These papers are available in English in L. Landau, *The Collected Papers of L.D. Landau*, Pergamon Press, 1965; A.B. Migdal, Phys. Rev. **103**, 1811 (1956).
46. S. Klein, Rev. Mod. Phys. **71**, 1501 (1999).
47. M.L. Ter-Mikaelian, SSSR **94**, 1033 (1954); M.L. Ter-Mikaelian, *High Energy Electromagnetic Processes in Condensed Media* (John Wiley and Sons, New York, 1972).
48. P. Anthony *et al.*, Phys. Rev. Lett. **76**, 3550 (1996).
49. H.W. Koch and J.W. Motz, Rev. Mod. Phys. **31**, 920 (1959).
50. M.J. Berger and S.M. Seltzer, "Tables of Energy Losses and Ranges of Electrons and Positrons," National Aeronautics and Space Administration Report NASA-SP-3012 (Washington DC 1964).
51. Data from J.H. Hubbell, H. Gimm, and I. Øverbø, J. Phys. Chem. Ref. Data **9**, 1023 (1980); parameters for $\sigma_{\text{g.d.r.}}$ from A. Veyssiere *et al.*, Nucl. Phys. **A159**, 561 (1970). Curves for these and other elements, compounds, and mixtures may be obtained from `http://physics.nist.gov/PhysRefData`. The photon total cross section is approximately flat for at least two decades beyond the energy range shown.
52. B.L. Berman and S.C. Fultz, Rev. Mod. Phys. **47**, 713 (1975).
53. J.W. Motz, H.A. Olsen, and H.W. Koch, Rev. Mod. Phys. **41**, 581 (1969).
54. P. Anthony *et al.*, Phys. Rev. Lett. **75**, 1949 (1995).
55. U.I. Uggerhoj, Rev. Mod. Phys. **77**, 1131 (2005).
56. L. Gerhardt and S.R. Klein, Phys. Rev. **D82**, 074017 (2010).
57. W.R. Nelson, H. Hirayama, and D.W.O. Rogers, "The EGS4 Code System," SLAC-265, Stanford Linear Accelerator Center (Dec. 1985).
58. *Experimental Techniques in High Energy Physics*, ed. T. Ferbel (Addison-Wesley, Menlo Park CA 1987).
59. U. Amaldi, Phys. Scripta **23**, 409 (1981).
60. E. Longo and I. Sestili, Nucl. Instrum. Methods **128**, 283 (1975).
61. G. Grindhammer *et al.*, in *Proceedings of the Workshop on Calorimetry for the Supercollider*, Tuscaloosa, AL, March 13–17, 1989, edited by R. Donaldson and M.G.D. Gilchriese (World Scientific, Teaneck, NJ, 1989), p. 151.
62. W.R. Nelson *et al.*, Phys. Rev. **149**, 201 (1966).
63. G. Bathow *et al.*, Nucl. Phys. **B20**, 592 (1970).

64. H.A. Bethe and W. Heitler, *Proc. Roy. Soc.* **A146**, 83 (1934); H.A. Bethe, *Proc. Cambridge Phil. Soc.* **30**, 542 (1934).
65. A.A. Petrukhin and V.V. Shestakov, Can. J. Phys. **46**, S377 (1968).
66. V.M. Galitskii and S.R. Kel'ner, Sov. Phys. JETP **25**, 948 (1967).
67. S.R. Kel'ner and Yu.D. Kotov, Sov. J. Nucl. Phys. **7**, 237 (1968).
68. R.P. Kokoulin and A.A. Petrukhin, in *Proceedings of the International Conference on Cosmic Rays*, Hobart, Australia, August 16–25, 1971, Vol. **4**, p. 2436.
69. A.I. Nikishov, Sov. J. Nucl. Phys. **27**, 677 (1978).
70. Y.M. Andreev *et al.*, Phys. Atom. Nucl. **57**, 2066 (1994).
71. L.B. Bezrukov and E.V. Bugaev, Sov. J. Nucl. Phys. **33**, 635 (1981).
72. N.V. Mokhov, "The MARS Code System User's Guide," Fermilab-FN-628 (1995);
N.V. Mokhov *et al.*, Radiation Protection and Dosimetry, vol. 116, part 2, pp. 99 (2005);
Fermilab-Conf-04/053 (2004);
N.V. Mokhov *et al.*, in *Proc. of Intl. Conf. on Nuclear Data for Science and Tech*, (Santa Fe, NM, 2004), AIP C onf. Proc. 769, part 2, p. 1618;
Fermilab-Conf-04/269-AD (2004);
`http://www-ap.fnal.gov/MARS/`.
73. P.H. Barrett *et al.*, Rev. Mod. Phys. **24**, 133 (1952).
74. A. Van Ginneken, Nucl. Instrum. Methods **A251**, 21 (1986).
75. U. Becker *et al.*, Nucl. Instrum. Methods **A253**, 15 (1986).
76. J.J. Eastman and S.C. Loken, in *Proceedings of the Workshop on Experiments, Detectors, and Experimental Areas for the Supercollider*, Berkeley, CA, July 7–17, 1987, edited by R. Donaldson and M.G.D. Gilchriese (World Scientific, Singapore, 1988), p. 542.
77. *Methods of Experimental Physics*, L.C.L. Yuan and C.-S. Wu, editors, Academic Press, 1961, Vol. 5A, p. 163.
78. W.W.M. Allison and P.R.S. Wright, "The Physics of Charged Particle Identification: dE/dx, Cherenkov Radiation, and Transition Radiation," p. 371 in *Experimental Techniques in High Energy Physics*, T. Ferbel, editor, (Addison-Wesley 1987).
79. E.R. Hayes, R.A. Schluter, and A. Tamosaitis, "Index and Dispersion of Some Cherenkov Counter Gases," ANL-6916 (1964).
80. T. Ypsilantis, "Particle Identification at Hadron Colliders," CERN-EP/89-150 (1989), or ECFA 89-124, **2** 661 (1989).
81. I. Tamm, J. Phys. U.S.S.R., **1**, 439 (1939).
82. H. Motz and L.I. Schiff, Am. J. Phys. **21**, 258 (1953).
83. B.N. Ratcliff, Nucl. Instrum and Meth. **A502**, 211 (2003).
84. S.K. Mandal, S.R. Klein, and J. D. Jackson, Phys. Rev. **D72**, 093003 (2005).
85. G.A. Askaryan, Sov. Phys. JETP **14**, 441 (1962).
86. P.W. Gorham *et al.*, Phys. Rev. **D72**, 023002 (2005).
87. E. Zas, F. Halzen, and T. Stanev, Phys. Rev. D 45,362(1992).
88. M.L. Cherry, Phys. Rev. **D10**, 3594–3607 (1974);
M.L. Cherry, Phys. Rev. **D17**, 2245–2260 (1978).
89. B. Dolgoshein, Nucl. Instrum. Methods **A326**, 434–469 (1993).

33. PARTICLE DETECTORS AT ACCELERATORS

Revised 2013. See the various sections for authors.

33.1. Introduction

This review summarizes the detector technologies employed at accelerator particle physics experiments. Several of these detectors are also used in a non-accelerator context and examples of such applications will be provided. The detector techniques which are specific to non-accelerator particle physics experiments are the subject of Chap. 34. More detailed discussions of detectors and their underlying physics can be found in books by Ferbel [1], Kleinknecht [2], Knoll [3], Green [4], Leroy & Rancoita [5], and Grupen [6].

In Table 33.1 are given typical resolutions and deadtimes of common charged particle detectors. The quoted numbers are usually based on typical devices, and should be regarded only as rough approximations for new designs. The spatial resolution refers to the intrinsic detector resolution, i.e. without multiple scattering. We note that analog detector readout can provide better spatial resolution than digital readout by measuring the deposited charge in neighboring channels. Quoted ranges attempt to be representative of both possibilities.The time resolution is defined by how accurately the time at which a particle crossed the detector can be determined. The deadtime is the minimum separation in time between two resolved hits on the same channel. Typical performance of calorimetry and particle identification are provided in the relevant sections below.

Table 33.1: Typical resolutions and deadtimes of common charged particle detectors. Revised November 2011.

Detector Type	Intrinsinc Spatial Resolution (rms)	Time Resolution	Dead Time
Resistive plate chamber	$\lesssim$10 mm	1–2 ns	—
Streamer chamber	300 μm[a]	2 μs	100 ms
Liquid argon drift [7]	∼175–450 μm	$\sim$ 200 ns	$\sim$ 2 μs
Scintillation tracker	∼100 μm	100 ps/n[b]	10 ns
Bubble chamber	10–150 μm	1 ms	50 ms[c]
Proportional chamber	50–100 μm[d]	2 ns	20-200 ns
Drift chamber	50–100 μm	2 ns[e]	20-100 ns
Micro-pattern gas detectors	30–40 μm	$<$ 10 ns	10-100 ns
Silicon strip	pitch/(3 to 7)[f]	few ns[g]	$\lesssim$50 ns[g]
Silicon pixel	$\lesssim$10 μm	few ns[g]	$\lesssim$50 ns[g]
Emulsion	1 μm	—	—

[a] 300 μm is for 1 mm pitch (wirespacing/$\sqrt{12}$).
[b] n = index of refraction.
[c] Multiple pulsing time.
[d] Delay line cathode readout can give ±150 μm parallel to anode wire.
[e] For two chambers.
[f] The highest resolution ("7") is obtained for small-pitch detectors ($\lesssim$25 μm) with pulse-height-weighted center finding.
[g] Limited by the readout electronics [8].

33.2. Photon detectors

Updated August 2011 by D. Chakraborty (Northern Illinois U) and T. Sumiyoshi (Tokyo Metro U).

Most detectors in high-energy, nuclear, and astrophysics rely on the detection of photons in or near the visible range, 100 nm $\lesssim \lambda \lesssim$ 1000 nm, or $E \approx$ a few eV. This range covers scintillation and Cherenkov radiation as well as the light detected in many astronomical observations.

Generally, photodetection involves generating a detectable electrical signal proportional to the (usually very small) number of incident photons. The process involves three distinct steps:

1. Generation of a primary photoelectron or electron-hole (e-h) pair by an incident photon by the photoelectric or photoconductive effect,

2. Amplification of the p.e. signal to detectable levels by one or more multiplicative bombardment steps and/or an avalanche process (usually), and,
3. Collection of the secondary electrons to form the electrical signal.

The important characteristics of a photodetector include the following in statistical averages:

1. Quantum efficiency (QE or ϵ_Q): the number of primary photoelectrons generated per incident photon ($0 \leq \epsilon_Q \leq 1$; in silicon more than one e-h pair per incident photon can be generated for $\lambda \lesssim 165$ nm),
2. Collection efficiency (CE or ϵ_C): the overall acceptance factor other than the generation of photoelectrons ($0 \leq \epsilon_C \leq 1$),
3. Gain (G): the number of electrons collected for each photoelectron generated,
4. Dark current or dark noise: the electrical signal when there is no photon,
5. Energy resolution: electronic noise (ENC or N_e) and statistical fluctuations in the amplification process compound the Poisson distribution of n_γ photons from a given source:

$$\frac{\sigma(E)}{\langle E \rangle} = \sqrt{\frac{f_N}{n_\gamma \epsilon_Q \epsilon_C} + \left(\frac{N_e}{G n_\gamma \epsilon_Q \epsilon_C}\right)^2}, \qquad (33.1)$$

where f_N, or the excess noise factor (ENF), is the contribution to the energy distribution variance due to amplification statistics [9],

6. Dynamic range: the maximum signal available from the detector (this is usually expressed in units of the response to noise-equivalent power, or NEP, which is the optical input power that produces a signal-to-noise ratio of 1),
7. Time dependence of the response: this includes the transit time, which is the time between the arrival of the photon and the electrical pulse, and the transit time spread, which contributes to the pulse rise time and width, and
8. Rate capability: inversely proportional to the time needed, after the arrival of one photon, to get ready to receive the next.

such as chemical composition, temperature, magnetic field, ambient background, as well as ambient radiation of different types and, mode of operation (continuous or triggered), bias (high-voltage) requirements, power consumption, calibration needs, aging, cost, and so on. Several technologies employing different phenomena for the three steps described above, and many variants within each, offer a wide range of solutions to choose from. The salient features of the main technologies and the common variants are described below. Some key characteristics are summarized in Table 33.2.

33.2.1. ***Vacuum photodetectors*** : Vacuum photodetectors can be broadly subdivided into three types: photomultiplier tubes, microchannel plates, and hybrid photodetectors.

33.2.1.1. *Photomultiplier tubes:* A versatile class of photon detectors, vacuum photomultiplier tubes (PMT) has been employed by a vast majority of all particle physics experiments to date [9]. Both "transmission-" and "reflection-type" PMT's are widely used. In the former, the photocathode material is deposited on the inside of a transparent window through which the photons enter, while in the latter, the photocathode material rests on a separate surface that the incident photons strike. The cathode material has a low work function, chosen for the wavelength band of interest. When a photon hits the cathode and liberates an electron (the photoelectric effect), the latter is accelerated and guided by electric fields to impinge on a secondary-emission electrode, or dynode, which then emits a few (~ 5) secondary electrons. The multiplication process is repeated typically 10 times in series to generate a sufficient number of electrons, which are collected at the anode for delivery to the external circuit. The total gain of a PMT depends on the applied high voltage V as $G = AV^{kn}$, where $k \approx 0.7$–0.8 (depending on the dynode material), n is the number of dynodes in the chain, and A a constant (which also depends on n). Typically, G is in the range of 10^5–10^6. Pulse risetimes are usually in the few nanosecond range. With *e.g.* two-level discrimination the effective time resolution can be much better.

Table 33.2: Representative characteristics of some photodetectors commonly used in particle physics. The time resolution of the devices listed here vary in the 10–2000 ps range.

Type	λ (nm)	$\epsilon_Q\,\epsilon_C$	Gain	Risetime (ns)	Area (mm^2)	1-p.e noise (Hz)	HV (V)	Price (USD)
PMT*	115–1700	0.15–0.25	10^3–10^7	0.7–10	10^2–10^5	10–10^4	500–3000	100–5000
MCP*	100–650	0.01–0.10	10^3–10^7	0.15–0.3	10^2–10^4	0.1–200	500–3500	10–6000
HPD*	115–850	0.1–0.3	10^3–10^4	7	10^2–10^5	10–10^3	$\sim 2 \times 10^4$	$\sim$600
GPM*	115–500	0.15–0.3	10^3–10^6	$O(0.1)$	$O(10)$	10–10^3	300–2000	$O(10)$
APD	300–1700	$\sim$0.7	10–10^8	$O(1)$	10–10^3	1–10^3	400–1400	$O(100)$
PPD	320–900	0.15–0.3	10^5–10^6	~ 1	1–10	$O(10^6)$	30–60	$O(100)$
VLPC	500–600	$\sim$0.9	$\sim 5 \times 10^4$	~ 10	1	$O(10^4)$	$\sim$7	$\sim$1

∗These devices often come in multi-anode configurations. In such cases, area, noise, and price are to be considered on a "per readout-channel" basis.

The QE is a strong function of the photon wavelength (λ), and is usually quoted at maximum, together with a range of λ where the QE is comparable to its maximum. Spatial uniformity and linearity with respect to the number of photons are highly desirable in a photodetector's response.

Optimization of these factors involves many trade-offs and vary widely between applications. For example, while a large gain is desirable, attempts to increase the gain for a given device also increases the ENF and after-pulsing ("echos" of the main pulse). In solid-state devices, a higher QE often requires a compromise in the timing properties. In other types, coverage of large areas by focusing increases the transit time spread.

Other important considerations also are highly application-specific. These include the photon flux and wavelength range, the total area to be covered and the efficiency required, the volume available to accommodate the detectors, characteristics of the environment

A large variety of PMT's, including many just recently developed, covers a wide span of wavelength ranges from infrared (IR) to extreme ultraviolet (XUV) [10]. They are categorized by the window materials, photocathode materials, dynode structures, anode configurations, *etc.* Common window materials are borosilicate glass for IR to near-UV, fused quartz and sapphire (Al_2O_3) for UV, and MgF_2 or LiF for XUV. The choice of photocathode materials include a variety of mostly Cs- and/or Sb-based compounds such as CsI, CsTe, bi-alkali (SbRbCs, SbKCs), multi-alkali ($SbNa_2KCs$), GaAs(Cs), GaAsP, *etc.* Sensitive wavelengths and peak quantum efficiencies for these materials are summarized in Table 33.3. Typical dynode structures used in PMT's are circular cage, line focusing, box and grid, venetian blind, and fine mesh. In some cases, limited spatial resolution can be obtained by using a mosaic of multiple anodes. Fast PMT's with very large windows—measuring up to 508 mm across—have been developed in recent years for detection of Cherenkov radiation in neutrino

experiments such as Super-Kamiokande and KamLAND among many others. Specially prepared low-radioactivity glass is used to make these PMT's, and they are also able to withstand the high pressure of the surrounding liquid.

PMT's are vulnerable to magnetic fields—sometimes even the geomagnetic field causes large orientation-dependent gain changes. A high-permeability metal shield is often necessary. However, proximity-focused PMT's, *e.g.* the fine-mesh types, can be used even in a high magnetic field (≥ 1 T) if the electron drift direction is parallel to the field. CMS uses custom-made vacuum phototriodes (VPT) mounted on the back face of projective lead tungstate crystals to detect scintillation light in the endcap sections of its electromagnetic calorimeters, which are inside a 3.8 T superconducting solenoid. A VPT employs a single dynode (thus, $G \approx 10$) placed close to the photocathode, and a mesh anode plane between the two, to help it cope with the strong magnetic field, which is not too unfavorably oriented with respect to the photodetector axis in the endcaps (within 25°), but where the radiation level is too high for Avalanche Photodiodes (APD's) like those used in the barrel section.

33.2.1.2. *Microchannel plates:* A typical Microchannel plate (MCP) photodetector consists of one or more ∼2 mm thick glass plates with densely packed $O(10\ \mu\text{m})$-diameter cylindrical holes, or "channels", sitting between the transmission-type photocathode and anode planes, separated by $O(1$ mm) gaps. Instead of discrete dynodes, the inner surface of each cylindrical tube serves as a continuous dynode for the entire cascade of multiplicative bombardments initiated by a photoelectron. Gain fluctuations can be minimized by operating in a saturation mode, whence each channel is only capable of a binary output, but the sum of all channel outputs remains proportional to the number of photons received so long as the photon flux is low enough to ensure that the probability of a single channel receiving more than one photon during a single time gate is negligible. MCP's are thin, offer good spatial resolution, have excellent time resolution (∼20 ps), and can tolerate random magnetic fields up to 0.1 T and axial fields up to ~ 1 T. However, they suffer from relatively long recovery time per channel and short lifetime. MCP's are widely employed as image-intensifiers, although not so much in HEP or astrophysics.

33.2.1.3. *Hybrid photon detectors:* Hybrid photon detectors (HPD) combine the sensitivity of a vacuum PMT with the excellent spatial and energy resolutions of a Si sensor [11]. A single photoelectron ejected from the photocathode is accelerated through a potential difference of ∼20 kV before it impinges on the silicon sensor/anode. The gain nearly equals the maximum number of e-h pairs that could be created from the entire kinetic energy of the accelerated electron: $G \approx \text{eV}/w$, where e is the electronic charge, V is the applied potential difference, and $w \approx 3.7$ eV is the mean energy required to create an e-h pair in Si at room temperature. Since the gain is achieved in a single step, one might expect to have the excellent resolution of a simple Poisson statistic with large mean, but in fact it is even better, thanks to the Fano effect discussed in Sec. 33.7.

Low-noise electronics must be used to read out HPD's if one intends to take advantage of the low fluctuations in gain, *e.g.* when counting small numbers of photons. HPD's can have the same $\epsilon_Q\,\epsilon_C$ and window geometries as PMT's and can be segmented down to ∼50 μm. However, they require rather high biases and will not function in a magnetic field. The exception is proximity-focused devices ($\Rightarrow$ no (de)magnification) in an axial field. With time resolutions of ∼10 ps and superior rate capability, proximity-focused HPD's can be an alternative to MCP's. Current applications of HPD's include the CMS hadronic calorimeter and the RICH detector in LHCb. Large-size HPD's with sophisticated focusing may be suitable for future water Cherenkov experiments.

Hybrid APD's (HAPD's) add an avalanche multiplication step following the electron bombardment to boost the gain by a factor of ∼50. This affords a higher gain and/or lower electrical bias, but also degrades the signal definition.

Table 33.3: Properties of photocathode and window materials commonly used in vacuum photodetectors [10].

Photocathode material	λ (nm)	Window material	Peak ϵ_Q (λ/nm)
CsI	115–200	MgF_2	0.11 (140)
CsTe	115–320	MgF_2	0.14 (240)
Bi-alkali	300–650	Borosilicate	0.27 (390)
	160-650	Synthetic Silica	0.27 (390)
"Ultra Bi-alkali"	300–650	Borosilicate	0.43 (350)
	160-650	Synthetic Silica	0.43 (350)
Multi-alkali	300–850	Borosilicate	0.20 (360)
	160-850	Synthetic Silica	0.20 (360)
GaAs(Cs)*	160–930	Synthetic Silica	0.23 (280)
GaAsP(Cs)	300-750	Borosilicate	0.50 (500)
InP/InGaAsP†	350-1700	Borosilicate	0.01 (1100)

*Reflection type photocathode is used. †Requires cooling to ~ -80°C.

33.2.2. ***Gaseous photon detectors*** : In gaseous photomultipliers (GPM) a photoelectron in a suitable gas mixture initiates an avalanche in a high-field region, producing a large number of secondary impact-ionization electrons. In principle the charge multiplication and collection processes are identical to those employed in gaseous tracking detectors such as multiwire proportional chambers, micromesh gaseous detectors (Micromegas), or gas electron multipliers (GEM). These are discussed in Sec. 33.6.4.

The devices can be divided into two types depending on the photocathode material. One type uses solid photocathode materials much in the same way as PMT's. Since it is resistant to gas mixtures typically used in tracking chambers, CsI is a common choice. In the other type, photoionization occurs on suitable molecules vaporized and mixed in the drift volume. Most gases have photoionization work functions in excess of 10 eV, which would limit their sensitivity to wavelengths far too short. However, vapors of TMAE (tetrakis dimethyl-amine ethylene) or TEA (tri-ethyl-amine), which have smaller work functions (5.3 eV for TMAE and 7.5 eV for TEA), are suited for XUV photon detection [12]. Since devices like GEM's offer sub-mm spatial resolution, GPM's are often used as position-sensitive photon detectors. They can be made into flat panels to cover large areas ($O(1\ \text{m}^2)$), can operate in high magnetic fields, and are relatively inexpensive. Many of the ring imaging Cherenkov (RICH) detectors to date have used GPM's for the detection of Cherenkov light [13]. Special care must be taken to suppress the photon-feedback process in GPM's. It is also important to maintain high purity of the gas as minute traces of O_2 can significantly degrade the detection efficiency.

33.2.3. ***Solid-state photon detectors*** : In a phase of rapid development, solid-state photodetectors are competing with vacuum- or gas-based devices for many existing applications and making way for a multitude of new ones. Compared to traditional vacuum- and gaseous photodetectors, solid-state devices are more compact, lightweight, rugged, tolerant to magnetic fields, and often cheaper. They also allow fine pixelization, are easy to integrate into large systems, and can operate at low electric potentials, while matching or exceeding most performance criteria. They are particularly well suited for detection of γ- and X-rays. Except for applications where coverage of very large areas or dynamic range is required, solid-state detectors are proving to be the better choice. Some hybrid devices attempt to combine the best features of different technologies while applications of nanotechnology are opening up exciting new possibilities.

Silicon photodiodes (PD) are widely used in high-energy physics as particle detectors and in a great number of applications (including solar cells!) as light detectors. The structure is discussed in some detail in Sec. 33.7. In its simplest form, the PD is a reverse-biased p-n junction. Photons with energies above the indirect bandgap energy (wavelengths shorter than about 1050 nm, depending on the temperature) can create e-h pairs (the photoconductive effect), which are collected on the p and n sides, respectively. Often, as in the PD's

used for crystal scintillator readout in CLEO, L3, Belle, BaBar, and GLAST, intrinsic silicon is doped to create a *p-i-n* structure. The reverse bias increases the thickness of the depleted region; in the case of these particular detectors, to full depletion at a depth of about 100 μm. Increasing the depletion depth decreases the capacitance (and hence electronic noise) and extends the red response. Quantum efficiency can exceed 90%, but falls toward the red because of the increasing absorption length of light in silicon. The absorption length reaches 100 μm at 985 nm. However, since $G = 1$, amplification is necessary. Optimal low-noise amplifiers are slow, but, even so, noise limits the minimum detectable signal in room-temperature devices to several hundred photons.

Very large arrays containing $O(10^7)$ of $O(10\ \mu\text{m}^2)$-sized photodiodes pixelizing a plane are widely used to photograph all sorts of things from everyday subjects at visible wavelengths to crystal structures with X-rays and astronomical objects from infrared to UV. To limit the number of readout channels, these are made into charge-coupled devices (CCD), where pixel-to-pixel signal transfer takes place over thousands of synchronous cycles with sequential output through shift registers [14]. Thus, high spatial resolution is achieved at the expense of speed and timing precision. Custom-made CCD's have virtually replaced photographic plates and other imagers for astronomy and in spacecraft. Typical QE's exceed 90% over much of the visible spectrum, and "thick" CCD's have useful QE up to $\lambda = 1\ \mu$m. Active Pixel Sensor (APS) arrays with a preamplifier on each pixel and CMOS processing afford higher speeds, but are challenged at longer wavelengths. Much R&D is underway to overcome the limitations of both CCD and CMOS imagers.

In APD's, an exponential cascade of impact ionizations initiated by the original photogenerated *e-h* pair under a large reverse-bias voltage leads to an avalanche breakdown [15]. As a result, detectable electrical response can be obtained from low-intensity optical signals down to single photons. Excellent junction uniformity is critical, and a guard ring is generally used as a protection against edge breakdown. Well-designed APD's, such as those used in CMS' crystal-based electromagnetic calorimeter, have achieved $\epsilon_Q\,\epsilon_C \approx 0.7$ with sub-ns response time. The sensitive wavelength window and gain depend on the semiconductor used. The gain is typically 10–200 in linear and up to 10^8 in Geiger mode of operation. Stability and close monitoring of the operating temperature are important for linear-mode operation, and substantial cooling is often necessary. Position-sensitive APD's use time information at multiple anodes to calculate the hit position.

One of the most promising recent developments in the field is that of devices consisting of large arrays ($O(10^3)$) of tiny APD's packed over a small area ($O(1\ \text{mm}^2)$) and operated in a limited Geiger mode [16]. Among different names used for this class of photodetectors, "PPD" (for "Pixelized Photon Detector") is most widely accepted (formerly "SiPM"). Although each cell only offers a binary output, linearity with respect to the number of photons is achieved by summing the cell outputs in the same way as with a MCP in saturation mode (see above). PPD's are being adopted as the preferred solution for various purposes including medical imaging, *e.g.* positron emission tomography (PET). These compact, rugged, and economical devices allow auto-calibration through decent separation of photoelectron peaks and offer gains of $O(10^6)$ at a moderate bias voltage (∼50 V). However, the single-photoelectron noise of a PPD, being the logical "or" of $O(10^3)$ Geiger APD's, is rather large: $O(1\ \text{MHz/mm}^2)$ at room temperature. PPD's are particularly well-suited for applications where triggered pulses of several photons are expected over a small area, *e.g.* fiber-guided scintillation light. Intense R&D is expected to lower the noise level and improve radiation hardness, resulting in coverage of larger areas and wider applications. Attempts are being made to combine the fabrication of the sensors and the front-end electronics (ASIC) in the same process with the goal of making PPD's and other finely pixelized solid-state photodetectors extremely easy to use.

Of late, much R&D has been directed to *p-i-n* diode arrays based on thin polycrystalline diamond films formed by chemical vapor deposition (CVD) on a hot substrate (∼1000 K) from a hydrocarbon-containing gas mixture under low pressure (∼100 mbar). These devices have maximum sensitivity in the extreme- to moderate-UV region [17]. Many desirable characteristics, including high tolerance to radiation and temperature fluctuations, low dark noise, blindness to most of the solar radiation spectrum, and relatively low cost make them ideal for space-based UV/XUV astronomy, measurement of synchrotron radiation, and luminosity monitoring at (future) lepton collider(s).

Visible-light photon counters (VLPC) utilize the formation of an impurity band only 50 meV below the conduction band in As-doped Si to generate strong ($G \approx 5 \times 10^4$) yet sharp response to single photons with $\epsilon_Q \approx 0.9$ [18]. The smallness of the band gap considerably reduces the gain dispersion. Only a very small bias (∼7 V) is needed, but high sensitivity to infrared photons requires cooling below 10 K. The dark noise increases sharply and exponentially with both temperature and bias. The Run 2 DØ detector used 86000 VLPC's to read the optical signal from its scintillating-fiber tracker and scintillator-strip preshower detectors.

33.3. Organic scintillators

Revised August 2011 by Kurtis F. Johnson (FSU).

Organic scintillators are broadly classed into three types, crystalline, liquid, and plastic, all of which utilize the ionization produced by charged particles (see Sec. 32.2 of this *Review*) to generate optical photons, usually in the blue to green wavelength regions [19]. Plastic scintillators are by far the most widely used, liquid organic scintillator is finding increased use, and crystal organic scintillators are practically unused in high-energy physics. Plastic scintillator densities range from 1.03 to 1.20 g cm^{-3}. Typical photon yields are about 1 photon per 100 eV of energy deposit [20]. A one-cm-thick scintillator traversed by a minimum-ionizing particle will therefore yield $\approx 2 \times 10^4$ photons. The resulting photoelectron signal will depend on the collection and transport efficiency of the optical package and the quantum efficiency of the photodetector.

Organic scintillator does not respond linearly to the ionization density. Very dense ionization columns emit less light than expected on the basis of dE/dx for minimum-ionizing particles. A widely used semi-empirical model by Birks posits that recombination and quenching effects between the excited molecules reduce the light yield [21]. These effects are more pronounced the greater the density of the excited molecules. Birks' formula is

$$\frac{d\mathscr{L}}{dx} = \mathscr{L}_0 \frac{dE/dx}{1 + k_B\, dE/dx}\ , \tag{33.2}$$

where $\mathscr{L}$ is the luminescence, $\mathscr{L}_0$ is the luminescence at low specific ionization density, and k_B is Birks' constant, which must be determined for each scintillator by measurement. Decay times are in the ns range; rise times are much faster. The high light yield and fast response time allow the possibility of sub-ns timing resolution [22]. The fraction of light emitted during the decay "tail" can depend on the exciting particle. This allows pulse shape discrimination as a technique to carry out particle identification. Because of the hydrogen content (carbon to hydrogen ratio ≈ 1) plastic scintillator is sensitive to proton recoils from neutrons. Ease of fabrication into desired shapes and low cost has made plastic scintillator a common detector element. In the form of scintillating fiber it has found widespread use in tracking and calorimetry [23].

Demand for large volume detectors has lead to increased use of liquid organic scintillator, which has the same scintillation mechanism as plastic scintillator, due to its cost advantage. The containment vessel defines the detector shape; photodetectors or waveshifters may be immersed in the liquid.

33.3.1. ***Scintillation mechanism*** :

A charged particle traversing matter leaves behind it a wake of excited molecules. Certain types of molecules, however, will release a small fraction ($\approx 3\%$) of this energy as optical photons. This process, scintillation, is especially marked in those organic substances which contain aromatic rings, such as polystyrene (PS) and polyvinyltoluene (PVT). Liquids which scintillate include toluene, xylene and pseudocumene.

In fluorescence, the initial excitation takes place via the absorption of a photon, and de-excitation by emission of a longer wavelength photon. Fluors are used as "waveshifters" to shift scintillation light to a more convenient wavelength. Occurring in complex molecules, the absorption and emission are spread out over a wide band of photon energies, and have some overlap, that is, there is some fraction of the emitted light which can be re-absorbed [24]. This "self-absorption" is undesirable for detector applications because it causes a shortened attenuation length. The wavelength difference between the major absorption and emission peaks is called the Stokes shift. It is usually the case that the greater the Stokes shift, the smaller the self absorption thus, a large Stokes shift is a desirable property for a fluor.

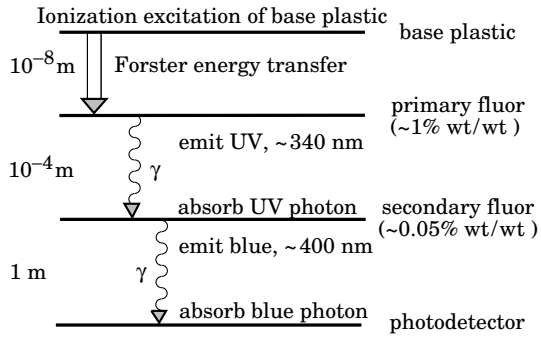

Figure 33.1: Cartoon of scintillation "ladder" depicting the operating mechanism of organic scintillator. Approximate fluor concentrations and energy transfer distances for the separate sub-processes are shown.

The plastic scintillators used in high-energy physics are binary or ternary solutions of selected fluors in a plastic base containing aromatic rings. (See the appendix in Ref. 25 for a comprehensive list of components.) Virtually all plastic scintillators contain as a base either PVT or PS. PVT-based scintillator can be up to 50% brighter.

Ionization in the plastic base produces UV photons with short attenuation length (several mm). Longer attenuation lengths are obtained by dissolving a "primary" fluor in high concentration (1% by weight) into the base, which is selected to efficiently re-radiate absorbed energy at wavelengths where the base is more transparent (see Fig. 33.1).

The primary fluor has a second important function. The decay time of the scintillator base material can be quite long – in pure polystyrene it is 16 ns, for example. The addition of the primary fluor in high concentration can shorten the decay time by an order of magnitude and increase the total light yield. At the concentrations used (1% and greater), the average distance between a fluor molecule and an excited base unit is around 100 Å, much less than a wavelength of light. At these distances the predominant mode of energy transfer from base to fluor is not the radiation of a photon, but a resonant dipole-dipole interaction, first described by Foerster, which strongly couples the base and fluor [26]. The strong coupling sharply increases the speed and the light yield of the plastic scintillators.

Unfortunately, a fluor which fulfills other requirements is usually not completely adequate with respect to emission wavelength or attenuation length, so it is necessary to add yet another waveshifter (the "secondary" fluor), at fractional percent levels, and occasionally a third (not shown in Fig. 33.1).

External wavelength shifters are widely used to aid light collection in complex geometries. Scintillation light is captured by a lightpipe comprising a wave-shifting fluor dissolved in a nonscintillating base. The wavelength shifter must be insensitive to ionizing radiation and Cherenkov light. A typical wavelength shifter uses an acrylic base because of its good optical qualities, a single fluor to shift the light emerging from the plastic scintillator to the blue-green, and contains ultra-violet absorbing additives to deaden response to Cherenkov light.

33.3.2. ***Caveats and cautions*** :

Plastic scintillators are reliable, robust, and convenient. However, they possess quirks to which the experimenter must be alert. Exposure to solvent vapors, high temperatures, mechanical flexing, irradiation, or rough handling will aggravate the process. A particularly fragile region is the surface which can "craze" develop microcracks which degrade its transmission of light by total internal reflection. Crazing is particularly likely where oils, solvents, or *fingerprints* have contacted the surface.

They have a long-lived luminescence which does not follow a simple exponential decay. Intensities at the 10^{-4} level of the initial fluorescence can persist for hundreds of ns [19,27].

They will decrease their light yield with increasing partial pressure of oxygen. This can be a 10% effect in an artificial atmosphere [28]. It is not excluded that other gases may have similar quenching effects.

Their light yield may be changed by a magnetic field. The effect is very nonlinear and apparently not all types of plastic scintillators are so affected. Increases of $\approx 3\%$ at 0.45 T have been reported [29]. Data are sketchy and mechanisms are not understood.

Irradiation of plastic scintillators creates color centers which absorb light more strongly in the UV and blue than at longer wavelengths. This poorly understood effect appears as a reduction both of light yield and attenuation length. Radiation damage depends not only on the integrated dose, but on the dose rate, atmosphere, and temperature, before, during and after irradiation, as well as the materials properties of the base such as glass transition temperature, polymer chain length, *etc.* Annealing also occurs, accelerated by the diffusion of atmospheric oxygen and elevated temperatures. The phenomena are complex, unpredictable, and not well understood [30]. Since color centers are less disruptive at longer wavelengths, the most reliable method of mitigating radiation damage is to shift emissions at every step to the longest practical wavelengths, *e.g.*, utilize fluors with large Stokes shifts (aka the "Better red than dead" strategy).

33.3.3. ***Scintillating and wavelength-shifting fibers*** :

The clad optical fiber comprising scintillator and wavelength shifter (WLS) is particularly useful [31]. Since the initial demonstration of the scintillating fiber (SCIFI) calorimeter [32], SCIFI techniques have become mainstream [33]. SCIFI calorimeters are fast, dense, radiation hard, and can have leadglass-like resolution. SCIFI trackers can handle high rates and are radiation tolerant, but the low photon yield at the end of a long fiber (see below) forces the use of sensitive photodetectors. WLS scintillator readout of a calorimeter allows a very high level of hermeticity since the solid angle blocked by the fiber on its way to the photodetector is very small. The sensitive region of scintillating fibers can be controlled by splicing them onto clear (non-scintillating/non-WLS) fibers.

A typical configuration would be fibers with a core of polystyrene-based scintillator or WLS (index of refraction $n = 1.59$), surrounded by a cladding of PMMA ($n = 1.49$) a few microns thick, or, for added light capture, with another cladding of fluorinated PMMA with $n = 1.42$, for an overall diameter of 0.5 to 1 mm. The fiber is drawn from a boule and great care is taken during production to ensure that the intersurface between the core and the cladding has the highest possible uniformity and quality, so that the signal transmission via total internal reflection has a low loss. The fraction of generated light which is transported down the optical pipe is denoted the capture fraction and is about 6% for the single-clad fiber and 10% for the double-clad fiber. The number of photons from the fiber available at the photodetector is always smaller than desired, and increasing the light yield has proven difficult. A minimum-ionizing particle traversing a high-quality 1 mm diameter fiber perpendicular to its axis will produce fewer than 2000 photons, of which about 200 are captured. Attenuation may eliminate 95% of these photons in a large collider tracker.

A scintillating or WLS fiber is often characterized by its attenuation

length, over which the signal is attenuated to $1/e$ of its original value. Many factors determine the attenuation length, including the importance of re-absorption of emitted photons by the polymer base or dissolved fluors, the level of crystallinity of the base polymer, and the quality of the total internal reflection boundary [34]. Attenuation lengths of several meters are obtained by high quality fibers. However, it should be understood that the attenuation length is not the sole measure of fiber quality. Among other things, it is not constant with distance from the excitation source and it is wavelength dependent.

33.4. Inorganic scintillators:

Revised September 2009 by R.-Y. Zhu (California Institute of Technology) and C.L. Woody (BNL).

Inorganic crystals form a class of scintillating materials with much higher densities than organic plastic scintillators (typically $\sim$ 4–8 g/cm^3) with a variety of different properties for use as scintillation detectors. Due to their high density and high effective atomic number, they can be used in applications where high stopping power or a high conversion efficiency for electrons or photons is required. These include total absorption electromagnetic calorimeters (see Sec. 33.9.1), which consist of a totally active absorber (as opposed to a sampling calorimeter), as well as serving as gamma ray detectors over a wide range of energies. Many of these crystals also have very high light output, and can therefore provide excellent energy resolution down to very low energies ($\sim$ few hundred keV).

Some crystals are intrinsic scintillators in which the luminescence is produced by a part of the crystal lattice itself. However, other crystals require the addition of a dopant, typically fluorescent ions such as thallium (Tl) or cerium (Ce) which is responsible for producing the scintillation light. However, in both cases, the scintillation mechanism is the same. Energy is deposited in the crystal by ionization, either directly by charged particles, or by the conversion of photons into electrons or positrons which subsequently produce ionization. This energy is transferred to the luminescent centers which then radiate scintillation photons. The efficiency η for the conversion of energy deposit in the crystal to scintillation light can be expressed by the relation [35]

$$\eta = \beta \cdot S \cdot Q \ . \tag{33.3}$$

where β is the efficiency of the energy conversion process, S is the efficiency of energy transfer to the luminescent center, and Q is the quantum efficiency of the luminescent center. The value of η ranges between 0.1 and $\sim$ 1 depending on the crystal, and is the main factor in determining the intrinsic light output of the scintillator. In addition, the scintillation decay time is primarily determined by the energy transfer and emission process. The decay time of the scintillator is mainly dominated by the decay time of the luminescent center. For example, in the case of thallium doped sodium iodide (NaI(Tl)), the value of η is $\sim$ 0.5, which results in a light output $\sim$ 40,000 photons per MeV of energy deposit. This high light output is largely due to the high quantum efficiency of the thallium ion (Q $\sim$ 1), but the decay time is rather slow ($\tau \sim 250$ ns).

Table 33.4 lists the basic properties of some commonly used inorganic crystal scintillators. NaI(Tl) is one of the most common and widely used scintillators, with an emission that is well matched to a bialkali photomultiplier tube, but it is highly hygroscopic and difficult to work with, and has a rather low density. CsI(Tl) has high light yield, an emission that is well matched to solid state photodiodes, and is mechanically robust (high plasticity and resistance to cracking). However, it needs careful surface treatment and is slightly hygroscopic. Compared with CsI(Tl), pure CsI has identical mechanical properties, but faster emission at shorter wavelengths and light output approximately an order of magnitude lower. BaF_2 has a fast component with a sub-nanosecond decay time, and is the fastest known scintillator. However, it also has a slow component with a much longer decay time ($\sim$ 630 ns). Bismuth gemanate ($Bi_4Ge_3O_{12}$ or BGO) has a high density, and consequently a short radiation length X_0 and Molière radius R_M. BGO's emission is well-matched to the spectral sensitivity of photodiodes, and it is easy to handle and not hygroscopic. Lead tungstate ($PbWO_4$ or PWO) has a very high density, with a very short X_0 and R_M, but its intrinsic light yield is rather low.

Cerium doped lutetium oxyorthosilicate (Lu_2SiO_5:Ce, or LSO:Ce) [36] and cerium doped lutetium-yttrium oxyorthosilicate ($Lu_{2(1-x)}Y_{2x}SiO_5$, LYSO:Ce) [37] are dense crystal scintillators which have a high light yield and a fast decay time. Only properties of LSO:Ce is listed in Table 33.4 since the properties of LYSO:Ce are similar to that of LSO:Ce except a little lower density than LSO:Ce depending on the yttrium fraction in LYSO:Ce. This material is also featured with excellent radiation hardness [38], so is expected to be used where extraordinary radiation hardness is required.

Table 33.4 also includes cerium doped lanthanum tri-halides, such as $LaBr_3$ [39], which is brighter and faster than LSO:Ce, but it is highly hygroscopic and has a lower density. The FWHM energy resolution measured for this material coupled to a PMT with bi-alkali photocathode for 0.662 MeV γ-rays from a ^{137}Cs source is about 3%, which is the best among all inorganic crystal scintillators. For this reason, $LaBr_3$ is expected to be widely used in applications where a good energy resolution for low energy photons are required, such as homeland security.

Beside the crystals listed in Table 33.4, a number of new crystals are being developed that may have potential applications in high energy or nuclear physics. Of particular interest is the family of yttrium and lutetium perovskites, which include YAP ($YAlO_3$:Ce) and LuAP ($LuAlO_3$:Ce) and their mixed compositions. These have been shown to be linear over a large energy range [40], and have the potential for providing extremely good intrinsic energy resolution. In addition, other fluoride crystals such as CeF_3 have been shown to provide excellent energy resolution in calorimeter applications.

Aiming at the best jet-mass resolution inorganic scintillators are being investigated for HEP calorimeters with dual readout for both Cherenkov and scintillation light to be used at future linear colliders. These materials may be used for an electromagnetic calorimeter [41] or a homogeneous hadronic calorimetry (HHCAL) detector concept, including both electromagnetic and hadronic parts [42]. Because of the unprecedented volume (70 to 100 m^3) foreseen for the HHCAL detector concept the materials must be (1) dense (to minimize the leakage) and (2) cost-effective. It should also be UV transparent (for effective collection of the Cherenkov light) and allow for a clear discrimination between the Cherenkov and scintillation light. The preferred scintillation light is thus at a longer wavelength, and not necessarily bright or fast. Dense crystals, scintillating glasses and ceramics offer a very attractive implementation for this detector concept. Inorganic crystals being investigated are lead fluoride (PbF_2), lead chroride fluoride (PbFCl) and BSO [43].

Table 33.4 gives the light output of other crystals relative to NaI(Tl) and their dependence to the temperature variations measured for crystal samples of 1.5 X_0 cube with a Tyvek paper wrapping and a full end face coupled to a photodetector [44]. The quantum efficiencies of the photodetector is taken out to facilitate a direct comparison of crystal's light output. However, the useful signal produced by a scintillator is usually quoted in terms of the number of photoelectrons per MeV produced by a given photodetector. The relationship between the number of photons/MeV produced and photoelectrons/MeV detected involves the factors for the light collection efficiency L and the quantum efficiency QE of the photodetector:

$$N_{\text{p.e.}}/\text{MeV} = L \cdot QE \cdot N_\gamma/\text{MeV} \tag{33.4}$$

L includes the transmission of scintillation light within the crystal (*i.e.*, the bulk attenuation length of the material), reflections and scattering from the surfaces, and the size and shape of the crystal. These factors can vary considerably depending on the sample, but can be in the range of $\sim$10–60%. The internal light transmission depends on the intrinsic properties of the material, e.g. the density and type of the scattering centers and defects that can produce internal absorption within the crystal, and can be highly affected by factors such as radiation damage, as discussed below.

The quantum efficiency depends on the type of photodetector used to detect the scintillation light, which is typically $\sim$15–20% for photomultiplier tubes and $\sim$70% for silicon photodiodes for visible wavelengths. The quantum efficiency of the detector is usually highly wavelength dependent and should be matched to the particular crystal of interest to give the highest quantum yield at the wavelength

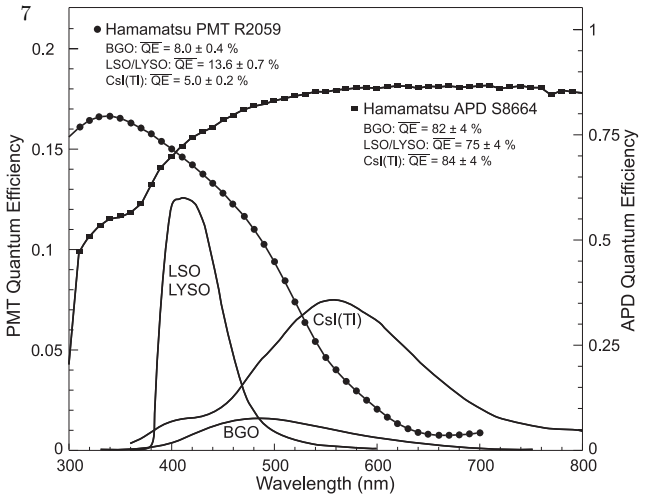

Figure 33.2: The quantum efficiencies of two photodetectors, a Hamamatsu R2059 PMT with bi-alkali cathode and a Hamamatsu S8664 avalanche photodiode (APD), are shown as a function of wavelength. Also shown in the figure are emission spectra of three crystal scintillators, BGO, LSO and CsI(Tl), and the numerical values of the emission weighted quantum efficiencies. The area under each emission spectrum is proportional to crystal's light yield.

corresponding to the peak of the scintillation emission. Fig. 33.2 shows the quantum efficiencies of two photodetectors, a Hamamatsu R2059 PMT with bi-alkali cathode and quartz window and a Hamamatsu S8664 avalanche photodiode (APD) as a function of wavelength. Also shown in the figure are emission spectra of three crystal scintillators, BGO, LSO:Ce/LYSO:Ce and CsI(Tl), and the numerical values of the emission weighted quantum efficiency. The area under each emission spectrum is proportional to crystal's light yield, as shown in Table 33.4, where the quantum efficiencies of the photodetector has been taken out. Results with different photodetectors can be significantly different. For example, the response of CsI(Tl) relative to NaI(Tl) with a standard photomultiplier tube with a bi-alkali photo-cathode, e.g. Hamamatsu R2059, would be 45 rather than 165 because of the photomultiplier's low quantum efficiency at longer wavelengths. For scintillators which emit in the UV, a detector with a quartz window should be used.

For very low energy applications (typically below 1 MeV), non-proportionality of the scintillation light yield may be important. It has been known for a long time that the conversion factor between the energy deposited in a crystal scintillator and the number of photons produced is not constant. It is also known that the energy resolution measured by all crystal scintillators for low energy γ-rays is significantly worse than the contribution from photo-electron statistics alone, indicating an intrinsic contribution from the scintillator itself. Precision measurement using low energy electron beam shows that this non-proportionality is crystal dependent [45]. Recent study on this issue also shows that this effect is also sample dependent even for the same crystal [46]. Further work is therefore needed to fully understand this subject.

One important issue related to the application of a crystal scintillator is its radiation hardness. Stability of its light output, or the ability to track and monitor the variation of its light output in a radiation environment, is required for high resolution and precision calibration [47]. All known crystal scintillators suffer from radiation damage. A common damage phenomenon is the appearance of radiation induced absorption caused by the formation of color centers originated from the impurities or point defects in the crystal. This radiation induced absorption reduces the light attenuation length in the crystal, and hence its light output. For crystals with high defect density, a severe reduction of light attenuation length may cause a distortion of the light response uniformity, leading to a degradation of the energy resolution. Additional radiation damage effects may include a reduced intrinsic scintillation light yield (damage to the luminescent centers) and an increased phosphorescence (afterglow). For crystals to be used in the construction a high precision calorimeter in a radiation environment, its scintillation mechanism must not be damaged and its light attenuation length in the expected radiation environment must be long enough so that its light response uniformity, and thus its energy resolution, does not change [48].

Table 33.4: Properties of several inorganic crystal scintillators. Most of the notation is defined in Sec. 6 of this *Review*.

Parameter:	ρ	MP	X_0^*	R_M^*	dE^*/dx	λ_I^*	$\tau_{\rm decay}$	$\lambda_{\rm max}$	$n^\natural$	Relative output†	Hygro-scopic?	$d({\rm LY})/dT$
Units:	g/cm^3	°C	cm	cm	MeV/cm	cm	ns	nm				%/°C‡
NaI(Tl)	3.67	651	2.59	4.13	4.8	42.9	245	410	1.85	100	yes	−0.2
BGO	7.13	1050	1.12	2.23	9.0	22.8	300	480	2.15	21	no	−0.9
BaF_2	4.89	1280	2.03	3.10	6.5	30.7	650^s	300^s	1.50	36^s	no	-1.9^s
							0.9^f	220^f		4.1^f		0.1^f
CsI(Tl)	4.51	621	1.86	3.57	5.6	39.3	1220	550	1.79	165	slight	0.4
CsI(pure)	4.51	621	1.86	3.57	5.6	39.3	30^s	420^s	1.95	3.6^s	slight	−1.4
							6^f	310^f		1.1^f		
$PbWO_4$	8.3	1123	0.89	2.00	10.1	20.7	30^s	425^s	2.20	0.3^s	no	−2.5
							10^f	420^f		0.077^f		
LSO(Ce)	7.40	2050	1.14	2.07	9.6	20.9	40	402	1.82	85	no	−0.2
$LaBr_3$(Ce)	5.29	788	1.88	2.85	6.9	30.4	20	356	1.9	130	yes	0.2

* Numerical values calculated using formulae in this review.
$^\natural$ Refractive index at the wavelength of the emission maximum.
† Relative light output measured for samples of 1.5 X_0 cube with a Tyvek paper wrapping and a full end face coupled to a photodetector. The quantum efficiencies of the photodetector are taken out.
‡ Variation of light yield with temperature evaluated at the room temperature.
f = fast component, s = slow component

Most of the crystals listed in Table 33.4 have been used in high energy or nuclear physics experiments when the ultimate energy resolution for electrons and photons is desired. Examples are the Crystal Ball NaI(Tl) calorimeter at SPEAR, the L3 BGO calorimeter at LEP, the CLEO CsI(Tl) calorimeter at CESR, the KTeV CsI calorimeter at the Tevatron, the BaBar, BELLE and BES II CsI(Tl) calorimeters at PEP-II, KEK and BEPC III. Because of its high density and relative low cost, PWO calorimeters are widely used by CMS and ALICE at LHC, by CLAS and PrimEx at CEBAF, and by PANDA at GSI. Recently, investigations have been made aiming at using LSO:Ce or LYSO:Ce crystals for future high energy or nuclear physics experiments [38].

33.5. Cherenkov detectors

Revised September 2009 by B.N. Ratcliff (SLAC).

Although devices using Cherenkov radiation are often thought of as only particle identification (PID) detectors, in practice they are used over a broader range of applications including; (1) fast particle counters; (2) hadronic PID; and (3) tracking detectors performing complete event reconstruction. Examples of applications from each category include; (1) the BaBar luminosity detector [49]; (2) the hadronic PID detectors at the B factory detectors—DIRC in BaBar [50] and the aerogel threshold Cherenkov in Belle [51]; and (3) large water Cherenkov counters such as Super-Kamiokande [53]. Cherenkov counters contain two main elements; (1) a radiator through which the charged particle passes, and (2) a photodetector. As Cherenkov radiation is a weak source of photons, light collection and detection must be as efficient as possible. The refractive index n and the particle's path length through the radiator L appear in the Cherenkov relations allowing the tuning of these quantities for particular applications.

Cherenkov detectors utilize one or more of the properties of Cherenkov radiation discussed in the Passages of Particles through Matter section (Sec. 32 of this *Review*): the prompt emission of a light pulse; the existence of a velocity threshold for radiation; and the dependence of the Cherenkov cone half-angle θ_c and the number of emitted photons on the velocity of the particle and the refractive index of the medium.

The number of photoelectrons ($N_{\rm p.e.}$) detected in a given device is

$$N_{\rm p.e.} = L\frac{\alpha^2 z^2}{r_e\, m_e c^2}\int \epsilon(E)\, \sin^2\theta_c(E) dE\ , \tag{33.5}$$

where ϵ(E) is the efficiency for collecting the Cherenkov light and transducing it into photoelectrons, and $\alpha^2/(r_e\, m_e c^2) = 370\ {\rm cm}^{-1}{\rm eV}^{-1}$.

The quantities ϵ and θ_c are functions of the photon energy E. As the typical energy dependent variation of the index of refraction is modest, a quantity called the *Cherenkov detector quality factor* N_0 can be defined as

$$N_0 = \frac{\alpha^2 z^2}{r_e\, m_e c^2}\ \int \epsilon\, dE\ , \tag{33.6}$$

so that, taking $z = 1$ (the usual case in high-energy physics),

$$N_{\rm p.e.} \approx L N_0 \langle \sin^2\theta_c\rangle\ . \tag{33.7}$$

This definition of the quality factor N_0 is not universal, nor, indeed, very useful for those common situations where ϵ factorizes as $\epsilon = \epsilon_{\rm coll}\epsilon_{\rm det}$ with the geometrical photon collection efficiency ($\epsilon_{\rm coll}$) varying substantially for different tracks while the photon detector efficiency ($\epsilon_{\rm det}$) remains nearly track independent. In this case, it can be useful to explicitly remove ($\epsilon_{\rm coll}$) from the definition of N_0. A typical value of N_0 for a photomultiplier (PMT) detection system working in the visible and near UV, and collecting most of the Cherenkov light, is about 100 cm^{-1}. Practical counters, utilizing a variety of different photodetectors, have values ranging between about 30 and 180 cm^{-1}. Radiators can be chosen from a variety of transparent materials (Sec. 32 of this *Review* and Table 6.1). In addition to refractive index, the choice requires consideration of factors such as material density, radiation length and radiation hardness, transmission bandwidth, absorption length, chromatic dispersion, optical workability (for solids), availability, and cost. When the momenta of particles to be identified is high, the refractive index must be set close to one, so that the photon yield per unit length is low and a long particle path in the radiator is required. Recently, the gap in refractive index that has traditionally existed between gases and liquid or solid materials has been partially closed with transparent *silica aerogels* with indices that range between about 1.007 and 1.13.

Cherenkov counters may be classified as either *imaging* or *threshold* types, depending on whether they do or do not make use of Cherenkov angle (θ_c) information. Imaging counters may be used to track particles as well as identify them. The recent development of very fast photodetectors such as micro-channel plate PMTs (MCP PMT) (see Sec. 33.2 of this *Review*) also potentially allows very fast Cherenkov based time of flight (TOF) detectors of either class [57].

Threshold Cherenkov detectors [54], in their simplest form, make a yes/no decision based on whether the particle is above or below the Cherenkov threshold velocity $\beta_t = 1/n$. A straightforward enhancement of such detectors uses the number of observed photoelectrons (or a calibrated pulse height) to discriminate between species or to set probabilities for each particle species [55]. This strategy can increase the momentum range of particle separation by a modest amount (to a momentum some 20% above the threshold momentum of the heavier particle in a typical case).

Careful designs give $\langle\epsilon_{\rm coll}\rangle \gtrsim 90\%$. For a photomultiplier with a typical bialkali cathode, $\int \epsilon_{\rm det} dE \approx 0.27$ eV, so that

$$N_{\rm p.e.}/L \approx 90\ {\rm cm}^{-1}\,\langle\sin^2\theta_c\rangle \quad (i.e.,\ N_0 = 90\ {\rm cm}^{-1})\ . \tag{33.8}$$

Suppose, for example, that n is chosen so that the threshold for species a is p_t; that is, at this momentum species a has velocity $\beta_a = 1/n$. A second, lighter, species b with the same momentum has velocity β_b, so $\cos\theta_c = \beta_a/\beta_b$, and

$$N_{\rm p.e.}/L \approx 90\ {\rm cm}^{-1}\,\frac{m_a^2 - m_b^2}{p_t^2 + m_a^2}\ . \tag{33.9}$$

For K/π separation at $p = p_t = 1(5)$ GeV/c, $N_{\rm p.e.}/L \approx 16(0.8)$ cm^{-1} for π's and (by design) 0 for K's.

For limited path lengths $N_{\rm p.e.}$ will usually be small. The overall efficiency of the device is controlled by Poisson fluctuations, which can be especially critical for separation of species where one particle type is dominant. Moreover, the effective number of photoelectrons is often less than the average number calculated above due to additional equivalent noise from the photodetector (see the discussion of the excess noise factor in Sec. 33.2 of this *Review*). It is common to design for at least 10 photoelectrons for the high velocity particle in order to obtain a robust counter. As rejection of the particle that is below threshold depends on *not* seeing a signal, electronic and other background noise can be important. Physics sources of light production for the below threshold particle, such as decay to an above threshold particle or the production of delta rays in the radiator, often limit the separation attainable, and need to be carefully considered. Well designed, modern multi-channel counters, such as the ACC at Belle [51], can attain adequate particle separation performance over a substantial momentum range for essentially the full solid angle of the spectrometer.

Imaging counters make the most powerful use of the information available by measuring the ring-correlated angles of emission of the individual Cherenkov photons. Since low-energy photon detectors can measure only the position (and, perhaps, a precise detection time) of the individual Cherenkov photons (not the angles directly), the photons must be "imaged" onto a detector so that their angles can be derived [56]. Typically the optics map the Cherenkov cone onto (a portion of) a distorted "circle" at the photodetector. Though the imaging process is directly analogous to familiar imaging techniques used in telescopes and other optical instruments, there is a somewhat bewildering variety of methods used in a wide variety of counter types with different names. Some of the imaging methods used include (1) focusing by a lens; (2) proximity focusing (i.e., focusing by limiting the emission region of the radiation); and (3) focusing through an aperture (a pinhole). In addition, the prompt Cherenkov emission coupled with the speed of modern photon detectors allows the use of (4) time imaging, a method which is little used in conventional imaging

technology. Finally, (5) correlated tracking (and event reconstruction) can be performed in large water counters by combining the individual space position and time of each photon together with the constraint that Cherenkov photons are emitted from each track at the same polar angle (Sec. 34.3.1 of this *Review*).

In a simple model of an imaging PID counter, the fractional error on the particle velocity (δ_β) is given by

$$\delta_\beta = \frac{\sigma_\beta}{\beta} = \tan\theta_c \sigma(\theta_c) \quad , \tag{33.10}$$

where

$$\sigma(\theta_c) = \frac{\langle\sigma(\theta_i)\rangle}{\sqrt{N_{\rm p.e.}}} \oplus C \ , \tag{33.11}$$

and $\langle\sigma(\theta_i)\rangle$ is the average single photoelectron resolution, as defined by the optics, detector resolution and the intrinsic chromaticity spread of the radiator index of refraction averaged over the photon detection bandwidth. C combines a number of other contributions to resolution including, (1) correlated terms such as tracking, alignment, and multiple scattering, (2) hit ambiguities, (3) background hits from random sources, and (4) hits coming from other tracks. The actual separation performance is also limited by physics effects such as decays in flight and particle interactions in the material of the detector. In many practical cases, the performance is limited by these effects.

For a $\beta \approx 1$ particle of momentum (p) well above threshold entering a radiator with index of refraction (n), the number of σ separation (N_σ) between particles of mass m_1 and m_2 is approximately

$$N_\sigma \approx \frac{|m_1^2 - m_2^2|}{2p^2\sigma(\theta_c)\sqrt{n^2-1}} \ . \tag{33.12}$$

In practical counters, the angular resolution term $\sigma(\theta_c)$ varies between about 0.1 and 5 mrad depending on the size, radiator, and photodetector type of the particular counter. The range of momenta over which a particular counter can separate particle species extends from the point at which the number of photons emitted becomes sufficient for the counter to operate efficiently as a threshold device (∼20% above the threshold for the lighter species) to the value in the imaging region given by the equation above. For example, for $\sigma(\theta_c) = 2$mrad, a fused silica radiator($n = 1.474$), or a fluorocarbon gas radiator (C_5F_{12}, $n = 1.0017$), would separate π/K's from the threshold region starting around 0.15(3) GeV/c through the imaging region up to about 4.2(18) GeV/c at better than 3σ.

Many different imaging counters have been built during the last several decades [57]. Among the earliest examples of this class of counters are the very limited acceptance Differential Cherenkov detectors, designed for particle selection in high momentum beam lines. These devices use optical focusing and/or geometrical masking to select particles having velocities in a specified region. With careful design, a velocity resolution of $\sigma_\beta/\beta \approx 10^{-4}$–$10^{-5}$ can be obtained [54].

Practical multi-track Ring-Imaging Cherenkov detectors (generically called RICH counters) are a more recent development. RICH counters are sometimes further classified by 'generations' that differ based on historical timing, performance, design, and photodetection techniques.

Prototypical examples of first generation RICH counters are those used in the DELPHI and SLD detectors at the LEP and SLC Z factory e^+e^- colliders [57]. They have both liquid (C_6F_{14}, $n = 1.276$) and gas (C_5F_{12}, $n = 1.0017$) radiators, the former being proximity imaged with the latter using mirrors. The phototransducers are a TPC/wire-chamber combination. They are made sensitive to photons by doping the TPC gas (usually, ethane/methane) with ∼ 0.05% TMAE (tetrakis(dimethylamino)ethylene). Great attention to detail is required, (1) to avoid absorbing the UV photons to which TMAE is sensitive, (2) to avoid absorbing the single photoelectrons as they drift in the long TPC, and (3) to keep the chemically active TMAE vapor from interacting with materials in the system. In spite of their unforgiving operational characteristics, these counters attained good $e/\pi/K/p$ separation over wide momentum ranges (from about 0.25 to 20 GeV/c) during several years of operation at LEP and SLC. Related but smaller acceptance devices include the OMEGA RICH at the CERN SPS, and the RICH in the balloon-borne CAPRICE detector [57].

Later generation counters [57] generally operate at much higher rates, with more detection channels, than the first generation detectors just described. They also utilize faster, more forgiving photon detectors, covering different photon detection bandwidths. Radiator choices have broadened to include materials such as lithium fluoride, fused silica, and aerogel. Vacuum based photodetection systems (*e.g.*, single or multi anode PMTs, MCP PMTs, or hybrid photodiodes (HPD)) have become increasingly common (see Sec. 33.2 of this *Review*). They handle high rates, and can be used with a wide choice of radiators. Examples include (1) the SELEX RICH at Fermilab, which mirror focuses the Cherenkov photons from a neon radiator onto a camera array made of ∼ 2000 PMTs to separate hadrons over a wide momentum range (to well above 200 GeV/c for heavy hadrons); (2) the HERMES RICH at HERA, which mirror focuses photons from C_4F_{10}($n = 1.00137$) and aerogel($n = 1.0304$) radiators within the same volume onto a PMT camera array to separate hadrons in the momentum range from 2 to 15 GeV/c; and (3) the LHCb detector now being brought into operation at the LHC. It uses two separate counters. One volume, like HERMES, contains two radiators (aerogel and C_4F_{10}) while the second volume contains CF_4. Photons are mirror focused onto detector arrays of HPDs to cover a π/K separation momentum range between 1 and 150 GeV/c.

Other fast detection systems that use solid cesium iodide (CsI) photocathodes or triethylamine (TEA) doping in proportional chambers are useful with certain radiator types and geometries. Examples include (1) the CLEO-III RICH at CESR that uses a LiF radiator with TEA doped proportional chambers; (2) the ALICE detector at the LHC that uses proximity focused liquid (C_6F_{14} radiators and solid CSI photocathodes (similar photodectors have been used for several years by the HADES and COMPASS detectors), and the hadron blind detector (HBD) in the PHENIX detector at RHIC that couples a low index CF_4 radiator to a photodetector based on electron multiplier (GEM) chambers with reflective CSI photocathodes [57].

A DIRC (Detection [of] Internally Reflected Cherenkov [light]) is a distinctive, compact RICH subtype first used in the BaBar detector [52]. A DIRC "inverts" the usual RICH principle for use of light from the radiator by collecting and imaging the total internally reflected light rather than the transmitted light. It utilizes the optical material of the radiator in two ways, simultaneously; first as a Cherenkov radiator, and second, as a light pipe. The magnitudes of the photon angles are preserved during transport by the flat, rectangular cross section radiators, allowing the photons to be efficiently transported to a detector outside the path of the particle where they may be imaged in up to three independent dimensions (the usual two in space and, due to the long photon paths lengths, one in time). Because the index of refraction in the radiator is large (∼ 1.48 for fused silica), the momentum range with good π/K separation is rather low. The BaBar DIRC range extends up to ∼ 4 GeV/c. It is plausible, but difficult, to extend it up to about 10 GeV/c with an improved design. New DIRC detectors are being developed that take advantage of the new, very fast, pixelated photodetectors becoming available, such as flat panel PMTs and MCP PMTs. They typically utilize either time imaging or mirror focused optics, or both, leading not only to a precision measurement of the Cherenkov angle, but in some cases, to a precise measurement of the particle time of flight, and/or to correction of the chromatic dispersion in the radiator. Examples include (1) the time of propagation (TOP) counter being developed for the BELLE-II upgrade at KEKB which emphasizes precision timing for both Cherenkov imaging and TOF; (2) the full 3-dimensional imaging FDIRC for the SuperB detector at the Italian SuperB collider which uses precision timing not only for improving the angle reconstruction and TOF, but also to correct the chromatic dispersion; and (3) the DIRCs being developed for the PANDA detector at FAIR that use elegant focusing optics and fast timing [57].

33.6. Gaseous detectors

33.6.1. ***Energy loss and charge transport in gases*** : Revised March 2010 by F. Sauli (CERN) and M. Titov (CEA Saclay).

Gas-filled detectors localize the ionization produced by charged particles, generally after charge multiplication. The statistics of ionization processes having asymmetries in the ionization trails, affect the coordinate determination deduced from the measurement of drift time, or of the center of gravity of the collected charge. For thin gas layers, the width of the energy loss distribution can be larger than its average, requiring multiple sample or truncated mean analysis to achieve good particle identification. In the truncated mean method for calculating $\langle dE/dx \rangle$, the ionization measurements along the track length are broken into many samples and then a fixed fraction of high-side (and sometimes also low-side) values are rejected [58].

The energy loss of charged particles and photons in matter is discussed in Sec. 32. Table 33.5 provides values of relevant parameters in some commonly used gases at NTP (normal temperature, 20° C, and pressure, 1 atm) for unit-charge minimum-ionizing particles (MIPs) [59–65]. Values often differ, depending on the source, so those in the table should be taken only as approximate. For different conditions and for mixtures, and neglecting internal energy transfer processes (*e.g.*, Penning effect), one can scale the density, N_P, and N_T with temperature and pressure assuming a perfect gas law.

Table 33.5: Properties of noble and molecular gases at normal temperature and pressure (NTP: 20° C, one atm). E_X, E_I: first excitation, ionization energy; W_I: average energy per ion pair; $dE/dx|_{\rm min}$, N_P, N_T: differential energy loss, primary and total number of electron-ion pairs per cm, for unit charge minimum ionizing particles.

Gas	Density, mg cm^{-3}	E_x eV	E_I eV	W_I eV	$dE/dx\|_{\rm min}$ keV cm^{-1}	N_P cm^{-1}	N_T cm^{-1}
He	0.179	19.8	24.6	41.3	0.32	3.5	8
Ne	0.839	16.7	21.6	37	1.45	13	40
Ar	1.66	11.6	15.7	26	2.53	25	97
Xe	5.495	8.4	12.1	22	6.87	41	312
CH_4	0.667	8.8	12.6	30	1.61	28	54
C_2H_6	1.26	8.2	11.5	26	2.91	48	112
iC_4H_{10}	2.49	6.5	10.6	26	5.67	90	220
CO_2	1.84	7.0	13.8	34	3.35	35	100
CF_4	3.78	10.0	16.0	54	6.38	63	120

When an ionizing particle passes through the gas it creates electron-ion pairs, but often the ejected electrons have sufficient energy to further ionize the medium. As shown in Table 33.5, the total number of electron-ion pairs (N_T) is usually a few times larger than the number of primaries (N_P).

The probability for a released electron to have an energy E or larger follows an approximate $1/E^2$ dependence (Rutherford law), shown in Fig. 33.3 for Ar/CH_4 at NTP (dotted line, left scale). More detailed estimates taking into account the electronic structure of the medium are shown in the figure, for three values of the particle velocity factor $\beta\gamma$ [60]. The dot-dashed line provides, on the right scale, the practical range of electrons (including scattering) of energy E. As an example, about 0.6% of released electrons have 1 keV or more energy, substantially increasing the ionization loss rate. The practical range of 1 keV electrons in argon (dot-dashed line, right scale) is 70 μm and this can contribute to the error in the coordinate determination.

The number of electron-ion pairs per primary ionization, or cluster size, has an exponentially decreasing probability; for argon, there is about 1% probability for primary clusters to contain ten or more electron-ion pairs [61].

Once released in the gas, and under the influence of an applied electric field, electrons and ions drift in opposite directions and diffuse towards the electrodes. The scattering cross section is determined by the details of atomic and molecular structure. Therefore, the drift velocity and diffusion of electrons depend very strongly on the

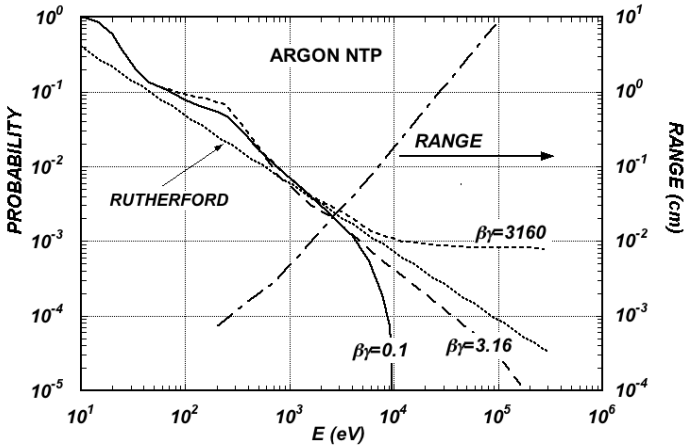

Figure 33.3: Probability of single collisions in which released electrons have an energy E or larger (left scale) and practical range of electrons in Ar/CH_4 (P10) at NTP (dot-dashed curve, right scale) [60].

nature of the gas, specifically on the inelastic cross-section involving the rotational and vibrational levels of molecules. In noble gases, the inelastic cross section is zero below excitation and ionization thresholds. Large drift velocities are achieved by adding polyatomic gases (usually CH_4, CO_2, or CF_4) having large inelastic cross sections at moderate energies, which results in "cooling" electrons into the energy range of the Ramsauer-Townsend minimum (at $\sim$0.5 eV) of the elastic cross-section of argon. The reduction in both the total electron scattering cross-section and the electron energy results in a large increase of electron drift velocity (for a compilation of electron-molecule cross sections see Ref. 62). Another principal role of the polyatomic gas is to absorb the ultraviolet photons emitted by the excited noble gas atoms. Extensive collections of experimental data [63] and theoretical calculations based on transport theory [64] permit estimates of drift and diffusion properties in pure gases and their mixtures. In a simple approximation, gas kinetic theory provides the drift velocity v as a function of the mean collision time τ and the electric field E: $v = eE\tau/m_e$ (Townsend's expression). Values of drift velocity and diffusion for some commonly used gases at NTP are given in Fig. 33.4 and Fig. 33.5. These have been computed with the MAGBOLTZ program [65]. For different conditions, the horizontal axis must be scaled inversely with the gas density. Standard deviations for longitudinal (σ_L) and transverse diffusion (σ_T) are given for one cm of drift, and scale with the the square root of the drift distance. Since the collection time is inversely proportional to the drift velocity, diffusion is less in gases such as CF_4 that have high drift velocities. In the presence of an external magnetic field, the Lorentz force acting on electrons between collisions deflects the drifting electrons and modifies the drift properties. The electron trajectories, velocities and diffusion parameters can be computed with MAGBOLTZ. A simple theory, the friction force model, provides an expression for the vector drift velocity $\boldsymbol{v}$ as a function of electric and magnetic field vectors $\boldsymbol{E}$ and $\boldsymbol{B}$, of the Larmor frequency $\omega = eB/m_e$, and of the mean collision time τ:

$$\boldsymbol{v} = \frac{e}{m_e}\frac{\tau}{1+\omega^2\tau^2}\left(\boldsymbol{E} + \frac{\omega\tau}{B}(\boldsymbol{E}\times\boldsymbol{B}) + \frac{\omega^2\tau^2}{B^2}(\boldsymbol{E}\cdot\boldsymbol{B})\boldsymbol{B}\right) \qquad (33.13)$$

To a good approximation, and for moderate fields, one can assume that the energy of the electrons is not affected by B, and use for τ the values deduced from the drift velocity at $B = 0$ (the Townsend expression). For $\boldsymbol{E}$ perpendicular to $\boldsymbol{B}$, the drift angle to the relative to the electric field vector is $\tan\theta_B = \omega\tau$ and $v = (E/B)(\omega\tau/\sqrt{1+\omega^2\tau^2})$. For parallel electric and magnetic fields, drift velocity and longitudinal diffusion are not affected, while the transverse diffusion can be strongly reduced: $\sigma_T(B) = \sigma_T(B=0)/\sqrt{1+\omega^2\tau^2}$. The dotted line in Fig. 33.5 represents σ_T for the classic Ar/CH_4 (90:10) mixture at 4 T. Large values of $\omega\tau \sim 20$ at 5 T are consistent with the measurement of diffusion coefficient in $Ar/CF_4/iC_4H_{10}$ (95:3:2). This reduction is

exploited in time projection chambers (Sec. 33.6.5) to improve spatial resolution.

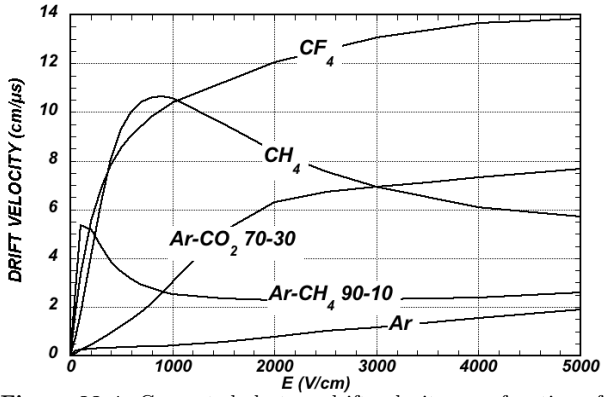

Figure 33.4: Computed electron drift velocity as a function of electric field in several gases at NTP and $B = 0$ [65].

In mixtures containing electronegative molecules, such as O_2 or H_2O, electrons can be captured to form negative ions. Capture cross-sections are strongly energy-dependent, and therefore the capture probability is a function of applied field. For example, the electron is attached to the oxygen molecule at energies below 1 eV. The three-body electron attachment coefficients may differ greatly for the same additive in different mixtures. As an example, at moderate fields (up to 1 kV/cm) the addition of 0.1% of oxygen to an Ar/CO_2 mixture results in an electron capture probability about twenty times larger than the same addition to Ar/CH_4.

Carbon tetrafluoride is not electronegative at low and moderate fields, making its use attractive as drift gas due to its very low diffusion. However, CF_4 has a large electron capture cross section at fields above $\sim$8 kV/cm, before reaching avalanche field strengths. Depending on detector geometry, some signal reduction and resolution loss can be expected using this gas.

If the electric field is increased sufficiently, electrons gain enough energy between collisions to ionize molecules. Above a gas-dependent threshold, the mean free path for ionization, λ_i, decreases exponentially with the field; its inverse, $\alpha = 1/\lambda_i$, is the first Townsend coefficient. In wire chambers, most of the increase of avalanche particle density occurs very close to the anode wires, and a simple electrostatic consideration shows that the largest fraction of the detected signal is due to the motion of positive ions receding from the wires. The electron component, although very fast, contributes very little to the signal. This determines the characteristic shape of the detected signals in the proportional mode: a fast rise followed by a gradual increase. The slow component, the so-called "ion tail" that limits the time resolution of the detector, is usually removed by differentiation of the signal. In uniform fields, N_0 initial electrons multiply over a length x forming an electron avalanche of size $N = N_0\, e^{\alpha x}$; N/N_0 is the gain of the detector. Fig. 33.6 shows examples of Townsend coefficients for several gas mixtures, computed with MAGBOLTZ [65].

Positive ions released by the primary ionization or produced in the avalanches drift and diffuse under the influence of the electric field. Negative ions may also be produced by electron attachment to gas molecules. The drift velocity of ions in the fields encountered in gaseous detectors (up to few kV/cm) is typically about three orders of magnitude less than for electrons. The ion mobility μ, the ratio of drift velocity to electric field, is constant for a given ion type up to very high fields. Values of mobility at NTP for ions in their own and other gases are given in Table 33.6 [66]. For different temperatures and pressures, the mobility can be scaled inversely with the density assuming an ideal gas law. For mixtures, due to a very effective charge transfer mechanism, only ions with the lowest ionization potential survive after a short path in the gas. Both the lateral and transverse diffusion of ions are proportional to the square root of the drift time, with a coefficient that depends on temperature but not on the ion mass. Accumulation of ions in the gas drift volume may induce field distortions (see Sec. 33.6.5).

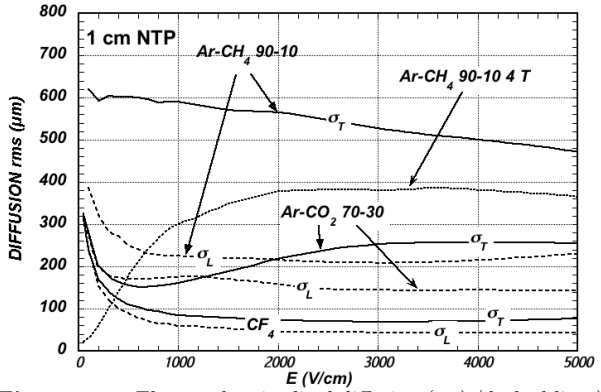

Figure 33.5: Electron longitudinal diffusion (σ_L) (dashed lines) and transverse diffusion (σ_T) (full lines) for 1 cm of drift at NTP and $B = 0$. The dotted line shows σ_T for the P10 mixture at 4 T [65].

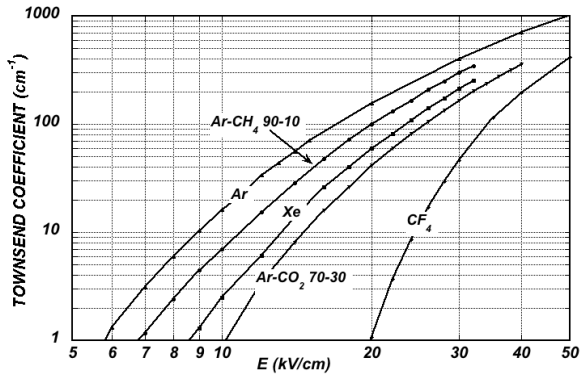

Figure 33.6: Computed first Townsend coefficient α as a function of electric field in several gases at NTP [65].

Table 33.6: Mobility of ions in gases at NTP [66].

Gas	Ion	Mobility μ ($cm^2\ V^{-1}\ s^{-1}$)
He	He^+	10.4
Ne	Ne^+	4.7
Ar	Ar^+	1.54
Ar/CH_4	CH_4^+	1.87
Ar/CO_2	CO_2^+	1.72
CH_4	CH_4^+	2.26
CO_2	CO_2^+	1.09

33.6.2. ***Multi-Wire Proportional and Drift Chambers*** : Revised March 2010 by Fabio Sauli (CERN) and Maxim Titov (CEA Saclay).

Single-wire counters that detect the ionization produced in a gas by a charged particle, followed by charge multiplication and collection around a thin wire have been used for decades. Good energy resolution is obtained in the proportional amplification mode, while very large saturated pulses can be detected in the streamer and Geiger modes [3].

Multiwire proportional chambers (MWPCs) [67,68], introduced in the late '60's, detect, localize and measure energy deposit by charged particles over large areas. A mesh of parallel anode wires at a suitable potential, inserted between two cathodes, acts almost as a set of independent proportional counters (see Fig. 33.7a). Electrons released in the gas volume drift towards the anodes and produce avalanches in the increasing field. Analytic expressions for the electric field can be found in many textbooks. The fields close to the wires $E(r)$, in the

drift region E_D, and the capacitance C per unit length of anode wire are approximately given by

$$E(r) = \frac{CV_0}{2\pi\epsilon_0}\frac{1}{r} \qquad E_D = \frac{CV_0}{2\epsilon_0 s} \qquad C = \frac{2\pi\epsilon_0}{\pi(\ell/s) - \ln(2\pi a/s)}\ , \quad (33.14)$$

where r is the distance from the center of the anode, s the wire spacing, ℓ and V_0 the distance and potential difference between anode and cathode, and a the anode wire radius.

Because of electrostatic forces, anode wires are in equilibrium only for a perfect geometry. Small deviations result in forces displacing the wires alternatively below and above the symmetry plane, sometimes with catastrophic results. These displacement forces are countered by the mechanical tension of the wire, up to a maximum unsupported stable length, L_M [58], above which the wire deforms:

$$L_M = \frac{s}{CV_0}\sqrt{4\pi\epsilon_0 T_M} \quad (33.15)$$

The maximum tension T_M depends on the wire diameter and modulus of elasticity. Table 33.7 gives approximate values for tungsten and the corresponding maximum stable wire length under reasonable assumptions for the operating voltage ($V_0 = 5\,\text{kV}$) [69]. Internal supports and spacers can be used in the construction of longer detectors to overcome limits on the wire length imposed by Eq. (33.15).

Table 33.7: Maximum tension T_M and stable unsupported length L_M for tungsten wires with spacing s, operated at $V_0 = 5$ kV. No safety factor is included.

Wire diameter (μm)	T_M (newton)	s (mm)	L_M (cm)
10	0.16	1	25
20	0.65	2	85

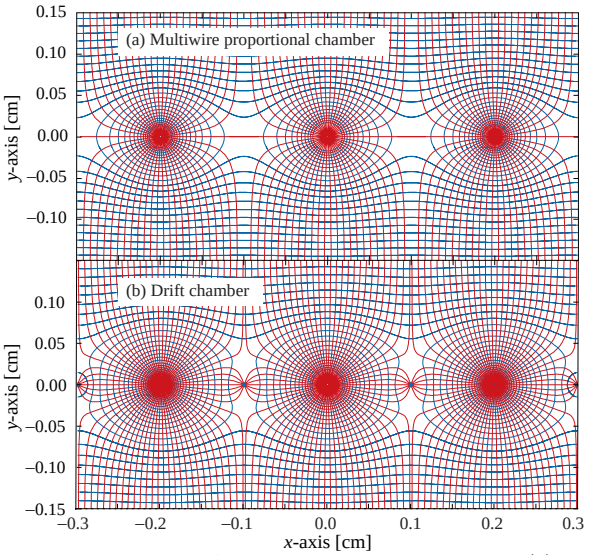

Figure 33.7: Electric field lines and equipotentials in (a) a multiwire proportional chamber and (b) a drift chamber.

Detection of charge on the wires over a predefined threshold provides the transverse coordinate to the wire with an accuracy comparable to that of the wire spacing. The coordinate along each wire can be obtained by measuring the ratio of collected charge at the two ends of resistive wires. Making use of the charge profile induced on segmented cathodes, the so-called center-of gravity (COG) method, permits localization of tracks to sub-mm accuracy. Due to the statistics of energy loss and asymmetric ionization clusters, the position accuracy is $\sim 50\,\mu$m rms for tracks perpendicular to the wire plane, but degrades to $\sim 250\,\mu$mat 30° to the normal [70]. The intrinsic bi-dimensional characteristic of the COG readout has found numerous applications in medical imaging.

Drift chambers, developed in the early '70's, can be used to estimate the longitudinal position of a track by exploiting the arrival time of electrons at the anodes if the time of interaction is known [71]. The distance between anode wires is usually several cm, allowing coverage of large areas at reduced cost. In the original design, a thicker wire (the field wire) at the proper voltage, placed between the anode wires, reduces the field at the mid-point between anodes and improves charge collection (Fig. 33.7b). In some drift chamber designs, and with the help of suitable voltages applied to field-shaping electrodes, the electric field structure is adjusted to improve the linearity of space-to-drift-time relation, resulting in better spatial resolution [72].

Drift chambers can reach a longitudinal spatial resolution from timing measurement of order 100 μm (rms) or better for minimum ionizing particles, depending on the geometry and operating conditions. However, a degradation of resolution is observed [73] due to primary ionization statistics for tracks close to the anode wires, caused by the spread in arrival time of the nearest ionization clusters. The effect can be reduced by operating the detector at higher pressures. Sampling the drift time on rows of anodes led to the concept of multiple arrays such as the multi-drift module [74] and the JET chamber [75]. A measurement of drift time, together with the recording of charge sharing from the two ends of the anode wires provides the coordinates of segments of tracks. The total charge gives information on the differential energy loss and is exploited for particle identification. The time projection chamber (TPC) [76] combines a measurement of drift time and charge induction on cathodes, to obtain excellent tracking for high multiplicity topologies occurring at moderate rates (see Sec. 33.6.5). In all cases, a good knowledge of electron drift velocity and diffusion properties is required. This has to be combined with the knowledge of the electric fields in the structures, computed with commercial or custom-developed software [65,77]. For an overview of detectors exploiting the drift time for coordinate measurement see Refs. 6 and 58.

Multiwire and drift chambers have been operated with a variety of gas fillings and operating modes, depending on experimental requirements. The so-called "Magic Gas," a mixture of argon, isobutane and Freon [68], permits very high and saturated gains ($\sim 10^6$). This gas mixture was used in early wire chambers, but was found to be susceptible to severe aging processes. With present-day electronics, proportional gains around 10^4 are sufficient for detection of minimum ionizing particles, and noble gases with moderate amounts of polyatomic gases, such as methane or carbon dioxide, are used.

Although very powerful in terms of performance, multi-wire structures have reliability problems when used in harsh or hard-to-access environments, since a single broken wire can disable the entire detector. Introduced in the '80's, straw and drift tube systems make use of large arrays of wire counters encased in individual enclosures, each acting as an independent wire counter [78]. Techniques for low-cost mass production of these detectors have been developed for large experiments, such as the Transition Radiation Tracker and the Drift Tubes arrays for CERN's LHC experiments [79].

33.6.3. ***High Rate Effects*** : Revised March 2010 by Fabio Sauli (CERN) and Maxim Titov (CEA Saclay).

The production of positive ions in the avalanches and their slow drift before neutralization result in a rate-dependent accumulation of positive charge in the detector. This may result in significant field distortion, gain reduction and degradation of spatial resolution. As shown in Fig. 33.8 [80], the proportional gain drops above a charge production rate around 10^9 electrons per second and mm of wire, independently of the avalanche size. For a proportional gain of 10^4 and 100 electrons per track, this corresponds to a particle flux of $10^3\,\text{s}^{-1}\text{mm}^{-1}$ (1 kHz/mm^2 for 1 mm wire spacing).

At high radiation fluxes, a fast degradation of detectors due to the formation of polymers deposits (aging) is often observed. The process has been extensively investigated, often with conflicting results. Several causes have been identified, including organic pollutants and silicone oils. Addition of small amounts of water in many (but not all) cases has been shown to extend the lifetime of the detectors. Addition of fluorinated gases (*e.g.*, CF_4) or oxygen may result in an

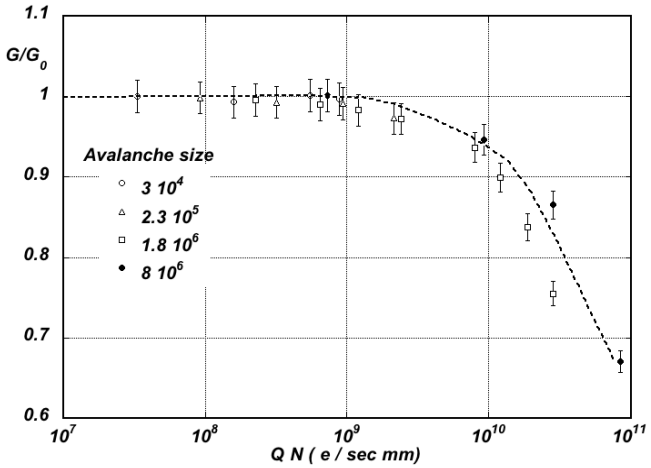

Figure 33.8: Charge rate dependence of normalized gas gain G/G_0 (relative to zero counting rate) in proportional thin-wire detectors [80]. Q is the total charge in single avalanche; N is the particle rate per wire length.

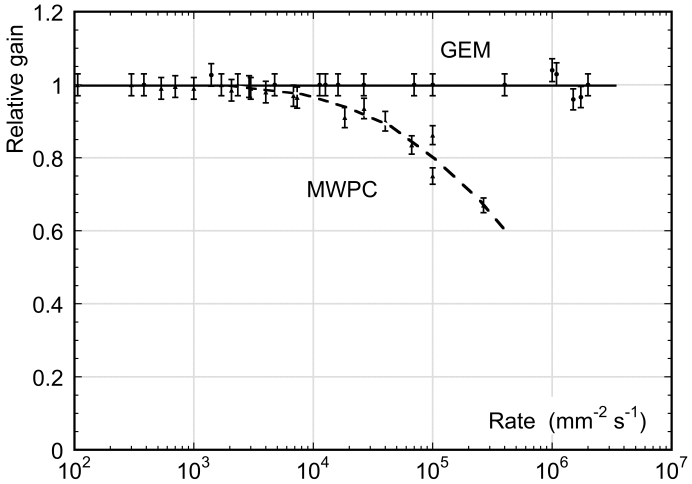

Figure 33.9: Normalized gas gain as a function of particle rate for MWPC [72] and GEM [86].

etching action that can overcome polymer formation, or even eliminate already existing deposits. However, the issue of long-term survival of gas detectors with these gases is controversial [81]. Under optimum operating conditions, a total collected charge of a few coulombs per cm of wire can usually be reached before noticeable degradation occurs. This corresponds, for one mm spacing and at a gain of 10^4, to a total particle flux of $\sim 10^{14}$ MIPs/cm^2.

33.6.4. ***Micro-Pattern Gas Detectors*** : Revised March 2010 by Fabio Sauli (CERN) and Maxim Titov (CEA Saclay)

Despite various improvements, position-sensitive detectors based on wire structures are limited by basic diffusion processes and space charge effects to localization accuracies of 50–100 μm [82]. Modern photolithographic technology led to the development of novel Micro-Pattern Gas Detector (MPGD) concepts [83], revolutionizing cell size limitations for many gas detector applications. By using pitch size of a few hundred μm, an order of magnitude improvement in granularity over wire chambers, these detectors offer intrinsic high rate capability ($> 10^6$ Hz/mm^2), excellent spatial resolution ($\sim$ 30 μm), multi-particle resolution ($\sim$ 500 μm), and single photo-electron time resolution in the ns range.

The Micro-Strip Gas Chamber (MSGC), invented in 1988, was the first of the micro-structure gas chambers [84]. It consists of a set of tiny parallel metal strips laid on a thin resistive support, alternatively connected as anodes and cathodes. Owing to the small anode-to-cathode distance ($\sim$ 100 μm), the fast collection of positive ions reduces space charge build-up, and provides a greatly increased rate capability. Unfortunately, the fragile electrode structure of the MSGC turned out to be easily destroyed by discharges induced by heavily ionizing particles [85]. Nevertheless, detailed studies of their properties, and in particular, on the radiation-induced processes leading to discharge breakdown, led to the development of the more powerful devices: GEM and Micromegas. These have improved reliability and radiation hardness. The absence of space-charge effects in GEM detectors at the highest rates reached so far and the fine granularity of MPGDs improve the maximum rate capability by more than two orders of magnitude (Fig. 33.9) [72,86]. Even larger rate capability has been reported for Micromegas [87].

The Gas Electron Multiplier (GEM) detector consists of a thin-foil copper-insulator-copper sandwich chemically perforated to obtain a high density of holes in which avalanches occur [88]. The hole diameter is typically between 25 μm and 150 μm, while the corresponding distance between holes varies between 50 μm and 200 μm. The central insulator is usually (in the original design) the polymer Kapton, with a thickness of 50 μm. Application of a potential difference between the two sides of the GEM generates the electric fields indicated in Fig. 33.10. Each hole acts as an independent proportional counter. Electrons released by the primary ionization particle in the upper conversion region (above the GEM foil) drift into the holes, where charge multiplication occurs in the high electric field (50–70 kV/cm). Most of avalanche electrons are transferred into the gap below the GEM. Several GEM foils can be cascaded, allowing the multi-layer GEM detectors to operate at overall gas gain above 10^4 in the presence of highly ionizing particles, while strongly reducing the risk of discharges. This is a major advantage of the GEM technology [89]. Localization can then be performed by collecting the charge on a patterned one- or two-dimensional readout board of arbitrary pattern, placed below the last GEM.

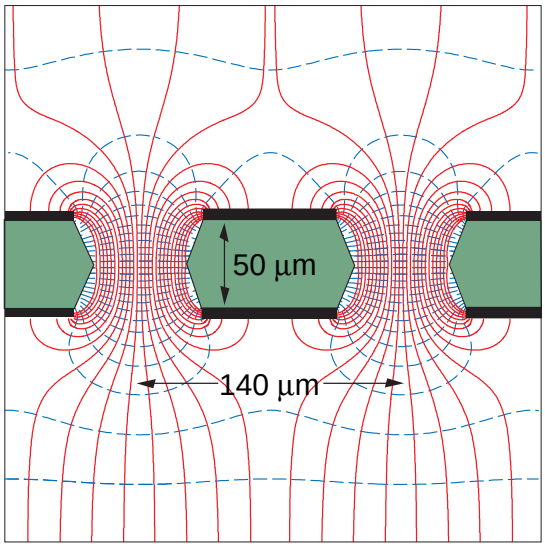

Figure 33.10: Schematic view and typical dimensions of the hole structure in the GEM amplification cell. Electric field lines (solid) and equipotentials (dashed) are shown.

The micro-mesh gaseous structure (Micromegas) is a thin parallel-plate avalanche counter, as shown in Fig. 33.11 [90]. It consists of a drift region and a narrow multiplication gap (25–150 μm) between a thin metal grid (micromesh) and the readout electrode (strips or pads of conductor printed on an insulator board). Electrons from the primary ionization drift through the holes of the mesh into the narrow multiplication gap, where they are amplified. The electric field is homogeneous both in the drift (electric field $\sim$1 kV/cm) and amplification (50–70 kV/cm) gaps. In the narrow multiplication region, gain variations due to small variations of the amplification gap are approximately compensated by an inverse variation of the amplification coefficient, resulting in a more uniform gain. The small

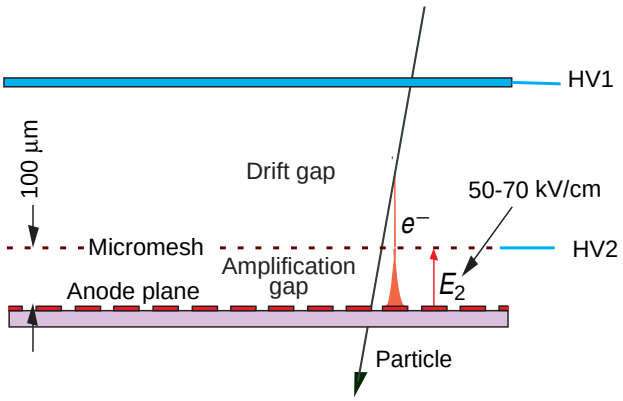

Figure 33.11: Schematic drawing of the Micromegas detector.

amplification gap produces a narrow avalanche, giving rise to excellent spatial resolution: 12 μm accuracy, limited by the micro-mesh pitch, has been achieved for MIPs, as well as very good time resolution and energy resolution ($\sim$12% FWHM with 6 keV x rays) [91].

The performance and robustness of GEM and Micromegas have encouraged their use in high-energy and nuclear physics, UV and visible photon detection, astroparticle and neutrino physics, neutron detection and medical physics. Most structures were originally optimized for high-rate particle tracking in nuclear and high-energy physics experiments. COMPASS, a high-luminosity experiment at CERN, pioneered the use of large-area ($\sim 40 \times 40$ cm^2) GEM and Micromegas detectors close to the beam line with particle rates of 25 kHz/mm^2. Both technologies achieved a tracking efficiency of close to 100% at gas gains of about 10^4, a spatial resolution of 70–100 μm and a time resolution of $\sim$10 ns. GEM detectors are also used for triggering in the LHCb Muon System and for tracking in the TOTEM Telescopes. Both GEM and Micromegas devices are foreseen for the upgrade of the LHC experiments and for one of the readout options for the Time Projection Chamber (TPC) at the International Linear Collider (ILC). The development of new fabrication techniques—"bulk" Micromegas technology [92] and single-mask GEMs [93] —is a big step toward industrial production of large-size MPGDs. In some applications requiring very large-area coverage with moderate spatial resolution, coarse macro-patterned detectors, such as Thick GEMs (THGEM) [94] or patterned resistive-plate devices [95] might offer economically interesting solutions.

Sensitive and low-noise electronics enlarge the range of the MPGD applications. Recently, the GEM and Micromegas detectors were read out by high-granularity ($\sim$50 μm pitch) CMOS chips assembled directly below the GEM or Micromegas amplification structures [96]. These detectors use the bump-bonding pads of a pixel chip as an integrated charge collecting anode. With this arrangement signals are induced at the input gate of a charge-sensitive preamplifier (top metal layer of the CMOS chip). Every pixel is then directly connected to the amplification and digitization circuits, integrated in the underlying active layers of the CMOS technology, yielding timing and charge measurements as well as precise spatial information in 3D.

The operation of a MPGD with a Timepix CMOS chip has demonstrated the possibility of reconstructing 3D-space points of individual primary electron clusters with $\sim$30 μm spatial resolution and event-time resolution with nanosecond precision. This has become indispensable for tracking and triggering and also for discriminating between ionizing tracks and photon conversions. The GEM, in conjunction with a CMOS ASIC,* can directly view the absorption process of a few keV x-ray quanta and simultaneously reconstruct the direction of emission, which is sensitive to the x-ray polarization. Thanks to these developments, a micro-pattern device with finely segmented CMOS readout can serve as a high-precision "electronic bubble chamber." This may open new opportunities for x-ray polarimeters, detection of weakly interacting massive particles (WIMPs) and axions, Compton telescopes, and 3D imaging of nuclear recoils.

* Application Specific Integrated Circuit

An elegant solution for the construction of the Micromegas with pixel readout is the integration of the amplification grid and CMOS chip by means of an advanced "wafer post-processing" technology [97]. This novel concept is called "Ingrid" (see Fig. 33.12). With this technique, the structure of a thin (1 μm) aluminum grid is fabricated on top of an array of insulating pillars. which stands $\sim$50 μm above the CMOS chip. The sub-μm precision of the grid dimensions and avalanche gap size results in a uniform gas gain. The grid hole size, pitch and pattern can be easily adapted to match the geometry of any pixel readout chip.

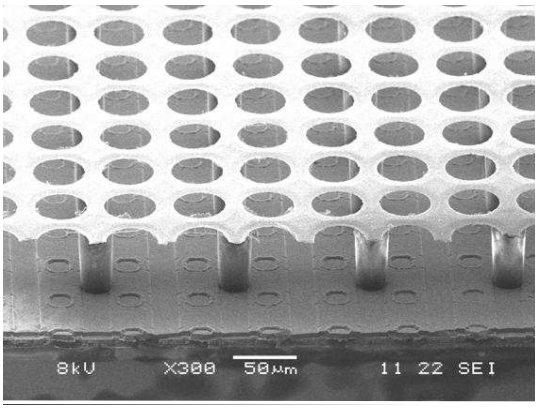

Figure 33.12: Photo of the Micromegas "Ingrid" detector. The grid holes can be accurately aligned with readout pixels of CMOS chip. The insulating pillars are centered between the grid holes, thus avoiding dead regions.

Recent developments in radiation hardness research with state-of-the-art MPGDs are reviewed in Ref. 98. Earlier aging studies of GEM and Micromegas concepts revealed that they might be even less vulnerable to radiation-induced performance degradation than standard silicon microstrip detectors.

The RD51 collaboration was established in 2008 to further advance technological developments of micro-pattern detectors and associated electronic-readout systems for applications in basic and applied research [99].

33.6.5. ***Time-projection chambers*** : Reviser October 2011 by D. Karlen (U. of Victoria and TRIUMF, Canada)

The Time Projection Chamber (TPC) concept, invented by David Nygren in the late 1970's [76], is the basis for charged particle tracking in a large number of particle and nuclear physics experiments. A uniform electric field drifts tracks of electrons produced by charged particles traversing a medium, either gas or liquid, towards a surface segmented into 2D readout pads. The signal amplitudes and arrival times are recorded to provide full 3D measurements of the particle trajectories. The intrinsic 3D segmentation gives the TPC a distinct advantage over other large volume tracking detector designs which record information only in a 2D projection with less overall segmentation, particularly for pattern recognition in events with large numbers of particles.

Gaseous TPC's are often designed to operate within a strong magnetic field (typically parallel to the drift field) so that particle momenta can be estimated from the track curvature. For this application, precise spatial measurements in the plane transverse to the magnetic field are most important. Since the amount of ionization along the length of the track depends on the velocity of the particle, ionization and momentum measurements can be combined to identify the types of particles observed in the TPC. The estimator for the energy deposit by a particle is usually formed as the truncated mean of the energy deposits, using the 50%–70% of the samples with the smallest signals. Variance due to energetic δ-ray production is thus reduced.

Gas amplification of 10^3–10^4 at the readout endplate is usually required in order to provide signals with sufficient amplitude for conventional electronics to sense the drifted ionization. Until recently,

the gas amplification system used in TPC's have exclusively been planes of anode wires operated in proportional mode placed close to the readout pads. Performance has been recently improved by replacing these wire planes with micro-pattern gas detectors, namely GEM [88] and Micromegas [90] devices. Advances in electronics miniaturization have been important in this development, allowing pad areas to be reduced to the 10 mm^2 scale or less, well matched to the narrow extent of signals produced with micro-pattern gas detectors. Presently, the ultimate in fine segmentation TPC readout are silicon sensors, with 0.05 mm × 0.05 mm pixels, in combination with GEM or Micromegas [100]. With such fine granularity it is possible to count the number of ionization clusters along the length of a track which, in principle, can improve the particle identification capability.

Examples of two modern large volume gaseous TPC's are shown in Fig. 33.13 and Fig. 33.14. The particle identification performance is illustrated in Fig. 33.15, for the original TPC in the PEP-4/9 experiment [101].

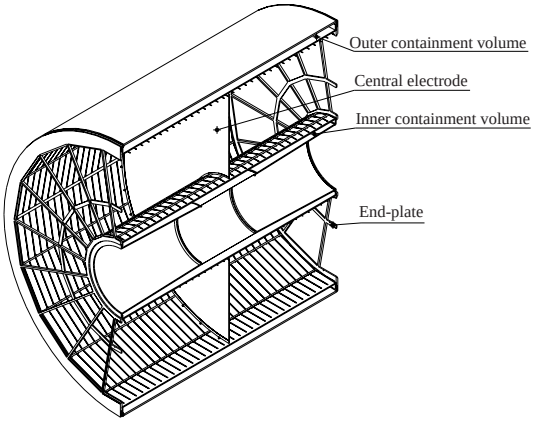

Figure 33.13: The ALICE TPC shown in a cutaway view [102]. The drift volume is 5 m long with a 5 m diameter. Gas amplification is provided by planes of anode wires.

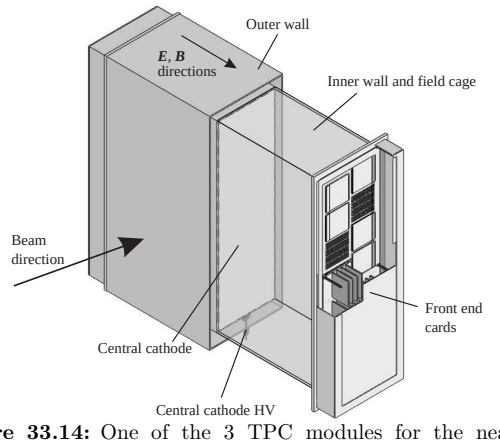

Figure 33.14: One of the 3 TPC modules for the near detector of the T2K experiment [103]. The drift volume is 2 m×2 m×0.8 m. Micromegas devices are used for gas amplification and readout.

The greatest challenges for a large TPC arise from the long drift distance, typically 100 times further than in a comparable wire chamber design. In particular, the long drift distance can make the device sensitive to small distortions in the electric field. Distortions can arise from a number of sources, such as imperfections in the TPC

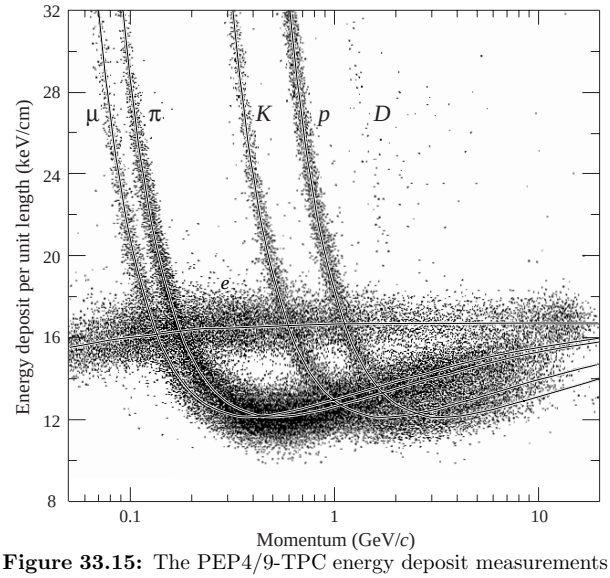

Figure 33.15: The PEP4/9-TPC energy deposit measurements (185 samples, 8.5 atm Ar-CH_4 80:20). The ionization rate at the Fermi plateau (at high β) is 1.4 times that for the minimum at lower β. This ratio increases to 1.6 at atmospheric pressure.

construction, deformations of the readout surface, or the presence of ions in the active medium.

For a gaseous TPC operated in a magnetic field, the electron drift velocity $\boldsymbol{v}$ is defined by Eq. (33.13). With a strong magnetic field parallel to the electric field and a gas with a large value of $\omega\tau$ (also favored to reduce transverse diffusion as discussed below), the transverse displacements of the drifting electrons due to electric field distortions are reduced. In this mode of operation, it is essential to precisely map the magnetic field as the electron drift lines closely follow the magnetic field lines. Corrections for electric and/or magnetic field non-uniformities can be determined from control samples of electrons produced by ionizing the gas with UV laser beams, from photoelectrons produced on the cathode, or from tracks emanating from calibration reactions.

The long drift distance means that there is a delay, typically 10–100 μs in a large gaseous TPC, for signals to arrive at the endplate. For experiments with shorter intervals between events, this can produce ambiguities in the starting time for the drift of ionization. This can be resolved by matching the TPC data with that from an auxiliary detector providing additional spatial or timing information.

In a gaseous TPC, the motion of positive ions is much slower than the electrons, and so the positive ions produced by many events may exist in the active volume. Of greatest concern is the ions produced in the gas amplification stage. Large gaseous TPC's built until now with wire planes have included a gating grid that prevent the positive ions from escaping into the drift volume in the interval between event triggers. Micro-pattern gas detectors release much less positive ions than wire planes operating at the same gain, which may allow operation of a TPC without a gating grid.

Given the long drift distance in a large TPC, the active medium must remain very pure, as small amounts of contamination can absorb the ionization signal. For example, in a typical large gaseous TPC, O_2 must be kept below a few parts in 10^5, otherwise a large fraction of the drifting electrons will become attached. Special attention must be made in the choice of construction materials in order to avoid the release of other electronegative contaminants.

Diffusion degrades the position information of ionization that drifts a long distance. For a gaseous TPC, the effect can be alleviated by the choice of a gas with low intrinsic diffusion or by operating in a strong magnetic field parallel to the drift field with a gas which exhibits a significant reduction in transverse diffusion with magnetic field. For typical operation without magnetic field, the transverse extent of the electrons, σ_{Dx}, is a few mm after drifting 1 m due to diffusion. With a strong magnetic field, σ_{Dx} can be reduced by as much as a factor of

10,

$$\sigma_{Dx}(B)/\sigma_{Dx}(0) = \frac{1}{\sqrt{1+\omega^2\tau^2}} \tag{33.16}$$

where $\omega\tau$ is defined above. The diffusion limited position resolution from the information collected by a single row of pads is

$$\sigma_x = \frac{\sigma_{Dx}}{\sqrt{n}} \tag{33.17}$$

where n is the effective number of electrons collected by the pad row, giving an ultimate single row resolution of order 100 μm.

Diffusion is significantly reduced in a negative-ion TPC [104], which uses a special gas mixture that attaches electrons immediately as they are produced. The drifting negative ions exhibit much less diffusion than electrons. The slow drift velocity and small $\omega\tau$ of negative ions must be compatible with the experimental environment.

The spatial resolution achieved by a TPC is determined by a number of factors in addition to diffusion. Non-uniform ionization along the length of the track is a particularly important factor, and is responsible for the so-called "track angle" and "$\boldsymbol{E}\times\boldsymbol{B}$" effects. If the boundaries between pads in a row are not parallel to the track, the ionization fluctuations will increase the variance in the position estimate from that row. For this reason, experiments with a preferred track direction should have pad boundaries aligned with that direction. Traditional TPC's with wire plane amplification suffer from the effects of non-parallel electric and magnetic fields near the wires that rotate ionization segments, thereby degrading the resolution because of the non-uniform ionization. Micro-pattern gas detectors exhibit a much smaller $\boldsymbol{E}\times\boldsymbol{B}$ effect, since their feature size is much smaller than that of a wire grid.

33.6.6. ***Transition radiation detectors (TRD's)*** : Revised August 2013 by P. Nevski (BNL) and A. Romaniouk (Moscow Eng. & Phys. Inst.)

Transition radiation (TR) X-rays are produced when a highly relativistic particle ($\gamma \gtrsim 10^3$) crosses a refractive index interface, as discussed in Sec. 32.7. The X-rays, ranging from a few keV to a few dozen keV or more, are emitted at a characteristic angle $1/\gamma$ from the particle trajectory. Since the TR yield is about 1% per boundary crossing, radiation from multiple surface crossings is used in practical detectors. In the simplest concept, a detector module might consist of low-Z foils followed by a high-Z active layer made of proportional counters filled with a Xe-rich gas mixture. The atomic number considerations follow from the dominant photoelectric absorption cross section per atom going roughly as Z^n/E_x^3, where n varies between 4 and 5 over the region of interest, and the X-ray energy is E_x.* To minimize self-absorption, materials such as polypropylene, Mylar, carbon, and (rarely) lithium are used as radiators. The TR signal in the active regions is in most cases superimposed upon the particle ionization losses, which are proportional to Z.

The TR intensity for a single boundary crossing always increases with γ, but, for multiple boundary crossings, interference leads to saturation above a Lorentz factor $\gamma_{\,\mathrm{sat}} = 0.6\ \omega_1\sqrt{\ell_1\ell_2}/c$ [105], where ω_1 is the radiator material plasma frequency, ℓ_1 is its thickness, and ℓ_2 the spacing. In most of the detectors used in particle physics the radiator parameters are chosen to provide $\gamma_{\,\mathrm{sat}} \approx 2000$. Those detectors normally work as threshold devices, ensuring the best electron/pion separation in the momentum range $1\ \mathrm{GeV}/c \lesssim p \lesssim 150\ \mathrm{GeV}/c$.

One can distinguish two design concepts—"thick" and "thin" detectors:

1. The radiator, optimized for a minimum total radiation length at maximum TR yield and total TR absorption, consists of few hundred foils (for instance 300 20 μm thick polypropylene foils). Most of the TR photons are absorbed in the radiator itself. To maximise the number of TR photons reaching the detector, part of the radiator far from the active layers is often made of thicker foils, which shifts the X-ray spectrum to higher energies. The detector thickness, about 2-4 cm for Xe-filled gas chambers, is optimized to absorb the incoming X-ray spectrum. A classical detector is composed of several similar modules which respond nearly independently. Such detectors were used in the UA2, NA34 and other experiments [106], and are being used in the ALICE experiment [107], [108].
2. In other TRD concepts a fine granular radiator/detector structure exploits the soft part of the TR spectrum more efficiently and thereby may act also as an integral part of the tracking detector. This can be achieved, for instance, by distributing small-diameter straw-tube detectors uniformly or in thin layers throughout the radiator material (foils or fibers). Even with a relatively thin radiator stack, radiation below 5 keV is mostly lost in the radiators themselves. However for photon energies above this value, the absorption is reduced and the radiation can be registered by several consecutive detector layers, thus creating a strong TR build-up effect. This approach allows to realise TRD as an integral part of the tracking detector. Descriptions of detectors using this approach can be found in both accelerator and space experiments [107] and [108]. For example, in the ATLAS TR tracker (TRT), charged particles cross about 35 effective straw tube layers embedded in the radiator material [107]. The effective thickness of the Xe gas per straw is about 2.2 mm and the average number of foils per straw is about 40 with an effective foil thickness of about 18 μm.

Both TR photon absorption and the TR build-up significantly affect the detector performance. Although the values mentioned above are typical for most of the plastic radiators used with Xe-based detectors, they vary significantly depending on the detector parameters: radiator material, thickness and spacing, the geometry and position of the sensitive chambers, *etc.* Thus careful simulations are usually needed to build a detector optimized for a particular application. For TRD simulation stand-alone codes based on GEANT3 program were usually used (P.Nevski in [107]) . TR simulation is now available in GEANT4 [112]. The most recent version of it (starting from release 9.5) shows a reasonable agreement with data (S. Furletov in [108] and [109]) .

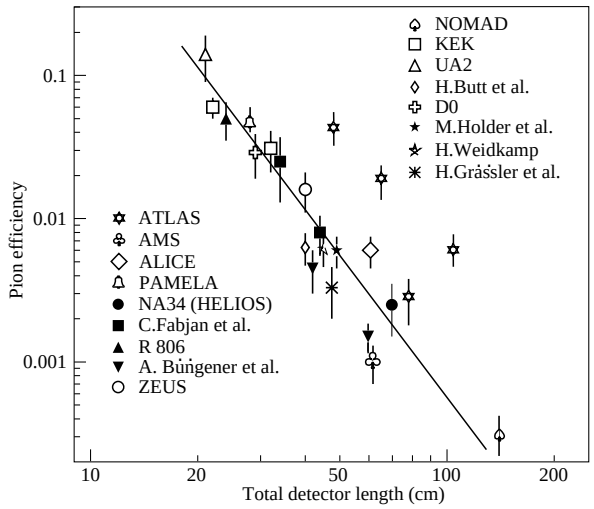

Figure 33.16: Pion efficiency measured (or predicted) for different TRDs as a function of the detector length for a fixed electron efficiency of 90%. The plot is taken from [106]. Results from more recent detectors are added from [107] and [108].

The discrimination between electrons and pions can be based on the charge deposition measured in each detection module, on the number of clusters – energy depositions observed above an optimal threshold (usually it is 5–7 keV), or on more sophisticated methods such as analyzing the pulse shape as a function of time. The total energy measurement technique is more suitable for thick gas volumes, which absorb most of the TR radiation and where the ionization loss fluctuations are small. The cluster-counting method works

* Photon absorption coefficients for the elements (via a NIST link), and $dE/dx|_{\mathrm{min}}$ and plasma energies for many materials are given in `pdg.lbl.gov/AtomicNuclearProperties`.

better for detectors with thin gas layers, where the fluctuations of the ionization losses are big. Cluster-counting replaces the Landau-Vavilov distribution of background ionization energy losses with the Poisson statistics of δ-electrons, responsible for the distribution tails. The latter distribution is narrower than the Landau-Vavilov distribution. In practice, most of the experiments use a likelihood method, which exploits detailed knowledge of the detector response for different particles and gives the best separation. The more parameters that are considered, the better separation power. The recent results of the TRD in the AMS experiment is a good example. In the real experiment the rejection power is better by almost one order of magnitude than that obtained in the beam test if stringent criteria for track selection are applied (see T. Kirn *et al.* in [108]) . Another example is a neural network method used by the ALICE TRD (ALICE point in Fig. 33.16) which gives another factor of 2–3 in rejecton power with respect to the likelihood method [110]) .

The major factor in the performance of any TRD is its overall length. This is illustrated in Fig. 33.16, which shows, for a variety of detectors, the pion efficiency at a fixed electron efficiency of 90% as a function of the overall detector length. The experimental data, covering a range of particle energies from 1 GeV to 40 GeV, are rescaled to an energy of 10 GeV when possible. Phenomenologically, the rejection power against pions increases as $5 \cdot 10^{L/38}$, where the range of validity is $L \approx$ 20–100 cm. Apart from the beam energy variations, the observed scattering of the points in the plot reflects how effectively the detector space is used and how well the exact response to different particles is taken into account in the analysis. For instance, the ATLAS TRT was built as a compromise between TR and tracking requirements; that is why the test-beam prototype result (lower point) is better than the real TRT performance at the LHC shown in Fig. 33.16 for different regions in the detector (in agreement with MC).

In most cases, recent TRDs combine particle identification with charged-track measurement in the same detector [107], [108] and [111]. This is particularly important for collider experiments, where the available space for the inner detector is very limited. For a modest increase of the radiation length due to the radiator (∼4% X0), a significant enhancement of the electron identification was obtained in the case of the ATLAS TRT. The combination of the two detector functions provides a powerful tool for electron identification even at very high particle densities.

In addition to the enhancement of the electron identification, one of the most important roles of the TRDs in the collider experiments is their participation in different trigger and data analysis algorithms. The ALICE experiment [108] is a good example of the use of the TRD in a First Level Trigger. In the ATLAS experiment, the TRT information is used in the High Level Trigger (HLT) algorithms. With continuous increase of instantaneous luminosity, the electron trigger output rate becomes so high, that a significant increase of the calorimeter energy threshold is required to keep it at an acceptable level. For luminosities above $2 \cdot 10^{34} cm^{-2} s^{-1}$ at the LHC this will affect the trigger efficiency of very important physics channels (e.g. $W \to e\nu$ inclusive decay). Even a very soft TR cut at HLT level, which preserves high electron efficiency (98%), allows to maintain a high trigger efficiency and its purity for physics events with a single electron in a final state. TRT also plays a crucial role in the studies where an electron suppression is required (e.g. hadronic mode of τ–decays). TR information is a completely independent tool for electron identification and allows to study systematic uncertainties of other electron reconstruction methods.

Electron identification is not the only TRD application. Recent TRDs for particle astrophysics are designed to directly measure the Lorentz factor of high-energy nuclei by using the quadratic dependence of the TR yield on nuclear charge; see Cherry and Müller papers in [107]. The radiator configuration (ℓ_1, ℓ_2) is tuned to extend the TR yield rise up to $\gamma \lesssim 10^5$ using the more energetic part of the TR spectrum (up to 100 keV). Large density radiator materials (such as Al) are the best for this purpose. Direct absorption of the TR-photons of these energies with thin detectors becomes problematic and TR detection methods based on Compton scattering have been proposed to use (M. Cherry in [107], [108]) .

In all cases to-date, the radiator properties have been the main limiting factor for the TRDs, and for future progress in this field, it is highly important to develop effective and compact radiators. By now, all traditional materials have been studied extensively, so new technologies must be invented. The properties of all radiators are defined by one basic parameter which is the plasma frequency of the radiator material – $\omega_1 \sim 1/m_e$ (see Eq. (32.48)). In semiconductor materials, a quantum mechanical treatment of the electron binding to the lattice leads to a small effective electron mass and correspondingly to large values of ω_1. All semiconductor materials have large Z and may not be good candidates as TR radiators, but new materials, such as graphene, may offer similar features at much lower Z (M. Cherry in [108]) . It might even be possible to produce graphene-based radiators with the required ω_1 value. One should take into account that TR cutoff energy – $E_c \sim \omega_1 \gamma$ and 95% of TR energy belongs to an interval of $0.1E_c$ to E_c. For large ω_1 the detector must have a larger thickness to absorb X-rays in this range. It would be important to control ω_1 during radiator production and use it as a free parameter in the detector optimization process.

Si-microstrip tracking detectors operating in a magnetic field can also be used for TR detection, even though the dE/dx losses in Si are much larger than the absorbed TR energy. The excellent spatial resolution of the Si detectors provides separation of the TR photons and dE/dx losses at relatively modest distances between radiator and detector. Simulations made on the basis of the beam-test data results has shown that in a magnetic field of 2 T and for the geometry of the ATLAS Si-tracker proposed for sLHC, a rejection factor of > 30 can be obtained for an electron efficiency above 90% over a particle momentum range 2-30 GeV/c (Brigida *et al.* in [107] and [108]) . New detector techniques for TRDs are also under development and among them one should mention GasPixel detectors which allow to obtain a space point accuracy of < 30 μm and exploit all details of the particle tracks to highlight individual TR clusters in the gas (F. Harjes *et al.* in [108]) . Thin films of heavy scintillators (V.V Berdnikov*et al.* in [108]) might be very attractive in a combination with new radiators mentioned above.

33.6.7. ***Resistive-plate chambers*** : Revised September 2007 by H.R. Band (U. Wisconsin).

The resistive-plate chamber (RPC) was developed by Santonico and Cardarelli in the early 1980's [113] as a low-cost alternative to large scintillator planes.* Most commonly, an RPC is constructed from two parallel high-resistivity (10^9–10^{13} Ω-cm) glass or phenolic (Bakelite)/melamine laminate plates with a few-mm gap between them which is filled with atmospheric-pressure gas. The gas is chosen to absorb UV photons in order to limit transverse growth of discharges. The backs of the plates are coated with a lower-resistivity paint or ink ($\sim 10^5\,\Omega/\Box$), and a high potential (7–12 kV) is maintained between them. The passage of a charged particle initiates an electric discharge, whose size and duration are limited since the current reduces the local potential to below that needed to maintain the discharge. The sensitivity of the detector outside of this region is unaffected. The signal readout is via capacitive coupling to metallic strips on both sides of the detector which are separated from the high voltage coatings by thin insulating sheets. The x and y position of the discharge can be measured if the strips on opposite sides of the gap are orthogonal. When operated in streamer mode, the induced signals on the strips can be quite large (∼300 mV), making sensitive electronics unnecessary. An example of an RPC structure is shown in Fig. 33.17.

RPC's have inherent rate limitations since the time needed to re-establish the field after a discharge is proportional to the chamber capacitance and plate resistance. The average charge per streamer is 100–1000 pC. Typically, the efficiency of streamer-mode glass RPC's begins to fall above ∼0.4 Hz/cm^2. Because of Bakelite's lower bulk resistivity, Bakelite RPC's can be efficient at 10–100 Hz/cm^2. The need for higher rate capability led to the development of avalanche-mode RPC's, in which the gas and high voltage have been tuned to limit the growth of the electric discharge, preventing streamer

* It was based on earlier work on a spark counter with one high-resistivity plate [114].

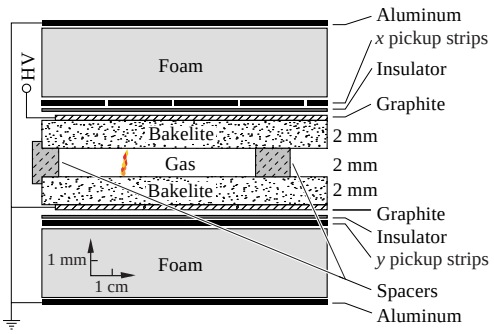

Figure 33.17: Schematic cross section of a typical RPC, in this case the single-gap streamer-mode BaBar RPC.

formation. Typical avalanche-mode RPC's have a signal charge of about 10 pC and can be efficient at 1 kHz/cm^2. The avalanche discharge produces a much smaller induced signal on the pickup strips ($\sim$1 mV) than streamers, and thus requires a more sophisticated and careful electronic design.

Many variations of the initial RPC design have been built for operation in either mode. Efficiencies of $\gtrsim 92\%$ for single gaps can be improved by the use of two or more gas gaps with shared pickup strips. Non-flammable and more environmentally friendly gas mixtures have been developed. In streamer mode, various mixtures of argon with isobutane and tetrafluoroethane have been used. For avalanche mode operation, a gas mixture of tetrafluoroethane ($C_2H_2F_4$) with 2–5% isobutane and 0.4–10% sulfur hexafluoride (SF_6) is typical. An example of large-scale RPC use is provided by the muon system being built for the ATLAS detector, where three layers of pairs of RPC's are used to trigger the drift tube arrays between the pairs. The total area is about 10,000 m^2. These RPC's provide a spatial resolution of 1 cm and a time resolution of 1 ns at an efficiency $\geq 99\%$.

Developments of multiple-gap RPC's [115] lead to RPC designs with much better timing resolution ($\sim$ 50 ps) for use in time-of-flight particle identification systems. A pioneering design used by the HARP experiment [116] has two sets of 2 thin gas gaps (0.3 mm) separated by thin(0.7 mm) glass plates. The outer plates are connected to high voltage and ground while the inner plate is electrically isolated and floats to a stable equilibrium potential. The observed RPC intrinsic time resolution of 127 ps may have been limited by amplifier noise. Fonte provides useful review [117] of other RPC designs.

Operational experience with RPC's has been mixed. Several experiments (*e.g.*, L3 and HARP) have reported reliable performance. However, the severe problems experienced with the BaBar RPC's have raised concerns about the long-term reliability of Bakelite RPC's.

Glass RPC's have had fewer problems, as seen by the history of the BELLE chambers. A rapid growth in the noise rate and leakage current in some of the BELLE glass RPC's was observed during commissioning. It was found that water vapor in the input gas was reacting with fluorine (produced by the disassociation of the tetrafluoroethane in the streamers) to produce hydrofluoric acid. The acid etched the glass surfaces, leading to increased noise rates and lower efficiencies. The use of copper gas piping to insure the dryness of the input gas stopped the problem. The BELLE RPC's have now operated reliably for more than 5 years.

Several different failure modes diagnosed in the first-generation BaBar Bakelite RPC's caused the average efficiency of the barrel RPC's to fall from $\gtrsim$90% to 35% in five years. The linseed oil which is used in Bakelite RPC's to coat the inner surface [118] had not been completely cured. Under warm conditions (32° C) and high voltage, oil collected on the spacers between the gaps or formed oil-drop bridges between the gaps. This led to large leakage currents (50–100 μA in some chambers) which persisted even when the temperature was regulated at 20° C. In addition, the graphite layer used to distribute the high voltage over the Bakelite became highly resistive (100 k$\Omega/\Box \rightarrow$ 10 M$\Omega/\Box$), resulting in lowered efficiency in some regions and the complete death of whole chambers.

The BaBar problems and the proposed use of Bakelite RPC's in the LHC detectors prompted detailed studies of RPC aging and have led to improved construction techniques and a better understanding of RPC operational limits. The graphite layer has been improved and should be stable with integrated currents of $\lesssim$600 mC/cm^2. Molded gas inlets and improved cleanliness during construction have reduced the noise rate of new chambers. Unlike glass RPC's, Bakelite RPC's have been found to require humid input gases to prevent drying of the Bakelite (increasing the bulk resistivity) which would decrease the rate capability. Second-generation BaBar RPC's incorporating many of the above improvements have performed reliably for over two years [119].

With many of these problems solved, new-generation RPC's are now being or soon will be used in about a dozen cosmic-ray and HEP detectors. Their comparatively low cost, ease of construction, good time resolution, high efficiency, and moderate spatial resolution make them attractive in many situations, particularly those requiring fast timing and/or large-area coverage.

33.7. Semiconductor detectors

Updated November 2013 by H. Spieler.

detectors provide a unique combination of energy and position resolution. In collider detectors they are most widely used as position sensing devices and photodetectors (Sec. 33.2). Integrated circuit technology allows the formation of high-density micron-scale electrodes on large (15–20 cm diameter) wafers, providing excellent position resolution. Furthermore, the density of silicon and its small ionization energy yield adequate signals with active layers only 100–300 μm thick, so the signals are also fast (typically tens of ns). The high energy resolution is a key parameter in x-ray, gamma, and charged particle spectroscopy, *e.g.*, in neutrinoless double beta decay searches. Silicon and germanium are the most commonly used materials, but gallium-arsenide, CdTe, CdZnTe, and other materials are also useful. CdZnTe provides a higher stopping power and the ratio of Cd to Zn concentrations changes the bandgap. Ge detectors are commonly operated at liquid nitrogen temperature to reduce the bias current, which depends exponentially on temperature. Semiconductor detectors depend crucially on low-noise electronics (see Sec. 33.8), so the detection sensitivity is determined by signal charge and capacitance. For a comprehensive discussion of semiconductor detectors and electronics see Ref. 120 or the tutorial website `http://www-physics.lbl.gov/spieler`.

33.7.1. *Materials Requirements* :

Semiconductor detectors are essentially solid state ionization chambers. Absorbed energy forms electron-hole pairs, *i.e.*, negative and positive charge carriers, which under an applied electric field move towards their respective collection electrodes, where they induce a signal current. The energy required to form an electron-hole pair is proportional to the bandgap. In tracking detectors the energy loss in the detector should be minimal, whereas for energy spectroscopy the stopping power should be maximized, so for gamma rays high-Z materials are desirable.

Measurements on silicon photodiodes [121] show that for photon energies below 4 eV one electron-hole (e-h) pair is formed per incident photon. The mean energy E_i required to produce an e-h pair peaks at 4.4 eV for a photon energy around 6 eV. Above $\sim$1.5 keV it assumes a constant value, 3.67 eV at room temperature. It is larger than the bandgap energy because momentum conservation requires excitation of lattice vibrations (phonons). For minimum-ionizing particles, the most probable charge deposition in a 300 μm thick silicon detector is about 3.5 fC (22000 electrons). Other typical ionization energies are 2.96 eV in Ge, 4.2 eV in GaAs, and 4.43 eV in CdTe.

Since both electronic and lattice excitations are involved, the variance in the number of charge carriers $N = E/E_i$ produced by an absorbed energy E is reduced by the Fano factor F (about 0.1 in Si and Ge). Thus, $\sigma_N = \sqrt{FN}$ and the energy resolution $\sigma_E/E = \sqrt{FE_i/E}$. However, the measured signal fluctuations are usually dominated by electronic noise or energy loss fluctuations in the detector. The electronic noise contributions depend on the pulse shaping in the signal processing electronics, so the choice of the shaping time is critical (see Sec. 33.8).

A smaller bandgap would produce a larger signal and improve energy resolution, but the intrinsic resistance of the material is critical. Thermal excitation, given by the Fermi-Dirac distribution, promotes

electrons into the conduction band, so the thermally excited carrier concentration increases exponentially with decreasing bandgaps. In pure Si the carrier concentration is $\sim 10^{10}\text{cm}^{-3}$ at 300 K, corresponding to a resistivity $\rho \approx 400\,\text{k}\Omega\,\text{cm}$. In reality, crystal imperfections and minute impurity concentrations limit Si carrier concentrations to $\sim 10^{11}$ cm^{-3} at 300 K, corresponding to a resistivity $\rho \approx 40\,\text{k}\Omega\,\text{cm}$. In practice, resistivities up to $20\,\text{k}\Omega\,\text{cm}$ are available, with mass production ranging from 5 to $10\,\text{k}\Omega\,\text{cm}$. Signal currents at keV scale energies are of order μA. However, for a resistivity of 10^4 Ωcm a 300 μm thick sensor with 1 cm^2 area would have a resistance of 300 Ω , so 30 V would lead to a current flow of 100 mA and a power dissipation of 3 W. On the other hand, high-quality single crystals of Si and Ge can be grown economically with suitably large volumes, so to mitigate the effect of resistivity one resorts to reverse-biased diode structures. Although this reduces the bias current relative to a resistive material, the thermally excited leakage current can still be excessive at room temperature, so Ge diodes are typically operated at liquid nitrogen temperature (77 K).

A major effort is to find high-Z materials with a bandgap that is sufficiently high to allow room-temperature operation while still providing good energy resolution. Compound semiconductors, *e.g.*, CdZnTe, can allow this, but typically suffer from charge collection problems, characterized by the product $\mu\tau$ of mobility and carrier lifetime. In Si and Ge $\mu\tau > 1\,\text{cm}^2\,\text{V}^{-1}$ for both electrons and holes, whereas in compound semiconductors it is in the range 10^{-3}–10^{-8}. Since for holes $\mu\tau$ is typically an order of magnitude smaller than for electrons, detector configurations where the electron contribution to the charge signal dominates—*e.g.*, strip or pixel structures—can provide better performance.

33.7.2. ***Detector Configurations*** :

A p-n junction operated at reverse bias forms a sensitive region depleted of mobile charge and sets up an electric field that sweeps charge liberated by radiation to the electrodes. Detectors typically use an asymmetric structure, *e.g.*, a highly doped p electrode and a lightly doped n region, so that the depletion region extends predominantly into the lightly doped volume.
In a planar device the thickness of the depleted region is

$$W = \sqrt{2\epsilon\,(V + V_{bi})/Ne} = \sqrt{2\rho\mu\epsilon(V + V_{bi})}\ , \tag{33.18}$$

where $V =$ external bias voltage
$V_{bi} =$ "built-in" voltage (≈ 0.5 V for resistivities typically used in Si detectors)
$N =$ doping concentration
$e =$ electronic charge
$\epsilon =$ dielectric constant $= 11.9\ \epsilon_0 \approx 1$ pF/cm in Si
$\rho =$ resistivity (typically 1–10 kΩ cm in Si)
$\mu =$ charge carrier mobility
$= 1350$ cm^2 V^{-1} s^{-1} for electrons in Si
$= 450$ cm^2 V^{-1} s^{-1} for holes in Si

In Si

$$W = 0.5\ [\mu\text{m}/\sqrt{\Omega\text{-cm}\cdot\text{V}}] \times \sqrt{\rho(V + V_{bi})}\ \text{ for } n\text{-type Si, and}$$

$$W = 0.3\ [\mu\text{m}/\sqrt{\Omega\text{-cm}\cdot\text{V}}] \times \sqrt{\rho(V + V_{bi})}\ \text{ for } p\text{-type Si.}$$

The conductive p and n regions together with the depleted volume form a capacitor with the capacitance per unit area

$$C = \epsilon/W \approx 1\,[\text{pF/cm}]\,/W \text{ in Si.} \tag{33.19}$$

In strip and pixel detectors the capacitance is dominated by the fringing capacitance to neighboring electrodes. For example, the strip-to-strip Si fringing capacitance is $\sim$ 1–1.5 pF cm^{-1} of strip length at a strip pitch of 25–50 μm.

Large volume ($\sim 10^2$–10^3 cm^3) Ge detectors are commonly configured as coaxial detectors, *e.g.*, a cylindrical n-type crystal with 5–10 cm diameter and 10 cm length with an inner 5–10 mm diameter n^+ electrode and an outer p^+ layer forming the diode junction. Ge can be grown with very low impurity levels, 10^9–$10^{10}\,\text{cm}^{-3}$ (HPGe), so these large volumes can be depleted with several kV.

33.7.3. ***Signal Formation*** :

The signal pulse shape depends on the instantaneous carrier velocity $v(x) = \mu E(x)$ and the electrode geometry, which determines the distribution of induced charge (*e.g.*, see Ref. 120, pp. 71–83). Charge collection time decreases with increasing bias voltage, and can be reduced further by operating the detector with "overbias," *i.e.*, a bias voltage exceeding the value required to fully deplete the device. Note that in partial depletion the electric field goes to zero, whereas going beyond full depletion adds a constantly distributed field. The collection time is limited by velocity saturation at high fields (in Si approaching 10^7 cm/s at $E > 10^4$ V/cm); at an average field of 10^4 V/cm the collection time is about 15 ps/μm for electrons and 30 ps/μm for holes. In typical fully-depleted detectors 300 μm thick, electrons are collected within about 10 ns, and holes within about 25 ns.

Position resolution is limited by transverse diffusion during charge collection (typically 5 μm for 300 μm thickness) and by knock-on electrons. Resolutions of 2–4 μm (rms) have been obtained in beam tests. In magnetic fields, the Lorentz drift deflects the electron and hole trajectories and the detector must be tilted to reduce spatial spreading (see "Hall effect" in semiconductor textbooks).

Electrodes can be in the form of cm-scale pads, strips, or μm-scale pixels. Various readout structures have been developed for pixels, *e.g.*, CCDs, DEPFETs, monolithic pixel devices that integrate sensor and electronics (MAPS), and hybrid pixel devices that utilize separate sensors and readout ICs connected by two-dimensional arrays of solder bumps. For an overview and further discussion see Ref. 120.

In gamma ray spectroscopy ($\text{E}_\gamma > 10^2$ keV) Compton scattering dominates, so for a significant fraction of events the incident gamma energy is not completely absorbed, *i.e.*, the Compton scattered photon escapes from the detector and the energy deposited by the Compton electron is only a fraction of the total. Distinguishing multi-interaction events, *e.g.*, multiple Compton scatters with a final photoelectric absorption, from single Compton scatters allows background suppression. Since the individual interactions take place in different parts of the detector volume, these events can be distinguished by segmenting the outer electrode of a coaxial detector and analyzing the current pulse shapes. The different collection times can be made more distinguishable by using "point" electrodes, where most of the signal is induced when charges are close to the electrode, similarly to strip or pixel detectors. Charge clusters arriving from different positions in the detector will arrive at different times and produce current pulses whose major components are separated in time. Point electrodes also reduce the electrode capacitance, which reduces electronic noise, but careful design is necessary to avoid low-field regions in the detector volume.

33.7.4. ***Radiation Damage*** : Radiation damage occurs through two basic mechanisms:

1. Bulk damage due to displacement of atoms from their lattice sites. This leads to increased leakage current, carrier trapping, and build-up of space charge that changes the required operating voltage. Displacement damage depends on the nonionizing energy loss and the energy imparted to the recoil atoms, which can initiate a chain of subsequent displacements, *i.e.*, damage clusters. Hence, it is critical to consider both particle type and energy.
2. Surface damage due to charge build-up in surface layers, which leads to increased surface leakage currents. In strip detectors the inter-strip isolation is affected. The effects of charge build-up are strongly dependent on the device structure and on fabrication details. Since the damage is proportional to the absorbed energy (when ionization dominates), the dose can be specified in rad (or Gray) independent of particle type.

The increase in reverse bias current due to bulk damage is $\Delta I_r = \alpha\Phi$ per unit volume, where Φ is the particle fluence and α the damage coefficient ($\alpha \approx 3 \times 10^{-17}$ A/cm for minimum ionizing protons and pions after long-term annealing; $\alpha \approx 2 \times 10^{-17}$ A/cm for 1 MeV neutrons). The reverse bias current depends strongly on temperature

$$\frac{I_R(T_2)}{I_R(T_1)} = \left(\frac{T_2}{T_1}\right)^2 \exp\left[-\frac{E}{2k}\left(\frac{T_1 - T_2}{T_1 T_2}\right)\right]\ , \tag{33.20}$$

where $E = 1.2$ eV, so rather modest cooling can reduce the current substantially ($\sim$ 6-fold current reduction in cooling from room temperature to 0°C).

Displacement damage forms acceptor-like states. These trap electrons, building up a negative space charge, which in turn requires an increase in the applied voltage to sweep signal charge through the detector thickness. This has the same effect as a change in resistivity, *i.e.*, the required voltage drops initially with fluence, until the positive and negative space charge balance and very little voltage is required to collect all signal charge. At larger fluences the negative space charge dominates, and the required operating voltage increases ($V \propto N$). The safe limit on operating voltage ultimately limits the detector lifetime. Strip detectors specifically designed for high voltages have been extensively operated at bias voltages >500 V. Since the effect of radiation damage depends on the electronic activity of defects, various techniques have been applied to neutralize the damage sites. For example, additional doping with oxygen can increase the allowable charged hadron fluence roughly three-fold [122]. Detectors with columnar electrodes normal to the surface can also extend operational lifetime [123]. The increase in leakage current with fluence, on the other hand, appears to be unaffected by resistivity and whether the material is n or p-type. At fluences beyond 10^{15} cm^{-2} decreased carrier lifetime becomes critical [124,125].

Strip and pixel detectors have remained functional at fluences beyond 10^{15} cm^{-2} for minimum ionizing protons. At this damage level, charge loss due to recombination and trapping becomes significant and the high signal-to-noise ratio obtainable with low-capacitance pixel structures extends detector lifetime. The higher mobility of electrons makes them less sensitive to carrier lifetime than holes, so detector configurations that emphasize the electron contribution to the charge signal are advantageous, *e.g.*, n^+ strips or pixels on a p- or n-substrate. The occupancy of the defect charge states is strongly temperature dependent; competing processes can increase or decrease the required operating voltage. It is critical to choose the operating temperature judiciously (−10 to 0°C in typical collider detectors) and limit warm-up periods during maintenance. For a more detailed summary see Ref. 126 and and the web-sites of the ROSE and RD50 collaborations at `http://RD48.web.cern.ch/rd48` and `http://RD50.web.cern.ch/rd50`. Materials engineering, *e.g.*, introducing oxygen interstitials, can improve certain aspects and is under investigation. At high fluences diamond is an alternative, but operates as an insulator rather than a reverse-biased diode.

Currently, the lifetime of detector systems is still limited by the detectors; in the electronics use of standard "deep submicron" CMOS fabrication processes with appropriately designed circuitry has increased the radiation resistance to fluences $> 10^{15}$ cm^{-2} of minimum ionizing protons or pions. For a comprehensive discussion of radiation effects see Ref. 127.

33.8. Low-noise electronics

Revised November 2013 by H. Spieler.

Many detectors rely critically on low-noise electronics, either to improve energy resolution or to allow a low detection threshold. A typical detector front-end is shown in Fig. 33.18.

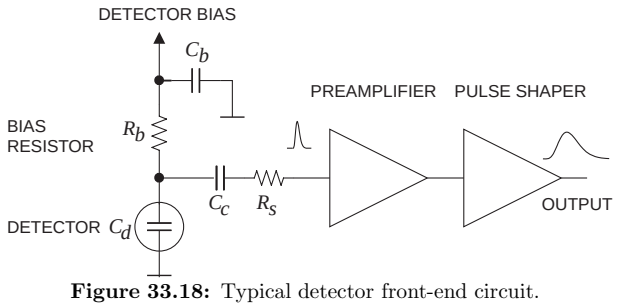

Figure 33.18: Typical detector front-end circuit.

The detector is represented by a capacitance C_d, a relevant model for most detectors. Bias voltage is applied through resistor R_b and the signal is coupled to the preamplifier through a blocking capacitor C_c. The series resistance R_s represents the sum of all resistances present in the input signal path, *e.g.* the electrode resistance, any input protection networks, and parasitic resistances in the input transistor. The preamplifier provides gain and feeds a pulse shaper, which tailors the overall frequency response to optimize signal-to-noise ratio while limiting the duration of the signal pulse to accommodate the signal pulse rate. Even if not explicitly stated, all amplifiers provide some form of pulse shaping due to their limited frequency response.

The equivalent circuit for the noise analysis (Fig. 33.19) includes both current and voltage noise sources. The leakage current of a semiconductor detector, for example, fluctuates due to continuous electron emission statistics. The statistical fluctuations in the charge measurement will scale with the square root of the total number of recorded charges, so this noise contribution increases with the width of the shaped output pulse. This "shot noise" i_{nd} is represented by a current noise generator in parallel with the detector. Resistors exhibit noise due to thermal velocity fluctuations of the charge carriers. This yields a constant noise power density vs. frequency, so increasing the bandwidth of the shaped output pulse, *i.e.* reducing the shaping time, will increase the noise. This noise source can be modeled either as a voltage or current generator. Generally, resistors shunting the input act as noise current sources and resistors in series with the input act as noise voltage sources (which is why some in the detector community refer to current and voltage noise as "parallel" and "series" noise). Since the bias resistor effectively shunts the input, as the capacitor C_b passes current fluctuations to ground, it acts as a current generator i_{nb} and its noise current has the same effect as the shot noise current from the detector. Any other shunt resistances can be incorporated in the same way. Conversely, the series resistor R_s acts as a voltage generator. The electronic noise of the amplifier is described fully by a combination of voltage and current sources at its input, shown as e_{na} and i_{na}.

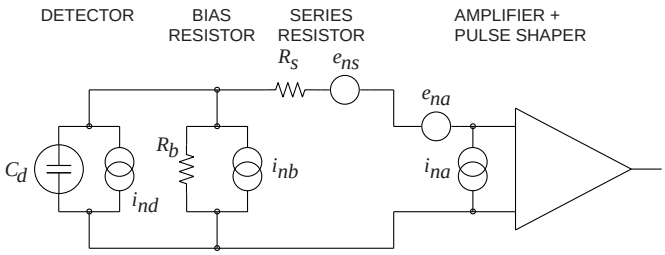

Figure 33.19: Equivalent circuit for noise analysis.

Shot noise and thermal noise have a "white" frequency distribution, *i.e.* the spectral power densities $dP_n/df \propto di_n^2/df \propto de_n^2/df$ are constant with the magnitudes

$$\begin{aligned} i_{nd}^2 &= 2eI_d \ , \\ i_{nb}^2 &= \frac{4kT}{R_b} \ , \\ e_{ns}^2 &= 4kTR_s \ , \end{aligned} \tag{33.21}$$

where e is the electronic charge, I_d the detector bias current, k the Boltzmann constant and T the temperature. Typical amplifier noise parameters e_{na} and i_{na} are of order nV/$\sqrt{\text{Hz}}$ and pA/$\sqrt{\text{Hz}}$. Trapping and detrapping processes in resistors, dielectrics and semiconductors can introduce additional fluctuations whose noise power frequently exhibits a $1/f$ spectrum. The spectral density of the $1/f$ noise voltage is

$$e_{nf}^2 = \frac{A_f}{f} \ , \tag{33.22}$$

where the noise coefficient A_f is device specific and of order 10^{-10}–10^{-12} V^2.

A fraction of the noise current flows through the detector capacitance, resulting in a frequency-dependent noise voltage $i_n/(\omega C_d)$, which is added to the noise voltage in the input circuit. Thus, the current noise contribution increases with lowering frequency, so its contribution increases with shaping pulse width. Since the

individual noise contributions are random and uncorrelated, they add in quadrature. The total noise at the output of the pulse shaper is obtained by integrating over the full bandwidth of the system. Superimposed on repetitive detector signal pulses of constant magnitude, purely random noise produces a Gaussian signal distribution.

Since radiation detectors typically convert the deposited energy into charge, the system's noise level is conveniently expressed as an equivalent noise charge Q_n, which is equal to the detector signal that yields a signal-to-noise ratio of one. The equivalent noise charge is commonly expressed in Coulombs, the corresponding number of electrons, or the equivalent deposited energy (eV). For a capacitive sensor

$$Q_n^2 = i_n^2 F_i T_S + e_n^2 F_v \frac{C^2}{T_S} + F_{vf} A_f C^2 \ , \tag{33.23}$$

where C is the sum of all capacitances shunting the input, F_i, F_v, and F_{vf} depend on the shape of the pulse determined by the shaper and T_s is a characteristic time, for example, the peaking time of a semi-gaussian pulse or the sampling interval in a correlated double sampler. The form factors F_i, F_v are easily calculated

$$F_i = \frac{1}{2T_S}\int_{-\infty}^{\infty} [W(t)]^2\, dt \ , \qquad F_v = \frac{T_S}{2}\int_{-\infty}^{\infty}\left[\frac{dW(t)}{dt}\right]^2 dt \ , \tag{33.24}$$

where for time-invariant pulse-shaping $W(t)$ is simply the system's impulse response (the output signal seen on an oscilloscope) for a short input pulse with the peak output signal normalized to unity. For more details see Refs. 128 and 129.

A pulse shaper formed by a single differentiator and integrator with equal time constants has $F_i = F_v = 0.9$ and $F_{vf} = 4$, independent of the shaping time constant. The overall noise bandwidth, however, depends on the time constant, *i.e.* the characteristic time T_s. The contribution from noise currents increases with shaping time, *i.e.*, pulse duration, whereas the voltage noise decreases with increasing shaping time, *i.e.* reduced bandwidth. Noise with a $1/f$ spectrum depends only on the ratio of upper to lower cutoff frequencies (integrator to differentiator time constants), so for a given shaper topology the $1/f$ contribution to Q_n is independent of T_s. Furthermore, the contribution of noise voltage sources to Q_n increases with detector capacitance. Pulse shapers can be designed to reduce the effect of current noise, *e.g.*, mitigate radiation damage. Increasing pulse symmetry tends to decrease F_i and increase F_v (*e.g.*, to 0.45 and 1.0 for a shaper with one CR differentiator and four cascaded integrators). For the circuit shown in Fig. 33.19,

$$\begin{aligned} Q_n^2 = &\left(2eI_d + 4kT/R_b + i_{na}^2\right) F_i T_S \\ &+ \left(4kTR_s + e_{na}^2\right) F_v C_d^2/T_S + F_{vf} A_f C_d^2 \ . \end{aligned} \tag{33.25}$$

As the characteristic time T_S is changed, the total noise goes through a minimum, where the current and voltage contributions are equal. Fig. 33.20 shows a typical example. At short shaping times the voltage noise dominates, whereas at long shaping times the current noise takes over. The noise minimum is flattened by the presence of $1/f$ noise. Increasing the detector capacitance will increase the voltage noise and shift the noise minimum to longer shaping times.

For quick estimates, one can use the following equation, which assumes an FET amplifier (negligible i_{na}) and a simple CR–RC shaper with time constants τ (equal to the peaking time):

$$\begin{aligned} (Q_n/e)^2 = &\ 12\left[\frac{1}{\mathrm{nA\cdot ns}}\right] I_d \tau + 6\times 10^5 \left[\frac{\mathrm{k\Omega}}{\mathrm{ns}}\right]\frac{\tau}{R_b} \\ &+ 3.6\times 10^4 \left[\frac{\mathrm{ns}}{(\mathrm{pF})^2(\mathrm{nV})^2/\mathrm{Hz}}\right] e_n^2 \frac{C^2}{\tau} \ . \end{aligned} \tag{33.26}$$

Noise is improved by reducing the detector capacitance and leakage current, judiciously selecting all resistances in the input circuit, and choosing the optimum shaping time constant. Another noise contribution to consider is that noise cross-couples from the neighboring front-ends in strip and pixel detectors through the inter-electrode capacitance.

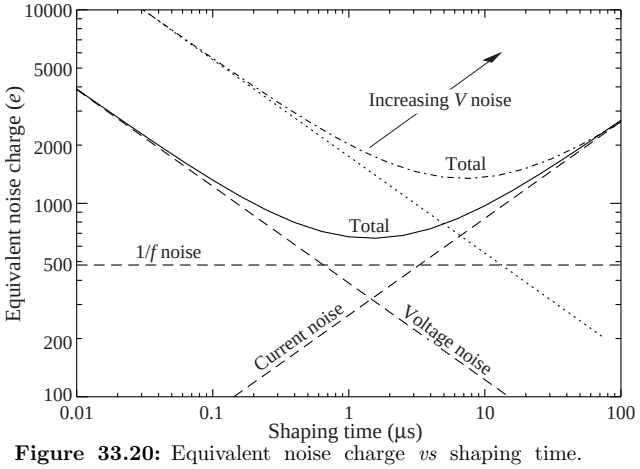

Figure 33.20: Equivalent noise charge *vs* shaping time. Changing the voltage or current noise contribution shifts the noise minimum. Increased voltage noise is shown as an example.

The noise parameters of the amplifier depend primarily on the input device. In field effect transistors, the noise current contribution is very small, so reducing the detector leakage current and increasing the bias resistance will allow long shaping times with correspondingly lower noise. In bipolar transistors, the base current sets a lower bound on the noise current, so these devices are best at short shaping times. In special cases where the noise of a transistor scales with geometry, *i.e.*, decreasing noise voltage with increasing input capacitance, the lowest noise is obtained when the input capacitance of the transistor is equal to the detector capacitance, albeit at the expense of power dissipation. Capacitive matching is useful with field-effect transistors, but not bipolar transistors. In bipolar transistors, the minimum obtainable noise is independent of shaping time, but only at the optimum collector current I_C, which does depend on shaping time.

$$Q_{n,\min}^2 = 4kT\frac{C}{\sqrt{\beta_{DC}}}\sqrt{F_i F_v} \ \text{ at } \ I_c = \frac{kT}{e} C\sqrt{\beta_{DC}}\sqrt{\frac{F_v}{F_i}}\frac{1}{T_S} \ , \tag{33.27}$$

where β_{DC} is the DC current gain. For a CR–RC shaper and $\beta_{DC} = 100$,

$$Q_{n,\min}/e \approx 250\sqrt{C/\mathrm{pF}} \ . \tag{33.28}$$

Practical noise levels range from $\sim 1e$ for CCD's at long shaping times to $\sim 10^4$ e in high-capacitance liquid argon calorimeters. Silicon strip detectors typically operate at $\sim 10^3$ electrons, whereas pixel detectors with fast readout provide noise of several hundred electrons.

In timing measurements, the slope-to-noise ratio must be optimized, rather than the signal-to-noise ratio alone, so the rise time t_r of the pulse is important. The "jitter" σ_t of the timing distribution is

$$\sigma_t = \frac{\sigma_n}{(dS/dt)_{S_T}} \approx \frac{t_r}{S/N} \ , \tag{33.29}$$

where σ_n is the rms noise and the derivative of the signal dS/dt is evaluated at the trigger level S_T. To increase dS/dt without incurring excessive noise, the amplifier bandwidth should match the rise-time of the detector signal. The 10 to 90% rise time of an amplifier with bandwidth f_U is $0.35/f_U$. For example, an oscilloscope with 350 MHz bandwidth has a 1 ns rise time. When amplifiers are cascaded, which is invariably necessary, the individual rise times add in quadrature.

$$t_r \approx \sqrt{t_{r1}^2 + t_{r2}^2 + ... + t_{rn}^2} \ . \tag{33.30}$$

Increasing signal-to-noise ratio also improves time resolution, so minimizing the total capacitance at the input is also important. At high signal-to-noise ratios, the time jitter can be much smaller than the rise time. The timing distribution may shift with signal level ("walk"), but this can be corrected by various means, either in hardware or software [8].

The basic principles discussed above apply to both analog and digital signal processing. In digital signal processing the pulse shaper

shown in Fig. 33.18 is replaced by an analog to digital converter (ADC) followed by a digital processor that determines the pulse shape. Digital signal processing allows great flexibility in implementing filtering functions. The software can be changed readily to adapt to a wide variety of operating conditions and it is possible to implement filters that are impractical or even impossible using analog circuitry. However, this comes at the expense of increased circuit complexity and increased demands on the ADC compared to analog shaping.

If the sampling rate of the ADC is too low, high frequency components will be transferred to lower frequencies ("aliasing"). The sampling rate of the ADC must be high enough to capture the maximum frequency component of the input signal. Apart from missing information on the fast components of the pulse, undersampling introduces spurious artifacts. If the frequency range of the input signal is much greater, the noise at the higher frequencies will be transferred to lower frequencies and increase the noise level in the frequency range of pulses formed in the subsequent digital shaper. The Nyquist criterion states that the sampling frequency must be at least twice the maximum relevant input frequency. This requires that the bandwith of the circuitry preceding the ADC must be limited. The most reliable technique is to insert a low-pass filter.

The digitization process also introduces inherent noise, since the voltage range ΔV corresponding to a minimum bit introduces quasi-random fluctuations relative to the exact amplitude

$$\sigma_n = \frac{\Delta V}{\sqrt{12}} \, . \tag{33.31}$$

When the Nyquist condition is fulfilled the noise bandwidth Δf_n is spread nearly uniformly and extends to 1/2 the sampling frequency f_S, so the spectral noise density

$$e_n = \frac{\sigma_n}{\sqrt{\Delta f_n}} = \frac{\Delta V}{\sqrt{12}} \cdot \frac{1}{\sqrt{f_S/2}} = \frac{\Delta V}{\sqrt{6 f_S}} \, . \tag{33.32}$$

Sampling at a higher frequency spreads the total noise over a larger frequency range, so oversampling can be used to increase the effective resolution. In practice, this quantization noise is increased by differential nonlinearity. Furthermore, the equivalent input noise of ADCs is often rather high, so the overall gain of the stages preceding the ADC must be sufficiently large for the preamplifier input noise to override.

When implemented properly, digital signal processing provides significant advantages in systems where the shape of detector signal pulses changes greatly, for example in large semiconductor detectors for gamma rays or in gaseous detectors (*e.g.* TPCs) where the duration of the current pulse varies with drift time, which can range over orders of magnitude. Where is analog signal processing best (most efficient)? In systems that require fast time response the high power requirements of high-speed ADCs are prohibitive. Systems that are not sensitive to pulse shape can use fixed shaper constants and rather simple filters, which can be either continuous or sampled. In high density systems that require small circuit area and low power (*e.g.* strip and pixel detectors), analog filtering often yields the required response and tends to be most efficient.

It is important to consider that additional noise is often introduced by external electronics, *e.g.* power supplies and digital systems. External noise can couple to the input. Often the "common grounding" allows additional noise current to couple to the current loop connecting the detector to the preamp. Recognizing additional noise sources and minimizing cross-coupling to the detector current loop is often important. Understanding basic physics and its practical effects is important in forming a broad view of the detector system and recognizing potential problems (*e.g.* modified data), rather than merely following standard recipes.

For a more detailed introduction to detector signal processing and electronics see Ref. 120 or the tutorial website `http://www-physics.lbl.gov/ spieler`.

33.9. Calorimeters

A calorimeter is designed to measure a particle's (or jet's) energy and direction for an (ideally) contained electromagnetic (EM) or hadronic shower. The characteristic interaction distance for an electromagnetic interaction is the radiation length X_0, which ranges from 13.8 g cm^{-2} in iron to 6.0 g cm^{-2} in uranium.* Similarly, the characteristic nuclear interaction length λ_I varies from 132.1 g cm^{-2} (Fe) to 209 g cm^{-2} (U).† In either case, a calorimeter must be many interaction lengths deep, where "many" is determined by physical size, cost, and other factors. EM calorimeters tend to be 15–30 X_0 deep, while hadronic calorimeters are usually compromised at 5–8 λ_I. In real experiments there is likely to be an EM calorimeter in front of the hadronic section, which in turn has less sampling density in the back, so the hadronic cascade occurs in a succession of different structures.

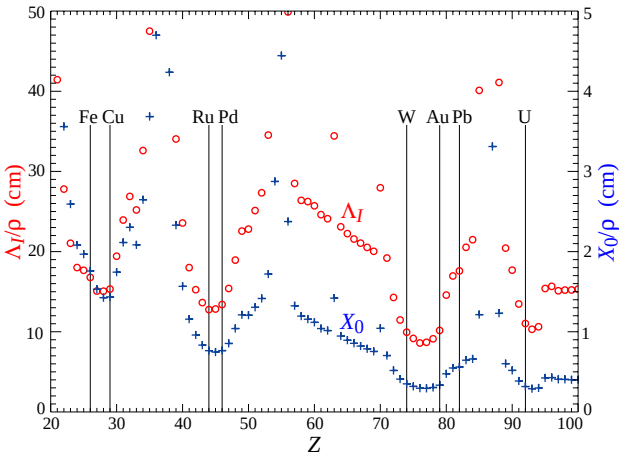

Figure 33.21: Nuclear interaction length λ_I/ρ (circles) and radiation length X_0/ρ (+'s) in cm for the chemical elements with $Z > 20$ and $\lambda_I < 50$ cm.

In all cases there is a premium on small λ_I/ρ and X_0/ρ (both with units of length). These quantities are shown for $Z > 20$ for the chemical elements in Fig. 33.21. For the hadronic case, metallic absorbers in the W–Au region are best, followed by U. The Ru–Pd region elements are rare and expensive. Lead is a bad choice. Given cost considerations, Fe and Cu might be appropriate choices. For EM calorimeters high Z is preferred, and lead is not a bad choice.

These considerations are for *sampling calorimeters* consisting of metallic absorber sandwiched or (threaded) with an active material which generates signal. The active medium may be a scintillator, an ionizing noble liquid, a gas chamber, a semiconductor, or a Cherenkov radiator. The average interaction length is thus greater than that of the absorber alone, sometimes substantially so.

There are also *homogeneous calorimeters,* in which the entire volume is sensitive, *i.e.*, contributes signal. Homogeneous calorimeters (so far usually electromagnetic) may be built with inorganic heavy (high density, high $\langle Z \rangle$) scintillating crystals, or non-scintillating Cherenkov radiators such as lead glass and lead fluoride. Scintillation light and/or ionization in noble liquids can be detected. Nuclear interaction lengths in inorganic crystals range from 17.8 cm ($LuAlO_3$) to 42.2 cm (NaI). Popular choices have been BGO with $\lambda_I = 22.3$ cm and $X_0 = 1.12$ cm, and $PbWO_4$ (20.3 cm and 0.89 cm). Properties of these and other commonly used inorganic crystal scintillators can be found in Table 33.4.

* $X_0 = 120 \ \mathrm{g\,cm^{-2}}\, Z^{-2/3}$ to better than 5% for $Z > 23$.

† $\lambda_I = 37.8 \ \mathrm{g\,cm^{-2}}\, A^{0.312}$ to within 0.8% for $Z > 15$.

See `pdg.lbl.gov/AtomicNuclearProperties` for actual values.

33.9.1. ***Electromagnetic calorimeters*** :
Revised October 2009 by R.-Y. Zhu (California Inst. of Technology).

The development of electromagnetic showers is discussed in the section on "Passage of Particles Through Matter" (Sec. 32 of this *Review*).

Formulae are given which approximately describe average showers, but since the physics of electromagnetic showers is well understood, detailed and reliable Monte Carlo simulation is possible. EGS4 [130] and GEANT [131] have emerged as the standards.

There are homogeneous and sampling electromagnetic calorimeters. In a homogeneous calorimeter the entire volume is sensitive, *i.e.*, contributes signal. Homogeneous electromagnetic calorimeters may be built with inorganic heavy (high-Z) scintillating crystals such as BGO, CsI, NaI, and PWO, non-scintillating Cherenkov radiators such as lead glass and lead fluoride, or ionizing noble liquids. Properties of commonly used inorganic crystal scintillators can be found in Table 33.4. A sampling calorimeter consists of an active medium which generates signal and a passive medium which functions as an absorber. The active medium may be a scintillator, an ionizing noble liquid, a gas chamber, or a semiconductor. The passive medium is usually a material of high density, such as lead, iron, copper, or depleted uranium.

The energy resolution σ_E/E of a calorimeter can be parametrized as $a/\sqrt{E}\oplus b\oplus c/E$, where $\oplus$ represents addition in quadrature and E is in GeV. The stochastic term a represents statistics-related fluctuations such as intrinsic shower fluctuations, photoelectron statistics, dead material at the front of the calorimeter, and sampling fluctuations. For a fixed number of radiation lengths, the stochastic term a for a sampling calorimeter is expected to be proportional to $\sqrt{t/f}$, where t is plate thickness and f is sampling fraction [132,133]. While a is at a few percent level for a homogeneous calorimeter, it is typically 10% for sampling calorimeters. The main contributions to the systematic, or constant, term b are detector non-uniformity and calibration uncertainty. In the case of the hadronic cascades discussed below, non-compensation also contributes to the constant term. One additional contribution to the constant term for calorimeters built for modern high-energy physics experiments, operated in a high-beam intensity environment, is radiation damage of the active medium. This can be minimized by developing radiation-hard active media [48] and by frequent *in situ* calibration and monitoring [47,133]. With effort, the constant term b can be reduced to below one percent. The term c is due to electronic noise summed over readout channels within a few Molière radii. The best energy resolution for electromagnetic shower measurement is obtained in total absorption homogeneous calorimeters, *e.g.* calorimeters built with heavy crystal scintillators. These are used when ultimate performance is pursued.

The position resolution depends on the effective Molière radius and the transverse granularity of the calorimeter. Like the energy resolution, it can be factored as $a/\sqrt{E}\oplus b$, where a is a few to 20 mm and b can be as small as a fraction of mm for a dense calorimeter with fine granularity. Electromagnetic calorimeters may also provide direction measurement for electrons and photons. This is important for photon-related physics when there are uncertainties in event origin, since photons do not leave information in the particle tracking system. Typical photon angular resolution is about 45 mrad$/\sqrt{E}$, which can be provided by implementing longitudinal segmentation [134] for a sampling calorimeter or by adding a preshower detector [135] for a homogeneous calorimeter without longitudinal segmentation.

Novel technologies have been developed for electromagnetic calorimetry. New heavy crystal scintillators, such as PWO and LSO:Ce (see Sec. 33.4), have attracted much attention for homogeneous calorimetry. In some cases, such as PWO, it has received broad applications in high-energy and nuclear physics experiments. The "spaghetti" structure has been developed for sampling calorimetry with scintillating fibers as the sensitive medium. The "accordion" structure has been developed for sampling calorimetry with ionizing noble liquid as the sensitive medium. Table 33.8 provides a brief description of typical electromagnetic calorimeters built recently for high-energy physics experiments. Also listed in this table are calorimeter depths in radiation lengths (X_0) and the achieved energy resolution. Whenever possible, the performance of calorimeters *in situ* is quoted, which is usually in good agreement with prototype test beam results as well as EGS or GEANT simulations, provided that all systematic effects are properly included. Detailed references on detector design and performance can be found in Appendix C of reference [133] and Proceedings of the International Conference series on Calorimetry in Particle Physics.

Table 33.8: Resolution of typical electromagnetic calorimeters. E is in GeV.

Technology (Experiment)	Depth	Energy resolution	Date
NaI(Tl) (Crystal Ball)	$20X_0$	$2.7\%/\mathrm{E}^{1/4}$	1983
$Bi_4Ge_3O_{12}$ (BGO) (L3)	$22X_0$	$2\%/\sqrt{E}\oplus 0.7\%$	1993
CsI (KTeV)	$27X_0$	$2\%/\sqrt{E}\oplus 0.45\%$	1996
CsI(Tl) (BaBar)	16–$18X_0$	$2.3\%/E^{1/4}\oplus 1.4\%$	1999
CsI(Tl) (BELLE)	$16X_0$	1.7% for $E_\gamma > 3.5$ GeV	1998
$PbWO_4$ (PWO) (CMS)	$25X_0$	$3\%/\sqrt{E}\oplus 0.5\%\oplus 0.2/E$	1997
Lead glass (OPAL)	$20.5X_0$	$5\%/\sqrt{E}$	1990
Liquid Kr (NA48)	$27X_0$	$3.2\%/\sqrt{E}\oplus 0.42\%\oplus 0.09/E$	1998
Scintillator/depleted U (ZEUS)	20–$30X_0$	$18\%/\sqrt{E}$	1988
Scintillator/Pb (CDF)	$18X_0$	$13.5\%/\sqrt{E}$	1988
Scintillator fiber/Pb spaghetti (KLOE)	$15X_0$	$5.7\%/\sqrt{E}\oplus 0.6\%$	1995
Liquid Ar/Pb (NA31)	$27X_0$	$7.5\%/\sqrt{E}\oplus 0.5\%\oplus 0.1/E$	1988
Liquid Ar/Pb (SLD)	$21X_0$	$8\%/\sqrt{E}$	1993
Liquid Ar/Pb (H1)	20–$30X_0$	$12\%/\sqrt{E}\oplus 1\%$	1998
Liquid Ar/depl. U (DØ)	$20.5X_0$	$16\%/\sqrt{E}\oplus 0.3\%\oplus 0.3/E$	1993
Liquid Ar/Pb accordion (ATLAS)	$25X_0$	$10\%/\sqrt{E}\oplus 0.4\%\oplus 0.3/E$	1996

33.9.2. ***Hadronic calorimeters*** : [1–5,133]
Revised September 2013 by D. E. Groom (LBNL).

Hadronic calorimetry is considerably more difficult than EM calorimetry. For the same cascade containment fraction discussed in the previous section, the calorimeter would need to be ∼30 times deeper. Electromagnetic energy deposit from the decay of a small number of π^0's are usually detected with greater efficiency than are the hadronic parts of the cascade, themselves subject to large fluctuations in neutron production, undetectable energy loss to nuclear disassociation, and other effects.

Most large hadron calorimeters are parts of large 4π detectors at colliding beam facilities. At present these are sampling calorimeters: plates of absorber (Fe, Pb, Cu, or occasionally U or W) alternating with plastic scintillators (plates, tiles, bars), liquid argon (LAr), or gaseous detectors. The ionization is measured directly, as in LAr calorimeters, or via scintillation light observed by photodetectors (usually PMT's or silicon photodiodes). Wavelength-shifting fibers are often used to solve difficult problems of geometry and light collection uniformity. Silicon sensors are being studied for ILC detectors; in this case e-h pairs are collected. There are as many variants of these schemes as there are calorimeters, including variations in geometry of the absorber and sensors, *e.g.*, scintillating fibers threading an absorber [136], and the "accordion" LAr detector [137]. The latter has zig-zag absorber plates to minimize channeling effects; the calorimeter is hermitic (no cracks), and plates are oriented so that cascades cross the same plate repeatedly. Another departure from the traditional sandwich structure is the LAr-tube design shown in Fig. 33.22(a) [138].

A relatively new variant in hadron calorimetry is the detection of Cerenkov light. Such a calorimeter is sensitive to relativistic $e^\pm$'s in the EM showers plus a few relativistic pions. An example is the radiation-hard forward calorimeter in CMS, with iron absorber and

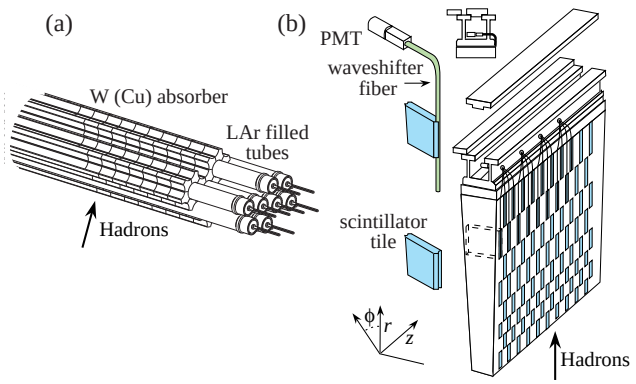

Figure 33.22: (a) ATLAS forward hadronic calorimeter structure (FCal2, 3) [138]. Tubes containing LAr are embedded in a mainly tungsten matrix. (b) ATLAS central calorimeter wedge; iron with plastic scintillator tile with wavelength-shifting fiber readout [139].

quartz fiber readout by PMT's [140].

Ideally the calorimeter is segmented in ϕ and θ (or $\eta = -\ln\tan(\theta/2)$). Fine segmentation, while desirable, is limited by cost, readout complexity, practical geometry, and the transverse size of the cascades—but see Ref. 141. An example, a wedge of the ATLAS central barrel calorimeter, is shown in Fig. 33.22(b) [139].

Much of the following discussion assumes an idealized calorimeter, with the same structure throughout and without leakage. "Real" calorimeters usually have an EM detector in front and a coarse "catcher" in the back. Complete containment is generally impractical.

In an inelastic hadronic collision a significant fraction f_{em} of the energy is removed from further hadronic interaction by the production of secondary π^0's and η's, whose decay photons generate high-energy electromagnetic (EM) showers. Charged secondaries ($\pi^{\pm}$, p, ...) deposit energy via ionization and excitation, but also interact with nuclei, producing spallation protons and neutrons, evaporation neutrons, and spallation products. The charged collision products produce detectable ionization, as do the showering γ-rays from the prompt de-excitation of highly excited nuclei. The recoiling nuclei generate little or no detectable signal. The neutrons lose kinetic energy in elastic collisions, thermalize on a time scale of several μs, and are captured, with the production of more γ-rays—usually outside the acceptance gate of the electronics. Between endothermic spallation losses, nuclear recoils, and late neutron capture, a significant fraction of the hadronic energy (20%–40%, depending on the absorber and energy of the incident particle) is used to overcome nuclear binding energies and is therefore lost or "invisible."

In contrast to EM showers, hadronic cascade processes are characterized by the production of relatively few high-energy particles. The lost energy and f_{em} are highly variable from event to event. Until there is event-by-event knowledge of both the EM fraction and the invisible energy loss, the energy resolution of a hadron calorimeter will remain significantly worse than that of its EM counterpart.

The efficiency e with which EM deposit is detected varies from event to event, but because of the large multiplicity in EM showers the variation is small. In contrast, because a variable fraction of the hadronic energy deposit is detectable, the efficiency h with which hadronic energy is detected is subject to considerably larger fluctuations. It thus makes sense to consider the ratio h/e as a stochastic variable.

Most energy deposit is by very low-energy electrons and charged hadrons. Because so many generations are involved in a high-energy cascade, the hadron spectra in a given material are essentially independent of energy except for overall normalization [143]. For this reason $\langle h/e\rangle$ is a robust concept, independently of hadron energy and species.

If the detection efficiency for the EM sector is e and that for the hadronic sector is h, then the ratio of the mean response to a pion relative to that for an electron is

$$\langle \pi/e\rangle = \langle f_{em}\rangle + \langle f_h\rangle\langle h/e\rangle^* = 1 - (1 - \langle h/e\rangle)\langle f_h\rangle \qquad (33.33)$$

It has been shown by a simple induction argument and verified by experiment, that the decrease in the average value of the hadronic energy fraction $\langle f_h\rangle = 1 - \langle f_{em}\rangle$ as the projectile energy E increases is fairly well described by the power law [142,143]

$$\langle f_h\rangle \approx (E/E_0)^{m-1} \qquad (\text{for } E > E_0)\ , \qquad (33.34)$$

at least up to a few hundred GeV. The exponent m depends logarithmically on the mean multiplicity and the mean fractional loss to π^0 production in a single interaction. It is in the range 0.80–0.87. E_0, roughly the energy for the onset of inelastic collisions, is 1 GeV or a little less for incident pions [142]. Both m and E_0 must be obtained experimentally for a given calorimeter configuration.

Only the product $(1 - \langle h/e\rangle)E_0^{1-m}$ can be obtained by measuring $\langle \pi/e\rangle$ as a function of energy. Since $1 - m$ is small and $E_0 \approx 1$ GeV for pion-induced cascades, this fact is usually ignored and $\langle h/e\rangle$ is reported.

In a hadron-nucleus collision a large fraction of the incident energy is carried by a "leading particle" with the same quark content as the incident hadron. If the projectile is a charged pion, the leading particle is usually a pion, which can be neutral and hence contributes to the EM sector. This is not true for incident protons. The result is an increased mean hadronic fraction for incident protons: $E_0 \approx 2.6$ GeV [142–145].

By definition, $0 \le f_{em} \le 1$. Its variance $\sigma^2_{f_{em}}$ changes only slowly with energy, but perforce $\langle f_{em}\rangle \to 1$ as the projectile energy increases. An empirical power law (unrelated to Eq. (33.33)) of the form $\sigma_{f_{em}} = (E/E_1)^{1-\ell}$ (where $\ell < 1$) describes the energy dependence of the variance adequately and has the right asymptotic properties [133]. For $\langle h/e\rangle \neq 1$ (*noncompensation*), fluctuations in f_{em} significantly contribute to or even dominate the resolution. Since the f_{em} distribution has a high-energy tail, the calorimeter response is non-Gaussian with a high-energy tail if $\langle h/e\rangle < 1$. Noncompensation thus seriously degrades resolution and produces a nonlinear response.

It is clearly desirable to *compensate* the response, *i.e.*, to design the calorimeter such that $\langle h/e\rangle = 1$. This is possible only with a sampling calorimeter, where several variables can be chosen or tuned:

1. Decrease the EM sensitivity. EM cross sections increase with Z,[†] and most of the energy in an EM shower is deposited by low-energy electrons. A disproportionate fraction of the EM energy is thus deposited in the higher-Z absorber. Lower-Z cladding, such as the steel cladding on ZEUS U plates, preferentially absorbs low-energy γ's in EM showers and thus also lowers the electronic response. G10 signal boards in the DØ calorimeters and G10 next to slicon readout detectors has the same effect. The degree of EM signal suppression can be somewhat controlled by tuning the sensor/absorber thickness ratio.
2. Increase the hadronic sensitivity. The abundant neutrons produced in the cascade have large n-p elastic scattering cross sections, so that low-energy scattered protons are produced in hydrogenous sampling materials such as butane-filled proportional counters or plastic scintillator. (The maximal fractional energy loss when a neutron scatters from a nucleus with mass number A is $4A/(1 + A)^2$.) The down side in the scintillator case is that the signal from a highly-ionizing stopping proton can be reduced by as much as 90% by recombination and quenching parameterized by Birks' Law (Eq. (33.2)).
3. Fabjan and Willis proposed that the additional signal generated in the aftermath of fission in ^{238}U absorber plates should compensate nuclear fluctuations [146]. The production of fission fragments due to fast n capture was later observed [147]. However, while a very large amount of energy is released, it is mostly carried by low-velocity, very highly ionizing fission fragments which produce very little observable signal because of recombination and quenching. But in fact much of the compensation observed with the ZEUS ^{238}U/scintillator calorimeter was mainly the result of methods 1 and 2 above.

* Technically, we should write $\langle f_h(h/e)\rangle$, but we approximate it as $\langle f_h\rangle\langle h/e\rangle$ to facilitate the rest of the discussion.

† The asymptotic pair-production cross section scales roughly as $Z^{0.75}$, and $|dE/dx|$ slowly decreases with increasing Z.

Motivated very much by the work of Brau, Gabriel, Brückmann, and Wigmans [148], several groups built calorimeters which were very nearly compensating. The degree of compensation was sensitive to the acceptance gate width, and so could be somewhat further tuned. These included

a) HELIOS with 2.5 mm thick scintillator plates sandwiched between 2 mm thick ^{238}U plates (one of several structures); $\sigma/E = 0.34/\sqrt{E}$ was obtained,
b) ZEUS, 2.6 cm thick scintillator plates between 3.3 mm ^{238}U plates; $\sigma/E = 0.35/\sqrt{E}$,
c) a ZEUS prototype with 10 mm Pb plates and 2.5 mm scintillator sheets; $\sigma/E = 0.44/\sqrt{E}$, and
d) DØ, where the sandwich cell consists of a 4–6 mm thick ^{238}U plate, 2.3 mm LAr, a G-10 signal board, and another 2.3 mm LAr gap; $\sigma/E \approx 0.45/\sqrt{E}$.

Given geometrical and cost constraints, the calorimeters used in modern collider detectors are not compensating: $\langle h/e\rangle \approx 0.7$, for the ATLAS central barrel calorimeter, is typical.

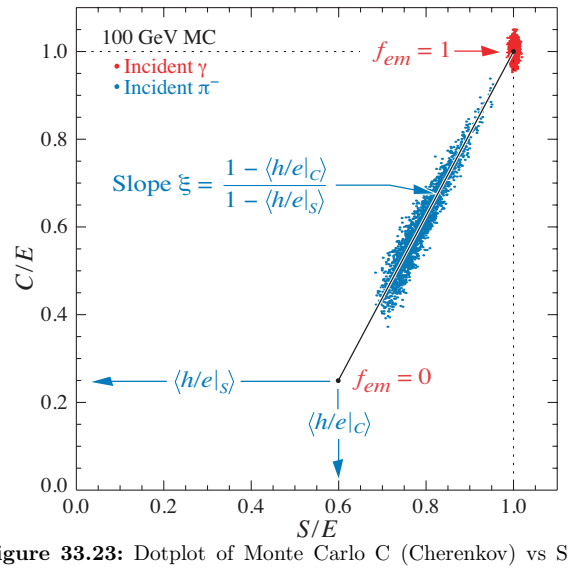

Figure 33.23: Dotplot of Monte Carlo C (Cherenkov) vs S (scintillator) signals for individual events in a dual readout calorimeter. Hadronic (π^-) induced events are shown in blue, and scatter about the indicated event locus. Electromagnetic events cluster about (C,S) = (0,0). In this case worse resolution (fewer p.e.'s) was assumed for the Cherenkov events, leading to the "elliptical" distribution.

A more versatile approach to compensation is provided by a *dual-readout calorimeter*, in which the signal is sensed by two readout systems with highly contrasting $\langle h/e\rangle$. Although the concept is more than two decades old [149], it was only recently been implemented by the DREAM collaboration [150]. The test beam calorimeter consisted of copper tubes, each filled with scintillator and quartz fibers. If the two signals C and S (quartz and scintillator) are both normalized to electron response, then for each event Eq. (33.33) takes the form

$$\begin{aligned} C &= E[f_{em} + \langle h/e\rangle|_C(1 - f_{em})] \\ S &= E[f_{em} + \langle h/e\rangle|_S(1 - f_{em})] \end{aligned} \qquad (33.35)$$

for the Cherenkov and scintillator responses. On a dotplot of C/E vs S/E, events scatter about a line-segment locus described in Fig. 33.23. With increasing energy the distribution moves upward along the locus and becomes tighter. Equations 33.35 are linear in $1/E$ and f_{em}, and are easily solved to obtain estimators of the *corrected* energy and f_{em} for each event. Both are subject to resolution effects, but contributions due to fluctuations in f_{em} are eliminated. The solution for the corrected energy is given by [143]:

$$E = \frac{\xi S - C}{\xi - 1}\ , \text{ where } \xi = \frac{1 - \langle h/e\rangle|_C}{1 - \langle h/e\rangle|_S} \qquad (33.36)$$

ξ is the energy-independent slope of the event locus on a plot of C vs S. It can be found either from the fitted slope or by measuring π/e as a function of E. Because we have no knowledge of h/e on an event-by-event basis, it has been replaced by $\langle h/e\rangle$ in Eq. (33.36). ξ must be as far from unity as possible to optimize resolution, which means in practical terms that the scintillator readout of the calorimeter must be as compensating as possible.

Although the usually-dominant contribution of the f_{em} distribution to the resolution can be minimized by compensation or the use of dual calorimetry, there remain significant contributions to the resolution:

1. Incomplete corrections for leakage, differences in light collection efficiency, and electronics calibration.
2. Readout transducer shot noise (usually photoelectron statistics), plus electronic noise.
3. Sampling fluctuations. Only a small part of the energy deposit takes place in the scintillator or other sensor, and that fraction is subject to large fluctuations. This can be as high as $40\%/\sqrt{E}$ (lead/scintillator). It is even greater in the Fe/scint case because of the very small sampling fraction (if the calorimeter is to be compensating), and substantially lower in a U/scint calorimeter. It is obviously zero for a homogeneous calorimeter.
4. Intrinisic fluctuations. The many ways ionization can be produced in a hadronic shower have different detection efficiencies and are subject to stochastic fluctuations. In particular, a very large fraction of the hadronic energy (∼20% for Fe/scint, ∼40% for U/scint) is "invisible," going into nuclear dissociation, thermalized neutrons, etc. The lost fraction depends on readout—it will be greater for a Cherenkov readout, less for an organic scintillator readout.

Except in a sampling calorimeter especially designed for the purpose, sampling and intrinsic resolution contributions cannot be separated. This may have been best studied by Drews *et al.* [151], who used a calorimeter in which even- and odd-numbered scintillators were separately read out. Sums and differences of the variances were used to separate sampling and intrinsic contributions.

The fractional energy resolution can be represented by

$$\frac{\sigma}{E} = \frac{a_1(E)}{\sqrt{E}} \oplus \left|1 - \langle\frac{h}{e}\rangle\right| \left(\frac{E}{E_1}\right)^{1-\ell} \qquad (33.37)$$

The coefficient a_1 is expected to have mild energy dependence for a number of reasons. For example, the sampling variance is $(\pi/e)E$ rather than E. The term $(E/E_1)^{1-\ell}$ is the parametrization of $\sigma_{f_{em}}$ discussed above. Usually a plot of $(\sigma/E)^2$ vs $1/E$ ia well-described by a straight line (constant a_1) with a finite intercept—the square of the right term in Eq. (33.37), is called "the constant term." Precise data show the slight downturn [136].

After the first interaction of the incident hadron, the average longitudinal distribution rises to a smooth peak. The peak position increases slowly with energy. The distribution becomes nearly exponential after several interaction lengths. Examples from the CDHS magnetized iron-scintillator sandwich calorimeter test beam calibration runs [152] are shown in Fig. 33.24. Proton-induced cascades are somewhat shorter and broader than pion-induced cascades [145]. A gamma distribution fairly well describes the longitudinal development of an EM shower, as discussed in Sec. 32.5. Following this logic, Bock *et al.* suggested that the profile of a hadronic cascade could be fitted by the sum of two Γ distributions, one with a characteristic length X_0 and the other with length λ_I [153]. Fits to this 4-parameter function are commonly used, *e.g.*, by the ATLAS Tilecal collaboration [145]. If the interaction point is not known (the usual case), the distribution must be convoluted with an exponential in the interaction length of the incident particle. Adragna *et al.* give an analytic form for the convoluted function [145].

The transverse energy deposit is characterized by a central core dominated by EM cascades, together with a wide "skirt" produced by wide-angle hadronic interactions [154].

The CALICE collaboration has tested a "tracking" calorimeter (AHCAL) with highly granular scintillator readout [141]. Since the position of the first interaction is observed, the average longitudinal and radial shower distributions are obtained.

While the average distributions might be useful in designing a calorimeter, they have little meaning for individual events, whose

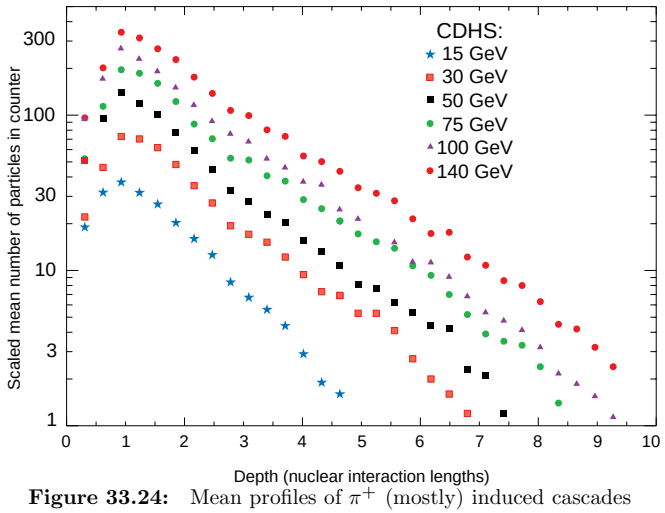

Figure 33.24: Mean profiles of π^+ (mostly) induced cascades in the CDHS neutrino detector [152].

distributions are extremely variable because of the small number of particles involved early in the cascade.

Particle identification, primarily e-π discrimination, is accomplished in most calorimeters by depth development. An EM shower is mostly contained in $15X_0$ while a hadronic shower takes about $4\lambda_I$. In high-A absorbers such as Pb, $X_0/\lambda_I \sim 0.03$. In a fiber calorimeter, such as the RD52 dual-readout calorimeter [155], e-π discrimination is achieved by differences in the Cerenkov and scintillation signals, lateral spread, and timing differences, ultimately achieving about 500:1 discrimination.

33.9.3. *Free electron drift velocities in liquid ionization chambers* :

Written August 2009 by W. Walkowiak (U. Siegen)

Drift velocities of free electrons in LAr [156] are given as a function of electric field strength for different temperatures of the medium in Fig. 33.25. The drift velocites in LAr have been measured using a double-gridded drift chamber with electrons produced by a laser pulse on a gold-plated cathode. The average temperature gradient of the drift velocity of the free electrons in LAr is described [156] by

$$\frac{\Delta v_d}{\Delta T\, v_d} = (-1.72 \pm 0.08)\ \%/\mathrm{K}.$$

Earlier measurements [157–160] used different techniques and show systematic deviations of the drift velocities for free electrons which cannot be explained by the temperature dependence mentioned above.

Drift velocities of free electrons in LXe [158] as a function of electric field strength are also displayed in Fig. 33.25. The drift velocity saturates for $|\boldsymbol{E}| > 3$ kV/cm, and decreases with increasing temperature for LXe as well as measured e.g. by [161].

The addition of small concentrations of other molecules like N_2, H_2 and CH_4 in solution to the liquid typically increases the drift velocities of free electrons above the saturation value [158,159], see example for CH_4 admixture to LAr in Fig. 33.25. Therefore, actual drift velocities are critically dependent on even small additions or contaminations.

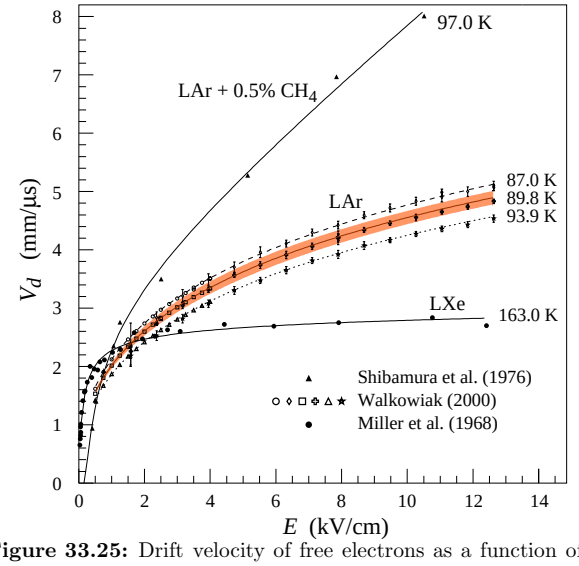

Figure 33.25: Drift velocity of free electrons as a function of electric field strength for LAr [156], LAr + 0.5% CH_4 [158] and LXe [157]. The average temperatures of the liquids are indicated. Results of a fit to an empirical function [162] are superimposed. In case of LAr at 91 K the error band for the global fit [156] including statistical and systematic errors as well as correlations of the data points is given. Only statistical errors are shown for the individual LAr data points.

33.10. Superconducting magnets for collider detectors

Revised September 2011 by A. Yamamoto (KEK); revised October 2001 by R.D. Kephart (FNAL)

33.10.1. *Solenoid Magnets* :

In all cases SI unit are assumed, so that the magnetic field, B, is in Tesla, the stored energy, E, is in joules, the dimensions are in meters, and $\mu_0 = 4\pi \times 10^{-7}$.

The magnetic field (B) in an ideal solenoid with a flux return iron yoke, in which the magnetic field is < 2 T, is given by

$$B = \mu_0\, n\, I \tag{33.38}$$

where n is the number of turns/meter and I is the current. In an air-core solenoid, the central field is given by

$$B(0,0) = \mu_0\, n\, I \frac{L}{\sqrt{L^2 + 4R^2}}\ , \tag{33.39}$$

where L is the coil length and R is the coil radius.

In most cases, momentum analysis is made by measuring the circular trajectory of the passing particles according to $p = mv\gamma = qrB$, where p is the momentum, m the mass, q the charge, r the bending radius. The sagitta, s, of the trajectory is given by

$$s = q\, B\, \ell^2/8p\ , \tag{33.40}$$

where ℓ is the path length in the magnetic field. In a practical momentum measurement in colliding beam detectors, it is more effective to increase the magnetic volume than the field strength, since

$$dp/p \propto p/B\,\ell^2\ , \tag{33.41}$$

where ℓ corresponds to the solenoid coil radius R. The energy stored in the magnetic field of any magnet is calculated by integrating B^2 over all space:

$$E = \frac{1}{2\mu_0}\int B^2 dV \tag{33.42}$$

If the coil thin, (which is the case if it is to superconducting coil), then

$$E \approx (B^2/2\mu_0)\pi R^2 L\ . \tag{33.43}$$

Table 33.9: Progress of superconducting magnets for particle physics detectors.

Experiment	Laboratory	B [T]	Radius [m]	Length [m]	Energy [MJ]	X/X_0	E/M [kJ/kg]
TOPAZ*	KEK	1.2	1.45	5.4	20	0.70	4.3
CDF*	Tsukuba/Fermi	1.5	1.5	5.07	30	0.84	5.4
VENUS*	KEK	0.75	1.75	5.64	12	0.52	2.8
AMY*	KEK	3	1.29	3	40	†	
CLEO-II*	Cornell	1.5	1.55	3.8	25	2.5	3.7
ALEPH*	Saclay/CERN	1.5	2.75	7.0	130	2.0	5.5
DELPHI*	RAL/CERN	1.2	2.8	7.4	109	1.7	4.2
ZEUS*	INFN/DESY	1.8	1.5	2.85	11	0.9	5.5
H1*	RAL/DESY	1.2	2.8	5.75	120	1.8	4.8
BaBar*	INFN/SLAC	1.5	1.5	3.46	27	†	3.6
D0*	Fermi	2.0	0.6	2.73	5.6	0.9	3.7
BELLE*	KEK	1.5	1.8	4	42	†	5.3
BES-III	IHEP	1.0	1.475	3.5	9.5	†	2.6
ATLAS-CS	ATLAS/CERN	2.0	1.25	5.3	38	0.66	7.0
ATLAS-BT	ATLAS/CERN	1	4.7–9.75	26	1080	(Toroid)†	
ATLAS-ET	ATLAS/CERN	1	0.825–5.35	5	2×250	(Toroid)†	
CMS	CMS/CERN	4	6	12.5	2600	†	12

* No longer in service

† EM calorimeter is inside solenoid, so small X/X_0 is not a goal

For a detector in which the calorimetry is outside the aperture of the solenoid, the coil must be thin in terms of radiation and absorption lengths. This usually means that the coil is superconducting and that the vacuum vessel encasing it is of minimum real thickness and fabricated of a material with long radiation length. There are two major contributors to the thickness of a thin solenoid:

1) The conductor consisting of the current-carrying superconducting material (usually NbTi/Cu) and the quench protecting stabilizer (usually aluminum) are wound on the inside of a structural support cylinder (usually aluminum also). The coil thickness scales as B^2R, so the thickness in radiation lengths (X_0) is

$$t_{\rm coil}/X_0 = (R/\sigma_h X_0)(B^2/2\mu_0) \ , \qquad (33.44)$$

where $t_{\rm coil}$ is the physical thickness of the coil, X_0 the average radiation length of the coil/stabilizer material, and σ_h is the hoop stress in the coil [165]. $B^2/2\mu_0$ is the magnetic pressure. In large detector solenoids, the aluminum stabilizer and support cylinders dominate the thickness; the superconductor (NbTI/Cu) contributes a smaller fraction. The main coil and support cylinder components typically contribute about 2/3 of the total thickness in radiation lengths.

2) Another contribution to the material comes from the outer cylindrical shell of the vacuum vessel. Since this shell is susceptible to buckling collapse, its thickness is determined by the diameter, length and the modulus of the material of which it is fabricated. The outer vacuum shell represents about 1/3 of the total thickness in radiation length.

33.10.2. ***Properties of collider detector magnets*** :

The physical dimensions, central field stored energy and thickness in radiation lengths normal to the beam line of the superconducting solenoids associated with the major collider are given in Table 33.9 [164]. Fig. 33.26 shows thickness in radiation lengths as a function of B^2R in various collider detector solenoids.

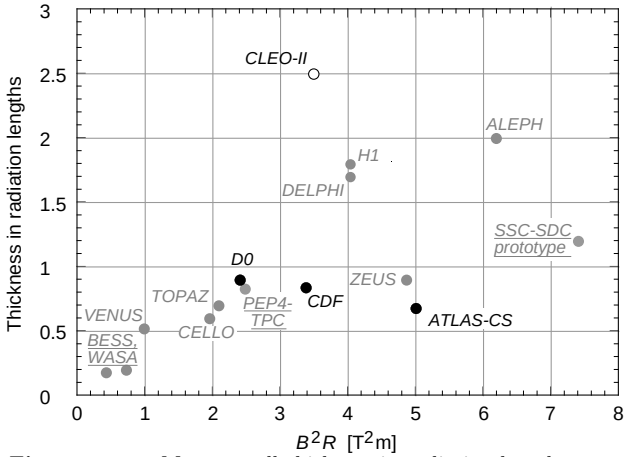

Figure 33.26: Magnet wall thickness in radiation length as a function of B^2R for various detector solenoids. Gray entries are for magnets no longer in use, and entries underlined are not listed in Table 33.9. Open circles are for magnets not designed to be "thin." The SSC-SDC prototype provided important R&D for LHC magnets.

The ratio of stored energy to cold mass (E/M) is a useful performance measure. It can also be expressed as the ratio of the stress, σ_h, to twice the equivalent density, ρ, in the coil [165]:

$$\frac{E}{M} = \frac{\int (B^2/2\mu_0) dV}{\rho\, V_{\rm coil}} \approx \frac{\sigma_h}{2\rho} \qquad (33.45)$$

The E/M ratio in the coil is approximately equivalent to H,* the enthalpy of the coil, and it determines the average coil temperature rise after energy absorption in a quench:

$$E/M = H(T_2) - H(T_1) \approx H(T_2) \tag{33.46}$$

where T_2 is the average coil temperature after the full energy absorption in a quench, and T_1 is the initial temperature. E/M ratios of 5, 10, and 20 kJ/kg correspond to ∼65, ∼80, and ∼100 K, respectively. The E/M ratios of various detector magnets are shown in Fig. 33.27 as a function of total stored energy. One would like the cold mass to be as small as possible to minimize the thickness, but temperature rise during a quench must also be minimized. An E/M ratio as large as 12 kJ/kg is designed into the CMS solenoid, with the possibility that about half of the stored energy can go to an external dump resistor. Thus the coil temperature can be kept below 80 K if the energy extraction system work well. The limit is set by the maximum temperature that the coil design can tolerate during a quench. This maximum local temperature should be <130 K (50 K + 80 K), so that thermal expansion effects in the coil are manageable.

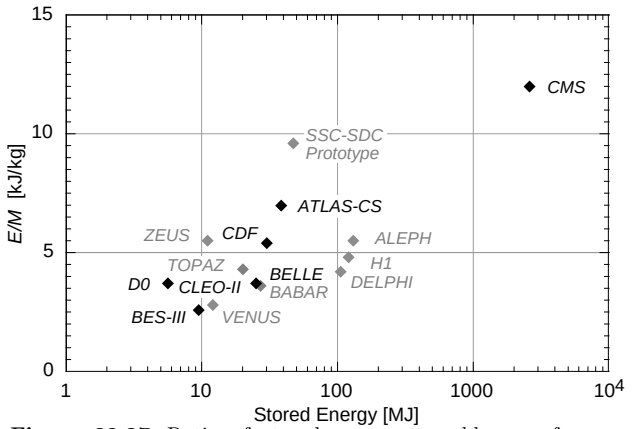

Figure 33.27: Ratio of stored energy to cold mass for major detector solenoids. Gray indicates magnets no longer in operation.

33.10.3. *Toroidal magnets* :

Toroidal coils uniquely provide a closed magnetic field without the necessity of an iron flux-return yoke. Because no field exists at the collision point and along the beam line, there is, in principle, no effect on the beam. On the other hand, the field profile generally has $1/r$ dependence. The particle momentum may be determined by measurements of the deflection angle combined with the sagitta. The deflection (bending) power BL is

$$BL \approx \int_{R_i}^{R_0} \frac{B_i R_i \, dR}{R \sin\theta} = \frac{B_i \, R_i}{\sin\theta} \ln(R_0/R_i) \ , \tag{33.47}$$

where R_i is the inner coil radius, R_0 is the outer coil radius, and θ is the angle between the particle trajectory and the beam line axis . The momentum resolution given by the deflection may be expressed as

$$\frac{\Delta p}{p} \propto \frac{p}{BL} \approx \frac{p \sin\theta}{B_i R_i \ln(R_0/R_i)} \ . \tag{33.48}$$

The momentum resolution is better in the forward/backward (smaller θ) direction. The geometry has been found to be optimal when $R_0/R_i \approx 3$–4. In practical designs, the coil is divided into 6–12 lumped coils in order to have reasonable acceptance and accessibility. This causes the coil design to be much more complex. The mechanical structure needs to sustain the decentering force between adjacent coils, and the peak field in the coil is 3–5 times higher than the useful magnetic field for the momentum analysis [163].

* The enthalpy, or heat content, is called H in the thermodynamics literature. It is not to be confused with the magnetic field intensity B/μ.

33.11. Measurement of particle momenta in a uniform magnetic field [166,167]

The trajectory of a particle with momentum p (in GeV/c) and charge ze in a constant magnetic field $\vec{B}$ is a helix, with radius of curvature R and pitch angle λ. The radius of curvature and momentum component perpendicular to $\vec{B}$ are related by

$$p \cos\lambda = 0.3 \, z \, B \, R \ , \tag{33.49}$$

where B is in tesla and R is in meters.

The distribution of measurements of the curvature $k \equiv 1/R$ is approximately Gaussian. The curvature error for a large number of uniformly spaced measurements on the trajectory of a charged particle in a uniform magnetic field can be approximated by

$$(\delta k)^2 = (\delta k_{\rm res})^2 + (\delta k_{\rm ms})^2 \ , \tag{33.50}$$

where $\delta k =$ curvature error
$\delta k_{\rm res} =$ curvature error due to finite measurement resolution
$\delta k_{\rm ms} =$ curvature error due to multiple scattering.

If many (≥ 10) uniformly spaced position measurements are made along a trajectory in a uniform medium,

$$\delta k_{\rm res} = \frac{\epsilon}{L'^2} \sqrt{\frac{720}{N+4}} \ , \tag{33.51}$$

where $N =$ number of points measured along track
$L' =$ the projected length of the track onto the bending plane
$\epsilon =$ measurement error for each point, perpendicular to the trajectory.

If a vertex constraint is applied at the origin of the track, the coefficient under the radical becomes 320.

For arbitrary spacing of coordinates s_i measured along the projected trajectory and with variable measurement errors ϵ_i the curvature error $\delta k_{\rm res}$ is calculated from:

$$(\delta k_{\rm res})^2 = \frac{4}{w} \ \frac{V_{ss}}{V_{ss} V_{s^2 s^2} - (V_{ss^2})^2} \ , \tag{33.52}$$

where V are covariances defined as $V_{s^m s^n} = \langle s^m s^n \rangle - \langle s^m \rangle \langle s^n \rangle$ with $\langle s^m \rangle = w^{-1} \sum (s_i{}^m / \epsilon_i{}^2)$ and $w = \sum \epsilon_i{}^{-2}$.

The contribution due to multiple Coulomb scattering is approximately

$$\delta k_{\rm ms} \approx \frac{(0.016)(\text{GeV}/c) z}{L p \beta \cos^2\lambda} \sqrt{\frac{L}{X_0}} \ , \tag{33.53}$$

where $p =$ momentum (GeV/c)
$z =$ charge of incident particle in units of e
$L =$ the total track length
$X_0 =$ radiation length of the scattering medium (in units of length; the X_0 defined elsewhere must be multiplied by density)
$\beta =$ the kinematic variable v/c.

More accurate approximations for multiple scattering may be found in the section on Passage of Particles Through Matter (Sec. 32 of this *Review*). The contribution to the curvature error is given approximately by $\delta k_{\rm ms} \approx 8 s^{\rm rms}_{\rm plane}/L^2$, where $s^{\rm rms}_{\rm plane}$ is defined there.

References:

1. *Experimental Techniques in High Energy Physics*, T. Ferbel (ed.) (Addison-Wesley, Menlo Park, CA, 1987).
2. K. Kleinknecht, *Detectors for Particle Radiation*, Cambridge University Press (1998).
3. G.F. Knoll, *Radiation Detection and Measurement*, 3nd edition, John Wiley & Sons, New York (1999).
4. D.R. Green, *The Physics of Particle Detectors,* Cambridge Monographs on Particle Physics, Nuclear Physics and Cosmology, # 12, Cambridge University Press (2000).
5. C. Leroy & P.-G. Rancoita, *Principles of Radiation Interaction in Matter and Detection*, (World Scientific, Singapore, 2004).
6. C. Grupen, *Particle Detectors, Cambridge Monographs on Particle Physics, Nuclear Physics and Cosmology*, Cambridge University Press (2008).
7. [Icarus Collab.], ICARUS-TM/2001-09; LGNS-EXP 13/89 add 2-01.

8. H. Spieler, IEEE Trans. **NS29**, 1142 (1982).
9. K. Arisaka, Nucl. Instrum. Methods **A442**, 80 (2000).
10. K.K. Hamamatsu, Electron Tube Division, *Photomultiplier Tubes: Basics and Applications*, 3rd edition (2006); Can be found under "Photomultiplier Tube Handbook" at `http://sales.hamamatsu.com/assets/applications/ETD/pmt_handbook/pmt_handbook_complete.pdf`.
11. A. Braem *et al.*, Nucl. Instrum. Methods **A518**, 574 (2004).
12. R. Arnold *et al.*, Nucl. Instrum. Methods **A314**, 465 (1992).
13. P. Mangeot *et al.*, Nucl. Instrum. Methods **A216**, 79 (1983); R. Apsimon *et al.*, IEEE. Trans. Nucl. Sci. **33**, 122 (1986); R. Arnold *et al.*, Nucl. Instrum. Methods **A270**, 255 (1988); D. Aston *et al.*, Nucl. Instrum. Methods **A283**, 582 (1989).
14. J. Janesick *Scientific charge-coupled devices*, SPIE Press, Bellingham, WA (2001).
15. R. Haitz *et al.*, J. Appl. Phys. **36**, 3123 (1965); R. McIntyre, IEEE Trans. Electron Devices **13**, 164 (1966); H. Dautet *et al.*, Applied Optics, **32**, (21), 3894 (1993); Perkin-Elmer Optoelectronics, *Avalanche Photodiodes: A User's Guide*.
16. P. Buzhan *et al.*, Nucl. Instrum. Methods **A504**, 48 (2003); Z. Sadygov *et al.*, Nucl. Instrum. Methods **A504**, 301 (2003); V. Golovin and V. Saveliev, Nucl. Instrum. Methods **A518**, 560 (2004).
17. M. Landstrass *et al.*, Diam. & Rel. Matter, **2**, 1033 (1993); R. McKeag and R. Jackman, Diam. & Rel. Matter, **7**, 513 (1998); R. Brascia *et al.*, Phys. Stat. Sol. **199**, 113 (2003).
18. M. Petrov, M. Stapelbroek, and W. Kleinhans, Appl. Phys. Lett. **51**, 406 (1987); M. Atac, M. Petrov, IEEE Trans. Nucl. Sci. **36**, 163 (1989); M. Atac *et al.*, Nucl. Instrum. Methods **A314**, 56 (1994).
19. J.B. Birks, *The Theory and Practice of Scintillation Counting*, (Pergamon, London, 1964).
20. D. Clark, Nucl. Instrum. Methods **117**, 295 (1974).
21. J.B. Birks, Proc. Phys. Soc. **A64**, 874 (1951).
22. B. Bengston and M. Moszynski, Nucl. Instrum. Methods **117**, 227 (1974); J. Bialkowski, *et al.*, Nucl. Instrum. Methods **117**, 221 (1974).
23. C. P. Achenbach, "Active optical fibres in modern particle physics experiments," `arXiv:nucl-ex/0404008v1`.
24. I.B. Berlman, *Handbook of Fluorescence Spectra of Aromatic Molecules*, 2nd edition (Academic Press, New York, 1971).
25. C. Zorn, in *Instrumentation in High Energy Physics,* ed. F. Sauli, (1992, World Scientific, Singapore) pp. 218–279.
26. T. Foerster, Ann. Phys. **2**, 55 (1948).
27. J.M. Fluornoy, *Conference on Radiation-Tolerant Plastic Scintillators and Detectors*, K.F. Johnson and R.L. Clough editors, Rad. Phys. and Chem., **41** 389 (1993).
28. D. Horstman and U. Holm, *ibid,* 395.
29. D. Blomker, *et al.*, Nucl. Instrum. Methods **A311**, 505 (1992); J. Mainusch, *et al.*, Nucl. Instrum. Methods **A312**, 451 (1992).
30. *Conference on Radiation-Tolerant Plastic Scintillators and Detectors*, K.F. Johnson and R.L. Clough editors, Rad. Phys. and Chem., **41** (1993).
31. S.R. Borenstein and R.C. Strand, IEEE Trans. Nuc. Sci. **NS-31(1)**, 396 (1984).
32. P. Sonderegger, Nucl. Instrum. Methods **A257**, 523 (1987).
33. Achenbach, *ibid.*
34. C.M. Hawkes, *et al.*, Nucl. Instrum. Methods **A292**, 329 (1990).
35. A. Lempicki *et al.*, Nucl. Instrum. Methods **A333**, 304 (1993); G. Blasse, *Proceedings of the Crystal 2000 International Workshop on Heavy Scintillators for Scientific and Industrial Applications*, Chamonix, France, Sept. (1992), Edition Frontieres.
36. C. Melcher and J. Schweitzer, Nucl. Instrum. Methods **A314**, 212 (1992).
37. D.W. Cooke *et al.*, J. Appl. Phys. **88**, 7360 (2000); T. Kimble, M Chou, and B.H.T. Chai, in *Proc. IEEE Nuclear Science Symposium Conference* (2002).
38. J.M. Chen *et al.*, IEEE Trans. Nuc. Sci. **NS-54(3)**, 718 (2007) and **NS-54(4)**, 1319 (2007).
39. E.V.D. van Loef *et al.*, Nucl. Instrum. Methods **A486**, 254 (2002).
40. C. Kuntner *et al.*, Nucl. Instrum. Methods **A493**, 131 (2002).
41. N. Akchurin *et al.*, Nucl. Instrum. Methods **A595**, 359 (2008).
42. A. Para, FERMILAB-CONF-11-519-CD; H. Wenzel *et al.*, FERMILAB-PUB-11-531-CD-E.
43. R.-Y. Zhu, Journal of Physics: Conference Series **160**, 012017 (2009).
44. R.H. Mao, L.Y. Zhang, and R.Y. Zhu, IEEE Trans. Nuc. Sci. **NS-55(4)**, 2425 (2008).
45. B.D. Rooney and J.D. Valentine, IEEE Trans. Nuc. Sci. **NS-44(3)**, 509 (1997).
46. W.W. Moses *et al.*, IEEE Trans. Nuc. Sci. **NS-55(3)**, 1049 (2008).
47. G. Gratta, H. Newman, and R.Y. Zhu, Ann. Rev. Nucl. and Part. Sci. **44**, 453 (1994).
48. R.Y. Zhu, Nucl. Instrum. Methods **A413**, 297 (1998).
49. S. Ecklund, *et al.*, Nucl. Instrum. Methods **A463**, 68 (2001).
50. B. Aubert, *et al.*, [BaBar Collab.], Nucl. Instrum. Methods **A479**, 1 (2002).
51. A. Abashian, *et al.*, Nucl. Instrum. Methods **A479**, 117 (2002).
52. I. Adam, *et al.*, Nucl. Instrum. Methods **A538**, 281 (2005).
53. M. Shiozawa, [Super-Kamiokande Collab.], Nucl. Instrum. Methods **A433**, 240 (1999).
54. J. Litt and R. Meunier, Ann. Rev. Nucl. Sci. **23**, 1 (1973).
55. D. Bartlett, *et al.*, Nucl. Instrum. Methods **A260**, 55 (1987).
56. B. Ratcliff, Nucl. Instrum. Methods **A502**, 211 (2003).
57. See the RICH Workshop series: Nucl. Instrum. Methods **A343**, 1 (1993); Nucl. Instrum. Methods **A371**, 1 (1996); Nucl. Instrum. Methods **A433**, 1 (1999); Nucl. Instrum. Methods **A502**, 1 (2003); Nucl. Instrum. Methods **A553**, 1 (2005); Nucl. Instrum. Methods **A595**, 1 (2008).
58. W. Blum, W. Riegler, and L. Rolandi, *Particle Detection with Drift Chambers* (Springer-Verlag, 2008).
59. L.G. Christophorou, *Atomic and Molecular Radiation Physics* (Wiley, 1971); I.B. Smirnov, Nucl. Instrum. Methods **A554**, 474 (2005); J. Berkowitz, *Atomic and Molecular Photo Absorption* (Academic Press, 2002); `http://pdg.lbl.gov/2007/AtomicNuclearProperties`.
60. H. Bichsel, Nucl. Instrum. Methods **A562**, 154 (2006).
61. H. Fischle *et al.*, Nucl. Instrum. Methods **A301**, 202 (1991).
62. `http://rjd.web.cern.ch/rjd/cgi-bin/cross`.
63. A. Peisert and F. Sauli, "Drift and Diffusion of Electrons in Gases," CERN 84-08 (1984).
64. S. Biagi, Nucl. Instrum. Methods **A421**, 234 (1999).
65. `http://consult.cern.ch/writeup/magboltz/`.
66. E. McDaniel and E. Mason, *The Mobility and Diffusion of Ions in Gases* (Wiley, 1973); G. Shultz *et al.*, Rev. Phys. Appl. **12**, 67 (1977).
67. G. Charpak *et al.*, Nucl. Instrum. Methods **A62**, 262 (1968).
68. G. Charpak and F. Sauli, Ann. Rev. Nucl. Sci. **34**, 285 (1984).
69. F. Sauli, "Principles of Operation of Multiwire Proportional and Drift Chambers," in *Experimental Techniques in High Energy Physics*, T. Ferbel (ed.) (Addison-Wesley, Menlo Park, CA, 1987).
70. G. Charpak *et al.*, Nucl. Instrum. Methods **A167**, 455 (1979).
71. A.H. Walenta *et al.*, Nucl. Instrum. Methods **A92**, 373 (1971).
72. A. Breskin *et al.*, Nucl. Instrum. Methods **A124**, 189 (1975).
73. A. Breskin *et al.*, Nucl. Instrum. Methods **A156**, 147 (1978).
74. R. Bouclier *et al.*, Nucl. Instrum. Methods **A265**, 78 (1988).
75. H. Drumm *et al.*, Nucl. Instrum. Methods **A176**, 333 (1980).
76. D.R. Nygren & J.N. Marx, Phys. Today **31N10**, 46 (1978).
77. `http://www.ansoft.com`.
78. P. Beringer *et al.*, Nucl. Instrum. Methods **A254**, 542 (1987).
79. J. Virdee, Phys. Rep. 403-404, 401 (2004).
80. H. Walenta, Phys. Scripta **23**, 354 (1981).

81. J. Va'vra, Nucl. Instrum. Methods **A515**, 1 (2003); M. Titov, "Radiation damage and long-term aging in gas detectors," arXiv:physics/0403055.
82. M. Aleksa *et al.*, Nucl. Instrum. Methods **A446**, 435 (2000).
83. F. Sauli and A. Sharma, Ann. Rev. Nucl. Part. Sci. **49**, 341 (1999).
84. A. Oed, Nucl. Instrum. Methods **A263**, 351 (1988); A. Barr *et al.*, Nucl. Phys. B (Proc. Suppl.), **61B**, 264 (1988).
85. Y. Bagaturia *et al.*, Nucl. Instrum. Methods **A490**, 223 (2002).
86. J. Benlloch *et al.*, IEEE Trans. Nucl. Sci., **NS-45** (1998) 234.
87. Y. Giomataris, Nucl. Instrum. Methods **A419**, 239 (1998).
88. F. Sauli, Nucl. Instrum. Methods **A386**, 531 (1997); A. Bressan *et al.*, Nucl. Instrum. Methods **A425**, 262 (1999).
89. S. Bachmann *et al.*, Nucl. Instrum. Methods **A479**, 294 (2002); A. Bressan *et al.*, Nucl. Instrum. Methods **A424**, 321 (1999).
90. Y. Giomataris *et al.*, Nucl. Instrum. Methods **A376**, 29 (1996).
91. J. Derre *et al.*, Nucl. Instrum. Methods **A459**, 523 (2001); G. Charpak *et al.*, Nucl. Instrum. Methods **A478**, 26 (2002).
92. I. Giomataris *et al.*, Nucl. Instrum. Methods **A560**, 405 (2006).
93. S. Duarte Pinto *et al.*, IEEE NSS/MIC Conference Record (2008).
94. L. Periale *et al.*, Nucl. Instrum. Methods **A478**, 377 (2002); R. Chechik *et al.*, Nucl. Instrum. Methods **A535**, 303 (2004); A. Breskin *et al.*, Nucl. Instrum. Methods **A598**, 107 (2009).
95. A. Di Mauro *et al.*, Nucl. Instrum. Methods **A581**, 225 (2007).
96. R. Bellazzini *et al.*, Nucl. Instrum. Methods **A535**, 477 (2004); M. Campbell *et al.*, Nucl. Instrum. Methods **A540**, 295 (2005); A. Bamberger *et al.*, Nucl. Instrum. Methods **A573**, 361 (2007); T.Kim *et al.*, Nucl. Instrum. Methods **A599**, 173 (2008).
97. M. Chefdeville *et al.*, Nucl. Instrum. Methods **A556**, 490 (2006).
98. M. Titov, arXiv: physics/0403055; *Proc. of the Workshop of the INFN ELOISATRON Project*, "Innovative Detectors For Super-Colliders," Erice, Italy, Sept. 28–Oct. 4 (2003).
99. http://rd51-public.web.cern.ch/RD51-Public.
100. P. Colas *et al.*, Nucl. Instrum. Methods **A535**, 506 (2004); M. Campbell *et al.*, Nucl. Instrum. Methods **A540**, 295 (2005).
101. H. Aihara *et al.*, IEEE Trans. **NS30**, 63 (1983).
102. J. Alme *et al.*, Nucl. Instrum. Methods **A622**, 316 (2010).
103. N. Abgrall *et al.*, Nucl. Instrum. Methods **A637**, 25 (2011).
104. C.J. Martoff *et al.*, Nucl. Instrum. Methods **A440**, 355 (2000).
105. X. Artru *et al.*, Phys. Rev. **D12**, 1289 (1975); G.M. Garibian *et al.*, Nucl. Instrum. Methods **125**, 133 (1975).
106. B. Dolgoshein, Nucl. Instrum. Methods **A326**, 434 (1993).
107. *TRDs for the Third Millenium: Proc. 2nd Workshop on Advanced Transition Radiation Detectors for Accelerator and Space Applications,* Nucl. Instrum. Methods **A522**, 1 (2004).
108. *TRDs for the Third Millenium: Proc. 4th Workshop on Advanced Transition Radiation Detectors for Accelerator and Space Applications,* Nucl. Instrum. Methods **A706**, 1 (2013).
109. B. Beischer *et al.*, Nucl. Instrum. Methods **A583**, 485 (2007).
110. A. Adronic and J.P Wessels, Nucl. Instrum. Methods **A666**, 130 (2012).
111. M. Petris *et al.*, Nucl. Instrum. Methods **A714**, 17 (2007).
112. J. Apostolakis *et al.*, Radiation Physics and Chemistry78,859(2009).
113. R. Santonico and R. Cardarelli, Nucl. Instrum. Methods **A187**, 377 (1981).
114. V.V. Parkhomchuck, Yu.N. Pestov, and N.V. Petrovykh, Nucl. Instrum. Methods **93**, 269 (1971).
115. E. Cerron Zeballos *et al.*, Nucl. Instrum. Methods **A374**, 132 (1996).
116. V. Ammosov *et al.*, Nucl. Instrum. Methods **A578**, 119 (2007).
117. P. Fonte, IEEE. Trans. Nucl. Sci. **49**, 881 (2002).
118. M. Abbrescia *et al.*, Nucl. Instrum. Methods **A394**, 13 (1997).
119. F. Anulli *et al.*, Nucl. Instrum. Methods **A552**, 276 (2005).
120. H. Spieler, *Semiconductor Detector Systems*, Oxford Univ. Press, Oxford (2005).
121. F. Scholze *et al.*, Nucl. Instrum. Methods **A439**, 208 (2000).
122. G. Lindström *et al.*, Nucl. Instrum. Methods **A465**, 60 (2001).
123. C. Da Via *et al.*, Nucl. Instrum. Methods **A509**, 86 (2003).
124. G. Kramberger *et al.*, Nucl. Instrum. Methods **A481**, 297 (2002).
125. O. Krasel *et al.*, IEEE Trans. Nucl. Sci NS-51/6,3055 (2004).
126. G. Lindström *et al.*, Nucl. Instrum. Methods **A426**, 1 (1999).
127. A. Holmes-Siedle and L. Adams, *Handbook of Radiation Effects*, 2nd ed., Oxford 2002.
128. V. Radeka, IEEE Trans. Nucl. Sci. **NS-15/3**, 455 (1968); V. Radeka, IEEE Trans. Nucl. Sci. **NS-21**, 51 (1974).
129. F.S. Goulding, Nucl. Instrum. Methods **100**, 493 (1972); F.S. Goulding and D.A. Landis, IEEE Trans. Nucl. Sci. **NS-29**, 1125 (1982).
130. W.R. Nelson, H. Hirayama, and D.W.O. Rogers, "The EGS4 Code System," SLAC-265, Stanford Linear Accelerator Center (Dec. 1985).
131. R. Brun *et al.*, *GEANT3*, CERN DD/EE/84-1 (1987).
132. D. Hitlin *et al.*, Nucl. Instrum. Methods **137**, 225 (1976). See also W. J. Willis and V. Radeka, Nucl. Instrum. Methods **120**, 221 (1974), for a more detailed discussion.
133. R. Wigmans, *Calorimetry: Energy Measurement in Particle Physics*, Inter. Series of Monographs on Phys. **107**, Clarendon, Oxford (2000).
134. ATLAS Collaboration, *The ATLAS Liquid Argon Calorimeter Technical Design Report*, CERN/LHCC 96-41 (1996).
135. CMS Collaboration, *The CMS Electromagnetic Calorimeter Technical Design Report*, CERN/LHCC 97-33 (1997).
136. N. Akchurin, *et al.*, Nucl. Instrum. Methods **A399**, 202 (1997).
137. B. Aubert,*et al.*, Nucl. Instrum. Methods **A321**, 467 (1992).
138. A. Artamonov, *et al.*, J. Inst. **3**, P02010.
139. F. Ariztizabal, *et al.*, Nucl. Instrum. Methods **A349**, 384 (1994).
140. S. Abdullin, *et al.*, Eur. Phys. J. **53** , 139 (2008).
141. M. Romalli, "Hadronic models validation in GEANT4 with CALICE highly granular calorimeters," *Proc. XVth Inter. Conf. on Calorimetry in High Energy Physics,* Santa Fe, NM, 4–8 June 2012, eds. N. Akchurin, S-W. Lee, & I. Volobouev, J. Phys. Conf. Series **404** (2012) 012050. See also C. Adloff, et al., arXiv:1306.3037.
142. T.A. Gabriel *et al.*, Nucl. Instrum. Methods **A338**, 336 (1994).
143. D.E. Groom, Nucl. Instrum. Methods **A572**, 633 (2007); Erratum: D.E. Groom, Nucl. Instrum. Methods **A593**, 638 (2008).
144. N. Akchurin, *et al.*, Nucl. Instrum. Methods **A408**, 380 (1998); An energy-independent analysis of these data is given in Ref. 143.
145. P. Adragna *et al.*, Nucl. Instrum. Methods **A615**, 158 (2010).
146. C.W. Fabjan *et al.*, Phys. Lett. **B60**, 105 (1975).
147. C. Leroy, J. Sirois, and R. Wigmans, Nucl. Instrum. Methods **A252**, 4 (1986).
148. J.E. Brau and T.A. Gabriel, Nucl. Instrum. Methods **A238**, 489 (1985); H. Brückmann and H. Kowalski, ZEUS Int. Note 86/026 DESY, Hamburg (1986); R. Wigmans, Nucl. Instrum. Methods **A259**, 389 (1987); R. Wigmans, Nucl. Instrum. Methods **A265**, 273 (1988).
149. P. Mockett, "A review of the physics and technology of high-energy calorimeter devices," *Proc. 11th SLAC Summer Inst. Part. Phy.,* July 1983, SLAC Report No. 267 (July 1983), p. 42, www.slac.stanford.edu/pubs/confproc/ssi83/ssi83-008.html.
150. R. Wigmans, "Quartz Fibers and the Prospects for Hadron Calorimetry at the 1% Resolution Level," *Proc. 7th Inter. Conf. on Calorimetry in High Energy Physics,* Tucson, AZ, Nov. 9–14, 1997, eds. E. Cheu *et al.*, (World Scientific, River Edge, NJ, 1998), p. 182; N. Akchurin *et al.*, Nucl. Instrum. Methods **A537**, 537 (2005).
151. G. Drews, *et al.*, Nucl. Instr. and Meth. A 335, 335 (1990).
152. M. Holder *et al.*, Nucl. Instrum. Methods **151**, 69 (1978).
153. R.K. Bock, T. Hansl-Kozanecka, and T.P. Shah, Nucl. Instrum. Methods **186**, 533 (1981);

Y.A. Kulchitsky and V.B. Vinogradov, Nucl. Instrum. Methods **A455**, 499 (2000).
154. D. Acosta *et al.*, Nucl. Instrum. Methods **A316**, 184 (1997).
155. N. Akchurin, *et al.*, Nucl. Instrum. Methods **A735**, 120 (2013).
156. W. Walkowiak, Nucl. Instrum. Methods **A449**, 288 (2000).
157. L.S. Miller *et al.*, Phys. Rev. **166**, 871 (1968).
158. E. Shibamura *et al.*, Nucl. Instrum. Methods **A316**, 184 (1975).
159. K. Yoshino *et al.*, Phys. Rev. **A14**, 438 (1976).
160. A.O. Allen *et al.*, "Drift mobilities and conduction band energies of excess electrons in dielectric liquids," NSRDS-NBS-58 (1976).
161. P. Benetti *et al.*, Nucl. Instrum. Methods **A32**, 361 (1993).
162. A.M. Kalinin *et al.*, "Temperature and electric field strength dependence of electron drift velocity in liquid argon," ATLAS Internal Note, ATLAS-LARG-NO-058, CERN (1996).
163. T. Taylor, Phys. Scr. **23**, 459 (1980).
164. A. Yamamoto, Nucl. Instr. Meth. **A494**, 255 (2003).
165. A. Yamamoto, Nucl. Instr. Meth. **A453**, 445 (2000).
166. R.L. Gluckstern, Nucl. Instrum. Methods **24**, 381 (1963).
167. V. Karimäki, Nucl. Instrum. Methods **A410**, 284 (1998).

34. PARTICLE DETECTORS FOR NON-ACCELERATOR PHYSICS

Updated 2013 (see the various sections for authors).

34.1. Introduction

Non-accelerator experiments have become increasingly important in particle physics. These include classical cosmic ray experiments, neutrino oscillation measurements, and searches for double-beta decay, dark matter candidates, and magnetic monopoles. The experimental methods are sometimes those familiar at accelerators (plastic scintillators, drift chambers, TRD's, *etc.*) but there is also instrumentation either not found at accelerators or applied in a radically different way. Examples are atmospheric scintillation detectors (Fly's Eye), massive Cherenkov detectors (Super-Kamiokande, IceCube), ultracold solid state detectors (CDMS). And, except for the cosmic ray detectors, radiologically ultra-pure materials are required.

In this section, some more important detectors special to terrestrial non-accelerator experiments are discussed. Techniques used in both accelerator and non-accelerator experiments are described in Sec. 28, Particle Detectors at Accelerators, some of which have been modified to accommodate the non-accelerator nuances.

Space-based detectors also use some unique instrumentation, but these are beyond the present scope of RPP.

34.2. High-energy cosmic-ray hadron and gamma-ray detectors

34.2.1. *Atmospheric fluorescence detectors* :

Updated August 2013 by L.R. Wiencke (Colorado School of Mines).

Cosmic-ray fluorescence detectors (FD) use the atmosphere as a giant calorimeter to measure isotropic scintillation light that traces the development profiles of extensive air showers (EAS). The EASs observed are produced by the interactions of high-energy ($E > 10^{17}$ eV) subatomic particles in the stratosphere and upper troposphere. These are the highest energy particles known to exist. The amount of scintillation light generated is proportional to energy deposited in the atmosphere and nearly independent of the primary species. Experiments with FDs include the pioneering Fly's Eye [1], HiRes [2], the Telescope Array [3], and the Pierre Auger Observatory (Auger) [4]. The Auger FD also measures the time development of a class of atmospheric transient luminous events called "Elves" that are created in the ionosphere above some thunderstorms [5]. The proposed JEM-EUSO [6] FD would tilt down to sweep across a much larger area from the international space station.

The scintillation light is emitted between 290 and 430 nm (Fig. 34.1), when relativistic charged particles, primarily electrons and positrons, excite nitrogen molecules in air, resulting in transitions of the 1P and 2P systems. Reviews and references for the pioneering and ongoing laboratory measurements of fluorescence yield, $Y(\lambda, P, T, u)$, including dependence on wavelength (λ), temperature (T), pressure (p), and humidity (u) may be found in Refs. 7–9.

An FD element (telescope) consists of a non-tracking spherical mirror (3.5–13 m^2 and less than astronomical quality), a close-packed "camera" of PMTs (for example, Hamamatsu R9508 or Photonis XP3062) near the focal plane, and a flash ADC readout system with a pulse and track-finding trigger scheme [10]. Simple reflector optics ($12^\circ \times 16^\circ$ degree field of view (FOV) on 256 PMTs) and Schmidt optics ($30^\circ \times 30^\circ$ FOV on 440 PMTs), including a correcting element, have been used. Segmented mirrors have been fabricated from slumped or slumped/polished glass with an anodized aluminium coating and from chemically anodized $AlMgSiO_5$ affixed to shaped aluminum. A broadband UV filter (custom fabricated or Schott MUG-6) reduces background light such as starlight, airglow, man-made light pollution, and airplane strobelights.

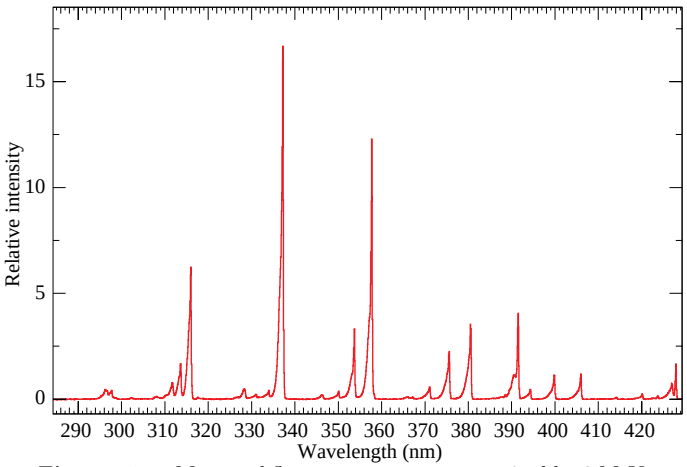

Figure 34.1: Measured fluorescence spectrum excited by 3 MeV electrons in dry air at 800 hPa and 293 K [11].

At 10^{20} eV, where the flux drops below 1 EAS/km^{2}century, the aperture for an eye of adjacent FD telescopes that span the horizon can reach 10^4 km^2 sr. FD operation requires (nearly) moonless nights and clear atmospheric conditions, which imposes a duty cycle of about 10%. Arrangements of LEDs, calibrated diffuse sources [12], pulsed UV lasers [13], LIDARs* and cloud monitors are used for photometric

* This acronym for "Light Detection and Ranging," refers here to systems that measure atmospheric properties from the light scattered backwards from laser pulses directed into the sky.

calibration, atmospheric calibration [14], and determination of exposure [15].

The EAS generates a track consistent with a light source moving at $v = c$ across the FOV. The number of photons (N_γ) as a function of atmospheric depth (X) can be expressed as [8]

$$\frac{\mathrm{d}N_\gamma}{\mathrm{d}X} = \frac{dE^{\mathrm{tot}}_{\mathrm{dep}}}{dX} \int Y(\lambda, P, T, u) \cdot \tau_{\mathrm{atm}}(\lambda, X) \cdot \varepsilon_{\mathrm{FD}}(\lambda)\mathrm{d}\lambda \quad , \qquad (34.1)$$

where $\tau_{atm}(\lambda, X)$ is atmospheric transmission, including wavelength (λ) dependence, and $\varepsilon_{\mathrm{FD}}(\lambda)$ is FD efficiency. $\varepsilon_{\mathrm{FD}}(\lambda)$ includes geometric factors and collection efficiency of the optics, quantum efficiency of the PMTs, and other throughput factors. The typical systematic uncertainties, Y (10%), τ_{atm} (10%) and $\varepsilon_{\mathrm{FD}}$ (photometric calibration 10%), currently dominate the total reconstructed EAS energy uncertainty. $\Delta E/E$ of 20–25% is possible, provided the geometric fit of the EAS axis is constrained by multi-eye stereo projection, or by timing from a colocated sparse array of surface detectors.

Analysis methods to reconstruct the EAS profile and deconvolute the contributions of re-scattered scintillation light, and direct and scattered Cherenkov light are described in [1] and more recently in [16]. The EAS energy is typically obtained by integrating over the Gaisser-Hillas function [17]

$$E_{\mathrm{cal}} = \int_0^\infty w_{\mathrm{max}} \left(\frac{X - X_0}{X_{\mathrm{max}} - X_0} \right)^{(X_{\mathrm{max}} - X_0)/\lambda} e^{(X_{\mathrm{max}} - X)/\lambda} \mathrm{d}X \quad , \qquad (34.2)$$

where X_{max} is the depth at which the shower reaches its maximum energy deposit w_{max}. X_0 and λ are two shape parameters.

34.2.2. *Atmospheric Cherenkov telescopes for high-energy γ-ray astronomy* :

Revised August 2013 by J. Holder (Dept. of Physics and Astronomy & Bartol Research Inst., Univ. of Delaware).

A wide variety of astrophysical objects are now known to produce high-energy γ-ray photons. Leptonic or hadronic particle populations, accelerated to relativistic energies in the source, produce γ rays typically through inverse Compton boosting of ambient photons, or through the decay of neutral pions produced in hadronic interactions. At energies below ∼30 GeV, γ-ray emission can be detected directly using satellite or balloon-borne instrumentation, with an effective area approximately equal to the size of the detector (< 1 m^2). At higher energies, a technique with much larger effective collection area is required to measure astrophysical γ-ray fluxes, which decrease rapidly with increasing energy. Atmospheric Cherenkov detectors achieve effective collection areas of $\sim 10^5$ m^2 by employing the Earth's atmosphere as an intrinsic part of the detection technique.

As described in Chapter 28, a hadronic cosmic ray or high energy γ-ray incident on the Earth's atmosphere triggers a particle cascade, or air shower. Relativistic charged particles in the cascade produce Cherenkov radiation, which is emitted along the shower direction, resulting in a light pool on the ground with a radius of ∼130 m. Cherenkov light is produced throughout the cascade development, with the maximum emission occurring when the number of particles in the cascade is largest, at an altitude of ∼10 km for primary energies of 100 GeV–1 TeV. Following absorption and scattering in the atmosphere, the Cherenkov light at ground level peaks at a wavelength, $\lambda \approx$ 300–350 nm. The photon density is typically ∼100 photons/m^2 at 1 TeV, arriving in a brief flash of a few nanoseconds duration. This Cherenkov pulse can be detected from any point within the light pool radius by using large reflecting surfaces to focus the Cherenkov light on to fast photon detectors (Fig. 34.2).

Modern atmospheric Cherenkov telescopes, such as those built and operated by the VERITAS [18], H.E.S.S. [19] and MAGIC [20] collaborations, consist of large ($> 100\,\mathrm{m}^2$) segmented mirrors on steerable altitude-azimuth mounts. A camera made from an array of up to 1000 photomultiplier tubes (PMTs) covering a field-of-view of up to 5.0° in diameter is placed at the mirror focus and used to record a Cherenkov image of each air shower. Images are recorded at a rate of a few hundred Hz, the vast majority of which are due to showers with hadronic cosmic-ray primaries. The shape and orientation of the Cherenkov images are used to discriminate γ-ray photon events from this cosmic-ray background, and to reconstruct the photon energy and arrival direction. γ-ray images result from purely electromagnetic cascades and appear as narrow, elongated ellipses in the camera plane. The long axis of the ellipse corresponds to the vertical extension of the air shower, and points back towards the source position in the field-of-view. If multiple telescopes are used to view the same shower ("stereoscopy"), the source position is simply the intersection point of the various image axes. Cosmic-ray primaries produce secondaries with large transverse momenta, which initiate sub-showers. Their images are consequently wider and less regular than those with γ-ray primaries and, since the original charged particle has been deflected by galactic magnetic fields before reaching the Earth, the images have no preferred orientation.

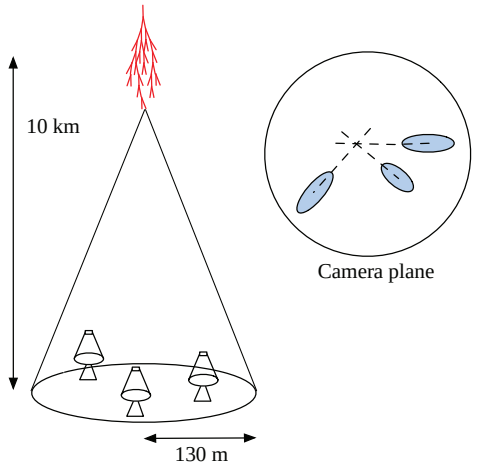

Figure 34.2: A schematic illustration of an atmospheric Cherenkov telescope array. The primary particle initiates an air shower, resulting in a cone of Cherenkov radiation. Telescopes within the Cherenkov light pool record elliptical images; the intersection of the long axes of these images indicates the arrival direction of the primary, and hence the location of a γ-ray source in the sky.

The measurable differences in Cherenkov image orientation and morphology provide the background discrimination which makes ground-based γ-ray astronomy possible. For point-like sources, such as distant Active Galactic Nuclei (AGNs), modern instruments can reject up to 99.999% of the triggered cosmic-ray events, while retaining up to 50% of the γ-ray population. In the case of spatially extended sources, such as Galactic supernova remnants (SNR), the background rejection is less efficient, but the technique can be used to produce γ-ray maps of the emission from the source. The angular resolution depends upon the energy of the primary γ-ray, but is typically 0.1° per event (68% containment radius) at energies above a few hundred GeV.

The total Cherenkov yield from the air shower is proportional to the energy of the primary particle. The image intensity, combined with the reconstructed distance of the shower core from each telescope, can therefore be used to estimate the primary energy. The energy resolution of this technique, also energy-dependent, is typically 15–20% at energies above a few hundred GeV. Energy spectra of γ-ray sources can be measured over a wide range; potentially from ∼50 GeV to ∼100 TeV, depending upon the instrument characteristics, source strength, and exposure time. To a first approximation, the lower energy threshold at the trigger level, E_T, depends upon the mirror area, A, the photon collection efficiency, $\eta(\lambda)$, the Cherenkov light yield, $C(\lambda)$, the night sky background light, $B(\lambda)$, the solid angle, Ω, and the trigger resolving time, τ, as follows [21]:

$$E_T \propto \frac{1}{C(\lambda)} \sqrt{\frac{B(\lambda)\Omega\tau}{\eta(\lambda)A}} \qquad (34.3)$$

In practice, this function may be modified by the properties of the detector; for example, by complex, multi-level, combinatorial trigger

systems and highly pixellated fields of view. In addition, the useful scientific threshold, after the application of analysis cuts to select γ-ray events, is always somewhat higher than this.

The first astrophysical source to be convincingly detected using the imaging atmospheric Cherenkov technique was the Crab Nebula [22], with a flux of 2.1×10^{-11} photons cm^{-2} s^{-1} above 1 TeV [23]. Modern arrays have sensitivity sufficient to detect sources with 1% of the Crab Nebula flux in a few tens of hours. The TeV source catalog now consists of more than 140 sources (see e.g. Ref. 24). The majority of these were detected by scanning the Galactic plane from the southern hemisphere with the H.E.S.S. telescope array [25].

Major upgrades of the existing arrays have recently been completed, including the addition of a 28 m diameter central telescope to H.E.S.S. (H.E.S.S. II). Prototyping is also underway for the next generation instrument, the Cherenkov Telescope Array (CTA), which will consist of a northern and a southern hemisphere observatory, with a combined total of more than 100 telescopes [26]. Telescopes of three different sizes are planned, spread over an area of > 1 km^2, providing wide energy coverage and an order of magnitude improvement in sensitivity. Baseline telescope designs are similar to existing devices, but technological developments such as dual mirror optics and silicon photo-detectors are also under investigation.

34.3. Large neutrino detectors

34.3.1. *Deep liquid detectors for rare processes* :

Revised September 2013 by K. Scholberg & C.W. Walter (Duke University)

Deep, large detectors for rare processes tend to be multi-purpose with physics reach that includes not only solar, reactor, supernova and atmospheric neutrinos, but also searches for baryon number violation, searches for exotic particles such as magnetic monopoles, and neutrino and cosmic-ray astrophysics in different energy regimes. The detectors may also serve as targets for long-baseline neutrino beams for neutrino oscillation physics studies. In general, detector design considerations can be divided into high-and low-energy regimes, for which background and event reconstruction issues differ. The high-energy regime, from about 100 MeV to a few hundred GeV, is relevant for proton decay searches, atmospheric neutrinos and high-energy astrophysical neutrinos. The low-energy regime (a few tens of MeV or less) is relevant for supernova, solar, reactor and geological neutrinos.

Table 34.1: Properties of large detectors for rare processes. If total target mass is divided into large submodules, the number of subdetectors is indicated in parentheses.

Detector	Mass, kton (modules)	PMTs (diameter, cm)	ξ	p.e./MeV	Dates
Baksan	0.33, scint (3150)	1/module (15)	segmented	40	1980–
MACRO	0.56, scint (476)	2-4/module (20)	segmented	18	1989–2000
LVD	1, scint. (840)	3/module (15)	segmented	15	1992–
KamLAND	0.41^f, scint	1325(43)+554(51)*	34%	460	2002–
Borexino	0.1^f, scint	2212 (20)	30%	500	2007–
SNO+	0.78, scint	9438 (20)	54%	400–900	2014–
CHOOZ	0.005, scint (Gd)	192 (20)	15%	130	1997–1998
Double Chooz	0.017, scint (Gd)(2)	534/module (20)	13%	180	2011–
Daya Bay	0.160, scint (Gd)(8)	192/module (20)	5.6%†	100	2011–
RENO	0.032, scint (Gd)(2)	342/module (25)	12.6%	100	2011–
IMB-1	3.3^f, H_2O	2048 (12.5)	1%	0.25	1982–1985
IMB-2	3.3^f, H_2O	2048 (20)	4.5%	1.1	1987–1990
Kam I	$0.88/0.78^f$, H_2O	1000/948 (50)	20%	3.4	1983–1985
Kam II	1.04^f, H_2O	948 (50)	20%	3.4	1986–1990
Kam III	1.04^f, H_2O	948 (50)	20%‡	4.3	1990–1995
SK I	22.5^f, H_2O	11146 (50)	39%	6	1996–2001
SK II	22.5^f, H_2O	5182 (50)	19%	3	2002–2005
SK III+	22.5^f, H_2O	11129 (50)	39%	6	2006–
SNO	1, D_2O/1.7, H_2O	9438 (20)	31% §	9	1999–2006

f indicates typical fiducial mass used for data analysis; this may vary by physics topic.

* The 51 cm PMTs were added in 2003.

† The effective Daya Bay coverage is 12% with top and bottom reflectors.

‡ The effective Kamiokande III coverage was 25% with light collectors.

§ The effective SNO coverage was 54% with light collectors.

Large water Cherenkov and scintillator detectors (see Table 34.1) usually consist of a volume of transparent liquid viewed by photomultiplier tubes (PMTs) (see Sec. 33.2); the liquid serves as active target. PMT hit charges and times are recorded and digitized, and triggering is usually based on coincidence of PMT hits within a time window comparable to the detector's light-crossing time. Because photosensors lining an inner surface represent a driving cost that scales as surface area, very large volumes can be used for comparatively reasonable cost. Some detectors are segmented into subvolumes individually viewed by PMTs, and may include other detector elements (*e.g.*, tracking detectors). Devices to increase light collection, *e.g.*, reflectors or waveshifter plates, may be employed. A common configuration is to have at least one concentric outer layer of liquid material separated from the inner part of the detector to serve as shielding against ambient background. If optically separated and instrumented with PMTs, an outer layer may also serve as an active veto against entering cosmic rays and other background events. The PMTs for large detectors typically range in size from 20 cm to 50 cm diameter, and typical quantum efficiencies are in the 20–25% range. The active liquid volume requires purification and there may be continuous recirculation of liquid. For large homogeneous detectors, the event interaction vertex is determined using relative timing of PMT hits, and energy deposition is determined from the number of recorded photoelectrons. A "fiducial volume" is usually defined within the full detector volume, some distance away from the PMT array. Inside the fiducial volume, enough PMTs are illuminated per event that reconstruction is considered reliable, and furthermore, entering background from the enclosing walls is suppressed by a buffer of self-shielding. PMT and detector optical parameters are calibrated using laser, LED, or other light sources. Quality of event reconstruction typically depends on photoelectron yield, pixelization and timing.

Because in most cases one is searching for rare events, large detectors are usually sited underground to reduce cosmic-ray-related background (see Chapter 28). The minimum depth required varies according to the physics goals [27].

34.3.1.1. *Liquid scintillator detectors:*

Past and current large underground detectors based on hydrocarbon scintillators include LVD, MACRO, Baksan, Borexino, KamLAND and SNO+. Experiments at nuclear reactors include CHOOZ, Double CHOOZ, Daya Bay, and RENO. Organic liquid scintillators (see Sec. 33.3.0) for large detectors are chosen for high light yield and attenuation length, good stability, compatibility with other detector materials, high flash point, low toxicity, appropriate density for mechanical stability, and low cost. They may be doped with waveshifters and stabilizing agents. Popular choices are pseudocumene (1,2,4-trimethylbenzene) with a few g/L of the PPO (2,5-diphenyloxazole) fluor, and linear alkylbenzene (LAB). In a typical detector configuration there will be active or passive regions of undoped scintillator, non-scintillating mineral oil or water surrounding the inner neutrino target volume. A thin vessel or balloon made of nylon, acrylic or other material transparent to scintillation light may contain the inner target; if the scintillator is buoyant with respect to its buffer, ropes may hold the balloon in place. For phototube surface coverages in the 20–40% range, yields in the few hundreds of photoelectrons per MeV of energy deposition can be obtained. Typical energy resolution is about $7\%/\sqrt{E(\mathrm{MeV})}$, and typical position reconstruction resolution is a few tens of cm at ~ 1 MeV, scaling as $\sim N^{-1/2}$, where N is the number of photoelectrons detected.

Shallow detectors for reactor neutrino oscillation experiments require excellent muon veto capabilities. For $\bar{\nu}_e$ detection via inverse beta decay on free protons, $\bar{\nu}_e + p \to n + e^+$, the neutron is captured by a proton on a $\sim$180 μs timescale, resulting in a 2.2 MeV γ ray, observable by Compton scattering and which can be used as a tag in coincidence with the positron signal. The positron annihilation γ rays may also contribute. Inverse beta decay tagging may be improved by addition of Gd at $\sim$0.1% by mass, which for natural isotope abundance has a $\sim$49,000 barn cross-section for neutron capture (in contrast to the 0.3 barn cross-section for capture on free protons). Gd capture takes $\sim$30 μs, and is followed by a cascade of γ rays adding up to about 8 MeV. Gadolinium doping of scintillator requires specialized formulation to ensure adequate attenuation length and stability.

Scintillation detectors have an advantage over water Cherenkov detectors in the lack of Cherenkov threshold and the high light yield. However, scintillation light emission is nearly isotropic, and therefore directional capabilities are relatively weak. Liquid scintillator is especially suitable for detection of low-energy events. Radioactive backgrounds are a serious issue, and include long-lived cosmogenics. To go below a few MeV, very careful selection of materials and purification of the scintillator is required (see Sec. 34.6). Fiducialization and tagging can reduce background. One can also dissolve neutrinoless double beta decay ($0\nu\beta\beta$) isotopes in scintillator. This has been realized by KamLAND-Zen, which deployed a 1.5 m-radius balloon containing enriched Xe dissolved in scintillator inside KamLAND, and ^{130}Te is considered for SNO+. Although energy resolution is poor compared to typical $0\nu\beta\beta$ search experiments, the quantity of isotope can be so large that the kinematic signature of $0\nu\beta\beta$ would be visible as a clear feature in the spectrum.

34.3.1.2. *Water Cherenkov detectors:*

Very large imaging water detectors reconstruct ten-meter-scale Cherenkov rings produced by charged particles (see Sec. 33.5.0). The first such large detectors were IMB and Kamiokande. The only currently existing instance of this class of detector, with fiducial volume of 22.5 kton and total mass of 50 kton, is Super-Kamiokande (Super-K). For volumes of this scale, absorption and scattering of Cherenkov light are non-negligible, and a wavelength-dependent factor $\exp(-d/L(\lambda))$ (where d is the distance from emission to the sensor and $L(\lambda)$ is the attenuation length of the medium) must be included in the integral of Eq. (33.5) for the photoelectron yield. Attenuation lengths on the order of 100 meters have been achieved.

Cherenkov detectors are excellent electromagnetic calorimeters, and the number of Cherenkov photons produced by an e/γ is nearly proportional to its kinetic energy. For massive particles, the number of photons produced is also related to the energy, but not linearly. For any type of particle, the *visible energy* E_{vis} is defined as the energy of an electron which would produce the same number of Cherenkov photons. The number of collected photoelectrons depends on the scattering and attenuation in the water along with the photocathode coverage, quantum efficiency and the optical parameters of any external light collection systems or protective material surrounding them. Event-by-event corrections are made for geometry and attenuation. For a typical case, in water $N_{\mathrm{p.e.}} \sim 15\,\xi\,E_{\mathrm{vis}}(\mathrm{MeV})$, where ξ is the effective fractional photosensor coverage. Cherenkov photoelectron yield per MeV of energy is relatively small compared to that for scintillator, *e.g.*, $\sim$ 6 pe/MeV for Super-K with a PMT surface coverage of $\sim$ 40%. In spite of light yield and Cherenkov threshold issues, the intrinsic directionality of Cherenkov light allows individual particle tracks to be reconstructed. Vertex and direction fits are performed using PMT hit charges and times, requiring that the hit pattern be consistent with a Cherenkov ring.

High-energy ($\sim$100 MeV or more) neutrinos from the atmosphere or beams interact with nucleons; for the nucleons bound inside the ^{16}O nucleus, nuclear effects must be considered both at the interaction and as the particles leave the nucleus. Various event topologies can be distinguished by their timing and fit patterns, and by presence or absence of light in a veto. "Fully-contained" events are those for which the neutrino interaction final state particles do not leave the inner part of the detector; these have their energies relatively well measured. Neutrino interactions for which the lepton is not contained in the inner detector sample have higher-energy parent neutrino energy distributions. For example, in "partially-contained" events, the neutrino interacts inside the inner part of the detector but the lepton (almost always a muon, since only muons are penetrating) exits. "Upward-going muons" can arise from neutrinos which interact in the rock below the detector and create muons which enter the detector and either stop, or go all the way through (entering downward-going muons cannot be distinguished from cosmic rays). At high energies, multi-photoelectron hits are likely and the charge collected by each PMT (rather than the number of PMTs firing) must be used; this degrades the energy resolution to approximately $2\%/\sqrt{\xi\,E_{\mathrm{vis}}(\mathrm{GeV})}$. The absolute energy scale in this regime can be known to $\approx$2–3% using cosmic-ray muon energy deposition, Michel electrons and π^0

from atmospheric neutrino interactions. Typical vertex resolutions for GeV energies are a few tens of cm [28]. Angular resolution for determination of the direction of a charged particle track is a few degrees. For a neutrino interaction, because some final-state particles are usually below Cherenkov threshold, knowledge of direction of the incoming neutrino direction itself is generally worse than that of the lepton direction, and dependent on neutrino energy.

Multiple particles in an interaction (so long as they are above Cherenkov threshold) may be reconstructed, allowing for the exclusive reconstruction of final states. In searches for proton decay, multiple particles can be kinematically reconstructed to form a decaying nucleon. High-quality particle identification is also possible: γ rays and electrons shower, and electrons scatter, which results in fuzzy rings, whereas muons, pions and protons make sharp rings. These patterns can be quantitatively separated with high reliability using maximum likelihood methods [29]. A e/μ misidentification probability of $\sim 0.4\%/\xi$ in the sub-GeV range is consistent with the performance of several experiments for $4\% < \xi < 40\%$. Sources of background for high energy interactions include misidentified cosmic muons and anomalous light patterns when the PMTs sometimes "flash" and emit photons themselves. The latter class of events can be removed using its distinctive PMT signal patterns, which may be repeated. More information about high energy event selection and reconstruction may be found in reference [30].

In spite of the fairly low light yield, large water Cherenkov detectors may be employed for reconstructing low-energy events, down to *e.g.* $\sim$ 4-5 MeV for Super-K [31]. Low-energy neutrino interactions of solar neutrinos in water are predominantly elastic scattering off atomic electrons; single electron events are then reconstructed. At solar neutrino energies, the visible energy resolution ($\sim 30\%/\sqrt{\xi\, E_{\rm vis}(\rm MeV)}$) is about 20% worse than photoelectron counting statistics would imply. Using an electron LINAC and/or nuclear sources, Approximately 0.5% determination of the absolute energy scale has been achieved at solar neutrino energies. Angular resolution is limited by multiple scattering in this energy regime (25–30°). At these energies, radioactive backgrounds become a dominant issue. These backgrounds include radon in the water itself or emanated by detector materials, and γ rays from the rock and detector materials. In the few to few tens of MeV range, radioactive products of cosmic-ray-muon-induced spallation are troublesome, and are removed by proximity in time and space to preceding muons, at some cost in dead time.

The Sudbury Neutrino Observatory (SNO) detector [32] is the only instance of a large heavy water detector and deserves mention here. In addition to an outer 1.7 kton of light water, SNO contained 1 kton of D_2O, giving it unique sensitivity to neutrino neutral current ($\nu_x + d \to \nu_x + p + n$), and charged current ($\nu_e + d \to p + p + e^-$) deuteron breakup reactions. The neutrons were detected in three ways: In the first phase, via the reaction $n + d \to t + \gamma + 6.25$ MeV; Cherenkov radiation from electrons Compton-scattered by the γ rays was observed. In the second phase, NaCl was dissolved in the water. ^{35}Cl captures neutrons, $n + {}^{35}\mathrm{Cl} \to {}^{36}\mathrm{Cl} + \gamma + 8.6$ MeV. The γ rays were observed via Compton scattering. In a final phase, specialized low-background ^{3}He counters ("neutral current detectors" or NCDs) were deployed in the detector. These counters detected neutrons via $n + {}^3\mathrm{He} \to p + t + 0.76$ MeV; ionization charge from energy loss of the products was recorded in proportional counters.

34.3.2. *Neutrino telescopes* :

Written Nov. 2013 by Ch. Spiering (DESY/Zeuthen) and U.F. Katz (Univ. Erlangen)

The primary goal of neutrino telescopes (NTs) is the detection of astrophysical neutrinos, in particularly those which are expected to accompany the production of high-energy cosmic rays in astrophysical accelerators. NTs in addition address a variety of other fundamental physics issues like indirect search for dark matter, study of neutrino oscillations, search for exotic particles like magnetic monopoles or study of cosmic rays and their interactions [33,34,35].

NTs are large-volume arrays of "optical modules" (OMs) installed in open transparent media like water or ice, at depths that completely block the daylight. The OMs record the Cherenkov light induced by charged secondary particles produced in reactions of high-energy neutrinos in or around the instrumented volume. The neutrino energy, E_ν, and direction can be reconstructed from the hit pattern recorded. NTs typically target an energy range $E_\nu \gtrsim 100\,\mathrm{GeV}$; sensitivity to lower energies is achieved in dedicated setups with denser instrumentation.

In detecting cosmic neutrinos, three sources of backgrounds have to be considered: (i) *atmospheric neutrinos* from cosmic-ray interactions in the atmosphere, which can be separated from cosmic neutrinos only on a statistical basis; (ii) down-going punch-through *atmospheric muons* from cosmic-ray interactions, which can be avoided/reduced by selecting upward-going or high-energy muons and are suppressed by several orders of magnitude with respect to the ground level due to the large detector depths; (iii) random backgrounds due to photomultiplier (PMT) dark counts, ^{40}K decays (mainly in sea water) or bioluminescence (only water), which impact adversely on event recognition and reconstruction. Note that atmospheric neutrinos and muons allow for investigating neutrino oscillations and cosmic ray anisotropies, respectively.

34.3.2.1. *Basic principles and parameters:*

Neutrinos can interact with target nucleons N through charged current ($\overset{(-)}{\nu}_\ell N \to \ell^\mp X$, CC) or neutral current ($\overset{(-)}{\nu}_\ell N \to \overset{(-)}{\nu}_\ell X$, NC) processes. A CC reaction of a $\overset{(-)}{\nu}_\mu$ produces a muon track and a hadronic particle cascade, whereas all NC reactions and CC reactions of $\overset{(-)}{\nu}_e$ produce particle cascades only. CC interactions of $\overset{(-)}{\nu}_\tau$ can have either signature, depending on the τ decay mode. In most astrophysical models, neutrinos are produced through the $\pi/K \to \mu \to e$ decay chain, *i.e.*, with a flavour ratio $\nu_e : \nu_\mu : \nu_\tau \approx 1 : 2 : 0$. For sources outside the solar system, neutrino oscillations turn this ratio to $\nu_e : \nu_\mu : \nu_\tau \approx 1 : 1 : 1$ upon arrival on Earth.

The total neutrino-nucleon cross section is about $10^{-35}\,\mathrm{cm}^2$ at $E_\nu = 1\,\mathrm{TeV}$ and rises roughly linearly with E_ν below this energy and as $E_\nu^{0.3-0.5}$ above, flattening out towards high energies. The CC:NC cross-section ratio is about 2:1. At energies above some TeV, neutrino absorption in the Earth becomes significant; for vertically upward-moving neutrinos (zenith angle $\theta = 180°$), the survival probability is $74\,(27, < 2)\%$ for $10\,(100, 1000)\,\mathrm{TeV}$. On average, between 50% (65%) and 75% of E_ν is transfered to the final-state lepton in neutrino (antineutrino) reactions between 100 GeV and 10 PeV.

The final-state lepton follows the initial neutrino direction with a RMS mismatch angle $\langle \phi_{\nu\ell} \rangle \approx 1.5°/\sqrt{E_\nu\,[\mathrm{TeV}]}$, indicating the intrinsic kinematic limit to the angular resolution of NTs. For CC $\overset{(-)}{\nu}_\mu$ reactions at energies above a few TeV, the angular resolution is dominated by the muon reconstruction accuracy of a few times 0.1° at most. For muon energies $E_\mu \gtrsim 1\,\mathrm{TeV}$, the increasing light emission due to radiative processes allows for reconstructing E_μ from the measured dE_μ/dx with an accuracy of $\sigma(\log E_\mu) \approx 0.3$; at lower energies, E_μ can be estimated from the length of the muon track if it is contained in the detector. These properties make CC $\overset{(-)}{\nu}_\mu$ reactions the prime channel for the identification of individual astrophysical neutrino sources.

Particle cascades at the relevant energies are 5–20 m long, *i.e.*, short compared to typical OM distances. The total amount of Cherenkov light provides a direct measurement of the cascade energy with an accuracy of about 30% (15% at high energies) for events contained in the instrumented volume. Neutrino flavour and reaction mechanism can, however, hardly be determined and neutrinos from NC reactions or τ decays may carry away significant "invisible" energy. The directional reconstruction accuracy of cascades is a few degrees at best. These features, together with the small background of atmospheric $\overset{(-)}{\nu}_e$ and $\overset{(-)}{\nu}_\tau$ events, makes the cascade channel particularly interesting for searches for a diffuse, high-energy excess of extraterrestrial over atmospheric neutrinos.

The detection efficiency of a NT is quantified by its effective area, *e.g.*, the fictitious area for which the full incoming neutrino flux would be recorded (see Fig. 34.3). The increase with E_ν is due to the rise of neutrino cross section and muon range, while neutrino absorption in the Earth causes the decrease at large θ. Identification of downward-going neutrinos requires strong cuts against atmospheric muons, hence the cut-off towards low E_ν. Due to the small cross section, the effective area is many orders of magnitude smaller than the geometrical dimension of the detector; a $\overset{(-)}{\nu}_\mu$ with 1 TeV can, *e.g.*, be detected with a probability of the order 10^{-6} if the telescope is on

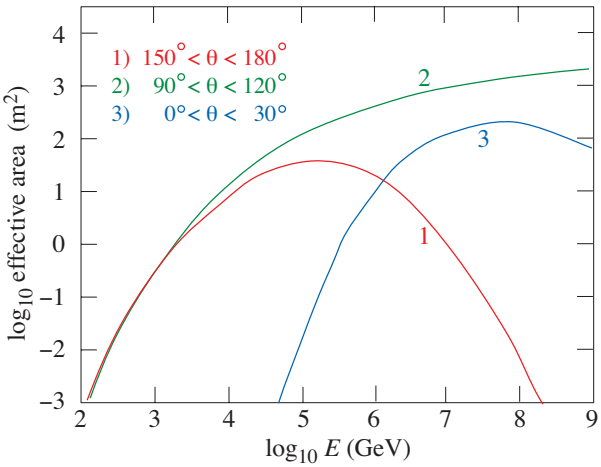

Figure 34.3: Effective $\overline{\nu}_\mu$ area for IceCube as an example of a cubic-kilometre NT, as a function of neutrino energy for three intervals of θ. The effective areas shown here correspond to a specific event selection for point source searches.

its path.

Note that the fields of view of NTs at the South Pole and in the Northern hemisphere are complementary for each reaction channel and neutrino energy.

34.3.2.2. *The Projects:*

Noise rates measured by 25 cm PMTs in deep polar ice are about 0.5 kHz per PMT and almost entirely due to radioactivity in the OM components. The corresponding rates in sea water are typically 60 kHz, mostly due to ^{40}K decays. Bioluminescence activity can temporarily cause rates on the MHz scale. Experience from ANTARES shows that these backgrounds are manageable without a major loss of efficiency or experimental resolution.

34.3.2.4. *Technical realisation:*

Optical modules (OMs) and PMTs: An OM is a pressure-tight glass sphere housing one or several PMTs with a time resolution in the nanosecond range, and in most cases also electronics for control, HV generation, operation of calibration LEDs, time synchronisation and signal digitisation.

Hybrid PMTs with 37 cm diameter have been used for NT-200, conventional hemispheric PMTs for AMANDA (20 cm) and for ANTARES and IceCube (25 cm). A novel concept has been chosen for KM3NeT. The OMs (43 cm) will be equipped with 31 PMTs (7.5 cm), plus control, calibration and digitisation electronics. The main advantages are that (i) the overall photocathode area exceeds that of a 25 cm PMT by more than a factor of 3; (ii) the individual readout of the PMTs results in a very good separation between one- and two-photoelectron signals which is essential for online data filtering and random background suppression; (iii) some directional information is provided; (iv) no mu-metal shielding against the Earth magnetic field is required. Figure 34.4 shows the OM designs of IceCube and KM3NeT.

Table 34.2: Past, present and future neutrino telescope projects and their main parameters. The milestone years give the times of project start, of first data taking with partial configurations, of detector completion, and of project termination. The size refers to the largest instrumented volume reached during the project development. See [35] for references to the different projects where unspecified.

Experiment	Milestones	Medium/Location	Size (km^3)	Remarks
DUMAND	1978/–/–/1995	Pacific/Hawaii		Terminated due to technical/funding problems
NT-200	1980/1993/1998/–	Lake Baikal	10^{-4}	First proof of principle
NESTOR	1991/–/–/–	Med. Sea		2004 data taking with prototype
NEMO	1998/–/–/–	Med. Sea		R&D project, prototype tests
AMANDA	1990/1996/2000/2009	Ice/South Pole	0.015	First deep-ice neutrino telescope
ANTARES	1997/2006/2008/–	Med. Sea	0.010	First deep-sea neutrino telescope
IceCube	2001/2005/2010/–	Ice/South Pole	1.0	First km^3-sized detector
KM3NeT	2013/(2015)/–/–	Med. Sea	3–4	First construction phase starts 2014
PINGU [36]	2014/–/–/–	Ice/South Pole	0.003	planned low-energy extension of IceCube
GVD	2012/(2015)/–/–	Lake Baikal	0.5–1.5	Sparse instrumentation, prototype tests ongoing

34.3.2.3. *Properties of media:*

The efficiency and quality of event reconstruction depend strongly on the optical properties (absorption and scattering length, intrinsic optical activity) of the medium in the spectral range of bialkali photocathodes (300–550 nm). Large absorption lengths result in a better light collection, large scattering lengths in superior angular resolution. Deep-sea sites typically have effective scattering lengths of > 100 m and, at their peak transparency around 450 nm, absorption lengths of 50–65 m. The absorption length for Lake Baikal is 22–24 m. The properties of South Polar ice vary strongly with depth; at the peak transparency wave length (400 nm), the scattering length is between 5 and 75 m and the absorption length between 15 and 250 m, with the best values in the depth region 2200–2450 m and the worst ones in the layer 1950–2100 m.

Readout and data filtering:

In current NTs the PMT data are digitised in situ, for ANTARES and Baikal-GVD in special electronics containers close to the OMs, for IceCube and KM3NeT inside the OMs. For IceCube, data are transmitted via electrical cables (2.5 km from OM to counting house), for ANTARES and KM3NeT optical fibre connections have been chosen (several 10 km).

The full digitised waveforms of the IceCube OMs are transmitted to the surface for pulses appearing in local coincidences on a string; for other pulses, only time and charge information is provided. For ANTARES (time and charge) and KM3NeT (time over threshold), all PMT signals above an adjustable noise threshold are sent to shore.

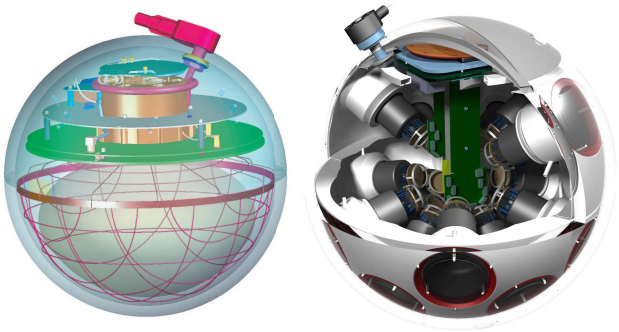

Figure 34.4: Schematic views of the digital OMs of IceCube (left) and KM3NeT (right).

The raw data are subsequently processed on online computer farms, where multiplicity and topology-driven filter algorithms are applied to select event candidates. The filter output data rate is about 10 GByte/day for ANTARES and of the order 1 TByte/day for IceCube (100 GByte/day transfered via satellite) and KM3NeT.
Calibration: For efficient event recognition and reconstruction, the OM timing must be synchronised at the few-nanosecond level and the OM positions and orientations must be known to a few 10 cm and a few degrees, respectively. Time calibration is achieved by sending synchronisation signals to the OM electronics and also by light calibration signals emitted by LED or laser flashers emitted in situ at known times (ANTARES, KM3NeT). Precise position calibration is achieved by measuring the travel time of light calibration signals sent from OM to OM (IceCube) or acoustic signals sent from transducers at the sea floor to receivers on the detector strings (ANTARES, KM3NeT).
Detector configurations: IceCube (see Fig. 34.5) consists of 5160 Digital OMs (DOMs) installed on 86 strings at depths of 1450 to 2450 m in the Antarctic ice; except for the DeepCore region, string distances are 125 m and vertical distances between OMs 17 m. 324 further DOMs are installed in IceTop, an array of detector stations on the ice surface above the strings. DeepCore is a high-density sub-array at large depths (*i.e.*, in the best ice layer) at the centre of IceCube.

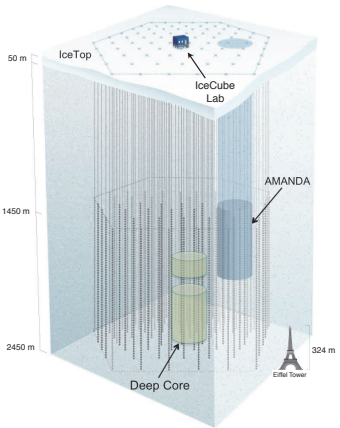

Figure 34.5: Schematic view of the IceCube NT. Operation of AMANDA was terminated in 2009.

The NT200 detector in Lake Baikal at a depth of 1100 m consists of 8 strings attached to an umbrella-like frame, with 12 pairs of OMs per string. The diameter of the instrumented volume is 42 m, its height 70 m. The Baikal collaboration is testing engineering setups for a cubic-kilometre array with several 1000 OMs (Gigaton Volume Detector, GVD).

ANTARES comprises 12 strings with lateral distances of 60–70 m, each carrying 25 triplets of OMs at vertical distances of 14.5 m. The OMs are located at depths 2.1–2.4 km, starting 100 m above the sea floor. A further string carries devices for calibration and environmental monitoring. A system to investigate the feasibility of acoustic neutrino detection is also implemented.

KM3NeT will be a distributed research infrastructure constructed at three sites (near Toulon; near Capo Passero, East of Sicily; near Pylos, West of the Peloponnesos). KM3NeT will consist of six building blocks of 115 strings each, with 18 OMs per string at vertical distances of 36 m. The lateral distance between adjacent strings will be 90 m. In a first construction phase starting in 2014 the shore and sea-bed infrastructure will be prepared at the Toulon and Capo Passero sites and about 40 strings will be deployed.

34.3.2.5. *Results:*
Atmospheric neutrino fluxes have been pecisely measured with AMANDA and ANTARES ($\overset{(-)}{\nu}_\mu$) and with IceCube ($\overset{(-)}{\nu}_\mu, \overset{(-)}{\nu}_e$); the results are in agreement with predicted spectra. No astrophysical point sources have been identified yet, and no indications of neutrino fluxes from dark matter annihilations or of exotic phenomena have been found (see [35] and references therein). A diffuse excess of track and cascade events between 30 TeV and 1 PeV has recently been reported by IceCube [37]; this analysis for the first time employs containment conditions and an atmospheric muon veto for suppression of down-going atmospheric neutrinos. The observed excess can hardly be explained by atmospheric neutrinos and misidentified atmospheric muons alone (see [38], Part II). At lower energies, down to 10 GeV, IceCube/DeepCore and ANTARES have identified clear signals of oscillations of atmospheric neutrinos. Also, IceCube has reported an energy-dependent anisotropy of cosmic-ray induced muons. See [38] and [39] for summaries of recent results.

34.3.2.6. *Future plans:*
As an extension of IceCube, further, substantially denser instrumentation of the DeepCore sub-volume is planned, leading to an E_ν threshold for neutrino detection of a few GeV. This project (Phased IceCube Next Generation Upgrade, PINGU) [36] primarily aims at measuring the neutrino mass hierarchy using matter-induced oscillation effects of atmospheric neutrinos in the Earth. A large-volume extension of IceCube is discussed internally. A case study for a dense deep-sea detector with similar physics reach as PINGU is performed in the KM3NeT framework (Oscillation Research with Atmospheric Neutrinos in the Abyss, ORCA).

34.3.3. ***Coherent radio Cherenkov radiation detectors*** :
Revised February 2013 by S.R. Klein (LBNL/UC Berkeley)

Radio detectors sensitive to coherent Cherenkov radiation provide an attractive way to search for ultra-high energy cosmic neutrinos. These neutrinos are the only long-range probe of the ultra-high energy cosmos. Protons and heavier nuclei with energies $\gtrsim 5 \times 10^{19}$ eV are limited to ranges of less than 100 Mpc by interactions (photo-excitation) with CMB photons (the GZK effect [40]), and gamma rays pair-produce from the CMB. When the photoexcited protons/nuclei decay, they produce neutrinos. To detect a useful number of these cosmogenic ("GZK neutrinos") annually (assuming that ultra-high energy cosmic rays are protons) requires a detector of about 100 km^3 in volume. Optical attenuation lengths are less than 200 m in ice or water, so a 100 km^3 detector would require a prohibitive number of sensors.

An alternative is to look for the radio waves from the charged particle showers that are produced when neutrinos interact in a non-conducting medium, as discussed in Sec. 32. As Gurgen Askaryan pointed out [41], particle showers contain more electrons than positrons, so, for wavelengths larger than their transverse size, emit coherent Cherenkov radiation. The electric field strength is proportional to the neutrino energy; the radiated power goes as its square. Detectors with antennas placed in the active volume have thresholds around 10^{17} eV.

Radiodetection requires a medium with a long absorption length for radio waves. The huge target volumes require that this be a commonly available natural material, usually Antarctic ice or the lunar regolith [44]. Underground salt domes were also considered, but they appear to have too short an attenuation length for radio waves.

The radiation is peaked at the Cherenkov angle (about 56^o in ice). There, the shower produces a short ($\approx$ 1 ns wide) radio pulse.

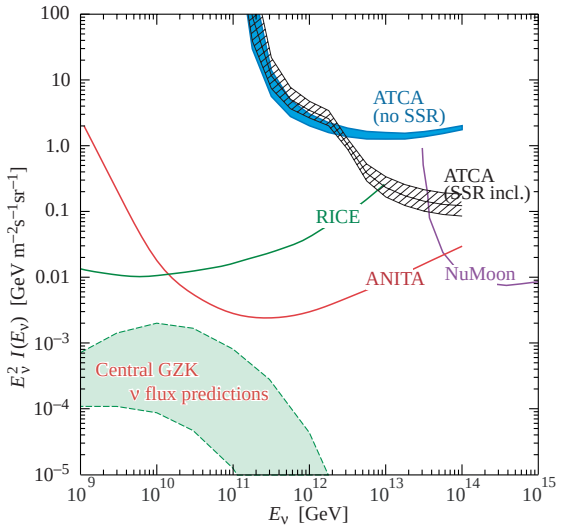

Figure 34.6: Representative ν flux limits from radio-detection experiments, illustrating the energy ranges for different techniques. Shown are limits from the Rice, ANITA, NuMoon and Lunaska (ATCA) collaborations. NuMoon and Lunaska are low and high frequency lunar scans respectively, showing the strengths of the two different frequency bands. The two limits for ATCA are for different models of the lunar regolith; their separation is a measure of the resultant uncertainty. Also shown, for comparison is the mid-range of flux predictions for GZK neutrinos from Ref. 47.

The electric field strength increases linearly with frequency, up to a cut-off wavelength set by the transverse size of the shower and the viewing angle [42,43]. The maximum cut-off is about 1 GHz in ice, and 2.5 GHz in rock/lunar regolith. Away from the Cherenkov angle, the spectrum cuts off at lower frequencies as the angular separation from the Cherenkov angle increases, and the pulse may be longer. The angular distribution broadens with decreasing frequency, and the frequency spectrum may be used to determine how close a detector is to the Cherenkov cone. This requires a broadband detector; it may also be necessary to account for dispersion and/or refraction as the signal travels from the interaction to the detector. The signal is linearly polarized pointing toward the shower axis. This polarization is a key diagnostic for radiodetection, and can be used to help determine the neutrino direction.

Radio detectors have observed cosmic-ray air showers in the atmosphere. The physics of radio-wave generation in air showers is more complex because there are contributions due to charge separation by charged particles, and from synchrotron radiation from $e^{\pm}$, both due to the Earth's magnetic field. Several experiments have also set limits on radiation due to magnetic monopoles.

34.3.3.1. *The Moon as a target:*

Because of its large size and non-conducting regolith, and the availability of large radio-telescopes, the Moon is an attractive target [45]. Several representative lunar experiments are listed in Table 34.3. Conventional radio-telescopes are reasonably well matched to lunar neutrino searches, with natural beam widths not too dissimilar from the size of the Moon. Still, there are some experimental challenges in understanding the signal. The composition of the lunar regolith is not well known, and the attenuation length for radio waves must be estimated. An attenuation length of 9/f(GHz) (m) is often used. The big limitation of lunar experiments is that the 240,000 km target-antenna separation leads to neutrino energy thresholds far above 10^{20} eV.

The frequency range affects the sensitive volume. At low frequencies, radiation is relatively isotropic, so signals can be detected from most of the Moon's surface, for most angles of incidence. At higher frequencies, the electric field is stronger, but radiation is concentrated near the Cherenkov angle, and the geometry limits the sensitivity to interactions near the Moon's limb, where the neutrino also arrives within a fairly narrow angular range. The larger high-frequency attenuation limits the depth below the surface that is probed.

Table 34.3: Experiments that have set limits on neutrino interactions in the Moon [44]. Some current limits are shown in Fig. 34.6.

Experiment	Year	Dish Size	Frequency	Bandwidth	Obs. Time
Parkes	1995	64 m	1425 MHz	500 MHz	10 hrs
Glue	1999+	70 m, 34 m	2200 MHz	40-150 MHz	120 hrs
NuMoon	2008	11×25 m	115–180 MHz	—	50 hrs
Lunaska	2008	3× 22 m	1200–1800 MHz	—	6 nights
Resun	2008	4× 25 m	1450 MHz	50 MHz	45 hours

So, higher frequency searches probe lower neutrino energies, but lower frequency searches can set tighter flux limits on high-energy neutrinos. An alternative approach, increasingly viable with modern technology, is to search over a wide frequency range. This introduces a technical challenge in the form of dispersion (frequency dependent time delays) in the ionosphere. The Parkes experiment pioneered the use of de-dispersion filters; this has been taken to a high art by the Lunaska collaboration.

Lunar experiments use several techniques to reject backgrounds, which are mostly anthropogenic. Many experiments use multiple antennas, separated by at least hundreds of meters; by requiring a coincidence within a small time window, anthropogenic noise can be rejected. An alternative approach is to use beam forming with multiple receivers in a single antenna, to ensure that the signal points back to the Moon. The limits set by representative lunar experiments are shown in Fig. 34.6.

In the near future, several large radio detector arrays should reach significantly lower limits. The LOFAR array is beginning to take data with 36 detector clusters spread over Northwest Europe [46]. In the longer term, the Square Kilometer Array (SKA) with 1 km^2 effective area will push thresholds down to near 10^{20} eV.

34.3.3.2. *The ANITA balloon experiment:*

To reduce the energy threshold, it is necessary to reduce the antenna-target separation. One such experiment is the ANITA balloon experiment which made two flights around Antarctica, floating at an altitude around 35 km [47]. Its 40 (32 in the first flight) dual-polarization horn antennas scanned the polar ice cap out to the horizon (650 km away). The smaller source-detector separation led to an energy threshold just above 10^{19} eV, slightly above the peak of the GZK neutrino spectrum.

Because of the small angle of incidence, ANITA was able to make use of polarization information; ν signals should be vertically polarized, while most background from cosmic-ray air showers is expected to be horizontally polarized. The analysis treated the multiple antennas as an interferometer; the several-meter separation between antennas led to a pointing accuracy of 0.2-0.4^0 in elevation, and 0.5-1.1^0 in azimuth. The collaboration verified the resolution using radio emitters that they buried in the ice. They then used pointing to eliminate possible anthropogenic backgrounds from inhabited areas of Antarctica.

Antarctic experiments must consider the inhomogeneities in the ice: varying density in the upper ice (the firn) and the variation in radio attenuation length with temperature. ANITA also had to consider the surface roughness, which affects the transition from ice to air. All of these affect the propagation of radio-waves.

The 'firn,' the top 100-200 m of Antarctic ice, marks a gradual transition from packed snow at the surface to solid ice (density 0.92 g/cm^3) below. The index of refraction depends on the density, so radio waves bend downward. This curvature reduces the field of view of surface or aerial antennas.

The radio attenuation length depends on the frequency and ice temperature, with attenuation higher in warmer ice. A recent measurement, by the ARA collaboration at the South Pole found an average attenuation length of 670^{+180}_{-66} m [48]. On the Ross Ice Shelf, where the ice is warmer, ARIANNA measures attenuation lengths of 300-500 m, depending on frequency [49].

ANITA has also recently observed radio waves from cosmic-ray air

showers; these showers are differentiated from neutrino showers on the basis of the radio polarization and zenith angle distribution [50].

34.3.3.3. *Active Volume Detectors:*

The use of radio antennas located in the active volume was pioneered by the RICE experiment, which buried radio antennas in holes drilled for AMANDA [51] at the South Pole. RICE was comprised of 18 half-wave dipole antennas, sensitive from 200 MHz to 1 GHz, buried between 100 and 300 m deep. Each antenna fed an in-situ preamplifier which transmitted the signals to surface digitizing electronics. The array triggered when four or more stations fired within 1.2 μs, giving it a threshold of about 10^{17} eV.

Two groups are prototyping detectors, with the goal of a detector with an active volume in the 100 km^3 range. Both techniques are modular, so the detector volume scales roughly linearly with the available funding. The Askaryan Radio Array (ARA) is located at the South Pole, while the Antarctic Ross Iceshelf ANtenna Neutrino Array (ARIANNA) is on the Ross Ice Shelf. Both experiments are built of largely independent modules (clusters or stations, respectively), with local triggers based on coincidence between multiple antennas in a module.

One difference between the two experiments is the depth of their antennas. The ARA buries antennas up to 200 m deep in the ice, to avoid the firn, and consequently limited field of view. However, drilling holes raises the costs, and the limited hole diameter (15 cm in ARA) requires compromises between antenna design (particularly for horizontally polarized waves), mechanical support, power and communications. In contrast, ARIANNA places antennas in shallow, near-surface holes. This greatly simplifies deployment and avoid limitations on antenna design, but at a cost of reduced sensitivity to near-surface neutrino interactions.

The current ARA proposal, ARA-37 [48], calls for an array of 37 stations, each consisting of 16 embedded antennas deployed up to 200 m deep below the firn) in several 15-cm diameter boreholes. ARA will detect signals in the frequency range from 150 to 850 MHz for vertical polarization, and 250 MHz to 850 MHz for horizontal polarization. ARA plans to use bicone antennas for vertical polarization, and quad-slotted cylinders for horizontal polarization. The collaboration uses notch filters and surface veto antennas to eliminate most anthropogenic noise, and vetos events when aircraft are in the area, or weather balloons are being launched.

ARIANNA will be located on the Ross Ice Shelf, where ≈ 575 m of ice sits atop the Ross Sea [49]. The site was chosen because the ice-seawater interface is smooth there, so the interface acts as a mirror for radio waves. The major advantage of this approach is that ARIANNA is sensitive to downward going neutrinos, and should be able to see more of the Cherenkov cone for horizontal neutrinos. One disadvantage of the site is that the ice is warmer, so the radio attenuation length will be shorter. Each ARIANNA station will use 8 log-periodic dipole antennas, pointing downward and arranged in an octagon. The multiple antennas allow for single-station directional and polarization measurements.

34.4. Large time-projection chambers for rare event detection

Written August 2009 by M. Heffner (LLNL).

The Time Projection Chamber (TPC) concept (Sec. 33.6.5) has been applied to many projects outside of particle physics and the accelerator-based experiments for which it was initially developed. TPCs in non-accelerator particle physics experiments are principally focused on rare event detection (*e.g.*, neutrino and dark matter experiments) and the physics of these experiments can place dramatically different constraints on the TPC design (only extensions of the traditional TPCs are discussed here). The drift gas or liquid is usually the target or matter under observation and due to very low signal rates a TPC with the largest possible active mass is desired. The large mass complicates particle tracking of short and sometimes very low-energy particles. Other special design issues include efficient light collection, background rejection, internal triggering, and optimal energy resolution.

Backgrounds from γ rays and neutrons are significant design issues in the construction of these TPCs. These are generally placed deep underground to shield them from cosmogenic particles and are surrounded with shielding to reduce radiation from the local surroundings. The construction materials are carefully screened for radiopurity, as they are in close contact with the active mass and can be a significant source of background. The TPC excels in reducing this internal background because the mass inside the field cage forms one monolithic volume from which fiducial cuts can be made *ex post facto* to isolate quiet drift mass. The liquid (gas) can be circulated and purified to a very high level. Self-shielding in these large mass systems can be significant and the effect improves with density and size. (See Sec. 34.6.)

The liquid-phase TPC can have a high density at low pressure that results in very good self-shielding and compact installation with lightweight containment. The down sides are the need for cryogenics, slower charge drift, tracks shorter than typical electron diffusion distances, lower-energy resolution (*e.g.*, xenon) and limited charge readout options. Slower charge drift requires long electron lifetimes, placing strict limits on the oxygen and other impurities with high electron affinity. A significant variation of the liquid-phase TPC that improves the charge readout is the dual-phase TPC, where a gas phase layer is formed above the liquid into which the drifting electrons are extracted and amplified, typically with electroluminescence (*i.e.*, secondary scintillation or proportional scintillation (Fig. 34.7)). The successful transfer of electrons across the phase boundary requires careful control of its position and setting up an appropriate electric field.

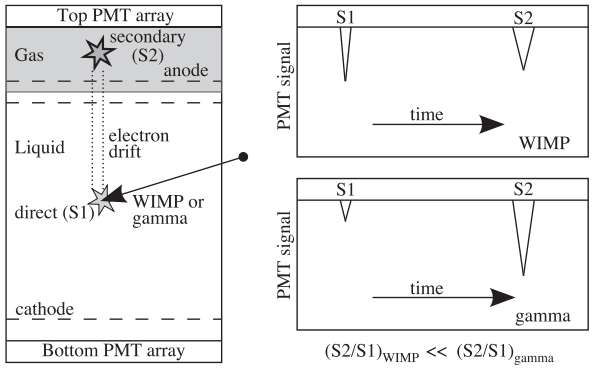

Figure 34.7: The configuration of a dual phase detector is shown on the left with the locations of where the primary and secondary light are generated. On the right is a schematic view of the signals of both an electron and nuclear interaction illustrating the discrimination power of this method. This figure is slightly modified from Ref. 52.

A high-pressure gas phase TPC has no cryogenics and density is easily optimized for the signal, but a large heavy-pressure vessel is required. Although self shielding is reduced, it can in some cases approach that of the liquid phase; in xenon at 50 atm the density is about half that of water or about 1/6 of liquid xenon. A significant feature of high pressure xenon gas is the energy resolution. Below a density of about 0.5 g cm^{-3} the intrinsic resolution is only a few times that of high purity germanium [53]. A neutrinoless double beta decay ($0\nu2\beta$) search with a TPC operated below this density limit could enjoy excellent energy resolution and maintain particle tracking for background rejection.

An observable interaction with the TPC results in a charged particle that travels in the drift matter, exciting and ionizing the atoms until the initial energy is converted into ionization, scintillation, or heat with relatively large fluctuations around the mean. Rare-event TPCs can be designed to detect scintillation light as well as charge to exploit the anti-correlation to improve energy resolution and/or signal to noise [54]. An electric drift field separates the electrons and positive ions from the ionization although the separation is not complete and some electrons are captured, exciting atoms and releasing more light than the primary excitation alone. The average partition between the scintillation and ionization can be manipulated to increase the ionization (at the expense of scintillation) by a number

of methods, such as increasing the strength of the electric field up to saturation of the ionization yield, increasing the temperature to enhance the diffusion of the ionized electrons, and adding dopants such as triethylamine that can be photoionized by the scintillation photons releasing more ionization.

Scintillation light is typically collected with photomultiplier tubes (PMTs) and avalanche photo diodes (APDs) although any fast (compared to the ionization drift speed) light collector capable of detecting the typically UV photons, maintaining high radiopurity, and perhaps withstanding pressure would work. (CCDs are slow and therefore only record two dimensions, integrating over the time direction. Some of the 3D information can be recovered by a few PMTs.) In most cases, coating the optics or adding a wavelength shifter is required [54], although some work has been done to directly readout the 175 nm light from xenon with a silicon detector. In a typical cylindrical geometry, the light detectors are placed at the ends on an equipotential of the field cage simplifying the design, but limiting the collection efficiency. The field cage can be made of UV-reflective materials such as Teflon, to increase the light-collection efficiency.

Charge collection can be accomplished with proportional avalanche in the manner used in a traditional TPC (even in the liquid state), although the final signal suffers from rather large fluctuations caused by small fluctuations early in the avalanche that are amplified by the process. Inductive readout of passing charges and direct collection of the unamplified charge do not rely on an avalanche, and are effective where energy resolution is of paramount importance, but depend on low-noise amplifiers and relatively large signals (*e.g.*, in $0\nu2\beta$ decay).

Electroluminescence can be used to proportionally amplify the the drifted ionization, and it does not suffer the fluctuations of an avalanche or the small signals of direct collection. It works by setting up at the positive end of the drift volume parallel meshes or wire arrays with an electric field larger than the drift field, but less than the field needed for avalanche. In xenon, this is 3–6 $\mathrm{kV\,cm^{-1}\,bar^{-1}}$ for good energy resolution. Eq. (34.4) shows the dependence of the yield (Y) in zenon in units of photons/(electron cm bar) as a function of pressure (p) in units of bar and electric field (E) in units of kV/cm [55]:

$$Y/p = 140\,E/p - 116\ . \tag{34.4}$$

The amplification can be adjusted with the length of the electroluminescence region, pressure and electric field.

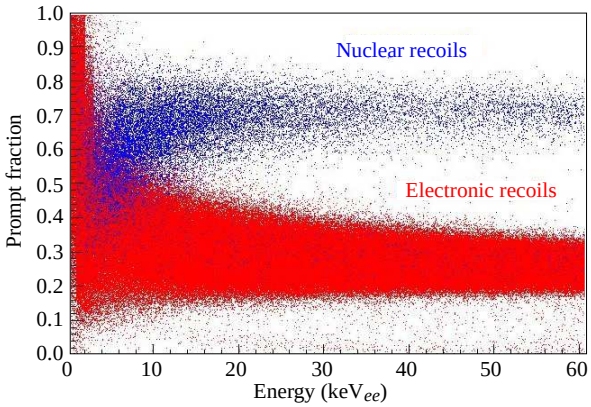

Figure 34.8: An example of pulse-shape discrimination of nuclear recoils and electrons in argon. The prompt fraction is a measure of the pulse shape that clearly separates the two interactions down to very low energy. Figure from Ref. 56.

Differentiation of nuclear and electron recoils at low-energy deposition is important as a means of background rejection. The nuclear recoil deposits a higher density of ionization than an electron recoil and this results in a higher geminate recombination resulting in a higher output of primary scintillation and lower charge. The ratio of scintillation to charge can be used to distinguish the two. In the case of an electroluminescence readout, this is done simply with the ratio of primary light to secondary light. Optically transparent grids with PMT or APD readout combine to make a elegant setup wherein the same array can measure the primary scintillation (S1), and the electroluminescence (S2) eliminating the necessity of two sets of readout detectors. Fig. 34.7 illustrates this method that works in the gas phase and in dual phase detectors. The time evolution of the primary light is also affected by the type of recoil that results from different populations of excimers in the singlet and triplet states [56]. This alone has resulted in excellent discrimination, particularly in gasses where the decay times are significantly different (see Table 34.4). An example of the discrimination is displayed in Fig. 34.8, where nuclear recoils and electrons can be identified down to 10's of keV$_{ee}$, in argon. Nuclear recoils deposit less ionization than electrons at a given energy. For this reason, nuclear recoil energy is typically reported in equivalent electron energy loss, keV$_{ee}$, when compared with electrons.

The composition of the drift matter is an important choice in TPC design, and the noble gasses are frequently selected as the bulk element in the mix (Table 34.4). The noble gases have no electron affinity in the ground state, resulting in good free-electron lifetime and a good amount of scintillation that is useful for particle identification and t_0 determination. In the case of argon and xenon, the low average energy to produce an ion pair results in good energy resolution. The noble gases are easily purified to a high level that, combined with moderate cost, enables the construction of large monolithic detectors. Of the noble gasses one isotope of xenon (^{136}Xe) is a candidate for ($0\nu2\beta$).

Table 34.4: Properties of the noble gasses typically used in non-accelerator TPCs [57,58]. W is the average energy spent to produce one electron ion pair.

Element	W (eV)	photon yield (γ/keV)	wave-length (nm)	decay time (fast/slow)	cost* ($/kg)
Helium	46.0	50	80	10 ns/1.6 μs	$52
Neon	36.6	30	77	10 ns/3.9 μs	$330
Argon	26.4	40	128	4 ns/1.6 μs	$5
Xenon	21.7	42	175	4 ns/22 ns	$1200

* Prices from `chemcool.com` as updated in 2011.

The negative-ion TPC [59] uses an electronegative gas (*e.g.*, CS_2) either as the drift gas or as a dopant to the drift gas that captures the primary electrons, forming negative ions that drift in the electric field. Upon reaching the gas-gain region of the TPC, the electron is stripped from the ion in the high electric field, and the electron avalanches in the normal manner. The larger mass of the the negative ion keeps the kinetic energy of the ion thermal at high electric fields, and therefore such a TPC exhibits far less diffusion. The reduction of diffusion over large distance (time) enables detailed tracking of small tracks in a large volume without the benefit of a magnetic field to limit diffusion (which would be prohibitively expensive for a large volume). The trade-off is orders-of-magnitude slower drift, placing a limit on the trigger rate.

34.5. Sub-Kelvin detectors

Written September 2009 by S. Golwala (Caltech).

Detectors operating below 1 K, also known as "low-temperature" or "cryogenic" detectors, use $\lesssim$meV quanta (phonons, superconducting quasiparticles) to provide better energy resolution than is typically available from conventional technologies. Such resolution can provide unique advantages to applications reliant on energy resolution, such as beta-decay experiments seeking to measure the ν_e mass or searches for neutrinoless double-beta decay. In addition, the sub-Kelvin mode is combined with conventional (eV quanta) ionization or scintillation measurements to provide discrimination of nuclear recoils from electron recoils, critical for searches for WIMP dark matter and for coherent neutrino-nucleus scattering. We describe the techniques in generic fashion in the text and provide a list of experiments using these techniques in An excellent review [60] is available that covers this material and other applications of low-temperature detectors.

The proceedings of the Low Temperature Detectors Workshops are also useful [61].

34.5.1. ***Thermal Phonons*** :

The most basic kind of low-temperature detector employs a dielectric absorber coupled to a thermal bath via a weak link. A thermistor monitors the temperature of the absorber. The energy E deposited by a particle interaction causes a calorimetric temperature change by increasing the population of thermal phonons. The fundamental sensitivity is

$$\sigma_E^2 = \xi^2 kT[T\,C(T) + \beta E] \ , \tag{34.5}$$

where C is the heat capacity of the detector, T is the temperature of operation, k is Boltzmann's constant, and ξ is a dimensionless factor of order unity that is precisely calculable from the nature of the thermal link and the non-thermodynamic noises (*e.g.*, Johnson and/or readout noise). The first term is imposed by statistical fluctuations in the number of thermally excited phonons and on the energy in the absorber due to exchange with the thermal bath (see, *e.g.*, Ref. 62 and references therein). The second term is due to statistical fluctuations in the number of phonons excited by the absorbed radiation. The factor β is also dimensionless and $\mathcal{O}(1)$ and is also precisely calculable from the nature of the thermal link. The ratio of the second term to the first term is equal to the fractional absorber temperature change due to an energy deposition. Thus, the second term becomes appreciable when this fractional temperature change is appreciable, at which point nonlinear effects also come into play. The energy resolution typically acquires an additional energy dependence due to deviations from an ideal calorimetric model that cause position and/or energy dependence in the signal shape.

The rise time of response is limited by the internal thermal conductivity of the absorber. The decay time constant, describing the time required for the absorbed energy to flow out to the bath, is $\tau = C/G$, where G is the thermal conductance of the weak link. The above formula immediately suggests the use of crystalline dielectric absorbers and low temperatures because of the linear factor of T and because C for crystalline dielectrics drops as T^3 for T well below the material's Debye temperature (Θ_D, typically hundreds of K). Specifically, the Debye model indicates that a crystal consisting of N atoms has

$$C = \frac{12\,\pi^4}{5}\,N\,k\left(\frac{T}{\Theta_D}\right)^3 \tag{34.6}$$

which gives $\sigma_E = 5.2\,\xi$ eV for 1 kg of germanium operated at $T = 10$ mK. (For a detector of this size the 2nd term in Eq. (34.5) is negligible.) In practice, a number of factors degrade the above result by about an order of magnitude (thermistor heat capacity and power dissipation, readout noise, *etc.*), but the predicted energy resolution for such a large mass remains attractive.

Neutron-transmutation-doped (NTD) germanium and implanted silicon semiconductors are used for thermistors. Conduction is via phonon-assisted hopping between impurity sites, yielding an exponentially decreasing resistance as a function of temperature, $R(T)$, with negative slope, dR/dT. Attachment to the absorber is usually by eutectic bonding or epoxy or by direct implantation into the absorber. Another type of temperature sensor is the superconducting phase-transition thermometers (SPT) or transition-edge sensor (TES). A SPT or TES is a superconducting film operated in the transition from superconductive to normal resistance at the transition temperature, T_c, where its resistance is a strong function of temperature with positive dR/dT. This can provide strong electrothermal negative feedback, which improves linearity, speeds up response, and mitigates variations in T_c among multiple TESs on the same absorber. Nb_xSi_{1-x} is another thermistor material that ranges between the semiconducting and superconducting regimes as a function of the stoichiometry (defined by x). SPTs/TESs and Nb_xSi_{1-x} thermistors are frequently deposited directly onto the absorber by sputtering or evaporation.

The readout method depends on the type of thermometer used. Doped semiconductors typically have high impedances and are well matched to low-noise JFET-based readout while SPTs/TESs are low-impedance devices requiring SQUID amplifiers.

34.5.2. ***Athermal Phonons and Superconducting Quasiparticles*** :

The advantage of thermal phonons is also a disadvantage: energy resolution degrades as $\sqrt{M}$ where M is the detector mass. This motivates the use of athermal phonons. There are three steps in the development of the phonon signal. The recoiling particle deposits energy along its track, with the majority going directly into phonons. (A minority of the energy goes directly into scintillation and ionization. Energy deposited in ionization is recovered when the carriers recombine.) The recoil and bandgap energy scales (keV and higher, and eV, respectively) are much larger than phonon energies (meV), so the full energy spectrum of phonons is populated, with phase space favoring the most energetic phonons. However, these initial energetic phonons do not propagate because of isotopic scattering (scattering due to variations in lattice ion atomic mass, rate $\propto \nu^4$ where ν is the phonon frequency) and anharmonic decay (scattering wherein a single phonon splits into two phonons, rate $\propto \nu^5$). Anharmonic decay downshifts the phonon spectrum, which increases the phonon mean free path, so that eventually phonons can propagate the characteristic dimension of the detector. These phonons travel quasiballistically, preserve information about the position of the parent interaction, and are not affected by an increase in detector mass (modulo the concomitant larger distance to the surface where they can be sensed). Anharmonic decay continues until a thermal distribution is reached (μeV at mK temperatures), which is exhibited as a thermal increase in the temperature of the detector. If one can detect the athermal phonons at the crystal surface, keep the density of such sensors fixed as the detector surface area increases with mass, and the crystals are pure enough that the athermal phonons can propagate to the surface prior to thermalization, then an increase in detector mass need not degrade energy resolution, and can in fact improve position reconstruction. Sensors for athermal phonons are similar to those for superconducting quasiparticles described below.

Another mode is detection of superconducting quasiparticles in superconducting crystals. Energy absorption breaks superconducting Cooper pairs and yields quasiparticles, electron-like excitations that can diffuse through the material and that recombine after the quasiparticle lifetime. In crystals with very large mean free path against scattering, the diffusion length (distance traveled in a quasiparticle lifetime) is large enough (mm to cm) that the quasiparticles reach the surface and can be detected, usually in a superconducting tunnel junction (STJ) or TES/SPT.

A similar technique is applied to detect athermal phonons. Athermal phonons reaching a superconducting film on the detector surface generate quasiparticles as above. Such thin films have diffusion lengths much shorter than for superconducting crystalline substrates, only of order 100 μm to 1 mm. Thus, the superconducting film must be segmented on this length scale and have a quasiparticle sensor for each segment. The sensors may, however, be connected in series or parallel in large groups to reduce readout channel count.

The readout for athermal phonon and quasiparticle sensing depends on the type of quasiparticle detector. Tunnel junctions match well to JFET-based readouts, while TESs/SPTs use SQUID amplifiers.

34.5.3. ***Ionization and Scintillation*** :

While ionization and scintillation detectors usually operate at much higher temperatures, ionization and scintillation can be measured at low temperature and can be combined with a "sub-Kelvin" technique to discriminate nuclear recoils from background interactions producing electron recoils, which is critical for WIMP searches and coherent neutrino-nucleus scattering. With ionization, such techniques are based on Lindhard theory [63], which predicts substantially reduced ionization yield for nuclear recoils relative to electron recoils. For scintillation, application of Birks' law (Sec. 33.3.0) yields a similar prediction. (The reduced ionization or scintillation yield for nuclear recoils is frequently referred to as "quenching".)

Table 34.5: Selected experiments using sub-Kelvin detectors. The table is not exhaustive. Operation mode, detector and excitation sensor construction, baseline energy resolution, and energy resolution at a particular energy of interest E_0 are given. We quote the energy and energy resolution for "total" phonon signal, where the total phonon signal includes both recoil energy and, where relevant, drift heating. Ionization and scintillation energies are normalized so that, for electron recoils, the energy in these channels is equal to the recoil energy ("electron-equivalent" energies). For scintillation energy, this is the electron-equivalent energy deposited in the target detector, not the energy received by the photon absorber. Approximate dates of operation are also given. Key to comments: "a-Si" and "a-Ge" = amorphous silicon or germanium layers in ionization electrodes. "H-a-Si" = hydrogenated amorphous silicon. "P-implanted" = phosphorous implantation. "Interdig." = interdigitated ionization electrode design that provides some z information from ionization signal asymmetry. "Surface-event discrimination" = ability to reject events near surfaces that suffer reduced ionization yield and can be misidentified as WIMPs. "w/phonons" = using athermal phonon pulse rising edge (faster for surface events). "w/ioniz. asym." = using the asymmetry of the ionization signal on electrodes on opposite faces of interdigitated-electrode detectors. "w/phonon asym." = using the asymmetry of the phonon signal detected on opposite detector faces. "U" = not known by author. SuperCDMS energy resolutions have not been fully reported yet but are likely no worse than CDMS II.

Experiment	technique	substrate + mass	sensor	ΔE_{FWHM} [keV] at E=0	at E_0	E_0 [keV]	comments
WIMP dark matter							
CDMS I (1996–2000)	thermal phonon, ionization	Ge 0.16 kg	NTD Ge thermistor, H-a-Si/Al electrode	0.3 0.9	0.7 1.1	12 10.4	nuclear recoil discrimination w/ionization yield
CDMS II (2001–2008)	athermal phonon, ionization	Ge 0.25 kg	tungsten TES, a-Si/Al electrode	0.4 0.7	2.4 0.8	20.7 10.4	CDMS I+ surface-event discrimination w/phonons
SuperCDMS-SNOLAB, in development	athermal phonon, ionization	Ge 0.64 kg	tungsten TES, a-Si/Al interdig.	0.4 0.7	U U	U U	CDMS II+ surface-event discr.w/ioniz.+ phonon z asym.
EDELWEISS I (1996–2005)	thermal phonon, ionization	Ge 0.32 kg	NTD Ge thermistor, a-Si/Al a-Ge/Al	2.3 1.1	2.3 1.1	24.2 10.4	nuclear recoil discrimination w/ionization yield
EDELWEISS II (2006–)	thermal phonon, ionization	Ge 0.4 kg	NTD Ge thermistor, a-Si/Al interdig.	3.6 1.0	3.6 1.0	38.0 10.4	EDELWEISS I +surface-event discrimination w/ioniz.asym.
CRESST I (1996–2002)	athermal phonon	Al_2O_3 0.26 kg	tungsten SPT	0.20	0.24	1.5	no NR discr.
CRESST II (2003–)	athermal phonon, scint.	$CaWO_4$ 0.3 kg ($ZnWO_4$)	tungsten SPT (target and photon abs.)	0.3 1.0	0.3 3.5	8.1 10	NR discr. w/scint. yield
α decay							
ROSEBUD (1996–)	athermal phonon, scint.	BGO 46 g	NTD Ge thermistor (target & photon abs.)	6 U	5500 U	18 U	α discr. w/scint. yield, first det. of ^{209}Bi α decay
β decay							
Oxford ^{63}Ni (1994–1995)	athermal phonon	InSb 3.3 g	Al STJ	1.24	1.24	67	
MARE (2009–)	thermal phonon	$AgReO_4$ 0.5 mg	P-implanted Si thermistor	U	0.033	2.6	
$0\nu\beta\beta$ decay							
CUORE (2003–)	thermal phonon	TeO_2* 0.75 kg	NTD Ge thermistor	U	7	2527	

* The CUORE energy resolution is worse than can be obtained with Ge diode detectors.

Specifically, consider the example of measuring thermal phonons and ionization. All the deposited energy eventually appears in the thermal phonon channel, regardless of recoil type (modulo some loss to permanent crystal defect creation). Thus, the ionization yield—the number of charge pairs detected per unit detected energy in phonons—provides a means to discriminate nuclear recoils from electron recoils. Similar discrimination is observed with athermal phonons and ionization and with phonons and scintillation.

In semiconducting materials of sufficient purity—germanium and silicon—electron-hole pairs created by recoiling particles can be drifted to surface electrodes by applying an electric field, similar to how this is done at 77 K in high-purity germanium photon spectrometers (Sec. 33.7). There are three important differences, however, that result in the use of low fields—of order 1 V/cm—instead of the hundreds to thousands of V/cm used in 77 K detectors. First, high fields are required at 77 K to deplete the active volume of thermally excited mobile carriers. At low temperature and in crystals of purity high enough to drift ionization with negligible trapping, the population of thermally excited carriers is exponentially suppressed due to the low ambient thermal energy. Second, high fields in 77 K operation prevent trapping of drifting carriers on ionized impurities and crystalline defects and/or overcome space charge effects. At low temperatures, ionized impurities and space charge can be neutralized (using free charge created by photons from LEDs or radioactive sources) and remain in this state for minutes to hours. This reduces trapping exponentially and allows low-field drift. Third, a high field in a sub-Kelvin detector would result in a massive phonon signal from the drifting carriers, fully correlated with the ionization signal and thereby eliminating nuclear recoil discrimination. Readout of the charge signal is typically done with a conventional JFET-based transimpedance amplifier.

A number of materials that scintillate on their own (*i.e.*, without doping) continue to do so at low temperatures, including BaF_2, BGO, $CaWO_4$, $ZnWO_4$, $PbWO_4$, and other tungstates and molybdates. In and of itself, there is little advantage to a low-temperature scintillation measurement because detecting the scintillation is nontrivial, the quanta are large, and the detection efficiency is usually poor. Such techniques are pursued only in order to obtain nuclear-recoil discrimination. Conventional photodetectors do not operate at such low temperatures, so one typically detects the scintillation photons in an adjacent low-temperature detector that is thermally disconnected from but resides in an optically reflective cavity with the target detector.

34.6. Low-radioactivity background techniques

Revised July 2013 by A. Piepke (University of Alabama).

The physics reach of low-energy rare event searches *e.g.* for dark matter, neutrino oscillations, or double beta decay is often limited by background caused by radioactivity. Depending on the chosen detector design, the separation of the physics signal from this unwanted interference can be achieved on an event-by-event basis by active event tagging, utilizing some unique event feature, or by reducing the radiation background by appropriate shielding and material selection. In both cases, the background rate is proportional to the flux of background-creating radiation. Its reduction is thus essential for realizing the full physics potential of the experiment. In this context, "low energy" may be defined as the regime of natural, anthropogenic, or cosmogenic radioactivity, all at energies up to about 10 MeV. See [64,65] for in-depth reviews of this subject. Following the classification of [64], sources of background may be categorized into the following classes:

1. environmental radioactivity,
2. radioimpurities in detector or shielding components,
3. radon and its progeny,
4. cosmic rays,
5. neutrons from natural fission, (α, n) reactions and from cosmic-ray muon spallation and capture.

34.6.1. ***Defining the problem*** : The application defines the requirements. Background goals can be as demanding as a few low-energy events per year in a ton-size detector. The strength of the physics signal to be measured can often be estimated theoretically or from limits derived by earlier experiments. The experiments are then designed for the desired signal-to-background ratio. This requires finding the right balance between clarity of measurement, ease of construction, and budget. In a practical sense, it is important to formulate background goals that are sufficient for the task at hand but doable, in a finite time. It is now standard practice to use a detector simulation to translate the background requirements into limits for the radioactivity content of various detector components, requirements for the radiation shielding, and allowable cosmic-ray flux. This strategy allows identifying the most critical components early and the allocation of analysis and development resources accordingly. The CERN code GEANT4 is a widely used tool for this task. It contains sufficient nuclear physics to allow accurate background estimations. Custom-written event generators, *e.g.*, modeling particle correlations in complex decay schemes, or deviations from allowed beta spectra are used as well.

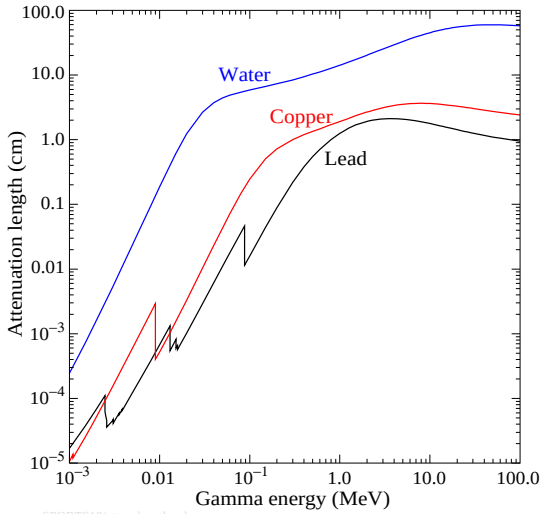

Figure 34.9: γ-ray attenuation lengths in some common shielding materials. The mass attenuation data has been taken from the NIST data base XCOM; see "Atomic Nuclear Properties" at `pdg.lbl.gov`.

34.6.2. ***Environmental radioactivity*** : The long-lived natural radioisotopes ^{40}K, ^{232}Th, and ^{238}U have average abundances of 1.6, 11.1 and 2.7 ppm in the earth's crust, with large local variations. In most applications, γ radiation emitted during the decay of natural radioactivity and its unstable daughters constitutes the dominant contribution to the local radiation field. Typical low-background applications require levels of natural radioactivity on the order of ppb or ppt in the detector components. Passive or active shielding is used to suppress external γ radiation down to that level. Fig. 34.9 shows the energy-dependent attenuation length $\lambda(E_\gamma)$ as a function of γ ray energy E_γ for three common shielding materials (water, copper, lead). The thickness ℓ required to reduce the external flux by a factor $f > 1$ is estimated assuming exponential damping:

$$\ell \;=\; \lambda(E_\gamma) \cdot \ln f \;. \tag{34.7}$$

At 100 keV, a typical energy scale for dark matter searches (or 2.615 MeV, for a typical double-beta decay experiment), attenuation by a factor $f = 10^5$ requires 67(269) cm of H_2O, 2.8(34) cm of Cu, or 0.18(23) cm of Pb. Such estimates allows for an order-of-magnitude determination of the experiment dimensions. A precise estimation of the leakage of external γ radiation, including scattering and the effect of energy cuts, requires Monte Carlo simulations and determination of the radioactivity present in the laboratory. Detailed modeling of the γ flux in a large laboratory, or inside hermetic shielding, needs to cope

with very small detector-hit efficiencies. It is often advantageous to calculate solid angle and mass attenuation separately. This approach reduces the computation time required for a statistically meaningful number of detector hits to manageable levels.

Because of its low density, water has relatively long attenuation lengths, resulting in rather voluminous shields. However, because water can be obtained relatively cheaply in large amounts, it has become the medium of choice for most large detectors. Water purification technology is effective and commercially available, an important consideration in view of the intrinsic radioactivity of the shield, to be discussed below. High-purity water, instrumented with photo multiplier tubes, can further serve as a Cherenkov cosmic-ray veto detector. Liquefied gases are being used for shielding as well.

34.6.3. ***Radioimpurities in detector or shielding components*** : After suppressing the effect of external radioactivity, radioactive impurities, contained in the detector components or attached to its surfaces, become important. Any material is radioactive at some level. The activity can be natural, cosmogenic, or man-made. The determination of the activity content of a specific material or component requires case-by-case analysis, and is almost never obtainable from the manufacturer. However, there are some general rules than can be used to guide the pre-selection. For detectors designed to look for electrons (for example in double-beta decay searches or neutrino detection via inverse beta decay or elastic scattering), this is the principal source of background. For devices detecting nuclear recoils (for example in dark matter searches), this is often of secondary importance as ionization signals can be actively suppressed on an event-by-event basis.

For natural radioactivity, a rule of thumb is that synthetic substances are cleaner than natural materials. Typically, more highly processed materials have lower activity content than raw substances. Substances with high electronegativity tend to be cleaner as the refining process tends to remove K, Th, and U. For example, Al is often found to contain considerable amounts of Th and U, while electrolytic Cu is very low in primordial activities. Plastics or liquid hydrocarbons, having been refined by distillation, are often quite radiopure. Tabulated radioactivity screening results for a wide range of materials can be found in Refs. 66 and 67.

The long-lived ^{238}U daughter ^{210}Pb ($T_{1/2}$=22.3 y) is found in all shielding lead, and is a background concern at low energies. This is due to the relatively high endpoint energy (Q_β=1.162 MeV) of its beta-unstable daughter ^{210}Bi. Lead parts made from selected low-U ores have specific activities of about 5–30 Bq/kg. For lower activity, ancient lead (for example from Roman ships) has been used. Because the ore processing and lead refining removed most of the ^{238}U, the ^{210}Pb decayed during the long waiting time to the level supported by the U-content of the refined lead. Lining the lead with copper to range out the low-energy radiation is another remedy. However, intermediate Z materials are an activation risk when handled above ground, as will be discussed below. ^{210}Pb is also found in solders.

The fission product ^{137}Cs can be found attached to the surface of materials. The radioactive noble gas ^{85}Kr, released into the atmosphere by nuclear reactors and nuclear fuel re-processing, is also important, especially due to its high solubility in organic materials. Post-World War II steel typically contains a few tens of mBq/kg of ^{60}Co.

Surface activity is not a material property but is added during manufacturing and handling. It can often be effectively removed by etching. Installation of low-background detectors is often done in clean rooms to avoid this contamination. Surface contamination can be quantified by means of wipe-testing with acid or alcohol wetted Whatman 41 filters. Pre-soaking of the filters in clean acid reduces the amount of Th and U contained in the paper and boosts analysis sensitivity. The paper filters are ashed after wiping and the residue is digested in acid. Subsequent analysis by means of mass spectroscopy or neutron activation analysis is capable of detecting less than 1 pg/cm^2 of Th and U. The most demanding low-rate experiments require screening of *all* components, which can be a time consuming task. The requirements for activity characterization depend on the experiment and the location and amount of a particular component. Monte Carlo simulations are used to quantify these requirements. Activities of the order μBq/kg or even below may need to be detected in the process. At such level of sensitivity, the characterization becomes a challenging problem in itself. Low-background α, β, and γ ray counting, mass spectroscopy, and neutron activation analysis are used.

34.6.4. ***Radon and its progeny*** : The noble gas ^{222}Rn, a pure α-emitter, is a ^{238}U decay product. Due to its relatively long half-life of 3.8 d it is released by surface soil and is found in the atmosphere everywhere. ^{220}Rn (^{232}Th decay product) is unimportant because of its short half-life. The ^{222}Rn activity in air ranges from 10 to 100 mBq/L outdoors and 100 to thousands of mBq/L indoors. The natural radon concentration depends on the weather and shows daily and seasonal variations. Radon levels are lowest above the oceans. For electron detectors, it is not the Rn itself that creates background, but its progeny ^{214}Pb, ^{214}Bi, ^{210}Bi, which emit energetic beta and γ radiation. Thus, not only the detector itself has to be separated from contact with air, but also internal voids in the shield which contain air can be a background concern. Radon is quite soluble in water and even more so in organic solvents. For large liquid scintillation detectors, radon mobility due to convection and diffusion is a concern. To define a scale: typical double-beta-decay searches are disturbed by a $\sim \mu$Bq (or 1 decay per 11.6 days) activity of ^{222}Rn contained in the detector medium. This corresponds to a steady-state population of 0.5 atoms or 50 μL of air (assuming 20 mBq/L of radon in the air). The criteria for leak tightness are thus quite demanding. The decay of Rn itself is a concern for some recoil type detectors, as nuclear recoil energies in α decays are substantial (76 keV in case of ^{222}Rn).

Low-activity detectors are often kept sealed from the air and continuously flushed with boil-off nitrogen, which contains only small amounts of Rn. For the most demanding applications, the nitrogen is purified by multiple distillations. Then only the Rn outgassing of the piping (due to its U internal content) determines the radon concentration. Radon diffuses readily through thin plastic barriers. If the detector is to be isolated from its environment by means of a membrane, the right choice of material is important [68].

If energies below 1 MeV are to be measured, additional care has to be taken to avoid plate-out of the long-lived radon daughter ^{210}Pb on the surfaces. The α-decay of ^{210}Po, accumulated on plastic surfaces due to prolonged exposure to air, can create energetic neutrons and gamma radiation through the reaction ^{13}C(α,n)^{16}O. In case plastic granules were exposed before the manufacture of the finished material, the ^{210}Po can also be present in the bulk. Careful air exposure management is the only way to reduce this source of background. This can be achieved by storing the parts under a protective low-radon cover gas.

Radon can be detected even at the level of few atoms with solid state, scintillation, or gas detectors by exploiting the fast decay sequences of ^{214}Bi and ^{214}Po. The efficiency of these devices is sometimes boosted by electrostatic collection of charged radon from a large gas volume into a small detector.

34.6.5. ***Cosmic rays*** : Cosmic radiation, discussed in detail in Chapter 28, is a source of background for just about any non-accelerator experiment. Primary cosmic rays are about 90% protons, 9% alpha particles, and the rest heavier nuclei (Fig. 28.1). They are totally attenuated within the first the first few hg/cm^2 of atmospheric thickness. At sea level secondary particles ($\pi^\pm : p : e^\pm : n : \mu^\pm$) are observed with relative intensities 1 : 13 : 340 : 480 : 1420 (Ref. 69; also see Fig. 28.4).

All but the muon and the neutron components are readily absorbed by overburden such as building ceilings and passive shielding. Only if there is very little overburden ($\lesssim$1 g/cm^2 or so) do pions and protons need to be considered when estimating the production rate of cosmogenic radioactivity.

Sensitive experiments are thus operated deep underground where essentially only muons penetrate. As shown in Fig. 28.7, the muon intensity falls off rapidly with depth. Active detection systems capable of tagging events correlated in time with cosmic-ray activity are needed, depending on the overburden. Such experiments are described in Sec. 34.3.1.

The muonic background is related to low-radioactivity techniques insofar as photonuclear interactions of muons can produce long-lived

radioactivity. This happens at any depth, and it constitutes an essentially irreducible background. Muon bremsstrahlung, created in high-Z shielding materials, contributes to the low energy background too. Active muon veto detection systems are effective in reducing this background.

Cosmogenic activation of components brought from the surface is also an issue. Proper management of parts and materials above ground during machining and detector assembly minimizes the accumulation of long-lived activity. Cosmogenic activation is most important for intermediate Z materials such as Cu and Fe. For the most demanding applications, metals are stored and transported under sufficient shielding to stop the hadronic component of the cosmic rays. Parts can be stored underground for long periods before being used. Underground machine shops are sometimes used to limit the duration of exposure at the surface.

34.6.6. ***Neutrons*** : Neutrons contribute to the background of low-energy experiments in different ways: directly through nuclear recoil in the detector medium, and indirectly, through the production of radio nuclides inside the detector and its components. The latter mechanism allows even remote materials to contribute to the background by means of penetrating γ radiation, since inelastic scattering of fast neutrons or radiative capture of slow neutrons can result in the emission of γ radiation. Neutrons are thus an important source of low-energy background. They are produced in different ways:

1. At the earth's surface the flux of cosmic-ray secondary neutrons is exceeded only by that of muons;
2. Energetic tertiary neutrons are produced by cosmic-ray muons in nuclear spallation reactions with the detector and laboratory walls;
3. In high Z materials, often used in radiation shields, nuclear capture of negative muons results in emission of neutrons;
4. Natural radioactivity has a neutron component through spontaneous fission and (α, n)-reactions.

A calculation with the hadronic simulation code FLUKA, using the known energy distribution of secondary neutrons at the earth's surface [70], yields a mass attenuation of 1.5 hg/cm^2 in concrete for secondary neutrons. If energy-dependent neutron-capture cross sections are known, then such calculations can be used to obtain the production rate of radio nuclides.

At an overburden of only few meters, water equivalent neutron production by muons becomes the dominant mechanism. Neutron production rates are high in high-Z shielding materials. A high-Z radiation shield, discussed earlier as being effective in reducing background due to external radioactivity, thus acts as a source for cosmogenic tertiary high-energy neutrons. Depending on the overburden and the radioactivity content of the laboratory, there is an optimal shielding thickness. Water shields, although bulky, are an attractive alternative due to their low neutron production yield and self-shielding.

Neutron shields made from plastic or water are commonly used to reduce the neutron flux. The shield is sometimes doped with a substance having a high thermal neutron capture cross section (such as boron) to absorb thermal neutrons more quickly. The hydrogen serves as a target for elastic scattering, and is effective in reducing the neutron energy. Neutrons from natural radioactivity have relatively low energies and can be effectively suppressed by a neutron shield. Such a neutron shield should be inside the lead to be effective for tertiary neutrons. However, this is rarely done as it increases the neutron production target (in form of the passive shield), and costs increase as the cube of the linear dimensions. An active cosmic-ray veto is an effective solution, correlating a neutron with its parent muon. This solution works best if the veto system is as far removed from the detector as feasible (outside the radiation shield) to correlate as many background-producing muons with neutrons as possible. The vetoed time after a muon hit needs to be sufficiently long to assure neutron thermalization. The average thermalization and capture time in lead is about 900 μs [64]. The veto-induced deadtime, and hence muon hit rate on the veto detector, is the limiting factor for the physical size of the veto system (besides the cost). The background caused by neutron-induced radioactivity with live times exceeding the veto time cannot be addressed in this way. Moving the detector deep underground, and thus reducing the muon flux, is the only technique addressing all sources of neutron background.

References:

1. R.M. Baltrusaitis *et al.*, Nucl. Instrum. Methods **A20**, 410 (1985).
2. T. Abu-Zayyad *et al.*, Nucl. Instrum. Methods **A450**, 253 (2000).
3. H. Tokuno *et al.*, Nucl. Instrum. Methods **A676**, 54 (2012).
4. J. Abraham *et al.*, [Pierre Auger Collab.], Nucl. Instrum. Methods **A620**, 227 (2010).
5. J. Abraham *et al.*, [Pierre Auger Collab.], Eur. Phys. J. Plus **127**, 94 (2012).
6. J.H. Adams Jr. *et al.*(JEM-EUSO Collab.), Astropart. Phys. **44**, 76 (2013).
7. F. Arqueros, J. Hrandel, and B. Keilhauer, Nucl. Instrum. Methods **A597**, 23 (2008).
8. F. Arqueros, J. Hrandel, and B. Keilhauer, Nucl. Instrum. Methods **A597**, 1 (2008).
9. J. Rosado, F. Blanco, and F. Arqueros, Astropart. Phys. **34**, 164 (2010).
10. J. Boyer *et al.*, Nucl. Instrum. Methods **A482**, 457 (2002); M. Kleifges for the Pierre Auger Collab., Nucl. Instrum. Methods **A518**, 180 (2004).
11. M. Ave *et al.*, [AIRFLY Collab.], Astropart. Phys. **28**, 41 (2007).
12. J.T. Brack *et al.*, Astropart. Phys. **20**, 653, (2004).
13. B. Fick *et al.*, JINST **1**, 11003, (2006).
14. J. Abraham *et al.*, [Pierre Auger Collab.], Astropart. Phys. **33**, 108 (2010).
15. J. Abraham *et al.*, [Pierre Auger Collab.], Astropart. Phys. **34**, 368 (2011).
16. M. Unger *et al.*, Nucl. Instrum. Methods **A588**, 433 (2008).
17. T.K. Gaisser and A.M. Hillas, *Proc. 15th Int. Cosmic Ray Conf.* (Plovdiv, Bulgaria, 13–26 Aug. 1977).
18. J. Holder *et al.*, *Proc. 4th International Meeting on High Energy Gamma-Ray Astron.*, eds. F.A. Aharonian, W. Hofmann & F. Rieger, AIP Conf. Proc. **1085**, 657 (2008).
19. J.A. Hinton, New Astron. Rev. **48**, 331 (2004).
20. J. Albert *et al.*, Astrophys. J. **674**, 1037 (2008).
21. `astro-ph/0508253` Lectures given at the International Heraeus Summer School, "Physics with Cosmic Accelerators," Bad Honnef, Germany, July 5–16 (2004).
22. T.C. Weekes *et al.*, Astrophys. J. **342**, 379 (1989).
23. A.M. Hillas *et al.*, Astrophys. J. **503**, 744 (1998).
24. J. Holder, Astropart. Phys. **39**, 61 (2012).
25. F.A. Aharonian, *et al.*, Astrophys. J. **636**, 777 (2006).
26. M. Actis, *et al.*, Experimental Astronomy **32**, 193 (2011).
27. L.A. Bernstein *et al.*, "Report on the Depth Requirements for a Massive Detector at Homestake" (2009); `arXiv:0907.4183`.
28. Y. Ashie *et al.*, Phys. Rev. **D71**, 112005 (2005).
29. S. Kasuga *et al.*, Phys. Lett. **B374**, 238 (1996).
30. M. Shiozawa, Nucl. Instrum. Methods **A433**, 240 (1999).
31. J. Hosaka *et al.*, Phys. Rev. **D73**, 112001 (2006).
32. J. Boger *et al.*, Nucl. Instrum. Methods **A449**, 172 (2000).
33. T.K. Gaisser, F. Halzen, and T. Stanev, Phys. Reports **258**, 17 (1995).
34. J.G. Learned and K. Mannheim, Ann. Rev. Nucl. and Part. Sci. **50**, 679 (2000).
35. U.F. Katz and C. Spiering, Prog. in Part. Nucl. Phys. **67**, 651 (2012).
36. M.G. Aartsen et al. (IceCube and PINGU Coll.), *Snowmass Proc.*, `arXiv:1306.5846 [astro-ph.IM]`.
37. M.G. Aartsen *et al.* (IceCube Coll.), Science **342**, 1242856 (2013).
38. M.G. Aartsen *et al.* (IceCube Coll.), contributions to ICRC13, `arXiv:1309.6979/7003/7006/7007/7008/7010 [astro-ph.HE]`.
39. P. Coyle for the ANTARES Coll., Nucl. Phys. (Proc. Suppl.) **B235-236**, 339 (2013).
40. K. Griesen, Phys. Rev. Lett. **16**, 748 (1966); G.T. Zatsepin and V.A. Kuzmin, JETP Lett. **4**, 78 (1966).

41. G.A. Askaryan, Sov. Phys. JETP **14**, 441 (1962); G.A. Askaryan Sov. Phys. JETP **21**, 658 (1965).
42. D. Saltzberg *et al.*, Phys. Rev. Lett. **86**, 2802 (2001); O. Scholten et al., J. Phys. Conf. Ser. **81**, 012004 (2007).
43. E. Zas, F. Halzen, and T. Stanev, Phys. Rev. **D45**, 362 (1992); J. Alvarez-Muniz, R. A. Vazques, and E. Zas, Phys. Rev. **D62**, 063001 (2000).
44. S.R. Klein, Nucl. Phys. B - Proc. Suppl. **229-232**, 284 (2012).
45. R.D. Dagkesamanskii and I.M. Zheleznykh, Sov. Phys. JETP Lett. **50**, 233 (1989).
46. S. Buitink *et al.*, `arXiv:1301.5185`.
47. P. Gorham *et al.*, Phys. Rev. **D82**, 022004 (2010); see also the erratum with updated limits, P. Gorham *et al.*, Phys. Rev. **D85**, 049901 (2012).
48. P. Allison *et al.*, Astropart. Phys. **35**, 457 (2012); P. Allison *et al.*, Nucl. Instrum. Methods **A604**, S64 (2009).
49. L. Gerhardt *et al.*, Nucl. Instrum. Methods **A624**, 85-91 (2010); S. Barwick, preprint `arXiv:astro-ph/0610631`; S. Klein, `arXiv:1207.3846`.
50. S. Hoover *et al.*, Phys. Rev. Lett. **105**, 151101 (2010).
51. I. Kravchenko *et al.*, Phys. Rev. **D73**, 082002 (2006); I. Kravchenko *et al.*, Astropart. Phys. **19**, 15 (2003).
52. M. Schaumann, "The XENON 100 Dark Matter Experiment," *10th Conf. on the Intersections of Part. & Nucl. Phys.,* (2009), to be published in AIP Conf. Proc.
53. A. Bolotnikov and B. Ramsey, Nucl. Instrum. Methods **A496**, 360 (1997).
54. E. Aprile *et al.*, Phys. Rev. **B76**, 014115 (2007).
55. C.M.B. Monteiro *et al.*, "Secondary scintillation yield in pure xenon," JINST 2 P05001 (2007), doi 10.1088/1748-0221/2/05/P05001.
56. W.H. Lippincott *et al.*, Phys. Rev. **C78**, 035801 (2008).
57. W. Blum and L. Rolandi, *Particle Detection with Drift Chambers,* Springer-Verlag (1994).
58. R.S. Chandrasekharan, "Noble Gas Scintillation-Based Radiation Portal Monitor and Active Interrogation Systems," IEEE Nucl. Sci. Symposium Conference Record (2006).
59. C.J. Martoff *et al.*, Nucl. Instrum. Methods **A440**, 355 (2000).
60. *Cryogenic Particle Detection*, ed. by C. Enss, (Springer-Verlag: Berlin, 2005).
61. *Proc. 13th Inter. Workshop on Low Temperature Detectors*, AIP Conference Proc. (2009); see also *Proceedings* of previous occurrences of this workshop.
62. S.H. Moseley, J.C. Mather, and D. McCammon, J. Appl. Phys. **56**, 1257 (1984).
63. J. Lindhard *et al.*, Mat. Fys. Medd. K. Dan. Vidensk. Selsk. **33**, 10 (1963).
64. G. Heusser, Ann. Rev. Nucl. and Part. Sci. **45**, 543 (1995).
65. J.A. Formaggio and C.J. Martoff, Ann. Rev. Nucl. and Part. Sci. **54**, 361 (2004).
66. P. Jagam and J.J. Simpson, Nucl. Instrum. Methods **A324**, 389 (1993).
67. D.S. Leonard *et al.*, Nucl. Instrum. Methods **A591**, 490 (2008).
68. M. Wojcik *et al.*, Nucl. Instrum. Methods **A449**, 158 (2000).
69. National Council on Radiation Protection and Measurement, Report 94, Bethesda, MD (1987).
70. M.S. Gordon *et al.*, IEEE Trans. **NS51**, 3427 (2004).

35. RADIOACTIVITY AND RADIATION PROTECTION

Revised August 2013 by S. Roesler and M. Silari (CERN).

35.1. Definitions [1,2]

It would be desirable if legal protection limits could be expressed in directly measurable *physical quantities*. However, this does not allow to quantify biological effects of the exposure of the human body to ionizing radiation.

For this reason, protection limits are expressed in terms of so-called *protection quantities* which, although calculable, are not measurable. Protection quantities quantify the extent of exposure of the human body to ionizing radiation from both whole and partial body external irradiation and from intakes of radionuclides.

In order to demonstrate compliance with dose limits, so-called *operational quantities* are typically used which aim at providing conservative estimates of protection quantities. Often radiation protection detectors used for individual and area monitoring are calibrated in terms of operational quantities and, thus, these quantities become "measurable".

35.1.1. *Physical quantities* :

• **Fluence,** Φ (unit: $1/\mathrm{m}^2$): The fluence is the quotient of dN by da, where dN is the number of particles incident upon a small sphere of cross-sectional area da

$$\Phi = dN/da \ . \tag{35.1}$$

In dosimetric calculations, fluence is frequently expressed in terms of the lengths of the particle trajectories. It can be shown that the fluence, Φ, is given by

$$\Phi = dl/dV,$$

where dl is the sum of the particle trajectory lengths in the volume dV.

• **Absorbed dose,** D (unit: gray, 1 Gy=1 J/kg=100 rad): The absorbed dose is the energy imparted by ionizing radiation in a volume element of a specified material divided by the mass of this volume element.

• **Kerma,** K (unit: gray): Kerma is the sum of the initial kinetic energies of all charged particles liberated by indirectly ionizing radiation in a volume element of the specified material divided by the mass of this volume element.

• **Linear energy transfer,** L **or** LET (unit: J/m, often given in keV/μm, 1 keV/μm$\approx 1.602 \times 10^{-10}$ J/m): The linear energy transfer is the mean energy, dE, lost by a charged particle owing to collisions with electrons in traversing a distance dl in matter. *Low-LET radiation:* X rays and gamma rays (accompanied by charged particles due to interactions with the surrounding medium) or light charged particles such as electrons that produce sparse ionizing events far apart at a molecular scale ($L < 10$ keV/μm). *High-LET radiation:* neutrons and heavy charged particles that produce ionizing events densely spaced at a molecular scale ($L > 10$ keV/μm).

• **Activity,** A (unit: becquerel, 1 Bq=1/s=27 pCi): Activity is the expectation value of the number of nuclear decays occurring in a given quantity of material per unit time.

35.1.2. *Protection quantities* :

• **Organ absorbed dose,** D_T (unit: gray): The mean absorbed dose in an organ or tissue T of mass m_T is defined as

$$D_T = \frac{1}{m_T} \int_{m_T} D dm \ .$$

• **Equivalent dose,** H_T (unit: sievert, 1 Sv=100 rem): The equivalent dose H_T in an organ or tissue T is equal to the sum of the absorbed doses $D_{T,R}$ in the organ or tissue caused by different radiation types R weighted with so-called radiation weighting factors w_R:

$$H_T = \sum_R w_R \times D_{T,R} \ . \tag{35.2}$$

Table 35.1: Radiation weighting factors, w_R.

Radiation type	w_R
Photons, electrons and muons	1
Neutrons, $E_n < 1$ MeV	$2.5 + 18.2 \times \exp[-(\ln E_n)^2/6]$
1 MeV $\leq E_n \leq$ 50 MeV	$5.0 + 17.0 \times \exp[-(\ln(2E_n))^2/6]$
$E_n >$ 50 MeV	$2.5 + 3.25 \times \exp[-(\ln(0.04E_n))^2/6]$
Protons and charged pions	2
Alpha particles, fission fragments, heavy ions	20

It expresses long-term risks (primarily cancer and leukemia) from low-level chronic exposure. The values for w_R recommended by ICRP [2] are given in Table 35.1.

• **Effective dose,** E (unit: sievert): The sum of the equivalent doses, weighted by the tissue weighting factors w_T ($\sum_T w_T = 1$) of several organs and tissues T of the body that are considered to be most sensitive [2], is called "effective dose":

$$E = \sum_T w_T \times H_T \ . \tag{35.3}$$

35.1.3. *Operational quantities* :

• **Ambient dose equivalent,** $H^*(10)$ (unit: sievert): The dose equivalent at a point in a radiation field that would be produced by the corresponding expanded and aligned field in a 30 cm diameter sphere of unit density tissue (ICRU sphere) at a depth of 10 mm on the radius vector opposing the direction of the aligned field. Ambient dose equivalent is the operational quantity for *area monitoring*.

• **Personal dose equivalent,** $H_p(d)$ (unit: sievert): The dose equivalent in ICRU tissue at an appropriate depth, d, below a specified point on the human body. The specified point is normally taken to be where the individual dosimeter is worn. For the assessment of effective dose, $H_p(10)$ with a depth $d = 10$ mm is chosen, and for the assessment of the dose to the skin and to the hands and feet the personal dose equivalent, $H_p(0.07)$, with a depth $d = 0.07$ mm, is used. Personal dose equivalent is the operational quantity for *individual monitoring*.

35.1.4. *Dose conversion coefficients* :

Dose conversion coefficients allow direct calculation of protection or operational quantities from particle fluence and are functions of particle type, energy and irradiation configuration. The most common coefficients are those for effective dose and ambient dose equivalent. The former are based on simulations in which the dose to organs of anthropomorphic phantoms is calculated for approximate actual conditions of exposure, such as irradiation of the front of the body (antero-posterior irradiation) or isotropic irradiation.

Conversion coefficients from fluence to effective dose are given for anterior-posterior irradiation and various particles in Fig. 35.1 [3]. For example, the effective dose from an anterior-posterior irradiation in a field of 1-MeV neutrons with a fluence of 1 neutron per cm^2 is about 290 pSv. In Monte Carlo simulations such coefficients allow multiplication with fluence at scoring time such that effective dose to a human body at the considered location is directly obtained.

35.2. Radiation levels [4]

• **Natural background radiation**: On a worldwide average, the annual whole-body dose equivalent due to all sources of natural background radiation ranges from 1.0 to 13 mSv (0.1–1.3 rem) with an annual average of 2.4 mSv [5]. In certain areas values up to 50 mSv (5 rem) have been measured. A large fraction (typically more than 50%) originates from inhaled natural radioactivity, mostly radon and radon daughters. The latter can vary by more than one order of magnitude: it is 0.1–0.2 mSv in open areas, 2 mSv on average in a house and more than 20 mSv in poorly ventilated mines.

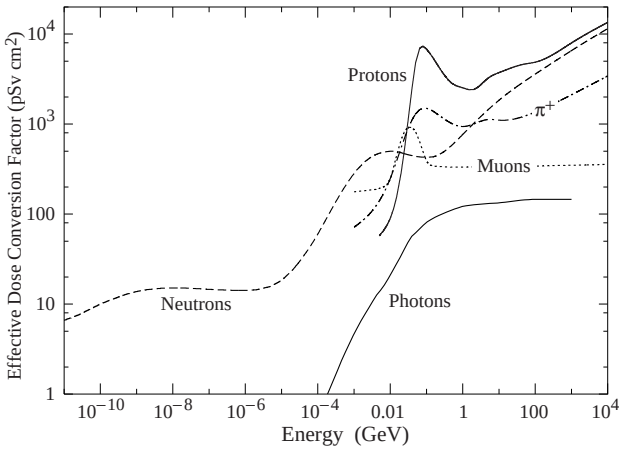

Figure 35.1: Fluence to effective dose conversion coefficients for anterior-posterior irradiation and various particles [3].

• **Cosmic ray background radiation**: At sea level, the whole-body dose equivalent due to cosmic ray background radiation is dominated by muons; at higher altitudes also nucleons contribute. Dose equivalent rates range from less than 0.1 μSv/h at sea level to a few μSv/h at aircraft altitudes. Details on cosmic ray fluence levels are given in the Cosmic Rays section (Sec. 28 of this *Review*).

• **Fluence to deposit one Gy**: *Charged particles:* The fluence necessary to deposit a dose of one Gy (in units of cm^{-2}) is about $6.24 \times 10^9/(dE/dx)$, where dE/dx (in units of MeV g^{-1} cm^2) is the mean energy loss rate that may be obtained from Figs. 32.2 and 32.4 in Sec. 32 of this *Review*, and from `http://pdg.lbl.gov/AtomicNuclearProperties`. For example, it is approximately 3.5×10^9 cm^{-2} for minimum-ionizing singly-charged particles in carbon. *Photons:* This fluence is about $6.24 \times 10^9/(Ef/\ell)$ for photons of energy E (in MeV), an attenuation length ℓ (in g cm^{-2}), and a fraction $f \lesssim 1$, expressing the fraction of the photon energy deposited in a small volume of thickness $\ll \ell$ but large enough to contain the secondary electrons. For example, it is approximately 2×10^{11} cm^{-2} for 1 MeV photons on carbon ($f \approx 1/2$).

35.3. Health effects of ionizing radiation

Radiation can cause two types of health effects, deterministic and stochastic:

• **Deterministic effects** are tissue reactions which cause injury to a population of cells if a given threshold of absorbed dose is exceeded. The severity of the reaction increases with dose. The quantity in use for tissue reactions is the absorbed dose, D. When particles other than photons and electrons (low-LET radiation) are involved, a Relative Biological Effectiveness (RBE)-weighted dose may be used. The RBE of a given radiation is the reciprocal of the ratio of the absorbed dose of that radiation to the absorbed dose of a reference radiation (usually X rays) required to produce the same degree of biological effect. It is a complex quantity that depends on many factors such as cell type, dose rate, fractionation, etc.

• **Stochastic effects** are malignant diseases and heritable effects for which the probability of an effect occurring, but not its severity, is a function of dose without threshold.

• **Lethal dose**: The whole-body dose from penetrating ionizing radiation resulting in 50% mortality in 30 days (assuming no medical treatment) is 2.5–4.5 Gy (250–450 rad)†, as measured internally on the body longitudinal center line. The surface dose varies due to variable body attenuation and may be a strong function of energy.

• **Cancer induction**: The cancer induction probability is about 5% per Sv on average for the entire population [2].

• **Recommended effective dose limits**: The International Commission on Radiological Protection (ICRP) recommends a limit for radiation workers of 20 mSv effective dose per year averaged over 5 years, with the provision that the dose should not exceed 50 mSv in any single year [2]. The limit in the EU-countries and Switzerland is 20 mSv per year, in the U.S. it is 50 mSv per year (5 rem per year). Many physics laboratories in the U.S. and elsewhere set lower limits. The effective dose limit for general public is typically 1 mSv per year.

† RBE-weighted when necessary

35.4. Prompt neutrons at accelerators

Neutrons dominate the particle environment outside thick shielding (*e.g.*, > 1 m of concrete) for high energy (> a few hundred MeV) electron and hadron accelerators. In addition, for accelerators with energies above about 10 GeV, muons contribute significantly at small angles with regard to the beam, even behind several meters of shielding. Another special case are synchrotron light sources where particular care has to be taken to shield the very intense low-energy photons extracted from the electron synchrotron into the experimental areas. Due to its importance at high energy accelerators this section focuses on prompt neutrons.

35.4.1. *Electron accelerators* :

At electron accelerators, neutrons are generated via photonuclear reactions from bremsstrahlung photons. Neutron production takes place above a threshold value which varies from 10 to 19 MeV for light nuclei (with important exceptions, such as 2.23 MeV for deuterium and 1.67 MeV for beryllium) and from 4 to 6 MeV for heavy nuclei. It is commonly described by different mechanisms depending on the photon energy: the giant dipole resonance interactions (from threshold up to about 30 MeV, often the dominant process), the quasi-deuteron effect (between 30 MeV and a few hundred MeV), the delta resonance mechanism (between 200 MeV and a few GeV) and the vector meson dominance model at higher energies.

The giant dipole resonance reaction consists in a collective excitation of the nucleus, in which neutrons and protons oscillate in the direction of the photon electric field. The oscillation is damped by friction in a few cycles, with the photon energy being transferred to the nucleus in a process similar to evaporation. Nucleons emitted in the dipolar interaction have an anisotropic angular distribution, with a maximum at 90°, while those leaving the nucleus as a result of evaporation are emitted isotropically with a Maxwellian energy distribution described as [6]:

$$\frac{dN}{dE_n} = \frac{E_n}{T^2} e^{-E_n/T} \ , \tag{35.4}$$

where T is a nuclear 'temperature' (in units of MeV) characteristic of the particular target nucleus and its excitation energy. For heavy nuclei the 'temperature' generally lies in the range of T = 0.5–1.0 MeV. Neutron yields from semi-infinite targets per kW of electron beam power are plotted in Fig. 35.2 as a function of the electron beam energy [6].

Typical neutron energy spectra outside of concrete (80 cm thick, 2.35 g/cm^3) and iron (40 cm thick) shields are shown in Fig. 35.3. In order to compare these spectra to those caused by proton beams (see below) the spectra are scaled by a factor of 100, which roughly corresponds to the difference in the high energy hadronic cross sections for photons and hadrons (*e.g.*, the fine structure constant). The shape of these spectra are generally characterized by a low-energy peak at around 1 MeV (evaporation neutrons) and a high-energy shoulder at around 70–80 MeV. In case of concrete shielding, the spectrum also shows a pronounced peak at thermal neutron energies.

35.4.2. *Proton accelerators* :

At proton accelerators, neutron yields emitted per incident proton by different target materials are roughly independent of proton energy between 20 MeV and 1 GeV, and are given by the ratio C : Al : Cu-Fe : Sn : Ta-Pb = 0.3 : 0.6 : 1.0 : 1.5 : 1.7 [9]. Above about 1 GeV, the neutron yield is proportional to E^m, where $0.80 \leq m \leq 0.85$ [10].

Typical neutron energy spectra outside of concrete and iron shielding are shown in Fig. 35.3. Here, the radiation fields are caused by a 25 GeV proton beam interacting with a thick copper target. The comparison of these spectra with those for an electron beam of the same energy reflects the difference in the hadronic cross sections

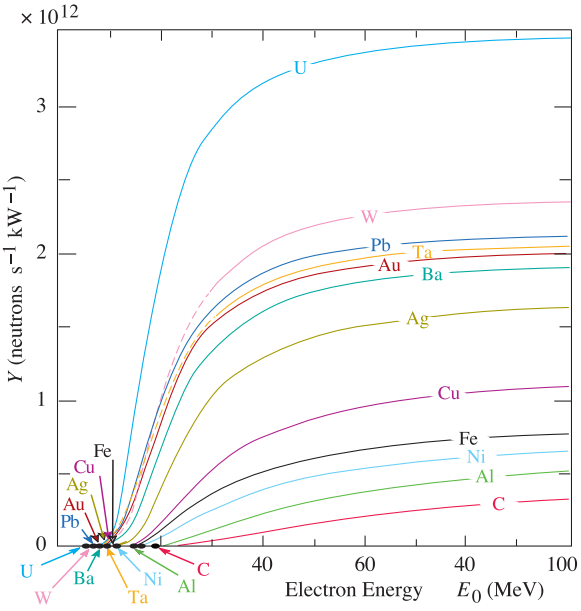

Figure 35.2: Neutron yields from semi-infinite targets per kW of electron beam power, as a function of the electron beam energy, disregarding target self-shielding [6].

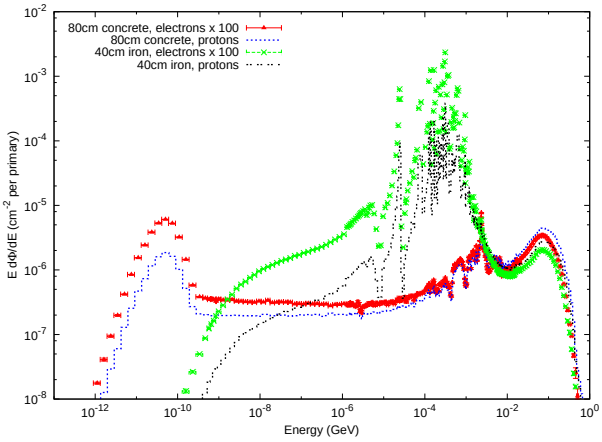

Figure 35.3: Neutron energy spectra calculated with the FLUKA code [7,8] from 25 GeV proton and electron beams on a thick copper target. Spectra are evaluated at 90° to the beam direction behind 80 cm of concrete or 40 cm of iron. All spectra are normalized per beam particle. In addition, spectra for electron beam are multiplied by a factor of 100.

between photons and hadrons above a few 100 MeV. Differences are increasing towards lower energies because of different interaction mechanisms. Furthermore, the slight shift in energy above about 100 MeV follows from the fact that the energies of the interacting photons are lower than 25 GeV. Apart from this the shapes of the two spectra are similar.

The neutron-attenuation length is shown in Fig. 35.4 for concrete and mono-energetic broad-beam conditions. As can be seen in the figure it reaches a value of about 117 g/cm^2 above 200 MeV. As the cascade through thick shielding is carried by high-energy particles this value is equal to the equilibrium attenuation length for particles emitted at 90 degrees in concrete.

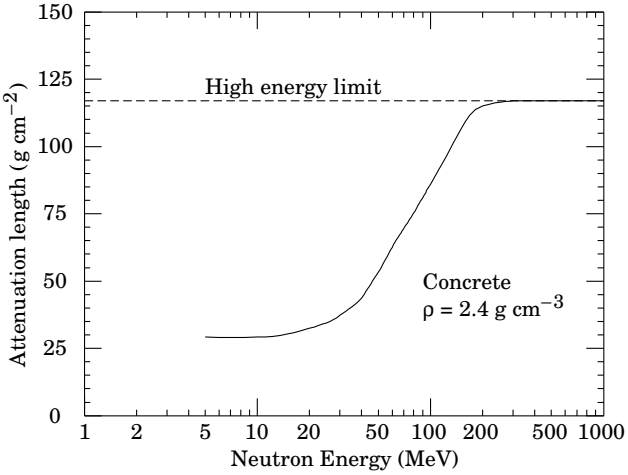

Figure 35.4: The variation of the attenuation length for mono-energetic neutrons in concrete as a function of neutron energy [9].

35.5. Photon sources

The dose equivalent rate in tissue (in mSv/h) from a gamma point source emitting one photon of energy E (in MeV) per second at a distance of 1 m is $4.6 \times 10^{-9}\,\mu_{en}/\rho\,E$, where μ_{en}/ρ is the mass energy absorption coefficient. The latter has a value of 0.029 ± 0.004 cm^2/g for photons in tissue over an energy range between 60 keV and 2 MeV (see Ref. 11 for tabulated values).

Similarly, the dose equivalent rate in tissue (in mSv/h) at the surface of a semi-infinite slab of uniformly activated material containing 1 Bq/g of a gamma emitter of energy E (in MeV) is $2.9 \times 10^{-4}\,R_\mu\,E$, where R_μ is the ratio of the mass energy absorption coefficients of the photons in tissue and in the material.

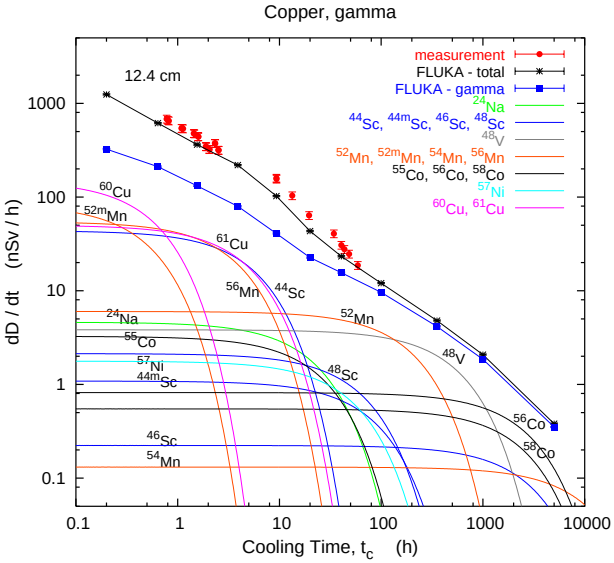

Figure 35.5: Contribution of individual gamma-emitting nuclides to the total dose rate at 12.4 cm distance to an activated copper sample [12].

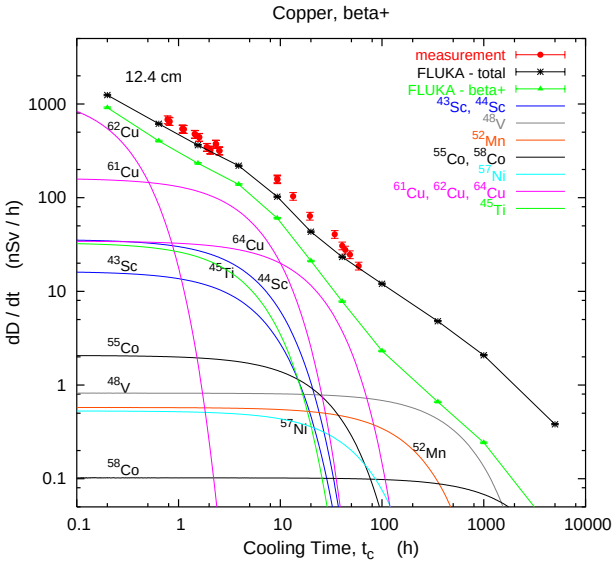

Figure 35.6: Contribution of individual positron-emitting nuclides to the total dose rate at 12.4 cm distance to an activated copper sample [12].

35.6. Accelerator-induced radioactivity

Typical medium- and long-lived activation products in metallic components of accelerators are ^{22}Na, ^{46}Sc, ^{48}V, ^{51}Cr, ^{54}Mn, ^{55}Fe, ^{59}Fe, ^{56}Co, ^{57}Co, ^{58}Co, ^{60}Co, ^{63}Ni and ^{65}Zn. Gamma-emitting nuclides dominate doses by external irradiation at longer decay times (more than one day) while at short decay times β^+ emitters are also important (through photons produced by β^+ annihilation). Due to their short range, β^- emitters are relevant, for example, only for dose to the skin and eyes or for doses due to inhalation or ingestion. Fig. 35.5 and Fig. 35.6 show the contributions of gamma and β^+ emitters to the total dose rate at 12.4 cm distance to a copper sample [12]. The sample was activated by the stray radiation field created by a 120 GeV mixed hadron beam dumped in a copper target during about 8 hours at intensities between $10^7 - 10^8$ hadrons per second. Typically, dose rates at a certain decay time are mainly determined by radionuclides having a half-life of the order of the decay time. Extended irradiation periods might be an exception to this general rule as in this case the activity of long-lived nuclides can build up sufficiently so that it dominates that one of short-lived even at short cooling times.

Activation in concrete is dominated by ^{24}Na (short decay times) and ^{22}Na (long decay times). Both nuclides can be produced either by low-energy neutron reactions on the sodium-component in the concrete or by spallation reactions on silicon, calcium and other consituents such as aluminum. At long decay times nuclides of radiological interest in activated concrete can also be ^{60}Co, ^{152}Eu, ^{154}Eu and ^{134}Cs, all of which produced by (n,γ)-reactions with traces of natural cobalt, europium and cesium, Thus, such trace elements might be important even if their content in concrete is only a few parts per million or less by weight.

The explicit simulation of radionuclide production with general-purpose Monte Carlo codes has become the most commonly applied method to calculate induced radioactivity and its radiological consequences. Nevertheless, other more approximative approaches, such as "ω-factors" [9], can still be useful for fast order-of-magnitude estimates. These ω-factors give the dose rate per unit star density (inelastic reactions above a certain energy threshold, *e.g.* 50 MeV) on contact to an extended, uniformly activated object after a 30-day irradiation and 1-day decay. For steel or iron, $\omega \simeq 3 \times 10^{-12}$ (Sv cm^3/star). This does not include possible contributions from thermal-neutron activation.

35.7. Radiation protection instrumentation

The capacity to distinguish and measure the high-LET (mostly neutrons) and the low-LET components (photons, electrons, muons) of the radiation field at workplaces is of primary importance to evaluate the exposure of personnel. At proton machines the prompt dose equivalent outside a shield is mainly due to neutrons, with some contribution from photons and, to a minor extent, charged particles. At high-energy electron accelerators the dominant stray radiation during operation consists of high-energy neutrons, because the shielding is normally thick enough to absorb most of the bremsstrahlung photons. Most of the personnel exposure at accelerator facilities is often received during maintenance interventions, and is due to gamma/beta radiation coming from residual radioactivity in accelerator components.

Radiation detectors used both for radiation surveys and area monitoring are normally calibrated in ambient dose equivalent $H^*(10)$.

35.7.1. *Neutron detectors* :

• **Rem counters:** A rem counter is a portable detector consisting of a thermal neutron counter embedded in a polyethylene moderator, with a response function that approximately follows the curve of the conversion coefficients from neutron fluence to $H^*(10)$ over a wide energy range. Conventional rem counters provide a response to neutrons up to approximately 10-15 MeV, extended-range units are heavier as they include a high-Z converter but correctly measure $H^*(10)$ up to several hundred MeV.

• **Bonner Sphere Spectrometer (BSS):** A BSS is made up of a thermal neutron detector at the centre of moderating spheres of different diameters made of polyethylene (PE) or a combination of PE and a high-Z material. Each sphere has a different response function versus neutron energy, and the neutron energy, at which the sensitivity peaks, increases with sphere diameter. The energy resolution of the system is rather low but satisfactory for radiation protection purposes. The neutron spectrum is obtained by unfolding the experimental counts of the BSS with its response matrix by a computer code that is often based on an iterative algorithm. BSS exist in active (using ^{3}He or BF_3 proportional counters or ^{6}LiI scintillators) and passive versions (using CR-39 track detectors or LiF), for use *e.g.* in strongly pulsed fields. With ^{3}He counters the discrimination with respect to gamma rays and noise is excellent.

• **Bubble detectors:** A bubble detector is a dosimeter based on a super-heated emulsion (super-heated droplets suspended in a gel) contained in a vial and acting as a continuously sensitive, miniature bubble chamber. The total number of bubbles evolved from the radiation-induced nucleation of drops gives an integrated measure of the total neutron exposure. Various techniques exist to record and count the bubbles, *e.g.*, visual inspection, automated reading with video cameras or acoustic counting. Bubble detectors are insensitive to low-LET radiation. Super-heated emulsions are used as personal, area and environmental dosimeters, as well as neutron spectrometers.

• **Track etched detectors:** Track etched detectors (TEDs) are based on the preferential dissolution of suitable, mostly insulator, materials along the damage trails of charged particles of sufficiently high-energy deposition density. The detectors are effectively not sensitive to radiation which deposits the energy through the interactions of particles with low LET. These dosimeters are generally able to determine neutron ambient dose equivalent down to around 100 μSv. They are used both as personal dosimeters and for area monitoring, *e.g.*, in BSS.

35.7.2. *Photon detectors* :

• **GM counters:** Geiger Müller (GM) counters are low cost devices and simple to operate. They work in pulse mode and since they only count radiation-induced events, any spectrometric information is lost. In general they are calibrated in terms of air kerma, for instance in a ^{60}Co field. The response of GM counters to photons is constant within 15% for energies up to 2 MeV and shows considerable energy dependence above.

• **Ionization chambers:** Ionization chambers are gas-filled detectors used both as hand-held instruments (*e.g.*, for radiation surveys)

and environmental monitors. They are normally operated in current mode although pulse-mode operation is also possible. They possess a relatively flat response to a wide range of X- and gamma ray energies (typically from 10 keV to several MeV), can measure radiation over a wide intensity range and are capable of discriminating between the beta and gamma components of a radiation field (by use of, *e.g.*, a beta window). Pressurized ion chambers (filled, *e.g.*, with Ar or H gas to several tens of bars) are used for environmental monitoring applications. They have good sensitivity to neutrons and charged hadrons in addition to low LET radiation (gammas and muons), with the response function to the former being strongly non-linear with energy.

• **Scintillators:** Scintillation-based detectors are used in radiation protection as hand-held probes and in fixed installations, *e.g.*, portal monitors. A scintillation detector or counter is obtained coupling a scintillator to an electronic light sensor such as a photomultiplier tube (PMT), a photodiode or a silicon photomultiplier (SiPM). There is a wide range of scintillating materials, inorganic (such as CsI and BGO), organic or plastic; they find application in both photon dosimetry and spectrometry.

35.7.3. *Personal dosimeters* :

Personal dosimeters, calibrated in $H_p(10)$, are worn by persons exposed to ionizing radiation for professional reasons to record the dose received. They are typically passive detectors, either film, track etched detectors, ^{6}Li/^{7}Li-based dosimeters (*e.g.* LiF), optically stimulated luminescense (OSL) or radiophotoluminescence detectors (RPL) but semi-active dosimeters using miniaturized ion-chambers also exist.

Electronic personal dosimeters are small active units for on-line monitoring of individual exposure, designed to be worn on the body. They can give an alarm on both the integral dose received or dose rate once a pre-set threshold is exceeded.

35.8. Monte Carlo codes for radiation protection studies

The use of general-purpose particle interaction and transport Monte Carlo codes is often the most accurate and efficient choice for assessing radiation protection quantities at accelerators. Due to the vast spread of such codes to all areas of particle physics and the associated extensive benchmarking with experimental data, the modeling has reached an unprecedented accuracy. Furthermore, most codes allow the user to simulate all aspects of a high energy particle cascade in one and the same run: from the first interaction of a TeV nucleus over the transport and re-interactions (hadronic and electromagnetic) of the produced secondaries, to detailed nuclear fragmentation, the calculation of radioactive decays and even of the electromagnetic shower caused by the radiation from such decays. A brief account of the codes most widely used for radiation protection studies at high energy accelerators is given in the following.

• **FLUKA [7,8]:** FLUKA is a general-purpose particle interaction and transport code. It comprises all features needed for radiation protection, such as detailed hadronic and nuclear interaction models up to 10 PeV, full coupling between hadronic and electromagnetic processes and numerous variance reduction options. The latter include weight windows, region importance biasing, and leading particle, interaction, and decay length biasing (among others). The capabilities of FLUKA are unique for studies of induced radioactivity, especially with regard to nuclide production, decay, and transport of residual radiation. In particular, particle cascades by prompt and residual radiation are simulated in parallel based on the microscopic models for nuclide production and a solution of the Bateman equations for activity build-up and decay.

• **GEANT4 [13,14]:** GEANT4 is an object-oriented toolkit consisting of a kernel that provides the framework for particle transport, including tracking, geometry description, material specifications, management of events and interfaces to external graphics systems. The kernel also provides interfaces to physics processes. It allows the user to freely select the physics models that best serve the particular application needs. Implementations of interaction models exist over an extended range of energies, from optical photons and thermal neutrons to high-energy interactions required for the simulation of accelerator and cosmic ray experiments. To facilitate the use of variance reduction techniques, general-purpose biasing methods such as importance biasing, weight windows, and a weight cut-off method have been introduced directly into the toolkit. Other variance reduction methods, such as leading particle biasing for hadronic processes, come with the respective physics packages.

• **MARS15 [15,16]:** The MARS15 code system is a set of Monte Carlo programs for the simulation of hadronic and electromagnetic cascades. It covers a wide energy range: 1 keV to 100 TeV for muons, charged hadrons, heavy ions and electromagnetic showers; and 0.00215 eV to 100 TeV for neutrons. Hadronic interactions above 5 GeV can be simulated with either an inclusive or an exclusive event generator. MARS15 is coupled to the MCNP4C code that handles all interactions of neutrons with energies below 14 MeV. Different variance reduction techniques, such as inclusive particle production, weight windows, particle splitting, and Russian roulette, are available in MARS15. A tagging module allows one to tag the origin of a given signal for source term or sensitivity analyses. Further features of MARS15 include a MAD-MARS Beam-Line Builder for a convenient creation of accelerator models.

• **MCNPX [17,18]:** MCNPX originates from the Monte Carlo N-Particle transport (MCNP) family of neutron interaction and transport codes and, therefore, features one of the most comprehensive and detailed descriptions of the related physical processes. Later it was extended to other particle types, including ions and electromagnetic particles. The neutron interaction and transport modules use standard evaluated data libraries mixed with physics models where such libraries are not available. The transport is continuous in energy. MCNPX contains one of the most powerful implementations of variance reduction techniques. Spherical mesh weight windows can be created by a generator in order to focus the simulation time on certain spatial regions of interest. In addition, a more generalized phase space biasing is also possible through energy- and time-dependent weight windows. Other biasing options include pulse-height tallies with variance reduction and criticality source convergence acceleration.

• **PHITS [19,20]:** The Particle and Heavy-Ion Transport code System PHITS was among the first general-purpose codes to simulate the transport and interactions of heavy ions in a wide energy range, from 10 MeV/nucleon to 100 GeV/nucleon. It is based on the high-energy hadron transport code NMTC/JAM that was extended to heavy ions. The transport of low-energy neutrons employs cross sections from evaluated nuclear data libraries such as ENDF and JENDL below 20 MeV and LA150 up to 150 MeV. Electromagnetic interactions are simulated based on the ITS code in the energy range between 1 keV and 1 GeV. Several variance reduction techniques, including weight windows and region importance biasing, are available in PHITS.

References:

1. International Commission on Radiation Units and Measurements, *Fundamental Quantities and Units for Ionizing Radiation*, ICRU Report 60 (1998).
2. ICRP Publication 103, *The 2007 Recommendations of the International Commission on Radiological Protection*, Annals of the ICRP, Elsevier (2007).
3. M. Pelliccioni, Radiation Protection Dosimetry **88**, 279 (2000).
4. E. Pochin, *Nuclear Radiation: Risks and Benefits*, Clarendon Press, Oxford, 1983.
5. United Nations, *Report of the United Nations Scientific Committee on the Effect of Atomic Radiation*, General Assembly, Official Records A/63/46 (2008).
6. W.P. Swanson, *Radiological Safety Aspects of the Operation of Electron Linear Accelerators*, IAEA Technical Reports Series No. 188 (1979).
7. A. Ferrari, *et al.*, FLUKA, A Multi-particle Transport Code (Program Version 2005), CERN-2005-010 (2005).
8. G. Battistoni, *et al.*, The FLUKA code: Description and benchmarking, *Proceedings of the Hadronic Shower Simulation Workshop 2006,* Fermilab 6–8 September 2006, M. Albrow, R. Raja, eds., *AIP Conference Proceeding 896*, 31–49, (2007).

9. R.H. Thomas and G.R. Stevenson, *Radiological Safety Aspects of the Operation of Proton Accelerators,* IAEA Technical Report Series No. 283 (1988).
10. T.A. Gabriel, *et al.*, Nucl. Instrum. Methods **A338**, 336 (1994).
11. `http://physics.nist.gov/PhysRefData/XrayMassCoef/cover.html`.
12. S. Roesler, *et al.*, "Simulation of Remanent Dose Rates and Benchmark Measurements at the CERN-EU High Energy Reference Field Facility," in *Proceedings of the Sixth International Meeting on Nuclear Applications of Accelerator Technology,* San Diego, CA, 1-5 June 2003, 655–662 (2003).
13. S. Agostinelli, *et al.*, Nucl. Instrum. Methods **A506**, 250 (2003).
14. J. Allison, *et al.*, IEEE Transactions on Nuclear Science **53**, 270 (2006).
15. N.V. Mokhov, S.I. Striganov, MARS15 Overview *Proceedings of the Hadronic Shower Simulation Workshop 2006,* Fermilab 6–8 September 2006, M. Albrow, R. Raja, eds., *AIP Conference Proceeding 896*, 50–60, (2007).
16. N.V. Mokhov, MARS Code System, Version 15 (2009), `www-ap.fnal.gov/MARS`.
17. D.B. Pelowitz, ed., Los Alamos National Laboratory report, LA-CP-05-0369 (2005).
18. G. McKinney, *et al.*, *Proceedings of the International Workshop on Fast Neutron Detectors* University of Cape Town, South Africa (2006).
19. H. Iwase, K. Niita, and T. Nakamura, Journal of Nuclear Science and Technology **39**, 1142 (2002).
20. K. Niita, *et al.*, Radiation Measurements **41**, 1080 (2006).

36. COMMONLY USED RADIOACTIVE SOURCES

Table 36.1. Revised November 1993 by E. Browne (LBNL).

			Particle		Photon	
		Type of	Energy	Emission	Energy	Emission
Nuclide	Half-life	decay	(MeV)	prob.	(MeV)	prob.
$^{22}_{11}$Na	2.603 y	β^+, EC	0.545	90%	0.511	Annih.
					1.275	100%
$^{54}_{25}$Mn	0.855 y	EC			0.835	100%
					Cr K x rays	26%
$^{55}_{26}$Fe	2.73 y	EC			Mn K x rays:	
					0.00590	24.4%
					0.00649	2.86%
$^{57}_{27}$Co	0.744 y	EC			0.014	9%
					0.122	86%
					0.136	11%
					Fe K x rays	58%
$^{60}_{27}$Co	5.271 y	β^-	0.316	100%	1.173	100%
					1.333	100%
$^{68}_{32}$Ge	0.742 y	EC			Ga K x rays	44%
$\rightarrow {}^{68}_{31}$Ga		β^+, EC	1.899	90%	0.511	Annih.
					1.077	3%
$^{90}_{38}$Sr	28.5 y	β^-	0.546	100%		
$\rightarrow {}^{90}_{39}$Y		β^-	2.283	100%		
$^{106}_{44}$Ru	1.020 y	β^-	0.039	100%		
$\rightarrow {}^{106}_{45}$Rh		β^-	3.541	79%	0.512	21%
					0.622	10%
$^{109}_{48}$Cd	1.267 y	EC	0.063 e^-	41%	0.088	3.6%
			0.084 e^-	45%	Ag K x rays	100%
			0.087 e^-	9%		
$^{113}_{50}$Sn	0.315 y	EC	0.364 e^-	29%	0.392	65%
			0.388 e^-	6%	In K x rays	97%
$^{137}_{55}$Cs	30.2 y	β^-	0.514	94%	0.662	85%
			1.176	6%		
$^{133}_{56}$Ba	10.54 y	EC	0.045 e^-	50%	0.081	34%
			0.075 e^-	6%	0.356	62%
					Cs K x rays	121%
$^{207}_{83}$Bi	31.8 y	EC	0.481 e^-	2%	0.569	98%
			0.975 e^-	7%	1.063	75%
			1.047 e^-	2%	1.770	7%
					Pb K x rays	78%
$^{228}_{90}$Th	1.912 y	6α:	5.341 to 8.785		0.239	44%
		3β^-:	0.334 to 2.246		0.583	31%
					2.614	36%
($\rightarrow {}^{224}_{88}$Ra	$\rightarrow {}^{220}_{86}$Rn	$\rightarrow {}^{216}_{84}$Po	$\rightarrow {}^{212}_{82}$Pb	$\rightarrow {}^{212}_{83}$Bi	$\rightarrow {}^{212}_{84}$Po)	
$^{241}_{95}$Am	432.7 y	α	5.443	13%	0.060	36%
			5.486	85%	Np L x rays	38%
$^{241}_{95}$Am/Be	432.2 y	6×10^{-5} neutrons (4–8 MeV) and				
		$4 \times 10^{-5}\gamma$'s (4.43 MeV) per Am decay				
$^{244}_{96}$Cm	18.11 y	α	5.763	24%	Pu L x rays	$\sim 9\%$
			5.805	76%		
$^{252}_{98}$Cf	2.645 y	α (97%)	6.076	15%		
			6.118	82%		
		Fission (3.1%)				
		$\approx 20\ \gamma$'s/fission; 80% < 1 MeV				
		≈ 4 neutrons/fission; $\langle E_n \rangle = 2.14$ MeV				

"Emission probability" is the probability per decay of a given emission; because of cascades these may total more than 100%. Only principal emissions are listed. EC means electron capture, and e^- means monoenergetic internal conversion (Auger) electron. The intensity of 0.511 MeV e^+e^- annihilation photons depends upon the number of stopped positrons. Endpoint $\beta^\pm$ energies are listed. In some cases when energies are closely spaced, the γ-ray values are approximate weighted averages. Radiation from short-lived daughter isotopes is included where relevant.

Half-lives, energies, and intensities are from E. Browne and R.B. Firestone, *Table of Radioactive Isotopes* (John Wiley & Sons, New York, 1986), recent *Nuclear Data Sheets*, and *X-ray and Gamma-ray Standards for Detector Calibration*, IAEA-TECDOC-619 (1991).

Neutron data are from *Neutron Sources for Basic Physics and Applications* (Pergamon Press, 1983).

37. PROBABILITY

Revised September 2013 by G. Cowan (RHUL).

37.1. General [1–8]

An abstract definition of probability can be given by considering a set S, called the sample space, and possible subsets $A, B, \ldots$, the interpretation of which is left open. The probability P is a real-valued function defined by the following axioms due to Kolmogorov [9]:

1. For every subset A in S, $P(A) \geq 0$;
2. For disjoint subsets (*i.e.*, $A \cap B = \emptyset$), $P(A \cup B) = P(A) + P(B)$;
3. $P(S) = 1$.

In addition, one defines the conditional probability $P(A|B)$ (read as P of A given B) as

$$P(A|B) = \frac{P(A \cap B)}{P(B)} \, . \tag{37.1}$$

From this definition and using the fact that $A \cap B$ and $B \cap A$ are the same, one obtains *Bayes' theorem*,

$$P(A|B) = \frac{P(B|A)P(A)}{P(B)} \, . \tag{37.2}$$

From the three axioms of probability and the definition of conditional probability, one obtains the *law of total probability*,

$$P(B) = \sum_i P(B|A_i)P(A_i) \, , \tag{37.3}$$

for any subset B and for disjoint A_i with $\cup_i A_i = S$. This can be combined with Bayes' theorem (Eq. (37.2)) to give

$$P(A|B) = \frac{P(B|A)P(A)}{\sum_i P(B|A_i)P(A_i)} \, , \tag{37.4}$$

where the subset A could, for example, be one of the A_i.

The most commonly used interpretation of the elements of the sample space are outcomes of a repeatable experiment. The probability $P(A)$ is assigned a value equal to the limiting frequency of occurrence of A. This interpretation forms the basis of *frequentist statistics*.

The elements of the sample space might also be interpreted as *hypotheses*, *i.e.*, statements that are either true or false, such as 'The mass of the W boson lies between 80.3 and 80.5 GeV.' Upon repetition of a measurement, however, such statements are either always true or always false, *i.e.*, the corresponding probabilities in the frequentist interpretation are either 0 or 1. Using *subjective probability*, however, $P(A)$ is interpreted as the degree of belief that the hypothesis A is true. Subjective probability is used in *Bayesian* (as opposed to frequentist) statistics. Bayes' theorem can be written

$$P(\text{theory}|\text{data}) \propto P(\text{data}|\text{theory})P(\text{theory}) \, , \tag{37.5}$$

where 'theory' represents some hypothesis and 'data' is the outcome of the experiment. Here $P(\text{theory})$ is the *prior* probability for the theory, which reflects the experimenter's degree of belief before carrying out the measurement, and $P(\text{data}|\text{theory})$ is the probability to have gotten the data actually obtained, given the theory, which is also called the *likelihood*.

Bayesian statistics provides no fundamental rule for obtaining the prior probability, which may depend on previous measurements, theoretical prejudices, *etc.* Once this has been specified, however, Eq. (37.5) tells how the probability for the theory must be modified in the light of the new data to give the *posterior* probability, $P(\text{theory}|\text{data})$. As Eq. (37.5) is stated as a proportionality, the probability must be normalized by summing (or integrating) over all possible hypotheses.

37.2. Random variables

A *random variable* is a numerical characteristic assigned to an element of the sample space. In the frequency interpretation of probability, it corresponds to an outcome of a repeatable experiment. Let x be a possible outcome of an observation. If x can take on any value from a continuous range, we write $f(x;\theta)dx$ as the probability that the measurement's outcome lies between x and $x + dx$. The function $f(x;\theta)$ is called the *probability density function* (p.d.f.), which may depend on one or more parameters θ. If x can take on only discrete values (*e.g.*, the non-negative integers), then we use $f(x;\theta)$ to denote the probability to find the value x. In the following the term p.d.f. is often taken to cover both the continuous and discrete cases, although technically the term density should only be used in the continuous case.

The p.d.f. is always normalized to unity. Both x and θ may have multiple components and are then often written as vectors. If θ is unknown, we may wish to estimate its value from a given set of measurements of x; this is a central topic of *statistics* (see Sec. 38).

The *cumulative distribution function* $F(a)$ is the probability that $x \leq a$:

$$F(a) = \int_{-\infty}^{a} f(x)\, dx \, . \tag{37.6}$$

Here and below, if x is discrete-valued, the integral is replaced by a sum. The endpoint a is expressly included in the integral or sum. Then $0 \leq F(x) \leq 1$, $F(x)$ is nondecreasing, and $P(a < x \leq b) = F(b) - F(a)$. If x is discrete, $F(x)$ is flat except at allowed values of x, where it has discontinuous jumps equal to $f(x)$.

Any function of random variables is itself a random variable, with (in general) a different p.d.f. The *expectation value* of any function $u(x)$ is

$$E[u(x)] = \int_{-\infty}^{\infty} u(x)\, f(x)\, dx \, , \tag{37.7}$$

assuming the integral is finite. The expectation value is linear, *i.e.*, for any two functions u and v of x and constants c_1 and c_2, $E[c_1 u + c_2 v] = c_1 E[u] + c_2 E[v]$.

The n^{th} moment of a random variable x is

$$\alpha_n \equiv E[x^n] = \int_{-\infty}^{\infty} x^n f(x)\, dx \, , \tag{37.8a}$$

and the n^{th} central moment of x (or moment about the mean, α_1) is

$$m_n \equiv E[(x - \alpha_1)^n] = \int_{-\infty}^{\infty} (x - \alpha_1)^n f(x)\, dx \, . \tag{37.8b}$$

The most commonly used moments are the mean μ and variance σ^2:

$$\mu \equiv \alpha_1 \, , \tag{37.9a}$$

$$\sigma^2 \equiv V[x] \equiv m_2 = \alpha_2 - \mu^2 \, . \tag{37.9b}$$

The mean is the location of the "center of mass" of the p.d.f., and the variance is a measure of the square of its width. Note that $V[cx+k] = c^2 V[x]$. It is often convenient to use the *standard deviation* of x, σ, defined as the square root of the variance.

Any odd moment about the mean is a measure of the skewness of the p.d.f. The simplest of these is the dimensionless coefficient of skewness $\gamma_1 = m_3/\sigma^3$.

The fourth central moment m_4 provides a convenient measure of the tails of a distribution. For the Gaussian distribution (see Sec. 37.4), one has $m_4 = 3\sigma^4$. The *kurtosis* is defined as $\gamma_2 = m_4/\sigma^4 - 3$, *i.e.*, it is zero for a Gaussian, positive for a *leptokurtic* distribution with longer tails, and negative for a *platykurtic* distribution with tails that die off more quickly than those of a Gaussian.

The *quantile* x_α is the value of the random variable x at which the cumulative distribution is equal to α. That is, the quantile is the inverse of the cumulative distribution function, *i.e.*, $x_\alpha = F^{-1}(\alpha)$. An important special case is the *median*, x_{med}, defined by $F(x_{\text{med}}) = 1/2$, *i.e.*, half the probability lies above and half lies below x_{med}.

(More rigorously, $x_{\rm med}$ is a median if $P(x \geq x_{\rm med}) \geq 1/2$ and $P(x \leq x_{\rm med}) \geq 1/2$. If only one value exists, it is called '*the* median.')

Under a monotonic change of variable $x \to y(x)$, the quantiles of a distribution (and hence also the median) obey $y_\alpha = y(x_\alpha)$. In general the expectation value and *mode* (most probable value) of a distribution do not, however, transform in this way.

Let x and y be two random variables with a *joint* p.d.f. $f(x,y)$. The *marginal* p.d.f. of x (the distribution of x with y unobserved) is

$$f_1(x) = \int_{-\infty}^{\infty} f(x,y)\,dy \;, \tag{37.10}$$

and similarly for the marginal p.d.f. $f_2(y)$. The *conditional* p.d.f. of y given fixed x (with $f_1(x) \neq 0$) is defined by $f_3(y|x) = f(x,y)/f_1(x)$, and similarly $f_4(x|y) = f(x,y)/f_2(y)$. From these, we immediately obtain Bayes' theorem (see Eqs. (37.2) and (37.4)),

$$f_4(x|y) = \frac{f_3(y|x)f_1(x)}{f_2(y)} = \frac{f_3(y|x)f_1(x)}{\int f_3(y|x')f_1(x')\,dx'} \;. \tag{37.11}$$

The mean of x is

$$\mu_x = \int_{-\infty}^{\infty}\int_{-\infty}^{\infty} x\, f(x,y)\,dx\,dy = \int_{-\infty}^{\infty} x\, f_1(x)\,dx \;, \tag{37.12}$$

and similarly for y. The *covariance* of x and y is

$$\mathrm{cov}[x,y] = E[(x-\mu_x)(y-\mu_y)] = E[xy] - \mu_x\mu_y \;. \tag{37.13}$$

A dimensionless measure of the covariance of x and y is given by the *correlation coefficient*,

$$\rho_{xy} = \mathrm{cov}[x,y]/\sigma_x\sigma_y \;, \tag{37.14}$$

where σ_x and σ_y are the standard deviations of x and y. It can be shown that $-1 \leq \rho_{xy} \leq 1$.

Two random variables x and y are *independent* if and only if

$$f(x,y) = f_1(x)f_2(y) \;. \tag{37.15}$$

If x and y are independent, then $\rho_{xy} = 0$; the converse is not necessarily true. If x and y are independent, $E[u(x)v(y)] = E[u(x)]E[v(y)]$, and $V[x+y] = V[x] + V[y]$; otherwise, $V[x+y] = V[x] + V[y] + 2\mathrm{cov}[x,y]$, and $E[uv]$ does not necessarily factorize.

Consider a set of n continuous random variables $\boldsymbol{x} = (x_1, \ldots, x_n)$ with joint p.d.f. $f(\boldsymbol{x})$, and a set of n new variables $\boldsymbol{y} = (y_1, \ldots, y_n)$, related to $\boldsymbol{x}$ by means of a function $\boldsymbol{y}(\boldsymbol{x})$ that is one-to-one, *i.e.*, the inverse $\boldsymbol{x}(\boldsymbol{y})$ exists. The joint p.d.f. for $\boldsymbol{y}$ is given by

$$g(\boldsymbol{y}) = f(\boldsymbol{x}(\boldsymbol{y}))|J| \;\;, \tag{37.16}$$

where $|J|$ is the absolute value of the determinant of the square matrix $J_{ij} = \partial x_i/\partial y_j$ (the Jacobian determinant). If the transformation from $\boldsymbol{x}$ to $\boldsymbol{y}$ is not one-to-one, the $\boldsymbol{x}$-space must be broken into regions where the function $\boldsymbol{y}(\boldsymbol{x})$ can be inverted, and the contributions to $g(\boldsymbol{y})$ from each region summed.

Given a set of functions $\boldsymbol{y} = (y_1, \ldots, y_m)$ with $m < n$, one can construct $n-m$ additional independent functions, apply the procedure above, then integrate the resulting $g(\boldsymbol{y})$ over the unwanted y_i to find the marginal distribution of those of interest.

For a one-to-one transformation of discrete random variables, the probability is obtained by simple substitution; no Jacobian is necessary because in this case f is a probability rather than a probability density. If the transformation is not one-to-one, then one must sum the probabilities for all values of the original variable that contribute to a given value of the transformed variable. If f depends on a set of parameters $\boldsymbol{\theta}$, a change to a different parameter set $\boldsymbol{\eta}(\boldsymbol{\theta})$ is made by simple substitution; no Jacobian is used.

37.3. Characteristic functions

The characteristic function $\phi(u)$ associated with the p.d.f. $f(x)$ is essentially its Fourier transform, or the expectation value of e^{iux}:

$$\phi(u) = E\left[e^{iux}\right] = \int_{-\infty}^{\infty} e^{iux} f(x)\,dx \;. \tag{37.17}$$

Once $\phi(u)$ is specified, the p.d.f. $f(x)$ is uniquely determined and vice versa; knowing one is equivalent to the other. Characteristic functions are useful in deriving a number of important results about moments and sums of random variables.

It follows from Eqs. (37.8a) and (37.17) that the n^{th} moment of a random variable x that follows $f(x)$ is given by

$$i^{-n}\left.\frac{d^n\phi}{du^n}\right|_{u=0} = \int_{-\infty}^{\infty} x^n f(x)\,dx = \alpha_n \;. \tag{37.18}$$

Thus it is often easy to calculate all the moments of a distribution defined by $\phi(u)$, even when $f(x)$ cannot be written down explicitly.

If the p.d.f.s $f_1(x)$ and $f_2(y)$ for independent random variables x and y have characteristic functions $\phi_1(u)$ and $\phi_2(u)$, then the characteristic function of the weighted sum $ax + by$ is $\phi_1(au)\phi_2(bu)$. The rules of addition for several important distributions (*e.g.*, that the sum of two Gaussian distributed variables also follows a Gaussian distribution) easily follow from this observation.

Let the (partial) characteristic function corresponding to the conditional p.d.f. $f_2(x|z)$ be $\phi_2(u|z)$, and the p.d.f. of z be $f_1(z)$. The characteristic function after integration over the conditional value is

$$\phi(u) = \int \phi_2(u|z)f_1(z)\,dz \;. \tag{37.19}$$

Suppose we can write ϕ_2 in the form

$$\phi_2(u|z) = A(u)e^{ig(u)z} \;. \tag{37.20}$$

Then

$$\phi(u) = A(u)\phi_1(g(u)) \;. \tag{37.21}$$

The cumulants (semi-invariants) κ_n of a distribution with characteristic function $\phi(u)$ are defined by the relation

$$\phi(u) = \exp\left[\sum_{n=1}^{\infty}\frac{\kappa_n}{n!}(iu)^n\right] = \exp\left(i\kappa_1 u - \tfrac{1}{2}\kappa_2 u^2 + \ldots\right) \;. \tag{37.22}$$

The values κ_n are related to the moments α_n and m_n. The first few relations are

$$\begin{aligned} &\kappa_1 = \alpha_1 \;(= \mu, \text{ the mean}) \\ &\kappa_2 = m_2 \;= \alpha_2 - \alpha_1^2 \;(= \sigma^2, \text{ the variance}) \\ &\kappa_3 = m_3 = \alpha_3 - 3\alpha_1\alpha_2 + 2\alpha_1^3 \;. \end{aligned} \tag{37.23}$$

37.4. Commonly used probability distributions

Table 37.1 gives a number of common probability density functions and corresponding characteristic functions, means, and variances. Further information may be found in Refs. [1– 8], [10], and [11], which has particularly detailed tables. Monte Carlo techniques for generating each of them may be found in our Sec. 39.4 and in Ref. [10]. We comment below on all except the trivial uniform distribution.

37.4.1. *Binomial and multinomial distributions* :

A random process with exactly two possible outcomes which occur with fixed probabilities is called a *Bernoulli* process. If the probability of obtaining a certain outcome (a "success") in an individual trial is p, then the probability of obtaining exactly r successes ($r = 0, 1, 2, \ldots, N$) in N independent trials, without regard to the order of the successes and failures, is given by the binomial distribution $f(r; N, p)$ in Table 37.1. If r and s are binomially distributed with parameters (N_r, p) and (N_s, p), then $t = r + s$ follows a binomial distribution with parameters $(N_r + N_s, p)$.

If there are are m possible outcomes for each trial having probabilities $p_1, p_2, \ldots, p_m$, then the joint probability to find $r_1, r_2, \ldots, r_m$ of each outcome after a total of N independent trials is given by the multinomial distribution as shown in Table 37.1. We can regard outcome i as "success" and all the rest as "failure", so individually, any of the r_i follow a binomial distribution for N trials and a success probability p_i.

37.4.2. ***Poisson distribution*** :

The Poisson distribution $f(n;\nu)$ gives the probability of finding exactly n events in a given interval of x (*e.g.*, space or time) when the events occur independently of one another and of x at an average rate of ν per the given interval. The variance σ^2 equals ν. It is the limiting case $p \to 0$, $N \to \infty$, $Np = \nu$ of the binomial distribution. The Poisson distribution approaches the Gaussian distribution for large ν.

For example, a large number of radioactive nuclei of a given type will result in a certain number of decays in a fixed time interval. If this interval is small compared to the mean lifetime, then the probability for a given nucleus to decay is small, and thus the number of decays in the time interval is well modeled as a Poisson variable.

37.4.3. ***Normal or Gaussian distribution*** :

The normal (or Gaussian) probability density function $f(x;\mu,\sigma^2)$ given in Table 37.1 has mean $E[x] = \mu$ and variance $V[x] = \sigma^2$. Comparison of the characteristic function $\phi(u)$ given in Table 37.1 with Eq. (37.22) shows that all cumulants κ_n beyond κ_2 vanish; this is a unique property of the Gaussian distribution. Some other properties are:

$P(x \text{ in range } \mu \pm \sigma) = 0.6827,$

$P(x \text{ in range } \mu \pm 0.6745\sigma) = 0.5,$

$E[|x-\mu|] = \sqrt{2/\pi}\sigma = 0.7979\sigma,$

half-width at half maximum $= \sqrt{2\ln 2}\,\sigma = 1.177\sigma.$

Table 37.1. Some common probability density functions, with corresponding characteristic functions and means and variances. In the Table, $\Gamma(k)$ is the gamma function, equal to $(k-1)!$ when k is an integer; ${}_1F_1$ is the confluent hypergeometric function of the 1st kind [11].

Distribution	Probability density function f (variable; parameters)	Characteristic function $\phi(u)$	Mean	Variance
Uniform	$f(x;a,b) = \begin{cases} 1/(b-a) & a \le x \le b \\ 0 & \text{otherwise} \end{cases}$	$\dfrac{e^{ibu} - e^{iau}}{(b-a)iu}$	$\dfrac{a+b}{2}$	$\dfrac{(b-a)^2}{12}$
Binomial	$f(r;N,p) = \dfrac{N!}{r!(N-r)!}\, p^r q^{N-r}$ $r = 0,1,2,\ldots,N\ ;\quad 0 \le p \le 1\ ;\quad q = 1-p$	$(q + pe^{iu})^N$	Np	Npq
Multinomial	$f(r_1,\ldots,r_m;N,p_1,\ldots,p_m) = \dfrac{N!}{r_1!\cdots r_m!} p_1^{r_1}\cdots p_m^{r_m}$ $r_k = 0,1,2,\ldots,N\ ;\quad 0 \le p_k \le 1\ ;\quad \sum_{k=1}^m r_k = N$	$\left(\sum_{k=1}^m p_k e^{iu_k}\right)^N$	$E[r_i] = Np_i$	$\mathrm{cov}[r_i,r_j] = Np_i(\delta_{ij} - p_j)$
Poisson	$f(n;\nu) = \dfrac{\nu^n e^{-\nu}}{n!}\ ;\quad n = 0,1,2,\ldots\ ;\quad \nu > 0$	$\exp[\nu(e^{iu}-1)]$	ν	ν
Normal (Gaussian)	$f(x;\mu,\sigma^2) = \dfrac{1}{\sigma\sqrt{2\pi}}\ \exp(-(x-\mu)^2/2\sigma^2)$ $-\infty < x < \infty\ ;\quad -\infty < \mu < \infty\ ;\quad \sigma > 0$	$\exp(i\mu u - \frac{1}{2}\sigma^2 u^2)$	μ	σ^2
Multivariate Gaussian	$f(\boldsymbol{x};\boldsymbol{\mu},V) = \dfrac{1}{(2\pi)^{n/2}\sqrt{\lvert V\rvert}}$ $\times \exp\left[-\frac{1}{2}(\boldsymbol{x}-\boldsymbol{\mu})^T V^{-1}(\boldsymbol{x}-\boldsymbol{\mu})\right]$ $-\infty < x_j < \infty;\quad -\infty < \mu_j < \infty;\quad \lvert V\rvert > 0$	$\exp\left[i\boldsymbol{\mu}\cdot\boldsymbol{u} - \frac{1}{2}\boldsymbol{u}^T V \boldsymbol{u}\right]$	$\boldsymbol{\mu}$	V_{jk}
Log-normal	$f(x;\mu,\sigma^2) = \dfrac{1}{\sigma\sqrt{2\pi}}\dfrac{1}{x}\ \exp(-(\ln x - \mu)^2/2\sigma^2)$ $0 < x < \infty\ ;\quad -\infty < \mu < \infty\ ;\quad \sigma > 0$	—	$\exp(\mu + \sigma^2/2)$	$\exp(2\mu+\sigma^2)$ $\times[\exp(\sigma^2) - 1]$
χ^2	$f(z;n) = \dfrac{z^{n/2-1}e^{-z/2}}{2^{n/2}\Gamma(n/2)}\ ;\quad z \ge 0$	$(1-2iu)^{-n/2}$	n	$2n$
Student's t	$f(t;n) = \dfrac{1}{\sqrt{n\pi}}\ \dfrac{\Gamma[(n+1)/2]}{\Gamma(n/2)}\left(1+\dfrac{t^2}{n}\right)^{-(n+1)/2}$ $-\infty < t < \infty\ ;\quad n$ not required to be integer	—	0 for $n > 1$	$n/(n-2)$ for $n > 2$
Gamma	$f(x;\lambda,k) = \dfrac{x^{k-1}\lambda^k e^{-\lambda x}}{\Gamma(k)}\ ;\quad 0 \le x < \infty\ ;$ k not required to be integer	$(1 - iu/\lambda)^{-k}$	k/λ	k/λ^2
Beta	$f(x;\alpha,\beta) = \dfrac{\Gamma(\alpha+\beta)}{\Gamma(\alpha)\Gamma(\beta)} x^{\alpha-1}(1-x)^{\beta-1}$ $0 \le x \le 1$	${}_1F_1(\alpha;\alpha+\beta;iu)$	$\dfrac{\alpha}{\alpha+\beta}$	$\dfrac{\alpha\beta}{(\alpha+\beta)^2(\alpha+\beta+1)}$

For a Gaussian with $\mu = 0$ and $\sigma^2 = 1$ (the *standard normal*) the cumulative distribution, often written $\Phi(x)$, is related to the error function erf by

$$F(x; 0, 1) \equiv \Phi(x) = \tfrac{1}{2}\left[1 + \mathrm{erf}(x/\sqrt{2})\right] . \quad (37.24)$$

The error function and standard Gaussian are tabulated in many references (*e.g.*, Ref. [11,12]) and are available in software packages such as ROOT [13]. For a mean μ and variance σ^2, replace x by $(x - \mu)/\sigma$. The probability of x in a given range can be calculated with Eq. (38.65).

For x and y independent and normally distributed, $z = ax + by$ follows a normal p.d.f. $f(z; a\mu_x + b\mu_y, a^2\sigma_x^2 + b^2\sigma_y^2)$; that is, the weighted means and variances add.

The Gaussian derives its importance in large part from the *central limit theorem*:

If independent random variables $x_1, \ldots, x_n$ are distributed according to *any* p.d.f. with finite mean and variance, then the sum $y = \sum_{i=1}^{n} x_i$ will have a p.d.f. that approaches a Gaussian for large n. If the p.d.f.s of the x_i are not identical, the theorem still holds under somewhat more restrictive conditions. The mean and variance are given by the sums of corresponding terms from the individual x_i. Therefore, the sum of a large number of fluctuations x_i will be distributed as a Gaussian, even if the x_i themselves are not.

For a set of n Gaussian random variables $\boldsymbol{x}$ with means $\boldsymbol{\mu}$ and covariances $V_{ij} = \mathrm{cov}[x_i, x_j]$, the p.d.f. for the one-dimensional Gaussian is generalized to

$$f(\boldsymbol{x}; \boldsymbol{\mu}, V) = \frac{1}{(2\pi)^{n/2}\sqrt{|V|}} \exp\left[-\tfrac{1}{2}(\boldsymbol{x} - \boldsymbol{\mu})^T V^{-1} (\boldsymbol{x} - \boldsymbol{\mu})\right] , \quad (37.25)$$

where the determinant $|V|$ must be greater than 0. For diagonal V (independent variables), $f(\boldsymbol{x}; \boldsymbol{\mu}, V)$ is the product of the p.d.f.s of n Gaussian distributions.

For $n = 2$, $f(\boldsymbol{x}; \boldsymbol{\mu}, V)$ is

$$f(x_1, x_2;\ \mu_1, \mu_2, \sigma_1, \sigma_2, \rho) = \frac{1}{2\pi\sigma_1\sigma_2\sqrt{1-\rho^2}}$$

$$\times \exp\left\{\frac{-1}{2(1-\rho^2)}\left[\frac{(x_1-\mu_1)^2}{\sigma_1^2} - \frac{2\rho(x_1-\mu_1)(x_2-\mu_2)}{\sigma_1\sigma_2} + \frac{(x_2-\mu_2)^2}{\sigma_2^2}\right]\right\} . \quad (37.26)$$

The characteristic function for the multivariate Gaussian is

$$\phi(\boldsymbol{u}; \boldsymbol{\mu}, V) = \exp\left[i\boldsymbol{\mu}\cdot\boldsymbol{u} - \tfrac{1}{2}\boldsymbol{u}^T V \boldsymbol{u}\right] . \quad (37.27)$$

If the components of $\boldsymbol{x}$ are independent, then Eq. (37.27) is the product of the characteristic functions of n Gaussians.

For an n-dimensional Gaussian distribution for $\boldsymbol{x}$ with mean $\boldsymbol{\mu}$ and covariance matrix V, the marginal distribution for any single x_i is is a one-dimensional Gaussian with mean μ_i and variance V_{ii}. The equation $(\boldsymbol{x} - \boldsymbol{a})^T V^{-1} (\boldsymbol{x} - \boldsymbol{a}) = C$, where C is any positive number, defines an n-dimensional ellipse centered about $\boldsymbol{a}$. If $\boldsymbol{a}$ is equal to the mean $\boldsymbol{\mu}$, then C is a random variable obeying the χ^2 distribution for n degrees of freedom, which is discussed in the following section. The probability that $\boldsymbol{x}$ lies outside the ellipsoid for a given value of C is given by $1 - F_{\chi^2}(C; n)$, where F_{χ^2} is the cumulative χ^2 distribution. This may be read from Fig. 38.1. For example, the "s-standard-deviation ellipsoid" occurs at $C = s^2$. For the two-variable case ($n = 2$), the point $\boldsymbol{x}$ lies outside the one-standard-deviation ellipsoid with 61% probability. The use of these ellipsoids as indicators of probable error is described in Sec. 38.4.2.2; the validity of those indicators assumes that $\boldsymbol{\mu}$ and V are correct.

37.4.4. *Log-normal distribution* :

If a random variable y follows a Gaussian distribution with mean μ and variance σ^2, then $x = e^y$ follows a log-normal distribution, as given in Table 37.1. As a consequence of the central limit theorem described in Sec. 37.4.3, the distribution of the product of a large number of positive random variables approaches a log-normal. It is bounded below by zero and is thus well suited for modeling quantities that are intrinsically non-negative such as an efficiency. One can implement a log-normal model for a random variable x by defining $y = \ln x$ so that y follows a Gaussian distribution.

37.4.5. χ^2 *distribution* :

If $x_1, \ldots, x_n$ are independent Gaussian random variables, the sum $z = \sum_{i=1}^{n} (x_i - \mu_i)^2/\sigma_i^2$ follows the χ^2 p.d.f. with n *degrees of freedom*, which we denote by $\chi^2(n)$. More generally, for n correlated Gaussian variables as components of a vector $\boldsymbol{X}$ with covariance matrix V, $z = \boldsymbol{X}^T V^{-1} \boldsymbol{X}$ follows $\chi^2(n)$ as in the previous section. For a set of z_i, each of which follows $\chi^2(n_i)$, $\sum z_i$ follows $\chi^2(\sum n_i)$. For large n, the χ^2 p.d.f. approaches a Gaussian with a mean and variance given by $\mu = n$ and $\sigma^2 = 2n$, respectively (here the formulae for μ and σ^2 are valid for all n).

The χ^2 p.d.f. is often used in evaluating the level of compatibility between observed data and a hypothesis for the p.d.f. that the data might follow. This is discussed further in Sec. 38.3.2 on significance tests.

37.4.6. *Student's t distribution* :

Suppose that y and $x_1, \ldots, x_n$ are independent and Gaussian distributed with mean 0 and variance 1. We then define

$$z = \sum_{i=1}^{n} x_i^2 \quad \text{and} \quad t = \frac{y}{\sqrt{z/n}} . \quad (37.28)$$

The variable z thus follows a $\chi^2(n)$ distribution. Then t is distributed according to Student's t distribution with n degrees of freedom, $f(t; n)$, given in Table 37.1.

If defined through gamma functions as in Table 37.1, the parameter n is not required to be an integer. As $n \to \infty$, the distribution approaches a Gaussian, and for $n = 1$ it is a *Cauchy* or *Breit–Wigner* distribution.

As an example, consider the *sample mean* $\overline{x} = \sum x_i/n$ and the *sample variance* $s^2 = \sum (x_i - \overline{x})^2/(n-1)$ for normally distributed x_i with unknown mean μ and variance σ^2. The sample mean has a Gaussian distribution with a variance σ^2/n, so the variable $(\overline{x} - \mu)/\sqrt{\sigma^2/n}$ is normal with mean 0 and variance 1. The quantity $(n-1)s^2/\sigma^2$ is independent of this and follows $\chi^2(n-1)$. The ratio

$$t = \frac{(\overline{x} - \mu)/\sqrt{\sigma^2/n}}{\sqrt{(n-1)s^2/\sigma^2(n-1)}} = \frac{\overline{x} - \mu}{\sqrt{s^2/n}} \quad (37.29)$$

is distributed as $f(t; n-1)$. The unknown variance σ^2 cancels, and t can be used to test the hypothesis that the true mean is some particular value μ.

37.4.7. *Gamma distribution* :

For a process that generates events as a function of x (*e.g.*, space or time) according to a Poisson distribution, the distance in x from an arbitrary starting point (which may be some particular event) to the k^{th} event follows a *gamma* distribution, $f(x; \lambda, k)$. The Poisson parameter μ is λ per unit x. The special case $k = 1$ (*i.e.*, $f(x; \lambda, 1) = \lambda e^{-\lambda x}$) is called the *exponential* distribution. A sum of k' exponential random variables x_i is distributed as $f(\sum x_i; \lambda, k')$.

The parameter k is not required to be an integer. For $\lambda = 1/2$ and $k = n/2$, the gamma distribution reduces to the $\chi^2(n)$ distribution.

37.4.8. ***Beta distribution*** :

The beta distribution describes a continuous random variable x in the interval $[0, 1]$. By scaling and translation one can easily generalize it to have arbitrary endpoints. In Bayesian inference about the parameter p of a binomial process, if the prior p.d.f. is a beta distribution $f(p; \alpha, \beta)$ then the observation of r successes out of N trials gives a posterior beta distribution $f(p; r+\alpha, N-r+\beta)$ (Bayesian methods are discussed further in Sec. 38). The uniform distribution is a beta distribution with $\alpha = \beta = 1$.

References:

1. H. Cramér, *Mathematical Methods of Statistics,* (Princeton Univ. Press, New Jersey, 1958).
2. A. Stuart and J.K. Ord, *Kendall's Advanced Theory of Statistics*, Vol. 1 *Distribution Theory* 6th Ed., (Halsted Press, New York, 1994), and earlier editions by Kendall and Stuart.
3. F.E. James, *Statistical Methods in Experimental Physics*, 2nd Ed., (World Scientific, Singapore, 2006).
4. L. Lyons, *Statistics for Nuclear and Particle Physicists*, (Cambridge University Press, New York, 1986).
5. B.R. Roe, *Probability and Statistics in Experimental Physics,* 2nd Ed., (Springer, New York, 2001).
6. R.J. Barlow, *Statistics: A Guide to the Use of Statistical Methods in the Physical Sciences*, (John Wiley, New York, 1989).
7. S. Brandt, *Data Analysis*, 3rd Ed., (Springer, New York, 1999).
8. G. Cowan, *Statistical Data Analysis*, (Oxford University Press, Oxford, 1998).
9. A.N. Kolmogorov, *Grundbegriffe der Wahrscheinlichkeitsrechnung*, (Springer, Berlin, 1933); *Foundations of the Theory of Probability*, 2nd Ed., (Chelsea, New York 1956).
10. Ch. Walck, *Hand-book on Statistical Distributions for Experimentalists*, University of Stockholm Internal Report SUF-PFY/96-01, available from `www.physto.se/~walck`.
11. M. Abramowitz and I. Stegun, eds., *Handbook of Mathematical Functions*, (Dover, New York, 1972).
12. F.W.J. Olver *et al.*, eds., NIST Handbook of Mathematical Functions, (Cambridge University Press, 2010); a companion Digital Library of Mathematical Functions is available at `dlmf.nist.gov`.
13. Rene Brun and Fons Rademakers, Nucl. Inst. Meth. A **389**, 81 (1997); see also `root.cern.ch`.
14. The CERN Program Library (CERNLIB); see `cernlib.web.cern.ch/cernlib`.

38. STATISTICS

Revised September 2013 by G. Cowan (RHUL).

This chapter gives an overview of statistical methods used in high-energy physics. In statistics, we are interested in using a given sample of data to make inferences about a probabilistic model, *e.g.*, to assess the model's validity or to determine the values of its parameters. There are two main approaches to statistical inference, which we may call frequentist and Bayesian.

In frequentist statistics, probability is interpreted as the frequency of the outcome of a repeatable experiment. The most important tools in this framework are parameter estimation, covered in Section 38.2, statistical tests, discussed in Section 38.3, and confidence intervals, which are constructed so as to cover the true value of a parameter with a specified probability, as described in Section 38.4.2. Note that in frequentist statistics one does not define a probability for a hypothesis or for the value of a parameter.

In Bayesian statistics, the interpretation of probability is more general and includes *degree of belief* (called subjective probability). One can then speak of a probability density function (p.d.f.) for a parameter, which expresses one's state of knowledge about where its true value lies. Bayesian methods provide a natural means to include additional information, which in general may be subjective; in fact they *require* prior probabilities for the hypotheses (or parameters) in question, *i.e.*, the degree of belief about the parameters' values before carrying out the measurement. Using Bayes' theorem (Eq. (37.4)), the prior degree of belief is updated by the data from the experiment. Bayesian methods for interval estimation are discussed in Sections 38.4.1 and 38.4.2.4.

For many inference problems, the frequentist and Bayesian approaches give similar numerical values, even though they answer different questions and are based on fundamentally different interpretations of probability. In some important cases, however, the two approaches may yield very different results. For a discussion of Bayesian vs. non-Bayesian methods, see references written by a statistician [1], by a physicist [2], or the more detailed comparison in Ref. 3.

Following common usage in physics, the word "error" is often used in this chapter to mean "uncertainty." More specifically it can indicate the size of an interval as in "the standard error" or "error propagation," where the term refers to the standard deviation of an estimator.

38.1. Fundamental concepts

Consider an experiment whose outcome is characterized by one or more data values, which we can write as a vector $\boldsymbol{x}$. A *hypothesis* H is a statement about the probability for the data, often written $P(\boldsymbol{x}|H)$. (We will usually use a capital letter for a probability and lower case for a probability density. Often the term p.d.f. is used loosely to refer to either a probability or a probability density.) This could, for example, define completely the p.d.f. for the data (a simple hypothesis), or it could specify only the functional form of the p.d.f., with the values of one or more parameters not determined (a composite hypothesis).

If the probability $P(\boldsymbol{x}|H)$ for data $\boldsymbol{x}$ is regarded as a function of the hypothesis H, then it is called the *likelihood* of H, usually written $L(H)$. Often the hypothesis is characterized by one or more parameters $\boldsymbol{\theta}$, in which case $L(\boldsymbol{\theta}) = P(\boldsymbol{x}|\boldsymbol{\theta})$ is called the likelihood function.

In some cases one can obtain at least approximate frequentist results using the likelihood evaluated only with the data obtained. In general, however, the frequentist approach requires a full specification of the probability model $P(\boldsymbol{x}|H)$ both as a function of the data $\boldsymbol{x}$ and hypothesis H.

In the Bayesian approach, inference is based on the posterior probability for H given the data $\boldsymbol{x}$, which represents one's degree of belief that H is true given the data. This is obtained from Bayes' theorem (37.4), which can be written

$$P(H|\boldsymbol{x}) = \frac{P(\boldsymbol{x}|H)\pi(H)}{\int P(\boldsymbol{x}|H')\pi(H')\,dH'} \,. \tag{38.1}$$

Here $P(\boldsymbol{x}|H)$ is the likelihood for H, which depends only on the data actually obtained. The quantity $\pi(H)$ is the prior probability for H, which represents one's degree of belief for H before carrying out the measurement. The integral in the denominator (or sum, for discrete hypotheses) serves as a normalization factor. If H is characterized by a continuous parameter θ then the posterior probability is a p.d.f. $p(\theta|\boldsymbol{x})$. Note that the likelihood function itself is not a p.d.f. for θ.

38.2. Parameter estimation

Here we review *point estimation* of parameters, first with an overview of the frequentist approach and its two most important methods, maximum likelihood and least squares, treated in Sections 38.2.2 and 38.2.3. The Bayesian approach is outlined in Sec. 38.2.4.

An *estimator* $\widehat{\theta}$ (written with a hat) is a function of the data used to estimate the value of the parameter θ. Sometimes the word 'estimate' is used to denote the value of the estimator when evaluated with given data. There is no fundamental rule dictating how an estimator must be constructed. One tries, therefore, to choose that estimator which has the best properties. The most important of these are (a) *consistency*, (b) *bias*, (c) *efficiency*, and (d) *robustness*.

(a) An estimator is said to be *consistent* if the estimate $\widehat{\theta}$ converges to the true value θ as the amount of data increases. This property is so important that it is possessed by all commonly used estimators.

(b) The *bias*, $b = E[\widehat{\theta}] - \theta$, is the difference between the expectation value of the estimator and the true value of the parameter. The expectation value is taken over a hypothetical set of similar experiments in which $\widehat{\theta}$ is constructed in the same way. When $b = 0$, the estimator is said to be unbiased. The bias depends on the chosen metric, *i.e.*, if $\widehat{\theta}$ is an unbiased estimator of θ, then $\widehat{\theta}^2$ is not in general an unbiased estimator for θ^2.

(c) *Efficiency* is the ratio of the minimum possible variance for any estimator of θ to the variance $V[\widehat{\theta}]$ of the estimator $\widehat{\theta}$. For the case of a single parameter, under rather general conditions the minimum variance is given by the Rao-Cramér-Fréchet bound,

$$\sigma^2_{\rm min} = \left(1 + \frac{\partial b}{\partial \theta}\right)^2 / I(\theta) \,, \tag{38.2}$$

where

$$I(\theta) = E\left[\left(\frac{\partial \ln L}{\partial \theta}\right)^2\right] = -E\left[\frac{\partial^2 \ln L}{\partial \theta^2}\right] \tag{38.3}$$

is the *Fisher information*, L is the likelihood, and the expectation value in (38.3) is carried out with respect to the data. For the final equality to hold, the range of allowed data values must not depend on θ.

The *mean-squared error*,

$$\text{MSE} = E[(\widehat{\theta} - \theta)^2] = V[\widehat{\theta}] + b^2 \,, \tag{38.4}$$

is a measure of an estimator's quality which combines bias and variance.

(d) *Robustness* is the property of being insensitive to departures from assumptions in the p.d.f., *e.g.*, owing to uncertainties in the distribution's tails.

It is not in general possible to optimize simultaneously for all the measures of estimator quality described above. For example, there is in general a trade-off between bias and variance. For some common estimators, the properties above are known exactly. More generally, it is possible to evaluate them by Monte Carlo simulation. Note that they will often depend on the unknown θ.

38.2.1. *Estimators for mean, variance, and median* :

Suppose we have a set of n independent measurements, $x_1, \ldots, x_n$, each assumed to follow a p.d.f. with unknown mean μ and unknown variance σ^2. The measurements do not necessarily have to follow a Gaussian distribution. Then

$$\widehat{\mu} = \frac{1}{n}\sum_{i=1}^{n} x_i \tag{38.5}$$

$$\widehat{\sigma^2} = \frac{1}{n-1}\sum_{i=1}^{n}(x_i - \widehat{\mu})^2 \tag{38.6}$$

are unbiased estimators of μ and σ^2. The variance of $\widehat{\mu}$ is σ^2/n and the variance of $\widehat{\sigma^2}$ is

$$V\left[\widehat{\sigma^2}\right] = \frac{1}{n}\left(m_4 - \frac{n-3}{n-1}\sigma^4\right) , \tag{38.7}$$

where m_4 is the 4th central moment of x (see Eq. (37.8b)). For Gaussian distributed x_i, this becomes $2\sigma^4/(n-1)$ for any $n \geq 2$, and for large n the standard deviation of $\widehat{\sigma}$ (the "error of the error") is $\sigma/\sqrt{2n}$. For any n and Gaussian x_i, $\widehat{\mu}$ is an efficient estimator for μ, and the estimators $\widehat{\mu}$ and $\widehat{\sigma^2}$ are uncorrelated. Otherwise the arithmetic mean (38.5) is not necessarily the most efficient estimator; this is discussed further in Sec. 8.7 of Ref. 4.

If σ^2 is known, it does not improve the estimate $\widehat{\mu}$, as can be seen from Eq. (38.5); however, if μ is known, one can substitute it for $\widehat{\mu}$ in Eq. (38.6) and replace $n-1$ by n to obtain an estimator of σ^2 still with zero bias but smaller variance. If the x_i have different, known variances σ_i^2, then the weighted average

$$\widehat{\mu} = \frac{1}{w}\sum_{i=1}^{n} w_i x_i , \tag{38.8}$$

where $w_i = 1/\sigma_i^2$ and $w = \sum_i w_i$, is an unbiased estimator for μ with a smaller variance than an unweighted average. The standard deviation of $\widehat{\mu}$ is $1/\sqrt{w}$.

As an estimator for the median $x_{\rm med}$, one can use the value $\widehat{x}_{\rm med}$ such that half the x_i are below and half above (the sample median). If the sample median lies between two observed values, it is set by convention halfway between them. If the p.d.f. of x has the form $f(x-\mu)$ and μ is both mean and median, then for large n the variance of the sample median approaches $1/[4nf^2(0)]$, provided $f(0) > 0$. Although estimating the median can often be more difficult computationally than the mean, the resulting estimator is generally more robust, as it is insensitive to the exact shape of the tails of a distribution.

38.2.2. *The method of maximum likelihood* :

Suppose we have a set of measured quantities $\boldsymbol{x}$ and the likelihood $L(\boldsymbol{\theta}) = P(\boldsymbol{x}|\boldsymbol{\theta})$ for a set of parameters $\boldsymbol{\theta} = (\theta_1, \ldots, \theta_N)$. The *maximum likelihood* (ML) estimators for $\boldsymbol{\theta}$ are defined as the values that give the maximum of L. Because of the properties of the logarithm, it is usually easier to work with $\ln L$, and since both are maximized for the same parameter values $\boldsymbol{\theta}$, the ML estimators can be found by solving the *likelihood equations*,

$$\frac{\partial \ln L}{\partial \theta_i} = 0 , \qquad i = 1, \ldots, N . \tag{38.9}$$

Often the solution must be found numerically. Maximum likelihood estimators are important because they are asymptotically unbiased and efficient for large data samples, under quite general conditions, and the method has a wide range of applicability.

In general the likelihood function is obtained from the probability of the data under assumption of the parameters. An important special case is when the data consist of *i.i.d.* (independent and identically distributed) values. Here one has a set of n statistically independent quantities $\boldsymbol{x} = (x_1, \ldots, x_n)$, where each component follows the same p.d.f. $f(x;\boldsymbol{\theta})$. In this case the joint p.d.f. of the data sample factorizes and the likelihood function is

$$L(\boldsymbol{\theta}) = \prod_{i=1}^{n} f(x_i;\boldsymbol{\theta}) . \tag{38.10}$$

In this case the number of events n is regarded as fixed. If however the probability to observe n events itself depends on the parameters $\boldsymbol{\theta}$, then this should be included in the likelihood. For example, if n follows a Poisson distribution with mean μ and the independent x values all follow $f(x;\boldsymbol{\theta})$, then the likelihood becomes

$$L(\boldsymbol{\theta}) = \frac{\mu^n}{n!}e^{-\mu}\prod_{i=1}^{n} f(x_i;\boldsymbol{\theta}) . \tag{38.11}$$

Equation. (38.11)) is often called the *extended likelihood* (see, *e.g.*, Refs. [6–8]) . In general μ is a function of $\boldsymbol{\theta}$, and including the probability for n given $\boldsymbol{\theta}$ in the likelihood provides additional information about the parameters and thus leads to a reduction in their statistical uncertainties.

In evaluating the likelihood function, it is important that any normalization factors in the p.d.f. that involve $\boldsymbol{\theta}$ be included. However, we will only be interested in the maximum of L and in ratios of L at different values of the parameters; hence any multiplicative factors that do not involve the parameters that we want to estimate may be dropped, including factors that depend on the data but not on $\boldsymbol{\theta}$.

Under a one-to-one change of parameters from $\boldsymbol{\theta}$ to $\boldsymbol{\eta}$, the ML estimators $\widehat{\boldsymbol{\theta}}$ transform to $\boldsymbol{\eta}(\widehat{\boldsymbol{\theta}})$. That is, the ML solution is invariant under change of parameter. However, other properties of ML estimators, in particular the bias, are not invariant under change of parameter.

The inverse V^{-1} of the covariance matrix $V_{ij} = \mathrm{cov}[\widehat{\theta}_i, \widehat{\theta}_j]$ for a set of ML estimators can be estimated by using

$$(\widehat{V}^{-1})_{ij} = -\left.\frac{\partial^2 \ln L}{\partial\theta_i \partial\theta_j}\right|_{\widehat{\theta}} ; \tag{38.12}$$

for finite samples, however, Eq. (38.12) can result in an underestimate of the variances. In the large sample limit (or in a linear model with Gaussian errors), L has a Gaussian form and $\ln L$ is (hyper)parabolic. In this case, it can be seen that a numerically equivalent way of determining s-standard-deviation errors is from the hypersurface defined by the $\boldsymbol{\theta'}$ such that

$$\ln L(\boldsymbol{\theta'}) = \ln L_{\rm max} - s^2/2 , \tag{38.13}$$

where $\ln L_{\rm max}$ is the value of $\ln L$ at the solution point (compare with Eq. (38.68)). The minimum and maximum values of θ_i on the hypersurface then give an approximate s-standard deviation confidence interval for θ_i (see Section 38.4.2.2).

38.2.2.1. *ML with binned data:*

If the total number of data values x_i, $i = 1, \ldots, n_{\rm tot}$, is small, the unbinned maximum likelihood method, *i.e.*, use of equation (38.10) (or (38.11) for extended ML), is preferred since binning can only result in a loss of information, and hence larger statistical errors for the parameter estimates. If the sample is large, it can be convenient to bin the values in a histogram with N bins, so that one obtains a vector of data $\boldsymbol{n} = (n_1, \ldots, n_N)$ with expectation values $\boldsymbol{\mu} = E[\boldsymbol{n}]$ and probabilities $f(\boldsymbol{n};\boldsymbol{\mu})$. Suppose the mean values $\boldsymbol{\mu}$ can be determined as a function of a set of parameters $\boldsymbol{\theta}$. Then one may maximize the likelihood function based on the contents of the bins.

As mentioned in Sec. 38.2.2, the total number of events $n_{\rm tot} = \sum_i n_i$ can be regarded as fixed or as a random variable. If it is fixed, the histogram follows a multinomial distribution,

$$f_{\rm M}(\boldsymbol{n};\boldsymbol{\theta}) = \frac{n_{\rm tot}!}{n_1! \cdots n_N!} p_1^{n_1} \cdots p_N^{n_N} , \tag{38.14}$$

where we assume the probabilities p_i are given functions of the parameters $\boldsymbol{\theta}$. The distribution can be written equivalently in terms of the expected number of events in each bin, $\mu_i = n_{\rm tot} p_i$. If the n_i are regarded as independent and Poisson distributed, then the data are described by a product of Poisson probabilities,

$$f_{\rm P}(\boldsymbol{n};\boldsymbol{\theta}) = \prod_{i=1}^{N} \frac{\mu_i^{n_i}}{n_i!} e^{-\mu_i} , \tag{38.15}$$

where the mean values μ_i are given functions of $\boldsymbol{\theta}$. The total number of events $n_{\rm tot}$ thus follows a Poisson distribution with mean $\mu_{\rm tot} = \sum_i \mu_i$.

When using maximum likelihood with binned data, one can find the ML estimators and at the same time obtain a statistic usable for a test of goodness-of-fit (see Sec. 38.3.2). Maximizing the likelihood $L(\boldsymbol{\theta}) = f_{\rm M/P}(\boldsymbol{n};\boldsymbol{\theta})$ is equivalent to maximizing the likelihood ratio $\lambda(\boldsymbol{\theta}) = f_{\rm M/P}(\boldsymbol{n};\boldsymbol{\theta})/f(\boldsymbol{n};\widehat{\boldsymbol{\mu}})$, where in the denominator $f(\boldsymbol{n};\boldsymbol{\mu})$ is a

model with an adjustable parameter for each bin, $\boldsymbol{\mu} = (\mu_1, \ldots, \mu_N)$, and the corresponding estimators are $\hat{\boldsymbol{\mu}} = (n_1, \ldots, n_N)$. Often one minimizes instead the equivalent quantity $-2\ln\lambda(\boldsymbol{\theta})$. For independent Poisson distributed n_i this is [9]

$$-2\ln\lambda(\boldsymbol{\theta}) = 2\sum_{i=1}^{N}\left[\mu_i(\boldsymbol{\theta}) - n_i + n_i\ln\frac{n_i}{\mu_i(\boldsymbol{\theta})}\right] , \qquad (38.16)$$

where for bins with $n_i = 0$, the last term in (38.16) is zero. The expression (38.16) without the terms $\mu_i - n_i$ also gives $-2\ln\lambda(\boldsymbol{\theta})$ for multinomially distributed n_i, *i.e.*, when the total number of entries is regarded as fixed. In the limit of zero bin width, maximizing (38.16) is equivalent to maximizing the unbinned extended likelihood function (38.11) or in the multinomial case without the $\mu_i - n_i$ terms one obtains Eq. (38.10).

A smaller value of $-2\ln\lambda(\widehat{\boldsymbol{\theta}})$ corresponds to better agreement between the data and the hypothesized form of $\boldsymbol{\mu}(\boldsymbol{\theta})$. The value of $-2\ln\lambda(\widehat{\boldsymbol{\theta}})$ can thus be translated into a p-value as a measure of goodness-of-fit, as described in Sec. 38.3.2. Assuming the model is correct, then according to Wilks' theorem, for sufficiently large μ_i and providing certain regularity conditions are met, the minimum of $-2\ln\lambda$ as defined by Eq. (38.16) follows a χ^2 distribution (see, *e.g.*, Ref. 9). If there are N bins and m fitted parameters, then the number of degrees of freedom for the χ^2 distribution is $N - m$ if the data are treated as Poisson-distributed, and $N - m - 1$ if the n_i are multinomially distributed.

Suppose the n_i are Poisson-distributed and the overall normalization $\mu_{\rm tot} = \sum_i \mu_i$ is taken as an adjustable parameter, so that $\mu_i = \mu_{\rm tot} p_i(\boldsymbol{\theta})$, where the probability to be in the ith bin, $p_i(\boldsymbol{\theta})$, does not depend on $\mu_{\rm tot}$. Then by minimizing Eq. (38.16), one obtains that the area under the fitted function is equal to the sum of the histogram contents, *i.e.*, $\sum_i \mu_i = \sum_i n_i$.

38.2.2.2. *Frequentist treatment of nuisance parameters:*

Suppose we want to determine the values of parameters $\boldsymbol{\theta}$ using a set of measurements $\boldsymbol{x}$ described by a probability model $P_x(\boldsymbol{x}|\boldsymbol{\theta})$. In general the model is not perfect, which is to say it can not provide an accurate description of the data even at the most optimal point of its parameter space. As a result, the estimated parameters can have a systematic bias.

One can in general improve the model by including in it additional parameters. That is, it is extended to $P_x(\boldsymbol{x}|\boldsymbol{\theta},\boldsymbol{\nu})$, which depends on parameters of interest $\boldsymbol{\theta}$ and *nuisance parameters* $\boldsymbol{\nu}$. The additional parameters are not of intrinsic interest but must be included for the model to be accurate for some point in the enlarged parameter space.

Although including additional parameters may eliminate or at least reduce the effect of systematic uncertainties, their presence will result in increased statistical uncertainties for the parameters of interest. This occurs because the estimators for the nuisance parameters and those of interest will in general be correlated, which results in an enlargement of the contour defined by Eq. (38.13).

To reduce the impact of the nuisance parameters one often tries to constrain their values by means of control or calibration measurements, say, having data $\boldsymbol{y}$. For example, some components of $\boldsymbol{y}$ could represent estimates of the nuisance parameters, often from separate experiments. Suppose the measurements $\boldsymbol{y}$ are statistically independent from $\boldsymbol{x}$ and are described by a model $P_y(\boldsymbol{y}|\boldsymbol{\nu})$. The joint model for both $\boldsymbol{x}$ and $\boldsymbol{y}$ is in this case therefore the product of the probabilities for $\boldsymbol{x}$ and $\boldsymbol{y}$, and thus the likelihood function for the full set of parameters is

$$L(\boldsymbol{\theta},\boldsymbol{\nu}) = P_x(\boldsymbol{x}|\boldsymbol{\theta},\boldsymbol{\nu})P_y(\boldsymbol{y}|\boldsymbol{\nu}) . \qquad (38.17)$$

Note that in this case if one wants to simulate the experiment by means of Monte Carlo, both the primary and control measurements, $\boldsymbol{x}$ and $\boldsymbol{y}$, must be generated for each repetition under assumption of fixed values for the parameters $\boldsymbol{\theta}$ and $\boldsymbol{\nu}$.

Using all of the parameters $(\boldsymbol{\theta},\boldsymbol{\nu})$ in Eq. (38.13) to find the statistical errors in the parameters of interest $\boldsymbol{\theta}$ is equivalent to using the *profile likelihood*, which depends only on $\boldsymbol{\theta}$. It is defined as

$$L_{\rm p}(\boldsymbol{\theta}) = L(\boldsymbol{\theta},\widehat{\widehat{\boldsymbol{\nu}}}(\boldsymbol{\theta})), \qquad (38.18)$$

where the double-hat notation indicates the profiled values of the parameters $\boldsymbol{\nu}$, defined as the values that maximize L for the specified $\boldsymbol{\theta}$. The profile likelihood is discussed further in Section 38.3.2.1 in connection with hypothesis tests.

38.2.3. ***The method of least squares*** :

The *method of least squares* (LS) coincides with the method of maximum likelihood in the following special case. Consider a set of N independent measurements y_i at known points x_i. The measurement y_i is assumed to be Gaussian distributed with mean $\mu(x_i;\boldsymbol{\theta})$ and known variance σ_i^2. The goal is to construct estimators for the unknown parameters $\boldsymbol{\theta}$. The likelihood function contains the sum of squares

$$\chi^2(\boldsymbol{\theta}) = -2\ln L(\boldsymbol{\theta}) + \text{ constant } = \sum_{i=1}^{N}\frac{(y_i - \mu(x_i;\boldsymbol{\theta}))^2}{\sigma_i^2} . \qquad (38.19)$$

The parameter values that maximize L are the same as those which minimize χ^2.

The minimum of Equation (38.19) defines the least-squares estimators $\widehat{\boldsymbol{\theta}}$ for the more general case where the y_i are not Gaussian distributed as long as they are independent. If they are not independent but rather have a covariance matrix $V_{ij} = \text{cov}[y_i, y_j]$, then the LS estimators are determined by the minimum of

$$\chi^2(\boldsymbol{\theta}) = (\boldsymbol{y} - \boldsymbol{\mu}(\boldsymbol{\theta}))^T V^{-1}(\boldsymbol{y} - \boldsymbol{\mu}(\boldsymbol{\theta})) , \qquad (38.20)$$

where $\boldsymbol{y} = (y_1, \ldots, y_N)$ is the (column) vector of measurements, $\boldsymbol{\mu}(\boldsymbol{\theta})$ is the corresponding vector of predicted values, and the superscript T denotes the transpose.

Often one further restricts the problem to the case where $\mu(x_i;\boldsymbol{\theta})$ is a linear function of the parameters, *i.e.*,

$$\mu(x_i;\boldsymbol{\theta}) = \sum_{j=1}^{m}\theta_j h_j(x_i) . \qquad (38.21)$$

Here the $h_j(x)$ are m linearly independent functions, *e.g.*, $1, x, x^2, \ldots, x^{m-1}$ or Legendre polynomials. We require $m < N$ and at least m of the x_i must be distinct.

Minimizing χ^2 in this case with m parameters reduces to solving a system of m linear equations. Defining $H_{ij} = h_j(x_i)$ and minimizing χ^2 by setting its derivatives with respect to the θ_i equal to zero gives the LS estimators,

$$\widehat{\boldsymbol{\theta}} = (H^T V^{-1} H)^{-1} H^T V^{-1}\boldsymbol{y} \equiv D\boldsymbol{y} . \qquad (38.22)$$

The covariance matrix for the estimators $U_{ij} = \text{cov}[\widehat{\theta}_i, \widehat{\theta}_j]$ is given by

$$U = DVD^T = (H^T V^{-1} H)^{-1} , \qquad (38.23)$$

or equivalently, its inverse U^{-1} can be found from

$$(U^{-1})_{ij} = \frac{1}{2}\frac{\partial^2\chi^2}{\partial\theta_i\partial\theta_j}\bigg|_{\theta=\widehat{\theta}} = \sum_{k,l=1}^{N} h_i(x_k)(V^{-1})_{kl}h_j(x_l) . \qquad (38.24)$$

The LS estimators can also be found from the expression

$$\widehat{\boldsymbol{\theta}} = U\boldsymbol{g} , \qquad (38.25)$$

where the vector $\boldsymbol{g}$ is defined by

$$g_i = \sum_{j,k=1}^{N} y_j h_i(x_k)(V^{-1})_{jk} . \qquad (38.26)$$

For the case of uncorrelated y_i, for example, one can use (38.25) with

$$(U^{-1})_{ij} = \sum_{k=1}^{N}\frac{h_i(x_k)h_j(x_k)}{\sigma_k^2} , \qquad (38.27)$$

$$g_i = \sum_{k=1}^{N}\frac{y_k h_i(x_k)}{\sigma_k^2} . \qquad (38.28)$$

Expanding $\chi^2(\boldsymbol{\theta})$ about $\widehat{\boldsymbol{\theta}}$, one finds that the contour in parameter space defined by

$$\chi^2(\boldsymbol{\theta}) = \chi^2(\widehat{\boldsymbol{\theta}}) + 1 = \chi^2_{\rm min} + 1 \qquad (38.29)$$

has tangent planes located at approximately plus-or-minus-one standard deviation $\sigma_{\widehat{\theta}}$ from the LS estimates $\widehat{\boldsymbol{\theta}}$.

In constructing the quantity $\chi^2(\boldsymbol{\theta})$ one requires the variances or, in the case of correlated measurements, the covariance matrix. Often these quantities are not known *a priori* and must be estimated from the data; an important example is where the measured value y_i represents the event count in a histogram bin. If, for example, y_i represents a Poisson variable, for which the variance is equal to the mean, then one can either estimate the variance from the predicted value, $\mu(x_i;\boldsymbol{\theta})$, or from the observed number itself, y_i. In the first option, the variances become functions of the fitted parameters, which may lead to calculational difficulties. The second option can be undefined if y_i is zero, and in both cases for small y_i, the variance will be poorly estimated. In either case, one should constrain the normalization of the fitted curve to the correct value, *i.e.*, one should determine the area under the fitted curve directly from the number of entries in the histogram (see Ref. 8, Section 7.4). As noted in Sec. 38.2.2.1, this issue is avoided when using the method of extended maximum likelihood with binned data by minimizing Eq. (38.16). In that case if the expected number of events $\mu_{\rm tot}$ does not depend on the other fitted parameters $\boldsymbol{\theta}$, then its extended ML estimator is equal to the observed total number of events.

As the minimum value of the χ^2 represents the level of agreement between the measurements and the fitted function, it can be used for assessing the goodness-of-fit; this is discussed further in Section 38.3.2.

38.2.4. *The Bayesian approach* :

In the frequentist methods discussed above, probability is associated only with data, not with the value of a parameter. This is no longer the case in Bayesian statistics, however, which we introduce in this section. For general introductions to Bayesian statistics see, *e.g.*, Refs. [22–25].

Suppose the outcome of an experiment is characterized by a vector of data $\boldsymbol{x}$, whose probability distribution depends on an unknown parameter (or parameters) $\boldsymbol{\theta}$ that we wish to determine. In Bayesian statistics, all knowledge about $\boldsymbol{\theta}$ is summarized by the posterior p.d.f. $p(\boldsymbol{\theta}|\boldsymbol{x})$, whose integral over any given region gives the degree of belief for $\boldsymbol{\theta}$ to take on values in that region, given the data $\boldsymbol{x}$. It is obtained by using Bayes' theorem,

$$p(\boldsymbol{\theta}|\boldsymbol{x}) = \frac{P(\boldsymbol{x}|\boldsymbol{\theta})\pi(\boldsymbol{\theta})}{\int P(\boldsymbol{x}|\boldsymbol{\theta}')\pi(\boldsymbol{\theta}')\,d\boldsymbol{\theta}'}\,, \qquad (38.30)$$

where $P(\boldsymbol{x}|\boldsymbol{\theta})$ is the likelihood function, *i.e.*, the joint p.d.f. for the data viewed as a function of $\boldsymbol{\theta}$, evaluated with the data actually obtained in the experiment, and $\pi(\boldsymbol{\theta})$ is the prior p.d.f. for $\boldsymbol{\theta}$. Note that the denominator in Eq. (38.30) serves to normalize the posterior p.d.f. to unity.

As it can be difficult to report the full posterior p.d.f. $p(\boldsymbol{\theta}|\boldsymbol{x})$, one would usually summarize it with statistics such as the mean (or median) values, and covariance matrix. In addition one may construct intervals with a given probability content, as is discussed in Sec. 38.4.1 on Bayesian interval estimation.

38.2.4.1. *Priors:*

Bayesian statistics supplies no unique rule for determining the prior $\pi(\boldsymbol{\theta})$; this reflects the analyst's subjective degree of belief (or state of knowledge) about $\boldsymbol{\theta}$ before the measurement was carried out. For the result to be of value to the broader community, whose members may not share these beliefs, it is important to carry out a sensitivity analysis, that is, to show how the result changes under a reasonable variation of the prior probabilities.

One might like to construct $\pi(\boldsymbol{\theta})$ to represent complete ignorance about the parameters by setting it equal to a constant. A problem here is that if the prior p.d.f. is flat in $\boldsymbol{\theta}$, then it is not flat for a nonlinear function of $\boldsymbol{\theta}$, and so a different parametrization of the problem would lead in general to a non-equivalent posterior p.d.f.

For the special case of a constant prior, one can see from Bayes' theorem (38.30) that the posterior is proportional to the likelihood, and therefore the mode (peak position) of the posterior is equal to the ML estimator. The posterior mode, however, will change in general upon a transformation of parameter. One may use as the Bayesian estimator a summary statistic other than the mode, such as the median, which is invariant under parameter transformation. But this will not in general coincide with the ML estimator.

The difficult and subjective nature of encoding personal knowledge into priors has led to what is called *objective Bayesian statistics*, where prior probabilities are based not on an actual degree of belief but rather derived from formal rules. These give, for example, priors which are invariant under a transformation of parameters, or ones which result in a maximum gain in information for a given set of measurements. For an extensive review see, *e.g.*, Ref. 26.

Objective priors do not in general reflect degree of belief, but they could in some cases be taken as possible, although perhaps extreme, subjective priors. The posterior probabilities as well therefore do not necessarily reflect a degree of belief. However one may regard investigating a variety of objective priors to be an important part of the sensitivity analysis. Furthermore, use of objective priors with Bayes' theorem can be viewed as a recipe for producing estimators or intervals which have desirable frequentist properties.

An important procedure for deriving objective priors is due to Jeffreys. According to *Jeffreys' rule* one takes the prior as

$$\pi(\boldsymbol{\theta}) \propto \sqrt{\det(I(\boldsymbol{\theta}))}\,, \qquad (38.31)$$

where

$$I_{ij}(\boldsymbol{\theta}) = -E\left[\frac{\partial^2 \ln P(\boldsymbol{x}|\boldsymbol{\theta})}{\partial\theta_i \partial\theta_j}\right] \qquad (38.32)$$

is the *Fisher information matrix*. One can show that the Jeffreys prior leads to inference that is invariant under a transformation of parameters. One should note that the Jeffreys prior depends on the likelihood function, and thus contains information about the measurement model itself, which goes beyond one's degree of belief about the value of a parameter. As examples, the Jeffreys prior for the mean μ of a Gaussian distribution is a constant, and for the mean of a Poisson distribution one finds $\pi(\mu) \propto 1/\sqrt{\mu}$.

Neither the constant nor $1/\sqrt{\mu}$ priors can be normalized to unit area and are therefore said to be *improper*. This can be allowed because the prior always appears multiplied by the likelihood function, and if the likelihood falls to zero sufficiently quickly then one may have a normalizable posterior density.

An important type of objective prior is the reference prior due to Bernardo and Berger [27]. To find the reference prior for a given problem one considers the Kullback-Leibler divergence $D_n[\pi, p]$ of the posterior $p(\boldsymbol{\theta}|\boldsymbol{x})$ relative to a prior $\pi(\boldsymbol{\theta})$, obtained from a set of i.i.d. data $\boldsymbol{x} = (x_1, \ldots, x_n)$:

$$D_n[\pi, p] = \int p(\boldsymbol{\theta}|\boldsymbol{x}) \ln \frac{p(\boldsymbol{\theta}|\boldsymbol{x})}{\pi(\boldsymbol{\theta})}\, d\boldsymbol{\theta}\,. \qquad (38.33)$$

This is effectively a measure of the gain in information provided by the data. The reference prior is chosen so that the expectation value of this information gain is maximized for the limiting case of $n \to \infty$, where the expectation is computed with respect to the marginal distribution of the data,

$$p(\boldsymbol{x}) = \int p(\boldsymbol{x}|\boldsymbol{\theta})\pi(\boldsymbol{\theta})\, d\boldsymbol{\theta}\,. \qquad (38.34)$$

For a single, continuous parameter the reference prior is usually identical to the Jeffreys prior. In the multiparameter case an iterative algorithm exists, which requires sorting the parameters by order of inferential importance. Often the result does not depend on this order, but when it does, this can be part of a robustness analysis. Further discussion and applications to particle physics problems can be found in Ref. 28.

38.2.4.2. *Bayesian treatment of nuisance parameters:*

As discussed in Sec. 38.2.2, a model may depend on parameters of interest $\boldsymbol{\theta}$ as well as on nuisance parameters $\boldsymbol{\nu}$, which must be included for an accurate description of the data. Knowledge about the values of $\boldsymbol{\nu}$ may be supplied by control measurements, theoretical insights, physical constraints, etc. Suppose, for example, one has data $\boldsymbol{y}$ from a control measurement which is characterized by a probability $P_y(\boldsymbol{y}|\boldsymbol{\nu})$. Suppose further that before carrying out the control measurement one's state of knowledge about $\boldsymbol{\nu}$ is described by an initial prior $\pi_0(\boldsymbol{\nu})$, which in practice is often taken to be a constant or in any case very broad. By using Bayes' theorem (38.1) one obtains the updated prior $\pi(\boldsymbol{\nu})$ (*i.e.*, now $\pi(\boldsymbol{\nu}) = \pi(\boldsymbol{\nu}|\boldsymbol{y})$, the probability for $\boldsymbol{\nu}$ given $\boldsymbol{y}$),

$$\pi(\boldsymbol{\nu}|\boldsymbol{y}) \propto P(\boldsymbol{y}|\boldsymbol{\nu})\pi_0(\boldsymbol{\nu}) \; . \tag{38.35}$$

In the absence of a model for $P(\boldsymbol{y}|\boldsymbol{\nu})$ one may make some reasonable but ad hoc choices. For a single nuisance parameter ν, for example, one might characterize the uncertainty in a nuisance parameter ν by a p.d.f. $\pi(\nu)$ centered about its nominal value with a certain standard deviation σ_ν. Often a Gaussian p.d.f. provides a reasonable model for one's degree of belief about a nuisance parameter; in other cases, more complicated shapes may be appropriate. If, for example, the parameter represents a non-negative quantity then a log-normal or gamma p.d.f. can be a more natural choice than a Gaussian truncated at zero. Note also that truncation of the prior of a nuisance parameter ν at zero will in general make $\pi(\nu)$ nonzero at $\nu = 0$, which can lead to an unnormalizable posterior for a parameter of interest that appears multiplied by ν.

The likelihood function, prior, and posterior p.d.f.s then all depend on both $\boldsymbol{\theta}$ and $\boldsymbol{\nu}$, and are related by Bayes' theorem, as usual. Note that the likelihood here only refers to the primary measurement $\boldsymbol{x}$. Once any control measurements $\boldsymbol{y}$ are used to find the updated prior $\pi(\boldsymbol{\nu})$ for the nuisance parameters, this information is fully encapsulated in $\pi(\boldsymbol{\nu})$ and the control measurements do not appear further.

One can obtain the posterior p.d.f. for $\boldsymbol{\theta}$ alone by integrating over the nuisance parameters, *i.e.*,

$$p(\boldsymbol{\theta}|\boldsymbol{x}) = \int p(\boldsymbol{\theta}, \boldsymbol{\nu}|\boldsymbol{x}) \, d\boldsymbol{\nu} \; . \tag{38.36}$$

Such integrals can often not be carried out in closed form, and if the number of nuisance parameters is large, then they can be difficult to compute with standard Monte Carlo methods. *Markov Chain Monte Carlo* (MCMC) techniques are often used for computing integrals of this type (see Sec. 39.5).

38.2.5. ***Propagation of errors*** :

Consider a set of n quantities $\boldsymbol{\theta} = (\theta_1, \ldots, \theta_n)$ and a set of m functions $\boldsymbol{\eta}(\boldsymbol{\theta}) = (\eta_1(\boldsymbol{\theta}), \ldots, \eta_m(\boldsymbol{\theta}))$. Suppose we have estimated $\widehat{\boldsymbol{\theta}} = (\widehat{\theta}_1, \ldots, \widehat{\theta}_n)$, using, say, maximum-likelihood or least-squares, and we also know or have estimated the covariance matrix $V_{ij} = \mathrm{cov}[\widehat{\theta}_i, \widehat{\theta}_j]$. The goal of *error propagation* is to determine the covariance matrix for the functions, $U_{ij} = \mathrm{cov}[\widehat{\eta}_i, \widehat{\eta}_j]$, where $\widehat{\boldsymbol{\eta}} = \boldsymbol{\eta}(\widehat{\boldsymbol{\theta}})$. In particular, the diagonal elements $U_{ii} = V[\widehat{\eta}_i]$ give the variances. The new covariance matrix can be found by expanding the functions $\boldsymbol{\eta}(\boldsymbol{\theta})$ about the estimates $\widehat{\boldsymbol{\theta}}$ to first order in a Taylor series. Using this one finds

$$U_{ij} \approx \sum_{k,l} \frac{\partial \eta_i}{\partial \theta_k} \frac{\partial \eta_j}{\partial \theta_l} \bigg|_{\widehat{\theta}} V_{kl} \; . \tag{38.37}$$

This can be written in matrix notation as $U \approx AVA^T$ where the matrix of derivatives A is

$$A_{ij} = \frac{\partial \eta_i}{\partial \theta_j} \bigg|_{\widehat{\theta}} \; , \tag{38.38}$$

and A^T is its transpose. The approximation is exact if $\boldsymbol{\eta}(\boldsymbol{\theta})$ is linear (it holds, for example, in equation (38.23)). If this is not the case, the approximation can break down if, for example, $\boldsymbol{\eta}(\boldsymbol{\theta})$ is significantly nonlinear close to $\widehat{\boldsymbol{\theta}}$ in a region of a size comparable to the standard deviations of $\widehat{\boldsymbol{\theta}}$.

38.3. Statistical tests

In addition to estimating parameters, one often wants to assess the validity of certain statements concerning the data's underlying distribution. Frequentist *hypothesis tests*, described in Sec. 38.3.1, provide a rule for accepting or rejecting hypotheses depending on the outcome of a measurement. In *significance tests*, covered in Sec. 38.3.2, one gives the probability to obtain a level of incompatibility with a certain hypothesis that is greater than or equal to the level observed with the actual data. In the Bayesian approach, the corresponding procedure is based fundamentally on the posterior probabilities of the competing hypotheses. In Sec. 38.3.3 we describe a related construct called the Bayes factor, which can be used to quantify the degree to which the data prefer one or another hypothesis.

38.3.1. ***Hypothesis tests*** :

A frequentist *test* of a hypothesis (often called the null hypothesis, H_0) is a rule that states for which data values $\boldsymbol{x}$ the hypothesis is rejected. A region of $\boldsymbol{x}$-space called the critical region, w, is specified such that such that there is no more than a given probability under H_0, α, called the *size* or *significance level* of the test, to find $\boldsymbol{x} \in w$. If the data are discrete, it may not be possible to find a critical region with exact probability content α, and thus we require $P(\boldsymbol{x} \in w|H_0) \leq \alpha$. If the data are observed in the critical region, H_0 is rejected.

The critical region is not unique. Choosing one should take into account the probabilities for the data predicted by some alternative hypothesis (or set of alternatives) H_1. Rejecting H_0 if it is true is called a *type-I error*, and occurs by construction with probability no greater than α. Not rejecting H_0 if an alternative H_1 is true is called a *type-II error*, and for a given test this will have a certain probability $\beta = P(\boldsymbol{x} \notin w|H_1)$. The quantity $1 - \beta$ is called the *power* of the test of H_0 with respect to the alternative H_1. A strategy for defining the critical region can therefore be to maximize the power with respect to some alternative (or alternatives) given a fixed size α.

In high-energy physics, the components of $\boldsymbol{x}$ might represent the measured properties of candidate events, and the critical region is defined by the cuts that one imposes in order to reject background and thus accept events likely to be of a certain desired type. Here H_0 could represent the background hypothesis and the alternative H_1 could represent the sought after signal. In other cases, H_0 could be the hypothesis that an entire event sample consists of background events only, and the alternative H_1 may represent the hypothesis of a mixture of background and signal.

Often rather than using the full set of quantities $\boldsymbol{x}$, it is convenient to define a scalar function of $\boldsymbol{x}$ called a *test statistic*, $t(\boldsymbol{x})$. The critical region in $\boldsymbol{x}$-space is bounded by a surface of constant $t(\boldsymbol{x})$. Once the function $t(\boldsymbol{x})$ is fixed, a given hypothesis for the distribution of $\boldsymbol{x}$ will determine a distribution for t.

To maximize the power of a test of H_0 with respect to the alternative H_1, the *Neyman–Pearson lemma* states that the critical region w should be chosen such that for all data values $\boldsymbol{x}$ inside w, the ratio

$$\lambda(\boldsymbol{x}) = \frac{f(\boldsymbol{x}|H_1)}{f(\boldsymbol{x}|H_0)} \; , \tag{38.39}$$

is greater than a given constant, the value of which is determined by the size of the test α. Here H_0 and H_1 must be simple hypotheses, i.e., they should not contain undetermined parameters.

The lemma is equivalent to the statement that (38.39) represents the optimal test statistic where the critical region is defined by a single cut on λ. This test will lead to the maximum power (*i.e.*, the maximum probability to reject H_0 if H_1 is true) for a given probability α to reject H_0 if H_0 is in fact true. It can be difficult in practice, however, to determine $\lambda(\boldsymbol{x})$, since this requires knowledge of the joint p.d.f.s $f(\boldsymbol{x}|H_0)$ and $f(\boldsymbol{x}|H_1)$.

In the usual case where the likelihood ratio (38.39) cannot be used explicitly, there exist a variety of other multivariate classifiers that effectively separate different types of events. Methods often used in HEP include *neural networks* or *Fisher discriminants* (see Ref. 10). Recently, further classification methods from machine-learning have been applied in HEP analyses; these include *probability density estimation (PDE)* techniques, *kernel-based PDE* (*KDE* or *Parzen*

window), *support vector machines*, and *decision trees*. Techniques such as "boosting" and "bagging" can be applied to combine a number of classifiers into a stronger one with greater stability with respect to fluctuations in the training data. Descriptions of these methods can be found in [11–13], and *Proceedings of the PHYSTAT* conference series [14]. Software for HEP includes the `TMVA` [15] and `StatPatternRecognition` [16] packages.

38.3.2. *Tests of significance (goodness-of-fit)* :

Often one wants to quantify the level of agreement between the data and a hypothesis without explicit reference to alternative hypotheses. This can be done by defining a statistic t, which is a function of the data whose value reflects in some way the level of agreement between the data and the hypothesis. The analyst must decide what values of the statistic correspond to better or worse levels of agreement with the hypothesis in question; the choice will in general depend on the relevant alternative hypotheses.

The hypothesis in question, H_0, will determine the p.d.f. $f(t|H_0)$ for the statistic. The significance of a discrepancy between the data and what one expects under the assumption of H_0 is quantified by giving the p-value, defined as the probability to find t in the region of equal or lesser compatibility with H_0 than the level of compatibility observed with the actual data. For example, if t is defined such that large values correspond to poor agreement with the hypothesis, then the p-value would be

$$p = \int_{t_{\rm obs}}^{\infty} f(t|H_0)\, dt \ , \tag{38.40}$$

where $t_{\rm obs}$ is the value of the statistic obtained in the actual experiment.

The p-value should not be confused with the size (significance level) of a test, or the confidence level of a confidence interval (Section 38.4), both of which are pre-specified constants. We may formulate a hypothesis test, however, by defining the critical region to correspond to the data outcomes that give the lowest p-values, so that finding $p \leq \alpha$ implies that the data outcome was in the critical region. When constructing a p-value, one generally chooses the region of data space deemed to have lower compatibility with the model being tested as one having higher compatibility with a given alternative, such that the corresponding test will have a high power with respect to this alternative.

The p-value is a function of the data, and is therefore itself a random variable. If the hypothesis used to compute the p-value is true, then for continuous data p will be uniformly distributed between zero and one. Note that the p-value is not the probability for the hypothesis; in frequentist statistics, this is not defined. Rather, the p-value is the probability, under the assumption of a hypothesis H_0, of obtaining data at least as incompatible with H_0 as the data actually observed.

When searching for a new phenomenon, one tries to reject the hypothesis H_0 that the data are consistent with known (*e.g.*, Standard Model) processes. If the p-value of H_0 is sufficiently low, then one is willing to accept that some alternative hypothesis is true. Often one converts the p-value into an equivalent significance Z, defined so that a Z standard deviation upward fluctuation of a Gaussian random variable would have an upper tail area equal to p, *i.e.*,

$$Z = \Phi^{-1}(1-p) \ . \tag{38.41}$$

Here Φ is the cumulative distribution of the Standard Gaussian, and Φ^{-1} is its inverse (quantile) function. Often in HEP the level of significance where an effect is said to qualify as a discovery is $Z = 5$, *i.e.*, a 5σ effect, corresponding to a p-value of 2.87×10^{-7}. One's actual degree of belief that a new process is present, however, will depend in general on other factors as well, such as the plausibility of the new signal hypothesis and the degree to which it can describe the data, one's confidence in the model that led to the observed p-value, and possible corrections for multiple observations out of which one focuses on the smallest p-value obtained (the "look-elsewhere effect", discussed in Section 38.3.2.2).

38.3.2.1. *Treatment of nuisance parameters for frequentist tests:*

Suppose one wants to test hypothetical values of parameters $\boldsymbol{\theta}$, but the model also contains nuisance parameters $\boldsymbol{\nu}$. To find a p-value for $\boldsymbol{\theta}$ we can construct a test statistic q_θ such that larger values constitute increasing incompatibility between the data and the hypothesis. Then for an observed value of the statistic $q_{\theta,\rm obs}$, the p-value of $\boldsymbol{\theta}$ is

$$p_\theta(\boldsymbol{\nu}) = \int_{q_{\theta,\rm obs}}^{\infty} f(q_\theta|\boldsymbol{\theta},\boldsymbol{\nu})\, dq_\theta \ , \tag{38.42}$$

which depends in general on the nuisance parameters $\boldsymbol{\nu}$. In the strict frequentist approach, $\boldsymbol{\theta}$ is rejected only if the p-value is less than α for all possible values of the nuisance parameters.

The difficulty described above is effectively solved if we can define the test statistic q_θ in such a way that its distribution $f(q_\theta|\boldsymbol{\theta})$ is independent of the nuisance parameters. Although exact independence is only found in special cases, it can be achieved approximately by use of the *profile likelihood ratio*. This is given by the profile likelihood from Eq.(38.18) divided by the value of the likelihood at its maximum, *i.e.*, when evaluated wit the ML estimators $\widehat{\boldsymbol{\theta}}$ and $\widehat{\boldsymbol{\nu}}$:

$$\lambda_p(\boldsymbol{\theta}) = \frac{L(\boldsymbol{\theta}, \widehat{\widehat{\boldsymbol{\nu}}}(\boldsymbol{\theta}))}{L(\widehat{\boldsymbol{\theta}}, \widehat{\boldsymbol{\nu}})} \ . \tag{38.43}$$

Wilks' theorem states that, providing certain general conditions are satisfied, the distribution of $-2\ln\lambda_{\rm p}(\boldsymbol{\theta})$, under assumption of $\boldsymbol{\theta}$, approaches a χ^2 distribution in the limit where the data sample is very large, independent of the values of the nuisance parameters $\boldsymbol{\nu}$. Here the number of degrees of freedom is equal to the number of components of $\boldsymbol{\theta}$. More details on use of the profile likelihood are given in Refs. [36–37] and in contributions to the PHYSTAT conferences [14]; explicit formulae for special cases can be found in Ref. 38. Further discussion on how to incorporate systematic uncertainties into p-values can be found in Ref. 17.

Even with use of the profile likelihood ratio, for a finite data sample the p-value of hypothesized parameters $\boldsymbol{\theta}$ will retain in general some dependence on the nuisance parameters $\boldsymbol{\nu}$. Ideally one would find the the maximum of $p_\theta(\boldsymbol{\nu})$ from Eq. (38.42) explicitly, but that is often impractical. An approximate and computationally feasible technique is to use $p_\theta(\widehat{\widehat{\boldsymbol{\nu}}}(\theta))$, where $\widehat{\widehat{\boldsymbol{\nu}}}(\theta)$ are the profiled values of the nuisance parameters as defined in Section 38.2.2.2. The resulting p-value is the correct if the true values of the nuisance parameters are equal to the profiled values used; otherwise it could be either too high or too low. This is discussed further in Section 38.4.2 on confidence intervals.

One may also treat model uncertainties in a Bayesian manner but then use the resulting model in a frequentist test. Suppose the uncertainty in a set of nuisance parameters $\boldsymbol{\nu}$ is characterized by a Bayesian prior p.d.f. $\pi(\boldsymbol{\nu})$. This can be used to construct the marginal (also called the prior predictive) model for the data $\boldsymbol{x}$ and parameters of interest $\boldsymbol{\theta}$,

$$P_{\rm m}(\boldsymbol{x}|\boldsymbol{\theta}) = \int P(\boldsymbol{x}|\boldsymbol{\theta},\boldsymbol{\nu})\pi(\boldsymbol{\nu})\, d\boldsymbol{\nu} \ . \tag{38.44}$$

The marginal model does not represent the probability of data that would be generated if on were really to repeat the experiment, as in that case one would assume that the nuisance parameters do not vary. Rather, the marginal model represents a situation in which every repetition of the experiment is carried out with new values of $\boldsymbol{\nu}$, randomly sampled from $\pi(\boldsymbol{\nu})$. It is in effect an average of models each with a given $\boldsymbol{\nu}$, where the average carried out with respect to the prior p.d.f. $\pi(\boldsymbol{\nu})$.

The marginal model for the data $\boldsymbol{x}$ can be used to determine the distribution of a test statistic Q, which can be written

$$P_{\rm m}(Q|\boldsymbol{\theta}) = \int P(Q|\boldsymbol{\theta},\boldsymbol{\nu})\pi(\boldsymbol{\nu})\, d\boldsymbol{\nu} \ . \tag{38.45}$$

In a search for a new signal process, the test statistic can be based on the ratio of likelihoods corresponding to the experiments where signal and background events are both present, L_{s+b}, to that of background only, L_b. Often the likelihoods are evaluated with the profiled values

of the nuisance parameters, which may give improved performance. It is important to note, however, that it is through use of the marginal model for the distribution of Q that the uncertainties related to the nuisance parameters are incorporated into the result of the test. Different choices for the test statistic itself only result in variations of the power of the test with respect to different alternatives.

38.3.2.2. *The look-elsewhere effect:*

The "look-elsewhere effect" relates to multiple measurements used to test a single hypothesis. The classic example is when one searches in a distribution for a peak whose position is not predicted in advance. Here the no-peak hypothesis is tested using data in a given range of the distribution. In the frequentist approach the correct p-value of the no-peak hypothesis is the probability, assuming background only, to find a signal as significant as the one found or more so anywhere in the search region. This can be substantially higher than the probability to find a peak of equal or greater significance in the particular place where it appeared. There is in general some ambiguity as to what constitutes the relevant search region or even the broader set of relevant measurements. Although the desired p-value is well defined once the search region has been fixed, an exact treatment can require extensive computation.

The "brute-force" solution to this problem by Monte Carlo involves generating data under the background-only hypothesis and for each data set, fitting a peak of unknown position and recording a measure of its significance. To establish a discovery one often requires a p-value less than 2.9×10^{-7}, corresponding to a 5σ or larger effect. Determining this with Monte Carlo thus requires generating and fitting a very large number of experiments, perhaps several times 10^7. In contrast, if the position of the peak is fixed, then the fit to the distribution is much easier, and furthermore one can in many cases use formulae valid for sufficiently large samples that bypass completely the need for Monte Carlo (see, e.g., [38]) . But this fixed-position or "local" p-value would not be correct in general, as it assumes the position of the peak was known in advance.

A method that allows one to modify the local p-value computed under assumption of a fixed position to obtain an approximation to the correct "global" value using a relatively simple calculation is described in Ref. 18. Suppose a test statistic q_0, defined so that larger values indicate increasing disagreement with the data, is observed to have a value u. Furthermore suppose the model contains a nuisance parameter θ (such as the peak position) which is only defined under the signal model (there is no peak in the background-only model). An approximation for the global p-value is found to be

$$p_{\text{global}} \approx p_{\text{local}} + \langle N_u \rangle \ , \tag{38.46}$$

where $\langle N_u \rangle$ is the mean number of "upcrossings" of the the statistic q_0 above the level u in the range of the nuisance parameter considered (e.g., the mass range).

The value of $\langle N_u \rangle$ can be estimated from the number of upcrossings $\langle N_{u_0} \rangle$ above some much lower value, u_0, by using a relation due to Davis [19],

$$\langle N_u \rangle \approx \langle N_{u_0} \rangle e^{-(u-u_0)/2} \ . \tag{38.47}$$

By choosing u_0 sufficiently low, the value of $\langle N_u \rangle$ can be estimated by simulating only a very small number of experiments or even from the observed data, rather than the 10^7 needed if one is dealing with a 5σ effect.

38.3.2.3. *Goodness-of-fit with the method of Least Squares:*

When estimating parameters using the method of least squares, one obtains the minimum value of the quantity χ^2 (38.19). This statistic can be used to test the *goodness-of-fit*, *i.e.*, the test provides a measure of the significance of a discrepancy between the data and the hypothesized functional form used in the fit. It may also happen that no parameters are estimated from the data, but that one simply wants to compare a histogram, *e.g.*, a vector of Poisson distributed numbers $\boldsymbol{n} = (n_1, \ldots, n_N)$, with a hypothesis for their expectation values $\mu_i = E[n_i]$. As the distribution is Poisson with variances $\sigma_i^2 = \mu_i$, the χ^2 (38.19) becomes *Pearson's* χ^2 *statistic*,

$$\chi^2 = \sum_{i=1}^{N} \frac{(n_i - \mu_i)^2}{\mu_i} \ . \tag{38.48}$$

If the hypothesis $\boldsymbol{\mu} = (\mu_1, \ldots, \mu_N)$ is correct, and if the expected values μ_i in (38.48) are sufficiently large (or equivalently, if the measurements n_i can be treated as following a Gaussian distribution), then the χ^2 statistic will follow the χ^2 p.d.f. with the number of degrees of freedom equal to the number of measurements N minus the number of fitted parameters.

Alternatively, one may fit parameters and evaluate goodness-of-fit by minimizing $-2 \ln \lambda$ from Eq. (38.16). One finds that the distribution of this statistic approaches the asymptotic limit faster than does Pearson's χ^2, and thus computing the p-value with the χ^2 p.d.f. will in general be better justified (see Ref. 9 and references therein).

Assuming the goodness-of-fit statistic follows a χ^2 p.d.f., the p-value for the hypothesis is then

$$p = \int_{\chi^2}^{\infty} f(z; n_{\text{d}})\, dz \ , \tag{38.49}$$

where $f(z; n_{\text{d}})$ is the χ^2 p.d.f. and n_{d} is the appropriate number of degrees of freedom. Values are shown in Fig. 38.1 or obtained from the ROOT function `TMath::Prob`. If the conditions for using the χ^2 p.d.f. do not hold, the statistic can still be defined as before, but its p.d.f. must be determined by other means in order to obtain the p-value, *e.g.*, using a Monte Carlo calculation.

Since the mean of the χ^2 distribution is equal to n_{d}, one expects in a "reasonable" experiment to obtain $\chi^2 \approx n_{\text{d}}$. Hence the quantity χ^2/n_{d} is sometimes reported. Since the p.d.f. of χ^2/n_{d} depends on n_{d}, however, one must report n_{d} as well if one wishes to determine the p-value. The p-values obtained for different values of χ^2/n_{d} are shown in Fig. 38.2.

If one finds a χ^2 value much greater than n_{d}, and a correspondingly small p-value, one may be tempted to expect a high degree of uncertainty for any fitted parameters. Poor goodness-of-fit, however, does not mean that one will have large statistical errors for parameter estimates. If, for example, the error bars (or covariance matrix) used in constructing the χ^2 are underestimated, then this will lead to underestimated statistical errors for the fitted parameters. The standard deviations of estimators that one finds from, say, Eq. (38.13) reflect how widely the estimates would be distributed if one were to repeat the measurement many times, assuming that the hypothesis and measurement errors used in the χ^2 are also correct. They do not include the systematic error which may result from an incorrect hypothesis or incorrectly estimated measurement errors in the χ^2.

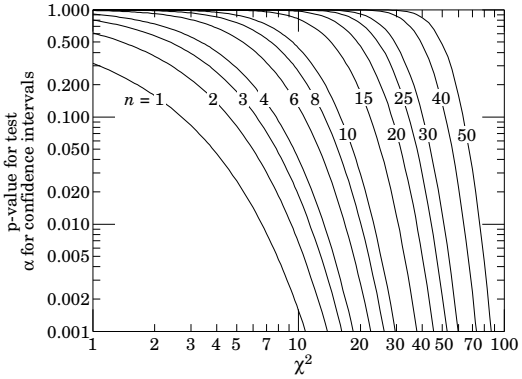

Figure 38.1: One minus the χ^2 cumulative distribution, $1 - F(\chi^2; n)$, for n degrees of freedom. This gives the p-value for the χ^2 goodness-of-fit test as well as one minus the coverage probability for confidence regions (see Sec. 38.4.2.2).

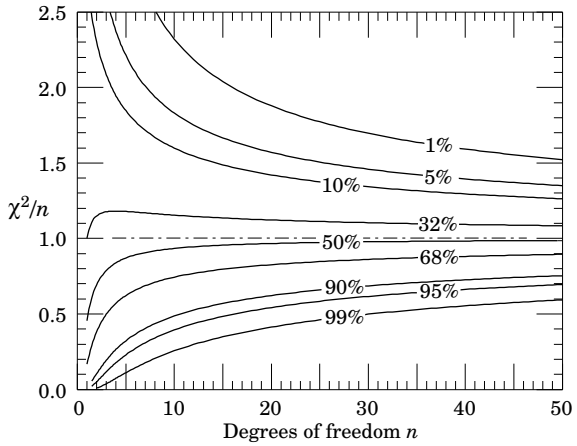

Figure 38.2: The 'reduced' χ^2, equal to χ^2/n, for n degrees of freedom. The curves show as a function of n the χ^2/n that corresponds to a given p-value.

38.3.3. ***Bayes factors*** :

In Bayesian statistics, all of one's knowledge about a model is contained in its posterior probability, which one obtains using Bayes' theorem (38.30). Thus one could reject a hypothesis H if its posterior probability $P(H|\boldsymbol{x})$ is sufficiently small. The difficulty here is that $P(H|\boldsymbol{x})$ is proportional to the prior probability $P(H)$, and there will not be a consensus about the prior probabilities for the existence of new phenomena. Nevertheless one can construct a quantity called the Bayes factor (described below), which can be used to quantify the degree to which the data prefer one hypothesis over another, and is independent of their prior probabilities.

Consider two models (hypotheses), H_i and H_j, described by vectors of parameters $\boldsymbol{\theta}_i$ and $\boldsymbol{\theta}_j$, respectively. Some of the components will be common to both models and others may be distinct. The full prior probability for each model can be written in the form

$$\pi(H_i, \boldsymbol{\theta}_i) = P(H_i)\pi(\boldsymbol{\theta}_i|H_i) \; . \tag{38.50}$$

Here $P(H_i)$ is the overall prior probability for H_i, and $\pi(\boldsymbol{\theta}_i|H_i)$ is the normalized p.d.f. of its parameters. For each model, the posterior probability is found using Bayes' theorem,

$$P(H_i|\boldsymbol{x}) = \frac{\int P(\boldsymbol{x}|\boldsymbol{\theta}_i, H_i)P(H_i)\pi(\boldsymbol{\theta}_i|H_i)\, d\boldsymbol{\theta}_i}{P(\boldsymbol{x})} \; , \tag{38.51}$$

where the integration is carried out over the internal parameters $\boldsymbol{\theta}_i$ of the model. The ratio of posterior probabilities for the models is therefore

$$\frac{P(H_i|\boldsymbol{x})}{P(H_j|\boldsymbol{x})} = \frac{\int P(\boldsymbol{x}|\boldsymbol{\theta}_i, H_i)\pi(\boldsymbol{\theta}_i|H_i)\, d\boldsymbol{\theta}_i}{\int P(\boldsymbol{x}|\boldsymbol{\theta}_j, H_j)\pi(\boldsymbol{\theta}_j|H_j)\, d\boldsymbol{\theta}_j} \frac{P(H_i)}{P(H_j)} \; . \tag{38.52}$$

The *Bayes factor* is defined as

$$B_{ij} = \frac{\int P(\boldsymbol{x}|\boldsymbol{\theta}_i, H_i)\pi(\boldsymbol{\theta}_i|H_i)\, d\boldsymbol{\theta}_i}{\int P(\boldsymbol{x}|\boldsymbol{\theta}_j, H_j)\pi(\boldsymbol{\theta}_j|H_j)\, d\boldsymbol{\theta}_j} \; . \tag{38.53}$$

This gives what the ratio of posterior probabilities for models i and j would be if the overall prior probabilities for the two models were equal. If the models have no nuisance parameters, *i.e.*, no internal parameters described by priors, then the Bayes factor is simply the likelihood ratio. The Bayes factor therefore shows by how much the probability ratio of model i to model j changes in the light of the data, and thus can be viewed as a numerical measure of evidence supplied by the data in favour of one hypothesis over the other.

Although the Bayes factor is by construction independent of the overall prior probabilities $P(H_i)$ and $P(H_j)$, it does require priors for all internal parameters of a model, *i.e.*, one needs the functions $\pi(\boldsymbol{\theta}_i|H_i)$ and $\pi(\boldsymbol{\theta}_j|H_j)$. In a Bayesian analysis where one is only interested in the posterior p.d.f. of a parameter, it may be acceptable to take an unnormalizable function for the prior (an improper prior) as long as the product of likelihood and prior can be normalized. But improper priors are only defined up to an arbitrary multiplicative constant, and so the Bayes factor would depend on this constant. Furthermore, although the range of a constant normalized prior is unimportant for parameter determination (provided it is wider than the likelihood), this is not so for the Bayes factor when such a prior is used for only one of the hypotheses. So to compute a Bayes factor, all internal parameters must be described by normalized priors that represent meaningful probabilities over the entire range where they are defined.

An exception to this rule may be considered when the identical parameter appears in the models for both numerator and denominator of the Bayes factor. In this case one can argue that the arbitrary constants would cancel. One must exercise some caution, however, as parameters with the same name and physical meaning may still play different roles in the two models.

Both integrals in equation (38.53) are of the form

$$m = \int P(\boldsymbol{x}|\boldsymbol{\theta})\pi(\boldsymbol{\theta})\, d\boldsymbol{\theta} \; , \tag{38.54}$$

which is the marginal likelihood seen previously in Eq. (38.44) (in some fields this quantity is called the *evidence*). A review of Bayes factors can be found in Ref. 30. Computing marginal likelihoods can be difficult; in many cases it can be done with the nested sampling algorithm [31] as implemented, *e.g.*, in the program `MultiNest` [32].

38.4. Intervals and limits

When the goal of an experiment is to determine a parameter θ, the result is usually expressed by quoting, in addition to the point estimate, some sort of interval which reflects the statistical precision of the measurement. In the simplest case, this can be given by the parameter's estimated value $\widehat{\theta}$ plus or minus an estimate of the standard deviation of $\widehat{\theta}$, $\widehat{\sigma}_{\widehat{\theta}}$. If, however, the p.d.f. of the estimator is not Gaussian or if there are physical boundaries on the possible values of the parameter, then one usually quotes instead an interval according to one of the procedures described below.

In reporting an interval or limit, the experimenter may wish to

- communicate as objectively as possible the result of the experiment;
- provide an interval that is constructed to cover the true value of the parameter with a specified probability;
- provide the information needed by the consumer of the result to draw conclusions about the parameter or to make a particular decision;
- draw conclusions about the parameter that incorporate stated prior beliefs.

With a sufficiently large data sample, the point estimate and standard deviation (or for the multiparameter case, the parameter estimates and covariance matrix) satisfy essentially all of these goals. For finite data samples, no single method for quoting an interval will achieve all of them.

In addition to the goals listed above, the choice of method may be influenced by practical considerations such as ease of producing an interval from the results of several measurements. Of course the experimenter is not restricted to quoting a single interval or limit; one may choose, for example, first to communicate the result with a confidence interval having certain frequentist properties, and then in addition to draw conclusions about a parameter using a judiciously chosen subjective Bayesian prior.

It is recommended, however, that there be a clear separation between these two aspects of reporting a result. In the remainder of this section, we assess the extent to which various types of intervals achieve the goals stated here.

38.4.1. ***Bayesian intervals*** :

As described in Sec. 38.2.4, a Bayesian posterior probability may be used to determine regions that will have a given probability of containing the true value of a parameter. In the single parameter case, for example, an interval (called a Bayesian or credible interval) $[\theta_{\rm lo}, \theta_{\rm up}]$ can be determined which contains a given fraction $1-\alpha$ of the posterior probability, *i.e.*,

$$1-\alpha = \int_{\theta_{\rm lo}}^{\theta_{\rm up}} p(\theta|\boldsymbol{x})\, d\theta \ . \tag{38.55}$$

Sometimes an upper or lower limit is desired, *i.e.*, $\theta_{\rm lo}$ or $\theta_{\rm up}$ can be set to a physical boundary or to plus or minus infinity. In other cases, one might be interested in the set of θ values for which $p(\theta|\boldsymbol{x})$ is higher than for any θ not belonging to the set, which may constitute a single interval or a set of disjoint regions; these are called highest posterior density (HPD) intervals. Note that HPD intervals are not invariant under a nonlinear transformation of the parameter.

If a parameter is constrained to be non-negative, then the prior p.d.f. can simply be set to zero for negative values. An important example is the case of a Poisson variable n, which counts signal events with unknown mean s, as well as background with mean b, assumed known. For the signal mean s, one often uses the prior

$$\pi(s) = \begin{cases} 0 & s < 0 \\ 1 & s \geq 0 \end{cases} \ . \tag{38.56}$$

This prior is regarded as providing an interval whose frequentist properties can be studied, rather than as representing a degree of belief. For example, to obtain an upper limit on s, one may proceed as follows. The likelihood for s is given by the Poisson distribution for n with mean $s+b$,

$$P(n|s) = \frac{(s+b)^n}{n!} e^{-(s+b)} \ , \tag{38.57}$$

along with the prior (38.56) in (38.30) gives the posterior density for s. An upper limit $s_{\rm up}$ at confidence level (or here, rather, credibility level) $1-\alpha$ can be obtained by requiring

$$1-\alpha = \int_{-\infty}^{s_{\rm up}} p(s|n) ds = \frac{\int_{-\infty}^{s_{\rm up}} P(n|s)\, \pi(s)\, ds}{\int_{-\infty}^{\infty} P(n|s)\, \pi(s)\, ds} \ , \tag{38.58}$$

where the lower limit of integration is effectively zero because of the cut-off in $\pi(s)$. By relating the integrals in Eq. (38.58) to incomplete gamma functions, the solution for the upper limit is found to be

$$s_{\rm up} = \tfrac{1}{2} F_{\chi^2}^{-1}\left[p, 2(n+1)\right] - b \ , \tag{38.59}$$

where $F_{\chi^2}^{-1}$ is the quantile of the χ^2 distribution (inverse of the cumulative distribution). Here the quantity p is

$$p = 1-\alpha\left(F_{\chi^2}\left[2b, 2(n+1)\right]\right) \ , \tag{38.60}$$

where F_{χ^2} is the cumulative χ^2 distribution. For both F_{χ^2} and $F_{\chi^2}^{-1}$ above, the argument $2(n+1)$ gives the number of degrees of freedom. For the special case of $b=0$, the limit reduces to

$$s_{\rm up} = \tfrac{1}{2} F_{\chi^2}^{-1}(1-\alpha; 2(n+1)) \ . \tag{38.61}$$

It happens that for the case of $b=0$, the upper limit from Eq. (38.61) coincides numerically with the frequentist upper limit discussed in Section 38.4.2.3. Values for $1-\alpha = 0.9$ and 0.95 are given by the values $\mu_{\rm up}$ in Table 38.3. The frequentist properties of confidence intervals for the Poisson mean found in this way are discussed in Refs. [2] and [21].

As in any Bayesian analysis, it is important to show how the result changes under assumption of different prior probabilities. For example, one could consider the Jeffreys prior as described in Sec. 38.2.4. For this problem one finds the Jeffreys prior $\pi(s) \propto 1/\sqrt{s+b}$ for $s \geq 0$ and zero otherwise. As with the constant prior, one would not regard this as representing one's prior beliefs about s, both because it is improper and also as it depends on b. Rather it is used with Bayes' theorem to produce an interval whose frequentist properties can be studied.

If the model contains nuisance parameters then these are eliminated by marginalizing, as in Eq. (38.36), to obtain the p.d.f. for the parameters of interest. For example, if the parameter b in the Poisson counting problem above were to be characterized by a prior p.d.f. $\pi(b)$, then one would first use Bayes' theorem to find $p(s,b|n)$. This is then marginalized to find $p(s|n) = \int p(s,b|n)\pi(b)\, db$, from which one may determine an interval for s. One may not be certain whether to extend a model by including more nuisance parameters. In this case, a Bayes factor may be used to determine to what extent the data prefer a model with additional parameters, as described in Section 38.3.3.

38.4.2. ***Frequentist confidence intervals*** :

The unqualified phrase "confidence intervals" refers to frequentist intervals obtained with a procedure due to Neyman [29], described below. These are intervals (or in the multiparameter case, regions) constructed so as to include the true value of the parameter with a probability greater than or equal to a specified level, called the *coverage probability*. It is important to note that in the frequentist approach, such coverage is not meaningful for a fixed interval. A confidence interval, however, depends on the data and thus would fluctuate if one were to repeat the experiment many times. The coverage probability refers to the fraction of intervals in such a set that contain the true parameter value. In this section, we discuss several techniques for producing intervals that have, at least approximately, this property.

38.4.2.1. *The Neyman construction for confidence intervals:*

Consider a p.d.f. $f(x;\theta)$ where x represents the outcome of the experiment and θ is the unknown parameter for which we want to construct a confidence interval. The variable x could (and often does) represent an estimator for θ. Using $f(x;\theta)$, we can find for a pre-specified probability $1-\alpha$, and for every value of θ, a set of values $x_1(\theta,\alpha)$ and $x_2(\theta,\alpha)$ such that

$$P(x_1 < x < x_2; \theta) = 1-\alpha = \int_{x_1}^{x_2} f(x;\theta)\, dx \ . \tag{38.62}$$

This is illustrated in Fig. 38.3: a horizontal line segment $[x_1(\theta,\alpha), x_2(\theta,\alpha)]$ is drawn for representative values of θ. The union of such intervals for all values of θ, designated in the figure as $D(\alpha)$, is known as the *confidence belt*. Typically the curves $x_1(\theta,\alpha)$ and $x_2(\theta,\alpha)$ are monotonic functions of θ, which we assume for this discussion.

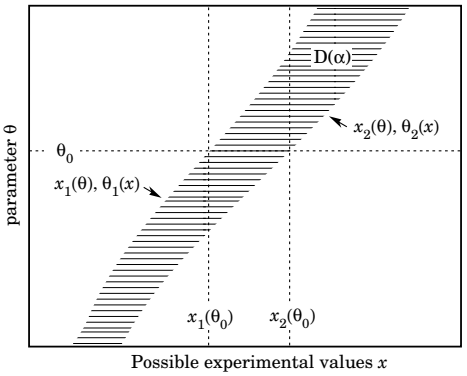

Figure 38.3: Construction of the confidence belt (see text).

Upon performing an experiment to measure x and obtaining a value x_0, one draws a vertical line through x_0. The confidence interval for θ is the set of all values of θ for which the corresponding line segment $[x_1(\theta,\alpha), x_2(\theta,\alpha)]$ is intercepted by this vertical line. Such confidence intervals are said to have a *confidence level* (CL) equal to $1-\alpha$.

Now suppose that the true value of θ is θ_0, indicated in the figure. We see from the figure that θ_0 lies between $\theta_1(x)$ and $\theta_2(x)$ if and

only if x lies between $x_1(\theta_0)$ and $x_2(\theta_0)$. The two events thus have the same probability, and since this is true for any value θ_0, we can drop the subscript 0 and obtain

$$1-\alpha = P(x_1(\theta) < x < x_2(\theta)) = P(\theta_2(x) < \theta < \theta_1(x)) \; . \qquad (38.63)$$

In this probability statement, $\theta_1(x)$ and $\theta_2(x)$, *i.e.*, the endpoints of the interval, are the random variables and θ is an unknown constant. If the experiment were to be repeated a large number of times, the interval $[\theta_1, \theta_2]$ would vary, covering the fixed value θ in a fraction $1-\alpha$ of the experiments.

The condition of coverage in Eq. (38.62) does not determine x_1 and x_2 uniquely, and additional criteria are needed. One possibility is to choose *central intervals* such that the probabilities excluded below x_1 and above x_2 are each $\alpha/2$. In other cases, one may want to report only an upper or lower limit, in which case the probability excluded below x_1 or above x_2 can be set to zero. Another principle based on *likelihood ratio ordering* for determining which values of x should be included in the confidence belt is discussed below.

When the observed random variable x is continuous, the coverage probability obtained with the Neyman construction is $1-\alpha$, regardless of the true value of the parameter. If x is discrete, however, it is not possible to find segments $[x_1(\theta,\alpha), x_2(\theta,\alpha)]$ that satisfy Eq. (38.62) exactly for all values of θ. By convention, one constructs the confidence belt requiring the probability $P(x_1 < x < x_2)$ to be *greater than or equal to* $1-\alpha$. This gives confidence intervals that include the true parameter with a probability greater than or equal to $1-\alpha$.

An equivalent method of constructing confidence intervals is to consider a test (see Sec. 38.3) of the hypothesis that the parameter's true value is θ (assume one constructs a test for all physical values of θ). One then excludes all values of θ where the hypothesis would be rejected in a test of size α or less. The remaining values constitute the confidence interval at confidence level $1-\alpha$. If the critical region of the test is characterized by having a p-value $p_\theta \leq \alpha$, then the endpoints of the confidence interval are found in practice by solving $p_\theta = \alpha$ for θ.

In this procedure, one is still free to choose the test to be used; this corresponds to the freedom in the Neyman construction as to which values of the data are included in the confidence belt. One possibility is to use a test statistic based on the *likelihood ratio*,

$$\lambda = \frac{f(x;\theta)}{f(x;\widehat{\theta}\,)} \; , \qquad (38.64)$$

where $\widehat{\theta}$ is the value of the parameter which, out of all allowed values, maximizes $f(x;\theta)$. This results in the intervals described in Ref. 33 by Feldman and Cousins. The same intervals can be obtained from the Neyman construction described above by including in the confidence belt those values of x which give the greatest values of λ.

If the model contains nuisance parameters $\boldsymbol{\nu}$, then these can be incorporated into the test (or the p-values) used to determine the limit by profiling as discussed in Section 38.3.2.1. As mentioned there, the strict frequentist approach is to regard the parameter of interest θ as excluded only if it is rejected for all possible values of $\boldsymbol{\nu}$. The resulting interval for θ will then cover then cover the true value with a probability greater than or equal to the nominal confidence level for all points in $\boldsymbol{\nu}$-space.

If the p-value is based on the profiled values of the nuisance parameters, *i.e.*, with $\boldsymbol{\nu} = \widehat{\widehat{\boldsymbol{\nu}}}(\theta)$ used in Eq. (38.42), then the resulting interval for the parameter of interest will have the correct coverage if the true values of $\boldsymbol{\nu}$ are equal to the profiled values. Otherwise the coverage probability may be too high or too low. This procedure has been called *profile construction* in HEP [20](see also [17]) .

38.4.2.2. *Gaussian distributed measurements:*

An important example of constructing a confidence interval is when the data consists of a single random variable x that follows a Gaussian distribution; this is often the case when x represents an estimator for a parameter and one has a sufficiently large data sample. If there is more than one parameter being estimated, the multivariate Gaussian is used. For the univariate case with known σ, the probability that the measured value x will fall within $\pm\delta$ of the true value μ is

$$1-\alpha = \frac{1}{\sqrt{2\pi}\sigma}\int_{\mu-\delta}^{\mu+\delta} e^{-(x-\mu)^2/2\sigma^2}\, dx = \mathrm{erf}\left(\frac{\delta}{\sqrt{2}\,\sigma}\right) = 2\Phi\left(\frac{\sigma}{\delta}\right) - 1 \; , \qquad (38.65)$$

where erf is the Gaussian error function, which is rewritten in the final equality using Φ, the Gaussian cumulative distribution. Fig. 38.4 shows a $\delta = 1.64\sigma$ confidence interval unshaded. The choice $\delta = \sigma$ gives an interval called the *standard error* which has $1-\alpha = 68.27\%$ if σ is known. Values of α for other frequently used choices of δ are given in Table 38.1.

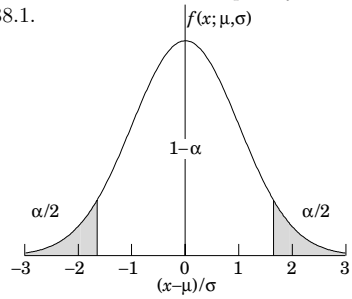

Figure 38.4: Illustration of a symmetric 90% confidence interval (unshaded) for a measurement of a single quantity with Gaussian errors. Integrated probabilities, defined by $\alpha = 0.1$, are as shown.

Table 38.1: Area of the tails α outside $\pm\delta$ from the mean of a Gaussian distribution.

α	δ	α	δ
0.3173	1σ	0.2	1.28σ
4.55×10^{-2}	2σ	0.1	1.64σ
2.7×10^{-3}	3σ	0.05	1.96σ
6.3×10^{-5}	4σ	0.01	2.58σ
5.7×10^{-7}	5σ	0.001	3.29σ
2.0×10^{-9}	6σ	10^{-4}	3.89σ

We can set a one-sided (upper or lower) limit by excluding above $x+\delta$ (or below $x-\delta$). The values of α for such limits are half the values in Table 38.1.

The relation (38.65) can be re-expressed using the cumulative distribution function for the χ^2 distribution as

$$\alpha = 1 - F(\chi^2; n) \; , \qquad (38.66)$$

for $\chi^2 = (\delta/\sigma)^2$ and $n = 1$ degree of freedom. This can be seen as the $n = 1$ curve in Fig. 38.1 or obtained by using the ROOT function `TMath::Prob`.

For multivariate measurements of, say, n parameter estimates $\widehat{\boldsymbol{\theta}} = (\widehat{\theta}_1, \ldots, \widehat{\theta}_n)$, one requires the full covariance matrix $V_{ij} = \mathrm{cov}[\widehat{\theta}_i, \widehat{\theta}_j]$, which can be estimated as described in Sections 38.2.2 and 38.2.3. Under fairly general conditions with the methods of maximum-likelihood or least-squares in the large sample limit, the estimators will be distributed according to a multivariate Gaussian centered about the true (unknown) values $\boldsymbol{\theta}$, and furthermore, the likelihood function itself takes on a Gaussian shape.

The standard error ellipse for the pair $(\widehat{\theta}_i, \widehat{\theta}_j)$ is shown in Fig. 38.5, corresponding to a contour $\chi^2 = \chi^2_{\mathrm{min}} + 1$ or $\ln L = \ln L_{\mathrm{max}} - 1/2$. The ellipse is centered about the estimated values $\widehat{\boldsymbol{\theta}}$, and the tangents to the ellipse give the standard deviations of the estimators, σ_i and σ_j. The angle of the major axis of the ellipse is given by

$$\tan 2\phi = \frac{2\rho_{ij}\sigma_i\sigma_j}{\sigma_j^2 - \sigma_i^2} \; , \qquad (38.67)$$

Table 38.2: Values of $\Delta\chi^2$ or $2\Delta\ln L$ corresponding to a coverage probability $1-\alpha$ in the large data sample limit, for joint estimation of m parameters.

$(1-\alpha)$ (%)	$m=1$	$m=2$	$m=3$
68.27	1.00	2.30	3.53
90.	2.71	4.61	6.25
95.	3.84	5.99	7.82
95.45	4.00	6.18	8.03
99.	6.63	9.21	11.34
99.73	9.00	11.83	14.16

where $\rho_{ij} = \mathrm{cov}[\widehat{\theta}_i, \widehat{\theta}_j]/\sigma_i\sigma_j$ is the correlation coefficient.

The correlation coefficient can be visualized as the fraction of the distance σ_i from the ellipse's horizontal center-line at which the ellipse becomes tangent to vertical, *i.e.*, at the distance $\rho_{ij}\sigma_i$ below the center-line as shown. As ρ_{ij} goes to $+1$ or -1, the ellipse thins to a diagonal line.

It could happen that one of the parameters, say, θ_j, is known from previous measurements to a precision much better than σ_j, so that the current measurement contributes almost nothing to the knowledge of θ_j. However, the current measurement of θ_i and its dependence on θ_j may still be important. In this case, instead of quoting both parameter estimates and their correlation, one sometimes reports the value of θ_i, which minimizes χ^2 at a fixed value of θ_j, such as the PDG best value. This θ_i value lies along the dotted line between the points where the ellipse becomes tangent to vertical, and has statistical error $\sigma_{\rm inner}$ as shown on the figure, where $\sigma_{\rm inner} = (1-\rho_{ij}^2)^{1/2}\sigma_i$. Instead of the correlation ρ_{ij}, one reports the dependency $d\widehat{\theta}_i/d\theta_j$ which is the slope of the dotted line. This slope is related to the correlation coefficient by $d\widehat{\theta}_i/d\theta_j = \rho_{ij} \times \frac{\sigma_i}{\sigma_j}$.

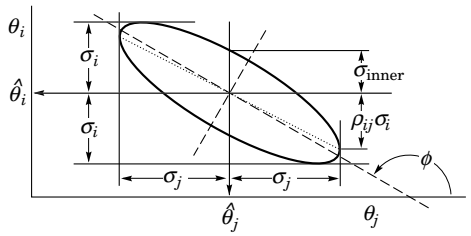

Figure 38.5: Standard error ellipse for the estimators $\widehat{\theta}_i$ and $\widehat{\theta}_j$. In this case the correlation is negative.

As in the single-variable case, because of the symmetry of the Gaussian function between $\boldsymbol{\theta}$ and $\widehat{\boldsymbol{\theta}}$, one finds that contours of constant $\ln L$ or χ^2 cover the true values with a certain, fixed probability. That is, the confidence region is determined by

$$\ln L(\boldsymbol{\theta}) \geq \ln L_{\rm max} - \Delta\ln L \ , \tag{38.68}$$

or where a χ^2 has been defined for use with the method of least-squares,

$$\chi^2(\boldsymbol{\theta}) \leq \chi^2_{\rm min} + \Delta\chi^2 \ . \tag{38.69}$$

Values of $\Delta\chi^2$ or $2\Delta\ln L$ are given in Table 38.2 for several values of the coverage probability and number of fitted parameters.

For non-Gaussian data samples, the probability for the regions determined by equations (38.68) or (38.69) to cover the true value of $\boldsymbol{\theta}$ becomes independent of $\boldsymbol{\theta}$ only in the large-sample limit. So for a finite data sample these are not exact confidence regions according to our previous definition. Nevertheless, they can still have a coverage probability only weakly dependent on the true parameter, and approximately as given in Table 38.2. In any case, the coverage probability of the intervals or regions obtained according to this procedure can in principle be determined as a function of the true parameter(s), for example, using a Monte Carlo calculation.

One of the practical advantages of intervals that can be constructed from the log-likelihood function or χ^2 is that it is relatively simple to produce the interval for the combination of several experiments. If N independent measurements result in log-likelihood functions $\ln L_i(\boldsymbol{\theta})$, then the combined log-likelihood function is simply the sum,

$$\ln L(\boldsymbol{\theta}) = \sum_{i=1}^{N} \ln L_i(\boldsymbol{\theta}) \ . \tag{38.70}$$

This can then be used to determine an approximate confidence interval or region with Eq. (38.68), just as with a single experiment.

38.4.2.3. *Poisson or binomial data:*

Another important class of measurements consists of counting a certain number of events, n. In this section, we will assume these are all events of the desired type, *i.e.*, there is no background. If n represents the number of events produced in a reaction with cross section σ, say, in a fixed integrated luminosity $\mathcal{L}$, then it follows a Poisson distribution with mean $\mu = \sigma\mathcal{L}$. If, on the other hand, one has selected a larger sample of N events and found n of them to have a particular property, then n follows a binomial distribution where the parameter p gives the probability for the event to possess the property in question. This is appropriate, *e.g.*, for estimates of branching ratios or selection efficiencies based on a given total number of events.

For the case of Poisson distributed n, the upper and lower limits on the mean value μ can be found from the Neyman procedure to be

$$\mu_{\rm lo} = \tfrac{1}{2}F^{-1}_{\chi^2}(\alpha_{\rm lo}; 2n) \ , \tag{38.71a}$$

$$\mu_{\rm up} = \tfrac{1}{2}F^{-1}_{\chi^2}(1-\alpha_{\rm up}; 2(n+1)) \ , \tag{38.71b}$$

where the upper and lower limits are at confidence levels of $1-\alpha_{\rm lo}$ and $1-\alpha_{\rm up}$, respectively, and $F^{-1}_{\chi^2}$ is the quantile of the χ^2 distribution (inverse of the cumulative distribution). The quantiles $F^{-1}_{\chi^2}$ can be obtained from standard tables or from the ROOT routine `TMath::ChisquareQuantile`. For central confidence intervals at confidence level $1-\alpha$, set $\alpha_{\rm lo} = \alpha_{\rm up} = \alpha/2$.

Table 38.3: Lower and upper (one-sided) limits for the mean μ of a Poisson variable given n observed events in the absence of background, for confidence levels of 90% and 95%.

	$1-\alpha$ =90%		$1-\alpha$ =95%	
n	$\mu_{\rm lo}$	$\mu_{\rm up}$	$\mu_{\rm lo}$	$\mu_{\rm up}$
0	–	2.30	–	3.00
1	0.105	3.89	0.051	4.74
2	0.532	5.32	0.355	6.30
3	1.10	6.68	0.818	7.75
4	1.74	7.99	1.37	9.15
5	2.43	9.27	1.97	10.51
6	3.15	10.53	2.61	11.84
7	3.89	11.77	3.29	13.15
8	4.66	12.99	3.98	14.43
9	5.43	14.21	4.70	15.71
10	6.22	15.41	5.43	16.96

It happens that the upper limit from Eq. (38.71*b*) coincides numerically with the Bayesian upper limit for a Poisson parameter, using a uniform prior p.d.f. for μ. Values for confidence levels of 90% and 95% are shown in Table 38.3. For the case of binomially distributed n successes out of N trials with probability of success p, the upper and lower limits on p are found to be

$$p_{\rm lo} = \frac{nF_F^{-1}[\alpha_{\rm lo}; 2n, 2(N-n+1)]}{N-n+1 \ + \ nF_F^{-1}[\alpha_{\rm lo}; 2n, 2(N-n+1)]} \ , \tag{38.72a}$$

$$p_{\rm up} = \frac{(n+1)F_F^{-1}[1-\alpha_{\rm up}; 2(n+1), 2(N-n)]}{(N-n) \ + \ (n+1)F_F^{-1}[1-\alpha_{\rm up}; 2(n+1), 2(N-n)]} \ . \tag{38.72b}$$

Here F_F^{-1} is the quantile of the F distribution (also called the Fisher–Snedecor distribution; see Ref. 4).

38.4.2.4. *Parameter exclusion in cases of low sensitivity:*

An important example of a statistical test arises in the search for a new signal process. Suppose the parameter μ is defined such that it is proportional to the signal cross section. A statistical test may be carried out for hypothesized values of μ, which may be done by computing a p-value, p_μ, for all μ. Those values not rejected in a test of size α, *i.e.*, for which one does not find $p_\mu \leq \alpha$, constitute a confidence interval with confidence level $1-\alpha$.

In general one will find that for some regions in the parameter space of the signal model, the predictions for data are almost indistinguishable from those of the background-only model. This corresponds to the case where μ is very small, as would occur, *e.g.*, if one searches for a new particle with a mass so high that its production rate in a given experiment is negligible. That is, one has essentially no experimental sensitivity to such a model.

One would prefer that if the sensitivity to a model (or a point in a model's parameter space) is very low, then it should not be excluded. Even if the outcomes predicted with or without signal are identical, however, the probability to reject the signal model will equal α, the type-I error rate. As one often takes α to be 5%, this would mean that in a large number of searches covering a broad range of a signal model's parameter space, there would inevitably be excluded regions in which the experimental sensitivity is very small, and thus one may question whether it is justified to regard such parameter values as disfavored.

Exclusion of models to which one has little or no sensitivity occurs, for example, if the data fluctuate very low relative to the expectation of the background-only hypothesis. In this case the resulting upper limit on the predicted rate (cross section) of a signal model may be anomalously low. As a means of controlling this effect one often determines the mean or median limit under assumption of the background-only hypothesis using a simplified Monte Carlo simulation of the experiment. An upper limit found significantly below the background-only expectation may indicate a strong downward fluctuation of the data, or perhaps as well an incorrect estimate of the background rate.

One way to mitigate the problem of excluding models to which one is not sensitive is the $\mathrm{CL_s}$ method, where the measure used to test a parameter is increased for decreasing sensitivity [34,35]. The procedure is based on a statistic called $\mathrm{CL_s}$, which is defined as

$$\mathrm{CL_s} = \frac{p_\mu}{1-p_\mathrm{b}} \,, \tag{38.73}$$

where p_b is the p-value of the background-only hypothesis. In the usual formulation of the method, both p_μ and p_b are defined using a single test statistic, and the definition of $\mathrm{CL_s}$ above assumes this statistic is continuous; more details can be found in Refs. [34,35].

A point in a model's parameter space is regarded as excluded if one finds $\mathrm{CL_s} \leq \alpha$. As the denominator in Eq. (38.73) is always less than or equal to unity, the exclusion criterion based on $\mathrm{CL_s}$ is more stringent than the usual requirement $p_\mu \leq \alpha$. In this sense the $\mathrm{CL_s}$ procedure is conservative, and the coverage probability of the corresponding intervals will exceed the nominal confidence level $1-\alpha$. If the experimental sensitivity to a given value of μ is very low, then one finds that as p_μ decreases, so does the denominator $1-p_\mathrm{b}$, and thus the condition $\mathrm{CL_s} \leq \alpha$ is effectively prevented from being satisfied. In this way the exclusion of parameters in the case of low sensitivity is suppressed.

The $\mathrm{CL_s}$ procedure has the attractive feature that the resulting intervals coincide with those obtained from the Bayesian method in two important cases: the mean value of a Poisson or Gaussian distributed measurement with a constant prior. The $\mathrm{CL_s}$ intervals overcover for all values of the parameter μ, however, by an amount that depends on μ.

The problem of excluding parameter values to which one has little sensitivity is particularly acute when one wants to set a one-sided limit, *e.g.*, an upper limit on a cross section. Here one tests a value of a rate parameter μ against the alternative of a lower rate, and therefore the critical region of the test is taken to correspond to data outcomes with a low event yield. If the number of events found in the search region fluctuates low enough, however, it can happen that all physically meaningful signal parameter values, including those to which one has very little sensitivity, are rejected by the test.

Another solution to this problem, therefore, is to replace the one-sided test by one based on the likelihood ratio, where the critical region is not restricted to low rates. This is the approach followed in the Feldman-Cousins procedure described in Section 38.4.2.1. The critical region for the test of a given value of μ contains data values characteristic of both higher and lower rates. As a result, for a given observed rate one can in general obtain a two-sided interval. If, however, the parameter estimate $\hat{\mu}$ is sufficiently close to the lower limit of zero, then only high values of μ are rejected, and the lower edge of the confidence interval is at zero. Note, however, that the coverage property of $1-\alpha$ pertains to the entire interval, not to the probability for the upper edge μ_up to be greater than the true value μ. For parameter estimates increasingly far away from the boundary, *i.e.*, for increasing signal significance, the point $\mu = 0$ is excluded and the interval has nonzero upper and lower edges.

An additional difficulty arises when a parameter estimate is not significantly far away from the boundary, in which case it is natural to report a one-sided confidence interval (often an upper limit). It is straightforward to force the Neyman prescription to produce only an upper limit by setting $x_2 = \infty$ in Eq. (38.62). Then x_1 is uniquely determined and the upper limit can be obtained. If, however, the data come out such that the parameter estimate is not so close to the boundary, one might wish to report a central confidence interval (*i.e.*, an interval based on a two-sided test with equal upper and lower tail areas). As pointed out by Feldman and Cousins [33], however, if the decision to report an upper limit or two-sided interval is made by looking at the data ("flip-flopping"), then in general there will be parameter values for which the resulting intervals have a coverage probability less than $1-\alpha$. With the confidence intervals suggested in [33], the prescription determines whether the interval is one- or two-sided in a way which preserves the coverage probability (and are thus said to be *unified*).

The intervals according to this method for the mean of Poisson variable in the absence of background are given in Table 38.4. (Note that α in Ref. 33 is defined following Neyman [29] as the coverage probability; this is opposite the modern convention used here in which the coverage probability is $1-\alpha$.) The values of $1-\alpha$ given here refer to the coverage of the true parameter by the whole interval $[\mu_1, \mu_2]$. In Table 38.3 for the one-sided upper limit, however, $1-\alpha$ refers to the probability to have $\mu_\mathrm{up} \geq \mu$ (or $\mu_\mathrm{lo} \leq \mu$ for lower limits).

Table 38.4: Unified confidence intervals $[\mu_1, \mu_2]$ for a the mean of a Poisson variable given n observed events in the absence of background, for confidence levels of 90% and 95%.

	$1-\alpha$ =90%		$1-\alpha$ =95%	
n	μ_1	μ_2	μ_1	μ_2
0	0.00	2.44	0.00	3.09
1	0.11	4.36	0.05	5.14
2	0.53	5.91	0.36	6.72
3	1.10	7.42	0.82	8.25
4	1.47	8.60	1.37	9.76
5	1.84	9.99	1.84	11.26
6	2.21	11.47	2.21	12.75
7	3.56	12.53	2.58	13.81
8	3.96	13.99	2.94	15.29
9	4.36	15.30	4.36	16.77
10	5.50	16.50	4.75	17.82

A potential difficulty with unified intervals arises if, for example, one constructs such an interval for a Poisson parameter s of some yet to be discovered signal process with, say, $1-\alpha = 0.9$. If the true signal parameter is zero, or in any case much less than the expected background, one will usually obtain a one-sided upper limit on s. In a certain fraction of the experiments, however, a two-sided interval for s will result. Since, however, one typically chooses $1-\alpha$ to be only 0.9 or 0.95 when setting limits, the value $s = 0$ may be found below the lower edge of the interval before the existence of the effect is well established. It must then be communicated carefully that in excluding $s = 0$ at, say, 90% or 95% confidence level from the interval, one is not necessarily claiming to have discovered the effect, for which one would usually require a higher level of significance (*e.g.*, 5 σ).

Another possibility is to construct a Bayesian interval as described in Section 38.4.1. The presence of the boundary can be incorporated simply by setting the prior density to zero in the unphysical region. More specifically, the prior may be chosen using formal rules such as the reference prior or Jeffreys prior mentioned in Sec. 38.2.4.

In HEP a widely used prior for the mean μ of a Poisson distributed measurement has been uniform for $\mu \geq 0$. This prior does not follow from any fundamental rule nor can it be regarded as reflecting a reasonable degree of belief, since the prior probability for μ to lie between any two finite limits is zero. It is more appropriately regarded as a procedure for obtaining intervals with frequentist properties that can be investigated. The resulting upper limits have a coverage probability that depends on the true value of the Poisson parameter, and is nowhere smaller than the stated probability content. Lower limits and two-sided intervals for the Poisson mean based on flat priors undercover, however, for some values of the parameter, although to an extent that in practical cases may not be too severe [2,21]. Intervals constructed in this way have the advantage of being easy to derive; if several independent measurements are to be combined then one simply multiplies the likelihood functions (cf. Eq. (38.70)).

In any case, it is important to always report sufficient information so that the result can be combined with other measurements. Often this means giving an unbiased estimator and its standard deviation, even if the estimated value is in the unphysical region.

It can also be useful with a frequentist interval to calculate its subjective probability content using the posterior p.d.f. based on one or several reasonable guesses for the prior p.d.f. If it turns out to be significantly less than the stated confidence level, this warns that it would be particularly misleading to draw conclusions about the parameter's value from the interval alone.

References:

1. B. Efron, Am. Stat. **40**, 11 (1986).
2. R.D. Cousins, Am. J. Phys. **63**, 398 (1995).
3. A. Stuart, J.K. Ord, and S. Arnold, *Kendall's Advanced Theory of Statistics*, Vol. 2A: *Classical Inference and the Linear Model*, 6th ed., Oxford Univ. Press (1999), and earlier editions by Kendall and Stuart. The likelihood-ratio ordering principle is described at the beginning of Ch. 23. Chapter 26 compares different schools of statistical inference.
4. F.E. James, *Statistical Methods in Experimental Physics*, 2nd ed., (World Scientific, Singapore, 2007).
5. H. Cramér, *Mathematical Methods of Statistics,* Princeton Univ. Press, New Jersey (1958).
6. L. Lyons, *Statistics for Nuclear and Particle Physicists*, (Cambridge University Press, New York, 1986).
7. R. Barlow, Nucl. Instrum. Methods **A297**, 496 (1990).
8. G. Cowan, *Statistical Data Analysis*, (Oxford University Press, Oxford, 1998).
9. For a review, see S. Baker and R. Cousins, Nucl. Instrum. Methods **221**, 437 (1984).
10. For information on neural networks and related topics, see *e.g.*, C.M. Bishop, *Neural Networks for Pattern Recognition*, Clarendon Press, Oxford (1995); C. Peterson and T. Rögnvaldsson, An Introduction to Artificial Neural Networks, in *Proceedings of the 1991 CERN School of Computing*, C. Verkerk (ed.), CERN 92-02 (1992).
11. T. Hastie, R. Tibshirani, and J. Friedman, *The Elements of Statistical Learning* (2nd edition, Springer, New York, 2009).
12. A. Webb, *Statistical Pattern Recognition*, 2nd ed., (Wiley, New York, 2002).
13. L.I. Kuncheva, *Combining Pattern Classifiers*, (Wiley, New York, 2004).
14. Links to the *Proceedings of the PHYSTAT* conference series (Durham 2002, Stanford 2003, Oxford 2005, and Geneva 2007, 2011) can be found at `phystat.org`.
15. A. Höcker *et al.*, *TMVA Users Guide*, `physics/0703039`(2007); software available from `tmva.sf.net`.
16. I. Narsky, *StatPatternRecognition: A C++ Package for Statistical Analysis of High Energy Physics Data*, `physics/0507143`(2005); software avail. from `sourceforge.net/projects/statpatrec`.
17. L. Demortier, *P-Values and Nuisance Parameters*, *Proceedings of PHYSTAT 2007*, CERN-2008-001, p. 23.
18. E. Gross and O. Vitells, Eur. Phys. J. **C70**, 525 (2010); `arXiv:1005.1891`.
19. R.B. Davis, Biometrica **74**, 33 (1987).
20. K. Cranmer, *Statistical Challenges for Searches for New Physics at the LHC*, in Proceedings of PHYSTSAT 2005, L. Lyons and m. Karagoz Unel (eds.), Oxford (2005); `arXiv:physics/0511028`.
21. B.P. Roe and M.B. Woodroofe, Phys. Rev. **D63**, 13009 (2000).
22. A. O'Hagan and J.J. Forster, *Bayesian Inference*, (2nd edition, volume 2B of *Kendall's Advanced Theory of Statistics*, Arnold, London, 2004).
23. D. Sivia and J. Skilling, *Data Analysis: A Bayesian Tutorial*, (Oxford University Press, 2006).
24. P.C. Gregory, *Bayesian Logical Data Analysis for the Physical Sciences*, (Cambridge University Press, 2005).
25. J.M. Bernardo and A.F.M. Smith, *Bayesian Theory*, (Wiley, 2000).
26. Robert E. Kass and Larry Wasserman, J. Am. Stat. Assoc. **91**, 1343 (1996).
27. J.M. Bernardo, J. R. Statist. Soc. **B41**, 113 (1979); J.M. Bernardo and J.O. Berger, J. Am. Stat. Assoc. **84**, 200 (1989). See also J.M. Bernardo, *Reference Analysis*, in *Handbook of Statistics*, 25 (D.K. Dey and C.R. Rao, eds.), 17-90, Elsevier (2005) and references therein.
28. L. Demortier, S. Jain, and H. Prosper, Phys. Rev. **D 82**, 034002 (2010); `arXiv:1002.1111`.
29. J. Neyman, Phil. Trans. Royal Soc. London, Series A, **236**, 333 (1937), reprinted in *A Selection of Early Statistical Papers on J. Neyman*, (University of California Press, Berkeley, 1967).
30. R. E. Kass and A. E. Raftery, J. Am. Stat. Assoc. **90**, 773 (1995).
31. J. Skilling, *Nested Sampling*, *AIP Conference Proceedings* **735**, 395405 (2004).
32. F. Feroz, M.P. Hobson, and M. Bridges, Mon. Not. Roy. Astron. Soc. **398**, 1601-1614 (2009); `arXiv:0809.3437`.
33. G.J. Feldman and R.D. Cousins, Phys. Rev. **D57**, 3873 (1998). This paper does not specify what to do if the ordering principle gives equal rank to some values of x. Eq. 21.6 of Ref. 3 gives the rule: all such points are included in the acceptance region (the domain $D(\alpha)$). Some authors have assumed the contrary, and shown that one can then obtain null intervals.
34. A.L. Read, *Modified frequentist analysis of search results (the CL_s method)*, in F. James, L. Lyons, and Y. Perrin (eds.), *Workshop on Confidence Limits*, CERN Yellow Report 2000-005, available through `cdsweb.cern.ch`.
35. T. Junk, Nucl. Instrum. Methods **A434**, 435 (1999).
36. N. Reid, *Likelihood Inference in the Presence of Nuisance Parameters*, *Proceedings of PHYSTAT2003*, L. Lyons, R. Mount, and R. Reitmeyer, eds., eConf C030908, Stanford, 2003.
37. W.A. Rolke, A.M. Lopez, and J. Conrad, Nucl. Instrum. Methods **A551**, 493 (2005); `physics/0403059`.
38. G. Cowan, K. Cranmer, E. Gross, and O. Vitells, Eur. Phys. J. **C71**, 1554 (2011).

39. MONTE CARLO TECHNIQUES

Revised September 2011 by G. Cowan (RHUL).

Monte Carlo techniques are often the only practical way to evaluate difficult integrals or to sample random variables governed by complicated probability density functions. Here we describe an assortment of methods for sampling some commonly occurring probability density functions.

39.1. Sampling the uniform distribution

Most Monte Carlo sampling or integration techniques assume a "random number generator," which generates uniform statistically independent values on the half open interval $[0, 1)$; for reviews see, *e.g.*, [1,2].

Uniform random number generators are available in software libraries such as CERNLIB [3], CLHEP [4], and ROOT [5]. For example, in addition to a basic congruential generator `TRandom` (see below), ROOT provides three more sophisticated routines: `TRandom1` implements the RANLUX generator [6] based on the method by Lüscher, and allows the user to select different quality levels, trading off quality with speed; `TRandom2` is based on the maximally equidistributed combined Tausworthe generator by L'Ecuyer [7]; the `TRandom3` generator implements the Mersenne twister algorithm of Matsumoto and Nishimura [8]. All of the algorithms produce a periodic sequence of numbers, and to obtain effectively random values, one must not use more than a small subset of a single period. The Mersenne twister algorithm has an extremely long period of $2^{19937} - 1$.

The performance of the generators can be investigated with tests such as DIEHARD [9] or TestU01 [10]. Many commonly available congruential generators fail these tests and often have sequences (typically with periods less than 2^{32}), which can be easily exhausted on modern computers. A short period is a problem for the `TRandom` generator in ROOT, which, however, has the advantage that its state is stored in a single 32-bit word. The generators `TRandom1`, `TRandom2`, or `TRandom3` have much longer periods, with `TRandom3` being recommended by the ROOT authors as providing the best combination of speed and good random properties. For further information see, *e.g.*, Ref. 11.

39.2. Inverse transform method

If the desired probability density function is $f(x)$ on the range $-\infty < x < \infty$, its cumulative distribution function (expressing the probability that $x \leq a$) is given by Eq. (37.6). If a is chosen with probability density $f(a)$, then the integrated probability up to point a, $F(a)$, is itself a random variable which will occur with uniform probability density on $[0, 1]$. Suppose u is generated according to a uniformly distributed in $(0, 1)$. If x can take on any value, and ignoring the endpoints, we can then find a unique x chosen from the p.d.f. $f(x)$ for a given u if we set

$$u = F(x) \ , \tag{39.1}$$

provided we can find an inverse of F, defined by

$$x = F^{-1}(u) \ . \tag{39.2}$$

This method is shown in Fig. 39.1a. It is most convenient when one can calculate by hand the inverse function of the indefinite integral of f. This is the case for some common functions $f(x)$ such as $\exp(x)$, $(1 - x)^n$, and $1/(1 + x^2)$ (Cauchy or Breit-Wigner), although it does not necessarily produce the fastest generator. Standard libraries contain software to implement this method numerically, working from functions or histograms in one or more dimensions, *e.g.*, the UNU.RAN package [12], available in ROOT.

For a discrete distribution, $F(x)$ will have a discontinuous jump of size $f(x_k)$ at each allowed $x_k, k = 1, 2, \cdots$. Choose u from a uniform distribution on (0,1) as before. Find x_k such that

$$F(x_{k-1}) < u \leq F(x_k) \equiv \text{Prob}\,(x \leq x_k) = \sum_{i=1}^{k} f(x_i) \ ; \tag{39.3}$$

then x_k is the value we seek (note: $F(x_0) \equiv 0$). This algorithm is illustrated in Fig. 39.1b.

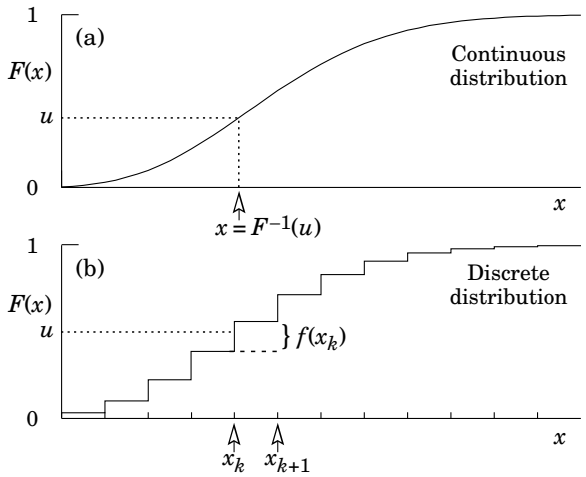

Figure 39.1: Use of a random number u chosen from a uniform distribution (0,1) to find a random number x from a distribution with cumulative distribution function $F(x)$.

39.3. Acceptance-rejection method (Von Neumann)

Very commonly an analytic form for $F(x)$ is unknown or too complex to work with, so that obtaining an inverse as in Eq. (39.2) is impractical. We suppose that for any given value of x, the probability density function $f(x)$ can be computed, and further that enough is known about $f(x)$ that we can enclose it entirely inside a shape which is C times an easily generated distribution $h(x)$, as illustrated in Fig. 39.2. That is, $Ch(x) \geq f(x)$ must hold for all x.

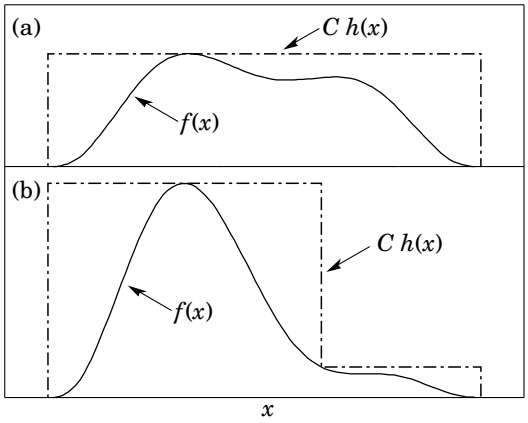

Figure 39.2: Illustration of the acceptance-rejection method. Random points are chosen inside the upper bounding figure, and rejected if the ordinate exceeds $f(x)$. The lower figure illustrates a method to increase the efficiency (see text).

Frequently $h(x)$ is uniform or is a normalized sum of uniform distributions. Note that both $f(x)$ and $h(x)$ must be normalized to unit area, and therefore, the proportionality constant $C > 1$. To generate $f(x)$, first generate a candidate x according to $h(x)$. Calculate $f(x)$ and the height of the envelope $C\,h(x)$; generate u and test if $uC\,h(x) \leq f(x)$. If so, accept x; if not reject x and try again. If we regard x and $uC\,h(x)$ as the abscissa and ordinate of a point in a two-dimensional plot, these points will populate the entire area $C\,h(x)$ in a smooth manner; then we accept those which fall under $f(x)$. The efficiency is the ratio of areas, which must equal $1/C$; therefore we must keep C as close as possible to 1.0. Therefore, we try to choose $C\,h(x)$ to be as close to $f(x)$ as convenience dictates, as in the lower part of Fig. 39.2.

39.4. Algorithms

Algorithms for generating random numbers belonging to many different distributions are given for example by Press [13], Ahrens and Dieter [14], Rubinstein [15], Devroye [16], Walck [17] and Gentle [18]. For many distributions, alternative algorithms exist, varying in complexity, speed, and accuracy. For time-critical applications, these algorithms may be coded in-line to remove the significant overhead often encountered in making function calls.

In the examples given below, we use the notation for the variables and parameters given in Table 37.1. Variables named "u" are assumed to be independent and uniform on [0,1). Denominators must be verified to be non-zero where relevant.

39.4.1. ***Exponential decay*** :

This is a common application of the inverse transform method, and uses the fact that if u is uniformly distributed in $[0,1]$, then $(1-u)$ is as well. Consider an exponential p.d.f. $f(t) = (1/\tau)\exp(-t/\tau)$ that is truncated so as to lie between two values, a and b, and renormalized to unit area. To generate decay times t according to this p.d.f., first let $\alpha = \exp(-a/\tau)$ and $\beta = \exp(-b/\tau)$; then generate u and let

$$t = -\tau \ln(\beta + u(\alpha - \beta)). \tag{39.4}$$

For $(a,b) = (0,\infty)$, we have simply $t = -\tau \ln u$. (See also Sec. 39.4.6.)

39.4.2. ***Isotropic direction in 3D*** :

Isotropy means the density is proportional to solid angle, the differential element of which is $d\Omega = d(\cos\theta)d\phi$. Hence $\cos\theta$ is uniform $(2u_1 - 1)$ and ϕ is uniform $(2\pi u_2)$. For alternative generation of $\sin\phi$ and $\cos\phi$, see the next subsection.

39.4.3. ***Sine and cosine of random angle in 2D*** :

Generate u_1 and u_2. Then $v_1 = 2u_1 - 1$ is uniform on (−1,1), and $v_2 = u_2$ is uniform on (0,1). Calculate $r^2 = v_1^2 + v_2^2$. If $r^2 > 1$, start over. Otherwise, the sine (S) and cosine (C) of a random angle (*i.e.*, uniformly distributed between zero and 2π) are given by

$$S = 2v_1v_2/r^2 \quad \text{and} \quad C = (v_1^2 - v_2^2)/r^2\ . \tag{39.5}$$

39.4.4. ***Gaussian distribution*** :

If u_1 and u_2 are uniform on (0,1), then

$$z_1 = \sin(2\pi u_1)\sqrt{-2\ln u_2} \quad \text{and} \quad z_2 = \cos(2\pi u_1)\sqrt{-2\ln u_2} \tag{39.6}$$

are independent and Gaussian distributed with mean 0 and $\sigma = 1$.

There are many variants of this basic algorithm, which may be faster. For example, construct $v_1 = 2u_1 - 1$ and $v_2 = 2u_2 - 1$, which are uniform on (−1,1). Calculate $r^2 = v_1^2 + v_2^2$, and if $r^2 > 1$ start over. If $r^2 < 1$, it is uniform on (0,1). Then

$$z_1 = v_1\sqrt{\frac{-2\ln r^2}{r^2}} \quad \text{and} \quad z_2 = v_2\sqrt{\frac{-2\ln r^2}{r^2}} \tag{39.7}$$

are independent numbers chosen from a normal distribution with mean 0 and variance 1. $z_i' = \mu + \sigma z_i$ distributes with mean μ and variance σ^2.

For a multivariate Gaussian with an $n \times n$ covariance matrix V, one can start by generating n independent Gaussian variables, $\{\eta_j\}$, with mean 0 and variance 1 as above. Then the new set $\{x_i\}$ is obtained as $x_i = \mu_i + \sum_j L_{ij}\eta_j$, where μ_i is the mean of x_i, and L_{ij} are the components of L, the unique lower triangular matrix that fulfils $V = LL^T$. The matrix L can be easily computed by the following recursive relation (Cholesky's method):

$$L_{jj} = \left(V_{jj} - \sum_{k=1}^{j-1} L_{jk}^2\right)^{1/2}\ , \tag{39.8a}$$

$$L_{ij} = \frac{V_{ij} - \sum_{k=1}^{j-1} L_{ik}L_{jk}}{L_{jj}}\ ,\ j = 1,...,n\ ;\ i = j+1,...,n, \tag{39.8b}$$

where $V_{ij} = \rho_{ij}\sigma_i\sigma_j$ are the components of V. For $n = 2$ one has

$$L = \begin{pmatrix} \sigma_1 & 0 \\ \rho\sigma_2 & \sqrt{1-\rho^2}\,\sigma_2 \end{pmatrix}\ , \tag{39.9}$$

and therefore the correlated Gaussian variables are generated as $x_1 = \mu_1 + \sigma_1\eta_1$, $x_2 = \mu_2 + \rho\sigma_2\eta_1 + \sqrt{1-\rho^2}\,\sigma_2\eta_2$.

39.4.5. **$\chi^2(n)$ distribution** :

To generate a variable following the χ^2 distribution for n degrees of freedom, use the Gamma distribution with $k = n/2$ and $\lambda = 1/2$ using the method of Sec. 39.4.6.

39.4.6. ***Gamma distribution*** :

All of the following algorithms are given for $\lambda = 1$. For $\lambda \neq 1$, divide the resulting random number x by λ.

- If $k = 1$ (the *exponential* distribution), accept $x = -\ln u$. (See also Sec. 39.4.1.)

- If $0 < k < 1$, initialize with $v_1 = (e + k)/e$ (with $e = 2.71828...$ being the natural log base). Generate u_1, u_2. Define $v_2 = v_1u_1$.

  Case 1: $v_2 \leq 1$. Define $x = v_2^{1/k}$. If $u_2 \leq e^{-x}$, accept x and stop, else restart by generating new u_1, u_2.
  Case 2: $v_2 > 1$. Define $x = -\ln([v_1 - v_2]/k)$. If $u_2 \leq x^{k-1}$, accept x and stop, else restart by generating new u_1, u_2. Note that, for $k < 1$, the probability density has a pole at $x = 0$, so that return values of zero due to underflow must be accepted or otherwise dealt with.

- Otherwise, if $k > 1$, initialize with $c = 3k - 0.75$. Generate u_1 and compute $v_1 = u_1(1 - u_1)$ and $v_2 = (u_1 - 0.5)\sqrt{c/v_1}$. If $x = k + v_2 - 1 \leq 0$, go back and generate new u_1; otherwise generate u_2 and compute $v_3 = 64v_1^3u_2^2$. If $v_3 \leq 1 - 2v_2^2/x$ **or** if $\ln v_3 \leq 2\{[k-1]\ln[x/(k-1)] - v_2\}$, accept x and stop; otherwise go back and generate new u_1.

39.4.7. ***Binomial distribution*** :

Begin with $k = 0$ and generate u uniform in $[0,1)$. Compute $P_k = (1-p)^n$ and store P_k into B. If $u \leq B$ accept $r_k = k$ and stop. Otherwise, increment k by one; compute the next P_k as $P_k \cdot (p/(1-p)) \cdot (n-k)/(k+1)$; add this to B. Again, if $u \leq B$, accept $r_k = k$ and stop, otherwise iterate until a value is accepted. If $p > 1/2$, it will be more efficient to generate r from $f(r; n, q)$, *i.e.*, with p and q interchanged, and then set $r_k = n - r$.

39.4.8. ***Poisson distribution*** :

Iterate until a successful choice is made: Begin with $k = 1$ and set $A = 1$ to start. Generate u. Replace A with uA; if now $A < \exp(-\mu)$, where μ is the Poisson parameter, accept $n_k = k - 1$ and stop. Otherwise increment k by 1, generate a new u and repeat, always starting with the value of A left from the previous try.

Note that the Poisson generator used in ROOT's `TRandom` classes before version 5.12 (including the derived classes `TRandom1, TRandom2, TRandom3`) as well as the routine `RNPSSN` from CERNLIB, use a Gaussian approximation when μ exceeds a given threshold. This may be satisfactory (and much faster) for some applications. To do this, generate z from a Gaussian with zero mean and unit standard deviation; then use $x = \max(0, [\mu + z\sqrt{\mu} + 0.5])$ where $[\ ]$ signifies the greatest integer $\leq$ the expression. The routines from Numerical Recipes [13] and CLHEP's routine `RandPoisson` do not make this approximation (see, *e.g.*, Ref. 11).

39.4.9. ***Student's t distribution*** :

Generate u_1 and u_2 uniform in $(0,1)$; then $t = \sin(2\pi u_1)[n(u_2^{-2/n} - 1)]^{1/2}$ follows the Student's t distribution for $n > 0$ degrees of freedom (n not necessarily an integer).

Alternatively, generate x from a Gaussian with mean 0 and $\sigma^2 = 1$ according to the method of 39.4.4. Next generate y, an independent gamma random variate, according to 39.4.6 with $\lambda = 1/2$ and $k = n/2$. Then $z = x/\sqrt{y/n}$ is distributed as a t with n degrees of freedom.

For the special case $n = 1$, the Breit-Wigner distribution, generate u_1 and u_2; set $v_1 = 2u_1 - 1$ and $v_2 = 2u_2 - 1$. If $v_1^2 + v_2^2 \leq 1$ accept $z = v_1/v_2$ as a Breit-Wigner distribution with unit area, center at 0.0, and FWHM 2.0. Otherwise start over. For center M_0 and FWHM Γ, use $W = z\Gamma/2 + M_0$.

39.4.10. ***Beta distribution*** :

The choice of an appropriate algorithm for generation of beta distributed random numbers depends on the values of the parameters α and β. For, *e.g.*, $\alpha = 1$, one can use the transformation method to find $x = 1 - u^{1/\beta}$, and similarly if $\beta = 1$ one has $x = u^{1/\alpha}$. For more general cases see, *e.g.*, Refs. [17,18] and references therein.

39.5. Markov Chain Monte Carlo

In applications involving generation of random numbers following a multivariate distribution with a high number of dimensions, the transformation method may not be possible and the acceptance-rejection technique may have too low of an efficiency to be practical. If it is not required to have independent random values, but only that they follow a certain distribution, then Markov Chain Monte Carlo (MCMC) methods can be used. In depth treatments of MCMC can be found, *e.g.*, in the texts by Robert and Casella [19], Liu [20], and the review by Neal [21].

MCMC is particularly useful in connection with Bayesian statistics, where a p.d.f. $p(\boldsymbol{\theta})$ for an n-dimensional vector of parameters $\boldsymbol{\theta} = (\theta_1, \ldots, \theta_n)$ is obtained, and one needs the marginal distribution of a subset of the components. Here one samples $\boldsymbol{\theta}$ from $p(\boldsymbol{\theta})$ and simply records the marginal distribution for the components of interest.

A simple and broadly applicable MCMC method is the Metropolis-Hastings algorithm, which allows one to generate multidimensional points $\boldsymbol{\theta}$ distributed according to a target p.d.f. that is proportional to a given function $p(\boldsymbol{\theta})$. It is not necessary to have $p(\boldsymbol{\theta})$ normalized to unit area, which is useful in Bayesian statistics, as posterior probability densities are often determined only up to an unknown normalization constant.

To generate points that follow $p(\boldsymbol{\theta})$, one first needs a proposal p.d.f. $q(\boldsymbol{\theta}; \boldsymbol{\theta}_0)$, which can be (almost) any p.d.f. from which independent random values $\boldsymbol{\theta}$ can be generated, and which contains as a parameter another point in the same space $\boldsymbol{\theta}_0$. For example, a multivariate Gaussian centered about $\boldsymbol{\theta}_0$ can be used. Beginning at an arbitrary starting point $\boldsymbol{\theta}_0$, the Hastings algorithm iterates the following steps:

1. Generate a value $\boldsymbol{\theta}$ using the proposal density $q(\boldsymbol{\theta}; \boldsymbol{\theta}_0)$;
2. Form the Hastings test ratio, $\alpha = \min\left[1, \dfrac{p(\boldsymbol{\theta}) q(\boldsymbol{\theta}_0; \boldsymbol{\theta})}{p(\boldsymbol{\theta}_0) q(\boldsymbol{\theta}; \boldsymbol{\theta}_0)}\right]$;
3. Generate a value u uniformly distributed in $[0, 1]$;
4. If $u \leq \alpha$, take $\boldsymbol{\theta}_1 = \boldsymbol{\theta}$. Otherwise, repeat the old point, *i.e.*, $\boldsymbol{\theta}_1 = \boldsymbol{\theta}_0$.
5. Set $\boldsymbol{\theta}_0 = \boldsymbol{\theta}_1$ and return to step 1.

If one takes the proposal density to be symmetric in $\boldsymbol{\theta}$ and $\boldsymbol{\theta}_0$, then this is the *Metropolis*-Hastings algorithm, and the test ratio becomes $\alpha = \min[1, p(\boldsymbol{\theta})/p(\boldsymbol{\theta}_0)]$. That is, if the proposed $\boldsymbol{\theta}$ is at a value of probability higher than $\boldsymbol{\theta}_0$, the step is taken. If the proposed step is rejected, the old point is repeated.

Methods for assessing and optimizing the performance of the algorithm are discussed in, *e.g.*, Refs. [19–21]. One can, for example, examine the autocorrelation as a function of the lag k, *i.e.*, the correlation of a sampled point with that k steps removed. This should decrease as quickly as possible for increasing k.

Generally one chooses the proposal density so as to optimize some quality measure such as the autocorrelation. For certain problems it has been shown that one achieves optimal performance when the acceptance fraction, that is, the fraction of points with $u \leq \alpha$, is around 40%. This can be adjusted by varying the width of the proposal density. For example, one can use for the proposal p.d.f. a multivariate Gaussian with the same covariance matrix as that of the target p.d.f., but scaled by a constant.

References:

1. F. James, Comp. Phys. Comm. **60**, 329 (1990).
2. P. L'Ecuyer, *Proc. 1997 Winter Simulation Conference*, IEEE Press, Dec. 1997, 127–134.
3. The CERN Program Library (CERNLIB); see `cernlib.web.cern.ch/cernlib`.
4. Leif Lönnblad, Comp. Phys. Comm. **84**, 307 (1994).
5. Rene Brun and Fons Rademakers, Nucl. Inst. Meth. **A389**, 81 (1997); see also `root.cern.ch`.
6. F. James, Comp. Phys. Comm. **79**, 111 (1994), based on M. Lüscher, Comp. Phys. Comm. **79**, 100 (1994).
7. P. L'Ecuyer, Mathematics of Computation, **65**, 213 (1996) and **65**, 225 (1999).
8. M. Matsumoto and T. Nishimura, *ACM Transactions on Modeling and Computer Simulation*, Vol. 8, No. 1, January 1998, 3–30.
9. Much of DIEHARD is described in: G. Marsaglia, *A Current View of Random Number Generators*, keynote address, *Computer Science and Statistics: 16th Symposium on the Interface*, Elsevier (1985).
10. P. L'Ecuyer and R. Simard, *ACM Transactions on Mathematical Software* 33, 4, Article 1, December 2007.
11. J. Heinrich, CDF Note CDF/MEMO/STATISTICS/PUBLIC /8032, 2006.
12. UNU.RAN is described at `statmath.wu.ac.at/software/unuran`; see also W. Hörmann, J. Leydold, and G. Derflinger, *Automatic Nonuniform Random Variate Generation*, (Springer, New York, 2004).
13. W.H. Press *et al.*, *Numerical Recipes*, 3rd edition, (Cambridge University Press, New York, 2007).
14. J.H. Ahrens and U. Dieter, Computing **12**, 223 (1974).
15. R.Y. Rubinstein, *Simulation and the Monte Carlo Method*, (John Wiley and Sons, Inc., New York, 1981).
16. L. Devroye, *Non-Uniform Random Variate Generation*, (Springer-Verlag, New York, 1986); available online at `cg.scs.carleton.ca/~luc/rnbookindex.html`.
17. C. Walck, *Handbook on Statistical Distributions for Experimentalists*, University of Stockholm Internal Report SUF-PFY/96-01, available from `www.physto.se/~walck`.
18. J.E. Gentle, *Random Number Generation and Monte Carlo Methods*, 2nd ed., (Springer, New York, 2003).
19. C.P. Robert and G. Casella, *Monte Carlo Statistical Methods*, 2nd ed., (Springer, New York, 2004).
20. J.S. Liu, *Monte Carlo Strategies in Scientific Computing*, (Springer, New York, 2001).
21. R.M. Neal, *Probabilistic Inference Using Markov Chain Monte Carlo Methods*, Technical Report CRG-TR-93-1, Dept. of Computer Science, University of Toronto, available from `www.cs.toronto.edu/~radford/res-mcmc.html`.

40. MONTE CARLO EVENT GENERATORS

Revised September 2013 by P. Nason (INFN, Milan) and P.Z. Skands (CERN)

General-purpose Monte Carlo (GPMC) generators like HERWIG [1], HERWIG++ [2], PYTHIA 6 [3], PYTHIA 8 [4], and SHERPA [5], provide fully exclusive simulations of high-energy collisions. They play an essential role in QCD modeling (in particular for aspects beyond fixed-order perturbative QCD), in data analysis, where they are used together with detector simulation to provide a realistic estimate of the detector response to collision events, and in the planning of new experiments, where they are used to estimate signals and backgrounds in high-energy processes. They are built from several components, that describe the physics starting from very short distance scales, up to the typical scale of hadron formation and decay. Since QCD is weakly interacting at short distances (below a femtometer), the components of the GPMC dealing with short-distance physics are based upon perturbation theory. At larger distances, all soft hadronic phenomena, like hadronization and the formation of the underlying event, cannot be computed from first principles, and one must rely upon QCD-inspired models.

The purpose of this review is to illustrate the main components of these generators. It is divided into four sections. The first one deals with short-distance, perturbative phenomena. The basic concepts leading to the simulations of the dominant QCD processes are illustrated here. In the second section, hadronization phenomena are treated. The two most popular hadronization models for the formation of primary hadrons, the string and cluster models, are illustrated. The basics of the implementation of primary-hadron decays into stable ones is also illustrated here. In the third section, models for soft hadron physics are discussed. These include models for the underlying event, and for minimum-bias interactions. Issues of Bose-Einstein and color-reconnection effects are also discussed here. The fourth section briefly introduces the problem of MC tuning.

We use natural units throughout, such that $c = 1$ and $\hbar = 1$, with energy, momenta and masses measured in GeV, and time and distances measured in GeV^{-1}.

40.1. Short-distance physics in GPMC generators

The short-distance components of a GPMC generator deal with the computation of the primary process at hand, with decays of short-lived particles, and with the generation of QCD and QED radiation, on time scales below $1/\Lambda$, with Λ denoting a typical hadronic scale of a few hundred MeV, corresponding roughly to an inverse femtometer. In e^+e^- annihilation, for example, the short-distance physics describes the evolution of the system from the instant when the e^+e^- pair annihilates up to a time when the size of the produced system is just below a femtometer.

In the present discussion we take the momentum scale of the primary process to be $Q \gg \Lambda$, so that the corresponding time and distance scale $1/Q$ is small. Soft- and collinear-safe inclusive observables, such as total decay widths or inclusive cross sections, can then be reliably computed in QCD perturbation theory (pQCD), with the perturbative expansion truncated at any fixed order n, and the remainder suppressed by $\alpha_S(Q)^{n+1}$.

Less inclusive observables, however, can receive large enhancements that destroy the convergence of the fixed-order expansion. This is due to the presence of collinear and infrared singularities in QCD. Thus, for example, a correction in which a parton from the primary interaction splits collinearly into two partons of comparable energy, is of order $\alpha_S(Q)\ln(Q/\Lambda)$, where the logarithm arises from an integral over a singularity regulated by the hadronic scale Λ. Since $\alpha_S(Q) \propto 1/\ln(Q/\Lambda)$, the corresponding cross section receives a correction of order unity. Two subsequent collinear splittings yield $\alpha_S^2(Q)\ln^2(Q/\Lambda)$, and so on. Thus, corrections of order unity arise at all orders in perturbation theory. The dominant region of phase space is the one where radiation is strongly ordered in a measure of hardness. This means that, from a typical final-state configuration, by clustering together final-state parton pairs with the smallest hardness recursively, we can reconstruct a branching tree, that may be viewed as the splitting history of the event. This history necessarily has some dependence on how we define hardness. For example, we can define it as the energy of the incoming parton times the splitting angle, or as its virtuality, or as the transverse momentum of the splitting partons with respect to the incoming one. These definitions, however, are all equivalent in the collinear region. In fact, in the small-angle limit, the virtuality of a parton of energy E, splitting into two on-shell partons, is given by

$$p^2 = E^2 z(1-z)(1-\cos\theta) \approx \frac{z(1-z)}{2} E^2\theta^2\,, \tag{40.1}$$

where z and $1-z$ are the energy fractions carried by the produced partons, and θ is their relative angle. The transverse momentum of the final partons relative to the direction of the incoming one is given by

$$p_T^2 \approx z^2(1-z)^2 E^2\theta^2. \tag{40.2}$$

Thus, significant differences between these measures only arise in regions with very small z or $1-z$ values. In QCD, because of soft divergences, these regions are in fact important, and the choice of the appropriate ordering variable is very relevant (see Sec. 40.3).

The so called KLN theorem [6,7] guarantees that large logarithmically divergent corrections, arising from final-state collinear splitting and from soft emissions, cancel against the virtual corrections in the total cross section, order by order in perturbation theory. Furthermore, the factorization theorem guarantees that initial-state collinear singularities can be factorized into the parton density functions (PDFs). Therefore, the cross section for the basic process remains accurate up to corrections of higher orders in $\alpha_S(Q)$, provided it is interpreted as an inclusive cross section, rather than as a bare partonic cross section. Thus, for example, the leading order (LO) cross section for $e^+e^- \to q\bar{q}$ is a good LO estimate of the e^+e^- cross section for the production of a pair of quarks accompanied by an arbitrary number of collinear and soft gluons, but is not a good estimate of the cross section for the production of a $q\bar{q}$ pair with no extra radiation.

Shower algorithms are used to compute the cross section for generic hard processes including all leading-logarithmic (LL) corrections. These algorithms begin with the generation of the kinematics of the basic process, performed with a probability proportional to its LO partonic cross section, which is interpreted physically as the inclusive cross section for the basic process, followed by an arbitrary sequence of shower splittings. A probability is then assigned to each splitting sequence. Thus, the initial LO cross section is partitioned into the cross sections for a multitude of final states of arbitrary multiplicity. The sum of all these partial cross sections equals that of the primary process. This property of the GPMCs reflects the KLN cancellation mentioned earlier, and it is often called "unitarity of the shower process", a name that reminds us that the KLN cancellation itself is a consequence of unitarity. The fact that a quantum mechanical process can be described in terms of composition of probabilities, rather than amplitudes, follows from the LL approximation. In fact, in the dominant, strongly ordered region, subsequent splittings are separated by increasingly large times and distances, and this suppresses interference effects.

We now illustrate the basic parton-shower algorithm, as first introduced in Ref. 8. The purpose of this illustration is to give a schematic representation of how shower algorithms work, to introduce some concepts that will be referred to in the following, and to show the relationship between shower algorithms and Feynman-diagram results. For simplicity, we consider the example of e^+e^- annihilation into $q\bar{q}$ pairs. With each dominant (i.e. strongly ordered) final-state configuration one can associate an ordered tree diagram, by recursively clustering together final-state parton pairs with the smallest hardness, and ending up with the hard production vertex (i.e. the $\gamma^* \to q\bar{q}$). The momenta of all intermediate lines of the tree diagram are then uniquely determined from the final-state momenta. Hardnesses in the graph are also strongly ordered. One assigns to each splitting vertex the hardness t, the energy fractions z and $1-z$ of the two generated partons, and the azimuth ϕ of the splitting process with respect to the momentum of the incoming parton. For definiteness, we assume that z and ϕ are defined in the center-of-mass (CM) frame of the e^+e^- collision, although other definitions are possible that differ only beyond the LL approximation. The differential cross section for a

given final state is given by the product of the differential cross section for the initial $e^+e^- \to q\bar{q}$ process, multiplied by a factor

$$\Delta_i(t,t')\frac{\alpha_S(t)}{2\pi}P_{i,jk}(z)\frac{dt}{t}dz\frac{d\phi}{2\pi} \tag{40.3}$$

for each intermediate line ending in a splitting vertex. We have denoted with t' the maximal hardness that is allowed for the line, with t its hardness, and z and ϕ refer to the splitting process. $\Delta(t,t')$ is the so-called Sudakov form factor

$$\Delta_i(t,t') = \exp\left[-\int_t^{t'}\frac{dq^2}{q^2}\,\frac{\alpha_S(q^2)}{2\pi}\sum_{jk}P_{i,jk}(z)dz\frac{d\phi}{2\pi}\right]. \tag{40.4}$$

The suffixes i and jk represent the parton species of the incoming and final partons, respectively, and $P_{i,jk}(z)$ are the Altarelli-Parisi [9] splitting kernels. Final-state lines that do not undergo any further splitting are associated with a factor

$$\Delta_i(t_0,t')\,, \tag{40.5}$$

where t_0 is an infrared cutoff defined by the shower hadronization scale (at which the charges are screened by hadronization) or, for an unstable particle, its width (a source cannot emit radiation with a period exceeding its lifetime).

Notice that the definition of the Sudakov form factor is such that

$$\Delta_i(t_2,t_1) + \int_{t_2}^{t_1}\frac{dt}{t}dz\frac{d\phi}{2\pi}\sum_{jk}\Delta_i(t,t_1)\frac{\alpha_S(t)}{2\pi}P_{i,jk}(z) = 1\,. \tag{40.6}$$

This implies that the cross section for developing the shower up to a given stage does not depend on what happens next, since subsequent factors for further splitting or not splitting add up to one.

The shower cross section can then be formulated in a probabilistic way. The Sudakov form factor $\Delta_i(t_2,t_1)$ is interpreted as the probability for a splitting *not* to occur, for a parton of type i, starting from a branching vertex at the scale t_1, down to a scale t_2. Notice that $0 < \Delta_i(t_2,t_1) \leq 1$, where the upper extreme is reached for $t_2 = t_1$, and the lower extreme is approached for $t_2 = t_0$. From Eq. (40.4), it seems that the Sudakov form factor should vanish if $t_2 = 0$. However, because of the presence of the running coupling in the integrand, t_2 cannot be taken smaller than some cutoff scale of the order of Λ, so that at its lower extreme the Sudakov form factor is small, but not zero. Event generation then proceeds as follows. One gets a uniform random number $0 \leq r \leq 1$, and seeks a solution of the equation $r = \Delta_i(t_2,t_1)$ as a function of t_2. If r is too small and no solution exists, no splitting is generated, and the line is interpreted as a final parton. If a solution t_2 exists, a branching is generated at the scale t_2. Its z value and the final parton species jk are generated with a probability proportional to $P_{i,jk}(z)$. The azimuth is generated uniformly. This procedure is started with each of the primary process partons, and is applied recursively to all generated partons. It may generate an arbitrary number of partons, and it stops when no final-state partons undergo further splitting.

The four-momenta of the final-state partons are reconstructed from the momenta of the initiating ones, and from the whole sequence of splitting variables, subject to overall momentum conservation. Different algorithms employ different strategies to treat recoil effects due to momentum conservation, which may be applied either locally for each parton or dipole splitting, or globally for the entire set of partons (a procedure called *momentum reshuffling*.) This has a subleading effect with respect to the collinear approximation.

We emphasize that the shower cross section described above can be derived from perturbative QCD by keeping only the collinear-dominant real and virtual contributions to the cross section. In particular, up to terms that vanish after azimuthal averaging, the product of the cross section for the basic process, times the factors

$$\frac{\alpha_S}{2\pi}\frac{dt}{t}dz\frac{d\phi}{2\pi}P_{i,jk}(z) \tag{40.7}$$

at each branching vertex, gives the leading collinear contribution to the tree-level cross section for the same process. The dominant virtual corrections in the same approximation are provided by the running coupling at each vertex and by the Sudakov form factors in the intermediate lines.

40.1.1. *Angular correlations* :

In gluon splitting processes ($g \to q\bar{q}$, $g \to gg$) in the collinear approximation, the distribution of the split pair is not uniform in azimuth, and the Altarelli-Parisi splitting functions are recovered only after azimuthal averaging. This dependence is due to the interference of positive and negative helicity states for the gluon that undergoes splitting. Spin correlations propagate through the splitting process, and determine acausal correlations of the EPR kind [10]. A method to partially account for these effects was introduced in Ref. 11, in which the azimuthal correlation between two successive splittings is computed by averaging over polarizations. This can then be applied at each branching step. Acausal correlations are argued to be small, and are discarded with this method, that is still used in the `PYTHIA` code [3]. A method that fully includes spin correlation effects was later proposed by Collins [12], and has been implemented in the fortran `HERWIG` code [13].

40.1.2. *Initial-state radiation* :

Initial-state radiation (ISR) arises because incoming charged particles can radiate before entering the hard-scattering process. In doing so, they acquire a non-vanishing transverse momentum, and their virtuality becomes negative (spacelike). The dominant logarithmic region is the collinear one, where virtualities become larger and larger in absolute value with each emission, up to a limit given by the hardness of the basic process itself. A shower that starts by considering the highest virtualities first would thus have to work backward in time for ISR. A corresponding backwards-evolution algorithm was formulated by Sjöstrand [14], and was basically adopted in all shower models.

The key point in backwards evolution is that the evolution probability depends on the amount of partons that could have given rise to the one being evolved. This is reflected by introducing the ratio of the PDF after the branching to the PDF before the branching in the definition of the backward-evolution Sudakov form factor,

$$\Delta_i^{\rm ISR}(t,t') = \exp\left[-\int_{t'}^{t}\frac{dt''}{t''}\frac{\alpha_S(t'')}{2\pi}\int_x^1\frac{dz}{z}\sum_{jk}P_{j,ik}(z)\frac{f_j(t'',x/z)}{f_i(t'',x)}\right]. \tag{40.8}$$

Notice that there are two uses of the PDFs: they are used to compute the cross section for the basic hard process, and they control ISR via backward evolution. Since the evolution is generated with leading-logarithmic accuracy, it is acceptable to use two different PDF sets for these two tasks, provided they agree at the LO level.

In the context of GPMC evolution, each ISR emission generates a finite amount of transverse momentum. Details on how the recoils generated by these transverse "kicks" are distributed among other partons in the event, in particular the ones involved in the hard process, constitute one of the main areas of difference between existing algorithms, see Ref. 15. An additional $\mathcal{O}(1\,\text{GeV})$ of "primordial k_T" is typically added, to represent the sum of unresolved and/or non-perturbative motion below the shower cutoff scale.

40.1.3. *Soft emissions and QCD coherence* :

In massless field theories like QCD, there are two sources of large logarithms of infrared origin. One has to do with collinear singularities, which arise when two final-state particles become collinear, or when a final-state particle becomes collinear to an initial-state one. The other has to do with the emission of soft gluons at arbitrary angles. Because of that, it turns out that in QCD perturbation theory two powers of large logarithms can arise for each power of α_S. The expansion in leading soft and collinear logarithms is often referred to as the double-logarithmic expansion.

Within the conventional parton-shower formalism, based on collinear factorization, it was shown in a sequel of publications (see Ref. 16 and references therein) that the double-logarithmic region can be correctly described by using the angle of the emissions as the ordering variable, rather than the virtuality, and that the argument of α_S at the splitting vertex should be the relative parton transverse momentum after the splitting. Physically, the ordering in angle approximates the coherent interference arising from large-angle

soft emission from a bunch of collinear partons. Without this effect, the particle multiplicity would grow too rapidly with energy, in conflict with e^+e^- data. For this reason, angular ordering is used as the evolution variable in both the HERWIG [16] and HERWIG++ [17] programs, and an angular veto is imposed on the virtuality-ordered evolution in PYTHIA 6 [18].

A radical alternative formulation of QCD cascades first proposed in Ref. 19 focuses upon soft emission, rather than collinear emission, as the basic splitting mechanism. It then becomes natural to consider a branching process where it is a parton pair (i.e. a dipole) rather than a single parton, that emits a soft parton. Adding a suitable correction for non-soft, collinear partons, one can achieve in this framework the correct logarithmic structure for both soft and collinear emissions in the limit of large number of colors N_c, without any explicit angular-ordering requirement. The ARIADNE [20] and VINCIA [21] programs are based on this approach. In SHERPA, the default shower [22] is also of a dipole type [23], while the $p_\perp$-ordered showers in PYTHIA 6 and 8 represent a hybrid, combining collinear splitting kernels with dipole kinematics [24].

40.1.4. ***Massive quarks*** :
Quark masses act as cut-off on collinear singularities. If the mass of a quark is below, or of the order of Λ, its effect in the shower is small. For larger quark masses, like in c, b, or t production, it is the mass, rather than the typical hadronic scale, that cuts off collinear radiation. For a quark with energy E and mass m_Q, the divergent behavior $d\theta/\theta$ of the collinear splitting process is regulated for $\theta \leq \theta_0 = m_Q/E$. We thus expect less collinear activity for heavy quarks than for light ones, which in turn is the reason why heavy quarks carry a larger fraction of the momentum acquired in the hard production process.

This feature can be implemented with different levels of sophistication. Using the fact that soft emission exhibits a zero at zero emission angle, older parton shower algorithms simply limited the shower emission to be not smaller than the angle θ_0. More modern approaches are used in both PYTHIA, where mass effects are included using a kind of matrix-element correction method [25], and in HERWIG++ and SHERPA, where a generalization of the Altarelli-Parisi splitting kernel is used for massive quarks [26].

40.1.5. ***Color information*** :
Shower MC generators track large-N_c color information during the development of the shower. In the large-N_c limit, quarks or antiquarks are represented by a color line, i.e. a line with an arrow indicating the direction of color flow. Gluons are represented by a pair of color lines with opposite arrows. The rules for color propagation are:

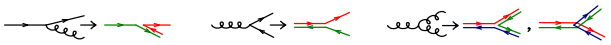

(40.9)

During the shower development, partons are connected by color lines. We can have a quark directly connected by a color line to an antiquark, or via an arbitrary number of intermediate gluons, as shown in Fig. 40.1.

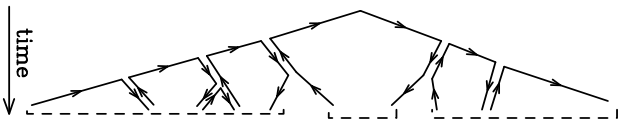

Figure 40.1: Color development of a shower in e^+e^- annihilation. Systems of color-connected partons are indicated by the dashed lines.

It is also possible for a set of gluons to be connected cyclically in color, as e.g. in the decay $\Upsilon \to ggg$.

The color information is used in angular-ordered showers, where the angle of color-connected partons determines the initial angle for the shower development, and in dipole showers, where dipoles are always color-connected partons. It is also used in hadronization models, where the initial strings or clusters used for hadronization are formed by systems of color-connected partons.

40.1.6. ***Electromagnetic corrections*** :
The physics of photon emission from light charged particles can also be treated with a shower MC algorithm. High-energy electrons and quarks, for example, are accompanied by bremsstrahlung photons. Also here, similarly to the QCD case, electromagnetic corrections are of order $\alpha_{\rm em}\ln(Q/m)$, where m is the mass of the radiating particle, or even of order $\alpha_{\rm em}\ln(Q/m)\ln(E_\gamma/E)$ in the region where soft photon emission is important, so that, especially for the case of electrons, their inclusion in the simulation process is mandatory. This is done in most of the GPMC's (for a recent comparative study see [27]) . The specialized generator PHOTOS [28] is sometimes used as an afterburner for an improved treatment of QED radiation in non-hadronic resonace decays.

In case of photons emitted by leptons the shower can be continued down to virtualities arbitrarily close to the lepton mass shell (unlike the case in QCD). In practice, photon radiation must be cut off below a certain energy, in order for the shower algorithm to terminate. Therefore, there is always a minimum energy for emitted photons that depends upon the implementations [27](and so does the MC truth for a charged lepton). In the case of electrons, this energy is typically of the order of its mass. Electromagnetic radiation below this scale is not enhanced by collinear singularities, and is thus bound to be soft, so that the electron momentum is not affected by it.

For photons emitted from quarks, we have instead the obvious limitation that the photon wavelength cannot exceed the typical hadronic size. Longer-wavelength photons are in fact emitted by hadrons, rather than quarks. This last effect is in practice never modeled by existing shower MC implementations. Thus, electromagnetic radiation from quarks is cut off at a typical hadronic scale. Finally, hadron (and τ) decays involving charged particles can produce additional soft bremsstrahlung. This is implemented in a general way in HERWIG++ [29] and SHERPA [30].

40.1.7. ***Beyond-the-Standard-Model Physics*** :
The inclusion of processes for physics beyond the Standard Model (BSM) in event generators is to some extent only a matter of implementing the relevant hard processes and (chains of) decays, with the level of difficulty depending on the complexity of the model and the degree of automation [31,32]. Notable exceptions are long-lived colored particles [33], particles in exotic color representations, and particles showering under new gauge symmetries, with a growing set of implementations documented in the individual GPMC manuals. Further complications that may be relevant are finite-width effects (discussed in Sec. 40.1.8) and the assumed threshold behavior.

In addition to code-specific implementations [15], there are a few commonly adopted standards that are useful for transferring information and events between codes. Currently, the most important of these is the Les Houches Event File (LHEF) standard [34], normally used to transfer parton-level events from a hard-process generator to a shower generator. Another important standard is the Supersymmetry Les Houches Accord (SLHA) format [35], originally used to transfer information on supersymmetric particle spectra and couplings, but by now extended to apply also to more general BSM frameworks and incorporated within the LHEF standard [36].

40.1.8. ***Decay Chains and Particle Widths*** :
In most BSM processes and some SM ones, an important aspect of the event simulation is how decays of short-lived particles, such as top quarks, EW and Higgs bosons, and new BSM resonances, are handled. We here briefly summarize the spectrum of possibilities, but emphasize that there is no universal standard. Users are advised to check whether the treatment of a given code is adequate for the physics study at hand.

The appearance of an unstable resonance as a physical particle at some intermediate stage of the event generation implies that its production and decay processes are treated as being factorized. This is valid up to corrections of order Γ/m_0, with Γ the width and m_0 the pole mass. States whose widths are a substantial fraction of their mass should not be treated as "physical particles," but rather as intrinsically off-shell internal propagator lines.

For states treated as physical particles, two aspects are relevant: the mass distribution of the decaying particle itself and the distributions

of its decay products. For the former, matrix-element generators often use a simple δ function at m_0. The next level up, typically used in GPMCs, is to use a Breit-Wigner distribution (relativistic or non-relativistic), which formally resums higher-order virtual corrections to the mass distribution. Note, however, that this still only generates an improved picture for *moderate* fluctuations away from m_0. Similarly to above, particles that are significantly off-shell (in units of Γ) should not be treated as resonant, but rather as internal off-shell propagator lines. In most GPMCs, further refinements are included, for instance by letting Γ be a function of m ("running widths") and by limiting the magnitude of the allowed fluctuations away from m_0.

For the distributions of the decay products, the simplest treatment is again to assign them their respective m_0 values, with a uniform phase-space distribution. A more sophisticated treatment distributes the decay products according to the differential decay matrix elements, capturing at least the internal dynamics and helicity structure of the decay process, including EPR-like correlations. Further refinements include polarizations of the external states [37] and assigning the decay products their own Breit-Wigner distributions, the latter of which opens the possibility to include also intrinsically off-shell decay channels, like $H \to WW^*$.

During subsequent showering of the decay products, most parton-shower models will preserve their total invariant mass, so as not to skew the original resonance shape.

When computing partial widths and/or modifying decay tables, one should be aware of the danger of double-counting intermediate on-shell particles, see Sec. 40.2.3.

40.1.9. *Matching with Matrix Elements* :

Shower algorithms are based upon a combination of the collinear (small-angle) and soft (small-energy) approximations and are thus inaccurate for hard, large-angle emissions. They also lack next-to-leading order (NLO) corrections to the basic process.

Traditional GPMCs, like `HERWIG` and `PYTHIA`, have included for a long time the so called Matrix Element Corrections (MEC), first formulated in Ref. 38 with later developments summarized in Ref. 15. They are available for processes involving two incoming and one outgoing or one incoming and two outgoing particles, like DIS, vector boson and Higgs production and decays, and top decays. The MEC corrects the emission of the hardest jet at large angles, so that it becomes exact at leading order.

In the past decade, considerable progress has taken place in order to improve the parton-shower description of hard collisions, in two different directions: the so called Matrix Elements and Parton Shower matching (ME+PS from now on), and the matching of NLO calculations and Parton Showers (NLO+PS).

The ME+PS method allows one to use tree-level matrix elements for hard, large-angle emissions. It was first formulated in the so-called CKKW paper [39], and several variants have appeared, including the CKKW-L, MLM, and pseudoshower methods, see Refs. 40, 15 for summaries. Truncated showers are required [41] in order to maintain color coherence when interfacing matrix-element calculations to angular-ordered parton showers using these methods. It is also important to ensure consistent α_S choices between the real (ME-driven) and virtual (PS-driven) corrections [42].

In the ME+PS method one typically starts by generating exact matrix elements for the production of the basic process plus a certain number $\leq n$ of other partons. A minimum separation is imposed on the produced partons, requiring, for example, that the relative transverse momentum in any pair of partons is above a given cut $Q_{\rm cut}$. One then reweights these amplitudes in such a way that, in the strongly ordered region, the virtual effects that are included in the shower algorithm (i.e. running couplings and Sudakov form factors) are also accounted for. At this stage, before parton showers are added, the generated configurations are tree-level accurate at large angle, and at small angle they match the results of the shower algorithm, except that there are no emissions below the scale $Q_{\rm cut}$, and no final states with more than n partons. These kinematic configurations are thus fed into a GPMC, that must generate all splittings with relative transverse momentum below the scale $Q_{\rm cut}$, for initial events with less than n partons, or below the scale of the smallest pair transverse momentum, for events with n partons. The matching parameter $Q_{\rm cut}$ must be chosen to be large enough for fixed-order perturbation theory to hold, but small enough so that the shower is accurate for emissions below it. Notice that the accuracy achieved with MEC is equivalent to that of ME+PS with $n = 1$, where MEC has the advantage of not having a matching parameter $Q_{\rm cut}$.

The popularity of the ME+PS method is due to the fact that processes with many jets appear often as backgrounds to new-physics searches. These jets are typically required to be well separated, and to have large transverse momenta. These kinematical configurations, away from the small-angle region, are precisely those where GPMCs fail to be accurate, and it is thus mandatory to describe them using at least tree-level accurate matrix elements.

The NLO+PS methods extend the accuracy of the generation of the basic process at the NLO level in QCD. They must thus include the radiation of an extra parton with tree-level accuracy, since this radiation constitutes a NLO correction to the basic process. They must also include NLO virtual corrections. They can be viewed as an extension of the MEC method with the inclusion of NLO virtual corrections. They are however more general, since they are applicable to processes of arbitrary complexity. Two of these methods are now widely used: `MC@NLO` [43] and `POWHEG` [41,44], with several alternative methods now also being pursued, see Ref. 15 and references therein.

NLO+PS generators produce NLO accurate distributions for inclusive quantities, and generate the hardest jet with tree-level accuracy even at large angle. It should be recalled, though, that in $2 \to 1$ processes like Z/W production, GPMCs including MEC and weighted by a constant K factor may perform nearly as well, and, if suitably tuned, may even yield a better description of data. It may thus be wise to consider tuning also the NLO+PS generators for these processes.

ME+PS generators should be preferred over NLO+PS ones when one needs an accurate description of more than one hard, large-angle jet associated with the primary process. In order to get event samples that have the advantage of both methods, several attempts to combine NLO+PS calculations at different multiplicities, possibly merged with ME+PS calculations for even higher multiplicities, have appeared recently, see refs [10]-[19] in Ref. 46.

Several ME+PS implementations use existing LO generators, like `ALPGEN` [47], `MADGRAPH` [48], and others summarized in Ref. 40, for the calculation of the matrix elements, and feed the partonic events to a GPMC like `PYTHIA` or `HERWIG` using the Les Houches Interface for User Processes (LHI/LHEF) [49,34]. `SHERPA` and `HERWIG++` also include their own matrix-element generators.

Several NLO+PS processes are implemented in the `MC@NLO` program [43], together with the new `AMC@NLO` development [50], and in the `POWHEG BOX` framework [44]. `HERWIG++` also includes its own `POWHEG` implementation, suitably adapted with the inclusion of vetoed and truncated showers, for several processes. `SHERPA` instead implements a variant of the `MC@NLO` method.

40.2. Hadronization Models

In the context of GPMCs, *hadronization* denotes the process by which a set of colored partons (*after* showering) is transformed into a set of color-singlet *primary* hadrons, which may then subsequently decay further (to *secondary* hadrons). This non-perturbative transition takes place at the *hadronization scale* $Q_{\rm had}$, which by construction is identical to the infrared cutoff of the parton shower. In the absence of a first-principles solution to the relevant dynamics, GPMCs use QCD-inspired phenomenological models to describe this transition.

A key difference between MC hadronization models and the fragmentation-function (FF) formalism used to describe inclusive hadron spectra in perturbative QCD (see Chap. 9 of PDG book) is that the former is always defined at the hadronization scale, while the latter can be defined at an arbitrary perturbative scale Q. They can therefore only be compared directly if the perturbative evolution between Q and $Q_{\rm had}$ is taken into account. FFs are calculable in

pQCD, given a non-perturbative initial condition obtained by fits to hadron spectra. In the MC context, one can prove that the correct QCD evolution of the FFs arises from the shower formalism, with the hadronization model providing an explicit parametrization of the non-perturbative component. It should be kept in mind, however, that the MC modeling of shower and hadronization includes much more information on the final state since it is fully exclusive (i.e., it addresses all particles in the final state explicitly), while FFs only describe inclusive spectra. This exclusivity also enables MC models to make use of the color-flow information coming from the perturbative shower evolution (see Sec. 40.1.5) to determine between which partons the confining potentials should arise.

If one had an exact hadronization model, its dependence upon the hadronization scale $Q_{\rm had}$ would be compensated by the corresponding scale dependence of the shower algorithm, which stops generating branchings at the scale $Q_{\rm had}$. However, due to their complicated and fully exclusive nature, it is generally not possible to enforce this compensation automatically in MC models of hadronization. One must therefore be aware that the model must be "retuned" by hand if changes are made to the perturbative evolution, in particular if the infrared cutoff is modified. Tuning is discussed briefly in Sec. 40.4.

An important result in "quenched" lattice QCD (see Chap. 18 of PDG book) is that the potential of the color-dipole field between a charge and an anticharge appears to grow linearly with the separation of the charges, at distances greater than about a femtometer. This is known as "linear confinement", and it forms the starting point for the *string model of hadronization*, discussed below in Sec. 40.2.1. Alternatively, a property of perturbative QCD called "preconfinement" is the basis of the *cluster model of hadronization*, discussed in Sec. 40.2.2.

Finally, it should be emphasized that the so-called "parton level" that can be obtained by switching off hadronization in a GPMC, is not a universal concept, since each model defines the hadronization scale differently (e.g. by a cutoff in $p_\perp$, invariant mass, etc., with different tunes using different values for the cutoff). Comparisons to distributions at this level may therefore be used to provide an idea of the overall impact of hadronization corrections within a given model, but should be avoided in the context of physical observables.

40.2.1. *The String Model* :

Starting from early concepts [51], several hadronization models based on strings have been proposed [15]. Of these, the most widely used today is the so-called Lund model [52,53], implemented in `PYTHIA` [3,4]. We concentrate on that particular model here, though many of the overall concepts would be shared by any string-inspired method.

Consider a color-connected quark-antiquark pair with no intermediate gluons emerging from the parton shower (like the $\bar{q}q$ pair in the center of Fig. 40.1), e.g. a red q and an antired $\bar{q}$. As the charges move apart, linear confinement implies that a potential $V(r) = \kappa\, r$ is reached for large distances r. (At short distances, there is a Coulomb term $\propto 1/r$ as well, but this is neglected in the Lund string.) This potential describes a string with tension $\kappa \sim 1\,\text{GeV/fm} \sim 0.2\,\text{GeV}^2$. The physical picture is that of a color flux tube being stretched between the q and the $\bar{q}$.

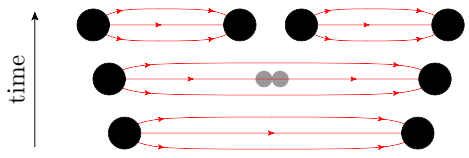

Figure 40.2: Illustration of string breaking by quark pair-creation in the string field.

As the string grows, the non-perturbative creation of quark-antiquark pairs can break the string, via the process $(q\bar{q}) \to (q\bar{q}') + (q'\bar{q})$, illustrated in Fig. 40.2. More complicated color-connected quark-antiquark configurations involving intermediate gluons (like the $\bar{q}gggq$ and $\bar{q}gq$ systems on the left and right part of Fig. 40.1) are treated by representing gluons as transverse "kinks." Thus soft gluons effectively build up a transverse structure in the originally one-dimensional object, with infinitely soft ones smoothly absorbed into the string. For strings with finite-energy kinks, the space-time evolution is slightly more involved [53], but the main point is that there are no separate free parameters for gluon jets. Differences with respect to quark fragmentation arise simply because quarks are only connected to a single string piece, while gluons have one on either side, increasing their relative energy loss (per unit invariant time) by a factor of 2, similar to the ratio of color Casimirs $C_A/C_F = 2.25$.

Since the string breaks are causally disconnected (as can be realized from space-time diagrams [53]) , they do not have to be considered in any specific time-ordered sequence. In the Lund model, the string breaks are generated starting with the leading ("outermost") hadrons, containing the endpoint quarks, and iterating inwards towards the center of the string, alternating randomly between the left and right sides. One can thereby split off a single on-shell hadron in each step, making it straightforward to ensure that only states consistent with known hadron states are produced.

For each breakup vertex, quantum mechanical tunneling is assumed to control the masses and $p_\perp$ kicks that can be produced, leading to a Gaussian suppression

$$\text{Prob}(m_q^2, p_{\perp q}^2) \;\propto\; \exp\left(\frac{-\pi m_q^2}{\kappa}\right) \exp\left(\frac{-\pi p_{\perp q}^2}{\kappa}\right) \;, \qquad (40.10)$$

where m_q is the mass of the produced quark flavor and $p_\perp$ is the non-perturbative transverse momentum imparted to it by the breakup process (the antiquark has the same mass and opposite $p_\perp$), with a universal average value of $\left\langle p_{\perp q}^2 \right\rangle = \kappa/\pi \sim (250\,\text{MeV})^2$. The charm and bottom masses are sufficiently heavy that they are not produced at all in the soft fragmentation. The transverse direction is defined with respect to the string axis, so the $p_\perp$ in a frame where the string is moving will be modified by a Lorentz boost. Note that the effective amount of "non-perturbative" $p_\perp$, in a Monte Carlo model with a fixed shower cutoff $Q_{\rm had}$, may be larger than the purely non-perturbative κ/π above, to account for effects of additional unresolved soft-gluon radiation below $Q_{\rm had}$. In principle, the magnitude of this additional component should scale with the cutoff, but in practice it is up to the user to enforce this by retuning the relevant parameter when changing the hadronization scale.

Since quark masses are difficult to define for light quarks, the value of the strangeness suppression is determined from experimental observables, such as the K/π and K^*/ρ ratios. Note that the parton-shower evolution generates a small amount of strangeness as well, through perturbative $g \to s\bar{s}$ splittings.

Baryon production can also be incorporated, by allowing string breaks to produce pairs of *diquarks*, loosely bound states of two quarks in an overall $\bar{3}$ representation. Again, since diquark masses are difficult to define, the relative rate of diquark to quark production is extracted, e.g. from the p/π ratio. Since the perturbative shower splittings do not produce diquarks, the optimal value for this parameter is mildly correlated with the amount of $g \to q\bar{q}$ splittings produced by the shower. More advanced scenarios for baryon production have also been proposed, see Ref. 53. Within the `PYTHIA` framework, a fragmentation model including baryon string junctions [54] is also available.

The next step of the algorithm is the assignment of the produced quarks within hadron multiplets. Using a nonrelativistic classification of spin states, the fragmenting q may combine with the $\bar{q}'$ from a newly created breakup to produce a meson — or baryon, if diquarks are involved — of a given spin S and angular momentum L. The lowest-lying pseudoscalar and vector meson multiplets, and spin-1/2 and -3/2 baryons, are assumed to dominate in a string framework[1],

[1] The `PYTHIA` implementation includes the lightest pseudoscalar and vector mesons, with the four $L = 1$ multiplets (scalar, tensor, and 2 pseudovectors) available but disabled by default, largely because sev-

but individual rates are not predicted by the model. This is therefore the sector that contains the largest amount of free parameters.

From spin counting, the ratio V/P of vectors to pseudoscalars is expected to be 3, but in practice this is only approximately true for B mesons. For lighter flavors, the difference in phase space caused by the V–P mass splittings implies a suppression of vector production. When extracting the corresponding parameters from data, it is advisable to begin with the heaviest states, since so-called feed-down from the decays of higher-lying hadron states complicates the extraction for lighter particles, see Sec. 40.2.3. For baryons, separate parameters control the relative rates of spin-1 diquarks vs. spin-0 ones and, likewise, have to be extracted from data.

With $p_\perp^2$ and m^2 now fixed, the final step is to select the fraction, z, of the fragmenting endpoint quark's longitudinal momentum that is carried by the created hadron, an aspect for which the string model is highly predictive. The requirement that the fragmentation be independent of the sequence in which breakups are considered (causality) imposes a "left-right symmetry" on the possible form of the fragmentation function, $f(z)$, with the solution

$$f(z) \propto \frac{1}{z}(1-z)^a \exp\left(-\frac{b\,(m_h^2 + p_{\perp h}^2)}{z}\right) \quad , \tag{40.11}$$

which is known as the Lund symmetric fragmentation function (normalized to unit integral). The dimensionless parameter a dampens the hard tail of the fragmentation function, towards $z \to 1$, and may in principle be flavor-dependent, while b, with dimension GeV^{-2}, is a universal constant related to the string tension [53] which determines the behavior in the soft limit, $z \to 0$. Note that the explicit mass dependence in $f(z)$ implies a harder fragmentation function for heavier hadrons (in the rest frame of the string).

As a by-product, the probability distribution in invariant time τ of $q'\bar{q}$ breakup vertices, or equivalently $\Gamma = (\kappa\tau)^2$, is also obtained, with $dP/d\Gamma \propto \Gamma^a \exp(-b\Gamma)$ implying an area law for the color flux, and the average breakup time lying along a hyperbola of constant invariant time $\tau_0 \sim 10^{-23}$s [53].

For massive endpoints (e.g. c and b quarks, or hypothetical hadronizing new-physics particles), which do not move along straight lightcone sections, the exponential suppression with string area leads to modifications of the form $f(z) \to f(z)/z^{b m_Q^2}$, with m_Q the mass of the heavy quark [55]. Although different forms can also be used to describe inclusive heavy-meson spectra (see Sec 20.9 of PDG book), such choices are not consistent with causality in the string framework and hence are theoretically disfavored in this context, one well-known example being the Peterson formula [56],

$$f(z) \propto \frac{1}{z}\left(1 - \frac{1}{z} - \frac{\epsilon_Q}{1-z}\right)^{-2} \quad , \tag{40.12}$$

with ϵ_Q a free parameter expected to scale $\propto 1/m_Q^2$.

40.2.2. *The Cluster Model* :

The cluster hadronization model is based on *preconfinement*, i.e., on the observation [57,58] that the color structure of a perturbative QCD shower evolution at any scale Q_0 is such that color-singlet subsystems of partons (labeled "clusters") occur with a universal invariant mass distribution that only depends on Q_0 and on Λ_{QCD}, not on the starting scale Q, for $Q \gg Q_0 \gg \Lambda_{\mathrm{QCD}}$. Further, this mass distribution is power-suppressed at large masses.

Following early models based on this universality [8,59], the cluster model developed by Webber [60] has for many years been a hallmark of the `HERWIG` and `HERWIG++` generators, with an alternative implementation [61] now available in the `SHERPA` generator. The key idea, in addition to preconfinement, is to force "by hand" all gluons to split into quark-antiquark pairs at the end of the parton shower. Compared with the string description, this effectively amounts to viewing gluons as "seeds" for string breaks, rather than as kinks in a continuous object. After the splittings, a new set of low-mass color-singlet clusters is obtained, formed only by quark-antiquark pairs. These can be decayed to on-shell hadrons in a simple manner.

The algorithm starts by generating the forced $g \to q\bar{q}$ breakups, and by assigning flavors and momenta to the produced quark pairs. For a typical shower cutoff corresponding to a gluon virtuality of $Q_{\mathrm{had}} \sim 1\,\mathrm{GeV}$, the $p_\perp$ generated by the splittings can be neglected. The constituent light-quark masses, $m_{u,d} \sim 300\,\mathrm{MeV}$ and $m_s \sim 450\,\mathrm{MeV}$, imply a suppression (typically even an absence) of strangeness production. In principle, the model also allows for diquarks to be produced at this stage, but due to the larger constituent masses this would only become relevant for shower cutoffs larger than 1 GeV.

If a cluster formed in this way has an invariant mass above some cutoff value, typically 3–4 GeV, it is forced to undergo sequential $1 \to 2$ cluster breakups, along an axis defined by the constituent partons of the original cluster, until all sub-cluster masses fall below the cutoff value. Due to the preservation of the original axis in these breakups, this treatment has some resemblance to the string-like picture.

Next, on the low-mass side of the spectrum, some clusters are allowed to decay directly to a single hadron, with nearby clusters absorbing any excess momentum. This improves the description of the high-z part of the fragmentation spectrum — where the hadron carries almost all the momentum of its parent jet — at the cost of introducing one additional parameter, controlling the probability for single-hadron cluster decay.

Having obtained a final distribution of small-mass clusters, now with a strict cutoff at 3–4 GeV and with the component destined to decay to single hadrons already removed, the remaining clusters are interpreted as a smoothed-out spectrum of excited mesons, each of which decays isotropically to two hadrons, with relative probabilities proportional to the available phase space for each possible two-hadron combination that is consistent with the cluster's internal flavors, including spin degeneracy. It is important that all the light members (containing only uds) of each hadron multiplet be included, as the absence of members can lead to unphysical isospin or SU(3) flavor violation. Typically, the lightest pseudoscalar, vector, scalar, even and odd charge conjugation pseudovector, and tensor multiplets of light mesons are included. In addition, some excited vector multiplets of light mesons may be available. For baryons, usually only the lightest flavor-octet, -decuplet and -singlet baryons are present, although both the `HERWIG++` and `SHERPA` implementations now include some heavier baryon multiplets as well.

Contrary to the case in the string model, the mechanism of phase-space suppression employed here leads to a natural enhancement of the lighter pseudoscalars, and no parameters beyond the spectrum of hadron masses need to be introduced at this point. The phase space also limits the transverse momenta of the produced hadrons relative to the jet axis.

Note that, since the masses and decays of excited heavy-flavor hadrons in particular are not well known, there is some freedom in the model to adjust these, which in turn will affect their relative phase-space populations.

40.2.3. *Hadron and τ Decays* :

Of the so-called primary hadrons, originating directly from string breaks and/or cluster decays (see above), many are unstable and so decay further, until a set of particles is obtained that can be considered stable on time scales relevant to the given measurement[2]. The decay modeling can therefore have a significant impact on final particle yields and spectra, especially for the lowest-lying hadronic states, which receive the largest relative contributions from decays (feed-down). Note that the interplay between primary production and feed-down implies that the hadronization parameters should be retuned if significant changes to the decay treatment are made.

eral states are poorly known and thus may result in a worse overall description when included. For baryons, the lightest spin-1/2 and -3/2 multiplets are included.

[2] E.g., a typical hadron-collider definition of a "stable particle" is $c\tau \geq 10\,\mathrm{mm}$, which includes the weakly-decaying strange hadrons (K, Λ, $\Sigma^\pm$, $\bar{\Sigma}^\pm$, Ξ, Ω).

Particle summary tables, such as those given elsewhere in this *Review*, represent a condensed summary of the available experimental measurements and hence may be incomplete and/or exhibit inconsistencies within the experimental precision. In an MC decay package, on the other hand, all information must be quantified and consistent, with all branching ratios summing to unity. When adapting particle summary information for use in a decay package, a number of choices must therefore be made. The amount of ambiguity increases as more excited hadron multiplets are added to the simulation, about which less and less is known from experiment, with each GPMC making its own choices.

A related choice is how to distribute the decay products differentially in phase space, in particular which matrix elements to use. Historically, MC generators contained matrix elements only for selected (generator-specific) classes of hadron and τ decays, coupled with a Breit-Wigner smearing of the masses, truncated at the edges of the physical decay phase space (the treatment of decay thresholds can be important for certain modes [15]) . A more sophisticated treatment can then be obtained by reweighting the generated events using the obtained particle four-momenta and/or by using specialized external packages such as `EVTGEN` [62] for hadron decays and `TAUOLA` [63] for τ decays.

More recently, `HERWIG++` and `SHERPA` include helicity-dependence in τ decays [64,65], with a more limited treatment available in `PYTHIA 8` [4]. The `HERWIG++` and `SHERPA` generators have also included significantly improved internal simulations of hadronic decays, which include spin correlations between those decays for which matrix elements are used. Photon-bremsstrahlung effects are discussed in Sec. 40.1.6.

`HERWIG++` and `PYTHIA` include the probability for B mesons to oscillate into $\bar{B}$ ones before decay. `SHERPA` and `EVTGEN` also include CP-violating effects and, for common decay modes of the neutral meson and its antiparticle, the interference between the direct decay and oscillation followed by decay.

We end on a note of warning on double counting. This may occur if a particle can decay via an intermediate on-shell resonance. An example is $a_1 \to \pi\pi\pi$ which may proceed via $a_1 \to \rho\pi$, $\rho \to \pi\pi$. If these decay channels of the a_1 are both included, each with their full partial width, a double counting of the on-shell $a_1 \to \rho\pi$ contribution would result. Such cases are normally dealt with consistently in the default MC generator packages, so this warning is mostly for users that wish to edit decay tables on their own.

40.3. Models for Soft Hadron-Hadron Physics

40.3.1. ***Minimum-Bias and Diffraction*** :
The term "minimum bias" (MB) originates from the experimental requirement of a minimal number of tracks (or hits) in a given instrumented region. In order to make MC predictions for such observables, all possible contributions to the relevant phase-space region must be accounted for. There are essentially four types of physics processes, which together make up the total hadron-hadron (hh) cross section: 1) elastic scattering[3]: $hh \to hh$, 2) single diffractive dissociation: $hh \to h + \text{gap} + X$, with X denoting anything that is not the original beam particle, and "gap" denoting a rapidity region devoid of observed activity; 3) double diffractive dissociation: $hh \to X + \text{gap} + X$, and 4) inelastic non-diffractive scattering: everything else. A fifth class may also be defined, called central diffraction ($hh \to h + \text{gap} + X + \text{gap} + h$). Some differences exist between theoretical and experimental terminology [66]. In the experimental setting, diffraction is defined by an observable gap, of some minimal size in rapidity. In the MC context, each diffractive physics process typically produces a whole spectrum of gaps, with small ones suppressed but not excluded.

The inelastic non-diffractive part of the cross section is typically modeled either by smoothly regulating and extending the perturbative QCD scattering cross sections all the way to zero $p_\perp$ [67] (`PYTHIA` 6, `PYTHIA` 8, and `SHERPA`), or by regulating the QCD cross sections with a sharp cutoff [68](`HERWIG+JIMMY`) and adding a separate class of intrinsically soft scatterings below that scale [69](`HERWIG++`). See also Sec. 40.3.2. In all cases, the three most important ingredients are: 1) the IR regularization of the perturbative scattering cross sections, including their PDF dependence, 2) the assumed matter distribution of the colliding hadrons, possibly including multi-parton correlations [54] and/or x dependence [70], and 3) additional soft-QCD effects such as color reconnections and/or other collective effects, discussed in Sec. 40.3.3.

Currently, there are essentially three methods for simulating diffraction in the main MC models: 1) in `PYTHIA` 6, one picks a diffractive mass according to parametrized cross sections $\propto \mathrm{d}M^2/M^2$ [71]. This mass is represented as a string, which is fragmented as described in Sec. 40.2.1, though differences in the effective scale of the hadronization may necessitate a (re)tuning of the fragmentation parameters for diffraction; 2) in `PYTHIA` 8, the high-mass tail beyond $M \sim 10\,\text{GeV}$ is augmented by a partonic description in terms of pomeron PDFs [72], allowing diffractive jet production including showers and underlying event [73]; 3) the `PHOJET` and `DPMJET` programs also include central diffraction and rely directly on a formulation in terms of pomerons (color-singlet multi-gluon states) [74–76]. Cut pomerons correspond to exchanges of soft gluons while uncut ones give elastic and diffractive topologies as well as virtual corrections that help preserve unitarity. So-called "hard pomerons" provide a transition to the perturbative regime. Fragmentation is still handled using the Lund string model, so there is some overlap with the above models at the hadronization stage. In addition, a pomeron-based package exists for `HERWIG` [77], and an effort is underway to construct an MC implementation of the "KMR" model [78] within the `SHERPA` generator. Color reconnections (Sec. 40.3.3) may also play a role in creating rapidity gaps and the underlying event (Sec. 40.3.2) in destroying them.

40.3.2. ***Underlying Event and Jet Pedestals*** :
In the GPMC context, the term underlying event (UE) denotes any additional activity *beyond* the basic process and its associated ISR and FSR activity. The dominant contribution to this is believed to come from additional color exchanges between the beam particles, which can be represented either as multiple parton-parton interactions (MPI) or as so-called cut pomerons (Sec. 40.3.1). The experimentally observed fact that the UE is more active than MB events at the same CM energy is called the "jet pedestal" effect.

The most clearly identifiable consequence of MPI is arguably the possibility of observing several hard parton-parton interactions in one and the same hadron-hadron event. This produces two or more back-to-back jet pairs, with each pair having a small value of $\text{sum}(\vec{p}_\perp)$. For comparison, jets from bremsstrahlung tend to be aligned with the direction of their parent initial- or final-state partons. The fraction of MPI that give rise to additional reconstructible jets is, however, quite small. Soft MPI that do not give rise to observable jets are much more plentiful, and can give significant corrections to the color flow and total scattered energy of the event. This affects the final-state activity in a more global way, increasing multiplicity and summed E_T distributions, and contributing to the break-up of the beam remnants in the forward direction.

The first detailed Monte Carlo model for perturbative MPI was proposed in Ref. 67, and with some variation this still forms the basis for most modern implementations. Some useful additional references can be found in Ref. 15. The first crucial observation is that the t-channel propagators appearing in perturbative QCD $2 \to 2$ scattering almost go on shell at low $p_\perp$, causing the differential cross sections to become very large, behaving roughly as

$$d\sigma_{2\to 2} \propto \frac{dt}{t^2} \sim \frac{dp_\perp^2}{p_\perp^4} \ . \tag{40.13}$$

This cross section is an inclusive number. Thus, if a single hadron-hadron event contains two parton-parton interactions, it will "count" twice in $\sigma_{2\to 2}$ but only once in σ_{tot}, and so on. In the limit that all the interactions are independent and equivalent, one would have

$$\sigma_{2\to 2}(p_{\perp\min}) = \langle n \rangle (p_{\perp\min})\ \sigma_{\text{tot}} \ , \tag{40.14}$$

[3] The QED elastic-scattering cross section diverges and is normally a non-default option in MC models.

with $\langle n\rangle(p_{\perp\min})$ giving the average of a Poisson distribution in the number of parton-parton interactions above $p_{\perp\min}$ per hadron-hadron collision,

$$\mathcal{P}_n(p_{\perp\min}) = (\langle n\rangle(p_{\perp\min}))^n \frac{\exp\left(-\langle n\rangle\ (p_{\perp\min})\right)}{n!} \quad . \tag{40.15}$$

This simple argument expresses unitarity; instead of the total interaction cross section diverging as $p_{\perp\min} \to 0$ (which would violate unitarity), we have restated the problem so that it is now the *number of MPI per collision* that diverges, with the total cross section remaining finite. At LHC energies, the $2 \to 2$ scattering cross sections computed using the full LO QCD cross section folded with modern PDFs becomes larger than the total pp one for $p_\perp$ values of order 4–5 GeV [79]. One therefore expects the average number of perturbative MPI to exceed unity at around that scale.

Two important ingredients remain to fully regulate the remaining divergence. Firstly, the interactions cannot use up more momentum than is available in the parent hadron. This suppresses the large-n tail of the estimate above. In `PYTHIA`-based models, the MPI are ordered in $p_\perp$, and the parton densities for each successive interaction are explicitly constructed so that the sum of x fractions can never be greater than unity. In the `HERWIG` models, instead the uncorrelated estimate of $\langle n\rangle$ above is used as an initial guess, but the generation of actual MPI is stopped once the energy-momentum conservation limit is reached.

The second ingredient invoked to suppress the number of interactions, at low $p_\perp$ and x, is color screening; if the wavelength $\sim 1/p_\perp$ of an exchanged colored parton becomes larger than a typical color-anticolor separation distance, it will only see an *average* color charge that vanishes in the limit $p_\perp \to 0$, hence leading to suppressed interactions. This provides an infrared cutoff for MPI similar to that provided by the hadronization scale for parton showers. A first estimate of the color-screening cutoff would be the proton size, $p_{\perp\min} \approx \hbar/r_p \approx 0.3\,\text{GeV} \approx \Lambda_{\text{QCD}}$, but empirically this appears to be far too low. In current models, one replaces the proton radius r_p in the above formula by a "typical color screening distance," i.e., an average size of a region within which the net compensation of a given color charge occurs. This number is not known from first principles [78] and is perceived of simply as an effective cutoff parameter. The simplest choice is to introduce a step function $\Theta(p_\perp - p_{\perp\min})$. Alternatively, one may note that the jet cross section is divergent like $\alpha_{\text{S}}^2(p_\perp^2)/p_\perp^4$, cf. Eq. (40.13), and that therefore a factor

$$\frac{\alpha_{\text{S}}^2(p_{\perp 0}^2 + p_\perp^2)}{\alpha_{\text{S}}^2(p_\perp^2)} \frac{p_\perp^4}{(p_{\perp 0}^2 + p_\perp^2)^2} \tag{40.16}$$

would smoothly regulate the divergences, now with $p_{\perp 0}$ as the free parameter. Regardless of whether it is imposed as a smooth (`PYTHIA` and `SHERPA`) or steep (`HERWIG++`) function, this is effectively the main "tuning" parameter in such models.

Note that the numerical value obtained for the cross section depends upon the PDF set used, and therefore the optimal value to use for the cutoff will also depend on this choice. Note also that the cutoff does not have to be energy-independent. Higher energies imply that parton densities can be probed at smaller x values, where the number of partons rapidly increases. Partons then become closer packed and the color screening distance d decreases. The uncertainty on the energy and/or x scaling of the cutoff is a major concern when extrapolating between different collider energies [80].

We now turn to the origin of the observational fact that hard jets appear to sit on top of a higher "pedestal" of underlying activity than events with no hard jets. This is interpreted as a consequence of impact-parameter-dependence: in peripheral collisions, only a small fraction of events contain any high-$p_\perp$ activity, whereas central collisions are more likely to contain at least one hard scattering; a high-$p_\perp$ triggered sample will therefore be biased towards small impact parameters, b. The ability of a model to describe the shape of the pedestal (e.g. to describe both MB and UE distributions simultaneously) therefore depends upon its modeling of the b-dependence, and correspondingly the impact-parameter shape constitutes another main tuning parameter.

For each impact parameter b, the number of interactions $\tilde{n}(b)$ can still be assumed to be distributed according to Eq. (40.15), again modulo momentum conservation, but now with the mean value of the Poisson distribution depending on impact parameter, $\langle\tilde{n}(b)\rangle$. This causes the final n-distribution (integrated over b) to be wider than a Poissonian.

Finally, there are two perturbative modeling aspects which go beyond the introduction of MPI themselves: 1) parton showers off the MPI, and 2) perturbative parton-rescattering effects. Without showers, MPI models would generate very sharp peaks for back-to-back MPI jets, caused by unshowered partons passed directly to the hadronization model. However, with the exception of the oldest `PYTHIA6` model, all GPMC models do include such showers [15], and hence should exhibit more realistic (i.e., broader and more decorrelated) MPI jets. On the initial-state side, the main questions are whether and how correlated multi-parton densities are taken into account and, as discussed previously, how the showers are regulated at low $p_\perp$ and/or low x. Although none of the MC models currently impose a rigorous correlated multi-parton evolution, all of them include some elementary aspects. The most significant for parton-level results is arguably momentum conservation, which is enforced explicitly in all the models. The so-called "interleaved" models [24] attempt to go a step further, generating an explicitly correlated multi-parton evolution in which flavor sum rules are imposed to conserve, e.g. the total numbers of valence and sea quarks [54].

Perturbative rescattering in the final state can occur if partons are allowed to undergo several distinct interactions, with showering activity possibly taking place in-between. This has so far not been studied extensively, but a first exploratory model is available [81]. In the initial state, parton rescattering/recombination effects have so far not been included in any of the GPMC models.

40.3.3. ***Bose-Einstein and Color-Reconnection Effects*** :
In the context of e^+e^- collisions, Bose-Einstein (BE) correlations have mostly been discussed as a source of uncertainty on high-precision W mass determinations at LEP [82]. In hadron-hadron (and nucleus-nucleus) collisions, however, BE correlations are used extensively to study the space-time structure of hadronizing matter ("femtoscopy").

In MC models of hadronization, each string break and/or particle/cluster decay is normally factorized from all other ones. This reduces the number of variables that must be considered simultaneously, but also makes the introduction of correlations among particles from different breaks/decays intrinsically difficult to address. In the context of GPMCs, a few semi-classical models are available within the `PYTHIA` 6 and 8 generators [83], in which the BE effect is mimicked by an attractive interaction between pairs of identical particles in the final state, with no higher correlations included. This "force" acts after the decays of very short-lived particles, like ρ, but before decays of longer-lived ones, like π^0. The main differences between the variants of this model is the assumed shape of the correlation function and how overall momentum conservation is handled.

As discussed in Sec. 40.2, leading-color ("planar") color flows are used to set up the hadronizing systems (clusters or strings) at the hadronization stage. If the systems do not overlap significantly in space and time, subleading-color ambiguities and/or non-perturbative reconnections are expected to be small. However, if the density of displaced color charges is sufficiently high that several systems can overlap significantly, full-color and/or reconnection effects should become progressively larger.

In the specific context of MPI, a crucial question is how color is neutralized *between* different MPI systems, including the remnants. The large rapidity differences involved imply large invariant masses (though normally low $p_\perp$), and hence large amounts of (soft) particle production. Indeed, in the context of soft-inclusive physics, it is these "inter-system" strings/clusters that furnish the dominant particle-production mechanism, and hence their modeling is an essential part of the soft-physics description, affecting topics such as MB/UE multiplicity and $p_\perp$ distributions, rapidity gaps, and precision mass measurements. A more comprehensive review of color-reconnection effects can be found in Ref. 15.

40.4. Parameters and Tuning

The accuracy of GPMC models depends both on the inclusiveness of the chosen observable and on the sophistication of the simulation. Improvements at the theoretical level is an important driver for the latter, but the achievable precision also depends crucially on the available constraints on the remaining free parameters. Using existing data to constrain these is referred to as generator tuning.

Although MC models may appear to have a bewildering array of adjustable parameters, most of them only control relatively small (exclusive) details of the event generation. The majority of the (inclusive) physics is determined by only a few, very important ones, such as the value of α_S, in the perturbative domain, and the properties of the non-perturbative fragmentation functions, in the non-perturbative one. One may therefore take a factorized approach, first constraining the perturbative parameters and thereafter the non-perturbative ones, each ordered in a measure of their relative significance to the overall modeling.

At LO×LL, perturbation theory is doing well if it agrees with an IR safe measurement within 10%. It would therefore not make much sense to tune a GPMC beyond roughly 5% (it might even be dangerous, due to overfitting). The advent of NLO Monte Carlos may reduce this number slightly, but only for quantities for which one expects NLO precision. For LO Monte Carlos, distributions should be normalized to unity, since the NLO normalization is not tunable. For quantities governed by non-perturbative physics, uncertainties are larger. For some quantities, e.g. ones for which the underlying modeling is known to be poor, an order-of-magnitude agreement or worse may have to be accepted.

In the context of LO×LL GPMC tuning, subleading aspects of coupling-constant and PDF choices are relevant. In particular, one should be aware that the choice of QCD Λ parameter $\Lambda_{\rm MC} = 1.569\Lambda_{\overline{\rm MS}}$ (for 5 active flavors) improves the predictions of coherent shower algorithms at the NLL level [84], and hence this scheme is typically considered the baseline for shower tuning. The question of LO vs. NLO PDFs is more involved [15], but it should be emphasized that the low-x gluon in particular is important for determining the level of the underlying event in MPI models (Sec. 40.3.2), and hence the MB/UE tuning (and energy scaling [80]) is linked to the choice of PDF in such models. Further issues and an example of a specific recipe that could be followed in a realistic set-up can be found in Ref. 85. A useful online resource can be found at the mcplots.cern.ch web site [86], based on the RIVET tool [87].

Recent years have seen the emergence of automated tools that attempt to reduce the amount of both computer and manpower required for tuning [88]. Automating the human expert input is more difficult. In the tools currently on the market, this is addressed by a combination of input solicited from the GPMC authors (e.g., which parameters and ranges to consider, which observables constitute a complete set, etc) and a set of weights determining the relative priority given to each bin in each distribution. The field is still burgeoning, however, and future sophistications are to be expected. Nevertheless, the overall quality of the automated tunes appear to at least be competitive with the manual ones.

References:

1. G. Corcella *et al.*, JHEP **0101**, 010 (2001), hep-ph/0011363.
2. M.Bähr *et al.*, Eur. Phys. J. **C58**, 639 (2008), arXiv:0803.0883.
3. T. Sjöstrand, S. Mrenna, and P. Z. Skands, JHEP **05**, 026 (2006), hep-ph/0603175.
4. T. Sjöstrand, S. Mrenna, and P. Z. Skands, Comp. Phys. Comm. **178**, 852 (2008), arXiv:0710.3820.
5. T. Gleisberg *et al.*, JHEP **0402**, 056 (2004), hep-ph/0311263.
6. T. Kinoshita, J. Math. Phys. **3**, 650 (1962).
7. T. Lee and M. Nauenberg, Phys. Rev. **133**, 1549 (1964).
8. G.C. Fox and S. Wolfram, Nucl. Phys. **B168**, 285 (1980).
9. G. Altarelli and G. Parisi, Nucl. Phys. **B126**, 298 (1977).
10. A. Einstein, B. Podolsky, and N. Rosen, Phys. Rev. **47**, 777 (1935).
11. B.R. Webber, Phys. Lett. **B193**, 91 (1987).
12. J.C. Collins, Nucl. Phys. **B304**, 794 (1988).
13. I.G. Knowles, Comp. Phys. Comm. **58**, 271 (1990).
14. T. Sjöstrand, Phys. Lett. **B157**, 321 (1985).
15. A. Buckley *et al.*, Phys. Reports **504**, 145 (2011), arXiv:1101.2599.
16. G. Marchesini and B.R. Webber, Nucl. Phys. **B310**, 461 (1988).
17. S. Gieseke, P. Stephens, and B. Webber, JHEP **0312**, 045 (2003), hep-ph/0310083.
18. M. Bengtsson and T. Sjöstrand, Nucl. Phys. **B289**, 810 (1987).
19. G. Gustafson and U. Pettersson, Nucl. Phys. **B306**, 746 (1988).
20. L. Lönnblad, Comp. Phys. Comm. **71**, 15 (1992).
21. W.T. Giele, D.A. Kosower, and P.Z. Skands, Phys. Rev. **D78**, 014026 (2008), arXiv:0707.3652.
22. S. Schumann and F. Krauss, JHEP **0803**, 038 (2008), arXiv:0709.1027.
23. Z. Nagy and D.E. Soper, JHEP **0510**, 024 (2005), hep-ph/0503053.
24. T. Sjöstrand and P.Z. Skands, Eur. Phys. J. **C39**, 129 (2005), hep-ph/0408302.
25. E. Norrbin and T. Sjöstrand, Nucl. Phys. **B603**, 297 (2001), hep-ph/0010012.
26. S. Catani *et al.*, Nucl. Phys. **B627**, 189 (2002), hep-ph/0201036.
27. J. Cembranos *et al.*, (2013), arXiv:1305.2124.
28. N. Davidson, T. Przedzinski, and Z. Was, (2010), arXiv:1011.0937.
29. K. Hamilton and P. Richardson, JHEP **0607**, 010 (2006), hep-ph/0603034.
30. M. Schönherr and F. Krauss, JHEP **0812**, 018 (2008), arXiv:0810.5071.
31. A. Semenov, Comp. Phys. Comm. **180**, 431 (2009), arXiv:0805.0555.
32. N.D. Christensen and C. Duhr, Comp. Phys. Comm. **180**, 1614 (2009), arXiv:0806.4194.
33. M. Fairbairn *et al.*, Phys. Reports **438**, 1 (2007), hep-ph/0611040.
34. J. Alwall *et al.*, Comp. Phys. Comm. **176**, 300 (2007), hep-ph/0609017.
35. P.Z. Skands *et al.*, JHEP **0407**, 036 (2004), hep-ph/0311123.
36. J. Alwall *et al.*, (2007), arXiv:0712.3311.
37. P. Richardson, JHEP **0111**, 029 (2001), hep-ph/0110108.
38. M. Bengtsson and T. Sjöstrand, Phys. Lett. **B185**, 435 (1987).
39. S. Catani *et al.*, JHEP **11**, 063 (2001), hep-ph/0109231.
40. J. Alwall *et al.*, Eur. Phys. J. **C53**, 473 (2008), arXiv:0706.2569.
41. P. Nason, JHEP **11**, 040 (2004), hep-ph/0409146.
42. B. Cooper *et al.*, Eur. Phys. J. **C72**, 2078 (2012), arXiv:1109.5295.
43. S. Frixione and B.R. Webber, JHEP **06**, 029 (2002), hep-ph/0204244.
44. S. Alioli *et al.*, JHEP **1006**, 043 (2010), arXiv:1002.2581.
45. S. Alioli, K. Hamilton, and E. Re, (2001), arXiv:1108.0909.
46. L. Hartgring, E. Laenen, and P. Skands, (2013), arXiv:1303.4974.
47. M.L. Mangano *et al.*, JHEP **0307**, 001 (2003), hep-ph/0206293.
48. J. Alwall *et al.*, JHEP **1106**, 128 (2011), arXiv:1106.0522.
49. E. Boos *et al.*, (2007), hep-ph/0109068.
50. V. Hirschi *et al.*, JHEP **1105**, 044 (2011), arXiv:1103.0621.
51. X. Artru and G. Mennessier, Nucl. Phys. **B70**, 93 (1974).
52. B. Andersson *et al.*, Phys. Reports **97**, 31 (1983).
53. B. Andersson, Camb. Monogr. Part. Phys. Nucl. Phys. Cosmol. **7** (1997).
54. T. Sjöstrand and P.Z. Skands, JHEP **0403**, 053 (2004), hep-ph/0402078.
55. M. Bowler, Z. Phys. **C11**, 169 (1981).
56. C. Peterson *et al.*, Phys. Rev. **D27**, 105 (1983).
57. D. Amati and G. Veneziano, Phys. Lett. **B83**, 87 (1979).
58. A. Bassetto, M. Ciafaloni, and G. Marchesini, Phys. Lett. **B83**, 207 (1979).
59. R.D. Field and S. Wolfram, Nucl. Phys. **B213**, 65 (1983).
60. B.R. Webber, Nucl. Phys. **B238**, 492 (1984).
61. J.-C. Winter, F. Krauss, and G. Soff, Eur. Phys. J. **C36**, 381 (2004), hep-ph/0311085.
62. D. Lange, Nucl. Instrum. Methods **A462**, 152 (2001).
63. S. Jadach *et al.*, Comp. Phys. Comm. **76**, 361 (1993).

64. D. Grellscheid and P. Richardson, (2007), arXiv:0710.1951.
65. T. Gleisberg *et al.*, JHEP **0902**, 007 (2009), arXiv:0811.4622.
66. V. Khoze *et al.*, Eur. Phys. J. **C69**, 85 (2010), arXiv:1005.4839.
67. T. Sjöstrand and M. van Zijl, Phys. Rev. **D36**, 2019 (1987).
68. J.M. Butterworth, J.R. Forshaw, and M.H. Seymour, Z. Phys. **C72**, 637 (1996), hep-ph/9601371.
69. M. Bähr *et al.*, (2009), arXiv:0905.4671.
70. R. Corke and T. Sjöstrand, JHEP **1105**, 009 (2011), 1101.5953.
71. G.A. Schuler and T. Sjöstrand, Phys. Rev. **D49**, 2257 (1994).
72. G. Ingelman and P. Schlein, Phys. Lett. **B152**, 256 (1985).
73. S. Navin, (2010), arXiv:1005.3894.
74. P. Aurenche *et al.*, Comp. Phys. Comm. **83**, 107 (1994), hep-ph/9402351.
75. F.W. Bopp, R. Engel, and J. Ranft, (1998), hep-ph/9803437.
76. S. Roesler, R. Engel, and J. Ranft, p. 1033 (2000), hep-ph/0012252.
77. B.E. Cox and J.R. Forshaw, Comp. Phys. Comm. **144**, 104 (2002), hep-ph/0010303.
78. M. Ryskin, A. Martin, and V. Khoze, Eur. Phys. J. **C71**, 1617 (2011), arXiv:1102.2844.
79. M. Bähr, J.M. Butterworth, and M.H. Seymour, JHEP **01**, 065 (2009), arXiv:0806.2949.
80. H. Schulz and P.Z. Skands, Eur. Phys. J. **C71**, 1644 (2011), arXiv:1103.3649.
81. R. Corke and T. Sjöstrand, JHEP **01**, 035 (2009), arXiv:0911.1901.
82. LEP Electroweak Working Group, (2005), hep-ex/0511027.
83. L. Lönnblad and T. Sjöstrand, Eur. Phys. J. **C2**, 165 (1998), hep-ph/9711460.
84. S. Catani, B. R. Webber, and G. Marchesini, Nucl. Phys. **B349**, 635 (1991).
85. P.Z. Skands, (2011), arXiv:1104.2863.
86. A. Karneyeu *et al.*, (2013), arXiv:1306.3436.
87. A. Buckley *et al.*, (2010), arXiv:1003.0694.
88. A. Buckley *et al.*, Eur. Phys. J. **C65**, 331 (2010), arXiv:0907.2973.

41. MONTE CARLO NEUTRINO EVENT GENERATORS

Written September 2013 by H. Gallagher (Tufts U.) and Y. Hayato (Tokyo U.)

Monte Carlo neutrino generators are programs or libraries which simulate neutrino interactions with electrons, nucleons and nuclei. In this capacity their usual task is to take an input neutrino and nucleus and produce a set of 4-vectors for particles emerging from the interaction, which are then input to full detector simulations. Since these generators have to simulate not only the initial interaction of neutrinos with target particles, but re-interactions of the generated particles in the nucleus, they contain a wide range of elementary particle and nuclear physics. Viewed more broadly, they are the access point for neutrino experimentalists to the theory inputs needed for analysis. Examples include cross section libraries for event rate calculations and parameter uncertainties and reweighting tools for systematic error evaluation.

Neutrino experiments typically operate in neutrino beams that are neither completely pure nor mono-energetic. Generators are a crucial component in the convolution of beam flux, neutrino interaction physics, and detector response that is necessary to make predictions about observable quantities. Similarly they are used to relate reconstructed quantities back to true quantities. In these various capacities they are used from the detector design stage through the extraction of physics measurements from reconstructed observables. Monte Carlo neutrino generators play unique and important roles in the experimental study of neutrino interactions and oscillations.

There are several neutrino event generators available, such as ANIS [1], GENIE [2], GiBUU [3], NEGN [4], NEUT [5], NUANCE [6], the FLUKA routines NUNDIS/NUNRES [7], and NuWRO [8]. Historically, experiments would develop their own generators. This was often because they were focused on a particular measurement, energy range, or target, and wanted to ensure that the best physics was included for it. These 'home-grown' generators were often tuned primarily or exclusively to the neutrino data most similar to the data that the experiment would be collecting. A major advance in the field was the introduction of conference series devoted to the topic of neutrino interaction physics, NuINT and NuFACT in particular. Event generator comparisons have been a regular staple of the NuINT conference series from its inception, and a great deal of information on this topic can be found in the Proceedings of these meetings. These meetings have facilitated experiment-theory discussions leading to the first generator developed by a theory group (NuWRO) [8], the extension of established nuclear interaction codes (FLUKA and GiBUU) to include neutrino-nuclear processes [3], [7], and inclusion of theorists in existing generator development teams.

These activites have led to more careful scrutiny of the crucial nuclear theory inputs to these generators, which is evaluated in particular through comparisons to electron-scattering data. At this point in time all simulation codes face challenges in describing the full extent of the lepton scattering data, and the tension between incorporating the best available theory versus obtaining the best agreement with the data plays out in a variety of ways within the field. For the field to make progress, inclusion of state of the art theory needs to be coupled to global analyses that correctly incorporate correlations between measurements. Given the rapid pace of new data and the complexity of analyses, this is a significant challenge for the field in the coming years.

There are many neutrino experiments which use various sources of neutrinos, from reactors, accelerators, the atmosphere, and astrophysical sources, thereby covering a range of energies from MeV to TeV. Much of the emphasis has been on the few-GeV region in the generators, as this is the relevant energy range for long-baseline neutrino oscillation experiments. These generators use the impulse approximation for most of the primary neutrino interactions and simulate the interactions of secondary particles in the nucleus in semi-classical ways in order to simulate a variety of nuclei in a single model, and for practical considerations as these approaches are fast. However, there are several challenges facing these simulations coming mainly from the complexity of the nuclear physics, and avoiding double counting in combining perturbative and non-perturbative models for the neutrino-nucleon scattering processes. While generators share many common ingredients, differences in implementation, parameter values, and approaches to avoid double counting can yield dramatically different predictions [9]. In the following sections, interaction models and their implementations including the interactions of generated particles in the nuclei are described.

In order to assure its reproducibility, neutrino event generators are tuned and validated against a wide variety of data, including data from photon, charged lepton, neutrino, and hadron probes. The results from these external data tuning exercises are important for experiments as they quantify the uncertainty on model paramaters, needed by experiments in the evaluation of generator-related systematic errors. Electron scattering data plays an important role in determining the vector contribution to the form-factors and structure functions, as well as in evaluating specific aspects of the nuclear model. Hadron scattering data is used in validating the nuclear model, in particular the modeling of final state interactions. Tuning of neutrino-nucleon scattering and hadronization models relies heavily on the previous generation of high energy neutrino scattering and hydrogen and deuterium bubble chamber experiments, and more recent data from the K2K, MiniBooNE, NOMAD, SciBooNE, MINOS, T2K, ArgoNEUT, and MINERvA experiments either has been, or will be, used for this purpose.

41.1. Neutrino-Nucleon Scattering

Event generators typically begin with free-nucleon cross sections which are then embedded into a nuclear physics model. The most important processes are quasi-elastic (elastic for NC) scattering, resonance production, and non-resonant inelastic scattering, which make comparable contributions for few-GeV interactions. The neutrino cross sections in this energy range can be seen in Figures 49.1 through 49.4 of this *Review*.

41.1.1. ***Quasi-Elastic Scattering*** : The cross section for the neutrino nucleon charged current quasi-elastic scattering is described in terms of the leptonic and hadronic weak currents, where dominant contributions to the hadronic current come from the vector and axial-vector form factors. There also exists the pseudo-scalar term (the pseudo-scalar form factor) in the hadronic current but this term is rather small for electron and muon neutrinos and usually related to the axial form factor assuming partially conserved axial current (PCAC). The vector form factors are measured by the recent precise electron scattering experiments and known to have some deviation from the simple dipole form [10]. Therefore, most of the generators use parametrizations of this form factor taken directly from the data. For the axial form factor there is no such precise experiment, and most of the generators use a dipole form. Generally, the value of axial form factor at $q^2 = 0$ is extracted from the polarized nucleon beta decay experiment. However, the selection of the axial vector mass parameter depends on each generator, with values typically around 1.00 GeV/c^2.

41.1.2. ***Resonance Production*** : Most generators use the calculation of Rein-Sehgal to simulate neutrino-induced single pion production [13]. To obtain the cross section for a particular channel, they calculate the amplitude for the production of each resonance multiplied by the probability for the decay of that resonance into that particular channel. Implementation differences include the number of resonances included, whether the amplitudes are added coherently or incoherently, the invariant mass range over which the model is used, how non-resonant backgrounds are included, inclusion of lepton mass terms, and the model parameter values (in particular the axial mass). In this model it is also possible to calculate the cross-sections of single photon, kaon and η productions by changing the decay probability of the resonances, which are included in some of the programs. However, it is known that discrepancies exist between the recent pion electro/photoproduction data and the results from the simulation data with the same framework, i.e. vector part of this model. There are several attempts to overcome this issue [12] and some of the generators started using more appropriate form factors. The GiBUU and NuWRO generators do not use the Rein-Sehgal model, and instead rely directly on electro-production data for the vector contribution and fit bubble chamber data to determine the remaining parameters for the axial contribution [14], [15], [16].

41.1.3. ***Deep and Shallow Inelastic Scattering*** : For this process the fundamental target shifts from the nucleon to its quark constituents. Therefore, the generators use the standard expression for the constructions for the nucleon structure functions F_2 and xF_3 from parton distributions for high Q^2 (the DIS regime) to calculate direction and momeuntum of lepton. The first challenge is in extending this picture to the lower values of Q^2 and W that dominate the available phase space for few-GeV interactions (the so-called 'shallow inelastic scattering', or SIS regime). The corrections proposed in [17] are widely used, while others [7] implement their own modifictions to the parton distributions at low Q^2. Both DIS and SIS generates hadrons but their production depends on each generator's implementation of a hadronization model as described in the next section. There are various difficulties not only in the actual hadronization but the relation with the single meson production. It is necessary to avoid double counting between the resonance and SIS/DIS models, and all generators are different in this regard. The scheme chosen can have a significant impact on the results of simulations at a few-GeV neutrino energies.

41.2. Hadronization Models

For hadrons produced via baryonic resonances, the underlying model amplitudes and resonance branching fractions can be used to fully characterize the hadronic system. For non-resonant production, a hadronization model is required. Most generators use PYTHIA [18] for this purpose, although some with modified parameters. In addition some implement their own models to handle invariant masses that are too low for PYTHIA, typically somwhere around 2.0 GeV/c^2. Such models rely heavily on measurements of neutrino hadro-production in high-resolution devices, such as bubble chambers and the CHORUS [19] and NOMAD experiments [20], to construct empirical parametrizations that reproduce the key features of the data [21], [22]. The basic ingredients are the emperical observations that average charged particle multiplicites increase logarithmically with the invariant mass of the hadronic system, and that the distribution of charged particle multiplicities about this average are described by a single function (an observation known as KNO scaling). Neutral particles are assumed to be produced with an average multiplicity that is 50% of the charged particle multiplicity. Simple parametrizations to more accurately reproduce differences observed in the forward/backward hemispheres of hadronic systems are included in GENIE, NEUT, and NuWRO.

41.3. Nuclear Physics

The nuclear physics relevant to neutrino-nucleus scattering at few-GeV energies is complicated, involving Fermi motion, nuclear binding, Pauli blocking, in-medium modifications of form factors and hadronization, intranuclear rescattering of hadrons, and many-body scattering mechanisms including long- and short-range nucleon-nucleon correlations.

41.3.1. ***Scattering Mechanisms*** :

Most of the models used for neutrino-nuclear scattering kinematics were developed in the context of few-GeV inclusive electron scattering, by experiments going back nearly 50 years. A topic of considerable discussion within this community has been to what extent the impulse approximation, whereby the nucleus is envisioned as collection of bound, moving, single nucleons, is appropriate. The question arose initially in the context of measurements of the quasi-elastic axial mass, with a number of recent experiments using nuclear targets measuring values that were significantly higher than those obtained by an earlier generation of bubble chamber experiments using hydrogen or deuterium [23]. These led to a revisitation of the role played by scattering from multi-particle/hole states in the nucleus. The contribution of these scattering processes is an extremely active area of theoretical research at present, with significant implications for generators and analyses [24]. The GiBUU, NuWRO, GENIE, and NEUT generators have all implemented, or are in the process of implementing, first models for these processes [25].

In order to obtain the cross-section off nucleons in the nucleus, it is necessary to take into account the in-medium effects. The basic models imployed in event generators rely on impulse approximation schemes, the most simple of which is the Relativistic Fermi Gas Model. The most common implementations are the Smith-Moniz [26] and Bodek-Ritchie [27] models. Within the electron scattering community, the analagous calculations have for decades relied on spectral functions, which incorpoate information about nucleon momenta and binding energies in the impulse approximation scheme. The NuWRO and GiBUU generators currently use spectral functions, they are incorporated into NEUT as an option, and several of the other generators are incorporating spectral function models at this time. It is known from photo and electro-nuclear scattering that the Delta width is affected by Pauli blocking and collisional broadening. These effects are included in some, but not all, generators.

When scattering from a nucleus, coherent scattering of various kinds is possible. Most simulations incorporate, at least, neutral and charged coherent coherent single pion production. While the interaction rate for these interactions is typically around a percent of the total yield, the unique kinematic features of these events can make them potential backgrounds for oscillation searches. Implemented in Monte Carlo are PCAC-based methods, while microscopic models are currently being incorporated into several generators as well. Reference [9] clearly demonstrates a point mentioned earlier, where generators implementing the same model [28] are seen to produce very different predictions.

41.3.2. ***Hadron Production in Nuclei*** :

Neutrino pion production is one of the dominant interactions in a few-GeV region and the interaction cross sections of pions in nucleus from those interactions are quite large. Therefore, the interactions of pions in nucleus changes the kinematics of the pions and can have large effects on the results of simulations at these energies. Most generators implement this physics through an intranculear cascade simulation. In generators which utilize cascade models, a hadron, which has been formed in the nucleus, is moved step by step until it interacts with the other nucleon or escapes from the nucleus. The probabilities of each interaction in nuclus are usually given as the mean free paths and used to determine whether the hadron is interacted or not. If the hadron is found to be interacted, appropriate interactions are selected and simulated. Usually, absorption, elastic, and inelastic scatterings including particle productions are simulated as secondary interactions. The determination method of the kinematics for the final state particles heavily depends on the generators but most of them use experimentally validated models to simulate hadron interactions in nucleus. No two interanuclear cascade simulations implemented in neutrino event generators are the same. In all cases hadrons propagate from an interaction vertex chosen based on the density distribution of the target nucleus. In determining the generated position of the hadrons in nucleus, the concept of the formation length is sometimes employed. Based on this idea, the hadronization process is not instantaneous and it takes some time before generating the hadrons [29]. The basis for formation times are measurements at relatively high energy and Q^2, and most generators that employ the concept do not apply them to resonance interactions, the exception is [29]. The intranuclear rescattering simulations are typically validated against hadron scattering data. In some simulations (e.g. NEUT) the pion-less Delta decay is also considered and 20% of the events do not have a pion and only the lepton and the nucleon are generated.

The exception is GiBUU, a semiclassical transport model in coupled channels that describes the space-time evolution of a manybody system in the presence of potentials and a collision term [3]. This approach assures consistency between nuclear effects in the initial state, such as Fermi motion, Pauli blocking, hadron self-energies, and modified cross sections, and the final state, such as particle reinteractions, since the two are derived from the same model. This model has been previously used to describe a wide variety of nuclear interaction data. Similarly, the hadronic simulation of the NUNDIS/NUNRES programs are handled by the well-established FLUKA hadronic simulation package [7].

References:

1. A. Gazizov and M. P. Kowalski, Comput. Phys. Commun. **172**, 203 (2005), astro-ph/0406439.
2. C. Andreopoulos *et al.*, Nucl. Instrum. Methods **A614**, 87 (2001), hep-ph/09052517.
3. O. Buss *et al.*, Phys. Reports **512**, 1 (2012), hep-ph/1106.1344.
4. D. Autiero, Nucl. Phys. Proc. Suppl. **139**, 253 (2005).
5. Y. Hayato, Nucl. Phys. (Proc. Supp.) **112**, 171 (2002).
6. D. Casper, Nucl. Phys. (Proc. Supp.) **112**, 161 (2002), hep-ph/0208030.
7. G. Battiston *et al.*, Acta Phys. Polon. **B40**, 2491 (2009).
8. C. Juszczak, J. A. Nowak, and J. T. Sobczyk, Nucl. Phys. (Proc. Supp.) **159**, 211 (2006), hep-ph/0512365.
9. S. Boyd *et al.*, AIP Conf. Proc. **1189**, 60 (2009).
10. A. Bodek *et al.*, Eur. Phys. J. **C53**, 349 (2008), hep-ex0708.1946/.
11. R. P. Feynman, M. Kislinger, and F. Ravndal, Phys. Rev. D **3**, 2706 (1971).
12. K. M. Graczyk and J. T. Sobczyk, Phys. Rev. D **77**, 053001 (2008) [Erratum-ibid. D **79**, 079903 (2009)] [arXiv:0707.3561 [hep-ph]].
13. D. Rein, and L. M. Sehgal, Ann. Phys. **133**, 79 (1981).
14. O. Lalakulich and E. A. Paschos, Phys. Rev. **D71**, 074003 (2005), hep-ph/0501109.
15. J. Nowak, Phys. Scripta **T127**, 70 (2006).
16. L. Alvarez-Ruso, S. K. Singh, and M. J. Vicente-Vacas, Phys. Rev. **C57**, 2693 (1998), nucl-th/9712058.
17. A. Bodek, and U. K. Yang, J. Phys. **G29**, 1899 (2003), hep-ex/0210024.
18. T. Sjostrand, S. Mrenna, and P. Skands, JHEP **05**, 26 (2006), hep-ph/0603175.
19. A. Kayis-Topaksu *et al.*, Eur. Phys. J. **C51**, 775 (2007), hep-ex/arXiv:0707.1586.
20. J. Altegoer *et al.*, Phys. Lett. **B445**, 439 (1999).
21. T. Yang *et al.*, Eur. Phys. J. **C63**, 1 (2009), hep-ph/0904.4043.
22. J. Nowak and J. Sobczyk, Acta Phys. Polon. **B37, 2371 (2006),** hep-ph/0608108.
23. H. Gallagher, G. Garvey, and G. Zeller, Ann. Rev. Nucl. and Part. Sci. **61**, 355 (2011).
24. O. Lalakulich, U. Mosel, and K. Gallmeister, Phys. Rev. **C86**, 054606 (2012), nucl-th/1208.3678.
25. T. Katori, nucl-th/1304.6014.
26. R. Smith and E. Moniz, Nucl. Phys. **B43**, 605 (1972).
27. A. Bodek and J. Ritchie, Phys. Rev. **D24**, 1400 (1981).
28. D. Rein and L. Sehgal, Nucl. Phys. **B223**, 29 (1983).
29. T. Golan, C. Juszczak and J. Sobczyk, Phys. Rev. **C86**, 015505 (2012), nucl-th/1202.4197.

42. MONTE CARLO PARTICLE NUMBERING SCHEME

Revised September 2013 by J.-F. Arguin LBNL), L. Garren (Fermilab), F. Krauss (Durham U.), C.-J. Lin (LBNL), S. Navas (U. Granada), P. Richardson (Durham U.), and T. Sjöstrand (Lund U.).

The Monte Carlo particle numbering scheme presented here is intended to facilitate interfacing between event generators, detector simulators, and analysis packages used in particle physics. The numbering scheme was introduced in 1988 [1] and a revised version [2,3] was adopted in 1998 in order to allow systematic inclusion of quark model states which are as yet undiscovered and hypothetical particles such as SUSY particles. The numbering scheme is used in several event generators, *e.g.* HERWIG, PYTHIA, and SHERPA, and interfaces, *e.g.* `/HEPEVT/` and HepMC.

The general form is a 7–digit number:

$$\pm n\, n_r\, n_L\, n_{q_1}\, n_{q_2}\, n_{q_3}\, n_J\ .$$

This encodes information about the particle's spin, flavor content, and internal quantum numbers. The details are as follows:

1. Particles are given positive numbers, antiparticles negative numbers. The PDG convention for mesons is used, so that K^+ and B^+ are particles.
2. Quarks and leptons are numbered consecutively starting from 1 and 11 respectively; to do this they are first ordered by family and within families by weak isospin.
3. In composite quark systems (diquarks, mesons, and baryons) $n_{q_{1-3}}$ are quark numbers used to specify the quark content, while the rightmost digit $n_J = 2J+1$ gives the system's spin (except for the K^0_S and K^0_L). The scheme does not cover particles of spin $J > 4$.
4. Diquarks have 4-digit numbers with $n_{q_1} \geq n_{q_2}$ and $n_{q_3} = 0$.
5. The numbering of mesons is guided by the nonrelativistic (L–S decoupled) quark model, as listed in Tables 15.2 and 15.3.
   a. The numbers specifying the meson's quark content conform to the convention $n_{q_1} = 0$ and $n_{q_2} \geq n_{q_3}$. The special case K^0_L is the sole exception to this rule.
   b. The quark numbers of flavorless, light (u, d, s) mesons are: 11 for the member of the isotriplet $(\pi^0, \rho^0, \ldots)$, 22 for the lighter isosinglet $(\eta, \omega, \ldots)$, and 33 for the heavier isosinglet $(\eta', \phi, \ldots)$. Since isosinglet mesons are often large mixtures of $u\overline{u} + d\overline{d}$ and $s\overline{s}$ states, 22 and 33 are assigned by mass and do not necessarily specify the dominant quark composition.
   c. The special numbers 310 and 130 are given to the K^0_S and K^0_L respectively.
   d. The fifth digit n_L is reserved to distinguish mesons of the same total (J) but different spin (S) and orbital (L) angular momentum quantum numbers. For $J > 0$ the numbers are: $(L, S) = (J-1, 1)$ $n_L = 0$, $(J, 0)$ $n_L = 1$, $(J, 1)$ $n_L = 2$ and $(J+1, 1)$ $n_L = 3$. For the exceptional case $J = 0$ the numbers are $(0, 0)$ $n_L = 0$ and $(1, 1)$ $n_L = 1$ (*i.e.* $n_L = L$). See Table 42.1.

Table 42.1: Meson numbering logic. Here qq stands for $n_{q2}\, n_{q3}$.

	$L = J-1$, $S = 1$			$L = J$, $S = 0$			$L = J$, $S = 1$			$L = J+1$, $S = 1$		
J	code	J^{PC}	L	code	J^{PC}	L	code	J^{PC}	L	code	J^{PC}	L
0	—	—	—	$00qq1$	0^{-+}	0	—	—	—	$10qq1$	0^{++}	1
1	$00qq3$	1^{--}	0	$10qq3$	1^{+-}	1	$20qq3$	1^{++}	1	$30qq3$	1^{--}	2
2	$00qq5$	2^{++}	1	$10qq5$	2^{-+}	2	$20qq5$	2^{--}	2	$30qq5$	2^{++}	3
3	$00qq7$	3^{--}	2	$10qq7$	3^{+-}	3	$20qq7$	3^{++}	3	$30qq7$	3^{--}	4
4	$00qq9$	4^{++}	3	$10qq9$	4^{-+}	4	$20qq9$	4^{--}	4	$30qq9$	4^{++}	5

   e. If a set of physical mesons correspond to a (non-negligible) mixture of basis states, differing in their internal quantum numbers, then the lightest physical state gets the smallest basis state number. For example the $K_1(1270)$ is numbered 10313 (1^1P_1 K_{1B}) and the $K_1(1400)$ is numbered 20313 (1^3P_1 K_{1A}).
   f. The sixth digit n_r is used to label mesons radially excited above the ground state.
   g. Numbers have been assigned for complete $n_r = 0$ S- and P-wave multiplets, even where states remain to be identified.
   h. In some instances assignments within the $q\bar{q}$ meson model are only tentative; here best guess assignments are made.
   i. Many states appearing in the Meson Listings are not yet assigned within the $q\bar{q}$ model. Here $n_{q_{2-3}}$ and n_J are assigned according to the state's likely flavors and spin; all such unassigned light isoscalar states are given the flavor code 22. Within these groups $n_L = 0, 1, 2, \ldots$ is used to distinguish states of increasing mass. These states are flagged using $n = 9$. It is to be expected that these numbers will evolve as the nature of the states are elucidated. Codes are assigned to all mesons which are listed in the one-page table at the end of the Meson Summary Table as long as they have a prefered or established spin. Additional heavy meson states expected from heavy quark spectroscopy are also assigned codes.
6. The numbering of baryons is again guided by the nonrelativistic quark model, see Table 15.6. This numbering scheme is illustrated through a few examples in Table 42.2.
   a. The numbers specifying a baryon's quark content are such that in general $n_{q_1} \geq n_{q_2} \geq n_{q_3}$.
   b. Two states exist for $J = 1/2$ baryons containing 3 different types of quarks. In the lighter baryon $(\Lambda, \Xi, \Omega, \ldots)$ the light quarks are in an antisymmetric ($J = 0$) state while for the heavier baryon $(\Sigma^0, \Xi', \Omega', \ldots)$ they are in a symmetric ($J = 1$) state. In this situation n_{q_2} and n_{q_3} are reversed for the lighter state, so that the smaller number corresponds to the lighter baryon.
   c. For excited baryons a scheme is adopted, where the n_r label is used to denote the excitation bands in the harmonic oscillator model, see Sec. 15.4. Using the notation employed there, n_r is given by the N-index of the D_N band identifier.
   d. Further degeneracies of excited hadron multiplets with the same excitation number n_r and spin J are lifted by labelling such multiplets with the n_L index according to their mass, as given by its N or Δ-equivalent.
   e. In such excited multiplets extra singlets may occur, the $\Lambda(1520)$ being a prominent example. In such cases the ordering is reversed such that the heaviest quark label is pushed to the last position: $n_{q_3} > n_{q_1} > n_{q_2}$.
   f. For pentaquark states $n = 9$, $n_r n_L n_{q_1} n_{q_2}$ gives the four quark numbers in order $n_r \geq n_L \geq n_{q_1} \geq n_{q_2}$, n_{q_3} gives the antiquark number, and $n_J = 2J+1$, with the assumption that $J = 1/2$ for the states currently reported.
7. The gluon, when considered as a gauge boson, has official number 21. In codes for glueballs, however, 9 is used to allow a notation in close analogy with that of hadrons.
8. The pomeron and odderon trajectories and a generic reggeon trajectory of states in QCD are assigned codes 990, 9990, and 110 respectively, where the final 0 indicates the indeterminate nature of the spin, and the other digits reflect the expected "valence" flavor content. We do not attempt a complete classification of all reggeon trajectories, since there is currently no need to distinguish a specific such trajectory from its lowest-lying member.
9. Two-digit numbers in the range 21–30 are provided for the Standard Model gauge bosons and Higgs.
10. Codes 81–100 are reserved for generator-specific pseudoparticles and concepts.
11. The search for physics beyond the Standard Model is an active area, so these codes are also standardized as far as possible.
    a. A standard fourth generation of fermions is included by analogy with the first three.
    b. The graviton and the boson content of a two-Higgs-doublet scenario and of additional SU(2)×U(1) groups are found in the range 31–40.
    c. "One-of-a-kind" exotic particles are assigned numbers in the range 41–80.
    d. Fundamental supersymmetric particles are identified by adding a nonzero n to the particle number. The superpartner of a boson or a left-handed fermion has $n = 1$ while the superpartner of a right-handed fermion has $n = 2$. When mixing occurs, such as between the winos and charged

Table 42.2: Some examples of octet (top) and decuplet (bottom) members for the numbering scheme for excited baryons. Here qqq stands for $n_{q_1}n_{q_2}n_{q_3}$. See the text for the definition of the notation. The numbers in parenthesis correspond to the mass of the baryons. The states marked as (?) are not experimentally confirmed.

J^P	(D, L_N^P)	$n_r n_L n_{q_1} n_{q_2} n_{q_3} n_J$	N	Λ_8	Σ	Ξ	Λ_1
Octet			211,221	312	311,321,322	331,332	213
$1/2^+$	$(\mathbf{56}, \mathbf{0_0^+})$	$00qqq2$	(939)	(1116)	(1193)	(1318)	—
$1/2^+$	$(\mathbf{56}, \mathbf{0_2^+})$	$20qqq2$	(1440)	(1600)	(1660)	(1690)	—
$1/2^+$	$(\mathbf{70}, \mathbf{0_2^+})$	$21qqq2$	(1710)	(1810)	(1880)	(?)	(?)
$1/2^-$	$(\mathbf{70}, \mathbf{1_1^-})$	$10qqq2$	(1535)	(1670)	(1620)	(1750)	(1405)
J^P	(D, L_N^P)	$n_r n_L n_{q_1} n_{q_2} n_{q_3} n_J$	Δ		Σ	Ξ	Ω
Decuplet			111,211,221,222		311,321,322	331,332	333
$3/2^+$	$(\mathbf{56}, \mathbf{0_0^+})$	$00qqq4$	(1232)		(1385)	(1530)	(1672)
$3/2^+$	$(\mathbf{56}, \mathbf{0_2^+})$	$20qqq4$	(1600)		(1690)	(?)	(?)
$1/2^-$	$(\mathbf{70}, \mathbf{1_1^-})$	$11qqq2$	(1620)		(1750)	(?)	(?)
$3/2^-$	$(\mathbf{70}, \mathbf{1_1^-})$	$12qqq4$	(1700)		(?)	(?)	(?)

Higgsinos to give charginos, or between left and right sfermions, the lighter physical state is given the smaller basis state number.

e. Technicolor states have $n = 3$, with technifermions treated like ordinary fermions. States which are ordinary color singlets have $n_r = 0$. Color octets have $n_r = 1$. If a state has non-trivial quantum numbers under the topcolor groups $SU(3)_1 \times SU(3)_2$, the quantum numbers are specified by tech,ij, where i and j are 1 or 2. n_L is then $2i + j$. The coloron, V_8, is a heavy gluon color octet and thus is 3100021.

f. Excited (composite) quarks and leptons are identified by setting $n = 4$ and $n_r = 0$.

g. Within several scenarios of new physics, it is possible to have colored particles sufficiently long-lived for color-singlet hadronic states to form around them. In the context of supersymmetric scenarios, these states are called R-hadrons, since they carry odd R-parity. R-hadron codes, defined here, should be viewed as templates for corresponding codes also in other scenarios, for any long-lived particle that is either an unflavored color octet or a flavored color triplet. The R-hadron code is obtained by combining the SUSY particle code with a code for the light degrees of freedom, with as many intermediate zeros removed from the former as required to make place for the latter at the end. (To exemplify, a sparticle $n00000n_{\tilde{q}}$ combined with quarks q_1 and q_2 obtains code $n00n_{\tilde{q}}n_{q_1}n_{q_2}n_J$.) Specifically, the new-particle spin decouples in the limit of large masses, so that the final n_J digit is defined by the spin state of the light-quark system alone. An appropriate number of n_q digits is used to define the ordinary-quark content. As usual, 9 rather than 21 is used to denote a gluon/gluino in composite states. The sign of the hadron agrees with that of the constituent new particle (a color triplet) where there is a distinct new antiparticle, and else is defined as for normal hadrons. Particle names are R with the flavor content as lower index.

h. A black hole in models with extra dimensions has code 5000040. Kaluza-Klein excitations in models with extra dimensions have $n = 5$ or $n = 6$, to distinquish excitations of left- or right-handed fermions or, in case of mixing, the lighter or heavier state (cf. 11d). The nonzero n_r digit gives the radial excitation number, in scenarios where the level spacing allow these to be distinguished. Should the model also contain supersymmetry, excited SUSY states would be denoted by an $n_r > 0$, with $n = 1$ or 2 as usual. Should some colored states be long-lived enough that hadrons would form around them, the coding strategy of 11g applies, with the initial two nn_r digits preserved in the combined code.

i. Magnetic monopoles and dyons are assumed to have one unit of Dirac monopole charge and a variable integer number $n_{q1}n_{q2}n_{q3}$ units of electric charge. Codes $411n_{q1}n_{q2}n_{q3}0$ are then used when the magnetic and electrical charge sign agree and $412n_{q1}n_{q2}n_{q3}0$ when they disagree, with the overall sign of the particle set by the magnetic charge. For now no spin information is provided.

12. Occasionally program authors add their own states. To avoid confusion, these should be flagged by setting $nn_r = 99$.
13. Concerning the non-99 numbers, it may be noted that only quarks, excited quarks, squarks, and diquarks have $n_{q_3} = 0$; only diquarks, baryons (including pentaquarks), and the odderon have $n_{q_1} \neq 0$; and only mesons, the reggeon, and the pomeron have $n_{q_1} = 0$ and $n_{q_2} \neq 0$. Concerning mesons (not antimesons), if n_{q_1} is odd then it labels a quark and an antiquark if even.
14. Nuclear codes are given as 10-digit numbers $\pm 10LZZZAAAI$. For a (hyper)nucleus consisting of n_p protons, n_n neutrons and n_Λ Λ's, $A = n_p + n_n + n_\Lambda$ gives the total baryon number, $Z = n_p$ the total charge and $L = n_\Lambda$ the total number of strange quarks. I gives the isomer level, with $I = 0$ corresponding to the ground state and $I > 0$ to excitations, see [4], where states denoted m, n, p, q translate to $I = 1 - 4$. As examples, the deuteron is 1000010020 and ^{235}U is 1000922350. To avoid ambiguities, nuclear codes should not be applied to a single hadron, like p, n or Λ^0, where quark-contents-based codes already exist.

This text and full lists of particle numbers, including excited baryons and particles from physics beyond the standard model, can be found online [5]. The StdHep Monte Carlo standardization project [6] maintains the list of PDG particle numbers, as well as numbering schemes from most event generators and software to convert between the different schemes.

References:

1. G.P. Yost *et al.*, Particle Data Group, Phys. Lett. **B204**, 1 (1988).
2. I.G. Knowles *et al.*, in *"Physics at LEP2"*, CERN 96-01, v. 2, p. 103.
3. C. Caso *et al.*, Particle Data Group, Eur. Phys. J. **C3**, 1 (1998).
4. G. Audi *et al.*, Nucl. Phys. **A729**, 3 (2003) See also `http://www.nndc.bnl.gov/amdc/web/nubase_en.html`.
5. `http://pdg.lbl.gov/current/mc-particle-id/`.
6. L. Garren, StdHep, *Monte Carlo Standardization at FNAL*, Fermilab PM0091 and StdHep WWW site: `http://cepa.fnal.gov/psm/stdhep/`.

QUARKS

d	1
u	2
s	3
c	4
b	5
t	6
b'	7
t'	8

LEPTONS

e^-	11
ν_e	12
μ^-	13
ν_μ	14
τ^-	15
ν_τ	16
τ'^-	17
$\nu_{\tau'}$	18

GAUGE AND HIGGS BOSONS

g	(9) 21
γ	22
Z^0	23
W^+	24
h^0/H_1^0	25
Z'/Z_2^0	32
Z''/Z_3^0	33
W'/W_2^+	34
H^0/H_2^0	35
A^0/H_3^0	36
H^+	37

SPECIAL PARTICLES

G (graviton)	39
R^0	41
LQ^c	42
reggeon	110
pomeron	990
odderon	9990

for MC internal use 81–100

DIQUARKS

$(dd)_1$	1103
$(ud)_0$	2101
$(ud)_1$	2103
$(uu)_1$	2203
$(sd)_0$	3101
$(sd)_1$	3103
$(su)_0$	3201
$(su)_1$	3203
$(ss)_1$	3303
$(cd)_0$	4101
$(cd)_1$	4103
$(cu)_0$	4201
$(cu)_1$	4203
$(cs)_0$	4301
$(cs)_1$	4303
$(cc)_1$	4403
$(bd)_0$	5101
$(bd)_1$	5103
$(bu)_0$	5201
$(bu)_1$	5203
$(bs)_0$	5301
$(bs)_1$	5303
$(bc)_0$	5401
$(bc)_1$	5403
$(bb)_1$	5503

SUSY PARTICLES

$\widetilde{d}_L$	1000001
$\widetilde{u}_L$	1000002
$\widetilde{s}_L$	1000003
$\widetilde{c}_L$	1000004
$\widetilde{b}_1$	1000005[a]
$\widetilde{t}_1$	1000006[a]
$\widetilde{e}_L^-$	1000011
$\widetilde{\nu}_{eL}$	1000012
$\widetilde{\mu}_L^-$	1000013
$\widetilde{\nu}_{\mu L}$	1000014
$\widetilde{\tau}_1^-$	1000015[a]
$\widetilde{\nu}_{\tau L}$	1000016
$\widetilde{d}_R$	2000001
$\widetilde{u}_R$	2000002
$\widetilde{s}_R$	2000003
$\widetilde{c}_R$	2000004
$\widetilde{b}_2$	2000005[a]
$\widetilde{t}_2$	2000006[a]
$\widetilde{e}_R^-$	2000011
$\widetilde{\mu}_R^-$	2000013
$\widetilde{\tau}_2^-$	2000015[a]
$\widetilde{g}$	1000021
$\widetilde{\chi}_1^0$	1000022[b]
$\widetilde{\chi}_2^0$	1000023[b]
$\widetilde{\chi}_1^+$	1000024[b]
$\widetilde{\chi}_3^0$	1000025[b]
$\widetilde{\chi}_4^0$	1000035[b]
$\widetilde{\chi}_2^+$	1000037[b]
$\widetilde{G}$	1000039

LIGHT $I = 1$ MESONS

π^0	111
π^+	211
$a_0(980)^0$	9000111
$a_0(980)^+$	9000211
$\pi(1300)^0$	100111
$\pi(1300)^+$	100211
$a_0(1450)^0$	10111
$a_0(1450)^+$	10211
$\pi(1800)^0$	9010111
$\pi(1800)^+$	9010211
$\rho(770)^0$	113
$\rho(770)^+$	213
$b_1(1235)^0$	10113
$b_1(1235)^+$	10213
$a_1(1260)^0$	20113
$a_1(1260)^+$	20213
$\pi_1(1400)^0$	9000113
$\pi_1(1400)^+$	9000213
$\rho(1450)^0$	100113
$\rho(1450)^+$	100213
$\pi_1(1600)^0$	9010113
$\pi_1(1600)^+$	9010213
$a_1(1640)^0$	9020113
$a_1(1640)^+$	9020213
$\rho(1700)^0$	30113
$\rho(1700)^+$	30213
$\rho(1900)^0$	9030113
$\rho(1900)^+$	9030213
$\rho(2150)^0$	9040113
$\rho(2150)^+$	9040213
$a_2(1320)^0$	115
$a_2(1320)^+$	215
$\pi_2(1670)^0$	10115
$\pi_2(1670)^+$	10215
$a_2(1700)^0$	9000115
$a_2(1700)^+$	9000215
$\pi_2(2100)^0$	9010115
$\pi_2(2100)^+$	9010215
$\rho_3(1690)^0$	117
$\rho_3(1690)^+$	217
$\rho_3(1990)^0$	9000117
$\rho_3(1990)^+$	9000217
$\rho_3(2250)^0$	9010117
$\rho_3(2250)^+$	9010217
$a_4(2040)^0$	119
$a_4(2040)^+$	219

LIGHT $I = 0$ MESONS
($u\overline{u}$, $d\overline{d}$, and $s\overline{s}$ Admixtures)

η	221
$\eta'(958)$	331
$f_0(600)$	9000221
$f_0(980)$	9010221
$\eta(1295)$	100221
$f_0(1370)$	10221
$\eta(1405)$	9020221
$\eta(1475)$	100331
$f_0(1500)$	9030221
$f_0(1710)$	10331
$\eta(1760)$	9040221
$f_0(2020)$	9050221
$f_0(2100)$	9060221
$f_0(2200)$	9070221
$\eta(2225)$	9080221
$\omega(782)$	223
$\phi(1020)$	333
$h_1(1170)$	10223
$f_1(1285)$	20223
$h_1(1380)$	10333
$f_1(1420)$	20333
$\omega(1420)$	100223
$f_1(1510)$	9000223
$h_1(1595)$	9010223
$\omega(1650)$	30223
$\phi(1680)$	100333
$f_2(1270)$	225
$f_2(1430)$	9000225
$f_2'(1525)$	335
$f_2(1565)$	9010225
$f_2(1640)$	9020225
$\eta_2(1645)$	10225
$f_2(1810)$	9030225
$\eta_2(1870)$	10335
$f_2(1910)$	9040225
$f_2(1950)$	9050225
$f_2(2010)$	9060225
$f_2(2150)$	9070225
$f_2(2300)$	9080225
$f_2(2340)$	9090225
$\omega_3(1670)$	227
$\phi_3(1850)$	337
$f_4(2050)$	229
$f_J(2220)$	9000229
$f_4(2300)$	9010229

STRANGE MESONS

K_L^0	130
K_S^0	310
K^0	311
K^+	321
$K_0^*(800)^0$	9000311
$K_0^*(800)^+$	9000321
$K_0^*(1430)^0$	10311
$K_0^*(1430)^+$	10321
$K(1460)^0$	100311
$K(1460)^+$	100321
$K(1830)^0$	9010311
$K(1830)^+$	9010321
$K_0^*(1950)^0$	9020311
$K_0^*(1950)^+$	9020321
$K^*(892)^0$	313
$K^*(892)^+$	323
$K_1(1270)^0$	10313
$K_1(1270)^+$	10323
$K_1(1400)^0$	20313
$K_1(1400)^+$	20323
$K^*(1410)^0$	100313
$K^*(1410)^+$	100323
$K_1(1650)^0$	9000313
$K_1(1650)^+$	9000323
$K^*(1680)^0$	30313
$K^*(1680)^+$	30323
$K_2^*(1430)^0$	315
$K_2^*(1430)^+$	325
$K_2(1580)^0$	9000315
$K_2(1580)^+$	9000325
$K_2(1770)^0$	10315
$K_2(1770)^+$	10325
$K_2(1820)^0$	20315
$K_2(1820)^+$	20325
$K_2^*(1980)^0$	9010315
$K_2^*(1980)^+$	9010325
$K_2(2250)^0$	9020315
$K_2(2250)^+$	9020325
$K_3^*(1780)^0$	317
$K_3^*(1780)^+$	327
$K_3(2320)^0$	9010317
$K_3(2320)^+$	9010327
$K_4^*(2045)^0$	319
$K_4^*(2045)^+$	329
$K_4(2500)^0$	9000319
$K_4(2500)^+$	9000329

CHARMED MESONS

D^+	411
D^0	421
$D_0^*(2400)^+$	10411
$D_0^*(2400)^0$	10421
$D^*(2010)^+$	413
$D^*(2007)^0$	423
$D_1(2420)^+$	10413
$D_1(2420)^0$	10423
$D_1(H)^+$	20413
$D_1(2430)^0$	20423
$D_2^*(2460)^+$	415
$D_2^*(2460)^0$	425
D_s^+	431
$D_{s0}^*(2317)^+$	10431
D_s^{*+}	433
$D_{s1}(2536)^+$	10433
$D_{s1}(2460)^+$	20433
$D_{s2}^*(2573)^+$	435

BOTTOM MESONS

B^0	511
B^+	521
B_0^{*0}	10511
B_0^{*+}	10521
B^{*0}	513
B^{*+}	523
$B_1(L)^0$	10513
$B_1(L)^+$	10523
$B_1(H)^0$	20513
$B_1(H)^+$	20523
B_2^{*0}	515
B_2^{*+}	525
B_s^0	531
B_{s0}^{*0}	10531
B_s^{*0}	533
$B_{s1}(L)^0$	10533
$B_{s1}(H)^0$	20533
B_{s2}^{*0}	535
B_c^+	541
B_{c0}^{*+}	10541
B_c^{*+}	543
$B_{c1}(L)^+$	10543
$B_{c1}(H)^+$	20543
B_{c2}^{*+}	545

$c\bar{c}$ MESONS

$\eta_c(1S)$	441
$\chi_{c0}(1P)$	10441
$\eta_c(2S)$	100441
$J/\psi(1S)$	443
$h_c(1P)$	10443
$\chi_{c1}(1P)$	20443
$\psi(2S)$	100443
$\psi(3770)$	30443
$\psi(4040)$	9000443
$\psi(4160)$	9010443
$\psi(4415)$	9020443
$\chi_{c2}(1P)$	445
$\chi_{c2}(2P)$	100445

$b\bar{b}$ MESONS

$\eta_b(1S)$	551
$\chi_{b0}(1P)$	10551
$\eta_b(2S)$	100551
$\chi_{b0}(2P)$	110551
$\eta_b(3S)$	200551
$\chi_{b0}(3P)$	210551
$\Upsilon(1S)$	553
$h_b(1P)$	10553
$\chi_{b1}(1P)$	20553
$\Upsilon_1(1D)$	30553
$\Upsilon(2S)$	100553
$h_b(2P)$	110553
$\chi_{b1}(2P)$	120553
$\Upsilon_1(2D)$	130553
$\Upsilon(3S)$	200553
$h_b(3P)$	210553
$\chi_{b1}(3P)$	220553
$\Upsilon(4S)$	300553
$\Upsilon(10860)$	9000553
$\Upsilon(11020)$	9010553
$\chi_{b2}(1P)$	555
$\eta_{b2}(1D)$	10555
$\Upsilon_2(1D)$	20555
$\chi_{b2}(2P)$	100555
$\eta_{b2}(2D)$	110555
$\Upsilon_2(2D)$	120555
$\chi_{b2}(3P)$	200555
$\Upsilon_3(1D)$	557
$\Upsilon_3(2D)$	100557

LIGHT BARYONS

p	2212
n	2112
Δ^{++}	2224
Δ^+	2214
Δ^0	2114
Δ^-	1114

STRANGE BARYONS

Λ	3122
Σ^+	3222
Σ^0	3212
Σ^-	3112
Σ^{*+}	3224^c
Σ^{*0}	3214^c
Σ^{*-}	3114^c
Ξ^0	3322
Ξ^-	3312
Ξ^{*0}	3324^c
Ξ^{*-}	3314^c
Ω^-	3334

CHARMED BARYONS

Λ_c^+	4122
Σ_c^{++}	4222
Σ_c^+	4212
Σ_c^0	4112
Σ_c^{*++}	4224
Σ_c^{*+}	4214
Σ_c^{*0}	4114
Ξ_c^+	4232
Ξ_c^0	4132
$\Xi_c^{\prime+}$	4322
$\Xi_c^{\prime0}$	4312
Ξ_c^{*+}	4324
Ξ_c^{*0}	4314
Ω_c^0	4332
Ω_c^{*0}	4334
Ξ_{cc}^+	4412
Ξ_{cc}^{++}	4422
Ξ_{cc}^{*+}	4414
Ξ_{cc}^{*++}	4424
Ω_{cc}^+	4432
Ω_{cc}^{*+}	4434
Ω_{ccc}^{++}	4444

BOTTOM BARYONS

Λ_b^0	5122
Σ_b^-	5112
Σ_b^0	5212
Σ_b^+	5222
Σ_b^{*-}	5114
Σ_b^{*0}	5214
Σ_b^{*+}	5224
Ξ_b^-	5132
Ξ_b^0	5232
$\Xi_b^{\prime-}$	5312
$\Xi_b^{\prime0}$	5322
Ξ_b^{*-}	5314
Ξ_b^{*0}	5324
Ω_b^-	5332
Ω_b^{*-}	5334
Ξ_{bc}^0	5142
Ξ_{bc}^+	5242
$\Xi_{bc}^{\prime0}$	5412
$\Xi_{bc}^{\prime+}$	5422
Ξ_{bc}^{*0}	5414
Ξ_{bc}^{*+}	5424
Ω_{bc}^0	5342
$\Omega_{bc}^{\prime0}$	5432
Ω_{bc}^{*0}	5434
Ω_{bcc}^+	5442
Ω_{bcc}^{*+}	5444
Ξ_{bb}^-	5512
Ξ_{bb}^0	5522
Ξ_{bb}^{*-}	5514
Ξ_{bb}^{*0}	5524
Ω_{bb}^-	5532
Ω_{bb}^{*-}	5534
Ω_{bbc}^0	5542
Ω_{bbc}^{*0}	5544
Ω_{bbb}^-	5554

Footnotes to the Tables:

a) Particulary in the third generation, the left and right sfermion states may mix, as shown. The lighter mixed state is given the smaller number.

b) The physical $\widetilde{\chi}$ states are admixtures of the pure $\widetilde{\gamma}$, $\widetilde{Z}^0$, $\widetilde{W}^+$, $\widetilde{H}_1^0$, $\widetilde{H}_2^0$, and $\widetilde{H}^+$ states.

c) Σ^* and Ξ^* are alternate names for $\Sigma(1385)$ and $\Xi(1530)$.

43. CLEBSCH-GORDAN COEFFICIENTS, SPHERICAL HARMONICS, AND *d* FUNCTIONS

Note: A square-root sign is to be understood over *every* coefficient, *e.g.*, for $-8/15$ read $-\sqrt{8/15}$.

Notation:

J	J	...
M	M	...

m_1	m_2	
m_1	m_2	Coefficients
.	.	
.	.	
.	.	

$1/2\times1/2$

1			
+1	1	0	
+1/2 +1/2	0	0	
+1/2 −1/2	1/2	1/2	1
−1/2 +1/2	1/2	−1/2	−1
	−1/2 −1/2		1

$1\times1/2$

3/2			
+3/2	3/2	1/2	
+1 +1/2	0	0	
+1 −1/2	1/3	2/3	3/2
0 +1/2	2/3	−1/3	−1/2
0 −1/2	2/3	1/3	3/2
−1 +1/2	1/3	−2/3	−3/2
	−1 −1/2		1

2×1

3				
+3	3	2		
+2 +1	0	0		
+2 0	1/3	2/3	3	2
+1 +1	2/3	−1/3	+1	+1
+2 −1	1/15	1/3	3/5	1
+1 0	8/15	1/6	−3/10	+1
0 +1	2/5	−1/2	1/10	0
	−1 −1			1

1×1

2					
+2	2	1			
+1 +1	0	0			
+1 0	1/2	1/2	2	1	0
0 +1	1/2	−1/2	0	0	0
+1 −1	1/6	1/2	1/3	2	1
0 0	2/3	0	−1/3	−1	−1
−1 +1	1/6	−1/2	1/3		
	0 −1	1/2	1/2	2	
	−1 0	1/2	−1/2	−2	
		−1 −1		1	

$2\times1/2$

5/2					
+5/2	5/2	3/2			
+2 +1/2	3/2	3/2			
+2 −1/2	1/5	4/5	5/2	3/2	
+1 +1/2	4/5	−1/5	1/2	1/2	
+1 −1/2	2/5	3/5	5/2	3/2	
0 +1/2	3/5	−2/5	−1/2	−1/2	
0 −1/2	3/5	2/5	5/2	3/2	
−1 +1/2	2/5	−3/5	−3/2	−3/2	
−1 −1/2	4/5	1/5	5/2		
−2 +1/2	1/5	−4/5	−5/2		
	−2 −1/2		1		

$3/2\times1/2$

2					
+2	2	1			
+3/2 +1/2	1	1			
+3/2 −1/2	1/4	3/4	2	1	
+1/2 +1/2	3/4	−1/4	0	0	
+1/2 −1/2	1/2	1/2	2	1	
−1/2 +1/2	1/2	−1/2	−1	−1	
−1/2 −1/2	3/4	1/4	2		
−3/2 +1/2	1/4	−3/4	−2		
	−3/2 −1/2		1		

$3/2\times1$

5/2						
+5/2	5/2	3/2				
+3/2 +1	1	+3/2				
+3/2 0	2/5	3/5	5/2	3/2	1/2	
+1/2 +1	3/5	−2/5	+1/2	+1/2	+1/2	
+3/2 −1	1/10	2/5	1/2			
+1/2 0	3/5	1/15	−1/3	5/2	3/2	1/2
−1/2 +1	3/10	−8/15	1/6	−1/2	−1/2	−1/2
+1/2 −1	3/10	8/15	1/6			
−1/2 0	3/5	−1/15	−1/3	5/2	3/2	
−3/2 +1	1/10	−2/5	1/2	−3/2	−3/2	
−1/2 −1	3/5	2/5	5/2			
−3/2 0	2/5	−3/5	−5/2			
	−3/2 −1		1			

$3/2\times3/2$

3						
+3	3	2				
+3/2 +3/2	1	+2				
+3/2 +1/2	1/2	1/2	3	2	1	
+1/2 +3/2	1/2	−1/2	+1	+1	+1	
+3/2 −1/2	1/5	1/2	3/10			
+1/2 +1/2	3/5	0	−2/5	3	2	1
−1/2 +3/2	1/5	−1/2	3/10	0	0	0
+3/2 −3/2	1/20	1/4	9/20	1/4		
+1/2 −1/2	9/20	1/4	−1/20	−1/4		
−1/2 +1/2	9/20	−1/4	−1/20	1/4		
−3/2 +3/2	1/20	−1/4	9/20	−1/4		
+1/2 −3/2	1/5	1/2	3/10			
−1/2 −1/2	3/5	0	−2/5	3	2	
−3/2 +1/2	1/5	−1/2	3/10	−2	−2	
−1/2 −3/2	1/2	1/2	3			
−3/2 −1/2	1/2	−1/2	−3			
	−3/2 −3/2		1			

2×2

4						
+4	4	3				
+2 +2	1	+3				
+2 +1	1/2	1/2	4	3	2	
+1 +2	1/2	−1/2	+2	+2	+2	
+2 0	3/14	1/2	2/7			
+1 +1	4/7	0	−3/7	4	3	2
0 +2	3/14	−1/2	2/7	+1	+1	+1
+2 −1	1/14	3/10	3/7	1/5		
+1 0	3/7	1/5	−1/14	−3/10		
0 +1	3/7	−1/5	−1/14	3/10		
−1 +2	1/14	−3/10	3/7	−1/5		
+2 −2	1/70	1/10	2/7	2/5	1/5	
+1 −1	8/35	2/5	1/14	−1/10	−1/5	
0 0	18/35	0	−2/7	0	1/5	
−1 +1	8/35	−2/5	1/14	1/10	−1/5	
−2 +2	1/70	−1/10	2/7	−2/5	1/5	
+1 −2	1/14	3/10	3/7	1/5		
0 −1	3/7	1/5	−1/14	−3/10		
−1 0	3/7	−1/5	−1/14	3/10		
−2 +1	1/14	−3/10	3/7	−1/5		
0 −2	3/14	1/2	2/7			
−1 −1	4/7	0	−3/7	4	3	
−2 0	3/14	−1/2	2/7	−3	−3	
−1 −2	1/2	1/2	4			
−2 −1	1/2	−1/2	−4			
	−2 −2		1			

$2\times3/2$

7/2						
+7/2	7/2	5/2				
+2+3/2	1	+5/2				
+2+1/2	3/7	4/7	7/2	5/2	3/2	
+1+3/2	4/7	−3/7	+3/2	+3/2	+3/2	
+2 −1/2	1/7	16/35	2/5			
+1 +1/2	4/7	1/35	−2/5	7/2	5/2	3/2
0 +3/2	2/7	−18/35	1/5	+1/2	+1/2	+1/2
+2 −3/2	1/35	6/35	2/5	2/5		
+1 −1/2	12/35	5/14	0	−3/10		
0 +1/2	18/35	−3/35	−1/5	1/5		
−1 +3/2	4/35	−27/70	2/5	−1/10		
+1 −3/2	4/35	27/70	2/5	1/10		
0 −1/2	18/35	3/35	−1/5	−1/5		
−1 +1/2	12/35	−5/14	0	3/10		
−2 +3/2	1/35	−6/35	2/5	−2/5		
0 −3/2	2/7	18/35	1/5			
−1 −1/2	4/7	−1/35	−2/5	7/2	5/2	
−2 +1/2	1/7	−16/35	2/5	−5/2	−5/2	
−1 −3/2	4/7	3/7	7/2			
−2 −1/2	3/7	−4/7	−7/2			
	−2 −3/2		1			

$3/2\times2$

5/2						
+5/2	5/2	3/2				
+2 +1/2	3/2	+3/2				
+2 −1/2	1/5	4/5	5/2	3/2		
+1 +1/2	4/5	−1/5	+1/2	+1/2		
+1 −1/2	2/5	3/5	5/2	3/2		
0 +1/2	3/5	−2/5	−1/2	−1/2		
0 −1/2	3/5	2/5	5/2	3/2		
−1 +1/2	2/5	−3/5	−3/2	−3/2		
−1 −1/2	4/5	1/5	5/2			
−2 +1/2	1/5	−4/5	−5/2			
	−2 −1/2		1			

$$Y_1^0 = \sqrt{\frac{3}{4\pi}}\cos\theta$$

$$Y_1^1 = -\sqrt{\frac{3}{8\pi}}\sin\theta\, e^{i\phi}$$

$$Y_2^0 = \sqrt{\frac{5}{4\pi}}\left(\frac{3}{2}\cos^2\theta - \frac{1}{2}\right)$$

$$Y_2^1 = -\sqrt{\frac{15}{8\pi}}\sin\theta\cos\theta\, e^{i\phi}$$

$$Y_2^2 = \frac{1}{4}\sqrt{\frac{15}{2\pi}}\sin^2\theta\, e^{2i\phi}$$

$$Y_\ell^{-m} = (-1)^m Y_\ell^{m*}$$

$$d^\ell_{m,0} = \sqrt{\frac{4\pi}{2\ell+1}}\, Y_\ell^m\, e^{-im\phi}$$

$$\langle j_1 j_2 m_1 m_2 | j_1 j_2 J M\rangle = (-1)^{J-j_1-j_2}\langle j_2 j_1 m_2 m_1 | j_2 j_1 J M\rangle$$

$$d^j_{m',m} = (-1)^{m-m'} d^j_{m,m'} = d^j_{-m,-m'}$$

$$d^1_{0,0} = \cos\theta \qquad d^{1/2}_{1/2,1/2} = \cos\frac{\theta}{2} \qquad d^1_{1,1} = \frac{1+\cos\theta}{2}$$

$$d^{1/2}_{1/2,-1/2} = -\sin\frac{\theta}{2} \qquad d^1_{1,0} = -\frac{\sin\theta}{\sqrt{2}}$$

$$d^1_{1,-1} = \frac{1-\cos\theta}{2}$$

$$d^{3/2}_{3/2,3/2} = \frac{1+\cos\theta}{2}\cos\frac{\theta}{2} \qquad d^{3/2}_{3/2,1/2} = -\sqrt{3}\frac{1+\cos\theta}{2}\sin\frac{\theta}{2} \qquad d^2_{2,2} = \left(\frac{1+\cos\theta}{2}\right)^2$$

$$d^{3/2}_{3/2,-1/2} = \sqrt{3}\frac{1-\cos\theta}{2}\cos\frac{\theta}{2} \qquad d^2_{2,1} = -\frac{1+\cos\theta}{2}\sin\theta$$

$$d^{3/2}_{3/2,-3/2} = -\frac{1-\cos\theta}{2}\sin\frac{\theta}{2} \qquad d^2_{2,0} = \frac{\sqrt{6}}{4}\sin^2\theta \qquad d^2_{1,1} = \frac{1+\cos\theta}{2}(2\cos\theta - 1)$$

$$d^{3/2}_{1/2,1/2} = \frac{3\cos\theta - 1}{2}\cos\frac{\theta}{2} \qquad d^2_{2,-1} = -\frac{1-\cos\theta}{2}\sin\theta \qquad d^2_{1,0} = -\sqrt{\frac{3}{2}}\sin\theta\cos\theta$$

$$d^{3/2}_{1/2,-1/2} = -\frac{3\cos\theta + 1}{2}\sin\frac{\theta}{2} \qquad d^2_{2,-2} = \left(\frac{1-\cos\theta}{2}\right)^2 \qquad d^2_{1,-1} = \frac{1-\cos\theta}{2}(2\cos\theta + 1) \qquad d^2_{0,0} = \left(\frac{3}{2}\cos^2\theta - \frac{1}{2}\right)$$

Figure 43.1: The sign convention is that of Wigner (*Group Theory*, Academic Press, New York, 1959), also used by Condon and Shortley (*The Theory of Atomic Spectra*, Cambridge Univ. Press, New York, 1953), Rose (*Elementary Theory of Angular Momentum*, Wiley, New York, 1957), and Cohen (*Tables of the Clebsch-Gordan Coefficients*, North American Rockwell Science Center, Thousand Oaks, Calif., 1974).

44. SU(3) ISOSCALAR FACTORS AND REPRESENTATION MATRICES

Written by R.L. Kelly (LBNL).

The most commonly used SU(3) isoscalar factors, corresponding to the singlet, octet, and decuplet content of $8 \otimes 8$ and $10 \otimes 8$, are shown at the right. The notation uses particle names to identify the coefficients, so that the pattern of relative couplings may be seen at a glance. We illustrate the use of the coefficients below. See J.J de Swart, Rev. Mod. Phys. **35**, 916 (1963) for detailed explanations and phase conventions.

A $\sqrt{\ }$ is to be understood over every integer in the matrices; the exponent 1/2 on each matrix is a reminder of this. For example, the $\Xi \to \Omega K$ element of the $10 \to 10 \otimes 8$ matrix is $-\sqrt{6}/\sqrt{24} = -1/2$.

Intramultiplet relative decay strengths may be read directly from the matrices. For example, in decuplet → octet + octet decays, the ratio of $\Omega^* \to \Xi\overline{K}$ and $\Delta \to N\pi$ partial widths is, from the $10 \to 8 \times 8$ matrix,

$$\frac{\Gamma\,(\Omega^* \to \Xi\overline{K})}{\Gamma\,(\Delta \to N\pi)} = \frac{12}{6} \times \text{ (phase space factors)} \; . \tag{44.1}$$

Including isospin Clebsch-Gordan coefficients, we obtain, *e.g.*,

$$\frac{\Gamma(\Omega^{*-} \to \Xi^0 K^-)}{\Gamma(\Delta^+ \to p\,\pi^0)} = \frac{1/2}{2/3} \times \frac{12}{6} \times p.s.f. = \frac{3}{2} \times p.s.f. \tag{44.2}$$

Partial widths for $8 \to 8 \otimes 8$ involve a linear superposition of 8_1 (symmetric) and 8_2 (antisymmetric) couplings. For example,

$$\Gamma(\Xi^* \to \Xi\pi) \sim \left(-\sqrt{\frac{9}{20}}\, g_1 + \sqrt{\frac{3}{12}}\, g_2 \right)^2 \; . \tag{44.3}$$

The relations between g_1 and g_2 (with de Swart's normalization) and the standard D and F couplings that appear in the interaction Lagrangian,

$$\mathscr{L} = -\sqrt{2}\, D\, Tr\,(\{\overline{B}, B\}M) + \sqrt{2}\, F\, Tr\,([\overline{B}, B]\, M) \; , \tag{44.4}$$

where $[\overline{B}, B] \equiv \overline{B}B - B\overline{B}$ and $\{\overline{B}, B\} \equiv \overline{B}B + B\overline{B}$, are

$$D = \frac{\sqrt{30}}{40}\, g_1 \; , \qquad F = \frac{\sqrt{6}}{24}\, g_2 \; . \tag{44.5}$$

Thus, for example,

$$\Gamma(\Xi^* \to \Xi\pi) \sim (F - D)^2 \sim (1 - 2\alpha)^2 \; , \tag{44.6}$$

where $\alpha \equiv F/(D + F)$. (This definition of α is de Swart's. The alternative $D/(D + F)$, due to Gell-Mann, is also used.)

The generators of SU(3) transformations, λ_a $(a = 1, 8)$, are 3×3 matrices that obey the following commutation and anticommutation relationships:

$$[\lambda_a,\ \lambda_b] \equiv \lambda_a\lambda_b - \lambda_b\lambda_a = 2i f_{abc}\lambda_c \tag{44.7}$$

$$\{\lambda_a,\ \lambda_b\} \equiv \lambda_a\lambda_b + \lambda_b\lambda_a = \frac{4}{3}\delta_{ab} I + 2 d_{abc}\lambda_c \; , \tag{44.8}$$

where I is the 3×3 identity matrix, and δ_{ab} is the Kronecker delta symbol. The f_{abc} are odd under the permutation of any pair of indices, while the d_{abc} are even. The nonzero values are

$\mathbf{1 \to 8 \otimes 8}$

$$\begin{pmatrix} \Lambda \end{pmatrix} \to \begin{pmatrix} N\overline{K} & \Sigma\pi & \Lambda\eta & \Xi K \end{pmatrix} = \frac{1}{\sqrt{8}} \begin{pmatrix} 2 & 3 & -1 & -2 \end{pmatrix}^{1/2}$$

$\mathbf{8_1 \to 8 \otimes 8}$

$$\begin{pmatrix} N \\ \Sigma \\ \Lambda \\ \Xi \end{pmatrix} \to \begin{pmatrix} N\pi & N\eta & \Sigma K & \Lambda K \\ N\overline{K} & \Sigma\pi & \Lambda\pi & \Sigma\eta & \Xi K \\ & N\overline{K} & \Sigma\pi & \Lambda\eta & \Xi K \\ & & \Sigma\overline{K} & \Lambda\overline{K} & \Xi\pi & \Xi\eta \end{pmatrix} = \frac{1}{\sqrt{20}} \begin{pmatrix} 9 & -1 & -9 & -1 \\ -6 & 0 & 4 & 4 & -6 \\ 2 & -12 & -4 & -2 \\ 9 & -1 & -9 & -1 \end{pmatrix}^{1/2}$$

$\mathbf{8_2 \to 8 \otimes 8}$

$$\begin{pmatrix} N \\ \Sigma \\ \Lambda \\ \Xi \end{pmatrix} \to \begin{pmatrix} N\pi & N\eta & \Sigma K & \Lambda K \\ N\overline{K} & \Sigma\pi & \Lambda\pi & \Sigma\eta & \Xi K \\ & N\overline{K} & \Sigma\pi & \Lambda\eta & \Xi K \\ & & \Sigma\overline{K} & \Lambda\overline{K} & \Xi\pi & \Xi\eta \end{pmatrix} = \frac{1}{\sqrt{12}} \begin{pmatrix} 3 & 3 & 3 & -3 \\ 2 & 8 & 0 & 0 & -2 \\ & 6 & 0 & 0 & 6 \\ & 3 & 3 & 3 & -3 \end{pmatrix}^{1/2}$$

$\mathbf{10 \to 8 \otimes 8}$

$$\begin{pmatrix} \Delta \\ \Sigma \\ \Xi \\ \Omega \end{pmatrix} \to \begin{pmatrix} N\pi & \Sigma K \\ N\overline{K} & \Sigma\pi & \Lambda\pi & \Sigma\eta & \Xi K \\ & \Sigma\overline{K} & \Lambda\overline{K} & \Xi\pi & \Xi\eta \\ & & \Xi\overline{K} \end{pmatrix} = \frac{1}{\sqrt{12}} \begin{pmatrix} -6 & 6 \\ -2 & 2 & -3 & 3 & 2 \\ & 3 & -3 & 3 & 3 \\ & & 12 \end{pmatrix}^{1/2}$$

$\mathbf{8 \to 10 \otimes 8}$

$$\begin{pmatrix} N \\ \Sigma \\ \Lambda \\ \Xi \end{pmatrix} \to \begin{pmatrix} \Delta\pi & \Sigma K \\ \Delta\overline{K} & \Sigma\pi & \Sigma\eta & \Xi K \\ & \Sigma\pi & \Xi K \\ \Sigma\overline{K} & \Xi\pi & \Xi\eta & \Omega K \end{pmatrix} = \frac{1}{\sqrt{15}} \begin{pmatrix} -12 & 3 \\ 8 & -2 & -3 & 2 \\ & -9 & 6 \\ 3 & -3 & -3 & 6 \end{pmatrix}^{1/2}$$

$\mathbf{10 \to 10 \otimes 8}$

$$\begin{pmatrix} \Delta \\ \Sigma \\ \Xi \\ \Omega \end{pmatrix} \to \begin{pmatrix} \Delta\pi & \Delta\eta & \Sigma K \\ \Delta\overline{K} & \Sigma\pi & \Sigma\eta & \Xi K \\ \Sigma\overline{K} & \Xi\pi & \Xi\eta & \Omega K \\ & \Xi\overline{K} & \Omega\eta \end{pmatrix} = \frac{1}{\sqrt{24}} \begin{pmatrix} 15 & 3 & -6 \\ 8 & 8 & 0 & -8 \\ 12 & 3 & -3 & -6 \\ & 12 & -12 \end{pmatrix}^{1/2}$$

abc	f_{abc}
123	1
147	1/2
156	−1/2
246	1/2
257	1/2
345	1/2
367	−1/2
458	$\sqrt{3}/2$
678	$\sqrt{3}/2$

abc	d_{abc}
118	$1/\sqrt{3}$
146	1/2
157	1/2
228	$1/\sqrt{3}$
247	−1/2
256	1/2
338	$1/\sqrt{3}$
344	1/2

abc	d_{abc}
355	1/2
366	−1/2
377	−1/2
448	$-1/(2\sqrt{3})$
558	$-1/(2\sqrt{3})$
668	$-1/(2\sqrt{3})$
778	$-1/(2\sqrt{3})$
888	$-1/\sqrt{3}$

The λ_a's are

$$\lambda_1 = \begin{pmatrix} 0 & 1 & 0 \\ 1 & 0 & 0 \\ 0 & 0 & 0 \end{pmatrix} \; \lambda_2 = \begin{pmatrix} 0 & -i & 0 \\ i & 0 & 0 \\ 0 & 0 & 0 \end{pmatrix} \; \lambda_3 = \begin{pmatrix} 1 & 0 & 0 \\ 0 & -1 & 0 \\ 0 & 0 & 0 \end{pmatrix}$$

$$\lambda_4 = \begin{pmatrix} 0 & 0 & 1 \\ 0 & 0 & 0 \\ 1 & 0 & 0 \end{pmatrix} \; \lambda_5 = \begin{pmatrix} 0 & 0 & -i \\ 0 & 0 & 0 \\ i & 0 & 0 \end{pmatrix} \; \lambda_6 = \begin{pmatrix} 0 & 0 & 0 \\ 0 & 0 & 1 \\ 0 & 1 & 0 \end{pmatrix}$$

$$\lambda_7 = \begin{pmatrix} 0 & 0 & 0 \\ 0 & 0 & -i \\ 0 & i & 0 \end{pmatrix} \; \lambda_8 = \frac{1}{\sqrt{3}} \begin{pmatrix} 1 & 0 & 0 \\ 0 & 1 & 0 \\ 0 & 0 & -2 \end{pmatrix}$$

Equation (44.7) defines the Lie algebra of SU(3). A general d-dimensional representation is given by a set of $d \times d$ matrices satisfying Eq. (44.7) with the f_{abc} given above. Equation (44.8) is specific to the defining 3-dimensional representation.

45. SU(n) MULTIPLETS AND YOUNG DIAGRAMS

Written by C.G. Wohl (LBNL).

This note tells (1) how SU(n) particle multiplets are identified or labeled, (2) how to find the number of particles in a multiplet from its label, (3) how to draw the Young diagram for a multiplet, and (4) how to use Young diagrams to determine the overall multiplet structure of a composite system, such as a 3-quark or a meson-baryon system.

In much of the literature, the word "representation" is used where we use "multiplet," and "tableau" is used where we use "diagram."

45.1. Multiplet labels

An SU(n) multiplet is uniquely identified by a string of (n−1) nonnegative integers: $(\alpha, \beta, \gamma, \ldots)$. Any such set of integers specifies a multiplet. For an SU(2) multiplet such as an isospin multiplet, the single integer α is the number of *steps* from one end of the multiplet to the other (*i.e.*, it is one fewer than the number of particles in the multiplet). In SU(3), the two integers α and β are the numbers of steps across the top and bottom levels of the multiplet diagram. Thus the labels for the SU(3) octet and decuplet

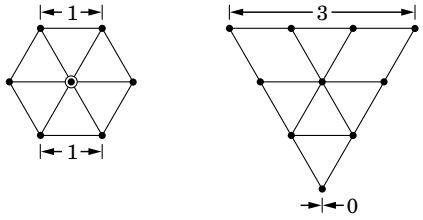

are (1,1) and (3,0). For larger n, the interpretation of the integers in terms of the geometry of the multiplets, which exist in an (n−1)-dimensional space, is not so readily apparent.

The label for the SU(n) singlet is $(0, 0, \ldots, 0)$. In a flavor SU(n), the n quarks together form a $(1, 0, \ldots, 0)$ multiplet, and the n antiquarks belong to a $(0, \ldots, 0, 1)$ multiplet. These two multiplets are *conjugate* to one another, which means their labels are related by $(\alpha, \beta, \ldots) \leftrightarrow (\ldots, \beta, \alpha)$.

45.2. Number of particles

The number of particles in a multiplet, $N = N(\alpha, \beta, \ldots)$, is given as follows (note the pattern of the equations).

In SU(2), $N = N(\alpha)$ is

$$N = \frac{(\alpha + 1)}{1} \, . \tag{45.1}$$

In SU(3), $N = N(\alpha, \beta)$ is

$$N = \frac{(\alpha + 1)}{1} \cdot \frac{(\beta + 1)}{1} \cdot \frac{(\alpha + \beta + 2)}{2} \, . \tag{45.2}$$

In SU(4), $N = N(\alpha, \beta, \gamma)$ is

$$N = \frac{(\alpha+1)}{1} \cdot \frac{(\beta+1)}{1} \cdot \frac{(\gamma+1)}{1} \cdot \frac{(\alpha+\beta+2)}{2} \cdot \frac{(\beta+\gamma+2)}{2} \cdot \frac{(\alpha+\beta+\gamma+3)}{3} \, . \tag{45.3}$$

Note that in Eq. (45.3) there is no factor with $(\alpha + \gamma + 2)$: only a *consecutive* sequence of the label integers appears in any factor. One more example should make the pattern clear for any SU(n). In SU(5), $N = N(\alpha, \beta, \gamma, \delta)$ is

$$N = \frac{(\alpha+1)}{1} \cdot \frac{(\beta+1)}{1} \cdot \frac{(\gamma+1)}{1} \cdot \frac{(\delta+1)}{1} \cdot \frac{(\alpha+\beta+2)}{2} \cdot \frac{(\beta+\gamma+2)}{2} \times \frac{(\gamma+\delta+2)}{2} \cdot \frac{(\alpha+\beta+\gamma+3)}{3} \cdot \frac{(\beta+\gamma+\delta+3)}{3} \cdot \frac{(\alpha+\beta+\gamma+\delta+4)}{4} \tag{45.4}$$

From the symmetry of these equations, it is clear that multiplets that are conjugate to one another have the same number of particles, but so can other multiplets. For example, the SU(4) multiplets (3,0,0) and (1,1,0) each have 20 particles. Try the equations and see.

45.3. Young diagrams

A Young diagram consists of an array of boxes (or some other symbol) arranged in one or more *left-justified* rows, with each row being *at least as long* as the row beneath. The correspondence between a diagram and a multiplet label is: The top row juts out α boxes to the right past the end of the second row, the second row juts out β boxes to the right past the end of the third row, *etc.* A diagram in SU(n) has at most n rows. There can be any number of "completed" columns of n boxes buttressing the left of a diagram; these don't affect the label. Thus in SU(3) the diagrams

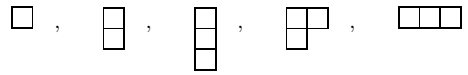

represent the multiplets (1,0), (0,1), (0,0), (1,1), and (3,0). In any SU(n), the quark multiplet is represented by a single box, the antiquark multiplet by a column of (n−1) boxes, and a singlet by a completed column of n boxes.

45.4. Coupling multiplets together

The following recipe tells how to find the multiplets that occur in coupling two multiplets together. To couple together more than two multiplets, first couple two, then couple a third with each of the multiplets obtained from the first two, *etc.*

First a definition: A sequence of the letters $a, b, c, \ldots$ is *admissible* if at any point in the sequence at least as many a's have occurred as b's, at least as many b's have occurred as c's, *etc.* Thus *abcd* and *aabcb* are admissible sequences and *abb* and *acb* are not. Now the recipe:

(a) Draw the Young diagrams for the two multiplets, but in one of the diagrams replace the boxes in the first row with a's, the boxes in the second row with b's, *etc.* Thus, to couple two SU(3) octets (such as the π-meson octet and the baryon octet), we start with  and  . The *unlettered* diagram forms the *upper left-hand corner* of all the enlarged diagrams constructed below.

(b) Add the a's from the lettered diagram to the right-hand ends of the rows of the unlettered diagram to form all possible legitimate Young diagrams that have no more than one a per column. In general, there will be several distinct diagrams, and all the a's appear in each diagram. At this stage, for the coupling of the two SU(3) octets, we have:

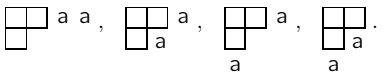

(c) Use the b's to further enlarge the diagrams already obtained, subject to the same rules. Then throw away any diagram in which the full sequence of letters formed by reading *right to left* in the first row, then the second row, *etc.*, is not admissible.

(d) Proceed as in (c) with the c's (if any), *etc.*

The final result of the coupling of the two SU(3) octets is:

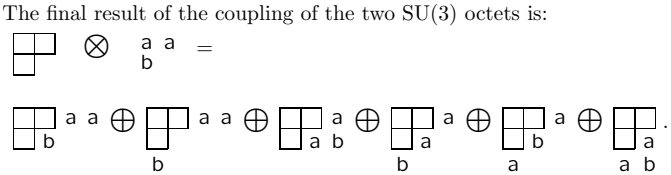

Here only the diagrams with admissible sequences of a's and b's and with fewer than four rows (since $n = 3$) have been kept. In terms of multiplet labels, the above may be written

$$(1,1) \otimes (1,1) = (2,2) \oplus (3,0) \oplus (0,3) \oplus (1,1) \oplus (1,1) \oplus (0,0) \, .$$

In terms of numbers of particles, it may be written

$$\mathbf{8} \otimes \mathbf{8} = \mathbf{27} \oplus \mathbf{10} \oplus \overline{\mathbf{10}} \oplus \mathbf{8} \oplus \mathbf{8} \oplus \mathbf{1} \, .$$

The product of the numbers on the left here is equal to the sum on the right, a useful check. (See also Sec. 15 on the Quark Model.)

46. KINEMATICS

Revised January 2000 by J.D. Jackson (LBNL) and June 2008 by D.R. Tovey (Sheffield).

Throughout this section units are used in which $\hbar = c = 1$. The following conversions are useful: $\hbar c = 197.3$ MeV fm, $(\hbar c)^2 = 0.3894$ (GeV)^2 mb.

46.1. Lorentz transformations

The energy E and 3-momentum $\boldsymbol{p}$ of a particle of mass m form a 4-vector $p = (E, \boldsymbol{p})$ whose square $p^2 \equiv E^2 - |\boldsymbol{p}|^2 = m^2$. The velocity of the particle is $\boldsymbol{\beta} = \boldsymbol{p}/E$. The energy and momentum $(E^*, \boldsymbol{p}^*)$ viewed from a frame moving with velocity $\boldsymbol{\beta}_f$ are given by

$$\begin{pmatrix} E^* \\ p^*_\parallel \end{pmatrix} = \begin{pmatrix} \gamma_f & -\gamma_f\beta_f \\ -\gamma_f\beta_f & \gamma_f \end{pmatrix} \begin{pmatrix} E \\ p_\parallel \end{pmatrix} , \quad p^*_T = p_T , \tag{46.1}$$

where $\gamma_f = (1-\beta_f^2)^{-1/2}$ and p_T ($p_\parallel$) are the components of $\boldsymbol{p}$ perpendicular (parallel) to $\boldsymbol{\beta}_f$. Other 4-vectors, such as the space-time coordinates of events, of course transform in the same way. The scalar product of two 4-momenta $p_1 \cdot p_2 = E_1E_2 - \boldsymbol{p}_1 \cdot \boldsymbol{p}_2$ is invariant (frame independent).

46.2. Center-of-mass energy and momentum

In the collision of two particles of masses m_1 and m_2 the total center-of-mass energy can be expressed in the Lorentz-invariant form

$$\begin{aligned} E_{\rm cm} &= \left[(E_1+E_2)^2 - (\boldsymbol{p}_1+\boldsymbol{p}_2)^2\right]^{1/2} , \\ &= \left[m_1^2 + m_2^2 + 2E_1E_2(1-\beta_1\beta_2\cos\theta)\right]^{1/2} , \end{aligned} \tag{46.2}$$

where θ is the angle between the particles. In the frame where one particle (of mass m_2) is at rest (lab frame),

$$E_{\rm cm} = (m_1^2 + m_2^2 + 2E_{1\,\rm lab}\, m_2)^{1/2} . \tag{46.3}$$

The velocity of the center-of-mass in the lab frame is

$$\boldsymbol{\beta}_{\rm cm} = \boldsymbol{p}_{\rm lab}/(E_{1\,\rm lab} + m_2) , \tag{46.4}$$

where $\boldsymbol{p}_{\rm lab} \equiv \boldsymbol{p}_{1\,\rm lab}$ and

$$\gamma_{\rm cm} = (E_{1\,\rm lab} + m_2)/E_{\rm cm} . \tag{46.5}$$

The c.m. momenta of particles 1 and 2 are of magnitude

$$p_{\rm cm} = p_{\rm lab}\frac{m_2}{E_{\rm cm}} . \tag{46.6}$$

For example, if a 0.80 GeV/c kaon beam is incident on a proton target, the center of mass energy is 1.699 GeV and the center of mass momentum of either particle is 0.442 GeV/c. It is also useful to note that

$$E_{\rm cm}\, dE_{\rm cm} = m_2\, dE_{1\,\rm lab} = m_2\, \beta_{1\,\rm lab}\, dp_{\rm lab} . \tag{46.7}$$

46.3. Lorentz-invariant amplitudes

The matrix elements for a scattering or decay process are written in terms of an invariant amplitude $-i\mathscr{M}$. As an example, the S-matrix for $2 \to 2$ scattering is related to $\mathscr{M}$ by

$$\begin{aligned} \langle p_1'p_2'\,|S|\,p_1p_2\rangle &= I - i(2\pi)^4\,\delta^4(p_1+p_2-p_1'-p_2') \\ &\times \frac{\mathscr{M}(p_1,\,p_2;\,p_1',\,p_2')}{(2E_1)^{1/2}\,(2E_2)^{1/2}\,(2E_1')^{1/2}\,(2E_2')^{1/2}} . \end{aligned} \tag{46.8}$$

The state normalization is such that

$$\langle p'|p\rangle = (2\pi)^3\delta^3(\boldsymbol{p}-\boldsymbol{p}') . \tag{46.9}$$

46.4. Particle decays

The partial decay rate of a particle of mass M into n bodies in its rest frame is given in terms of the Lorentz-invariant matrix element $\mathscr{M}$ by

$$d\Gamma = \frac{(2\pi)^4}{2M}\,|\mathscr{M}|^2\,d\Phi_n\,(P;\,p_1,\,\ldots,\,p_n), \tag{46.10}$$

where $d\Phi_n$ is an element of n-body phase space given by

$$d\Phi_n(P;\,p_1,\,\ldots,\,p_n) = \delta^4\,(P - \sum_{i=1}^n p_i)\,\prod_{i=1}^n \frac{d^3p_i}{(2\pi)^3 2E_i} . \tag{46.11}$$

This phase space can be generated recursively, viz.

$$\begin{aligned} d\Phi_n(P;\,p_1,\,\ldots,\,p_n) &= d\Phi_j(q;\,p_1,\,\ldots,\,p_j) \\ &\times\; d\Phi_{n-j+1}\,(P;\,q,\,p_{j+1},\,\ldots,\,p_n)(2\pi)^3dq^2 , \end{aligned} \tag{46.12}$$

where $q^2 = (\sum_{i=1}^j E_i)^2 - \left|\sum_{i=1}^j \boldsymbol{p}_i\right|^2$. This form is particularly useful in the case where a particle decays into another particle that subsequently decays.

46.4.1. ***Survival probability*** : If a particle of mass M has mean proper lifetime τ $(= 1/\Gamma)$ and has momentum $(E, \boldsymbol{p})$, then the probability that it lives for a time t_0 or greater before decaying is given by

$$P(t_0) = e^{-t_0\,\Gamma/\gamma} = e^{-Mt_0\,\Gamma/E} , \tag{46.13}$$

and the probability that it travels a distance x_0 or greater is

$$P(x_0) = e^{-Mx_0\,\Gamma/|\boldsymbol{p}|} . \tag{46.14}$$

46.4.2. ***Two-body decays*** :

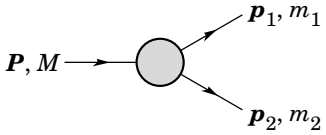

Figure 46.1: Definitions of variables for two-body decays.

In the rest frame of a particle of mass M, decaying into 2 particles labeled 1 and 2,

$$E_1 = \frac{M^2 - m_2^2 + m_1^2}{2M} , \tag{46.15}$$

$$\begin{aligned} |\boldsymbol{p}_1| &= |\boldsymbol{p}_2| \\ &= \frac{\left[\left(M^2 - (m_1+m_2)^2\right)\left(M^2 - (m_1-m_2)^2\right)\right]^{1/2}}{2M} , \end{aligned} \tag{46.16}$$

and

$$d\Gamma = \frac{1}{32\pi^2}\,|\mathscr{M}|^2\,\frac{|\boldsymbol{p}_1|}{M^2}\,d\Omega , \tag{46.17}$$

where $d\Omega = d\phi_1 d(\cos\theta_1)$ is the solid angle of particle 1. The invariant mass M can be determined from the energies and momenta using Eq. (46.2) with $M = E_{\rm cm}$.

46.4.3. ***Three-body decays*** :

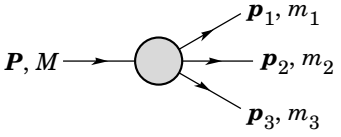

Figure 46.2: Definitions of variables for three-body decays.

Defining $p_{ij} = p_i + p_j$ and $m_{ij}^2 = p_{ij}^2$, then $m_{12}^2 + m_{23}^2 + m_{13}^2 = M^2 + m_1^2 + m_2^2 + m_3^2$ and $m_{12}^2 = (P - p_3)^2 = M^2 + m_3^2 - 2ME_3$, where E_3 is the energy of particle 3 in the rest frame of M. In that frame, the momenta of the three decay particles lie in a plane. The relative orientation of these three momenta is fixed if their energies are known. The momenta can therefore be specified in space by giving three Euler angles (α, β, γ) that specify the orientation of the final system relative to the initial particle [1]. Then

$$d\Gamma = \frac{1}{(2\pi)^5} \frac{1}{16M} |\mathscr{M}|^2 \, dE_1 \, dE_2 \, d\alpha \, d(\cos\beta) \, d\gamma \, . \tag{46.18}$$

Alternatively

$$d\Gamma = \frac{1}{(2\pi)^5} \frac{1}{16M^2} |\mathscr{M}|^2 \, |\boldsymbol{p}_1^*| \, |\boldsymbol{p}_3| \, dm_{12} \, d\Omega_1^* \, d\Omega_3 \, , \tag{46.19}$$

where $(|\boldsymbol{p}_1^*|, \Omega_1^*)$ is the momentum of particle 1 in the rest frame of 1 and 2, and Ω_3 is the angle of particle 3 in the rest frame of the decaying particle. $|\boldsymbol{p}_1^*|$ and $|\boldsymbol{p}_3|$ are given by

$$|\boldsymbol{p}_1^*| = \frac{\left[\left(m_{12}^2 - (m_1 + m_2)^2\right)\left(m_{12}^2 - (m_1 - m_2)^2\right)\right]^{1/2}}{2m_{12}} \, , \tag{46.20a}$$

and

$$|\boldsymbol{p}_3| = \frac{\left[\left(M^2 - (m_{12} + m_3)^2\right)\left(M^2 - (m_{12} - m_3)^2\right)\right]^{1/2}}{2M} \, . \tag{46.20b}$$

[Compare with Eq. (46.16).]

If the decaying particle is a scalar or we average over its spin states, then integration over the angles in Eq. (46.18) gives

$$d\Gamma = \frac{1}{(2\pi)^3} \frac{1}{8M} \overline{|\mathscr{M}|^2} \, dE_1 \, dE_2$$

$$= \frac{1}{(2\pi)^3} \frac{1}{32M^3} \overline{|\mathscr{M}|^2} \, dm_{12}^2 \, dm_{23}^2 \, . \tag{46.21}$$

This is the standard form for the Dalitz plot.

46.4.3.1. *Dalitz plot:* For a given value of m_{12}^2, the range of m_{23}^2 is determined by its values when $\boldsymbol{p}_2$ is parallel or antiparallel to $\boldsymbol{p}_3$:

$$(m_{23}^2)_{\rm max} =$$

$$(E_2^* + E_3^*)^2 - \left(\sqrt{E_2^{*2} - m_2^2} - \sqrt{E_3^{*2} - m_3^2}\right)^2 \, , \tag{46.22a}$$

$$(m_{23}^2)_{\rm min} =$$

$$(E_2^* + E_3^*)^2 - \left(\sqrt{E_2^{*2} - m_2^2} + \sqrt{E_3^{*2} - m_3^2}\right)^2 \, . \tag{46.22b}$$

Here $E_2^* = (m_{12}^2 - m_1^2 + m_2^2)/2m_{12}$ and $E_3^* = (M^2 - m_{12}^2 - m_3^2)/2m_{12}$ are the energies of particles 2 and 3 in the m_{12} rest frame. The scatter plot in m_{12}^2 and m_{23}^2 is called a Dalitz plot. If $\overline{|\mathscr{M}|^2}$ is constant, the allowed region of the plot will be uniformly populated with events [see Eq. (46.21)]. A nonuniformity in the plot gives immediate information on $|\mathscr{M}|^2$. For example, in the case of $D \to K\pi\pi$, bands appear when $m_{(K\pi)} = m_{K^*(892)}$, reflecting the appearance of the decay chain $D \to K^*(892)\pi \to K\pi\pi$.

46.4.4. *Kinematic limits* :

46.4.4.1. *Three-body decays:* In a three-body decay (Fig. 46.2) the maximum of $|\boldsymbol{p}_3|$, [given by Eq. (46.20)], is achieved when $m_{12} = m_1 + m_2$, *i.e.*, particles 1 and 2 have the same vector velocity in the rest frame of the decaying particle. If, in addition, $m_3 > m_1, m_2$, then $|\boldsymbol{p}_3|_{\rm max} > |\boldsymbol{p}_1|_{\rm max}$, $|\boldsymbol{p}_2|_{\rm max}$. The distribution of m_{12} values possesses an end-point or maximum value at $m_{12} = M - m_3$. This can be used to constrain the mass difference of a parent particle and one invisible decay product.

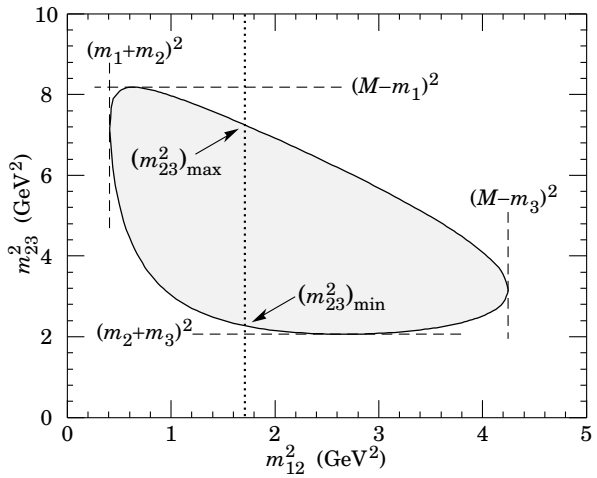

Figure 46.3: Dalitz plot for a three-body final state. In this example, the state is $\pi^+\overline{K}^0 p$ at 3 GeV. Four-momentum conservation restricts events to the shaded region.

46.4.4.2. *Sequential two-body decays:*

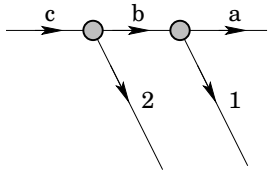

Figure 46.4: Particles participating in sequential two-body decay chain. Particles labeled 1 and 2 are visible while the particle terminating the chain (a) is invisible.

When a heavy particle initiates a sequential chain of two-body decays terminating in an invisible particle, constraints on the masses of the states participating in the chain can be obtained from end-points and thresholds in invariant mass distributions of the aggregated decay products. For the two-step decay chain depicted in Fig. 46.4 the invariant mass distribution of the two visible particles possesses an end-point given by:

$$(m_{12}^{\rm max})^2 = \frac{(m_{\rm c}^2 - m_{\rm b}^2)(m_{\rm b}^2 - m_{\rm a}^2)}{m_{\rm b}^2} \, , \tag{46.23}$$

provided particles 1 and 2 are massless. If visible particle 1 has non-zero mass m_1 then Eq. (46.23) is replaced by

$$(m_{12}^{\rm max})^2 = m_1^2 + \frac{(m_{\rm c}^2 - m_{\rm b}^2)}{2m_{\rm b}^2} \times$$

$$\left(m_1^2 + m_{\rm b}^2 - m_{\rm a}^2 + \sqrt{(-m_1^2 + m_{\rm b}^2 - m_{\rm a}^2)^2 - 4m_1^2 m_{\rm a}^2}\right) . \tag{46.24}$$

See Refs. 2 and 3 for other cases.

46.4.5. *Multibody decays* :

The above results may be generalized to final states containing any number of particles by combining some of the particles into "effective particles" and treating the final states as 2 or 3 "effective particle" states. Thus, if $p_{ijk\ldots} = p_i + p_j + p_k + \ldots$, then

$$m_{ijk\ldots} = \sqrt{p^2_{ijk\ldots}} \, , \tag{46.25}$$

and $m_{ijk\ldots}$ may be used in place of *e.g.*, m_{12} in the relations in Sec. 46.4.3 or Sec. 46.4.4 above.

46.5. Cross sections

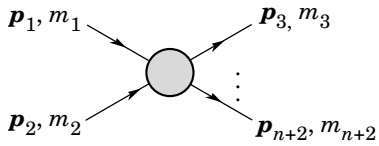

Figure 46.5: Definitions of variables for production of an n-body final state.

The differential cross section is given by

$$d\sigma = \frac{(2\pi)^4 |\mathscr{M}|^2}{4\sqrt{(p_1 \cdot p_2)^2 - m_1^2 m_2^2}} \times d\Phi_n(p_1 + p_2;\, p_3, \ldots, p_{n+2}) \; . \tag{46.26}$$

[See Eq. (46.11).] In the rest frame of m_2(lab),

$$\sqrt{(p_1 \cdot p_2)^2 - m_1^2 m_2^2} = m_2 p_{1\,\mathrm{lab}} \; ; \tag{46.27a}$$

while in the center-of-mass frame

$$\sqrt{(p_1 \cdot p_2)^2 - m_1^2 m_2^2} = p_{1\mathrm{cm}} \sqrt{s} \; . \tag{46.27b}$$

46.5.1. ***Two-body reactions*** :

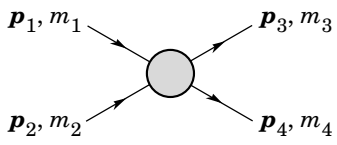

Figure 46.6: Definitions of variables for a two-body final state.

Two particles of momenta p_1 and p_2 and masses m_1 and m_2 scatter to particles of momenta p_3 and p_4 and masses m_3 and m_4; the Lorentz-invariant Mandelstam variables are defined by

$$\begin{aligned} s &= (p_1 + p_2)^2 = (p_3 + p_4)^2 \\ &= m_1^2 + 2E_1E_2 - 2\boldsymbol{p}_1 \cdot \boldsymbol{p}_2 + m_2^2 \; , \end{aligned} \tag{46.28}$$

$$\begin{aligned} t &= (p_1 - p_3)^2 = (p_2 - p_4)^2 \\ &= m_1^2 - 2E_1E_3 + 2\boldsymbol{p}_1 \cdot \boldsymbol{p}_3 + m_3^2 \; , \end{aligned} \tag{46.29}$$

$$\begin{aligned} u &= (p_1 - p_4)^2 = (p_2 - p_3)^2 \\ &= m_1^2 - 2E_1E_4 + 2\boldsymbol{p}_1 \cdot \boldsymbol{p}_4 + m_4^2 \; , \end{aligned} \tag{46.30}$$

and they satisfy

$$s + t + u = m_1^2 + m_2^2 + m_3^2 + m_4^2 \; . \tag{46.31}$$

The two-body cross section may be written as

$$\frac{d\sigma}{dt} = \frac{1}{64\pi s} \, \frac{1}{|\boldsymbol{p}_{1\mathrm{cm}}|^2} \, |\mathscr{M}|^2 \; . \tag{46.32}$$

In the center-of-mass frame

$$\begin{aligned} t = (E_{1\mathrm{cm}} - E_{3\mathrm{cm}})^2 - (p_{1\mathrm{cm}} - p_{3\mathrm{cm}})^2 \quad &- 4p_{1\mathrm{cm}}\, p_{3\mathrm{cm}}\, \sin^2(\theta_{\mathrm{cm}}/2) \\ = t_0 - 4p_{1\mathrm{cm}}\, p_{3\mathrm{cm}}\, \sin^2(\theta_{\mathrm{cm}}/2) \; , \end{aligned} \tag{46.33}$$

where θ_{cm} is the angle between particle 1 and 3. The limiting values t_0 ($\theta_{\mathrm{cm}} = 0$) and t_1 ($\theta_{\mathrm{cm}} = \pi$) for $2 \to 2$ scattering are

$$t_0(t_1) = \left[\frac{m_1^2 - m_3^2 - m_2^2 + m_4^2}{2\sqrt{s}} \right]^2 - (p_{1\,\mathrm{cm}} \mp p_{3\,\mathrm{cm}})^2 \; . \tag{46.34}$$

In the literature the notation $t_{\min}$ ($t_{\max}$) for t_0 (t_1) is sometimes used, which should be discouraged since $t_0 > t_1$. The center-of-mass energies and momenta of the incoming particles are

$$E_{1\mathrm{cm}} = \frac{s + m_1^2 - m_2^2}{2\sqrt{s}} \; , \qquad E_{2\mathrm{cm}} = \frac{s + m_2^2 - m_1^2}{2\sqrt{s}} \; , \tag{46.35}$$

For $E_{3\mathrm{cm}}$ and $E_{4\mathrm{cm}}$, change m_1 to m_3 and m_2 to m_4. Then

$$p_{i\,\mathrm{cm}} = \sqrt{E_{i\,\mathrm{cm}}^2 - m_i^2} \text{ and } p_{1\mathrm{cm}} = \frac{p_{1\,\mathrm{lab}}\, m_2}{\sqrt{s}} \; . \tag{46.36}$$

Here the subscript lab refers to the frame where particle 2 is at rest. [For other relations see Eqs. (46.2)–(46.4).]

46.5.2. ***Inclusive reactions*** : Choose some direction (usually the beam direction) for the z-axis; then the energy and momentum of a particle can be written as

$$E = m_T \cosh y \; , \; p_x \; , \; p_y \; , \; p_z = m_T \sinh y \; , \tag{46.37}$$

where m_T, conventionally called the 'transverse mass', is given by

$$m_T^2 = m^2 + p_x^2 + p_y^2 \; . \tag{46.38}$$

and the rapidity y is defined by

$$y = \frac{1}{2} \ln \left(\frac{E + p_z}{E - p_z} \right)$$

$$= \ln \left(\frac{E + p_z}{m_T} \right) = \tanh^{-1} \left(\frac{p_z}{E} \right) \; . \tag{46.39}$$

Note that the definition of the transverse mass in Eq. (46.38) differs from that used by experimentalists at hadron colliders (see Sec. 46.6.1 below). Under a boost in the z-direction to a frame with velocity β, $y \to y - \tanh^{-1}\beta$. Hence the shape of the rapidity distribution dN/dy is invariant, as are differences in rapidity. The invariant cross section may also be rewritten

$$E \frac{d^3\sigma}{d^3p} = \frac{d^3\sigma}{d\phi\, dy\, p_T dp_T} \Longrightarrow \frac{d^2\sigma}{\pi\, dy\, d(p_T^2)} \; . \tag{46.40}$$

The second form is obtained using the identity $dy/dp_z = 1/E$, and the third form represents the average over ϕ.

Feynman's x variable is given by

$$x = \frac{p_z}{p_{z\,\max}} \approx \frac{E + p_z}{(E + p_z)_{\max}} \quad (p_T \ll |p_z|) \; . \tag{46.41}$$

In the c.m. frame,

$$x \approx \frac{2p_{z\,\mathrm{cm}}}{\sqrt{s}} = \frac{2m_T \sinh y_{\mathrm{cm}}}{\sqrt{s}} \tag{46.42}$$

and

$$= (y_{\mathrm{cm}})_{\max} = \ln(\sqrt{s}/m) \; . \tag{46.43}$$

The invariant mass M of the two-particle system described in Sec. 46.4.2 can be written in terms of these variables as

$$M^2 = m_1^2 + m_2^2 + 2[E_T(1)E_T(2)\cosh\Delta y - \boldsymbol{p}_T(1) \cdot \boldsymbol{p}_T(2)] \; , \tag{46.44}$$

where

$$E_T(i) = \sqrt{|\boldsymbol{p}_T(i)|^2 + m_i^2} \; , \tag{46.45}$$

and $\boldsymbol{p}_T(i)$ denotes the transverse momentum vector of particle i.

For $p \gg m$, the rapidity [Eq. (46.39)] may be expanded to obtain

$$y = \frac{1}{2} \ln \frac{\cos^2(\theta/2) + m^2/4p^2 + \ldots}{\sin^2(\theta/2) + m^2/4p^2 + \ldots}$$

$$\approx -\ln \tan(\theta/2) \equiv \eta \tag{46.46}$$

where $\cos\theta = p_z/p$. The pseudorapidity η defined by the second line is approximately equal to the rapidity y for $p \gg m$ and $\theta \gg 1/\gamma$, and in any case can be measured when the mass and momentum of the particle are unknown. From the definition one can obtain the identities

$$\sinh\eta = \cot\theta \; , \quad \cosh\eta = 1/\sin\theta \; , \quad \tanh\eta = \cos\theta \; . \tag{46.47}$$

46.5.3. ***Partial waves*** : The amplitude in the center of mass for elastic scattering of spinless particles may be expanded in Legendre polynomials

$$f(k,\theta) = \frac{1}{k}\sum_{\ell}(2\ell+1)a_\ell P_\ell(\cos\theta) \ , \tag{46.48}$$

where k is the c.m. momentum, θ is the c.m. scattering angle, $a_\ell = (\eta_\ell e^{2i\delta_\ell} - 1)/2i$, $0 \le \eta_\ell \le 1$, and δ_ℓ is the phase shift of the ℓ^{th} partial wave. For purely elastic scattering, $\eta_\ell = 1$. The differential cross section is

$$\frac{d\sigma}{d\Omega} = |f(k,\theta)|^2 \ . \tag{46.49}$$

The optical theorem states that

$$\sigma_{\rm tot} = \frac{4\pi}{k}{\rm Im}\, f(k,0) \ , \tag{46.50}$$

and the cross section in the ℓ^{th} partial wave is therefore bounded:

$$\sigma_\ell = \frac{4\pi}{k^2}(2\ell+1)|a_\ell|^2 \le \frac{4\pi(2\ell+1)}{k^2} \ . \tag{46.51}$$

The evolution with energy of a partial-wave amplitude a_ℓ can be displayed as a trajectory in an Argand plot, as shown in Fig. 46.7.

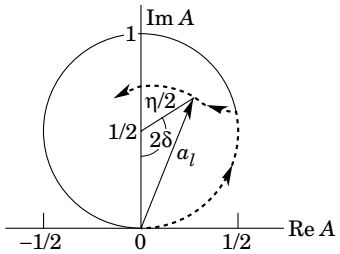

Figure 46.7: Argand plot showing a partial-wave amplitude a_ℓ as a function of energy. The amplitude leaves the unitary circle where inelasticity sets in ($\eta_\ell < 1$).

The usual Lorentz-invariant matrix element $\mathscr{M}$ (see Sec. 46.3 above) for the elastic process is related to $f(k,\theta)$ by

$$\mathscr{M} = -8\pi\sqrt{s}\, f(k,\theta) \ , \tag{46.52}$$

so

$$\sigma_{\rm tot} = -\frac{1}{2p_{\rm lab}\, m_2}\,{\rm Im}\,\mathscr{M}(t=0) \ , \tag{46.53}$$

where s and t are the center-of-mass energy squared and momentum transfer squared, respectively (see Sec. 46.4.1).

46.5.3.1. *Resonances:* The Breit-Wigner (nonrelativistic) form for an elastic amplitude a_ℓ with a resonance at c.m. energy E_R, elastic width $\Gamma_{\rm el}$, and total width $\Gamma_{\rm tot}$ is

$$a_\ell = \frac{\Gamma_{\rm el}/2}{E_R - E - i\Gamma_{\rm tot}/2} \ , \tag{46.54}$$

where E is the c.m. energy. As shown in Fig. 46.8, in the absence of background the elastic amplitude traces a counterclockwise circle with center $ix_{\rm el}/2$ and radius $x_{\rm el}/2$, where the elasticity $x_{\rm el} = \Gamma_{\rm el}/\Gamma_{\rm tot}$. The amplitude has a pole at $E = E_R - i\Gamma_{\rm tot}/2$.

The spin-averaged Breit-Wigner cross section for a spin-J resonance produced in the collision of particles of spin S_1 and S_2 is

$$\sigma_{BW}(E) = \frac{(2J+1)}{(2S_1+1)(2S_2+1)}\ \frac{\pi}{k^2}\ \frac{B_{\rm in}B_{\rm out}\Gamma_{\rm tot}^2}{(E-E_R)^2+\Gamma_{\rm tot}^2/4} \ , \tag{46.55}$$

where k is the c.m. momentum, E is the c.m. energy, and $B_{\rm in}$ and $B_{\rm out}$ are the branching fractions of the resonance into the entrance and exit channels. The $2S+1$ factors are the multiplicities of the incident spin states, and are replaced by 2 for photons. This expression is valid only for an isolated state. If the width is not small, $\Gamma_{\rm tot}$ cannot be treated as a constant independent of E. There are many other forms for σ_{BW}, all of which are equivalent to the one given here in the narrow-width case. Some of these forms may be more appropriate if the resonance is broad.

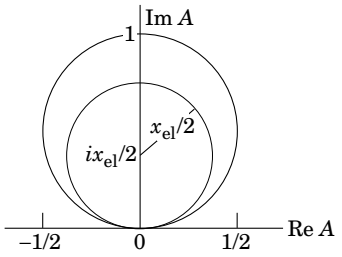

Figure 46.8: Argand plot for a resonance.

The relativistic Breit-Wigner form corresponding to Eq. (46.54) is:

$$a_\ell = \frac{-m\Gamma_{\rm el}}{s - m^2 + im\Gamma_{\rm tot}} \ . \tag{46.56}$$

A better form incorporates the known kinematic dependences, replacing $m\Gamma_{\rm tot}$ by $\sqrt{s}\,\Gamma_{\rm tot}(s)$, where $\Gamma_{\rm tot}(s)$ is the width the resonance particle would have if its mass were $\sqrt{s}$, and correspondingly $m\Gamma_{\rm el}$ by $\sqrt{s}\,\Gamma_{\rm el}(s)$ where $\Gamma_{\rm el}(s)$ is the partial width in the incident channel for a mass $\sqrt{s}$:

$$a_\ell = \frac{-\sqrt{s}\,\Gamma_{\rm el}(s)}{s - m^2 + i\sqrt{s}\,\Gamma_{\rm tot}(s)} \ . \tag{46.57}$$

For the Z boson, all the decays are to particles whose masses are small enough to be ignored, so on dimensional grounds $\Gamma_{\rm tot}(s) = \sqrt{s}\,\Gamma_0/m_Z$, where Γ_0 defines the width of the Z, and $\Gamma_{\rm el}(s)/\Gamma_{\rm tot}(s)$ is constant. A full treatment of the line shape requires consideration of dynamics, not just kinematics. For the Z this is done by calculating the radiative corrections in the Standard Model.

46.6. Transverse variables

At hadron colliders, a significant and unknown proportion of the energy of the incoming hadrons in each event escapes down the beam-pipe. Consequently if invisible particles are created in the final state, their net momentum can only be constrained in the plane transverse to the beam direction. Defining the z-axis as the beam direction, this net momentum is equal to the missing transverse energy vector

$$\boldsymbol{E}_T^{\rm miss} = -\sum_i \boldsymbol{p}_T(i) \ , \tag{46.58}$$

where the sum runs over the transverse momenta of all visible final state particles.

46.6.1. ***Single production with semi-invisible final state*** :

Consider a single heavy particle of mass M produced in association with visible particles which decays as in Fig. 46.1 to two particles, of which one (labeled particle 1) is invisible. The mass of the parent particle can be constrained with the quantity M_T defined by

$$\begin{aligned} M_T^2 &\equiv [E_T(1)+E_T(2)]^2 - [\boldsymbol{p}_T(1)+\boldsymbol{p}_T(2)]^2 \\ &= m_1^2 + m_2^2 + 2[E_T(1)E_T(2) - \boldsymbol{p}_T(1)\cdot\boldsymbol{p}_T(2)] \ , \end{aligned} \tag{46.59}$$

where

$$\boldsymbol{p}_T(1) = \boldsymbol{E}_T^{\rm miss} \ . \tag{46.60}$$

This quantity is called the 'transverse mass' by hadron collider experimentalists but it should be noted that it is quite different from that used in the description of inclusive reactions [Eq. (46.38)]. The distribution of event M_T values possesses an end-point at $M_T^{\rm max} = M$. If $m_1 = m_2 = 0$ then

$$M_T^2 = 2|\boldsymbol{p}_T(1)||\boldsymbol{p}_T(2)|(1-\cos\phi_{12}) \ , \tag{46.61}$$

where ϕ_{ij} is defined as the angle between particles i and j in the transverse plane.

46.6.2. ***Pair production with semi-invisible final states*** :

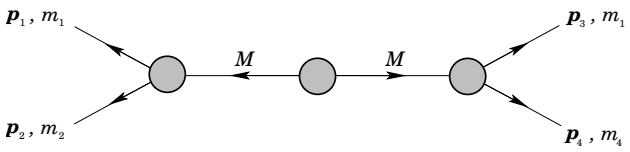

Figure 46.9: Definitions of variables for pair production of semi-invisible final states. Particles 1 and 3 are invisible while particles 2 and 4 are visible.

Consider two identical heavy particles of mass M produced such that their combined center-of-mass is at rest in the transverse plane (Fig. 46.9). Each particle decays to a final state consisting of an invisible particle of fixed mass m_1 together with an additional visible particle. M and m_1 can be constrained with the variables M_{T2} and M_{CT} which are defined in Refs. [4] and [5].

References:

1. See, for example, J.J. Sakurai, *Modern Quantum Mechanics*, Addison-Wesley (1985), p. 172, or D.M. Brink and G.R. Satchler, *Angular Momentum*, 2nd ed., Oxford University Press (1968), p. 20.
2. I. Hinchliffe *et al.*, Phys. Rev. **D55**, 5520 (1997).
3. B.C. Allanach *et al.*, JHEP **0009**, 004 (2000).
4. C.G. Lester and D.J. Summers, Phys. Lett. **B463**, 99 (1999).
5. D.R. Tovey, JHEP **0804**, 034 (2008).

47. RESONANCES

Written 2013 by D. Asner (Pacific Northwest National Laboratory), C. Hanhart (Forschungszentrum Jülich) and E. Klempt (Bonn).

47.1. General Considerations

For simplicity, throughout this review the formulas are given for distinguishable, scalar particles. The additional complications that appear in the presence of spins can be controlled in the helicity framework developed by Jacob and Wick [1], or in a non-relativistic [2] or relativistic [3] tensor operator formalism. Within these frames, sequential (cascade) decays are commonly treated as a coherent sum of two-body interactions. Therefore below most explicit expressions are given for two–body kinematics.

47.1.1. *Properties of the S-matrix* :

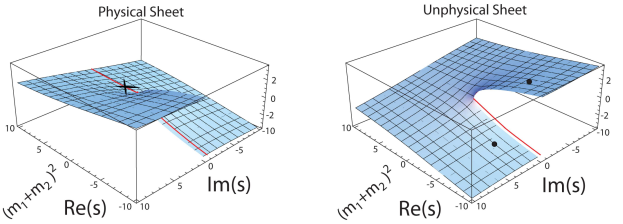

Figure 47.1: Sketch of the imaginary part of a typical single–channel amplitude in the complex s-plane. The solid dots indicate allowed positions for resonance poles, the cross for a bound state. The solid line is the physical axis (shifted by $i\epsilon$ into the physical sheet). The two sheets are connected smoothly along their discontinuities.

The unitary operator that connects asymptotic *in* and *out* states is called the S–matrix. It is an analytic function in the Mandelstam plane up to its branch points and poles. Branch points appear whenever there is a channel opening — at each threshold the number of Riemann sheets doubles. Poles refer either to bound states or to resonances. The former poles are located on the physical sheet, the latter are located on the unphysical sheet closest to the physical one, often called the second sheet; each can be accompanied by mirror poles. If there are resonances in subsystems of multi–particle states, branch points appear in the complex plane of the unphysical sheet(s). Any of these singularities leads to some structure in the observables (see also Ref. [4]). In a partial wave decomposed amplitude additional singularities not related to resonance physics may emerge as a result of the partial-wave projection. For a discussion see, e.g., Ref. [5].

If for simplicity we now restrict ourselves to reactions involving four particles, the kinematics of the reaction are fully described by the Mandelstam variables s, t and u, only two of them being independent (cf. Eqs. (28)-(31) of the kinematics review). Bound state poles are allowed only on the real s–axis below the lowest threshold. There is no restriction for the location of poles on the unphysical sheets — only that analyticity requires that, if there is a pole at some complex value of s, there must also be a pole at s^*. The pole with a negative imaginary part is closer to the physical axis and thus influences the observables in the vicinity of the resonance region more strongly, however, at the threshold both poles are always equally important. This is illustrated in Fig. 47.1.

The S-matrix is related to the scattering matrix $\mathscr{M}$ (c.f. Eq. (8) of the kinematics review). For two–body scattering it can be cast into the form

$$S_{ab} = I_{ab} - 2i\sqrt{\rho_a}\mathscr{M}_{ab}\sqrt{\rho_b}\,. \tag{47.1}$$

$\mathscr{M}$ is a matrix in channel space and depends, for two–body scattering, on both s and t. The channel indices a and b are multi–indices specifying all properties of the channel including the conserved quantum numbers. The two-body phase-space ρ is given (cf. Eq. 12 of the kinematics review) by

$$\rho_a(s) = \frac{1}{16\pi}\frac{2|\vec{q}_a|}{\sqrt{s}}\,. \tag{47.2}$$

with q_a denoting the relative momentum of the decay particles of channel a, with masses m_1 and m_2, cf. Eq. (20a) of the kinematics review.

As discussed below, unitarity puts strong constraints on the scattering matrix. Further constraints may be imposed, e.g., from crossing symmetry and duality [6].

47.1.2. *Consequences from unitarity* :

In what follows, scattering amplitudes $\mathscr{M}$ and decay amplitudes $\mathcal{A}$ will be distinguished, since unitarity puts different constraints on these. The discontinuity of the scattering amplitude from channel a to channel b [7] is constrained by unitarity to

$$i\,[\mathscr{M}_{ba} - \mathscr{M}^*_{ab}] = (2\pi)^4 \sum_c \int d\Phi_c \mathscr{M}^*_{cb}\mathscr{M}_{ca}\,. \tag{47.3}$$

Using $\mathrm{Disc}(\mathscr{M}(s)) = 2i\,\mathrm{Im}(\mathscr{M}(s+i\epsilon))$ the optical theorem follows

$$\mathrm{Im}\,(\mathscr{M}_{aa}|_{\mathrm{forward}}) = 2q_a\sqrt{s}\,\sigma_{\mathrm{tot}}(a \to \mathrm{anything})\,. \tag{47.4}$$

The unitarity relation for a decay amplitude of a heavy state H into a channel a is given by

$$i\left[\mathcal{A}^H_a - \mathcal{A}^{H\,*}_a\right] = (2\pi)^4 \sum_c \int d\Phi_c \mathscr{M}^*_{ca}\mathcal{A}^H_c\,. \tag{47.5}$$

From Eq. (47.5) the Watson theorem follows straightforwardly: the phase of $\mathcal{A}$ agrees with that of $\mathscr{M}$ as long as only a single channel contributes. For systems where the phase shifts are known like $\pi\pi$ in S– and P–waves for low energies, $\mathcal{A}^H$ can be calculated in a model-independent way using dispersion theory [8]. Those methods can also be generalized to three–body final states [9] and were applied to $\eta \to \pi\pi\pi$ in Refs. [10,11,12] and to ϕ and ω to 3π in Ref. [13].

47.1.3. *Partial-wave decomposition* :

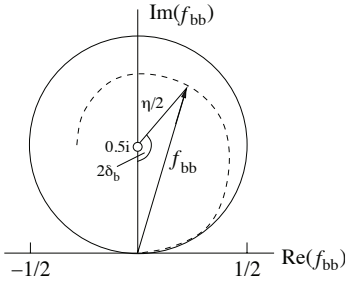

Figure 47.2: Argand plot showing a diagonal element of a partial-wave amplitude, a_{bb}, as a function of energy. The amplitude leaves the unitary circle (solid line) as soon as inelasticity sets in, $\eta < 1$ (dashed line).

In general, a physical amplitude $\mathscr{M}$ (c.f. Eq. (8) of the kinematics review) is a matrix in channel space. It depends, for two–body scattering, on both s and t. It is often convenient to expand the amplitudes in partial waves. For this purpose one defines for the transition matrix from channel a to channel b

$$\mathscr{M}_{ba}(s,t) = \sum_{L=0}^{\infty}(2L+1)\mathscr{M}^L_{ba}(s)P_L(\cos(\theta))\,, \tag{47.6}$$

where L denotes the angular momentum—in the presence of spins the initial and final value of L does not need to be equal. To simplify notations below we will drop the label L. The function $\mathscr{M}_{ba}(s)$ is expressed in terms of the partial-wave amplitudes $f_{ba}(s)$ via

$$\mathscr{M}_{ba}(s) = -f_{ba}(s)/\sqrt{\rho_a\rho_b}\,. \tag{47.7}$$

The partial-wave amplitudes f_{ba} depend on s only. Using $S_{ba} = \delta_{ba} + 2if_{ba}$ one gets from the unitarity of the S-matrix

$$f_{bb} = (\eta\exp(2i\delta_b) - 1)/2i\,, \tag{47.8}$$

where δ_b (η) denotes the phase shift (elasticity parameter — also called inelasticity) for the scattering from channel b to channel b. One has $0 \leq \eta \leq 1$, where $\eta = 1$ refers to purely elastic scattering. The evolution with energy of a partial-wave amplitude a_{bb} can be displayed as a trajectory in an Argand plot, as shown in Fig. 47.2. In case of a two–channel problem the off–diagonal element is typically parametrized as $f_{ba} = \sqrt{1-\eta^2}/2\, \exp(i(\delta_b + \delta_a))$.

47.1.4. ***Explicit parametrizations for scattering and production amplitudes*** :

It is often convenient to decompose the physical amplitude $\mathscr{M}$ into a pole part and a non–pole part, often called background

$$\mathscr{M} = \mathscr{M}^{\rm b.g.} + \mathscr{M}^{\rm pole} \ . \tag{47.9}$$

The splitting given in Eq. (47.9) is not unique and reaction dependent, such that some resonances show up differently in different reactions. What are independent of the reaction, however, are the location of the pole of a given resonance R in the complex s-plane, $s_{\rm R}$, and its residues, or, more accurately, the pole couplings introduced in the last section of this review. Those parameters capture all the properties of a given resonance. The decomposition of Eq. (47.9) is employed, e.g., in Ref. [14] to study the lineshape of $\psi(3770)$ and in Refs. [15,16] to investigate πN scattering. Traditionally one introduces the notation

$$\sqrt{s_{\rm R}} = M_{\rm R} - i\Gamma_{\rm R}/2 \ , \tag{47.10}$$

where $M_{\rm R}$ and $\Gamma_{\rm R}$ are referred to as mass and total width of the resonance R, respectively. Note, the standard Breit-Wigner parameters $M_{\rm BW}$ and $\Gamma_{\rm BW}$, also introduced below, agree to $M_{\rm R}$ and $\Gamma_{\rm R}$ only for narrow, well-separated resonances far away from the opening of decay channels.

If there are N resonances in a particular channel,

$$\mathscr{M}^{\rm pole}_{ba}(s) = \gamma_b(s)[1 - V^{\rm R}(s)\Sigma(s)]^{-1}_{bc} V^{\rm R}_{ca}(s)\gamma_a(s) \ . \tag{47.11}$$

where all ingredients are matrices in channel space. Especially

$$V^{\rm R}_{ab}(s) = -\sum_{n=1}^{N} \frac{g_{n\,b}\ g_{n\,a}}{s - M_n^2} \ , \tag{47.12}$$

γ_a and Σ_a denote the normalized vertex function and the self-energy, respectively, while $g_{n\,a}$ denotes the coupling of the resonance $\rm R_n$ to channel a and M_n its mass parameter (not to be confused with the pole position). The sign in Eq. (47.12) is necessary to render the g–parameters real. A relation analogous to Eq. (47.5) holds for any kind of production amplitude — especially also for the normalized vertex functions, however, with the final state interaction provided by $\mathscr{M}^{\rm b.g.}$

$$i\,[\gamma_a - \gamma_a^*] = (2\pi)^4 \sum_c d\Phi_c \left(\mathscr{M}^{\rm b.g.}\right)^*_{ca} \gamma_c \ . \tag{47.13}$$

The discontinuity of the self-energy $\Sigma_a(s)$ is

$$i\,[\Sigma_a - \Sigma_a^*] = (2\pi)^4 \int d\Phi_a |\gamma_a|^2 \ . \tag{47.14}$$

The real part of Σ_a can be calculated from Eq. (47.14) via a properly subtracted dispersion integral. If $\mathscr{M}^{\rm b.g.}$ is unitary, the use of Eq. (47.11) leads to a unitary full amplitude, cf. Eq. (47.9).

For a single resonance ($N = 1$) Eq. (47.11) reads

$$\mathscr{M}_{\rm pole}(s)_{ba}\big|_{N=1} = -\gamma_b(s) \frac{g_b\ g_a}{s - \hat{M}_{\rm R}(s)^2 + i\sqrt{s}\Gamma^{\rm R}(s)_{\rm tot}} \gamma_a(s) \ , \tag{47.15}$$

where the mass function $\hat{M}_{\rm R}(s)^2 = M^2 + \sum_c g_c^2 {\rm Re}(\Sigma_c)$. The imaginary part of the self-energy gives the width of the resonance via

$$\Gamma^{\rm R}_c(s) = \frac{(2\pi)^4}{2\sqrt{s}} g_c^2 \int d\Phi_c |\gamma_c|^2; \ \Gamma^{\rm R}(s)_{\rm tot} = \sum_c \Gamma^{\rm R}_c(s) \ . \tag{47.16}$$

Here the sum runs over all channels. Eq. (47.16) agrees with Eq. (10) of the kinematics review.

In the absence of left–hand cuts in the production mechanism, the decay amplitude $\mathcal{A}^H$ can be written as

$$\mathcal{A}^H_a(s) = \gamma_a(s) \left[1 - V^{\rm R}(s)\Sigma(s)\right]^{-1}_{ab} \mathcal{P}^H_b(s) \ , \tag{47.17}$$

where $\mathcal{P}^H$ is a vector in channel space that may be parametrized as

$$\mathcal{P}^H_b(s) = p_b(s) - \sum_{n=1}^{N} \frac{g_{n\,b}\ \alpha^H_n}{s - M_n^2} \tag{47.18}$$

and the masses M_n need to agree with those in $V_{\rm R}$. The function $p_a(s)$ is a background term and the α^H_n denote the coupling of the heavy state H to the particular resonance $\rm R_n$. If there are additional particles in the final state of the studied decay of heavy state H, not included in the non-perturbative treatment of Eq. (47.17), then they also contain the corresponding kinematic factors related to their coupling. If these additional particles are interacting strongly, a complete few–body treatment of the final state becomes necessary, especially since rescattering effects can introduce additional complex phases [17]. However, in practice those effects as well as those from missing channels are often parametrized by choosing the parameters α^H_n complex valued. With some additional assumptions, Eq. (47.9) and Eq. (47.17) were employed in Ref. [18] to study the pion vector form factor. An alternative parametrization for the production amplitude that is convenient, if the full matrix $\mathscr{M}$ — including the resonances — is known, cf. Ref. [19]

$$\mathcal{A}^H_a(s) = \mathscr{M}_{ab}(s) \tilde{\mathcal{P}}^H_b(s) \ . \tag{47.19}$$

The function $\tilde{\mathcal{P}}_H(s)_b$ needs to cancel the left–hand cuts of $\mathscr{M}$ and therefore could be strongly energy dependent. In actual applications a low-order polynomial turned out to be sufficient — c.f. Ref. [20,21] for a study of $\gamma\gamma \to \pi\pi$. As above, to preserve unitarity the coefficients of $\tilde{\mathcal{P}}_H(s)_b$ need to real, however, in practice rescattering effects or missing channels are parametrized by complex valued parameters.

Three-body decays are often represented by Dalitz plots. It is often of interest to quantify the contribution of a single amplitude $\mathcal{A}^H_a$ to the decay of a heavy resonance H, where now $\mathcal{A}^H_a$ needs to be generalized to three body kinematics either completely by considering the full three–body final state interactions or effectively by choosing complex vertex parameters. Then fractional contributions are introduced (since different intermediate states leading to the same final state interfere, the assignment of branching ratios is to be taken with some caution) via

$${\rm F}^H_a = \frac{\int d\Phi |\mathcal{A}^H_a|^2}{\int d\Phi |\sum_a \mathcal{A}^H_a|^2} \tag{47.20}$$

where the space space integral $d\Phi$ extends over the Dalitz plot region and the angular dependence of the subsystems needs to be kept (cf. Eq. (47.6)). Typically the effect of interference terms in the denominator is small.

The formulas given so far are completely general. However, they require as input, e.g., information on the non–resonant scattering in the various channels. It is therefore often necessary and appropriate to find approximations/parametrizations.

47.2. Common parametrizations for resonances

In most common parametrizations the non–pole interaction, $\mathscr{M}^{\rm b.g.}$, is omitted. While this is a bad approximation for, e.g., scalar–isoscalar $\pi\pi$ interactions at very low energies [22], under more favorable conditions this can be justified. Thus in what follows we will assume $\mathscr{M}^{\rm b.g.} = 0$, which leads to real vertex functions. For two–body channels one writes

$$\gamma(s)_a = q_a^{L_a} F_{L_a}(q_a, q_{\rm o}) \ ,$$

where L_a denotes the angular momentum of the decay products, giving rise to the centrifugal barrier $q_a^{L_a}$, where q_a denotes the relative momentum of the outgoing particle pair defined in the rest frame of the decaying particle, cf. Eq. (20a) of the kinematics

review. Often one introduces a phenomenological form factor, here denoted by $F_{L_a}(q_a, q_o)$. It depends on the channel momentum as well as some intrinsic scale q_o. Often the Blatt-Weisskopf form is chosen [23,24], where, e.g., $F_0^2 = 1$, $F_1^2 = 2/(q_a + q_o)$ and $F_2^2 = 13/((q_a - 3q_o)^2 + 9q_a q_o)$. In addition, for isolated, narrow resonances the couplings g_a can be related to the partial widths, $\Gamma_{R\to a}$, via

$$g_a = \frac{1}{\gamma_a(s_R)} \sqrt{\frac{M_R \Gamma_{R\to a}}{\rho_a}} , \qquad (47.21)$$

where M_R was defined in Eq. (47.10).

47.2.1. ***The Breit–Wigner and Flatté Parametrizations*** :

If there is only a single resonance present and all relevant thresholds are far away, then one may replace $\Gamma_R(s)_{tot}$ with a constant, Γ_{BW}. Under these conditions also the real part of Σ is a constant that can be absorbed into the mass parameter and Eq. (47.15) simplifies to

$$\mathscr{M}_{ba}^{pole}\Big|_{N=1} = -\frac{g_b\, g_a}{s - M_{BW}^2 + i\sqrt{s}\Gamma_{BW}} , \qquad (47.22)$$

which is the standard Breit–Wigner parametrization. For a narrow resonance it is common to replace $\sqrt{s}$ by M_{BW}. If there are nearby relevant thresholds, Γ_{BW} needs to be replaced by $\Gamma(s)$. For two–body decays one writes

$$\Gamma(s) = \sum_c \Gamma_{R\to c} \left(\frac{q_c}{q_{R\,c}}\right)^{2L_c+1} \left(\frac{F_{L_c}(q_c, q_o)}{F_{L_c}(q_{R\,c}, q_o)}\right)^2 , \qquad (47.23)$$

where $q_{R\,c} = q(M_{BW})_c$ denotes the decay momentum of resonance R into channel c. The Breit-Wigner parameters M_{BW} and Γ_{BW} agree with the pole parameters only if $M_R\Gamma(M_R) \ll M_{thr.}^2 - M_R^2$, with $M_{thr.}$ for the closest relevant threshold. Otherwise the Breit-Wigner parameters deviate from the pole parameters and are reaction dependent.

If there is more than one resonance in one partial wave that significantly couples to the same channels, it is in general incorrect to use a sum of Breit-Wigner functions, for it may violate unitarity constraints. Then more refined methods should be used, like the K–matrix approximation described in the next section.

Below the corresponding threshold, q_c in Eq. (47.23) must be continued analytically: if, e.g., the particles in channel c have equal mass m_c, then

$$q_c = \frac{i}{2}\sqrt{4m_c^2 - s} \quad \text{for} \quad \sqrt{s} < 2m_c . \qquad (47.24)$$

The resulting line shape above and below the threshold of channel c is called Flatté parametrization [25]. If the coupling of a resonance to the channel opening nearby is very strong, the Flatté parametrization shows a scaling invariance and does not allow for an extraction of individual partial decay widths, but only of ratios [26].

47.2.2. ***The K–matrix approximation*** :

As soon as there is more than one resonance in one channel, the use of the K–matrix approximation should be preferred compared to the Breit–Wigner parametrization discussed above. From the considerations formulated in Eq. (47.11), the K–matrix approximation follows straightforwardly by replacing the self-energy Σ_c by its imaginary part in the absence of $\mathscr{M}^{b.g.}$, but keeping the full matrix structure of V^R. Thus, for two–body intermediate states one writes within this scheme for the self-energy

$$\Sigma(s)_c \to i\rho_c\, \gamma(s)_c^2 . \qquad (47.25)$$

However, in distinction to the Breit-Wigner approach, V^R, then called K–matrix, is kept in the form of Eq. (47.12). The decay amplitude given in Eq. (47.17) then takes the form of the standard P–vector formalism introduced in Ref. [27]. For $N = 1$ the amplitude derived from the K–matrix is identical to that of Eq. (47.22).

Some authors use the analytic continuation of ρ_c below the threshold via the analytic continuation of the particle momentum as described above [28,29].

47.2.3. ***Further improvements*** :

The K–matrix described above usually allows one to get a proper fit of physical amplitudes and it is easy to deal with, however, it also has an important deficit: it violates constraints from analyticity — e.g., ρ_a, defined in Eq. (47.2), is ill-defined at $s = 0$ and for unequal masses develops an unphysical cut. In addition, the analytic continuation of the amplitudes into the complex plane is not controlled and typically the parameters of broad resonances come out wrong (see, e.g., minireview on scalar mesons). A method to improve the analytic properties was suggested in Refs. [30,31,32,33]. It basically amounts to replacing the phase-space factor $i\rho_a$ in Eq. (47.25) by an analytic function that produces the identical imaginary part on the right-hand cut. In the simplest case of a channel with equal masses the expressions that can be used for real values of s read

$$-\frac{\hat\rho_a}{\pi}\log\left|\frac{1+\hat\rho_a}{1-\hat\rho_a}\right| , \; -\frac{2\hat\rho_a}{\pi}\arctan\left(\frac{1}{\hat\rho_a}\right) , \; -\frac{\hat\rho_a}{\pi}\log\left|\frac{1+\hat\rho_a}{1-\hat\rho_a}\right| + i\hat\rho_a$$

for $s < 0$, $0 < s < 4m_a^2$, and $4m_a^2 < s$, respectively, with $\hat\rho_a = \sqrt{|1 - 4m_a^2/s|}$ for all values of s, extending the expression of Eq. (47.2) into the regime below threshold. The more complicated expression for the case of different masses can be found, e.g., in Ref. [31].

If there is only a single resonance in a given channel, it is possible to feed the imaginary part of the Breit-Wigner function, Eq. (47.22) with an energy-dependent width, directly into a dispersion integral to get a resonance propagator with the correct analytic structure [34,35].

47.3. Properties of resonances

A resonance is characterized not only by is complex pole position but also by its residues that quantify its couplings to the various channels and allow one to define a branching ratio also for broader resonances. In the Meson Particle Listings the two-photon width of $f_0(500)$ is defined in terms of the corresponding residue. The Baryon Particle Listings give the elastic pole residues and normalized transition residues. However, different conventions are used in the two sectors, which are shortly outlined here.

In the close vicinity of a pole the scattering matrix $\mathscr{M}$ can be written as

$$\lim_{s\to s_R} \mathscr{M}_{ba} = -\frac{\mathscr{R}_{ba}}{s - s_R} , \qquad (47.26)$$

where s_R denotes the pole position of the resonance R. The sign convention in Eq. (47.26) is consistent with that of Eq. (47.12). The residues may be calculated via an integration along a closed contour around the pole using

$$\mathscr{R}_{ba} = \frac{i}{2\pi}\oint ds \mathscr{M}_{ba} .$$

The factorization of the residue $(\mathscr{R}_{ba})^2 = \mathscr{R}_{aa} \times \mathscr{R}_{bb}$ allows one to introduce pole couplings according to

$$\tilde g_a = \mathscr{R}_{ba}/\sqrt{\mathscr{R}_{bb}} . \qquad (47.27)$$

The pole couplings are the only reaction independent quantities that allow one quantify the transition strength of a given resonance to some channel a. For a single, narrow state with an energy-independent background in the resonance region, far away from all relevant thresholds one finds $\tilde g_a = \gamma_a(s_R) g_a$ with the real valued resonance couplings g_a defined in Eq. (47.12) accompanied by the complex valued vertex functions γ_a introduced in Eq. (47.11). Based on this observation one may use the straightforward generalization of Eq. (47.21) to define a partial width and a branching fraction even for a broad resonance via

$$\Gamma_{R\to a} = \frac{|\tilde g_a|^2}{M_R}\rho_a(M_R^2) \quad \text{and} \quad Br_a = \Gamma_{R\to a}/\Gamma_R , \qquad (47.28)$$

where M_R and Γ_R where introduced in Eq. (47.10). This expression was used to define a two–photon width for the broad $f_0(500)$ (also called σ) [20,21]. Eq. (47.28) defines a partial decay width

independent of the reaction used to extract the parameters. It maps smoothly onto the standard definitions for narrow resonances — cf. Eq. (47.16). There are cases where a resonance couples to a channel that opens only above $M_{\rm R}$. A prominent example for this being $f_0(980)$ to $\bar{K}K$. If one wants to define a branching fraction that also captures this situation one may define

$$Br'_a = \int\limits_{\rm threshold}^{\infty} \frac{ds}{\pi} \frac{|\tilde{g}_a|^2 \rho(s)}{|D(s)|^2} \ . \tag{47.29}$$

Here one needs to assume a line shape for the resonance R. A possible choice is a Flatté form $|D(s)|^2 = (M_{\rm R}^2 - s)^2 + (\sum_a |\tilde{g}_a|^2 \rho_a(s))^2$. The only model-independent quantities are the pole couplings/residues — both forms, Eq. (47.28) and Eq. (47.29), are in general not directly related to observables but meant to quantify the effect of the pole couplings by employing better known quantities.

In the baryon sector it is common to define the residue with respect to the partial-wave amplitudes $f_{ba}(s)$ defined in Eq. (47.7) and with respect to $\sqrt{s}$ instead of s. The two definitions are related via

$$Res(a \to b) = -\sqrt{\frac{\rho_a(s_{\rm R})\rho_b(s_{\rm R})}{4 s_{\rm R}}}\, \mathscr{R}_{ba} \ , \tag{47.30}$$

where the phase space factors are to be evaluated at the pole. The elastic pole residues for $a \to a$ scattering, in the baryon listings called r, are

$$r = -Res(a \to a) \ . \tag{47.31}$$

One may now define the partial decay widths and the branching ratios of a resonance R into channel a at its pole position on the basis of the residues introduced in Eq. (47.30)

$$\Gamma_{{\rm R}\to a} = 2\,|Res(a \to b)| \quad \text{and} \quad BR_a = 2|\,Res(a \to a)|/\Gamma_{\rm R}. \tag{47.32}$$

The only difference between the definitions of the branching ratio of Eq. (47.28) and Eq. (47.32) is that for the former the phase space factors are evaluated on the real axis while for the latter they are evaluated at the pole. The Baryon Particle Listings give information on the πN elastic residues, r, on various normalized $\pi N \to a$ transition residues, and on branching ratios.

References:

1. M. Jacob and G. C. Wick, Annals Phys. **7**, 404 (1959) [Annals Phys. **281**, 774 (2000)].
2. C. Zemach, Phys. Rev. **140B**, 97, 109 (1965).
3. A. V. Anisovich *et al.*, J. Phys. G **28**, 15 (2002), Eur. Phys. J. A **24**, 111 (2005).
4. A rapid change in an amplitude is not an unambiguous signal of a singularity of the S–matrix [36], however, for realistic interactions this connection holds.
5. G. Höhler, *Pion-Nucleon Scattering – Methods and Results of Phenomenological Analyses*, Springer-Verlag Berlin, Heidelberg, New York, 1983.
6. M. Fukugita and K. Igi, Phys. Rept. **31** (1977) 237.
7. M. P. Peskin and D. V. Schroeder, *An Introduction to Quantum Field Theory*, Westview Press, 1995.
8. R. Omnes, Nuovo Cim. **8**, 316 (1958).
9. N. N. Khuri and S. B. Treiman, Phys. Rev. **119**, 1115 (1960).
10. J. Kambor, C. Wiesendanger, and D. Wyler, Nucl. Phys. B **465**, 215 (1996).
11. A. V. Anisovich and H. Leutwyler, Phys. Lett. B **375**, 335 (1996).
12. S. P. Schneider, B. Kubis, and C. Ditsche, JHEP **1102**, 028 (2011).
13. F. Niecknig, B. Kubis, and S. P. Schneider, Eur. Phys. J. C **72**, 2014 (2012).
14. N. N. Achasov and G. N. Shestakov, Phys. Rev. D **86**, 114013 (2012).
15. A. Matsuyama, T. Sato, and T. -S. H. Lee, Phys. Rept. **439**, 193 (2007).
16. M. Döring et al., Phys. Lett. B **681**, 26 (2009).
17. I. Caprini, Phys. Lett. B **638**, 468 (2006).
18. C. Hanhart, Phys. Lett. B **715**, 170 (2012).
19. K. L. Au, D. Morgan, and M. R. Pennington, Phys. Rev. D **35**, 1633 (1987).
20. D. Morgan and M. R. Pennington, Z. Phys. C **37** (1988) 431 [Erratum-*ibid.,* C **39** (1988) 590].
21. D. Morgan and M. R. Pennington, Z. Phys. **C48**, 623 (1990).
22. J. Gasser and U. G. Meißner, Nucl. Phys. B **357**, 90 (1991).
23. J. Blatt and V. Weisskopf, *Theoretical Nuclear Physics*, New York: John Wiley & Sons (1952).
24. S. U. Chung *et al.*, Annalen Phys. **4**, 404 (1995).
25. S.M. Flatté, Phys. Lett. B **63**, 224 (1976).
26. V. Baru *et al.*, Eur. Phys. J. A **23**, 523 (2005).
27. I.J.R. Aitchison, Nucl. Phys. **A189**, 417 (1972).
28. J. H. Reid and N. N. Trofimenkoff, J. Math. Phys. **25**, 3540 (1984).
29. V.V. Anisovich and A.V. Sarantsev, Eur. Phys. J. A **16**, 229 (2003).
30. M. R. Pennington *et al.*, Eur. Phys. J. **C56**, 1 (2008).
31. J. A. Oller and E. Oset, Phys. Rev. D **60**, 074023 (1999).
32. N. N. Achasov and A. V. Kiselev, Phys. Rev. D **83**, 054008 (2011).
33. A. V. Anisovich *et al.*, Phys. Rev. D **84**, 076001 (2011).
34. E. L. Lomon and S. Pacetti, Phys. Rev. D **85**, 113004 (2012) [Erratum-*ibid.,* D **86**, 039901 (2012)].
35. B. Moussallam, `arXiv:1305.3143 [hep-ph]`.
36. G. Calucci, L. Fonda, and G. C. Ghirardi, Phys. Rev. **166**, 1719 (1968).

48. CROSS-SECTION FORMULAE FOR SPECIFIC PROCESSES

Revised October 2009 by H. Baer (University of Oklahoma) and R.N. Cahn (LBNL).

PART I: STANDARD MODEL PROCESSES

Setting aside leptoproduction (for which, see Sec. 16 of this *Review*), the cross sections of primary interest are those with light incident particles, e^+e^-, $\gamma\gamma$, $q\overline{q}$, gq , gg, *etc.*, where g and q represent gluons and light quarks. The produced particles include both light particles and heavy ones - t, W, Z, and the Higgs boson H. We provide the production cross sections calculated within the Standard Model for several such processes.

48.1. Resonance Formation

Resonant cross sections are generally described by the Breit-Wigner formula (Sec. 19 of this *Review*).

$$\sigma(E) = \frac{2J+1}{(2S_1+1)(2S_2+1)}\frac{4\pi}{k^2}\left[\frac{\Gamma^2/4}{(E-E_0)^2+\Gamma^2/4}\right]B_{in}B_{out}, \quad (48.1)$$

where E is the c.m. energy, J is the spin of the resonance, and the number of polarization states of the two incident particles are $2S_1+1$ and $2S_2+1$. The c.m. momentum in the initial state is k, E_0 is the c.m. energy at the resonance, and Γ is the full width at half maximum height of the resonance. The branching fraction for the resonance into the initial-state channel is B_{in} and into the final-state channel is B_{out}. For a narrow resonance, the factor in square brackets may be replaced by $\pi\Gamma\delta(E-E_0)/2$.

48.2. Production of light particles

The production of point-like, spin-1/2 fermions in e^+e^- annihilation through a virtual photon, $e^+e^- \to \gamma^* \to f\overline{f}$, at c.m. energy squared s is given by

$$\frac{d\sigma}{d\Omega} = N_c\frac{\alpha^2}{4s}\beta\left[1+\cos^2\theta+(1-\beta^2)\sin^2\theta\right]Q_f^2 \ , \quad (48.2)$$

where β is v/c for the produced fermions in the c.m., θ is the c.m. scattering angle, and Q_f is the charge of the fermion. The factor N_c is 1 for charged leptons and 3 for quarks. In the ultrarelativistic limit, $\beta \to 1$,

$$\sigma = N_cQ_f^2\frac{4\pi\alpha^2}{3s} = N_cQ_f^2\frac{86.8\text{ nb}}{s\,(\text{GeV}^2)} \ . \quad (48.3)$$

The cross section for the annihilation of a $q\overline{q}$ pair into a distinct pair $q'\overline{q}'$ through a gluon is completely analogous up to color factors, with the replacement $\alpha \to \alpha_s$. Treating all quarks as massless, averaging over the colors of the initial quarks and defining $t = -s\sin^2(\theta/2)$, $u = -s\cos^2(\theta/2)$, one finds [1]

$$\frac{d\sigma}{d\Omega}(q\overline{q} \to q'\overline{q}') = \frac{\alpha_s^2}{9s}\frac{t^2+u^2}{s^2} \ . \quad (48.4)$$

Crossing symmetry gives

$$\frac{d\sigma}{d\Omega}(qq' \to qq') = \frac{\alpha_s^2}{9s}\frac{s^2+u^2}{t^2} \ . \quad (48.5)$$

If the quarks q and q' are identical, we have

$$\frac{d\sigma}{d\Omega}(q\overline{q} \to q\overline{q}) = \frac{\alpha_s^2}{9s}\left[\frac{t^2+u^2}{s^2}+\frac{s^2+u^2}{t^2}-\frac{2u^2}{3st}\right] \ , \quad (48.6)$$

and by crossing

$$\frac{d\sigma}{d\Omega}(qq \to qq) = \frac{\alpha_s^2}{9s}\left[\frac{t^2+s^2}{u^2}+\frac{s^2+u^2}{t^2}-\frac{2s^2}{3ut}\right] . \quad (48.7)$$

Annihilation of e^+e^- into $\gamma\gamma$ has the cross section

$$\frac{d\sigma}{d\Omega}(e^+e^- \to \gamma\gamma) = \frac{\alpha^2}{2s}\frac{u^2+t^2}{tu} \ . \quad (48.8)$$

The related QCD process also has a triple-gluon coupling. The cross section is

$$\frac{d\sigma}{d\Omega}(q\overline{q} \to gg) = \frac{8\alpha_s^2}{27s}(t^2+u^2)\left(\frac{1}{tu}-\frac{9}{4s^2}\right) \ . \quad (48.9)$$

The crossed reactions are

$$\frac{d\sigma}{d\Omega}(qg \to qg) = \frac{\alpha_s^2}{9s}(s^2+u^2)(-\frac{1}{su}+\frac{9}{4t^2}) \quad (48.10)$$

and

$$\frac{d\sigma}{d\Omega}(gg \to q\overline{q}) = \frac{\alpha_s^2}{24s}(t^2+u^2)(\frac{1}{tu}-\frac{9}{4s^2}) \ . \quad (48.11)$$

Finally,

$$\frac{d\sigma}{d\Omega}(gg \to gg) = \frac{9\alpha_s^2}{8s}(3-\frac{ut}{s^2}-\frac{su}{t^2}-\frac{st}{u^2}) \ . \quad (48.12)$$

Lepton-quark scattering is analogous (neglecting Z exchange)

$$\frac{d\sigma}{d\Omega}(eq \to eq) = \frac{\alpha^2}{2s}e_q^2\frac{s^2+u^2}{t^2} \ . \quad (48.13)$$

where e_q is the charge of the quark. For neutrino scattering with the four-Fermi interaction

$$\frac{d\sigma}{d\Omega}(\nu d \to \ell^- u) = \frac{G_F^2 s}{4\pi^2} \ , \quad (48.14)$$

where the Cabibbo angle suppression is ignored. Similarly

$$\frac{d\sigma}{d\Omega}(\nu\overline{u} \to \ell^-\overline{d}) = \frac{G_F^2 s}{4\pi^2}\frac{(1+\cos\theta)^2}{4} \ . \quad (48.15)$$

To obtain the formulae for deep inelastic scattering (presented in more detail in Section 16) we consider quarks of type i carrying a fraction $x = Q^2/(2M\nu)$ of the nucleon's energy, where $\nu = E-E'$ is the energy lost by the lepton in the nucleon rest frame. With $y = \nu/E$ we have the correspondences

$$1+\cos\theta \to 2(1-y) \ ,$$
$$d\Omega_{cm} \to 4\pi f_i(x)dx\,dy \ , \quad (48.16)$$

where the latter incorporates the quark distribution, $f_i(x)$. In this way we find

$$\frac{d\sigma}{dx\,dy}(eN \to eX) = \frac{4\pi\alpha^2 xs}{Q^4}\frac{1}{2}\left[1+(1-y)^2\right] \quad (48.17)$$
$$\times\ \left[\frac{4}{9}(u(x)+\overline{u}(x)+\ldots)+\frac{1}{9}(d(x)+\overline{d}(x)+\ldots)\right]$$

where now $s = 2ME$ is the cm energy squared for the electron-nucleon collision and we have suppressed contributions from higher mass quarks.

Similarly,

$$\frac{d\sigma}{dx\,dy}(\nu N \to \ell^- X) = \frac{G_F^2 xs}{\pi}[(d(x)+\ldots)+(1-y)^2(\overline{u}(x)+\ldots)] \quad (48.18)$$

and

$$\frac{d\sigma}{dx\,dy}(\overline{\nu}N \to \ell^+ X) = \frac{G_F^2 xs}{\pi}[(\overline{d}(x)+\ldots)+(1-y)^2(u(x)+\ldots)] \ . \quad (48.19)$$

Quasi-elastic neutrino scattering ($\nu_\mu n \to \mu^- p$, $\overline{\nu}_\mu p \to \mu^+ n$) is directly related to the crossed reaction, neutron decay. The formula for the differential cross section is presented, for example, in N.J. Baker *et al.*, Phys. Rev. **D23**, 2499 (1981).

48.3. Hadroproduction of heavy quarks

For hadroproduction of heavy quarks $Q = c,\ b,\ t$, it is important to include mass effects in the formulae. For $q\bar{q} \to Q\bar{Q}$, one has

$$\frac{d\sigma}{d\Omega}(q\bar{q} \to Q\bar{Q}) = \frac{\alpha_s^2}{9s^3}\sqrt{1-\frac{4m_Q^2}{s}}\left[(m_Q^2-t)^2+(m_Q^2-u)^2+2m_Q^2 s\right], \tag{48.20}$$

while for $gg \to Q\bar{Q}$ one has

$$\begin{aligned}\frac{d\sigma}{d\Omega}(gg \to Q\bar{Q}) = \frac{\alpha_s^2}{32s}\sqrt{1-\frac{4m_Q^2}{s}}\Bigg[&\frac{6}{s^2}(m_Q^2-t)(m_Q^2-u)\\ &-\frac{m_Q^2(s-4m_Q^2)}{3(m_Q^2-t)(m_Q^2-u)}\\ &+\frac{4}{3}\frac{(m_Q^2-t)(m_Q^2-u)-2m_Q^2(m_Q^2+t)}{(m_Q^2-t)^2}\\ &+\frac{4}{3}\frac{(m_Q^2-t)(m_Q^2-u)-2m_Q^2(m_Q^2+u)}{(m_Q^2-u)^2}\\ &-3\,\frac{(m_Q^2-t)(m_Q^2-u)+m_Q^2(u-t)}{s(m_Q^2-t)}\\ &-3\,\frac{(m_Q^2-t)(m_Q^2-u)+m_Q^2(t-u)}{s(m_Q^2-u)}\Bigg].\end{aligned} \tag{48.21}$$

48.4. Production of Weak Gauge Bosons

48.4.1. *W and Z resonant production* :

Resonant production of a single W or Z is governed by the partial widths

$$\Gamma(W \to \ell_i\overline{\nu}_i) = \frac{\sqrt{2}G_F m_W^3}{12\pi} \tag{48.22}$$

$$\Gamma(W \to q_i\overline{q}_j) = 3\frac{\sqrt{2}G_F|V_{ij}|^2 m_W^3}{12\pi} \tag{48.23}$$

$$\begin{aligned}\Gamma(Z \to f\overline{f}) = N_c&\frac{\sqrt{2}G_F m_Z^3}{6\pi}\\ &\times\left[(T_3 - Q_f\sin^2\theta_W)^2+(Q_f\sin\theta_W)^2\right].\end{aligned} \tag{48.24}$$

The weak mixing angle is θ_W. The CKM matrix elements are indicated by V_{ij} and N_c is 3 for $q\overline{q}$ final states and 1 for leptonic final states.

The full differential cross section for $f_i\overline{f}_j \to (W,Z) \to f_{i'}\overline{f}_{j'}$ is given by

$$\begin{aligned}\frac{d\sigma}{d\Omega} = \frac{N_c^f}{N_c^i}\cdot\frac{1}{256\pi^2 s}\cdot\frac{s^2}{(s-M^2)^2+s\Gamma^2}\\ \times\Big[(L^2+R^2)(L'^2+R'^2)(1+\cos^2\theta)\\ +(L^2-R^2)(L'^2-R'^2)2\,cos\theta\Big]\end{aligned} \tag{48.25}$$

where M is the mass of the W or Z. The couplings for the W are $L = (8G_F m_W^2/\sqrt{2})^{1/2}V_{ij}/\sqrt{2}; R = 0$ where V_{ij} is the corresponding CKM matrix element, with an analogous expression for L' and R'. For Z, the couplings are $L = (8G_F m_Z^2/\sqrt{2})^{1/2}(T_3 - \sin^2\theta_W Q); R = -(8G_F m_Z^2/\sqrt{2})^{1/2}\sin^2\theta_W Q$, where T_3 is the weak isospin of the initial left-handed fermion and Q is the initial fermion's electric charge. The expressions for L' and R' are analogous. The color factors $N_c^{i,f}$ are 3 for initial or final quarks and 1 for initial or final leptons.

48.4.2. *Production of pairs of weak gauge bosons* :

The cross section for $f\overline{f} \to W^+W^-$ is given in term of the couplings of the left-handed and right-handed fermion f, $\ell = 2(T_3 - Qx_W)$, $r = -2Qx_W$, where T_3 is the third component of weak isospin for the left-handed f, Q is its electric charge (in units of the proton charge), and $x_W = \sin^2\theta_W$:

$$\begin{aligned}\frac{d\sigma}{dt} = \frac{2\pi\alpha^2}{N_c s^2}\Bigg\{&\left[\left(Q+\frac{\ell+r}{4x_W}\frac{s}{s-m_Z^2}\right)^2+\left(\frac{\ell-r}{4x_W}\frac{s}{s-m_Z^2}\right)^2\right]A(s,t,u)\\ &+\frac{1}{2x_W}\left(Q+\frac{\ell}{2x_W}\frac{s}{s-m_Z^2}\right)(\Theta(-Q)I(s,t,u)-\Theta(Q)I(s,u,t))\\ &+\frac{1}{8x_W^2}(\Theta(-Q)E(s,t,u)+\Theta(Q)E(s,u,t))\Bigg\},\end{aligned} \tag{48.26}$$

where $\Theta(x)$ is 1 for $x > 0$ and 0 for $x < 0$, and where

$$\begin{aligned}A(s,t,u) &= \left(\frac{tu}{m_W^4}-1\right)\left(\frac{1}{4}-\frac{m_W^2}{s}+3\frac{m_W^4}{s^2}\right)+\frac{s}{m_W^2}-4,\\ I(s,t,u) &= \left(\frac{tu}{m_W^4}-1\right)\left(\frac{1}{4}-\frac{m_W^2}{2s}-\frac{m_W^4}{st}\right)+\frac{s}{m_W^2}-2+2\frac{m_W^2}{t},\\ E(s,t,u) &= \left(\frac{tu}{m_W^4}-1\right)\left(\frac{1}{4}+\frac{m_W^4}{t^2}\right)+\frac{s}{m_W^2},\end{aligned} \tag{48.27}$$

and s,t,u are the usual Mandelstam variables with $s = (p_f + p_{\overline{f}})^2, t = (p_f - p_{W^-})^2, u = (p_f - p_{W^+})^2$. The factor N_c is 3 for quarks and 1 for leptons.

The analogous cross-section for $q_i\overline{q}_j \to W^\pm Z^0$ is

$$\begin{aligned}\frac{d\sigma}{dt} = \frac{\pi\alpha^2|V_{ij}|^2}{6s^2x_W^2}\Bigg\{&\left(\frac{1}{s-m_W^2}\right)^2\left[\left(\frac{9-8x_W}{4}\right)\left(ut-m_W^2m_Z^2\right)\right.\\ &\left.+(8x_W-6)\,s\left(m_W^2+m_Z^2\right)\right]\\ &+\left[\frac{ut-m_W^2m_Z^2-s(m_W^2+m_Z^2)}{s-m_W^2}\right]\left[\frac{\ell_j}{t}-\frac{\ell_i}{u}\right]\\ &+\frac{ut-m_W^2m_Z^2}{4(1-x_W)}\left[\frac{\ell_j^2}{t^2}+\frac{\ell_i^2}{u^2}\right]+\frac{s(m_W^2+m_Z^2)}{2(1-x_W)}\frac{\ell_i\ell_j}{tu}\Bigg\},\end{aligned} \tag{48.28}$$

where ℓ_i and ℓ_j are the couplings of the left-handed q_i and q_j as defined above. The CKM matrix element between q_i and q_j is V_{ij}.

The cross section for $q_i\overline{q}_i \to Z^0Z^0$ is

$$\frac{d\sigma}{dt} = \frac{\pi\alpha^2}{96}\frac{\ell_i^4+r_i^4}{x_W^2(1-x_W^2)^2s^2}\left[\frac{t}{u}+\frac{u}{t}+\frac{4m_Z^2s}{tu}-m_Z^4\left(\frac{1}{t^2}+\frac{1}{u^2}\right)\right]. \tag{48.29}$$

48.5. Production of Higgs Bosons

48.5.1. *Resonant Production* :

The Higgs boson of the Standard Model can be produced resonantly in the collisions of quarks, leptons, W or Z bosons, gluons, or photons. The production cross section is thus controlled by the partial width of the Higgs boson into the entrance channel and its total width. The branching fractions for the Standard Model Higgs boson are shown in Fig. 1 of the "Searches for Higgs bosons" review in the Particle Listings section, as a function of the Higgs boson mass. The partial widths are given by the relations

$$\Gamma(H \to f\overline{f}) = \frac{G_F m_f^2 m_H N_c}{4\pi\sqrt{2}} \left(1 - 4m_f^2/m_H^2\right)^{3/2}, \quad (48.30)$$

$$\Gamma(H \to W^+W^-) = \frac{G_F m_H^3 \beta_W}{32\pi\sqrt{2}} \left(4 - 4a_W + 3a_W^2\right), \quad (48.31)$$

$$\Gamma(H \to ZZ) = \frac{G_F m_H^3 \beta_Z}{64\pi\sqrt{2}} \left(4 - 4a_Z + 3a_Z^2\right), \quad (48.32)$$

where N_c is 3 for quarks and 1 for leptons and where $a_W = 1 - \beta_W^2 = 4m_W^2/m_H^2$ and $a_Z = 1 - \beta_Z^2 = 4m_Z^2/m_H^2$. The decay to two gluons proceeds through quark loops, with the t quark dominating [2]. Explicitly,

$$\Gamma(H \to gg) = \frac{\alpha_s^2 G_F m_H^3}{36\pi^3\sqrt{2}} \left|\sum_q I(m_q^2/m_H^2)\right|^2, \quad (48.33)$$

where $I(z)$ is complex for $z < 1/4$. For $z < 2 \times 10^{-3}$, $|I(z)|$ is small so the light quarks contribute negligibly. For $m_H < 2m_t$, $z > 1/4$ and

$$I(z) = 3\left[2z + 2z(1-4z)\left(\sin^{-1}\frac{1}{2\sqrt{z}}\right)^2\right], \quad (48.34)$$

which has the limit $I(z) \to 1$ as $z \to \infty$.

48.5.2. *Higgs Boson Production in W^* and Z^* decay* :

The Standard Model Higgs boson can be produced in the decay of a virtual W or Z ("Higgstrahlung") [3,4]: In particular, if k is the c.m. momentum of the Higgs boson,

$$\sigma(q_i\overline{q}_j \to WH) = \frac{\pi\alpha^2|V_{ij}|^2}{36\sin^4\theta_W} \frac{2k}{\sqrt{s}} \frac{k^2 + 3m_W^2}{(s - m_W^2)^2} \quad (48.35)$$

$$\sigma(f\overline{f} \to ZH) = \frac{2\pi\alpha^2(\ell_f^2 + r_f^2)}{48N_c\sin^4\theta_W\cos^4\theta_W} \frac{2k}{\sqrt{s}} \frac{k^2 + 3m_Z^2}{(s - m_Z^2)^2}, \quad (48.36)$$

where ℓ and r are defined as above.

48.5.3. *W and Z Fusion* :

Just as high-energy electrons can be regarded as sources of virtual photon beams, at very high energies they are sources of virtual W and Z beams. For Higgs boson production, it is the longitudinal components of the Ws and Zs that are important [5]. The distribution of longitudinal Ws carrying a fraction y of the electron's energy is [6]

$$f(y) = \frac{g^2}{16\pi^2}\frac{1-y}{y}, \quad (48.37)$$

where $g = e/\sin\theta_W$. In the limit $s \gg m_H \gg m_W$, the partial decay rate is $\Gamma(H \to W_L W_L) = (g^2/64\pi)(m_H^3/m_W^2)$ and in the equivalent W approximation [7]

$$\sigma(e^+e^- \to \overline{\nu}_e\nu_e H) = \frac{1}{16m_W^2}\left(\frac{\alpha}{\sin^2\theta_W}\right)^3 \times \left[\left(1 + \frac{m_H^2}{s}\right)\log\frac{s}{m_H^2} - 2 + 2\frac{m_H^2}{s}\right]. \quad (48.38)$$

There are significant corrections to this relation when m_H is not large compared to m_W [8]. For $m_H = 150$ GeV, the estimate is too high by 51% for $\sqrt{s} = 1000$ GeV, 32% too high at $\sqrt{s} = 2000$ GeV, and 22% too high at $\sqrt{s} = 4000$ GeV. Fusion of ZZ to make a Higgs boson can be treated similarly. Identical formulae apply for Higgs production in the collisions of quarks whose charges permit the emission of a W^+ and a W^-, except that QCD corrections and CKM matrix elements are required. Even in the absence of QCD corrections, the fine-structure constant ought to be evaluated at the scale of the collision, say m_W. All quarks contribute to the ZZ fusion process.

48.6. Inclusive hadronic reactions

One-particle inclusive cross sections $Ed^3\sigma/d^3p$ for the production of a particle of momentum p are conveniently expressed in terms of rapidity y (see above) and the momentum p_T transverse to the beam direction (in the c.m.):

$$E\frac{d^3\sigma}{d^3p} = \frac{d^3\sigma}{d\phi\, dy\, p_T dp_T^2}. \quad (48.39)$$

In appropriate circumstances, the cross section may be decomposed as a partonic cross section multiplied by the probabilities of finding partons of the prescribed momenta:

$$\sigma_{\text{hadronic}} = \sum_{ij}\int dx_1\, dx_2\, f_i(x_1)\, f_j(x_2)\, d\hat{\sigma}_{\text{partonic}}, \quad (48.40)$$

The probability that a parton of type i carries a fraction of the incident particle's that lies between x_1 and $x_1 + dx_1$ is $f_i(x_1)dx_1$ and similarly for partons in the other incident particle. The partonic collision is specified by its c.m. energy squared $\hat{s} = x_1x_2s$ and the momentum transfer squared $\hat{t}$. The final hadronic state is more conveniently specified by the rapidities y_1, y_2 of the two jets resulting from the collision and the transverse momentum p_T. The connection between the differentials is

$$dx_1dx_2d\hat{t} = dy_1dy_2\frac{\hat{s}}{s}dp_T^2, \quad (48.41)$$

so that

$$\frac{d^3\sigma}{dy_1dy_2dp_T^2} = \frac{\hat{s}}{s}\left[f_i(x_1)f_j(x_2)\frac{d\hat{\sigma}}{d\hat{t}}(\hat{s},\hat{t},\hat{u}) + f_i(x_2)f_j(x_1)\frac{d\hat{\sigma}}{d\hat{t}}(\hat{s},\hat{u},\hat{t})\right], \quad (48.42)$$

where we have taken into account the possibility that the incident parton types might arise from either incident particle. The second term should be dropped if the types are identical: $i = j$.

48.7. Two-photon processes

In the Weizsäcker-Williams picture, a high-energy electron beam is accompanied by a spectrum of virtual photons of energies ω and invariant-mass squared $q^2 = -Q^2$, for which the photon number density is

$$dn = \frac{\alpha}{\pi}\left[1 - \frac{\omega}{E} + \frac{\omega^2}{E^2} - \frac{m_e^2\,\omega^2}{Q^2E^2}\right]\frac{d\omega}{\omega}\frac{dQ^2}{Q^2}, \quad (48.43)$$

where E is the energy of the electron beam. The cross section for $e^+e^- \to e^+e^-X$ is then [9]

$$d\sigma_{e^+e^-\to e^+e^-X}(s) = dn_1dn_2d\sigma_{\gamma\gamma\to X}(W^2), \quad (48.44)$$

where $W^2 = m_X^2$. Integrating from the lower limit $Q^2 = m_e^2\frac{\omega_i^2}{E_i(E_i - \omega_i)}$ to a maximum Q^2 gives

$$\sigma_{e^+e^-\to e^+e^-X}(s) = \frac{\alpha^2}{\pi^2}\int_{z_{th}}^1\frac{dz}{z} \times \left[\left(\ln\frac{Q_{max}^2}{zm_e^2} - 1\right)^2 f(z) + \frac{1}{3}(\ln z)^3\right]\sigma_{\gamma\gamma\to X}(zs), \quad (48.45)$$

where

$$f(z) = \left(1 + \tfrac{1}{2}z\right)^2\ln(1/z) - \tfrac{1}{2}(1-z)(3+z). \quad (48.46)$$

The appropriate value of Q_{max}^2 depends on the properties of the produced system X. For production of hadronic systems, $Q_{max}^2 \approx m_\rho^2$,

while for lepton-pair production, $Q^2 \approx W^2$. For production of a resonance with spin $J \neq 1$, we have

$$\sigma_{e^+e^-\to e^+e^-R}(s) = (2J+1)\frac{8\alpha^2\Gamma_{R\to\gamma\gamma}}{m_R^3} \times \left[f(m_R^2/s)\left(\ln\frac{m_V^2 s}{m_e^2 m_R^2} - 1\right)^2 - \frac{1}{3}\left(\ln\frac{s}{M_R^2}\right)^3\right], \quad (48.47)$$

where m_V is the mass that enters into the form factor for the $\gamma\gamma \to R$ transition, typically m_ρ.

PART II: PROCESSES BEYOND THE STANDARD MODEL

48.8. Production of supersymmetric particles

In supersymmetric (SUSY) theories (see Supersymmetric Particle Searches in this *Review*), every boson has a fermionic superpartner, and every fermion has a bosonic superpartner. The minimal supersymmetric Standard Model (MSSM) is a direct supersymmetrization of the Standard Model (SM), although a second Higgs doublet is needed to avoid triangle anomalies [10]. Under *soft* SUSY breaking, superpartner masses are lifted above the SM particle masses. In weak scale SUSY, the superpartners are invoked to stabilize the weak scale under radiative corrections, so the superpartners are expected to have masses of order the TeV scale.

48.8.1. *Gluino and squark production* :

The superpartners of gluons are the color octet, spin$-\frac{1}{2}$ gluinos ($\tilde{g}$), while each helicity component of quark flavor has a spin-0 *squark* partner, *e.g.* $\tilde{q}_L$ and $\tilde{q}_R$. Third generation left- and right- squarks are expected to have large mixing, resulting in mass eigenstates $\tilde{q}_1$ and $\tilde{q}_2$, with $m_{\tilde{q}_1} < m_{\tilde{q}_2}$ (here, q denotes any of the SM flavors of quarks and $\tilde{q}_i$ the corresponding flavor and type ($i = L, R$ or $1, 2$) of squark). Gluino pair production ($\tilde{g}\tilde{g}$) takes place via either glue-glue or quark-antiquark annihilation [11].

The subprocess cross sections are usually presented as differential distributions in the Mandelstam variables s, t and u. Note that for a $2 \to 2$ scattering subprocess $ab \to cd$, the Mandelstam variable $s = (p_a + p_b)^2 = (p_c + p_d)^2$, where p_a is the 4-momentum of particle a, and so forth. The variable $t = (p_c - p_a)^2$, where c and a are taken conventionally to be the most similar particles in the subprocess. The variable u would then be equal to $(p_d - p_a)^2$. Note that since s, t and u are squares of 4-vectors, they are invariants in any inertial reference frame.

Gluino pair production at hadron colliders is described by:

$$\frac{d\sigma}{dt}(gg \to \tilde{g}\tilde{g}) = \frac{9\pi\alpha_s^2}{4s^2}\left\{\frac{2(m_{\tilde{g}}^2 - t)(m_{\tilde{g}}^2 - u)}{s^2} + \frac{(m_{\tilde{g}}^2 - t)(m_{\tilde{g}}^2 - u) - 2m_{\tilde{g}}^2(m_{\tilde{g}}^2 + t)}{(m_{\tilde{g}}^2 - t)^2} + \frac{(m_{\tilde{g}}^2 - t)(m_{\tilde{g}}^2 - u) - 2m_{\tilde{g}}^2(m_{\tilde{g}}^2 + u)}{(m_{\tilde{g}}^2 - u)^2} + \frac{m_{\tilde{g}}^2(s - 4m_{\tilde{g}}^2)}{(m_{\tilde{g}}^2 - t)(m_{\tilde{g}}^2 - u)} - \frac{(m_{\tilde{g}}^2 - t)(m_{\tilde{g}}^2 - u) + m_{\tilde{g}}^2(u - t)}{s(m_{\tilde{g}}^2 - t)} - \frac{(m_{\tilde{g}}^2 - t)(m_{\tilde{g}}^2 - u) + m_{\tilde{g}}^2(t - u)}{s(m_{\tilde{g}}^2 - u)}\right\}, \quad (48.48)$$

where α_s is the strong fine structure constant. Also,

$$\frac{d\sigma}{dt}(q\bar{q} \to \tilde{g}\tilde{g}) = \frac{8\pi\alpha_s^2}{9s^2}\left\{\frac{4}{3}\left(\frac{m_{\tilde{g}}^2 - t}{m_{\tilde{q}}^2 - t}\right)^2 + \frac{4}{3}\left(\frac{m_{\tilde{g}}^2 - u}{m_{\tilde{q}}^2 - u}\right)^2 + \frac{3}{s^2}\left[(m_{\tilde{g}}^2 - t)^2 + (m_{\tilde{g}}^2 - u)^2 + 2m_{\tilde{g}}^2 s\right] - 3\frac{\left[(m_{\tilde{g}}^2 - t)^2 + m_{\tilde{g}}^2 s\right]}{s(m_{\tilde{q}}^2 - t)} - 3\frac{\left[(m_{\tilde{g}}^2 - u)^2 + m_{\tilde{g}}^2 s\right]}{s(m_{\tilde{q}}^2 - u)} + \frac{1}{3}\frac{m_{\tilde{g}}^2 s}{(m_{\tilde{q}}^2 - t)(m_{\tilde{q}}^2 - u)}\right\}. \quad (48.49)$$

Gluinos can also be produced in association with squarks: $\tilde{g}\tilde{q}_i$ production, where $\tilde{q}_i$ represents any of the various types (left-, right- or mixed) and flavors of squarks. The subprocess cross section is independent of whether the squark is the right-, left- or mixed type:

$$\frac{d\sigma}{dt}(gq \to \tilde{g}\tilde{q}_i) = \frac{\pi\alpha_s^2}{24s^2}\frac{\left[\frac{16}{3}(s^2 + (m_{\tilde{q}_i}^2 - u)^2) + \frac{4}{3}s(m_{\tilde{q}_i}^2 - u)\right]}{s(m_{\tilde{g}}^2 - t)(m_{\tilde{q}_i}^2 - u)^2} \times \left((m_{\tilde{g}}^2 - u)^2 + (m_{\tilde{q}_i}^2 - m_{\tilde{g}}^2)^2 + \frac{2sm_{\tilde{g}}^2(m_{\tilde{q}_i}^2 - m_{\tilde{g}}^2)}{(m_{\tilde{g}}^2 - t)}\right). \quad (48.50)$$

There are many different subprocesses for production of squark pairs. Since left- and right- squarks generally have different masses and different decay patterns, we present the differential cross section for each subprocess of $\tilde{q}_i$ ($i = L,\ R$ or $1,\ 2$) separately. (In early literature, the following formulae were often combined into a single equation which didn't differentiate the various squark types.) The result for $gg \to \tilde{q}_i\bar{\tilde{q}}_i$ is:

$$\frac{d\sigma}{dt}(gg \to \tilde{q}_i\bar{\tilde{q}}_i) = \frac{\pi\alpha_s^2}{4s^2}\left\{\frac{1}{3}\left(\frac{m_{\tilde{q}}^2 + t}{m_{\tilde{q}}^2 - t}\right)^2 + \frac{1}{3}\left(\frac{m_{\tilde{q}}^2 + u}{m_{\tilde{q}}^2 - u}\right)^2 + \frac{3}{32s^2}\left(8s(4m_{\tilde{q}}^2 - s) + 4(u - t)^2\right) + \frac{7}{12} - \frac{1}{48}\frac{(4m_{\tilde{q}}^2 - s)^2}{(m_{\tilde{q}}^2 - t)(m_{\tilde{q}}^2 - u)} + \frac{3}{32}\frac{\left[(t - u)(4m_{\tilde{q}}^2 + 4t - s) - 2(m_{\tilde{q}}^2 - u)(6m_{\tilde{q}}^2 + 2t - s)\right]}{s(m_{\tilde{q}}^2 - t)} + \frac{3}{32}\frac{\left[(u - t)(4m_{\tilde{q}}^2 + 4u - s) - 2(m_{\tilde{q}}^2 - t)(6m_{\tilde{q}}^2 + 2u - s)\right]}{s(m_{\tilde{q}}^2 - u)} + \frac{7}{96}\frac{\left[4m_{\tilde{q}}^2 + 4t - s\right]}{m_{\tilde{q}}^2 - t} + \frac{7}{96}\frac{\left[4m_{\tilde{q}}^2 + 4u - s\right]}{m_{\tilde{q}}^2 - u}\right\}, \quad (48.51)$$

which has an obvious $u \leftrightarrow t$ symmetry.

For $q\bar{q} \to \tilde{q}_i\bar{\tilde{q}}_i$ with the same initial and final state flavors, we have

$$\frac{d\sigma}{dt}(q\bar{q} \to \tilde{q}_i\bar{\tilde{q}}_i) = \frac{2\pi\alpha_s^2}{9s^2}\left\{\frac{1}{(t - m_{\tilde{g}}^2)^2} + \frac{2}{s^2} - \frac{2/3}{s(t - m_{\tilde{g}}^2)}\right\} \times \left[-st - (t - m_{\tilde{q}_i}^2)^2\right], \quad (48.52)$$

while if initial and final state flavors are different ($q\bar{q} \to \tilde{q}_i'\bar{\tilde{q}}_i'$) we instead have

$$\frac{d\sigma}{dt}(q\bar{q} \to \tilde{q}_i'\bar{\tilde{q}}_i') = \frac{4\pi\alpha_s^2}{9s^4}\left[-st - (t - m_{\tilde{q}_i'}^2)^2\right]. \quad (48.53)$$

If the two initial state quarks are of different flavors, then we have

$$\frac{d\sigma}{dt}(q\bar{q}' \to \tilde{q}_i\bar{\tilde{q}}_i') = \frac{2\pi\alpha_s^2}{9s^2}\frac{-st - (t - m_{\tilde{q}_i}^2)^2}{(t - m_{\tilde{g}}^2)^2}. \quad (48.54)$$

If the initial quarks are of different flavor and final state squarks are of different type ($i \neq j$) then

$$\frac{d\sigma}{dt}(q\bar{q}' \to \tilde{q}_i\bar{\tilde{q}}_j') = \frac{2\pi\alpha_s^2}{9s^2}\frac{m_{\tilde{g}}^2 s}{(t - m_{\tilde{g}}^2)^2}. \quad (48.55)$$

For same-flavor initial state quarks, but final state unlike-type squarks, we also have

$$\frac{d\sigma}{dt}(q\bar{q} \to \tilde{q}_i\bar{\tilde{q}}_j) = \frac{2\pi\alpha_s^2}{9s^2}\frac{m_{\tilde{g}}^2 s}{(t - m_{\tilde{g}}^2)^2}. \quad (48.56)$$

There also exist cross sections for quark-quark annihilation to squark pairs. For same flavor quark-quark annihilation to same flavor/same type final state squarks,

$$\frac{d\sigma}{dt}(qq \to \tilde{q}_i\tilde{q}_i) =$$

$$= \frac{\pi\alpha_s^2}{9s^2} m_{\tilde{g}}^2 s \left\{ \frac{1}{(t-m_{\tilde{g}}^2)^2} + \frac{1}{(u-m_{\tilde{g}}^2)^2} - \frac{2/3}{(t-m_{\tilde{g}}^2)(u-m_{\tilde{g}}^2)} \right\}, \quad (48.57)$$

while if the final type squarks are different ($i \neq j$), we have

$$\frac{d\sigma}{dt}(qq \to \tilde{q}_i\tilde{q}_j) =$$

$$\frac{2\pi\alpha_s^2}{9s^2} \left\{ \frac{[-st-(t-m_{\tilde{q}_i}^2)(t-m_{\tilde{q}_j}^2)]}{(t-m_{\tilde{g}}^2)} + \frac{[-su-(u-m_{\tilde{q}_i}^2)(u-m_{\tilde{q}_j}^2)]}{(u-m_{\tilde{g}}^2)} \right\}. \quad (48.58)$$

If initial/final state flavors are different, but final state squark types are the same, then

$$\frac{d\sigma}{dt}(qq' \to \tilde{q}_i\tilde{q}_i') = \frac{2\pi\alpha_s^2}{9s^2} \frac{m_{\tilde{g}}^2 s}{(t-m_{\tilde{g}}^2)^2}. \quad (48.59)$$

If initial quark flavors are different and final squark types are different, then

$$\frac{d\sigma}{dt}(qq' \to \tilde{q}_i\tilde{q}_j') = \frac{2\pi\alpha_s^2}{9s^2} \frac{-st-(t-m_{\tilde{q}_i}^2)(t-m_{\tilde{q}_j}^2)}{(t-m_{\tilde{g}}^2)^2}. \quad (48.60)$$

48.8.2. *Gluino and squark associated production* :

In the MSSM, the charged spin-$\frac{1}{2}$ winos and higgsinos mix to make chargino states $\chi_1^\pm$ and $\chi_2^\pm$, with $m_{\chi_1^\pm} < m_{\chi_2^\pm}$. The spin$-\frac{1}{2}$ neutral bino, wino and higgsino fields mix to give four neutralino mass eigenstates $\chi_{1,2,3,4}^0$ ordered according to mass. We sometimes denote the charginos and neutralinos collectively as -inos for notational simplicity

For gluino and squark production in association with charginos and neutralinos [12], the quark-squark-neutralino couplings* are defined by the interaction Lagrangian terms $\mathcal{L}_{\bar{f}f\chi_i^0} = \left[iA_{\tilde{\chi}_i^0}^f \tilde{f}_L^\dagger \bar{\tilde{\chi}}_i^0 P_L f + iB_{\tilde{\chi}_i^0}^f \tilde{f}_R^\dagger \bar{\tilde{\chi}}_i^0 P_R f + \text{h.c.} \right]$, where $A_{\tilde{\chi}_i^0}^f$ and $B_{\tilde{\chi}_i^0}^f$ are coupling constants involving gauge couplings, neutralino mixing elements and in the case of third generation fermions, Yukawa couplings. Their form depends on the conventions used for setting up the MSSM Lagrangian, and can be found in various reviews [13] and textbooks [14,15]. P_L and P_R are the usual left- and right-spinor projection operators and f denotes any of the SM fermions $u,\ d,\ e,\ \nu_e, \cdots$. The fermion-sfermion- chargino couplings have the form $\mathcal{L} = \left[iA_{\tilde{\chi}_i^-}^d \tilde{u}_L^\dagger \overline{\tilde{\chi}_i^-} P_L d + iA_{\tilde{\chi}_i^-}^u \tilde{d}_L^\dagger \overline{\tilde{\chi}_i^c} P_L u + \text{h.c.} \right]$ for u and d quarks, where the $A_{\tilde{\chi}_i^-}^d$ and $A_{\tilde{\chi}_i^-}^u$ couplings are again convention-dependent, and can be found in textbooks. The superscript c denotes "charge conjugate spinor", defined by $\psi^c \equiv C\bar{\psi}^T$.

The subprocess cross sections for chargino-squark associated production occur via squark exchange and are given by

$$\frac{d\sigma}{dt}(\bar{u}g \to \tilde{\chi}_i^- \bar{\tilde{d}}_L) = \frac{\alpha_s}{24s^2} |A_{\tilde{\chi}_i^-}^u|^2 \psi(m_{\tilde{d}_L}, m_{\tilde{\chi}_i^-}, t), \quad (48.61)$$

$$\frac{d\sigma}{dt}(dg \to \tilde{\chi}_i^- \tilde{u}_L) = \frac{\alpha_s}{24s^2} |A_{\tilde{\chi}_i^-}^d|^2 \psi(m_{\tilde{u}_L}, m_{\tilde{\chi}_i^-}, t), \quad (48.62)$$

while neutralino-squark production is given by

$$\frac{d\sigma}{dt}(qg \to \tilde{\chi}_i^0 \tilde{q}) = \frac{\alpha_s}{24s^2} \left(|A_{\tilde{\chi}_i^0}^q|^2 + |B_{\tilde{\chi}_i^0}^q|^2 \right) \psi(m_{\tilde{q}}, m_{\tilde{\chi}_i^0}, t), \quad (48.63)$$

where

$$\psi(m_1, m_2, t) = \frac{s+t-m_1^2}{2s} - \frac{m_1^2(m_2^2-t)}{(m_1^2-t)^2} + \frac{t(m_2^2-m_1^2)+m_2^2(s-m_2^2+m_1^2)}{s(m_1^2-t)}. \quad (48.64)$$

Here, the variable t is given by the square of "squark-minus-quark" four-momentum. The neutralino-gluino associated production cross section also occurs via squark exchange and is given by

$$\frac{d\sigma}{dt}(q\bar{q} \to \tilde{\chi}_i^0 \tilde{g}) = \frac{\alpha_s}{18s^2} \left(|A_{\tilde{\chi}_i^0}^q|^2 + |B_{\tilde{\chi}_i^0}^q|^2 \right) \left[\frac{(m_{\tilde{\chi}_i^0}^2 - t)(m_{\tilde{g}}^2 - t)}{(m_{\tilde{q}}^2 - t)^2} + \frac{(m_{\tilde{\chi}_i^0}^2 - u)(m_{\tilde{g}}^2 - u)}{(m_{\tilde{q}}^2 - u)^2} - \frac{2\eta_i\eta_{\tilde{g}} m_{\tilde{g}} m_{\tilde{\chi}_i^0} s}{(m_{\tilde{q}}^2 - t)(m_{\tilde{q}}^2 - u)} \right], \quad (48.65)$$

where η_i is the sign of the neutralino mass eigenvalue and $\eta_{\tilde{g}}$ is the sign of the gluino mass eigenvalue. We also have chargino-gluino associated production:

$$\frac{d\sigma}{dt}(\bar{u}d \to \tilde{\chi}_i^- \tilde{g}) = \frac{\alpha_s}{18s^2} \left[|A_{\tilde{\chi}_i^-}^u|^2 \frac{(m_{\tilde{\chi}_i^-}^2 - t)(m_{\tilde{g}}^2 - t)}{(m_{\tilde{d}_L}^2 - t)^2} + |A_{\tilde{\chi}_i^-}^d|^2 \frac{(m_{\tilde{\chi}_i^-}^2 - u)(m_{\tilde{g}}^2 - u)}{(m_{\tilde{u}_L}^2 - u)^2} + \frac{2\eta_{\tilde{g}} Re(A_{\tilde{\chi}_i^-}^u A_{\tilde{\chi}_i^-}^{d*}) m_{\tilde{g}} m_{\tilde{\chi}_i} s}{(m_{\tilde{d}_L}^2 - t)(m_{\tilde{u}_L}^2 - u)} \right], \quad (48.66)$$

where $\hat{t} = (\tilde{g} - d)^2$ and in the third term one must take the real part of the in general complex coupling constant product.

48.8.3. *Slepton and sneutrino production* :

The subprocess cross section for $\tilde{\ell}_L\bar{\tilde{\nu}}_{\ell_L}$ production ($\ell = e$ or μ) occurs via s-channel W exchange and is given by

$$\frac{d\sigma}{dt}(d\bar{u} \to \tilde{\ell}_L\bar{\tilde{\nu}}_{\ell_L}) = \frac{g^4 |D_W(s)|^2}{192\pi s^2} \left(tu - m_{\tilde{\ell}_L}^2 m_{\tilde{\nu}_{\ell_L}}^2 \right), \quad (48.67)$$

where $D_W(s) = 1/(s - M_W^2 + iM_W\Gamma_W)$ is the W-boson propagator denominator. The production of $\tilde{\tau}_1\bar{\tilde{\nu}}_\tau$ is given as above, but replacing $m_{\tilde{\ell}_L} \to m_{\tilde{\tau}_1}$, $m_{\tilde{\nu}_{\ell_L}} \to m_{\tilde{\nu}_\tau}$ and multiplying by an overall factor of $\cos^2\theta_\tau$ (where θ_τ is the tau-slepton mixing angle). Similar substitutions hold for $\tilde{\tau}_2\bar{\tilde{\nu}}_\tau$ production, except the overall factor is $\sin^2\theta_\tau$.

Table 48.1: The constants α_f and β_f that appear in in the SM neutral current Lagrangian. Here $t \equiv \tan\theta_W$ and $c \equiv \cot\theta_W$.

f	q_f	α_f	β_f
ℓ	-1	$\frac{1}{4}(3t-c)$	$\frac{1}{4}(t+c)$
ν_ℓ	0	$\frac{1}{4}(t+c)$	$-\frac{1}{4}(t+c)$
u	$\frac{2}{3}$	$-\frac{5}{12}t+\frac{1}{4}c$	$-\frac{1}{4}(t+c)$
d	$-\frac{1}{3}$	$\frac{1}{12}t-\frac{1}{4}c$	$\frac{1}{4}(t+c)$

* The couplings $A_{\tilde{\chi}_i^0}^f$ and $B_{\tilde{\chi}_i^0}^f$ are given explicitly in Ref. 15 in Eq. (8.87). Also, the couplings $A_{\tilde{\chi}_i^-}^d$ and $A_{\tilde{\chi}_i^-}^u$ are given in Eq. (8.93). The couplings X_i^j and Y_i^j are given by Eq. (8.103), while the x_i and y_i couplings are given in Eq. (8.100). Finally, the couplings W_{ij} are given in Eq. (8.101).

The subprocess cross section for $\tilde{\ell}_L\bar{\tilde{\ell}}_L$ production occurs via s-channel γ and Z exchange, and depends on the neutral current interaction, with fermion couplings to γ and Z^0 given by $\mathcal{L}_{\rm neutral} = -eq_f\bar{f}\gamma^\mu f A_\mu + e\bar{f}\gamma^\mu(\alpha_f+\beta_f\gamma_5)fZ_\mu$ (with values of q_f, α_f, and β_f given in Table 48.1.

The subprocess cross section is given by

$$\frac{d\sigma}{dt}(q\bar{q}\to\tilde{\ell}_L\bar{\tilde{\ell}}_L) = \frac{e^4}{24\pi s^2}\left(tu-m^4_{\tilde{\ell}_L}\right)\times$$

$$\left\{\frac{q_\ell^2 q_q^2}{s^2}+(\alpha_\ell-\beta_\ell)^2(\alpha_q^2+\beta_q^2)|D_Z(s)|^2\right.$$

$$\left.+\frac{2q_\ell q_q\alpha_q(\alpha_\ell-\beta_\ell)(s-M_Z^2)}{s}|D_Z(s)|^2\right\}, \qquad (48.68)$$

where $D_Z(s) = 1/(s-M_Z^2+iM_Z\Gamma_Z)$. The cross section for sneutrino production is given by the same formula, but with α_ℓ, β_ℓ, q_ℓ and $m_{\tilde{\ell}_L}$ replaced by α_ν, β_ν, 0 and $m_{\tilde{\nu}_L}$, respectively. The cross section for $\tilde{\tau}_1\bar{\tilde{\tau}}_1$ production is obtained by replacing $m_{\tilde{\ell}_L}\to m_{\tilde{\tau}_1}$ and $\beta_\ell\to\beta_\ell\cos 2\theta_\tau$. The cross section for $\tilde{\ell}_R\bar{\tilde{\ell}}_R$ production is given by substituting $\alpha_\ell-\beta_\ell\to\alpha_\ell+\beta_\ell$ and $m_{\tilde{\ell}_L}\to m_{\tilde{\ell}_R}$ in the equation above. The cross section for $\tilde{\tau}_2\bar{\tilde{\tau}}_2$ production is obtained from the formula for $\tilde{\ell}_R\bar{\tilde{\ell}}_R$ production by replacing $m_{\tilde{\ell}_R}\to m_{\tilde{\tau}_2}$ and $\beta_\ell\to\beta_\ell\cos 2\theta_\tau$.

Finally, the cross section for $\tilde{\tau}_1\bar{\tilde{\tau}}_2$ production occurs only via Z exchange, and is given by

$$\frac{d\sigma}{dt}(q\bar{q}\to\tilde{\tau}_1\bar{\tilde{\tau}}_2) = \frac{d\sigma}{dt}(q\bar{q}\to\bar{\tilde{\tau}}_1\tilde{\tau}_2) =$$

$$\frac{e^4}{24\pi s^2}(\alpha_q^2+\beta_q^2)\beta_\ell^2\sin^2 2\theta_\tau|D_Z(s)|^2(ut-m^2_{\tilde{\tau}_1}m^2_{\tilde{\tau}_2}). \qquad (48.69)$$

48.8.4. *Chargino and neutralino pair production* :

48.8.4.1. $\tilde{\chi}_i^-\tilde{\chi}_j^0$ *production:*

The subprocess cross section for $d\bar{u}\to\tilde{\chi}_i^-\tilde{\chi}_j^0$ depends on Lagrangian couplings $\mathcal{L}_{W\bar{u}d} = -\frac{g}{\sqrt{2}}\bar{u}\gamma_\mu P_L d W^{+\mu}$ + h.c., $\mathcal{L}_{W\tilde{\chi}_i^-\tilde{\chi}_j^0} = -g(-i)^{\theta_j}\overline{\tilde{\chi}^-}_i[X_i^j+Y_i^j\gamma_5]\gamma_\mu\tilde{\chi}_j^0 W^{-\mu}$ + h.c., $\mathcal{L}_{q\tilde{q}\tilde{\chi}_i^-} = iA^d_{\tilde{\chi}_i^-}\tilde{u}_L^\dagger\overline{\tilde{\chi}_i^-}P_L d + iA^u_{\tilde{\chi}_i^-}\tilde{d}_L^\dagger\overline{\tilde{\chi}_i^c}P_L u$ +h.c. and $\mathcal{L}_{q\tilde{q}\tilde{\chi}_j^0} = iA^q_{\tilde{\chi}_j^0}\tilde{q}_L^\dagger\overline{\tilde{\chi}^0}_j P_L q$ +h.c.. Contributing diagrams include W exchange and also $\tilde{d}_L$ and $\tilde{u}_L$ squark exchange. The X_i^j and Y_i^j couplings are new, and again convention-dependent: the cross section formulae works if the interaction Lagrangian is written in the above form, so that the couplings can be suitably extracted. The term $\theta_j = 0$ (1) if $m_{\tilde{\chi}_j^0} > 0$ (< 0); it comes about because the neutralino field must be re-defined by a $-i\gamma_5$ transformation if its mass eigenvalue is negative [15]. The subprocess cross section is given in terms of dot products of four momenta, where particle labels are used to denote their four-momenta; note that all mass terms in the cross section formulae are positive definite, so that the signs of mass eigenstates have been absorbed into the Lagrangian couplings, as for instance in Ref. [15]. We then have

$$\frac{d\sigma}{dt}(d\bar{u}\to\tilde{\chi}_i^-\tilde{\chi}_j^0) = \frac{1}{192\pi s^2}$$

$$\left[T_W + T_{\tilde{d}_L} + T_{\tilde{u}_L} + T_{W\tilde{d}_L} + T_{W\tilde{u}_L} + T_{\tilde{d}_L\tilde{u}_L}\right] \qquad (48.70)$$

where

$$T_W = 8g^4|D_W(s)|^2\left\{[X_i^{j2}+Y_i^{j2}](\tilde{\chi}_j^0\cdot d\tilde{\chi}_i^-\cdot\overline{u}+\tilde{\chi}_j^0\cdot\overline{u}\tilde{\chi}_i^-\cdot d)\right.$$
$$\left.+2(X_i^jY_i^j)(\tilde{\chi}_j^0\cdot d\tilde{\chi}_i^-\cdot\overline{u}-\tilde{\chi}_j^0\cdot\overline{u}\tilde{\chi}_i^-\cdot d)+[X_i^{j2}-Y_i^{j2}]m_{\tilde{\chi}_i^-}m_{\tilde{\chi}_j^0}d\cdot\overline{u}\right\}, \qquad (48.71)$$

$$T_{\tilde{d}_L} = \frac{4|A^u_{\tilde{\chi}_i^-}|^2|A^d_{\tilde{\chi}_j^0}|^2}{[(\tilde{\chi}_i^- - \overline{u})^2 - m^2_{\tilde{d}_L}]^2}\; d\cdot\tilde{\chi}_j^0\tilde{\chi}_i^-\cdot\overline{u}, \qquad (48.72)$$

$$T_{\tilde{u}_L} = \frac{4|A^d_{\tilde{\chi}_i^-}|^2|A^u_{\tilde{\chi}_j^0}|^2}{[(\tilde{\chi}_j^0 - \overline{u})^2 - m^2_{\tilde{u}_L}]^2}\; \overline{u}\cdot\tilde{\chi}_j^0\tilde{\chi}_i^-\cdot d \qquad (48.73)$$

$$T_{W\tilde{d}_L} = \frac{-\sqrt{2}g^2 Re[A^{d*}_{\tilde{\chi}_j^0}A^u_{\tilde{\chi}_i^-}(-i)^{\theta_j}](s-M_W^2)|D_W(s)|^2}{(\tilde{\chi}_i^- - \overline{u})^2 - m^2_{\tilde{d}_L}}$$
$$\times\left\{8(X_i^j+Y_i^j)\tilde{\chi}_j^0\cdot d\overline{u}\cdot\tilde{\chi}_i^- + 4(X_i^j-Y_i^j)m_{\tilde{\chi}_i^-}m_{\tilde{\chi}_j^0}d\cdot\overline{u}\right\} \qquad (48.74)$$

$$T_{W\tilde{u}_L} = \frac{\sqrt{2}g^2 Re[A^{d*}_{\tilde{\chi}_i^-}A^u_{\tilde{\chi}_j^0}(-i)^{\theta_j}](s-M_W^2)|D_W(s)|^2}{(\tilde{\chi}_j^0 - \overline{u})^2 - m^2_{\tilde{u}_L}}$$
$$\times\left\{8(X_i^j-Y_i^j)\tilde{\chi}_j^0\cdot\overline{u}d\cdot\tilde{\chi}_i^- + 4(X_i^j+Y_i^j)m_{\tilde{\chi}_i^-}m_{\tilde{\chi}_j^0}d\cdot\overline{u}\right\} \qquad (48.75)$$

and

$$T_{\tilde{d}_L\tilde{u}_L} = -\frac{4Re[A^d_{\tilde{\chi}_j^0}A^{u*}_{\tilde{\chi}_i^-}A^{d*}_{\tilde{\chi}_i^-}A^u_{\tilde{\chi}_j^0}]m_{\tilde{\chi}_i^-}m_{\tilde{\chi}_j^0}d\cdot\overline{u}}{[(\tilde{\chi}_i^- - \overline{u})^2 - m^2_{\tilde{d}_L}][(\tilde{\chi}_j^0 - \overline{u})^2 - m^2_{\tilde{u}_L}]}. \qquad (48.76)$$

48.8.4.2. *Chargino pair production:*

The subprocess cross section for $d\bar{d}\to\tilde{\chi}_i^-\tilde{\chi}_i^+$ $(i=1,2)$ depends on Lagrangian couplings $\mathcal{L} = e\overline{\tilde{\chi}_i^-}\gamma_\mu\tilde{\chi}_i^- A^\mu - e\cot\theta_W\overline{\tilde{\chi}_i^-}\gamma_\mu(x_i-y_i\gamma_5)\tilde{\chi}_i^- Z^\mu$ and also $\mathcal{L}\ni iA^d_{\tilde{\chi}_i^-}\tilde{u}_L^\dagger\overline{\tilde{\chi}_i^-}P_L d + iA^u_{\tilde{\chi}_i^-}\tilde{d}_L^\dagger\overline{\tilde{\chi}_i^{-c}}P_L u$ + h.c.. Contributing diagrams include s-channel γ, Z^0 exchange and t-channel $\tilde{u}_L$ exchange [16,17]. The couplings x_i and y_i are again new and as usual convention-dependent.

The subprocess cross section is given by

$$\frac{d\sigma}{dt}(d\bar{d}\to\tilde{\chi}_i^-\tilde{\chi}_i^+) = \frac{1}{192\pi s^2}\left[T_\gamma + T_Z + T_{\tilde{u}_L} + T_{\gamma Z} + T_{\gamma\tilde{u}_L} + T_{Z\tilde{u}_L}\right] \qquad (48.77)$$

where

$$T_\gamma = \frac{32e^4q_d^2}{s^2}\left[d\cdot\tilde{\chi}_i^+\overline{d}\cdot\tilde{\chi}_i^- + d\cdot\tilde{\chi}_i^-\overline{d}\cdot\tilde{\chi}_i^+ + m^2_{\tilde{\chi}_i^-}d\cdot\overline{d}\right] \qquad (48.78)$$

$$T_Z = 32e^4\cot^2\theta_W|D_Z(s)|^2$$
$$\left\{(\alpha_d^2+\beta_d^2)(x_i^2+y_i^2)\left[d\cdot\tilde{\chi}_i^+\overline{d}\cdot\tilde{\chi}_i^- + d\cdot\tilde{\chi}_i^-\overline{d}\cdot\tilde{\chi}_i^+ + m^2_{\tilde{\chi}_i^-}d\cdot\overline{d}\right]\right.$$
$$\left.\mp 4\alpha_d\beta_d x_i y_i\left[d\cdot\tilde{\chi}_i^+\overline{d}\cdot\tilde{\chi}_i^- - d\cdot\tilde{\chi}_i^-\overline{d}\cdot\tilde{\chi}_i^+\right] - 2y_i^2(\alpha_d^2+\beta_d^2)m^2_{\tilde{\chi}_i^-}d\cdot\overline{d}\right\}, \qquad (48.79)$$

$$T_{\tilde{u}_L} = \frac{4|A^d_{\tilde{\chi}_i^-}|^4}{[(d-\tilde{\chi}_i^-)^2 - m^2_{\tilde{u}_L}]^2}\; d\cdot\tilde{\chi}_i^-\overline{d}\cdot\tilde{\chi}_i^+ \qquad (48.80)$$

$$T_{\gamma Z} = \frac{64e^4\cot\theta_W q_d(s-M_Z^2)|D_Z(s)|^2}{s}\times$$
$$\left\{\alpha_d x_i\left(d\cdot\tilde{\chi}_i^+\overline{d}\cdot\tilde{\chi}_i^- + d\cdot\tilde{\chi}_i^-\overline{d}\cdot\tilde{\chi}_i^+ + m^2_{\tilde{\chi}_i^-}d\cdot\overline{d}\right)\right.$$
$$\left.\pm\beta_d y_i\left(d\cdot\tilde{\chi}_i^-\overline{d}\cdot\tilde{\chi}_i^+ - d\cdot\tilde{\chi}_i^+\overline{d}\cdot\tilde{\chi}_i^-\right)\right\} \qquad (48.81)$$

$$T_{\gamma\tilde{u}_L} = \mp\frac{8e^2q_d}{s}\frac{|A^d_{\tilde{\chi}_i^-}|^2}{[(d-\tilde{\chi}_i^-)^2 - m^2_{\tilde{u}_L}]}\left\{2\overline{d}\cdot\tilde{\chi}_i^+ d\cdot\tilde{\chi}_i^- + m^2_{\tilde{\chi}_i^-}d\cdot\overline{d}\right\} \qquad (48.82)$$

and

$$T_{Z\tilde{u}_L} = \mp 8e^2 \cot\theta_W |D_Z(s)|^2 \frac{|A^d_{\tilde{\chi}_i^-}|^2 (s-M_Z^2)}{[(d-\tilde{\chi}_i^-)^2 - m^2_{\tilde{u}_L}]} (\alpha_d - \beta_d) \times \left\{ 2(x_i \mp y_i) d\cdot\tilde{\chi}_i^- \overline{d}\cdot\tilde{\chi}_i^+ + m^2_{\tilde{\chi}_i^-}(x_i \pm y_i) d\cdot\overline{d} \right\} \quad (48.83)$$

using the upper of the sign choices.

The cross section for $u\overline{u} \to \tilde{\chi}_i^+ \tilde{\chi}_i^-$ can be obtained from the above by replacing $\alpha_d \to \alpha_u$, $\beta_d \to \beta_u$, $q_d \to q_u$, $\tilde{u}_L \to \tilde{d}_L$, $A^d_{\tilde{\chi}_i^-} \to A^u_{\tilde{\chi}_i^-}$, $d \to \overline{u}$, $\overline{d} \to u$ and adopting the lower of the sign choices everywhere.

The cross section for $q\bar{q} \to \tilde{\chi}_1^- \tilde{\chi}_2^+$, $\tilde{\chi}_1^+ \tilde{\chi}_2^-$ can occur via Z and $\tilde{q}_L$ exchange. It is usually much smaller than $\tilde{\chi}^-_{1,2}\tilde{\chi}^+_{1,2}$ production, so the cross section will not be presented here. It can be found in Appendix A of Ref. 15.

48.8.4.3. *Neutralino pair production:*

Neutralino pair production via $q\bar{q}$ fusion takes place via s-channel Z exchange plus t- and u-channel left- and right- squark exchange (5 diagrams) [17,18]. The Lagrangian couplings (see previous footnote*) needed include terms given above plus terms of the form $\mathcal{L} = W_{ij}\overline{\tilde{\chi}^0}_i \gamma_\mu (\gamma_5)^{\theta_i+\theta_j+1} \tilde{\chi}^0_j Z^\mu$. The couplings W_{ij} depend only on the *higgsino* components of the neutralinos i and j. The subprocess cross section is given by:

$$\frac{d\sigma}{dt}(q\bar{q} \to \tilde{\chi}_i^0 \tilde{\chi}_j^0) = \frac{1}{192\pi s^2} \left[T_Z + T_{\tilde{q}_L} + T_{\tilde{q}_R} + T_{Z\tilde{q}_L} + T_{Z\tilde{q}_R} \right] \quad (48.84)$$

where

$$T_Z = 128e^2 |W_{ij}|^2 (\alpha_q^2 + \beta_q^2) |D_Z(s)|^2 \left[q\cdot\tilde{\chi}_i^0 \bar{q}\cdot\tilde{\chi}_j^0 + q\cdot\tilde{\chi}_j^0 \bar{q}\cdot\tilde{\chi}_i^0 - \eta_i\eta_j m_{\tilde{\chi}_i^0} m_{\tilde{\chi}_j^0} q\cdot\bar{q} \right], \quad (48.85)$$

$$T_{\tilde{q}_L} = 4|A^q_{\tilde{\chi}_i^0}|^2 |A^q_{\tilde{\chi}_j^0}|^2 \left\{ \frac{q\cdot\tilde{\chi}_i^0 \bar{q}\cdot\tilde{\chi}_j^0}{[(\tilde{\chi}_i^0 - q)^2 - m^2_{\tilde{q}_L}]^2} + \frac{q\cdot\tilde{\chi}_j^0 \bar{q}\cdot\tilde{\chi}_i^0}{[(\tilde{\chi}_j^0 - q)^2 - m^2_{\tilde{q}_L}]^2} - \eta_i\eta_j \frac{m_{\tilde{\chi}_i^0} m_{\tilde{\chi}_j^0} q\cdot\bar{q}}{[(\tilde{\chi}_i^0 - q)^2 - m^2_{\tilde{q}_L}][(\tilde{\chi}_j^0 - q)^2 - m^2_{\tilde{q}_L}]} \right\} \quad (48.86)$$

$$T_{\tilde{q}_R} = 4|B^q_{\tilde{\chi}_i^0}|^2 |B^q_{\tilde{\chi}_j^0}|^2 \left\{ \frac{q\cdot\tilde{\chi}_i^0 \bar{q}\cdot\tilde{\chi}_j^0}{[(\tilde{\chi}_i^0 - q)^2 - m^2_{\tilde{q}_R}]^2} + \frac{q\cdot\tilde{\chi}_j^0 \bar{q}\cdot\tilde{\chi}_i^0}{[(\tilde{\chi}_j^0 - q)^2 - m^2_{\tilde{q}_R}]^2} - \eta_i\eta_j \frac{m_{\tilde{\chi}_i^0} m_{\tilde{\chi}_j^0} q\cdot\bar{q}}{[(\tilde{\chi}_i^0 - q)^2 - m^2_{\tilde{q}_R}][(\tilde{\chi}_j^0 - q)^2 - m^2_{\tilde{q}_R}]} \right\} \quad (48.87)$$

$$T_{Z\tilde{q}_L} = 16e(\alpha_q - \beta_q)(s - M_Z^2) |D_Z(s)|^2 \left\{ \frac{Re(W_{ij} A^{q*}_{\tilde{\chi}_i^0} A^q_{\tilde{\chi}_j^0})}{[(\tilde{\chi}_i^0 - q)^2 - m^2_{\tilde{q}_L}]} \left[2q\cdot\tilde{\chi}_i^0 \bar{q}\cdot\tilde{\chi}_j^0 - \eta_i\eta_j m_{\tilde{\chi}_i^0} m_{\tilde{\chi}_j^0} q\cdot\bar{q} \right] + \eta_i\eta_j \frac{Re(W_{ij} A^q_{\tilde{\chi}_i^0} A^{q*}_{\tilde{\chi}_j^0})}{[(\tilde{\chi}_j^0 - q)^2 - m^2_{\tilde{q}_L}]} \left[2q\cdot\tilde{\chi}_j^0 \bar{q}\cdot\tilde{\chi}_i^0 - \eta_i\eta_j m_{\tilde{\chi}_i^0} m_{\tilde{\chi}_j^0} q\cdot\bar{q} \right] \right\} \quad (48.88)$$

$$T_{Z\tilde{q}_R} = 16e(\alpha_q + \beta_q)(s - M_Z^2) |D_Z(s)|^2 \left\{ \frac{Re(W_{ij} B^{q*}_{\tilde{\chi}_i^0} B^q_{\tilde{\chi}_j^0})}{[(\tilde{\chi}_i^0 - q)^2 - m^2_{\tilde{q}_R}]} \left[2q\cdot\tilde{\chi}_i^0 \bar{q}\cdot\tilde{\chi}_j^0 - \eta_i\eta_j m_{\tilde{\chi}_i^0} m_{\tilde{\chi}_j^0} q\cdot\bar{q} \right] - \frac{Re(W_{ij} B^q_{\tilde{\chi}_i^0} B^{q*}_{\tilde{\chi}_j^0})}{[(\tilde{\chi}_j^0 - q)^2 - m^2_{\tilde{q}_R}]} \left[2q\cdot\tilde{\chi}_j^0 \bar{q}\cdot\tilde{\chi}_i^0 - \eta_i\eta_j m_{\tilde{\chi}_i^0} m_{\tilde{\chi}_j^0} q\cdot\bar{q} \right] \right\}. \quad (48.89)$$

As before, $\eta_i = \pm 1$ corresponding to whether the neutralino mass eigenvalue is positive or negative. When $i = j$ in the above formula, one must remember to integrate over just 2π steradians of solid angle to avoid double counting in the total cross section.

48.9. Universal extra dimensions

In the Universal Extra Dimension (UED) model of Ref. [19] (see Ref. [20] for a review of models with extra spacetime dimensions), the Standard Model is embedded in a five dimensional theory, where the fifth dimension is compactified on an S_1/Z_2 orbifold. Each SM chirality state is then the zero mode of an infinite tower of Kaluza-Klein excitations labelled by $n = 0 - \infty$. A KK parity is usually assumed to hold, where each state is assigned KK-parity $P = (-1)^n$. If the compactification scale is around a TeV, then the $n = 1$ (or even higher) KK modes may be accessible to collider searches.

Of interest for hadron colliders are the production of massive $n \geq 1$ quark or gluon pairs. These production cross sections have been calculated in Ref. [21,22]. We list here results for the $n = 1$ case only with $M_1 = 1/R$ (R is the compactification radius) and s, t and u are the usual Mandelstam variables; more general formulae can be found in Ref. [22]. The superscript $*$ stands for any KK excited state, while $\bullet$ stands for left chirality states and $\circ$ stands for right chirality states.

$$\frac{d\sigma}{dt} = \frac{1}{16\pi s^2} T \quad (48.90)$$

where

$$T(q\bar{q} \to g^* g^*) = \frac{2g_s^4}{27} \left[M_1^2 \left(-\frac{4s^3}{t'^2 u'^2} + \frac{57s}{t'u'} - \frac{108}{s} \right) + \frac{20s^2}{t'u'} - 93 + \frac{108 t'u'}{s^2} \right] \quad (48.91)$$

and

$$T(gg \to g^* g^*) = \frac{9g_s^4}{27} \left[3M_1^4 \frac{s^2 + t'^2 + u'^2}{t'^2 u'^2} - 3M_1^2 \frac{s^2 + t'^2 + u'^2}{st'u'} + 1 + \frac{(s^2 + t'^2 + u'^2)^3}{4s^2 t'^2 u'^2} - \frac{t'u'}{s^2} \right] \quad (48.92)$$

where $t' = t - M_1^2$ and $u' = u - M_1^2$.

Also,

$$T(q\bar{q} \to q_1^{*\prime} \bar{q}_1^{*\prime}) = \frac{4g_s^4}{9} \left[\frac{2M_1^2}{s} + \frac{t'^2 + u'^2}{s^2} \right],$$

$$T(q\bar{q} \to q_1^* \bar{q}_1^*) = \frac{g_2^4}{9} \left[2M_1^2 \left(\frac{4}{s} + \frac{s}{t'^2} - \frac{1}{t'} \right) + \frac{23}{6} + \frac{2s^2}{t'^2} + \frac{8s}{3t'} + \frac{6t'}{s} + \frac{8t'^2}{s^2} \right],$$

$$T(qq \to q_1^* q_1^*) = \frac{g_s^4}{27} \left[M_1^2 \left(6\frac{t'}{u'^2} + 6\frac{u'}{t'^2} - \frac{s}{t'u'} \right) + 2 \left(3\frac{t'^2}{u'^2} + 3\frac{u'^2}{t'^2} + 4\frac{s^2}{t'u'} - 5 \right) \right],$$

$$T(gg \to q_1^* \bar{q}_1^*) = g_s^4 \left[M_1^4 \frac{-4}{t'u'} \left(\frac{s^2}{6t'u'} - \frac{3}{8} \right) + M_1^2 \frac{4}{s} \left(\frac{s^2}{6t'u'} - \frac{3}{8} \right) + \frac{s^2}{6t'u'} - \frac{17}{24} + \frac{3t'u'}{4s^2} \right],$$

$$T(gq \to g^* q_1^*) = \frac{-g_s^4}{3} \left[\frac{5s^2}{12t'^2} + \frac{s^3}{t'^2 u'} + \frac{11su'}{6t'^2} + \frac{5u'^2}{12t'^2} + \frac{u'^3}{st'^2} \right],$$

$$T(q\bar{q}' \to q_1^* \bar{q}_1^{*\prime}) = \frac{g_s^4}{18} \left[4M_1^4 \frac{s}{t'^2} + 5 + 4\frac{s^2}{t'^2} + 8\frac{s}{t'} \right],$$

$$T(qq' \to q_1^* q_1^{*\prime}) = \frac{2g_s^4}{9} \left[-M_1^2 \frac{s}{t'^2} + \frac{1}{4} + \frac{s^2}{t'^2} \right],$$

$$T(qq \to q_1^\bullet q_1^\circ) = \frac{g_s^4}{9}\left[M_1^2\left(\frac{2s^3}{t'^2u'^2} - \frac{4s}{t'u'}\right) + 2\frac{s^4}{t'^2u'^2} - 8\frac{s^2}{t'u'} + 5\right],$$

$$T(q\bar{q}' \to q_1^\bullet \bar{q}_1'^\circ) = \frac{g_s^4}{9}\left[2M_1^2\left(\frac{1}{t'} + \frac{u'}{t'^2}\right) + \frac{5}{2} + \frac{4u'}{t'} + \frac{2u'^2}{t'^2}\right],$$

and

$$T(qq' \to q_1^\bullet q_1'^\circ) = \frac{g_s^4}{9}\left[-2M_1^2\left(\frac{1}{t'} + \frac{u'}{t'^2}\right) + \frac{1}{2} + \frac{2u'^2}{t'^2}\right].$$

48.10. Large extra dimensions

In the ADD theory [23] with large extra dimensions (LED), the SM particles are confined to a 3-brane, while gravity propagates in the bulk. It is assumed that the n extra dimensions are compactified on an n-dimensional torus of volume $(2\pi r)^n$, so that the fundamental $4+n$ dimensional Planck scale M_* is related to the usual 4-dimensional Planck scale M_{Pl} by $M_{Pl}^2 = M_*^{n+2}(2\pi r)^n$. If $M_* \sim 1$ TeV, then the $M_W - M_{Pl}$ hierarchy problem is just due to gravity propagating in the large extra dimensions.

In these theories, the KK-excited graviton states $G_{\mu\nu}^n$ for $n = 1-\infty$ can be produced at collider experiments. The graviton couplings to matter are suppressed by $1/M_{Pl}$, so that graviton emission cross sections $d\sigma/dt \sim 1/M_{Pl}^2$. However, the mass splittings between the excited graviton states can be tiny, so the graviton eigenstates are usually approximated by a continuum distribution. A summation (integration) over all allowed graviton emissions ends up cancelling the $1/M_{Pl}^2$ factor, so that observable cross section rates can be attained. Some of the fundamental production formulae for a KK graviton (denoted G) of mass m at hadron colliders include the subprocesses

$$\frac{d\sigma_m}{dt}(f\bar{f} \to \gamma G) = \frac{\alpha Q_f^2}{16N_f}\frac{1}{sM_{Pl}^2}F_1(\frac{t}{s}, \frac{m^2}{s}), \tag{48.93}$$

where Q_f is the charge of fermion f and N_f is the number of QCD colors of f. Also,

$$\frac{d\sigma_m}{dt}(q\bar{q} \to gG) = \frac{\alpha_s}{36}\frac{1}{sM_{Pl}^2}F_1(\frac{t}{s}, \frac{m^2}{s}), \tag{48.94}$$

$$\frac{d\sigma_m}{dt}(qg \to qG) = \frac{\alpha_s}{96}\frac{1}{sM_{Pl}^2}F_2(\frac{t}{s}, \frac{m^2}{s}), \tag{48.95}$$

$$\frac{d\sigma_m}{dt}(gg \to gG) = \frac{3\alpha_s}{16}\frac{1}{sM_{Pl}^2}F_3(\frac{t}{s}, \frac{m^2}{s}), \tag{48.96}$$

where

$$F_1(x,y) = \frac{1}{x(y-1-x)}\Big[-4x(1+x)(1+2x+2x^2) + y(1+6x+18x^2+16x^3) - 6y^2x(1+2x) + y^3(1+4x)\Big] \tag{48.97}$$

$$F_2(x,y) = -(y-1-x)F_1\left(\frac{x}{y-1-x}, \frac{y}{y-1-x}\right) \tag{48.98}$$

and

$$F_3(x,y) = \frac{1}{x(y-1-x)}\Big[1+2x+3x^2+2x^3+x^4 - 2y(1+x^3) + 3y^2(1+x^2) - 2y^3(1+x) + y^4\Big]. \tag{48.99}$$

These formulae must then be multiplied by the graviton density of states formula $dN = S_{n-1}\frac{M_{Pl}^2}{M_*^{n+2}}m^{n-1}dm$ to gain the cross section

$$\frac{d^2\sigma}{dtdm} = S_{n-1}\frac{M_{Pl}^2}{M_*^{n+2}}m^{n-1}\frac{d\sigma_m}{dt} \tag{48.100}$$

where $S_n = \frac{(2\pi)^{n/2}}{\Gamma(n/2)}$ is the surface area of an n-dimensional sphere of unit radius.

Virtual graviton processes can also be searched for at colliders. For instance, in Ref. [24] the cross section for Drell-Yan production of lepton pairs via gluon fusion was calculated, where it is found that, in the center-of-mass system

$$\frac{d\sigma}{dz}(gg \to \ell^+\ell^-) = \frac{\lambda^2 s^3}{64\pi M_*^8}(1-z^2)(1+z^2) \tag{48.101}$$

where $z = \cos\theta$ and λ is a model-dependent coupling constant ~ 1. Formulae for Drell-Yan production via $q\bar{q}$ fusion can also be found in Refs. [24,25].

48.11. Warped extra dimensions

In the Randall-Sundrum model [26] of warped extra dimensions, the arena for physics is a 5-d anti-deSitter (AdS_5) spacetime, for which a non-factorizable metric exists with a metric warp factor $e^{-2\sigma(\phi)}$. It is assumed that two opposite tension 3-branes exist within AdS_5 at the two ends of an S_1/Z_2 orbifold parametrized by co-ordinate ϕ which runs from $0-\pi$. The 4-D solution of the Einstein equations yields $\sigma(\phi) = kr_c|\phi|$, where r_c is the compactification radius of the extra dimension and $k \sim M_{Pl}$. The 4-D effective action allows one to identify $\overline{M}_{Pl}^2 = \frac{M^3}{k}(1 - e^{-2kr_c\pi})$, where M is the 5-D Planck scale. Physical particles on the TeV scale (SM) brane have mass $m = e^{-kr_c\pi}m_0$, where m_0 is a fundamental mass of order the Planck scale. Thus, the weak scale-Planck scale hierarchy occurs due to the existence of the exponential warp factor if $kr_c \sim 12$.

In the simplest versions of the RS model, the TeV-scale brane contains only SM particles plus a tower of KK gravitons. The RS gravitons have mass $m_n = kx_ne^{-kr_c\pi}$, where the x_i are roots of Bessel functions $J_1(x_n) = 0$, with $x_1 \simeq 3.83$, $x_2 \simeq 7.02$ etc. While the RS zero-mode graviton couplings suppressed by $1/\overline{M}_{Pl}$ and are thus inconsequential for collider searches, the $n=1$ and higher modes have couplings suppressed instead by $\Lambda_\pi = e^{-kr_c\pi}\overline{M}_{Pl} \sim TeV$. The $n=1$ RS graviton should have width $\Gamma_1 = \rho m_1 x_1^2(k/\overline{M}_{Pl})^2$, where ρ is a constant depending on how many decay modes are open. The formulae for dilepton production via virtual RS graviton exchange can be gained from the above formulae for the ADD scenario via the replacement [27]

$$\frac{\lambda}{M_*^4} \to \frac{i^2}{8\Lambda_\pi^2}\sum_{n=1}^{\infty}\frac{1}{s - m_n^2 + im_n\Gamma_n}. \tag{48.102}$$

References:

1. J.F. Owens *et al.*, Phys. Rev. **D18**, 1501 (1978). Note that cross section given in previous editions of RPP for $gg \to q\overline{q}$ lacked a factor of π.
2. F. Wilczek, Phys. Rev. Lett. **39**, 1304 (1977).
3. B.L. Ioffe and V.Khoze, Leningrad Report 274, 1976; Sov. J. Nucl. Phys. **9**, 50 (1978).
4. J. Ellis *et al.*, Nucl. Phys. **B106**, 292 (1976).
5. R.N. Cahn and S. Dawson, Phys. Lett. **B136**, 196 (1984), erratum, Phys. Lett. **B138**, 464 (1984).
6. S. Dawson, Nucl. Phys. **B249**, 42 (1985).
7. M.S. Chanowitz and M.K. Gaillard, Phys. Lett. **B142**, 85 (1984).
8. R.N. Cahn, Nucl. Phys. **B255**, 341 (1985).
9. For an exhaustive treatment, see V.M. Budnev *et al.*, Phys. Reports **15C**, 181(1975).
10. See *e.g.* H. Haber, *Supersymmetry, Part I (Theory)*, this review.
11. P. R. Harrison and C. H. Llewellyn Smith, Nucl. Phys. **B213**, 223 (1983), Erratum-*ibid.*, **B223**, 542 (1983); S. Dawson, E. Eichten, and C. Quigg, Phys. Rev. **D31**, 1581 (1985); V. Barger *et al.*, Phys. Rev. **D31**, 528 (1985); H. Baer and X. Tata, Phys. Lett. **B160**, 159 (1985).
12. H. Baer, D. Karatas, and X. Tata, Phys. Rev. **D42**, 2259 (1990).
13. H. Haber and G. Kane, Phys. Rept. **117**, 75 (1985).
14. Theory and Phenomenology of Sparticles, M. Drees, R. Godbole, and P. Roy (World Scientific) 2005.

15. Weak Scale Supersymmetry: From Superfields to Scattering Events, H. Baer and X. Tata (Cambridge University Press) 2006.
16. A. Bartl, H. Fraas, and W. Majerotto, Z. Phys. **C30**, 441 (1986).
17. H. Baer *et al.*, Int. J. Mod. Phys. **A4**, 4111 (1989).
18. A. Bartl, H. Fraas, and W. Majerotto, Nucl. Phys. **B278**, 1 (1986).
19. T. Appelquist, H.C. Cheng, and B. Dobrescu, Phys. Rev. **D64**, 035002 (2001).
20. For a review of models with extra spacetime dimensions, see G. Giudice and J. Wells, *Extra Dimensions*, this *Review*.
21. J.M. Smillie and B.R. Webber, JHEP **0510**, 069 (2005).
22. C. Macesanu, C.D. McMullen, and S. Nandi, Phys. Rev. **D66**, 015009 (2002).
23. N. Arkani-Hamed, S. Dimopoulos, and G. Dvali, Phys. Lett. **B429**, 263 (1998) and Phys. Rev. **D59**, 086004 (1999).
24. J. L. Hewett, Phys. Rev. Lett. **82**, 4765 (1999).
25. G. Giudice, R. Rattazzi, and J. Wells, Nucl. Phys. **B544**, 3 (1999); E.A. Mirabelli, M. Perelstein, and M.E. Peskin, Phys. Rev. Lett. **82**, 2236 (1999); T. Han, J. Lykken, and R. Zhang, Phys. Rev. **D59**, 105006 (1999).
26. L. Randall and R.S. Sundrum, Phys. Rev. Lett. **83**, 3370 (1999).
27. H. Davoudiasl, J.L. Hewett, and T.G. Rizzo, Phys. Rev. Lett. **84**, 2080 (2000).

49. NEUTRINO CROSS SECTION MEASUREMENTS

Revised January 2014 by G.P. Zeller (Fermilab)

Neutrino cross sections are an essential ingredient in all neutrino experiments. Interest in neutrino scattering has recently increased due to the need for such information in the interpretation of neutrino oscillation data. Historically, neutrino scattering results on both charged current (CC) and neutral current (NC) channels have been collected over many decades using a variety of targets, analysis techniques, and detector technologies. With the advent of intense neutrino sources constructed for neutrino oscillation investigations, experiments are now remeasuring these cross sections with a renewed appreciation for nuclear effects[†] and the importance of improved neutrino flux calculations. This work summarizes accelerator-based neutrino cross section measurements performed in the $\sim 0.1-300$ GeV range with an emphasis on inclusive, quasi-elastic, and single-pion production processes, areas where we have the most experimental input at present (Table 49.1). For a more comprehensive discussion of neutrino cross sections, including neutrino-electron elastic scattering and lower energy measurements, the reader is directed to a recent review of this subject [1]. Here, we survey existing experimental data on neutrino interactions and do not attempt to provide a census of the associated theoretical calculations, which are both important and plentiful.

49.1. Inclusive Scattering

Over the years, many experiments have measured the total inclusive cross section for neutrino ($\nu_\mu N \to \mu^- X$) and antineutrino ($\overline{\nu}_\mu N \to \mu^+ X$) scattering off nucleons covering a broad range of neutrino energies. As can be seen in Fig. 49.1, the inclusive cross section approaches a linear dependence on neutrino energy. Such behavior is expected for point-like scattering of neutrinos from quarks, an assumption which breaks down at lower energies. To provide a more complete picture, differential cross sections for such inclusive scattering processes have been reported - these include measurements on iron from NuTeV [29] and, more recently, at lower energies on argon from ArgoNeuT [2] and carbon from T2K [28]. MINERvA has also provided new measurements of the ratios of the CC inclusive scattering cross section on a variety of targets (lead, iron, plastic) [30]. At high energy, the inclusive cross section is dominated by deep inelastic scattering (DIS). Several high energy neutrino experiments have measured the DIS cross sections for specific final states, for example opposite-sign dimuon production. The most recent dimuon cross section measurements include those from CHORUS [31], NOMAD [32], and NuTeV [33]. At lower neutrino energies, the inclusive cross section is an additionally complex combination of quasi-elastic scattering and resonance production processes, two areas we discuss next.

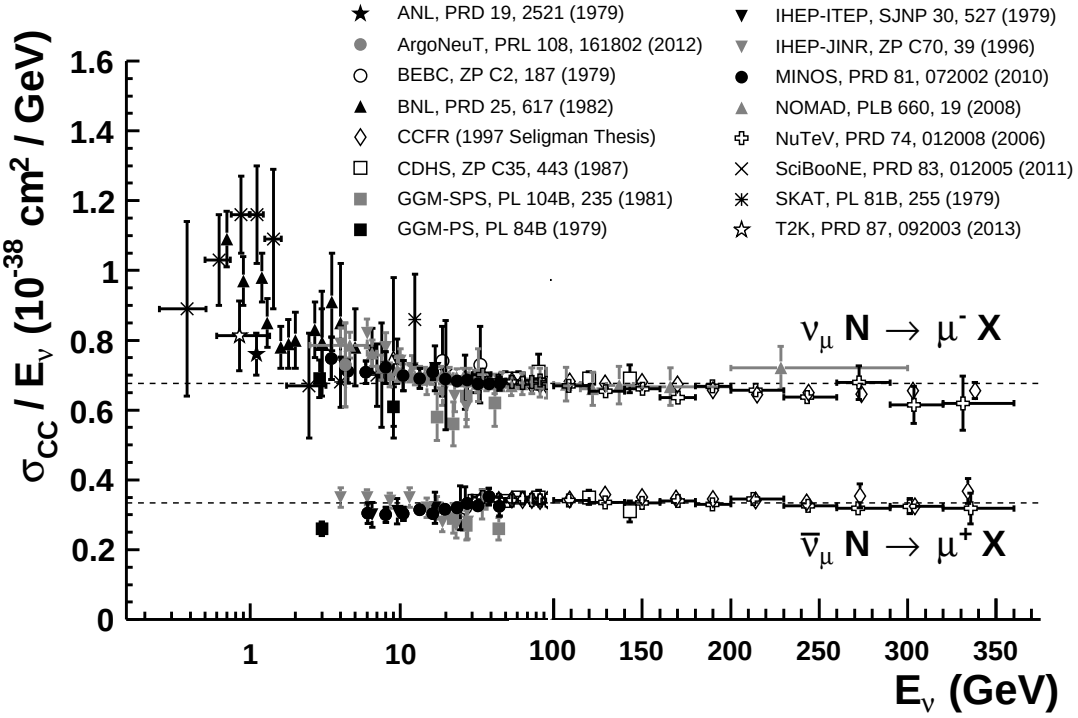

Fig. 49.1: Measurements of ν_μ and $\overline{\nu}_\mu$ CC inclusive scattering cross sections divided by neutrino energy as a function of neutrino energy. Note the transition between logarithmic and linear scales occurring at 100 GeV. Neutrino cross sections are typically twice as large as their corresponding antineutrino counterparts, although this difference can be larger at lower energies. NC cross sections (not shown) are generally smaller but non-negligible compared to the CC scattering case.

[†] Nuclear effects refer to kinematic and final state effects which impact neutrino scattering off nuclei. Such effects can be significant and are particularly relevant given that modern neutrino experiments make use of nuclear targets to increase their event yields.

Table 49.1: Summary of modern accelerator-based experiments and their published results on neutrino CC inclusive, quasi-elastic (QE) scattering, and pion production cross sections. MINOS, NOvA, and T2K refer to their near detector data.

Experiment	beam	$\langle E_\nu \rangle$ GeV	neutrino target(s)	run period	σ_ν publications by topic
ArgoNeuT	$\nu, \overline{\nu}$	3.3	Ar	2009 – 2010	CC [2]
ICARUS	ν	20.0	Ar	2010 – present	
K2K	ν	1.3	CH, H_2O	2003 – 2004	QE [3], π [4,5,6,7]
MicroBooNE	ν	0.8	Ar	scheduled 2014	
MINERνA	$\nu, \overline{\nu}$	3.3, 6.5	He, C, O, Fe, Pb	2009 – present	QE [8,9]
MiniBooNE	$\nu, \overline{\nu}$	0.8	CH_2	2002 – 2012	QE [10,11,12,13,14], π [15,16,17,18,19]
MINOS	$\nu, \overline{\nu}$	3.3, 6.5	Fe	2004 – present	CC [20]
NOMAD	$\nu, \overline{\nu}$	26.0	C	1995 – 1998	CC [21], QE [22], π [23]
NOvA (+ NDOS)	$\nu, \overline{\nu}$	2.0	CH_2	2010 – present	
SciBooNE	$\nu, \overline{\nu}$	0.8	CH	2007 – 2008	CC [24], π [25,26,27]
T2K	ν, $\overline{\nu}$	0.85	CH, H_2O	2010 – present	CC [28]

49.2. Quasi-elastic scattering

Quasi-elastic (QE) scattering is the dominant neutrino interaction for neutrino energies less than ~ 1 GeV and represents a large fraction of the signal samples in many neutrino oscillation experiments. Historically, neutrino (antineutrino) quasi-elastic scattering refers to the process, $\nu_\mu n \to \mu^- p$ ($\overline{\nu}_\mu p \to \mu^+ n$), where a charged lepton and single nucleon are ejected in the elastic interaction of a neutrino (or antineutrino) with a nucleon in the target material. This is the final state one would strictly observe, for example, in scattering off of a free nucleon target. Fig. 49.2 displays the current status of existing measurements of ν_μ and $\overline{\nu}_\mu$ QE scattering cross sections as a function of neutrino energy. In this plot, and all others in this review, the prediction from a representative neutrino event generator (NUANCE) [34] provides a theoretical comparator. Other generators and more sophisticated calculations exist which can yield significantly different predictions [35]. Note that modern experiments have recently opted to report QE cross sections as a function of final state muon or proton kinematics [12,11,36]. Such distributions are harder to compare between experiments but are much less model-dependent and provide more stringent tests of the theory than cross sections as a function of neutrino energy.

In many of these initial measurements of the neutrino QE cross section, bubble chamber experiments employed light targets (H_2 or D_2) and required both the detection of the final state muon and single nucleon‡; thus the final state was clear and elastic kinematic conditions could be verified. The situation is more complicated, of course, for heavier nuclear targets. In this case, nuclear effects can impact the size and shape of the cross section as well as the final state kinematics and topology. Due to intranuclear hadron rescattering and the possible effects of correlations between target nucleons, additional nucleons may be ejected in the final state; hence, a QE interaction on a nuclear target does not always imply the ejection of a *single* nucleon. One therefore needs to take some care in defining what one means by neutrino QE scattering when scattering off targets heavier than H_2 or D_2. Adding to the complexity, recent MiniBooNE measurements of the ν_μ and $\overline{\nu}_\mu$ QE scattering cross sections on carbon near 1 GeV have revealed a significantly larger cross section than originally anticipated [11,12]. Such an enhancement was observed many years prior in electron-nucleus scattering [45] and is believed to be due to the presence of correlations between target nucleons in the nucleus. As a result, the impact of such nuclear effects on neutrino QE scattering has recently been the subject of intense experimental and theoretical scrutiny with potential implications on event rates, nucleon emission, neutrino energy reconstruction, and neutrino/antineutrino ratios. The reader is referred to a recent review of the situation in [46].

‡ In the case of D_2, many experiments additionally observed the spectator proton.

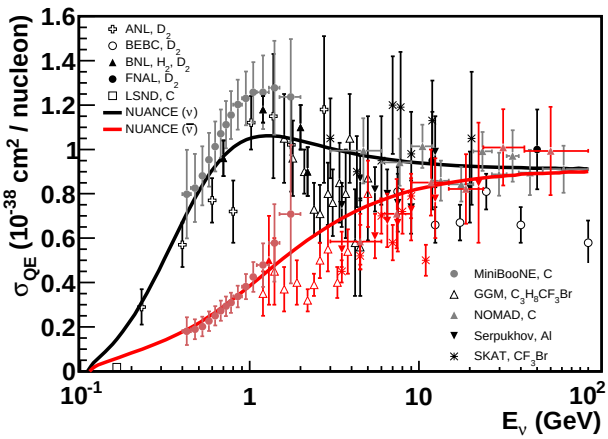

Figure 49.2: Measurements of ν_μ (black) and $\overline{\nu}_\mu$ (red) QE scattering cross sections (per nucleon) as a function of neutrino energy. Data on a variety of nuclear targets are shown, including measurements from ANL [37], BEBC [38], BNL [39], FNAL [40], GGM [41], LSND [42], MiniBooNE [11,12], NOMAD [22], Serpukhov [43], and SKAT [44]. Shown is the QE free nucleon scattering prediction from NUANCE [34] assuming $M_A = 1.0$ GeV. This prediction is significantly altered by nuclear effects in the case of neutrino-nucleus scattering. Although plotted together, care should be taken in interpreting measurements performed on targets heavier than D_2 due to possible differences in QE identification and kinematics.

Additional measurements are clearly needed before a complete understanding is achieved. To help drive further progress, neutrino-nucleus QE cross sections have been reported for the first time in the form of double-differential distributions in muon kinematics, $d^2\sigma/dT_\mu d\cos\theta_\mu$, by MiniBooNE [11,12] thus reducing the model-dependence of the reported data and allowing a more detailed 2-dimensional test of the underlying nuclear theory. Experiments such as ArgoNeuT have begun to provide the first measurements of proton multiplicities in neutrino-argon QE scattering [36], a critical ingredient in understanding the hadronic side of these interactions and final state effects. Both MINOS and NOvA have started to study QE interactions in their near detectors with sizable statistics [47,48]. Most recently, MINERvA has measured the differential cross section, $d\sigma/dQ^2_{QE}$, and vertex energy in both ν_μ and $\overline{\nu}_\mu$ QE interactions in hydrocarbon [8,9], with future results expected on numerous nuclear targets. With the MiniBooNE results having recently revealed this additional physics, measurements from other neutrino experiments

are crucial for getting a better handle on the complex underlying nuclear physics impacting neutrino-nucleus interactions. What we once thought was "simple" QE scattering is in fact not so simple.

In addition to such charged current investigations, measurements of the neutral current counterpart of this channel have also been performed. The most recent NC elastic scattering cross section measurements include those from BNL E734 [49] and MiniBooNE [10,13]. A number of measurements of the Cabibbo-suppressed antineutrino QE hyperon production cross section have additionally been reported [44,50], although not in recent years.

49.3. Pion Production

In addition to such elastic processes, neutrinos can also inelastically scatter producing a nucleon excited state (Δ, N^*). Such baryonic resonances quickly decay, most often to a nucleon and single-pion final state. Fig. 49.3 and Fig. 49.4 show a collection of historical resonantly-produced single-pion cross section data for both CC and NC neutrino scattering. Decades ago, BEBC, FNAL, Gargamelle, and SKAT also performed similar measurements for antineutrinos [51]. Most often, these experiments reported measurements of NC/CC single-pion cross section ratios [52].

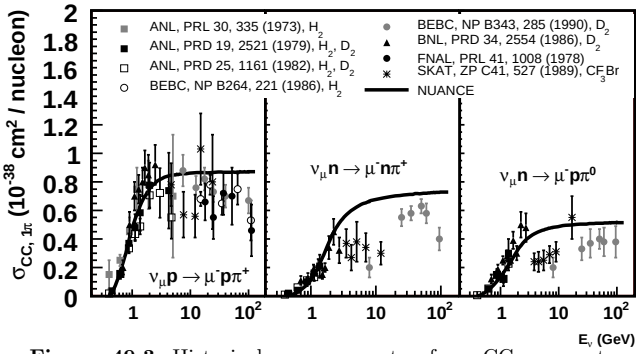

Figure 49.3: Historical measurements of ν_μ CC resonant single-pion production. The data appear as reported by the experiments; no additional corrections have been applied to account for differing nuclear targets or invariant mass selections. The free scattering curve from NUANCE assumes $M_A = 1.1$ GeV [34]. Note that other absolute measurements have been made by MiniBooNE [15,16] but cannot be directly compared with this historical data - such modern measurements are more inclusive and have quantified the production of pions leaving the target nucleus rather than specific $\pi + N$ final states as identified at the neutrino interaction vertex.

It should be noted that baryonic resonances can also decay to multi-pion, other mesonic (K, η, ρ, etc.), and even photon final states. Experimental results for these channels are typically sparse or non-existent [1]; however, photon production processes can be an important background for $\nu_\mu \to \nu_e$ appearance searches and thus have become the focus of some recent experimental investigations; for example, in NOMAD [53].

In addition to resonance production processes, neutrinos can also coherently scatter off of the entire nucleus and produce a distinctly forward-scattered single-pion final state. Both CC ($\nu_\mu\, A \to \mu^-\, A\, \pi^+$, $\overline{\nu}_\mu\, A \to \mu^+\, A\, \pi^-$) and NC ($\nu_\mu\, A \to \nu_\mu\, A\pi^0$, $\overline{\nu}_\mu\, A \to \overline{\nu}_\mu\, A\pi^0$) processes are possible in this case. The level of coherent pion production is predicted to be small compared to incoherent processes, but observations exist across a broad energy range and on multiple nuclear targets [23,55,56]. Most of these measurements have been performed at energies above 2 GeV, but several modern experiments have started to search for coherent pion production at lower neutrino energies, including K2K [7], MiniBooNE [19], and SciBooNE [25,27].

As with QE scattering, a new appreciation for the significance of nuclear effects has surfaced in pion production channels, again due to the use of heavy nuclear targets in modern neutrino experiments. Many experiments have been careful to report cross sections for various detected final states, thereby not correcting for large and uncertain nuclear effects (e.g., pion rescattering, charge exchange, and absorption) which can introduce unwanted sources of uncertainty and model dependence. Recent measurements of single-pion cross sections, as published by K2K [4–6], MiniBooNE [18], and SciBooNE [26], take the form of ratios with respect to QE or CC inclusive scattering samples. Providing the most comprehensive survey of neutrino single-pion production to date, MiniBooNE has recently published a total of 16 single- and double-differential cross sections for both the final state muon (in the case of CC scattering) and pion in these interactions; thus, providing the first measurements of these distributions [15–17]. Regardless of the interaction channel, such differential cross section measurements (in terms of observed final state particle kinematics) are now preferred for their reduced model dependence and for the additional kinematic information they provide. Such a new direction has been the focus of modern measurements as opposed to the reporting of more model-dependent, historical cross sections as a function of E_ν or Q^2. Together with similar results for other interaction channels, a better understanding and modeling of nuclear effects will be possible moving forward.

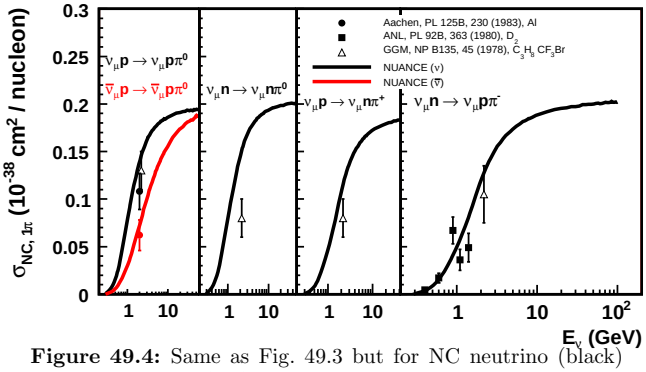

Figure 49.4: Same as Fig. 49.3 but for NC neutrino (black) and antineutrino (red) scattering. The Gargamelle (GGM) measurements come from a re-analysis of this data [54]. Note that more recent measurements of this absolute cross section exist [17] but cannot be directly compared with this historical data for the same reasons as in Fig. 49.3.

49.4. Outlook

Coming soon, additional neutrino and antineutrino cross section measurements in the few-GeV energy range are anticipated from MiniBooNE, MINOS, NOMAD, and SciBooNE. In addition, a few new experiments are now collecting data or will soon be commissioning their detectors. Analysis of a broad energy range of data on a variety of targets in the MINERνA experiment will provide the most detailed analysis yet of nuclear effects in neutrino interactions. Data from ArgoNeuT, ICARUS, and MicroBooNE will probe deeper into complex neutrino final states using the superior capabilities of liquid argon time projection chambers, while the T2K and NOvA near detectors will collect high statistics samples in intense neutrino beams. Together, these investigations should significantly advance our understanding of neutrino-nucleus scattering in the years to come.

49.5. Acknowledgments

The author thanks Anne Schukraft (Fermilab) for help in updating the plots contained in this review.

References:

1. J.A. Formaggio and G.P. Zeller, Rev. Mod. Phys. **84**, 1307 (2012).
2. C. Anderson *et al.*, Phys. Rev. Lett. **108**, 161802 (2012).
3. R. Gran *et al.*, Phys. Rev. **D74**, 052002 (2006).
4. C. Mariani *et al.*, Phys. Rev. **D83**, 054023 (2011).
5. A. Rodriguez *et al.*, Phys. Rev. **D78**, 032003 (2008).
6. S. Nakayama *et al.*, Phys. Lett. **B619**, 255 (2005).
7. M. Hasegawa *et al.*, Phys. Rev. Lett. **95**, 252301 (2005).

8. G.A. Fiorentini *et al.*, Phys. Rev. Lett. **111**, 022502 (2013).
9. L. Fields *et al.*, Phys. Rev. Lett. **111**, 022501 (2013).
10. A.A. Aguilar-Arevalo *et al.*, arXiv:1309.7257 [hep-ex], submitted to Phys. Rev. D.
11. A.A. Aguilar-Arevalo *et al.*, Phys. Rev. **D88**, 032001 (2013).
12. A.A. Aguilar-Arevalo *et al.*, Phys. Rev. **D81**, 092005 (2010).
13. A.A. Aguilar-Arevalo *et al.*, Phys. Rev. **D82**, 092005 (2010).
14. A.A. Aguilar-Arevalo *et al.*, Phys. Rev. Lett. **100**, 032301 (2008).
15. A.A. Aguilar-Arevalo *et al.*, Phys. Rev. **D83**, 052009 (2011).
16. A.A. Aguilar-Arevalo *et al.*, Phys. Rev. **D83**, 052007 (2011).
17. A.A. Aguilar-Arevalo *et al.*, Phys. Rev. **D81**, 013005 (2010).
18. A.A. Aguilar-Arevalo *et al.*, Phys. Rev. Lett. **103**, 081801 (2009).
19. A.A. Aguilar-Arevalo *et al.*, Phys. Lett. **B664**, 41 (2008).
20. P. Adamson *et al.*, Phys. Rev. **D81**, 072002 (2010).
21. Q. Wu *et al.*, Phys. Lett. **B660**, 19 (2008).
22. V. Lyubushkin *et al.*, Eur. Phys. J. **C63**, 355 (2009).
23. C.T. Kullenberg *et al.*, Phys. Lett. **B682**, 177 (2009).
24. Y. Nakajima *et al.*, Phys. Rev. **D83**, 12005 (2011).
25. Y. Kurimoto *et al.*, Phys. Rev. **D81**, 111102 (R) (2010).
26. Y. Kurimoto *et al.*, Phys. Rev. **D81**, 033004 (2010).
27. K. Hiraide *et al.*, Phys. Rev. **D78**, 112004 (2008).
28. K. Abe *et al.*, Phys. Rev. **D87**, 092003 (2013).
29. M. Tzanov *et al.*, Phys. Rev. **D74**, 012008 (2006).
30. B. Tice, Ph.D. thesis, Rutgers University, 2014.
31. A. Kayis-Topaksu *et al.*, Nucl. Phys. **B798**, 1 (2008).
32. O. Samoylov *et al.*, Nucl. Phys. **B876**, 339 (2013).
33. D. Mason *et al.*, Phys. Rev. Lett. **99**, 192001 (2007).
34. D. Casper, Nucl. Phys. (Proc. Supp.) **112**, 161 (2002), default v3 NUANCE.
35. R. Tacik, AIP Conf. Proc. **1405**, 229 (2011); S. Boyd *et al.*, AIP Conf. Proc. **1189**, 60 (2009).
36. O. Palamara *et al.*, arXiv:1309.7480 [physics.ins-det].
37. S.J. Barish *et al.*, Phys. Rev. **D16**, 3103 (1977).
38. D. Allasia *et al.*, Nucl. Phys. **B343**, 285 (1990).
39. N.J. Baker *et al.*, Phys. Rev. **D23**, 2499 (1981); G. Fanourakis *et al.*, Phys. Rev. **D21**, 562 (1980).
40. T. Kitagaki *et al.*, Phys. Rev. **D28**, 436 (1983).
41. S. Bonetti *et al.*, Nuovo Cimento **A38**, 260 (1977); N. Armenise *et al.*, Nucl. Phys. **B152**, 365 (1979).
42. L.B. Auerbach *et al.*, Phys. Rev. **C66**, 015501 (2002).
43. S.V. Belikov *et al.*, Z. Phys. **A320**, 625 (1985).
44. J. Brunner *et al.*, Z. Phys. **C45**, 551 (1990).
45. J. Carlson *et al.*, Phys. Rev. **C65**, 024002 (2002).
46. H. Gallagher *et al.*, Ann. Rev. Nucl. and Part. Sci. **61**, 355 (2011).
47. N. Mayer and N. Graf, AIP Conf. Proc. **1405**, 41 (2011).
48. M. Betancourt, "Study of Quasi-Elastic Scattering in the NOvA Detector Prototype," Ph.D. thesis, University of Minnesota, 2013, http://lss.fnal.gov/archive/thesis/2000/fermilab-thesis-2013-10.pdf.
49. L.A. Ahrens *et al.*, Phys. Rev. **D35**, 785 (1987).
50. V.V. Ammosov *et al.*, Z. Phys. **C36**, 377 (1987); O. Erriques *et al.*, Phys. Lett. **70B**, 383 (1977); T. Eichten *et al.*, Phys. Lett. **40B**, 593 (1972).
51. D. Allasia *et al.*, Nucl. Phys. **B343**, 285 (1990); H.J. Grabosch *et al.*, Z. Phys. **C41**, 527 (1989); G.T. Jones *et al.*, Z. Phys. **C43**, 527 (1998); P. Allen *et al.*, Nucl. Phys. **B264**, 221 (1986); S.J. Barish *et al.*, Phys. Lett. **B91**, 161 (1980); T. Bolognese *et al.*, Phys. Lett. **B81**, 393 (1979).
52. M. Derrick *et al.*, Phys. Rev. **D23**, 569 (1981); W. Krenz *et al.*, Nucl. Phys. **B135**, 45 (1978); W. Lee *et al.*, Phys. Rev. Lett. **38**, 202 (1977); S.J. Barish *et al.*, Phys. Rev. Lett. **33**, 448 (1974).
53. C.T. Kullenberg *et al.*, Phys. Lett. **B706**, 268 (2012).
54. E. Hawker, *Proceedings of the 2nd International Workshop on Neutrino-Nucleus Interactions in the Few-GeV Region,* Irvine, CA, 2002, unpublished, http://www.ps.uci.edu/ nuint/proceedings/hawker.pdf.
55. For a compilation of historical coherent pion production data, please see P. Villain *et al.*, Phys. Lett. **B313**, 267 (1993).
56. D. Cherdack, AIP Conf. Proc. **1405**, 115 (2011).

50. PLOTS OF CROSS SECTIONS AND RELATED QUANTITIES

(For neutrino plots, see review article "Neutrino Cross Section Measurements" by G.P. Zeller in this edition of RPP)

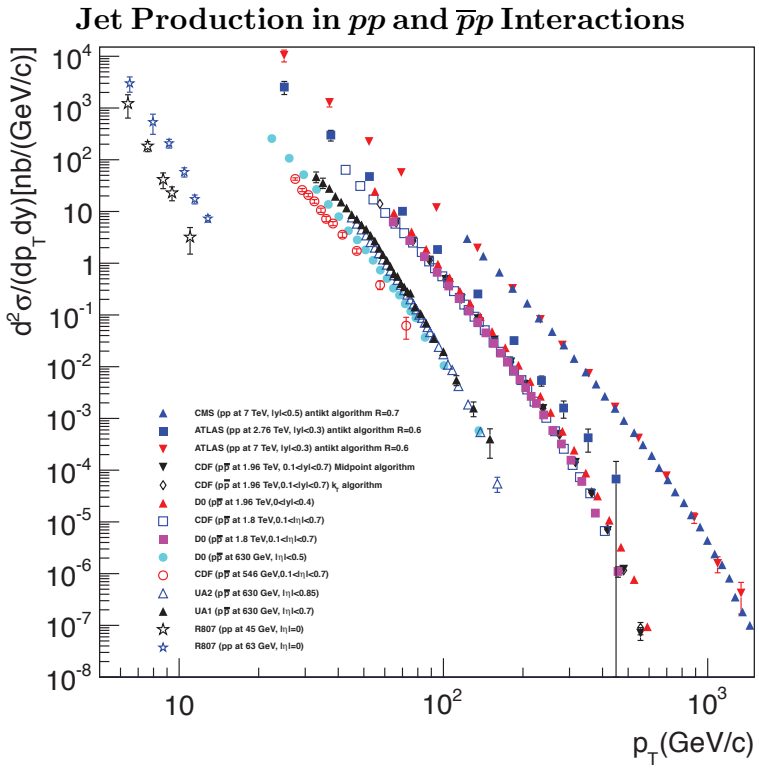

Figure 50.1: Inclusive differential jet cross sections, in the central rapidity region, plotted as a function of the jet transverse momentum. Results earlier than from the Tevatron Run 2 used transverse energy rather than transverse momentum and pseudo-rapidity η rather than rapidity y, but p_T and y are used for all results shown here for simplicity. The error bars plotted are in most cases the experimental stat. and syst. errors added in quadrature. The CDF and D0 measurements use jet sizes of 0.7 (JetClu for CDF Run 1, and Midpoint and k_T for CDF Run 2, a cone algorithm for D0 in Run 1 and the Midpoint algorithm in Run 2). The ATLAS results are plotted for the antikT algorithm for R=0.4, while the CMS results also use antikT, but with R=0.5. NLO QCD predictions in general provide a good description of the Tevatron and LHC data; the Tevatron jet data in fact are crucial components of global PDF fits, and the LHC data are starting to be used as well. Comparisons with the older cross sections are more difficult due to the nature of the jet algorithms used. **ATLAS**:Phys. Rev. **D86**, 014022 (2012), Eur. Phys. J **C73**, 2509 (2013); **CMS**: Phys. Rev. **D84**, 052011 (2011); **CDF**: Phys. Rev. **D75**, 092006 (2007), Phys. Rev. **D64**, 032001 (2001), Phys. Rev. Lett. **70**, 1376 (1993); **D0**: Phys. Rev. **D64**, 032003 (2001); **UA2**: Phys. Lett. **B257**, 232 (1991); **UA1**: Phys. Lett. **172**, 461 (1986); **R807**: Phys. Lett. **B123**, 133 (1983). (Courtesy of J. Huston, Michigan State University, 2013.)

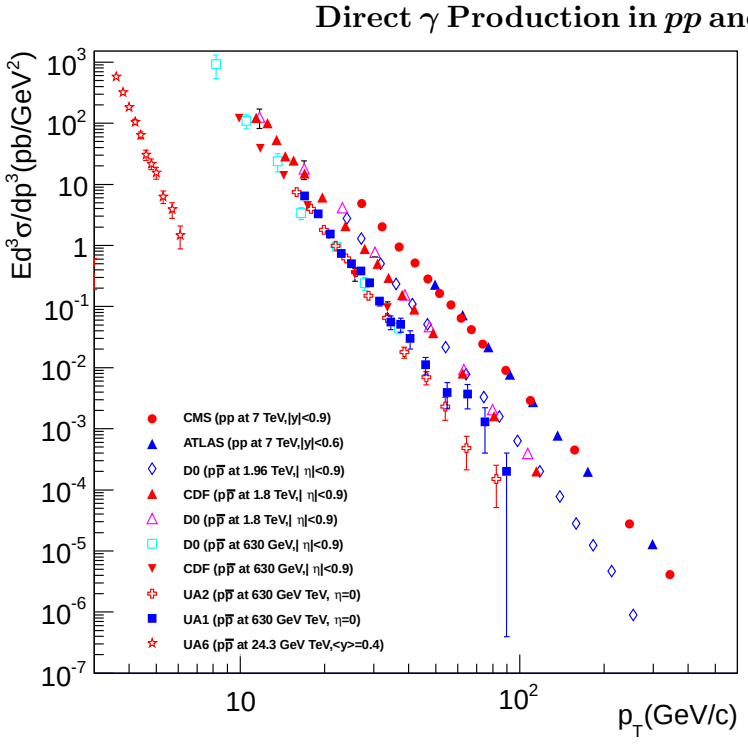

Figure 50.2: Isolated photon cross sections plotted as a function of the photon transverse momentum. The errors are either statistical only, or statistical and systematic added in quadrature. **ATLAS**: Phys. Lett. **B706**, 150 (2011); **CMS**: Phys. Rev. **D84**, 052011 (2011); **D0** : Phys. Lett. **B639**, 151 (2006), Phys. Rev. Lett. **87**, 251805 (2001); **CDF**: Phys. Rev. **D65**, 112003 (2002); **UA6**: Phys. Lett. **B206**, 163 (1988); **UA1**: Phys. Lett. **B209**, 385 (1988); **UA2**: Phys. Lett. **B288**, 386 (1992). (Courtesy of J. Huston, Michigan State University, 2013).

Differential Cross Section for W and Z Boson Production

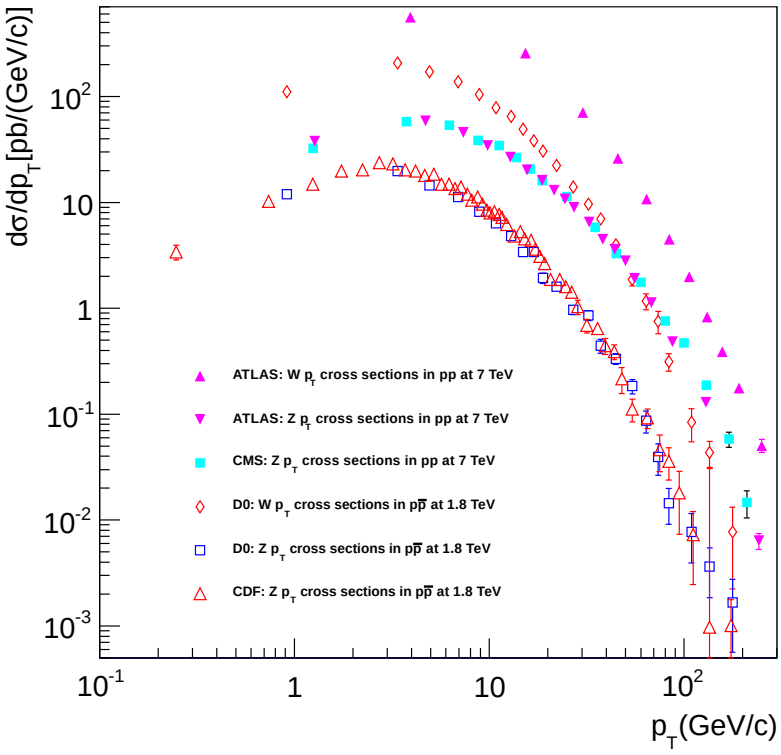

Figure 50.3: Differential cross sections for W and Z production shown as a function of the boson transverse momentum. The errors plotted are either statistical only or statistical and systematic added in quadrature. The results are in good agreement with theoretical predictions that include both the effects of NLO corrections and of q_T resummation. **ATLAS**: Phys. Rev. **D85**, 012005 (2012), Phys. Lett. **B705**, 415 (2011); **CMS**: Phys. Rev. **D85**, 032002 (2012); **D0**: Phys. Lett. **B513**, 292 (2001), Phys. Rev. Lett. **84**, 2792 (2000); **CDF**: Phys. Rev. Lett. **84**, 845 (2000). (Courtesy of J. Huston, Michigan State University, 2013.)

Pseudorapidity Distributions in pp and $\overline{p}p$ Interactions

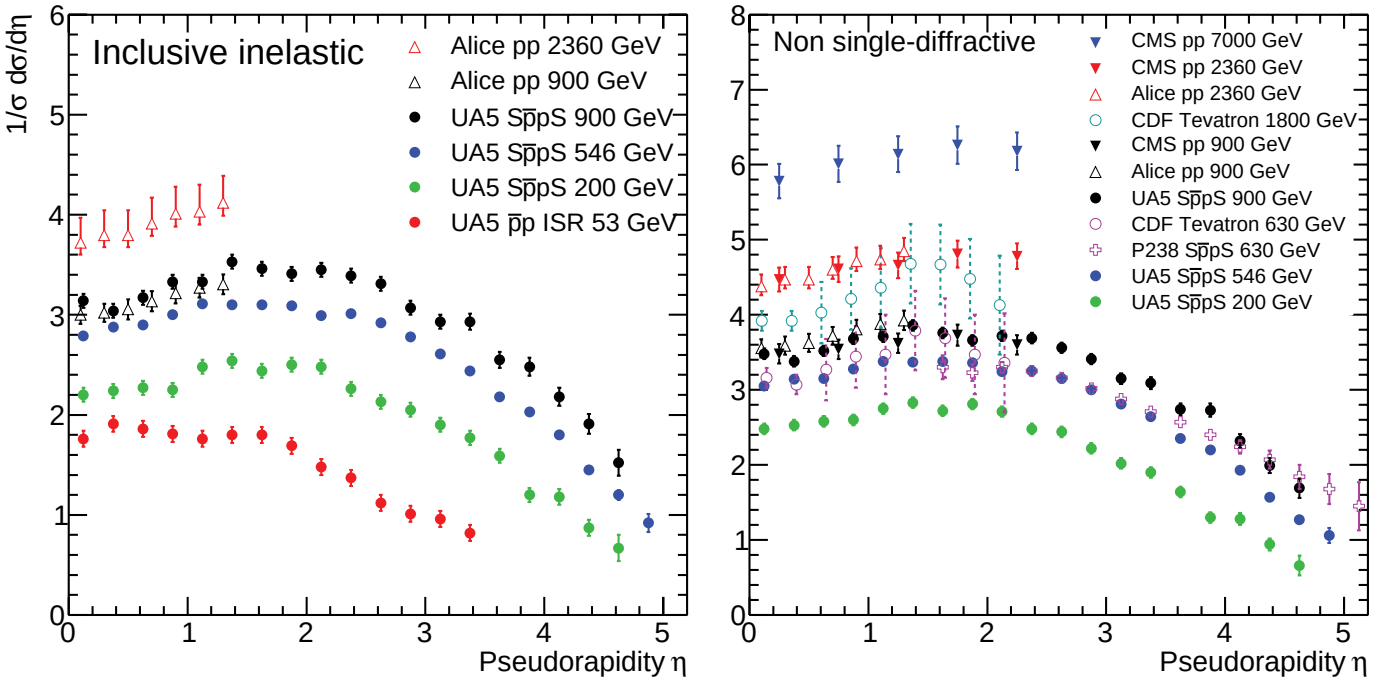

Figure 50.4: Charged particle pseudorapidity distributions in $p\overline{p}$ collisions for 53 GeV $\leq \sqrt{s} \leq$ 1800 GeV. UA5 data from the S$p\overline{p}$S are taken from G.J.Alner *et al.*, Z. Phys. **C33**, 1 (1986), and from the ISR from K.Alpgøard *et al.*, Phys.Lett. 112B 193 (1982). The UA5 data are shown for both the full inelastic cross-section and with singly diffractive events excluded. Additional non single-diffractive measurements are available from CDF at the Tevatron, F.Abe *et al.*, Phys. Rev. **D41**, 2330 (1990) and from P238 at the S$p\overline{p}$S, R.Harr *et al.*, Phys. Lett. **B401**, 176 (1997). These may be compared with both inclusive and non single-diffractive measurements in pp collisions at the LHC from ALICE, K.Aamodt *et al.*, Eur. Phys. J. **C68**, 89 (2010) and for non single-diffractive interactions from CMS , V.Khachatryan *et al.*, JHEP 1002:041 (2010), Phys. Rev. Lett. **105**, 022002 (2010). (Courtesy of D.R. Ward, Cambridge Univ., 2013)

Average Hadron Multiplicities in Hadronic e^+e^- Annihilation Events

Table 50.1: Average hadron multiplicities per hadronic e^+e^- annihilation event at $\sqrt{s} \approx 10$, 29–35, 91, and 130–200 GeV. The rates given include decay products from resonances with $c\tau < 10$ cm, and include the corresponding anti-particle state. Correlations of the systematic uncertainties were considered for the calculation of the averages. (Updated August 2013 by O. Biebel, LMU, Munich)

Particle	$\sqrt{s} \approx 10$ GeV	$\sqrt{s} = 29$–35 GeV	$\sqrt{s} = 91$ GeV	$\sqrt{s} = 130$–200 GeV
Pseudoscalar mesons:				
π^+	6.52 ± 0.11	10.3 ± 0.4	17.02 ± 0.19	21.24 ± 0.39
π^0	3.2 ± 0.3	5.83 ± 0.28	9.42 ± 0.32	
K^+	0.953 ± 0.018	1.48 ± 0.09	2.228 ± 0.059	2.82 ± 0.19
K^0	0.91 ± 0.05	1.48 ± 0.07	2.049 ± 0.026	2.10 ± 0.12
η	0.20 ± 0.04	0.61 ± 0.07	1.049 ± 0.080	
$\eta'(958)$	0.03 ± 0.01	0.26 ± 0.10	0.152 ± 0.020	
D^+	$0.194 \pm 0.019^{(a)}$	0.17 ± 0.03	0.175 ± 0.016	
D^0	$0.446 \pm 0.032^{(a)}$	0.45 ± 0.07	0.454 ± 0.030	
D_s^+	$0.063 \pm 0.014^{(a)}$	$0.45 \pm 0.20^{(b)}$	0.131 ± 0.021	
$B^{(c)}$	—	—	$0.165 \pm 0.026^{(d)}$	
B^+	—	—	$0.178 \pm 0.006^{(d)}$	
B_s^0	—	—	$0.057 \pm 0.013^{(d)}$	
Scalar mesons:				
$f_0(980)$	0.024 ± 0.006	$0.05 \pm 0.02^{(e)}$	0.146 ± 0.012	
$a_0(980)^\pm$	—	—	$0.27 \pm 0.11^{(f)}$	
Vector mesons:				
$\rho(770)^0$	0.35 ± 0.04	0.81 ± 0.08	1.231 ± 0.098	
$\rho(770)^\pm$	—	—	$2.40 \pm 0.43^{(f)}$	
$\omega(782)$	0.30 ± 0.08	—	1.016 ± 0.065	
$K^*(892)^+$	0.27 ± 0.03	0.64 ± 0.05	0.715 ± 0.059	
$K^*(892)^0$	0.29 ± 0.03	0.56 ± 0.06	0.738 ± 0.024	
$\phi(1020)$	0.044 ± 0.003	0.085 ± 0.011	0.0963 ± 0.0032	
$D^*(2010)^+$	$0.177 \pm 0.022^{(a)}$	0.43 ± 0.07	$0.1937 \pm 0.0057^{(g)}$	
$D^*(2007)^0$	$0.168 \pm 0.019^{(a)}$	0.27 ± 0.11	—	
$D_s^*(2112)^+$	$0.048 \pm 0.014^{(a)}$	—	$0.101 \pm 0.048^{(h)}$	
$B^{*\ (i)}$	—	—	0.288 ± 0.026	
$J/\psi(1S)$	$0.00050 \pm 0.00005^{(a)}$	—	$0.0052 \pm 0.0004^{(j)}$	
$\psi(2S)$	—	—	$0.0023 \pm 0.0004^{(j)}$	
$\Upsilon(1S)$	—	—	$0.00014 \pm 0.00007^{(j)}$	
Pseudovector mesons:				
$f_1(1285)$	—	—	0.165 ± 0.051	
$f_1(1420)$	—	—	0.056 ± 0.012	
$\chi_{c1}(3510)$	—	—	$0.0041 \pm 0.0011^{(j)}$	
Tensor mesons:				
$f_2(1270)$	0.09 ± 0.02	0.14 ± 0.04	0.166 ± 0.020	
$f_2'(1525)$	—	—	0.012 ± 0.006	
$K_2^*(1430)^+$	—	0.09 ± 0.03	—	
$K_2^*(1430)^0$	—	0.12 ± 0.06	0.084 ± 0.022	
$B^{**\ (k)}$	—	—	0.118 ± 0.024	
$D_{s1}^\pm$	—	—	$0.0052 \pm 0.0011^{(\ell)}$	
$D_{s2}^{*\pm}$	—	—	$0.0083 \pm 0.0031^{(\ell)}$	
Baryons:				
p	0.266 ± 0.008	0.640 ± 0.050	1.050 ± 0.032	1.41 ± 0.18
Λ	0.080 ± 0.007	0.205 ± 0.010	0.3915 ± 0.0065	0.39 ± 0.03
Σ^0	0.023 ± 0.008	—	0.076 ± 0.011	
Σ^-	—	—	0.081 ± 0.010	
Σ^+	—	—	0.107 ± 0.011	
$\Sigma^\pm$	—	—	0.174 ± 0.009	
Ξ^-	0.0059 ± 0.0007	0.0176 ± 0.0027	0.0258 ± 0.0010	
$\Delta(1232)^{++}$	0.040 ± 0.010	—	0.085 ± 0.014	
$\Sigma(1385)^-$	0.006 ± 0.002	0.017 ± 0.004	0.0240 ± 0.0017	
$\Sigma(1385)^+$	0.005 ± 0.001	0.017 ± 0.004	0.0239 ± 0.0015	
$\Sigma(1385)^\pm$	0.0106 ± 0.0020	0.033 ± 0.008	0.0462 ± 0.0028	
$\Xi(1530)^0$	0.0015 ± 0.0006	—	0.0068 ± 0.0006	
Ω^-	0.0007 ± 0.0004	0.014 ± 0.007	0.0016 ± 0.0003	
Λ_c^+	$0.074 \pm 0.031^{(m)}$	0.110 ± 0.050	0.078 ± 0.017	
Λ_b^0	—	—	0.031 ± 0.016	
$\Sigma_c^{++}, \Sigma_c^0$	0.014 ± 0.007	—	—	
$\Lambda(1520)$	0.008 ± 0.002	—	0.0222 ± 0.0027	

Notes for Table 50.1:

(*a*) $\sigma_{\rm had} = 3.33 \pm 0.05 \pm 0.21$ nb (**CLEO**: Phys. Rev. **D29**, 1254 (1984)) has been used in converting the measured cross sections to average hadron multiplicities.

(*b*) B($D_s \to \eta\pi,\ \eta'\pi$) was used (RPP 1994).

(*c*) Comprises both charged and neutral B meson states.

(*d*) The Standard Model B($Z \to b\overline{b}$) = 0.217 was used.

(*e*) $x_p = p/p_{\rm beam} > 0.1$ only.

(*f*) Both charge states.

(*g*) B($D^*(2010)^+ \to D^0\pi^+$) × B($D^0 \to K^-\pi^+$) has been used (RPP 2000).

(*h*) B($D_s^* \to D_S^+\gamma$), B($D_s^+ \to \phi\pi^+$), B($\phi \to K^+K^-$) have been used (RPP 1998).

(*i*) Any charge state (*i.e.*, B_d^*, B_u^*, or B_s^*).

(*j*) B($Z \to$ hadrons) = 0.699 was used (RPP 1994).

(*k*) Any charge state (*i.e.*, B_d^{**}, B_u^{**}, or B_s^{**}).

(*ℓ*) Assumes B($D_{s1}^+ \to D^{*+}K^0 + D^{*0}K+$) = 100% and B($D_{s2}^+ \to D^0K^+$) = 45%.

(*m*) The value was derived from the cross section of $\Lambda_c^+ \to p\pi K$ using (*a*) and assuming the branching fraction to be (5.0 ± 1.3)% (RPP 2004).

References for Table 50.1:

RPP 1992: Phys. Rev. **D45** (1992); **RPP 1994**: Phys. Rev. **D50**, 1173 (1994); **RPP 1996**: Phys. Rev. **D54**, 1 (1996); **RPP 1998**: Eur. Phys. J. **C3**, 1 (1998); **RPP 2000**: Eur. Phys. J. **C15**, 1 (2000); **RPP 2002**: Phys. Rev. **D66**, 010001 (2002); **RPP 2004**: Phys. Lett. **B592**, 1 (2004); **RPP 2006**: J. Phys. **G33**, 1 (2006); **RPP 2008**: Phys. Lett. **B667**, 1 (2008); **RPP 2010**: J. Phys. **G37**, 075021 (2010); **RPP 2012**: Phys. Rev. D 86,010001(2012) and references therein.

R. Marshall, Rept. on Prog. in Phys. **52**, 1329 (1989). A. De Angelis, J. Phys. **G19**, 1233 (1993) and references therein.

ALEPH: D. Buskulic *et al.*: Phys. Lett. **B295**, 396 (1992); Z. Phys. **C64**, 361 (1994); **C69**, 15 (1996); **C69**, 379 (1996); **C73**, 409 (1997); and R. Barate *et al.*: Z. Phys. **C74**, 451 (1997); Phys. Reports **294**, 1 (1998); Eur. Phys. J. **C5**, 205 (1998); **C16**, 597 (2000); **C16**, 613 (2000); and A. Heister *et al.*: Phys. Lett. **B526**, 34 (2002); **B528**, 19 (2002).

ARGUS: H. Albrecht *et al.*: Phys. Lett. **230B**, 169 (1989); Z. Phys. **C44**, 547 (1989); **C46**, 15 (1990); **C54**, 1 (1992); **C58**, 199 (1993); **C61**, 1 (1994); Phys. Rep. **276**, 223 (1996).

BaBar: B. Aubert *et al.*: Phys. Rev. Lett. **87**, 162002 (2001); Phys. Rev. **D65**, 091104 (2002); J.P. Lees *et al.*: SLAC-PUB-15524, `arXiv:1306.2895`.

Belle: K. Abe *et al.*, Phys. Rev. Lett. **88**, 052001 (2002); and R. Seuster *et al.*, Phys. Rev. **D73**, 032002 (2006).

CELLO: H.J. Behrend *et al.*: Z. Phys. **C46**, 397 (1990); **C47**, 1 (1990).

CLEO: D. Bortoletto *et al.*, Phys. Rev. **D37**, 1719 (1988); erratum *ibid.* **D39**, 1471 (1989); and M. Artuso *et al.*, Phys. Rev. **D70**, 112001 (2004).

Crystal Ball: Ch. Bieler *et al.*, Z. Phys. **C49**, 225 (1991).

DELPHI: P. Abreu *et al.*: Z. Phys. **C57**, 181 (1993); **C59**, 533 (1993); **C61**, 407 (1994); **C65**, 587 (1995); **C67**, 543 (1995); **C68**, 353 (1995); **C73**, 61 (1996); Nucl. Phys. **B444**, 3 (1995); Phys. Lett. **B341**, 109 (1994); **B345**, 598 (1995); **B361**, 207 (1995); **B372**, 172 (1996); **B379**, 309 (1996); **B416**, 233 (1998); **B449**, 364 (1999); **B475**, 429 (2000); Eur. Phys. J. **C6**, 19 (1999); **C5**, 585 (1998); **C18**, 203 (2000); and J. Abdallah *et al.*, Phys. Lett. **B569**, 129 (2003); Phys. Lett. **B576**, 29 (2003); Eur. Phys. J. **C44**, 299 (2005); and W. Adam *et al.*: Z. Phys. **C69**, 561 (1996); **C70**, 371 (1996).

HRS: S. Abachi *et al.*, Phys. Rev. Lett. **57**, 1990 (1986); and M. Derrick *et al.*, Phys. Rev. **D35**, 2639 (1987).

L3: M. Acciarri *et al.*: Phys. Lett. **B328**, 223 (1994); **B345**, 589 (1995); **B371**, 126 (1996); **B371**, 137 (1996); **B393**, 465 (1997); **B404**, 390 (1997); **B407**, 351 (1997); **B407**, 389 (1997), erratum *ibid.* **B427**, 409 (1998); **B453**, 94 (1999); **B479**, 79 (2000).

MARK II: H. Schellman *et al.*, Phys. Rev. **D31**, 3013 (1985); and G. Wormser *et al.*, Phys. Rev. Lett. **61**, 1057 (1988).

JADE: W. Bartel *et al.*, Z. Phys. **C20**, 187 (1983); and D.D. Pietzl *et al.*, Z. Phys. **C46**, 1 (1990).

OPAL: R. Akers *et al.*: Z. Phys. **C63**, 181 (1994); **C66**, 555 (1995); **C67**, 389 (1995); **C68**, 1 (1995); and G. Alexander *et al.*: Phys. Lett. **B358**, 162 (1995); Z. Phys. **C70**, 197 (1996); **C72**, 1 (1996); **C72**, 191 (1996); **C73**, 569 (1997); **C73**, 587 (1997); Phys. Lett. **B370**, 185 (1996); and K. Ackerstaff *et al.*: Z. Phys. **C75**, 192 (1997); Phys. Lett. **B412**, 210 (1997); Eur. Phys. J. **C1**, 439 (1998); **C4**, 19 (1998); **C5**, 1 (1998); **C5**, 411 (1998); and G. Abbiendi *et al.*: Eur. Phys. J. **C16**, 185 (2000); **C17**, 373 (2000).

PLUTO: Ch. Berger *et al.*, Phys. Lett. **104B**, 79 (1981).

SLD: K. Abe, Phys. Rev. **D59**, 052001 (1999); Phys. Rev. **D69**, 072003 (2004).

TASSO: H. Aihara *et al.*, Z. Phys. **C27**, 27 (1985).

TPC: H. Aihara *et al.*, Phys. Rev. Lett. **53**, 2378 (1984).

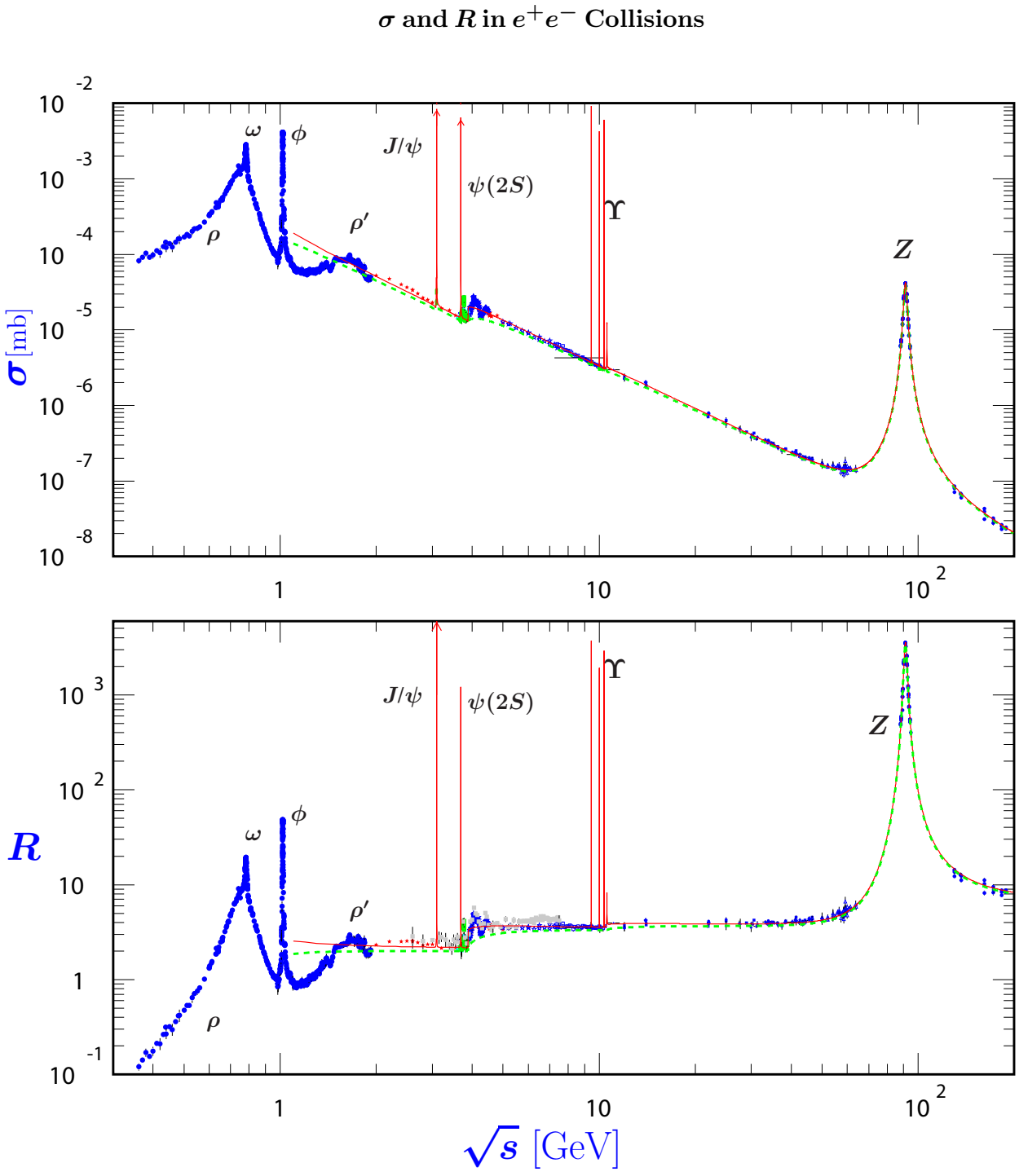

Figure 50.5: World data on the total cross section of $e^+e^- \to hadrons$ and the ratio $R(s) = \sigma(e^+e^- \to hadrons, s)/\sigma(e^+e^- \to \mu^+\mu^-, s)$. $\sigma(e^+e^- \to hadrons, s)$ is the experimental cross section corrected for initial state radiation and electron-positron vertex loops, $\sigma(e^+e^- \to \mu^+\mu^-, s) = 4\pi\alpha^2(s)/3s$. Data errors are total below 2 GeV and statistical above 2 GeV. The curves are an educative guide: the broken one (green) is a naive quark-parton model prediction, and the solid one (red) is 3-loop pQCD prediction (see "Quantum Chromodynamics" section of this *Review*, Eq. (9.7) or, for more details, K. G. Chetyrkin *et al.*, Nucl. Phys. **B586**, 56 (2000) (Erratum *ibid.* **B634**, 413 (2002)). Breit-Wigner parameterizations of J/ψ, $\psi(2S)$, and $\Upsilon(nS), n = 1, 2, 3, 4$ are also shown. The full list of references to the original data and the details of the R ratio extraction from them can be found in `[arXiv:hep-ph/0312114]`. Corresponding computer-readable data files are available at `http://pdg.lbl.gov/current/xsect/`. (Courtesy of the COMPAS (Protvino) and HEPDATA (Durham) Groups, May 2010.)

R in Light-Flavor, Charm, and Beauty Threshold Regions

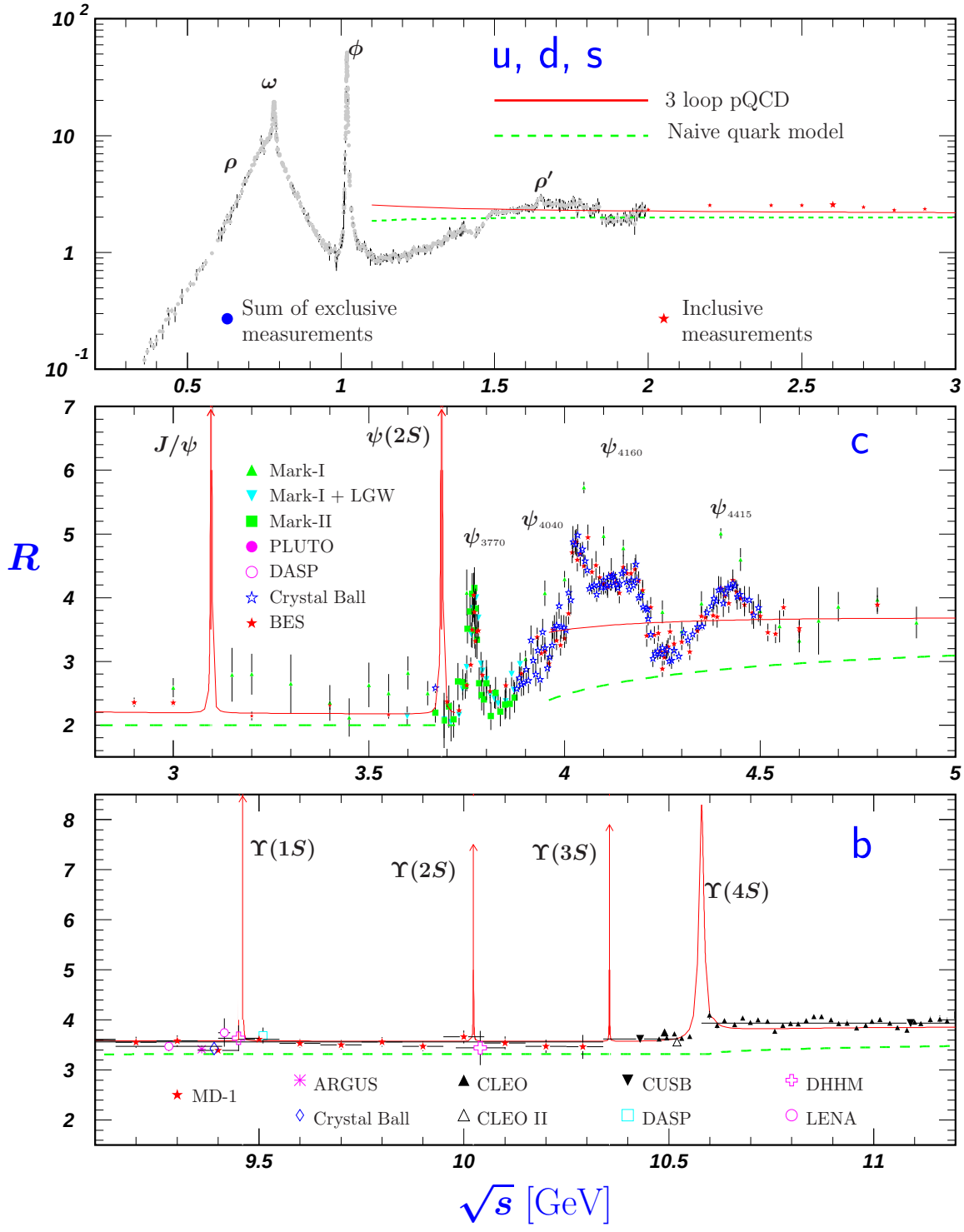

Figure 50.6: R in the light-flavor, charm, and beauty threshold regions. Data errors are total below 2 GeV and statistical above 2 GeV. The curves are the same as in Fig. 50.5. **Note:** CLEO data above $\Upsilon(4S)$ were not fully corrected for radiative effects, and we retain them on the plot only for illustrative purposes with a normalization factor of 0.8. The full list of references to the original data and the details of the R ratio extraction from them can be found in `[arXiv:hep-ph/0312114]`. The computer-readable data are available at `http://pdg.lbl.gov/current/xsect/`. (Courtesy of the COMPAS (Protvino) and HEPDATA (Durham) Groups, May 2010.)

Annihilation Cross Section Near M_Z

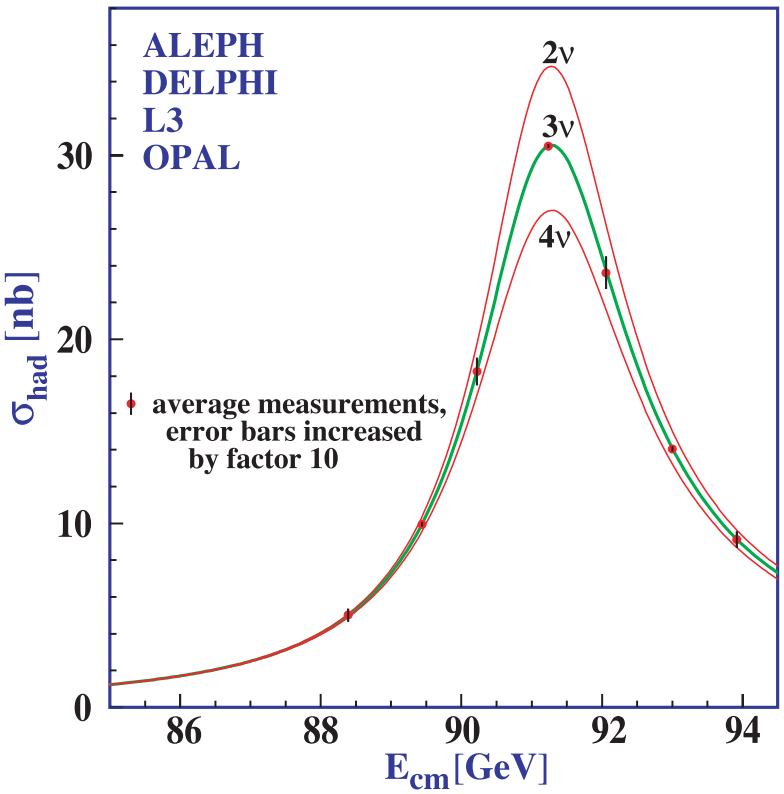

Figure 50.7: Combined data from the ALEPH, DELPHI, L3, and OPAL Collaborations for the cross section in e^+e^- annihilation into hadronic final states as a function of the center-of-mass energy near the Z pole. The curves show the predictions of the Standard Model with two, three, and four species of light neutrinos. The asymmetry of the curve is produced by initial-state radiation. Note that the error bars have been increased by a factor ten for display purposes. References:

ALEPH: R. Barate *et al.*, Eur. Phys. J. **C14**, 1 (2000).
DELPHI: P. Abreu *et al.*, Eur. Phys. J. **C16**, 371 (2000).
L3: M. Acciarri *et al.*, Eur. Phys. J. **C16**, 1 (2000).
OPAL: G. Abbiendi *et al.*, Eur. Phys. J. **C19**, 587 (2001).
Combination: The ALEPH, DELPHI, L3, OPAL, SLD Collaborations, the LEP Electroweak Working Group, and the SLD Electroweak and Heavy Flavor Groups, Phys. Rept. **427**, 257 (2006) [arXiv:hep-ex/0509008].

(Courtesy of M. Grünewald and the LEP Electroweak Working Group, 2007)

Total Hadronic Cross Sections

(Updated September 2013, COMPAS group, IHEP, Protvino)

This updated version of the total hadronic cross sections review is based on the first half of 2013 update of the database for total cross section and the ratio of the real-to-imaginary parts of the forward elastic scattering hadronic amplitudes. New data on total pp collisions cross sections from CERN-LHC-TOTEM [1] and new data from cosmic rays experiment PAO [2] were added.

We use a procedure for ranking models as described in [3] to identify the safest parameterizations for extrapolations. Incidentally, the models giving the best fit of accelerator data also reproduce the experimental cosmic ray nucleon–nucleon data extracted from nucleon–air data with no need of any extra phenomenological corrections to the data.

The statement in [3] that the models with universal (across of collision initial states) $B\log^2(s/s_0)$ asymptotic term work much better than the models with $B\log(s/s_0)$ or $B(s/s_0)^{\Delta}$ terms was confirmed in [4–8] based on matching traditional asymptotic parameterizations with low energy data in different ways. However in these references the scale parameter s_0 was still claimed to be dependent on the colliding particles as it should be for the asymptotic form of parameterizations constructed by the Regge-Gribov phenomenology prescriptions.

The possibility of the universal $\log^2(s/s_0)$ rise of the hadronic total cross sections for different colliding particles was first pointed out by W. Heisenberg [9–10] and discussed many times (see for example [11] and more recent [12–14], and references therein). In [13] the universality of the asymptotic total collision cross sections has been advocated for hadron-nucleus collisions. In [14] additional indications to the universal asymptotic high-energy behavior for hadronic total collision cross sections in form $B\log^2(s/s_0)$ were obtained from lattice QCD.

In this review we use $\mathrm{HPR_1R_2}$ model of highest COMPETE–rank modified (as in 2012 version) to save the universality of the rising part in new form that explicitly includes dependence of the s_0 and B on the initial state mass parameters and the new scale parameter M.

$$\sigma^{a^{\mp}b} = H\log^2\left(\frac{s}{s_M^{ab}}\right) + P^{ab} + R_1^{ab}\left(\frac{s}{s_M^{ab}}\right)^{-\eta_1} \pm R_2^{ab}\left(\frac{s}{s_M^{ab}}\right)^{-\eta_2};$$

$$\rho^{a^{\mp}b} = \frac{1}{\sigma^{a^{\mp}b}}\left[\pi H\log\left(\frac{s}{s_M^{ab}}\right) - R_1^{ab}\left(\frac{s}{s_M^{ab}}\right)^{-\eta_1}\tan\left(\frac{\eta_1\pi}{2}\right) \pm R_2^{ab}\left(\frac{s}{s_M^{ab}}\right)^{-\eta_2}\cot\left(\frac{\eta_2\pi}{2}\right)\right],$$

where upper signs in formulas are for particles and lower signs for antiparticles. The adjustable parameters are as follows:

$H = \pi\frac{(\hbar c)^2}{M^2}$ in mb, where notation H[§] is after Heisenberg(1952,1975);

P^{ab} in mb, are Pomeranchuk's(1958) constant terms;

R_i^{ab} in mb are the intensities of the effective secondary Regge pole contributions named after Regge-Gribov(1961);

s, $s_M^{ab} = (m_a + m_b + M)^2$ are in GeV^2 ;

m_a, m_b, $(m_{\gamma^*} = m_{\rho(770)})$ are the masses of initial state particles, and M – the mass parameter defining the rate of universal rise of the cross sections are all in GeV. Parameters M, η_1 and η_2 are universal for all collisions considered.

Exact factorization hypothesis was used for both $H\log^2(\frac{s}{s_M^{ab}})$ and P^{ab} to extend the universal rise of the total hadronic cross sections to the $\gamma(p,d) \to hadrons$ and $\gamma\gamma \to hadrons$ collisions. This results in one additional adjustable parameter δ with substitutions:

$$\pi H\log^2\left(\frac{s}{s_M^{\gamma(p,d)}}\right) + P^{\gamma(p,d)} \Rightarrow \delta\left[\pi(1,\lambda)H\log^2\left(\frac{s}{s_M^{\gamma(p,d)}}\right) + P^{p(p,d)}\right];$$

$$\pi H\log^2\left(\frac{s}{s_M^{\gamma\gamma}}\right) + P^{\gamma\gamma} \quad \Rightarrow \quad \delta^2\left[\pi H\log^2\left(\frac{s}{s_M^{\gamma\gamma}}\right) + P^{pp}\right] \quad .$$

These parameterizations were used for simultaneous fit with **35** adjustable parameters to the data on collisions:

$$(\overline{p},p)\ (p,n,d);\quad \Sigma^- p;\quad \pi^{\mp}\ (p,n,d);\quad K^{\mp}\ (p,n,d);\quad \gamma\ p;\quad \gamma\ \gamma;\quad \gamma\ d.$$

To trace the variation of the range of applicability of simultaneous fit results, several fits were produced with lower energy $\sqrt{s} \geq 5, \geq 6, \geq 7, \ldots$ GeV cutoffs until the uniformity of the fit across different collision became acceptable with good value of FQ.

The results of the fits are presented in the following tables and figures. In the tables, two values of the fit quality indicator $\mathrm{FQ} = \chi^2/(\mathrm{Npt}-35)$ are reported in the last element of the first row for each case of energy cutoff, where **Npt** is the number of data points in corresponding sample. $\mathrm{FQ_{INT}}$ calculated with "internal" parameter values of machine precision (16 digits) and $\mathrm{FQ_{EXT}}$ calculated with rounded parameter values as displayed in the table in accordance with PDG rules (Section 5.3 of J. Beringer *et al.*, (Particle Data Group), Phys. Rev. **D86**, 010001 (2012)), recent metrology recommendations [15] and rules for safe uniform rounding of correlated data [16]. The uniformity of the quality of data description across different collisions is shown in the last two columns of each $\sqrt{s}$ subtable; **npt** is the number of data points in a subsample and χ^2/npt is the contribution of the subsample to the global χ^2 reduced to **npt**. The values of the fit quality indicators and uniformity of model descriptions improve with higher collision energy cuts. The uniformity is excellent for 7 GeV cut. All fits were performed with NonlinearModelFit package in *Mathematica* 8^+, which gives the statistically complete presentation of the fit results: best fit parameter values and estimated parameter uncertainties covariance matrix calculated as inverse $Hessian/2$ matrix at the best fit parameter values which is perfect for linearized in parameters fits, but can produce overestimated covariance matrix for nonlinear optimization task.

---

§ *For collisions with deuteron target H_d=λ H where dimensionless parameter λ is introduced to test the universality of the Heisenberg rise for particle−nuclear and nuclear−nuclear collisions.*

HPR$_1$R$_2$ at $\sqrt{s} \geq 5$GeV	**M**=2.127 ± 0.015 **[GeV]** **H**=0.2704 ± 0.0038 **[mb]** $\eta_1 = 0.451 \pm 0.013$ $\eta_2 = 0.5490 \pm 0.0070$ $\delta = (\mathbf{3.060 \pm 0.021}) \times \mathbf{10^{-3}}$ $\lambda = 1.626 \pm 0.049$				**FQ$_{\mathbf{INT}}$ = 0.96** **FQ$_{\mathbf{EXT}}$ = 0.96**
P[mb]	R_1**[mb]**	R_2**[mb]**	**Beam/Target**	**Npt=1046**	χ^2/npt **by Groups**
34.49 ± 0.21	12.98 ± 0.26	7.38 ± 0.11	$\bar{p}(p)/p$	*256*	*1.15*
34.79 ± 0.25	12.44 ± 0.48	6.65 ± 0.22	$\bar{p}(p)/n$	*67*	*0.48*
34.7 ± 2.0	$-48. \pm 30.$	$-50. \pm 30.$	Σ^-/p	*9*	*0.37*
18.82 ± 0.18	9.48 ± 0.22	1.763 ± 0.042	$\pi^{\mp}/p$	*183*	*1.02*
16.41 ± 0.13	4.22 ± 0.19	3.403 ± 0.060	$K^{\mp}/p$	*121*	*0.81*
16.35 ± 0.14	3.64 ± 0.27	1.82 ± 0.10	$K^{\mp}/n$	*64*	*0.58*
	0.0137 ± 0.0017		γ/p	*41*	*0.62*
	$(-4. \pm 25.) \times 10^{-6}$		γ/γ	*37*	*0.75*
	0.0367 ± 00028		γ/d	*13*	*0.9*
64.59 ± 0.53	29.51 ± 0.61	14.93 ± 0.24	$\bar{p}(p)/d$	*85*	*1.51*
36.75 ± 0.41	18.64 ± 0.58	0.34 ± 0.12	$\pi^{\mp}/d$	*92*	*0.72*
32.13 ± 0.32	7.61 ± 0.48	5.61 ± 0.12	$K\mp/d$	*78*	*0.79*

HPR$_1$R$_2$ at $\sqrt{s} \geq 6$GeV	**M**=2.081 ± 0.016 **[GeV]** **H**=0.2824 ± 0.0044 **[mb]** $\eta_1 = 0.409 \pm 0.016$ $\eta_2 = 0.5566 \pm 0.0083$ $\delta = (\mathbf{3.097 \pm 0.026}) \times \mathbf{10^{-3}}$ $\lambda = 1.496 \pm 0.053$				**FQ$_{\mathbf{INT}}$ = 0.9** **FQ$_{\mathbf{EXT}}$ = 0.9**
P[mb]	R_1**[mb]**	R_2**[mb]**	**Beam/Target**	**Npt=933**	χ^2/npt **by Groups**
34.70 ± 0.31	13.72 ± 0.32	7.58 ± 0.14	$\bar{p}(p)/p$	*243*	*1.13*
34.03 ± 0.34	13.16 ± 0.54	6.88 ± 0.25	$\bar{p}(p)/n$	*58*	*0.45*
34.5 ± 2.1	$-29. \pm 20.$	$-32. \pm 20.$	Σ^-/p	*9*	*0.38*
18.15 ± 0.26	10.20 ± 0.29	1.855 ± 0.055	$\pi^{\mp}/p$	*157*	*0.99*
15.90 ± 0.19	4.93 ± 0.25	3.466 ± 0.077	$K^{\mp}/p$	*99*	*0.7*
15.86 ± 0.20	4.38 ± 0.34	1.83 ± 0.12	$K^{\mp}/n$	*55*	*0.58*
	0.0146 ± 0.0021		γ/p	*35*	*0.59*
	$(-18. \pm 27.) \times 10^{-6}$		γ/γ	*34*	*0.75*
	0.0315 ± 00035		γ/d	*6*	*1.06*
64.48 ± 0.68	27.53 ± 0.78	15.36 ± 0.33	$\bar{p}(p)/d$	*77*	*1.06*
36.43 ± 0.56	18.19 ± 0.72	0.38 ± 0.13	$\pi^{\mp}/d$	*87*	*0.7*
32.97 ± 0.32	7.36 ± 0.60	5.71 ± 0.14	$K\mp/d$	*73*	*0.72*

HPR$_1$R$_2$ at $\sqrt{s} \geq 7$GeV	**M**=2.076 ± 0.016 **[GeV]** **H**=0.2838 ± 0.0045 **[mb]** $\eta_1 = 0.412 \pm 0.017$ $\eta_2 = 0.5626 \pm 0.0092$ $\delta = (\mathbf{3.112 \pm 0.027}) \times \mathbf{10^{-3}}$ $\lambda = 1.456 \pm 0.058$				**FQ$_{\mathbf{INT}}$ = 0.86** **FQ$_{\mathbf{EXT}}$ = 0.87**
P[mb]	R_1**[mb]**	R_2**[mb]**	**Beam/Target**	**Npt=933**	χ^2/npt **by Groups**
33.73 ± 0.33	13.67 ± 0.33	7.77 ± 0.18	$\bar{p}(p)/p$	*219*	*1.09*
33.77 ± 0.38	14.05 ± 0.63	6.93 ± 0.29	$\bar{p}(p)/n$	*48*	*0.39*
33.2 ± 3.9	$-14. \pm 47.$	$-15. \pm 52.$	Σ^-/p	*8*	*0.41*
18.08 ± 0.29	10.44 ± 0.32	1.977 ± 0.078	$\pi^{\mp}/p$	*137*	*0.91*
15.84 ± 0.20	5.12 ± 0.28	3.538 ± 0.095	$K^{\mp}/p$	*85*	*0.76*
15.73 ± 0.22	4.81 ± 0.40	1.86 ± 0.13	$K^{\mp}/n$	*48*	*0.56*
	0.0132 ± 0.0023		γ/p	*34*	*0.56*
	$(-60. \pm 33.) \times 10^{-6}$		γ/γ	*31*	*0.68*
	0.0256 ± 00044		γ/d	*3*	*0.31*
64.79 ± 0.75	27.06 ± 0.85	15.46 ± 0.37	$\bar{p}(p)/d$	*75*	*0.97*
36.66 ± 0.62	17.89 ± 0.82	0.38 ± 0.14	$\pi^{\mp}/d$	*81*	*0.71*
32.28 ± 0.46	7.02 ± 0.71	5.74 ± 0.16	$K\mp/d$	*67*	*0.67*

Cut in GeV	Λ_5^{min}	CN_5	Λ_6^{min}	CN_6	Λ_7^{min}	CN_7
Hessian	*0.000093*	*137197*	*0.000190*	*69375*	*0.000034*	*353613*
Monte Carlo	*0.00047*	*27022*	*0.00090*	*14345*	*0.00086*	*14452*
$\mid MC_{cut} \mid$	*1000000*		*200000*		*300000*	

To construct the parameter scatter region we follow Section 38.4.2.2 of J. Beringer *et al.*. (Particle Data Group), Phys. Rev. **D86**, 010001 (2012) and recent metrology JCGM 101:2008 recommendations and produce the direct Monte Carlo propagation of uncertainties from experimental data to the uncertainties of the best fit parameters. To do this we interpret the whole input data sample as statistically independent sample with total experimental uncertainty at each experimental data point being a Gaussian standard deviation. This technical assumption allows us to generate MC sampling of experimental data and to obtain at each MC trial new "biased" best fit parameters belonging to scatter region of the initial best fit parameters values. These biased best fit parameters constitute the MC-samples of cardinalities $|MC_{cut}|$ at each $\sqrt{s}$ cutoff and are the basis for construction of three 35-dimensional empirical parameter distributions. These distributions were used to estimate correlation matrices and compare their characteristics: minimal eigenvalues Λ_{cut}^{min} and condition numbers defined as $CN_{cut} = \Lambda_{cut}^{max}/\Lambda_{cut}^{min}$ with that of estimates obtained by Hessian method (see the bottom subtable). The results show that the MC-matrices are better than the Hessian matrices in all the cases. Condition numbers are much smaller.

It should be stressed that almost all best fit parameters are monotonously shifted as the lower $\sqrt{s}$ cutoff increases. The shifts are within 2 to 3 standard deviations and in "expected" directions. Indeed:

• λ is expected from [13] to weakly depend on atomic numbers of colliding nuclei and asymptotically tend to 1 as $\sqrt{s} \to \infty$, its $\sqrt{s}$ dependence being quite weak;

• Rate H of Heisenberg rise is increasing;

• Scale M (defining the starting point $s = s_M^{ab}$ of Heisenberg's rise) is decreasing towards the possible mass of lightest glueball or alternatively towards the $s_M^{ab} = m_a \cdot m_b$. Regge-Gribov prescriptions to construct asymptotic hadronic scattering amplitudes is based on transition to complex valued $z_t \gg 1$ (z_t– the cosine of t-channel scattering angle expressed in s-channel Mandelstam variables). Condition $z_t \gg 1$ for s-channel forward scattering amplitudes is equivalent to $\frac{s}{m_a \cdot m_b} \gg 1$. Thus, the energy scale in all nonlinear entries of z_t in asymptotic expressions is fixed. This "expected" monotonic evolution of asymptotic parameters with growth of $\sqrt{s}$ cutoff indicates that hadronic "asymptopia" clearly starts above the 7 GeV border. The rise of H with $\sqrt{s}$ cut could be treated as indication to the possible changes in the functional energy dependence of the leading asymptotic term to the $log^c(s/s_0)$ with $c > 2$ or even to temporal power behavior $(s/s_0)^{\Delta}$. In a recent paper [17] the asymptotic bounds (Froissart, Martin) on the possible rise of the total collision cross sections in the form $log^2(s/s_0)$ was questioned in favour of possible faster rising forms. It was supported by the fits presented in [18] where the form $\log^c(s/s_0)$ with adjustable c was tested on $(\bar{p})pp$ data only and it was claimed that values of c obtained in number of different fits are statistically compatible with $c \in [2.2, 2.4]$.

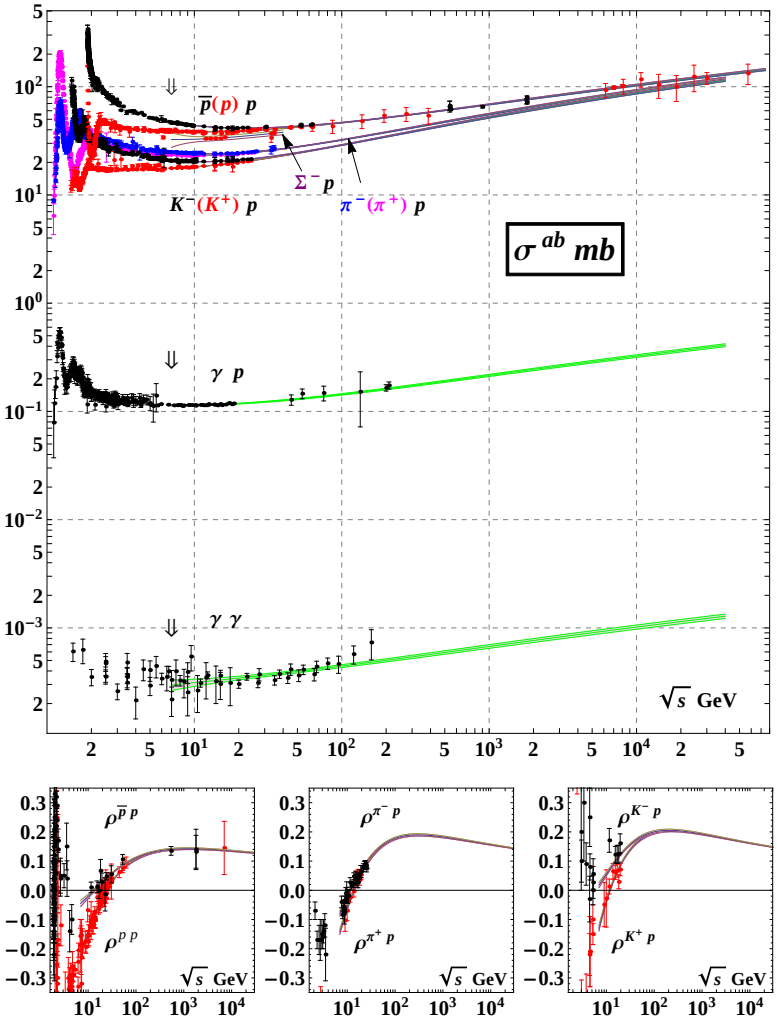

Figure 50.8: Summary of $h^{\mp}p \to anything$, $\gamma p \to hadrons$, $\gamma\gamma \to hadrons$ total cross sections σ^{ab} in mb and $\rho^{h^{\mp}p}$ the ratio of real to imaginary parts of the forward hadronic amplitudes. Also for qualitative comparison of the uniformity of data description by HPR_1R_2–model across the different collisions and observables. The uncertainties for the experimental data points include both the statistical and systematic errors. Curves, corresponding to fit above 7 GeV cut, are plotted with error bands calculated with parameter covariance matrix constructed on MC-propagated vectors from 95% quantile of the empirical distribution.

We have performed our global fit with adjustable c to the total cross sections and available ρ–parameters (as of August 2013) including TOTEM data point at 8 TeV [18]. For this fit we have 37 adjustable parameters. Fit was done with all data at $\sqrt{s} \geq 5$ GeV with $FQ = 0.87$. We have obtained value $c = 1.98 \pm 0.01$ (Hessian error) which is in two standard deviation lower than $c = 2$(exact) and possibly could be tentatively interpreted as an indication to the slower universal rising total cross sections as it was proposed 33 years ago by Cheng and Wu in the form $\log^2\left(\frac{(s/s_0)^a}{\log^2(s/s_0)}\right)$ in their seminal paper [20]. However, to notice this difference much experimental, theoretical, and modelling work has to be done. In conclusion, the Heisenberg prediction of the universal $\log^2(s/s_M)$ form of asymptotic rise of the hadronic collision total cross sections is still actual and should be tested in all aspects at available colliders operating with $(\bar{p}, p, nuclei)$ beams and in experiments with cosmic rays.

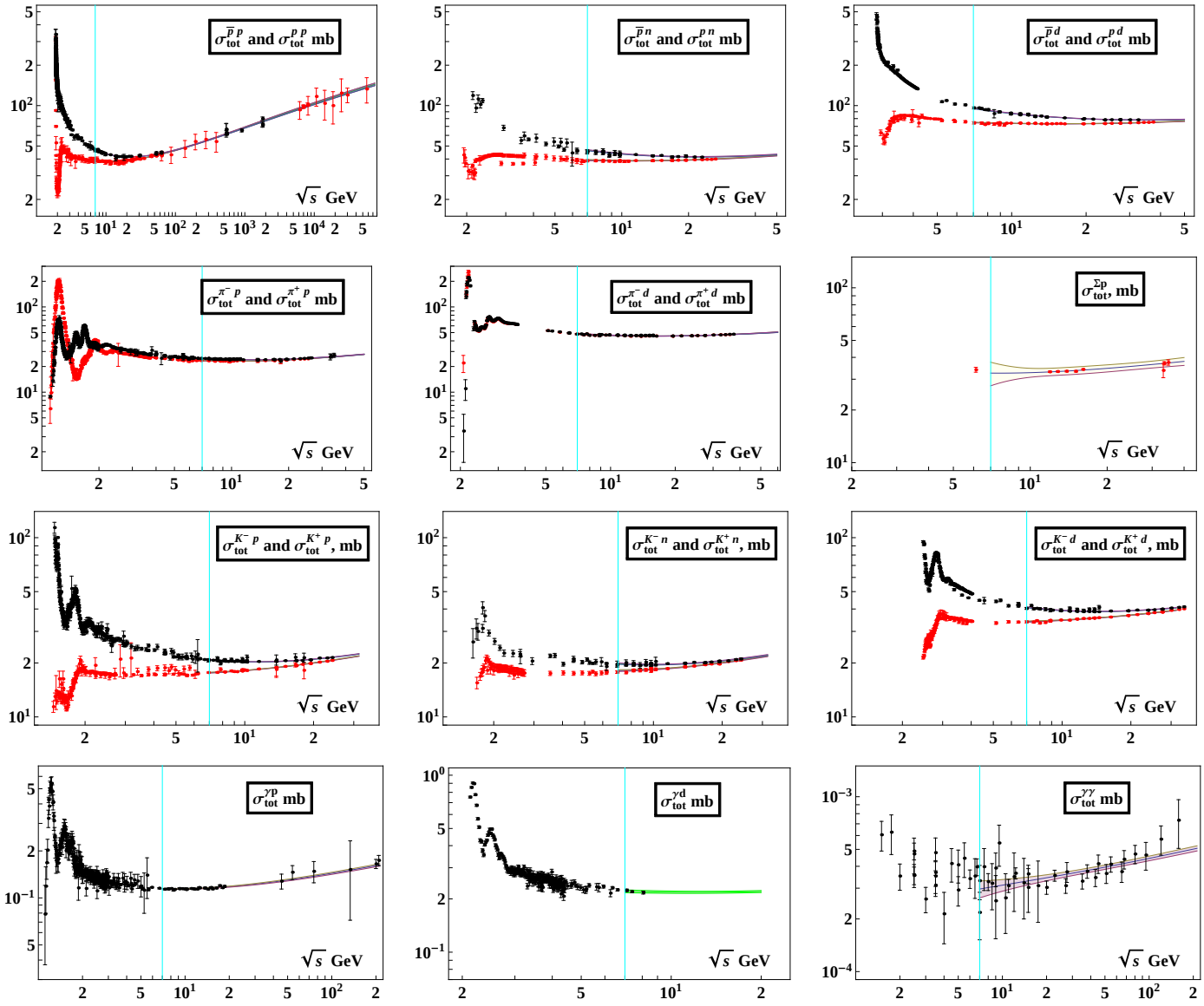

Figure 50.9: Summary of all total collision cross sections jointly fitted with available hadronic ρ parameter data. Corresponding computer-readable data files may be found at http://pdg.lbl.gov/xsect/contents.html

References

[1] G. Antchev *et al.*, Europhys. Lett. **101**, 21004 (2013).

[2] P. Abreu *et al.*, Phys. Rev. Lett. **109**, 062002 (2012).

[3] J.R. Cudell *et al.*: Phys. Rev. **D65**, 074024 (2002); Phys. Rev. Lett. **89**, 201801 (2002).

[4] K. Igi and M. Ishida: Phys. Rev. **D66**, 034023 (2002); Phys. Lett. **B622**, 286 (2005).

[5] M.M. Bock and F. Halzen: Phys. Rev. **D72**, 036006 (2005); Phys. Rev. **D72**, 039902 (2005).

[6] M. Ishida and K. Igi, Prog. Theor. Phys. Suppl. **187**, 297 (2011).

[7] M. Ishida and V. Barger, Phys. Rev. **D84**, 014027 (2011).

[8] F. Halzen *et al.*, Phys. Rev. **D85**, 074020 (2012).

[9] W. Heisenberg, Z. Phys. **133**, 65 (1952).

[10] W. Heisenberg, *Fourteenth Int. Cosm. Ray Conference*, Vol.11, München 1975, 3461-3474;

[11] S.S. Gershtein and A.A. Logunov, Sov. J. Nucl. Phys. **39**, 960 (1984).

[12] E. Iancu and R. Venugopalan, R.C. Hwa (ed.) *et al.*, [hep-ph/0303204].

[13] L. Frankfurt, M. Strikman, and M. Zhalov, Phys. Lett. **B616**, 59 (2005).

[14] M. Giordano, E. Meggiolaro, and N. Moretti, JHEP **1209**, 031 (2012).

[15] JCGM 100:2008, JCGM 101:2008, JCGM 104:2009, JCGM 102:2011 via www.bipm.org/en/publications/guides/gum.html

[16] V.V. Ezhela, Data Science Journal **6**, PS676 (2007).

[17] Y.I. Azimov, Phys. Rev. **D84**, 056012 (2011).

[18] D.A. Fagundes, M.J. Menon, and P.V.R.G. Silva, J. Phys. **G40**, 065005 (2013).

[19] G. Antchev *et al.*, Phys. Rev. Lett. **111**, 012001 (2013).

[20] H. Cheng and T.T. Wu, Phys. Rev. Lett. **24**, 1456 (1970).

High Energy Elastic $\bar{p}\,p$ and $p\,p$ Differential Cross Sections

(Updated September 2013, COMPAS group, IHEP, Protvino)

Using new results from FNAL-COLLIDER-D0 experiment in $\bar{p}\,p$ elastic collisions at $\sqrt{s} = 1.96$ TeV [1], CERN-LHC-TOTEM experiment in $p\,p$ elastic collisions at $\sqrt{s} = 7$, 8 TeV [2–3] and PAO experiment in proton-air collisions at 57 TeV [4] the amplitudes of the elastic $\bar{p}\,p$ and $p\,p$ collisions are investigated in a most broad region in $\sqrt{s}$ and t via three observables $d\sigma/dt(s,t)$, $\sigma^{tot}(s)$, and $\rho(s)$. The summary of the database for $d\sigma/dt(s,t)$ is presented in Figure 50.10, where projection of the $d\sigma/dt(\sqrt{s},t)$ to the $(d\sigma/dt, -t)$ plane orthogonal to the $\sqrt{s}$ axis is displayed.

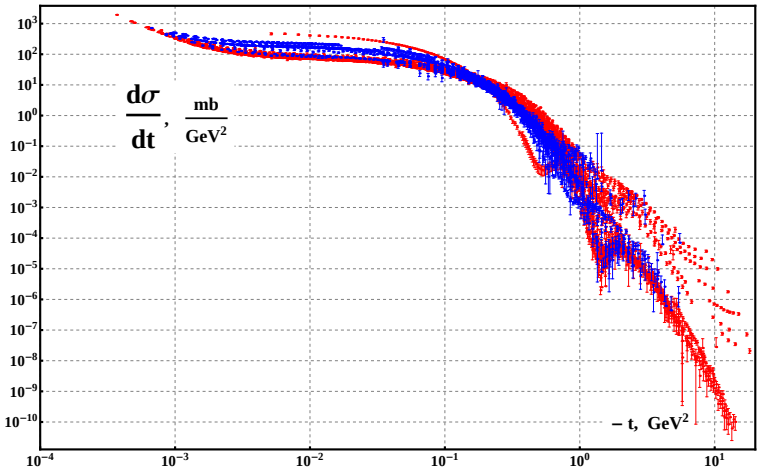

Figure 50.10: Cumulative plots of data on $d\sigma/dt$ for $\bar{p}\,p$ (blue) and $p\,p$ (red) elastic collisions at $\sqrt{s} \geq 2.99$ GeV. Number of data points $Ntot = 6629$

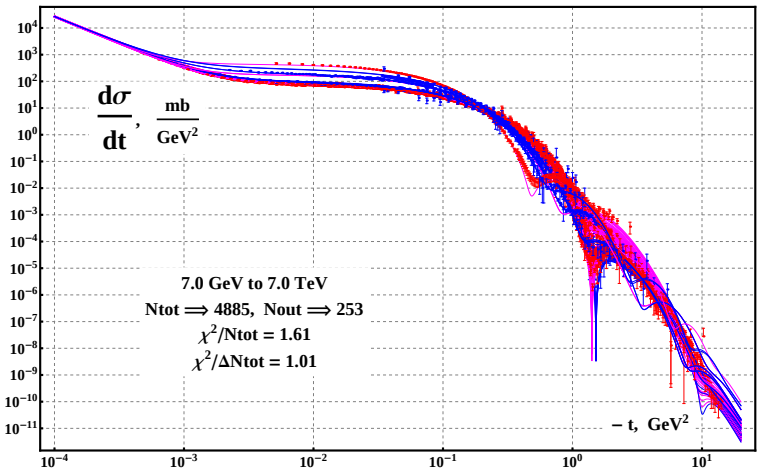

Figure 50.11: Cumulative plots of data on $d\sigma/dt$ and model description for $\bar{p}\,p$ (blue,blue) and $p\,p$ (red,magenta) elastic collisions at $\sqrt{s} \geq 7$ GeV.

All characteristic features of the $d\sigma/dt(\sqrt{s},t)$ behavior in $-t$ and $\sqrt{s}$ are clearly seen:

- The energy-dependent Coulomb-Nuclear Interference (CNI) effects at small $-t$;
- Diffractive peaks with crossover effect at $-t \approx 0.16\,\mathrm{GeV}^2$ for particle-antiparticle data at same energies;
- The first dip/shoulder moving to the left with growing $\sqrt{s}$. New data on $d\sigma/dt$ in $\bar{p}\,p$ and $p\,p$ elastic collisions at highest accelerator energies have challenged all previous model predictions that gave "not so bad qualitative agreement" with previously available data on $d\sigma/dt$. There is a need to reveal a quantitative and statistically complete picture of the data description by at least one model with most ambitious claim on the "best known description". There are several conceptually related papers with such a claims [5–7] but with different areas of applicability and without treatment of the CNI region. Description of $d\sigma/dt$ by our model (a variation of AGNM [7] parameterization) at $\sqrt{s} \geq 7$ GeV is displyed on Figure 50.11. Our model which includes terms responsible for the CNI effects gives stable fit quality (FQ) for the whole sample with all available values of $-t$. Overall $FQ = 1.51$ and reduced to $d\sigma/dt$ $FQ(d\sigma/dt) \approx 1.61$.

Historically the most complete compilations on $d\sigma/dt$ data expressed in Mandelstam variables $\sqrt{s}$ and t were published in Landolt-Börnstein volumes (now available in digital form) up to 1981 [8]. Updated (in high energy part) analogous CLM-compilation [9] (available in computer readable form) was compiled with help of HEPDATA and COMPAS databases and released in 2006. In our fits we use the CLM-compilation with minor corrections, filled detected gaps, and updated with new data published up to August 2013. We performed simultaneous fits to the sample of data on $d\sigma/dt(s,t)$, $\sigma^{tot}(s)$, and $\rho(s)$ in $\bar{p}\,p$ and $p\,p$ collisions at $7\,\mathrm{GeV} \leq \sqrt{s} \leq 8\,\mathrm{TeV}$ and all available t. Overall fit quality $FQ = \chi^2(Ntot)/(Ntot - Npar) = 1.51$, which is unreliable for our number of degrees of freedom. Removing contributions to $\chi^2(d\sigma/dt)$ from $Nout = 253$ points with $\chi^2(point) > (2.4)^2$ (of 2.4×standard deviation (**std**) – randomly scattered outliers) we have $\chi^2(\Delta Ntot)/(\Delta Ntot) = 1.01$, where $\Delta Ntot = Ntot - Nout$. The uniformity level of the fit quality in different intervals of $\sqrt{s}$ is shown on Figure 50.12.

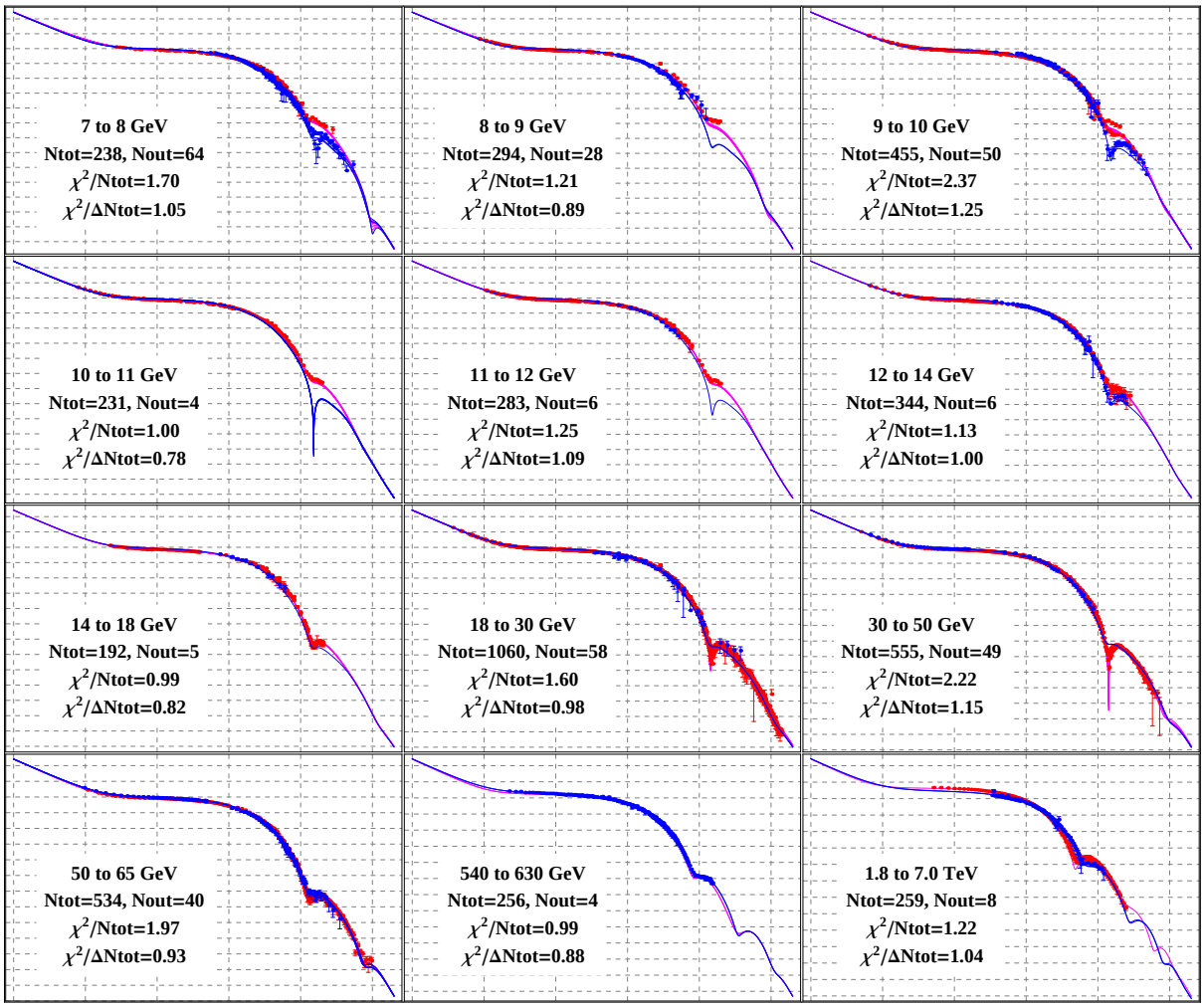

Figure 50.12: All 12 energy intervals are non overlapping and cover all data points. All panels have axis labelled as in Figure 50.11. All data sets corresponding to the same energy have model curve drawn. Some panels have no red or blue data points. In such a cases we add the curve as prediction of the model.

To reveal a more complete picture of phenomenological description of the elastic scattering data we originally selected the most flexible model (43 parameters) from [7] with most broad claimed area of applicability. It turns out that without partial removal of some data (made in [7]) the claimed solution cannot be used even as starting point for adjustments, most probably, because of over-rounded published parameter values, or misprints in parameter tables, or strong parameter correlations. Moreover, numerous fits with different starting points failed to find any locally stable solution with physically reasonable adjustable parameter values. We obtain a stable solution only with addition of data in CNI region and with slightly modified parameterization to reduce the number of adjustable parameters from 43 to 37. Our expressions for observables $\sigma_{\pm}^{tot}(s)$, $\rho_{\pm}(s)$, and $d\sigma_{\pm}/dt(s,t)$ with sign "+" for pp and sign "−" for $\bar{p}p$ collisions are constructed (in notations of [7]) using corresponding scattering amplitudes: nuclear $T_{\pm}(s,t)$ and Coulomb $T_{\pm}^{c}(s,t)$ both in mb $\cdot$ GeV^2 as follows:

$$\sigma_{\pm}^{tot}(s) = \frac{Im\ T_{\pm}(s,0)}{\sqrt{s(s-4m_p^2)}}, \qquad \rho_{\pm}(s) = \frac{Re\ T_{\pm}(s,0)}{Im\ T_{\pm}(s,0)}, \qquad \frac{d\sigma_{\pm}}{dt}(s,t) = \frac{\left|T_{\pm}(s,t)+T_{\pm}^{c}(s,t)\right|^2}{16\pi(\hbar c)^2 s(s-4m_p^2)},$$

where constants: m_p stands for proton mass, and $(\hbar c)^2$ for mb-to-GeV^2 conversion factor. Nuclear amplitudes $T_{\pm}(s,t)$ are linearly combined crossing even $F_{+}(\hat{s},t)$ and crossing odd $F_{-}(\hat{s},t)$ functions.

$$T_{\pm}(s,t) = [F_{+}(\hat{s},t) \mp F_{-}(\hat{s},t)],$$

$$F_{+}(\hat{s},t) = F_{+}^{H}(\hat{s},t) + F_{+}^{P}(\hat{s},t) + F_{+}^{PP}(\hat{s},t) + F_{+}^{R}(\hat{s},t) + F_{+}^{RP}(\hat{s},t) + N_{+}(s,t),$$

$$F_{-}(\hat{s},t) = F_{-}^{MO}(\hat{s},t) + F_{-}^{O}(\hat{s},t) + F_{-}^{OP}(\hat{s},t) + F_{-}^{R}(\hat{s},t) + F_{-}^{RP}(\hat{s},t) + N_{-}(s,t),$$

$$F_{+}^{H}(\hat{s},t) = i\hat{s}\left\{\begin{array}{c} H_1\dfrac{2J_1(K_+\tilde{\tau})}{K_+\tilde{\tau}}\cdot e^{b_{+1}t}\ln^2\tilde{s}\ + \\ H_2 J_0(K_+\tilde{\tau})\cdot e^{b_{+2}t}\ln\tilde{s}\quad + \\ H_3\left[J_0(K_+\tilde{\tau}) - K_+\tilde{\tau}J_1(K_+\tilde{\tau})\right]\cdot e^{b_{+3}t} \end{array}\right\}, \qquad F_{-}^{MO}(\hat{s},t) = \hat{s}\left\{\begin{array}{c} O_1\dfrac{\sin(K_-\tilde{\tau})}{K_-\tilde{\tau}}e^{b_{-1}t}\cdot\ln^2\tilde{s}\ + \\ O_2\cos(K_-\tilde{\tau})e^{b_{-2}t}\cdot\ln\tilde{s}\quad + \\ O_3\ e^{b_{-3}t} \end{array}\right\},$$

$$F_+^P(\hat{s},t) = -C_P e^{b_P t} e^{-i\frac{\pi}{2}\alpha_P(t)}\,(\hat{s})^{\alpha_P(t)}\,, \qquad F_-^O(\hat{s},t) = -iC_O e^{b_O t} e^{-i\frac{\pi}{2}\alpha_O(t)}\,(\hat{s})^{\alpha_O(t)}\,(1+A_O t),$$

$$F_+^{PP}(\hat{s},t) = -\frac{C_{PP}}{\ln\tilde{s}} e^{b_{PP} t} e^{-i\frac{\pi}{2}\alpha_{PP}(t)}\,(\hat{s})^{\alpha_{PP}(t)}\,, \quad F_-^{OP}(\hat{s},t) = -i\frac{C_{OP}}{\ln\tilde{s}} e^{b_{OP} t} e^{-i\frac{\pi}{2}\alpha_{OP}(t)}\,(\hat{s})^{\alpha_{OP}(t)}\,,$$

$$F_\pm^{RP}(\hat{s},t) = \frac{tC_{RP}^\pm}{\ln\tilde{s}} e^{b_{RP}^\pm t} i\frac{-1\pm1}{2}\, e^{-i\frac{\pi}{2}\alpha_{RP}^\pm(t)}\,(\hat{s})^{\alpha_{RP}^\pm(t)}\,, \quad F_\pm^R(\hat{s},t) = \mp C_R^\pm e^{b_R^\pm t} i\frac{-1\pm1}{2}\, e^{-i\frac{\pi}{2}\alpha_R^\pm(t)}\,(\hat{s})^{\alpha_R^\pm(t)}\,,$$

$$N_\pm(s,t) = -i^{\frac{1\pm1}{2}}\cdot\hat{s}\cdot N_\pm\cdot(\ln\tilde{s})\,\frac{t}{t_0}\cdot(1-t/t_\pm)^{-5},$$

$$\alpha_P(t) = 1+\alpha'_P\cdot t; \quad \alpha_R^\pm(t) = \alpha_R^\pm(0)+\alpha_R^{\pm\prime}\cdot t; \quad \alpha_O(t) = 1+\alpha'_O\cdot t\ ,$$

$$\alpha_{OP}(t) = 1+\frac{\alpha'_P\alpha'_O}{\alpha'_P+\alpha'_O}\cdot t; \quad \alpha_{PP}(t) = 1+\frac{\alpha'_P}{2}\cdot t; \quad \alpha_{RP}^\pm(t) = \alpha_R^\pm(0)+\frac{\alpha_P{}'\alpha_R^{\pm\prime}}{\alpha_P{}'+\alpha_R^{\pm\prime}}\cdot t\ ,$$

$$\hat{s}(s,t)\equiv\hat{s} = (-t+2s-4m_p^2)/(2s_0), \ \ s_0 = 1\ \text{GeV}^2; \quad \tilde{s} = \ln\hat{s} - i\frac{\pi}{2}; \quad \tilde{\tau} = \sqrt{-t/t_0}\ln\tilde{s}, \ \ t_0 = 1\ \text{GeV}^2.$$

Coulomb amplitudes are taken with dipole electric nucleon form factor

$$T_\pm^c(s,t) = \mp e^{\left[\pm i\alpha\Phi_\pm^{NC}(s,t)\right]}\cdot 8\pi(\hbar c)^2\alpha\cdot\frac{s}{t}\cdot\left(1-\frac{t}{\Lambda^2}\right)^{-4},$$

where: $\Phi_\pm^{CN}(s,t) = \ln\left[-\frac{t}{2}\left(B_\pm(s)+\frac{8}{\Lambda^2}\right)\right]+\gamma-\frac{4t}{\Lambda^2}\ln\left(-\frac{4t}{\Lambda^2}\right)-\frac{2t}{\Lambda^2}$ is the CNI phase in the R. Cahn form [10]; $\Lambda = \sqrt{0.71}$ GeV; α – fine structure constant; γ – Euler constant. Instead of the traditional definition of the $d\sigma_\pm/dt(s,t)$ slope function $B_\pm(s) = \left[\frac{d}{dt}\ln\left(\frac{d\sigma_\pm}{dt}(s,t)\right)\right]_{t=0}$, we set $B_\pm(s) = \frac{\sigma_\pm(s)}{4\pi(\hbar c)^2}$ to simplify calculations and to get faster minimization procedures. Solution obtained with this simplification is presented in the Table of independently rounded best fit parameter values and their standard deviations.

Name	**Unit**	**Value**	**±Vstd**	**Name**	**Unit**	**Value**	**±Vstd**
H_1	*mb GeV*^{2}	*0.2478*	*0.0014*	O_1	*mb GeV*^{2}	*0.*	*(fix)*
H_2	*mb GeV*^{2}	*0.0078*	*0.0011*	O_2	*mb GeV*^{2}	*0.686*	*0.049*
H_3	*mb GeV*^{2}	*11.22*	*0.32*	O_3	*mb GeV*^{2}	*-3.82*	*0.51*
K_+		*0.3076*	*0.0017*	K_-		*0.0998*	*0.0029*
C_P	*mb GeV*^{2}	*-0.150*	*0.026*	C_O	*mb GeV*^{2}	*-8.60*	*0.44*
C_{PP}	*mb GeV*^{2}	*148.4*	*2.8*	C_{OP}	*mb GeV*^{2}	*64.1*	*2.3*
C_R^+	*mb GeV*^{2}	*-26.6*	*2.3*	C_R^-	*mb GeV*^{2}	*99.1*	*3.7*
C_{RP}^+	*mb GeV*^{2}	*-1.5*	*1.0*	C_{RP}^-	*mb GeV*^{2}	*-58.0*	*10.0*
$\alpha_R^+(0)$		*0.614*	*0.022*	$\alpha_R^-(0)$		*0.444*	*0.011*
$\alpha_R^{+\prime}$	*GeV*$^{-2}$	*0.8*	*(fix)*	$\alpha_R^{-\prime}$	*GeV*$^{-2}$	*0.8*	*(fix)*
$\alpha_P{}'$	*GeV*$^{-2}$	*0.151*	*0.013*	$\alpha_O{}'$	*GeV*$^{-2}$	*0.947*	*0.099*
b_{+1}	*GeV*$^{-2}$	*3.592*	*0.053*	b_{-1}	*GeV*$^{-2}$	*0.*	*(fix)*
b_{+2}	*GeV*$^{-2}$	*0.622*	*0.021*	b_{-2}	*GeV*$^{-2}$	*3.013*	*0.054*
b_{+3}	*GeV*$^{-2}$	*5.44*	*0.13*	b_{-3}	*GeV*$^{-2}$	*2.572*	*0.069*
b_P	*GeV*$^{-2}$	*0.205*	*0.070*	b_O	*GeV*$^{-2}$	*12.25*	*0.53*
b_{PP}	*GeV*$^{-2}$	*5.643*	*0.071*	b_{OP}	*GeV*$^{-2}$	*2.611*	*0.049*
b_R^+	*GeV*$^{-2}$	*1.92*	*0.13*	b_R^-	*GeV*$^{-2}$	*11.28*	*0.43*
b_{RP}^+	*GeV*$^{-2}$	*0.41*	*0.14*	b_{RP}^-	*GeV*$^{-2}$	*1.27*	*0.14*
N_+	*mb GeV*^{2}	*-0.0441*	*0.0073*	N_-	*mb GeV*^{2}	*9.5*	*2.4*
t_+	*GeV*^{2}	*1.678*	*0.072*	t_-	*GeV*^{2}	*0.190*	*0.014*
				A_O	*GeV*$^{-2}$	*-26.1*	*2.3*

Estimates of the std were obtained by the MC-propagation of the assumed Gaussian distribution for each individual data point. Despite of poor MC statistics, the obtained "propagated" covariance matrix is in good conditions [11] and gives reasonable std estimates. The quality of the fit reduced to the $\sigma_\mp^{tot}(s)$ and $\rho_\mp(s)$ is presented on the Figure 50.13. Error bands were calculated by propagation of the parameter scatter region to the scatter region of these observables.

In summary, the solution obtained gives satisfactory picture of the used parametric description of the current database on observables related to elastic (anti)proton–proton scattering amplitudes, and reveals problems with lack of good data at the pre-asymptotic energies. Indeed:

1. Noisy data in dip/shoulder regions does not allow to tune parameters to give credible description of the depth of dips;

2. All frames in Figure 50.12 with $\sqrt{s}\le 12$ GeV apparently show that there is an urgent need in $\bar{p}p$ data at CNI as well as at the first dip/shoulder "$-t$" intervals;

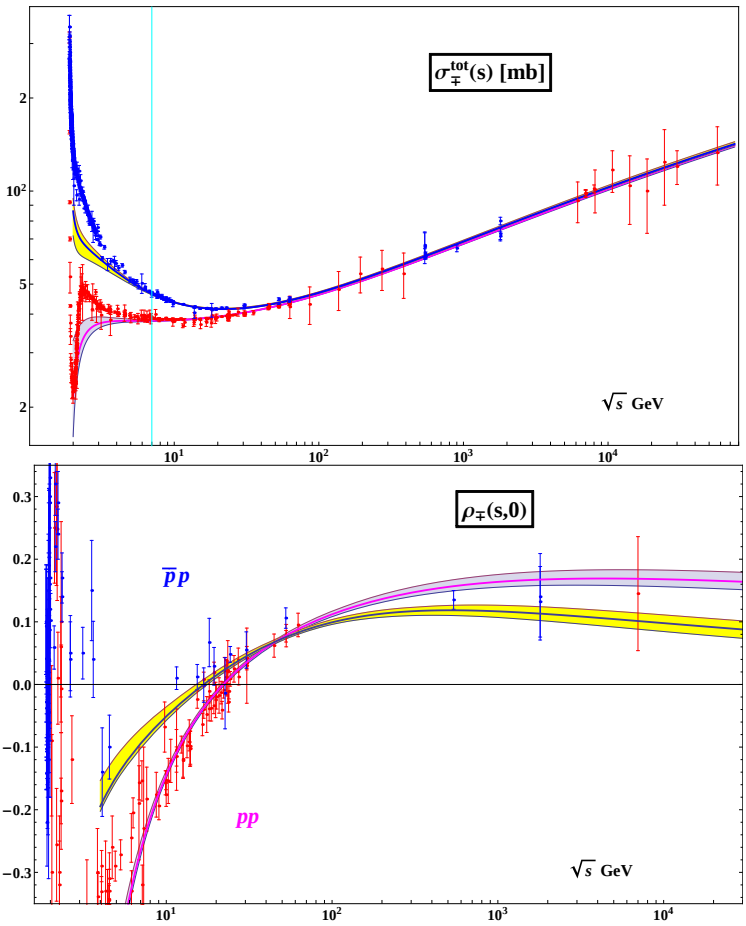

Figure 50.13: Descriptions of $\sigma^{tot}_{\mp}(s)$ and $\rho_{\mp}(s)$ data using our model which is based on AGNM [7] parametrization.

3. Frame marked as "9 to 10 GeV" shows some contradictory data samples in pp collisions (48 "2.4–std outliers" out of 565 data points). There are no model independent resolution of these contradictions other than remeasurements with much higher statistics and more precise measuring systems. New accurate experimental data are highly desirable;

4. There is a sharp difference in descriptions of ρ parameter data from our global fits with HPR_1R_2 model without odderon contribution (non-intersecting $\rho_{\mp}$ curves) and model RPP2013 with odderons (intersecting $\rho_{\mp}$ curves). Further modelling is needed to remove this difference.

In paper [12] the simultaneous description of $\sigma_{\mp}$ and $\rho_{\mp}$ in the interval $5.\text{GeV} \le \sqrt{s} \le 7.\text{TeV}$ and $d\sigma_{\mp}/dt$ in the region $(19.\,\text{GeV} \le \sqrt{s} \le 7.\,\text{TeV}) \otimes (0.01\,\text{GeV}^2 \le -t \le 14.2\,\text{GeV}^2)$ by a hybrid model of [6] and [7] with triple pole odderon switched off at $t = 0$ was claimed to be good enough. It gives nonintersecting $\rho_{\mp}$ curves. Unfortunately the poorly specified pre–filtered experimental data sample to fit, and no evidence of the results stability did not allow us to reproduce claimed results.

Interesting indication on a possible second dip/shoulder "activity" effects at higher values of "$-t$" is visible (on RPP2013 curves) on the first three low energy panels of Figure 50.12 and more pronounced on the last four highest energy panels. The possibility of the multiple dips on the $d\sigma/dt$ at large $|t|$ has been broadly discussed earlier in context of the geometrical picture of diffractive scattering (see, for example, paper [13] and its citations). This could be possibly tested in a dedicated experiments on the high intensity ($\bar{p}$) and p fixed target accelerators and at active colliders. New high precision elastic data at Serpukhov, RHIC, and FNAL energies will be helpful to clarify the situation with multiple dips and odderons in continuing frontier studies by the TOTEM collaboration at CERN-LHC.

References

[1] V.M. Abazov *et al.*, Phys. Rev. **D86**, 012009 (2012);

[2] G. Antchev *et al.*, Europhys. Lett.:**111**, 012001 (2013); **101**, 21004 (2013); **101**, 21002 (2013); **96**, 21002 (2011).

[3] G. Antchev *et al.*, Europhys. Lett. **95**, 41001 (2011).

[4] P. Abreu *et al.*, Phys. Rev. Lett. **109**, 062002 (2012).

[5] R. Avila, P. Gauron, and B. Nicolescu, Eur. Phys. J. **C49**, 581 (2007).

[6] E. Martynov, Phys. Rev. **D76**, 074030 (2007).

[7] E. Martynov and B. Nicolescu, Eur. Phys. J. **C56**, 57 (2008).

[8] In Landolt-Börnstein, Group I: P.J. Carson, v.9, 675 (1980); R.R. Shubert, v.9, 216 (1980); P.J. Carlson, v.7, 109 (1973); A.N. Diddens, v.7, 27 (1973).

[9] J. R. Cudell, A. Lengyel, and E. Martynov, Phys. Rev. **D73**, 034008 (2006).

[10] R. Cahn, Z. Phys. **C15**, 253 (1982).

[11] Our sample contains 656 37-dimensional vectors in the scatter region. Minimal eigenvalue of the correlation matrix is 8.1×10^{-4}, its condition number is 1.04×10^4.

[12] E. Martynov, Phys. Rev. **D87**, 114018 (2013).

[13] T.T. Chou and C.N. Yang, Phys. Rev. **D19**, 3268 (1979).

INTRODUCTION TO THE PARTICLE LISTINGS

Illustrative Key to the Particle Listings

Name of particle. "Old" name used before 1986 renaming scheme also given if different. See the section "Naming Scheme for Hadrons" for details.

Particle quantum numbers (where known).

Indicates particle omitted from Particle Physics Summary Table, implying particle's existence is not confirmed.

Quantity tabulated below.

General comments on particle.

Top line gives our best value (and error) of quantity tabulated here, based on weighted average of measurements used. Could also be from fit, best limit, estimate, or other evaluation. See next page for details.

"Document id" for this result; full reference given below.

Footnote number linking measurement to text of footnote.

Measurement technique. (See abbreviations on next page.)

Number of events *above background*.

Measured value used in averages, fits, limits, etc.

Scale factor > 1 indicates possibly inconsistent data.

Reaction producing particle, or general comments.

Error in measured value (often statistical only; followed by systematic if separately known; the two are combined in quadrature for averaging and fitting.)

"Change bar" indicates result added or changed since previous edition.

Measured value *not used* in averages, fits, limits, etc. See the Introductory Text for explanations.

Charge(s) of particle(s) detected.

Arrow points to weighted average.

Ideogram to display possibly inconsistent data. Curve is sum of Gaussians, one for each experiment (area of Gaussian = 1/error; width of Gaussian = ±error). See Introductory Text for discussion.

Shaded pattern extends $\pm 1\sigma$ (scaled by "scale factor" S) from weighted average.

Value and error for each experiment.

Contribution of experiment to χ^2 (if no entry present, experiment not used in calculating χ^2 or scale factor because of very large error).

Partial decay mode (labeled by Γ_i).

Our best value for branching fraction as determined from data averaging, fitting, evaluating, limit selection, etc. This list is basically a compact summary of results in the Branching Ratio section below.

Branching ratio.

Our best value (and error) of quantity tabulated, as determined from constrained fit (using *all significant* measured branching ratios for this particle).

Weighted average of measurements of this ratio only.

Footnote (referring to LYNCH 81).

Branching ratio in terms of partial decay mode(s) Γ_i above.

Confidence level for measured upper limit.

References, ordered inversely by year, then author.

Partial list of author(s) in addition to first author.

"Document id" used on data entries above.

Quantum number determinations in this reference.

Journal, report, preprint, etc. (See abbreviations on next page.)

Institution(s) of author(s). (See abbreviations on next page.)

$a_0(1200)$

$I^G(J^{PC}) = 1^-(0^{++})$

OMITTED FROM SUMMARY TABLE

Evidence not compelling, may be a kinematic effect.

$a_0(1200)$ MASS

VALUE (MeV)	EVTS	DOCUMENT ID		TECN	CHG	COMMENT
1206± 7 OUR AVERAGE						
1210± 8±9	3000	FENNER	87	MMS	−	3.5 $\pi^- p$
1198±10		PIERCE	83	ASPK	+	2.1 $K^- p$
1216±11±9	1500	[1] MERRILL	81	HBC	0	3.2 $K^- p$
• • • We do not use the following data for averages, fits, limits, etc. • • •						
1192±16	200	LYNCH	81	HBC	±	2.7 $\pi^- p$

[1] Systematic error was added quadratically by us in our 1986 edition.

$a_0(1200)$ WIDTH

VALUE (MeV)	EVTS	DOCUMENT ID		TECN	CHG	COMMENT
41±11 OUR AVERAGE Error includes scale factor of 1.8. See the ideogram below.						
50± 8		PIERCE	83	ASPK	+	2.1 $K^- p$
70^{+30}_{-20}	200	LYNCH	81	HBC	±	2.7 $\pi^- p$
25± 5±7		MERRILL	81	HBC	0	3.2 $K^- p$
• • • We do not use the following data for averages, fits, limits, etc. • • •						
<60		FENNER	87	MMS	−	3.5 $\pi^- p$

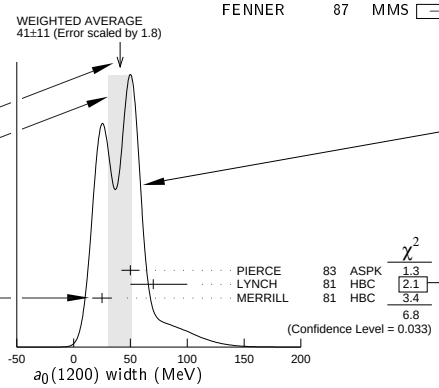

$a_0(1200)$ DECAY MODES

Mode	Fraction (Γ_i/Γ)	Scale factor/ Confidence level
Γ_1 3π	(65.2±1.3) %	S=1.7
Γ_2 $K\overline{K}$	(34.8±1.3) %	S=1.7
Γ_3 $\eta\pi^\pm$	< 4.9 $\times 10^{-4}$	CL=95%

$a_0(1200)$ BRANCHING RATIOS

$\Gamma(3\pi)/\Gamma_{total}$ Γ_1/Γ

VALUE	DOCUMENT ID		TECN	CHG	COMMENT
0.652±0.013 OUR FIT Error includes scale factor of 1.7.					
0.643±0.010 OUR AVERAGE					
0.64 ±0.01	PIERCE	83	ASPK	+	2.1 $K^- p$
0.74 ±0.06	MERRILL	81	HBC	0	3.2 $K^- p$
• • • We do not use the following data for averages, fits, limits, etc. • • •					
0.48 ±0.15	[2] LYNCH	81	HBC	±	2.7 $\pi^- p$

[2] Data has questionable background subtraction.

$\Gamma(K\overline{K})/\Gamma_{total}$ Γ_2/Γ

VALUE	DOCUMENT ID	TECN	CHG	COMMENT
0.348±0.013 OUR FIT Error includes scale factor of 1.7.				
0.35 ±0.05	PIERCE 83	ASPK	+	2.1 $K^- p$

$\Gamma(K\overline{K})/\Gamma(3\pi)$ Γ_2/Γ_1

VALUE	DOCUMENT ID	TECN	CHG	COMMENT
0.535±0.030 OUR FIT Error includes scale factor of 1.7.				
0.50 ±0.03	MERRILL 81	HBC	0	3.2 $K^- p$

$\Gamma(\eta(\text{neutral decay})\pi^\pm)/\Gamma_{total}$ $0.71\Gamma_3/\Gamma$

VALUE (units 10^{-4})	CL%	DOCUMENT ID	TECN	CHG	COMMENT
<3.5	95	PIERCE 83	ASPK	+	2.1 $K^- p$

$a_0(1200)$ REFERENCES

FENNER	87	PRL 55 14	H. Fenner *et al.*	(SLAC)	
PIERCE	83	PL 123B 230	J.H. Pierce	(FNAL)	UP
LYNCH	81	PR D24 610	G.R. Lynch *et al.*	(CLEO Collab.)	
MERRILL	81	PRL 47 143	D.W. Merrill *et al.*	(SACL, CERN)	

Abbreviations Used in the Particle Listings

Indicator of Procedure Used to Obtain Our Result

OUR AVERAGE	From a weighted average of selected data.
OUR FIT	From a constrained or overdetermined multiparameter fit of selected data.
OUR EVALUATION	Not from a direct measurement, but evaluated from measurements of other quantities.
OUR ESTIMATE	Based on the observed range of the data. Not from a formal statistical procedure.
OUR LIMIT	For special cases where the limit is evaluated by us from measured ratios or other data. Not from a direct measurement.

Measurement Techniques (i.e., Detectors and Methods of Analysis)

ACCM	ACCMOR Collaboration
ADMX	Axion Dark Matter Experiment
AEMS	Argonne effective mass spectrometer
ALEP	ALEPH – CERN LEP detector
ALPS	Photon regeneration experiment
AMND	AMANDA South Pole neutrino detector
AMY	AMY detector at KEK-TRISTAN
ANIT	Antarctic Impulsive Transient Antenna balloon mission
ANTR	ANTARES underwater neutrino telescope in the Western Mediterranean Sea
APEX	FNAL APEX Collab.
ARG	ARGUS detector at DORIS
ARGD	Fit to semicircular amplitude path on Argand diagram
ASP	Anomalous single-photon detector
ASPK	Automatic spark chambers
ASTE	ASTERIX detector at LEAR
ASTR	Astronomy
ATLS	ATLAS detector at CERN LHC
B787	BNL experiment 787 detector
B791	BNL experiment 791 detector
B845	BNL experiment 845 detector
B852	BNL E-852
B865	BNL E865 detector
B871	BNL experiment 871 detector
B949	BNL E949 detector at AGS
BABR	BaBar Collab.
BAKS	Baksan underground scintillation telescope
BC	Bubble chamber
BDMP	Beam dump
BEAT	CERN BEATRICE Collab.
BEBC	Big European bubble chamber at CERN
BELL	Belle Collab.
BES	BES Beijing Spectrometer at Beijing Electron-Positron Collider
BES2	BES Beijing Spectrometer at Beijing Electron-Positron Collider
BES3	BES Beijing Spectrometer at Beijing Electron-Positron Collider
BIS2	BIS-2 spectrometer at Serpukhov
BKEI	BENKEI spectrometer system at KEK Proton Synchroton
BOLO	Bolometer, a cryogenic thermal detector
BONA	Bonanza nonmagnetic detector at DORIS
BORX	BOREXINO
BPWA	Barrelet-zero partial-wave analysis
CALO	Calorimeter
CAST	CAST experiment at CERN
CBAL	Crystal Ball detector at SLAC-SPEAR or DORIS
CBAR	Crystal Barrel detector at CERN-LEAR
CBOX	Crystal Box at LAMPF
CBTP	CBELSA/TAPS Collaboration
CC	Cloud chamber
CCFR	Columbia-Chicago-Fermilab-Rochester detector
CDEX	China Dark Matter Experiment
CDF	Collider detector at Fermilab
CDF2	CDF-II Collab.
CDHS	CDHS neutrino detector at CERN
CDM2	CDMS II, Cryogenic Dark Matter Search at Soudan Underground Lab.
CDMS	CDMS Collab.
CELL	CELLO detector at DESY
CGNT	CoGeNT dark matter search experiment
CHER	Cherenkov detector
CHM2	CHARM-II neutrino detector (glass) at CERN
CHOZ	Nuclear Power Station near Chooz, France
CHRM	CHARM neutrino detector (marble) at CERN
CHRS	CHORUS Collaboration – CERNS SPS
CIB	Cosmic Infrared Background
CIBS	CERN-IHEP boson spectrometer
CLAS	Jefferson CLAS Collab.
CLE2	CLEO II detector at CESR
CLE3	CLEO III detector at CESR
CLEO	Cornell magnetic detector at CESR
CMB	Cosmic Microwave Background
CMD	Cryogenic magnetic detector at VEPP-2M, Novosibirsk
CMD2	Cryogenic magnetic detector 2 at VEPP-2M, Novosibirsk
CMD3	Cryogenic magnetic detector 3 at VEPP-2000, Novosibirsk
CMS	CMS detector at CERN LHC
CNTR	Counters
COMB	Combined analysis of data from independent experiments.
COMP	COMPASS experiment at the CERN SPS
COSM	Cosmology and astrophysics
COSY	COSY-TOF Collaboration
COUP	COUPP (the Chicagoland Observatory for Underground Particle Physics) Collab.
CPLR	CPLEAR Collaboration
CRBT	Crystal Ball and TAPS detector at MAMI
CRES	CRESST cryogenic detector
CRYB	Crystal Ball at BNL
CRYM	Crystal Ball detector at Mainz Microtron MAMI
CSB2	Columbia U. - Stony Brook BGO calorimeter inserted in NaI array
CSME	COSME Collaboration
CUOR	CUORICINO experiment at Gran Sasso Laboratory.
CUSB	Columbia U. - Stony Brook segmented NaI detector at CESR
D0	D0 detector at Fermilab Tevatron Collider
DAMA	DAMA, dark matter detector at Gran Sasso National Lab.
DASP	DESY double-arm spectrometer
DAYA	Daya Bay Collaboration
DBC	Deuterium bubble chamber
DCHZ	Double Chooz Collaboration
DLCO	DELCO detector at SLAC-SPEAR or SLAC-PEP
DLPH	DELPHI detector at LEP
DM1	Magnetic detector no. 1 at Orsay DCI collider
DM2	Magnetic detector no. 2 at Orsay DCI collider
DMIC	DAMIC Dark Matter in CCD experiment at Fermilab
DMTP	Dark Matter Time Projection Chamber (DMTPC) directional detection experiment
DONU	DONUT Collab.
DPWA	Energy-dependent partial-wave analysis
DRFT	Directional dark matter detector at Boulby Underground Science Facility
E621	Fermilab E621 detector
E653	Fermilab E653 detector
E665	Fermilab E665 detector
E687	Fermilab E687 detector
E691	Fermilab E691 detector
E705	Fermilab E705 Spectrometer-Calorimeter
E731	Fermilab E731 Spectrometer-Calorimeter
E756	Fermilab E756 detector
E760	Fermilab E760 detector
E761	Fermilab E761 detector
E771	Fermilab E771 detector
E773	Fermilab E773 Spectrometer-Calorimeter
E789	Fermilab E789 detector
E791	Fermilab E791 detector
E799	Fermilab E799 Spectrometer-Calorimeter
E835	Fermilab E835 detector
EDE2	EDELWEISS II dark matter search Collaboration
EDEL	EDELWEISS dark matter search Collaboration
EHS	Four-pi detector at CERN
ELEC	Electronic combination
EMC	European muon collaboration detector at CERN
EMUL	Emulsions
FAST	Fiber Active Scintillator Target detector at PSI
FBC	Freon bubble chamber
FENI	FENICE (at the ADONE collider of Frascati)
FIT	Fit to previously existing data
FLAT	Large Area Telescope onboard the Fermi Gamma-Ray Space Telescope
FMPS	Fermilab Multiparticle Spectrometer
FOCS	FNAL E831 FOCUS Collab.
FRAB	ADONE $B\overline{B}$ group detector
FRAG	ADONE $\gamma\gamma$ group detector
FRAM	ADONE MEA group detector
FREJ	FREJUS Collaboration – modular flash chamber detector (calorimeter)

Abbreviations Used in the Particle Listings

FRMI	Fermi large area telescope (Fermi-LAT)
GA24	Hodoscope Cherenkov γ calorimeter (IHEP GAMS-2000) (CERN GAMS-4000)
GALX	GALLEX solar neutrino detector in the Gran Sasso Underground Lab.
GAM2	IHEP hodoscope Cherenkov γ calorimeter GAMS-2000
GAM4	CERN hodoscope Cherenkov γ calorimeter GAMS-4000
GAMS	IHEP hodoscope Cherenkov γ calorimeter GAMS-4π
GNO	Gallium Neutrino Observatory in the Gran Sasso Underground Lab.
GOLI	CERN Goliath spectrometer
GRAL	GRAAL Collaboration
H1	H1 detector at DESY/HERA
HBC	Hydrogen bubble chamber
HDBC	Hydrogen and deuterium bubble chambers
HDMO	Heidelberg-Moscow Experiment
HDMS	Heidelberg Dark Matter Search Experiment
HEBC	Helium bubble chamber
HEPT	Helium proportional tubes
HERB	HERA-B detector at DESY/HERA
HERM	HERMES detector at DESY/HERA
HESS	High Energy Stereoscopic System gamma-ray instrument
HFS	Hyperfine structure
HLBC	Heavy-liquid bubble chamber
HOME	Homestake underground scintillation detector
HPGE	High-purity Germanium detector
HPW	Harvard-Pennsylvania-Wisconsin detector
HRS	SLAC high-resolution spectrometer
HYBR	Hybrid: bubble chamber + electronics
HYCP	HyperCP Collab. (FNAL E-871)
IACT	Imaging Air Cherenkov Telescope
ICAR	ICARUS experiment at Gran Sasso Laboratory.
ICCB	IceCube neutrino detector at South Pole
IGEX	IGEX Collab.
IMB	Irvine-Michigan-Brookhaven underground Cherenkov detector
IMB3	Irvine-Michigan-Brookhaven underground Cherenkov detector
INDU	Magnetic induction
IPWA	Energy-independent partial-wave analysis
ISTR	IHEP ISTRA+ spectrometer-calorimeter
JADE	JADE detector at DESY
K246	KEK E246 detector with polarimeter
K2K	KEK to Super-Kamiokande
K391	KEK E391a detector
K470	KEK-E470 Stopping K detector
KAM2	KAMIOKANDE-II underground Cherenkov detector
KAMI	KAMIOKANDE underground Cherenkov detector
KAR2	KARMEN2 calorimeter at the ISIS neutron spallation source at Rutherford
KARM	KARMEN calorimeter at the ISIS neutron spallation source at Rutherford
KEDR	detector operating at VEPP-4M collider (Novosibirsk)
KIMS	Korea Invisible Mass Search experiment at YangYang, Korea
KLND	KamLand Collab. (Japan)
KLOE	KLOE detector at DAFNE (the Frascati e+e- collider Italy)
KOLR	Kolar Gold Field underground detector
KTEV	KTeV Collaboration
L3	L3 detector at LEP
LASR	Laser
LASS	Large-angle superconducting solenoid spectrometer at SLAC
LATT	Lattice calculations
LEBC	Little European bubble chamber at CERN
LEGS	BNL LEGS Collab.
LENA	Nonmagnetic lead-glass NaI detector at DORIS
LEP	From combination of all 4 LEP experiments: ALEPH, DELPHI, L3, OPAL
LEPS	Low-Energy Pion Spectrometer at the Paul Scherrer Institute
LGW	Lead Glass Wall collaboration at SPEAR/SLAC
LHCB	LHCb detector at CERN LHC
LSD	Mont Blanc liquid scintillator detector
LSND	Liquid Scintillator Neutrino Detector
LSW	Light Shining through a Wall
MAC	MAC detector at PEP/SLAC
MBOO	Fermilab MiniBooNE neutrino experiment
MBR	Molecular beam resonance technique
MCRO	MACRO detector in Gran Sasso
MD1	Magnetic detector at VEPP-4, Novosibirsk
MDRP	Millikan drop measurement
MEG	Muon to electron conversion detector at PSI
MICA	Underground mica deposits
MINS	Fermilab MINOS experiment
MIRA	MIRABELLE Liquid-hydrogen bubble chamber
MLEV	Magnetic levitation
MMS	Missing mass spectrometer
MPS	Multiparticle spectrometer at BNL
MPS2	Multiparticle spectrometer upgrade at BNL
MPSF	Multiparticle spectrometer at Fermilab
MPWA	Model-dependent partial-wave analysis
MRK1	SLAC Mark-I detector
MRK2	SLAC Mark-II detector
MRK3	SLAC Mark-III detector
MRKJ	Mark-J detector at DESY
MRS	Magnetic resonance spectrometer
MUG2	MUON(g-2)
MWPC	Multi-Wire Proportional Chamber
NA14	CERN NA14
NA31	CERN NA31 Spectrometer-Calorimeter
NA32	CERN NA32 Spectrometer
NA48	CERN NA48 Collaboration
NA49	CERN NA49 Collaboration
NA60	CERN NA60 Collaboration
NA62	CERN NA62 Experiment
NAGE	NEWAGE, New generation WIMP-search experiment with advanced gaseous tracking
NAIA	NAIAD (NaI Advanced Detector) dark matter search experiment
ND	NaI detector at VEPP-2M, Novosibirsk
NICE	Serpukhov nonmagnetic precision spectrometer
NMR	Nuclear magnetic resonance
NOMD	NOMAD Collaboration, CERN SPS
NTEV	NuTeV Collab. at Fermilab
nTRV	neutron Time-Reversal Violation
NUSX	Mont Blanc NUSEX underground detector
OBLX	OBELIX detector at LEAR
OLYA	Detector at VEPP-2M and VEPP-4, Novosibirsk
OMEG	CERN OMEGA spectrometer
OPAL	OPAL detector at LEP
OPER	OPERA experiment with emulsion tracking at Gran Sasso
OSPK	Optical spark chamber
PIBE	The PIBETA detector at the Paul Scherrer Institute (PSI), Switzerland.
PICA	PICASSO dark matter search experiment
PLAS	Plastic detector
PLUT	DESY PLUTO detector
PRMX	The PRIMEX detector in Hall B at TJNAF
PWA	Partial-wave analysis
REDE	Resonance depolarization
RENO	RENO Collaboration
RICE	Radio Ice Cherenkov Experiment
RVUE	Review of previous data
SAGE	US - Russian Gallium Experiment
SELX	FNAL SELEX Collab.
SFM	CERN split-field magnet
SHF	SLAC Hybrid Facility Photon Collaboration
SIGM	Serpukhov CERN-IHEP magnetic spectrometer (SIGMA)
SILI	Silicon detector
SIMP	SIMPLE, dark matter detector at Laboratori Nazionali del Sud
SKAM	Super-Kamiokande Collab.
SLAX	Solar Axion Experiment in Canfranc Underground Laboratory
SLD	SLC Large Detector for e^+e^- colliding beams at SLAC
SMPL	SIMPLE, Superheated Instrument for Massive ParticLe Experiments
SND	Novosibirisk Spherical neutral detector at VEPP-2M
SNDR	SINDRUM spectrometer at PSI
SNO	SNO Collaboration (Sudbury Neutrino Observatory)
SOU2	Soudan 2 underground detector
SOUD	Soudan underground detector
SPEC	Spectrometer
SPED	From maximum of speed plot or resonant amplitude
SPHR	Bonn SAPHIR Collab.
SPNX	SPHINX spectrometer at IHEP accelerator
SPRK	Spark chamber
SQID	SQUID device
STRC	Streamer chamber
SVD2	SVD-2 experiment at IHEP, Protvino
T2K	T2K Collaboration

TASS	DESY TASSO detector
TEVA	Combined analysis of CDF and DØ experiments
TEXO	TEXONO Collab., ultra low energy Ge detector at Kuo-Sheng Laboratory
THEO	Theoretical or heavily model-dependent result
TNF	TNF-IHEP facility at 70 GeV IHEP accelerator
TOF	Time-of-flight
TOPZ	TOPAZ detector at KEK-TRISTAN
TPC	TPC detector at PEP/SLAC
TPS	Tagged photon spectrometer at Fermilab
TRAP	Penning trap
TWST	TWIST spectrometer at TRIUMF
UA1	UA1 detector at CERN
UA2	UA2 detector at CERN
UA5	UA5 detector at CERN
UCNA	UCNA collaboration using polarizeed ultracold neutrons at LANSCE
UKDM	UK Dark Matter Collab.
VES	Vertex Spectrometer Facility at 70 GeV IHEP accelerator
VLBI	Very Long Baseline Interferometer
VNS	VENUS detector at KEK-TRISTAN
VRTS	Very Energetic Radiation Imaging Telescope Array System (VERITAS)
WA75	CERN WA75 experiment
WA82	CERN WA82 experiment
WA89	CERN WA89 experiment
WARP	Liquid argon detector for CDM searches at Gran Sasso
WASA	WASA detector at CELSIUS, Uppsala and at COSY, Juelich
WIRE	Wire chamber
X100	XENON100 dark matter search experiment at Gran Sasso National Laboratory
XE10	XENON10 experiment at Gran Sasso National Laboratory
XEBC	Xenon bubble chamber
XMAS	XMASS, liquid xenon scintillation detector at Kamioka Observatory
ZEP2	ZEPLIN-II dark matter detector
ZEP3	ZEPLIN-III dark matter detector at Palmer Underground Lab.
ZEPL	ZEPLIN-I galactic dark matter detector
ZEUS	ZEUS detector at DESY/HERA

Conferences

Conferences are generally referred to by the location at which they were held (e.g., HAMBURG, TORONTO, CORNELL, BRIGHTON, etc.).

Journals

AA	Astronomy and Astrophysics
ADVP	Advances in Physics
AFIS	Anales de Fisica
AJP	American Journal of Physics
AL	Astronomy Letters
ANP	Annals of Physics
ANPL	Annals of Physics (Leipzig)
ANYAS	Annals of the New York Academy of Sciences
AP	Atomic Physics
APAH	Acta Physica Academiae Scientiarum Hungaricae
APJ	Astrophysical Journal
APJS	Astrophysical Journal Suppl.
APP	Acta Physica Polonica
APS	Acta Physica Slovaca
ARNPS	Annual Review of Nuclear and Particle Science
ARNS	Annual Review of Nuclear Science
ASP	Astroparticle Physics
BAPS	Bulletin of the American Physical Society
BASUP	Bulletin of the Academy of Science, USSR (Physics)
CJNP	Chinese Journal of Nuclear Physics
CJP	Canadian Journal of Physics
CNPP	Comments on Nuclear and Particle Physics
CP	Chinese Physics
CTP	Communications in Theoretical Physics
CZJP	Czechoslovak Journal of Physics
DANS	Doklady Akademii nauk SSSR
EPJ	The European Physical Journal
EPL	Europhysics Letters
FECAY	Fizika Elementarnykh Chastits i Atomnogo Yadra
HADJ	Hadronic Journal
IJMP	International Journal of Modern Physics
JAP	Journal of Applied Physics
JCAP	Journal of Cosmology and Astroparticle Physics
JETP	English Translation of Soviet Physics ZETF
JETPL	English Translation of Soviet Physics ZETF Letters
JHEP	Journal of High Energy Physics
JINR	Joint Inst. for Nuclear Research
JINRRC	JINR Rapid Communications
JP	Journal of Physics (generic for all A,B,E,G)
JPA	Journal of Physics, A
JPB	Journal of Physics, B
JPCRD	Journal of Physical and Chemical Reference Data
JPG	Journal of Physics, G
JPSJ	Journal of the Physical Society of Japan
LNC	Lettere Nuovo Cimento
MNRAS	Monthly Notices of the Royal Astronomical Society
MPL	Modern Physics Letters
NAST	New Astronomy
NAT	Nature
NC	Nuovo Cimento
NIM	Nuclear Instruments and Methods
NJP	New Journal of Physics
NP	Nuclear Physics
NPBPS	Nuclear Physics B Proceedings Supplement
PAN	Physics of Atomic Nuclei (formerly SJNP)
PD	Physics Doklady (Magazine)
PDAT	Physik Daten
PL	Physics Letters
PN	Particles and Nuclei
PPCF	Plasma Physics and Controlled Fusion
PPN	Physics of Particles and Nuclei (formerly SJPN)
PPNL	Physics of Particles and Nuclei Letters
PPNP	Progress in Particles and Nuclear Physics
PPSL	Proc. of the Physical Society of London
PR	Physical Review
PRAM	Pramana
PRL	Physical Review Letters
PRPL	Physics Reports (Physics Letters C)
PRSE	Proc. of the Royal Society of Edinburgh
PRSL	Proc. of the Royal Society of London, Section A
PS	Physica Scripta
PTEP	Progress of Theoretical and Experimental Physics
PTP	Progress of Theoretical Physics
PTPS	Progress of Theoretical Physics Supplement
PTRSL	Phil. Trans. Royal Society of London
RA	Radiochimica Acta
RMP	Reviews of Modern Physics
RNC	La Rivista del Nuovo Cimento
RPP	Reports on Progress in Physics
RRP	Revue Roumaine de Physique
SCI	Science
SJNP	Soviet Journal of Nuclear Physics
SJPN	Soviet Journal of Particles and Nuclei
SPD	Soviet Physics Doklady (Magazine)
SPU	Soviet Physics - Uspekhi
UFN	Usp. Fiz. Nauk – Russian version of SPU
YAF	Yadernaya Fizika
ZETF	Zhurnal Eksperimental'noi i Teoreticheskoi Fiziki
ZETFP	Zhurnal Eksperimental'noi i Teoreticheskoi Fiziki, Pis'ma v Redakts
ZNAT	Zeitschrift fur Naturforschung
ZPHY	Zeitschrift fur Physik

Institutions

AACH	Phys. Inst. der Techn. Hochschule **Aachen** (Historical, use for general Inst. der Techn. Hochschule)	Aachen, Germany
AACH1	I Phys. Inst. B, RWTH **Aachen**	Aachen, Germany
AACH3	III Phys. Inst. A, RWTH **Aachen** Univ.	Aachen, Germany
AACHT	Inst. für Theoretische Teilchenphysik & Kosmologie, RWTH **Aachen**	Aachen, Germany
AARH	Univ. of **Aarhus**	Aarhus C, Denmark
ABO	**Åbo** Akademi Univ.	Turku, Finland
ADEL	**Adelphi** Univ.	Garden City, NY, USA
ADLD	The Univ. of **Adelaide**	Adelaide, SA, Australia

Abbreviations Used in the Particle Listings

AERE	Atomic Energy Research Estab.	Didcot, United Kingdom
AFRR	**Armed Forces** Radiobiology Res. Inst.	Bethesda, MD, USA
AHMED	Physical Research Lab.	**Ahmedabad**, Gujarat, India
AICH	**Aichi** Univ. of Education	Aichi, Japan
AKIT	**Akita** Univ.	Akita, Japan
ALAH	Univ. of **Alabama (Huntsville)**	Huntsville, AL, USA
ALAT	Univ. of **Alabama (Tuscaloosa)**	Tuscaloosa, AL, USA
ALBA	**SUNY at Albany**	Albany, NY, USA
ALBE	Univ. of **Alberta**	Edmonton, AB, Canada
AMES	**Ames Lab.**	Ames, IA, USA
AMHT	**Amherst** College	Amherst, MA, USA
AMST	Univ. van **Amsterdam**	GL Amsterdam, The Netherlands
ANIK	**NIKHEF**	**Amsterdam**, The Netherlands
ANKA	**Middle East** Technical Univ.; Dept. of Physics; Experimental HEP Lab	Ankara, Turkey
ANL	**Argonne** National Lab.; High Energy Physics Division, Bldg. 362; Physics Division, Bldg. 203	Argonne, IL, USA
ANSM	**St. Anselm** Coll.	Manchester, NH, USA
ARCBO	**Arecibo** Observatory	Arecibo, PR, USA
ARIZ	Univ. of **Arizona**	Tucson, AZ, USA
ARZS	**Arizona State** Univ.	Tempe, AZ, USA
ASCI	Russian Academy of Sciences	**Moscow**, Russian Federation
AST	**Academia Sinica**	Nankang, Taipei, Taiwan
ATEN	NCSR **"Demokritos"**	**Aghia** Paraskevi , Greece
ATHU	Univ. of **Athens**	Athens, Greece
AUCK	Univ. of **Auckland**	Auckland, New Zealand
BAKU	**Natl. Azerbaijan Academy of Sciences**, Inst. of Physics	**Baku**, Azerbaijan
BANG	Indian Inst. of Science	**Bangalore**, India
BANGB	**Bangabasi** College	Calcutta, India
BARC	Univ. Autónoma de **Barcelona**	Bellaterra (Barcelona), Spain
BARI	Univ. e del Politecnico di **Bari**	Bari, Italy
BART	Univ. of **Delaware**; **Bartol** Research Inst.	Newark, DE, USA
BASL	Inst. für Physik der Univ. **Basel**	Basel, Switzerland
BAYR	Univ. **Bayreuth**	Bayreuth, Germany
BCEN	Centre d'Etudes Nucleaires de **Bordeaux-Gradignan**	Gradignan, France
BCIP	Natl. Inst. for Physics & Nuclear Eng. "Horia Hulubei" **(IFIN-HH)**	**Bucharest**-Magurele, Romania
BEIJ	**Beijing** Univ.	Beijing, China
BEIJT	**Inst. of Theoretical Physics**	**Beijing**, China
BELG	Inter-University Inst. for High Energies (ULB-VUB)	**Brussel**, Belgium
BELL	AT & T **Bell** Labs	Murray Hill, NJ, USA
BERG	Univ. of **Bergen**	Bergen, Norway
BERL	**DESY**, Deutsches Elektronen-Synchrotron	**Zeuthen**, Germany
BERN	Univ. of **Berne**	Berne, Switzerland
BGNA	Univ. di **Bologna**, & **INFN**, Sezione di Bologna; Via Irnerio, 46, I-40126 Bologna; Viale C. Berti Pichat, n. 6/2	Bologna, Italy
BHAB	**Bhabha Atomic** Research Center	Trombay, Bombay, India
BHEP	**Inst. of High Energy Physics**	**Beijing**, China
BIEL	Univ. **Bielefeld**	Bielefeld, Germany
BING	**SUNY at Binghamton**	Binghamton, NY, USA
BIRK	**Birkbeck** College, Univ. of London	London, United Kingdom
BIRM	Univ. of **Birmingham**	Edgbaston, Birmingham, United Kingdom
BLSU	**Bloomsburg** Univ.	Bloomsburg, PA, USA
BNL	**Brookhaven National Lab.**	Upton, NY, USA
BOCH	**Ruhr** Univ. **Bochum**	Bochum, Germany
BOHR	**Niels Bohr Inst.**	Copenhagen Ø, Denmark
BOIS	**Boise** State Univ.	Boise, ID, USA
BOMB	Univ. of **Bombay**	Bombay, India
BONN	**Univ. of Bonn**	Bonn, Germany
BORD	Centre d'Etudes Nucléaires de **Bordeaux** Gradignan **(CENBG)**	Gradignan, France
BOSE	S.N. **Bose** National Centre for Basis Sciences	Calcutta, India
BOSK	**"Rudjer Bošković"** Inst.	Zagreb, Croatia
BOST	**Boston** Univ.	Boston, MA, USA
BRAN	**Brandeis** Univ.	Waltham, MA, USA
BRCO	Univ. of **British Columbia**	Vancouver, BC, Canada
BRIS	Univ. of **Bristol**	Bristol, United Kingdom
BROW	**Brown** Univ.	Providence, RI, USA
BRUN	**Brunel** Univ.	Uxbridge, Middlesex, United Kingdom
BRUX	Univ. Libre de **Bruxelles**; Physique des Particules Elémentaires	Bruxelles, Belgium
BRUXT	Univ. Libre de **Bruxelles**; Physique Théorique	Bruxelles, Belgium
BUCH	Univ. of **Bucharest**	Bucharest-Magurele, Romania
BUDA	**Wigner** Research Centre for Physics	**Budapest**, Hungary
BUFF	**SUNY at Buffalo**	Buffalo, NY, USA
BURE	Inst. des Hautes Etudes Scientifiques	**Bures-sur-Yvette**, France
CAEN	Lab. de Physique Corpusculaire, **ENSICAEN**	**Caen**, France
CAGL	Univ. degli Studi di **Cagliari**	Monserrato (CA), Italy
CAIR	**Cairo** University	Orman, Giza, Cairo, Egypt
CAIW	**Carnegie Inst.** of Washington	Washington, DC, USA
CALB	Univ. della **Calabria**	Cosenza, Italy
CALC	Univ. of **Calcutta**	Calcutta, India
CAMB	**DAMTP**	Cambridge, United Kingdom
CAMP	Univ. Estadual de **Campinas** (UNICAMP)	**Campinas**, SP, Brasil
CANB	**Australian National Univ.**	Canberra, ACT, Australia
CANTB	Inst. de Física de Cantabria (CSIC–Univ. **Cantabria**)	Santander, Spain
CAPE	University of **Cape Town**	Rondebosch, Cape Town, South Africa
CARA	Univ. Central de **Venezuela**	Caracas, Venezuela
CARL	**Carleton** Univ.	Ottawa, ON, Canada
CARLC	**Carleton** College	Northfield, MN, USA
CASE	**Case** Western Reserve Univ.	Cleveland, OH, USA
CAST	**China** Center of Advanced Science and Technology	Beijing, China
CATA	Univ. di **Catania**	Catania, Italy
CATH	**Catholic** Univ. of America	Washington, DC, USA
CAVE	**Cavendish** Lab.	Cambridge, United Kingdom
CBNM	CBNM	**Geel**, Belgium
CCAC	**Allegheny** College	Meadville, PA, USA
CDEF	**Univ. Paris VII, Denis Diderot**	Paris, France
CEA	Cambridge Electron Accelerator (Historical in *Review*)	**Cambridge, MA**, USA
CEADE	Center for Apl. Studies for Nuclear Physics	Havana, Cuba
CEBAF	**Jefferson Lab—Thomas Jefferson National Accelerator Facility**	**Newport News**, VA, USA
CENG	Centre d'Etudes Nucleaires	**Grenoble**, France
CERN	**CERN**, European Organization for Nuclear Research	Genève, Switzerland
CFPA	Univ. of **California, (Berkeley)**	Berkeley, CA, USA
CHIC	Univ. of **Chicago**	Chicago, IL, USA
CIAE	**State Nuclear Power Research Inst.**	**Beijing**, China
CINC	Univ. of **Cincinnati**	Cincinnati, OH, USA
CINV	**CINVESTAV-IPN** Centro de Investigacion y de Estudios Avanzados del IPN	**México**, DF, Mexico
CIT	**California Inst. of Tech.**	Pasadena, CA, USA
CLER	Univ. de **Clermont-Ferrand**	Aubière, France
CLEV	**Cleveland** State Univ.	Cleveland, OH, USA
CMNS	**Comenius** Univ. (FMFI UK)	**Bratislava**, Slovakia

Abbreviations Used in the Particle Listings

CMU	**Carnegie Mellon** Univ.	Pittsburgh, PA, USA
CNEA	**Comisión Nacional de Energía Atómica**	Buenos Aires, Argentina
CNRC	Centre for Research in Particle Physics	Ottawa, ON, Canada
COIM	Univ. de Coimbra	**Coimbra**, Portugal
COLO	Univ. of **Colorado**	Boulder, CO, USA
COLU	**Columbia** Univ.	New York, NY, USA
CONC	**Concordia** University	Montreal, PQ, Canada
CORN	**Cornell** Univ.	Ithaca, NY, USA
COSU	**Colorado State** Univ.	Fort Collins, CO, USA
CPPM	Centre National de la Recherche Scientifique, Luminy	**Marseille**, France
CRAC	Henryk Niewodnicza'nski Inst. of Nuclear Physics	**Kraków**, Poland
CRNL	**Chalk River** Labs.	Chalk River, ON, Canada
CSOK	**Oklahoma** Central State Univ.	Edmond, OK, USA
CST	Univ. of **Science and Technology** of China	**Hefei**, Anhui 230026, China
CSULB	**California** State Univ.	Long Beach, CA, USA
CSUS	**California** State Univ.	Sacramento, CA, USA
CUNY	**City College** of **New York**	New York, NY, USA
CURCP	**Univ. Pierre et Marie Curie** (Paris VI), LCP	Paris, France
CURIN	**Univ. Pierre et Marie Curie** (Paris VI), LPNHE	Paris, France
CURIT	**Univ. Pierre et Marie Curie** (Paris VI), LPTHE	Paris, France
DALH	**Dalhousie** Univ.	Halifax, NS, Canada
DALI	**Dalian** Univ. of Tech.	Dalian, China
DARE	**Daresbury** Lab	Cheshire, United Kingdom
DARM	Tech. Hochschule **Darmstadt**	Darmstadt, Germany
DELA	Univ. of **Delaware**; Dept. of Physics & Astronomy	Newark, DE, USA
DELH	Univ. of **Delhi**	Delhi, India
DESY	**DESY**, Deutsches Elektronen-Synchrotron	**Hamburg**, Germany
DFAB	Escuela de Ingenieros	**Bilbao**, Spain
DOE	**Department of Energy**	Washington, DC, USA
DORT	Technische Univ. **Dortmund**	Dortmund, Germany
DUKE	**Duke** Univ.	Durham, NC, USA
DURH	Univ. of **Durham**	Durham , United Kingdom
DUUC	**University College** Dublin	Dublin, Ireland
EDIN	Univ. of **Edinburgh**	Edinburgh, United Kingdom
EFI	Univ. of Chicago, **The Enrico Fermi Inst.**	**Chicago**, IL, USA
ELMT	**Elmhurst** College	Elmhurst, IL, USA
ENSP	**l'Ecole Normale Supérieure**	**Paris**, France
EOTV	**Eötvös** University	Budapest, Hungary
EPOL	**École Polytechnique**	**Palaiseau**, France
ERLA	Univ. **Erlangen-Nurnberg**	Erlangen, Germany
ETH	**Univ. Zürich**	Zürich, Switzerland
FERR	Univ. di **Ferrara**	Ferrara, Italy
FIRZ	Univ. degli Studi di **Firenze**	Sesto Fiorentino, Italy
FISK	**Fisk** Univ.	Nashville, TN, USA
FLOR	Univ. of **Florida**	Gainesville, FL, USA
FNAL	**Fermilab**	Batavia, IL, USA
FOM	**FOM**, Stichting voor Fundamenteel Onderzoek der Materie	JP **Utrecht**, The Netherlands
FRAN	**Frankfurt Inst. for Advanced Studies (FIAS)**	Frankfurt am Main, Germany
FRAS	Lab. Nazionali di **Frascati** dell'**INFN**	Frascati (Roma), Italy
FREIB	**Albert-Ludwigs** Univ.	**Freiburg**, Germany
FREIE	**Freie Univ. Berlin**	Berlin, Germany
FRIB	Univ. de **Fribourg**	Fribourg, Switzerland
FSU	**Florida State** Univ.; High Energy Physics	Tallahassee, FL, USA
FSUSC	**Florida State** Univ.; SCS (School of Computational Science)	Tallahassee, FL, USA
FUKI	**Fukui** Univ.	Fukui, Japan
FUKU	**Fukushima** Univ.	Fukushima, Japan
GENO	Univ. di **Genova**	Genova, Italy
GEOR	**E. Andronikashvili Inst. of Physics**	Tbilisi, Republic of Georgia
GESC	**General Electric** Co.	Schenectady, NY, USA
GEVA	Univ. de **Genève**	Genève, Switzerland
GIES	Univ. **Giessen**	Giessen, Germany
GIFU	**Gifu** Univ.	Gifu, Japan
GLAS	Univ. of **Glasgow**	Glasgow, United Kingdom
GMAS	**George Mason** Univ.	Fairfax, VA, USA
GOET	Univ. **Göttingen**	Göttingen, Germany
GRAN	Univ. de **Granada**	Granada, Spain
GRAZ	Univ. **Graz**	Graz, Austria
GRON	Univ. of **Groningen**	Groningen, The Netherlands
GSCO	**Geological Survey of Canada**	Ottawa, ON, Canada
GSI	GSI Helmholtzzentrum für Schwerionenforschung GmbH	**Darmstadt**, Germany
GUAN	Univ. de **Guanajuato**	León, Gto., Mexico
GUEL	Univ. of **Guelph**	Guelph, ON, Canada
GWU	**George Washington** Univ.	Washington, DC, USA
HAHN	**Hahn-Meitner** Inst. Berlin GmbH	Berlin, Germany
HAIF	**Technion** – Israel Inst. of Tech.	Technion, Haifa, Israel
HAMB	Univ. **Hamburg**	Hamburg, Germany
HANN	Univ. **Hannover**	Hannover, Germany
HARC	**Houston Advanced Research Ctr.**	The Woodlands, TX, USA
HARV	**Harvard** Univ.	Cambridge, MA, USA
HARV	**Harvard** Univ. (LPPC)	Cambridge, MA, USA
HAWA	Univ. of **Hawai'i**	Honolulu, HI, USA
HEBR	**Hebrew** Univ.	Jerusalem, Israel
HEID	Univ. **Heidelberg**; (unspecified division) (Historical in *Review*)	Heidelberg, Germany
HEIDH	Ruprecht-Karls Univ. **Heidelberg**	Heidelberg, Germany
HEIDP	Univ. **Heidelberg**; Physics Inst.	Heidelberg, Germany
HEIDT	Ruprecht-Karls-Univ. **Heidelberg**	Heidelberg, Germany
HELS	Univ. of **Helsinki**	University of Helsinki, Finland
HIRO	**Hiroshima** Univ.	Higashi-Hiroshima, Japan
HOUS	Univ. of **Houston**	Houston, TX, USA
HPC	**Hewlett-Packard** Corp.	Cupertino, CA, USA
HSCA	**Harvard-Smithsonian** Center for Astrophysics	Cambridge, MA, USA
IAS	**Inst. for Advanced Study**	Princeton, NJ, USA
IASD	**Dublin** Inst. for Advanced Studies	Dublin, Ireland
IBAR	**Ibaraki** Univ.	Ibaraki, Japan
IBM	**IBM** Corp.	Palo Alto, CA, USA
IBMY	**IBM**	Yorktown Heights, NY, USA
IBS	Inst. for **Boson Studies**	Pasadena, CA, USA
ICEPP	The Univ. of **Tokyo**	Tokyo, Japan
ICRR	Univ. of **Tokyo**	Chiba, Japan
ICTP	**Abdus Salam** International Centre for Theoretical Physics	**Trieste**, Italy
IFIC	**IFIC** (Instituto de Física Corpuscular)	**Paterna (Valencia)**, Spain
IFRJ	Univ. Federal do **Rio de Janeiro**	Rio de Janeiro, RJ, Brasil
IIT	**Illinois Inst. of Tech.**	Chicago, IL, USA
ILL	Univ. of **Illinois at Urbana-Champaign**	Urbana, IL, USA
ILLC	Univ. of **Illinois at Chicago**	Chicago, IL, USA
ILLG	Inst. **Laue-Langevin**	Grenoble, France
IND	**Indiana** Univ.	Bloomington, IN, USA
INEL	E G and G **Idaho**, Inc.	Idaho Falls, ID, USA
INFN	Ist. Nazionale di Fisica Nuclear (Generic INFN, unknown location)	Various places, Italy
INNS	Univ. of **Innsbruck**	**Innsbruck**, Austria
INPK	Henryk Niewodniczański Inst. of Nuclear Physics	**Kraków**, Poland
INRM	**INR**, Inst. for Nucl. Research	**Moscow**, Russian Federation
INUS	**KEK**, High Energy Accelerator Research Organization	Tokyo, Japan
IOAN	Univ. of **Ioannina**	Ioannina, Greece

Abbreviations Used in the Particle Listings

IOFF	A.F. **Ioffe** Phys. Tech. Inst.	St. **Petersburg**, Russian Federation
IOWA	Univ. of **Iowa**	Iowa City, IA, USA
IPN	**IPN**, Inst. de Phys. Nucl.	**Orsay**, France
IPNP	Univ. Pierre et Marie Curie (**Paris** VI)	Paris, France
IRAD	Inst. du Radium (Historical)	**Paris**, France
ISNG	Lab. de Physique Subatomique et de Cosmologie **(LPSC)**	**Grenoble**, France
ISU	**Iowa State** Univ.	Ames, IA, USA
ISUT	Isfahan University of Technology	Isfahan, Iran
ITEP	**ITEP**, Inst. of Theor. and Exp. Physics	**Moscow**, Russian Federation
ITHA	**Ithaca** College	Ithaca, NY, USA
IUPU	**Indiana** Univ., **Purdue** Univ. **Indianapolis**	Indianapolis, IN, USA
JADA	**Jadavpur** Univ.	Calcutta, India
JAGL	**Jagiellonian** Univ.	Kraków, Poland
JHU	**Johns Hopkins** Univ.	Baltimore, MD, USA
JINR	**JINR**, Joint Inst. for Nucl. Research	**Dubna**, Russian Federation
JULI	Forschungszentrum **Jülich**	Jülich, Germany
JYV	Univ. of **Jyväskylä**	Jyväskylä, Finland
KAGO	Univ. of **Kagoshima**	Kagoshima-shi, Japan
KAIST	**Korea** Advanced Inst. of Science and Technology	Yusung ku, Daejon, Republic of Korea
KANS	Univ. of **Kansas**	Lawrence, KS, USA
KARL	Univ. **Karlsruhe** (Historical in *Review*)	Karlsruhe, Germany
KARLE	**Karlsruhe** Inst. of Technology (KIT); Inst. for Experimental Nuclear Physics	Karlsruhe, Germany
KARLK	**Karlsruhe** Inst. of Technology (KIT)	Eggenstein-Leopoldshafen, Germany
KARLT	**Karlsruhe** Inst. of Technology (KIT); Inst. for Theoretical Physics	Karlsruhe, Germany
KAZA	**Kazakh** Inst. of High Energy Physics	Alma Ata, Kazakhstan
KEK	**KEK**, High Energy Accelerator Research Organization	Ibaraki-ken, Japan
KENT	Univ. of **Kent**	Canterbury, United Kingdom
KEYN	**Open** Univ.	Milton Keynes, United Kingdom
KFTI	**Kharkov** Inst. of Physics and Tech. (NSC KIPT)	Kharkov, Ukraine
KIAE	**Kurchatov** Inst.	**Moscow**, Russian Federation
KIAM	**Keldysh** Inst. of Applied Math., Acad. Sci., Russia	Moscow, Russian Federation
KIDR	**Vinča Inst. of Nuclear Sciences**	Belgrade, Serbia
KIEV	**Institute for Nuclear Research**	**Kyiv**, Ukraine
KINK	**Kinki** Univ.	Osaka, Japan
KNTY	Univ. of **Kentucky**	Lexington, KY, USA
KOBE	**Kobe** Univ.	Kobe, Japan
KOMAB	Univ. of **Tokyo, Komaba**	Tokyo, Japan
KONAN	**Konan** Univ.	Kobe, Japan
KOSI	Inst. of Experimental Physics SAS	**Košice**, Slovakia
KYOT	**Kyoto** Univ.; Dept. of Physics, Graduate School of Science	Kyoto, Japan
KYOTU	**Kyoto** Univ.; **Yukawa** Inst. for Theor. Physics	Kyoto, Japan
KYUN	**Kyungpook** National Univ.	Daegu, Republic of Korea
KYUSH	**Kyushu** Univ.; Elementary ParticleTheory Group; Exp. Particle Physics Group; Research Center for Advanced Particle Physics	Fukuoka, Japan
LALO	**LAL**, Laboratoire de l'Accélérateur Linéaire	**Orsay**, France
LANC	**Lancaster** Univ.	Lancaster, United Kingdom
LANL	**Los Alamos National Lab.** (LANL)	Los Alamos, NM, USA
LAPL	Univ. Nacional de **La Plata**	La Plata, Argentina
LAPP	**LAPP**, Lab. d'Annecy-le-Vieux de Phys. des Particules	**Annecy-le-Vieux**, France
LASL	U.C. **Los Alamos Scientific** Lab. (Old name for LANL)	Los Alamos, NM, USA
LATV	**Latvian** State Univ.	Riga, Latvia
LAUS	EPFL **Lausanne**	Lausanne, Switzerland
LAVL	Univ. **Laval**	Quebec, QC, Canada
LBL	**Lawrence Berkeley National Lab.**	Berkeley, CA, USA
LCGT	Univ. di **Torino**	Turin, Italy
LEBD	**Lebedev** Physical Inst.	**Moscow**, Russian Federation
LECE	Univ. di **Lecce**	Lecce, Italy
LEED	Univ. of **Leeds**	Leeds, United Kingdom
LEGN	Lab. Naz. di Legnaro	**Legnaro**, Italy
LEHI	**Lehigh** Univ.	Bethlehem, PA, USA
LEHM	**Lehman** College of CUNY	Bronx, NY, USA
LEID	Univ. **Leiden**	Leiden, The Netherlands
LEMO	**Le Moyne** Coll.	Syracuse, NY, USA
LEUV	Katholieke Univ. **Leuven**	Leuven, Belgium
LIEG	Univ. de **Liège**	Liège, Belgium
LINZ	Univ. **Linz**	Linz, Austria
LISB	Inst. Nacional de Investigacion Cientifica	**Lisboa** CODEX, Portugal
LISBT	Centro de Física Teórica de Partículas **(CFTP)**	**Lisboa**, Portugal
LIVP	Univ. of **Liverpool**	Liverpool, United Kingdom
LLL	**Lawrence Livermore Lab.** (Old name for LLNL)	Livermore, CA, USA
LLNL	**Lawrence Livermore National Lab.**	Livermore, CA, USA
LOCK	**Lockheed** Palo Alto Res. Lab	Palo Alto, CA, USA
LOIC	**Imperial** College of Science Tech. & Medicine	London, United Kingdom
LOQM	Queen Mary, **Univ. of London**	London, United Kingdom
LOUC	**University College** London	London, United Kingdom
LOUV	Univ. Catholique de **Louvain**	Louvain-la-Neuve, Belgium
LOWC	**Westfield** College (Historical, see LOQM (Queen Mary and Westfield joined))	London, United Kingdom
LRL	U.C. Lawrence Radiation Lab. (Old name for LBL)	**Berkeley**, CA, USA
LSU	**Louisiana** State Univ.	Baton Rouge, LA, USA
LUND	**Fysiska Institutionen**	**Lund**, Sweden
LUND	**Lund** Univ.	Lund, Sweden
LYON	Institute de Physique Nucléaire de **Lyon** (IPN)	Villeurbanne, France
MADE	**UAM/CSIC**, Inst. de Física Teórica	**Madrid**, Cantoblanco, Spain
MADR	**C.I.E.M.A.T**	**Madrid**, Spain
MADU	Univ. Autónoma de **Madrid**	Cantoblanco, Madrid, Spain
MANI	Univ. of **Manitoba**	Winnipeg, MB, Canada
MANZ	**Johannes-Gutenberg-Univ.**; Inst. für Kernphysik, J.-J.-Becher-Weg 45; Inst. für Physik, Staudingerweg 7	**Mainz**, Germany
MARB	Univ. **Marburg**	Marburg, Germany
MARS	Centre de Physique des Particules de **Marseille**	Marseille, France
MASA	Univ. of **Massachusetts** Amherst	**Amherst**, MA, USA
MASB	Univ. of **Massachusetts** Boston	**Boston**, MA, USA
MASD	Univ. of **Massachusetts** Dartmouth	North **Dartmouth**, MA, USA
MCGI	**McGill** Univ.	Montreal, QC, Canada
MCHS	Univ. of **Manchester**	Manchester, United Kingdom
MCMS	**McMaster** Univ.	Hamilton, ON, Canada
MEHTA	**Harish-Chandra** Research Inst.	Allahabad, India
MEIS	**Meisei** Univ.	Tokyo, Japan
MELB	Univ. of **Melbourne**	Victoria, Australia
MEUD	Observatoire de **Meudon**	Meudon, France
MICH	Univ. of **Michigan**	Ann Arbor, MI, USA
MILA	Univ. di **Milano**	Milano, Italy
MILAI	**INFN**, Sez. di **Milano**	Milano, Italy
MINN	Univ. of **Minnesota**	Minneapolis, MN, USA
MIPT	Moscow Institute of Physics and Technology	Moscow, Russian Federation

Abbreviations Used in the Particle Listings

MISS	Univ. of **Mississippi**	University, MS, USA
MISSR	Univ. of **Missouri**	Rolla, MO, USA
MIT	**MIT Massachusetts Inst. of Technology**	Cambridge, MA, USA
MIU	**Maharishi** International Univ.	Fairfield, IA, USA
MIYA	**Miyazaki** Univ.	Miyazaki-shi, Japan
MONP	Univ. de **Montpellier** II	Montpellier, France
MONS	Univ. of **Mons**	**Mons**, Belgium
MONT	Univ. de **Montréal**; Pavillon René-J.-A.-Lévesque	Montréal, PQ, Canada
MONTC	Univ. de **Montréal**; Centre de recherches mathématiques	Montréal, PQ, Canada
MOSU	**Skobeltsyn** Inst. of Nuclear Physics, Lomonosov Moscow State Univ.; Experimental HEP Division; Theoretical HEP Division	**Moscow**, Russian Federation
MPCM	Max Planck Inst. fur Chemie	**Mainz**, Germany
MPEI	**Moscow Physical Engineering** Inst.	Moscow, Russian Federation
MPIG	**Max-Planck**-Institute für Astrophysik	Garching, Germany
MPIH	**Max-Planck-Inst.** für Kernphysik	**Heidelberg**, Germany
MPIM	**Max-Planck-Inst.** für Physik	**München**, Germany
MSST	Mississippi State University	Mississippi State, MS, USA
MSU	**Michigan State** Univ.	East Lansing, MI, USA
MTHO	**Mount Holyoke** College	South Hadley, MA, USA
MULH	Centre Univ. du **Haut-Rhin**	Mulhouse, France
MUNI	**Ludwig-Maximilians-Univ. München**	Garching, Germany
MUNT	Tech. Univ. **München**	Garching, Germany
MURA	**Midwestern** Univ. Research Assoc. (Historical in *Review*)	Stroughton, WI, USA
MURC	Univ. of Murcia	Murcia, Spain
NAAS	North Americal Aviation Science Center (Historical in *Review*)	Thousand Oaks, CA, USA
NAGO	**Nagoya** Univ.	Nagoya, Japan
NAPL	Univ. di **Napoli** "Federico II"	Napoli, Italy
NASA	**NASA**	Greenbelt, MD, USA
NBS	U.S **National Bureau of Standards** (Old name for NIST)	Gaithersburg, MD, USA
NBSB	**National Inst. Standards Tech.**	Boulder, CO, USA
NCAR	**National Center for Atmospheric Research**	Boulder, CO, USA
NCSU	**North Carolina** State Univ.	**Raleigh**, NC, USA
NDAM	Univ. of **Notre Dame**	Notre Dame, IN, USA
NEAS	**Northeastern** Univ.	Boston, MA, USA
NEBR	Univ. of **Nebraska**	Lincoln, NE, USA
NEUC	Univ. de **Neuchâtel**	Neuchâtel, Switzerland
NICEA	Univ. de **Nice**	Nice, France
NICEO	Observatoire de **Nice**	Nice, France
NIHO	**Nihon** Univ.	Tokyo, Japan
NIIG	**Niigata** Univ.	Niigata, Japan
NIJM	**Radboud** Univ. Nijmegen	AJ **Nijmegen**, The Netherlands
NIRS	Nat. Inst. Radiological Sciences	**Chiba**, Japan
NIST	**National Institute of Standards & Technology**	Gaithersburg, MD, USA
NIU	**Northern Illinois** Univ.	De Kalb, IL, USA
NMSU	**New Mexico** State Univ.; Dept. of Physics, MSC 3D; Part. & Nucl. Phys. Group, Box 30001/Dept.	Las Cruces, NM, USA
NORD	**Nordita**	Stockholm, Sweden
NOTT	Univ. of **Nottingham**	Nottingham, United Kingdom
NOVM	Inst. of Mathematics	**Novosibirsk**, Russian Federation
NOVO	BINP, **Budker** Inst. of Nuclear Physics	**Novosibirsk**, Russian Federation
NPOL	Polytechnic of **North London**	London, United Kingdom
NRL	**Naval Research** Lab	Washington, DC, USA
NSF	**National Science Foundation**	Arlington, VA, USA
NTHU	**National Tsing Hua** Univ.	Hsinchu, Taiwan
NTUA	**National Tech. Univ. of Athens**	Athens, Greece
NWES	**Northwestern** Univ.	Evanston, IL, USA
NYU	**New York** Univ.	New York, NY, USA
OBER	**Oberlin** College	Oberlin, OH, USA
OCH	**Ochanomizu** Univ.	Tokyo, Japan
OHIO	**Ohio** Univ.	Athens, OH, USA
OKAY	**Okayama** Univ.	Okayama, Japan
OKLA	Univ. of **Oklahoma**	Norman, OK, USA
OKSU	**Oklahoma State** Univ.	Stillwater, OK, USA
OREG	Univ. of **Oregon**; Inst. of Theoretical Science; U.O. Center for High Energy Physics	Eugene, OR, USA
ORNL	**Oak Ridge** National Laboratory	Oak Ridge, TN, USA
ORSAY	Univ. de **Paris Sud** 11	**Orsay** CEDEX, France
ORST	**Oregon State** Univ.	Corvallis, OR, USA
OSAK	**Osaka** Univ.	Osaka, Japan
OSKC	**Osaka City** Univ.	Osaka, Japan
OSLO	Univ. of **Oslo**	Oslo, Norway
OSU	**Ohio State** Univ.	Columbus, OH, USA
OTTA	Univ. of **Ottawa**	Ottawa, ON, Canada
OXF	University of **Oxford**	Oxford, United Kingdom
OXFTP	Univ. of **Oxford**	Oxford, United Kingdom
PADO	Univ. degli Studi di **Padova**	Padova, Italy
PARIN	**LPNHE**, IN^2P^3/CNRS	Paris, France
PARIS	Univ. de Paris (Historical)	**Paris**, France
PARIT	**Univ. Paris VII**, LPTHE	Paris, France
PARM	**INFN**, Gruppo Collegato di **Parma**	Parma, Italy
PAST	Institut **Pasteur**	**Paris**, France
PATR	Univ. of **Patras**	Patras, Greece
PAVI	Univ. di **Pavia**	Pavia, Italy
PAVII	INFN, Sez. di **Pavia**	**Pavia**, Italy
PENN	Univ. of **Pennsylvania**	Philadelphia, PA, USA
PGIA	**INFN**, Sezione di **Perugia**	Perugia, Italy
PISA	Univ. di **Pisa**	Pisa, Italy
PISAI	**INFN**, Sez. di **Pisa**	Pisa, Italy
PITT	Univ. of **Pittsburgh**	Pittsburgh, PA, USA
PLAT	**SUNY at Plattsburgh**	Plattsburgh, NY, USA
PLRM	Univ. di **Palermo**	Palermo, Italy
PNL	**Battelle Memorial** Inst.	Richland, WA, USA
PNPI	**Petersburg** Nuclear Physics Inst. of Russian Academy of Sciences	Gatchina, Russian Federation
PPA	Princeton-Penn. Proton Accelerator (Historical in *Review*)	Princeton, NJ, USA
PRAG	Inst. of Physics, **ASCR**	**Prague**, Czech Republic
PRIN	**Princeton** Univ.	Princeton, NJ, USA
PSI	Paul Scherrer Inst.	**Villigen** PSI, Switzerland
PSLL	**Physical Science Lab**	Las Cruces, NM, USA
PSU	**Penn State** Univ.	University Park, PA, USA
PUCB	**Pontifícia Univ. Católica do Rio de Janeiro**	Rio de Janeiro, RJ, Brasil
PUEB	Univ. Autonoma de **Puebla**	**Puebla**, Pue, Mexico
PURD	**Purdue** Univ.	West Lafayette, IN, USA
QUKI	**Queen's** Univ.	Kingston, ON, Canada
RAL	**STFC Rutherford Appleton** Lab.	Chilton, Didcot, Oxfordshire, United Kingdom
REGE	Univ. **Regensburg**	Regensburg, Germany
REHO	**Weizmann** Inst. of Science	Rehovot, Israel
REZ	Nuclear Physics Inst. **AVČR**	**Řež**, Czech Republic
RGSUL	Univ. Federal do **Rio Grande do Sul** (UFRGS)	Porto Alegre, RS, Brasil
RHBL	**Royal Holloway, Univ. of London**	Egham, Surrey, United Kingdom
RHEL	**Rutherford** High Energy Lab (Old name for RAL)	Chilton, Didcot, Oxon., United Kingdom
RICE	**Rice** Univ.	Houston, TX, USA
RIKEN	**Riken** Nishina Center for Accelerator-Based Science	Saitama, Japan
RIKK	**Rikkyo** Univ.	Tokyo, Japan
RIS	**Rowland** Inst. for Science	Cambridge, MA, USA
RISC	**Rockwell** International	Thousand Oaks, CA, USA

Abbreviations Used in the Particle Listings

RISL	**Universities Research Reactor**	**Risley**, Warrington, United Kingdom
RISO	**Riso** National Laboratory	Roskilde, Denmark
RL	**Rutherford** High Energy Lab (Old name for RAL)	Chilton, Didcot, Oxon., United Kingdom
RMCS	**Royal Military** Coll. of Science	Swindon, Wilts., United Kingdom
ROCH	Univ. of **Rochester**	Rochester, NY, USA
ROCK	**Rockefeller** Univ.	New York, NY, USA
ROMA	Univ. di **Roma** (Historical)	**Roma**, Italy
ROMA2	Univ. di **Roma**, "Tor Vergata"	Roma, Italy
ROMA3	**INFN, Sez. di Roma Tre**	**Roma**, Italy
ROMAI	**INFN, Sez. di Roma**	Roma, Italy
ROSE	**Rose-Hulman** Inst. of Technology	Terre Haute, IN, USA
RPI	**Rensselaer Polytechnic** Inst.	Troy, NY, USA
RUTG	**Rutgers**, the State Univ. of New Jersey	Piscataway, NJ, USA
S0GA	**Sogang** University	Seoul, Republic of Korea
SACL	**CEA Saclay**, IRFU	Gif-sur-Yvette, France
SACLD	**CEA Saclay** (Essonne)	Gif-sur-Yvette, France
SAGA	**Saga** Univ.	Saga-shi, Japan
SAHA	**Saha** Inst. of Nuclear Physics	Bidhan Nagar, Calcutta, India
SANG	**Kyoto Sangyo** Univ.	Kyoto-shi, Japan
SANI	Ist. Superiore di Sanità	**Roma**, Italy
SASK	Univ. of **Saskatchewan**	Saskatoon, SK, Canada
SASSO	Lab. Naz. **Gran Sasso** dell'INFN	**Assergi** (AQ), Italy
SAVO	Univ. de **Savoie**	Chambery, France
SBER	**California** State Univ.	**San Bernardino**, CA, USA
SCHAF	W.J. **Schafer** Assoc.	Livermore, DA, USA
SCIT	**Science** Univ. of **Tokyo**	Tokyo, Japan
SCOT	**Scottish** Univ. Research and Reactor Ctr.	Glasgow, United Kingdom
SCUC	Univ. of **South Carolina**	Columbia, SC, USA
SEAT	**Seattle Pacific** Coll.	Seattle, WA, USA
SEIB	Austrian Research Center, **Seibersdorf** LTD.	Seibersdorf, Austria
SEOU	**Korea** Univ.; Dept. of Physics; HEP Group	Seoul, Republic of Korea
SEOUL	**Seoul** National Univ.; Center for Theoretical Physics; Dept. of Physics & Astronomy, Coll. of Natural Sciences	Seoul, Republic of Korea
SERP	**IHEP**, Inst. for High Energy Physics	Protvino, Russian Federation
SETO	**Seton Hall** Univ.	South Orange, NJ, USA
SFLA	Univ. of **South Florida**	Tampa, FL, USA
SFRA	**Simon Fraser University**	Burnaby, BC, Canada
SFSU	**California** State Univ.	**San Francisco**, CA, USA
SHAMS	**Ain Shams** University	Abbassia, Cairo, Egypt
SHEF	Univ. of **Sheffield**	Sheffield, United Kingdom
SHMP	Univ. of **Southampton**	Southampton, United Kingdom
SHRZ	**Shiraz** Univ.	Shiraz, Iran
SIEG	Univ. **Siegen**	Siegen, Germany
SILES	Univ. of **Silesia**	Katowice, Poland
SIN	Swiss Inst. of Nuclear Research (Old name for VILL)	**Villigen**, Switzerland
SING	**National Univ.** of Singapore	Kent Ridge, Singapore
SISSA	Scuola Internazionale Superiore di Studi Avanzati	**Trieste**, Italy
SLAC	**SLAC National Accelerator Laboratory**	Menlo Park, CA, USA
SLOV	Inst. of Physics, Slovak Acad. of Sciences	**Bratislava** 45, Slovakia
SMU	**Southern Methodist** Univ.	Dallas, TX, USA
SNSP	**Scuola Normale Superiore**	**Pisa**, Italy
SOFI	Inst. for Nuclear Research and Nuclear Energy	**Sofia**, Bulgaria
SOFU	Univ. of **Sofia** "St. Kliment Ohridski"	Sofia, Bulgaria
SPAUL	Univ. de **São Paulo**	São Paulo, SP, Brasil
SPIFT	Inst. de Física Teórica (**IFT**)	**São Paulo**, SP, Brasil
SSL	Univ. of **California (Berkeley)**	Berkeley, CA, USA
STAN	**Stanford** Univ.	Stanford, CA, USA
STEV	**Stevens** Inst. of Tech.	Hoboken, NJ, USA
STFN	**Jožef Stefan** Institute	**Ljubljana**, Slovenia
STLO	**St. Louis** Univ.	St. Louis, MO, USA
STOH	**Stockholm** Univ.	Stockholm, Sweden
STON	**SUNY at Stony Brook**	Stony Brook, NY, USA
STRB	Inst. Pluridisciplinaire Hubert Curien (**CNRS**)	**Strasbourg**, France
STUT	Univ. **Stuttgart**	Stuttgart, Germany
STUTM	Max-Planck-Inst.	**Stuttgart**, Germany
SUGI	**Sugiyama Jogakuen** Univ.	Aichi, Japan
SURR	Univ. of **Surrey**	Guildford, Surrey, United Kingdom
SUSS	Univ. of **Sussex**	Brighton, United Kingdom
SVR	**Savannah** River Labs.	Aiken, SC, USA
SYDN	Univ. of **Sydney**	Sydney, NSW, Australia
SYRA	**Syracuse** Univ.	Syracuse, NY, USA
TAJK	Acad. Sci., Tadzhik SSR	**Dushanbe**, Tadzhikstan
TAMU	**Texas A&M** Univ.	College Station, TX, USA
TATA	**Tata** Inst. of Fundamental Research	Bombay, India
TBIL	**Tbilisi State University**	Tbilisi, Republic of Georgia
TELA	**Tel-Aviv** Univ.	Tel Aviv, Israel
TELE	**Teledyne Brown** Engineering	Huntsville, AL, USA
TEMP	**Temple** Univ.	Philadelphia, PA, USA
TENN	Univ. of **Tennessee**	Knoxville, TN, USA
TEXA	Univ. of **Texas** at **Austin**	Austin, TX, USA
TGAK	**Tokyo Gakugei** Univ.	Tokyo, Japan
TGU	**Tohoku Gakuin** Univ.	Miyagi, Japan
THES	Aristotle Univ. of **Thessaloniki** (AUTh)	Thessaloniki, Greece
TINT	**Tokyo Inst. of Technology**	Tokyo, Japan
TISA	**Sagamihara** Inst. of Space & Astronautical Sci.	Kanagawa, Japan
TMSK	**Tomsk** Polytechnic Univ.	**Tomsk**, Russian Federation
TMTC	**Tokyo Metropolitan** Coll. Tech.	Tokyo, Japan
TMU	**Tokyo Metropolitan Univ.**	Tokyo, Japan
TNTO	Univ. of **Toronto**	Toronto, ON, Canada
TOHO	**Toho** Univ.	Chiba, Japan
TOHOK	**Tohoku** Univ.	Sendai, Japan
TOKA	**Tokai** Univ.	Shimizu, Japan
TOKAH	**Tokai** Univ.	Hiratsuka, Japan
TOKMS	Univ. of **Tokyo**; Meson Science Laboratory	Tokyo, Japan
TOKU	Univ. of **Tokushima**	Tokushima-shi, Japan
TOKY	Univ. of **Tokyo**; High-Energy Physics Theory Group	Tokyo, Japan
TOKYC	Univ. of **Tokyo**; Dept. of Chemistry	Tokyo, Japan
TORI	Univ. degli Studi di **Torino**	Torino, Italy
TPTI	**Uzbek** Academy of Sciences	**Tashkent**, Republic of Uzbekistan
TRIN	Trinity College **Dublin**	Dublin, Ireland
TRIU	**TRIUMF**	Vancouver, BC, Canada
TRST	Univ. di **Trieste**	Trieste, Italy
TRSTI	**INFN**, Sez. di **Trieste**	Trieste, Italy
TRSTT	Univ. degli Studi di **Trieste**	**Trieste**, Italy
TSUK	Univ. of **Tsukuba**	Ibaraki-ken, Japan
TTAM	**Tamagawa** Univ.	Tokyo, Japan
TUAT	**Tokyo** Univ. of Agriculture Tech.	Tokyo, Japan
TUBIN	Univ. **Tübingen**	Tübingen, Germany
TUFTS	**Tufts** Univ.	Medford, MA, USA
TUW	**Technische** Univ. **Wien**	Vienna, Austria
TUZL	**Tuzla** Univ.	Tuzla, Argentina
UBA	Univ. de **Buenos Aires**	Buenos Aires, Argentina
UCB	Univ. of **California (Berkeley)**	Berkeley, CA, USA
UCD	Univ. of **California (Davis)**	Davis, CA, USA
UCI	Univ. of **California (Irvine)**	Irvine, CA, USA
UCLA	Univ. of **California (Los Angeles)**	Los Angeles, CA, USA
UCND	**Union Carbide** Corp.	Oak Ridge, TN, USA
UCR	Univ. of **California (Riverside)**	Riverside, CA, USA

Abbreviations Used in the Particle Listings

UCSB	Univ. of **California (Santa Barbara)**; Physics Dept., High Energy Physics Experiment	Santa Barbara, CA, USA
UCSBT	Univ. of **California (Santa Barbara)**; Kavli Inst. for Theoretical Physics	Santa Barbara, CA, USA
UCSC	Univ. of **California (Santa Cruz)**	Santa Cruz, CA, USA
UCSD	Univ. of **California (San Diego)**	La Jolla, CA, USA
UGAZ	Univ. of **Gaziantep**	Gaziantep, Turkey
UMD	Univ. of **Maryland**	College Park, MD, USA
UNAM	Univ. Nac. Autónoma de México (**UNAM**)	**México**, DF, Mexico
UNAM	Univ. Nacional Autónoma de México (**UNAM**)	**México**, DF, Mexico
UNC	Univ. of **North Carolina**	Greensboro, NC, USA
UNCCH	Univ. of **North Carolina** at **Chapel Hill**	Chapel Hill, NC, USA
UNCS	**Union** College	Schenectady, NY, USA
UNESP	UNESP	Botucatu, Brasil
UNH	Univ. of **New Hampshire**	Durham, NH, USA
UNM	Univ. of **New Mexico**	Albuquerque, NM, USA
UOEH	Univ. of Occupational and Environmental Health	**Kitakyushu**, Japan
UPNJ	**Upsala** College	East Orange, NJ, USA
UPPS	**Uppsala** Univ.	**Uppsala**, Sweden
UPR	Univ. of **Puerto Rico**	**San Juan**, PR, USA
URI	Univ. of **Rhode Island**	Kingston, RI, USA
USC	Univ. of **Southern California**	Los Angeles, CA, USA
USF	Univ. of **San Francisco**	San Francisco, CA, USA
UTAH	Univ. of **Utah**	Salt Lake City, UT, USA
UTRE	Univ. of **Utrecht**	Utrecht, The Netherlands
UTRO	**Norwegian Univ. of Science & Technology**	Trondheim, Norway
UVA	Univ. of **Virginia**	Charlottesville, VA, USA
UZINR	Acad. Sci., **Ukrainian** SSR	**Uzhgorod**, Ukraine
VALE	Univ. de **Valencia**	Burjassot, **Valencia**, Spain
VALP	**Valparaiso** Univ.	Valparaiso, IN, USA
VAND	**Vanderbilt** Univ.	Nashville, TN, USA
VASS	**Vassar** College	Poughkeepsie, NY, USA
VICT	Univ. of **Victoria**	Victoria, BC, Canada
VIEN	Inst. für Hochenergiephysik (HEPHY)	**Vienna**, Austria
VILL	**ETH Zürich**	Zürich, Switzerland
VPI	**Virginia Tech.**	Blacksburg, VA, USA
VRIJ	**Vrije** Univ.	HV **Amsterdam**, The Netherlands
WABRN	Eidgenossisches Amt für Messwesen	**Waber**, Switzerland
WARS	Univ. of **Warsaw**	Warsaw, Poland
WASCR	**Waseda** Univ.; Cosmic Ray Division	Tokyo, Japan
WASH	Univ. of **Washington**; Elem. Particle Experiment (EPE); Particle Astrophysics (PA)	Seattle, WA, USA
WASU	**Waseda** Univ.; Dept. of Physics, High Energy Physics Group	Tokyo, Japan
WAYN	**Wayne** State Univ.	Detroit, MI, USA
WESL	**Wesleyan** Univ.	Middletown, CT, USA
WIEN	Univ. **Wien**	Vienna, Austria
WILL	Coll. of **William and Mary**	Williamsburg, VA, USA
WINR	National Centre for Nuclear Research	**Warsaw**, Poland
WISC	Univ. of **Wisconsin**	Madison, WI, USA
WITW	Univ. of the **Witwatersrand**	Wits, South Africa
WMIU	**Western Michigan** Univ.	Kalamazoo, MI, USA
WONT	The Univ. of **Western Ontario**	London, ON, Canada
WOOD	**Woodstock** College (No longer in existence)	Woodstock, MD, USA
WUPP	**Bergische** Univ. Wuppertal	**Wuppertal**, Germany
WURZ	Univ. **Würzburg**	Würzburg, Germany
WUSL	**Washington** Univ.	St. Louis, MO, USA
WYOM	Univ. of **Wyoming**	Laramie, WY, USA
YALE	**Yale** Univ.	New Haven, CT, USA
YARO	**Yaroslavl** State Univ.	Yaroslavl, Russian Federation
YCC	**Yokohama** Coll. of Commerce	Yokohama, Japan
YERE	**Yerevan** Physics Inst.	Yerevan, Armenia
YOKO	**Yokohama National** Univ.	Yokohama-shi, Japan
YORKC	**York** Univ.	Toronto, Canada
ZAGR	**Zagreb** Univ.	Zagreb, Croatia
ZARA	Univ. de **Zaragoza**	Zaragoza, Spain
ZEEM	Univ. van **Amsterdam**	TV Amsterdam, The Netherlands
ZHON	**Zhongshan** (Sun Yat-Sen) Univ.	Guangzhou, China
ZHZH	**Zhengzhou** Univ.	Zhengzhou, Henan, China
ZURI	Univ. **Zürich**	Zürich, Switzerland

GAUGE AND HIGGS BOSONS

Notes in the Gauge and Higgs Boson Listings

GAUGE AND HIGGS BOSONS

γ

$I(J^{PC}) = 0,1(1^{--})$

γ MASS

Results prior to 2008 are critiqued in GOLDHABER 10. All experimental results published prior to 2005 are summarized in detail by TU 05.

The following conversions are useful: 1 eV = 1.783×10^{-33} g = 1.957×10^{-6} m_e; $\lambda\!\!\!^{-}_C = (1.973 \times 10^{-7}$ m)×(1 eV/m_γ).

VALUE (eV)	CL%	DOCUMENT ID		TECN	COMMENT
<1 × 10^{-18}		[1] RYUTOV	07		MHD of solar wind
• • • We do not use the following data for averages, fits, limits, etc. • • •					
		[2] ACCIOLY	10		Anomalous mag. mom.
<1 × 10^{-26}		[3] ADELBERGER	07A		Proca galactic field
no limit feasible		[3] ADELBERGER	07A		γ as Higgs particle
<1 × 10^{-19}		[4] TU	06		Torque on rotating magnetized toroid
<1.4 × 10^{-7}		ACCIOLY	04		Dispersion of GHz radio waves by sun
<2 × 10^{-16}		[5] FULLEKRUG	04		Speed of 5-50 Hz radiation in atmosphere
<7 × 10^{-19}		[6] LUO	03		Torque on rotating magnetized toroid
<1 × 10^{-17}		[7] LAKES	98		Torque on toroid balance
<6 × 10^{-17}		[8] RYUTOV	97		MHD of solar wind
<8 × 10^{-16}	90	[9] FISCHBACH	94		Earth magnetic field
<5 × 10^{-13}		[10] CHERNIKOV	92	SQID	Ampere-law null test
<1.5 × 10^{-9}	90	[11] RYAN	85		Coulomb-law null test
<3 × 10^{-27}		[12] CHIBISOV	76		Galactic magnetic field
<6 × 10^{-16}	99.7	[13] DAVIS	75		Jupiter magnetic field
<7.3 × 10^{-16}		HOLLWEG	74		Alfven waves
<6 × 10^{-17}		[14] FRANKEN	71		Low freq. res. cir.
<2.4 × 10^{-13}		[15] KROLL	71A		Dispersion in atmosphere
<1 × 10^{-14}		[16] WILLIAMS	71	CNTR	Tests Gauss law
<2.3 × 10^{-15}		GOLDHABER	68		Satellite data

[1] RYUTOV 07 extends the method of RYUTOV 97 to the radius of Pluto's orbit.

[2] ACCIOLY 10 limits come from possible alterations of anomalous magnetic moment of electron and gravitational deflection of electromagnetic radiation. Reported limits are not "claimed" by the authors and in any case are not competitive.

[3] When trying to measure m one must distinguish between measurements performed on large and small scales. If the photon acquires mass by the Higgs mechanism, the large-scale behavior of the photon might be effectively Maxwellian. If, on the other hand, one postulates the Proca regime for all scales, the very existence of the galactic field implies $m < 10^{-26}$ eV, as correctly calculated by YAMAGUCHI 59 and CHIBISOV 76.

[4] TU 06 continues the work of LUO 03, with extended LAKES 98 method, reporting the improved limit $\mu^2 A = (0.7 \pm 1.7) \times 10^{-13}$ T/m if $A = 0.2$ μG out to 4×10^{22} m. Reported result $\mu = (0.9 \pm 1.5) \times 10^{-52}$ g reduces to the frequentist mass limit 1.2×10^{-19} eV (FELDMAN 98).

[5] FULLEKRUG 04 adopted KROLL 71A method with newer and better Schummann resonance data. Result questionable because assumed frequency shift with photon mass is assumed to be linear. It is quadratic according to theorem by GOLDHABER 71B, KROLL 71, and PARK 71.

[6] LUO 03 extends LAKES 98 technique to set a limit on $\mu^2 A$, where μ^{-1} is the Compton wavelength $\lambda\!\!\!^{-}_C$ of the massive photon and A is the ambient vector potential. The important departure is that the apparatus rotates, removing sensitivity to the direction of A. They take $A = 10^{12}$ Tm, due to "cluster level fields." But see comment of GOLDHABER 03 and reply by LUO 03B.

[7] LAKES 98 reports limits on torque on a toroid Cavendish balance, obtaining a limit on $\mu^2 A < 2 \times 10^{-9}$ Tm/m^2 via the Maxwell-Proca equations, where μ^{-1} is the characteristic length associated with the photon mass and A is the ambient vector potential in the Lorentz gauge. Assuming $A \approx 1 \times 10^{12}$ Tm due to cluster fields he obtains $\mu^{-1} > 2 \times 10^{10}$ m, corresponding to $\mu < 1 \times 10^{-17}$ eV. A more conservative limit, using $A \approx (1$ μG)×(600 pc) based on the galactic field, is $\mu^{-1} > 1 \times 10^{9}$ m or $\mu < 2 \times 10^{-16}$ eV.

[8] RYUTOV 97 uses a magnetohydrodynamics argument concerning survival of the Sun's field to the radius of the Earth's orbit. "To reconcile observations to theory, one has to reduce [the photon mass] by approximately an order of magnitude compared with" per DAVIS 75. "Secure limit, best by this method" (per GOLDHABER 10).

[9] FISCHBACH 94 analysis is based on terrestrial magnetic fields; approach analogous to DAVIS 75. Similar result based on a much smaller planet probably follows from more precise B field mapping. "Secure limit, best by this method" (per GOLDHABER 10).

[10] CHERNIKOV 92, motivated by possibility that photon exhibits mass only below some unknown critical temperature, searches for departure from Ampere's Law at 1.24 K. See also RYAN 85.

[11] RYAN 85, motivated by possibility that photon exhibits mass only below some unknown critical temperature, sets mass limit at $< (1.5 \pm 1.4) \times 10^{-42}$ g based on Coulomb's Law departure limit at 1.36 K. We report the result as frequentist 90% CL (FELDMAN 98).

[12] CHIBISOV 76 depends in critical way on assumptions such as applicability of virial theorem. Some of the arguments given only in unpublished references.

[13] DAVIS 75 analysis of Pioneer-10 data on Jupiter's magnetic field. "Secure limit, best by this method" (per GOLDHABER 10).

[14] FRANKEN 71 method is of dubious validity (KROLL 71A, JACKSON 99, GOLDHABER 10, and references therein).

[15] KROLL 71A used low frequency Schumann resonances in cavity between the conducting earth and resistive ionosphere, overcoming objections to resonant-cavity methods (JACKSON 99, GOLDHABER 10, and references therein). "Secure limit, best by this method" (per GOLDHABER 10).

[16] WILLIAMS 71 is landmark test of Coulomb's law. "Secure limit, best by this method" (per GOLDHABER 10).

γ CHARGE

OKUN 06 has argued that schemes in which all photons are charged are inconsistent. He says that if a neutral photon is also admitted to avoid this problem, then other problems emerge, such as those connected with the emission and absorption of charged photons by charged particles. He concludes that in the absence of a self-consistent phenomenological basis, interpretation of experimental data is at best difficult.

VALUE (e)	CHARGE	DOCUMENT ID		TECN	COMMENT
<1 × 10^{-46}	**mixed**	[1] ALTSCHUL	07B	VLBI	Aharonov-Bohm effect
<1 × 10^{-35}	**single**	[2] CAPRINI	05	CMB	Isotropy constraint
• • • We do not use the following data for averages, fits, limits, etc. • • •					
<1 × 10^{-32}	single	[1] ALTSCHUL	07B	VLBI	Aharonov-Bohm effect
<3 × 10^{-33}	mixed	[3] KOBYCHEV	05	VLBI	Smear as function of B·E_γ
<4 × 10^{-31}	single	[3] KOBYCHEV	05	VLBI	Deflection as function of B·E_γ
<8.5 × 10^{-17}		[4] SEMERTZIDIS	03		Laser light deflection in B-field
<3 × 10^{-28}	single	[5] SIVARAM	95	CMB	For $\Omega_M = 0.3$, $h^2 = 0.5$
<5 × 10^{-30}		[6] RAFFELT	94	TOF	Pulsar $f_1 - f_2$
<2 × 10^{-28}		[7] COCCONI	92		VLBA radio telescope resolution
<2 × 10^{-32}		COCCONI	88	TOF	Pulsar $f_1 - f_2$ TOF

[1] ALTSCHUL 07B looks for Aharonov-Bohm phase shift in addition to geometric phase shift in radio interference fringes (VSOP mission).

[2] CAPRINI 05 uses isotropy of the cosmic microwave background to place stringent limits on possible charge asymmetry of the Universe. Charge limits are set on the photon, neutrino, and dark matter particles. Valid if charge asymmetries produced by different particles are not anticorrelated.

[3] KOBYCHEV 05 considers a variety of observable effects of photon charge for extragalactic compact radio sources. Best limits if source observed through a foreground cluster of galaxies.

[4] SEMERTZIDIS 03 reports the first laboratory limit on the photon charge in the last 30 years. Straightforward improvements in the apparatus could attain a sensitivity of 10^{-20} e.

[5] SIVARAM 95 requires that CMB photon charge density not overwhelm gravity. Result scales as $\Omega_M h^2$.

[6] RAFFELT 94 notes that COCCONI 88 neglects the fact that the time delay due to dispersion by free electrons in the interstellar medium has the same photon energy dependence as that due to bending of a charged photon in the magnetic field. His limit is based on the assumption that the entire observed dispersion is due to photon charge. It is a factor of 200 less stringent than the COCCONI 88 limit.

[7] See COCCONI 92 for less stringent limits in other frequency ranges. Also see RAFFELT 94 note.

γ REFERENCES

ACCIOLY	10	PR D82 065026	A. Accioly, J. Helayel-Neto, E. Scatena (LABEX+)
GOLDHABER	10	RMP 82 939	A.F. Goldhaber, M.M. Nieto (STON, LANL)
ADELBERGER	07A	PRL 98 010402	E. Adelberger, G. Dvali, A. Gruzinov (WASH, NYU)
ALTSCHUL	07B	PRL 98 261801	B. Altschul (IND)
Also		ASP 29 290	B. Altschul (SCUC)
RYUTOV	07	PPCF 49 B429	D.D. Ryutov (LLNL)
OKUN	06	APP B37 565	L.B. Okun (ITEP)
TU	06	PL A352 267	L.-C. Tu *et al.*
CAPRINI	05	JCAP 0502 006	C. Caprini, P.G. Ferreira (GEVA, OXFTP)
KOBYCHEV	05	AL 31 147	V.V. Kobychev, S.B. Popov (KIEV, PADO)
TU	05	RPP 68 77	L.-C. Tu, J. Luo, G.T. Gillies
ACCIOLY	04	PR D69 107501	A. Accioly, R. Paszko
FULLEKRUG	04	PRL 93 043901	M. Fullekrug
GOLDHABER	03	PRL 91 149101	A.S. Goldhaber, M.M. Nieto
LUO	03	PRL 90 081801	J. Luo *et al.*
LUO	03B	PRL 91 149102	J. Luo *et al.*
SEMERTZIDIS	03	PR D67 017701	Y.K. Semertzidis, G.T. Danby, D.M. Lazarus
JACKSON	99	Classical Electrodynamics	J.D. Jackson (3rd ed., J. Wiley and Sons (1999))
FELDMAN	98	PR D57 3873	G.J. Feldman, R.D. Cousins
LAKES	98	PRL 80 1826	R. Lakes (WISC)
RYUTOV	97	PPCF 39 A73	D.D. Ryutov (LLNL)
SIVARAM	95	AJP 63 473	C. Sivaram (BANG)
FISCHBACH	94	PRL 73 514	E. Fischbach *et al.* (PURD, JHU+)
RAFFELT	94	PR D50 7729	G. Raffelt (MPIM)
CHERNIKOV	92	PRL 68 3383	M.A. Chernikov *et al.* (ETH)
Also		PRL 69 2999 (erratum)	M.A. Chernikov *et al.* (ETH)
COCCONI	92	AJP 60 750	G. Cocconi (CERN)
COCCONI	88	PL B206 705	G. Cocconi (CERN)
RYAN	85	PR D32 802	J.J. Ryan, F. Accetta, R.H. Austin (PRIN)
CHIBISOV	76	SPU 19 624	G.V. Chibisov (LEBD)
		Translated from UFN 119 551.	
DAVIS	75	PRL 35 1402	L. Davis, A.S. Goldhaber, M.M. Nieto (CIT, STON+)
HOLLWEG	74	PRL 32 961	J.V. Hollweg (NCAR)
FRANKEN	71	PRL 26 115	P.A. Franken, G.W. Ampulski (MICH)
GOLDHABER	71B	RMP 43 277	A.S. Goldhaber, M.M. Nieto (STON, BOHR, UCSB)
KROLL	71	PRL 26 1395	N.M. Kroll (SLAC)
KROLL	71A	PRL 27 340	N.M. Kroll (SLAC)
PARK	71	PRL 26 1393	D. Park, E.R. Williams (WILC)
WILLIAMS	71	PRL 26 721	E.R. Williams, J.E. Faller, H.A. Hill (WESL)
GOLDHABER	68	PRL 21 567	A.S. Goldhaber, M.M. Nieto (STON)
YAMAGUCHI	59	PTPS 11 37	Y. Yamaguchi

Gauge & Higgs Boson Particle Listings

g, graviton, W

g or gluon

$I(J^P) = 0(1^-)$

SU(3) color octet

Mass $m = 0$. Theoretical value. A mass as large as a few MeV may not be precluded, see YNDURAIN 95.

VALUE	DOCUMENT ID		TECN	COMMENT
• • • We do not use the following data for averages, fits, limits, etc. • • •				
	ABREU	92E	DLPH	Spin 1, not 0
	ALEXANDER	91H	OPAL	Spin 1, not 0
	BEHREND	82D	CELL	Spin 1, not 0
	BERGER	80D	PLUT	Spin 1, not 0
	BRANDELIK	80C	TASS	Spin 1, not 0

gluon REFERENCES

YNDURAIN	95	PL B345 524	F.J. Yndurain	(MADU)
ABREU	92E	PL B274 498	P. Abreu *et al.*	(DELPHI Collab.)
ALEXANDER	91H	ZPHY C52 543	G. Alexander *et al.*	(OPAL Collab.)
BEHREND	82D	PL B110 329	H.J. Behrend *et al.*	(CELLO Collab.)
BERGER	80D	PL B97 459	C. Berger *et al.*	(PLUTO Collab.)
BRANDELIK	80C	PL B97 453	R. Brandelik *et al.*	(TASSO Collab.)

graviton

$J = 2$

graviton MASS

In 1970 van Dam amd Veltman (VANDAM 70) showed that "... there is a discrete difference between the theory with zero-mass and a theory with finite mass, no matter how small as compared to all external momenta. ... We may conclude that the graviton has rigorously zero mass." However, see GOLDHABER 10 and references therein. It has been of interest to set experimental limits, whether or not a finite mass can exist. In most (but not all) cases limits have been set on the distance without evidence for a Yukawa cutoff. h_0 is the Hubble constant in units of 100 km s^{-1} Mpc^{-1}.

The following conversions are useful: 1 eV = 1.783×10^{-33} g = 1.957×10^{-6} m_e; $\lambda\!\!\!^{-}_C = (1.973 \times 10^{-7}$ m)$\times$(1 eV/m_g).

VALUE (eV)	DOCUMENT ID		COMMENT
$< 6 \times 10^{-32}$	[1] CHOUDHURY	04	Weak gravitational lensing
• • • We do not use the following data for averages, fits, limits, etc. • • •			
$< 5 \times 10^{-23}$	[2] BRITO	13	Spinning black holes bounds
$< 4 \times 10^{-25}$	[3] BASKARAN	08	Graviton phase velocity fluctuations
$< 6 \times 10^{-32}$	[4] GRUZINOV	05	Solar System observations
$> 6 \times 10^{-34}$	[5] DVALI	03	Horizon scales
$< 8 \times 10^{-20}$	[6,7] FINN	02	Binary pulsar orbital period decrease
	[7,8] DAMOUR	91	Binary pulsar PSR 1913+16
$< 2 \times 10^{-29}$ h_0^{-1}	GOLDHABER	74	Rich clusters
$< 7 \times 10^{-28}$	HARE	73	Galaxy
$< 8 \times 10^{4}$	HARE	73	2γ decay

[1] CHOUDHURY 04 concludes from a study of weak-lensing data that masses heavier than about the inverse of 100 Mpc seem to be ruled out if the gravitation field has the Yukawa form.

[2] BRITO 13 explore massive graviton (spin-2) fluctuations around rotating black holes.

[3] BASKARAN 08 consider fluctuations in pulsar timing due to photon interactions ("surfing") with background gravitational waves.

[4] GRUZINOV 05 uses the DGP model (DVALI 00) showing that non-perturbative effects restore continuity with Einstein's equations as the gravition mass approaches 0, then bases his limit on Solar System observations.

[5] DVALI 03 suggest scale of horizon distance via DGP model (DVALI 00). For a horizon distance of 3×10^{26} m (about age of Universe/c; GOLDHABER 10) this graviton mass limit is implied.

[6] FINN 02 analyze the orbital decay rates of PSR B1913+16 and PSR B1534+12 with a possible graviton mass as a parameter. The combined frequentist mass limit is at 90%CL.

[7] As of 2014, limits on dP/dt are now about 0.1% (see T. Damour, "Experimental tests of gravitational theory," in this *Review*).

[8] DAMOUR 91 is an analysis of the orbital period change in binary pulsar PSR 1913+16, and confirms the general relativity prediction to 0.8%. "The theoretical importance of the [rate of orbital period decay] measurement has long been recognized as a direct confirmation that the gravitational interaction propagates with velocity c (which is the immediate cause of the appearance of a damping force in the binary pulsar system) and thereby as a test of the existence of gravitational radiation and of its quadrupolar nature." TAYLOR 93 adds that orbital parameter studies now agree with general relativity to 0.5%, and set limits on the level of scalar contribution in the context of a family of tensor [spin 2]-biscalar theories.

graviton REFERENCES

BRITO	13	PR D88 023514	R. Brito, V. Cardoso, P. Pani	(LISB, MISS, HSCA+)
GOLDHABER	10	RMP 82 939	A.F. Goldhaber, M.M. Nieto	(STON, LANL)
BASKARAN	08	PR D78 044018	D. Baskaran *et al.*	
GRUZINOV	05	NAST 10 311	A. Gruzinov	(NYU)
CHOUDHURY	04	ASP 21 559	S.R. Choudhury *et al.*	(DELPH, MELB)
DVALI	03	PR D68 024012	G.R. Dvali, A. Grizinov, M. Zaldarriaga	(NYU)
FINN	02	PR D65 044022	L.S. Finn, P.J. Sutton	
DVALI	00	PL B485 208	G.R. Dvali, G. Gabadadze, M. Porrati	(NYU)
TAYLOR	93	NAT 355 132	J.N. Taylor *et al.*	(PRIN, ARCBO, BURE+) J
DAMOUR	91	APJ 366 501	T. Damour, J.H. Taylor	(BURE, MEUD, PRIN)
GOLDHABER	74	PR D9 1119	A.S. Goldhaber, M.M. Nieto	(LANL, STON)
HARE	73	CJP 51 431	M.G. Hare	(SASK)
VANDAM	70	NP B22 397	H. van Dam, M. Veltman	(UTRE)

W

$J = 1$

THE MASS AND WIDTH OF THE W BOSON

Revised September 2013 by M.W. Grünewald (U. College Dublin and U. Ghent) and A. Gurtu (Formerly Tata Inst.).

Precision determination of the W-mass is of great importance in testing the internal consistency of the Standard Model. From the time of its discovery in 1983, the W-boson has been studied and its mass determined in $p\bar{p}$ and e^+e^- interactions; it is currently studied in pp interactions at the LHC. The W mass and width definition used here corresponds to a Breit-Wigner with mass-dependent width.

Production of on-shell W bosons at hadron colliders is tagged by the high p_T charged lepton from its decay. Owing to the unknown parton-parton effective energy and missing energy in the longitudinal direction, the collider experiments reconstruct the transverse mass of the W, and derive the W mass from comparing the transverse mass distribution with Monte Carlo predictions as a function of M_W. These analyses use the electron and muon decay modes of the W boson.

In the e^+e^- collider (LEP) a precise knowledge of the beam energy enables one to determine the $e^+e^- \to W^+W^-$ cross section as a function of center of mass energy, as well as to reconstruct the W mass precisely from its decay products, even if one of them decays leptonically. Close to the W^+W^- threshold (161 GeV), the dependence of the W-pair production cross section on M_W is large, and this was used to determine M_W. At higher energies (172 to 209 GeV) this dependence is much weaker and W-bosons were directly reconstructed and the mass determined as the invariant mass of its decay products, improving the resolution with a kinematic fit.

In order to compute the LEP average W mass, each experiment provided its measured W mass for the $q\bar{q}q\bar{q}$ and $q\bar{q}\ell\overline{\nu_\ell}$, $\ell = e, \mu, \tau$ channels at each center-of-mass energy, along with a detailed break-up of errors: statistical, uncorrelated, partially correlated and fully correlated systematics [1]. These have been combined to obtain a LEP W mass of $M_W = 80.376 \pm 0.033$ GeV. Errors due to uncertainties in LEP energy (9 MeV), and possible effect of color reconnection (CR) and Bose-Einstein correlations (BEC) between quarks from different W's (8 MeV) are included. The mass difference between $q\bar{q}q\bar{q}$ and $q\bar{q}\ell\overline{\nu_\ell}$ final states (due to possible CR and BEC effects) is -12 ± 45 MeV. In a similar manner, the width results obtained at LEP have been combined, resulting in $\Gamma_W = 2.195 \pm 0.083$ GeV [1].

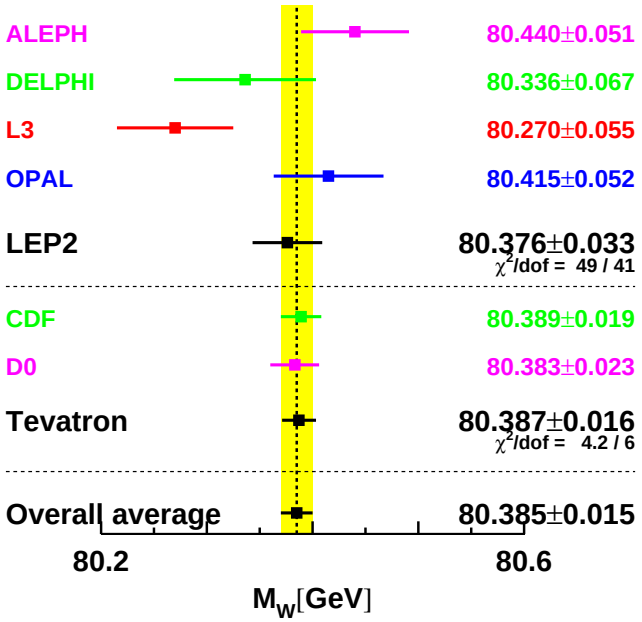

Figure 1: Measurements of the W-boson mass by the LEP and Tevatron experiments.

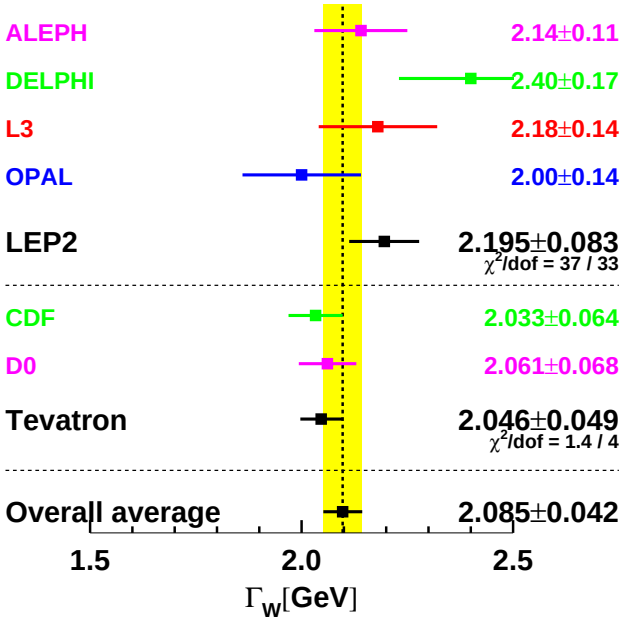

Figure 2: Measurements of the W-boson width by the LEP and Tevatron experiments.

The two Tevatron experiments have also identified common systematic errors. Between the two experiments, uncertainties due to the parton distribution functions, radiative corrections, and choice of mass (width) in the width (mass) measurements are treated as correlated. An average W width of $\Gamma_W = 2.046 \pm 0.049$ GeV [2] is obtained. Errors of 20 MeV and 7 MeV accounting for PDF and radiative correction uncertainties in this width combination dominate the correlated uncertainties. At the 2012 winter conferences, the CDF and D0 experiments have presented new results for the mass of the W boson based on $2-4$ fb^{-1} of Run-II data, 80.387 ± 0.019 GeV [3] and 80.375 ± 0.023 GeV [4], respectively. The W-mass determination from the Tevatron experiments has thus become very precise. Combining all Tevatron results from Run-I and Run-II using an improved treatment of correlations, a new average of 80.387 ± 0.016 GeV is obtained [5], with common uncertainties of 10 MeV (PDF) and 4 MeV (radiative corrections).

The LEP and Tevatron results on mass and width, which are based on all results available, are compared in Fig. 1 and Fig. 2. Good agreement between the results is observed. Combining these results, assuming no common systematic uncertainties between the LEP and the Tevatron measurements, yields an average W mass of $M_W = 80.385 \pm 0.015$ GeV and a W width of $\Gamma_W = 2.085 \pm 0.042$ GeV.

The Standard Model prediction from the electroweak fit, using Z-pole data plus $m_{\rm top}$ measurement, gives a W-boson mass of $M_W = 80.363 \pm 0.020$ GeV and a W-boson width of $\Gamma_W = 2.091 \pm 0.002$ GeV [1].

References

1. The LEP Collaborations: ALEPH, DELPHI, L3, OPAL, the LEP Electroweak Working Group, CERN-PH-EP/2013-022, arXiv:1302.3415 [hep-ex], Phys.Rept. 532 (2013) 119-244.
2. The Tevatron Electroweak Working Group, for the CDF and D0 Collaborations: *Combination of CDF and D0 Results on the Width of the W Boson*, March 2010, arXiv:1003.2826 [hep-ex].
3. The CDF Collaboration, *Precise measurement of the W-boson mass with the CDF II detector*, arXiv:1203.0275 [hep-ex], Phys. Rev. Lett. **108**, 151803 (2012).
4. The D0 Collaboration, *Measurement of the W Boson Mass with the D0 Detector*, arXiv:1203.0293 [hep-ex], Phys. Rev. Lett. **108**, 151804 (2012).
5. The CDF and D0 Collabs: *Combination of CDF and D0 W-Boson Mass Measurements*, July 2013, arXiv:1307.7627 [hep-ex], Phys. Rev. **D88**, 052018 (2013).

W MASS

The *W*-mass listed here corresponds to the mass parameter in a Breit-Wigner distribution with mass-dependent width. To obtain the world average, common systematic uncertainties between experiments are properly taken into account. The LEP-2 average *W* mass based on published results is 80.376 ± 0.033 GeV [SCHAEL 13A]. The combined Tevatron data yields an average *W* mass of 80.387 ± 0.016 GeV [AALTONEN 13N].

OUR FIT uses these average LEP and Tevatron mass values and combines them assuming no correlations.

VALUE (GeV)	EVTS	DOCUMENT ID		TECN	COMMENT
80.385± 0.015 OUR FIT					
80.387± 0.019	1095k	[1] AALTONEN	12E	CDF	$E_{\rm cm}^{p\overline{p}}$ = 1.96 TeV
80.367± 0.026	1677k	[2] ABAZOV	12F	D0	$E_{\rm cm}^{p\overline{p}}$ = 1.96 TeV
80.401± 0.043	500k	[3] ABAZOV	09AB	D0	$E_{\rm cm}^{p\overline{p}}$ = 1.96 TeV
80.336± 0.055±0.039	10.3k	[4] ABDALLAH	08A	DLPH	$E_{\rm cm}^{ee}$ = 161–209 GeV
80.415± 0.042±0.031	11830	[5] ABBIENDI	06	OPAL	$E_{\rm cm}^{ee}$ = 170–209 GeV
80.270± 0.046±0.031	9909	[6] ACHARD	06	L3	$E_{\rm cm}^{ee}$ = 161–209 GeV
80.440± 0.043±0.027	8692	[7] SCHAEL	06	ALEP	$E_{\rm cm}^{ee}$ = 161–209 GeV
80.483± 0.084	49247	[8] ABAZOV	02D	D0	$E_{\rm cm}^{p\overline{p}}$ = 1.8 TeV
80.433± 0.079	53841	[9] AFFOLDER	01E	CDF	$E_{\rm cm}^{p\overline{p}}$ = 1.8 TeV

Gauge & Higgs Boson Particle Listings

W

• • • We do not use the following data for averages, fits, limits, etc. • • •

80.413 ± 0.034 ± 0.034	115k	[10] AALTONEN	07F	CDF	$E_{cm}^{p\overline{p}}$ = 1.96 TeV
82.87 ± 1.82 $^{+0.30}_{-0.16}$	1500	[11] AKTAS	06	H1	$e^{\pm}p \to \overline{\nu}_e(\nu_e)X$, $\sqrt{s} \approx$ 300 GeV
80.3 ± 2.1 ± 1.2 ± 1.0	645	[12] CHEKANOV	02C	ZEUS	$e^-p \to \nu_e X$, $\sqrt{s}$= 318 GeV
81.4 $^{+2.7}_{-2.6}$ ± 2.0 $^{+3.3}_{-3.0}$	1086	[13] BREITWEG	00D	ZEUS	$e^+p \to \overline{\nu}_e X$, $\sqrt{s} \approx$ 300 GeV
80.84 ± 0.22 ± 0.83	2065	[14] ALITTI	92B	UA2	See W/Z ratio below
80.79 ± 0.31 ± 0.84		[15] ALITTI	90B	UA2	$E_{cm}^{p\overline{p}}$ = 546,630 GeV
80.0 ± 3.3 ± 2.4	22	[16] ABE	89I	CDF	$E_{cm}^{p\overline{p}}$ = 1.8 TeV
82.7 ± 1.0 ± 2.7	149	[17] ALBAJAR	89	UA1	$E_{cm}^{p\overline{p}}$ = 546,630 GeV
81.8 $^{+6.0}_{-5.3}$ ± 2.6	46	[18] ALBAJAR	89	UA1	$E_{cm}^{p\overline{p}}$ = 546,630 GeV
89 ± 3 ± 6	32	[19] ALBAJAR	89	UA1	$E_{cm}^{p\overline{p}}$ = 546,630 GeV
81. ± 5.	6	ARNISON	83	UA1	$E_{cm}^{e\overline{e}}$ = 546 GeV
80. $^{+10.}_{-6.}$	4	BANNER	83B	UA2	Repl. by ALITTI 90B

[1] AALTONEN 12E select 470k $W \to e\nu$ decays and 625k $W \to \mu\nu$ decays in 2.2 fb^{-1} of Run-II data. The mass is determined using the transverse mass, transverse lepton momentum and transverse missing energy distributions, accounting for correlations. This result superseeds AALTONEN 07F.

[2] ABAZOV 12F select 1677k $W \to e\nu$ decays in 4.3 fb^{-1} of Run-II data. The mass is determined using the transverse mass and transverse lepton momentum distributions, accounting for correlations.

[3] ABAZOV 09AB study the transverse mass, transverse electron momentum, and transverse missing energy in a sample of 0.5 million $W \to e\nu$ decays selected in Run-II data. The quoted result combines all three methods, accounting for correlations.

[4] ABDALLAH 08A use direct reconstruction of the kinematics of $W^+W^- \to q\overline{q}\ell\nu$ and $W^+W^- \to q\overline{q}q\overline{q}$ events for energies 172 GeV and above. The W mass was also extracted from the dependence of the WW cross section close to the production threshold and combined appropriately to obtain the final result. The systematic error includes ±0.025 GeV due to final state interactions and ±0.009 GeV due to LEP energy uncertainty.

[5] ABBIENDI 06 use direct reconstruction of the kinematics of $W^+W^- \to q\overline{q}\ell\nu_\ell$ and $W^+W^- \to q\overline{q}q\overline{q}$ events. The result quoted here is obtained combining this mass value with the results using $W^+W^- \to \ell\nu_\ell\ell'\nu_{\ell'}$ events in the energy range 183–207 GeV (ABBIENDI 03C) and the dependence of the WW production cross-section on m_W at threshold. The systematic error includes ±0.009 GeV due to the uncertainty on the LEP beam energy.

[6] ACHARD 06 use direct reconstruction of the kinematics of $W^+W^- \to q\overline{q}\ell\nu_\ell$ and $W^+W^- \to q\overline{q}q\overline{q}$ events in the C.M. energy range 189–209 GeV. The result quoted here is obtained combining this mass value with the results obtained from a direct W mass reconstruction at 172 and 183 GeV and with those from the dependence of the WW production cross-section on m_W at 161 and 172 GeV (ACCIARRI 99).

[7] SCHAEL 06 use direct reconstruction of the kinematics of $W^+W^- \to q\overline{q}\ell\nu_\ell$ and $W^+W^- \to q\overline{q}q\overline{q}$ events in the C.M. energy range 183–209 GeV. The result quoted here is obtained combining this mass value with those obtained from the dependence of the W pair production cross-section on m_W at 161 and 172 GeV (BARATE 97 and BARATE 97S respectively). The systematic error includes ±0.009 GeV due to possible effects of final state interactions in the $q\overline{q}q\overline{q}$ channel and ±0.009 GeV due to the uncertainty on the LEP beam energy.

[8] ABAZOV 02D improve the measurement of the W-boson mass including $W \to e\nu_e$ events in which the electron is close to a boundary of a central electromagnetic calorimeter module. Properly combining the results obtained by fitting $m_T(W)$, $p_T(e)$, and $p_T(\nu)$, this sample provides a mass value of 80.574 ± 0.405 GeV. The value reported here is a combination of this measurement with all previous DØ W-boson mass measurements.

[9] AFFOLDER 01E fit the transverse mass spectrum of 30115 $W \to e\nu_e$ events (M_W= 80.473 ± 0.065 ± 0.092 GeV) and of 14740 $W \to \mu\nu_\mu$ events (M_W= 80.465 ± 0.100 ± 0.103 GeV) obtained in the run IB (1994-95). Combining the electron and muon results, accounting for correlated uncertainties, yields M_W= 80.470 ± 0.089 GeV. They combine this value with their measurement of ABE 95P reported in run IA (1992-93) to obtain the quoted value.

[10] AALTONEN 07F obtain high purity $W \to e\nu_e$ and $W \to \mu\nu_\mu$ candidate samples totaling 63,964 and 51,128 events respectively. The W mass value quoted above is derived by simultaneously fitting the transverse mass and the lepton, and neutrino p_T distributions.

[11] AKTAS 06 fit the Q^2 dependence ($300 < Q^2 < 30{,}000$ GeV^2) of the charged-current differential cross section with a propagator mass. The first error is experimental and the second corresponds to uncertainties due to input parameters and model assumptions.

[12] CHEKANOV 02C fit the Q^2 dependence ($200 < Q^2 < 60000$ GeV^2) of the charged-current differential cross sections with a propagator mass fit. The last error is due to the uncertainty on the probability density functions.

[13] BREITWEG 00D fit the Q^2 dependence ($200 < Q^2 < 22500$ GeV^2) of the charged-current differential cross sections with a propagator mass fit. The last error is due to the uncertainty on the probability density functions.

[14] ALITTI 92B result has two contributions to the systematic error (±0.83); one (±0.81) cancels in m_W/m_Z and one (±0.17) is noncancelling. These were added in quadrature. We choose the ALITTI 92B value without using the LEP m_Z value, because we perform our own combined fit.

[15] There are two contributions to the systematic error (±0.84): one (±0.81) which cancels in m_W/m_Z and one (±0.21) which is non-cancelling. These were added in quadrature.

[16] ABE 89I systematic error dominated by the uncertainty in the absolute energy scale.

[17] ALBAJAR 89 result is from a total sample of 299 $W \to e\nu$ events.

[18] ALBAJAR 89 result is from a total sample of 67 $W \to \mu\nu$ events.

[19] ALBAJAR 89 result is from $W \to \tau\nu$ events.

W/Z MASS RATIO

VALUE	EVTS	DOCUMENT ID		TECN	COMMENT
0.8819 ±0.0012 OUR AVERAGE					
0.8821 ±0.0011 ±0.0008	28323	[1] ABBOTT	98N	D0	$E_{cm}^{p\overline{p}}$= 1.8 TeV
0.88114 ± 0.00154 ± 0.00252	5982	[2] ABBOTT	98P	D0	$E_{cm}^{p\overline{p}}$= 1.8 TeV
0.8813 ±0.0036 ±0.0019	156	[3] ALITTI	92B	UA2	$E_{cm}^{p\overline{p}}$= 630 GeV

[1] ABBOTT 98N obtain this from a study of 28323 $W \to e\nu_e$ and 3294 $Z \to e^+e^-$ decays. Of this latter sample, 2179 events are used to calibrate the electron energy scale.

[2] ABBOTT 98P obtain this from a study of 5982 $W \to e\nu_e$ events. The systematic error includes an uncertainty of ±0.00175 due to the electron energy scale.

[3] Scale error cancels in this ratio.

$m_Z - m_W$

VALUE (GeV)	DOCUMENT ID		TECN	COMMENT
10.4±1.4±0.8	ALBAJAR	89	UA1	$E_{cm}^{p\overline{p}}$= 546,630 GeV
• • • We do not use the following data for averages, fits, limits, etc. • • •				
11.3±1.3±0.9	ANSARI	87	UA2	$E_{cm}^{p\overline{p}}$= 546,630 GeV

$m_{W^+} - m_{W^-}$

Test of CPT invariance.

VALUE (GeV)	EVTS	DOCUMENT ID		TECN	COMMENT
−0.19±0.58	1722	ABE	90G	CDF	$E_{cm}^{p\overline{p}}$= 1.8 TeV

W WIDTH

The W width listed here corresponds to the width parameter in a Breit-Wigner distribution with mass-dependent width. To obtain the world average, common systematic uncertainties between experiments are properly taken into account. The LEP-2 average W width based on published results is 2.195 ± 0.083 GeV [SCHAEL 13A]. The combined Tevatron data yields an average W width of 2.046±0.049 GeV [FERMILAB-TM-2460-E].

OUR FIT uses these average LEP and Tevatron width values and combines them assuming no correlations.

VALUE (GeV)	EVTS	DOCUMENT ID		TECN	COMMENT
2.085±0.042 OUR FIT					
2.028±0.072	5272	[1] ABAZOV	09AK	D0	$E_{cm}^{p\overline{p}}$ = 1.96 GeV
2.032±0.045±0.057	6055	[2] AALTONEN	08B	CDF	$E_{cm}^{p\overline{p}}$ = 1.96 TeV
2.404±0.140±0.101	10.3k	[3] ABDALLAH	08A	DLPH	E_{cm}^{ee}= 183–209 GeV
1.996±0.096±0.102	10729	[4] ABBIENDI	06	OPAL	E_{cm}^{ee}= 170–209 GeV
2.18 ±0.11 ±0.09	9795	[5] ACHARD	06	L3	E_{cm}^{ee}= 172–209 GeV
2.14 ±0.09 ±0.06	8717	[6] SCHAEL	06	ALEP	E_{cm}^{ee}= 183–209 GeV
2.23 $^{+0.15}_{-0.14}$ ±0.10	294	[7] ABAZOV	02E	D0	Direct meas.
2.05 ±0.10 ±0.08	662	[8] AFFOLDER	00M	CDF	Direct meas.
• • • We do not use the following data for averages, fits, limits, etc. • • •					
2.152±0.066	79176	[9] ABBOTT	00B	D0	Extracted value
2.064±0.060±0.059		[10] ABE	95W	CDF	Extracted value
2.10 $^{+0.14}_{-0.13}$ ±0.09	3559	[11] ALITTI	92	UA2	Extracted value
2.18 $^{+0.26}_{-0.24}$ ±0.04		[12] ALBAJAR	91	UA1	Extracted value

[1] ABAZOV 09AK obtain this result fitting the high-end tail (100-200 GeV) of the transverse mass spectrum in $W \to e\nu$ decays.

[2] AALTONEN 08B obtain this result fitting the high-end tail (90–200 GeV) of the transverse mass spectrum in semileptonic $W \to e\nu_e$ and $W \to \mu\nu_\mu$ decays.

[3] ABDALLAH 08A use direct reconstruction of the kinematics of $W^+W^- \to q\overline{q}\ell\nu$ and $W^+W^- \to q\overline{q}q\overline{q}$ events. The systematic error includes ±0.065 GeV due to final state interactions.

[4] ABBIENDI 06 use direct reconstruction of the kinematics of $W^+W^- \to q\overline{q}\ell\nu_\ell$ and $W^+W^- \to q\overline{q}q\overline{q}$ events. The systematic error includes ±0.003 GeV due to the uncertainty on the LEP beam energy.

[5] ACHARD 06 use direct reconstruction of the kinematics of $W^+W^- \to q\overline{q}\ell\nu_\ell$ and $W^+W^- \to q\overline{q}q\overline{q}$ events in the C.M. energy range 189–209 GeV. The result quoted here is obtained combining this value of the width with the result obtained from a direct W mass reconstruction at 172 and 183 GeV (ACCIARRI 99).

[6] SCHAEL 06 use direct reconstruction of the kinematics of $W^+W^- \to q\overline{q}\ell\nu_\ell$ and $W^+W^- \to q\overline{q}q\overline{q}$ events. The systematic error includes ±0.05 GeV due to possible effects of final state interactions in the $q\overline{q}q\overline{q}$ channel and ±0.01 GeV due to the uncertainty on the LEP beam energy.

[7] ABAZOV 02E obtain this result fitting the high-end tail (90–200 GeV) of the transverse-mass spectrum in semileptonic $W \to e\nu_e$ decays.

[8] AFFOLDER 00M fit the high transverse mass (100–200 GeV) $W \to e\nu_e$ and $W \to \mu\nu_\mu$ events to obtain $\Gamma(W)$= 2.04 ± 0.11(stat)±0.09(syst) GeV. This is combined with the earlier CDF measurement (ABE 95C) to obtain the quoted result.

[9] ABBOTT 00B measure $R = 10.43 \pm 0.27$ for the $W \to e\nu_e$ decay channel. They use the SM theoretical predictions for $\sigma(W)/\sigma(Z)$ and $\Gamma(W \to e\nu_e)$ and the world average for $B(Z \to ee)$. The value quoted here is obtained combining this result (2.169 ± 0.070 GeV) with that of ABBOTT 99H.

[10] ABE 95W measured $R = 10.90 \pm 0.32 \pm 0.29$. They use m_W=80.23 ± 0.18 GeV, $\sigma(W)/\sigma(Z) = 3.35 \pm 0.03$, $\Gamma(W \to e\nu) = 225.9 \pm 0.9$ MeV, $\Gamma(Z \to e^+e^-) = 83.98 \pm 0.18$ MeV, and $\Gamma(Z) = 2.4969 \pm 0.0038$ GeV.

[11] ALITTI 92 measured $R = 10.4^{+0.7}_{-0.6} \pm 0.3$. The values of $\sigma(Z)$ and $\sigma(W)$ come from $O(\alpha_s^2)$ calculations using $m_W = 80.14 \pm 0.27$ GeV, and $m_Z = 91.175 \pm 0.021$ GeV along with the corresponding value of $\sin^2\theta_W = 0.2274$. They use $\sigma(W)/\sigma(Z) = 3.26 \pm 0.07 \pm 0.05$ and $\Gamma(Z) = 2.487 \pm 0.010$ GeV.

[12] ALBAJAR 91 measured $R = 9.5^{+1.1}_{-1.0}$ (stat. + syst.). $\sigma(W)/\sigma(Z)$ is calculated in QCD at the parton level using $m_W = 80.18 \pm 0.28$ GeV and $m_Z = 91.172 \pm 0.031$ GeV along with $\sin^2\theta_W = 0.2322 \pm 0.0014$. They use $\sigma(W)/\sigma(Z) = 3.23 \pm 0.05$ and $\Gamma(Z) = 2.498 \pm 0.020$ GeV. This measurement is obtained combining both the electron and muon channels.

W^+ DECAY MODES

W^- modes are charge conjugates of the modes below.

	Mode		Fraction (Γ_i/Γ)		Confidence level
Γ_1	$\ell^+\nu$	[a]	(10.86 ± 0.09) %		
Γ_2	$e^+\nu$		(10.71 ± 0.16) %		
Γ_3	$\mu^+\nu$		(10.63 ± 0.15) %		
Γ_4	$\tau^+\nu$		(11.38 ± 0.21) %		
Γ_5	hadrons		(67.41 ± 0.27) %		
Γ_6	$\pi^+\gamma$		< 7	$\times 10^{-5}$	95%
Γ_7	$D_s^+\gamma$		< 1.3	$\times 10^{-3}$	95%
Γ_8	cX		(33.3 ± 2.6) %		
Γ_9	$c\overline{s}$		$(31\ ^{+13}_{-11})$ %		
Γ_{10}	invisible	[b]	(1.4 ± 2.9) %		

[a] ℓ indicates each type of lepton (e, μ, and τ), not sum over them.

[b] This represents the width for the decay of the W boson into a charged particle with momentum below detectability, p< 200 MeV.

W PARTIAL WIDTHS

Γ(invisible) Γ_{10}

This represents the width for the decay of the W boson into a charged particle with momentum below detectability, p< 200 MeV.

VALUE (MeV)	DOCUMENT ID		TECN	COMMENT
$\mathbf{30^{+52}_{-48} \pm 33}$	[1] BARATE	99I	ALEP	E^{ee}_{cm}= 161+172+183 GeV
• • • We do not use the following data for averages, fits, limits, etc. • • •				
	[2] BARATE	99L	ALEP	E^{ee}_{cm}= 161+172+183 GeV

[1] BARATE 99I measure this quantity using the dependence of the total cross section σ_{WW} upon a change in the total width. The fit is performed to the WW measured cross sections at 161, 172, and 183 GeV. This partial width is < 139 MeV at 95%CL.

[2] BARATE 99L use W-pair production to search for effectively invisible W decays, tagging with the decay of the other W boson to Standard Model particles. The partial width for effectively invisible decay is < 27 MeV at 95%CL.

W BRANCHING RATIOS

Overall fits are performed to determine the branching ratios of the W boson. Averages on $W \to e\nu$, $W \to \mu\nu$, and $W \to \tau\nu$, and their correlations are obtained by combining results from the four LEP experiments properly taking into account the common systematic uncertainties and their correlations [SCHAEL 13A]. A first fit determines the three individual leptonic braching ratios B($W \to e\nu$), B($W \to \mu\nu$), and B($W \to \tau\nu$). This fit has a $\chi^2 = 6.3$ for 9 degrees of freedom. The correlation coefficients between the bracnching fractions are 0.14 ($e-\mu$), −0.20 ($e-\tau$), −0.12 ($\mu-\tau$). A second fit assumes lepton universality and determines the leptonic branching ratio br$W \to \ell\nu$ and the hadronic branching ratio is derived as B($W \to$ hadrons) = 1–3 br$W \to \ell$. This fit has a χ^2 = 15.4 for 11 degrees of freedom.

$\Gamma(\ell^+\nu)/\Gamma_{total}$ Γ_1/Γ

ℓ indicates average over e, μ, and τ modes, not sum over modes.

VALUE (units 10^{-2})	EVTS	DOCUMENT ID		TECN	COMMENT
10.86±0.09 OUR FIT					
10.86±0.12±0.08	16438	ABBIENDI	07A	OPAL	E^{ee}_{cm}= 161–209 GeV
10.85±0.14±0.08	13600	ABDALLAH	04G	DLPH	E^{ee}_{cm}= 161–209 GeV
10.83±0.14±0.10	11246	ACHARD	04J	L3	E^{ee}_{cm}= 161–209 GeV
10.96±0.12±0.05	16116	SCHAEL	04A	ALEP	E^{ee}_{cm}= 183–209 GeV
• • • We do not use the following data for averages, fits, limits, etc. • • •					
11.02±0.52	11858	[1] ABBOTT	99H	D0	$E^{p\overline{p}}_{cm}$= 1.8 TeV
10.4 ±0.8	3642	[2] ABE	92I	CDF	$E^{p\overline{p}}_{cm}$= 1.8 TeV

[1] ABBOTT 99H measure $R \equiv [\sigma_W \text{ B}(W \to \ell\nu_\ell)]/[\sigma_Z \text{ B}(Z \to \ell\ell)] = 10.90 \pm 0.52$ combining electron and muon channels. They use $M_W = 80.39 \pm 0.06$ GeV and the SM theoretical predictions for $\sigma(W)/\sigma(Z)$ and B($Z \to \ell\ell$).

[2] $1216 \pm 38^{+27}_{-31}$ $W \to \mu\nu$ events from ABE 92I and 2426 $W \to e\nu$ events of ABE 91C. ABE 92I give the inverse quantity as 9.6 ± 0.7 and we have inverted.

$\Gamma(e^+\nu)/\Gamma_{total}$ Γ_2/Γ

VALUE (units 10^{-2})	EVTS	DOCUMENT ID		TECN	COMMENT
10.71±0.16 OUR FIT					
10.71±0.25±0.11	2374	ABBIENDI	07A	OPAL	E^{ee}_{cm}= 161–209 GeV
10.55±0.31±0.14	1804	ABDALLAH	04G	DLPH	E^{ee}_{cm}= 161–209 GeV
10.78±0.29±0.13	1576	ACHARD	04J	L3	E^{ee}_{cm}= 161–209 GeV
10.78±0.27±0.10	2142	SCHAEL	04A	ALEP	E^{ee}_{cm}= 183–209 GeV
• • • We do not use the following data for averages, fits, limits, etc. • • •					
10.61±0.28		[1] ABAZOV	04D	TEVA	$E^{p\overline{p}}_{cm}$= 1.8 TeV

[1] ABAZOV 04D take into account all correlations to properly combine the CDF (ABE 95W) and DØ (ABBOTT 00B) measurements of the ratio R in the electron channel. The ratio R is defined as $[\sigma_W \cdot \text{B}(W \to e\nu_e)] / [\sigma_Z \cdot \text{B}(Z \to ee)]$. The combination gives $R^{Tevatron} = 10.59 \pm 0.23$. σ_W / σ_Z is calculated at next–to–next–to–leading order (3.360 ± 0.051). The branching fraction B($Z \to ee$) is taken from this *Review* as (3.363 ± 0.004)%.

$\Gamma(\mu^+\nu)/\Gamma_{total}$ Γ_3/Γ

VALUE (units 10^{-2})	EVTS	DOCUMENT ID		TECN	COMMENT
10.63±0.15 OUR FIT					
10.78±0.24±0.10	2397	ABBIENDI	07A	OPAL	E^{ee}_{cm}= 161–209 GeV
10.65±0.26±0.08	1998	ABDALLAH	04G	DLPH	E^{ee}_{cm} = 161–209 GeV
10.03±0.29±0.12	1423	ACHARD	04J	L3	E^{ee}_{cm} = 161–209 GeV
10.87±0.25±0.08	2216	SCHAEL	04A	ALEP	E^{ee}_{cm} = 183–209 GeV

$\Gamma(\tau^+\nu)/\Gamma_{total}$ Γ_4/Γ

VALUE (units 10^{-2})	EVTS	DOCUMENT ID		TECN	COMMENT
11.38±0.21 OUR FIT					
11.14±0.31±0.17	2177	ABBIENDI	07A	OPAL	E^{ee}_{cm}= 161–209 GeV
11.46±0.39±0.19	2034	ABDALLAH	04G	DLPH	E^{ee}_{cm} = 161–209 GeV
11.89±0.40±0.20	1375	ACHARD	04J	L3	E^{ee}_{cm} = 161–209 GeV
11.25±0.32±0.20	2070	SCHAEL	04A	ALEP	E^{ee}_{cm} = 183–209 GeV

Γ(hadrons)/Γ_{total} Γ_5/Γ

OUR FIT value is obtained by a fit to the lepton branching ratio data assuming lepton universality.

VALUE (units 10^{-2})	EVTS	DOCUMENT ID		TECN	COMMENT
67.41±0.27 OUR FIT					
67.41±0.37±0.23	16438	ABBIENDI	07A	OPAL	E^{ee}_{cm}= 161–209 GeV
67.45±0.41±0.24	13600	ABDALLAH	04G	DLPH	E^{ee}_{cm} = 161–209 GeV
67.50±0.42±0.30	11246	ACHARD	04J	L3	E^{ee}_{cm} = 161–209 GeV
67.13±0.37±0.15	16116	SCHAEL	04A	ALEP	E^{ee}_{cm} = 183–209 GeV

$\Gamma(\mu^+\nu)/\Gamma(e^+\nu)$ Γ_3/Γ_2

VALUE	EVTS	DOCUMENT ID		TECN	COMMENT
0.993±0.019 OUR FIT					
0.89 ±0.10	13k	[1] ABACHI	95D	D0	$E^{p\overline{p}}_{cm}$= 1.8 TeV
1.02 ±0.08	1216	[2] ABE	92I	CDF	$E^{p\overline{p}}_{cm}$= 1.8 TeV
1.00 ±0.14 ±0.08	67	ALBAJAR	89	UA1	$E^{p\overline{p}}_{cm}$= 546,630 GeV
• • • We do not use the following data for averages, fits, limits, etc. • • •					
$1.24\ ^{+0.6}_{-0.4}$	14	ARNISON	84D	UA1	Repl. by ALBAJAR 89

[1] ABACHI 95D obtain this result from the measured σ_WB($W \to \mu\nu$)= 2.09 ± 0.23 ± 0.11 nb and σ_WB($W \to e\nu$)= 2.36 ± 0.07 ± 0.13 nb in which the first error is the combined statistical and systematic uncertainty, the second reflects the uncertainty in the luminosity.

[2] ABE 92I obtain σ_WB($W \to \mu\nu$)= 2.21 ± 0.07 ± 0.21 and combine with ABE 91C σ_W B(($W \to e\nu$)) to give a ratio of the couplings from which we derive this measurement.

$\Gamma(\tau^+\nu)/\Gamma(e^+\nu)$ Γ_4/Γ_2

VALUE	EVTS	DOCUMENT ID		TECN	COMMENT
1.063±0.027 OUR FIT					
0.961±0.061	980	[1] ABBOTT	00D	D0	$E^{p\overline{p}}_{cm}$= 1.8 TeV
0.94 ±0.14	179	[2] ABE	92E	CDF	$E^{p\overline{p}}_{cm}$= 1.8 TeV
1.04 ±0.08 ±0.08	754	[3] ALITTI	92F	UA2	$E^{p\overline{p}}_{cm}$= 630 GeV
1.02 ±0.20 ±0.12	32	ALBAJAR	89	UA1	$E^{p\overline{p}}_{cm}$= 546,630 GeV
• • • We do not use the following data for averages, fits, limits, etc. • • •					
0.995±0.112±0.083	198	ALITTI	91C	UA2	Repl. by ALITTI 92F
1.02 ±0.20 ±0.10	32	ALBAJAR	87	UA1	Repl. by ALBAJAR 89

[1] ABBOTT 00D measure $\sigma_W \times$B($W \to \tau\nu_\tau$) = 2.22 ± 0.09 ± 0.10 ± 0.10 nb. Using the ABBOTT 00B result $\sigma_W \times$B($W \to e\nu_e$) = 2.31 ± 0.01 ± 0.05 ± 0.10 nb, they quote the ratio of the couplings from which we derive this measurement.

[2] ABE 92E use two procedures for selecting $W \to \tau\nu_\tau$ events. The missing E_T trigger leads to 132 ± 14 ± 8 events and the τ trigger to 47 ± 9 ± 4 events. Proper statistical and systematic correlations are taken into account to arrive at σB($W \to \tau\nu$) = 2.05 ± 0.27 nb. Combined with ABE 91C result on σB($W \to e\nu$), ABE 92E quote a ratio of the couplings from which we derive this measurement.

[3] This measurement is derived by us from the ratio of the couplings of ALITTI 92F.

$\Gamma(\pi^+\gamma)/\Gamma(e^+\nu)$ Γ_6/Γ_2

VALUE	CL%	DOCUMENT ID		TECN	COMMENT
< 7 × 10⁻⁴	95	ABE	98H	CDF	$E_{cm}^{p\overline{p}}$ = 1.8 TeV
< 4.9 × 10⁻³	95	[1] ALITTI	92D	UA2	$E_{cm}^{p\overline{p}}$ = 630 GeV
<58 × 10⁻³	95	[2] ALBAJAR	90	UA1	$E_{cm}^{p\overline{p}}$ = 546, 630 GeV

[1] ALITTI 92D limit is 3.8×10^{-3} at 90%CL.
[2] ALBAJAR 90 obtain < 0.048 at 90%CL.

$\Gamma(D_s^+\gamma)/\Gamma(e^+\nu)$ Γ_7/Γ_2

VALUE	CL%	DOCUMENT ID		TECN	COMMENT
<1.2 × 10⁻²	95	ABE	98P	CDF	$E_{cm}^{p\overline{p}}$ = 1.8 TeV

$\Gamma(cX)/\Gamma(\text{hadrons})$ Γ_8/Γ_5

VALUE	EVTS	DOCUMENT ID		TECN	COMMENT
0.49 ±0.04 OUR AVERAGE					
0.481±0.042±0.032	3005	[1] ABBIENDI	00V	OPAL	E_{cm}^{ee} = 183 + 189 GeV
0.51 ±0.05 ±0.03	746	[2] BARATE	99M	ALEP	E_{cm}^{ee} = 172 + 183 GeV

[1] ABBIENDI 00V tag $W \to cX$ decays using measured jet properties, lifetime information, and leptons produced in charm decays. From this result, and using the additional measurements of $\Gamma(W)$ and $B(W \to \text{hadrons})$, $|V_{cs}|$ is determined to be 0.969 ± 0.045 ± 0.036.
[2] BARATE 99M tag c jets using a neural network algorithm. From this measurement $|V_{cs}|$ is determined to be 1.00 ± 0.11 ± 0.07.

$R_{cs} = \Gamma(c\overline{s})/\Gamma(\text{hadrons})$ Γ_9/Γ_5

VALUE	DOCUMENT ID		TECN	COMMENT
$0.46^{+0.18}_{-0.14} \pm 0.07$	[1] ABREU	98N	DLPH	E_{cm}^{ee} = 161+172 GeV

[1] ABREU 98N tag c and s jets by identifying a charged kaon as the highest momentum particle in a hadronic jet. They also use a lifetime tag to independently identify a c jet, based on the impact parameter distribution of charged particles in a jet. From this measurement $|V_{cs}|$ is determined to be $0.94^{+0.32}_{-0.26} \pm 0.13$.

AVERAGE PARTICLE MULTIPLICITIES IN HADRONIC *W* DECAY

Summed over particle and antiparticle, when appropriate.

$\langle N_{\pi^\pm} \rangle$

VALUE	DOCUMENT ID		TECN	COMMENT
15.70±0.35	[1] ABREU,P	00F	DLPH	E_{cm}^{ee} = 189 GeV

[1] ABREU,P 00F measure $\langle N_{\pi^\pm} \rangle$ = 31.65 ± 0.48 ± 0.76 and 15.51 ± 0.38 ± 0.40 in the fully hadronic and semileptonic final states respectively. The value quoted is a weighted average without assuming any correlations.

$\langle N_{K^\pm} \rangle$

VALUE	DOCUMENT ID		TECN	COMMENT
2.20±0.19	[1] ABREU,P	00F	DLPH	E_{cm}^{ee} = 189 GeV

[1] ABREU,P 00F measure $\langle N_{K^\pm} \rangle$ = 4.38 ± 0.42 ± 0.12 and 2.23 ± 0.32 ± 0.17 in the fully hadronic and semileptonic final states respectively. The value quoted is a weighted average without assuming any correlations.

$\langle N_p \rangle$

VALUE	DOCUMENT ID		TECN	COMMENT
0.92±0.14	[1] ABREU,P	00F	DLPH	E_{cm}^{ee} = 189 GeV

[1] ABREU,P 00F measure $\langle N_p \rangle$ = 1.82 ± 0.29 ± 0.16 and 0.94 ± 0.23 ± 0.06 in the fully hadronic and semileptonic final states respectively. The value quoted is a weighted average without assuming any correlations.

$\langle N_{\text{charged}} \rangle$

VALUE	DOCUMENT ID		TECN	COMMENT
19.39±0.08 OUR AVERAGE				
19.38±0.05±0.08	[1] ABBIENDI	06A	OPAL	E_{cm}^{ee} = 189–209 GeV
19.44±0.17	[2] ABREU,P	00F	DLPH	E_{cm}^{ee} = 183+189 GeV
19.3 ±0.3 ±0.3	[3] ABBIENDI	99N	OPAL	E_{cm}^{ee} = 183 GeV
19.23±0.74	[4] ABREU	98C	DLPH	E_{cm}^{ee} = 172 GeV

[1] ABBIENDI 06A measure $\langle N_{\text{charged}} \rangle$ = 38.74 ± 0.12 ± 0.26 when both W bosons decay hadronically and $\langle N_{\text{charged}} \rangle$ = 19.39 ± 0.11 ± 0.09 when one W boson decays semileptonically. The value quoted here is obtained under the assumption that there is no color reconnection between W bosons; the value is a weighted average taking into account correlations in the systematic uncertainties.
[2] ABREU,P 00F measure $\langle N_{\text{charged}} \rangle$ = 39.12 ± 0.33 ± 0.36 and 38.11 ± 0.57 ± 0.44 in the fully hadronic final states at 189 and 183 GeV respectively, and $\langle N_{\text{charged}} \rangle$ = 19.49 ± 0.31 ± 0.27 and 19.78 ± 0.49 ± 0.43 in the semileptonic final states. The value quoted is a weighted average without assuming any correlations.
[3] ABBIENDI 99N use the final states $W^+W^- \to q\overline{q}\ell\overline{\nu}_\ell$ to derive this value.
[4] ABREU 98C combine results from both the fully hadronic as well semileptonic WW final states after demonstrating that the W decay charged multiplicity is independent of the topology within errors.

TRIPLE GAUGE COUPLINGS (TGC'S)

Revised September 2013 by M.W. Grünewald (U. College Dublin and U. Ghent) and A. Gurtu (Formerly Tata Inst.).

Fourteen independent couplings, seven each for ZWW and γWW, completely describe the VWW vertices within the most general framework of the electroweak Standard Model (SM) consistent with Lorentz invariance and U(1) gauge invariance. Of each of the seven TGCs, three conserve C and P individually, three violate CP, and one violates C and P individually while conserving CP. Assumption of C and P conservation and electromagnetic gauge invariance reduces the number of independent VWW couplings to five: one common set [1,2] is $(\kappa_\gamma, \kappa_Z, \lambda_\gamma, \lambda_Z, g_1^Z)$, where $\kappa_\gamma = \kappa_Z = g_1^Z = 1$ and $\lambda_\gamma = \lambda_Z = 0$ in the Standard Model at tree level. The parameters κ_Z and λ_Z are related to the other three due to constraints of gauge invariance as follows: $\kappa_Z = g_1^Z - (\kappa_\gamma - 1)\tan^2\theta_W$ and $\lambda_Z = \lambda_\gamma$, where θ_W is the weak mixing angle. The W magnetic dipole moment, μ_W, and the W electric quadrupole moment, q_W, are expressed as $\mu_W = e\,(1 + \kappa_\gamma + \lambda_\gamma)/2M_W$ and $q_W = -e\,(\kappa_\gamma - \lambda_\gamma)/M_W^2$.

Precision measurements of suitable observables at LEP1 has already led to an exploration of much of the TGC parameter space. At LEP2, the VWW coupling arises in W-pair production via s-channel exchange, or in single W production via the radiation of a virtual photon off the incident e^+ or e^-. At the Tevatron and the LHC, hard-photon bremsstrahlung off a produced W or Z signals the presence of a triple-gauge vertex. In order to extract the value of one TGC, the others are generally kept fixed to their SM values. While most analyses use the above gauge constraints in the extraction of TGCs, one analysis of W-pair events also determines the real and imaginary parts of all 14 couplings using unconstrained single-parameter fits [3]. The results are consistent. Some experiments have determined limits on the couplings under various non-LEP scenarios and assuming different values of the form factor Λ. For practical reasons it is not possible to quote all such determinations in the listings. For that the individual papers may be consulted.

References

1. K. Hagiwara *et al.*, Nucl. Phys. **B282**, 253 (1987).
2. G. Gounaris *et al.*, CERN 96-01 p. 525.
3. S. Schael *et al.* (ALEPH Collab.), Phys. Lett. **B614**, 7 (2005).

g_1^Z

OUR FIT below is taken from [SCHAEL 13A].

VALUE	EVTS	DOCUMENT ID		TECN	COMMENT
$0.984^{+0.018}_{-0.020}$ OUR FIT					
$0.975^{+0.033}_{-0.030}$	7872	[1] ABDALLAH	10	DLPH	E_{cm}^{ee} = 189–209 GeV
1.001±0.027±0.013	9310	[2] SCHAEL	05A	ALEP	E_{cm}^{ee} = 183–209 GeV
$0.987^{+0.034}_{-0.033}$	9800	[3] ABBIENDI	04D	OPAL	E_{cm}^{ee} = 183–209 GeV
$0.966^{+0.034}_{-0.032} \pm 0.015$	8325	[4] ACHARD	04D	L3	E_{cm}^{ee} = 161–209 GeV

• • • We do not use the following data for averages, fits, limits, etc. • • •

		[5] AAD	13AL	ATLS	E_{cm}^{pp} = 7 TeV	
		[6] CHATRCHYAN	13BF	CMS	E_{cm}^{pp} = 7 TeV	
		[7] AAD	12CD	ATLS	E_{cm}^{pp} = 7 TeV	
		[8] AALTONEN	12AC	CDF	$E_{cm}^{p\overline{p}}$ = 1.96 TeV	
		[9] ABAZOV	12AG	D0	$E_{cm}^{p\overline{p}}$ = 1.96 TeV	
	34	[10] ABAZOV	11	D0	$E_{cm}^{p\overline{p}}$ = 1.96 TeV	
	334	[11] AALTONEN	10K	CDF	$E_{cm}^{p\overline{p}}$ = 1.96 TeV	
1.04 ±0.09		[12] ABAZOV	09AD	D0	$E_{cm}^{p\overline{p}}$ = 1.96 TeV	
		[13] ABAZOV	09AJ	D0	$E_{cm}^{p\overline{p}}$ = 1.96 TeV	
$1.07\ ^{+0.08}_{-0.12}$	1880	[14] ABDALLAH	08C	DLPH	Superseded by ABDALLAH 10	
	13	[15] ABAZOV	07Z	D0	$E_{cm}^{p\overline{p}}$ = 1.96 TeV	
	2.3	[16] ABAZOV	05S	D0	$E_{cm}^{p\overline{p}}$ = 1.96 TeV	
0.98 ±0.07 ±0.01	2114	[17] ABREU	01I	DLPH	E_{cm}^{ee} = 183+189 GeV	
	331	[18] ABBOTT	99I	D0	$E_{cm}^{p\overline{p}}$ = 1.8 TeV	

[1] ABDALLAH 10 use data on the final states $e^+e^- \to jj\ell\nu$, $jjjj$, jjX, ℓX, at center-of-mass energies between 189–209 GeV at LEP2, where j = jet, ℓ = lepton, and X represents missing momentum. The fit is carried out keeping all other parameters fixed at their SM values.

[2] SCHAEL 05A study single–photon, single–W, and WW–pair production from 183 to 209 GeV. The result quoted here is derived from the WW–pair production sample. Each parameter is determined from a single–parameter fit in which the other parameters assume their Standard Model values.

[3] ABBIENDI 04D combine results from W^+W^- in all decay channels. Only *CP*-conserving couplings are considered and each parameter is determined from a single-parameter fit in which the other parameters assume their Standard Model values. The 95% confidence interval is $0.923 < g_1^Z < 1.054$.

[4] ACHARD 04D study WW–pair production, single–W production and single–photon production with missing energy from 189 to 209 GeV. The result quoted here is obtained from the WW–pair production sample including data from 161 to 183 GeV, ACCIARRI 99Q. Each parameter is determined from a single–parameter fit in which the other parameters assume their Standard Model values.

[5] AAD 13AL study WW production in pp collisions and select 1325 WW candidates in decay modes with electrons or muons with an expected background of 369 ± 61 events. Assuming the LEP formulation and setting the form-factor Λ = infinity, a fit to the transverse momentum distribution of the leading charged lepton, leads to a 95% C.L. range of $0.961 < g_1^Z < 1.052$. Supersedes AAD 12AC.

[6] CHATRCHYAN 13BF determine the W^+W^- production cross section using unlike sign di-lepton (e or μ) events with high $\not{p}_T$. The leptons have $p_T > 20$ GeV/c and are isolated. 1134 candidate events are observed with an expected SM background of 247 ± 34. The p_T distribution of the leading lepton is fitted to obtain 95% C.L. limits of $0.905 \le g_1^Z \le 1.095$.

[7] AAD 12CD study WZ production in pp collisions and select 317 WZ candidates in three $\ell\nu$ decay modes with an expected background of 68.0 ± 10.0 events. The resulting 95% C.L. range is: $0.943 < g_1^Z < 1.093$. Supersedes AAD 12V.

[8] AALTONEN 12AC study WZ production in $p\overline{p}$ collisions and select 63 WZ candidates in three $\ell\nu$ decay modes with an expected background of 7.9 ± 1.0 events. Based on the cross section and shape of the Z transverse momentum spectrum, the following 95% C.L. range is reported: $0.92 < g_1^Z < 1.20$ for a form factor of Λ = 2 TeV.

[9] ABAZOV 12AG combine new results with already published results on $W\gamma$, WW and WZ production in order to determine the couplings with increased precision, superseeding ABAZOV 08R, ABAZOV 11AC, ABAZOV 09AJ, ABAZOV 09AD. The 68% C.L. result for a formfactor cutoff of Λ = 2 TeV is $g_1^Z = 1.022^{+0.032}_{-0.030}$.

[10] ABAZOV 11 study the $p\overline{p} \to 3\ell\nu$ process arising in WZ production. They observe 34 WZ candidates with an estimated background of 6 events. An analysis of the p_T spectrum of the Z boson leads to a 95% C.L. limit of $0.944 < g_1^Z < 1.154$, for a form factor Λ = 2 TeV.

[11] AALTONEN 10K study $p\overline{p} \to W^+W^-$ with $W \to e/\mu\nu$. The p_T of the leading (second) lepton is required to be > 20 (10) GeV. The final number of events selected is 654 of which 320 ± 47 are estimated to be background. The 95% C.L. interval is $0.76 < g_1^Z < 1.34$ for Λ = 1.5 TeV and $0.78 < g_1^Z < 1.30$ for Λ = 2 TeV.

[12] ABAZOV 09AD study the $p\overline{p} \to \ell\nu$ 2jet process arising in WW and WZ production. They select 12,473 (14,392) events in the electron (muon) channel with an expected di-boson signal of 436 (527) events. The results on the anomalous couplings are derived from an analysis of the p_T spectrum of the 2-jet system and quoted at 68% C.L. and for a form factor of 2 TeV. This measurement is not used for obtaining the mean as it is for a specific form factor. The 95% confidence interval is $0.88 < g_1^Z < 1.20$.

[13] ABAZOV 09AJ study the $p\overline{p} \to 2\ell 2\nu$ process arising in WW production. They select 100 events with an expected WW signal of 65 events. An analysis of the p_T spectrum of the two charged leptons leads to 95% C.L. limits of $0.86 < g_1^Z < 1.3$, for a form factor Λ = 2 TeV.

[14] ABDALLAH 08C determine this triple gauge coupling from the measurement of the spin density matrix elements in $e^+e^- \to W^+W^- \to (q\overline{q})(\ell\nu)$, where $\ell = e$ or μ. Values of all other couplings are fixed to their standard model values.

[15] ABAZOV 07Z set limits on anomalous TGCs using the measured cross section and $p_T(Z)$ distribution in WZ production with both the W and the Z decaying leptonically into electrons and muons. Setting the other couplings to their standard model values, the 95% C.L. limit for a form factor scale Λ = 2 TeV is $0.86 < g_1^Z < 1.35$.

[16] ABAZOV 05S study $\overline{p}p \to WZ$ production with a subsequent trilepton decay to $\ell\nu\ell'\overline{\ell}'$ (ℓ and ℓ' = e or μ). Three events (estimated background 0.71 ± 0.08 events) with WZ decay characteristics are observed from which they derive limits on the anomalous WWZ couplings. The 95% CL limit for a form factor scale Λ = 1.5 TeV is $0.51 < g_1^Z < 1.66$, fixing λ_Z and κ_Z to their Standard Model values.

[17] ABREU 01I combine results from e^+e^- interactions at 189 GeV leading to W^+W^- and $We\nu_e$ final states with results from ABREU 99L at 183 GeV. The 95% confidence interval is $0.84 < g_1^Z < 1.13$.

[18] ABBOTT 99I perform a simultaneous fit to the $W\gamma$, $WW \to$ dilepton, $WW/WZ \to e\nu jj$, $WW/WZ \to \mu\nu jj$, and $WZ \to$ trilepton data samples. For Λ = 2.0 TeV, the 95%CL limits are $0.63 < g_1^Z < 1.57$, fixing λ_Z and κ_Z to their Standard Model values, and assuming Standard Model values for the $WW\gamma$ couplings.

κ_γ

OUR FIT below is taken from [SCHAEL 13A].

VALUE	*EVTS*	*DOCUMENT ID*		*TECN*	*COMMENT*
0.982±0.042 OUR FIT					
$1.024^{+0.077}_{-0.081}$	7872	[1] ABDALLAH	10	DLPH	E_{cm}^{ee} = 189–209 GeV
0.971 ±0.055 ±0.030	10689	[2] SCHAEL	05A	ALEP	E_{cm}^{ee} = 183–209 GeV
$0.88\ ^{+0.09}_{-0.08}$	9800	[3] ABBIENDI	04D	OPAL	E_{cm}^{ee} = 183–209 GeV
$1.013^{+0.067}_{-0.064}$ ±0.026	10575	[4] ACHARD	04D	L3	E_{cm}^{ee} = 161–209 GeV

• • • We do not use the following data for averages, fits, limits, etc. • • •

		[5] AAD	13AN	ATLS	E_{cm}^{pp} = 7 TeV	
		[6] CHATRCHYAN	13BF	CMS	E_{cm}^{pp} = 7 TeV	
		[7] ABAZOV	12AG	D0	$E_{cm}^{p\overline{p}}$ = 1.96 TeV	
		[8] ABAZOV	11AC	D0	$E_{cm}^{p\overline{p}}$ = 1.96 TeV	
		[9] CHATRCHYAN	11M	CMS	E_{cm}^{pp} = 7 TeV	
	334	[10] AALTONEN	10K	CDF	$E_{cm}^{p\overline{p}}$ = 1.96 TeV	
	53	[11] AARON	09B	H1	E_{cm}^{ep} = 0.3 TeV	
$1.07\ ^{+0.26}_{-0.29}$		[12] ABAZOV	09AD	D0	$E_{cm}^{p\overline{p}}$ = 1.96 TeV	
		[13] ABAZOV	09AJ	D0	$E_{cm}^{p\overline{p}}$ = 1.96 TeV	
		[14] ABAZOV	08R	D0	$E_{cm}^{p\overline{p}}$ = 1.96 TeV	
$0.68\ ^{+0.17}_{-0.15}$	1880	[15] ABDALLAH	08C	DLPH	Superseded by ABDALLAH 10	
	1617	[16] AALTONEN	07L	CDF	$E_{cm}^{p\overline{p}}$ = 1.96 GeV	
	17	[17] ABAZOV	06H	D0	$E_{cm}^{p\overline{p}}$ = 1.96 TeV	
	141	[18] ABAZOV	05J	D0	$E_{cm}^{p\overline{p}}$ = 1.96 TeV	
$1.25\ ^{+0.21}_{-0.20}$ ±0.06	2298	[19] ABREU	01I	DLPH	E_{cm}^{ee} = 183+189 GeV	
		[20] BREITWEG	00	ZEUS	$e^+p \to e^+W^{\pm}X$, $\sqrt{s} \approx$ 300 GeV	
0.92 ±0.34	331	[21] ABBOTT	99I	D0	$E_{cm}^{p\overline{p}}$ = 1.8 TeV	

[1] ABDALLAH 10 use data on the final states $e^+e^- \to jj\ell\nu$, $jjjj$, jjX, ℓX, at center-of-mass energies between 189–209 GeV at LEP2, where j = jet, ℓ = lepton, and X represents missing momentum. The fit is carried out keeping all other parameters fixed at their SM values.

[2] SCHAEL 05A study single–photon, single–W, and WW–pair production from 183 to 209 GeV. Each parameter is determined from a single–parameter fit in which the other parameters assume their Standard Model values.

[3] ABBIENDI 04D combine results from W^+W^- in all decay channels. Only *CP*-conserving couplings are considered and each parameter is determined from a single-parameter fit in which the other parameters assume their Standard Model values. The 95% confidence interval is $0.73 < \kappa_\gamma < 1.07$.

[4] ACHARD 04D study WW–pair production, single–W production and single–photon production with missing energy from 189 to 209 GeV. The result quoted here is obtained including data from 161 to 183 GeV, ACCIARRI 99Q. Each parameter is determined from a single–parameter fit in which the other parameters assume their Standard Model values.

[5] AAD 13AN study $W\gamma$ production in pp collisions. In events with no additional jet, 4449 (6578) W decays to electron (muon) are selected, with an expected background of 1662 ± 262 (2538 ± 362) events. Analysing the photon p_T spectrum above 100 GeV yields a 95% C.L. limit of $0.59 < \kappa_\gamma < 1.46$. Supersedes AAD 12BX.

[6] CHATRCHYAN 13BF determine the W^+W^- production cross section using unlike sign di-lepton (e or μ) events with high $\not{p}_T$. The leptons have $p_T > 20$ GeV/c and are isolated. 1134 candidate events are observed with an expected SM background of 247 ± 34. The p_T distribution of the leading lepton is fitted to obtain 95% C.L. limits of $0.79 \le k_\gamma \le 1.22$.

[7] ABAZOV 12AG combine new results with already published results on $W\gamma$, WW and WZ production in order to determine the couplings with increased precision, superseeding ABAZOV 08R, ABAZOV 11AC, ABAZOV 09AJ, ABAZOV 09AD. The 68% C.L. result for a formfactor cutoff of Λ = 2 TeV is $\kappa_\gamma = 1.048^{+0.106}_{-0.105}$.

[8] ABAZOV 11AC study $W\gamma$ production in $p\overline{p}$ collisions at 1.96 TeV, with the W decay products containing an electron or a muon. They select 196 (363) events in the electron (muon) mode, with a SM expectation of 190 (372) events. A likelihood fit to the photon E_T spectrum above 15 GeV yields at 95% C.L. the result: $0.6 < \kappa_\gamma < 1.4$ for a formfactor Λ = 2 TeV.

[9] CHATRCHYAN 11M study $W\gamma$ production in pp collisions at $\sqrt{s}$ = 7 TeV using 36 pb^{-1} pp data with the W decaying to electron and muon. The total cross section is measured for photon transverse energy $E_T^\gamma > 10$ GeV and spatial separation from charged leptons in the plane of pseudo rapidity and azimuthal angle $\Delta R(\ell,\gamma) > 0.7$. The number of candidate (background) events is 452 (228 ± 21) for the electron channel and 520 (277 ± 25) for the muon channel. Setting other couplings to their standard model value, they derive a 95% CL limit of $-0.11 < \kappa_\gamma < 2.04$.

[10] AALTONEN 10K study $p\overline{p} \to W^+W^-$ with $W \to e/\mu\nu$. The p_T of the leading (second) lepton is required to be > 20 (10) GeV. The final number of events selected is 654 of which 320 ± 47 are estimated to be background. The 95% C.L. interval is $0.37 < \kappa_\gamma < 1.72$ for Λ = 1.5 TeV and $0.43 < \kappa_\gamma < 1.65$ for Λ = 2 TeV.

[11] AARON 09B study single-W production in ep collisions at 0.3 TeV C.M. energy. They select 53 $W \to e/\mu$ events with a standard model expectation of 54.1 ± 7.4 events. Fitting the transverse momentum spectrum of the hadronic recoil system they obtain a 95% C.L. limit of $-3.7 < \kappa_\gamma < -1.5$ or $0.3 < \kappa_\gamma < 1.5$, where the ambiguity is due to the quadratic dependence of the cross section to the coupling parameter.

[12] ABAZOV 09AD study the $p\overline{p} \to \ell\nu$ 2jet process arising in WW and WZ production. They select 12,473 (14,392) events in the electron (muon) channel with an expected di-boson signal of 436 (527) events. The results on the anomalous couplings are derived from an analysis of the p_T spectrum of the 2-jet system and quoted at 68% C.L. and for a form factor of 2 TeV. This measurement is not used for obtaining the mean as it is for a specific form factor. The 95% confidence interval is $0.56 < \kappa_\gamma < 1.55$.

[13] ABAZOV 09AJ study the $p\overline{p} \to 2\ell 2\nu$ process arising in WW production. They select 100 events with an expected WW signal of 65 events. An analysis of the p_T spectrum of the two charged leptons leads to 95% C.L. limits of $0.46 < \kappa_\gamma < 1.83$, for a form factor $\Lambda = 2$ TeV.

[14] ABAZOV 08R use 0.7 fb^{-1} $p\overline{p}$ data at $\sqrt{s} = 1.96$ TeV to select 263 $W\gamma + X$ events, of which 187 constitute signal, with the W decaying into an electron or a muon, which is required to be well separated from a photon with $E_T > 9$ GeV. A likelihood fit to the photon E_T spectrum yields a 95% CL limit $0.49 < \kappa_\gamma < 1.51$ with other couplings fixed to their Standard Model values.

[15] ABDALLAH 08C determine this triple gauge coupling from the measurement of the spin density matrix elements in $e^+e^- \to W^+W^- \to (qq)(\ell\nu)$, where $\ell = e$ or μ. Values of all other couplings are fixed to their standard model values.

[16] AALTONEN 07L set limits on anomalous TGCs using the $p_T(W)$ distribution in WW and WZ production with the W decaying to an electron or muon and the Z to 2 jets. Setting other couplings to their standard model value, the 95% C.L. limits are $0.54 < \kappa_\gamma < 1.39$ for a form factor scale $\Lambda = 1.5$ TeV.

[17] ABAZOV 06H study $\overline{p}p \to WW$ production with a subsequent decay $WW \to e^+\nu_e e^-\overline{\nu}_e$, $WW \to e^\pm\nu_e\mu^\mp\nu_\mu$ or $WW \to \mu^+\nu_\mu\mu^-\overline{\nu}_\mu$. The 95% C.L. limit for a form factor scale $\Lambda = 1$ TeV is $-0.05 < \kappa_\gamma < 2.29$, fixing $\lambda_\gamma = 0$. With the assumption that the $WW\gamma$ and WWZ couplings are equal the 95% C.L. one-dimensional limit ($\Lambda = 2$ TeV) is $0.68 < \kappa < 1.45$.

[18] ABAZOV 05J perform a likelihood fit to the photon E_T spectrum of $W\gamma + X$ events, where the W decays to an electron or muon which is required to be well separated from the photon. For $\Lambda = 2.0$ TeV the 95% CL limits are $0.12 < \kappa_\gamma < 1.96$. In the fit λ_γ is kept fixed to its Standard Model value.

[19] ABREU 01I combine results from e^+e^- interactions at 189 GeV leading to W^+W^-, $We\nu_e$, and $\nu\overline{\nu}\gamma$ final states with results from ABREU 99L at 183 GeV. The 95% confidence interval is $0.87 < \kappa_\gamma < 1.68$.

[20] BREITWEG 00 search for W production in events with large hadronic p_T. For $p_T > 20$ GeV, the upper limit on the cross section gives the 95%CL limit $-3.7 < \kappa_\gamma < 2.5$ (for $\lambda_\gamma = 0$).

[21] ABBOTT 99I perform a simultaneous fit to the $W\gamma$, $WW \to$ dilepton, $WW/WZ \to e\nu jj$, $WW/WZ \to \mu\nu jj$, and $WZ \to$ trilepton data samples. For $\Lambda = 2.0$ TeV, the 95%CL limits are $0.75 < \kappa_\gamma < 1.39$.

λ_γ

OUR FIT below is taken from [SCHAEL 13A].

VALUE	EVTS	DOCUMENT ID		TECN	COMMENT
-0.022 ± 0.019 OUR FIT					
0.002 ± 0.035	7872	[1] ABDALLAH	10	DLPH	$E_{cm}^{ee} = 189$–209 GeV
$-0.012 \pm 0.027 \pm 0.011$	10689	[2] SCHAEL	05A	ALEP	$E_{cm}^{ee} = 183$–209 GeV
$-0.060^{+0.034}_{-0.033}$	9800	[3] ABBIENDI	04D	OPAL	$E_{cm}^{ee} = 183$–209 GeV
$-0.021^{+0.035}_{-0.034} \pm 0.017$	10575	[4] ACHARD	04D	L3	$E_{cm}^{ee} = 161$–209 GeV
• • • We do not use the following data for averages, fits, limits, etc. • • •					
		[5] AAD	13AN	ATLS	$E_{cm}^{pp} = 7$ TeV
		[6] ABAZOV	12AG	D0	$E_{cm}^{p\overline{p}} = 1.96$ TeV
		[7] ABAZOV	11AC	D0	$E_{cm}^{p\overline{p}} = 1.96$ TeV
		[8] CHATRCHYAN	11M	CMS	$E_{cm}^{pp} = 7$ TeV
	53	[9] AARON	09B	H1	$E_{cm}^{ep} = 0.3$ TeV
0.00 ± 0.06		[10] ABAZOV	09AD	D0	$E_{cm}^{p\overline{p}} = 1.96$ TeV
		[11] ABAZOV	09AJ	D0	$E_{cm}^{p\overline{p}} = 1.96$ TeV
		[12] ABAZOV	08R	D0	$E_{cm}^{p\overline{p}} = 1.96$ TeV
$0.16^{+0.12}_{-0.13}$	1880	[13] ABDALLAH	08C	DLPH	Superseded by ABDALLAH 10
	1617	[14] AALTONEN	07L	CDF	$E_{cm}^{p\overline{p}} = 1.96$ GeV
	17	[15] ABAZOV	06H	D0	$E_{cm}^{p\overline{p}} = 1.96$ TeV
	141	[16] ABAZOV	05J	D0	$E_{cm}^{p\overline{p}} = 1.96$ TeV
$0.05 \pm 0.09 \pm 0.01$	2298	[17] ABREU	01I	DLPH	$E_{cm}^{ee} = 183$+189 GeV
		[18] BREITWEG	00	ZEUS	$e^+p \to e^+W^\pm X$, $\sqrt{s} \approx 300$ GeV
$0.00^{+0.10}_{-0.09}$	331	[19] ABBOTT	99I	D0	$E_{cm}^{p\overline{p}} = 1.8$ TeV

[1] ABDALLAH 10 use data on the final states $e^+e^- \to jj\ell\nu$, $jjjj$, jjX, ℓX, at center-of-mass energies between 189–209 GeV at LEP2, where j = jet, ℓ = lepton, and X represents missing momentum. The fit is carried out keeping all other parameters fixed at their SM values.

[2] SCHAEL 05A study single–photon, single–W, and WW–pair production from 183 to 209 GeV. Each parameter is determined from a single–parameter fit in which the other parameters assume their Standard Model values.

[3] ABBIENDI 04D combine results from W^+W^- in all decay channels. Only CP-conserving couplings are considered and each parameter is determined from a single-parameter fit in which the other parameters assume their Standard Model values. The 95% confidence interval is $-0.13 < \lambda_\gamma < 0.01$.

[4] ACHARD 04D study WW–pair production, single–W production and single–photon production with missing energy from 189 to 209 GeV. The result quoted here is obtained including data from 161 to 183 GeV, ACCIARRI 99Q. Each parameter is determined from a single–parameter fit in which the other parameters assume their Standard Model values.

[5] AAD 13AN study $W\gamma$ production in pp collisions. In events with no additional jet, 4449 (6578) W decays to electron (muon) are selected, with an expected background of 1662 ± 262 (2538 ± 362) events. Analysing the photon p_T spectrum above 100 GeV yields a 95% C.L. limit of $-0.065 < \lambda_\gamma < 0.061$. Supersedes AAD 12BX.

[6] ABAZOV 12AG combine new results with already published results on $W\gamma$, WW and WZ production in order to determine the couplings with increased precision, superseeding ABAZOV 08R, ABAZOV 11AC, ABAZOV 09AJ, ABAZOV 09AD. The 68% C.L. result for a formfactor cutoff of $\Lambda = 2$ TeV is $\lambda_\gamma = 0.007^{+0.021}_{-0.022}$.

[7] ABAZOV 11AC study $W\gamma$ production in $p\overline{p}$ collisions at 1.96 TeV, with the W decay products containing an electron or a muon. They select 196 (363) events in the electron (muon) mode, with a SM expectation of 190 (372) events. A likelihood fit to the photon E_T spectrum above 15 GeV yields at 95% C.L. the result: $-0.08 < \lambda_\gamma < 0.07$ for a formfactor $\Lambda = 2$ TeV.

[8] CHATRCHYAN 11M study $W\gamma$ production in pp collisions at $\sqrt{s} = 7$ TeV using 36 pb^{-1} pp data with the W decaying to electron and muon. The total cross section is measured for photon transverse energy $E_T^\gamma > 10$ GeV and spatial separation from charged leptons in the plane of pseudo rapidity and azimuthal angle $\Delta R(\ell,\gamma) > 0.7$. The number of candidate (background) events is 452 (228 ± 21) for the electron channel and 520 (277 ± 25) for the muon channel. Setting other couplings to their standard model value, they derive a 95% CL limit of $-0.18 < \lambda_\gamma < 0.17$.

[9] AARON 09B study single-W production in ep collisions at 0.3 TeV C.M. energy. They select 53 $W \to e/\mu$ events with a standard model expectation of 54.1 ± 7.4 events. Fitting the transverse momentum spectrum of the hadronic recoil system they obtain a 95% C.L. limit of $-2.5 < \lambda_\gamma < 2.5$.

[10] ABAZOV 09AD study the $p\overline{p} \to \ell\nu$ 2jet process arising in WW and WZ production. They select 12,473 (14,392) events in the electron (muon) channel with an expected di-boson signal of 436 (527) events. The results on the anomalous couplings are derived from an analysis of the p_T spectrum of the 2-jet system and quoted at 68% C.L. and for a form factor of 2 TeV. This measurement is not used for obtaining the mean as it is for a specific form factor. The 95% confidence interval is $-0.10 < \lambda_\gamma < 0.11$.

[11] ABAZOV 09AJ study the $p\overline{p} \to 2\ell 2\nu$ process arising in WW production. They select 100 events with an expected WW signal of 65 events. An analysis of the p_T spectrum of the two charged leptons leads to 95% C.L. limits of $-0.14 < \lambda_\gamma < 0.18$, for a form factor $\Lambda = 2$ TeV.

[12] ABAZOV 08R use 0.7 fb^{-1} $p\overline{p}$ data at $\sqrt{s} = 1.96$ TeV to select 263 $W\gamma + X$ events, of which 187 constitute signal, with the W decaying into an electron or a muon, which is required to be well separated from a photon with $E_T > 9$ GeV. A likelihood fit to the photon E_T spectrum yields a 95% CL limit $-0.12 < \lambda_\gamma < 0.13$ with other couplings fixed to their Standard Model values.

[13] ABDALLAH 08C determine this triple gauge coupling from the measurement of the spin density matrix elements in $e^+e^- \to W^+W^- \to (qq)(\ell\nu)$, where $\ell = e$ or μ. Values of all other couplings are fixed to their standard model values.

[14] AALTONEN 07L set limits on anomalous TGCs using the $p_T(W)$ distribution in WW and WZ production with the W decaying to an electron or muon and the Z to 2 jets. Setting other couplings to their standard model value, the 95% C.L. limits are $-0.18 < \lambda_\gamma < 0.17$ for a form factor scale $\Lambda = 1.5$ TeV.

[15] ABAZOV 06H study $\overline{p}p \to WW$ production with a subsequent decay $WW \to e^+\nu_e e^-\overline{\nu}_e$, $WW \to e^\pm\nu_e\mu^\mp\nu_\mu$ or $WW \to \mu^+\nu_\mu\mu^-\overline{\nu}_\mu$. The 95% C.L. limit for a form factor scale $\Lambda = 1$ TeV is $-0.97 < \lambda_\gamma < 1.04$, fixing $\kappa_\gamma = 1$. With the assumption that the $WW\gamma$ and WWZ couplings are equal the 95% C.L. one-dimensional limit ($\Lambda = 2$ TeV) is $-0.29 < \lambda < 0.30$.

[16] ABAZOV 05J perform a likelihood fit to the photon E_T spectrum of $W\gamma + X$ events, where the W decays to an electron or muon which is required to be well separated from the photon. For $\Lambda = 2.0$ TeV the 95% CL limits are $-0.20 < \lambda_\gamma < 0.20$. In the fit κ_γ is kept fixed to its Standard Model value.

[17] ABREU 01I combine results from e^+e^- interactions at 189 GeV leading to W^+W^-, $We\nu_e$, and $\nu\overline{\nu}\gamma$ final states with results from ABREU 99L at 183 GeV. The 95% confidence interval is $-0.11 < \lambda_\gamma < 0.23$.

[18] BREITWEG 00 search for W production in events with large hadronic p_T. For $p_T > 20$ GeV, the upper limit on the cross section gives the 95%CL limit $-3.2 < \lambda_\gamma < 3.2$ for κ_γ fixed to its Standard Model value.

[19] ABBOTT 99I perform a simultaneous fit to the $W\gamma$, $WW \to$ dilepton, $WW/WZ \to e\nu jj$, $WW/WZ \to \mu\nu jj$, and $WZ \to$ trilepton data samples. For $\Lambda = 2.0$ TeV, the 95%CL limits are $-0.18 < \lambda_\gamma < 0.19$.

κ_Z

This coupling is CP-conserving (C- and P- separately conserving).

VALUE	EVTS	DOCUMENT ID		TECN	COMMENT
$0.924^{+0.059}_{-0.056} \pm 0.024$	7171	[1] ACHARD	04D	L3	$E_{cm}^{ee} = 189$–209 GeV
• • • We do not use the following data for averages, fits, limits, etc. • • •					
		[2] AAD	13AL	ATLS	$E_{cm}^{pp} = 7$ TeV
		[3] AAD	12CD	ATLS	$E_{cm}^{pp} = 7$ TeV
		[4] AALTONEN	12AC	CDF	$E_{cm}^{p\overline{p}} = 1.96$ TeV
	34	[5] ABAZOV	11	D0	$E_{cm}^{p\overline{p}} = 1.96$ TeV
	17	[6] ABAZOV	06H	D0	$E_{cm}^{p\overline{p}} = 1.96$ TeV
	2.3	[7] ABAZOV	05S	D0	$E_{cm}^{p\overline{p}} = 1.96$ TeV

[1] ACHARD 04D study WW–pair production, single–W production and single–photon production with missing energy from 189 to 209 GeV. The result quoted here is obtained using the WW–pair production sample. Each parameter is determined from a single–parameter fit in which the other parameters assume their Standard Model values.

[2] AAD 13AL study WW production in pp collisions and select 1325 WW candidates in decay modes with electrons or muons with an expected background of 369 ± 61 events. Assuming the LEP formulation and setting the form-factor Λ = infinity, a fit to the transverse momentum distribution of the leading charged lepton, leads to a 95% C.L. range of $0.957 < \kappa_Z < 1.043$. Supersedes AAD 12AC.

[3] AAD 12CD study WZ production in pp collisions and select 317 WZ candidates in three $\ell\nu$ decay modes with an expected background of 68.0 ± 10.0 events. The resulting 95% C.L. range is: $0.63 < \kappa_Z < 1.57$. Supersedes AAD 12V.

[4] AALTONEN 12AC study WZ production in $p\overline{p}$ collisions and select 63 WZ candidates in three $\ell\nu$ decay modes with an expected background of 7.9 ± 1.0 events. Based on the cross section and shape of the Z transverse momentum spectrum, the following 95% C.L. range is reported: $0.61 < \kappa_Z < 1.90$ for a form factor of Λ = 2 TeV.

[5] ABAZOV 11 study the $p\overline{p} \rightarrow 3\ell\nu$ process arising in WZ production. They observe 34 WZ candidates with an estimated background of 6 events. An analysis of the p_T spectrum of the Z boson leads to a 95% C.L. limit of $0.600 < \kappa_Z < 1.675$, for a form factor Λ = 2 TeV.

[6] ABAZOV 06H study $\overline{p}p \rightarrow WW$ production with a subsequent decay $WW \rightarrow e^+\nu_e e^-\overline{\nu}_e$, $WW \rightarrow e^\pm\nu_e\mu^\mp\nu_\mu$ or $WW \rightarrow \mu^+\nu_\mu\mu^-\overline{\nu}_\mu$. The 95% C.L. limit for a form factor scale Λ = 2 TeV is $0.55 < \kappa_Z < 1.55$, fixing λ_Z=0. With the assumption that the $WW\gamma$ and WWZ couplings are equal the 95% C.L. one-dimensional limit (Λ = 2 TeV) is $0.68 < \kappa < 1.45$.

[7] ABAZOV 05S study $\overline{p}p \rightarrow WZ$ production with a subsequent trilepton decay to $\ell\nu\ell'\overline{\ell}'$ (ℓ and ℓ' = e or μ). Three events (estimated background 0.71 ± 0.08 events) with WZ decay characteristics are observed from which they derive limits on the anomalous WWZ couplings. The 95% CL limit for a form factor scale Λ = 1 TeV is $-1.0 < \kappa_Z < 3.4$, fixing λ_Z and g_1^Z to their Standard Model values.

λ_Z

This coupling is *CP*-conserving (*C*- and *P*- separately conserving).

VALUE	EVTS	DOCUMENT ID		TECN	COMMENT
$-0.088^{+0.060}_{-0.057} \pm 0.023$	7171	[1] ACHARD	04D	L3	E_{cm}^{ee} = 189–209 GeV
• • • We do not use the following data for averages, fits, limits, etc. • • •					
		[2] AAD	13AL	ATLS	E_{cm}^{pp} = 7 TeV
		[3] CHATRCHYAN	13BF	CMS	E_{cm}^{pp} = 7 TeV
		[4] AAD	12CD	ATLS	E_{cm}^{pp} = 7 TeV
		[5] AALTONEN	12AC	CDF	$E_{cm}^{p\overline{p}}$ = 1.96 TeV
34		[6] ABAZOV	11	D0	$E_{cm}^{p\overline{p}}$ = 1.96 TeV
334		[7] AALTONEN	10K	CDF	$E_{cm}^{p\overline{p}}$ = 1.96 TeV
13		[8] ABAZOV	07Z	D0	$E_{cm}^{p\overline{p}}$ = 1.96 TeV
17		[9] ABAZOV	06H	D0	$E_{cm}^{p\overline{p}}$ = 1.96 TeV
2.3		[10] ABAZOV	05S	D0	$E_{cm}^{p\overline{p}}$ = 1.96 TeV

[1] ACHARD 04D study WW–pair production, single–W production and single–photon production with missing energy from 189 to 209 GeV. The result quoted here is obtained using the WW–pair production sample. Each parameter is determined from a single–parameter fit in which the other parameters assume their Standard Model values.

[2] AAD 13AL study WW production in pp collisions and select 1325 WW candidates in decay modes with electrons or muons with an expected background of 369 ± 61 events. Assuming the LEP formulation and setting the form-factor Λ = infinity, a fit to the transverse momentum distribution of the leading charged lepton, leads to a 95% C.L. range of $-0.062 < \lambda_Z < 0.059$. Supersedes AAD 12AC.

[3] CHATRCHYAN 13BF determine the W^+W^- production cross section using unlike sign di-lepton (e or μ) events with high $\not{p}_T$. The leptons have $p_T > 20$ GeV/c and are isolated. 1134 candidate events are observed with an expected SM background of 247 ± 34. The p_T distribution of the leading lepton is fitted to obtain 95% C.L. limits of $-0.048 \leq \lambda_Z \leq 0.048$.

[4] AAD 12CD study WZ production in pp collisions and select 317 WZ candidates in three $\ell\nu$ decay modes with an expected background of 68.0 ± 10.0 events. The resulting 95% C.L. range is: $-0.046 < \lambda_Z < 0.047$. Supersedes AAD 12V.

[5] AALTONEN 12AC study WZ production in $p\overline{p}$ collisions and select 63 WZ candidates in three $\ell\nu$ decay modes with an expected background of 7.9 ± 1.0 events. Based on the cross section and shape of the Z transverse momentum spectrum, the following 95% C.L. range is reported: $-0.08 < \lambda_Z < 0.10$ for a form factor of Λ = 2 TeV.

[6] ABAZOV 11 study the $p\overline{p} \rightarrow 3\ell\nu$ process arising in WZ production. They observe 34 WZ candidates with an estimated background of 6 events. An analysis of the p_T spectrum of the Z boson leads to a 95% C.L. limit of $-0.077 < \lambda_Z < 0.093$, for a form factor Λ = 2 TeV.

[7] AALTONEN 10K study $p\overline{p} \rightarrow W^+W^-$ with $W \rightarrow e/\mu\nu$. The p_T of the leading (second) lepton is required to be > 20 (10) GeV. The final number of events selected is 654 of which 320 ± 47 are estimated to be background. The 95% C.L. interval is $-0.16 < \lambda_Z < 0.16$ for Λ = 1.5 TeV and $-0.14 < \lambda_Z < 0.15$ for Λ = 2 TeV.

[8] ABAZOV 07Z set limits on anomalous TGCs using the measured cross section and $p_T(Z)$ distribution in WZ production with both the W and the Z decaying leptonically into electrons and muons. Setting the other couplings to their standard model values, the 95% C.L. limit for a form factor scale Λ = 2 TeV is $-0.17 < \lambda_Z < 0.21$.

[9] ABAZOV 06H study $\overline{p}p \rightarrow WW$ production with a subsequent decay $WW \rightarrow e^+\nu_e e^-\overline{\nu}_e$, $WW \rightarrow e^\pm\nu_e\mu^\mp\nu_\mu$ or $WW \rightarrow \mu^+\nu_\mu\mu^-\overline{\nu}_\mu$. The 95% C.L. limit for a form factor scale Λ = 2 TeV is $-0.39 < \lambda_Z < 0.39$, fixing κ_Z=1. With the assumption that the $WW\gamma$ and WWZ couplings are equal the 95% C.L. one-dimensional limit (Λ = 2 TeV) is $-0.29 < \lambda < 0.30$.

[10] ABAZOV 05S study $\overline{p}p \rightarrow WZ$ production with a subsequent trilepton decay to $\ell\nu\ell'\overline{\ell}'$ (ℓ and ℓ' = e or μ). Three events (estimated background 0.71 ± 0.08 events) with WZ decay characteristics are observed from which they derive limits on the anomalous WWZ couplings. The 95% CL limit for a form factor scale Λ = 1.5 TeV is $-0.48 < \lambda_Z < 0.48$, fixing g_1^Z and κ_Z to their Standard Model values.

g_5^Z

This coupling is *CP*-conserving but *C*- and *P*-violating.

VALUE	EVTS	DOCUMENT ID		TECN	COMMENT
−0.07 ± 0.09 OUR AVERAGE		Error includes scale factor of 1.1.			
$-0.04^{+0.13}_{-0.12}$	9800	[1] ABBIENDI	04D	OPAL	E_{cm}^{ee} = 183–209 GeV
$0.00 \pm 0.13 \pm 0.05$	7171	[2] ACHARD	04D	L3	E_{cm}^{ee} = 189–209 GeV
$-0.44^{+0.23}_{-0.22} \pm 0.12$	1154	[3] ACCIARRI	99Q	L3	E_{cm}^{ee} = 161+172+ 183 GeV
• • • We do not use the following data for averages, fits, limits, etc. • • •					
-0.31 ± 0.23		[4] EBOLI	00	THEO	LEP1, SLC+ Tevatron

[1] ABBIENDI 04D combine results from W^+W^- in all decay channels. Only *CP*-conserving couplings are considered and each parameter is determined from a single-parameter fit in which the other parameters assume their Standard Model values. The 95% confidence interval is $-0.28 < g_5^Z < +0.21$.

[2] ACHARD 04D study WW–pair production, single–W production and single–photon production with missing energy from 189 to 209 GeV. The result quoted here is obtained using the WW–pair production sample. Each parameter is determined from a single–parameter fit in which the other parameters assume their Standard Model values.

[3] ACCIARRI 99Q study W-pair, single-W, and single photon events.

[4] EBOLI 00 extract this indirect value of the coupling studying the non-universal one-loop contributions to the experimental value of the $Z \rightarrow b\overline{b}$ width (Λ=1 TeV is assumed).

g_4^Z

This coupling is *CP*-violating (*C*-violating and *P*-conserving).

VALUE	EVTS	DOCUMENT ID		TECN	COMMENT
−0.30 ± 0.17 OUR AVERAGE					
$-0.39^{+0.19}_{-0.20}$	1880	[1] ABDALLAH	08C	DLPH	E_{cm}^{ee} = 189–209 GeV
$-0.02^{+0.32}_{-0.33}$	1065	[2] ABBIENDI	01H	OPAL	E_{cm}^{ee} = 189 GeV

[1] ABDALLAH 08C determine this triple gauge coupling from the measurement of the spin density matrix elements in $e^+e^- \rightarrow W^+W^- \rightarrow (qq)(\ell\nu)$, where ℓ = e or μ. Values of all other couplings are fixed to their standard model values.

[2] ABBIENDI 01H study W-pair events, with one leptonically and one hadronically decaying W. The coupling is extracted using information from the W production angle together with decay angles from the leptonically decaying W.

$\tilde{\kappa}_Z$

This coupling is *CP*-violating (*C*-conserving and *P*-violating).

VALUE	EVTS	DOCUMENT ID		TECN	COMMENT
$\mathbf{-0.12^{+0.06}_{-0.04}}$ **OUR AVERAGE**					
$-0.09^{+0.08}_{-0.05}$	1880	[1] ABDALLAH	08C	DLPH	E_{cm}^{ee} = 189–209 GeV
$-0.20^{+0.10}_{-0.07}$	1065	[2] ABBIENDI	01H	OPAL	E_{cm}^{ee} = 189 GeV
• • • We do not use the following data for averages, fits, limits, etc. • • •					
		[3] BLINOV	11	LEP	E_{cm}^{ee} = 183–207 GeV

[1] ABDALLAH 08C determine this triple gauge coupling from the measurement of the spin density matrix elements in $e^+e^- \rightarrow W^+W^- \rightarrow (qq)(\ell\nu)$, where ℓ = e or μ. Values of all other couplings are fixed to their standard model values.

[2] ABBIENDI 01H study W-pair events, with one leptonically and one hadronically decaying W. The coupling is extracted using information from the W production angle together with decay angles from the leptonically decaying W.

[3] BLINOV 11 use the LEP-average $e^+e^- \rightarrow W^+W^-$ cross section data for $\sqrt{s}$ = 183–207 GeV to determine an upper limit on the TGC $\tilde{\kappa}_Z$. The average values of the cross sections as well as their correlation matrix, and standard model expectations of the cross sections are taken from the LEPEWWG note hep-ex/0612034. At 95% confidence level $|\tilde{\kappa}_Z| < 0.13$.

$\tilde{\lambda}_Z$

This coupling is *CP*-violating (*C*-conserving and *P*-violating).

VALUE	EVTS	DOCUMENT ID		TECN	COMMENT
−0.09 ± 0.07 OUR AVERAGE					
-0.08 ± 0.07	1880	[1] ABDALLAH	08C	DLPH	E_{cm}^{ee} = 189–209 GeV
$-0.18^{+0.24}_{-0.16}$	1065	[2] ABBIENDI	01H	OPAL	E_{cm}^{ee} = 189 GeV
• • • We do not use the following data for averages, fits, limits, etc. • • •					
		[3] BLINOV	11	LEP	E_{cm}^{ee} = 183–207 GeV

[1] ABDALLAH 08C determine this triple gauge coupling from the measurement of the spin density matrix elements in $e^+e^- \rightarrow W^+W^- \rightarrow (qq)(\ell\nu)$, where ℓ = e or μ. Values of all other couplings are fixed to their standard model values.

[2] ABBIENDI 01H study W-pair events, with one leptonically and one hadronically decaying W. The coupling is extracted using information from the W production angle together with decay angles from the leptonically decaying W.

[3] BLINOV 11 use the LEP-average $e^+e^- \rightarrow W^+W^-$ cross section data for $\sqrt{s}$ = 183–207 GeV to determine an upper limit on the TGC $\tilde{\lambda}_Z$. The average values of the cross sections as well as their correlation matrix, and standard model expectations of the cross sections are taken from the LEPEWWG note hep-ex/0612034. At 95% confidence level $|\tilde{\lambda}_Z| < 0.31$.

W ANOMALOUS MAGNETIC MOMENT

The full magnetic moment is given by $\mu_W = e(1+\kappa+\lambda)/2m_W$. In the Standard Model, at tree level, $\kappa = 1$ and $\lambda = 0$. Some papers have defined $\Delta\kappa = 1-\kappa$ and assume that $\lambda = 0$. Note that the electric quadrupole moment is given by $-e(\kappa-\lambda)/m_W^2$. A description of the parameterization of these moments and additional references can be found in HAGIWARA 87 and BAUR 88. The parameter Λ appearing in the theoretical limits below

is a regularization cutoff which roughly corresponds to the energy scale where the structure of the W boson becomes manifest.

VALUE ($e/2m_W$)	*EVTS*	*DOCUMENT ID*		*TECN*	*COMMENT*
$2.22^{+0.20}_{-0.19}$	2298	[1] ABREU	01I	DLPH	$E_{\rm cm}^{ee}$= 183+189 GeV
• • • We do not use the following data for averages, fits, limits, etc. • • •					
		[2] ABE	95G	CDF	
		[3] ALITTI	92C	UA2	
		[4] SAMUEL	92	THEO	
		[5] SAMUEL	91	THEO	
		[6] GRIFOLS	88	THEO	
		[7] GROTCH	87	THEO	
		[8] VANDERBIJ	87	THEO	
		[9] GRAU	85	THEO	
		[10] SUZUKI	85	THEO	
		[11] HERZOG	84	THEO	

[1] ABREU 01I combine results from e^+e^- interactions at 189 GeV leading to W^+W^-, $We\nu_e$, and $\nu\overline{\nu}\gamma$ final states with results from ABREU 99L at 183 GeV to determine Δg_1^Z, $\Delta\kappa_\gamma$, and λ_γ. $\Delta\kappa_\gamma$ and λ_γ are simultaneously floated in the fit to determine μ_W.

[2] ABE 95G report $-1.3 < \kappa < 3.2$ for λ=0 and $-0.7 < \lambda < 0.7$ for κ=1 in $p\overline{p} \to e\nu_e\gamma$X and $\mu\nu_\mu\gamma$X at $\sqrt{s} = 1.8$ TeV.

[3] ALITTI 92C measure $\kappa = 1^{+2.6}_{-2.2}$ and $\lambda = 0^{+1.7}_{-1.8}$ in $p\overline{p} \to e\nu\gamma+$ X at $\sqrt{s} = 630$ GeV. At 95%CL they report $-3.5 < \kappa < 5.9$ and $-3.6 < \lambda < 3.5$.

[4] SAMUEL 92 use preliminary CDF and UA2 data and find $-2.4 < \kappa < 3.7$ at 96%CL and $-3.1 < \kappa < 4.2$ at 95%CL respectively. They use data for $W\gamma$ production and radiative W decay.

[5] SAMUEL 91 use preliminary CDF data for $p\overline{p} \to W\gamma$X to obtain $-11.3 \leq \Delta\kappa \leq 10.9$. Note that their $\kappa = 1-\Delta\kappa$.

[6] GRIFOLS 88 uses deviation from ρ parameter to set limit $\Delta\kappa \lesssim 65$ (M_W^2/Λ^2).

[7] GROTCH 87 finds the limit $-37 < \Delta\kappa < 73.5$ (90% CL) from the experimental limits on $e^+e^- \to \nu\overline{\nu}\gamma$ assuming three neutrino generations and $-19.5 < \Delta\kappa < 56$ for four generations. Note their $\Delta\kappa$ has the opposite sign as our definition.

[8] VANDERBIJ 87 uses existing limits to the photon structure to obtain $|\Delta\kappa| < 33$ (m_W/Λ). In addition VANDERBIJ 87 discusses problems with using the ρ parameter of the Standard Model to determine $\Delta\kappa$.

[9] GRAU 85 uses the muon anomaly to derive a coupled limit on the anomalous magnetic dipole and electric quadrupole (λ) moments $1.05 > \Delta\kappa \ln(\Lambda/m_W) + \lambda/2 > -2.77$. In the Standard Model $\lambda = 0$.

[10] SUZUKI 85 uses partial-wave unitarity at high energies to obtain $|\Delta\kappa| \lesssim 190\ (m_W/\Lambda)^2$. From the anomalous magnetic moment of the muon, SUZUKI 85 obtains $|\Delta\kappa| \lesssim 2.2/\ln(\Lambda/m_W)$. Finally SUZUKI 85 uses deviations from the ρ parameter and obtains a very qualitative, order-of-magnitude limit $|\Delta\kappa| \lesssim 150\ (m_W/\Lambda)^4$ if $|\Delta\kappa| \ll 1$.

[11] HERZOG 84 consider the contribution of W-boson to muon magnetic moment including anomalous coupling of $WW\gamma$. Obtain a limit $-1 < \Delta\kappa < 3$ for $\Lambda \gtrsim 1$ TeV.

ANOMALOUS *W/Z* QUARTIC COUPLINGS

Revised September 2013 by M.W. Grünewald (U. College Dublin and U. Ghent) and A. Gurtu (Formerly Tata Inst.).

The Standard Model quartic couplings, $WWWW$, $WWZZ$, $WWZ\gamma$, $WW\gamma\gamma$, and $ZZ\gamma\gamma$, lead to negligible effects at LEP energies, while they are important at a TeV Linear Collider. Outside the Standard Model framework, possible quartic couplings, a_0, a_c, a_n, are expressed in terms of the following dimension-6 operators [1,2];

$$L_6^0 = -\frac{e^2}{16\Lambda^2}\, a_0\, F^{\mu\nu}\, F_{\mu\nu}\vec{W}^\alpha \cdot \vec{W}_\alpha$$
$$L_6^c = -\frac{e^2}{16\Lambda^2}\, a_c\, F^{\mu\alpha}\, F_{\mu\beta}\vec{W}^\beta \cdot \vec{W}_\alpha$$
$$L_6^n = -i\frac{e^2}{16\Lambda^2}\, a_n \epsilon_{ijk}\, W_{\mu\alpha}^{(i)}\, W_\nu^{(j)}\, W^{(k)\alpha} F^{\mu\nu}$$
$$\widetilde{L}_6^0 = -\frac{e^2}{16\Lambda^2}\, \widetilde{a}_0\, F^{\mu\nu}\, \widetilde{F}_{\mu\nu}\vec{W}^\alpha \cdot \vec{W}_\alpha$$
$$\widetilde{L}_6^n = -i\frac{e^2}{16\Lambda^2}\, \widetilde{a}_n \epsilon_{ijk}\, W_{\mu\alpha}^{(i)}\, W_\nu^{(j)}\, W^{(k)\alpha} \widetilde{F}^{\mu\nu}$$

where F, W are photon and W fields, L_6^0 and L_6^c conserve C, P separately ($\widetilde{L}_6^0$ conserves only C) and generate anomalous $W^+W^-\gamma\gamma$ and $ZZ\gamma\gamma$ couplings, L_6^n violates CP ($\widetilde{L}_6^n$ violates both C and P) and generates an anomalous $W^+W^-Z\gamma$ coupling, and Λ is an energy scale for new physics. For the $ZZ\gamma\gamma$ coupling the CP-violating term represented by L_6^n does not contribute. These couplings are assumed to be real and to vanish at tree level in the Standard Model.

Within the same framework as above, a more recent description of the quartic couplings [3] treats the anomalous parts of the $WW\gamma\gamma$ and $ZZ\gamma\gamma$ couplings separately, leading to two sets parameterized as a_0^V/Λ^2 and a_c^V/Λ^2, where $V = W$ or Z.

At LEP the processes studied in search of these quartic couplings are $e^+e^- \to WW\gamma$, $e^+e^- \to \gamma\gamma\nu\overline{\nu}$, and $e^+e^- \to Z\gamma\gamma$ and limits are set on the quantities $a_0^W/\Lambda^2, a_c^W/\Lambda^2, a_n/\Lambda^2$. The characteristics of the first process depend on all the three couplings whereas those of the latter two depend only on the two CP-conserving couplings. The sensitive measured variables are the cross sections for these processes as well as the energy and angular distributions of the photon and recoil mass to the photon pair. At hadron colliders, tri-boson production $VV\gamma$ as well as di-boson scattering $\gamma\gamma \to VV$ is analysed to set limits on anomalous QGCs.

References

1. G. Belanger and F. Boudjema, Phys. Lett. **B288**, 201 (1992).
2. J.W. Stirling and A. Werthenbach, Eur. Phys. J. **C14**, 103 (2000);
   J.W. Stirling and A. Werthenbach, Phys. Lett. **B466**, 369 (1999);
   A. Denner *et al.*, Eur. Phys. J. **C20**, 201 (2001);
   G. Montagna *et al.*, Phys. Lett. **B515**, 197 (2001).
3. G. Belanger *et al.*, Eur. Phys. J. **C13**, 283 (2000).

a_0/Λ^2, a_c/Λ^2, a_n/Λ^2

Using the $WW\gamma$ final state, the LEP combined 95% CL limits on the anomalous contributions to the $WW\gamma\gamma$ and $WWZ\gamma$ vertices (as of summer 2003) are given below:

(See P. Wells, "Experimental Tests of the Standard Model," Int. Europhysics Conference on High-Energy Physics, Aachen, Germany, 17–23 July 2003)

$$-0.02 < a_0^W/\Lambda^2 < 0.02\ \text{GeV}^{-2},$$
$$-0.05 < a_c^W/\Lambda^2 < 0.03\ \text{GeV}^{-2},$$
$$-0.15 < a_n/\Lambda^2 < 0.15\ \text{GeV}^{-2}.$$

VALUE	*DOCUMENT ID*		*TECN*
• • • We do not use the following data for averages, fits, limits, etc. • • •			
	[1] ABAZOV	13D	D0
	[2] CHATRCHYAN	13AA	CMS
	[3] ABBIENDI	04B	OPAL
	[4] ABBIENDI	04L	OPAL
	[5] HEISTER	04A	ALEP
	[6] ABDALLAH	03I	DLPH
	[7] ACHARD	02F	L3

[1] ABAZOV 13D searches for anomalous $WW\gamma\gamma$ quartic gauge couplings in the two-photon-mediated process $pp \to ppWW$, assuming the $WW\gamma$ triple gauge boson couplings to be at their Standard Model values. 946 events containing an e^+e^- pair with missing energy are selected in a total luminosity of 9.7 fb^{-1}, with an expectation of 983 ± 108 events from Standard-Model processes. The following 1-parameter limits at 95% CL are otained: $|a_0^W/\Lambda^2| < 4.3\times10^{-4}$ GeV^{-2} ($a_c^W = 0$), $|a_c^W/\Lambda^2| < 1.5\times10^{-3}$ GeV^{-2} ($a_0^W = 0$).

[2] CHATRCHYAN 13AA searches for anomalous $WW\gamma\gamma$ quartic gauge couplings in the two-photon-mediated process $pp \to ppWW$, assuming the $WW\gamma$ triple gauge boson couplings to be at their Standard Model values. 2 events containing an $e^\pm\mu^\mp$ pair with $p_T(e,\mu) > 30$ GeV are selected in a total luminosity of 5.05 fb^{-1}, with an expected $ppWW$ signal of 2.2 ± 0.4 events and an expected background of 0.84 ± 0.15 events. The following 1-parameter limits at 95% CL are otained from the $p_T(e,\mu)$ spectrum: $|a_0^W/\Lambda^2| < 4.0\times10^{-6}$ GeV^{-2} ($a_c^W = 0$), $|a_c^W/\Lambda^2| < 1.5\times10^{-5}$ GeV^{-2} ($a_0^W = 0$).

[3] ABBIENDI 04B select 187 $e^+e^- \to W^+W^-\gamma$ events in the C.M. energy range 180–209 GeV, where E_γ >2.5 GeV, the photon has a polar angle $|\cos\theta_\gamma| < 0.975$ and is well isolated from the nearest jet and charged lepton, and the effective masses of both fermion-antifermion systems agree with the W mass within 3 Γ_W. The measured differential cross section as a function of the photon energy and photon polar angle is used to extract the 95% CL limits: -0.020 GeV^{-2} $<a_0/\Lambda^2 < 0.020$ GeV^{-2}, -0.053 GeV^{-2} $<a_c/\Lambda^2 < 0.037$ GeV^{-2} and -0.16 GeV^{-2} $<a_n/\Lambda^2 < 0.15$ GeV^{-2}.

[4] ABBIENDI 04L select 20 $e^+e^- \to \nu\overline{\nu}\gamma\gamma$ acoplanar events in the energy range 180–209 GeV and 176 $e^+e^- \to q\overline{q}\gamma\gamma$ events in the energy range 130–209 GeV. These samples are used to constrain possible anomalous $W^+W^-\gamma\gamma$ and $ZZ\gamma\gamma$ quartic couplings.

Further combining with the $W^+W^-\gamma$ sample of ABBIENDI 04B the following one–parameter 95% CL limits are obtained: $-0.007 < a_0^Z/\Lambda^2 < 0.023$ GeV^{-2}, $-0.029 < a_c^Z/\Lambda^2 < 0.029$ GeV^{-2}, $-0.020 < a_0^W/\Lambda^2 < 0.020$ GeV^{-2}, $-0.052 < a_c^W/\Lambda^2 < 0.037$ GeV^{-2}.

[5] In the CM energy range 183 to 209 GeV HEISTER 04A select 30 $e^+e^- \to \nu\overline{\nu}\gamma\gamma$ events with two acoplanar, high energy and high transverse momentum photons. The photon–photon acoplanarity is required to be $> 5^\circ$, $E_\gamma/\sqrt{s} > 0.025$ (the more energetic photon having energy $> 0.2\sqrt{s}$), $p_{T_\gamma}/E_{\rm beam} > 0.05$ and $|\cos\theta_\gamma| < 0.94$. A likelihood fit to the photon energy and recoil missing mass yields the following one–parameter 95% CL limits: $-0.012 < a_0^Z/\Lambda^2 < 0.019$ GeV^{-2}, $-0.041 < a_c^Z/\Lambda^2 < 0.044$ GeV^{-2}, $-0.060 < a_0^W/\Lambda^2 < 0.055$ GeV^{-2}, $-0.099 < a_c^W/\Lambda^2 < 0.093$ GeV^{-2}.

[6] ABDALLAH 03I select 122 $e^+e^- \to W^+W^-\gamma$ events in the C.M. energy range 189–209 GeV, where $E_\gamma > 5$ GeV, the photon has a polar angle $|\cos\theta_\gamma| < 0.95$ and is well isolated from the nearest charged fermion. A fit to the photon energy spectra yields $a_c/\Lambda^2 = 0.000^{+0.019}_{-0.040}$ GeV^{-2}, $a_0/\Lambda^2 = -0.004^{+0.018}_{-0.010}$ GeV^{-2}, $\tilde{a}_0/\Lambda^2 = -0.007^{+0.019}_{-0.008}$ GeV^{-2}, $a_n/\Lambda^2 = -0.09^{+0.16}_{-0.05}$ GeV^{-2}, and $\tilde{a}_n/\Lambda^2 = +0.05^{+0.07}_{-0.15}$ GeV^{-2}, keeping the other parameters fixed to their Standard Model values (0). The 95% CL limits are: -0.063 GeV$^{-2} < a_c/\Lambda^2 < +0.032$ GeV^{-2}, -0.020 GeV$^{-2} < a_0/\Lambda^2 < +0.020$ GeV^{-2}, -0.020 GeV$^{-2} < \tilde{a}_0/\Lambda^2 < +0.020$ GeV^{-2}, -0.18 GeV$^{-2} < a_n/\Lambda^2 < +0.14$ GeV^{-2}, -0.16 GeV$^{-2} < \tilde{a}_n/\Lambda^2 < +0.17$ GeV^{-2}.

[7] ACHARD 02F select 86 $e^+e^- \to W^+W^-\gamma$ events at 192–207 GeV, where $E_\gamma > 5$ GeV and the photon is well isolated. They also select 43 acoplanar $e^+e^- \to \nu\overline{\nu}\gamma\gamma$ events in this energy range, where the photon energies are >5 GeV and >1 GeV and the photon polar angles are between 14° and 166°. All these 43 events are in the recoil mass region corresponding to the Z (75–110 GeV). Using the shape and normalization of the photon spectra in the $W^+W^-\gamma$ events, and combining with the 42 event sample from 189 GeV data (ACCIARRI 00T), they obtain: $a_0/\Lambda^2 = 0.000 \pm 0.010$ GeV^{-2}, $a_c/\Lambda^2 = -0.013 \pm 0.023$ GeV^{-2}, and $a_n/\Lambda^2 = -0.002 \pm 0.076$ GeV^{-2}. Further combining the analyses of $W^+W^-\gamma$ events with the low recoil mass region of $\nu\overline{\nu}\gamma\gamma$ events (including samples collected at $183 + 189$ GeV), they obtain the following one-parameter 95% CL limits: -0.015 GeV$^{-2} < a_0/\Lambda^2 < 0.015$ GeV^{-2}, -0.048 GeV$^{-2} < a_c/\Lambda^2 < 0.026$ GeV^{-2}, and -0.14 GeV$^{-2} < a_n/\Lambda^2 < 0.13$ GeV^{-2}.

W REFERENCES

AAD 13AL PR D87 112001 G. Aad *et al.* (ATLAS Collab.)
Also PR D88 079906 (errat.) G. Aad *et al.* (ATLAS Collab.)
AAD 13AN PR D87 112003 G. Aad *et al.* (ATLAS Collab.)
AALTONEN 13N PR D88 052018 T. Aaltonen *et al.* (CDF Collab.)
ABAZOV 13D PR D88 012005 V.M. Abazov *et al.* (D0 Collab.)
CHATRCHYAN 13AA JHEP 1307 116 S. Chatrchyan *et al.* (CMS Collab.)
CHATRCHYAN 13BF EPJ C73 2610 S. Chatrchyan *et al.* (CMS Collab.)
SCHAEL 13A PRPL 532 119 S. Schael *et al.* (ALEPH, DELPHI, L3, OPAL+)
AAD 12AC PL B712 289 G. Aad *et al.* (ATLAS Collab.)
AAD 12BX PL B717 49 G. Aad *et al.* (ATLAS Collab.)
AAD 12CD EPJ C72 2173 G. Aad *et al.* (ATLAS Collab.)
AAD 12V PL B709 341 G. Aad *et al.* (ATLAS Collab.)
AALTONEN 12AC PR D86 031104 T. Aaltonen *et al.* (CDF Collab.)
AALTONEN 12E PRL 108 151803 T. Aaltonen *et al.* (CDF Collab.)
ABAZOV 12AG PL B718 451 V.M. Abazov *et al.* (D0 Collab.)
ABAZOV 12F PRL 108 151804 V.M. Abazov *et al.* (D0 Collab.)
ABAZOV 11 PL B695 67 V.M. Abazov *et al.* (D0 Collab.)
ABAZOV 11AC PRL 107 241803 V.M. Abazov *et al.* (D0 Collab.)
BLINOV 11 PL B699 287 A.E. Blinov, A.S. Rudenko (NOVO)
CHATRCHYAN 11M PL B701 535 S. Chatrchyan *et al.* (CMS Collab.)
AALTONEN 10K PRL 104 201801 T. Aaltonen *et al.* (CDF Collab.)
Also PRL 105 019905(errat) T. Aaltonen *et al.* (CDF Collab.)
ABDALLAH 10 EPJ C66 35 J. Abdallah *et al.* (DELPHI Collab.)
AARON 09B EPJ C64 251 F.D. Aaron *et al.* (H1 Collab.)
ABAZOV 09AB PRL 103 141801 V.M. Abazov *et al.* (D0 Collab.)
ABAZOV 09AD PR D80 053012 V.M. Abazov *et al.* (D0 Collab.)
ABAZOV 09AJ PRL 103 191801 V.M. Abazov *et al.* (D0 Collab.)
ABAZOV 09AK PRL 103 231802 V.M. Abazov *et al.* (D0 Collab.)
AALTONEN 08B PRL 100 071801 T. Aaltonen *et al.* (CDF Collab.)
ABAZOV 08R PRL 100 241805 V.M. Abazov *et al.* (D0 Collab.)
ABDALLAH 08A EPJ C55 1 J. Abdallah *et al.* (DELPHI Collab.)
ABDALLAH 08C EPJ C54 345 J. Abdallah *et al.* (DELPHI Collab.)
AALTONEN 07F PRL 99 151801 T. Aaltonen *et al.* (CDF Collab.)
Also PR D77 112001 T. Aaltonen *et al.* (CDF Collab.)
AALTONEN 07L PR D76 111103 T. Aaltonen *et al.* (CDF Collab.)
ABAZOV 07Z PR D76 111104 V.M. Abazov *et al.* (D0 Collab.)
ABBIENDI 07A EPJ C52 767 G. Abbiendi *et al.* (OPAL Collab.)
ABAZOV 06H PR D74 057101 V.M. Abazov *et al.* (D0 Collab.)
Also PR D74 059904(errat) V.M. Abazov *et al.* (D0 Collab.)
ABBIENDI 06 EPJ C45 307 G. Abbiendi *et al.* (OPAL Collab.)
ABBIENDI 06A EPJ C45 291 G. Abbiendi *et al.* (OPAL Collab.)
ACHARD 06 EPJ C45 569 P. Achard *et al.* (L3 Collab.)
AKTAS 06 PL B632 35 A. Aktas *et al.* (H1 Collab.)
SCHAEL 06 EPJ C47 309 S. Schael *et al.* (ALEPH Collab.)
ABAZOV 05J PR D71 091108 V.M. Abazov *et al.* (D0 Collab.)
ABAZOV 05S PRL 95 141802 V.M. Abazov *et al.* (D0 Collab.)
SCHAEL 05A PL B614 7 S. Schael *et al.* (ALEPH Collab.)
ABAZOV 04D PR D70 092008 V.M. Abazov *et al.* (CDF, D0 Collab.)
ABBIENDI 04B PL B580 17 G. Abbiendi *et al.* (OPAL Collab.)
ABBIENDI 04D EPJ C33 463 G. Abbiendi *et al.* (OPAL Collab.)
ABBIENDI 04L PR D70 032005 G. Abbiendi *et al.* (OPAL Collab.)
ABDALLAH 04G EPJ C34 127 J. Abdallah *et al.* (DELPHI Collab.)
ACHARD 04D PL B586 151 P. Achard *et al.* (L3 Collab.)
ACHARD 04J PL B600 22 P. Achard *et al.* (L3 Collab.)
HEISTER 04A PL B602 31 A. Heister *et al.* (ALEPH Collab.)
SCHAEL 04A EPJ C38 147 S. Schael *et al.* (ALEPH Collab.)
ABBIENDI 03C EPJ C26 321 G. Abbiendi *et al.* (OPAL Collab.)
ABDALLAH 03I EPJ C31 139 J. Abdallah *et al.* (DELPHI Collab.)
ABAZOV 02D PR D66 012001 V.M. Abazov *et al.* (D0 Collab.)
ABAZOV 02E PR D66 032008 V.M. Abazov *et al.* (D0 Collab.)
ACHARD 02F PL B527 29 P. Achard *et al.* (L3 Collab.)
CHEKANOV 02C PL B539 197 S. Chekanov *et al.* (ZEUS Collab.)
ABBIENDI 01H EPJ C19 229 G. Abbiendi *et al.* (OPAL Collab.)
ABREU 01I PL B502 9 P. Abreu *et al.* (DELPHI Collab.)
AFFOLDER 01E PR D64 052001 T. Affolder *et al.* (CDF Collab.)
ABBIENDI 00V PL B490 71 G. Abbiendi *et al.* (OPAL Collab.)
ABBOTT 00B PR D61 072001 B. Abbott *et al.* (D0 Collab.)
ABBOTT 00D PRL 84 5710 B. Abbott *et al.* (D0 Collab.)
ABREU,P 00F EPJ C18 203 P. Abreu *et al.* (DELPHI Collab.)
Also EPJ C25 493 (errat) P. Abreu *et al.* (DELPHI Collab.)
ACCIARRI 00T PL B490 187 M. Acciarri *et al.* (L3 Collab.)
AFFOLDER 00M PRL 85 3347 T. Affolder *et al.* (CDF Collab.)
BREITWEG 00 PL B471 411 J. Breitweg *et al.* (ZEUS Collab.)
BREITWEG 00D EPJ C12 411 J. Breitweg *et al.* (ZEUS Collab.)
EBOLI 00 MPL A15 1 O. Eboli, M. Gonzalez-Garcia, S. Novaes
ABBIENDI 99N PL B453 153 G. Abbiendi *et al.* (OPAL Collab.)
ABBOTT 99H PR D60 052003 B. Abbott *et al.* (D0 Collab.)
ABBOTT 99I PR D60 072002 B. Abbott *et al.* (D0 Collab.)
ABREU 99L PL B459 382 P. Abreu *et al.* (DELPHI Collab.)
ACCIARRI 99 PL B454 386 M. Acciarri *et al.* (L3 Collab.)
ACCIARRI 99Q PL B467 171 M. Acciarri *et al.* (L3 Collab.)
BARATE 99I PL B453 107 R. Barate *et al.* (ALEPH Collab.)
BARATE 99L PL B462 389 R. Barate *et al.* (ALEPH Collab.)
BARATE 99M PL B465 349 R. Barate *et al.* (ALEPH Collab.)
ABBOTT 98N PR D58 092003 B. Abbott *et al.* (D0 Collab.)
ABBOTT 98P PR D58 012002 B. Abbott *et al.* (D0 Collab.)
ABE 98H PR D58 031101 F. Abe *et al.* (CDF Collab.)
ABE 98P PR D58 091101 F. Abe *et al.* (CDF Collab.)
ABREU 98C PL B416 233 P. Abreu *et al.* (DELPHI Collab.)
ABREU 98N PL B439 209 P. Abreu *et al.* (DELPHI Collab.)
BARATE 97 PL B401 347 R. Barate *et al.* (ALEPH Collab.)
BARATE 97S PL B415 435 R. Barate *et al.* (ALEPH Collab.)
ABACHI 95D PRL 75 1456 S. Abachi *et al.* (D0 Collab.)
ABE 95C PRL 74 341 F. Abe *et al.* (CDF Collab.)
ABE 95G PRL 74 1936 F. Abe *et al.* (CDF Collab.)
ABE 95P PRL 75 11 F. Abe *et al.* (CDF Collab.)
Also PR D52 4784 F. Abe *et al.* (CDF Collab.)
ABE 95W PR D52 2624 F. Abe *et al.* (CDF Collab.)
Also PRL 73 220 F. Abe *et al.* (CDF Collab.)
ABE 92E PRL 68 3398 F. Abe *et al.* (CDF Collab.)
ABE 92I PRL 69 28 F. Abe *et al.* (CDF Collab.)
ALITTI 92 PL B276 365 J. Alitti *et al.* (UA2 Collab.)
ALITTI 92B PL B276 354 J. Alitti *et al.* (UA2 Collab.)
ALITTI 92C PL B277 194 J. Alitti *et al.* (UA2 Collab.)
ALITTI 92D PL B277 203 J. Alitti *et al.* (UA2 Collab.)
ALITTI 92F PL B280 137 J. Alitti *et al.* (UA2 Collab.)
SAMUEL 92 PL B280 124 M.A. Samuel *et al.* (OKSU, CARL)
ABE 91C PR D44 29 F. Abe *et al.* (CDF Collab.)
ALBAJAR 91 PL B253 503 C. Albajar *et al.* (UA1 Collab.)
ALITTI 91C ZPHY C52 209 J. Alitti *et al.* (UA2 Collab.)
SAMUEL 91 PRL 67 9 M.A. Samuel *et al.* (OKSU, CARL)
Also PRL 67 2920 (erratum) M.A. Samuel *et al.*
ABE 90G PRL 65 2243 F. Abe *et al.* (CDF Collab.)
Also PR D43 2070 F. Abe *et al.* (CDF Collab.)
ALBAJAR 90 PL B241 283 C. Albajar *et al.* (UA1 Collab.)
ALITTI 90B PL B241 150 J. Alitti *et al.* (UA2 Collab.)
ABE 89I PRL 62 1005 F. Abe *et al.* (CDF Collab.)
ALBAJAR 89 ZPHY C44 15 C. Albajar *et al.* (UA1 Collab.)
BAUR 88 NP B308 127 U. Baur, D. Zeppenfeld (FSU, WISC)
GRIFOLS 88 IJMP A3 225 J.A. Grifols, S. Peris, J. Sola (BARC, DESY)
Also PL B197 437 J.A. Grifols, S. Peris, J. Sola (BARC, DESY)
ALBAJAR 87 PL B185 233 C. Albajar *et al.* (UA1 Collab.)
ANSARI 87 PL B186 440 R. Ansari *et al.* (UA2 Collab.)
GROTCH 87 PR D36 2153 H. Grotch, R.W. Robinett (PSU)
HAGIWARA 87 NP B282 253 K. Hagiwara *et al.* (KEK, UCLA, FSU)
VANDERBIJ 87 PR D35 1088 J.J. van der Bij (FNAL)
GRAU 85 PL 154B 283 A. Grau, J.A. Grifols (BARC)
SUZUKI 85 PL 153B 289 M. Suzuki (LBL)
ARNISON 84D PL 134B 469 G.T.J. Arnison *et al.* (UA1 Collab.)
HERZOG 84 PL 148B 355 F. Herzog (WISC)
Also PL 155B 468 (erratum) F. Herzog (WISC)
ARNISON 83 PL 122B 103 G.T.J. Arnison *et al.* (UA1 Collab.)
BANNER 83B PL 122B 476 M. Banner *et al.* (UA2 Collab.)

Z

$J = 1$

THE *Z* BOSON

Revised September 2013 by M.W. Grünewald (U. College Dublin and U. Ghent), and A. Gurtu (Formerly Tata Inst.).

Precision measurements at the Z-boson resonance using electron–positron colliding beams began in 1989 at the SLC and at LEP. During 1989–95, the four LEP experiments (ALEPH, DELPHI, L3, OPAL) made high-statistics studies of the production and decay properties of the Z. Although the SLD experiment at the SLC collected much lower statistics, it was able to match the precision of LEP experiments in determining the effective electroweak mixing angle $\sin^2\overline{\theta}_W$ and the rates of Z decay to b- and c-quarks, owing to availability of polarized electron beams, small beam size, and stable beam spot.

The Z-boson properties reported in this section may broadly be categorized as:

- The standard 'lineshape' parameters of the Z consisting of its mass, M_Z, its total width, Γ_Z, and its partial decay widths, Γ(hadrons), and $\Gamma(\ell\overline{\ell})$ where $\ell = e, \mu, \tau, \nu$;
- Z asymmetries in leptonic decays and extraction of Z couplings to charged and neutral leptons;
- The b- and c-quark-related partial widths and charge asymmetries which require special techniques;
- Determination of Z decay modes and the search for modes that violate known conservation laws;
- Average particle multiplicities in hadronic Z decay;
- Z anomalous couplings.

The effective vector and axial-vector coupling constants describing the Z-to-fermion coupling are also measured in $p\bar{p}$ and ep collisions at the Tevatron and at HERA. The corresponding cross-section formulae are given in Section 39 (Cross-section formulae for specific processes) and Section 16 (Structure Functions) in this *Review*. In this minireview, we concentrate on the measurements in e^+e^- collisions at LEP and SLC.

The standard 'lineshape' parameters of the Z are determined from an analysis of the production cross sections of these final states in e^+e^- collisions. The $Z \to \nu\overline{\nu}(\gamma)$ state is identified directly by detecting single photon production and indirectly by subtracting the visible partial widths from the total width. Inclusion in this analysis of the forward-backward asymmetry of charged leptons, $A_{FB}^{(0,\ell)}$, of the τ polarization, $P(\tau)$, and its forward-backward asymmetry, $P(\tau)^{fb}$, enables the separate determination of the effective vector ($\overline{g}_V$) and axial vector ($\overline{g}_A$) couplings of the Z to these leptons and the ratio ($\overline{g}_V/\overline{g}_A$), which is related to the effective electroweak mixing angle $\sin^2\overline{\theta}_W$ (see the "Electroweak Model and Constraints on New Physics" review).

Determination of the b- and c-quark-related partial widths and charge asymmetries involves tagging the b and c quarks for which various methods are employed: requiring the presence of a high momentum prompt lepton in the event with high transverse momentum with respect to the accompanying jet; impact parameter and lifetime tagging using precision vertex measurement with high-resolution detectors; application of neural-network techniques to classify events as b or non-b on a statistical basis using event–shape variables; and using the presence of a charmed meson (D/D^*) or a kaon as a tag.

Z-parameter determination

LEP was run at energy points on and around the Z mass (88–94 GeV) constituting an energy 'scan.' The shape of the cross-section variation around the Z peak can be described by a Breit-Wigner *ansatz* with an energy-dependent total width [1–3]. The **three** main properties of this distribution, viz., the **position** of the peak, the **width** of the distribution, and the **height** of the peak, determine respectively the values of M_Z, Γ_Z, and $\Gamma(e^+e^-) \times \Gamma(f\overline{f})$, where $\Gamma(e^+e^-)$ and $\Gamma(f\overline{f})$ are the electron and fermion partial widths of the Z. The quantitative determination of these parameters is done by writing analytic expressions for these cross sections in terms of the parameters, and fitting the calculated cross sections to the measured ones by varying these parameters, taking properly into account all the errors. Single-photon exchange (σ_γ^0) and γ-Z interference ($\sigma_{\gamma Z}^0$) are included, and the large ($\sim$25 %) initial-state radiation (ISR) effects are taken into account by convoluting the analytic expressions over a 'Radiator Function' [1–5] $H(s, s')$. Thus for the process $e^+e^- \to f\overline{f}$:

$$\sigma_f(s) = \int H(s, s')\ \sigma_f^0(s')\ ds' \tag{1}$$

$$\sigma_f^0(s) = \sigma_Z^0 + \sigma_\gamma^0 + \sigma_{\gamma Z}^0 \tag{2}$$

$$\sigma_Z^0 = \frac{12\pi}{M_Z^2}\ \frac{\Gamma(e^+e^-)\Gamma(f\overline{f})}{\Gamma_Z^2}\ \frac{s\ \Gamma_Z^2}{(s - M_Z^2)^2\ +\ s^2\Gamma_Z^2/M_Z^2} \tag{3}$$

$$\sigma_\gamma^0 = \frac{4\pi\alpha^2(s)}{3s}\ Q_f^2 N_c^f \tag{4}$$

$$\sigma_{\gamma Z}^0 = -\frac{2\sqrt{2}\alpha(s)}{3}\ (Q_f G_F N_c^f \mathcal{G}_V^e \mathcal{G}_V^f) \times \frac{(s - M_Z^2)M_Z^2}{(s - M_Z^2)^2 + s^2\Gamma_Z^2/M_Z^2} \tag{5}$$

where Q_f is the charge of the fermion, $N_c^f = 3$ for quarks and 1 for leptons, and $\mathcal{G}_V^f$ is the vector coupling of the Z to the fermion-antifermion pair $f\overline{f}$.

Since $\sigma_{\gamma Z}^0$ is expected to be much less than σ_Z^0, the LEP Collaborations have generally calculated the interference term in the framework of the Standard Model. This fixing of $\sigma_{\gamma Z}^0$ leads to a tighter constraint on M_Z, and consequently a smaller error on its fitted value. It is possible to relax this constraint and carry out the fit within the S-matrix framework, which is briefly described in the next section.

In the above framework, the QED radiative corrections have been explicitly taken into account by convoluting over the ISR and allowing the electromagnetic coupling constant to run [6]: $\alpha(s) = \alpha/(1 - \Delta\alpha)$. On the other hand, weak radiative corrections that depend upon the assumptions of the electroweak theory and on the values of $M_{\rm top}$ and $M_{\rm Higgs}$ are accounted for by **absorbing them into the couplings**, which are then called the *effective* couplings $\mathcal{G}_V$ and $\mathcal{G}_A$ (or alternatively the effective parameters of the $\star$ scheme of Kennedy and Lynn [7].)

$\mathcal{G}_V^f$ and $\mathcal{G}_A^f$ are complex numbers with small imaginary parts. As experimental data does not allow simultaneous extraction of both real and imaginary parts of the effective couplings, the convention $g_A^f = \mathrm{Re}(\mathcal{G}_A^f)$ and $g_V^f = \mathrm{Re}(\mathcal{G}_V^f)$ is used and the imaginary parts are added in the fitting code [4].

Defining

$$A_f = 2\frac{g_V^f \cdot g_A^f}{(g_V^f)^2 + (g_A^f)^2} \tag{6}$$

the lowest-order expressions for the various lepton-related asymmetries on the Z pole are [8–10] $A_{FB}^{(0,\ell)} = (3/4)A_e A_f$, $P(\tau) = -A_\tau$, $P(\tau)^{fb} = -(3/4)A_e$, $A_{LR} = A_e$. The full analysis takes into account the energy-dependence of the asymmetries. Experimentally A_{LR} is defined as $(\sigma_L - \sigma_R)/(\sigma_L + \sigma_R)$,

where $\sigma_{L(R)}$ are the $e^+e^- \to Z$ production cross sections with left- (right)-handed electrons.

The definition of the partial decay width of the Z to $f\overline{f}$ includes the effects of QED and QCD final-state corrections, as well as the contribution due to the imaginary parts of the couplings:

$$\Gamma(f\overline{f}) = \frac{G_F M_Z^3}{6\sqrt{2}\pi}\, N_c^f (\left|\mathcal{G}_A^f\right|^2 R_A^f + \left|\mathcal{G}_V^f\right|^2 R_V^f) + \Delta_{ew/\mathrm{QCD}} \quad (7)$$

where R_V^f and R_A^f are radiator factors to account for final state QED and QCD corrections, as well as effects due to nonzero fermion masses, and $\Delta_{ew/\mathrm{QCD}}$ represents the non-factorizable electroweak/QCD corrections.

S-matrix approach to the Z

While most experimental analyses of LEP/SLC data have followed the 'Breit-Wigner' approach, an alternative S-matrix-based analysis is also possible. The Z, like all unstable particles, is associated with a complex pole in the S matrix. The pole position is process-independent and gauge-invariant. The mass, $\overline{M}_Z$, and width, $\overline{\Gamma}_Z$, can be defined in terms of the pole in the energy plane via [11–14]

$$\overline{s} = \overline{M}_Z^2 - i\overline{M}_Z\overline{\Gamma}_Z \quad (8)$$

leading to the relations

$$\overline{M}_Z = M_Z/\sqrt{1+\Gamma_Z^2/M_Z^2} \approx M_Z - 34.1 \text{ MeV} \quad (9)$$

$$\overline{\Gamma}_Z = \Gamma_Z/\sqrt{1+\Gamma_Z^2/M_Z^2} \approx \Gamma_Z - 0.9 \text{ MeV} . \quad (10)$$

The LEP collaborations [15] have analyzed their data using the S–matrix approach as defined in Eq. (8), in addition to the conventional one. They observe a downward shift in the Z mass as expected.

Handling the large-angle e^+e^- final state

Unlike other $f\overline{f}$ decay final states of the Z, the e^+e^- final state has a contribution not only from the s-channel but also from the t-channel and s-t interference. The full amplitude is not amenable to fast calculation, which is essential if one has to carry out minimization fits within reasonable computer time. The usual procedure is to calculate the non-s channel part of the cross section separately using the Standard Model programs ALIBABA [16] or TOPAZ0 [17], with the measured value of M_{top}, and $M_{\mathrm{Higgs}} = 150$ GeV, and add it to the s-channel cross section calculated as for other channels. This leads to two additional sources of error in the analysis: firstly, the theoretical calculation in ALIBABA itself is known to be accurate to $\sim 0.5\%$, and secondly, there is uncertainty due to the error on M_{top} and the unknown value of M_{Higgs} (100–1000 GeV). These errors are propagated into the analysis by including them in the systematic error on the e^+e^- final state. As these errors are common to the four LEP experiments, this is taken into account when performing the LEP average.

Errors due to uncertainty in LEP energy determination [18–23]

The systematic errors related to the LEP energy measurement can be classified as:

- The absolute energy scale error;
- Energy-point-to-energy-point errors due to the non-linear response of the magnets to the exciting currents;
- Energy-point-to-energy-point errors due to possible higher-order effects in the relationship between the dipole field and beam energy;
- Energy reproducibility errors due to various unknown uncertainties in temperatures, tidal effects, corrector settings, RF status, *etc.*

Precise energy calibration was done outside normal data-taking using the resonant depolarization technique. Run-time energies were determined every 10 minutes by measuring the relevant machine parameters and using a model which takes into account all the known effects, including leakage currents produced by trains in the Geneva area and the tidal effects due to gravitational forces of the Sun and the Moon. The LEP Energy Working Group has provided a covariance matrix from the determination of LEP energies for the different running periods during 1993–1995 [18].

Choice of fit parameters

The LEP Collaborations have chosen the following primary set of parameters for fitting: M_Z, Γ_Z, $\sigma^0_{\mathrm{hadron}}$, $R(\mathrm{lepton})$, $A_{FB}^{(0,\ell)}$, where $R(\mathrm{lepton}) = \Gamma(\mathrm{hadrons})/\Gamma(\mathrm{lepton})$, $\sigma^0_{\mathrm{hadron}} = 12\pi\Gamma(e^+e^-)\Gamma(\mathrm{hadrons})/M_Z^2\Gamma_Z^2$. With a knowledge of these fitted parameters and their covariance matrix, any other parameter can be derived. The main advantage of these parameters is that they form a physics motivated set of parameters with much reduced correlations.

Thus, the most general fit carried out to cross section and asymmetry data determines the **nine parameters**: M_Z, Γ_Z, $\sigma^0_{\mathrm{hadron}}$, $R(e)$, $R(\mu)$, $R(\tau)$, $A_{FB}^{(0,e)}$, $A_{FB}^{(0,\mu)}$, $A_{FB}^{(0,\tau)}$. Assumption of lepton universality leads to a **five-parameter fit** determining M_Z, Γ_Z, $\sigma^0_{\mathrm{hadron}}$, $R(\mathrm{lepton})$, $A_{FB}^{(0,\ell)}$.

Combining results from LEP and SLC experiments

With a steady increase in statistics over the years and improved understanding of the common systematic errors between LEP experiments, the procedures for combining results have evolved continuously [24]. The Line Shape Sub-group of the LEP Electroweak Working Group investigated the effects of these common errors, and devised a combination procedure for the precise determination of the Z parameters from LEP experiments. Using these procedures, this note also gives the results after combining the final parameter sets from the four experiments, and these are the results quoted as the fit results in the Z listings below. Transformation of variables leads

to values of derived parameters like partial decay widths and branching ratios to hadrons and leptons. Finally, transforming the LEP combined nine parameter set to (M_Z, Γ_Z, $\sigma^\circ_{\rm hadron}$, g^f_A, g^f_V, $f = e, \mu, \tau$) using the average values of lepton asymmetry parameters (A_e, A_μ, A_τ) as constraints, leads to the best fitted values of the vector and axial-vector couplings (g_V, g_A) of the charged leptons to the Z.

Brief remarks on the handling of common errors and their magnitudes are given below. The identified common errors are those coming from

(a) LEP energy-calibration uncertainties, and

(b) the theoretical uncertainties in (i) the luminosity determination using small angle Bhabha scattering, (ii) estimating the non-s channel contribution to large angle Bhabha scattering, (iii) the calculation of QED radiative effects, and (iv) the parametrization of the cross section in terms of the parameter set used.

Common LEP energy errors

All the collaborations incorporate in their fit the full LEP energy error matrix as provided by the LEP energy group for their intersection region [18]. The effect of these errors is separated out from that of other errors by carrying out fits with energy errors scaled up and down by $\sim 10\%$ and redoing the fits. From the observed changes in the overall error matrix, the covariance matrix of the common energy errors is determined. Common LEP energy errors lead to uncertainties on M_Z, Γ_Z, and $\sigma^\circ_{\rm hadron}$ of 1.7, 1.2 MeV, and 0.011 nb, respectively.

Common luminosity errors

BHLUMI 4.04 [25] is used by all LEP collaborations for small-angle Bhabha scattering leading to a common uncertainty in their measured cross sections of 0.061% [26]. BHLUMI does not include a correction for production of light fermion pairs. OPAL explicitly corrects for this effect and reduces their luminosity uncertainty to 0.054%, which is taken fully correlated with the other experiments. The other three experiments among themselves have a common uncertainty of 0.061%.

Common non-s channel uncertainties

The same standard model programs ALIBABA [16] and TOPAZ0 [17] are used to calculate the non-s channel contribution to the large angle Bhabha scattering [27]. As this contribution is a function of the Z mass, which itself is a variable in the fit, it is parametrized as a function of M_Z by each collaboration to properly track this contribution as M_Z varies in the fit. The common errors on R_e and $A^{(0,e)}_{FB}$ are 0.024 and 0.0014 respectively, and are correlated between them.

Common theoretical uncertainties: QED

There are large initial-state photon and fermion pair radiation effects near the Z resonance, for which the best currently available evaluations include contributions up to $\mathcal{O}(\alpha^3)$. To estimate the remaining uncertainties, different schemes are incorporated in the standard model programs ZFITTER [5], TOPAZ0 [17], and MIZA [28]. Comparing the different options leads to error estimates of 0.3 and 0.2 MeV on M_Z and Γ_Z respectively, and of 0.02% on $\sigma^\circ_{\rm hadron}$.

Common theoretical uncertainties: parametrization of lineshape and asymmetries

To estimate uncertainties arising from ambiguities in the model-independent parametrization of the differential cross-section near the Z resonance, results from TOPAZ0 and ZFITTER were compared by using ZFITTER to fit the cross sections and asymmetries calculated using TOPAZ0. The resulting uncertainties on M_Z, Γ_Z, $\sigma^\circ_{\rm hadron}$, R(lepton), and $A^{(0,\ell)}_{FB}$ are 0.1 MeV, 0.1 MeV, 0.001 nb, 0.004, and 0.0001 respectively.

Thus, the overall theoretical errors on M_Z, Γ_Z, $\sigma^\circ_{\rm hadron}$ are 0.3 MeV, 0.2 MeV, and 0.008 nb respectively; on each R(lepton) is 0.004 and on each $A^{(0,\ell)}_{FB}$ is 0.0001. Within the set of three R(lepton)'s and the set of three $A^{(0,\ell)}_{FB}$'s, the respective errors are fully correlated.

All the theory-related errors mentioned above utilize Standard Model programs which need the Higgs mass and running electromagnetic coupling constant as inputs; uncertainties on these inputs will also lead to common errors. All LEP collaborations used the same set of inputs for Standard Model calculations: $M_Z = 91.187$ GeV, the Fermi constant $G_F = (1.16637 \pm 0.00001) \times 10^{-5}$ GeV^{-2} [29], $\alpha^{(5)}(M_Z) = 1/128.877 \pm 0.090$ [30], $\alpha_s(M_Z) = 0.119$ [31], $M_{\rm top} = 174.3 \pm 5.1$ GeV [31] and $M_{\rm Higgs} = 150$ GeV. The only observable effect, on M_Z, is due to the variation of $M_{\rm Higgs}$ between 100–1000 GeV (due to the variation of the γ/Z interference term which is taken from the Standard Model): M_Z changes by +0.23 MeV per unit change in $\log_{10} M_{\rm Higgs}/{\rm GeV}$, which is not an error but a correction to be applied once $M_{\rm Higgs}$ is determined. The effect is much smaller than the error on M_Z (± 2.1 MeV).

Methodology of combining the LEP experimental results

The LEP experimental results actually used for combination are slightly modified from those published by the experiments (which are given in the Listings below). This has been done in order to facilitate the procedure by making the inputs more consistent. These modified results are given explicitly in [24]. The main differences compared to the published results are (a) consistent use of ZFITTER 6.23 and TOPAZ0 (the published ALEPH results used ZFITTER 6.10); (b) use of the combined energy-error matrix, which makes a difference of 0.1 MeV on the M_Z and Γ_Z for L3 only as at that intersection the RF modeling uncertainties are the largest.

Thus, nine-parameter sets from all four experiments with their covariance matrices are used together with all the common errors correlations. A grand covariance matrix, V, is constructed and a combined nine-parameter set is obtained by minimizing $\chi^2 = \Delta^T V^{-1} \Delta$, where Δ is the vector of residuals of the combined parameter set to the results of individual experiments. Imposing lepton universality in the combination results in the combined five parameter set.

Study of $Z \to b\overline{b}$ and $Z \to c\overline{c}$

In the sector of c- and b-physics, the LEP experiments have measured the ratios of partial widths $R_b = \Gamma(Z \to b\overline{b})/\Gamma(Z \to$ hadrons), and $R_c = \Gamma(Z \to c\overline{c})/\Gamma(Z \to$ hadrons), and the forward-backward (charge) asymmetries $A_{FB}^{b\overline{b}}$ and $A_{FB}^{c\overline{c}}$. The SLD experiment at SLC has measured the ratios R_c and R_b and, utilizing the polarization of the electron beam, was able to obtain the final state coupling parameters A_b and A_c from a measurement of the left-right forward-backward asymmetry of $b-$ and $c-$quarks. The high precision measurement of R_c at SLD was made possible owing to the small beam size and very stable beam spot at SLC, coupled with a highly precise CCD pixel detector. Several of the analyses have also determined other quantities, in particular the semileptonic branching ratios, $B(b \to \ell^-)$, $B(b \to c \to \ell^+)$, and $B(c \to \ell^+)$, the average time-integrated $B^0\overline{B}^0$ mixing parameter $\overline{\chi}$ and the probabilities for a c–quark to fragment into a D^+, a D_s, a D^{*+} , or a charmed baryon. The latter measurements do not concern properties of the Z boson, and hence they do not appear in the Listing below. However, for completeness, we will report at the end of this minireview their values as obtained fitting the data contained in the Z section. All these quantities are correlated with the electroweak parameters, and since the mixture of b hadrons is different from the one at the $\Upsilon(4S)$, their values might differ from those measured at the $\Upsilon(4S)$.

All the above quantities are correlated to each other since:

- Several analyses (for example the lepton fits) determine more than one parameter simultaneously;
- Some of the electroweak parameters depend explicitly on the values of other parameters (for example R_b depends on R_c);
- Common tagging and analysis techniques produce common systematic uncertainties.

The LEP Electroweak Heavy Flavour Working Group has developed [32] a procedure for combining the measurements taking into account known sources of correlation. The combining procedure determines fourteen parameters: the six parameters of interest in the electroweak sector, R_b, R_c, $A_{FB}^{b\overline{b}}$, $A_{FB}^{c\overline{c}}$, A_b and A_c and, in addition, $B(b \to \ell^-)$, $B(b \to c \to \ell^+)$, $B(c \to \ell^+)$, $\overline{\chi}$, $f(D^+)$, $f(D_s)$, $f(c_{\rm baryon})$ and $P(c \to D^{*+}) \times B(D^{*+} \to \pi^+ D^0)$, to take into account their correlations with the electroweak parameters. Before the fit both the peak and off-peak asymmetries are translated to the common energy $\sqrt{s} = 91.26$ GeV using the predicted energy-dependence from ZFITTER [5].

Summary of the measurements and of the various kinds of analysis

The measurements of R_b and R_c fall into two classes. In the first, named single-tag measurement, a method for selecting b and c events is applied and the number of tagged events is counted. A second technique, named double-tag measurement, has the advantage that the tagging efficiency is directly derived from the data thereby reducing the systematic error on the measurement.

The measurements in the b- and c-sector can be essentially grouped in the following categories:

- Lifetime (and lepton) double-tagging measurements of R_b. These are the most precise measurements of R_b and obviously dominate the combined result. The main sources of systematics come from the charm contamination and from estimating the hemisphere b-tagging efficiency correlation;
- Analyses with $D/D^{*\pm}$ to measure R_c. These measurements make use of several different tagging techniques (inclusive/exclusive double tag, exclusive double tag, reconstruction of all weakly decaying charmed states) and no assumptions are made on the energy-dependence of charm fragmentation;
- A measurement of R_c using single leptons and assuming $B(b \to c \to \ell^+)$;
- Lepton fits which use hadronic events with one or more leptons in the final state to measure the asymmetries $A_{FB}^{b\overline{b}}$ and $A_{FB}^{c\overline{c}}$. Each analysis usually gives several other electroweak parameters. The dominant sources of systematics are due to lepton identification, to other semileptonic branching ratios and to the modeling of the semileptonic decay;
- Measurements of $A_{FB}^{b\overline{b}}$ using lifetime tagged events with a hemisphere charge measurement. These measurements dominate the combined result;
- Analyses with $D/D^{*\pm}$ to measure $A_{FB}^{c\overline{c}}$ or simultaneously $A_{FB}^{b\overline{b}}$ and $A_{FB}^{c\overline{c}}$;
- Measurements of A_b and A_c from SLD, using several tagging methods (lepton, kaon, D/D^*, and vertex mass). These quantities are directly extracted from a measurement of the left–right forward–backward asymmetry in $c\overline{c}$ and $b\overline{b}$ production using a polarized electron beam.

Averaging procedure

All the measurements are provided by the LEP and SLD Collaborations in the form of tables with a detailed breakdown of the systematic errors of each measurement and its dependence on other electroweak parameters.

The averaging proceeds via the following steps:

- Define and propagate a consistent set of external inputs such as branching ratios, hadron lifetimes, fragmentation models *etc.* All the measurements are checked to ensure that all use a common set of assumptions (for instance, since the QCD corrections for the forward–backward asymmetries are strongly dependent on the experimental conditions, the data are corrected before combining);
- Form the full (statistical and systematic) covariance matrix of the measurements. The systematic correlations between different analyses are calculated from the detailed error breakdown in the measurement tables. The correlations relating several

measurements made by the same analysis are also used;

- Take into account any explicit dependence of a measurement on the other electroweak parameters. As an example of this dependence, we illustrate the case of the double-tag measurement of R_b, where c-quarks constitute the main background. The normalization of the charm contribution is not usually fixed by the data and the measurement of R_b depends on the assumed value of R_c, which can be written as:

$$R_b = R_b^{\rm meas} + a(R_c)\frac{(R_c - R_c^{\rm used})}{R_c} \ , \qquad (11)$$

where $R_b^{\rm meas}$ is the result of the analysis which assumed a value of $R_c = R_c^{\rm used}$ and $a(R_c)$ is the constant which gives the dependence on R_c;

- Perform a χ^2 minimization with respect to the combined electroweak parameters.

After the fit the average peak asymmetries $A_{FB}^{c\bar{c}}$ and $A_{FB}^{b\bar{b}}$ are corrected for the energy shift from 91.26 GeV to M_Z and for QED (initial state radiation), γ exchange, and γZ interference effects, to obtain the corresponding pole asymmetries $A_{FB}^{0,c}$ and $A_{FB}^{0,b}$.

This averaging procedure, using the fourteen parameters described above, and applied to the data contained in the Z particle listing below, gives the following results (where the last 8 parameters do not depend directly on the Z):

$$\begin{aligned}
R_b^0 &= 0.21629 \pm 0.00066 \\
R_c^0 &= 0.1721 \pm 0.0030 \\
A_{FB}^{0,b} &= 0.0992 \pm 0.0016 \\
A_{FB}^{0,c} &= 0.0707 \pm 0.0035 \\
A_b &= 0.923 \pm 0.020 \\
A_c &= 0.670 \pm 0.027 \\
\\
B(b \to \ell^-) &= 0.1071 \pm 0.0022 \\
{\rm B}(b \to c \to \ell^+) &= 0.0801 \pm 0.0018 \\
B(c \to \ell^+) &= 0.0969 \pm 0.0031 \\
\overline{\chi} &= 0.1250 \pm 0.0039 \\
f(D^+) &= 0.235 \pm 0.016 \\
f(D_s) &= 0.126 \pm 0.026 \\
f(c_{\rm baryon}) &= 0.093 \pm 0.022 \\
P(c \to D^{*+}) \times {\rm B}(D^{*+} \to \pi^+ D^0) &= 0.1622 \pm 0.0048
\end{aligned}$$

Among the non–electroweak observables, the B semileptonic branching fraction $B(b \to \ell^-)$ is of special interest, since the dominant error source on this quantity is the dependence on the semileptonic decay model for $b \to \ell^-$, with $\Delta B(b \to \ell^-)_{b\to\ell^- -{\rm model}} = 0.0012$. Extensive studies have been made to understand the size of this error. Among the electroweak quantities, the quark asymmetries with leptons depend also on the semileptonic decay model, while the asymmetries using other methods usually do not. The fit implicitely requires that the different methods give consistent results and this effectively constrains the decay model, and thus reduces in principle the error from this source in the fit result.

To obtain a conservative estimate of the modelling error, the above fit has been repeated removing all asymmetry measurements. The results of the fit on B–decay related observables are [24]: $B(b \to \ell^-) = 0.1069 \pm 0.0022$, with $\Delta B(b \to \ell^-)_{b\to\ell^- -{\rm model}} = 0.0013$, $B(b \to c \to \ell^+) = 0.0802 \pm 0.0019$ and $\overline{\chi} = 0.1259 \pm 0.0042$.

References

1. R.N. Cahn, Phys. Rev. **D36**, 2666 (1987).
2. F.A. Berends *et al.*, "Z Physics at LEP 1," CERN Report 89-08 (1989), Vol. 1, eds. G. Altarelli, R. Kleiss, and C. Verzegnassi, p. 89.
3. A. Borrelli *et al.*, Nucl. Phys. **B333**, 357 (1990).
4. D. Bardin and G. Passarino, "Upgrading of Precision Calculations for Electroweak Observables," `hep-ph/9803425`; D. Bardin, G. Passarino, and M. Grünewald, "Precision Calculation Project Report," `hep-ph/9902452`.
5. D. Bardin *et al.*, Z. Phys. **C44**, 493 (1989); Comp. Phys. Comm. **59**, 303 (1990); D. Bardin *et al.*, Nucl. Phys. **B351**, 1 (1991); Phys. Lett. **B255**, 290 (1991), and CERN-TH/6443/92 (1992); Comp. Phys. Comm. **133**, 229 (2001).
6. G. Burgers *et al.*, "Z Physics at LEP 1," CERN Report 89-08 (1989), Vol. 1, eds. G. Altarelli, R. Kleiss, and C. Verzegnassi, p. 55.
7. D.C. Kennedy and B.W. Lynn, Nucl. Phys. **B322**, 1 (1989).
8. M. Consoli *et al.*, "Z Physics at LEP 1," CERN Report 89-08 (1989), Vol. 1, eds. G. Altarelli, R. Kleiss, and C. Verzegnassi, p. 7.
9. M. Bohm *et al.*, *ibid*, p. 203.
10. S. Jadach *et al.*, *ibid*, p. 235.
11. R. Stuart, Phys. Lett. **B262**, 113 (1991).
12. A. Sirlin, Phys. Rev. Lett. **67**, 2127 (1991).
13. A. Leike, T. Riemann, and J. Rose, Phys. Lett. **B273**, 513 (1991).
14. See also D. Bardin *et al.*, Phys. Lett. **B206**, 539 (1988).
15. The LEP Collaborations: ALEPH, DELPHI, L3, OPAL, the LEP Electroweak Working Group, CERN-PH-EP/2013-022, `arXiv:1302.3415 [hep-ex]`, Phys.Rept. 532 (2013) 119-244.
16. W. Beenakker, F.A. Berends, and S.C. van der Marck, Nucl. Phys. **B349**, 323 (1991).
17. G. Montagna *et al.*, Nucl. Phys. **B401**, 3 (1993); Comp. Phys. Comm. **76**, 328 (1993); Comp. Phys. Comm. **93**, 120 (1996); G. Montagna *et al.*, Comp. Phys. Comm. **117**, 278 (1999).

18. R. Assmann *et al.*, (Working Group on LEP Energy), Eur. Phys. J. **C6**, 187 (1999).
19. R. Assmann *et al.*, (Working Group on LEP Energy), Z. Phys. **C66**, 567 (1995).
20. L. Arnaudon *et al.*, (Working Group on LEP Energy and LEP Collabs.), Phys. Lett. **B307**, 187 (1993).
21. L. Arnaudon *et al.*, (Working Group on LEP Energy), CERN-PPE/92-125 (1992).
22. L. Arnaudon *et al.*, Phys. Lett. **B284**, 431 (1992).
23. R. Bailey *et al.*, 'LEP Energy Calibration' CERN-SL-90-95-AP, *Proceedings of the "2nd European Particle Accelerator Conference,"* Nice, France, 12–16 June 1990, pp. 1765-1767.
24. The LEP Collabs.: ALEPH, DELPHI, L3, OPAL, the LEP Electroweak Working Group, and the SLD Heavy Flavour Group: Phys. Reports **427**, 257 (2006).
25. S. Jadach *et al.*, BHLUMI 4.04, Comp. Phys. Comm. **102**, 229 (1997);
S. Jadach and O. Nicrosini, Event generators for Bhabha scattering, in Physics at LEP2, CERN-96-01 Vol. 2, February 1996.
26. B.F.L. Ward *et al.*, Phys. Lett. **B450**, 262 (1999).
27. W. Beenakker and G. Passarino, Phys. Lett. **B425**, 199 (1998).
28. M. Martinez *et al.*, Z. Phys. **C49**, 645 (1991);
M. Martinez and F. Teubert, Z. Phys. **C65**, 267 (1995), updated with results summarized in S. Jadach, B. Pietrzyk, and M. Skrzypek, Phys. Lett. **B456**, 77 (1999) and Reports of the working group on precision calculations for the Z resonance, CERN 95-03, ed. D. Bardin, W. Hollik, and G. Passarino, and references therein.
29. T. van Ritbergen and R. Stuart, Phys. Lett. **B437**, 201 (1998); Phys. Rev. Lett. **82**, 488 (1999).
30. S. Eidelman and F. Jegerlehner, Z. Phys. **C67**, 585 (1995); M. Steinhauser, Phys. Lett. **B429**, 158 (1998).
31. Particle Data Group (D.E. Groom *et al.*), Eur. Phys. J. **C15**, 1 (2000).
32. The LEP Experiments: ALEPH, DELPHI, L3, and OPAL Nucl. Instrum. Methods **A378**, 101 (1996).

Z MASS

OUR FIT is obtained using the fit procedure and correlations as determined by the LEP Electroweak Working Group (see the note "The Z boson" and ref. LEP-SLC 06). The fit is performed using the Z mass and width, the Z hadronic pole cross section, the ratios of hadronic to leptonic partial widths, and the Z pole forward-backward lepton asymmetries. This set is believed to be most free of correlations.

The Z-boson mass listed here corresponds to the mass parameter in a Breit-Wigner distribution with mass dependent width. The value is 34 MeV greater than the real part of the position of the pole (in the energy-squared plane) in the Z-boson propagator. Also the LEP experiments have generally assumed a fixed value of the $\gamma - Z$ interferences term based on the standard model. Keeping this term as free parameter leads to a somewhat larger error on the fitted Z mass. See ACCIARRI 00Q and ABBIENDI 04G for a detailed investigation of both these issues.

VALUE (GeV)	EVTS	DOCUMENT ID		TECN	COMMENT
91.1876±0.0021 OUR FIT					
91.1852±0.0030	4.57M	[1] ABBIENDI	01A	OPAL	E^{ee}_{cm}= 88–94 GeV
91.1863±0.0028	4.08M	[2] ABREU	00F	DLPH	E^{ee}_{cm}= 88–94 GeV
91.1898±0.0031	3.96M	[3] ACCIARRI	00C	L3	E^{ee}_{cm}= 88–94 GeV
91.1885±0.0031	4.57M	[4] BARATE	00C	ALEP	E^{ee}_{cm}= 88–94 GeV
• • • We do not use the following data for averages, fits, limits, etc. • • •					
91.1872±0.0033		[5] ABBIENDI	04G	OPAL	E^{ee}_{cm}= LEP1 + 130–209 GeV
91.272 ±0.032 ±0.033		[6] ACHARD	04C	L3	E^{ee}_{cm}= 183–209 GeV
91.1875±0.0039	3.97M	[7] ACCIARRI	00Q	L3	E^{ee}_{cm}= LEP1 + 130–189 GeV
91.151 ±0.008		[8] MIYABAYASHI	95	TOPZ	E^{ee}_{cm}= 57.8 GeV
91.74 ±0.28 ±0.93	156	[9] ALITTI	92B	UA2	$E^{p\overline{p}}_{cm}$= 630 GeV
90.9 ±0.3 ±0.2	188	[10] ABE	89C	CDF	$E^{p\overline{p}}_{cm}$= 1.8 TeV
91.14 ±0.12	480	[11] ABRAMS	89B	MRK2	E^{ee}_{cm}= 89–93 GeV
93.1 ±1.0 ±3.0	24	[12] ALBAJAR	89	UA1	$E^{p\overline{p}}_{cm}$= 546,630 GeV

[1] ABBIENDI 01A error includes approximately 2.3 MeV due to statistics and 1.8 MeV due to LEP energy uncertainty.
[2] The error includes 1.6 MeV due to LEP energy uncertainty.
[3] The error includes 1.8 MeV due to LEP energy uncertainty.
[4] BARATE 00C error includes approximately 2.4 MeV due to statistics, 0.2 MeV due to experimental systematics, and 1.7 MeV due to LEP energy uncertainty.
[5] ABBIENDI 04G obtain this result using the S–matrix formalism for a combined fit to their cross section and asymmetry data at the Z peak and their data at 130–209 GeV. The authors have corrected the measurement for the 34 MeV shift with respect to the Breit–Wigner fits.
[6] ACHARD 04C select $e^+e^- \to Z\gamma$ events with hard initial–state radiation. Z decays to $q\overline{q}$ and muon pairs are considered. The fit results obtained in the two samples are found consistent to each other and combined considering the uncertainty due to ISR modelling as fully correlated.
[7] ACCIARRI 00Q interpret the s-dependence of the cross sections and lepton forward-backward asymmetries in the framework of the S-matrix formalism. They fit to their cross section and asymmetry data at high energies, using the results of S-matrix fits to Z-peak data (ACCIARRI 00C) as constraints. The 130–189 GeV data constrains the γ/Z interference term. The authors have corrected the measurement for the 34.1 MeV shift with respect to the Breit-Wigner fits. The error contains a contribution of ±2.3 MeV due to the uncertainty on the γZ interference.
[8] MIYABAYASHI 95 combine their low energy total hadronic cross-section measurement with the ACTON 93D data and perform a fit using an S-matrix formalism. As expected, this result is below the mass values obtained with the standard Breit-Wigner parametrization.
[9] Enters fit through W/Z mass ratio given in the W Particle Listings. The ALITTI 92B systematic error (±0.93) has two contributions: one (±0.92) cancels in m_W/m_Z and one (±0.12) is noncancelling. These were added in quadrature.
[10] First error of ABE 89 is combination of statistical and systematic contributions; second is mass scale uncertainty.
[11] ABRAMS 89B uncertainty includes 35 MeV due to the absolute energy measurement.
[12] ALBAJAR 89 result is from a total sample of 33 $Z \to e^+e^-$ events.

Z WIDTH

OUR FIT is obtained using the fit procedure and correlations as determined by the LEP Electroweak Working Group (see the note "The Z boson" and ref. LEP-SLC 06).

VALUE (GeV)	EVTS	DOCUMENT ID		TECN	COMMENT
2.4952±0.0023 OUR FIT					
2.4948±0.0041	4.57M	[1] ABBIENDI	01A	OPAL	E^{ee}_{cm}= 88–94 GeV
2.4876±0.0041	4.08M	[2] ABREU	00F	DLPH	E^{ee}_{cm}= 88–94 GeV
2.5024±0.0042	3.96M	[3] ACCIARRI	00C	L3	E^{ee}_{cm}= 88–94 GeV
2.4951±0.0043	4.57M	[4] BARATE	00C	ALEP	E^{ee}_{cm}= 88–94 GeV
• • • We do not use the following data for averages, fits, limits, etc. • • •					
2.4943±0.0041		[5] ABBIENDI	04G	OPAL	E^{ee}_{cm}= LEP1 + 130–209 GeV
2.5025±0.0041	3.97M	[6] ACCIARRI	00Q	L3	E^{ee}_{cm}= LEP1 + 130–189 GeV
2.50 ±0.21 ±0.06		[7] ABREU	96R	DLPH	E^{ee}_{cm}= 91.2 GeV
3.8 ±0.8 ±1.0	188	ABE	89C	CDF	$E^{p\overline{p}}_{cm}$= 1.8 TeV
2.42 $^{+0.45}_{-0.35}$	480	[8] ABRAMS	89B	MRK2	E^{ee}_{cm}= 89–93 GeV
2.7 $^{+1.2}_{-1.0}$ ±1.3	24	[9] ALBAJAR	89	UA1	$E^{p\overline{p}}_{cm}$= 546,630 GeV
2.7 ±2.0 ±1.0	25	[10] ANSARI	87	UA2	$E^{p\overline{p}}_{cm}$= 546,630 GeV

[1] ABBIENDI 01A error includes approximately 3.6 MeV due to statistics, 1 MeV due to event selection systematics, and 1.3 MeV due to LEP energy uncertainty.
[2] The error includes 1.2 MeV due to LEP energy uncertainty.
[3] The error includes 1.3 MeV due to LEP energy uncertainty.
[4] BARATE 00C error includes approximately 3.8 MeV due to statistics, 0.9 MeV due to experimental systematics, and 1.3 MeV due to LEP energy uncertainty.
[5] ABBIENDI 04G obtain this result using the S–matrix formalism for a combined fit to their cross section and asymmetry data at the Z peak and their data at 130–209 GeV. The authors have corrected the measurement for the 1 MeV shift with respect to the Breit–Wigner fits.
[6] ACCIARRI 00Q interpret the s-dependence of the cross sections and lepton forward-backward asymmetries in the framework of the S-matrix formalism. They fit to their cross section and asymmetry data at high energies, using the results of S-matrix fits to Z-peak data (ACCIARRI 00C) as constraints. The 130–189 GeV data constrains the γ/Z interference term. The authors have corrected the measurement for the 0.9 MeV shift with respect to the Breit-Wigner fits.
[7] ABREU 96R obtain this value from a study of the interference between initial and final state radiation in the process $e^+e^- \to Z \to \mu^+\mu^-$.
[8] ABRAMS 89B uncertainty includes 50 MeV due to the miniSAM background subtraction error.
[9] ALBAJAR 89 result is from a total sample of 33 $Z \to e^+e^-$ events.

[10] Quoted values of ANSARI 87 are from direct fit. Ratio of Z and W production gives either $\Gamma(Z) < (1.09 \pm 0.07) \times \Gamma(W)$, CL = 90% or $\Gamma(Z) = (0.82^{+0.19}_{-0.14} \pm 0.06) \times \Gamma(W)$. Assuming Standard-Model value $\Gamma(W) = 2.65$ GeV then gives $\Gamma(Z) < 2.89 \pm 0.19$ or $= 2.17^{+0.50}_{-0.37} \pm 0.16$.

Z DECAY MODES

	Mode		Fraction (Γ_i/Γ)	Scale factor/ Confidence level
Γ_1	$e^+ e^-$		(3.363 ±0.004) %	
Γ_2	$\mu^+ \mu^-$		(3.366 ±0.007) %	
Γ_3	$\tau^+ \tau^-$		(3.370 ±0.008) %	
Γ_4	$\ell^+ \ell^-$	[a]	(3.3658±0.0023) %	
Γ_5	$\ell^+ \ell^- \ell^+ \ell^-$	[b]	(4.2 $^{+0.9}_{-0.8}$) $\times 10^{-6}$	
Γ_6	invisible		(20.00 ±0.06) %	
Γ_7	hadrons		(69.91 ±0.06) %	
Γ_8	$(u\overline{u}+c\overline{c})/2$		(11.6 ±0.6) %	
Γ_9	$(d\overline{d}+s\overline{s}+b\overline{b})/3$		(15.6 ±0.4) %	
Γ_{10}	$c\overline{c}$		(12.03 ±0.21) %	
Γ_{11}	$b\overline{b}$		(15.12 ±0.05) %	
Γ_{12}	$b\overline{b}b\overline{b}$		(3.6 ±1.3) $\times 10^{-4}$	
Γ_{13}	ggg		< 1.1 %	CL=95%
Γ_{14}	$\pi^0\gamma$		< 5.2 $\times 10^{-5}$	CL=95%
Γ_{15}	$\eta\gamma$		< 5.1 $\times 10^{-5}$	CL=95%
Γ_{16}	$\omega\gamma$		< 6.5 $\times 10^{-4}$	CL=95%
Γ_{17}	$\eta'(958)\gamma$		< 4.2 $\times 10^{-5}$	CL=95%
Γ_{18}	$\gamma\gamma$		< 5.2 $\times 10^{-5}$	CL=95%
Γ_{19}	$\gamma\gamma\gamma$		< 1.0 $\times 10^{-5}$	CL=95%
Γ_{20}	$\pi^\pm W^\mp$	[c]	< 7 $\times 10^{-5}$	CL=95%
Γ_{21}	$\rho^\pm W^\mp$	[c]	< 8.3 $\times 10^{-5}$	CL=95%
Γ_{22}	$J/\psi(1S)$X		(3.51 $^{+0.23}_{-0.25}$) $\times 10^{-3}$	S=1.1
Γ_{23}	$\psi(2S)$X		(1.60 ±0.29) $\times 10^{-3}$	
Γ_{24}	$\chi_{c1}(1P)$X		(2.9 ±0.7) $\times 10^{-3}$	
Γ_{25}	$\chi_{c2}(1P)$X		< 3.2 $\times 10^{-3}$	CL=90%
Γ_{26}	$\Upsilon(1S)$ X + $\Upsilon(2S)$ X + $\Upsilon(3S)$ X		(1.0 ±0.5) $\times 10^{-4}$	
Γ_{27}	$\Upsilon(1S)$X		< 4.4 $\times 10^{-5}$	CL=95%
Γ_{28}	$\Upsilon(2S)$X		< 1.39 $\times 10^{-4}$	CL=95%
Γ_{29}	$\Upsilon(3S)$X		< 9.4 $\times 10^{-5}$	CL=95%
Γ_{30}	$(D^0/\overline{D}^0)$ X		(20.7 ±2.0) %	
Γ_{31}	$D^\pm$X		(12.2 ±1.7) %	
Γ_{32}	$D^*(2010)^\pm$X	[c]	(11.4 ±1.3) %	
Γ_{33}	$D_{s1}(2536)^\pm$X		(3.6 ±0.8) $\times 10^{-3}$	
Γ_{34}	$D_{sJ}(2573)^\pm$X		(5.8 ±2.2) $\times 10^{-3}$	
Γ_{35}	$D^{*\prime}(2629)^\pm$X		searched for	
Γ_{36}	BX			
Γ_{37}	B^*X			
Γ_{38}	B^+X	[d]	(6.08 ±0.13) %	
Γ_{39}	B^0_sX	[d]	(1.59 ±0.13) %	
Γ_{40}	B^+_cX		searched for	
Γ_{41}	Λ^+_cX		(1.54 ±0.33) %	
Γ_{42}	Ξ^0_cX		seen	
Γ_{43}	Ξ_bX		seen	
Γ_{44}	b-baryon X	[d]	(1.38 ±0.22) %	
Γ_{45}	anomalous γ+ hadrons	[e]	< 3.2 $\times 10^{-3}$	CL=95%
Γ_{46}	$e^+ e^- \gamma$	[e]	< 5.2 $\times 10^{-4}$	CL=95%
Γ_{47}	$\mu^+ \mu^- \gamma$	[e]	< 5.6 $\times 10^{-4}$	CL=95%
Γ_{48}	$\tau^+ \tau^- \gamma$	[e]	< 7.3 $\times 10^{-4}$	CL=95%
Γ_{49}	$\ell^+ \ell^- \gamma\gamma$	[f]	< 6.8 $\times 10^{-6}$	CL=95%
Γ_{50}	$q\overline{q}\gamma\gamma$	[f]	< 5.5 $\times 10^{-6}$	CL=95%
Γ_{51}	$\nu\overline{\nu}\gamma\gamma$	[f]	< 3.1 $\times 10^{-6}$	CL=95%
Γ_{52}	$e^\pm \mu^\mp$	LF [c]	< 1.7 $\times 10^{-6}$	CL=95%
Γ_{53}	$e^\pm \tau^\mp$	LF [c]	< 9.8 $\times 10^{-6}$	CL=95%
Γ_{54}	$\mu^\pm \tau^\mp$	LF [c]	< 1.2 $\times 10^{-5}$	CL=95%
Γ_{55}	pe	L,B	< 1.8 $\times 10^{-6}$	CL=95%
Γ_{56}	$p\mu$	L,B	< 1.8 $\times 10^{-6}$	CL=95%

[a] ℓ indicates each type of lepton (e, μ, and τ), not sum over them.

[b] Here ℓ indicates e or μ.

[c] The value is for the sum of the charge states or particle/antiparticle states indicated.

[d] This value is updated using the product of (i) the $Z \to b\overline{b}$ fraction from this listing and (ii) the b-hadron fraction in an unbiased sample of weakly decaying b-hadrons produced in Z-decays provided by the Heavy Flavor Averaging Group (HFAG, http://www.slac.stanford.edu/xorg/hfag/osc/PDG_2009/#FRACZ).

[e] See the Particle Listings below for the γ energy range used in this measurement.

[f] For $m_{\gamma\gamma} = (60 \pm 5)$ GeV.

Z PARTIAL WIDTHS

Γ(e⁺e⁻) Γ1

For the LEP experiments, this parameter is not directly used in the overall fit but is derived using the fit results; see the note "The Z boson" and ref. LEP-SLC 06.

VALUE (MeV)	EVTS	DOCUMENT ID		TECN	COMMENT
83.91±0.12 OUR FIT					
83.66±0.20	137.0K	ABBIENDI	01A	OPAL	E^{ee}_{cm}= 88–94 GeV
83.54±0.27	117.8k	ABREU	00F	DLPH	E^{ee}_{cm}= 88–94 GeV
84.16±0.22	124.4k	ACCIARRI	00C	L3	E^{ee}_{cm}= 88–94 GeV
83.88±0.19		BARATE	00C	ALEP	E^{ee}_{cm}= 88–94 GeV
82.89±1.20±0.89		[1] ABE	95J	SLD	E^{ee}_{cm}= 91.31 GeV

[1] ABE 95J obtain this measurement from Bhabha events in a restricted fiducial region to improve systematics. They use the values 91.187 and 2.489 GeV for the Z mass and total decay width to extract this partial width.

Γ(μ⁺μ⁻) Γ2

This parameter is not directly used in the overall fit but is derived using the fit results; see the note "The Z boson" and ref. LEP-SLC 06.

VALUE (MeV)	EVTS	DOCUMENT ID		TECN	COMMENT
83.99±0.18 OUR FIT					
84.03±0.30	182.8K	ABBIENDI	01A	OPAL	E^{ee}_{cm}= 88–94 GeV
84.48±0.40	157.6k	ABREU	00F	DLPH	E^{ee}_{cm}= 88–94 GeV
83.95±0.44	113.4k	ACCIARRI	00C	L3	E^{ee}_{cm}= 88–94 GeV
84.02±0.28		BARATE	00C	ALEP	E^{ee}_{cm}= 88–94 GeV

Γ(τ⁺τ⁻) Γ3

This parameter is not directly used in the overall fit but is derived using the fit results; see the note "The Z boson" and ref. LEP-SLC 06.

VALUE (MeV)	EVTS	DOCUMENT ID		TECN	COMMENT
84.08±0.22 OUR FIT					
83.94±0.41	151.5K	ABBIENDI	01A	OPAL	E^{ee}_{cm}= 88–94 GeV
83.71±0.58	104.0k	ABREU	00F	DLPH	E^{ee}_{cm}= 88–94 GeV
84.23±0.58	103.0k	ACCIARRI	00C	L3	E^{ee}_{cm}= 88–94 GeV
84.38±0.31		BARATE	00C	ALEP	E^{ee}_{cm}= 88–94 GeV

Γ(ℓ⁺ℓ⁻) Γ4

In our fit $\Gamma(\ell^+\ell^-)$ is defined as the partial Z width for the decay into a pair of massless charged leptons. This parameter is not directly used in the 5-parameter fit assuming lepton universality but is derived using the fit results. See the note "The Z boson" and ref. LEP-SLC 06.

VALUE (MeV)	EVTS	DOCUMENT ID		TECN	COMMENT
83.984±0.086 OUR FIT					
83.82 ±0.15	471.3K	ABBIENDI	01A	OPAL	E^{ee}_{cm}= 88–94 GeV
83.85 ±0.17	379.4k	ABREU	00F	DLPH	E^{ee}_{cm}= 88–94 GeV
84.14 ±0.17	340.8k	ACCIARRI	00C	L3	E^{ee}_{cm}= 88–94 GeV
84.02 ±0.15	500k	BARATE	00C	ALEP	E^{ee}_{cm}= 88–94 GeV

Γ(invisible) Γ6

We use only direct measurements of the invisible partial width using the single photon channel to obtain the average value quoted below. OUR FIT value is obtained as a difference between the total and the observed partial widths assuming lepton universality.

VALUE (MeV)	EVTS	DOCUMENT ID		TECN	COMMENT
499.0± 1.5 OUR FIT					
503 ±16 OUR AVERAGE Error includes scale factor of 1.2.					
498 ±12 ±12	1791	ACCIARRI	98G	L3	E^{ee}_{cm}= 88–94 GeV
539 ±26 ±17	410	AKERS	95C	OPAL	E^{ee}_{cm}= 88–94 GeV
450 ±34 ±34	258	BUSKULIC	93L	ALEP	E^{ee}_{cm}= 88–94 GeV
540 ±80 ±40	52	ADEVA	92	L3	E^{ee}_{cm}= 88–94 GeV
• • • We do not use the following data for averages, fits, limits, etc. • • •					
498.1± 2.6		[1] ABBIENDI	01A	OPAL	E^{ee}_{cm}= 88–94 GeV
498.1± 3.2		[1] ABREU	00F	DLPH	E^{ee}_{cm}= 88–94 GeV
499.1± 2.9		[1] ACCIARRI	00C	L3	E^{ee}_{cm}= 88–94 GeV
499.1± 2.5		[1] BARATE	00C	ALEP	E^{ee}_{cm}= 88–94 GeV

[1] This is an indirect determination of Γ(invisible) from a fit to the visible Z decay modes.

Γ(hadrons) Γ7

This parameter is not directly used in the 5-parameter fit assuming lepton universality, but is derived using the fit results. See the note "The *Z* boson" and ref. LEP-SLC 06.

VALUE (MeV)	EVTS	DOCUMENT ID		TECN	COMMENT
1744.4±2.0 OUR FIT					
1745.4±3.5	4.10M	ABBIENDI	01A	OPAL	E_{cm}^{ee}= 88–94 GeV
1738.1±4.0	3.70M	ABREU	00F	DLPH	E_{cm}^{ee}= 88–94 GeV
1751.1±3.8	3.54M	ACCIARRI	00C	L3	E_{cm}^{ee}= 88–94 GeV
1744.0±3.4	4.07M	BARATE	00C	ALEP	E_{cm}^{ee}= 88–94 GeV

Z BRANCHING RATIOS

OUR FIT is obtained using the fit procedure and correlations as determined by the LEP Electroweak Working Group (see the note "The *Z* boson" and ref. LEP-SLC 06).

Γ(hadrons)/Γ(e+ e−) Γ7/Γ1

VALUE	EVTS	DOCUMENT ID		TECN	COMMENT
20.804± 0.050 OUR FIT					
20.902± 0.084	137.0K	[1] ABBIENDI	01A	OPAL	E_{cm}^{ee}= 88–94 GeV
20.88 ± 0.12	117.8k	ABREU	00F	DLPH	E_{cm}^{ee}= 88–94 GeV
20.816± 0.089	124.4k	ACCIARRI	00C	L3	E_{cm}^{ee}= 88–94 GeV
20.677± 0.075		[2] BARATE	00C	ALEP	E_{cm}^{ee}= 88–94 GeV
• • • We do not use the following data for averages, fits, limits, etc. • • •					
27.0 $^{+11.7}_{-8.8}$	12	[3] ABRAMS	89D	MRK2	E_{cm}^{ee}= 89–93 GeV

[1] ABBIENDI 01A error includes approximately 0.067 due to statistics, 0.040 due to event selection systematics, 0.027 due to the theoretical uncertainty in *t*-channel prediction, and 0.014 due to LEP energy uncertainty.
[2] BARATE 00C error includes approximately 0.062 due to statistics, 0.033 due to experimental systematics, and 0.026 due to the theoretical uncertainty in *t*-channel prediction.
[3] ABRAMS 89D have included both statistical and systematic uncertainties in their quoted errors.

Γ(hadrons)/Γ(μ+ μ−) Γ7/Γ2

OUR FIT is obtained using the fit procedure and correlations as determined by the LEP Electroweak Working Group (see the note "The *Z* boson" and ref. LEP-SLC 06).

VALUE	EVTS	DOCUMENT ID		TECN	COMMENT
20.785±0.033 OUR FIT					
20.811±0.058	182.8K	[1] ABBIENDI	01A	OPAL	E_{cm}^{ee}= 88–94 GeV
20.65 ±0.08	157.6k	ABREU	00F	DLPH	E_{cm}^{ee}= 88–94 GeV
20.861±0.097	113.4k	ACCIARRI	00C	L3	E_{cm}^{ee}= 88–94 GeV
20.799±0.056		[2] BARATE	00C	ALEP	E_{cm}^{ee}= 88–94 GeV
• • • We do not use the following data for averages, fits, limits, etc. • • •					
18.9 $^{+7.1}_{-5.3}$	13	[3] ABRAMS	89D	MRK2	E_{cm}^{ee}= 89–93 GeV

[1] ABBIENDI 01A error includes approximately 0.050 due to statistics and 0.027 due to event selection systematics.
[2] BARATE 00C error includes approximately 0.053 due to statistics and 0.021 due to experimental systematics.
[3] ABRAMS 89D have included both statistical and systematic uncertainties in their quoted errors.

Γ(hadrons)/Γ(τ+ τ−) Γ7/Γ3

OUR FIT is obtained using the fit procedure and correlations as determined by the LEP Electroweak Working Group (see the note "The *Z* boson" and ref. LEP-SLC 06).

VALUE	EVTS	DOCUMENT ID		TECN	COMMENT
20.764±0.045 OUR FIT					
20.832±0.091	151.5K	[1] ABBIENDI	01A	OPAL	E_{cm}^{ee}= 88–94 GeV
20.84 ±0.13	104.0k	ABREU	00F	DLPH	E_{cm}^{ee}= 88–94 GeV
20.792±0.133	103.0k	ACCIARRI	00C	L3	E_{cm}^{ee}= 88–94 GeV
20.707±0.062		[2] BARATE	00C	ALEP	E_{cm}^{ee}= 88–94 GeV
• • • We do not use the following data for averages, fits, limits, etc. • • •					
15.2 $^{+4.8}_{-3.9}$	21	[3] ABRAMS	89D	MRK2	E_{cm}^{ee}= 89–93 GeV

[1] ABBIENDI 01A error includes approximately 0.055 due to statistics and 0.071 due to event selection systematics.
[2] BARATE 00C error includes approximately 0.054 due to statistics and 0.033 due to experimental systematics.
[3] ABRAMS 89D have included both statistical and systematic uncertainties in their quoted errors.

Γ(hadrons)/Γ(ℓ+ ℓ−) Γ7/Γ4

ℓ indicates each type of lepton (*e*, μ, and τ), not sum over them.

Our fit result is obtained requiring lepton universality.

VALUE	EVTS	DOCUMENT ID		TECN	COMMENT
20.767±0.025 OUR FIT					
20.823±0.044	471.3K	[1] ABBIENDI	01A	OPAL	E_{cm}^{ee}= 88–94 GeV
20.730±0.060	379.4k	ABREU	00F	DLPH	E_{cm}^{ee}= 88–94 GeV
20.810±0.060	340.8k	ACCIARRI	00C	L3	E_{cm}^{ee}= 88–94 GeV
20.725±0.039	500k	[2] BARATE	00C	ALEP	E_{cm}^{ee}= 88–94 GeV
• • • We do not use the following data for averages, fits, limits, etc. • • •					
18.9 $^{+3.6}_{-3.2}$	46	ABRAMS	89B	MRK2	E_{cm}^{ee}= 89–93 GeV

[1] ABBIENDI 01A error includes approximately 0.034 due to statistics and 0.027 due to event selection systematics.
[2] BARATE 00C error includes approximately 0.033 due to statistics, 0.020 due to experimental systematics, and 0.005 due to the theoretical uncertainty in *t*-channel prediction.

Γ(hadrons)/Γtotal Γ7/Γ

This parameter is not directly used in the overall fit but is derived using the fit results; see the note "The *Z* boson" and ref. LEP-SLC 06.

VALUE (%)	DOCUMENT ID
69.911±0.056 OUR FIT	

Γ(e+ e−)/Γtotal Γ1/Γ

This parameter is not directly used in the overall fit but is derived using the fit results; see the note "The *Z* boson" and ref. LEP-SLC 06.

VALUE (%)	DOCUMENT ID
(3363.2±4.2) × 10−3 OUR FIT	

Γ(μ+ μ−)/Γtotal Γ2/Γ

This parameter is not directly used in the overall fit but is derived using the fit results; see the note "The *Z* boson" and ref. LEP-SLC 06.

VALUE (%)	DOCUMENT ID
(3366.2±6.6) × 10−3 OUR FIT	

Γ(μ+ μ−)/Γ(e+ e−) Γ2/Γ1

This parameter is not directly used in the overall fit but is derived using the fit results; see the note "The *Z* boson" and ref. LEP-SLC 06.

VALUE	DOCUMENT ID
1.0009±0.0028 OUR FIT	

Γ(τ+ τ−)/Γtotal Γ3/Γ

This parameter is not directly used in the overall fit but is derived using the fit results; see the note "The *Z* boson" and ref. LEP-SLC 06.

VALUE (%)	DOCUMENT ID
(3369.6±8.3) × 10−3 OUR FIT	

Γ(τ+ τ−)/Γ(e+ e−) Γ3/Γ1

This parameter is not directly used in the overall fit but is derived using the fit results; see the note "The *Z* boson" and ref. LEP-SLC 06.

VALUE	DOCUMENT ID
1.0019±0.0032 OUR FIT	

Γ(ℓ+ ℓ−)/Γtotal Γ4/Γ

ℓ indicates each type of lepton (*e*, μ, and τ), not sum over them.

Our fit result assumes lepton universality.

This parameter is not directly used in the overall fit but is derived using the fit results; see the note "The *Z* boson" and ref. LEP-SLC 06.

VALUE (%)	DOCUMENT ID
(3365.8±2.3) × 10−3 OUR FIT	

Γ(ℓ+ ℓ− ℓ+ ℓ−)/Γtotal Γ5/Γ

Here ℓ indicates either *e* or μ.

VALUE (units 10^{-6})	EVTS	DOCUMENT ID	TECN	COMMENT
4.2$^{+0.9}_{-0.8}$±0.2	28	CHATRCHYAN 12BN	CMS	E_{cm}^{pp} = 7 TeV

Γ(invisible)/Γtotal Γ6/Γ

See the data, the note, and the fit result for the partial width, Γ_6, above.

VALUE (%)	DOCUMENT ID
20.000±0.055 OUR FIT	

Γ((u u¯ + c c¯)/2)/Γ(hadrons) Γ8/Γ7

This quantity is the branching ratio of $Z \to$ "up-type" quarks to $Z \to$ hadrons. Except ACKERSTAFF 97T the values of $Z \to$ "up-type" and $Z \to$ "down-type" branchings are extracted from measurements of Γ(hadrons), and $\Gamma(Z \to \gamma +$ jets) where γ is a high-energy (>5 or 7 GeV) isolated photon. As the experiments use different procedures and slightly different values of M_Z, Γ(hadrons) and α_s in their extraction procedures, our average has to be taken with caution.

VALUE	DOCUMENT ID		TECN	COMMENT
0.166±0.009 OUR AVERAGE				
0.172$^{+0.011}_{-0.010}$	[1] ABBIENDI	04E	OPAL	E_{cm}^{ee} = 91.2 GeV
0.160±0.019±0.019	[2] ACKERSTAFF	97T	OPAL	E_{cm}^{ee}= 88–94 GeV
0.137$^{+0.038}_{-0.054}$	[3] ABREU	95X	DLPH	E_{cm}^{ee}= 88–94 GeV
0.137±0.033	[4] ADRIANI	93	L3	E_{cm}^{ee}= 91.2 GeV

[1] ABBIENDI 04E select photons with energy > 7 GeV and use Γ(hadrons) = 1744.4 ± 2.0 MeV and α_s = 0.1172 ± 0.002 to obtain $\Gamma_u = 300^{+19}_{-18}$ MeV.
[2] ACKERSTAFF 97T measure $\Gamma_{u\overline{u}}/(\Gamma_{d\overline{d}}+\Gamma_{u\overline{u}}+\Gamma_{s\overline{s}})$ = 0.258 ± 0.031 ± 0.032. To obtain this branching ratio authors use R_c+R_b = 0.380 ± 0.010. This measurement is fully negatively correlated with the measurement of $\Gamma_{d\overline{d},s\overline{s}}/(\Gamma_{d\overline{d}}+\Gamma_{u\overline{u}}+\Gamma_{s\overline{s}})$ given in the next data block.
[3] ABREU 95X use M_Z = 91.187 ± 0.009 GeV, Γ(hadrons) = 1725 ± 12 MeV and α_s = 0.123 ± 0.005. To obtain this branching ratio we divide their value of $C_{2/3} = 91^{+0.25}_{-0.36}$ by their value of $(3C_{1/3} + 2C_{2/3})$ = 6.66 ± 0.05.
[4] ADRIANI 93 use M_Z = 91.181 ± 0.022 GeV, Γ(hadrons) = 1742 ± 19 MeV and α_s = 0.125 ± 0.009. To obtain this branching ratio we divide their value of $C_{2/3}$ = 0.92 ± 0.22 by their value of $(3C_{1/3} + 2C_{2/3})$ = 6.720 ± 0.076.

Gauge & Higgs Boson Particle Listings

Z

$\Gamma((d\overline{d}+s\overline{s}+b\overline{b})/3)/\Gamma(\text{hadrons})$ Γ_9/Γ_7

This quantity is the branching ratio of $Z \to$ "down-type" quarks to $Z \to$ hadrons. Except ACKERSTAFF 97T the values of $Z \to$ "up-type" and $Z \to$ "down-type" branchings are extracted from measurements of Γ(hadrons), and $\Gamma(Z \to \gamma +$ jets) where γ is a high-energy (>5 or 7 GeV) isolated photon. As the experiments use different procedures and slightly different values of M_Z, Γ(hadrons) and α_s in their extraction procedures, our average has to be taken with caution.

VALUE	DOCUMENT ID		TECN	COMMENT
0.223±0.006 OUR AVERAGE				
0.218±0.007	[1] ABBIENDI	04E	OPAL	$E_{\rm cm}^{ee}$ = 91.2 GeV
0.230±0.010±0.010	[2] ACKERSTAFF	97T	OPAL	$E_{\rm cm}^{ee}$ = 88–94 GeV
$0.243^{+0.036}_{-0.026}$	[3] ABREU	95X	DLPH	$E_{\rm cm}^{ee}$ = 88–94 GeV
0.243±0.022	[4] ADRIANI	93	L3	$E_{\rm cm}^{ee}$ = 91.2 GeV

[1] ABBIENDI 04E select photons with energy > 7 GeV and use Γ(hadrons) = 1744.4 ± 2.0 MeV and α_s = 0.1172 ± 0.002 to obtain Γ_d = 381 ± 12 MeV.

[2] ACKERSTAFF 97T measure $\Gamma_{d\overline{d},s\overline{s}}/(\Gamma_{d\overline{d}}+\Gamma_{u\overline{u}}+\Gamma_{s\overline{s}})$ = 0.371 ± 0.016 ± 0.016. To obtain this branching ratio authors use R_c+R_b = 0.380 ± 0.010. This measurement is fully negatively correlated with the measurement of $\Gamma_{u\overline{u}}/(\Gamma_{d\overline{d}}+\Gamma_{u\overline{u}}+\Gamma_{s\overline{s}})$ presented in the previous data block.

[3] ABREU 95X use M_Z = 91.187 ± 0.009 GeV, Γ(hadrons) = 1725 ± 12 MeV and α_S = 0.123 ± 0.005. To obtain this branching ratio we divide their value of $C_{1/3} = 1.62^{+0.24}_{-0.17}$ by their value of $(3C_{1/3} + 2C_{2/3})$ = 6.66 ± 0.05.

[4] ADRIANI 93 use M_Z = 91.181 ± 0.022 GeV, Γ(hadrons) = 1742 ± 19 MeV and α_S = 0.125 ± 0.009. To obtain this branching ratio we divide their value of $C_{1/3}$ = 1.63 ± 0.15 by their value of $(3C_{1/3} + 2C_{2/3})$ = 6.720 ± 0.076.

$R_c = \Gamma(c\overline{c})/\Gamma(\text{hadrons})$ Γ_{10}/Γ_7

OUR FIT is obtained by a simultaneous fit to several c- and b-quark measurements as explained in the note "The Z boson" and ref. LEP-SLC 06.

The Standard Model predicts R_c = 0.1723 for m_t = 174.3 GeV and M_H = 150 GeV.

VALUE	DOCUMENT ID		TECN	COMMENT
0.1721±0.0030 OUR FIT				
0.1744±0.0031±0.0021	[1] ABE	05F	SLD	$E_{\rm cm}^{ee}$=91.28 GeV
0.1665±0.0051±0.0081	[2] ABREU	00	DLPH	$E_{\rm cm}^{ee}$ = 88–94 GeV
0.1698±0.0069	[3] BARATE	00B	ALEP	$E_{\rm cm}^{ee}$ = 88–94 GeV
0.180 ±0.011 ±0.013	[4] ACKERSTAFF	98E	OPAL	$E_{\rm cm}^{ee}$ = 88–94 GeV
0.167 ±0.011 ±0.012	[5] ALEXANDER	96R	OPAL	$E_{\rm cm}^{ee}$ = 88–94 GeV
• • • We do not use the following data for averages, fits, limits, etc. • • •				
0.1623±0.0085±0.0209	[6] ABREU	95D	DLPH	$E_{\rm cm}^{ee}$ = 88–94 GeV

[1] ABE 05F use hadronic Z decays collected during 1996–98 to obtain an enriched sample of $c\overline{c}$ events using a double tag method. The single c-tag is obtained with a neural network trained to perform flavor discrimination using as input several signatures (corrected secondary vertex mass, vertex decay length, multiplicity and total momentum of the hemisphere). A multitag approach is used, defining 4 regions of the output value of the neural network and R_c is extracted from a simultaneous fit to the count rates of the 4 different tags. The quoted systematic error includes an uncertainty of ±0.0006 due to the uncertainty on R_b.

[2] ABREU 00 obtain this result properly combining the measurement from the D^{*+} production rate (R_c= 0.1610 ± 0.0104 ± 0.0077 ± 0.0043 (BR)) with that from the overall charm counting (R_c= 0.1692 ± 0.0047 ± 0.0063 ± 0.0074 (BR)) in $c\overline{c}$ events. The systematic error includes an uncertainty of ±0.0054 due to the uncertainty on the charmed hadron branching fractions.

[3] BARATE 00B use exclusive decay modes to independently determine the quantities $R_c \times$f($c \to$ X), X=D^0, D^+, D_s^+, and Λ_c. Estimating $R_c \times$f($c \to \Xi_c/\Omega_c$)= 0.0034, they simply sum over all the charm decays to obtain R_c= 0.1738 ± 0.0047 ± 0.0088 ± 0.0075(BR). This is combined with all previous ALEPH measurements (BARATE 98T and BUSKULIC 94G, R_c= 0.1681 ± 0.0054 ± 0.0062) to obtain the quoted value.

[4] ACKERSTAFF 98E use an inclusive/exclusive double tag. In one jet $D^{*\pm}$ mesons are exclusively reconstructed in several decay channels and in the opposite jet a slow pion (opposite charge inclusive $D^{*\pm}$) tag is used. The b content of this sample is measured by the simultaneous detection of a lepton in one jet and an inclusively reconstructed $D^{*\pm}$ meson in the opposite jet. The systematic error includes an uncertainty of ±0.006 due to the external branching ratios.

[5] ALEXANDER 96R obtain this value via direct charm counting, summing the partial contributions from D^0, D^+, D_s^+, and Λ_c^+, and assuming that strange-charmed baryons account for the 15% of the Λ_c^+ production. An uncertainty of ±0.005 due to the uncertainties in the charm hadron branching ratios is included in the overall systematics.

[6] ABREU 95D perform a maximum likelihood fit to the combined p and p_T distributions of single and dilepton samples. The second error includes an uncertainty of ±0.0124 due to models and branching ratios.

$R_b = \Gamma(b\overline{b})/\Gamma(\text{hadrons})$ Γ_{11}/Γ_7

OUR FIT is obtained by a simultaneous fit to several c- and b-quark measurements as explained in the note "The Z boson" and ref. LEP-SLC 06.

The Standard Model predicts R_b=0.21581 for m_t=174.3 GeV and M_H=150 GeV.

VALUE	DOCUMENT ID		TECN	COMMENT
0.21629±0.00066 OUR FIT				
0.21594±0.00094±0.00075	[1] ABE	05F	SLD	$E_{\rm cm}^{ee}$=91.28 GeV
0.2174 ±0.0015 ±0.0028	[2] ACCIARRI	00	L3	$E_{\rm cm}^{ee}$= 89–93 GeV
0.2178 ±0.0011 ±0.0013	[3] ABBIENDI	99B	OPAL	$E_{\rm cm}^{ee}$ = 88–94 GeV
0.21634±0.00067±0.00060	[4] ABREU	99B	DLPH	$E_{\rm cm}^{ee}$ = 88–94 GeV
0.2159 ±0.0009 ±0.0011	[5] BARATE	97F	ALEP	$E_{\rm cm}^{ee}$ = 88–94 GeV
• • • We do not use the following data for averages, fits, limits, etc. • • •				
0.2145 ±0.0089 ±0.0067	[6] ABREU	95D	DLPH	$E_{\rm cm}^{ee}$ = 88–94 GeV
0.219 ±0.006 ±0.005	[7] BUSKULIC	94G	ALEP	$E_{\rm cm}^{ee}$ = 88–94 GeV
0.251 ±0.049 ±0.030	[8] JACOBSEN	91	MRK2	$E_{\rm cm}^{ee}$ = 91 GeV

[1] ABE 05F use hadronic Z decays collected during 1996–98 to obtain an enriched sample of $b\overline{b}$ events using a double tag method. The single b–tag is obtained with a neural network trained to perform flavor discrimination using as input several signatures (corrected secondary vertex mass, vertex decay length, multiplicity and total momentum of the hemisphere; the key tag is obtained requiring the secondary vertex corrected mass to be above the D–meson mass). ABE 05F obtain R_b =0.21604 ± 0.00098 ± 0.00074 where the systematic error includes an uncertainty of ±0.00012 due to the uncertainty on R_c. The value reported here is obtained properly combining with ABE 98D. The quoted systematic error includes an uncertainty of ±0.00012 due to the uncertainty on R_c.

[2] ACCIARRI 00 obtain this result using a double-tagging technique, with a high p_T lepton tag and an impact parameter tag in opposite hemispheres.

[3] ABBIENDI 99B tag $Z \to b\overline{b}$ decays using leptons and/or separated decay vertices. The b-tagging efficiency is measured directly from the data using a double-tagging technique.

[4] ABREU 99B obtain this result combining in a multivariate analysis several tagging methods (impact parameter and secondary vertex reconstruction, complemented by event shape variables). For R_c different from its Standard Model value of 0.172, R_b varies as $-0.024\times(R_c - 0.172)$.

[5] BARATE 97F combine the lifetime-mass hemisphere tag (BARATE 97E) with event shape information and lepton tag to identify $Z \to b\overline{b}$ candidates. They further use c- and uds-selection tags to identify the background. For R_c different from its Standard Model value of 0.172, R_b varies as $-0.019\times(R_c - 0.172)$.

[6] ABREU 95D perform a maximum likelihood fit to the combined p and p_T distributions of single and dilepton samples. The second error includes an uncertainty of ±0.0023 due to models and branching ratios.

[7] BUSKULIC 94G perform a simultaneous fit to the p and p_T spectra of both single and dilepton events.

[8] JACOBSEN 91 tagged $b\overline{b}$ events by requiring coincidence of $\geq$ 3 tracks with significant impact parameters using vertex detector. Systematic error includes lifetime and decay uncertainties (±0.014).

$\Gamma(b\overline{b}b\overline{b})/\Gamma(\text{hadrons})$ Γ_{12}/Γ_7

VALUE (units 10^{-4})	DOCUMENT ID		TECN	COMMENT
5.2±1.9 OUR AVERAGE				
3.6±1.7±2.7	[1] ABBIENDI	01G	OPAL	$E_{\rm cm}^{ee}$ = 88–94 GeV
6.0±1.9±1.4	[2] ABREU	99U	DLPH	$E_{\rm cm}^{ee}$ = 88–94 GeV

[1] ABBIENDI 01G use a sample of four-jet events from hadronic Z decays. To enhance the $b\overline{b}b\overline{b}$ signal, at least three of the four jets are required to have a significantly detached secondary vertex.

[2] ABREU 99U force hadronic Z decays into 3 jets to use all the available phase space and require a b tag for every jet. This decay mode includes primary and secondary $4b$ production, *e.g.*, from gluon splitting to $b\overline{b}$.

$\Gamma(ggg)/\Gamma(\text{hadrons})$ Γ_{13}/Γ_7

VALUE	CL%	DOCUMENT ID		TECN	COMMENT
<1.6 × 10⁻²	95	[1] ABREU	96S	DLPH	$E_{\rm cm}^{ee}$ = 88–94 GeV

[1] This branching ratio is slightly dependent on the jet-finder algorithm. The value we quote is obtained using the JADE algorithm, while using the DURHAM algorithm ABREU 96S obtain an upper limit of 1.5×10^{-2}.

$\Gamma(\pi^0\gamma)/\Gamma_{\text{total}}$ Γ_{14}/Γ

VALUE	CL%	DOCUMENT ID		TECN	COMMENT
<5.2 × 10⁻⁵	95	[1] ACCIARRI	95G	L3	$E_{\rm cm}^{ee}$ = 88–94 GeV
$<5.5 \times 10^{-5}$	95	ABREU	94B	DLPH	$E_{\rm cm}^{ee}$ = 88–94 GeV
$<2.1 \times 10^{-4}$	95	DECAMP	92	ALEP	$E_{\rm cm}^{ee}$ = 88–94 GeV
$<1.4 \times 10^{-4}$	95	AKRAWY	91F	OPAL	$E_{\rm cm}^{ee}$ = 88–94 GeV

[1] This limit is for both decay modes $Z \to \pi^0\gamma/\gamma\gamma$ which are indistinguishable in ACCIARRI 95G.

$\Gamma(\eta\gamma)/\Gamma_{\text{total}}$ Γ_{15}/Γ

VALUE	CL%	DOCUMENT ID		TECN	COMMENT
$<7.6 \times 10^{-5}$	95	ACCIARRI	95G	L3	$E_{\rm cm}^{ee}$ = 88–94 GeV
$<8.0 \times 10^{-5}$	95	ABREU	94B	DLPH	$E_{\rm cm}^{ee}$ = 88–94 GeV
<5.1 × 10⁻⁵	95	DECAMP	92	ALEP	$E_{\rm cm}^{ee}$ = 88–94 GeV
$<2.0 \times 10^{-4}$	95	AKRAWY	91F	OPAL	$E_{\rm cm}^{ee}$ = 88–94 GeV

$\Gamma(\omega\gamma)/\Gamma_{\text{total}}$ Γ_{16}/Γ

VALUE	CL%	DOCUMENT ID		TECN	COMMENT
<6.5 × 10⁻⁴	95	ABREU	94B	DLPH	$E_{\rm cm}^{ee}$ = 88–94 GeV

$\Gamma(\eta'(958)\gamma)/\Gamma_{\text{total}}$ Γ_{17}/Γ

VALUE	CL%	DOCUMENT ID		TECN	COMMENT
<4.2 × 10⁻⁵	95	DECAMP	92	ALEP	$E_{\rm cm}^{ee}$ = 88–94 GeV

$\Gamma(\gamma\gamma)/\Gamma_{\text{total}}$ Γ_{18}/Γ

This decay would violate the Landau-Yang theorem.

VALUE	CL%	DOCUMENT ID		TECN	COMMENT
<5.2 × 10⁻⁵	95	[1] ACCIARRI	95G	L3	$E_{\rm cm}^{ee}$ = 88–94 GeV
$<5.5 \times 10^{-5}$	95	ABREU	94B	DLPH	$E_{\rm cm}^{ee}$ = 88–94 GeV
$<1.4 \times 10^{-4}$	95	AKRAWY	91F	OPAL	$E_{\rm cm}^{ee}$ = 88–94 GeV

[1] This limit is for both decay modes $Z \to \pi^0\gamma/\gamma\gamma$ which are indistinguishable in ACCIARRI 95G.

$\Gamma(\gamma\gamma\gamma)/\Gamma_{total}$ Γ_{19}/Γ

VALUE	CL%	DOCUMENT ID		TECN	COMMENT
$<1.0\times10^{-5}$	95	[1] ACCIARRI	95C	L3	E_{cm}^{ee}= 88–94 GeV
$<1.7\times10^{-5}$	95	[1] ABREU	94B	DLPH	E_{cm}^{ee}= 88–94 GeV
$<6.6\times10^{-5}$	95	AKRAWY	91F	OPAL	E_{cm}^{ee}= 88–94 GeV

[1] Limit derived in the context of composite Z model.

$\Gamma(\pi^{\pm}W^{\mp})/\Gamma_{total}$ Γ_{20}/Γ

The value is for the sum of the charge states indicated.

VALUE	CL%	DOCUMENT ID		TECN	COMMENT
$<7\times10^{-5}$	95	DECAMP	92	ALEP	E_{cm}^{ee}= 88–94 GeV

$\Gamma(\rho^{\pm}W^{\mp})/\Gamma_{total}$ Γ_{21}/Γ

The value is for the sum of the charge states indicated.

VALUE	CL%	DOCUMENT ID		TECN	COMMENT
$<8.3\times10^{-5}$	95	DECAMP	92	ALEP	E_{cm}^{ee}= 88–94 GeV

$\Gamma(J/\psi(1S)X)/\Gamma_{total}$ Γ_{22}/Γ

VALUE (units 10^{-3})	EVTS	DOCUMENT ID		TECN	COMMENT
$3.51^{+0.23}_{-0.25}$ OUR AVERAGE Error includes scale factor of 1.1.					
$3.21\pm0.21^{+0.19}_{-0.28}$	553	[1] ACCIARRI	99F	L3	E_{cm}^{ee}= 88–94 GeV
$3.9\ \pm0.2\ \pm0.3$	511	[2] ALEXANDER	96B	OPAL	E_{cm}^{ee}= 88–94 GeV
$3.73\pm0.39\pm0.36$	153	[3] ABREU	94P	DLPH	E_{cm}^{ee}= 88–94 GeV

[1] ACCIARRI 99F combine $\mu^+\mu^-$ and e^+e^- $J/\psi(1S)$ decay channels. The branching ratio for prompt $J/\psi(1S)$ production is measured to be $(2.1\pm0.6\pm0.4^{+0.4}_{-0.2}\text{(theor.)})\times10^{-4}$.

[2] ALEXANDER 96B identify $J/\psi(1S)$ from the decays into lepton pairs. (4.8 ± 2.4)% of this branching ratio is due to prompt $J/\psi(1S)$ production (ALEXANDER 96N).

[3] Combining $\mu^+\mu^-$ and e^+e^- channels and taking into account the common systematic errors. $(7.7^{+6.3}_{-5.4})$% of this branching ratio is due to prompt $J/\psi(1S)$ production.

$\Gamma(\psi(2S)X)/\Gamma_{total}$ Γ_{23}/Γ

VALUE (units 10^{-3})	EVTS	DOCUMENT ID		TECN	COMMENT
1.60±0.29 OUR AVERAGE					
$1.6\ \pm0.5\ \pm0.3$	39	[1] ACCIARRI	97J	L3	E_{cm}^{ee}= 88–94 GeV
$1.6\ \pm0.3\ \pm0.2$	46.9	[2] ALEXANDER	96B	OPAL	E_{cm}^{ee}= 88–94 GeV
$1.60\pm0.73\pm0.33$	5.4	[3] ABREU	94P	DLPH	E_{cm}^{ee}= 88–94 GeV

[1] ACCIARRI 97J measure this branching ratio via the decay channel $\psi(2S)\to\ell^+\ell^-$ ($\ell=\mu, e$).

[2] ALEXANDER 96B measure this branching ratio via the decay channel $\psi(2S)\to J/\psi\pi^+\pi^-$, with $J/\psi\to\ell^+\ell^-$.

[3] ABREU 94P measure this branching ratio via decay channel $\psi(2S)\to J/\psi\pi^+\pi^-$, with $J/\psi\to\mu^+\mu^-$.

$\Gamma(\chi_{c1}(1P)X)/\Gamma_{total}$ Γ_{24}/Γ

VALUE (units 10^{-3})	EVTS	DOCUMENT ID		TECN	COMMENT
2.9±0.7 OUR AVERAGE					
$2.7\pm0.6\pm0.5$	33	[1] ACCIARRI	97J	L3	E_{cm}^{ee}= 88–94 GeV
$5.0\pm2.1^{+1.5}_{-0.9}$	6.4	[2] ABREU	94P	DLPH	E_{cm}^{ee}= 88–94 GeV

[1] ACCIARRI 97J measure this branching ratio via the decay channel $\chi_{c1}\to J/\psi+\gamma$, with $J/\psi\to\ell^+\ell^-$ ($\ell=\mu, e$). The $M(\ell^+\ell^-\gamma)$–$M(\ell^+\ell^-)$ mass difference spectrum is fitted with two gaussian shapes for χ_{c1} and χ_{c2}.

[2] This branching ratio is measured via the decay channel $\chi_{c1}\to J/\psi+\gamma$, with $J/\psi\to\mu^+\mu^-$.

$\Gamma(\chi_{c2}(1P)X)/\Gamma_{total}$ Γ_{25}/Γ

VALUE	CL%	DOCUMENT ID		TECN	COMMENT
$<3.2\times10^{-3}$	90	[1] ACCIARRI	97J	L3	E_{cm}^{ee}= 88–94 GeV

[1] ACCIARRI 97J derive this limit via the decay channel $\chi_{c2}\to J/\psi+\gamma$, with $J/\psi\to\ell^+\ell^-$ ($\ell=\mu, e$). The $M(\ell^+\ell^-\gamma)$–$M(\ell^+\ell^-)$ mass difference spectrum is fitted with two gaussian shapes for χ_{c1} and χ_{c2}.

$\Gamma(\Upsilon(1S)X+\Upsilon(2S)X+\Upsilon(3S)X)/\Gamma_{total}$ $\Gamma_{26}/\Gamma=(\Gamma_{27}+\Gamma_{28}+\Gamma_{29})/\Gamma$

VALUE (units 10^{-4})	EVTS	DOCUMENT ID		TECN	COMMENT
1.0±0.4±0.22	6.4	[1] ALEXANDER	96F	OPAL	E_{cm}^{ee}= 88–94 GeV

[1] ALEXANDER 96F identify the Υ (which refers to any of the three lowest bound states) through its decay into e^+e^- and $\mu^+\mu^-$. The systematic error includes an uncertainty of ±0.2 due to the production mechanism.

$\Gamma(\Upsilon(1S)X)/\Gamma_{total}$ Γ_{27}/Γ

VALUE	CL%	DOCUMENT ID		TECN	COMMENT
$<4.4\times10^{-5}$	95	[1] ACCIARRI	99F	L3	E_{cm}^{ee}= 88–94 GeV

[1] ACCIARRI 99F search for $\Upsilon(1S)$ through its decay into $\ell^+\ell^-$ ($\ell=e$ or μ).

$\Gamma(\Upsilon(2S)X)/\Gamma_{total}$ Γ_{28}/Γ

VALUE	CL%	DOCUMENT ID		TECN	COMMENT
$<13.9\times10^{-5}$	95	[1] ACCIARRI	97R	L3	E_{cm}^{ee}= 88–94 GeV

[1] ACCIARRI 97R search for $\Upsilon(2S)$ through its decay into $\ell^+\ell^-$ ($\ell=e$ or μ).

$\Gamma(\Upsilon(3S)X)/\Gamma_{total}$ Γ_{29}/Γ

VALUE	CL%	DOCUMENT ID		TECN	COMMENT
$<9.4\times10^{-5}$	95	[1] ACCIARRI	97R	L3	E_{cm}^{ee}= 88–94 GeV

[1] ACCIARRI 97R search for $\Upsilon(3S)$ through its decay into $\ell^+\ell^-$ ($\ell=e$ or μ).

$\Gamma((D^0/\overline{D}^0)X)/\Gamma(\text{hadrons})$ Γ_{30}/Γ_7

VALUE	EVTS	DOCUMENT ID		TECN	COMMENT
0.296±0.019±0.021	369	[1] ABREU	93I	DLPH	E_{cm}^{ee}= 88–94 GeV

[1] The $(D^0/\overline{D}^0)$ states in ABREU 93I are detected by the $K\pi$ decay mode. This is a corrected result (see the erratum of ABREU 93I).

$\Gamma(D^{\pm}X)/\Gamma(\text{hadrons})$ Γ_{31}/Γ_7

VALUE	EVTS	DOCUMENT ID		TECN	COMMENT
0.174±0.016±0.018	539	[1] ABREU	93I	DLPH	E_{cm}^{ee}= 88–94 GeV

[1] The $D^{\pm}$ states in ABREU 93I are detected by the $K\pi\pi$ decay mode. This is a corrected result (see the erratum of ABREU 93I).

$\Gamma(D^*(2010)^{\pm}X)/\Gamma(\text{hadrons})$ Γ_{32}/Γ_7

The value is for the sum of the charge states indicated.

VALUE	EVTS	DOCUMENT ID		TECN	COMMENT
0.163±0.019 OUR AVERAGE		Error includes scale factor of 1.3.			
$0.155\pm0.010\pm0.013$	358	[1] ABREU	93I	DLPH	E_{cm}^{ee}= 88–94 GeV
$0.21\ \pm0.04$	362	[2] DECAMP	91J	ALEP	E_{cm}^{ee}= 88–94 GeV

[1] $D^*(2010)^{\pm}$ in ABREU 93I are reconstructed from $D^0\pi^{\pm}$, with $D^0\to K^-\pi^+$. The new CLEO II measurement of $B(D^{*\pm}\to D^0\pi^{\pm})=(68.1\pm1.6)$ % is used. This is a corrected result (see the erratum of ABREU 93I).

[2] DECAMP 91J report $B(D^*(2010)^+\to D^0\pi^+)\ B(D^0\to K^-\pi^+)\ \Gamma(D^*(2010)^{\pm}X)\ /\ \Gamma(\text{hadrons})=(5.11\pm0.34)\times10^{-3}$. They obtained the above number assuming $B(D^0\to K^-\pi^+)=(3.62\pm0.34\pm0.44)$% and $B(D^*(2010)^+\to D^0\pi^+)=(55\pm4)$%. We have rescaled their original result of 0.26 ± 0.05 taking into account the new CLEO II branching ratio $B(D^*(2010)^+\to D^0\pi^+)=(68.1\pm1.6)$%.

$\Gamma(D_{s1}(2536)^{\pm}X)/\Gamma(\text{hadrons})$ Γ_{33}/Γ_7

$D_{s1}(2536)^{\pm}$ is an expected orbitally-excited state of the D_s meson.

VALUE (%)	EVTS	DOCUMENT ID		TECN	COMMENT
0.52±0.09±0.06	92	[1] HEISTER	02B	ALEP	E_{cm}^{ee}= 88–94 GeV

[1] HEISTER 02B reconstruct this meson in the decay modes $D_{s1}(2536)^{\pm}\to D^{*\pm}K^0$ and $D_{s1}(2536)^{\pm}\to D^{*0}K^{\pm}$. The quoted branching ratio assumes that the decay width of the $D_{s1}(2536)$ is saturated by the two measured decay modes.

$\Gamma(D_{sJ}(2573)^{\pm}X)/\Gamma(\text{hadrons})$ Γ_{34}/Γ_7

$D_{sJ}(2573)^{\pm}$ is an expected orbitally-excited state of the D_s meson.

VALUE (%)	EVTS	DOCUMENT ID		TECN	COMMENT
$0.83\pm0.29^{+0.07}_{-0.13}$	64	[1] HEISTER	02B	ALEP	E_{cm}^{ee}= 88–94 GeV

[1] HEISTER 02B reconstruct this meson in the decay mode $D_{s2}^*(2573)^{\pm}\to D^0K^{\pm}$. The quoted branching ratio assumes that the detected decay mode represents 45% of the full decay width.

$\Gamma(D^{*\prime}(2629)^{\pm}X)/\Gamma(\text{hadrons})$ Γ_{35}/Γ_7

$D^{*\prime}(2629)^{\pm}$ is a predicted radial excitation of the $D^*(2010)^{\pm}$ meson.

VALUE	DOCUMENT ID		TECN	COMMENT
searched for	[1] ABBIENDI	01N	OPAL	E_{cm}^{ee}= 88–94 GeV

[1] ABBIENDI 01N searched for the decay mode $D^{*\prime}(2629)^{\pm}\to D^{*\pm}\pi^+\pi^-$ with $D^{*+}\to D^0\pi^+$, and $D^0\to K^-\pi^+$. They quote a 95% CL limit for $Z\to D^{*\prime}(2629)^{\pm}\times B(D^{*\prime}(2629)^+\to D^{*+}\pi^+\pi^-)<3.1\times10^{-3}$.

$\Gamma(B^*X)/[\Gamma(BX)+\Gamma(B^*X)]$ $\Gamma_{37}/(\Gamma_{36}+\Gamma_{37})$

As the experiments assume different values of the b-baryon contribution, our average should be taken with caution.

VALUE	EVTS	DOCUMENT ID		TECN	COMMENT
0.75 ±0.04 OUR AVERAGE					
$0.760\pm0.036\pm0.083$		[1] ACKERSTAFF	97M	OPAL	E_{cm}^{ee}= 88–94 GeV
$0.771\pm0.026\pm0.070$		[2] BUSKULIC	96D	ALEP	E_{cm}^{ee}= 88–94 GeV
$0.72\ \pm0.03\ \pm0.06$		[3] ABREU	95R	DLPH	E_{cm}^{ee}= 88–94 GeV
$0.76\ \pm0.08\ \pm0.06$	1378	[4] ACCIARRI	95B	L3	E_{cm}^{ee}= 88–94 GeV

[1] ACKERSTAFF 97M use an inclusive B reconstruction method and assume a (13.2 ± 4.1)% b-baryon contribution. The value refers to a b-flavored meson mixture of B_u, B_d, and B_s.

[2] BUSKULIC 96D use an inclusive reconstruction of B hadrons and assume a (12.2 ± 4.3)% b-baryon contribution. The value refers to a b-flavored mixture of B_u, B_d, and B_s.

[3] ABREU 95R use an inclusive B-reconstruction method and assume a (10 ± 4)% b-baryon contribution. The value refers to a b-flavored meson mixture of B_u, B_d, and B_s.

[4] ACCIARRI 95B assume a 9.4% b-baryon contribution. The value refers to a b-flavored mixture of B_u, B_d, and B_s.

$\Gamma(B^+X)/\Gamma(\text{hadrons})$ Γ_{38}/Γ_7

"OUR EVALUATION" is obtained using our current values for $f(\overline{b} \to B^+)$ and R_b = $\Gamma(b\overline{b})/\Gamma(\text{hadrons})$. We calculate $\Gamma(B^+X)/\Gamma(\text{hadrons}) = R_b \times f(\overline{b} \to B^+)$. The decay fraction $f(\overline{b} \to B^+)$ was provided by the Heavy Flavor Averaging Group (HFAG, http://www.slac.stanford.edu/xorg/hfag/osc/PDG_2009/#FRACZ).

VALUE	DOCUMENT ID		TECN	COMMENT
0.0869±0.0019 OUR EVALUATION				
0.0887±0.0030	[1] ABDALLAH	03K	DLPH	E^{ee}_{cm} = 88–94 GeV

[1] ABDALLAH 03K measure the production fraction of B^+ mesons in hadronic Z decays $f(B^+) = (40.99 \pm 0.82 \pm 1.11)\%$. The value quoted here is obtained multiplying this production fraction by our value of $R_b = \Gamma(\overline{b}b)/\Gamma(\text{hadrons})$.

$\Gamma(B^0_sX)/\Gamma(\text{hadrons})$ Γ_{39}/Γ_7

"OUR EVALUATION" is obtained using our current values for $f(\overline{b} \to B^0_s)$ and R_b = $\Gamma(b\overline{b})/\Gamma(\text{hadrons})$. We calculate $\Gamma(B^0_s)/\Gamma(\text{hadrons}) = R_b \times f(\overline{b} \to B^0_s)$. The decay fraction $f(\overline{b} \to B^0_s)$ was provided by the Heavy Flavor Averaging Group (HFAG, http://www.slac.stanford.edu/xorg/hfag/osc/PDG_2009/#FRACZ).

VALUE	DOCUMENT ID		TECN	COMMENT
0.0227±0.0019 OUR EVALUATION				
seen	[1] ABREU	92M	DLPH	E^{ee}_{cm}= 88–94 GeV
seen	[2] ACTON	92N	OPAL	E^{ee}_{cm}= 88–94 GeV
seen	[3] BUSKULIC	92E	ALEP	E^{ee}_{cm}= 88–94 GeV

[1] ABREU 92M reported value is $\Gamma(B^0_sX)*B(B^0_s \to D_s\mu\nu_\mu X)*B(D_s \to \phi\pi)/\Gamma(\text{hadrons}) = (18 \pm 8) \times 10^{-5}$.

[2] ACTON 92N find evidence for B^0_s production using D_s-ℓ correlations, with $D^+_s \to \phi\pi^+$ and $K^*(892)\,K^+$. Assuming R_b from the Standard Model and averaging over the e and μ channels, authors measure the product branching fraction to be $f(\overline{b} \to B^0_s)\times B(B^0_s \to D^-_s \ell^+ \nu_\ell X)\times B(D^-_s \to \phi\pi^-) = (3.9 \pm 1.1 \pm 0.8) \times 10^{-4}$.

[3] BUSKULIC 92E find evidence for B^0_s production using D_s-ℓ correlations, with $D^+_s \to \phi\pi^+$ and $K^*(892)\,K^+$. Using $B(D^+_s \to \phi\pi^+) = (2.7 \pm 0.7)\%$ and summing up the e and μ channels, the weighted average product branching fraction is measured to be $B(\overline{b} \to B^0_s)\times B(B^0_s \to D^-_s \ell^+ \nu_\ell X) = 0.040 \pm 0.011^{+0.010}_{-0.012}$.

$\Gamma(B^+_cX)/\Gamma(\text{hadrons})$ Γ_{40}/Γ_7

VALUE	DOCUMENT ID		TECN	COMMENT
searched for	[1] ACKERSTAFF	98O	OPAL	E^{ee}_{cm}= 88–94 GeV
searched for	[2] ABREU	97E	DLPH	E^{ee}_{cm}= 88–94 GeV
searched for	[3] BARATE	97H	ALEP	E^{ee}_{cm}= 88–94 GeV

[1] ACKERSTAFF 98O searched for the decay modes $B_c \to J/\psi\pi^+$, $J/\psi a^+_1$, and $J/\psi\ell^+\nu_\ell$, with $J/\psi \to \ell^+\ell^-$, $\ell = e,\mu$. The number of candidates (background) for the three decay modes is 2 (0.63 ± 0.2), 0 (1.10 ± 0.22), and 1 (0.82 ± 0.19) respectively. Interpreting the $2\,B_c \to J/\psi\pi^+$ candidates as signal, they report $\Gamma(B^+_cX)\times B(B_c \to J/\psi\pi^+)/\Gamma(\text{hadrons}) = (3.8^{+5.0}_{-2.4} \pm 0.5)\times 10^{-5}$. Interpreted as background, the 90% CL bounds are $\Gamma(B^+_cX)*B(B_c \to J/\psi\pi^+)/\Gamma(\text{hadrons}) < 1.06\times 10^{-4}$, $\Gamma(B^+_cX)*B(B_c \to J/\psi a^+_1)/\Gamma(\text{hadrons}) < 5.29 \times 10^{-4}$, $\Gamma(B^+_cX)*B(B_c \to J/\psi\ell^+\nu_\ell)/\Gamma(\text{hadrons}) < 6.96 \times 10^{-5}$.

[2] ABREU 97E searched for the decay modes $B_c \to J/\psi\pi^+$, $J/\psi\ell^+\nu_\ell$, and $J/\psi(3\pi)^+$, with $J/\psi \to \ell^+\ell^-$, $\ell = e,\mu$. The number of candidates (background) for the three decay modes is 1 (1.7), 0 (0.3), and 1 (2.3) respectively. They report the following 90% CL limits: $\Gamma(B^+_cX)*B(B_c \to J/\psi\pi^+)/\Gamma(\text{hadrons}) < (1.05\text{–}0.84)\times 10^{-4}$, $\Gamma(B^+_cX)*B(B_c \to J/\psi\ell\nu_\ell)/\Gamma(\text{hadrons}) < (5.8\text{–}5.0)\times 10^{-5}$, $\Gamma(B^+_cX)*B(B_c \to J/\psi(3\pi)^+)/\Gamma(\text{hadrons}) < 1.75 \times 10^{-4}$, where the ranges are due to the predicted B_c lifetime (0.4–1.4) ps.

[3] BARATE 97H searched for the decay modes $B_c \to J/\psi\pi^+$ and $J/\psi\ell^+\nu_\ell$ with $J/\psi \to \ell^+\ell^-$, $\ell = e,\mu$. The number of candidates (background) for the two decay modes is 0 (0.44) and 2 (0.81) respectively. They report the following 90% CL limits: $\Gamma(B^+_cX)*B(B_c \to J/\psi\pi^+)/\Gamma(\text{hadrons}) < 3.6 \times 10^{-5}$ and $\Gamma(B^+_cX)*B(B_c \to J/\psi\ell^+\nu_\ell)/\Gamma(\text{hadrons}) < 5.2 \times 10^{-5}$.

$\Gamma(\Lambda^+_cX)/\Gamma(\text{hadrons})$ Γ_{41}/Γ_7

VALUE	DOCUMENT ID		TECN	COMMENT
0.022±0.005 OUR AVERAGE				
0.024±0.005±0.006	[1] ALEXANDER	96R	OPAL	E^{ee}_{cm} = 88–94 GeV
0.021±0.003±0.005	[2] BUSKULIC	96Y	ALEP	E^{ee}_{cm} = 88–94 GeV

[1] ALEXANDER 96R measure $R_b \times f(b \to \Lambda^+_cX) \times B(\Lambda^+_c \to pK^-\pi^+) = (0.122 \pm 0.023 \pm 0.010)\%$ in hadronic Z decays; the value quoted here is obtained using our best value $B(\Lambda^+_c \to pK^-\pi^+) = (5.0 \pm 1.3)\%$. The first error is the total experiment's error and the second error is the systematic error due to the branching fraction uncertainty.

[2] BUSKULIC 96Y obtain the production fraction of Λ^+_c baryons in hadronic Z decays $f(b \to \Lambda^+_cX) = 0.110 \pm 0.014 \pm 0.006$ using $B(\Lambda^+_c \to pK^-\pi^+) = (4.4 \pm 0.6)\%$; we have rescaled using our best value $B(\Lambda^+_c \to pK^-\pi^+) = (5.0 \pm 1.3)\%$ obtaining $f(b \to \Lambda^+_cX) = 0.097 \pm 0.013 \pm 0.025$ where the first error is their total experiment's error and the second error is the systematic error due to the branching fraction uncertainty. The value quoted here is obtained multiplying this production fraction by our value of $R_b = \Gamma(b\overline{b})/\Gamma(\text{hadrons})$.

$\Gamma(\Xi^0_cX)/\Gamma(\text{hadrons})$ Γ_{42}/Γ_7

VALUE	DOCUMENT ID		TECN	COMMENT
• • • We do not use the following data for averages, fits, limits, etc. • • •				
seen	[1] ABDALLAH	05C	DLPH	E^{ee}_{cm} = 88–94 GeV

[1] ABDALLAH 05C searched for the charmed strange baryon Ξ^0_c in the decay channel $\Xi^0_c \to \Xi^-\pi^+$ ($\Xi^- \to \Lambda\pi^-$). The production rate is measured to be $f_{\Xi^0_c} \times B(\Xi^0_c \to \Xi^-\pi^+) = (4.7 \pm 1.4 \pm 1.1) \times 10^{-4}$ per hadronic Z decay.

$\Gamma(\Xi_bX)/\Gamma(\text{hadrons})$ Γ_{43}/Γ_7

Here Ξ_b is used as a notation for the strange b-baryon states Ξ^-_b and Ξ^0_b.

VALUE	DOCUMENT ID		TECN	COMMENT
• • • We do not use the following data for averages, fits, limits, etc. • • •				
seen	[1] ABDALLAH	05C	DLPH	E^{ee}_{cm} = 88–94 GeV
seen	[2] BUSKULIC	96T	ALEP	E^{ee}_{cm} = 88–94 GeV
seen	[3] ABREU	95V	DLPH	E^{ee}_{cm} = 88–94 GeV

[1] ABDALLAH 05C searched for the beauty strange baryon Ξ_b in the inclusive semileptonic decay channel $\Xi_b \to \Xi^-\ell^-\overline{\nu}_\ell X$. Evidence for the Ξ_b production is seen from the observation of $\Xi^{\mp}$ production accompanied by a lepton of the same sign. From the excess of "right-sign" pairs $\Xi^{\mp}\ell^{\mp}$ compared to "wrong-sign" pairs $\Xi^{\mp}\ell^{\pm}$ the production rate is measured to be $B(b \to \Xi_b) \times B(\Xi_b \to \Xi^-\ell^-X) = (3.0 \pm 1.0 \pm 0.3) \times 10^{-4}$ per lepton species, averaged over electrons and muons.

[2] BUSKULIC 96T investigate Ξ-lepton correlations and find a significant excess of "right–sign" pairs $\Xi^{\mp}\ell^{\mp}$ compared to "wrong–sign" pairs $\Xi^{\mp}\ell^{\pm}$. This excess is interpreted as evidence for Ξ_b semileptonic decay. The measured product branching ratio is $B(b \to \Xi_b) \times B(\Xi_b \to X_c X\ell^-\overline{\nu}_\ell) \times B(X_c \to \Xi^-X') = (5.4 \pm 1.1 \pm 0.8) \times 10^{-4}$ per lepton species, averaged over electrons and muons, with X_c a charmed baryon.

[3] ABREU 95V observe an excess of "right-sign" pairs $\Xi^{\mp}\ell^{\mp}$ compared to "wrong-sign" pairs $\Xi^{\mp}\ell^{\pm}$ in jets: this excess is interpreted as evidence for the beauty strange baryon Ξ_b production, with $\Xi_b \to \Xi^-\ell^-\overline{\nu}_\ell X$. They find that the probability for this signal to come from non b-baryon decays is less than 5×10^{-4} and that Λ_b decays can account for less than 10% of these events. The Ξ_b production rate is then measured to be $B(b \to \Xi_b) \times B(\Xi_b \to \Xi^-\ell^-X) = (5.9 \pm 2.1 \pm 1.0) \times 10^{-4}$ per lepton species, averaged over electrons and muons.

$\Gamma(b\text{-baryon}\,X)/\Gamma(\text{hadrons})$ Γ_{44}/Γ_7

"OUR EVALUATION" is obtained using our current values for $f(b \to b\text{-baryon})$ and R_b = $\Gamma(b\overline{b})/\Gamma(\text{hadrons})$. We calculate $\Gamma(b\text{-baryon}\,X)/\Gamma(\text{hadrons}) = R_b \times f(b \to b\text{-baryon})$. The decay fraction $f(b \to b\text{-baryon})$ was provided by the Heavy Flavor Averaging Group (HFAG, http://www.slac.stanford.edu/xorg/hfag/osc/PDG_2009).

VALUE	DOCUMENT ID		TECN	COMMENT
0.0197±0.0032 OUR EVALUATION				
0.0221±0.0015±0.0058	[1] BARATE	98V	ALEP	E^{ee}_{cm}= 88–94 GeV

[1] BARATE 98V use the overall number of identified protons in b-hadron decays to measure $f(b \to b\text{-baryon}) = 0.102 \pm 0.007 \pm 0.027$. They assume $BR(b\text{-baryon} \to pX) = (58 \pm 6)\%$ and $BR(B^0_s \to pX) = (8.0 \pm 4.0)\%$. The value quoted here is obtained multiplying this production fraction by our value of $R_b = \Gamma(b\overline{b})/\Gamma(\text{hadrons})$.

$\Gamma(\text{anomalous}\,\gamma + \text{hadrons})/\Gamma_{\text{total}}$ Γ_{45}/Γ

Limits on additional sources of prompt photons beyond expectations for final-state bremsstrahlung.

VALUE	CL%	DOCUMENT ID		TECN	COMMENT
<3.2 × 10⁻³	95	[1] AKRAWY	90J	OPAL	E^{ee}_{cm}= 88–94 GeV

[1] AKRAWY 90J report $\Gamma(\gamma X) < 8.2$ MeV at 95%CL. They assume a three-body $\gamma q\overline{q}$ distribution and use $E(\gamma) > 10$ GeV.

$\Gamma(e^+e^-\gamma)/\Gamma_{\text{total}}$ Γ_{46}/Γ

VALUE	CL%	DOCUMENT ID		TECN	COMMENT
<5.2 × 10⁻⁴	95	[1] ACTON	91B	OPAL	E^{ee}_{cm}= 91.2 GeV

[1] ACTON 91B looked for isolated photons with E>2% of beam energy (> 0.9 GeV).

$\Gamma(\mu^+\mu^-\gamma)/\Gamma_{\text{total}}$ Γ_{47}/Γ

VALUE	CL%	DOCUMENT ID		TECN	COMMENT
<5.6 × 10⁻⁴	95	[1] ACTON	91B	OPAL	E^{ee}_{cm}= 91.2 GeV

[1] ACTON 91B looked for isolated photons with E>2% of beam energy (> 0.9 GeV).

$\Gamma(\tau^+\tau^-\gamma)/\Gamma_{\text{total}}$ Γ_{48}/Γ

VALUE	CL%	DOCUMENT ID		TECN	COMMENT
<7.3 × 10⁻⁴	95	[1] ACTON	91B	OPAL	E^{ee}_{cm}= 91.2 GeV

[1] ACTON 91B looked for isolated photons with E>2% of beam energy (> 0.9 GeV).

$\Gamma(\ell^+\ell^-\gamma\gamma)/\Gamma_{\text{total}}$ Γ_{49}/Γ

The value is the sum over $\ell = e,\ \mu,\ \tau$.

VALUE	CL%	DOCUMENT ID		TECN	COMMENT
<6.8 × 10⁻⁶	95	[1] ACTON	93E	OPAL	E^{ee}_{cm}= 88–94 GeV

[1] For $m_{\gamma\gamma} = 60 \pm 5$ GeV.

$\Gamma(q\overline{q}\gamma\gamma)/\Gamma_{\text{total}}$ Γ_{50}/Γ

VALUE	CL%	DOCUMENT ID		TECN	COMMENT
<5.5 × 10⁻⁶	95	[1] ACTON	93E	OPAL	E^{ee}_{cm}= 88–94 GeV

[1] For $m_{\gamma\gamma} = 60 \pm 5$ GeV.

$\Gamma(\nu\overline{\nu}\gamma\gamma)/\Gamma_{total}$ Γ_{51}/Γ

VALUE	CL%	DOCUMENT ID		TECN	COMMENT
$<3.1\times10^{-6}$	95	[1] ACTON	93E	OPAL	E_{cm}^{ee}= 88–94 GeV

[1] For $m_{\gamma\gamma}=60\pm5$ GeV.

$\Gamma(e^{\pm}\mu^{\mp})/\Gamma_{total}$ Γ_{52}/Γ

Test of lepton family number conservation. The value is for the sum of the charge states indicated.

VALUE	CL%	DOCUMENT ID		TECN	COMMENT
$<2.5\times10^{-6}$	95	ABREU	97C	DLPH	E_{cm}^{ee}= 88–94 GeV
$<1.7\times10^{-6}$	95	AKERS	95W	OPAL	E_{cm}^{ee}= 88–94 GeV
$<0.6\times10^{-5}$	95	ADRIANI	93I	L3	E_{cm}^{ee}= 88–94 GeV
$<2.6\times10^{-5}$	95	DECAMP	92	ALEP	E_{cm}^{ee}= 88–94 GeV

$\Gamma(e^{\pm}\mu^{\mp})/\Gamma(e^{+}e^{-})$ Γ_{52}/Γ_{1}

Test of lepton family number conservation. The value is for the sum of the charge states indicated.

VALUE	CL%	DOCUMENT ID		TECN	COMMENT
<0.07	90	ALBAJAR	89	UA1	$E_{cm}^{p\overline{p}}$= 546,630 GeV

$\Gamma(e^{\pm}\tau^{\mp})/\Gamma_{total}$ Γ_{53}/Γ

Test of lepton family number conservation. The value is for the sum of the charge states indicated.

VALUE	CL%	DOCUMENT ID		TECN	COMMENT
$<2.2\times10^{-5}$	95	ABREU	97C	DLPH	E_{cm}^{ee}= 88–94 GeV
$<9.8\times10^{-6}$	95	AKERS	95W	OPAL	E_{cm}^{ee}= 88–94 GeV
$<1.3\times10^{-5}$	95	ADRIANI	93I	L3	E_{cm}^{ee}= 88–94 GeV
$<1.2\times10^{-4}$	95	DECAMP	92	ALEP	E_{cm}^{ee}= 88–94 GeV

$\Gamma(\mu^{\pm}\tau^{\mp})/\Gamma_{total}$ Γ_{54}/Γ

Test of lepton family number conservation. The value is for the sum of the charge states indicated.

VALUE	CL%	DOCUMENT ID		TECN	COMMENT
$<1.2\times10^{-5}$	95	ABREU	97C	DLPH	E_{cm}^{ee}= 88–94 GeV
$<1.7\times10^{-5}$	95	AKERS	95W	OPAL	E_{cm}^{ee}= 88–94 GeV
$<1.9\times10^{-5}$	95	ADRIANI	93I	L3	E_{cm}^{ee}= 88–94 GeV
$<1.0\times10^{-4}$	95	DECAMP	92	ALEP	E_{cm}^{ee}= 88–94 GeV

$\Gamma(pe)/\Gamma_{total}$ Γ_{55}/Γ

Test of baryon number and lepton number conservations. Charge conjugate states are implied.

VALUE	CL%	DOCUMENT ID		TECN	COMMENT
$<1.8\times10^{-6}$	95	[1] ABBIENDI	99I	OPAL	E_{cm}^{ee}= 88–94 GeV

[1] ABBIENDI 99I give the 95%CL limit on the partial width $\Gamma(Z^0\rightarrow pe)<4.6$ KeV and we have transformed it into a branching ratio.

$\Gamma(p\mu)/\Gamma_{total}$ Γ_{56}/Γ

Test of baryon number and lepton number conservations. Charge conjugate states are implied.

VALUE	CL%	DOCUMENT ID		TECN	COMMENT
$<1.8\times10^{-6}$	95	[1] ABBIENDI	99I	OPAL	E_{cm}^{ee}= 88–94 GeV

[1] ABBIENDI 99I give the 95%CL limit on the partial width $\Gamma(Z^0\rightarrow p\mu)<4.4$ KeV and we have transformed it into a branching ratio.

AVERAGE PARTICLE MULTIPLICITIES IN HADRONIC *Z* DECAY

Summed over particle and antiparticle, when appropriate.

$\langle N_\gamma\rangle$

VALUE	DOCUMENT ID		TECN	COMMENT
20.97±0.02±1.15	ACKERSTAFF	98A	OPAL	E_{cm}^{ee}= 91.2 GeV

$\langle N_{\pi^\pm}\rangle$

VALUE	DOCUMENT ID		TECN	COMMENT
17.03 ±0.16 OUR AVERAGE				
17.007±0.209	ABE	04C	SLD	E_{cm}^{ee}= 91.2 GeV
17.26 ±0.10 ±0.88	ABREU	98L	DLPH	E_{cm}^{ee}= 91.2 GeV
17.04 ±0.31	BARATE	98V	ALEP	E_{cm}^{ee}= 91.2 GeV
17.05 ±0.43	AKERS	94P	OPAL	E_{cm}^{ee}= 91.2 GeV

$\langle N_{\pi^0}\rangle$

VALUE	DOCUMENT ID		TECN	COMMENT
9.76±0.26 OUR AVERAGE				
9.55±0.06±0.75	ACKERSTAFF	98A	OPAL	E_{cm}^{ee}= 91.2 GeV
9.63±0.13±0.63	BARATE	97J	ALEP	E_{cm}^{ee}= 91.2 GeV
9.90±0.02±0.33	ACCIARRI	96	L3	E_{cm}^{ee}= 91.2 GeV
9.2 ±0.2 ±1.0	ADAM	96	DLPH	E_{cm}^{ee}= 91.2 GeV

$\langle N_\eta\rangle$

VALUE	DOCUMENT ID		TECN	COMMENT
1.01±0.08 OUR AVERAGE Error includes scale factor of 1.3. See the ideogram below.				
1.20±0.04±0.11	HEISTER	02C	ALEP	E_{cm}^{ee}= 91.2 GeV
0.97±0.03±0.11	ACKERSTAFF	98A	OPAL	E_{cm}^{ee}= 91.2 GeV
0.93±0.01±0.09	ACCIARRI	96	L3	E_{cm}^{ee}= 91.2 GeV

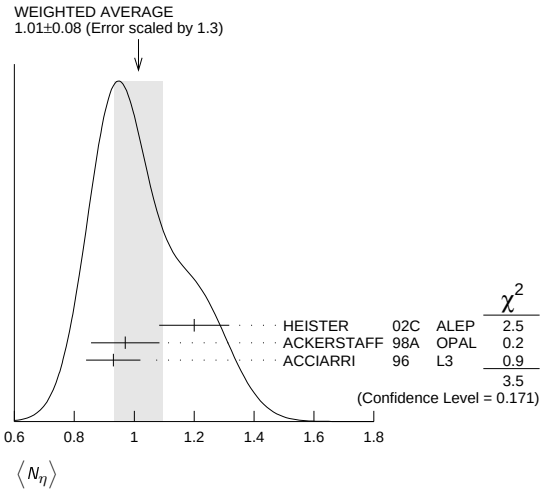

$\langle N_{\rho^\pm}\rangle$

VALUE	DOCUMENT ID		TECN	COMMENT
2.57±0.15 OUR AVERAGE				
2.59±0.03±0.16	[1] BEDDALL	09		ALEPH archive, E_{cm}^{ee}= 91.2 GeV
2.40±0.06±0.43	ACKERSTAFF	98A	OPAL	E_{cm}^{ee}= 91.2 GeV

[1] BEDDALL 09 analyse 3.2 million hadronic Z decays as archived by ALEPH collaboration and report a value of $2.59\pm0.03\pm0.15\pm0.04$. The first error is statistical, the second systematic, and the third arises from extrapolation to full phase space. We combine the systematic errors in quadrature.

$\langle N_{\rho^0}\rangle$

VALUE	DOCUMENT ID		TECN	COMMENT
1.24±0.10 OUR AVERAGE Error includes scale factor of 1.1.				
1.19±0.10	ABREU	99J	DLPH	E_{cm}^{ee}= 91.2 GeV
1.45±0.06±0.20	BUSKULIC	96H	ALEP	E_{cm}^{ee}= 91.2 GeV

$\langle N_\omega\rangle$

VALUE	DOCUMENT ID		TECN	COMMENT
1.02±0.06 OUR AVERAGE				
1.00±0.03±0.06	HEISTER	02C	ALEP	E_{cm}^{ee}= 91.2 GeV
1.04±0.04±0.14	ACKERSTAFF	98A	OPAL	E_{cm}^{ee}= 91.2 GeV
1.17±0.09±0.15	ACCIARRI	97D	L3	E_{cm}^{ee}= 91.2 GeV

$\langle N_{\eta'}\rangle$

VALUE	DOCUMENT ID		TECN	COMMENT
0.17 ±0.05 OUR AVERAGE Error includes scale factor of 2.4.				
0.14 ±0.01 ±0.02	ACKERSTAFF	98A	OPAL	E_{cm}^{ee}= 91.2 GeV
0.25 ±0.04	[1] ACCIARRI	97D	L3	E_{cm}^{ee}= 91.2 GeV
• • • We do not use the following data for averages, fits, limits, etc. • • •				
0.068±0.018±0.016	[2] BUSKULIC	92D	ALEP	E_{cm}^{ee}= 91.2 GeV

[1] ACCIARRI 97D obtain this value averaging over the two decay channels $\eta'\rightarrow\pi^+\pi^-\eta$ and $\eta'\rightarrow\rho^0\gamma$.

[2] BUSKULIC 92D obtain this value for $x>0.1$.

$\langle N_{f_0(980)}\rangle$

VALUE	DOCUMENT ID		TECN	COMMENT
0.147±0.011 OUR AVERAGE				
0.164±0.021	ABREU	99J	DLPH	E_{cm}^{ee}= 91.2 GeV
0.141±0.007±0.011	ACKERSTAFF	98Q	OPAL	E_{cm}^{ee}= 91.2 GeV

$\langle N_{a_0(980)^\pm}\rangle$

VALUE	DOCUMENT ID		TECN	COMMENT
0.27±0.04±0.10	ACKERSTAFF	98A	OPAL	E_{cm}^{ee}= 91.2 GeV

$\langle N_\phi \rangle$

VALUE	DOCUMENT ID		TECN	COMMENT
0.098±0.006 OUR AVERAGE	Error includes scale factor of 2.0.			See the ideogram below.
0.105±0.008	ABE	99E	SLD	E_{cm}^{ee}= 91.2 GeV
0.091±0.002±0.003	ACKERSTAFF	98Q	OPAL	E_{cm}^{ee}= 91.2 GeV
0.104±0.003±0.007	ABREU	96U	DLPH	E_{cm}^{ee}= 91.2 GeV
0.122±0.004±0.008	BUSKULIC	96H	ALEP	E_{cm}^{ee}= 91.2 GeV

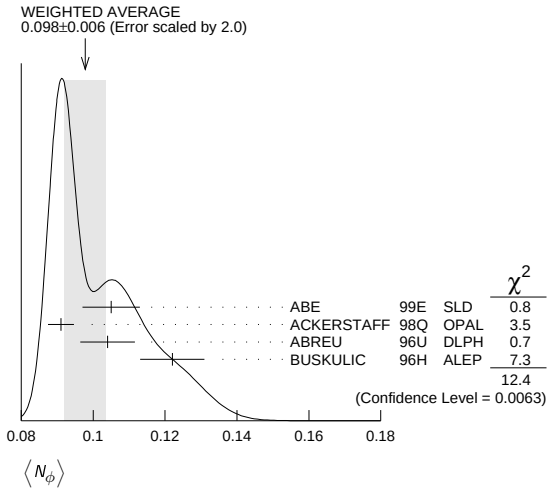

$\langle N_{f_2(1270)} \rangle$

VALUE	DOCUMENT ID		TECN	COMMENT
0.169±0.025 OUR AVERAGE	Error includes scale factor of 1.4.			
0.214±0.038	ABREU	99J	DLPH	E_{cm}^{ee}= 91.2 GeV
0.155±0.011±0.018	ACKERSTAFF	98Q	OPAL	E_{cm}^{ee}= 91.2 GeV

$\langle N_{f_1(1285)} \rangle$

VALUE	DOCUMENT ID		TECN	COMMENT
0.165±0.051	[1] ABDALLAH	03H	DLPH	E_{cm}^{ee}= 91.2 GeV

[1] ABDALLAH 03H assume a $K\overline{K}\pi$ branching ratio of (9.0 ± 0.4)%.

$\langle N_{f_1(1420)} \rangle$

VALUE	DOCUMENT ID		TECN	COMMENT
0.056±0.012	[1] ABDALLAH	03H	DLPH	E_{cm}^{ee}= 91.2 GeV

[1] ABDALLAH 03H assume a $K\overline{K}\pi$ branching ratio of 100%.

$\langle N_{f_2'(1525)} \rangle$

VALUE	DOCUMENT ID		TECN	COMMENT
0.012±0.006	ABREU	99J	DLPH	E_{cm}^{ee}= 91.2 GeV

$\langle N_{K^\pm} \rangle$

VALUE	DOCUMENT ID		TECN	COMMENT
2.24 ±0.04 OUR AVERAGE				
2.203±0.071	ABE	04C	SLD	E_{cm}^{ee}= 91.2 GeV
2.21 ±0.05 ±0.05	ABREU	98L	DLPH	E_{cm}^{ee}= 91.2 GeV
2.26 ±0.12	BARATE	98V	ALEP	E_{cm}^{ee}= 91.2 GeV
2.42 ±0.13	AKERS	94P	OPAL	E_{cm}^{ee}= 91.2 GeV

$\langle N_{K^0} \rangle$

VALUE	DOCUMENT ID		TECN	COMMENT
2.039±0.025 OUR AVERAGE	Error includes scale factor of 1.3.			See the ideogram below.
2.093±0.004±0.029	BARATE	00O	ALEP	E_{cm}^{ee}= 91.2 GeV
2.01 ±0.08	ABE	99E	SLD	E_{cm}^{ee}= 91.2 GeV
2.024±0.006±0.042	ACCIARRI	97L	L3	E_{cm}^{ee}= 91.2 GeV
1.962±0.022±0.056	ABREU	95L	DLPH	E_{cm}^{ee}= 91.2 GeV
1.99 ±0.01 ±0.04	AKERS	95U	OPAL	E_{cm}^{ee}= 91.2 GeV

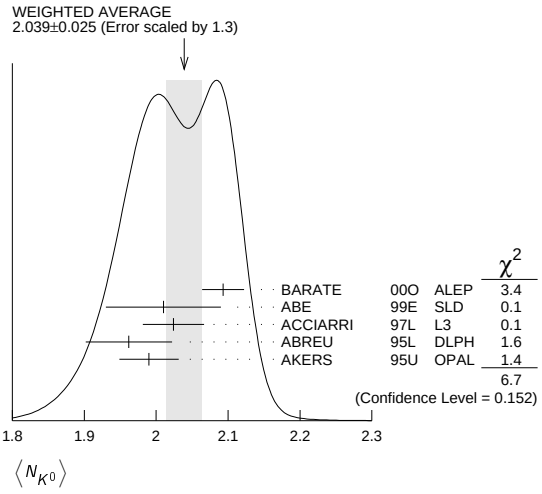

$\langle N_{K^*(892)^\pm} \rangle$

VALUE	DOCUMENT ID		TECN	COMMENT
0.72 ±0.05 OUR AVERAGE				
0.712±0.031±0.059	ABREU	95L	DLPH	E_{cm}^{ee}= 91.2 GeV
0.72 ±0.02 ±0.08	ACTON	93	OPAL	E_{cm}^{ee}= 91.2 GeV

$\langle N_{K^*(892)^0} \rangle$

VALUE	DOCUMENT ID		TECN	COMMENT
0.739±0.022 OUR AVERAGE				
0.707±0.041	ABE	99E	SLD	E_{cm}^{ee}= 91.2 GeV
0.74 ±0.02 ±0.02	ACKERSTAFF	97S	OPAL	E_{cm}^{ee}= 91.2 GeV
0.77 ±0.02 ±0.07	ABREU	96U	DLPH	E_{cm}^{ee}= 91.2 GeV
0.83 ±0.01 ±0.09	BUSKULIC	96H	ALEP	E_{cm}^{ee}= 91.2 GeV
0.97 ±0.18 ±0.31	ABREU	93	DLPH	E_{cm}^{ee}= 91.2 GeV

$\langle N_{K_2^*(1430)} \rangle$

VALUE	DOCUMENT ID		TECN	COMMENT
0.073±0.023	ABREU	99J	DLPH	E_{cm}^{ee}= 91.2 GeV
• • • We do not use the following data for averages, fits, limits, etc. • • •				
0.19 ±0.04 ±0.06	[1] AKERS	95X	OPAL	E_{cm}^{ee}= 91.2 GeV

[1] AKERS 95X obtain this value for $x < 0.3$.

$\langle N_{D^\pm} \rangle$

VALUE	DOCUMENT ID		TECN	COMMENT
0.187±0.020 OUR AVERAGE	Error includes scale factor of 1.5.			See the ideogram below.
0.170±0.009±0.014	ALEXANDER	96R	OPAL	E_{cm}^{ee}= 91.2 GeV
0.251±0.026±0.025	BUSKULIC	94J	ALEP	E_{cm}^{ee}= 91.2 GeV
0.199±0.019±0.024	[1] ABREU	93I	DLPH	E_{cm}^{ee}= 91.2 GeV

[1] See ABREU 95 (erratum).

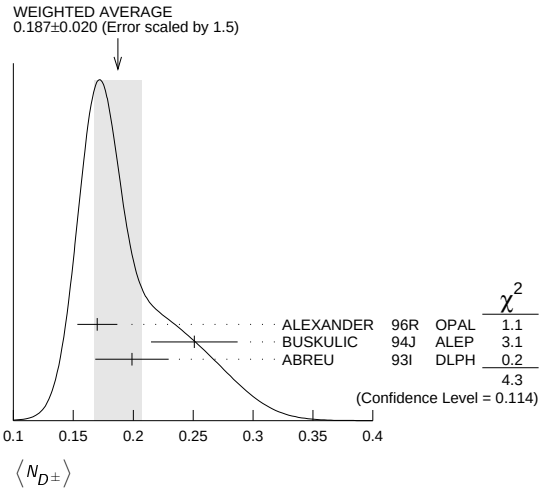

$\langle N_{D^0} \rangle$

VALUE	DOCUMENT ID		TECN	COMMENT
0.462±0.026 OUR AVERAGE				
0.465±0.017±0.027	ALEXANDER	96R	OPAL	E_{cm}^{ee}= 91.2 GeV
0.518±0.052±0.035	BUSKULIC	94J	ALEP	E_{cm}^{ee}= 91.2 GeV
0.403±0.038±0.044	[1] ABREU	93I	DLPH	E_{cm}^{ee}= 91.2 GeV

[1] See ABREU 95 (erratum).

$\langle N_{D_s^\pm} \rangle$

VALUE	DOCUMENT ID		TECN	COMMENT
0.131±0.010±0.018	ALEXANDER	96R	OPAL	E_{cm}^{ee}= 91.2 GeV

$\langle N_{D^*(2010)^\pm} \rangle$

VALUE	DOCUMENT ID		TECN	COMMENT
0.183 ±0.008 OUR AVERAGE				
0.1854±0.0041±0.0091	[1] ACKERSTAFF	98E	OPAL	E_{cm}^{ee}= 91.2 GeV
0.187 ±0.015 ±0.013	BUSKULIC	94J	ALEP	E_{cm}^{ee}= 91.2 GeV
0.171 ±0.012 ±0.016	[2] ABREU	93I	DLPH	E_{cm}^{ee}= 91.2 GeV

[1] ACKERSTAFF 98E systematic error includes an uncertainty of ±0.0069 due to the branching ratios $B(D^{*+} \to D^0\pi^+) = 0.683\pm0.014$ and $B(D^0 \to K^-\pi^+) = 0.0383\pm0.0012$.

[2] See ABREU 95 (erratum).

$\langle N_{D_{s1}(2536)^+} \rangle$

VALUE (units 10^{-3})	DOCUMENT ID		TECN	COMMENT
• • • We do not use the following data for averages, fits, limits, etc. • • •				
$2.9^{+0.7}_{-0.6}\pm0.2$	[1] ACKERSTAFF	97W	OPAL	E_{cm}^{ee}= 91.2 GeV

[1] ACKERSTAFF 97W obtain this value for $x > 0.6$ and with the assumption that its decay width is saturated by the D^*K final states.

$\langle N_{B^*} \rangle$

VALUE	DOCUMENT ID		TECN	COMMENT
0.28±0.01±0.03	[1] ABREU	95R	DLPH	E_{cm}^{ee}= 91.2 GeV

[1] ABREU 95R quote this value for a flavor-averaged excited state.

$\langle N_{J/\psi(1S)} \rangle$

VALUE	DOCUMENT ID		TECN	COMMENT
0.0056±0.0003±0.0004	[1] ALEXANDER	96B	OPAL	E_{cm}^{ee}= 91.2 GeV

[1] ALEXANDER 96B identify $J/\psi(1S)$ from the decays into lepton pairs.

$\langle N_{\psi(2S)} \rangle$

VALUE	DOCUMENT ID		TECN	COMMENT
0.0023±0.0004±0.0003	ALEXANDER	96B	OPAL	E_{cm}^{ee}= 91.2 GeV

$\langle N_p \rangle$

VALUE	DOCUMENT ID		TECN	COMMENT
1.046±0.026 OUR AVERAGE				
1.054±0.035	ABE	04C	SLD	E_{cm}^{ee}= 91.2 GeV
1.08 ±0.04 ±0.03	ABREU	98L	DLPH	E_{cm}^{ee}= 91.2 GeV
1.00 ±0.07	BARATE	98V	ALEP	E_{cm}^{ee}= 91.2 GeV
0.92 ±0.11	AKERS	94P	OPAL	E_{cm}^{ee}= 91.2 GeV

$\langle N_{\Delta(1232)^{++}} \rangle$

VALUE	DOCUMENT ID		TECN	COMMENT
0.087±0.033 OUR AVERAGE	Error includes scale factor of 2.4.			
0.079±0.009±0.011	ABREU	95W	DLPH	E_{cm}^{ee}= 91.2 GeV
0.22 ±0.04 ±0.04	ALEXANDER	95D	OPAL	E_{cm}^{ee}= 91.2 GeV

$\langle N_\Lambda \rangle$

VALUE	DOCUMENT ID		TECN	COMMENT
0.388±0.009 OUR AVERAGE	Error includes scale factor of 1.7.			See the ideogram below.
0.404±0.002±0.007	BARATE	00O	ALEP	E_{cm}^{ee}= 91.2 GeV
0.395±0.022	ABE	99E	SLD	E_{cm}^{ee}= 91.2 GeV
0.364±0.004±0.017	ACCIARRI	97L	L3	E_{cm}^{ee}= 91.2 GeV
0.374±0.002±0.010	ALEXANDER	97D	OPAL	E_{cm}^{ee}= 91.2 GeV
0.357±0.003±0.017	ABREU	93L	DLPH	E_{cm}^{ee}= 91.2 GeV

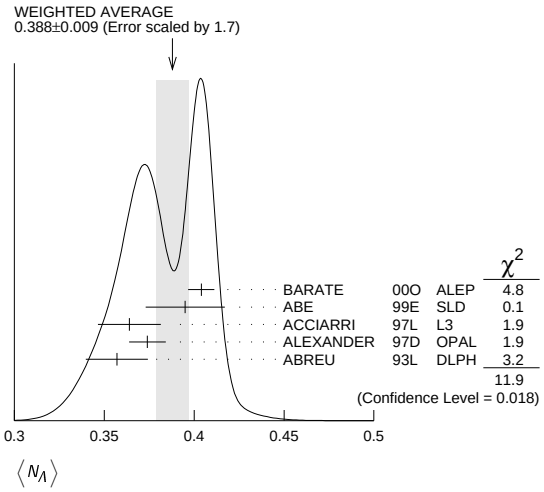

$\langle N_{\Lambda(1520)} \rangle$

VALUE	DOCUMENT ID		TECN	COMMENT
0.0224±0.0027 OUR AVERAGE				
0.029 ±0.005 ±0.005	ABREU	00P	DLPH	E_{cm}^{ee}= 91.2 GeV
0.0213±0.0021±0.0019	ALEXANDER	97D	OPAL	E_{cm}^{ee}= 91.2 GeV

$\langle N_{\Sigma^+} \rangle$

VALUE	DOCUMENT ID		TECN	COMMENT
0.107±0.010 OUR AVERAGE				
0.114±0.011±0.009	ACCIARRI	00J	L3	E_{cm}^{ee}= 91.2 GeV
0.099±0.008±0.013	ALEXANDER	97E	OPAL	E_{cm}^{ee}= 91.2 GeV

$\langle N_{\Sigma^-} \rangle$

VALUE	DOCUMENT ID		TECN	COMMENT
0.082±0.007 OUR AVERAGE				
0.081±0.002±0.010	ABREU	00P	DLPH	E_{cm}^{ee}= 91.2 GeV
0.083±0.006±0.009	ALEXANDER	97E	OPAL	E_{cm}^{ee}= 91.2 GeV

$\langle N_{\Sigma^+ + \Sigma^-} \rangle$

VALUE	DOCUMENT ID		TECN	COMMENT
0.181±0.018 OUR AVERAGE				
0.182±0.010±0.016	[1] ALEXANDER	97E	OPAL	E_{cm}^{ee}= 91.2 GeV
0.170±0.014±0.061	ABREU	95O	DLPH	E_{cm}^{ee}= 91.2 GeV

[1] We have combined the values of $\langle N_{\Sigma^+} \rangle$ and $\langle N_{\Sigma^-} \rangle$ from ALEXANDER 97E adding the statistical and systematic errors of the two final states separately in quadrature. If isospin symmetry is assumed this value becomes 0.174 ± 0.010 ± 0.015.

$\langle N_{\Sigma^0} \rangle$

VALUE	DOCUMENT ID		TECN	COMMENT
0.076±0.010 OUR AVERAGE				
0.095±0.015±0.013	ACCIARRI	00J	L3	E_{cm}^{ee}= 91.2 GeV
0.071±0.012±0.013	ALEXANDER	97E	OPAL	E_{cm}^{ee}= 91.2 GeV
0.070±0.010±0.010	ADAM	96B	DLPH	E_{cm}^{ee}= 91.2 GeV

$\langle N_{(\Sigma^+ + \Sigma^- + \Sigma^0)/3} \rangle$

VALUE	DOCUMENT ID		TECN	COMMENT
0.084±0.005±0.008	ALEXANDER	97E	OPAL	E_{cm}^{ee}= 91.2 GeV

$\langle N_{\Sigma(1385)^+} \rangle$

VALUE	DOCUMENT ID		TECN	COMMENT
0.0239±0.0009±0.0012	ALEXANDER	97D	OPAL	E_{cm}^{ee}= 91.2 GeV

$\langle N_{\Sigma(1385)^-} \rangle$

VALUE	DOCUMENT ID		TECN	COMMENT
0.0240±0.0010±0.0014	ALEXANDER	97D	OPAL	E_{cm}^{ee}= 91.2 GeV

$\langle N_{\Sigma(1385)^+ + \Sigma(1385)^-} \rangle$

VALUE	DOCUMENT ID		TECN	COMMENT
0.046 ±0.004 OUR AVERAGE	Error includes scale factor of 1.6.			
0.0479±0.0013±0.0026	ALEXANDER	97D	OPAL	E_{cm}^{ee}= 91.2 GeV
0.0382±0.0028±0.0045	ABREU	95O	DLPH	E_{cm}^{ee}= 91.2 GeV

$\langle N_{\Xi^-} \rangle$

VALUE	DOCUMENT ID		TECN	COMMENT
0.0258±0.0009 OUR AVERAGE				
0.0247±0.0009±0.0025	ABDALLAH	06E	DLPH	E_{cm}^{ee} = 91.2 GeV
0.0259±0.0004±0.0009	ALEXANDER	97D	OPAL	E_{cm}^{ee} = 91.2 GeV

$\langle N_{\Xi(1530)^0} \rangle$

VALUE	DOCUMENT ID		TECN	COMMENT
0.0059±0.0011 OUR AVERAGE	Error includes scale factor of 2.3.			
0.0045±0.0005±0.0006	ABDALLAH	05C	DLPH	E_{cm}^{ee}= 91.2 GeV
0.0068±0.0005±0.0004	ALEXANDER	97D	OPAL	E_{cm}^{ee}= 91.2 GeV

$\langle N_{\Omega^-} \rangle$

VALUE	DOCUMENT ID		TECN	COMMENT
0.00164±0.00028 OUR AVERAGE				
0.0018 ±0.0003 ±0.0002	ALEXANDER	97D	OPAL	E_{cm}^{ee}= 91.2 GeV
0.0014 ±0.0002 ±0.0004	ADAM	96B	DLPH	E_{cm}^{ee}= 91.2 GeV

$\langle N_{\Lambda_c^+} \rangle$

VALUE	DOCUMENT ID		TECN	COMMENT
0.078±0.012±0.012	ALEXANDER	96R	OPAL	E_{cm}^{ee}= 91.2 GeV

$\langle N_{\overline{D}} \rangle$

VALUE (units 10^{-6})	DOCUMENT ID		TECN	COMMENT
• • • We do not use the following data for averages, fits, limits, etc. • • •				
5.9±1.8±0.5	[1] SCHAEL	06A	ALEP	E_{cm}^{ee} = 91.2 GeV

[1] SCHAEL 06A obtain this anti-deuteron production rate per hadronic Z decay in the anti-deuteron momentum range from 0.62 to 1.03 GeV/c.

$\langle N_{charged} \rangle$

VALUE	DOCUMENT ID		TECN	COMMENT
20.76±0.16 OUR AVERAGE	Error includes scale factor of 2.1. See the ideogram below.			
20.46±0.01±0.11	ACHARD	03G	L3	E_{cm}^{ee}= 91.2 GeV
21.21±0.01±0.20	ABREU	99	DLPH	E_{cm}^{ee}= 91.2 GeV
21.05±0.20	AKERS	95Z	OPAL	E_{cm}^{ee}= 91.2 GeV
20.91±0.03±0.22	BUSKULIC	95R	ALEP	E_{cm}^{ee}= 91.2 GeV
21.40±0.43	ACTON	92B	OPAL	E_{cm}^{ee}= 91.2 GeV
20.71±0.04±0.77	ABREU	91H	DLPH	E_{cm}^{ee}= 91.2 GeV
20.7 ±0.7	ADEVA	91I	L3	E_{cm}^{ee}= 91.2 GeV
20.1 ±1.0 ±0.9	ABRAMS	90	MRK2	E_{cm}^{ee}= 91.1 GeV

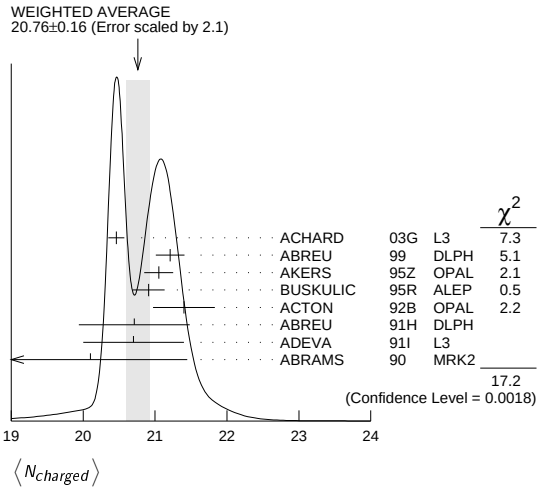

Z HADRONIC POLE CROSS SECTION

OUR FIT is obtained using the fit procedure and correlations as determined by the LEP Electroweak Working Group (see the note "The Z boson" and ref. LEP-SLC 06). This quantity is defined as

$$\sigma_h^0 = \frac{12\pi}{M_Z^2} \frac{\Gamma(e^+e^-)\Gamma(\text{hadrons})}{\Gamma_Z^2}$$

It is one of the parameters used in the Z lineshape fit.

VALUE (nb)	EVTS	DOCUMENT ID		TECN	COMMENT
41.541±0.037 OUR FIT					
41.501±0.055	4.10M	[1] ABBIENDI	01A	OPAL	E_{cm}^{ee}= 88–94 GeV
41.578±0.069	3.70M	ABREU	00F	DLPH	E_{cm}^{ee}= 88–94 GeV
41.535±0.055	3.54M	ACCIARRI	00C	L3	E_{cm}^{ee}= 88–94 GeV
41.559±0.058	4.07M	[2] BARATE	00C	ALEP	E_{cm}^{ee}= 88–94 GeV
• • • We do not use the following data for averages, fits, limits, etc. • • •					
42 ±4	450	ABRAMS	89B	MRK2	E_{cm}^{ee}= 89.2–93.0 GeV

[1] ABBIENDI 01A error includes approximately 0.031 due to statistics, 0.033 due to event selection systematics, 0.029 due to uncertainty in luminosity measurement, and 0.011 due to LEP energy uncertainty.
[2] BARATE 00C error includes approximately 0.030 due to statistics, 0.026 due to experimental systematics, and 0.025 due to uncertainty in luminosity measurement.

Z VECTOR COUPLINGS

These quantities are the effective vector couplings of the Z to charged leptons. Their magnitude is derived from a measurement of the Z lineshape and the forward-backward lepton asymmetries as a function of energy around the Z mass. The relative sign among the vector to axial-vector couplings is obtained from a measurement of the Z asymmetry parameters, A_e, A_μ, and A_τ. By convention the sign of g_A^e is fixed to be negative (and opposite to that of g^{ν_e} obtained using ν_e scattering measurements). For the light quarks, the sign of the couplings is assigned consistently with this assumption. The fit values quoted below correspond to global nine- or five-parameter fits to lineshape, lepton forward-backward asymmetry, and A_e, A_μ, and A_τ measurements. See the note "The Z boson" and ref. LEP-SLC 06 for details. Where $p\overline{p}$ and ep data is quoted, OUR FIT value corresponds to a weighted average of this with the LEP/SLD fit result.

g_V^e

VALUE	EVTS	DOCUMENT ID		TECN	COMMENT
−0.03817±0.00047 OUR FIT					
−0.058 ±0.016 ±0.007	5026	[1] ACOSTA	05M	CDF	$E_{cm}^{p\overline{p}}$= 1.96 TeV
−0.0346 ±0.0023	137.0K	[2] ABBIENDI	01O	OPAL	E_{cm}^{ee}= 88–94 GeV
−0.0412 ±0.0027	124.4k	[3] ACCIARRI	00C	L3	E_{cm}^{ee}= 88–94 GeV
−0.0400 ±0.0037		BARATE	00C	ALEP	E_{cm}^{ee}= 88–94 GeV
−0.0414 ±0.0020		[4] ABE	95J	SLD	E_{cm}^{ee}= 91.31 GeV

[1] ACOSTA 05M determine the forward–backward asymmetry of e^+e^- pairs produced via $q\overline{q} \to Z/\gamma^* \to e^+e^-$ in 15 M(e^+e^-) effective mass bins ranging from 40 GeV to 600 GeV. These results are used to obtain the vector and axial–vector couplings of the Z to e^+e^-, assuming the quark couplings are as predicted by the standard model. Higher order radiative corrections have not been taken into account.
[2] ABBIENDI 01O use their measurement of the τ polarization in addition to the lineshape and forward-backward lepton asymmetries.
[3] ACCIARRI 00C use their measurement of the τ polarization in addition to forward-backward lepton asymmetries.
[4] ABE 95J obtain this result combining polarized Bhabha results with the A_{LR} measurement of ABE 94C. The Bhabha results alone give −0.0507 ± 0.0096 ± 0.0020.

g_V^μ

VALUE	EVTS	DOCUMENT ID		TECN	COMMENT
−0.0367±0.0023 OUR FIT					
$-0.0388^{+0.0060}_{-0.0064}$	182.8K	[1] ABBIENDI	01O	OPAL	E_{cm}^{ee}= 88–94 GeV
−0.0386±0.0073	113.4k	[2] ACCIARRI	00C	L3	E_{cm}^{ee}= 88–94 GeV
−0.0362±0.0061		BARATE	00C	ALEP	E_{cm}^{ee}= 88–94 GeV
• • • We do not use the following data for averages, fits, limits, etc. • • •					
−0.0413±0.0060	66143	[3] ABBIENDI	01K	OPAL	E_{cm}^{ee}= 89–93 GeV

[1] ABBIENDI 01O use their measurement of the τ polarization in addition to the lineshape and forward-backward lepton asymmetries.
[2] ACCIARRI 00C use their measurement of the τ polarization in addition to forward-backward lepton asymmetries.
[3] ABBIENDI 01K obtain this from an angular analysis of the muon pair asymmetry which takes into account effects of initial state radiation on an event by event basis and of initial-final state interference.

g_V^τ

VALUE	EVTS	DOCUMENT ID		TECN	COMMENT
−0.0366±0.0010 OUR FIT					
−0.0365±0.0023	151.5K	[1] ABBIENDI	01O	OPAL	E_{cm}^{ee}= 88–94 GeV
−0.0384±0.0026	103.0k	[2] ACCIARRI	00C	L3	E_{cm}^{ee}= 88–94 GeV
−0.0361±0.0068		BARATE	00C	ALEP	E_{cm}^{ee}= 88–94 GeV

[1] ABBIENDI 01O use their measurement of the τ polarization in addition to the lineshape and forward-backward lepton asymmetries.
[2] ACCIARRI 00C use their measurement of the τ polarization in addition to forward-backward lepton asymmetries.

g_V^ℓ

VALUE	EVTS	DOCUMENT ID		TECN	COMMENT
−0.03783±0.00041 OUR FIT					
−0.0358 ±0.0014	471.3K	[1] ABBIENDI	01O	OPAL	E_{cm}^{ee}= 88–94 GeV
−0.0397 ±0.0020	379.4k	[2] ABREU	00F	DLPH	E_{cm}^{ee}= 88–94 GeV
−0.0397 ±0.0017	340.8k	[3] ACCIARRI	00C	L3	E_{cm}^{ee}= 88–94 GeV
−0.0383 ±0.0018	500k	BARATE	00C	ALEP	E_{cm}^{ee}= 88–94 GeV

[1] ABBIENDI 01O use their measurement of the τ polarization in addition to the lineshape and forward-backward lepton asymmetries.
[2] Using forward-backward lepton asymmetries.
[3] ACCIARRI 00C use their measurement of the τ polarization in addition to forward-backward lepton asymmetries.

g_V^u

VALUE	EVTS	DOCUMENT ID		TECN	COMMENT
0.25 $^{+0.07}_{-0.06}$ OUR AVERAGE					
0.201±0.112	156k	[1] ABAZOV	11D	D0	$E_{cm}^{p\overline{p}}$ = 1.97 TeV
0.27 ±0.13	1500	[2] AKTAS	06	H1	$e^\pm p \to \overline{\nu}_e(\nu_e)X$, $\sqrt{s} \approx 300$ GeV
0.24 $^{+0.28}_{-0.11}$		[3] LEP-SLC	06		E_{cm}^{ee} = 88–94 GeV
$0.399^{+0.152}_{-0.188}$±0.066	5026	[4] ACOSTA	05M	CDF	$E_{cm}^{p\overline{p}}$= 1.96 TeV

[1] ABAZOV 11D study $p\overline{p} \to Z/\gamma^* e^+ e^-$ events using 5 fb^{-1} data at $\sqrt{s} = 1.96$ TeV. The candidate events are selected by requiring two isolated electromagnetic showers with $E_T > 25$ GeV, at least one electron in the central region and the di-electron mass in the range 50–1000 GeV. From the forward-backward asymmetry, determined as a function of the di-electron mass, they derive the axial and vector couplings of the u- and d- quarks and the value of $\sin^2\theta^\ell_{eff} = 0.2309 \pm 0.0008(\text{stat}) \pm 0.0006(\text{syst})$.

[2] AKTAS 06 fit the neutral current ($1.5 \leq Q^2 \leq 30{,}000$ GeV^2) and charged current ($1.5 \leq Q^2 \leq 15{,}000$ GeV^2) differential cross sections. In the determination of the u-quark couplings the electron and d-quark couplings are fixed to their standard model values.

[3] LEP-SLC 06 is a combination of the results from LEP and SLC experiments using light quark tagging. s- and d-quark couplings are assumed to be identical.

[4] ACOSTA 05M determine the forward-backward asymmetry of e^+e^- pairs produced via $q\overline{q} \to Z/\gamma^* \to e^+e^-$ in 15 M(e^+e^-) effective mass bins ranging from 40 GeV to 600 GeV. These results are used to obtain the vector and axial-vector couplings of the Z to the light quarks, assuming the electron couplings are as predicted by the Standard Model. Higher order radiative corrections have not been taken into account.

g_V^d

VALUE	EVTS	DOCUMENT ID		TECN	COMMENT
$-0.33\ ^{+0.05}_{-0.06}$ OUR AVERAGE					
-0.351 ± 0.251	156k	[1] ABAZOV	11D	D0	$E^{p\overline{p}}_{\text{cm}} = 1.97$ TeV
-0.33 ± 0.33	1500	[2] AKTAS	06	H1	$e^\pm p \to \overline{\nu}_e(\nu_e)X$, $\sqrt{s} \approx 300$ GeV
$-0.33\ ^{+0.05}_{-0.07}$		[3] LEP-SLC	06		$E^{ee}_{\text{cm}} = 88$–94 GeV
$-0.226\ ^{+0.635}_{-0.290} \pm 0.090$	5026	[4] ACOSTA	05M	CDF	$E^{p\overline{p}}_{\text{cm}} = 1.96$ TeV

[1] ABAZOV 11D study $p\overline{p} \to Z/\gamma^* e^+ e^-$ events using 5 fb^{-1} data at $\sqrt{s} = 1.96$ TeV. The candidate events are selected by requiring two isolated electromagnetic showers with $E_T > 25$ GeV, at least one electron in the central region and the di-electron mass in the range 50–1000 GeV. From the forward-backward asymmetry, determined as a function of the di-electron mass, they derive the axial and vector couplings of the u- and d- quarks and the value of $\sin^2\theta^\ell_{eff} = 0.2309 \pm 0.0008(\text{stat}) \pm 0.0006(\text{syst})$.

[2] AKTAS 06 fit the neutral current ($1.5 \leq Q^2 \leq 30{,}000$ GeV^2) and charged current ($1.5 \leq Q^2 \leq 15{,}000$ GeV^2) differential cross sections. In the determination of the d-quark couplings the electron and u-quark couplings are fixed to their standard model values.

[3] LEP-SLC 06 is a combination of the results from LEP and SLC experiments using light quark tagging. s- and d-quark couplings are assumed to be identical.

[4] ACOSTA 05M determine the forward-backward asymmetry of e^+e^- pairs produced via $q\overline{q} \to Z/\gamma^* \to e^+e^-$ in 15 M(e^+e^-) effective mass bins ranging from 40 GeV to 600 GeV. These results are used to obtain the vector and axial-vector couplings of the Z to the light quarks, assuming the electron couplings are as predicted by the Standard Model. Higher order radiative corrections have not been taken into account.

Z AXIAL-VECTOR COUPLINGS

These quantities are the effective axial-vector couplings of the Z to charged leptons. Their magnitude is derived from a measurement of the Z line-shape and the forward-backward lepton asymmetries as a function of energy around the Z mass. The relative sign among the vector to axial-vector couplings is obtained from a measurement of the Z asymmetry parameters, A_e, A_μ, and A_τ. By convention the sign of g_A^e is fixed to be negative (and opposite to that of g^{ν_e} obtained using ν_e scattering measurements). For the light quarks, the sign of the couplings is assigned consistently with this assumption. The fit values quoted below correspond to global nine- or five-parameter fits to lineshape, lepton forward-backward asymmetry, and A_e, A_μ, and A_τ measurements. See the note "The Z boson" and ref. LEP-SLC 06 for details. Where $p\overline{p}$ and ep data is quoted, OUR FIT value corresponds to a weighted average of this with the LEP/SLD fit result.

g_A^e

VALUE	EVTS	DOCUMENT ID		TECN	COMMENT
-0.50111 ± 0.00035 OUR FIT					
$-0.528 \pm 0.123 \pm 0.059$	5026	[1] ACOSTA	05M	CDF	$E^{p\overline{p}}_{\text{cm}} = 1.96$ TeV
-0.50062 ± 0.00062	137.0K	[2] ABBIENDI	01O	OPAL	$E^{ee}_{\text{cm}} = 88$–94 GeV
-0.5015 ± 0.0007	124.4k	[3] ACCIARRI	00C	L3	$E^{ee}_{\text{cm}} = 88$–94 GeV
-0.50166 ± 0.00057		BARATE	00C	ALEP	$E^{ee}_{\text{cm}} = 88$–94 GeV
-0.4977 ± 0.0045		[4] ABE	95J	SLD	$E^{ee}_{\text{cm}} = 91.31$ GeV

[1] ACOSTA 05M determine the forward–backward asymmetry of e^+e^- pairs produced via $q\overline{q} \to Z/\gamma^* \to e^+e^-$ in 15 M(e^+e^-) effective mass bins ranging from 40 GeV to 600 GeV. These results are used to obtain the vector and axial–vector couplings of the Z to e^+e^-, assuming the quark couplings are as predicted by the standard model. Higher order radiative corrections have not been taken into account.

[2] ABBIENDI 01O use their measurement of the τ polarization in addition to the lineshape and forward-backward lepton asymmetries.

[3] ACCIARRI 00C use their measurement of the τ polarization in addition to forward-backward lepton asymmetries.

[4] ABE 95J obtain this result combining polarized Bhabha results with the A_{LR} measurement of ABE 94C. The Bhabha results alone give $-0.4968 \pm 0.0039 \pm 0.0027$.

g_A^μ

VALUE	EVTS	DOCUMENT ID		TECN	COMMENT
-0.50120 ± 0.00054 OUR FIT					
-0.50117 ± 0.00099	182.8K	[1] ABBIENDI	01O	OPAL	$E^{ee}_{\text{cm}} = 88$–94 GeV
-0.5009 ± 0.0014	113.4k	[2] ACCIARRI	00C	L3	$E^{ee}_{\text{cm}} = 88$–94 GeV
-0.50046 ± 0.00093		BARATE	00C	ALEP	$E^{ee}_{\text{cm}} = 88$–94 GeV
• • • We do not use the following data for averages, fits, limits, etc. • • •					
-0.520 ± 0.015	66143	[3] ABBIENDI	01K	OPAL	$E^{ee}_{\text{cm}} = 89$–93 GeV

[1] ABBIENDI 01O use their measurement of the τ polarization in addition to the lineshape and forward-backward lepton asymmetries.

[2] ACCIARRI 00C use their measurement of the τ polarization in addition to forward-backward lepton asymmetries.

[3] ABBIENDI 01K obtain this from an angular analysis of the muon pair asymmetry which takes into account effects of initial state radiation on an event by event basis and of initial-final state interference.

g_A^τ

VALUE	EVTS	DOCUMENT ID		TECN	COMMENT
-0.50204 ± 0.00064 OUR FIT					
-0.50165 ± 0.00124	151.5K	[1] ABBIENDI	01O	OPAL	$E^{ee}_{\text{cm}} = 88$–94 GeV
-0.5023 ± 0.0017	103.0k	[2] ACCIARRI	00C	L3	$E^{ee}_{\text{cm}} = 88$–94 GeV
-0.50216 ± 0.00100		BARATE	00C	ALEP	$E^{ee}_{\text{cm}} = 88$–94 GeV

[1] ABBIENDI 01O use their measurement of the τ polarization in addition to the lineshape and forward-backward lepton asymmetries.

[2] ACCIARRI 00C use their measurement of the τ polarization in addition to forward-backward lepton asymmetries.

g_A^ℓ

VALUE	EVTS	DOCUMENT ID		TECN	COMMENT
-0.50123 ± 0.00026 OUR FIT					
-0.50089 ± 0.00045	471.3K	[1] ABBIENDI	01O	OPAL	$E^{ee}_{\text{cm}} = 88$–94 GeV
-0.5007 ± 0.0005	379.4k	ABREU	00F	DLPH	$E^{ee}_{\text{cm}} = 88$–94 GeV
-0.50153 ± 0.00053	340.8k	[2] ACCIARRI	00C	L3	$E^{ee}_{\text{cm}} = 88$–94 GeV
-0.50150 ± 0.00046	500k	BARATE	00C	ALEP	$E^{ee}_{\text{cm}} = 88$–94 GeV

[1] ABBIENDI 01O use their measurement of the τ polarization in addition to the lineshape and forward-backward lepton asymmetries.

[2] ACCIARRI 00C use their measurement of the τ polarization in addition to forward-backward lepton asymmetries.

g_A^u

VALUE	EVTS	DOCUMENT ID		TECN	COMMENT
$0.50\ ^{+0.04}_{-0.06}$ OUR AVERAGE					
0.501 ± 0.110	156k	[1] ABAZOV	11D	D0	$E^{p\overline{p}}_{\text{cm}} = 1.97$ TeV
0.57 ± 0.08	1500	[2] AKTAS	06	H1	$e^\pm p \to \overline{\nu}_e(\nu_e)X$, $\sqrt{s} \approx 300$ GeV
$0.47\ ^{+0.05}_{-0.33}$		[3] LEP-SLC	06		$E^{ee}_{\text{cm}} = 88$–94 GeV
$0.441\ ^{+0.207}_{-0.173} \pm 0.067$	5026	[4] ACOSTA	05M	CDF	$E^{p\overline{p}}_{\text{cm}} = 1.96$ TeV

[1] ABAZOV 11D study $p\overline{p} \to Z/\gamma^* e^+ e^-$ events using 5 fb^{-1} data at $\sqrt{s} = 1.96$ TeV. The candidate events are selected by requiring two isolated electromagnetic showers with $E_T > 25$ GeV, at least one electron in the central region and the di-electron mass in the range 50–1000 GeV. From the forward-backward asymmetry, determined as a function of the di-electron mass, they derive the axial and vector couplings of the u- and d- quarks and the value of $\sin^2\theta^\ell_{eff} = 0.2309 \pm 0.0008(\text{stat}) \pm 0.0006(\text{syst})$.

[2] AKTAS 06 fit the neutral current ($1.5 \leq Q^2 \leq 30{,}000$ GeV^2) and charged current ($1.5 \leq Q^2 \leq 15{,}000$ GeV^2) differential cross sections. In the determination of the u-quark couplings the electron and d-quark couplings are fixed to their standard model values.

[3] LEP-SLC 06 is a combination of the results from LEP and SLC experiments using light quark tagging. s- and d-quark couplings are assumed to be identical.

[4] ACOSTA 05M determine the forward-backward asymmetry of e^+e^- pairs produced via $q\overline{q} \to Z/\gamma^* \to e^+e^-$ in 15 M(e^+e^-) effective mass bins ranging from 40 GeV to 600 GeV. These results are used to obtain the vector and axial-vector couplings of the Z to the light quarks, assuming the electron couplings are as predicted by the Standard Model. Higher order radiative corrections have not been taken into account.

g_A^d

VALUE	EVTS	DOCUMENT ID		TECN	COMMENT
$-0.523\ ^{+0.050}_{-0.029}$ OUR AVERAGE					
-0.497 ± 0.165	156k	[1] ABAZOV	11D	D0	$E^{p\overline{p}}_{\text{cm}} = 1.97$ TeV
-0.80 ± 0.24	1500	[2] AKTAS	06	H1	$e^\pm p \to \overline{\nu}_e(\nu_e)X$, $\sqrt{s} \approx 300$ GeV
$-0.52\ ^{+0.05}_{-0.03}$		[3] LEP-SLC	06		$E^{ee}_{\text{cm}} = 88$–94 GeV
$-0.016\ ^{+0.346}_{-0.536} \pm 0.091$	5026	[4] ACOSTA	05M	CDF	$E^{p\overline{p}}_{\text{cm}} = 1.96$ TeV

[1] ABAZOV 11D study $p\overline{p} \to Z/\gamma^* e^+ e^-$ events using 5 fb^{-1} data at $\sqrt{s} = 1.96$ TeV. The candidate events are selected by requiring two isolated electromagnetic showers with $E_T > 25$ GeV, at least one electron in the central region and the di-electron mass in the range 50–1000 GeV. From the forward-backward asymmetry, determined as a function of the di-electron mass, they derive the axial and vector couplings of the u- and d- quarks and the value of $\sin^2\theta^\ell_{eff} = 0.2309 \pm 0.0008(\text{stat}) \pm 0.0006(\text{syst})$.

[2] AKTAS 06 fit the neutral current ($1.5 \leq Q^2 \leq 30{,}000$ GeV^2) and charged current ($1.5 \leq Q^2 \leq 15{,}000$ GeV^2) differential cross sections. In the determination of the d-quark couplings the electron and u-quark couplings are fixed to their standard model values.

[3] LEP-SLC 06 is a combination of the results from LEP and SLC experiments using light quark tagging. s- and d-quark couplings are assumed to be identical.

[4] ACOSTA 05M determine the forward-backward asymmetry of e^+e^- pairs produced via $q\overline{q} \rightarrow Z/\gamma^* \rightarrow e^+e^-$ in 15 M(e^+e^-) effective mass bins ranging from 40 GeV to 600 GeV. These results are used to obtain the vector and axial-vector couplings of the Z to the light quarks, assuming the electron couplings are as predicted by the Standard Model. Higher order radiative corrections have not been taken into account.

Z COUPLINGS TO NEUTRAL LEPTONS

Averaging over neutrino species, the invisible Z decay width determines the effective neutrino coupling g^{ν_ℓ}. For g^{ν_e} and g^{ν_μ}, $\nu_e e$ and $\nu_\mu e$ scattering results are combined with g^e_A and g^e_V measurements at the Z mass to obtain g^{ν_e} and g^{ν_μ} following NOVIKOV 93C.

g^{ν_ℓ}

VALUE	DOCUMENT ID		COMMENT
0.50076±0.00076	[1] LEP-SLC	06	$E^{ee}_{\rm cm}$ = 88–94 GeV

[1] From invisible Z-decay width.

g^{ν_e}

VALUE	DOCUMENT ID		TECN	COMMENT
0.528±0.085	[1] VILAIN	94	CHM2	From $\nu_\mu e$ and $\nu_e e$ scattering

[1] VILAIN 94 derive this value from their value of g^{ν_μ} and their ratio $g^{\nu_e}/g^{\nu_\mu} = 1.05^{+0.15}_{-0.18}$.

g^{ν_μ}

VALUE	DOCUMENT ID		TECN	COMMENT
0.502±0.017	[1] VILAIN	94	CHM2	From $\nu_\mu e$ scattering

[1] VILAIN 94 derive this value from their measurement of the couplings $g_A^{e\nu_\mu} = -0.503 \pm 0.017$ and $g_V^{e\nu_\mu} = -0.035 \pm 0.017$ obtained from $\nu_\mu e$ scattering. We have re-evaluated this value using the current PDG values for g^e_A and g^e_V.

Z ASYMMETRY PARAMETERS

For each fermion-antifermion pair coupling to the Z these quantities are defined as

$$A_f = \frac{2g_V^f g_A^f}{(g_V^f)^2 + (g_A^f)^2}$$

where g_V^f and g_A^f are the effective vector and axial-vector couplings. For their relation to the various lepton asymmetries see the note "The Z boson" and ref. LEP-SLC 06.

A_e

Using polarized beams, this quantity can also be measured as $(\sigma_L - \sigma_R)/(\sigma_L + \sigma_R)$, where σ_L and σ_R are the e^+e^- production cross sections for Z bosons produced with left-handed and right-handed electrons respectively.

VALUE	EVTS	DOCUMENT ID		TECN	COMMENT
0.1515±0.0019 OUR AVERAGE					
0.1454±0.0108±0.0036	144810	[1] ABBIENDI	01O	OPAL	$E^{ee}_{\rm cm}$ = 88–94 GeV
0.1516±0.0021	559000	[2] ABE	01B	SLD	$E^{ee}_{\rm cm}$ = 91.24 GeV
0.1504±0.0068±0.0008		[3] HEISTER	01	ALEP	$E^{ee}_{\rm cm}$ = 88–94 GeV
0.1382±0.0116±0.0005	105000	[4] ABREU	00E	DLPH	$E^{ee}_{\rm cm}$ = 88–94 GeV
0.1678±0.0127±0.0030	137092	[5] ACCIARRI	98H	L3	$E^{ee}_{\rm cm}$ = 88–94 GeV
0.162 ±0.041 ±0.014	89838	[6] ABE	97	SLD	$E^{ee}_{\rm cm}$ = 91.27 GeV
0.202 ±0.038 ±0.008		[7] ABE	95J	SLD	$E^{ee}_{\rm cm}$ = 91.31 GeV

[1] ABBIENDI 01O fit for A_e and A_τ from measurements of the τ polarization at varying τ production angles. The correlation between A_e and A_τ is less than 0.03.

[2] ABE 01B use the left-right production and left-right forward-backward decay asymmetries in leptonic Z decays to obtain a value of 0.1544 ± 0.0060. This is combined with left-right production asymmetry measurement using hadronic Z decays (ABE 00B) to obtain the quoted value.

[3] HEISTER 01 obtain this result fitting the τ polarization as a function of the polar production angle of the τ.

[4] ABREU 00E obtain this result fitting the τ polarization as a function of the polar τ production angle. This measurement is a combination of different analyses (exclusive τ decay modes, inclusive hadronic 1-prong reconstruction, and a neural network analysis).

[5] Derived from the measurement of forward-backward τ polarization asymmetry.

[6] ABE 97 obtain this result from a measurement of the observed left-right charge asymmetry, $A_Q^{\rm obs} = 0.225 \pm 0.056 \pm 0.019$, in hadronic Z decays. If they combine this value of $A_Q^{\rm obs}$ with their earlier measurement of $A_{LR}^{\rm obs}$ they determine A_e to be $0.1574 \pm 0.0197 \pm 0.0067$ independent of the beam polarization.

[7] ABE 95J obtain this result from polarized Bhabha scattering.

A_μ

This quantity is directly extracted from a measurement of the left-right forward-backward asymmetry in $\mu^+\mu^-$ production at SLC using a polarized electron beam. This double asymmetry eliminates the dependence on the Z-e-e coupling parameter A_e.

VALUE	EVTS	DOCUMENT ID		TECN	COMMENT
0.142±0.015	16844	[1] ABE	01B	SLD	$E^{ee}_{\rm cm}$ = 91.24 GeV

[1] ABE 01B obtain this direct measurement using the left-right production and left-right forward-backward polar angle asymmetries in $\mu^+\mu^-$ decays of the Z boson obtained with a polarized electron beam.

A_τ

The LEP Collaborations derive this quantity from the measurement of the τ polarization in $Z \rightarrow \tau^+\tau^-$. The SLD Collaboration directly extracts this quantity from its measured left-right forward-backward asymmetry in $Z \rightarrow \tau^+\tau^-$ produced using a polarized e^- beam. This double asymmetry eliminates the dependence on the Z-e-e coupling parameter A_e.

VALUE	EVTS	DOCUMENT ID		TECN	COMMENT
0.143 ±0.004 OUR AVERAGE					
0.1456±0.0076±0.0057	144810	[1] ABBIENDI	01O	OPAL	$E^{ee}_{\rm cm}$ = 88–94 GeV
0.136 ±0.015	16083	[2] ABE	01B	SLD	$E^{ee}_{\rm cm}$ = 91.24 GeV
0.1451±0.0052±0.0029		[3] HEISTER	01	ALEP	$E^{ee}_{\rm cm}$ = 88–94 GeV
0.1359±0.0079±0.0055	105000	[4] ABREU	00E	DLPH	$E^{ee}_{\rm cm}$ = 88–94 GeV
0.1476±0.0088±0.0062	137092	ACCIARRI	98H	L3	$E^{ee}_{\rm cm}$ = 88–94 GeV

[1] ABBIENDI 01O fit for A_e and A_τ from measurements of the τ polarization at varying τ production angles. The correlation between A_e and A_τ is less than 0.03.

[2] ABE 01B obtain this direct measurement using the left-right production and left-right forward-backward polar angle asymmetries in $\tau^+\tau^-$ decays of the Z boson obtained with a polarized electron beam.

[3] HEISTER 01 obtain this result fitting the τ polarization as a function of the polar production angle of the τ.

[4] ABREU 00E obtain this result fitting the τ polarization as a function of the polar τ production angle. This measurement is a combination of different analyses (exclusive τ decay modes, inclusive hadronic 1-prong reconstruction, and a neural network analysis).

A_s

The SLD Collaboration directly extracts this quantity by a simultaneous fit to four measured s-quark polar angle distributions corresponding to two states of e^- polarization (positive and negative) and to the K^+K^- and $K^\pm K^0_S$ strange particle tagging modes in the hadronic final states.

VALUE	EVTS	DOCUMENT ID		TECN	COMMENT
0.895±0.066±0.062	2870	[1] ABE	00D	SLD	$E^{ee}_{\rm cm}$ = 91.2 GeV

[1] ABE 00D tag $Z \rightarrow s\overline{s}$ events by an absence of B or D hadrons and the presence in each hemisphere of a high momentum $K^\pm$ or K^0_S.

A_c

This quantity is directly extracted from a measurement of the left-right forward-backward asymmetry in $c\overline{c}$ production at SLC using polarized electron beam. This double asymmetry eliminates the dependence on the Z-e-e coupling parameter A_e. OUR FIT is obtained by a simultaneous fit to several c- and b-quark measurements as explained in the note "The Z boson" and ref. LEP-SLC 06.

VALUE	DOCUMENT ID		TECN	COMMENT
0.670 ±0.027 OUR FIT				
0.6712±0.0224±0.0157	[1] ABE	05	SLD	$E^{ee}_{\rm cm}$ = 91.24 GeV
• • • We do not use the following data for averages, fits, limits, etc. • • •				
0.583 ±0.055 ±0.055	[2] ABE	02G	SLD	$E^{ee}_{\rm cm}$ = 91.24 GeV
0.688 ±0.041	[3] ABE	01C	SLD	$E^{ee}_{\rm cm}$ = 91.25 GeV

[1] ABE 05 use hadronic Z decays collected during 1996–98 to obtain an enriched sample of $c\overline{c}$ events tagging on the invariant mass of reconstructed secondary decay vertices. The charge of the underlying c–quark is obtained with an algorithm that takes into account the net charge of the vertex as well as the charge of tracks emanating from the vertex and identified as kaons. This yields (9970 events) $A_c = 0.6747 \pm 0.0290 \pm 0.0233$. Taking into account all correlations with earlier results reported in ABE 02G and ABE 01C, they obtain the quoted overall SLD result.

[2] ABE 02G tag b and c quarks through their semileptonic decays into electrons and muons. A maximum likelihood fit is performed to extract simultaneously A_b and A_c.

[3] ABE 01C tag $Z \rightarrow c\overline{c}$ events using two techniques: exclusive reconstruction of D^{*+}, D^+ and D^0 mesons and the soft pion tag for $D^{*+} \rightarrow D^0\pi^+$. The large background from D mesons produced in $b\overline{b}$ events is separated efficiently from the signal using precision vertex information. When combining the A_c values from these two samples, care is taken to avoid double counting of events common to the two samples, and common systematic errors are properly taken into account.

A_b

This quantity is directly extracted from a measurement of the left-right forward-backward asymmetry in $b\overline{b}$ production at SLC using polarized electron beam. This double asymmetry eliminates the dependence on the Z-e-e coupling parameter A_e. OUR FIT is obtained by a simultaneous fit to several c- and b-quark measurements as explained in the note "The Z boson" and ref. LEP-SLC 06.

VALUE	EVTS	DOCUMENT ID		TECN	COMMENT
0.923 ±0.020 OUR FIT					
0.9170±0.0147±0.0145		[1] ABE	05	SLD	$E^{ee}_{\rm cm}$ = 91.24 GeV
• • • We do not use the following data for averages, fits, limits, etc. • • •					
0.907 ±0.020 ±0.024	48028	[2] ABE	03F	SLD	$E^{ee}_{\rm cm}$ = 91.24 GeV
0.919 ±0.030 ±0.024		[3] ABE	02G	SLD	$E^{ee}_{\rm cm}$ = 91.24 GeV
0.855 ±0.088 ±0.102	7473	[4] ABE	99L	SLD	$E^{ee}_{\rm cm}$ = 91.27 GeV

[1] ABE 05 use hadronic Z decays collected during 1996–98 to obtain an enriched sample of $b\overline{b}$ events tagging on the invariant mass of reconstructed secondary decay vertices. The charge of the underlying b–quark is obtained with an algorithm that takes into account the net charge of the vertex as well as the charge of tracks emanating from the vertex and identified as kaons. This yields (25917 events) $A_b = 0.9173 \pm 0.0184 \pm 0.0173$. Taking into account all correlations with earlier results reported in ABE 03F, ABE 02G and ABE 99L, they obtain the quoted overall SLD result.

[2] ABE 03F obtain an enriched sample of $b\overline{b}$ events tagging on the invariant mass of a 3-dimensional topologically reconstructed secondary decay. The charge of the underlying b quark is obtained using a self-calibrating track-charge method. For the 1996–1998 data sample they measure $A_b = 0.906 \pm 0.022 \pm 0.023$. The value quoted here is obtained combining the above with the result of ABE 98I (1993–1995 data sample).

[3] ABE 02G tag b and c quarks through their semileptonic decays into electrons and muons. A maximum likelihood fit is performed to extract simultaneously A_b and A_c.

[4] ABE 99L obtain an enriched sample of $b\overline{b}$ events tagging with an inclusive vertex mass cut. For distinguishing b and $\overline{b}$ quarks they use the charge of identified $K^{\pm}$.

TRANSVERSE SPIN CORRELATIONS IN $Z \to \tau^+\tau^-$

The correlations between the transverse spin components of $\tau^+\tau^-$ produced in Z decays may be expressed in terms of the vector and axial-vector couplings:

$$C_{TT} = \frac{|g_A^\tau|^2 - |g_V^\tau|^2}{|g_A^\tau|^2 + |g_V^\tau|^2}$$

$$C_{TN} = -2\frac{|g_A^\tau||g_V^\tau|}{|g_A^\tau|^2 + |g_V^\tau|^2}\sin(\Phi_{g_V^\tau} - \Phi_{g_A^\tau})$$

C_{TT} refers to the transverse-transverse (within the collision plane) spin correlation and C_{TN} refers to the transverse-normal (to the collision plane) spin correlation.

The longitudinal τ polarization P_τ $(= -A_\tau)$ is given by:

$$P_\tau = -2\frac{|g_A^\tau||g_V^\tau|}{|g_A^\tau|^2 + |g_V^\tau|^2}\cos(\Phi_{g_V^\tau} - \Phi_{g_A^\tau})$$

Here Φ is the phase and the phase difference $\Phi_{g_V^\tau} - \Phi_{g_A^\tau}$ can be obtained using both the measurements of C_{TN} and P_τ.

C_{TT}

VALUE	EVTS	DOCUMENT ID		TECN	COMMENT
1.01±0.12 OUR AVERAGE					
$0.87 \pm 0.20^{+0.10}_{-0.12}$	9.1k	ABREU	97G	DLPH	E_{cm}^{ee}= 91.2 GeV
$1.06 \pm 0.13 \pm 0.05$	120k	BARATE	97D	ALEP	E_{cm}^{ee}= 91.2 GeV

C_{TN}

VALUE	EVTS	DOCUMENT ID		TECN	COMMENT
0.08±0.13±0.04	120k	[1] BARATE	97D	ALEP	E_{cm}^{ee}= 91.2 GeV

[1] BARATE 97D combine their value of C_{TN} with the world average $P_\tau = -0.140 \pm 0.007$ to obtain $\tan(\Phi_{g_V^\tau} - \Phi_{g_A^\tau}) = -0.57 \pm 0.97$.

FORWARD-BACKWARD $e^+e^- \to f\overline{f}$ CHARGE ASYMMETRIES

These asymmetries are experimentally determined by tagging the respective lepton or quark flavor in e^+e^- interactions. Details of heavy flavor (c- or b-quark) tagging at LEP are described in the note on "The Z boson" and ref. LEP-SLC 06. The Standard Model predictions for LEP data have been (re)computed using the ZFITTER package (version 6.36) with input parameters M_Z=91.187 GeV, M_{top}=174.3 GeV, M_{Higgs}=150 GeV, α_s=0.119, $\alpha^{(5)}$ (M_Z)= 1/128.877 and the Fermi constant $G_F = 1.16637 \times 10^{-5}$ GeV^{-2} (see the note on "The Z boson" for references). For non-LEP data the Standard Model predictions are as given by the authors of the respective publications.

$A_{FB}^{(0,e)}$ CHARGE ASYMMETRY IN $e^+e^- \to e^+e^-$

OUR FIT is obtained using the fit procedure and correlations as determined by the LEP Electroweak Working Group (see the note "The Z boson" and ref. LEP-SLC 06). For the Z peak, we report the pole asymmetry defined by $(3/4)A_e^2$ as determined by the nine-parameter fit to cross-section and lepton forward-backward asymmetry data.

ASYMMETRY (%)	STD. MODEL	$\sqrt{s}$ (GeV)	DOCUMENT ID		TECN
1.45±0.25 OUR FIT					
0.89 ± 0.44	1.57	91.2	[1] ABBIENDI	01A	OPAL
1.71 ± 0.49	1.57	91.2	ABREU	00F	DLPH
1.06 ± 0.58	1.57	91.2	ACCIARRI	00C	L3
1.88 ± 0.34	1.57	91.2	[2] BARATE	00C	ALEP

[1] ABBIENDI 01A error includes approximately 0.38 due to statistics, 0.16 due to event selection systematics, and 0.18 due to the theoretical uncertainty in t-channel prediction.

[2] BARATE 00C error includes approximately 0.31 due to statistics, 0.06 due to experimental systematics, and 0.13 due to the theoretical uncertainty in t-channel prediction.

$A_{FB}^{(0,\mu)}$ CHARGE ASYMMETRY IN $e^+e^- \to \mu^+\mu^-$

OUR FIT is obtained using the fit procedure and correlations as determined by the LEP Electroweak Working Group (see the note "The Z boson" and ref. LEP-SLC 06). For the Z peak, we report the pole asymmetry defined by $(3/4)A_eA_\mu$ as determined by the nine-parameter fit to cross-section and lepton forward-backward asymmetry data.

ASYMMETRY (%)	STD. MODEL	$\sqrt{s}$ (GeV)	DOCUMENT ID		TECN
1.69± 0.13 OUR FIT					
1.59 ± 0.23	1.57	91.2	[1] ABBIENDI	01A	OPAL
1.65 ± 0.25	1.57	91.2	ABREU	00F	DLPH
1.88 ± 0.33	1.57	91.2	ACCIARRI	00C	L3
1.71 ± 0.24	1.57	91.2	[2] BARATE	00C	ALEP
• • • We do not use the following data for averages, fits, limits, etc. • • •					
9 ± 30	-1.3	20	[3] ABREU	95M	DLPH
7 ± 26	-8.3	40	[3] ABREU	95M	DLPH
-11 ± 33	-24.1	57	[3] ABREU	95M	DLPH
-62 ± 17	-44.6	69	[3] ABREU	95M	DLPH
-56 ± 10	-63.5	79	[3] ABREU	95M	DLPH
-13 ± 5	-34.4	87.5	[3] ABREU	95M	DLPH
$-29.0 \pm {}^{5.0}_{4.8} \pm 0.5$	-32.1	56.9	[4] ABE	90I	VNS
$-9.9 \pm 1.5 \pm 0.5$	-9.2	35	HEGNER	90	JADE
0.05 ± 0.22	0.026	91.14	[5] ABRAMS	89D	MRK2
-43.4 ± 17.0	-24.9	52.0	[6] BACALA	89	AMY
-11.0 ± 16.5	-29.4	55.0	[6] BACALA	89	AMY
-30.0 ± 12.4	-31.2	56.0	[6] BACALA	89	AMY
-46.2 ± 14.9	-33.0	57.0	[6] BACALA	89	AMY
-29 ± 13	-25.9	53.3	ADACHI	88C	TOPZ
$+5.3 \pm 5.0 \pm 0.5$	-1.2	14.0	ADEVA	88	MRKJ
$-10.4 \pm 1.3 \pm 0.5$	-8.6	34.8	ADEVA	88	MRKJ
$-12.3 \pm 5.3 \pm 0.5$	-10.7	38.3	ADEVA	88	MRKJ
$-15.6 \pm 3.0 \pm 0.5$	-14.9	43.8	ADEVA	88	MRKJ
-1.0 ± 6.0	-1.2	13.9	BRAUNSCH...	88D	TASS
$-9.1 \pm 2.3 \pm 0.5$	-8.6	34.5	BRAUNSCH...	88D	TASS
$-10.6 \pm {}^{2.2}_{2.3} \pm 0.5$	-8.9	35.0	BRAUNSCH...	88D	TASS
$-17.6 \pm {}^{4.4}_{4.3} \pm 0.5$	-15.2	43.6	BRAUNSCH...	88D	TASS
$-4.8 \pm 6.5 \pm 1.0$	-11.5	39	BEHREND	87C	CELL
$-18.8 \pm 4.5 \pm 1.0$	-15.5	44	BEHREND	87C	CELL
$+2.7 \pm 4.9$	-1.2	13.9	BARTEL	86C	JADE
$-11.1 \pm 1.8 \pm 1.0$	-8.6	34.4	BARTEL	86C	JADE
$-17.3 \pm 4.8 \pm 1.0$	-13.7	41.5	BARTEL	86C	JADE
$-22.8 \pm 5.1 \pm 1.0$	-16.6	44.8	BARTEL	86C	JADE
$-6.3 \pm 0.8 \pm 0.2$	-6.3	29	ASH	85	MAC
$-4.9 \pm 1.5 \pm 0.5$	-5.9	29	DERRICK	85	HRS
-7.1 ± 1.7	-5.7	29	LEVI	83	MRK2
-16.1 ± 3.2	-9.2	34.2	BRANDELIK	82C	TASS

[1] ABBIENDI 01A error is almost entirely on account of statistics.

[2] BARATE 00C error is almost entirely on account of statistics.

[3] ABREU 95M perform this measurement using radiative muon-pair events associated with high-energy isolated photons.

[4] ABE 90I measurements in the range $50 \leq \sqrt{s} \leq 60.8$ GeV.

[5] ABRAMS 89D asymmetry includes both 9 $\mu^+\mu^-$ and 15 $\tau^+\tau^-$ events.

[6] BACALA 89 systematic error is about 5%.

$A_{FB}^{(0,\tau)}$ CHARGE ASYMMETRY IN $e^+e^- \to \tau^+\tau^-$

OUR FIT is obtained using the fit procedure and correlations as determined by the LEP Electroweak Working Group (see the note "The Z boson" and ref. LEP-SLC 06). For the Z peak, we report the pole asymmetry defined by $(3/4)A_eA_\tau$ as determined by the nine-parameter fit to cross-section and lepton forward-backward asymmetry data.

ASYMMETRY (%)	STD. MODEL	$\sqrt{s}$ (GeV)	DOCUMENT ID		TECN
1.88± 0.17 OUR FIT					
1.45 ± 0.30	1.57	91.2	[1] ABBIENDI	01A	OPAL
2.41 ± 0.37	1.57	91.2	ABREU	00F	DLPH
2.60 ± 0.47	1.57	91.2	ACCIARRI	00C	L3
1.70 ± 0.28	1.57	91.2	[2] BARATE	00C	ALEP
• • • We do not use the following data for averages, fits, limits, etc. • • •					
$-32.8 \pm {}^{6.4}_{6.2} \pm 1.5$	-32.1	56.9	[3] ABE	90I	VNS
$-8.1 \pm 2.0 \pm 0.6$	-9.2	35	HEGNER	90	JADE
-18.4 ± 19.2	-24.9	52.0	[4] BACALA	89	AMY
-17.7 ± 26.1	-29.4	55.0	[4] BACALA	89	AMY
-45.9 ± 16.6	-31.2	56.0	[4] BACALA	89	AMY
-49.5 ± 18.0	-33.0	57.0	[4] BACALA	89	AMY
-20 ± 14	-25.9	53.3	ADACHI	88C	TOPZ
$-10.6 \pm 3.1 \pm 1.5$	-8.5	34.7	ADEVA	88	MRKJ

− 8.5 ± 6.6 ±1.5	−15.4	43.8	ADEVA	88	MRKJ
− 6.0 ± 2.5 ±1.0	8.8	34.6	BARTEL	85F	JADE
−11.8 ± 4.6 ±1.0	14.8	43.0	BARTEL	85F	JADE
− 5.5 ± 1.2 ±0.5	−0.063	29.0	FERNANDEZ	85	MAC
− 4.2 ± 2.0	0.057	29	LEVI	83	MRK2
−10.3 ± 5.2	−9.2	34.2	BEHREND	82	CELL
− 0.4 ± 6.6	−9.1	34.2	BRANDELIK	82C	TASS

[1] ABBIENDI 01A error includes approximately 0.26 due to statistics and 0.14 due to event selection systematics.
[2] BARATE 00C error includes approximately 0.26 due to statistics and 0.11 due to experimental systematics.
[3] ABE 90I measurements in the range $50 \leq \sqrt{s} \leq 60.8$ GeV.
[4] BACALA 89 systematic error is about 5%.

$A_{FB}^{(0,\ell)}$ CHARGE ASYMMETRY IN $e^+e^- \to \ell^+\ell^-$

For the Z peak, we report the pole asymmetry defined by $(3/4)A_\ell^2$ as determined by the five-parameter fit to cross-section and lepton forward-backward asymmetry data assuming lepton universality. For details see the note "The Z boson" and ref. LEP-SLC 06.

ASYMMETRY (%)	STD. MODEL	$\sqrt{s}$ (GeV)	DOCUMENT ID		TECN
1.71±0.10 OUR FIT					
1.45±0.17	1.57	91.2	[1] ABBIENDI	01A	OPAL
1.87±0.19	1.57	91.2	ABREU	00F	DLPH
1.92±0.24	1.57	91.2	ACCIARRI	00C	L3
1.73±0.16	1.57	91.2	[2] BARATE	00C	ALEP

[1] ABBIENDI 01A error includes approximately 0.15 due to statistics, 0.06 due to event selection systematics, and 0.03 due to the theoretical uncertainty in t-channel prediction.
[2] BARATE 00C error includes approximately 0.15 due to statistics, 0.04 due to experimental systematics, and 0.02 due to the theoretical uncertainty in t-channel prediction.

$A_{FB}^{(0,u)}$ CHARGE ASYMMETRY IN $e^+e^- \to u\overline{u}$

ASYMMETRY (%)	STD. MODEL	$\sqrt{s}$ (GeV)	DOCUMENT ID		TECN
4.0±6.7±2.8	**7.2**	**91.2**	[1] ACKERSTAFF	97T	OPAL

[1] ACKERSTAFF 97T measure the forward-backward asymmetry of various fast hadrons made of light quarks. Then using SU(2) isospin symmetry and flavor independence for down and strange quarks authors solve for the different quark types.

$A_{FB}^{(0,s)}$ CHARGE ASYMMETRY IN $e^+e^- \to s\overline{s}$

The s-quark asymmetry is derived from measurements of the forward-backward asymmetry of fast hadrons containing an s quark.

ASYMMETRY (%)	STD. MODEL	$\sqrt{s}$ (GeV)	DOCUMENT ID		TECN
9.8 ±1.1 OUR AVERAGE					
10.08±1.13±0.40	10.1	91.2	[1] ABREU	00B	DLPH
6.8 ±3.5 ±1.1	10.1	91.2	[2] ACKERSTAFF	97T	OPAL

[1] ABREU 00B tag the presence of an s quark requiring a high-momentum-identified charged kaon. The s-quark pole asymmetry is extracted from the charged-kaon asymmetry taking the expected d- and u-quark asymmetries from the Standard Model and using the measured values for the c- and b-quark asymmetries.
[2] ACKERSTAFF 97T measure the forward-backward asymmetry of various fast hadrons made of light quarks. Then using SU(2) isospin symmetry and flavor independence for down and strange quarks authors solve for the different quark types. The value reported here corresponds then to the forward-backward asymmetry for "down-type" quarks.

$A_{FB}^{(0,c)}$ CHARGE ASYMMETRY IN $e^+e^- \to c\overline{c}$

OUR FIT, which is obtained by a simultaneous fit to several c- and b-quark measurements as explained in the note "The Z boson" and ref. LEP-SLC 06, refers to the **Z pole** asymmetry. The experimental values, on the other hand, correspond to the measurements carried out at the respective energies.

ASYMMETRY (%)	STD. MODEL	$\sqrt{s}$ (GeV)	DOCUMENT ID		TECN
7.07± 0.35 OUR FIT					
6.31± 0.93±0.65	6.35	91.26	[1] ABDALLAH	04F	DLPH
5.68± 0.54±0.39	6.3	91.25	[2] ABBIENDI	03P	OPAL
6.45± 0.57±0.37	6.10	91.21	[3] HEISTER	02H	ALEP
6.59± 0.94±0.35	6.2	91.235	[4] ABREU	99Y	DLPH
6.3 ± 0.9 ±0.3	6.1	91.22	[5] BARATE	98O	ALEP
6.3 ± 1.2 ±0.6	6.1	91.22	[6] ALEXANDER	97C	OPAL
8.3 ± 3.8 ±2.7	6.2	91.24	[7] ADRIANI	92D	L3
• • • We do not use the following data for averages, fits, limits, etc. • • •					
3.1 ± 3.5 ±0.5	−3.5	89.43	[1] ABDALLAH	04F	DLPH
11.0 ± 2.8 ±0.7	12.3	92.99	[1] ABDALLAH	04F	DLPH
− 6.8 ± 2.5 ±0.9	−3.0	89.51	[2] ABBIENDI	03P	OPAL
14.6 ± 2.0 ±0.8	12.2	92.95	[2] ABBIENDI	03P	OPAL
−12.4 ±15.9 ±2.0	−9.6	88.38	[3] HEISTER	02H	ALEP
− 2.3 ± 2.6 ±0.2	−3.8	89.38	[3] HEISTER	02H	ALEP
− 0.3 ± 8.3 ±0.6	0.9	90.21	[3] HEISTER	02H	ALEP
10.6 ± 7.7 ±0.7	9.6	92.05	[3] HEISTER	02H	ALEP
11.9 ± 2.1 ±0.6	12.2	92.94	[3] HEISTER	02H	ALEP
12.1 ±11.0 ±1.0	14.2	93.90	[3] HEISTER	02H	ALEP
− 4.96± 3.68±0.53	−3.5	89.434	[4] ABREU	99Y	DLPH
11.80± 3.18±0.62	12.3	92.990	[4] ABREU	99Y	DLPH
− 1.0 ± 4.3 ±1.0	−3.9	89.37	[5] BARATE	98O	ALEP
11.0 ± 3.3 ±0.8	12.3	92.96	[5] BARATE	98O	ALEP
3.9 ± 5.1 ±0.9	−3.4	89.45	[6] ALEXANDER	97C	OPAL
15.8 ± 4.1 ±1.1	12.4	93.00	[6] ALEXANDER	97C	OPAL
−12.9 ± 7.8 ±5.5	−13.6	35	BEHREND	90D	CELL
7.7 ±13.4 ±5.0	−22.1	43	BEHREND	90D	CELL
−12.8 ± 4.4 ±4.1	−13.6	35	ELSEN	90	JADE
−10.9 ±12.9 ±4.6	−23.2	44	ELSEN	90	JADE
−14.9 ± 6.7	−13.3	35	OULD-SAADA	89	JADE

[1] ABDALLAH 04F tag b– and c–quarks using semileptonic decays combined with charge flow information from the hemisphere opposite to the lepton. Enriched samples of $c\overline{c}$ and $b\overline{b}$ events are obtained using lifetime information.
[2] ABBIENDI 03P tag heavy flavors using events with one or two identified leptons. This allows the simultaneous fitting of the b and c quark forward-backward asymmetries as well as the average B^0-$\overline{B}^0$ mixing.
[3] HEISTER 02H measure simultaneously b and c quark forward-backward asymmetries using their semileptonic decays to tag the quark charge. The flavor separation is obtained with a discriminating multivariate analysis.
[4] ABREU 99Y tag $Z \to b\overline{b}$ and $Z \to c\overline{c}$ events by an exclusive reconstruction of several D meson decay modes (D^{*+}, D^0, and D^+ with their charge-conjugate states).
[5] BARATE 98O tag $Z \to c\overline{c}$ events requiring the presence of high-momentum reconstructed D^{*+}, D^+, or D^0 mesons.
[6] ALEXANDER 97C identify the b and c events using a D/D^* tag.
[7] ADRIANI 92D use both electron and muon semileptonic decays.

$A_{FB}^{(0,b)}$ CHARGE ASYMMETRY IN $e^+e^- \to b\overline{b}$

OUR FIT, which is obtained by a simultaneous fit to several c- and b-quark measurements as explained in the note "The Z boson" and ref. LEP-SLC 06, refers to the **Z pole** asymmetry. The experimental values, on the other hand, correspond to the measurements carried out at the respective energies.

ASYMMETRY (%)	STD. MODEL	$\sqrt{s}$ (GeV)	DOCUMENT ID		TECN
9.92± 0.16 OUR FIT					
9.58± 0.32± 0.14	9.68	91.231	[1] ABDALLAH	05	DLPH
10.04± 0.56± 0.25	9.69	91.26	[2] ABDALLAH	04F	DLPH
9.72± 0.42± 0.15	9.67	91.25	[3] ABBIENDI	03P	OPAL
9.77± 0.36± 0.18	9.69	91.26	[4] ABBIENDI	02I	OPAL
9.52± 0.41± 0.17	9.59	91.21	[5] HEISTER	02H	ALEP
10.00± 0.27± 0.11	9.63	91.232	[6] HEISTER	01D	ALEP
7.62± 1.94± 0.85	9.64	91.235	[7] ABREU	99Y	DLPH
9.60± 0.66± 0.33	9.69	91.26	[8] ACCIARRI	99D	L3
9.31± 1.01± 0.55	9.65	91.24	[9] ACCIARRI	98U	L3
9.4 ± 2.7 ± 2.2	9.61	91.22	[10] ALEXANDER	97C	OPAL
• • • We do not use the following data for averages, fits, limits, etc. • • •					
6.37± 1.43± 0.17	5.8	89.449	[1] ABDALLAH	05	DLPH
10.41± 1.15± 0.24	12.1	92.990	[1] ABDALLAH	05	DLPH
6.7 ± 2.2 ± 0.2	5.7	89.43	[2] ABDALLAH	04F	DLPH
11.2 ± 1.8 ± 0.2	12.1	92.99	[2] ABDALLAH	04F	DLPH
4.7 ± 1.8 ± 0.1	5.9	89.51	[3] ABBIENDI	03P	OPAL
10.3 ± 1.5 ± 0.2	12.0	92.95	[3] ABBIENDI	03P	OPAL
5.82± 1.53± 0.12	5.9	89.50	[4] ABBIENDI	02I	OPAL
12.21± 1.23± 0.25	12.0	92.91	[4] ABBIENDI	02I	OPAL
−13.1 ±13.5 ± 1.0	3.2	88.38	[5] HEISTER	02H	ALEP
5.5 ± 1.9 ± 0.1	5.6	89.38	[5] HEISTER	02H	ALEP
− 0.4 ± 6.7 ± 0.8	7.5	90.21	[5] HEISTER	02H	ALEP
11.1 ± 6.4 ± 0.5	11.0	92.05	[5] HEISTER	02H	ALEP
10.4 ± 1.5 ± 0.3	12.0	92.94	[5] HEISTER	02H	ALEP
13.8 ± 9.3 ± 1.1	12.9	93.90	[5] HEISTER	02H	ALEP
4.36± 1.19± 0.11	5.8	89.472	[6] HEISTER	01D	ALEP
11.72± 0.97± 0.11	12.0	92.950	[6] HEISTER	01D	ALEP
5.67± 7.56± 1.17	5.7	89.434	[7] ABREU	99Y	DLPH
8.82± 6.33± 1.22	12.1	92.990	[7] ABREU	99Y	DLPH
6.11± 2.93± 0.43	5.9	89.50	[8] ACCIARRI	99D	L3
13.71± 2.40± 0.44	12.2	93.10	[8] ACCIARRI	99D	L3
4.95± 5.23± 0.40	5.8	89.45	[9] ACCIARRI	98U	L3
11.37± 3.99± 0.65	12.1	92.99	[9] ACCIARRI	98U	L3
− 8.6 ±10.8 ± 2.9	5.8	89.45	[10] ALEXANDER	97C	OPAL
− 2.1 ± 9.0 ± 2.6	12.1	93.00	[10] ALEXANDER	97C	OPAL
−71 ±34 $^{+\ 7}_{-\ 8}$	−58	58.3	SHIMONAKA	91	TOPZ
−22.2 ± 7.7 ± 3.5	−26.0	35	BEHREND	90D	CELL
−49.1 ±16.0 ± 5.0	−39.7	43	BEHREND	90D	CELL
−28 ±11	−23	35	BRAUNSCH...	90	TASS
−16.6 ± 7.7 ± 4.8	−24.3	35	ELSEN	90	JADE
−33.6 ±22.2 ± 5.2	−39.9	44	ELSEN	90	JADE
3.4 ± 7.0 ± 3.5	−16.0	29.0	BAND	89	MAC
−72 ±28 ±13	−56	55.2	SAGAWA	89	AMY

[1] ABDALLAH 05 obtain an enriched samples of $b\overline{b}$ events using lifetime information. The quark (or antiquark) charge is determined with a neural network using the secondary vertex charge, the jet charge and particle identification.
[2] ABDALLAH 04F tag b– and c–quarks using semileptonic decays combined with charge flow information from the hemisphere opposite to the lepton. Enriched samples of $c\overline{c}$ and $b\overline{b}$ events are obtained using lifetime information.

[3] ABBIENDI 03P tag heavy flavors using events with one or two identified leptons. This allows the simultaneous fitting of the b and c quark forward-backward asymmetries as well as the average B^0-$\overline{B}^0$ mixing.

[4] ABBIENDI 02I tag $Z^0 \to b\overline{b}$ decays using a combination of secondary vertex and lepton tags. The sign of the b-quark charge is determined using an inclusive tag based on jet, vertex, and kaon charges.

[5] HEISTER 02H measure simultaneously b and c quark forward-backward asymmetries using their semileptonic decays to tag the quark charge. The flavor separation is obtained with a discriminating multivariate analysis.

[6] HEISTER 01D tag $Z \to b\overline{b}$ events using the impact parameters of charged tracks complemented with information from displaced vertices, event shape variables, and lepton identification. The b-quark direction and charge is determined using the hemisphere charge method along with information from fast kaon tagging and charge estimators of primary and secondary vertices. The change in the quoted value due to variation of A_{FB}^c and R_b is given as $+0.103\ (A_{FB}^c - 0.0651) - 0.440\ (R_b - 0.21585)$.

[7] ABREU 99Y tag $Z \to b\overline{b}$ and $Z \to c\overline{c}$ events by an exclusive reconstruction of several D meson decay modes (D^{*+}, D^0, and D^+ with their charge-conjugate states).

[8] ACCIARRI 99D tag $Z \to b\overline{b}$ events using high p and p_T leptons. The analysis determines simultaneously a mixing parameter $\chi_b = 0.1192 \pm 0.0068 \pm 0.0051$ which is used to correct the observed asymmetry.

[9] ACCIARRI 98U tag $Z \to b\overline{b}$ events using lifetime and measure the jet charge using the hemisphere charge.

[10] ALEXANDER 97C identify the b and c events using a D/D^* tag.

CHARGE ASYMMETRY IN $e^+e^- \to q\overline{q}$

Summed over five lighter flavors.

Experimental and Standard Model values are somewhat event-selection dependent. Standard Model expectations contain some assumptions on B^0-$\overline{B}^0$ mixing and on other electroweak parameters.

ASYMMETRY (%)	STD. MODEL	$\sqrt{s}$ (GeV)	DOCUMENT ID		TECN
• • • We do not use the following data for averages, fits, limits, etc. • • •					
$-0.76 \pm 0.12 \pm 0.15$		91.2	[1] ABREU	92I	DLPH
$4.0 \pm 0.4 \pm 0.63$	4.0	91.3	[2] ACTON	92L	OPAL
$9.1 \pm 1.4 \pm 1.6$	9.0	57.9	ADACHI	91	TOPZ
$-0.84 \pm 0.15 \pm 0.04$		91	DECAMP	91B	ALEP
$8.3 \pm 2.9 \pm 1.9$	8.7	56.6	STUART	90	AMY
$11.4 \pm 2.2 \pm 2.1$	8.7	57.6	ABE	89L	VNS
6.0 ± 1.3	5.0	34.8	GREENSHAW	89	JADE
8.2 ± 2.9	8.5	43.6	GREENSHAW	89	JADE

[1] ABREU 92I has 0.14 systematic error due to uncertainty of quark fragmentation.

[2] ACTON 92L use the weight function method on 259k selected $Z \to$ hadrons events. The systematic error includes a contribution of 0.2 due to B^0-$\overline{B}^0$ mixing effect, 0.4 due to Monte Carlo (MC) fragmentation uncertainties and 0.3 due to MC statistics. ACTON 92L derive a value of $\sin^2\theta_W^{\rm eff}$ to be $0.2321 \pm 0.0017 \pm 0.0028$.

CHARGE ASYMMETRY IN $p\overline{p} \to Z \to e^+e^-$

ASYMMETRY (%)	STD. MODEL	$\sqrt{s}$ (GeV)	DOCUMENT ID		TECN
• • • We do not use the following data for averages, fits, limits, etc. • • •					
$5.2 \pm 5.9 \pm 0.4$		91	ABE	91E	CDF

ANOMALOUS $ZZ\gamma$, $Z\gamma\gamma$, AND ZZV COUPLINGS

Revised September 2013 by M.W. Grünewald (U. College Dublin and U. Ghent) and A. Gurtu (Formerly Tata Inst.).

In on-shell $Z\gamma$ production, deviations from the Standard Model for the $Z\gamma\gamma^*$ and $Z\gamma Z^*$ couplings may be described in terms of eight parameters, h_i^V $(i = 1, 4;\ V = \gamma, Z)$ [1]. The parameters h_i^γ describe the $Z\gamma\gamma^*$ couplings and the parameters h_i^Z the $Z\gamma Z^*$ couplings. In this formalism h_1^V and h_2^V lead to CP-violating and h_3^V and h_4^V to CP-conserving effects. All these anomalous contributions to the cross section increase rapidly with center-of-mass energy. In order to ensure unitarity, these parameters are usually described by a form-factor representation, $h_i^V(s) = h_{io}^V/(1 + s/\Lambda^2)^n$, where Λ is the energy scale for the manifestation of a new phenomenon and n is a sufficiently large power. By convention one uses $n = 3$ for $h_{1,3}^V$ and $n = 4$ for $h_{2,4}^V$. Usually limits on h_i^V's are put assuming some value of Λ, sometimes ∞.

In on-shell ZZ production, deviations from the Standard Model for the $ZZ\gamma^*$ and ZZZ^* couplings may be described by means of four anomalous couplings f_i^V $(i = 4, 5; V = \gamma, Z)$ [2]. As above, the parameters f_i^γ describe the $ZZ\gamma^*$ couplings and the parameters f_i^Z the ZZZ^* couplings. The anomalous couplings f_5^V lead to violation of C and P symmetries while f_4^V introduces CP violation. Also here, formfactors depending on a scale Λ are used.

All these couplings h_i^V and f_i^V are zero at tree level in the Standard Model; they are measured in e^+e^-, $p\overline{p}$ and pp collisions at LEP, Tevatron and LHC.

References

1. U. Baur and E.L. Berger Phys. Rev. **D47**, 4889 (1993).
2. K. Hagiwara *et al.*, Nucl. Phys. **B282**, 253 (1987).

h_i^V

Combining the LEP-2 results taking into account the correlations, the following 95% CL limits are derived [SCHAEL 13A]:

$$-0.12 < h_1^Z < +0.11, \quad -0.07 < h_2^Z < +0.07,$$
$$-0.19 < h_3^Z < +0.06, \quad -0.04 < h_4^Z < +0.13,$$
$$-0.05 < h_1^\gamma < +0.05, \quad -0.04 < h_2^\gamma < +0.02,$$
$$-0.05 < h_3^\gamma < +0.00, \quad +0.01 < h_4^\gamma < +0.05.$$

VALUE	DOCUMENT ID		TECN	COMMENT
• • • We do not use the following data for averages, fits, limits, etc. • • •				
[1] AAD	13AN	ATLS		$E_{\rm cm}^{pp} = 7$ TeV
[2] CHATRCHYAN	13BI	CMS		$E_{\rm cm}^{pp} = 7$ TeV
[3] ABAZOV	12S	D0		$E_{\rm cm}^{p\overline{p}} = 1.96$ TeV
[4] AALTONEN	11S	CDF		$E_{\rm cm}^{p\overline{p}} = 1.96$ TeV
[5] CHATRCHYAN	11M	CMS		$E_{\rm cm}^{pp} = 7$ TeV
[6] ABAZOV	09L	D0		$E_{\rm cm}^{p\overline{p}} = 1.96$ TeV
[7] ABAZOV	07M	D0		$E_{\rm cm}^{p\overline{p}} = 1.96$ TeV
[8] ABDALLAH	07C	DLPH		$E_{\rm cm}^{ee} = 183$–208 GeV
[9] ACHARD	04H	L3		$E_{\rm cm}^{ee} = 183$–208 GeV
[10] ABBIENDI,G	00C	OPAL		$E_{\rm cm}^{ee} = 189$ GeV
[11] ABBOTT	98M	D0		$E_{\rm cm}^{p\overline{p}} = 1.8$ TeV
[12] ABREU	98K	DLPH		$E_{\rm cm}^{ee} = 161, 172$ GeV

[1] AAD 13AN study $Z\gamma$ production in pp collisions. In events with no additional jet, 1417 (2031) Z decays to electron (muon) pairs are selected, with an expected background of 156 ± 54 (244 ± 64) events, as well as 662 Z decays to neutrino pairs with an expected background of 302 ± 42 events. Analysing the photon p_T spectrum above 100 GeV yields the 95% C.L. limts: $-0.013 < h_3^Z < 0.014$, $-8.7 \times 10^{-5} < h_4^Z < 8.7 \times 10^{-5}$, $-0.015 < h_\gamma^3 < 0.016$, $-9.4 \times 10^{-5} < h_\gamma^4 < 9.2 \times 10^{-5}$. Supersedes AAD 12BX.

[2] CHATRCHYAN 13BI determine the $Z\gamma \to \nu\overline{\nu}\gamma$ cross section by selecting events with a photon of $E_T > 145$ GeV and a $\not{E}_T > 130$ GeV. 73 candidate events are observed with an expected SM background of 30.2 ± 6.5. The E_T spectrum of the photon is used to set 95% C.L. limits as follows: $|h_3^Z| < 2.7 \times 10^{-3}$, $|h_4^Z| < 1.3 \times 10^{-5}$, $|h_3^\gamma| < 2.9 \times 10^{-3}$, $|h_4^\gamma| < 1.5 \times 10^{-5}$.

[3] ABAZOV 12S study $Z\gamma$ production in $p\overline{p}$ collisions at $\sqrt{s} = 1.96$ TeV using 6.2 fb^{-1} of data where the Z decays to electron (muon) pairs and the photon has at least 10 GeV of transverse momentum. In data, 304 (308) di-electron (di-muon) events are observed with an expected background of 255 ± 16 (285 ± 24) events. Based on the photon p_T spectrum, and including also earlier data and the $Z \to \nu\overline{\nu}$ decay mode (from ABAZOV 09L), the following 95% C.L. limits are reported: $|h_{03}^Z| < 0.026$, $|h_{04}^Z| < 0.0013$, $|h_{03}^\gamma| < 0.027$, $|h_{04}^\gamma| < 0.0014$ for a form factor scale of $\Lambda = 1.5$ TeV.

[4] AALTONEN 11S study $Z\gamma$ events in $p\overline{p}$ interactions at $\sqrt{s} = 1.96$ TeV with integrated luminosity 5.1 fb^{-1} for $Z \to e^+e^-/\mu^+\mu^-$ and 4.9 fb^{-1} for $Z \to \nu\overline{\nu}$. For the charged lepton case, the two leptons must be of the same flavor with the transverse momentum/energy of one > 20 GeV and the other > 10 GeV. The isolated photon must have $E_T > 50$ GeV. They observe 91 events with 87.2 ± 7.8 events expected from standard model processes. For the $\nu\overline{\nu}$ case they require solitary photons with $E_T > 25$ GeV and missing $E_T > 25$ GeV and observe 85 events with standard model expectation of 85.9 ± 5.6 events. Taking the form factor $\Lambda = 1.5$ TeV they derive 95% C.L. limits as $|h_3^{\gamma,Z}| < 0.022$ and $|h_4^{\gamma,Z}| < 0.0009$.

[5] CHATRCHYAN 11M study $Z\gamma$ production in pp collisions at $\sqrt{s} = 7$ TeV using 36 pb^{-1} pp data, where the Z decays to e^+e^- or $\mu^+\mu^-$. The total cross sections are measured for photon transverse energy $E_T^\gamma > 10$ GeV and spatial separation from charged leptons in the plane of pseudo rapidity and azimuthal angle $\Delta R(\ell,\gamma) > 0.7$ with the dilepton invariant mass requirement of $M_{\ell\ell} > 50$ GeV. The number of $e^+e^-\gamma$ and $\mu^+\mu^-\gamma$ candidates is 81 and 90 with estimated backgrounds of 20.5 ± 2.5 and 27.3 ± 3.2 events respectively. The 95% CL limits for $ZZ\gamma$ couplings are $-0.05 < h_3^Z < 0.06$

and $-0.0005 < h_4^Z < 0.0005$, and for $Z\gamma\gamma$ couplings are $-0.07 < h_3^\gamma < 0.07$ and $-0.0005 < h_4^\gamma < 0.0006$.

[6] ABAZOV 09L study $Z\gamma$, $Z \to \nu\overline{\nu}$ production in $p\overline{p}$ collisions at 1.96 TeV C.M. energy. They select 51 events with a photon of transverse energy E_T larger than 90 GeV, with an expected background of 17 events. Based on the photon E_T spectrum and including also Z decays to charged leptons (from ABAZOV 07M), the following 95% CL limits are reported: $|h_{30}^\gamma| < 0.033$, $|h_{40}^\gamma| < 0.0017$, $|h_{30}^Z| < 0.033$, $|h_{40}^Z| < 0.0017$.

[7] ABAZOV 07M use 968 $p\overline{p} \to e^+e^-/\mu^+\mu^-\gamma X$ candidates, at 1.96 TeV center of mass energy, to tag $p\overline{p} \to Z\gamma$ events by requiring $E_T(\gamma) > 7$ GeV, lepton-gamma separation $\Delta R_{\ell\gamma} > 0.7$, and di-lepton invariant mass > 30 GeV. The cross section is in agreement with the SM prediction. Using these $Z\gamma$ events they obtain 95% C.L. limits on each h_i^V, keeping all others fixed at their SM values. They report: $-0.083 < h_{30}^Z < 0.082$, $-0.0053 < h_{40}^Z < 0.0054$, $-0.085 < h_{30}^\gamma < 0.084$, $-0.0053 < h_{40}^\gamma < 0.0054$, for the form factor scale $\Lambda = 1.2$ TeV.

[8] Using data collected at $\sqrt{s} = 183$–208, ABDALLAH 07C select 1,877 $e^+e^- \to Z\gamma$ events with $Z \to q\overline{q}$ or $\nu\overline{\nu}$, 171 $e^+e^- \to ZZ$ events with $Z \to q\overline{q}$ or lepton pair (except an explicit τ pair), and 74 $e^+e^- \to Z\gamma^*$ events with a $q\overline{q}\mu^+\mu^-$ or $q\overline{q}e^+e^-$ signature, to derive 95% CL limits on h_i^V. Each limit is derived with other parameters set to zero. They report: $-0.23 < h_1^Z < 0.23$, $-0.30 < h_3^Z < 0.16$, $-0.14 < h_1^\gamma < 0.14$, $-0.049 < h_3^\gamma < 0.044$.

[9] ACHARD 04H select 3515 $e^+e^- \to Z\gamma$ events with $Z \to q\overline{q}$ or $\nu\overline{\nu}$ at $\sqrt{s} = 189$–209 GeV to derive 95% CL limits on h_i^V. For deriving each limit the other parameters are fixed at zero. They report: $-0.153 < h_1^Z < 0.141$, $-0.087 < h_2^Z < 0.079$, $-0.220 < h_3^Z < 0.112$, $-0.068 < h_4^Z < 0.148$, $-0.057 < h_1^\gamma < 0.057$, $-0.050 < h_2^\gamma < 0.023$, $-0.059 < h_3^\gamma < 0.004$, $-0.004 < h_4^\gamma < 0.042$.

[10] ABBIENDI,G 00C study $e^+e^- \to Z\gamma$ events (with $Z \to q\overline{q}$ and $Z \to \nu\overline{\nu}$) at 189 GeV to obtain the central values (and 95% CL limits) of these couplings: $h_1^Z = 0.000 \pm 0.100$ $(-0.190, 0.190)$, $h_2^Z = 0.000 \pm 0.068$ $(-0.128, 0.128)$, $h_3^Z = -0.074^{+0.102}_{-0.103}$ $(-0.269, 0.119)$, $h_4^Z = 0.046 \pm 0.068$ $(-0.084, 0.175)$, $h_1^\gamma = 0.000 \pm 0.061$ $(-0.115, 0.115)$, $h_2^\gamma = 0.000 \pm 0.041$ $(-0.077, 0.077)$, $h_3^\gamma = -0.080^{+0.039}_{-0.041}$ $(-0.164, -0.006)$, $h_4^\gamma = 0.064^{+0.033}_{-0.030}$ $(+0.007, +0.134)$. The results are derived assuming that only one coupling at a time is different from zero.

[11] ABBOTT 98M study $p\overline{p} \to Z\gamma + X$, with $Z \to e^+e^-$, $\mu^+\mu^-$, $\overline{\nu}\nu$ at 1.8 TeV, to obtain 95% CL limits at $\Lambda = 750$ GeV: $|h_{30}^Z| < 0.36$, $|h_{40}^Z| < 0.05$ (keeping $h_i^\gamma = 0$), and $|h_{30}^\gamma| < 0.37$, $|h_{40}^\gamma| < 0.05$ (keeping $h_i^Z = 0$). Limits on the CP-violating couplings are $|h_{10}^Z| < 0.36$, $|h_{20}^Z| < 0.05$ (keeping $h_i^\gamma = 0$), and $|h_{10}^\gamma| < 0.37$, $|h_{20}^\gamma| < 0.05$ (keeping $h_i^Z = 0$).

[12] ABREU 98K determine a 95% CL upper limit on $\sigma(e^+e^- \to \gamma +$ invisible particles$) < 2.5$ pb using 161 and 172 GeV data. This is used to set 95% CL limits on $|h_{30}^\gamma| < 0.8$ and $|h_{30}^Z| < 1.3$, derived at a scale $\Lambda = 1$ TeV and with $n = 3$ in the form factor representation.

f_i^V

Combining the LEP-2 results taking into account the correlations, the following 95% CL limits are derived [SCHAEL 13A]:

$$-0.28 < f_4^Z < +0.32, \qquad -0.34 < f_5^Z < +0.35,$$
$$-0.17 < f_4^\gamma < +0.19, \qquad -0.35 < f_5^\gamma < +0.32.$$

VALUE	DOCUMENT ID		TECN	COMMENT
• • • We do not use the following data for averages, fits, limits, etc. • • •				
	[1] AAD	13Z	ATLS	$E_{cm}^{pp} = 7$ TeV
	[2] CHATRCHYAN	13B	CMS	$E_{cm}^{pp} = 7$ TeV
	[3] SCHAEL	09	ALEP	$E_{cm}^{ee} = 192$–209 GeV
	[4] ABAZOV	08K	D0	$E_{cm}^{p\overline{p}} = 1.96$ TeV
	[5] ABDALLAH	07C	DLPH	$E_{cm}^{ee} = 183$–208 GeV
	[6] ABBIENDI	04C	OPAL	
	[7] ACHARD	03D	L3	

[1] AAD 13Z study ZZ production in pp collisions at $\sqrt{s} = 7$ TeV. In the $ZZ \to \ell^+\ell^-\ell'^+\ell'^-$ final state they observe a total of 66 events with an expected background of 0.9 ± 1.3. In the $ZZ \to \ell^+\ell^-\nu\nu$ final state they observe a total of 87 events with an expected background of 46.9 ± 5.2. The limits on anomalous TGCs are determined using the observed and expected numbers of these ZZ events binned in p_T^Z. The 95% C.L. are as follows: for form factor scale $\Lambda = \infty$, $-0.015 < f_4^\gamma < 0.015$, $-0.013 < f_4^Z < 0.013$, $-0.016 < f_5^\gamma < 0.015$, $-0.013 < f_5^Z < 0.013$; for form factor scale $\Lambda = 3$ TeV, $-0.022 < f_4^\gamma < 0.023$, $-0.019 < f_4^Z < 0.019$, $-0.023 < f_5^\gamma < 0.023$, $-0.020 < f_5^Z < 0.019$.

[2] CHATRCHYAN 13B study ZZ production in pp collisions and select 54 ZZ candidates in the Z decay channel with electrons or muons with an expected background of 1.4 ± 0.5 events. The resulting 95% C.L. ranges are: $-0.013 < f_4^\gamma < 0.015$, $-0.011 < f_4^Z < 0.012$, $-0.014 < f_5^\gamma < 0.014$, $-0.012 < f_5^Z < 0.012$.

[3] Using data collected in the center of mass energy range 192–209 GeV, SCHAEL 09 select 318 $e^+e^- \to ZZ$ events with 319.4 expected from the standard model. Using this data they derive the following 95% CL limits: $-0.321 < f_4^\gamma < 0.318$, $-0.534 < f_4^Z < 0.534$, $-0.724 < f_5^\gamma < 0.733$, $-1.194 < f_5^Z < 1.190$.

[4] ABAZOV 08K search for ZZ and $Z\gamma^*$ events with 1 fb^{-1} $p\overline{p}$ data at $\sqrt{s} = 1.96$ TeV in $(ee)(ee)$, $(\mu\mu)(\mu\mu)$, $(ee)(\mu\mu)$ final states requiring the lepton pair masses to be > 30 GeV. They observe 1 event, which is consistent with an expected signal of 1.71 ± 0.15 events and a background of 0.13 ± 0.03 events. From this they derive the following limits, for a form factor (Λ) value of 1.2 TeV: $-0.28 < f_{40}^Z < 0.28$, $-0.31 < f_{50}^Z < 0.29$, $-0.26 < f_{40}^\gamma < 0.26$, $-0.30 < f_{50}^\gamma < 0.28$.

[5] Using data collected at $\sqrt{s} = 183$–208 GeV, ABDALLAH 07C select 171 $e^+e^- \to ZZ$ events with $Z \to q\overline{q}$ or lepton pair (except an explicit τ pair), and 74 $e^+e^- \to Z\gamma^*$ events with a $q\overline{q}\mu^+\mu^-$ or $q\overline{q}e^+e^-$ signature, to derive 95% CL limits on f_i^V. Each limit is derived with other parameters set to zero. They report: $-0.40 < f_4^Z < 0.42$, $-0.38 < f_5^Z < 0.62$, $-0.23 < f_4^\gamma < 0.25$, $-0.52 < f_5^\gamma < 0.48$.

[6] ABBIENDI 04C study ZZ production in e^+e^- collisions in the C.M. energy range 190–209 GeV. They select 340 events with an expected background of 180 events. Including the ABBIENDI 00N data at 183 and 189 GeV (118 events with an expected background of 65 events) they report the following 95% CL limits: $-0.45 < f_4^Z < 0.58$, $-0.94 < f_5^Z < 0.25$, $-0.32 < f_4^\gamma < 0.33$, and $-0.71 < f_5^\gamma < 0.59$.

[7] ACHARD 03D study Z-boson pair production in e^+e^- collisions in the C.M. energy range 200–209 GeV. They select 549 events with an expected background of 432 events. Including the ACCIARRI 99G and ACCIARRI 99O data (183 and 189 GeV respectively, 286 events with an expected background of 241 events) and the 192–202 GeV ACCIARRI 01I results (656 events, expected background of 512 events), they report the following 95% CL limits: $-0.48 \le f_4^Z \le 0.46$, $-0.36 \le f_5^Z \le 1.03$, $-0.28 \le f_4^\gamma \le 0.28$, and $-0.40 \le f_5^\gamma \le 0.47$.

ANOMALOUS W/Z QUARTIC COUPLINGS

Revised September 2013 by M.W. Grünewald (U. College Dublin and U. Ghent) and A. Gurtu (Formerly Tata Inst.).

The Standard Model quartic couplings, $WWWW$, $WWZZ$, $WWZ\gamma$, $WW\gamma\gamma$, and $ZZ\gamma\gamma$, lead to negligible effects at LEP energies, while they are important at a TeV Linear Collider. Outside the Standard Model framework, possible quartic couplings, a_0, a_c, a_n, are expressed in terms of the following dimension-6 operators [1,2];

$$L_6^0 = -\frac{e^2}{16\Lambda^2}\, a_0\, F^{\mu\nu}\, F_{\mu\nu}\vec{W}^\alpha \cdot \vec{W}_\alpha$$
$$L_6^c = -\frac{e^2}{16\Lambda^2}\, a_c\, F^{\mu\alpha}\, F_{\mu\beta}\vec{W}^\beta \cdot \vec{W}_\alpha$$
$$L_6^n = -i\frac{e^2}{16\Lambda^2}\, a_n \epsilon_{ijk}\, W_{\mu\alpha}^{(i)}\, W_\nu^{(j)}\, W^{(k)\alpha} F^{\mu\nu}$$
$$\widetilde{L}_6^0 = -\frac{e^2}{16\Lambda^2}\, \widetilde{a}_0\, F^{\mu\nu}\, \widetilde{F}_{\mu\nu}\vec{W}^\alpha \cdot \vec{W}_\alpha$$
$$\widetilde{L}_6^n = -i\frac{e^2}{16\Lambda^2}\, \widetilde{a}_n \epsilon_{ijk}\, W_{\mu\alpha}^{(i)}\, W_\nu^{(j)}\, W^{(k)\alpha} \widetilde{F}^{\mu\nu}$$

where F, W are photon and W fields, L_6^0 and L_6^c conserve C, P separately ($\widetilde{L}_6^0$ conserves only C) and generate anomalous $W^+W^-\gamma\gamma$ and $ZZ\gamma\gamma$ couplings, L_6^n violates CP ($\widetilde{L}_6^n$ violates both C and P) and generates an anomalous $W^+W^-Z\gamma$ coupling, and Λ is an energy scale for new physics. For the $ZZ\gamma\gamma$ coupling the CP-violating term represented by L_6^n does not contribute. These couplings are assumed to be real and to vanish at tree level in the Standard Model.

Within the same framework as above, a more recent description of the quartic couplings [3] treats the anomalous parts of the $WW\gamma\gamma$ and $ZZ\gamma\gamma$ couplings separately, leading to two sets parameterized as a_0^V/Λ^2 and a_c^V/Λ^2, where $V = W$ or Z.

At LEP the processes studied in search of these quartic couplings are $e^+e^- \to WW\gamma$, $e^+e^- \to \gamma\gamma\nu\overline{\nu}$, and $e^+e^- \to Z\gamma\gamma$ and limits are set on the quantities $a_0^W/\Lambda^2, a_c^W/\Lambda^2, a_n/\Lambda^2$. The characteristics of the first process depend on all the three couplings whereas those of the latter two depend only on the two CP-conserving couplings. The sensitive measured variables are the cross sections for these processes as well as the energy and angular distributions of the photon and recoil mass to the photon pair. At hadron colliders, tri-boson production $VV\gamma$ as

well as di-boson scattering $\gamma\gamma \to VV$ is analysed to set limits on anomalous QGCs.

References

1. G. Belanger and F. Boudjema, Phys. Lett. **B288**, 201 (1992).
2. J.W. Stirling and A. Werthenbach, Eur. Phys. J. **C14**, 103 (2000);
J.W. Stirling and A. Werthenbach, Phys. Lett. **B466**, 369 (1999);
A. Denner *et al.*, Eur. Phys. J. **C20**, 201 (2001);
G. Montagna *et al.*, Phys. Lett. **B515**, 197 (2001).
3. G. Belanger *et al.*, Eur. Phys. J. **C13**, 283 (2000).

a_0/Λ^2, a_c/Λ^2

Combining published and unpublished preliminary LEP results the following 95% CL intervals for the QGCs associated with the $ZZ\gamma\gamma$ vertex are derived (CERN-PH-EP/2005-051 or hep-ex/0511027):

$$-0.008 < a_0^Z/\Lambda^2 < +0.021$$
$$-0.029 < a_c^Z/\Lambda^2 < +0.039$$

VALUE	*DOCUMENT ID*	*TECN*
• • • We do not use the following data for averages, fits, limits, etc. • • •		
[1] ABBIENDI	04L	OPAL
[2] HEISTER	04A	ALEP
[3] ACHARD	02G	L3

[1] ABBIENDI 04L select 20 $e^+e^- \to \nu\overline{\nu}\gamma\gamma$ acoplanar events in the energy range 180–209 GeV and 176 $e^+e^- \to q\overline{q}\gamma\gamma$ events in the energy range 130–209 GeV. These samples are used to constrain possible anomalous $W^+W^-\gamma\gamma$ and $ZZ\gamma\gamma$ quartic couplings. Further combining with the $W^+W^-\gamma$ sample of ABBIENDI 04B the following one–parameter 95% CL limits are obtained: $-0.007 < a_0^Z/\Lambda^2 < 0.023$ GeV^{-2}, $-0.029 < a_c^Z/\Lambda^2 < 0.029$ GeV^{-2}, $-0.020 < a_0^W/\Lambda^2 < 0.020$ GeV^{-2}, $-0.052 < a_c^W/\Lambda^2 < 0.037$ GeV^{-2}.

[2] In the CM energy range 183 to 209 GeV HEISTER 04A select 30 $e^+e^- \to \nu\overline{\nu}\gamma\gamma$ events with two acoplanar, high energy and high transverse momentum photons. The photon–photon acoplanarity is required to be $> 5^\circ$, $E_\gamma/\sqrt{s} > 0.025$ (the more energetic photon having energy $> 0.2\ \sqrt{s}$), $p_{T_\gamma}/E_{beam} > 0.05$ and $|\cos\theta_\gamma| < 0.94$. A likelihood fit to the photon energy and recoil missing mass yields the following one–parameter 95% CL limits: $-0.012 < a_0^Z/\Lambda^2 < 0.019$ GeV^{-2}, $-0.041 < a_c^Z/\Lambda^2 < 0.044$ GeV^{-2}, $-0.060 < a_0^W/\Lambda^2 < 0.055$ GeV^{-2}, $-0.099 < a_c^W/\Lambda^2 < 0.093$ GeV^{-2}.

[3] ACHARD 02G study $e^+e^- \to Z\gamma\gamma \to q\overline{q}\gamma\gamma$ events using data at center-of-mass energies from 200 to 209 GeV. The photons are required to be isolated, each with energy >5 GeV and $|\cos\theta| < 0.97$, and the di-jet invariant mass to be compatible with that of the Z boson (74–111 GeV). Cuts on Z velocity ($\beta < 0.73$) and on the energy of the most energetic photon reduce the backgrounds due to non-resonant production of the $q\overline{q}\gamma\gamma$ state and due to ISR respectively, yielding a total of 40 candidate events of which 8.6 are expected to be due to background. The energy spectra of the least energetic photon are fitted for all ten center-of-mass energy values from 130 GeV to 209 GeV (as obtained adding to the present analysis 130–202 GeV data of ACCIARRI 01E, for a total of 137 events with an expected background of 34.1 events) to obtain the fitted values $a_0/\Lambda^2 = 0.00^{+0.02}_{-0.01}$ GeV^{-2} and $a_c/\Lambda^2 = 0.03^{+0.01}_{-0.02}$ GeV^{-2}, where the other parameter is kept fixed to its Standard Model value (0). A simultaneous fit to both parameters yields the 95% CL limits -0.02 GeV$^{-2} < a_0/\Lambda^2 < 0.03$ GeV^{-2} and -0.07 GeV$^{-2} < a_c/\Lambda^2 < 0.05$ GeV^{-2}.

Z REFERENCES

AAD	13AN	PR D87 112003	G. Aad *et al.*	(ATLAS Collab.)
AAD	13Z	JHEP 1303 128	G. Aad *et al.*	(ATLAS Collab.)
CHATRCHYAN	13B	JHEP 1301 063	S. Chatrchyan *et al.*	(CMS Collab.)
CHATRCHYAN	13BI	JHEP 1310 164	S. Chatrchyan *et al.*	(CMS Collab.)
SCHAEL	13A	PRPL 532 119	S. Schael *et al.*	(ALEPH, DELPHI, L3, OPAL+)
AAD	12BX	PL B717 49	G. Aad *et al.*	(ATLAS Collab.)
ABAZOV	12S	PR D85 052001	V.M. Abazov *et al.*	(D0 Collab.)
CHATRCHYAN	12BN	JHEP 1212 034	S. Chatrchyan *et al.*	(CMS Collab.)
AALTONEN	11S	PRL 107 051802	T. Aaltonen *et al.*	(CDF Collab.)
ABAZOV	11D	PR D84 012007	V.M. Abazov *et al.*	(D0 Collab.)
CHATRCHYAN	11M	PL B701 535	S. Chatrchyan *et al.*	(CMS Collab.)
ABAZOV	09L	PRL 102 201802	V.M. Abazov *et al.*	(D0 Collab.)
BEDDALL	09	PL B670 300	A. Beddall, A. Beddall, A. Bingul	(UGAZ)
SCHAEL	09	JHEP 0904 124	S. Schael *et al.*	(ALEPH Collab.)
ABAZOV	08K	PRL 100 131801	V.M. Abazov *et al.*	(D0 Collab.)
ABAZOV	07M	PL B653 378	V.M. Abazov *et al.*	(D0 Collab.)
ABDALLAH	07C	EPJ C51 525	J. Abdallah *et al.*	(DELPHI Collab.)
ABDALLAH	06E	PL B639 179	J. Abdallah *et al.*	(DELPHI Collab.)
AKTAS	06	PL B632 35	A. Aktas *et al.*	(H1 Collab.)
LEP-SLC	06	PRPL 427 257	ALEPH, DELPHI, L3, OPAL, SLD and working groups	
SCHAEL	06A	PL B639 192	S. Schael *et al.*	(ALEPH Collab.)
ABDALLAH	05	EPJ C40 1	J. Abdallah *et al.*	(DELPHI Collab.)
ABDALLAH	05C	EPJ C44 299	J. Abdallah *et al.*	(DELPHI Collab.)
ABE	05	PRL 94 091801	K. Abe *et al.*	(SLD Collab.)
ABE	05F	PR D71 112004	K. Abe *et al.*	(SLD Collab.)
ACOSTA	05M	PR D71 052002	D. Acosta *et al.*	(CDF Collab.)
ABBIENDI	04B	PL B580 17	G. Abbiendi *et al.*	(OPAL Collab.)
ABBIENDI	04C	EPJ C32 303	G. Abbiendi *et al.*	(OPAL Collab.)
ABBIENDI	04E	PL B586 167	G. Abbiendi *et al.*	(OPAL Collab.)
ABBIENDI	04G	EPJ C33 173	G. Abbiendi *et al.*	(OPAL Collab.)
ABBIENDI	04L	PR D70 032005	G. Abbiendi *et al.*	(OPAL Collab.)
ABDALLAH	04F	EPJ C34 109	J. Abdallah *et al.*	(DELPHI Collab.)
ABE	04C	PR D69 072003	K. Abe *et al.*	(SLD Collab.)
ACHARD	04C	PL B585 42	P. Achard *et al.*	(L3 Collab.)
ACHARD	04H	PL B597 119	P. Achard *et al.*	(L3 Collab.)
HEISTER	04A	PL B602 31	A. Heister *et al.*	(ALEPH Collab.)
ABBIENDI	03P	PL B577 18	G. Abbiendi *et al.*	(OPAL Collab.)
ABDALLAH	03H	PL B569 129	J. Abdallah *et al.*	(DELPHI Collab.)
ABDALLAH	03K	PL B576 29	J. Abdallah *et al.*	(DELPHI Collab.)
ABE	03F	PRL 90 141804	K. Abe *et al.*	(SLD Collab.)
ACHARD	03D	PL B572 133	P. Achard *et al.*	(L3 Collab.)
ACHARD	03G	PL B577 109	P. Achard *et al.*	(L3 Collab.)
ABBIENDI	02I	PL B546 29	G. Abbiendi *et al.*	(OPAL Collab.)
ABE	02G	PRL 88 151801	K. Abe *et al.*	(SLD Collab.)
ACHARD	02G	PL B540 43	P. Achard *et al.*	(L3 Collab.)
HEISTER	02B	PL B526 34	A. Heister *et al.*	(ALEPH Collab.)
HEISTER	02C	PL B528 19	A. Heister *et al.*	(ALEPH Collab.)
HEISTER	02H	EPJ C24 177	A. Heister *et al.*	(ALEPH Collab.)
ABBIENDI	01A	EPJ C19 587	G. Abbiendi *et al.*	(OPAL Collab.)
ABBIENDI	01G	EPJ C18 447	G. Abbiendi *et al.*	(OPAL Collab.)
ABBIENDI	01K	PL B516 1	G. Abbiendi *et al.*	(OPAL Collab.)
ABBIENDI	01N	EPJ C20 445	G. Abbiendi *et al.*	(OPAL Collab.)
ABBIENDI	01O	EPJ C21 1	G. Abbiendi *et al.*	(OPAL Collab.)
ABE	01B	PRL 86 1162	K. Abe *et al.*	(SLD Collab.)
ABE	01C	PR D63 032005	K. Abe *et al.*	(SLD Collab.)
ACCIARRI	01E	PL B505 47	M. Acciarri *et al.*	(L3 Collab.)
ACCIARRI	01I	PL B497 23	M. Acciarri *et al.*	(L3 Collab.)
HEISTER	01	EPJ C20 401	A. Heister *et al.*	(ALEPH Collab.)
HEISTER	01D	EPJ C22 201	A. Heister *et al.*	(ALEPH Collab.)
ABBIENDI	00N	PL B476 256	G. Abbiendi *et al.*	(OPAL Collab.)
ABBIENDI,G	00C	EPJ C17 553	G. Abbiendi *et al.*	(OPAL Collab.)
ABE	00B	PRL 84 5945	K. Abe *et al.*	(SLD Collab.)
ABE	00D	PRL 85 5059	K. Abe *et al.*	(SLD Collab.)
ABREU	00	EPJ C12 225	P. Abreu *et al.*	(DELPHI Collab.)
ABREU	00B	EPJ C14 613	P. Abreu *et al.*	(DELPHI Collab.)
ABREU	00E	EPJ C14 585	P. Abreu *et al.*	(DELPHI Collab.)
ABREU	00F	EPJ C16 371	P. Abreu *et al.*	(DELPHI Collab.)
ABREU	00P	PL B475 429	P. Abreu *et al.*	(DELPHI Collab.)
ACCIARRI	00	EPJ C13 47	M. Acciarri *et al.*	(L3 Collab.)
ACCIARRI	00C	EPJ C16 1	M. Acciarri *et al.*	(L3 Collab.)
ACCIARRI	00J	PL B479 79	M. Acciarri *et al.*	(L3 Collab.)
ACCIARRI	00Q	PL B489 93	M. Acciarri *et al.*	(L3 Collab.)
BARATE	00B	EPJ C16 597	R. Barate *et al.*	(ALEPH Collab.)
BARATE	00C	EPJ C14 1	R. Barate *et al.*	(ALEPH Collab.)
BARATE	00O	EPJ C16 613	R. Barate *et al.*	(ALEPH Collab.)
ABBIENDI	99B	EPJ C8 217	G. Abbiendi *et al.*	(OPAL Collab.)
ABBIENDI	99I	PL B447 157	G. Abbiendi *et al.*	(OPAL Collab.)
ABE	99E	PR D59 052001	K. Abe *et al.*	(SLD Collab.)
ABE	99L	PRL 83 1902	K. Abe *et al.*	(SLD Collab.)
ABREU	99	EPJ C6 19	P. Abreu *et al.*	(DELPHI Collab.)
ABREU	99B	EPJ C10 415	P. Abreu *et al.*	(DELPHI Collab.)
ABREU	99J	PL B449 364	P. Abreu *et al.*	(DELPHI Collab.)
ABREU	99U	PL B462 425	P. Abreu *et al.*	(DELPHI Collab.)
ABREU	99Y	EPJ C10 219	P. Abreu *et al.*	(DELPHI Collab.)
ACCIARRI	99D	PL B448 152	M. Acciarri *et al.*	(L3 Collab.)
ACCIARRI	99F	PL B453 94	M. Acciarri *et al.*	(L3 Collab.)
ACCIARRI	99G	PL B450 281	M. Acciarri *et al.*	(L3 Collab.)
ACCIARRI	99O	PL B465 363	M. Acciarri *et al.*	(L3 Collab.)
ABBOTT	98M	PR D57 R3817	B. Abbott *et al.*	(D0 Collab.)
ABE	98D	PRL 80 660	K. Abe *et al.*	(SLD Collab.)
ABE	98I	PRL 81 942	K. Abe *et al.*	(SLD Collab.)
ABREU	98K	PL B423 194	P. Abreu *et al.*	(DELPHI Collab.)
ABREU	98L	EPJ C5 585	P. Abreu *et al.*	(DELPHI Collab.)
ACCIARRI	98G	PL B431 199	M. Acciarri *et al.*	(L3 Collab.)
ACCIARRI	98H	PL B429 387	M. Acciarri *et al.*	(L3 Collab.)
ACCIARRI	98U	PL B439 225	M. Acciarri *et al.*	(L3 Collab.)
ACKERSTAFF	98A	EPJ C5 411	K. Ackerstaff *et al.*	(OPAL Collab.)
ACKERSTAFF	98E	EPJ C1 439	K. Ackerstaff *et al.*	(OPAL Collab.)
ACKERSTAFF	98O	PL B420 157	K. Ackerstaff *et al.*	(OPAL Collab.)
ACKERSTAFF	98Q	EPJ C4 19	K. Ackerstaff *et al.*	(OPAL Collab.)
BARATE	98O	PL B434 415	R. Barate *et al.*	(ALEPH Collab.)
BARATE	98T	EPJ C4 557	R. Barate *et al.*	(ALEPH Collab.)
BARATE	98V	EPJ C5 205	R. Barate *et al.*	(ALEPH Collab.)
ABE	97	PRL 78 17	K. Abe *et al.*	(SLD Collab.)
ABREU	97C	ZPHY C73 243	P. Abreu *et al.*	(DELPHI Collab.)
ABREU	97E	PL B398 207	P. Abreu *et al.*	(DELPHI Collab.)
ABREU	97G	PL B404 194	P. Abreu *et al.*	(DELPHI Collab.)
ACCIARRI	97D	PL B393 465	M. Acciarri *et al.*	(L3 Collab.)
ACCIARRI	97J	PL B407 351	M. Acciarri *et al.*	(L3 Collab.)
ACCIARRI	97L	PL B407 389	M. Acciarri *et al.*	(L3 Collab.)
ACCIARRI	97R	PL B413 167	M. Acciarri *et al.*	(L3 Collab.)
ACKERSTAFF	97M	ZPHY C74 413	K. Ackerstaff *et al.*	(OPAL Collab.)
ACKERSTAFF	97S	PL B412 210	K. Ackerstaff *et al.*	(OPAL Collab.)
ACKERSTAFF	97T	ZPHY C76 387	K. Ackerstaff *et al.*	(OPAL Collab.)
ACKERSTAFF	97W	ZPHY C76 425	K. Ackerstaff *et al.*	(OPAL Collab.)
ALEXANDER	97C	ZPHY C73 379	G. Alexander *et al.*	(OPAL Collab.)
ALEXANDER	97D	ZPHY C73 569	G. Alexander *et al.*	(OPAL Collab.)
ALEXANDER	97E	ZPHY C73 587	G. Alexander *et al.*	(OPAL Collab.)
BARATE	97D	PL B405 191	R. Barate *et al.*	(ALEPH Collab.)
BARATE	97E	PL B401 150	R. Barate *et al.*	(ALEPH Collab.)
BARATE	97F	PL B401 163	R. Barate *et al.*	(ALEPH Collab.)
BARATE	97H	PL B402 213	R. Barate *et al.*	(ALEPH Collab.)
BARATE	97J	ZPHY C74 451	R. Barate *et al.*	(ALEPH Collab.)
ABREU	96R	ZPHY C72 31	P. Abreu *et al.*	(DELPHI Collab.)
ABREU	96S	PL B389 405	P. Abreu *et al.*	(DELPHI Collab.)
ABREU	96U	ZPHY C73 61	P. Abreu *et al.*	(DELPHI Collab.)
ACCIARRI	96	PL B371 126	M. Acciarri *et al.*	(L3 Collab.)
ADAM	96	ZPHY C69 561	W. Adam *et al.*	(DELPHI Collab.)
ADAM	96B	ZPHY C70 371	W. Adam *et al.*	(DELPHI Collab.)
ALEXANDER	96B	ZPHY C70 197	G. Alexander *et al.*	(OPAL Collab.)
ALEXANDER	96F	PL B370 185	G. Alexander *et al.*	(OPAL Collab.)
ALEXANDER	96N	PL B384 343	G. Alexander *et al.*	(OPAL Collab.)
ALEXANDER	96R	ZPHY C72 1	G. Alexander *et al.*	(OPAL Collab.)
BUSKULIC	96D	ZPHY C69 393	D. Buskulic *et al.*	(ALEPH Collab.)
BUSKULIC	96H	ZPHY C69 379	D. Buskulic *et al.*	(ALEPH Collab.)
BUSKULIC	96T	PL B384 449	D. Buskulic *et al.*	(ALEPH Collab.)
BUSKULIC	96Y	PL B388 648	D. Buskulic *et al.*	(ALEPH Collab.)
ABE	95J	PRL 74 2880	K. Abe *et al.*	(SLD Collab.)
ABREU	95	ZPHY C65 709 (erratum)	P. Abreu *et al.*	(DELPHI Collab.)
ABREU	95D	ZPHY C66 323	P. Abreu *et al.*	(DELPHI Collab.)
ABREU	95L	ZPHY C65 587	P. Abreu *et al.*	(DELPHI Collab.)
ABREU	95M	ZPHY C65 603	P. Abreu *et al.*	(DELPHI Collab.)
ABREU	95O	ZPHY C67 543	P. Abreu *et al.*	(DELPHI Collab.)
ABREU	95R	ZPHY C68 353	P. Abreu *et al.*	(DELPHI Collab.)
ABREU	95V	ZPHY C68 541	P. Abreu *et al.*	(DELPHI Collab.)
ABREU	95W	PL B361 207	P. Abreu *et al.*	(DELPHI Collab.)
ABREU	95X	ZPHY C69 1	P. Abreu *et al.*	(DELPHI Collab.)
ACCIARRI	95B	PL B345 589	M. Acciarri *et al.*	(L3 Collab.)
ACCIARRI	95C	PL B345 609	M. Acciarri *et al.*	(L3 Collab.)
ACCIARRI	95G	PL B353 136	M. Acciarri *et al.*	(L3 Collab.)
AKERS	95C	ZPHY C65 47	R. Akers *et al.*	(OPAL Collab.)
AKERS	95U	ZPHY C67 389	R. Akers *et al.*	(OPAL Collab.)
AKERS	95W	ZPHY C67 555	R. Akers *et al.*	(OPAL Collab.)

AKERS	95X	ZPHY C68 1	R. Akers *et al.*	(OPAL Collab.)
AKERS	95Z	ZPHY C68 203	R. Akers *et al.*	(OPAL Collab.)
ALEXANDER	95D	PL B358 162	G. Alexander *et al.*	(OPAL Collab.)
BUSKULIC	95R	ZPHY C69 15	D. Buskulic *et al.*	(ALEPH Collab.)
MIYABAYASHI	95	PL B347 171	K. Miyabayashi *et al.*	(TOPAZ Collab.)
ABE	94C	PRL 73 25	K. Abe *et al.*	(SLD Collab.)
ABREU	94B	PL B327 386	P. Abreu *et al.*	(DELPHI Collab.)
ABREU	94P	PL B341 109	P. Abreu *et al.*	(DELPHI Collab.)
AKERS	94P	ZPHY C63 181	R. Akers *et al.*	(OPAL Collab.)
BUSKULIC	94G	ZPHY C62 179	D. Buskulic *et al.*	(ALEPH Collab.)
BUSKULIC	94J	ZPHY C62 1	D. Buskulic *et al.*	(ALEPH Collab.)
VILAIN	94	PL B320 203	P. Vilain *et al.*	(CHARM II Collab.)
ABREU	93	PL B298 236	P. Abreu *et al.*	(DELPHI Collab.)
ABREU	93I	ZPHY C59 533	P. Abreu *et al.*	(DELPHI Collab.)
Also		ZPHY C65 709 (erratum)	P. Abreu *et al.*	(DELPHI Collab.)
ABREU	93L	PL B318 249	P. Abreu *et al.*	(DELPHI Collab.)
ACTON	93	PL B305 407	P.D. Acton *et al.*	(OPAL Collab.)
ACTON	93D	ZPHY C58 219	P.D. Acton *et al.*	(OPAL Collab.)
ACTON	93E	PL B311 391	P.D. Acton *et al.*	(OPAL Collab.)
ADRIANI	93	PL B301 136	O. Adriani *et al.*	(L3 Collab.)
ADRIANI	93I	PL B316 427	O. Adriani *et al.*	(L3 Collab.)
BUSKULIC	93L	PL B313 520	D. Buskulic *et al.*	(ALEPH Collab.)
NOVIKOV	93C	PL B298 453	V.A. Novikov, L.B. Okun, M.I. Vysotsky	(ITEP)
ABREU	92I	PL B277 371	P. Abreu *et al.*	(DELPHI Collab.)
ABREU	92M	PL B289 199	P. Abreu *et al.*	(DELPHI Collab.)
ACTON	92B	ZPHY C53 539	D.P. Acton *et al.*	(OPAL Collab.)
ACTON	92L	PL B294 436	P.D. Acton *et al.*	(OPAL Collab.)
ACTON	92N	PL B295 357	P.D. Acton *et al.*	(OPAL Collab.)
ADEVA	92	PL B275 209	B. Adeva *et al.*	(L3 Collab.)
ADRIANI	92D	PL B292 454	O. Adriani *et al.*	(L3 Collab.)
ALITTI	92B	PL B276 354	J. Alitti *et al.*	(UA2 Collab.)
BUSKULIC	92D	PL B292 210	D. Buskulic *et al.*	(ALEPH Collab.)
BUSKULIC	92E	PL B294 145	D. Buskulic *et al.*	(ALEPH Collab.)
DECAMP	92	PRPL 216 253	D. Decamp *et al.*	(ALEPH Collab.)
ABE	91E	PRL 67 1502	F. Abe *et al.*	(CDF Collab.)
ABREU	91H	ZPHY C50 185	P. Abreu *et al.*	(DELPHI Collab.)
ACTON	91B	PL B273 338	D.P. Acton *et al.*	(OPAL Collab.)
ADACHI	91	PL B255 613	I. Adachi *et al.*	(TOPAZ Collab.)
ADEVA	91I	PL B259 199	B. Adeva *et al.*	(L3 Collab.)
AKRAWY	91F	PL B257 531	M.Z. Akrawy *et al.*	(OPAL Collab.)
DECAMP	91B	PL B259 377	D. Decamp *et al.*	(ALEPH Collab.)
DECAMP	91J	PL B266 218	D. Decamp *et al.*	(ALEPH Collab.)
JACOBSEN	91	PRL 67 3347	R.G. Jacobsen *et al.*	(Mark II Collab.)
SHIMONAKA	91	PL B268 457	A. Shimonaka *et al.*	(TOPAZ Collab.)
ABE	90I	ZPHY C48 13	K. Abe *et al.*	(VENUS Collab.)
ABRAMS	90	PRL 64 1334	G.S. Abrams *et al.*	(Mark II Collab.)
AKRAWY	90J	PL B246 285	M.Z. Akrawy *et al.*	(OPAL Collab.)
BEHREND	90D	ZPHY C47 333	H.J. Behrend *et al.*	(CELLO Collab.)
BRAUNSCH...	90	ZPHY C48 433	W. Braunschweig *et al.*	(TASSO Collab.)
ELSEN	90	ZPHY C46 349	E. Elsen *et al.*	(JADE Collab.)
HEGNER	90	ZPHY C46 547	S. Hegner *et al.*	(JADE Collab.)
STUART	90	PRL 64 983	D. Stuart *et al.*	(AMY Collab.)
ABE	89	PRL 62 613	F. Abe *et al.*	(CDF Collab.)
ABE	89C	PRL 63 720	F. Abe *et al.*	(CDF Collab.)
ABE	89L	PL B232 425	K. Abe *et al.*	(VENUS Collab.)
ABRAMS	89B	PRL 63 2173	G.S. Abrams *et al.*	(Mark II Collab.)
ABRAMS	89D	PRL 63 2780	G.S. Abrams *et al.*	(Mark II Collab.)
ALBAJAR	89	ZPHY C44 15	C. Albajar *et al.*	(UA1 Collab.)
BACALA	89	PL B218 112	A. Bacala *et al.*	(AMY Collab.)
BAND	89	PL B218 369	H.R. Band *et al.*	(MAC Collab.)
GREENSHAW	89	ZPHY C42 1	T. Greenshaw *et al.*	(JADE Collab.)
OULD-SAADA	89	ZPHY C44 567	F. Ould-Saada *et al.*	(JADE Collab.)
SAGAWA	89	PRL 63 2341	H. Sagawa *et al.*	(AMY Collab.)
ADACHI	88C	PL B208 319	I. Adachi *et al.*	(TOPAZ Collab.)
ADEVA	88	PR D38 2665	B. Adeva *et al.*	(Mark-J Collab.)
BRAUNSCH...	88D	ZPHY C40 163	W. Braunschweig *et al.*	(TASSO Collab.)
ANSARI	87	PL B186 440	R. Ansari *et al.*	(UA2 Collab.)
BEHREND	87C	PL B191 209	H.J. Behrend *et al.*	(CELLO Collab.)
BARTEL	86C	ZPHY C30 371	W. Bartel *et al.*	(JADE Collab.)
Also		ZPHY C26 507	W. Bartel *et al.*	(JADE Collab.)
Also		PL 108B 140	W. Bartel *et al.*	(JADE Collab.)
ASH	85	PRL 55 1831	W.W. Ash *et al.*	(MAC Collab.)
BARTEL	85F	PL 161B 188	W. Bartel *et al.*	(JADE Collab.)
DERRICK	85	PR D31 2352	M. Derrick *et al.*	(HRS Collab.)
FERNANDEZ	85	PRL 54 1624	E. Fernandez *et al.*	(MAC Collab.)
LEVI	83	PRL 51 1941	M.E. Levi *et al.*	(Mark II Collab.)
BEHREND	82	PL 114B 282	H.J. Behrend *et al.*	(CELLO Collab.)
BRANDELIK	82C	PL 110B 173	R. Brandelik *et al.*	(TASSO Collab.)

H^0

$J = 0$

In the following H^0 refers to the signal that has been discovered in the Higgs searches. Whereas the observed signal is labeled as a spin 0 particle and is called a Higgs Boson, the detailed properties of H^0 and its role in the context of electroweak symmetry breaking need to be further clarified. These issues are addressed by the measurements listed below.

Concerning mass limits and cross section limits that have been obtained in the searches for neutral and charged Higgs bosons, see the sections "Searches for Neutral Higgs Bosons" and "Searches for Charged Higgs Bosons ($H^{\pm}$ and $H^{\pm\pm}$)", respectively.

H^0 MASS

A combination of the results from ATLAS and CMS, where a recent unpublished result from CMS is used, yields an average value of 125.6 ± 0.3 GeV, see the review on "Status of Higgs Boson Physics."

VALUE (GeV)	*DOCUMENT ID*		*TECN*	*COMMENT*
125.7±0.4 OUR AVERAGE				
$125.5 \pm 0.2 ^{+0.5}_{-0.6}$	[1,2] AAD	13AK	ATLS	pp, 7 and 8 TeV
125.8 ± 0.4 ± 0.4	[1,3] CHATRCHYAN	13J	CMS	pp, 7 and 8 TeV
126.8 ± 0.2 ± 0.7	[2] AAD	13AK	ATLS	pp, 7 and 8 TeV, $\gamma\gamma$
$124.3 ^{+0.6}_{-0.5} ^{+0.5}_{-0.3}$	[2] AAD	13AK	ATLS	pp, 7, 8 TeV, $ZZ^* \to 4\ell$
126.2 ± 0.6 ± 0.2	[3] CHATRCHYAN	13J	CMS	pp, 7, 8 TeV, $ZZ^* \to 4\ell$
126.0 ± 0.4 ± 0.4	[1,4] AAD	12AI	ATLS	pp, 7 and 8 TeV
125.3 ± 0.4 ± 0.5	[1,5] CHATRCHYAN	12N	CMS	pp, 7 and 8 TeV

• • • We do not use the following data for averages, fits, limits, etc. • • •

[1] Combined value from $\gamma\gamma$ and $ZZ^* \to 4\ell$ final states.

[2] AAD 13AK use 4.7 fb^{-1} of pp collisions at E_{cm}=7 TeV and 20.7 fb^{-1} at E_{cm}=8 TeV.

[3] CHATRCHYAN 13J use 5.1 fb^{-1} of pp collisions at E_{cm} = 7 TeV and 12.2 fb^{-1} at E_{cm} = 8 TeV.

[4] AAD 12AI obtain results based on 4.6–4.8 fb^{-1} of pp collisions at E_{cm} = 7 TeV and 5.8–5.9 fb^{-1} at E_{cm} = 8 TeV. An excess of events over background with a local significance of 5.9 σ is observed at m_{H^0} = 126 GeV. See also AAD 12DA.

[5] CHATRCHYAN 12N obtain results based on 4.9–5.1 fb^{-1} of pp collisions at E_{cm} = 7 TeV and 5.1–5.3 fb^{-1} at E_{cm} = 8 TeV. An excess of events over background with a local significance of 5.0 σ is observed at about m_{H^0} = 125 GeV. See also CHATRCHYAN 12BY and CHATRCHYAN 13Y.

H^0 SPIN AND CP PROPERTIES

The observation of the signal in the $\gamma\gamma$ final state rules out the possibility that the discovered particle has spin 1, as a consequence of the Landau-Yang theorem. This argument relies on the assumptions that the decaying particle is an on-shell resonance and that the decay products are indeed two photons rather than two pairs of boosted photons, which each could in principle be misidentified as a single photon.

Concerning distinguishing the spin 0 hypothesis from a spin 2 hypothesis, some care has to be taken in modelling the latter in order to ensure that the discriminating power is actually based on the spin properties rather than on unphysical behavior that may affect the model of the spin 2 state.

Under the assumption that the observed signal consists of a single state rather than an overlap of more than one resonance, it is sufficient to discriminate between distinct hypotheses in the spin analyses. On the other hand, the determination of the CP properties is in general much more difficult since in principle the observed state could consist of any admixture of CP-even and CP-odd components. As a first step, the compatibility of the data with distinct hypotheses of pure CP-even and pure CP-odd states with different spin assignments has been investigated. In CHATRCHYAN 13J angular distributions of the lepton pairs have been studied in the ZZ^* channel where both Z bosons decay to e or μ pairs. Under the assumption that the observed particle has spin 0, the data are found to be consistent with the pure CP-even hypothesis, while the pure CP-odd hypothesis is disfavored. In AAD 13AJ the spin 0, CP-even hypothesis has been compared with specific alternative hypotheses of spin 0, CP-odd, spin 1, CP-even and CP-odd, and spin 2, CP-even models using the Higgs boson decays $H \to \gamma\gamma$, $H \to ZZ^* \to 4\ell$ and $H \to WW^* \to \ell\nu\ell\nu$ and combinations thereof. The data are compatible with the spin 0, CP-even hypothesis, while all other tested hypotheses are excluded at confidence levels above 97.8%.

H^0 DECAY WIDTH

The total decay width for a light Higgs boson with a mass in the observed range is not expected to be directly observable at the LHC. For the case of the Standard Model the prediction for the total width is about 4 MeV, which is three orders of magnitude smaller than the experimental mass resolution. There is no indication from the results observed so far that the natural width is broadened by new physics effects to such an extent that it could be directly observable. Furthermore, as all LHC Higgs channels rely on the identification of Higgs decay products, the total Higgs width cannot be measured indirectly without additional assumptions. The different dependence of on-peak and off-peak contributions on the total width in Higgs decays to ZZ^* and interference effects between signal and background in Higgs decays to $\gamma\gamma$ can provide additional information in this context. Without an experimental determination of the total width or further theoretical assumptions, only ratios of couplings can be determined at the LHC rather than absolute values of couplings.

H^0 DECAY MODES

	Mode
Γ_1	WW^*
Γ_2	ZZ^*
Γ_3	$\gamma\gamma$
Γ_4	$b\overline{b}$
Γ_5	$\tau^+\tau^-$
Γ_6	$Z\gamma$

H^0 SIGNAL STRENGTHS IN DIFFERENT CHANNELS

The H^0 signal strength in a particular final state xx is given by the cross section times branching ratio in this channel normalized to the Standard Model (SM) value, $\sigma \cdot B(H^0 \to xx) / (\sigma \cdot B(H^0 \to xx))_{SM}$, for the specified mass value of H^0.

Combined Final States

VALUE	*DOCUMENT ID*		*TECN*	*COMMENT*
1.17±0.17 OUR AVERAGE	Error includes scale factor of 1.2.			
$1.33 ^{+0.14}_{-0.10} \pm 0.15$	[1] AAD	13AK	ATLS	pp, 7 and 8 TeV

$1.44^{+0.59}_{-0.56}$	[2] AALTONEN	13M	TEVA	$p\overline{p} \to H^0 X$, 1.96 TeV	
0.87 ± 0.23	[3] CHATRCHYAN	12N	CMS	$pp \to H^0 X$, 7, 8 TeV	
• • • We do not use the following data for averages, fits, limits, etc. • • •					
$1.54^{+0.77}_{-0.73}$	[4] AALTONEN	13L	CDF	$p\overline{p} \to H^0 X$, 1.96 TeV	
$1.40^{+0.92}_{-0.88}$	[5] ABAZOV	13L	D0	$p\overline{p} \to H^0 X$, 1.96 TeV	
1.4 ± 0.3	[6] AAD	12AI	ATLS	$pp \to H^0 X$, 7, 8 TeV	
1.2 ± 0.4	[6] AAD	12AI	ATLS	$pp \to H^0 X$, 7 TeV	
1.5 ± 0.4	[6] AAD	12AI	ATLS	$pp \to H^0 X$, 8 TeV	

[1] AAD 13AK use 4.7 fb^{-1} of pp collisions at E_{cm} = 7 TeV and 20.7 fb^{-1} at E_{cm} = 8 TeV. The combined signal strength is based on the $\gamma\gamma$, $ZZ^* \to 4\ell$, and $WW^* \to \ell\nu\ell\nu$ channels. The quoted signal strength is given for m_{H^0} = 125.5 GeV. Reported statistical error value modified following private communication with the experiment.

[2] AALTONEN 13M combine all Tevatron data from the CDF and D0 Collaborations with up to 10.0 fb^{-1} and 9.7 fb^{-1}, respectively, of $p\overline{p}$ collisions at E_{cm} = 1.96 TeV. The quoted signal strength is given for m_{H^0} = 125 GeV.

[3] CHATRCHYAN 12N obtain results based on 4.9–5.1 fb^{-1} of pp collisions at E_{cm} = 7 TeV and 5.1–5.3 fb^{-1} at E_{cm} = 8 TeV. An excess of events over background with a local significance of 5.0 σ is observed at about m_{H^0} = 125 GeV. The combined signal strength is based on the $\gamma\gamma$, ZZ^*, WW^*, $\tau^+\tau^-$, and $b\overline{b}$ channels. The quoted signal strength is given for m_{H^0} = 125.5 GeV. See also CHATRCHYAN 13Y.

[4] AALTONEN 13L combine all CDF results with 9.45–10.0 fb^{-1} of $p\overline{p}$ collisions at E_{cm} = 1.96 TeV. The quoted signal strength is given for m_{H^0} = 125 GeV.

[5] ABAZOV 13L combine all D0 results with up to 9.7 fb^{-1} of $p\overline{p}$ collisions at E_{cm} = 1.96 TeV. The quoted signal strength is given for m_{H^0} = 125 GeV.

[6] AAD 12AI obtain results based on 4.6–4.8 fb^{-1} of pp collisions at E_{cm} = 7 TeV and 5.8–5.9 fb^{-1} at E_{cm} = 8 TeV. An excess of events over background with a local significance of 5.9 σ is observed at m_{H^0} = 126 GeV. The quoted signal strengths are given for m_{H^0} = 126 GeV. See also AAD 12DA.

WW^* Final State

VALUE	DOCUMENT ID		TECN	COMMENT
$0.87^{+0.24}_{-0.22}$ OUR AVERAGE				
$0.99^{+0.31}_{-0.28}$	[1] AAD	13AK	ATLS	pp, 7 and 8 TeV
$0.94^{+0.85}_{-0.83}$	[2] AALTONEN	13M	TEVA	$p\overline{p} \to H^0 X$, 1.96 TeV
$0.60^{+0.42}_{-0.37}$	[3] CHATRCHYAN	12N	CMS	$pp \to H^0 X$, 7, 8 TeV
• • • We do not use the following data for averages, fits, limits, etc. • • •				
$0.00^{+1.78}_{-0.00}$	[4] AALTONEN	13L	CDF	$p\overline{p} \to H^0 X$, 1.96 TeV
$1.90^{+1.63}_{-1.52}$	[5] ABAZOV	13L	D0	$p\overline{p} \to H^0 X$, 1.96 TeV
1.3 ± 0.5	[6] AAD	12AI	ATLS	$pp \to H^0 X$, 7, 8 TeV
0.5 ± 0.6	[6] AAD	12AI	ATLS	$pp \to H^0 X$, 7 TeV
1.9 ± 0.7	[6] AAD	12AI	ATLS	$pp \to H^0 X$, 8 TeV

[1] AAD 13AK use 4.7 fb^{-1} of pp collisions at E_{cm} = 7 TeV and 20.7 fb^{-1} at E_{cm} = 8 TeV. The quoted signal strength is given for m_{H^0} = 125.5 GeV.

[2] AALTONEN 13M combine all Tevatron data from the CDF and D0 Collaborations with up to 10.0 fb^{-1} and 9.7 fb^{-1}, respectively, of $p\overline{p}$ collisions at E_{cm} = 1.96 TeV. The quoted signal strength is given for m_{H^0} = 125 GeV.

[3] CHATRCHYAN 12N obtain results based on 4.9 fb^{-1} of pp collisions at E_{cm} = 7 TeV and 5.1 fb^{-1} at E_{cm} = 8 TeV. The quoted signal strength is given for m_{H^0} = 125.5 GeV. See also CHATRCHYAN 13Y.

[4] AALTONEN 13L combine all CDF results with 9.45–10.0 fb^{-1} of $p\overline{p}$ collisions at E_{cm} = 1.96 TeV. The quoted signal strength is given for m_{H^0} = 125 GeV.

[5] ABAZOV 13L combine all D0 results with up to 9.7 fb^{-1} of $p\overline{p}$ collisions at E_{cm} = 1.96 TeV. The quoted signal strength is given for m_{H^0} = 125 GeV.

[6] AAD 12AI obtain results based on 4.7 fb^{-1} of pp collisions at E_{cm} = 7 TeV and 5.8 fb^{-1} at E_{cm} = 8 TeV. The quoted signal strengths are given for m_{H^0} = 126 GeV. See also AAD 12DA.

ZZ^* Final State

VALUE	DOCUMENT ID		TECN	COMMENT
$1.11^{+0.34}_{-0.28}$ OUR AVERAGE Error includes scale factor of 1.3.				
$1.43^{+0.40}_{-0.35}$	[1] AAD	13AK	ATLS	pp, 7 and 8 TeV
$0.80^{+0.35}_{-0.28}$	[2] CHATRCHYAN	13J	CMS	$pp \to H^0 X$, 7, 8 TeV
• • • We do not use the following data for averages, fits, limits, etc. • • •				
1.2 ± 0.6	[3] AAD	12AI	ATLS	$pp \to H^0 X$, 7, 8 TeV
1.4 ± 1.1	[3] AAD	12AI	ATLS	$pp \to H^0 X$, 7 TeV
1.1 ± 0.8	[3] AAD	12AI	ATLS	$pp \to H^0 X$, 8 TeV
$0.73^{+0.45}_{-0.33}$	[4] CHATRCHYAN	12N	CMS	$pp \to H^0 X$, 7, 8 TeV

[1] AAD 13AK use 4.7 fb^{-1} of pp collisions at E_{cm} = 7 TeV and 20.7 fb^{-1} at E_{cm} = 8 TeV. The quoted signal strength is given for m_{H^0} = 125.5 GeV.

[2] CHATRCHYAN 13J obtain results based on $ZZ \to 4\ell$ final states in 5.1 fb^{-1} of pp collisions at E_{cm} = 7 TeV and 12.2 fb^{-1} at E_{cm} = 8 TeV. The quoted signal strength is given for m_{H^0} = 125.8 GeV.

[3] AAD 12AI obtain results based on 4.7–4.8 fb^{-1} of pp collisions at E_{cm} = 7 TeV and 5.8 fb^{-1} at E_{cm} = 8 TeV. The quoted signal strengths are given for m_{H^0} = 126 GeV. See also AAD 12DA.

[4] CHATRCHYAN 12N obtain results based on 4.9–5.1 fb^{-1} of pp collisions at E_{cm} = 7 TeV and 5.1–5.3 fb^{-1} at E_{cm} = 8 TeV. An excess of events over background with a local significance of 5.0 σ is observed at about m_{H^0} = 125 GeV. The quoted signal strengths are given for m_{H^0} = 125.5 GeV. See also CHATRCHYAN 12BY and CHATRCHYAN 13Y.

$\gamma\gamma$ Final State

VALUE	DOCUMENT ID		TECN	COMMENT
$1.58^{+0.27}_{-0.23}$ OUR AVERAGE				
$1.55^{+0.33}_{-0.28}$	[1] AAD	13AK	ATLS	pp, 7 and 8 TeV
$5.97^{+3.39}_{-3.12}$	[2] AALTONEN	13M	TEVA	$p\overline{p} \to H^0 X$, 1.96 TeV
$1.54^{+0.46}_{-0.42}$	[3] CHATRCHYAN	12N	CMS	$pp \to H^0 X$, 7, 8 TeV
• • • We do not use the following data for averages, fits, limits, etc. • • •				
$7.81^{+4.61}_{-4.42}$	[4] AALTONEN	13L	CDF	$p\overline{p} \to H^0 X$, 1.96 TeV
$4.20^{+4.60}_{-4.20}$	[5] ABAZOV	13L	D0	$p\overline{p} \to H^0 X$, 1.96 TeV
1.8 ± 0.5	[6] AAD	12AI	ATLS	$pp \to H^0 X$, 7, 8 TeV
2.2 ± 0.7	[6] AAD	12AI	ATLS	$pp \to H^0 X$, 7 TeV
1.5 ± 0.6	[6] AAD	12AI	ATLS	$pp \to H^0 X$, 8 TeV

[1] AAD 13AK use 4.7 fb^{-1} of pp collisions at E_{cm} = 7 TeV and 20.7 fb^{-1} at E_{cm} = 8 TeV. The quoted signal strength is given for m_{H^0} = 125.5 GeV.

[2] AALTONEN 13M combine all Tevatron data from the CDF and D0 Collaborations with up to 10.0 fb^{-1} and 9.7 fb^{-1}, respectively, of $p\overline{p}$ collisions at E_{cm} = 1.96 TeV. The quoted signal strength is given for m_{H^0} = 125 GeV.

[3] CHATRCHYAN 12N obtain results based on 5.1 fb^{-1} of pp collisions at E_{cm}=7 TeV and 5.3 fb^{-1} at E_{cm}=8 TeV. The quoted signal strength is given for m_{H^0}=125.5 GeV. See also CHATRCHYAN 13Y.

[4] AALTONEN 13L combine all CDF results with 9.45–10.0 fb^{-1} of $p\overline{p}$ collisions at E_{cm} = 1.96 TeV. The quoted signal strength is given for m_{H^0} = 125 GeV.

[5] ABAZOV 13L combine all D0 results with up to 9.7 fb^{-1} of $p\overline{p}$ collisions at E_{cm} = 1.96 TeV. The quoted signal strength is given for m_{H^0} = 125 GeV.

[6] AAD 12AI obtain results based on 4.8 fb^{-1} of pp collisions at E_{cm} = 7 TeV and 5.9 fb^{-1} at E_{cm} = 8 TeV. The quoted signal strengths are given for m_{H^0} = 126 GeV. See also AAD 12DA.

$b\overline{b}$ Final State

VALUE	CL%	DOCUMENT ID		TECN	COMMENT
1.1 ± 0.5 OUR AVERAGE					
$1.59^{+0.69}_{-0.72}$		[1] AALTONEN	13M	TEVA	$p\overline{p} \to H^0 X$, 1.96 TeV
0.5 ± 2.2		[2] AAD	12AI	ATLS	$pp \to H^0 WX$, $H^0 ZX$, 7 TeV
$0.48^{+0.81}_{-0.70}$		[3] CHATRCHYAN	12N	CMS	$pp \to H^0 WX$, $H^0 ZX$, 7, 8 TeV
• • • We do not use the following data for averages, fits, limits, etc. • • •					
$1.72^{+0.92}_{-0.87}$		[4] AALTONEN	13L	CDF	$p\overline{p} \to H^0 X$, 1.96 TeV
$9.49^{+6.60}_{-6.28}$		[4] AALTONEN	13L	CDF	$p\overline{p} \to H^0 t\overline{t} X$, 1.96 TeV
$1.23^{+1.24}_{-1.17}$		[5] ABAZOV	13L	D0	$p\overline{p} \to H^0 X$, 1.96 TeV
< 5.8	95	[6] CHATRCHYAN	13X	CMS	$pp \to H^0 t\overline{t} X$
		[7] AALTONEN	12P	CDF	$p\overline{p} \to H^0 WX$, $H^0 ZX$, 1.96 TeV
		[8] AALTONEN	12T	TEVA	$p\overline{p} \to H^0 WX$, $H^0 ZX$, 1.96 TeV
1.2 ± 1.2		[9] ABAZOV	12N	D0	$p\overline{p} \to H^0 WX$, $H^0 ZX$, 1.96 TeV

[1] AALTONEN 13M combine all Tevatron data from the CDF and D0 Collaborations with up to 10.0 fb^{-1} and 9.7 fb^{-1}, respectively, of $p\overline{p}$ collisions at E_{cm} = 1.96 TeV. The quoted signal strength is given for m_{H^0} = 125 GeV.

[2] AAD 12AI obtain results based on 4.6–4.8 fb^{-1} of pp collisions at E_{cm} = 7 TeV. The quoted signal strengths are given in their Fig. 10 for m_{H^0} = 126 GeV. See also Fig. 13 of AAD 12DA.

[3] CHATRCHYAN 12N obtain results based on 5.0 fb^{-1} of pp collisions at E_{cm}=7 TeV and 5.1 fb^{-1} at E_{cm}=8 TeV. The quoted signal strength is given for m_{H^0}=125.5 GeV. See also CHATRCHYAN 13Y.

[4] AALTONEN 13L combine all CDF results with 9.45–10.0 fb^{-1} of $p\overline{p}$ collisions at E_{cm} = 1.96 TeV. The quoted signal strength is given for m_{H^0} = 125 GeV.

[5] ABAZOV 13L combine all D0 results with up to 9.7 fb^{-1} of $p\overline{p}$ collisions at E_{cm} = 1.96 TeV. The quoted signal strength is given for m_{H^0} = 125 GeV.

[6] CHATRCHYAN 13X search for $H^0 t\overline{t}$ production followed by $H^0 \to b\overline{b}$, one top decaying to $\ell\nu$ and the other to either $\ell\nu$ or $q\overline{q}$ in 5.0 fb^{-1} and 5.1 fb^{-1} of pp collisions at E_{cm} = 7 and 8 TeV. A limit on cross section times branching ratio which corresponds to (4.0–8.6) times the expected Standard Model cross section is given for m_{H^0} = 110–140 GeV at 95% CL. The quoted limit is given for m_{H^0} = 125 GeV, where 5.2 is expected for no signal.

[7] AALTONEN 12P combine AALTONEN 12Q, AALTONEN 12R, and AALTONEN 12S. An excess of events over background is observed in the region m_{H^0} = 100–150 GeV, with a local significance of 2.7 σ for m_{H^0} = 125 GeV. This corresponds to $(\sigma(H^0 W) + \sigma(H^0 Z)) \cdot B(H^0 \to b\overline{b}) = (291^{+118}_{-113})$ fb. Superseded by AALTONEN 13L.

[8] AALTONEN 12T combine AALTONEN 12Q, AALTONEN 12R, AALTONEN 12S, ABAZOV 12O, ABAZOV 12P, and ABAZOV 12K. An excess of events over background is observed which is most significant in the region m_{H^0} = 120–135 GeV, with a local significance of up to 3.3 σ. The local significance at m_{H^0} = 125 GeV is 2.8 σ, which corresponds to $(\sigma(H^0 W) + \sigma(H^0 Z)) \cdot B(H^0 \to b\overline{b}) = (0.23^{+0.09}_{-0.08})$ pb, compared to the Standard Model expectation at m_{H^0} = 125 GeV of 0.12 ± 0.01 pb. Superseded by AALTONEN 13M.

[9] ABAZOV 12N combine ABAZOV 12O, ABAZOV 12P, and ABAZOV 12K. An excess of events over background is observed in the region m_{H^0} = 120–145 GeV with a local significance of 1.0–1.7 σ. The quoted signal strength is given for m_{H^0} = 125 GeV. Superseded by ABAZOV 13L.

$\tau^+\tau^-$ Final State

VALUE	DOCUMENT ID		TECN	COMMENT
0.4 ±0.6 OUR AVERAGE				
$1.68^{+2.28}_{-1.68}$	[1] AALTONEN	13M	TEVA	$p\overline{p} \to H^0 X$, 1.96 TeV
$0.4^{+1.6}_{-2.0}$	[2] AAD	12AI	ATLS	$pp \to H^0 X$, 7 TeV
$0.09^{+0.76}_{-0.74}$	[3] CHATRCHYAN	12N	CMS	$pp \to H^0 X$, 7, 8 TeV
• • • We do not use the following data for averages, fits, limits, etc. • • •				
$0.00^{+8.44}_{-0.00}$	[4] AALTONEN	13L	CDF	$p\overline{p} \to H^0 X$, 1.96 TeV
$3.96^{+4.11}_{-3.38}$	[5] ABAZOV	13L	D0	$p\overline{p} \to H^0 X$, 1.96 TeV

[1] AALTONEN 13M combine all Tevatron data from the CDF and D0 Collaborations with up to 10.0 fb^{-1} and 9.7 fb^{-1}, respectively, of $p\overline{p}$ collisions at E_{cm} = 1.96 TeV. The quoted signal strength is given for m_{H^0} = 125 GeV.

[2] AAD 12AI obtain results based on 4.7 fb^{-1} of pp collisions at E_{cm} = 7 TeV. The quoted signal strengths are given in their Fig. 10 for m_{H^0} = 126 GeV. See also Fig. 13 of AAD 12DA.

[3] CHATRCHYAN 12N obtain results based on 4.9 fb^{-1} of pp collisions at E_{cm}=7 TeV and 5.1 fb^{-1} at E_{cm}=8 TeV. The quoted signal strength is given for m_{H^0}=125.5 GeV. See also CHATRCHYAN 13Y .

[4] AALTONEN 13L combine all CDF results with 9.45–10.0 fb^{-1} of $p\overline{p}$ collisions at E_{cm} = 1.96 TeV. The quoted signal strength is given for m_{H^0} = 125 GeV.

[5] ABAZOV 13L combine all D0 results with up to 9.7 fb^{-1} of $p\overline{p}$ collisions at E_{cm} = 1.96 TeV. The quoted signal strength is given for m_{H^0} = 125 GeV.

$Z\gamma$ Final State

VALUE	CL%	DOCUMENT ID		TECN	COMMENT
<9.5	95	[1] CHATRCHYAN	13BK	CMS	$pp \to H^0 X$, 7, 8 TeV

[1] CHATRCHYAN 13BK search for $H^0 \to Z\gamma \to \ell\ell\gamma$ in 5.0 fb^{-1} of pp collisions at E_{cm} = 7 TeV and 19.6 fb^{-1} at E_{cm} = 8 TeV. A limit on cross section times branching ratio which corresponds to (4–25) times the expected Standard Model cross section is given in the range m_{H^0} = 120–160 GeV at 95% CL. The quoted limit is given for m_{H^0} = 125 GeV, where 10 is expected for no signal.

H^0 REFERENCES

AAD	13AJ	PL B726 120	G. Aad *et al.*	(ATLAS Collab.)
AAD	13AK	PL B726 88	G. Aad *et al.*	(ATLAS Collab.)
AALTONEN	13L	PR D88 052013	T. Aaltonen *et al.*	(CDF Collab.)
AALTONEN	13M	PR D88 052014	T. Aaltonen *et al.*	(CDF and D0 Collab.)
ABAZOV	13L	PR D88 052011	V.M. Abazov *et al.*	(D0 Collab.)
CHATRCHYAN	13BK	PL B726 587	S. Chatrchyan *et al.*	(CMS Collab.)
CHATRCHYAN	13J	PRL 110 081803	S. Chatrchyan *et al.*	(CMS Collab.)
CHATRCHYAN	13X	JHEP 1305 145	S. Chatrchyan *et al.*	(CMS Collab.)
CHATRCHYAN	13Y	JHEP 1306 081	S. Chatrchyan *et al.*	(CMS Collab.)
AAD	12AI	PL B716 1	G. Aad *et al.*	(ATLAS Collab.)
AAD	12DA	SCI 338 1576	G. Aad *et al.*	(ATLAS Collab.)
AALTONEN	12P	PRL 109 111802	T. Aaltonen *et al.*	(CDF Collab.)
AALTONEN	12Q	PRL 109 111803	T. Aaltonen *et al.*	(CDF Collab.)
AALTONEN	12R	PRL 109 111804	T. Aaltonen *et al.*	(CDF Collab.)
AALTONEN	12S	PRL 109 111805	T. Aaltonen *et al.*	(CDF Collab.)
AALTONEN	12T	PRL 109 071804	T. Aaltonen *et al.*	(CDF and D0 Collab.)
ABAZOV	12K	PL B716 285	V.M. Abazov *et al.*	(D0 Collab.)
ABAZOV	12N	PRL 109 121802	V.M. Abazov *et al.*	(D0 Collab.)
ABAZOV	12O	PRL 109 121803	V.M. Abazov *et al.*	(D0 Collab.)
ABAZOV	12P	PRL 109 121804	V.M. Abazov *et al.*	(D0 Collab.)
CHATRCHYAN	12BY	SCI 338 1569	S. Chatrchyan *et al.*	(CMS Collab.)
CHATRCHYAN	12N	PL B716 30	S. Chatrchyan *et al.*	(CMS Collab.)

Neutral Higgs Bosons, Searches for

CONTENTS:

MASS LIMITS FOR NEUTRAL HIGGS BOSONS IN SUPERSYMMETRIC MODELS

The minimal supersymmetric model has two complex doublets of Higgs bosons. The resulting physical states are two scalars [H_1^0 and H_2^0, where we define $m_{H_1^0} < m_{H_2^0}$], a pseudoscalar (A^0), and a charged Higgs pair ($H^\pm$). H_1^0 and H_2^0 are also called h and H in the literature. There are two free parameters in the Higgs sector which can be chosen to be m_{A^0} and $\tan\beta = v_2/v_1$, the ratio of vacuum expectation values of the two Higgs doublets. Tree-level Higgs masses are constrained by the model to be $m_{H_1^0} \leq m_Z$, $m_{H_2^0} \geq m_Z$, $m_{A^0} \geq m_{H_1^0}$, and $m_{H^\pm} \geq m_W$. However, as described in the review on "Status of Higgs Boson Physics" in this Volume these relations are violated by radiative corrections.

Unless otherwise noted, the experiments in e^+e^- collisions search for the processes $e^+e^- \to H_1^0 Z^0$ in the channels used for the Standard Model Higgs searches and $e^+e^- \to H_1^0 A^0$ in the final states $b\overline{b}b\overline{b}$ and $b\overline{b}\tau^+\tau^-$. In $p\overline{p}$ and pp collisions the experiments search for a variety of processes, as explicitly specified for each entry. Limits on the A^0 mass arise from these direct searches, as well as from the relations valid in the minimal supersymmetric model between m_{A^0} and $m_{H_1^0}$. As discussed in the review on "Status of Higgs Boson Physics" in this Volume, these relations depend, via potentially large radiative corrections, on the mass of the t quark and on the supersymmetric parameters, in particular those of the stop sector. These indirect limits are weaker for larger t and $\bar{t}$ masses. To include the radiative corrections to the Higgs masses, unless otherwise stated, the listed papers use theoretical predictions incorporating two-loop corrections, and the results are given for the m_h^{max} benchmark scenario, which gives rise to the most conservative upper bound on the mass of H_1^0 for given values of m_{A^0} and $\tan\beta$, see CARENA 99B, CARENA 03, and CARENA 13.

Limits in the low-mass region of H_1^0, as well as other by now obsolete limits from different techniques, have been removed from this compilation, and can be found in earlier editions of this Review. Unless otherwise stated, the following results assume no invisible H_1^0 or A^0 decays.

The observed signal at about 126 GeV, see section "H^0", can be interpreted as one of the neutral Higgs bosons of supersymmetric models.

Mass Limits for H_1^0 (Higgs Boson) in Supersymmetric Models

VALUE (GeV)	CL%	DOCUMENT ID		TECN	COMMENT
>89.7		[1] ABDALLAH	08B	DLPH	$E_{cm} \leq 209$ GeV
>92.8	95	[2] SCHAEL	06B	LEP	$E_{cm} \leq 209$ GeV
>84.5	95	[3,4] ABBIENDI	04M	OPAL	$E_{cm} \leq 209$ GeV
>86.0	95	[3,5] ACHARD	02H	L3	$E_{cm} \leq 209$ GeV, $\tan\beta > 0.4$
• • • We do not use the following data for averages, fits, limits, etc. • • •					
		[6] AAD	13O	ATLS	$pp \to H_{1,2}^0/A^0 + X$, $H_{1,2}^0/A^0 \to \tau^+\tau^-, \mu^+\mu^-$
		[7] AAIJ	13T	LHCB	$pp \to H_{1,2}^0/A^0 + X$, $H_{1,2}^0/A^0 \to \tau^+\tau^-$
		[8] CHATRCHYAN	13AG	CMS	$pp \to H_{1,2}^0/A^0 + b + X$, $H_{1,2}^0/A^0 \to b\overline{b}$
		[9] AALTONEN	12AQ	TEVA	$p\overline{p} \to H_{1,2}^0/A^0 + b + X$, $H_{1,2}^0/A^0 \to b\overline{b}$
		[10] AALTONEN	12X	CDF	$p\overline{p} \to H_{1,2}^0/A^0 + b + X$, $H_{1,2}^0/A^0 \to b\overline{b}$
		[11] ABAZOV	12	D0	$p\overline{p} \to H_{1,2}^0/A^0 + X$, $H_{1,2}^0/A^0 \to \tau^+\tau^-$
		[12] ABAZOV	12G	D0	$p\overline{p} \to H_{1,2}^0/A^0 + X$, $H_{1,2}^0/A^0 \to \tau^+\tau^-$

		[13] CHATRCHYAN	12K	CMS	$pp \to H^0_{1,2}/A^0 + X$, $H^0_{1,2}/A^0 \to \tau^+\tau^-$
		[14] AAD	11R	ATLS	$pp \to H^0_{1,2}/A^0 + X$, $H^0_{1,2}/A^0 \to \tau^+\tau^-$
		[15] ABAZOV	11K	D0	$p\overline{p} \to H^0_{1,2}/A^0 + b + X$, $H^0_{1,2}/A^0 \to b\overline{b}$
		[16] ABAZOV	11W	D0	$p\overline{p} \to H^0_{1,2}/A^0 + b + X$, $H^0_{1,2}/A^0 \to \tau^+\tau^-$
		[17] CHATRCHYAN	11H	CMS	$pp \to H^0_{1,2}/A^0 + X$, $H^0_{1,2}/A^0 \to \tau^+\tau^-$
		[18] AALTONEN	09AR	CDF	$p\overline{p} \to H^0_{1,2}/A^0 + X$, $H^0_{1,2}/A^0 \to \tau^+\tau^-$
		[19] ABAZOV	08W	D0	$p\overline{p} \to H^0_{1,2}/A^0 + X$, $H^0_{1,2}/A^0 \to \tau^+\tau^-$
		[20] ABBIENDI	03G	OPAL	$H^0_1 \to A^0A^0$
>89.8	95	[3,21] HEISTER	02	ALEP	$E_{cm} \leq 209$ GeV, $\tan\beta > 0.5$

[1] ABDALLAH 08B give limits in eight *CP*-conserving benchmark scenarios and some *CP*-violating scenarios. See paper for excluded regions for each scenario. Supersedes ABDALLAH 04.

[2] SCHAEL 06B make a combined analysis of the LEP data. The quoted limit is for the m_h^{max} scenario with $m_t = 174.3$ GeV. In the *CP*-violating CPX scenario no lower bound on $m_{H^0_1}$ can be set at 95% CL. See paper for excluded regions in various scenarios. See Figs. 2–6 and Tabs. 14–21 for limits on $\sigma(ZH^0)\cdot$B($H^0 \to b\overline{b}, \tau^+\tau^-$) and $\sigma(H^0_1H^0_2)\cdot$B(H^0_1,$H^0_2 \to b\overline{b}$,$\tau^+\tau^-$).

[3] Search for $e^+e^- \to H^0_1A^0$ in the final states $b\overline{b}b\overline{b}$ and $b\overline{b}\tau^+\tau^-$, and $e^+e^- \to H^0_1Z$. Universal scalar mass of 1 TeV, SU(2) gaugino mass of 200 GeV, and $\mu = -200$ GeV are assumed, and two-loop radiative corrections incorporated. The limits hold for m_t=175 GeV, and for the m_h^{max} scenario.

[4] ABBIENDI 04M exclude $0.7 < \tan\beta < 1.9$, assuming $m_t = 174.3$ GeV. Limits for other MSSM benchmark scenarios, as well as for *CP* violating cases, are also given.

[5] ACHARD 02H also search for the final state $H^0_1Z \to 2A^0q\overline{q}$, $A^0 \to q\overline{q}$. In addition, the MSSM parameter set in the "large-μ" and "no-mixing" scenarios are examined.

[6] AAD 13O search for production of a Higgs boson in the decay $H^0_{1,2}/A^0 \to \tau^+\tau^-$ and $\mu^+\mu^-$ with 4.7–4.8 fb^{-1} of pp collisions at $E_{cm} = 7$ TeV. See their Fig. 6 for the excluded region in the MSSM parameter space and their Fig. 7 for the limits on cross section times branching ratio. For $m_{A^0} = 110$–170 GeV, $\tan\beta \gtrsim 10$ is excluded, and for $\tan\beta = 50$, m_{A^0} below 470 GeV is excluded at 95% CL in the m_h^{max} scenario.

[7] AAIJ 13T search for production of a Higgs boson in the forward region in the decay $H^0_{1,2}/A^0 \to \tau^+\tau^-$ in 1.0 fb^{-1} of pp collisions at $E_{cm} = 7$ TeV. See their Fig. 2 for the limits on cross section times branching ratio and the excluded region in the MSSM parameter space.

[8] CHATRCHYAN 13AG search for production of a Higgs boson in association with a b quark in the decay $H^0_{1,2}/A^0 \to b\overline{b}$ in 2.7–4.8 fb^{-1} of pp collisions at $E_{cm} = 7$ TeV. See their Fig. 6 for the excluded region in the MSSM parameter space and Fig. 5 for the limits on cross section times branching ratio. For $m_{A^0} = 90$–350 GeV, upper bounds on $\tan\beta$ of 18–42 at 95% CL are obtained in the m_h^{max} scenario with $\mu = +200$ GeV.

[9] AALTONEN 12AQ combine AALTONEN 12X and ABAZOV 11K. See their Table I and Fig. 1 for the limit on cross section times branching ratio and Fig. 2 for the excluded region in the MSSM parameter space.

[10] AALTONEN 12X search for associated production of a Higgs boson and a b quark in the decay $H^0_{1,2}/A^0 \to b\overline{b}$, with 2.6 fb^{-1} of $p\overline{p}$ collisions at $E_{cm} = 1.96$ TeV. See their Table III and Fig. 15 for the limit on cross section times branching ratio and Figs. 17, 18 for the excluded region in the MSSM parameter space.

[11] ABAZOV 12 search for production of a Higgs boson followed by the decay $H^0_{1,2}/A^0 \to \tau^+\tau^-$ in 5.4 fb^{-1} of $p\overline{p}$ collisions at $E_{cm} = 1.96$ TeV. See their Fig. 2 for the limit on cross section times branching ratio and Fig. 3 for the excluded region in the MSSM parameter space. Superseded by ABAZOV 12G.

[12] ABAZOV 12G search for production of a Higgs boson in the decay $H^0_{1,2}/A^0 \to \tau^+\tau^-$ with 7.3 fb^{-1} of $p\overline{p}$ collisions at $E_{cm} = 1.96$ TeV and combine with ABAZOV 11W and ABAZOV 11K. See their Figs. 4, 5, and 6 for the excluded region in the MSSM parameter space. For $m_{A^0} = 90$–180 GeV, $\tan\beta \gtrsim 30$ is excluded at 95% CL. in the m_h^{max} scenario.

[13] CHATRCHYAN 12K search for production of a Higgs boson in the decay $H^0_{1,2}/A^0 \to \tau^+\tau^-$ with 4.6 fb^{-1} of pp collisions at $E_{cm} = 7$ TeV. See their Fig. 3 and Table 4 for the excluded region in the MSSM parameter space. For $m_{A^0} = 160$ GeV, the region $\tan\beta > 7.1$ is excluded at 95% CL in the m_h^{max} scenario.

[14] AAD 11R search for production of a Higgs boson followed by the decay $H^0_{1,2}/A^0 \to \tau^+\tau^-$ in 36 pb^{-1} of pp collisions at $E_{cm} = 7$ TeV. See their Fig. 3 for the limit on cross section times branching ratio and for the excluded region in the MSSM parameter space. Superseded by AAD 13O.

[15] ABAZOV 11K search for associated production of a Higgs boson and a b quark, followed by the decay $H^0_{1,2}/A^0 \to b\overline{b}$, in 5.2 fb^{-1} of $p\overline{p}$ collisions at $E_{cm} = 1.96$ TeV. See their Fig. 5/Table 2 for the limit on cross section times branching ratio and Fig. 6 for the excluded region in the MSSM parameter space for $\mu = -200$ GeV.

[16] ABAZOV 11W search for associated production of a Higgs boson and a b quark, followed by the decay $H^0_{1,2}/A^0 \to \tau\tau$, in 7.3 fb^{-1} of $p\overline{p}$ collisions at $E_{cm} = 1.96$ TeV. See their Fig. 2 for the limit on cross section times branching ratio and for the excluded region in the MSSM parameter space.

[17] CHATRCHYAN 11H search for production of a Higgs boson followed by the decay $H^0_{1,2}/A^0 \to \tau^+\tau^-$ in 36 pb^{-1} of pp collisions at $E_{cm} = 7$ TeV. See their Fig. 2 for the limit on cross section times branching ratio and Fig. 3 for the excluded region in the MSSM parameter space. Superseded by CHATRCHYAN 12K.

[18] AALTONEN 09AR search for Higgs bosons decaying to $\tau^+\tau^-$ in two doublet models in 1.8 fb^{-1} of $p\overline{p}$ collisions at $E_{cm} = 1.96$ TeV. See their Fig. 2 for the limit on $\sigma\cdot$B($H^0_{1,2}/A^0 \to \tau^+\tau^-$) for different Higgs masses, and see their Fig. 3 for the excluded region in the MSSM parameter space.

[19] ABAZOV 08W search for Higgs boson production in $p\overline{p}$ collisions at $E_{cm} = 1.96$ TeV with the decay $H^0_{1,2}/A^0 \to \tau^+\tau^-$. See their Fig. 3 for the limit on $\sigma\cdot$B($H^0_{1,2}/A^0 \to \tau^+\tau^-$) for different Higgs masses, and see their Fig. 4 for the excluded region in the MSSM parameter space. Superseded by ABAZOV 12.

[20] ABBIENDI 03G search for $e^+e^- \to H^0_1Z$ followed by $H^0_1 \to A^0A^0$, $A^0 \to c\overline{c}$, gg, or $\tau^+\tau^-$. In the no-mixing scenario, the region $m_{H^0_1}$ = 45–85 GeV and m_{A^0} = 2–9.5 GeV is excluded at 95% CL.

[21] HEISTER 02 excludes the range $0.7 < \tan\beta < 2.3$. A wider range is excluded with different stop mixing assumptions. Updates BARATE 01C.

Mass Limits for A^0 (Pseudoscalar Higgs Boson) in Supersymmetric Models

VALUE (GeV)	CL%	DOCUMENT ID		TECN	COMMENT
>90.4		[1] ABDALLAH	08B	DLPH	$E_{cm} \leq 209$ GeV
>93.4	95	[2] SCHAEL	06B	LEP	$E_{cm} \leq 209$ GeV
>85.0	95	[3,4] ABBIENDI	04M	OPAL	$E_{cm} \leq 209$ GeV
>86.5	95	[3,5] ACHARD	02H	L3	$E_{cm} \leq 209$ GeV, $\tan\beta > 0.4$
>90.1	95	[3,6] HEISTER	02	ALEP	$E_{cm} \leq 209$ GeV, $\tan\beta > 0.5$

• • • We do not use the following data for averages, fits, limits, etc. • • •

		[7] AAD	13O	ATLS	$pp \to H^0_{1,2}/A^0 + X$, $H^0_{1,2}/A^0 \to \tau^+\tau^-, \mu^+\mu^-$
		[8] AAIJ	13T	LHCB	$pp \to H^0_{1,2}/A^0 + X$, $H^0_{1,2}/A^0 \to \tau^+\tau^-$
		[9] CHATRCHYAN	13AG	CMS	$pp \to H^0_{1,2}/A^0 + b + X$, $H^0_{1,2}/A^0 \to b\overline{b}$
		[10] AALTONEN	12AQ	TEVA	$p\overline{p} \to H^0_{1,2}/A^0 + b + X$, $H^0_{1,2}/A^0 \to b\overline{b}$
		[11] AALTONEN	12X	CDF	$p\overline{p} \to H^0_{1,2}/A^0 + b + X$, $H^0_{1,2}/A^0 \to b\overline{b}$
		[12] ABAZOV	12	D0	$p\overline{p} \to H^0_{1,2}/A^0 + X$, $H^0_{1,2}/A^0 \to \tau^+\tau^-$
		[13] ABAZOV	12G	D0	$p\overline{p} \to H^0_{1,2}/A^0 + X$, $H^0_{1,2}/A^0 \to \tau^+\tau^-$
		[14] CHATRCHYAN	12K	CMS	$pp \to H^0_{1,2}/A^0 + X$, $H^0_{1,2}/A^0 \to \tau^+\tau^-$
		[15] AAD	11R	ATLS	$pp \to H^0_{1,2}/A^0 + X$, $H^0_{1,2}/A^0 \to \tau^+\tau^-$
		[16] ABAZOV	11K	D0	$p\overline{p} \to H^0_{1,2}/A^0 + b + X$, $H^0_{1,2}/A^0 \to b\overline{b}$
		[17] ABAZOV	11W	D0	$p\overline{p} \to H^0_{1,2}/A^0 + b + X$, $H^0_{1,2}/A^0 \to \tau^+\tau^-$
		[18] CHATRCHYAN	11H	CMS	$pp \to H^0_{1,2}/A^0 + X$, $H^0_{1,2}/A^0 \to \tau^+\tau^-$
		[19] AALTONEN	09AR	CDF	$p\overline{p} \to H^0_{1,2}/A^0 + X$, $H^0_{1,2}/A^0 \to \tau^+\tau^-$
		[20] ACOSTA	05Q	CDF	$p\overline{p} \to H^0_{1,2}/A^0 + X$
		[21] ABBIENDI	03G	OPAL	$H^0_1 \to A^0A^0$
		[22] AKEROYD	02	RVUE	

[1] ABDALLAH 08B give limits in eight *CP*-conserving benchmark scenarios and some *CP*-violating scenarios. See paper for excluded regions for each scenario. Supersedes ABDALLAH 04.

[2] SCHAEL 06B make a combined analysis of the LEP data. The quoted limit is for the m_h^{max} scenario with $m_t = 174.3$ GeV. In the *CP*-violating CPX scenario no lower bound on $m_{H^0_1}$ can be set at 95% CL. See paper for excluded regions in various scenarios. See Figs. 2–6 and Tabs. 14–21 for limits on $\sigma(ZH^0)\cdot$B($H^0 \to b\overline{b}, \tau^+\tau^-$) and $\sigma(H^0_1H^0_2)\cdot$B(H^0_1,$H^0_2 \to b\overline{b}$,$\tau^+\tau^-$).

[3] Search for $e^+e^- \to H^0_1A^0$ in the final states $b\overline{b}b\overline{b}$ and $b\overline{b}\tau^+\tau^-$, and $e^+e^- \to H^0_1Z$. Universal scalar mass of 1 TeV, SU(2) gaugino mass of 200 GeV, and $\mu = -200$ GeV are assumed, and two-loop radiative corrections incorporated. The limits hold for m_t=175 GeV, and for the m_h^{max} scenario.

[4] ABBIENDI 04M exclude $0.7 < \tan\beta < 1.9$, assuming $m_t = 174.3$ GeV. Limits for other MSSM benchmark scenarios, as well as for *CP* violating cases, are also given.

[5] ACHARD 02H also search for the final state $H^0_1Z \to 2A^0q\overline{q}$, $A^0 \to q\overline{q}$. In addition, the MSSM parameter set in the "large-μ" and "no-mixing" scenarios are examined.

[6] HEISTER 02 excludes the range $0.7 < \tan\beta < 2.3$. A wider range is excluded with different stop mixing assumptions. Updates BARATE 01C.

[7] AAD 13O search for production of a Higgs boson in the decay $H^0_{1,2}/A^0 \to \tau^+\tau^-$ and $\mu^+\mu^-$ with 4.7–4.8 fb^{-1} of pp collisions at E_{cm} = 7 TeV. See their Fig. 6 for the excluded region in the MSSM parameter space and their Fig. 7 for the limits on cross section times branching ratio. For m_{A^0} = 110–170 GeV, tan$\beta \gtrsim$ 10 is excluded, and for tanβ = 50, m_{A^0} below 470 GeV is excluded at 95% CL in the m_h^{max} scenario.

[8] AAIJ 13T search for production of a Higgs boson in the forward region in the decay $H^0_{1,2}/A^0 \to \tau^+\tau^-$ in 1.0 fb^{-1} of pp collisions at E_{cm} = 7 TeV. See their Fig. 2 for the limits on cross section times branching ratio and the excluded region in the MSSM parameter space.

[9] CHATRCHYAN 13AG search for production of a Higgs boson in association with a b quark in the decay $H^0_{1,2}/A^0 \to b\overline{b}$ in 2.7–4.8 fb^{-1} of pp collisions at E_{cm} = 7 TeV. See their Fig. 6 for the excluded region in the MSSM parameter space and Fig. 5 for the limits on cross section times branching ratio. For m_{A^0} = 90–350 GeV, upper bounds on tanβ of 18–42 at 95% CL are obtained in the m_h^{max} scenario with μ = +200 GeV.

[10] AALTONEN 12AQ combine AALTONEN 12X and ABAZOV 11K. See their Table I and Fig. 1 for the limit on cross section times branching ratio and Fig. 2 for the excluded region in the MSSM parameter space.

[11] AALTONEN 12X search for associated production of a Higgs boson and a b quark in the decay $H^0_{1,2}/A^0 \to b\overline{b}$, with 2.6 fb^{-1} of $p\overline{p}$ collisions at E_{cm} = 1.96 TeV. See their Table III and Fig. 15 for the limit on cross section times branching ratio and Figs. 17, 18 for the excluded region in the MSSM parameter space.

[12] ABAZOV 12 search for production of a Higgs boson followed by the decay $H^0_{1,2}/A^0 \to \tau^+\tau^-$ in 5.4 fb^{-1} of $p\overline{p}$ collisions at E_{cm} = 1.96 TeV. See their Fig. 2 for the limit on cross section times branching ratio and Fig. 3 for the excluded region in the MSSM parameter space. Superseded by ABAZOV 12G.

[13] ABAZOV 12G search for production of a Higgs boson in the decay $H^0_{1,2}/A^0 \to \tau^+\tau^-$ with 7.3 fb^{-1} of $p\overline{p}$ collisions at E_{cm} = 1.96 TeV and combine with ABAZOV 11W and ABAZOV 11K. See their Figs. 4, 5, and 6 for the excluded region in the MSSM parameter space. For m_{A^0} = 90–180 GeV, tan$\beta \gtrsim$ 30 is excluded at 95% CL. in the m_h^{max} scenario.

[14] CHATRCHYAN 12K search for production of a Higgs boson in the decay $H^0_{1,2}/A^0 \to \tau^+\tau^-$ with 4.6 fb^{-1} of pp collisions at E_{cm} = 7 TeV. See their Fig. 3 and Table 4 for the excluded region in the MSSM parameter space. For m_{A^0} = 160 GeV, the region tanβ > 7.1 is excluded at 95% CL in the m_h^{max} scenario.

[15] AAD 11R search for production of a Higgs boson followed by the decay $H^0_{1,2}/A^0 \to \tau^+\tau^-$ in 36 pb^{-1} of pp collisions at E_{cm} = 7 TeV. See their Fig. 3 for the limit on cross section times branching ratio and for the excluded region in the MSSM parameter space. Superseded by AAD 13O.

[16] ABAZOV 11K search for associated production of a Higgs boson and a b quark, followed by the decay $H^0_{1,2}/A^0 \to b\overline{b}$, in 5.2 fb^{-1} of $p\overline{p}$ collisions at E_{cm} = 1.96 TeV. See their Fig. 5/Table 2 for the limit on cross section times branching ratio and Fig. 6 for the excluded region in the MSSM parameter space for $\mu = -200$ GeV.

[17] ABAZOV 11W search for associated production of a Higgs boson and a b quark, followed by the decay $H^0_{1,2}/A^0 \to \tau\tau$, in 7.3 fb^{-1} of $p\overline{p}$ collisions at E_{cm} = 1.96 TeV. See their Fig. 2 for the limit on cross section times branching ratio and for the excluded region in the MSSM parameter space.

[18] CHATRCHYAN 11H search for production of a Higgs boson followed by the decay $H^0_{1,2}/A^0 \to \tau^+\tau^-$ in 36 pb^{-1} of pp collisions at E_{cm} = 7 TeV. See their Fig. 2 for the limit on cross section times branching ratio and Fig. 3 for the excluded region in the MSSM parameter space. Superseded by CHATRCHYAN 12K.

[19] AALTONEN 09AR search for Higgs bosons decaying to $\tau^+\tau^-$ in two doublet models in 1.8 fb^{-1} of $p\overline{p}$ collisions at E_{cm} = 1.96 TeV. See their Fig. 2 for the limit on $\sigma \cdot$ B($H^0_{1,2}/A^0 \to \tau^+\tau^-$) for different Higgs masses, and see their Fig. 3 for the excluded region in the MSSM parameter space.

[20] ACOSTA 05Q search for $H^0_{1,2}/A^0$ production in $p\overline{p}$ collisions at E_{cm} = 1.8 TeV with $H^0_{1,2}/A^0 \to \tau^+\tau^-$. At m_{A^0} = 100 GeV, the obtained cross section upper limit is above theoretical expectation.

[21] ABBIENDI 03G search for $e^+e^- \to H^0_1 Z$ followed by $H^0_1 \to A^0A^0$, $A^0 \to c\overline{c}$, gg, or $\tau^+\tau^-$. In the no-mixing scenario, the region $m_{H^0_1}$ = 45-85 GeV and m_{A^0} = 2-9.5 GeV is excluded at 95% CL.

[22] AKEROYD 02 examine the possibility of a light A^0 with tanβ <1. Electroweak measurements are found to be inconsistent with such a scenario.

MASS LIMITS FOR NEUTRAL HIGGS BOSONS IN EXTENDED HIGGS MODELS

This Section covers models which do not fit into either the Standard Model or its simplest minimal Supersymmetric extension (MSSM), leading to anomalous production rates, or nonstandard final states and branching ratios. In particular, this Section covers limits which may apply to generic two-Higgs-doublet models (2HDM), or to special regions of the MSSM parameter space where decays to invisible particles or to photon pairs are dominant (see the review on "Status of Higgs Boson Physics"). Concerning the mass limits for H^0 and A^0 listed below, see the footnotes or the comment lines for details on the nature of the models to which the limits apply.

The observed signal at about 126 GeV, see section "H^{0}", can be interpreted as one of the neutral Higgs bosons of an extended Higgs sector.

Mass Limits in General two-Higgs-doublet Models

VALUE (GeV)	CL%	DOCUMENT ID		TECN	COMMENT
• • • We do not use the following data for averages, fits, limits, etc. • • •					
	95	[1] AALTONEN	09AR	CDF	$p\overline{p} \to H^0_{1,2}/A^0 + X$, $H^0_{1,2}/A^0 \to \tau^+\tau^-$
none 1–55	95	[2] ABBIENDI	05A	OPAL	H^0_1, Type II model
>110.6	95	[3] ABDALLAH	05D	DLPH	$H^0 \to$ 2 jets
		[4] ABDALLAH	04O	DLPH	$Z \to f\overline{f}H$
		[5] ABDALLAH	04O	DLPH	$e^+e^- \to H^0Z$, H^0A^0
		[6] ABBIENDI	02D	OPAL	$e^+e^- \to b\overline{b}H$
none 1–44	95	[7] ABBIENDI	01E	OPAL	H^0_1, Type-II model
> 68.0	95	[8] ABBIENDI	99E	OPAL	tanβ > 1
		[9] ABREU	95H	DLPH	$Z \to H^0Z^*$, H^0A^0
		[10] PICH	92	RVUE	Very light Higgs

[1] AALTONEN 09AR search for Higgs bosons decaying to $\tau^+\tau^-$ in two doublet models in 1.8 fb^{-1} of $p\overline{p}$ collisions at E_{cm} = 1.96 TeV. See their Fig. 2 for the limit on $\sigma \cdot$ B($H^0_{1,2}/A^0 \to \tau^+\tau^-$) for different Higgs masses, and see their Fig. 3 for the excluded region in the MSSM parameter space.

[2] ABBIENDI 05A search for $e^+e^- \to H^0_1A^0$ in general Type-II two-doublet models, with decays H^0_1, $A^0 \to q\overline{q}$, gg, $\tau^+\tau^-$, and $H^0_1 \to A^0A^0$.

[3] ABDALLAH 05D search for $e^+e^- \to H^0Z$ and H^0A^0 with H^0, A^0 decaying to two jets of any flavor including gg. The limit is for SM H^0Z production cross section with B($H^0 \to jj$) = 1.

[4] ABDALLAH 04O search for $Z \to b\overline{b}H^0$, $b\overline{b}A^0$, $\tau^+\tau^-H^0$ and $\tau^+\tau^-A^0$ in the final states 4b, $b\overline{b}\tau^+\tau^-$, and 4$\tau$. See paper for limits on Yukawa couplings.

[5] ABDALLAH 04O search for $e^+e^- \to H^0Z$ and H^0A^0, with H^0, A^0 decaying to $b\overline{b}$, $\tau^+\tau^-$, or $H^0 \to A^0A^0$ at E_{cm} = 189–208 GeV. See paper for limits on couplings.

[6] ABBIENDI 02D search for $Z \to b\overline{b}H^0_1$ and $b\overline{b}A^0$ with $H^0_1/A^0 \to \tau^+\tau^-$, in the range 4<$m_H$ <12 GeV. See their Fig. 8 for limits on the Yukawa coupling.

[7] ABBIENDI 01E search for neutral Higgs bosons in general Type-II two-doublet models, at $E_{cm} \leq$ 189 GeV. In addition to usual final states, the decays H^0_1, $A^0 \to q\overline{q}$, gg are searched for. See their Figs. 15,16 for excluded regions.

[8] ABBIENDI 99E search for $e^+e^- \to H^0A^0$ and H^0Z at E_{cm} = 183 GeV. The limit is with m_H=m_A in general two Higgs-doublet models. See their Fig. 18 for the exclusion limit in the m_H-m_A plane. Updates the results of ACKERSTAFF 98S.

[9] See Fig. 4 of ABREU 95H for the excluded region in the $m_{H^0} - m_{A^0}$ plane for general two-doublet models. For tanβ >1, the region $m_{H^0}+m_{A^0} \lesssim$ 87 GeV, m_{H^0} <47 GeV is excluded at 95% CL.

[10] PICH 92 analyse H^0 with $m_{H^0} < 2m_\mu$ in general two-doublet models. Excluded regions in the space of mass-mixing angles from LEP, beam dump, and $\pi^\pm$, η rare decays are shown in Figs. 3,4. The considered mass region is not totally excluded.

Mass Limits for H^0 with Vanishing Yukawa Couplings

These limits assume that H^0 couples to gauge bosons with the same strength as the Standard Model Higgs boson, but has no coupling to quarks and leptons (this is often referred to as "fermiophobic").

VALUE (GeV)	CL%	DOCUMENT ID		TECN	COMMENT
• • • We do not use the following data for averages, fits, limits, etc. • • •					
	95	[1] AALTONEN	13K	CDF	$H^0 \to WW^{(*)}$
none 100–113	95	[2] AALTONEN	13L	CDF	$H^0 \to \gamma\gamma$, WW^*, ZZ^*
none 100–116	95	[3] AALTONEN	13M	TEVA	$H^0 \to \gamma\gamma$, WW^*, ZZ^*
		[4] ABAZOV	13G	D0	$H^0 \to WW^{(*)}$
none 100–113	95	[5] ABAZOV	13H	D0	$H^0 \to \gamma\gamma$
		[6] ABAZOV	13I	D0	$H^0 \to WW^{(*)}$
		[7] ABAZOV	13J	D0	$H^0 \to WW^{(*)}$, $ZZ^{(*)}$
none 100–114	95	[8] ABAZOV	13L	D0	$H^0 \to \gamma\gamma$, WW^*, ZZ^*
none 110–147	95	[9] CHATRCHYAN	13AL	CMS	$H^0 \to \gamma\gamma$
none 110–118, 119.5–121	95	[10] AAD	12N	ATLS	$H^0 \to \gamma\gamma$
none 100–114	95	[11] AALTONEN	12	CDF	$H^0 \to \gamma\gamma$
none 100–114	95	[12] AALTONEN	12AN	CDF	$H^0 \to \gamma\gamma$
none 110–194	95	[13] CHATRCHYAN	12AO	CMS	$H^0 \to \gamma\gamma$, $WW^{(*)}$, $ZZ^{(*)}$
none 100–112.9	95	[14] ABAZOV	11Y	D0	$H^0 \to \gamma\gamma$
none 70–106	95	[15] AALTONEN	09AB	CDF	$H^0 \to \gamma\gamma$
none 70–100	95	[16] ABAZOV	08U	D0	$H^0 \to \gamma\gamma$
>105.8	95	[17] SCHAEL	07	ALEP	$e^+e^- \to H^0Z$, $H^0 \to WW^*$
>104.1	95	[18,19] ABDALLAH	04L	DLPH	$e^+e^- \to H^0Z$, $H^0 \to \gamma\gamma$
>107	95	[20] ACHARD	03C	L3	$H^0 \to WW^*$,ZZ^*, $\gamma\gamma$
>105.5	95	[18,21] ABBIENDI	02F	OPAL	$H^0 \to \gamma\gamma$
>105.4	95	[22] ACHARD	02C	L3	$H^0 \to \gamma\gamma$
none 60–82	95	[23] AFFOLDER	01H	CDF	$p\overline{p} \to H^0$ W/Z, $H^0 \to \gamma\gamma$
> 94.9	95	[24] ACCIARRI	00S	L3	$e^+e^- \to H^0Z$, $H^0 \to \gamma\gamma$
>100.7	95	[25] BARATE	00L	ALEP	$e^+e^- \to H^0Z$, $H^0 \to \gamma\gamma$
> 96.2	95	[26] ABBIENDI	99O	OPAL	$e^+e^- \to H^0Z$, $H^0 \to \gamma\gamma$
> 78.5	95	[27] ABBOTT	99B	D0	$p\overline{p} \to H^0W/Z$, $H^0 \to \gamma\gamma$
		[28] ABREU	99P	DLPH	$e^+e^- \to H^0\gamma$ and/or $H^0 \to \gamma\gamma$

[1] AALTONEN 13K search for $H^0 \to WW^{(*)}$ in 9.7 fb^{-1} of $p\overline{p}$ collisions at E_{cm} = 1.96 TeV. A limit on cross section times branching ratio which corresponds to (1.3–6.6) times the expected cross section is given in the range m_{H^0} = 110–200 GeV at 95% CL.

[2] AALTONEN 13L combine all CDF searches with 9.45–10.0 fb^{-1} of $p\overline{p}$ collisions at E_{cm} = 1.96 TeV.

[3] AALTONEN 13M combine all Tevatron data from the CDF and D0 Collaborations of $p\overline{p}$ collisions at E_{cm} = 1.96 TeV.

[4] ABAZOV 13G search for $H^0 \to WW^{(*)}$ in 9.7 fb^{-1} of $p\overline{p}$ collisions at E_{cm} = 1.96 TeV. A limit on cross section times branching ratio which corresponds to (2–9) times the expected cross section is given for m_{H^0} = 100–200 GeV at 95% CL.

[5] ABAZOV 13H search for $H^0 \to \gamma\gamma$ in 9.6 fb^{-1} of $p\overline{p}$ collisions at E_{cm} = 1.96 TeV.

[6] ABAZOV 13I search for H^0 production in the final state with one lepton and two or more jets plus missing E_T in 9.7 fb^{-1} of $p\overline{p}$ collisions at E_{cm} = 1.96 TeV. The search is sensitive to WH^0, ZH^0 and vector-boson fusion Higgs production with $H^0 \to WW^{(*)}$. A limit on cross section times branching ratio which corresponds to (8–30) times the expected cross section is given in the range m_{H^0} = 100–200 GeV at 95% CL.

[7] ABAZOV 13J search for H^0 production in the final states $e e\mu$, $e\mu\mu$, $\mu\tau\tau$, and $e^{\pm}\mu^{\pm}$ in 8.6–9.7 fb^{-1} of $p\overline{p}$ collisions at E_{cm} = 1.96 TeV. The search is sensitive to WH^0, ZH^0 production with $H^0 \to WW^{(*)}$, $ZZ^{(*)}$, decaying to leptonic final states. A limit on cross section times branching ratio which corresponds to (2.4–13.0) times the expected cross section is given in the range m_{H^0} = 100–200 GeV at 95% CL.

[8] ABAZOV 13L combine all D0 results with up to 9.7 fb^{-1} of $p\overline{p}$ collisions at E_{cm} = 1.96 TeV.

[9] CHATRCHYAN 13AL search for $H^0 \to \gamma\gamma$ in 5.1 fb^{-1} and 5.3 fb^{-1} of pp collisions at E_{cm} = 7 and 8 TeV.

[10] AAD 12N search for $H^0 \to \gamma\gamma$ with 4.9 fb^{-1} of pp collisions at E_{cm} = 7 TeV in the mass range m_{H^0} = 110–150 GeV.

[11] AALTONEN 12 search for $H^0 \to \gamma\gamma$ in 7.0 fb^{-1} of $p\overline{p}$ collisions at E_{cm} = 1.96 TeV in the mass range m_{H^0} = 100–150 GeV. Superseded by AALTONEN 12AN.

[12] AALTONEN 12AN search for $H^0 \to \gamma\gamma$ with 10 fb^{-1} of $p\overline{p}$ collisions at E_{cm} = 1.96 TeV in the mass range m_{H^0} = 100–150 GeV.

[13] CHATRCHYAN 12AO use data from CHATRCHYAN 12G, CHATRCHYAN 12E, CHATRCHYAN 12H, CHATRCHYAN 12I, CHATRCHYAN 12D, and CHATRCHYAN 12C.

[14] ABAZOV 11Y search for $H^0 \to \gamma\gamma$ in 8.2 fb^{-1} of $p\overline{p}$ collisions at E_{cm} = 1.96 TeV in the mass range m_{H^0} = 100–150 GeV.

[15] AALTONEN 09AB search for $H^0 \to \gamma\gamma$ in 3.0 fb^{-1} of $p\overline{p}$ collisions at E_{cm} = 1.96 TeV in the mass range m_{H^0} = 70–150 GeV. Associated H^0W, H^0Z production and WW, ZZ fusion are considered.

[16] ABAZOV 08U search for $H^0 \to \gamma\gamma$ in $p\overline{p}$ collisions at E_{cm} = 1.96 TeV in the mass range m_{H^0} = 70–150 GeV. Associated H^0W, H^0Z production and WW, ZZ fusion are considered. See their Tab. 1 for the limit on $\sigma \cdot B(H^0 \to \gamma\gamma)$, and see their Fig. 3 for the excluded region in the m_{H^0} — $B(H^0 \to \gamma\gamma)$ plane.

[17] SCHAEL 07 search for Higgs bosons in association with a fermion pair and decaying to WW^*. The limit is from this search and HEISTER 02L for a H^0 with SM production cross section.

[18] Search for associated production of a $\gamma\gamma$ resonance with a Z boson, followed by $Z \to q\overline{q}$, $\ell^+\ell^-$, or $\nu\overline{\nu}$, at $E_{cm} \leq$ 209 GeV. The limit is for a H^0 with SM production cross section.

[19] Updates ABREU 01F.

[20] ACHARD 03C search for $e^+e^- \to ZH^0$ followed by $H^0 \to WW^*$ or ZZ^* at E_{cm}= 200-209 GeV and combine with the ACHARD 02C result. The limit is for a H^0 with SM production cross section. For $B(H^0 \to WW^*) + B(H^0 \to ZZ^*) = 1$, $m_{H^0} > 108.1$ GeV is obtained. See fig. 6 for the limits under different BR assumptions.

[21] For $B(H^0 \to \gamma\gamma)$=1, m_{H^0} >117 GeV is obtained.

[22] ACHARD 02C search for associated production of a $\gamma\gamma$ resonance with a Z boson, followed by $Z \to q\overline{q}$, $\ell^+\ell^-$, or $\nu\overline{\nu}$, at $E_{cm} \leq$ 209 GeV. The limit is for a H^0 with SM production cross section. For $B(H^0 \to \gamma\gamma)$=1, m_{H^0} >114 GeV is obtained.

[23] AFFOLDER 01H search for associated production of a $\gamma\gamma$ resonance and a W or Z (tagged by two jets, an isolated lepton, or missing E_T). The limit assumes Standard Model values for the production cross section and for the couplings of the H^0 to W and Z bosons. See their Fig. 11 for limits with $B(H^0 \to \gamma\gamma) < 1$.

[24] ACCIARRI 00S search for associated production of a $\gamma\gamma$ resonance with a $q\overline{q}$, $\nu\overline{\nu}$, or $\ell^+\ell^-$ pair in e^+e^- collisions at E_{cm}= 189 GeV. The limit is for a H^0 with SM production cross section. For $B(H^0 \to \gamma\gamma)$=1, $m_{H^0} > 98$ GeV is obtained. See their Fig. 5 for limits on $B(H \to \gamma\gamma)\cdot\sigma(e^+e^- \to Hf\overline{f})/\sigma(e^+e^- \to Hf\overline{f})$ (SM).

[25] BARATE 00L search for associated production of a $\gamma\gamma$ resonance with a $q\overline{q}$, $\nu\overline{\nu}$, or $\ell^+\ell^-$ pair in e^+e^- collisions at E_{cm}= 88–202 GeV. The limit is for a H^0 with SM production cross section. For $B(H^0 \to \gamma\gamma)$=1, $m_{H^0} > 109$ GeV is obtained. See their Fig. 3 for limits on $B(H \to \gamma\gamma)\cdot\sigma(e^+e^- \to Hf\overline{f})/\sigma(e^+e^- \to Hf\overline{f})$ (SM).

[26] ABBIENDI 99O search for associated production of a $\gamma\gamma$ resonance with a $q\overline{q}$, $\nu\overline{\nu}$, or $\ell^+\ell^-$ pair in e^+e^- collisions at 189 GeV. The limit is for a H^0 with SM production cross section. See their Fig. 4 for limits on $\sigma(e^+e^- \to H^0Z^0)\times B(H^0 \to \gamma\gamma)\times B(X^0 \to f\overline{f})$ for various masses. Updates the results of ACKERSTAFF 98Y.

[27] ABBOTT 99B search for associated production of a $\gamma\gamma$ resonance and a dijet pair. The limit assumes Standard Model values for the production cross section and for the couplings of the H^0 to W and Z bosons. Limits in the range of $\sigma(H^0 + Z/W)\cdot B(H^0 \to \gamma\gamma)$= 0.80–0.34 pb are obtained in the mass range m_{H^0}= 65–150 GeV.

[28] ABREU 99P search for $e^+e^- \to H^0\gamma$ with $H^0 \to b\overline{b}$ or $\gamma\gamma$, and $e^+e^- \to H^0q\overline{q}$ with $H^0 \to \gamma\gamma$. See their Fig. 4 for limits on $\sigma\times$B. Explicit limits within an effective interaction framework are also given.

Mass Limits for H^0 Decaying to Invisible Final States

These limits are for a neutral scalar H^0 which predominantly decays to invisible final states. Standard Model values are assumed for the couplings of H^0 to ordinary particles unless otherwise stated.

VALUE (GeV)	CL%	DOCUMENT ID		TECN	COMMENT
• • • We do not use the following data for averages, fits, limits, etc. • • •					
		[1] AAD	13AG	ATLS	secondary vertex
		[2] AAD	13AT	ATLS	electron jets
		[3] CHATRCHYAN	13BJ	CMS	
		[4] AAD	12AQ	ATLS	secondary vertex
		[5] AALTONEN	12AB	CDF	secondary vertex
		[6] AALTONEN	12U	CDF	secondary vertex
>108.2	95	[7] ABBIENDI	10	OPAL	
		[8] ABBIENDI	07	OPAL	large width
>112.3	95	[9] ACHARD	05	L3	
>112.1	95	[9] ABDALLAH	04B	DLPH	
>114.1	95	[9] HEISTER	02	ALEP	$E_{cm} \leq$ 209 GeV
>106.4	95	[9] BARATE	01C	ALEP	$E_{cm} \leq$ 202 GeV
> 89.2	95	[10] ACCIARRI	00M	L3	

[1] AAD 13AG search for H^0 production in the decay mode $H^0 \to X^0X^0$, where X^0 is a long-lived particle which decays to $\mu^+\mu^-X'^0$, in 1.9 fb^{-1} of pp collisions at E_{cm} = 7 TeV. See their Fig. 7 for limits on cross section times branching ratio.

[2] AAD 13AT search for H^0 production in the decay $H^0 \to X^0X^0$, where X^0 eventually decays to clusters of collimated e^+e^- pairs, in 2.04 fb^{-1} of pp collisions at E_{cm} = 7 TeV. See their Fig. 3 for limits on cross section times branching ratio.

[3] CHATRCHYAN 13BJ search for H^0 production in the decay chain $H^0 \to X^0X^0$, $X^0 \to \mu^+\mu^-X'^0$ in 5.3 fb^{-1} of pp collisions at E_{cm} = 7 TeV. See their Fig. 2 for limits on cross section times branching ratio.

[4] AAD 12AQ search for H^0 production in the decay mode $H^0 \to X^0X^0$, where X^0 is a long-lived particle which decays mainly to $b\overline{b}$ in the muon detector, in 1.94 fb^{-1} of pp collisions at E_{cm} = 7 TeV. See their Fig. 3 for limits on cross section times branching ratio for m_{H^0} = 120, 140 GeV, m_{X^0} = 20, 40 GeV in the $c\tau$ range of 0.5–35 m.

[5] AALTONEN 12AB search for H^0 production in the decay $H^0 \to X^0X^0$, where X^0 eventually decays to clusters of collimated $\ell^+\ell^-$ pairs, in 5.1 fb^{-1} of $p\overline{p}$ collisions at E_{cm} = 1.96 TeV. Cross section limits are provided for a benchmark MSSM model incorporating the parameters given in Table VI.

[6] AALTONEN 12U search for H^0 production in the decay mode $H^0 \to X^0X^0$, where X^0 is a long-lived particle with $c\tau \approx$ 1 cm which decays mainly to $b\overline{b}$, in 3.2 fb^{-1} of $p\overline{p}$ collisions at E_{cm} = 1.96 TeV. See their Figs. 9 and 10 for limits on cross section times branching ratio for m_{H^0} = (130–170) GeV, m_{X^0} = 20, 40 GeV.

[7] ABBIENDI 10 search for $e^+e^- \to H^0Z$ with H^0 decaying invisibly. The limit assumes SM production cross section and $B(H^0 \to$ invisible) = 1.

[8] ABBIENDI 07 search for $e^+e^- \to H^0Z$ with $Z \to q\overline{q}$ and H^0 decaying to invisible final states. The H^0 width is varied between 1 GeV and 3 TeV. A limit $\sigma\cdot B(H^0 \to$ invisible) < (0.07–0.57) pb (95%CL) is obtained at E_{cm} = 206 GeV for m_{H^0} = 60–114 GeV.

[9] Search for $e^+e^- \to H^0Z$ with H^0 decaying invisibly. The limit assumes SM production cross section and $B(H^0 \to$ invisible) = 1.

[10] ACCIARRI 00M search for $e^+e^- \to ZH^0$ with H^0 decaying invisibly at E_{cm}=183–189 GeV. The limit assumes SM production cross section and $B(H^0 \to$ invisible)=1. See their Fig. 6 for limits for smaller branching ratios.

Mass Limits for Light A^0

These limits are for a pseudoscalar A^0 in the mass range below $\mathcal{O}(10)$ GeV.

VALUE (GeV)	CL%	DOCUMENT ID		TECN	COMMENT
• • • We do not use the following data for averages, fits, limits, etc. • • •					
		[1] LEES	13C	BABR	$\Upsilon(1S) \to A^0\gamma$
		[2] LEES	13L	BABR	$\Upsilon(1S) \to A^0\gamma$
		[3] LEES	13R	BABR	$\Upsilon(1S) \to A^0\gamma$
		[4] CHATRCHYAN	12V	CMS	$A^0 \to \mu^+\mu^-$
		[5] AALTONEN	11P	CDF	$t \to bH^+$, $H^+ \to W^+A^0$
		[6,7] ABOUZAID	11A	KTEV	$K_L \to \pi^0\pi^0A^0$, $A^0 \to \mu^+\mu^-$
		[8] DEL-AMO-SA..	11J	BABR	$\Upsilon(1S) \to A^0\gamma$
		[9] LEES	11H	BABR	$\Upsilon(2S,3S) \to A^0\gamma$
		[10] ANDREAS	10	RVUE	
		[7,11] HYUN	10	BELL	$B^0 \to K^{*0}A^0$, $A^0 \to \mu^+\mu^-$
		[7,12] HYUN	10	BELL	$B^0 \to \rho^0A^0$, $A^0 \to \mu^+\mu^-$
		[13] AUBERT	09P	BABR	$\Upsilon(3S) \to A^0\gamma$
		[14] AUBERT	09Z	BABR	$\Upsilon(2S) \to A^0\gamma$
		[15] AUBERT	09Z	BABR	$\Upsilon(3S) \to A^0\gamma$
		[7,16] TUNG	09	K391	$K_L \to \pi^0\pi^0A^0$, $A^0 \to \gamma\gamma$
		[17] LOVE	08	CLEO	$\Upsilon(1S) \to A^0\gamma$
		[18] BESSON	07	CLEO	$\Upsilon(1S) \to \eta_b\gamma$
		[19] PARK	05	HYCP	$\Sigma^+ \to pA^0$, $A^0 \to \mu^+\mu^-$
$<1.5 \times 10^{-5}$	90	[20] BALEST	95	CLE2	$\Upsilon(1S) \to A^0\gamma$, $m_{A^0} < 5$ GeV
$<5.6 \times 10^{-5}$	90	[21] ANTREASYAN	90C	CBAL	$\Upsilon(1S) \to A^0\gamma$, $m_{A^0} < 7.2$ GeV

[1] LEES 13C search for the process $\Upsilon(2S,3S) \to \Upsilon(1S)\pi^+\pi^- \to A^0\gamma\pi^+\pi^-$ with A^0 decaying to $\mu^+\mu^-$ and give limits on $B(\Upsilon(1S) \to A^0\gamma)\cdot B(A^0 \to \mu^+\mu^-)$ in the range $(0.3–9.7) \times 10^{-6}$ (90% CL) for $0.212 \leq m_{A^0} \leq 9.20$ GeV. See their Fig. 5(e) for limits on the $b-A^0$ Yukawa coupling derived by combining this result with AUBERT 09Z.

[2] LEES 13L search for the process $\Upsilon(2S) \to \Upsilon(1S)\pi^+\pi^- \to A^0\gamma\pi^+\pi^-$ with A^0 decaying to gg or $s\overline{s}$ and give limits on $B(\Upsilon(1S) \to A^0\gamma)\cdot B(A^0 \to gg)$ between 10^{-6} and 10^{-2} (90% CL) for $0.5 \leq m_{A^0} \leq 9.0$ GeV, and $B(\Upsilon(1S) \to A^0\gamma)\cdot B(A^0 \to s\overline{s})$ between 10^{-5} and 10^{-3} (90%CL) for $1.5 \leq m_{A^0} \leq 9.0$ GeV.

Gauge & Higgs Boson Particle Listings

Neutral Higgs Bosons, Searches for

[3] LEES 13R search for the process $\Upsilon(2S) \to \Upsilon(1S)\pi^+\pi^- \to A^0\gamma\pi^+\pi^-$ with A^0 decaying to $\tau^+\tau^-$ and give limits on $B(\Upsilon(1S) \to A^0\gamma)\cdot B(A^0 \to \tau^+\tau^-)$ in the range $0.9–13\times10^{-5}$ (90% CL) for $3.6 \le m_{A^0} \le 9.2$ GeV. See their Fig. 4 for limits on the $b-A^0$ Yukawa coupling derived by combining this result with AUBERT 09P.

[4] CHATRCHYAN 12V search for A^0 production in the decay $A^0 \to \mu^+\mu^-$ with 1.3 fb^{-1} of pp collisions at $E_{cm} = 7$ TeV. A limit on $\sigma(A^0)\cdot B(A^0 \to \mu^+\mu^-)$ in the range (1.5–7.5) pb is given for m_{A^0} = (5.5–8.7) and (11.5–14) GeV at 95% CL.

[5] AALTONEN 11P search in 2.7 fb^{-1} of $p\overline{p}$ collisions at $E_{cm} = 1.96$ TeV for the decay chain $t \to bH^+$, $H^+ \to W^+A^0$, $A^0 \to \tau^+\tau^-$ with m_{A^0} between 4 and 9 GeV. See their Fig. 4 for limits on $B(t \to bH^+)$ for $90 < m_{H^+} < 160$ GeV.

[6] ABOUZAID 11A search for the decay chain $K_L \to \pi^0\pi^0A^0$, $A^0 \to \mu^+\mu^-$ and give a limit $B(K_L \to \pi^0\pi^0A^0)\cdot B(A^0 \to \mu^+\mu^-) < 1.0\times10^{-10}$ at 90% CL for m_{A^0} = 214.3 MeV.

[7] The search was motivated by PARK 05.

[8] DEL-AMO-SANCHEZ 11J search for the process $\Upsilon(2S) \to \Upsilon(1S)\pi^+\pi^- \to A^0\gamma\pi^+\pi^-$ with A^0 decaying to invisible final states. They give limits on $B(\Upsilon(1S) \to A^0\gamma)\cdot B(A^0 \to$ invisible) in the range $(1.9–4.5)\times10^{-6}$ (90% CL) for $0 \le m_{A^0} \le 8.0$ GeV, and $(2.7–37)\times10^{-6}$ for $8.0 \le m_{A^0} \le 9.2$ GeV.

[9] LEES 11H search for the process $\Upsilon(2S,3S) \to A^0\gamma$ with A^0 decaying hadronically and give limits on $B(\Upsilon(2S,3S) \to A^0\gamma)\cdot B(A^0 \to$ hadrons) in the range 1×10^{-6}–8×10^{-5} (90% CL) for $0.3 < m_{A^0} < 7$ GeV. The decay rates for $\Upsilon(2S)$ and $\Upsilon(3S)$ are assumed to be equal up to the phase space factor.

[10] ANDREAS 10 analyze constraints from rare decays and other processes on a light A^0 with $m_{A^0} < 2m_\mu$ and give limits on its coupling to fermions at the level of 10^{-4} times the Standard Model value.

[11] HYUN 10 search for the decay chain $B^0 \to K^{*0}A^0$, $A^0 \to \mu^+\mu^-$ and give a limit on $B(B^0 \to K^{*0}A^0)\cdot B(A^0 \to \mu^+\mu^-)$ in the range $(2.26–5.53)\times10^{-8}$ at 90%CL for m_{A^0} = 212–300 MeV. The limit for $m_{A^0} = 214.3$ MeV is 2.26×10^{-8}.

[12] HYUN 10 search for the decay chain $B^0 \to \rho^0A^0$, $A^0 \to \mu^+\mu^-$ and give a limit on $B(B^0 \to \rho^0A^0)\cdot B(A^0 \to \mu^+\mu^-)$ in the range $(1.73–4.51)\times10^{-8}$ at 90%CL for m_{A^0} = 212–300 MeV. The limit for $m_{A^0} = 214.3$ MeV is 1.73×10^{-8}.

[13] AUBERT 09P search for the process $\Upsilon(3S) \to A^0\gamma$ with $A^0 \to \tau^+\tau^-$ for $4.03 < m_{A^0} < 9.52$ and $9.61 < m_{A^0} < 10.10$ GeV, and give limits on $B(\Upsilon(3S) \to A^0\gamma)\cdot B(A^0 \to \tau^+\tau^-)$ in the range $(1.5–16)\times10^{-5}$ (90% CL).

[14] AUBERT 09Z search for the process $\Upsilon(2S) \to A^0\gamma$ with $A^0 \to \mu^+\mu^-$ for $0.212 < m_{A^0} < 9.3$ GeV and give limits on $B(\Upsilon(2S) \to A^0\gamma)\cdot B(A^0 \to \mu^+\mu^-)$ in the range $(0.3–8)\times10^{-6}$ (90% CL).

[15] AUBERT 09Z search for the process $\Upsilon(3S) \to A^0\gamma$ with $A^0 \to \mu^+\mu^-$ for $0.212 < m_{A^0} < 9.3$ GeV and give limits on $B(\Upsilon(3S) \to A^0\gamma)\cdot B(A^0 \to \mu^+\mu^-)$ in the range $(0.3–5)\times10^{-6}$ (90% CL).

[16] TUNG 09 search for the decay chain $K_L \to \pi^0\pi^0A^0$, $A^0 \to \gamma\gamma$ and give a limit on $B(K_L \to \pi^0\pi^0A^0)\cdot B(A^0 \to \gamma\gamma)$ in the range $(2.4–10.7)\times10^{-7}$ at 90%CL for m_{A^0} = 194.3–219.3 MeV. The limit for $m_{A^0} = 214.3$ MeV is 2.4×10^{-7}.

[17] LOVE 08 search for the process $\Upsilon(1S) \to A^0\gamma$ with $A^0 \to \mu^+\mu^-$ (for $m_{A^0} < 2m_\tau$) and $A^0 \to \tau^+\tau^-$. Limits on $B(\Upsilon(1S) \to A^0\gamma)\cdot B(A^0 \to \ell^+\ell^-)$ in the range 10^{-6}–10^{-4} (90% CL) are given.

[18] BESSON 07 give a limit $B(\Upsilon(1S) \to \eta_b\gamma)\cdot B(\eta_b \to \tau^+\tau^-) < 0.27\%$ (95% CL), which constrains a possible A^0 exchange contribution to the η_b decay.

[19] PARK 05 found three candidate events for $\Sigma^+ \to p\mu^+\mu^-$ in the HyperCP experiment. Due to a narrow spread in dimuon mass, they hypothesize the events as a possible signal of a new boson. It can be interpreted as a neutral particle with $m_{A^0} = 214.3 \pm 0.5$ MeV and the branching fraction $B(\Sigma^+ \to pA^0)\cdot B(A^0 \to \mu^+\mu^-) = (3.1^{+2.4}_{-1.9}\pm1.5)\times10^{-8}$.

[20] BALEST 95 two-body limit is for pseudoscalar A^0. The limit becomes $< 10^{-4}$ for $m_{A^0} < 7.7$ GeV.

[21] ANTREASYAN 90C assume that A^0 does not decay in the detector.

Other Mass Limits

VALUE (GeV)	CL%	DOCUMENT ID		TECN	COMMENT
• • • We do not use the following data for averages, fits, limits, etc. • • •					
		[1] AALTONEN	13P	CDF	$H'^0 \to H^\pm W^\mp \to H^0W^+W^-$
		[2] CHATRCHYAN	13BJ	CMS	$H^0 \to A^0A^0$
		[3] AALTONEN	11P	CDF	$t \to bH^+$, $H^+ \to W^+A^0$
		[4] ABBIENDI	10	OPAL	$H^0 \to \tilde{\chi}^0_1\tilde{\chi}^0_2$
		[5] SCHAEL	10	ALEP	$H^0 \to A^0A^0$
		[6] ABAZOV	09V	D0	$H^0 \to A^0A^0$
none 3–63	95	[7] ABBIENDI	05A	OPAL	A^0, Type II model
>104	95	[8] ABBIENDI	04K	OPAL	$H^0 \to$ 2 jets
		[9] ABDALLAH	04	DLPH	H^0VV couplings
>110.3	95	[10] ACHARD	04B	L3	$H^0 \to$ 2 jets
		[11] ACHARD	04F	L3	Anomalous coupling
		[12] ABBIENDI	03F	OPAL	$e^+e^- \to H^0Z$, $H^0 \to$ any
		[13] ABBIENDI	03G	OPAL	$H^0_1 \to A^0A^0$
>105.4	95	[14,15] HEISTER	02L	ALEP	$H^0_1 \to \gamma\gamma$
>109.1	95	[16] HEISTER	02M	ALEP	$H^0 \to$ 2 jets or $\tau^+\tau^-$
none 12–56	95	[17] ABBIENDI	01E	OPAL	A^0, Type-II model
		[18] ACCIARRI	00R	L3	$e^+e^- \to H^0\gamma$ and/or $H^0 \to \gamma\gamma$
		[19] ACCIARRI	00R	L3	$e^+e^- \to e^+e^-H^0$
		[20] GONZALEZ-G..	98B	RVUE	Anomalous coupling
		[21] KRAWCZYK	97	RVUE	$(g-2)_\mu$
		[22] ALEXANDER	96H	OPAL	$Z \to H^0\gamma$

[1] AALTONEN 13P search for production of a heavy Higgs boson H'^0 that decays into a charged Higgs boson $H^\pm$ and a lighter Higgs boson H^0 via the decay chain $H'^0 \to H^\pm W^\mp$, $H^\pm \to W^\pm H^0$, $H^0 \to b\overline{b}$ in the final state $\ell\nu$ plus 4 jets in 8.7 fb^{-1} of $p\overline{p}$ collisions at $E_{cm} = 1.96$ TeV. See their Fig. 4 for limits on cross section times branching ratio in the $m_{H^\pm}$–$m_{H'^0}$ plane for $m_{H^0} = 126$ GeV.

[2] CHATRCHYAN 13BJ search for H^0 production in the decay chain $H^0 \to A^0A^0$, $A^0 \to \mu^+\mu^-$ in 5.3 fb^{-1} of pp collisions at $E_{cm} = 7$ TeV. See their Fig. 2 for limits on cross section times branching ratio.

[3] AALTONEN 11P search in 2.7 fb^{-1} of $p\overline{p}$ collisions at $E_{cm} = 1.96$ TeV for the decay chain $t \to bH^+$, $H^+ \to W^+A^0$, $A^0 \to \tau^+\tau^-$ with m_{A^0} between 4 and 9 GeV. See their Fig. 4 for limits on $B(t \to bH^+)$ for $90 < m_{H^+} < 160$ GeV.

[4] ABBIENDI 10 search for $e^+e^- \to ZH^0$ with the decay chain $H^0 \to \tilde{\chi}^0_1\tilde{\chi}^0_2$, $\tilde{\chi}^0_2 \to \tilde{\chi}^0_1 + (\gamma$ or $Z^*)$, when $\tilde{\chi}^0_1$ and $\tilde{\chi}^0_2$ are nearly degenerate. For a mass difference of 2 (4) GeV, a lower limit on m_{H^0} of 108.4 (107.0) GeV (95% CL) is obtained for SM ZH^0 cross section and $B(H^0 \to \tilde{\chi}^0_1\tilde{\chi}^0_2) = 1$.

[5] SCHAEL 10 search for the process $e^+e^- \to H^0Z$ followed by the decay chain $H^0 \to A^0A^0 \to \tau^+\tau^-\tau^+\tau^-$ with $Z \to \ell^+\ell^-$, $\nu\overline{\nu}$ at $E_{cm} = 183–209$ GeV. For a H^0ZZ coupling equal to the SM value, $B(H^0 \to A^0A^0) = B(A^0 \to \tau^+\tau^-) = 1$, and m_{A^0} = 4–10 GeV, m_{H^0} up to 107 GeV is excluded at 95% CL.

[6] ABAZOV 09V search for H^0 production followed by the decay chain $H^0 \to A^0A^0 \to \mu^+\mu^-\mu^+\mu^-$ or $\mu^+\mu^-\tau^+\tau^-$ in 4.2 fb^{-1} of $p\overline{p}$ collisions at $E_{cm} = 1.96$ TeV. See their Fig. 3 for limits on $\sigma(H^0)\cdot B(H^0 \to A^0A^0)$ for m_{A^0} = 3.6–19 GeV.

[7] ABBIENDI 05A search for $e^+e^- \to H^0_1A^0$ in general Type-II two-doublet models, with decays H^0_1, $A^0 \to q\overline{q}$, gg, $\tau^+\tau^-$, and $H^0_1 \to A^0A^0$.

[8] ABBIENDI 04K search for $e^+e^- \to H^0Z$ with H^0 decaying to two jets of any flavor including gg. The limit is for SM production cross section with $B(H^0 \to jj) = 1$.

[9] ABDALLAH 04 consider the full combined LEP and LEP2 datasets to set limits on the Higgs coupling to W or Z bosons, assuming SM decays of the Higgs. Results in Fig. 26.

[10] ACHARD 04B search for $e^+e^- \to H^0Z$ with H^0 decaying to $b\overline{b}$, $c\overline{c}$, or gg. The limit is for SM production cross section with $B(H^0 \to jj) = 1$.

[11] ACHARD 04F search for H^0 with anomalous coupling to gauge boson pairs in the processes $e^+e^- \to H^0\gamma$, $e^+e^-H^0$, H^0Z with decays $H^0 \to f\overline{f}$, $\gamma\gamma$, $Z\gamma$, and W^*W at E_{cm} = 189–209 GeV. See paper for limits.

[12] ABBIENDI 03F search for $H^0 \to$ anything in $e^+e^- \to H^0Z$, using the recoil mass spectrum of $Z \to e^+e^-$ or $\mu^+\mu^-$. In addition, it searched for $Z \to \nu\overline{\nu}$ and $H^0 \to e^+e^-$ or photons. Scenarios with large width or continuum H^0 mass distribution are considered. See their Figs. 11–14 for the results.

[13] ABBIENDI 03G search for $e^+e^- \to H^0_1Z$ followed by $H^0_1 \to A^0A^0$, $A^0 \to c\overline{c}$, gg, or $\tau^+\tau^-$ in the region $m_{H^0_1}$ = 45-86 GeV and m_{A^0} = 2-11 GeV. See their Fig. 7 for the limits.

[14] Search for associated production of a $\gamma\gamma$ resonance with a Z boson, followed by $Z \to q\overline{q}$, $\ell^+\ell^-$, or $\nu\overline{\nu}$, at $E_{cm} \le 209$ GeV. The limit is for a H^0 with SM production cross section and $B(H^0 \to f\overline{f})$=0 for all fermions f.

[15] For $B(H^0 \to \gamma\gamma)$=1, $m_{H^0} > 113.1$ GeV is obtained.

[16] HEISTER 02M search for $e^+e^- \to H^0Z$, assuming that H^0 decays to $q\overline{q}$, gg, or $\tau^+\tau^-$ only. The limit assumes SM production cross section.

[17] ABBIENDI 01E search for neutral Higgs bosons in general Type-II two-doublet models, at $E_{cm} \le 189$ GeV. In addition to usual final states, the decays H^0_1, $A^0 \to q\overline{q}$, gg are searched for. See their Figs. 15,16 for excluded regions.

[18] ACCIARRI 00R search for $e^+e^- \to H^0\gamma$ with $H^0 \to b\overline{b}$, $Z\gamma$, or $\gamma\gamma$. See their Fig. 3 for limits on $\sigma\cdot B$. Explicit limits within an effective interaction framework are also given, for which the Standard Model Higgs search results are used in addition.

[19] ACCIARRI 00R search for the two-photon type processes $e^+e^- \to e^+e^-H^0$ with $H^0 \to b\overline{b}$ or $\gamma\gamma$. See their Fig. 4 for limits on $\Gamma(H^0 \to \gamma\gamma)\cdot B(H^0 \to \gamma\gamma$ or $b\overline{b})$ for m_{H^0}=70–170 GeV.

[20] GONZALEZ-GARCIA 98B use DØ limit for $\gamma\gamma$ events with missing E_T in $p\overline{p}$ collisions (ABBOTT 98) to constrain possible ZH or WH production followed by unconventional $H \to \gamma\gamma$ decay which is induced by higher-dimensional operators. See their Figs. 1 and 2 for limits on the anomalous couplings.

[21] KRAWCZYK 97 analyse the muon anomalous magnetic moment in a two-doublet Higgs model (with type II Yukawa couplings) assuming no H^0_1ZZ coupling and obtain $m_{H^0_1} \gtrsim 5$ GeV or $m_{A^0} \gtrsim 5$ GeV for $\tan\beta > 50$. Other Higgs bosons are assumed to be much heavier.

[22] ALEXANDER 96H give $B(Z \to H^0\gamma)\times B(H^0 \to q\overline{q}) < 1–4\times10^{-5}$ (95%CL) and $B(Z \to H^0\gamma)\times B(H^0 \to b\overline{b}) < 0.7–2\times10^{-5}$ (95%CL) in the range $20 < m_{H^0} < 80$ GeV.

SEARCHES FOR A HIGGS BOSON WITH STANDARD MODEL COUPLINGS

These listings are based on experimental searches for a scalar boson whose couplings to W, Z and fermions are precisely those of the Higgs boson predicted by the three-generation Standard Model with the minimal Higgs sector.

For a review and a bibliography, see the review on "Status of Higgs Boson Physics."

Direct Mass Limits for H^0

The mass limits shown below apply to a Higgs boson H^0 with Standard Model couplings whose mass is a priori unknown. These mass limits are compatible with and independent of the observed signal at about 126 GeV. In particular, the symbol H^0 employed below does not in general refer to the observed signal at about 126 GeV.

The cross section times branching ratio limits quoted in the footnotes below are typically given relative to those of a Standard Model Higgs boson of the relevant mass. These limits can be reinterpreted in terms of more general models (e.g. extended Higgs sectors) in which the Higgs couplings to W, Z and fermions are re-scaled from their Standard Model values.

All data that have been superseded by newer results are marked as "not used" or have been removed from this compilation, and are documented in previous editions of this *Review* of Particle Physics.

VALUE (GeV)	CL%	DOCUMENT ID		TECN	COMMENT
> 122 and none 128–710 (CL = 95%)					
none 90–102, 149–172	95	[1] AALTONEN	13L	CDF	$pp \to H^0 X$, combined
none 90–109, 149–182	95	[2] AALTONEN	13M	TEVA	Tevatron combined
none 90–101, 157–178	95	[3] ABAZOV	13L	D0	$p\overline{p} \to H^0 X$, combined
none 145–710	95	[4] CHATRCHYAN	13Q	CMS	$pp \to H^0 X$ combined
none 111–122, 131–559	95	[5] AAD	12AI	ATLS	$pp \to H^0 X$ combined
none 110–121.5, 128–145	95	[6] CHATRCHYAN	12N	CMS	$pp \to H^0 X$ combined
>114.1	95	[7] ABDALLAH	04	DLPH	$e^+e^- \to H^0 Z$
>112.7	95	[7] ABBIENDI	03B	OPAL	$e^+e^- \to H^0 Z$
>114.4	95	[7,8] HEISTER	03D	LEP	$e^+e^- \to H^0 Z$
>111.5	95	[7,9] HEISTER	02	ALEP	$e^+e^- \to H^0 Z$
>112.0	95	[7] ACHARD	01C	L3	$e^+e^- \to H^0 Z$
• • • We do not use the following data for averages, fits, limits, etc. • • •					
		[10] AALTONEN	13B	CDF	$p\overline{p} \to H^0 ZX, H^0 WX, H^0 \to b\overline{b}$
		[11] AALTONEN	13C	CDF	$p\overline{p} \to H^0 X, H^0 \to b\overline{b}$
none 149–172	95	[12] AALTONEN	13K	CDF	$p\overline{p} \to H^0 X, H^0 \to WW^{(*)}$
		[13] ABAZOV	13E	D0	$p\overline{p} \to H^0 X, 4\ell$
		[14] ABAZOV	13F	D0	$p\overline{p} \to H^0 X, \ell\tau jj$
none 159–176	95	[15] ABAZOV	13G	D0	$p\overline{p} \to H^0 X, H^0 \to WW^{(*)}$
		[16] ABAZOV	13H	D0	$p\overline{p} \to H^0 X, H^0 \to \gamma\gamma$
		[17] ABAZOV	13I	D0	$p\overline{p} \to H^0 X, \ell\nu jj$
		[18] ABAZOV	13J	D0	$p\overline{p} \to H^0 X$, leptonic
		[19] ABAZOV	13K	D0	$p\overline{p} \to H^0 ZX$
		[20] CHATRCHYAN	13AL	CMS	$pp \to H^0 X, H^0 \to \tau\tau, WW^{(*)}, ZZ^{(*)}$
		[21] CHATRCHYAN	13BK	CMS	$pp \to H^0 X, H^0 \to Z\gamma$
		[22] CHATRCHYAN	13X	CMS	$pp \to H^0 t\overline{t}X$
none 113–122, 128–133, 138–149	95	[23] CHATRCHYAN	13Y	CMS	$pp \to H^0 X, H^0 \to \gamma\gamma$
none 130–164, 170–180	95	[24] CHATRCHYAN	13Y	CMS	$pp \to H^0 X, H^0 \to ZZ^*$
none 129–160	95	[25] CHATRCHYAN	13Y	CMS	$pp \to H^0 X, H^0 \to WW^*$
		[26] AAD	12	ATLS	$pp \to H^0 X, H^0 \to ZZ$
none 133–261	95	[27] AAD	12AJ	ATLS	$pp \to H^0 X, H^0 \to WW^{(*)}$
none 111.4–116.6, 119.4–122.1, 129.2–541	95	[28] AAD	12BD	ATLS	$pp \to H^0 X$
		[29] AAD	12BU	ATLS	$pp \to H^0 X, H^0 \to \tau^+\tau^-$
none 319–558	95	[30] AAD	12BZ	ATLS	$pp \to H^0 X, H^0 \to ZZ$
none 300–322, 353–410	95	[31] AAD	12CA	ATLS	$pp \to H^0 X, H^0 \to ZZ$
		[32] AAD	12CN	ATLS	$pp \to H^0 WX, H^0 ZX, H^0 \to b\overline{b}$
		[33] AAD	12CO	ATLS	$pp \to H^0 X, H^0 \to WW$
none 134–156, 182–233, 256–265, 268–415	95	[34] AAD	12D	ATLS	$pp \to H^0 X, H^0 \to ZZ^{(*)}$
none 112.9–115.5, 131–238, 251–466	95	[35] AAD	12E	ATLS	$pp \to H^0 X$
none 145–206	95	[36] AAD	12F	ATLS	$pp \to H^0 X, H^0 \to WW^{(*)}$
none 113–115, 134.5–136	95	[37] AAD	12G	ATLS	$pp \to H^0 X, H^0 \to \gamma\gamma$
		[38] AALTONEN	12	CDF	$H^0 \to \gamma\gamma$
		[39] AALTONEN	12AA	CDF	$p\overline{p} \to H^0 WX, H^0 \to b\overline{b}$
		[40] AALTONEN	12AE	CDF	$p\overline{p} \to H^0 WX, H^0 \to b\overline{b}$
		[41] AALTONEN	12AK	CDF	$p\overline{p} \to H^0 t\overline{t}X$
		[42] AALTONEN	12AM	CDF	$p\overline{p} \to H^0 X$, inclusive 4ℓ
		[43] AALTONEN	12AN	CDF	$p\overline{p} \to H^0 X, H^0 \to \gamma\gamma$
		[44] AALTONEN	12H	CDF	$p\overline{p} \to H^0 ZX, H^0 \to b\overline{b}$
		[45] AALTONEN	12J	CDF	$p\overline{p} \to H^0 X, H^0 \to \tau\tau$
none 90–96	95	[46] AALTONEN	12P	CDF	$p\overline{p} \to H^0 WX, H^0 ZX, H^0 \to b\overline{b}$
		[47] AALTONEN	12Q	CDF	$p\overline{p} \to H^0 ZX, H^0 \to b\overline{b}$
		[48] AALTONEN	12R	CDF	$p\overline{p} \to H^0 WX, H^0 \to b\overline{b}$
		[49] AALTONEN	12S	CDF	$p\overline{p} \to H^0 ZX, H^0 WX, H^0 \to b\overline{b}$
none 100–106	95	[50] AALTONEN	12T	TEVA	$p\overline{p} \to H^0 WX, H^0 ZX, H^0 \to b\overline{b}$
		[51] AALTONEN	12Y	CDF	$p\overline{p} \to H^0 WX, H^0 \to b\overline{b}$
		[52] ABAZOV	12J	D0	$p\overline{p} \to H^0 X, \tau$
		[53] ABAZOV	12K	D0	$p\overline{p} \to H^0 ZX, H^0 WX, H^0 \to b\overline{b}$
none 100–102	95	[54] ABAZOV	12N	D0	$p\overline{p} \to H^0 WX, H^0 ZX, H^0 \to b\overline{b}$
		[55] ABAZOV	12O	D0	$p\overline{p} \to H^0 ZX, H^0 \to b\overline{b}$
		[56] ABAZOV	12P	D0	$p\overline{p} \to H^0 WX, H^0 \to b\overline{b}$
		[57] ABAZOV	12V	D0	$p\overline{p} \to H^0 WX, H^0 \to b\overline{b}$
		[58] ABAZOV	12W	D0	$p\overline{p} \to H^0 X, H^0 \to WW^{(*)}$
		[59,60] CHATRCHYAN	12AY	CMS	$pp \to H^0 WX, H^0 ZX$
none 127–600	95	[61] CHATRCHYAN	12B	CMS	$pp \to H^0 X$ combined
		[62] CHATRCHYAN	12C	CMS	$pp \to H^0 X, H^0 \to ZZ$
		[63] CHATRCHYAN	12D	CMS	$pp \to H^0 X, H^0 \to ZZ^{(*)}$
none 129–270	95	[64] CHATRCHYAN	12E	CMS	$pp \to H^0 X, H^0 \to WW^{(*)}$
		[65] CHATRCHYAN	12F	CMS	$pp \to H^0 WX, H^0 ZX$
none 128–132	95	[66] CHATRCHYAN	12G	CMS	$pp \to H^0 X, H^0 \to \gamma\gamma$
none 134–158, 180–305, 340–465	95	[67] CHATRCHYAN	12H	CMS	$pp \to H^0 X, H^0 \to ZZ^{(*)}$
none 270–440	95	[68] CHATRCHYAN	12I	CMS	$pp \to H^0 X, H^0 \to ZZ$
		[69] CHATRCHYAN	12K	CMS	$pp \to H^0 X, H^0 \to \tau^+\tau^-$
		[70] AAD	11AB	ATLS	$pp \to H^0 X, H^0 \to WW$
none 340–450	95	[71] AAD	11V	ATLS	$pp \to H^0 X, H^0 \to ZZ$
		[72] AAD	11W	ATLS	$pp \to H^0 X$
		[73] AALTONEN	11AA	CDF	$p\overline{p} \to H^0 WX, H^0 ZX, H^0 q\overline{q}X$
		[74] ABAZOV	11AB	D0	$p\overline{p} \to H^0 WX, H^0 ZX$
		[75] ABAZOV	11G	D0	$p\overline{p} \to H^0 X, H^0 \to WW^{(*)}$
		[76] ABAZOV	11J	D0	$p\overline{p} \to H^0 WX, H^0 \to b\overline{b}$
		[77] ABAZOV	11Y	D0	$H^0 \to \gamma\gamma$
		[78] CHATRCHYAN	11J	CMS	$pp \to H^0 X, H^0 \to WW$
		[79] AALTONEN	10AD	CDF	$p\overline{p} \to H^0 ZX$
none 162–166	95	[80] AALTONEN	10F	TEVA	$p\overline{p} \to H^0 X, H^0 \to WW^{(*)}$
		[81] AALTONEN	10G	CDF	$p\overline{p} \to H^0 X, H^0 \to WW^{(*)}$
		[82] AALTONEN	10J	CDF	$p\overline{p} \to H^0 ZX, H^0 WX$
		[83] AALTONEN	10M	TEVA	$p\overline{p} \to ggX \to H^0 X, H^0 \to WW^{(*)}$
		[84] ABAZOV	10B	D0	$p\overline{p} \to H^0 X, H^0 \to WW^{(*)}$
		[85] ABAZOV	10C	D0	$p\overline{p} \to H^0 ZX, H^0 WX$
		[86] ABAZOV	10T	D0	$p\overline{p} \to H^0 ZX$
		[87] AALTONEN	09A	CDF	$p\overline{p} \to H^0 X, H^0 \to WW^{(*)}$
		[88] AALTONEN	09AI	CDF	$p\overline{p} \to H^0 WX$
		[89] ABAZOV	09U	D0	$H^0 \to \tau^+\tau^-$
		[90] ABAZOV	08Y	D0	$p\overline{p} \to H^0 WX$
		[91] ABAZOV	06	D0	$p\overline{p} \to H^0 X, H^0 \to WW^*$
		[92] ABAZOV	06O	D0	$p\overline{p} \to H^0 WX, H^0 \to WW^*$

[1] AALTONEN 13L combine all CDF searches with 9.45–10.0 fb^{-1} of $p\overline{p}$ collisions at E_{cm} = 1.96 TeV. A limit on cross section times branching ratio which corresponds to (0.45–4.8) times the expected Standard Model cross section is given for m_{H^0} = 90–200 GeV at 95 %CL. An excess of events over background is observed with a local significance of 2.0 σ at m_{H^0} = 125 GeV. In the Standard Model with an additional generation of heavy quarks and leptons which receive their masses via the Higgs mechanism, m_{H^0} values between 124 and 203 GeV are excluded at 95% CL.

[2] AALTONEN 13M combine all Tevatron data from the CDF and D0 Collaborations. A limit on cross section times branching ratio which corresponds to (0.37–3.1) times the expected Standard Model cross section is given for m_{H^0} = 90–200 GeV at 95% CL. An excess of events over background is observed with a local significance of 3.0σ at m_{H^0} = 125 GeV. In the Standard Model with an additional generation of heavy quarks and leptons which receive their masses via the Higgs mechanism, m_{H^0} values between 121 and 225 GeV are excluded at 95% CL.

[3] ABAZOV 13L combine all D0 results with up to 9.7 fb^{-1} of $p\overline{p}$ collisions at E_{cm} = 1.96 TeV. A limit on cross section times branching ratio which corresponds to (0.66–3.1) times the expected Standard Model cross section is given in the range m_{H^0} = 90–200 GeV at 95% CL. An excess of events over background is observed with a local significance of 1.7σ at m_{H^0} = 125 GeV. In the Standard Model with an additional generation of heavy quarks and leptons which receive their masses via the Higgs mechanism, m_{H^0} values between 125 and 218 GeV are excluded at 95% CL.

[4] CHATRCHYAN 13Q search for H^0 production in the decays $H \to W^+W^- \to \ell\nu\ell\nu$, $\ell\nu qq$ and $H \to ZZ \to 4\ell$, $\ell\ell\tau\tau$, $\ell\ell\nu\nu$, and $\ell\ell qq$ in up to 5.1 fb^{-1} of pp collisions at E_{cm}=7 TeV and up to 5.3 fb^{-1} at E_{cm}=8 TeV in the range m_{H^0} = 145–1000 GeV.

[5] AAD 12AI search for H^0 production in pp collisions for the final states $H^0 \to ZZ^{(*)}$, $\gamma\gamma$, $WW^{(*)}$, $b\overline{b}$, $\tau\tau$ with 4.6–4.8 fb^{-1} at E_{cm} = 7 TeV, and $H^0 \to ZZ^{(*)} \to 4\ell$, $\gamma\gamma$, $WW^{(*)} \to e\nu\mu\nu$ with 5.8–5.9 fb^{-1} at E_{cm} = 8 TeV. The 99% CL excluded range is 113–114, 117–121, and 132–527 GeV. An excess of events over background with a local significance of 5.9 σ is observed at m_{H^0} = 126 GeV.

[6] CHATRCHYAN 12N search for H^0 production in the decays $H \to \gamma\gamma$, $ZZ^* \to 4\ell$, $WW^* \to \ell\nu\ell\nu$, $\tau\tau$, and $b\overline{b}$ in 4.9–5.1 fb^{-1} of pp collisions at E_{cm} = 7 TeV and 5.1–5.3 fb^{-1} at E_{cm} = 8 TeV. The expected exclusion region for no signal is 110–145 GeV at 99.9% CL. See also CHATRCHYAN 13Y.

[7] Search for $e^+e^- \to H^0 Z$ at $E_{cm} \leq$ 209 GeV in the final states $H^0 \to b\overline{b}$ with $Z \to \ell\overline{\ell}$, $\nu\overline{\nu}$, $q\overline{q}$, $\tau^+\tau^-$ and $H^0 \to \tau^+\tau^-$ with $Z \to q\overline{q}$.

[8] Combination of the results of all LEP experiments.

[9] A 3σ excess of candidate events compatible with m_{H^0} near 114 GeV is observed in the combined channels $q\overline{q}q\overline{q}$, $q\overline{q}\ell\overline{\ell}$, $q\overline{q}\tau^+\tau^-$.

[10] AALTONEN 13B search for associated $H^0 Z$ production in the final state $H^0 \to b\overline{b}$, $Z \to \nu\overline{\nu}$, and $H^0 W$ production in $H^0 \to b\overline{b}$, $W \to \ell\nu$ (ℓ not identified) with an improved b identification algorithm in 9.45 fb^{-1} of $p\overline{p}$ collisions at E_{cm} = 1.96 TeV. A limit on cross section times branching ratio which corresponds to (0.72–11.8) times the expected Standard Model cross section is given for m_{H^0} = 90–150 GeV at 95%CL. The limit for m_{H^0} = 125 GeV is 3.06, where 3.33 is expected for no signal.

[11] AALTONEN 13C search for associated $H^0 W$ and $H^0 Z$ as well as vector-boson fusion $H^0 q\overline{q}'$ production in the final state $H^0 \to b\overline{b}$, $W/Z \to q\overline{q}$ with 9.45 fb^{-1} of $p\overline{p}$ collisions at E_{cm} = 1.96 TeV. A limit on cross section times branching ratio which is (7.0–64.6) times larger than the expected Standard Model cross section is given in the range m_{H^0} = 100–150 GeV at 95% CL. The limit for m_{H^0} = 125 GeV is 9.0, where 11.0 is expected for no signal.

[12] AALTONEN 13K search for H^0 production (with a possible additional W or Z) in the final state $H^0 \to WW^{(*)} \to \ell\nu\ell\nu$ in 9.7 fb^{-1} of $p\overline{p}$ collisions at E_{cm} = 1.96 TeV. A limit on cross section times branching ratio which corresponds to (0.49–14.1) times the expected Standard Model cross section is given in the range m_{H^0} = 110–200 GeV at 95% CL. The limit at m_{H^0} = 125 GeV is 3.26, where 3.25 is expected for no signal. In the Standard Model with an additional generation of heavy quarks and leptons which receive their masses via the Higgs mechanism, m_{H^0} values between 124 and 200 GeV are excluded at 95% CL.

[13] ABAZOV 13E search for H^0 production in four-lepton final states from $H^0 \to ZZ^{(*)}$ and $H^0 Z$ in 9.6–9.8 fb^{-1} of $p\overline{p}$ collisions at E_{cm} = 1.96 TeV. A limit on cross section times branching ratio which corresponds to (8.6–78.9) times the expected Standard Model cross section is given in the range m_{H^0} = 115–200 GeV at 95% CL. The limit for m_{H^0} = 125 GeV is 42.3, where 42.8 is expected for no signal.

[14] ABAZOV 13F search for H^0 production in final states $e\tau jj$ and $\mu\tau jj$ in 9.7 fb^{-1} of $p\overline{p}$ collisions at E_{cm} = 1.96 TeV. The search is sensitive to $H \to \tau\tau$ and $H \to WW^{(*)}$. A limit on cross section times branching ratio which corresponds to (9.4–17.9) times the expected Standard Model cross section is given in the range m_{H^0} = 105–150 GeV at 95% CL. The limit for m_{H^0} = 125 GeV is 11.3, where 9.0 is expected for no signal.

[15] ABAZOV 13G search for H^0 production in final states $H^0 \to WW^{(*)} \to \ell^+\nu\ell^-\nu$ in 9.7 fb^{-1} of $p\overline{p}$ collisions at E_{cm} = 1.96 TeV and give a limit on cross section times branching ratio for m_{H^0} = 100–150 GeV at 95% CL. The limit for m_{H^0} = 125 GeV is 4.1, where 3.4 is expected for no signal. In the Standard Model with an additional generation of heavy quarks and leptons which receive their masses via the Higgs mechanism, m_{H^0} values between 125 and 218 GeV are excluded at 95% CL.

[16] ABAZOV 13H search for H^0 production with the decay $H^0 \to \gamma\gamma$ in 9.6 fb^{-1} of $p\overline{p}$ collisions at E_{cm} = 1.96 TeV. A limit on cross section times branching ratio which corresponds to (8.3–25.4) times the expected Standard Model cross section is given in the range m_{H^0} = 100–150 GeV at 95% CL. The limit for m_{H^0} = 125 GeV is 12.8, where 8.7 is expected for no signal.

[17] ABAZOV 13I search for H^0 production in the final state with one lepton and two or more jets plus missing E_T with b identification in 9.7 fb^{-1} of $p\overline{p}$ collisions at E_{cm} = 1.96 TeV. The search is mainly sensitive to $H^0 W \to b\overline{b}\ell\nu$, $H^0 \to WW^{(*)} \to \ell\nu q\overline{q}$, and $H^0 V \to VWW^{(*)} \to \ell\nu q\overline{q}q\overline{q}$ ($V = W, Z$). A limit on cross section times branching ratio which corresponds to (1.3–11.4) times the expected Standard Model cross section is given in the range m_{H^0} = 90–200 GeV at 95% CL. The limit for m_{H^0} = 125 GeV is 5.8, where 4.7 is expected for no signal. In the Standard Model with an additional generation of heavy quarks and leptons which receive their masses via the Higgs mechanism, m_{H^0} values between 150 and 188 GeV are excluded at 95% CL.

[18] ABAZOV 13J search for H^0 production in the final states $ee\mu$, $e\mu\mu$, $\mu\tau\tau$, and $e^{\pm}\mu^{\pm}$ in 8.6–9.7 fb^{-1} of $p\overline{p}$ collisions at E_{cm} = 1.96 TeV. The search is sensitive to WH^0, ZH^0 and gluon fusion production with $H^0 \to WW^{(*)}$, $ZZ^{(*)}$, decaying to leptonic final states, and to WH^0, ZH^0 production with $H^0 \to \tau^+\tau^-$. A limit on cross section times branching ratio which corresponds to (4.4–12.7) times the expected Standard Model cross section is given in the range m_{H^0} = 100–200 GeV at 95% CL. The limit for m_{H^0} = 125 GeV is 8.4, where 6.3 is expected for no signal.

[19] ABAZOV 13K search for associated $H^0 Z$ production in the final states $\ell\ell bb$ with b identification in 9.7 fb^{-1} of $p\overline{p}$ collisions at E_{cm} = 1.96 TeV. A limit on cross section times branching ratio which corresponds to (1.8–53) times the expected Standard Model cross section is given for m_{H^0} = 90–150 GeV at 95% CL. The limit for m_{H^0} = 125 GeV is 7.1, where 5.1 is expected for no signal.

[20] CHATRCHYAN 13AL search for $H^0 \to \tau^+\tau^-$, $WW^{(*)}$, and $ZZ^{(*)}$ in 5.1 fb^{-1} and 5.3 fb^{-1} of pp collisions at E_{cm} = 7 and 8 TeV. In the Standard Model with an additional generation of heavy quarks and leptons which receive their masses via the Higgs mechanism, m_{H^0} values between 110 and 600 GeV are excluded at 99% CL.

[21] CHATRCHYAN 13BK search for $H^0 \to Z\gamma \to \ell\ell\gamma$ in 5.0 fb^{-1} of pp collisions at E_{cm} = 7 TeV and 19.6 fb^{-1} at E_{cm} = 8 TeV. A limit on cross section times branching ratio which corresponds to (4–25) times the expected Standard Model cross section is given in the range m_{H^0} = 120–160 GeV at 95% CL. The limit for m_{H^0} = 125 GeV is 9.5, where 10 is expected for no signal.

[22] CHATRCHYAN 13X search for $H^0 t\overline{t}$ production followed by $H^0 \to b\overline{b}$, one top decaying to $\ell\nu$ and the other to either $\ell\nu$ or $q\overline{q}$ in 5.0 fb^{-1} and 5.1 fb^{-1} of pp collisions at E_{cm} = 7 and 8 TeV. A limit on cross section times branching ratio which corresponds to (4.0–8.6) times the expected Standard Model cross section is given for m_{H^0} = 110–140 GeV at 95% CL. The limit for m_{H^0} = 125 GeV is 5.8, where 5.2 is expected for no signal.

[23] CHATRCHYAN 13Y search for H^0 production in the decay $H \to \gamma\gamma$ in 5.1 fb^{-1} of pp collisions at E_{cm} = 7 TeV and 5.3 fb^{-1} at E_{cm} = 8 TeV. The expected exclusion region for no signal is 110–144 GeV at 95% CL.

[24] CHATRCHYAN 13Y search for H^0 production in the decay $H \to ZZ^* \to 4\ell$ in 5.0 fb^{-1} of pp collisions at E_{cm} = 7 TeV and 5.3 fb^{-1} at E_{cm} = 8 TeV. The expected exclusion region for no signal is 120–180 GeV at 95% CL.

[25] CHATRCHYAN 13Y search for H^0 production in the decay $H \to WW^* \to \ell\nu\ell\nu$ in 4.9 fb^{-1} of pp collisions at E_{cm} = 7 TeV and 5.3 fb^{-1} at E_{cm} = 8 TeV. The expected exclusion region for no signal is 122–160 GeV at 95% CL.

[26] AAD 12 search for H^0 production with $H \to ZZ \to \ell^+\ell^- q\overline{q}$ in 1.04 fb^{-1} of pp collisions at E_{cm} = 7 TeV. A limit on cross section times branching ratio which is (1.7–13) times larger than the expected Standard Model cross section is given for m_{H^0} = 200–600 GeV at 95% CL. The best limit is at m_{H^0} = 360 GeV. Superseded by AAD 12CA.

[27] AAD 12AJ search for H^0 production in the decay $H^0 \to WW^{(*)} \to \ell\nu\ell\nu$ with 4.7 fb^{-1} of pp collisions at E_{cm} = 7 TeV. A limit on cross section times branching ratio which corresponds to (0.2–10) times the expected Standard Model cross section is given for m_{H^0} = 110–600 GeV at 95% CL.

[28] AAD 12BD search for H^0 production in the decay modes $H^0 \to \gamma\gamma$, $WW^{(*)}$, $ZZ^{(*)}$, $\tau^+\tau^-$, and $b\overline{b}$ with 4.6 to 4.9 fb^{-1} of pp collisions at E_{cm} = 7 TeV. The 99% CL excluded range is 130.7–506 GeV. A limit on cross section times branching ratio which corresponds to (0.2–2) times the expected Standard Model cross section is given for m_{H^0} = 110–600 GeV at 95% CL. An excess of events over background with a local significance of 2.9 σ is observed at about m_{H^0} = 126 GeV. Superseded by AAD 12AI.

[29] AAD 12BU search for H^0 production in the decay $H \to \tau^+\tau^-$ with 4.7 fb^{-1} of pp collisions at E_{cm} = 7 TeV. A limit on cross section times branching ratio which is (2.9–11.7) times larger than the expected Standard Model cross section is given for m_{H^0} = 100–150 GeV at 95% CL.

[30] AAD 12BZ search for H^0 production in the decay $H \to ZZ \to \ell^+\ell^-\nu\overline{\nu}$ with 4.7 fb^{-1} of pp collisions at E_{cm} = 7 TeV. A limit on cross section times branching ratio which corresponds to (0.2–4) times the expected Standard Model cross section is given for m_{H^0} = 200–600 GeV at 95% CL.

[31] AAD 12CA search for H^0 production in the decay $H \to ZZ \to \ell^+\ell^- q\overline{q}$ with 4.7 fb^{-1} of pp collisions at E_{cm} = 7 TeV. A limit on cross section times branching ratio which corresponds to (0.7–9) times the expected Standard Model cross section is given for m_{H^0} = 200–600 GeV at 95% CL.

[32] AAD 12CN search for associated $H^0 W$ and $H^0 Z$ production in the channels $W \to \ell\nu$, $Z \to \ell^+\ell^-$, $\nu\overline{\nu}$, and $H^0 \to b\overline{b}$, with 4.7 fb^{-1} of pp collisions at E_{cm} = 7 TeV. A limit on cross section times branching ratio which is (2.5–5.5) times larger than the expected Standard Model cross section is given for m_{H^0} = 110–130 GeV at 95% CL.

[33] AAD 12CO search for H^0 production in the decay $H \to WW \to \ell\nu q\overline{q}$ with 4.7 fb^{-1} of pp collisions at E_{cm} = 7 TeV. A limit on cross section times branching ratio which is (1.9–10) times larger than the expected Standard Model cross section is given for m_{H^0} = 300–600 GeV at 95% CL.

[34] AAD 12D search for H^0 production with $H \to ZZ^{(*)} \to 4\ell$ in 4.8 fb^{-1} of pp collisions at E_{cm} = 7 TeV in the mass range m_{H^0} = 110–600 GeV. An excess of events over background with a local significance of 2.1 σ is observed at 125 GeV.

[35] AAD 12E combine data from AAD 11V, AAD 11AB, AAD 12, AAD 12D, AAD 12F, AAD 12G. The 99% CL exclusion range is 133–230 and 260–437 GeV. An excess of events over background with a local significance of 3.5 σ is observed at about m_{H^0} = 126 GeV. Superseded by AAD 12AI.

[36] AAD 12F search for H^0 production with $H \to WW^{(*)} \to \ell^+\nu\ell^-\overline{\nu}$ in 2.05 fb^{-1} of pp collisions at E_{cm} = 7 TeV in the mass range m_{H^0} = 110–300 GeV. Superseded by AAD 12AJ.

[37] AAD 12G search for H^0 production with $H \to \gamma\gamma$ in 4.9 fb^{-1} of pp collisions at E_{cm} = 7 TeV in the mass range m_{H^0} = 110–150 GeV. An excess of events over background with a local significance of 2.8 σ is observed at 126.5 GeV.

[38] AALTONEN 12 search for $H^0 \to \gamma\gamma$ in 7.0 fb^{-1} of $p\overline{p}$ collisions at E_{cm} = 1.96 TeV. A limit on cross section times branching ratio which is (8.5–29) times larger than the expected Standard Model cross section is given for m_{H^0} = 100–150 GeV at 95% CL. Superseded by AALTONEN 12AN.

[39] AALTONEN 12AA search for associated $H^0 W$ production in the final state $H^0 \to b\overline{b}$, $W \to \ell\nu$ with 5.6 fb^{-1} of $p\overline{p}$ collisions at E_{cm} = 1.96 TeV. A limit on cross section times branching ratio which is (2.1–35.3) times larger than the expected Standard Model cross section is given for m_{H^0} = 100–150 GeV at 95% CL. Superseded by AALTONEN 12AE.

[40] AALTONEN 12AE search for associated $H^0 W$ production in the final state $H^0 \to b\overline{b}$, $W \to \ell\nu$ with 7.5 fb^{-1} of $p\overline{p}$ collisions at E_{cm} = 1.96 TeV. A limit on cross section times branching ratio which is (1.1–34.4) times larger than the expected Standard Model cross section is given for m_{H^0} = 100–150 GeV at 95% CL. The limit for m_{H^0} = 125 GeV is 4.4, where 3.7 is expected. Superseded by AALTONEN 12R.

[41] AALTONEN 12AK search for associated $H^0 t\overline{t}$ production in the decay chain $t\overline{t} \to WWbb \to \ell\nu qqbb$ with 9.45 fb^{-1} of $p\overline{p}$ collisions at E_{cm} = 1.96 TeV. A limit on cross section times branching ratio which is (10–40) times larger than the expected Standard Model cross section is given for m_{H^0} = 100–150 GeV at 95% CL. The limit for m_{H^0} = 125 GeV is 20.5, where 12.6 is expected.

[42] AALTONEN 12AM search for H^0 production in inclusive four-lepton final states coming from $H^0 \to ZZ$, $H^0 Z \to WW^{(*)}\ell\ell$, or $H^0 Z \to \tau\tau\ell\ell$, with 9.7 fb^{-1} of $p\overline{p}$ collisions at E_{cm} = 1.96 TeV. A limit on cross section times branching ratio which is (7.2–42.4) times larger than the expected Standard Model cross section is given for m_{H^0} = 120–300 GeV at 95% CL. The best limit is for m_{H^0} = 200 GeV.

[43] AALTONEN 12AN search for H^0 production in the decay $H^0 \to \gamma\gamma$ with 10 fb^{-1} of $p\overline{p}$ collisions at E_{cm} = 1.96 TeV. A limit on cross section times branching ratio which is (7.7–21.3) times larger than the expected Standard Model cross section is given for m_{H^0} = 100–150 GeV at 95% CL. The limit for m_{H^0} = 125 GeV is 17.0, where 9.9 is expected.

[44] AALTONEN 12H search for associated $H^0 Z$ production in the final state $Z \to \ell^+\ell^-$, $H^0 \to b\overline{b}$ with 7.9 fb^{-1} of $p\overline{p}$ collisions at E_{cm} = 1.96 TeV. A limit on cross section times branching ratio which is (2.8–22) times larger than the expected Standard Model cross section is given for m_{H^0} = 100–150 GeV at 95% CL. The best limit is for m_{H^0} = 100 GeV. Superseded by AALTONEN 12Q.

[45] AALTONEN 12J search for H^0 production in the decay $H^0 \to \tau^+\tau^-$ (one leptonic, the other hadronic) with 6.0 fb^{-1} of $p\overline{p}$ collisions at E_{cm} = 1.96 TeV. A limit on cross section times branching ratio which is (14.6–70.2) times larger than the expected Standard Model cross section is given for m_{H^0} = 100–150 GeV at 95% CL. The best limit is for m_{H^0} = 120 GeV.

[46] AALTONEN 12P combine AALTONEN 12Q, AALTONEN 12R, and AALTONEN 12S. An excess of events over background is observed in the region m_{H^0} = 100–150 GeV, with a local significance of 2.7 σ for m_{H^0} = 125 GeV. This corresponds to $(\sigma(H^0 W) + \sigma(H^0 Z))\cdot B(H^0 \to b\overline{b}) = (291^{+118}_{-113})$ fb. Superseded by AALTONEN 13L.

[47] AALTONEN 12Q search for associated $H^0 Z$ production in the final state $H^0 \to b\overline{b}$, $Z \to \ell^+\ell^-$ with 9.45 fb^{-1} of $p\overline{p}$ collisions at $E_{cm} = 1.96$ TeV. A limit on cross section times branching ratio which corresponds to (1.0–37.5) times the expected Standard Model cross section is given for $m_{H^0} = 90$–150 GeV at 95% CL. The limit for $m_{H^0} = 125$ GeV is 7.1, where 3.9 is expected. A broad excess of events for $m_{H^0} > 110$ GeV is observed, with a local significance of 2.4 σ at $m_{H^0} = 135$ GeV.

[48] AALTONEN 12R search for associated $H^0 W$ production in the final state $H^0 \to b\overline{b}$, $W \to \ell\nu$ with 9.45 fb^{-1} of $p\overline{p}$ collisions at $E_{cm} = 1.96$ TeV. A limit on cross section times branching ratio which is (1.4–21.7) times larger than the expected Standard Model cross section is given for $m_{H^0} = 90$–150 GeV at 95% CL. The limit for $m_{H^0} = 125$ GeV is 4.9, where 2.8 is expected. Superseded by AALTONEN 13B.

[49] AALTONEN 12S search for associated $H^0 Z$ production in the final state $H^0 \to b\overline{b}$, $Z \to \nu\overline{\nu}$, and $H^0 W$ production in $H^0 \to b\overline{b}$, $W \to \ell\nu$ (ℓ not identified) with 9.45 fb^{-1} of $p\overline{p}$ collisions at $E_{cm} = 1.96$ TeV. A limit on cross section times branching ratio which is (1.7–27.2) times larger than the expected Standard Model cross section is given for $m_{H^0} = 90$–150 GeV at 95% CL. The limit for $m_{H^0} = 125$ GeV is 6.7, where 3.6 is expected. Superseded by AALTONEN 13B.

[50] AALTONEN 12T combine AALTONEN 12Q, AALTONEN 12R, AALTONEN 12S, ABAZOV 12O, ABAZOV 12P, and ABAZOV 12K. An excess of events over background is observed which is most significant in the region $m_{H^0} = 120$–135 GeV, with a local significance of up to 3.3 σ. The local significance at $m_{H^0} = 125$ GeV is 2.8 σ, which corresponds to $(\sigma(H^0 W) + \sigma(H^0 Z))\ \mathrm{B}(H^0 \to b\overline{b})) = (0.23^{+0.09}_{-0.08})$ pb, compared to the Standard Model expectation at $m_{H^0} = 125$ GeV of 0.12 ± 0.01 pb.

[51] AALTONEN 12Y search for associated $H^0 W$ production in the final state $H^0 \to b\overline{b}$, $W \to \ell\nu$ with 2.7 fb^{-1} of $p\overline{p}$ collisions at $E_{cm} = 1.96$ TeV. A limit on cross section times branching ratio which is (3.6–61.1) times larger than the expected Standard Model cross section is given for $m_{H^0} = 100$–150 GeV at 95% CL. Superseded by AALTONEN 12AA.

[52] ABAZOV 12J search for H^0 and associated $H^0 W$, $H^0 Z$ production, in the final state including a τ and e/μ with 7.3 fb^{-1} of $p\overline{p}$ collisions at $E_{cm} = 1.96$ TeV. A limit on cross section times branching ratio which is (6.8–29.9) times larger than the expected Standard Model cross section is given for $m_{H^0} = 105$–200 GeV at 95% CL. The limit for $m_{H^0} = 125$ GeV is 15.7, where 12.8 is expected. Superseded by ABAZOV 13F.

[53] ABAZOV 12K search for associated $H^0 Z$ production in the final state $H^0 \to b\overline{b}$, $Z \to \nu\overline{\nu}$, and $H^0 W$ production with $W \to \ell\nu$ (ℓ not identified) with 9.5 fb^{-1} of $p\overline{p}$ collisions at $E_{cm} = 1.96$ TeV. A limit on cross section times branching ratio which is (1.9–16.8) times larger than the expected Standard Model cross section is given for $m_{H^0} = 100$–150 GeV at 95% CL. The limit for $m_{H^0} = 125$ GeV is 4.3, where 3.9 is expected.

[54] ABAZOV 12N combine ABAZOV 12O, ABAZOV 12P, and ABAZOV 12K. A limit on cross section times branching ratio which corresponds to (0.94–14) times the expected Standard Model cross section is given for $m_{H^0} = 100$–150 GeV at 95% CL. An excess of events over background is observed in the region $m_{H^0} = 120$–145 GeV with a local significance of 1.0–1.7 σ. Superseded by ABAZOV 13L.

[55] ABAZOV 12O search for associated $H^0 Z$ production in the final state $H^0 \to b\overline{b}$, $Z \to \ell^+\ell^-$ with 9.7 fb^{-1} of $p\overline{p}$ collisions at $E_{cm} = 1.96$ TeV. A limit on cross section times branching ratio which is (1.8–53) times larger than the expected Standard Model cross section is given for $m_{H^0} = 90$–150 GeV at 95% CL. The limit for $m_{H^0} = 125$ GeV is 7.1, where 5.1 is expected. Superseded by ABAZOV 13K.

[56] ABAZOV 12P search for associated $H^0 W$ production in the final state $H^0 \to b\overline{b}$, $W \to \ell\nu$ with 9.7 fb^{-1} of $p\overline{p}$ collisions at $E_{cm} = 1.96$ TeV. A limit on cross section times branching ratio which is (2.6–21.8) times larger than the expected Standard Model cross section is given for $m_{H^0} = 100$–150 GeV at 95% CL. The limit for $m_{H^0} = 125$ GeV is 5.2, where 4.7 is expected. Superseded by ABAZOV 13I.

[57] ABAZOV 12V search for associated $H^0 W$ production in the final state $H^0 \to b\overline{b}$, $W \to \ell\nu$ with 5.3 fb^{-1} of $p\overline{p}$ collisions at $E_{cm} = 1.96$ TeV. A limit on cross section times branching ratio which is (2.7–30.4) times larger than the expected Standard Model cross section is given for $m_{H^0} = 100$–150 GeV at 95% CL. The limit for $m_{H^0} = 125$ GeV is 6.6, where 6.8 is expected. Superseded by ABAZOV 12P.

[58] ABAZOV 12W search for H^0 production in the decay $H^0 \to WW^{(*)} \to \ell\nu\ell\nu$ with 8.6 fb^{-1} of $p\overline{p}$ collisions at $E_{cm} = 1.96$ TeV. A limit on cross section times branching ratio which is (1.1–13.3) times larger than the expected Standard Model cross section is given for $m_{H^0} = 115$–200 GeV at 95% CL. The best limit is at $m_{H^0} = 160$ GeV. The limit for $m_{H^0} = 125$ GeV is 5.0, where 3.8 is expected. Superseded by ABAZOV 13G.

[59] CHATRCHYAN 12AY search for associated $H^0 W$ and $H^0 Z$ production in the channels $W \to \ell\nu$, $Z \to \ell^+\ell^-$, and $H^0 \to \tau\tau$, $WW^{(*)}$, with 5 fb^{-1} of pp collisions at $E_{cm} = 7$ TeV. A limit on cross section times branching ratio which is (3.1–9.1) times larger than the expected Standard Model cross section is given for $m_{H^0} = 110$–200 GeV at 95% CL.

[60] CHATRCHYAN 12AY combine CHATRCHYAN 12F and CHATRCHYAN 12AO in addition and give a limit on cross section times branching ratio which is (2.1–3.7) times larger than the expected Standard Model cross section for $m_{H^0} = 110$–170 GeV at 95% CL. The limit for $m_{H^0} = 125$ GeV is 3.3.

[61] CHATRCHYAN 12B combine CHATRCHYAN 12E, CHATRCHYAN 12F, CHATRCHYAN 12G, CHATRCHYAN 12H, CHATRCHYAN 12I, CHATRCHYAN 12C, CHATRCHYAN 12D, as well as a search in the decay mode $H^0 \to \tau\tau$. The 99% CL exclusion range is 129–525 GeV. An excess of events over background with a local significance of 3.1 σ is observed at about $m_{H^0} = 124$ GeV. Superseded by CHATRCHYAN 12N and CHATRCHYAN 13Q.

[62] CHATRCHYAN 12C search for H^0 production with $H \to ZZ \to \ell^+\ell^-\tau^+\tau^-$ in 4.7 fb^{-1} of pp collisions at $E_{cm} = 7$ TeV. A limit on cross section times branching ratio which is (4–12) times larger than the expected Standard Model cross section is given for $m_{H^0} = 190$–600 GeV at 95% CL. The best limit is at $m_{H^0} = 200$ GeV.

[63] CHATRCHYAN 12D search for H^0 production with $H \to ZZ^{(*)} \to \ell^+\ell^- q\overline{q}$ in 4.6 fb^{-1} of pp collisions at $E_{cm} = 7$ TeV. A limit on cross section times branching ratio which corresponds to (1–22) times the expected Standard Model cross section is given for $m_{H^0} = 130$–164 GeV, 200–600 GeV at 95% CL. The best limit is at $m_{H^0} = 230$ GeV. In the Standard Model with an additional generation of heavy quarks and leptons which receive their masses via the Higgs mechanism, m_{H^0} values in the ranges $m_{H^0} = 154$–161 GeV and 200–470 GeV are excluded at 95% CL.

[64] CHATRCHYAN 12E search for H^0 production with $H \to WW^{(*)} \to \ell^+\nu\ell^-\overline{\nu}$ in 4.6 fb^{-1} of pp collisions at $E_{cm} = 7$ TeV in the mass range $m_{H^0} = 110$–600 GeV.

[65] CHATRCHYAN 12F search for associated $H^0 W$ and $H^0 Z$ production followed by $W \to \ell\nu$, $Z \to \ell^+\ell^-$, $\nu\overline{\nu}$, and $H^0 \to b\overline{b}$, in 4.7 fb^{-1} of pp collisions at $E_{cm} = 7$ TeV. A limit on cross section times branching ratio which is (3.1–9.0) times larger than the expected Standard Model cross section is given for $m_{H^0} = 110$–135 GeV at 95% CL. The best limit is at $m_{H^0} = 110$ GeV.

[66] CHATRCHYAN 12G search for H^0 production with $H \to \gamma\gamma$ in 4.8 fb^{-1} of pp collisions at $E_{cm} = 7$ TeV in the mass range $m_{H^0} = 110$–150 GeV. An excess of events over background with a local significance of 3.1 σ is observed at 124 GeV.

[67] CHATRCHYAN 12H search for H^0 production with $H \to ZZ^{(*)} \to 4\ell$ in 4.7 fb^{-1} of pp collisions at $E_{cm} = 7$ TeV in the mass range $m_{H^0} = 110$–600 GeV. Excesses of events over background are observed around 119, 126 and 320 GeV. The region $m_{H^0} = 114.4$–134 GeV remains consistent with the expectation for the production of a SM-like Higgs boson.

[68] CHATRCHYAN 12I search for H^0 production with $H \to ZZ \to \ell^+\ell^-\nu\overline{\nu}$ in 4.6 fb^{-1} of pp collisions at $E_{cm} = 7$ TeV in the mass range $m_{H^0} = 250$–600 GeV.

[69] CHATRCHYAN 12K search for H^0 production in the decay $H \to \tau^+\tau^-$ with 4.6 fb^{-1} of pp collisions at $E_{cm} = 7$ TeV. A limit on cross section times branching ratio which is (3.2–7.0) times larger than the expected Standard Model cross section is given for $m_{H^0} = 110$–145 GeV at 95% CL.

[70] AAD 11AB search for H^0 production with $H \to W^+W^- \to \ell\nu q\overline{q}$ in 1.04 fb^{-1} of pp collisions at $E_{cm} = 7$ TeV. A limit on cross section times branching ratio which is (2.7–20) times larger than the expected Standard Model cross section is given for $m_{H^0} = 240$–600 GeV at 95% CL. The best limit is at $m_{H^0} = 400$ GeV. Superseded by AAD 12CO.

[71] AAD 11V search for H^0 production with $H \to ZZ \to \ell^+\ell^-\nu\overline{\nu}$ in 1.04 fb^{-1} of pp collisions at $E_{cm} = 7$ TeV. A limit on cross section times branching ratio which corresponds to (0.6–6) times the expected Standard Model cross section is given for $m_{H^0} = 200$–600 GeV at 95% CL. Superseded by AAD 12BZ.

[72] AAD 11W search for Higgs boson production in the decay channels $\gamma\gamma$, $ZZ^{(*)} \to 4\ell$, $ZZ \to \ell\ell\nu\nu$, $ZZ \to \ell\ell qq$, $WW^{(*)} \to \ell\ell\nu\nu$, $WW^{(*)} \to \ell\nu qq$ in 35–40 pb^{-1} of pp collisions at $E_{cm} = 7$ TeV. A limit on cross section times branching ratio which is (2–40) times larger than the expected Standard Model cross section is given for $m_{H^0} = 110$–600 GeV at 95% CL. In the Standard Model with an additional generation of heavy quarks and leptons which receive their masses via the Higgs mechanism, m_{H^0} values between 140 and 185 GeV are excluded at 95% CL. The results for the Standard Model Higgs are superseded by AAD 12E.

[73] AALTONEN 11AA search in 4.0 fb^{-1} of $p\overline{p}$ collisions at $E_{cm} = 1.96$ TeV for associated $H^0 W$ and $H^0 Z$ production followed by $W/Z \to q\overline{q}$, and for $p\overline{p} \to H^0 q\overline{q}X$ (vector boson fusion), both with $H^0 \to b\overline{b}$. A limit on cross section times branching ratio which is (9–100) times larger than the expected Standard Model cross section is given for $m_{H^0} = 100$–150 GeV at 95% CL. The best limit is at $m_{H^0} = 115$ GeV. Superseded by AALTONEN 13C.

[74] ABAZOV 11AB search for associated $H^0 W$ and $H^0 Z$ production followed by $H^0 \to WW^{(*)}$ in like-sign dilepton final states using 5.3 fb^{-1} of $p\overline{p}$ collisions at $E_{cm} = 1.96$ TeV. A limit on cross section times branching ratio which is (6.4–18) times larger than the expected Standard Model cross section is given for $m_{H^0} = 115$–200 GeV at 95% CL. The best limit is for $m_{H^0} = 135$ and 165 GeV. Superseded by ABAZOV 13J.

[75] ABAZOV 11G search for H^0 production in 5.4 fb^{-1} of $p\overline{p}$ collisions at $E_{cm} = 1.96$ TeV in the decay mode $H^0 \to WW^{(*)} \to \ell\nu q\overline{q}'$ (and processes with similar final states). A limit on cross section times branching ratio which is (3.9–37) times larger than the expected Standard Model cross section is given for $m_{H^0} = 115$–200 GeV at 95% CL. The best limit is at $m_{H^0} = 160$ GeV.

[76] ABAZOV 11J search for associated $H^0 W$ production in 5.3 fb^{-1} of $p\overline{p}$ collisions at $E_{cm} = 1.96$ TeV in the final state $H^0 \to b\overline{b}$, $W \to \ell\nu$. A limit on cross section times branching ratio which is (2.7–30) times larger than the expected Standard Model cross section is given for $m_{H^0} = 100$–150 GeV at 95% CL. The limit at $m_{H^0} = 115$ GeV is 4.5 times larger than the expected Standard Model cross section. Superseded by ABAZOV 12P.

[77] ABAZOV 11Y search for $H^0 \to \gamma\gamma$ in 8.2 fb^{-1} of $p\overline{p}$ collisions at $E_{cm} = 1.96$ TeV. A limit on cross section times branching ratio which is (10–25) times larger than the expected Standard Model cross section is given for $m_{H^0} = 100$–150 GeV at 95% CL. Superseded by ABAZOV 13H.

[78] CHATRCHYAN 11J search for H^0 production with $H \to W^+W^- \to \ell\ell\nu\nu$ in 36 pb^{-1} of pp collisions at $E_{cm} = 7$ TeV. See their Fig. 6 for a limit on cross section times branching ratio for $m_{H^0} = 120$–600 GeV at 95% CL. In the Standard Model with an additional generation of heavy quarks and leptons which receive their masses via the Higgs mechanism, m_{H^0} values between 144 and 207 GeV are excluded at 95% CL.

[79] AALTONEN 10AD search for associated $H^0 Z$ production in 4.1 fb^{-1} of $p\overline{p}$ collisions at $E_{cm} = 1.96$ TeV in the decay mode $H^0 \to b\overline{b}$, $Z \to \ell^+\ell^-$. A limit $\sigma \cdot \mathrm{B}(H^0 \to b\overline{b}) <$ (4.5–43) $\sigma \cdot \mathrm{B}_{(SM)}$ (95% CL) is given for $m_{H^0} = 100$–150 GeV. The limit for $m_{H^0} = 115$ GeV is 5.9 times larger than the expected Standard Model cross section. Superseded by AALTONEN 12H.

[80] AALTONEN 10F combine searches for H^0 decaying to W^+W^- in $p\overline{p}$ collisions at $E_{cm} = 1.96$ TeV with 4.8 fb^{-1} (CDF) and 5.4 fb^{-1} (DØ).

[81] AALTONEN 10G search for H^0 production in 4.8 fb^{-1} of $p\overline{p}$ collisions at $E_{cm} = 1.96$ TeV in the decay mode $H^0 \to WW^{(*)}$. A limit on $\sigma(H^0)$ which is (1.3–39) times larger than the expected Standard Model cross section is given for $m_{H^0} = 110$–200 GeV at 95% CL. The best limit is obtained for $m_{H^0} = 165$ GeV. Superseded by AALTONEN 13K.

[82] AALTONEN 10J search for associated $H^0 W$ and $H^0 Z$ production in 2.1 fb^{-1} of $p\overline{p}$ collisions at $E_{cm} = 1.96$ TeV in the final state with (b) jets and missing p_T. A limit $\sigma <$ (5.8–50) σ_{SM} (95% CL) is given for $m_{H^0} = 110$–150 GeV. The limit for $m_{H^0} = 115$ GeV is 6.9 times larger than the expected Standard Model cross section. Superseded by AALTONEN 12S.

[83] AALTONEN 10M combine searches for H^0 decaying to W^+W^- in $p\overline{p}$ collisions at $E_{cm} = 1.96$ TeV with 4.8 fb^{-1} (CDF) and 5.4 fb^{-1} (DØ) and derive limits $\sigma(p\overline{p} \to H^0) \cdot \mathrm{B}(H^0 \to W^+W^-) <$ (1.75–0.38) pb for $m_H = 120$–165 GeV, where H^0 is produced

in gg fusion. In the Standard Model with an additional generation of heavy quarks, m_{H^0} between 131 and 204 GeV is excluded at 95% CL.

[84] ABAZOV 10B search for H^0 production in 5.4 fb^{-1} of $p\overline{p}$ collisions at $E_{cm} = 1.96$ TeV in the decay mode $H^0 \to WW^{(*)}$. A limit on $\sigma(H^0)$ which is (1.6–21) times larger than the expected Standard Model cross section is given for $m_{H^0} = 115$–200 GeV at 95% CL. The best limit is obtained for $m_{H^0} = 165$ GeV. Superseded by ABAZOV 12W.

[85] ABAZOV 10C search for associated H^0Z and H^0W production in 5.2 fb^{-1} of $p\overline{p}$ collisions at $E_{cm} = 1.96$ TeV in the final states $H^0 \to b\overline{b}$, $Z \to \nu\overline{\nu}$, and $W \to (\ell)\nu$, where ℓ is not identified. A limit $\sigma \cdot B(H^0 \to b\overline{b}) <$ (3.4–38) $\sigma \cdot B_{(SM)}$ (95% CL) is given for $m_{H^0} = 100$–150 GeV. The limit for $m_{H^0} = 115$ GeV is 3.7 times larger than the expected Standard Model cross section. Superseded by ABAZOV 12K.

[86] ABAZOV 10T search for associated H^0Z production in 4.2 fb^{-1} of $p\overline{p}$ collisions at E_{cm} = 1.96 TeV in the decay mode $H^0 \to b\overline{b}$, $Z \to \ell^+\ell^-$. A limit $\sigma \cdot B(H^0 \to b\overline{b}) <$ (3.0–49) $\sigma \cdot B_{(SM)}$ (95% CL) is given for $m_{H^0} = 100$–150 GeV. The limit for $m_{H^0} =$ 115 GeV is 5.9 times larger than the expected Standard Model cross section. Superseded by ABAZOV 12O.

[87] AALTONEN 09A search for H^0 production in $p\overline{p}$ collisions at E_{cm} =1.96 TeV in the decay mode $H^0 \to WW^{(*)} \to \ell^+\ell^-\nu\overline{\nu}$. A limit on $\sigma(H^0) \cdot B(H^0 \to WW^{(*)})$ between 0.7 and 2.5 pb (95% CL) is given for $m_{H^0} = 110$–200 GeV, which is 1.7–45 times larger than the expected Standard Model cross section. The best limit is obtained for $m_{H^0} = 160$ GeV.

[88] AALTONEN 09AI search for associated H^0W production in 2.7 fb^{-1} of $p\overline{p}$ collisions at $E_{cm} = 1.96$ TeV in the decay mode $H^0 \to b\overline{b}$, $W \to \ell\nu$. A limit on $\sigma(H^0W) \cdot B(H^0 \to b\overline{b})$ (95% CL) is given for $m_{H^0} = 100$–150 GeV, which is 3.3–75.5 times larger than the expected Standard Model cross section. The limit for $m_{H^0} = 115$ GeV is 5.6 times larger than the expected Standard Model cross section. Superseded by AALTONEN 12AA.

[89] ABAZOV 09U search for $H^0 \to \tau^+\tau^-$ with $\tau \to$ hadrons in 1 fb^{-1} of $p\overline{p}$ collisions at $E_{cm} = 1.96$ TeV. The production mechanisms include associated $W/Z+H^0$ production, weak boson fusion, and gluon fusion. A limit (95% CL) is given for $m_{H^0} = 105$–145 GeV, which is 20–82 times larger than the expected Standard Model cross section. The limit for $m_{H^0} = 115$ GeV is 29 times larger than the expected Standard Model cross section.

[90] ABAZOV 08Y search for associated H^0W production in $p\overline{p}$ collisions at $E_{cm} = 1.96$ TeV in the decay mode $H^0 \to b\overline{b}$, $W \to \ell\nu$. A limit $\sigma(H^0W) \cdot B(H^0 \to b\overline{b}) <$ (1.9–1.6) pb (95% CL) is given for $m_{H^0} = 105$–145 GeV, which is 10–93 times larger than the expected Standard Model cross section. These results are combined with ABAZOV 06, ABAZOV 06O, ABAZOV 06Q, and ABAZOV 07X to give cross section limits for $m_{H^0} = 100$–200 GeV which are 6–24 times larger than the Standard Model expectation. Superseded by ABAZOV 12N.

[91] ABAZOV 06 search for Higgs boson production in $p\overline{p}$ collisions at $E_{cm} = 1.96$ TeV with the decay chain $H^0 \to WW^* \to \ell^\pm\nu\ell'^\mp\overline{\nu}$. A limit $\sigma(H^0) \cdot B(H^0 \to WW^*) <$ (5.6–3.2) pb (95 %CL) is given for $m_{H^0} = 120$–200 GeV, which far exceeds the expected Standard Model cross section.

[92] ABAZOV 06O search for associated H^0W production in $p\overline{p}$ collisions at $E_{cm} = 1.96$ TeV with the decay $H^0 \to WW^*$, in the final states $\ell^\pm\ell'^\mp\nu\nu'X$ where $\ell = e$, μ. A limit $\sigma(H^0W) \cdot B(H^0 \to WW^*) <$ (3.2–2.8) pb (95 %CL) is given for $m_{H^0} =$ 115–175 GeV, which far exceeds the expected Standard Model cross section.

Indirect Mass Limits for H^0 from Electroweak Analysis

The mass limits shown below apply to a Higgs boson H^0 with Standard Model couplings whose mass is a priori unknown.

For limits obtained before the direct measurement of the top quark mass, see the 1996 (Physical Review **D54** 1 (1996)) Edition of this Review. Other studies based on data available prior to 1996 can be found in the 1998 Edition (The European Physical Journal **C3** 1 (1998)) of this Review.

VALUE (GeV)	*DOCUMENT ID*		*TECN*
$\mathbf{94^{+25}_{-22}}$	[1] BAAK	12A	RVUE
• • • We do not use the following data for averages, fits, limits, etc. • • •			
91^{+30}_{-23}	[2] BAAK	12	RVUE
91^{+31}_{-24}	[3] ERLER	10A	RVUE
80^{+30}_{-23}	[4] FLACHER	09	RVUE
129^{+74}_{-49}	[5] LEP-SLC	06	RVUE

[1] BAAK 12A make Standard Model fits to Z and neutral current parameters, m_t, m_W, and Γ_W measurements available in 2012 (using also preliminary data). The quoted result is obtained from a fit that does not include the measured mass value of the signal observed at the LHC and also no limits from direct Higgs searches.

[2] BAAK 12 make Standard Model fits to Z and neutral current parameters, m_t, m_W, and Γ_W measurements available in 2010 (using also preliminary data). The quoted result is obtained from a fit that does not include the limit from the direct Higgs searches. The result including direct search data from LEP2, the Tevatron and the LHC is 120^{+12}_{-5} GeV.

[3] ERLER 10A makes Standard Model fits to Z and neutral current parameters, m_t, m_W measurements available in 2009 (using also preliminary data). The quoted result is obtained from a fit that does not include the limits from the direct Higgs searches. With direct search data from LEP2 and Tevatron added to the fit, the 90% CL (99% CL) interval is 115–148 (114–197) GeV.

[4] FLACHER 09 make Standard Model fits to Z and neutral current parameters, m_t, m_W, and Γ_W measurements available in 2008 (using also preliminary data). The 2σ (3σ) interval is 39–155 (26–209) GeV. The quoted results are obtained from a fit that does not include the limit from the direct Higgs searches. Superseded by BAAK 12.

[5] LEP-SLC 06 make Standard Model fits to Z parameters from LEP/SLC and m_t, m_W, and Γ_W measurements available in 2005 with $\Delta\alpha^{(5)}_{had}(m_Z) = 0.02758 \pm 0.00035$. The 95% CL limit is 285 GeV.

SEARCHES FOR NEUTRAL HIGGS BOSONS REFERENCES

AAD	13AG	PL B721 32	G. Aad *et al.* (ATLAS Collab.)
AAD	13AT	NJP 15 043009	G. Aad *et al.* (ATLAS Collab.)
AAD	13O	JHEP 1302 095	G. Aad *et al.* (ATLAS Collab.)
AAIJ	13T	JHEP 1305 132	R. Aaij *et al.* (LHCb Collab.)
AALTONEN	13B	PR D87 052008	T. Aaltonen *et al.* (CDF Collab.)
AALTONEN	13C	JHEP 1302 004	T. Aaltonen *et al.* (CDF Collab.)
AALTONEN	13K	PR D88 052012	T. Aaltonen *et al.* (CDF Collab.)
AALTONEN	13L	PR D88 052013	T. Aaltonen *et al.* (CDF Collab.)
AALTONEN	13M	PR D88 052014	T. Aaltonen *et al.* (CDF and D0 Collab.)
AALTONEN	13P	PRL 110 121801	T. Aaltonen *et al.* (CDF Collab.)
ABAZOV	13E	PR D88 032008	V.M. Abazov *et al.* (D0 Collab.)
ABAZOV	13F	PR D88 052005	V.M. Abazov *et al.* (D0 Collab.)
ABAZOV	13G	PR D88 052006	V.M. Abazov *et al.* (D0 Collab.)
ABAZOV	13H	PR D88 052007	V.M. Abazov *et al.* (D0 Collab.)
ABAZOV	13I	PR D88 052008	V.M. Abazov *et al.* (D0 Collab.)
ABAZOV	13J	PR D88 052009	V.M. Abazov *et al.* (D0 Collab.)
ABAZOV	13K	PR D88 052010	V.M. Abazov *et al.* (D0 Collab.)
ABAZOV	13L	PR D88 052011	V.M. Abazov *et al.* (D0 Collab.)
CARENA	13	EPJ C73 2552	M. Carena *et al.*
CHATRCHYAN	13AG	PL B722 207	S. Chatrchyan *et al.* (CMS Collab.)
CHATRCHYAN	13AL	PL B725 36	S. Chatrchyan *et al.* (CMS Collab.)
CHATRCHYAN	13BJ	PL B726 564	S. Chatrchyan *et al.* (CMS Collab.)
CHATRCHYAN	13BK	PL B726 587	S. Chatrchyan *et al.* (CMS Collab.)
CHATRCHYAN	13Q	EPJ C73 2469	S. Chatrchyan *et al.* (CMS Collab.)
CHATRCHYAN	13X	JHEP 1305 145	S. Chatrchyan *et al.* (CMS Collab.)
CHATRCHYAN	13Y	JHEP 1306 081	S. Chatrchyan *et al.* (CMS Collab.)
LEES	13C	PR D87 031102	J.P. Lees *et al.* (BABAR Collab.)
LEES	13L	PR D88 031701	J.P. Lees *et al.* (BABAR Collab.)
LEES	13R	PR D88 071102	J.P. Lees *et al.* (BABAR Collab.)
AAD	12	PL B707 27	G. Aad *et al.* (ATLAS Collab.)
AAD	12AI	PL B716 1	G. Aad *et al.* (ATLAS Collab.)
AAD	12AJ	PL B716 62	G. Aad *et al.* (ATLAS Collab.)
AAD	12AQ	PRL 108 251801	G. Aad *et al.* (ATLAS Collab.)
AAD	12BD	PR D86 032003	G. Aad *et al.* (ATLAS Collab.)
AAD	12BU	JHEP 1209 070	G. Aad *et al.* (ATLAS Collab.)
AAD	12BZ	PL B717 29	G. Aad *et al.* (ATLAS Collab.)
AAD	12CA	PL B717 70	G. Aad *et al.* (ATLAS Collab.)
AAD	12CN	PL B718 369	G. Aad *et al.* (ATLAS Collab.)
AAD	12CO	PL B718 391	G. Aad *et al.* (ATLAS Collab.)
AAD	12D	PL B710 383	G. Aad *et al.* (ATLAS Collab.)
AAD	12E	PL B710 49	G. Aad *et al.* (ATLAS Collab.)
AAD	12F	PRL 108 111802	G. Aad *et al.* (ATLAS Collab.)
AAD	12G	PRL 108 111803	G. Aad *et al.* (ATLAS Collab.)
AAD	12N	EPJ C72 2157	G. Aad *et al.* (ATLAS Collab.)
AALTONEN	12	PRL 108 011801	T. Aaltonen *et al.* (CDF Collab.)
AALTONEN	12AA	PR D85 072001	T. Aaltonen *et al.* (CDF Collab.)
AALTONEN	12AB	PR D85 092001	T. Aaltonen *et al.* (CDF Collab.)
AALTONEN	12AE	PR D86 032011	T. Aaltonen *et al.* (CDF Collab.)
AALTONEN	12AK	PRL 109 181802	T. Aaltonen *et al.* (CDF Collab.)
AALTONEN	12AM	PR D86 072012	T. Aaltonen *et al.* (CDF Collab.)
AALTONEN	12AN	PL B717 173	T. Aaltonen *et al.* (CDF Collab.)
AALTONEN	12AQ	PR D86 091101	T. Aaltonen *et al.* (CDF and D0 Collabs.)
AALTONEN	12H	PL B715 98	T. Aaltonen *et al.* (CDF Collab.)
AALTONEN	12J	PRL 108 181804	T. Aaltonen *et al.* (CDF Collab.)
AALTONEN	12P	PRL 109 111802	T. Aaltonen *et al.* (CDF Collab.)
AALTONEN	12Q	PRL 109 111803	T. Aaltonen *et al.* (CDF Collab.)
AALTONEN	12R	PRL 109 111804	T. Aaltonen *et al.* (CDF Collab.)
AALTONEN	12S	PRL 109 111805	T. Aaltonen *et al.* (CDF Collab.)
AALTONEN	12T	PRL 109 071804	T. Aaltonen *et al.* (CDF and D0 Collab.)
AALTONEN	12U	PR D85 012007	T. Aaltonen *et al.* (CDF Collab.)
AALTONEN	12X	PR D85 032005	T. Aaltonen *et al.* (CDF Collab.)
AALTONEN	12Y	PR D85 052002	T. Aaltonen *et al.* (CDF Collab.)
ABAZOV	12	PL B707 323	V.M. Abazov *et al.* (D0 Collab.)
ABAZOV	12G	PL B710 569	V.M. Abazov *et al.* (D0 Collab.)
ABAZOV	12J	PL B714 237	V.M. Abazov *et al.* (D0 Collab.)
ABAZOV	12K	PL B716 285	V.M. Abazov *et al.* (D0 Collab.)
ABAZOV	12N	PRL 109 121802	V.M. Abazov *et al.* (D0 Collab.)
ABAZOV	12O	PRL 109 121803	V.M. Abazov *et al.* (D0 Collab.)
ABAZOV	12P	PRL 109 121804	V.M. Abazov *et al.* (D0 Collab.)
ABAZOV	12V	PR D86 032005	V.M. Abazov *et al.* (D0 Collab.)
ABAZOV	12W	PR D86 032010	V.M. Abazov *et al.* (D0 Collab.)
BAAK	12	EPJ C72 2003	M. Baak *et al.* (Gfitter Group)
BAAK	12A	EPJ C72 2205	M. Baak *et al.* (Gfitter Group)
CHATRCHYAN	12AO	JHEP 1209 111	S. Chatrchyan *et al.* (CMS Collab.)
CHATRCHYAN	12AY	JHEP 1211 088	S. Chatrchyan *et al.* (CMS Collab.)
CHATRCHYAN	12B	PL B710 26	S. Chatrchyan *et al.* (CMS Collab.)
CHATRCHYAN	12C	JHEP 1203 081	S. Chatrchyan *et al.* (CMS Collab.)
CHATRCHYAN	12D	JHEP 1204 036	S. Chatrchyan *et al.* (CMS Collab.)
CHATRCHYAN	12E	PL B710 91	S. Chatrchyan *et al.* (CMS Collab.)
CHATRCHYAN	12F	PL B710 284	S. Chatrchyan *et al.* (CMS Collab.)
CHATRCHYAN	12G	PL B710 403	S. Chatrchyan *et al.* (CMS Collab.)
CHATRCHYAN	12H	PRL 108 111804	S. Chatrchyan *et al.* (CMS Collab.)
CHATRCHYAN	12I	JHEP 1203 040	S. Chatrchyan *et al.* (CMS Collab.)
CHATRCHYAN	12K	PL B713 68	S. Chatrchyan *et al.* (CMS Collab.)
CHATRCHYAN	12N	PL B716 30	S. Chatrchyan *et al.* (CMS Collab.)
CHATRCHYAN	12V	PRL 109 121801	S. Chatrchyan *et al.* (CMS Collab.)
AAD	11AB	PRL 107 231801	G. Aad *et al.* (ATLAS Collab.)
AAD	11R	PL B705 174	G. Aad *et al.* (ATLAS Collab.)
AAD	11V	PRL 107 221802	G. Aad *et al.* (ATLAS Collab.)
AAD	11W	EPJ C71 1728	G. Aad *et al.* (ATLAS Collab.)
AALTONEN	11AA	PR D84 052010	T. Aaltonen *et al.* (CDF Collab.)
AALTONEN	11P	PRL 107 031801	T. Aaltonen *et al.* (CDF Collab.)
ABAZOV	11AB	PR D84 092002	V.M. Abazov *et al.* (D0 Collab.)
ABAZOV	11G	PRL 106 171802	V.M. Abazov *et al.* (D0 Collab.)
ABAZOV	11J	PL B698 6	V.M. Abazov *et al.* (D0 Collab.)
ABAZOV	11K	PL B698 97	V.M. Abazov *et al.* (D0 Collab.)
ABAZOV	11W	PRL 107 121801	V.M. Abazov *et al.* (D0 Collab.)
ABAZOV	11Y	PRL 107 151801	V.M. Abazov *et al.* (D0 Collab.)
ABOUZAID	11A	PRL 107 201803	E. Abouzaid *et al.* (KTeV Collab.)
CHATRCHYAN	11H	PRL 106 231801	S. Chatrchyan *et al.* (CMS Collab.)
CHATRCHYAN	11J	PL B699 25	S. Chatrchyan *et al.* (CMS Collab.)
DEL-AMO-SA...	11J	PRL 107 021804	P. del Amo Sanchez *et al.* (BABAR Collb.)
LEES	11H	PRL 107 221803	J.P. Lees *et al.* (BABAR Collab.)
AALTONEN	10AD	PRL 105 251802	T. Aaltonen *et al.* (CDF Collab.)
AALTONEN	10F	PRL 104 061802	T. Aaltonen *et al.* (CDF and D0 Collab.)
AALTONEN	10G	PRL 104 061803	T. Aaltonen *et al.* (CDF Collab.)
AALTONEN	10J	PRL 104 141801	T. Aaltonen *et al.* (CDF Collab.)
AALTONEN	10M	PR D82 011102	T. Aaltonen *et al.* (CDF and D0 Collab.)
ABAZOV	10B	PRL 104 061804	V.M. Abazov *et al.* (D0 Collab.)
ABAZOV	10C	PRL 104 071801	V.M. Abazov *et al.* (D0 Collab.)
ABAZOV	10T	PRL 105 251801	V.M. Abazov *et al.* (D0 Collab.)
ABBIENDI	10	PL B682 381	G. Abbiendi *et al.* (OPAL Collab.)
ANDREAS	10	JHEP 1008 003	S. Andreas *et al.* (DESY)
ERLER	10A	PR D81 051301	J. Erler (UNAM)
HYUN	10	PRL 105 091801	H.J. Hyun *et al.* (BELLE Collab.)
SCHAEL	10	JHEP 1005 049	S. Schael *et al.* (ALEPH Collab.)
AALTONEN	09A	PRL 102 021802	T. Aaltonen *et al.* (CDF Collab.)
AALTONEN	09AB	PRL 103 061803	T. Aaltonen *et al.* (CDF Collab.)
AALTONEN	09AI	PRL 103 101802	T. Aaltonen *et al.* (CDF Collab.)
AALTONEN	09AR	PRL 103 201801	T. Aaltonen *et al.* (CDF Collab.)

ABAZOV 09U PRL 102 251801 V.M. Abazov *et al.* (D0 Collab.)
ABAZOV 09V PRL 103 061801 V.M. Abazov *et al.* (D0 Collab.)
AUBERT 09P PRL 103 181801 B. Aubert *et al.* (BABAR Collab.)
AUBERT 09Z PRL 103 081803 B. Aubert *et al.* (BABAR Collab.)
FLACHER 09 EPJ C60 543 H. Flacher *et al.* (CERN, DESY, HAMB)
TUNG 09 PRL 102 051802 Y.C. Tung *et al.* (KEK E391a Collab.)
ABAZOV 08U PRL 101 051801 V.M. Abazov *et al.* (D0 Collab.)
ABAZOV 08W PRL 101 071804 V.M. Abazov *et al.* (D0 Collab.)
ABAZOV 08Y PL B663 26 V.M. Abazov *et al.* (D0 Collab.)
ABDALLAH 08B EPJ C54 1 J. Abdallah *et al.* (DELPHI Collab.)
Also EPJ C56 165 (errat) J. Abdallah *et al.* (DELPHI Collab.)
LOVE 08 PRL 101 151802 W. Love *et al.* (CLEO Collab.)
ABAZOV 07X PL B655 209 V.M. Abazov *et al.* (D0 Collab.)
ABBIENDI 07 EPJ C49 457 G. Abbiendi *et al.* (OPAL Collab.)
BESSON 07 PRL 98 052002 D. Besson *et al.* (CLEO Collab.)
SCHAEL 07 EPJ C49 439 S. Schael *et al.* (ALEPH Collab.)
ABAZOV 06 PRL 96 011801 V.M. Abazov *et al.* (D0 Collab.)
ABAZOV 06O PRL 97 151804 V.M. Abazov *et al.* (D0 Collab.)
ABAZOV 06Q PRL 97 161803 V.M. Abazov *et al.* (D0 Collab.)
LEP-SLC 06 PRPL 427 257 ALEPH, DELPHI, L3, OPAL, SLD and working groups
SCHAEL 06B EPJ C47 547 S. Schael *et al.* (LEP Collabs.)
ABBIENDI 05A EPJ C40 317 G. Abbiendi *et al.* (OPAL Collab.)
ABDALLAH 05D EPJ C44 147 J. Abdallah *et al.* (DELPHI Collab.)
ACHARD 05 PL B609 35 P. Achard *et al.* (L3 Collab.)
ACOSTA 05Q PR D72 072004 D. Acosta *et al.* (CDF Collab.)
PARK 05 PRL 94 021801 H.K. Park *et al.* (FNAL HyperCP Collab.)
ABBIENDI 04K PL B597 11 G. Abbiendi *et al.* (OPAL Collab.)
ABBIENDI 04M EPJ C37 49 G. Abbiendi *et al.* (OPAL Collab.)
ABDALLAH 04 EPJ C32 145 J. Abdallah *et al.* (DELPHI Collab.)
ABDALLAH 04B EPJ C32 475 J. Abdallah *et al.* (DELPHI Collab.)
ABDALLAH 04L EPJ C35 313 J. Abdallah *et al.* (DELPHI Collab.)
ABDALLAH 04O EPJ C38 1 J. Abdallah *et al.* (DELPHI Collab.)
ACHARD 04B PL B583 14 P. Achard *et al.* (L3 Collab.)
ACHARD 04F PL B589 89 P. Achard *et al.* (L3 Collab.)
ABBIENDI 03B EPJ C26 479 G. Abbiendi *et al.* (OPAL Collab.)
ABBIENDI 03F EPJ C27 311 G. Abbiendi *et al.* (OPAL Collab.)
ABBIENDI 03G EPJ C27 483 G. Abbiendi *et al.* (OPAL Collab.)
ACHARD 03C PL B568 191 P. Achard *et al.* (L3 Collab.)
CARENA 03 EPJ C26 601 M.S. Carena *et al.*
HEISTER 03D PL B565 61 A. Heister *et al.* (ALEPH, DELPHI, L3+)
ALEPH, DELPHI, L3, OPAL, LEP Higgs Working Group
ABBIENDI 02D EPJ C23 397 G. Abbiendi *et al.* (OPAL Collab.)
ABBIENDI 02F PL B544 44 G. Abbiendi *et al.* (OPAL Collab.)
ACHARD 02C PL B534 28 P. Achard *et al.* (L3 Collab.)
ACHARD 02H PL B545 30 P. Achard *et al.* (L3 Collab.)
AKEROYD 02 PR D66 037702 A.G. Akeroyd *et al.*
HEISTER 02 PL B526 191 A. Heister *et al.* (ALEPH Collab.)
HEISTER 02L PL B544 16 A. Heister *et al.* (ALEPH Collab.)
HEISTER 02M PL B544 25 A. Heister *et al.* (ALEPH Collab.)
ABBIENDI 01E EPJ C18 425 G. Abbiendi *et al.* (OPAL Collab.)
ABREU 01F PL B507 89 P. Abreu *et al.* (DELPHI Collab.)
ACHARD 01C PL B517 319 P. Achard *et al.* (L3 Collab.)
AFFOLDER 01H PR D64 092002 T. Affolder *et al.* (CDF Collab.)
BARATE 01C PL B499 53 R. Barate *et al.* (ALEPH Collab.)
ACCIARRI 00M PL B485 85 M. Acciarri *et al.* (L3 Collab.)
ACCIARRI 00R PL B489 102 M. Acciarri *et al.* (L3 Collab.)
ACCIARRI 00S PL B489 115 M. Acciarri *et al.* (L3 Collab.)
BARATE 00L PL B487 241 R. Barate *et al.* (ALEPH Collab.)
ABBIENDI 99E EPJ C7 407 G. Abbiendi *et al.* (OPAL Collab.)
ABBIENDI 99O PL B464 311 G. Abbiendi *et al.* (OPAL Collab.)
ABBOTT 99B PRL 82 2244 B. Abbott *et al.* (D0 Collab.)
ABREU 99P PL B458 431 P. Abreu *et al.* (DELPHI Collab.)
CARENA 99B hep-ph/9912223 M.S. Carena *et al.*
CERN-TH/99-374
ABBOTT 98 PRL 80 442 B. Abbott *et al.* (D0 Collab.)
ACKERSTAFF 98S EPJ C5 19 K. Ackerstaff *et al.* (OPAL Collab.)
ACKERSTAFF 98Y PL B437 218 K. Ackerstaff *et al.* (OPAL Collab.)
GONZALEZ-G... 98B PR D57 7045 M.C. Gonzalez-Garcia, S.M. Lietti, S.F. Novaes
PDG 98 EPJ C3 1 C. Caso *et al.* (PDG Collab.)
KRAWCZYK 97 PR D55 6968 M. Krawczyk, J. Zochowski (WARS)
ALEXANDER 96H ZPHY C71 1 G. Alexander *et al.* (OPAL Collab.)
PDG 96 PR D54 1 R. M. Barnett *et al.* (PDG Collab.)
ABREU 95H ZPHY C67 69 P. Abreu *et al.* (DELPHI Collab.)
BALEST 95 PR D51 2053 R. Balest *et al.* (CLEO Collab.)
PICH 92 NP B388 31 A. Pich, J. Prades, P. Yepes (CERN, CPPM)
ANTREASYAN 90C PL B251 204 D. Antreasyan *et al.* (Crystal Ball Collab.)

Charged Higgs Bosons ($H^{\pm}$ & $H^{\pm\pm}$), Searches for

CONTENTS:

$H^{\pm}$ (Charged Higgs) MASS LIMITS

Unless otherwise stated, the limits below assume $B(H^+ \to \tau^+\nu)+B(H^+ \to c\overline{s})=1$, and hold for all values of $B(H^+ \to \tau^+\nu_\tau)$, and assume H^+ weak isospin of $T_3=+1/2$. In the following, $\tan\beta$ is the ratio of the two vacuum expectation values in two-doublet models (2HDM).

The limits are also applicable to point-like technipions. For a discussion of techniparticles, see the Review of Dynamical Electroweak Symmetry Breaking in this Review.

For limits obtained in hadronic collisions before the observation of the top quark, and based on the top mass values inconsistent with the current measurements, see the 1996 (Physical Review **D54** 1 (1996)) Edition of this Review.

Searches in e^+e^- collisions at and above the Z pole have conclusively ruled out the existence of a charged Higgs in the region $m_{H^+} \lesssim 45$ GeV, and are meanwhile superseded by the searches in higher energy e^+e^- collisions at LEP. Results that are by now obsolete are therefore not included in this compilation, and can be found in a previous Edition (The European Physical Journal **C15** 1 (2000)) of this Review.

In the following, and unless otherwise stated, results from the LEP experiments (ALEPH, DELPHI, L3, and OPAL) are assumed to derive from the study of the $e^+e^- \to H^+H^-$ process. Limits from $b \to s\gamma$ decays are usually stronger in generic 2HDM models than in Supersymmetric models.

VALUE (GeV)	*CL%*	*DOCUMENT ID*		*TECN*	*COMMENT*
> 80	95	[1] LEP	13	LEP	$e^+e^- \to H^+H^-, E_{cm} \leq$ 209GeV
> 76.3	95	[2] ABBIENDI	12	OPAL	$e^+e^- \to H^+H^-, E_{cm} \leq$ 209GeV
> 74.4	95	ABDALLAH	04I	DLPH	$E_{cm} \leq 209$ GeV
> 76.5	95	ACHARD	03E	L3	$E_{cm} \leq 209$ GeV
> 79.3	95	HEISTER	02P	ALEP	$E_{cm} \leq 209$ GeV
• • • We do not use the following data for averages, fits, limits, etc. • • •					
		[3] AAD	13AC	ATLS	$t \to bH^+$
		[4] AAD	13V	ATLS	$t \to bH^+$, lepton non-universality
		[5] AAD	12BH	ATLS	$t \to bH^+$
		[6] CHATRCHYAN	12AA	CMS	$t \to bH^+$
		[7] AALTONEN	11P	CDF	$t \to bH^+, H^+ \to W^+A^0$
>316	95	[8] DESCHAMPS	10	RVUE	Type II, flavor physics data
		[9] AALTONEN	09AJ	CDF	$t \to bH^+$
		[10] ABAZOV	09AC	D0	$t \to bH^+$
		[11] ABAZOV	09AG	D0	$t \to bH^+$
		[12] ABAZOV	09AI	D0	$t \to bH^+$
		[13] ABAZOV	09P	D0	$H^+ \to t\overline{b}$
>240	95	[14] FLACHER	09	RVUE	Type II, flavor physics data
		[15] ABULENCIA	06E	CDF	$t \to bH^+$
> 92.0	95	ABBIENDI	04	OPAL	$B(\tau\nu) = 1$
> 76.7	95	[16] ABDALLAH	04I	DLPH	Type I
		[17] ABBIENDI	03	OPAL	$\tau \to \mu\overline{\nu}\nu, e\overline{\nu}\nu$
		[18] ABAZOV	02B	D0	$t \to bH^+, H \to \tau\nu$
		[19] BORZUMATI	02	RVUE	
		[20] ABBIENDI	01Q	OPAL	$B \to \tau\nu_\tau X$
		[21] BARATE	01E	ALEP	$B \to \tau\nu_\tau$
>315	99	[22] GAMBINO	01	RVUE	$b \to s\gamma$
		[23] AFFOLDER	00I	CDF	$t \to bH^+, H \to \tau\nu$
> 59.5	95	ABBIENDI	99E	OPAL	$E_{cm} \leq 183$ GeV
		[24] ABBOTT	99E	D0	$t \to bH^+$
		[25] ACKERSTAFF	99D	OPAL	$\tau \to e\nu\nu, \mu\nu\nu$
		[26] ACCIARRI	97F	L3	$B \to \tau\nu_\tau$
		[27] AMMAR	97B	CLEO	$\tau \to \mu\nu\nu$
		[28] COARASA	97	RVUE	$B \to \tau\nu_\tau X$
		[29] GUCHAIT	97	RVUE	$t \to bH^+, H \to \tau\nu$
		[30] MANGANO	97	RVUE	$B_{u(c)} \to \tau\nu_\tau$
		[31] STAHL	97	RVUE	$\tau \to \mu\nu\nu$
>244	95	[32] ALAM	95	CLE2	$b \to s\gamma$
		[33] BUSKULIC	95	ALEP	$b \to \tau\nu_\tau X$

[1] The limit refers to the Type II scenario. The limit for $B(H^+ \to \tau\nu) = 1$ is 94 GeV (95% CL), and for $B(H^+ \to cs) = 1$ the region below 80.5 as well as the region 83–88 GeV is excluded (95% CL). LEP 13 also search for the decay mode $H^+ \to A^0W^*$ with $A^0 \to b\overline{b}$, which is not negligible in Type I models. The limit in Type I models is 72.5 GeV (95% CL) if $m_{A^0} > 12$ GeV.

[2] ABBIENDI 12 also search for the decay mode $H^+ \to A^0W^*$ with $A^0 \to b\overline{b}$.

[3] AAD 13AC search for $t\overline{t}$ production followed by $t \to bH^+$, $H^+ \to c\overline{s}$ (flavor unidentified) in 4.7 fb^{-1} of pp collisions at $E_{cm} = 7$ TeV. Upper limits on $B(t \to bH^+)$ between 0.05 and 0.01 (95%CL) are given for m_{H^+}=90–150 GeV and $B(H^+ \to c\overline{s})$=1.

[4] AAD 13V search for $t\overline{t}$ production followed by $t \to bH^+$, $H^+ \to \tau^+\nu$ through violation of lepton universality with 4.6 fb^{-1} of pp collisions at $E_{cm} = 7$ TeV. Upper limits on $B(t \to bH^+)$ between 0.032 and 0.044 (95% CL) are given for m_{H^+} = 90–140 GeV and $B(H^+ \to \tau^+\nu) = 1$. By combining with AAD 12BH, the limits improve to 0.008 to 0.034 for m_{H^+} = 90–160 GeV. See their Fig. 7 for the excluded region in the m_h^{max} scenario of the MSSM.

[5] AAD 12BH search for $t\overline{t}$ production followed by $t \to bH^+$, $H^+ \to \tau^+\nu$ with 4.6 fb^{-1} of pp collisions at $E_{cm} = 7$ TeV. Upper limits on $B(t \to bH^+)$ between 0.01 and 0.05 (95% CL) are given for m_{H^+} = 90–160 GeV and $B(H^+ \to \tau^+\nu) = 1$. See their Fig. 8 for the excluded region in the m_h^{max} scenario of the MSSM.

[6] CHATRCHYAN 12AA search for $t\overline{t}$ production followed by $t \to bH^+$, $H^+ \to \tau^+\nu$ with 2 fb^{-1} of pp collisions at $E_{cm} = 7$ TeV. Upper limits on $B(t \to bH^+)$ between 0.019 and 0.041 (95% CL) are given for m_{H^+} = 80–160 GeV and $B(H^+ \to \tau^+\nu)$=1.

[7] AALTONEN 11P search in 2.7 fb^{-1} of $p\overline{p}$ collisions at $E_{cm} = 1.96$ TeV for the decay chain $t \to bH^+$, $H^+ \to W^+A^0$, $A^0 \to \tau^+\tau^-$ with m_{A^0} between 4 and 9 GeV. See their Fig. 4 for limits on $B(t \to bH^+)$ for $90 < m_{H^+} < 160$ GeV.

[8] DESCHAMPS 10 make Type II two Higgs doublet model fits to weak leptonic and semileptonic decays, $b \to s\gamma$, B, B_s mixings, and $Z \to b\overline{b}$. The limit holds irrespective of $\tan\beta$.

[9] AALTONEN 09AJ search for $t \to bH^+$, $H^+ \to c\overline{s}$ in $t\overline{t}$ events in 2.2 fb^{-1} of $p\overline{p}$ collisions at E_{cm} = 1.96 TeV. Upper limits on B($t \to bH^+$) between 0.08 and 0.32 (95% CL) are given for m_{H^+} = 60–150 GeV and B($H^+ \to c\overline{s}$) = 1.

[10] ABAZOV 09AC search for $t \to bH^+$, $H^+ \to \tau^+\nu$ in $t\overline{t}$ events in 0.9 fb^{-1} of $p\overline{p}$ collisions at E_{cm} = 1.96 TeV. Upper limits on B($t \to bH^+$) between 0.19 and 0.25 (95% CL) are given for m_{H^+} = 80–155 GeV and B($H^+ \to \tau^+\nu$) = 1. See their Fig. 4 for an excluded region in a MSSM scenario.

[11] ABAZOV 09AG measure $t\overline{t}$ cross sections in final states with ℓ + jets (ℓ = e, μ), $\ell\ell$, and $\tau\ell$ in 1 fb^{-1} of $p\overline{p}$ collisions at E_{cm} = 1.96 TeV, which constrains possible $t \to bH^+$ branching fractions. Upper limits (95% CL) on B($t \to bH^+$) between 0.15 and 0.40 (0.48 and 0.57) are given for B($H^+ \to \tau^+\nu$) = 1 (B($H^+ \to c\overline{s}$) = 1) for m_{H^+} = 80–155 GeV.

[12] ABAZOV 09AI search for $t \to bH^+$ in $t\overline{t}$ events in 1 fb^{-1} of $p\overline{p}$ collisions at E_{cm} = 1.96 TeV. Final states with ℓ + jets (ℓ = e, μ), $\ell\ell$, and $\tau\ell$ are examined. Upper limits on B($t \to bH^+$) (95% CL) between 0.15 and 0.19 (0.19 and 0.22) are given for B($H^+ \to \tau^+\nu$) = 1 (B($H^+ \to c\overline{s}$) = 1) for m_{H^+} = 80–155 GeV. For B($H^+ \to \tau^+\nu$) = 1 also a simultaneous extraction of B($t \to bH^+$) and the $t\overline{t}$ cross section is performed, yielding a limit on B($t \to bH^+$) between 0.12 and 0.26 for m_{H^+} = 80–155 GeV. See their Figs. 5–8 for excluded regions in several MSSM scenarios.

[13] ABAZOV 09P search for H^+ production by $q\overline{q}'$ annihilation followed by $H^+ \to t\overline{b}$ decay in 0.9 fb^{-1} of $p\overline{p}$ collisions at E_{cm} = 1.96 TeV. Cross section limits in several two-doublet models are given for m_{H^+} = 180–300 GeV. A region with 20 $\lesssim \tan\beta \lesssim$ 70 is excluded (95% CL) for 180 GeV $\lesssim m_{H^+} \lesssim$ 184 GeV in type-I models.

[14] FLACHER 09 make Type II two Higgs doublet model fits to weak leptonic and semileptonic decays, $b \to s\gamma$, and $Z \to b\overline{b}$. The limit holds irrespective of tanβ.

[15] ABULENCIA 06E search for associated H^0W production in $p\overline{p}$ collisions at E_{cm} = 1.96 TeV. A fit is made for $t\overline{t}$ production processes in dilepton, lepton + jets, and lepton + τ final states, with the decays $t \to W^+b$ and $t \to H^+b$ followed by $H^+ \to \tau^+\nu$, $c\overline{s}$, $t^*\overline{b}$, or W^+H^0. Within the MSSM the search is sensitive to the region tan$\beta < 1$ or > 30 in the mass range m_{H^+} = 80–160 GeV. See Fig. 2 for the excluded region in a certain MSSM scenario.

[16] ABDALLAH 04I search for $e^+e^- \to H^+H^-$ with $H^\pm$ decaying to $\tau\nu$, cs, or W^*A^0 in Type-I two-Higgs-doublet models.

[17] ABBIENDI 03 give a limit $m_{H^+} > 1.28\tan\beta$ GeV (95%CL) in Type II two-doublet models.

[18] ABAZOV 02B search for a charged Higgs boson in top decays with $H^+ \to \tau^+\nu$ at E_{cm}=1.8 TeV. For m_{H^+}=75 GeV, the region tan$\beta > 32.0$ is excluded at 95%CL. The excluded mass region extends to over 140 GeV for tanβ values above 100.

[19] BORZUMATI 02 point out that the decay modes such as $b\overline{b}W$, A^0W, and supersymmetric ones can have substantial branching fractions in the mass range explored at LEP II and Tevatron.

[20] ABBIENDI 01Q give a limit tan$\beta/m_{H^+} < 0.53$ GeV^{-1} (95%CL) in Type II two-doublet models.

[21] BARATE 01E give a limit tan$\beta/m_{H^+} < 0.40$ GeV^{-1} (90% CL) in Type II two-doublet models. An independent measurement of $B \to \tau\nu_\tau X$ gives tan$\beta/m_{H^+} < 0.49$ GeV^{-1} (90% CL).

[22] GAMBINO 01 use the world average data in the summer of 2001 B($b \to s\gamma$)= (3.23 ± 0.42) × 10^{-4}. The limit applies for Type-II two-doublet models.

[23] AFFOLDER 00I search for a charged Higgs boson in top decays with $H^+ \to \tau^+\nu$ in $p\overline{p}$ collisions at E_{cm}=1.8 TeV. The excluded mass region extends to over 120 GeV for tanβ values above 100 and B($\tau\nu$)=1. If B($t \to bH^+$) $\gtrsim$ 0.6, m_{H^+} up to 160 GeV is excluded. Updates ABE 97L.

[24] ABBOTT 99E search for a charged Higgs boson in top decays in $p\overline{p}$ collisions at E_{cm}=1.8 TeV, by comparing the observed $t\overline{t}$ cross section (extracted from the data assuming the dominant decay $t \to bW^+$) with theoretical expectation. The search is sensitive to regions of the domains tan$\beta \lesssim$1, 50 <m_{H^+}(GeV) $\lesssim$120 and tan$\beta \gtrsim$40, 50 <m_{H^+} (GeV) $\lesssim$160. See Fig. 3 for the details of the excluded region.

[25] ACKERSTAFF 99D measure the Michel parameters ρ, ξ, η, and $\xi\delta$ in leptonic τ decays from $Z \to \tau\tau$. Assuming e-μ universality, the limit $m_{H^+} > 0.97$ tanβ GeV (95%CL) is obtained for two-doublet models in which only one doublet couples to leptons.

[26] ACCIARRI 97F give a limit $m_{H^+} > 2.6$ tanβ GeV (90% CL) from their limit on the exclusive $B \to \tau\nu_\tau$ branching ratio.

[27] AMMAR 97B measure the Michel parameter ρ from $\tau \to e\nu\nu$ decays and assumes e/μ universality to extract the Michel η parameter from $\tau \to \mu\nu\nu$ decays. The measurement is translated to a lower limit on m_{H^+} in a two-doublet model $m_{H^+} > 0.97$ tanβ GeV (90% CL).

[28] COARASA 97 reanalyzed the constraint on the ($m_{H^\pm}$,tanβ) plane derived from the inclusive $B \to \tau\nu_\tau X$ branching ratio in GROSSMAN 95B and BUSKULIC 95. They show that the constraint is quite sensitive to supersymmetric one-loop effects.

[29] GUCHAIT 97 studies the constraints on m_{H^+} set by Tevatron data on $\ell\tau$ final states in $t\overline{t} \to (Wb)(Hb)$, $W \to \ell\nu$, $H \to \tau\nu_\tau$. See Fig. 2 for the excluded region.

[30] MANGANO 97 reconsiders the limit in ACCIARRI 97F including the effect of the potentially large $B_c \to \tau\nu_\tau$ background to $B_u \to \tau\nu_\tau$ decays. Stronger limits are obtained.

[31] STAHL 97 fit τ lifetime, leptonic branching ratios, and the Michel parameters and derive limit $m_{H^+} > 1.5$ tanβ GeV (90% CL) for a two-doublet model. See also STAHL 94.

[32] ALAM 95 measure the inclusive $b \to s\gamma$ branching ratio at $\Upsilon(4S)$ and give B($b \to s\gamma$)< 4.2×10^{-4} (95% CL), which translates to the limit m_{H^+} >[244 + 63/(tanβ)$^{1.3}$] GeV in the Type II two-doublet model. Light supersymmetric particles can invalidate this bound.

[33] BUSKULIC 95 give a limit $m_{H^+} > 1.9$ tanβ GeV (90% CL) for Type-II models from $b \to \tau\nu_\tau X$ branching ratio, as proposed in GROSSMAN 94.

MASS LIMITS for $H^{\pm\pm}$ (doubly-charged Higgs boson)

This section covers searches for a doubly-charged Higgs boson with couplings to lepton pairs. Its weak isospin T_3 is thus restricted to two possibilities depending on lepton chiralities: $T_3(H^{\pm\pm}) = \pm 1$, with the coupling $g_{\ell\ell}$ to $\ell_L^-\ell_L'^-$ and $\ell_R^+\ell_R'^+$ ("left-handed") and $T_3(H^{\pm\pm}) = 0$, with the coupling to $\ell_R^-\ell_R'^-$ and $\ell_L^+\ell_L'^+$ ("right-handed"). These Higgs bosons appear in some left-right symmetric models based on the gauge group $SU(2)_L \times SU(2)_R \times U(1)$. These two cases are listed separately in the following. Unless noted, one of the lepton flavor combinations is assumed to be dominant in the decay.

LIMITS for $H^{\pm\pm}$ with $T_3 = \pm 1$

VALUE (GeV)	CL%	DOCUMENT ID		TECN	COMMENT
>398	95	[1] AAD	12CQ	ATLS	$\mu\mu$
>375	95	[1] AAD	12CQ	ATLS	$e\mu$
>409	95	[1] AAD	12CQ	ATLS	ee
>169	95	[2] CHATRCHYAN	12AU	CMS	$\tau\tau$
>300	95	[2] CHATRCHYAN	12AU	CMS	$\mu\tau$
>293	95	[2] CHATRCHYAN	12AU	CMS	$e\tau$
>395	95	[2] CHATRCHYAN	12AU	CMS	$\mu\mu$
>391	95	[2] CHATRCHYAN	12AU	CMS	$e\mu$
>382	95	[2] CHATRCHYAN	12AU	CMS	ee
> 98.1	95	[3] ABDALLAH	03	DLPH	$\tau\tau$
> 99.0	95	[4] ABBIENDI	02C	OPAL	$\tau\tau$
• • • We do not use the following data for averages, fits, limits, etc. • • •					
>330	95	[5] AAD	13Y	ATLS	$\mu\mu$
>237	95	[5] AAD	13Y	ATLS	$\mu\tau$
>355	95	[6] AAD	12AY	ATLS	$\mu\mu$
>128	95	[7] ABAZOV	12A	D0	$\tau\tau$
>144	95	[7] ABAZOV	12A	D0	$\mu\tau$
>245	95	[8] AALTONEN	11AF	CDF	$\mu\mu$
>210	95	[8] AALTONEN	11AF	CDF	$e\mu$
>225	95	[8] AALTONEN	11AF	CDF	ee
>114	95	[9] AALTONEN	08AA	CDF	$e\tau$
>112	95	[9] AALTONEN	08AA	CDF	$\mu\tau$
>168	95	[10] ABAZOV	08V	D0	$\mu\mu$
		[11] AKTAS	06A	H1	single $H^{\pm\pm}$
>133	95	[12] ACOSTA	05L	CDF	stable
>118.4	95	[13] ABAZOV	04E	D0	$\mu\mu$
		[14] ABBIENDI	03Q	OPAL	$E_{cm} \leq 209$ GeV, single $H^{\pm\pm}$
		[15] GORDEEV	97	SPEC	muonium conversion
		[16] ASAKA	95	THEO	
> 45.6	95	[17] ACTON	92M	OPAL	
> 30.4	95	[18] ACTON	92M	OPAL	
none 6.5–36.6	95	[19] SWARTZ	90	MRK2	

[1] AAD 12CQ search for $H^{++}H^{--}$ production with 4.7 fb^{-1} of pp collisions at E_{cm} = 7 TeV. The limit assumes 100% branching ratio to the specified final state. See their Table 1 for limits assuming smaller branching ratios.

[2] CHATRCHYAN 12AU search for $H^{++}H^{--}$ production with 4.9 fb^{-1} of pp collisions at E_{cm} = 7 TeV. The limit assumes 100% branching ratio to the specified final state. See their Table 6 for limits including associated $H^{++}H^-$ production or assuming different scenarios.

[3] ABDALLAH 03 search for $H^{++}H^{--}$ pair production either followed by $H^{++} \to \tau^+\tau^+$, or decaying outside the detector.

[4] ABBIENDI 02C searches for pair production of $H^{++}H^{--}$, with $H^{\pm\pm} \to \ell^\pm\ell^\pm$ (ℓ,ℓ' = e,μ,τ). The limit holds for ℓ=ℓ'=τ, and becomes stronger for other combinations of leptonic final states. To ensure the decay within the detector, the limit only applies for $g(H\ell\ell) \gtrsim 10^{-7}$.

[5] AAD 13Y search for $H^{++}H^{--}$ production in a generic search of events with three charged leptons in 4.6 fb^{-1} of pp collisions at E_{cm} = 7 TeV. The limit assumes 100% branching ratio to the specified final state.

[6] AAD 12AY search for $H^{++}H^{--}$ production with 1.6 fb^{-1} of pp collisions at E_{cm} = 7 TeV. The limit assumes 100% branching ratio to the specified final state.

[7] ABAZOV 12A search for $H^{++}H^{--}$ production in 7.0 fb^{-1} of $p\overline{p}$ collisions at E_{cm} = 1.96 TeV.

[8] AALTONEN 11AF search for $H^{++}H^{--}$ production in 6.1 fb^{-1} of $p\overline{p}$ collisions at E_{cm} = 1.96 TeV.

[9] AALTONEN 08AA search for $H^{++}H^{--}$ production in $p\overline{p}$ collisions at E_{cm} = 1.96 TeV. The limit assumes 100% branching ratio to the specified final state.

[10] ABAZOV 08V search for $H^{++}H^{--}$ production in $p\overline{p}$ collisions at E_{cm}= 1.96 TeV. The limit is for B($H \to \mu\mu$) = 1. The limit is updated in ABAZOV 12A.

[11] AKTAS 06A search for single $H^{\pm\pm}$ production in ep collisions at HERA. Assuming that H^{++} only couples to $e^+\mu^+$ with $g_{e\mu}$ = 0.3 (electromagnetic strength), a limit $m_{H^{++}} > 141$ GeV (95% CL) is derived. For the case where H^{++} couples to $e\tau$ only the limit is 112 GeV.

[12] ACOSTA 05L search for $H^{++}H^{--}$ pair production in $p\overline{p}$ collisions. The limit is valid for $g_{\ell\ell'} < 10^{-8}$ so that the Higgs decays outside the detector.

[13] ABAZOV 04E search for $H^{++}H^{--}$ pair production in $H^{\pm\pm} \to \mu^\pm\mu^\pm$. The limit is valid for $g_{\mu\mu} \gtrsim 10^{-7}$.

[14] ABBIENDI 03Q searches for single $H^{\pm\pm}$ via direct production in $e^+e^- \to e^\mp e^\mp H^{\pm\pm}$, and via t-channel exchange in $e^+e^- \to e^+e^-$. In the direct case, and assuming B($H^{\pm\pm} \to \ell^\pm\ell^\pm$) = 1, a 95% CL limit on $h_{ee} < 0.071$ is set for $m_{H^{\pm\pm}} < 160$ GeV (see Fig. 6). In the second case, indirect limits on h_{ee} are set for $m_{H^{\pm\pm}} < 2$ TeV (see Fig. 8).

[15] GORDEEV 97 search for muonium-antimuonium conversion and find $G_{M\overline{M}}/G_F < 0.14$ (90% CL), where $G_{M\overline{M}}$ is the lepton-flavor violating effective four-fermion coupling. This limit may be converted to $m_{H^{++}} > 210$ GeV if the Yukawa couplings of H^{++} to ee and $\mu\mu$ are as large as the weak gauge coupling. For similar limits on muonium-antimuonium conversion, see the muon Particle Listings.

[16] ASAKA 95 point out that H^{++} decays dominantly to four fermions in a large region of parameter space where the limit of ACTON 92M from the search of dilepton modes does not apply.

[17] ACTON 92M limit assumes $H^{\pm\pm} \to \ell^{\pm}\ell^{\pm}$ or $H^{\pm\pm}$ does not decay in the detector. Thus the region $g_{\ell\ell} \approx 10^{-7}$ is not excluded.

[18] ACTON 92M from $\Delta\Gamma_Z$ <40 MeV.

[19] SWARTZ 90 assume $H^{\pm\pm} \to \ell^{\pm}\ell^{\pm}$ (any flavor). The limits are valid for the Higgs-lepton coupling $g(H\ell\ell) \gtrsim 7.4\times10^{-7}/[m_H/\text{GeV}]^{1/2}$. The limits improve somewhat for ee and $\mu\mu$ decay modes.

LIMITS for $H^{\pm\pm}$ with $T_3 = 0$

VALUE (GeV)	CL%	DOCUMENT ID		TECN	COMMENT
>306	95	[1] AAD	12CQ	ATLS	$\mu\mu$
>310	95	[1] AAD	12CQ	ATLS	$e\mu$
>322	95	[1] AAD	12CQ	ATLS	ee
> 97.3	95	[2] ABDALLAH	03	DLPH	$\tau\tau$
> 97.3	95	[3] ACHARD	03F	L3	$\tau\tau$
> 98.5	95	[4] ABBIENDI	02C	OPAL	$\tau\tau$
• • • We do not use the following data for averages, fits, limits, etc. • • •					
>251	95	[5] AAD	12AY	ATLS	$\mu\mu$
>113	95	[6] ABAZOV	12A	D0	$\mu\tau$
>205	95	[7] AALTONEN	11AF	CDF	$\mu\mu$
>190	95	[7] AALTONEN	11AF	CDF	$e\mu$
>205	95	[7] AALTONEN	11AF	CDF	ee
>145	95	[8] ABAZOV	08V	D0	$\mu\mu$
		[9] AKTAS	06A	H1	single $H^{\pm\pm}$
>109	95	[10] ACOSTA	05L	CDF	stable
> 98.2	95	[11] ABAZOV	04E	D0	$\mu\mu$
		[12] ABBIENDI	03Q	OPAL	$E_{\text{cm}} \le 209$ GeV, single $H^{\pm\pm}$
		[13] GORDEEV	97	SPEC	muonium conversion
> 45.6	95	[14] ACTON	92M	OPAL	
> 25.5	95	[15] ACTON	92M	OPAL	
none 7.3–34.3	95	[16] SWARTZ	90	MRK2	

[1] AAD 12CQ search for $H^{++}H^{--}$ production with 4.7 fb^{-1} of pp collisions at E_{cm} = 7 TeV. The limit assumes 100% branching ratio to the specified final state. See their Table 1 for limits assuming smaller branching ratios.

[2] ABDALLAH 03 search for $H^{++}H^{--}$ pair production either followed by $H^{++} \to \tau^+\tau^+$, or decaying outside the detector.

[3] ACHARD 03F search for $e^+e^- \to H^{++}H^{--}$ with $H^{\pm\pm} \to \ell^{\pm}\ell'^{\pm}$. The limit holds for $\ell = \ell' = \tau$, and slightly different limits apply for other flavor combinations. The limit is valid for $g_{\ell\ell'} \gtrsim 10^{-7}$.

[4] ABBIENDI 02C searches for pair production of $H^{++}H^{--}$, with $H^{\pm\pm} \to \ell^{\pm}\ell^{\pm}$ (ℓ,ℓ' = e,μ,τ). the limit holds for ℓ=ℓ'=τ, and becomes stronger for other combinations of leptonic final states. To ensure the decay within the detector, the limit only applies for $g(H\ell\ell) \gtrsim 10^{-7}$.

[5] AAD 12AY search for $H^{++}H^{--}$ production with 1.6 fb^{-1} of pp collisions at E_{cm} = 7 TeV. The limit assumes 100% branching ratio to the specified final state.

[6] ABAZOV 12A search for $H^{++}H^{--}$ production in 7.0 fb^{-1} of $p\overline{p}$ collisions at E_{cm} = 1.96 TeV.

[7] AALTONEN 11AF search for $H^{++}H^{--}$ production in 6.1 fb^{-1} of $p\overline{p}$ collisions at E_{cm} = 1.96 TeV.

[8] ABAZOV 08V search for $H^{++}H^{--}$ production in $p\overline{p}$ collisions at E_{cm}= 1.96 TeV. The limit is for B($H \to \mu\mu$) = 1. The limit is updated in ABAZOV 12A.

[9] AKTAS 06A search for single $H^{\pm\pm}$ production in ep collisions at HERA. Assuming that H^{++} only couples to $e^+\mu^+$ with $g_{e\mu} = 0.3$ (electromagnetic strength), a limit $m_{H^{++}} > 141$ GeV (95% CL) is derived. For the case where H^{++} couples to $e\tau$ only the limit is 112 GeV.

[10] ACOSTA 05L search for $H^{++}H^{--}$ pair production in $p\overline{p}$ collisions. The limit is valid for $g_{\ell\ell'} < 10^{-8}$ so that the Higgs decays outside the detector.

[11] ABAZOV 04E search for $H^{++}H^{--}$ pair production in $H^{\pm\pm} \to \mu^{\pm}\mu^{\pm}$. The limit is valid for $g_{\mu\mu} \gtrsim 10^{-7}$.

[12] ABBIENDI 03Q searches for single $H^{\pm\pm}$ via direct production in $e^+e^- \to e^{\mp}e^{\mp}H^{\pm\pm}$, and via t-channel exchange in $e^+e^- \to e^+e^-$. In the direct case, and assuming B($H^{\pm\pm} \to \ell^{\pm}\ell^{\pm}$) = 1, a 95% CL limit on $h_{ee} < 0.071$ is set for $m_{H^{\pm\pm}} < 160$ GeV (see Fig. 6). In the second case, indirect limits on h_{ee} are set for $m_{H^{\pm\pm}} < 2$ TeV (see Fig. 8).

[13] GORDEEV 97 search for muonium-antimuonium conversion and find $G_{M\overline{M}}/G_F < 0.14$ (90% CL), where $G_{M\overline{M}}$ is the lepton-flavor violating effective four-fermion coupling. This limit may be converted to $m_{H^{++}} > 210$ GeV if the Yukawa couplings of H^{++} to ee and $\mu\mu$ are as large as the weak gauge coupling. For similar limits on muonium-antimuonium conversion, see the muon Particle Listings.

[14] ACTON 92M limit assumes $H^{\pm\pm} \to \ell^{\pm}\ell^{\pm}$ or $H^{\pm\pm}$ does not decay in the detector. Thus the region $g_{\ell\ell} \approx 10^{-7}$ is not excluded.

[15] ACTON 92M from $\Delta\Gamma_Z$ <40 MeV.

[16] SWARTZ 90 assume $H^{\pm\pm} \to \ell^{\pm}\ell^{\pm}$ (any flavor). The limits are valid for the Higgs-lepton coupling $g(H\ell\ell) \gtrsim 7.4\times10^{-7}/[m_H/\text{GeV}]^{1/2}$. The limits improve somewhat for ee and $\mu\mu$ decay modes.

$H^{\pm}$ and $H^{\pm\pm}$ REFERENCES

AAD	13AC	EPJ C73 2465	G. Aad *et al.*	(ATLAS Collab.)
AAD	13V	JHEP 1303 076	G. Aad *et al.*	(ATLAS Collab.)
AAD	13Y	PR D87 052002	G. Aad *et al.*	(ATLAS Collab.)
LEP	13	EPJ C73 2463	LEP Collabs	(ALEPH, DELPHI, L3, OPAL, LEP)
AAD	12AY	PR D85 032004	G. Aad *et al.*	(ATLAS Collab.)
AAD	12BH	JHEP 1206 039	G. Aad *et al.*	(ATLAS Collab.)
AAD	12CQ	EPJ C72 2244	G. Aad *et al.*	(ATLAS Collab.)
ABAZOV	12A	PRL 108 021801	V.M. Abazov *et al.*	(D0 Collab.)
ABBIENDI	12	EPJ C72 2076	G. Abbiendi *et al.*	(OPAL Collab.)
CHATRCHYAN	12AA	JHEP 1207 143	S. Chatrchyan *et al.*	(CMS Collab.)
CHATRCHYAN	12AU	EPJ C72 2189	S. Chatrchyan *et al.*	(CMS Collab.)
AALTONEN	11AF	PRL 107 181801	T. Aaltonen *et al.*	(CDF Collab.)
AALTONEN	11P	PRL 107 031801	T. Aaltonen *et al.*	(CDF Collab.)
DESCHAMPS	10	PR D82 073012	O. Deschamps *et al.*	(CLER, ORSAY, LAPP)
AALTONEN	09AJ	PRL 103 101803	T. Aaltonen *et al.*	(CDF Collab.)
ABAZOV	09AC	PR D80 051107	V.M. Abazov *et al.*	(D0 Collab.)
ABAZOV	09AG	PR D80 071102	V.M. Abazov *et al.*	(D0 Collab.)
ABAZOV	09AI	PL B682 278	V.M. Abazov *et al.*	(D0 Collab.)
ABAZOV	09P	PRL 102 191802	V.M. Abazov *et al.*	(D0 Collab.)
FLACHER	09	EPJ C60 543	H. Flacher *et al.*	(CERN, DESY, HAMB)
AALTONEN	08AA	PRL 101 121801	T. Aaltonen *et al.*	(CDF Collab.)
ABAZOV	08V	PRL 101 071803	V.M. Abazov *et al.*	(D0 Collab.)
ABULENCIA	06E	PRL 96 042003	A. Abulencia *et al.*	(CDF Collab.)
AKTAS	06A	PL B638 432	A. Aktas *et al.*	(H1 Collab.)
ACOSTA	05L	PRL 95 071801	D. Acosta *et al.*	(CDF Collab.)
ABAZOV	04E	PRL 93 141801	V.M. Abazov *et al.*	(D0 Collab.)
ABBIENDI	04	EPJ C32 453	G. Abbiendi *et al.*	(OPAL Collab.)
ABDALLAH	04I	EPJ C34 399	J. Abdallah *et al.*	(DELPHI Collab.)
ABBIENDI	03	PL B551 35	G. Abbiendi *et al.*	(OPAL Collab.)
ABBIENDI	03Q	PL B577 93	G. Abbiendi *et al.*	(OPAL Collab.)
ABDALLAH	03	PL B552 127	J. Abdallah *et al.*	(DELPHI Collab.)
ACHARD	03E	PL B575 208	P. Achard *et al.*	(L3 Collab.)
ACHARD	03F	PL B576 18	P. Achard *et al.*	(L3 Collab.)
ABAZOV	02B	PRL 88 151803	V.M. Abazov *et al.*	(D0 Collab.)
ABBIENDI	02C	PL B526 221	G. Abbiendi *et al.*	(OPAL Collab.)
BORZUMATI	02	PL B549 170	F.M. Borzumati, A. Djouadi	
HEISTER	02P	PL B543 1	A. Heister *et al.*	(ALEPH Collab.)
ABBIENDI	01Q	PL B520 1	G. Abbiendi *et al.*	(OPAL Collab.)
BARATE	01E	EPJ C19 213	R. Barate *et al.*	(ALEPH Collab.)
GAMBINO	01	NP B611 338	P. Gambino, M. Misiak	
AFFOLDER	00I	PR D62 012004	T. Affolder *et al.*	(CDF Collab.)
PDG	00	EPJ C15 1	D.E. Groom *et al.*	(PDG Collab.)
ABBIENDI	99E	EPJ C7 407	G. Abbiendi *et al.*	(OPAL Collab.)
ABBOTT	99E	PRL 82 4975	B. Abbott *et al.*	(D0 Collab.)
ACKERSTAFF	99D	EPJ C8 3	K. Ackerstaff *et al.*	(OPAL Collab.)
ABE	97L	PRL 79 357	F. Abe *et al.*	(CDF Collab.)
ACCIARRI	97F	PL B396 327	M. Acciarri *et al.*	(L3 Collab.)
AMMAR	97B	PRL 78 4686	R. Ammar *et al.*	(CLEO Collab.)
COARASA	97	PL B406 337	J.A. Coarasa, R.A. Jimenez, J. Sola	
GORDEEV	97	PAN 60 1164	V.A. Gordeev *et al.*	(PNPI)
		Translated from YAF 60 1291.		
GUCHAIT	97	PR D55 7263	M. Guchait, D.P. Roy	(TATA)
MANGANO	97	PL B410 299	M. Mangano, S. Slabospitsky	
STAHL	97	ZPHY C74 73	A. Stahl, H. Voss	(BONN)
PDG	96	PR D54 1	R. M. Barnett *et al.*	(PDG Collab.)
ALAM	95	PRL 74 2885	M.S. Alam *et al.*	(CLEO Collab.)
ASAKA	95	PL B345 36	T. Asaka, K.I. Hikasa	(TOHOK)
BUSKULIC	95	PL B343 444	D. Buskulic *et al.*	(ALEPH Collab.)
GROSSMAN	95B	PL B357 630	Y. Grossman, H. Haber, Y. Nir	
GROSSMAN	94	PL B332 373	Y. Grossman, Z. Ligeti	
STAHL	94	PL B324 121	A. Stahl	(BONN)
ACTON	92M	PL B295 347	P.D. Acton *et al.*	(OPAL Collab.)
SWARTZ	90	PRL 64 2877	M.L. Swartz *et al.*	(Mark II Collab.)

New Heavy Bosons (W', Z', leptoquarks, etc.), Searches for

We list here various limits on charged and neutral heavy vector bosons (other than W's and Z's), heavy scalar bosons (other than Higgs bosons), vector or scalar leptoquarks, and axigluons. The latest unpublished results are described in "W' Searches" and "Z' Searches" reviews.

CONTENTS:

W'-BOSON SEARCHES

Revised November 2013 by G. Brooijmans (Columbia University), M.-C. Chen (UC Irvine) and B.A. Dobrescu (Fermilab).

The W' boson is a massive hypothetical particle of charge ±1 and spin 1, predicted in various extensions of the Standard Model (SM).

W' couplings to quarks and leptons. The Lagrangian terms describing couplings of a W'^{+} boson to fermions are given by

$$\frac{W'^{+}_{\mu}}{\sqrt{2}}\Big[\overline{u}_i\Big(C^{R}_{q_{ij}}P_R+C^{L}_{q_{ij}}P_L\Big)\gamma^{\mu}d_j+\overline{\nu}_i\Big(C^{R}_{l_{ij}}P_R+C^{L}_{l_{ij}}P_L\Big)\gamma^{\mu}e_j\Big]\,. \quad (1)$$

Here u, d, ν and e are the SM fermions in the mass eigenstate basis, $i, j = 1, 2, 3$ label the fermion generation, and $P_{R,L} = (1 \pm \gamma_5)/2$. The coefficients $C^{L}_{q_{ij}}$, $C^{R}_{q_{ij}}$, $C^{L}_{l_{ij}}$, $C^{R}_{l_{ij}}$ are complex dimensionless parameters. If $C^{R}_{l_{ij}} \neq 0$, then the ith generation includes a right-handed neutrino. Using this notation, the SM W couplings are $C^{L}_{q} = gV_{\rm CKM}$, $C^{L}_{l} = g$ and $C^{R}_{q} = C^{R}_{l} = 0$.

Unitarity considerations imply that the W' boson is associated with a spontaneously-broken gauge symmetry. This is true even when it is a composite particle (*e.g.*, $\rho^{\pm}$-like bound states [1]) if its mass is much smaller than the compositeness scale, or a Kaluza-Klein mode in theories where the W boson propagates in extra dimensions [2]. The simplest extension of the electroweak gauge group that includes a W' boson is $SU(2)_1 \times SU(2)_2 \times U(1)$, but larger groups are encountered in some theories. A generic property of these gauge theories is that they also include a Z' boson [3]; whether the W' boson can be discovered first depends on theoretical and experimental details.

The renormalizable photon-W' coupling is fixed by electromagnetic gauge invariance. By contrast, the $W'WZ$ and $W'W'Z$ couplings as well as the W' boson couplings to Z' or Higgs bosons are model-dependent.

A tree-level mass mixing may be induced between the electrically-charged gauge bosons. Upon diagonalization of their mass matrix, the $W - Z$ mass ratio and the couplings of the observed W boson are shifted from the SM values. Their measurements imply that the $W - W'$ mixing angle must be smaller than about 10^{-2}. Similarly, a $Z - Z'$ mixing is induced in generic theories, leading to even tighter constraints. There are, however, theories in which these mixings are negligible (*e.g.* due to a new parity [4]), even when the W' and Z' masses are below the electroweak scale.

A popular model [5] is based on the "left-right symmetric" gauge group, $SU(2)_L \times SU(2)_R \times U(1)_{B-L}$, with the SM fermions that couple to the W boson transforming as doublets under $SU(2)_L$, and the other ones transforming as doublets under $SU(2)_R$. In this model the W' boson couples primarily to right-handed fermions, and its coupling to left-handed fermions arises solely due to $W - W'$ mixing. As a result, C^{L}_{q} is proportional to the CKM matrix, and its elements are much smaller than the diagonal elements of C^{R}_{q}.

There are many other models based on the $SU(2)_1 \times SU(2)_2 \times U(1)$ gauge symmetry. In the "alternate left-right" model [6], all the couplings shown in Eq. (1) vanish, but there are some new fermions such that the W' boson couples to pairs involving a SM fermion and a new fermion. In the "ununified SM" [7], the left-handed quarks are doublets under one $SU(2)$, and the left-handed leptons are doublets under a different $SU(2)$, leading to a mostly leptophobic W' boson: $C^{L}_{l_{ij}} \ll C^{L}_{q_{ij}}$ and $C^{R}_{q_{ij}} = C^{R}_{l_{ij}} = 0$. Fermions of different generations may also transform as doublets under different $SU(2)$ gauge groups [8]. In particular, the couplings to third generation quarks may be enhanced [9].

It is also possible that the W' couplings to SM fermions are highly suppressed. For example, if the quarks and leptons are singlets under one $SU(2)$ [10] , then the couplings are proportional to a mixing angle that could be very small. Similar suppressions may arise if some vectorlike fermions mix with the SM ones [11].

Gauge groups that embed the electroweak symmetry, such as $SU(3)_W \times U(1)$ or $SU(4)_W \times U(1)$, also include one or more W' bosons [12].

Collider searches. At LEP-II, W' bosons could have been produced in pairs via their photon and Z couplings. The production cross section depends only on the W' mass, and is large enough to rule out $M_{W'} \leq \sqrt{s}/2 \approx 105$ GeV for most patterns of decay modes.

At hadron colliders, W' bosons can be detected through resonant pair production of fermions or electroweak bosons. Assuming that the W' width is much smaller than its mass, the contribution of the s-channel W' boson exchange to the total rate for $pp \to f\bar{f}'X$, where f and f' are fermions whose electric charges differ by ±1, and X is any final state, may be approximated by the branching fraction $B(W' \to f\bar{f}')$ times the production cross section

$$\sigma\big(pp\to W'X\big) \simeq \frac{\pi}{48\,s}\sum_{i,j}\Big[(C^{L}_{q_{ij}})^2+(C^{R}_{q_{ij}})^2\Big]\,w_{ij}\big(M^2_{W'}/s, M_{W'}\big)\,. \quad (2)$$

The functions w_{ij} include the information about proton structure, and are given to leading order in α_s by

$$w_{ij}(z,\mu) = \int_z^1 \frac{dx}{x}\Big[u_i(x,\mu)\,\overline{d}_j\Big(\frac{z}{x},\mu\Big)+\overline{u}_i(x,\mu)\,d_j\Big(\frac{z}{x},\mu\Big)\Big]\,, \quad (3)$$

where $u_i(x,\mu)$ and $d_i(x,\mu)$ are the parton distributions inside the proton, at the factorization scale μ and parton momentum fraction x, for the up- and down-type quark of the ith generation, respectively. QCD corrections to W' production are sizable (they also include quark-gluon initial states), but preserve the above factorization of couplings at next-to-leading order [13].

The most commonly studied W' signal consists of a high-energy electron or muon and large missing transverse energy, with the transverse mass distribution forming a Jacobian peak with its endpoint at $M_{W'}$ (see Fig. 2 of Ref. 14) Given that the branching fractions for $W' \to e\nu$ and $W' \to \mu\nu$ could be

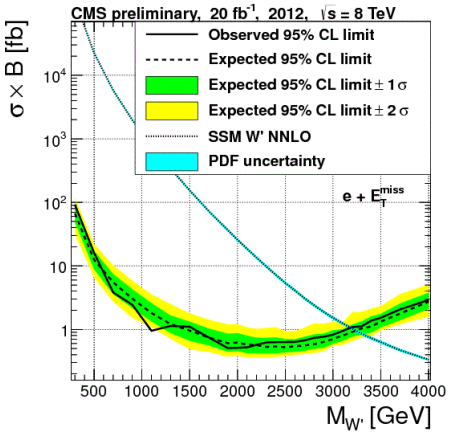

Figure 1: 95% CL limit on $\sigma(pp \to W'X) \times B(W' \to e\nu)$ from CMS [16]. The theoretical prediction (dotted line) is for $C_q^R = gV_{\rm CKM}$, $C_l^R = g$, $C_q^L = C_l^L = 0$.

very different, these channels should be analyzed separately. Searches in these channels often assume that the left-handed couplings vanish (no interference between W and W'), and that the right-handed neutrino of the first generation is light compared to $M_{W'}$ and escapes the detector. However, if a W' boson were discovered and the final state fermions have left-handed helicity, then the effects of $W - W'$ interference could be observed [15], providing useful information about the W' couplings.

In the $e\nu$ channel, the CMS Collab. has set limits [16] for $M_{W'}$ in the $0.3 - 4$ TeV range, based on 20 fb^{-1} of LHC data at $\sqrt{s} = 8$ TeV, as shown in Fig. 1. For $M_{W'}$ in the $500 - 600$ GeV range, the limits on W' couplings set by CDF [17] are also stringent (for a comparison, see Fig. 4 of Ref. 14). The limits are much weaker for $M_{W'}$ in the $200 - 300$ GeV range because these were obtained using only 0.2 fb^{-1} of Tevatron data [18], while the $105 - 200$ GeV range has been even less explored (see the UA1 and UA2 references in Ref. 19).

In the $\mu\nu$ channel, the most stringent limits in the $0.3 - 4$ TeV range are set by CMS [16] using the $\sqrt{s} = 8$ TeV data. When combined with the $e\nu$ channel, the limit varies between 71 and 1.7 fb. The ATLAS $\mu\nu$ limit [14] uses the 7 TeV data set. For $M_{W'}$ in the $200 - 300$ GeV range there are only weak limits on the W' couplings from Run I [20] of the Tevatron. There are no direct limits on $W' \to \mu\nu$ for $M_{W'}$ in the $105 - 200$ GeV range. Note that masses of the order of the electroweak scale are interesting from a theory point of view, while lepton universality does not necessarily apply to a W' boson.

Dedicated searches for the $W' \to \tau\nu$ decay have not yet been performed, but limits can be derived from some searches in the $\ell + \not{E}_T$ channel as well as from charged-Higgs searches such as $pp \to t\bar{b}\tau\nu X$.

The W' decay into a lepton and a right-handed neutrino, ν_R, may also be followed by the ν_R decay through a virtual W' boson into a lepton and two quark jets. The CMS [21] and

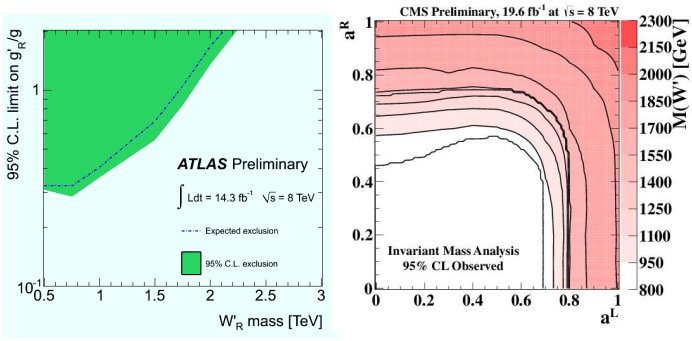

Figure 2: 95% CL upper limits on W' couplings using the $t\bar{b}$ and $\bar{t}b$ final states, assuming that the diagonal couplings are generation independent. Left panel: ATLAS [23] limit on C_{q11}^R/g. Right panel: CMS [24] limit on $M_{W'}$ as contours in the C_{q11}^R/g – C_{q11}^L/g plane.

ATLAS [22] searches in the $eejj$, $\mu\mu jj$ and $\tau\tau jj$ channels have set limits on various quantities for $M_{W'}$ in the $0.6 - 3$ TeV range.

The $t\bar{b}$ channel is particularly important because a W' boson that couples only to right-handed fermions cannot decay to leptons when the right-handed neutrinos are heavier than $M_{W'}$ (additional motivations are provided by a W' boson with enhanced couplings to the third generation [9], and by a leptophobic W' boson). The usual signal consists of a leptonically decaying W boson and two b-jets. Upper limits on the W' couplings to right- and left-handed quarks normalized to the SM W couplings, have been set by ATLAS [23] and CMS [24] as shown in Fig. 2. The best limits on the couplings to right-handed quarks for $M_{W'}$ in the 300–500 GeV range have been set by CDF with 1.9 fb^{-1} [25], while on couplings to left-handed quarks for $M_{W'}$ in the 600–800 GeV range have been set by DØ with 2.3 fb^{-1} [26]. For $M_{W'} \gg m_t$, one could also use hadronic W boson decays to search for $W' \to t\bar{b}$ with a boosted top quark. Finally, if W' couplings to left-handed quarks are large, then interference effects modify the SM s-channel single-top production [27].

Searches for dijet resonances may be used to set limits on $W' \to q\bar{q}'$. The best limits on W' couplings to quarks have been set by UA2 [28] in the $140 - 250$ GeV mass range, by CDF [29] in the $250 - 900$ GeV range, and by CMS [30] in the $\sim 1 - 3$ TeV range.

In some theories [4], the W' couplings to SM fermions are suppressed by discrete symmetries. W' production then occurs in pairs, through a photon or Z boson. The decay modes are model-dependent and often involve other new particles. The ensuing collider signals arise from cascade decays and typically include missing transverse energy.

Searches for WZ resonances at the LHC have focused on the process $pp \to W' \to WZ$ with the production mainly from $u\bar{d} \to W'$ assuming SM-like couplings to quarks. CMS [32] and ATLAS [33] have set upper limits on the $W'WZ$ coupling for $M_{W'}$ in the $170 - 2000$ GeV range. Similar searches have also been performed at the Tevatron [34].

A fermiophobic W' boson that couples to WZ may be produced at hadron colliders in association with a Z boson, or via WZ fusion. This would give rise to $(WZ)Z$ and $(WZ)jj$ final states, where the parentheses represent a resonance [31].

Low-energy constraints. The properties of W' bosons are also constrained by measurements of processes at energies much below $M_{W'}$. The bounds on $W-W'$ mixing [19] are mostly due to the change in W properties compared to the SM. Limits on deviations in the ZWW couplings provide a leading constraint for fermiophobic W' bosons [11].

Constraints arising from low-energy effects of W' exchange are strongly model-dependent. If the W' couplings to quarks are not suppressed, then box diagrams involving a W and a W' boson contribute to neutral meson-mixing. In the case of W' couplings to right-handed quarks as in the left-right symmetric model, the limit from $K_L - K_S$ mixing is severe: $M_{W'} > 2.5$ TeV [35]. However, if no correlation between $C^R_{q_{ij}}$ and $C^R_{l_{ij}}$ is assumed, then the limit on $M_{W'}$ may be significantly relaxed [36].

W' exchange also contributes at tree level to various low-energy processes. In particular, it would impact the measurement of the Fermi constant G_F in muon decay, which in turn would change the predictions of many other electroweak processes. A recent test of parity violation in polarized muon decay [37] has set limits of about 600 GeV on $M_{W'}$, assuming W' couplings to right-handed leptons as in left-right symmetric models. There are also W' contributions to the neutron electric dipole moment, β decays, and other processes [19].

If right-handed neutrinos have Majorana masses, then there are tree-level contributions to neutrinoless double-beta decay, and a limit on $M_{W'}$ versus the ν_R mass may be derived [38]. For ν_R masses below a few GeV, the W' boson contributes to leptonic and semileptonic B meson decays, so that limits may be placed on various combinations of W' parameters [36]. For ν_R masses below $\sim$30 MeV, most stringent constraints on $M_{W'}$ are due to the limits on ν_R emission from supernovae.

References

1. M. Bando, T. Kugo, and K. Yamawaki, Phys. Rept. **164**, 217 (1988).
2. H.C. Cheng *et al*, Phys. Rev. D**64**, 065007 (2001).
3. See the Section on "Z' searches" in this *Review*.
4. H.C. Cheng and I. Low, JHEP **0309**, 051 (2003).
5. R.N. Mohapatra and J.C. Pati, Phys. Rev. D**11**, 566 (1975). G. Senjanovic and R.N. Mohapatra, Phys. Rev. D**12**, 1502 (1975).
6. K.S. Babu, X.G. He, and E. Ma, Phys. Rev. D**36**, 878 (1987).
7. H. Georgi, E.E. Jenkins, and E.H. Simmons, Nucl. Phys. B**331**, 541 (1990).
8. See, *e.g.*, X.y. Li and E. Ma, J. Phys. G**19**, 1265 (1993).
9. D.J. Muller and S. Nandi, Phys. Lett. B**383**, 345 (1996). E. Malkawi, T. Tait, and C.P. Yuan, Phys. Lett. B**385**, 304 (1996).
10. A. Donini *et al*, Nucl. Phys. B**507**, 51 (1997).
11. R.S. Chivukula *et al*, Phys. Rev. D**74**, 075011 (2006). H.J. He, T. Tait, and C.P. Yuan, Phys. Rev. D**62**, 011702 (2000).
12. F. Pisano and V. Pleitez, Phys. Rev. D**46**, 410 (1992); **51**, 3865 (1995).
13. Z. Sullivan, Phys. Rev. D**66**, 075011 (2002).
14. G. Aad *et al.* [ATLAS Collab.], Eur. Phys. J. C **72**, 2241 (2012).
15. T.G. Rizzo, JHEP **0705**, 037 (2007). E. Boos *et al*, Phys. Lett. B**655**, 245 (2007).
16. CMS Collab., note PAS-EXO-12-060, March 2013, updated in July 2013.
17. T. Aaltonen *et al.* [CDF Collab.], Phys. Rev. D **83**, 031102 (2011).
18. A. Abulencia *et al.* [CDF Collab.], Phys. Rev. **D75**, 091101 (2007).
19. See the particle listings for W' in this *Review*.
20. F. Abe *et al.* [CDF Collab.], Phys. Rev. Lett. **84**, 5716 (2000).
21. CMS Collab., note PAS-EXO-12-017, updated July 2013.
22. G. Aad *et al.* [ATLAS Collab.], Eur. Phys. J. C **72**, 2056 (2012).
23. ATLAS Collab., note ATLAS-CONF-2013-050.
24. S. Chatrchyan *et al.* [CMS Collab.], Phys. Lett. B **718**, 1229 (2013); note PAS-B2G-12-010, March 2013.
25. T. Aaltonen *et al.* [CDF Collab.], Phys. Rev. Lett. **103**, 041801 (2009).
26. V. M. Abazov *et al.* [D0 Collab.], Phys. Lett. **B699**, 145 (2011).
27. T.M.P. Tait, C.-P. Yuan, Phys. Rev. **D63**, 014018 (2000).
28. J. Alitti *et al.* [UA2 Collab.], Nucl. Phys. B **400**, 3 (1993).
29. T. Aaltonen *et al.* [CDF Collab.], Phys. Rev. D **79**, 112002 (2009).
30. CMS Collab., note PAS-EXO-12-059, Feb. 2013; S. Chatrchyan *et al* [CMS Collab.], `arXiv:1302.4794`; see also G. Aad *et al.* [ATLAS Collab.], JHEP **1301**, 029 (2013).
31. H.J. He *et al.*, Phys. Rev. D**78**, 031701 (2008).
32. CMS Collab., note PAS-EXO-12-025, Jun. 2013.
33. ATLAS Collab., note ATLAS-CONF-2013-015, Mar. 2013.
34. V. M. Abazov *et al.* [D0 Collab.], Phys. Rev. Lett. **107**, 011801 (2011); T. Aaltonen *et al.* [CDF Collab.], Phys. Rev. Lett. **104** (2010) 241801.
35. Y. Zhang *et al*, Phys. Rev. D**76**, 091301 (2007).
36. P. Langacker and S.U. Sankar, Phys. Rev. D**40**, 1569 (1989).
37. J. F. Bueno *et al.* [TWIST Collab.], Phys. Rev. D **84**, 032005 (2011).
38. See Fig. 5 of G. Prezeau, M. Ramsey-Musolf, and P. Vogel, Phys. Rev. D**68**, 034016 (2003).

MASS LIMITS for W' (Heavy Charged Vector Boson Other Than W) in Hadron Collider Experiments

Couplings of W' to quarks and leptons are taken to be identical with those of W. The following limits are obtained from $p\overline{p}$ or $pp \to W'X$ with W' decaying to the mode indicated in the comments. New decay channels (*e.g.*, $W' \to WZ$) are assumed to be suppressed. The most recent preliminary results can be found in the "W'-boson searches" review above.

VALUE (GeV)	*CL%*	*DOCUMENT ID*		*TECN*	*COMMENT*
> 950	95	[1] AAD	13AO	ATLS	$W' \to WZ$
>1680	95	AAD	13D	ATLS	$W' \to q\overline{q}$
>1920	95	CHATRCHYAN	13A	CMS	$W' \to q\overline{q}$
>2900	95	[2] CHATRCHYAN	13AQ	CMS	$W' \to e\nu,\ \mu\nu$
>1510	95	[3] CHATRCHYAN	13E	CMS	$W' \to tb$

>1130	95	[4] AAD	12AV	ATLS	$W' \to t b$
> 760	95	[5] AAD	12BB	ATLS	$W' \to WZ$
>2550	95	AAD	12CR	ATLS	$W' \to e\nu, \mu\nu$
>2630	95	[6] CHATRCHYAN	12AB	CMS	$W' \to e\nu, \mu\nu$
>1143	95	[5] CHATRCHYAN	12AF	CMS	$W' \to WZ$
• • • We do not use the following data for averages, fits, limits, etc. • • •					
		[7] CHATRCHYAN	13AJ	CMS	$W' \to WZ$
none 1000–1730	95	[8] CHATRCHYAN	13AS	CMS	$W' \to q\overline{q}$
none 700–940	95	[9] CHATRCHYAN	13U	CMS	$W' \to WZ$
		[10] AAD	12CK	ATLS	$W' \to \overline{t}q$
		[11] AAD	12M	ATLS	$W' \to N\ell \to \ell\ell jj$
		[12] AALTONEN	12N	CDF	$W' \to \overline{t}d$
		[13] CHATRCHYAN	12AR	CMS	$W' \to \overline{t}d$
		[14] CHATRCHYAN	12BG	CMS	$W' \to N\ell \to \ell\ell jj$
>1490	95	AAD	11M	ATLS	$W' \to e\nu, \mu\nu$
>2150	95	AAD	11Q	ATLS	$W' \to e\nu, \mu\nu$
>1120	95	AALTONEN	11C	CDF	$W' \to e\nu$
none 180–690	95	[15] ABAZOV	11H	D0	$W' \to WZ$
> 863	95	[16] ABAZOV	11L	D0	$W' \to t b$
>1580	95	CHATRCHYAN	11K	CMS	$W' \to e\nu, \mu\nu$
>1400	95	CHATRCHYAN	11K	CMS	$W' \to \mu\nu$
>1510	95	CHATRCHYAN	11Y	CMS	$W' \to q\overline{q}$
>1360	95	KHACHATRY...	11H	CMS	$W' \to e\nu$
none 285–516	95	[17] AALTONEN	10N	CDF	$W' \to WZ$
none 188–520	95	[18] ABAZOV	10A	D0	$W' \to WZ$
> 800	95	[19] AALTONEN	09AA	CDF	$W' \to t b$
none 280–840	95	[20] AALTONEN	09AC	CDF	$W' \to q\overline{q}$
>1000	95	ABAZOV	08C	D0	$W' \to e\nu$
> 731	95	[21] ABAZOV	08P	D0	$W' \to t b$
> 788	95	ABULENCIA	07K	CDF	$W' \to e\nu$
none 200–610	95	[22] ABAZOV	06N	D0	$W' \to t b$
> 800	95	ABAZOV	04C	D0	$W' \to q\overline{q}$
225–536	95	[23] ACOSTA	03B	CDF	$W' \to t b$
none 200–480	95	[24] AFFOLDER	02C	CDF	$W' \to WZ$
> 786	95	[25] AFFOLDER	01I	CDF	$W' \to e\nu, \mu\nu$
> 660	95	[26] ABE	00	CDF	$W' \to \mu\nu$
none 300–420	95	[27] ABE	97G	CDF	$W' \to q\overline{q}$
> 720	95	[28] ABACHI	96C	D0	$W' \to e\nu$
> 610	95	[29] ABACHI	95E	D0	$W' \to e\nu, \tau\nu$
> 652	95	[30] ABE	95M	CDF	$W' \to e\nu$
none 260–600	95	[31] RIZZO	93	RVUE	$W' \to q\overline{q}$

[1] AAD 13AO search for W' decaying into the WZ final state with $W \to \ell\nu$, $Z \to 2j$. The quoted limit assumes $g_{W'WZ}/g_{WWZ} = (M_W/M_{W'})^2$.

[2] CHATRCHYAN 13AQ limit is for W' with SM-like coupling which interferes with the SM W boson.

[3] CHATRCHYAN 13E limit is for W' with SM-like coupling which intereferes with the SM W boson. For W' with right-handed coupling, the bound becomes >1850 GeV (>1910 GeV) if W' decays to both leptons and quarks (only to quarks). If both left- and right-handed couplings are present, the limit becomes >1640 GeV.

[4] The AAD 12AV quoted limit is for a SM-like right-handed W'. $W' \to \ell\nu$ decay is assumed to be forbidden.

[5] The quoted limit assumes $g_{W'WZ}/g_{WWZ} = (M_W/M_{W'})^2$.

[6] CHATRCHYAN 12AB limit is for W' with SM-like coupling which interferes with the SM W boson constructively. For W' with right-handed coupling, the bound becomes >2.5 TeV.

[7] CHATRCHYAN 13AJ search for resonances decaying to WZ pair, using the hadronic decay modes of W and Z. See their Fig. 7 for the limit on the cross section.

[8] CHATRCHYAN 13AS search for new resonance decaying to dijets in pp collisions at $\sqrt{s}$ = 8 TeV.

[9] CHATRCHYAN 13U search for W' decaying to the WZ final state, with W decaying into jets. The quoted limit assumes $g_{W'WZ}/g_{WWZ} = (M_W/M_{W'})^2$.

[10] AAD 12CK search for $pp \to tW'$, $W' \to \overline{t}q$ events in pp collisions. See their Fig. 5 for the limit on $\sigma \cdot$ B.

[11] AAD 12M search for right-handed W_R in pp collisionsat $\sqrt{s}$ = 7 TeV. W_R is assumed to decay into ℓ and hypothetical heavy neutrino N, with N decaying into ℓjj. See their Fig. 4 for the limit in the $m_N - m_{W'}$ plane.

[12] AALTONEN 12N search for $p\overline{p} \to tW'$, $W' \to \overline{t}d$ events in $p\overline{p}$ collisions. See their Fig. 3 for the limit on $\sigma \cdot$ B.

[13] CHATRCHYAN 12AR search for $pp \to tW'$, $W' \to \overline{t}d$ events in pp collisions. See their Fig. 2 for the limit on $\sigma \cdot$ B.

[14] CHATRCHYAN 12BG search for right-handed W_R in pp collisions $\sqrt{s}$ = 7 TeV. W_R is assumed to decay into ℓ and hypothetical heavy neutrino N, with N decaying into ℓjj. See their Fig. 3 for the limit in the $m_N - m_{W'}$ plane.

[15] The quoted limit is obtained assuming $W'WZ$ coupling strength is the same as the ordinary WWZ coupling strength in the Standard Model.

[16] ABAZOV 11L limit is for W' with SM-like coupling which interferes with the SM W boson. For W' with right-handed coupling, the bound becomes >885 GeV (>890 GeV) if W' decays to both leptons and quarks (only to quarks). If both left- and right-handed couplings present, the limit becomes >916 GeV.

[17] The quoted limit assumes $g_{W'WZ}/g_{WWZ} = (M_W/M_{W'})^2$. See their Fig. 4 for limits in mass-coupling plane.

[18] The quoted limit assumes $g_{W'WZ}/g_{WWZ} = (M_W/M_{W'})^2$. See their Fig. 3 for limits in mass-coupling plane.

[19] The AALTONEN 09AA quoted limit is for a right-handed W' with SM-like coupling allowing $W' \to \ell\nu$ decays.

[20] AALTONEN 09AC search for new particle decaying to dijets.

[21] The ABAZOV 08P quoted limit is for W' with SM-like coupling which interferes with the SM W boson. For W' with right-handed coupling, the bound becomes >739 GeV (>768 GeV) if W' decays to both leptons and quarks (only to quarks).

[22] The ABAZOV 06N quoted limit is for W' with SM-like coupling which interferes with the SM W boson. For W' with right-handed coupling, $M_{W'}$ between 200 and 630 (670) GeV is excluded for $M_{\nu_R} \ll M_{W'}$ ($M_{\nu_R} > M_{W'}$).

[23] The ACOSTA 03B quoted limit is for $M_{W'} \gg M_{\nu_R}$. For $M_{W'} < M_{\nu_R}$, $M_{W'}$ between 225 and 566 GeV is excluded.

[24] The quoted limit is obtained assuming $W'WZ$ coupling strength is the same as the ordinary WWZ coupling strength in the Standard Model. See their Fig. 2 for the limits on the production cross sections as a function of the W' width.

[25] AFFOLDER 01I combine a new bound on $W' \to e\nu$ of 754 GeV with the bound of ABE 00 on $W' \to \mu\nu$ to obtain quoted bound.

[26] ABE 00 assume that the neutrino from W' decay is stable and has a mass significantly less than $m_{W'}$.

[27] ABE 97G search for new particle decaying to dijets.

[28] For bounds on W_R with nonzero right-handed mass, see Fig. 5 from ABACHI 96C.

[29] ABACHI 95E assume that the decay $W' \to WZ$ is suppressed and that the neutrino from W' decay is stable and has a mass significantly less $m_{W'}$.

[30] ABE 95M assume that the decay $W' \to WZ$ is suppressed and the (right-handed) neutrino is light, noninteracting, and stable. If m_ν=60 GeV, for example, the effect on the mass limit is negligible.

[31] RIZZO 93 analyses CDF limit on possible two-jet resonances. The limit is sensitive to the inclusion of the assumed K factor.

W_R (Right-Handed W Boson) MASS LIMITS

Assuming a light right-handed neutrino, except for BEALL 82, LANGACKER 89B, and COLANGELO 91. $g_R = g_L$ assumed. [Limits in the section MASS LIMITS for W' below are also valid for W_R if $m_{\nu_R} \ll m_{W_R}$.] Some limits assume manifest left-right symmetry, *i.e.*, the equality of left- and right Cabibbo-Kobayashi-Maskawa matrices. For a comprehensive review, see LANGACKER 89B. Limits on the W_L-W_R mixing angle ζ are found in the next section. Values in brackets are from cosmological and astrophysical considerations and assume a light right-handed neutrino.

VALUE (GeV)	CL%	DOCUMENT ID		TECN	COMMENT
> 592	90	[1] BUENO	11	TWST	μ decay
> 715	90	[2] CZAKON	99	RVUE	Electroweak
• • • We do not use the following data for averages, fits, limits, etc. • • •					
> 245	90	[3] WAUTERS	10	CNTR	^{60}Co β decay
> 180	90	[4] MELCONIAN	07	CNTR	^{37}K β^+ decay
> 290.7	90	[5] SCHUMANN	07	CNTR	Polarized neutron decay
[> 3300]	95	[6] CYBURT	05	COSM	Nucleosynthesis; light ν_R
> 310	90	[7] THOMAS	01	CNTR	β^+ decay
> 137	95	[8] ACKERSTAFF	99D	OPAL	τ decay
>1400	68	[9] BARENBOIM	98	RVUE	Electroweak, Z-Z' mixing
> 549	68	[10] BARENBOIM	97	RVUE	μ decay
> 220	95	[11] STAHL	97	RVUE	τ decay
> 220	90	[12] ALLET	96	CNTR	β^+ decay
> 281	90	[13] KUZNETSOV	95	CNTR	Polarized neutron decay
> 282	90	[14] KUZNETSOV	94B	CNTR	Polarized neutron decay
> 439	90	[15] BHATTACH...	93	RVUE	Z-Z' mixing
> 250	90	[16] SEVERIJNS	93	CNTR	β^+ decay
		[17] IMAZATO	92	CNTR	K^+ decay
> 475	90	[18] POLAK	92B	RVUE	μ decay
> 240	90	[19] AQUINO	91	RVUE	Neutron decay
> 496	90	[19] AQUINO	91	RVUE	Neutron and muon decay
> 700		[20] COLANGELO	91	THEO	$m_{K_L^0} - m_{K_S^0}$
> 477	90	[21] POLAK	91	RVUE	μ decay
[none 540–23000]		[22] BARBIERI	89B	ASTR	SN 1987A; light ν_R
> 300	90	[23] LANGACKER	89B	RVUE	General
> 160	90	[24] BALKE	88	CNTR	$\mu \to e\nu\overline{\nu}$
> 406	90	[25] JODIDIO	86	ELEC	Any ζ
> 482	90	[25] JODIDIO	86	ELEC	$\zeta = 0$
> 800		MOHAPATRA	86	RVUE	$SU(2)_L \times SU(2)_R \times U(1)$
> 400	95	[26] STOKER	85	ELEC	Any ζ
> 475	95	[26] STOKER	85	ELEC	ζ <0.041
		[27] BERGSMA	83	CHRM	$\nu_\mu e \to \mu\nu_e$
> 380	90	[28] CARR	83	ELEC	μ^+ decay
>1600		[29] BEALL	82	THEO	$m_{K_L^0} - m_{K_S^0}$

[1] The quoted limit is for manifest left-right symmetric model.

[2] CZAKON 99 perform a simultaneous fit to charged and neutral sectors.

[3] WAUTERS 10 limit is from a measurement of the asymmetry parameter of polarized ^{60}Co β decays. The listed limit assumes no mixing.

[4] MELCONIAN 07 measure the neutrino angular asymmetry in β^+-decays of polarized ^{37}K, stored in a magneto-optical trap. Result is consistent with SM prediction and does not constrain the $W_L - W_R$ mixing angle appreciably.

[5] SCHUMANN 07 limit is from measurements of the asymmetry $\langle \vec{p}_\nu \cdot \sigma_n \rangle$ in the β decay of polarized neutrons. Zero mixing is assumed.

[6] CYBURT 05 limit follows by requiring that three light ν_R's decouple when $T_{dec} > 140$ MeV. For different T_{dec}, the bound becomes $M_{W_R} > 3.3$ TeV $(T_{dec} / 140\ \text{MeV})^{3/4}$.

[7] THOMAS 01 limit is from measurement of β^+ polarization in decay of polarized ^{12}N. The listed limit assumes no mixing.

[8] ACKERSTAFF 99D limit is from τ decay parameters. Limit increase to 145 GeV for zero mixing.

[9] BARENBOIM 98 assumes minimal left-right model with Higgs of $SU(2)_R$ in $SU(2)_L$ doublet. For Higgs in $SU(2)_L$ triplet, m_{W_R} >1100 GeV. Bound calculated from effect of corresponding Z_{LR} on electroweak data through Z–Z_{LR} mixing.

[10] The quoted limit is from μ decay parameters. BARENBOIM 97 also evaluate limit from K_L-K_S mass difference.

[11] STAHL 97 limit is from fit to τ-decay parameters.

[12] ALLET 96 measured polarization-asymmetry correlation in $^{12}N\beta^+$ decay. The listed limit assumes zero L-R mixing.

[13] KUZNETSOV 95 limit is from measurements of the asymmetry $\langle \vec{p}_\nu \cdot \sigma_n \rangle$ in the β decay of polarized neutrons. Zero mixing assumed. See also KUZNETSOV 94B.

[14] KUZNETSOV 94B limit is from measurements of the asymmetry $\langle \vec{p}_\nu \cdot \sigma_n \rangle$ in the β decay of polarized neutrons. Zero mixing assumed.

[15] BHATTACHARYYA 93 uses Z-Z' mixing limit from LEP '90 data, assuming a specific Higgs sector of $SU(2)_L \times SU(2)_R \times U(1)$ gauge model. The limit is for m_t=200 GeV and slightly improves for smaller m_t.

[16] SEVERIJNS 93 measured polarization-asymmetry correlation in $^{107}In\,\beta^+$ decay. The listed limit assumes zero L-R mixing. Value quoted here is from SEVERIJNS 94 erratum.

[17] IMAZATO 92 measure positron asymmetry in $K^+ \to \mu^+\nu_\mu$ decay and obtain $\xi P_\mu > 0.990$ (90% CL). If W_R couples to $u\overline{s}$ with full weak strength (V^R_{us}=1), the result corresponds to m_{W_R} >653 GeV. See their Fig. 4 for m_{W_R} limits for general $|V^R_{us}|^2$=1−$|V^R_{ud}|^2$.

[18] POLAK 92B limit is from fit to muon decay parameters and is essentially determined by JODIDIO 86 data assuming ζ=0. Supersedes POLAK 91.

[19] AQUINO 91 limits obtained from neutron lifetime and asymmetries together with unitarity of the CKM matrix. Manifest left-right symmetry assumed. Stronger of the two limits also includes muon decay results.

[20] COLANGELO 91 limit uses hadronic matrix elements evaluated by QCD sum rule and is less restrictive than BEALL 82 limit which uses vacuum saturation approximation. Manifest left-right symmetry assumed.

[21] POLAK 91 limit is from fit to muon decay parameters and is essentially determined by JODIDIO 86 data assuming ζ=0. Superseded by POLAK 92B.

[22] BARBIERI 89B limit holds for $m_{\nu_R} \leq 10$ MeV.

[23] LANGACKER 89B limit is for any ν_R mass (either Dirac or Majorana) and for a general class of right-handed quark mixing matrices.

[24] BALKE 88 limit is for $m_{\nu_{eR}} = 0$ and $m_{\nu_{\mu R}} \leq 50$ MeV. Limits come from precise measurements of the muon decay asymmetry as a function of the positron energy.

[25] JODIDIO 86 is the same TRIUMF experiment as STOKER 85 (and CARR 83); however, it uses a different technique. The results given here are combined results of the two techniques. The technique here involves precise measurement of the end-point e^+ spectrum in the decay of the highly polarized μ^+.

[26] STOKER 85 is same TRIUMF experiment as CARR 83. Here they measure the decay e^+ spectrum asymmetry above 46 MeV/c using a muon-spin-rotation technique. Assumed a light right-handed neutrino. Quoted limits are from combining with CARR 83.

[27] BERGSMA 83 set limit m_{W_2}/m_{W_1} >1.9 at CL = 90%.

[28] CARR 83 is TRIUMF experiment with a highly polarized μ^+ beam. Looked for deviation from $V-A$ at the high momentum end of the decay e^+ energy spectrum. Limit from previous world-average muon polarization parameter is m_{W_R} >240 GeV. Assumes a light right-handed neutrino.

[29] BEALL 82 limit is obtained assuming that W_R contribution to K^0_L-K^0_S mass difference is smaller than the standard one, neglecting the top quark contributions. Manifest left-right symmetry assumed.

Limit on W_L-W_R Mixing Angle ζ

Lighter mass eigenstate $W_1 = W_L\cos\zeta - W_R\sin\zeta$. Light ν_R assumed unless noted. Values in brackets are from cosmological and astrophysical considerations.

VALUE	CL%	DOCUMENT ID		TECN	COMMENT
• • • We do not use the following data for averages, fits, limits, etc. • • •					
−0.020 to 0.017	90	BUENO	11	TWST	$\mu \to e\nu\overline{\nu}$
< 0.022	90	MACDONALD	08	TWST	$\mu \to e\nu\overline{\nu}$
< 0.12	95	[1] ACKERSTAFF	99D	OPAL	τ decay
< 0.013	90	[2] CZAKON	99	RVUE	Electroweak
< 0.0333		[3] BARENBOIM	97	RVUE	μ decay
< 0.04	90	[4] MISHRA	92	CCFR	νN scattering
−0.0006 to 0.0028	90	[5] AQUINO	91	RVUE	
[none 0.00001–0.02]		[6] BARBIERI	89B	ASTR	SN 1987A
< 0.040	90	[7] JODIDIO	86	ELEC	μ decay
−0.056 to 0.040	90	[7] JODIDIO	86	ELEC	μ decay

[1] ACKERSTAFF 99D limit is from τ decay parameters.

[2] CZAKON 99 perform a simultaneous fit to charged and neutral sectors.

[3] The quoted limit is from μ decay parameters. BARENBOIM 97 also evaluate limit from K_L-K_S mass difference.

[4] MISHRA 92 limit is from the absence of extra large-x, large-y $\overline{\nu}_\mu N \to \overline{\nu}_\mu X$ events at Tevatron, assuming left-handed ν and right-handed $\overline{\nu}$ in the neutrino beam. The result gives $\zeta^2(1-2m^2_{W_1}/m^2_{W_2})$< 0.0015. The limit is independent of ν_R mass.

[5] AQUINO 91 limits obtained from neutron lifetime and asymmetries together with unitarity of the CKM matrix. Manifest left-right asymmetry is assumed.

[6] BARBIERI 89B limit holds for $m_{\nu_R} \leq 10$ MeV.

[7] First JODIDIO 86 result assumes m_{W_R}=∞, second is for unconstrained m_{W_R}.

Z'-BOSON SEARCHES

Revised November 2013 by G. Brooijmans (Columbia University), M.-C. Chen (UC Irvine), and B.A. Dobrescu (Fermilab).

The Z' boson is a massive, electrically-neutral and color-singlet hypothetical particle of spin 1. This particle is predicted in many extensions of the Standard Model (SM), and has been the object of extensive phenomenological studies [1].

Z' boson couplings to quarks and leptons. The couplings of a Z' boson to the first-generation fermions are given by

$$Z'_\mu \left(g^L_u \overline{u}_L \gamma^\mu u_L + g^L_d \overline{d}_L \gamma^\mu d_L + g^R_u \overline{u}_R \gamma^\mu u_R + g^R_d \overline{d}_R \gamma^\mu d_R \right.$$
$$\left. + g^L_\nu \overline{\nu}_L \gamma^\mu \nu_L + g^L_e \overline{e}_L \gamma^\mu e_L + g^R_e \overline{e}_R \gamma^\mu e_R \right) \ , \qquad (1)$$

where u, d, ν and e are the quark and lepton fields in the mass eigenstate basis, and the coefficients g^L_u, g^L_d, g^R_u, g^R_d, g^L_ν, g^L_e, g^R_e are real dimensionless parameters. If the Z' couplings to quarks and leptons are generation-independent, then these seven parameters describe the couplings of the Z' boson to all SM fermions. More generally, however, the Z' couplings to fermions are generation-dependent, in which case Eq. (1) may be written with generation indices $i, j = 1, 2, 3$ labeling the quark and lepton fields, and with the seven coefficients promoted to 3×3 Hermitian matrices (*e.g.*, $g^L_{eij}\,\overline{e}^i_L \gamma^\mu e^j_L$, where e^2_L is the left-handed muon, etc.).

These parameters describing the Z' boson interactions with quarks and leptons are subject to some theoretical constraints. Quantum field theories that include a heavy spin-1 particle are well behaved at high energies only if that particle is a gauge boson associated with a spontaneously broken gauge symmetry. Quantum effects preserve the gauge symmetry only if the couplings of the gauge boson to fermions satisfy anomaly cancellation conditions. Furthermore, the fermion charges under the new gauge symmetry are constrained by the requirement that the quarks and leptons get masses from gauge-invariant interactions with Higgs fields.

The relation between the couplings displayed in Eq. (1) and the gauge charges z^L_{fi} and z^R_{fi} of the fermions $f = u, d, \nu, e$ involves the unitary 3×3 matrices V^L_f and V^R_f that transform the gauge eigenstate fermions f^i_L and f^i_R, respectively, into the mass eigenstates. In addition, the Z' couplings are modified if the new gauge boson in the gauge eigenstate basis ($\tilde{Z}'_\mu$) has a kinetic mixing $(-\chi/2)B^{\mu\nu}\tilde{Z}'_{\mu\nu}$ with the hypercharge gauge boson B^μ (due to a dimension-4 or 6 operator, depending on whether the new gauge symmetry is Abelian or not), or a mass mixing $\delta M^2 \tilde{Z}^\mu \tilde{Z}'_\mu$ with the linear combination ($\tilde{Z}_\mu$) of neutral bosons that couples as the SM Z boson [2]. Since both the kinetic and mass mixings shift the mass and couplings of the Z boson, electroweak measurements impose upper limits on χ and $\delta M^2/(M^2_{Z'} - M^2_Z)$ of the order of 10^{-3} [3]. Keeping only

Table 1: Examples of generation-independent $U(1)'$ charges for quarks and leptons. The parameter x is an arbitrary rational number. Anomaly cancellation requires certain new fermions [4].

fermion	$U(1)_{B-xL}$	$U(1)_{10+x\bar{5}}$	$U(1)_{d-xu}$	$U(1)_{q+xu}$
(u_L, d_L)	$1/3$	$1/3$	0	$1/3$
u_R	$1/3$	$-1/3$	$-x/3$	$x/3$
d_R	$1/3$	$-x/3$	$1/3$	$(2-x)/3$
(ν_L, e_L)	$-x$	$x/3$	$(-1+x)/3$	-1
e_R	$-x$	$-1/3$	$x/3$	$-(2+x)/3$

linear terms in these two small quantities, the couplings of the mass-eigenstate Z' boson are given by

$$g^L_{f_{ij}} = g_z V^L_{fii'} z^L_{f_{i'}} \left(V^L_f\right)^\dagger_{i'j} + \frac{e}{c_W}\left(\frac{s_W \chi M^2_{Z'} + \delta M^2}{2 s_W \left(M^2_{Z'} - M^2_Z\right)}\sigma^3_f - \epsilon\, Q_f\right) \ ,$$

$$g^R_{f_{ij}} = g_z V^R_{fii'} z^R_{f_{i'}} \left(V^R_f\right)^\dagger_{i'j} - \frac{e}{c_W}\,\epsilon\, Q_f \ , \qquad (2)$$

where g_z is the new gauge coupling, Q_f is the electric charge of f, e is the electromagnetic gauge coupling, s_W and c_W are the sine and cosine of the weak mixing angle, $\sigma^3_f = +1$ for $f = u, \nu$ and $\sigma^3_f = -1$ for $f = d, e$, and

$$\epsilon = \frac{\chi\left(M^2_{Z'} - c^2_W M^2_Z\right) + s_W \delta M^2}{M^2_{Z'} - M^2_Z} \ . \qquad (3)$$

While an interaction of a Z' boson with a pair of W bosons is also allowed, its coupling is typically smaller than the $\tilde{Z}^\mu \tilde{Z}'_\mu$ mixing.

U*(1) *gauge groups. A simple origin of a Z' boson is a new $U(1)'$ gauge symmetry. In that case, the matricial equalities $z^L_u = z^L_d$ and $z^L_\nu = z^L_e$ are required by the SM $SU(2)_W$ gauge symmetry. Given that the $U(1)'$ interaction is not asymptotically free, the theory may be well-behaved at high energies (for example, by embedding $U(1)'$ in a non-Abelian gauge group) only if the Z' couplings are commensurate numbers, *i.e.* any ratio of couplings is a rational number. Satisfying the anomaly cancellation conditions (which include an equation cubic in charges) with rational numbers is highly nontrivial, and in general new fermions charged under $U(1)'$ are necessary.

Consider first the case where the couplings are generation-independent (the V_f matrices then disappear from Eq. (2)), so that there are five commensurate couplings: g^L_q, g^R_u, g^R_d, g^L_l, g^R_e. Four sets of charges are displayed in Table 1, each of them spanned by one free parameter, x [4]. The first set, labelled $B - xL$, has charges proportional to the baryon number minus x times the lepton number. These charges allow all SM Yukawa couplings to a Higgs doublet which is neutral under $U(1)_{B-xL}$, so that there is no tree-level $\tilde{Z} - \tilde{Z}'$ mixing. For $x = 1$ one recovers the $U(1)_{B-L}$ group, which is non-anomalous in the presence of one "right-handed neutrino" (a chiral fermion that is a singlet under the SM gauge group) per generation. For $x \neq 1$, it is necessary to include some fermions that are vector-like (*i.e.* their mass terms are gauge invariant) with respect to the electroweak gauge group and chiral with respect to $U(1)_{B-xL}$. In the particular cases $x = 0$ or $x \gg 1$ the Z' is leptophobic or quark-phobic, respectively.

The second set, $U(1)_{10+x\bar{5}}$, has charges that commute with the representations of the $SU(5)$ grand unified group. Here x is related to the mixing angle between the two $U(1)$ bosons encountered in the $E_6 \to SU(5) \times U(1) \times U(1)$ symmetry breaking patterns of grand unified theories [1,5]. This set leads to $\tilde{Z} - \tilde{Z}'$ mass mixing at tree level, such that for a Z' mass close to the electroweak scale, the measurements at the Z-pole require some fine tuning between the charges and VEVs of the two Higgs doublets. Vector-like fermions charged under the electroweak gauge group and also carrying color are required (except for $x = -3$) to make this set anomaly free. The particular cases $x = -3, 1, -1/2$ are usually labelled $U(1)_\chi$, $U(1)_\psi$, and $U(1)_\eta$, respectively. Under the third set, $U(1)_{d-xu}$, the weak-doublet quarks are neutral, and the ratio of u_R and d_R charges is $-x$. For $x = 1$ this is the "right-handed" group $U(1)_R$. For $x = 0$, the charges are those of the E_6-inspired $U(1)_I$ group, which requires new quarks and leptons. Other generation-independent sets of $U(1)'$ charges are given in [6].

In the absence of new fermions charged under the SM group, the most general generation-independent charge assignment is $U(1)_{q+xu}$, which is a linear combination of hypercharge and $B - L$. Many other anomaly-free solutions exist if generation-dependent charges are allowed. An example is $B - xL_e - yL_\mu + (y-3)L_\tau$, with x, y free parameters. This allows all fermion masses to be generated by Yukawa couplings to a single Higgs doublet, without inducing tree-level flavor-changing neutral current (FCNC) processes. There are also lepton-flavor dependent charges that allow neutrino masses to arise only from operators of high dimensionality [7].

If the $SU(2)_W$-doublet quarks have generation-dependent $U(1)'$ charges, then the mass eigenstate quarks have flavor off-diagonal couplings to the Z' boson (see Eq. (1), and note that $V^L_u \left(V^L_d\right)^\dagger$ is the CKM matrix). These are severely constrained by measurements of FCNC processes, which in this case are mediated at tree-level by Z' boson exchange [8]. The constraints are relaxed if the first and second generation charges are the same, although they are increasingly tightened by the measurements of B meson properties [9]. If only the $SU(2)_W$-singlet quarks have generation-dependent $U(1)'$ charges, there is more freedom in adjusting the flavor off-diagonal couplings because the $V^R_{u,d}$ matrices are not observable in the SM.

The anomaly cancellation conditions for $U(1)'$ could be relaxed only if there is an axion with certain dimension-5 couplings to the gauge bosons. However, such a scenario violates unitarity unless the quantum field theory description breaks down at a scale near $M_{Z'}$ [10].

Other models. Z' bosons may also arise from larger gauge groups. These may be orthogonal to the electroweak group, as in

$SU(2)_W \times U(1)_Y \times SU(2)'$, or may embed the electroweak group, as in $SU(3)_W \times U(1)$ [11]. If the larger group is spontaneously broken down to $SU(2)_W \times U(1)_Y \times U(1)'$ at a scale $v_\star \gg M_{Z'}/g_z$, then the above discussion applies up to corrections of order $M_{Z'}^2/(g_z v_\star)^2$. For $v_\star \sim M_{Z'}/g_z$, additional gauge bosons have masses comparable to $M_{Z'}$, including at least a W' boson [11]. If the larger gauge group breaks together with the electroweak symmetry directly to the electromagnetic $U(1)_{\rm em}$, then the left-handed fermion charges are no longer correlated ($z_u^L \neq z_d^L$, $z_\nu^L \neq z_e^L$) and a $Z'W^+W^-$ coupling is induced.

If the electroweak gauge bosons propagate in extra dimensions, then their Kaluza-Klein (KK) excitations include a series of Z' boson pairs. Each of these pairs can be associated with a different $SU(2) \times U(1)$ gauge group in four dimensions. The properties of the KK particles depend strongly on the extra-dimensional theory [12]. For example, in universal extra dimensions there is a parity that forces all couplings of Eq. (1) to vanish in the case of the lightest KK bosons, while allowing couplings to pairs of fermions involving a SM and a heavy vector-like fermion. There are also 4-dimensional gauge theories (*e.g.* little Higgs with T parity) with Z' bosons exhibiting similar properties. By contrast, in a warped extra dimension, the couplings of Eq. (1) may be sizable even when SM fields propagate along the extra dimension.

Z' bosons may also be composite particles. For example, in confining gauge theories [13], the ρ-like bound state is a spin-1 boson that may be interpreted as arising from a spontaneously broken gauge symmetry [14].

Resonances versus cascade decays. In the presence of the couplings shown in Eq. (1), the Z' boson may be produced in the s-channel at colliders, and would decay to pairs of fermions. The decay width into a pair of electrons is given by

$$\Gamma\left(Z' \to e^+e^-\right) \simeq \left[\left(g_e^L\right)^2 + \left(g_e^R\right)^2\right] \frac{M_{Z'}}{24\pi} \ , \qquad (4)$$

where small corrections from electroweak loops are not included. The decay width into $q\bar{q}$ is similar, except for an additional color factor of 3, QCD radiative corrections, and fermion mass corrections. Thus, one may compute the Z' branching fractions in terms of the couplings of Eq. (1). However, other decay channels, such as WW or a pair of new particles, could have large widths and need to be added to the total decay width.

As mentioned above, there are theories in which the Z' couplings are controlled by a discrete symmetry which does not allow decay into a pair of SM particles. Typically, such theories involve several new particles, which may be produced only in pairs and undergo cascade decays through Z' bosons, leading to signals involving some missing (transverse) energy. Given that the cascade decays depend on the properties of new particles other than the Z' boson, this case is not discussed further here.

LEP-II limits. The Z' contribution to the cross sections for $e^+e^- \to f\bar{f}$ proceeds through an s-channel Z' exchange (when $f = e$, there are also t- and u-channel exchanges). For $M_{Z'} < \sqrt{s}$, the Z' appears as an $f\bar{f}$ resonance in the radiative return process where photon emission tunes the effective center-of-mass energy to $M_{Z'}$. The agreement between the LEP-II measurements and the SM predictions implies that either the Z' couplings are smaller than or of order 10^{-2}, or else $M_{Z'}$ is above 209 GeV, the maximum energy of LEP-II. In the latter case, the Z' effects may be approximated up to corrections of order $s/M_{Z'}^2$ by the contact interactions

$$\frac{g_z^2}{M_{Z'}^2 - s} \left[\bar{e}\gamma_\mu \left(z_e^L P_L + z_e^R P_R\right) e\right] \left[\bar{f}\gamma^\mu \left(z_f^L P_L + z_f^R P_R\right) f\right] \ , \qquad (5)$$

where $P_{L,R}$ are chirality projection operators, and the relation between Z' couplings and charges (see Eq. (2) in the limit where the mass and kinetic mixings are neglected) is used, assuming generation-independent charges. The four LEP collaborations have set limits on the coefficients of such operators for all possible chiral structures and for various combinations of fermions [15]. Thus, one may derive bounds on $(M_{Z'}/g_z)|z_e^L z_f^L|^{-1/2}$ and the analogous combinations of LR, RL and RR charges, which are typically on the order of a few TeV. LEP-II limits were derived [4] on the four sets of charges shown in Table 1.

Somewhat stronger bounds can be set on $M_{Z'}/g_z$ for specific sets of Z' couplings if the effects of several operators from Eq. (5) are combined. Dedicated analyses by the LEP collaborations have set limits on Z' bosons for particular values of the gauge coupling (see section 3.5.2 of [15]).

Searches at hadron colliders. Z' bosons with couplings to quarks (see Eq. (1)) may be produced at hadron colliders in the s-channel, and would show up as resonances in the invariant mass distribution of the decay products. The cross section for producing a Z' boson at the LHC which then decays to some $f\bar{f}$ final state takes the form

$$\sigma\left(pp \to Z'X \to f\bar{f}X\right) \simeq \frac{\pi}{48\,s} \sum_q c_q^f \, w_q\big(s, M_{Z'}^2\big) \qquad (6)$$

for flavor-diagonal couplings to quarks. Here we have neglected the interference with the SM contribution to $f\bar{f}$ production, which is a good approximation for a narrow Z' resonance (deviations from the narrow width approximation are discussed in [16]). The coefficients

$$c_q^f = \left[\left(g_q^L\right)^2 + \left(g_q^R\right)^2\right] B(Z' \to f\bar{f}) \qquad (7)$$

contain all the dependence on the Z' couplings, while the functions w_q include all the information about parton distributions and QCD corrections [4,6]. This factorization holds exactly to NLO, and the deviations from it induced at NNLO are very small. Note that the w_u and w_d functions are substantially larger than the w_q functions for the other quarks. Eq. (6) also applies to the Tevatron, except for changing the pp initial state to $p\bar{p}$, which implies that the $w_q(s, M_{Z'}^2)$ functions are replaced by some other functions $\bar{w}_q((1.96\,\text{TeV})^2, M_{Z'}^2)$.

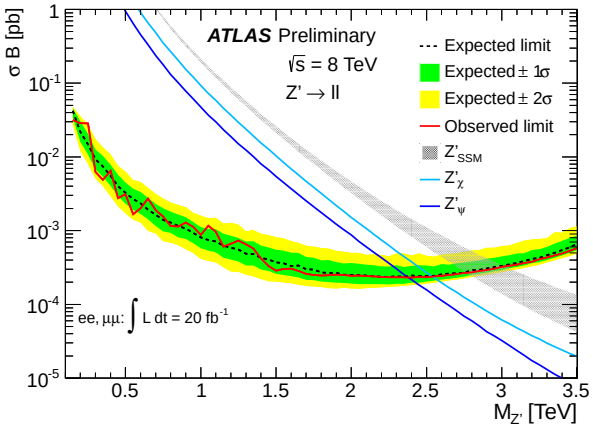

Figure 1: Upper limit on $\sigma(pp \to Z'X \to \ell^+\ell^- X)$ with $\ell = e$ or μ as a function of $M_{Z'}$ [17], assuming equal couplings for electrons and muons. The lines labelled by Z'_ψ and Z'_χ are theoretical predictions for the $U(1)_{10+x\bar{5}}$ models in Table 1 with $x = -3$ and $x = +1$, respectively, for g_z fixed by an E_6 unification condition. The $Z'_{\rm SSM}$ line corresponds to Z' couplings equal to those of the Z boson.

It is common to present results of Z' searches as limits on the cross section versus $M_{Z'}$ (see for example Fig. 1). An alternative is to plot exclusion curves for fixed $M_{Z'}$ values in the $c_u^f - c_d^f$ planes, allowing a simple derivation of the mass limit within any Z' model. LHC limits in the $c_u^\ell - c_d^\ell$ plane ($\ell = e$ or μ) for different $M_{Z'}$ are shown in Fig. 2 (for Tevatron limits, see [18,6]).

The discovery of a dilepton resonance at the LHC would determine the Z' mass and width. A measurement of the total cross section would define a band in the $c_u^\ell - c_d^\ell$ plane. Angular distributions can be used to measure several combinations of Z' parameters (an example of how angular distributions improve the Tevatron sensitivity is given in [19]). Even though the original quark direction in a pp collider is unknown, the leptonic forward-backward asymmetry $A_{\rm FB}^\ell$ can be extracted from the kinematics of the dilepton system, and is sensitive to parity-violating couplings. A fit to the Z' rapidity distribution can distinguish between the couplings to up and down quarks. These measurements, combined with off-peak observables, have the potential to differentiate among various Z' models [20]. For example, the couplings of a Z' boson with mass below 1.5 TeV can be well determined with 100 fb^{-1} of data at $\sqrt{s} = 14$ TeV. With this amount of data, the spin of the Z' boson may be determined for $M_{Z'} \leq 3$ TeV [21], and the expected sensitivity extends to $M_{Z'} \sim 4 - 5$ TeV for many models [22].

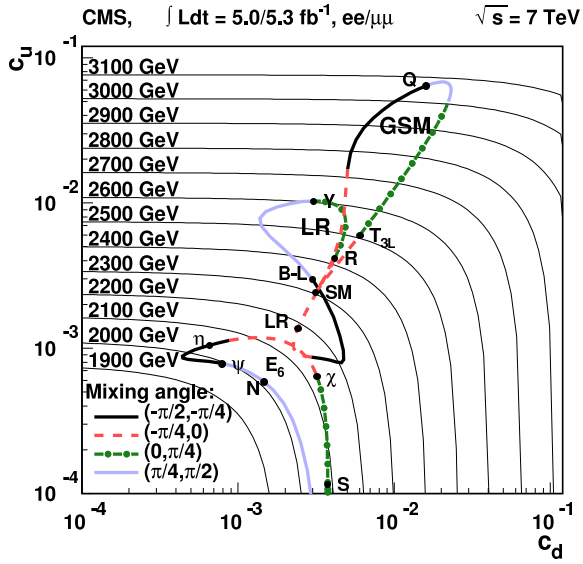

Figure 2: CMS results from [23]. Limits in the $c_u^\ell - c_d^\ell$ plane ($\ell = e$ or μ) are shown as thin lines for certain $M_{Z'}$ values. For specific sets of charges (described in [6]), parametrized by a mixing angle, the mass limit is given by the intersection of the thick and thin lines.

The Z' decays into e^+e^- and $\mu^+\mu^-$ are useful due to relatively good mass resolution and large acceptance. The Z' decays into $e\mu$ and $\tau^+\tau^-$, along with $t\bar{t}$, $b\bar{b}$ and jj which suffer from larger backgrounds, are also important as they probe various combinations of Z' couplings to fermions. The ATLAS and CMS Collaborations have performed Z' searches at the LHC in all these fermionic final states: e^+e^- and $\mu^+\mu^-$ [17,24], $e^\pm\mu^\mp$ [25], $\tau^+\tau^-$ [26], $t\bar{t}$ [27], $b\bar{b}$ [28] and jj [29].

The $pp \to Z'X \to W^+W^-X$ process may also be explored at the LHC. The Z' boson may be produced in this process through its couplings to either quarks [30] or W bosons [31].

At the Tevatron, the CDF and DØ Collaborations have searched for Z' bosons in the e^+e^- [32], $\mu^+\mu^-$ [33], $e^\pm\mu^\mp$ [34], $\tau^+\tau^-$ [35], $t\bar{t}$ [36], jj [37] and WW [38] final states. Although these limits have been often superseded by the LHC results, the Tevatron limits on certain Z' couplings (most notably, those arising from jj resonance searches [39]) remain the most stringent ones for low M'_Z.

Low-energy constraints. Z' boson properties are also constrained by a variety of low-energy experiments [40]. Polarized electron-nucleon scattering and atomic parity violation are sensitive to electron-quark contact interactions, which get contributions from Z' exchange that can be expressed in terms of the couplings introduced in Eq. (1) and M'_Z. Further corrections to the electron-quark contact interactions are induced in the presence of $\tilde{Z} - \tilde{Z}'$ mixing because of the shifts in the Z couplings to quarks and leptons [2]. Deep-inelastic neutrino-nucleon scattering is similarly affected by Z' bosons. Other low-energy observables are discussed in [3]. In some models, the lower limits on $M_{Z'}$ set by low energy data are above 1 TeV.

Although the LHC data are most constraining for many Z' models, one should be careful in assessing the relative reach of various experiments given the freedom in Z' couplings. For example, a Z' coupled to $B - yL_\mu + (y-3)L_\tau$ has implications for the muon $g-2$, neutrino oscillations or τ decays, and would be hard to see in processes involving first-generation fermions. Moreover, the combination of LHC searches and low-energy measurements could allow a precise determination of the Z' parameters [41].

References

1. For reviews, see P. Langacker, Rev. Mod. Phys. **81**, 1199 (2009); A. Leike, Phys. Rept. **317**, 143 (1999); J. Hewett and T. Rizzo, Phys. Rept. **183**, 193 (1989).
2. K.S. Babu *et al.*, Phys. Rev. **D57**, 6788 (1998); B. Holdom, Phys. Lett. **B259**, 329 (1991).
3. J. Erler *et al.*, JHEP **0908**, 017 (2009).
4. M.S. Carena *et al.*, Phys. Rev. D**70**, 093009 (2004).
5. See, *e.g.*, F. Del Aguila *et al.*, Phys. Rev. D**52**, 37 (1995).
6. E. Accomando *et al.*, Phys. Rev. **D83**, 075012 (2011).
7. M.-C. Chen *et al.*, Phys. Rev. D**75**, 055009 (2007).
8. P. Langacker and M. Plumacher, Phys. Rev. D**62**, 013006 (2000); R.S. Chivukula and E.H. Simmons, Phys. Rev. D**66**, 015006 (2002).
9. A. J. Buras, F. De Fazio, and J. Girrbach, JHEP **1302**, 116 (2013).
10. L.E. Ibanez and G.G. Ross, Phys. Lett. B**332**, 100 (1994).
11. See the Section on "W' searches" in this *Review*.
12. J. Parsons and A. Pomarol, "Extra dimensions" in this *Review*.
13. R.S. Chivukula *et al.*, "Dynamical electroweak symmetry breaking" in this *Review*.
14. M. Bando *et al.*, Phys. Rept. **164**, 217 (1988).
15. J. Alcaraz *et al.* [ALEPH, DELPHI, L3, OPAL Collabs., LEP Electroweak Working Group], hep-ex/0612034.
16. E. Accomando *et al.*, JHEP **1310**, 153 (2013).
17. ATLAS Collab., note ATLAS-CONF-2013-017, Mar. 2013.
18. A. Abulencia *et al.* [CDF Collab.], Phys. Rev. Lett. **95**, 252001 (2005).
19. A. Abulencia *et al.* [CDF Collab.], Phys. Rev. Lett. **96**, 211801 (2006).
20. F. Petriello and S. Quackenbush, Phys. Rev. D**77**, 115004 (2008).
21. P. Osland *et al*, Phys. Rev. D**79**, 115021 (2009).
22. G.L. Bayatian *et al.* [CMS Collab.], J. Phys. G**34**, 995 (2007).
23. S. Chatrchyan *et al.* [CMS Collab.], Phys. Lett. B**714**, 158 (2012).
24. CMS Collab., note PAS-EXO-12-061, Feb. 2013.
25. G. Aad *et al.* [ATLAS Collab.], Eur. Phys. J. C**71**, 1809 (2011).
26. S. Chatrchyan *et al.* [CMS Collab.], Phys. Lett. B**716**, 82 (2012); G. Aad *et al.* [ATLAS Collab.], Phys. Lett. B**719**, 242 (2013); note ATLAS-CONF-2013-066, July 2013.
27. G. Aad *et al.* [ATLAS Collab.], JHEP **1301**, 116 (2013); note ATLAS-CONF-2013-052, May 2013; S. Chatrchyan *et al.* [CMS Collab.], arXiv:1309.2030.
28. CMS Collab., note PAS-EXO-12-023, Apr. 2013.
29. S. Chatrchyan *et al.* [CMS Collab.], arXiv:1302.4794; JHEP 1301, 013 (2013); note PAS-EXO-12-059, Feb. 2013; note PAS-EXO-11-094, July 2012.
30. A. Alves *et al.*, Phys. Rev. D**80**, 073011 (2009).
31. H. J. He *et al.*, Phys. Rev. D**78**, 031701 (2008).
32. V. M. Abazov *et al.* [D0 Collab.], Phys. Lett. B**695**, 88 (2011); T. Aaltonen *et al.* [CDF Collab.], Phys. Rev. Lett. **102**, 031801 (2009).
33. T. Aaltonen *et al.* [CDF Collab.], Phys. Rev. Lett. **106**, 121801 (2011).
34. A. Abulencia *et al.* [CDF Collab.], Phys. Rev. Lett. **96**, 211802 (2006); V. M. Abazov *et al.* [D0 Collab.], Phys. Rev. Lett. **105**, 191802 (2010).
35. D. Acosta *et al.* [CDF Collab.], Phys. Rev. Lett. **95**, 131801 (2005).
36. T. Aaltonen *et al.* [CDF Collab.], Phys. Rev. D**84**, 072004 (2011); V. M. Abazov *et al.* [D0 Collab.], Phys. Rev. D**85**, 051101 (2012).
37. T. Aaltonen *et al.* [CDF Collab.], Phys. Rev. D**79**, 112002 (2009).
38. T. Aaltonen *et al.* [CDF Collab.], Phys. Rev. Lett. **104**, 241801 (2010).
39. B.A. Dobrescu and F. Yu, Phys. Rev. D**88**, 035021 (2013).
40. See, *e.g.*, V.D. Barger *et al.*, Phys. Rev. D**57**, 391 (1998); J. Erler and M.J. Ramsey-Musolf, Prog. Part. Nucl. Phys. **54**, 351 (2005).
41. Y. Li *et al.*, Phys. Rev. D**80**, 055018 (2009).

MASS LIMITS for Z' (Heavy Neutral Vector Boson Other Than Z)

Limits for Z'_{SM}

Z'_{SM} is assumed to have couplings with quarks and leptons which are identical to those of Z, and decays only to known fermions. The most recent preliminary results can be found in the "Z'-boson searches" review above.

VALUE (GeV)	CL%	DOCUMENT ID		TECN	COMMENT
>1400	95	[1] AAD	13S	ATLS	pp; $Z'_{SM} \to \tau^+\tau^-$
>1470	95	CHATRCHYAN	13A	CMS	pp; $Z'_{SM} \to q\overline{q}$
>2590	95	[2] CHATRCHYAN	13AF	CMS	pp; $Z'_{SM} \to e^+e^-, \mu^+\mu^-$
none 1000–1620	95	[3] CHATRCHYAN	13AS	CMS	pp; $Z'_{SM} \to q\overline{q}$
>2220	95	[4] AAD	12CC	ATLS	pp; $Z'_{SM} \to e^+e^-, \mu^+\mu^-$
>1400	95	[5] CHATRCHYAN	12O	CMS	pp; $Z'_{SM} \to \tau^+\tau^-$
>1500	95	[6] CHEUNG	01B	RVUE	Electroweak
• • • We do not use the following data for averages, fits, limits, etc. • • •					
>2330	95	[7] CHATRCHYAN	12M	CMS	pp; $Z'_{SM} \to e^+e^-, \mu^+\mu^-$
>1830	95	[8] AAD	11AD	ATLS	pp; $Z'_{SM} \to e^+e^-, \mu^+\mu^-$
>1048	95	[9] AAD	11J	ATLS	pp, $Z'_{SM} \to e^+e^-, \mu^+\mu^-$
>1071	95	[10] AALTONEN	11I	CDF	$p\overline{p}$; $Z'_{SM} \to \mu^+\mu^-$
>1023	95	[11] ABAZOV	11A	D0	$p\overline{p}$; $Z'_{SM} \to e^+e^-$
>1140	95	[12] CHATRCHYAN	11	CMS	pp, $Z'_{SM} \to e^+e^-, \mu^+\mu^-$
none 247–544	95	[13] AALTONEN	10N	CDF	$Z' \to WW$
none 320–740	95	[14] AALTONEN	09AC	CDF	$Z' \to q\overline{q}$
> 963	95	[11] AALTONEN	09T	CDF	$p\overline{p}$; $Z'_{SM} \to e^+e^-$
>1030	95	[15] AALTONEN	09V	CDF	$p\overline{p}$; $Z'_{SM} \to \mu^+\mu^-$
>1403	95	[16] ERLER	09	RVUE	Electroweak
> 923	95	[11] AALTONEN	07H	CDF	Repl. by AALTONEN 09T
>1305	95	[17] ABDALLAH	06C	DLPH	e^+e^-
> 850		[11] ABULENCIA	06L	CDF	Repl. by AALTONEN 07H
> 825	95	[18] ABULENCIA	05A	CDF	$p\overline{p}$; $Z'_{SM} \to e^+e^-, \mu^+\mu^-$
> 399	95	[19] ACOSTA	05R	CDF	$\overline{p}p$: $Z'_{SM} \to \tau^+\tau^-$
none 400–640	95	ABAZOV	04C	D0	$p\overline{p}$: $Z'_{SM} \to q\overline{q}$
>1018	95	[20] ABBIENDI	04G	OPAL	e^+e^-
> 670	95	[21] ABAZOV	01B	D0	$p\overline{p}$, $Z'_{SM} \to e^+e^-$
> 710	95	[22] ABREU	00S	DLPH	e^+e^-
> 898	95	[23] BARATE	00I	ALEP	e^+e^-
> 809	95	[24] ERLER	99	RVUE	Electroweak

> 690	95	[25] ABE	97S	CDF	$p\overline{p}$; $Z'_{SM} \to e^+e^-$, $\mu^+\mu^-$
> 490	95	ABACHI	96D	D0	$p\overline{p}$; $Z'_{SM} \to e^+e^-$
> 398	95	[26] VILAIN	94B	CHM2	$\nu_\mu e \to \nu_\mu e$ and $\overline{\nu}_\mu e \to \overline{\nu}_\mu e$
> 237	90	[27] ALITTI	93	UA2	$p\overline{p}$; $Z'_{SM} \to q\overline{q}$
none 260–600	95	[28] RIZZO	93	RVUE	$p\overline{p}$; $Z'_{SM} \to q\overline{q}$
> 426	90	[29] ABE	90F	VNS	e^+e^-

[1] AAD 13S search for resonances decaying to $\tau^+\tau^-$ in pp collisions at $\sqrt{s}$ = 7 TeV.
[2] CHATRCHYAN 13AF search for resonances decaying to e^+e^-, $\mu^+\mu^-$ in pp collisions at $\sqrt{s}$ = 7 TeV and 8 TeV.
[3] CHATRCHYAN 13AS search for new resonance decaying to dijets in pp collisions at $\sqrt{s}$ = 8 TeV.
[4] AAD 12CC search for resonances decaying to e^+e^-, $\mu^+\mu^-$ in pp collisions at $\sqrt{s}$ = 7 TeV.
[5] CHATRCHYAN 12O search for resonances decaying to $\tau^+\tau^-$ in pp collisions at $\sqrt{s}$ = 7 TeV.
[6] CHEUNG 01B limit is derived from bounds on contact interactions in a global electroweak analysis.
[7] CHATRCHYAN 12M search for resonances decaying to e^+e^- or $\mu^+\mu^-$ in pp collisions at $\sqrt{s}$ = 7 TeV.
[8] AAD 11AD search for resonances decaying to e^+e^-, $\mu^+\mu^-$ in pp collisions at $\sqrt{s}$ = 7 TeV.
[9] AAD 11J search for resonances decaying to e^+e^- or $\mu^+\mu^-$ in pp collisions at $\sqrt{s}$ = 7 TeV.
[10] AALTONEN 11I search for resonances decaying to $\mu^+\mu^-$ in $p\overline{p}$ collisions at $\sqrt{s}$ = 1.96 TeV.
[11] ABAZOV 11A, AALTONEN 09T, AALTONEN 07H, and ABULENCIA 06L search for resonances decaying to e^+e^- in $p\overline{p}$ collisions at $\sqrt{s}$ = 1.96 TeV.
[12] CHATRCHYAN 11 search for resonances decaying to e^+e^- or $\mu^+\mu^-$ in pp collisions at $\sqrt{s}$ = 7 TeV.
[13] The quoted limit assumes $g_{WWZ'}/g_{WWZ} = (M_W/M_{Z'})^2$. See their Fig. 4 for limits in mass-coupling plane.
[14] AALTONEN 09AC search for new particle decaying to dijets.
[15] AALTONEN 09V search for resonances decaying to $\mu^+\mu^-$ in $p\overline{p}$ collisions at $\sqrt{s}$ = 1.96 TeV.
[16] ERLER 09 give 95% CL limit on the Z-Z' mixing $-0.0026 < \theta < 0.0006$.
[17] ABDALLAH 06C use data $\sqrt{s}$ = 130–207 GeV.
[18] ABULENCIA 05A search for resonances decaying to electron or muon pairs in $p\overline{p}$ collisions at $\sqrt{s}$ = 1.96 TeV.
[19] ACOSTA 05R search for resonances decaying to tau lepton pairs in $\overline{p}p$ collisions at $\sqrt{s}$ = 1.96 TeV.
[20] ABBIENDI 04G give 95% CL limit on Z-Z' mixing $-0.00422 < \theta < 0.00091$. $\sqrt{s}$ = 91 to 207 GeV.
[21] ABAZOV 01B search for resonances in $p\overline{p} \to e^+e^-$ at $\sqrt{s}$=1.8 TeV. They find $\sigma \cdot$ B($Z' \to ee$)< 0.06 pb for $M_{Z'} > 500$ GeV.
[22] ABREU 00S uses LEP data at $\sqrt{s}$=90 to 189 GeV.
[23] BARATE 00I search for deviations in cross section and asymmetries in $e^+e^- \to$ fermions at $\sqrt{s}$=90 to 183 GeV. Assume θ=0. Bounds in the mass-mixing plane are shown in their Figure 18.
[24] ERLER 99 give 90%CL limit on the Z-Z' mixing $-0.0041 < \theta < 0.0003$. ρ_0=1 is assumed.
[25] ABE 97S find $\sigma(Z')\times$B(e^+e^-,$\mu^+\mu^-$)< 40 fb for $m_{Z'} > 600$ GeV at $\sqrt{s}$= 1.8 TeV.
[26] VILAIN 94B assume m_t = 150 GeV.
[27] ALITTI 93 search for resonances in the two-jet invariant mass. The limit assumes B($Z' \to q\overline{q}$)=0.7. See their Fig. 5 for limits in the $m_{Z'}$–B($q\overline{q}$) plane.
[28] RIZZO 93 analyses CDF limit on possible two-jet resonances.
[29] ABE 90F use data for R, $R_{\ell\ell}$, and $A_{\ell\ell}$. They fix m_W = 80.49 ± 0.43 ± 0.24 GeV and m_Z = 91.13 ± 0.03 GeV.

Limits for Z_{LR}

Z_{LR} is the extra neutral boson in left-right symmetric models. $g_L = g_R$ is assumed unless noted. Values in parentheses assume stronger constraint on the Higgs sector, usually motivated by specific left-right symmetric models (see the Note on the W'). Values in brackets are from cosmological and astrophysical considerations and assume a light right-handed neutrino. Direct search bounds assume decays to Standard Model fermions only, unless noted.

VALUE (GeV)	CL%	DOCUMENT ID		TECN	COMMENT
>1162	95	[1] DEL-AGUILA	10	RVUE	Electroweak
> 630	95	[2] ABE	97S	CDF	$p\overline{p}$; $Z'_{LR} \to e^+e^-$, $\mu^+\mu^-$
• • • We do not use the following data for averages, fits, limits, etc. • • •					
> 998	95	[3] ERLER	09	RVUE	Electroweak
> 600	95	SCHAEL	07A	ALEP	e^+e^-
> 455	95	[4] ABDALLAH	06C	DLPH	e^+e^-
> 518	95	[5] ABBIENDI	04G	OPAL	e^+e^-
> 860	95	[6] CHEUNG	01B	RVUE	Electroweak
> 380	95	[7] ABREU	00S	DLPH	e^+e^-
> 436	95	[8] BARATE	00I	ALEP	Repl. by SCHAEL 07A
> 550	95	[9] CHAY	00	RVUE	Electroweak
		[10] ERLER	00	RVUE	Cs
		[11] CASALBUONI	99	RVUE	Cs
(> 1205)	90	[12] CZAKON	99	RVUE	Electroweak
> 564	95	[13] ERLER	99	RVUE	Electroweak
(> 1673)	95	[14] ERLER	99	RVUE	Electroweak
(> 1700)	68	[15] BARENBOIM	98	RVUE	Electroweak
> 244	95	[16] CONRAD	98	RVUE	$\nu_\mu N$ scattering
> 253	95	[17] VILAIN	94B	CHM2	$\nu_\mu e \to \nu_\mu e$ and $\overline{\nu}_\mu e \to \overline{\nu}_\mu e$
none 200–600	95	[18] RIZZO	93	RVUE	$p\overline{p}$; $Z_{LR} \to q\overline{q}$
[> 2000]		WALKER	91	COSM	Nucleosynthesis; light ν_R
none 200–500		[19] GRIFOLS	90	ASTR	SN 1987A; light ν_R
none 350–2400		[20] BARBIERI	89B	ASTR	SN 1987A; light ν_R

[1] DEL-AGUILA 10 give 95% CL limit on the Z-Z' mixing $-0.0012 < \theta < 0.0004$.
[2] ABE 97S find $\sigma(Z')\times$B(e^+e^-,$\mu^+\mu^-$)< 40 fb for $m_{Z'} > 600$ GeV at $\sqrt{s}$= 1.8 TeV.
[3] ERLER 09 give 95% CL limit on the Z-Z' mixing $-0.0013 < \theta < 0.0006$.
[4] ABDALLAH 06C give 95% CL limit $|\theta| < 0.0028$. See their Fig. 14 for limit contours in the mass-mixing plane.
[5] ABBIENDI 04G give 95% CL limit on Z-Z' mixing $-0.00098 < \theta < 0.00190$. See their Fig. 20 for the limit contour in the mass-mixing plane. $\sqrt{s}$ = 91 to 207 GeV.
[6] CHEUNG 01B limit is derived from bounds on contact interactions in a global electroweak analysis.
[7] ABREU 00S give 95% CL limit on Z-Z' mixing $|\theta| < 0.0018$. See their Fig. 6 for the limit contour in the mass-mixing plane. $\sqrt{s}$=90 to 189 GeV.
[8] BARATE 00I search for deviations in cross section and asymmetries in $e^+e^- \to$ fermions at $\sqrt{s}$=90 to 183 GeV. Assume θ=0. Bounds in the mass-mixing plane are shown in their Figure 18.
[9] CHAY 00 also find $-0.0003 < \theta < 0.0019$. For g_R free, $m_{Z'} > 430$ GeV.
[10] ERLER 00 discuss the possibility that a discrepancy between the observed and predicted values of Q_W(Cs) is due to the exchange of Z'. The data are better described in a certain class of the Z' models including Z_{LR} and Z_χ.
[11] CASALBUONI 99 discuss the discrepancy between the observed and predicted values of Q_W(Cs). It is shown that the data are better described in a class of models including the Z_{LR} model.
[12] CZAKON 99 perform a simultaneous fit to charged and neutral sectors. Assumes manifest left-right symmetric model. Finds $|\theta| < 0.0042$.
[13] ERLER 99 give 90% CL limit on the Z-Z' mixing $-0.0009 < \theta < 0.0017$.
[14] ERLER 99 assumes 2 Higgs doublets, transforming as 10 of SO(10), embedded in E_6.
[15] BARENBOIM 98 also gives 68% CL limits on the Z-Z' mixing $-0.0005 < \theta < 0.0033$. Assumes Higgs sector of minimal left-right model.
[16] CONRAD 98 limit is from measurements at CCFR, assuming no Z-Z' mixing.
[17] VILAIN 94B assume m_t = 150 GeV and θ=0. See Fig. 2 for limit contours in the mass-mixing plane.
[18] RIZZO 93 analyses CDF limit on possible two-jet resonances.
[19] GRIFOLS 90 limit holds for $m_{\nu_R} \lesssim 1$ MeV. A specific Higgs sector is assumed. See also GRIFOLS 90D, RIZZO 91.
[20] BARBIERI 89B limit holds for $m_{\nu_R} \leq 10$ MeV. Bounds depend on assumed supernova core temperature.

Limits for Z_χ

Z_χ is the extra neutral boson in SO(10) → SU(5) × U(1)$_\chi$. $g_\chi = e/\cos\theta_W$ is assumed unless otherwise stated. We list limits with the assumption $\rho = 1$ but with no further constraints on the Higgs sector. Values in parentheses assume stronger constraint on the Higgs sector motivated by superstring models. Values in brackets are from cosmological and astrophysical considerations and assume a light right-handed neutrino.

VALUE (GeV)	CL%	DOCUMENT ID		TECN	COMMENT
>1970	95	[1] AAD	12CC	ATLS	pp, $Z'_\chi \to e^+e^-$, $\mu^+\mu^-$
>1141	95	[2] ERLER	09	RVUE	Electroweak
• • • We do not use the following data for averages, fits, limits, etc. • • •					
>1640	95	[3] AAD	11AD	ATLS	pp; $Z'_\chi \to e^+e^-$, $\mu^+\mu^-$
> 900	95	[4] AAD	11J	ATLS	pp, $Z'_\chi \to e^+e^-$, $\mu^+\mu^-$
> 930	95	[5] AALTONEN	11I	CDF	$p\overline{p}$; $Z'_\chi \to \mu^+\mu^-$
> 903	95	[6] ABAZOV	11A	D0	$p\overline{p}$, $Z'_\chi \to e^+e^-$
>1022	95	[7] DEL-AGUILA	10	RVUE	Electroweak
> 862	95	[6] AALTONEN	09T	CDF	$p\overline{p}$, $Z'_\chi \to e^+e^-$
> 892	95	[8] AALTONEN	09V	CDF	$p\overline{p}$; $Z'_\chi \to \mu^+\mu^-$
> 822	95	[6] AALTONEN	07H	CDF	Repl. by AALTONEN 09T
> 680	95	SCHAEL	07A	ALEP	e^+e^-
> 545	95	[9] ABDALLAH	06C	DLPH	e^+e^-
> 740		[6] ABULENCIA	06L	CDF	Repl. by AALTONEN 07H
> 690	95	[10] ABULENCIA	05A	CDF	$p\overline{p}$; $Z'_\chi \to e^+e^-$, $\mu^+\mu^-$
> 781	95	[11] ABBIENDI	04G	OPAL	e^+e^-
>2100		[12] BARGER	03B	COSM	Nucleosynthesis; light ν_R
> 680	95	[13] CHEUNG	01B	RVUE	Electroweak
> 440	95	[14] ABREU	00S	DLPH	e^+e^-
> 533	95	[15] BARATE	00I	ALEP	Repl. by SCHAEL 07A
> 554	95	[16] CHO	00	RVUE	Electroweak
		[17] ERLER	00	RVUE	Cs
		[18] ROSNER	00	RVUE	Cs
> 545	95	[19] ERLER	99	RVUE	Electroweak
(> 1368)	95	[20] ERLER	99	RVUE	Electroweak
> 215	95	[21] CONRAD	98	RVUE	$\nu_\mu N$ scattering
> 595	95	[22] ABE	97S	CDF	$p\overline{p}$; $Z'_\chi \to e^+e^-$, $\mu^+\mu^-$
> 190	95	[23] ARIMA	97	VNS	Bhabha scattering
> 262	95	[24] VILAIN	94B	CHM2	$\nu_\mu e \to \nu_\mu e$; $\overline{\nu}_\mu e \to \overline{\nu}_\mu e$
[>1470]		[25] FARAGGI	91	COSM	Nucleosynthesis; light ν_R
> 231	90	[26] ABE	90F	VNS	e^+e^-
[> 1140]		[27] GONZALEZ-G..	90D	COSM	Nucleosynthesis; light ν_R
[> 2100]		[28] GRIFOLS	90	ASTR	SN 1987A; light ν_R

[1] AAD 12CC search for resonances decaying to e^+e^-, $\mu^+\mu^-$ in pp collisions at $\sqrt{s}=7$ TeV.
[2] ERLER 09 give 95% CL limit on the Z-Z' mixing $-0.0016<\theta<0.0006$.
[3] AAD 11AD search for resonances decaying to e^+e^-, $\mu^+\mu^-$ in pp collisions at $\sqrt{s}=7$ TeV.
[4] AAD 11J search for resonances decaying to e^+e^- or $\mu^+\mu^-$ in pp collisions at $\sqrt{s}=7$ TeV.
[5] AALTONEN 11I search for resonances decaying to $\mu^+\mu^-$ in $p\overline{p}$ collisions at $\sqrt{s}=1.96$ TeV.
[6] ABAZOV 11A, AALTONEN 09T, AALTONEN 07H, and ABULENCIA 06L search for resonances decaying to e^+e^- in $p\overline{p}$ collisions at $\sqrt{s}=1.96$ TeV.
[7] DEL-AGUILA 10 give 95% CL limit on the Z-Z' mixing $-0.0011<\theta<0.0007$.
[8] AALTONEN 09V search for resonances decaying to $\mu^+\mu^-$ in $p\overline{p}$ collisions at $\sqrt{s}=1.96$ TeV.
[9] ABDALLAH 06C give 95% CL limit $|\theta|<0.0031$. See their Fig. 14 for limit contours in the mass-mixing plane.
[10] ABULENCIA 05A search for resonances decaying to electron or muon pairs in $p\overline{p}$ collisions at $\sqrt{s}=1.96$ TeV.
[11] ABBIENDI 04G give 95% CL limit on Z-Z' mixing $-0.00099<\theta<0.00194$. See their Fig. 20 for the limit contour in the mass-mixing plane. $\sqrt{s}=91$ to 207 GeV.
[12] BARGER 03B limit is from the nucleosynthesis bound on the effective number of light neutrino δN_ν <1. The quark-hadron transition temperature T_C=150 MeV is assumed. The limit with T_C=400 MeV is >4300 GeV.
[13] CHEUNG 01B limit is derived from bounds on contact interactions in a global electroweak analysis.
[14] ABREU 00S give 95% CL limit on Z-Z' mixing $|\theta|<0.0017$. See their Fig. 6 for the limit contour in the mass-mixing plane. $\sqrt{s}$=90 to 189 GeV.
[15] BARATE 00I search for deviations in cross section and asymmetries in $e^+e^-\to$ fermions at $\sqrt{s}$=90 to 183 GeV. Assume θ=0. Bounds in the mass-mixing plane are shown in their Figure 18.
[16] CHO 00 use various electroweak data to constrain Z' models assuming m_H=100 GeV. See Fig. 3 for limits in the mass-mixing plane.
[17] ERLER 00 discuss the possibility that a discrepancy between the observed and predicted values of Q_W(Cs) is due to the exchange of Z'. The data are better described in a certain class of the Z' models including Z_{LR} and Z_χ.
[18] ROSNER 00 discusses the possibility that a discrepancy between the observed and predicted values of Q_W(Cs) is due to the exchange of Z'. The data are better described in a certain class of the Z' models including Z_χ.
[19] ERLER 99 give 90% CL limit on the Z-Z' mixing $-0.0020<\theta<0.0015$.
[20] ERLER 99 assumes 2 Higgs doublets, transforming as 10 of SO(10), embedded in E_6.
[21] CONRAD 98 limit is from measurements at CCFR, assuming no Z-Z' mixing.
[22] ABE 97S find $\sigma(Z')\times$B(e^+e^-,$\mu^+\mu^-$)< 40 fb for $m_{Z'}>600$ GeV at $\sqrt{s}$= 1.8 TeV.
[23] Z-Z' mixing is assumed to be zero. $\sqrt{s}$= 57.77 GeV.
[24] VILAIN 94B assume $m_t=150$ GeV and θ=0. See Fig. 2 for limit contours in the mass-mixing plane.
[25] FARAGGI 91 limit assumes the nucleosynthesis bound on the effective number of neutrinos $\Delta N_\nu<0.5$ and is valid for $m_{\nu_R}<1$ MeV.
[26] ABE 90F use data for R, $R_{\ell\ell}$, and $A_{\ell\ell}$. ABE 90F fix $m_W=80.49\pm0.43\pm0.24$ GeV and $m_Z=91.13\pm0.03$ GeV.
[27] Assumes the nucleosynthesis bound on the effective number of light neutrinos ($\delta N_\nu<1$) and that ν_R is light ($\lesssim$ 1 MeV).
[28] GRIFOLS 90 limit holds for $m_{\nu_R}\lesssim$ 1 MeV. See also GRIFOLS 90D, RIZZO 91.

Limits for Z_ψ

Z_ψ is the extra neutral boson in $E_6\to SO(10)\times U(1)_\psi$. $g_\psi=e/\cos\theta_W$ is assumed unless otherwise stated. We list limits with the assumption $\rho=1$ but with no further constraints on the Higgs sector. Values in brackets are from cosmological and astrophysical considerations and assume a light right-handed neutrino.

VALUE (GeV)	CL%	DOCUMENT ID		TECN	COMMENT
>2260	95	[1] CHATRCHYAN	13AF	CMS	pp, $Z'_\psi\to e^+e^-$, $\mu^+\mu^-$
>1790	95	[2] AAD	12CC	ATLS	pp, $Z'_\psi\to e^+e^-$, $\mu^+\mu^-$
>1100	95	[3] CHATRCHYAN	12O	CMS	pp, $Z'_\psi\to\tau^+\tau^-$
> 476	95	[4] DEL-AGUILA	10	RVUE	Electroweak
• • • We do not use the following data for averages, fits, limits, etc. • • •					
>2000	95	[5] CHATRCHYAN	12M	CMS	pp, $Z'_\psi\to e^+e^-$, $\mu^+\mu^-$
>1490	95	[6] AAD	11AD	ATLS	pp; $Z'_\psi\to e^+e^-$, $\mu^+\mu^-$
> 738	95	[7] AAD	11J	ATLS	pp; $Z'_\psi\to e^+e^-$, $\mu^+\mu^-$
> 917	95	[8] AALTONEN	11I	CDF	$p\overline{p}$; $Z'_\psi\to\mu^+\mu^-$
> 891	95	[9] ABAZOV	11A	D0	$p\overline{p}$; $Z'_\psi\to e^+e^-$
> 887	95	[10] CHATRCHYAN	11	CMS	pp, $Z'_\psi\to e^+e^-$, $\mu^+\mu^-$
> 851	95	[9] AALTONEN	09T	CDF	$p\overline{p}$, $Z'_\psi\to e^+e^-$
> 878	95	[11] AALTONEN	09V	CDF	$p\overline{p}$; $Z'_\psi\to\mu^+\mu^-$
> 147	95	[12] ERLER	09	RVUE	Electroweak
> 822	95	[9] AALTONEN	07H	CDF	Repl. by AALTONEN 09T
> 410	95	SCHAEL	07A	ALEP	e^+e^-
> 475	95	[13] ABDALLAH	06C	DLPH	e^+e^-
> 725		[9] ABULENCIA	06L	CDF	Repl. by AALTONEN 07H
> 675	95	[14] ABULENCIA	05A	CDF	$p\overline{p}$; $Z'_\psi\to e^+e^-$, $\mu^+\mu^-$
> 366	95	[15] ABBIENDI	04G	OPAL	e^+e^-
> 600		[16] BARGER	03B	COSM	Nucleosynthesis; light ν_R
> 350	95	[17] ABREU	00S	DLPH	e^+e^-
> 294	95	[18] BARATE	00I	ALEP	Repl. by SCHAEL 07A
> 137	95	[19] CHO	00	RVUE	Electroweak
> 146	95	[20] ERLER	99	RVUE	Electroweak
> 54	95	[21] CONRAD	98	RVUE	$\nu_\mu N$ scattering
> 590	95	[22] ABE	97S	CDF	$p\overline{p}$; $Z'_\psi\to e^+e^-$, $\mu^+\mu^-$
> 135	95	[23] VILAIN	94B	CHM2	$\nu_\mu e\to\nu_\mu e$; $\overline{\nu}_\mu e\to\overline{\nu}_\mu e$
> 105	90	[24] ABE	90F	VNS	e^+e^-
[> 160]		[25] GONZALEZ-G..	90D	COSM	Nucleosynthesis; light ν_R
[> 2000]		[26] GRIFOLS	90D	ASTR	SN 1987A; light ν_R

[1] CHATRCHYAN 13AF search for resonances decaying to e^+e^-, $\mu^+\mu^-$ in pp collisions at $\sqrt{s}=7$ TeV and 8 TeV.
[2] AAD 12CC search for resonances decaying to e^+e^-, $\mu^+\mu^-$ in pp collisions at $\sqrt{s}=7$ TeV.
[3] CHATRCHYAN 12O search for resonances decaying to $\tau^+\tau^-$ in pp collisions at $\sqrt{s}=7$ TeV.
[4] DEL-AGUILA 10 give 95% CL limit on the Z-Z' mixing $-0.0019<\theta<0.0007$.
[5] CHATRCHYAN 12M search for resonances decaying to e^+e^- or $\mu^+\mu^-$ in pp collisions at $\sqrt{s}=7$ TeV.
[6] AAD 11AD search for resonances decaying to e^+e^-, $\mu^+\mu^-$ in pp collisions at $\sqrt{s}=7$ TeV.
[7] AAD 11J search for resonances decaying to e^+e^- or $\mu^+\mu^-$ in pp collisions at $\sqrt{s}=7$ TeV.
[8] AALTONEN 11I search for resonances decaying to $\mu^+\mu^-$ in $p\overline{p}$ collisions at $\sqrt{s}=1.96$ TeV.
[9] ABAZOV 11A, AALTONEN 09T, AALTONEN 07H, and ABULENCIA 06L search for resonances decaying to e^+e^- in $p\overline{p}$ collisions at $\sqrt{s}=1.96$ TeV.
[10] CHATRCHYAN 11 search for resonances decaying to e^+e^- or $\mu^+\mu^-$ in pp collisions at $\sqrt{s}=7$ TeV.
[11] AALTONEN 09V search for resonances decaying to $\mu^+\mu^-$ in $p\overline{p}$ collisions at $\sqrt{s}=1.96$ TeV.
[12] ERLER 09 give 95% CL limit on the Z-Z' mixing $-0.0018<\theta<0.0009$.
[13] ABDALLAH 06C give 95% CL limit $|\theta|<0.0027$. See their Fig. 14 for limit contours in the mass-mixing plane.
[14] ABULENCIA 05A search for resonances decaying to electron or muon pairs in $p\overline{p}$ collisions at $\sqrt{s}=1.96$ TeV.
[15] ABBIENDI 04G give 95% CL limit on Z-Z' mixing $-0.00129<\theta<0.00258$. See their Fig. 20 for the limit contour in the mass-mixing plane. $\sqrt{s}=91$ to 207 GeV.
[16] BARGER 03B limit is from the nucleosynthesis bound on the effective number of light neutrino δN_ν <1. The quark-hadron transition temperature T_C=150 MeV is assumed. The limit with T_C=400 MeV is >1100 GeV.
[17] ABREU 00S give 95% CL limit on Z-Z' mixing $|\theta|<0.0018$. See their Fig. 6 for the limit contour in the mass-mixing plane. $\sqrt{s}$=90 to 189 GeV.
[18] BARATE 00I search for deviations in cross section and asymmetries in $e^+e^-\to$ fermions at $\sqrt{s}$=90 to 183 GeV. Assume θ=0. Bounds in the mass-mixing plane are shown in their Figure 18.
[19] CHO 00 use various electroweak data to constrain Z' models assuming m_H=100 GeV. See Fig. 3 for limits in the mass-mixing plane.
[20] ERLER 99 give 90% CL limit on the Z-Z' mixing $-0.0013<\theta<0.0024$.
[21] CONRAD 98 limit is from measurements at CCFR, assuming no Z-Z' mixing.
[22] ABE 97S find $\sigma(Z')\times$B(e^+e^-,$\mu^+\mu^-$)< 40 fb for $m_{Z'}>600$ GeV at $\sqrt{s}$= 1.8 TeV.
[23] VILAIN 94B assume $m_t=150$ GeV and θ=0. See Fig. 2 for limit contours in the mass-mixing plane.
[24] ABE 90F use data for R, $R_{\ell\ell}$, and $A_{\ell\ell}$. ABE 90F fix $m_W=80.49\pm0.43\pm0.24$ GeV and $m_Z=91.13\pm0.03$ GeV.
[25] Assumes the nucleosynthesis bound on the effective number of light neutrinos ($\delta N_\nu<1$) and that ν_R is light ($\lesssim$ 1 MeV).
[26] GRIFOLS 90D limit holds for $m_{\nu_R}\lesssim$ 1 MeV. See also RIZZO 91.

Limits for Z_η

Z_η is the extra neutral boson in E_6 models, corresponding to $Q_\eta=\sqrt{3/8}\,Q_\chi-\sqrt{5/8}\,Q_\psi$. $g_\eta=e/\cos\theta_W$ is assumed unless otherwise stated. We list limits with the assumption $\rho=1$ but with no further constraints on the Higgs sector. Values in parentheses assume stronger constraint on the Higgs sector motivated by superstring models. Values in brackets are from cosmological and astrophysical considerations and assume a light right-handed neutrino.

VALUE (GeV)	CL%	DOCUMENT ID		TECN	COMMENT
>1870	95	[1] AAD	12CC	ATLS	pp, $Z'_\eta\to e^+e^-$, $\mu^+\mu^-$
> 619	95	[2] CHO	00	RVUE	Electroweak
• • • We do not use the following data for averages, fits, limits, etc. • • •					
>1540	95	[3] AAD	11AD	ATLS	pp; $Z'_\eta\to e^+e^-$, $\mu^+\mu^-$
> 771	95	[4] AAD	11J	ATLS	pp, $Z'_\eta\to e^+e^-$, $\mu^+\mu^-$
> 938	95	[5] AALTONEN	11I	CDF	$p\overline{p}$; $Z'_\eta\to\mu^+\mu^-$
> 923	95	[6] ABAZOV	11A	D0	$p\overline{p}$, $Z'_\eta\to e^+e^-$
> 488	95	[7] DEL-AGUILA	10	RVUE	Electroweak
> 877	95	[6] AALTONEN	09T	CDF	$p\overline{p}$, $Z'_\eta\to e^+e^-$
> 904	95	[8] AALTONEN	09V	CDF	$p\overline{p}$; $Z'_\eta\to\mu^+\mu^-$
> 427	95	[9] ERLER	09	RVUE	Electroweak
> 891	95	[6] AALTONEN	07H	CDF	Repl. by AALTONEN 09T
> 350	95	SCHAEL	07A	ALEP	e^+e^-
> 360	95	[10] ABDALLAH	06C	DLPH	e^+e^-
> 745		[6] ABULENCIA	06L	CDF	Repl. by AALTONEN 07H
> 720	95	[11] ABULENCIA	05A	CDF	$p\overline{p}$; $Z'_\eta\to e^+e^-$, $\mu^+\mu^-$

> 515	95	[12] ABBIENDI	04G	OPAL	e^+e^-	
>1600		[13] BARGER	03B	COSM	Nucleosynthesis; light ν_R	
> 310	95	[14] ABREU	00S	DLPH	e^+e^-	
> 329	95	[15] BARATE	00I	ALEP	Repl. by SCHAEL 07A	
> 365	95	[16] ERLER	99	RVUE	Electroweak	
> 87	95	[17] CONRAD	98	RVUE	$\nu_\mu N$ scattering	
> 620	95	[18] ABE	97S	CDF	$p\overline{p}$; $Z'_\eta \to e^+e^-, \mu^+\mu^-$	
> 100	95	[19] VILAIN	94B	CHM2	$\nu_\mu e \to \nu_\mu e$; $\overline{\nu}_\mu e \to \overline{\nu}_\mu e$	
> 125	90	[20] ABE	90F	VNS	e^+e^-	
[> 820]		[21] GONZALEZ-G..	90D	COSM	Nucleosynthesis; light ν_R	
[> 3300]		[22] GRIFOLS	90	ASTR	SN 1987A; light ν_R	
[> 1040]		[21] LOPEZ	90	COSM	Nucleosynthesis; light ν_R	

[1] AAD 12CC search for resonances decaying to e^+e^-, $\mu^+\mu^-$ in pp collisions at $\sqrt{s} = 7$ TeV.

[2] CHO 00 use various electroweak data to constrain Z' models assuming m_H=100 GeV. See Fig. 3 for limits in the mass-mixing plane.

[3] AAD 11AD search for resonances decaying to e^+e^-, $\mu^+\mu^-$ in pp collisions at $\sqrt{s} = 7$ TeV.

[4] AAD 11J search for resonances decaying to e^+e^- or $\mu^+\mu^-$ in pp collisions at $\sqrt{s} = 7$ TeV.

[5] AALTONEN 11I search for resonances decaying to $\mu^+\mu^-$ in $p\overline{p}$ collisions at $\sqrt{s} = 1.96$ TeV.

[6] ABAZOV 11A, AALTONEN 09T, AALTONEN 07H, and ABULENCIA 06L search for resonances decaying to e^+e^- in $p\overline{p}$ collisions at $\sqrt{s} = 1.96$ TeV.

[7] DEL-AGUILA 10 give 95% CL limit on the Z-Z' mixing $-0.0023 < \theta < 0.0027$.

[8] AALTONEN 09V search for resonances decaying to $\mu^+\mu^-$ in $p\overline{p}$ collisions at $\sqrt{s} = 1.96$ TeV.

[9] ERLER 09 give 95% CL limit on the Z-Z' mixing $-0.0047 < \theta < 0.0021$.

[10] ABDALLAH 06C give 95% CL limit $|\theta| < 0.0092$. See their Fig. 14 for limit contours in the mass-mixing plane.

[11] ABULENCIA 05A search for resonances decaying to electron or muon pairs in $p\overline{p}$ collisions at $\sqrt{s} = 1.96$ TeV.

[12] ABBIENDI 04G give 95% CL limit on Z-Z' mixing $-0.00447 < \theta < 0.00331$. See their Fig. 20 for the limit contour in the mass-mixing plane. $\sqrt{s} = 91$ to 207 GeV.

[13] BARGER 03B limit is from the nucleosynthesis bound on the effective number of light neutrino δN_ν <1. The quark-hadron transition temperature T_c=150 MeV is assumed. The limit with T_c=400 MeV is >3300 GeV.

[14] ABREU 00S give 95% CL limit on Z-Z' mixing $|\theta| < 0.0024$. See their Fig. 6 for the limit contour in the mass-mixing plane. $\sqrt{s}$=90 to 189 GeV.

[15] BARATE 00I search for deviations in cross section and asymmetries in $e^+e^- \to$ fermions at $\sqrt{s}$=90 to 183 GeV. Assume θ=0. Bounds in the mass-mixing plane are shown in their Figure 18.

[16] ERLER 99 give 90% CL limit on the Z-Z' mixing $-0.0062 < \theta < 0.0011$.

[17] CONRAD 98 limit is from measurements at CCFR, assuming no Z-Z' mixing.

[18] ABE 97S find $\sigma(Z') \times B(e^+e^-, \mu^+\mu^-) < 40$ fb for $m_{Z'} > 600$ GeV at $\sqrt{s} = 1.8$ TeV.

[19] VILAIN 94B assume $m_t = 150$ GeV and θ=0. See Fig. 2 for limit contours in the mass-mixing plane.

[20] ABE 90F use data for R, $R_{\ell\ell}$, and $A_{\ell\ell}$. ABE 90F fix $m_W = 80.49 \pm 0.43 \pm 0.24$ GeV and $m_Z = 91.13 \pm 0.03$ GeV.

[21] These authors claim that the nucleosynthesis bound on the effective number of light neutrinos ($\delta N_\nu < 1$) constrains Z' masses if ν_R is light ($\lesssim$ 1 MeV).

[22] GRIFOLS 90 limit holds for $m_{\nu_R} \lesssim 1$ MeV. See also GRIFOLS 90D, RIZZO 91.

Limits for other Z'

VALUE (GeV)	CL%	DOCUMENT ID		TECN	COMMENT
• • • We do not use the following data for averages, fits, limits, etc. • • •					
		[1] AAD	13AI	ATLS	$Z' \to e\mu$, $e\tau$, $\mu\tau$
none 500–1740	95	[2] AAD	13AQ	ATLS	$Z' \to t\overline{t}$
>1320 or 1000–1280	95	[3] AAD	13G	ATLS	$Z' \to t\overline{t}$
> 915	95	[3] AALTONEN	13A	CDF	$Z' \to t\overline{t}$
>1300	95	[4] CHATRCHYAN	13AP	CMS	$Z' \to t\overline{t}$
>2100	95	[3] CHATRCHYAN	13BM	CMS	$Z' \to t\overline{t}$
		[5] AAD	12BV	ATLS	$Z' \to t\overline{t}$
		[6] AAD	12K	ATLS	$Z' \to t\overline{t}$
		[7] AALTONEN	12AR	CDF	Chromophilic
		[8] AALTONEN	12N	CDF	$Z' \to \overline{t}u$
> 835	95	[9] ABAZOV	12R	D0	$Z' \to t\overline{t}$
		[10] CHATRCHYAN	12AI	CMS	$Z' \to t\overline{u}$
		[11] CHATRCHYAN	12AQ	CMS	$Z' \to t\overline{t}$
>1490	95	[3] CHATRCHYAN	12BL	CMS	$Z' \to t\overline{t}$
		[12] AAD	11H	ATLS	$Z' \to e\mu$
		[13] AAD	11Z	ATLS	$Z' \to e\mu$
		[14] AALTONEN	11AD	CDF	$Z' \to t\overline{t}$
		[15] AALTONEN	11AE	CDF	$Z' \to t\overline{t}$
		[16] CHATRCHYAN	11O	CMS	$pp \to tt$
		[17] AALTONEN	08D	CDF	$Z' \to t\overline{t}$
		[17] AALTONEN	08Y	CDF	$Z' \to t\overline{t}$
		[17] ABAZOV	08AA	D0	$Z' \to t\overline{t}$
		[18] ABULENCIA	06M	CDF	$Z' \to e\mu$
		[19] ABAZOV	04A	D0	Repl. by ABAZOV 08AA
		[20] BARGER	03B	COSM	Nucleosynthesis; light ν_R
		[21] CHO	00	RVUE	E_6-motivated
		[22] CHO	98	RVUE	E_6-motivated
		[23] ABE	97G	CDF	$Z' \to \overline{q}q$

[1] AAD 13AI search for new particle with lepton flavor violating decay in pp collisions at $\sqrt{s} = 7$ TeV. See their Fig. 2 for limits on $\sigma \cdot B$.

[2] AAD 13AQ search for a leptophobic top-color Z' decaying to $t\overline{t}$. The quoted limit assumes that $\Gamma_{Z'}/m_{Z'} = 0.012$.

[3] Search for top-color Z' decaying to $t\overline{t}$. The quoted limit is for $\Gamma_{Z'}/m_{Z'} = 0.012$.

[4] CHATRCHYAN 13AP search for top-color leptophobic Z' decaying to $t\overline{t}$. The quoted limit is for $\Gamma_{Z'}/m_{Z'} = 0.012$.

[5] Search for narrow resonance decaying to $t\overline{t}$. See their Fig. 7 for limit on $\sigma \cdot B$.

[6] Search for narrow resonance decaying to $t\overline{t}$. See their Fig. 5 for limit on $\sigma \cdot B$.

[7] AALTONEN 12AR search for chromophilic Z' in $p\overline{p}$ collisions at $\sqrt{s} = 1.96$ TeV. See their Fig. 5 for limit on $\sigma \cdot B$.

[8] AALTONEN 12N search for $p\overline{p} \to tZ'$, $Z' \to \overline{t}u$ events in $p\overline{p}$ collisions. See their Fig. 3 for the limit on $\sigma \cdot B$.

[9] ABAZOV 12R search for top-color Z' boson decaying exclusively to $t\overline{t}$. The quoted limit is for $\Gamma_{Z'}/m_{Z'} = 0.012$.

[10] CHATRCHYAN 12AI search for $pp \to tt$ events and give constraints on a Z' model having $Z'\overline{u}t$ coupling. See their Fig. 4 for the limit in mass-coupling plane.

[11] Search for resonance decaying to $t\overline{t}$. See their Fig. 6 for limit on $\sigma \cdot B$.

[12] AAD 11H search for new particle with lepton flavor violating decay in pp collisions at $\sqrt{s} = 7$ TeV. See their Fig. 3 for exclusion plot on the production cross section.

[13] AAD 11Z search for new particle with lepton flavor violating decay in pp collisions at $\sqrt{s} = 7$ TeV. See their Fig. 3 for limit on $\sigma \cdot B$.

[14] Search for narrow resonance decaying to $t\overline{t}$. See their Fig. 4 for limit on $\sigma \cdot B$.

[15] Search for narrow resonance decaying to $t\overline{t}$. See their Fig. 3 for limit on $\sigma \cdot B$.

[16] CHATRCHYAN 11O search for same-sign top production in pp collisions induced by a hypothetical FCNC Z' at $\sqrt{s} = 7$ TeV. See their Fig. 3 for limit in mass-coupling plane.

[17] Search for narrow resonance decaying to $t\overline{t}$. See their Fig. 3 for limit on $\sigma \cdot B$.

[18] ABULENCIA 06M search for new particle with lepton flavor violating decay at $\sqrt{s} = 1.96$ TeV. See their Fig. 4 for an exclusion plot on a mass-coupling plane.

[19] Search for narrow resonance decaying to $t\overline{t}$. See their Fig. 2 for limit on $\sigma \cdot B$.

[20] BARGER 03B use the nucleosynthesis bound on the effective number of light neutrino δN_ν. See their Figs. 4–5 for limits in general E_6 motivated models.

[21] CHO 00 use various electroweak data to constrain Z' models assuming m_H=100 GeV. See Fig. 2 for limits in general E_6-motivated models.

[22] CHO 98 study constraints on four-Fermi contact interactions obtained from low-energy electroweak experiments, assuming no Z-Z' mixing.

[23] Search for Z' decaying to dijets at $\sqrt{s}$=1.8 TeV. For Z' with electromagnetic strength coupling, no bound is obtained.

Indirect Constraints on Kaluza-Klein Gauge Bosons

Bounds on a Kaluza-Klein excitation of the Z boson or photon in d=1 extra dimension. These bounds can also be interpreted as a lower bound on $1/R$, the size of the extra dimension. Unless otherwise stated, bounds assume all fermions live on a single brane and all gauge fields occupy the $4+d$-dimensional bulk. See also the section on "Extra Dimensions" in the "Searches" Listings in this *Review*.

VALUE (TeV)	CL%	DOCUMENT ID		TECN	COMMENT
• • • We do not use the following data for averages, fits, limits, etc. • • •					
> 4.7		[1] MUECK	02	RVUE	Electroweak
> 3.3	95	[2] CORNET	00	RVUE	$e\nu qq'$
>5000		[3] DELGADO	00	RVUE	ϵ_K
> 2.6	95	[4] DELGADO	00	RVUE	Electroweak
> 3.3	95	[5] RIZZO	00	RVUE	Electroweak
> 2.9	95	[6] MARCIANO	99	RVUE	Electroweak
> 2.5	95	[7] MASIP	99	RVUE	Electroweak
> 1.6	90	[8] NATH	99	RVUE	Electroweak
> 3.4	95	[9] STRUMIA	99	RVUE	Electroweak

[1] MUECK 02 limit is 2σ and is from global electroweak fit ignoring correlations among observables. Higgs is assumed to be confined on the brane and its mass is fixed. For scenarios of bulk Higgs, of brane-SU(2)$_L$, bulk-U(1)$_Y$, and of bulk-SU(2)$_L$, brane-U(1)$_Y$, the corresponding limits are > 4.6 TeV, > 4.3 TeV and > 3.0 TeV, respectively.

[2] Bound is derived from limits on $e\nu qq'$ contact interaction, using data from HERA and the Tevatron.

[3] Bound holds only if first two generations of quarks lives on separate branes. If quark mixing is not complex, then bound lowers to 400 TeV from Δm_K.

[4] See Figs. 1 and 2 of DELGADO 00 for several model variations. Special boundary conditions can be found which permit KK states down to 950 GeV and that agree with the measurement of Q_W(Cs). Quoted bound assumes all Higgs bosons confined to brane; placing one Higgs doublet in the bulk lowers bound to 2.3 TeV.

[5] Bound is derived from global electroweak analysis assuming the Higgs field is trapped on the matter brane. If the Higgs propagates in the bulk, the bound increases to 3.8 TeV.

[6] Bound is derived from global electroweak analysis but considering only presence of the KK W bosons.

[7] Global electroweak analysis used to obtain bound independent of position of Higgs on brane or in bulk.

[8] Bounds from effect of KK states on G_F, α, M_W, and M_Z. Hard cutoff at string scale determined using gauge coupling unification. Limits for d=2,3,4 rise to 3.5, 5.7, and 7.8 TeV.

[9] Bound obtained for Higgs confined to the matter brane with m_H=500 GeV. For Higgs in the bulk, the bound increases to 3.5 TeV.

LEPTOQUARKS

Updated August 2013 by S. Rolli (US Department of Energy) and M. Tanabashi (Nagoya U.)

Table 1: Possible leptoquarks and their quantum numbers.

Leptoquarks	Spin	$3B+L$	$SU(3)_c$	$SU(2)_W$	$U(1)_Y$	Allowed coupling
$S_0^\dagger$	0	-2	$\bar{3}$	1	1/3	$\bar{q}_L^c \ell_L$ or $\bar{u}_R^c e_R$
$\tilde{S}_0^\dagger$	0	-2	$\bar{3}$	1	4/3	$\bar{d}_R^c e_R$
$S_1^\dagger$	0	-2	$\bar{3}$	3	1/3	$\bar{q}_L^c \ell_L$
$V_{1/2}^\dagger$	1	-2	$\bar{3}$	2	5/6	$\bar{q}_L^c \gamma^\mu e_R$ or $\bar{d}_R^c \gamma^\mu \ell_L$
$\tilde{V}_{1/2}^\dagger$	1	-2	$\bar{3}$	2	$-1/6$	$\bar{u}_R^c \gamma^\mu \ell_L$
$S_{1/2}^\dagger$	0	0	3	2	7/6	$\bar{q}_L e_R$ or $\bar{u}_R \ell_L$
$\tilde{S}_{1/2}^\dagger$	0	0	3	2	1/6	$\bar{d}_R \ell_L$
$V_0^\dagger$	1	0	3	1	2/3	$\bar{q}_L \gamma^\mu \ell_L$ or $\bar{d}_R \gamma^\mu e_R$
$\tilde{V}_0^\dagger$	1	0	3	1	5/3	$\bar{u}_R \gamma^\mu e_R$
$V_1^\dagger$	1	0	3	3	2/3	$\bar{q}_L \gamma^\mu \ell_L$

Leptoquarks are hypothetical particles carrying both baryon number (B) and lepton number (L). The possible quantum numbers of leptoquark states can be restricted by assuming that their direct interactions with the ordinary SM fermions are dimensionless and invariant under the standard model (SM) gauge group. Table 1 shows the list of all possible quantum numbers with this assumption [1]. The columns of $SU(3)_C$, $SU(2)_W$, and $U(1)_Y$ in Table 1 indicate the QCD representation, the weak isospin representation, and the weak hypercharge, respectively. The spin of a leptoquark state is taken to be 1 (vector leptoquark) or 0 (scalar leptoquark).

If we do not require leptoquark states to couple directly with SM fermions, different assignments of quantum numbers become possible [2,3].

Leptoquark states are expected to exist in various extensions of SM. The Pati-Salam model [4] is an example predicting the existence of a leptoquark state. Vector leptoquark states also exist in grand unification theories based on $SU(5)$ [5], $SO(10)$ [6], which includes Pati-Salam color $SU(4)$, and larger gauge groups. Scalar quarks in supersymmetric models with R-parity violation may also have leptoquark-type Yukawa couplings. The bounds on the leptoquark states can therefore be applied to constrain R-parity-violating supersymmetric models [7]. Scalar leptoquarks are expected to exist at TeV scale in extended technicolor models [8,9], where leptoquark states appear as the bound states of techni-fermions. Compositeness of quarks and leptons also provides examples of models which may have light leptoquark states [10].

Bounds on leptoquark states are obtained both directly and indirectly. Direct limits are from their production cross sections at colliders, while indirect limits are calculated from the bounds on the leptoquark-induced four-fermion interactions, which are obtained from low-energy experiments, or from collider experiments below threshold.

If a leptoquark couples to fermions belonging to more than a single generation in the mass eigenbasis of the SM fermions, it can induce four-fermion interactions causing flavor-changing neutral currents and lepton-family-number violations. The quantum number assignment of Table 1 allows several leptoquark states to couple to both left- and right-handed quarks simultaneously. Such leptoquark states are called non-chiral and may cause four-fermion interactions affecting the $(\pi \to e\nu)/(\pi \to \mu\nu)$ ratio [11]. Non-chiral scalar leptoquarks also contribute to the muon anomalous magnetic moment [12,13]. Since indirect limits provide more stringent constraints on these types of leptoquarks, it is often assumed that a leptoquark state couples only to a single generation in a chiral interaction, for which indirect limits become much weaker. Additionally, this assumption gives strong constraints on concrete models of leptoquarks.

Leptoquark states which couple only to left- or right-handed quarks are called chiral leptoquarks. Leptoquark states which couple only to the first (second, third) generation are referred as the first- (second-, third-) generation leptoquarks. Refs. [14,15] give extensive lists of the bounds on the leptoquark-induced four-fermion interactions. For the isoscalar, scalar and vector leptoquarks S_0 and V_0, for example, which couple with the first- (second-) generation left-handed quark, and the first-generation left-handed lepton, the bounds of Ref. 14 read $\lambda^2 < 0.03 \times (M_{\rm LQ}/300\ {\rm GeV})^2$ for S_0, and $\lambda^2 < 0.02 \times (M_{\rm LQ}/300\ {\rm GeV})^2$ for V_0 ($\lambda^2 < 5 \times (M_{\rm LQ}/300\ {\rm GeV})^2$ for S_0, and $\lambda^2 < 3 \times (M_{\rm LQ}/300\ {\rm GeV})^2$ for V_0) with λ being the leptoquark coupling strength. The e^+e^- experiments are sensitive to the indirect effects coming from t- and u-channel exchanges of leptoquarks in the $e^+e^- \to q\bar{q}$ process. The HERA experiments give bounds on the leptoquark-induced four-fermion interaction. For detailed bounds obtained in this way, see the Boson Particle Listings for "Indirect Limits for Leptoquarks" and its references.

Collider experiments provide direct limits on the leptoquark states through limits on the pair- and single-production cross sections. The leading-order cross sections of the parton processes

$$\begin{aligned} &q + \bar{q} \to LQ + \overline{LQ} \\ &g + g \to LQ + \overline{LQ} \\ &e + q \to LQ \end{aligned} \tag{1}$$

may be written as [16]

$$\begin{aligned} \hat{\sigma}_{\rm LO}\Big[q\bar{q} \to {\rm LQ} + \overline{\rm LQ}\Big] &= \frac{2\alpha_s^2\pi}{27\hat{s}}\beta^3, \\ \hat{\sigma}_{\rm LO}\Big[gg \to {\rm LQ} + \overline{\rm LQ}\Big] &= \frac{\alpha_s^2\pi}{96\hat{s}} \\ &\quad \times \Big[\beta(41 - 31\beta^2) + (18\beta^2 - \beta^4 - 17)\log\frac{1+\beta}{1-\beta}\Big], \\ \hat{\sigma}_{\rm LO}\Big[eq \to {\rm LQ}\Big] &= \frac{\pi\lambda^2}{4}\delta(\hat{s} - M_{\rm LQ}^2) \end{aligned} \tag{2}$$

for a scalar leptoquark. Here $\sqrt{\hat{s}}$ is the invariant energy of the parton subprocess, and $\beta \equiv \sqrt{1-4M_{\rm LQ}^2/\hat{s}}$. Leptoquarks are also produced singly at hadron colliders through $g+q \to LQ+\ell$ [17], which allows extending to higher masses the collider reach in the leptoquark search [18], depending on the leptoquark Yukawa coupling.

The LHC, Tevatron and LEP experiments have searched for pair production of the leptoquark states, which arises from the leptoquark gauge interaction. The searches are carried on in signatures including high P_T leptons, E_T jets and large missing transverse energy, due to the typical decay of the leptoquark. The gauge couplings of a scalar leptoquark are determined uniquely according to its quantum numbers in Table 1. Since all of the leptoquark states belong to color-triplet representation, the scalar leptoquark pair-production cross section at the Tevatron and LHC is essentially independent from the leptoquark Yukawa coupling and can be determined solely as a function of the leptoquark mass. This is in contrast to the indirect or single-production limits, which give constraints in the leptoquark mass-coupling plane. For the first- and second-generation scalar leptoquark states with decaying branching fraction $\beta = B(eq) = 1$ and $\beta = B(\mu q) = 1$, the CDF and DØ experiments obtain the lower bounds on the leptoquark mass > 236 GeV (first generation, CDF) [19], > 299 GeV (first generation, DØ) [20], > 226 GeV (second generation, CDF) [21], and > 316 GeV (second generation, DØ) [22] at 95% CL. Third generation leptoquark mass bounds come from the DØ experiment [23] which sets a limit at 247 GeV for a charge $-1/3$ third generation scalar leptoquark, at 95% C.L.

Recent results from the LHC proton-proton collider, running at a center of mass energy of 7 TeV, extend previous Tevatron mass limits for scalar leptoquarks to > 830 GeV (first generation, CMS, β =1) and > 640 GeV(first generation, CMS, β =0.5) [24]; > 660 GeV (first generation, ATLAS, β =1) and > 607 GeV (first generation, ATLAS, β =0.5) [25]; > 1070 GeV (second generation, CMS, β =1) [26] and > 785 GeV (second generation, CMS, β =0.5) [26]; and > 685 GeV (second generation, ATLAS, β =1) and > 594 GeV (second generation, ATLAS, β =0.5) [27]. All limits are at 95% C.L.

Finally new measurements performed by the CMS experiment extend the mass limit to 450 GeV (β =0.5) [28] and 525 GeV (β =1) [29] for third generation scalar leptoquarks, at 95% C.L. The ATLAS collaboration published a similar limit on third generation scalar leptoquark for the case of β =1 of 525 GeV [30].

The magnetic-dipole-type and the electric-quadrupole-type interactions of a vector leptoquark are not determined even if we fix its gauge quantum numbers as listed in the Table [31]. The production of vector leptoquarks depends in general on additional assumptions that the leptoquark couplings and their pair-production cross sections are enhanced relative to the scalar leptoquark contributions. At the Tevatron for instance, since the acceptance for vector and scalar leptoquark detection is similar, limits on the vector leptoquark mass will be

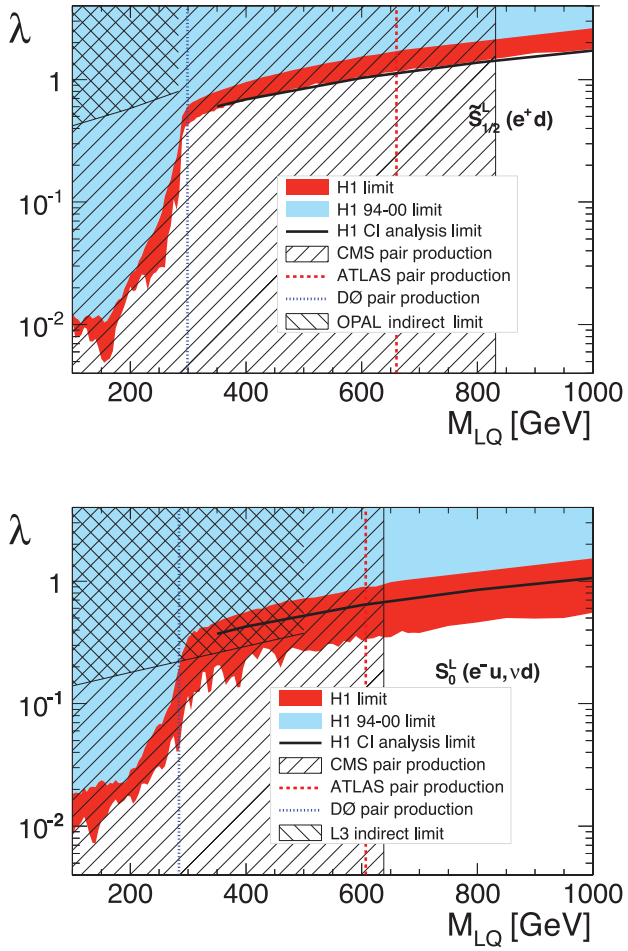

Figure 1: Limits on two typical first-generation scalar leptoquark states in the mass-coupling plane. The upper figure is for a weak-isodoublet, weak-hypercharge 7/6, $3B + L = 0$ leptoquark state, while the lower figure for a weak-isosinglet, weak-hypercharge $-1/3$, $3B + L = 2$ state. Figure adopted from Ref. 36.

more stringent (see for example [37,20]) . The leptoquark pair-production cross sections in e^+e^- collisions depend on the leptoquark $SU(2)_W \times U(1)_Y$ quantum numbers and Yukawa coupling with electron [32]. The OPAL experiment sets mass bounds on various leptoquark states from the pair-production cross sections [33]. For a second-generation weak-isosinglet weak-hypercharge $-4/3$ scalar-leptoquark state, for example, the OPAL pair-production bound is $M_{\rm LQ} > 100$ GeV/c^2 at 95% C.L. The LEP experiments also searched for the single production of the leptoquark states from the process $e\gamma \to LQ + q$.

The most stringent searches for the leptoquark single production are performed by the HERA experiments. Since the leptoquark single-production cross section depends on its Yukawa coupling, the leptoquark mass limits from HERA are usually displayed in the mass-coupling plane. For leptoquark Yukawa coupling $\lambda = 0.1$, the ZEUS bounds on the first-generation

leptoquarks range from 248 to 290 GeV, depending on the leptoquark species [34]. Recently the H1 Collab. released a comprehensive summary of searches for first generation leptoquarks using the full data sample collected in *ep* collisions at HERA (446 pb^{-1}). No evidence of production of leptoquarks is observed in final states with a large transverse momentum electron or large missing transverse momentum. For a coupling strength $\lambda = 0.3$, first generation leptoquarks with masses up to 800 GeV are excluded at 95% C.L. [36].

Fig. 1 summarizes ATLAS, CMS, DØ, LEP, and H1 limits on two typical first-generation scalar-leptoquark states in the mass-coupling plane [36].

The search for LQ will be continued with more LHC data. Early feasability studies by the LHC experiments ATLAS [38] and CMS [39] indicate that clear signals can be established for masses up to about M(LQ) 1.3 to 1.4 TeV for first- and second-generation scalar LQ, with a likely final reach 1.5 TeV, for collisions at 14 TeV in the center of mass.

Reference

1. W. Buchmüller, R. Rückl, and D. Wyler, Phys. Lett. **B191**, 442 (1987).
2. K. S. Babu, C. F. Kolda, and J. March-Russell, Phys. Lett. **B408**, 261 (1997).
3. J. L. Hewett and T. G. Rizzo, Phys. Rev. **D58**, 055005 (1998).
4. J.C. Pati and A. Salam, Phys. Rev. **D10**, 275 (1974).
5. H. Georgi and S.L. Glashow, Phys. Rev. Lett. **32**, 438 (1974).
6. H. Georgi, *AIP Conf. Proc.* **23**, 575 (1975); H. Fritzsch and P. Minkowski, Ann. Phys. **93**, 193 (1975).
7. R. Barbieri *et al.*, Phys. Reports **420**, 1 (2005).
8. For a review, see, E. Farhi and L. Susskind, Phys. Reports **74**, 277 (1981).
9. K. Lane and M. Ramana, Phys. Rev. **D44**, 2678 (1991).
10. See, for example, B. Schremp and F. Schremp, Phys. Lett. **153B**, 101 (1985).
11. O. Shanker, Nucl. Phys. **B204**, 375, (1982).
12. U. Mahanta, Eur. Phys. J. **C21**, 171 (2001) [Phys. Lett. **B515**, 111 (2001)].
13. K. Cheung, Phys. Rev. **D64**, 033001 (2001).
14. S. Davidson, D.C. Bailey, and B.A. Campbell, Z. Phys. **C61**, 613 (1994).
15. M. Leurer, Phys. Rev. **D49**, 333 (1994); Phys. Rev. **D50**, 536 (1994).
16. T. Plehn *et al.*, Z. Phys. **C74**, 611 (1997); M. Kramer *et al.*, Phys. Rev. Lett. **79**, 341 (1997); and references therein.
17. J.L. Hewett and S. Pakvasa, Phys. Rev. **D37**, 3165 (1988); O.J.P. Eboli and A.V. Olinto, Phys. Rev. **D38**, 3461 (1988); A. Dobado, M.J. Herrero, and C. Muñoz, Phys. Lett. **207B**, 97 (1988); V.D. Barger *et al.*, Phys. Lett. **B220**, 464 (1989); M. De Montigny and L. Marleau, Phys. Rev. **D40**, 2869 (1989) [Erratum-*ibid.* **D56**, 3156 (1997)].
18. A. Belyaev *et al.*, JHEP **0509**, 005 (2005).
19. D. Acosta *et al.*, [CDF Collab.], Phys. Rev. **D72**, 051107 (2005).
20. V.M. Abazov *et al.*, [DØCollab.], Phys. Lett. **B681**, 224 (2009).
21. A. Abulencia *et al.*, [CDF Collab.], Phys. Rev. **D73**, 051102 (2006).
22. V.M. Abazov *et al.*, [DØCollab.], Phys. Lett. **B671**, 224 (2009).
23. V.Abazov *et al.*, [DØCollab.] Phys. Lett. **B693**, 95 (2010).
24. S. Chatrchyan *et al.*, [CMS Collab.], Phys. Rev. **D86**, 052013 (2012).
25. G.Aad *et al.*, [ATLAS Collab.] Phys. Lett. **B709**, 158 (2012).
26. S. Chatrchyan *et al.*, [CMS Collab.], CMS PAS EXO-12-042 (2013).
27. G.Aad *et al.*, [ATLAS Collab.] Eur. Phys. J. **C72**, 2151 (2012).
28. S. Chatrchyan *et al.*, [CMS Collab.], JHEP **012**, 055 (2012).
29. S. Chatrchyan *et al.*, [CMS Collab.], Phys. Rev. Lett. **110**, 081801 (2013).
30. G. Aad *et al.*, [ATLAS Collab.], JHEP **06**, 033 (2013).
31. J. Blümlein, E. Boos, and A. Kryukov, Z. Phys. **C76**, 137 (1997).
32. J. Blümlein and R. Ruckl, Phys. Lett. **B304**, 337 (1993).
33. G. Abbiendi *et al.*, [OPAL Collab.], Eur. Phys. J. **C31**, 281 (2003).
34. S. Chekanov *et al.*, [ZEUS Collab.], Phys. Rev. **D68**, 052004 (2003).
35. A. Aktas *et al.*, [H1 Collab.], Phys. Lett. **B629**, 9 (2005).
36. F.D. Aaron *et al.*, H1 Collab. arXiv:1107.3716.
37. T. Aalton *et al.*, [CDF Collab.] Phys. Rev. **D77**, 091105 (2008).
38. V.A. Mitsou *et al.*, Czech. J. Phys. **55** B659, 2005.
39. S. Abdulin and F. Charles, Phys. Lett. **B464**, 223 (1999).

MASS LIMITS for Leptoquarks from Pair Production

These limits rely only on the color or electroweak charge of the leptoquark.

VALUE (GeV)	CL%	DOCUMENT ID		TECN	COMMENT
>534	95	[1] AAD	13AE	ATLS	Third generation
>525	95	[2] CHATRCHYAN	13M	CMS	Third generation
>660	95	[3] AAD	12H	ATLS	First generation
>830	95	[4] CHATRCHYAN	12AG	CMS	First generation
>840	95	[5] CHATRCHYAN	12AG	CMS	Second generation
>422	95	[6] AAD	11D	ATLS	Second generation
• • • We do not use the following data for averages, fits, limits, etc. • • •					
>685	95	[7] AAD	12O	ATLS	Second generation
>450	95	[8] CHATRCHYAN	12BO	CMS	Third generation
>376	95	[9] AAD	11D	ATLS	First generation
>326	95	[10] ABAZOV	11V	D0	First generation
>339	95	[11] CHATRCHYAN	11N	CMS	First generation
>384	95	[12] KHACHATRY...	11D	CMS	First generation
>394	95	[13] KHACHATRY...	11E	CMS	Second generation
>247	95	[14] ABAZOV	10L	D0	Third generation
>316	95	[15] ABAZOV	09	D0	Second generation
>299	95	[16] ABAZOV	09AF	D0	First generation
		[17] AALTONEN	08P	CDF	Third generation
>153	95	[18] AALTONEN	08Z	CDF	Third generation
>205	95	[19] ABAZOV	08AD	D0	All generations
>210	95	[18] ABAZOV	08AN	D0	Third generation
>229	95	[20] ABAZOV	07J	D0	Third generation
>251	95	[21] ABAZOV	06A	D0	Superseded by ABAZOV 09
>136	95	[22] ABAZOV	06L	D0	Superseded by ABAZOV 08AD
>226	95	[23] ABULENCIA	06T	CDF	Second generation
>256	95	[24] ABAZOV	05H	D0	First generation
>117	95	[19] ACOSTA	05I	CDF	First generation
>236	95	[25] ACOSTA	05P	CDF	First generation
> 99	95	[26] ABBIENDI	03R	OPAL	First generation

>100	95	[26] ABBIENDI	03R	OPAL	Second generation
> 98	95	[26] ABBIENDI	03R	OPAL	Third generation
> 98	95	[27] ABAZOV	02	D0	All generations
>225	95	[28] ABAZOV	01D	D0	First generation
> 85.8	95	[29] ABBIENDI	00M	OPAL	Superseded by ABBIENDI 03R
> 85.5	95	[29] ABBIENDI	00M	OPAL	Superseded by ABBIENDI 03R
> 82.7	95	[29] ABBIENDI	00M	OPAL	Superseded by ABBIENDI 03R
>200	95	[30] ABBOTT	00C	D0	Second generation
>123	95	[31] AFFOLDER	00K	CDF	Second generation
>148	95	[32] AFFOLDER	00K	CDF	Third generation
>160	95	[33] ABBOTT	99J	D0	Second generation
>225	95	[34] ABBOTT	98E	D0	First generation
> 94	95	[35] ABBOTT	98J	D0	Third generation
>202	95	[36] ABE	98S	CDF	Second generation
>242	95	[37] GROSS-PILCH..98			First generation
> 99	95	[38] ABE	97F	CDF	Third generation
>213	95	[39] ABE	97X	CDF	First generation
> 45.5	95	[40,41] ABREU	93J	DLPH	First + second generation
> 44.4	95	[42] ADRIANI	93M	L3	First generation
> 44.5	95	[42] ADRIANI	93M	L3	Second generation
> 45	95	[42] DECAMP	92	ALEP	Third generation
none 8.9–22.6	95	[43] KIM	90	AMY	First generation
none 10.2–23.2	95	[43] KIM	90	AMY	Second generation
none 5–20.8	95	[44] BARTEL	87B	JADE	
none 7–20.5	95	[45] BEHREND	86B	CELL	

[1] AAD 13AE search for scalar leptoquarks using $\tau\tau bb$ events in pp collisions at E_{cm} = 7 TeV. The limit above assumes B(τb) = 1.

[2] CHATRCHYAN 13M search for scalar and vector leptoquarks decaying to τb in pp collisions at E_{cm} = 7 TeV. The limit above is for scalar leptoquarks with B(τb) = 1.

[3] AAD 12H search for scalar leptoquarks using $eejj$ and $e\nu jj$ events in pp collisions at E_{cm} = 7 TeV. The limit above assumes B(eq) = 1. For B(eq) = 0.5, the limit becomes 607 GeV.

[4] CHATRCHYAN 12AG search for scalar leptoquarks using $eejj$ and $e\nu jj$ events in pp collisions at E_{cm} = 7 TeV. The limit above assumes B(eq) = 1. For B(eq) = 0.5, the limit becomes 640 GeV.

[5] CHATRCHYAN 12AG search for scalar leptoquarks using $\mu jujj$ and $\mu\nu jj$ events in pp collisions at E_{cm} = 7 TeV. The limit above assumes B(μq) = 1. For B(μq) = 0.5, the limit becomes 650 GeV.

[6] AAD 11D search for scalar leptoquarks using $\mu\mu jj$ and $\mu\nu jj$ events in pp collisions at E_{cm} = 7 TeV. The limit above assumes B(μq) = 1. For B(μq) = 0.5, the limit becomes 362 GeV.

[7] AAD 12O search for scalar leptoquarks using $\mu\mu jj$ and $\mu\nu jj$ events in pp collisions at E_{cm} = 7 TeV. The limit above assumes B(μq) = 1. For B(μq) = 0.5, the limit becomes 594 GeV.

[8] CHATRCHYAN 12BO search for scalar leptoquarks decaying to νb in pp collisions at $\sqrt{s}$ = 7 TeV. The limit above assumes B(νb) = 1.

[9] AAD 11D search for scalar leptoquarks using $eejj$ and $e\nu jj$ events in pp collisions at E_{cm} = 7 TeV.The limit above assumes B(eq) = 1. For B(eq) = 0.5, the limit becomes 319 GeV.

[10] ABAZOV 11V search for scalar leptoquarks using $e\nu jj$ events in $p\overline{p}$ collisions at E_{cm} = 1.96 TeV. The limit above assumes B(eq) = 0.5.

[11] CHATRCHYAN 11N search for scalar leptoquarks using $e\nu jj$ events in pp collisions at E_{cm} = 7 TeV. The limit above assumes B(eq) = 0.5.

[12] KHACHATRYAN 11D search for scalar leptoquarks using $eejj$ events in pp collisions at E_{cm} = 7 TeV. The limit above assumes B(eq) = 1.

[13] KHACHATRYAN 11E search for scalar leptoquarks using $\mu\mu jj$ events in pp collisions at E_{cm} = 7 TeV. The limit above assumes $B(\mu q) = 1$.

[14] ABAZOV 10L search for pair productions of scalar leptoquark state decaying to νb in $p\overline{p}$ collisions at E_{cm} = 1.96 TeV. The limit above assumes B(νb) = 1.

[15] ABAZOV 09 search for scalar leptoquarks using $\mu\mu jj$ and $\mu\nu jj$ events in $p\overline{p}$ collisions at E_{cm} = 1.96 TeV. The limit above assumes B(μq) = 1. For B(μq) = 0.5, the limit becomes 270 GeV.

[16] ABAZOV 09AF search for scalar leptoquarks using $eejj$ and $e\nu jj$ events in $p\overline{p}$ collisions at E_{cm} = 1.96 TeV. The limit above assumes B(eq) = 1. For B(eq) = 0.5 the bound becomes 284 GeV.

[17] AALTONEN 08P search for vector leptoquarks using $\tau^+\tau^- b\overline{b}$ events in $p\overline{p}$ collisions at E_{cm} = 1.96 TeV. Assuming Yang-Mills (minimal) couplings, the mass limit is >317 GeV (251 GeV) at 95% CL for B(τb) = 1.

[18] Search for pair production of scalar leptoquark state decaying to τb in $p\overline{p}$ collisions at E_{cm}= 1.96 TeV. The limit above assumes B(τb) = 1.

[19] Search for scalar leptoquarks using $\nu\nu jj$ events in $\overline{p}p$ collisions at E_{cm} = 1.96 TeV. The limit above assumes B(νq) = 1.

[20] ABAZOV 07J search for pair productions of scalar leptoquark state decaying to νb in $p\overline{p}$ collisions at E_{cm} = 1.96 TeV. The limit above assumes B(νb) = 1.

[21] ABAZOV 06A search for scalar leptoquarks using $\mu\mu jj$ events in $p\overline{p}$ collisions at E_{cm} = 1.8 TeV and 1.96 TeV. The limit above assumes B(μq) = 1. For B(μq) = 0.5, the limit becomes 204 GeV.

[22] ABAZOV 06L search for scalar leptoquarks using $\nu\nu jj$ events in $p\overline{p}$ collisions at E_{cm} = 1.8 TeV and at 1.96 TeV. The limit above assumes B(νq) = 1.

[23] ABULENCIA 06T search for scalar leptoquarks using $\mu\mu jj$, $\mu\nu jj$, and $\nu\nu jj$ events in $p\overline{p}$ collisions at E_{cm} = 1.96 TeV. The quoted limit assumes B(μq) = 1. For B(μq) = 0.5 or 0.1, the bound becomes 208 GeV or 143 GeV, respectively. See their Fig. 4 for the exclusion limit as a function of B(μq).

[24] ABAZOV 05H search for scalar leptoquarks using $eejj$ and $e\nu jj$ events in $\overline{p}p$ collisions at E_{cm} = 1.8 TeV and 1.96 TeV. The limit above assumes B(eq) = 1. For B(eq) = 0.5 the bound becomes 234 GeV.

[25] ACOSTA 05P search for scalar leptoquarks using $eejj$, $e\nu jj$ events in $\overline{p}p$ collisions at E_{cm} = 1.96TeV. The limit above assumes B(eq) = 1. For B(eq) = 0.5 and 0.1, the bound becomes 205 GeV and 145 GeV, respectively.

[26] ABBIENDI 03R search for scalar/vector leptoquarks in e^+e^- collisions at $\sqrt{s}$ = 189–209 GeV. The quoted limits are for charge $-4/3$ isospin 0 scalar-leptoquark with B(ℓq) = 1. See their table 12 for other cases.

[27] ABAZOV 02 search for scalar leptoquarks using $\nu\nu jj$ events in $\overline{p}p$ collisions at E_{cm}=1.8 TeV. The bound holds for all leptoquark generations. Vector leptoquarks are likewise constrained to lie above 200 GeV.

[28] ABAZOV 01D search for scalar leptoquarks using $e\nu jj$, $eejj$, and $\nu\nu jj$ events in $p\overline{p}$ collisions at E_{cm}=1.8 TeV. The limit above assumes B(eq)=1. For B(eq)=0.5 and 0, the bound becomes 204 and 79 GeV, respectively. Bounds for vector leptoquarks are also given. Supersedes ABBOTT 98E.

[29] ABBIENDI 00M search for scalar/vector leptoquarks in e^+e^- collisions at $\sqrt{s}$=183 GeV. The quoted limits are for charge $-4/3$ isospin 0 scalar-leptoquarks with B(ℓq)=1. See their Table 8 and Figs. 6–9 for other cases.

[30] ABBOTT 00C search for scalar leptoquarks using $\mu\mu jj$, $\mu\nu jj$, and $\nu\nu jj$ events in $p\overline{p}$ collisions at E_{cm}=1.8 TeV. The limit above assumes B(μq)=1. For B(μq)=0.5 and 0, the bound becomes 180 and 79 GeV respectively. Bounds for vector leptoquarks are also given.

[31] AFFOLDER 00K search for scalar leptoquark using $\nu\nu cc$ events in $p\overline{p}$ collisions at E_{cm}=1.8 TeV. The quoted limit assumes B(νc)=1. Bounds for vector leptoquarks are also given.

[32] AFFOLDER 00K search for scalar leptoquark using $\nu\nu bb$ events in $p\overline{p}$ collisions at E_{cm}=1.8 TeV. The quoted limit assumes B(νb)=1. Bounds for vector leptoquarks are also given.

[33] ABBOTT 99J search for leptoquarks using $\mu\nu jj$ events in $p\overline{p}$ collisions at E_{cm}= 1.8TeV. The quoted limit is for a scalar leptoquark with B(μq) = B(νq) = 0.5. Limits on vector leptoquarks range from 240 to 290 GeV.

[34] ABBOTT 98E search for scalar leptoquarks using $e\nu jj$, $eejj$, and $\nu\nu jj$ events in $p\overline{p}$ collisions at E_{cm}=1.8 TeV. The limit above assumes B(eq)=1. For B(eq)=0.5 and 0, the bound becomes 204 and 79 GeV, respectively.

[35] ABBOTT 98J search for charge $-1/3$ third generation scalar and vector leptoquarks in $p\overline{p}$ collisions at E_{cm}= 1.8 TeV. The quoted limit is for scalar leptoquark with B(νb)=1.

[36] ABE 98S search for scalar leptoquarks using $\mu\mu jj$ events in $p\overline{p}$ collisions at E_{cm}= 1.8 TeV. The limit is for B(μq)= 1. For B(μq)=B(νq)=0.5, the limit is > 160 GeV.

[37] GROSS-PILCHER 98 is the combined limit of the CDF and DØ Collaborations as determined by a joint CDF/DØ working group and reported in this FNAL Technical Memo. Original data published in ABE 97X and ABBOTT 98E.

[38] ABE 97F search for third generation scalar and vector leptoquarks in $p\overline{p}$ collisions at E_{cm} = 1.8 TeV. The quoted limit is for scalar leptoquark with B(τb) = 1.

[39] ABE 97X search for scalar leptoquarks using $eejj$ events in $p\overline{p}$ collisions at E_{cm}=1.8 TeV. The limit is for B(eq)=1.

[40] Limit is for charge $-1/3$ isospin-0 leptoquark with B(ℓq) = 2/3.

[41] First and second generation leptoquarks are assumed to be degenerate. The limit is slightly lower for each generation.

[42] Limits are for charge $-1/3$, isospin-0 scalar leptoquarks decaying to $\ell^- q$ or νq with any branching ratio. See paper for limits for other charge-isospin assignments of leptoquarks.

[43] KIM 90 assume pair production of charge 2/3 scalar-leptoquark via photon exchange. The decay of the first (second) generation leptoquark is assumed to be any mixture of de^+ and $u\overline{\nu}$ ($s\mu^+$ and $c\overline{\nu}$). See paper for limits for specific branching ratios.

[44] BARTEL 87B limit is valid when a pair of charge 2/3 spinless leptoquarks X is produced with point coupling, and when they decay under the constraint B(X $\rightarrow$ $c\overline{\nu}_\mu$) + B(X $\rightarrow$ $s\mu^+$) = 1.

[45] BEHREND 86B assumed that a charge 2/3 spinless leptoquark, χ, decays either into $s\mu^+$ or $c\overline{\nu}$: B($\chi \rightarrow s\mu^+$) + B($\chi \rightarrow c\overline{\nu}$) = 1.

MASS LIMITS for Leptoquarks from Single Production

These limits depend on the q-ℓ-leptoquark coupling g_{LQ}. It is often assumed that $g^2_{LQ}/4\pi$=1/137. Limits shown are for a scalar, weak isoscalar, charge $-1/3$ leptoquark.

VALUE (GeV)	CL%	DOCUMENT ID		TECN	COMMENT
>304	95	[1] ABRAMOWICZ	12A	ZEUS	First generation
> 73	95	[2] ABREU	93J	DLPH	Second generation
• • • We do not use the following data for averages, fits, limits, etc. • • •					
		[3] AARON	11A	H1	Lepton-flavor violation
>300	95	[4] AARON	11B	H1	First generation
		[5] ABAZOV	07E	D0	Second generation
>295	95	[6] AKTAS	05B	H1	First generation
		[7] CHEKANOV	05A	ZEUS	Lepton-flavor violation
>298	95	[8] CHEKANOV	03B	ZEUS	First generation
>197	95	[9] ABBIENDI	02B	OPAL	First generation
		[10] CHEKANOV	02	ZEUS	Repl. by CHEKANOV 05A
>290	95	[11] ADLOFF	01C	H1	First generation
>204	95	[12] BREITWEG	01	ZEUS	First generation
		[13] BREITWEG	00E	ZEUS	First generation
>161	95	[14] ABREU	99G	DLPH	First generation
>200	95	[15] ADLOFF	99	H1	First generation
		[16] DERRICK	97	ZEUS	Lepton-flavor violation
>168	95	[17] DERRICK	93	ZEUS	First generation

[1] ABRAMOWICZ 12A limit is for a scalar, weak isoscalar, charge $-1/3$ leptoquark coupled with e_R. See their Figs. 12–17 and Table 4 for states with different quantum numbers.

[2] Limit from single production in Z decay. The limit is for a leptoquark coupling of electromagnetic strength and assumes B(ℓq) = 2/3. The limit is 77 GeV if first and second leptoquarks are degenerate.

[3] AARON 11A search for various leptoquarks with lepton-flavor violating couplings. See their Figs. 2–3 and Tables 1–4 for detailed limits.

[4] The quoted limit is for a scalar, weak isoscalar, charge $-1/3$ leptoquark coupled with e_R. See their Figs. 3–5 for limits on states with different quantum numbers.

[5] ABAZOV 07E search for leptoquark single production through qg fusion process in $p\overline{p}$ collisions. See their Fig. 4 for exclusion plot in mass-coupling plane.

[6] AKTAS 05B limit is for a scalar, weak isoscalar, charge $-1/3$ leptoquark coupled with e_R. See their Fig. 3 for limits on states with different quantum numbers.

[7] CHEKANOV 05 search for various leptoquarks with lepton-flavor violating couplings. See their Figs.6–10 and Tables 1–8 for detailed limits.

[8] CHEKANOV 03B limit is for a scalar, weak isoscalar, charge $-1/3$ leptoquark coupled with e_R. See their Figs. 11–12 and Table 5 for limits on states with different quantum numbers.
[9] For limits on states with different quantum numbers and the limits in the mass-coupling plane, see their Fig. 4 and Fig. 5.
[10] CHEKANOV 02 search for various leptoquarks with lepton-flavor violating couplings. See their Figs. 6–7 and Tables 5–6 for detailed limits.
[11] For limits on states with different quantum numbers and the limits in the mass-coupling plane, see their Fig. 3.
[12] See their Fig. 14 for limits in the mass-coupling plane.
[13] BREITWEG 00E search for F=0 leptoquarks in e^+p collisions. For limits in mass-coupling plane, see their Fig. 11.
[14] ABREU 99G limit obtained from process $e\gamma \to LQ+q$. For limits on vector and scalar states with different quantum numbers and the limits in the coupling-mass plane, see their Fig. 4 and Table 2.
[15] For limits on states with different quantum numbers and the limits in the mass-coupling plane, see their Fig. 13 and Fig. 14. ADLOFF 99 also search for leptoquarks with lepton-flavor violating couplings. ADLOFF 99 supersedes AID 96B.
[16] DERRICK 97 search for various leptoquarks with lepton-flavor violating couplings. See their Figs. 5–8 and Table 1 for detailed limits.
[17] DERRICK 93 search for single leptoquark production in ep collisions with the decay eq and νq. The limit is for leptoquark coupling of electromagnetic strength and assumes $B(eq) = B(\nu q) = 1/2$. The limit for $B(eq) = 1$ is 176 GeV. For limits on states with different quantum numbers, see their Table 3.

Indirect Limits for Leptoquarks

VALUE (TeV)	CL%	DOCUMENT ID		TECN	COMMENT
• • • We do not use the following data for averages, fits, limits, etc. • • •					
		[1] SAKAKI	13	RVUE	$B \to D^{(*)}\tau\overline{\nu}$, $B \to X_s\nu\overline{\nu}$
		[2] KOSNIK	12	RVUE	$b \to s\ell^+\ell^-$
> 2.5	95	[3] AARON	11C	H1	First generation
		[4] DORSNER	11	RVUE	scalar, weak singlet, charge 4/3
		[5] AKTAS	07A	H1	Lepton-flavor violation
> 0.49	95	[6] SCHAEL	07A	ALEP	$e^+e^- \to q\overline{q}$
		[7] SMIRNOV	07	RVUE	$K \to e\mu$, $B \to e\tau$
		[8] CHEKANOV	05A	ZEUS	Lepton-flavor violation
> 1.7	96	[9] ADLOFF	03	H1	First generation
> 46	90	[10] CHANG	03	BELL	Pati-Salam type
		[11] CHEKANOV	02	ZEUS	Repl. by CHEKANOV 05A
> 1.7	95	[12] CHEUNG	01B	RVUE	First generation
> 0.39	95	[13] ACCIARRI	00P	L3	$e^+e^- \to qq$
> 1.5	95	[14] ADLOFF	00	H1	First generation
> 0.2	95	[15] BARATE	00I	ALEP	Repl. by SCHAEL 07A
		[16] BARGER	00	RVUE	Cs
		[17] GABRIELLI	00	RVUE	Lepton flavor violation
> 0.74	95	[18] ZARNECKI	00	RVUE	S_1 leptoquark
		[19] ABBIENDI	99	OPAL	
> 19.3	95	[20] ABE	98V	CDF	$B_s \to e^\pm\mu^\mp$, Pati-Salam type
		[21] ACCIARRI	98J	L3	$e^+e^- \to q\overline{q}$
		[22] ACKERSTAFF	98V	OPAL	$e^+e^- \to q\overline{q}$, $e^+e^- \to b\overline{b}$
> 0.76	95	[23] DEANDREA	97	RVUE	$\tilde{R}_2$ leptoquark
		[24] DERRICK	97	ZEUS	Lepton-flavor violation
		[25] GROSSMAN	97	RVUE	$B \to \tau^+\tau^-$(X)
		[26] JADACH	97	RVUE	$e^+e^- \to q\overline{q}$
>1200		[27] KUZNETSOV	95B	RVUE	Pati-Salam type
		[28] MIZUKOSHI	95	RVUE	Third generation scalar leptoquark
> 0.3	95	[29] BHATTACH...	94	RVUE	Spin-0 leptoquark coupled to $\overline{e}_R\, t_L$
		[30] DAVIDSON	94	RVUE	
> 18		[31] KUZNETSOV	94	RVUE	Pati-Salam type
> 0.43	95	[32] LEURER	94	RVUE	First generation spin-1 leptoquark
> 0.44	95	[32] LEURER	94B	RVUE	First generation spin-0 leptoquark
		[33] MAHANTA	94	RVUE	P and T violation
> 1		[34] SHANKER	82	RVUE	Nonchiral spin-0 leptoquark
> 125		[34] SHANKER	82	RVUE	Nonchiral spin-1 leptoquark

[1] SAKAKI 13 explain the $B \to D^{(*)}\tau\overline{\nu}$ anomaly using Wilson coefficients of leptoquark-induced four-fermion operators.
[2] KOSNIK 12 obtains limits on leptoquark induced four-fermion interactions from $b \to s\ell^+\ell^-$ decays.
[3] AARON 11C limit is for weak isotriplet spin-0 leptoquark at strong coupling $\lambda = \sqrt{4\pi}$. For the limits of leptoquarks with different quantum numbers, see their Table 3. Limits are derived from bounds of eq contact intereractions.
[4] DORSNER 11 give bounds on scalar, weak singlet, charge 4/3 leptoquark from K, B, τ decays, meson mixings, LFV, $g-2$ and $Z \to b\overline{b}$.
[5] AKTAS 07A search for lepton-flavor violation in ep collision. See their Tables 4–7 for limits on lepton-flavor violating four-fermion interactions induced by various leptoquarks.
[6] SCHAEL 07A limit is for the weak-isoscalar spin-0 left-handed leptoquark with the coupling of electromagnetic strength. For the limits of leptoquarks with different quantum numbers, see their Table 35.
[7] SMIRNOV 07 obtains mass limits for the vector and scalar chiral leptoquark states from $K \to e\mu$, $B \to e\tau$ decays.
[8] CHEKANOV 05 search for various leptoquarks with lepton-flavor violating couplings. See their Figs. 6–10 and Tables 1–8 for detailed limits.
[9] ADLOFF 03 limit is for the weak isotriplet spin-0 leptoquark at strong coupling $\lambda = \sqrt{4\pi}$. For the limits of leptoquarks with different quantum numbers, see their Table 3. Limits are derived from bounds on $e^\pm q$ contact interactions.
[10] The bound is derived from $B(B^0 \to e^\pm\mu^\mp) < 1.7 \times 10^{-7}$.
[11] CHEKANOV 02 search for lepton-flavor violation in ep collisions. See their Tables 1–4 for limits on lepton-flavor violating and four-fermion interactions induced by various leptoquarks.
[12] CHEUNG 01B quoted limit is for a scalar, weak isoscalar, charge $-1/3$ leptoquark with a coupling of electromagnetic strength. The limit is derived from bounds on contact interactions in a global electroweak analysis. For the limits of leptoquarks with different quantum numbers, see Table 5.
[13] ACCIARRI 00P limit is for the weak isoscalar spin-0 leptoquark with the coupling of electromagnetic strength. For the limits of leptoquarks with different quantum numbers, see their Table 4.
[14] ADLOFF 00 limit is for the weak isotriplet spin-0 leptoquark at strong coupling, $\lambda = \sqrt{4\pi}$. For the limits of leptoquarks with different quantum numbers, see their Table 2. ADLOFF 00 limits are from the Q^2 spectrum measurement of $e^+p \to e^+$X.
[15] BARATE 00I search for deviations in cross section and jet-charge asymmetry in $e^+e^- \to \overline{q}q$ due to t-channel exchange of a leptoquark at $\sqrt{s}$=130 to 183 GeV. Limits for other scalar and vector leptoquarks are also given in their Table 22.
[16] BARGER 00 explain the deviation of atomic parity violation in cesium atoms from prediction is explained by scalar leptoquark exchange.
[17] GABRIELLI 00 calculate various process with lepton flavor violation in leptoquark models.
[18] ZARNECKI 00 limit is derived from data of HERA, LEP, and Tevatron and from various low-energy data including atomic parity violation. Leptoquark coupling with electromagnetic strength is assumed.
[19] ABBIENDI 99 limits are from $e^+e^- \to q\overline{q}$ cross section at 130–136, 161–172, 183 GeV. See their Fig. 8 and Fig. 9 for limits in mass-coupling plane.
[20] ABE 98V quoted limit is from $B(B_s \to e^\pm\mu^\mp) < 8.2 \times 10^{-6}$. ABE 98V also obtain a similar limit on $M_{LQ} > 20.4$ TeV from $B(B_d \to e^\pm\mu^\mp) < 4.5 \times 10^{-6}$. Both bounds assume the non-canonical association of the b quark with electrons or muons under SU(4).
[21] ACCIARRI 98J limit is from $e^+e^- \to q\overline{q}$ cross section at $\sqrt{s}$= 130–172 GeV which can be affected by the t- and u-channel exchanges of leptoquarks. See their Fig. 4 and Fig. 5 for limits in the mass-coupling plane.
[22] ACKERSTAFF 98V limits are from $e^+e^- \to q\overline{q}$ and $e^+e^- \to b\overline{b}$ cross sections at $\sqrt{s}$ = 130–172 GeV, which can be affected by the t- and u-channel exchanges of leptoquarks. See their Fig. 21 and Fig. 22 for limits of leptoquarks in mass-coupling plane.
[23] DEANDREA 97 limit is for $\tilde{R}_2$ leptoquark obtained from atomic parity violation (APV). The coupling of leptoquark is assumed to be electromagnetic strength. See Table 2 for limits of the four-fermion interactions induced by various scalar leptoquark exchange. DEANDREA 97 combines APV limit and limits from Tevatron and HERA. See Fig. 1–4 for combined limits of leptoquark in mass-coupling plane.
[24] DERRICK 97 search for lepton-flavor violation in ep collision. See their Tables 2–5 for limits on lepton-flavor violating four-fermion interactions induced by various leptoquarks.
[25] GROSSMAN 97 estimate the upper bounds on the branching fraction $B \to \tau^+\tau^-$(X) from the absence of the B decay with large missing energy. These bounds can be used to constrain leptoquark induced four-fermion interactions.
[26] JADACH 97 limit is from $e^+e^- \to q\overline{q}$ cross section at $\sqrt{s}$=172.3 GeV which can be affected by the t- and u-channel exchanges of leptoquarks. See their Fig. 1 for limits on vector leptoquarks in mass-coupling plane.
[27] KUZNETSOV 95B use π, K, B, τ decays and μe conversion and give a list of bounds on the leptoquark mass and the fermion mixing matrix in the Pati-Salam model. The quoted limit is from $K_L \to \mu e$ decay assuming zero mixing.
[28] MIZUKOSHI 95 calculate the one-loop radiative correction to the Z-physics parameters in various scalar leptoquark models. See their Fig. 4 for the exclusion plot of third generation leptoquark models in mass-coupling plane.
[29] BHATTACHARYYA 94 limit is from one-loop radiative correction to the leptonic decay width of the Z. m_H=250 GeV, $\alpha_s(m_Z)$=0.12, m_t=180 GeV, and the electroweak strength of leptoquark coupling are assumed. For leptoquark coupled to $\overline{e}_L\, t_R$, $\overline{\mu}t$, and $\overline{\tau}t$, see Fig. 2 in BHATTACHARYYA 94B erratum and Fig. 3.
[30] DAVIDSON 94 gives an extensive list of the bounds on leptoquark-induced four-fermion interactions from π, K, D, B, μ, τ decays and meson mixings, *etc.* See Table 15 of DAVIDSON 94 for detail.
[31] KUZNETSOV 94 gives mixing independent bound of the Pati-Salam leptoquark from the cosmological limit on $\pi^0 \to \overline{\nu}\nu$.
[32] LEURER 94, LEURER 94B limits are obtained from atomic parity violation and apply to any chiral leptoquark which couples to the first generation with electromagnetic strength. For a nonchiral leptoquark, universality in $\pi_{\ell 2}$ decay provides a much more stringent bound.
[33] MAHANTA 94 gives bounds of P- and T-violating scalar-leptoquark couplings from atomic and molecular experiments.
[34] From $(\pi \to e\nu)/(\pi \to \mu\nu)$ ratio. SHANKER 82 assumes the leptoquark induced four-fermion coupling $4g^2/M^2\ (\overline{\nu}_{eL}\ u_R)\ (\overline{d}_L\, e_R)$with g=0.004 for spin-0 leptoquark and $g^2/M^2\ (\overline{\nu}_{eL}\ \gamma_\mu u_L)\ (\overline{d}_R\ \gamma^\mu e_R)$ with $g \simeq$ 0.6 for spin-1 leptoquark.

MASS LIMITS for Diquarks

VALUE (GeV)	CL%	DOCUMENT ID		TECN	COMMENT
>3750	95	[1] CHATRCHYAN	13A	CMS	E_6 diquark
none 1000–4280	95	[2] CHATRCHYAN	13AS	CMS	E_6 diquark
• • • We do not use the following data for averages, fits, limits, etc. • • •					
>3520	95	[3] CHATRCHYAN	11Y	CMS	E_6 diquark
none 970–1080, 1450–1600	95	[4] KHACHATRY...10		CMS	E_6 diquark
none 290–630	95	[5] AALTONEN	09AC	CDF	E_6 diquark
none 290–420	95	[6] ABE	97G	CDF	E_6 diquark
none 15–31.7	95	[7] ABREU	94O	DLPH	SUSY E_6 diquark

[1] CHATRCHYAN 13A search for new resonance decaying to dijets in pp collisions at $\sqrt{s}$ = 7 TeV.
[2] CHATRCHYAN 13AS search for new resonance decaying to dijets in pp collisions at $\sqrt{s}$ = 8 TeV.
[3] CHATRCHYAN 11Y search for new resonance decaying to dijets in pp collisions at $\sqrt{s}$ = 7 TeV.
[4] KHACHATRYAN 10 search for new resonance decaying to dijets in pp collisions at $\sqrt{s}$ = 7 TeV.
[5] AALTONEN 09AC search for new narrow resonance decaying to dijets.
[6] ABE 97G search for new particle decaying to dijets.
[7] ABREU 94O limit is from $e^+e^- \to \overline{cs}cs$. Range extends up to 43 GeV if diquarks are degenerate in mass.

MASS LIMITS for g_A (axigluon) and Other Color-Octet Gauge Bosons

Axigluons are massive color-octet gauge bosons in chiral color models and have axial-vector coupling to quarks with the same coupling strength as gluons.

VALUE (GeV)	CL%	DOCUMENT ID		TECN	COMMENT
>3360	95	[1] CHATRCHYAN	13A	CMS	$pp \to g_A X, g_A \to 2$ jets
none 1000–3270	95	[2] CHATRCHYAN	13AS	CMS	$pp \to g_A X, g_A \to 2$ jets
• • • We do not use the following data for averages, fits, limits, etc. • • •					
		[3] AALTONEN	13R	CDF	$p\overline{p} \to g_A X, g_A \to \sigma\sigma$, $\sigma \to 2$ jets
none 250–740	95	[4] CHATRCHYAN	13AU	CMS	$pp \to 2g_A X, g_A \to 2$ jets
> 775	95	[5] ABAZOV	12R	D0	$p\overline{p} \to g_A X, g_A \to t\overline{t}$
>2470	95	[6] CHATRCHYAN	11Y	CMS	$pp \to g_A X, g_A \to 2$ jets
		[7] AALTONEN	10L	CDF	$p\overline{p} \to g_A X, g_A \to t\overline{t}$
none 1470–1520	95	[8] KHACHATRY...10		CMS	$pp \to g_A X, g_A \to 2$ jets
none 260–1250	95	[9] AALTONEN	09AC	CDF	$p\overline{p} \to g_A X, g_A \to 2$ jets
> 910	95	[10] CHOUDHURY	07	RVUE	$p\overline{p} \to t\overline{t}X$
> 365	95	[11] DONCHESKI	98	RVUE	$\Gamma(Z \to$ hadron)
none 200–980	95	[12] ABE	97G	CDF	$p\overline{p} \to g_A X, g_A \to 2$ jets
none 200–870	95	[13] ABE	95N	CDF	$p\overline{p} \to g_A X, g_A \to q\overline{q}$
none 240–640	95	[14] ABE	93G	CDF	$p\overline{p} \to g_A X, g_A \to 2$jets
> 50	95	[15] CUYPERS	91	RVUE	$\sigma(e^+e^- \to$ hadrons)
none 120–210	95	[16] ABE	90H	CDF	$p\overline{p} \to g_A X, g_A \to 2$jets
> 29		[17] ROBINETT	89	THEO	Partial-wave unitarity
none 150–310	95	[18] ALBAJAR	88B	UA1	$p\overline{p} \to g_A X, g_A \to 2$jets
> 20		BERGSTROM	88	RVUE	$p\overline{p} \to \Upsilon X$ via $g_A g$
> 9		[19] CUYPERS	88	RVUE	Υ decay
> 25		[20] DONCHESKI	88B	RVUE	Υ decay

[1] CHATRCHYAN 13A search for new resonance decaying to dijets in pp collisions at $\sqrt{s}$ = 7 TeV.

[2] CHATRCHYAN 13AS search for new resonance decaying to dijets in pp collisions at $\sqrt{s}$ = 8 TeV.

[3] AALTONEN 13R search for new resonance decaying to $\sigma\sigma$, with hypothetical strongly interacting σ particle subsequently decaying to 2 jets, in $p\overline{p}$ collisions at $\sqrt{s} = 1.96$ TeV, using data corresponding to an integrated luminosity of 6.6 fb^{-1}. For 50 GeV $< m_\sigma <$ $m_{g_A}/2$, axigluons in mass range 150–400 GeV are excluded.

[4] CHATRCHYAN 13AU search for the pair produced color-octet vector bosons decaying to $q\overline{q}$ pairs in pp collisions. The quoted limit is for B($g_A \to q\overline{q}$) = 1.

[5] ABAZOV 12R search for massive color octet vector particle decaying to $t\overline{t}$. The quoted limit assumes g_A couplings with light quarks are suppressed by 0.2.

[6] CHATRCHYAN 11Y search for new resonance decaying to dijets in pp collisions at $\sqrt{s} = 7$ TeV.

[7] AALTONEN 10L search for massive color octet non-chiral vector particle decaying into $t\overline{t}$ pair with mass in the range 400 GeV $<$ M $<$ 800 GeV. See their Fig. 6 for limit in the mass-coupling plane.

[8] KHACHATRYAN 10 search for new resonance decaying to dijets in pp collisions at $\sqrt{s} = 7$ TeV.

[9] AALTONEN 09AC search for new narrow resonance decaying to dijets.

[10] CHOUDHURY 07 limit is from the $t\overline{t}$ production cross section measured at CDF.

[11] DONCHESKI 98 compare α_s derived from low-energy data and that from $\Gamma(Z \to$ hadrons$)/\Gamma(Z \to$ leptons).

[12] ABE 97G search for new particle decaying to dijets.

[13] ABE 95N assume axigluons decaying to quarks in the Standard Model only.

[14] ABE 93G assume $\Gamma(g_A) = N\alpha_s m_{g_A}/6$ with $N = 10$.

[15] CUYPERS 91 compare α_s measured in Υ decay and that from R at PEP/PETRA energies.

[16] ABE 90H assumes $\Gamma(g_A) = N\alpha_s m_{g_A}/6$ with $N = 5$ ($\Gamma(g_A) = 0.09 m_{g_A}$). For $N = 10$, the excluded region is reduced to 120–150 GeV.

[17] ROBINETT 89 result demands partial-wave unitarity of $J = 0$ $t\overline{t} \to t\overline{t}$ scattering amplitude and derives a limit $m_{g_A} > 0.5\, m_t$. Assumes $m_t > 56$ GeV.

[18] ALBAJAR 88B result is from the nonobservation of a peak in two-jet invariant mass distribution. $\Gamma(g_A) < 0.4\, m_{g_A}$ assumed. See also BAGGER 88.

[19] CUYPERS 88 requires $\Gamma(\Upsilon \to g g g_A) < \Gamma(\Upsilon \to g g g)$. A similar result is obtained by DONCHESKI 88.

[20] DONCHESKI 88B requires $\Gamma(\Upsilon \to g q\overline{q})/\Gamma(\Upsilon \to g g g) < 0.25$, where the former decay proceeds via axigluon exchange. A more conservative estimate of < 0.5 leads to $m_{g_A} > 21$ GeV.

MASS LIMITS for Color-Octet Scalar Bosons

VALUE (GeV)	CL%	DOCUMENT ID		TECN	COMMENT
• • • We do not use the following data for averages, fits, limits, etc. • • •					
none 150–287	95	[1] AAD	13K	ATLS	$pp \to S_8 S_8 X, S_8 \to 2$ jets

[1] AAD 13K search for pair production of color-octet scalar particles in pp collisions at $\sqrt{s}$ = 7 TeV. Cross section limits are interpreted as mass limits on scalar partners of a Dirac gluino.

X^0 (Heavy Boson) Searches in Z Decays

Searches for radiative transition of Z to a lighter spin-0 state X^0 decaying to hadrons, a lepton pair, a photon pair, or invisible particles as shown in the comments. The limits are for the product of branching ratios.

VALUE	CL%	DOCUMENT ID		TECN	COMMENT
• • • We do not use the following data for averages, fits, limits, etc. • • •					
		[1] BARATE	98U	ALEP	$X^0 \to \ell\overline{\ell}$, $q\overline{q}$, gg, $\gamma\gamma$, $\nu\overline{\nu}$
		[2] ACCIARRI	97Q	L3	$X^0 \to$ invisible particle(s)
		[3] ACTON	93E	OPAL	$X^0 \to \gamma\gamma$
		[4] ABREU	92D	DLPH	$X^0 \to$ hadrons
		[5] ADRIANI	92F	L3	$X^0 \to$ hadrons
		[6] ACTON	91	OPAL	$X^0 \to$ anything
$<1.1 \times 10^{-4}$	95	[7] ACTON	91B	OPAL	$X^0 \to e^+e^-$
$<9 \times 10^{-5}$	95	[7] ACTON	91B	OPAL	$X^0 \to \mu^+\mu^-$
$<1.1 \times 10^{-4}$	95	[7] ACTON	91B	OPAL	$X^0 \to \tau^+\tau^-$
$<2.8 \times 10^{-4}$	95	[8] ADEVA	91D	L3	$X^0 \to e^+e^-$
$<2.3 \times 10^{-4}$	95	[8] ADEVA	91D	L3	$X^0 \to \mu^+\mu^-$
$<4.7 \times 10^{-4}$	95	[9] ADEVA	91D	L3	$X^0 \to$ hadrons
$<8 \times 10^{-4}$	95	[10] AKRAWY	90J	OPAL	$X^0 \to$ hadrons

[1] BARATE 98U obtain limits on B($Z \to \gamma X^0$)B($X^0 \to \ell\overline{\ell}$, $q\overline{q}$, gg, $\gamma\gamma$, $\nu\overline{\nu}$). See their Fig. 17.

[2] See Fig. 4 of ACCIARRI 97Q for the upper limit on B($Z \to \gamma X^0$; $E_\gamma > E_{\min}$) as a function of $E_{\min}$.

[3] ACTON 93E give $\sigma(e^+e^- \to X^0\gamma)$·B($X^0 \to \gamma\gamma$)$<$ 0.4 pb (95%CL) for m_{X^0}=60 ± 2.5 GeV. If the process occurs via s-channel γ exchange, the limit translates to $\Gamma(X^0)$·B($X^0 \to \gamma\gamma$)^2 $<$20 MeV for $m_{X^0} = 60 \pm 1$ GeV.

[4] ABREU 92D give $\sigma_Z \cdot$ B($Z \to \gamma X^0$) · B($X^0 \to$ hadrons) $<$(3–10) pb for m_{X^0} = 10–78 GeV. A very similar limit is obtained for spin-1 X^0.

[5] ADRIANI 92F search for isolated γ in hadronic Z decays. The limit $\sigma_Z \cdot$ B($Z \to \gamma X^0$) · B($X^0 \to$ hadrons) $<$(2–10) pb (95%CL) is given for m_{X^0} = 25–85 GeV.

[6] ACTON 91 searches for $Z \to Z^* X^0$, $Z^* \to e^+e^-$, $\mu^+\mu^-$, or $\nu\overline{\nu}$. Excludes any new scalar X^0 with $m_{X^0} < 9.5$ GeV/c if it has the same coupling to ZZ^* as the MSM Higgs boson.

[7] ACTON 91B limits are for m_{X^0} = 60–85 GeV.

[8] ADEVA 91D limits are for m_{X^0} = 30–89 GeV.

[9] ADEVA 91D limits are for m_{X^0} = 30–86 GeV.

[10] AKRAWY 90J give $\Gamma(Z \to \gamma X^0)$·B($X^0 \to$ hadrons) $<$ 1.9 MeV (95%CL) for m_{X^0} = 32–80 GeV. We divide by $\Gamma(Z)$ = 2.5 GeV to get product of branching ratios. For nonresonant transitions, the limit is B($Z \to \gamma q\overline{q}$) $<$ 8.2 MeV assuming three-body phase space distribution.

MASS LIMITS for a Heavy Neutral Boson Coupling to e^+e^-

VALUE (GeV)	CL%	DOCUMENT ID		TECN	COMMENT
• • • We do not use the following data for averages, fits, limits, etc. • • •					
none 55–61		[1] ODAKA	89	VNS	$\Gamma(X^0 \to e^+e^-)$ · B($X^0 \to$ had.) $\gtrsim$ 0.2 MeV
>45	95	[2] DERRICK	86	HRS	$\Gamma(X^0 \to e^+e^-)$=6 MeV
>46.6	95	[3] ADEVA	85	MRKJ	$\Gamma(X^0 \to e^+e^-)$=10 keV
>48	95	[3] ADEVA	85	MRKJ	$\Gamma(X^0 \to e^+e^-)$=4 MeV
		[4] BERGER	85B	PLUT	
none 39.8–45.5		[5] ADEVA	84	MRKJ	$\Gamma(X^0 \to e^+e^-)$=10 keV
>47.8	95	[5] ADEVA	84	MRKJ	$\Gamma(X^0 \to e^+e^-)$=4 MeV
none 39.8–45.2		[5] BEHREND	84C	CELL	
>47	95	[5] BEHREND	84C	CELL	$\Gamma(X^0 \to e^+e^-)$=4 MeV

[1] ODAKA 89 looked for a narrow or wide scalar resonance in $e^+e^- \to$ hadrons at $E_{\rm cm}$ = 55.0–60.8 GeV.

[2] DERRICK 86 found no deviation from the Standard Model Bhabha scattering at $E_{\rm cm}$= 29 GeV and set limits on the possible scalar boson e^+e^- coupling. See their figure 4 for excluded region in the $\Gamma(X^0 \to e^+e^-)$-m_{X^0} plane. Electronic chiral invariance requires a parity doublet of X^0, in which case the limit applies for $\Gamma(X^0 \to e^+e^-)$ = 3 MeV.

[3] ADEVA 85 first limit is from 2γ, $\mu^+\mu^-$, hadrons assuming X^0 is a scalar. Second limit is from e^+e^- channel. $E_{\rm cm}$ = 40–47 GeV. Supersedes ADEVA 84.

[4] BERGER 85B looked for effect of spin-0 boson exchange in $e^+e^- \to e^+e^-$ and $\mu^+\mu^-$ at $E_{\rm cm}$ = 34.7 GeV. See Fig. 5 for excluded region in the m_{X^0} – $\Gamma(X^0)$ plane.

[5] ADEVA 84 and BEHREND 84C have $E_{\rm cm}$ = 39.8–45.5 GeV. MARK-J searched X^0 in $e^+e^- \to$ hadrons, 2γ, $\mu^+\mu^-$, e^+e^- and CELLO in the same channels plus τ pair. No narrow or broad X^0 is found in the energy range. They also searched for the effect of X^0 with $m_X > E_{\rm cm}$. The second limits are from Bhabha data and for spin-0 singlet. The same limits apply for $\Gamma(X^0 \to e^+e^-) = 2$ MeV if X^0 is a spin-0 doublet. The second limit of BEHREND 84C was read off from their figure 2. The original papers also list limits in other channels.

Search for X^0 Resonance in e^+e^- Collisions

The limit is for $\Gamma(X^0 \to e^+e^-)$ · B($X^0 \to f$), where f is the specified final state. Spin 0 is assumed for X^0.

VALUE (keV)	CL%	DOCUMENT ID		TECN	COMMENT
• • • We do not use the following data for averages, fits, limits, etc. • • •					
$<10^3$	95	[1] ABE	93C	VNS	$\Gamma(ee)$
<(0.4–10)	95	[2] ABE	93C	VNS	$f = \gamma\gamma$
<(0.3–5)	95	[3,4] ABE	93D	TOPZ	$f = \gamma\gamma$
<(2–12)	95	[3,4] ABE	93D	TOPZ	$f =$ hadrons
<(4–200)	95	[4,5] ABE	93D	TOPZ	$f = ee$
<(0.1–6)	95	[4,5] ABE	93D	TOPZ	$f = \mu\mu$
<(0.5–8)	90	[6] STERNER	93	AMY	$f = \gamma\gamma$

Gauge & Higgs Boson Particle Listings

New Heavy Bosons

[1] Limit is for $\Gamma(X^0 \to e^+e^-)$ m_{X^0} = 56–63.5 GeV for $\Gamma(X^0)$ = 0.5 GeV.
[2] Limit is for m_{X^0} = 56–61.5 GeV and is valid for $\Gamma(X^0) \ll 100$ MeV. See their Fig. 5 for limits for Γ = 1,2 GeV.
[3] Limit is for m_{X^0} = 57.2–60 GeV.
[4] Limit is valid for $\Gamma(X^0) \ll 100$ MeV. See paper for limits for Γ = 1 GeV and those for J = 2 resonances.
[5] Limit is for m_{X^0} = 56.6–60 GeV.
[6] STERNER 93 limit is for m_{X^0} = 57–59.6 GeV and is valid for $\Gamma(X^0)$<100 MeV. See their Fig. 2 for limits for Γ = 1,3 GeV.

Search for X^0 Resonance in ep Collisions

VALUE	DOCUMENT ID		TECN	COMMENT
• • • We do not use the following data for averages, fits, limits, etc. • • •				
	[1] CHEKANOV	02B	ZEUS	$X \to jj$

[1] CHEKANOV 02B search for photoproduction of X decaying into dijets in ep collisions. See their Fig. 5 for the limit on the photoproduction cross section.

Search for X^0 Resonance in Two-Photon Process

The limit is for $\Gamma(X^0) \cdot B(X^0 \to \gamma\gamma)^2$. Spin 0 is assumed for X^0.

VALUE (MeV)	CL%	DOCUMENT ID		TECN	COMMENT
• • • We do not use the following data for averages, fits, limits, etc. • • •					
<2.6	95	[1] ACTON	93E	OPAL	m_{X^0}=60 ± 1 GeV
<2.9	95	BUSKULIC	93F	ALEP	$m_{X^0} \sim 60$ GeV

[1] ACTON 93E limit for a J = 2 resonance is 0.8 MeV.

Search for X^0 Resonance in $e^+e^- \to X^0\gamma$

VALUE (GeV)	DOCUMENT ID		TECN	COMMENT
• • • We do not use the following data for averages, fits, limits, etc. • • •				
	[1] ABBIENDI	03D	OPAL	$X^0 \to \gamma\gamma$
	[2] ABREU	00Z	DLPH	X^0 decaying invisibly
	[3] ADAM	96C	DLPH	X^0 decaying invisibly

[1] ABBIENDI 03D measure the $e^+e^- \to \gamma\gamma\gamma$ cross section at $\sqrt{s}$=181–209 GeV. The upper bound on the production cross section, $\sigma(e^+e^- \to X^0\gamma)$ times the branching ratio for $X^0 \to \gamma\gamma$, is less than 0.03 pb at 95%CL for X^0 masses between 20 and 180 GeV. See their Fig. 9b for the limits in the mass-cross section plane.
[2] ABREU 00Z is from the single photon cross section at $\sqrt{s}$=183, 189 GeV. The production cross section upper limit is less than 0.3 pb for X^0 mass between 40 and 160 GeV. See their Fig. 4 for the limit in mass-cross section plane.
[3] ADAM 96C is from the single photon production cross at $\sqrt{s}$=130, 136 GeV. The upper bound is less than 3 pb for X^0 masses between 60 and 130 GeV. See their Fig. 5 for the exact bound on the cross section $\sigma(e^+e^- \to \gamma X^0)$.

Search for X^0 Resonance in $Z \to f\bar{f}X^0$

The limit is for $B(Z \to f\bar{f}X^0) \cdot B(X^0 \to F)$ where f is a fermion and F is the specified final state. Spin 0 is assumed for X^0.

VALUE	CL%	DOCUMENT ID		TECN	COMMENT
• • • We do not use the following data for averages, fits, limits, etc. • • •					
		[1] ABREU	96T	DLPH	f=e,μ,τ; F=$\gamma\gamma$
$<3.7 \times 10^{-6}$	95	[2] ABREU	96T	DLPH	f=ν; F=$\gamma\gamma$
		[3] ABREU	96T	DLPH	f=q; F=$\gamma\gamma$
$<6.8 \times 10^{-6}$	95	[2] ACTON	93E	OPAL	f=e,μ,τ; F=$\gamma\gamma$
$<5.5 \times 10^{-6}$	95	[2] ACTON	93E	OPAL	f=q; F=$\gamma\gamma$
$<3.1 \times 10^{-6}$	95	[2] ACTON	93E	OPAL	f=ν; F=$\gamma\gamma$
$<6.5 \times 10^{-6}$	95	[2] ACTON	93E	OPAL	f=e,μ; F=$\ell\bar{\ell}$, $q\bar{q}$, $\nu\bar{\nu}$
$<7.1 \times 10^{-6}$	95	[2] BUSKULIC	93F	ALEP	f=e,μ; F=$\ell\bar{\ell}$, $q\bar{q}$, $\nu\bar{\nu}$
		[4] ADRIANI	92F	L3	f=q; F=$\gamma\gamma$

[1] ABREU 96T obtain limit as a function of m_{X^0}. See their Fig. 6.
[2] Limit is for m_{X^0} around 60 GeV.
[3] ABREU 96T obtain limit as a function of m_{X^0}. See their Fig. 15.
[4] ADRIANI 92F give $\sigma_Z \cdot B(Z \to q\bar{q}X^0) \cdot B(X^0 \to \gamma\gamma)$<(0.75–1.5) pb (95%CL) for m_{X^0} = 10–70 GeV. The limit is 1 pb at 60 GeV.

Search for X^0 Resonance in WX^0 final state

VALUE (MeV)	DOCUMENT ID		TECN	COMMENT
• • • We do not use the following data for averages, fits, limits, etc. • • •				
	[1] AALTONEN	13AA	CDF	$X^0 \to jj$
	[2] CHATRCHYAN	12BR	CMS	$X^0 \to jj$
	[3] ABAZOV	11I	D0	$X^0 \to jj$
	[4] ABE	97W	CDF	$X^0 \to b\bar{b}$

[1] AALTONEN 13AA search for X^0 production associated with W (or Z) in $p\bar{p}$ collisions at E_{cm} = 1.96 TeV. The upper limit on the cross section $\sigma(p\bar{p} \to WX^0)$ is 2.2 pb for M_{X^0} = 145 GeV.
[2] CHATRCHYAN 12BR search for X^0 production associated with W in pp collisions at E_{cm} = 7 TeV. The upper limit on the cross section is 5.0 pb at 95% CL for m_{X^0} = 150 GeV.
[3] ABAZOV 11I search for X^0 production associated with W in $p\bar{p}$ collisions at E_{cm} = 1.96 TeV. The 95% CL upper limit on the cross section ranges from 2.57 to 1.28 pb for X^0 mass between 110 and 170 GeV.
[4] ABE 97W search for X^0 production associated with W in $p\bar{p}$ collisions at E_{cm}=1.8 TeV. The 95%CL upper limit on the production cross section times the branching ratio for $X^0 \to b\bar{b}$ ranges from 14 to 19 pb for X^0 mass between 70 and 120 GeV. See their Fig. 3 for upper limits of the production cross section as a function of m_{X^0}.

Search for X^0 Resonance in Quarkonium Decays

Limits are for branching ratios to modes shown. Spin 1 is assumed for X^0.

VALUE	CL%	DOCUMENT ID		TECN	COMMENT
• • • We do not use the following data for averages, fits, limits, etc. • • •					
$< 3 \times 10^{-5}$–6×10^{-3}	90	[1] BALEST	95	CLE2	$\Upsilon(1S) \to X^0\overline{X}{}^0\gamma$, $m_{X^0} < 3.9$ GeV

[1] BALEST 95 three-body limit is for phase-space photon energy distribution and angular distribution same as for $\Upsilon \to gg\gamma$.

REFERENCES FOR Searches for New Heavy Bosons (W', Z', leptoquarks, etc.)

AAD	13AE	JHEP 1306 033	G. Aad *et al.* (ATLAS Collab.)
AAD	13AI	PL B723 15	G. Aad *et al.* (ATLAS Collab.)
AAD	13AO	PR D87 112006	G. Aad *et al.* (ATLAS Collab.)
AAD	13AQ	PR D88 012004	G. Aad *et al.* (ATLAS Collab.)
AAD	13D	JHEP 1301 029	G. Aad *et al.* (ATLAS Collab.)
AAD	13G	JHEP 1301 116	G. Aad *et al.* (ATLAS Collab.)
AAD	13K	EPJ C73 2263	G. Aad *et al.* (ATLAS Collab.)
AAD	13S	PL B719 242	G. Aad *et al.* (ATLAS Collab.)
AALTONEN	13A	PRL 110 121802	T. Aaltonen *et al.* (CDF Collab.)
AALTONEN	13AA	PR D88 092004	T. Aaltonen *et al.* (CDF Collab.)
AALTONEN	13R	PRL 111 031802	T. Aaltonen *et al.* (CDF Collab.)
CHATRCHYAN	13A	JHEP 1301 013	S. Chatrchyan *et al.* (CMS Collab.)
CHATRCHYAN	13AF	PL B720 63	S. Chatrchyan *et al.* (CMS Collab.)
CHATRCHYAN	13AJ	PL B723 280	S. Chatrchyan *et al.* (CMS Collab.)
CHATRCHYAN	13AP	PR D87 072002	S. Chatrchyan *et al.* (CMS Collab.)
CHATRCHYAN	13AQ	PR D87 072005	S. Chatrchyan *et al.* (CMS Collab.)
CHATRCHYAN	13AS	PR D87 114015	S. Chatrchyan *et al.* (CMS Collab.)
CHATRCHYAN	13AU	PRL 110 141802	S. Chatrchyan *et al.* (CMS Collab.)
CHATRCHYAN	13BM	PRL 111 211804	S. Chatrchyan *et al.* (CMS Collab.)
CHATRCHYAN	13E	PL B718 1229	S. Chatrchyan *et al.* (CMS Collab.)
CHATRCHYAN	13M	PRL 110 081801	S. Chatrchyan *et al.* (CMS Collab.)
CHATRCHYAN	13U	JHEP 1302 036	S. Chatrchyan *et al.* (CMS Collab.)
SAKAKI	13	PR D88 094012	Y. Sakaki *et al.*
AAD	12AV	PRL 109 081801	G. Aad *et al.* (ATLAS Collab.)
AAD	12BB	PR D85 112012	G. Aad *et al.* (ATLAS Collab.)
AAD	12BV	JHEP 1209 041	G. Aad *et al.* (ATLAS Collab.)
AAD	12CC	JHEP 1211 138	G. Aad *et al.* (ATLAS Collab.)
AAD	12CK	PR D86 091103	G. Aad *et al.* (ATLAS Collab.)
AAD	12CR	EPJ C72 2241	G. Aad *et al.* (ATLAS Collab.)
AAD	12H	PL B709 158	G. Aad *et al.* (ATLAS Collab.)
Also		PL B711 442 (errat.)	G. Aad *et al.* (ATLAS Collab.)
AAD	12K	EPJ C72 2083	G. Aad *et al.* (ATLAS Collab.)
AAD	12M	EPJ C72 2056	G. Aad *et al.* (ATLAS Collab.)
AAD	12O	EPJ C72 2151	G. Aad *et al.* (ATLAS Collab.)
AALTONEN	12AR	PR D86 112002	T. Aaltonen *et al.* (CDF Collab.)
AALTONEN	12N	PRL 108 211805	T. Aaltonen *et al.* (CDF Collab.)
ABAZOV	12R	PR D85 051101	V.M. Abazov *et al.* (D0 Collab.)
ABRAMOWICZ	12A	PR D86 012005	H. Abramowicz *et al.* (ZEUS Collab.)
CHATRCHYAN	12AB	JHEP 1208 023	S. Chatrchyan *et al.* (CMS Collab.)
CHATRCHYAN	12AF	PRL 109 141801	S. Chatrchyan *et al.* (CMS Collab.)
CHATRCHYAN	12AG	PR D86 052013	S. Chatrchyan *et al.* (CMS Collab.)
CHATRCHYAN	12AI	JHEP 1208 110	S. Chatrchyan *et al.* (CMS Collab.)
CHATRCHYAN	12AQ	JHEP 1209 029	S. Chatrchyan *et al.* (CMS Collab.)
CHATRCHYAN	12AR	PL B717 351	S. Chatrchyan *et al.* (CMS Collab.)
CHATRCHYAN	12BG	PRL 109 261802	S. Chatrchyan *et al.* (CMS Collab.)
CHATRCHYAN	12BL	JHEP 1212 015	S. Chatrchyan *et al.* (CMS Collab.)
CHATRCHYAN	12BO	JHEP 1212 055	S. Chatrchyan *et al.* (CMS Collab.)
CHATRCHYAN	12BR	PRL 109 251801	S. Chatrchyan *et al.* (CMS Collab.)
CHATRCHYAN	12M	PL B714 158	S. Chatrchyan *et al.* (CMS Collab.)
CHATRCHYAN	12O	PL B716 82	S. Chatrchyan *et al.* (CMS Collab.)
KOSNIK	12	PR D86 055004	N. Kosnik (LALO, STFN)
AAD	11AD	PRL 107 272002	G. Aad *et al.* (ATLAS Collab.)
AAD	11D	PR D83 112006	G. Aad *et al.* (ATLAS Collab.)
AAD	11H	PRL 106 251801	G. Aad *et al.* (ATLAS Collab.)
AAD	11J	PL B700 163	G. Aad *et al.* (ATLAS Collab.)
AAD	11M	PL B701 50	G. Aad *et al.* (ATLAS Collab.)
AAD	11Q	PL B705 28	G. Aad *et al.* (ATLAS Collab.)
AAD	11Z	EPJ C71 1809	G. Aad *et al.* (ATLAS Collab.)
AALTONEN	11AD	PR D84 072003	T. Aaltonen *et al.* (CDF Collab.)
AALTONEN	11AE	PR D84 072004	T. Aaltonen *et al.* (CDF Collab.)
AALTONEN	11C	PR D83 031102	T. Aaltonen *et al.* (CDF Collab.)
AALTONEN	11I	PRL 106 121801	T. Aaltonen *et al.* (CDF Collab.)
AARON	11A	PL B701 20	F. D. Aaron *et al.* (H1 Collab.)
AARON	11B	PL B704 388	F. D. Aaron *et al.* (H1 Collab.)
AARON	11C	PL B705 52	F. D. Aaron *et al.* (H1 Collab.)
ABAZOV	11A	PL B695 88	V.M. Abazov *et al.* (D0 Collab.)
ABAZOV	11H	PRL 107 011801	V. M. Abazov *et al.* (D0 Collab.)
ABAZOV	11I	PRL 107 011804	V. M. Abazov *et al.* (D0 Collab.)
ABAZOV	11L	PL B699 145	V. M. Abazov *et al.* (D0 Collab.)
ABAZOV	11V	PR D84 071104	V. M. Abazov *et al.* (D0 Collab.)
BUENO	11	PR D84 032005	J.F. Bueno *et al.* (TWIST Collab.)
Also		PR D85 039908 (errat.)	J.F. Bueno *et al.* (TWIST Collab.)
CHATRCHYAN	11	JHEP 1105 093	S. Chatrchyan *et al.* (CMS Collab.)
CHATRCHYAN	11K	PL B701 160	S. Chatrchyan *et al.* (CMS Collab.)
CHATRCHYAN	11N	PL B703 246	S. Chatrchyan *et al.* (CMS Collab.)
CHATRCHYAN	11O	JHEP 1108 005	S. Chatrchyan *et al.* (CMS Collab.)
CHATRCHYAN	11Y	PL B704 123	S. Chatrchyan *et al.* (CMS Collab.)
DORSNER	11	JHEP 1111 002	I. Dorsner *et al.*
KHACHATRY...	11D	PRL 106 201802	V. Khachatryan *et al.* (CMS Collab.)
KHACHATRY...	11E	PRL 106 201803	V. Khachatryan *et al.* (CMS Collab.)
KHACHATRY...	11H	PL B698 21	V. Khachatryan *et al.* (CMS Collab.)
AALTONEN	10L	PL B691 183	T. Aaltonen *et al.* (CDF Collab.)
AALTONEN	10N	PRL 104 241801	T. Aaltonen *et al.* (CDF Collab.)
ABAZOV	10A	PRL 104 061801	V.M. Abazov *et al.* (D0 Collab.)
ABAZOV	10L	PL B693 95	V.M. Abazov *et al.* (D0 Collab.)

DEL-AGUILA	10	JHEP 1009 033	F. del Aguila, J. de Blas, M. Perez-Victoria	(GRAN)
KHACHATRY...	10	PRL 105 211801	V. Khachatryan *et al.*	(CMS Collab.)
Also		PRL 106 029902	V. Khachatryan *et al.*	(CMS Collab.)
WAUTERS	10	PR C82 055502	F. Wauters *et al.*	(REZ, TAMU)
AALTONEN	09AA	PRL 103 041801	T. Aaltonen *et al.*	(CDF Collab.)
AALTONEN	09AC	PR D79 112002	T. Aaltonen *et al.*	(CDF Collab.)
AALTONEN	09T	PRL 102 031801	T. Aaltonen *et al.*	(CDF Collab.)
AALTONEN	09V	PRL 102 091805	T. Aaltonen *et al.*	(CDF Collab.)
ABAZOV	09	PL B671 224	V.M. Abazov *et al.*	(D0 Collab.)
ABAZOV	09AF	PL B681 224	V.M. Abazov *et al.*	(D0 Collab.)
ERLER	09	JHEP 0908 017	J. Erler *et al.*	
AALTONEN	08D	PR D77 051102	T. Aaltonen *et al.*	(CDF Collab.)
AALTONEN	08P	PR D77 091105	T. Aaltonen *et al.*	(CDF Collab.)
AALTONEN	08Y	PRL 100 231801	T. Aaltonen *et al.*	(CDF Collab.)
AALTONEN	08Z	PRL 101 071802	T. Aaltonen *et al.*	(CDF Collab.)
ABAZOV	08AA	PL B668 98	V.M. Abazov *et al.*	(D0 Collab.)
ABAZOV	08AD	PL B668 357	V.M. Abazov *et al.*	(D0 Collab.)
ABAZOV	08AN	PRL 101 241802	V.M. Abazov *et al.*	(D0 Collab.)
ABAZOV	08C	PRL 100 031804	V.M. Abazov *et al.*	(D0 Collab.)
ABAZOV	08P	PRL 100 211803	V.M. Abazov *et al.*	(D0 Collab.)
MACDONALD	08	PR D78 032010	R.P. MacDonald *et al.*	(TWIST Collab.)
AALTONEN	07H	PRL 99 171802	T. Aaltonen *et al.*	(CDF Collab.)
ABAZOV	07E	PL B647 74	V.M. Abazov *et al.*	(D0 Collab.)
ABAZOV	07J	PRL 99 061801	V.M. Abazov *et al.*	(D0 Collab.)
ABULENCIA	07K	PR D75 091101	A. Abulencia *et al.*	(CDF Collab.)
AKTAS	07A	EPJ C52 833	A. Aktas *et al.*	(H1 Collab.)
CHOUDHURY	07	PL B657 69	D. Choudhury *et al.*	
MELCONIAN	07	PL B649 370	D. Melconian *et al.*	(TRIUMF)
SCHAEL	07A	EPJ C49 411	S. Schael *et al.*	(ALEPH Collab.)
SCHUMANN	07	PRL 99 191803	M. Schumann *et al.*	(HEID, ILLG, KARL+)
SMIRNOV	07	MPL A22 2353	A.D. Smirnov	
ABAZOV	06A	PL B636 183	V.M. Abazov *et al.*	(D0 Collab.)
ABAZOV	06L	PL B640 230	V.M. Abazov *et al.*	(D0 Collab.)
ABAZOV	06N	PL B641 423	V.M. Abazov *et al.*	(D0 Collab.)
ABDALLAH	06C	EPJ C45 589	J. Abdallah *et al.*	(DELPHI Collab.)
ABULENCIA	06L	PRL 96 211801	A. Abulencia *et al.*	(CDF Collab.)
ABULENCIA	06M	PRL 96 211802	A. Abulencia *et al.*	(CDF Collab.)
ABULENCIA	06T	PR D73 051102	A. Abulencia *et al.*	(CDF Collab.)
ABAZOV	05H	PR D71 071104	V.M. Abazov *et al.*	(D0 Collab.)
ABULENCIA	05A	PRL 95 252001	A. Abulencia *et al.*	(CDF Collab.)
ACOSTA	05I	PR D71 112001	D. Acosta *et al.*	(CDF Collab.)
ACOSTA	05P	PR D72 051107	D. Acosta *et al.*	(CDF Collab.)
ACOSTA	05R	PRL 95 131801	D. Acosta *et al.*	(CDF Collab.)
AKTAS	05B	PL B629 9	A. Aktas *et al.*	(H1 Collab.)
CHEKANOV	05	PL B610 212	S. Chekanov *et al.*	(HERA ZEUS Collab.)
CHEKANOV	05A	EPJ C44 463	S. Chekanov *et al.*	(ZEUS Collab.)
CYBURT	05	ASP 23 313	R.H. Cyburt *et al.*	
ABAZOV	04A	PRL 92 221801	V.M. Abazov *et al.*	(D0 Collab.)
ABAZOV	04C	PR D69 111101	V.M. Abazov *et al.*	(D0 Collab.)
ABBIENDI	04G	EPJ C33 173	G. Abbiendi *et al.*	(OPAL Collab.)
ABBIENDI	03D	EPJ C26 331	G. Abbiendi *et al.*	(OPAL Collab.)
ABBIENDI	03R	EPJ C31 281	G. Abbiendi *et al.*	(OPAL)
ACOSTA	03B	PRL 90 081802	D. Acosta *et al.*	(CDF Collab.)
ADLOFF	03	PL B568 35	C. Adloff *et al.*	(H1 Collab.)
BARGER	03B	PR D67 075009	V. Barger, P. Langacker, H. Lee	
CHANG	03	PR D68 111101	M.-C. Chang *et al.*	(BELLE Collab.)
CHEKANOV	03B	PR D68 052004	S. Chekanov *et al.*	(ZEUS Collab.)
ABAZOV	02	PRL 88 191801	V.M. Abazov *et al.*	(D0 Collab.)
ABBIENDI	02B	PL B526 233	G. Abbiendi *et al.*	(OPAL Collab.)
AFFOLDER	02C	PRL 88 071806	T. Affolder *et al.*	(CDF Collab.)
CHEKANOV	02	PR D65 092004	S. Chekanov *et al.*	(ZEUS Collab.)
CHEKANOV	02B	PL B531 9	S. Chekanov *et al.*	(ZEUS Collab.)
MUECK	02	PR D65 085037	A. Mueck, A. Pilaftsis, R. Rueckl	
ABAZOV	01B	PRL 87 061802	V.M. Abazov *et al.*	(D0 Collab.)
ABAZOV	01D	PR D64 092004	V.M. Abazov *et al.*	(D0 Collab.)
ADLOFF	01C	PL B523 234	C. Adloff *et al.*	(H1 Collab.)
AFFOLDER	01I	PRL 87 231803	T. Affolder *et al.*	(CDF Collab.)
BREITWEG	01	PR D63 052002	J. Breitweg *et al.*	(ZEUS Collab.)
CHEUNG	01B	PL B517 167	K. Cheung	
THOMAS	01	NP A694 559	E. Thomas *et al.*	
ABBIENDI	00M	EPJ C13 15	G. Abbiendi *et al.*	(OPAL Collab.)
ABBOTT	00C	PRL 84 2088	B. Abbott *et al.*	(D0 Collab.)
ABE	00	PRL 84 5716	F. Abe *et al.*	(CDF Collab.)
ABREU	00S	PL B485 45	P. Abreu *et al.*	(DELPHI Collab.)
ABREU	00Z	EPJ C17 53	P. Abreu *et al.*	(DELPHI Collab.)
ACCIARRI	00P	PL B489 81	M. Acciarri *et al.*	(L3 Collab.)
ADLOFF	00	PL B479 358	C. Adloff *et al.*	(H1 Collab.)
AFFOLDER	00K	PRL 85 2056	T. Affolder *et al.*	(CDF Collab.)
BARATE	00I	EPJ C12 183	R. Barate *et al.*	(ALEPH Collab.)
BARGER	00	PL B480 149	V. Barger, K. Cheung	
BREITWEG	00E	EPJ C16 253	J. Breitweg *et al.*	(ZEUS Collab.)
CHAY	00	PR D61 035002	J. Chay, K.Y. Lee, S. Nam	
CHO	00	MPL A15 311	G. Cho	
CORNET	00	PR D61 037701	F. Cornet, M. Relano, J. Rico	
DELGADO	00	JHEP 0001 030	A. Delgado, A. Pomarol, M. Quiros	
ERLER	00	PRL 84 212	J. Erler, P. Langacker	
GABRIELLI	00	PR D62 055009	E. Gabrielli	
RIZZO	00	PR D61 016007	T.G. Rizzo, J.D. Wells	
ROSNER	00	PR D61 016006	J.L. Rosner	
ZARNECKI	00	EPJ C17 695	A. Zarnecki	
ABBIENDI	99	EPJ C6 1	G. Abbiendi *et al.*	(OPAL Collab.)
ABBOTT	99J	PRL 83 2896	B. Abbott *et al.*	(D0 Collab.)
ABREU	99G	PL B446 62	P. Abreu *et al.*	(DELPHI Collab.)
ACKERSTAFF	99D	EPJ C8 3	K. Ackerstaff *et al.*	(OPAL Collab.)
ADLOFF	99	EPJ C11 447	C. Adloff *et al.*	(H1 Collab.)
Also		EPJ C14 553 (errat)	C. Adloff *et al.*	(H1 Collab.)
CASALBUONI	99	PL B460 135	R. Casalbuoni *et al.*	
CZAKON	99	PL B458 355	M. Czakon, J. Gluza, M. Zralek	
ERLER	99	PL B456 68	J. Erler, P. Langacker	
MARCIANO	99	PR D60 093006	W. Marciano	
MASIP	99	PR D60 096005	M. Masip, A. Pomarol	
NATH	99	PR D60 116004	P. Nath, M. Yamaguchi	
STRUMIA	99	PL B466 107	A. Strumia	
ABBOTT	98E	PRL 80 2051	B. Abbott *et al.*	(D0 Collab.)
ABBOTT	98J	PRL 81 38	B. Abbott *et al.*	(D0 Collab.)
ABE	98S	PRL 81 4806	F. Abe *et al.*	(CDF Collab.)
ABE	98V	PRL 81 5742	F. Abe *et al.*	(CDF Collab.)
ACCIARRI	98J	PL B433 163	M. Acciarri *et al.*	(L3 Collab.)
ACKERSTAFF	98V	EPJ C2 441	K. Ackerstaff *et al.*	(OPAL Collab.)
BARATE	98U	EPJ C4 571	R. Barate *et al.*	(ALEPH Collab.)
BARENBOIM	98	EPJ C1 369	G. Barenboim	
CHO	98	EPJ C5 155	G. Cho, K. Hagiwara, S. Matsumoto	
CONRAD	98	RMP 70 1341	J.M. Conrad, M.H. Shaevitz, T. Bolton	
DONCHESKI	98	PR D58 097702	M.A. Doncheski, R.W. Robinett	
GROSS-PILCH...	98	hep-ex/9810015	C. Grosso-Pilcher, G. Landsberg, M. Paterno	
ABE	97F	PRL 78 2906	F. Abe *et al.*	(CDF Collab.)
ABE	97G	PR D55 R5263	F. Abe *et al.*	(CDF Collab.)
ABE	97S	PRL 79 2192	F. Abe *et al.*	(CDF Collab.)
ABE	97W	PRL 79 3819	F. Abe *et al.*	(CDF Collab.)
ABE	97X	PRL 79 4327	F. Abe *et al.*	(CDF Collab.)
ACCIARRI	97Q	PL B412 201	M. Acciarri *et al.*	(L3 Collab.)
ARIMA	97	PR D55 19	T. Arima *et al.*	(VENUS Collab.)
BARENBOIM	97	PR D55 4213	G. Barenboim *et al.*	(VALE, IFIC)
DEANDREA	97	PL B409 277	A. Deandrea	(MARS)
DERRICK	97	ZPHY C73 613	M. Derrick *et al.*	(ZEUS Collab.)
GROSSMAN	97	PR D55 2768	Y. Grossman, Z. Ligeti, E. Nardi	(REHO, CIT)
JADACH	97	PL B408 281	S. Jadach, B.F.L. Ward, Z. Was	(CERN, INPK+)
STAHL	97	ZPHY C74 73	A. Stahl, H. Voss	(BONN)
ABACHI	96C	PRL 76 3271	S. Abachi *et al.*	(D0 Collab.)
ABACHI	96D	PL B385 471	S. Abachi *et al.*	(D0 Collab.)
ABREU	96T	ZPHY C72 179	P. Abreu *et al.*	(DELPHI Collab.)
ADAM	96C	PL B380 471	W. Adam *et al.*	(DELPHI Collab.)
AID	96B	PL B369 173	S. Aid *et al.*	(H1 Collab.)
ALLET	96	PL B383 139	M. Allet *et al.*	(VILL, LEUV, LOUV, WISC)
ABACHI	95E	PL B358 405	S. Abachi *et al.*	(D0 Collab.)
ABE	95M	PRL 74 2900	F. Abe *et al.*	(CDF Collab.)
ABE	95N	PRL 74 3538	F. Abe *et al.*	(CDF Collab.)
BALEST	95	PR D51 2053	R. Balest *et al.*	(CLEO Collab.)
KUZNETSOV	95	PRL 75 794	I.A. Kuznetsov *et al.*	(PNPI, KIAE, HARV+)
KUZNETSOV	95B	PAN 58 2113	A.V. Kuznetsov, N.V. Mikheev	(YARO)
		Translated from YAF 58 2228.		
MIZUKOSHI	95	NP B443 20	J.K. Mizukoshi, O.J.P. Eboli, M.C. Gonzalez-Garcia	
ABREU	94O	ZPHY C64 183	P. Abreu *et al.*	(DELPHI Collab.)
BHATTACH...	94	PL B336 100	G. Bhattacharyya, J. Ellis, K. Sridhar	(CERN)
Also		PL B338 522 (erratum)	G. Bhattacharyya, J. Ellis, K. Sridhar	(CERN)
BHATTACH...	94B	PL B338 522 (erratum)	G. Bhattacharyya, J. Ellis, K. Sridhar	(CERN)
DAVIDSON	94	ZPHY C61 613	S. Davidson, D. Bailey, B.A. Campbell	(CFPA+)
KUZNETSOV	94	PL B329 295	A.V. Kuznetsov, N.V. Mikheev	(YARO)
KUZNETSOV	94B	JETPL 60 315	I.A. Kuznetsov *et al.*	(PNPI, KIAE, HARV+)
		Translated from ZETFP 60 311.		
LEURER	94	PR D50 536	M. Leurer	(REHO)
LEURER	94B	PR D49 333	M. Leurer	(REHO)
Also		PRL 71 1324	M. Leurer	(REHO)
MAHANTA	94	PL B337 128	U. Mahanta	(MEHTA)
SEVERIJNS	94	PRL 73 611 (erratum)	N. Severijns *et al.*	(LOUV, WISC, LEUV+)
VILAIN	94B	PL B332 465	P. Vilain *et al.*	(CHARM II Collab.)
ABE	93C	PL B302 119	K. Abe *et al.*	(VENUS Collab.)
ABE	93D	PL B304 373	T. Abe *et al.*	(TOPAZ Collab.)
ABE	93G	PRL 71 2542	F. Abe *et al.*	(CDF Collab.)
ABREU	93J	PL B316 620	P. Abreu *et al.*	(DELPHI Collab.)
ACTON	93E	PL B311 391	P.D. Acton *et al.*	(OPAL Collab.)
ADRIANI	93M	PRPL 236 1	O. Adriani *et al.*	(L3 Collab.)
ALITTI	93	NP B400 3	J. Alitti *et al.*	(UA2 Collab.)
BHATTACH...	93	PR D47 R3693	G. Bhattacharyya *et al.*	(CALC, JADA, ICTP+)
BUSKULIC	93F	PL B308 425	D. Buskulic *et al.*	(ALEPH Collab.)
DERRICK	93	PL B306 173	M. Derrick *et al.*	(ZEUS Collab.)
RIZZO	93	PR D48 4470	T.G. Rizzo	(ANL)
SEVERIJNS	93	PRL 70 4047	N. Severijns *et al.*	(LOUV, WISC, LEUV+)
Also		PRL 73 611 (erratum)	N. Severijns *et al.*	(LOUV, WISC, LEUV+)
STERNER	93	PL B303 385	K.L. Sterner *et al.*	(AMY Collab.)
ABREU	92D	ZPHY C53 555	P. Abreu *et al.*	(DELPHI Collab.)
ADRIANI	92F	PL B292 472	O. Adriani *et al.*	(L3 Collab.)
DECAMP	92	PRPL 216 253	D. Decamp *et al.*	(ALEPH Collab.)
IMAZATO	92	PRL 69 877	J. Imazato *et al.*	(KEK, INUS, TOKY+)
MISHRA	92	PRL 68 3499	S.R. Mishra *et al.*	(COLU, CHIC, FNAL+)
POLAK	92B	PR D46 3871	J. Polak, M. Zralek	(SILES)
ACTON	91	PL B268 122	D.P. Acton *et al.*	(OPAL Collab.)
ACTON	91B	PL B273 338	D.P. Acton *et al.*	(OPAL Collab.)
ADEVA	91D	PL B262 155	B. Adeva *et al.*	(L3 Collab.)
AQUINO	91	PL B261 280	M. Aquino, A. Fernandez, A. Garcia	(CINV, PUEB)
COLANGELO	91	PL B253 154	P. Colangelo, G. Nardulli	(BARI)
CUYPERS	91	PL B259 173	F. Cuypers, A.F. Falk, P.H. Frampton	(DURH, HARV+)
FARAGGI	91	MPL A6 61	A.E. Faraggi, D.V. Nanopoulos	(TAMU)
POLAK	91	NP B363 385	J. Polak, M. Zralek	(SILES)
RIZZO	91	PR D44 202	T.G. Rizzo	(WISC, ISU)
WALKER	91	APJ 376 51	T.P. Walker *et al.*	(HSCA, OSU, CHIC+)
ABE	90F	PL B246 297	K. Abe *et al.*	(VENUS Collab.)
ABE	90H	PR D41 1722	F. Abe *et al.*	(CDF Collab.)
AKRAWY	90J	PL B246 285	M.Z. Akrawy *et al.*	(OPAL Collab.)
GONZALEZ-G...	90D	PL B240 163	M.C. Gonzalez-Garcia, J.W.F. Valle	(VALE)
GRIFOLS	90	NP B331 244	J.A. Grifols, E. Masso	(BARC)
GRIFOLS	90D	PR D42 3293	J.A. Grifols, E. Masso, T.G. Rizzo	(BARC, CERN+)
KIM	90	PL B240 243	G.N. Kim *et al.*	(AMY Collab.)
LOPEZ	90	PL B241 392	J.L. Lopez, D.V. Nanopoulos	(TAMU)
BARBIERI	89B	PR D39 1229	R. Barbieri, R.N. Mohapatra	(PISA, UMD)
LANGACKER	89B	PR D40 1569	P. Langacker, S. Uma Sankar	(PENN)
ODAKA	89	JPSJ 58 3037	S. Odaka *et al.*	(VENUS Collab.)
ROBINETT	89	PR D39 834	R.W. Robinett	(PSU)
ALBAJAR	88B	PL B209 127	C. Albajar *et al.*	(UA1 Collab.)
BAGGER	88	PR D37 1188	J. Bagger, C. Schmidt, S. King	(HARV, BOST)
BALKE	88	PR D37 587	B. Balke *et al.*	(LBL, UCB, COLO, NWES+)
BERGSTROM	88	PL B212 386	L. Bergstrom	(STOH)
CUYPERS	88	PRL 60 1237	F. Cuypers, P.H. Frampton	(UNCCH)
DONCHESKI	88	PL B206 137	M.A. Doncheski, H. Grotch, R. Robinett	(PSU)
DONCHESKI	88B	PR D38 412	M.A. Doncheski, H. Grotch, R.W. Robinett	(PSU)
BARTEL	87B	ZPHY C36 15	W. Bartel *et al.*	(JADE Collab.)
BEHREND	86B	PL B178 452	H.J. Behrend *et al.*	(CELLO Collab.)
DERRICK	86	PL 166B 463	M. Derrick *et al.*	(HRS Collab.)
Also		PR D34 3286	M. Derrick *et al.*	(HRS Collab.)
JODIDIO	86	PR D34 1967	A. Jodidio *et al.*	(LBL, NWES, TRIU)
Also		PR D37 237 (erratum)	A. Jodidio *et al.*	(LBL, NWES, TRIU)
MOHAPATRA	86	PR D34 909	R.N. Mohapatra	(UMD)
ADEVA	85	PL 152B 439	B. Adeva *et al.*	(Mark-J Collab.)
BERGER	85B	ZPHY C27 341	C. Berger *et al.*	(PLUTO Collab.)
STOKER	85	PRL 54 1887	D.P. Stoker *et al.*	(LBL, NWES, TRIU)
ADEVA	84	PRL 53 134	B. Adeva *et al.*	(Mark-J Collab.)
BEHREND	84C	PL 140B 130	H.J. Behrend *et al.*	(CELLO Collab.)
BERGSMA	83	PL 122B 465	F. Bergsma *et al.*	(CHARM Collab.)
CARR	83	PRL 51 627	J. Carr *et al.*	(LBL, NWES, TRIU)
BEALL	82	PRL 48 848	G. Beall, M. Bander, A. Soni	(UCI, UCLA)
SHANKER	82	NP B204 375	O. Shanker	(TRIU)

Axions (A^0) and Other Very Light Bosons, Searches for

AXIONS AND OTHER SIMILAR PARTICLES

Revised April 2014 by A. Ringwald (DESY), L.J Rosenberg and G. Rybka (U. of Washington).

Introduction

In this section, we list coupling-strength and mass limits for light neutral scalar or pseudoscalar bosons that couple weakly to normal matter and radiation. Such bosons may arise from a global spontaneously broken U(1) symmetry, resulting in a massless Nambu-Goldstone (NG) boson. If there is a small explicit symmetry breaking, either already in the Lagrangian or due to quantum effects such as anomalies, the boson acquires a mass and is called a pseudo-NG boson. Typical examples are axions (A^0) [1,2], familons [3] and Majorons [4], associated, respectively, with a spontaneously broken Peccei-Quinn, family and lepton-number symmetry.

A common characteristic among these light bosons ϕ is that their coupling to Standard-Model particles is suppressed by the energy scale that characterizes the symmetry breaking, *i.e.*, the decay constant f. The interaction Lagrangian is

$$\mathcal{L} = f^{-1} J^\mu \partial_\mu \phi \,, \tag{1}$$

where J^μ is the Noether current of the spontaneously broken global symmetry. If f is very large, these new particles interact very weakly. Detecting them would provide a window to physics far beyond what can be probed at accelerators.

Axions are of particular interest because the Peccei-Quinn (PQ) mechanism remains perhaps the most credible scheme to preserve CP in QCD. Moreover, the cold dark matter of the universe may well consist of axions and they are searched for in dedicated experiments with a realistic chance of discovery.

Originally it was assumed that the PQ scale f_A was related to the electroweak symmetry-breaking scale $v_{\rm weak} = (\sqrt{2}G_{\rm F})^{-1/2} = 247$ GeV. However, the associated "standard" and "variant" axions were quickly excluded—we refer to the Listings for detailed limits. Here we focus on "invisible axions" with $f_A \gg v_{\rm weak}$ as the main possibility.

Axions have a characteristic two-photon vertex, inherited from their mixing with π^0 and η. It allows for the main search strategy based on axion-photon conversion in external magnetic fields [5], an effect that also can be of astrophysical interest. While for axions the product "$A\gamma\gamma$ interaction strength $\times$ mass" is essentially fixed by the corresponding π^0 properties, one may consider more general axion-like particles (ALPs) where the two parameters are independent. Several experiments have recently explored this more general parameter space. ALPs populating the latter are predicted to arise generically, in addition to the axion, in low-energy effective field theories emerging from string theory [6]. The latter often contain also very light Abelian vector bosons under which the Standard-Model particles are not charged: so-called hidden-sector photons, dark photons or paraphotons. They share a lot of the phenomenological features with the axion and ALPs, notably the possibility of hidden photon - photon conversion. Their physics case and the current constraints are compiled in Ref. [7].

I. THEORY

I.1 Peccei-Quinn mechanism and axions

The QCD Lagrangian includes a CP-violating term $\mathcal{L}_\Theta = \bar{\Theta}\,(\alpha_s/8\pi)\,G^{\mu\nu a}\tilde{G}^a_{\mu\nu}$, where $-\pi \le \bar{\Theta} \le +\pi$ is the effective Θ parameter after diagonalizing quark masses, G is the color field strength tensor, and $\tilde{G}$ its dual. Limits on the neutron electric dipole moment [8] imply $|\bar{\Theta}| \lesssim 10^{-10}$ even though $\bar{\Theta} = \mathcal{O}(1)$ is otherwise completely satisfactory. The spontaneously broken global Peccei-Quinn symmetry $\mathrm{U(1)_{PQ}}$ was introduced to solve this "strong CP problem" [1], an axion being the pseudo-NG boson of $\mathrm{U(1)_{PQ}}$ [2]. This symmetry is broken due to the axion's anomalous triangle coupling to gluons,

$$\mathcal{L} = \left(\bar{\Theta} - \frac{\phi_A}{f_A}\right) \frac{\alpha_s}{8\pi} G^{\mu\nu a}\tilde{G}^a_{\mu\nu} \,, \tag{2}$$

where ϕ_A is the axion field and f_A the axion decay constant. Color anomaly factors have been absorbed in the normalization of f_A which is defined by this Lagrangian. Thus normalized, f_A is the quantity that enters all low-energy phenomena [9]. Non-perturbative QCD effects induce a potential for ϕ_A whose minimum is at $\phi_A = \bar{\Theta}\, f_A$, thereby canceling the $\bar{\Theta}$ term in the QCD Lagrangian and thus restoring CP symmetry.

The resulting axion mass is given by $m_A f_A \approx m_\pi f_\pi$ where $m_\pi = 135$ MeV and $f_\pi \approx 92$ MeV. In more detail one finds

$$m_A = \frac{z^{1/2}}{1+z}\,\frac{f_\pi m_\pi}{f_A} = \frac{0.60\ \text{meV}}{f_A/10^{10}\,\text{GeV}} \,, \tag{3}$$

where $z = m_u/m_d$. We have used the canonical value $z = 0.56$ [10], although the range $z = 0.35$–0.60 is plausible [11].

Originally one assumed $f_A \sim v_{\rm weak}$ [1,2]. Tree-level flavor conservation fixes the axion properties in terms of a single parameter $\tan\beta$, the ratio of the vacuum expectation values of two Higgs fields that appear as a minimal ingredient. This "standard axion" is excluded after extensive searches [12]. A narrow peak structure observed in positron spectra from heavy ion collisions [13] suggested an axion-like particle of mass 1.8 MeV that decays into e^+e^-, but extensive follow-up searches were negative. "Variant axion models" were proposed which keep $f_A \sim v_{\rm weak}$ while dropping the constraint of tree-level flavor conservation [14], but these models are also excluded [15].

Axions with $f_A \gg v_{\rm weak}$ evade all current experimental limits. One generic class of models invokes "hadronic axions" where new heavy quarks carry $\mathrm{U(1)_{PQ}}$ charges, leaving ordinary quarks and leptons without tree-level axion couplings. The prototype is the KSVZ model [16], where in addition the heavy quarks are electrically neutral. Another generic class requires at least two Higgs doublets and ordinary quarks and leptons carry PQ charges, the prototype being the DFSZ model [17]. All of these models contain at least one electroweak singlet

scalar that acquires a vacuum expectation value and thereby breaks the PQ symmetry. The KSVZ and DFSZ models are frequently used as generic examples, but other models exist where both heavy quarks and Higgs doublets carry PQ charges. In supersymmetric models, the axion is part of a supermultiplet and thus inevitably accompanied by a spin-0 saxion and a spin-1 axino, which both also have couplings suppressed by f_A, but are expected to have large masses due to supersymmetry breaking [18].

I.2 Model-dependent axion couplings

Although the generic axion interactions scale approximately with f_π/f_A from the corresponding π^0 couplings, there are non-negligible model-dependent factors and uncertainties. The axion's two-photon interaction plays a key role for many searches,

$$\mathcal{L}_{A\gamma\gamma} = \frac{G_{A\gamma\gamma}}{4} F_{\mu\nu}\tilde{F}^{\mu\nu}\phi_A = -G_{A\gamma\gamma}\mathbf{E}\cdot\mathbf{B}\,\phi_A\,, \tag{4}$$

where F is the electromagnetic field-strength tensor and $\tilde{F}$ its dual. The coupling constant is

$$\begin{aligned} G_{A\gamma\gamma} &= \frac{\alpha}{2\pi f_A}\left(\frac{E}{N} - \frac{2}{3}\frac{4+z}{1+z}\right) \\ &= \frac{\alpha}{2\pi}\left(\frac{E}{N} - \frac{2}{3}\frac{4+z}{1+z}\right)\frac{1+z}{z^{1/2}}\frac{m_A}{m_\pi f_\pi}\,, \end{aligned} \tag{5}$$

where E and N are the electromagnetic and color anomalies of the axial current associated with the axion. In grand unified models, and notably for DFSZ [17], $E/N = 8/3$, whereas for KSVZ [16] $E/N = 0$ if the electric charge of the new heavy quark is taken to vanish. In general, a broad range of E/N values is possible [19], as indicated by the yellow band in Figure 1. The two-photon decay width is

$$\Gamma_{A\to\gamma\gamma} = \frac{G^2_{A\gamma\gamma}m_A^3}{64\,\pi} = 1.1\times10^{-24}\ \text{s}^{-1}\left(\frac{m_A}{\text{eV}}\right)^5. \tag{6}$$

The second expression uses Eq. (5) with $z = 0.56$ and $E/N = 0$. Axions decay faster than the age of the universe if $m_A \gtrsim 20$ eV.

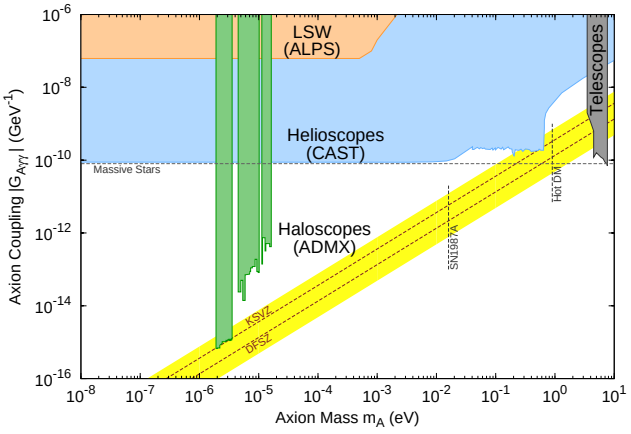

Figure 1: Exclusion plot for axion-like particles as described in the text.

The interaction with fermions f has derivative form and is invariant under a shift $\phi_A \to \phi_A + \phi_0$ as behooves a NG boson,

$$\mathcal{L}_{Aff} = \frac{C_f}{2f_A}\,\bar{\Psi}_f\gamma^\mu\gamma_5\Psi_f\partial_\mu\phi_A\,. \tag{7}$$

Here, Ψ_f is the fermion field, m_f its mass, and C_f a model-dependent coefficient. The dimensionless combination $g_{Aff} \equiv C_f m_f/f_A$ plays the role of a Yukawa coupling and $\alpha_{Aff} \equiv g^2_{Aff}/4\pi$ of a "fine-structure constant." The often-used pseudoscalar form $\mathcal{L}_{Aff} = -\mathrm{i}\,(C_f m_f/f_A)\,\bar{\Psi}_f\gamma_5\Psi_f\phi_A$ need not be equivalent to the appropriate derivative structure, for example when two NG bosons are attached to one fermion line as in axion emission by nucleon bremsstrahlung [20].

In the DFSZ model [17], the tree-level coupling coefficient to electrons is

$$C_e = \frac{\cos^2\beta}{3}\,, \tag{8}$$

where $\tan\beta$ is the ratio of two Higgs vacuum expectation values that are generic to this and similar models.

For nucleons, $C_{n,p}$ are related to axial-vector current matrix elements by generalized Goldberger-Treiman relations,

$$\begin{aligned} C_p &= (C_u - \eta)\Delta u + (C_d - \eta z)\Delta d + (C_s - \eta w)\Delta s\,, \\ C_n &= (C_u - \eta)\Delta d + (C_d - \eta z)\Delta u + (C_s - \eta w)\Delta s\,. \end{aligned} \tag{9}$$

Here, $\eta = (1+z+w)^{-1}$ with $z = m_u/m_d$ and $w = m_u/m_s \ll z$ and the Δq are given by the axial vector current matrix element $\Delta q\, S_\mu = \langle p|\bar{q}\gamma_\mu\gamma_5 q|p\rangle$ with S_μ the proton spin.

Neutron beta decay and strong isospin symmetry considerations imply $\Delta u - \Delta d = F + D = 1.269 \pm 0.003$, whereas hyperon decays and flavor SU(3) symmetry imply $\Delta u + \Delta d - 2\Delta s = 3F - D = 0.586 \pm 0.031$ [21]. The strange-quark contribution is $\Delta s = -0.08 \pm 0.01_{\text{stat}} \pm 0.05_{\text{syst}}$ from the COMPASS experiment [22], and $\Delta s = -0.085 \pm 0.008_{\text{exp}} \pm 0.013_{\text{theor}} \pm 0.009_{\text{evol}}$ from HERMES [21], in agreement with each other and with an early estimate of $\Delta s = -0.11 \pm 0.03$ [23]. We thus adopt $\Delta u = 0.84 \pm 0.02$, $\Delta d = -0.43 \pm 0.02$ and $\Delta s = -0.09 \pm 0.02$, very similar to what was used in the axion literature.

The uncertainty of the axion-nucleon couplings is dominated by the uncertainty $z = m_u/m_d = 0.35$–0.60 that we mentioned earlier. For hadronic axions $C_{u,d,s} = 0$ so that $-0.51 < C_p < -0.36$ and $0.10 > C_n > -0.05$. Therefore it is well possible that $C_n = 0$ whereas C_p does not vanish within the plausible z range. In the DFSZ model, $C_u = \frac{1}{3}\sin^2\beta$ and $C_d = \frac{1}{3}\cos^2\beta$ and C_n and C_p as functions of β and z do not vanish simultaneously.

The axion-pion interaction is given by the Lagrangian [24]

$$\mathcal{L}_{A\pi} = \frac{C_{A\pi}}{f_\pi f_A}\left(\pi^0\pi^+\partial_\mu\pi^- + \pi^0\pi^-\partial_\mu\pi^+ - 2\pi^+\pi^-\partial_\mu\pi^0\right)\partial_\mu\phi_A\,, \tag{10}$$

where $C_{A\pi} = (1-z)/[3(1+z)]$ in hadronic models. The chiral symmetry-breaking Lagrangian provides an additional term $\mathcal{L}'_{A\pi} \propto (m_\pi^2/f_\pi f_A)\,(\pi^0\pi^0 + 2\pi^-\pi^+)\,\pi^0\phi_A$. For hadronic axions it vanishes identically, in contrast to the DFSZ model (Roberto Peccei, private communication).

II. LABORATORY SEARCHES

II.1 Light shining through walls

Searching for "invisible axions" is extremely challenging. The most promising approaches rely on the axion-two-photon vertex, allowing for axion-photon conversion in external electric or magnetic fields [5]. For the Coulomb field of a charged particle, the conversion is best viewed as a scattering process, $\gamma + Ze \leftrightarrow Ze + A$, called Primakoff effect [25]. In the other extreme of a macroscopic field, usually a large-scale B-field, the momentum transfer is small, the interaction coherent over a large distance, and the conversion is best viewed as an axion-photon oscillation phenomenon in analogy to neutrino flavor oscillations [26].

Photons propagating through a transverse magnetic field, with incident $\mathbf{E}_\gamma$ and magnet $\mathbf{B}$ parallel, may convert into axions. For $m_A^2 L/2\omega \ll 2\pi$, where L is the length of the B field region and ω the photon energy, the resultant axion beam is coherent with the incident photon beam and the conversion probability is $\Pi \sim (1/4)(G_{A\gamma\gamma}BL)^2$. A practical realization uses a laser beam propagating down the bore of a superconducting dipole magnet (like the bending magnets in high-energy accelerators). If another magnet is in line with the first, but shielded by an optical barrier, then photons may be regenerated from the pure axion beam [27]. The overall probability is $P(\gamma \to A \to \gamma) = \Pi^2$.

The first such experiment utilized two magnets of length $L = 4.4$ m and $B = 3.7$ T and found $G_{A\gamma\gamma} < 6.7 \times 10^{-7}$ GeV^{-1} at 95% CL for $m_A < 1$ meV [28]. More recently, several such experiments were performed (see Listings) [29,30]. The current best limit, $G_{A\gamma\gamma} < 0.7 \times 10^{-7}$ GeV^{-1} at 95% CL for $m_A \lesssim 0.5$ meV, has been achieved by the ALPS (Any Light Particle Search) experiment, which exploited a superconducting HERA dipole magnet and a Fabry-Perot cavity to enhance the laser power on the production side [30], cf. Figure 1. Some of these experiments have also reported limits for scalar bosons where the photon $\mathbf{E}_\gamma$ must be chosen perpendicular to the magnet $\mathbf{B}$.

The concept of resonantly enhanced photon regeneration may open unexplored regions of coupling strength [31]. In this scheme, both the production and detection magnets are within Fabry-Perot optical cavities and actively locked in frequency. The $\gamma \to A \to \gamma$ rate is enhanced by a factor $2\mathcal{F}\mathcal{F}'/\pi^2$ relative to a single-pass experiment, where $\mathcal{F}$ and $\mathcal{F}'$ are the finesses of the two cavities. The resonant enhancement could be of order $10^{(10-12)}$, improving the $G_{A\gamma\gamma}$ sensitivity by $10^{(2.5-3)}$. A detailed technical design for ALPS-II, based on this concept and aiming at an improvement of the current laboratory bound on $G_{A\gamma\gamma}$ by a factor $\sim 3 \times 10^3$, has recently been published [32].

Resonantly enhanced photon regeneration has already been exploited in experiments searching for "radiowaves shining through a shielding" [33,34]. For $m_A \lesssim 10^{-5}$ eV, the upper bound on $G_{A\gamma\gamma}$ established by the CROWS (CERN Resonant Weakly Interacting sub-eV Particle Search) experiment [35] is comparable to the one set by ALPS.

II.2 Photon polarization

An alternative to regenerating the lost photons is to use the beam itself to detect conversion: the polarization of light propagating through a transverse B field suffers dichroism and birefringence [36]. Dichroism: The $E_\parallel$ component, but not $E_\perp$, is depleted by axion production, causing a small rotation of linearly polarized light. For $m_A^2 L/2\omega \ll 2\pi$, the effect is independent of m_A. For heavier axions, it oscillates and diminishes as m_A increases, and it vanishes for $m_A > \omega$. Birefringence: This rotation occurs because there is mixing of virtual axions in the $E_\parallel$ state, but not for $E_\perp$. Hence, linearly polarized light will develop elliptical polarization. Higher-order QED also induces vacuum birefringence. A search for these effects was performed in the same dipole magnets in the early experiment above [37]. The dichroic rotation gave a stronger limit than the ellipticity rotation: $G_{A\gamma\gamma} < 3.6 \times 10^{-7}$ GeV^{-1} at 95% CL for $m_A < 5 \times 10^{-4}$ eV. The ellipticity limits are better at higher masses, as they fall off smoothly and do not terminate at m_A.

In 2006 the PVLAS collaboration reported a signature of magnetically induced vacuum dichroism that could be interpreted as the effect of a pseudoscalar with $m_A = 1$–1.5 meV and $G_{A\gamma\gamma} = (1.6$–$5) \times 10^{-6}$ GeV^{-1} [38]. Since then, these findings are attributed to instrumental artifacts [39]. This particle interpretation is also excluded by the above photon regeneration searches that were perhaps inspired by the original PVLAS result.

II.3 Long-range forces

New bosons would mediate long-range forces, which are severely constrained by "fifth force" experiments [40]. Those looking for new mass-spin couplings provide significant constraints on pseudoscalar bosons [41]. Presently, the most restrictive limits are obtained from combining long-range force measurements with stellar cooling arguments [42]. For the moment, any of these limits are far from realistic values expected for axions. Still, these efforts provide constraints on more general low-mass bosons.

III. AXIONS FROM ASTROPHYSICAL SOURCES

III.1 Stellar energy-loss limits:

Low-mass weakly-interacting particles (neutrinos, gravitons, axions, baryonic or leptonic gauge bosons, *etc.*) are produced in hot astrophysical plasmas, and can thus transport energy out of stars. The coupling strength of these particles with normal matter and radiation is bounded by the constraint that stellar lifetimes or energy-loss rates not conflict with observation [43–45].

We begin this discussion with our Sun and concentrate on hadronic axions. They are produced predominantly by the Primakoff process $\gamma + Ze \to Ze + A$. Integrating over a standard solar model yields the axion luminosity [46]

$$L_A = G_{10}^2\, 1.85 \times 10^{-3}\, L_\odot\,, \tag{11}$$

where $G_{10} = G_{A\gamma\gamma} \times 10^{10}$ GeV. The maximum of the spectrum is at 3.0 keV, the average at 4.2 keV, and the number flux at Earth is G_{10}^2 3.75×10^{11} cm^{-2} s^{-1}. The solar photon luminosity is fixed, so axion losses require enhanced nuclear energy production and thus enhanced neutrino fluxes. The all-flavor measurements by SNO together with a standard solar model imply $L_A \lesssim 0.10\, L_\odot$, corresponding to $G_{10} \lesssim 7$ [47], mildly superseding a similar limit from helioseismology [48].

A more restrictive limit derives from globular-cluster (GC) stars that allow for detailed tests of stellar-evolution theory. The stars on the horizontal branch (HB) in the color-magnitude diagram have reached helium burning with a core-averaged energy release of about 80 erg g^{-1} s^{-1}, compared to Primakoff axion losses of $G_{10}^2\, 30$ erg g^{-1} s^{-1}. The accelerated consumption of helium reduces the HB lifetime by about $80/(80{+}30\, G_{10}^2)$. Number counts of HB stars in 15 GCs compared with the number of red giants (that are not much affected by Primakoff losses) reveal agreement with expectations within 20–40% in any one GC and overall on the 10% level [44]. Therefore, a reasonably conservative limit is

$$G_{A\gamma\gamma} \lesssim 1 \times 10^{-10}\ \text{GeV}^{-1}\,, \qquad (12)$$

although a detailed error budget is not available.

Recently, it has been argued that for $G_{A\gamma\gamma} > 0.8 \times 10^{-10}$ GeV^{-1} the Primakoff flux of axions would shorten the helium-burning phase of massive stars so much that Cepheids could not be observed, thereby excluding such values of the photon coupling [49], cf. Figure 1.

We translate the conservative constraint, Equation 12, on $G_{A\gamma\gamma}$ to $f_A > 2.3 \times 10^7$ GeV ($m_A < 0.3$ eV), using $z = 0.56$ and $E/N = 0$ as in the KSVZ model, and show the excluded range in Figure 2. For the DFSZ model with $E/N = 8/3$, the corresponding limits are slightly less restrictive, $f_A > 0.8 \times 10^7$ GeV ($m_A < 0.7$ eV). The exact high-mass end of the exclusion range has not been determined. The relevant temperature is around 10 keV and the average photon energy is therefore around 30 keV. The excluded m_A range thus certainly extends beyond the shown 100 keV.

If axions couple directly to electrons, the dominant emission processes are atomic axio-recombination and axio-deexcitation, axio-bremsstrahlung in electron-ion or electron-electron collisions, and Compton scattering [51]. Bremsstrahlung is efficient in white dwarfs (WDs), where the Primakoff and Compton processes are suppressed by the large plasma frequency. The enhanced energy losses would delay helium ignition in GC stars, implying $\alpha_{Aee} \lesssim 0.5 \times 10^{-26}$ [52]. Enhanced WD cooling led to a similar limit from the WD luminosity function [53]. Based on much better data and detailed WD cooling treatment, today it appears that the WD luminosity function fits better with a new energy-loss channel that can be interpreted in terms of axion losses corresponding to $\alpha_{Aee} \sim 10^{-27}$ [54]. For pulsationally unstable WDs (ZZ Ceti stars), the period decrease $\dot{P}/P$ is a measure of the cooling speed. The corresponding observations of the pulsating WDs G117-B15A and R548 imply

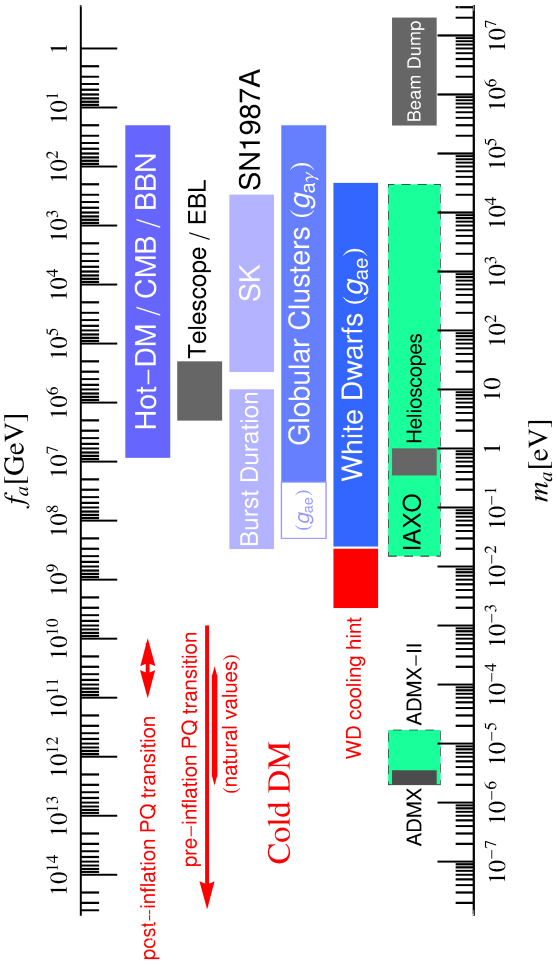

Figure 2: Exclusion ranges as described in the text. The dark intervals are the approximate CAST and ADMX search ranges, with green regions indicating the planned reach of future upgrades. Limits on coupling strengths are translated into limits on m_A and f_A using $z = 0.56$ and the KSVZ values for the coupling strengths. The "Beam Dump" bar is a rough representation of the exclusion range for standard or variant axions. The "Globular Clusters" and "White Dwarfs" ranges uses the DFSZ model with an axion-electron coupling corresponding to $\cos^2\beta = 1/2$. The Cold Dark Matter exclusion range is particularly uncertain; ranges for pre-inflation and post-inflation Peccei-Quinn transitions are shown. Figure adapted from [49].

additional cooling that can be interpreted in terms of similar axion losses [55]. At the moment we prefer to interpret these results as an upper limit $\alpha_{Aee} \lesssim 10^{-27}$ shown in Figure 2.

Similar constraints derive from the measured duration of the neutrino signal of the supernova SN 1987A. Numerical simulations for a variety of cases, including axions and Kaluza-Klein gravitons, reveal that the energy-loss rate of a nuclear medium at the density 3×10^{14} g cm^{-3} and temperature 30 MeV should

not exceed about 1×10^{19} erg g^{-1} s^{-1} [44]. The energy-loss rate from nucleon bremsstrahlung, $N + N \to N + N + A$, is $(C_N/2f_A)^2(T^4/\pi^2 m_N)\,F$. Here F is a numerical factor that represents an integral over the dynamical spin-density structure function because axions couple to the nucleon spin. For realistic conditions, even after considerable effort, one is limited to a heuristic estimate leading to $F \approx 1$ [45].

The SN 1987A limits are of particular interest for hadronic axions where the bounds on α_{Aee} are moot. Within uncertainties of $z = m_u/m_d$ a reasonable choice for the coupling constants is then $C_p = -0.4$ and $C_n = 0$. Using a proton fraction of 0.3, $F = 1$, and $T = 30$ MeV one finds [45]

$$f_A \gtrsim 4 \times 10^8 \text{ GeV} \qquad \text{and} \qquad m_A \lesssim 16 \text{ meV}\,. \tag{13}$$

If axions interact sufficiently strongly they are trapped. Only about three orders of magnitude in g_{ANN} or m_A are excluded, a range shown somewhat schematically in Figure 2. For even larger couplings, the axion flux would have been negligible, yet it would have triggered additional events in the detectors, excluding a further range [56]. A possible gap between these two SN 1987A arguments was discussed as the "hadronic axion window" under the assumption that $G_{A\gamma\gamma}$ was anomalously small [57]. This range is now excluded by hot dark matter bounds (see below).

The very tentative indication for additional WD cooling by axion emission described above is not in conflict with SN 1987A bounds. Still, if the WD interpretation were correct, SNe would lose a large fraction of their energy as axions. This would lead to a diffuse SN axion background (DSAB) in the universe with an energy density comparable to the extra-galactic background light [58]. However, there is no apparent way of detecting it or the axion burst from the next nearby SN.

III.2 Searches for solar axions and ALPs

Instead of using stellar energy losses to derive axion limits, one can also search directly for these fluxes, notably from the Sun. The main focus has been on axion-like particles with a two-photon vertex. They are produced by the Primakoff process with a flux given by Equation 11 and an average energy of 4.2 keV, and can be detected at Earth with the reverse process in a macroscopic B-field ("axion helioscope") [5]. In order to extend the sensitivity in mass towards larger values, one can endow the photon with an effective mass in a gas, $m_\gamma = \omega_{\rm plas}$, thus matching the axion and photon dispersion relations [59].

An early implementation of these ideas used a conventional dipole magnet, with a conversion volume of variable-pressure gas with a xenon proportional chamber as x-ray detector [60]. The conversion magnet was fixed in orientation and collected data for about 1000 s/day. Axions were excluded for $G_{A\gamma\gamma} < 3.6 \times 10^{-9}$ GeV^{-1} for $m_A < 0.03$ eV, and $G_{A\gamma\gamma} < 7.7 \times 10^{-9}$ GeV^{-1} for $0.03 < m_A < 0.11$ eV at 95% CL.

Later, the Tokyo axion helioscope used a superconducting magnet on a tracking mount, viewing the Sun continuously. They reported $G_{A\gamma\gamma} < 6 \times 10^{-10}$ GeV^{-1} for $m_A < 0.3$ eV [61]. This experiment was recommissioned and a similar limit for masses around 1 eV was reported [62].

The most recent helioscope CAST (CERN Axion Solar Telescope) uses a decommissioned LHC dipole magnet on a tracking mount. The hardware includes grazing-incidence x-ray optics with solid-state x-ray detectors, as well as a novel x-ray Micromegas position-sensitive gaseous detector. CAST has established a 95% CL limit $G_{A\gamma\gamma} < 8.8 \times 10^{-11}$ GeV^{-1} for $m_A < 0.02$ eV [46]. To cover larger masses, the magnet bores are filled with a gas at varying pressure. The runs with ^{4}He cover masses up to about 0.4 eV [63], providing the ^{4}He limits shown in Figure 1. To cover yet larger masses, ^{3}He was used to achieve a larger pressure at cryogenic temperatures. Limits up to 1.17 eV were recently published [64], allowing CAST to "cross the axion line" for the KSVZ model (Figure 1).

Going to yet larger masses in a helioscope search is not well motivated because of the cosmic hot dark matter bound of $m_A \lesssim 0.7$ eV (see below). Sensitivity to significantly smaller values of $G_{A\gamma\gamma}$ can be achieved with a next-generation axion helioscope with a much larger magnetic-field cross section. Realistic design options for this "International Axion Observatory" (IAXO) have been studied in some detail [65]. Such a next-generation axion helioscope may also push the sensitivity in the product of couplings to photons and to electrons, $G_{A\gamma\gamma}g_{Aee}$, into a range beyond stellar energy-loss limits and test the hypothesis that WD cooling is dominated by axion emission [66].

Other Primakoff searches for solar axions and ALPs have been carried out using crystal detectors, exploiting the coherent conversion of axions into photons when the axion angle of incidence satisfies a Bragg condition with a crystal plane [67]. However, none of these limits is more restrictive than the one derived from the constraint on the solar axion luminosity ($L_A \lesssim 0.10\,L_\odot$) discussed earlier.

Another idea is to look at the Sun with an x-ray satellite when the Earth is in between. Solar axions and ALPs would convert in the Earth magnetic field on the far side and could be detected [68]. The sensitivity to $G_{A\gamma\gamma}$ could be comparable to CAST, but only for much smaller m_A. Deep solar x-ray measurements with existing satellites, using the solar magnetosphere as conversion region, have reported preliminary limits on $G_{A\gamma\gamma}$ [69].

III.3 Conversion of astrophysical photon fluxes

Large-scale B fields exist in astrophysics that can induce axion-photon oscillations. In practical cases, B is much smaller than in the laboratory, whereas the conversion region L is much larger. Therefore, while the product BL can be large, realistic sensitivities are usually restricted to very low-mass particles, far away from the "axion band" in a plot like Figure 1.

One example is SN 1987A, which would have emitted a burst of axion-like particles (ALPs) due to the Primakoff production in its core. They would have partially converted into γ-rays in the galactic B-field. The absence of a γ-ray

burst in coincidence with SN 1987A neutrinos provides a limit $G_{A\gamma\gamma} \lesssim 1 \times 10^{-11}$ GeV^{-1} for $m_A \lesssim 10^{-9}$ eV [70].

Magnetically induced oscillations between photons and axion-like particles (ALPs) can modify the photon fluxes from distant sources in various ways, featuring (i) frequency-dependent dimming, (ii) modified polarization, and (iii) avoiding absorption by propagation in the form of axions.

For example, dimming of SNe Ia could influence the interpretation in terms of cosmic acceleration [71], although it has become clear that photon-ALP conversion could only be a subdominant effect [72]. Searches for linearly polarised emission from magnetised white dwarfs [73] and changes of the linear polarisation from radio galaxies (see, e.g., Ref. [74]) provide limits close to $G_{A\gamma\gamma} \sim 10^{-11}$ GeV^{-1}, for masses $m_A \lesssim 10^{-7}$ eV and $m_A \lesssim 10^{-15}$ eV, respectively, albeit with uncertainties related to the underlying assumptions. Even stronger limits, $G_{A\gamma\gamma} \lesssim 2 \times 10^{-13}$ GeV^{-1}, for $m_A \lesssim 10^{-14}$ eV, have been obtained by exploiting high-precision measurements of quasar polarisations [75].

Remarkably, it appears that the universe could be too transparent to TeV γ-rays that should be absorbed by pair production on the extra-galactic background light [76]. The situation is not conclusive at present, but the possible role of photon-ALP oscillations in TeV γ-ray astronomy is tantalizing [77]. Fortunately, the region in ALP parameter space, $G_{A\gamma\gamma} \sim 10^{-12} - 10^{-10}$ GeV^{-1} for $m_A \lesssim 10^{-7}$ eV [78], required to explain the anomalous TeV transparency of the universe, could be conceivably probed by the next generation of laboratory experiments (ALPS-II) and helioscopes (IAXO) mentioned above.

IV. COSMIC AXIONS

IV.1 Cosmic axion populations

In the early universe, axions are produced by processes involving quarks and gluons [79]. After color confinement, the dominant thermalization process is $\pi + \pi \leftrightarrow \pi + A$ [24]. The resulting axion population would contribute a hot dark matter component in analogy to massive neutrinos. Cosmological precision data provide restrictive constraints on a possible hot dark-matter fraction that translate into $m_A \lesssim 0.9$ eV [80], but in detail depend on the used data set and assumed cosmological model.

For $m_A \gtrsim 20$ eV, axions decay fast on a cosmic time scale, removing the axion population while injecting photons. This excess radiation provides additional limits up to very large axion masses [81]. An anomalously small $G_{A\gamma\gamma}$ provides no loophole because suppressing decays leads to thermal axions overdominating the mass density of the universe.

The main cosmological interest in axions derives from their possible role as cold dark matter (CDM). In addition to thermal processes, axions are abundantly produced by the "vacuum realignment mechanism" [82] and the decay of topological defects (axion strings and domain walls) [83]. After the breakdown of the PQ symmetry, the axion field relaxes somewhere in the "bottom of the wine bottle" potential. Near the QCD epoch, instanton effects explicitly break the PQ symmetry, the very effect that causes dynamical PQ symmetry restoration. This "tilting of the wine bottle" drives the axion field toward the CP-conserving minimum, thereby exciting coherent oscillations of the axion field that ultimately represent a condensate of CDM, with a density that depends on the initial value of the field before the start of the oscillations, $-\pi \leq \bar{\Theta}_{\rm i} = \phi_A(t_{\rm i})/f_A \leq \pi$. Moreover, discrete domains, with vacuum angles differing by 2π, form after the QCD transition and at their borders topological defects form. These defects decay and radiate non-relativistic axions which eventually add up to the re-alignment population.

The expected cosmic mass density axions depends on whether inflation happens after or before the PQ symmetry breakdown. In the former case, the topological defects are diluted away and the fractional cosmic mass density in axions is solely produced by the vacuum re-alignment mechanism [84],

$$\begin{aligned}\Omega_A^{\rm vr} h^2 &\approx 0.11 \left(\frac{f_A}{5\times 10^{11}\ {\rm GeV}}\right)^{1.184} F\,\bar{\Theta}_{\rm i}^2 \\ &= 0.11 \left(\frac{12\ \mu{\rm eV}}{m_A}\right)^{1.184} F\,\bar{\Theta}_{\rm i}^2\,,\end{aligned} \tag{14}$$

and depends on the initial value $\bar{\Theta}_{\rm i}$ attained in the causally connected region which evolved into today's observable universe. Here, h is today's Hubble expansion parameter in units of 100 km s^{-1} Mpc^{-1}, and $F = F(\bar{\Theta}_{\rm i}, f_A)$ is a factor accounting for anharmonicities in the axion potential. For $F\bar{\Theta}_{\rm i}^2 = \mathcal{O}(1)$, m_A should be above $\sim 10\,\mu$eV in order that the cosmic axion density does not exceed the observed CDM density, $\Omega_{\rm CDM}h^2 = 0.11$. However, much smaller axion masses (much higher PQ scales) would still be possible if the initial value $\bar{\Theta}_{\rm i}$ was small ("anthropic axion window" [85]) .

However, this window may have been closed recently by measurements of fluctuations in the cosmic microwave background. In fact, if the PQ phase transition happens before inflation, the axion field is present during inflation and thus subject to quantum fluctuations, leading to isocurvature fluctuations that are severely constrained by observations [86]. These isocurvature constraints, combined with the recent measurement of a tensor to scalar ratio $r = 0.2^{+0.07}_{-0.05}$ by the cosmic microwave background polarimeter experiment BICEP2 [87] strongly disfavor scenarios with preinflationary PQ symmetry breaking [88], i.e. for which

$$f_A > \frac{H_I}{2\pi} \simeq 1.8\times 10^{13}\,{\rm GeV}\left(\frac{r}{0.2}\right)^{1/2},\ m_A \lesssim 0.3\ \mu{\rm eV}\left(\frac{r}{0.2}\right)^{-1/2},$$

where H_I is the Hubble scale during inflation. It remains to be seen whether the BICEP2 observations will be confirmed by PLANCK later in this year.

This tentatively leaves us either with scenarios in which there is no PQ symmetry during inflation and no phase transition at all [89] or scenarios in which the PQ symmetry breakdown takes place after inflation. In the latter case, $\bar{\Theta}_{\rm i}$

will take on different values in different patches of the universe, resulting in an average contribution from the vacuum re-alignment mechanism of [84]

$$\Omega_A^{\rm vr} h^2 \approx 0.11 \left(\frac{40\ \mu{\rm eV}}{m_A}\right)^{1.184} . \qquad (15)$$

However, the additional contribution from the decay of topological defects suffers from significant uncertainties. According to Sikivie and collaborators, these populations are comparable to the re-alignment contribution [83]. Other groups find a significantly enhanced axion density [90] or rather, a larger m_A value for axions providing CDM,

$$\Omega_A^{\rm td} h^2 \approx 0.11 \left(\frac{400\ \mu{\rm eV}}{m_A}\right)^{1.184} . \qquad (16)$$

Moreover, the spatial axion density variations are large at the QCD transition and they are not erased by free streaming. When matter begins to dominate the universe, gravitationally bound "axion mini clusters" form promptly [91]. A significant fraction of CDM axions can reside in these bound objects.

In R-parity conserving supersymmetric models, more possibilities arise: cold dark matter might be a mixture of axions along with the lightest SUSY particle (LSP) [18]. Candidates for the LSP include the lightest neutralino, the gravitino, the axino, or a sneutrino. In the case of a neutralino LSP, saxion and axino production in the early universe have a strong impact on the neutralino and axion abundance. The former almost always gets increased beyond its thermal-production-only value, favoring then models with higgsino-like or wino-like neutralinos [92]. For large values of f_A, saxions from the vacuum re-alignment mechanism may produce large relic dilution via entropy dumping, thus allowing for much larger values of f_A, sometimes as high as approaching the GUT scale, $\sim 10^{16}$ GeV, for natural values of the initial re-alignment angle. Then the dark matter may be either neutralino- or axion-dominated, or a comparable mixture. In such scenarios, one might expect eventual direct detection of both relic neutralinos and relic axions.

Finally, it is worth mentioning that the non-thermal production mechanisms attributed to axions are indeed generic to bosonic weakly interacting ultra-light particles such as ALPs: a wide range in $G_{A\gamma\gamma}$ – m_A parameter space outside the axion band can generically contain models with adequate CDM density [93].

IV.2 Telescope searches

The two-photon decay is extremely slow for axions with masses in the CDM regime, but could be detectable for eV masses. The signature would be a quasi-monochromatic emission line from galaxies and galaxy clusters. The expected optical line intensity for DFSZ axions is similar to the continuum night emission. An early search in three rich Abell clusters [94], and a recent search in two rich Abell clusters [95], exclude the "Telescope" range in Figure 1 and Figure 2 unless the axion-photon coupling is strongly suppressed. Of course, axions in this mass range would anyway provide an excessive hot DM contribution.

Very low-mass axions in halos produce a weak quasi-monochromatic radio line. Virial velocities in undisrupted dwarf galaxies are very low, and the axion decay line would therefore be extremely narrow. A search with the Haystack radio telescope on three nearby dwarf galaxies provided a limit $G_{A\gamma\gamma} < 1.0 \times 10^{-9}$ GeV^{-1} at 96% CL for $298 < m_A < 363$ μeV [96]. However, this combination of m_A and $G_{\rm A\gamma\gamma}$ does not exclude plausible axion models.

IV.3 Microwave cavity experiments

The limits of Figure 2 suggest that axions, if they exist, provide a significant fraction or even perhaps all of the cosmic CDM. In a broad range of the plausible m_A range for CDM, galactic halo axions may be detected by their resonant conversion into a quasi-monochromatic microwave signal in a high-Q electromagnetic cavity permeated by a strong static B field [5,97]. The cavity frequency is tunable, and the signal is maximized when the frequency is the total axion energy, rest mass plus kinetic energy, of $\nu = (m_A/2\pi)\,[1 + \mathcal{O}(10^{-6})]$, the width above the rest mass representing the virial distribution in the galaxy. The frequency spectrum may also contain finer structure from axions more recently fallen into the galactic potential and not yet completely virialized [98].

The feasibility of this technique was established in early experiments of relatively small sensitive volume, $\mathcal{O}(1$ liter), with HFET-based amplifiers, setting limits in the range $4.5 < m_A < 16.3$ μeV [99], but lacking by 2–3 orders of magnitude the sensitivity required to detect realistic axions. Later, ADMX ($B \sim 8$ T, $V \sim 200$ liters) has achieved sensitivity to KSVZ axions, assuming they saturate the local dark matter density and are well virialized, over the mass range 1.9–3.3 μeV [100]. Should halo axions have a significant component not yet virialized, ADMX is sensitive to DFSZ axions [101]. The corresponding 90% CL exclusion regions shown in Figure 3 are normalized to an assumed local CDM density of 7.5×10^{-25} g cm^{-3} (450 MeV cm^{-3}). More recently the ADMX experiment commissioned an upgrade [102] that replaces the microwave HFET amplifiers by near quantum-limited low-noise dc SQUID microwave amplifiers [103], allowing for a significantly improved sensitivity [104]. This apparatus is also sensitive to other hypothetical light bosons, such as hidden photons or chameleons, over a limited parameter space [93,105]. Alternatively, a Rydberg atom single-photon detector [106] can in principle evade the standard quantum limit for coherent photon detection.

Other new concepts for searching for axion dark matter are also being investigated. Photons from dark matter axions or ALPs could be focused in a manner similar to a dish antenna instead of a resonant cavity [107]. The oscillating galactic dark matter axion field induces extremely small oscillating nuclear electric dipole moments. Conceivably these could be detected by exploiting NMR techniques or molecular interferometry [108], which are most sensitive in the range of low

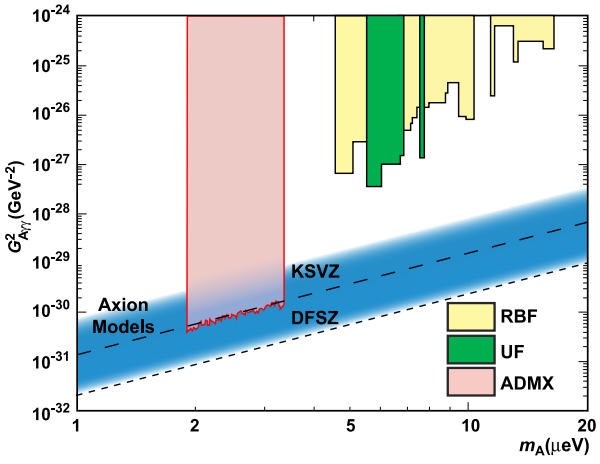

Figure 3: Exclusion region reported from the microwave cavity experiments RBF and UF [99] and ADMX [100]. A local dark-matter density of 450 MeV cm^{-3} is assumed.

oscillation frequencies corresponding to sub-neV axion masses. The reach of these techniques in practice remains to be seen.

Conclusions

There is a strengthening physics case for very weakly coupled ultralight particles beyond the Standard Model. The elegant solution of the strong CP problem proposed by Peccei and Quinn yields a particularly strong motivation for the axion. In many theoretically appealing ultraviolet completions of the Standard Model axions and axion-like particles occur automatically. Moreover, they are natural cold dark matter candidates. May be the first hints of their existence has already been seen in the anomalous cooling of white dwarfs and the anomalous transparency of the Universe for VHE gamma rays. Interestingly, a significant portion of previously unexplored, but phenomenologically very interesting and theoretically very well motivated axion and ALP parameter space can be tackled in the foreseeable future by a number of terrestrial experiments searching for axion/ALP dark matter, for solar axions/ALPs, and for light apparently shining through a wall.

References

1. R.D. Peccei and H. Quinn, Phys. Rev. Lett. **38**, 1440 (1977); Phys. Rev. **D16**, 1791 (1977).
2. S. Weinberg, Phys. Rev. Lett. **40**, 223 (1978); F. Wilczek, Phys. Rev. Lett. **40**, 279 (1978).
3. F. Wilczek, Phys. Rev. Lett. **49**, 1549 (1982).
4. Y. Chikashige, R.N. Mohapatra, and R.D. Peccei, Phys. Lett. **B98**, 265 (1981); G.B. Gelmini and M. Roncadelli, Phys. Lett. **B99**, 411 (1981).
5. P. Sikivie, Phys. Rev. Lett. **51**, 1415 (1983) and Erratum *ibid.*, **52**, 695 (1984).
6. K. -S. Choi *et al.*, Phys. Lett. **B675**, 381 (2009); A. Arvanitaki *et al.*, Phys. Rev. **D81**, 123530 (2010); B.S. Acharya, K. Bobkov, and P. Kumar, JHEP **1011**, 105 (2010); M. Cicoli, M. Goodsell, and A. Ringwald, JHEP **1210**, 146 (2012).
7. J. Jaeckel and A. Ringwald, Ann. Rev. Nucl. and Part. Sci. **60**, 405 (2010); J. Jaeckel, Frascati Phys. Ser. **56**, 172 (2013).
8. C.A. Baker *et al.*, Phys. Rev. Lett. **97**, 131801 (2006).
9. H. Georgi, D.B. Kaplan, and L. Randall, Phys. Lett. **B169**, 73 (1986).
10. H. Leutwyler, Phys. Lett. **B378**, 313 (1996).
11. Mini review on Quark Masses in: C. Amsler *et al.* (Particle Data Group), Phys. Lett. **B667**, 1 (2008).
12. T.W. Donnelly *et al.*, Phys. Rev. **D18**, 1607 (1978); S. Barshay *et al.*, Phys. Rev. Lett. **46**, 1361 (1981); A. Barroso and N.C. Mukhopadhyay, Phys. Lett. **B106**, 91 (1981); R.D. Peccei, in *Proceedings of Neutrino '81*, Honolulu, Hawaii, Vol. 1, p. 149 (1981); L.M. Krauss and F. Wilczek, Phys. Lett. **B173**, 189 (1986).
13. J. Schweppe *et al.*, Phys. Rev. Lett. **51**, 2261 (1983); T. Cowan *et al.*, Phys. Rev. Lett. **54**, 1761 (1985).
14. R.D. Peccei, T.T. Wu, and T. Yanagida, Phys. Lett. **B172**, 435 (1986).
15. W.A. Bardeen, R.D. Peccei, and T. Yanagida, Nucl. Phys. **B279**, 401 (1987).
16. J.E. Kim, Phys. Rev. Lett. **43**, 103 (1979); M.A. Shifman, A.I. Vainstein, and V.I. Zakharov, Nucl. Phys. **B166**, 493 (1980).
17. M. Dine, W. Fischler, and M. Srednicki, Phys. Lett. **B104**, 199 (1981); A.R. Zhitnitsky, Sov. J. Nucl. Phys. **31**, 260 (1980).
18. J.E. Kim and G. Carosi, Rev. Mod. Phys. **82**, 557 (2010).
19. J.E. Kim, Phys. Rev. **D58**, 055006 (1998).
20. G. Raffelt and D. Seckel, Phys. Rev. Lett. **60**, 1793 (1988); M. Carena and R.D. Peccei, Phys. Rev. **D40**, 652 (1989); K. Choi, K. Kang, and J.E. Kim, Phys. Rev. Lett. **62**, 849 (1989).
21. A. Airapetian *et al.* (HERMES Collab.), Phys. Rev. **D75**, 012007 (2007) and Erratum *ibid.*, **D76**, 039901 (2007).
22. V.Y. Alexakhin *et al.* (COMPASS Collab.), Phys. Lett. **B647**, 8 (2007).
23. J.R. Ellis and M. Karliner, in: *The spin structure of the nucleon: International school of nucleon structure* (3–10 August 1995, Erice, Italy), ed. by B. Frois, V.W. Hughes, and N. De Groot (World Scientific, Singapore, 1997) [hep-ph/9601280].
24. S. Chang and K. Choi, Phys. Lett. **B316**, 51 (1993).
25. D.A. Dicus *et al.*, Phys. Rev. **D18**, 1829 (1978).
26. G. Raffelt and L. Stodolsky, Phys. Rev. **D37**, 1237 (1988).
27. A.A. Anselm, Yad. Fiz. **42**, 1480 (1985); K. van Bibber *et al.*, Phys. Rev. Lett. **59**, 759 (1987).
28. G. Ruoso *et al.*, Z. Phys. **C56**, 505 (1992); R. Cameron *et al.*, Phys. Rev. **D47**, 3707 (1993).
29. M. Fouche *et al.* (BMV Collab.), Phys. Rev. **D78**, 032013 (2008); P. Pugnat *et al.* (OSQAR Collab.), Phys. Rev. **D78**, 092003 (2008); A. Chou *et al.* (GammeV T-969 Collab), Phys. Rev. Lett.

100, 080402 (2008);
A. Afanasev *et al.* (LIPSS Collab.), Phys. Rev. Lett. **101**, 120401 (2008);
P. Pugnat *et al.* (OSQAR Collab.), arXiv:1306.0443.

30. K. Ehret *et al.* (ALPS Collab.), Phys. Lett. **B689**, 149 (2010).
31. F. Hoogeveen and T. Ziegenhagen , Nucl. Phys. **B358**, 3 (1991);
P. Sikivie, D. Tanner, and K. van Bibber, Phys. Rev. Lett. **98**, 172002 (2007);
G. Mueller *et al.*, Phys. Rev. **D80**, 072004 (2009).
32. R. Baehre *et al.* (ALPS Collab.), JINST **1308**, T09001 (2013).
33. F. Hoogeveen, Phys. Lett. **B288**, 195 (1992);
J. Jaeckel and A. Ringwald, Phys. Lett. **B659**, 509 (2008);
F. Caspers, J. Jaeckel, and A. Ringwald, JINST **0904**, P11013 (2009).
34. R. Povey, J. Hartnett, and M. Tobar, Phys. Rev. **D82**, 052003 (2010);
A. Wagner *et al.*, Phys. Rev. Lett. **105**, 171801 (2010).
35. M. Betz *et al.*, Phys. Rev. **D88**, 075014 (2013).
36. L. Maiani *et al.*, Phys. Lett. **B175**, 359 (1986).
37. Y. Semertzidis *et al.*, Phys. Rev. Lett. **64**, 2988 (1990).
38. E. Zavattini *et al.* (PVLAS Collab.), Phys. Rev. Lett. **96**, 110406 (2006).
39. E. Zavattini *et al.* (PVLAS Collab.), Phys. Rev. **D77**, 032006 (2008).
40. E. Fischbach and C. Talmadge, Nature **356**, 207 (1992).
41. J.E. Moody and F. Wilczek, Phys. Rev. D 30, 130(1984);
A.N. Youdin *et al.*, Phys. Rev. Lett. **77**, 2170 (1996);
Wei-Tou Ni *et al.*, Phys. Rev. Lett. **82**, 2439 (1999);
D.F. Phillips *et al.*, Phys. Rev. **D63**, 111101 (R)(2001);
B.R. Heckel *et al.*, (Eöt-Wash Collab.), Phys. Rev. Lett. **97**, 021603 (2006);
S.A. Hoedl *et al.*, Phys. Rev. Lett. **106**, 041801 (2011).
42. G. Raffelt, Phys. Rev. **D86**, 015001 (2012).
43. M.S. Turner, Phys. Reports **197**, 67 (1990);
G.G. Raffelt, Phys. Reports **198**, 1 (1990).
44. G.G. Raffelt, *Stars as Laboratories for Fundamental Physics*, (Univ. of Chicago Press, Chicago, 1996).
45. G.G. Raffelt, Lect. Notes Phys. **741**, 51 (2008).
46. S. Andriamonje *et al.* (CAST Collab.), JCAP **0704**, 010 (2007).
47. P. Gondolo and G. Raffelt, Phys. Rev. **D79**, 107301 (2009).
48. H. Schlattl, A. Weiss, and G. Raffelt, Astropart. Phys. **10**, 353 (1999).
49. A. Friedland, M. Giannotti, and M. Wise, Phys. Rev. Lett. **110**, 061101 (2013).
50. R. Essig *et al.*, arXiv:1311.0029.
51. J. Redondo, arXiv:1310.0823.
52. G. Raffelt and A. Weiss, Phys. Rev. **D51**, 1495 (1995);
M. Catelan, J.A. de Freitas Pacheco, and J.E. Horvath, Astrophys. J. **461**, 231 (1996).
53. G.G. Raffelt, Phys. Lett. **B166**, 402 (1986);
S.I. Blinnikov and N.V. Dunina-Barkovskaya, Mon. Not. R. Astron. Soc. **266**, 289 (1994).
54. J. Isern *et al.*, Astrophys. J. Lett. **682**, L109 (2008);
J. Isern *et al.*, J. Phys. Conf. Ser. **172**, 012005 (2009).
55. J. Isern *et al.*, Astron. Astrophys. **512**, A86 (2010);
A.H. Córsico *et al.*, arXiv:1205.6180;
A.H. Córsico *et al.*, JCAP **1212**, 010 (2012).
56. J. Engel, D. Seckel, and A.C. Hayes, Phys. Rev. Lett. **65**, 960 (1990).
57. T. Moroi and H. Murayama, Phys. Lett. **B440**, 69 (1998).
58. G.G. Raffelt, J. Redondo, and N. Viaux Maira, Phys. Rev. **D84**, 103008 (2011).
59. K. van Bibber *et al.*, Phys. Rev. **D39**, 2089 (1989).
60. D. Lazarus *et al.*, Phys. Rev. Lett. **69**, 2333 (1992).
61. S. Moriyama *et al.*, Phys. Lett. **B434**, 147 (1998);
Y. Inoue *et al.*, Phys. Lett. **B536**, 18 (2002).
62. M. Minowa *et al.*, Phys. Lett. **B668**, 93 (2008).
63. E. Arik *et al.*, (CAST Collab.), JCAP **0902**, 008 (2009).
64. E. Arik *et al.* (CAST Collab.), Phys. Rev. Lett. **107**, 261302 (2011);
E. Arik *et al.* (CAST Collab.), arXiv:1307.1985.
65. I. Irastorza *et al.*, JCAP **0611**, 013 (2011).
66. K. Barth *et al.*, JCAP **1305**, 010 (2013).
67. F.T. Avignone III *et al.*, Phys. Rev. Lett. **81**, 5068 (1998);
S. Cebrian *et al.*, Astropart. Phys. **10**, 397 (1999);
A. Morales *et al.* (COSME Collab.), Astropart. Phys. **16**, 325 (2002);
R. Bernabei *et al.*, Phys. Lett. **B515**, 6 (2001);
Z. Ahmed *et al.* (CDMS Collab.), Phys. Rev. Lett. **103**, 141802 (2009);
E. Armengaud *et al.* (EDELWEISS Collab.), arXiv:1307.1488.
68. H. Davoudiasl and P. Huber, Phys. Rev. Lett. **97**, 141302 (2006).
69. H.S. Hudson *et al.*, arXiv:1201.4607.
70. J.W. Brockway, E.D. Carlson, and G.G. Raffelt, Phys. Lett. **B383**, 439 (1996);
J.A. Grifols, E.Massó, and R. Toldrà, Phys. Rev. Lett. **77**, 2372 (1996).
71. C. Csaki, N. Kaloper, and J. Terning, Phys. Rev. Lett. **88**, 161302 (2002).
72. A. Mirizzi, G.G. Raffelt, and P.D. Serpico, Lect. Notes Phys. **741**, 115 (2008).
73. R. Gill and J.S. Heyl, Phys. Rev. **D84**, 085001 (2011).
74. D. Horns *et al.*, Phys. Rev. **D85**, 085021 (2012).
75. A. Payez, J.R. Cudell, and D. Hutsemekers, JCAP **1207**, 041 (2012).
76. D. Horns and M. Meyer, JCAP **1202**, 033 (2012).
77. A. De Angelis, G. Galanti, and M. Roncadelli, Phys. Rev. **D84**, 105030 (2011);
M. Simet, D. Hooper, and P.D. Serpico, Phys. Rev. **D77**, 063001 (2008);
M.A. Sanchez-Conde *et al.*, Phys. Rev. **D79**, 123511 (2009).
78. M. Meyer, D. Horns, and M. Raue, Phys. Rev. **D87**, 035027 (2013).
79. M.S. Turner, Phys. Rev. Lett. **59**, 2489 (1987) and Erratum *ibid.*, **60**, 1101 (1988);
E. Massó, F. Rota, and G. Zsembinszki, Phys. Rev. **D66**, 023004 (2002);
P. Graf and F.D. Steffen, Phys. Rev. **D83**, 075011 (2011).
80. S. Hannestad *et al.*, JCAP **1008**, 001 (2010);
M. Archidiacono *et al.*, arXiv:1307.0615.

81. E. Massó and R. Toldra, Phys. Rev. **D55**, 7967 (1997); D. Cadamuro and J. Redondo, JCAP **1202**, 032 (2012).
82. J. Preskill, M.B. Wise, and F. Wilczek, Phys. Lett. **B120**, 127 (1983); L.F. Abbott and P. Sikivie, Phys. Lett. **B120**, 133 (1983); M. Dine and W. Fischler, Phys. Lett. **B120**, 137 (1983).
83. P. Sikivie, Lect. Notes Phys. **741**, 19 (2008).
84. K.J. Bae, J.-H. Huh, and J.E. Kim, JCAP **0809**, 005 (2008); L. Visinelli and P. Gondolo, Phys. Rev. **D80**, 035024 (2009).
85. M. Tegmark *et al.*, Phys. Rev. **D73**, 023505 (2006); K. Mack, JCAP **1107**, 021 (2011).
86. M. Beltrán, J. García-Bellido, and J. Lesgourgues, Phys. Rev. **D75**, 103507 (2007); M.P. Hertzberg, M. Tegmark, and F. Wilczek, Phys. Rev. **D78**, 083507 (2008); J. Hamann *et al.*, JCAP **0906**, 022 (2009); P.A.R. Ade *et al.* [Planck Collab.], arXiv:1303.5082.
87. P.A.R. Ade *et al.* [BICEP2 Collab.], arXiv:1403.3985.
88. P. Fox, A. Pierce, and S.D. Thomas, hep-th/0409059; T. Higaki, K.S. Jeong, F. Takahashi, arXiv:1403.4186; D.J.E. Marsh, *et al.*, arXiv:1403.4216; L. Visinelli and P. Gondolo, arXiv:1403.4594.
89. M. Dine and A. Anisimov, JCAP **0507**, 009 (2005).
90. O. Wantz and E.P.S. Shellard, Phys. Rev. **D82**, 123508 (2010); T. Hiramatsu *et al.*, Phys. Rev. **D83**, 123531 (2011); T. Hiramatsu *et al.*, Phys. Rev. **D85**, 105020 (2012) and Erratum *ibid.*, **86**, 089902 (2012).
91. E.W. Kolb and I.I. Tkachev, Phys. Rev. Lett. **71**, 3051 (1993), Astrophys. J. **460**, L25 (1996); K.M. Zurek, C.J. Hogan, and T.R. Quinn, Phys. Rev. **D75**, 043511 (2007).
92. K.J. Bae, H. Baer, and A. Lessa, JCAP **1304**, 041 (2013); K.J. Bae, H. Baer, and E.J. Chun, arXiv:1309.0519; K.J. Bae, H. Baer, and E.J. Chun, arXiv:1309.5365.
93. P. Arias *et al.*, JCAP **1206**, 013 (2012).
94. M. Bershady *et al.*, Phys. Rev. Lett. **66**, 1398 (1991); M. Ressell, Phys. Rev. **D44**, 3001 (1991).
95. D. Grin *et al.*, Phys. Rev. **D75**, 105018 (2007).
96. B.D. Blout *et al.*, Astrophys. J. **546**, 825 (2001).
97. P. Sikivie, Phys. Rev. **D32**, 2988 (1985); L. Krauss *et al.*, Phys. Rev. Lett. **55**, 1797 (1985); R. Bradley *et al.*, Rev. Mod. Phys. **75**, 777 (2003).
98. P. Sikivie and J. Ipser, Phys. Lett. **B291**, 288 (1992); P. Sikivie *et al.*, Phys. Rev. Lett. **75**, 2911 (1995).
99. S. DePanfilis *et al.*, Phys. Rev. Lett. **59**, 839 (1987); W. Wuensch *et al.*, Phys. Rev. **D40**, 3153 (1989); C. Hagmann *et al.*, Phys. Rev. **D42**, 1297 (1990).
100. S. Asztalos *et al.*, Phys. Rev. **D69**, 011101 (2004).
101. L. Duffy *et al.*, Phys. Rev. Lett. **95**, 091304 (2005); J. Hoskins *et al.*, Phys. Rev. **D84**, 121302 (2011).
102. S.J. Asztalos *et al.* (ADMX Collab.), arXiv:0910.5914.
103. S.J. Asztalos *et al.*, Nucl. Instrum. Methods **A656**, 39 (2011).
104. S.J. Asztalos *et al.*, Phys. Rev. Lett. **104**, 041301 (2010).
105. G. Rybka *et al.*, Phys. Rev. Lett. **105**, 051801 (2010); A. Wagner *et al.*, Phys. Rev. Lett. **105**, 171801 (2010).
106. I. Ogawa, S. Matsuki, and K. Yamamoto, Phys. Rev. **D53**, 1740 (1996); Y. Kishimoto *et al.*, Phys. Lett. **A303**, 279 (2002); M. Tada *et al.*, Phys. Lett. **A303**, 285 (2002); T.Haseyama *et al.*, J. Low Temp. Phys. **150**, 549 (2008).
107. D. Horns *et al.*, JCAP **1304**, 016 (2013).
108. P.W. Graham and S. Rajendran, Phys. Rev. **D84**, 055013 (2011); P.W. Graham and S. Rajendran, Phys. Rev. **D88**, 035023 (2013); D. Budker *et al.*, arXiv:1306.6089.

A^0 (Axion) MASS LIMITS from Astrophysics and Cosmology

These bounds depend on model-dependent assumptions (i.e. — on a combination of axion parameters).

VALUE (MeV)	DOCUMENT ID		TECN	COMMENT
• • • We do not use the following data for averages, fits, limits, etc. • • •				
>0.2	BARROSO	82	ASTR	Standard Axion
>0.25	[1] RAFFELT	82	ASTR	Standard Axion
>0.2	[2] DICUS	78C	ASTR	Standard Axion
	MIKAELIAN	78	ASTR	Stellar emission
>0.3	[2] SATO	78	ASTR	Standard Axion
>0.2	VYSOTSKII	78	ASTR	Standard Axion

[1] Lower bound from 5.5 MeV γ-ray line from the sun.
[2] Lower bound from requiring the red giants' stellar evolution not be disrupted by axion emission.

A^0 (Axion) and Other Light Boson (X^0) Searches in Hadron Decays

Limits are for branching ratios.

VALUE	CL%	DOCUMENT ID		TECN	COMMENT
• • • We do not use the following data for averages, fits, limits, etc. • • •					
$<1.5\times10^{-6}$	90	[1] ADLARSON	13	WASA	$\pi^0\to\gamma X^0$ ($X^0\to e^+e^-$), $m_{X^0}=100$ MeV
$<2\times10^{-8}$	90	[2] BABUSCI	13B	KLOE	$\phi\to\eta X^0$ ($X^0\to e^+e^-$)
		[3] ARCHILLI	12	KLOE	$\phi\to\eta X_0$, $X_0\to e^+e^-$
$<2\times10^{-15}$	90	[4] GNINENKO	12A	BDMP	$\pi^0\to\gamma X^0$ ($X^0\to e^+e^-$)
$<3\times10^{-14}$	90	[5] GNINENKO	12B	BDMP	$\eta(\eta')\to\gamma X^0$ ($X^0\to e^+e^-$)
$<7\times10^{-10}$	90	[6] ADLER	04	B787	$K^+\to\pi^+X^0$
$<7.3\times10^{-11}$	90	[7] ANISIMOVSK...	04	B949	$K^+\to\pi^+X^0$
$<4.5\times10^{-11}$	90	[8] ADLER	02C	B787	$K^+\to\pi^+X^0$
$<4\times10^{-5}$	90	[9] ADLER	01	B787	$K^+\to\pi^+\pi^0A^0$
$<4.9\times10^{-5}$	90	AMMAR	01B	CLEO	$B^\pm\to\pi^\pm(K^\pm)X^0$
$<5.3\times10^{-5}$	90	AMMAR	01B	CLEO	$B^0\to K^0_SX^0$
$<3.3\times10^{-5}$	90	[10] ALTEGOER	98	NOMD	$\pi^0\to\gamma X^0$, $m_{X^0}<120$ MeV
$<5.0\times10^{-8}$	90	[11] KITCHING	97	B787	$K^+\to\pi^+X^0$ ($X^0\to\gamma\gamma$)
$<5.2\times10^{-10}$	90	[12] ADLER	96	B787	$K^+\to\pi^+X^0$
$<2.8\times10^{-4}$	90	[13] AMSLER	96B	CBAR	$\pi^0\to\gamma X^0$, $m_{X^0}<65$ MeV
$<3\times10^{-4}$	90	[13] AMSLER	96B	CBAR	$\eta\to\gamma X^0$, m_{X^0}= 50–200 MeV
$<4\times10^{-5}$	90	[13] AMSLER	96B	CBAR	$\eta'\to\gamma X^0$, m_{X^0}= 50–925 MeV
$<6\times10^{-5}$	90	[13] AMSLER	94B	CBAR	$\pi^0\to\gamma X^0$, m_{X^0}=65–125 MeV
$<6\times10^{-5}$	90	[13] AMSLER	94B	CBAR	$\eta\to\gamma X^0$, m_{X^0}=200–525 MeV
$<7\times10^{-3}$	90	[14] MEIJERDREES	94	CNTR	$\pi^0\to\gamma X^0$, m_{X^0}=25 MeV
$<2\times10^{-3}$	90	[14] MEIJERDREES	94	CNTR	$\pi^0\to\gamma X^0$, m_{X^0}=100 MeV
$<2\times10^{-7}$	90	[15] ATIYA	93B	B787	Sup. by ADLER 04
$<3\times10^{-13}$		[16] NG	93	COSM	$\pi^0\to\gamma X^0$
$<1.1\times10^{-8}$	90	[17] ALLIEGRO	92	SPEC	$K^+\to\pi^+X^0$ ($X^0\to e^+e^-$)
$<5\times10^{-4}$	90	[18] ATIYA	92	B787	$\pi^0\to\gamma X^0$
$<4\times10^{-6}$	90	[19] MEIJERDREES	92	SPEC	$\pi^0\to\gamma X^0$, $X^0\to e^+e^-$, m_{X^0}= 100 MeV
$<1\times10^{-7}$	90	[20] ATIYA	90B	B787	Sup. by KITCHING 97
$<1.3\times10^{-8}$	90	[21] KORENCHE...	87	SPEC	$\pi^+\to e^+\nu A^0$ ($A^0\to e^+e^-$)
$<1\times10^{-9}$	90	[22] EICHLER	86	SPEC	Stopped $\pi^+\to e^+\nu A^0$
$<2\times10^{-5}$	90	[23] YAMAZAKI	84	SPEC	For 160<m<260 MeV
$<(1.5–4)\times10^{-6}$	90	[23] YAMAZAKI	84	SPEC	K decay, $m_{X^0}\ll100$ MeV
		[24] ASANO	82	CNTR	Stopped $K^+\to\pi^+X^0$
		[25] ASANO	81B	CNTR	Stopped $K^+\to\pi^+X^0$
		[26] ZHITNITSKII	79		Heavy axion

[1] Limits between 2.0×10^{-5} and 1.5×10^{-6} are obtained for m_{X^0} = 20–100 MeV (see their Fig. 8). Angular momentum conservation requires that X^0 has spin ≥ 1.
[2] The limit is for B($\phi\to\eta X^0$)·B($X^0\to e^+e^-$) and applies to $m_{X^0}=410$ MeV. It is derived by analyzing $\eta\to\pi^0\pi^0\pi^0$ and $\pi^-\pi^+\pi^0$. Limits between 1×10^{-6} and 2×10^{-8} are obtained for $m_{X^0}\leq450$ MeV (see their Fig. 6).

Gauge & Higgs Boson Particle Listings

Axions (A^0) and Other Very Light Bosons

[3] ARCHILLI 12 analyzed $\eta \to \pi^+\pi^-\pi^0$ decays. Derived limits on $\alpha'/\alpha < 2\times10^{-5}$ for m_{X^0} = 50–420 MeV at 90% CL. See their Fig. 8 for mass-dependent limits.

[4] This limit is for B($\pi^0 \to \gamma X^0$)·B($X^0 \to e^+e^-$) and applies for m_{X^0} = 90 MeV and $\tau_{X^0} \simeq 1\times10^{-8}$ sec. Limits between 10^{-8} and 2×10^{-15} are obtained for m_{X^0} = 3–120 MeV and $\tau_{X^0} = 1\times10^{-11}$–1 sec. See their Fig. 3 for limits at different masses and lifetimes.

[5] This limit is for B($\eta \to \gamma X^0$)·B($x^0 \to e^+e^-$) and applies for m_{X^0} = 100 MeV and $\tau_{X^0} \simeq 6\times10^{-9}$ sec. Limits between 10^{-5} and 3×10^{-14} are obtained for $m_{X^0} \lesssim$ 550 MeV and $\tau_{X^0} = 10^{-10}$–10 sec. See their Fig. 5 for limits at different mass and lifetime and for η' decays.

[6] This limit applies for a mass near 180 MeV. For other masses in the range m_{X^0} = 150–250 MeV the limit is less restrictive, but still improves ADLER 02C and ATIYA 93B.

[7] ANISIMOVSKY 04 bound is for m_{X^0}=0.

[8] ADLER 02C bound is for m_{X^0} <60 MeV. See Fig. 2 for limits at higher masses.

[9] The quoted limit is for m_{X^0} = 0–80 MeV. See their Fig. 5 for the limit at higher mass. The branching fraction limit assumes pure phase space decay distributions.

[10] ALTEGOER 98 looked for X^0 from π^0 decay which penetrate the shielding and convert to π^0 in the external Coulomb field of a nucleus.

[11] KITCHING 97 limit is for B($K^+ \to \pi^+X^0$)·B($X^0 \to \gamma\gamma$) and applies for $m_{X^0} \simeq$ 50 MeV, $\tau_{X^0} < 10^{-10}$ s. Limits are provided for 0<m_{X^0} < 100 MeV, $\tau_{X^0} < 10^{-8}$ s.

[12] ADLER 96 looked for a peak in missing-mass distribution. This work is an update of ATIYA 93. The limit is for massless stable X^0 particles and extends to m_{X^0}=80 MeV at the same level. See paper for dependence on finite lifetime.

[13] AMSLER 94B and AMSLER 96B looked for a peak in missing-mass distribution.

[14] The MEIJERDREES 94 limit is based on inclusive photon spectrum and is independent of X^0 decay modes. It applies to $\tau(X^0) > 10^{-23}$ sec.

[15] ATIYA 93B looked for a peak in missing mass distribution. The bound applies for stable X^0 of m_{X^0}=150–250 MeV, and the limit becomes stronger (10^{-8}) for m_{X^0}=180–240 MeV.

[16] NG 93 studied the production of X^0 via $\gamma\gamma \to \pi^0 \to \gamma X^0$ in the early universe at $T \simeq 1$ MeV. The bound on extra neutrinos from nucleosynthesis $\Delta N_\nu < 0.3$ (WALKER 91) is employed. It applies to $m_{X^0} \ll 1$ MeV in order to be relativistic down to nucleosynthesis temperature. See paper for heavier X^0.

[17] ALLIEGRO 92 limit applies for m_{X^0}=150–340 MeV and is the branching ratio times the decay probability. Limit is $< 1.5\times10^{-8}$ at 99%CL.

[18] ATIYA 92 looked for a peak in missing mass distribution. The limit applies to m_{X^0}=0–130 MeV in the narrow resonance limit. See paper for the dependence on lifetime. Covariance requires X^0 to be a vector particle.

[19] MEIJERDREES 92 limit applies for $\tau_{X^0} = 10^{-23}$–10^{-11} sec. Limits between 2×10^{-4} and 4×10^{-6} are obtained for m_{X^0} = 25–120 MeV. Angular momentum conservation requires that X^0 has spin ≥ 1.

[20] ATIYA 90B limit is for B($K^+ \to \pi^+X^0$)·B($X^0 \to \gamma\gamma$) and applies for m_{X^0} = 50 MeV, $\tau_{X^0} < 10^{-10}$ s. Limits are also provided for $0 < m_{X^0} < 100$ MeV, $\tau_{X^0} < 10^{-8}$ s.

[21] KORENCHENKO 87 limit assumes $m_{A^0} = 1.7$ MeV, $\tau_{A^0} \lesssim 10^{-12}$ s, and B($A^0 \to e^+e^-$) = 1.

[22] EICHLER 86 looked for $\pi^+ \to e^+\nu A^0$ followed by $A^0 \to e^+e^-$. Limits on the branching fraction depend on the mass and and lifetime of A^0. The quoted limits are valid when $\tau(A^0) \gtrsim 3.\times10^{-10}$s if the decays are kinematically allowed.

[23] YAMAZAKI 84 looked for a discrete line in $K^+ \to \pi^+$X. Sensitive to wide mass range (5–300 MeV), independent of whether X decays promptly or not.

[24] ASANO 82 at KEK set limits for B($K^+ \to \pi^+X^0$) for m_{X^0} <100 MeV as BR $< 4.\times10^{-8}$ for $\tau(X^0 \to n\gamma$'s) $> 1.\times10^{-9}$ s, BR $< 1.4\times10^{-6}$ for $\tau < 1.\times10^{-9}$s.

[25] ASANO 81B is KEK experiment. Set B($K^+ \to \pi^+X^0$) $< 3.8\times10^{-8}$ at CL = 90%.

[26] ZHITNITSKII 79 argue that a heavy axion predicted by YANG 78 (3 <m <40 MeV) contradicts experimental muon anomalous magnetic moments.

A^0 (Axion) Searches in Quarkonium Decays

Decay or transition of quarkonium. Limits are for branching ratio.

VALUE	CL%	DOCUMENT ID		TECN	COMMENT
• • • We do not use the following data for averages, fits, limits, etc. • • •					
$<4.0\times10^{-5}$	90	[1] ANTREASYAN	90C	CBAL	$\Upsilon(1S) \to A^0\gamma$
$<5\times10^{-5}$	90	[2] DRUZHININ	87	ND	$\phi \to A^0\gamma$ ($A^0 \to e^+e^-$)
$<2\times10^{-3}$	90	[3] DRUZHININ	87	ND	$\phi \to A^0\gamma$ ($A^0 \to \gamma\gamma$)
$<7\times10^{-6}$	90	[4] DRUZHININ	87	ND	$\phi \to A^0\gamma$ ($A^0 \to$ missing)
$<1.4\times10^{-5}$	90	[5] EDWARDS	82	CBAL	$J/\psi \to A^0\gamma$

[1] ANTREASYAN 90C assume that A^0 does not decay in the detector.

[2] The first DRUZHININ 87 limit is valid when $\tau_{A^0}/m_{A^0} < 3\times10^{-13}$ s/MeV and $m_{A^0} < 20$ MeV.

[3] The second DRUZHININ 87 limit is valid when $\tau_{A^0}/m_{A^0} < 5\times10^{-13}$ s/MeV and $m_{A^0} < 20$ MeV.

[4] The third DRUZHININ 87 limit is valid when $\tau_{A^0}/m_{A^0} > 7\times10^{-12}$ s/MeV and $m_{A^0} < 200$ MeV.

[5] EDWARDS 82 looked for $J/\psi \to \gamma A^0$ decays by looking for events with a single γ [of energy $\sim 1/2$ the $J/\psi(1S)$ mass], plus nothing else in the detector. The limit is inconsistent with the axion interpretation of the FAISSNER 81B result.

A^0 (Axion) Searches in Positronium Decays

Decay or transition of positronium. Limits are for branching ratio.

VALUE	CL%	DOCUMENT ID		TECN	COMMENT
• • • We do not use the following data for averages, fits, limits, etc. • • •					
$<4.4\times10^{-5}$	90	[1] BADERT...	02	CNTR	o-Ps $\to \gamma X_1 X_2$, $m_{X_1}+m_{X_2} \leq$ 900 keV
$<2\times10^{-4}$	90	MAENO	95	CNTR	o-Ps $\to A^0\gamma$ m_{A^0}=850–1013 keV
$<3.0\times10^{-4}$	90	[2] ASAI	94	CNTR	o-Ps $\to A^0\gamma$ m_{A^0}=30–500 keV
$<2.8\times10^{-5}$	90	[3] AKOPYAN	91	CNTR	o-Ps $\to A^0\gamma$ ($A^0 \to \gamma\gamma$), m_{A^0} < 30 keV
$<1.1\times10^{-6}$	90	[4] ASAI	91	CNTR	o-Ps $\to A^0\gamma$, m_{A^0} < 800 keV
$<3.8\times10^{-4}$	90	GNINENKO	90	CNTR	o-Ps $\to A^0\gamma$, m_{A^0} < 30 keV
$<(1–5)\times10^{-4}$	95	[5] TSUCHIAKI	90	CNTR	o-Ps $\to A^0\gamma$, m_{A^0} = 300–900 keV
$<6.4\times10^{-5}$	90	[6] ORITO	89	CNTR	o-Ps $\to A^0\gamma$, m_{A^0} < 30 keV
		[7] AMALDI	85	CNTR	Ortho-positronium
		[8] CARBONI	83	CNTR	Ortho-positronium

[1] BADERTSCHER 02 looked for a three-body decay of ortho-positronium into a photon and two penetrating (neutral or milli-charged) particles.

[2] The ASAI 94 limit is based on inclusive photon spectrum and is independent of A^0 decay modes.

[3] The AKOPYAN 91 limit applies for a short-lived A^0 with $\tau_{A^0} < 10^{-13}\ m_{A^0}$ [keV]s.

[4] ASAI 91 limit translates to $g^2_{A^0e^+e^-}/4\pi < 1.1\times10^{-11}$ (90% CL) for $m_{A^0} < 800$ keV.

[5] The TSUCHIAKI 90 limit is based on inclusive photon spectrum and is independent of A^0 decay modes.

[6] ORITO 89 limit translates to $g^2_{A^0ee}/4\pi < 6.2\times10^{-10}$. Somewhat more sensitive limits are obtained for larger m_{A^0}: $B < 7.6\times10^{-6}$ at 100 keV.

[7] AMALDI 85 set limits B($A^0\gamma$) / B($\gamma\gamma\gamma$) < (1–5) $\times10^{-6}$ for m_{A^0} = 900–100 keV which are about 1/10 of the CARBONI 83 limits.

[8] CARBONI 83 looked for orthopositronium $\to A^0\gamma$. Set limit for A^0 electron coupling squared, $g(eeA^0)^2/(4\pi) < 6.\times10^{-10}$–$7.\times10^{-9}$ for m_{A^0} from 150–900 keV (CL = 99.7%). This is about 1/10 of the bound from $g-2$ experiments.

A^0 (Axion) Search in Photoproduction

VALUE	DOCUMENT ID		COMMENT
• • • We do not use the following data for averages, fits, limits, etc. • • •			
	[1] BASSOMPIE...	95	$m_{A^0} = 1.8 \pm 0.2$ MeV

[1] BASSOMPIERRE 95 is an extension of BASSOMPIERRE 93. They looked for a peak in the invariant mass of e^+e^- pairs in the region $m_{e^+e^-} = 1.8 \pm 0.2$ MeV. They obtained bounds on the production rate A^0 for $\tau(A^0) = 10^{-18}$–10^{-9} sec. They also found an excess of events in the range $m_{e^+e^-} = 2.1$–3.5 MeV.

A^0 (Axion) Production in Hadron Collisions

Limits are for $\sigma(A^0)$ / $\sigma(\pi^0)$.

VALUE	CL%	EVTS	DOCUMENT ID		TECN	COMMENT
• • • We do not use the following data for averages, fits, limits, etc. • • •						
			[1] JAIN	07	CNTR	$A^0 \to e^+e^-$
			[2] AHMAD	97	SPEC	e^+ production
			[3] LEINBERGER	97	SPEC	$A^0 \to e^+e^-$
			[4] GANZ	96	SPEC	$A^0 \to e^+e^-$
			[5] KAMEL	96	EMUL	^{32}S emulsion, $A^0 \to e^+e^-$
			[6] BLUEMLEIN	92	BDMP	$A^0N_Z \to \ell^+\ell^-N_Z$
			[7] MEIJERDREES	92	SPEC	$\pi^-p \to nA^0$, $A^0 \to e^+e^-$
			[8] BLUEMLEIN	91	BDMP	$A^0 \to e^+e^-$, 2γ
			[9] FAISSNER	89	OSPK	Beam dump, $A^0 \to e^+e^-$
			[10] DEBOER	88	RVUE	$A^0 \to e^+e^-$
			[11] EL-NADI	88	EMUL	$A^0 \to e^+e^-$
			[12] FAISSNER	88	OSPK	Beam dump, $A^0 \to 2\gamma$
			[13] BADIER	86	BDMP	$A^0 \to e^+e^-$
$<2.\times10^{-11}$	90	0	[14] BERGSMA	85	CHRM	CERN beam dump
$<1.\times10^{-13}$	90	0	[14] BERGSMA	85	CHRM	CERN beam dump
		24	[15] FAISSNER	83	OSPK	Beam dump, $A^0 \to 2\gamma$
			[16] FAISSNER	83B	RVUE	LAMPF beam dump
			[17] FRANK	83B	RVUE	LAMPF beam dump
			[18] HOFFMAN	83	CNTR	$\pi p \to nA^0$ ($A^0 \to e^+e^-$)
			[19] FETSCHER	82	RVUE	See FAISSNER 81B
		12	[20] FAISSNER	81	OSPK	CERN PS ν wideband
		15	[21] FAISSNER	81B	OSPK	Beam dump, $A^0 \to 2\gamma$
		8	[22] KIM	81	OSPK	26 GeV $pN \to A^0$X
		0	[23] FAISSNER	80	OSPK	Beam dump, $A^0 \to e^+e^-$
$<1.\times10^{-8}$	90		[24] JACQUES	80	HLBC	28 GeV protons
$<1.\times10^{-14}$	90		[24] JACQUES	80	HLBC	Beam dump
			[25] SOUKAS	80	CALO	28 GeV p beam dump
			[26] BECHIS	79	CNTR	
$<1.\times10^{-8}$	90		[27] COTEUS	79	OSPK	Beam dump
$<1.\times10^{-3}$	95		[28] DISHAW	79	CALO	400 GeV pp
$<1.\times10^{-8}$	90		ALIBRAN	78	HYBR	Beam dump
$<6.\times10^{-9}$	95		ASRATYAN	78B	CALO	Beam dump

$<1.5\times10^{-8}$	90	[29] BELLOTTI	78	HLBC	Beam dump
$<5.4\times10^{-14}$	90	[29] BELLOTTI	78	HLBC	m_{A^0}=1.5 MeV
$<4.1\times10^{-9}$	90	[29] BELLOTTI	78	HLBC	m_{A^0}=1 MeV
$<1.\times10^{-8}$	90	[30] BOSETTI	78B	HYBR	Beam dump
		[31] DONNELLY	78		
$<0.5\times10^{-8}$	90	HANSL	78D	WIRE	Beam dump
		[32] MICELMAC...	78		
		[33] VYSOTSKII	78		

[1] JAIN 07 claims evidence for $A^0 \to e^+e^-$ produced in ^{207}Pb collision on nuclear emulsion (Ag/Br) for $m(A^0) = 7\pm1$ or 19 ± 1 MeV and $\tau(A^0) \le 10^{-13}$ s.

[2] AHMAD 97 reports a result of APEX Collaboration which studied positron production in ^{238}U+^{232}Ta and ^{238}U+^{181}Ta collisions, without requiring a coincident electron. No narrow lines were found for $250 < E_{e^+} < 750$ keV.

[3] LEINBERGER 97 (ORANGE Collaboration) at GSI looked for a narrow sum-energy e^+e^--line at $\sim$ 635 keV in ^{238}U+^{181}Ta collision. Limits on the production probability for a narrow sum-energy e^+e^- line are set. See their Table 2.

[4] GANZ 96 (EPos II Collaboration) has placed upper bounds on the production cross section of e^+e^- pairs from ^{238}U+^{181}Ta and ^{238}U+^{232}Th collisions at GSI. See Table 2 for limits both for back-to-back and isotropic configurations of e^+e^- pairs. These limits rule out the existence of peaks in the e^+e^- sum-energy distribution, reported by an earlier version of this experiment.

[5] KAMEL 96 looked for e^+e^- pairs from the collision of ^{32}S (200 GeV/nucleon) and emulsion. No evidence of mass peaks is found in the region of sensitivity $m_{ee} > 2$ MeV.

[6] BLUEMLEIN 92 is a proton beam dump experiment at Serpukhov with a secondary target to induce Bethe-Heitler production of e^+e^- or $\mu^+\mu^-$ from the produce A^0. See Fig. 5 for the excluded region in m_{A^0}-x plane. For the standard axion, $0.3 < x < 25$ is excluded at 95% CL. If combined with BLUEMLEIN 91, $0.008 < x < 32$ is excluded.

[7] MEIJERDREES 92 give $\Gamma(\pi^- p \to n A^0)\cdot B(A^0 \to e^+e^-)/\Gamma(\pi^- p \to \text{all}) < 10^{-5}$ (90% CL) for $m_{A^0} = 100$ MeV, $\tau_{A^0} = 10^{-11}$–10^{-23} sec. Limits ranging from 2.5×10^{-3} to 10^{-7} are given for $m_{A^0} = 25$–136 MeV.

[8] BLUEMLEIN 91 is a proton beam dump experiment at Serpukhov. No candidate event for $A^0 \to e^+e^-$, 2γ are found. Fig. 6 gives the excluded region in m_{A^0}-x plane ($x = \tan\beta = v_2/v_1$). Standard axion is excluded for $0.2 < m_{A^0} < 3.2$ MeV for most $x > 1$, 0.2–11 MeV for most $x < 1$.

[9] FAISSNER 89 searched for $A^0 \to e^+e^-$ in a proton beam dump experiment at SIN. No excess of events was observed over the background. A standard axion with mass $2m_e$–20 MeV is excluded. Lower limit on f_{A^0} of $\simeq 10^4$ GeV is given for $m_{A^0} = 2m_e$–20 MeV.

[10] DEBOER 88 reanalyze EL-NADI 88 data and claim evidence for three distinct states with mass $\sim$ 1.1, $\sim$ 2.1, and $\sim$ 9 MeV, lifetimes 10^{-16}–10^{-15} s decaying to e^+e^- and note the similarity of the data with those of a cosmic-ray experiment by Bristol group (B.M. Anand, Proc. of the Royal Society of London, Section A **A22** 183 (1953)). For a criticism see PERKINS 89, who suggests that the events are compatible with π^0 Dalitz decay. DEBOER 89B is a reply which contests the criticism.

[11] EL-NADI 88 claim the existence of a neutral particle decaying into e^+e^- with mass 1.60 ± 0.59 MeV, lifetime $(0.15\pm0.01)\times10^{-14}$ s, which is produced in heavy ion interactions with emulsion nuclei at $\sim$ 4 GeV/c/nucleon.

[12] FAISSNER 88 is a proton beam dump experiment at SIN. They found no candidate event for $A^0 \to \gamma\gamma$. A standard axion decaying to 2γ is excluded except for a region $x \simeq 1$. Lower limit on f_{A^0} of 10^2–10^3 GeV is given for $m_{A^0} = 0.1$–1 MeV.

[13] BADIER 86 did not find long-lived A^0 in 300 GeV π^- Beam Dump Experiment that decays into e^+e^- in the mass range $m_{A^0} = (20$–$200)$ MeV, which excludes the A^0 decay constant $f(A^0)$ in the interval (60–600) GeV. See their figure 6 for excluded region on $f(A^0)$-m_{A^0} plane.

[14] BERGSMA 85 look for $A^0 \to 2\gamma$, e^+e^-, $\mu^+\mu^-$. First limit above is for $m_{A^0} = 1$ MeV; second is for 200 MeV. See their figure 4 for excluded region on f_{A^0}–m_{A^0} plane, where f_{A^0} is A^0 decay constant. For Peccei-Quinn PECCEI 77 A^0, $m_{A^0} < 180$ keV and $\tau > 0.037$ s. (CL = 90%). For the axion of FAISSNER 81B at 250 keV, BERGSMA 85 expect 15 events but observe zero.

[15] FAISSNER 83 observed 19 1-γ and 12 2-γ events where a background of 4.8 and 2.3 respectively is expected. A small-angle peak is observed even if iron wall is set in front of the decay region.

[16] FAISSNER 83B extrapolate SIN γ signal to LAMPF ν experimental condition. Resulting 370 γ's are not at variance with LAMPF upper limit of 450 γ's. Derived from LAMPF limit that $[d\sigma(A^0)/d\omega$ at $90^\circ] m_{A^0}/\tau_{A^0} < 14\times10^{-35}$ cm^2 sr^{-1} MeV ms^{-1}. See comment on FRANK 83B.

[17] FRANK 83B stress the importance of LAMPF data bins with negative net signal. By statistical analysis say that LAMPF and SIN-A0 are at variance when extrapolation by phase-space model is done. They find LAMPF upper limit is 248 not 450 γ's. See comment on FAISSNER 83B.

[18] HOFFMAN 83 set CL = 90% limit $d\sigma/dt\ B(e^+e^-) < 3.5\times10^{-32}$ cm^2/GeV^2 for $140 < m_{A^0} < 160$ MeV. Limit assumes $\tau(A^0) < 10^{-9}$ s.

[19] FETSCHER 82 reanalyzes SIN beam-dump data of FAISSNER 81. Claims no evidence for axion since 2-γ peak rate remarkably decreases if iron wall is set in front of the decay region.

[20] FAISSNER 81 see excess μe events. Suggest axion interactions.

[21] FAISSNER 81B is SIN 590 MeV proton beam dump. Observed 14.5 ± 5.0 events of 2γ decay of long-lived neutral penetrating particle with $m_{2\gamma} \lesssim 1$ MeV. Axion interpretation with η-A^0 mixing gives $m_{A^0} = 250\pm25$ keV, $\tau_{(2\gamma)} = (7.3\pm3.7)\times10^{-3}$ s from above rate. See critical remarks below in comments of FETSCHER 82, FAISSNER 83, FAISSNER 83B, FRANK 83B, and BERGSMA 85. Also see in the next subsection ALEKSEEV 82B, CAVAIGNAC 83, and ANANEV 85.

[22] KIM 81 analyzed 8 candidates for $A^0 \to 2\gamma$ obtained by Aachen-Padova experiment at CERN with 26 GeV protons on Be. Estimated axion mass is about 300 keV and lifetime is $(0.86\sim5.6)\times10^{-3}$ s depending on models. Faissner (private communication), says axion production underestimated and mass overestimated. Correct value around 200 keV.

[23] FAISSNER 80 is SIN beam dump experiment with 590 MeV protons looking for $A^0 \to e^+e^-$ decay. Assuming $A^0/\pi^0 = 5.5\times10^{-7}$, obtained decay rate limit 20/(A^0 mass) MeV/s (CL = 90%), which is about 10^{-7} below theory and interpreted as upper limit to $m_{A^0} < 2m_{e^-}$.

[24] JACQUES 80 is a BNL beam dump experiment. First limit above comes from nonobservation of excess neutral-current-type events $[\sigma(\text{production})\sigma(\text{interaction}) < 7.\times10^{-68}$ cm^4, CL = 90%]. Second limit is from nonobservation of axion decays into 2γ's or e^+e^-, and for axion mass a few MeV.

[25] SOUKAS 80 at BNL observed no excess of neutral-current-type events in beam dump.

[26] BECHIS 79 looked for the axion production in low energy electron Bremsstrahlung and the subsequent decay into either 2γ or e^+e^-. No signal found. CL = 90% limits for model parameter(s) are given.

[27] COTEUS 79 is a beam dump experiment at BNL.

[28] DISHAW 79 is a calorimetric experiment and looks for low energy tail of energy distributions due to energy lost to weakly interacting particles.

[29] BELLOTTI 78 first value comes from search for $A^0 \to e^+e^-$. Second value comes from search for $A^0 \to 2\gamma$, assuming mass $< 2m_{e^-}$. For any mass satisfying this, limit is above value$\times$(mass^{-4}). Third value uses data of PL 60B 401 and quotes $\sigma(\text{production})\sigma(\text{interaction}) < 10^{-67}$ cm^4.

[30] BOSETTI 78B quotes $\sigma(\text{production})\sigma(\text{interaction}) < 2.\times10^{-67}$ cm^4.

[31] DONNELLY 78 examines data from reactor neutrino experiments of REINES 76 and GURR 74 as well as SLAC beam dump experiment. Evidence is negative.

[32] MICELMACHER 78 finds no evidence of axion existence in reactor experiments of REINES 76 and GURR 74. (See reference under DONNELLY 78 below).

[33] VYSOTSKII 78 derived lower limit for the axion mass 25 keV from luminosity of the sun and 200 keV from red supergiants.

A^0 (Axion) Searches in Reactor Experiments

VALUE		DOCUMENT ID		TECN	COMMENT
• • • We do not use the following data for averages, fits, limits, etc. • • •					
		[1] CHANG	07		Primakoff or Compton
		[2] ALTMANN	95	CNTR	Reactor; $A^0 \to e^+e^-$
		[3] KETOV	86	SPEC	Reactor, $A^0 \to \gamma\gamma$
		[4] KOCH	86	SPEC	Reactor; $A^0 \to \gamma\gamma$
		[5] DATAR	82	CNTR	Light water reactor
		[6] VUILLEUMIER	81	CNTR	Reactor, $A^0 \to 2\gamma$

[1] CHANG 07 looked for monochromatic photons from Primakoff or Compton conversion of axions from the Kuo-Sheng reactor due to axion coupling to photon or electron, respectively. The search places model-independent limits on the products $G_{A\gamma\gamma}G_{ANN}$ and $G_{Aee}G_{ANN}$ for $m(A^0)$ less than the MeV range.

[2] ALTMANN 95 looked for A^0 decaying into e^+e^- from the Bugey 5 nuclear reactor. They obtain an upper limit on the A^0 production rate of $\omega(A^0)/\omega(\gamma) \times B(A^0 \to e^+e^-) < 10^{-16}$ for $m_{A^0} = 1.5$ MeV at 90% CL. The limit is weaker for heavier A^0. In the case of a standard axion, this limit excludes a mass in the range $2m_e < m_{A^0} < 4.8$ MeV at 90% CL. See Fig. 5 of their paper for exclusion limits of axion-like resonances Z^0 in the (m_{X^0},f_{X^0}) plane.

[3] KETOV 86 searched for A^0 at the Rovno nuclear power plant. They found an upper limit on the A^0 production probability of $0.8\ [100\text{ keV}/m_{A^0}]^6 \times 10^{-6}$ per fission. In the standard axion model, this corresponds to $m_{A^0} > 150$ keV. Not valid for $m_{A^0} \gtrsim 1$ MeV.

[4] KOCH 86 searched for $A^0 \to \gamma\gamma$ at nuclear power reactor Biblis A. They found an upper limit on the A^0 production rate of $\omega(A^0)/\omega(\gamma(M1)) < 1.5\times10^{-10}$ (CL=95%). Standard axion with $m_{A^0} = 250$ keV gives 10^{-5} for the ratio. Not valid for $m_{A^0} > 1022$ keV.

[5] DATAR 82 looked for $A^0 \to 2\gamma$ in neutron capture ($np \to dA^0$) at Tarapur 500 MW reactor. Sensitive to sum of $I = 0$ and $I = 1$ amplitudes. With ZEHNDER 81 $[(I = 0) - (I = 1)]$ result, assert nonexistence of standard A^0.

[6] VUILLEUMIER 81 is at Grenoble reactor. Set limit $m_{A^0} < 280$ keV.

A^0 (Axion) and Other Light Boson (X^0) Searches in Nuclear Transitions

Limits are for branching ratio.

VALUE	CL%	DOCUMENT ID		TECN	COMMENT
• • • We do not use the following data for averages, fits, limits, etc. • • •					
$< 8.5\times10^{-6}$	90	[1] DERBIN	02	CNTR	^{125m}Te decay
		[2] DEBOER	97C	RVUE	M1 transitions
$< 5.5\times10^{-10}$	95	[3] TSUNODA	95	CNTR	^{252}Cf fission, $A^0 \to ee$
$< 1.2\times10^{-6}$	95	[4] MINOWA	93	CNTR	^{139}La$^* \to {}^{139}$LaA^0
$< 2\times10^{-4}$	90	[5] HICKS	92	CNTR	^{35}S decay, $A^0 \to \gamma\gamma$
$< 1.5\times10^{-9}$	95	[6] ASANUMA	90	CNTR	^{241}Am decay
$<(0.4$–$10)\times10^{-3}$	95	[7] DEBOER	90	CNTR	^{8}Be$^* \to {}^8$BeA^0, $A^0 \to e^+e^-$
$<(0.2$–$1)\times10^{-3}$	90	[8] BINI	89	CNTR	^{16}O$^* \to {}^{16}$OX^0, $X^0 \to e^+e^-$
		[9] AVIGNONE	88	CNTR	Cu$^* \to$ CuA^0 ($A^0 \to 2\gamma$, $A^0 e \to \gamma e$, $A^0 Z \to \gamma Z$)
$< 1.5\times10^{-4}$	90	[10] DATAR	88	CNTR	^{12}C$^* \to {}^{12}$CA^0, $A^0 \to e^+e^-$
$< 5\times10^{-3}$	90	[11] DEBOER	88C	CNTR	^{16}O$^* \to {}^{16}$OX^0, $X^0 \to e^+e^-$
$< 3.4\times10^{-5}$	95	[12] DOEHNER	88	SPEC	^{2}H*, $A^0 \to e^+e^-$
$< 4\times10^{-4}$	95	[13] SAVAGE	88	CNTR	Nuclear decay (isovector)

Gauge & Higgs Boson Particle Listings

Axions (A^0) and Other Very Light Bosons

$< 3 \times 10^{-3}$	95	[13] SAVAGE	88	CNTR	Nuclear decay (isoscalar)
$<10.6 \times 10^{-2}$	90	[14] HALLIN	86	SPEC	^{6}Li isovector decay
<10.8	90	[14] HALLIN	86	SPEC	^{10}B isoscalar decays
< 2.2	90	[14] HALLIN	86	SPEC	^{14}N isoscalar decays
$< 4 \times 10^{-4}$	90	[15] SAVAGE	86B	CNTR	^{14}N*
		[16] ANANEV	85	CNTR	Li*, deut* $A^0 \rightarrow 2\gamma$
		[17] CAVAIGNAC	83	CNTR	^{97}Nb*, deut* transition $A^0 \rightarrow 2\gamma$
		[18] ALEKSEEV	82B	CNTR	Li*, deut* transition $A^0 \rightarrow 2\gamma$
		[19] LEHMANN	82	CNTR	Cu* $\rightarrow$ Cu A^0 ($A^0 \rightarrow 2\gamma$)
		[20] ZEHNDER	82	CNTR	Li*, Nb* decay, n-capt.
		[21] ZEHNDER	81	CNTR	Ba* $\rightarrow$ Ba A^0 ($A^0 \rightarrow 2\gamma$)
		[22] CALAPRICE	79		Carbon

[1] DERBIN 02 looked for the axion emission in an M1 transition in ^{125m}Te decay. They looked for a possible presence of a shifted energy spectrum in gamma rays due to the undetected axion.

[2] DEBOER 97C reanalyzed the existent data on Nuclear M1 transitions and find that a 9 MeV boson decaying into e^+e^- would explain the excess of events with large opening angles. See also DEBOER 01 for follow-up experiments.

[3] TSUNODA 95 looked for axion emission when ^{252}Cf undergoes a spontaneous fission, with the axion decaying into e^+e^-. The bound is for m_{A^0}=40 MeV. It improves to 2.5×10^{-5} for m_{A^0}=200 MeV.

[4] MINOWA 93 studied chain process, ^{139}Ce $\rightarrow$ ^{139}La* by electron capture and M1 transition of ^{139}La* to the ground state. It does not assume decay modes of A^0. The bound applies for $m_{A^0} < 166$ keV.

[5] HICKS 92 bound is applicable for $\tau_{X^0} < 4 \times 10^{-11}$ sec.

[6] The ASANUMA 90 limit is for the branching fraction of X^0 emission per ^{241}Am α decay and valid for $\tau_{X^0} < 3 \times 10^{-11}$ s.

[7] The DEBOER 90 limit is for the branching ratio ^{8}Be* (18.15 MeV, 1^+) $\rightarrow$ ^{8}BeA^0, $A^0 \rightarrow e^+e^-$ for the mass range m_{A^0} = 4–15 MeV.

[8] The BINI 89 limit is for the branching fraction of ^{16}O*(6.05 MeV, 0^+) $\rightarrow$ ^{16}OX^0, $X^0 \rightarrow e^+e^-$ for m_X = 1.5–3.1 MeV. $\tau_{X^0} \lesssim 10^{-11}$ s is assumed. The spin-parity of X is restricted to 0^+ or 1^-.

[9] AVIGNONE 88 looked for the 1115 keV transition C* $\rightarrow$ CuA^0, either from $A^0 \rightarrow 2\gamma$ in-flight decay or from the secondary A^0 interactions by Compton and by Primakoff processes. Limits for axion parameters are obtained for $m_{A^0} < 1.1$ MeV.

[10] DATAR 88 rule out light pseudoscalar particle emission through its decay $A^0 \rightarrow e^+e^-$ in the mass range 1.02–2.5 MeV and lifetime range 10^{-13}–10^{-8} s. The above limit is for $\tau = 5 \times 10^{-13}$ s and m = 1.7 MeV; see the paper for the τ-m dependence of the limit.

[11] The limit is for the branching fraction of ^{16}O*(6.05 MeV, 0^+) $\rightarrow$ ^{16}OX^0, $X^0 \rightarrow e^+e^-$ against internal pair conversion for m_{X^0} = 1.7 MeV and $\tau_{X^0} < 10^{-11}$ s. Similar limits are obtained for m_{X^0} = 1.3–3.2 MeV. The spin parity of X^0 must be either 0^+ or 1^-. The limit at 1.7 MeV is translated into a limit for the X^0-nucleon coupling constant: $g^2_{X^0NN}/4\pi < 2.3 \times 10^{-9}$.

[12] The DOEHNER 88 limit is for m_{A^0} = 1.7 MeV, $\tau(A^0) < 10^{-10}$ s. Limits less than 10^{-4} are obtained for m_{A^0} = 1.2–2.2 MeV.

[13] SAVAGE 88 looked for A^0 that decays into e^+e^- in the decay of the 9.17 MeV $J^P = 2^+$ state in ^{14}N, 17.64 MeV state $J^P = 1^+$ in ^{8}Be, and the 18.15 MeV state $J^P = 1^+$ in ^{8}Be. This experiment constrains the isovector coupling of A^0 to hadrons, if m_{A^0} = (1.1 $\rightarrow$ 2.2) MeV and the isoscalar coupling of A^0 to hadrons, if m_{A^0} = (1.1 $\rightarrow$ 2.6) MeV. Both limits are valid only if $\tau(A^0) \lesssim 1 \times 10^{-11}$ s.

[14] Limits are for $\Gamma(A^0(1.8\text{ MeV}))/\Gamma(\pi\text{M1})$; i.e., for 1.8 MeV axion emission normalized to the rate for internal emission of e^+e^- pairs. Valid for $\tau_{A^0} < 2 \times 10^{-11}$s. ^{6}Li isovector decay data strongly disfavor PECCEI 86 model I, whereas the ^{10}B and ^{14}N isoscalar decay data strongly reject PECCEI 86 model II and III.

[15] SAVAGE 86B looked for A^0 that decays into e^+e^- in the decay of the 9.17 MeV $J^P = 2^+$ state in ^{14}N. Limit on the branching fraction is valid if $\tau_{A^0} \lesssim 1. \times 10^{-11}$s for m_{A^0} = (1.1–1.7) MeV. This experiment constrains the iso-vector coupling of A^0 to hadrons.

[16] ANANEV 85 with IBR-2 pulsed reactor exclude standard A^0 at CL = 95% masses below 470 keV (Li* decay) and below $2m_e$ for deuteron* decay.

[17] CAVAIGNAC 83 at Bugey reactor exclude axion at any $m_{^{97}\text{Nb*decay}}$ and axion with m_{A^0} between 275 and 288 keV (deuteron* decay).

[18] ALEKSEEV 82 with IBR-2 pulsed reactor exclude standard A^0 at CL = 95% mass-ranges m_{A^0} <400 keV (Li* decay) and 330 keV <m_{A^0} <2.2 MeV. (deuteron* decay).

[19] LEHMANN 82 obtained $A^0 \rightarrow 2\gamma$ rate $< 6.2 \times 10^{-5}$/s (CL = 95%) excluding m_{A^0} between 100 and 1000 keV.

[20] ZEHNDER 82 used Gosgen 2.8GW light-water reactor to check A^0 production. No 2γ peak in Li*, Nb* decay (both single p transition) nor in n capture (combined with previous Ba* negative result) rules out standard A^0. Set limit m_{A^0} <60 keV for any A^0.

[21] ZEHNDER 81 looked for Ba* $\rightarrow$ A^0Ba transition with $A^0 \rightarrow 2\gamma$. Obtained 2γ coincidence rate $< 2.2 \times 10^{-5}$/s (CL = 95%) excluding m_{A^0} >160 keV (or 200 keV depending on Higgs mixing). However, see BARROSO 81.

[22] CALAPRICE 79 saw no axion emission from excited states of carbon. Sensitive to axion mass between 1 and 15 MeV.

A^0 (Axion) Limits from Its Electron Coupling

Limits are for $\tau(A^0 \rightarrow e^+e^-)$.

VALUE (s)	CL%	DOCUMENT ID	TECN	COMMENT
• • • We do not use the following data for averages, fits, limits, etc. • • •				
none 4×10^{-16}–4.5×10^{-12}	90	[1] BROSS 91	BDMP	$eN \rightarrow eA^0N$ ($A^0 \rightarrow ee$)
		[2] GUO 90	BDMP	$eN \rightarrow eA^0N$ ($A^0 \rightarrow ee$)
		[3] BJORKEN 88	CALO	$A \rightarrow e^+e^-$ or 2γ
		[4] BLINOV 88	MD1	$ee \rightarrow eeA^0$ ($A^0 \rightarrow ee$)
none 1×10^{-14}–1×10^{-10}	90	[5] RIORDAN 87	BDMP	$eN \rightarrow eA^0N$ ($A^0 \rightarrow ee$)
none 1×10^{-14}–1×10^{-11}	90	[6] BROWN 86	BDMP	$eN \rightarrow eA^0N$ ($A^0 \rightarrow ee$)
none 6×10^{-14}–9×10^{-11}	95	[7] DAVIER 86	BDMP	$eN \rightarrow eA^0N$ ($A^0 \rightarrow ee$)
none 3×10^{-13}–1×10^{-7}	90	[8] KONAKA 86	BDMP	$eN \rightarrow eA^0N$ ($A^0 \rightarrow ee$)

[1] The listed BROSS 91 limit is for m_{A^0} = 1.14 MeV. B($A^0 \rightarrow e^+e^-$) =1 assumed. Excluded domain in the τ_{A^0}–m_{A^0} plane extends up to $m_{A^0} \approx 7$ MeV (see Fig. 5). Combining with electron $g-2$ constraint, axions coupling only to e^+e^- ruled out for $m_{A^0} < 4.8$ MeV (90% CL).

[2] GUO 90 use the same apparatus as BROWN 86 and improve the previous limit in the shorter lifetime region. Combined with $g-2$ constraint, axions coupling only to e^+e^- are ruled out for $m_{A^0} < 2.7$ MeV (90% CL).

[3] BJORKEN 88 reports limits on axion parameters (f_A, m_A, τ_A) for $m_{A^0} < 200$ MeV from electron beam-dump experiment with production via Primakoff photoproduction, bremsstrahlung from electrons, and resonant annihilation of positrons on atomic electrons.

[4] BLINOV 88 assume zero spin, m = 1.8 MeV and lifetime $< 5 \times 10^{-12}$ s and find $\Gamma(A^0 \rightarrow \gamma\gamma)$B($A^0 \rightarrow e^+e^-$) < 2 eV (CL=90%).

[5] Assumes $A^0\gamma\gamma$ coupling is small and hence Primakoff production is small. Their figure 2 shows limits on axions for $m_{A^0} < 15$ MeV.

[6] Uses electrons in hadronic showers from an incident 800 GeV proton beam. Limits for $m_{A^0} < 15$ MeV are shown in their figure 3.

[7] m_{A^0} = 1.8 MeV assumed. The excluded domain in the τ_{A^0}–m_{A^0} plane extends up to $m_{A^0} \approx 14$ MeV, see their figure 4.

[8] The limits are obtained from their figure 3. Also given is the limit on the $A^0\gamma\gamma$–$A^0e^+e^-$ coupling plane by assuming Primakoff production.

Search for A^0 (Axion) Resonance in Bhabha Scattering

The limit is for $\Gamma(A^0)$[B($A^0 \rightarrow e^+e^-$)]^2.

VALUE (10^{-3} eV)	CL%	DOCUMENT ID	TECN	COMMENT
• • • We do not use the following data for averages, fits, limits, etc. • • •				
< 1.3	97	[1] HALLIN 92	CNTR	m_{A^0} = 1.75–1.88 MeV
none 0.0016–0.47	90	[2] HENDERSON 92C	CNTR	m_{A^0}= 1.5–1.86 MeV
< 2.0	90	[3] WU 92	CNTR	m_{A^0}= 1.56–1.86 MeV
< 0.013	95	TSERTOS 91	CNTR	m_{A^0} = 1.832 MeV
none 0.19–3.3	95	[4] WIDMANN 91	CNTR	m_{A^0}= 1.78–1.92 MeV
< 5	97	BAUER 90	CNTR	m_{A^0} = 1.832 MeV
none 0.09–1.5	95	[5] JUDGE 90	CNTR	m_{A^0} = 1.832 MeV, elastic
< 1.9	97	[6] TSERTOS 89	CNTR	m_{A^0} = 1.82 MeV
<(10–40)	97	[6] TSERTOS 89	CNTR	m_{A^0} = 1.51–1.65 MeV
<(1–2.5)	97	[6] TSERTOS 89	CNTR	m_{A^0} = 1.80–1.86 MeV
< 31	95	LORENZ 88	CNTR	m_{A^0} = 1.646 MeV
< 94	95	LORENZ 88	CNTR	m_{A^0} = 1.726 MeV
< 23	95	LORENZ 88	CNTR	m_{A^0} = 1.782 MeV
< 19	95	LORENZ 88	CNTR	m_{A^0} = 1.837 MeV
< 3.8	97	[7] TSERTOS 88	CNTR	m_{A^0} = 1.832 MeV
		[8] VANKLINKEN 88	CNTR	
		[9] MAIER 87	CNTR	
<2500	90	MILLS 87	CNTR	m_{A^0} = 1.8 MeV
		[10] VONWIMMER..87	CNTR	

[1] HALLIN 92 quote limits on lifetime, $8 \times 10^{-14} - 5 \times 10^{-13}$ sec depending on mass, assuming B($A^0 \rightarrow e^+e^-$) = 100%. They say that TSERTOS 91 overstated their sensitivity by a factor of 3.

[2] HENDERSON 92C exclude axion with lifetime τ_{A^0}=$1.4 \times 10^{-12} - 4.0 \times 10^{-10}$ s, assuming B($A^0 \rightarrow e^+e^-$)=100%. HENDERSON 92C also exclude a vector boson with τ=$1.4 \times 10^{-12} - 6.0 \times 10^{-10}$ s.

[3] WU 92 quote limits on lifetime $> 3.3 \times 10^{-13}$s assuming B($A^0 \rightarrow e^+e^-$)=100%. They say that TSERTOS 89 overestimate the limit by a factor of $\pi/2$. WU 92 also quote a bound for vector boson, $\tau > 8.2 \times 10^{-13}$s.

[4] WIDMANN 91 bound applies exclusively to the case B($A^0 \rightarrow e^+e^-$)=1, since the detection efficiency varies substantially as $\Gamma(A^0)_{\text{total}}$ changes. See their Fig. 6.

[5] JUDGE 90 excludes an elastic pseudoscalar e^+e^- resonance for $4.5 \times 10^{-13} < \tau(A^0) < 7.5 \times 10^{-12}$ s (95% CL) at m_{A^0} = 1.832 MeV. Comparable limits can be set for m_{A^0} = 1.776–1.856 MeV.

[6] See also TSERTOS 88B in references.

[7] The upper limit listed in TSERTOS 88 is too large by a factor of 4. See TSERTOS 88B, footnote 3.

[8] VANKLINKEN 88 looked for relatively long-lived resonance ($\tau = 10^{-10}$–10^{-12} s). The sensitivity is not sufficient to exclude such a narrow resonance.

[9] MAIER 87 obtained limits $R\Gamma \lesssim 60$ eV (100 eV) at $m_{A^0} \simeq 1.64$ MeV (1.83 MeV) for energy resolution $\Delta E_{\text{cm}} \simeq 3$ keV, where R is the resonance cross section normalized

to that of Bhabha scattering, and $\Gamma = \Gamma^2_{ee}/\Gamma_{\rm total}$. For a discussion implying that $\Delta E_{\rm cm} \simeq 10$ keV, see TSERTOS 89.

[10] VONWIMMERSPERG 87 measured Bhabha scattering for $E_{\rm cm}$ = 1.37–1.86 MeV and found a possible peak at 1.73 with $\int \sigma dE_{\rm cm} = 14.5 \pm 6.8$ keV·b. For a comment and a reply, see VANKLINKEN 88B and VONWIMMERSPERG 88. Also see CONNELL 88.

Search for A^0 (Axion) Resonance in $e^+e^- \to \gamma\gamma$

The limit is for $\Gamma(A^0 \to e^+e^-)\cdot\Gamma(A^0 \to \gamma\gamma)/\Gamma_{\rm total}$

VALUE (10^{-3} eV)	CL%	DOCUMENT ID		TECN	COMMENT
• • • We do not use the following data for averages, fits, limits, etc. • • •					
< 0.18	95	VO	94	CNTR	m_{A^0}=1.1 MeV
< 1.5	95	VO	94	CNTR	m_{A^0}=1.4 MeV
<12	95	VO	94	CNTR	m_{A^0}=1.7 MeV
< 6.6	95	[1] TRZASKA	91	CNTR	m_{A^0} = 1.8 MeV
< 4.4	95	WIDMANN	91	CNTR	m_{A^0}= 1.78–1.92 MeV
		[2] FOX	89	CNTR	
< 0.11	95	[3] MINOWA	89	CNTR	m_{A^0} = 1.062 MeV
<33	97	CONNELL	88	CNTR	m_{A^0} = 1.580 MeV
<42	97	CONNELL	88	CNTR	m_{A^0} = 1.642 MeV
<73	97	CONNELL	88	CNTR	m_{A^0} = 1.782 MeV
<79	97	CONNELL	88	CNTR	m_{A^0} = 1.832 MeV

[1] TRZASKA 91 also give limits in the range (6.6–30) $\times 10^{-3}$ eV (95%CL) for m_{A^0} = 1.6–2.0 MeV.

[2] FOX 89 measured positron annihilation with an electron in the source material into two photons and found no signal at 1.062 MeV ($< 9\times10^{-5}$ of two-photon annihilation at rest).

[3] Similar limits are obtained for m_{A^0} = 1.045–1.085 MeV.

Search for X^0 (Light Boson) Resonance in $e^+e^- \to \gamma\gamma\gamma$

The limit is for $\Gamma(X^0 \to e^+e^-)\cdot\Gamma(X^0 \to \gamma\gamma\gamma)/\Gamma_{\rm total}$. C invariance forbids spin-0 X^0 coupling to both e^+e^- and $\gamma\gamma\gamma$.

VALUE (10^{-3} eV)	CL%	DOCUMENT ID		TECN	COMMENT
• • • We do not use the following data for averages, fits, limits, etc. • • •					
< 0.2	95	[1] VO	94	CNTR	m_{X^0}=1.1–1.9 MeV
< 1.0	95	[2] VO	94	CNTR	m_{X^0}=1.1 MeV
< 2.5	95	[2] VO	94	CNTR	m_{X^0}=1.4 MeV
<120	95	[2] VO	94	CNTR	m_{X^0}=1.7 MeV
< 3.8	95	[3] SKALSEY	92	CNTR	m_{X^0}= 1.5 MeV

[1] VO 94 looked for $X^0 \to \gamma\gamma\gamma$ decaying at rest. The precise limits depend on m_{X^0}. See Fig. 2(b) in paper.

[2] VO 94 looked for $X^0 \to \gamma\gamma\gamma$ decaying in flight.

[3] SKALSEY 92 also give limits 4.3 for m_{X^0} = 1.54 and 7.5 for 1.64 MeV. The spin of X^0 is assumed to be one.

Light Boson (X^0) Search in Nonresonant e^+e^- Annihilation at Rest

Limits are for the ratio of $n\gamma + X^0$ production relative to $\gamma\gamma$.

VALUE (units 10^{-6})	CL%	DOCUMENT ID		TECN	COMMENT
• • • We do not use the following data for averages, fits, limits, etc. • • •					
< 4.2	90	[1] MITSUI	96	CNTR	γX^0
< 4	68	[2] SKALSEY	95	CNTR	γX^0
<40	68	[3] SKALSEY	95	RVUE	γX^0
< 0.18	90	[4] ADACHI	94	CNTR	$\gamma\gamma X^0$, $X^0 \to \gamma\gamma$
< 0.26	90	[5] ADACHI	94	CNTR	$\gamma\gamma X^0$, $X^0 \to \gamma\gamma$
< 0.33	90	[6] ADACHI	94	CNTR	γX^0, $X^0 \to \gamma\gamma\gamma$

[1] MITSUI 96 looked for a monochromatic γ. The bound applies for a vector X^0 with C=−1 and m_{X^0} <200 keV. They derive an upper bound on eeX^0 coupling and hence on the branching ratio B(o-Ps $\to \gamma\gamma X^0$)< 6.2×10^{-6}. The bounds weaken for heavier X^0.

[2] SKALSEY 95 looked for a monochromatic γ without an accompanying γ in e^+e^- annihilation. The bound applies for scalar and vector X^0 with $C = -1$ and m_{X^0} = 100–1000 keV.

[3] SKALSEY 95 reinterpreted the bound on γA^0 decay of o-Ps by ASAI 91 where 3% of delayed annihilations are not from $^3S_1$ states. The bound applies for scalar and vector X^0 with $C = -1$ and m_{X^0} = 0–800 keV.

[4] ADACHI 94 looked for a peak in the $\gamma\gamma$ invariant mass distribution in $\gamma\gamma\gamma\gamma$ production from e^+e^- annihilation. The bound applies for m_{X^0} = 70–800 keV.

[5] ADACHI 94 looked for a peak in the missing-mass mass distribution in $\gamma\gamma$ channel, using $\gamma\gamma\gamma\gamma$ production from e^+e^- annihilation. The bound applies for m_{X^0} <800 keV.

[6] ADACHI 94 looked for a peak in the missing mass distribution in $\gamma\gamma\gamma$ channel, using $\gamma\gamma\gamma\gamma$ production from e^+e^- annihilation. The bound applies for m_{X^0} = 200–900 keV.

Searches for Goldstone Bosons (X^0)

(Including Horizontal Bosons and Majorons.) Limits are for branching ratios.

VALUE	CL%	DOCUMENT ID		TECN	COMMENT
• • • We do not use the following data for averages, fits, limits, etc. • • •					
		[1] LATTANZI	13	COSM	Majoron dark matter decay
		[2] LESSA	07	RVUE	Meson, ℓ decays to Majoron
		[3] DIAZ	98	THEO	$H^0 \to X^0X^0$, $A^0 \to X^0X^0X^0$, Majoron
		[4] BOBRAKOV	91		Electron quasi-magnetic interaction
$<3.3\times10^{-2}$	95	[5] ALBRECHT	90E	ARG	$\tau \to \mu X^0$. Familon
$<1.8\times10^{-2}$	95	[5] ALBRECHT	90E	ARG	$\tau \to e X^0$. Familon
$<6.4\times10^{-9}$	90	[6] ATIYA	90	B787	$K^+ \to \pi^+X^0$. Familon
$<1.1\times10^{-9}$	90	[7] BOLTON	88	CBOX	$\mu^+ \to e^+\gamma X^0$. Familon
		[8] CHANDA	88	ASTR	Sun, Majoron
		[9] CHOI	88	ASTR	Majoron, SN 1987A
$<5\times10^{-6}$	90	[10] PICCIOTTO	88	CNTR	$\pi \to e\nu X^0$, Majoron
$<1.3\times10^{-9}$	90	[11] GOLDMAN	87	CNTR	$\mu \to e\gamma X^0$. Familon
$<3\times10^{-4}$	90	[12] BRYMAN	86B	RVUE	$\mu \to e X^0$. Familon
$<1\times10^{-10}$	90	[13] EICHLER	86	SPEC	$\mu^+ \to e^+X^0$. Familon
$<2.6\times10^{-6}$	90	[14] JODIDIO	86	SPEC	$\mu^+ \to e^+X^0$. Familon
		[15] BALTRUSAIT...	85	MRK3	$\tau \to \ell X^0$. Familon
		[16] DICUS	83	COSM	ν(hvy) $\to \nu$(light)X^0

[1] LATTANZI 13 use WMAP 9 year data as well as X-ray and γ-ray observations to derive limits on decaying majoron dark matter. A limit on the decay width $\Gamma(X^0 \to \nu\overline{\nu})$ $< 6.4\times10^{-19}$ s^{-1} at 95% CL is found if majorons make up all of the dark matter.

[2] LESSA 07 consider decays of the form Meson $\to \ell\nu$Majoron and $\ell \to \ell'\nu\overline{\nu}$Majoron and use existing data to derive limits on the neutrino-Majoron Yukawa couplings $g_{\alpha\beta}$ (α,β=e,μ,τ). Their best limits are $|g_{e\alpha}|^2 < 5.5\times10^{-6}$, $|g_{\mu\alpha}|^2 < 4.5\times10^{-5}$, $|g_{\tau\alpha}|^2 < 5.5\times10^{-2}$ at CL = 90%.

[3] DIAZ 98 studied models of spontaneously broken lepton number with both singlet and triplet Higgses. They obtain limits on the parameter space from invisible decay $Z \to H^0A^0 \to X^0X^0X^0X^0X^0$ and $e^+e^- \to ZH^0$ with $H^0 \to X^0X^0$.

[4] BOBRAKOV 91 searched for anomalous magnetic interactions between polarized electrons expected from the exchange of a massless pseudoscalar boson (arion). A limit $x_e^2 < 2\times10^{-4}$ (95%CL) is found for the effective anomalous magneton parametrized as $x_e(G_F/8\pi\sqrt{2})^{1/2}$.

[5] ALBRECHT 90E limits are for B($\tau \to \ell X^0$)/B($\tau \to \ell\nu\overline{\nu}$). Valid for $m_{X^0} < 100$ MeV. The limits rise to 7.1% (for μ), 5.0% (for e) for m_{X^0} = 500 MeV.

[6] ATIYA 90 limit is for $m_{X^0} = 0$. The limit B $< 1\times10^{-8}$ holds for $m_{X^0} < 95$ MeV. For the reduction of the limit due to finite lifetime of X^0, see their Fig. 3.

[7] BOLTON 88 limit corresponds to $F > 3.1\times10^9$ GeV, which does not depend on the chirality property of the coupling.

[8] CHANDA 88 find $v_T < 10$ MeV for the weak-triplet Higgs vacuum expectation value in Gelmini-Roncadelli model, and $v_S > 5.8\times10^6$ GeV in the singlet Majoron model.

[9] CHOI 88 used the observed neutrino flux from the supernova SN1987A to exclude the neutrino Majoron Yukawa coupling h in the range $2\times10^{-5} < h < 3\times10^{-4}$ for the interaction $L_{\rm int} = \frac{1}{2}ih\overline{\psi}^c_\nu\gamma_5\psi_\nu\phi_X$. For several families of neutrinos, the limit applies for $(\Sigma h_i^4)^{1/4}$.

[10] PICCIOTTO 88 limit applies when $m_{X^0} < 55$ MeV and $\tau_{X^0} > 2$ns, and it decreases to 4×10^{-7} at m_{X^0} = 125 MeV, beyond which no limit is obtained.

[11] GOLDMAN 87 limit corresponds to $F > 2.9\times10^9$ GeV for the family symmetry breaking scale from the Lagrangian $L_{\rm int} = (1/F)\overline{\psi}_\mu\gamma^\mu(a+b\gamma_5)\psi_e\partial_\mu\phi_{X^0}$ with $a^2+b^2 = 1$. This is not as sensitive as the limit $F > 9.9\times10^9$ GeV derived from the search for $\mu^+ \to e^+X^0$ by JODIDIO 86, but does not depend on the chirality property of the coupling.

[12] Limits are for $\Gamma(\mu \to eX^0)/\Gamma(\mu \to e\nu\overline{\nu})$. Valid when m_{X^0} = 0–93.4, 98.1–103.5 MeV.

[13] EICHLER 86 looked for $\mu^+ \to e^+X^0$ followed by $X^0 \to e^+e^-$. Limits on the branching fraction depend on the mass and and lifetime of X^0. The quoted limits are valid when $\tau_{X^0} \lesssim 3.\times10^{-10}$ s if the decays are kinematically allowed.

[14] JODIDIO 86 corresponds to $F > 9.9\times10^9$ GeV for the family symmetry breaking scale with the parity-conserving effective Lagrangian $L_{\rm int} = (1/F)\ \overline{\psi}_\mu\gamma^\mu\psi_e\partial^\mu\phi_{X^0}$.

[15] BALTRUSAITIS 85 search for light Goldstone boson(X^0) of broken U(1). CL = 95% limits are B($\tau \to \mu^+X^0$)/B($\tau \to \mu^+\nu\nu$) <0.125 and B($\tau \to e^+X^0$)/B($\tau \to e^+\nu\nu$) <0.04. Inferred limit for the symmetry breaking scale is m >3000 TeV.

[16] The primordial heavy neutrino must decay into ν and familon, f_A, early so that the red-shifted decay products are below critical density, see their table. In addition, $K \to \pi f_A$ and $\mu \to e f_A$ are unseen. Combining these excludes $m_{{\rm heavy}\nu}$ between 5×10^{-5} and 5×10^{-4} MeV (μ decay) and $m_{{\rm heavy}\nu}$ between 5×10^{-5} and 0.1 MeV (K-decay).

Majoron Searches in Neutrinoless Double β Decay

Limits are for the half-life of neutrinoless $\beta\beta$ decay with a Majoron emission. No experiment currently claims any such evidence. Only the best or comparable limits for each isotope are reported. Also see the reviews ZUBER 98 and FAESSLER 98B.

$t_{1/2}(10^{21}$ yr)	CL%	ISOTOPE	TRANSITION	METHOD	DOCUMENT ID	
>7200	**90**	**^{128}Te**		**CNTR**	[1] BERNATOW...	92
• • • We do not use the following data for averages, fits, limits, etc. • • •						
>2600	90	^{136}Xe	$0\nu\chi$	KamLAND-Zen	[2] GANDO	12
> 16	90	^{130}Te	$0\nu\chi$	NEMO-3	[3] ARNOLD	11
> 1.9	90	^{96}Zr	$2\nu1\chi$	NEMO-3	[4] ARGYRIADES	10
> 1.52	90	^{150}Nd	$0\nu1\chi$	NEMO-3	[5] ARGYRIADES	09
> 27	90	^{100}Mo	$0\nu1\chi$	NEMO-3	[6] ARNOLD	06
> 15	90	^{82}Se	$0\nu1\chi$	NEMO-3	[7] ARNOLD	06
> 14	90	^{100}Mo	$0\nu1\chi$	NEMO-3	[8] ARNOLD	04
> 12	90	^{82}Se	$0\nu1\chi$	NEMO-3	[9] ARNOLD	04

Gauge & Higgs Boson Particle Listings

Axions (A^0) and Other Very Light Bosons

> 2.2	90	^{130}Te	$0\nu 1\chi$	Cryog. det.	[10] ARNABOLDI	03
> 0.9	90	^{130}Te	$0\nu 2\chi$	Cryog. det.	[11] ARNABOLDI	03
> 8	90	^{116}Cd	$0\nu 1\chi$	$CdWO_4$ scint.	[12] DANEVICH	03
> 0.8	90	^{116}Cd	$0\nu 2\chi$	$CdWO_4$ scint.	[13] DANEVICH	03
> 500	90	^{136}Xe	$0\nu\chi$	Liquid Xe Scint.	[14] BERNABEI	02D
> 5.8	90	^{100}Mo	$0\nu\chi$	ELEGANT V	[15] FUSHIMI	02
> 0.32	90	^{100}Mo	$0\nu\chi$	Liq. Ar ioniz.	[16] ASHITKOV	01
> 0.0035	90	^{160}Gd	$0\nu\chi$	$^{160}Gd_2SiO_5$:Ce	[17] DANEVICH	01
> 0.013	90	^{160}Gd	$0\nu 2\chi$	$^{160}Gd_2SiO_5$:Ce	[18] DANEVICH	01
> 2.3	90	^{82}Se	$0\nu\chi$	NEMO 2	[19] ARNOLD	00
> 0.31	90	^{96}Zr	$0\nu\chi$	NEMO 2	[20] ARNOLD	00
> 0.63	90	^{82}Se	$0\nu 2\chi$	NEMO 2	[21] ARNOLD	00
> 0.063	90	^{96}Zr	$0\nu 2\chi$	NEMO 2	[21] ARNOLD	00
> 0.16	90	^{100}Mo	$0\nu 2\chi$	NEMO 2	[21] ARNOLD	00
> 2.4	90	^{82}Se	$0\nu\chi$	NEMO 2	[22] ARNOLD	98
> 7.2	90	^{136}Xe	$0\nu 2\chi$	TPC	[23] LUESCHER	98
> 7.91	90	^{76}Ge		SPEC	[24] GUENTHER	96
> 17	90	^{76}Ge		CNTR	BECK	93

[1] BERNATOWICZ 92 studied double-β decays of ^{128}Te and ^{130}Te, and found the ratio $\tau(^{130}\text{Te})/\tau(^{128}\text{Te}) = (3.52 \pm 0.11) \times 10^{-4}$ in agreement with relatively stable theoretical predictions. The bound is based on the requirement that Majoron-emitting decay cannot be larger than the observed double-beta rate of ^{128}Te of $(7.7 \pm 0.4) \times 10^{24}$ year. We calculated 90% CL limit as $(7.7\text{–}1.28 \times 0.4{=}7.2) \times 10^{24}$.

[2] GANDO 12 use the KamLAND-Zen detector to obtain the limit on the $0\nu\chi$ decay with Majoron emission. It implies that the coupling constant $g_{\nu\chi} < 0.8\text{–}1.6 \times 10^{-5}$ depending on the nuclear matrix elements used.

[3] ARNOLD 11 use the NEMO-3 detector to obtain the reported limit on Majoron emission. It implies that the coupling constant $g_{\nu\chi} < 0.6\text{–}1.6 \times 10^{-4}$ depending on the nuclear matrix element used. Supercedes ARNABOLDI 03.

[4] ARGYRIADES 10 use the NEMO-3 tracking detector and ^{96}Zr to derive the reported limit. No limit for the Majoron electron coupling is given.

[5] ARGYRIADES 09 use ^{150}Nd data taken with the NEMO-3 tracking detector. The reported limit corresponds to $\langle g_{\nu\chi} \rangle < 1.7\text{–}3.0 \times 10^{-4}$ using a range of nuclear matrix elements that include the effect of nuclear deformation.

[6] ARNOLD 06 use ^{100}Mo data taken with the NEMO-3 tracking detector. The reported limit corresponds to $\langle g_{\nu\chi} \rangle < (0.4\text{–}1.8) \times 10^{-4}$ using a range of matrix element calculations. Supersedes ARNOLD 04.

[7] NEMO-3 tracking calorimeter is used in ARNOLD 06 . Reported half-life limit for ^{82}Se corresponds to $\langle g_{\nu\chi} \rangle < (0.66\text{–}1.9) \times 10^{-4}$ using a range of matrix element calculations. Supersedes ARNOLD 04.

[8] ARNOLD 04 use the NEMO-3 tracking detector. The limit corresponds to $\langle g_{\nu\chi} \rangle < (0.5\text{–}0.9) 10^{-4}$ using the matrix elements of SIMKOVIC 99, STOICA 01 and CIVITARESE 03.

[9] ARNOLD 04 use the NEMO-3 tracking detector. The limit corresponds to $\langle g_{\nu\chi} \rangle < (0.7\text{–}1.6) 10^{-4}$ using the matrix elements of SIMKOVIC 99, STOICA 01 and CIVITARESE 03.

[10] Supersedes ALESSANDRELLO 00. Array of TeO_2 crystals in high resolution cryogenic calorimeter. Some enriched in ^{130}Te. Derive $\langle g_{\nu\chi} \rangle < 17\text{–}33 \times 10^{-5}$ depending on matrix element.

[11] Supersedes ALESSANDRELLO 00. Cryogenic calorimeter search.

[12] Limit for the $0\nu\chi$ decay with Majoron emission of ^{116}Cd using enriched $CdWO_4$ scintillators. $\langle g_{\nu\chi} \rangle < 4.6\text{–}8.1 \times 10^{-5}$ depending on the matrix element. Supersedes DANEVICH 00.

[13] Limit for the $0\nu 2\chi$ decay of ^{116}Cd. Supersedes DANEVICH 00.

[14] BERNABEI 02D obtain limit for $0\nu\chi$ decay with Majoron emission of ^{136}Xe using liquid Xe scintillation detector. They derive $\langle g_{\nu\chi} \rangle < 2.0\text{–}3.0 \times 10^{-5}$ with several nuclear matrix elements.

[15] Replaces TANAKA 93. FUSHIMI 02 derive half-life limit for the $0\nu\chi$ decay by means of tracking calorimeter ELEGANT V. Considering various matrix element calculations, a range of limits for the Majoron-neutrino coupling is given: $\langle g_{\nu\chi} \rangle < (6.3\text{–}360) \times 10^{-5}$.

[16] ASHITKOV 01 result for $0\nu\chi$ of ^{100}Mo is less stringent than ARNOLD 00.

[17] DANEVICH 01 obtain limit for the $0\nu\chi$ decay with Majoron emission of ^{160}Gd using Gd_2SiO_5:Ce crystal scintillators.

[18] DANEVICH 01 obtain limit for the $0\nu 2\chi$ decay with 2 Majoron emission of ^{160}Gd.

[19] ARNOLD 00 reports limit for the $0\nu\chi$ decay with Majoron emission derived from tracking calorimeter NEMO 2. Using ^{82}Se source: $\langle g_{\nu\chi} \rangle < 1.6 \times 10^{-4}$. Matrix element from GUENTHER 96.

[20] Using ^{96}Zr source: $\langle g_{\nu\chi} \rangle < 2.6 \times 10^{-4}$. Matrix element from ARNOLD 99.

[21] ARNOLD 00 reports limit for the $0\nu 2\chi$ decay with two Majoron emission derived from tracking calorimeter NEMO 2.

[22] ARNOLD 98 determine the limit for $0\nu_\chi$ decay with Majoron emission of ^{82}Se using the NEMO-2 tracking detector. They derive $\langle g_{\nu_\chi} \rangle < 2.3\text{–}4.3 \times 10^{-4}$ with several nuclear matrix elements.

[23] LUESCHER 98 report a limit for the 0ν decay with Majoron emission of ^{136}Xe using Xe TPC. This result is more stringent than BARABASH 89. Using the matrix elements of ENGEL 88, they obtain a limit on $\langle g_{\nu\chi} \rangle$ of 2.0×10^{-4}.

[24] See Table 1 in GUENTHER 96 for limits on the Majoron coupling in different models.

Invisible A^0 (Axion) MASS LIMITS from Astrophysics and Cosmology

$v_1 = v_2$ is usually assumed (v_i = vacuum expectation values). For a review of these limits, see RAFFELT 91 and TURNER 90. In the comment lines below, D and K refer to DFSZ and KSVZ axion types, discussed in the above minireview.

VALUE (eV)	CL%	DOCUMENT ID	TECN	COMMENT
• • • We do not use the following data for averages, fits, limits, etc. • • •				
< 0.67	95	[1] ARCHIDIACO...13A	COSM	K, hot dark matter
none $0.7\text{–}3 \times 10^5$		[2] CADAMURO 11	COSM	D abundance
< 105	90	[3] DERBIN 11A	CNTR	D, solar axion
		[4] ANDRIAMON...10	CAST	K, solar axions
< 0.72	95	[5] HANNESTAD 10	COSM	K, hot dark matter
		[6] ANDRIAMON...09	CAST	K, solar axions
< 191	90	[7] DERBIN 09A	CNTR	K, solar axions
< 334	95	[8] KEKEZ 09	HPGE	K, solar axions
< 1.02	95	[9] HANNESTAD 08	COSM	K, hot dark matter
< 1.2	95	[10] HANNESTAD 07	COSM	K, hot dark matter
< 0.42	95	[11] MELCHIORRI 07A	COSM	K, hot dark matter
< 1.05	95	[12] HANNESTAD 05A	COSM	K, hot dark matter
3 to 20		MOROI 98	COSM	K, hot dark matter
< 0.007		BORISOV 97	ASTR	D, neutron star
< 4		KACHELRIESS 97	ASTR	D, neutron star cooling
$< (0.5\text{–}6) \times 10^{-3}$		KEIL 97	ASTR	SN 1987A
< 0.018		RAFFELT 95	ASTR	D, red giant
< 0.010		ALTHERR 94	ASTR	D, red giants, white dwarfs
		CHANG 93	ASTR	K, SN 1987A
< 0.01		WANG 92	ASTR	D, white dwarf
< 0.03		WANG 92C	ASTR	D, C-O burning
none 3–8		BERSHADY 91	ASTR	D, K, intergalactic light
< 10		KIM 91C	COSM	D, K, mass density of the universe, supersymmetry
$< 1 \times 10^{-3}$		RAFFELT 91B	ASTR	D,K, SN 1987A
none 10^{-3}–3		RESSELL 91	ASTR	K, intergalactic light
		BURROWS 90	ASTR	D,K, SN 1987A
< 0.02		ENGEL 90	ASTR	D,K, SN 1987A
$< 1 \times 10^{-3}$		RAFFELT 90D	ASTR	D, red giant
$< (1.4\text{–}10) \times 10^{-3}$		BURROWS 89	ASTR	D,K, SN 1987A
$< 3.6 \times 10^{-4}$		ERICSON 89	ASTR	D,K, SN 1987A
< 12		MAYLE 89	ASTR	D,K, SN 1987A
$< 1 \times 10^{-3}$		CHANDA 88	ASTR	D, Sun
		RAFFELT 88	ASTR	D,K, SN 1987A
< 0.07		RAFFELT 88B	ASTR	red giant
< 0.7		FRIEMAN 87	ASTR	D, red giant
$< 2\text{–}5$		RAFFELT 87	ASTR	K, red giant
< 0.01		TURNER 87	COSM	K, thermal production
< 0.06		DEARBORN 86	ASTR	D, red giant
< 0.7		RAFFELT 86	ASTR	D, red giant
< 0.03		RAFFELT 86	ASTR	K, red giant
< 1		RAFFELT 86B	ASTR	D, white dwarf
$< 0.003\text{–}0.02$		KAPLAN 85	ASTR	K, red giant
$> 1 \times 10^{-5}$		IWAMOTO 84	ASTR	D, K, neutron star
		ABBOTT 83	COSM	D,K, mass density of the universe
$> 1 \times 10^{-5}$		DINE 83	COSM	D,K, mass density of the universe
< 0.04		ELLIS 83B	ASTR	D, red giant
$> 1 \times 10^{-5}$		PRESKILL 83	COSM	D,K, mass density of the universe
< 0.1		BARROSO 82	ASTR	D, red giant
< 1		FUKUGITA 82	ASTR	D, stellar cooling
< 0.07		FUKUGITA 82B	ASTR	D, red giant

[1] ARCHIDIACONO 13A is analogous to HANNESTAD 05A. The limit is based on the CMB temperature power spectrum of the Planck data, the CMB polarization from the WMAP 9-yr data, the matter power spectrum from SDSS-DR7, and the local Hubble parameter measurement by the Carnegie Hubble program.

[2] CADAMURO 11 use the deuterium abundance to show that the m_{A^0} range 0.7 eV – 300 keV is excluded for axions, complementing HANNESTAD 10.

[3] DERBIN 11A look for solar axions produced by Compton and bremsstrahlung processes, in the resonant excitation of ^{169}Tm, constraining the axion-electron $\times$ axion nucleon couplings.

[4] ANDRIAMONJE 10 search for solar axions produced from ^{7}Li (478 keV) and D$(p,\gamma)^3$He (5.5 MeV) nuclear transitions. They show limits on the axion-photon coupling for two reference values of the axion-nucleon coupling for $m_A < 100$ eV.

[5] This is an update of HANNESTAD 08 including 7 years of WMAP data.

[6] ANDRIAMONJE 09 look for solar axions produced from the thermally excited 14.4 keV level of ^{57}Fe. They show limits on the axion-nucleon $\times$ axion-photon coupling assuming $m_A < 0.03$ eV.

[7] DERBIN 09A look for Primakoff-produced solar axions in the resonant excitation of ^{169}Tm, constraining the axion-photon $\times$ axion-nucleon couplings.

[8] KEKEZ 09 look at axio-electric effect of solar axions in HPGe detectors. The one-loop axion-electron coupling for hadronic axions is used.

[9] This is an update of HANNESTAD 07 including 5 years of WMAP data.

[10] This is an update of HANNESTAD 05A with new cosmological data, notably WMAP (3 years) and baryon acoustic oscillations (BAO). Lyman-α data are left out, in contrast to HANNESTAD 05A and MELCHIORRI 07A, because it is argued that systematic errors are large. It uses Bayesian statistics and marginalizes over a possible neutrino hot dark matter component.

[11] MELCHIORRI 07A is analogous to HANNESTAD 05A, with updated cosmological data, notably WMAP (3 years). Uses Bayesian statistics and marginalizes over a possible neutrino hot dark matter component. Leaving out Lyman-α data, a conservative limit is 1.4 eV.

[12] HANNESTAD 05A puts an upper limit on the mass of hadronic axion because in this mass range it would have been thermalized and contribute to the hot dark matter component of the universe. The limit is based on the CMB anisotropy from WMAP, SDSS large

scale structure, Lyman α, and the prior Hubble parameter from HST Key Project. A χ^2 statistic is used. Neutrinos are assumed not to contribute to hot dark matter.

[13] MOROI 98 points out that a KSVZ axion of this mass range (see CHANG 93) can be a viable hot dark matter of Universe, as long as the model-dependent $g_{A\gamma}$ is accidentally small enough as originally emphasized by KAPLAN 85; see Fig. 1.

[14] BORISOV 97 bound is on the axion-electron coupling $g_{ae} < 1\times10^{-13}$ from the photo-production of axions off of magnetic fields in the outer layers of neutron stars.

[15] KACHELRIESS 97 bound is on the axion-electron coupling $g_{ae} < 1\times10^{-10}$ from the production of axions in strongly magnetized neutron stars. The authors also quote a stronger limit, $g_{ae} < 9\times10^{-13}$ which is strongly dependent on the strength of the magnetic field in white dwarfs.

[16] KEIL 97 uses new measurements of the axial-vector coupling strength of nucleons, as well as a reanalysis of many-body effects and pion-emission processes in the core of the neutron star, to update limits on the invisible-axion mass.

[17] RAFFELT 95 reexamined the constraints on axion emission from red giants due to the axion-electron coupling. They improve on DEARBORN 86 by taking into proper account degeneracy effects in the bremsstrahlung rate. The limit comes from requiring the red giant core mass at helium ignition not to exceed its standard value by more than 5% (0.025 solar masses).

[18] ALTHERR 94 bound is on the axion-electron coupling $g_{ae} < 1.5\times10^{-13}$, from energy loss via axion emission.

[19] CHANG 93 updates ENGEL 90 bound with the Kaplan-Manohar ambiguity in $z=m_u/m_d$ (see the Note on the Quark Masses in the Quark Particle Listings). It leaves the window $f_A=3\times10^5$–3×10^6 GeV open. The constraint from Big-Bang Nucleosynthesis is satisfied in this window as well.

[20] BERSHADY 91 searched for a line at wave length from 3100–8300 Å expected from 2γ decays of relic thermal axions in intergalactic light of three rich clusters of galaxies.

[21] KIM 91C argues that the bound from the mass density of the universe will change drastically for the supersymmetric models due to the entropy production of saxion (scalar component in the axionic chiral multiplet) decay. Note that it is an *upperbound* rather than a lowerbound.

[22] RAFFELT 91B argue that previous SN 1987A bounds must be relaxed due to corrections to nucleon bremsstrahlung processes.

[23] RESSELL 91 uses absence of any intracluster line emission to set limit.

[24] ENGEL 90 rule out $10^{-10} \lesssim g_{AN} \lesssim 10^{-3}$, which for a hadronic axion with EMC motivated axion-nucleon couplings corresponds to 2.5×10^{-3} eV $\lesssim m_{A^0} \lesssim 2.5\times10^4$ eV. The constraint is loose in the middle of the range, i.e. for $g_{AN}\sim10^{-6}$.

[25] RAFFELT 90D is a re-analysis of DEARBORN 86.

[26] The region $m_{A^0} \gtrsim 2$ eV is also allowed.

[27] ERICSON 89 considered various nuclear corrections to axion emission in a supernova core, and found a reduction of the previous limit (MAYLE 88) by a large factor.

[28] MAYLE 89 limit based on naive quark model couplings of axion to nucleons. Limit based on couplings motivated by EMC measurements is 2–4 times weaker. The limit from axion-electron coupling is weak: see HATSUDA 88B.

[29] RAFFELT 88B derives a limit for the energy generation rate by exotic processes in helium-burning stars $\epsilon < 100$ erg g^{-1} s^{-1}, which gives a firmer basis for the axion limits based on red giant cooling.

[30] RAFFELT 87 also gives a limit $g_{A\gamma} < 1\times10^{-10}$ GeV^{-1}.

[31] DEARBORN 86 also gives a limit $g_{A\gamma} < 1.4\times10^{-11}$ GeV^{-1}.

[32] RAFFELT 86 gives a limit $g_{A\gamma} < 1.1\times10^{-10}$ GeV^{-1} from red giants and $< 2.4\times10^{-9}$ GeV^{-1} from the sun.

[33] KAPLAN 85 says $m_{A^0} < 23$ eV is allowed for a special choice of model parameters.

[34] FUKUGITA 82 gives a limit $g_{A\gamma} < 2.3\times10^{-10}$ GeV^{-1}.

Search for Relic Invisible Axions

Limits are for $[G_{A\gamma\gamma}/m_{A^0}]^2\rho_A$ where $G_{A\gamma\gamma}$ denotes the axion two-photon coupling, $L_{\rm int} = -\frac{G_{A\gamma\gamma}}{4}\phi_A F_{\mu\nu}\tilde{F}^{\mu\nu} = G_{A\gamma\gamma}\phi_A \mathbf{E}\cdot\mathbf{B}$, and ρ_A is the axion energy density near the earth.

VALUE	CL%	DOCUMENT ID		TECN	COMMENT
• • • We do not use the following data for averages, fits, limits, etc. • • •					
		[1] BECK	13		m_{A^0} = 0.11 meV
$<3.5\times10^{-43}$		[2] HOSKINS	11	ADMX	m_{A^0} = 3.3–3.69 $\times10^{-6}$ eV
$<2.9\times10^{-43}$	90	[3] ASZTALOS	10	ADMX	m_{A^0} = 3.34–3.53 $\times10^{-6}$ eV
$<1.9\times10^{-43}$	97.7	[4] DUFFY	06	ADMX	m_{A^0} = 1.98–2.17 $\times10^{-6}$ eV
$<5.5\times10^{-43}$	90	[5] ASZTALOS	04	ADMX	m_{A^0} = 1.9–3.3 $\times10^{-6}$ eV
		[6] KIM	98	THEO	
$<2\times10^{-41}$		[7] HAGMANN	90	CNTR	m_{A^0} = (5.4–5.9)10^{-6} eV
$<1.3\times10^{-42}$	95	[8] WUENSCH	89	CNTR	m_{A^0} = (4.5–10.2)10^{-6} eV
$<2\times10^{-41}$	95	[8] WUENSCH	89	CNTR	m_{A^0} = (11.3–16.3)10^{-6} eV

[1] BECK 13 argues that dark-matter axions passing through Earth may generate a small observable signal in resonant S/N/S Josephson junctions. A measurement by HOFFMANN 04 [Physical Review **B70** 180503 (2004)] is interpreted in terms of subdominant dark matter axions with m_{A^0} = 0.11 meV.

[2] HOSKINS 11 is analogous to DUFFY 06. See Fig. 4 for the mass-dependent limit in terms of the local density.

[3] ASZTALOS 10 used the upgraded detector of ASZTALOS 04 to search for halo axions. See their Fig. 5 for the m_{A^0} dependence of the limit.

[4] DUFFY 06 used the upgraded detector of ASZTALOS 04, while assuming a smaller velocity dispersion than the isothermal model as in Eq. (8) of their paper. See Fig. 10 of their paper on the axion mass dependence of the limit.

[5] ASZTALOS 04 looked for a conversion of halo axions to microwave photons in magnetic field. At 90% CL, the KSVZ axion cannot have a local halo density more than 0.45 GeV/cm^3 in the quoted mass range. See Fig. 7 of their paper on the axion mass dependence of the limit.

[6] KIM 98 calculated the axion-to-photon couplings for various axion models and compared them to the HAGMANN 90 bounds. This analysis demonstrates a strong model dependence of $G_{A\gamma\gamma}$ and hence the bound from relic axion search.

[7] HAGMANN 90 experiment is based on the proposal of SIKIVIE 83.

[8] WUENSCH 89 looks for condensed axions near the earth that could be converted to photons in the presence of an intense electromagnetic field via the Primakoff effect, following the proposal of SIKIVIE 83. The theoretical prediction with $[G_{A\gamma\gamma}/m_{A^0}]^2 = 2\times10^{-14}$ MeV^{-4} (the three generation DFSZ model) and $\rho_A = 300$ MeV/cm^3 that makes up galactic halos gives $(G_{A\gamma\gamma}/m_{A^0})^2\,\rho_A = 4\times10^{-44}$. Note that our definition of $G_{A\gamma\gamma}$ is $(1/4\pi)$ smaller than that of WUENSCH 89.

Invisible A^0 (Axion) Limits from Photon Coupling

Limits are for the axion-two-photon coupling $G_{A\gamma\gamma}$ defined by $L = G_{A\gamma\gamma}\phi_A \mathbf{E}\cdot\mathbf{B}$. For scalars S^0 the limit is on the coupling constant in $L = G_{S\gamma\gamma}\phi_S(\mathbf{E}^2-\mathbf{B}^2)$.

VALUE (GeV^{-1})	CL%	DOCUMENT ID		TECN	COMMENT
• • • We do not use the following data for averages, fits, limits, etc. • • •					
$<2.1\times10^{-11}$	95	[1] ABRAMOWSKI	13A	IACT	m_{A^0} = 15–60 neV
$<2.15\times10^{-9}$	95	[2] ARMENGAUD	13	EDEL	$m_{A^0} < 200$ eV
$<4.5\times10^{-8}$	95	[3] BETZ	13	LSW	$m_{A^0} = 7.2\times10^{-6}$ eV
$<8\times10^{-11}$		[4] FRIEDLAND	13	ASTR	Red giants
$>2\times10^{-11}$		[5] MEYER	13	ASTR	$m_{A^0} < 1\times10^{-7}$ eV
		[6] CADAMURO	12	COSM	Axion-like particles
$<2.5\times10^{-13}$	95	[7] PAYEZ	12	ASTR	$m_{A^0} < 4.2\times10^{-14}$ eV
$<2.3\times10^{-10}$	95	[8] ARIK	11	CAST	m_{A^0} = 0.39–0.64 eV
$<6.5\times10^{-8}$	95	[9] EHRET	10	ALPS	$m_{A^0} < 0.7$ meV
$<2.4\times10^{-9}$	95	[10] AHMED	09A	CDMS	$m_{A^0} < 100$ eV
<1.2–2.8×10^{-10}	95	[11] ARIK	09	CAST	m_{A^0} = 0.02–0.39 eV
		[12] CHOU	09		Chameleons
$<7\times10^{-10}$		[13] GONDOLO	09	ASTR	m_{A^0} < few keV
$<1.3\times10^{-6}$	95	[14] AFANASEV	08		$m_{S^0} < 1$ meV
$<3.5\times10^{-7}$	99.7	[15] CHOU	08		$m_{A^0} < 0.5$ meV
$<1.1\times10^{-6}$	99.7	[16] FOUCHE	08		$m_{A^0} < 1$ meV
<5.6–13.4×10^{-10}	95	[17] INOUE	08		m_{A^0} = 0.84–1.00 eV
$<5\times10^{-7}$		[18] ZAVATTINI	08		$m_{A^0} < 1$ meV
$<8.8\times10^{-11}$	95	[19] ANDRIAMON...	07	CAST	$m_{A^0} < 0.02$ eV
$<1.25\times10^{-6}$	95	[20] ROBILLIARD	07		$m_{A^0} < 1$ meV
2–5×10^{-6}		[21] ZAVATTINI	06		m_{A^0} = 1–1.5 meV
$<1.1\times10^{-9}$	95	[22] INOUE	02		m_{A^0}= 0.05–0.27 eV
$<2.78\times10^{-9}$	95	[23] MORALES	02B		m_{A^0} <1 keV
$<1.7\times10^{-9}$	90	[24] BERNABEI	01B		m_{A^0} <100 eV
$<1.5\times10^{-4}$	90	[25] ASTIER	00B	NOMD	m_{A^0} <40 eV
		[26] MASSO	00	THEO	induced γ coupling
$<2.7\times10^{-9}$	95	[27] AVIGNONE	98	SLAX	$m_{A^0} < 1$ keV
$<6.0\times10^{-10}$	95	[28] MORIYAMA	98		$m_{A^0} < 0.03$ eV
$<3.6\times10^{-7}$	95	[29] CAMERON	93		$m_{A^0} < 10^{-3}$ eV, optical rotation
$<6.7\times10^{-7}$	95	[30] CAMERON	93		$m_{A^0} < 10^{-3}$ eV, photon regeneration
$<3.6\times10^{-9}$	99.7	[31] LAZARUS	92		$m_{A^0} < 0.03$ eV
$<7.7\times10^{-9}$	99.7	[31] LAZARUS	92		m_{A^0}= 0.03–0.11 eV
$<7.7\times10^{-7}$	99	[32] RUOSO	92		$m_{A^0} < 10^{-3}$ eV
$<2.5\times10^{-6}$		[33] SEMERTZIDIS	90		$m_{A^0} < 7\times10^{-4}$ eV

[1] ABRAMOWSKI 13A look for irregularities in the energy spectrum of the BL Lac object PKS 2155–304 measured by H.E.S.S. The limits depend on assumed magnetic field around the source. See their Fig. 7 for mass-dependent limits.

[2] ARMENGAUD 13 is analogous to AVIGNONE 98. See Fig. 6 for the limit.

[3] BETZ 13 performed a microwave-based light shining through the wall experiment. See their Fig. 13 for mass-dependent limits.

[4] FRIEDLAND 13 derived the limit by considering blue-loop suppression of the evolution of red giants with 7–12 solar masses.

[5] MEYER 13 attributed to axion-photon oscillations the observed excess of very high-energy γ-rays with respect to predictions based on extragalactic background light models. See their Fig.4 for mass-dependent lower limits for various magnetic field configurations.

[6] CADAMURO 12 derived cosmological limits on $G_{A\gamma\gamma}$ for axion-like particles. See their Fig. 1 for mass-dependent limits.

[7] PAYEZ 12 derive limits from polarization measurements of quasar light (see their Fig. 3). The limits depend on assumed magnetic field strength in galaxy clusters. The limits depend on assumed magnetic field and electron density in the local galaxy supercluster.

[8] ARIK 11 search for solar axions using ^{3}He buffer gas in CAST, continuing from the ^{4}He version of ARIK 09. See Fig. 2 for the exact mass-dependent limits.

[9] ALPS is a photon regeneration experiment. See their Fig. 4 for mass-dependent limits on scalar and pseudoscalar bosons.

[10] AHMED 09A is analogous to AVIGNONE 98.

[11] ARIK 09 is the ^{4}He filling version of the CAST axion helioscope in analogy to INOUE 02 and INOUE 08. See their Fig. 7 for mass-dependent limits.

[12] CHOU 09 use the GammeV apparatus in the afterglow mode to search for chameleons, (pseudo)scalar bosons with a mass depending on the environment. For pseudoscalars they exclude at 3σ the range 2.6×10^{-7} GeV$^{-1} < G_{A\gamma\gamma} < 4.2\times10^{-6}$ GeV^{-1} for vacuum m_{A^0} roughly below 6 meV for density scaling index exceeding 0.8.

[13] GONDOLO 09 use the all-flavor measured solar neutrino flux to constrain solar interior temperature and thus energy losses.

[14] LIPSS photon regeneration experiment, assuming scalar particle S^0. See Fig. 4 for mass-dependent limits.

Gauge & Higgs Boson Particle Listings

Axions (A^0) and Other Very Light Bosons

[15] CHOU 08 perform a variable-baseline photon regeneration experiment. See their Fig. 3 for mass-dependent limits. Excludes the PVLAS result of ZAVATTINI 06.
[16] FOUCHE 08 is an update of ROBILLIARD 07. See their Fig. 12 for mass-dependent limits.
[17] INOUE 08 is an extension of INOUE 02 to larger axion masses, using the Tokyo axion helioscope. See their Fig. 4 for mass-dependent limits.
[18] ZAVATTINI 08 is an upgrade of ZAVATTINI 06, see their Fig. 8 for mass-dependent limits. They now exclude the parameter range where ZAVATTINI 06 had seen a positive signature.
[19] ANDRIAMONJE 07 looked for Primakoff conversion of solar axions in 9T superconducting magnet into X-rays. Supersedes ZIOUTAS 05.
[20] ROBILLIARD 07 perform a photon regeneration experiment with a pulsed laser and pulsed magnetic field. See their Fig. 4 for mass-dependent limits. Excludes the PVLAS result of ZAVATTINI 06 with a CL exceeding 99.9%.
[21] ZAVATTINI 06 propagate a laser beam in a magnetic field and observe dichroism and birefringence effects that could be attributed to an axion-like particle. This result is now excluded by ROBILLIARD 07, ZAVATTINI 08, and CHOU 08.
[22] INOUE 02 looked for Primakoff conversion of solar axions in 4T superconducting magnet into X ray.
[23] MORALES 02B looked for the coherent conversion of solar axions to photons via the Primakoff effect in Germanium detector.
[24] BERNABEI 01B looked for Primakoff coherent conversion of solar axions into photons via Bragg scattering in NaI crystal in DAMA dark matter detector.
[25] ASTIER 00B looked for production of axions from the interaction of high-energy photons with the horn magnetic field and their subsequent re-conversion to photons via the interaction with the NOMAD dipole magnetic field.
[26] MASSO 00 studied limits on axion-proton coupling using the induced axion-photon coupling through the proton loop and CAMERON 93 bound on the axion-photon coupling using optical rotation. They obtained the bound $g_p^2/4\pi < 1.7 \times 10^{-9}$ for the coupling $g_p \overline{p} \gamma_5 p \phi_A$.
[27] AVIGNONE 98 result is based on the coherent conversion of solar axions to photons via the Primakoff effect in a single crystal germanium detector.
[28] Based on the conversion of solar axions to X-rays in a strong laboratory magnetic field.
[29] Experiment based on proposal by MAIANI 86.
[30] Experiment based on proposal by VANBIBBER 87.
[31] LAZARUS 92 experiment is based on proposal found in VANBIBBER 89.
[32] RUOSO 92 experiment is based on the proposal by VANBIBBER 87.
[33] SEMERTZIDIS 90 experiment is based on the proposal of MAIANI 86. The limit is obtained by taking the noise amplitude as the upper limit. Limits extend to $m_{A^0} = 4 \times 10^{-3}$ where $G_{A\gamma\gamma} < 1 \times 10^{-4}$ GeV^{-1}.

Limit on Invisible A^0 (Axion) Electron Coupling

The limit is for $G_{Aee} \partial_\mu \phi_A \overline{e} \gamma^\mu \gamma_5 e$ in GeV^{-1}, or equivalently, the dipole-dipole potential $\frac{G^2_{Aee}}{4\pi}$ $((\boldsymbol{\sigma}_1 \cdot \boldsymbol{\sigma}_2) - 3(\boldsymbol{\sigma}_1 \cdot \boldsymbol{n})(\boldsymbol{\sigma}_2 \cdot \boldsymbol{n}))/r^3$ where $\boldsymbol{n} = \boldsymbol{r}/r$.

VALUE (GeV^{-1})	CL%	DOCUMENT ID		TECN	COMMENT
• • • We do not use the following data for averages, fits, limits, etc. • • •					
$<5.3 \times 10^{-8}$	90	[1] ABE	13D	XMAS	Solar axions
$<1.05 \times 10^{-9}$	90	[2] ARMENGAUD	13	EDEL	$m_{A^0} = 12.5$ keV
$<2.53 \times 10^{-8}$	90	[3] ARMENGAUD	13	EDEL	Solar axion
		[4] BARTH	13	CAST	Solar axions
< 1.4–9.5×10^{-4}	90	[5] DERBIN	13	CNTR	$m_{A^0} = 0.1$–1 MeV
$<2.9 \times 10^{-5}$	68	[6] HECKEL	13		$m_{A^0} \leq 0.1$ μeV
$<4.2 \times 10^{-10}$	95	[7] VIAUX	13A	ASTR	Low-mass red giants
$<7 \times 10^{-10}$	95	[8] CORSICO	12	ASTR	White dwarf cooling
$<2.2 \times 10^{-7}$	90	[9] DERBIN	12	CNTR	Solar axions
< 0.02–1×10^{-7}	90	[10] AALSETH	11	CNTR	$m_{A^0} = 0.3$–8 keV
$<1.4 \times 10^{-9}$	90	[11] AHMED	09A	CDMS	$m_{A^0} = 2.5$ keV
$<3 \times 10^{-6}$		[12] DAVOUDIASL	09	ASTR	Earth cooling
$<5.3 \times 10^{-5}$	66	[13] NI	94		Induced magnetism
$<6.7 \times 10^{-5}$	66	[13] CHUI	93		Induced magnetism
$<3.6 \times 10^{-4}$	66	[14] PAN	92		Torsion pendulum
$<2.7 \times 10^{-5}$	95	[13] BOBRAKOV	91		Induced magnetism
$<1.9 \times 10^{-3}$	66	[15] WINELAND	91	NMR	
$<8.9 \times 10^{-4}$	66	[14] RITTER	90		Torsion pendulum
$<6.6 \times 10^{-5}$	95	[13] VOROBYOV	88		Induced magnetism

[1] ABE 13D is analogous to DERBIN 12, using the XMASS detector.
[2] ARMENGAUD 13 is similar to AALSETH 11. See their Fig. 10 for limits between 3 keV $< m_{A^0} <$ 100 keV.
[3] ARMENGAUD 13 is similar to DERBIN 12, and take account of axio-recombination and axio-deexcitation effects. See their Fig. 12 for mass-dependent limits.
[4] BARTH 13 search for solar axions produced by axion-electron coupling, and obtained the limit, $G_{Aee} \cdot G_{A\gamma\gamma} < 7.9 \times 10^{-20}$ GeV^{-2} at 95%CL.
[5] DERBIN 13 looked for 5.5 MeV solar axions produced in $pd \rightarrow {}^3\mathrm{He}\, A^0$ in a BGO detector through the axioelectric effect. See their Fig. 4 for mass-dependent limits.
[6] HECKEL 13 studied the influence of 2 or 4 stationary sources each containing 6.0×10^{24} polarized electrons, on a rotating torsion pendulum containing 9.8×10^{24} polarized electrons. See their Fig. 4 for mass-dependent limits.
[7] VIAUX 13A constrain axion emission using the observed brightness of the tip of the red-giant branch in the globular cluster M5.
[8] CORSICO 12 attributed the excessive cooling rate of the pulsating white dwarf R548 to emission of axions with $G_{Aee} \simeq 5 \times 10^{-10}$.
[9] DERBIN 12 look for solar axions with the axio-electric effect in a Si(Li) detector. The solar production is based on Compton and bremsstrahlung processes.
[10] AALSETH 11 is analogous to AHMED 09A. See their Fig. 4 for mass-dependent limits.
[11] AHMED 09A assume keV-mass pseudoscalars are the local dark matter and constrain the axio-electric effect in the CDMS detector. See their Fig. 5 for mass-dependent limits.
[12] DAVOUDIASL 09 use geophysical constraints on Earth cooling by axion emission.
[13] These experiments measured induced magnetization of a bulk material by the spin-dependent potential generated from other bulk material with aligned electron spins, where the magnetic field is shielded with superconductor.
[14] These experiments used a torsion pendulum to measure the potential between two bulk matter objects where the spins are polarized but without a net magnetic field in either of them.
[15] WINELAND 91 looked for an effect of bulk matter with aligned electron spins on atomic hyperfine splitting using nuclear magnetic resonance.

Invisible A^0 (Axion) Limits from Nucleon Coupling

Limits are for the axion mass in eV.

VALUE (eV)	CL%	DOCUMENT ID		TECN	COMMENT
• • • We do not use the following data for averages, fits, limits, etc. • • •					
$<2.50 \times 10^2$	95	[1] ALESSANDRIA	13	CNTR	Solar axion
$<1.55 \times 10^2$	90	[2] ARMENGAUD	13	EDEL	Solar axion
$<8.6 \times 10^3$	90	[3] BELLI	12	CNTR	Solar axion
$<1.41 \times 10^2$	90	[4] BELLINI	12B	BORX	Solar axion
$<1.45 \times 10^2$	95	[5] DERBIN	11	CNTR	Solar axion
		[6] BELLINI	08	CNTR	Solar axion
		[7] ADELBERGER	07		Test of Newton's law

[1] ALESSANDRIA 13 used the CUORE experiment to look for 14.4 keV solar axions produced from the M1 transition of thermally excited ^{57}Fe nuclei in the solar core, using the axio-electric effect. The limit assumes the hadronic axion model. See their Fig. 4 for the limit on product of axion couplings to electrons and nucleons.
[2] ARMENGAUD 13 is analogous to ALESSANDRIA 13. The limit assumes the hadronic axion model. See their Fig. 8 for the limit on product of axion couplings to electrons and nucleons.
[3] BELLI 12 looked for solar axions emitted by the M1 transition of ^{7}Li* (478 keV) after the electron capture of ^{7}Be, using the resonant excitation ^{7}Li in the LiF crystal. The mass bound assumes $m_u/m_d = 0.55$, $m_u/m_s = 0.029$, and the flavor-singlet axial vector matrix element $S = 0.4$.
[4] BELLINI 12B looked for 5.5 MeV solar axions produced in the $pd \rightarrow {}^3\mathrm{He}\, A^0$. The limit assumes the hadronic axion model. See their Figs. 4 and 5 for mass-dependent limits on products of axion couplings to photons, electrons, and nucleons.
[5] DERBIN 11 looked for solar axions emitted by the M1 transition of thermally excited ^{57}Fe nuclei in the Sun, using their possible resonant capture on ^{57}Fe in the laboratory. The mass bound assumes $m_u/m_d = 0.56$ and the flavor-singlet axial vector matrix element $S = 3F - D \simeq 0.5$.
[6] BELLINI 08 consider solar axions emitted in the M1 transition of ^{7}Li* (478 keV) and look for a peak at 478 keV in the energy spectra of the Counting Test Facility (CTF), a Borexino prototype. For $m_{A^0} < 450$ keV they find mass-dependent limits on products of axion couplings to photons, electrons, and nucleons.
[7] ADELBERGER 07 use precision tests of Newton's law to constrain a force contribution from the exchange of two pseudoscalars. See their Fig. 5 for limits on the pseudoscalar coupling to nucleons, relevant for m_{A^0} below about 1 meV.

Axion Limits from T-violating Medium-Range Forces

The limit is for the coupling $g = g_p\, g_s$ in a T-violating potential between nucleons or nucleon and electron of the form $V = \frac{g\hbar^2}{8\pi m_p} (\boldsymbol{\sigma} \cdot \hat{\boldsymbol{r}}) \left(\frac{1}{r^2} + \frac{1}{\lambda r}\right) e^{-r/\lambda}$, where g_p and g_s are dimensionless scalar and pseudoscalar coupling constants and $\lambda = \hbar/(m_A c)$ is the range of the force.

VALUE	DOCUMENT ID		TECN	COMMENT
• • • We do not use the following data for averages, fits, limits, etc. • • •				
	[1] BULATOWICZ	13	NMR	polarized ^{129}Xe and ^{131}Xe
	[2] CHU	13		polarized ^{3}He
	[3] RAFFELT	12		stellar energy loss
	[4] HOEDL	11		torsion pendulum
	[5] PETUKHOV	10		polarized ^{3}He
	[6] SEREBROV	10		ultracold neutrons
	[7] IGNATOVICH	09	RVUE	ultracold neutrons
	[8] SEREBROV	09	RVUE	ultracold neutrons
	[9] BAESSLER	07		ultracold neutrons
	[10] HECKEL	06		torsion pendulum
	[11] NI	99		paramagnetic Tb F_3
	[12] POSPELOV	98	THEO	neutron EDM
	[13] YOUDIN	96		
	[14] RITTER	93		torsion pendulum
	[15] VENEMA	92		nuclear spin-precession frequencies
	[16] WINELAND	91	NMR	

[1] BULATOWICZ 13 looked for NMR frequency shifts in polarized ^{129}Xe and ^{131}Xe when a zirconia rod is positioned near the NMR cell, and find $g < 1 \times 10^{-19}$–1×10^{-24} for $\lambda = 0.01$–1 cm. See their Fig. 4 for their limits.
[2] CHU 13 look for a shift of the spin precession frequency of polarized ^{3}He in the presence of an unpolarized mass, in analogy to YOUDIN 96. See Fig. 3 for limits on g in the approximate m_{A^0} range 0.02–2 meV.
[3] RAFFELT 12 show that the pseudoscalar couplings to electron and nucleon and the scalar coupling to nucleon are individually constrained by stellar energy-loss arguments and searches for anomalous monopole-monopole forces, together providing restrictive constraints on g. See their Figs. 2 and 3 for results.
[4] HOEDL 11 use a novel torsion pendulum to study the force by the polarized electrons of an external magnet. In their Fig. 3 they show restrictive limits on g in the approximate m_{A^0} range 0.03–10 meV.

[5] PETUKHOV 10 use spin relaxation of polarized ^{3}He and find $g < 3\times10^{-23}$ (cm/λ)^2 at 95% CL for the force range $\lambda = 10^{-4}$–1 cm.

[6] SEREBROV 10 use spin precession of ultracold neutrons close to bulk matter and find $g < 2\times10^{-21}$ (cm/λ)^2 at 95% CL for the force range $\lambda = 10^{-4}$–1 cm.

[7] IGNATOVICH 09 use data on depolarization of ultracold neutrons in material traps. They show λ-dependent limits in their Fig. 1.

[8] SEREBROV 09 uses data on depolarization of ultracold neutrons stored in material traps and finds $g < 2.96\times10^{-21}$ (cm/λ)^2 for the force range $\lambda = 10^{-3}$–1 cm and $g < 3.9\times10^{-22}$ (cm/λ)^2 for $\lambda = 10^{-4}$–10^{-3} cm, each time at 95% CL, significantly improving on BAESSLER 07.

[9] BAESSLER 07 use the observation of quantum states of ultracold neutrons in the Earth's gravitational field to constrain g for an interaction range 1 μm–a few mm. See their Fig. 3 for results.

[10] HECKEL 06 studied the influence of unpolarized bulk matter, including the laboratory's surroundings or the Sun, on a torsion pendulum containing about 9×10^{22} polarized electrons. See their Fig. 4 for limits on g as a function of interaction range.

[11] NI 99 searched for a T-violating medium-range force acting on paramagnetic Tb F_3 salt. See their Fig. 1 for the result.

[12] POSPELOV 98 studied the possible contribution of T-violating Medium-Range Force to the neutron electric dipole moment, which is possible when axion interactions violate CP. The size of the force among nucleons must be smaller than gravity by a factor of 2×10^{-10} (1 cm/λ_A), where $\lambda_A = \hbar/m_A c$.

[13] YOUDIN 96 compared the precession frequencies of atomic ^{199}Hg and Cs when a large mass is positioned near the cells, relative to an applied magnetic field. See Fig. 3 for their limits.

[14] RITTER 93 studied the influence of bulk mass with polarized electrons on an unpolarized torsion pendulum, providing limits in the interaction range from 1 to 100 cm.

[15] VENEMA 92 looked for an effect of Earth's gravity on nuclear spin-precession frequencies of ^{199}Hg and ^{201}Hg atoms.

[16] WINELAND 91 looked for an effect of bulk matter with aligned electron spins on atomic hyperfine resonances in stored ^{9}Be$^+$ ions using nuclear magnetic resonance.

Hidden Photons: Kinetic Mixing Parameter Limits

Hidden photons limits are listed for the first time, including only the most recent papers. Suggestions for previous important results are welcome. Limits are on the kinetic mixing parameter χ which is defined by the Lagrangian

$$L = -\tfrac{1}{4} F_{\mu\nu}F^{\mu\nu} - \tfrac{1}{4} F'_{\mu\nu}F'^{\mu\nu} - \tfrac{\chi}{2} F_{\mu\nu}F'^{\mu\nu} + \frac{m^2_{\gamma'}}{2} A'_\mu A'^\mu,$$

where A_μ and A'_μ are the photon and hidden-photon fields with field strengths $F_{\mu\nu}$ and $F'_{\mu\nu}$, respectively, and $m_{\gamma'}$ is the hidden-photon mass.

VALUE	CL%	DOCUMENT ID		TECN	COMMENT
• • • We do not use the following data for averages, fits, limits, etc. • • •					
$<3\times10^{-15}$		[1] AN	13B	ASTR	$m_{\gamma'} = 2$ keV
$<7\times10^{-14}$		[2] AN	13C	XE10	$m_{\gamma'} = 100$ eV
$<2.2\times10^{-13}$		[3] HORVAT	13	HPGE	$m_{\gamma'} = 230$ eV
$<8.06\times10^{-5}$	95	[4] INADA	13	LSW	$m_{\gamma'} = 0.04$ eV–26 keV
$<2\times10^{-10}$	95	[5] MIZUMOTO	13		$m_{\gamma'} = 1$ eV
$<1.7\times10^{-7}$		[6] PARKER	13	LSW	$m_{\gamma'} = 53\ \mu$eV
$<5.32\times10^{-15}$		[7] PARKER	13		$m_{\gamma'} = 53\ \mu$eV
$<1\times10^{-15}$		[8] REDONDO	13	ASTR	$m_{\gamma'} = 2$ keV

[1] AN 13B examined the stellar production of hidden photons, correcting an important error of the production rate of the longitudinal mode which now dominates. See their Fig. 2 for mass-dependent limits based on solar energy loss.

[2] AN 13C use the solar flux of hidden photons to set a limit on the atomic ionization rate in the XENON10 experiment. They find $\chi < 3\times10^{-12}$ ($m_{\gamma'}$/1 eV) for $m_{\gamma'} < 1$ eV. See their Fig. 2 for mass-dependent limits.

[3] HORVAT 13 look for hidden-photo-electric effect in HPGe detectors induced by solar hidden photons. See their Fig. 3 for mass-dependent limits.

[4] INADA 13 search for hidden photons using an intense X-ray beamline at SPring-8. See their Fig. 4 for mass-dependent limits.

[5] MIZUMOTO 13 look for solar hidden photons. See their Fig. 5 for mass-dependent limits.

[6] PARKER 13 look for hidden photons using a cryogenic resonant microwave cavity. See their Fig.5 for mass-dependent limits.

[7] PARKER 13 derived a limit for the hidden photon CDM with a randomly oriented hidden photon field.

[8] REDONDO 13 examined the solar emission of hidden photons including the enhancement factor for the longitudinal mode pointed out by AN 13B, and also updated stellar-energy loss arguments. See their Fig.3 for mass-dependent limits, including a review of the currently best limits from other arguments.

REFERENCES FOR Searches for Axions (A^0) and Other Very Light Bosons

ABE	13D	PL B724 46	K. Abe *et al.*	(XMASS Collab.)
ABRAMOWSKI	13A	PR D88 102003	A. Abramowski *et al.*	(H.E.S.S. Collab.)
ADLARSON	13	PL B726 187	P. Adlarson *et al.*	(WASA-at-COSY Collab.)
ALESSANDRIA	13	JCAP 1305 007	F. Alessandria *et al.*	(CUORE Collab.)
AN	13B	PL B725 190	H. An, M. Pospelov, J. Pradler	
AN	13C	PRL 111 041302	H. An, M. Pospelov, J. Pradler	
ARCHIDIACO...	13A	JCAP 1310 020	M. Archidiacono *et al.*	
ARMENGAUD	13	JCAP 1311 067	E. Armengaud *et al.*	(EDELWEISS-II Collab.)
BABUSCI	13B	PL B720 111	D. Babusci *et al.*	(KLOE-2 Collab.)
BARTH	13	JCAP 1305 010	K. Barth *et al.*	(CAST Collab.)
BECK	13	PRL 111 231801	C. Beck	
BETZ	13	PR D88 075014	M. Betz *et al.*	(CROWS Collab.)
BULATOWICZ	13	PRL 111 102001	M. Bulatowicz *et al.*	
CHU	13	PR D87 011105	P.-H. Chu *et al.*	(DUKE, IND, SJTU)
DERBIN	13	EPJ C73 2490	A. V. Derbin *et al.*	
FRIEDLAND	13	PRL 110 061101	A. Friedland, M. Giannotti, M. Wise	
HECKEL	13	PRL 111 151802	B. R. Heckel *et al.*	
HORVAT	13	PL B721 220	R. Horvat *et al.*	
INADA	13	PL B722 301	T. Inada *et al.*	
LATTANZI	13	PR D88 063528	M. Lattanzi *et al.*	
MEYER	13	PR D87 035027	M. Meyer, D. Horns, M. Raue	
MIZUMOTO	13	JCAP 1307 013	T. Mizumoto *et al.*	
PARKER	13	PR D88 112004	S. Parker *et al.*	
REDONDO	13	JCAP 1308 034	J. Redondo, G. Raffelt	
VIAUX	13A	PRL 111 231301	N. Viaux *et al.*	
ARCHILLI	12	PL B706 251	F. Archilli *et al.*	(KLOE-2 Collab.)
BELLI	12	PL B711 41	P. Belli *et al.*	(DAMA-KIEV)
BELLINI	12B	PR D85 092003	G. Bellini *et al.*	(Borexino Collab.)
CADAMURO	12	JCAP 1202 032	D. Cadamuro *et al.*	(MPIM)
CORSICO	12	JCAP 1212 010	A.H. Corsico *et al.*	(LAPL, RGSUL, WASH+)
DERBIN	12	JETPL 95 339 Translated from ZETFP 95 379.	A.V. Derbin *et al.*	(PNPI)
GANDO	12	PR C86 021601	A. Gando *et al.*	(KamLAND-Zen Collab.)
GNINENKO	12A	PR D85 055027	S.N. Gninenko	(INRM)
GNINENKO	12B	PL B713 244	S.N. Gninenko	(INRM)
PAYEZ	12	JCAP 1207 041	A. Payez *et al.*	(LIEG)
RAFFELT	12	PR D86 015001	G. Raffelt	(MPIM)
AALSETH	11	PRL 106 131301	C.E. Aalseth *et al.*	(CoGeNT Collab.)
ARIK	11	PRL 107 261302	M. Arik *et al.*	(CAST Collb.)
ARNOLD	11	PRL 107 062504	R. Arnold *et al.*	(NEMO-3 Collab.)
CADAMURO	11	JCAP 1102 003	D. Cadamuro *et al.*	(MPIM, AARHUS)
DERBIN	11	PAN 74 596 Translated from YAF 74 620.	A.V. Derbin *et al.*	(PNPI)
DERBIN	11A	PR D83 023505	A.V. Derbin *et al.*	(PNPI)
HOEDL	11	PRL 106 041801	S.A. Hoedl *et al.*	(WASH)
HOSKINS	11	PR D84 121302	J. Hoskins *et al.*	(ADMX Collab.)
ANDRIAMON...	10	JCAP 1003 032	S. Andriamonje *et al.*	(CAST Collab.)
ARGYRIADES	10	NP A847 168	J. Argyriades *et al.*	(NEMO-3 Collab.)
ASZTALOS	10	PRL 104 041301	S.J. Asztalos *et al.*	(ADMX Collab.)
EHRET	10	PL B689 149	K. Ehret *et al.*	(ALPS Collab.)
HANNESTAD	10	JCAP 1008 001	S. Hannestad *et al.*	
PETUKHOV	10	PRL 105 170401	A.K. Petukhov *et al.*	
SEREBROV	10	JETPL 91 6 Translated from ZETFP 91 8.	A. Serebrov *et al.*	
AHMED	09A	PRL 103 141802	Z. Ahmed *et al.*	(CDMS Collab.)
ANDRIAMON...	09	JCAP 0912 002	S. Andriamonje *et al.*	
ARGYRIADES	09	PR C80 032501	J. Argyriades *et al.*	(NEMO-3 Collab.)
ARIK	09	JCAP 0902 008	E. Arik *et al.*	(CAST Collab.)
CHOU	09	PRL 102 030402	A.S. Chou *et al.*	(GammeV Collab.)
DAVOUDIASL	09	PR D79 095024	H. Davoudiasl, P. Huber	
DERBIN	09A	PL B678 181	A.V. Derbin *et al.*	
GONDOLO	09	PR D79 107301	P. Gondolo, G. Raffelt	(UTAH, MPIM)
IGNATOVICH	09	EPJ C64 19	V.K. Ignatovich, Y.N. Pokotilovski	(JINR)
KEKEZ	09	PL B671 345	D. Kekez *et al.*	
SEREBROV	09	PL B680 423	A. Serebrov	(PNPI)
AFANASEV	08	PRL 101 120401	A. Afanasev *et al.*	
BELLINI	08	EPJ C54 61	G. Bellini *et al.*	(Borexino Collab.)
CHOU	08	PRL 100 080402	A.S. Chou *et al.*	(GammeV Collab.)
FOUCHE	08	PR D78 032013	M. Fouche *et al.*	
HANNESTAD	08	JCAP 0804 019	S. Hannestad *et al.*	
INOUE	08	PL B668 93	Y. Inoue *et al.*	
ZAVATTINI	08	PR D77 032006	E. Zavattini *et al.*	(PVLAS Collab.)
ADELBERGER	07	PRL 98 131104	E.G. Adelberger *et al.*	
ANDRIAMON...	07	JCAP 0704 010	S. Andriamonje *et al.*	(CAST Collab.)
BAESSLER	07	PR D75 075006	S. Baessler *et al.*	
CHANG	07	PR D75 052004	H.M. Chang *et al.*	(TEXONO Collab.)
HANNESTAD	07	JCAP 0708 015	S. Hannestad *et al.*	
JAIN	07	JP G34 129	P.L. Jain, G. Singh	
LESSA	07	PR D75 094001	A.P. Lessa, O.L.G. Peres	
MELCHIORRI	07A	PR D76 041303	A. Melchiorri, O. Mena, A. Slosar	
ROBILLIARD	07	PRL 99 190403	C. Robilliard *et al.*	
ARNOLD	06	NP A765 483	R. Arnold *et al.*	(NEMO-3 Collab.)
DUFFY	06	PR D74 012006	L.D. Duffy *et al.*	
HECKEL	06	PRL 97 021603	B.R. Heckel *et al.*	
ZAVATTINI	06	PRL 96 110406	E. Zavattini *et al.*	(PVLAS Collab.)
HANNESTAD	05A	JCAP 0507 002	S. Hannestad, A. Mirizzi, G. Raffelt	
ZIOUTAS	05	PRL 94 121301	K. Zioutas *et al.*	(CAST Collab.)
ADLER	04	PR D70 037102	S. Adler *et al.*	(BNL E787 Collab.)
ANISIMOVSK...	04	PRL 93 031801	V.V. Anisimovsky *et al.*	(BNL E949 Collab.)
ARNOLD	04	JETPL 80 377 Translated from ZETFP 80 429.	R. Arnold *et al.*	(NEMO3 Detector Collab.)
ASZTALOS	04	PR D69 011101	S.J. Asztalos *et al.*	
HOFFMANN	04	PR B70 180503	C. Hoffmann *et al.*	
ARNABOLDI	03	PL B557 167	C. Arnaboldi *et al.*	
CIVITARESE	03	NP A729 867	O. Civitarese, J. Suhonen	
DANEVICH	03	PR C68 035501	F.A. Danevich *et al.*	
ADLER	02C	PL B537 211	S. Adler *et al.*	(BNL E787 Collab.)
BADERT...	02	PL B542 29	A. Badertscher *et al.*	
BERNABEI	02D	PL B546 23	R. Bernabei *et al.*	(DAMA Collab.)
DERBIN	02	PAN 65 1302 Translated from YAF 65 1335.	A.V. Derbin *et al.*	
FUSHIMI	02	PL B531 190	K. Fushimi *et al.*	(ELEGANT V Collab.)
INOUE	02	PL B536 18	Y. Inoue *et al.*	
MORALES	02B	ASP 16 325	A. Morales *et al.*	(COSME Collab.)
ADLER	01	PR D63 032004	S. Adler *et al.*	(BNL E787 Collab.)
AMMAR	01B	PRL 87 271801	R. Ammar *et al.*	(CLEO Collab.)
ASHITKOV	01	JETPL 74 529 Translated from ZETFP 74 601.	V.D. Ashitkov *et al.*	
BERNABEI	01B	PL B515 6	R. Bernabei *et al.*	(DAMA Collab.)
DANEVICH	01	NP A694 375	F.A. Danevich *et al.*	
DEBOER	01	JP G27 L29	F.W.N. de Boer *et al.*	
STOICA	01	NP A694 269	S. Stoica, H.V. Klapdor-Kleingrothous	
ALESSAND...	00	PL B486 13	A. Alessandrello *et al.*	
ARNOLD	00	NP A678 341	R. Arnold *et al.*	
ASTIER	00B	PL B479 371	P. Astier *et al.*	(NOMAD Collab.)
DANEVICH	00	PR C62 045501	F.A. Danevich *et al.*	
MASSO	00	PR D61 011701	E. Masso	
ARNOLD	99	NP A658 299	R. Arnold *et al.*	(NEMO Collab.)
NI	99	PRL 82 2439	W.-T. Ni *et al.*	
SIMKOVIC	99	PR C60 055502	F. Simkovic *et al.*	
ALTEGOER	98	PL B428 197	J. Altegoer *et al.*	
ARNOLD	98	NP A636 209	R. Arnold *et al.*	(NEMO-2 Collab.)
AVIGNONE	98	PRL 81 5068	F.T. Avignone *et al.*	(Solar Axion Experiment)
DIAZ	98	NP B527 44	M.A. Diaz *et al.*	
FAESSLER	98B	JP G24 2139	A. Faessler, F. Simkovic	
KIM	98	PR D58 055006	J.E. Kim	
LUESCHER	98	PL B434 407	R. Luescher *et al.*	
MORIYAMA	98	PL B434 147	S. Moriyama *et al.*	
MOROI	98	PL B440 69	T. Moroi, H. Murayama	
POSPELOV	98	PR D58 097703	M. Pospelov	
ZUBER	98	PRPL 305 295	K. Zuber	
AHMAD	97	PRL 78 618	I. Ahmad *et al.*	(APEX Collab.)
BORISOV	97	JETP 83 868	A.V. Borisov, V.Y. Grishinia	(MOSU)
DEBOER	97C	JP G23 L85	F.W.N. de Boer *et al.*	
KACHELRIESS	97	PR D56 1313	M. Kachelriess, C. Wilke, G. Wunner	(BOCH)
KEIL	97	PR D56 2419	W. Keil *et al.*	
KITCHING	97	PRL 79 4079	P. Kitching *et al.*	(BNL E787 Collab.)
LEINBERGER	97	PL B394 16	U. Leinberger *et al.*	(ORANGE Collab.)
ADLER	96	PRL 76 1421	S. Adler *et al.*	(BNL E787 Collab.)
AMSLER	96B	ZPHY C70 219	C. Amsler *et al.*	(Crystal Barrel Collab.)

Gauge & Higgs Boson Particle Listings

Axions (A^0) and Other Very Light Bosons

GANZ 96 PL B389 4 R. Ganz *et al.* (GSI, HEID, FRAN, JAGL+)
GUENTHER 96 PR D54 3641 M. Gunther *et al.* (MPIH, SASSO)
KAMEL 96 PL B368 291 S. Kamel (SHAMS)
MITSUI 96 EPL 33 111 T. Mitsui *et al.* (TOKY)
YOUDIN 96 PRL 77 2170 A.N. Youdin *et al.* (AMHT, WASH)
ALTMANN 95 ZPHY C68 221 M. Altmann *et al.* (MUNT, LAPP, CPPM)
BASSOMPIE... 95 PL B355 584 G. Bassompierre *et al.* (LAPP, LCGT, LYON)
MAENO 95 PL B351 574 T. Maeno *et al.* (TOKY)
RAFFELT 95 PR D51 1495 G. Raffelt, A. Weiss (MPIM, MPIG)
SKALSEY 95 PR D51 6292 M. Skalsey, R.S. Conti (MICH)
TSUNODA 95 EPL 30 273 T. Tsunoda *et al.* (TOKY)
ADACHI 94 PR A49 3201 S. Adachi *et al.* (TMU)
ALTHERR 94 ASP 2 175 T. Altherr, E. Petitgirard, T. del Rio Gaztelurrutia
AMSLER 94B PL B333 271 C. Amsler *et al.* (Crystal Barrel Collab.)
ASAI 94 PL B323 90 S. Asai *et al.* (TOKY)
MEIJERDREES 94 PR D49 4937 M.R. Drees *et al.* (BRCO, OREG, TRIU)
NI 94 Physica B194 153 W.T. Ni *et al.* (NTHU)
VO 94 PR C49 1551 D.T. Vo *et al.* (ISU, LBL, LLNL, UCD)
ATIYA 93 PRL 70 2521 M.S. Atiya *et al.* (BNL E787 Collab.)
Also PRL 71 305 (erratum) M.S. Atiya *et al.* (BNL E787 Collab.)
ATIYA 93B PR D48 R1 M.S. Atiya *et al.* (BNL E787 Collab.)
BASSOMPIE... 93 EPL 22 239 G. Bassompierre *et al.* (LAPP, TORI, LYON)
BECK 93 PRL 70 2853 M. Beck *et al.* (MPIH, KIAE, SASSO)
CAMERON 93 PR D47 3707 R.E. Cameron *et al.* (ROCH, BNL, FNAL+)
CHANG 93 PL B316 51 S. Chang, K. Choi
CHUI 93 PRL 71 3247 T.C.P. Chui, W.T. Ni (NTHU)
MINOWA 93 PRL 71 4120 M. Minowa *et al.* (TOKY)
NG 93 PR D48 2941 K.W. Ng (AST)
RITTER 93 PRL 70 701 R.C. Ritter *et al.*
TANAKA 93 PR D48 5412 J. Tanaka, H. Ejiri (OSAK)
ALLIEGRO 92 PRL 68 278 C. Alliegro *et al.* (BNL, FNAL, PSI+)
ATIYA 92 PRL 69 733 M.S. Atiya *et al.* (BNL, LANL, PRIN+)
BERNATOW... 92 PRL 69 2341 T. Bernatowicz *et al.* (WUSL, TATA)
BLUEMLEIN 92 IJMP A7 3835 J. Blumlein *et al.* (BERL, BUDA, JINR+)
HALLIN 92 PR D45 3955 A.L. Hallin *et al.* (PRIN)
HENDERSON 92C PRL 69 1733 S.D. Henderson *et al.* (YALE, BNL)
HICKS 92 PL B276 423 K.H. Hicks, D.E. Alburger (OHIO, BNL)
LAZARUS 92 PRL 69 2333 D.M. Lazarus *et al.* (BNL, ROCH, FNAL)
MEIJERDREES 92 PRL 68 3845 R. Meijer Drees *et al.* (SINDRUM I Collab.)
PAN 92 MPL A7 1287 S.S. Pan, W.T. Ni, S.C. Chen (NTHU)
RUOSO 92 ZPHY C56 505 G. Ruoso *et al.* (ROCH, BNL, FNAL, TRST)
SKALSEY 92 PRL 68 456 M. Skalsey, J.J. Kolata (MICH, NDAM)
VENEMA 92 PRL 68 135 B.J. Venema *et al.*
WANG 92 MPL A7 1497 J. Wang (ILL)
WANG 92C PL B291 97 J. Wang (ILL)
WU 92 PRL 69 1729 X.Y. Wu *et al.* (BNL, YALE, CUNY)
AKOPYAN 91 PL B272 443 M.V. Akopyan *et al.* (INRM)
ASAI 91 PRL 66 2440 S. Asai *et al.* (ICEPP)
BERSHADY 91 PRL 66 1398 M.A. Bershady, M.T. Ressell, M.S. Turner (CHIC+)
BLUEMLEIN 91 ZPHY C51 341 J. Blumlein *et al.* (BERL, BUDA, JINR+)
BOBRAKOV 91 JETPL 53 294 V.F. Bobrakov *et al.* (PNPI)
Translated from ZETFP 53 283.
BROSS 91 PRL 67 2942 A.D. Bross *et al.* (FNAL, ILL)
KIM 91C PRL 67 3465 J.E. Kim (SEOUL)
RAFFELT 91 PRPL 198 1 G.G. Raffelt (MPIM)
RAFFELT 91B PRL 67 2605 G. Raffelt, D. Seckel (MPIM, BART)
RESSELL 91 PR D44 3001 M.T. Ressell (CHIC, FNAL)
TRZASKA 91 PL B269 54 W.H. Trzaska *et al.* (TAMU)
TSERTOS 91 PL B266 259 H. Tsertos *et al.* (ILLG, GSI)
WALKER 91 APJ 376 51 T.P. Walker *et al.* (HSCA, OSU, CHIC+)
WIDMANN 91 ZPHY A340 209 E. Widmann *et al.* (STUT, GSI, STUTM)
WINELAND 91 PRL 67 1735 D.J. Wineland *et al.* (NBSB)
ALBRECHT 90E PL B246 278 H. Albrecht *et al.* (ARGUS Collab.)
ANTREASYAN 90C PL B251 204 D. Antreasyan *et al.* (Crystal Ball Collab.)
ASANUMA 90 PL B237 588 T. Asanuma *et al.* (TOKY)
ATIYA 90 PRL 64 21 M.S. Atiya *et al.* (BNL E787 Collab.)
ATIYA 90B PRL 65 1188 M.S. Atiya *et al.* (BNL E787 Collab.)
BAUER 90 NIM B50 300 W. Bauer *et al.* (STUT, VILL, GSI)
BURROWS 90 PR D42 3297 A. Burrows, M.T. Ressell, M.S. Turner (ARIZ+)
DEBOER 90 JP G16 L1 F.W.N. de Boer, J. Lehmann, J. Steyaert (LOUV)
ENGEL 90 PRL 65 960 J. Engel, D. Seckel, A.C. Hayes (BART, LANL)
GNINENKO 90 PL B237 287 S.N. Gninenko *et al.* (INRM)
GUO 90 PR D41 2924 R. Guo *et al.* (NIU, LANL, FNAL, CASE+)
HAGMANN 90 PR D42 1297 C. Hagmann *et al.* (FLOR)
JUDGE 90 PRL 65 972 S.M. Judge *et al.* (ILLG, GSI)
RAFFELT 90D PR D41 1324 G.G. Raffelt (MPIM)
RITTER 90 PR D42 977 R.C. Ritter *et al.* (UVA)
SEMERTZIDIS 90 PRL 64 2988 Y.K. Semertzidis *et al.* (ROCH, BNL, FNAL+)
TSUCHIAKI 90 PL B236 81 M. Tsuchiaki *et al.* (ICEPP)
TURNER 90 PRPL 197 67 M.S. Turner (FNAL)
BARABASH 89 PL B223 273 A.S. Barabash *et al.* (ITEP, INRM)
BINI 89 PL B221 99 M. Bini *et al.* (FIRZ, CERN, AARH)
BURROWS 89 PR D39 1020 A. Burrows, M.S. Turner, R.P. Brinkmann (ARIZ+)
Also PRL 60 1797 M.S. Turner (FNAL, EFI)
DEBOER 89B PRL 62 2639 F.W.N. de Boer, R. van Dantzig (ANIK)
ERICSON 89 PL B219 507 T.E.O. Ericson, J.F. Mathiot (CERN, IPN)
FAISSNER 89 ZPHY C44 557 H. Faissner *et al.* (AACH3, BERL, PSI)
FOX 89 PR C39 288 J.D. Fox *et al.* (FSU)
MAYLE 89 PL B219 515 R. Mayle *et al.* (LLL, CERN, MINN, FNAL+)
Also PL B203 188 R. Mayle *et al.* (LLL, CERN, MINN, FNAL+)
MINOWA 89 PRL 62 1091 H. Minowa *et al.* (ICEPP)
ORITO 89 PRL 63 597 S. Orito *et al.* (ICEPP)
PERKINS 89 PRL 62 2638 D.H. Perkins (OXF)
TSERTOS 89 PR D40 1397 H. Tsertos *et al.* (GSI, ILLG)
VANBIBBER 89 PR D39 2089 K. van Bibber *et al.* (LLL, TAMU, LBL)
WUENSCH 89 PR D40 3153 W.U. Wuensch *et al.* (ROCH, BNL, FNAL)
Also PRL 59 839 S. de Panfilis *et al.* (ROCH, BNL, FNAL)
AVIGNONE 88 PR D37 618 F.T. Avignone *et al.* (PRIN, SCUC, ORNL+)
BJORKEN 88 PR D38 3375 J.D. Bjorken *et al.* (FNAL, SLAC, VPI)
BLINOV 88 SJNP 47 563 A.E. Blinov *et al.* (NOVO)
Translated from YAF 47 889.
BOLTON 88 PR D38 2077 R.D. Bolton *et al.* (LANL, STAN, CHIC+)
Also PRL 56 2461 R.D. Bolton *et al.* (LANL, STAN, CHIC+)
Also PRL 57 3241 D. Grosnick *et al.* (CHIC, LANL, STAN+)
CHANDA 88 PR D37 2714 R. Chanda, J.F. Nieves, P.B. Pal (UMD, UPR+)
CHOI 88 PR D37 3225 K. Choi *et al.* (JHU)
CONNELL 88 PRL 60 2242 S.H. Connell *et al.* (WITW)
DATAR 88 PR C37 250 V.M. Datar *et al.* (IPN)
DEBOER 88 PRL 61 1274 F.W.N. de Boer, R. van Dantzig (ANIK)
Also PRL 62 2644 (erratum) F.W.N. de Boer, R. van Dantzig (ANIK)
Also PR D62 2638 D.H. Perkins (OXF)
Also PRL 62 2639 F.W.N. de Boer, R. van Dantzig (ANIK)
DEBOER 88C JP G14 L131 F.W.N. de Boer *et al.* (LOUV)
DOEHNER 88 PR D38 2722 J. Dohner *et al.* (HEIDP, ANL, ILLG)
EL-NADI 88 PRL 61 1271 M. el Nadi, O.E. Badawy (CAIR)
ENGEL 88 PR C37 731 J. Engel, P. Vogel, M.R. Zirnbauer
FAISSNER 88 ZPHY C37 231 H. Faissner *et al.* (AACH3, BERL, SIN)
HATSUDA 88B PL B203 469 T. Hatsuda, M. Yoshimura (KEK)
LORENZ 88 PL B214 10 E. Lorenz *et al.* (MPIM, PSI)
MAYLE 88 PL B203 188 R. Mayle *et al.* (LLL, CERN, MINN, FNAL+)
PICCIOTTO 88 PR D37 1131 C.E. Picciotto *et al.* (TRIU, CNRC)
RAFFELT 88 PRL 60 1793 G. Raffelt, D. Seckel (UCB, LLL, UCSC)
RAFFELT 88B PR D37 549 G.G. Raffelt, D.S.P. Dearborn (UCB, LLL)
SAVAGE 88 PR D37 1134 M.J. Savage, B.W. Filippone, L.W. Mitchell (CIT)
TSERTOS 88 PL B207 273 A. Tsertos *et al.* (GSI, ILLG)
TSERTOS 88B ZPHY A331 103 A. Tsertos *et al.* (GSI, ILLG)
VANKLINKEN 88 PL B205 223 J. van Klinken *et al.* (GRON, GSI)
VANKLINKEN 88B PRL 60 2442 J. van Klinken (GRON)
VONWIMMER...88 PRL 60 2443 U. von Wimmersperg (BNL)
VOROBYOV 88 PL B208 146 P.V. Vorobiev, Y.I. Gitarts (NOVO)
DRUZHININ 87 ZPHY C37 1 V.P. Druzhinin *et al.* (NOVO)
FRIEMAN 87 PR D36 2201 J.A. Frieman, S. Dimopoulos, M.S. Turner (SLAC+)
GOLDMAN 87 PR D36 1543 T. Goldman *et al.* (LANL, CHIC, STAN+)
KORENCHE... 87 SJNP 46 192 S.M. Korenchenko *et al.* (JINR)
Translated from YAF 46 313.
MAIER 87 ZPHY A326 527 K. Maier *et al.* (STUT, GSI)
MILLS 87 PR D36 707 A.P. Mills, J. Levy (BELL)
RAFFELT 87 PR D36 2211 G.G. Raffelt, D.S.P. Dearborn (LLL, UCB)
RIORDAN 87 PRL 59 755 E.M. Riordan *et al.* (ROCH, CIT+)
TURNER 87 PRL 59 2489 M.S. Turner (FNAL, EFI)
VANBIBBER 87 PRL 59 759 K. van Bibber *et al.* (LLL, CIT, MIT+)
VONWIMMER...87 PRL 59 266 U. von Wimmersperg *et al.* (WITW)
BADIER 86 ZPHY C31 21 J. Badier *et al.* (NA3 Collab.)
BROWN 86 PRL 57 2101 C.N. Brown *et al.* (FNAL, WASH, KYOT+)
BRYMAN 86B PRL 57 2787 D.A. Bryman, E.T.H. Clifford (TRIU)
DAVIER 86 PL B180 295 M. Davier, J. Jeanjean, H. Nguyen Ngoc (LALO)
DEARBORN 86 PRL 56 26 D.S.P. Dearborn, D.N. Schramm, G. Steigman (LLL+)
EICHLER 86 PL B175 101 R.A. Eichler *et al.* (SINDRUM Collab.)
HALLIN 86 PRL 57 2105 A.L. Hallin *et al.* (PRIN)
JODIDIO 86 PR D34 1967 A. Jodidio *et al.* (LBL, NWES, TRIU)
Also PR D37 237 (erratum) A. Jodidio *et al.* (LBL, NWES, TRIU)
KETOV 86 JETPL 44 146 S.N. Ketov *et al.* (KIAE)
Translated from ZETFP 44 114.
KOCH 86 NC 96A 182 H.R. Koch, O.W.B. Schult (JULI)
KONAKA 86 PRL 57 659 A. Konaka *et al.* (KYOT, KEK)
MAIANI 86 PL B175 359 L. Maiani, R. Petronzio, E. Zavattini (CERN)
PECCEI 86 PL B172 435 R.D. Peccei, T.T. Wu, T. Yanagida (DESY)
RAFFELT 86 PR D33 897 G.G. Raffelt (MPIM)
RAFFELT 86B PL 166B 402 G.G. Raffelt (MPIM)
SAVAGE 86B PRL 57 178 M.J. Savage *et al.* (CIT)
AMALDI 85 PL 153B 444 U. Amaldi *et al.* (CERN)
ANANEV 85 SJNP 41 585 V.D. Ananev *et al.* (JINR)
Translated from YAF 41 912.
BALTRUSAIT... 85 PRL 55 1842 R.M. Baltrusaitis *et al.* (Mark III Collab.)
BERGSMA 85 PL 157B 458 F. Bergsma *et al.* (CHARM Collab.)
KAPLAN 85 NP B260 215 D.B. Kaplan (HARV)
IWAMOTO 84 PRL 53 1198 N. Iwamoto (UCSB, WUSL)
YAMAZAKI 84 PRL 52 1089 T. Yamazaki *et al.* (INUS, KEK)
ABBOTT 83 PL 120B 133 L.F. Abbott, P. Sikivie (BRAN, FLOR)
CARBONI 83 PL 123B 349 G. Carboni, W. Dahme (CERN, MUNI)
CAVAIGNAC 83 PL 121B 193 J.F. Cavaignac *et al.* (ISNG, LAPP)
DICUS 83 PR D28 1778 D.A. Dicus, V.L. Teplitz (TEXA, UMD)
DINE 83 PL 120B 137 M. Dine, W. Fischler (IAS, PENN)
ELLIS 83B NP B223 252 J. Ellis, K.A. Olive (CERN)
FAISSNER 83 PR D28 1198 H. Faissner *et al.* (AACH)
FAISSNER 83B PR D28 1787 H. Faissner *et al.* (AACH3)
FRANK 83B PR D28 1790 J.S. Frank *et al.* (LANL, YALE, LBL+)
HOFFMAN 83 PR D28 660 C.M. Hoffman *et al.* (LANL, ARZS)
PRESKILL 83 PL 120B 127 J. Preskill, M.B. Wise, F. Wilczek (HARV, UCSBT)
SIKIVIE 83 PRL 51 1415 P. Sikivie (FLOR)
Also PRL 52 695 (erratum) P. Sikivie (FLOR)
ALEKSEEV 82 JETP 55 591 E.A. Alekseeva *et al.* (KIAE)
Translated from ZETF 82 1007.
ALEKSEEV 82B JETPL 36 116 G.D. Alekseev *et al.* (MOSU, JINR)
Translated from ZETFP 36 94.
ASANO 82 PL 113B 195 Y. Asano *et al.* (KEK, TOKY, INUS, OSAK)
BARROSO 82 PL 116B 247 A. Barroso, G.C. Branco (LISB)
DATAR 82 PL 114B 63 V.M. Datar *et al.* (BHAB)
EDWARDS 82 PRL 48 903 C. Edwards *et al.* (Crystal Ball Collab.)
FETSCHER 82 JP G8 L147 W. Fetscher (ETH)
FUKUGITA 82 PRL 48 1522 M. Fukugita, S. Watamura, M. Yoshimura (KEK)
FUKUGITA 82B PR D26 1840 M. Fukugita, S. Watamura, M. Yoshimura (KEK)
LEHMANN 82 PL 115B 270 P. Lehmann *et al.* (SACL)
RAFFELT 82 PL 119B 323 G. Raffelt, L. Stodolsky (MPIM)
ZEHNDER 82 PL 110B 419 A. Zehnder, K. Gabathuler, J.L. Vuilleumier (ETH+)
ASANO 81B PL 107B 159 Y. Asano *et al.* (KEK, TOKY, INUS, OSAK)
BARROSO 81 PL 106B 91 A. Barroso, N.C. Mukhopadhyay (SIN)
FAISSNER 81 ZPHY C10 95 H. Faissner *et al.* (AACH3)
FAISSNER 81B PL 103B 234 H. Faissner *et al.* (AACH3)
KIM 81 PL 105B 55 B.R. Kim, C. Stamm (AACH3)
VUILLEUMIER 81 PL 101B 341 J.L. Vuilleumier *et al.* (CIT, MUNI)
ZEHNDER 81 PL 104B 494 A. Zehnder (ETH)
FAISSNER 80 PL 96B 201 H. Faissner *et al.* (AACH3)
JACQUES 80 PR D21 1206 P.F. Jacques *et al.* (RUTG, STEV, COLU)
SOUKAS 80 PRL 44 564 A. Soukas *et al.* (BNL, HARV, ORNL, PENN)
BECHIS 79 PRL 42 1511 D.J. Bechis *et al.* (UMD, COLU, AFRR)
CALAPRICE 79 PR D20 2708 F.P. Calaprice *et al.* (PRIN)
COTEUS 79 PRL 42 1438 P. Coteus *et al.* (COLU, ILL, BNL)
DISHAW 79 PL 85B 142 J.P. Dishaw *et al.* (SLAC, CIT)
ZHITNITSKII 79 SJNP 29 517 A.R. Zhitnitsky, Y.I. Skovpen (NOVO)
Translated from YAF 29 1001.
ALIBRAN 78 PL 74B 134 P. Alibran *et al.* (Gargamelle Collab.)
ASRATYAN 78B PL 79B 497 A.E. Asratyan *et al.* (ITEP, SERP)
BELLOTTI 78 PL 76B 223 E. Bellotti, E. Fiorini, L. Zanotti (MILA)
BOSETTI 78B PL 74B 143 P.C. Bosetti *et al.* (BEBC Collab.)
DICUS 78C PR D18 1829 D.A. Dicus *et al.* (TEXA, VPI, STAN)
DONNELLY 78 PR D18 1607 T.W. Donnelly *et al.* (STAN)
Also PRL 37 315 F. Reines, H.S. Gurr, H.W. Sobel (UCI)
Also PRL 33 179 H.S. Gurr, F. Reines, H.W. Sobel (UCI)
HANSL 78D PL 74B 139 T. Hansl *et al.* (CDHS Collab.)
MICELMAC... 78 LNC 21 441 G.V. Mitselmakher, B. Pontecorvo (JINR)
MIKAELIAN 78 PR D18 3605 K.O. Mikaelian (FNAL, NWES)
SATO 78 PTP 60 1942 K. Sato (KYOT)
VYSOTSKII 78 JETPL 27 502 M.I. Vysotsky *et al.* (ASCI)
Translated from ZETFP 27 533.
YANG 78 PRL 41 523 T.C. Yang (MASA)
PECCEI 77 PR D16 1791 R.D. Peccei, H.R. Quinn (STAN, SLAC)
Also PRL 38 1440 R.D. Peccei, H.R. Quinn (STAN, SLAC)
REINES 76 PRL 37 315 F. Reines, H.S. Gurr, H.W. Sobel (UCI)
GURR 74 PRL 33 179 H.S. Gurr, F. Reines, H.W. Sobel (UCI)
ANAND 53 PRSL A22 183 B.M. Anand

OTHER RELATED PAPERS

SREDNICKI 85 NP B260 689 M. Srednicki (UCSB)
BARDEEN 78 PL 74B 229 W.A. Bardeen, S.-H.H. Tye (FNAL)

LEPTONS

Notes in the Lepton Listings

LEPTONS

e $J = \frac{1}{2}$

e MASS (atomic mass units u)

The primary determination of an electron's mass comes from measuring the ratio of the mass to that of a nucleus, so that the result is obtained in u (atomic mass units). The conversion factor to MeV is more uncertain than the mass of the electron in u; indeed, the recent improvements in the mass determination are not evident when the result is given in MeV. In this datablock we give the result in u, and in the following datablock in MeV.

VALUE (10^{-6} u)	DOCUMENT ID		TECN	COMMENT
548.57990946±0.00000022	MOHR	12	RVUE	2010 CODATA value
• • • We do not use the following data for averages, fits, limits, etc. • • •				
548.57990943±0.00000023	MOHR	08	RVUE	2006 CODATA value
548.57990945±0.00000024	MOHR	05	RVUE	2002 CODATA value
548.5799092 ±0.0000004	[1] BEIER	02	CNTR	Penning trap
548.5799110 ±0.0000012	MOHR	99	RVUE	1998 CODATA value
548.5799111 ±0.0000012	[2] FARNHAM	95	CNTR	Penning trap
548.579903 ±0.000013	COHEN	87	RVUE	1986 CODATA value

[1] BEIER 02 compares Larmor frequency of the electron bound in a $^{12}C^{5+}$ ion with the cyclotron frequency of a single trapped $^{12}C^{5+}$ ion.
[2] FARNHAM 95 compares cyclotron frequency of trapped electrons with that of a single trapped $^{12}C^{6+}$ ion.

e MASS

2010 CODATA (MOHR 12) gives the conversion factor from u (atomic mass units, see the above datablock) to MeV as 931.494 061 (21). Earlier values use the then-current conversion factor. The conversion error dominates the uncertainty of the masses given below.

VALUE (MeV)	DOCUMENT ID		TECN	COMMENT
0.510998928±0.000000011	MOHR	12	RVUE	2010 CODATA value
• • • We do not use the following data for averages, fits, limits, etc. • • •				
0.510998910±0.000000013	MOHR	08	RVUE	2006 CODATA value
0.510998918±0.000000044	MOHR	05	RVUE	2002 CODATA value
0.510998901±0.000000020	[3,4] BEIER	02	CNTR	Penning trap
0.510998902±0.000000021	MOHR	99	RVUE	1998 CODATA value
0.510998903±0.000000020	[3,5] FARNHAM	95	CNTR	Penning trap
0.510998895±0.000000024	[3] COHEN	87	RVUE	1986 CODATA value
0.5110034 ±0.0000014	COHEN	73	RVUE	1973 CODATA value

[3] Converted to MeV using the 1998 CODATA value of the conversion constant, 931.494013 ± 0.000037 MeV/u.
[4] BEIER 02 compares Larmor frequency of the electron bound in a $^{12}C^{5+}$ ion with the cyclotron frequency of a single trapped $^{12}C^{5+}$ ion.
[5] FARNHAM 95 compares cyclotron frequency of trapped electrons with that of a single trapped $^{12}C^{6+}$ ion.

$(m_{e^+} - m_{e^-}) / m_{average}$

A test of CPT invariance.

VALUE	CL%	DOCUMENT ID		TECN	COMMENT
$<8\times10^{-9}$	90	[6] FEE	93	CNTR	Positronium spectroscopy
• • • We do not use the following data for averages, fits, limits, etc. • • •					
$<4\times10^{-8}$	90	CHU	84	CNTR	Positronium spectroscopy

[6] FEE 93 value is obtained under the assumption that the positronium Rydberg constant is exactly half the hydrogen one.

$|q_{e^+} + q_{e^-}|/e$

A test of CPT invariance. See also similar tests involving the proton.

VALUE	DOCUMENT ID		TECN	COMMENT
$<4\times10^{-8}$	[7] HUGHES	92	RVUE	
• • • We do not use the following data for averages, fits, limits, etc. • • •				
$<2\times10^{-18}$	[8] SCHAEFER	95	THEO	Vacuum polarization
$<1\times10^{-18}$	[9] MUELLER	92	THEO	Vacuum polarization

[7] HUGHES 92 uses recent measurements of Rydberg-energy and cyclotron-frequency ratios.
[8] SCHAEFER 95 removes model dependency of MUELLER 92.
[9] MUELLER 92 argues that an inequality of the charge magnitudes would, through higher-order vacuum polarization, contribute to the net charge of atoms.

e MAGNETIC MOMENT ANOMALY

$\mu_e/\mu_B - 1 = (g-2)/2$

VALUE (units 10^{-6})	DOCUMENT ID		TECN	CHG	COMMENT
1159.65218076±0.00000027	MOHR	12	RVUE		2010 CODATA value
• • • We do not use the following data for averages, fits, limits, etc. • • •					
1159.65218073±0.00000028	HANNEKE	08	MRS		Single electron
1159.65218111±0.00000074	[10] MOHR	08	RVUE		2006 CODATA value
1159.65218085±0.00000076	[11] ODOM	06	MRS	−	Single electron
1159.65218591 ±0.0000038	MOHR	05	RVUE		2002 CODATA value
1159.65218691 ±0.0000041	MOHR	99	RVUE		1998 CODATA value
1159.652193 ±0.000010	COHEN	87	RVUE		1986 CODATA value
1159.65221884 ±0.0000043	VANDYCK	87	MRS	−	Single electron
1159.65221879 ±0.0000043	VANDYCK	87	MRS	+	Single positron

[10] MOHR 08 average is dominated by ODOM 06.
[11] Superseded by HANNEKE 08 per private communication with Gerald Gabrielse.

$(g_{e^+} - g_{e^-}) / g_{average}$

A test of CPT invariance.

VALUE (units 10^{-12})	CL%	DOCUMENT ID		TECN	COMMENT
− 0.5± 2.1		[12] VANDYCK	87	MRS	Penning trap
• • • We do not use the following data for averages, fits, limits, etc. • • •					
< 12	95	[13] VASSERMAN	87	CNTR	Assumes $m_{e^+} = m_{e^-}$
22 ±64		SCHWINBERG	81	MRS	Penning trap

[12] VANDYCK 87 measured $(g_-/g_+)-1$ and we converted it.
[13] VASSERMAN 87 measured $(g_+ - g_-)/(g-2)$. We multiplied by $(g-2)/g = 1.2\times10^{-3}$.

e ELECTRIC DIPOLE MOMENT (d)

A nonzero value is forbidden by both T invariance and P invariance.

VALUE (10^{-28} ecm)	CL%	DOCUMENT ID		TECN	COMMENT
< 10.5	90	[14] HUDSON	11	NMR	YbF molecules
• • • We do not use the following data for averages, fits, limits, etc. • • •					
< 6050	90	[15] ECKEL	12	CNTR	$Eu_{0.5}Ba_{0.5}TiO_3$ molecules
6.9± 7.4		REGAN	02	MRS	^{205}Tl beams
18 ± 12 ± 10		[16] COMMINS	94	MRS	^{205}Tl beams
− 27 ± 83		[16] ABDULLAH	90	MRS	^{205}Tl beams
− 1400 ± 2400		CHO	89	NMR	Tl F molecules
− 150 ± 550 ±150		MURTHY	89		Cesium, no B field
− 5000 ±11000		LAMOREAUX	87	NMR	^{199}Hg
19000 ±34000	90	SANDARS	75	MRS	Thallium
7000 ±22000	90	PLAYER	70	MRS	Xenon
< 30000	90	WEISSKOPF	68	MRS	Cesium

[14] HUDSON 11 gives a measurement corresponding to this limit as $(-2.4\pm5.7\pm1.5)\times10^{-28}$ ecm.
[15] ECKEL 12 gives a measurement corresponding to this limit as $(-1.07\pm3.06\pm1.74)\times10^{-25}$ ecm.
[16] ABDULLAH 90, COMMINS 94, and REGAN 02 use the relativistic enhancement of a valence electron's electric dipole moment in a high-Z atom.

e^- MEAN LIFE / BRANCHING FRACTION

A test of charge conservation. See the "Note on Testing Charge Conservation and the Pauli Exclusion Principle" following this section in our 1992 edition (Physical Review **D45** S1 (1992), p. VI.10).

Most of these experiments are one of three kinds: Attempts to observe (a) the 255.5 keV gamma ray produced in $e^- \to \nu_e\gamma$, (b) the (K) shell x ray produced when an electron decays without additional energy deposit, e.g., $e^- \to \nu_e\overline{\nu}_e\nu_e$ ("disappearance" experiments), and (c) nuclear de-excitation gamma rays after the electron disappears from an atomic shell and the nucleus is left in an excited state. The last can include both weak boson and photon mediating processes. We use the best $e^- \to \nu_e\gamma$ limit for the Summary Tables.

Note that we use the mean life rather than the half life, which is often reported.

$e \to \nu_e\gamma$ and astrophysical limits

VALUE (yr)	CL%	DOCUMENT ID		TECN	COMMENT
>4.6 $\times10^{26}$	90	BACK	02	BORX	$e^- \to \nu\gamma$
• • • We do not use the following data for averages, fits, limits, etc. • • •					
>1.22 $\times10^{26}$	68	[17] KLAPDOR-K...	07	CNTR	$e^- \to \nu\gamma$
>3.4 $\times10^{26}$	68	BELLI	00B	DAMA	$e^- \to \nu\gamma$, liquid Xe
>3.7 $\times10^{25}$	68	AHARONOV	95B	CNTR	$e^- \to \nu\gamma$
>2.35 $\times10^{25}$	68	BALYSH	93	CNTR	$e^- \to \nu\gamma$, ^{76}Ge detector
>1.5 $\times10^{25}$	68	AVIGNONE	86	CNTR	$e^- \to \nu\gamma$
>1 $\times10^{39}$		[18] ORITO	85	ASTR	Astrophysical argument
>3 $\times10^{23}$	68	BELLOTTI	83B	CNTR	$e^- \to \nu\gamma$

[17] The authors of A. Derbin et al, arXiv:0704.2047v1 argue that this limit is overestimated by at least a factor of 5.
[18] ORITO 85 assumes that electromagnetic forces extend out to large enough distances and that the age of our galaxy is 10^{10} years.

Disappearance and nuclear-de-excitation experiments

VALUE (yr)	CL%	DOCUMENT ID		TECN	COMMENT
$>6.4\times10^{24}$	68	[19] BELLI	99B	DAMA	De-excitation of ^{129}Xe
• • • We do not use the following data for averages, fits, limits, etc. • • •					
$>4.2\times10^{24}$	68	BELLI	99	DAMA	Iodine L-shell disappearance
$>2.4\times10^{23}$	90	[20] BELLI	99D	DAMA	De-excitation of ^{127}I (in NaI)
$>4.3\times10^{23}$	68	AHARONOV	95B	CNTR	Ge K-shell disappearance
$>2.7\times10^{23}$	68	REUSSER	91	CNTR	Ge K-shell disappearance
$>2\ \times10^{22}$	68	BELLOTTI	83B	CNTR	Ge K-shell disappearance

[19] BELLI 99B limit on charge nonconserving e^- capture involving excitation of the 236.1 keV nuclear state of ^{129}Xe; the 90% CL limit is 3.7×10^{24} yr. Less stringent limits for other states are also given.

[20] BELLI 99D limit on charge nonconserving e^- capture involving excitation of the 57.6 keV nuclear state of ^{127}I. Less stringent limits for the other states and for the state of ^{23}Na are also given.

LIMITS ON LEPTON-FLAVOR VIOLATION IN PRODUCTION

Forbidden by lepton family number conservation.

This section was added for the 2008 edition of this *Review* and is not complete. For a list of further measurements see references in the papers listed below.

$\sigma(e^+e^-\to e^\pm\tau^\mp)\,/\,\sigma(e^+e^-\to\mu^+\mu^-)$

VALUE	CL%	DOCUMENT ID		TECN	COMMENT
$<8.9\times10^{-6}$	95	AUBERT	07P	BABR	e^+e^- at $E_{cm}=10.58$ GeV
• • • We do not use the following data for averages, fits, limits, etc. • • •					
$<1.8\times10^{-3}$	95	GOMEZ-CAD...	91	MRK2	e^+e^- at $E_{cm}=29$ GeV

$\sigma(e^+e^-\to\mu^\pm\tau^\mp)\,/\,\sigma(e^+e^-\to\mu^+\mu^-)$

VALUE	CL%	DOCUMENT ID		TECN	COMMENT
$<4.0\times10^{-6}$	95	AUBERT	07P	BABR	e^+e^- at $E_{cm}=10.58$ GeV
• • • We do not use the following data for averages, fits, limits, etc. • • •					
$<6.1\times10^{-3}$	95	GOMEZ-CAD...	91	MRK2	e^+e^- at $E_{cm}=29$ GeV

e REFERENCES

ECKEL	12	PRL 109 193003	S. Eckel, A.O. Sushkov, S.K. Lamoreaux	(YALE)
MOHR	12	RMP 84 1527	P.J. Mohr, B.N. Taylor, D.B. Newell	(NIST)
HUDSON	11	NAT 473 493	J.J. Hadson *et al.*	(LOIC)
HANNEKE	08	PRL 100 120801	D. Hanneke, S. Fogwell, G. Gabrielse	(HARV)
MOHR	08	RMP 80 633	P.J. Mohr, B.N. Taylor, D.B. Newell	(NIST)
AUBERT	07P	PR D75 031103	B. Aubert *et al.*	(BABAR Collab.)
KLAPDOR-K...	07	PL B644 109	H.V. Klapdor-Kleingrothaus, I.V. Krivosheina, I.V. Titkova	
ODOM	06	PRL 97 030801	B. Odom *et al.*	(HARV)
MOHR	05	RMP 77 1	P.J. Mohr, B.N. Taylor	(NIST)
BACK	02	PL B525 29	H.O. Back *et al.*	(BOREXINO/SASSO Collab.)
BEIER	02	PRL 88 011603	T. Beier *et al.*	
REGAN	02	PRL 88 071805	B.C. Regan *et al.*	
BELLI	00B	PR D61 117301	P. Belli *et al.*	(DAMA Collab.)
BELLI	99	PL B460 236	P. Belli *et al.*	(DAMA Collab.)
BELLI	99B	PL B465 315	P. Belli *et al.*	(DAMA Collab.)
BELLI	99D	PR C60 065501	P. Belli *et al.*	(DAMA Collab.)
MOHR	99	JPCRD 28 1713	P.J. Mohr, B.N. Taylor	(NIST)
Also		RMP 72 351	P.J. Mohr, B.N. Taylor	(NIST)
AHARONOV	95B	PR D52 3785	Y. Aharonov *et al.*	(SCUC, PNL, ZARA+)
Also		PL B353 168	Y. Aharonov *et al.*	(SCUC, PNL, ZARA+)
FARNHAM	95	PRL 75 3598	D.L. Farnham, R.S. van Dyck, P.B. Schwinberg	(WASH)
SCHAEFER	95	PR A51 838	A. Schaefer, J. Reinhardt	(FRAN)
COMMINS	94	PR A50 2960	E.D. Commins *et al.*	
BALYSH	93	PL B298 278	A. Balysh *et al.*	(KIAE, MPIH, SASSO)
FEE	93	PR A48 192	M.S. Fee *et al.*	
HUGHES	92	PRL 69 578	R.J. Hughes, B.I. Deutch	(LANL, AARH)
MUELLER	92	PRL 69 3432	B. Muller, M.H. Thoma	(DUKE)
PDG	92	PR D45 S1	K. Hikasa *et al.*	(KEK, LBL, BOST+)
GOMEZ-CAD...	91	PRL 66 1007	J.J. Gomez-Cadenas *et al.*	(SLAC MARK-2 Collab.)
REUSSER	91	PL B255 143	D. Reusser *et al.*	(NEUC, CIT, PSI)
ABDULLAH	90	PRL 65 2347	K. Abdullah *et al.*	(LBL, UCB)
CHO	89	PRL 63 2559	D. Cho, K. Sangster, E.A. Hinds	(YALE)
MURTHY	89	PRL 63 965	S.A. Murthy *et al.*	(AMHT)
COHEN	87	RMP 59 1121	E.R. Cohen, B.N. Taylor	(RISC, NBS)
LAMOREAUX	87	PRL 59 2275	S.K. Lamoreaux *et al.*	(WASH)
VANDYCK	87	PRL 59 26	R.S. van Dyck, P.B. Schwinberg, H.G. Dehmelt	(WASH)
VASSERMAN	87	PL B198 302	I.B. Vasserman *et al.*	(NOVO)
Also		PL B187 172	I.B. Vasserman *et al.*	(NOVO)
AVIGNONE	86	PR D34 97	F.T. Avignone *et al.*	(PNL, SCUC)
ORITO	85	PRL 54 2457	S. Orito, M. Yoshimura	(TOKY, KEK)
CHU	84	PRL 52 1689	S. Chu, A.P. Mills, J.L. Hall	(BELL, NBS, COLO)
BELLOTTI	83B	PL 124B 435	E. Bellotti *et al.*	(MILA)
SCHWINBERG	81	PRL 47 1679	P.B. Schwinberg, R.S. van Dyck, H.G. Dehmelt	(WASH)
SANDARS	75	PR A11 473	P.G.H. Sandars, D.M. Sternheimer	(OXF, BNL)
COHEN	73	JPCRD 2 664	E.R. Cohen, B.N. Taylor	(RISC, NBS)
PLAYER	70	JP B3 1620	M.A. Player, P.G.H. Sandars	(OXF)
WEISSKOPF	68	PRL 21 1645	M.C. Weisskopf *et al.*	(BRAN)

μ

$J = \frac{1}{2}$

μ MASS (atomic mass units u)

The muon's mass is obtained from the muon-electron mass ratio as determined from the measurement of Zeeman transition frequencies in muonium (μ^+e^- atom). Since the electron's mass is most accurately known in u, the muon's mass is also most accurately known in u. The conversion factor to MeV has approximately the same relative uncertainty as the mass of the muon in u. In this datablock we give the result in u, and in the following datablock in MeV.

VALUE (u)		DOCUMENT ID		TECN	COMMENT
0.1134289267±0.0000000029		MOHR	12	RVUE	2010 CODATA value
• • • We do not use the following data for averages, fits, limits, etc. • • •					
0.1134289256±0.0000000029		MOHR	08	RVUE	2006 CODATA value
0.1134289264±0.0000000030		MOHR	05	RVUE	2002 CODATA value
0.1134289168±0.0000000034	[1]	MOHR	99	RVUE	1998 CODATA value
0.113428913 ±0.000000017	[2]	COHEN	87	RVUE	1986 CODATA value

[1] MOHR 99 make use of other 1998 CODATA entries below.
[2] COHEN 87 make use of other 1986 CODATA entries below.

μ MASS

2010 CODATA (MOHR 12) gives the conversion factor from u (atomic mass units, see the above datablock) to MeV as 931.494 061 (21). Earlier values use the then-current conversion factor. The conversion error contributes significantly to the uncertainty of the masses given below.

VALUE (MeV)		DOCUMENT ID		TECN	CHG	COMMENT
105.6583715±0.0000035		MOHR	12	RVUE		2010 CODATA value
• • • We do not use the following data for averages, fits, limits, etc. • • •						
105.6583668±0.0000038		MOHR	08	RVUE		2006 CODATA value
105.6583692±0.0000094		MOHR	05	RVUE		2002 CODATA value
105.6583568±0.0000052		MOHR	99	RVUE		1998 CODATA value
105.658353 ±0.000016	[3]	COHEN	87	RVUE		1986 CODATA value
105.658386 ±0.000044	[4]	MARIAM	82	CNTR	+	
105.65836 ±0.00026	[5]	CROWE	72	CNTR		
105.65865 ±0.00044	[6]	CRANE	71	CNTR		

[3] Converted to MeV using the 1998 CODATA value of the conversion constant, 931.494013 ± 0.000037 MeV/u.
[4] MARIAM 82 give $m_\mu/m_e = 206.768259(62)$.
[5] CROWE 72 give $m_\mu/m_e = 206.7682(5)$.
[6] CRANE 71 give $m_\mu/m_e = 206.76878(85)$.

μ MEAN LIFE τ

Measurements with an error $> 0.001\times10^{-6}$ s have been omitted.

VALUE (10^{-6} s)		DOCUMENT ID		TECN	CHG	COMMENT
2.1969811±0.0000022 OUR AVERAGE						
2.1969803±0.0000021±0.0000007	[7]	TISHCHENKO	13	CNTR	+	Surface μ^+ at PSI
2.197083 ±0.000032 ±0.000015		BARCZYK	08	CNTR	+	Muons from π^+ decay at rest
2.197013 ±0.000021 ±0.000011		CHITWOOD	07	CNTR	+	Surface μ^+ at PSI
2.197078 ±0.000073		BARDIN	84	CNTR	+	
2.197025 ±0.000155		BARDIN	84	CNTR	−	
2.19695 ±0.00006		GIOVANETTI	84	CNTR	+	
2.19711 ±0.00008		BALANDIN	74	CNTR	+	
2.1973 ±0.0003		DUCLOS	73	CNTR	+	
• • • We do not use the following data for averages, fits, limits, etc. • • •						
2.1969803±0.0000022		WEBBER	11	CNTR	+	Surface μ^+ at PSI

[7] TISHCHENKO 13 uses 1.6×10^{12} μ^+ events and supersedes WEBBER 11.

$\tau_{\mu^+}/\tau_{\mu^-}$ MEAN LIFE RATIO

A test of CPT invariance.

VALUE	DOCUMENT ID		TECN	COMMENT
1.000024±0.000078	BARDIN	84	CNTR	
• • • We do not use the following data for averages, fits, limits, etc. • • •				
1.0008 ±0.0010	BAILEY	79	CNTR	Storage ring
1.000 ±0.001	MEYER	63	CNTR	Mean life μ^+/μ^-

$(\tau_{\mu^+}-\tau_{\mu^-})\,/\,\tau_{\text{average}}$

A test of CPT invariance. Calculated from the mean-life ratio, above.

VALUE	DOCUMENT ID
$(2\pm8)\times10^{-5}$ OUR EVALUATION	

μ/p MAGNETIC MOMENT RATIO

This ratio is used to obtain a precise value of the muon mass and to reduce experimental muon Larmor frequency measurements to the muon magnetic moment anomaly. Measurements with an error > 0.00001 have been omitted. By convention, the minus sign on this ratio is omitted. CODATA values were fitted using their selection of data, plus other data from multiparameter fits.

VALUE		DOCUMENT ID		TECN	CHG	COMMENT
3.183345137 ± 0.000000085		MOHR	08	RVUE		2006 CODATA value
• • • We do not use the following data for averages, fits, limits, etc. • • •						
3.183345118	±0.000000089	MOHR	05	RVUE		2002 CODATA value
3.18334513	±0.00000039	LIU	99	CNTR	+	HFS in muonium
3.18334539	±0.00000010	MOHR	99	RVUE		1998 CODATA value
3.18334547	±0.00000047	COHEN	87	RVUE		1986 CODATA value
3.1833441	±0.0000017	KLEMPT	82	CNTR	+	Precession strob
3.1833461	±0.0000011	MARIAM	82	CNTR	+	HFS splitting
3.1833448	±0.0000029	CAMANI	78	CNTR	+	See KLEMPT 82
3.1833403	±0.0000044	CASPERSON	77	CNTR	+	HFS splitting
3.1833402	±0.0000072	COHEN	73	RVUE		1973 CODATA value
3.1833467	±0.0000082	CROWE	72	CNTR	+	Precession phase

THE MUON ANOMALOUS MAGNETIC MOMENT

Updated August 2013 by A. Hoecker (CERN), and W.J. Marciano (BNL).

The Dirac equation predicts a muon magnetic moment, $\vec{M} = g_\mu \frac{e}{2m_\mu}\vec{S}$, with gyromagnetic ratio $g_\mu = 2$. Quantum loop effects lead to a small calculable deviation from $g_\mu = 2$, parameterized by the anomalous magnetic moment

$$a_\mu \equiv \frac{g_\mu - 2}{2} \ . \tag{1}$$

That quantity can be accurately measured and, within the Standard Model (SM) framework, precisely predicted. Hence, comparison of experiment and theory tests the SM at its quantum loop level. A deviation in $a_\mu^{\rm exp}$ from the SM expectation would signal effects of new physics, with current sensitivity reaching up to mass scales of $\mathcal{O}$(TeV) [1,2]. For recent and very thorough muon $g-2$ reviews, see Refs. [3–5].

The E821 experiment at Brookhaven National Lab (BNL) studied the precession of μ^+ and μ^- in a constant external magnetic field as they circulated in a confining storage ring. It found [7] [1]

$$\begin{aligned} a_{\mu^+}^{\rm exp} &= 11\,659\,204(6)(5) \times 10^{-10}\,, \\ a_{\mu^-}^{\rm exp} &= 11\,659\,215(8)(3) \times 10^{-10}\,, \end{aligned} \tag{2}$$

where the first errors are statistical and the second systematic. Assuming CPT invariance and taking into account correlations between systematic uncertainties, one finds for their average [6,7]

$$a_\mu^{\rm exp} = 11\,659\,209.1(5.4)(3.3) \times 10^{-10} \ . \tag{3}$$

These results represent about a factor of 14 improvement over the classic CERN experiments of the 1970's [8]. Improvement of the measurement in Eq. (3) by a factor of four by moving the E821 storage ring to Fermilab, and utilizing a cleaner and more intense muon beam is in progress. An even more ambitious precision goal is set by an experiment based on a beam of ultra-cold muons proposed at the Japan Proton Accelerator Research Complex.

[1] The original results reported by the experiment have been updated in Eq. (2) and Eq. (3) to the newest value for the absolute muon-to-proton magnetic ratio $\lambda = 3.183\,345\,107(84)$ [6]. The change induced in $a_\mu^{\rm exp}$ with respect to the value of $\lambda = 3.183\,345\,39(10)$ used in Ref. 7 amounts to $+1.12 \times 10^{-10}$.

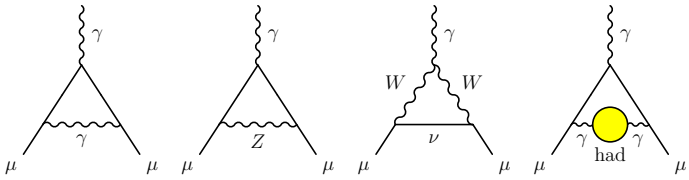

Figure 1: Representative diagrams contributing to $a_\mu^{\rm SM}$. From left to right: first order QED (Schwinger term), lowest-order weak, lowest-order hadronic.

The SM prediction for $a_\mu^{\rm SM}$ is generally divided into three parts (see Fig. 1 for representative Feynman diagrams)

$$a_\mu^{\rm SM} = a_\mu^{\rm QED} + a_\mu^{\rm EW} + a_\mu^{\rm Had} \ . \tag{4}$$

The QED part includes all photonic and leptonic (e, μ, τ) loops starting with the classic $\alpha/2\pi$ Schwinger contribution. It has been computed through 5 loops [9]

$$\begin{aligned} a_\mu^{\rm QED} =& \frac{\alpha}{2\pi} + 0.765\,857\,425(17)\left(\frac{\alpha}{\pi}\right)^2 + 24.050\,509\,96(32)\left(\frac{\alpha}{\pi}\right)^3 \\ &+ 130.879\,6(6\,3)\left(\frac{\alpha}{\pi}\right)^4 + 753.3(1.0)\left(\frac{\alpha}{\pi}\right)^5 + \cdots \end{aligned} \tag{5}$$

with a few significant changes in the coefficients since our previous update of this review in 2011. Employing[2] $\alpha^{-1} = 137.035\,999\,049(90)$, obtained [6] from the precise measurements of $h/m_{\rm Rb}$ [11], the Rydberg constant and $m_{\rm Rb}/m_e$ [6], leads to [9]

$$a_\mu^{\rm QED} = 116\,584\,718.95(0.08) \times 10^{-11}\,, \tag{6}$$

where the small error results mainly from the uncertainty in α.

Loop contributions involving heavy $W^\pm, Z$ or Higgs particles are collectively labeled as $a_\mu^{\rm EW}$. They are suppressed by at least a factor of $\frac{\alpha}{\pi}\frac{m_\mu^2}{m_W^2} \simeq 4 \times 10^{-9}$. At 1-loop order [12]

$$\begin{aligned} a_\mu^{\rm EW}[\text{1-loop}] &= \frac{G_\mu m_\mu^2}{8\sqrt{2}\pi^2}\left[\frac{5}{3} + \frac{1}{3}\left(1 - 4\sin^2\theta_{\rm W}\right)^2 \right. \\ &\quad \left. + \mathcal{O}\left(\frac{m_\mu^2}{M_W^2}\right) + \mathcal{O}\left(\frac{m_\mu^2}{m_H^2}\right)\right], \\ &= 194.8 \times 10^{-11}\,, \end{aligned} \tag{7}$$

for $\sin^2\theta_{\rm W} \equiv 1 - M_W^2/M_Z^2 \simeq 0.223$, and where $G_\mu \simeq 1.166 \times 10^{-5}$ GeV^{-2} is the Fermi coupling constant. Two-loop

[2] In the previous versions of this review we used the precise α value determined from the electron a_e measurement [9,10]. With the new measurement [11] of the recoil velocity of Rubidium, $h/m_{\rm Rb}$, an a_e-independent determination of α with sufficient precision is available and preferred.

corrections are relatively large and negative [13]. For a Higgs boson mass of ≃126 GeV [13]

$$a_\mu^{\rm EW}[\text{2-loop}] = -41.2(1.0)\times 10^{-11}\,, \tag{8}$$

where the uncertainty stems from quark triangle loops. The 3-loop leading logarithms are negligible [13,14], $\mathcal{O}(10^{-12})$, implying in total

$$a_\mu^{\rm EW} = 153.6(1.0)\times 10^{-11}\ . \tag{9}$$

Hadronic (quark and gluon) loop contributions to $a_\mu^{\rm SM}$ give rise to its main theoretical uncertainties. At present, those effects are not calculable from first principles, but such an approach, at least partially, may become possible as lattice QCD matures. Instead, one currently relies on a dispersion relation approach to evaluate the lowest-order (*i.e.*, $\mathcal{O}(\alpha^2)$) hadronic vacuum polarization contribution $a_\mu^{\rm Had}$[LO] from corresponding cross section measurements [15]

$$a_\mu^{\rm Had}[\text{LO}] = \frac{1}{3}\left(\frac{\alpha}{\pi}\right)^2\int_{m_\pi^2}^{\infty} ds\,\frac{K(s)}{s}R^{(0)}(s)\,, \tag{10}$$

where $K(s)$ is a QED kernel function [16], and where $R^{(0)}(s)$ denotes the ratio of the bare[3] cross section for e^+e^- annihilation into hadrons to the pointlike muon-pair cross section at center-of-mass energy $\sqrt{s}$. The function $K(s)\sim 1/s$ in Eq. (10) gives a strong weight to the low-energy part of the integral. Hence, $a_\mu^{\rm Had}$[LO] is dominated by the $\rho(770)$ resonance.

Currently, the available $\sigma(e^+e^-\to\text{hadrons})$ data give a leading-order hadronic vacuum polarization (representative) contribution of [17]

$$a_\mu^{\rm Had}[\text{LO}] = 6\,923(42)(3)\times 10^{-11}\,, \tag{11}$$

where the first error is experimental (dominated by systematic uncertainties), and the second due to perturbative QCD, which is used at intermediate and large energies to predict the contribution from the quark-antiquark continuum. New multi-hadron data from the BABAR experiment have increased the constraints on unmeasured exclusive final states and led to a small reduction in the hadronic contribution compared to the 2009 PDG value.

Alternatively, one can use precise vector spectral functions from $\tau\to\nu_\tau+\text{hadrons}$ decays [18] that can be related to isovector $e^+e^-\to$ hadrons cross sections by isospin symmetry. Replacing e^+e^- data in the two-pion and four-pion channels by the corresponding isospin-transformed τ data, and applying isospin-violating corrections (from QED and $m_d-m_u\neq 0$), one finds [17]

$$a_\mu^{\rm Had}[\text{LO}] = 7\,015(42)(19)(3)\times 10^{-11}\ (\tau)\,, \tag{12}$$

where the first error is experimental, the second estimates the uncertainty in the isospin-breaking corrections applied to the τ data, and the third error is due to perturbative QCD. The current discrepancy between the e^+e^- and τ-based determinations of $a_\mu^{\rm Had}$[LO] has been reduced to 1.8σ with respect to earlier evaluations. New e^+e^- and τ data from the B-factory experiments BABAR and Belle have increased the experimental information. Reevaluated isospin-breaking corrections have also contributed to this improvement [19]. BABAR reported good agreement with the τ data in the most important two-pion channel [20]. The remaining discrepancy with the older e^+e^- and τ datasets may be indicative of problems with one or both data sets. It may also suggest the need for additional isospin-violating corrections to the τ data. Several evaluations of $a_\mu^{\rm Had}$[LO] have been published leading to similar results (see Fig. 2). The low-energy contribution to $a_\mu^{\rm Had}$[LO] has also been evaluated with the use of additional theory or model constraints in Refs. [22] and [23], respectively.

Higher order, $\mathcal{O}(\alpha^3)$, hadronic contributions are obtained from dispersion relations using the same $e^+e^-\to$ hadrons data [18,21,24], giving $a_\mu^{\rm Had,Disp}[\text{NLO}] = (-98.4\pm 0.6)\times 10^{-11}$, along with model-dependent estimates of the hadronic light-by-light scattering contribution, $a_\mu^{\rm Had,LBL}$[NLO], motivated by large-N_C QCD [25–31]. [4] Following [29], one finds for the sum of the two terms

$$a_\mu^{\rm Had}[\text{NLO}] = 7(26)\times 10^{-11}\,, \tag{13}$$

where the error is dominated by hadronic light-by-light uncertainties.

Adding Eqs. (6), (9), (11) and (13) gives the representative e^+e^- data based SM prediction

$$a_\mu^{\rm SM} = 116\,591\,803(1)(42)(26)\times 10^{-11}\,, \tag{14}$$

where the errors are due to the electroweak, lowest-order hadronic, and higher-order hadronic contributions, respectively. The difference between experiment and theory

$$\Delta a_\mu = a_\mu^{\rm exp} - a_\mu^{\rm SM} = 288(63)(49)\times 10^{-11}\,, \tag{15}$$

(with all errors combined in quadrature) represents an interesting but not yet conclusive discrepancy of 3.6 times the estimated 1σ error. All the recent estimates for the hadronic contribution compiled in Fig. 2 exhibit similar discrepancies. Switching to τ data reduces the discrepancy to 2.4σ, assuming the isospin-violating corrections are under control within the estimated uncertainties (see Ref. 32 for an analysis leading to a different conclusion).

An alternate interpretation is that Δa_μ may be a new physics signal with supersymmetric particle loops as the leading candidate explanation. Such a scenario is quite natural, since

[3] The bare cross section is defined as the measured cross section corrected for initial-state radiation, electron-vertex loop contributions and vacuum-polarization effects in the photon propagator. However, QED effects in the hadron vertex and final state, as photon radiation, are included.

[4] Some representative recent estimates of the hadronic light-by-light scattering contribution, $a_\mu^{\rm Had,LBL}$[NLO], that followed after the sign correction of [27], are: $105(26)\times 10^{-11}$ [29], $110(40)\times 10^{-11}$ [25], $136(25)\times 10^{-11}$ [26].

See key on page 547

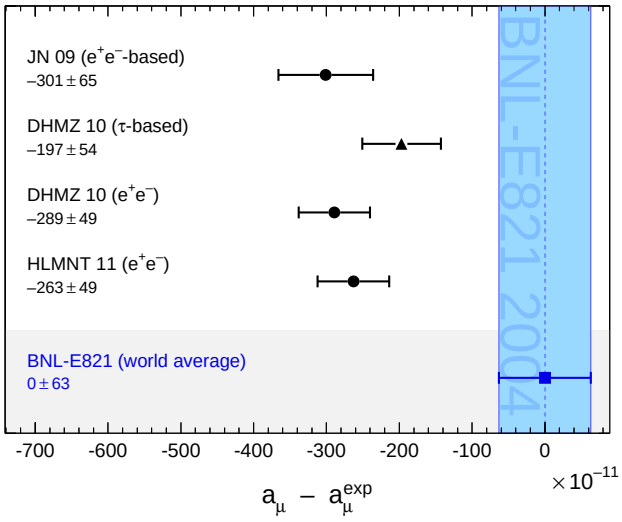

Figure 2: Compilation of recent published results for a_μ (in units of 10^{-11}), subtracted by the central value of the experimental average (3). The shaded band indicates the size of the experimental uncertainty. The SM predictions are taken from: JN [4], DHMZ [17], HMNT [21]. Note that the quoted errors in the figure do not include the uncertainty on the subtracted experimental value. To obtain for each theory calculation a result equivalent to Eq. (15), the errors from theory and experiment must be added in quadrature.

generically, supersymmetric models predict [1] an additional contribution to $a_\mu^{\rm SM}$

$$a_\mu^{\rm SUSY} \simeq {\rm sign}(\mu) \cdot 130 \times 10^{-11} \cdot \left(\frac{100\ {\rm GeV}}{m_{\rm SUSY}}\right)^2 \tan\beta\,, \qquad (16)$$

where $m_{\rm SUSY}$ is a representative supersymmetric mass scale, $\tan\beta \simeq$ 3–40 a potential enhancement factor, and ${\rm sign}(\mu) = \pm 1$. Supersymmetric particles in the mass range 100–500 GeV could be the source of the deviation Δa_μ. If so, those particles should be directly observed at the Large Hadron Collider at CERN.

New physics effects [1] other than supersymmetry could also explain a non-vanishing Δa_μ. A recent popular scenario involves the "dark photon", a relatively light hypothetical vector boson from the dark matter sector that couples to our world of particle physics through mixing with the ordinary photon [33–35]. As a result, it couples to ordinary charged particles with strength $\varepsilon \cdot e$ and gives rise to an additional muon anomalous magnetic moment contribution

$$a_\mu^{\rm dark\ photon} = \frac{\alpha}{2\pi}\varepsilon^2 F(m_V/m_\mu)\,, \qquad (17)$$

where $F(x) = \int_0^1 2z(1-z)^2/[(1-z)^2 + x^2 z]\,dz$. For values of $\varepsilon \sim 1$–$2 \cdot 10^{-3}$ and $m_V \sim$ 10–100 MeV, the dark photon, which was originally motivated by cosmology, can provide a viable solution to the muon $g-2$ discrepancy. Searches for the dark photon in that mass range are currently underway at Jefferson Lab, USA, and MAMI in Mainz, Germany.

References

1. A. Czarnecki and W.J. Marciano, Phys. Rev. **D64**, 013014 (2001).
2. M. Davier and W.J. Marciano, Ann. Rev. Nucl. and Part. Sci. **54**, 115 (2004).
3. J. Miller, E. de Rafael, and B. Lee Roberts, Rept. Prog. Phys. **70**, 795 (2007).
4. F. Jegerlehner and A. Nyffeler, Phys. Reports **477**, 1 (2009).
5. J.P. Miller *et al.*, Ann. Rev. Nucl. and Part. Sci. **62**, 237 (2012).
6. P.J. Mohr, B.N. Taylor, and D.B. Newell, CODATA Group, Rev. Mod. Phys. **84**, 1527 (2012).
7. G.W. Bennett *et al.*, Phys. Rev. Lett. **89**, 101804 (2002); Erratum *ibid.* Phys. Rev. Lett. **89**, 129903 (2002); G.W. Bennett *et al.*, Phys. Rev. Lett. **92**, 161802 (2004); G.W. Bennett *et al.*, Phys. Rev. **D73**, 072003 (2006).
8. J. Bailey *et al.*, Nucl. Phys. **B150**, 1 (1979).
9. T. Aoyama *et al.*, Phys. Rev. Lett. **109**, 111808 (2012); T. Aoyama *et al.*, Phys. Rev. Lett. **109**, 111807 (2012); T. Kinoshita and M. Nio, Phys. Rev. **D73**, 013003 (2006); T. Aoyama *et al.*, Phys. Rev. Lett. **99**, 110406 (2007); T. Kinoshita and M. Nio, Phys. Rev. **D70**, 113001 (2004); T. Kinoshita, Nucl. Phys. **B144**, 206 (2005)(Proc. Supp.); T. Kinoshita and M. Nio, Phys. Rev. **D73**, 053007 (2006); A.L. Kataev, `arXiv:hep-ph/0602098` (2006); M. Passera, J. Phys. **G31**, 75 (2005).
10. G. Gabrielse et al., Phys. Rev. Lett. **97**, 030802 (2006); Erratum *ibid.* Phys. Rev. Lett. **99**, 039902 (2007); D. Hanneke, S. Fogwell, and G. Gabrielse, Phys. Rev. Lett. **100**, 120801 (2008).
11. R. Bouchendira *et al.*, Phys. Rev. Lett. **106**, 080801 (2011).
12. R. Jackiw and S. Weinberg, Phys. Rev. **D5**, 2396 (1972); G. Altarelli *et al.*, Phys. Lett. **B40**, 415 (1972); I. Bars and M. Yoshimura, Phys. Rev. **D6**, 374 (1972); K. Fujikawa, B.W. Lee, and A.I. Sanda, Phys. Rev. **D6**, 2923 (1972).
13. C. Gnendiger, D. Stöckinger, H. Stöckinger-Kim, Phys. Rev. **D88**, 053005 (2013); A. Czarnecki *et al.*, Phys. Rev. **D67**, 073006 (2003), Erratum *ibid.* Phys. Rev. **D73**, 119901 (2006); S. Heinemeyer, D. Stockinger, and G. Weiglein, Nucl. Phys. **B699**, 103 (2004); T. Gribouk and A. Czarnecki, Phys. Rev. **D72**, 053016 (2005); A. Czarnecki, B. Krause, and W.J. Marciano, Phys. Rev. Lett. **76**, 3267 (1996); A. Czarnecki, B. Krause, and W.J. Marciano, Phys. Rev. **D52**, 2619, (1995); S. Peris, M. Perrottet, and E. de Rafael, Phys. Lett. **B355**, 523 (1995); T. Kukhto et al, Nucl. Phys. **B371**, 567 (1992).
14. G. Degrassi and G.F. Giudice, Phys. Rev. **D58**, 053007 (1998).
15. C. Bouchiat and L. Michel, J. Phys. Radium **22**, 121 (1961); M. Gourdin and E. de Rafael, Nucl. Phys. **B10**, 667 (1969).
16. S.J. Brodsky and E. de Rafael, Phys. Rev. **168**, 1620 (1968).
17. M. Davier *et al.*, Eur. Phys. J. **C71**, 1515 (2011).

18. R. Alemany *et al.*, Eur. Phys. J. **C2**, 123 (1998).
19. M. Davier *et al.*, Eur. Phys. J. **C66**, 127 (2010).
20. BABAR Collaboration (B. Aubert *et al.*), Phys. Rev. Lett. **103**, 231801 (2009).
21. K. Hagiwara *et al.*, JPHGB **G38**, 085003 (2011).
22. S. Bodenstein *et al.*, Phys. Rev. **D88**, 014005 (2013).
23. M. Benayoun *et al.*, Eur. Phys. J. **C73**, 2453 (2013).
24. B.Krause, Phys. Lett. **B390**, 392 (1997).
25. J. Bijnens and J. Prades, Mod. Phys. Lett. **A22**, 767 (2007).
26. K. Melnikov and A. Vainshtein, Phys. Rev. **D70**, 113006 (2004).
27. M. Knecht and A. Nyffeler, Phys. Rev. **D65**, 073034 (2002);
M. Knecht *et al.*, Phys. Rev. Lett. **88**, 071802 (2002).
28. J. Bijnens *et al.*, Nucl. Phys. **B626**, 410 (2002).
29. J. Prades, E. de Rafael, and A. Vainshtein,
Advanced series on directions in high energy physics 20,
Editors B.L. Roberts and W. Marciano,
arXiv:0901.0306 [hep-ph] (2009).
30. J. Hayakawa and T. Kinoshita, Erratum Phys. Rev. **D66**, 019902 (2002).
31. E. de Rafael, Phys. Lett. **B322**, 239 (1994).
32. F. Jegerlehner and R. Szafron, Eur. Phys. J. **C71**, 1632 (2011).
33. P. Fayet, Phys. Rev. **D75**, 115017 (2007).
34. M. Pospelov, Phys. Rev. **D80**, 095002 (2009).
35. D. Tucker-Smith and I. Yavin, Phys. Rev. **D83**, 101702 (R)(2011).

μ MAGNETIC MOMENT ANOMALY

The parity-violating decay of muons in a storage ring is observed. The difference frequency ω_a between the muon spin precision and the orbital angular frequency $(e/m_\mu c)\langle B\rangle$ is measured, as is the free proton NMR frequency ω_p, thus determining the ratio $R=\omega_a/\omega_p$. Given the magnetic moment ratio $\lambda=\mu_\mu/\mu_p$ (from hyperfine structure in muonium), $(g-2)/2 = R/(\lambda-R)$.

$\mu_\mu/(e\hbar/2m_\mu)-1 = (g_\mu-2)/2$

VALUE (units 10^{-10})			DOCUMENT ID		TECN	CHG	COMMENT
11659208.9±		**5.4±3.3**	[8] BENNETT	06	MUG2		Average μ^+ and μ^-
• • • We do not use the following data for averages, fits, limits, etc. • • •							
11659208	±	6	BENNETT	04	MUG2		Average μ^+ and μ^-
11659214	±	8 ±3	BENNETT	04	MUG2	−	Storage ring
11659203	±	6 ±5	BENNETT	04	MUG2	+	Storage ring
11659204	±	7 ±5	BENNETT	02	MUG2	+	Storage ring
11659202	±	14 ±6	BROWN	01	MUG2	+	Storage ring
11659191	±	59	BROWN	00	MUG2	+	
11659100	±	110	[9] BAILEY	79	CNTR	+	Storage ring
11659360	±	120	[9] BAILEY	79	CNTR	−	Storage ring
11659230	±	85	[9] BAILEY	79	CNTR	±	Storage ring
11620000	±5000		CHARPAK	62	CNTR	+	

[8] BENNETT 06 reports $(g_\mu-2)/2 = (11659208.0 \pm 5.4 \pm 3.3)\times 10^{-10}$. We rescaled this value using μ/p magnetic moment ratio of 3.183345137(85) from MOHR 08.
[9] BAILEY 79 values recalculated by HUGHES 99 using the COHEN 87 μ/p magnetic moment. The improved MOHR 99 value does not change the result.

$(g_{\mu^+} - g_{\mu^-}) / g_{\text{average}}$

A test of CPT invariance.

VALUE (units 10^{-8})	DOCUMENT ID		TECN
−0.11±0.12	BENNETT	04	MUG2
• • • We do not use the following data for averages, fits, limits, etc. • • •			
−2.6 ±1.6	BAILEY	79	CNTR

μ ELECTRIC DIPOLE MOMENT (d)

A nonzero value is forbidden by both T invariance and P invariance.

VALUE (10^{-19} e cm)	DOCUMENT ID		TECN	CHG	COMMENT
−0.1±0.9	[10] BENNETT	09	MUG2	±	Storage ring
• • • We do not use the following data for averages, fits, limits, etc. • • •					
−0.1±1.0	BENNETT	09	MUG2	+	Storage ring
−0.1±0.7	BENNETT	09	MUG2	−	Storage ring
−3.7±3.4	[11] BAILEY	78	CNTR	±	Storage ring
8.6±4.5	BAILEY	78	CNTR	+	Storage ring
0.8±4.3	BAILEY	78	CNTR	−	Storage ring

[10] This is the combination of the two BENNETT 09 results quoted here separately for μ^+ and μ^-. BENNETT 09 uses the convention $d = 1/2\cdot(d_{\mu^-} - d_{\mu^+})$.
[11] This is the combination of the two BAILEY 78 results quoted here separately for μ^+ and μ^-. BAILEY 78 uses the convention $d = 1/2\cdot(d_{\mu^+} - d_{\mu^-})$ and reports 3.7 ± 3.4. We convert their result to use the same convention as BENNETT 09.

MUON-ELECTRON CHARGE RATIO ANOMALY $q_{\mu^+}/q_{e^-} + 1$

VALUE	DOCUMENT ID		TECN	CHG	COMMENT
(1.1±2.1) × 10^{-9}	[12] MEYER	00	CNTR	+	1s–2s muonium interval

[12] MEYER 00 measure the 1s–2s muonium interval, and then interpret the result in terms of muon-electron charge ratio q_{μ^+}/q_{e^-}.

μ^- DECAY MODES

μ^+ modes are charge conjugates of the modes below.

	Mode		Fraction (Γ_i/Γ)		Confidence level
Γ_1	$e^-\overline{\nu}_e\nu_\mu$		$\approx 100\%$		
Γ_2	$e^-\overline{\nu}_e\nu_\mu\gamma$		[a] (1.4 ± 0.4) %		
Γ_3	$e^-\overline{\nu}_e\nu_\mu e^+e^-$		[b] $(3.4\pm0.4)\times10^{-5}$		
	Lepton Family number (LF) violating modes				
Γ_4	$e^-\nu_e\overline{\nu}_\mu$	LF	[c] < 1.2	%	90%
Γ_5	$e^-\gamma$	LF	< 5.7	$\times10^{-13}$	90%
Γ_6	$e^-e^+e^-$	LF	< 1.0	$\times10^{-12}$	90%
Γ_7	$e^-2\gamma$	LF	< 7.2	$\times10^{-11}$	90%

[a] This only includes events with the γ energy > 10 MeV. Since the $e^-\overline{\nu}_e\nu_\mu$ and $e^-\overline{\nu}_e\nu_\mu\gamma$ modes cannot be clearly separated, we regard the latter mode as a subset of the former.
[b] See the Particle Listings below for the energy limits used in this measurement.
[c] A test of additive vs. multiplicative lepton family number conservation.

μ^- BRANCHING RATIOS

$\Gamma(e^-\overline{\nu}_e\nu_\mu\gamma)/\Gamma_{\text{total}}$ Γ_2/Γ

VALUE	EVTS	DOCUMENT ID		TECN	COMMENT
0.014 ±0.004		CRITTENDEN	61	CNTR	γ KE > 10 MeV
• • • We do not use the following data for averages, fits, limits, etc. • • •					
	862	BOGART	67	CNTR	γ KE > 14.5 MeV
0.0033±0.0013		CRITTENDEN	61	CNTR	γ KE > 20 MeV
	27	ASHKIN	59	CNTR	

$\Gamma(e^-\overline{\nu}_e\nu_\mu e^+e^-)/\Gamma_{\text{total}}$ Γ_3/Γ

VALUE (units 10^{-5})	EVTS	DOCUMENT ID		TECN	CHG	COMMENT
3.4±0.2±0.3	7443	[13] BERTL	85	SPEC	+	SINDRUM
• • • We do not use the following data for averages, fits, limits, etc. • • •						
2.2±1.5	7	[14] CRITTENDEN	61	HLBC	+	$E(e^+e^-) > 10$ MeV
2	1	[15] GUREVICH	60	EMUL	+	
1.5±1.0	3	[16] LEE	59	HBC	+	

[13] BERTL 85 has transverse momentum cut $p_T > 17$ MeV/c. Systematic error was increased by us.
[14] CRITTENDEN 61 count only those decays where total energy of either (e^+, e^-) combination is >10 MeV.
[15] GUREVICH 60 interpret their event as either virtual or real photon conversion. e^+ and e^- energies not measured.
[16] In the three LEE 59 events, the sum of energies $E(e^+) + E(e^-) + E(e^+)$ was 51 MeV, 55 MeV, and 33 MeV.

$\Gamma(e^-\nu_e\overline{\nu}_\mu)/\Gamma_{\text{total}}$ Γ_4/Γ

Forbidden by the additive conservation law for lepton family number. A multiplicative law predicts this branching ratio to be 1/2. For a review see NEMETHY 81.

VALUE	CL%	DOCUMENT ID		TECN	CHG	COMMENT
< 0.012	90	[17] FREEDMAN	93	CNTR	+	ν oscillation search
• • • We do not use the following data for averages, fits, limits, etc. • • •						
< 0.018	90	KRAKAUER	91B	CALO	+	
< 0.05	90	[18] BERGSMA	83	CALO		$\overline{\nu}_\mu e \to \mu^-\overline{\nu}_e$
< 0.09	90	JONKER	80	CALO		See BERGSMA 83
−0.001±0.061		WILLIS	80	CNTR	+	
0.13 ±0.15		BLIETSCHAU	78	HLBC	±	Avg. of 4 values
< 0.25	90	EICHTEN	73	HLBC	+	

[17] FREEDMAN 93 limit on $\overline{\nu}_e$ observation is here interpreted as a limit on lepton family number violation.
[18] BERGSMA 83 gives a limit on the inverse muon decay cross-section ratio $\sigma(\overline{\nu}_\mu e^- \to \mu^- \overline{\nu}_e)/\sigma(\nu_\mu e^- \to \mu^- \nu_e)$, which is essentially equivalent to $\Gamma(e^- \nu_e \overline{\nu}_\mu)/\Gamma_{\text{total}}$ for small values like that quoted.

$\Gamma(e^-\gamma)/\Gamma_{\text{total}}$ Γ_5/Γ

Forbidden by lepton family number conservation.

VALUE (units 10^{-11})	CL%	DOCUMENT ID		TECN	CHG	COMMENT
< 0.057	90	ADAM	13B	SPEC	+	MEG at PSI
• • • We do not use the following data for averages, fits, limits, etc. • • •						
< 0.24	90	ADAM	11	SPEC	+	MEG at PSI
< 2.8	90	ADAM	10	SPEC	+	MEG at PSI
< 1.2	90	AHMED	02	SPEC	+	MEGA
< 1.2	90	BROOKS	99	SPEC	+	LAMPF
< 4.9	90	BOLTON	88	CBOX	+	LAMPF
<100	90	AZUELOS	83	CNTR	+	TRIUMF
< 17	90	KINNISON	82	SPEC	+	LAMPF
<100	90	SCHAAF	80	ELEC	+	SIN

$\Gamma(e^- e^+ e^-)/\Gamma_{\text{total}}$ Γ_6/Γ

Forbidden by lepton family number conservation.

VALUE (units 10^{-12})	CL%	DOCUMENT ID		TECN	CHG	COMMENT
< 1.0	90	[19] BELLGARDT	88	SPEC	+	SINDRUM
• • • We do not use the following data for averages, fits, limits, etc. • • •						
< 36	90	BARANOV	91	SPEC	+	ARES
< 35	90	BOLTON	88	CBOX	+	LAMPF
< 2.4	90	[19] BERTL	85	SPEC	+	SINDRUM
<160	90	[19] BERTL	84	SPEC	+	SINDRUM
<130	90	[19] BOLTON	84	CNTR		LAMPF

[19] These experiments assume a constant matrix element.

$\Gamma(e^- 2\gamma)/\Gamma_{\text{total}}$ Γ_7/Γ

Forbidden by lepton family number conservation.

VALUE (units 10^{-11})	CL%	DOCUMENT ID		TECN	CHG	COMMENT
< 7.2	90	BOLTON	88	CBOX	+	LAMPF
• • • We do not use the following data for averages, fits, limits, etc. • • •						
< 840	90	[20] AZUELOS	83	CNTR	+	TRIUMF
<5000	90	[21] BOWMAN	78	CNTR		DEPOMMIER 77 data

[20] AZUELOS 83 uses the phase space distribution of BOWMAN 78.
[21] BOWMAN 78 assumes an interaction Lagrangian local on the scale of the inverse μ mass.

LIMIT ON $\mu^- \to e^-$ CONVERSION

Forbidden by lepton family number conservation.

$\sigma(\mu^- {}^{32}\text{S} \to e^- {}^{32}\text{S}) / \sigma(\mu^- {}^{32}\text{S} \to \nu_\mu {}^{32}\text{P}^*)$

VALUE	CL%	DOCUMENT ID		TECN	COMMENT
$<7 \times 10^{-11}$	90	BADERT...	80	STRC	SIN
• • • We do not use the following data for averages, fits, limits, etc. • • •					
$<4 \times 10^{-10}$	90	BADERT...	77	STRC	SIN

$\sigma(\mu^- \text{Cu} \to e^- \text{Cu}) / \sigma(\mu^- \text{Cu} \to \text{capture})$

VALUE	CL%	DOCUMENT ID		TECN
• • • We do not use the following data for averages, fits, limits, etc. • • •				
$<1.6 \times 10^{-8}$	90	BRYMAN	72	SPEC

$\sigma(\mu^- \text{Ti} \to e^- \text{Ti}) / \sigma(\mu^- \text{Ti} \to \text{capture})$

VALUE	CL%	DOCUMENT ID		TECN	COMMENT
$<4.3 \times 10^{-12}$	90	[22] DOHMEN	93	SPEC	SINDRUM II
• • • We do not use the following data for averages, fits, limits, etc. • • •					
$<4.6 \times 10^{-12}$	90	AHMAD	88	TPC	TRIUMF
$<1.6 \times 10^{-11}$	90	BRYMAN	85	TPC	TRIUMF

[22] DOHMEN 93 assumes $\mu^- \to e^-$ conversion leaves the nucleus in its ground state, a process enhanced by coherence and expected to dominate.

$\sigma(\mu^- \text{Pb} \to e^- \text{Pb}) / \sigma(\mu^- \text{Pb} \to \text{capture})$

VALUE	CL%	DOCUMENT ID		TECN	COMMENT
$<4.6 \times 10^{-11}$	90	HONECKER	96	SPEC	SINDRUM II
• • • We do not use the following data for averages, fits, limits, etc. • • •					
$<4.9 \times 10^{-10}$	90	AHMAD	88	TPC	TRIUMF

$\sigma(\mu^- \text{Au} \to e^- \text{Au}) / \sigma(\mu^- \text{Au} \to \text{capture})$

VALUE	CL%	DOCUMENT ID		TECN	CHG	COMMENT
$<7 \times 10^{-13}$	90	BERTL	06	SPEC	–	SINDRUM II

LIMIT ON $\mu^- \to e^+$ CONVERSION

Forbidden by total lepton number conservation.

$\sigma(\mu^- {}^{32}\text{S} \to e^+ {}^{32}\text{Si}^*) / \sigma(\mu^- {}^{32}\text{S} \to \nu_\mu {}^{32}\text{P}^*)$

VALUE	CL%	DOCUMENT ID		TECN	COMMENT
$<9 \times 10^{-10}$	90	BADERT...	80	STRC	SIN
• • • We do not use the following data for averages, fits, limits, etc. • • •					
$<1.5 \times 10^{-9}$	90	BADERT...	78	STRC	SIN

$\sigma(\mu^- {}^{127}\text{I} \to e^+ {}^{127}\text{Sb}^*) / \sigma(\mu^- {}^{127}\text{I} \to \text{anything})$

VALUE	CL%	DOCUMENT ID		TECN	COMMENT
$<3 \times 10^{-10}$	90	[23] ABELA	80	CNTR	Radiochemical tech.

[23] ABELA 80 is upper limit for $\mu^- e^+$ conversion leading to particle-stable states of ^{127}Sb. Limit for total conversion rate is higher by a factor less than 4 (G. Backenstoss, private communication).

$\sigma(\mu^- \text{Cu} \to e^+ \text{Co}) / \sigma(\mu^- \text{Cu} \to \nu_\mu \text{Ni})$

VALUE	CL%	DOCUMENT ID		TECN
• • • We do not use the following data for averages, fits, limits, etc. • • •				
$<2.6 \times 10^{-8}$	90	BRYMAN	72	SPEC
$<2.2 \times 10^{-7}$	90	CONFORTO	62	OSPK

$\sigma(\mu^- \text{Ti} \to e^+ \text{Ca}) / \sigma(\mu^- \text{Ti} \to \text{capture})$

VALUE	CL%	EVTS		DOCUMENT ID		TECN	CHG	COMMENT
$<3.6 \times 10^{-11}$	90	1	[24,25]	KAULARD	98	SPEC	–	SINDRUM II
• • • We do not use the following data for averages, fits, limits, etc. • • •								
$<1.7 \times 10^{-12}$	90	1	[25,26]	KAULARD	98	SPEC	–	SINDRUM II
$<4.3 \times 10^{-12}$	90		[26]	DOHMEN	93	SPEC		SINDRUM II
$<8.9 \times 10^{-11}$	90		[24]	DOHMEN	93	SPEC		SINDRUM II
$<1.7 \times 10^{-10}$	90		[27]	AHMAD	88	TPC		TRIUMF

[24] This limit assumes a giant resonance excitation of the daughter Ca nucleus (mean energy and width both 20 MeV).
[25] KAULARD 98 obtained these same limits using the unified classical analysis of FELDMAN 98.
[26] This limit assumes the daughter Ca nucleus is left in the ground state. However, the probability of this is unknown.
[27] Assuming a giant-resonance-excitation model.

LIMIT ON MUONIUM → ANTIMUONIUM CONVERSION

Forbidden by lepton family number conservation.

$R_g = G_C / G_F$

The effective Lagrangian for the $\mu^+ e^- \to \mu^- e^+$ conversion is assumed to be

$$\mathcal{L} = 2^{-1/2}\, G_C\, [\overline{\psi}_\mu \gamma_\lambda\, (1-\gamma_5)\, \psi_e]\, [\overline{\psi}_\mu \gamma_\lambda\, (1-\gamma_5)\, \psi_e] + \text{h.c.}$$

The experimental result is then an upper limit on G_C/G_F, where G_F is the Fermi coupling constant.

VALUE	CL%	EVTS		DOCUMENT ID		TECN	CHG	COMMENT
< 0.0030	90	1	[28]	WILLMANN	99	SPEC	+	μ^+ at 26 GeV/c
• • • We do not use the following data for averages, fits, limits, etc. • • •								
< 0.14	90	1	[29]	GORDEEV	97	SPEC	+	JINR phasotron
< 0.018	90	0	[30]	ABELA	96	SPEC	+	μ^+ at 24 MeV
< 6.9	90			NI	93	CBOX		LAMPF
< 0.16	90			MATTHIAS	91	SPEC		LAMPF
< 0.29	90			HUBER	90B	CNTR		TRIUMF
<20	95			BEER	86	CNTR		TRIUMF
<42	95			MARSHALL	82	CNTR		

[28] WILLMANN 99 quote both probability $P_{M\overline{M}} < 8.3 \times 10^{-11}$ at 90%CL in a 0.1 T field and $R_g = G_C/G_F$.
[29] GORDEEV 97 quote limits on both $f = G_{MM}/GF$ and the probability $W_{MM} < 4.7 \times 10^{-7}$ (90% CL).
[30] ABELA 96 quote both probability $P_{M\overline{M}} < 8 \times 10^{-9}$ at 90% CL and $R_g = G_C/G_F$.

MUON DECAY PARAMETERS

Revised September 2013 by W. Fetscher and H.-J. Gerber (ETH Zürich).

Introduction: All measurements in direct muon decay, $\mu^- \to e^- + 2$ neutrals, and its inverse, $\nu_\mu + e^- \to \mu^- +$ neutral, are successfully described by the "V-A interaction," which is a particular case of a local, derivative-free, lepton-number-conserving, four-fermion interaction [1]. As shown below, within this framework, the Standard Model assumptions, such as the V-A form and the nature of the neutrals (ν_μ and $\bar{\nu}_e$), and hence the doublet assignments $(\nu_e\ e^-)_L$ and $(\nu_\mu\ \mu^-)_L$, have been determined from experiments [2,3]. All considerations on muon decay are valid for the leptonic tau decays $\tau \to \ell + \nu_\tau + \bar{\nu}_e$ with the replacements $m_\mu \to m_\tau$, $m_e \to m_\ell$.

Parameters: The differential decay probability to obtain an $e^\pm$ with (reduced) energy between x and $x + \mathrm{d}x$, emitted in the direction $\hat{\boldsymbol{x}}_3$ at an angle between ϑ and $\vartheta + \mathrm{d}\vartheta$ with respect to the muon polarization vector $\boldsymbol{P}_\mu$, and with its spin parallel

to the arbitrary direction $\widehat{\boldsymbol{\zeta}}$, neglecting radiative corrections, is given by

$$\frac{\mathrm{d}^2\Gamma}{\mathrm{d}x\ \mathrm{d}\cos\vartheta} = \frac{m_\mu}{4\pi^3}\ W_{e\mu}^4\ G_\mathrm{F}^2\ \sqrt{x^2-x_0^2} \times (F_\mathrm{IS}(x) \pm P_\mu \cos\vartheta\ F_\mathrm{AS}(x)) \times \left[1+\widehat{\boldsymbol{\zeta}}\cdot\boldsymbol{P}_e(x,\vartheta)\right]\ . \quad (1)$$

Here, $W_{e\mu} = \max(E_e) = (m_\mu^2+m_e^2)/2m_\mu$ is the maximum $e^\pm$ energy, $x = E_e/W_{e\mu}$ is the reduced energy, $x_0 = m_e/W_{e\mu} = 9.67\times10^{-3}$, and $P_\mu = |\boldsymbol{P}_\mu|$ is the degree of muon polarization. $\widehat{\boldsymbol{\zeta}}$ is the direction in which a perfect polarization-sensitive electron detector is most sensitive. The isotropic part of the spectrum, $F_\mathrm{IS}(x)$, the anisotropic part $F_\mathrm{AS}(x)$, and the electron polarization, $\boldsymbol{P}_e(x,\vartheta)$, may be parametrized by the Michel parameter ρ [1], by η [4], by ξ and δ [5,6], *etc.* These are bilinear combinations of the coupling constants $g^\gamma_{\varepsilon\mu}$, which occur in the matrix element (given below).

If the masses of the neutrinos as well as x_0^2 are neglected, the energy and angular distribution of the electron in the rest frame of a muon ($\mu^\pm$) measured by a polarization insensitive detector, is given by

$$\frac{\mathrm{d}^2\Gamma}{\mathrm{d}x\ \mathrm{d}\cos\vartheta} \sim x^2\cdot\left\{3(1-x)+\frac{2\rho}{3}(4x-3)+3\eta\ x_0(1-x)/x \pm P_\mu\cdot\xi\cdot\cos\vartheta\left[1-x+\frac{2\delta}{3}(4x-3)\right]\right\}\ . \quad (2)$$

Here, ϑ is the angle between the electron momentum and the muon spin, and $x \equiv 2E_e/m_\mu$. For the Standard Model coupling, we obtain $\rho = \xi\delta = 3/4$, $\xi = 1$, $\eta = 0$ and the differential decay rate is

$$\frac{\mathrm{d}^2\Gamma}{\mathrm{d}x\ \mathrm{d}\cos\vartheta} = \frac{G_\mathrm{F}^2 m_\mu^5}{192\pi^3}\ [3-2x\pm P_\mu\cos\vartheta(2x-1)]\ x^2\quad . \quad (3)$$

The coefficient in front of the square bracket is the total decay rate.

If only the neutrino masses are neglected, and if the $e^\pm$ polarization is detected, then the functions in Eq. (1) become

$$\begin{aligned} F_\mathrm{IS}(x) &= x(1-x)+\tfrac{2}{9}\ \rho(4x^2-3x-x_0^2)+\eta\cdot x_0(1-x)\\ F_\mathrm{AS}(x) &= \tfrac{1}{3}\xi\ \sqrt{x^2-x_0^2}\\ &\quad\times[1-x+\tfrac{2}{3}\delta(4x-3+(\sqrt{1-x_0^2}-1))]\\ \boldsymbol{P}_e(x,\vartheta) &= P_\mathrm{T_1}\cdot\widehat{\boldsymbol{x}}_1+P_\mathrm{T_2}\cdot\widehat{\boldsymbol{x}}_2+P_L\cdot\widehat{\boldsymbol{x}}_3\ . \end{aligned} \quad (4)$$

Here $\widehat{\boldsymbol{x}}_1$, $\widehat{\boldsymbol{x}}_2$, and $\widehat{\boldsymbol{x}}_3$ are orthogonal unit vectors defined as follows:

$\widehat{\boldsymbol{x}}_3$	is along the e momentum $\boldsymbol{p}_e$
$\dfrac{\widehat{\boldsymbol{x}}_3\times\boldsymbol{P}_\mu}{\lvert\widehat{\boldsymbol{x}}_2\times\boldsymbol{P}_\mu\rvert} = \widehat{\boldsymbol{x}}_2$	is transverse to $\boldsymbol{p}_e$ and perpendicular to the "decay plane"
$\widehat{\boldsymbol{x}}_2\times\widehat{\boldsymbol{x}}_3 = \widehat{\boldsymbol{x}}_1$	is transverse to the $\boldsymbol{p}_e$ and in the "decay plane."

The components of $\boldsymbol{P}_e$ then are given by

$$\begin{aligned} P_\mathrm{T_1}(x,\vartheta) &= P_\mu\sin\vartheta\cdot F_\mathrm{T_1}(x)/\left(F_\mathrm{IS}(x)\pm P_\mu\cos\vartheta\cdot F_\mathrm{AS}(x)\right)\\ P_\mathrm{T_2}(x,\vartheta) &= P_\mu\sin\vartheta\cdot F_\mathrm{T_2}(x)/\left(F_\mathrm{IS}(x)\pm P_\mu\cos\vartheta\cdot F_\mathrm{AS}(x)\right)\\ P_L(x,\vartheta) &= \Big(\pm F_\mathrm{IP}(x)+P_\mu\cos\vartheta\\ &\quad\times F_\mathrm{AP}(x)\Big)/\left(F_\mathrm{IS}(x)\pm P_\mu\cos\vartheta\cdot F_\mathrm{AS}(x)\right)\ , \end{aligned}$$

where

$$\begin{aligned} F_\mathrm{T_1}(x) &= \tfrac{1}{12}\left\{-2\left[\xi''+12(\rho-\tfrac{3}{4})\right](1-x)x_0\right.\\ &\quad\left.-3\eta(x^2-x_0^2)+\eta''(-3x^2+4x-x_0^2)\right\}\\ F_\mathrm{T_2}(x) &= \tfrac{1}{3}\sqrt{x^2-x_0^2}\left\{3\frac{\alpha'}{A}(1-x)+2\frac{\beta'}{A}\sqrt{1-x_0^2}\right\}\\ F_\mathrm{IP}(x) &= \tfrac{1}{54}\sqrt{x^2-x_0^2}\left\{9\xi'\left(-2x+2+\sqrt{1-x_0^2}\right)\right.\\ &\quad\left.+4\xi(\delta-\tfrac{3}{4})(4x-4+\sqrt{1-x_0^2})\right\}\\ F_\mathrm{AP}(x) &= \tfrac{1}{6}\left\{\xi''(2x^2-x-x_0^2)+4(\rho-\tfrac{3}{4})\left(4x^2-3x-x_0^2\right)\right.\\ &\quad\left.+2\eta''(1-x)x_0\right\}\ . \end{aligned} \quad (5)$$

For the experimental values of the parameters ρ, ξ, ξ', ξ'', δ, η, η'', α/A, β/A, α'/A, β'/A, which are not all independent, see the Data Listings below. Experiments in the past have also been analyzed using the parameters a, b, c, a', b', c', α/A, β/A, α'/A, β'/A (and $\eta = (\alpha-2\beta)/2A$), as defined by Kinoshita and Sirlin [5,6]. They serve as a model-independent summary of all possible measurements on the decay electron (see Listings below). The relations between the two sets of parameters are

$$\begin{aligned} \rho-\tfrac{3}{4} &= \tfrac{3}{4}(-a+2c)/A\ ,\\ \eta &= (\alpha-2\beta)/A\ ,\\ \eta'' &= (3\alpha+2\beta)/A\ ,\\ \delta-\tfrac{3}{4} &= \tfrac{9}{4}\cdot\frac{(a'-2c')/A}{1-[a+3a'+4(b+b')+6c-14c']/A}\ ,\\ 1-\xi\frac{\delta}{\rho} &= 4\ \frac{[(b+b')+2(c-c')]/A}{1-(a-2c)/A}\ ,\\ 1-\xi' &= [(a+a')+4(b+b')+6(c+c')]/A\ ,\\ 1-\xi'' &= (-2a+20c)/A\ , \end{aligned}$$

where

$$A = a + 4b + 6c\ . \quad (6)$$

The differential decay probability to obtain a *left-handed* ν_e with (reduced) energy between y and $y+dy$, neglecting radiative corrections as well as the masses of the electron and of the neutrinos, is given by [7]

$$\frac{\mathrm{d}\Gamma}{\mathrm{d}y} = \frac{m_\mu^5\ G_F^2}{16\pi^3}\ \cdot\ Q_L^{\nu_e}\ \cdot y^2\left\{(1-y)-\omega_L\cdot(y-\tfrac{3}{4})\right\}\ . \quad (7)$$

Here, $y = 2\ E_{\nu_e}/m_\mu$. $Q_L^{\nu_e}$ and ω_L are parameters. ω_L is the neutrino analog of the spectral shape parameter ρ of Michel. Since in the Standard Model, $Q_L^{\nu_e} = 1$, $\omega_L = 0$, the measurement of $d\Gamma/dy$ has allowed a null-test of the Standard Model (see Listings below).

Matrix element: All results in direct muon decay (energy spectra of the electron and of the neutrinos, polarizations, and angular distributions), and in inverse muon decay (the reaction cross section) at energies well below $m_W c^2$, may be parametrized in terms of amplitudes $g^{\gamma}_{\varepsilon\mu}$ and the Fermi coupling constant G_F, using the matrix element

$$\frac{4G_F}{\sqrt{2}} \sum_{\substack{\gamma=S,V,T \\ \varepsilon,\mu=R,L}} g^{\gamma}_{\varepsilon\mu} \langle \bar{e}_{\varepsilon} | \Gamma^{\gamma} | (\nu_e)_n \rangle \langle (\bar{\nu}_{\mu})_m | \Gamma_{\gamma} | \mu_{\mu} \rangle . \tag{8}$$

We use the notation of Fetscher *et al.* [2], who in turn use the sign conventions and definitions of Scheck [8]. Here, $\gamma = S, V, T$ indicates a scalar, vector, or tensor interaction; and $\varepsilon, \mu = R, L$ indicate a right- or left-handed chirality of the electron or muon. The chiralities n and m of the ν_e and $\bar{\nu}_{\mu}$ are then determined by the values of γ, ε, and μ. The particles are represented by fields of definite chirality [9].

As shown by Langacker and London [10], explicit lepton-number nonconservation still leads to a matrix element equivalent to Eq. (8). They conclude that it is not possible, even in principle, to test lepton-number conservation in (leptonic) muon decay if the final neutrinos are massless and are not observed.

The ten complex amplitudes $g^{\gamma}_{\varepsilon\mu}$ (g^{T}_{RR} and g^{T}_{LL} are identically zero) and G_F constitute 19 independent (real) parameters to be determined by experiment. The Standard Model interaction corresponds to one single amplitude g^{V}_{LL} being unity and all the others being zero.

The (direct) muon decay experiments are compatible with an arbitrary mix of the scalar and vector amplitudes g^{S}_{LL} and g^{V}_{LL} – in the extreme even with purely scalar $g^{S}_{LL} = 2$, $g^{V}_{LL} = 0$. The decision in favour of the Standard Model comes from the quantitative observation of inverse muon decay, which would be forbidden for pure g^{S}_{LL} [2].

Experimental determination of V–A: In order to determine the amplitudes $g^{\gamma}_{\varepsilon\mu}$ uniquely from experiment, the following set of equations, where the left-hand sides represent experimental results, has to be solved.

$$\begin{aligned}
a &= 16(|g^{V}_{RL}|^2 + |g^{V}_{LR}|^2) + |g^{S}_{RL} + 6g^{T}_{RL}|^2 + |g^{S}_{LR} + 6g^{T}_{LR}|^2 \\
a' &= 16(|g^{V}_{RL}|^2 - |g^{V}_{LR}|^2) + |g^{S}_{RL} + 6g^{T}_{RL}|^2 - |g^{S}_{LR} + 6g^{T}_{LR}|^2 \\
\alpha &= 8\mathrm{Re}\left\{ g^{V}_{RL}(g^{S*}_{LR} + 6g^{T*}_{LR}) + g^{V}_{LR}(g^{S*}_{RL} + 6g^{T*}_{RL}) \right\} \\
\alpha' &= 8\mathrm{Im}\left\{ g^{V}_{LR}(g^{S*}_{RL} + 6g^{T*}_{RL}) - g^{V}_{RL}(g^{S*}_{LR} + 6g^{T*}_{LR}) \right\} \\
b &= 4(|g^{V}_{RR}|^2 + |g^{V}_{LL}|^2) + |g^{S}_{RR}|^2 + |g^{S}_{LL}|^2 \\
b' &= 4(|g^{V}_{RR}|^2 - |g^{V}_{LL}|^2) + |g^{S}_{RR}|^2 - |g^{S}_{LL}|^2 \\
\beta &= -4\mathrm{Re}\left\{ g^{V}_{RR} g^{S*}_{LL} + g^{V}_{LL} g^{S*}_{RR} \right\} \\
\beta' &= 4\mathrm{Im}\left\{ g^{V}_{RR} g^{S*}_{LL} - g^{V}_{LL} g^{S*}_{RR} \right\} \\
c &= \tfrac{1}{2}\left\{ |g^{S}_{RL} - 2g^{T}_{RL}|^2 + |g^{S}_{LR} - 2g^{T}_{LR}|^2 \right\} \\
c' &= \tfrac{1}{2}\left\{ |g^{S}_{RL} - 2g^{T}_{RL}|^2 - |g^{S}_{LR} - 2g^{T}_{LR}|^2 \right\}
\end{aligned}$$

and

$$\begin{aligned}
Q^{\nu_e}_{L} &= 1 - \left\{ \tfrac{1}{4}|g^{S}_{LR}|^2 + \tfrac{1}{4}|g^{S}_{LL}|^2 + |g^{V}_{RR}|^2 + |g^{V}_{RL}|^2 + 3|g^{T}_{LR}|^2 \right\} \\
\omega_L &= \tfrac{3}{4}\, \frac{\{|g^{S}_{RR}|^2 + 4|g^{V}_{LR}|^2 + |g^{S}_{RL} + 2g^{T}_{RL}|^2\}}{|g^{S}_{RL}|^2 + |g^{S}_{RR}|^2 + 4|g^{V}_{LL}|^2 + 4|g^{V}_{LR}|^2 + 12|g^{T}_{RL}|^2\}} \, .
\end{aligned}$$

It has been noted earlier by C. Jarlskog [11], that certain experiments observing the decay electron are especially informative if they yield the V-A values. The complete solution is now found as follows. Fetscher *et al.* [2] introduced four probabilities $Q_{\varepsilon\mu}(\varepsilon, \mu = R, L)$ for the decay of a μ-handed muon into an ε-handed electron, and showed that there exist upper bounds on Q_{RR}, Q_{LR}, and Q_{RL}, and a lower bound on Q_{LL}. These probabilities are given in terms of the $g^{\gamma}_{\varepsilon\mu}$'s by

$$Q_{\varepsilon\mu} = \tfrac{1}{4}|g^{S}_{\varepsilon\mu}|^2 + |g^{V}_{\varepsilon\mu}|^2 + 3(1 - \delta_{\varepsilon\mu})|g^{T}_{\varepsilon\mu}|^2 \, , \tag{9}$$

where $\delta_{\varepsilon\mu} = 1$ for $\varepsilon = \mu$, and $\delta_{\varepsilon\mu} = 0$ for $\varepsilon \neq \mu$. They are related to the parameters a, b, c, a', b', and c' by

$$\begin{aligned}
Q_{RR} &= 2(b + b')/A \, , \\
Q_{LR} &= [(a - a') + 6(c - c')]/2A \, , \\
Q_{RL} &= [(a + a') + 6(c + c')]/2A \, , \\
Q_{LL} &= 2(b - b')/A \, ,
\end{aligned} \tag{10}$$

with $A = 16$. In the Standard Model, $Q_{LL} = 1$ and the others are zero.

Since the upper bounds on Q_{RR}, Q_{LR}, and Q_{RL} are found to be small, and since the helicity of the ν_{μ} in pion decay is known from experiment [12,13] to very high precision to be -1 [14], the cross section S of *inverse* muon decay, normalized to the V-A value, yields [2]

$$|g^{S}_{LL}|^2 \leq 4(1 - S) \tag{11}$$

and

$$|g^{V}_{LL}|^2 \;=\; S \, . \tag{12}$$

Thus the Standard Model assumption of a pure V-A leptonic charged weak interaction of e and μ is derived (within errors) from experiments at energies far below mass of the $W^{\pm}$: Eq. (12) gives a lower limit for V-A, and Eqs. (9) and (11) give upper limits for the other four-fermion interactions. The existence of such upper limits may also be seen from $Q_{RR} + Q_{RL} = (1 - \xi')/2$ and $Q_{RR} + Q_{LR} = \frac{1}{2}(1 + \xi/3 - 16\ \xi\delta/9)$. Table 1 gives the current experimental limits on the magnitudes of the $g^{\gamma}_{\varepsilon\mu}$'s. More stringent limits on the six coupling constants g^{S}_{LR}, g^{V}_{LR}, g^{T}_{LR}, g^{S}_{RL}, g^{V}_{RL}, and g^{T}_{RL} have been derived from upper limits on the neutrino mass [18]. Limits on the "charge retention" coordinates, as used in the older literature (*e.g.*, Ref. 19), are given by Burkard *et al.* [20].

Lepton Particle Listings

μ

Table 1. Coupling constants $g^{\gamma}_{\varepsilon\mu}$ and some combinations of them. Ninety-percent confidence level experimental limits. The limits on $|g^S_{LL}|$ and $|g^V_{LL}|$ are from Ref. 15, and the others from a general analysis of muon decay measurements. Top three rows: Ref. 22, fourth row: Ref. 16, next three rows: Ref. 17, last row: Ref. 21. The experimental uncertainty on the muon polarization in pion decay is included. Note that, by definition, $|g^S_{\varepsilon\mu}| \leq 2$, $|g^V_{\varepsilon\mu}| \leq 1$ and $|g^T_{\varepsilon\mu}| \leq 1/\sqrt{3}$.

$\lvert g^S_{RR}\rvert < 0.035$	$\lvert g^V_{RR}\rvert < 0.017$	$\lvert g^T_{RR}\rvert \equiv 0$
$\lvert g^S_{LR}\rvert < 0.050$	$\lvert g^V_{LR}\rvert < 0.023$	$\lvert g^T_{LR}\rvert < 0.015$
$\lvert g^S_{RL}\rvert < 0.420$	$\lvert g^V_{RL}\rvert < 0.105$	$\lvert g^T_{RL}\rvert < 0.105$
$\lvert g^S_{LL}\rvert < 0.550$	$\lvert g^V_{LL}\rvert > 0.960$	$\lvert g^T_{LL}\rvert \equiv 0$
$\lvert g^S_{LR} + 6g^T_{LR}\rvert < 0.143$	$\lvert g^S_{RL} + 6g^T_{RL}\rvert < 0.418$	
$\lvert g^S_{LR} + 2g^T_{LR}\rvert < 0.108$	$\lvert g^S_{RL} + 2g^T_{RL}\rvert < 0.417$	
$\lvert g^S_{LR} - 2g^T_{LR}\rvert < 0.070$	$\lvert g^S_{RL} - 2g^T_{RL}\rvert < 0.418$	
$Q_{RR} + Q_{LR} < 8.2 \times 10^{-4}$		

References

1. L. Michel, Proc. Phys. Soc. **A63**, 514 (1950).
2. W. Fetscher, H.-J. Gerber, and K.F. Johnson, Phys. Lett. **B173**, 102 (1986).
3. P. Langacker, Comm. Nucl. Part. Phys. **19**, 1 (1989).
4. C. Bouchiat and L. Michel, Phys. Rev. **106**, 170 (1957).
5. T. Kinoshita and A. Sirlin, Phys. Rev. **107**, 593 (1957).
6. T. Kinoshita and A. Sirlin, Phys. Rev. **108**, 844 (1957).
7. W. Fetscher, Phys. Rev. **D49**, 5945 (1994).
8. F. Scheck, in *Electroweak and Strong Interactions* (Springer Verlag, 1996).
9. K. Mursula and F. Scheck, Nucl. Phys. **B253**, 189 (1985).
10. P. Langacker and D. London, Phys. Rev. **D39**, 266 (1989).
11. C. Jarlskog, Nucl. Phys. **75**, 659 (1966).
12. A. Jodidio *et al.*, Phys. Rev. **D34**, 1967 (1986); A. Jodidio *et al.*, Phys. Rev. **D37**, 237 (1988).
13. L.Ph. Roesch *et al.*, Helv. Phys. Acta **55**, 74 (1982).
14. W. Fetscher, Phys. Lett. **140B**, 117 (1984).
15. S.R. Mishra *et al.*, Phys. Lett. **B252**, 170 (1990); S.R. Mishra, private communication; See also P. Vilain *et al.*, Phys. Lett. **B364**, 121 (1995).
16. R.P. MacDonald *et al.*, Phys. Rev. **D78**, 032010 (2008).
17. C.A. Gagliardi, R.E. Tribble, and N.J. Williams, Phys. Rev. **D72**, 073002 (2005).
18. G. Prézeau and A. Kurylov, Phys. Rev. Lett. **95**, 101802 (2005).
19. S.E. Derenzo, Phys. Rev. **181**, 1854 (1969).
20. H. Burkard *et al.*, Phys. Lett. **160B**, 343 (1985).
21. R. Bayes *et al.*, Phys. Rev. Lett. **106**, 041804 (2011).
22. A. Hillairet *et al.*, Phys. Rev. **D85**, 092013 (2012).

μ DECAY PARAMETERS

ρ PARAMETER

($V-A$) theory predicts $\rho = 0.75$.

VALUE	EVTS	DOCUMENT ID		TECN	CHG	COMMENT
0.74979±0.00026 OUR AVERAGE						
0.74977±0.00012±0.00023		[31] BAYES	11	TWST	+	Surface μ^+
0.7518 ±0.0026		DERENZO	69	RVUE		
• • • We do not use the following data for averages, fits, limits, etc. • • •						
0.75014±0.00017±0.00045		[32] MACDONALD	08	TWST	+	Surface μ^+
0.75080±0.00032±0.00100	6G	[33] MUSSER	05	TWST	+	Surface μ^+
0.72 ±0.06 ±0.08		AMORUSO	04	ICAR		Liquid Ar TPC
0.762 ±0.008	170k	[34] FRYBERGER	68	ASPK	+	25–53 MeV e^+
0.760 ±0.009	280k	[34] SHERWOOD	67	ASPK	+	25–53 MeV e^+
0.7503 ±0.0026	800k	[34] PEOPLES	66	ASPK	+	20–53 MeV e^+

[31] The quoted systematic error includes a contribution of 0.00013 (added in quadrature) from uncertainties on radiative corrections and on the Michel parameter η.
[32] The quoted systematic error includes a contribution of 0.00011 (added in quadrature) from the dependence on the Michel parameter η.
[33] The quoted systematic error includes a contribution of 0.00023 (added in quadrature) from the dependence on the Michel parameter η.
[34] η constrained = 0. These values incorporated into a two parameter fit to ρ and η by DERENZO 69.

η PARAMETER

($V-A$) theory predicts $\eta = 0$.

VALUE	EVTS	DOCUMENT ID		TECN	CHG	COMMENT
0.057 ±0.034 OUR AVERAGE						
0.071 ±0.037 ±0.005	30M	DANNEBERG	05	CNTR	+	7–53 MeV e^+
0.011 ±0.081 ±0.026	5.3M	[35] BURKARD	85B	CNTR	+	9–53 MeV e^+
−0.12 ±0.21	6346	DERENZO	69	HBC	+	1.6–6.8 MeV e^+
• • • We do not use the following data for averages, fits, limits, etc. • • •						
−0.0021±0.0070±0.0010	30M	[36] DANNEBERG	05	CNTR	+	7–53 MeV e^+
−0.012 ±0.015 ±0.003	5.3M	[36] BURKARD	85B	CNTR	+	9–53 MeV e^+
−0.007 ±0.013	5.3M	[37] BURKARD	85B	FIT	+	9–53 MeV e^+
−0.7 ±0.5	170k	[38] FRYBERGER	68	ASPK	+	25–53 MeV e^+
−0.7 ±0.6	280k	[38] SHERWOOD	67	ASPK	+	25–53 MeV e^+
0.05 ±0.5	800k	[38] PEOPLES	66	ASPK	+	20–53 MeV e^+
−2.0 ±0.9	9213	[39] PLANO	60	HBC	+	Whole spectrum

[35] Previously we used the global fit result from BURKARD 85B in OUR AVERAGE, we now only include their actual measurement.
[36] $\alpha = \alpha' = 0$ assumed.
[37] Global fit to all measured parameters. The fit correlation coefficients are given in BURKARD 85B.
[38] ρ constrained = 0.75.
[39] Two parameter fit to ρ and η; PLANO 60 discounts value for η.

δ PARAMETER

($V-A$) theory predicts $\delta = 0.75$.

VALUE	EVTS	DOCUMENT ID		TECN	CHG	COMMENT
0.75047±0.00034 OUR AVERAGE						
0.75049±0.00021±0.00027		[40] BAYES	11	TWST	+	Surface μ^+
0.7486 ±0.0026 ±0.0028		[41] BALKE	88	SPEC	+	Surface μ^+
• • • We do not use the following data for averages, fits, limits, etc. • • •						
0.75067±0.00030±0.00067		MACDONALD	08	TWST	+	Surface μ^+
0.74964±0.00066±0.00112	6G	GAPONENKO	05	TWST	+	Surface μ^+
		[42] VOSSLER	69			
0.752 ±0.009	490k	FRYBERGER	68	ASPK	+	25–53 MeV e^+
0.782 ±0.031		KRUGER	61			
0.78 ±0.05	8354	PLANO	60	HBC	+	Whole spectrum

[40] The quoted systematic error includes a contribution of 0.00006 (added in quadrature) from uncertainties on radiative corrections and on the Michel parameter η.
[41] BALKE 88 uses $\rho = 0.752 \pm 0.003$.
[42] VOSSLER 69 has measured the asymmetry below 10 MeV. See comments about radiative corrections in VOSSLER 69.

|(ξ PARAMETER)×(μ LONGITUDINAL POLARIZATION)|

($V-A$) theory predicts $\xi = 1$, longitudinal polarization = 1.

VALUE	DOCUMENT ID		TECN	CHG	COMMENT
1.0009 $^{+0.0016}_{-0.0007}$ OUR AVERAGE					
1.00084±0.00029$^{+0.00165}_{-0.00063}$	BUENO	11	TWST		Surface μ^+ beam
1.0027 ±0.0079 ±0.0030	BELTRAMI	87	CNTR		SIN, π decay in flight
• • • We do not use the following data for averages, fits, limits, etc. • • •					
1.0003 ±0.0006 ±0.0038	JAMIESON	06	TWST	+	surface μ^+ beam
1.0013 ±0.0030 ±0.0053	[43] IMAZATO	92	SPEC	+	$K^+ \to \mu^+ \nu_\mu$
0.975 ±0.015	AKHMANOV	68	EMUL		140 kG
0.975 ±0.030	GUREVICH	64	EMUL		See AKHMANOV 68
0.903 ±0.027	[44] ALI-ZADE	61	EMUL	+	27 kG
0.93 ±0.06	PLANO	60	HBC	+	8.8 kG
0.97 ±0.05	BARDON	59	CNTR		Bromoform target

[43] The corresponding 90% confidence limit from IMAZATO 92 is $|\xi P_\mu| > 0.990$. This measurement is of K^+ decay, not π^+ decay, so we do not include it in an average, nor do we yet set up a separate data block for K results.
[44] Depolarization by medium not known sufficiently well.

ξ × (μ LONGITUDINAL POLARIZATION) × δ / ρ

VALUE	CL%	DOCUMENT ID		TECN	CHG	COMMENT
1.00179 $^{+0.00156}_{-0.00071}$		[45] BAYES	11	TWST	+	Surface μ^+ beam
• • • We do not use the following data for averages, fits, limits, etc. • • •						
>0.99682	90	[46] JODIDIO	86	SPEC	+	TRIUMF
>0.9966	90	[47] STOKER	85	SPEC	+	μ-spin rotation
>0.9959	90	CARR	83	SPEC	+	11 kG

[45] BAYES 11 obtains the limit > 0.99909 (90% CL) with the constraint that $\xi\times(\mu$ LONGITUDINAL POLARIZATION$)\times\delta/\rho \leq 1.0$.

[46] JODIDIO 86 includes data from CARR 83 and STOKER 85. The value here is from the erratum.

[47] STOKER 85 find $(\xi P_\mu \delta/\rho) > 0.9955$ and > 0.9966, where the first limit is from new μ spin-rotation data and the second is from combination with CARR 83 data. In $V-A$ theory, $(\delta/\rho) = 1.0$.

ξ' = LONGITUDINAL POLARIZATION OF e^+

($V-A$) theory predicts the longitudinal polarization $= \pm 1$ for $e^\pm$, respectively. We have flipped the sign for e^- so our programs can average.

VALUE	EVTS	DOCUMENT ID		TECN	CHG	COMMENT
1.00 ±0.04 OUR AVERAGE						
0.998±0.045	1M	BURKARD	85	CNTR	+	Bhabha + annihil
0.89 ±0.28	29k	SCHWARTZ	67	OSPK	−	Moller scattering
0.94 ±0.38		BLOOM	64	CNTR	+	Brems. transmiss.
1.04 ±0.18		DUCLOS	64	CNTR	+	Bhabha scattering
1.05 ±0.30		BUHLER	63	CNTR	+	Annihilation

ξ'' PARAMETER

VALUE	EVTS	DOCUMENT ID		TECN	CHG	COMMENT
0.65±0.36	326k	[48] BURKARD	85	CNTR	+	Bhabha + annihil

[48] BURKARD 85 measure $(\xi''-\xi\xi')/\xi$ and ξ' and set $\xi = 1$.

TRANSVERSE e^+ POLARIZATION IN PLANE OF μ SPIN, e^+ MOMENTUM

VALUE (units 10^{-3})	EVTS	DOCUMENT ID		TECN	CHG	COMMENT
7 ± 8 OUR AVERAGE						
6.3± 7.7± 3.4	30M	DANNEBERG	05	CNTR	+	7–53 MeV e^+
16 ±21 ±10	5.3M	BURKARD	85B	CNTR	+	Annihil 9–53 MeV

TRANSVERSE e^+ POLARIZATION NORMAL TO PLANE OF μ SPIN, e^+ MOMENTUM

Zero if T invariance holds.

VALUE (units 10^{-3})	EVTS	DOCUMENT ID		TECN	CHG	COMMENT
−2 ± 8 OUR AVERAGE						
−3.7± 7.7±3.4	30M	DANNEBERG	05	CNTR	+	7–53 MeV e^+
7 ±22 ±7	5.3M	BURKARD	85B	CNTR	+	Annihil 9–53 MeV

α/A

VALUE (units 10^{-3})	EVTS	DOCUMENT ID		TECN	CHG	COMMENT
0.4± 4.3		[49] BURKARD	85B	FIT		
• • • We do not use the following data for averages, fits, limits, etc. • • •						
15 ±50 ±14	5.3M	BURKARD	85B	CNTR	+	9–53 MeV e^+

[49] Global fit to all measured parameters. Correlation coefficients are given in BURKARD 85B.

α'/A

Zero if T invariance holds.

VALUE (units 10^{-3})	EVTS	DOCUMENT ID		TECN	CHG	COMMENT
−10 ±20 OUR AVERAGE						
− 3.4±21.3± 4.9	30M	DANNEBERG	05	CNTR	+	7–53 MeV e^+
−47 ±50 ±14	5.3M	[50] BURKARD	85B	CNTR	+	9–53 MeV e^+
• • • We do not use the following data for averages, fits, limits, etc. • • •						
− 0.2± 4.3		[51] BURKARD	85B	FIT		

[50] Previously we used the global fit result from BURKARD 85B in OUR AVERAGE, we now only include their actual measurement. BURKARD 85B measure e^+ polarizations P_{T_1} and P_{T_2} versus e^+ energy.

[51] Global fit to all measured parameters. The fit correlation coefficients are given in BURKARD 85B.

β/A

VALUE (units 10^{-3})	EVTS	DOCUMENT ID		TECN	CHG	COMMENT
3.9± 6.2		[52] BURKARD	85B	FIT		
• • • We do not use the following data for averages, fits, limits, etc. • • •						
2 ±17 ±6	5.3M	BURKARD	85B	CNTR	+	9–53 MeV e^+

[52] Global fit to all measured parameters. The fit correlation coefficients are given in BURKARD 85B.

β'/A

Zero if T invariance holds.

VALUE (units 10^{-3})	EVTS	DOCUMENT ID		TECN	CHG	COMMENT
2 ± 7 OUR AVERAGE						
− 0.5± 7.8±1.8	30M	DANNEBERG	05	CNTR	+	7–53 MeV e^+
17 ±17 ±6	5.3M	[53] BURKARD	85B	CNTR	+	9–53 MeV e^+
• • • We do not use the following data for averages, fits, limits, etc. • • •						
− 1.3± 3.5±0.6	30M	[54] DANNEBERG	05	CNTR	+	7–53 MeV e^+
1.5± 6.3		[55] BURKARD	85B	FIT		

[53] Previously we used the global fit result from BURKARD 85B in OUR AVERAGE, we now only include their actual measurement. BURKARD 85B measure e^+ polarizations P_{T_1} and P_{T_2} versus e^+ energy.

[54] $\alpha = \alpha' = 0$ assumed.

[55] Global fit to all measured parameters. The fit correlation coefficients are given in BURKARD 85B.

a/A

This comes from an alternative parameterization to that used in the Summary Table (see the "Note on Muon Decay Parameters" above).

VALUE (units 10^{-3})	CL%	DOCUMENT ID		TECN
• • • We do not use the following data for averages, fits, limits, etc. • • •				
<15.9	90	[56] BURKARD	85B	FIT

[56] Global fit to all measured parameters. Correlation coefficients are given in BURKARD 85B.

a'/A

This comes from an alternative parameterization to that used in the Summary Table (see the "Note on Muon Decay Parameters" above).

VALUE (units 10^{-3})	DOCUMENT ID		TECN
• • • We do not use the following data for averages, fits, limits, etc. • • •			
5.3±4.1	[57] BURKARD	85B	FIT

[57] Global fit to all measured parameters. Correlation coefficients are given in BURKARD 85B.

$(b'+b)/A$

This comes from an alternative parameterization to that used in the Summary Table (see the "Note on Muon Decay Parameters" above).

VALUE (units 10^{-3})	CL%	DOCUMENT ID		TECN
• • • We do not use the following data for averages, fits, limits, etc. • • •				
<1.04	90	[58] BURKARD	85B	FIT

[58] Global fit to all measured parameters. Correlation coefficients are given in BURKARD 85B.

c/A

This comes from an alternative parameterization to that used in the Summary Table (see the "Note on Muon Decay Parameters" above).

VALUE (units 10^{-3})	CL%	DOCUMENT ID		TECN
• • • We do not use the following data for averages, fits, limits, etc. • • •				
<6.4	90	[59] BURKARD	85B	FIT

[59] Global fit to all measured parameters. Correlation coefficients are given in BURKARD 85B.

c'/A

This comes from an alternative parameterization to that used in the Summary Table (see the "Note on Muon Decay Parameters" above).

VALUE (units 10^{-3})	DOCUMENT ID		TECN
• • • We do not use the following data for averages, fits, limits, etc. • • •			
3.5±2.0	[60] BURKARD	85B	FIT

[60] Global fit to all measured parameters. Correlation coefficients are given in BURKARD 85B.

$\overline{\eta}$ PARAMETER

($V-A$) theory predicts $\overline{\eta} = 0$. $\overline{\eta}$ affects spectrum of radiative muon decay.

VALUE	DOCUMENT ID		TECN	CHG	COMMENT
0.02 ±0.08 OUR AVERAGE					
−0.014±0.090	EICHENBER...	84	ELEC	+	ρ free
+0.09 ±0.14	BOGART	67	CNTR	+	
• • • We do not use the following data for averages, fits, limits, etc. • • •					
−0.035±0.098	EICHENBER...	84	ELEC	+	ρ=0.75 assumed

μ REFERENCES

ADAM	13B	PRL 110 201801	J. Adam *et al.* (MEG Collab.)
TISHCHENKO	13	PR D87 052003	V. Tishchenko *et al.* (MuLan Collab.)
MOHR	12	RMP 84 1527	P.J. Mohr, B.N. Taylor, D.B. Newell (NIST)
ADAM	11	PRL 107 171801	J. Adam *et al.* (MEG Collab.)
BAYES	11	PRL 106 041804	R. Bayes *et al.* (TWIST Collab.)
Also		PR D85 092013	A. Hillairet *et al.* (TWIST Collab.)
BUENO	11	PR D84 032005	J.F. Bueno *et al.* (TWIST Collab.)
Also		PR D85 039908 (errat)	J.F. Bueno *et al.* (TWIST Collab.)
WEBBER	11	PRL 106 041803	D.M. Webber *et al.* (MuLan Collab.)
Also		PRL 106 079901 (errat)	D.M. Webber *et al.* (MuLan Collab.)
ADAM	10	NP B834 1	J. Adam *et al.* (MEG Collab.)
BENNETT	09	PR D80 052008	G.W. Bennett *et al.* (MUG-2 Collab.)
BARCZYK	08	PL B663 172	A. Barczyk *et al.* (FAST Collab.)
MACDONALD	08	PR D78 032010	R.P. MacDonald *et al.* (TWIST Collab.)
MOHR	08	RMP 80 633	P.J. Mohr, B.N. Taylor, D.B. Newell (NIST)
CHITWOOD	07	PRL 99 032001	D.B. Chitwood *et al.* (MULAN Collab.)
BENNETT	06	PR D73 072003	G.W. Bennett *et al.* (MUG-2 Collab.)
BERTL	06	EPJ C47 337	W. Bertl *et al.* (SINDRUM II Collab.)
JAMIESON	06	PR D74 072007	B. Jamieson *et al.* (TWIST Collab.)
DANNEBERG	05	PRL 94 021802	N. Danneberg *et al.* (ETH, JAGL, PSI+)
GAPONENKO	05	PR D71 071101	A. Gaponenko *et al.* (TWIST Collab.)
MOHR	05	RMP 77 1	P.J. Mohr, B.N. Taylor (NIST)
MUSSER	05	PRL 94 101805	J.R. Musser *et al.* (TWIST Collab.)
AMORUSO	04	EPJ C33 233	S. Amoruso *et al.* (ICARUS Collab.)
BENNETT	04	PRL 92 161802	G.W. Bennett *et al.* (Muon(g-2) Collab.)
AHMED	02	PR D65 112002	M. Ahmed *et al.* (MEGA Collab.)
BENNETT	02	PRL 89 101804	G.W. Bennett *et al.* (Muon(g-2) Collab.)
BROWN	01	PRL 86 2227	H.N. Brown *et al.* (Muon(g-2) Collab.)
BROWN	00	PR D62 091101	H.N. Brown *et al.* (BNL/G-2 Collab.)
MEYER	00	PRL 84 1136	V. Meyer *et al.*
BROOKS	99	PRL 83 1521	M.L. Brooks *et al.* (MEGA/LAMPF Collab.)
HUGHES	99	RMP 71 S133	V.W. Hughes, T. Kinoshita
LIU	99	PRL 82 711	W. Liu *et al.* (LAMPF Collab.)
MOHR	99	JPCRD 28 1713	P.J. Mohr, B.N. Taylor (NIST)
Also		RMP 72 351	P.J. Mohr, B.N. Taylor (NIST)
WILLMANN	99	PRL 82 49	L. Willmann *et al.*
FELDMAN	98	PR D57 3873	G.J. Feldman, R.D. Cousins
KAULARD	98	PL B422 334	J. Kaulard *et al.* (SINDRUM-II Collab.)
GORDEEV	97	PAN 60 1164	V.A. Gordeev *et al.* (PNPI)

Translated from YAF 60 1291.

ABELA 96 PRL 77 1950 R. Abela *et al.* (PSI, ZURI, HEIDH, TBIL+)
HONECKER 96 PRL 76 200 W. Honecker *et al.* (SINDRUM II Collab.)
DOHMEN 93 PL B317 631 C. Dohmen *et al.* (PSI SINDRUM-II Collab.)
FREEDMAN 93 PR D47 811 S.J. Freedman *et al.* (LAMPF E645 Collab.)
NI 93 PR D48 1976 B. Ni *et al.* (LAMPF Crystal-Box Collab.)
IMAZATO 92 PRL 69 877 J. Imazato *et al.* (KEK, INUS, TOKY+)
BARANOV 91 SJNP 53 802 V.A. Baranov *et al.* (JINR)
Translated from YAF 53 1302.
KRAKAUER 91B PL B263 534 D.A. Krakauer *et al.* (UMD, UCI, LANL)
MATTHIAS 91 PRL 66 2716 B.E. Matthias *et al.* (YALE, HEIDP, WILL+)
Also PRL 67 932 (erratum) B.E. Matthias *et al.* (YALE, HEIDP, WILL+)
HUBER 90B PR D41 2709 T.M. Huber *et al.* (WYOM, VICT, ARIZ+)
AHMAD 88 PR D38 2102 S. Ahmad *et al.* (TRIU, VICT, VPI, BRCO+)
Also PRL 59 970 S. Ahmad *et al.* (TRIU, VPI, VICT, BRCO+)
BALKE 88 PR D37 587 B. Balke *et al.* (LBL, UCB, COLO, NWES+)
BELLGARDT 88 NP B299 1 U. Bellgardt *et al.* (SINDRUM Collab.)
BOLTON 88 PR D38 2077 R.D. Bolton *et al.* (LANL, STAN, CHIC+)
Also PRL 56 2461 R.D. Bolton *et al.* (LANL, STAN, CHIC+)
Also PRL 57 3241 D. Grosnick *et al.* (CHIC, LANL, STAN+)
BELTRAMI 87 PL B194 326 I. Beltrami *et al.* (ETH, SIN, MANZ)
COHEN 87 RMP 59 1121 E.R. Cohen, B.N. Taylor (RISC, NBS)
BEER 86 PRL 57 671 G.A. Beer *et al.* (VICT, TRIU, WYOM)
JODIDIO 86 PR D34 1967 A. Jodidio *et al.* (LBL, NWES, TRIU)
Also PR D37 237 (erratum) A. Jodidio *et al.* (LBL, NWES, TRIU)
BERTL 85 NP B260 1 W. Bertl *et al.* (SINDRUM Collab.)
BRYMAN 85 PRL 55 465 D.A. Bryman *et al.* (TRIU, CNRC, BRCO+)
BURKARD 85 PL 150B 242 H. Burkhardt *et al.* (ETH, SIN, MANZ)
BURKARD 85B PL 160B 343 H. Burkhardt *et al.* (ETH, SIN, MANZ)
Also PR D24 2004 F. Corriveau *et al.* (ETH, SIN, MANZ)
Also PL 129B 260 F. Corriveau *et al.* (ETH, SIN, MANZ)
STOKER 85 PRL 54 1887 D.P. Stoker *et al.* (LBL, NWES, TRIU)
BARDIN 84 PL 137B 135 G. Bardin *et al.* (SACL, CERN, BGNA, FIRZ)
BERTL 84 PL 140B 299 W. Bertl *et al.* (SINDRUM Collab.)
BOLTON 84 PRL 53 1415 R.D. Bolton *et al.* (LANL, CHIC, STAN+)
EICHENBER... 84 NP A412 523 W. Eichenberger, R. Engfer, A. van der Schaff
GIOVANETTI 84 PR D29 343 K.L. Giovanetti *et al.* (WILL)
AZUELOS 83 PRL 51 164 G. Azuelos *et al.* (MONT, TRIU, BRCO)
Also PRL 39 1113 P. Depommier *et al.* (MONT, BRCO, TRIU+)
BERGSMA 83 PL 122B 465 F. Bergsma *et al.* (CHARM Collab.)
CARR 83 PRL 51 627 J. Carr *et al.* (LBL, NWES, TRIU)
KINNISON 82 PR D25 2846 W.W. Kinnison *et al.* (EFI, STAN, LANL)
Also PRL 42 556 J.D. Bowman *et al.* (LASL, EFI, STAN)
KLEMPT 82 PR D25 652 E. Klempt *et al.* (MANZ, ETH)
MARIAM 82 PRL 49 993 F.G. Mariam *et al.* (YALE, HEIDH, BERN)
MARSHALL 82 PR D25 1174 G.M. Marshall *et al.* (BRCO)
NEMETHY 81 CNPP 10 147 P. Nemethy, V.W. Hughes (LBL, YALE)
ABELA 80 PL 95B 318 R. Abela *et al.* (BASL, KARLK, KARLE)
BADERT... 80 LNC 28 401 A. Badertscher *et al.* (BERN)
Also NP A377 406 A. Badertscher *et al.* (BERN)
JONKER 80 PL 93B 203 M. Jonker *et al.* (CHARM Collab.)
SCHAAF 80 NP A340 249 A. van der Schaaf *et al.* (ZURI, ETH+)
Also PL 72B 183 H.P. Povel *et al.* (ZURI, ETH, SIN)
WILLIS 80 PRL 44 522 S.E. Willis *et al.* (YALE, LBL, LASL+)
Also PRL 45 1370 S.E. Willis *et al.* (YALE, LBL, LASL+)
BAILEY 79 NP B150 1 J.M. Bailey (CERN, DARE, MANZ)
BADERT... 78 PL 79B 371 A. Badertscher *et al.* (BERN)
BAILEY 78 JP G4 345 J.M. Bailey (DARE, BERN, SHEF, MANZ, RMCS+)
Also NP B150 1 J.M. Bailey (CERN, DARE, MANZ)
BLIETSCHAU 78 NP B133 205 J. Blietschau *et al.* (Gargamelle Collab.)
BOWMAN 78 PRL 41 442 J.D. Bowman *et al.* (LASL, IAS, CMU+)
CAMANI 78 PL 77B 326 M. Camani *et al.* (ETH, MANZ)
BADERT... 77 PRL 39 1385 A. Badertscher *et al.* (BERN)
CASPERSON 77 PRL 38 956 D.E. Casperson *et al.* (BERN, HEIDH, LASL+)
DEPOMMIER 77 PRL 39 1113 P. Depommier *et al.* (MONT, BRCO, TRIU+)
BALANDIN 74 JETP 40 811 M.P. Balandin *et al.* (JINR)
Translated from ZETF 67 1631.
COHEN 73 JPCRD 2 664 E.R. Cohen, B.N. Taylor (RISC, NBS)
DUCLOS 73 PL 47B 491 J. Duclos, A. Magnon, J. Picard (SACL)
EICHTEN 73 PL 46B 281 T. Eichten *et al.* (Gargamelle Collab.)
BRYMAN 72 PRL 28 1469 D.A. Bryman *et al.* (VPI)
CROWE 72 PR D5 2145 K.M. Crowe *et al.* (LBL, WASH)
CRANE 71 PRL 27 474 T. Crane *et al.* (YALE)
DERENZO 69 PR 181 1854 S.E. Derenzo (EFI)
VOSSLER 69 NC 63A 423 C. Vossler (EFI)
AKHMANOV 68 SJNP 6 230 V.V. Akhmanov *et al.* (KIAE)
Translated from YAF 6 316.
FRYBERGER 68 PR 166 1379 D. Fryberger (EFI)
BOGART 67 PR 156 1405 E. Bogart *et al.* (COLU)
SCHWARTZ 67 PR 162 1306 D.M. Schwartz (EFI)
SHERWOOD 67 PR 156 1475 B.A. Sherwood (EFI)
PEOPLES 66 Nevis 147 unpub. J. Peoples (COLU)
BLOOM 64 PL 8 87 S. Bloom *et al.* (CERN)
DUCLOS 64 PL 9 62 J. Duclos *et al.* (CERN)
GUREVICH 64 PL 11 185 I.I. Gurevich *et al.* (KIAE)
BUHLER 63 PL 7 368 A. Buhler-Broglin *et al.* (CERN)
MEYER 63 PR 132 2693 S.L. Meyer *et al.* (COLU)
CHARPAK 62 PL 1 16 G. Charpak *et al.* (CERN)
CONFORTO 62 NC 26 261 G. Conforto *et al.* (INFN, ROMA, CERN)
ALI-ZADE 61 JETP 13 313 S.A. Ali-Zade, I.I. Gurevich, B.A. Nikolsky
Translated from ZETF 40 452.
CRITTENDEN 61 PR 121 1823 R.R. Crittenden, W.D. Walker, J. Ballam (WISC+)
KRUGER 61 UCRL 9322 unpub. H. Kruger (LRL)
GUREVICH 60 JETP 10 225 I.I. Gurevich, B.A. Nikolsky, L.V. Surkova (ITEP)
Translated from ZETF 37 318.
PLANO 60 PR 119 1400 R.J. Plano (COLU)
ASHKIN 59 NC 14 1266 J. Ashkin *et al.* (CERN)
BARDON 59 PRL 2 56 M. Bardon, D. Berley, L.M. Lederman (COLU)
LEE 59 PRL 3 55 J. Lee, N.P. Samios (COLU)

τ

$J = \frac{1}{2}$

τ discovery paper was PERL 75. $e^+e^- \to \tau^+\tau^-$ cross-section threshold behavior and magnitude are consistent with pointlike spin-1/2 Dirac particle. BRANDELIK 78 ruled out pointlike spin-0 or spin-1 particle. FELDMAN 78 ruled out $J = 3/2$. KIRKBY 79 also ruled out J=integer, $J = 3/2$.

τ MASS

VALUE (MeV)	EVTS	DOCUMENT ID		TECN	COMMENT
1776.82±0.16 OUR AVERAGE					
$1776.68 \pm 0.12 \pm 0.41$	682k	[1] AUBERT	09AK	BABR	423 fb^{-1}, $E^{ee}_{\rm cm}$=10.6 GeV
$1776.81^{+0.25}_{-0.23} \pm 0.15$	81	ANASHIN	07	KEDR	6.7 pb^{-1}, $E^{ee}_{\rm cm}$ = 3.54–3.78 GeV
$1776.61 \pm 0.13 \pm 0.35$		[1] BELOUS	07	BELL	414 fb^{-1} $E^{ee}_{\rm cm}$=10.6 GeV
$1775.1 \pm 1.6 \pm 1.0$	13.3k	[2] ABBIENDI	00A	OPAL	1990–1995 LEP runs
$1778.2 \pm 0.8 \pm 1.2$		ANASTASSOV	97	CLEO	$E^{ee}_{\rm cm}$ = 10.6 GeV
$1776.96^{+0.18}_{-0.21} {}^{+0.25}_{-0.17}$	65	[3] BAI	96	BES	$E^{ee}_{\rm cm}$ = 3.54–3.57 GeV
$1776.3 \pm 2.4 \pm 1.4$	11k	[4] ALBRECHT	92M	ARG	$E^{ee}_{\rm cm}$ = 9.4–10.6 GeV
$1783 \; {}^{+3}_{-4}$	692	[5] BACINO	78B	DLCO	$E^{ee}_{\rm cm}$ = 3.1–7.4 GeV
• • • We do not use the following data for averages, fits, limits, etc. • • •					
$1777.8 \pm 0.7 \pm 1.7$	35k	[6] BALEST	93	CLEO	Repl. by ANASTASSOV 97
$1776.9 \; {}^{+0.4}_{-0.5} \pm 0.2$	14	[7] BAI	92	BES	Repl. by BAI 96

[1] AUBERT 09AK and BELOUS 07 fit τ pseudomass spectrum in $\tau \to \pi\pi^+\pi^-\nu_\tau$ decays. Result assumes $m_{\nu_\tau} = 0$.

[2] ABBIENDI 00A fit τ pseudomass spectrum in $\tau \to \pi^\pm \leq 2\pi^0\nu_\tau$ and $\tau \to \pi^\pm\pi^+\pi^- \leq 1\pi^0\nu_\tau$ decays. Result assumes m_{ν_τ}=0.

[3] BAI 96 fit $\sigma(e^+e^- \to \tau^+\tau^-)$ at different energies near threshold.

[4] ALBRECHT 92M fit τ pseudomass spectrum in $\tau^- \to 2\pi^-\pi^+\nu_\tau$ decays. Result assumes m_{ν_τ}=0.

[5] BACINO 78B value comes from $e^\pm X^\mp$ threshold. Published mass 1782 MeV increased by 1 MeV using the high precision $\psi(2S)$ mass measurement of ZHOLENTZ 80 to eliminate the absolute SPEAR energy calibration uncertainty.

[6] BALEST 93 fit spectra of minimum kinematically allowed τ mass in events of the type $e^+e^- \to \tau^+\tau^- \to (\pi^+ n\pi^0\nu_\tau)(\pi^- m\pi^0\nu_\tau)$ $n \leq 2$, $m \leq 2$, $1 \leq n+m \leq 3$. If $m_{\nu_\tau} \neq 0$, result increases by $(m^2_{\nu_\tau}/1100$ MeV).

[7] BAI 92 fit $\sigma(e^+e^- \to \tau^+\tau^-)$ near threshold using $e\mu$ events.

$(m_{\tau^+} - m_{\tau^-})/m_{\rm average}$

A test of CPT invariance.

VALUE	CL%	DOCUMENT ID		TECN	COMMENT
$<2.8 \times 10^{-4}$	90	BELOUS	07	BELL	414 fb^{-1}, $E^{ee}_{\rm cm}$=10.6 GeV
• • • We do not use the following data for averages, fits, limits, etc. • • •					
$<5.5 \times 10^{-4}$	90	[1] AUBERT	09AK	BABR	423 fb^{-1}, $E^{ee}_{\rm cm}$=10.6 GeV
$<3.0 \times 10^{-3}$	90	ABBIENDI	00A	OPAL	1990–1995 LEP runs

[1] AUBERT 09AK quote both the listed upper limit and $(m_{\tau^+} - m_{\tau^-})/m_{\rm average} = (-3.4 \pm 1.3 \pm 0.3) \times 10^{-4}$.

τ MEAN LIFE

VALUE (10^{-15} s)	EVTS	DOCUMENT ID		TECN	COMMENT
290.3 ± 0.5 OUR AVERAGE					
$290.17 \pm 0.53 \pm 0.33$	1.1M	BELOUS	14	BELL	711 fb^{-1} $E^{ee}_{\rm cm}$=10.6 GeV
$290.9 \pm 1.4 \pm 1.0$		ABDALLAH	04T	DLPH	1991–1995 LEP runs
$293.2 \pm 2.0 \pm 1.5$		ACCIARRI	00B	L3	1991–1995 LEP runs
$290.1 \pm 1.5 \pm 1.1$		BARATE	97R	ALEP	1989–1994 LEP runs
$289.2 \pm 1.7 \pm 1.2$		ALEXANDER	96E	OPAL	1990–1994 LEP runs
$289.0 \pm 2.8 \pm 4.0$	57.4k	BALEST	96	CLEO	$E^{ee}_{\rm cm}$= 10.6 GeV
• • • We do not use the following data for averages, fits, limits, etc. • • •					
$291.2 \pm 2.0 \pm 1.2$		BARATE	97I	ALEP	Repl. by BARATE 97R
291.4 ± 3.0		ABREU	96B	DLPH	Repl. by ABDALLAH 04T
290.1 ± 4.0	34k	ACCIARRI	96K	L3	Repl. by ACCIARRI 00B
$297 \pm 9 \pm 5$	1671	ABE	95Y	SLD	1992–1993 SLC runs
$304 \pm 14 \pm 7$	4100	BATTLE	92	CLEO	$E^{ee}_{\rm cm}$= 10.6 GeV
301 ± 29	3780	KLEINWORT	89	JADE	$E^{ee}_{\rm cm}$= 35–46 GeV
$288 \pm 16 \pm 17$	807	AMIDEI	88	MRK2	$E^{ee}_{\rm cm}$= 29 GeV
$306 \pm 20 \pm 14$	695	BRAUNSCH...	88C	TASS	$E^{ee}_{\rm cm}$= 36 GeV
$299 \pm 15 \pm 10$	1311	ABACHI	87C	HRS	$E^{ee}_{\rm cm}$= 29 GeV
$295 \pm 14 \pm 11$	5696	ALBRECHT	87P	ARG	$E^{ee}_{\rm cm}$= 9.3–10.6 GeV
$309 \pm 17 \pm 7$	3788	BAND	87B	MAC	$E^{ee}_{\rm cm}$= 29 GeV
$325 \pm 14 \pm 18$	8470	BEBEK	87C	CLEO	$E^{ee}_{\rm cm}$= 10.5 GeV
460 ± 190	102	FELDMAN	82	MRK2	$E^{ee}_{\rm cm}$= 29 GeV

$(\tau_{\tau^+} - \tau_{\tau^-}) / \tau_{\rm average}$

Test of CPT invariance.

VALUE	CL%	DOCUMENT ID		TECN	COMMENT
$<7.0 \times 10^{-3}$	90	[1] BELOUS	14	BELL	711 fb^{-1} $E^{ee}_{\rm cm}$ = 10.6 GeV

[1] BELOUS 14 quote limit on the absolute value of the relative lifetime difference.

τ MAGNETIC MOMENT ANOMALY

The q^2 dependence is expected to be small providing no thresholds are nearby.

$\mu_\tau/(e\hbar/2m_\tau) - 1 = (g_\tau - 2)/2$

For a theoretical calculation [$(g_\tau - 2)/2 = 117\,721(5) \times 10^{-8}$], see EIDELMAN 07.

VALUE	CL%	DOCUMENT ID		TECN	COMMENT
> -0.052 and < 0.013 (CL = 95%) OUR LIMIT					
> -0.052 and < 0.013	95	[1] ABDALLAH	04K	DLPH	$e^+e^- \to e^+e^-\tau^+\tau^-$ at LEP2

• • • We do not use the following data for averages, fits, limits, etc. • • •

<0.107	95	[2] ACHARD	04G	L3	$e^+e^- \to e^+e^-\tau^+\tau^-$ at LEP2
> -0.007 and < 0.005	95	[3] GONZALEZ-S...00		RVUE	$e^+e^- \to \tau^+\tau^-$ and $W \to \tau\nu_\tau$
> -0.052 and < 0.058	95	[4] ACCIARRI	98E	L3	1991–1995 LEP runs
> -0.068 and < 0.065	95	[5] ACKERSTAFF	98N	OPAL	1990–1995 LEP runs
> -0.004 and < 0.006	95	[6] ESCRIBANO	97	RVUE	$Z \to \tau^+\tau^-$ at LEP
<0.01	95	[7] ESCRIBANO	93	RVUE	$Z \to \tau^+\tau^-$ at LEP
<0.12	90	GRIFOLS	91	RVUE	$Z \to \tau\tau\gamma$ at LEP
<0.023	95	[8] SILVERMAN	83	RVUE	$e^+e^- \to \tau^+\tau^-$ at PETRA

[1] ABDALLAH 04K limit is derived from $e^+e^- \to e^+e^-\tau^+\tau^-$ total cross-section measurements at $\sqrt{s}$ between 183 and 208 GeV. In addition to the limits, the authors also quote a value of -0.018 ± 0.017.

[2] ACHARD 04G limit is derived from $e^+e^- \to e^+e^-\tau^+\tau^-$ total cross-section measurements at $\sqrt{s}$ between 189 and 206 GeV, and is on the absolute value of the magnetic moment anomaly.

[3] GONZALEZ-SPRINBERG 00 use data on tau lepton production at LEP1, SLC, and LEP2, and data from colliders and LEP2 to determine limits. Assume imaginary component is zero.

[4] ACCIARRI 98E use $Z \to \tau^+\tau^-\gamma$ events. In addition to the limits, the authors also quote a value of $0.004 \pm 0.027 \pm 0.023$.

[5] ACKERSTAFF 98N use $Z \to \tau^+\tau^-\gamma$ events. The limit applies to an average of the form factor for off-shell τ's having p^2 ranging from m_τ^2 to $(M_Z - m_\tau)^2$.

[6] ESCRIBANO 97 use preliminary experimental results.

[7] ESCRIBANO 93 limit derived from $\Gamma(Z \to \tau^+\tau^-)$, and is on the absolute value of the magnetic moment anomaly.

[8] SILVERMAN 83 limit is derived from $e^+e^- \to \tau^+\tau^-$ total cross-section measurements for q^2 up to (37 GeV)^2.

τ ELECTRIC DIPOLE MOMENT (d_τ)

A nonzero value is forbidden by both T invariance and P invariance.

The q^2 dependence is expected to be small providing no thresholds are nearby.

Re(d_τ)

VALUE (10^{-16} ecm)	CL%	DOCUMENT ID		TECN	COMMENT
-0.22 to 0.45	95	[1] INAMI	03	BELL	$E_{\rm cm}^{ee} = 10.6$ GeV

• • • We do not use the following data for averages, fits, limits, etc. • • •

< 2.3	90	[2] GROZIN	09A	RVUE	From e EDM limit
< 3.7	95	[3] ABDALLAH	04K	DLPH	$e^+e^- \to e^+e^-\tau^+\tau^-$ at LEP2
< 11.4	95	[4] ACHARD	04G	L3	$e^+e^- \to e^+e^-\tau^+\tau^-$ at LEP2
< 4.6	95	[5] ALBRECHT	00	ARG	$E_{\rm cm}^{ee} = 10.4$ GeV
> -3.1 and < 3.1	95	ACCIARRI	98E	L3	1991–1995 LEP runs
> -3.8 and < 3.6	95	[6] ACKERSTAFF	98N	OPAL	1990–1995 LEP runs
< 0.11	95	[7,8] ESCRIBANO	97	RVUE	$Z \to \tau^+\tau^-$ at LEP
< 0.5	95	[9] ESCRIBANO	93	RVUE	$Z \to \tau^+\tau^-$ at LEP
< 7	90	GRIFOLS	91	RVUE	$Z \to \tau\tau\gamma$ at LEP
< 1.6	90	DELAGUILA	90	RVUE	$e^+e^- \to \tau^+\tau^-$ $E_{\rm cm}^{ee} = 35$ GeV

[1] INAMI 03 use $e^+e^- \to \tau^+\tau^-$ events.

[2] GROZIN 09A calculate the contribution to the electron electric dipole moment from the τ electric dipole moment appearing in loops, which is $\Delta d_e = 6.9 \times 10^{-12}\ d_\tau$. Dividing the REGAN 02 upper limit $|d_e| \le 1.6 \times 10^{-27}$ e cm at CL=90% by 6.9×10^{-12} gives this limit.

[3] ABDALLAH 04K limit is derived from $e^+e^- \to e^+e^-\tau^+\tau^-$ total cross-section measurements at $\sqrt{s}$ between 183 and 208 GeV and is on the absolute value of d_τ.

[4] ACHARD 04G limit is derived from $e^+e^- \to e^+e^-\tau^+\tau^-$ total cross-section measurements at $\sqrt{s}$ between 189 and 206 GeV, and is on the absolute value of d_τ.

[5] ALBRECHT 00 use $e^+e^- \to \tau^+\tau^-$ events. Limit is on the absolute value of Re(d_τ).

[6] ACKERSTAFF 98N use $Z \to \tau^+\tau^-\gamma$ events. The limit applies to an average of the form factor for off-shell τ's having p^2 ranging from m_τ^2 to $(M_Z - m_\tau)^2$.

[7] ESCRIBANO 97 derive the relationship $|d_\tau| = \cot\theta_W\, |d_\tau^W|$ using effective Lagrangian methods, and use a conference result $|d_\tau^W| < 5.8 \times 10^{-18}$ e cm at 95% CL (L. Silvestris, ICHEP96) to obtain this result.

[8] ESCRIBANO 97 use preliminary experimental results.

[9] ESCRIBANO 93 limit derived from $\Gamma(Z \to \tau^+\tau^-)$, and is on the absolute value of the electric dipole moment.

Im(d_τ)

VALUE (10^{-16} ecm)	CL%	DOCUMENT ID		TECN	COMMENT
-0.25 to 0.008	95	[1] INAMI	03	BELL	$E_{\rm cm}^{ee} = 10.6$ GeV

• • • We do not use the following data for averages, fits, limits, etc. • • •

< 1.8	95	[2] ALBRECHT	00	ARG	$E_{\rm cm}^{ee} = 10.4$ GeV

[1] INAMI 03 use $e^+e^- \to \tau^+\tau^-$ events.

[2] ALBRECHT 00 use $e^+e^- \to \tau^+\tau^-$ events. Limit is on the absolute value of Im(d_τ).

τ WEAK DIPOLE MOMENT (d_τ^W)

A nonzero value is forbidden by CP invariance.

The q^2 dependence is expected to be small providing no thresholds are nearby.

Re(d_τ^W)

VALUE (10^{-17} ecm)	CL%	DOCUMENT ID		TECN	COMMENT
<0.50	95	[1] HEISTER	03F	ALEP	1990–1995 LEP runs

• • • We do not use the following data for averages, fits, limits, etc. • • •

<3.0	90	[1] ACCIARRI	98C	L3	1991–1995 LEP runs
<0.56	95	ACKERSTAFF	97L	OPAL	1991–1995 LEP runs
<0.78	95	[2] AKERS	95F	OPAL	Repl. by ACKERSTAFF 97L
<1.5	95	[2] BUSKULIC	95C	ALEP	Repl. by HEISTER 03F
<7.0	95	[2] ACTON	92F	OPAL	$Z \to \tau^+\tau^-$ at LEP
<3.7	95	[2] BUSKULIC	92J	ALEP	Repl. by BUSKULIC 95C

[1] Limit is on the absolute value of the real part of the weak dipole moment.

[2] Limit is on the absolute value of the real part of the weak dipole moment, and applies for $q^2 = m_Z^2$.

Im(d_τ^W)

VALUE (10^{-17} ecm)	CL%	DOCUMENT ID		TECN	COMMENT
<1.1	95	[1] HEISTER	03F	ALEP	1990–1995 LEP runs

• • • We do not use the following data for averages, fits, limits, etc. • • •

<1.5	95	ACKERSTAFF	97L	OPAL	1991–1995 LEP runs
<4.5	95	[2] AKERS	95F	OPAL	Repl. by ACKERSTAFF 97L

[1] HEISTER 03F limit is on the absolute value of the imaginary part of the weak dipole moment.

[2] Limit is on the absolute value of the imaginary part of the weak dipole moment, and applies for $q^2 = m_Z^2$.

τ WEAK ANOMALOUS MAGNETIC DIPOLE MOMENT (a_τ^W)

Electroweak radiative corrections are expected to contribute at the 10^{-6} level. See BERNABEU 95.

The q^2 dependence is expected to be small providing no thresholds are nearby.

Re(a_τ^W)

VALUE		CL%	DOCUMENT ID		TECN	COMMENT
$<1.1 \times 10^{-3}$		95	[1] HEISTER	03F	ALEP	1990–1995 LEP runs

• • • We do not use the following data for averages, fits, limits, etc. • • •

> -0.0024 and < 0.0025	95	[2] GONZALEZ-S...00		RVUE	$e^+e^- \to \tau^+\tau^-$ and $W \to \tau\nu_\tau$
$<4.5 \times 10^{-3}$	90	[1] ACCIARRI	98C	L3	1991–1995 LEP runs

[1] Limit is on the absolute value of the real part of the weak anomalous magnetic dipole moment.

[2] GONZALEZ-SPRINBERG 00 use data on tau lepton production at LEP1, SLC, and LEP2, and data from colliders and LEP2 to determine limits. Assume imaginary component is zero.

Im(a_τ^W)

VALUE	CL%	DOCUMENT ID		TECN	COMMENT
$<2.7 \times 10^{-3}$	95	[1] HEISTER	03F	ALEP	1990–1995 LEP runs

• • • We do not use the following data for averages, fits, limits, etc. • • •

$<9.9 \times 10^{-3}$	90	[1] ACCIARRI	98C	L3	1991–1995 LEP runs

[1] Limit is on the absolute value of the imaginary part of the weak anomalous magnetic dipole moment.

τ^- DECAY MODES

τ^+ modes are charge conjugates of the modes below. "$h^\pm$" stands for $\pi^\pm$ or $K^\pm$. "ℓ" stands for e or μ. "Neutrals" stands for γ's and/or π^0's.

	Mode		Fraction (Γ_i/Γ)	Scale factor/ Confidence level
	Modes with one charged particle			
Γ_1	particle$^- \ge 0$ neutrals $\ge 0 K^0 \nu_\tau$ ("1-prong")		(85.35 $\pm$0.07) %	S=1.3
Γ_2	particle$^- \ge 0$ neutrals $\ge 0 K_L^0 \nu_\tau$		(84.71 $\pm$0.08) %	S=1.3
Γ_3	$\mu^- \overline{\nu}_\mu \nu_\tau$	[a]	(17.41 $\pm$0.04) %	S=1.1
Γ_4	$\mu^- \overline{\nu}_\mu \nu_\tau \gamma$	[b]	(3.6 $\pm$0.4) $\times 10^{-3}$	
Γ_5	$e^- \overline{\nu}_e \nu_\tau$	[a]	(17.83 $\pm$0.04) %	
Γ_6	$e^- \overline{\nu}_e \nu_\tau \gamma$	[b]	(1.75 $\pm$0.18) %	
Γ_7	$h^- \ge 0 K_L^0 \nu_\tau$		(12.06 $\pm$0.06) %	S=1.2
Γ_8	$h^- \nu_\tau$		(11.53 $\pm$0.06) %	S=1.2
Γ_9	$\pi^- \nu_\tau$	[a]	(10.83 $\pm$0.06) %	S=1.2
Γ_{10}	$K^- \nu_\tau$	[a]	(7.00 $\pm$0.10) $\times 10^{-3}$	S=1.1
Γ_{11}	$h^- \ge 1$ neutrals ν_τ		(37.10 $\pm$0.10) %	S=1.2
Γ_{12}	$h^- \ge 1\pi^0 \nu_\tau$ (ex.K^0)		(36.58 $\pm$0.10) %	S=1.2
Γ_{13}	$h^- \pi^0 \nu_\tau$		(25.95 $\pm$0.09) %	S=1.1

Γ_{14}	$\pi^-\pi^0\nu_\tau$	[a]	(25.52 ±0.09) %		S=1.1
Γ_{15}	$\pi^-\pi^0$ non-$\rho(770)\,\nu_\tau$		(3.0 ±3.2) $\times 10^{-3}$		
Γ_{16}	$K^-\pi^0\nu_\tau$	[a]	(4.29 ±0.15) $\times 10^{-3}$		
Γ_{17}	$h^- \geq 2\pi^0\nu_\tau$		(10.87 ±0.11) %		S=1.2
Γ_{18}	$h^-2\pi^0\nu_\tau$		(9.52 ±0.11) %		S=1.1
Γ_{19}	$h^-2\pi^0\nu_\tau$(ex.K^0)		(9.36 ±0.11) %		S=1.2
Γ_{20}	$\pi^-2\pi^0\nu_\tau$(ex.K^0)	[a]	(9.30 ±0.11) %		S=1.2
Γ_{21}	$\pi^-2\pi^0\nu_\tau$(ex.K^0), scalar	<	9	$\times 10^{-3}$	CL=95%
Γ_{22}	$\pi^-2\pi^0\nu_\tau$(ex.K^0), vector	<	7	$\times 10^{-3}$	CL=95%
Γ_{23}	$K^-2\pi^0\nu_\tau$(ex.K^0)	[a]	(6.5 ±2.3) $\times 10^{-4}$		
Γ_{24}	$h^- \geq 3\pi^0\nu_\tau$		(1.35 ±0.07) %		S=1.1
Γ_{25}	$h^- \geq 3\pi^0\nu_\tau$(ex. K^0)		(1.26 ±0.07) %		S=1.1
Γ_{26}	$h^-3\pi^0\nu_\tau$		(1.19 ±0.07) %		
Γ_{27}	$\pi^-3\pi^0\nu_\tau$(ex.K^0)	[a]	(1.05 ±0.07) %		
Γ_{28}	$K^-3\pi^0\nu_\tau$(ex.K^0, η)	[a]	(4.8 ±2.2) $\times 10^{-4}$		
Γ_{29}	$h^-4\pi^0\nu_\tau$(ex.K^0)		(1.6 ±0.4) $\times 10^{-3}$		
Γ_{30}	$h^-4\pi^0\nu_\tau$(ex.K^0,η)	[a]	(1.1 ±0.4) $\times 10^{-3}$		
Γ_{31}	$K^- \geq 0\pi^0 \geq 0K^0 \geq 0\gamma\ \nu_\tau$		(1.572±0.033) %		S=1.1
Γ_{32}	$K^- \geq 1$ (π^0 or K^0 or γ) ν_τ		(8.72 ±0.32) $\times 10^{-3}$		S=1.1

Modes with K^0's

Γ_{33}	K^0_S(particles)$^-\nu_\tau$		(9.2 ±0.4) $\times 10^{-3}$		S=1.5
Γ_{34}	$h^-\overline{K}^0\nu_\tau$		(1.00 ±0.05) %		S=1.8
Γ_{35}	$\pi^-\overline{K}^0\nu_\tau$	[a]	(8.4 ±0.4) $\times 10^{-3}$		S=2.1
Γ_{36}	$\pi^-\overline{K}^0$(non-$K^*(892)^-$)ν_τ		(5.4 ±2.1) $\times 10^{-4}$		
Γ_{37}	$K^-K^0\nu_\tau$	[a]	(1.59 ±0.16) $\times 10^{-3}$		
Γ_{38}	$K^-K^0 \geq 0\pi^0\nu_\tau$		(3.18 ±0.23) $\times 10^{-3}$		
Γ_{39}	$h^-\overline{K}^0\pi^0\nu_\tau$		(5.6 ±0.4) $\times 10^{-3}$		
Γ_{40}	$\pi^-\overline{K}^0\pi^0\nu_\tau$	[a]	(4.0 ±0.4) $\times 10^{-3}$		
Γ_{41}	$\overline{K}^0\rho^-\nu_\tau$		(2.2 ±0.5) $\times 10^{-3}$		
Γ_{42}	$K^-K^0\pi^0\nu_\tau$	[a]	(1.59 ±0.20) $\times 10^{-3}$		
Γ_{43}	$\pi^-\overline{K}^0 \geq 1\pi^0\nu_\tau$		(3.2 ±1.0) $\times 10^{-3}$		
Γ_{44}	$\pi^-\overline{K}^0\pi^0\pi^0\nu_\tau$		(2.6 ±2.4) $\times 10^{-4}$		
Γ_{45}	$K^-K^0\pi^0\pi^0\nu_\tau$	<	1.6	$\times 10^{-4}$	CL=95%
Γ_{46}	$\pi^-K^0\overline{K}^0\nu_\tau$		(1.7 ±0.4) $\times 10^{-3}$		S=1.8
Γ_{47}	$\pi^-K^0_SK^0_S\nu_\tau$	[a]	(2.31 ±0.17) $\times 10^{-4}$		S=1.9
Γ_{48}	$\pi^-K^0_SK^0_L\nu_\tau$	[a]	(1.2 ±0.4) $\times 10^{-3}$		S=1.8
Γ_{49}	$\pi^-K^0\overline{K}^0\pi^0\nu_\tau$		(3.1 ±2.3) $\times 10^{-4}$		
Γ_{50}	$\pi^-K^0_SK^0_S\pi^0\nu_\tau$		(1.60 ±0.30) $\times 10^{-4}$		
Γ_{51}	$\pi^-K^0_SK^0_L\pi^0\nu_\tau$		(3.1 ±1.2) $\times 10^{-4}$		
Γ_{52}	$K^-K^0_SK^0_S\nu_\tau$	<	6.3	$\times 10^{-7}$	CL=90%
Γ_{53}	$K^-K^0_SK^0_S\pi^0\nu_\tau$	<	4.0	$\times 10^{-7}$	CL=90%
Γ_{54}	$K^0h^+h^-h^- \geq 0$ neutrals ν_τ	<	1.7	$\times 10^{-3}$	CL=95%
Γ_{55}	$K^0h^+h^-h^-\nu_\tau$		(2.3 ±2.0) $\times 10^{-4}$		

Modes with three charged particles

Γ_{56}	$h^-h^-h^+ \geq 0$ neutrals $\geq 0K^0_L\nu_\tau$		(15.20 ±0.08) %		S=1.3
Γ_{57}	$h^-h^-h^+ \geq 0$ neutrals ν_τ (ex. $K^0_S \to \pi^+\pi^-$) ("3-prong")		(14.57 ±0.07) %		S=1.3
Γ_{58}	$h^-h^-h^+\nu_\tau$		(9.80 ±0.07) %		S=1.2
Γ_{59}	$h^-h^-h^+\nu_\tau$(ex.K^0)		(9.46 ±0.06) %		S=1.2
Γ_{60}	$h^-h^-h^+\nu_\tau$(ex.K^0,ω)		(9.42 ±0.06) %		S=1.2
Γ_{61}	$\pi^-\pi^+\pi^-\nu_\tau$		(9.31 ±0.06) %		S=1.2
Γ_{62}	$\pi^-\pi^+\pi^-\nu_\tau$(ex.K^0)		(9.02 ±0.06) %		S=1.1
Γ_{63}	$\pi^-\pi^+\pi^-\nu_\tau$(ex.K^0), non-axial vector	<	2.4	%	CL=95%
Γ_{64}	$\pi^-\pi^+\pi^-\nu_\tau$(ex.K^0,ω)	[a]	(8.99 ±0.06) %		S=1.1
Γ_{65}	$h^-h^-h^+ \geq 1$ neutrals ν_τ		(5.39 ±0.07) %		S=1.2
Γ_{66}	$h^-h^-h^+ \geq 1\pi^0\nu_\tau$(ex. K^0)		(5.09 ±0.06) %		S=1.2
Γ_{67}	$h^-h^-h^+\pi^0\nu_\tau$		(4.76 ±0.06) %		S=1.2
Γ_{68}	$h^-h^-h^+\pi^0\nu_\tau$(ex.K^0)		(4.57 ±0.06) %		S=1.2
Γ_{69}	$h^-h^-h^+\pi^0\nu_\tau$(ex. K^0, ω)		(2.79 ±0.08) %		S=1.2
Γ_{70}	$\pi^-\pi^+\pi^-\pi^0\nu_\tau$		(4.62 ±0.06) %		S=1.2
Γ_{71}	$\pi^-\pi^+\pi^-\pi^0\nu_\tau$(ex.$K^0$)		(4.48 ±0.06) %		S=1.2
Γ_{72}	$\pi^-\pi^+\pi^-\pi^0\nu_\tau$(ex.$K^0$,$\omega$)	[a]	(2.70 ±0.08) %		S=1.2
Γ_{73}	$h^-\rho\pi^0\nu_\tau$				
Γ_{74}	$h^-\rho^+h^-\nu_\tau$				
Γ_{75}	$h^-\rho^-h^+\nu_\tau$				
Γ_{76}	$h^-h^-h^+ \geq 2\pi^0\nu_\tau$(ex. K^0)		(5.21 ±0.32) $\times 10^{-3}$		
Γ_{77}	$h^-h^-h^+2\pi^0\nu_\tau$		(5.08 ±0.32) $\times 10^{-3}$		
Γ_{78}	$h^-h^-h^+2\pi^0\nu_\tau$(ex.K^0)		(4.98 ±0.32) $\times 10^{-3}$		
Γ_{79}	$h^-h^-h^+2\pi^0\nu_\tau$(ex.K^0,ω,η)	[a]	(1.0 ±0.4) $\times 10^{-3}$		
Γ_{80}	$h^-h^-h^+3\pi^0\nu_\tau$	[a]	(2.3 ±0.6) $\times 10^{-4}$		S=1.2
Γ_{81}	$2\pi^-\pi^+3\pi^0\nu_\tau$(ex.$K^0$)		(2.1 ±0.4) $\times 10^{-4}$		
Γ_{82}	$2\pi^-\pi^+3\pi^0\nu_\tau$(ex.$K^0$, η, $f_1(1285)$)		(1.7 ±0.4) $\times 10^{-4}$		
Γ_{83}	$2\pi^-\pi^+3\pi^0\nu_\tau$(ex.$K^0$, η, ω, $f_1(1285)$)	<	5.8	$\times 10^{-5}$	CL=90%
Γ_{84}	$K^-h^+h^- \geq 0$ neutrals ν_τ		(6.35 ±0.24) $\times 10^{-3}$		S=1.5
Γ_{85}	$K^-h^+\pi^-\nu_\tau$(ex.K^0)		(4.38 ±0.19) $\times 10^{-3}$		S=2.7
Γ_{86}	$K^-h^+\pi^-\pi^0\nu_\tau$(ex.K^0)		(8.7 ±1.2) $\times 10^{-4}$		S=1.1
Γ_{87}	$K^-\pi^+\pi^- \geq 0$ neutrals ν_τ		(4.85 ±0.21) $\times 10^{-3}$		S=1.4
Γ_{88}	$K^-\pi^+\pi^- \geq 0\pi^0\nu_\tau$(ex.$K^0$)		(3.75 ±0.19) $\times 10^{-3}$		S=1.5
Γ_{89}	$K^-\pi^+\pi^-\nu_\tau$		(3.49 ±0.16) $\times 10^{-3}$		S=1.9
Γ_{90}	$K^-\pi^+\pi^-\nu_\tau$(ex.K^0)	[a]	(2.94 ±0.15) $\times 10^{-3}$		S=2.2
Γ_{91}	$K^-\rho^0\nu_\tau \to K^-\pi^+\pi^-\nu_\tau$		(1.4 ±0.5) $\times 10^{-3}$		
Γ_{92}	$K^-\pi^+\pi^-\pi^0\nu_\tau$		(1.35 ±0.14) $\times 10^{-3}$		
Γ_{93}	$K^-\pi^+\pi^-\pi^0\nu_\tau$(ex.$K^0$)		(8.1 ±1.2) $\times 10^{-4}$		
Γ_{94}	$K^-\pi^+\pi^-\pi^0\nu_\tau$(ex.$K^0$,$\eta$)	[a]	(7.8 ±1.2) $\times 10^{-4}$		
Γ_{95}	$K^-\pi^+\pi^-\pi^0\nu_\tau$(ex.$K^0$,$\omega$)		(3.7 ±0.9) $\times 10^{-4}$		
Γ_{96}	$K^-\pi^+K^- \geq 0$ neut. ν_τ	<	9	$\times 10^{-4}$	CL=95%
Γ_{97}	$K^-K^+\pi^- \geq 0$ neut. ν_τ		(1.50 ±0.06) $\times 10^{-3}$		S=1.8
Γ_{98}	$K^-K^+\pi^-\nu_\tau$	[a]	(1.44 ±0.05) $\times 10^{-3}$		S=1.9
Γ_{99}	$K^-K^+\pi^-\pi^0\nu_\tau$	[a]	(6.1 ±2.5) $\times 10^{-5}$		S=1.4
Γ_{100}	$K^-K^+K^-\nu_\tau$		(2.1 ±0.8) $\times 10^{-5}$		S=5.4
Γ_{101}	$K^-K^+K^-\nu_\tau$(ex. ϕ)	<	2.5	$\times 10^{-6}$	CL=90%
Γ_{102}	$K^-K^+K^-\pi^0\nu_\tau$	<	4.8	$\times 10^{-6}$	CL=90%
Γ_{103}	$\pi^-K^+\pi^- \geq 0$ neut. ν_τ	<	2.5	$\times 10^{-3}$	CL=95%
Γ_{104}	$e^-e^-e^+\overline{\nu}_e\nu_\tau$		(2.8 ±1.5) $\times 10^{-5}$		
Γ_{105}	$\mu^-e^-e^+\overline{\nu}_\mu\nu_\tau$	<	3.6	$\times 10^{-5}$	CL=90%

Modes with five charged particles

Γ_{106}	$3h^-2h^+ \geq 0$ neutrals ν_τ (ex. $K^0_S \to \pi^-\pi^+$) ("5-prong")		(1.02 ±0.04) $\times 10^{-3}$		S=1.1
Γ_{107}	$3h^-2h^+\nu_\tau$(ex.K^0)	[a]	(8.39 ±0.35) $\times 10^{-4}$		S=1.1
Γ_{108}	$3\pi^-2\pi^+\nu_\tau$(ex.K^0, ω)		(8.3 ±0.4) $\times 10^{-4}$		
Γ_{109}	$3\pi^-2\pi^+\nu_\tau$(ex.K^0, ω, $f_1(1285)$)		(7.7 ±0.4) $\times 10^{-4}$		
Γ_{110}	$K^-2\pi^-2\pi^+\nu_\tau$	<	2.4	$\times 10^{-6}$	CL=90%
Γ_{111}	$K^+3\pi^-\pi^+\nu_\tau$	<	5.0	$\times 10^{-6}$	CL=90%
Γ_{112}	$K^+K^-2\pi^-\pi^+\nu_\tau$	<	4.5	$\times 10^{-7}$	CL=90%
Γ_{113}	$3h^-2h^+\pi^0\nu_\tau$(ex.K^0)	[a]	(1.78 ±0.27) $\times 10^{-4}$		
Γ_{114}	$3\pi^-2\pi^+\pi^0\nu_\tau$(ex.$K^0$)		(1.65 ±0.10) $\times 10^{-4}$		
Γ_{115}	$3\pi^-2\pi^+\pi^0\nu_\tau$(ex.$K^0$, η, $f_1(1285)$)		(1.11 ±0.10) $\times 10^{-4}$		
Γ_{116}	$3\pi^-2\pi^+\pi^0\nu_\tau$(ex.$K^0$, η, ω, $f_1(1285)$)		(3.6 ±0.9) $\times 10^{-5}$		
Γ_{117}	$K^-2\pi^-2\pi^+\pi^0\nu_\tau$	<	1.9	$\times 10^{-6}$	CL=90%
Γ_{118}	$K^+3\pi^-\pi^+\pi^0\nu_\tau$	<	8	$\times 10^{-7}$	CL=90%
Γ_{119}	$3h^-2h^+2\pi^0\nu_\tau$	<	3.4	$\times 10^{-6}$	CL=90%

Miscellaneous other allowed modes

Γ_{120}	$(5\pi)^-\nu_\tau$		(7.6 ±0.5) $\times 10^{-3}$		
Γ_{121}	$4h^-3h^+ \geq 0$ neutrals ν_τ ("7-prong")	<	3.0	$\times 10^{-7}$	CL=90%
Γ_{122}	$4h^-3h^+\nu_\tau$	<	4.3	$\times 10^{-7}$	CL=90%
Γ_{123}	$4h^-3h^+\pi^0\nu_\tau$	<	2.5	$\times 10^{-7}$	CL=90%
Γ_{124}	$X^-(S=-1)\nu_\tau$		(2.87 ±0.07) %		S=1.3
Γ_{125}	$K^*(892)^- \geq 0$ neutrals $\geq 0K^0_L\nu_\tau$		(1.42 ±0.18) %		S=1.4
Γ_{126}	$K^*(892)^-\nu_\tau$		(1.20 ±0.07) %		S=1.8
Γ_{127}	$K^*(892)^-\nu_\tau \to \pi^-\overline{K}^0\nu_\tau$		(7.9 ±0.5) $\times 10^{-3}$		
Γ_{128}	$K^*(892)^0K^- \geq 0$ neutrals ν_τ		(3.2 ±1.4) $\times 10^{-3}$		
Γ_{129}	$K^*(892)^0K^-\nu_\tau$		(2.1 ±0.4) $\times 10^{-3}$		
Γ_{130}	$\overline{K}^*(892)^0\pi^- \geq 0$ neutrals ν_τ		(3.8 ±1.7) $\times 10^{-3}$		
Γ_{131}	$\overline{K}^*(892)^0\pi^-\nu_\tau$		(2.2 ±0.5) $\times 10^{-3}$		
Γ_{132}	$(\overline{K}^*(892)\pi)^-\nu_\tau \to \pi^-\overline{K}^0\pi^0\nu_\tau$		(1.0 ±0.4) $\times 10^{-3}$		
Γ_{133}	$K_1(1270)^-\nu_\tau$		(4.7 ±1.1) $\times 10^{-3}$		
Γ_{134}	$K_1(1400)^-\nu_\tau$		(1.7 ±2.6) $\times 10^{-3}$		S=1.7
Γ_{135}	$K^*(1410)^-\nu_\tau$		(1.5 $^{+1.4}_{-1.0}$) $\times 10^{-3}$		
Γ_{136}	$K^*_0(1430)^-\nu_\tau$	<	5	$\times 10^{-4}$	CL=95%
Γ_{137}	$K^*_2(1430)^-\nu_\tau$	<	3	$\times 10^{-3}$	CL=95%
Γ_{138}	$a_0(980)^- \geq 0$ neutrals ν_τ				
Γ_{139}	$\eta\pi^-\nu_\tau$	<	9.9	$\times 10^{-5}$	CL=95%
Γ_{140}	$\eta\pi^-\pi^0\nu_\tau$	[a]	(1.39 ±0.10) $\times 10^{-3}$		S=1.4

See key on page 547

Γ_{141}	$\eta\pi^-\pi^0\pi^0\nu_\tau$		(1.81	±0.31)	$\times 10^{-4}$	
Γ_{142}	$\eta K^-\nu_\tau$	[a]	(1.52	±0.08)	$\times 10^{-4}$	
Γ_{143}	$\eta K^*(892)^-\nu_\tau$		(1.38	±0.15)	$\times 10^{-4}$	
Γ_{144}	$\eta K^-\pi^0\nu_\tau$		(4.8	±1.2)	$\times 10^{-5}$	
Γ_{145}	$\eta K^-\pi^0$(non-$K^*(892)$)ν_τ		< 3.5		$\times 10^{-5}$	CL=90%
Γ_{146}	$\eta\overline{K}^0\pi^-\nu_\tau$		(9.3	±1.5)	$\times 10^{-5}$	
Γ_{147}	$\eta\overline{K}^0\pi^-\pi^0\nu_\tau$		< 5.0		$\times 10^{-5}$	CL=90%
Γ_{148}	$\eta K^-K^0\nu_\tau$		< 9.0		$\times 10^{-6}$	CL=90%
Γ_{149}	$\eta\pi^+\pi^-\pi^-\geq 0$ neutrals ν_τ		< 3		$\times 10^{-3}$	CL=90%
Γ_{150}	$\eta\pi^-\pi^+\pi^-\nu_\tau$(ex.$K^0$)		(2.25	±0.13)	$\times 10^{-4}$	
Γ_{151}	$\eta\pi^-\pi^+\pi^-\nu_\tau$(ex.$K^0$,$f_1(1285)$)		(9.9	±1.6)	$\times 10^{-5}$	
Γ_{152}	$\eta a_1(1260)^-\nu_\tau \to \eta\pi^-\rho^0\nu_\tau$		< 3.9		$\times 10^{-4}$	CL=90%
Γ_{153}	$\eta\eta\pi^-\nu_\tau$		< 7.4		$\times 10^{-6}$	CL=90%
Γ_{154}	$\eta\eta\pi^-\pi^0\nu_\tau$		< 2.0		$\times 10^{-4}$	CL=95%
Γ_{155}	$\eta\eta K^-\nu_\tau$		< 3.0		$\times 10^{-6}$	CL=90%
Γ_{156}	$\eta'(958)\pi^-\nu_\tau$		< 4.0		$\times 10^{-6}$	CL=90%
Γ_{157}	$\eta'(958)\pi^-\pi^0\nu_\tau$		< 1.2		$\times 10^{-5}$	CL=90%
Γ_{158}	$\eta'(958)K^-\nu_\tau$		< 2.4		$\times 10^{-6}$	CL=90%
Γ_{159}	$\phi\pi^-\nu_\tau$		(3.4	±0.6)	$\times 10^{-5}$	
Γ_{160}	$\phi K^-\nu_\tau$		(3.70	±0.33)	$\times 10^{-5}$	S=1.3
Γ_{161}	$f_1(1285)\pi^-\nu_\tau$		(3.9	±0.5)	$\times 10^{-4}$	S=1.9
Γ_{162}	$f_1(1285)\pi^-\nu_\tau \to \eta\pi^-\pi^+\pi^-\nu_\tau$		(1.18	±0.07)	$\times 10^{-4}$	S=1.3
Γ_{163}	$f_1(1285)\pi^-\nu_\tau \to 3\pi^-2\pi^+\nu_\tau$		(5.2	±0.5)	$\times 10^{-5}$	
Γ_{164}	$\pi(1300)^-\nu_\tau \to (\rho\pi)^-\nu_\tau \to (3\pi)^-\nu_\tau$		< 1.0		$\times 10^{-4}$	CL=90%
Γ_{165}	$\pi(1300)^-\nu_\tau \to ((\pi\pi)_{S-\text{wave}}\ \pi)^-\nu_\tau \to (3\pi)^-\nu_\tau$		< 1.9		$\times 10^{-4}$	CL=90%
Γ_{166}	$h^-\omega\geq 0$ neutrals ν_τ		(2.41	±0.09)	%	S=1.2
Γ_{167}	$h^-\omega\nu_\tau$	[a]	(2.00	±0.08)	%	S=1.3
Γ_{168}	$K^-\omega\nu_\tau$		(4.1	±0.9)	$\times 10^{-4}$	
Γ_{169}	$h^-\omega\pi^0\nu_\tau$	[a]	(4.1	±0.4)	$\times 10^{-3}$	
Γ_{170}	$h^-\omega 2\pi^0\nu_\tau$		(1.4	±0.5)	$\times 10^{-4}$	
Γ_{171}	$\pi^-\omega 2\pi^0\nu_\tau$		(7.3	±1.7)	$\times 10^{-5}$	
Γ_{172}	$h^-2\omega\nu_\tau$		< 5.4		$\times 10^{-7}$	CL=90%
Γ_{173}	$2h^-h^+\omega\nu_\tau$		(1.20	±0.22)	$\times 10^{-4}$	
Γ_{174}	$2\pi^-\pi^+\omega\nu_\tau$		(8.4	±0.7)	$\times 10^{-5}$	

Lepton Family number (*LF*), Lepton number (*L*), or Baryon number (*B*) violating modes

L means lepton number violation (*e.g.* $\tau^- \to e^+\pi^-\pi^-$). Following common usage, *LF* means lepton family violation *and not* lepton number violation (*e.g.* $\tau^- \to e^-\pi^+\pi^-$). *B* means baryon number violation.

Γ_{175}	$e^-\gamma$	*LF*	< 3.3		$\times 10^{-8}$	CL=90%
Γ_{176}	$\mu^-\gamma$	*LF*	< 4.4		$\times 10^{-8}$	CL=90%
Γ_{177}	$e^-\pi^0$	*LF*	< 8.0		$\times 10^{-8}$	CL=90%
Γ_{178}	$\mu^-\pi^0$	*LF*	< 1.1		$\times 10^{-7}$	CL=90%
Γ_{179}	$e^-K^0_S$	*LF*	< 2.6		$\times 10^{-8}$	CL=90%
Γ_{180}	$\mu^-K^0_S$	*LF*	< 2.3		$\times 10^{-8}$	CL=90%
Γ_{181}	$e^-\eta$	*LF*	< 9.2		$\times 10^{-8}$	CL=90%
Γ_{182}	$\mu^-\eta$	*LF*	< 6.5		$\times 10^{-8}$	CL=90%
Γ_{183}	$e^-\rho^0$	*LF*	< 1.8		$\times 10^{-8}$	CL=90%
Γ_{184}	$\mu^-\rho^0$	*LF*	< 1.2		$\times 10^{-8}$	CL=90%
Γ_{185}	$e^-\omega$	*LF*	< 4.8		$\times 10^{-8}$	CL=90%
Γ_{186}	$\mu^-\omega$	*LF*	< 4.7		$\times 10^{-8}$	CL=90%
Γ_{187}	$e^-K^*(892)^0$	*LF*	< 3.2		$\times 10^{-8}$	CL=90%
Γ_{188}	$\mu^-K^*(892)^0$	*LF*	< 5.9		$\times 10^{-8}$	CL=90%
Γ_{189}	$e^-\overline{K}^*(892)^0$	*LF*	< 3.4		$\times 10^{-8}$	CL=90%
Γ_{190}	$\mu^-\overline{K}^*(892)^0$	*LF*	< 7.0		$\times 10^{-8}$	CL=90%
Γ_{191}	$e^-\eta'(958)$	*LF*	< 1.6		$\times 10^{-7}$	CL=90%
Γ_{192}	$\mu^-\eta'(958)$	*LF*	< 1.3		$\times 10^{-7}$	CL=90%
Γ_{193}	$e^-f_0(980) \to e^-\pi^+\pi^-$	*LF*	< 3.2		$\times 10^{-8}$	CL=90%
Γ_{194}	$\mu^-f_0(980) \to \mu^-\pi^+\pi^-$	*LF*	< 3.4		$\times 10^{-8}$	CL=90%
Γ_{195}	$e^-\phi$	*LF*	< 3.1		$\times 10^{-8}$	CL=90%
Γ_{196}	$\mu^-\phi$	*LF*	< 8.4		$\times 10^{-8}$	CL=90%
Γ_{197}	$e^-e^+e^-$	*LF*	< 2.7		$\times 10^{-8}$	CL=90%
Γ_{198}	$e^-\mu^+\mu^-$	*LF*	< 2.7		$\times 10^{-8}$	CL=90%
Γ_{199}	$e^+\mu^-\mu^-$	*LF*	< 1.7		$\times 10^{-8}$	CL=90%
Γ_{200}	$\mu^-e^+e^-$	*LF*	< 1.8		$\times 10^{-8}$	CL=90%
Γ_{201}	$\mu^+e^-e^-$	*LF*	< 1.5		$\times 10^{-8}$	CL=90%
Γ_{202}	$\mu^-\mu^+\mu^-$	*LF*	< 2.1		$\times 10^{-8}$	CL=90%
Γ_{203}	$e^-\pi^+\pi^-$	*LF*	< 2.3		$\times 10^{-8}$	CL=90%
Γ_{204}	$e^+\pi^-\pi^-$	*L*	< 2.0		$\times 10^{-8}$	CL=90%
Γ_{205}	$\mu^-\pi^+\pi^-$	*LF*	< 2.1		$\times 10^{-8}$	CL=90%
Γ_{206}	$\mu^+\pi^-\pi^-$	*L*	< 3.9		$\times 10^{-8}$	CL=90%
Γ_{207}	$e^-\pi^+K^-$	*LF*	< 3.7		$\times 10^{-8}$	CL=90%
Γ_{208}	$e^-\pi^-K^+$	*LF*	< 3.1		$\times 10^{-8}$	CL=90%
Γ_{209}	$e^+\pi^-K^-$	*L*	< 3.2		$\times 10^{-8}$	CL=90%
Γ_{210}	$e^-K^0_SK^0_S$	*LF*	< 7.1		$\times 10^{-8}$	CL=90%
Γ_{211}	$e^-K^+K^-$	*LF*	< 3.4		$\times 10^{-8}$	CL=90%
Γ_{212}	$e^+K^-K^-$	*L*	< 3.3		$\times 10^{-8}$	CL=90%
Γ_{213}	$\mu^-\pi^+K^-$	*LF*	< 8.6		$\times 10^{-8}$	CL=90%
Γ_{214}	$\mu^-\pi^-K^+$	*LF*	< 4.5		$\times 10^{-8}$	CL=90%
Γ_{215}	$\mu^+\pi^-K^-$	*L*	< 4.8		$\times 10^{-8}$	CL=90%
Γ_{216}	$\mu^-K^0_SK^0_S$	*LF*	< 8.0		$\times 10^{-8}$	CL=90%
Γ_{217}	$\mu^-K^+K^-$	*LF*	< 4.4		$\times 10^{-8}$	CL=90%
Γ_{218}	$\mu^+K^-K^-$	*L*	< 4.7		$\times 10^{-8}$	CL=90%
Γ_{219}	$e^-\pi^0\pi^0$	*LF*	< 6.5		$\times 10^{-6}$	CL=90%
Γ_{220}	$\mu^-\pi^0\pi^0$	*LF*	< 1.4		$\times 10^{-5}$	CL=90%
Γ_{221}	$e^-\eta\eta$	*LF*	< 3.5		$\times 10^{-5}$	CL=90%
Γ_{222}	$\mu^-\eta\eta$	*LF*	< 6.0		$\times 10^{-5}$	CL=90%
Γ_{223}	$e^-\pi^0\eta$	*LF*	< 2.4		$\times 10^{-5}$	CL=90%
Γ_{224}	$\mu^-\pi^0\eta$	*LF*	< 2.2		$\times 10^{-5}$	CL=90%
Γ_{225}	$p\mu^-\mu^-$	*L*,*B*	< 4.4		$\times 10^{-7}$	CL=90%
Γ_{226}	$\overline{p}\mu^+\mu^-$	*L*,*B*	< 3.3		$\times 10^{-7}$	CL=90%
Γ_{227}	$\overline{p}\gamma$	*L*,*B*	< 3.5		$\times 10^{-6}$	CL=90%
Γ_{228}	$\overline{p}\pi^0$	*L*,*B*	< 1.5		$\times 10^{-5}$	CL=90%
Γ_{229}	$\overline{p}2\pi^0$	*L*,*B*	< 3.3		$\times 10^{-5}$	CL=90%
Γ_{230}	$\overline{p}\eta$	*L*,*B*	< 8.9		$\times 10^{-6}$	CL=90%
Γ_{231}	$\overline{p}\pi^0\eta$	*L*,*B*	< 2.7		$\times 10^{-5}$	CL=90%
Γ_{232}	$\Lambda\pi^-$	*L*,*B*	< 7.2		$\times 10^{-8}$	CL=90%
Γ_{233}	$\overline{\Lambda}\pi^-$	*L*,*B*	< 1.4		$\times 10^{-7}$	CL=90%
Γ_{234}	e^-light boson	*LF*	< 2.7		$\times 10^{-3}$	CL=95%
Γ_{235}	μ^-light boson	*LF*	< 5		$\times 10^{-3}$	CL=95%

[a] Basis mode for the τ.

[b] See the Particle Listings below for the energy limits used in this measurement.

CONSTRAINED FIT INFORMATION

An overall fit to 66 branching ratios uses 139 measurements and one constraint to determine 31 parameters. The overall fit has a $\chi^2 = 128.9$ for 109 degrees of freedom.

The following *off-diagonal* array elements are the correlation coefficients $\langle \delta x_i \delta x_j \rangle / (\delta x_i \cdot \delta x_j)$, in percent, from the fit to the branching fractions, $x_i \equiv \Gamma_i/\Gamma_{\rm total}$. The fit constrains the x_i whose labels appear in this array to sum to one.

x_5	13									
x_9	−13	8								
x_{10}	11	0	−5							
x_{14}	−15	−18	−15	−3						
x_{16}	0	0	−1	−1	−7					
x_{20}	−1	−7	−15	−3	−48	−2				
x_{23}	−1	0	0	−1	−1	−11	−10			
x_{27}	−1	−4	−11	−1	1	0	−28	−1		
x_{28}	−1	0	1	−1	1	−10	−6	−18	−11	
x_{30}	−1	−4	−12	0	−10	0	10	−2	−41	1
x_{35}	−9	−7	−5	−2	−2	0	−12	0	−4	0
x_{37}	−2	−2	−1	−1	0	−6	−1	−10	1	−10
x_{40}	−7	−6	−4	−1	−2	1	−9	2	−6	2
x_{42}	−1	−1	−1	−1	1	−8	1	−13	1	−13
x_{47}	0	0	0	0	0	0	0	0	0	0
x_{48}	−7	−6	−4	−2	−2	1	−10	1	−3	1
x_{64}	−10	−8	3	−2	0	0	−21	1	−12	1
x_{72}	−4	−5	−5	0	−7	1	−2	1	−3	0
x_{79}	2	0	−3	0	−2	0	3	−1	3	−1
x_{80}	0	0	0	0	1	0	−2	0	−1	0
x_{90}	−3	−2	−1	−1	1	0	−10	0	−4	0
x_{94}	−1	0	1	0	2	0	−4	0	−2	0
x_{98}	−3	−2	−1	−1	1	0	−9	0	−4	0
x_{99}	0	0	0	0	0	0	−1	0	0	0
x_{107}	1	1	0	0	−1	−1	2	−1	2	−1
x_{113}	0	0	−1	0	−2	0	2	0	1	0
x_{140}	−1	−1	0	0	0	0	−3	0	0	0
x_{142}	0	0	0	0	0	0	0	0	0	0
x_{167}	−4	−4	−4	0	−4	0	−5	0	−3	0
x_{169}	0	−2	−5	−1	−3	0	1	−1	3	−2
	x_3	x_5	x_9	x_{10}	x_{14}	x_{16}	x_{20}	x_{23}	x_{27}	x_{28}

x_{35}	−1									
x_{37}	0	−3								
x_{40}	0	−10	0							
x_{42}	0	−2	−17	−18						
x_{47}	0	−1	0	0	0					
x_{48}	−1	−24	−7	−18	−5	−1				
x_{64}	−7	−1	−1	−1	0	0	−1			
x_{72}	3	3	1	3	0	0	2	−11		
x_{79}	3	−1	0	−1	0	0	−1	−2	−7	
x_{80}	−1	0	0	0	0	0	0	0	−1	−1
x_{90}	−2	−2	0	−1	0	0	−2	10	−3	−1
x_{94}	−1	−1	0	−1	0	0	−1	−2	−7	−1
x_{98}	−2	−2	0	−1	0	0	−1	9	−3	−1
x_{99}	0	0	0	0	0	0	0	0	−1	0
x_{107}	0	−2	0	−2	0	0	−2	−3	−2	1
x_{113}	−1	0	0	0	0	0	0	−2	−1	1
x_{140}	−3	−1	0	−1	0	0	−1	0	0	−7
x_{142}	0	0	0	0	0	0	0	0	0	0
x_{167}	1	0	0	0	0	0	0	−7	−69	−4
x_{169}	3	−3	0	−2	0	0	−2	−3	−9	−62
	x_{30}	x_{35}	x_{37}	x_{40}	x_{42}	x_{47}	x_{48}	x_{64}	x_{72}	x_{79}

x_{90}	0									
x_{94}	−1	−2								
x_{98}	0	76	−1							
x_{99}	0	0	−3	0						
x_{107}	0	−2	−1	−2	0					
x_{113}	0	−1	0	−1	0	−5				
x_{140}	0	0	0	0	0	0	0			
x_{142}	0	0	−2	0	0	0	0	0		
x_{167}	−1	−2	3	−2	1	−1	−1	0	0	
x_{169}	−2	−2	−2	−2	0	1	1	−1	0	−5
	x_{80}	x_{90}	x_{94}	x_{98}	x_{99}	x_{107}	x_{113}	x_{140}	x_{142}	x_{167}

τ BRANCHING FRACTIONS

Revised September 2013 by K.G. Hayes (Hillsdale College).

There are now 42 measurements and 23 upper limits from Belle and BaBar on branching fractions of conventional τ-decay modes, up from 1 measurement and 3 upper limits in the 2006 edition of this Review. Eighteen of these measurements are used in the constrained fit to τ branching fractions, and 22 are for τ-decay modes for which older non-B-factory measurements exist. For those 22 measurements, the new B-factory measurements have on average about sixty times the number of events as the most precise earlier measurements, and the statistical uncertainties on the B-factory measurements are on average about eight times smaller. However, the systematic uncertainties now greatly exceed the statistical uncertainties of all B-factory branching fraction measurements of major τ-decay modes. For example, the average ratio of systematic to statistical uncertainty of the B-factory measurements of τ branching fractions larger than 10^{-3} is 17.6, while the average ratio for branching fractions smaller than 10^{-4} is 0.9. Thus, the total uncertainty on the branching fraction measurements from B-factories is on average only about 3.8 times smaller than the previous most precise non-B-factory measurements.

The constrained fit to τ branching fractions: The Lepton Summary Table and the List of τ-Decay Modes contain branching fractions for 131 conventional τ-decay modes and upper limits on the branching fractions for 39 other conventional τ-decay modes. Of the 131 modes with branching fractions, 82 are derived from a constrained fit to τ branching fraction data. The goal of the constrained fit is to make optimal use of the experimental data to determine τ branching fractions. For example, the branching fractions for the decay mode $\tau^- \to \pi^-\pi^+\pi^-\pi^0\nu_\tau$ is determined mostly from experimental measurements of the branching fraction for $\tau^- \to h^-h^-h^+\pi^0\nu_\tau$ and measurements of exclusive branching fractions for 3-prong modes containing charged kaons and 1 π^0.

Branching fractions from the constrained fit are derived from a set of basis modes. The basis modes form an exclusive set whose branching fractions are constrained to sum exactly to one. The set of selected basis modes expands as branching fraction measurements for new τ-decay modes are published. The number of basis modes has expanded from 12 in the year 1994 fit to 31 in the 2002 through 2013 fits. The 31 basis modes selected for the 2013 fit are listed in Table 1. See the

See key on page 547

1996 edition of this *Review* [1] for a complete description of our notation for naming τ-decay modes and the selection of the basis modes. For each edition since the 1996 edition, the changes in the selected basis modes from the previous edition are described in the τ Branching Fractions Review. Figure 1 illustrates the basis mode branching fractions from the 2013 fit.

Table 1: Basis modes and fit values(%) for the 2013 fit to τ branching fraction data.

$e^-\overline{\nu}_e\nu_\tau$	17.83 ± 0.04
$\mu^-\overline{\nu}_\mu\nu_\tau$	17.41 ± 0.04
$\pi^-\nu_\tau$	10.83 ± 0.06
$\pi^-\pi^0\nu_\tau$	25.52 ± 0.09
$\pi^-2\pi^0\nu_\tau$ (ex. K^0)	9.30 ± 0.11
$\pi^-3\pi^0\nu_\tau$ (ex. K^0)	1.05 ± 0.07
$h^-4\pi^0\nu_\tau$ (ex. K^0, η)	0.11 ± 0.04
$K^-\nu_\tau$	0.700 ± 0.010
$K^-\pi^0\nu_\tau$	0.429 ± 0.015
$K^-2\pi^0\nu_\tau$ (ex. K^0)	0.065 ± 0.023
$K^-3\pi^0\nu_\tau$ (ex. K^0, η)	0.048 ± 0.022
$\pi^-\overline{K}^0\nu_\tau$	0.84 ± 0.04
$\pi^-\overline{K}^0\pi^0\nu_\tau$	0.40 ± 0.04
$\pi^-K^0_SK^0_S\nu_\tau$	0.023 ± 0.002
$\pi^-K^0_SK^0_L\nu_\tau$	0.12 ± 0.04
$K^-K^0\nu_\tau$	0.159 ± 0.016
$K^-K^0\pi^0\nu_\tau$	0.159 ± 0.020
$\pi^-\pi^+\pi^-\nu_\tau$ (ex. K^0, ω)	8.99 ± 0.06
$\pi^-\pi^+\pi^-\pi^0\nu_\tau$ (ex. K^0, ω)	2.70 ± 0.08
$K^-\pi^+\pi^-\nu_\tau$ (ex. K^0)	0.294 ± 0.015
$K^-\pi^+\pi^-\pi^0\nu_\tau$ (ex. K^0, η)	0.078 ± 0.012
$K^-K^+\pi^-\nu_\tau$	0.144 ± 0.005
$K^-K^+\pi^-\pi^0\nu_\tau$	0.0061 ± 0.0025
$h^-h^-h^+2\pi^0\nu_\tau$ (ex. K^0, ω, η)	0.10 ± 0.04
$h^-h^-h^+3\pi^0\nu_\tau$	0.023 ± 0.006
$3h^-2h^+\nu_\tau$ (ex. K^0)	0.0839 ± 0.0035
$3h^-2h^+\pi^0\nu_\tau$ (ex. K^0)	0.0178 ± 0.0027
$h^-\omega\nu_\tau$	2.00 ± 0.08
$h^-\omega\pi^0\nu_\tau$	0.41 ± 0.04
$\eta\pi^-\pi^0\nu_\tau$	0.139 ± 0.010
$\eta K^-\nu_\tau$	0.0152 ± 0.0008

In selecting the basis modes, assumptions and choices must be made. For example, we assume the decays $\tau^- \to \pi^-K^+\pi^- \geq 0\pi^0\nu_\tau$ and $\tau^- \to \pi^+K^-K^- \geq 0\pi^0\nu\tau$ have negligible branching fractions. This is consistent with standard model predictions for τ decay, although the experimental limits for these branching fractions are not very stringent. The 95% confidence level upper limits for these branching fractions in the current Listings are $\mathrm{B}(\tau^- \to \pi^-K^+\pi^- \geq 0\pi^0\nu_\tau) < 0.25\%$ and $\mathrm{B}(\tau^- \to \pi^+K^-K^- \geq 0\pi^0\nu_\tau) < 0.09\%$, values not so different from measured branching fractions for allowed 3-prong modes containing charged kaons. Although our usual goal is to impose

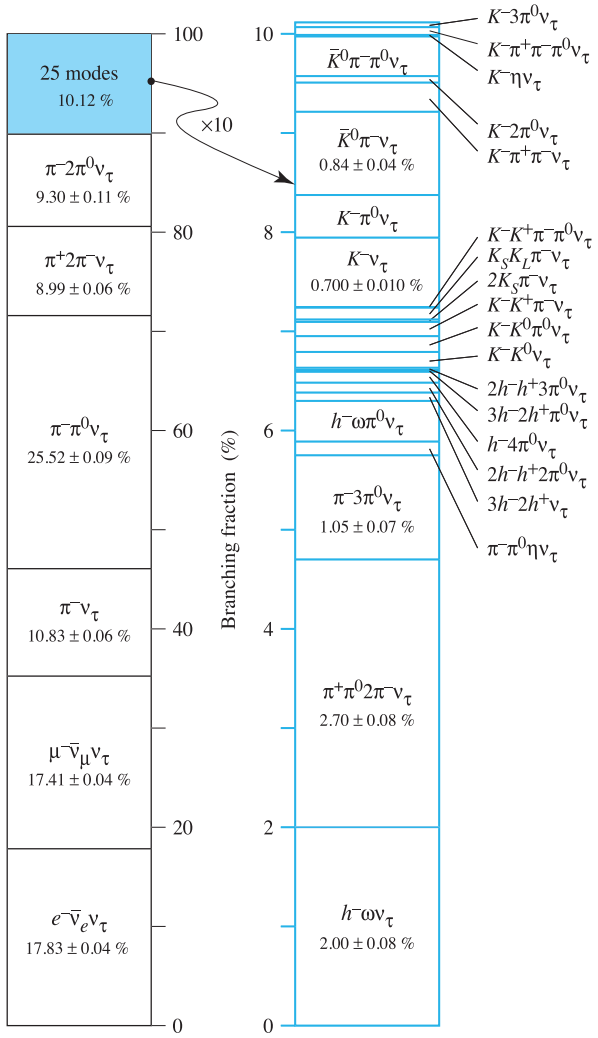

Figure 1: Basis mode branching fractions of the τ. Six modes account for 90% of the decays, 25 modes account for the last 10%. The list of excluded intermediate states for each basis mode has been suppressed.

as few theoretical constraints as possible so that the world averages and fit results can be used to test the theoretical constraints (*i.e.*, we do not make use of the theoretical constraint from lepton universality on the ratio of the τ-leptonic branching fractions $\mathrm{B}(\tau^- \to \mu^-\overline{\nu}_\mu\nu_\tau)/\ \mathrm{B}(\tau^- \to e^-\overline{\nu}_e\nu_\tau) = 0.9726$), the experimental challenge to identify charged prongs in 3-prong τ decays is sufficiently difficult that experimenters have been forced to make these assumptions when measuring the branching fractions of the allowed decays. We are constrained by the assumptions made by the experimenters.

There are several τ-decay modes with small but well-measured (> 2.5 sigma from zero) branching fractions [2] which cannot be expressed in terms of the selected basis modes and are therefore left out of the fit:

$$\begin{aligned}
\mathrm{B}(\tau^- \to \pi^- K_S^0 K_L^0 \pi^0 \nu_\tau) &= (3.1 \pm 1.2) \times 10^{-4} \\
\mathrm{B}(\tau^- \to 2K^- K^+ \nu_\tau) &= (0.21 \pm 0.08) \times 10^{-4} \\
\mathrm{B}(\tau^- \to \eta K^- \pi^0 \nu_\tau) &= (0.48 \pm 0.12) \times 10^{-4} \\
\mathrm{B}(\tau^- \to \eta \overline{K}{}^0 \pi^- \nu_\tau) &= (0.93 \pm 0.15) \times 10^{-4}.
\end{aligned}$$

Certain components of other small but well-measured τ-decay modes cannot be expressed in terms of the selected basis modes and therefore are also left out of the fit:

$$\begin{aligned}
&\mathrm{B}(\tau^- \to \eta\pi^-\pi^0\pi^0\nu_\tau)\times \\
&\quad \mathrm{B}(\eta\to\gamma\gamma \text{ or } \eta\to\pi^+\pi^-\gamma \text{ or } \eta \to 3\pi^0) = (1.4 \pm 0.2) \times 10^{-4}, \\
&\mathrm{B}(\tau^- \to \eta\pi^-\pi^+\pi^-\nu_\tau)\times \\
&\quad \mathrm{B}(\eta \to \gamma\gamma \text{ or } \eta \to \pi^+\pi^-\gamma) = (0.99 \pm 0.06) \times 10^{-4}, \\
&\mathrm{B}(\tau^- \to \phi K^- \nu_\tau)\times \\
&\quad \mathrm{B}(\phi \to K_S^0 K_L^0 \text{ or } \phi \to \eta\gamma) = (0.13 \pm 0.01) \times 10^{-4}, \\
&\mathrm{B}(\tau^-\to f_1(1285)\pi^-\nu_\tau)\mathrm{B}(f_1(1285)\to\rho^0\gamma) = (0.22 \pm 0.06) \times 10^{-4}, \\
&\mathrm{B}(\tau^- \to h^-\omega\pi^0\pi^0\nu_\tau)\mathrm{B}(\omega \to \pi^0\gamma) = (0.12 \pm 0.04) \times 10^{-4}, \\
&\mathrm{B}(\tau^- \to 2h^-h^+\omega\nu_\tau)\mathrm{B}(\omega \to \pi^0\gamma) = (0.10 \pm 0.02) \times 10^{-4}.
\end{aligned}$$

The sum of these excluded branching fractions is $(0.08 \pm 0.01)\%$. This is near our goal of 0.1% for the internal consistency of the τ Listings for this edition, and thus for simplicity we do not include these small branching fraction decay modes in the basis set.

Beginning with the 2002 edition, the fit algorithm has been improved to allow for correlations between branching fraction measurements used in the fit. If only a few measurements are correlated, the correlation coefficients are listed in the footnote for each measurement. If a large number of measurements are correlated, then the full correlation matrix is listed in the footnote to the measurement that first appears in the τ Listings. Footnotes to the other measurements refer to the first measurement. For example, the large correlation matrices for the branching fraction measurements contained in Refs. [3,4] are listed in Footnotes to the $\Gamma(e^-\overline{\nu}_e\nu_\tau)/\Gamma_{\mathrm{total}}$ and $\Gamma(h^-\nu_\tau)/\Gamma_{\mathrm{total}}$ measurements respectively. Sometimes experimental papers contain correlation coefficients between measurements using only statistical errors without including systematic errors. We usually cannot make use of these correlation coefficients.

The 2013 constrained fit has a χ^2 of 128.9 for 109 degrees of freedom, and is essentially unchanged from the 2012 fit.

Inconsistencies in the τlepton Branching Fraction Data: Several inconsistencies are known to exist in the branching fraction measurements that are used to determine the τ-lepton branching fractions. The sources of the inconsistencies are unknown. The treatment of discrepant data used for fits and averages is described in the introduction of this *Review*. Of the 82 branching fractions that are derived from the constrained fit, 12 (15%) have scale factors that are 1.5 or larger, and the largest is 2.7. Of the 49 branching fractions that are not derived from the constrained fit, 32 make use of only one measurement. Of the 17 averages that make use of more than one measurement, 4 (24%) have scale factors that are 1.5 or larger, and the largest is 5.4. Ideograms for 8 branching fractions are currently displayed in the τ Listings.

The τ branching fraction measurements by BaBar and Belle tend to be smaller than the non-B-factory measurements. There are 22 B-factory branching fraction measurements of τ-decay modes for which older non-B-factory measurements exist. Comparing the B-factory branching fraction measurements to the earlier non-B-factory measurements reveals a systematic discrepancy between the two sets of measurements. Figure 2 shows a histogram of the normalized difference ((B-factory value minus non-B-factory value)/estimated uncertainty in the difference) for the 22 measurements. The value used for the non-B-factory measurement is the value listed in the latest edition of this *Review* prior to the first B-factory measurement for that decay mode. Nineteen of the 22 B-factory branching fraction measurements are smaller than the non-B-factory values. The average normalized difference between the two sets of measurements is -1.08 (-1.41 for the 11 Belle measurements and -0.75 for the 11 BaBar measurements). The Heavy Flavor Averaging Group (HFAG) analysis of τ branching fractions includes a similar comparison of the B-factory and non-B-factory measurements [6].

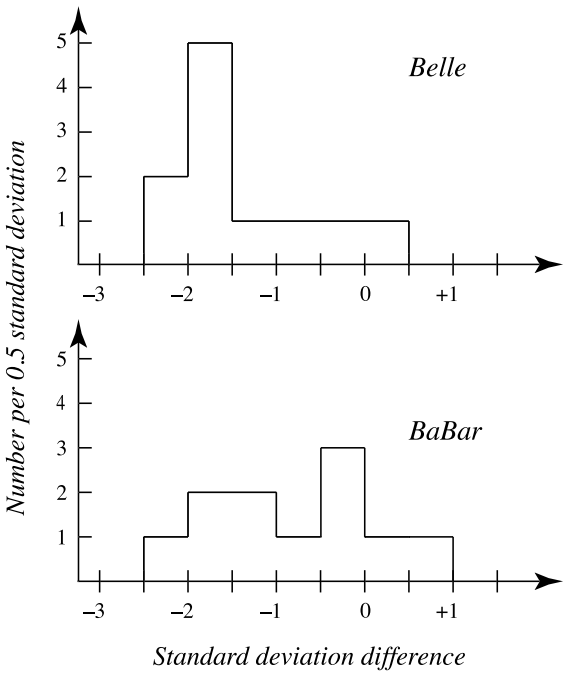

Figure 2: Distribution of the normalized difference between the 22 B-factory measurements of conventional τ-decay branching fractions and non-B-factory measurements. The Belle and BaBar collaborations have each published 11 measurements of τ-decay branching fractions for which older non-B-factory measurements exist.

See key on page 547

Belle and BaBar have each published branching fraction measurements for the six τ-decay modes listed in Table 2. The normalized difference between the two measured values is calculated by subtracting the Belle value from the BaBar value and dividing this difference by the quadratic sum of the statistical and systematic errors for each measurement. When a measurement has asymmetric errors, the larger of the two values is used in the quadratic sum. It is apparent from the values in Table 2 that the Belle and BaBar values differ significantly for several of the τ-decay modes.

Table 2: Comparison of the Belle and Babar branching fraction measurements for the six τ-decay modes that both experiments have measured. The normalized difference is the difference between the Belle and BaBar branching fraction values divided by the quadratic sum of the statistical and systematic errors for both measurements.

Mode	BaBar − Belle Normalized Difference ($\#\sigma$)
$\pi^-\pi^+\pi^-\nu_\tau$ (ex. K^0)	+1.4
$K^-\pi^+\pi^-\nu_\tau$ (ex. K^0)	−2.9
$K^-K^+\pi^-\nu_\tau$	−2.9
$K^-K^+K^-\nu_\tau$	−5.4
$\eta\ K^-\nu_\tau$	−1.0
$\phi\ K^-\nu_\tau$	−1.3

Overconsistency of Leptonic Branching Fraction Measurements: To minimize the effects of older experiments which often have larger systematic errors and sometimes make assumptions that have later been shown to be invalid, we exclude old measurements in decay modes which contain at least several newer data of much higher precision. As a rule, we exclude those experiments with large errors which together would contribute no more than 5% of the weight in the average. This procedure leaves five measurements for $B_e \equiv B(\tau^- \to e^-\overline{\nu}_e\nu_\tau)$ and five measurements for $B_\mu \equiv B(\tau^- \to \mu^-\overline{\nu}_\mu\nu_\tau)$. For both B_e and B_μ, the selected measurements are considerably more consistent with each other than should be expected from the quoted errors on the individual measurements. The χ^2 from the calculation of the average of the selected measurements is 0.34 for B_e and 0.08 for B_μ. Assuming normal errors, the probability of a smaller χ^2 is 1.3% for B_e and 0.08% for B_μ.

References

1. R.M. Barnett *et al.* (Particle Data Group), *Review of Particle Physics*, Phys. Rev. **D54**, 1 (1996).
2. See the τ Listings for references.
3. S. Schael *et al.* (ALEPH Collab.), Phys. Rep. **421**, 191 (2005).
4. J. Abdallah *et al.* (DELPHI Collab.), Eur. Phys. J. **C46**, 1 (2006).
5. B. Aubert *et al.* (BaBar Collab.), Phys. Rev. Lett. **105**, 051602 (2010).
6. S. Banerjee *et al.* (HFAG), http://arxiv.org/pdf/1101.5138v1.pdf.

$(\Gamma(\tau^+) - \Gamma(\tau^-)) / (\Gamma(\tau^+) + \Gamma(\tau^-))$

$\tau^\pm \to \pi^\pm K^0_S \nu_\tau$ (RATE DIFFERENCE) / (RATE SUM)

VALUE (%)	DOCUMENT ID		TECN	COMMENT
−0.36±0.23±0.11	LEES	12M	BABR	476 fb^{-1} E^{ee}_{cm} = 10.6 GeV

τ^- BRANCHING RATIOS

$\Gamma(\text{particle}^- \geq 0 \text{ neutrals } \geq 0K^0\nu_\tau(\text{"1-prong"}))/\Gamma_{total}$ Γ_1/Γ

$\Gamma_1/\Gamma = (\Gamma_3+\Gamma_5+\Gamma_9+\Gamma_{10}+\Gamma_{14}+\Gamma_{16}+\Gamma_{20}+\Gamma_{23}+\Gamma_{27}+\Gamma_{28}+\Gamma_{30}+\Gamma_{35}+\Gamma_{37}+\Gamma_{40}+\Gamma_{42}+2\Gamma_{47}+\Gamma_{48}+0.708\Gamma_{140}+0.715\Gamma_{142}+0.09\Gamma_{167}+0.09\Gamma_{169})/\Gamma$

The charged particle here can be e, μ, or hadron. In many analyses, the sum of the topological branching fractions (1, 3, and 5 prongs) is constrained to be unity. Since the 5-prong fraction is very small, the measured 1-prong and 3-prong fractions are highly correlated and cannot be treated as independent quantities in our overall fit. We arbitrarily choose to use the 3-prong fraction in our fit, and leave the 1-prong fraction out. We do, however, use these 1-prong measurements in our average below. The measurements used only for the average are marked "avg," whereas "f&a" marks a result used for the fit and the average.

VALUE (%)	EVTS	DOCUMENT ID		TECN	COMMENT
85.35 ±0.07 OUR FIT Error includes scale factor of 1.3.					
85.26 ±0.13 OUR AVERAGE Error includes scale factor of 1.6. See the ideogram below.					
• • • We use the following data for averages but not for fits. • • •					
85.316±0.093±0.049	78k	[1] ABREU	01M	DLPH	1992–1995 LEP runs
85.274±0.105±0.073		[2] ACHARD	01D	L3	1992–1995 LEP runs
84.48 ±0.27 ±0.23		ACTON	92H	OPAL	1990–1991 LEP runs
• • • We do not use the following data for averages, fits, limits, etc. • • •					
85.45 $^{+0.69}_{-0.73}$ ±0.65		DECAMP	92C	ALEP	Repl. by SCHAEL 05C

[1] The correlation coefficients between this measurement and the ABREU 01M measurements of B($\tau \to$ 3-prong) and B($\tau \to$ 5-prong) are −0.98 and −0.08 respectively.
[2] The correlation coefficients between this measurement and the ACHARD 01D measurements of B($\tau \to$ "3-prong") and B($\tau \to$ "5-prong") are −0.978 and −0.082 respectively.

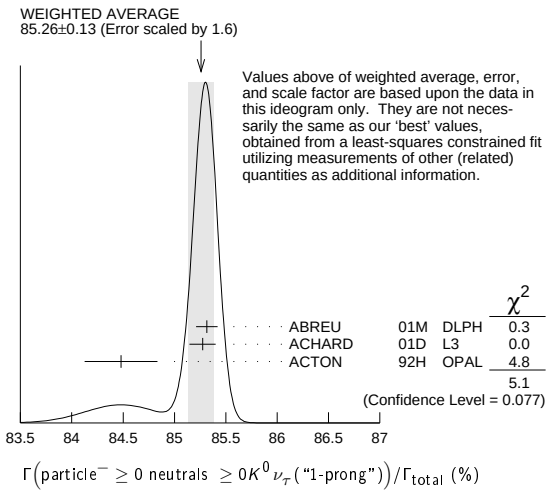

$\Gamma(\text{particle}^- \geq 0 \text{ neutrals } \geq 0K^0_L\nu_\tau)/\Gamma_{total}$ Γ_2/Γ

$\Gamma_2/\Gamma = (\Gamma_3+\Gamma_5+\Gamma_9+\Gamma_{10}+\Gamma_{14}+\Gamma_{16}+\Gamma_{20}+\Gamma_{23}+\Gamma_{27}+\Gamma_{28}+\Gamma_{30}+0.6569\Gamma_{35}+0.6569\Gamma_{37}+0.6569\Gamma_{40}+0.6569\Gamma_{42}+1.0985\Gamma_{47}+0.3139\Gamma_{48}+0.708\Gamma_{140}+0.715\Gamma_{142}+0.09\Gamma_{167}+0.09\Gamma_{169})/\Gamma$

VALUE (%)	EVTS	DOCUMENT ID		TECN	COMMENT
84.71±0.08 OUR FIT Error includes scale factor of 1.3.					
85.1 ±0.4 OUR AVERAGE					
• • • We use the following data for averages but not for fits. • • •					
85.6 ±0.6 ±0.3	3300	[1] ADEVA	91F	L3	E^{ee}_{cm}= 88.3–94.3 GeV
84.9 ±0.4 ±0.3		BEHREND	89B	CELL	E^{ee}_{cm}= 14–47 GeV
84.7 ±0.8 ±0.6		[2] AIHARA	87B	TPC	E^{ee}_{cm}= 29 GeV

• • • We do not use the following data for averages, fits, limits, etc. • • •

86.4 ±0.3 ±0.3			ABACHI	89B	HRS	E_{cm}^{ee}= 29 GeV
87.1 ±1.0 ±0.7		[3]	BURCHAT	87	MRK2	E_{cm}^{ee}= 29 GeV
87.2 ±0.5 ±0.8			SCHMIDKE	86	MRK2	E_{cm}^{ee}= 29 GeV
84.7 ±1.1 $^{+1.6}_{-1.3}$	169	[4]	ALTHOFF	85	TASS	E_{cm}^{ee}= 34.5 GeV
86.1 ±0.5 ±0.9			BARTEL	85F	JADE	E_{cm}^{ee}= 34.6 GeV
87.8 ±1.3 ±3.9		[5]	BERGER	85	PLUT	E_{cm}^{ee}= 34.6 GeV
86.7 ±0.3 ±0.6			FERNANDEZ	85	MAC	E_{cm}^{ee}= 29 GeV

[1] Not independent of ADEVA 91F $\Gamma(h^-h^-h^+ \geq 0 \text{ neutrals } \geq 0K_L^0\nu_\tau)/\Gamma_{total}$ value.

[2] Not independent of AIHARA 87B $\Gamma(\mu^-\overline{\nu}_\mu\nu_\tau)/\Gamma_{total}$, $\Gamma(e^-\overline{\nu}_e\nu_\tau)/\Gamma_{total}$, and $\Gamma(h^- \geq 0 \text{ neutrals } \geq 0K_L^0\ \nu_\tau)/\Gamma_{total}$ values.

[3] Not independent of SCHMIDKE 86 value (also not independent of BURCHAT 87 value for $\Gamma(h^-h^-h^+ \geq 0 \text{ neutrals } \geq 0K_L^0\nu_\tau)/\Gamma_{total}$.

[4] Not independent of ALTHOFF 85 $\Gamma(\mu^-\overline{\nu}_\mu\nu_\tau)/\Gamma_{total}$, $\Gamma(e^-\overline{\nu}_e\nu_\tau)/\Gamma_{total}$, $\Gamma(h^- \geq 0 \text{ neutrals } \geq 0K_L^0\ \nu_\tau)/\Gamma_{total}$, and $\Gamma(h^-h^-h^+ \geq 0 \text{ neutrals } \geq 0K_L^0\nu_\tau)/\Gamma_{total}$ values.

[5] Not independent of (1-prong + $0\pi^0$) and (1-prong + $\geq 1\pi^0$) values.

$\Gamma(\mu^-\overline{\nu}_\mu\nu_\tau)/\Gamma_{total}$ Γ_3/Γ

To minimize the effect of experiments with large systematic errors, we exclude experiments which together would contribute 5% of the weight in the average.

VALUE (%)	EVTS		DOCUMENT ID		TECN	COMMENT
17.41 ±0.04 OUR FIT Error includes scale factor of 1.1.						
17.33 ±0.05 OUR AVERAGE						
17.319±0.070±0.032	54k	[1]	SCHAEL	05C	ALEP	1991-1995 LEP runs
17.34 ±0.09 ±0.06	31.4k		ABBIENDI	03	OPAL	1990-1995 LEP runs
17.342±0.110±0.067	21.5k	[2]	ACCIARRI	01F	L3	1991-1995 LEP runs
17.325±0.095±0.077	27.7k		ABREU	99X	DLPH	1991-1995 LEP runs
• • • We use the following data for averages but not for fits. • • •						
17.37 ±0.08 ±0.18		[3]	ANASTASSOV 97		CLEO	E_{cm}^{ee}= 10.6 GeV
• • • We do not use the following data for averages, fits, limits, etc. • • •						
17.31 ±0.11 ±0.05	20.7k		BUSKULIC	96C	ALEP	Repl. by SCHAEL 05C
17.02 ±0.19 ±0.24	6586		ABREU	95T	DLPH	Repl. by ABREU 99X
17.36 ±0.27	7941		AKERS	95I	OPAL	Repl. by ABBIENDI 03
17.6 ±0.4 ±0.4	2148		ADRIANI	93M	L3	Repl. by ACCIARRI 01F
17.4 ±0.3 ±0.5		[4]	ALBRECHT	93G	ARG	E_{cm}^{ee}= 9.4–10.6 GeV
17.35 ±0.41 ±0.37			DECAMP	92C	ALEP	1989-1990 LEP runs
17.7 ±0.8 ±0.4	568		BEHREND	90	CELL	E_{cm}^{ee}= 35 GeV
17.4 ±1.0	2197		ADEVA	88	MRKJ	E_{cm}^{ee}= 14–16 GeV
17.7 ±1.2 ±0.7			AIHARA	87B	TPC	E_{cm}^{ee}= 29 GeV
18.3 ±0.9 ±0.8			BURCHAT	87	MRK2	E_{cm}^{ee}= 29 GeV
18.6 ±0.8 ±0.7	558	[5]	BARTEL	86D	JADE	E_{cm}^{ee}= 34.6 GeV
12.9 ±1.7 $^{+0.7}_{-0.5}$			ALTHOFF	85	TASS	E_{cm}^{ee}= 34.5 GeV
18.0 ±0.9 ±0.5	473	[5]	ASH	85B	MAC	E_{cm}^{ee}= 29 GeV
18.0 ±1.0 ±0.6		[6]	BALTRUSAIT...85		MRK3	E_{cm}^{ee}= 3.77 GeV
19.4 ±1.6 ±1.7	153		BERGER	85	PLUT	E_{cm}^{ee}= 34.6 GeV
17.6 ±2.6 ±2.1	47		BEHREND	83C	CELL	E_{cm}^{ee}= 34 GeV
17.8 ±2.0 ±1.8			BERGER	81B	PLUT	E_{cm}^{ee}= 9–32 GeV

[1] See footnote to SCHAEL 05C $\Gamma(\tau^- \to e^-\overline{\nu}_e\nu_\tau)/\Gamma_{total}$ measurement for correlations with other measurements.

[2] The correlation coefficient between this measurement and the ACCIARRI 01F measurement of $B(\tau^- \to e^-\overline{\nu}_e\nu_\tau)$ is 0.08.

[3] The correlation coefficients between this measurement and the ANASTASSOV 97 measurements of $B(e\overline{\nu}_e\nu_\tau)$, $B(\mu\overline{\nu}_\mu\nu_\tau)/B(e\overline{\nu}_e\nu_\tau)$, $B(h^-\nu_\tau)$, and $B(h^-\nu_\tau)/B(e\overline{\nu}_e\nu_\tau)$ are 0.50, 0.58, 0.50, and 0.08 respectively.

[4] Not independent of ALBRECHT 92D $\Gamma(\mu^-\overline{\nu}_\mu\nu_\tau)/\Gamma(e^-\overline{\nu}_e\nu_\tau)$ and ALBRECHT 93G $\Gamma(\mu^-\overline{\nu}_\mu\nu_\tau) \times \Gamma(e^-\overline{\nu}_e\nu_\tau)/\Gamma_{total}^2$ values.

[5] Modified using $B(e^-\overline{\nu}_e\nu_\tau)/B(\text{“1 prong”})$ and B(“1 prong”) ,= 0.855.

[6] Error correlated with BALTRUSAITIS 85 $e\nu\overline{\nu}$ value.

$\Gamma(\mu^-\overline{\nu}_\mu\nu_\tau\gamma)/\Gamma_{total}$ Γ_4/Γ

VALUE (%)	EVTS		DOCUMENT ID		TECN	COMMENT
0.361±0.016±0.035		[1]	BERGFELD	00	CLEO	E_{cm}^{ee}= 10.6 GeV
• • • We do not use the following data for averages, fits, limits, etc. • • •						
0.30 ±0.04 ±0.05	116	[2]	ALEXANDER	96S	OPAL	1991–1994 LEP runs
0.23 ±0.10	10	[3]	WU	90	MRK2	E_{cm}^{ee}= 29 GeV

[1] BERGFELD 00 impose requirements on detected γ's corresponding to a τ-rest-frame energy cutoff $E_\gamma^* > 10$ MeV. For $E_\gamma^* > 20$ MeV, they quote $(3.04 \pm 0.14 \pm 0.30) \times 10^{-3}$.

[2] ALEXANDER 96S impose requirements on detected γ's corresponding to a τ-rest-frame energy cutoff E_γ >20 MeV.

[3] WU 90 reports $\Gamma(\mu^-\overline{\nu}_\mu\nu_\tau\gamma)/\Gamma(\mu^-\overline{\nu}_\mu\nu_\tau) = 0.013 \pm 0.006$, which is converted to $\Gamma(\mu^-\overline{\nu}_\mu\nu_\tau\gamma)/\Gamma_{total}$ using $\Gamma(\mu^-\overline{\nu}_\mu\nu_\tau\gamma)/\Gamma_{total} = 17.35\%$. Requirements on detected γ's correspond to a τ rest frame energy cutoff $E_\gamma > 37$ MeV.

$\Gamma(e^-\overline{\nu}_e\nu_\tau)/\Gamma_{total}$ Γ_5/Γ

To minimize the effect of experiments with large systematic errors, we exclude experiments which together would contribute 5% of the weight in the average.

VALUE (%)	EVTS		DOCUMENT ID		TECN	COMMENT
17.83 ±0.04 OUR FIT						
17.82 ±0.05 OUR AVERAGE						
17.837±0.072±0.036	56k	[1]	SCHAEL	05C	ALEP	1991-1995 LEP runs
17.806±0.104±0.076	24.7k	[2]	ACCIARRI	01F	L3	1991–1995 LEP runs
17.81 ±0.09 ±0.06	33.1k		ABBIENDI	99H	OPAL	1991–1995 LEP runs
17.877±0.109±0.110	23.3k		ABREU	99X	DLPH	1991–1995 LEP runs
17.76 ±0.06 ±0.17		[3]	ANASTASSOV 97		CLEO	E_{cm}^{ee}= 10.6 GeV
• • • We do not use the following data for averages, fits, limits, etc. • • •						
17.78 ±0.10 ±0.09	25.3k		ALEXANDER	96D	OPAL	Repl. by ABBIENDI 99H
17.79 ±0.12 ±0.06	20.6k		BUSKULIC	96C	ALEP	Repl. by SCHAEL 05C
17.51 ±0.23 ±0.31	5059		ABREU	95T	DLPH	Repl.. by ABREU 99X
17.9 ±0.4 ±0.4	2892		ADRIANI	93M	L3	Repl. by ACCIARRI 01F
17.5 ±0.3 ±0.5		[4]	ALBRECHT	93G	ARG	E_{cm}^{ee}= 9.4–10.6 GeV
17.97 ±0.14 ±0.23	3970		AKERIB	92	CLEO	Repl. by ANASTASSOV 97
19.1 ±0.4 ±0.6	2960	[5]	AMMAR	92	CLEO	E_{cm}^{ee}= 10.5–10.9 GeV
18.09 ±0.45 ±0.45			DECAMP	92C	ALEP	Repl. by SCHAEL 05C
17.0 ±0.5 ±0.6	1.7k		ABACHI	90	HRS	E_{cm}^{ee}= 29 GeV
18.4 ±0.8 ±0.4	644		BEHREND	90	CELL	E_{cm}^{ee}= 35 GeV
16.3 ±0.3 ±3.2			JANSSEN	89	CBAL	E_{cm}^{ee}= 9.4–10.6 GeV
18.4 ±1.2 ±1.0			AIHARA	87B	TPC	E_{cm}^{ee}= 29 GeV
19.1 ±0.8 ±1.1			BURCHAT	87	MRK2	E_{cm}^{ee}= 29 GeV
16.8 ±0.7 ±0.9	515	[5]	BARTEL	86D	JADE	E_{cm}^{ee}= 34.6 GeV
20.4 ±3.0 $^{+1.4}_{-0.9}$			ALTHOFF	85	TASS	E_{cm}^{ee}= 34.5 GeV
17.8 ±0.9 ±0.6	390	[5]	ASH	85B	MAC	E_{cm}^{ee}= 29 GeV
18.2 ±0.7 ±0.5		[6]	BALTRUSAIT...85		MRK3	E_{cm}^{ee}= 3.77 GeV
13.0 ±1.9 ±2.9			BERGER	85	PLUT	E_{cm}^{ee}= 34.6 GeV
18.3 ±2.4 ±1.9	60		BEHREND	83C	CELL	E_{cm}^{ee}= 34 GeV
16.0 ±1.3	459	[7]	BACINO	78B	DLCO	E_{cm}^{ee}= 3.1–7.4 GeV

[1] Correlation matrix for SCHAEL 05C branching fractions, in percent:

(1) $\Gamma(\tau^- \to e^-\overline{\nu}_e\nu_\tau)/\Gamma_{total}$
(2) $\Gamma(\tau^- \to \mu^-\overline{\nu}_\mu\nu_\tau)/\Gamma_{total}$
(3) $\Gamma(\tau^- \to \pi^-\nu_\tau)/\Gamma_{total}$
(4) $\Gamma(\tau^- \to \pi^-\pi^0\nu_\tau)/\Gamma_{total}$
(5) $\Gamma(\tau^- \to \pi^-2\pi^0\nu_\tau(\text{ex. } K^0))/\Gamma_{total}$
(6) $\Gamma(\tau^- \to \pi^-3\pi^0\nu_\tau(\text{ex. } K^0))/\Gamma_{total}$
(7) $\Gamma(\tau^- \to h^-4\pi^0\nu_\tau(\text{ex. } K^0,\eta))/\Gamma_{total}$
(8) $\Gamma(\tau^- \to \pi^-\pi^+\pi^-\nu_\tau(\text{ex. } K^0,\omega))/\Gamma_{total}$
(9) $\Gamma(\tau^- \to \pi^-\pi^+\pi^-\pi^0\nu_\tau(\text{ex. } K^0))/\Gamma_{total}$
(10) $\Gamma(\tau^- \to h^-h^-h^+2\pi^0\nu_\tau(\text{ex. } K^0))/\Gamma_{total}$
(11) $\Gamma(\tau^- \to h^-h^-h^+3\pi^0\nu_\tau)/\Gamma_{total}$
(12) $\Gamma(\tau^- \to 3h^-2h^+\nu_\tau(\text{ex. } K^0))/\Gamma_{total}$
(13) $\Gamma(\tau^- \to 3h^-2h^+\pi^0\nu_\tau(\text{ex. } K^0))/\Gamma_{total}$

	(1)	(2)	(3)	(4)	(5)	(6)	(7)	(8)	(9)	(10)	(11)	(12)
(2)	-20											
(3)	-9	-6										
(4)	-16	-12	2									
(5)	-5	-5	-17	-37								
(6)	0	-4	-15	2	-27							
(7)	-2	-4	-24	-15	20	-47						
(8)	-14	-9	15	-5	-17	-14	-8					
(9)	-13	-12	-25	-30	4	-2	16	-15				
(10)	0	-2	-23	-14	4	10	13	-6	-17			
(11)	1	0	-5	1	4	6	0	-9	-2	-11		
(12)	0	1	9	4	-8	-4	-6	9	-5	-4	-2	
(13)	1	-4	-3	-5	3	2	-4	-3	-1	4	1	-24

[2] The correlation coefficient between this measurement and the ACCIARRI 01F measurement of $B(\tau^- \to \mu^-\overline{\nu}_\mu\nu_\tau)$ is 0.08.

[3] The correlation coefficients between this measurement and the ANASTASSOV 97 measurements of $B(\mu\overline{\nu}_\mu\nu_\tau)$, $B(\mu\overline{\nu}_\mu\nu_\tau)/B(e\overline{\nu}_e\nu_\tau)$, $B(h^-\nu_\tau)$, and $B(h^-\nu_\tau)/B(e\overline{\nu}_e\nu_\tau)$ are 0.50, −0.42, 0.48, and −0.39 respectively.

[4] Not independent of ALBRECHT 92D $\Gamma(\mu^-\overline{\nu}_\mu\nu_\tau)/\Gamma(e^-\overline{\nu}_e\nu_\tau)$ and ALBRECHT 93G $\Gamma(\mu^-\overline{\nu}_\mu\nu_\tau) \times \Gamma(e^-\overline{\nu}_e\nu_\tau)/\Gamma_{total}^2$ values.

[5] Modified using $B(e^-\overline{\nu}_e\nu_\tau)/B(\text{“1 prong”})$ and B(“1 prong”) ,= 0.855.

[6] Error correlated with BALTRUSAITIS 85 $\Gamma(\mu^-\overline{\nu}_\mu\nu_\tau)/\Gamma_{total}$.

[7] BACINO 78B value comes from fit to events with $e^\pm$ and one other nonelectron charged prong.

$\Gamma(\mu^-\overline{\nu}_\mu\nu_\tau)/\Gamma(e^-\overline{\nu}_e\nu_\tau)$ Γ_3/Γ_5

Standard Model prediction including mass effects is 0.9726.

VALUE	EVTS		DOCUMENT ID		TECN	COMMENT
0.9764±0.0030 OUR FIT Error includes scale factor of 1.1.						
0.979 ±0.004 OUR AVERAGE						
0.9796±0.0016±0.0036	731k	[1]	AUBERT	10F	BABR	467 fb^{-1} E_{cm}^{ee}= 10.6 GeV
0.9777±0.0063±0.0087		[2]	ANASTASSOV 97		CLEO	E_{cm}^{ee}= 10.6 GeV
0.997 ±0.035 ±0.040			ALBRECHT	92D	ARG	E_{cm}^{ee}= 9.4–10.6 GeV

[1] Correlation matrix for AUBERT 10F branching fractions:
(1) $\Gamma(\tau^- \to \mu^- \overline{\nu}_\mu \nu_\tau)$ / $\Gamma(\tau^- \to e^- \overline{\nu}_e \nu_\tau)$
(2) $\Gamma(\tau^- \to \pi^- \nu_\tau)$ / $\Gamma(\tau^- \to e^- \overline{\nu}_e \nu_\tau)$
(3) $\Gamma(\tau^- \to K^- \nu_\tau)$ / $\Gamma(\tau^- \to e^- \overline{\nu}_e \nu_\tau)$

	(1)	(2)
(2)	0.25	
(3)	0.12	0.33

[2] The correlation coefficients between this measurement and the ANASTASSOV 97 measurements of $B(\mu\overline{\nu}_\mu\nu_\tau)$, $B(e\overline{\nu}_e\nu_\tau)$, $B(h^-\nu_\tau)$, and $B(h^-\nu_\tau)/B(e\overline{\nu}_e\nu_\tau)$ are 0.58, −0.42, 0.07, and 0.45 respectively.

$\Gamma(e^-\overline{\nu}_e\nu_\tau\gamma)/\Gamma_{total}$ Γ_6/Γ

VALUE (%)	DOCUMENT ID		TECN	COMMENT
1.75±0.06±0.17	[1] BERGFELD	00	CLEO	E^{ee}_{cm}= 10.6 GeV

[1] BERGFELD 00 impose requirements on detected γ's corresponding to a τ-rest-frame energy cutoff $E^*_\gamma > 10$ MeV.

$\Gamma(h^- \geq 0K^0_L\,\nu_\tau)/\Gamma_{total}$ Γ_7/Γ

$\Gamma_7/\Gamma = (\Gamma_9+\Gamma_{10}+\frac{1}{2}\Gamma_{35}+\frac{1}{2}\Gamma_{37}+\Gamma_{47})/\Gamma$

VALUE (%)	EVTS	DOCUMENT ID		TECN	COMMENT
12.06±0.06 OUR FIT	Error includes scale factor of 1.2.				
12.2 ±0.4 OUR AVERAGE					
12.47±0.26±0.43	2967	[1] ACCIARRI	95	L3	1992 LEP run
12.4 ±0.7 ±0.7	283	[2] ABREU	92N	DLPH	1990 LEP run
12.1 ±0.7 ±0.5	309	ALEXANDER	91D	OPAL	1990 LEP run
• • • We use the following data for averages but not for fits. • • •					
11.3 ±0.5 ±0.8	798	[3] FORD	87	MAC	E^{ee}_{cm}= 29 GeV
• • • We do not use the following data for averages, fits, limits, etc. • • •					
12.44±0.11±0.11	15k	[4] BUSKULIC	96	ALEP	Repl. by SCHAEL 05C
11.7 ±0.6 ±0.8		[5] ALBRECHT	92D	ARG	E^{ee}_{cm}= 9.4–10.6 GeV
12.98±0.44±0.33		[6] DECAMP	92C	ALEP	Repl. by SCHAEL 05C
12.3 ±0.9 ±0.5	1338	BEHREND	90	CELL	E^{ee}_{cm}= 35 GeV
11.1 ±1.1 ±1.4		[7] BURCHAT	87	MRK2	E^{ee}_{cm}= 29 GeV
12.3 ±0.6 ±1.1	328	[8] BARTEL	86D	JADE	E^{ee}_{cm}= 34.6 GeV
13.0 ±2.0 ±4.0		BERGER	85	PLUT	E^{ee}_{cm}= 34.6 GeV
11.2 ±1.7 ±1.2	34	[9] BEHREND	83C	CELL	E^{ee}_{cm}= 34 GeV

[1] ACCIARRI 95 with 0.65% added to remove their correction for $\pi^- K^0_L$ backgrounds.
[2] ABREU 92N with 0.5% added to remove their correction for $K^*(892)^-$ backgrounds.
[3] FORD 87 result for $B(\pi^-\nu_\tau)$ with 0.67% added to remove their K^- correction and adjusted for 1992 B("1 prong").
[4] BUSKULIC 96 quote 11.78 ± 0.11 ± 0.13 We add 0.66 to undo their correction for unseen K^0_L and modify the systematic error accordingly.
[5] Not independent of ALBRECHT 92D $\Gamma(\mu^-\overline{\nu}_\mu\nu_\tau)/\Gamma(e^-\overline{\nu}_e\nu_\tau)$, $\Gamma(\mu^-\overline{\nu}_\mu\nu_\tau)\times\Gamma(e^-\overline{\nu}_e\nu_\tau)$, and $\Gamma(h^-\geq 0K^0_L\nu_\tau)/\Gamma(e^-\overline{\nu}_e\nu_\tau)$ values.
[6] DECAMP 92C quote $B(h^-\geq 0K^0_L \geq 0(K^0_S\to\pi^+\pi^-)\nu_\tau) = 13.32\pm0.44\pm0.33$. We subtract 0.35 to correct for their inclusion of the K^0_S decays.
[7] BURCHAT 87 with 1.1% added to remove their correction for K^- and $K^*(892)^-$ backgrounds.
[8] BARTEL 86D result for $B(\pi^-\nu_\tau)$ with 0.59% added to remove their K^- correction and adjusted for 1992 B("1 prong").
[9] BEHREND 83C quote $B(\pi^-\nu_\tau) = 9.9\pm1.7\pm1.3$ after subtracting 1.3 ± 0.5 to correct for $B(K^-\nu_\tau)$.

$\Gamma(h^-\nu_\tau)/\Gamma_{total}$ $\Gamma_8/\Gamma = (\Gamma_9+\Gamma_{10})/\Gamma$

VALUE (%)	EVTS	DOCUMENT ID		TECN	COMMENT
11.53 ±0.06 OUR FIT	Error includes scale factor of 1.2.				
11.63 ±0.12 OUR AVERAGE	Error includes scale factor of 1.4. See the ideogram below.				
11.571±0.120±0.114	19k	[1] ABDALLAH	06A	DLPH	1992–1995 LEP runs
11.98 ±0.13 ±0.16		ACKERSTAFF	98M	OPAL	1991–1995 LEP runs
11.52 ±0.05 ±0.12		[2] ANASTASSOV	97	CLEO	E^{ee}_{cm}= 10.6 GeV

[1] Correlation matrix for ABDALLAH 06A branching fractions, in percent:
(1) $\Gamma(\tau^-\to h^-\nu_\tau)/\Gamma_{total}$
(2) $\Gamma(\tau^-\to h^-\pi^0\nu_\tau)/\Gamma_{total}$
(3) $\Gamma(\tau^-\to h^-\geq 1\pi^0\nu_\tau(\text{ex. }K^0))/\Gamma_{total}$
(4) $\Gamma(\tau^-\to h^-2\pi^0\nu_\tau(\text{ex. }K^0))/\Gamma_{total}$
(5) $\Gamma(\tau^-\to h^-\geq 3\pi^0\nu_\tau(\text{ex. }K^0))/\Gamma_{total}$
(6) $\Gamma(\tau^-\to h^-h^-h^+\nu_\tau(\text{ex. }K^0))/\Gamma_{total}$
(7) $\Gamma(\tau^-\to h^-h^-h^+\pi^0\nu_\tau(\text{ex. }K^0))/\Gamma_{total}$
(8) $\Gamma(\tau^-\to h^-h^-h^+\geq 1\pi^0\nu_\tau(\text{ex. }K^0))/\Gamma_{total}$
(9) $\Gamma(\tau^-\to h^-h^-h^+\geq 2\pi^0\nu_\tau(\text{ex. }K^0))/\Gamma_{total}$
(10) $\Gamma(\tau^-\to 3h^-2h^+\nu_\tau(\text{ex. }K^0))/\Gamma_{total}$
(11) $\Gamma(\tau^-\to 3h^-2h^+\pi^0\nu_\tau(\text{ex. }K^0))/\Gamma_{total}$

	(1)	(2)	(3)	(4)	(5)	(6)	(7)	(8)	(9)	(10)
(2)	–34									
(3)	–47	56								
(4)	6	–66	15							
(5)	–6	38	11	–86						
(6)	–7	–8	15	0	–2					
(7)	–2	–1	–5	–3	3	–53				
(8)	–4	–4	–13	–4	–2	–56	75			
(9)	–1	–1	–4	3	–6	26	–78	–16		
(10)	–1	–1	1	0	0	–2	–3	–1	3	
(11)	0	0	0	0	0	1	0	–5	5	–57

[2] The correlation coefficients between this measurement and the ANASTASSOV 97 measurements of $B(\mu\overline{\nu}_\mu\nu_\tau)$, $B(e\overline{\nu}_e\nu_\tau)$, $B(\mu\overline{\nu}_\mu\nu_\tau)/B(e\overline{\nu}_e\nu_\tau)$, and $B(h^-\nu_\tau)/B(e\overline{\nu}_e\nu_\tau)$ are 0.50, 0.48, 0.07, and 0.63 respectively.

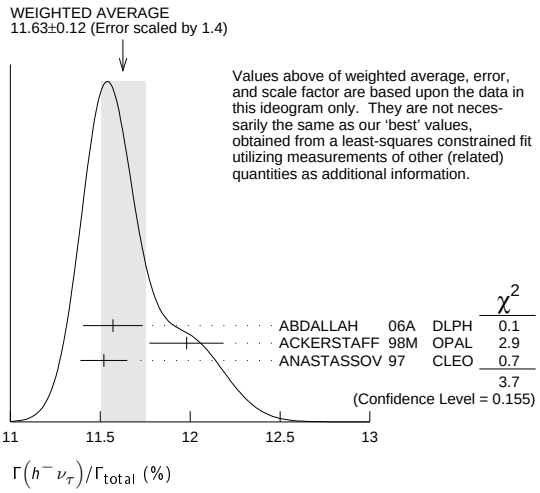

$\Gamma(h^-\nu_\tau)/\Gamma(e^-\overline{\nu}_e\nu_\tau)$ $\Gamma_8/\Gamma_5 = (\Gamma_9+\Gamma_{10})/\Gamma_5$

VALUE	EVTS	DOCUMENT ID		TECN	COMMENT
0.647 ±0.004 OUR FIT	Error includes scale factor of 1.1.				
0.640 ±0.007 OUR AVERAGE	Error includes scale factor of 1.6.				
• • • We use the following data for averages but not for fits. • • •					
0.6333±0.0014±0.0061	394k	[1] AUBERT	10F	BABR	467 fb^{-1} E^{ee}_{cm}=10.6 GeV
0.6484±0.0041±0.0060		[2] ANASTASSOV	97	CLEO	E^{ee}_{cm}= 10.6 GeV

[1] Not independent of AUBERT 10F $\Gamma(\tau^-\to\pi^-\nu_\tau)/\Gamma(\tau^-\to e^-\overline{\nu}_e\nu_\tau)$ and $\Gamma(\tau^-\to K^-\nu_\tau)/\Gamma(\tau^-\to e^-\overline{\nu}_e\nu_\tau)$.
[2] The correlation coefficients between this measurement and the ANASTASSOV 97 measurements of $B(\mu\overline{\nu}_\mu\nu_\tau)$, $B(e\overline{\nu}_e\nu_\tau)$, $B(\mu\overline{\nu}_\mu\nu_\tau)/B(e\overline{\nu}_e\nu_\tau)$, and $B(h^-\nu_\tau)$ are 0.08, −0.39, 0.45, and 0.63 respectively.

$\Gamma(\pi^-\nu_\tau)/\Gamma_{total}$ Γ_9/Γ

VALUE (%)	EVTS	DOCUMENT ID		TECN	COMMENT
10.83 ±0.06 OUR FIT	Error includes scale factor of 1.2.				
10.828±0.070±0.078	38k	[1] SCHAEL	05C	ALEP	1991–1995 LEP runs
• • • We do not use the following data for averages, fits, limits, etc. • • •					
11.06 ±0.11 ±0.14		[2] BUSKULIC	96	ALEP	Repl. by SCHAEL 05C
11.7 ±0.4 ±1.8	1138	BLOCKER	82D	MRK2	E^{ee}_{cm}= 3.5–6.7 GeV

[1] See footnote to SCHAEL 05C $\Gamma(\tau^-\to e^-\overline{\nu}_e\nu_\tau)/\Gamma_{total}$ measurement for correlations with other measurements.
[2] Not independent of BUSKULIC 96 $B(h^-\nu_\tau)$ and $B(K^-\nu_\tau)$ values.

$\Gamma(\pi^-\nu_\tau)/\Gamma(e^-\overline{\nu}_e\nu_\tau)$ Γ_9/Γ_5

VALUE	EVTS	DOCUMENT ID		TECN	COMMENT
0.607 ±0.004 OUR FIT	Error includes scale factor of 1.1.				
0.5945±0.0014±0.0061	369k	[1] AUBERT	10F	BABR	467 fb^{-1} E^{ee}_{cm}= 10.6 GeV

[1] See footnote to AUBERT 10F $\Gamma(\tau^-\to\mu^-\overline{\nu}_\mu\nu_\tau)/\Gamma(\tau^-\to e^-\overline{\nu}_e\nu_\tau)$ for correlations with other measurements.

$\Gamma(K^-\nu_\tau)/\Gamma_{total}$ Γ_{10}/Γ

VALUE (%)	EVTS	DOCUMENT ID		TECN	COMMENT
0.700±0.010 OUR FIT	Error includes scale factor of 1.1.				
0.685±0.023 OUR AVERAGE					
0.658±0.027±0.029		[1] ABBIENDI	01J	OPAL	1990–1995 LEP runs
0.696±0.025±0.014	2032	BARATE	99K	ALEP	1991–1995 LEP runs
0.85 ±0.18	27	ABREU	94K	DLPH	LEP 1992 Z data
0.66 ±0.07 ±0.09	99	BATTLE	94	CLEO	$E^{ee}_{cm} \approx$ 10.6 GeV
• • • We do not use the following data for averages, fits, limits, etc. • • •					
0.72 ±0.04 ±0.04	728	BUSKULIC	96	ALEP	Repl. by BARATE 99K
0.59 ±0.18	16	MILLS	84	DLCO	E^{ee}_{cm}= 29 GeV
1.3 ±0.5	15	BLOCKER	82B	MRK2	E^{ee}_{cm}= 3.9–6.7 GeV

[1] The correlation coefficient between this measurement and the ABBIENDI 01J $B(\tau^-\to K^-\geq 0\pi^0\geq 0K^0\geq 0\gamma\,\nu_\tau)$ is 0.60.

$\Gamma(K^-\nu_\tau)/\Gamma(e^-\overline{\nu}_e\nu_\tau)$ Γ_{10}/Γ_5

VALUE (units 10^{-2})	EVTS	DOCUMENT ID		TECN	COMMENT
3.93 ±0.06 OUR FIT	Error includes scale factor of 1.1.				
3.882±0.032±0.057	25k	[1] AUBERT	10F	BABR	467 fb^{-1} E_{cm}^{ee}= 10.6 GeV

[1] See footnote to AUBERT 10F $\Gamma(\tau^-\to\mu^-\overline{\nu}_\mu\nu_\tau)/\Gamma(\tau^-\to e^-\overline{\nu}_e\nu_\tau)$ for correlations with other measurements.

$\Gamma(K^-\nu_\tau)/\Gamma(\pi^-\nu_\tau)$ Γ_{10}/Γ_9

VALUE (units 10^{-2})	DOCUMENT ID		TECN	COMMENT
6.46 ±0.10 OUR FIT	Error includes scale factor of 1.1.			
• • • We use the following data for averages but not for fits. • • •				
6.531±0.056±0.093	[1] AUBERT	10F	BABR	467 fb^{-1} E_{cm}^{ee}= 10.6 GeV

[1] Not independent of AUBERT 10F $\Gamma(\tau^-\to\pi^-\nu_\tau)/\Gamma(\tau^-\to e^-\overline{\nu}_e\nu_\tau)$ and $\Gamma(\tau^-\to K^-\nu_\tau)/\Gamma(\tau^-\to e^-\overline{\nu}_e\nu_\tau)$.

$\Gamma(h^-\geq 1\text{ neutrals}\,\nu_\tau)/\Gamma_{total}$ Γ_{11}/Γ

$\Gamma_{11}/\Gamma=(\Gamma_{14}+\Gamma_{16}+\Gamma_{20}+\Gamma_{23}+\Gamma_{27}+\Gamma_{28}+\Gamma_{30}+0.157\Gamma_{35}+0.157\Gamma_{37}+0.157\Gamma_{40}+0.157\Gamma_{42}+0.0985\Gamma_{47}+0.708\Gamma_{140}+0.715\Gamma_{142}+0.09\Gamma_{167}+0.09\Gamma_{169})/\Gamma$

VALUE (%)	DOCUMENT ID		TECN	COMMENT
37.10±0.10 OUR FIT	Error includes scale factor of 1.2.			
• • • We do not use the following data for averages, fits, limits, etc. • • •				
36.14±0.33±0.58	[1] AKERS	94E	OPAL	1991–1992 LEP runs
38.4 ±1.2 ±1.0	[2] BURCHAT	87	MRK2	E_{cm}^{ee}= 29 GeV
42.7 ±2.0 ±2.9	BERGER	85	PLUT	E_{cm}^{ee}= 34.6 GeV

[1] Not independent of ACKERSTAFF 98M $B(h^-\pi^0\nu_\tau)$ and $B(h^-\geq 2\pi^0\nu_\tau)$ values.
[2] BURCHAT 87 quote for $B(\pi^\pm\geq 1\text{ neutral}\,\nu_\tau)=0.378\pm0.012\pm0.010$. We add 0.006 to account for contribution from $(K^{*-}\nu_\tau)$ which they fixed at BR = 0.013.

$\Gamma(h^-\geq 1\pi^0\nu_\tau(\text{ex.}K^0))/\Gamma_{total}$
$\Gamma_{12}/\Gamma=(\Gamma_{14}+\Gamma_{16}+\Gamma_{20}+\Gamma_{23}+\Gamma_{27}+\Gamma_{28}+\Gamma_{30}+0.325\Gamma_{140}+0.325\Gamma_{142})/\Gamma$

VALUE (%)	EVTS	DOCUMENT ID		TECN	COMMENT
36.58 ±0.10 OUR FIT	Error includes scale factor of 1.2.				
• • • We use the following data for averages but not for fits. • • •					
36.641±0.155±0.127	45k	[1] ABDALLAH	06A	DLPH	1992–1995 LEP runs

[1] See footnote to ABDALLAH 06A $\Gamma(\tau^-\to h^-\nu_\tau)/\Gamma_{total}$ measurement for correlations with other measurements.

$\Gamma(h^-\pi^0\nu_\tau)/\Gamma_{total}$ $\Gamma_{13}/\Gamma=(\Gamma_{14}+\Gamma_{16})/\Gamma$

VALUE (%)	EVTS	DOCUMENT ID		TECN	COMMENT
25.95 ±0.09 OUR FIT	Error includes scale factor of 1.1.				
25.73 ±0.16 OUR AVERAGE					
25.67 ±0.01 ±0.39	5.4M	FUJIKAWA	08	BELL	72 fb^{-1} E_{cm}^{ee}=10.6GeV
25.740±0.201±0.138	35k	[1] ABDALLAH	06A	DLPH	1992–1995 LEP runs
25.89 ±0.17 ±0.29		ACKERSTAFF	98M	OPAL	1991–1995 LEP runs
25.05 ±0.35 ±0.50	6613	ACCIARRI	95	L3	1992 LEP run
25.87 ±0.12 ±0.42	51k	[2] ARTUSO	94	CLEO	E_{cm}^{ee}= 10.6 GeV
• • • We do not use the following data for averages, fits, limits, etc. • • •					
25.76 ±0.15 ±0.13	31k	BUSKULIC	96	ALEP	Repl. by SCHAEL 05C
25.98 ±0.36 ±0.52		[3] AKERS	94E	OPAL	Repl. by ACKER-STAFF 98M
22.9 ±0.8 ±1.3	283	[4] ABREU	92N	DLPH	E_{cm}^{ee}= 88.2–94.2 GeV
23.1 ±0.4 ±0.9	1249	[5] ALBRECHT	92Q	ARG	E_{cm}^{ee}= 10 GeV
25.02 ±0.64 ±0.88	1849	DECAMP	92C	ALEP	1989–1990 LEP runs
22.0 ±0.8 ±1.9	779	ANTREASYAN	91	CBAL	E_{cm}^{ee}= 9.4–10.6 GeV
22.6 ±1.5 ±0.7	1101	BEHREND	90	CELL	E_{cm}^{ee}= 35 GeV
23.1 ±1.9 ±1.6		BEHREND	84	CELL	E_{cm}^{ee}= 14,22 GeV

[1] See footnote to ABDALLAH 06A $\Gamma(\tau^-\to h^-\nu_\tau)/\Gamma_{total}$ measurement for correlations with other measurements.
[2] ARTUSO 94 reports the combined result from three independent methods, one of which (23% of the $\tau^-\to h^-\pi^0\nu_\tau$) is normalized to the inclusive one-prong branching fraction, taken as 0.854 ± 0.004. Renormalization to the present value causes negligible change.
[3] AKERS 94E quote $(26.25\pm0.36\pm0.52)\times10^{-2}$; we subtract 0.27% from their number to correct for $\tau^-\to h^-K_L^0\nu_\tau$.
[4] ABREU 92N with 0.5% added to remove their correction for $K^*(892)^-$ backgrounds.
[5] ALBRECHT 92Q with 0.5% added to remove their correction for $\tau^-\to K^*(892)^-\nu_\tau$ background.

$\Gamma(\pi^-\pi^0\nu_\tau)/\Gamma_{total}$ Γ_{14}/Γ

VALUE (%)	EVTS	DOCUMENT ID		TECN	COMMENT
25.52 ±0.09 OUR FIT	Error includes scale factor of 1.1.				
25.46 ±0.12 OUR AVERAGE					
25.471±0.097±0.085	81k	[1] SCHAEL	05C	ALEP	1991-1995 LEP runs
• • • We use the following data for averages but not for fits. • • •					
25.36 ±0.44		[2] ARTUSO	94	CLEO	E_{cm}^{ee}= 10.6 GeV
• • • We do not use the following data for averages, fits, limits, etc. • • •					
25.30 ±0.15 ±0.13		[3] BUSKULIC	96	ALEP	Repl. by SCHAEL 05C
21.5 ±0.4 ±1.9	4400	[4,5] ALBRECHT	88L	ARG	E_{cm}^{ee}= 10 GeV
23.0 ±1.3 ±1.7	582	ADLER	87B	MRK3	E_{cm}^{ee}= 3.77 GeV
25.8 ±1.7 ±2.5		[6] BURCHAT	87	MRK2	E_{cm}^{ee}= 29 GeV
22.3 ±0.6 ±1.4	629	[5] YELTON	86	MRK2	E_{cm}^{ee}= 29 GeV

[1] See footnote to SCHAEL 05C $\Gamma(\tau^-\to e^-\overline{\nu}_e\nu_\tau)/\Gamma_{total}$ measurement for correlations with other measurements.
[2] Not independent of ARTUSO 94 $B(h^-\pi^0\nu_\tau)$ and BATTLE 94 $B(K^-\pi^0\nu_\tau)$ values.
[3] Not independent of BUSKULIC 96 $B(h^-\pi^0\nu_\tau)$ and $B(K^-\pi^0\nu_\tau)$ values.
[4] The authors divide by $(\Gamma_3+\Gamma_5+\Gamma_9+\Gamma_{10})/\Gamma=0.467$ to obtain this result.
[5] Experiment had no hadron identification. Kaon corrections were made, but insufficient information is given to permit their removal.
[6] BURCHAT 87 value is not independent of YELTON 86 value. Nonresonant decays included.

$\Gamma(\pi^-\pi^0\text{ non-}\rho(770)\nu_\tau)/\Gamma_{total}$ Γ_{15}/Γ

VALUE (%)	DOCUMENT ID		TECN	COMMENT
0.3±0.1±0.3	[1] BEHREND	84	CELL	E_{cm}^{ee}= 14,22 GeV

[1] BEHREND 84 assume a flat nonresonant mass distribution down to the $\rho(770)$ mass, using events with mass above 1300 to set the level.

$\Gamma(K^-\pi^0\nu_\tau)/\Gamma_{total}$ Γ_{16}/Γ

VALUE (%)	EVTS	DOCUMENT ID		TECN	COMMENT
0.429±0.015 OUR FIT					
0.426±0.016 OUR AVERAGE					
0.416±0.003±0.018	78k	AUBERT	07AP	BABR	230 fb^{-1} E_{cm}^{ee}= 10.6 GeV
0.471±0.059±0.023	360	ABBIENDI	04J	OPAL	1991-1995 LEP runs
0.444±0.026±0.024	923	BARATE	99K	ALEP	1991-1995 LEP runs
0.51 ±0.10 ±0.07	37	BATTLE	94	CLEO	$E_{cm}^{ee}\approx$ 10.6 GeV
• • • We do not use the following data for averages, fits, limits, etc. • • •					
0.52 ±0.04 ±0.05	395	BUSKULIC	96	ALEP	Repl. by BARATE 99K

$\Gamma(h^-\geq 2\pi^0\nu_\tau)/\Gamma_{total}$ Γ_{17}/Γ

$\Gamma_{17}/\Gamma=(\Gamma_{20}+\Gamma_{23}+\Gamma_{27}+\Gamma_{28}+\Gamma_{30}+0.157\Gamma_{35}+0.157\Gamma_{37}+0.157\Gamma_{40}+0.157\Gamma_{42}+0.0985\Gamma_{47}+0.319\Gamma_{140}+0.322\Gamma_{142})/\Gamma$

VALUE (%)	EVTS	DOCUMENT ID		TECN	COMMENT
10.87±0.11 OUR FIT	Error includes scale factor of 1.2.				
9.91±0.31±0.27		ACKERSTAFF	98M	OPAL	1991–1995 LEP runs
• • • We do not use the following data for averages, fits, limits, etc. • • •					
9.89±0.34±0.55		[1] AKERS	94E	OPAL	Repl. by ACKER-STAFF 98M
14.0 ±1.2 ±0.6	938	[2] BEHREND	90	CELL	E_{cm}^{ee}= 35 GeV
12.0 ±1.4 ±2.5		[3] BURCHAT	87	MRK2	E_{cm}^{ee}= 29 GeV
13.9 ±2.0 $^{+1.9}_{-2.2}$		[4] AIHARA	86E	TPC	E_{cm}^{ee}= 29 GeV

[1] AKERS 94E not independent of AKERS 94E $B(h^-\geq1\pi^0\nu_\tau)$ and $B(h^-\pi^0\nu_\tau)$ measurements.
[2] No independent of BEHREND 90 $\Gamma(h^-2\pi^0\nu_\tau(\text{exp. }K^0))$ and $\Gamma(h^-\geq3\pi^0\nu_\tau)$.
[3] Error correlated with BURCHAT 87 $\Gamma(\rho^-\nu_e)/\Gamma(\text{total})$ value.
[4] AIHARA 86E (TPC) quote $B(2\pi^0\pi^-\nu_\tau)+1.6B(3\pi^0\pi^-\nu_\tau)+1.1B(\pi^0\eta\pi^-\nu_\tau)$.

$\Gamma(h^-2\pi^0\nu_\tau)/\Gamma_{total}$ Γ_{18}/Γ

$\Gamma_{18}/\Gamma=(\Gamma_{20}+\Gamma_{23}+0.157\Gamma_{35}+0.157\Gamma_{37})/\Gamma$

VALUE (%)	EVTS	DOCUMENT ID		TECN	COMMENT
9.52±0.11 OUR FIT	Error includes scale factor of 1.1.				
• • • We do not use the following data for averages, fits, limits, etc. • • •					
9.48±0.13±0.10	12k	[1] BUSKULIC	96	ALEP	Repl. by SCHAEL 05C

[1] BUSKULIC 96 quote 9.29 ± 0.13 ± 0.10. We add 0.19 to undo their correction for $\tau^-\to h^-K^0\nu_\tau$.

$\Gamma(h^-2\pi^0\nu_\tau(\text{ex.}K^0))/\Gamma_{total}$ Γ_{19}/Γ

$\Gamma_{19}/\Gamma=(\Gamma_{20}+\Gamma_{23})/\Gamma$

VALUE (%)	EVTS	DOCUMENT ID		TECN	COMMENT
9.36 ±0.11 OUR FIT	Error includes scale factor of 1.2.				
9.17 ±0.27 OUR AVERAGE					
9.498±0.320±0.275	9.5k	[1] ABDALLAH	06A	DLPH	1992–1995 LEP runs
8.88 ±0.37 ±0.42	1060	ACCIARRI	95	L3	1992 LEP run
• • • We use the following data for averages but not for fits. • • •					
8.96 ±0.16 ±0.44		[2] PROCARIO	93	CLEO	$E_{cm}^{ee}\approx$ 10.6 GeV
• • • We do not use the following data for averages, fits, limits, etc. • • •					
10.38 ±0.66 ±0.82	809	[3] DECAMP	92C	ALEP	Repl. by SCHAEL 05C
5.7 ±0.5 $^{+1.7}_{-1.0}$	133	[4] ANTREASYAN	91	CBAL	E_{cm}^{ee}= 9.4–10.6 GeV
10.0 ±1.5 ±1.1	333	[5] BEHREND	90	CELL	E_{cm}^{ee}= 35 GeV
8.7 ±0.4 ±1.1	815	[6] BAND	87	MAC	E_{cm}^{ee}= 29 GeV
6.2 ±0.6 ±1.2		[7] GAN	87	MRK2	E_{cm}^{ee}= 29 GeV
6.0 ±3.0 ±1.8		BEHREND	84	CELL	E_{cm}^{ee}= 14,22 GeV

[1] See footnote to ABDALLAH 06A $\Gamma(\tau^-\to h^-\nu_\tau)/\Gamma_{total}$ measurement for correlations with other measurements.
[2] PROCARIO 93 entry is obtained from $B(h^-2\pi^0\nu_\tau)/B(h^-\pi^0\nu_\tau)$ using ARTUSO 94 result for $B(h^-\pi^0\nu_\tau)$.
[3] We subtract 0.0015 to account for $\tau^-\to K^*(892)^-\nu_\tau$ contribution.
[4] ANTREASYAN 91 subtract 0.001 to account for the $\tau^-\to K^*(892)^-\nu_\tau$ contribution.
[5] BEHREND 90 subtract 0.002 to account for the $\tau^-\to K^*(892)^-\nu_\tau$ contribution.
[6] BAND 87 assume $B(\pi^-3\pi^0\nu_\tau)=0.01$ and $B(\pi^-\pi^0\eta\nu_\tau)=0.005$.
[7] GAN 87 analysis use photon multiplicity distribution.

$\Gamma(h^-2\pi^0\nu_\tau(\text{ex.}K^0))/\Gamma(h^-\pi^0\nu_\tau)$ Γ_{19}/Γ_{13}

$\Gamma_{19}/\Gamma_{13}=(\Gamma_{20}+\Gamma_{23})/(\Gamma_{14}+\Gamma_{16})$

VALUE	DOCUMENT ID	TECN	COMMENT
0.361±0.005 OUR FIT	Error includes scale factor of 1.1.		
0.342±0.006±0.016	[1] PROCARIO 93	CLEO	$E_{cm}^{ee}\approx$ 10.6 GeV

[1] PROCARIO 93 quote 0.345 ± 0.006 ± 0.016 after correction for 2 kaon backgrounds assuming B($K^{*-}\nu_\tau$)=1.42 ± 0.18% and B($h^-K^0\pi^0\nu_\tau$)=0.48 ± 0.48%. We multiply by 0.990 ± 0.010 to remove these corrections to B($h^-\pi^0\nu_\tau$).

$\Gamma(\pi^-2\pi^0\nu_\tau(\text{ex.}K^0))/\Gamma_{\text{total}}$ Γ_{20}/Γ

VALUE (%)	EVTS	DOCUMENT ID	TECN	COMMENT
9.30 ±0.11 OUR FIT	Error includes scale factor of 1.2.			
9.239±0.086±0.090	31k	[1] SCHAEL 05C	ALEP	1991–1995 LEP runs
• • • We do not use the following data for averages, fits, limits, etc. • • •				
9.21 ±0.13 ±0.11		[2] BUSKULIC 96	ALEP	Repl. by SCHAEL 05C

[1] See footnote to SCHAEL 05C $\Gamma(\tau^-\to e^-\overline{\nu}_e\nu_\tau)/\Gamma_{\text{total}}$ measurement for correlations with other measurements.
[2] Not independent of BUSKULIC 96 B($h^-2\pi^0\nu_\tau$(ex. K^0)) and B($K^-2\pi^0\nu_\tau$(ex. K^0)) values.

$\Gamma(\pi^-2\pi^0\nu_\tau(\text{ex.}K^0),\text{scalar})/\Gamma(\pi^-2\pi^0\nu_\tau(\text{ex.}K^0))$ Γ_{21}/Γ_{20}

VALUE	CL%	DOCUMENT ID	TECN	COMMENT
<0.094	95	[1] BROWDER 00	CLEO	4.7 fb^{-1} E_{cm}^{ee}= 10.6 GeV

[1] Model-independent limit from structure function analysis on contribution to B($\tau^-\to\pi^-2\pi^0\nu_\tau$(ex. K^0)) from scalars.

$\Gamma(\pi^-2\pi^0\nu_\tau(\text{ex.}K^0),\text{vector})/\Gamma(\pi^-2\pi^0\nu_\tau(\text{ex.}K^0))$ Γ_{22}/Γ_{20}

VALUE	CL%	DOCUMENT ID	TECN	COMMENT
<0.073	95	[1] BROWDER 00	CLEO	4.7 fb^{-1} E_{cm}^{ee}= 10.6 GeV

[1] Model-independent limit from structure function analysis on contribution to B($\tau^-\to\pi^-2\pi^0\nu_\tau$(ex. K^0)) from vectors.

$\Gamma(K^-2\pi^0\nu_\tau(\text{ex.}K^0))/\Gamma_{\text{total}}$ Γ_{23}/Γ

VALUE (units 10^{-4})	EVTS	DOCUMENT ID	TECN	COMMENT
6.5± 2.3 OUR FIT				
5.8± 2.4 OUR AVERAGE				
5.6± 2.0±1.5	131	BARATE 99K	ALEP	1991–1995 LEP runs
9 ±10 ±3	3	[1] BATTLE 94	CLEO	$E_{cm}^{ee}\approx$ 10.6 GeV
• • • We do not use the following data for averages, fits, limits, etc. • • •				
8 ± 2 ±2	59	BUSKULIC 96	ALEP	Repl. by BARATE 99K

[1] BATTLE 94 quote $(14\pm10\pm3)\times10^{-4}$ or $<30\times10^{-4}$ at 90% CL. We subtract $(5\pm2)\times10^{-4}$ to account for $\tau^-\to K^-(K^0\to\pi^0\pi^0)\nu_\tau$ background.

$\Gamma(h^-\geq3\pi^0\nu_\tau)/\Gamma_{\text{total}}$ Γ_{24}/Γ

$\Gamma_{24}/\Gamma=(\Gamma_{27}+\Gamma_{28}+\Gamma_{30}+0.157\Gamma_{40}+0.157\Gamma_{42}+0.0985\Gamma_{47}+0.319\Gamma_{140}+0.322\Gamma_{142})/\Gamma$

VALUE (%)	EVTS	DOCUMENT ID	TECN	COMMENT
1.35±0.07 OUR FIT	Error includes scale factor of 1.1.			
• • • We do not use the following data for averages, fits, limits, etc. • • •				
1.53±0.40±0.46	186	DECAMP 92C	ALEP	Repl. by SCHAEL 05C
3.2 ±1.0 ±1.0		BEHREND 90	CELL	E_{cm}^{ee}= 35 GeV

$\Gamma(h^-\geq3\pi^0\nu_\tau(\text{ex. }K^0))/\Gamma_{\text{total}}$ $\Gamma_{25}/\Gamma=(\Gamma_{27}+\Gamma_{28}+\Gamma_{30}+0.325\Gamma_{140}+0.325\Gamma_{142})/\Gamma$

VALUE (%)	EVTS	DOCUMENT ID	TECN	COMMENT
1.26 ±0.07 OUR FIT	Error includes scale factor of 1.1.			
1.403±0.214±0.224	1.1k	[1] ABDALLAH 06A	DLPH	1992–1995 LEP runs

[1] See footnote to ABDALLAH 06A $\Gamma(\tau^-\to h^-\nu_\tau)/\Gamma_{\text{total}}$ measurement for correlations with other measurements.

$\Gamma(h^-3\pi^0\nu_\tau)/\Gamma_{\text{total}}$ Γ_{26}/Γ

$\Gamma_{26}/\Gamma=(\Gamma_{27}+\Gamma_{28}+0.157\Gamma_{40}+0.157\Gamma_{42}+0.322\Gamma_{142})/\Gamma$

VALUE (%)	EVTS	DOCUMENT ID	TECN	COMMENT
1.19±0.07 OUR FIT				
1.21±0.17 OUR AVERAGE	Error includes scale factor of 1.2.			
1.70±0.24±0.38	293	ACCIARRI 95	L3	1992 LEP run
• • • We use the following data for averages but not for fits. • • •				
1.15±0.08±0.13		[1] PROCARIO 93	CLEO	$E_{cm}^{ee}\approx$ 10.6 GeV
• • • We do not use the following data for averages, fits, limits, etc. • • •				
1.24±0.09±0.11	2.3k	[2] BUSKULIC 96	ALEP	Repl. by SCHAEL 05C
0.0 $^{+1.4}_{-0.1}$ $^{+1.1}_{-0.1}$		[3] GAN 87	MRK2	E_{cm}^{ee}= 29 GeV

[1] PROCARIO 93 entry is obtained from B($h^-3\pi^0\nu_\tau$)/B($h^-\pi^0\nu_\tau$) using ARTUSO 94 result for B($h^-\pi^0\nu_\tau$).
[2] BUSKULIC 96 quote B($h^-3\pi^0\nu_\tau$(ex. K^0)) = 1.17 ± 0.09 ± 0.11. We add 0.07 to remove their correction for K^0 backgrounds.
[3] Highly correlated with GAN 87 $\Gamma(\eta\pi^-\pi^0\nu_\tau)/\Gamma_{\text{total}}$ value. Authors quote B($\pi^\pm3\pi^0\nu_\tau$) + 0.67B($\pi^\pm\eta\pi^0\nu_\tau$) = 0.047 ± 0.010 ± 0.011.

$\Gamma(h^-3\pi^0\nu_\tau)/\Gamma(h^-\pi^0\nu_\tau)$ Γ_{26}/Γ_{13}

$\Gamma_{26}/\Gamma_{13}=(\Gamma_{27}+\Gamma_{28}+0.157\Gamma_{40}+0.157\Gamma_{42}+0.322\Gamma_{142})/(\Gamma_{14}+\Gamma_{16})$

VALUE	DOCUMENT ID	TECN	COMMENT
0.0459±0.0029 OUR FIT			
0.044 ±0.003 ±0.005	[1] PROCARIO 93	CLEO	$E_{cm}^{ee}\approx$ 10.6 GeV

[1] PROCARIO 93 quote 0.041 ± 0.003 ± 0.005 after correction for 2 kaon backgrounds assuming B($K^{*-}\nu_\tau$)=1.42 ± 0.18% and B($h^-K^0\pi^0\nu_\tau$)=0.48 ± 0.48%. We add 0.003 ± 0.003 and multiply the sum by 0.990 ± 0.010 to remove these corrections.

$\Gamma(\pi^-3\pi^0\nu_\tau(\text{ex.}K^0))/\Gamma_{\text{total}}$ Γ_{27}/Γ

VALUE (%)	EVTS	DOCUMENT ID	TECN	COMMENT
1.05 ±0.07 OUR FIT				
0.977±0.069±0.058	6.1k	[1] SCHAEL 05C	ALEP	1991–1995 LEP runs

[1] See footnote to SCHAEL 05C $\Gamma(\tau^-\to e^-\overline{\nu}_e\nu_\tau)/\Gamma_{\text{total}}$ measurement for correlations with other measurements.

$\Gamma(K^-3\pi^0\nu_\tau(\text{ex.}K^0,\eta))/\Gamma_{\text{total}}$ Γ_{28}/Γ

VALUE (units 10^{-4})	EVTS	DOCUMENT ID	TECN	COMMENT
4.8± 2.2 OUR FIT				
3.7± 2.1±1.1	22	BARATE 99K	ALEP	1991–1995 LEP runs
• • • We do not use the following data for averages, fits, limits, etc. • • •				
5 ±13		[1] BUSKULIC 94E	ALEP	Repl. by BARATE 99K

[1] BUSKULIC 94E quote B($K^-\geq0\pi^0\geq0K^0\nu_\tau$) − [B($K^-\nu_\tau$) + B($K^-\pi^0\nu_\tau$) + B($K^-K^0\nu_\tau$) + B($K^-\pi^0\pi^0\nu_\tau$) + B($K^-\pi^0K^0\nu_\tau$)] = (5 ± 13) × 10^{-4} accounting for common systematic errors in BUSKULIC 94E and BUSKULIC 94F measurements of these modes. We assume B($K^-\geq2K^0\nu_\tau$) and B($K^-\geq4\pi^0\nu_\tau$) are negligible.

$\Gamma(h^-4\pi^0\nu_\tau(\text{ex.}K^0))/\Gamma_{\text{total}}$ Γ_{29}/Γ

$\Gamma_{29}/\Gamma=(\Gamma_{30}+0.319\Gamma_{140})/\Gamma$

VALUE (%)	EVTS	DOCUMENT ID	TECN	COMMENT
0.16±0.04 OUR FIT				
0.16±0.05±0.05		[1] PROCARIO 93	CLEO	$E_{cm}^{ee}\approx$ 10.6 GeV
• • • We do not use the following data for averages, fits, limits, etc. • • •				
0.16±0.04±0.09	232	[2] BUSKULIC 96	ALEP	Repl. by SCHAEL 05C

[1] PROCARIO 93 quotes B($h^-4\pi^0\nu_\tau$)/B($h^-\pi^0\nu_\tau$) =0.006±0.002±0.002. We multiply by the ARTUSO 94 result for B($h^-\pi^0\nu_\tau$) to obtain B($h^-4\pi^0\nu_\tau$). PROCARIO 93 assume B($h^-\geq5\ \pi^0\nu_\tau$) is small and do not correct for it.
[2] BUSKULIC 96 quote result for $\tau^-\to h^-\geq4\pi^0\nu_\tau$. We assume B($h^-\geq5\pi^0\nu_\tau$) is negligible.

$\Gamma(h^-4\pi^0\nu_\tau(\text{ex.}K^0,\eta))/\Gamma_{\text{total}}$ Γ_{30}/Γ

VALUE (%)	EVTS	DOCUMENT ID	TECN	COMMENT
0.11 ±0.04 OUR FIT				
0.112±0.037±0.035	957	[1] SCHAEL 05C	ALEP	1991–1995 LEP runs

[1] See footnote to SCHAEL 05C $\Gamma(\tau^-\to e^-\overline{\nu}_e\nu_\tau)/\Gamma_{\text{total}}$ measurement for correlations with other measurements.

$\Gamma(K^-\geq0\pi^0\geq0K^0\geq0\gamma\ \nu_\tau)/\Gamma_{\text{total}}$ Γ_{31}/Γ

$\Gamma_{31}/\Gamma=(\Gamma_{10}+\Gamma_{16}+\Gamma_{23}+\Gamma_{28}+\Gamma_{37}+\Gamma_{42}+0.715\Gamma_{142})/\Gamma$

VALUE (%)	EVTS	DOCUMENT ID	TECN	COMMENT
1.572±0.033 OUR FIT	Error includes scale factor of 1.1.			
1.53 ±0.04 OUR AVERAGE				
1.528±0.039±0.040		[1] ABBIENDI 01J	OPAL	1990–1995 LEP runs
1.54 ±0.24		ABREU 94K	DLPH	LEP 1992 Z data
1.70 ±0.12 ±0.19	202	[2] BATTLE 94	CLEO	$E_{cm}^{ee}\approx$ 10.6 GeV
• • • We use the following data for averages but not for fits. • • •				
1.520±0.040±0.041	4006	[3] BARATE 99K	ALEP	1991–1995 LEP runs
• • • We do not use the following data for averages, fits, limits, etc. • • •				
1.70 ±0.05 ±0.06	1610	[4] BUSKULIC 96	ALEP	Repl. by BARATE 99K
1.6 ±0.4 ±0.2	35	AIHARA 87B	TPC	E_{cm}^{ee}= 29 GeV
1.71 ±0.29	53	MILLS 84	DLCO	E_{cm}^{ee}= 29 GeV

[1] The correlation coefficient between this measurement and the ABBIENDI 01J B($\tau^-\to K^-\nu_\tau$) is 0.60.
[2] BATTLE 94 quote 1.60 ± 0.12 ± 0.19. We add 0.10 ± 0.02 to correct for their rejection of $K_S^0\to\pi^+\pi^-$ decays.
[3] Not independent of BARATE 99K B($K^-\nu_\tau$), B($K^-\pi^0\nu_\tau$), B($K^-2\pi^0\nu_\tau$(ex. K^0)), B($K^-3\pi^0\nu_\tau$(ex. K^0)), B($K^-K^0\nu_\tau$), and B($K^-K^0\pi^0\nu_\tau$) values.
[4] Not independent of BUSKULIC 96 B($K^-\nu_\tau$), B($K^-\pi^0\nu_\tau$), B($K^-2\pi^0\nu_\tau$), B($K^-K^0\nu_\tau$), and B($K^-K^0\pi^0\nu_\tau$) values.

$\Gamma(K^-\geq1(\pi^0\text{ or }K^0\text{ or }\gamma)\ \nu_\tau)/\Gamma_{\text{total}}$ Γ_{32}/Γ

$\Gamma_{32}/\Gamma=(\Gamma_{16}+\Gamma_{23}+\Gamma_{28}+\Gamma_{37}+\Gamma_{42}+0.715\Gamma_{142})/\Gamma$

VALUE (%)	EVTS	DOCUMENT ID	TECN	COMMENT
0.872±0.032 OUR FIT	Error includes scale factor of 1.1.			
0.86 ±0.05 OUR AVERAGE				
• • • We use the following data for averages but not for fits. • • •				
0.869±0.031±0.034		[1] ABBIENDI 01J	OPAL	1990–1995 LEP runs
0.69 ±0.25		[2] ABREU 94K	DLPH	LEP 1992 Z data
• • • We do not use the following data for averages, fits, limits, etc. • • •				
1.2 ±0.5 $^{+0.2}_{-0.4}$	9	AIHARA 87B	TPC	E_{cm}^{ee}= 29 GeV

[1] Not independent of ABBIENDI 01J B($\tau^-\to K^-\nu_\tau$) and B($\tau^-\to K^-\geq0\pi^0\geq0K^0\geq0\gamma\ \nu_\tau$) values.
[2] Not independent of ABREU 94K B($K^-\nu_\tau$) and B($K^-\geq0$ neutralsν_τ) measurements.

$\Gamma(K^0_S(\text{particles})^-\nu_\tau)/\Gamma_{\text{total}}$ Γ_{33}/Γ

$\Gamma_{33}/\Gamma = (\frac{1}{2}\Gamma_{35}+\frac{1}{2}\Gamma_{37}+\frac{1}{2}\Gamma_{40}+\frac{1}{2}\Gamma_{42}+\Gamma_{47}+\Gamma_{48})/\Gamma$

VALUE (%)	EVTS	DOCUMENT ID		TECN	COMMENT
0.92 ±0.04 OUR FIT		Error includes scale factor of 1.5.			
0.97 ±0.07 OUR AVERAGE					
0.970±0.058±0.062	929	BARATE	98E	ALEP	1991–1995 LEP runs
0.97 ±0.09 ±0.06	141	AKERS	94G	OPAL	E^{ee}_{cm}= 88–94 GeV

$\Gamma(h^-\overline{K}^0\nu_\tau)/\Gamma_{\text{total}}$ $\Gamma_{34}/\Gamma = (\Gamma_{35}+\Gamma_{37})/\Gamma$

VALUE (%)	EVTS	DOCUMENT ID		TECN	COMMENT
1.00 ±0.05 OUR FIT		Error includes scale factor of 1.8.			
0.90 ±0.07 OUR AVERAGE					
0.855±0.036±0.073	1242	COAN	96	CLEO	$E^{ee}_{\text{cm}} \approx$ 10.6 GeV
• • • We use the following data for averages but not for fits. • • •					
1.01 ±0.11 ±0.07	555	[1] BARATE	98E	ALEP	1991–1995 LEP runs

[1] Not independent of BARATE 98E B($\tau^- \to \pi^-\overline{K}^0\nu_\tau$) and B($\tau^- \to K^-K^0\nu_\tau$) values.

$\Gamma(\pi^-\overline{K}^0\nu_\tau)/\Gamma_{\text{total}}$ Γ_{35}/Γ

VALUE (%)	EVTS	DOCUMENT ID		TECN	COMMENT
0.84 ±0.04 OUR FIT		Error includes scale factor of 2.1.			
0.831±0.030 OUR AVERAGE		Error includes scale factor of 1.4. See the ideogram below.			
0.808±0.004±0.026	53k	EPIFANOV	07	BELL	351 fb^{-1} E^{ee}_{cm}=10.6 GeV
0.933±0.068±0.049	377	ABBIENDI	00C	OPAL	1991–1995 LEP runs
0.928±0.045±0.034	937	[1] BARATE	99K	ALEP	1991–1995 LEP runs
0.95 ±0.15 ±0.06		[2] ACCIARRI	95F	L3	1991–1993 LEP runs
• • • We use the following data for averages but not for fits. • • •					
0.855±0.117±0.066	509	[3] BARATE	98E	ALEP	1991–1995 LEP runs
0.704±0.041±0.072		[4] COAN	96	CLEO	$E^{ee}_{\text{cm}} \approx$ 10.6 GeV
• • • We do not use the following data for averages, fits, limits, etc. • • •					
0.79 ±0.10 ±0.09	98	[5] BUSKULIC	96	ALEP	Repl. by BARATE 99K

[1] BARATE 99K measure K^0's by detecting K^0_L's in their hadron calorimeter.
[2] ACCIARRI 95F do not identify π^-/K^- and assume B($K^-K^0\nu_\tau$) = (0.29 ± 0.12)%.
[3] BARATE 98E reconstruct K^0's using $K^0_S \to \pi^+\pi^-$ decays. Not independent of BARATE 98E B(K^0particles$^-\nu_\tau$) value.
[4] Not independent of COAN 96 B($h^-K^0\nu_\tau$) and B($K^-K^0\nu_\tau$) measurements.
[5] BUSKULIC 96 measure K^0's by detecting K^0_L's in their hadron calorimeter.

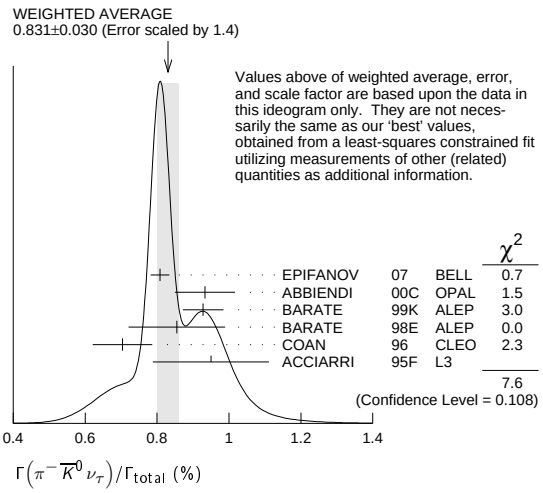

$\Gamma(\pi^-\overline{K}^0(\text{non-}K^*(892)^-)\nu_\tau)/\Gamma_{\text{total}}$ Γ_{36}/Γ

VALUE (units 10^{-4})	CL%	DOCUMENT ID		TECN	COMMENT
5.4±2.1		[1] EPIFANOV	07	BELL	351 fb^{-1} E^{ee}_{cm}= 10.6 GeV
• • • We do not use the following data for averages, fits, limits, etc. • • •					
<17	95	ACCIARRI	95F	L3	1991–1993 LEP runs

[1] EPIFANOV 07 quote B($\tau^- \to K^*(892)^-\nu_\tau$) B($K^*(892)^- \to K^0_S\pi^-$) / B($\tau^- \to K^0_S\pi^-\nu_\tau$) = 0.933 ± 0.027. We multiply their B($\tau^- \to \overline{K}^0\pi^-\nu_\tau$) by [1−(0.933 ± 0.027)] to obtain this result.

$\Gamma(K^-K^0\nu_\tau)/\Gamma_{\text{total}}$ Γ_{37}/Γ

VALUE (%)	EVTS	DOCUMENT ID		TECN	COMMENT
0.159±0.016 OUR FIT					
0.158±0.017 OUR AVERAGE					
0.162±0.021±0.011	150	[1] BARATE	99K	ALEP	1991–1995 LEP runs
0.158±0.042±0.017	46	[2] BARATE	98E	ALEP	1991–1995 LEP runs
0.151±0.021±0.022	111	COAN	96	CLEO	$E^{ee}_{\text{cm}} \approx$ 10.6 GeV
• • • We do not use the following data for averages, fits, limits, etc. • • •					
0.26 ±0.09 ±0.02	13	[3] BUSKULIC	96	ALEP	Repl. by BARATE 99K

[1] BARATE 99K measure K^0's by detecting K^0_L's in their hadron calorimeter.
[2] BARATE 98E reconstruct K^0's using $K^0_S \to \pi^+\pi^-$ decays.
[3] BUSKULIC 96 measure K^0's by detecting K^0_L's in their hadron calorimeter.

$\Gamma(K^-K^0 \geq 0\pi^0\nu_\tau)/\Gamma_{\text{total}}$ $\Gamma_{38}/\Gamma = (\Gamma_{37}+\Gamma_{42})/\Gamma$

VALUE (%)	EVTS	DOCUMENT ID		TECN	COMMENT
0.318±0.023 OUR FIT					
0.330±0.055±0.039	124	ABBIENDI	00C	OPAL	1991–1995 LEP runs

$\Gamma(h^-\overline{K}^0\pi^0\nu_\tau)/\Gamma_{\text{total}}$ $\Gamma_{39}/\Gamma = (\Gamma_{40}+\Gamma_{42})/\Gamma$

VALUE (%)	EVTS	DOCUMENT ID		TECN	COMMENT
0.56 ±0.04 OUR FIT					
0.50 ±0.06 OUR AVERAGE		Error includes scale factor of 1.2.			
0.562±0.050±0.048	264	COAN	96	CLEO	$E^{ee}_{\text{cm}} \approx$ 10.6 GeV
• • • We use the following data for averages but not for fits. • • •					
0.446±0.052±0.046	157	[1] BARATE	98E	ALEP	1991–1995 LEP runs

[1] Not independent of BARATE 98E B($\tau^- \to \pi^-\overline{K}^0\pi^0\tau$) and B($\tau^- \to K^-K^0\pi^0\nu_\tau$) values.

$\Gamma(\pi^-\overline{K}^0\pi^0\nu_\tau)/\Gamma_{\text{total}}$ Γ_{40}/Γ

VALUE (%)	EVTS	DOCUMENT ID		TECN	COMMENT
0.40 ±0.04 OUR FIT					
0.36 ±0.04 OUR AVERAGE					
0.347±0.053±0.037	299	[1] BARATE	99K	ALEP	1991–1995 LEP runs
0.294±0.073±0.037	142	[2] BARATE	98E	ALEP	1991–1995 LEP runs
0.41 ±0.12 ±0.03		[3] ACCIARRI	95F	L3	1991–1993 LEP runs
• • • We use the following data for averages but not for fits. • • •					
0.417±0.058±0.044		[4] COAN	96	CLEO	$E^{ee}_{\text{cm}} \approx$ 10.6 GeV
• • • We do not use the following data for averages, fits, limits, etc. • • •					
0.32 ±0.11 ±0.05	23	[5] BUSKULIC	96	ALEP	Repl. by BARATE 99K

[1] BARATE 99K measure K^0's by detecting K^0_L's in their hadron calorimeter.
[2] BARATE 98E reconstruct K^0's using $K^0_S \to \pi^+\pi^-$ decays.
[3] ACCIARRI 95F do not identify π^-/K^- and assume B($K^-K^0\pi^0\nu_\tau$) = (0.05 ± 0.05)%.
[4] Not independent of COAN 96 B($h^-K^0\pi^0\nu_\tau$) and B($K^-K^0\pi^0\nu_\tau$) measurements.
[5] BUSKULIC 96 measure K^0's by detecting K^0_L's in their hadron calorimeter.

$\Gamma(\overline{K}^0\rho^-\nu_\tau)/\Gamma_{\text{total}}$ Γ_{41}/Γ

VALUE (%)	DOCUMENT ID		TECN	COMMENT
0.22 ±0.05 OUR AVERAGE				
0.250±0.057±0.044	[1] BARATE	99K	ALEP	1991–1995 LEP runs
0.188±0.054±0.038	[2] BARATE	98E	ALEP	1991–1995 LEP runs

[1] BARATE 99K measure K^0's by detecting K^0_L's in hadron calorimeter. They determine the $\overline{K}^0\rho^-$ fraction in $\tau^- \to \pi^-\overline{K}^0\pi^0\nu_\tau$ decays to be (0.72 ± 0.12 ± 0.10) and multiply their B($\pi^-\overline{K}^0\pi^0\nu_\tau$) measurement by this fraction to obtain the quoted result.
[2] BARATE 98E reconstruct K^0's using $K^0_S \to \pi^+\pi^-$ decays. They determine the $\overline{K}^0\rho^-$ fraction in $\tau^- \to \pi^-\overline{K}^0\pi^0\nu_\tau$ decays to be (0.64 ± 0.09 ± 0.10) and multiply their B($\pi^-\overline{K}^0\pi^0\nu_\tau$) measurement by this fraction to obtain the quoted result.

$\Gamma(K^-K^0\pi^0\nu_\tau)/\Gamma_{\text{total}}$ Γ_{42}/Γ

VALUE (%)	EVTS	DOCUMENT ID		TECN	COMMENT
0.159±0.020 OUR FIT					
0.144±0.023 OUR AVERAGE					
0.143±0.025±0.015	78	[1] BARATE	99K	ALEP	1991–1995 LEP runs
0.152±0.076±0.021	15	[2] BARATE	98E	ALEP	1991–1995 LEP runs
0.145±0.036±0.020	32	COAN	96	CLEO	$E^{ee}_{\text{cm}} \approx$ 10.6 GeV
• • • We do not use the following data for averages, fits, limits, etc. • • •					
0.10 ±0.05 ±0.03	5	[3] BUSKULIC	96	ALEP	Repl. by BARATE 99K

[1] BARATE 99K measure K^0's by detecting K^0_L's in their hadron calorimeter.
[2] BARATE 98E reconstruct K^0's using $K^0_S \to \pi^+\pi^-$ decays.
[3] BUSKULIC 96 measure K^0's by detecting K^0_L's in their hadron calorimeter.

$\Gamma(\pi^-\overline{K}^0 \geq 1\pi^0\nu_\tau)/\Gamma_{\text{total}}$ $\Gamma_{43}/\Gamma = (\Gamma_{40}+\Gamma_{44})/\Gamma$

VALUE (%)	EVTS	DOCUMENT ID		TECN	COMMENT
0.324±0.074±0.066	148	ABBIENDI	00C	OPAL	1991–1995 LEP runs

$\Gamma(\pi^-\overline{K}^0\pi^0\pi^0\nu_\tau)/\Gamma_{\text{total}}$ Γ_{44}/Γ

VALUE (units 10^{-3})	CL%	EVTS	DOCUMENT ID		TECN	COMMENT
0.26±0.24			[1] BARATE	99R	ALEP	1991–1995 LEP runs
• • • We do not use the following data for averages, fits, limits, etc. • • •						
<0.66	95	17	[2] BARATE	99K	ALEP	1991–1995 LEP runs
0.58±0.33±0.14		5	[3] BARATE	98E	ALEP	1991–1995 LEP runs

[1] BARATE 99R combine the BARATE 98E and BARATE 99K measurements to obtain this value.
[2] BARATE 99K measure K^0's by detecting K^0_L's in their hadron calorimeter.
[3] BARATE 98E reconstruct K^0's using $K^0_S \to \pi^+\pi^-$ decays.

$\Gamma(K^-K^0\pi^0\pi^0\nu_\tau)/\Gamma_{\text{total}}$ Γ_{45}/Γ

VALUE	CL%	DOCUMENT ID		TECN	COMMENT
<0.16 × 10^{-3}	95	[1] BARATE	99R	ALEP	1991–1995 LEP runs
• • • We do not use the following data for averages, fits, limits, etc. • • •					
<0.18 × 10^{-3}	95	[2] BARATE	99K	ALEP	1991–1995 LEP runs
<0.39 × 10^{-3}	95	[3] BARATE	98E	ALEP	1991–1995 LEP runs

[1] BARATE 99R combine the BARATE 98E and BARATE 99K bounds to obtain this value.
[2] BARATE 99K measure K^0's by detecting K^0_L's in hadron calorimeter.
[3] BARATE 98E reconstruct K^0's by using $K^0_S \to \pi^+\pi^-$ decays.

$\Gamma(\pi^- K^0 \overline{K}^0 \nu_\tau)/\Gamma_{total}$ $\Gamma_{46}/\Gamma = (2\Gamma_{47}+\Gamma_{48})/\Gamma$

VALUE (%)	EVTS	DOCUMENT ID		TECN	COMMENT
0.17 ±0.04 OUR FIT	Error includes scale factor of 1.8.				
• • • We use the following data for averages but not for fits. • • •					
0.153±0.030±0.016	74	[1] BARATE	98E	ALEP	1991–1995 LEP runs
• • • We do not use the following data for averages, fits, limits, etc. • • •					
0.31 ±0.12 ±0.04		[2] ACCIARRI	95F	L3	1991–1993 LEP runs

[1] BARATE 98E obtain this value by adding twice their $B(\pi^- K^0_S K^0_S \nu_\tau)$ value to their $B(\pi^- K^0_S K^0_L \nu_\tau)$ value.
[2] ACCIARRI 95F assume $B(\pi^- K^0_S K^0_S \nu) = B(\pi^- K^0_S K^0_L \nu) = 1/2 B(\pi^- K^0_S K^0_L \nu)$.

$\Gamma(\pi^- K^0_S K^0_S \nu_\tau)/\Gamma_{total}$ Γ_{47}/Γ

Bose-Einstein correlations might make the mixing fraction different than 1/4.

VALUE (units 10^{-4})	EVTS	DOCUMENT ID		TECN	COMMENT
2.31±0.17 OUR FIT	Error includes scale factor of 1.9.				
2.31±0.09 OUR AVERAGE					
2.31±0.04±0.08	5.0k	LEES	12Y	BABR	468 fb^{-1} E^{ee}_{cm}=10.6 GeV
2.6 ±1.0 ±0.5	6	BARATE	98E	ALEP	1991–1995 LEP runs
2.3 ±0.5 ±0.3	42	COAN	96	CLEO	$E^{ee}_{cm} \approx$ 10.6 GeV

$\Gamma(\pi^- K^0_S K^0_L \nu_\tau)/\Gamma_{total}$ Γ_{48}/Γ

VALUE (units 10^{-4})	EVTS	DOCUMENT ID		TECN	COMMENT
12 ±4 OUR FIT	Error includes scale factor of 1.8.				
10.1±2.3±1.3	68	BARATE	98E	ALEP	1991–1995 LEP runs

$\Gamma(\pi^- K^0 \overline{K}^0 \pi^0 \nu_\tau)/\Gamma_{total}$ Γ_{49}/Γ

VALUE	DOCUMENT ID		TECN	COMMENT
(0.31±0.23) × 10^{-3}	[1] BARATE	99R	ALEP	1991–1995 LEP runs

[1] BARATE 99R combine BARATE 98E $\Gamma(\pi^- K^0_S K^0_S \pi^0 \nu_\tau)/\Gamma_{total}$ and $\Gamma(\pi^- K^0_S K^0_L \pi^0 \nu_\tau)/\Gamma_{total}$ measurements to obtain this value.

$\Gamma(\pi^- K^0_S K^0_S \pi^0 \nu_\tau)/\Gamma_{total}$ Γ_{50}/Γ

VALUE (units 10^{-4})	CL%	EVTS	DOCUMENT ID		TECN	COMMENT
1.60±0.20±0.22		409	LEES	12Y	BABR	468 fb^{-1} E^{ee}_{cm}=10.6 GeV
• • • We do not use the following data for averages, fits, limits, etc. • • •						
<2.0	95		BARATE	98E	ALEP	1991–1995 LEP runs

$\Gamma(\pi^- K^0_S K^0_L \pi^0 \nu_\tau)/\Gamma_{total}$ Γ_{51}/Γ

VALUE (units 10^{-4})	EVTS	DOCUMENT ID		TECN	COMMENT
3.1±1.1±0.5	11	BARATE	98E	ALEP	1991–1995 LEP runs

$\Gamma(K^- K^0_S K^0_S \nu_\tau)/\Gamma_{total}$ Γ_{52}/Γ

VALUE	CL%	DOCUMENT ID		TECN	COMMENT
<6.3 × 10^{-7}	90	LEES	12Y	BABR	468 fb^{-1} E^{ee}_{cm}=10.6 GeV

$\Gamma(K^- K^0_S K^0_S \pi^0 \nu_\tau)/\Gamma_{total}$ Γ_{53}/Γ

VALUE	CL%	DOCUMENT ID		TECN	COMMENT
<4.0 × 10^{-7}	90	LEES	12Y	BABR	468 fb^{-1} E^{ee}_{cm}=10.6 GeV

$\Gamma(K^0 h^+ h^- h^- \geq 0 \text{ neutrals } \nu_\tau)/\Gamma_{total}$ Γ_{54}/Γ

VALUE (%)	CL%	DOCUMENT ID		TECN	COMMENT
<0.17	95	TSCHIRHART	88	HRS	E^{ee}_{cm}= 29 GeV
• • • We do not use the following data for averages, fits, limits, etc. • • •					
<0.27	90	BELTRAMI	85	HRS	E^{ee}_{cm}= 29 GeV

$\Gamma(K^0 h^+ h^- h^- \nu_\tau)/\Gamma_{total}$ Γ_{55}/Γ

VALUE (units 10^{-4})	EVTS	DOCUMENT ID		TECN	COMMENT
2.3±1.9±0.7	6	[1] BARATE	98E	ALEP	1991–1995 LEP runs

[1] BARATE 98E reconstruct K^0's using $K^0_S \to \pi^+ \pi^-$ decays.

$\Gamma(h^- h^- h^+ \geq 0 \text{ neutrals } \geq 0 K^0_L \nu_\tau)/\Gamma_{total}$ Γ_{56}/Γ

$\Gamma_{56}/\Gamma = (0.3431\Gamma_{35}+0.3431\Gamma_{37}+0.3431\Gamma_{40}+0.3431\Gamma_{42}+0.4307\Gamma_{47}+0.6861\Gamma_{48}+\Gamma_{64}+\Gamma_{72}+\Gamma_{79}+\Gamma_{80}+\Gamma_{90}+\Gamma_{94}+\Gamma_{98}+\Gamma_{99}+0.285\Gamma_{140}+0.285\Gamma_{142}+0.9101\Gamma_{167}+0.9101\Gamma_{169})/\Gamma$

VALUE (%)	EVTS	DOCUMENT ID		TECN	COMMENT
15.20± 0.08 OUR FIT	Error includes scale factor of 1.3.				
14.8 ± 0.4 OUR AVERAGE					
14.4 ± 0.6 ±0.3		ADEVA	91F	L3	E^{ee}_{cm}= 88.3–94.3 GeV
15.0 ± 0.4 ±0.3		BEHREND	89B	CELL	E^{ee}_{cm}= 14–47 GeV
15.1 ± 0.8 ±0.6		AIHARA	87B	TPC	E^{ee}_{cm}= 29 GeV
• • • We do not use the following data for averages, fits, limits, etc. • • •					
13.5 ± 0.3 ±0.3		ABACHI	89B	HRS	E^{ee}_{cm}= 29 GeV
12.8 ± 1.0 ±0.7		[1] BURCHAT	87	MRK2	E^{ee}_{cm}= 29 GeV
12.1 ± 0.5 ±1.2		RUCKSTUHL	86	DLCO	E^{ee}_{cm}= 29 GeV
12.8 ± 0.5 ±0.8	1420	SCHMIDKE	86	MRK2	E^{ee}_{cm}= 29 GeV
15.3 ± 1.1 $^{+1.3}_{-1.6}$	367	ALTHOFF	85	TASS	E^{ee}_{cm}= 34.5 GeV
13.6 ± 0.5 ±0.8		BARTEL	85F	JADE	E^{ee}_{cm}= 34.6 GeV
12.2 ± 1.3 ±3.9		[2] BERGER	85	PLUT	E^{ee}_{cm}= 34.6 GeV
13.3 ± 0.3 ±0.6		FERNANDEZ	85	MAC	E^{ee}_{cm}= 29 GeV
24 ± 6	35	BRANDELIK	80	TASS	E^{ee}_{cm}= 30 GeV
32 ± 5	692	[3] BACINO	78B	DLCO	E^{ee}_{cm}= 3.1–7.4 GeV
35 ±11		[3] BRANDELIK	78	DASP	Assumes $V-A$ decay
18 ± 6.5	33	[3] JAROS	78	LGW	$E^{ee}_{cm} > 6$ GeV

[1] BURCHAT 87 value is not independent of SCHMIDKE 86 value.
[2] Not independent of BERGER 85 $\Gamma(\mu^- \overline{\nu}_\mu \nu_\tau)/\Gamma_{total}$, $\Gamma(e^- \overline{\nu}_e \nu_\tau)/\Gamma_{total}$, $\Gamma(h^- \geq 1 \text{ neutrals} \nu_\tau)/\Gamma_{total}$, and $\Gamma(h^- \geq 0 K^0_L \nu_\tau)/\Gamma_{total}$, and therefore not used in the fit.
[3] Low energy experiments are not in average or fit because the systematic errors in background subtraction are judged to be large.

$\Gamma(h^- h^- h^+ \geq 0 \text{ neutrals } \nu_\tau \text{ (ex. } K^0_S \to \pi^+ \pi^-) \text{(“3-prong”)})/\Gamma_{total}$ Γ_{57}/Γ

$\Gamma_{57}/\Gamma = (\Gamma_{64}+\Gamma_{72}+\Gamma_{79}+\Gamma_{80}+\Gamma_{90}+\Gamma_{94}+\Gamma_{98}+\Gamma_{99}+0.285\Gamma_{140}+0.285\Gamma_{142}+0.9101\Gamma_{167}+0.9101\Gamma_{169})/\Gamma$

VALUE (%)	EVTS	DOCUMENT ID		TECN	COMMENT
14.57 ±0.07 OUR FIT	Error includes scale factor of 1.3.				
14.61 ±0.06 OUR AVERAGE					
14.556±0.105±0.076		[1] ACHARD	01D	L3	1992–1995 LEP runs
14.96 ±0.09 ±0.22	10.4k	AKERS	95Y	OPAL	1991–1994 LEP runs
• • • We use the following data for averages but not for fits. • • •					
14.652±0.067±0.086		SCHAEL	05C	ALEP	1991–1995 LEP runs
14.569±0.093±0.048	23k	[2] ABREU	01M	DLPH	1992–1995 LEP runs
14.22 ±0.10 ±0.37		[3] BALEST	95C	CLEO	$E^{ee}_{cm} \approx$ 10.6 GeV
• • • We do not use the following data for averages, fits, limits, etc. • • •					
15.26 ±0.26 ±0.22		ACTON	92H	OPAL	Repl. by AKERS 95Y
13.3 ±0.3 ±0.8		[4] ALBRECHT	92D	ARG	E^{ee}_{cm}= 9.4–10.6 GeV
14.35 $^{+0.40}_{-0.45}$ ±0.24		DECAMP	92C	ALEP	1989–1990 LEP runs

[1] The correlation coefficients between this measurement and the ACHARD 01D measurements of $B(\tau \to$ “1-prong”) and $B(\tau \to$ “5-prong”) are −0.978 and −0.19 respectively.
[2] The correlation coefficients between this measurement and the ABREU 01M measurements of $B(\tau \to$ 1-prong) and $B(\tau \to$ 5-prong) are −0.98 and −0.08 respectively.
[3] Not independent of BALEST 95C $B(h^- h^- h^+ \nu_\tau)$ and $B(h^- h^- h^+ \pi^0 \nu_\tau)$ values, and BORTOLETTO 93 $B(h^- h^- h^+ 2\pi^0 \nu_\tau)/B(h^- h^- h^+ \geq 0 \text{ neutrals } \nu_\tau)$ value.
[4] This ALBRECHT 92D value is not independent of their $\Gamma(\mu^- \overline{\nu}_\mu \nu_\tau)\Gamma(e^- \overline{\nu}_e \nu_\tau)/\Gamma^2_{total}$ value.

$\Gamma(h^- h^- h^+ \nu_\tau)/\Gamma_{total}$ Γ_{58}/Γ

$\Gamma_{58}/\Gamma = (0.3431\Gamma_{35}+0.3431\Gamma_{37}+\Gamma_{64}+\Gamma_{90}+\Gamma_{98}+0.017\Gamma_{167})/\Gamma$

VALUE (%)	EVTS	DOCUMENT ID		TECN	COMMENT
9.80±0.07 OUR FIT	Error includes scale factor of 1.2.				
• • • We use the following data for averages but not for fits. • • •					
7.6 ±0.1 ±0.5	7.5k	[1] ALBRECHT	96E	ARG	E^{ee}_{cm}= 9.4–10.6 GeV
• • • We do not use the following data for averages, fits, limits, etc. • • •					
9.92±0.10±0.09	11.2k	[2] BUSKULIC	96	ALEP	Repl. by SCHAEL 05C
9.49±0.36±0.63		DECAMP	92C	ALEP	Repl. by SCHAEL 05C
8.7 ±0.7 ±0.3	694	[3] BEHREND	90	CELL	E^{ee}_{cm}= 35 GeV
7.0 ±0.3 ±0.7	1566	[4] BAND	87	MAC	E^{ee}_{cm}= 29 GeV
6.7 ±0.8 ±0.9		[5] BURCHAT	87	MRK2	E^{ee}_{cm}= 29 GeV
6.4 ±0.4 ±0.9		[6] RUCKSTUHL	86	DLCO	E^{ee}_{cm}= 29 GeV
7.8 ±0.5 ±0.8	890	SCHMIDKE	86	MRK2	E^{ee}_{cm}= 29 GeV
8.4 ±0.4 ±0.7	1255	[6] FERNANDEZ	85	MAC	E^{ee}_{cm}= 29 GeV
9.7 ±2.0 ±1.3		BEHREND	84	CELL	E^{ee}_{cm}= 14,22 GeV

[1] ALBRECHT 96E not independent of ALBRECHT 93C $\Gamma(h^- h^- h^+ \nu_\tau \text{(ex. } K^0) \times \Gamma(\text{particle}^- \geq 0 \text{ neutrals } \geq 0 K^0_L \nu_\tau)/\Gamma^2_{total}$ value.
[2] BUSKULIC 96 quote $B(h^- h^- h^+ \nu_\tau \text{(ex. } K^0)) = 9.50 \pm 0.10 \pm 0.11$. We add 0.42 to remove their K^0 correction and reduce the systematic error accordingly.
[3] BEHREND 90 subtract 0.3% to account for the $\tau^- \to K^*(892)^- \nu_\tau$ contribution to measured events.
[4] BAND 87 subtract for charged kaon modes; not independent of FERNANDEZ 85 value.
[5] BURCHAT 87 value is not independent of SCHMIDKE 86 value.
[6] Value obtained by multiplying paper's $R = B(h^- h^- h^+ \nu_\tau)/B(\text{3-prong})$ by B(3-prong) = 0.143 and subtracting 0.3% for $K^*(892)$ background.

$\Gamma(h^- h^- h^+ \nu_\tau \text{(ex.} K^0))/\Gamma_{total}$ Γ_{59}/Γ

$\Gamma_{59}/\Gamma = (\Gamma_{64}+\Gamma_{90}+\Gamma_{98}+0.017\Gamma_{167})/\Gamma$

VALUE (%)	EVTS	DOCUMENT ID		TECN	COMMENT
9.46 ±0.06 OUR FIT	Error includes scale factor of 1.2.				
9.44 ±0.14 OUR AVERAGE	Error includes scale factor of 1.4. See the ideogram below.				
9.317±0.090±0.082	12.2k	[1] ABDALLAH	06A	DLPH	1992–1995 LEP runs
9.51 ±0.07 ±0.20	37.7k	BALEST	95C	CLEO	$E^{ee}_{cm} \approx$ 10.6 GeV
• • • We use the following data for averages but not for fits. • • •					
9.87 ±0.10 ±0.24		[2] AKERS	95Y	OPAL	1991–1994 LEP runs
• • • We do not use the following data for averages, fits, limits, etc. • • •					
9.50 ±0.10 ±0.11	11.2k	[3] BUSKULIC	96	ALEP	Repl. by SCHAEL 05C

[1] See footnote to ABDALLAH 06A $\Gamma(\tau^- \to h^- \nu_\tau)/\Gamma_{\rm total}$ measurement for correlations with other measurements.
[2] Not independent of AKERS 95Y B($h^- h^- h^+ \geq 0$ neutrals ν_τ(ex. $K^0_S \to \pi^+\pi^-$)) and B($h^- h^- h^+ \nu_\tau$(ex. K^0))/B($h^- h^- h^+ \geq 0$ neutrals ν_τ(ex. $K^0_S \to \pi^+\pi^-$)) values.
[3] Not independent of BUSKULIC 96 B($h^- h^- h^+ \nu_\tau$) value.

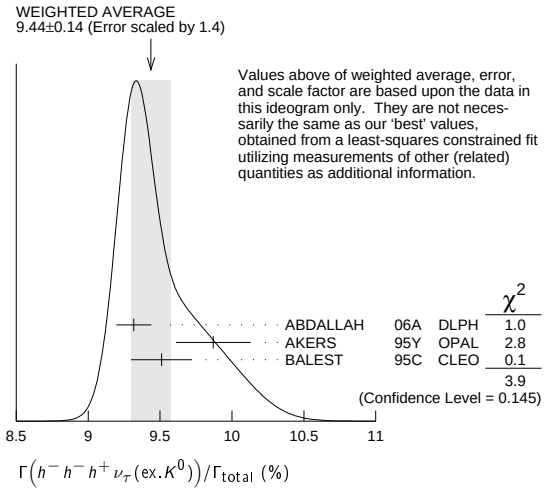

$\Gamma(h^- h^- h^+ \nu_\tau(\text{ex.}K^0))/\Gamma(h^- h^- h^+ \geq 0 \text{ neutrals } \nu_\tau(\text{ex. } K^0_S \to \pi^+\pi^-)$ ("3-prong")) Γ_{59}/Γ_{57}

$\Gamma_{59}/\Gamma_{57} = (\Gamma_{64}+\Gamma_{90}+\Gamma_{98}+0.017\Gamma_{167})/(\Gamma_{64}+\Gamma_{72}+\Gamma_{79}+\Gamma_{80}+\Gamma_{90}+\Gamma_{94}+\Gamma_{98}+\Gamma_{99}+0.285\Gamma_{140}+0.285\Gamma_{142}+0.9101\Gamma_{167}+0.9101\Gamma_{169})$

VALUE	DOCUMENT ID	TECN	COMMENT
0.6492±0.0034 OUR FIT	Error includes scale factor of 1.1.		
0.660 ±0.004 ±0.014	AKERS 95Y	OPAL	1991–1994 LEP runs

$\Gamma(h^- h^- h^+ \nu_\tau(\text{ex.}K^0,\omega))/\Gamma_{\rm total}$ $\Gamma_{60}/\Gamma = (\Gamma_{64}+\Gamma_{90}+\Gamma_{98})/\Gamma$

VALUE (%)	DOCUMENT ID
9.42±0.06 OUR FIT	Error includes scale factor of 1.2.

$\Gamma(\pi^-\pi^+\pi^-\nu_\tau)/\Gamma_{\rm total}$ $\Gamma_{61}/\Gamma = (0.3431\Gamma_{35}+\Gamma_{64}+0.017\Gamma_{167})/\Gamma$

VALUE (%)	DOCUMENT ID
9.31±0.06 OUR FIT	Error includes scale factor of 1.2.

$\Gamma(\pi^-\pi^+\pi^-\nu_\tau(\text{ex.}K^0))/\Gamma_{\rm total}$ $\Gamma_{62}/\Gamma = (\Gamma_{64}+0.017\Gamma_{167})/\Gamma$

VALUE (%)	EVTS	DOCUMENT ID	TECN	COMMENT
9.02±0.06 OUR FIT	Error includes scale factor of 1.1.			
8.77±0.13 OUR AVERAGE	Error includes scale factor of 1.1.			
$8.42\pm0.00^{+0.26}_{-0.25}$	8.9M	[1] LEE 10	BELL	666 fb^{-1} $E^{ee}_{\rm cm}$ = 10.6 GeV
8.83±0.01±0.13	1.6M	[2] AUBERT 08	BABR	342 fb^{-1} $E^{ee}_{\rm cm}$ = 10.6 GeV
9.13±0.05±0.46	43k	[3] BRIERE 03	CLE3	$E^{ee}_{\rm cm}$= 10.6 GeV

[1] Quoted statistical error is 0.003%. Correlation matrix for LEE 10 branching fractions:
(1) $\Gamma(\tau^- \to \pi^-\pi^+\pi^-\nu_\tau(\text{ex.}K^0))/\Gamma_{\rm total}$
(2) $\Gamma(\tau^- \to K^-\pi^+\pi^-\nu_\tau(\text{ex.}K^0))/\Gamma_{\rm total}$
(3) $\Gamma(\tau^- \to K^-K^+\pi^-\nu_\tau)/\Gamma_{\rm total}$
(4) $\Gamma(\tau^- \to K^-K^+K^-\nu_\tau)/\Gamma_{\rm total}$

	(1)	(2)	(3)
(2)	0.175		
(3)	0.049	0.080	
(4)	-0.053	0.035	-0.008

[2] Correlation matrix for AUBERT 08 branching fractions:
(1) $\Gamma(\tau^- \to \pi^-\pi^+\pi^-\nu_\tau(\text{ex.}K^0))/\Gamma_{\rm total}$
(2) $\Gamma(\tau^- \to K^-\pi^+\pi^-\nu_\tau(\text{ex.}K^0))/\Gamma_{\rm total}$
(3) $\Gamma(\tau^- \to K^-K^+\pi^-\nu_\tau)/\Gamma_{\rm total}$
(4) $\Gamma(\tau^- \to K^-K^+K^-\nu_\tau)/\Gamma_{\rm total}$

	(1)	(2)	(3)
(2)	0.544		
(3)	0.390	0.177	
(4)	0.031	0.093	0.087

[3] 47% correlated with BRIERE 03 $\tau^- \to K^-\pi^+\pi^-\nu_\tau$ and 71% correlated with $\tau^- \to K^-K^+\pi^-\nu_\tau$ because of a common 5% normalization error.

$\Gamma(\pi^-\pi^+\pi^-\nu_\tau(\text{ex.}K^0)\text{, non-axial vector})/\Gamma(\pi^-\pi^+\pi^-\nu_\tau(\text{ex.}K^0))$ $\Gamma_{63}/\Gamma_{62} = \Gamma_{63}/(\Gamma_{64}+0.017\Gamma_{167})$

VALUE	CL%	DOCUMENT ID	TECN	COMMENT
<0.261	95	[1] ACKERSTAFF 97R	OPAL	1992–1994 LEP runs

[1] Model-independent limit from structure function analysis on contribution to B($\tau^- \to \pi^-\pi^+\pi^-\nu_\tau$(ex. K^0)) from non-axial vectors.

$\Gamma(\pi^-\pi^+\pi^-\nu_\tau(\text{ex.}K^0,\omega))/\Gamma_{\rm total}$ Γ_{64}/Γ

VALUE (%)	EVTS	DOCUMENT ID	TECN	COMMENT
8.99 ±0.06 OUR FIT	Error includes scale factor of 1.1.			
9.041±0.060±0.076	29k	[1] SCHAEL 05C	ALEP	1991–1995 LEP runs

[1] See footnote to SCHAEL 05C $\Gamma(\tau^- \to e^-\overline{\nu}_e\nu_\tau)/\Gamma_{\rm total}$ measurement for correlations with other measurements.

$\Gamma(h^- h^- h^+ \geq 1 \text{ neutrals } \nu_\tau)/\Gamma_{\rm total}$ Γ_{65}/Γ

$\Gamma_{65}/\Gamma = (0.3431\Gamma_{40}+0.3431\Gamma_{42}+0.4307\Gamma_{47}+0.6861\Gamma_{48}+\Gamma_{72}+\Gamma_{79}+\Gamma_{80}+\Gamma_{94}+\Gamma_{99}+0.285\Gamma_{140}+0.285\Gamma_{142}+0.888\Gamma_{167}+0.9101\Gamma_{169})/\Gamma$

VALUE (%)	EVTS	DOCUMENT ID	TECN	COMMENT
5.39±0.07 OUR FIT	Error includes scale factor of 1.2.			
• • • We do not use the following data for averages, fits, limits, etc. • • •				
5.6 ±0.7 ±0.3	352	[1] BEHREND 90	CELL	$E^{ee}_{\rm cm}$= 35 GeV
4.2 ±0.5 ±0.9	203	[2] ALBRECHT 87L	ARG	$E^{ee}_{\rm cm}$= 10 GeV
6.1 ±0.8 ±0.9		[3] BURCHAT 87	MRK2	$E^{ee}_{\rm cm}$= 29 GeV
7.6 ±0.4 ±0.9		[4,5] RUCKSTUHL 86	DLCO	$E^{ee}_{\rm cm}$= 29 GeV
4.7 ±0.5 ±0.8	530	[6] SCHMIDKE 86	MRK2	$E^{ee}_{\rm cm}$= 29 GeV
5.6 ±0.4 ±0.7		[5] FERNANDEZ 85	MAC	$E^{ee}_{\rm cm}$= 29 GeV
6.2 ±2.3 ±1.7		BEHREND 84	CELL	$E^{ee}_{\rm cm}$= 14,22 GeV

[1] BEHREND 90 value is not independent of BEHREND 90 B($3h\nu_\tau \geq 1$ neutrals) + B(5-prong).
[2] ALBRECHT 87L measure the product of branching ratios B($3\pi^\pm\pi^0\nu_\tau$) B(($e\overline{\nu}$or$\mu\overline{\nu}$orπor$K$or$\rho)\nu_\tau$) = 0.029 and use the PDG 86 values for the second branching ratio which sum to 0.69 ± 0.03 to get the quoted value.
[3] BURCHAT 87 value is not independent of SCHMIDKE 86 value.
[4] Contributions from kaons and from $>1\pi^0$ are subtracted. Not independent of (3-prong + $0\pi^0$) and (3-prong + $\geq 0\pi^0$) values.
[5] Value obtained using paper's R = B($h^- h^- h^+\nu_\tau$)/B(3-prong) and current B(3-prong) = 0.143.
[6] Not independent of SCHMIDKE 86 $h^- h^- h^+\nu_\tau$ and $h^- h^- h^+(\geq 0\pi^0)\nu_\tau$ values.

$\Gamma(h^- h^- h^+ \geq 1\pi^0\nu_\tau(\text{ex. } K^0))/\Gamma_{\rm total}$ Γ_{66}/Γ

$\Gamma_{66}/\Gamma = (\Gamma_{72}+\Gamma_{79}+\Gamma_{80}+\Gamma_{94}+\Gamma_{99}+0.226\Gamma_{140}+0.226\Gamma_{142}+0.888\Gamma_{167}+0.9101\Gamma_{169})/\Gamma$

VALUE (%)	EVTS	DOCUMENT ID	TECN	COMMENT
5.09 ±0.06 OUR FIT	Error includes scale factor of 1.2.			
5.10 ±0.12 OUR AVERAGE				
• • • We use the following data for averages but not for fits. • • •				
5.106±0.083±0.103	10.1k	[1] ABDALLAH 06A	DLPH	1992–1995 LEP runs
5.09 ±0.10 ±0.23		[2] AKERS 95Y	OPAL	1991–1994 LEP runs
• • • We do not use the following data for averages, fits, limits, etc. • • •				
4.95 ±0.29 ±0.65	570	DECAMP 92C	ALEP	Repl. by SCHAEL 05C

[1] See footnote to ABDALLAH 06A $\Gamma(\tau^- \to h^-\nu_\tau)/\Gamma_{\rm total}$ measurement for correlations with other measurements.
[2] Not independent of AKERS 95Y B($h^- h^- h^+ \geq 0$ neutrals ν_τ(ex. $K^0_S \to \pi^+\pi^-$)) and B($h^- h^- h^+ \geq 0$ neutrals ν_τ(ex. K^0))/B($h^- h^- h^+ \geq 0$ neutrals ν_τ(ex. $K^0_S \to \pi^+\pi^-$)) values.

$\Gamma(h^- h^- h^+\pi^0\nu_\tau)/\Gamma_{\rm total}$ Γ_{67}/Γ

$\Gamma_{67}/\Gamma = (0.3431\Gamma_{40}+0.3431\Gamma_{42}+\Gamma_{72}+\Gamma_{94}+\Gamma_{99}+0.226\Gamma_{142}+0.888\Gamma_{167}+0.017\Gamma_{169})/\Gamma$

VALUE (%)	EVTS	DOCUMENT ID	TECN	COMMENT
4.76±0.06 OUR FIT	Error includes scale factor of 1.2.			
• • • We do not use the following data for averages, fits, limits, etc. • • •				
4.45±0.09±0.07	6.1k	[1] BUSKULIC 96	ALEP	Repl. by SCHAEL 05C

[1] BUSKULIC 96 quote B($h^- h^- h^+\pi^0\nu_\tau$(ex. K^0)) = 4.30 ± 0.09 ± 0.09. We add 0.15 to remove their K^0 correction and reduce the systematic error accordingly.

$\Gamma(h^- h^- h^+\pi^0\nu_\tau(\text{ex.}K^0))/\Gamma_{\rm total}$ Γ_{68}/Γ

$\Gamma_{68}/\Gamma = (\Gamma_{72}+\Gamma_{94}+\Gamma_{99}+0.226\Gamma_{142}+0.888\Gamma_{167}+0.017\Gamma_{169})/\Gamma$

VALUE (%)	EVTS	DOCUMENT ID	TECN	COMMENT
4.57 ±0.06 OUR FIT	Error includes scale factor of 1.2.			
4.45 ±0.14 OUR AVERAGE	Error includes scale factor of 1.2.			
4.545±0.106±0.103	8.9k	[1] ABDALLAH 06A	DLPH	1992–1995 LEP runs
4.23 ±0.06 ±0.22	7.2k	BALEST 95C	CLEO	$E^{ee}_{\rm cm} \approx$ 10.6 GeV

[1] See footnote to ABDALLAH 06A $\Gamma(\tau^- \to h^-\nu_\tau)/\Gamma_{\rm total}$ measurement for correlations with other measurements.

$\Gamma(h^- h^- h^+\pi^0\nu_\tau(\text{ex. } K^0,\omega))/\Gamma_{\rm total}$ $\Gamma_{69}/\Gamma = (\Gamma_{72}+\Gamma_{94}+\Gamma_{99}+0.226\Gamma_{142})/\Gamma$

VALUE (%)	DOCUMENT ID
2.79±0.08 OUR FIT	Error includes scale factor of 1.2.

$\Gamma(\pi^-\pi^+\pi^-\pi^0\nu_\tau)/\Gamma_{\rm total}$ $\Gamma_{70}/\Gamma = (0.3431\Gamma_{40}+\Gamma_{72}+0.888\Gamma_{167}+0.017\Gamma_{169})/\Gamma$

VALUE (%)	DOCUMENT ID
4.62±0.06 OUR FIT	Error includes scale factor of 1.2.

$\Gamma(\pi^-\pi^+\pi^-\pi^0\nu_\tau(\text{ex.}K^0))/\Gamma_{\text{total}}$ $\Gamma_{71}/\Gamma=(\Gamma_{72}+0.888\Gamma_{167}+0.017\Gamma_{169})/\Gamma$

VALUE (%)	EVTS	DOCUMENT ID	TECN	COMMENT
4.48 ±0.06 OUR FIT		Error includes scale factor of 1.2.		
4.55 ±0.13 OUR AVERAGE		Error includes scale factor of 1.6.		
4.598±0.057±0.064	16k	[1] SCHAEL	05C ALEP	1991-1995 LEP runs
4.19 ±0.10 ±0.21		[2] EDWARDS	00A CLEO	4.7 fb^{-1} E_{cm}^{ee}= 10.6 GeV

[1] SCHAEL 05C quote (4.590±0.057±0.064)%. We add 0.008% to remove their correction for $\tau^-\to\pi^-\pi^0\omega\nu_\tau\to\pi^-\pi^0\pi^+\pi^-\nu_\tau$ decays. See footnote to SCHAEL 05C $\Gamma(\tau^-\to e^-\overline{\nu}_e\nu_\tau)/\Gamma_{\text{total}}$ measurement for correlations with other measurements.

[2] EDWARDS 00A quote $(4.19\pm0.10)\times10^{-2}$ with a 5% systematic error.

$\Gamma(\pi^-\pi^+\pi^-\pi^0\nu_\tau(\text{ex.}K^0,\omega))/\Gamma_{\text{total}}$ Γ_{72}/Γ

VALUE (%)	DOCUMENT ID
2.70±0.08 OUR FIT	Error includes scale factor of 1.2.

$\Gamma(h^-\rho\pi^0\nu_\tau)/\Gamma(h^-h^-h^+\pi^0\nu_\tau)$ Γ_{73}/Γ_{67}

VALUE	EVTS	DOCUMENT ID	TECN	COMMENT
• • • We do not use the following data for averages, fits, limits, etc. • • •				
0.30±0.04±0.02	393	ALBRECHT	91D ARG	E_{cm}^{ee}= 9.4–10.6 GeV

$\Gamma(h^-\rho^+h^-\nu_\tau)/\Gamma(h^-h^-h^+\pi^0\nu_\tau)$ Γ_{74}/Γ_{67}

VALUE	EVTS	DOCUMENT ID	TECN	COMMENT
• • • We do not use the following data for averages, fits, limits, etc. • • •				
0.10±0.03±0.04	142	ALBRECHT	91D ARG	E_{cm}^{ee}= 9.4–10.6 GeV

$\Gamma(h^-\rho^-h^+\nu_\tau)/\Gamma(h^-h^-h^+\pi^0\nu_\tau)$ Γ_{75}/Γ_{67}

VALUE	EVTS	DOCUMENT ID	TECN	COMMENT
• • • We do not use the following data for averages, fits, limits, etc. • • •				
0.26±0.05±0.01	370	ALBRECHT	91D ARG	E_{cm}^{ee}= 9.4–10.6 GeV

$\Gamma(h^-h^-h^+\geq2\pi^0\nu_\tau(\text{ex. }K^0))/\Gamma_{\text{total}}$ $\Gamma_{76}/\Gamma=(\Gamma_{79}+\Gamma_{80}+0.226\Gamma_{140}+0.888\Gamma_{169})/\Gamma$

VALUE (%)	EVTS	DOCUMENT ID	TECN	COMMENT
0.521±0.032 OUR FIT				
0.561±0.068±0.095	1.3k	[1] ABDALLAH	06A DLPH	1992–1995 LEP runs

[1] See footnote to ABDALLAH 06A $\Gamma(\tau^-\to h^-\nu_\tau)/\Gamma_{\text{total}}$ measurement for correlations with other measurements.

$\Gamma(h^-h^-h^+2\pi^0\nu_\tau)/\Gamma_{\text{total}}$ Γ_{77}/Γ

$\Gamma_{77}/\Gamma=(0.4307\Gamma_{47}+\Gamma_{79}+0.226\Gamma_{140}+0.888\Gamma_{169})/\Gamma$

VALUE (%)	DOCUMENT ID
0.508±0.032 OUR FIT	

$\Gamma(h^-h^-h^+2\pi^0\nu_\tau(\text{ex.}K^0))/\Gamma_{\text{total}}$ Γ_{78}/Γ

$\Gamma_{78}/\Gamma=(\Gamma_{79}+0.226\Gamma_{140}+0.888\Gamma_{169})/\Gamma$

VALUE (%)	EVTS	DOCUMENT ID	TECN	COMMENT
0.498±0.032 OUR FIT				
0.435±0.030±0.035	2.6k	[1] SCHAEL	05C ALEP	1991-1995 LEP runs
• • • We do not use the following data for averages, fits, limits, etc. • • •				
0.50 ±0.07 ±0.07	1.8k	BUSKULIC	96 ALEP	Repl. by SCHAEL 05C

[1] SCHAEL 05C quote (0.392 ± 0.030 ± 0.035)%. We add 0.043% to remove their correction for $\tau^-\to\pi^-\eta\pi^0\nu_\tau\to\pi^-\pi^+\pi^-2\pi^0\nu_\tau$ and $\tau^-\to K^*(892)^-\eta\nu_\tau\to K^-\pi^+\pi^-2\pi^0\nu_\tau$ decays. See footnote to SCHAEL 05C $\Gamma(\tau^-\to e^-\overline{\nu}_e\nu_\tau)/\Gamma_{\text{total}}$ measurement for correlations with other measurements.

$\Gamma(h^-h^-h^+2\pi^0\nu_\tau(\text{ex.}K^0))/\Gamma(h^-h^-h^+\geq0\text{ neutrals }\geq0K_L^0\nu_\tau)$ Γ_{78}/Γ_{56}

$\Gamma_{78}/\Gamma_{56}=(\Gamma_{79}+0.226\Gamma_{140}+0.888\Gamma_{169})/(0.3431\Gamma_{35}+0.3431\Gamma_{37}+0.3431\Gamma_{40}+0.3431\Gamma_{42}+0.4307\Gamma_{47}+0.6861\Gamma_{48}+\Gamma_{64}+\Gamma_{72}+\Gamma_{79}+\Gamma_{80}+\Gamma_{90}+\Gamma_{94}+\Gamma_{98}+\Gamma_{99}+0.285\Gamma_{140}+0.285\Gamma_{142}+0.9101\Gamma_{167}+0.9101\Gamma_{169})$

VALUE	EVTS	DOCUMENT ID	TECN	COMMENT
0.0328±0.0021 OUR FIT				
0.034 ±0.002 ±0.003	668	BORTOLETTO93	CLEO	$E_{\text{cm}}^{ee}\approx10.6$ GeV

$\Gamma(h^-h^-h^+2\pi^0\nu_\tau(\text{ex.}K^0,\omega,\eta))/\Gamma_{\text{total}}$ Γ_{79}/Γ

VALUE (units 10^{-4})	DOCUMENT ID
10±4 OUR FIT	

$\Gamma(h^-h^-h^+3\pi^0\nu_\tau)/\Gamma_{\text{total}}$ Γ_{80}/Γ

VALUE (units 10^{-4})	CL%	EVTS	DOCUMENT ID	TECN	COMMENT
2.3 ±0.6 OUR FIT			Error includes scale factor of 1.2.		
2.2 ±0.3 ±0.4		139	ANASTASSOV 01	CLEO	E_{cm}^{ee}= 10.6 GeV
• • • We do not use the following data for averages, fits, limits, etc. • • •					
< 4.9	95		SCHAEL	05C ALEP	1991-1995 LEP runs
2.85±0.56±0.51		57	ANDERSON	97 CLEO	Repl. by ANASTASSOV 01
11 ±4 ±5		440	[1] BUSKULIC	96 ALEP	Repl. by SCHAEL 05C

[1] BUSKULIC 96 state their measurement is for $B(h^-h^-h^+\geq3\pi^0\nu_\tau)$. We assume that $B(h^-h^-h^+\geq4\pi^0\nu_\tau)$ is very small.

$\Gamma(2\pi^-\pi^+3\pi^0\nu_\tau(\text{ex.}K^0))/\Gamma_{\text{total}}$ Γ_{81}/Γ

VALUE (units 10^{-4})	DOCUMENT ID	TECN	COMMENT
2.07±0.18±0.37	[1] LEES	12X BABR	468 fb^{-1} E_{cm}^{ee} = 10.6 GeV

[1] Not independent of LEES 12X $\Gamma(\tau^-\to\eta\pi^-\pi^+\pi^-\nu_\tau(\text{ex.}K^0))/\Gamma$, $\Gamma(\tau^-\to\eta\pi^-\pi^0\pi^0\nu_\tau)/\Gamma$, $\Gamma(\tau^-\to\pi^-\omega2\pi^0\nu_\tau)/\Gamma$, and $\Gamma(\tau^-\to f_1(1285)\pi^-\nu_\tau\to\eta\pi^-\pi^+\pi^-\nu_\tau)/\Gamma$ values.

$\Gamma(2\pi^-\pi^+3\pi^0\nu_\tau(\text{ex.}K^0,\eta,f_1(1285)))/\Gamma_{\text{total}}$ Γ_{82}/Γ

VALUE (units 10^{-4})	DOCUMENT ID	TECN	COMMENT
1.69±0.08±0.43	LEES	12X BABR	468 fb^{-1} E_{cm}^{ee} = 10.6 GeV

$\Gamma(2\pi^-\pi^+3\pi^0\nu_\tau(\text{ex.}K^0,\eta,\omega,f_1(1285)))/\Gamma_{\text{total}}$ Γ_{83}/Γ

VALUE	CL%	DOCUMENT ID	TECN	COMMENT
<5.8 × 10^{-5}	90	[1] LEES	12X BABR	468 fb^{-1} E_{cm}^{ee} = 10.6 GeV

[1] LEES 12X also quote $(1.0\pm0.8\pm3.0)\times10^{-5}$ for this branching fraction.

$\Gamma(K^-h^+h^-\geq0\text{ neutrals }\nu_\tau)/\Gamma_{\text{total}}$ $\Gamma_{84}/\Gamma=(0.3431\Gamma_{37}+0.3431\Gamma_{42}+\Gamma_{90}+\Gamma_{94}+\Gamma_{98}+\Gamma_{99}+0.285\Gamma_{142})/\Gamma$

VALUE (%)	CL%	DOCUMENT ID	TECN	COMMENT
0.635±0.024 OUR FIT		Error includes scale factor of 1.5.		
<0.6	90	AIHARA	84C TPC	E_{cm}^{ee}= 29 GeV

$\Gamma(K^-h^+\pi^-\nu_\tau(\text{ex.}K^0))/\Gamma_{\text{total}}$ $\Gamma_{85}/\Gamma=(\Gamma_{90}+\Gamma_{98})/\Gamma$

VALUE (%)	DOCUMENT ID
0.438±0.019 OUR FIT	Error includes scale factor of 2.7.

$\Gamma(K^-h^+\pi^-\nu_\tau(\text{ex.}K^0))/\Gamma(\pi^-\pi^+\pi^-\nu_\tau(\text{ex.}K^0))$ $\Gamma_{85}/\Gamma_{62}=(\Gamma_{90}+\Gamma_{98})/(\Gamma_{64}+0.017\Gamma_{167})$

VALUE (%)	EVTS	DOCUMENT ID	TECN	COMMENT
4.85±0.22 OUR FIT		Error includes scale factor of 2.7.		
5.44±0.21±0.53	7.9k	RICHICHI	99 CLEO	E_{cm}^{ee}= 10.6 GeV

$\Gamma(K^-h^+\pi^-\pi^0\nu_\tau(\text{ex.}K^0))/\Gamma_{\text{total}}$ $\Gamma_{86}/\Gamma=(\Gamma_{94}+\Gamma_{99}+0.226\Gamma_{142})/\Gamma$

VALUE (units 10^{-4})	DOCUMENT ID
8.7±1.2 OUR FIT	Error includes scale factor of 1.1.

$\Gamma(K^-h^+\pi^-\pi^0\nu_\tau(\text{ex.}K^0))/\Gamma(\pi^-\pi^+\pi^-\pi^0\nu_\tau(\text{ex.}K^0))$ $\Gamma_{86}/\Gamma_{71}=(\Gamma_{94}+\Gamma_{99}+0.226\Gamma_{142})/(\Gamma_{72}+0.888\Gamma_{167}+0.017\Gamma_{169})$

VALUE (%)	EVTS	DOCUMENT ID	TECN	COMMENT
1.94±0.27 OUR FIT				
2.61±0.45±0.42	719	RICHICHI	99 CLEO	E_{cm}^{ee}= 10.6 GeV

$\Gamma(K^-\pi^+\pi^-\geq0\text{ neutrals }\nu_\tau)/\Gamma_{\text{total}}$ $\Gamma_{87}/\Gamma=(0.3431\Gamma_{37}+0.3431\Gamma_{42}+\Gamma_{90}+\Gamma_{94}+0.285\Gamma_{142})/\Gamma$

VALUE (%)	EVTS	DOCUMENT ID	TECN	COMMENT
0.485±0.021 OUR FIT		Error includes scale factor of 1.4.		
0.58 $^{+0.15}_{-0.13}$ ±0.12	20	[1] BAUER	94 TPC	E_{cm}^{ee}= 29 GeV
• • • We do not use the following data for averages, fits, limits, etc. • • •				
0.22 $^{+0.16}_{-0.13}$ ±0.05	9	[2] MILLS	85 DLCO	E_{cm}^{ee}= 29 GeV

[1] We multiply 0.58% by 0.20, the relative systematic error quoted by BAUER 94, to obtain the systematic error.

[2] Error correlated with MILLS 85 ($KK\pi\nu$) value. We multiply 0.22% by 0.23, the relative systematic error quoted by MILLS 85, to obtain the systematic error.

$\Gamma(K^-\pi^+\pi^-\geq0\pi^0\nu_\tau(\text{ex.}K^0))/\Gamma_{\text{total}}$ $\Gamma_{88}/\Gamma=(\Gamma_{90}+\Gamma_{94}+0.226\Gamma_{142})/\Gamma$

VALUE (%)	DOCUMENT ID	TECN	COMMENT
0.375±0.019 OUR FIT	Error includes scale factor of 1.5.		
0.30 ±0.05 OUR AVERAGE			
• • • We use the following data for averages but not for fits. • • •			
0.343±0.073±0.031	ABBIENDI	00D OPAL	1990–1995 LEP runs
0.275±0.064	[1] BARATE	98 ALEP	1991–1995 LEP runs

[1] Not independent of BARATE 98 $\Gamma(\tau^-\to K^-\pi^+\pi^-\nu_\tau)/\Gamma_{\text{total}}$ and $\Gamma(\tau^-\to K^-\pi^+\pi^-\pi^0\nu_\tau)/\Gamma_{\text{total}}$ values.

$\Gamma(K^-\pi^+\pi^-\nu_\tau)/\Gamma_{\text{total}}$ $\Gamma_{89}/\Gamma=(0.3431\Gamma_{37}+\Gamma_{90})/\Gamma$

VALUE (%)	DOCUMENT ID
0.349±0.016 OUR FIT	Error includes scale factor of 1.9.

$\Gamma(K^-\pi^+\pi^-\nu_\tau(\text{ex.}K^0))/\Gamma_{\text{total}}$ Γ_{90}/Γ

VALUE (%)	EVTS	DOCUMENT ID	TECN	COMMENT
0.294±0.015 OUR FIT		Error includes scale factor of 2.2.		
0.290±0.018 OUR AVERAGE		Error includes scale factor of 2.4. See the ideogram below.		
0.330±0.001 $^{+0.016}_{-0.017}$	794k	[1] LEE	10 BELL	666 fb^{-1} E_{cm}^{ee}=10.6 GeV
0.273±0.002±0.009	70k	[2] AUBERT	08 BABR	342 fb^{-1} E_{cm}^{ee}=10.6 GeV
0.415±0.053±0.040	269	ABBIENDI	04J OPAL	1991-1995 LEP runs
0.384±0.014±0.038	3.5k	[3] BRIERE	03 CLE3	E_{cm}^{ee}= 10.6 GeV
0.214±0.037±0.029		BARATE	98 ALEP	1991–1995 LEP runs
• • • We use the following data for averages but not for fits. • • •				
0.346±0.023±0.056	158	[4] RICHICHI	99 CLEO	E_{cm}^{ee}= 10.6 GeV
• • • We do not use the following data for averages, fits, limits, etc. • • •				
0.360±0.082±0.048		ABBIENDI	00D OPAL	1990–1995 LEP runs

[1] See footnote to LEE 10 $\Gamma(\tau^- \to \pi^-\pi^+\pi^-\nu_\tau(\text{ex.}K^0))/\Gamma_{\text{total}}$ measurement for correlations with other measurements. Not independent of LEE 10 $\Gamma(\tau^- \to K^-\pi^+\pi^-\nu_\tau(\text{ex.}K^0))/\Gamma(\tau^- \to \pi^-\pi^+\pi^-\nu_\tau(\text{ex.}K^0))$ value.

[2] See footnote to AUBERT 08 $\Gamma(\tau^- \to \pi^-\pi^+\pi^-\nu_\tau(\text{ex.}K^0))/\Gamma_{\text{total}}$ measurement for correlations with other measurements.

[3] 47% correlated with BRIERE 03 $\tau^- \to \pi^-\pi^+\pi^-\nu_\tau$ and 34% correlated with $\tau^- \to K^-K^+\pi^-\nu_\tau$ because of a common 5% normalization error.

[4] Not independent of RICHICHI 99 $\Gamma(\tau^- \to K^-h^+\pi^-\nu_\tau(\text{ex.}K^0))/\Gamma(\tau^- \to \pi^-\pi^+\pi^-\nu_\tau(\text{ex.}K^0))$, $\Gamma(\tau^- \to K^-K^+\pi^-\nu_\tau)/\Gamma(\tau^- \to \pi^-\pi^+\pi^-\nu_\tau(\text{ex.}K^0))$ and BALEST 95C $\Gamma(\tau^- \to h^-h^-h^+\nu_\tau(\text{ex.}K^0))/\Gamma_{\text{total}}$ values.

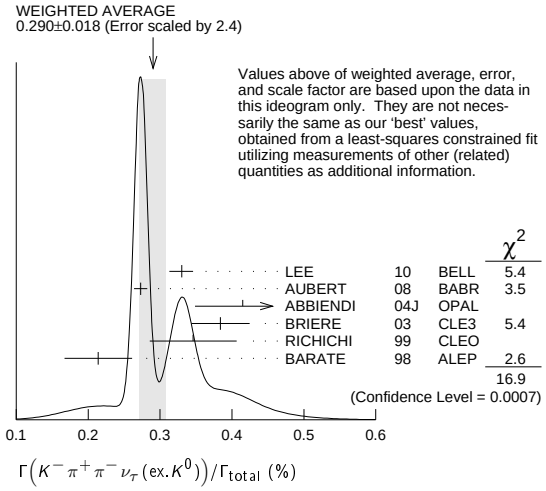

$\Gamma(K^-\pi^+\pi^-\nu_\tau(\text{ex.}K^0))/\Gamma(\pi^-\pi^+\pi^-\nu_\tau(\text{ex.}K^0))$ $\Gamma_{90}/\Gamma_{62} = \Gamma_{90}/(\Gamma_{64}+0.017\Gamma_{167})$

VALUE (units 10^{-2})	EVTS	DOCUMENT ID		TECN	COMMENT
3.26±0.17 OUR FIT	Error includes scale factor of 2.3.				
• • • We use the following data for averages but not for fits. • • •					
$3.92\pm0.02^{+0.15}_{-0.16}$	794k	[1] LEE	10	BELL	666 fb^{-1} E^{ee}_{cm} = 10.6 GeV

[1] Not independent of LEE 10 $\Gamma(\tau^- \to K^-\pi^+\pi^-\nu_\tau(\text{ex.}K^0))/\Gamma_{\text{total}}$ and $\Gamma(\tau^- \to \pi^-\pi^+\pi^-\nu_\tau(\text{ex.}K^0))/\Gamma_{\text{total}}$ values.

$\Gamma(K^-\rho^0\nu_\tau \to K^-\pi^+\pi^-\nu_\tau)/\Gamma(K^-\pi^+\pi^-\nu_\tau(\text{ex.}K^0))$ Γ_{91}/Γ_{90}

VALUE	DOCUMENT ID		TECN	COMMENT
0.48±0.14±0.10	[1] ASNER	00B	CLEO	E^{ee}_{cm} = 10.6 GeV
• • • We do not use the following data for averages, fits, limits, etc. • • •				
0.39±0.14	[2] BARATE	99R	ALEP	1991–1995 LEP runs

[1] ASNER 00B assume $\tau^- \to K^-\pi^+\pi^-\nu_\tau$ (ex. K^0) decays proceed only through $K\rho$ and $K^*\pi$ intermediate states. They assume the resonance structure of $\tau^- \to K^-\pi^+\pi^-\nu_\tau$ (ex. K^0) decays is dominated by $K_1(1270)^-$ and $K_1(1400)^-$ resonances, and assume $B(K_1(1270) \to K^*(892)\pi) = (16 \pm 5)\%$, $B(K_1(1270) \to K\rho) = (42 \pm 6)\%$, and $B(K_1(1400) \to K\rho) = 0$.

[2] BARATE 99R assume $\tau^- \to K^-\pi^+\pi^-\nu_\tau$ (ex. K^0) decays proceed only through $K\rho$ and $K^*\pi$ intermediate states. The quoted error is statistical only.

$\Gamma(K^-\pi^+\pi^-\pi^0\nu_\tau)/\Gamma_{\text{total}}$ $\Gamma_{92}/\Gamma = (0.3431\Gamma_{42}+\Gamma_{94}+0.226\Gamma_{142})/\Gamma$

VALUE (units 10^{-4})	DOCUMENT ID
13.5±1.4 OUR FIT	

$\Gamma(K^-\pi^+\pi^-\pi^0\nu_\tau(\text{ex.}K^0))/\Gamma_{\text{total}}$ $\Gamma_{93}/\Gamma = (\Gamma_{94}+0.226\Gamma_{142})/\Gamma$

VALUE (units 10^{-4})	CL%	DOCUMENT ID		TECN	COMMENT
8.1±1.2 OUR FIT					
7.3±1.2 OUR AVERAGE					
7.4±0.8±1.1		[1] ARMS	05	CLE3	7.6 fb^{-1}, E^{ee}_{cm} = 10.6 GeV
6.1±3.9±1.8		BARATE	98	ALEP	1991–1995 LEP runs
• • • We use the following data for averages but not for fits. • • •					
7.5±2.6±1.8		[2] RICHICHI	99	CLEO	E^{ee}_{cm} = 10.6 GeV
• • • We do not use the following data for averages, fits, limits, etc. • • •					
<17	95	ABBIENDI	00D	OPAL	1990–1995 LEP runs

[1] Not independent of ARMS 05 $\Gamma(\tau^- \to K^-\pi^+\pi^-\pi^0\nu_\tau(\text{ex.}K^0,\omega))$ / Γ_{total} and $\Gamma(\tau^- \to K^-\omega\nu_\tau)$ / Γ_{total} values.

[2] Not independent of RICHICHI 99 $\Gamma(\tau^- \to K^-h^+\pi^-\nu_\tau(\text{ex.}K^0))/\Gamma(\tau^- \to \pi^-\pi^+\pi^-\nu_\tau(\text{ex.}K^0))$, $\Gamma(\tau^- \to K^-K^+\pi^-\nu_\tau)/\Gamma(\tau^- \to \pi^-\pi^+\pi^-\nu_\tau(\text{ex.}K^0))$ and BALEST 95C $\Gamma(\tau^- \to h^-h^-h^+\nu_\tau(\text{ex.}K^0))/\Gamma_{\text{total}}$ values.

$\Gamma(K^-\pi^+\pi^-\pi^0\nu_\tau(\text{ex.}K^0,\eta))/\Gamma_{\text{total}}$ Γ_{94}/Γ

VALUE (units 10^{-4})	DOCUMENT ID
7.8±1.2 OUR FIT	

$\Gamma(K^-\pi^+\pi^-\pi^0\nu_\tau(\text{ex.}K^0,\omega))/\Gamma_{\text{total}}$ Γ_{95}/Γ

VALUE (units 10^{-4})	EVTS	DOCUMENT ID		TECN	COMMENT
3.7±0.5±0.8	833	ARMS	05	CLE3	7.6 fb^{-1}, E^{ee}_{cm} = 10.6 GeV

$\Gamma(K^-\pi^+K^- \geq 0 \text{ neut. } \nu_\tau)/\Gamma_{\text{total}}$ Γ_{96}/Γ

VALUE (%)	CL%	DOCUMENT ID		TECN	COMMENT
<0.09	95	BAUER	94	TPC	E^{ee}_{cm} = 29 GeV

$\Gamma(K^-K^+\pi^- \geq 0 \text{ neut. } \nu_\tau)/\Gamma_{\text{total}}$ $\Gamma_{97}/\Gamma = (\Gamma_{98}+\Gamma_{99})/\Gamma$

VALUE (%)	EVTS	DOCUMENT ID		TECN	COMMENT
0.150±0.006 OUR FIT	Error includes scale factor of 1.8.				
0.203±0.031 OUR AVERAGE					
0.159±0.053±0.020		ABBIENDI	00D	OPAL	1990–1995 LEP runs
$0.15\ ^{+0.09}_{-0.07}\pm0.03$	4	[1] BAUER	94	TPC	E^{ee}_{cm} = 29 GeV
• • • We use the following data for averages but not for fits. • • •					
0.238±0.042		[2] BARATE	98	ALEP	1991–1995 LEP runs

[1] We multiply 0.15% by 0.20, the relative systematic error quoted by BAUER 94, to obtain the systematic error.

[2] Not independent of BARATE 98 $\Gamma(\tau^- \to K^-K^+\pi^-\nu_\tau)/\Gamma_{\text{total}}$ and $\Gamma(\tau^- \to K^-K^+\pi^-\pi^0\nu_\tau)/\Gamma_{\text{total}}$ values.

$\Gamma(K^-K^+\pi^-\nu_\tau)/\Gamma_{\text{total}}$ Γ_{98}/Γ

VALUE (units 10^{-3})	EVTS	DOCUMENT ID		TECN	COMMENT
1.44 ±0.05 OUR FIT	Error includes scale factor of 1.9.				
1.43 ±0.07 OUR AVERAGE	Error includes scale factor of 2.4. See the ideogram below.				
1.55 ±0.01 $^{+0.06}_{-0.05}$	108k	[1] LEE	10	BELL	666 fb^{-1} E^{ee}_{cm}=10.6 GeV
1.346±0.010±0.036	18k	[2] AUBERT	08	BABR	342 fb^{-1} E^{ee}_{cm} = 10.6 GeV
1.55 ±0.06 ±0.09	932	[3] BRIERE	03	CLE3	E^{ee}_{cm} = 10.6 GeV
1.63 ±0.21 ±0.17		BARATE	98	ALEP	1991–1995 LEP runs
• • • We use the following data for averages but not for fits. • • •					
0.87 ±0.56 ±0.40		ABBIENDI	00D	OPAL	1990–1995 LEP runs
1.45 ±0.13 ±0.28	2.3k	[4] RICHICHI	99	CLEO	E^{ee}_{cm} = 10.6 GeV
• • • We do not use the following data for averages, fits, limits, etc. • • •					
2.2 $^{+1.7}_{-1.1}$ ±0.5	9	[5] MILLS	85	DLCO	E^{ee}_{cm} = 29 GeV

[1] See footnote to LEE 10 $\Gamma(\tau^- \to \pi^-\pi^+\pi^-\nu_\tau(\text{ex.}K^0))/\Gamma_{\text{total}}$ measurement for correlations with other measurements. Not independent of LEE 10 $\Gamma(\tau^- \to K^-K^+\pi^-\nu_\tau)/\Gamma(\tau^- \to \pi^-\pi^+\pi^-\nu_\tau(\text{ex.}K^0))$ value.

[2] See footnote to AUBERT 08 $\Gamma(\tau^- \to \pi^-\pi^+\pi^-\nu_\tau(\text{ex.}K^0))/\Gamma_{\text{total}}$ measurement for correlations with other measurements.

[3] 71% correlated with BRIERE 03 $\tau^- \to \pi^-\pi^+\pi^-\nu_\tau$ and 34% correlated with $\tau \to K^-\pi^+\pi^-\nu_\tau$ because of a common 5% normalization error.

[4] Not independent of RICHICHI 99 $\Gamma(\tau^- \to K^-K^+\pi^-\nu_\tau)/\Gamma(\tau^- \to \pi^-\pi^+\pi^-\nu_\tau(\text{ex.}K^0))$ and BALEST 95C $\Gamma(\tau^- \to h^-h^-h^+\nu_\tau(\text{ex.}K^0))/\Gamma_{\text{total}}$ values.

[5] Error correlated with MILLS 85 ($K\pi\pi\pi^0\nu$) value. We multiply 0.22% by 0.23, the relative systematic error quoted by MILLS 85, to obtain the systematic error.

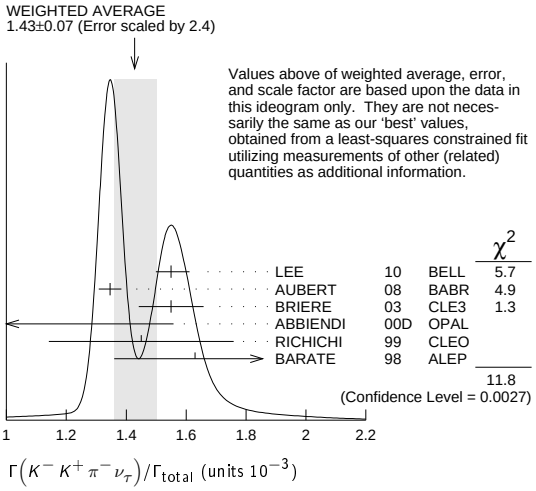

$\Gamma(K^-K^+\pi^-\nu_\tau)/\Gamma(\pi^-\pi^+\pi^-\nu_\tau(\text{ex.}K^0))$ $\Gamma_{98}/\Gamma_{62}=\Gamma_{98}/(\Gamma_{64}+0.017\Gamma_{167})$

VALUE (%)	EVTS	DOCUMENT ID		TECN	COMMENT
1.60±0.06 OUR FIT	Error includes scale factor of 1.9.				
1.83±0.05 OUR AVERAGE					
1.60±0.15±0.30	2.3k	RICHICHI	99	CLEO	E_{cm}^{ee}= 10.6 GeV
• • • We use the following data for averages but not for fits. • • •					
1.84±0.01±0.05	108k	[1] LEE	10	BELL	666 fb^{-1} E_{cm}^{ee}= 10.6 GeV

[1] Not independent of LEE 10 $\Gamma(\tau^- \to K^-K^+\pi^-\nu_\tau)/\Gamma_{total}$ and $\Gamma(\tau^- \to \pi^-\pi^+\pi^-\nu_\tau(\text{ex.}K^0))/\Gamma_{total}$ values.

$\Gamma(K^-K^+\pi^-\pi^0\nu_\tau)/\Gamma_{total}$ Γ_{99}/Γ

VALUE (units 10^{-4})	CL%	EVTS	DOCUMENT ID		TECN	COMMENT
0.61±0.25 OUR FIT	Error includes scale factor of 1.4.					
0.60±0.18 OUR AVERAGE						
0.55±0.14±0.12		48	ARMS	05	CLE3	7.6 fb^{-1},E_{cm}^{ee}=10.6 GeV
7.5 ±2.9 ±1.5			BARATE	98	ALEP	1991–1995 LEP runs
• • • We use the following data for averages but not for fits. • • •						
3.3 ±1.8 ±0.7		158	[1] RICHICHI	99	CLEO	E_{cm}^{ee}= 10.6 GeV
• • • We do not use the following data for averages, fits, limits, etc. • • •						
<27		95	ABBIENDI	00D	OPAL	1990–1995 LEP runs

[1] Not independent of RICHICHI 99 $\Gamma(\tau^- \to K^-K^+\pi^-\nu_\tau)/\Gamma(\tau^- \to \pi^-\pi^+\pi^-\nu_\tau(\text{ex.}K^0))$ and BALEST 95C $\Gamma(\tau^- \to h^-h^-h^+\nu_\tau(\text{ex.}K^0))/\Gamma_{total}$ values.

$\Gamma(K^-K^+\pi^-\pi^0\nu_\tau)/\Gamma(\pi^-\pi^+\pi^-\pi^0\nu_\tau(\text{ex.}K^0))$ $\Gamma_{99}/\Gamma_{71}=\Gamma_{99}/(\Gamma_{72}+0.888\Gamma_{167}+0.017\Gamma_{169})$

VALUE (%)	EVTS	DOCUMENT ID		TECN	COMMENT
0.14±0.05 OUR FIT	Error includes scale factor of 1.4.				
0.79±0.44±0.16	158	[1] RICHICHI	99	CLEO	E_{cm}^{ee}= 10.6 GeV

[1] RICHICHI 99 also quote a 95%CL upper limit of 0.0157 for this measurement.

$\Gamma(K^-K^+K^-\nu_\tau)/\Gamma_{total}$ Γ_{100}/Γ

VALUE (units 10^{-5})	CL%	EVTS	DOCUMENT ID		TECN	COMMENT
2.1 ±0.8 OUR AVERAGE	Error includes scale factor of 5.4.					
$3.29\pm0.17^{+0.19}_{-0.20}$		3.2k	[1] LEE	10	BELL	666 fb^{-1} E_{cm}^{ee} = 10.6 GeV
1.58±0.13±0.12		275	[2] AUBERT	08	BABR	342 fb^{-1} E_{cm}^{ee}= 10.6 GeV
• • • We do not use the following data for averages, fits, limits, etc. • • •						
< 3.7	90		BRIERE	03	CLE3	E_{cm}^{ee}= 10.6 GeV
< 19	90		BARATE	98	ALEP	1991–1995 LEP runs

[1] See footnote to LEE 10 $\Gamma(\tau^- \to \pi^-\pi^+\pi^-\nu_\tau(\text{ex.}K^0))/\Gamma_{total}$ measurement for correlations with other measurements. Not independent of LEE 10 $\Gamma(\tau^- \to K^-K^+K^-\nu_\tau)/\Gamma(\tau^- \to \pi^-\pi^+\pi^-\nu_\tau(\text{ex.}K^0))$ value.

[2] See footnote to AUBERT 08 $\Gamma(\tau^- \to \pi^-\pi^+\pi^-\nu_\tau(\text{ex.}K^0))/\Gamma_{total}$ measurement for correlations with other measurements.

$\Gamma(K^-K^+K^-\nu_\tau)/\Gamma(\pi^-\pi^+\pi^-\nu_\tau(\text{ex.}K^0))$ Γ_{100}/Γ_{62}

VALUE (units 10^{-4})	EVTS	DOCUMENT ID		TECN	COMMENT
• • • We do not use the following data for averages, fits, limits, etc. • • •					
$3.90\pm0.02^{+0.22}_{-0.23}$	3.2k	[1] LEE	10	BELL	666 fb^{-1} E_{cm}^{ee} = 10.6 GeV

[1] Not independent of LEE 10 $\Gamma(\tau^- \to K^-K^+K^-\nu_\tau)/\Gamma_{total}$ and $\Gamma(\tau^- \to \pi^-\pi^+\pi^-\nu_\tau(\text{ex.}K^0))/\Gamma_{total}$ values.

$\Gamma(K^-K^+K^-\nu_\tau(\text{ex. }\phi))/\Gamma_{total}$ Γ_{101}/Γ

VALUE	CL%	DOCUMENT ID		TECN	COMMENT
<2.5 × 10^{-6}	90	AUBERT	08	BABR	342 fb^{-1} E_{cm}^{ee} = 10.6 GeV

$\Gamma(K^-K^+K^-\pi^0\nu_\tau)/\Gamma_{total}$ Γ_{102}/Γ

VALUE	CL%	DOCUMENT ID		TECN	COMMENT
<4.8 × 10^{-6}	90	ARMS	05	CLE3	7.6 fb^{-1}, E_{cm}^{ee}= 10.6 GeV

$\Gamma(\pi^-K^+\pi^-\geq 0\text{ neut. }\nu_\tau)/\Gamma_{total}$ Γ_{103}/Γ

VALUE (%)	CL%	DOCUMENT ID		TECN	COMMENT
<0.25	95	BAUER	94	TPC	E_{cm}^{ee}= 29 GeV

$\Gamma(e^-e^-e^+\overline{\nu}_e\nu_\tau)/\Gamma_{total}$ Γ_{104}/Γ

VALUE (units 10^{-5})	EVTS	DOCUMENT ID		TECN	COMMENT
2.8±1.4±0.4	5	ALAM	96	CLEO	E_{cm}^{ee}= 10.6 GeV

$\Gamma(\mu^-e^-e^+\overline{\nu}_\mu\nu_\tau)/\Gamma_{total}$ Γ_{105}/Γ

VALUE (units 10^{-5})	CL%	DOCUMENT ID		TECN	COMMENT
<3.6	90	ALAM	96	CLEO	E_{cm}^{ee}= 10.6 GeV

$\Gamma(3h^-2h^+\geq 0\text{ neutrals }\nu_\tau(\text{ex. }K_S^0\to\pi^-\pi^+)(\text{"5-prong"}))/\Gamma_{total}$ Γ_{106}/Γ

$\Gamma_{106}/\Gamma=(\Gamma_{107}+\Gamma_{113})/\Gamma$

VALUE (%)	EVTS	DOCUMENT ID		TECN	COMMENT
0.102±0.004 OUR FIT	Error includes scale factor of 1.1.				
0.107±0.007 OUR AVERAGE	Error includes scale factor of 1.1.				
0.170±0.022±0.026		[1] ACHARD	01D	L3	1992–1995 LEP runs
0.097±0.005±0.011	419	GIBAUT	94B	CLEO	E_{cm}^{ee}= 10.6 GeV
0.102±0.029	13	BYLSMA	87	HRS	E_{cm}^{ee}= 29 GeV
• • • We use the following data for averages but not for fits. • • •					
0.093±0.009±0.012		SCHAEL	05C	ALEP	1991-1995 LEP runs
0.115±0.013±0.006	112	[2] ABREU	01M	DLPH	1992–1995 LEP runs
0.119±0.013±0.008	119	[3] ACKERSTAFF	99E	OPAL	1991–1995 LEP runs
• • • We do not use the following data for averages, fits, limits, etc. • • •					
0.26 ±0.06 ±0.05		ACTON	92H	OPAL	E_{cm}^{ee}= 88.2–94.2 GeV
$0.10\ ^{+0.05}_{-0.04}$ ±0.03		DECAMP	92C	ALEP	1989–1990 LEP runs
0.16 ±0.13 ±0.04		BEHREND	89B	CELL	E_{cm}^{ee}= 14–47 GeV
0.3 ±0.1 ±0.2		BARTEL	85F	JADE	E_{cm}^{ee}= 34.6 GeV
0.13 ±0.04	10	BELTRAMI	85	HRS	Repl. by BYLSMA 87
0.16 ±0.08 ±0.04	4	BURCHAT	85	MRK2	E_{cm}^{ee}= 29 GeV
1.0 ±0.4	10	BEHREND	82	CELL	Repl. by BEHREND 89B

[1] The correlation coefficients between this measurement and the ACHARD 01D measurements of B($\tau \to$ "1-prong") and B($\tau \to$ "3-prong") are −0.082 and −0.19 respectively.

[2] The correlation coefficients between this measurement and the ABREU 01M measurements of B($\tau \to$ 1-prong) and B($\tau \to$ 3-prong) are −0.08 and −0.08 respectively.

[3] Not independent of ACKERSTAFF 99E B($\tau^- \to 3h^-2h^+\nu_\tau$(ex. K^0)) and B($\tau^- \to 3h^-2h^+\pi^0\nu_\tau$(ex. K^0)) measurements.

$\Gamma(3h^-2h^+\nu_\tau(\text{ex.}K^0))/\Gamma_{total}$ Γ_{107}/Γ

VALUE (units 10^{-4})	EVTS	DOCUMENT ID		TECN	COMMENT
8.39±0.35 OUR FIT	Error includes scale factor of 1.1.				
8.32±0.35 OUR AVERAGE					
9.7 ±1.5 ±0.5	96	[1] ABDALLAH	06A	DLPH	1992–1995 LEP runs
8.56±0.05±0.42	34k	AUBERT,B	05W	BABR	232 fb^{-1}, E_{cm}^{ee}= 10.6 GeV
7.2 ±0.9 ±1.2	165	[2] SCHAEL	05C	ALEP	1991-1995 LEP runs
9.1 ±1.4 ±0.6	97	ACKERSTAFF	99E	OPAL	1991–1995 LEP runs
7.7 ±0.5 ±0.9	295	GIBAUT	94B	CLEO	E_{cm}^{ee}= 10.6 GeV
6.4 ±2.3 ±1.0	12	ALBRECHT	88B	ARG	E_{cm}^{ee}= 10 GeV
5.1 ±2.0	7	BYLSMA	87	HRS	E_{cm}^{ee}= 29 GeV
• • • We do not use the following data for averages, fits, limits, etc. • • •					
8.0 ±1.1 ±1.3	58	BUSKULIC	96	ALEP	Repl. by SCHAEL 05C
6.7 ±3.0	5	[3] BELTRAMI	85	HRS	Repl. by BYLSMA 87

[1] See footnote to ABDALLAH 06A $\Gamma(\tau^- \to h^-\nu_\tau)/\Gamma_{total}$ measurement for correlations with other measurements.

[2] See footnote to SCHAEL 05C $\Gamma(\tau^- \to e^-\overline{\nu}_e\nu_\tau)/\Gamma_{total}$ measurement for correlations with other measurements.

[3] The error quoted is statistical only.

$\Gamma(3\pi^-2\pi^+\nu_\tau(\text{ex.}K^0,\omega))/\Gamma_{total}$ Γ_{108}/Γ

VALUE (units 10^{-4})	DOCUMENT ID		TECN	COMMENT
8.33±0.04±0.43	[1] LEES	12X	BABR	468 fb^{-1} E_{cm}^{ee} = 10.6 GeV

[1] Not independent of LEES 12X $\Gamma(\tau^- \to f_1(1285)\pi^-\nu_\tau \to 3\pi^-2\pi^+\nu_\tau)/\Gamma$ and $\Gamma(\tau^- \to 3\pi^-2\pi^+\nu_\tau(\text{ex.}K^0,\omega,f_1(1285)))/\Gamma$ values.

$\Gamma(3\pi^-2\pi^+\nu_\tau(\text{ex.}K^0,\omega,f_1(1285)))/\Gamma_{total}$ Γ_{109}/Γ

VALUE (units 10^{-4})	EVTS	DOCUMENT ID		TECN	COMMENT
7.68±0.04±0.40	69k	LEES	12X	BABR	468 fb^{-1} E_{cm}^{ee} = 10.6 GeV

$\Gamma(K^-2\pi^-2\pi^+\nu_\tau)/\Gamma_{total}$ Γ_{110}/Γ

VALUE	CL%	DOCUMENT ID		TECN	COMMENT
<2.4 × 10^{-6}	90	LEES	12X	BABR	468 fb^{-1} E_{cm}^{ee} = 10.6 GeV

$\Gamma(K^+3\pi^-\pi^+\nu_\tau)/\Gamma_{total}$ Γ_{111}/Γ

VALUE	CL%	DOCUMENT ID		TECN	COMMENT
<5.0 × 10^{-6}	90	LEES	12X	BABR	468 fb^{-1} E_{cm}^{ee} = 10.6 GeV

$\Gamma(K^+K^-2\pi^-\pi^+\nu_\tau)/\Gamma_{total}$ Γ_{112}/Γ

VALUE	CL%	DOCUMENT ID		TECN	COMMENT
<4.5 × 10^{-7}	90	LEES	12X	BABR	468 fb^{-1} E_{cm}^{ee} = 10.6 GeV

$\Gamma(3h^-2h^+\pi^0\nu_\tau(\text{ex.}K^0))/\Gamma_{total}$ Γ_{113}/Γ

VALUE (units 10^{-4})	EVTS	DOCUMENT ID		TECN	COMMENT
1.78±0.27 OUR FIT					
1.74±0.27 OUR AVERAGE					
1.6 ±1.2 ±0.6	13	[1] ABDALLAH	06A	DLPH	1992–1995 LEP runs
2.1 ±0.7 ±0.9	95	[2] SCHAEL	05C	ALEP	1991-1995 LEP runs
1.7 ±0.2 ±0.2	231	ANASTASSOV	01	CLEO	E_{cm}^{ee}= 10.6 GeV
2.7 ±1.8 ±0.9	23	ACKERSTAFF	99E	OPAL	1991–1995 LEP runs

• • • We do not use the following data for averages, fits, limits, etc. • • •

1.8 ±0.7 ±1.2	18	BUSKULIC	96	ALEP	Repl. by SCHAEL 05C
1.9 ±0.4 ±0.4	31	GIBAUT	94B	CLEO	Repl. by ANASTASSOV 01
5.1 ±2.2	6	BYLSMA	87	HRS	E^{ee}_{cm}= 29 GeV
6.7 ±3.0	5 [3]	BELTRAMI	85	HRS	Repl. by BYLSMA 87

[1] See footnote to ABDALLAH 06A $\Gamma(\tau^- \to h^- \nu_\tau)/\Gamma_{total}$ measurement for correlations with other measurements.
[2] SCHAEL 05C quote $(1.4 \pm 0.7 \pm 0.9) \times 10^{-4}$. We add 0.7×10^{-4} to remove their correction for $\tau^- \to \eta\pi^-\pi^+\pi^-\nu_\tau \to 3\pi^-2\pi^+\pi^0\nu_\tau$ and $\tau^- \to K^*(892)^-\eta\nu_\tau \to 3\pi^-2\pi^+\pi^0\nu_\tau$ decays. See footnote to SCHAEL 05C $\Gamma(\tau^- \to e^-\overline{\nu}_e\nu_\tau)/\Gamma_{total}$ measurement for correlations with other measurements.
[3] The error quoted is statistical only.

$\Gamma(3\pi^-2\pi^+\pi^0\nu_\tau\,(\text{ex.}K^0))/\Gamma_{total}$ Γ_{114}/Γ

VALUE (units 10^{-4})	DOCUMENT ID		TECN	COMMENT
1.65±0.05±0.09	[1] LEES	12X	BABR	468 fb^{-1} E^{ee}_{cm} = 10.6 GeV

[1] Not independent of LEES 12X measurements of $\Gamma(\tau^- \to 2\pi^-\pi^+\omega\nu_\tau)/\Gamma$, $\Gamma(\tau^- \to \eta\pi^-\pi^+\pi^-\nu_\tau(\text{ex.}K^0))/\Gamma$, and $\Gamma(\tau^- \to 3\pi^-2\pi^+\pi^0\nu_\tau(\text{ex.}K^0, \eta, \omega, f_1(1285)))/\Gamma$.

$\Gamma(3\pi^-2\pi^+\pi^0\nu_\tau\,(\text{ex.}K^0, \eta, f_1(1285)))/\Gamma_{total}$ Γ_{115}/Γ

VALUE (units 10^{-4})	DOCUMENT ID		TECN	COMMENT
1.11±0.04±0.09	[1] LEES	12X	BABR	468 fb^{-1} E^{ee}_{cm} = 10.6 GeV

[1] Not independent of LEES 12X $\Gamma(\tau^- \to 2\pi^-\pi^+\omega\nu_\tau)/\Gamma$ and $\Gamma(\tau^- \to 3\pi^-2\pi^+\pi^0\nu_\tau(\text{ex.}K^0, \eta, \omega, f_1(1285)))/\Gamma$ values.

$\Gamma(3\pi^-2\pi^+\pi^0\nu_\tau\,(\text{ex.}K^0, \eta, \omega, f_1(1285)))/\Gamma_{total}$ Γ_{116}/Γ

VALUE (units 10^{-4})	EVTS	DOCUMENT ID		TECN	COMMENT
0.36±0.03±0.09	7.3k	LEES	12X	BABR	468 fb^{-1} E^{ee}_{cm} = 10.6 GeV

$\Gamma(K^-2\pi^-2\pi^+\pi^0\nu_\tau)/\Gamma_{total}$ Γ_{117}/Γ

VALUE	CL%	DOCUMENT ID		TECN	COMMENT
<1.9 × 10^{-6}	90	LEES	12X	BABR	468 fb^{-1} E^{ee}_{cm} = 10.6 GeV

$\Gamma(K^+3\pi^-\pi^+\pi^0\nu_\tau)/\Gamma_{total}$ Γ_{118}/Γ

VALUE	CL%	DOCUMENT ID		TECN	COMMENT
<8 × 10^{-7}	90	LEES	12X	BABR	468 fb^{-1} E^{ee}_{cm} = 10.6 GeV

$\Gamma(3h^-2h^+2\pi^0\nu_\tau)/\Gamma_{total}$ Γ_{119}/Γ

VALUE	CL%	DOCUMENT ID		TECN	COMMENT
<3.4 × 10^{-6}	90	AUBERT,B	06	BABR	232 fb^{-1} E^{ee}_{cm} = 10.6 GeV
• • • We do not use the following data for averages, fits, limits, etc. • • •					
<1.1 × 10^{-4}	90	GIBAUT	94B	CLEO	E^{ee}_{cm}= 10.6 GeV

$\Gamma((5\pi)^-\nu_\tau)/\Gamma_{total}$ Γ_{120}/Γ

$\Gamma_{120}/\Gamma = (\Gamma_{30}+\Gamma_{47}+\Gamma_{79}+\Gamma_{107}+0.553\Gamma_{140}+0.888\Gamma_{169})/\Gamma$

VALUE (%)	DOCUMENT ID		TECN	COMMENT
0.76±0.05 OUR FIT				
• • • We use the following data for averages but not for fits. • • •				
0.61±0.06±0.08	[1] GIBAUT	94B	CLEO	E^{ee}_{cm}= 10.6 GeV

[1] Not independent of GIBAUT 94B B($3h^-2h^+\nu_\tau$), PROCARIO 93 B($h^-4\pi^0\nu_\tau$), and BORTOLETTO 93 B($2h^-h^+2\pi^0\nu_\tau$)/B("3prong") measurements. Result is corrected for η contributions.

$\Gamma(4h^-3h^+ \geq 0 \text{ neutrals } \nu_\tau(\text{"7-prong"}))/\Gamma_{total}$ Γ_{121}/Γ

VALUE	CL%	DOCUMENT ID		TECN	COMMENT
<3.0 × 10^{-7}	90	AUBERT,B	05F	BABR	232 fb^{-1}, E^{ee}_{cm}= 10.6 GeV
• • • We do not use the following data for averages, fits, limits, etc. • • •					
<1.8 × 10^{-5}	95	ACKERSTAFF	97J	OPAL	1990–1995 LEP runs
<2.4 × 10^{-6}	90	EDWARDS	97B	CLEO	E^{ee}_{cm}= 10.6 GeV
<2.9 × 10^{-4}	90	BYLSMA	87	HRS	E^{ee}_{cm}= 29 GeV

$\Gamma(4h^-3h^+\nu_\tau)/\Gamma_{total}$ Γ_{122}/Γ

VALUE	CL%	DOCUMENT ID		TECN	COMMENT
<4.3 × 10^{-7}	90	AUBERT,B	05F	BABR	232 fb^{-1}, E^{ee}_{cm}= 10.6 GeV

$\Gamma(4h^-3h^+\pi^0\nu_\tau)/\Gamma_{total}$ Γ_{123}/Γ

VALUE	CL%	DOCUMENT ID		TECN	COMMENT
<2.5 × 10^{-7}	90	AUBERT,B	05F	BABR	232 fb^{-1}, E^{ee}_{cm}= 10.6 GeV

$\Gamma(X^-(S=-1)\nu_\tau)/\Gamma_{total}$

$\Gamma_{124}/\Gamma = (\Gamma_{10}+\Gamma_{16}+\Gamma_{23}+\Gamma_{28}+\Gamma_{35}+\Gamma_{40}+\Gamma_{90}+\Gamma_{94}+\Gamma_{142})/\Gamma$

VALUE (%)	DOCUMENT ID		TECN	COMMENT
2.87±0.07 OUR FIT Error includes scale factor of 1.3.				
• • • We use the following data for averages but not for fits. • • •				
2.87±0.12	[1] BARATE	99R	ALEP	1991–1995 LEP runs

[1] BARATE 99R perform a combined analysis of all ALEPH LEP 1 data on τ branching fraction measurements for decay modes having total strangeness equal to −1.

$\Gamma(K^*(892)^- \geq 0 \text{ neutrals } \geq 0K^0_L\nu_\tau)/\Gamma_{total}$ Γ_{125}/Γ

VALUE (%)	EVTS	DOCUMENT ID		TECN	COMMENT
1.42±0.18 OUR AVERAGE Error includes scale factor of 1.4. See the ideogram below.					
$1.19\pm0.15^{+0.13}_{-0.18}$	104	ALBRECHT	95H	ARG	E^{ee}_{cm}= 9.4–10.6 GeV
1.94±0.27±0.15	74	[1] AKERS	94G	OPAL	E^{ee}_{cm}= 88–94 GeV
1.43±0.11±0.13	475	[2] GOLDBERG	90	CLEO	E^{ee}_{cm}= 9.4–10.9 GeV

[1] AKERS 94G reject events in which a K^0_S accompanies the $K^*(892)^-$. We do not correct for them.
[2] GOLDBERG 90 estimates that 10% of observed $K^*(892)$ are accompanied by a π^0.

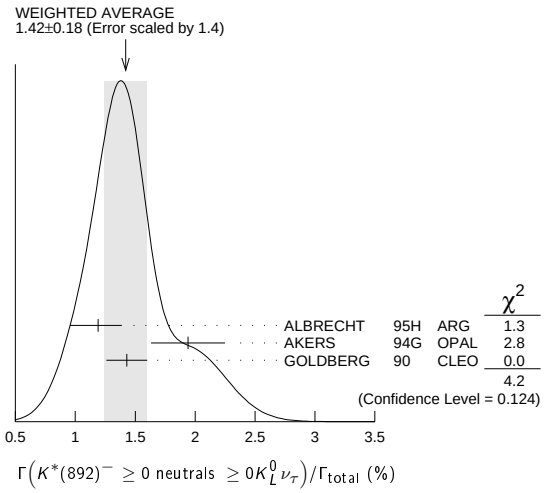

$\Gamma(K^*(892)^-\nu_\tau)/\Gamma_{total}$ Γ_{126}/Γ

VALUE (%)	EVTS	DOCUMENT ID		TECN	COMMENT
1.20 ±0.07 OUR AVERAGE Error includes scale factor of 1.8. See the ideogram below.					
1.131±0.006±0.051	49k	[1] EPIFANOV	07	BELL	351 fb^{-1} E^{ee}_{cm}=10.6 GeV
1.326±0.063		BARATE	99R	ALEP	1991–1995 LEP runs
1.11 ±0.12		[2] COAN	96	CLEO	$E^{ee}_{cm} \approx$ 10.6 GeV
1.42 ±0.22 ±0.09		[3] ACCIARRI	95F	L3	1991–1993 LEP runs
• • • We do not use the following data for averages, fits, limits, etc. • • •					
1.39 ±0.09 ±0.10		[4] BUSKULIC	96	ALEP	Repl. by BARATE 99R
1.45 ±0.13 ±0.11	273	[5] BUSKULIC	94F	ALEP	Repl. by BUSKULIC 96
1.23 ±0.21 $^{+0.11}_{-0.21}$	54	[6] ALBRECHT	88L	ARG	E^{ee}_{cm}= 10 GeV
1.9 ±0.3 ±0.4	44	[7] TSCHIRHART	88	HRS	E^{ee}_{cm}= 29 GeV
1.5 ±0.4 ±0.4	15	[8] AIHARA	87C	TPC	E^{ee}_{cm}= 29 GeV
1.3 ±0.3 ±0.3	31	YELTON	86	MRK2	E^{ee}_{cm}= 29 GeV
1.7 ±0.7	11	DORFAN	81	MRK2	E^{ee}_{cm}= 4.2–6.7 GeV

[1] EPIFANOV 07 quote B($\tau^- \to K^*(892)^-\nu_\tau$) B($K^*(892)^- \to K^0_S\pi^-$) = (3.77 ± 0.02(stat) ±0.12(syst) ±0.12(mod)) × 10^{-3}. We add the systematic and model uncertainties in quadrature and divide by B($K^*(892)^- \to K^0_S\pi^-$) = 0.3333.
[2] Not independent of COAN 96 B($\pi^-\overline{K}^0\nu_\tau$) and BATTLE 94 B($K^-\pi^0\nu_\tau$) measurements. $K\pi$ final states are consistent with and assumed to originate from $K^*(892)^-$ production.
[3] This result is obtained from their B($\pi^-\overline{K}^0\nu_\tau$) assuming all those decays originate in $K^*(892)^-$ decays.
[4] Not independent of BUSKULIC 96 B($\pi^-\overline{K}^0\nu_\tau$) and B($K^-\pi^0\nu_\tau$) measurements.
[5] BUSKULIC 94F obtain this result from BUSKULIC 94F B($\overline{K}^0\pi^-\nu_\tau$) and BUSKULIC 94E B($K^-\pi^0\nu_\tau$) assuming all of those decays originate in $K^*(892)^-$ decays.
[6] The authors divide by Γ_2/Γ = 0.865 to obtain this result.
[7] Not independent of TSCHIRHART 88 $\Gamma(\tau^- \to h^-\overline{K}^0 \geq 0 \text{ neutrals } \geq 0K^0_L\nu_\tau)$ / Γ.
[8] Decay π^- identified in this experiment, is assumed in the others.

See key on page 547

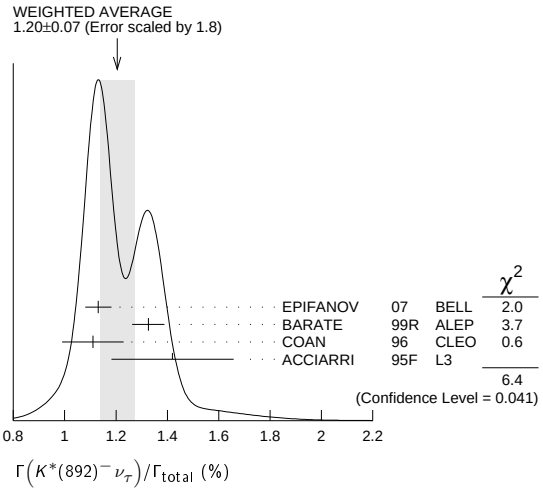

$\Gamma(K^*(892)^-\nu_\tau)/\Gamma(\pi^-\pi^0\nu_\tau)$ Γ_{126}/Γ_{14}

VALUE	DOCUMENT ID		TECN	COMMENT
0.075±0.027	[1] ABREU	94K	DLPH	LEP 1992 Z data

[1] ABREU 94K quote $B(\tau^- \to K^*(892)^-\nu_\tau)B(K^*(892)^- \to K^-\pi^0)/B(\tau^- \to \rho^-\nu_\tau) = 0.025 \pm 0.009$. We divide by $B(K^*(892)^- \to K^-\pi^0) = 0.333$ to obtain this result.

$\Gamma(K^*(892)^-\nu_\tau \to \pi^-\overline{K}^0\nu_\tau)/\Gamma(\pi^-\overline{K}^0\nu_\tau)$ Γ_{127}/Γ_{35}

VALUE	EVTS	DOCUMENT ID		TECN	COMMENT
0.933±0.027	49k	EPIFANOV	07	BELL	351 fb^{-1} E^{ee}_{cm}= 10.6 GeV

$\Gamma(K^*(892)^0K^- \geq 0 \text{ neutrals } \nu_\tau)/\Gamma_{total}$ Γ_{128}/Γ

VALUE (%)	EVTS	DOCUMENT ID		TECN	COMMENT
0.32±0.08±0.12	119	GOLDBERG	90	CLEO	E^{ee}_{cm}= 9.4–10.9 GeV

$\Gamma(K^*(892)^0K^-\nu_\tau)/\Gamma_{total}$ Γ_{129}/Γ

VALUE (%)	EVTS	DOCUMENT ID		TECN	COMMENT
0.21 ±0.04 OUR AVERAGE					
0.213±0.048		[1] BARATE	98	ALEP	1991–1995 LEP runs
0.20 ±0.05 ±0.04	47	ALBRECHT	95H	ARG	E^{ee}_{cm}= 9.4–10.6 GeV

[1] BARATE 98 measure the K^- ($\rho^0 \to \pi^+\pi^-$) fraction in $\tau^- \to K^-\pi^+\pi^-\nu_\tau$ decays to be (35 ± 11)% and derive this result from their measurement of $\Gamma(\tau^- \to K^-\pi^+\pi^-\nu_\tau)/\Gamma_{total}$ assuming the intermediate states are all $K^-\rho$ and $K^-K^*(892)^0$.

$\Gamma(\overline{K}^*(892)^0\pi^- \geq 0 \text{ neutrals } \nu_\tau)/\Gamma_{total}$ Γ_{130}/Γ

VALUE (%)	EVTS	DOCUMENT ID		TECN	COMMENT
0.38±0.11±0.13	105	GOLDBERG	90	CLEO	E^{ee}_{cm}= 9.4–10.9 GeV

$\Gamma(\overline{K}^*(892)^0\pi^-\nu_\tau)/\Gamma_{total}$ Γ_{131}/Γ

VALUE (%)	EVTS	DOCUMENT ID		TECN	COMMENT
0.22 ±0.05 OUR AVERAGE					
0.209±0.058		[1] BARATE	98	ALEP	1991–1995 LEP runs
0.25 ±0.10 ±0.05	27	ALBRECHT	95H	ARG	E^{ee}_{cm}= 9.4–10.6 GeV

[1] BARATE 98 measure the $K^-K^*(892)^0$ fraction in $\tau^- \to K^-K^+\pi^-\nu_\tau$ decays to be (87 ± 13)% and derive this result from their measurement of $\Gamma(\tau^- \to K^-K^+\pi^-\nu_\tau)/\Gamma_{total}$.

$\Gamma((\overline{K}^*(892)\pi)^-\nu_\tau \to \pi^-\overline{K}^0\pi^0\nu_\tau)/\Gamma_{total}$ Γ_{132}/Γ

VALUE (%)	DOCUMENT ID		TECN	COMMENT
0.10 ±0.04 OUR AVERAGE				
0.097±0.044±0.036	[1] BARATE	99K	ALEP	1991–1995 LEP runs
0.106±0.037±0.032	[2] BARATE	98E	ALEP	1991–1995 LEP runs

[1] BARATE 99K measure K^0's by detecting K^0_L's in their hadron calorimeter. They determine the $\overline{K}^0\rho^-$ fraction in $\tau^- \to \pi^-\overline{K}^0\pi^0\nu_\tau$ decays to be (0.72 ± 0.12 ± 0.10) and multiply their $B(\pi^-\overline{K}^0\pi^0\nu_\tau)$ measurement by one minus this fraction to obtain the quoted result.

[2] BARATE 98E reconstruct K^0's using $K^0_S \to \pi^+\pi^-$ decays. They determine the $\overline{K}^0\rho^-$ fraction in $\tau^- \to \pi^-\overline{K}^0\pi^0\nu_\tau$ decays to be (0.64 ± 0.09 ± 0.10) and multiply their $B(\pi^-\overline{K}^0\pi^0\nu_\tau)$ measurement by one minus this fraction to obtain the quoted result.

$\Gamma(K_1(1270)^-\nu_\tau)/\Gamma_{total}$ Γ_{133}/Γ

VALUE (%)	EVTS	DOCUMENT ID		TECN	COMMENT
0.47±0.11 OUR AVERAGE					
0.48±0.11		BARATE	99R	ALEP	1991–1995 LEP runs
$0.41^{+0.41}_{-0.35}\pm0.10$	5	[1] BAUER	94	TPC	E^{ee}_{cm}= 29 GeV

[1] We multiply 0.41% by 0.25, the relative systematic error quoted by BAUER 94, to obtain the systematic error.

$\Gamma(K_1(1400)^-\nu_\tau)/\Gamma_{total}$ Γ_{134}/Γ

VALUE (%)	EVTS	DOCUMENT ID		TECN	COMMENT
0.17±0.26 OUR AVERAGE Error includes scale factor of 1.7.					
0.05±0.17		BARATE	99R	ALEP	1991–1995 LEP runs
$0.76^{+0.40}_{-0.33}\pm0.20$	11	[1] BAUER	94	TPC	E^{ee}_{cm}= 29 GeV

[1] We multiply 0.76% by 0.25, the relative systematic error quoted by BAUER 94, to obtain the systematic error.

$[\Gamma(K_1(1270)^-\nu_\tau) + \Gamma(K_1(1400)^-\nu_\tau)]/\Gamma_{total}$ $(\Gamma_{133}+\Gamma_{134})/\Gamma$

VALUE (%)	EVTS	DOCUMENT ID		TECN	COMMENT
$\mathbf{1.17^{+0.41}_{-0.37}\pm0.29}$	16	[1] BAUER	94	TPC	E^{ee}_{cm}= 29 GeV

[1] We multiply 1.17% by 0.25, the relative systematic error quoted by BAUER 94, to obtain the systematic error. Not independent of BAUER 94 $B(K_1(1270)^-\nu_\tau)$ and BAUER 94 $B(K_1(1400)^-\nu_\tau)$ measurements.

$\Gamma(K_1(1270)^-\nu_\tau)/[\Gamma(K_1(1270)^-\nu_\tau) + \Gamma(K_1(1400)^-\nu_\tau)]$ $\Gamma_{133}/(\Gamma_{133}+\Gamma_{134})$

VALUE	DOCUMENT ID		TECN	COMMENT
0.69±0.15 OUR AVERAGE				
0.71±0.16±0.11	[1] ABBIENDI	00D	OPAL	1990–1995 LEP runs
0.66±0.19±0.13	[2] ASNER	00B	CLEO	E^{ee}_{cm}= 10.6 GeV

[1] ABBIENDI 00D assume the resonance structure of $\tau^- \to K^-\pi^+\pi^-\nu_\tau$ decays is dominated by the $K_1(1270)^-$ and $K_1(1400)^-$ resonances.

[2] ASNER 00B assume the resonance structure of $\tau^- \to K^-\pi^+\pi^-\nu_\tau$ (ex. K^0) decays is dominated by $K_1(1270)^-$ and $K_1(1400)^-$ resonances.

$\Gamma(K^*(1410)^-\nu_\tau)/\Gamma_{total}$ Γ_{135}/Γ

VALUE (units 10^{-3})	DOCUMENT ID		TECN	COMMENT
$\mathbf{1.5^{+1.4}_{-1.0}}$	BARATE	99R	ALEP	1991–1995 LEP runs

$\Gamma(K_0^*(1430)^-\nu_\tau)/\Gamma_{total}$ Γ_{136}/Γ

VALUE (units 10^{-3})	CL%	DOCUMENT ID		TECN	COMMENT
<0.5	95	BARATE	99R	ALEP	1991–1995 LEP runs

$\Gamma(K_2^*(1430)^-\nu_\tau)/\Gamma_{total}$ Γ_{137}/Γ

VALUE (%)	CL%	EVTS	DOCUMENT ID		TECN	COMMENT
<0.3	95		TSCHIRHART	88	HRS	E^{ee}_{cm}= 29 GeV
• • • We do not use the following data for averages, fits, limits, etc. • • •						
<0.33	95		[1] ACCIARRI	95F	L3	1991–1993 LEP runs
<0.9	95	0	DORFAN	81	MRK2	E^{ee}_{cm}= 4.2–6.7 GeV

[1] ACCIARRI 95F quote $B(\tau^- \to K^*(1430)^- \to \pi^-\overline{K}^0\nu_\tau) < 0.11\%$. We divide by $B(K^*(1430)^- \to \pi^-\overline{K}^0) = 0.33$ to obtain the limit shown.

$\Gamma(a_0(980)^- \geq 0 \text{ neutrals } \nu_\tau)/\Gamma_{total} \times B(a_0(980) \to K^0K^-)$ $\Gamma_{138}/\Gamma \times B$

VALUE (units 10^{-4})	CL%	DOCUMENT ID		TECN	COMMENT
<2.8	90	GOLDBERG	90	CLEO	E^{ee}_{cm}= 9.4–10.9 GeV

$\Gamma(\eta\pi^-\nu_\tau)/\Gamma_{total}$ Γ_{139}/Γ

VALUE (units 10^{-4})	CL%	EVTS	DOCUMENT ID		TECN	COMMENT
< 0.99	95		[1] DEL-AMO-SA...11E		BABR	470 fb^{-1} E^{ee}_{cm}= 10.6 GeV
• • • We do not use the following data for averages, fits, limits, etc. • • •						
< 6.2	95		BUSKULIC	97C	ALEP	1991–1994 LEP runs
< 1.4	95	0	BARTELT	96	CLEO	$E^{ee}_{cm} \approx$ 10.6 GeV
< 3.4	95		ARTUSO	92	CLEO	$E^{ee}_{cm} \approx$ 10.6 GeV
< 90	95		ALBRECHT	88M	ARG	$E^{ee}_{cm} \approx$ 10 GeV
<140	90		BEHREND	88	CELL	E^{ee}_{cm}= 14–46.8 GeV
<180	95		BARINGER	87	CLEO	E^{ee}_{cm}= 10.5 GeV
<250	90	0	COFFMAN	87	MRK3	E^{ee}_{cm}= 3.77 GeV
510 ±100±120	65		DERRICK	87	HRS	E^{ee}_{cm}= 29 GeV
<100	95		GAN	87B	MRK2	E^{ee}_{cm}= 29 GeV

[1] DEL-AMO-SANCHEZ 11E also quote $B(\tau^- \to \eta\pi^-\nu_\tau) = (3.4 \pm 3.4 \pm 2.1) \times 10^{-5}$.

$\Gamma(\eta\pi^-\pi^0\nu_\tau)/\Gamma_{total}$ Γ_{140}/Γ

VALUE (units 10^{-3})	CL%	EVTS	DOCUMENT ID		TECN	COMMENT
1.39± 0.10 OUR FIT Error includes scale factor of 1.4.						
1.38± 0.09 OUR AVERAGE Error includes scale factor of 1.2.						
1.35± 0.03± 0.07		6.0k	INAMI	09	BELL	490 fb^{-1} E^{ee}_{cm}= 10.6 GeV
1.8 ± 0.4 ± 0.2			BUSKULIC	97C	ALEP	1991–1994 LEP runs
1.7 ± 0.2 ± 0.2		125	ARTUSO	92	CLEO	$E^{ee}_{cm} \approx$ 10.6 GeV
• • • We do not use the following data for averages, fits, limits, etc. • • •						
< 11.0	95		ALBRECHT	88M	ARG	$E^{ee}_{cm} \approx$ 10 GeV
< 21.0	95		BARINGER	87	CLEO	E^{ee}_{cm}= 10.5 GeV
42.0 $^{+\ 7.0}_{-12.0}$ ±16.0			[1] GAN	87	MRK2	E^{ee}_{cm}= 29 GeV

[1] Highly correlated with GAN 87 $\Gamma(\pi^-3\pi^0\nu_\tau)/\Gamma(\text{total})$ value.

$\Gamma(\eta\pi^-\pi^0\pi^0\nu_\tau)/\Gamma_{total}$ Γ_{141}/Γ

VALUE (units 10^{-4})	CL%	EVTS	DOCUMENT ID		TECN	COMMENT
1.81±0.31 OUR AVERAGE						
2.01±0.34±0.22		381	LEES	12X	BABR	468 fb^{-1} E_{cm}^{ee} = 10.6 GeV
1.5 ±0.5		30	[1] ANASTASSOV	01	CLEO	E_{cm}^{ee} = 10.6 GeV
• • • We do not use the following data for averages, fits, limits, etc. • • •						
1.4 ±0.6 ±0.3		15	[2] BERGFELD	97	CLEO	Repl. by ANASTASSOV 01
< 4.3	95		ARTUSO	92	CLEO	$E_{cm}^{ee} \approx$ 10.6 GeV
<120	95		ALBRECHT	88M	ARG	$E_{cm}^{ee} \approx$ 10 GeV

[1] Weighted average of BERGFELD 97 and ANASTASSOV 01 value of $(1.5 \pm 0.6 \pm 0.3) \times 10^{-4}$ obtained using η's reconstructed from $\eta \to \pi^+\pi^-\pi^0$ decays.
[2] BERGFELD 97 reconstruct η's using $\eta \to \gamma\gamma$ decays.

$\Gamma(\eta K^-\nu_\tau)/\Gamma_{total}$ Γ_{142}/Γ

VALUE (units 10^{-4})	CL%	EVTS	DOCUMENT ID		TECN	COMMENT
1.52±0.08 OUR FIT						
1.52±0.08 OUR AVERAGE						
1.42±0.11±0.07		690	DEL-AMO-SA..11E		BABR	470 fb^{-1} E_{cm}^{ee}= 10.6 GeV
1.58±0.05±0.09		1.6k	INAMI	09	BELL	490 fb^{-1} E_{cm}^{ee}= 10.6 GeV
• • • We do not use the following data for averages, fits, limits, etc. • • •						
2.9 $^{+1.3}_{-1.2}$ ±0.7			BUSKULIC	97C	ALEP	1991–1994 LEP runs
2.6 ±0.5 ±0.5		85	BARTELT	96	CLEO	$E_{cm}^{ee} \approx$ 10.6 GeV
< 4.7	95		ARTUSO	92	CLEO	$E_{cm}^{ee} \approx$ 10.6 GeV

$\Gamma(\eta K^*(892)^-\nu_\tau)/\Gamma_{total}$ Γ_{143}/Γ

VALUE (units 10^{-4})	EVTS	DOCUMENT ID		TECN	COMMENT
1.38±0.15 OUR AVERAGE					
1.34±0.12±0.09	245	[1] INAMI	09	BELL	490 fb^{-1} E_{cm}^{ee}= 10.6 GeV
2.90±0.80±0.42	25	BISHAI	99	CLEO	E_{cm}^{ee}= 10.6 GeV

[1] Not independent of INAMI 09 B($\tau^- \to \eta K^-\pi^0\nu_\tau$) and B($\tau^- \to \eta\overline{K}^0\pi^-\nu_\tau$) values.

$\Gamma(\eta K^-\pi^0\nu_\tau)/\Gamma_{total}$ Γ_{144}/Γ

VALUE (units 10^{-4})	EVTS	DOCUMENT ID		TECN	COMMENT
0.48±0.12 OUR AVERAGE					
0.46±0.11±0.04	270	INAMI	09	BELL	490 fb^{-1} E_{cm}^{ee}= 10.6 GeV
1.77±0.56±0.71	36	BISHAI	99	CLEO	E_{cm}^{ee}= 10.6 GeV

$\Gamma(\eta K^-\pi^0(\text{non-}K^*(892))\nu_\tau)/\Gamma_{total}$ Γ_{145}/Γ

VALUE	CL%	DOCUMENT ID		TECN	COMMENT
<3.5 × 10^{-5}	90	INAMI	09	BELL	490 fb^{-1} E_{cm}^{ee}= 10.6 GeV

$\Gamma(\eta\overline{K}^0\pi^-\nu_\tau)/\Gamma_{total}$ Γ_{146}/Γ

VALUE (units 10^{-4})	EVTS	DOCUMENT ID		TECN	COMMENT
0.93±0.15 OUR AVERAGE					
0.88±0.14±0.06	161	[1] INAMI	09	BELL	490 fb^{-1} E_{cm}^{ee}= 10.6 GeV
2.20±0.70±0.22	15	[2] BISHAI	99	CLEO	E_{cm}^{ee}= 10.6 GeV

[1] We multiply the INAMI 09 measurement B($\tau^- \to \eta K_S^0\pi^-\nu_\tau$) = (0.44 ± 0.07 ± 0.03) × 10^{-4} by 2 to obtain the listed value.
[2] We multiply the BISHAI 99 measurement B($\tau^- \to \eta K_S^0\pi^-\nu_\tau$) = (1.10 ± 0.35 ± 0.11) × 10^{-4} by 2 to obtain the listed value.

$\Gamma(\eta\overline{K}^0\pi^-\pi^0\nu_\tau)/\Gamma_{total}$ Γ_{147}/Γ

VALUE	CL%	DOCUMENT ID		TECN	COMMENT
<5.0 × 10^{-5}	90	[1] INAMI	09	BELL	490 fb^{-1} E_{cm}^{ee}= 10.6 GeV

[1] We multiply the INAMI 09 measurement B($\tau^- \to \eta K_S^0\pi^-\pi^0\nu_\tau$) < 2.5 × 10^{-5} by 2 to obtain the listed value.

$\Gamma(\eta K^-K^0\nu_\tau)/\Gamma_{total}$ Γ_{148}/Γ

VALUE	CL%	DOCUMENT ID		TECN	COMMENT
<9.0 × 10^{-6}	90	[1] INAMI	09	BELL	490 fb^{-1} E_{cm}^{ee}= 10.6 GeV

[1] We multiply the INAMI 09 measurement B($\tau^- \to \eta K^-K_S^0\nu_\tau$) < 4.5 × 10^{-6} by 2 to obtain the listed value.

$\Gamma(\eta\pi^+\pi^-\pi^- \geq 0 \text{ neutrals } \nu_\tau)/\Gamma_{total}$ Γ_{149}/Γ

VALUE (%)	CL%	DOCUMENT ID		TECN	COMMENT
<0.3	90	ABACHI	87B	HRS	E_{cm}^{ee}= 29 GeV

$\Gamma(\eta\pi^-\pi^+\pi^-\nu_\tau(\text{ex.}K^0))/\Gamma_{total}$ Γ_{150}/Γ

VALUE (units 10^{-4})	EVTS	DOCUMENT ID		TECN	COMMENT
2.25±0.13 OUR AVERAGE					
2.25±0.07±0.12	4.6k	LEES	12X	BABR	468 fb^{-1} E_{cm}^{ee} = 10.6 GeV
2.3 ±0.5	170	[1] ANASTASSOV	01	CLEO	E_{cm}^{ee}= 10.6 GeV
• • • We do not use the following data for averages, fits, limits, etc. • • •					
1.60±0.05±0.11	1.8 k	AUBERT	08AE	BABR	Repl. by LEES 12X
3.4 $^{+0.6}_{-0.5}$ ±0.6	89	[2] BERGFELD	97	CLEO	Repl. by ANASTASSOV 01

[1] Weighted average of BERGFELD 97 and ANASTASSOV 01 measurements using η's reconstructed from $\eta \to \pi^+\pi^-\pi^0$ and $\eta \to 3\pi^0$ decays.
[2] BERGFELD 97 reconstruct η's using $\eta \to \gamma\gamma$ and $\eta \to 3\pi^0$ decays.

$\Gamma(\eta\pi^-\pi^+\pi^-\nu_\tau(\text{ex.}K^0,f_1(1285)))/\Gamma_{total}$ Γ_{151}/Γ

VALUE (units 10^{-4})	DOCUMENT ID		TECN	COMMENT
0.99±0.09±0.13	[1] LEES	12X	BABR	468 fb^{-1} E_{cm}^{ee} = 10.6 GeV

[1] LEES 12X obtain this result by subtracting their B($\tau^- \to f_1(1285)\pi^-\nu_\tau \to \eta\pi^-\pi^+\pi^-\nu_\tau$) measurement from their B($\tau^- \to \eta\pi^-\pi^+\pi^-\nu_\tau$(ex.$K^0$)) measurement.

$\Gamma(\eta a_1(1260)^-\nu_\tau \to \eta\pi^-\rho^0\nu_\tau)/\Gamma_{total}$ Γ_{152}/Γ

VALUE	CL%	DOCUMENT ID		TECN	COMMENT
<3.9 × 10^{-4}	90	BERGFELD	97	CLEO	E_{cm}^{ee}= 10.6 GeV

$\Gamma(\eta\eta\pi^-\nu_\tau)/\Gamma_{total}$ Γ_{153}/Γ

VALUE	CL%	DOCUMENT ID		TECN	COMMENT
<7.4 × 10^{-6}	90	INAMI	09	BELL	490 fb^{-1} E_{cm}^{ee}= 10.6 GeV
• • • We do not use the following data for averages, fits, limits, etc. • • •					
<1.1 × 10^{-4}	95	ARTUSO	92	CLEO	$E_{cm}^{ee} \approx$ 10.6 GeV
<8.3 × 10^{-3}	95	ALBRECHT	88M	ARG	$E_{cm}^{ee} \approx$ 10 GeV

$\Gamma(\eta\eta\pi^-\pi^0\nu_\tau)/\Gamma_{total}$ Γ_{154}/Γ

VALUE (units 10^{-4})	CL%	DOCUMENT ID		TECN	COMMENT
< 2.0	95	ARTUSO	92	CLEO	$E_{cm}^{ee} \approx$ 10.6 GeV
• • • We do not use the following data for averages, fits, limits, etc. • • •					
<90	95	ALBRECHT	88M	ARG	$E_{cm}^{ee} \approx$ 10 GeV

$\Gamma(\eta\eta K^-\nu_\tau)/\Gamma_{total}$ Γ_{155}/Γ

VALUE	CL%	DOCUMENT ID		TECN	COMMENT
<3.0 × 10^{-6}	90	INAMI	09	BELL	490 fb^{-1} E_{cm}^{ee}= 10.6 GeV

$\Gamma(\eta'(958)\pi^-\nu_\tau)/\Gamma_{total}$ Γ_{156}/Γ

VALUE	CL%	DOCUMENT ID		TECN	COMMENT
<4.0 × 10^{-6}	90	LEES	12X	BABR	468 fb^{-1} E_{cm}^{ee} = 10.6 GeV
• • • We do not use the following data for averages, fits, limits, etc. • • •					
<7.2 × 10^{-6}	90	AUBERT	08AE	BABR	384 fb^{-1}, E_{cm}^{ee}= 10.6 GeV
<7.4 × 10^{-5}	90	BERGFELD	97	CLEO	E_{cm}^{ee}= 10.6 GeV

$\Gamma(\eta'(958)\pi^-\pi^0\nu_\tau)/\Gamma_{total}$ Γ_{157}/Γ

VALUE	CL%	DOCUMENT ID		TECN	COMMENT
<1.2 × 10^{-5}	90	LEES	12X	BABR	468 fb^{-1} E_{cm}^{ee} = 10.6 GeV
• • • We do not use the following data for averages, fits, limits, etc. • • •					
<8.0 × 10^{-5}	90	BERGFELD	97	CLEO	E_{cm}^{ee}= 10.6 GeV

$\Gamma(\eta'(958)K^-\nu_\tau)/\Gamma_{total}$ Γ_{158}/Γ

VALUE	CL%	DOCUMENT ID		TECN	COMMENT
<2.4 × 10^{-6}	90	LEES	12X	BABR	468 fb^{-1} E_{cm}^{ee} = 10.6 GeV

$\Gamma(\phi\pi^-\nu_\tau)/\Gamma_{total}$ Γ_{159}/Γ

VALUE (units 10^{-5})	CL%	EVTS	DOCUMENT ID		TECN	COMMENT
3.42±0.55±0.25		344	AUBERT	08	BABR	342 fb^{-1} E_{cm}^{ee} = 10.6 GeV
• • • We do not use the following data for averages, fits, limits, etc. • • •						
< 20	90		[1] AVERY	97	CLEO	E_{cm}^{ee}= 10.6 GeV
< 35	90		ALBRECHT	95H	ARG	E_{cm}^{ee}= 9.4–10.6 GeV

[1] AVERY 97 limit varies from (1.2–2.0) × 10^{-4} depending on decay model assumptions.

$\Gamma(\phi K^-\nu_\tau)/\Gamma_{total}$ Γ_{160}/Γ

VALUE (units 10^{-5})	CL%	EVTS	DOCUMENT ID		TECN	COMMENT
3.70±0.33 OUR AVERAGE Error includes scale factor of 1.3.						
3.39±0.20±0.28		274	AUBERT	08	BABR	342 fb^{-1} E_{cm}^{ee} = 10.6 GeV
4.05±0.25±0.26		551	INAMI	06	BELL	401 fb^{-1} E_{cm}^{ee} =10.6 GeV
• • • We do not use the following data for averages, fits, limits, etc. • • •						
<6.7	90		[1] AVERY	97	CLEO	E_{cm}^{ee}= 10.6 GeV

[1] AVERY 97 limit varies from (5.4–6.7) × 10^{-5} depending on decay model assumptions.

$\Gamma(f_1(1285)\pi^-\nu_\tau)/\Gamma_{total}$ Γ_{161}/Γ

VALUE (units 10^{-4})	EVTS	DOCUMENT ID		TECN	COMMENT
3.9 ±0.5 OUR AVERAGE Error includes scale factor of 1.9.					
4.73±0.28±0.45	3.7k	[1] LEES	12X	BABR	468 fb^{-1} E_{cm}^{ee} = 10.6 GeV
3.60±0.18±0.23	2.5k	[2] LEES	12X	BABR	468 fb^{-1} E_{cm}^{ee} = 10.6 GeV
• • • We do not use the following data for averages, fits, limits, etc. • • •					
3.19±0.18±1.00	1.3 k	[3] AUBERT	08AE	BABR	Repl. by LEES 12X
3.9 ±0.7 ±0.5	1.4 k	[4] AUBERT,B	05W	BABR	Repl. by LEES 12X
5.8 $^{+1.4}_{-1.3}$ ±1.8	54	[5] BERGFELD	97	CLEO	E_{cm}^{ee}= 10.6 GeV

[1] LEES 12X obtain this value by dividing their $B(\tau^- \to f_1(1285)\pi^-\nu_\tau \to 3\pi^-2\pi^+\nu_\tau)$ measurement by the PDG 12 value of $B(f_1(1285) \to 2\pi^+2\pi^-) = 0.111^{+0.007}_{-0.006}$.

[2] LEES 12X obtain this value by dividing their $B(\tau^- \to f_1(1285)\pi^-\nu_\tau \to \eta\pi^-\pi^+\pi^-\nu_\tau)$ measurement by 2/3 of the PDG 12 value of $B(f_1(1285) \to \eta\pi\pi) = 0.524^{+0.019}_{-0.021}$.

[3] AUBERT 08AE obtain this value by dividing their $B(\tau^- \to f_1(1285)\pi^-\nu_\tau \to \eta\pi^-\pi^+\pi^-\nu_\tau)$ measurement by the PDG 06 value of $B(f_1(1285) \to \eta\pi^-\pi^+) = 0.35 \pm 0.11$. The quote $(3.19 \pm 0.18 \pm 0.16 \pm 0.99) \times 10^{-4}$ where the final error is due to the uncertainty on $B(f_1(1285) \to \eta\pi^-\pi^+)$. We combine the two systematic errors in quadrature.

[4] AUBERT,B 05W use the $f_1(1285) \to 2\pi^+2\pi^-$ decay mode and the PDG 04 value of $B(f_1(1285) \to 2\pi^+2\pi^-) = 0.110^{+0.007}_{-0.006}$.

[5] BERGFELD 97 use the $f_1(1285) \to \eta\pi^+\pi^-$ decay mode.

$\Gamma(f_1(1285)\pi^-\nu_\tau \to \eta\pi^-\pi^+\pi^-\nu_\tau)/\Gamma_{total}$ Γ_{162}/Γ

VALUE (units 10^{-4})	EVTS	DOCUMENT ID		TECN	COMMENT
1.18±0.07 OUR AVERAGE		Error includes scale factor of 1.3.			
1.26±0.06±0.06	2.5k	LEES	12X	BABR	468 fb^{-1} E^{ee}_{cm} = 10.6 GeV
1.11±0.06±0.05	1.3 k	AUBERT	08AE	BABR	384 fb^{-1}, E^{ee}_{cm} = 10.6 GeV

$\Gamma(f_1(1285)\pi^-\nu_\tau \to \eta\pi^-\pi^+\pi^-\nu_\tau)/\Gamma(\eta\pi^-\pi^+\pi^-\nu_\tau(ex.K^0))$ $\Gamma_{162}/\Gamma_{150}$

VALUE	DOCUMENT ID		TECN	COMMENT
0.69±0.01±0.05	[1] AUBERT	08AE	BABR	384 fb^{-1}, E^{ee}_{cm} = 10.6 GeV
• • • We do not use the following data for averages, fits, limits, etc. • • •				
0.55±0.14	BERGFELD	97	CLEO	E^{ee}_{cm} = 10.6 GeV

[1] Not independent of AUBERT 08AE $B(\tau^- \to f_1(1285)\pi^-\nu_\tau \to \eta\pi^-\pi^+\pi^-\nu_\tau)$ and $B(\tau^- \to \eta\pi^-\pi^+\pi^-\nu_\tau(ex.K^0))$ values.

$\Gamma(f_1(1285)\pi^-\nu_\tau \to 3\pi^-2\pi^+\nu_\tau)/\Gamma_{total}$ Γ_{163}/Γ

VALUE (units 10^{-4})	EVTS	DOCUMENT ID		TECN	COMMENT
0.520±0.031±0.037	3.7k	LEES	12X	BABR	468 fb^{-1} E^{ee}_{cm}=10.6 GeV

$\Gamma(\pi(1300)^-\nu_\tau \to (\rho\pi)^-\nu_\tau \to (3\pi)^-\nu_\tau)/\Gamma_{total}$ Γ_{164}/Γ

VALUE	CL%	DOCUMENT ID		TECN	COMMENT
<1.0 × 10^{-4}	90	ASNER	00	CLEO	E^{ee}_{cm}= 10.6 GeV

$\Gamma(\pi(1300)^-\nu_\tau \to ((\pi\pi)_{S-wave}\,\pi)^-\nu_\tau \to (3\pi)^-\nu_\tau)/\Gamma_{total}$ Γ_{165}/Γ

VALUE	CL%	DOCUMENT ID		TECN	COMMENT
<1.9 × 10^{-4}	90	ASNER	00	CLEO	E^{ee}_{cm}= 10.6 GeV

$\Gamma(h^-\omega \geq 0 \text{ neutrals } \nu_\tau)/\Gamma_{total}$ Γ_{166}/Γ

$\Gamma_{166}/\Gamma = (\Gamma_{167}+\Gamma_{169})/\Gamma$

VALUE (%)	EVTS	DOCUMENT ID		TECN	COMMENT
2.41±0.09 OUR FIT		Error includes scale factor of 1.2.			
• • • We use the following data for averages but not for fits. • • •					
1.65±0.3 ±0.2	1513	ALBRECHT	88M	ARG	E^{ee}_{cm} ≈ 10 GeV

$\Gamma(h^-\omega\nu_\tau)/\Gamma_{total}$ Γ_{167}/Γ

VALUE (%)	EVTS	DOCUMENT ID		TECN	COMMENT
2.00±0.08 OUR FIT		Error includes scale factor of 1.3.			
1.92±0.07 OUR AVERAGE					
1.91±0.07±0.06	5803	BUSKULIC	97C	ALEP	1991–1994 LEP runs
1.60±0.27±0.41	139	BARINGER	87	CLEO	E^{ee}_{cm}= 10.5 GeV
• • • We use the following data for averages but not for fits. • • •					
1.95±0.07±0.11	2223	[1] BALEST	95C	CLEO	E^{ee}_{cm} ≈ 10.6 GeV

[1] Not independent of BALEST 95C $B(\tau^- \to h^-\omega\nu_\tau)/B(\tau^- \to h^-h^-h^+\pi^0\nu_\tau)$ value.

$\Gamma(h^-\omega\nu_\tau)/\Gamma(h^-h^-h^+\pi^0\nu_\tau(ex.K^0))$ Γ_{167}/Γ_{68}

$\Gamma_{167}/\Gamma_{68} = \Gamma_{167}/(\Gamma_{72}+\Gamma_{94}+\Gamma_{99}+0.226\Gamma_{142}+0.888\Gamma_{167}+0.017\Gamma_{169})$

VALUE	EVTS	DOCUMENT ID		TECN	COMMENT
0.437±0.017 OUR FIT		Error includes scale factor of 1.2.			
0.453±0.019 OUR AVERAGE					
0.431±0.033	2350	[1] BUSKULIC	96	ALEP	LEP 1991–1993 data
0.464±0.016±0.017	2223	[2] BALEST	95C	CLEO	E^{ee}_{cm} ≈ 10.6 GeV
• • • We do not use the following data for averages, fits, limits, etc. • • •					
0.37 ±0.05 ±0.02	458	[3] ALBRECHT	91D	ARG	E^{ee}_{cm}= 9.4–10.6 GeV

[1] BUSKULIC 96 quote the fraction of $\tau \to h^-h^-h^+\pi^0\nu_\tau$(ex. K^0) decays which originate in a $h^-\omega$ final state = 0.383 ± 0.029. We divide this by the $\omega(782) \to \pi^+\pi^-\pi^0$ branching fraction (0.888).

[2] BALEST 95C quote the fraction of $\tau^- \to h^-h^-h^+\pi^0\nu_\tau$ (ex. K^0) decays which originate in a $h^-\omega$ final state equals 0.412 ± 0.014 ± 0.015. We divide this by the $\omega(782) \to \pi^+\pi^-\pi^0$ branching fraction (0.888).

[3] ALBRECHT 91D quote the fraction of $\tau^- \to h^-h^-h^+\pi^0\nu_\tau$ decays which originate in a $\pi^-\omega$ final state equals 0.33 ± 0.04 ± 0.02. We divide this by the $\omega(782) \to \pi^+\pi^-\pi^0$ branching fraction (0.888).

$\Gamma(K^-\omega\nu_\tau)/\Gamma_{total}$ Γ_{168}/Γ

VALUE (units 10^{-4})	EVTS	DOCUMENT ID		TECN	COMMENT
4.1±0.6±0.7	500	ARMS	05	CLE3	7.6 fb^{-1}, E^{ee}_{cm}= 10.6 GeV

$\Gamma(h^-\omega\pi^0\nu_\tau)/\Gamma_{total}$ Γ_{169}/Γ

VALUE (%)	EVTS	DOCUMENT ID		TECN	COMMENT
0.41±0.04 OUR FIT					
0.43±0.06±0.05	7283	BUSKULIC	97C	ALEP	1991–1994 LEP runs

$\Gamma(h^-\omega\pi^0\nu_\tau)/\Gamma(h^-h^-h^+ \geq 0 \text{ neutrals } \geq 0K^0_L\nu_\tau)$ Γ_{169}/Γ_{56}

$\Gamma_{169}/\Gamma_{56} = \Gamma_{169}/(0.3431\Gamma_{35}+0.3431\Gamma_{37}+0.3431\Gamma_{40}+0.3431\Gamma_{42}+0.4307\Gamma_{47}+0.6861\Gamma_{48}+\Gamma_{64}+\Gamma_{72}+\Gamma_{79}+\Gamma_{80}+\Gamma_{90}+\Gamma_{94}+\Gamma_{98}+\Gamma_{99}+0.285\Gamma_{140}+0.285\Gamma_{142}+0.9101\Gamma_{167}+0.9101\Gamma_{169})$

VALUE	EVTS	DOCUMENT ID		TECN	COMMENT
0.0271±0.0028 OUR FIT					
• • • We use the following data for averages but not for fits. • • •					
0.028 ±0.003 ±0.003	430	[1] BORTOLETTO	93	CLEO	$E^{ee}_{cm} \approx 10.6$ GeV

[1] Not independent of BORTOLETTO 93 $\Gamma(\tau^- \to h^-\omega\pi^0\nu_\tau)/\Gamma(\tau^- \to h^-h^-h^+2\pi^0\nu_\tau(ex.K^0))$ value.

$\Gamma(h^-\omega\pi^0\nu_\tau)/\Gamma(h^-h^-h^+2\pi^0\nu_\tau(ex.K^0))$ Γ_{169}/Γ_{78}

$\Gamma_{169}/\Gamma_{78} = \Gamma_{169}/(\Gamma_{79}+0.226\Gamma_{140}+0.888\Gamma_{169})$

VALUE	DOCUMENT ID		TECN	COMMENT
0.83±0.08 OUR FIT				
0.81±0.06±0.06	BORTOLETTO93		CLEO	$E^{ee}_{cm} \approx 10.6$ GeV

$\Gamma(h^-\omega2\pi^0\nu_\tau)/\Gamma_{total}$ Γ_{170}/Γ

VALUE (units 10^{-4})	EVTS	DOCUMENT ID		TECN	COMMENT
1.4 ±0.4 ±0.3	53	ANASTASSOV	01	CLEO	E^{ee}_{cm}= 10.6 GeV
• • • We do not use the following data for averages, fits, limits, etc. • • •					
1.89$^{+0.74}_{-0.67}$±0.40	19	ANDERSON	97	CLEO	Repl. by ANASTASSOV 01

$\Gamma(\pi^-\omega2\pi^0\nu_\tau)/\Gamma_{total}$ Γ_{171}/Γ

VALUE (units 10^{-4})	EVTS	DOCUMENT ID		TECN	COMMENT
0.73±0.12±0.12	1.1k	LEES	12X	BABR	468 fb^{-1} E^{ee}_{cm} = 10.6 GeV

$\Gamma(h^-2\omega\nu_\tau)/\Gamma_{total}$ Γ_{172}/Γ

VALUE	CL%	DOCUMENT ID		TECN	COMMENT
<5.4 × 10^{-7}	90	AUBERT,B	06	BABR	232 fb^{-1} E^{ee}_{cm} = 10.6 GeV

$\Gamma(2h^-h^+\omega\nu_\tau)/\Gamma_{total}$ Γ_{173}/Γ

VALUE (units 10^{-4})	EVTS	DOCUMENT ID		TECN	COMMENT
1.2±0.2±0.1	110	ANASTASSOV	01	CLEO	E^{ee}_{cm}= 10.6 GeV

$\Gamma(2\pi^-\pi^+\omega\nu_\tau)/\Gamma_{total}$ Γ_{174}/Γ

VALUE (units 10^{-4})	EVTS	DOCUMENT ID		TECN	COMMENT
0.84±0.04±0.06	2.4k	LEES	12X	BABR	468 fb^{-1} E^{ee}_{cm} = 10.6 GeV

$\Gamma(e^-\gamma)/\Gamma_{total}$ Γ_{175}/Γ

Test of lepton family number conservation.

VALUE	CL%	DOCUMENT ID		TECN	COMMENT
<3.3 × 10^{-8}	90	AUBERT	10B	BABR	516 fb^{-1}, E^{ee}_{cm}=10.6 GeV
• • • We do not use the following data for averages, fits, limits, etc. • • •					
<1.2 × 10^{-7}	90	HAYASAKA	08	BELL	535 fb^{-1}, E^{ee}_{cm}= 10.6 GeV
<1.1 × 10^{-7}	90	AUBERT	06C	BABR	232 fb^{-1}, E^{ee}_{cm}= 10.6 GeV
<3.9 × 10^{-7}	90	HAYASAKA	05	BELL	86.7 fb^{-1}, E^{ee}_{cm}=10.6 GeV
<2.7 × 10^{-6}	90	EDWARDS	97	CLEO	
<1.1 × 10^{-4}	90	ABREU	95U	DLPH	1990–1993 LEP runs
<1.2 × 10^{-4}	90	ALBRECHT	92K	ARG	E^{ee}_{cm}= 10 GeV
<2.0 × 10^{-4}	90	KEH	88	CBAL	E^{ee}_{cm}= 10 GeV
<6.4 × 10^{-4}	90	HAYES	82	MRK2	E^{ee}_{cm}= 3.8–6.8 GeV

$\Gamma(\mu^-\gamma)/\Gamma_{total}$ Γ_{176}/Γ

Test of lepton family number conservation.

VALUE	CL%	DOCUMENT ID		TECN	COMMENT
< 4.4 × 10^{-8}	90	AUBERT	10B	BABR	516 fb^{-1}, E^{ee}_{cm}=10.6 GeV
• • • We do not use the following data for averages, fits, limits, etc. • • •					
< 4.5 × 10^{-8}	90	HAYASAKA	08	BELL	535 fb^{-1}, E^{ee}_{cm} = 10.6 GeV
< 6.8 × 10^{-8}	90	AUBERT,B	05A	BABR	232 fb^{-1}, E^{ee}_{cm}= 10.6 GeV
< 3.1 × 10^{-7}	90	ABE	04B	BELL	86.3 fb^{-1}, E^{ee}_{cm} = 10.6 GeV
< 1.1 × 10^{-6}	90	AHMED	00	CLEO	E^{ee}_{cm}= 10.6 GeV
< 3.0 × 10^{-6}	90	EDWARDS	97	CLEO	
< 6.2 × 10^{-5}	90	ABREU	95U	DLPH	1990–1993 LEP runs
< 0.42 × 10^{-5}	90	BEAN	93	CLEO	E^{ee}_{cm}= 10.6 GeV
< 3.4 × 10^{-5}	90	ALBRECHT	92K	ARG	E^{ee}_{cm}= 10 GeV
<55 × 10^{-5}	90	HAYES	82	MRK2	E^{ee}_{cm}= 3.8–6.8 GeV

Lepton Particle Listings

τ

$\Gamma(e^-\pi^0)/\Gamma_{total}$ Γ_{177}/Γ

Test of lepton family number conservation.

VALUE	CL%	DOCUMENT ID		TECN	COMMENT
< 8.0×10^{-8}	90	MIYAZAKI	07	BELL	401 fb^{-1}, E^{ee}_{cm}=10.6 GeV
• • • We do not use the following data for averages, fits, limits, etc. • • •					
< 1.3×10^{-7}	90	AUBERT	07I	BABR	339 fb^{-1}, E^{ee}_{cm}=10.6 GeV
< 1.9×10^{-7}	90	ENARI	05	BELL	154 fb^{-1}, E^{ee}_{cm}= 10.6 GeV
< 3.7×10^{-6}	90	BONVICINI	97	CLEO	E^{ee}_{cm}= 10.6 GeV
< 17 $\times10^{-5}$	90	ALBRECHT	92K	ARG	E^{ee}_{cm}= 10 GeV
< 14 $\times10^{-5}$	90	KEH	88	CBAL	E^{ee}_{cm}= 10 GeV
<210 $\times10^{-5}$	90	HAYES	82	MRK2	E^{ee}_{cm}= 3.8–6.8 GeV

$\Gamma(\mu^-\pi^0)/\Gamma_{total}$ Γ_{178}/Γ

Test of lepton family number conservation.

VALUE	CL%	DOCUMENT ID		TECN	COMMENT
< 1.1×10^{-7}	90	AUBERT	07I	BABR	339 fb^{-1}, E^{ee}_{cm}=10.6 GeV
• • • We do not use the following data for averages, fits, limits, etc. • • •					
< 1.2×10^{-7}	90	MIYAZAKI	07	BELL	401 fb^{-1}, E^{ee}_{cm}=10.6 GeV
< 4.1×10^{-7}	90	ENARI	05	BELL	154 fb^{-1}, E^{ee}_{cm}= 10.6 GeV
< 4.0×10^{-6}	90	BONVICINI	97	CLEO	E^{ee}_{cm}= 10.6 GeV
< 4.4×10^{-5}	90	ALBRECHT	92K	ARG	E^{ee}_{cm}= 10 GeV
<82 $\times10^{-5}$	90	HAYES	82	MRK2	E^{ee}_{cm}= 3.8–6.8 GeV

$\Gamma(e^- K^0_S)/\Gamma_{total}$ Γ_{179}/Γ

Test of lepton family number conservation.

VALUE	CL%	DOCUMENT ID		TECN	COMMENT
<2.6×10^{-8}	90	MIYAZAKI	10A	BELL	671 fb^{-1} E^{ee}_{cm} = 10.6 GeV
• • • We do not use the following data for averages, fits, limits, etc. • • •					
<3.3×10^{-8}	90	AUBERT	09D	BABR	469 fb^{-1} E^{ee}_{cm} = 10.6 GeV
<5.6×10^{-8}	90	MIYAZAKI	06A	BELL	281 fb^{-1} E^{ee}_{cm} = 10.6 GeV
<9.1×10^{-7}	90	CHEN	02C	CLEO	E^{ee}_{cm}= 10.6 GeV
<1.3×10^{-3}	90	HAYES	82	MRK2	E^{ee}_{cm}= 3.8–6.8 GeV

$\Gamma(\mu^- K^0_S)/\Gamma_{total}$ Γ_{180}/Γ

Test of lepton family number conservation.

VALUE	CL%	DOCUMENT ID		TECN	COMMENT
<2.3×10^{-8}	90	MIYAZAKI	10A	BELL	671 fb^{-1} E^{ee}_{cm} = 10.6 GeV
• • • We do not use the following data for averages, fits, limits, etc. • • •					
<4.0×10^{-8}	90	AUBERT	09D	BABR	469 fb^{-1} E^{ee}_{cm} = 10.6 GeV
<4.9×10^{-8}	90	MIYAZAKI	06A	BELL	281 fb^{-1} E^{ee}_{cm} = 10.6 GeV
<9.5×10^{-7}	90	CHEN	02C	CLEO	E^{ee}_{cm}= 10.6 GeV
<1.0×10^{-3}	90	HAYES	82	MRK2	E^{ee}_{cm}= 3.8–6.8 GeV

$\Gamma(e^-\eta)/\Gamma_{total}$ Γ_{181}/Γ

Test of lepton family number conservation.

VALUE	CL%	DOCUMENT ID		TECN	COMMENT
< 9.2×10^{-8}	90	MIYAZAKI	07	BELL	401 fb^{-1}, E^{ee}_{cm}=10.6 GeV
• • • We do not use the following data for averages, fits, limits, etc. • • •					
< 1.6×10^{-7}	90	AUBERT	07I	BABR	339 fb^{-1}, E^{ee}_{cm}=10.6 GeV
< 2.4×10^{-7}	90	ENARI	05	BELL	154 fb^{-1}, E^{ee}_{cm}= 10.6 GeV
< 8.2×10^{-6}	90	BONVICINI	97	CLEO	E^{ee}_{cm}= 10.6 GeV
< 6.3×10^{-5}	90	ALBRECHT	92K	ARG	E^{ee}_{cm}= 10 GeV
<24 $\times10^{-5}$	90	KEH	88	CBAL	E^{ee}_{cm}= 10 GeV

$\Gamma(\mu^-\eta)/\Gamma_{total}$ Γ_{182}/Γ

Test of lepton family number conservation.

VALUE	CL%	DOCUMENT ID		TECN	COMMENT
<6.5×10^{-8}	90	MIYAZAKI	07	BELL	401 fb^{-1}, E^{ee}_{cm}=10.6 GeV
• • • We do not use the following data for averages, fits, limits, etc. • • •					
<1.5×10^{-7}	90	AUBERT	07I	BABR	339 fb^{-1}, E^{ee}_{cm}=10.6 GeV
<1.5×10^{-7}	90	ENARI	05	BELL	154 fb^{-1}, E^{ee}_{cm}= 10.6 GeV
<3.4×10^{-7}	90	ENARI	04	BELL	84.3 fb^{-1}, E^{ee}_{cm}=10.6 GeV
<9.6×10^{-6}	90	BONVICINI	97	CLEO	E^{ee}_{cm}= 10.6 GeV
<7.3×10^{-5}	90	ALBRECHT	92K	ARG	E^{ee}_{cm}= 10 GeV

$\Gamma(e^-\rho^0)/\Gamma_{total}$ Γ_{183}/Γ

Test of lepton family number conservation.

VALUE	CL%	DOCUMENT ID		TECN	COMMENT
< 1.8×10^{-8}	90	MIYAZAKI	11	BELL	854 fb^{-1} E^{ee}_{cm} = 10.6 GeV
• • • We do not use the following data for averages, fits, limits, etc. • • •					
< 4.6×10^{-8}	90	AUBERT	09W	BABR	451 fb^{-1} E^{ee}_{cm} = 10.6 GeV
< 6.3×10^{-8}	90	NISHIO	08	BELL	543 fb^{-1} E^{ee}_{cm} = 10.6 GeV
< 6.5×10^{-7}	90	YUSA	06	BELL	158 fb^{-1} E^{ee}_{cm} = 10.6 GeV
< 2.0×10^{-6}	90	BLISS	98	CLEO	E^{ee}_{cm}= 10.6 GeV
< 4.2×10^{-6}	90	[1] BARTELT	94	CLEO	Repl. by BLISS 98
< 1.9×10^{-5}	90	ALBRECHT	92K	ARG	E^{ee}_{cm}= 10 GeV
<37 $\times10^{-5}$	90	HAYES	82	MRK2	E^{ee}_{cm}= 3.8–6.8 GeV

[1] BARTELT 94 assume phase space decays.

$\Gamma(\mu^-\rho^0)/\Gamma_{total}$ Γ_{184}/Γ

Test of lepton family number conservation.

VALUE	CL%	DOCUMENT ID		TECN	COMMENT
< 1.2×10^{-8}	90	MIYAZAKI	11	BELL	854 fb^{-1} E^{ee}_{cm} = 10.6 GeV
• • • We do not use the following data for averages, fits, limits, etc. • • •					
< 2.6×10^{-8}	90	AUBERT	09W	BABR	451 fb^{-1} E^{ee}_{cm} = 10.6 GeV
< 6.8×10^{-8}	90	NISHIO	08	BELL	543 fb^{-1} E^{ee}_{cm} = 10.6 GeV
< 2.0×10^{-7}	90	YUSA	06	BELL	158 fb^{-1} E^{ee}_{cm} = 10.6 GeV
< 6.3×10^{-6}	90	BLISS	98	CLEO	E^{ee}_{cm}= 10.6 GeV
< 5.7×10^{-6}	90	[1] BARTELT	94	CLEO	Repl. by BLISS 98
< 2.9×10^{-5}	90	ALBRECHT	92K	ARG	E^{ee}_{cm}= 10 GeV
<44 $\times10^{-5}$	90	HAYES	82	MRK2	E^{ee}_{cm}= 3.8–6.8 GeV

[1] BARTELT 94 assume phase space decays.

$\Gamma(e^-\omega)/\Gamma_{total}$ Γ_{185}/Γ

VALUE	CL%	DOCUMENT ID		TECN	COMMENT
<4.8×10^{-8}	90	MIYAZAKI	11	BELL	854 fb^{-1} E^{ee}_{cm} = 10.6 GeV
• • • We do not use the following data for averages, fits, limits, etc. • • •					
<1.1×10^{-7}	90	AUBERT	08K	BABR	384 fb^{-1} E^{ee}_{cm} = 10.6 GeV
<1.8×10^{-7}	90	NISHIO	08	BELL	543 fb^{-1} E^{ee}_{cm} = 10.6 GeV

$\Gamma(\mu^-\omega)/\Gamma_{total}$ Γ_{186}/Γ

VALUE	CL%	DOCUMENT ID		TECN	COMMENT
<4.7×10^{-8}	90	MIYAZAKI	11	BELL	854 fb^{-1} E^{ee}_{cm} = 10.6 GeV
• • • We do not use the following data for averages, fits, limits, etc. • • •					
<1.0×10^{-7}	90	AUBERT	08K	BABR	384 fb^{-1} E^{ee}_{cm} = 10.6 GeV
<8.9×10^{-8}	90	NISHIO	08	BELL	543 fb^{-1} E^{ee}_{cm} = 10.6 GeV

$\Gamma(e^- K^*(892)^0)/\Gamma_{total}$ Γ_{187}/Γ

Test of lepton family number conservation.

VALUE	CL%	DOCUMENT ID		TECN	COMMENT
<3.2×10^{-8}	90	MIYAZAKI	11	BELL	854 fb^{-1} E^{ee}_{cm} = 10.6 GeV
• • • We do not use the following data for averages, fits, limits, etc. • • •					
<5.9×10^{-8}	90	AUBERT	09W	BABR	451 fb^{-1} E^{ee}_{cm} = 10.6 GeV
<7.8×10^{-8}	90	NISHIO	08	BELL	543 fb^{-1} E^{ee}_{cm} = 10.6 GeV
<3.0×10^{-7}	90	YUSA	06	BELL	158 fb^{-1} E^{ee}_{cm} = 10.6 GeV
<5.1×10^{-6}	90	BLISS	98	CLEO	E^{ee}_{cm}= 10.6 GeV
<6.3×10^{-6}	90	[1] BARTELT	94	CLEO	Repl. by BLISS 98
<3.8×10^{-5}	90	ALBRECHT	92K	ARG	E^{ee}_{cm}= 10 GeV

[1] BARTELT 94 assume phase space decays.

$\Gamma(\mu^- K^*(892)^0)/\Gamma_{total}$ Γ_{188}/Γ

Test of lepton family number conservation.

VALUE	CL%	DOCUMENT ID		TECN	COMMENT
<5.9×10^{-8}	90	NISHIO	08	BELL	543 fb^{-1} E^{ee}_{cm} = 10.6 GeV
• • • We do not use the following data for averages, fits, limits, etc. • • •					
<7.2×10^{-8}	90	MIYAZAKI	11	BELL	854 fb^{-1} E^{ee}_{cm} = 10.6 GeV
<1.7×10^{-7}	90	AUBERT	09W	BABR	451 fb^{-1} E^{ee}_{cm} = 10.6 GeV
<3.9×10^{-7}	90	YUSA	06	BELL	158 fb^{-1} E^{ee}_{cm} = 10.6 GeV
<7.5×10^{-6}	90	BLISS	98	CLEO	E^{ee}_{cm}= 10.6 GeV
<9.4×10^{-6}	90	[1] BARTELT	94	CLEO	Repl. by BLISS 98
<4.5×10^{-5}	90	ALBRECHT	92K	ARG	E^{ee}_{cm}= 10 GeV

[1] BARTELT 94 assume phase space decays.

$\Gamma(e^-\overline{K}^*(892)^0)/\Gamma_{total}$ Γ_{189}/Γ

Test of lepton family number conservation.

VALUE	CL%	DOCUMENT ID		TECN	COMMENT
<3.4×10^{-8}	90	MIYAZAKI	11	BELL	854 fb^{-1} E^{ee}_{cm} = 10.6 GeV
• • • We do not use the following data for averages, fits, limits, etc. • • •					
<4.6×10^{-8}	90	AUBERT	09W	BABR	451 fb^{-1} E^{ee}_{cm} = 10.6 GeV
<7.7×10^{-8}	90	NISHIO	08	BELL	543 fb^{-1} E^{ee}_{cm} = 10.6 GeV
<4.0×10^{-7}	90	YUSA	06	BELL	158 fb^{-1} E^{ee}_{cm} = 10.6 GeV
<7.4×10^{-6}	90	BLISS	98	CLEO	E^{ee}_{cm}= 10.6 GeV
<1.1×10^{-5}	90	[1] BARTELT	94	CLEO	Repl. by BLISS 98

[1] BARTELT 94 assume phase space decays.

$\Gamma(\mu^-\overline{K}^*(892)^0)/\Gamma_{total}$ Γ_{190}/Γ

Test of lepton family number conservation.

VALUE	CL%	DOCUMENT ID		TECN	COMMENT
<7.0×10^{-8}	90	MIYAZAKI	11	BELL	854 fb^{-1} E^{ee}_{cm} = 10.6 GeV
• • • We do not use the following data for averages, fits, limits, etc. • • •					
<7.3×10^{-8}	90	AUBERT	09W	BABR	451 fb^{-1} E^{ee}_{cm} = 10.6 GeV
<1.0×10^{-7}	90	NISHIO	08	BELL	543 fb^{-1} E^{ee}_{cm} = 10.6 GeV
<4.0×10^{-7}	90	YUSA	06	BELL	158 fb^{-1} E^{ee}_{cm} = 10.6 GeV
<7.5×10^{-6}	90	BLISS	98	CLEO	E^{ee}_{cm}= 10.6 GeV
<8.7×10^{-6}	90	[1] BARTELT	94	CLEO	Repl. by BLISS 98

[1] BARTELT 94 assume phase space decays.

$\Gamma(e^-\eta'(958))/\Gamma_{total}$ Γ_{191}/Γ

VALUE	CL%	DOCUMENT ID		TECN	COMMENT
$< 1.6 \times 10^{-7}$	90	MIYAZAKI	07	BELL	401 fb^{-1}, E_{cm}^{ee}=10.6 GeV
• • • We do not use the following data for averages, fits, limits, etc. • • •					
$< 2.4 \times 10^{-7}$	90	AUBERT	07I	BABR	339 fb^{-1}, E_{cm}^{ee}=10.6 GeV
$<10. \times 10^{-7}$	90	ENARI	05	BELL	154 fb^{-1}, E_{cm}^{ee}= 10.6 GeV

$\Gamma(\mu^-\eta'(958))/\Gamma_{total}$ Γ_{192}/Γ

VALUE	CL%	DOCUMENT ID		TECN	COMMENT
$<1.3 \times 10^{-7}$	90	MIYAZAKI	07	BELL	401 fb^{-1}, E_{cm}^{ee}=10.6 GeV
• • • We do not use the following data for averages, fits, limits, etc. • • •					
$<1.4 \times 10^{-7}$	90	AUBERT	07I	BABR	339 fb^{-1}, E_{cm}^{ee}=10.6 GeV
$<4.7 \times 10^{-7}$	90	ENARI	05	BELL	154 fb^{-1}, E_{cm}^{ee}= 10.6 GeV

$\Gamma(e^- f_0(980) \to e^-\pi^+\pi^-)/\Gamma_{total}$ Γ_{193}/Γ

VALUE	CL%	DOCUMENT ID		TECN	COMMENT
$<3.2 \times 10^{-8}$	90	MIYAZAKI	09	BELL	671 fb^{-1} E_{cm}^{ee}= 10.6 GeV

$\Gamma(\mu^- f_0(980) \to \mu^-\pi^+\pi^-)/\Gamma_{total}$ Γ_{194}/Γ

VALUE	CL%	DOCUMENT ID		TECN	COMMENT
$<3.4 \times 10^{-8}$	90	MIYAZAKI	09	BELL	671 fb^{-1} E_{cm}^{ee}= 10.6 GeV

$\Gamma(e^-\phi)/\Gamma_{total}$ Γ_{195}/Γ

Test of lepton family number conservation.

VALUE	CL%	DOCUMENT ID		TECN	COMMENT
$<3.1 \times 10^{-8}$	90	MIYAZAKI	11	BELL	854 fb^{-1} E_{cm}^{ee} = 10.6 GeV
$<3.1 \times 10^{-8}$	90	AUBERT	09W	BABR	451 fb^{-1} E_{cm}^{ee} = 10.6 GeV
• • • We do not use the following data for averages, fits, limits, etc. • • •					
$<7.3 \times 10^{-8}$	90	NISHIO	08	BELL	543 fb^{-1} E_{cm}^{ee} = 10.6 GeV
$<7.3 \times 10^{-7}$	90	YUSA	06	BELL	158 fb^{-1} E_{cm}^{ee} = 10.6 GeV
$<6.9 \times 10^{-6}$	90	BLISS	98	CLEO	E_{cm}^{ee}= 10.6 GeV

$\Gamma(\mu^-\phi)/\Gamma_{total}$ Γ_{196}/Γ

Test of lepton family number conservation.

VALUE	CL%	DOCUMENT ID		TECN	COMMENT
$<8.4 \times 10^{-8}$	90	MIYAZAKI	11	BELL	854 fb^{-1} E_{cm}^{ee} = 10.6 GeV
• • • We do not use the following data for averages, fits, limits, etc. • • •					
$<1.9 \times 10^{-7}$	90	AUBERT	09W	BABR	451 fb^{-1} E_{cm}^{ee} = 10.6 GeV
$<1.3 \times 10^{-7}$	90	NISHIO	08	BELL	543 fb^{-1} E_{cm}^{ee} = 10.6 GeV
$<7.7 \times 10^{-7}$	90	YUSA	06	BELL	158 fb^{-1} E_{cm}^{ee} = 10.6 GeV
$<7.0 \times 10^{-6}$	90	BLISS	98	CLEO	E_{cm}^{ee}= 10.6 GeV

$\Gamma(e^- e^+ e^-)/\Gamma_{total}$ Γ_{197}/Γ

Test of lepton family number conservation.

VALUE	CL%	DOCUMENT ID		TECN	COMMENT
$< 2.7 \times 10^{-8}$	90	HAYASAKA	10	BELL	782 fb^{-1} E_{cm}^{ee}= 10.6 GeV
• • • We do not use the following data for averages, fits, limits, etc. • • •					
$< 2.9 \times 10^{-8}$	90	LEES	10A	BABR	468 fb^{-1} E_{cm}^{ee}= 10.6 GeV
$< 3.6 \times 10^{-8}$	90	MIYAZAKI	08	BELL	535 fb^{-1} E_{cm}^{ee}= 10.6 GeV
$< 4.3 \times 10^{-8}$	90	AUBERT	07BK	BABR	376 fb^{-1} E_{cm}^{ee}= 10.6 GeV
$< 2.0 \times 10^{-7}$	90	AUBERT	04J	BABR	91.5 fb^{-1} E_{cm}^{ee}= 10.6 GeV
$< 3.5 \times 10^{-7}$	90	YUSA	04	BELL	87.1 fb^{-1} E_{cm}^{ee}= 10.6 GeV
$< 2.9 \times 10^{-6}$	90	BLISS	98	CLEO	E_{cm}^{ee}= 10.6 GeV
$< 0.33 \times 10^{-5}$	90	[1] BARTELT	94	CLEO	Repl. by BLISS 98
$< 1.3 \times 10^{-5}$	90	ALBRECHT	92K	ARG	E_{cm}^{ee}= 10 GeV
$< 2.7 \times 10^{-5}$	90	BOWCOCK	90	CLEO	E_{cm}^{ee}= 10.4–10.9
$<40 \times 10^{-5}$	90	HAYES	82	MRK2	E_{cm}^{ee}= 3.8–6.8 GeV

[1] BARTELT 94 assume phase space decays.

$\Gamma(e^-\mu^+\mu^-)/\Gamma_{total}$ Γ_{198}/Γ

Test of lepton family number conservation.

VALUE	CL%	DOCUMENT ID		TECN	COMMENT
$< 2.7 \times 10^{-8}$	90	HAYASAKA	10	BELL	782 fb^{-1} E_{cm}^{ee}= 10.6 GeV
• • • We do not use the following data for averages, fits, limits, etc. • • •					
$< 3.2 \times 10^{-8}$	90	LEES	10A	BABR	468 fb^{-1} E_{cm}^{ee}= 10.6 GeV
$< 4.1 \times 10^{-8}$	90	MIYAZAKI	08	BELL	535 fb^{-1} E_{cm}^{ee}= 10.6 GeV
$< 3.7 \times 10^{-8}$	90	AUBERT	07BK	BABR	376 fb^{-1} E_{cm}^{ee}= 10.6 GeV
$< 3.3 \times 10^{-7}$	90	AUBERT	04J	BABR	91.5 fb^{-1} E_{cm}^{ee}= 10.6 GeV
$< 2.0 \times 10^{-7}$	90	YUSA	04	BELL	87.1 fb^{-1} E_{cm}^{ee}= 10.6 GeV
$< 1.8 \times 10^{-6}$	90	BLISS	98	CLEO	E_{cm}^{ee}= 10.6 GeV
$< 0.36 \times 10^{-5}$	90	[1] BARTELT	94	CLEO	Repl. by BLISS 98
$< 1.9 \times 10^{-5}$	90	ALBRECHT	92K	ARG	E_{cm}^{ee}= 10 GeV
$< 2.7 \times 10^{-5}$	90	BOWCOCK	90	CLEO	E_{cm}^{ee}= 10.4–10.9
$<33 \times 10^{-5}$	90	HAYES	82	MRK2	E_{cm}^{ee}= 3.8–6.8 GeV

[1] BARTELT 94 assume phase space decays.

$\Gamma(e^+\mu^-\mu^-)/\Gamma_{total}$ Γ_{199}/Γ

Test of lepton family number conservation.

VALUE	CL%	DOCUMENT ID		TECN	COMMENT
$<1.7 \times 10^{-8}$	90	HAYASAKA	10	BELL	782 fb^{-1} E_{cm}^{ee}= 10.6 GeV
• • • We do not use the following data for averages, fits, limits, etc. • • •					
$<2.6 \times 10^{-8}$	90	LEES	10A	BABR	468 fb^{-1} E_{cm}^{ee}= 10.6 GeV
$<2.3 \times 10^{-8}$	90	MIYAZAKI	08	BELL	535 fb^{-1} E_{cm}^{ee}= 10.6 GeV
$<5.6 \times 10^{-8}$	90	AUBERT	07BK	BABR	376 fb^{-1} E_{cm}^{ee}= 10.6 GeV
$<1.3 \times 10^{-7}$	90	AUBERT	04J	BABR	91.5 fb^{-1} E_{cm}^{ee}= 10.6 GeV
$<2.0 \times 10^{-7}$	90	YUSA	04	BELL	87.1 fb^{-1} E_{cm}^{ee}= 10.6 GeV
$<1.5 \times 10^{-6}$	90	BLISS	98	CLEO	E_{cm}^{ee}= 10.6 GeV
$<0.35 \times 10^{-5}$	90	[1] BARTELT	94	CLEO	Repl. by BLISS 98
$<1.8 \times 10^{-5}$	90	ALBRECHT	92K	ARG	E_{cm}^{ee}= 10 GeV
$<1.6 \times 10^{-5}$	90	BOWCOCK	90	CLEO	E_{cm}^{ee}= 10.4–10.9

[1] BARTELT 94 assume phase space decays.

$\Gamma(\mu^- e^+ e^-)/\Gamma_{total}$ Γ_{200}/Γ

Test of lepton family number conservation.

VALUE	CL%	DOCUMENT ID		TECN	COMMENT
$< 1.8 \times 10^{-8}$	90	HAYASAKA	10	BELL	782 fb^{-1} E_{cm}^{ee}= 10.6 GeV
• • • We do not use the following data for averages, fits, limits, etc. • • •					
$< 2.2 \times 10^{-8}$	90	LEES	10A	BABR	468 fb^{-1} E_{cm}^{ee}= 10.6 GeV
$< 2.7 \times 10^{-8}$	90	MIYAZAKI	08	BELL	535 fb^{-1} E_{cm}^{ee}= 10.6 GeV
$< 8.0 \times 10^{-8}$	90	AUBERT	07BK	BABR	376 fb^{-1} E_{cm}^{ee}= 10.6 GeV
$< 2.7 \times 10^{-7}$	90	AUBERT	04J	BABR	91.5 fb^{-1} E_{cm}^{ee}= 10.6 GeV
$< 1.9 \times 10^{-7}$	90	YUSA	04	BELL	87.1 fb^{-1} E_{cm}^{ee}= 10.6 GeV
$< 1.7 \times 10^{-6}$	90	BLISS	98	CLEO	E_{cm}^{ee}= 10.6 GeV
$< 0.34 \times 10^{-5}$	90	[1] BARTELT	94	CLEO	Repl. by BLISS 98
$< 1.4 \times 10^{-5}$	90	ALBRECHT	92K	ARG	E_{cm}^{ee}= 10 GeV
$< 2.7 \times 10^{-5}$	90	BOWCOCK	90	CLEO	E_{cm}^{ee}= 10.4–10.9
$<44 \times 10^{-5}$	90	HAYES	82	MRK2	E_{cm}^{ee}= 3.8–6.8 GeV

[1] BARTELT 94 assume phase space decays.

$\Gamma(\mu^+ e^- e^-)/\Gamma_{total}$ Γ_{201}/Γ

Test of lepton family number conservation.

VALUE	CL%	DOCUMENT ID		TECN	COMMENT
$<1.5 \times 10^{-8}$	90	HAYASAKA	10	BELL	782 fb^{-1} E_{cm}^{ee}= 10.6 GeV
• • • We do not use the following data for averages, fits, limits, etc. • • •					
$<1.8 \times 10^{-8}$	90	LEES	10A	BABR	468 fb^{-1} E_{cm}^{ee}= 10.6 GeV
$<2.0 \times 10^{-8}$	90	MIYAZAKI	08	BELL	535 fb^{-1} E_{cm}^{ee}= 10.6 GeV
$<5.8 \times 10^{-8}$	90	AUBERT	07BK	BABR	376 fb^{-1} E_{cm}^{ee}= 10.6 GeV
$<1.1 \times 10^{-7}$	90	AUBERT	04J	BABR	91.5 fb^{-1} E_{cm}^{ee}= 10.6 GeV
$<2.0 \times 10^{-7}$	90	YUSA	04	BELL	87.1 fb^{-1} E_{cm}^{ee}= 10.6 GeV
$<1.5 \times 10^{-6}$	90	BLISS	98	CLEO	E_{cm}^{ee}= 10.6 GeV
$<0.34 \times 10^{-5}$	90	[1] BARTELT	94	CLEO	Repl. by BLISS 98
$<1.4 \times 10^{-5}$	90	ALBRECHT	92K	ARG	E_{cm}^{ee}= 10 GeV
$<1.6 \times 10^{-5}$	90	BOWCOCK	90	CLEO	E_{cm}^{ee}= 10.4–10.9

[1] BARTELT 94 assume phase space decays.

$\Gamma(\mu^-\mu^+\mu^-)/\Gamma_{total}$ Γ_{202}/Γ

Test of lepton family number conservation.

VALUE	CL%	DOCUMENT ID		TECN	COMMENT
$< 2.1 \times 10^{-8}$	90	HAYASAKA	10	BELL	782 fb^{-1} E_{cm}^{ee}= 10.6 GeV
• • • We do not use the following data for averages, fits, limits, etc. • • •					
$< 8.0 \times 10^{-8}$	90	AAIJ	13AH	LHCB	1.0 fb^{-1}, $\sqrt{s}$ = 7 TeV
$< 3.3 \times 10^{-8}$	90	LEES	10A	BABR	468 fb^{-1} E_{cm}^{ee}= 10.6 GeV
$< 3.2 \times 10^{-8}$	90	MIYAZAKI	08	BELL	535 fb^{-1} E_{cm}^{ee}= 10.6 GeV
$< 5.3 \times 10^{-8}$	90	AUBERT	07BK	BABR	376 fb^{-1} E_{cm}^{ee}= 10.6 GeV
$< 1.9 \times 10^{-7}$	90	AUBERT	04J	BABR	91.5 fb^{-1} E_{cm}^{ee}= 10.6 GeV
$< 2.0 \times 10^{-7}$	90	YUSA	04	BELL	87.1 fb^{-1} E_{cm}^{ee}= 10.6 GeV
$< 1.9 \times 10^{-6}$	90	BLISS	98	CLEO	E_{cm}^{ee}= 10.6 GeV
$< 0.43 \times 10^{-5}$	90	[1] BARTELT	94	CLEO	Repl. by BLISS 98
$< 1.9 \times 10^{-5}$	90	ALBRECHT	92K	ARG	E_{cm}^{ee}= 10 GeV
$< 1.7 \times 10^{-5}$	90	BOWCOCK	90	CLEO	E_{cm}^{ee}= 10.4–10.9
$<49 \times 10^{-5}$	90	HAYES	82	MRK2	E_{cm}^{ee}= 3.8–6.8 GeV

[1] BARTELT 94 assume phase space decays.

$\Gamma(e^-\pi^+\pi^-)/\Gamma_{total}$ Γ_{203}/Γ

Test of lepton family number conservation.

VALUE	CL%	DOCUMENT ID		TECN	COMMENT
$<2.3 \times 10^{-8}$	90	MIYAZAKI	13	BELL	854 fb^{-1} E_{cm}^{ee} = 10.6 GeV
• • • We do not use the following data for averages, fits, limits, etc. • • •					
$<4.4 \times 10^{-8}$	90	MIYAZAKI	10	BELL	Repl. by MIYAZAKI 13
$<7.3 \times 10^{-7}$	90	YUSA	06	BELL	158 fb^{-1} E_{cm}^{ee} = 10.6 GeV
$<1.2 \times 10^{-7}$	90	AUBERT,BE	05D	BABR	221 fb^{-1}, E_{cm}^{ee} = 10.6 GeV
$<2.2 \times 10^{-6}$	90	BLISS	98	CLEO	E_{cm}^{ee}= 10.6 GeV
$<4.4 \times 10^{-6}$	90	[1] BARTELT	94	CLEO	Repl. by BLISS 98
$<2.7 \times 10^{-5}$	90	ALBRECHT	92K	ARG	E_{cm}^{ee}= 10 GeV
$<6.0 \times 10^{-5}$	90	BOWCOCK	90	CLEO	E_{cm}^{ee}= 10.4–10.9

[1] BARTELT 94 assume phase space decays.

$\Gamma(e^+\pi^-\pi^-)/\Gamma_{total}$ Γ_{204}/Γ

Test of lepton number conservation.

VALUE	CL%	DOCUMENT ID		TECN	COMMENT
$<2.0\times10^{-8}$	90	MIYAZAKI	13	BELL	854 fb^{-1} E_{cm}^{ee} = 10.6 GeV
• • • We do not use the following data for averages, fits, limits, etc. • • •					
$<8.8\times10^{-8}$	90	MIYAZAKI	10	BELL	Repl. by MIYAZAKI 13
$<2.0\times10^{-7}$	90	YUSA	06	BELL	158 fb^{-1} E_{cm}^{ee} = 10.6 GeV
$<2.7\times10^{-7}$	90	AUBERT,BE	05D	BABR	221 fb^{-1}, E_{cm}^{ee} = 10.6 GeV
$<1.9\times10^{-6}$	90	BLISS	98	CLEO	E_{cm}^{ee} = 10.6 GeV
$<4.4\times10^{-6}$	90	[1] BARTELT	94	CLEO	Repl. by BLISS 98
$<1.8\times10^{-5}$	90	ALBRECHT	92K	ARG	E_{cm}^{ee} = 10 GeV
$<1.7\times10^{-5}$	90	BOWCOCK	90	CLEO	E_{cm}^{ee} = 10.4–10.9

[1] BARTELT 94 assume phase space decays.

$\Gamma(\mu^-\pi^+\pi^-)/\Gamma_{total}$ Γ_{205}/Γ

Test of lepton family number conservation.

VALUE	CL%	DOCUMENT ID		TECN	COMMENT
$<2.1\times10^{-8}$	90	MIYAZAKI	13	BELL	854 fb^{-1} E_{cm}^{ee} = 10.6 GeV
• • • We do not use the following data for averages, fits, limits, etc. • • •					
$<3.3\times10^{-8}$	90	MIYAZAKI	10	BELL	Repl. by MIYAZAKI 13
$<4.8\times10^{-7}$	90	YUSA	06	BELL	158 fb^{-1} E_{cm}^{ee} = 10.6 GeV
$<2.9\times10^{-7}$	90	AUBERT,BE	05D	BABR	221 fb^{-1}, E_{cm}^{ee} = 10.6 GeV
$<8.2\times10^{-6}$	90	BLISS	98	CLEO	E_{cm}^{ee} = 10.6 GeV
$<7.4\times10^{-6}$	90	[1] BARTELT	94	CLEO	Repl. by BLISS 98
$<3.6\times10^{-5}$	90	ALBRECHT	92K	ARG	E_{cm}^{ee} = 10 GeV
$<3.9\times10^{-5}$	90	BOWCOCK	90	CLEO	E_{cm}^{ee} = 10.4–10.9

[1] BARTELT 94 assume phase space decays.

$\Gamma(\mu^+\pi^-\pi^-)/\Gamma_{total}$ Γ_{206}/Γ

Test of lepton number conservation.

VALUE	CL%	DOCUMENT ID		TECN	COMMENT
$<3.9\times10^{-8}$	90	MIYAZAKI	13	BELL	854 fb^{-1} E_{cm}^{ee} = 10.6 GeV
• • • We do not use the following data for averages, fits, limits, etc. • • •					
$<3.7\times10^{-8}$	90	MIYAZAKI	10	BELL	Repl. by MIYAZAKI 13
$<3.4\times10^{-7}$	90	YUSA	06	BELL	158 fb^{-1} E_{cm}^{ee} = 10.6 GeV
$<7\times10^{-8}$	90	AUBERT,BE	05D	BABR	221 fb^{-1}, E_{cm}^{ee} = 10.6 GeV
$<3.4\times10^{-6}$	90	BLISS	98	CLEO	E_{cm}^{ee} = 10.6 GeV
$<6.9\times10^{-6}$	90	[1] BARTELT	94	CLEO	Repl. by BLISS 98
$<6.3\times10^{-5}$	90	ALBRECHT	92K	ARG	E_{cm}^{ee} = 10 GeV
$<3.9\times10^{-5}$	90	BOWCOCK	90	CLEO	E_{cm}^{ee} = 10.4–10.9

[1] BARTELT 94 assume phase space decays.

$\Gamma(e^-\pi^+K^-)/\Gamma_{total}$ Γ_{207}/Γ

Test of lepton family number conservation.

VALUE	CL%	DOCUMENT ID		TECN	COMMENT
$<3.7\times10^{-8}$	90	MIYAZAKI	13	BELL	854 fb^{-1} E_{cm}^{ee} = 10.6 GeV
• • • We do not use the following data for averages, fits, limits, etc. • • •					
$<5.8\times10^{-8}$	90	MIYAZAKI	10	BELL	Repl. by MIYAZAKI 13
$<7.2\times10^{-7}$	90	YUSA	06	BELL	158 fb^{-1} E_{cm}^{ee} = 10.6 GeV
$<3.2\times10^{-7}$	90	AUBERT,BE	05D	BABR	221 fb^{-1}, E_{cm}^{ee} = 10.6 GeV
$<6.4\times10^{-6}$	90	BLISS	98	CLEO	E_{cm}^{ee} = 10.6 GeV
$<7.7\times10^{-6}$	90	[1] BARTELT	94	CLEO	Repl. by BLISS 98
$<2.9\times10^{-5}$	90	ALBRECHT	92K	ARG	E_{cm}^{ee} = 10 GeV
$<5.8\times10^{-5}$	90	BOWCOCK	90	CLEO	E_{cm}^{ee} = 10.4–10.9

[1] BARTELT 94 assume phase space decays.

$\Gamma(e^-\pi^-K^+)/\Gamma_{total}$ Γ_{208}/Γ

Test of lepton family number conservation.

VALUE	CL%	DOCUMENT ID		TECN	COMMENT
$<3.1\times10^{-8}$	90	MIYAZAKI	13	BELL	854 fb^{-1} E_{cm}^{ee} = 10.6 GeV
• • • We do not use the following data for averages, fits, limits, etc. • • •					
$<5.2\times10^{-8}$	90	MIYAZAKI	10	BELL	Repl. by MIYAZAKI 13
$<1.6\times10^{-7}$	90	YUSA	06	BELL	158 fb^{-1} E_{cm}^{ee} = 10.6 GeV
$<1.7\times10^{-7}$	90	AUBERT,BE	05D	BABR	221 fb^{-1}, E_{cm}^{ee} = 10.6 GeV
$<3.8\times10^{-6}$	90	BLISS	98	CLEO	E_{cm}^{ee} = 10.6 GeV
$<4.6\times10^{-6}$	90	[1] BARTELT	94	CLEO	Repl. by BLISS 98
$<5.8\times10^{-5}$	90	BOWCOCK	90	CLEO	E_{cm}^{ee} = 10.4–10.9

[1] BARTELT 94 assume phase space decays.

$\Gamma(e^+\pi^-K^-)/\Gamma_{total}$ Γ_{209}/Γ

Test of lepton number conservation.

VALUE	CL%	DOCUMENT ID		TECN	COMMENT
$<3.2\times10^{-8}$	90	MIYAZAKI	13	BELL	854 fb^{-1} E_{cm}^{ee} = 10.6 GeV
• • • We do not use the following data for averages, fits, limits, etc. • • •					
$<6.7\times10^{-8}$	90	MIYAZAKI	10	BELL	Repl. by MIYAZAKI 13
$<1.9\times10^{-7}$	90	YUSA	06	BELL	158 fb^{-1} E_{cm}^{ee} = 10.6 GeV
$<1.8\times10^{-7}$	90	AUBERT,BE	05D	BABR	221 fb^{-1}, E_{cm}^{ee} = 10.6 GeV
$<2.1\times10^{-6}$	90	BLISS	98	CLEO	E_{cm}^{ee} = 10.6 GeV
$<4.5\times10^{-6}$	90	[1] BARTELT	94	CLEO	Repl. by BLISS 98
$<2.0\times10^{-5}$	90	ALBRECHT	92K	ARG	E_{cm}^{ee} = 10 GeV
$<4.9\times10^{-5}$	90	BOWCOCK	90	CLEO	E_{cm}^{ee} = 10.4–10.9

[1] BARTELT 94 assume phase space decays.

$\Gamma(e^-K_S^0K_S^0)/\Gamma_{total}$ Γ_{210}/Γ

Test of lepton family number conservation.

VALUE	CL%	DOCUMENT ID		TECN	COMMENT
$<7.1\times10^{-8}$	90	MIYAZAKI	10A	BELL	671 fb^{-1} E_{cm}^{ee} = 10.6 GeV
• • • We do not use the following data for averages, fits, limits, etc. • • •					
$<2.2\times10^{-6}$	90	CHEN	02C	CLEO	E_{cm}^{ee} = 10.6 GeV

$\Gamma(e^-K^+K^-)/\Gamma_{total}$ Γ_{211}/Γ

Test of lepton family number conservation.

VALUE	CL%	DOCUMENT ID		TECN	COMMENT
$<3.4\times10^{-8}$	90	MIYAZAKI	13	BELL	854 fb^{-1} E_{cm}^{ee} = 10.6 GeV
• • • We do not use the following data for averages, fits, limits, etc. • • •					
$<5.4\times10^{-8}$	90	MIYAZAKI	10	BELL	Repl. by MIYAZAKI 13
$<3.0\times10^{-7}$	90	YUSA	06	BELL	158 fb^{-1} E_{cm}^{ee} = 10.6 GeV
$<1.4\times10^{-7}$	90	AUBERT,BE	05D	BABR	221 fb^{-1}, E_{cm}^{ee} = 10.6 GeV
$<6.0\times10^{-6}$	90	BLISS	98	CLEO	E_{cm}^{ee} = 10.6 GeV

$\Gamma(e^+K^-K^-)/\Gamma_{total}$ Γ_{212}/Γ

Test of lepton number conservation.

VALUE	CL%	DOCUMENT ID		TECN	COMMENT
$<3.3\times10^{-8}$	90	MIYAZAKI	13	BELL	854 fb^{-1} E_{cm}^{ee} = 10.6 GeV
• • • We do not use the following data for averages, fits, limits, etc. • • •					
$<6.0\times10^{-8}$	90	MIYAZAKI	10	BELL	Repl. by MIYAZAKI 13
$<3.1\times10^{-7}$	90	YUSA	06	BELL	158 fb^{-1} E_{cm}^{ee} = 10.6 GeV
$<1.5\times10^{-7}$	90	AUBERT,BE	05D	BABR	221 fb^{-1}, E_{cm}^{ee} = 10.6 GeV
$<3.8\times10^{-6}$	90	BLISS	98	CLEO	E_{cm}^{ee} = 10.6 GeV

$\Gamma(\mu^-\pi^+K^-)/\Gamma_{total}$ Γ_{213}/Γ

Test of lepton family number conservation.

VALUE	CL%	DOCUMENT ID		TECN	COMMENT
$<8.6\times10^{-8}$	90	MIYAZAKI	13	BELL	854 fb^{-1} E_{cm}^{ee} = 10.6 GeV
• • • We do not use the following data for averages, fits, limits, etc. • • •					
$<1.6\times10^{-7}$	90	MIYAZAKI	10	BELL	Repl. by MIYAZAKI 13
$<2.7\times10^{-7}$	90	YUSA	06	BELL	158 fb^{-1} E_{cm}^{ee} = 10.6 GeV
$<2.6\times10^{-7}$	90	AUBERT,BE	05D	BABR	221 fb^{-1}, E_{cm}^{ee} = 10.6 GeV
$<7.5\times10^{-6}$	90	BLISS	98	CLEO	E_{cm}^{ee} = 10.6 GeV
$<8.7\times10^{-6}$	90	[1] BARTELT	94	CLEO	Repl. by BLISS 98
$<11\times10^{-5}$	90	ALBRECHT	92K	ARG	E_{cm}^{ee} = 10 GeV
$<7.7\times10^{-5}$	90	BOWCOCK	90	CLEO	E_{cm}^{ee} = 10.4–10.9

[1] BARTELT 94 assume phase space decays.

$\Gamma(\mu^-\pi^-K^+)/\Gamma_{total}$ Γ_{214}/Γ

Test of lepton family number conservation.

VALUE	CL%	DOCUMENT ID		TECN	COMMENT
$<4.5\times10^{-8}$	90	MIYAZAKI	13	BELL	854 fb^{-1} E_{cm}^{ee} = 10.6 GeV
• • • We do not use the following data for averages, fits, limits, etc. • • •					
$<1.0\times10^{-7}$	90	MIYAZAKI	10	BELL	Repl. by MIYAZAKI 13
$<7.3\times10^{-7}$	90	YUSA	06	BELL	158 fb^{-1} E_{cm}^{ee} = 10.6 GeV
$<3.2\times10^{-7}$	90	AUBERT,BE	05D	BABR	221 fb^{-1}, E_{cm}^{ee} = 10.6 GeV
$<7.4\times10^{-6}$	90	BLISS	98	CLEO	E_{cm}^{ee} = 10.6 GeV
$<1.5\times10^{-5}$	90	[1] BARTELT	94	CLEO	Repl. by BLISS 98
$<7.7\times10^{-5}$	90	BOWCOCK	90	CLEO	E_{cm}^{ee} = 10.4–10.9

[1] BARTELT 94 assume phase space decays.

$\Gamma(\mu^+\pi^-K^-)/\Gamma_{total}$ Γ_{215}/Γ

Test of lepton number conservation.

VALUE	CL%	DOCUMENT ID		TECN	COMMENT
$<4.8\times10^{-8}$	90	MIYAZAKI	13	BELL	854 fb^{-1} E_{cm}^{ee} = 10.6 GeV
• • • We do not use the following data for averages, fits, limits, etc. • • •					
$<9.4\times10^{-8}$	90	MIYAZAKI	10	BELL	Repl. by MIYAZAKI 13
$<2.9\times10^{-7}$	90	YUSA	06	BELL	158 fb^{-1} E_{cm}^{ee} = 10.6 GeV
$<2.2\times10^{-7}$	90	AUBERT,BE	05D	BABR	221 fb^{-1}, E_{cm}^{ee} = 10.6 GeV
$<7.0\times10^{-6}$	90	BLISS	98	CLEO	E_{cm}^{ee} = 10.6 GeV
$<2.0\times10^{-5}$	90	[1] BARTELT	94	CLEO	Repl. by BLISS 98
$<5.8\times10^{-5}$	90	ALBRECHT	92K	ARG	E_{cm}^{ee} = 10 GeV
$<4.0\times10^{-5}$	90	BOWCOCK	90	CLEO	E_{cm}^{ee} = 10.4–10.9

[1] BARTELT 94 assume phase space decays.

$\Gamma(\mu^- K_S^0 K_S^0)/\Gamma_{total}$ Γ_{216}/Γ

VALUE	CL%	DOCUMENT ID		TECN	COMMENT
$<8.0\times10^{-8}$	90	MIYAZAKI	10A	BELL	671 fb^{-1} E_{cm}^{ee}= 10.6 GeV
• • • We do not use the following data for averages, fits, limits, etc. • • •					
$<3.4\times10^{-6}$	90	CHEN	02C	CLEO	E_{cm}^{ee}= 10.6 GeV

$\Gamma(\mu^- K^+ K^-)/\Gamma_{total}$ Γ_{217}/Γ

Test of lepton family number conservation.

VALUE	CL%	DOCUMENT ID		TECN	COMMENT
$<4.4\times10^{-8}$	90	MIYAZAKI	13	BELL	854 fb^{-1} E_{cm}^{ee} = 10.6 GeV
• • • We do not use the following data for averages, fits, limits, etc. • • •					
$<6.8\times10^{-8}$	90	MIYAZAKI	10	BELL	Repl. by MIYAZAKI 13
$<8.0\times10^{-7}$	90	YUSA	06	BELL	158 fb^{-1} E_{cm}^{ee} = 10.6 GeV
$<2.5\times10^{-7}$	90	AUBERT,BE	05D	BABR	221 fb^{-1}, E_{cm}^{ee}= 10.6 GeV
$<15\times10^{-6}$	90	BLISS	98	CLEO	E_{cm}^{ee}= 10.6 GeV

$\Gamma(\mu^+ K^- K^-)/\Gamma_{total}$ Γ_{218}/Γ

Test of lepton number conservation.

VALUE	CL%	DOCUMENT ID		TECN	COMMENT
$<4.7\times10^{-8}$	90	MIYAZAKI	13	BELL	854 fb^{-1} E_{cm}^{ee} = 10.6 GeV
• • • We do not use the following data for averages, fits, limits, etc. • • •					
$<9.6\times10^{-8}$	90	MIYAZAKI	10	BELL	Repl. by MIYAZAKI 13
$<4.4\times10^{-7}$	90	YUSA	06	BELL	158 fb^{-1} E_{cm}^{ee} = 10.6 GeV
$<4.8\times10^{-7}$	90	AUBERT,BE	05D	BABR	221 fb^{-1}, E_{cm}^{ee}= 10.6 GeV
$<6.0\times10^{-6}$	90	BLISS	98	CLEO	E_{cm}^{ee}= 10.6 GeV

$\Gamma(e^- \pi^0 \pi^0)/\Gamma_{total}$ Γ_{219}/Γ

Test of lepton family number conservation.

VALUE	CL%	DOCUMENT ID		TECN	COMMENT
$<6.5\times10^{-6}$	90	BONVICINI	97	CLEO	E_{cm}^{ee}= 10.6 GeV

$\Gamma(\mu^- \pi^0 \pi^0)/\Gamma_{total}$ Γ_{220}/Γ

Test of lepton family number conservation.

VALUE	CL%	DOCUMENT ID		TECN	COMMENT
$<14\times10^{-6}$	90	BONVICINI	97	CLEO	E_{cm}^{ee}= 10.6 GeV

$\Gamma(e^- \eta\eta)/\Gamma_{total}$ Γ_{221}/Γ

Test of lepton family number conservation.

VALUE	CL%	DOCUMENT ID		TECN	COMMENT
$<35\times10^{-6}$	90	BONVICINI	97	CLEO	E_{cm}^{ee}= 10.6 GeV

$\Gamma(\mu^- \eta\eta)/\Gamma_{total}$ Γ_{222}/Γ

Test of lepton family number conservation.

VALUE	CL%	DOCUMENT ID		TECN	COMMENT
$<60\times10^{-6}$	90	BONVICINI	97	CLEO	E_{cm}^{ee}= 10.6 GeV

$\Gamma(e^- \pi^0 \eta)/\Gamma_{total}$ Γ_{223}/Γ

Test of lepton family number conservation.

VALUE	CL%	DOCUMENT ID		TECN	COMMENT
$<24\times10^{-6}$	90	BONVICINI	97	CLEO	E_{cm}^{ee}= 10.6 GeV

$\Gamma(\mu^- \pi^0 \eta)/\Gamma_{total}$ Γ_{224}/Γ

Test of lepton family number conservation.

VALUE	CL%	DOCUMENT ID		TECN	COMMENT
$<22\times10^{-6}$	90	BONVICINI	97	CLEO	E_{cm}^{ee}= 10.6 GeV

$\Gamma(p\mu^- \mu^-)/\Gamma_{total}$ Γ_{225}/Γ

VALUE	CL%	DOCUMENT ID		TECN	COMMENT
$<4.4\times10^{-7}$	90	AAIJ	13AH	LHCB	1.0 fb^{-1}, $\sqrt{s}$ = 7 TeV

$\Gamma(\overline{p}\mu^+ \mu^-)/\Gamma_{total}$ Γ_{226}/Γ

VALUE	CL%	DOCUMENT ID		TECN	COMMENT
$<3.3\times10^{-7}$	90	AAIJ	13AH	LHCB	1.0 fb^{-1}, $\sqrt{s}$ = 7 TeV

$\Gamma(\overline{p}\gamma)/\Gamma_{total}$ Γ_{227}/Γ

Test of lepton number and baryon number conservation.

VALUE	CL%	DOCUMENT ID		TECN	COMMENT
$<3.5\times10^{-6}$	90	GODANG	99	CLEO	E_{cm}^{ee}= 10.6 GeV
• • • We do not use the following data for averages, fits, limits, etc. • • •					
$<29\times10^{-5}$	90	ALBRECHT	92K	ARG	E_{cm}^{ee}= 10 GeV

$\Gamma(\overline{p}\pi^0)/\Gamma_{total}$ Γ_{228}/Γ

Test of lepton number and baryon number conservation.

VALUE	CL%	DOCUMENT ID		TECN	COMMENT
$<15\times10^{-6}$	90	GODANG	99	CLEO	E_{cm}^{ee}= 10.6 GeV
• • • We do not use the following data for averages, fits, limits, etc. • • •					
$<66\times10^{-5}$	90	ALBRECHT	92K	ARG	E_{cm}^{ee}= 10 GeV

$\Gamma(\overline{p}2\pi^0)/\Gamma_{total}$ Γ_{229}/Γ

Test of lepton number and baryon number conservation.

VALUE	CL%	DOCUMENT ID		TECN	COMMENT
$<33\times10^{-6}$	90	GODANG	99	CLEO	E_{cm}^{ee}= 10.6 GeV

$\Gamma(\overline{p}\eta)/\Gamma_{total}$ Γ_{230}/Γ

Test of lepton number and baryon number conservation.

VALUE	CL%	DOCUMENT ID		TECN	COMMENT
$<8.9\times10^{-6}$	90	GODANG	99	CLEO	E_{cm}^{ee}= 10.6 GeV
• • • We do not use the following data for averages, fits, limits, etc. • • •					
$<130\times10^{-5}$	90	ALBRECHT	92K	ARG	E_{cm}^{ee}= 10 GeV

$\Gamma(\overline{p}\pi^0\eta)/\Gamma_{total}$ Γ_{231}/Γ

Test of lepton number and baryon number conservation.

VALUE	CL%	DOCUMENT ID		TECN	COMMENT
$<27\times10^{-6}$	90	GODANG	99	CLEO	E_{cm}^{ee}= 10.6 GeV

$\Gamma(\Lambda\pi^-)/\Gamma_{total}$ Γ_{232}/Γ

Test of lepton number and baryon number conservation.

VALUE	CL%	DOCUMENT ID		TECN	COMMENT
$<0.72\times10^{-7}$	90	MIYAZAKI	06	BELL	154 fb^{-1}, E_{cm}^{ee}= 10.6 GeV

$\Gamma(\overline{\Lambda}\pi^-)/\Gamma_{total}$ Γ_{233}/Γ

Test of lepton number and baryon number conservation.

VALUE	CL%	DOCUMENT ID		TECN	COMMENT
$<1.4\times10^{-7}$	90	MIYAZAKI	06	BELL	154 fb^{-1}, E_{cm}^{ee}= 10.6 GeV

$\Gamma(e^-$ light boson$)/\Gamma(e^- \overline{\nu}_e \nu_\tau)$ Γ_{234}/Γ_5

Test of lepton family number conservation.

VALUE	CL%	DOCUMENT ID		TECN	COMMENT
<0.015	95	[1] ALBRECHT	95G	ARG	E_{cm}^{ee}= 9.4–10.6 GeV
• • • We do not use the following data for averages, fits, limits, etc. • • •					
<0.018	95	[2] ALBRECHT	90E	ARG	E_{cm}^{ee}= 9.4–10.6 GeV
<0.040	95	[3] BALTRUSAIT...85		MRK3	E_{cm}^{ee}= 3.77 GeV

[1] ALBRECHT 95G limit holds for bosons with mass < 0.4 GeV. The limit rises to 0.036 for a mass of 1.0 GeV, then falls to 0.006 at the upper mass limit of 1.6 GeV.
[2] ALBRECHT 90E limit applies for spinless boson with mass < 100 MeV, and rises to 0.050 for mass = 500 MeV.
[3] BALTRUSAITIS 85 limit applies for spinless boson with mass < 100 MeV.

$\Gamma(\mu^-$ light boson$)/\Gamma(e^- \overline{\nu}_e \nu_\tau)$ Γ_{235}/Γ_5

Test of lepton family number conservation.

VALUE	CL%	DOCUMENT ID		TECN	COMMENT
<0.026	95	[1] ALBRECHT	95G	ARG	E_{cm}^{ee}= 9.4–10.6 GeV
• • • We do not use the following data for averages, fits, limits, etc. • • •					
<0.033	95	[2] ALBRECHT	90E	ARG	E_{cm}^{ee}= 9.4–10.6 GeV
<0.125	95	[3] BALTRUSAIT...85		MRK3	E_{cm}^{ee}= 3.77 GeV

[1] ALBRECHT 95G limit holds for bosons with mass < 1.3 GeV. The limit rises to 0.034 for a mass of 1.4 GeV, then falls to 0.003 at the upper mass limit of 1.6 GeV.
[2] ALBRECHT 90E limit applies for spinless boson with mass < 100 MeV, and rises to 0.071 for mass = 500 MeV.
[3] BALTRUSAITIS 85 limit applies for spinless boson with mass < 100 MeV.

τ-DECAY PARAMETERS

τ-LEPTON DECAY PARAMETERS

Updated August 2011 by A. Stahl (RWTH Aachen).

The purpose of the measurements of the decay parameters (*i.e.*, Michel parameters) of the τ is to determine the structure (spin and chirality) of the current mediating its decays.

Leptonic Decays: The Michel parameters are extracted from the energy spectrum of the charged daughter lepton $\ell = e, \mu$ in the decays $\tau \to \ell\nu_\ell\nu_\tau$. Ignoring radiative corrections, neglecting terms of order $(m_\ell/m_\tau)^2$ and $(m_\tau/\sqrt{s})^2$, and setting the neutrino masses to zero, the spectrum in the laboratory frame reads

$$\frac{d\Gamma}{dx} = \frac{G_{\tau\ell}^2\, m_\tau^5}{192\ \pi^3} \times \left\{ f_0(x) + \rho f_1(x) + \eta \frac{m_\ell}{m_\tau} f_2(x) - P_\tau \left[\xi g_1(x) + \xi\delta g_2(x) \right] \right\} , \quad (1)$$

with

$$f_0(x) = 2 - 6x^2 + 4x^3$$
$$f_1(x) = -\frac{4}{9} + 4x^2 - \frac{32}{9}x^3 \qquad g_1(x) = -\frac{2}{3} + 4x - 6x^2 + \frac{8}{3}x^3$$
$$f_2(x) = 12(1-x)^2 \qquad g_2(x) = \frac{4}{9} - \frac{16}{3}x + 12x^2 - \frac{64}{9}x^3 .$$

The quantity x is the fractional energy of the daughter lepton ℓ, *i.e.*, $x = E_\ell/E_{\ell,max} \approx E_\ell/(\sqrt{s}/2)$ and P_τ is the polarization of the tau leptons. The integrated decay width is given by

$$\Gamma = \frac{G_{\tau\ell}^2 \ m_\tau^5}{192 \ \pi^3} \left(1 + 4\,\eta \ \frac{m_\ell}{m_\tau}\right) \ . \tag{2}$$

The situation is similar to muon decays $\mu \to e\nu_e\nu_\mu$. The generalized matrix element with the couplings $g_{\varepsilon\mu}^\gamma$ and their relations to the Michel parameters ρ, η, ξ, and δ have been described in the "Note on Muon Decay Parameters." The Standard Model expectations are 3/4, 0, 1, and 3/4, respectively. For more details, see Ref. 1.

Hadronic Decays: In the case of hadronic decays $\tau \to h\nu_\tau$, with $h = \pi$, ρ, or a_1, the ansatz is restricted to purely vectorial currents. The matrix element is

$$\frac{G_{\tau h}}{\sqrt{2}} \sum_{\lambda=R,L} g_\lambda \ \langle \ \overline{\Psi}_\omega(\nu_\tau) \ | \ \gamma^\mu \ | \ \Psi_\lambda(\tau) \ \rangle \quad J_\mu^h \tag{3}$$

with the hadronic current J_μ^h. The neutrino chirality ω is uniquely determined from λ. The spectrum depends only on a single parameter ξ_h

$$\frac{d^n\Gamma}{dx_1 dx_2 \ldots dx_n} = f\left(\vec{x}\right) + \xi_h P_\tau g\left(\vec{x}\right) \ , \tag{4}$$

with f and g being channel-dependent functions of the n observables $\vec{x} = (x_1, x_2, \ldots, x_n)$ (see Ref. 2). The parameter ξ_h is related to the couplings through

$$\xi_h = |g_L|^2 - |g_R|^2 \ . \tag{5}$$

ξ_h is the negative of the chirality of the τ neutrino in these decays. In the Standard Model, $\xi_h = 1$. Also included in the Data Listings for ξ_h are measurements of the neutrino helicity which coincide with ξ_h, if the neutrino is massless (ASNER 00, ACKERSTAFF 97R, AKERS 95P, ALBRECHT 93C, and ALBRECHT 90I).

Combination of Measurements: The individual measurements are combined, taking into account the correlations between the parameters. In a first fit, universality between the two leptonic decays, and between all hadronic decays, is assumed. A second fit is made without these assumptions. The results of the two fits are provided as OUR FIT in the Data Listings below in the tables whose title includes "(e or mu)" or "(all hadronic modes)," and "(e)," "(mu)" *etc.*, respectively. The measurements show good agreement with the Standard Model. The χ^2 values with respect to the Standard model predictions are 24.1 for 41 degrees of freedom and 26.8 for 56 degrees of freedom, respectively. The correlations are reduced through this combination to less than 20%, with the exception of ρ and η which are correlated by +23%, for the fit with universality and by +70% for $\tau \to \mu\nu_\mu\nu_\tau$.

Model-independent Analysis: From the Michel parameters, limits can be derived on the couplings $g_{\varepsilon\lambda}^\kappa$ without further model assumptions. In the Standard model $g_{LL}^V = 1$ (leptonic decays), and $g_L = 1$ (hadronic decays) and all other couplings vanish. First, the partial decay widths have to be compared to the Standard Model predictions to derive limits on the normalization of the couplings $A_x = G_{\tau x}^2/G_F^2$ with Fermi's constant G_F:

$$\begin{aligned} A_e &= 1.0029 \pm 0.0046 \ , \\ A_\mu &= 0.981 \pm 0.018 \ , \\ A_\pi &= 1.0020 \pm 0.0073 \ . \end{aligned} \tag{6}$$

Then limits on the couplings (95% CL) can be extracted (see Ref. 3 and Ref. 4). Without the assumption of universality, the limits given in Table 1 are derived.

Table 1: Coupling constants $g_{\varepsilon\mu}^\gamma$. 95% confidence level experimental limits. The limits include the quoted values of A_e, A_μ, and A_π and assume $A_\rho = A_{a_1} = 1$.

$\tau \to e\nu_e\nu_\tau$		
$\lvert g_{RR}^S\rvert < 0.70$	$\lvert g_{RR}^V\rvert < 0.17$	$\lvert g_{RR}^T\rvert \equiv 0$
$\lvert g_{LR}^S\rvert < 0.99$	$\lvert g_{LR}^V\rvert < 0.13$	$\lvert g_{LR}^T\rvert < 0.082$
$\lvert g_{RL}^S\rvert < 2.01$	$\lvert g_{RL}^V\rvert < 0.52$	$\lvert g_{RL}^T\rvert < 0.51$
$\lvert g_{LL}^S\rvert < 2.01$	$\lvert g_{LL}^V\rvert < 1.005$	$\lvert g_{LL}^T\rvert \equiv 0$
$\tau \to \mu\nu_\mu\nu_\tau$		
$\lvert g_{RR}^S\rvert < 0.72$	$\lvert g_{RR}^V\rvert < 0.18$	$\lvert g_{RR}^T\rvert \equiv 0$
$\lvert g_{LR}^S\rvert < 0.95$	$\lvert g_{LR}^V\rvert < 0.12$	$\lvert g_{LR}^T\rvert < 0.079$
$\lvert g_{RL}^S\rvert < 2.01$	$\lvert g_{RL}^V\rvert < 0.52$	$\lvert g_{RL}^T\rvert < 0.51$
$\lvert g_{LL}^S\rvert < 2.01$	$\lvert g_{LL}^V\rvert < 1.005$	$\lvert g_{LL}^T\rvert \equiv 0$
$\tau \to \pi\nu_\tau$		
$\lvert g_R^V\rvert < 0.15$	$\lvert g_L^V\rvert > 0.992$	
$\tau \to \rho\nu_\tau$		
$\lvert g_R^V\rvert < 0.10$	$\lvert g_L^V\rvert > 0.995$	
$\tau \to a_1\nu_\tau$		
$\lvert g_R^V\rvert < 0.16$	$\lvert g_L^V\rvert > 0.987$	

Model-dependent Interpretation: More stringent limits can be derived assuming specific models. For example, in the framework of a two Higgs doublet model, the measurements correspond to a limit of $m_{H^\pm} > 1.9$ GeV $\times \tan\beta$ on the mass of the charged Higgs boson, or a limit of 253 GeV on the mass of the second W boson in left-right symmetric models for arbitrary mixing (both 95% CL). See Ref. 4 and Ref. 5.

Footnotes and References

1. F. Scheck, Phys. Reports **44**, 187 (1978);
W. Fetscher and H.J. Gerber in *Precision Tests of the Standard Model*, edited by P. Langacker, World Scientific,

1993;
A. Stahl, *Physics with τ Leptons*, Springer Tracts in Modern Physics.

2. M. Davier *et al.*, Phys. Lett. **B306**, 411 (1993).
3. OPAL Collab., K. Ackerstaff *et al.*, Eur. Phys. J. **C8**, 3 (1999).
4. A. Stahl, Nucl. Phys. (Proc. Supp.) **B76**, 173 (1999).
5. M.-T. Dova *et al.*, Phys. Rev. **D58**, 015005 (1998); T. Hebbeker and W. Lohmann, Z. Phys. **C74**, 399 (1997); A. Pich and J.P. Silva, Phys. Rev. **D52**, 4006 (1995).

$\rho(e \text{ or } \mu)$ PARAMETER

($V-A$) theory predicts $\rho = 0.75$.

VALUE	EVTS	DOCUMENT ID		TECN	COMMENT
0.745±0.008 OUR FIT					
0.749±0.008 OUR AVERAGE					
0.742±0.014±0.006	81k	HEISTER	01E	ALEP	1991–1995 LEP runs
0.775±0.023±0.020	36k	ABREU	00L	DLPH	1992–1995 runs
0.781±0.028±0.018	46k	ACKERSTAFF	99D	OPAL	1990–1995 LEP runs
0.762±0.035	54k	ACCIARRI	98R	L3	1991–1995 LEP runs
0.731±0.031		[1] ALBRECHT	98	ARG	E^{ee}_{cm}= 9.5–10.6 GeV
0.72 ±0.09 ±0.03		[2] ABE	97O	SLD	1993–1995 SLC runs
0.747±0.010±0.006	55k	ALEXANDER	97F	CLEO	E^{ee}_{cm}= 10.6 GeV
0.79 ±0.10 ±0.10	3732	FORD	87B	MAC	E^{ee}_{cm}= 29 GeV
0.71 ±0.09 ±0.03	1426	BEHRENDS	85	CLEO	e^+e^- near $\Upsilon(4S)$
• • • We do not use the following data for averages, fits, limits, etc. • • •					
0.735±0.013±0.008	31k	AMMAR	97B	CLEO	Repl. by ALEXANDER 97F
0.794±0.039±0.031	18k	ACCIARRI	96H	L3	Repl. by ACCIARRI 98R
0.732±0.034±0.020	8.2k	[3] ALBRECHT	95	ARG	E^{ee}_{cm}= 9.5–10.6 GeV
0.738±0.038		[4] ALBRECHT	95C	ARG	Repl. by ALBRECHT 98
0.751±0.039±0.022		BUSKULIC	95D	ALEP	Repl. by HEISTER 01E
0.742±0.035±0.020	8000	ALBRECHT	90E	ARG	E^{ee}_{cm}= 9.4–10.6 GeV

[1] Combined fit to ARGUS tau decay parameter measurements in ALBRECHT 98, ALBRECHT 95C, ALBRECHT 93G, and ALBRECHT 94E. ALBRECHT 98 use tau pair events of the type $\tau^-\tau^+ \to (\ell^-\overline{\nu}_\ell\nu_\tau)(\pi^+\pi^0\overline{\nu}_\tau)$, and their charged conjugates.

[2] ABE 97O assume $\eta = 0$ in their fit. Letting η vary in the fit gives a ρ value of 0.69 ± 0.13 ± 0.05.

[3] Value is from a simultaneous fit for the ρ and η decay parameters to the lepton energy spectrum. Not independent of ALBRECHT 90E $\rho(e$ or $\mu)$ value which assumes $\eta = 0$. Result is strongly correlated with ALBRECHT 95C.

[4] Combined fit to ARGUS tau decay parameter measurements in ALBRECHT 95C, ALBRECHT 93G, and ALBRECHT 94E.

$\rho(e)$ PARAMETER

($V-A$) theory predicts $\rho = 0.75$.

VALUE	EVTS	DOCUMENT ID		TECN	COMMENT
0.747±0.010 OUR FIT					
0.744±0.010 OUR AVERAGE					
0.747±0.019±0.014	44k	HEISTER	01E	ALEP	1991–1995 LEP runs
0.744±0.036±0.037	17k	ABREU	00L	DLPH	1992–1995 runs
0.779±0.047±0.029	25k	ACKERSTAFF	99D	OPAL	1990–1995 LEP runs
0.68 ±0.04 ±0.07		[1] ALBRECHT	98	ARG	E^{ee}_{cm}= 9.5–10.6 GeV
0.71 ±0.14 ±0.05		ABE	97O	SLD	1993–1995 SLC runs
0.747±0.012±0.004	34k	ALEXANDER	97F	CLEO	E^{ee}_{cm}= 10.6 GeV
0.735±0.036±0.020	4.7k	[2] ALBRECHT	95	ARG	E^{ee}_{cm}= 9.5–10.6 GeV
0.79 ±0.08 ±0.06	3230	[3] ALBRECHT	93G	ARG	E^{ee}_{cm}= 9.4–10.6 GeV
0.64 ±0.06 ±0.07	2753	JANSSEN	89	CBAL	E^{ee}_{cm}= 9.4–10.6 GeV
0.62 ±0.17 ±0.14	1823	FORD	87B	MAC	E^{ee}_{cm}= 29 GeV
0.60 ±0.13	699	BEHRENDS	85	CLEO	e^+e^- near $\Upsilon(4S)$
0.72 ±0.10 ±0.11	594	BACINO	79B	DLCO	E^{ee}_{cm}= 3.5–7.4 GeV
• • • We do not use the following data for averages, fits, limits, etc. • • •					
0.732±0.014±0.009	19k	AMMAR	97B	CLEO	Repl. by ALEXANDER 97F
0.793±0.050±0.025		BUSKULIC	95D	ALEP	Repl. by HEISTER 01E
0.747±0.045±0.028	5106	ALBRECHT	90E	ARG	Repl. by ALBRECHT 95

[1] ALBRECHT 98 use tau pair events of the type $\tau^-\tau^+ \to (\ell^-\overline{\nu}_\ell\nu_\tau)(\pi^+\pi^0\overline{\nu}_\tau)$, and their charged conjugates.

[2] ALBRECHT 95 use tau pair events of the type $\tau^-\tau^+ \to (\ell^-\overline{\nu}_\ell\nu_\tau)(h^+h^-h^+(\pi^0)\overline{\nu}_\tau)$ and their charged conjugates.

[3] ALBRECHT 93G use tau pair events of the type $\tau^-\tau^+ \to (\mu^-\overline{\nu}_\mu\nu_\tau)(e^+\nu_e\overline{\nu}_\tau)$ and their charged conjugates.

$\rho(\mu)$ PARAMETER

($V-A$) theory predicts $\rho = 0.75$.

VALUE	EVTS	DOCUMENT ID		TECN	COMMENT
0.763±0.020 OUR FIT					
0.770±0.022 OUR AVERAGE					
0.776±0.045±0.019	46k	HEISTER	01E	ALEP	1991–1995 LEP runs
0.999±0.098±0.045	22k	ABREU	00L	DLPH	1992–1995 runs
0.777±0.044±0.016	27k	ACKERSTAFF	99D	OPAL	1990–1995 LEP runs
0.69 ±0.06 ±0.06		[1] ALBRECHT	98	ARG	E^{ee}_{cm}= 9.5–10.6 GeV
0.54 ±0.28 ±0.14		ABE	97O	SLD	1993–1995 SLC runs
0.750±0.017±0.045	22k	ALEXANDER	97F	CLEO	E^{ee}_{cm}= 10.6 GeV
0.76 ±0.07 ±0.08	3230	ALBRECHT	93G	ARG	E^{ee}_{cm}= 9.4–10.6 GeV
0.734±0.055±0.027	3041	ALBRECHT	90E	ARG	E^{ee}_{cm}= 9.4–10.6 GeV
0.89 ±0.14 ±0.08	1909	FORD	87B	MAC	E^{ee}_{cm}= 29 GeV
0.81 ±0.13	727	BEHRENDS	85	CLEO	e^+e^- near $\Upsilon(4S)$
• • • We do not use the following data for averages, fits, limits, etc. • • •					
0.747±0.048±0.044	13k	AMMAR	97B	CLEO	Repl. by ALEXANDER 97F
0.693±0.057±0.028		BUSKULIC	95D	ALEP	Repl. by HEISTER 01E

[1] ALBRECHT 98 use tau pair events of the type $\tau^-\tau^+ \to (\ell^-\overline{\nu}_\ell\nu_\tau)(\pi^+\pi^0\overline{\nu}_\tau)$, and their charged conjugates.

$\xi(e \text{ or } \mu)$ PARAMETER

($V-A$) theory predicts $\xi = 1$.

VALUE	EVTS	DOCUMENT ID		TECN	COMMENT
0.985±0.030 OUR FIT					
0.981±0.031 OUR AVERAGE					
0.986±0.068±0.031	81k	HEISTER	01E	ALEP	1991–1995 LEP runs
0.929±0.070±0.030	36k	ABREU	00L	DLPH	1992–1995 runs
0.98 ±0.22 ±0.10	46k	ACKERSTAFF	99D	OPAL	1990–1995 LEP runs
0.70 ±0.16	54k	ACCIARRI	98R	L3	1991–1995 LEP runs
1.03 ±0.11		[1] ALBRECHT	98	ARG	E^{ee}_{cm}= 9.5–10.6 GeV
1.05 ±0.35 ±0.04		[2] ABE	97O	SLD	1993–1995 SLC runs
1.007±0.040±0.015	55k	ALEXANDER	97F	CLEO	E^{ee}_{cm}= 10.6 GeV
• • • We do not use the following data for averages, fits, limits, etc. • • •					
0.94 ±0.21 ±0.07	18k	ACCIARRI	96H	L3	Repl. by ACCIARRI 98R
0.97 ±0.14		[3] ALBRECHT	95C	ARG	Repl. by ALBRECHT 98
1.18 ±0.15 ±0.16		BUSKULIC	95D	ALEP	Repl. by HEISTER 01E
0.90 ±0.15 ±0.10	3230	[4] ALBRECHT	93G	ARG	E^{ee}_{cm}= 9.4–10.6 GeV

[1] Combined fit to ARGUS tau decay parameter measurements in ALBRECHT 98, ALBRECHT 95C, ALBRECHT 93G, and ALBRECHT 94E. ALBRECHT 98 use tau pair events of the type $\tau^-\tau^+ \to (\ell^-\overline{\nu}_\ell\nu_\tau)(\pi^+\pi^0\overline{\nu}_\tau)$, and their charged conjugates.

[2] ABE 97O assume $\eta = 0$ in their fit. Letting η vary in the fit gives a ξ value of 1.02 ± 0.36 ± 0.05.

[3] Combined fit to ARGUS tau decay parameter measurements in ALBRECHT 95C, ALBRECHT 93G, and ALBRECHT 94E. ALBRECHT 95C uses events of the type $\tau^-\tau^+ \to (\ell^-\overline{\nu}_\ell\nu_\tau)(h^+h^-h^+\overline{\nu}_\tau)$ and their charged conjugates.

[4] ALBRECHT 93G measurement determines $|\xi|$ for the case $\xi(e) = \xi(\mu)$, but the authors point out that other LEP experiments determine the sign to be positive.

$\xi(e)$ PARAMETER

($V-A$) theory predicts $\xi = 1$.

VALUE	EVTS	DOCUMENT ID		TECN	COMMENT
0.994±0.040 OUR FIT					
1.00 ±0.04 OUR AVERAGE					
1.011±0.094±0.038	44k	HEISTER	01E	ALEP	1991–1995 LEP runs
1.01 ±0.12 ±0.05	17k	ABREU	00L	DLPH	1992–1995 runs
1.13 ±0.39 ±0.14	25k	ACKERSTAFF	99D	OPAL	1990–1995 LEP runs
1.11 ±0.20 ±0.08		[1] ALBRECHT	98	ARG	E^{ee}_{cm}= 9.5–10.6 GeV
1.16 ±0.52 ±0.06		ABE	97O	SLD	1993–1995 SLC runs
0.979±0.048±0.016	34k	ALEXANDER	97F	CLEO	E^{ee}_{cm}= 10.6 GeV
• • • We do not use the following data for averages, fits, limits, etc. • • •					
1.03 ±0.23 ±0.09		BUSKULIC	95D	ALEP	Repl. by HEISTER 01E

[1] ALBRECHT 98 use tau pair events of the type $\tau^-\tau^+ \to (\ell^-\overline{\nu}_\ell\nu_\tau)(\pi^+\pi^0\overline{\nu}_\tau)$, and their charged conjugates.

$\xi(\mu)$ PARAMETER

($V-A$) theory predicts $\xi = 1$.

VALUE	EVTS	DOCUMENT ID		TECN	COMMENT
1.030±0.059 OUR FIT					
1.06 ±0.06 OUR AVERAGE					
1.030±0.120±0.050	46k	HEISTER	01E	ALEP	1991–1995 LEP runs
1.16 ±0.19 ±0.06	22k	ABREU	00L	DLPH	1992–1995 runs
0.79 ±0.41 ±0.09	27k	ACKERSTAFF	99D	OPAL	1990–1995 LEP runs
1.26 ±0.27 ±0.14		[1] ALBRECHT	98	ARG	E^{ee}_{cm}= 9.5–10.6 GeV
0.75 ±0.50 ±0.14		ABE	97O	SLD	1993–1995 SLC runs
1.054±0.069±0.047	22k	ALEXANDER	97F	CLEO	E^{ee}_{cm}= 10.6 GeV
• • • We do not use the following data for averages, fits, limits, etc. • • •					
1.23 ±0.22 ±0.10		BUSKULIC	95D	ALEP	Repl. by HEISTER 01E

[1] ALBRECHT 98 use tau pair events of the type $\tau^-\tau^+ \to (\ell^-\overline{\nu}_\ell\nu_\tau)(\pi^+\pi^0\overline{\nu}_\tau)$, and their charged conjugates.

$\eta(e \text{ or } \mu)$ PARAMETER

($V-A$) theory predicts $\eta = 0$.

VALUE	EVTS	DOCUMENT ID		TECN	COMMENT
0.013±0.020 OUR FIT					
0.015±0.021 OUR AVERAGE					
0.012±0.026±0.004	81k	HEISTER	01E	ALEP	1991–1995 LEP runs
−0.005±0.036±0.037		ABREU	00L	DLPH	1992–1995 runs
0.027±0.055±0.005	46k	ACKERSTAFF	99D	OPAL	1990–1995 LEP runs
0.27 ±0.14	54k	ACCIARRI	98R	L3	1991–1995 LEP runs
−0.13 ±0.47 ±0.15		ABE	97O	SLD	1993–1995 SLC runs
−0.015±0.061±0.062	31k	AMMAR	97B	CLEO	$E^{ee}_{\rm cm}$= 10.6 GeV
0.03 ±0.18 ±0.12	8.2k	ALBRECHT	95	ARG	$E^{ee}_{\rm cm}$= 9.5–10.6 GeV
• • • We do not use the following data for averages, fits, limits, etc. • • •					
0.25 ±0.17 ±0.11	18k	ACCIARRI	96H	L3	Repl. by ACCIARRI 98R
−0.04 ±0.15 ±0.11		BUSKULIC	95D	ALEP	Repl. by HEISTER 01E

$\eta(\mu)$ PARAMETER

($V-A$) theory predicts $\eta = 0$.

VALUE	EVTS	DOCUMENT ID		TECN	COMMENT
0.094±0.073 OUR FIT					
0.17 ±0.15 OUR AVERAGE Error includes scale factor of 1.2.					
0.160±0.150±0.060	46k	HEISTER	01E	ALEP	1991–1995 LEP runs
0.72 ±0.32 ±0.15		ABREU	00L	DLPH	1992–1995 runs
−0.59 ±0.82 ±0.45		[1] ABE	97O	SLD	1993–1995 SLC runs
0.010±0.149±0.171	13k	[2] AMMAR	97B	CLEO	$E^{ee}_{\rm cm}$= 10.6 GeV
• • • We do not use the following data for averages, fits, limits, etc. • • •					
0.010±0.065±0.001	27k	[3] ACKERSTAFF	99D	OPAL	1990–1995 LEP runs
−0.24 ±0.23 ±0.18		BUSKULIC	95D	ALEP	Repl. by HEISTER 01E

[1] Highly correlated (corr. = 0.92) with ABE 97O $\rho(\mu)$ measurement.
[2] Highly correlated (corr. = 0.949) with AMMAR 97B $\rho(\mu)$ value.
[3] ACKERSTAFF 99D result is dominated by a constraint on η from the OPAL measurements of the τ lifetime and B($\tau^- \to \mu^- \overline{\nu}_\mu \nu_\tau$) assuming lepton universality for the total coupling strength.

$(\delta\xi)(e \text{ or } \mu)$ PARAMETER

($V-A$) theory predicts $(\delta\xi) = 0.75$.

VALUE	EVTS	DOCUMENT ID		TECN	COMMENT
0.746±0.021 OUR FIT					
0.744±0.022 OUR AVERAGE					
0.776±0.045±0.024	81k	HEISTER	01E	ALEP	1991–1995 LEP runs
0.779±0.070±0.028	36k	ABREU	00L	DLPH	1992–1995 runs
0.65 ±0.14 ±0.07	46k	ACKERSTAFF	99D	OPAL	1990–1995 LEP runs
0.70 ±0.11	54k	ACCIARRI	98R	L3	1991–1995 LEP runs
0.63 ±0.09		[1] ALBRECHT	98	ARG	$E^{ee}_{\rm cm}$= 9.5–10.6 GeV
0.88 ±0.27 ±0.04		[2] ABE	97O	SLD	1993–1995 SLC runs
0.745±0.026±0.009	55k	ALEXANDER	97F	CLEO	$E^{ee}_{\rm cm}$= 10.6 GeV
• • • We do not use the following data for averages, fits, limits, etc. • • •					
0.81 ±0.14 ±0.06	18k	ACCIARRI	96H	L3	Repl. by ACCIARRI 98R
0.65 ±0.12		[3] ALBRECHT	95C	ARG	Repl. by ALBRECHT 98
0.88 ±0.11 ±0.07		BUSKULIC	95D	ALEP	Repl. by HEISTER 01E

[1] Combined fit to ARGUS tau decay parameter measurements in ALBRECHT 98, ALBRECHT 95C, ALBRECHT 93G, and ALBRECHT 94E. ALBRECHT 98 use tau pair events of the type $\tau^-\tau^+ \to (\ell^- \overline{\nu}_\ell \nu_\tau)(\pi^+\pi^0\overline{\nu}_\tau)$, and their charged conjugates.
[2] ABE 97O assume $\eta = 0$ in their fit. Letting η vary in the fit gives a $(\delta\xi)$ value of 0.87 ± 0.27 ± 0.04.
[3] Combined fit to ARGUS tau decay parameter measurements in ALBRECHT 95C, ALBRECHT 93G, and ALBRECHT 94E. ALBRECHT 95C uses events of the type $\tau^-\tau^+ \to (\ell^- \overline{\nu}_\ell \nu_\tau)\ (h^+h^-h^+\overline{\nu}_\tau)$ and their charged conjugates.

$(\delta\xi)(e)$ PARAMETER

($V-A$) theory predicts $(\delta\xi) = 0.75$.

VALUE	EVTS	DOCUMENT ID		TECN	COMMENT
0.734±0.028 OUR FIT					
0.731±0.029 OUR AVERAGE					
0.778±0.066±0.024	44k	HEISTER	01E	ALEP	1991–1995 LEP runs
0.85 ±0.12 ±0.04	17k	ABREU	00L	DLPH	1992–1995 runs
0.72 ±0.31 ±0.14	25k	ACKERSTAFF	99D	OPAL	1990–1995 LEP runs
0.56 ±0.14 ±0.06		[1] ALBRECHT	98	ARG	$E^{ee}_{\rm cm}$= 9.5–10.6 GeV
0.85 ±0.43 ±0.08		ABE	97O	SLD	1993–1995 SLC runs
0.720±0.032±0.010	34k	ALEXANDER	97F	CLEO	$E^{ee}_{\rm cm}$= 10.6 GeV
• • • We do not use the following data for averages, fits, limits, etc. • • •					
1.11 ±0.17 ±0.07		BUSKULIC	95D	ALEP	Repl. by HEISTER 01E

[1] ALBRECHT 98 use tau pair events of the type $\tau^-\tau^+ \to (\ell^- \overline{\nu}_\ell \nu_\tau)(\pi^+\pi^0\overline{\nu}_\tau)$, and their charged conjugates.

$(\delta\xi)(\mu)$ PARAMETER

($V-A$) theory predicts $(\delta\xi) = 0.75$.

VALUE	EVTS	DOCUMENT ID		TECN	COMMENT
0.778±0.037 OUR FIT					
0.79 ±0.04 OUR AVERAGE					
0.786±0.066±0.028	46k	HEISTER	01E	ALEP	1991–1995 LEP runs
0.86 ±0.13 ±0.04	22k	ABREU	00L	DLPH	1992–1995 runs
0.63 ±0.23 ±0.05	27k	ACKERSTAFF	99D	OPAL	1990–1995 LEP runs
0.73 ±0.18 ±0.10		[1] ALBRECHT	98	ARG	$E^{ee}_{\rm cm}$= 9.5–10.6 GeV
0.82 ±0.32 ±0.07		ABE	97O	SLD	1993–1995 SLC runs
0.786±0.041±0.032	22k	ALEXANDER	97F	CLEO	$E^{ee}_{\rm cm}$= 10.6 GeV
• • • We do not use the following data for averages, fits, limits, etc. • • •					
0.71 ±0.14 ±0.06		BUSKULIC	95D	ALEP	Repl. by HEISTER 01E

[1] ALBRECHT 98 use tau pair events of the type $\tau^-\tau^+ \to (\ell^- \overline{\nu}_\ell \nu_\tau)(\pi^+\pi^0\overline{\nu}_\tau)$, and their charged conjugates.

$\xi(\pi)$ PARAMETER

($V-A$) theory predicts $\xi(\pi) = 1$.

VALUE	EVTS	DOCUMENT ID		TECN	COMMENT
0.993±0.022 OUR FIT					
0.994±0.023 OUR AVERAGE					
0.994±0.020±0.014	27k	HEISTER	01E	ALEP	1991–1995 LEP runs
0.81 ±0.17 ±0.02		ABE	97O	SLD	1993–1995 SLC runs
1.03 ±0.06 ±0.04	2.0k	COAN	97	CLEO	$E^{ee}_{\rm cm}$= 10.6 GeV
• • • We do not use the following data for averages, fits, limits, etc. • • •					
0.987±0.057±0.027		BUSKULIC	95D	ALEP	Repl. by HEISTER 01E
0.95 ±0.11 ±0.05		[1] BUSKULIC	94D	ALEP	1990+1991 LEP run

[1] Superseded by BUSKULIC 95D.

$\xi(\rho)$ PARAMETER

($V-A$) theory predicts $\xi(\rho) = 1$.

VALUE	EVTS	DOCUMENT ID		TECN	COMMENT
0.994±0.008 OUR FIT					
0.994±0.009 OUR AVERAGE					
0.987±0.012±0.011	59k	HEISTER	01E	ALEP	1991–1995 LEP runs
0.99 ±0.12 ±0.04		ABE	97O	SLD	1993–1995 SLC runs
0.995±0.010±0.003	66k	ALEXANDER	97F	CLEO	$E^{ee}_{\rm cm}$= 10.6 GeV
1.022±0.028±0.030	1.7k	[1] ALBRECHT	94E	ARG	$E^{ee}_{\rm cm}$= 9.4–10.6 GeV
• • • We do not use the following data for averages, fits, limits, etc. • • •					
1.045±0.058±0.032		BUSKULIC	95D	ALEP	Repl. by HEISTER 01E
1.03 ±0.11 ±0.05		[2] BUSKULIC	94D	ALEP	1990+1991 LEP run

[1] ALBRECHT 94E measure the square of this quantity and use the sign determined by ALBRECHT 90I to obtain the quoted result.
[2] Superseded by BUSKULIC 95D.

$\xi(a_1)$ PARAMETER

($V-A$) theory predicts $\xi(a_1) = 1$.

VALUE	EVTS	DOCUMENT ID		TECN	COMMENT
1.001±0.027 OUR FIT					
1.002±0.028 OUR AVERAGE					
1.000±0.016±0.024	35k	[1] HEISTER	01E	ALEP	1991–1995 LEP runs
1.02 ±0.13 ±0.03	17.2k	ASNER	00	CLEO	$E^{ee}_{\rm cm}$= 10.6 GeV
1.29 ±0.26 ±0.11	7.4k	[2] ACKERSTAFF	97R	OPAL	1992–1994 LEP runs
0.85 $^{+0.15}_{-0.17}$ ±0.05		ALBRECHT	95C	ARG	$E^{ee}_{\rm cm}$= 9.5–10.6 GeV
1.25 ±0.23 $^{+0.15}_{-0.08}$	7.5k	ALBRECHT	93C	ARG	$E^{ee}_{\rm cm}$= 9.4–10.6 GeV
• • • We do not use the following data for averages, fits, limits, etc. • • •					
1.08 $^{+0.46}_{-0.41}$ $^{+0.14}_{-0.25}$	2.6k	[3] AKERS	95P	OPAL	Repl. by ACKERSTAFF 97R
0.937±0.116±0.064		BUSKULIC	95D	ALEP	Repl. by HEISTER 01E

[1] HEISTER 01E quote 1.000 ± 0.016 ± 0.013 ± 0.020 where the errors are statistical, systematic, and an uncertainty due to the final state model. We combine the systematic error and model uncertainty.
[2] ACKERSTAFF 97R obtain this result with a model independent fit to the hadronic structure functions. Fitting with the model of Kuhn and Santamaria (ZPHY **C48**, 445 (1990)) gives 0.87 ± 0.16 ± 0.04, and with the model of of Isgur *et al.* (PR **D39**,1357 (1989)) they obtain 1.20 ± 0.21 ± 0.14.
[3] AKERS 95P obtain this result with a model independent fit to the hadronic structure functions. Fitting with the model of Kuhn and Santamaria (ZPHY **C48**, 445 (1990)) gives 0.87 ± 0.27 $^{+0.05}_{-0.06}$, and with the model of of Isgur *et al.* (PR **D39**,1357 (1989)) they obtain 1.10 ± 0.31 $^{+0.13}_{-0.14}$.

ξ(all hadronic modes) PARAMETER

($V-A$) theory predicts $\xi = 1$.

VALUE	EVTS	DOCUMENT ID		TECN	COMMENT
0.995±0.007 OUR FIT					
0.997±0.007 OUR AVERAGE					
0.992±0.007±0.008	102k	[1] HEISTER	01E	ALEP	1991–1995 LEP runs
0.997±0.027±0.011	39k	[2] ABREU	00L	DLPH	1992–1995 runs
1.02 ±0.13 ±0.03	17.2k	[3] ASNER	00	CLEO	$E^{ee}_{\rm cm}$= 10.6 GeV
1.032±0.031	37k	[4] ACCIARRI	98R	L3	1991–1995 LEP runs
0.93 ±0.10 ±0.04		ABE	97O	SLD	1993–1995 SLC runs
1.29 ±0.26 ±0.11	7.4k	[5] ACKERSTAFF	97R	OPAL	1992–1994 LEP runs
0.995±0.010±0.003	66k	[6] ALEXANDER	97F	CLEO	$E^{ee}_{\rm cm}$= 10.6 GeV
1.03 ±0.06 ±0.04	2.0k	[7] COAN	97	CLEO	$E^{ee}_{\rm cm}$= 10.6 GeV
1.017±0.039		[8] ALBRECHT	95C	ARG	$E^{ee}_{\rm cm}$= 9.5–10.6 GeV
1.25 ±0.23 $^{+0.15}_{-0.08}$	7.5k	[9] ALBRECHT	93C	ARG	$E^{ee}_{\rm cm}$= 9.4–10.6 GeV
• • • We do not use the following data for averages, fits, limits, etc. • • •					
0.970±0.053±0.011	14k	[10] ACCIARRI	96H	L3	Repl. by ACCIARRI 98R
1.08 $^{+0.46}_{-0.41}$ $^{+0.14}_{-0.25}$	2.6k	[11] AKERS	95P	OPAL	Repl. by ACKERSTAFF 97R
1.006±0.032±0.019		[12] BUSKULIC	95D	ALEP	Repl. by HEISTER 01E
1.022±0.028±0.030	1.7k	[13] ALBRECHT	94E	ARG	$E^{ee}_{\rm cm}$= 9.4–10.6 GeV
0.99 ±0.07 ±0.04		[14] BUSKULIC	94D	ALEP	1990+1991 LEP run

[1] HEISTER 01E quote $0.992 \pm 0.007 \pm 0.006 \pm 0.005$ where the errors are statistical, systematic, and an uncertainty due to the final state model. We combine the systematic error and model uncertainty. They use $\tau \to \pi\nu_\tau$, $\tau \to K\nu_\tau$, $\tau \to \rho\nu_\tau$, and $\tau \to a_1\nu_\tau$ decays.

[2] ABREU 00L use $\tau^- \to h^- \geq 0\pi^0\nu_\tau$ decays.

[3] ASNER 00 use $\tau^- \to \pi^- 2\pi^0\nu_\tau$ decays.

[4] ACCIARRI 98R use $\tau \to \pi\nu_\tau$, $\tau \to K\nu_\tau$, and $\tau \to \rho\nu_\tau$ decays.

[5] ACKERSTAFF 97R use $\tau \to a_1\nu_\tau$ decays.

[6] ALEXANDER 97F use $\tau \to \rho\nu_\tau$ decays.

[7] COAN 97 use h^+h^- energy correlations.

[8] Combined fit to ARGUS tau decay parameter measurements in ALBRECHT 95C, ALBRECHT 93G, and ALBRECHT 94E.

[9] Uses $\tau \to a_1\nu_\tau$ decays. Replaced by ALBRECHT 95C.

[10] ACCIARRI 96H use $\tau \to \pi\nu_\tau$, $\tau \to K\nu_\tau$, and $\tau \to \rho\nu_\tau$ decays.

[11] AKERS 95P use $\tau \to a_1\nu_\tau$ decays.

[12] BUSKULIC 95D use $\tau \to \pi\nu_\tau$, $\tau \to \rho\nu_\tau$, and $\tau \to a_1\nu_\tau$ decays.

[13] ALBRECHT 94E measure the square of this quantity and use the sign determined by ALBRECHT 90I to obtain the quoted result. Uses $\tau \to a_1\nu_\tau$ decays. Replaced by ALBRECHT 95C.

[14] BUSKULIC 94D use $\tau \to \pi\nu_\tau$ and $\tau \to \rho\nu_\tau$ decays. Superseded by BUSKULIC 95D.

τ REFERENCES

BELOUS	14	PRL 112 031801	K. Belous *et al.*	(BELLE Collab.)
AAIJ	13AH	PL B724 36	R. Aaij *et al.*	(LHCb Collab.)
MIYAZAKI	13	PL B719 346	Y. Miyazaki *et al.*	(BELLE Collab.)
LEES	12M	PR D85 031102	J.P. Lees *et al.*	(BABAR Collab.)
Also		PR D85 099904 (errat)	J.P. Lees *et al.*	(BABAR Collab.)
LEES	12X	PR D86 092010	J.P. Lees *et al.*	(BABAR Collab.)
LEES	12Y	PR D86 092013	J.P. Lees *et al.*	(BABAR Collab.)
PDG	12	PR D86 010001	J. Beringer *et al.*	(PDG Collab.)
DEL-AMO-SA...	11E	PR D83 032002	P. del Amo Sanchez *et al.*	(BABAR Collab.)
MIYAZAKI	11	PL B699 251	Y. Miyazaki *et al.*	(BELLE Collab.)
AUBERT	10B	PRL 104 021802	B. Aubert *et al.*	(BABAR Collab.)
AUBERT	10F	PRL 105 051602	B. Aubert *et al.*	(BABAR Collab.)
HAYASAKA	10	PL B687 139	K. Hayasaka *et al.*	(BELLE Collab.)
LEE	10	PR D81 113007	M.J. Lee *et al.*	(BELLE Collab.)
LEES	10A	PR D81 111101	J.P. Lees *et al.*	(BABAR Collab.)
MIYAZAKI	10	PL B682 355	Y. Miyazaki *et al.*	(BELLE Collab.)
MIYAZAKI	10A	PL B692 4	Y. Miyazaki *et al.*	(BELLE Collab.)
AUBERT	09AK	PR D80 092005	B. Aubert *et al.*	(BABAR Collab.)
AUBERT	09D	PR D79 012004	B. Aubert *et al.*	(BABAR Collab.)
AUBERT	09W	PRL 103 021801	B. Aubert *et al.*	(BABAR Collab.)
GROZIN	09A	PAN 72 1203	A.G. Grozin, I.B. Khriplovich, A.S. Rudenko	(NOVO)
INAMI	09	PL B672 209	K. Inami *et al.*	(BELLE Collab.)
MIYAZAKI	09	PL B672 317	Y. Miyazaki *et al.*	(BELLE Collab.)
AUBERT	08	PRL 100 011801	B. Aubert *et al.*	(BABAR Collab.)
AUBERT	08AE	PR D77 112002	B. Aubert *et al.*	(BABAR Collab.)
AUBERT	08K	PRL 100 071802	B. Aubert *et al.*	(BABAR Collab.)
FUJIKAWA	08	PR D78 072006	M. Fujikawa *et al.*	(BELLE Collab.)
HAYASAKA	08	PL B666 16	K. Hayasaka *et al.*	(BELLE Collab.)
MIYAZAKI	08	PL B660 154	Y. Miyazaki *et al.*	(BELLE Collab.)
NISHIO	08	PL B664 35	Y. Nishio *et al.*	(BELLE Collab.)
ANASHIN	07	JETPL 85 347	V.V. Anashin *et al.*	(KEDR Collab.)
		Translated from ZETFP 85 429.		
AUBERT	07AP	PR D76 051104	B. Aubert *et al.*	(BABAR Collab.)
AUBERT	07BK	PRL 99 251803	B. Aubert *et al.*	(BABAR Collab.)
AUBERT	07I	PRL 98 061803	B. Aubert *et al.*	(BABAR Collab.)
BELOUS	07	PRL 99 011801	K. Belous *et al.*	(BELLE Collab.)
EIDELMAN	07	MPL A22 159	S. Eidelman, M. Passera	(NOVO, PADO)
EPIFANOV	07	PL B654 65	D. Epifanov *et al.*	(BELLE Collab.)
MIYAZAKI	07	PL B648 341	Y. Miyazaki *et al.*	(BELLE Collab.)
ABDALLAH	06A	EPJ C46 1	J. Abdallah *et al.*	(DELPHI Collab.)
AUBERT	06C	PRL 96 041801	B. Aubert *et al.*	(BABAR Collab.)
AUBERT,B	06	PR D73 112003	B. Aubert *et al.*	(BABAR Collab.)
INAMI	06	PL B643 5	K. Inami *et al.*	(BELLE Collab.)
MIYAZAKI	06	PL B632 51	Y. Miyazaki *et al.*	(BELLE Collab.)
MIYAZAKI	06A	PL B639 159	Y. Miyazaki *et al.*	(BELLE Collab.)
PDG	06	JP G33 1	W.-M. Yao *et al.*	(PDG Collab.)
YUSA	06	PL B640 138	Y. Yusa *et al.*	(BELLE Collab.)
ARMS	05	PRL 94 241802	K. Arms *et al.*	(CLEO Collab.)
AUBERT,B	05A	PRL 95 041802	B. Aubert *et al.*	(BABAR Collab.)
AUBERT,B	05F	PR D72 012003	B. Aubert *et al.*	(BABAR Collab.)
AUBERT,B	05W	PR D72 072001	B. Aubert *et al.*	(BABAR Collab.)
AUBERT,BE	05D	PRL 95 191801	B. Aubert *et al.*	(BABAR Collab.)
ENARI	05	PL B622 218	Y. Enari *et al.*	(BELLE Collab.)
HAYASAKA	05	PL B613 20	K. Hayasaka *et al.*	(BELLE Collab.)
SCHAEL	05C	PRPL 421 191	S. Schael *et al.*	(ALEPH Collab.)
ABBIENDI	04J	EPJ C35 437	G. Abbiendi *et al.*	(OPAL Collab.)
ABDALLAH	04K	EPJ C35 159	J. Abdallah *et al.*	(DELPHI Collab.)
ABDALLAH	04T	EPJ C36 283	J. Abdallah *et al.*	(DELPHI Collab.)
ABE	04B	PRL 92 171802	K. Abe *et al.*	(BELLE Collab.)
ACHARD	04G	PL B585 53	P. Achard *et al.*	(L3 Collab.)
AUBERT	04J	PRL 92 121801	B. Aubert *et al.*	(BABAR Collab.)
ENARI	04	PRL 93 081803	Y. Enari *et al.*	(BELLE Collab.)
PDG	04	PL B592 1	S. Eidelman *et al.*	(PDG Collab.)
YUSA	04	PL B589 103	Y. Yusa *et al.*	(BELLE Collab.)
ABBIENDI	03	PL B551 35	G. Abbiendi *et al.*	(OPAL Collab.)
BRIERE	03	PRL 90 181802	R. A. Briere *et al.*	(CLEO Collab.)
HEISTER	03F	EPJ C30 291	A. Heister *et al.*	(ALEPH Collab.)
INAMI	03	PL B551 16	K. Inami *et al.*	(BELLE Collab.)
CHEN	02C	PR D66 071101	S. Chen *et al.*	(CLEO Collab.)
REGAN	02	PRL 88 071805	B.C. Regan *et al.*	
ABBIENDI	01J	EPJ C19 653	G. Abbiendi *et al.*	(OPAL Collab.)
ABREU	01M	EPJ C20 617	P. Abreu *et al.*	(DELPHI Collab.)
ACCIARRI	01F	PL B507 47	M. Acciarri *et al.*	(L3 Collab.)
ACHARD	01D	PL B519 189	P. Achard *et al.*	(L3 Collab.)
ANASTASSOV	01	PRL 86 4467	A. Anastassov *et al.*	(CLEO Collab.)
HEISTER	01E	EPJ C22 217	A. Heister *et al.*	(ALEPH Collab.)
ABBIENDI	00A	PL B492 23	G. Abbiendi *et al.*	(OPAL Collab.)
ABBIENDI	00C	EPJ C13 213	G. Abbiendi *et al.*	(OPAL Collab.)
ABBIENDI	00D	EPJ C13 197	G. Abbiendi *et al.*	(OPAL Collab.)
ABREU	00L	EPJ C16 229	P. Abreu *et al.*	(DELPHI Collab.)
ACCIARRI	00B	PL B479 67	M. Acciarri *et al.*	(L3 Collab.)
AHMED	00	PR D61 071101	S. Ahmed *et al.*	(CLEO Collab.)
ALBRECHT	00	PL B485 37	H. Albrecht *et al.*	(ARGUS Collab.)
ASNER	00	PR D61 012002	D.M. Asner *et al.*	(CLEO Collab.)
ASNER	00B	PR D62 072006	D.M. Asner *et al.*	(CLEO Collab.)
BERGFELD	00	PRL 84 830	T. Bergfeld *et al.*	(CLEO Collab.)
BROWDER	00	PR D61 052004	T.E. Browder *et al.*	(CLEO Collab.)
EDWARDS	00A	PR D61 072003	K.W. Edwards *et al.*	(CLEO Collab.)
GONZALEZ-S...	00	NP B582 3	G.A. Gonzalez-Sprinberg *et al.*	
ABBIENDI	99H	PL B447 134	G. Abbiendi *et al.*	(OPAL Collab.)
ABREU	99X	EPJ C10 201	P. Abreu *et al.*	(DELPHI Collab.)
ACKERSTAFF	99D	EPJ C8 3	K. Ackerstaff *et al.*	(OPAL Collab.)
ACKERSTAFF	99E	EPJ C8 183	K. Ackerstaff *et al.*	(OPAL Collab.)
BARATE	99K	EPJ C10 1	R. Barate *et al.*	(ALEPH Collab.)
BARATE	99R	EPJ C11 599	R. Barate *et al.*	(ALEPH Collab.)
BISHAI	99	PRL 82 281	M. Bishai *et al.*	(CLEO Collab.)
GODANG	99	PR D59 091303	R. Godang *et al.*	(CLEO Collab.)
RICHICHI	99	PR D60 112002	S.J. Richichi *et al.*	(CLEO Collab.)
ACCIARRI	98C	PL B426 207	M. Acciarri *et al.*	(L3 Collab.)
ACCIARRI	98E	PL B434 169	M. Acciarri *et al.*	(L3 Collab.)
ACCIARRI	98R	PL B438 405	M. Acciarri *et al.*	(L3 Collab.)
ACKERSTAFF	98M	EPJ C4 193	K. Ackerstaff *et al.*	(OPAL Collab.)
ACKERSTAFF	98N	PL B431 188	K. Ackerstaff *et al.*	(OPAL Collab.)
ALBRECHT	98	PL B431 179	H. Albrecht *et al.*	(ARGUS Collab.)
BARATE	98	EPJ C1 65	R. Barate *et al.*	(ALEPH Collab.)
BARATE	98E	EPJ C4 29	R. Barate *et al.*	(ALEPH Collab.)
BLISS	98	PR D57 5903	D.W. Bliss *et al.*	(CLEO Collab.)
ABE	97O	PRL 78 4691	K. Abe *et al.*	(SLD Collab.)
ACKERSTAFF	97J	PL B404 213	K. Ackerstaff *et al.*	(OPAL Collab.)
ACKERSTAFF	97L	ZPHY C74 403	K. Ackerstaff *et al.*	(OPAL Collab.)
ACKERSTAFF	97R	ZPHY C75 593	K. Ackerstaff *et al.*	(OPAL Collab.)
ALEXANDER	97F	PR D56 5320	J.P. Alexander *et al.*	(CLEO Collab.)
AMMAR	97B	PRL 78 4686	R. Ammar *et al.*	(CLEO Collab.)
ANASTASSOV	97	PR D55 2559	A. Anastassov *et al.*	(CLEO Collab.)
Also		PR D58 119903 (erratum)	A. Anastassov *et al.*	(CLEO Collab.)
ANDERSON	97	PRL 79 3814	S. Anderson *et al.*	(CLEO Collab.)
AVERY	97	PR D55 R1119	P. Avery *et al.*	(CLEO Collab.)
BARATE	97I	ZPHY C74 387	R. Barate *et al.*	(ALEPH Collab.)
BARATE	97R	PL B414 362	R. Barate *et al.*	(ALEPH Collab.)
BERGFELD	97	PRL 79 2406	T. Bergfeld *et al.*	(CLEO Collab.)
BONVICINI	97	PRL 79 1221	G. Bonvicini *et al.*	(CLEO Collab.)
BUSKULIC	97C	ZPHY C74 263	D. Buskulic *et al.*	(ALEPH Collab.)
COAN	97	PR D55 7291	T.E. Coan *et al.*	(CLEO Collab.)
EDWARDS	97	PR D55 R3919	K.W. Edwards *et al.*	(CLEO Collab.)
EDWARDS	97B	PR D56 R5297	K.W. Edwards *et al.*	(CLEO Collab.)
ESCRIBANO	97	PL B395 369	R. Escribano, E. Masso	(BARC, PARIT)
ABREU	96B	PL B365 448	P. Abreu *et al.*	(DELPHI Collab.)
ACCIARRI	96H	PL B377 313	M. Acciarri *et al.*	(L3 Collab.)
ACCIARRI	96K	PL B389 187	M. Acciarri *et al.*	(L3 Collab.)
ALAM	96	PRL 76 2637	M.S. Alam *et al.*	(CLEO Collab.)
ALBRECHT	96E	PRPL 276 223	H. Albrecht *et al.*	(ARGUS Collab.)
ALEXANDER	96D	PL B369 163	G. Alexander *et al.*	(OPAL Collab.)
ALEXANDER	96E	PL B374 341	G. Alexander *et al.*	(OPAL Collab.)
ALEXANDER	96S	PL B388 437	G. Alexander *et al.*	(OPAL Collab.)
BAI	96	PR D53 20	J.Z. Bai *et al.*	(BES Collab.)
BALEST	96	PL B388 402	R. Balest *et al.*	(CLEO Collab.)
BARTELT	96	PRL 76 4119	J.E. Bartelt *et al.*	(CLEO Collab.)
BUSKULIC	96	ZPHY C70 579	D. Buskulic *et al.*	(ALEPH Collab.)
BUSKULIC	96C	ZPHY C70 561	D. Buskulic *et al.*	(ALEPH Collab.)
COAN	96	PR D53 6037	T.E. Coan *et al.*	(CLEO Collab.)
ABE	95Y	PR D52 4828	K. Abe *et al.*	(SLD Collab.)
ABREU	95T	PL B357 715	P. Abreu *et al.*	(DELPHI Collab.)
ABREU	95U	PL B359 411	P. Abreu *et al.*	(DELPHI Collab.)
ACCIARRI	95	PL B345 93	M. Acciarri *et al.*	(L3 Collab.)
ACCIARRI	95F	PL B352 487	M. Acciarri *et al.*	(L3 Collab.)
AKERS	95F	ZPHY C66 31	R. Akers *et al.*	(OPAL Collab.)
AKERS	95I	ZPHY C66 543	R. Akers *et al.*	(OPAL Collab.)
AKERS	95P	ZPHY C67 45	R. Akers *et al.*	(OPAL Collab.)
AKERS	95Y	ZPHY C68 555	R. Akers *et al.*	(OPAL Collab.)
ALBRECHT	95	PL B341 441	H. Albrecht *et al.*	(ARGUS Collab.)
ALBRECHT	95C	PL B349 576	H. Albrecht *et al.*	(ARGUS Collab.)
ALBRECHT	95G	ZPHY C68 25	H. Albrecht *et al.*	(ARGUS Collab.)
ALBRECHT	95H	ZPHY C68 215	H. Albrecht *et al.*	(ARGUS Collab.)
BALEST	95C	PRL 75 3809	R. Balest *et al.*	(CLEO Collab.)
BERNABEU	95	NP B436 474	J. Bernabeu *et al.*	
BUSKULIC	95C	PL B346 371	D. Buskulic *et al.*	(ALEPH Collab.)
BUSKULIC	95D	PL B346 379	D. Buskulic *et al.*	(ALEPH Collab.)
Also		PL B363 265 (erratum)	D. Buskulic *et al.*	(ALEPH Collab.)
ABREU	94K	PL B334 435	P. Abreu *et al.*	(DELPHI Collab.)
AKERS	94E	PL B328 207	R. Akers *et al.*	(OPAL Collab.)
AKERS	94G	PL B339 278	R. Akers *et al.*	(OPAL Collab.)
ALBRECHT	94E	PL B337 383	H. Albrecht *et al.*	(ARGUS Collab.)
ARTUSO	94	PRL 72 3762	M. Artuso *et al.*	(CLEO Collab.)
BARTELT	94	PRL 73 1890	J.E. Bartelt *et al.*	(CLEO Collab.)
BATTLE	94	PRL 73 1079	M. Battle *et al.*	(CLEO Collab.)
BAUER	94	PR D50 R13	D.A. Bauer *et al.*	(TPC/2gamma Collab.)
BUSKULIC	94D	PL B321 168	D. Buskulic *et al.*	(ALEPH Collab.)
BUSKULIC	94E	PL B332 209	D. Buskulic *et al.*	(ALEPH Collab.)
BUSKULIC	94F	PL B332 219	D. Buskulic *et al.*	(ALEPH Collab.)
GIBAUT	94B	PRL 73 934	D. Gibaut *et al.*	(CLEO Collab.)
ADRIANI	93M	PRPL 236 1	O. Adriani *et al.*	(L3 Collab.)
ALBRECHT	93C	ZPHY C58 61	H. Albrecht *et al.*	(ARGUS Collab.)
ALBRECHT	93G	PL B316 608	H. Albrecht *et al.*	(ARGUS Collab.)
BALEST	93	PR D47 R3671	R. Balest *et al.*	(CLEO Collab.)
BEAN	93	PRL 70 138	A. Bean *et al.*	(CLEO Collab.)
BORTOLETTO	93	PRL 71 1791	D. Bortoletto *et al.*	(CLEO Collab.)
ESCRIBANO	93	PL B301 419	R. Escribano, E. Masso	(BARC)
PROCARIO	93	PRL 70 1207	M. Procario *et al.*	(CLEO Collab.)
ABREU	92N	ZPHY C55 555	P. Abreu *et al.*	(DELPHI Collab.)
ACTON	92F	PL B281 405	D.P. Acton *et al.*	(OPAL Collab.)
ACTON	92H	PL B288 373	P.D. Acton *et al.*	(OPAL Collab.)
AKERIB	92	PRL 69 3610	D.S. Akerib *et al.*	(CLEO Collab.)
Also		PRL 71 3395 (erratum)	D.S. Akerib *et al.*	(CLEO Collab.)
ALBRECHT	92D	ZPHY C53 367	H. Albrecht *et al.*	(ARGUS Collab.)
ALBRECHT	92K	ZPHY C55 179	H. Albrecht *et al.*	(ARGUS Collab.)
ALBRECHT	92M	PL B292 221	H. Albrecht *et al.*	(ARGUS Collab.)
ALBRECHT	92Q	ZPHY C56 339	H. Albrecht *et al.*	(ARGUS Collab.)
AMMAR	92	PR D45 3976	R. Ammar *et al.*	(CLEO Collab.)
ARTUSO	92	PRL 69 3278	M. Artuso *et al.*	(CLEO Collab.)
BAI	92	PRL 69 3021	J.Z. Bai *et al.*	(BES Collab.)
BATTLE	92	PL B291 488	M. Battle *et al.*	(CLEO Collab.)
BUSKULIC	92J	PL B297 459	D. Buskulic *et al.*	(ALEPH Collab.)
DECAMP	92C	ZPHY C54 211	D. Decamp *et al.*	(ALEPH Collab.)
ADEVA	91F	PL B265 451	B. Adeva *et al.*	(L3 Collab.)
ALBRECHT	91D	PL B260 259	H. Albrecht *et al.*	(ARGUS Collab.)
ALEXANDER	91D	PL B266 201	G. Alexander *et al.*	(OPAL Collab.)
ANTREASYAN	91	PL B259 216	D. Antreasyan *et al.*	(Crystal Ball Collab.)
GRIFOLS	91	PL B255 611	J.A. Grifols, A. Mendez	(BARC)
ABACHI	90	PR D41 1414	S. Abachi *et al.*	(HRS Collab.)
ALBRECHT	90E	PL B246 278	H. Albrecht *et al.*	(ARGUS Collab.)
ALBRECHT	90I	PL B250 164	H. Albrecht *et al.*	(ARGUS Collab.)
BEHREND	90	ZPHY C46 537	H.J. Behrend *et al.*	(CELLO Collab.)
BOWCOCK	90	PR D41 805	T.J.V. Bowcock *et al.*	(CLEO Collab.)
DELAGUILA	90	PL B252 116	F. del Aguila, M. Sher	(BARC, WILL)
GOLDBERG	90	PL B251 223	M. Goldberg *et al.*	(CLEO Collab.)
WU	90	PR D41 2339	D.Y. Wu *et al.*	(Mark II Collab.)
ABACHI	89B	PR D40 902	S. Abachi *et al.*	(HRS Collab.)
BEHREND	89B	PL B222 163	H.J. Behrend *et al.*	(CELLO Collab.)
JANSSEN	89	PL B228 273	H. Janssen *et al.*	(Crystal Ball Collab.)
KLEINWORT	89	ZPHY C42 7	C. Kleinwort *et al.*	(JADE Collab.)
ADEVA	88	PR D38 2665	B. Adeva *et al.*	(Mark-J Collab.)
ALBRECHT	88B	PL B202 149	H. Albrecht *et al.*	(ARGUS Collab.)

Lepton Particle Listings

τ, Heavy Charged Lepton Searches

ALBRECHT	88L	ZPHY C41 1	H. Albrecht *et al.*	(ARGUS Collab.)
ALBRECHT	88M	ZPHY C41 405	H. Albrecht *et al.*	(ARGUS Collab.)
AMIDEI	88	PR D37 1750	D. Amidei *et al.*	(Mark II Collab.)
BEHREND	88	PL B200 226	H.J. Behrend *et al.*	(CELLO Collab.)
BRAUNSCH...	88C	ZPHY C39 331	W. Braunschweig *et al.*	(TASSO Collab.)
KEH	88	PL B212 123	S. Keh *et al.*	(Crystal Ball Collab.)
TSCHIRHART	88	PL B205 407	R. Tschirhart *et al.*	(HRS Collab.)
ABACHI	87B	PL B197 291	S. Abachi *et al.*	(HRS Collab.)
ABACHI	87C	PRL 59 2519	S. Abachi *et al.*	(HRS Collab.)
ADLER	87B	PRL 59 1527	J. Adler *et al.*	(Mark III Collab.)
AIHARA	87B	PR D35 1553	H. Aihara *et al.*	(TPC Collab.)
AIHARA	87C	PRL 59 751	H. Aihara *et al.*	(TPC Collab.)
ALBRECHT	87L	PL B185 223	H. Albrecht *et al.*	(ARGUS Collab.)
ALBRECHT	87P	PL B199 580	H. Albrecht *et al.*	(ARGUS Collab.)
BAND	87	PL B198 297	H.R. Band *et al.*	(MAC Collab.)
BAND	87B	PRL 59 415	H.R. Band *et al.*	(MAC Collab.)
BARINGER	87	PRL 59 1993	P. Baringer *et al.*	(CLEO Collab.)
BEBEK	87C	PR D36 690	C. Bebek *et al.*	(CLEO Collab.)
BURCHAT	87	PR D35 27	P.R. Burchat *et al.*	(Mark II Collab.)
BYLSMA	87	PR D35 2269	B.G. Bylsma *et al.*	(HRS Collab.)
COFFMAN	87	PR D36 2185	D.M. Coffman *et al.*	(Mark III Collab.)
DERRICK	87	PL B189 260	M. Derrick *et al.*	(HRS Collab.)
FORD	87	PR D35 408	W.T. Ford *et al.*	(MAC Collab.)
FORD	87B	PR D36 1971	W.T. Ford *et al.*	(MAC Collab.)
GAN	87	PRL 59 411	K.K. Gan *et al.*	(Mark II Collab.)
GAN	87B	PL B197 561	K.K. Gan *et al.*	(Mark II Collab.)
AIHARA	86E	PRL 57 1836	H. Aihara *et al.*	(TPC Collab.)
BARTEL	86D	PL B182 216	W. Bartel *et al.*	(JADE Collab.)
PDG	86	PL 170B 1	M. Aguilar-Benitez *et al.*	(CERN, CIT+)
RUCKSTUHL	86	PRL 56 2132	W. Ruckstuhl *et al.*	(DELCO Collab.)
SCHMIDKE	86	PRL 57 527	W.B. Schmidke *et al.*	(Mark II Collab.)
YELTON	86	PRL 56 812	J.M. Yelton *et al.*	(Mark II Collab.)
ALTHOFF	85	ZPHY C26 521	M. Althoff *et al.*	(TASSO Collab.)
ASH	85B	PRL 55 2118	W.W. Ash *et al.*	(MAC Collab.)
BALTRUSAIT...	85	PRL 55 1842	R.M. Baltrusaitis *et al.*	(Mark III Collab.)
BARTEL	85F	PL 161B 188	W. Bartel *et al.*	(JADE Collab.)
BEHRENDS	85	PR D32 2468	S. Behrends *et al.*	(CLEO Collab.)
BELTRAMI	85	PRL 54 1775	I. Beltrami *et al.*	(HRS Collab.)
BERGER	85	ZPHY C28 1	C. Berger *et al.*	(PLUTO Collab.)
BURCHAT	85	PRL 54 2489	P.R. Burchat *et al.*	(Mark II Collab.)
FERNANDEZ	85	PRL 54 1624	E. Fernandez *et al.*	(MAC Collab.)
MILLS	85	PRL 54 624	G.B. Mills *et al.*	(DELCO Collab.)
AIHARA	84C	PR D30 2436	H. Aihara *et al.*	(TPC Collab.)
BEHREND	84	ZPHY C23 103	H.J. Behrend *et al.*	(CELLO Collab.)
MILLS	84	PRL 52 1944	G.B. Mills *et al.*	(DELCO Collab.)
BEHREND	83C	PL 127B 270	H.J. Behrend *et al.*	(CELLO Collab.)
SILVERMAN	83	PR D27 1196	D.J. Silverman, G.L. Shaw	(UCI)
BEHREND	82	PL 114B 282	H.J. Behrend *et al.*	(CELLO Collab.)
BLOCKER	82B	PRL 48 1586	C.A. Blocker *et al.*	(Mark II Collab.)
BLOCKER	82D	PL 109B 119	C.A. Blocker *et al.*	(Mark II Collab.) J
FELDMAN	82	PRL 48 66	G.J. Feldman *et al.*	(Mark II Collab.)
HAYES	82	PR D25 2869	K.G. Hayes *et al.*	(Mark II Collab.)
BERGER	81B	PL 99B 489	C. Berger *et al.*	(PLUTO Collab.)
DORFAN	81	PRL 46 215	J.M. Dorfan *et al.*	(Mark II Collab.)
BRANDELIK	80	PL 92B 199	R. Brandelik *et al.*	(TASSO Collab.)
ZHOLENTZ	80	PL 96B 214	A.A. Zholents *et al.*	(NOVO)
Also		SJNP 34 814	A.A. Zholents *et al.*	(NOVO)
		Translated from YAF 34 1471.		
BACINO	79B	PRL 42 749	W.J. Bacino *et al.*	(DELCO Collab.)
KIRKBY	79	SLAC-PUB-2419	J. Kirkby	(SLAC) J
		Batavia Lepton Photon Conference.		
BACINO	78B	PRL 41 13	W.J. Bacino *et al.*	(DELCO Collab.) J
Also		Tokyo Conf. 249	J. Kirz	(STON)
Also		PL 96B 214	A.A. Zholents *et al.*	(NOVO)
BRANDELIK	78	PL 73B 109	R. Brandelik *et al.*	(DASP Collab.) J
FELDMAN	78	Tokyo Conf. 777	G.J. Feldman	(SLAC) J
JAROS	78	PRL 40 1120	J. Jaros *et al.*	(LGW Collab.)
PERL	75	PRL 35 1489	M.L. Perl *et al.*	(LBL, SLAC)

OTHER RELATED PAPERS

DAVIER	06	RMP 78 1043	M. Davier, A. Hocker, Z. Zhang	(LALO, PARIN+)
RAHAL-CAL...	98	IJMP A13 695	G. Rahal-Callot	(ETH)
GENTILE	96	PRPL 274 287	S. Gentile, M. Pohl	(ROMAI, ETH)
WEINSTEIN	93	ARNPS 43 457	A.J. Weinstein, R. Stroynowski	(CIT, SMU)
PERL	92	RPP 55 653	M.L. Perl	(SLAC)
PICH	90	MPL A5 1995	A. Pich	(VALE)
BARISH	88	PRPL 157 1	B.C. Barish, R. Stroynowski	(CIT)
GAN	88	IJMP A3 531	K.K. Gan, M.L. Perl	(SLAC)
HAYES	88	PR D38 3351	K.G. Hayes, M.L. Perl	(SLAC)
PERL	80	ARNPS 30 299	M.L. Perl	(SLAC)

Heavy Charged Lepton Searches

Charged Heavy Lepton MASS LIMITS

Sequential Charged Heavy Lepton ($L^{\pm}$) MASS LIMITS

These experiments assumed that a fourth generation $L^{\pm}$ decayed to a fourth generation ν_L (or L^0) where ν_L was stable, or that $L^{\pm}$ decays to a light ν_ℓ via mixing.

See the "Quark and Lepton Compositeness, Searches for" Listings for limits on radiatively decaying excited leptons, *i.e.* $\ell^* \to \ell\gamma$. See the "WIMPs and other Particle Searches" section for heavy charged particle search limits in which the charged particle could be a lepton.

VALUE (GeV)	CL%	DOCUMENT ID		TECN	COMMENT
>100.8	95	ACHARD	01B	L3	Decay to νW
>101.9	95	ACHARD	01B	L3	$m_L - m_{L^0} > 15$ GeV
• • • We do not use the following data for averages, fits, limits, etc. • • •					
> 81.5	95	ACKERSTAFF	98C	OPAL	Assumed $m_{L^\pm} - m_{L^0} > 8.4$ GeV
> 80.2	95	ACKERSTAFF	98C	OPAL	$m_{L^0} > m_{L^\pm}$ and $L^\pm \to \nu W$
< 48 or > 61	95	[1] ACCIARRI	96G	L3	
> 63.9	95	ALEXANDER	96P	OPAL	Decay to massless ν's
> 63.5	95	BUSKULIC	96S	ALEP	$m_L - m_{L^0} > 7$ GeV
> 65	95	BUSKULIC	96S	ALEP	Decay to massless ν's
none 10–225		[2] AHMED	94	CNTR	H1 Collab. at HERA
none 12.6–29.6	95	KIM	91B	AMY	Massless ν assumed
> 44.3	95	AKRAWY	90G	OPAL	
none 0.5–10	95	[3] RILES	90	MRK2	For $(m_{L^0}$-$m_{L^0})>$ 0.25–0.4 GeV
> 8		[4] STOKER	89	MRK2	For $(m_{L^+} - m_{L^0}) =$ 0.4 GeV
> 12		[4] STOKER	89	MRK2	For m_{L^0}=0.9 GeV
none 18.4–27.6	95	[5] ABE	88	VNS	
> 25.5	95	[6] ADACHI	88B	TOPZ	
none 1.5–22.0	95	BEHREND	88C	CELL	
> 41	90	[7] ALBAJAR	87B	UA1	
> 22.5	95	[8] ADEVA	85	MRKJ	
> 18.0	95	[9] BARTEL	83	JADE	
none 4–14.5	95	[10] BERGER	81B	PLUT	
> 15.5	95	[11] BRANDELIK	81	TASS	
> 13.		[12] AZIMOV	80		
> 16.	95	[13] BARBER	80B	CNTR	
> 0.490		[14] ROTHE	69	RVUE	

[1] ACCIARRI 96G assumes LEP result that the associated neutral heavy lepton mass > 40 GeV.

[2] The AHMED 94 limits are from a search for neutral and charged sequential heavy leptons at HERA via the decay channels $L^- \to e\gamma$, $L^- \to \nu W^-$, $L^- \to eZ$; and $L^0 \to \nu\gamma$, $L^0 \to e^- W^+$, $L^- \to \nu Z$, where the W decays to $\ell\nu_\ell$, or to jets, and Z decays to $\ell^+\ell^-$ or jets.

[3] RILES 90 limits were the result of a special analysis of the data in the case where the mass difference $m_{L^-} - m_{L^0}$ was allowed to be quite small, where L^0 denotes the neutrino into which the sequential charged lepton decays. With a slightly reduced $m_{L^\pm}$ range, the mass difference extends to about 4 GeV.

[4] STOKER 89 (Mark II at PEP) gives bounds on charged heavy lepton (L^+) mass for the generalized case in which the corresponding neutral heavy lepton (L^0) in the SU(2) doublet is not of negligible mass.

[5] ABE 88 search for L^+ and L^- hadrons looking for acoplanar jets. The bound is valid for $m_\nu < 10$ GeV.

[6] ADACHI 88B search for hadronic decays giving acoplanar events with large missing energy. $E_{cm}^{ee} = 52$ GeV.

[7] Assumes associated neutrino is approximately massless.

[8] ADEVA 85 analyze one-isolated-muon data and sensitive to τ <10 nanosec. Assume B(lepton) = 0.30. $E_{cm} = 40$–47 GeV.

[9] BARTEL 83 limit is from PETRA e^+e^- experiment with average $E_{cm} = 34.2$ GeV.

[10] BERGER 81B is DESY DORIS and PETRA experiment. Looking for $e^+e^- \to L^+L^-$.

[11] BRANDELIK 81 is DESY-PETRA experiment. Looking for $e^+e^- \to L^+L^-$.

[12] AZIMOV 80 estimated probabilities for $M + N$ type events in $e^+e^- \to L^+L^-$ deducing semi-hadronic decay multiplicities of L from e^+e^- annihilation data at $E_{cm} = (2/3)m_L$. Obtained above limit comparing these with e^+e^- data (BRANDELIK 80).

[13] BARBER 80B looked for $e^+e^- \to L^+L^-$, $L \to \nu_L^+ X$ with MARK-J at DESY-PETRA.

[14] ROTHE 69 examines previous data on μ pair production and π and K decays.

Stable Charged Heavy Lepton ($L^{\pm}$) MASS LIMITS

VALUE (GeV)	CL%	DOCUMENT ID		TECN
>102.6	95	ACHARD	01B	L3
• • • We do not use the following data for averages, fits, limits, etc. • • •				
> 28.2	95	[15] ADACHI	90C	TOPZ
none 18.5–42.8	95	AKRAWY	90O	OPAL
> 26.5	95	DECAMP	90F	ALEP
none m_μ–36.3	95	SODERSTROM	90	MRK2

[15] ADACHI 90C put lower limits on the mass of stable charged particles with electric charge Q satisfying $2/3 < Q/e < 4/3$ and with spin 0 or 1/2. We list here the special case for a stable charged heavy lepton.

Charged Long-Lived Heavy Lepton MASS LIMITS

VALUE (GeV)	CL%	DOCUMENT ID		TECN	CHG	COMMENT
• • • We do not use the following data for averages, fits, limits, etc. • • •						
>574	95	CHATRCHYAN	13AB	CMS		Leptons singlet model
>102.0	95	ABBIENDI	03L	OPAL		pair produced in e^+e^-
> 0.1		[16] ANSORGE	73B	HBC	–	Long-lived
none 0.55–4.5		[17] BUSHNIN	73	CNTR	–	Long-lived
none 0.2–0.92		[18] BARNA	68	CNTR	–	Long-lived
none 0.97–1.03		[18] BARNA	68	CNTR	–	Long-lived

[16] ANSORGE 73B looks for electron pair production and electron-like Bremsstrahlung.

[17] BUSHNIN 73 is SERPUKHOV 70 GeV p experiment. Masses assume mean life above 7×10^{-10} and 3×10^{-8} respectively. Calculated from cross section (see "Charged Quasi-Stable Lepton Production Differential Cross Section" below) and 30 GeV muon pair production data.

[18] BARNA 68 is SLAC photoproduction experiment.

Doubly-Charged Heavy Lepton MASS LIMITS

VALUE (GeV)	CL%	DOCUMENT ID		TECN	CHG
• • • We do not use the following data for averages, fits, limits, etc. • • •					
none 1–9 GeV	90	[19] CLARK	81	SPEC	++

[19] CLARK 81 is FNAL experiment with 209 GeV muons. Bounds apply to μ_P which couples with full weak strength to muon. See also section on "Doubly-Charged Lepton Production Cross Section."

Doubly-Charged Lepton Production Cross Section (μN Scattering)

VALUE (cm^2)	EVTS	DOCUMENT ID		TECN	CHG
• • • We do not use the following data for averages, fits, limits, etc. • • •					
$<6. \times 10^{-38}$	0	[20] CLARK	81	SPEC	++

[20] CLARK 81 is FNAL experiment with 209 GeV muon. Looked for μ^+ nucleon $\rightarrow \overline{\mu}_P^0$ X, $\overline{\mu}_P^0 \rightarrow \mu^+\mu^-\overline{\nu}_\mu$ and $\mu^+ n \rightarrow \mu_P^{++}$ X, $\mu_P^{++} \rightarrow 2\mu^+\nu_\mu$. Above limits are for $\sigma\times$BR taken from their mass-dependence plot figure 2.

REFERENCES FOR Heavy Charged Lepton Searches

CHATRCHYAN	13AB	JHEP 1307 122	S. Chatrchyan *et al.*	(CMS Collab.)
ABBIENDI	03L	PL B572 8	G. Abbiendi *et al.*	(OPAL Collab.)
ACHARD	01B	PL B517 75	P. Achard *et al.*	(L3 Collab.)
ACKERSTAFF	98C	EPJ C1 45	K. Ackerstaff *et al.*	(OPAL Collab.)
ACCIARRI	96G	PL B377 304	M. Acciarri *et al.*	(L3 Collab.)
ALEXANDER	96P	PL B385 433	G. Alexander *et al.*	(OPAL Collab.)
BUSKULIC	96S	PL B384 439	D. Buskulic *et al.*	(ALEPH Collab.)
AHMED	94	PL B340 205	T. Ahmed *et al.*	(H1 Collab.)
KIM	91B	IJMP A6 2583	G.N. Kim *et al.*	(AMY Collab.)
ADACHI	90C	PL B244 352	I. Adachi *et al.*	(TOPAZ Collab.)
AKRAWY	90G	PL B240 250	M.Z. Akrawy *et al.*	(OPAL Collab.)
AKRAWY	90O	PL B252 290	M.Z. Akrawy *et al.*	(OPAL Collab.)
DECAMP	90F	PL B236 511	D. Decamp *et al.*	(ALEPH Collab.)
RILES	90	PR D42 1	K. Riles *et al.*	(Mark II Collab.)
SODERSTROM	90	PRL 64 2980	E. Soderstrom *et al.*	(Mark II Collab.)
STOKER	89	PR D39 1811	D.P. Stoker *et al.*	(Mark II Collab.)
ABE	88	PRL 61 915	K. Abe *et al.*	(VENUS Collab.)
ADACHI	88B	PR D37 1339	I. Adachi *et al.*	(TOPAZ Collab.)
BEHREND	88C	ZPHY C41 7	H.J. Behrend *et al.*	(CELLO Collab.)
ALBAJAR	87B	PL B185 241	C. Albajar *et al.*	(UA1 Collab.)
ADEVA	85	PL 152B 439	B. Adeva *et al.*	(Mark-J Collab.)
Also		PRPL 109 131	B. Adeva *et al.*	(Mark-J Collab.)
BARTEL	83	PL 123B 353	W. Bartel *et al.*	(JADE Collab.)
BERGER	81B	PL 99B 489	C. Berger *et al.*	(PLUTO Collab.)
BRANDELIK	81	PL 99B 163	R. Brandelik *et al.*	(TASSO Collab.)
CLARK	81	PRL 46 299	A.R. Clark *et al.*	(UCB, LBL, FNAL+)
Also		PR D25 2762	W.H. Smith *et al.*	(LBL, FNAL, PRIN)
AZIMOV	80	JETPL 32 664	Y.I. Azimov, V.A. Khoze	(PNPI)
		Translated from ZETFP 32 677.		
BARBER	80B	PRL 45 1904	D.P. Barber *et al.*	(Mark-J Collab.)
BRANDELIK	80	PL 92B 199	R. Brandelik *et al.*	(TASSO Collab.)
ANSORGE	73B	PR D7 26	R.E. Ansorge *et al.*	(CAVE)
BUSHNIN	73	NP B58 476	Y.B. Bushnin *et al.*	(SERP)
Also		PL 42B 136	S.V. Golovkin *et al.*	(SERP)
ROTHE	69	NP B10 241	K.W. Rothe, A.M. Wolsky	(PENN)
BARNA	68	PR 173 1391	A. Barna *et al.*	(SLAC, STAN)

OTHER RELATED PAPERS

PERL	81	SLAC-PUB-2752	M.L. Perl	(SLAC)

Physics in Collision Conference.

Neutrino Properties

INTRODUCTION TO THE NEUTRINO PROPERTIES LISTINGS

Revised August 2013 by P. Vogel (Caltech) and A. Piepke (University of Alabama).

The following Listings concern measurements of various properties of neutrinos. Nearly all of the measurements, all of which so far are limits, actually concern superpositions of the mass eigenstates ν_i, which are in turn related to the weak eigenstates ν_ℓ, via the neutrino mixing matrix

$$|\nu_\ell\rangle = \sum_i U_{\ell i}\,|\nu_i\rangle \ .$$

In the analogous case of quark mixing via the CKM matrix, the smallness of the off-diagonal terms (small mixing angles) permits a "dominant eigenstate" approximation. However, the results of neutrino oscillation searches show that the mixing matrix contains two large mixing angles and a third angle that is not exceedingly small. We cannot, therefore, associate any particular state $|\nu_i\rangle$ with any particular lepton label e, μ or τ. Nevertheless, note that in the standard labeling the $|\nu_1\rangle$ has the largest $|\nu_e\rangle$ component ($\sim 2/3$), $|\nu_2\rangle$ contains $\sim 1/3$ of the $|\nu_e\rangle$ component and $|\nu_3\rangle$ contains only a small $\sim 2.5\%$ $|\nu_e\rangle$ component.

Neutrinos are produced in weak decays with a definite lepton flavor, and are typically detected by the charged current weak interaction again associated with a specific lepton flavor. Hence, the listings for the neutrino mass that follow are separated into the three associated charged lepton categories. Other properties (mean lifetime, magnetic moment, charge and charge radius) are no longer separated this way. If needed, the associated lepton flavor is reported in the footnotes.

Measured quantities (mass-squared, magnetic moments, mean lifetimes, *etc.*) all depend upon the mixing parameters $|U_{\ell i}|^2$, but to some extent also on experimental conditions (*e.g.*, on energy resolution). Most of these observables, in particular mass-squared, cannot distinguish between Dirac and Majorana neutrinos, and are unaffected by CP phases.

Direct neutrino mass measurements are usually based on the analysis of the kinematics of charged particles (leptons, pions) emitted together with neutrinos (flavor states) in various weak decays. The most sensitive neutrino mass measurement to date, involving electron type antineutrinos, is based on fitting the shape of the beta spectrum. The quantity $\langle m_\beta^2\rangle = \sum_i |U_{ei}|^2 m_{\nu_i}^2$ is determined or constrained, where the sum is over all mass eigenvalues m_{ν_i} that are too close together to be resolved experimentally. If the energy resolution is better than $\Delta m_{ij}^2 \equiv m_{\nu_i}^2 - m_{\nu_j}^2$, the corresponding heavier m_{ν_i} and mixing parameter could be determined by fitting the resulting spectral anomaly (step or kink).

A limit on $\langle m_\beta^2\rangle$ implies an upper limit on the minimum value m_{min}^2 of $m_{\nu_i}^2$, independent of the mixing parameters U_{ei}: $m_{min}^2 \leq \langle m_\beta^2\rangle$. However, if and when the value of $\langle m_\beta^2\rangle$ is determined then its combination with the results derived from neutrino oscillations that give us the values of the neutrino mass-squared differences $\Delta m_{ij}^2 \equiv m_i^2 - m_j^2$ and the mixing parameters $|U_{ei}|^2$, the individual neutrino mass squares $m_{\nu_j}^2 = \langle m_\beta^2\rangle - \sum_i |U_{ei}|^2 \Delta m_{ij}^2$ can be determined.

So far solar, reactor, atmospheric and accelerator neutrino oscillation experiments can be consistently described using three active neutrino flavors, i.e. two mass splittings and three mixing angles. However, several experiments with radioactive sources, reactors, and accelerators imply the possible existence of one or more non-interacting neutrino species that might be observable since they couple weakly to the flavor neutrinos $|\nu_l\rangle$.

Combined three neutrino analyses determine the squared mass differences and all three mixing angles to within reasonable accuracy. For given $|\Delta m_{ij}^2|$ a limit on $\langle m_\beta^2\rangle$ from beta decay defines an upper limit on the maximum value m_{max} of m_{ν_i}: $m_{max}^2 \leq \langle m_\beta^2\rangle + \sum_{i<j} |\Delta m_{ij}^2|$. The analysis of the low energy beta decay of tritium, combined with the oscillation results, thus limits all active neutrino masses. Traditionally, experimental neutrino mass limits obtained from pion decay $\pi^+ \rightarrow \mu^+ + \nu_\mu$ or the shape of the spectrum of decay products of the τ lepton did not distinguish between flavor and mass eigenstates. These results are reported as limits of the μ and τ based neutrino mass. After the determination of the $|\Delta m_{ij}^2|$'s and the mixing angles θ_{ij}, the corresponding neutrino mass limits are no longer competitive with those derived from low energy beta decays.

Lepton Particle Listings

Neutrino Properties

The spread of arrival times of the neutrinos from SN1987A, coupled with the measured neutrino energies, provided a time-of-flight limit on a quantity similar to $\langle m_\beta \rangle \equiv \sqrt{\langle m_\beta^2 \rangle}$. This statement, clothed in various degrees of sophistication, has been the basis for a very large number of papers. The resulting limits, however, are no longer comparable with the limits from tritium beta decay.

Constraint on the sum of the neutrino masses can be obtained from the analysis of the cosmic microwave background anisotropy, combined with the galaxy redshift surveys and other data. These limits are reported in a separate table (Sum of Neutrino Masses, m_{tot}). Discussion concerning the model dependence of this limit is continuing.

$\overline{\nu}$ MASS (electron based)

Those limits given below are for the square root of $m^{2(\text{eff})}_{\nu_e} \equiv \sum_i |U_{ei}|^2\ m^2_{\nu_i}$. Limits that come from the kinematics of $^3\text{H}\,\beta^-\overline{\nu}$ decay are the square roots of the limits for $m^{2(\text{eff})}_{\nu_e}$. Obtained from the measurements reported in the Listings for "$\overline{\nu}$ Mass Squared," below.

VALUE (eV)	CL%	DOCUMENT ID		TECN	COMMENT
< 2 OUR EVALUATION					
< 2.05	95	[1] ASEEV	11	SPEC	^{3}H β decay
< 2.3	95	[2] KRAUS	05	SPEC	^{3}H β decay
• • • We do not use the following data for averages, fits, limits, etc. • • •					
< 5.8	95	[3] PAGLIAROLI	10	ASTR	SN1987A
<21.7	90	[4] ARNABOLDI	03A	BOLO	^{187}Re β-decay
< 5.7	95	[5] LOREDO	02	ASTR	SN1987A
< 2.5	95	[6] LOBASHEV	99	SPEC	^{3}H β decay
< 2.8	95	[7] WEINHEIMER	99	SPEC	^{3}H β decay
< 4.35	95	[8] BELESEV	95	SPEC	^{3}H β decay
<12.4	95	[9] CHING	95	SPEC	^{3}H β decay
<92	95	[10] HIDDEMANN	95	SPEC	^{3}H β decay
$15\ {}^{+32}_{-15}$		HIDDEMANN	95	SPEC	^{3}H β decay
<19.6	95	KERNAN	95	ASTR	SN 1987A
< 7.0	95	[11] STOEFFL	95	SPEC	^{3}H β decay
< 7.2	95	[12] WEINHEIMER	93	SPEC	^{3}H β decay
<11.7	95	[13] HOLZSCHUH	92B	SPEC	^{3}H β decay
<13.1	95	[14] KAWAKAMI	91	SPEC	^{3}H β decay
< 9.3	95	[15] ROBERTSON	91	SPEC	^{3}H β decay
<14	95	AVIGNONE	90	ASTR	SN 1987A
<16		SPERGEL	88	ASTR	SN 1987A
17 to 40		[16] BORIS	87	SPEC	^{3}H β decay

[1] ASEEV 11 report the analysis of the entire beta endpoint data, taken with the Troitsk integrating electrostatic spectrometer between 1997 and 2002 (some of the earlier runs were rejected), using a windowless gaseous tritium source. The fitted value of m_ν, based on the method of Feldman and Cousins, is obtained from the upper limit of the fit for m^2_ν. Previous analysis problems were resolved by careful monitoring of the tritium gas column density. Supersedes LOBASHEV 99 and BELESEV 95.

[2] KRAUS 05 is a continuation of the work reported in WEINHEIMER 99. This result represents the final analysis of data taken from 1997 to 2001. Various sources of systematic uncertainties have been identified and quantified. The background has been reduced compared to the initial running period. A spectral anomaly at the endpoint, reported in LOBASHEV 99, was not observed.

[3] PAGLIAROLI 10 is critical of the likelihood method used by LOREDO 02.

[4] ARNABOLDI 03A *et al.* report kinematical neutrino mass limit using β-decay of ^{187}Re. Bolometric $AgReO_4$ micro-calorimeters are used. Mass bound is substantially weaker than those derived from tritium β-decays but has different systematic uncertainties.

[5] LOREDO 02 updates LOREDO 89.

[6] LOBASHEV 99 report a new measurement which continues the work reported in BELESEV 95. This limit depends on phenomenological fit parameters used to derive their best fit to m^2_ν, making unambiguous interpretation difficult. See the footnote under "$\overline{\nu}$ Mass Squared."

[7] WEINHEIMER 99 presents two analyses which exclude the spectral anomaly and result in an acceptable m^2_ν. We report the most conservative limit, but the other is nearly the same. See the footnote under "$\overline{\nu}$ Mass Squared."

[8] BELESEV 95 (Moscow) use an integral electrostatic spectrometer with adiabatic magnetic collimation and a gaseous tritium sources. A fit to a normal Kurie plot above 18300–18350 eV (to avoid a low-energy anomaly) plus a monochromatic line 7–15 eV below the endpoint yields $m^2_\nu = -4.1 \pm 10.9$ eV^2, leading to this Bayesian limit.

[9] CHING 95 quotes results previously given by SUN 93; no experimental details are given. A possible explanation for consistently negative values of m^2_ν is given.

[10] HIDDEMANN 95 (Munich) experiment uses atomic tritium embedded in a metal-dioxide lattice. Bayesian limit calculated from the weighted mean $m^2_\nu = 221 \pm 4244$ eV^2 from the two runs listed below.

[11] STOEFFL 95 (LLNL) result is the Bayesian limit obtained from the m^2_ν errors given below but with m^2_ν set equal to 0. The anomalous endpoint accumulation leads to a value of m^2_ν which is negative by more than 5 standard deviations.

[12] WEINHEIMER 93 (Mainz) is a measurement of the endpoint of the tritium β spectrum using an electrostatic spectrometer with a magnetic guiding field. The source is molecular tritium frozen onto an aluminum substrate.

[13] HOLZSCHUH 92B (Zurich) result is obtained from the measurement $m^2_\nu = -24 \pm 48 \pm 61$ (1σ errors), in eV^2, using the PDG prescription for conversion to a limit in m_ν.

[14] KAWAKAMI 91 (Tokyo) experiment uses tritium-labeled arachidic acid. This result is the Bayesian limit obtained from the m^2_ν limit with the errors combined in quadrature. This was also done in ROBERTSON 91, although the authors report a different procedure.

[15] ROBERTSON 91 (LANL) experiment uses gaseous molecular tritium. The result is in strong disagreement with the earlier claims by the ITEP group [LUBIMOV 80, BORIS 87 (+ BORIS 88 erratum)] that m_ν lies between 17 and 40 eV. However, the probability of a positive m^2 is only 3% if statistical and systematic error are combined in quadrature.

[16] See also comment in BORIS 87B and erratum in BORIS 88.

$\overline{\nu}$ MASS SQUARED (electron based)

Given troubling systematics which result in improbably negative estimators of $m^{2(\text{eff})}_{\nu_e} \equiv \sum_i |U_{ei}|^2\ m^2_{\nu_i}$, in many experiments, we use only KRAUS 05 and LOBASHEV 99 for our average.

VALUE (eV^2)	CL%	DOCUMENT ID		TECN	COMMENT
− 0.6 ± 1.9 OUR AVERAGE					
− 0.67± 2.53		[1] ASEEV	11	SPEC	^{3}H β decay
− 0.6 ± 2.2 ± 2.1		[2] KRAUS	05	SPEC	^{3}H β decay
• • • We do not use the following data for averages, fits, limits, etc. • • •					
− 1.9 ± 3.4 ± 2.2		[3] LOBASHEV	99	SPEC	^{3}H β decay
− 3.7 ± 5.3 ± 2.1		[4] WEINHEIMER	99	SPEC	^{3}H β decay
− 22 ± 4.8		[5] BELESEV	95	SPEC	^{3}H β decay
129 ±6010		[6] HIDDEMANN	95	SPEC	^{3}H β decay
313 ±5994		[6] HIDDEMANN	95	SPEC	^{3}H β decay
−130 ± 20 ±15	95	[7] STOEFFL	95	SPEC	^{3}H β decay
− 31 ± 75 ±48		[8] SUN	93	SPEC	^{3}H β decay
− 39 ± 34 ±15		[9] WEINHEIMER	93	SPEC	^{3}H β decay
− 24 ± 48 ±61		[10] HOLZSCHUH	92B	SPEC	^{3}H β decay
− 65 ± 85 ±65		[11] KAWAKAMI	91	SPEC	^{3}H β decay
−147 ± 68 ±41		[12] ROBERTSON	91	SPEC	^{3}H β decay

[1] ASEEV 11 report the analysis of the entire beta endpoint data, taken with the Troitsk integrating electrostatic spectrometer between 1997 and 2002, using a windowless gaseous tritium source. The analysis does not use the two additional fit parameters (see LOBASHEV 99) for a step-like structure near the endpoint. Using only the runs where the tritium gas column density was carefully monitored the need for such parameters was eliminated. Supersedes LOBASHEV 99 and BELESEV 95.

[2] KRAUS 05 is a continuation of the work reported in WEINHEIMER 99. This result represents the final analysis of data taken from 1997 to 2001. Problems with significantly negative squared neutrino masses, observed in some earlier experiments, have been resolved in this work.

[3] LOBASHEV 99 report a new measurement which continues the work reported in BELESEV 95. The data were corrected for electron trapping effects in the source, eliminating the dependence of the fitted neutrino mass on the fit interval. The analysis assuming a pure beta spectrum yields significantly negative fitted $m^2_\nu \approx -(20\text{–}10)$ eV^2. This problem is attributed to a discrete spectral anomaly of about 6×10^{-11} intensity with a time-dependent energy of 5–15 eV below the endpoint. The data analysis accounts for this anomaly by introducing two extra phenomenological fit parameters resulting in a best fit of $m^2_\nu = -1.9 \pm 3.4 \pm 2.2$eV^2 which is used to derive a neutrino mass limit. However, the introduction of phenomenological fit parameters which are correlated with the derived m^2_ν limit makes unambiguous interpretation of this result difficult.

[4] WEINHEIMER 99 is a continuation of the work reported in WEINHEIMER 93 . Using a lower temperature of the frozen tritium source eliminated the dewetting of the T_2 film, which introduced a dependence of the fitted neutrino mass on the fit interval in the earlier work. An indication for a spectral anomaly reported in LOBASHEV 99 has been seen, but its time dependence does not agree with LOBASHEV 99. Two analyses, which exclude the spectral anomaly either by choice of the analysis interval or by using a particular data set which does not exhibit the anomaly, result in acceptable m^2_ν fits and are used to derive the neutrino mass limit published by the authors. We list the most conservative of the two.

[5] BELESEV 95 (Moscow) use an integral electrostatic spectrometer with adiabatic magnetic collimation and a gaseous tritium sources. This value comes from a fit to a normal Kurie plot above 18300–18350 eV (to avoid a low-energy anomaly), including the effects of an apparent peak 7–15 eV below the endpoint.

[6] HIDDEMANN 95 (Munich) experiment uses atomic tritium embedded in a metal-dioxide lattice. They quote measurements from two data sets.

[7] STOEFFL 95 (LLNL) uses a gaseous source of molecular tritium. An anomalous pileup of events at the endpoint leads to the negative value for m^2_ν. The authors acknowledge that "the negative value for the best fit of m^2_ν has no physical meaning" and discuss possible explanations for this effect.

[8] SUN 93 uses a tritiated hydrocarbon source. See also CHING 95.

[9] WEINHEIMER 93 (Mainz) is a measurement of the endpoint of the tritium β spectrum using an electrostatic spectrometer with a magnetic guiding field. The source is molecular tritium frozen onto an aluminum substrate.

[10] HOLZSCHUH 92B (Zurich) source is a monolayer of tritiated hydrocarbon.

[11] KAWAKAMI 91 (Tokyo) experiment uses tritium-labeled arachidic acid.

[12] ROBERTSON 91 (LANL) experiment uses gaseous molecular tritium. The result is in strong disagreement with the earlier claims by the ITEP group [LUBIMOV 80, BORIS 87 (+ BORIS 88 erratum)] that m_ν lies between 17 and 40 eV. However, the probability of a positive m_ν^2 is only 3% if statistical and systematic error are combined in quadrature.

ν MASS (electron based)

These are measurement of m_ν (in contrast to $m_{\overline{\nu}}$, given above). The masses can be different for a Dirac neutrino in the absence of CPT invariance. The possible distinction between ν and $\overline{\nu}$ properties is usually ignored elsewhere in these Listings.

VALUE (eV)	CL%	DOCUMENT ID		TECN	COMMENT
<460	68	YASUMI	94	CNTR	^{163}Ho decay
<225	95	SPRINGER	87	CNTR	^{163}Ho decay

ν MASS (muon based)

Limits given below are for the square root of $m^{2(\text{eff})}_{\nu_\mu} \equiv \sum_i |U_{\mu i}|^2\ m^2_{\nu_i}$.

In some of the COSM papers listed below, the authors did not distinguish between weak and mass eigenstates.

OUR EVALUATION is based on OUR AVERAGE for the $\pi^\pm$ mass and the ASSAMAGAN 96 value for the muon momentum for the π^+ decay at rest. The limit is calculated using the unified classical analysis of FELDMAN 98 for a Gaussian distribution near a physical boundary. WARNING: since $m^{2(\text{eff})}_{\nu_\mu}$ is calculated from the differences of large numbers, it and the corresponding limits are extraordinarily sensitive to small changes in the pion mass, the decay muon momentum, and their errors. For example, the limits obtained using JECKELMANN 94, LENZ 98, and the weighted averages are 0.15, 0.29, and 0.19 MeV, respectively.

VALUE (MeV)	CL%	DOCUMENT ID		TECN	COMMENT
<0.19 (CL = 90%) OUR EVALUATION					
<0.17	90	[1] ASSAMAGAN	96	SPEC	$m^2_\nu = -0.016 \pm 0.023$
• • • We do not use the following data for averages, fits, limits, etc. • • •					
<0.15		[2] DOLGOV	95	COSM	Nucleosynthesis
<0.48		[3] ENQVIST	93	COSM	Nucleosynthesis
<0.3		[4] FULLER	91	COSM	Nucleosynthesis
<0.42		[4] LAM	91	COSM	Nucleosynthesis
<0.50	90	[5] ANDERHUB	82	SPEC	$m^2_\nu = -0.14 \pm 0.20$
<0.65	90	CLARK	74	ASPK	$K_{\mu 3}$ decay

[1] ASSAMAGAN 96 measurement of p_μ from $\pi^+ \to \mu^+\nu$ at rest combined with JECKELMANN 94 Solution B pion mass yields $m^2_\nu = -0.016 \pm 0.023$ with corresponding Bayesian limit listed above. If Solution A is used, $m^2_\nu = -0.143 \pm 0.024$ MeV^2. Replaces ASSAMAGAN 94.

[2] DOLGOV 95 removes earlier assumptions (DOLGOV 93) about thermal equilibrium below T_{QCD} for wrong-helicity Dirac neutrinos (ENQVIST 93, FULLER 91) to set more stringent limits.

[3] ENQVIST 93 bases limit on the fact that thermalized wrong-helicity Dirac neutrinos would speed up expansion of early universe, thus reducing the primordial abundance. FULLER 91 exploits the same mechanism but in the older calculation obtains a larger production rate for these states, and hence a lower limit. Neutrino lifetime assumed to exceed nucleosynthesis time, ~ 1 s.

[4] Assumes neutrino lifetime >1 s. For Dirac neutrinos only. See also ENQVIST 93.

[5] ANDERHUB 82 kinematics is insensitive to the pion mass.

ν MASS (tau based)

The limits given below are the square roots of limits for $m^{2(\text{eff})}_{\nu_\tau} \equiv \sum_i |U_{\tau i}|^2\ m^2_{\nu_i}$.

In some of the ASTR and COSM papers listed below, the authors did not distinguish between weak and mass eigenstates.

VALUE (MeV)	CL%	EVTS	DOCUMENT ID		TECN	COMMENT
< 18.2	95		[1] BARATE	98F	ALEP	1991–1995 LEP runs
• • • We do not use the following data for averages, fits, limits, etc. • • •						
< 28	95		[2] ATHANAS	00	CLEO	E^{ee}_{cm}= 10.6 GeV
< 27.6	95		[3] ACKERSTAFF	98T	OPAL	1990–1995 LEP runs
< 30	95	473	[4] AMMAR	98	CLEO	$E^{ee}_{\text{cm}} = 10.6$ GeV
< 60	95		[5] ANASTASSOV	97	CLEO	E^{ee}_{cm}= 10.6 GeV
< 0.37 or >22			[6] FIELDS	97	COSM	Nucleosynthesis
< 68	95		[7] SWAIN	97	THEO	m_τ, τ_τ, τ partial widths
< 29.9	95		[8] ALEXANDER	96M	OPAL	1990–1994 LEP runs
<149			[9] BOTTINO	96	THEO	π, μ, τ leptonic decays
<1 or >25			[10] HANNESTAD	96C	COSM	Nucleosynthesis
< 71	95		[11] SOBIE	96	THEO	m_τ, τ_τ, B($\tau^- \to e^-\overline{\nu}_e\nu_\tau$)
< 24	95	25	[12] BUSKULIC	95H	ALEP	1991–1993 LEP runs
< 0.19			[13] DOLGOV	95	COSM	Nucleosynthesis
< 3			[14] SIGL	95	ASTR	SN 1987A
< 0.4 or > 30			[15] DODELSON	94	COSM	Nucleosynthesis
< 0.1 or > 50			[16] KAWASAKI	94	COSM	Nucleosynthesis
155–225			[17] PERES	94	THEO	π,K,μ,τ weak decays
< 32.6	95	113	[18] CINABRO	93	CLEO	$E^{ee}_{\text{cm}} \approx 10.6$ GeV
< 0.3 or > 35			[19] DOLGOV	93	COSM	Nucleosynthesis
< 0.74			[20] ENQVIST	93	COSM	Nucleosynthesis
< 31	95	19	[21] ALBRECHT	92M	ARG	E^{ee}_{cm}= 9.4–10.6 GeV
< 0.3			[22] FULLER	91	COSM	Nucleosynthesis
< 0.5 or > 25			[23] KOLB	91	COSM	Nucleosynthesis
< 0.42			[22] LAM	91	COSM	Nucleosynthesis

[1] BARATE 98F result based on kinematics of 2939 $\tau^- \to 2\pi^-\pi^+\nu_\tau$ and 52 $\tau^- \to 3\pi^- 2\pi^+(\pi^0)\nu_\tau$ decays. If possible 2.5% excited a_1 decay is included in 3-prong sample analysis, limit increases to 19.2 MeV.

[2] ATHANAS 00 bound comes from analysis of $\tau^- \to \pi^-\pi^+\pi^-\pi^0\nu_\tau$ decays.

[3] ACKERSTAFF 98T use $\tau \to 5\pi^\pm\nu_\tau$ decays to obtain a limit of 43.2 MeV (95%CL). They combine this with ALEXANDER 96M value using $\tau \to 3h^\pm\nu_\tau$ decays to obtain quoted limit.

[4] AMMAR 98 limit comes from analysis of $\tau^- \to 3\pi^- 2\pi^+\nu_\tau$ and $\tau^- \to 2\pi^-\pi^+ 2\pi^0\nu_\tau$ decay modes.

[5] ANASTASSOV 97 derive limit by comparing their m_τ measurement (which depends on m_{ν_τ}) to BAI 96 m_τ threshold measurement.

[6] FIELDS 97 limit for a Dirac neutrino. For a Majorana neutrino the mass region < 0.93 or >31 MeV is excluded. These bounds assume N_ν <4 from nucleosynthesis; a wider excluded region occurs with a smaller N_ν upper limit.

[7] SWAIN 97 derive their limit from the Standard Model relationships between the tau mass, lifetime, branching fractions for $\tau^- \to e^-\overline{\nu}_e\nu_\tau$, $\tau^- \to \mu^-\overline{\nu}_\mu\nu_\tau$, $\tau^- \to \pi^-\nu_\tau$, and $\tau^- \to K^-\nu_\tau$, and the muon mass and lifetime by assuming lepton universality and using world average values. Limit is reduced to 48 MeV when the CLEO τ mass measurement (BALEST 93) is included; see CLEO's more recent m_{ν_τ} limit (ANASTASSOV 97). Consideration of mixing with a fourth generation heavy neutrino yields $\sin^2\theta_L < 0.016$ (95%CL).

[8] ALEXANDER 96M bound comes from analyses of $\tau^- \to 3\pi^- 2\pi^+\nu_\tau$ and $\tau^- \to h^-h^-h^+\nu_\tau$ decays.

[9] BOTTINO 96 assumes three generations of neutrinos with mixing, finds consistency with massless neutrinos with no mixing based on 1995 data for masses, lifetimes, and leptonic partial widths.

[10] HANNESTAD 96C limit is on the mass of a Majorana neutrino. This bound assumes $N_\nu < 4$ from nucleosynthesis. A wider excluded region occurs with a smaller N_ν upper limit. This paper is the corrected version of HANNESTAD 96; see the erratum: HANNESTAD 96B.

[11] SOBIE 96 derive their limit from the Standard Model relationship between the tau mass, lifetime, and leptonic branching fraction, and the muon mass and lifetime, by assuming lepton universality and using world average values.

[12] BUSKULIC 95H bound comes from a two-dimensional fit of the visible energy and invariant mass distribution of $\tau \to 5\pi(\pi^0)\nu_\tau$ decays. Replaced by BARATE 98F.

[13] DOLGOV 95 removes earlier assumptions (DOLGOV 93) about thermal equilibrium below T_{QCD} for wrong-helicity Dirac neutrinos (ENQVIST 93, FULLER 91) to set more stringent limits. DOLGOV 96 argues that a possible window near 20 MeV is excluded.

[14] SIGL 95 exclude massive Dirac or Majorana neutrinos with lifetimes between 10^{-3} and 10^8 seconds if the decay products are predominantly γ or e^+e^-.

[15] DODELSON 94 calculate constraints on ν_τ mass and lifetime from nucleosynthesis for 4 generic decay modes. Limits depend strongly on decay mode. Quoted limit is valid for all decay modes of Majorana neutrinos with lifetime greater than about 300 s. For Dirac neutrinos limits change to < 0.3 or > 33.

[16] KAWASAKI 94 excluded region is for Majorana neutrino with lifetime >1000 s. Other limits are given as a function of ν_τ lifetime for decays of the type $\nu_\tau \to \nu_\mu\phi$ where ϕ is a Nambu-Goldstone boson.

[17] PERES 94 used PDG 92 values for parameters to obtain a value consistent with mixing. Reexamination by BOTTINO 96 which included radiative corrections and 1995 PDG parameters resulted in two allowed regions, m_3 < 70 MeV and 140 MeV m_3 < 149 MeV.

[18] CINABRO 93 bound comes from analysis of $\tau^- \to 3\pi^- 2\pi^+\nu_\tau$ and $\tau^- \to 2\pi^-\pi^+ 2\pi^0\nu_\tau$ decay modes.

[19] DOLGOV 93 assumes neutrino lifetime >100 s. For Majorana neutrinos, the low mass limit is 0.5 MeV. KAWANO 92 points out that these bounds can be overcome for a Dirac neutrino if it possesses a magnetic moment. See also DOLGOV 96.

[20] ENQVIST 93 bases limit on the fact that thermalized wrong-helicity Dirac neutrinos would speed up expansion of early universe, thus reducing the primordial abundance. FULLER 91 exploits the same mechanism but in the older calculation obtains a larger production rate for these states, and hence a lower limit. Neutrino lifetime assumed to exceed nucleosynthesis time, ~ 1 s.

[21] ALBRECHT 92M reports measurement of a slightly lower τ mass, which has the effect of reducing the ν_τ mass reported in ALBRECHT 88B. Bound is from analysis of $\tau^- \to 3\pi^- 2\pi^+ \nu_\tau$ mode.

[22] Assumes neutrino lifetime >1 s. For Dirac neutrinos. See also ENQVIST 93.

[23] KOLB 91 exclusion region is for Dirac neutrino with lifetime >1 s; other limits are given.

Revised September 2013 by K.A. Olive (University of Minnesota).

The limits on low mass ($m_\nu \lesssim$ 1 MeV) neutrinos apply to $m_{\rm tot}$ given by

$$m_{\rm tot} = \sum_\nu (g_\nu/2) m_\nu \ ,$$

where g_ν is the number of spin degrees of freedom for ν plus $\overline{\nu}$: $g_\nu = 4$ for neutrinos with Dirac masses; $g_\nu = 2$ for Majorana neutrinos. Stable neutrinos in this mass range make a contribution to the total energy density of the Universe which is given by

$$\rho_\nu = m_{\rm tot} n_\nu = m_{\rm tot}(3/11) n_\gamma \ ,$$

where the factor 3/11 is the ratio of (light) neutrinos to photons. Writing $\Omega_\nu = \rho_\nu/\rho_c$, where ρ_c is the critical energy density of the Universe, and using $n_\gamma = 412$ cm^{-3}, we have

$$\Omega_\nu h^2 = m_{\rm tot}/(94 \ {\rm eV}) \ .$$

While an upper limit to the matter density of $\Omega_m h^2 < 0.12$ would constrain $m_{\rm tot} < 11$ eV, much stronger constraints are obtained from a combination of observations of the CMB, the amplitude of density fluctuations on smaller scales from the clustering of galaxies and the Lyman-α forest, baryon acoustic oscillations, and new Hubble parameter data. These combine to give an upper limit of around 0.3 eV, and may, in the near future, be able to provide a lower bound on the sum of the neutrino masses.

SUM OF THE NEUTRINO MASSES, $m_{\rm tot}$

(Defined in the above note), of effectively stable neutrinos (i.e., those with mean lives greater than or equal to the age of the universe). These papers assumed Dirac neutrinos. When necessary, we have generalized the results reported so they apply to $m_{\rm tot}$. For other limits, see SZALAY 76, VYSOTSKY 77, BERNSTEIN 81, FREESE 84, SCHRAMM 84, and COWSIK 85.

VALUE (eV)	CL%	DOCUMENT ID		TECN	COMMENT
• • • We do not use the following data for averages, fits, limits, etc. • • •					
< 0.39	95	[1] GIUSARMA	13	COSM	
< 0.24	68	[2] MORESCO	12	COSM	
< 0.60	95	[3] RIEMER-SOR...	12	COSM	
< 0.29	95	[4] XIA	12	COSM	
< 0.81	95	[5] SAITO	11	COSM	SDSS
< 0.44	95	[6] HANNESTAD	10	COSM	
< 0.6	95	[7] SEKIGUCHI	10	COSM	
< 0.28	95	[8] THOMAS	10	COSM	
< 1.1		[9] ICHIKI	09	COSM	
< 1.3	95	[10] KOMATSU	09	COSM	WMAP
< 1.2		[11] TERENO	09	COSM	
< 0.33		[12] VIKHLININ	09	COSM	
< 0.28		[13] BERNARDIS	08	COSM	
< 0.17–2.3		[14] FOGLI	07	COSM	
< 0.42	95	[15] KRISTIANSEN	07	COSM	
< 0.63–2.2		[16] ZUNCKEL	07	COSM	
< 0.24	95	[17] CIRELLI	06	COSM	
< 0.62	95	[18] HANNESTAD	06	COSM	
< 1.2		[19] SANCHEZ	06	COSM	
< 0.17	95	[17] SELJAK	06	COSM	
< 2.0	95	[20] ICHIKAWA	05	COSM	
< 0.75		[21] BARGER	04	COSM	
< 1.0		[22] CROTTY	04	COSM	
< 0.7		[23] SPERGEL	03	COSM	WMAP
< 0.9		[24] LEWIS	02	COSM	
< 4.2		[25] WANG	02	COSM	CMB
< 2.7		[26] FUKUGITA	00	COSM	
< 5.5		[27] CROFT	99	ASTR	Ly α power spec
<180		SZALAY	74	COSM	
<132		COWSIK	72	COSM	
<280		MARX	72	COSM	
<400		GERSHTEIN	66	COSM	

[1] Constrains the total mass of neutrinos from Planck CMB data combined with galaxy clustering data from BOSS. Limit is relaxed to 0.49 eV if the dark energy equation of state is allowed to vary.

[2] Constrains the total mass of neutrinos from observational Hubble parameter data with seven-year WMAP data and the most recent estimate of H_0.

[3] Constrains the total mass of neutrinos from the WiggleZ high redshift galaxy sample when combined with seven-year WMAP data. Limit is improved to < 0.29 eV when further combined with a prior on the Hubble parameter and baryon acoustic oscillations.

[4] Constrains the total mass of neutrinos from the CFHTLS combined with seven-year WMAP data and a prior on the Hubble parameter. Limit is relaxed to 0.41 eV when small scales affected by non-linearities are removed.

[5] Constrains the total mass of neutrinos from the Sloan Digital Sky Survey and the five-year WMAP data.

[6] Constrains the total mass of neutrinos from the 7-year WMAP data including SDSS and HST data. Limit relaxes to 1.19 eV when CMB data is used alone. Supersedes HANNESTAD 06.

[7] Constrains the total mass of neutrinos from a combination of CMB data, a recent measurement of H_0 (SHOES), and baryon acoustic oscillation data from SDSS.

[8] Constrains the total mass of neutrinos from SDSS MegaZ LRG DR7 galaxy clustering data combined with CMB, HST, supernovae and baryon acoustic oscillation data. Limit relaxes to 0.47 eV when the equation of state parameter, $w \neq 1$.

[9] Constrains the total mass of neutrinos from weak lensing measurements when combined with CMB. Limit improves to 0.54 eV when supernovae and baryon acoustic oscillation observations are included. Assumes ΛCDM model.

[10] Constrains the total mass of neutrinos from five-year WMAP data. Limit improves to 0.67 eV when supernovae and baryon acoustic oscillation observations are included. Limits quoted assume the ΛCDM model. Supersedes SPERGEL 07.

[11] Constrains the total mass of neutrinos from weak lensing measurements when combined with CMB. Limit improves to $0.03 < \Sigma m_\nu < 0.54$ eV when supernovae and baryon acoustic oscillation observations are included. The slight preference for massive neutrinos at the two-sigma level disappears when systematic errors are taken into account. Assumes ΛCDM model.

[12] Constrains the total mass of neutrinos from recent Chandra X-ray observations of galaxy clusters when combined with CMB, supernovae, and baryon acoustic oscillation measurements. Assumes flat universe and constant dark-energy equation of state, w.

[13] Constraints the total mass of neutrinos from recent CMB and SOSS LRG power spectrum data along with bias mass relations from SDSS, DEEP2, and Lyman-Break Galaxies. It assumes ΛCDM model. Limit degrades to 0.59 eV in a more general wCDM model.

[14] Constrains the total mass of neutrinos from neutrino oscillation experiments and cosmological data. The most conservative limit uses only WMAP three-year data, while the most stringent limit includes CMB, large-scale structure, supernova, and Lyman-alpha data.

[15] Constrains the total mass of neutrinos from recent CMB, large scale structure, SN1a, and baryon acoustic oscillation data. The limit relaxes to 1.75 when WMAP data alone is used with no prior. Paper shows results with several combinations of data sets. Supersedes KRISTIANSEN 06.

[16] Constrains the total mass of neutrinos from the CMB and the large scale structure data. The most conservative limit is obtained when generic initial conditions are allowed.

[17] Constrains the total mass of neutrinos from recent CMB, large scale structure, Lyman-alpha forest, and SN1a data.

[18] Constrains the total mass of neutrinos from recent CMB and large scale structure data. See also GOOBAR 06. Superseded by HANNESTAD 10.

[19] Constrains the total mass of neutrinos from the CMB and the final 2dF Galaxy Redshift Survey.

[20] Constrains the total mass of neutrinos from the CMB experiments alone, assuming ΛCDM Universe. FUKUGITA 06 show that this result is unchanged by the 3-year WMAP data.

[21] Constrains the total mass of neutrinos from the power spectrum of fluctuations derived from the Sloan Digital Sky Survey and the 2dF galaxy redshift survey, WMAP and 27 other CMB experiments and measurements by the HST Key project.

[22] Constrains the total mass of neutrinos from the power spectrum of fluctuations derived from the Sloan Digital Sky Survey, the 2dF galaxy redshift survey, WMAP and ACBAR. The limit is strengthened to 0.6 eV when measurements by the HST Key project and supernovae data are included.

[23] Constrains the fractional contribution of neutrinos to the total matter density in the Universe from WMAP data combined with other CMB measurements, the 2dfGRS data, and Lyman α data. The limit does not noticeably change if the Lyman α data are not used.

[24] LEWIS 02 constrains the total mass of neutrinos from the power spectrum of fluctuations derived from the CMB, HST Key project, 2dF galaxy redshift survey, supernovae type Ia, and BBN.

[25] WANG 02 constrains the total mass of neutrinos from the power spectrum of fluctuations derived from the CMB and other cosmological data sets such as galaxy clustering and the Lyman α forest.

[26] FUKUGITA 00 is a limit on neutrino masses from structure formation. The constraint is based on the clustering scale σ_8 and the COBE normalization and leads to a conservative limit of 0.9 eV assuming 3 nearly degenerate neutrinos. The quoted limit is on the sum of the light neutrino masses.

[27] CROFT 99 result based on the power spectrum of the Ly α forest. If $\Omega_{\rm matter} < 0.5$, the limit is improved to $m_\nu < 2.4\ (\Omega_{\rm matter}/0.17\text{–}1)$ eV.

Limits on MASSES of Light Stable Right-Handed ν (with necessarily suppressed interaction strengths)

VALUE (eV)		DOCUMENT ID		TECN	COMMENT
• • • We do not use the following data for averages, fits, limits, etc. • • •					
<100–200		[1] OLIVE	82	COSM	Dirac ν
<200–2000		[1] OLIVE	82	COSM	Majorana ν

[1] Depending on interaction strength G_R where $G_R < G_F$.

Limits on MASSES of Heavy Stable Right-Handed ν (with necessarily suppressed interaction strengths)

VALUE (GeV)		DOCUMENT ID		TECN	COMMENT
• • • We do not use the following data for averages, fits, limits, etc. • • •					
> 10		[1] OLIVE	82	COSM	G_R/G_F <0.1
>100		[1] OLIVE	82	COSM	G_R/G_F <0.01

[1] These results apply to heavy Majorana neutrinos and are summarized by the equation: m_ν >1.2 GeV (G_F/G_R). The bound saturates, and if G_R is too small no mass range is allowed.

ν CHARGE

VALUE (units: electron charge)	CL%	DOCUMENT ID		TECN	COMMENT
• • • We do not use the following data for averages, fits, limits, etc. • • •					
$<3.7\times10^{-12}$	90	[1] GNINENKO	07	RVUE	Nuclear reactor
$<2\ \times10^{-14}$		[2] RAFFELT	99	ASTR	Red giant luminosity
$<6\ \times10^{-14}$		[3] RAFFELT	99	ASTR	Solar cooling
$<4\ \times10^{-4}$		[4] BABU	94	RVUE	BEBC beam dump
$<3\ \times10^{-4}$		[5] DAVIDSON	91	RVUE	SLAC e^- beam dump
$<2\ \times10^{-15}$		[6] BARBIELLINI	87	ASTR	SN 1987A
$<1\ \times10^{-13}$		[7] BERNSTEIN	63	ASTR	Solar energy losses

[1] GNINENKO 07 use limit on $\overline{\nu}_e$ magnetic moment from LI 03B to derive this result. The limit is considerably weaker than the limits on the charge of ν_e and $\overline{\nu}_e$ from various astrophysics considerations.

[2] This RAFFELT 99 limit applies to all neutrino flavors which are light enough (<5 keV) to be emitted from globular-cluster red giants.

[3] This RAFFELT 99 limit is derived from the helioseismological limit on a new energy-loss channel of the Sun, and applies to all neutrino flavors which are light enough (<1 keV) to be emitted from the sun.

[4] BABU 94 use COOPER-SARKAR 92 limit on ν magnetic moment to derive quoted result. It applies to ν_τ.

[5] DAVIDSON 91 use data from early SLAC electron beam dump experiment to derive charge limit as a function of neutrino mass. It applies to ν_τ.

[6] Exact BARBIELLINI 87 limit depends on assumptions about the intergalactic or galactic magnetic fields and about the direct distance and time through the field. It applies to ν_e.

[7] The limit applies to all flavors.

ν (MEAN LIFE) / MASS

Measures $\left[\sum|U_{\ell j}|^2\,\Gamma_j\,m_j\right]^{-1}$, where the sum is over mass eigenstates which cannot be resolved experimentally. Some of the limits constrain the radiative decay and are based on the limit of the corresponding photon flux. Other apply to the decay of a heavier neutrino into the lighter one and a Majoron or other invisible particle. Many of these limits apply to any ν within the indicated mass range.

Limits on the radiative decay are either directly based on the limits of the corresponding photon flux, or are derived from the limits on the neutrino magnetic moments. In the later case the transition rate for $\nu_i \to \nu_j + \gamma$ is constrained by $\Gamma_{ij} = \frac{1}{\tau_{ij}} = \frac{(m_i^2-m_j^2)^3}{m_i^3}\,\mu_{ij}^2$ where μ_{ij} is the neutrino transition moment in the mass eigenstates basis. Typically, the limits on lifetime based on the magnetic moments are many orders of magnitude more restrictive than limits based on the nonobservation of photons.

VALUE (s/eV)	CL%	DOCUMENT ID		TECN	COMMENT
> 15.4	90	[1] KRAKAUER	91	CNTR	ν_μ, $\overline{\nu}_\mu$ at LAMPF
> 7 $\times10^9$		[2] RAFFELT	85	ASTR	
> 300	90	[3] REINES	74	CNTR	$\overline{\nu}_e$
• • • We do not use the following data for averages, fits, limits, etc. • • •					
$>10^5-10^{10}$	95	[4] CECCHINI	11	ASTR	$\nu_2\to\nu_1$ radiative decay
	90	[5] MIRIZZI	07	CMB	radiative decay
	90	[6] MIRIZZI	07	CIB	radiative decay
		[7] WONG	07	CNTR	Reactor $\overline{\nu}_e$
> 0.11	90	[8] XIN	05	CNTR	Reactor ν_e
		[9] XIN	05	CNTR	Reactor ν_e
> 0.004	90	[10] AHARMIM	04	SNO	quasidegen. ν masses
> 4.4 $\times10^{-5}$	90	[10] AHARMIM	04	SNO	hierarchical ν masses
$\gtrsim$ 100	95	[11] CECCHINI	04	ASTR	Radiative decay for ν mass > 0.01 eV
> 0.067	90	[12] EGUCHI	04	KLND	quasidegen. ν masses
> 1.1 $\times10^{-3}$	90	[12] EGUCHI	04	KLND	hierarchical ν masses
> 8.7 $\times10^{-5}$	99	[13] BANDYOPA...	03	FIT	nonradiative decay
$\geq$ 4200	90	[14] DERBIN	02B	CNTR	Solar pp and Be ν
> 2.8 $\times10^{-5}$	99	[15] JOSHIPURA	02B	FIT	nonradiative decay
		[16] DOLGOV	99	COSM	
		[17] BILLER	98	ASTR	m_ν= 0.05–1 eV
> 2.8 $\times10^{15}$		[18,19] BLUDMAN	92	ASTR	$m_\nu < 50$ eV
none 10^{-12} – 5×10^4		[20] DODELSON	92	ASTR	m_ν=1–300 keV
$< 10^{-12}$ or $> 5\times10^4$		[20] DODELSON	92	ASTR	m_ν=1–300 keV
		[21] GRANEK	91	COSM	Decaying L^0
> 6.4	90	[22] KRAKAUER	91	CNTR	ν_e at LAMPF
> 1.1 $\times10^{15}$		[23] WALKER	90	ASTR	m_ν= 0.03 – ~ 2 MeV
> 6.3 $\times10^{15}$		[19,24] CHUPP	89	ASTR	$m_\nu < 20$ eV
> 1.7 $\times10^{15}$		[19] KOLB	89	ASTR	$m_\nu < 20$ eV
		[25] RAFFELT	89	RVUE	$\overline{\nu}$ (Dirac, Majorana)
		[26] RAFFELT	89B	ASTR	
> 8.3 $\times10^{14}$		[27] VONFEILIT...	88	ASTR	
> 22	68	[28] OBERAUER	87		$\overline{\nu}_R$ (Dirac)
> 38	68	[28] OBERAUER	87		$\overline{\nu}$ (Majorana)
> 59	68	[28] OBERAUER	87		$\overline{\nu}_L$ (Dirac)
> 30	68	KETOV	86	CNTR	$\overline{\nu}$ (Dirac)
> 20	68	KETOV	86	CNTR	$\overline{\nu}$ (Majorana)
		[29] BINETRUY	84	COSM	$m_\nu\sim$ 1 MeV
> 0.11	90	[30] FRANK	81	CNTR	$\nu\overline{\nu}$ LAMPF
> 2 $\times10^{21}$		[31] STECKER	80	ASTR	m_ν= 10–100 eV
> 1.0 $\times10^{-2}$	90	[30] BLIETSCHAU	78	HLBC	ν_μ, CERN GGM
> 1.7 $\times10^{-2}$	90	[30] BLIETSCHAU	78	HLBC	$\overline{\nu}_\mu$, CERN GGM
< 3 $\times10^{-11}$		[32] FALK	78	ASTR	m_ν <10 MeV
> 2.2 $\times10^{-3}$	90	[30] BARNES	77	DBC	ν, ANL 12-ft
		[33] COWSIK	77	ASTR	
> 3. $\times10^{-3}$	90	[30] BELLOTTI	76	HLBC	ν, CERN GGM
> 1.3 $\times10^{-2}$	90	[30] BELLOTTI	76	HLBC	$\overline{\nu}$, CERN GGM

[1] KRAKAUER 91 quotes the limit $\tau/m_{\nu_1} > (0.75a^2 + 21.65a + 26.3)$ s/eV, where a is a parameter describing the asymmetry in the neutrino decay defined as $dN_\gamma/d\cos\theta = (1/2)(1 + a\cos\theta)$ The parameter $a = 0$ for a Majorana neutrino, but can vary from -1 to 1 for a Dirac neutrino. The bound given by the authors is the most conservative (which applies for $a = -1$).

[2] RAFFELT 85 limit on the radiative decay is from solar x- and γ-ray fluxes. Limit depends on ν flux from pp, now established from GALLEX and SAGE to be > 0.5 of expectation.

[3] REINES 74 looked for ν of nonzero mass decaying radiatively to a neutral of lesser mass + γ. Used liquid scintillator detector near fission reactor. Finds lab lifetime 6×10^7 s or more. Above value of (mean life)/mass assumes average effective neutrino energy of 0.2 MeV. To obtain the limit 6×10^7 s REINES 74 assumed that the full $\overline{\nu}_e$ reactor flux could be responsible for yielding decays with photon energies in the interval 0.1 MeV – 0.5 MeV. This represents some overestimate so their lower limit is an over-estimate of the lab lifetime (VOGEL 84). If so, OBERAUER 87 may be comparable or better.

[4] CECCHINI 11 search for radiative decays of solar neutrinos into visible photons during the 2006 total solar eclipse. The range of (mean life)/mass values corresponds to a range of ν_1 masses between 10^{-4} and 0.1 eV.

[5] MIRIZZI 07 determine a limit on the neutrino radiative decay from analysis of the maximum allowed distortion of the CMB spectrum as measured by the COBE/FIRAS. For the decay $\nu_2 \to \nu_1$ the lifetime limit is $\lesssim 4\times10^{20}$ s for $m_{min} \lesssim 0.14$ eV. For transition with the $|\Delta m_{31}|$ mass difference the lifetime limit is $\sim 2\times10^{19}$ s for $m_{min} \lesssim 0.14$ eV and $\sim 5\times10^{20}$ s for $m_{min} \gtrsim 0.14$ eV.

[6] MIRIZZI 07 determine a limit on the neutrino radiative decay from analysis of the cosmic infrared background (CIB) using the Spitzer Observatory data. For transition with the $|\Delta m_{31}|$ mass difference they obtain the lifetime limit $\sim 10^{20}$ s for $m_{min} \lesssim 0.14$ eV.

[7] WONG 07 use their limit on the neutrino magnetic moment together with the assumed experimental value of $\Delta m^2_{13} \sim 2\times10^{-3}$ eV^2 to obtain $\tau_{13}/m_1^3 > 3.2\times10^{27}$ s/eV^3 for the radiative decay in the case of the inverted mass hierarchy. Similarly to RAFFELT 89 this limit can be violated if electric and magnetic moments are equal to each other. Analogous, but numerically somewhat different limits are obtained for τ_{23} and τ_{21}.

[8] XIN 05 search for the γ from radiative decay of ν_e produced by the electron capture on ^{51}Cr. No events were seen and the limit on τ/m_ν was derived. This is a weaker limit on the decay of ν_e than KRAKAUER 91.

[9] XIN 05 use their limit on the neutrino magnetic moment of ν_e together with the assumed experimental value of $\Delta m^2_{1,3} \sim 2\times10^{-3}$ eV^2 to obtain $\tau_{13}/m_1^3 > 1\times10^{23}$ s/eV^3 for the radiative decay in the case of the inverted mass hierarchy. Similarly to RAFFELT 89 this limit can be violated if electric and magnetic moments are equal to each other. Analogous, but numerically somewhat different limits are obtained for τ_{23} and τ_{21}. Again, this limit is specific for ν_e.

[10] AHARMIM 04 obtained these results from the solar $\overline{\nu}_e$ flux limit set by the SNO measurement assuming ν_2 decay through nonradiative process $\nu_2 \to \overline{\nu}_1 X$, where X is a Majoron or other invisible particle. Limits are given for the cases of quasidegenerate and hierarchical neutrino masses.

[11] CECCHINI 04 obtained this bound through the observations performed on the occasion of the 21 June 2001 total solar eclipse, looking for visible photons from radiative decays of solar neutrinos. Limit is a τ/m_{ν_2} in $\nu_2 \to \nu_1\gamma$. Limit ranges from $\sim$ 100 to 10^7 s/eV for $0.01 < m_{\nu_1} < 0.1$ eV.

[12] EGUCHI 04 obtained these results from the solar $\overline{\nu}_e$ flux limit set by the KamLAND measurement assuming ν_2 decay through nonradiative process $\nu_2 \to \overline{\nu}_1 X$, where X is a Majoron or other invisible particle. Limits are given for the cases of quasidegenerate and hierarchical neutrino masses.

[13] The ratio of the lifetime over the mass derived by BANDYOPADHYAY 03 is for ν_2. They obtained this result using the following solar-neutrino data: total rates measured in Cl and Ga experiments, the Super-Kamiokande's zenith-angle spectra, and SNO's day and night spectra. They assumed that ν_1 is the lowest mass, stable or nearly stable neutrino state and ν_2 decays through nonradiative Majoron emission process, $\nu_2 \to \overline{\nu}_1 + J$, or through nonradiative process with all the final state particles being sterile. The best fit is obtained in the region of the LMA solution.

[14] DERBIN 02B (also BACK 03B) obtained this bound for the radiative decay from the results of background measurements with Counting Test Facility (the prototype of the Borexino detector). The laboratory gamma spectrum is given as $dN_\gamma/d\cos\theta = (1/2)(1 + \alpha\cos\theta)$ with α=0 for a Majorana neutrino, and α varying to -1 to 1 for a Dirac neutrino. The listed bound is for the case of α=0. The most conservative bound 1.5×10^3 s eV^{-1} is obtained for the case of α=-1.

[15] The ratio of the lifetime over the mass derived by JOSHIPURA 02B is for ν_2. They obtained this result from the total rates measured in all solar neutrino experiments. They assumed that ν_1 is the lowest mass, stable or nearly stable neutrino state and ν_2 decays through nonradiative process like Majoron emission decay, $\nu_2 \to \nu_1' + J$ where ν_1' state is sterile. The exact limit depends on the specific solution of the solar neutrino problem. The quoted limit is for the LMA solution.

[16] DOLGOV 99 places limits in the (Majorana) τ-associated ν mass-lifetime plane based on nucleosynthesis. Results would be considerably modified if neutrino oscillations exist.

[17] BILLER 98 use the observed TeV γ-ray spectra to set limits on the mean life of any radiatively decaying neutrino between 0.05 and 1 eV. Curve shows $\tau_\nu/B_\gamma > 0.15\times10^{21}$ s at 0.05 eV, $> 1.2\times10^{21}$ s at 0.17 eV, $> 3\times10^{21}$ s at 1 eV, where B_γ is the branching ratio to photons.

[18] BLUDMAN 92 sets additional limits by this method for higher mass ranges. Cosmological limits are also obtained.

[19] Limit on the radiative decay based on nonobservation of γ's in coincidence with ν's from SN 1987A.

[20] DODELSON 92 range is for wrong-helicity keV mass Dirac ν's from the core of neutron star in SN 1987A decaying to ν's that would have interacted in KAM2 or IMB detectors.

[21] GRANEK 91 considers heavy neutrino decays to $\gamma\nu_L$ and $3\nu_L$, where m_{ν_L} <100 keV. Lifetime is calculated as a function of heavy neutrino mass, branching ratio into $\gamma\nu_L$, and m_{ν_L}.

[22] KRAKAUER 91 quotes the limit for ν_e, $\tau/m_\nu > (0.3a^2 + 9.8a + 15.9)$ s/eV, where a is a parameter describing the asymmetry in the radiative neutrino decay defined as $dN_\gamma/d\cos\theta = (1/2)(1 + a\cos\theta)$ a=0 for a Majorana neutrino, but can vary from -1 to 1 for a Dirac neutrino. The bound given by the authors is the most conservative (which applies for $a = -1$).

[23] WALKER 90 uses SN 1987A γ flux limits after 289 days.

[24] CHUPP 89 should be multiplied by a branching ratio (about 1) and a detection efficiency (about 1/4), and pertains to radiative decay of any neutrino to a lighter or sterile neutrino.

[25] RAFFELT 89 uses KYULDJIEV 84 to obtain $\tau m^3 > 3\times10^{18}$ s eV^3 (based on $\overline{\nu}_e e^-$ cross sections). The bound for the radiative decay is not valid if electric and magnetic transition moments are equal for Dirac neutrinos.

[26] RAFFELT 89B analyze stellar evolution and exclude the region $3\times10^{12} < \tau m^3 < 3\times10^{21}$ s eV^3.

[27] Model-dependent theoretical analysis of SN 1987A neutrinos. Quoted limit is for $\left[\sum_j |U_{\ell j}|^2\, \Gamma_j\, m_j\right]^{-1}$, where ℓ=μ, τ. Limit is 3.3×10^{14} s/eV for ℓ=e.

[28] OBERAUER 87 looks for photons and e^+e^- pairs from radiative decays of reactor neutrinos.

[29] BINETRUY 84 finds $\tau < 10^8$ s for neutrinos in a radiation-dominated universe.

[30] These experiments look for $\nu_k \to \nu_j\gamma$ or $\overline{\nu}_k \to \overline{\nu}_j\gamma$.

[31] STECKER 80 limit based on UV background; result given is $\tau > 4\times10^{22}$ s at m_ν=20 eV.

[32] FALK 78 finds lifetime constraints based on supernova energetics.

[33] COWSIK 77 considers variety of scenarios. For neutrinos produced in the big bang, present limits on optical photon flux require $\tau > 10^{23}$ s for $m_\nu \sim 1$ eV. See also COWSIK 79 and GOLDMAN 79.

ν MAGNETIC MOMENT

The coupling of neutrinos to an electromagnetic field is a characterized by a 3×3 matrix λ of the magnetic (μ) and electric (d) dipole moments ($\lambda = \mu - id$). For Majorana neutrinos the matrix λ is antisymmetric and only transition moments are allowed, while for Dirac neutrinos λ is a general 3×3 matrix. In the standard electroweak theory extended to include neutrino masses (see FUJIKAWA 80) $\mu_\nu = 3eG_F m_\nu/(8\pi^2\sqrt{2}) = 3.2\times10^{-19}(m_\nu/\text{eV})\mu_B$, i.e. it is unobservably small given the known small neutrino masses. In more general models there is no longer a proportionality between neutrino mass and its magnetic moment, even though only massive neutrinos have nonvanishing magnetic moments without fine tuning.

Laboratory bounds on λ are obtained via elastic ν-e scattering, where the scattered neutrino is not observed. The combinations of matrix elements of λ that are constrained by various experiments depend on the initial neutrino flavor and on its propagation between source and detector (e.g., solar ν_e and reactor $\overline{\nu}_e$ do not constrain the same combinations). The listings below therefore identify the initial neutrino flavor.

Other limits, e.g. from various stellar cooling processes, apply to all neutrino flavors. Analogous flavor independent, but weaker, limits are obtained from the analysis of $e^+e^- \to \nu\overline{\nu}\gamma$ collider experiments.

VALUE (10^{-10} μ_B)	CL%	DOCUMENT ID		TECN	COMMENT
< 0.29	90	[1] BEDA	13	CNTR	Reactor $\overline{\nu}_e$
< 6.8	90	[2] AUERBACH	01	LSND	$\nu_e e$, $\nu_\mu e$ scattering
< 3900	90	[3] SCHWIENHO...	01	DONU	$\nu_\tau e^- \to \nu_\tau e^-$
• • • We do not use the following data for averages, fits, limits, etc. • • •					
< 0.045	95	[4] VIAUX	13A	ASTR	Globular cluster M5
< 0.32	90	[5] BEDA	10	CNTR	Reactor $\overline{\nu}_e$
< 2.2	90	[6] DENIZ	10	TEXO	Reactor $\overline{\nu}_e$
< 0.011–0.027		[7] KUZNETSOV	09	ASTR	$\nu_L \to \nu_R$ in SN1987A
< 0.54	90	[8] ARPESELLA	08A	BORX	Solar ν spectrum shape
< 0.58	90	[9] BEDA	07	CNTR	Reactor $\overline{\nu}_e$
< 0.74	90	[10] WONG	07	CNTR	Reactor $\overline{\nu}_e$
< 0.9	90	[11] DARAKTCH...	05		Reactor $\overline{\nu}_e$
< 130	90	[12] XIN	05	CNTR	Reactor ν_e
< 37	95	[13] GRIFOLS	04	FIT	Solar ^{8}B ν (SNO NC)
< 3.6	90	[14] LIU	04	SKAM	Solar ν spectrum shape
< 1.1	90	[15] LIU	04	SKAM	Solar ν spectrum shape (LMA region)
< 5.5	90	[16] BACK	03B	CNTR	Solar pp and Be ν
< 1.0	90	[17] DARAKTCH...	03		Reactor $\overline{\nu}_e$
< 1.3	90	[18] LI	03B	CNTR	Reactor $\overline{\nu}_e$
< 2	90	[19] GRIMUS	02	FIT	solar + reactor (Majorana ν)
<80000	90	[20] TANIMOTO	00	RVUE	$e^+e^- \to \nu\overline{\nu}\gamma$
< 0.01–0.04		[21] AYALA	99	ASTR	$\nu_L \to \nu_R$ in SN 1987A
< 1.5	90	[22] BEACOM	99	SKAM	ν spectrum shape
< 0.03		[23] RAFFELT	99	ASTR	Red giant luminosity
< 4		[24] RAFFELT	99	ASTR	Solar cooling
<44000	90	ABREU	97J	DLPH	$e^+e^- \to \nu\overline{\nu}\gamma$ at LEP
<33000	90	[25] ACCIARRI	97Q	L3	$e^+e^- \to \nu\overline{\nu}\gamma$ at LEP
< 0.62		[26] ELMFORS	97	COSM	Depolarization in early universe plasma
<27000	95	[27] ESCRIBANO	97	RVUE	$\Gamma(Z \to \nu\nu)$ at LEP
< 30	90	VILAIN	95B	CHM2	$\nu_\mu e \to \nu_\mu e$
<55000	90	GOULD	94	RVUE	$e^+e^- \to \nu\overline{\nu}\gamma$ at LEP
< 1.9	95	[28] DERBIN	93	CNTR	Reactor $\overline{\nu}e \to \overline{\nu}e$
< 5400	90	[29] COOPER-...	92	BEBC	$\nu_\tau e^- \to \nu_\tau e^-$
< 2.4	90	[30] VIDYAKIN	92	CNTR	Reactor $\overline{\nu}e \to \overline{\nu}e$
<56000	90	DESHPANDE	91	RVUE	$e^+e^- \to \nu\overline{\nu}\gamma$
< 100	95	[31] DORENBOS...	91	CHRM	$\nu_\mu e \to \nu_\mu e$
< 8.5	90	AHRENS	90	CNTR	$\nu_\mu e \to \nu_\mu e$
< 10.8	90	[32] KRAKAUER	90	CNTR	LAMPF $\nu e \to \nu e$
< 7.4	90	[32] KRAKAUER	90	CNTR	LAMPF $(\nu_\mu, \overline{\nu}_\mu)e$ elast.
< 0.02		[33] RAFFELT	90	ASTR	Red giant luminosity
< 0.1		[34] RAFFELT	89B	ASTR	Cooling helium stars
		[35] FUKUGITA	88	COSM	Primordial magn. fields
<40000	90	[36] GROTCH	88	RVUE	$e^+e^- \to \nu\overline{\nu}\gamma$
≤ .3		[34] RAFFELT	88B	ASTR	He burning stars
< 0.11		[34] FUKUGITA	87	ASTR	Cooling helium stars
< 0.0006		[37] NUSSINOV	87	ASTR	Cosmic EM backgrounds
< 0.1–0.2		MORGAN	81	COSM	^{4}He abundance
< 0.85		BEG	78	ASTR	Stellar plasmons
< 0.6		[38] SUTHERLAND	76	ASTR	Red giants + degenerate dwarfs
< 81		[39] KIM	74	RVUE	$\overline{\nu}_\mu e \to \overline{\nu}_\mu e$
< 1		BERNSTEIN	63	ASTR	Solar cooling
< 14		COWAN	57	CNTR	Reactor $\overline{\nu}$

[1] BEDA 13 report $\overline{\nu}_e e^-$ scattering results, using the Kalinin Nuclear Power Plant and a shielded Ge detector. The recoil electron spectrum is analyzed between 2.5 and 55 keV. Supersedes BEDA 07. Supersedes BEDA 10. This is the most stringent limit on the magnetic moment of reactor $\overline{\nu}_e$.

[2] AUERBACH 01 limit is based on the LSND ν_e and ν_μ electron scattering measurements. The limit is slightly more stringent than KRAKAUER 90.

[3] SCHWIENHORST 01 quote an experimental sensitivity of 4.9×10^{-7}.

[4] VIAUX 13A constrains the neutrino magnetic moment from observations of the globular cluster M5.

[5] BEDA 10 report $\overline{\nu}_e e^-$ scattering results, using the Kalinin Nuclear Power Plant and a shielded Ge detector. The recoil electron spectrum is analyzed between 2.9 and 45 keV. Supersedes BEDA 07. Superseded by BEDA 13.

[6] DENIZ 10 observe reactor $\overline{\nu}_e e$ scattering with recoil kinetic energies 3–8 MeV using CsI(Tl) detectors. The observed rate and spectral shape are consistent with the Standard Model prediction, leading to the reported constraint on $\overline{\nu}_e$ magnetic moment.

[7] KUZNETSOV 09 obtain a limit on the flavor averaged magnetic moment of Dirac neutrinos from the time averaged neutrino signal of SN1987A. Improves and supersedes the analysis of BARBIERI 88 and AYALA 99.

[8] ARPESELLA 08A obtained this limit using the shape of the recoil electron energy spectrum from the Borexino 192 live days of solar neutrino data.

[9] BEDA 07 performed search for electromagnetic $\overline{\nu}_e$-e scattering at Kalininskaya nuclear reactor. A Ge detector with active and passive shield was used and the electron recoil spectrum between 3.0 and 61.3 keV analyzed. Superseded by BEDA 10.

[10] WONG 07 performed search for non-standard $\overline{\nu}_e$-e scattering at the Kuo-Sheng nuclear reactor. Ge detector equipped with active anti-Compton shield is used. Most stringent laboratory limit on magnetic moment of reactor $\overline{\nu}_e$. Supersedes LI 03B.

[11] DARAKTCHIEVA 05 present the final analysis of the search for non-standard $\overline{\nu}_e$-e scattering component at Bugey nuclear reactor. Full kinematical event reconstruction of both the kinetic energy above 700 keV and scattering angle of the recoil electron, by use of TPC. Most stringent laboratory limit on magnetic moment. Supersedes DARAKTCHIEVA 03.

[12] XIN 05 evaluated the ν_e flux at the Kuo-Sheng nuclear reactor and searched for non-standard ν_e-e scattering. Ge detector equipped with active anti-Compton shield was used. This laboratory limit on magnetic moment is considerably less stringent than the limits for reactor $\overline{\nu}_e$, but is specific to ν_e.

[13] GRIFOLS 04 obtained this bound using the SNO data of the solar ^{8}B neutrino flux measured with deuteron breakup. This bound applies to $\mu_{\rm eff} = (\mu_{21}^2 + \mu_{22}^2 + \mu_{23}^2)^{1/2}$.

[14] LIU 04 obtained this limit using the shape of the recoil electron energy spectrum from the Super-Kamiokande-I 1496 days of solar neutrino data. Neutrinos are assumed to have only diagonal magnetic moments, $\mu_{\nu 1} = \mu_{\nu 2}$. This limit corresponds to the oscillation parameters in the vacuum oscillation region.

[15] LIU 04 obtained this limit using the shape of the recoil electron energy spectrum from the Super-Kamiokande-I 1496 live-day solar neutrino data, by limiting the oscillation parameter region in the LMA region allowed by solar neutrino experiments plus KamLAND. $\mu_{\nu 1} = \mu_{\nu 2}$ is assumed. In the LMA region, the same limit would be obtained even if neutrinos have off-diagonal magnetic moments.

[16] BACK 03B obtained this bound from the results of background measurements with Counting Test Facility (the prototype of the Borexino detector). Standard Solar Model flux was assumed. This μ_ν can be different from the reactor μ_ν in certain oscillation scenarios (see BEACOM 99).

[17] DARAKTCHIEVA 03 searched for non-standard $\overline{\nu}_e$-e scattering component at Bugey nuclear reactor. Full kinematical event reconstruction by use of TPC. Superseded by DARAKTCHIEVA 05.

[18] LI 03B used Ge detector in active shield near nuclear reactor to test for nonstandard $\overline{\nu}_e$-e scattering.

[19] GRIMUS 02 obtain stringent bounds on all Majorana neutrino transition moments from a simultaneous fit of LMA-MSW oscillation parameters and transition moments to global solar neutrino data + reactor data. Using only solar neutrino data, a 90% CL bound of $6.3 \times 10^{-10} \mu_B$ is obtained.

[20] TANIMOTO 00 combined $e^+e^- \to \nu\overline{\nu}\gamma$ data from VENUS, TOPAZ, and AMY.

[21] AYALA 99 improves the limit of BARBIERI 88.

[22] BEACOM 99 obtain the limit using the shape, but not the absolute magnitude which is affected by oscillations, of the solar neutrino spectrum obtained by Superkamiokande (825 days). This μ_ν can be different from the reactor μ_ν in certain oscillation scenarios.

[23] RAFFELT 99 is an update of RAFFELT 90. This limit applies to all neutrino flavors which are light enough (< 5 keV) to be emitted from globular-cluster red giants. This limit pertains equally to electric dipole moments and magnetic transition moments, and it applies to both Dirac and Majorana neutrinos.

[24] RAFFELT 99 is essentially an update of BERNSTEIN 63, but is derived from the helioseismological limit on a new energy-loss channel of the Sun. This limit applies to all neutrino flavors which are light enough (<1 keV) to be emitted from the Sun. This limit pertains equally to electric dipole and magnetic transition moments, and it applies to both Dirac and Majorana neutrinos.

[25] ACCIARRI 97Q result applies to both direct and transition magnetic moments and for q^2=0.

[26] ELMFORS 97 calculate the rate of depolarization in a plasma for neutrinos with a magnetic moment and use the constraints from a big-bang nucleosynthesis on additional degrees of freedom.

[27] Applies to absolute value of magnetic moment.

[28] DERBIN 93 determine the cross section for 0.6–2.0 MeV electron energy as $(1.28 \pm 0.63) \times \sigma_{\rm weak}$. However, the (reactor on – reactor off)/(reactor off) is only $\sim 1/100$.

[29] COOPER-SARKAR 92 assume $f_{D_s}/f_\pi = 2$ and D_s, $\overline{D}_s$ production cross section = 2.6 μb to calculate ν flux.

[30] VIDYAKIN 92 limit is from a $e\overline{\nu}_e$ elastic scattering experiment. No experimental details are given except for the cross section from which this limit is derived. Signal/noise was 1/10. The limit uses $\sin^2\theta_W = 0.23$ as input.

[31] DORENBOSCH 91 corrects an incorrect statement in DORENBOSCH 89 that the ν magnetic moment is $< 1 \times 10^{-9}$ at the 95%CL. DORENBOSCH 89 measures both $\nu_\mu e$ and $\overline{\nu} e$ elastic scattering and assume $\mu(\nu) = \mu(\overline{\nu})$.

[32] KRAKAUER 90 experiment fully reported in ALLEN 93.

[33] RAFFELT 90 limit applies for a diagonal magnetic moment of a Dirac neutrino, or for a transition magnetic moment of a Majorana neutrino. In the latter case, the same analysis gives $< 1.4 \times 10^{-12}$. Limit at 95%CL obtained from δM_C.

[34] Significant dependence on details of stellar models.

[35] FUKUGITA 88 find magnetic dipole moments of any two neutrino species are bounded by $\mu < 10^{-16}$ $[10^{-9}\ G/B_0]$ where B_0 is the present-day intergalactic field strength.

[36] GROTCH 88 combined data from MAC, ASP, CELLO, and Mark J.

[37] For m_ν = 8–200 eV. NUSSINOV 87 examines transition magnetic moments for $\nu_\mu \to \nu_e$ and obtain $< 3 \times 10^{-15}$ for $m_\nu > 16$ eV and $< 6 \times 10^{-14}$ for $m_\nu > 4$ eV.

[38] We obtain above limit from SUTHERLAND 76 using their limit $f < 1/3$.

[39] KIM 74 is a theoretical analysis of $\overline{\nu}_\mu$ reaction data.

NEUTRINO CHARGE RADIUS SQUARED

We report limits on the so-called neutrino charge radius squared. While the straight-forward definition of a neutrino charge radius has been proven to be gauge-dependent and, hence, unphysical (LEE 77C), there have been recent attempts to define a physically observable neutrino charge radius (BERNABEU 00, BERNABEU 02). The issue is still controversial (FUJIKAWA 03, BERNABEU 03). A more general interpretation of the experimental results is that they are limits on certain nonstandard contributions to neutrino scattering.

VALUE (10^{-32} cm^2)	CL%	DOCUMENT ID		TECN	COMMENT
−2.1 to 3.3	90	[1] DENIZ	10	TEXO	Reactor $\overline{\nu}_e e$
• • • We do not use the following data for averages, fits, limits, etc. • • •					
−0.53 to 0.68	90	[2] HIRSCH	03		$\nu_\mu e$ scat.
−8.2 to 9.9	90	[3] HIRSCH	03		anomalous $e^+e^- \to \nu\overline{\nu}\gamma$
−2.97 to 4.14	90	[4] AUERBACH	01	LSND	$\nu_e e \to \nu_e e$
−0.6 to 0.6	90	VILAIN	95B	CHM2	$\nu_\mu e$ elastic scat.
0.9 ±2.7		ALLEN	93	CNTR	LAMPF $\nu e \to \nu e$
< 2.3	95	MOURAO	92	ASTR	HOME/KAM2 ν rates
< 7.3	90	[5] VIDYAKIN	92	CNTR	Reactor $\overline{\nu}e \to \overline{\nu}e$
1.1 ±2.3		ALLEN	91	CNTR	Repl. by ALLEN 93
−1.1 ±1.0		[6] AHRENS	90	CNTR	$\nu_\mu e$ elastic scat.
−0.3 ±1.5		[6] DORENBOS...	89	CHRM	$\nu_\mu e$ elastic scat.
		[7] GRIFOLS	89B	ASTR	SN 1987A

[1] DENIZ 10 observe reactor $\overline{\nu}_e e$ scattering with recoil kinetic energies 3–8 MeV using CsI(Tl) detectors. The observed rate and spectral shape are consistent with the Standard Model prediction, leading to the reported constraint on $\overline{\nu}_e$ charge radius.

[2] Based on analysis of CCFR 98 results. Limit is on $\langle r_V^2 \rangle + \langle r_A^2 \rangle$. The CHARM II and E734 at BNL results are reanalyzed, and weaker bounds on the charge radius squared than previously published are obtained. The NuTeV result is discussed; when tentatively interpreted as ν_μ charge radius it implies $\langle r_V^2 \rangle + \langle r_A^2 \rangle = (4.20 \pm 1.64) \times 10^{-33}$ cm^2.

[3] Results of LEP-2 are interpreted as limits on the axial-vector charge radius squared of a Majorana ν_τ. Slightly weaker limits for both vector and axial-vector charge radius squared are obtained for the Dirac case, and somewhat weaker limits are obtained from the analysis of lower energy data (LEP-1.5 and TRISTAN).

[4] AUERBACH 01 measure $\nu_e e$ elastic scattering with LSND detector. The cross section agrees with the Standard Model expectation, including the charge and neutral current interference. The 90% CL applies to the range shown.

[5] VIDYAKIN 92 limit is from a $e\overline{\nu}$ elastic scattering experiment. No experimental details are given except for the cross section from which this limit is derived. Signal/noise was 1/10. The limit uses $\sin^2\theta_W = 0.23$ as input.

[6] Result is obtained from reanalysis given in ALLEN 91, followed by our reduction to obtain $1\,\sigma$ errors.

[7] GRIFOLS 89B sets a limit of $\langle r^2 \rangle < 0.2 \times 10^{-32}$ cm^2 for right-handed neutrinos.

REFERENCES FOR Neutrino Properties

BEDA	13	PPNL 10 139	A.G. Beda *et al.*	(GEMMA Collab.)
GIUSARMA	13	PR D88 063515	E. Giusarma *et al.*	
VIAUX	13A	PRL 111 231301	N. Viaux *et al.*	
MORESCO	12	JCAP 1207 053	M. Moresco *et al.*	
RIEMER-SOR...	12	PR D85 081101	S. Riemer-Sorensen *et al.*	
XIA	12	JCAP 1206 010	J.-Q. Xia *et al.*	
ASEEV	11	PR D84 112003	V.N. Aseev *et al.*	
CECCHINI	11	ASP 34 486	S. Cecchini *et al.*	
SAITO	11	PR D83 043529	S. Saito, M. Takada, A. Taruya	
BEDA	10	PPNL 7 406	A.G. Beda *et al.*	(GEMMA Collab.)
DENIZ	10	PR D81 072001	M. Deniz *et al.*	(TEXONO Collab.)
HANNESTAD	10	JCAP 1008 001	S. Hannestad *et al.*	
PAGLIAROLI	10	ASP 33 287	G. Pagliaroli, F. Rossi-Torres, E. Vissani	(INFN+)
SEKIGUCHI	10	JCAP 1003 015	T. Sekiguchi *et al.*	
THOMAS	10	PRL 105 031301	S.A. Thomas, F.B. Abdalla, O. Lahav	(LOUC)
ICHIKI	09	PR D79 023520	K. Ichiki, M. Takada, T. Takahashi	
KOMATSU	09	APJS 180 330	E. Komatsu *et al.*	
KUZNETSOV	09	IJMP A24 5977	A.V. Kuznetsov, N.V. Mikheev, A.A. Okrugin	(YARO)
TERENO	09	AA 500 657	I. Tereno *et al.*	
VIKHLININ	09	APJ 692 1060	A. Vikhlinin *et al.*	
ARPESELLA	08A	PRL 101 091302	C. Arpesella *et al.*	(Borexino Collab.)
BERNARDIS	08	PR D78 083535	F. De Bernardis *et al.*	
BEDA	07	PAN 70 1873	A.G. Beda *et al.*	
		Translated from YAF 70 1925.		
FOGLI	07	PR D75 053001	G.L. Fogli *et al.*	
GNINENKO	07	PR D75 075014	S.N. Gninenko, N.V. Krasnikov, A. Rubbia	
KRISTIANSEN	07	PR D75 083510	J. Kristiansen, O. Elgaroy, H. Dahle	
MIRIZZI	07	PR D76 053007	A. Mirizzi, D. Montanino, P.D. Serpico	
SPERGEL	07	APJS 170 377	D.N. Spergel *et al.*	
WONG	07	PR D75 012001	H.T. Wong *et al.*	(TEXONO Collab.)
ZUNCKEL	07	JCAP 0708 004	C. Zunckel, P. Ferreira	
CIRELLI	06	JCAP 0612 013	M. Cirelli *et al.*	
FUKUGITA	06	PR D74 027302	M. Fukugita *et al.*	
GOOBAR	06	JCAP 0606 019	A. Goobar *et al.*	
HANNESTAD	06	JCAP 0611 016	S. Hannestad, G. Raffelt	
KRISTIANSEN	06	PR D74 123005	J. Kristiansen, O. Elgaroy, H. Eriksen	
SANCHEZ	06	MNRAS 366 189	A.G. Sanchez *et al.*	
SELJAK	06	JCAP 0610 014	U. Seljak, A. Slosar, P. McDonald	
DARAKTCH...	05	PL B615 153	Z. Daraktchieva *et al.*	(MUNU Collab.)
ICHIKAWA	05	PR D71 043001	K. Ichikawa, M. Fukugita, M. Kawasaki	(ICRR)
KRAUS	05	EPJ C40 447	Ch. Kraus *et al.*	
XIN	05	PR D72 012006	B. Xin *et al.*	(TEXONO Collab.)
AHARMIM	04	PR D70 093014	B. Aharmim *et al.*	(SNO Collab.)
BARGER	04	PL B595 55	V. Barger, D. Marfatia, A. Tregre	
CECCHINI	04	ASP 21 183	S. Cecchini *et al.*	(BGNA+)
CROTTY	04	PR D69 123007	P. Crotty, J. Lesgourgues, S. Pastor	
EGUCHI	04	PRL 92 071301	K. Eguchi *et al.*	(KamLAND Collab.)
GRIFOLS	04	PL B587 184	J.A. Grifols, E. Masso, S. Mohanty	(BARC, AHMED)
LIU	04	PRL 93 021802	D.W. Liu *et al.*	(Super-Kamiokande Collab.)
ARNABOLDI	03A	PRL 91 161802	C. Arnaboldi *et al.*	

BACK	03B	PL B563 35	H.O. Back *et al.*	(Borexino Collab.)
BANDYOPA...	03	PL B555 33	A. Bandyopadhyay, S. Choubey, S. Goswami	(SAHA+)
BERNABEU	03	hep-ph/0303202	J. Bernabeu, J. Papavassiliou, J. Vidal	
DARAKTCH...	03	PL B564 190	Z. Daraktchieva *et al.*	(MUNU Collab.)
FUJIKAWA	03	hep-ph/0303188	K. Fujikawa, R. Shrock	
HIRSCH	03	PR D67 033005	M. Hirsch *et al.*	
LI	03B	PRL 90 131802	H.B. Li *et al.*	(TEXONO Collab.)
SPERGEL	03	APJS 148 175	D.N. Spergel *et al.*	
BERNABEU	02	PRL 89 101802	J. Bernabeu, J. Papavassiliou, J. Vidal	
Also		PRL 89 229902 (errat)	J. Bernabeu, J. Papavassiliou, J. Vidal	
DERBIN	02B	JETPL 76 409	A.V. Derbin, O.Ju. Smirnov	
		Translated from ZETFP 76 483.		
GRIMUS	02	NP B648 376	W. Grimus *et al.*	
JOSHIPURA	02B	PR D66 113008	A.S. Joshipura, E. Masso, S. Mohanty	
LEWIS	02	PR D66 103511	A. Lewis, S. Bridle	
LOREDO	02	PR D65 063002	T.J. Loredo, D.Q. Lamb	
WANG	02	PR D65 123001	X. Wang, M. Tegmark, M. Zaldarriaga	
AUERBACH	01	PR D63 112001	L.B. Auerbach *et al.*	(LSND Collab.)
SCHWIENHO...	01	PL B513 23	R. Schwienhorst *et al.*	(DONUT Collab.)
ATHANAS	00	PR D61 052002	M. Athanas *et al.*	(CLEO Collab.)
BERNABEU	00	PR D62 113012	J. Bernabeu *et al.*	
FUKUGITA	00	PRL 84 1082	M. Fukugita, G.C. Liu, N. Sugiyama	
TANIMOTO	00	PL B478 1	N. Tanimoto *et al.*	
AYALA	99	PR D59 111901	A. Ayala, J.C. D'Olivo, M. Torres	
BEACOM	99	PRL 83 5222	J.F. Beacom, P. Vogel	
CROFT	99	PRL 83 1092	R.A.C. Croft, W. Hu, R. Dave	
DOLGOV	99	NP B548 385	A.D. Dolgov *et al.*	
LOBASHEV	99	PL B460 227	V.M. Lobashev *et al.*	
RAFFELT	99	PRPL 320 319	G.G. Raffelt	
WEINHEIMER	99	PL B460 219	Ch. Weinheimer *et al.*	
ACKERSTAFF	98T	EPJ C5 229	K. Ackerstaff *et al.*	(OPAL Collab.)
AMMAR	98	PL B431 209	R. Ammar *et al.*	(CLEO Collab.)
BARATE	98F	EPJ C2 395	R. Barate *et al.*	(ALEPH Collab.)
BILLER	98	PRL 80 2992	S.D. Biller *et al.*	(WHIPPLE Collab.)
FELDMAN	98	PR D57 3873	G.J. Feldman, R.D. Cousins	
LENZ	98	PL B416 50	S. Lenz *et al.*	
ABREU	97J	ZPHY C74 577	P. Abreu *et al.*	(DELPHI Collab.)
ACCIARRI	97Q	PL B412 201	M. Acciarri *et al.*	(L3 Collab.)
ANASTASSOV	97	PR D55 2559	A. Anastassov *et al.*	(CLEO Collab.)
Also		PR D58 119903 (erratum)	A. Anastassov *et al.*	(CLEO Collab.)
ELMFORS	97	NP B503 3	P. Elmfors *et al.*	
ESCRIBANO	97	PL B395 369	R. Escribano, E. Masso	(BARC, PARIT)
FIELDS	97	ASP 6 169	B.D. Fields, K. Kainulainen, K.A. Olive	(NDAM+)
SWAIN	97	PR D55 R1	J. Swain, L. Taylor	(NEAS)
ALEXANDER	96M	ZPHY C72 231	G. Alexander *et al.*	(OPAL Collab.)
ASSAMAGAN	96	PR D53 6065	K.A. Assamagan *et al.*	(PSI, ZURI, VILL+)
BAI	96	PR D53 20	J.Z. Bai *et al.*	(BES Collab.)
BOTTINO	96	PR D53 6361	A. Bottino *et al.*	
DOLGOV	96	PL B383 193	A.D. Dolgov, S. Pastor, J.W.F. Valle	(IFIC, VALE)
HANNESTAD	96	PRL 76 2848	S. Hannestad, J. Madsen	(AARH)
HANNESTAD	96B	PRL 77 5148 (erratum)	S. Hannestad, J. Madsen	(AARH)
HANNESTAD	96C	PR D54 7894	S. Hannestad, J. Madsen	(AARH)
SOBIE	96	ZPHY C70 383	R.J. Sobie, R.K. Keeler, I. Lawson	(VICT)
BELESEV	95	PL B350 263	A.I. Belesev *et al.*	(INRM, KIAE)
BUSKULIC	95H	PL B349 585	D. Buskulic *et al.*	(ALEPH Collab.)
CHING	95	IJMP A10 2841	C.R. Ching *et al.*	(CST, BEIJT, CIAE)
DOLGOV	95	PR D51 4129	A.D. Dolgov, K. Kainulainen, I.Z. Rothstein	(MICH+)
HIDDEMANN	95	JP G21 639	K.H. Hiddemann, H. Daniel, O. Schwentker	(MUNT)
KERNAN	95	NP B437 243	P.J. Kernan, L.M. Krauss	(CASE)
SIGL	95	PR D51 1499	G. Sigl, M.S. Turner	(FNAL, EFI)
STOEFFL	95	PRL 75 3237	W. Stoeffl, D.J. Decman	(LLNL)
VILAIN	95B	PL B345 115	P. Vilain *et al.*	(CHARM II Collab.)
ASSAMAGAN	94	PL B335 231	K.A. Assamagan *et al.*	(PSI, ZURI, VILL+)
BABU	94	PL B321 140	K.S. Babu, T.M. Gould, I.Z. Rothstein	(BART+)
DODELSON	94	PR D49 5068	S. Dodelson, G. Gyuk, M.S. Turner	(FNAL, CHIC+)
GOULD	94	PL B333 545	T.M. Gould, I.Z. Rothstein	(JHU, MICH)
JECKELMANN	94	PL B335 326	B. Jeckelmann, P.F.A. Goudsmit, H.J. Leisi	(WABRN+)
KAWASAKI	94	NP B419 105	M. Kawasaki *et al.*	(OSU)
PERES	94	PR D50 513	O.L.G. Peres, V. Pleitez, R. Zukanovich Funchal	
YASUMI	94	PL B334 229	S. Yasumi *et al.*	(KEK, TSUK, KYOT+)
ALLEN	93	PR D47 11	R.C. Allen *et al.*	(UCI, LANL, ANL+)
BALEST	93	PR D47 R3671	R. Balest *et al.*	(CLEO Collab.)
CINABRO	93	PRL 70 3700	D. Cinabro *et al.*	(CLEO Collab.)
DERBIN	93	JETPL 57 768	A.V. Derbin *et al.*	(PNPI)
		Translated from ZETFP 57 755.		
DOLGOV	93	PRL 71 476	A.D. Dolgov, I.Z. Rothstein	(MICH)
ENQVIST	93	PL B301 376	K. Enqvist, H. Uibo	(NORD)
SUN	93	CJNP 15 261	H.C. Sun *et al.*	(CIAE, CST, BEIJT)
WEINHEIMER	93	PL B300 210	C. Weinheimer *et al.*	(MANZ)
ALBRECHT	92M	PL B292 221	H. Albrecht *et al.*	(ARGUS Collab.)
BLUDMAN	92	PR D45 4720	S.A. Bludman	(CFPA)
COOPER-...	92	PL B280 153	A.M. Cooper-Sarkar *et al.*	(BEBC WA66 Collab.)
DODELSON	92	PRL 68 2572	S. Dodelson, J.A. Frieman, M.S. Turner	(FNAL+)
HOLZSCHUH	92B	PL B287 381	E. Holzschuh, M. Fritschi, W. Kundig	(ZURI)
KAWANO	92	PL B275 487	L.H. Kawano *et al.*	(CIT, UCSD, LLL+)
MOURAO	92	PL B285 364	A.M. Mourao, J. Pulido, J.P. Ralston	(LISB, LISBT+)
PDG	92	PR D45 S1	K. Hikasa *et al.*	(KEK, LBL, BOST+)
VIDYAKIN	92	JETPL 55 206	G.S. Vidyakin *et al.*	(KIAE)
		Translated from ZETFP 55 212.		
ALLEN	91	PR D43 R1	R.C. Allen *et al.*	(UCI, LANL, UMD)
DAVIDSON	91	PR D43 2314	S. Davidson, B.A. Campbell, D. Bailey	(ALBE+)
DESHPANDE	91	PR D43 943	N.G. Deshpande, K.V.L. Sarma	(OREG, TATA)
DORENBOS...	91	ZPHY C51 142 (erratum)	J. Dorenbosch *et al.*	(CHARM Collab.)
FULLER	91	PR D43 3136	G.M. Fuller, R.A. Malaney	(UCSD)
GRANEK	91	IJMP A6 2387	H. Granek, B.H.J. McKellar	(MELB)
KAWAKAMI	91	PL B256 105	H. Kawakami *et al.*	(INUS, TOHOK, TINT+)
KOLB	91	PRL 67 533	E.W. Kolb *et al.*	(FNAL, CHIC)
KRAKAUER	91	PR D44 R6	D.A. Krakauer *et al.*	(LAMPF E225 Collab.)
LAM	91	PR D44 3345	W.P. Lam, K.W. Ng	(AST)
ROBERTSON	91	PRL 67 957	R.G.H. Robertson *et al.*	(LASL, LLL)
AHRENS	90	PR D41 3297	L.A. Ahrens *et al.*	(BNL, BROW, HIRO+)
AVIGNONE	90	PR D41 682	F.T. Avignone, J.I. Collar	(SCUC)
KRAKAUER	90	PL B252 177	D.A. Krakauer *et al.*	(LAMPF E225 Collab.)
RAFFELT	90	PRL 64 2856	G.G. Raffelt	(MPIM)
WALKER	90	PR D41 689	T.P. Walker	(HARV)
CHUPP	89	PRL 62 505	E.L. Chupp, W.T. Vestrand, C. Reppin	(UNH, MPIM)
DORENBOS...	89	ZPHY C41 567	J. Dorenbosch *et al.*	(CHARM Collab.)
GRIFOLS	89B	PR D40 3819	J.A. Grifols, E. Masso	(BARC)
KOLB	89	PRL 62 509	E.W. Kolb, M.S. Turner	(CHIC, FNAL)
LOREDO	89	ANYAS 571 601	T.J. Loredo, D.Q. Lamb	(CHIC)
RAFFELT	89	PR D39 2066	G.G. Raffelt	(PRIN, UCB)
RAFFELT	89B	APJ 336 61	G. Raffelt, D. Dearborn, J. Silk	(UCB, LLL)
ALBRECHT	88B	PL B202 149	H. Albrecht *et al.*	(ARGUS Collab.)
BARBIERI	88	PRL 61 27	R. Barbieri, R.N. Mohapatra	(PISA, UMD)
BORIS	88	PRL 61 245 (erratum)	S.D. Boris *et al.*	(ITEP, ASCI)
FUKUGITA	88	PRL 60 879	M. Fukugita *et al.*	(KYOTU, MPIM, UCB)
GROTCH	88	ZPHY C39 553	H. Grotch, R.W. Robinett	(PSU)
RAFFELT	88B	PR D37 549	G.G. Raffelt, D.S.P. Dearborn	(UCB, LLL)
SPERGEL	88	PL B200 366	D.N. Spergel, J.N. Bahcall	(IAS)
VONFEILIT...	88	PL B200 580	F. von Feilitzsch, L. Oberauer	(MUNT)
BARBIELLINI	87	NAT 329 21	G. Barbiellini, G. Cocconi	(CERN)
BORIS	87	PRL 58 2019	S.D. Boris *et al.*	(ITEP, ASCI)
Also		PRL 61 245 (erratum)	S.D. Boris *et al.*	(ITEP, ASCI)
BORIS	87B	JETPL 45 333	S.D. Boris *et al.*	(ITEP)
		Translated from ZETFP 45 267.		
FUKUGITA	87	PR D36 3817	M. Fukugita, S. Yazaki	(KYOTU, TOKY)
NUSSINOV	87	PR D36 2278	S. Nussinov, Y. Rephaeli	(TELA)
OBERAUER	87	PL B198 113	L.F. Oberauer, F. von Feilitzsch, R.L. Mossbauer	
SPRINGER	87	PR A35 679	P.T. Springer *et al.*	(LLNL)
KETOV	86	JETPL 44 146	S.N. Ketov *et al.*	(KIAE)
		Translated from ZETFP 44 114.		
COWSIK	85	PL 151B 62	R. Cowsik	(TATA)
RAFFELT	85	PR D31 3002	G.G. Raffelt	(MPIM)
BINETRUY	84	PL 134B 174	P. Binetruy, G. Girardi, P. Salati	(LAPP)
FREESE	84	NP B233 167	K. Freese, D.N. Schramm	(CHIC, FNAL)
KYULDJIEV	84	NP B243 387	A.V. Kyuldjiev	(SOFI)
SCHRAMM	84	PL 141B 337	D.N. Schramm, G. Steigman	(FNAL, BART)
VOGEL	84	PR D30 1505	P. Vogel	
ANDERHUB	82	PL 114B 76	H.B. Anderhub *et al.*	(ETH, SIN)
OLIVE	82	PR D25 213	K.A. Olive, M.S. Turner	(CHIC, UCSB)
BERNSTEIN	81	PL 101B 39	J. Bernstein, G. Feinberg	(STEV, COLU)
FRANK	81	PR D24 2001	J.S. Frank *et al.*	(LASL, YALE, MIT+)
MORGAN	81	PL 102B 247	J.A. Morgan	(SUSS)
FUJIKAWA	80	PRL 45 963	K. Fujikawa, R. Shrock	(STON)
LUBIMOV	80	PL 94B 266	V.A. Lyubimov *et al.*	(ITEP)
STECKER	80	PRL 45 1460	F.W. Stecker	(NASA)
COWSIK	79	PR D19 2219	R. Cowsik	(TATA)
GOLDMAN	79	PR D19 2215	T. Goldman, G.J. Stephenson	(LASL)
BEG	78	PR D17 1395	M.A.B. Beg, W.J. Marciano, M. Ruderman	(ROCK+)
BLIETSCHAU	78	NP B133 205	J. Blietschau *et al.*	(Gargamelle Collab.)
FALK	78	PL 79B 511	S.W. Falk, D.N. Schramm	(CHIC)
BARNES	77	PRL 38 1049	V.E. Barnes *et al.*	(PURD, ANL)
COWSIK	77	PRL 39 784	R. Cowsik	(MPIM, TATA)
LEE	77C	PR D16 1444	B.W. Lee, R.E. Shrock	(STON)
VYSOTSKY	77	JETPL 26 188	M.I. Vysotsky, A.D. Dolgov, Y.B. Zeldovich	(ITEP)
		Translated from ZETFP 26 200.		
BELLOTTI	76	LNC 17 553	E. Bellotti *et al.*	(MILA)
SUTHERLAND	76	PR D13 2700	P. Sutherland *et al.*	(PENN, COLU, NYU)
SZALAY	76	AA 49 437	A.S. Szalay, G. Marx	(EOTV)
CLARK	74	PR D9 533	A.R. Clark *et al.*	(LBL)
KIM	74	PR D9 3050	J.E. Kim, V.S. Mathur, S. Okubo	(ROCH)
REINES	74	PRL 32 180	F. Reines, H.W. Sobel, H.S. Gurr	(UCI)
SZALAY	74	APAH 35 8	A.S. Szalay, G. Marx	(EOTV)
COWSIK	72	PRL 29 669	R. Cowsik, J. McClelland	(UCB)
MARX	72	Nu Conf. Budapest	G. Marx, A.S. Szalay	(EOTV)
GERSHTEIN	66	JETPL 4 120	S.S. Gershtein, Y.B. Zeldovich	(KIAM)
		Translated from ZETFP 4 189.		
BERNSTEIN	63	PR 132 1227	J. Bernstein, M. Ruderman, G. Feinberg	(NYU+)
COWAN	57	PR 107 528	C.L. Cowan, F. Reines	(LANL)

Number of Neutrino Types

The neutrinos referred to in this section are those of the Standard SU(2)×U(1) Electroweak Model possibly extended to allow nonzero neutrino masses. Light neutrinos are those with $m < m_Z/2$. The limits are on the number of neutrino mass eigenstates, including ν_1, ν_2, and ν_3.

THE NUMBER OF LIGHT NEUTRINO TYPES FROM COLLIDER EXPERIMENTS

Revised March 2008 by D. Karlen (University of Victoria and TRIUMF).

The most precise measurements of the number of light neutrino types, N_ν, come from studies of Z production in e^+e^- collisions. The invisible partial width, $\Gamma_{\rm inv}$, is determined by subtracting the measured visible partial widths, corresponding to Z decays into quarks and charged leptons, from the total Z width. The invisible width is assumed to be due to N_ν light neutrino species each contributing the neutrino partial width Γ_ν as given by the Standard Model. In order to reduce the model dependence, the Standard Model value for the ratio of the neutrino to charged leptonic partial widths, $(\Gamma_\nu/\Gamma_\ell)_{\rm SM} = 1.991 \pm 0.001$, is used instead of $(\Gamma_\nu)_{\rm SM}$ to determine the number of light neutrino types:

$$N_\nu = \frac{\Gamma_{\rm inv}}{\Gamma_\ell}\left(\frac{\Gamma_\ell}{\Gamma_\nu}\right)_{\rm SM} \ . \qquad (1)$$

The combined result from the four LEP experiments is $N_\nu = 2.984 \pm 0.008$ [1].

In the past, when only small samples of Z decays had been recorded by the LEP experiments and by the Mark II at SLC, the uncertainty in N_ν was reduced by using Standard Model

fits to the measured hadronic cross sections at several center-of-mass energies near the Z resonance. Since this method is much more dependent on the Standard Model, the approach described above is favored.

Before the advent of the SLC and LEP, limits on the number of neutrino generations were placed by experiments at lower-energy e^+e^- colliders by measuring the cross section of the process $e^+e^- \to \nu\overline{\nu}\gamma$. The ASP, CELLO, MAC, MARK J, and VENUS experiments observed a total of 3.9 events above background [2], leading to a 95% CL limit of $N_\nu < 4.8$. This process has a much larger cross section at center-of-mass energies near the Z mass and has been measured at LEP by the ALEPH, DELPHI, L3, and OPAL experiments [3]. These experiments have observed several thousand such events, and the combined result is $N_\nu = 3.00 \pm 0.08$. The same process has also been measured by the LEP experiments at much higher center-of-mass energies, between 130 and 208 GeV, in searches for new physics [4]. Combined with the lower energy data, the result is $N_\nu = 2.92 \pm 0.05$.

Experiments at $p\overline{p}$ colliders also placed limits on N_ν by determining the total Z width from the observed ratio of $W^\pm \to \ell^\pm\nu$ to $Z \to \ell^+\ell^-$ events [5]. This involved a calculation that assumed Standard Model values for the total W width and the ratio of W and Z leptonic partial widths, and used an estimate of the ratio of Z to W production cross sections. Now that the Z width is very precisely known from the LEP experiments, the approach is now one of those used to determine the W width.

References

1. ALEPH, DELPHI, L3, OPAL, and SLD Collaborations, and LEP Electroweak Working Group, and SLD Electroweak Group, and SLD Heavy Flavour Group, Phys. Reports **427**, 257 (2006).
2. VENUS: K. Abe *et al.*, Phys. Lett. **B232**, 431 (1989); ASP: C. Hearty *et al.*, Phys. Rev. **D39**, 3207 (1989); CELLO: H.J. Behrend *et al.*, Phys. Lett. **B215**, 186 (1988); MAC: W.T. Ford *et al.*, Phys. Rev. **D33**, 3472 (1986); MARK J: H. Wu, Ph.D. Thesis, Univ. Hamburg (1986).
3. L3: M. Acciarri *et al.*, Phys. Lett. **B431**, 199 (1998); DELPHI: P. Abreu *et al.*, Z. Phys. **C74**, 577 (1997); OPAL: R. Akers *et al.*, Z. Phys. **C65**, 47 (1995); ALEPH: D. Buskulic *et al.*, Phys. Lett. **B313**, 520 (1993).
4. DELPHI: J. Abdallah *et al.*, Eur. Phys. J. **C38**, 395 (2005); L3: P. Achard *et al.*, Phys. Lett. **B587**, 16 (2004); ALEPH: A. Heister *et al.*, Eur. Phys. J. **C28**, 1 (2003); OPAL: G. Abbiendi *et al.*, Eur. Phys. J. **C18**, 253 (2000).
5. UA1: C. Albajar *et al.*, Phys. Lett. **B198**, 271 (1987); UA2: R. Ansari *et al.*, Phys. Lett. **B186**, 440 (1987).

Number from e^+e^- Colliders

Number of Light ν Types

VALUE		DOCUMENT ID		TECN
2.9840±0.0082	[1]	LEP-SLC	06	RVUE
• • • We do not use the following data for averages, fits, limits, etc. • • •				
3.00 ±0.05	[2]	LEP	92	RVUE

[1] Combined fit from ALEPH, DELPHI, L3 and OPAL Experiments.

[2] Simultaneous fits to all measured cross section data from all four LEP experiments.

Number of Light ν Types from Direct Measurement of Invisible Z Width

In the following, the invisible Z width is obtained from studies of single-photon events from the reaction $e^+e^- \to \nu\overline{\nu}\gamma$. All are obtained from LEP runs in the E^{ee}_{cm} range 88–209 GeV.

VALUE	DOCUMENT ID		TECN	COMMENT
2.92±0.05 OUR AVERAGE Error includes scale factor of 1.2.				
2.84±0.10±0.14	ABDALLAH	05B	DLPH	$\sqrt{s}$ = 180–209 GeV
2.98±0.05±0.04	ACHARD	04E	L3	1990-2000 LEP runs
2.86±0.09	HEISTER	03C	ALEP	$\sqrt{s}$ = 189–209 GeV
2.69±0.13±0.11	ABBIENDI,G	00D	OPAL	1998 LEP run
2.89±0.32±0.19	ABREU	97J	DLPH	1993–1994 LEP runs
3.23±0.16±0.10	AKERS	95C	OPAL	1990–1992 LEP runs
2.68±0.20±0.20	BUSKULIC	93L	ALEP	1990–1991 LEP runs
• • • We do not use the following data for averages, fits, limits, etc. • • •				
2.84±0.15±0.14	ABREU	00Z	DLPH	1997–1998 LEP runs
3.01±0.08	ACCIARRI	99R	L3	1991–1998 LEP runs
3.1 ±0.6 ±0.1	ADAM	96C	DLPH	$\sqrt{s}$ = 130, 136 GeV

Limits from Astrophysics and Cosmology

Number of Light ν Types

("light" means < about 1 MeV). See also OLIVE 81. For a review of limits based on Nucleosynthesis, Supernovae, and also on terrestial experiments, see DENEGRI 90. Also see "Big-Bang Nucleosynthesis" in this *Review*.

VALUE	CL%	DOCUMENT ID		TECN	COMMENT
• • • We do not use the following data for averages, fits, limits, etc. • • •					
< 4.10	95	[3] MORESCO	12	COSM	
< 5.79	95	[4] XIA	12	COSM	
< 4.08	95	MANGANO	11	COSM	BBN
$0.9 < N_\nu < 8.2$		[5] ICHIKAWA	07	COSM	
$3 < N_\nu < 7$	95	[6] CIRELLI	06	COSM	
$2.7 < N_\nu < 4.6$	95	[7] HANNESTAD	06	COSM	
$3.6 < N_\nu < 7.4$	95	[6] SELJAK	06	COSM	
< 4.4		[8] CYBURT	05	COSM	
< 3.3		[9] BARGER	03C	COSM	
$1.4 < N_\nu < 6.8$		[10] CROTTY	03	COSM	
$1.9 < N_\nu < 6.6$		[10] PIERPAOLI	03	COSM	
$2 < N_\nu < 4$		LISI	99	COSM	BBN
< 4.3		OLIVE	99	COSM	BBN
< 4.9		COPI	97		Cosmology
< 3.6		HATA	97B		High D/H quasar abs.
< 4.0		OLIVE	97		BBN; high ^{4}He and ^{7}Li
< 4.7		CARDALL	96B	COSM	High D/H quasar abs.
< 3.9		FIELDS	96	COSM	BBN; high ^{4}He and ^{7}Li
< 4.5		KERNAN	96	COSM	High D/H quasar abs.
< 3.6		OLIVE	95		BBN; ≥ 3 massless ν
< 3.3		WALKER	91		Cosmology
< 3.4		OLIVE	90		Cosmology
< 4		YANG	84		Cosmology
< 4		YANG	79		Cosmology
< 7		STEIGMAN	77		Cosmology
		PEEBLES	71		Cosmology
<16	[11]	SHVARTSMAN	69		Cosmology
		HOYLE	64		Cosmology

[3] Limit on the number of light neutrino types from observational Hubble parameter data with seven-year WMAP data, SPT, and the most recent estimate of H_0. Best fit is 3.45 ± 0.65.

[4] Limit on the number of light neutrino types from the CFHTLS combined with seven-year WMAP data and a prior on the Hubble parameter. Best fit is $4.17^{+1.62}_{-1.26}$. Limit is relaxed to $3.98^{+2.02}_{-1.20}$ when small scales affected by non-linearities are removed.

[5] Constrains the number of neutrino types from recent CMB and large scale structure data. No priors on other cosmological parameters are used.

[6] Constrains the number of neutrino types from recent CMB, large scale structure, Lyman-alpha forest, and SN1a data. The slight preference for $N_\nu > 3$ comes mostly from the Lyman-alpha forest data.

[7] Constrains the number of neutrino types from recent CMB and large scale structure data. See also HAMANN 07.

[8] Limit on the number of neutrino types based on ^{4}He and D/H abundance assuming a baryon density fixed to the WMAP data. Limit relaxes to 4.6 if D/H is not used or to 5.8 if only D/H and the CMB are used. See also CYBURT 01 and CYBURT 03.

[9] Limit on the number of neutrino types based on combination of WMAP data and big-bang nucleosynthesis. The limit from WMAP data alone is 8.3. See also KNELLER 01. $N_\nu \geq 3$ is assumed to compute the limit.

[10] 95% confidence level range on the number of neutrino flavors from WMAP data combined with other CMB measurements, the 2dfGRS data, and HST data.

[11] SHVARTSMAN 69 limit inferred from his equations.

Number Coupling with Less Than Full Weak Strength

VALUE	DOCUMENT ID		TECN
• • • We do not use the following data for averages, fits, limits, etc. • • •			
<20	[12] OLIVE	81C	COSM
<20	[12] STEIGMAN	79	COSM

[12] Limit varies with strength of coupling. See also WALKER 91.

REFERENCES FOR Limits on Number of Neutrino Types

MORESCO	12	JCAP 1207 053	M. Moresco *et al.*	
XIA	12	JCAP 1206 010	J.-Q. Xia *et al.*	
MANGANO	11	PL B701 296	G. Mangano, P. Serpico	
HAMANN	07	JCAP 0708 021	J. Hamann *et al.*	
ICHIKAWA	07	JCAP 0705 007	K. Ichikawa, M. Kawasaki, F. Takahashi	
CIRELLI	06	JCAP 0612 013	M. Cirelli *et al.*	
HANNESTAD	06	JCAP 0611 016	S. Hannestad, G. Raffelt	
LEP-SLC	06	PRPL 427 257	ALEPH, DELPHI, L3, OPAL, SLD and working groups	
SELJAK	06	JCAP 0610 014	U. Seljak, A. Slosar, P. McDonald	
ABDALLAH	05B	EPJ C38 395	J. Abdallah *et al.*	(DELPHI Collab.)
CYBURT	05	ASP 23 313	R.H. Cyburt *et al.*	
ACHARD	04E	PL B587 16	P. Achard *et al.*	(L3 Collab.)
BARGER	03C	PL B566 8	V. Barger *et al.*	
CROTTY	03	PR D67 123005	P. Crotty, J. Lesgourgues, S. Pastor	
CYBURT	03	PL B567 227	R.H. Cyburt, B.D. Fields, K.A. Olive	
HEISTER	03C	EPJ C28 1	A. Heister *et al.*	(ALEPH Collab.)
PIERPAOLI	03	MNRAS 342 L63	E. Pierpaoli	
CYBURT	01	ASP 17 87	R.H. Cyburt, B.D. Fields, K.A. Olive	
KNELLER	01	PR D64 123506	J.P. Kneller *et al.*	
ABBIENDI,G	00D	EPJ C18 253	G. Abbiendi *et al.*	(OPAL Collab.)
ABREU	00Z	EPJ C17 53	P. Abreu *et al.*	(DELPHI Collab.)
ACCIARRI	99R	PL B470 268	M. Acciarri *et al.*	(L3 Collab.)
LISI	99	PR D59 123520	E. Lisi, S. Sarkar, F.L. Villante	
OLIVE	99	ASP 11 403	K.A. Olive, D. Thomas	
ABREU	97J	ZPHY C74 577	P. Abreu *et al.*	(DELPHI Collab.)
COPI	97	PR D55 3389	C.J. Copi, D.N. Schramm, M.S. Turner	(CHIC)
HATA	97B	PR D55 540	N. Hata *et al.*	(OSU, PENN)
OLIVE	97	ASP 7 27	K.A. Olive, D. Thomas	(MINN, FLOR)
ADAM	96C	PL B380 471	W. Adam *et al.*	(DELPHI Collab.)
CARDALL	96B	APJ 472 435	C.Y. Cardall, G.M. Fuller	(UCSD)
FIELDS	96	New Ast 1 77	B.D. Fields *et al.*	(NDAM, CERN, MINN+)
KERNAN	96	PR D54 3681	P.S. Kernan, S. Sarkar	(CASE, OXFTP)
AKERS	95C	ZPHY C65 47	R. Akers *et al.*	(OPAL Collab.)
OLIVE	95	PL B354 357	K.A. Olive, G. Steigman	(MINN, OSU)
BUSKULIC	93L	PL B313 520	D. Buskulic *et al.*	(ALEPH Collab.)
LEP	92	PL B276 247	LEP Collabs.	(LEP, ALEPH, DELPHI, L3, OPAL)
WALKER	91	APJ 376 51	T.P. Walker *et al.*	(HSCA, OSU, CHIC+)
DENEGRI	90	RMP 62 1	D. Denegri, B. Sadoulet, M. Spiro	(CERN, UCB+)
OLIVE	90	PL B236 454	K.A. Olive *et al.*	(MINN, CHIC, OSU+)
YANG	84	APJ 281 493	J. Yang *et al.*	(CHIC, BART)
OLIVE	81	APJ 246 557	K.A. Olive *et al.*	(CHIC, BART)
OLIVE	81C	NP B180 497	K.A. Olive, D.N. Schramm, G. Steigman	(EFI+)
STEIGMAN	79	PRL 43 239	G. Steigman, K.A. Olive, D.N. Schramm	(BART+)
YANG	79	APJ 227 697	J. Yang *et al.*	(CHIC, YALE, UVA)
STEIGMAN	77	PL 66B 202	G. Steigman, D.N. Schramm, J.E. Gunn	(YALE, CHIC+)
PEEBLES	71	Physical Cosmology Princeton Univ. Press (1971)	P.Z. Peebles	(PRIN)
SHVARTSMAN	69	JETPL 9 184 Translated from ZETFP 9 315.	V.F. Shvartsman	(MOSU)
HOYLE	64	NAT 203 1108	F. Hoyle, R.J. Tayler	(CAMB)

Double-β Decay

OMITTED FROM SUMMARY TABLE

NEUTRINOLESS DOUBLE-β DECAY

Revised August 2013 by P. Vogel (Caltech) and A. Piepke (University of Alabama).

Neutrinoless double-beta ($0\nu\beta\beta$) decay would signal violation of total lepton number conservation. The process can be mediated by an exchange of a light Majorana neutrino, or by an exchange of other particles. However, the existence of $0\nu\beta\beta$-decay requires Majorana neutrino mass, no matter what the actual mechanism is. As long as only a limit on the lifetime is available, limits on the effective Majorana neutrino mass, on the lepton-number violating right-handed current or other possible mechanisms mediating $0\nu\beta\beta$-decay can be obtained, independently of the actual mechanism. These limits are listed in the next three tables, together with a claimed $0\nu\beta\beta$-decay signal reported by part of the Heidelberg-Moscow collaboration. There is tension between that claim and several recent experiments which did not find evidence for $0\nu\beta\beta$ decay. In the following we assume that the exchange of light Majorana neutrinos ($m_{\nu_i} \leq 10$ MeV) contributes dominantly to the decay rate.

Besides a dependence on the phase space ($G^{0\nu}$) and the nuclear matrix element ($M^{0\nu}$), the observable $0\nu\beta\beta$-decay rate is proportional to the square of the effective Majorana mass $\langle m_{\beta\beta}\rangle$, $(T^{0\nu}_{1/2})^{-1} = G^{0\nu} \cdot |M^{0\nu}|^2 \cdot \langle m_{\beta\beta}\rangle^2$, with $\langle m_{\beta\beta}\rangle^2 = |\sum_i U^2_{ei} m_{\nu_i}|^2$. The sum contains, in general, complex CP-phases in U^2_{ei}, *i.e.*, cancellations may occur. For three neutrino flavors, there are three physical phases for Majorana neutrinos. There is only one phase if neutrinos are Dirac particles. The two additional Majorana phase differences affect only processes to which lepton-number-changing amplitudes contribute. Given the general 3×3 mixing matrix for Majorana neutrinos, one can construct other analogous lepton number violating quantities, $\langle m_{\ell\ell'}\rangle = \sum_i U_{\ell i} U_{\ell' i} m_{\nu_i} (l \text{ or } l' \neq e)$. However, these are currently much less constrained than $\langle m_{\beta\beta}\rangle$.

Nuclear structure calculations are needed to deduce $\langle m_{\beta\beta}\rangle$ from the decay rate. While $G^{0\nu}$ can be calculated, the computation of $M^{0\nu}$ is subject to uncertainty. Comparing different nuclear model evaluations indicates a factor ∼2 to 3 spread in the calculated nuclear matrix elements. The particle physics quantities to be determined are thus nuclear model-dependent, so the half-life measurements are listed first. Where possible, we reference the nuclear matrix elements used in the subsequent analysis. Since rates for the more conventional $2\nu\beta\beta$ decay serve to calibrate some nuclear models (e.g. QRPA-based calculations), results for this process are also given.

Oscillation experiments utilizing atmospheric-, accelerator-, solar-, and reactor-produced neutrinos and anti-neutrinos yield strong evidence that at least some neutrinos are massive. However, these findings shed no light on the mass hierarchy (*i.e.*, on the sign of Δm^2_{31}), the absolute neutrino mass values or the properties of neutrinos under CPT-conjugation (Dirac or Majorana).

All confirmed oscillation experiments can be consistently described using three interacting neutrino species with two mass splittings and three mixing angles. Full three flavor analyses such as *e.g.* [1] yield: $|\Delta m^2_{31}| = 2.55^{+0.06}_{-0.09}$ $(2.43^{+0.07}_{-0.06}) \times 10^{-3}$ eV^2 and $\sin^2\theta_{23} = 0.613^{+0.022}_{-0.040}$ $(0.600^{+0.026}_{-0.031})$ for the parameters observed in atmospheric and accelerator experiments, where the values correspond to the normal (inverted) hierarchies. Observations of solar ν_e and reactor $\bar{\nu}_e$ lead to $\Delta m^2_{21} = 7.62^{+0.19}_{-0.19} \times 10^{-5}$ eV^2 and $\sin^2\theta_{12} = 0.320^{+0.016}_{-0.017}$. The investigation of reactor $\bar{\nu}_e$ at ∼1.5 km baseline shows that electron type neutrinos couple only weakly to the third mass eigenstate with $\sin^2\theta_{13} = 0.0246^{+0.0029}_{-0.0028}$ $(0.0250^{+0.0026}_{-0.0027})$. (All errors correspond to 1σ.)

Based on the 3-neutrino analysis: $\langle m_{\beta\beta}\rangle^2 = |\cos^2\theta_{13}\cos^2\theta_{12} m_1 + e^{i\Delta\alpha_{21}}\cos^2\theta_{13}\sin^2\theta_{12} m_2 + e^{i\Delta\alpha_{31}}\sin^2\theta_{13} m_3|^2$, with $\Delta\alpha_{21}, \Delta\alpha_{31}$ denoting the physically relevant Majorana CP-phase differences (possible Dirac phase δ is absorbed in these $\Delta\alpha$). Given the present knowledge of the neutrino oscillation parameters one can derive the relation between the effective Majorana mass and the mass of the lightest neutrino, as illustrated in the left panel of Fig. 1. The three mass hierarchies

See key on page 547

allowed by the oscillation data: normal ($m_1 < m_2 < m_3$), inverted ($m_3 < m_1 < m_2$), and degenerate ($m_1 \approx m_2 \approx m_3$), result in different projections. The width of the innermost hatched bands reflects the uncertainty introduced by the unknown Majorana and Dirac phases. If the experimental errors of the oscillation parameters are taken into account, then the allowed areas are widened as shown by the outer bands of Fig. 1. Because of the overlap of the different mass scenarios a measurement of $\langle m_{\beta\beta}\rangle$ in the degenerate or inversely hierarchical ranges would not determine the hierarchy. The middle panel of Fig. 1 depicts the relation of $\langle m_{\beta\beta}\rangle$ with the summed neutrino mass $m_{tot} = m_1 + m_2 + m_3$, constrained by observational cosmology. The oscillation data thus allow to test whether observed values of $\langle m_{\beta\beta}\rangle$ and m_{tot} are consistent within the 3 neutrino framework and the light neutrino-exchange dominance assumption. The right hand panel of Fig. 1, finally, shows $\langle m_{\beta\beta}\rangle$ as a function of the kinematical mass $\langle m_\beta\rangle = [\Sigma|U_{ei}|^2 m_{\nu_i}^2]^{1/2}$ determined through the analysis of the electron energy distribution in low energy beta decays. The rather large intrinsic width of the $\beta\beta$-decay constraint essentially does not allow to positively identify the inverted hierarchy, and thus the sign of Δm^2_{31}, even in combination with these other observables. Naturally, if the value of $\langle m_{\beta\beta}\rangle \leq 0.01$ eV, but non-zero is ever established then normal hierarchy becomes the only possible scenario.

It should be noted that systematic uncertainties of the nuclear matrix elements are not folded into the mass projections shown in Fig. 1. Taking this additional uncertainty into account would further widen the allowed areas. The uncertainties in oscillation parameters affect the width of the allowed bands in an asymmetric manner, as shown in Fig. 1. For example, for the degenerate mass pattern ($\langle m_{\beta\beta}\rangle \geq 0.1$ eV) the upper edge is simply $\langle m_{\beta\beta}\rangle \sim m$, where m is the common mass of the degenerate multiplet, independent of the oscillation parameters, while the lower edge is $m\cos(2\theta_{12})$. Similar arguments explain the other features of Fig. 1.

If the neutrinoless double-beta decay is observed, it will be possible to fix a range of absolute values of the masses m_{ν_i}. Unlike the direct neutrino mass measurements, however, a limit on $\langle m_{\beta\beta}\rangle$ does not allow one to constrain the individual mass values m_{ν_i} even when the mass differences Δm^2 are known.

Neutrino oscillation data imply, for the first time, the existence of a lower limit ~ 0.013 eV for the Majorana neutrino mass for the inverted hierarchy mass pattern while $\langle m_{\beta\beta}\rangle$ could, by fine tuning, vanish in the case of the normal mass hierarchy. Several new double beta searches have been proposed to probe the interesting $\langle m_{\beta\beta}\rangle$ mass range, with the prospect of full coverage of the inverted mass hierarchy region within the next decade.

If lepton-number-violating right-handed current weak interactions exist, their strength can be characterized by the phenomenological coupling constants η and λ (η describes the coupling between the right-handed lepton current and left-handed quark current while λ describes the coupling when both currents are right-handed). The $0\nu\beta\beta$ decay rate then depends on $\langle\eta\rangle = \eta\sum_i U_{ei}V_{ei}$ and $\langle\lambda\rangle = \lambda\sum_i U_{ei}V_{ei}$ that vanish for massless or unmixed neutrinos ($V_{\ell j}$ is a matrix analogous to $U_{\ell j}$ but describing the mixing with the hypothetical right-handed neutrinos). This mechanism of the $0\nu\beta\beta$ decay could be, in principle, distinguished from the light Majorana neutrino exchange by the observation of the single electron spectra. The limits on $\langle\eta\rangle$ and $\langle\lambda\rangle$ are listed in a separate table. The reader is cautioned that a number of earlier experiments did not distinguish between η and λ. In addition, see the section on Majoron searches for additional limits set by these experiments.

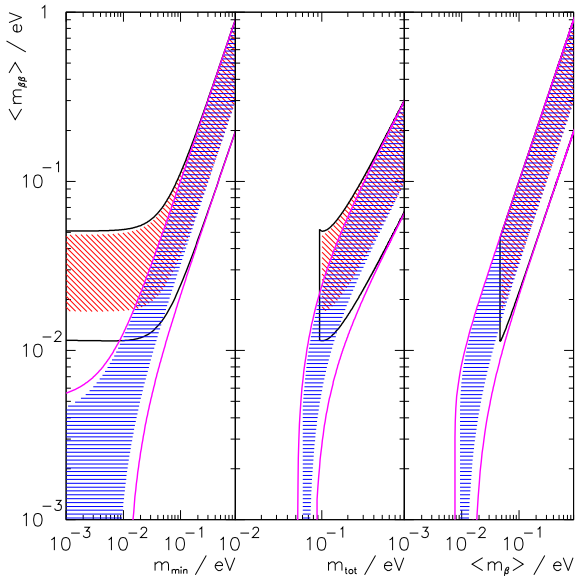

Figure 1: The left panel shows the dependence of $\langle m_{\beta\beta}\rangle$ on the absolute mass of the lightest neutrino m_{min}. The middle panel shows $\langle m_{\beta\beta}\rangle$ as a function of the summed neutrino mass m_{tot}, while the right panel depicts $\langle m_{\beta\beta}\rangle$ as a function of the mass $\langle m_\beta\rangle$. In all panels the width of the hatched areas is due to the unknown Majorana phases and thus irreducible. The allowed areas given by the solid lines are obtained by taking into account the errors of the oscillation parameters (at the 3σ level [1]) . The two sets of solid lines correspond to the normal and inverted hierarchies. These sets merge into each other for $\langle m_{\beta\beta}\rangle \geq 0.1$ eV, which corresponds to the degenerate mass pattern.

References

1. D.V. Forero, M. Tortola, and J.W.F. Valle, Phys. Rev. **D86**, 073012 (2012).

Half-life Measurements and Limits for Double-β Decay

In most cases the transitions (Z,A) $\rightarrow$ (Z+2,A) + $2e^-$ + (0 or 2) $\overline{\nu}_e$ to the 0^+ ground state of the final nucleus are listed. However, we also list transitions that increase the nuclear charge ($2e^+$, e^+/EC and ECEC) and transitions to excited states of the final nuclei (0^+_i, 2^+, and 2^+_i). In the following Listings, only best or comparable limits or lifetimes for each isotope are reported and only those with $T_{1/2} > 10^{20}$ years that are relevant for particle physics. For 2ν decay, which is well established, only measured half-lives are reported.

$t_{1/2}(10^{21}$ yr)	CL%	ISOTOPE	TRANSITION	METHOD	DOCUMENT ID		
• • • We do not use the following data for averages, fits, limits, etc. • • •							
$2.165 \pm 0.016 \pm 0.059$		^{136}Xe	2ν g.s.$\rightarrow$ g.s.	EXO-200	[1] ALBERT	14	
$1.84^{+0.14}_{-0.10}$		^{76}Ge	2ν g.s.$\rightarrow$ g.s.	GERDA	[2] AGOSTINI	13	
> 21000	90	^{76}Ge	0ν g.s.$\rightarrow$ g.s.	GERDA	[3] AGOSTINI	13A	
> 0.13	90	^{96}Ru	$0\nu+2\nu$ $2\beta^+$, g.s	Ge counting	[4] BELLI	13A	
> 0.23	90	^{96}Ru	$0\nu+2\nu$ β^+EC, g.s.$\rightarrow 2^+_1$		[5] BELLI	13A	
> 0.65	90	^{104}Ru	$0\nu+2\nu$ g.s.$\rightarrow 2^+_1$		[6] BELLI	13A	
> 19000	90	^{136}Xe	0ν g.s.$\rightarrow$ g.s.	KamLAND-Zen	[7] GANDO	13A	
$9.2^{+5.5}_{-2.6} \pm 1.3$		^{78}Kr	2ν2K g.s.$\rightarrow$ g.s.	BAKSAN	[8] GAVRILYAK	13	
> 5.4	90	^{78}Kr	0ν2K g.s.$\rightarrow 2^+$	BAKSAN	[9] GAVRILYAK	13	
> 940	90	^{130}Te	0ν $0^+ \rightarrow 0^+_1$	CUORICINO	[10] ANDREOTTI	12	
> 16000	90	^{136}Xe	0ν g.s.$\rightarrow$ g.s.	EXO-200	[11] AUGER	12	
> 1.0	90	^{106}Cd	0ν ECEC, g.s.	$^{106}CdWO_4$ scint.	[12] BELLI	12A	
> 2.2	90	^{106}Cd	0ν β^+EC, g.s.	$^{106}CdWO_4$ scint.	[13] BELLI	12A	
> 1.2	90	^{106}Cd	0ν $2\beta^+$, g.s.	$^{106}CdWO_4$ scint.	[14] BELLI	12A	
$2.38 \pm 0.02 \pm 0.14$		^{136}Xe	2ν g.s.$\rightarrow$ g.s.	KamLAND-Zen	[15] GANDO	12A	
> 5700	90	^{136}Xe	0ν g.s.$\rightarrow$ g.s.	KamLAND-Zen	[16] GANDO	12A	
$2.11 \pm 0.04 \pm 0.21$		^{136}Xe	2ν	EXO-200	[17] ACKERMAN	11	
$0.7 \pm 0.09 \pm 0.11$		^{130}Te	2ν	NEMO-3	[18] ARNOLD	11	
> 130	90	^{130}Te	0ν	NEMO-3	[19] ARNOLD	11	
> 1.3	90	^{112}Sn	0ν $0^+ \rightarrow 0^+_3$	γ Ge det.	[20] BARABASH	11	
> 0.69	90	^{112}Sn	0ν $0^+ \rightarrow 0^+_2$	γ Ge det.	[21] BARABASH	11	
> 1.3	90	^{112}Sn	0ν $0^+ \rightarrow 0^+_1$	γ Ge det.	[22] BARABASH	11	
> 1.06	90	^{112}Sn	0ν	γ Ge det.	[23] BARABASH	11	
$(2.8 \pm 0.1 \pm 0.3)$E-2		^{116}Cd	2ν	NEMO-3	[24] BARABASH	11A	
$(4.4^{+0.5}_{-0.4} \pm 0.4)$E-2		^{48}Ca	2ν	NEMO-3	[25,26] BARABASH	11A	
$(69 \pm 9 \pm 10)$E-2		^{130}Te	2ν	NEMO-3	[26,27] BARABASH	11A	
> 1100	90	^{100}Mo	0ν	NEMO-3	[26,28] BARABASH	11A	
> 360	90	^{82}Se	0ν	NEMO-3	[26,29] BARABASH	11A	
> 100	90	^{130}Te	0ν	NEMO-3	[26,30] BARABASH	11A	
> 16	90	^{116}Cd	0ν	NEMO-3	[26,31] BARABASH	11A	
> 13	90	^{48}Ca	0ν	NEMO-3	[26,32] BARABASH	11A	
> 0.32	90	^{64}Zn	0ν ECEC, g.s.	$ZnWO_4$ scint.	[33] BELLI	11D	
> 0.85	90	^{64}Zn	0ν β^+EC, g.s.	$ZnWO_4$ scint.	[33] BELLI	11D	
> 0.11	90	^{106}Cd	0ν $0^+ \rightarrow 4^+$	TGV2 det.	[34] RUKHADZE	11	
$(2.35 \pm 0.14 \pm 0.16)$E-2		^{96}Zr	2ν	NEMO-3	[35] ARGYRIADES	10	
> 9.2	90	^{96}Zr	0ν	NEMO-3	[36] ARGYRIADES	10	
> 0.22	90	^{96}Zr	0ν $0^+ \rightarrow 0^+_1$	NEMO-3	[37] ARGYRIADES	10	
$0.69^{+0.10}_{-0.08} \pm 0.07$		^{100}Mo	2ν $0^+ \rightarrow 0^+_1$	Ge coinc.	[38] BELLI	10	
> 18.0	90	^{150}Nd	0ν	NEMO-3	[39] ARGYRIADES	09	
$(9.11^{+0.25}_{-0.22} \pm 0.63)$E-3		^{150}Nd	2ν	NEMO-3	[40] ARGYRIADES	09	
> 0.43	90	^{64}Zn	0ν β^+EC	$ZnW0_4$ scint.	[41] BELLI	09A	
> 0.11	90	^{64}Zn	0ν ECEC	$ZnW0_4$ scint.	[42] BELLI	09A	
$0.55^{+0.12}_{-0.09}$		^{100}Mo	$2\nu+0\nu$ $0^+ \rightarrow 0^+_1$	Ge coincidence	[43] KIDD	09	
> 3000	90	^{130}Te	0ν	TeO_2 bolometer	[44] ARNABOLDI	08	
> 0.22	90	^{64}Zn	0ν	$ZnWO_4$ scint.	[45] BELLI	08	
> 1.1	90	^{114}Cd	0ν 2β	$CdWO_4$ scint.	[46] BELLI	08B	
> 58	90	^{48}Ca	0ν	CaF_2 scint.	[47] UMEHARA	08	
$0.57^{+0.13}_{-0.09} \pm 0.08$		^{100}Mo	2ν $0^+ \rightarrow 0^+_1$	NEMO-3	[48] ARNOLD	07	
> 89	90	^{100}Mo	0ν $0^+ \rightarrow 0^+_1$	NEMO-3	[49] ARNOLD	07	
> 160	90	^{100}Mo	0ν $0^+ \rightarrow 2^+$	NEMO-3	[50] ARNOLD	07	
> 0.0019	90	^{74}Se	$0\nu+2\nu$	γ in Ge det.	[51] BARABASH	07	
> 0.0055	90	^{74}Se	$0\nu+2\nu$ $0^+ \rightarrow 2^+_2$	γ in Ge det.	[52] BARABASH	07	
22300^{+4400}_{-3100}		^{76}Ge	0ν	Enriched HPGe	[53] KLAPDOR-K...	06A	
> 1800	90	^{130}Te	0ν	Cryog. det.	[54] ARNABOLDI	05	
> 460	90	^{100}Mo	0ν	NEMO-3	[55] ARNOLD	05A	
> 100	90	^{82}Se	0ν	NEMO-3	[56] ARNOLD	05A	
$(7.11 \pm 0.02 \pm 0.54)$E-3		^{100}Mo	2ν	NEMO-3	[57] ARNOLD	05A	
$(9.6 \pm 0.3 \pm 1.0)$E-2		^{82}Se	2ν	NEMO-3	[58] ARNOLD	05A	
> 140	90	^{82}Se	0ν	NEMO-3	[59] ARNOLD	04	
$(7.68 \pm 0.02 \pm 0.54)$E-3		^{100}Mo	2ν	NEMO-3	[60] ARNOLD	04	
$0.14^{+0.04}_{-0.02} \pm 0.03$		^{150}Nd	$0\nu+2\nu$ $0^+ \rightarrow 0^+_1$	γ in Ge det.	[61] BARABASH	04	
> 31	90	^{130}Te	0ν $0^+ \rightarrow 2^+$	Cryog. det.	[62] ARNABOLDI	03	
$0.61 \pm 0.14^{+0.29}_{-0.35}$		^{130}Te	2ν	Cryog. det.	[63] ARNABOLDI	03	
> 110	90	^{128}Te	0ν	Cryog. det.	[64] ARNABOLDI	03	
$(0.029^{+0.004}_{-0.003})$		^{116}Cd	2ν	$^{116}CdWO_4$ scint.	[65] DANEVICH	03	
> 170	90	^{116}Cd	0ν	$^{116}CdWO_4$ scint.	[66] DANEVICH	03	
> 29	90	^{116}Cd	0ν $0^+ \rightarrow 2^+$	$^{116}CdWO_4$ scint.	[67] DANEVICH	03	
> 14	90	^{116}Cd	0ν $0^+ \rightarrow 0^+_1$	$^{116}CdWO_4$ scint.	[68] DANEVICH	03	
> 6	90	^{116}Cd	0ν $0^+ \rightarrow 0^+_2$	$^{116}CdWO_4$ scint.	[69] DANEVICH	03	
> 1.1	90	^{186}W	0ν	$CdWO_4$ scint.	[70] DANEVICH	03	
> 1.1	90	^{186}W	0ν $0^+ \rightarrow 2^+$	$CdWO_4$ scint.	[71] DANEVICH	03	
$1.74 \pm 0.01^{+0.18}_{-0.16}$		^{76}Ge	2ν	Enriched HPGe	[72] DOERR	03	
>15700	90	^{76}Ge	0ν	Enriched HPGe	[73] AALSETH	02B	
> 58	90	^{134}Xe	0ν	Liquid Xe Scint.	[74] BERNABEI	02D	
> 1200	90	^{136}Xe	0ν	Liquid Xe Scint.	[75] BERNABEI	02D	
> 4.9	90	^{100}Mo	0ν	Liq. Ar ioniz.	[76] ASHITKOV	01	
> 1.3	90	^{160}Gd	0ν	Gd_2SiO_5:Ce	[77] DANEVICH	01	
> 1.3	90	^{160}Gd	0ν $0^+ \rightarrow 2^+$	Gd_2SiO_5:Ce	[78] DANEVICH	01	
$0.59^{+0.17}_{-0.11} \pm 0.06$		^{100}Mo	$0\nu+2\nu$ $0^+ \rightarrow 0^+_1$	Ge coinc.	[79] DEBRAECKEL.	01	
> 19000	90	^{76}Ge	0ν	Enriched HPGe	[80] KLAPDOR-K...	01	
(9.4 ± 3.2)E-3		^{96}Zr	$0\nu+2\nu$	Geochem	[81] WIESER	01	
$0.042^{+0.033}_{-0.013}$		^{48}Ca	2ν	Ge spectrometer	[82] BRUDANIN	00	
$0.021^{+0.008}_{-0.004} \pm 0.002$		^{96}Zr	2ν	NEMO-2	[83] ARNOLD	99	
$(8.3 \pm 1.0 \pm 0.7)$E-2		^{82}Se	2ν	NEMO-2	[84] ARNOLD	98	
> 2.8	90	^{82}Se	0ν $0^+ \rightarrow 2^+$	NEMO-2	[85] ARNOLD	98	
$(7.6^{+2.2}_{-1.4})$E-3		^{100}Mo	2ν	Si(Li)	[86] ALSTON-...	97	
$(6.82^{+0.38}_{-0.53} \pm 0.68)$E-3		^{100}Mo	2ν	TPC	[87] DESILVA	97	
$(6.75^{+0.37}_{-0.42} \pm 0.68)$E-3		^{150}Nd	2ν	TPC	[88] DESILVA	97	
$(3.75 \pm 0.35 \pm 0.21)$E-2		^{116}Cd	2ν $0^+ \rightarrow 0^+$	NEMO 2	[89] ARNOLD	96	
$0.043^{+0.024}_{-0.011} \pm 0.014$		^{48}Ca	2ν	TPC	[90] BALYSH	96	
0.79 ± 0.10		^{130}Te	$0\nu+2\nu$	Geochem	[91] TAKAOKA	96	
$0.61^{+0.18}_{-0.11}$		^{100}Mo	$0\nu+2\nu$ $0^+ \rightarrow 0^+_1$	γ in HPGe	[92] BARABASH	95	
$0.026^{+0.009}_{-0.005}$		^{116}Cd	2ν $0^+ \rightarrow 0^+$	ELEGANT IV	EJIRI	95	
$0.017^{+0.010}_{-0.005} \pm 0.0035$		^{150}Nd	2ν $0^+ \rightarrow 0^+$	TPC	ARTEMEV	93	
0.039 ± 0.009		^{96}Zr	$0\nu+2\nu$	Geochem	KAWASHIMA	93	
2.7 ± 0.1		^{130}Te	$0\nu+2\nu$	Geochem	BERNATOW...	92	
7200 ± 400		^{128}Te	$0\nu+2\nu$	Geochem	[93] BERNATOW...	92	
$0.108^{+0.026}_{-0.006}$		^{82}Se	2ν $0^+ \rightarrow 0^+$	TPC	ELLIOTT	92	
2.0 ± 0.6		^{238}U	$0\nu+2\nu$	Radiochem	[94] TURKEVICH	91	
$0.12 \pm 0.01 \pm 0.04$		^{82}Se	$0\nu+2\nu$	Geochem.	[95] LIN	88	
$0.75 \pm 0.03 \pm 0.23$		^{130}Te	$0\nu+2\nu$	Geochem.	[96] LIN	88	
1800 ± 700		^{128}Te	$0\nu+2\nu$	Geochem.	[97] LIN	88B	
2.60 ± 0.28		^{130}Te	$0\nu+2\nu$	Geochem	[98] KIRSTEN	83	

[1] ALBERT 14 use the EXO-200 tracking detector for a re-measurement of the $2\nu\beta\beta$-half life of ^{136}Xe. A nuclear matrix element of 0.0218 ± 0.0003 MeV^{-1} is derived from this data. Supersedes ACKERMAN 11.

[2] AGOSTINI 13 use 5.04 kg yr of data collected with bare enriched Ge diodes operated in a liquid argon shield, to determine the half life for the $0\nu\beta\beta$ decay of ^{76}Ge. This result is in agreement, and more accurate, than DOERR 03.

[3] AGOSTINI 13A use 21.6 kg yr of data, collected with GERDA detector array, to place a lower limit on the $0\nu\beta\beta$-half life of ^{76}Ge. This result is in tension with the evidence for $0\nu\beta\beta$-decay reported in KLAPDOR-KLEINGROTHAUS 06A. This half-life limit exceeds the limit reported in KLAPDOR-KLEINGROTHAUS 01.

[4] BELLI 13A use an underground Ge detector to search for the $2\beta^+$-decay of ^{96}Ru via the intensity of the annihilation peak. This method cannot distinguish two from zero neutrino decay.

[5] BELLI 13A use an underground Ge detector to search for the ECβ^+-decay of ^{96}Ru via the intensity of the 778 keV γ de-excitation peak. This method cannot distinguish two from zero neutrino decay. The same analysis provides several limits, (~ 0.1 - 0.3) 10^{21} years, for the β^+EC mode leading to the excited 0^+ and 2^+ states.

[6] BELLI 13A use an underground Ge detector to search for the $\beta\beta$-decay of ^{104}Ru via the intensity of the 556 keV γ de-excitation peak. This method cannot distinguish two from zero neutrino decay.

[7] GANDO 13A use the KamLAND detector to search for $0\nu\beta\beta$-decay of ^{136}Xe based on an exposure of 89.5 kg yr. This result is in tension with the evidence of $0\nu\beta\beta$ reported in KLAPDOR-KLEINGROTHAUS 06A and earier references to that work. Supersedes GANDO 12A and is more sensitive than BERNABEI 02D.

[8] GAVRILYAK 13 use a proportional counter filled with Kr gas to search for the 2ν2K decay of ^{78}Kr. Data with the enriched and depleted Kr were used to determine signal and background. A 2.5σ excess of events obtained with the enriched sample is interpreted as an indication for the presence of this decay.

[9] GAVRILYAK 13 use a proportional counter filled with Kr gas to search for the 0ν2K decay of ^{78}Kr into 2828 keV excited state of ^{78}Se. This transition could be subject to resonant rate enhancement. Data obtained with the enriched and depleted Kr were used to determine signal and background.

[10] ANDREOTTI 12 use high resolution TeO_2 bolometric calorimeter to search for the $0\nu\beta\beta$ decay of ^{130}Te leading to the excited 0^+_1 state at 1793.5 keV.

[11] AUGER 12 use EXO-200 liquid Xe TPC filled with 79.4 kg (fiducial mass) of ^{136}Xe to constrain the $0\nu\beta\beta$-decay halflife of ^{136}Xe. This result is more sensitive than BERNABEI 02D and GANDO 12A.

[12] BELLI 12A use $^{106}CdWO_4$ 215 g crystal scintillator to search for various $\beta\beta$ decay modes. The limit for the ECEC mode is derived from the fit to the background spectrum in the 1.8–3.2 MeV energy interval in the run of 6590 hours. The same analysis provides several limits ($\sim$ 2–5 $\times 10^{20}$ years) for the ECEC mode leading to the excited 0^+ and 2^+ states. Also a similar size limits for the possible resonance process populating states at 2718 keV, 2741 keV, and 2748 keV were obtained.

[13] BELLI 12A use $^{106}CdWO_4$ 215 g crystal scintillator to search for various $\beta\beta$ decay modes. The limit for the ECβ^+ mode is derived from the fit to the background spectrum in the 2.0–3.0 MeV energy interval in the run of 6590 hours. The same analysis provides several limits ($\sim$ 0.5–1.3 $\times 10^{21}$ years) for the ECβ^+ mode leading to the excited 0^+ and 2^+ states.

[14] BELLI 12A use $^{106}CdWO_4$ 215 g crystal scintillator to search for various $\beta\beta$ decay modes. The limit for the $\beta^+\beta^+$ mode is derived from the fit to the background spectrum in the 0.76–2.8 MeV energy interval in the run of 6590 hours. The same analysis provides the limit (1.2×10^{21} years) for the $\beta^+\beta^+$ mode leading to the first excited 2^+ state.

[15] GANDO 12A use a modification of the existing KamLAND detector. The $\beta\beta$ decay source/detector is 13 tons of enriched ^{136}Xe-loaded scintillator contained in an inner balloon. The $2\nu\beta\beta$ decay rate is derived from the fit to the spectrum between 0.5 and 4.8 MeV. This result is in agreement with ACKERMAN 11.

[16] GANDO 12A use a modification of the existing KamLAND detector. The $\beta\beta$ decay source/detector is 13 tons of enriched ^{136}Xe-loaded scintillator contained in an inner balloon. The $0\nu\beta\beta$ decay rate is derived from the fit where the background rates were allowed to float. Superseded by GANDO 13A.

[17] ACKERMAN 11 use the EXO-200 liquid Xe TPC filled with $\sim$ 175 kg of enriched ^{136}Xe to determine the 2ν half-life of ^{136}Xe. Superseded by ALBERT 14.

[18] ARNOLD 11 use enriched ^{130}Te in the NEMO-3 detector to measure the 2ν $\beta\beta$ decay rate. This result is in agreement with, but more accurate than ARNABOLDI 03.

[19] ARNOLD 11 use the NEMO-3 detector to obtain a limit for the 0ν $\beta\beta$ decay.This result is less significant than ARNABOLDI 05.

[20] BARABASH 11 use 100 g of enriched ^{112}Sn to determine a limit for the ECEC 0ν decay to the 0^+_3 state of ^{112}Cd by searching for the de-excitation γ with a Ge detector. This decay mode is a candidate for resonant rate enhancement.

[21] BARABASH 11 use 100 g of enriched ^{112}Sn to determine a limit for the ECEC 0ν decay to the 0^+_2 state of ^{112}Cd by searching for the de-excitation γ with a Ge detector.

[22] BARABASH 11 use 100 g of enriched ^{112}Sn to determine a limit for the ECEC 0ν decay to the 0^+_1 state of ^{112}Cd by searching for the de-excitation γ with a Ge detector.

[23] BARABASH 11 use 100 g of enriched ^{112}Sn to determine a limit for the ECEC 0ν decay to the ground state of ^{112}Cd by searching for the de-excitation γ with a Ge detector.

[24] Supersedes DANEVICH 03 and ARNOLD 96.

[25] Supersedes BRUDANIN 00 and BALYSH 96.

[26] BARABASH 11A use the NEMO-3 detector to measure $\beta\beta2\nu$ rates and place limits on $\beta\beta0\nu$ half lives for various nuclides.

[27] Supersedes ARNABOLDI 03.

[28] Supersedes ARNOLD 05A, ARNOLD 04, ASHITKOV 01, EJIRI 01, and DASSIE 95.

[29] Supersedes ARNOLD 05A, ARNOLD 04, ARNOLD 98, and ELLIOTT 92.

[30] Less restrictive than ARNABOLDI 08.

[31] Less restrictive than DANEVICH 03.

[32] Less restrictive than UMEHARA 08 and OGAWA 04.

[33] BELLI 11D use $ZnWO_4$ scintillator calorimeters to search for various $\beta\beta$ decay modes of ^{64}Zn, ^{70}Zn, ^{180}W, and ^{186}W.

[34] RUKHADZE 11 uses 13.6 g of enriched ^{106}Cd to search for the neutrinoless ECEC decay into an excited state of ^{106}Pd and its characteristic γ-radiation using the TGV2 detector. This decay mode is a candidate for resonant rate enhancement, however, hindered by the large spin difference.

[35] ARGYRIADES 10 use 9.4 $\pm$ 0.2 g of ^{96}Zr in NEMO-3 detector and identify its $2\nu\beta\beta$ decay. The result is in agreement and supersedes ARNOLD 99.

[36] ARGYRIADES 10 use 9.4 $\pm$ 0.2 g of ^{96}Zr in NEMO-3 detector and obtain a limit of the $0\nu\beta\beta$ decay. The result is in agreement and supersedes ARNOLD 99.

[37] ARGYRIADES 10 use 9.4 $\pm$ 0.2 g of ^{96}Zr in NEMO-3 detector and obtain a limit of the $0\nu\beta\beta$ decay into the first excited 0^+_1 state in ^{96}Mo.

[38] BELLI 10 use enriched ^{100}Mo with 4 HP Ge detectors to record the 590.8 and 539.5 keV γ rays from the decay of the 0^+_1 state in ^{100}Ru both in singles and coincidences. This result confirms the measurement of KIDD 09 and ARNOLD 07 and supersedes them.

[39] ARGYRIADES 09 use the NEMO-3 tracking calorimeter containing 36.5 g of ^{150}Nd, a total exposure of 924.7 days, to derive a limit for the $0\nu\beta\beta$ half-life. Supersedes DESILVA 97.

[40] ARGYRIADES 09 use the NEMO-3 tracking calorimeter containing 36.5 g of ^{150}Nd, a total exposure of 924.7 days, to determine the value of the $2\nu\beta\beta$ half-life. This result is in marginal agreement, but has somewhat smaller error bars, than DESILVA 97.

[41] BELLI 09A use $ZnWO_4$ scintillating crystals to search for various modes of $\beta\beta$ decay. This work improves the limits for different modes of ^{64}Zn decay into the ground state of ^{64}Ni, in this case for the 0ν β^+EC mode. Supersedes BELLI 08.

[42] BELLI 09A use $ZnWO_4$ scintillating crystals to search for various modes of $\beta\beta$ decay. This work improves the limits for different modes of ^{64}Zn decay into the ground state of ^{64}Ni, in this case for the 0ν ECEC mode. Supersedes BELLI 08.

[43] KIDD 09 combine past and new data with an improved coincidence detection efficiency determination. The result agrees with ARNOLD 95. Supersedes DEBRAECKELEER 01 and BARABASH 95.

[44] ARNABOLDI 08 use high resolution TeO_2 bolometer calorimeter to search for double beta decay of ^{130}Te. Supersedes ARNABOLDI 05.

[45] BELLI 08 use $ZnWO_4$ scintillation calorimeter to search for neutrinoless β^+ plus electron capture decay of ^{64}Zn. The halflife limit for the 2ν mode is 2.1×10^{20} years.

[46] BELLI 08B use $CdWO_4$ scintillation calorimeter to search for 0ν $\beta\beta$ decay of ^{114}Cd.

[47] UMEHARA 08 use CaF_2 scintillation calorimeter to search for double beta decay of ^{48}Ca. Limit is significantly more stringent than quoted sensitivity: 18×10^{21} years.

[48] First exclusive measurement of 2ν-decay to the first excited 0^+_1-state of daughter nucleus. ARNOLD 07 use the NEMO-3 tracking calorimeter to detect all particles emitted in decay. Result agrees with the inclusive ($0\nu + 2\nu$) measurement of DEBRAECKELEER 01.

[49] Limit on 0ν-decay to the first excited 0^+_1-state of daughter nucleus using NEMO-3 tracking calorimeter. Supersedes DASSIE 95.

[50] Limit on 0ν-decay to the first excited 2^+-state of daughter nucleus using NEMO-3 tracking calorimeter.

[51] BARABASH 07 use Ge calorimeter to search for γ-radiation following double electron capture or β^+ plus electron capture decays of ^{74}Se to the ground state of ^{74}Ge. This limit is based on the search for the 511 keV annihilation radiation. Various other limits, for the capture from different atomic shells and also to the excited states, are reported in the paper.

[52] BARABASH 07 use Ge calorimeter to search for γ-radiation following double electron capture decay of ^{74}Se into the second excited 2^+-state of ^{74}Ge. That transition has been considered due to a possible resonance enhancement. The 2ν mode would be suppressed for this decay by its extremely small phase space factor.

[53] KLAPDOR-KLEINGROTHAUS 06A present re-analysis of data originally published in KLAPDOR-KLEINGROTHAUS 04A. Modified pulse shape analysis leads the authors to claim improved 6σ statistical evidence for observation of 0ν-decay, compared to 4.2σ in KLAPDOR-KLEINGROTHAUS 04A. Analysis of the systematic uncertainty is not presented. This re-analysis is disputed in AGOSTINI 13A and SCHWINGENHEUER 13.

[54] Supersedes ARNABOLDI 04. Bolometric TeO_2 detector array CUORICINO is used for high resolution search for $0\nu\beta\beta$ decay. The half-life limit is derived from 3.09 kg yr ^{130}Te exposure.

[55] NEMO-3 tracking calorimeter containing 6.9 kg of enriched ^{100}Mo is used in ARNOLD 05A. A limit for $0\nu\beta\beta$ half-life of ^{100}Mo is reported. Supersedes ARNOLD 04.

[56] NEMO-3 tracking calorimeter is used in ARNOLD 05A to place limit on $0\nu\beta\beta$ half-life of ^{82}Se. Detector contains 0.93 kg of enriched ^{82}Se. Supersedes ARNOLD 04.

[57] ARNOLD 05A use the NEMO-3 tracking calorimeter to determine the $2\nu\beta\beta$ half-life of ^{100}Mo with high statistics and low background (389 days of data taking). Supersedes ARNOLD 04.

[58] ARNOLD 05A use the NEMO-3 tracking detector to determine the $2\nu\beta\beta$ half-life of ^{82}Se with high statistics and low background (389 days of data taking). Supersedes ARNOLD 04.

[59] ARNOLD 04 use the NEMO-3 tracking detector to determine the limit for $0\nu\beta\beta$ halflife of ^{82}Se. This represents an improvement, by a factor of $\sim$ 10, when compared with ELLIOTT 92. It supersedes the limit of ARNOLD 98 for this decay using NEMO-2.

[60] ARNOLD 04 use the NEMO-3 tracking detector to determine the $2\nu\beta\beta$ halflife of ^{100}Mo with high statistics and low background. The halflife is determined assuming the Single State Dominance. It is in agreement with, and more accurate than, previous determinations. Supersedes DASSIE 95 determination of this quantity with NEMO-2.

[61] BARABASH 04 perform an inclusive measurement of the $\beta\beta$ decay of ^{150}Nd into the first excited (0^+_1) state of ^{150}Sm. Gamma radiation emitted in decay of the excited state is detected.

[62] Decay into first excited state of daughter nucleus.

[63] Two neutrino decay into ground state. Relatively large error mainly due to uncertainties in background determination. Reported value is shorter than the geochemical measurements of KIRSTEN 83 and BERNATOWICZ 92 but in agreement with LIN 88 and TAKAOKA 96.

[64] Supersedes ALESSANDRELLO 00. Array of TeO_2 crystals in high resolution cryogenic calorimeter. Some enriched in ^{128}Te. Ground state to ground state decay.

[65] Calorimetric measurement of 2ν ground state decay of ^{116}Cd using enriched $CdWO_4$ scintillators. Agrees with EJIRI 95 and ARNOLD 96. Supersedes DANEVICH 00.

[66] Limit on 0ν decay of ^{116}Cd using enriched $CdWO_4$ scintillators. Supersedes DANEVICH 00.

[67] Limit on 0ν decay of ^{116}Cd into first excited 2^+ state of daughter nucleus using enriched $CdWO_4$ scintillators. Supersedes DANEVICH 00.

[68] Limit on 0ν decay of ^{116}Cd into first excited 0^+ state of daughter nucleus using enriched $CdWO_4$ scintillators. Supersedes DANEVICH 00.

[69] Limit on 0ν decay of ^{116}Cd into second excited 0^+ state of daughter nucleus using enriched $CdWO_4$ scintillators. Supersedes DANEVICH 00.

[70] Limit on the 0ν ground state decay of ^{186}W using enriched $CdWO_4$ scintillators.

[71] Limit on the 0ν decay of ^{186}W to the first excited 2^+ state of the daughter nucleus using enriched $CdWO_4$ scintillators.

[72] Results of the Heidelberg-Moscow experiment (KLAPDOR-KLEINGROTHAUS 01 and GUENTHER 97) are reanalyzed using a new simulation of the complete background spectrum. The $\beta\beta2\nu$-decay rate is deduced from a 41.57 kg-y exposure. The result is in agreement and supersedes the above referenced halflives with similar statistical and systematic errors.

[73] AALSETH 02B limit is based on 117 mol-yr of data using enriched Ge detectors. Background reduction by means of pulse shape analysis is applied to part of the data set. Reported limit is slightly less restrictive than that in KLAPDOR-KLEINGROTHAUS 01 However, it excludes part of the allowed half-life range reported in KLAPDOR-KLEINGROTHAUS 01B for the same nuclide. The analysis has been criticized in KLAPDOR-KLEINGROTHAUS 04B. The criticism was addressed and disputed in AALSETH 04.

[74] BERNABEI 02D report a limit for the 0ν, $0^+ \rightarrow 0^+$ decay of ^{134}Xe, present in the source at 17%, by considering the maximum number of events for this mode compatible with the fitted smooth background.

[75] BERNABEI 02D report a limit for the 0ν, $0^+ \rightarrow 0^+$ decay of ^{136}Xe, by considering the maximum number of events for this mode compatible with the fitted smooth background. The quoted sensitivity is 450×10^{21} yr. The Feldman and Cousins method is used to obtain the quoted limit.

[76] ASHITKOV 01 result for 0ν of ^{100}Mo is less stringent than EJIRI 01.

[77] DANEVICH 01 place limit on 0ν decay of ^{160}Gd using Gd_2SiO_5:Ce crystal scintillators. The limit is more stringent than KOBAYASHI 95.

[78] DANEVICH 01 place limits on 0ν decay of ^{160}Gd into excited 2^+ state of daughter nucleus using Gd_2SiO_5:Ce crystal scintillators.

[79] DEBRAECKELEER 01 performed an inclusive measurement of the $\beta\beta$ decay into the second excited state of the daughter nucleus. A novel coincidence technique counting the de-excitation photons is employed. The result agrees with BARABASH 95.

[80] KLAPDOR-KLEINGROTHAUS 01 is a continuation of the work published in BAUDIS 99. Isotopically enriched Ge detectors are used in calorimetric measurement. The most stringent bound is derived from the data set in which pulse-shape analysis has been used to reduce background. Exposure time is 35.5 kg y. Supersedes BAUDIS 99 as most stringent result.

[81] WIESER 01 reports an inclusive geochemical measurement of ^{96}Zr $\beta\beta$ half life. Their result agrees within 2σ with ARNOLD 99 but only marginally, within 3σ, with KAWASHIMA 93.

[82] BRUDANIN 00 determine the 2ν halflife of ^{48}Ca. Their value is less accurate than BALYSH 96.

[83] ARNOLD 99 measure directly the 2ν decay of Zr for the first time, using the NEMO-2 tracking detector and an isotopically enriched source. The lifetime is more accurate than the geochemical result of KAWASHIMA 93.

[84] ARNOLD 98 measure the 2ν decay of ^{82}Se by comparing the spectra in an enriched and natural selenium source using the NEMO-2 tracking detector. The measured half-life is in agreement, perhaps slightly shorter, than ELLIOTT 92.

[85] ARNOLD 98 determine the limit for 0ν decay to the excited 2^+ state of ^{82}Se using the NEMO-2 tracking detector.

[86] ALSTON-GARNJOST 97 report evidence for 2ν decay of ^{100}Mo. This decay has been also observed by EJIRI 91, DASSIE 95, and DESILVA 97.

[87] DESILVA 97 result for 2ν decay of ^{100}Mo is in agreement with ALSTON-GARNJOST 97 and DASSIE 95. This measurement has the smallest errors.

[88] DESILVA 97 result for 2ν decay of ^{150}Nd is in marginal agreement with ARTEMEV 93. It has smaller errors.

[89] ARNOLD 96 measure the 2ν decay of ^{116}Cd. This result is in agreement with EJIRI 95, but has smaller errors. Supersedes ARNOLD 95.

[90] BALYSH 96 measure the 2ν decay of ^{48}Ca, using a passive source of enriched ^{48}Ca in a TPC.

[91] TAKAOKA 96 measure the geochemical half-life of ^{130}Te. Their value is in disagreement with the quoted values of BERNATOWICZ 92 and KIRSTEN 83; but agrees with several other unquoted determinations, e.g., MANUEL 91.

[92] BARABASH 95 cannot distinguish 0ν and 2ν, but it is inferred indirectly that the 0ν mode accounts for less than 0.026% of their event sample. They also note that their result disagrees with the previous experiment by the NEMO group (BLUM 92).

[93] BERNATOWICZ 92 finds ^{128}Te/^{130}Te activity ratio from slope of ^{128}Xe/^{132}Xe vs ^{130}Xe/^{132}Xe ratios during extraction, and normalizes to lead-dated ages for the ^{130}Te lifetime. The authors state that their results imply that "(a) the double beta decay of ^{128}Te has been firmly established and its half-life has been determined ... without any ambiguity due to trapped Xe interferences... (b) Theoretical calculations ... underestimate the [long half-lives of ^{128}Te ^{130}Te] by 1 or 2 orders of magnitude, pointing to a real suppression in the 2ν decay rate of these isotopes. (c) Despite [this], most $\beta\beta$-models predict a *ratio* of 2ν decay widths ... in fair agreement with observation." Further details of the experiment are given in BERNATOWICZ 93. Our listed half-life has been revised downward from the published value by the authors, on the basis of reevaluated cosmic-ray ^{128}Xe production corrections.

[94] TURKEVICH 91 observes activity in old U sample. The authors compare their results with theoretical calculations. They state "Using the phase-space factors of Boehm and Vogel (BOEHM 87) leads to matrix element values for the ^{238}U transition in the same range as deduced for ^{130}Te and ^{76}Ge. On the other hand, the latest theoretical estimates (STAUDT 90) give an upper limit that is 10 times lower. This large discrepancy implies either a defect in the calculations or the presence of a faster path than the standard two-neutrino mode in this case." See BOEHM 87 and STAUDT 90.

[95] Result agrees with direct determination of ELLIOTT 92.

[96] Inclusive half life inferred from mass spectroscopic determination of abundance of $\beta\beta$-decay product ^{130}Te in mineral kitkaite (NiTeSe). Systematic uncertainty reflects variations in U-Xe gas-retention-age derived from different uranite samples. Agrees with geochemical determination of TAKAOKA 96 and direct measurement of ARNABOLDI 03. Inconsistent with results of KIRSTEN 83 and BERNATOWICZ 92.

[97] Ratio of inclusive double beta half lives of ^{128}Te and ^{130}Te determined from minerals melonite ($NiTe_2$) and altaite (PbTe) by means of mass spectroscopic measurement of abundance of $\beta\beta$-decay products. As gas-retention-age could not be determined the authors use half life of ^{130}Te (LIN 88) to infer the half life of ^{128}Te. No estimate of the systematic uncertainty of this method is given. The directly determined half life ratio agrees with BERNATOWICZ 92. However, the inferred ^{128}Te half life disagrees with KIRSTEN 83 and BERNATOWICZ 92.

[98] KIRSTEN 83 reports "2σ" error. References are given to earlier determinations of the ^{130}Te lifetime.

$\langle m_\nu \rangle$, The Effective Weighted Sum of Majorana Neutrino Masses Contributing to Neutrinoless Double-β Decay

$\langle m_\nu \rangle = |\Sigma\ U^2_{1j} m_{\nu_j}|$, where the sum goes from 1 to n and where n = number of neutrino generations, and ν_j is a Majorana neutrino. Note that U^2_{ej}, not $|U_{ej}|^2$, occurs in the sum. The possibility of cancellations has been stressed. In the following Listings, only best or comparable limits or lifetimes for each isotope are reported.

VALUE (eV)	CL%	ISOTOPE	TRANSITION	METHOD	DOCUMENT ID	
• • • We do not use the following data for averages, fits, limits, etc. • • •						
< 0.2–0.4	90	^{76}Ge	0ν	GERDA	[1] AGOSTINI	13A
< 0.12–0.25	90	^{136}Xe	0ν,g.s.→ g.s.	KamLAND-Zen	[2] GANDO	13A
< 0.14–0.38	90	^{136}Xe	0ν,g.s.→ g.s.	EXO-200	[3] AUGER	12
< 0.3–0.6	90	^{136}Xe	0ν,g.s.→ g.s.	KamLAND-Zen	[4] GANDO	12A
< 0.45–0.93	90	^{100}Mo	0ν	NEMO-3	[5] BARABASH	11A
< 0.89–2.43	90	^{82}Se	0ν	NEMO-3	[6] BARABASH	11A
< 7.2–19.5	90	^{96}Zr	0ν	NEMO-3	[7] ARGYRIADES	10
< 4.0–6.8	90	^{150}Nd	0ν	NEMO-3	[8] ARGYRIADES	09
< 0.19–0.68	90	^{130}Te	0ν	TeO_2 bolometer	[9] ARNABOLDI	08
< 3.5–22	90	^{48}Ca	0ν	CaF_2 scint.	[10] UMEHARA	08
< 9.3–60	90	^{100}Mo	$0^+ \rightarrow 0^+_1$	NEMO-3	[11] ARNOLD	07
< 6500	90	^{100}Mo	$0^+ \rightarrow 2^+$	NEMO-3	[12] ARNOLD	07
0.32 ± 0.03	68	^{76}Ge	0ν	Enriched HPGe	[13] KLAPDOR-K...	06A
< 0.2–1.1	90	^{130}Te		Cryog. det.	[14] ARNABOLDI	05
< 0.7–2.8	90	^{100}Mo	0ν	NEMO-3	[15] ARNOLD	05A
< 1.7–4.9	90	^{82}Se	0ν	NEMO-3	[16] ARNOLD	05A
< 0.37–1.9	90	^{130}Te		Cryog. det.	[17] ARNABOLDI	04
< 0.8–1.2	90	^{100}Mo	0ν	NEMO-3	[18] ARNOLD	04
< 1.5–3.1	90	^{82}Se	0ν	NEMO-3	[18] ARNOLD	04
0.1–0.9	99.7	^{76}Ge		Enriched HP Ge	[19] KLAPDOR-K...	04A
< 7.2–44.7	90	^{48}Ca		CaF_2 scint.	[20] OGAWA	04
< 1.1–2.6	90	^{130}Te		Cryog. det.	[21] ARNABOLDI	03
< 1.5–1.7	90	^{116}Cd	0ν	$^{116}CdWO_4$ scint.	[22] DANEVICH	03
< 0.33–1.35	90			Enriched HPGe	[23] AALSETH	02B
<2.9	90	^{136}Xe	0ν	Liquid Xe Scint.	[24] BERNABEI	02D
$0.39^{+0.17}_{-0.28}$		^{76}Ge	0ν	Enriched HPGe	[25] KLAPDOR-K...	02D
< 2.1–4.8	90	^{100}Mo	0ν	ELEGANT V	[26] EJIRI	01
< 0.35	90	^{76}Ge		Enriched HPGe	[27] KLAPDOR-K...	01
<23	90	^{96}Zr		NEMO-2	[28] ARNOLD	99
< 1.1–1.5		^{128}Te		Geochem	[29] BERNATOW...	92
<5	68	^{82}Se		TPC	[30] ELLIOTT	92
<8.3	76	^{48}Ca	0ν	CaF_2 scint.	YOU	91

[1] AGOSTINI 13A is based on 21.6 kg yr of data collected by the GERDA detector. The reported range reflects different nuclear matrix elements. This result is in tension with the evidence for $0\nu\beta\beta$-decay reported in KLAPDOR-KLEINGROTHAUS 06A and earlier references to that work.

[2] GANDO 13A limit is based on a combination of KamLAND-Zen and EXO-200 (AUGER 12) data. The reported range reflects different nuclear matrix elements. Supersedes GANDO 12A.

[3] AUGER 12 limit is based on the EXO-200 data. The reported range reflects different nuclear matrix elements.

[4] GANDO 12A limit is based on the KamLAND-Zen data. The reported range reflects different nuclear matrix elements. Superseded by GANDO 13A.

[5] BARABASH 11A limit is based on NEMO-3 data for ^{100}Mo. The reported range reflects different nuclear matrix elements. Supersedes ARNOLD 05A and ARNOLD 04.

[6] BARABASH 11A limit is based on NEMO-3 data for ^{82}Se. The reported range reflects different nuclear matrix elements. Supersedes ARNOLD 05A and ARNOLD 04.

[7] ARGYRIADES 10 use ^{96}Zr and the NEMO-3 tracking detector to obtain the reported mass limit. The range reflects the fluctuation of the nuclear matrix elements considered.

[8] ARGYRIADES 09 limit is based on data taken with the NEMO-3 detector and ^{150}Nd. A range of nuclear matrix elements that include the effect of nuclear deformation have been used.

[9] Limit was obtained using high resolution TeO_2 bolometer calorimeter to search for double beta decay of ^{130}Te. Reported range of limits reflects spread of matrix element calculations used. Supersedes ARNABOLDI 05.

[10] Limit was obtained using CaF_2 scintillation calorimeter to search for double beta decay of ^{48}Ca. Reported range of limits reflects spread of QRPA and SM matrix element calculations used. Supersedes OGAWA 04.

[11] ARNOLD 07 use NEMO-3 half life limit for 0ν-decay of ^{100}Mo to the first excited 0^+_1-state of daughter nucleus to obtain neutrino mass limit. The spread reflects the choice of two different nuclear matrix elements. This limit is not competitive when compared to the decay to the ground state.

[12] ARNOLD 07 use NEMO-3 half life limit for 0ν-decay of ^{100}Mo to the first excited 2^+-state of daughter nucleus to obtain neutrino mass limit. This limit is not competitive when compared to the decay to the ground state.

[13] Re-analysis of data originally published in KLAPDOR-KLEINGROTHAUS 04A. Modified pulse shape analysis leads the authors to claim 6σ statistical evidence for observation of 0ν-decay. Authors use matrix element of STAUDT 90. Uncertainty of nuclear matrix element is not reflected in stated error. Supersedes KLAPDOR-KLEINGROTHAUS 04A.

[14] Supersedes ARNABOLDI 04. Reported range of limits due to use of different nuclear matrix element calculations.

[15] Mass limits reported in ARNOLD 05A are derived from ^{100}Mo data, obtained by the NEMO-3 collaboration. The range reflects the spread of matrix element calculations considered in this work. Supersedes ARNOLD 04.

[16] Neutrino mass limits based on ^{82}Se data utilizing the NEMO-3 detector. The range reported in ARNOLD 05A reflects the spread of matrix element calculations considered in this work. Supersedes ARNOLD 04.

[17] Supersedes ARNABOLDI 03. Reported range of limits due to use of different nuclear matrix element calculations.

[18] ARNOLD 04 limit is based on the nuclear matrix elements of SIMKOVIC 99, STOICA 01 and CIVITARESE 03.

[19] Supersedes KLAPDOR-KLEINGROTHAUS 02D. Event excess at $\beta\beta$-decay energy is used to derive Majorana neutrino mass using the nuclear matrix elements of STAUDT 90. The mass range shown is based on the authors evaluation of the uncertainties of the STAUDT 90 matrix element calculation. If this uncertainty is neglected, and only statistical errors are considered, the range in $\langle m \rangle$ becomes (0.2–0.6) eV at the 3 σ level.

[20] Calorimetric CaF_2 scintillator. Range of limits reflects authors' estimate of the uncertainty of the nuclear matrix elements. Replaces YOU 91 as the most stringest limit based on ^{48}Ca.

[21] Supersedes ALESSANDRELLO 00. Cryogenic calorimeter search. Reported a range reflecting uncertainty in nuclear matrix element calculations.

[22] Limit for $\langle m_\nu \rangle$ is based on the nuclear matrix elements of STAUDT 90 and ARNOLD 96. Supersedes DANEVICH 00.

[23] AALSETH 02B reported range of limits on $\langle m_\nu \rangle$ reflects the spread of theoretical nuclear matrix elements. Excludes part of allowed mass range reported in KLAPDOR-KLEINGROTHAUS 01B.

[24] BERNABEI 02D limit is based on the matrix elements of SIMKOVIC 02. The range of neutrino masses based on a variety of matrix elements is 1.1–2.9 eV.

[25] KLAPDOR-KLEINGROTHAUS 02D is a detailed description of the analysis of the data collected by the Heidelberg-Moscow experiment, previously presented in KLAPDOR-KLEINGROTHAUS 01B. Matrix elements in STAUDT 90 have been used. See the footnote in the preceding table for further details. See also KLAPDOR-KLEINGROTHAUS 02B.

[26] The range of the reported $\langle m_\nu \rangle$ values reflects the spread of the nuclear matrix elements. On axis value assuming $\langle \lambda \rangle = \langle \eta \rangle = 0$.

[27] KLAPDOR-KLEINGROTHAUS 01 uses the calculation by STAUDT 90. Using several other models in the literature could worsen the limit up to 1.2eV. This is the most stringent experimental bound on m_ν. It supersedes BAUDIS 99B.

[28] ARNOLD 99 limit based on the nuclear matrix elements of STAUDT 90.

[29] BERNATOWICZ 92 finds these majorana neutrino mass limits assuming that the measured geochemical decay width is a limit on the 0ν decay width. The range is the range found using matrix elements from HAXTON 84, TOMODA 87, and SUHONEN 91. Further details of the experiment are given in BERNATOWICZ 93.

[30] ELLIOTT 92 uses the matrix elements of HAXTON 84.

Limits on Lepton-Number Violating ($V+A$) Current Admixture

For reasons given in the discussion at the beginning of this section, we list only results from 1989 and later. $\langle \lambda \rangle = \lambda \sum U_{ej} V_{ej}$ and $\langle \eta \rangle = \eta \sum U_{ej} V_{ej}$, where the sum is over the number of neutrino generations. This sum vanishes for massless or unmixed neutrinos. In the following Listings, only best or comparable limits or lifetimes for each isotope are reported.

$\langle \lambda \rangle$ (10^{-6})	CL%	$\langle \eta \rangle$ (10^{-8})	CL%	ISOTOPE	METHOD	DOCUMENT ID	
• • • We do not use the following data for averages, fits, limits, etc. • • •							
<120	90			^{100}Mo	$0^+ \to 2^+$	[1] ARNOLD	07
$0.692^{+0.058}_{-0.056}$	68	$0.305^{+0.026}_{-0.025}$	68	^{76}Ge	Enriched HPGe	[2] KLAPDOR-K...	06A
< 2.5	90			^{100}Mo	0ν, NEMO-3	[3] ARNOLD	05A
< 3.8	90			^{82}Se	0ν, NEMO-3	[4] ARNOLD	05A
< 1.5–2.0	90			^{100}Mo	0ν, NEMO-3	[5] ARNOLD	04
< 3.2–3.8	90			^{82}Se	0ν, NEMO-3	[6] ARNOLD	04
< 1.6–2.4	90	< 0.9–5.3	90	^{130}Te	Cryog. det.	[7] ARNABOLDI	03
< 2.2	90	<2.5	90	^{116}Cd	$^{116}CdWO_4$ scint.	[8] DANEVICH	03
< 3.2–4.7	90	< 2.4–2.7	90	^{100}Mo	ELEGANT V	[9] EJIRI	01
< 1.1	90	<0.64	90	^{76}Ge	Enriched HPGe	[10] GUENTHER	97
< 4.4	90	<2.3	90	^{136}Xe	TPC	[11] VUILLEUMIER	93
		<5.3		^{128}Te	Geochem	[12] BERNATOW...	92

[1] ARNOLD 07 use NEMO-3 half life limit for 0ν-decay of ^{100}Mo to the first excited 2^+-state of daughter nucleus to limit the right-right handed admixture of weak currents $\langle \lambda \rangle$. This limit is not competitive when compared to the decay to the ground state.

[2] Re-analysis of data originally published in KLAPDOR-KLEINGROTHAUS 04A. Modified pulse shape analysis leads the authors to claim 6σ statistical evidence for observation of 0ν-decay. Authors use matrix element of MUTO 89 to determine $\langle \lambda \rangle$ and $\langle \eta \rangle$. Uncertainty of nuclear matrix element is not reflected in stated errors.

[3] ARNOLD 05A derive limit for $\langle \lambda \rangle$ based on ^{100}Mo data collected with NEMO-3 detector. No limit for $\langle \eta \rangle$ is given. Supersedes ARNOLD 04.

[4] ARNOLD 05A derive limit for $\langle \lambda \rangle$ based on ^{82}Se data collected with NEMO-3 detector. No limit for $\langle \eta \rangle$ is given. Supersedes ARNOLD 04.

[5] ARNOLD 04 use the matrix elements of SUHONEN 94 to obtain a limit for $\langle \lambda \rangle$, no limit for $\langle \eta \rangle$ is given. This limit is more stringent than the limit in EJIRI 01 for the same nucleus.

[6] ARNOLD 04 use the matrix elements of TOMODA 91 and SUHONEN 91 to obtain a limit for $\langle \lambda \rangle$, no limit for $\langle \eta \rangle$ is given.

[7] Supersedes ALESSANDRELLO 00. Cryogenic calorimeter search. Reported a range reflecting uncertainty in nuclear matrix element calculations.

[8] Limits for $\langle \lambda \rangle$ and $\langle \eta \rangle$ are based on nuclear matrix elements of STAUDT 90. Supersedes DANEVICH 00.

[9] The range of the reported $\langle \lambda \rangle$ and $\langle \eta \rangle$ values reflects the spread of the nuclear matrix elements. On axis value assuming $\langle m_\nu \rangle = 0$ and $\langle \lambda \rangle = \langle \eta \rangle = 0$, respectively.

[10] GUENTHER 97 limits use the matrix elements of STAUDT 90. Supersedes BALYSH 95 and BALYSH 92.

[11] VUILLEUMIER 93 uses the matrix elements of MUTO 89. Based on a half-life limit 2.6×10^{23} y at 90%CL.

[12] BERNATOWICZ 92 takes the measured geochemical decay width as a limit on the 0ν width, and uses the SUHONEN 91 coefficients to obtain the least restrictive limit on η. Further details of the experiment are given in BERNATOWICZ 93.

Double-β Decay REFERENCES

ALBERT	14	PR C89 015502	J. Albert *et al.*	(EXO-200 Collab.)
AGOSTINI	13	JP G40 035110	M. Agostini *et al.*	(GERDA Collab.)
AGOSTINI	13A	PRL 111 122503	M. Agostini *et al.*	(GERDA Collab.)
BELLI	13A	PR C87 034607	P. Belli *et al.*	(DAMA-INR Collab.)
GANDO	13A	PRL 110 062502	A. Gando *et al.*	(KamLAND-Zen Collab.)
GAVRILYAK	13	PR C87 035501	Yu.M. Gavrilyuk *et al.*	
SCHWINGEN...	13	ANP 525 269	B. Schwingenheuer	(MPIH)
ANDREOTTI	12	PR C85 045503	E. Andreotti *et al.*	(CUORICINO Collab.)
AUGER	12	PRL 109 032505	M. Auger *et al.*	(EXO-200 Collab.)
BELLI	12A	PR C85 044610	P. Belli *et al.*	
GANDO	12A	PR C85 045504	A. Gando *et al.*	(KamLAND-Zen Collab.)
ACKERMAN	11	PRL 107 212501	N. Ackerman *et al.*	(EXO Collab.)
ARNOLD	11	PRL 107 062504	R. Arnold *et al.*	(NEMO-3 Collab.)
BARABASH	11	PR C83 045503	A.S. Barabash *et al.*	
BARABASH	11A	PAN 74 312	A.S. Barabash *et al.*	(NEMO-3 Collab.)
		Translated from YAF 74 330.		
BELLI	11D	JP G38 115107	P. Belli *et al.*	(DAMA-INR Collab.)
RUKHADZE	11	NP A852 197	N.I. Rukhadze *et al.*	(TGV-2 Collab.)
ARGYRIADES	10	NP A847 168	J. Argyriades *et al.*	(NEMO-3 Collab.)
BELLI	10	NP A846 143	P. Belli *et al.*	(DAMA-INR Collab.)
ARGYRIADES	09	PR C80 032501	J. Argyriades *et al.*	(NEMO-3 Collab.)
BELLI	09A	NP A826 256	P. Belli *et al.*	(DAMA-INR Collab.)
KIDD	09	NP A821 251	M. Kidd *et al.*	
ARNABOLDI	08	PR C78 035502	C. Arnaboldi *et al.*	
BELLI	08	PL B658 193	P. Belli *et al.*	(DAMA-INR Collab.)
BELLI	08B	EPJ A36 167	P. Belli *et al.*	
UMEHARA	08	PR C78 058501	S. Umehara *et al.*	
ARNOLD	07	NP A781 209	R. Arnold *et al.*	(NEMO-3 Collab.)
BARABASH	07	NP A785 371	A.S. Barabash *et al.*	
KLAPDOR-K...	06A	MPL A21 1547	H.V. Klapdor-Kleingrothaus, I.V. Krivosheina	
ARNABOLDI	05	PRL 95 142501	C. Arnaboldi *et al.*	(CUORICINO Collab.)
ARNOLD	05A	PRL 95 182302	R. Arnold *et al.*	(NEMO-3 Collab.)
AALSETH	04	PR D70 078302	C.E. Aalseth *et al.*	
ARNABOLDI	04	PL B584 260	C. Arnaboldi *et al.*	
ARNOLD	04	JETPL 80 377	R. Arnold *et al.*	(NEMO3 Detector Collab.)
		Translated from ZETFP 80 429.		
BARABASH	04	JETPL 79 10	A.S. Barabash *et al.*	
KLAPDOR-K...	04A	PL B586 198	H.V. Klapdor-Kleingrothaus *et al.*	
KLAPDOR-K...	04B	PR D70 078301	H.V. Klapdor-Kleingrothaus, A. Dietz, I.V. Krivosheina	
OGAWA	04	NP A730 215	I. Ogawa *et al.*	
ARNABOLDI	03	PL B557 167	C. Arnaboldi *et al.*	
CIVITARESE	03	NP A729 867	O. Civitarese, J. Suhonen	
DANEVICH	03	PR C68 035501	F.A. Danevich *et al.*	
DOERR	03	NIM A513 596	C. Doerr, H.V. Klapdor-Kleingrothaus	
AALSETH	02B	PR D65 092007	C.E. Aalseth *et al.*	(IGEX Collab.)
BERNABEI	02D	PL B546 23	R. Bernabei *et al.*	(DAMA Collab.)
KLAPDOR-K...	02B	PPNL 110 57	H.V. Klapdor-Kleingrothaus, A. Dietz, I.V. Krivosheina	
KLAPDOR-K...	02D	FP 32 1181	H.V. Klapdor-Kleingrothaus, A. Dietz, I.V. Krivosheina	
SIMKOVIC	02	hep-ph/0204278	F. Simkovic, P. Domin, A. Faessler	
ASHITKOV	01	JETPL 74 529	V.D. Ashitkov *et al.*	
		Translated from ZETFP 74 601.		
DANEVICH	01	NP A694 375	F.A. Danevich *et al.*	
DEBRAECKEL...	01	PRL 86 3510	L. De Braeckeleer *et al.*	
EJIRI	01	PR C63 065501	H. Ejiri *et al.*	
KLAPDOR-K...	01	EPJ A12 147	H.V. Klapdor-Kleingrothaus *et al.*	
KLAPDOR-K...	01B	MPL A16 2409	H.V. Klapdor-Kleingrothaus *et al.*	
STOICA	01	NP A694 269	S. Stoica, H.V. Klapdor-Kleingrothous	
WIESER	01	PR C64 024308	M.E. Wieser, J.R. De Laeter	
ALESSAND...	00	PL B486 13	A. Alessandrello *et al.*	
BRUDANIN	00	PL B495 63	V.B. Brudanin *et al.*	(TGV Collab.)
DANEVICH	00	PR C62 045501	F.A. Danevich *et al.*	
ARNOLD	99	NP A658 299	R. Arnold *et al.*	(NEMO Collab.)
BAUDIS	99	PR D59 022001	L. Baudis *et al.*	(Heidelberg-Moscow Collab.)
BAUDIS	99B	PRL 83 41	L. Baudis *et al.*	(Heidelberg-Moscow Collab.)
SIMKOVIC	99	PR C60 055502	F. Simkovic *et al.*	
ARNOLD	98	NP A636 209	R. Arnold *et al.*	(NEMO-2 Collab.)
ALSTON-...	97	PR C55 474	M. Alston-Garnjost *et al.*	(LBL, MTHO+)
DESILVA	97	PR C56 2451	A. de Silva *et al.*	(UCI)
GUENTHER	97	PR D55 54	M. Gunther *et al.*	(Heidelberg-Moscow Collab.)
ARNOLD	96	ZPHY C72 239	R. Arnold *et al.*	(BCEN, CAEN, JINR+)
BALYSH	96	PRL 77 5186	A. Balysh *et al.*	(KIAE, UCI, CIT)
TAKAOKA	96	PR C53 1557	N. Takaoka, Y. Motomura, K. Nagao	(KYUSH, OKAY)
ARNOLD	95	JETPL 61 170	R.G. Arnold *et al.*	(NEMO Collab.)
		Translated from ZETFP 61 168.		
BALYSH	95	PL B356 450	A. Balysh *et al.*	(Heidelberg-Moscow Collab.)
BARABASH	95	PL B345 408	A.S. Barabash *et al.*	(ITEP, SCUC, PNL+)
DASSIE	95	PR D51 2090	D. Dassie *et al.*	(NEMO Collab.)
EJIRI	95	JPSJ 64 339	H. Ejiri *et al.*	(OSAK, KIEV)
KOBAYASHI	95	NP A586 457	M. Kobayashi, M. Kobayashi	(KEK, SAGA)
SUHONEN	94	PR C49 3055	J. Suhonen, O. Civitarese	
ARTEMEV	93	JETPL 58 262	V.A. Artemiev *et al.*	(ITEP, INRM)
		Translated from ZETFP 58 256.		
BERNATOW...	93	PR C47 806	T. Bernatowicz *et al.*	(WUSL, TATA)
KAWASHIMA	93	PR C47 R2452	A. Kawashima, K. Takahashi, A. Masuda	(TOKYC+)
VUILLEUMIER	93	PR D48 1009	J.C. Vuilleumier *et al.*	(NEUC, CIT, VILL)
BALYSH	92	PL B283 32	A. Balysh *et al.*	(MPIH, KIAE, SASSO)
BERNATOW...	92	PRL 69 2341	T. Bernatowicz *et al.*	(WUSL, TATA)
BLUM	92	PL B275 506	D. Blum *et al.*	(NEMO Collab.)
ELLIOTT	92	PR C46 1535	S.R. Elliott *et al.*	(UCI)
EJIRI	91	PL B258 17	H. Ejiri *et al.*	(OSAK)
MANUEL	91	JP G17 S221	O.K. Manuel	(MISSR)
SUHONEN	91	NP A535 509	J. Suhonen, S.B. Khadkikar, A. Faessler	(JYV+)
TOMODA	91	RPP 54 53	T. Tomoda	
TURKEVICH	91	PRL 67 3211	A. Turkevich, T.E. Economou, G.A. Cowan	(CHIC+)
YOU	91	PL B265 53	K. You *et al.*	(BHEP, CAST+)
STAUDT	90	EPL 13 31	A. Staudt, K. Muto, H.V. Klapdor-Kleingrothaus	
MUTO	89	ZPHY A334 187	K. Muto, E. Bender, H.V. Klapdor	(TINT, MPIH)
LIN	88	NP A481 477	W.J. Lin *et al.*	
LIN	88B	NP A481 484	W.J. Lin *et al.*	

Lepton Particle Listings

Double-β Decay, Neutrino Mixing

BOEHM 87 Massive Neutrinos F. Bohm, P. Vogel (CIT)
Cambridge Univ. Press, Cambridge
TOMODA 87 PL B199 475 T. Tomoda, A. Faessler (TUBIN)
HAXTON 84 PPNP 12 409 W.C. Haxton, G.J. Stevenson
KIRSTEN 83 PRL 50 474 T. Kirsten, H. Richter, E. Jessberger (MPIH)

Neutrino Mixing

With the exception of a few possible anomalies such as LSND, current neutrino data can be described within the framework of a 3×3 mixing matrix between the flavor eigenstates ν_e, ν_μ, and ν_τ and the mass eigenstates ν_1, ν_2, and ν_3. (See Eq. (14.78) of the review "Neutrino Mass, Mixing, and Oscillations" by K. Nakamura and S.T. Petcov.) The Listings are divided into the following sections:

(A) Neutrino fluxes and event ratios: shows measurements which correspond to various oscillation tests for Accelerator, Reactor, Atmospheric, and Solar neutrino experiments. Typically ratios involve a measurement in a realm sensitive to oscillations compared to one for which no oscillation effect is expected.

(B) Three neutrino mixing parameters: shows measurements of $\sin^2(2\theta_{12})$, $\sin^2(2\theta_{23})$, Δm^2_{21}, Δm^2_{32}, and $\sin^2(2\theta_{13})$ which are all interpretations of data based on the three neutrino mixing scheme described in the review "Neutrino Mass, Mixing, and Oscillations." by K. Nakamura and S.T. Petcov. Many parameters have been calculated in the two-neutrino approximation.

(C) Other neutrino mixing results: shows measurements and limits for the probability of oscillation for experiments which might be relevant to the LSND oscillation claim. Included are experiments which are sensitive to $\nu_\mu \to \nu_e$, $\bar{\nu}_\mu \to \bar{\nu}_e$, sterile neutrinos, and CPT tests.

(A) Neutrino fluxes and event ratios

Events (observed/expected) from accelerator ν_μ experiments.

Some neutrino oscillation experiments compare the flux in two or more detectors. This is usually quoted as the ratio of the event rate in the far detector to the expected rate based on an extrapolation from the near detector in the absence of oscillations.

VALUE	DOCUMENT ID		TECN	COMMENT
• • • We do not use the following data for averages, fits, limits, etc. • • •				
0.71 ± 0.08	[1] AHN	06A	K2K	K2K to Super-K
0.64 ± 0.05	[2] MICHAEL	06	MINS	All charged current events
$0.71^{+0.08}_{-0.09}$	[3] ALIU	05	K2K	KEK to Super-K
$0.70^{+0.10}_{-0.11}$	[4] AHN	03	K2K	KEK to Super-K

[1] Based on the observation of 112 events when $158.1^{+9.2}_{-8.6}$ were expected without oscillations. Including not only the number of events but also the shape of the energy distribution, the evidence for oscillation is at the level of about 4.3 σ. Supersedes ALIU 05.

[2] This ratio is based on the observation of 215 events compared to an expectation of 336 ± 14 without oscillations. See also ADAMSON 08.

[3] This ratio is based on the observation of 107 events at the far detector 250 km away from KEK, and an expectation of 151^{+12}_{-10}.

[4] This ratio is based on the observation of 56 events with an expectation of $80.1^{+6.2}_{-5.4}$.

Events (observed/expected) from reactor $\overline{\nu}_e$ experiments.

The quoted values are the ratios of the measured reactor $\overline{\nu}_e$ event rate at the quoted distances, and the rate expected without oscillations. The expected rate is based on the experimental data for the most significant reactor fuels (^{235}U, ^{239}Pu, ^{241}Pu) and on calculations for ^{238}U.

A recent re-evaluation of the spectral conversion of electron to $\overline{\nu}_e$ in MUELLER 11 results in an upward shift of the reactor $\overline{\nu}_e$ spectrum by 3% and, thus, might require revisions to the ratios listed in this table.

VALUE	DOCUMENT ID		TECN	COMMENT
$0.944 \pm 0.007 \pm 0.003$	[1] AN	13	DAYA	DayaBay, LIng Ao/Ao II reactors
• • • We do not use the following data for averages, fits, limits, etc. • • •				
$0.944 \pm 0.016 \pm 0.040$	[2] ABE	12	DCHZ	Chooz reactors
$0.920 \pm 0.009 \pm 0.014$	[3] AHN	12	RENO	Yonggwang reactors
$0.940 \pm 0.011 \pm 0.004$	[4] AN	12	DAYA	DayaBay, LIng Ao/Ao II reactors
$1.08 \pm 0.21 \pm 0.16$	[5] DENIZ	10	TEXO	Kuo-Sheng reactor, 28 m
$0.658 \pm 0.044 \pm 0.047$	[6] ARAKI	05	KLND	Japanese react. $\sim$ 180 km
$0.611 \pm 0.085 \pm 0.041$	[7] EGUCHI	03	KLND	Japanese react. $\sim$ 180 km
$1.01 \pm 0.024 \pm 0.053$	[8] BOEHM	01		Palo Verde react. 0.75–0.89 km
$1.01 \pm 0.028 \pm 0.027$	[9] APOLLONIO	99	CHOZ	Chooz reactors 1 km
$0.987 \pm 0.006 \pm 0.037$	[10] GREENWOOD	96		Savannah River, 18.2 m
$0.988 \pm 0.004 \pm 0.05$	ACHKAR	95	CNTR	Bugey reactor, 15 m
$0.994 \pm 0.010 \pm 0.05$	ACHKAR	95	CNTR	Bugey reactor, 40 m
$0.915 \pm 0.132 \pm 0.05$	ACHKAR	95	CNTR	Bugey reactor, 95 m
$0.987 \pm 0.014 \pm 0.027$	[11] DECLAIS	94	CNTR	Bugey reactor, 15 m
$0.985 \pm 0.018 \pm 0.034$	KUVSHINN...	91	CNTR	Rovno reactor
$1.05 \pm 0.02 \pm 0.05$	VUILLEUMIER	82		Gösgen reactor
$0.955 \pm 0.035 \pm 0.110$	[12] KWON	81		$\overline{\nu}_e p \to e^+ n$
0.89 ± 0.15	[12] BOEHM	80		$\overline{\nu}_e p \to e^+ n$

[1] AN 13 use six identical detectors, with three placed near the reactor cores (flux-weighted baselines of 470 and 576 m) and the remaining three at the far hall (at the flux averaged distance of 1648 m from all six reactor cores) to determine the mixing angle θ_{13} using the $\overline{\nu}_e$ observed interaction rate ratios. This rate-only analysis excludes the no-oscillation hypothesis at 7.7 standard deviations. The value of $\Delta m^2_{31} = 2.32 \times 10^{-3}$ eV^2 was assumed in the analysis. This is an improved result (2.5 times increase in statistics) compared to AN 12.

[2] ABE 12 determine the $\overline{\nu}_e$ interaction rate in a single detector, located 1050 m from the cores of two reactors. The rate normalization is fixed by the results of the Bugey4 reactor experiment, thus avoiding any dependence on possible very short baseline oscillations.

[3] AHN 12 use two identical detectors, placed at flux weighted distances of 408.56 m and 1433.99m from six reactor cores, to determine the $\overline{\nu}_e$ interaction rate ratio.

[4] AN 12 use six identical detectors with three placed near the reactor cores (flux-weighted baselines of 470 m and 576 m) and the remaining three at the far hall (at the flux averaged distance of 1648 m from all six reactor cores) to determine the $\overline{\nu}_e$ interaction rate ratios. Superseded by AN 13.

[5] DENIZ 10 observe reactor $\overline{\nu}_e e$ scattering with recoil kinetic energies 3–8 MeV using CsI(Tl) detectors. The observed rate is consistent with the Standard Model prediction, leading to a constraint on $\sin^2\theta_W = 0.251 \pm 0.031(\text{stat}) \pm 0.024(\text{sys})$.

[6] Updated result of KamLAND, including the data used in EGUCHI 03. Note that the survival probabilities for different periods are not directly comparable because the effective baseline varies with power output of the reactor sources involved, and there were large variations in the reactor power production in Japan in 2003.

[7] EGUCHI 03 observe reactor neutrino disappearance at $\sim$ 180 km baseline to various Japanese nuclear power reactors.

[8] BOEHM 01 search for neutrino oscillations at 0.75 and 0.89 km distance from the Palo Verde reactors.

[9] APOLLONIO 99, APOLLONIO 98 search for neutrino oscillations at 1.1 km fixed distance from Chooz reactors. They use $\overline{\nu}_e p \to e^+ n$ in Gd-loaded scintillator target. APOLLONIO 99 supersedes APOLLONIO 98. See also APOLLONIO 03 for detailed description.

[10] GREENWOOD 96 search for neutrino oscillations at 18 m and 24 m from the reactor at Savannah River.

[11] DECLAIS 94 result based on integral measurement of neutrons only. Result is ratio of measured cross section to that expected in standard *V-A* theory. Replaced by ACHKAR 95.

[12] KWON 81 represents an analysis of a larger set of data from the same experiment as BOEHM 80.

Atmospheric neutrinos

Neutrinos and antineutrinos produced in the atmosphere induce μ-like and e-like events in underground detectors. The ratio of the numbers of the two kinds of events is defined as μ/e. It has the advantage that systematic effects, such as flux uncertainty, tend to cancel, for both experimental and theoretical values of the ratio. The "ratio of the ratios" of experimental to theoretical μ/e, $R(\mu/e)$, or that of experimental to theoretical μ/total, $R(\mu/\text{total})$ with total $= \mu + e$, is reported below. If the actual value is not unity, the value obtained in a given experiment may depend on the experimental conditions. In addition, the measured "up-down asymmetry" for μ ($N_{up}(\mu)/N_{down}(\mu)$) or e ($N_{up}(e)/N_{down}(e)$) is reported. The expected "up-down asymmetry" is nearly unity if there is no neutrino oscillation.

R(μ/e) = (Measured Ratio μ/e) / (Expected Ratio μ/e)

VALUE	DOCUMENT ID		TECN	COMMENT
• • • We do not use the following data for averages, fits, limits, etc. • • •				
$0.658 \pm 0.016 \pm 0.035$	[1] ASHIE	05	SKAM	sub-GeV
$0.702^{+0.032}_{-0.030} \pm 0.101$	[2] ASHIE	05	SKAM	multi-GeV
$0.69 \pm 0.10 \pm 0.06$	[3] SANCHEZ	03	SOU2	Calorimeter raw data
	[4] FUKUDA	96B	KAMI	Water Cherenkov

$1.00 \pm 0.15 \pm 0.08$	[5] DAUM	95	FREJ	Calorimeter
$0.60 \pm 0.06 \pm 0.05$	[6] FUKUDA	94	KAMI	sub-GeV
$0.57 \pm 0.08 \pm 0.07$	[7] FUKUDA	94	KAMI	multi-Gev
	[8] BECKER-SZ...	92B	IMB	Water Cherenkov

[1] ASHIE 05 results are based on an exposure of 92 kton yr during the complete Super-Kamiokande I running period. The analyzed data sample consists of fully-contained single-ring e-like events with 0.1 GeV/c $< p_e$ and μ-like events 0.2 GeV/c $< p_\mu$, both having a visible energy $<$ 1.33 GeV. These criteria match the definition used by FUKUDA 94.

[2] ASHIE 05 results are based on an exposure of 92 kton yr during the complete Super-Kamiokande I running period. The analyzed data sample consists of fully-contained single-ring events with visible energy $>$ 1.33 GeV and partially-contained events. All partially-contained events are classified as μ-like.

[3] SANCHEZ 03 result is based on an exposure of 5.9 kton yr, and updates ALLISON 99 result. The analyzed data sample consists of fully-contained e-flavor and μ-flavor events having lepton momentum $>$ 0.3 GeV/c.

[4] FUKUDA 96B studied neutron background in the atmospheric neutrino sample observed in the Kamiokande detector. No evidence for the background contamination was found.

[5] DAUM 95 results are based on an exposure of 2.0 kton yr which includes the data used by BERGER 90B. This ratio is for the contained and semicontained events. DAUM 95 also report $R(\mu/e) = 0.99 \pm 0.13 \pm 0.08$ for the total neutrino induced data sample which includes upward going stopping muons and horizontal muons in addition to the contained and semicontained events.

[6] FUKUDA 94 result is based on an exposure of 7.7 kton yr and updates the HIRATA 92 result. The analyzed data sample consists of fully-contained e-like events with 0.1 $< p_e <$ 1.33 GeV/c and fully-contained μ-like events with 0.2 $< p_\mu <$ 1.5 GeV/c.

[7] FUKUDA 94 analyzed the data sample consisting of fully contained events with visible energy $>$ 1.33 GeV and partially contained μ-like events.

[8] BECKER-SZENDY 92B reports the fraction of nonshowering events (mostly muons from atmospheric neutrinos) as $0.36 \pm 0.02 \pm 0.02$, as compared with expected fraction $0.51 \pm 0.01 \pm 0.05$. After cutting the energy range to the Kamiokande limits, BEIER 92 finds $R(\mu/e)$ very close to the Kamiokande value.

R(ν_μ) = (Measured Flux of ν_μ) / (Expected Flux of ν_μ)

VALUE	DOCUMENT ID		TECN	COMMENT
• • • We do not use the following data for averages, fits, limits, etc. • • •				
0.84 ± 0.12	[1] ADAMSON	06	MINS	MINOS atmospheric
$0.72 \pm 0.026 \pm 0.13$	[2] AMBROSIO	01	MCRO	upward through-going
$0.57 \pm 0.05 \pm 0.15$	[3] AMBROSIO	00	MCRO	upgoing partially contained
$0.71 \pm 0.05 \pm 0.19$	[4] AMBROSIO	00	MCRO	downgoing partially contained + upgoing stopping
$0.74 \pm 0.036 \pm 0.046$	[5] AMBROSIO	98	MCRO	Streamer tubes
	[6] CASPER	91	IMB	Water Cherenkov
	[7] AGLIETTA	89	NUSX	
0.95 ± 0.22	[8] BOLIEV	81		Baksan
0.62 ± 0.17	CROUCH	78		Case Western/UCI

[1] ADAMSON 06 uses a measurement of 107 total neutrinos compared to an expected rate of 127 $\pm$ 13 without oscillations.

[2] AMBROSIO 01 result is based on the upward through-going muon tracks with $E_\mu > 1$ GeV. The data came from three different detector configurations, but the statistics is largely dominated by the full detector run, from May 1994 to December 2000. The total live time, normalized to the full detector configuration, is 6.17 years. The first error is the statistical error, the second is the systematic error, dominated by the theoretical error in the predicted flux.

[3] AMBROSIO 00 result is based on the upgoing partially contained event sample. It came from 4.1 live years of data taking with the full detector, from April 1994 to February 1999. The average energy of atmospheric muon neutrinos corresponding to this sample is 4 GeV. The first error is statistical, the second is the systematic error, dominated by the 25% theoretical error in the rate (20% in the flux and 15% in the cross section, added in quadrature). Within statistics, the observed deficit is uniform over the zenith angle.

[4] AMBROSIO 00 result is based on the combined samples of downgoing partially contained events and upgoing stopping events. These two subsamples could not be distinguished due to the lack of timing information. The result came from 4.1 live years of data taking with the full detector, from April 1994 to February 1999. The average energy of atmospheric muon neutrinos corresponding to this sample is 4 GeV. The first error is statistical, the second is the systematic error, dominated by the 25% theoretical error in the rate (20% in the flux and 15% in the cross section, added in quadrature). Within statistics, the observed deficit is uniform over the zenith angle.

[5] AMBROSIO 98 result is for all nadir angles and updates AHLEN 95 result. The lower cutoff on the muon energy is 1 GeV. In addition to the statistical and systematic errors, there is a Monte Carlo flux error (theoretical error) of $\pm$0.13. With a neutrino oscillation hypothesis, the fit either to the flux or zenith distribution independently yields $\sin^2 2\theta$=1.0 and $\Delta(m^2) \sim$ a few times 10^{-3} eV^2. However, the fit to the observed zenith distribution gives a maximum probability for χ^2 of only 5% for the best oscillation hypothesis.

[6] CASPER 91 correlates showering/nonshowering signature of single-ring events with parent atmospheric-neutrino flavor. They find nonshowering ($\approx \nu_\mu$ induced) fraction is $0.41 \pm 0.03 \pm 0.02$, as compared with expected 0.51 ± 0.05 (syst).

[7] AGLIETTA 89 finds no evidence for any anomaly in the neutrino flux. They define ρ = (measured number of ν_e's)/(measured number of ν_μ's). They report ρ(measured)=ρ(expected) $= 0.96^{+0.32}_{-0.28}$.

[8] From this data BOLIEV 81 obtain the limit $\Delta(m^2) \leq 6 \times 10^{-3}$ eV^2 for maximal mixing, $\nu_\mu \not\to \nu_\mu$ type oscillation.

R(μ/total) = (Measured Ratio μ/total) / (Expected Ratio μ/total)

VALUE	DOCUMENT ID		TECN	COMMENT
• • • We do not use the following data for averages, fits, limits, etc. • • •				
$1.1^{+0.07}_{-0.12} \pm 0.11$	[1] CLARK	97	IMB	multi-GeV

[1] CLARK 97 obtained this result by an analysis of fully contained and partially contained events in the IMB water-Cherenkov detector with visible energy $>$ 0.95 GeV.

$N_{up}(\mu)/N_{down}(\mu)$

VALUE	DOCUMENT ID		TECN	COMMENT
• • • We do not use the following data for averages, fits, limits, etc. • • •				
0.71 ± 0.06	[1] ADAMSON	12B	MINS	contained-vertex muons
$0.551^{+0.035}_{-0.033} \pm 0.004$	[2] ASHIE	05	SKAM	multi-GeV

[1] ADAMSON 12B reports the atmospheric neutrino results obtained with MINOS far detector in 2,553 live days (an exposure of 37.9 kton-yr). This result is obtained with a sample of high resolution contained-vertex muons. The quoted error is statistical only.

[2] ASHIE 05 results are based on an exposure of 92 kton yr during the complete Super-Kamiokande I running period. The analyzed data sample consists of fully-contained single-ring μ-like events with visible energy $>$ 1.33 GeV and partially-contained events. All partially-contained events are classified as μ-like. Upward-going events are those with $-1 <$ cos(zenith angle) < -0.2 and downward-going events are those with 0.2$<$ cos(zenith angle) $<$1. The μ-like up-down ratio for the multi-GeV data deviates from 1 (the expectation for no atmospheric ν_μ oscillations) by more than 12 standard deviations.

$N_{up}(e)/N_{down}(e)$

VALUE	DOCUMENT ID		TECN	COMMENT
• • • We do not use the following data for averages, fits, limits, etc. • • •				
$0.961^{+0.086}_{-0.079} \pm 0.016$	[1] ASHIE	05	SKAM	multi-GeV

[1] ASHIE 05 results are based on an exposure of 92 kton yr during the complete Super-Kamiokande I running period. The analyzed data sample consists of fully-contained single-ring e-like events with visible energy $>$ 1.33 GeV. Upward-going events are those with $-1 <$ cos(zenith angle) < -0.2 and downward-going events are those with 0.2 $<$ cos(zenith angle) $<$ 1. The e-like up-down ratio for the multi-GeV data is consistent with 1 (the expectation for no atmospheric ν_e oscillations).

R(up/down; μ) = (Measured up/down; μ) / (Expected up/down; μ)

VALUE	DOCUMENT ID		TECN	COMMENT
• • • We do not use the following data for averages, fits, limits, etc. • • •				
$0.62 \pm 0.05 \pm 0.02$	[1] ADAMSON	12B	MINS	contained-vertex muons
$0.62^{+0.19}_{-0.14} \pm 0.02$	[2] ADAMSON	06	MINS	atmospheric ν with far detector

[1] ADAMSON 12B reports the atmospheric neutrino results obtained with MINOS far detector in 2,553 live days (an exposure of 37.9 kton-yr). This result is obtained with a sample of high resolution contained-vertex muons. The expected ratio is calculated with no neutrino oscillation.

[2] ADAMSON 06 result is obtained with the MINOS far detector with an exposure of 4.54 kton yr. The expected ratio is calculated with no neutrino oscillation.

N(μ^+)/N(μ^-)

VALUE	DOCUMENT ID		TECN	COMMENT
• • • We do not use the following data for averages, fits, limits, etc. • • •				
$0.46^{+0.05}_{-0.04}$	[1,2] ADAMSON	12B	MINS	contained-vertex muons
$0.63^{+0.09}_{-0.08}$	[1,3] ADAMSON	12B	MINS	ν-induced rock-muons

[1] ADAMSON 12B reports the atmospheric neutrino results obtained with MINOS far detector in 2,553 live days (an exposure of 37.9 kton-yr). The muon charge ratio N(μ^+)/N(μ^-) represents the $\overline{\nu}_\mu/\nu_\mu$ ratio.

[2] This result is obtained with a charge-separated sample of high resolution contained-vertex muons. The quoted error is statistical only.

[3] This result is obtained with a charge-separated sample of high resolution neutrino-induced rock-muons. The quoted error is statistical only.

R(μ^+/μ^-) = (Measured N(μ^+)/N(μ^-)) / (Expected N(μ^+)/N(μ^-))

VALUE	DOCUMENT ID		TECN	COMMENT
• • • We do not use the following data for averages, fits, limits, etc. • • •				
$0.93 \pm 0.09 \pm 0.09$	[1,2] ADAMSON	12B	MINS	contained-vertex muons
$1.29^{+0.19}_{-0.17} \pm 0.16$	[1,3] ADAMSON	12B	MINS	ν-induced rock-muons
$1.03 \pm 0.08 \pm 0.08$	[1,4] ADAMSON	12B	MINS	contained
$1.39^{+0.35+0.08}_{-0.46-0.14}$	[5] ADAMSON	07	MINS	Upward and horizontal μ with far detector
$0.96^{+0.38}_{-0.27} \pm 0.15$	[6] ADAMSON	06	MINS	atmospheric ν with far detector

[1] ADAMSON 12B reports the atmospheric neutrino results obtained with MINOS far detector in 2,553 live days (an exposure of 37.9 kton·yr). The muon charge ratio $N(\mu^+)/N(\mu^-)$ represents the $\overline{\nu}_\mu/\nu_\mu$ ratio. As far as the same oscillation parameters are used for νs and $\overline{\nu}$s, the expected $\overline{\nu}_\mu/\nu_\mu$ ratio is almost entirely independent of any input oscillations.

[2] This result is obtained with a charge-separated sample of high resolution contained-vertex muons.

[3] This result is obtained with a charge-separated sample of high resolution neutrino-induced rock-muons.

[4] The charge-separated samples of high resolution contained-vertex muons and neutrino-induced rock-muons are combined to obtain this result which is consistent with unity.

[5] ADAMSON 07 result is obtained with the MINOS far detector in 854.24 live days, based on neutrino-induced upward-going and horizontal muons. This result is consistent with *CPT* conservation.

[6] ADAMSON 06 result is obtained with the MINOS far detector with an exposure of 4.54 kton yr, based on contained events. The expected ratio is calculated by assuming the same oscillation parameters for neutrinos and antineutrinos.

Solar neutrinos

Solar neutrinos are produced by thermonuclear fusion reactions in the Sun. Radiochemical experiments measure particular combinations of fluxes from various neutrino-producing reactions, whereas water-Cherenkov experiments mainly measure a flux of neutrinos from decay of ^{8}B. Solar neutrino fluxes are composed of all active neutrino species, ν_e, ν_μ, and ν_τ. In addition, some other mechanisms may cause antineutrino components in solar neutrino fluxes. Each measurement method is sensitive to a particular component or a combination of components of solar neutrino fluxes. For details, see Section 13.4 of Reviews, Tables, and Plots.

ν_e Capture Rates from Radiochemical Experiments

1 SNU (Solar Neutrino Unit) = 10^{-36} captures per atom per second.

VALUE (SNU)		DOCUMENT ID		TECN	COMMENT
• • • We do not use the following data for averages, fits, limits, etc. • • •					
$73.4\ ^{+6.1}_{-6.0}\ ^{+3.7}_{-4.1}$		[1] KAETHER	10		GALX reanalysis
$67.6 \pm 4.0 \pm 3.2$		[2] KAETHER	10		GNO+GALX reanalysis combined
$65.4\ ^{+3.1}_{-3.0}\ ^{+2.6}_{-2.8}$		[3] ABDURASHI...	09	SAGE	^{71}Ga → ^{71}Ge
$62.9\ ^{+5.5}_{-5.3} \pm 2.5$		[4] ALTMANN	05	GNO	^{71}Ga → ^{71}Ge
$69.3 \pm 4.1 \pm 3.6$		[5] ALTMANN	05	GNO	GNO + GALX combined
$77.5 \pm 6.2\ ^{+4.3}_{-4.7}$		[6] HAMPEL	99	GALX	^{71}Ga → ^{71}Ge
$2.56 \pm 0.16 \pm 0.16$		[7] CLEVELAND	98	HOME	^{37}Cl → ^{37}Ar

[1] KAETHER 10 reports the reanalysis results of a complete GALLEX data (GALLEX I+II+III+IV, reported in HAMPEL 99) based on the event selection with a new pulse shape analysis, which provides a better background reduction than the rise time analysis adopted in HAMPEL 99.

[2] Combined result of GALLEX I+II+III+IV reanalysis and GNO I+II+III (ALTMANN 05).

[3] ABDURASHITOV 09 reports a combined analysis of 168 extractions of the SAGE solar neutrino experiment during the period January 1990 through December 2007, and updates the ABDURASHITOV 02 result. The data are consistent with the assumption that the solar neutrino production rate is constant in time. Note that a $\sim$ 15% systematic uncertainty in the overall normalization may be added to the ABDURASHITOV 09 result, because calibration experiments for gallium solar neutrino measurements using intense ^{51}Cr (twice by GALLEX and once by SAGE) and ^{37}Ar (by SAGE) result in an average ratio of 0.87 ± 0.05 of the observed to calculated rates.

[4] ALTMANN 05 reports the complete result from the GNO solar neutrino experiment (GNO I+II+III), which is the successor project of GALLEX. Experimental technique of GNO is essentially the same as that of GALLEX. The run data cover the period 20 May 1998 through 9 April 2003.

[5] Combined result of GALLEX I+II+III+IV (HAMPEL 99) and GNO I+II+III.

[6] HAMPEL 99 report the combined result for GALLEX I+II+III+IV (65 runs in total), which update the HAMPEL 96 result. The GALLEX IV result (12 runs) is 118.4 ± 17.8 ± 6.6 SNU. (HAMPEL 99 discuss the consistency of partial results with the mean.) The GALLEX experimental program has been completed with these runs. The total run data cover the period 14 May 1991 through 23 January 1997. A total of 300 ^{71}Ge events were observed. Note that a $\sim$ 15% systematic uncertainty in the overall normalization may be added to the HAMPEL 99 result, because calibration experiments for gallium solar neutrino measurements using intense ^{51}Cr (twice by GALLEX and once by SAGE) and ^{37}Ar (by SAGE) result in an average ratio of 0.87 ± 0.05 of the observed to calculated rates.

[7] CLEVELAND 98 is a detailed report of the ^{37}Cl experiment at the Homestake Mine. The average solar neutrino-induced ^{37}Ar production rate from 108 runs between 1970 and 1994 updates the DAVIS 89 result.

ϕ_{ES} (^{8}B)

^{8}B solar-neutrino flux measured via νe elastic scattering. This process is sensitive to all active neutrino flavors, but with reduced sensitivity to ν_μ, ν_τ due to the cross-section difference, $\sigma(\nu_{\mu,\tau} e) \sim 0.16\sigma(\nu_e e)$. If the ^{8}B solar-neutrino flux involves nonelectron flavor active neutrinos, their contribution to the flux is $\sim$ 0.16 times of ν_e.

VALUE (10^6 cm^{-2}s^{-1})	DOCUMENT ID		TECN	COMMENT
• • • We do not use the following data for averages, fits, limits, etc. • • •				
$2.32 \pm 0.04 \pm 0.05$	[1] ABE	11	SKAM	SK-III average flux
$2.41 \pm 0.05\ ^{+0.16}_{-0.15}$	[2] ABE	11	SKAM	SK-II average flux
$2.38 \pm 0.02 \pm 0.08$	[3] ABE	11	SKAM	SK-I average flux
$2.77 \pm 0.26 \pm 0.32$	[4] ABE	11B	KLND	average flux
$2.4 \pm 0.4 \pm 0.1$	[5] BELLINI	10A	BORX	average flux
$1.77\ ^{+0.24}_{-0.21}\ ^{+0.09}_{-0.10}$	[6] AHARMIM	08	SNO	Phase III
$2.38 \pm 0.05\ ^{+0.16}_{-0.15}$	[7] CRAVENS	08	SKAM	average flux
$2.35 \pm 0.02 \pm 0.08$	[8] HOSAKA	06	SKAM	average flux
$2.35 \pm 0.22 \pm 0.15$	[9] AHARMIM	05A	SNO	Salty D_2O; ^{8}B shape not constrained
$2.34 \pm 0.23\ ^{+0.15}_{-0.14}$	[9] AHARMIM	05A	SNO	Salty D_2O; ^{8}B shape constrained
$2.39\ ^{+0.24}_{-0.23} \pm 0.12$	[10] AHMAD	02	SNO	average flux
$2.39 \pm 0.34\ ^{+0.16}_{-0.14}$	[11] AHMAD	01	SNO	average flux
$2.80 \pm 0.19 \pm 0.33$	[12] FUKUDA	96	KAMI	average flux
2.70 ± 0.27	[12] FUKUDA	96	KAMI	day flux
$2.87\ ^{+0.27}_{-0.26}$	[12] FUKUDA	96	KAMI	night flux

[1] ABE 11 reports the Super-Kamiokande-III results for 548 live days from August 4, 2006 to August 18, 2008. The analysis threshold is 5.0 MeV, but the event sample in the 5.0–6.5 MeV total electron range has a total live time of 298 days.

[2] ABE 11 recalculated the Super-Kamiokande-II results using ^{8}B spectrum of WINTER 06A.

[3] ABE 11 recalculated the Super-Kamiokande-I results using ^{8}B spectrum of WINTER 06A.

[4] ABE 11B use a 123 kton·day exposure of the KamLAND liquid scintillation detector to measure the ^{8}B solar neutrino flux. They utilize $\nu - e$ elastic scattering above a reconstructed-energy threshold of 5.5 MeV, corresponding to 5 MeV electron recoil energy. 299 electron recoil candidate events are reported, of which 157 ± 23.6 are assigned to background.

[5] BELLINI 10A reports the Borexino result with 3 MeV energy threshold for scattered electrons. The data correspond to 345.3 live days with a target mass of 100 t, between July 15, 2007 and August 23, 2009.

[6] AHARMIM 08 reports the results from SNO Phase III measurement using an array of ^{3}He proportional counters to measure the rate of NC interactions in heavy water, over the period between November 27, 2004 and November 28, 2006, corresponding to 385.17 live days. A simultaneous fit was made for the number of NC events detected by the proportional counters and the numbers of NC, CC, and ES events detected by the PMTs, where the spectral distributions of the ES and CC events were not constrained to the ^{8}B shape.

[7] CRAVENS 08 reports the Super-Kamiokande-II results for 791 live days from December 2002 to October 2005. The photocathode coverage of the detector is 19% (reduced from 40% of that of Super-Kamiokande-I due to an accident in 2001). The analysis threshold for the average flux is 7 MeV.

[8] HOSAKA 06 reports the final results for 1496 live days with Super-Kamiokande-I between May 31, 1996 and July 15, 2001, and replace FUKUDA 02 results. The analysis threshold is 5 MeV except for the first 280 live days (6.5 MeV).

[9] AHARMIM 05A measurements were made with dissolved NaCl (0.195% by weight) in heavy water over the period between July 26, 2001 and August 28, 2003, corresponding to 391.4 live days, and update AHMED 04A. The *CC*, *ES*, and *NC* events were statistically separated. In one method, the ^{8}B energy spectrum was not constrained. In the other method, the constraint of an undistorted ^{8}B energy spectrum was added for comparison with AHMAD 02 results.

[10] AHMAD 02 reports the ^{8}B solar-neutrino flux measured via νe elastic scattering above the kinetic energy threshold of 5 MeV. The data correspond to 306.4 live days with SNO between November 2, 1999 and May 28, 2001, and updates AHMAD 01 results.

[11] AHMAD 01 reports the ^{8}B solar-neutrino flux measured via νe elastic scattering above the kinetic energy threshold of 6.75 MeV. The data correspond to 241 live days with SNO between November 2, 1999 and January 15, 2001.

[12] FUKUDA 96 results are for a total of 2079 live days with Kamiokande II and III from January 1987 through February 1995, covering the entire solar cycle 22, with threshold $E_e > 9.3$ MeV (first 449 days), > 7.5 MeV (middle 794 days), and > 7.0 MeV (last 836 days). These results update the HIRATA 90 result for the average ^{8}B solar-neutrino flux and HIRATA 91 result for the day-night variation in the ^{8}B solar-neutrino flux. The total data sample was also analyzed for short-term variations: within experimental errors, no strong correlation of the solar-neutrino flux with the sunspot numbers was found.

ϕ_{CC} (^{8}B)

^{8}B solar-neutrino flux measured with charged-current reaction which is sensitive exclusively to ν_e.

VALUE (10^6 cm^{-2}s^{-1})	DOCUMENT ID		TECN	COMMENT
• • • We do not use the following data for averages, fits, limits, etc. • • •				
$1.67\ ^{+0.05}_{-0.04}\ ^{+0.07}_{-0.08}$	[1] AHARMIM	08	SNO	Phase III
$1.68 \pm 0.06\ ^{+0.08}_{-0.09}$	[2] AHARMIM	05A	SNO	Salty D_2O; ^{8}B shape not const.
$1.72 \pm 0.05 \pm 0.11$	[2] AHARMIM	05A	SNO	Salty D_2O; ^{8}B shape constrained
$1.76\ ^{+0.06}_{-0.05} \pm 0.09$	[3] AHMAD	02	SNO	average flux
$1.75 \pm 0.07\ ^{+0.12}_{-0.11} \pm 0.05$	[4] AHMAD	01	SNO	average flux

[1] AHARMIM 08 reports the results from SNO Phase III measurement using an array of ^{3}He proportional counters to measure the rate of NC interactions in heavy water, over the period between November 27, 2004 and November 28, 2006, corresponding to 385.17 live days. A simultaneous fit was made for the number of NC events detected by the proportional counters and the numbers of NC, CC, and ES events detected by the PMTs, where the spectral distributions of the ES and CC events were not constrained to the ^{8}B shape.

[2] AHARMIM 05A measurements were made with dissolved NaCl (0.195% by weight) in heavy water over the period between July 26, 2001 and August 28, 2003, corresponding to 391.4 live days, and update AHMED 04A. The *CC*, *ES*, and *NC* events were statistically separated. In one method, the ^{8}B energy spectrum was not constrained. In the other method, the constraint of an undistorted ^{8}B energy spectrum was added for comparison with AHMAD 02 results.

[3] AHMAD 02 reports the SNO result of the ^{8}B solar-neutrino flux measured with charged-current reaction on deuterium, $\nu_e d \rightarrow pp e^-$, above the kinetic energy threshold of 5 MeV. The data correspond to 306.4 live days with SNO between November 2, 1999 and May 28, 2001, and updates AHMAD 01 results. The complete description of the SNO Phase I data set is given in AHARMIM 07.

[4] AHMAD 01 reports the first SNO result of the ^{8}B solar-neutrino flux measured with the charged-current reaction on deuterium, $\nu_e d \rightarrow pp e^-$, above the kinetic energy threshold of 6.75 MeV. The data correspond to 241 live days with SNO between November 2, 1999 and January 15, 2001.

ϕ_{NC} (^{8}B)

^{8}B solar neutrino flux measured with neutral-current reaction, which is equally sensitive to ν_e, ν_μ, and ν_τ.

VALUE (10^6 cm^{-2}s^{-1})	DOCUMENT ID		TECN	COMMENT
• • • We do not use the following data for averages, fits, limits, etc. • • •				
$5.25 \pm 0.16\ ^{+0.11}_{-0.13}$	[1] AHARMIM	13	SNO	All three phases combined
$5.140^{+0.160}_{-0.158}{}^{+0.132}_{-0.117}$	[2] AHARMIM	10	SNO	Phase I+II, low threshold
$5.54\ ^{+0.33}_{-0.31}\ ^{+0.36}_{-0.34}$	[3] AHARMIM	08	SNO	Phase III, prop. counter + PMT
$4.94 \pm 0.21\ ^{+0.38}_{-0.34}$	[4] AHARMIM	05A	SNO	Salty D_2O; ^{8}B shape not const.
$4.81 \pm 0.19\ ^{+0.28}_{-0.27}$	[4] AHARMIM	05A	SNO	Salty D_2O; ^{8}B shape constrained
$5.09\ ^{+0.44}_{-0.43}\ ^{+0.46}_{-0.43}$	[5] AHMAD	02	SNO	average flux; ^{8}B shape const.
$6.42 \pm 1.57\ ^{+0.55}_{-0.58}$	[5] AHMAD	02	SNO	average flux; ^{8}B shape not const.

[1] AHARMIM 13 obtained this result from a combined analysis of the data from all three phases, SNO-I, II, and III. The measurement of the ^{8}B flux mostly comes from the NC signal, however, CC contribution is included in the fit.

[2] AHARMIM 10 reports this result from a joint analysis of SNO Phase I+II data with the "effective electron kinetic energy" threshold of 3.5 MeV. This result is obtained with a "binned-histogram unconstrained fit" where binned probability distribution functions of the neutrino signal observables were used without any model constraints on the shape of the neutrino spectrum.

[3] AHARMIM 08 reports the results from SNO Phase III measurement using an array of ^{3}He proportional counters to measure the rate of NC interactions in heavy water, over the period between November 27, 2004 and November 28, 2006, corresponding to 385.17 live days. A simultaneous fit was made for the number of NC events detected by the proportional counters and the numbers of NC, CC, and ES events detected by the PMTs, where the spectral distributions of the ES and CC events were not constrained to the ^{8}B shape.

[4] AHARMIM 05A measurements were made with dissolved NaCl (0.195% by weight) in heavy water over the period between July 26, 2001 and August 28, 2003, corresponding to 391.4 live days, and update AHMED 04A. The *CC*, *ES*, and *NC* events were statistically separated. In one method, the ^{8}B energy spectrum was not constrained. In the other method, the constraint of an undistorted ^{8}B energy spectrum was added for comparison with AHMAD 02 results.

[5] AHMAD 02 reports the first SNO result of the ^{8}B solar-neutrino flux measured with the neutral-current reaction on deuterium, $\nu_\ell d \rightarrow np\nu_\ell$, above the neutral-current reaction threshold of 2.2 MeV. The data correspond to 306.4 live days with SNO between November 2, 1999 and May 28, 2001. The complete description of the SNO Phase I data set is given in AHARMIM 07.

$\phi_{\nu_\mu+\nu_\tau}$ (^{8}B)

Nonelectron-flavor active neutrino component (ν_μ and ν_τ) in the ^{8}B solar-neutrino flux.

VALUE (10^6 cm^{-2}s^{-1})	DOCUMENT ID		TECN	COMMENT
• • • We do not use the following data for averages, fits, limits, etc. • • •				
$3.26 \pm 0.25 \pm ^{0.40}_{0.35}$	[1] AHARMIM	05A	SNO	From ϕ_{NC}, ϕ_{CC}, and ϕ_{ES}; ^{8}B shape not const.
$3.09 \pm 0.22 \pm ^{0.30}_{0.27}$	[1] AHARMIM	05A	SNO	From ϕ_{NC}, ϕ_{CC}, and ϕ_{ES}; ^{8}B shape constrained
$3.41 \pm 0.45 \pm ^{0.48}_{0.45}$	[2] AHMAD	02	SNO	From ϕ_{NC}, ϕ_{CC}, and ϕ_{ES}
3.69 ± 1.13	[3] AHMAD	01		Derived from SNO+SuperKam, water Cherenkov

[1] AHARMIM 05A measurements were made with dissolved NaCl (0.195% by weight) in heavy water over the period between July 26, 2001 and August 28, 2003, corresponding to 391.4 live days, and update AHMED 04A. The *CC*, *ES*, and *NC* events were statistically separated. In one method, the ^{8}B energy spectrum was not constrained. In the other method, the constraint of an undistorted ^{8}B energy spectrum was added for comparison with AHMAD 02 results.

[2] AHMAD 02 deduced the nonelectron-flavor active neutrino component (ν_μ and ν_τ) in the ^{8}B solar-neutrino flux, by combining the charged-current result, the νe elastic-scattering result and the neutral-current result. The complete description of the SNO Phase I data set is given in AHARMIM 07.

[3] AHMAD 01 deduced the nonelectron-flavor active neutrino component (ν_μ and ν_τ) in the ^{8}B solar-neutrino flux, by combining the SNO charged-current result (AHMAD 01) and the Super-Kamiokande νe elastic-scattering result (FUKUDA 01).

Total Flux of Active ^{8}B Solar Neutrinos

Total flux of active neutrinos (ν_e, ν_μ, and ν_τ).

VALUE (10^6 cm^{-2}s^{-1})	DOCUMENT ID		TECN	COMMENT
• • • We do not use the following data for averages, fits, limits, etc. • • •				
$5.25 \pm 0.16\ ^{+0.11}_{-0.13}$	[1] AHARMIM	13	SNO	All three phases combined
$5.046^{+0.159}_{-0.152}{}^{+0.107}_{-0.123}$	[2] AHARMIM	10	SNO	From ϕ_{NC} in Phase I+II, low threshold
$5.54\ ^{+0.33}_{-0.31}\ ^{+0.36}_{-0.34}$	[3] AHARMIM	08	SNO	ϕ_{NC} in Phase III
$4.94 \pm 0.21\ ^{+0.38}_{-0.34}$	[4] AHARMIM	05A	SNO	From ϕ_{NC}; ^{8}B shape not const.
$4.81 \pm 0.19\ ^{+0.28}_{-0.27}$	[4] AHARMIM	05A	SNO	From ϕ_{NC}; ^{8}B shape constrained
$5.09\ ^{+0.44}_{-0.43}\ ^{+0.46}_{-0.43}$	[5] AHMAD	02	SNO	Direct measurement from ϕ_{NC}
5.44 ± 0.99	[6] AHMAD	01		Derived from SNO+SuperKam, water Cherenkov

[1] AHARMIM 13 obtained this result from a combined analysis of the data from all three phases, SNO-I, II, and III. The measurement of the ^{8}B flux mostly comes from the NC signal, however, CC contribution is included in the fit.

[2] AHARMIM 10 reports this result from a joint analysis of SNO Phase I+II data with the "effective electron kinetic energy" threshold of 3.5 MeV. This result is obtained with the assumption of unitarity, which relates the NC, CC, and ES rates. The data were fit with the free parameters directly describing the total ^{8}B neutrino flux and the energy-dependent ν_e survival probability.

[3] AHARMIM 08 reports the results from SNO Phase III measurement using an array of ^{3}He proportional counters to measure the rate of NC interactions in heavy water, over the period between November 27, 2004 and November 28, 2006, corresponding to 385.17 live days. A simultaneous fit was made for the number of NC events detected by the proportional counters and the numbers of NC, CC, and ES events detected by the PMTs, where the spectral distributions of the ES and CC events were not constrained to the ^{8}B shape.

[4] AHARMIM 05A measurements were made with dissolved NaCl (0.195% by weight) in heavy water over the period between July 26, 2001 and August 28, 2003, corresponding to 391.4 live days, and update AHMED 04A. The CC, ES, and NC events were statistically separated. In one method, the ^{8}B energy spectrum was not constrained. In the other method, the constraint of an undistorted ^{8}B energy spectrum was added for comparison with AHMAD 02 results.

[5] AHMAD 02 determined the total flux of active ^{8}B solar neutrinos by directly measuring the neutral-current reaction, $\nu_\ell d \rightarrow np\nu_\ell$, which is equally sensitive to ν_e, ν_μ, and ν_τ. The complete description of the SNO Phase I data set is given in AHARMIM 07.

[6] AHMAD 01 deduced the total flux of active ^{8}B solar neutrinos by combining the SNO charged-current result (AHMAD 01) and the Super-Kamiokande νe elastic-scattering result (FUKUDA 01).

Day-Night Asymmetry (^{8}B)

$A = (\phi_{\text{night}} - \phi_{\text{day}}) / \phi_{\text{average}}$

VALUE	DOCUMENT ID		TECN	COMMENT
• • • We do not use the following data for averages, fits, limits, etc. • • •				
$0.063 \pm 0.042 \pm 0.037$	[1] CRAVENS	08	SKAM	Based on ϕ_{ES}
$0.021 \pm 0.020 \pm ^{0.012}_{0.013}$	[2] HOSAKA	06	SKAM	Based on ϕ_{ES}
$0.017 \pm 0.016 \pm ^{0.012}_{0.013}$	[3] HOSAKA	06	SKAM	Fitted in the LMA region
$-0.056 \pm 0.074 \pm 0.053$	[4] AHARMIM	05A	SNO	From salty SNO ϕ_{CC}
$-0.037 \pm 0.063 \pm 0.032$	[4] AHARMIM	05A	SNO	From salty SNO ϕ_{CC}; const. of no ϕ_{NC} asymmetry
$0.14 \pm 0.063 \pm ^{0.015}_{0.014}$	[5] AHMAD	02B	SNO	Derived from SNO ϕ_{CC}
$0.07 \pm 0.049 \pm ^{0.013}_{0.012}$	[6] AHMAD	02B	SNO	Const. of no ϕ_{NC} asymmetry

[1] CRAVENS 08 reports the Super-Kamiokande-II results for 791 live days from December 2002 to October 2005. The photocathode coverage of the detector is 19% (reduced from 40% of that of Super-Kamiokande-I due to an accident in 2001). The analysis threshold for the day and night fluxes is 7.5 MeV.

[2] HOSAKA 06 reports the final results for 1496 live days with Super-Kamiokande-I between May 31, 1996 and July 15, 2001, and replace FUKUDA 02 results. The analysis threshold is 5 MeV except for the first 280 live days (6.5 MeV).

[3] This result with reduced statistical uncertainty is obtained by assuming two-neutrino oscillations within the LMA (large mixing angle) region and by fitting the time variation of

the solar neutrino flux measured via ν_e elastic scattering to the variations expected from neutrino oscillations. For details, see SMY 04. There is an additional small systematic error of ± 0.0004 coming from uncertainty of oscillation parameters.

[4] AHARMIM 05A measurements were made with dissolved NaCl (0.195% by weight) in heavy water over the period between July 26, 2001 and August 28, 2003, with 176.5 days of the live time recorded during the day and 214.9 days during the night. This result is obtained with the spectral distribution of the CC events not constrained to the ^{8}B shape.

[5] AHMAD 02B results are based on the charged-current interactions recorded between November 2, 1999 and May 28, 2001, with the day and night live times of 128.5 and 177.9 days, respectively. The complete description of the SNO Phase I data set is given in AHARMIM 07.

[6] AHMAD 02B results are derived from the charged-current interactions, neutral-current interactions, and νe elastic scattering, with the total flux of active neutrinos constrained to have no asymmetry. The data were recorded between November 2, 1999 and May 28, 2001, with the day and night live times of 128.5 and 177.9 days, respectively. The complete description of the SNO Phase I data set is given in AHARMIM 07.

ϕ_{ES} (^{7}Be)

^{7}Be solar-neutrino flux measured via ν_e elastic scattering. This process is sensitive to all active neutrino flavors, but with reduced sensitivity to ν_μ, ν_τ due to the cross-section difference, $\sigma(\nu_{\mu,\tau}\, e) \sim 0.2\ \sigma(\nu_e\, e)$. If the ^{7}Be solar-neutrino flux involves nonelectron flavor active neutrinos, their contribution to the flux is ~ 0.2 times that of ν_e.

VALUE (10^9 cm^{-2} s^{-1})	DOCUMENT ID		TECN	COMMENT
• • • We do not use the following data for averages, fits, limits, etc. • • •				
3.10 ± 0.15	[1] BELLINI	11A	BORX	average flux

[1] BELLINI 11A reports the ^{7}Be solar neutrino flux measured via $\nu - e$ elastic scattering. The data correspond to 740.7 live days between May 16, 2007 and May 8, 2010, and also correspond to 153.6 ton·year fiducial exposure. BELLINI 11A measured the 862 keV ^{7}Be solar neutrino flux, which is an 89.6% branch of the ^{7}Be solar neutrino flux, to be $(2.78 \pm 0.13) \times 10^9$ cm^{-2} s^{-1}. Supercedes ARPESELLA 08A.

ϕ_{ES} (pep)

pep solar-neutrino flux measured via ν_e elastic scattering. This process is sensitive to all active neutrino flavors, but with reduced sensitivity to ν_μ, ν_τ due to the cross section difference, $\sigma(\nu_{\mu,\tau}\, e) \sim 0.2\ \sigma(\nu_e e)$. If the pep solar-neutrino flux involves non-electron flavor active neutrinos, their contribution to the flux is ~ 0.2 times that of ν_e.

VALUE (10^8 cm^{-2}s^{-1})	DOCUMENT ID		TECN	COMMENT
• • • We do not use the following data for averages, fits, limits, etc. • • •				
1.0 ± 0.2	[1] BELLINI	12A	BORX	average flux

[1] BELLINI 12A reports 1.44 MeV pep solar-neutrino flux measured via ν_e elastic scattering. The data were collected between January 13, 2008 and May 9, 2010, corresponding to 20,4009 ton·day fiducial exposure. The listed flux value is calculated from the observed rate of pep solar neutrino interactions in Borexino ($3.1 \pm 0.6 \pm 0.3$ counts/(day·100 ton)) and the corresponding rate expected for no neutrino flavor oscillations (4.47 ± 0.05 counts/(day·100 ton)), using the SSM prediction for the pep solar neutrino flux of $(1.441 \pm 0.012) \times 10^8$ cm^{-2}s^{-1}.

ϕ_{ES} (CNO)

CNO solar-neutrino flux measured via ν_e elastic scattering. This process is sensitive to all active neutrino flavors, but with reduced sensitivity to ν_μ, ν_τ due to the cross section difference, $\sigma(\nu_{\mu,\tau}\, e) \sim 0.2\ \sigma(\nu_e\, e)$. If the CNO solar-neutrino flux involves non-electron flavor active neutrinos, their contribution to the flux is ~ 0.2 times that of ν_e.

VALUE (10^8 cm^{-2}s^{-1})	CL%	DOCUMENT ID		TECN	COMMENT
• • • We do not use the following data for averages, fits, limits, etc. • • •					
<7.7	90	[1] BELLINI	12A	BORX	MSW-LMA solution assumed

[1] BELLINI 12A reports an upper limit of the CNO solar neutrino flux measured via ν_e elastic scattering. The data were collected between January 13, 2008 and May 9, 2010, corresponding to 20,409 ton·day fiducial exposure.

$\phi_{CC}(pp)$

pp solar-neutrino flux measured with charged-current reaction which is sensitive exclusively to ν_e.

VALUE (10^{10} cm^{-2} s^{-1})	DOCUMENT ID		TECN	COMMENT
• • • We do not use the following data for averages, fits, limits, etc. • • •				
3.38 ± 0.47	[1] ABDURASHI...	09	FIT	Fit existing solar-ν data

[1] ABDURASHITOV 09 reports the pp solar-neutrino flux derived from the Ga solar neutrino capture rate by subtracting contributions from ^{8}B, ^{7}Be, pep and CNO solar neutrino fluxes determined by other solar neutrino experiments as well as neutrino oscillation parameters determined from available world neutrino oscillation data.

ϕ_{ES} (hep)

hep solar-neutrino flux measured via νe elastic scattering. This process is sensitive to all active neutrino flavors, but with reduced sensitivity to ν_μ, ν_τ due to the cross-section difference, $\sigma(\nu_{\mu,\tau}\, e) \sim 0.16\sigma(\nu_e\, e)$. If the hep solar-neutrino flux involves nonelectron flavor active neutrinos, their contribution to the flux is ~ 0.16 times of ν_e.

VALUE (10^3 cm^{-2}s^{-1})	CL%	DOCUMENT ID		TECN
• • • We do not use the following data for averages, fits, limits, etc. • • •				
<73	90	[1] HOSAKA	06	SKAM

[1] HOSAKA 06 result is obtained from the recoil electron energy window of 18–21 MeV, and updates FUKUDA 01 result.

$\phi_{\overline{\nu}_e}$ (^{8}B)

Searches are made for electron antineutrino flux from the Sun. Flux limits listed here are derived relative to the BS05(OP) Standard Solar Model ^{8}B solar neutrino flux (5.69×10^6 cm^{-2} s^{-1}), with an assumption that solar $\overline{\nu}_e$s follow an unoscillated ^{8}B neutrino spectrum.

VALUE (%)	CL%	DOCUMENT ID		TECN	COMMENT
• • • We do not use the following data for averages, fits, limits, etc. • • •					
<0.013	90	BELLINI	11	BORX	$E_{\overline{\nu}_e} > 1.8$ MeV
<1.9	90	[1] BALATA	06	CNTR	$1.8 < E_{\overline{\nu}_e} < 20.0$ MeV
<0.72	90	AHARMIM	04	SNO	$4.0 < E_{\overline{\nu}_e} < 14.8$ MeV
<0.022	90	EGUCHI	04	KLND	$8.3 < E_{\overline{\nu}_e} < 14.8$ MeV
<0.7	90	GANDO	03	SKAM	$8.0 < E_{\overline{\nu}_e} < 20.0$ MeV
<1.7	90	AGLIETTA	96	LSD	$7 < E_{\overline{\nu}_e} < 17$ MeV

[1] BALATA 06 obtained this result from the search for $\overline{\nu}_e$ interactions with Counting Test Facility (the prototype of the Borexino detector).

(B) Three-neutrino mixing parameters

INTRODUCTION TO THREE-NEUTRINO MIXING PARAMETERS LISTINGS

Updated January 2014 by M. Goodman (ANL).

Introduction and Notation: With the exception of possible short-baseline anomalies (such as LSND), current accelerator, reactor, solar and atmospheric neutrino data can be described within the framework of a 3×3 mixing matrix between the flavor eigenstates ν_e, ν_μ and ν_τ and mass eigenstates ν_1, ν_2 and ν_3. (See equation 14.78 of the review "Neutrino Mass, Mixing and Oscillations" by K. Nakamura and S.T. Petcov.) Whether or not this is the ultimately correct framework, it is currently widely used to parametrize neutrino mixing data and to plan new experiments.

The mass differences are called $\Delta m^2_{21} \equiv m^2_2 - m^2_1$ and $\Delta m^2_{32} \equiv m^2_3 - m^2_2$. In these listings, we assume

$$\Delta m^2_{32} \sim \Delta m^2_{31} \tag{1}$$

even though the experimental error is comparable to the difference $\Delta m^2_{31} - \Delta m^2_{32} = \Delta m^2_{21}$. The measurements made by ν_μ disappearance at accelerators and by ν_e disappearance at reactors are slightly different mixtures of Δm^2_{32} and Δm^2_{31}. The angles are labeled θ_{12}, θ_{23} and θ_{13}. The CP violating phase is called δ, but that does not yet appear in the listings. The familiar two neutrino form for oscillations is

$$P(\nu_a \to \nu_b; a \neq b) = \sin^2(2\theta) \sin^2(\Delta m^2 L/4E). \tag{2}$$

Despite the fact that the mixing angles have been measured to be much larger than in the quark sector, the two neutrino form is often a very good approximation and is used in many situations.

The angles appear in the equations below in many forms. They most often appear as $\sin^2(2\theta)$. The listings currently use this convention.

Accelerator neutrino experiments: Ignoring Δm^2_{21}, *CP* violation, and matter effects, the equations for the probability of appearance in an accelerator oscillation experiment are:

$$P(\nu_\mu \to \nu_\tau) = \sin^2(2\theta_{23})\cos^4(\theta_{13})\sin^2(\Delta m^2_{32}L/4E) \quad (3)$$
$$P(\nu_\mu \to \nu_e) = \sin^2(2\theta_{13})\sin^2(\theta_{23})\sin^2(\Delta m^2_{32}L/4E) \quad (4)$$
$$P(\nu_e \to \nu_\mu) = \sin^2(2\theta_{13})\sin^2(\theta_{23})\sin^2(\Delta m^2_{32}L/4E) \quad (5)$$
$$P(\nu_e \to \nu_\tau) = \sin^2(2\theta_{13})\cos^2(\theta_{23})\sin^2(\Delta m^2_{32}L/4E)\ . \quad (6)$$

Current and future long-baseline accelerator experiments are studying non-zero θ_{13} through $P(\nu_\mu \to \nu_e)$. Including the CP terms and low mass scale, the equation for neutrino oscillation in vacuum is:

$$\begin{aligned} P(\nu_\mu \to \nu_e) &= P1 + P2 + P3 + P4 \\ P1 &= \sin^2(\theta_{23})\sin^2(2\theta_{13})\sin^2(\Delta m^2_{32}L/4E) \\ P2 &= \cos^2(\theta_{23})\sin^2(2\theta_{13})\sin^2(\Delta m^2_{21}L/4E) \\ P3 &= -/+ J\sin(\delta)\sin(\Delta m^2_{32}L/4E) \\ P4 &= J\cos(\delta)\cos(\Delta m^2_{32}L/4E) \end{aligned} \quad (7)$$

where

$$\begin{aligned} J = &\cos(\theta_{13})\sin(2\theta_{12})\sin(2\theta_{13})\sin(2\theta_{23})\times \\ &\sin(\Delta m^2_{32}L/4E)\sin(\Delta m^2_{21}L/4E) \end{aligned} \quad (8)$$

and the sign in P3 is negative for neutrinos and positive for antineutrinos respectively. For most new long-baseline accelerator experiments, P2 can safely be neglected but the other three terms could be comparable. Also, depending on the distance and the mass hierarchy, matter effects will need to be included.

Reactor neutrino experiments: Nuclear reactors are prolific sources of $\bar{\nu}_e$ with an energy near 4 MeV. The oscillation probability can be expressed

$$\begin{aligned} P(\bar{\nu}_e \to \bar{\nu}_e) = 1 &- \cos^4(\theta_{13})\sin^2(2\theta_{12})\sin^2(\Delta m^2_{21}L/4E) \\ &- \cos^2(\theta_{12})\sin^2(2\theta_{13})\sin^2(\Delta m^2_{31}L/4E) \\ &- \sin^2(\theta_{12})\sin^2(2\theta_{13})\sin^2(\Delta m^2_{32}L/4E) \end{aligned} \quad (9)$$

not using the approximation in Eq. (1). For short distances (L<5 km) we can ignore the second term on the right and can reimpose approximation Eq. (1). This takes the familiar two neutrino form with θ_{13} and Δm^2_{32}:

$$P(\bar{\nu}_e \to \bar{\nu}_e) = 1 - \sin^2(2\theta_{13})\sin^2(\Delta m^2_{32}L/4E). \quad (10)$$

Solar and Atmospheric neutrino experiments: Solar neutrino experiments are sensitive to ν_e disappearance and have allowed the measurement of θ_{12} and Δm^2_{21}. They are also sensitive to θ_{13}. We identify $\Delta m^2_\odot = \Delta m^2_{21}$ and $\theta_\odot = \theta_{12}$.

Atmospheric neutrino experiments are primarily sensitive to ν_μ disappearance through $\nu_\mu \to \nu_\tau$ oscillations, and have allowed the measurement of θ_{23} and Δm^2_{32}. We identify $\Delta m^2_A = \Delta m^2_{32}$ and $\theta_A = \theta_{23}$. Despite the large ν_e component of the atmospheric neutrino flux, it is difficult to measure Δm^2_{21} effects. This is because of a cancellation between $\nu_\mu \to \nu_e$ and $\nu_e \to \nu_\mu$ together with the fact that the ratio of ν_μ and ν_e atmospheric fluxes, which arise from sequential π and μ decay, is near 2.

Oscillation Parameter Listings: In Section (B) we encode the three mixing angles θ_{12}, θ_{23}, θ_{13} and two mass squared differences Δm^2_{21} and Δm^2_{32}. Our knowledge of θ_{12} and Δm^2_{21} comes from the KamLAND reactor neutrino experiment together with solar neutrino experiments. Our knowledge of θ_{23} and Δm^2_{32} comes from atmospheric neutrino experiments and long-baseline accelerator experiments. Results on θ_{13} come from reactor antineutrino disappearance experiments. There are also results from long-baseline accelerator experiments looking for ν_e appearance. The interpretation of both kinds of results depends on Δm^2_{32}, and the accelerator results also depend on the mass hierarchy, θ_{23} and the CP violating phase δ. We present values for θ_{13} at the current best fit value of Δm^2_{32}, but they are not symmetric around that best fit value.

Accelerator and atmospheric experiments are beginning to have some sensitivity to the CP violation phase δ through Eq. (7). Note that P3 depends on the sign of Δm^2_{32} so the sensitivity depends on the mass hierarchy. For non-maximal θ_{13} mixing, it also depends on the octant of θ_{13}, i.e. whether $\theta_{13} > \pi/4$ or $\theta_{13} < \pi/4$.

$\sin^2(2\theta_{12})$

VALUE	DOCUMENT ID		TECN	COMMENT
$0.846^{+0.021}_{-0.021}$	[1] GANDO	13	FIT	KamLAND + global solar + SBL + accelerator: 3ν
• • • We do not use the following data for averages, fits, limits, etc. • • •				
$0.839^{+0.021}_{-0.023}$	[2,3] AHARMIM	13	FIT	global solar: 2ν
$0.846^{+0.033}_{-0.029}$	[3,4] AHARMIM	13	FIT	global solar: 3ν
$0.851^{+0.023}_{-0.020}$	[3,5] AHARMIM	13	FIT	KamLAND + global solar: 3ν
0.847 ± 0.021	[6] GANDO	13	FIT	KamLAND + global solar: 3ν
$0.877^{+0.049}_{-0.060}$	[7] GANDO	13	FIT	KamLAND: 3ν
$0.85\ \pm0.02$	[8] ABE	11	FIT	KamLAND + global solar: 2ν
$0.84\ ^{+0.03}_{-0.02}$	[9] ABE	11	FIT	global solar: 2ν
$0.85\ ^{+0.04}_{-0.03}$	[10] ABE	11	FIT	KamLAND + global solar: 3ν
$0.85\ ^{+0.04}_{-0.05}$	[11] ABE	11	FIT	global solar: 3ν
$0.861^{+0.022}_{-0.018}$	[12] BELLINI	11A	FIT	KamLAND + global solar: 2ν
$0.869^{+0.024}_{-0.022}$	[13] BELLINI	11A	FIT	global solar: 2ν
$0.857^{+0.023}_{-0.025}$	[14] GANDO	11	FIT	KamLAND + solar: 3ν
$0.846^{+0.064}_{-0.073}$	[15] GANDO	11	FIT	KamLAND: 3ν
$0.861^{+0.026}_{-0.022}$	[16,17] AHARMIM	10	FIT	KamLAND + global solar: 2ν
$0.861^{+0.024}_{-0.031}$	[16,18] AHARMIM	10	FIT	global solar: 2ν
$0.869^{+0.026}_{-0.024}$	[16,19] AHARMIM	10	FIT	KamLAND + global solar: 3ν
$0.869^{+0.031}_{-0.037}$	[16,20] AHARMIM	10	FIT	global solar: 3ν
$0.92\ \pm0.05$	[21] ABE	08A	FIT	KamLAND
$0.87\ \pm0.04$	[22] ABE	08A	FIT	KamLAND + global fit
$0.87\ \pm0.03$	[23] AHARMIM	08	FIT	KamLAND + global solar
$0.85\ ^{+0.04}_{-0.06}$	[24] HOSAKA	06	FIT	KamLAND + global solar
$0.85\ ^{+0.06}_{-0.05}$	[25] HOSAKA	06	FIT	SKAM+SNO+KamLAND

$0.86\ ^{+0.05}_{-0.07}$	[26] HOSAKA	06	FIT	SKAM+SNO
$0.86\ ^{+0.03}_{-0.04}$	[27] AHARMIM	05A	FIT	KamLAND + global solar
0.75–0.95	[28] AHARMIM	05A	FIT	global solar
$0.82\ \pm0.05$	[29] ARAKI	05	FIT	KamLAND + global solar
$0.82\ \pm0.04$	[30] AHMED	04A	FIT	KamLAND + global solar
0.71–0.93	[31] AHMED	04A	FIT	global solar
$0.85\ ^{+0.05}_{-0.07}$	[32] SMY	04	FIT	KamLAND + global solar
$0.83\ ^{+0.06}_{-0.08}$	[33] SMY	04	FIT	global solar
$0.87\ ^{+0.07}_{-0.08}$	[34] SMY	04	FIT	SKAM + SNO
0.62–0.88	[35] AHMAD	02B	FIT	global solar
0.62–0.95	[36] FUKUDA	02	FIT	global solar

[1] GANDO 13 obtained this result by a three-neutrino oscillation analysis using KamLAND, global solar neutrino, short-baseline (SBL) reactor, and accelerator data, assuming CPT invariance. Supersedes GANDO 11.

[2] AHARMIM 13 obtained this result by a two-neutrino oscillation analysis using global solar neutrino data.

[3] AHARMIM 13 global solar neutrino data include SNO's all-phases-combined analysis results on the total active ^{8}B neutrino flux and energy-dependent ν_e survival probability parameters, measurements of Cl (CLEVELAND 98), Ga (ABDURASHITOV 09 which contains combined analysis with GNO (ALTMANN 05 and Ph.D. thesis of F. Kaether)), and ^{7}Be (BELLINI 11A) rates, and ^{8}B solar-neutrino recoil electron measurements of SK-I (HOSAKA 06) zenith, SK-II (CRAVENS 08) and SK-III (ABE 11) day/night spectra, and Borexino (BELLINI 10A) spectra.

[4] AHARMIM 13 obtained this result by a three-neutrino oscillation analysis with the value of Δm^2_{32} fixed to 2.45×10^{-3} eV^2, using global solar neutrino data.

[5] AHARMIM 13 obtained this result by a three-neutrino oscillation analysis with the value of Δm^2_{32} fixed to 2.45×10^{-3} eV^2, using global solar neutrino and KamLAND (GANDO 11) data. CPT invariance is assumed.

[6] GANDO 13 obtained this result by a three-neutrino oscillation analysis using KamLAND and global solar neutrino data, assuming CPT invariance. Supersedes GANDO 11.

[7] GANDO 13 obtained this result by a three-neutrino oscillation analysis using KamLAND data. Supersedes GANDO 11.

[8] ABE 11 obtained this result by a two-neutrino oscillation analysis using solar neutrino data including Super-Kamiokande, SNO, Borexino (ARPESELLA 08A), Homestake, GALLEX/GNO, SAGE, and KamLAND data. CPT invariance is assumed.

[9] ABE 11 obtained this result by a two-neutrino oscillation analysis using solar neutrino data including Super-Kamiokande, SNO, Borexino (ARPESELLA 08A), Homestake, GALLEX/GNO, and SAGE data.

[10] ABE 11 obtained this result by a three-neutrino oscillation analysis with the value of Δm^2_{32} fixed to 2.4×10^{-3} eV^2, using solar neutrino data including Super-Kamiokande, SNO, Borexino (ARPESELLA 08A), Homestake, GALLEX/GNO, SAGE, and KamLAND data. The normal neutrino mass hierarchy and CPT invariance are assumed.

[11] ABE 11 obtained this result by a three-neutrino oscillation analysis with the value of Δm^2_{32} fixed to 2.4×10^{-3} eV^2, using solar neutrino data including Super-Kamiokande, SNO, Borexino (ARPESELLA 08A), Homestake, and GALLEX/GNO data. The normal neutrino mass hierarchy is assumed.

[12] BELLINI 11A obtained this result by a two-neutrino oscillation analysis using KamLAND, Homestake, SAGE, Gallex, GNO, Kamiokande, Super-Kamiokande, SNO, and Borexino (BELLINI 11A) data and the SSM flux prediction in SERENELLI 11 (Astrophysical Journal **743** 24 (2011)) with the exception that the ^{8}B flux was left free. CPT invariance is assumed.

[13] BELLINI 11A obtained this result by a two-neutrino oscillation analysis using Homestake, SAGE, Gallex, GNO, Kamiokande, Super-Kamiokande, SNO, and Borexino (BELLINI 11A) data and the SSM flux prediction in SERENELLI 11 (Astrophysical Journal **743** 24 (2011)) with the exception that the ^{8}B flux was left free.

[14] GANDO 11 obtain this result with three-neutrino fit using the KamLAND + solar data. Superseded by GANDO 13.

[15] GANDO 11 obtain this result with three-neutrino fit using the KamLAND data only. Superseded by GANDO 13.

[16] AHARMIM 10 global solar neutrino data include SNO's low-energy-threshold analysis survival probability day/night curves, SNO Phase III integral rates (AHARMIM 08), Cl (CLEVELAND 98), SAGE (ABDURASHITOV 09), Gallex/GNO (HAMPEL 99, ALTMANN 05), Borexino (ARPESELLA 08A), SK-I zenith (HOSAKA 06), and SK-II day/night spectra (CRAVENS 08).

[17] AHARMIM 10 obtained this result by a two-neutrino oscillation analysis using global solar neutrino data and KamLAND data (ABE 08A). *CPT* invariance is assumed.

[18] AHARMIM 10 obtained this result by a two-neutrino oscillation analysis using global solar neutrino data.

[19] AHARMIM 10 obtained this result by a three-neutrino oscillation analysis with the value of Δm^2_{31} fixed to 2.3×10^{-3} eV^2, using global solar neutrino data and KamLAND data (ABE 08A). *CPT* invariance is assumed.

[20] AHARMIM 10 obtained this result by a three-neutrino oscillation analysis with the value of Δm^2_{31} fixed to 2.3×10^{-3} eV^2, using global solar neutrino data.

[21] ABE 08A obtained this result by a rate + shape + time combined geoneutrino and reactor two-neutrino fit for Δm^2_{21} and $\tan^2\theta_{12}$, using KamLAND data only. Superseded by GANDO 11.

[22] ABE 08A obtained this result by means of a two-neutrino fit using KamLAND, Homestake, SAGE, GALLEX, GNO, SK (zenith angle and E-spectrum), the SNO χ^2-map, and solar flux data. *CPT* invariance is assumed. Superseded by GANDO 11.

[23] The result given by AHARMIM 08 is $\theta = (34.4^{+1.3}_{-1.2})^\circ$. This result is obtained by a two-neutrino oscillation analysis using solar neutrino data including those of Borexino (ARPESELLA 08A) and Super-Kamiokande-I (HOSAKA 06), and KamLAND data (ABE 08A). *CPT* invariance is assumed.

[24] HOSAKA 06 obtained this result by a two-neutrino oscillation analysis using SK ν_e data, CC data from other solar neutrino experiments, and KamLAND data (ARAKI 05). *CPT* invariance is assumed.

[25] HOSAKA 06 obtained this result by a two-neutrino oscillation analysis using the data from Super-Kamiokande, SNO (AHMAD 02 and AHMAD 02B), and KamLAND (ARAKI 05) experiments. *CPT* invariance is assumed.

[26] HOSAKA 06 obtained this result by a two-neutrino oscillation analysis using the Super-Kamiokande and SNO (AHMAD 02 and AHMAD 02B) solar neutrino data.

[27] The result given by AHARMIM 05A is $\theta = (33.9 \pm 1.6)^\circ$. This result is obtained by a two-neutrino oscillation analysis using SNO pure deuteron and salt phase data, SK ν_e data, Cl and Ga CC data, and KamLAND data (ARAKI 05). *CPT* invariance is assumed. AHARMIM 05A also quotes $\theta = (33.9^{+2.4}_{-2.2})^\circ$ as the error enveloping the 68% CL two-dimensional region. This translates into $\sin^2 2\,\theta = 0.86^{+0.05}_{-0.06}$.

[28] AHARMIM 05A obtained this result by a two-neutrino oscillation analysis using the data from all solar neutrino experiments. The listed range of the parameter envelops the 95% CL two-dimensional region shown in figure 35a of AHARMIM 05A. AHARMIM 05A also quotes $\tan^2\theta = 0.45^{+0.09}_{-0.08}$ as the error enveloping the 68% CL two-dimensional region. This translates into $\sin^2 2\,\theta = 0.86^{+0.05}_{-0.07}$.

[29] ARAKI 05 obtained this result by a two-neutrino oscillation analysis using KamLAND and solar neutrino data. *CPT* invariance is assumed. The 1σ error shown here is translated from the number provided by the KamLAND collaboration, $\tan^2\theta = 0.40^{+0.07}_{-0.05}$. The corresponding number quoted in ARAKI 05 is $\tan^2\theta = 0.40^{+0.10}_{-0.07}$ ($\sin^2 2\,\theta = 0.82 \pm 0.07$), which envelops the 68% CL two-dimensional region.

[30] The result given by AHMED 04A is $\theta = (32.5^{+1.7}_{-1.6})^\circ$. This result is obtained by a two-neutrino oscillation analysis using solar neutrino and KamLAND data (EGUCHI 03). *CPT* invariance is assumed. AHMED 04A also quotes $\theta = (32.5^{+2.4}_{-2.3})^\circ$ as the error enveloping the 68% CL two-dimensional region. This translates into $\sin^2 2\,\theta = 0.82 \pm 0.06$.

[31] AHMED 04A obtained this result by a two-neutrino oscillation analysis using the data from all solar neutrino experiments. The listed range of the parameter envelops the 95% CL two-dimensional region shown in Fig. 5(a) of AHMED 04A. The best-fit point is $\Delta(m^2) = 6.5\times10^{-5}$ eV^2, $\tan^2\theta = 0.40$ ($\sin^2 2\,\theta = 0.82$).

[32] The result given by SMY 04 is $\tan^2\theta = 0.44 \pm 0.08$. This result is obtained by a two-neutrino oscillation analysis using solar neutrino and KamLAND data (IANNI 03). *CPT* invariance is assumed.

[33] SMY 04 obtained this result by a two-neutrino oscillation analysis using the data from all solar neutrino experiments. The 1σ errors are read from Fig. 6(a) of SMY 04.

[34] SMY 04 obtained this result by a two-neutrino oscillation analysis using the Super-Kamiokande and SNO (AHMAD 02 and AHMAD 02B) solar neutrino data. The 1σ errors are read from Fig. 6(a) of SMY 04.

[35] AHMAD 02B obtained this result by a two-neutrino oscillation analysis using the data from all solar neutrino experiments. The listed range of the parameter envelops the 95% CL two-dimensional region shown in Fig. 4(b) of AHMAD 02B. The best fit point is $\Delta(m^2) = 5.0\times10^{-5}$ eV^2 and $\tan\theta = 0.34$ ($\sin^2 2\,\theta = 0.76$).

[36] FUKUDA 02 obtained this result by a two-neutrino oscillation analysis using the data from all solar neutrino experiments. The listed range of the parameter envelops the 95% CL two-dimensional region shown in Fig. 4 of FUKUDA 02. The best fit point is $\Delta(m^2) = 6.9\times10^{-5}$ eV^2 and $\tan^2\theta = 0.38$ ($\sin^2 2\,\theta = 0.80$).

Δm^2_{21}

VALUE (10^{-5} eV^2)	*DOCUMENT ID*		*TECN*	*COMMENT*
7.53±0.18	[1] GANDO	13	FIT	KamLAND + global solar + SBL + accelerator: 3ν
• • • We do not use the following data for averages, fits, limits, etc. • • •				
$5.13^{+1.29}_{-0.96}$	[2,3] AHARMIM	13	FIT	global solar: 2ν
$5.13^{+1.49}_{-0.98}$	[3,4] AHARMIM	13	FIT	global solar: 3ν
$7.46^{+0.20}_{-0.19}$	[3,5] AHARMIM	13	FIT	KamLAND + global solar: 3ν
$7.53^{+0.19}_{-0.18}$	[6] GANDO	13	FIT	KamLAND + global solar: 3ν
$7.54^{+0.19}_{-0.18}$	[7] GANDO	13	FIT	KamLAND: 3ν
$7.6\ \pm0.2$	[8] ABE	11	FIT	KamLAND + global solar: 2ν
$6.2\ ^{+1.1}_{-1.9}$	[9] ABE	11	FIT	global solar: 2ν
$7.7\ \pm0.3$	[10] ABE	11	FIT	KamLAND + global solar: 3ν
$6.0\ ^{+2.2}_{-2.5}$	[11] ABE	11	FIT	global solar: 3ν
$7.50^{+0.16}_{-0.24}$	[12] BELLINI	11A	FIT	KamLAND + global solar: 2ν
$5.2\ ^{+1.5}_{-0.9}$	[13] BELLINI	11A	FIT	global solar: 2ν
$7.50^{+0.19}_{-0.20}$	[14] GANDO	11	FIT	KamLAND + solar: 3ν
7.49 ± 0.20	[15] GANDO	11	FIT	KamLAND: 3ν
$7.59^{+0.20}_{-0.21}$	[16,17] AHARMIM	10	FIT	KamLAND + global solar: 2ν
$5.89^{+2.13}_{-2.16}$	[16,18] AHARMIM	10	FIT	global solar: 2ν
7.59 ± 0.21	[16,19] AHARMIM	10	FIT	KamLAND + global solar: 3ν
$6.31^{+2.49}_{-2.58}$	[16,20] AHARMIM	10	FIT	global solar: 3ν
$7.58^{+0.14}_{-0.13}\pm0.15$	[21] ABE	08A	FIT	KamLAND

7.59 ± 0.21	[22] ABE	08A	FIT	KamLAND + global solar
$7.59^{+0.19}_{-0.21}$	[23] AHARMIM	08	FIT	KamLAND + global solar
8.0 ± 0.3	[24] HOSAKA	06	FIT	KamLAND + global solar
8.0 ± 0.3	[25] HOSAKA	06	FIT	SKAM+SNO+KamLAND
$6.3\ ^{+3.7}_{-1.5}$	[26] HOSAKA	06	FIT	SKAM+SNO
5–12	[27] HOSAKA	06	FIT	SKAM day/night in the LMA region
$8.0\ ^{+0.4}_{-0.3}$	[28] AHARMIM	05A	FIT	KamLAND + global solar LMA
3.3–14.4	[29] AHARMIM	05A	FIT	global solar
$7.9\ ^{+0.4}_{-0.3}$	[30] ARAKI	05	FIT	KamLAND + global solar
$7.1\ ^{+1.0}_{-0.3}$	[31] AHMED	04A	FIT	KamLAND + global solar
3.2–13.7	[32] AHMED	04A	FIT	global solar
$7.1\ ^{+0.6}_{-0.5}$	[33] SMY	04	FIT	KamLAND + global solar
$6.0\ ^{+1.7}_{-1.6}$	[34] SMY	04	FIT	global solar
$6.0\ ^{+2.5}_{-1.6}$	[35] SMY	04	FIT	SKAM + SNO
2.8–12.0	[36] AHMAD	02B	FIT	global solar
3.2–19.1	[37] FUKUDA	02	FIT	global solar

[1] GANDO 13 obtained this result by a three-neutrino oscillation analysis using KamLAND, global solar neutrino, short-baseline (SBL) reactor, and accelerator data, assuming CPT invariance. Supersedes GANDO 11.

[2] AHARMIM 13 obtained this result by a two-neutrino oscillation analysis using global solar neutrino data.

[3] AHARMIM 13 global solar neutrino data include SNO's all-phases-combined analysis results on the total active ^{8}B neutrino flux and energy-dependent ν_e survival probability parameters, measurements of Cl (CLEVELAND 98), Ga (ABDURASHITOV 09 which contains combined analysis with GNO (ALTMANN 05 and Ph.D. thesis of F. Kaether)), and ^{7}Be (BELLINI 11A) rates, and ^{8}B solar-neutrino recoil electron measurements of SK-I (HOSAKA 06) zenith, SK-II (CRAVENS 08), and SK-III (ABE 11) day/night spectra, and Borexino (BELLINI 10A) spectra.

[4] AHARMIM 13 obtained this result by a three-neutrino oscillation analysis with the value of Δm^2_{31} fixed to 2.45×10^{-3} eV^2, using global solar neutrino data.

[5] AHARMIM 13 obtained this result by a three-neutrino oscillation analysis with the value of Δm^2_{31} fixed to 2.45×10^{-3} eV^2, using global solar neutrino and KamLAND data (GANDO 11). CPT invariance is assumed.

[6] GANDO 13 obtained this result by a three-neutrino oscillation analysis using KamLAND and global solar neutrino data, assuming CPT invariance. Supersedes GANDO 11.

[7] GANDO 13 obtained this result by a three-neutrino oscillation analysis using KamLAND data. Supersedes GANDO 11.

[8] ABE 11 obtained this result by a two-neutrino oscillation analysis using solar neutrino data including Super-Kamiokande, SNO, Borexino (ARPESELLA 08A), Homestake, GALLEX/GNO, SAGE, and KamLAND data. CPT invariance is assumed.

[9] ABE 11 obtained this result by a two-neutrino oscillation analysis using solar neutrino data including Super-Kamiokande, SNO, Borexino (ARPESELLA 08A), Homestake, GALLEX/GNO, and SAGE data.

[10] ABE 11 obtained this result by a three-neutrino oscillation analysis with the value of Δm^2_{32} fixed to 2.4×10^{-3} eV^2, using solar neutrino data including Super-Kamiokande, SNO, Borexino (ARPESELLA 08A), Homestake, GALLEX/GNO, SAGE, and KamLAND data. The normal neutrino mass hierarchy and CPT invariance are assumed.

[11] ABE 11 obtained this result by a three-neutrino oscillation analysis with the value of Δm^2_{32} fixed to 2.4×10^{-3} eV^2, using solar neutrino data including Super-Kamiokande, SNO, Borexino (ARPESELLA 08A), Homestake, and GALLEX/GNO data. The normal neutrino mass hierarchy is assumed.

[12] BELLINI 11A obtained this result by a two-neutrino oscillation analysis using KamLAND, Homestake, SAGE, Gallex, GNO, Kamiokande, Super-Kamiokande, SNO, and Borexino (BELLINI 11A) data and the SSM flux prediction in SERENELLI 11 (Astrophysical Journal **743** 24 (2011)) with the exception that the ^{8}B flux was left free. CPT invariance is assumed.

[13] BELLINI 11A obtained this result by a two-neutrino oscillation analysis using Homestake, SAGE, Gallex, GNO, Kamiokande, Super-Kamiokande, SNO, and Borexino (BELLINI 11A) data and the SSM flux prediction in SERENELLI 11 (Astrophysical Journal **743** 24 (2011)) with the exception that the ^{8}B flux was left free.

[14] GANDO 11 obtain this result with three-neutrino fit using the KamLAND + solar data. Superseded by GANDO 13.

[15] GANDO 11 obtain this result with three-neutrino fit using the KamLAND data only. Supersedes ABE 08A.

[16] AHARMIM 10 global solar neutrino data include SNO's low-energy-threshold analysis survival probability day/night curves, SNO Phase III integral rates (AHARMIM 08), Cl (CLEVELAND 98), SAGE (ABDURASHITOV 09), Gallex/GNO (HAMPEL 99, ALTMANN 05), Borexino (ARPESELLA 08A), SK-I zenith (HOSAKA 06), and SK-II day/night spectra (CRAVENS 08).

[17] AHARMIM 10 obtained this result by a two-neutrino oscillation analysis using global solar neutrino data and KamLAND data (ABE 08A). *CPT* invariance is assumed.

[18] AHARMIM 10 obtained this result by a two-neutrino oscillation analysis using global solar neutrino data.

[19] AHARMIM 10 obtained this result by a three-neutrino oscillation analysis with the value of Δm^2_{31} fixed to 2.3×10^{-3} eV^2, using global solar neutrino data and KamLAND data (ABE 08A). *CPT* invariance is assumed.

[20] AHARMIM 10 obtained this result by a three-neutrino oscillation analysis with the value of Δm^2_{31} fixed to 2.3×10^{-3} eV^2, using global solar neutrino data.

[21] ABE 08A obtained this result by a rate + shape + time combined geoneutrino and reactor two-neutrino fit for Δm^2_{21} and $\tan^2\theta_{12}$, using KamLAND data only. Superseded by GANDO 11.

[22] ABE 08A obtained this result by means of a two-neutrino fit using KamLAND, Homestake, SAGE, GALLEX, GNO, SK (zenith angle and E-spectrum), the SNO χ^2-map, and solar flux data. *CPT* invariance is assumed. Superseded by GANDO 11.

[23] AHARMIM 08 obtained this result by a two-neutrino oscillation analysis using all solar neutrino data including those of Borexino (ARPESELLA 08A) and Super-Kamiokande-I (HOSAKA 06), and KamLAND data (ABE 08A). *CPT* invariance is assumed.

[24] HOSAKA 06 obtained this result by a two-neutrino oscillation analysis using solar neutrino and KamLAND data (ARAKI 05). *CPT* invariance is assumed.

[25] HOSAKA 06 obtained this result by a two-neutrino oscillation analysis using the data from Super-Kamiokande, SNO (AHMAD 02 and AHMAD 02B), and KamLAND (ARAKI 05) experiments. *CPT* invariance is assumed.

[26] HOSAKA 06 obtained this result by a two-neutrino oscillation analysis using the Super-Kamiokande and SNO (AHMAD 02 and AHMAD 02B) solar neutrino data.

[27] HOSAKA 06 obtained this result from the consistency between the observed and expected day-night flux asymmetry amplitude. The listed 68% CL range is derived from the 1σ boundary of the amplitude fit to the data. Oscillation parameters are constrained to be in the LMA region. The mixing angle is fixed at $\tan^2\theta = 0.44$ because the fit depends only very weekly on it.

[28] AHARMIM 05A obtained this result by a two-neutrino oscillation analysis using solar neutrino and KamLAND data (ARAKI 05). *CPT* invariance is assumed. AHARMIM 05A also quotes $\Delta(m^2) = (8.0^{+0.6}_{-0.4}) \times 10^{-5}$ eV^2 as the error enveloping the 68% CL two-dimensional region.

[29] AHARMIM 05A obtained this result by a two-neutrino oscillation analysis using the data from all solar neutrino experiments. The listed range of the parameter envelops the 95% CL two-dimensional region shown in figure 35a of AHARMIM 05A. AHARMIM 05A also quotes $\Delta(m^2) = (6.5^{+4.4}_{-2.3}) \times 10^{-5}$ eV^2 as the error enveloping the 68% CL two-dimensional region.

[30] ARAKI 05 obtained this result by a two-neutrino oscillation analysis using KamLAND and solar neutrino data. *CPT* invariance is assumed. The 1σ error shown here is provided by the KamLAND collaboration. The error quoted in ARAKI 05, $\Delta(m^2) = (7.9^{+0.6}_{-0.5}) \times 10^{-5}$, envelops the 68% CL two-dimensional region.

[31] AHMED 04A obtained this result by a two-neutrino oscillation analysis using solar neutrino and KamLAND data (EGUCHI 03). *CPT* invariance is assumed. AHMED 04A also quotes $\Delta(m^2) = (7.1^{+1.2}_{-0.6}) \times 10^{-5}$ eV^2 as the error enveloping the 68% CL two-dimensional region.

[32] AHMED 04A obtained this result by a two-neutrino oscillation analysis using the data from all solar neutrino experiments. The listed range of the parameter envelops the 95% CL two-dimensional region shown in Fig. 5(a) of AHMED 04A. The best-fit point is $\Delta(m^2) = 6.5 \times 10^{-5}$ eV^2, $\tan^2\theta = 0.40$ ($\sin^2 2\,\theta = 0.82$).

[33] SMY 04 obtained this result by a two-neutrino oscillation analysis using solar neutrino and KamLAND data (IANNI 03). *CPT* invariance is assumed.

[34] SMY 04 obtained this result by a two-neutrino oscillation analysis using the data from all solar neutrino experiments. The 1σ errors are read from Fig. 6(a) of SMY 04.

[35] SMY 04 obtained this result by a two-neutrino oscillation analysis using the Super-Kamiokande and SNO (AHMAD 02 and AHMAD 02B) solar neutrino data. The 1σ errors are read from Fig. 6(a) of SMY 04.

[36] AHMAD 02B obtained this result by a two-neutrino oscillation analysis using the data from all solar neutrino experiments. The listed range of the parameter envelops the 95% CL two-dimensional region shown in Fig. 4(b) of AHMAD 02B. The best fit point is $\Delta(m^2) = 5.0 \times 10^{-5}$ eV^2 and $\tan\theta = 0.34$ ($\sin^2 2\,\theta = 0.76$).

[37] FUKUDA 02 obtained this result by a two-neutrino oscillation analysis using the data from all solar neutrino experiments. The listed range of the parameter envelops the 95% CL two-dimensional region shown in Fig. 4 of FUKUDA 02. The best fit point is $\Delta(m^2) = 6.9 \times 10^{-5}$ eV^2 and $\tan^2\theta = 0.38$ ($\sin^2 2\,\theta = 0.80$).

$\sin^2(2\theta_{23})$

The reported limits below correspond to the projection onto the $\sin^2(2\theta_{23})$ axis of the 90% CL contours in the $\sin^2(2\theta_{23}) - \Delta m^2_{32}$ plane presented by the authors. Unless otherwise specified, the limits are 90% CL and the reported uncertainties are 68% CL. If the result is reported as $\sin^2(\theta_{23})$ we convert it to $\sin^2(2\theta_{23})$ and choose the quadrant that represents the more conservative value.

VALUE	CL%	DOCUMENT ID		TECN	COMMENT
$\mathbf{0.999^{+0.001}_{-0.018}}$		[1] ABE	14	T2K	3ν osc.; normal mass hierarchy
$\mathbf{1.000^{+0.000}_{-0.017}}$		[1] ABE	14	T2K	3ν osc.; inverted mass hierarchy
• • • We do not use the following data for averages, fits, limits, etc. • • •					
$0.97\ ^{+0.03}_{-0.06}$	90	[2] ADAMSON	14	MINS	3ν osc., normal hierarchy
$0.97\ ^{+0.03}_{-0.09}$	90	[2] ADAMSON	14	MINS	3ν osc.; inverted mass hierarchy
>0.73		[3] AARTSEN	13B	ICCB	DeepCore, 2ν oscillation
>0.963	68	[4] ABE	13G	T2K	3ν osc.; normal mass hierarchy
$0.95\ ^{+0.035}_{-0.036}$		[5] ADAMSON	13B	MINS	Beam + Atmospheric; identical ν & $\overline{\nu}$
0.84 - 1.0		[6] ABE	12A	T2K	off-axis beam
>0.75		[7] ADAMSON	12	MINS	$\overline{\nu}$ beam
>0.815		[8,9] ADAMSON	12B	MINS	MINOS atmospheric
>0.78		[8,10] ADAMSON	12B	MINS	MINOS pure atmospheric ν
>0.67		[8,10] ADAMSON	12B	MINS	MINOS pure atmospheric $\overline{\nu}$

>0.51	[11] ADRIAN-MAR..12	ANTR		atmospheric ν with deep see telescope
>0.95	[12] ABE	11C	SKAM	Super-Kamiokande
>0.90	ADAMSON	11	MINS	2ν osc.; maximal mixing
$0.86\ ^{+0.11}_{-0.12}$	[13] ADAMSON	11B	MINS	$\overline{\nu}$ beam
>0.965	[14] WENDELL	10	SKAM	3ν osc. with solar terms; θ_{13}=0
>0.95	[15] WENDELL	10	SKAM	3ν osc.; normal mass hierarchy
>0.93	[16] WENDELL	10	SKAM	3ν osc.; inverted mass hierarchy
>0.85	ADAMSON	08A	MINS	MINOS
>0.2	[17] ADAMSON	06	MINS	atmospheric ν with far detector
>0.59	[18] AHN	06A	K2K	KEK to Super-K
>0.7	[19] MICHAEL	06	MINS	MINOS
>0.58	[20] ALIU	05	K2K	KEK to Super-K
>0.6	[21] ALLISON	05	SOU2	
>0.92	[22] ASHIE	05	SKAM	Super-Kamiokande
>0.80	[23] AMBROSIO	04	MCRO	MACRO
>0.90	[24] ASHIE	04	SKAM	L/E distribution
>0.30	[25] AHN	03	K2K	KEK to Super-K
>0.45	[26] AMBROSIO	03	MCRO	MACRO
>0.77	[27] AMBROSIO	03	MCRO	MACRO
>0.50	[28] SANCHEZ	03	SOU2	Soudan-2 Atmospheric
>0.80	[29] AMBROSIO	01	MCRO	upward μ
>0.82	[30] AMBROSIO	01	MCRO	upward μ
>0.45	[31] FUKUDA	99C	SKAM	upward μ
>0.70	[32] FUKUDA	99D	SKAM	upward μ
>0.30	[33] FUKUDA	99D	SKAM	stop μ / through
>0.82	[34] FUKUDA	98C	SKAM	Super-Kamiokande
>0.30	[35] HATAKEYAMA	98	KAMI	Kamiokande
>0.73	[36] HATAKEYAMA	98	KAMI	Kamiokande
>0.65	[37] FUKUDA	94	KAMI	Kamiokande

[1] ABE 14 results are based on ν_μ disappearance using three-neutrino oscillation fit. The confidence intervals are derived from one dimensional profiled likelihoods. ABE 14 reported results as $\sin^2(\theta_{23}) = 0.514\ ^{+0.055}_{-0.056}$ (0.511 ± 0.055), assuming normal (inverted) mass hierarchy.

[2] ADAMSON 14 uses a complete set of accelerator and atmospheric data. The analysis combines the ν_μ disappearance and ν_e appearance data using three-neutrino oscillation fit. The fit results are obtained for normal and inverted mass hierarchy assumptions. The best fit is for lower θ_{23} quadrant and inverted mass hierarchy.

[3] AARTSEN 13B obtained this result by a two-neutrino oscillation analysis using 20–100 GeV muon neutrino sample from a total of 318.9 days of live-time measurement with the low-energy subdetector DeepCore of the IceCube neutrino telescope.

[4] The best fit value is $\sin^2(\theta_{23}) = 0.514 \pm 0.082$. Superseded by ABE 14.

[5] ADAMSON 13B obtained this result from ν_μ and $\overline{\nu}_\mu$ disappearance using ν_μ (10.71×10^{20} POT) and $\overline{\nu}_\mu$ (3.36×10^{20} POT) beams, and atmospheric (37.88kton-years) data from MINOS The fit assumed two-flavor neutrino hypothesis and identical ν_μ and $\overline{\nu}_\mu$ oscillation parameters. Superseded by ADAMSON 14.

[6] ABE 12A obtained this result by a two-neutrino oscillation analysis. The best-fit point is $\sin^2(2\theta_{23}) = 0.98$.

[7] ADAMSON 12 is a two-neutrino oscillation analysis using antineutrinos. The best fit value is $\sin^2(2\theta_{23}) = 0.95\ ^{+0.10}_{-0.11} \pm 0.01$.

[8] ADAMSON 12B obtained this result by a two-neutrino oscillation analysis of the L/E distribution using 37.9 kton-yr atmospheric neutrino data with the MINOS far detector.

[9] The best fit point is $\Delta m^2 = 0.0019$ eV^2 and $\sin^2 2\theta = 0.99$. The 90% single-parameter confidence interval at the best fit point is $\sin^2 2\theta > 0.86$.

[10] The data are separated into pure samples of νs and $\overline{\nu}$s, and separate oscillation parameters for νs and $\overline{\nu}$s are fit to the data. The best fit point is (Δm^2, $\sin^2 2\theta$) = (0.0022 eV^2, 0.99) and ($\Delta\overline{m}^2$, $\sin^2 2\overline{\theta}$) = (0.0016 eV^2, 1.00). The quoted result is taken from the 90% C.L. contour in the (Δm^2, $\sin^2 2\theta$) plane obtained by minimizing the four parameter log-likelihood function with respect to the other oscillation parameters.

[11] ADRIAN-MARTINEZ 12 measured the oscillation parameters of atmospheric neutrinos with the ANTARES deep sea neutrino telescope using the data taken from 2007 to 2010 (863 days of total live time).

[12] ABE 11C obtained this result by a two-neutrino oscillation analysis using the Super-Kamiokande-I+II+III atmospheric neutrino data. ABE 11C also reported results under a two-neutrino disappearance model with separate mixing parameters between ν and $\overline{\nu}$, and obtained $\sin^2 2\theta > 0.93$ for ν and $\sin^2 2\theta > 0.83$ for $\overline{\nu}$ at 90% C.L.

[13] ADAMSON 11B obtained this result by a two-neutrino oscillation analysis of antineutrinos in an antineutrino enhanced beam with 1.71×10^{20} protons on target. This results is consistent with the neutrino measurements of ADAMSON 11 at 2% C.L.

[14] WENDELL 10 obtained this result ($\sin^2\theta_{23} = 0.407$–$0.583$) by a three-neutrino oscillation analysis using the Super-Kamiokande-I+II+III atmospheric neutrino data, assuming $\theta_{13} = 0$ but including the solar oscillation parameters Δm^2_{21} and $\sin^2\theta_{12}$ in the fit.

[15] WENDELL 10 obtained this result ($\sin^2\theta_{23} = 0.43$–0.61) by a three-neutrino oscillation analysis with one mass scale dominance ($\Delta m^2_{21} = 0$) using the Super-Kamiokande-I+II+III atmospheric neutrino data, and updates the HOSAKA 06A result.

[16] WENDELL 10 obtained this result ($\sin^2\theta_{23} = 0.44$–0.63) by a three-neutrino oscillation analysis with one mass scale dominance ($\Delta m^2_{21} = 0$) using the Super-Kamiokande-I+II+III atmospheric neutrino data, and updates the HOSAKA 06A result.

[17] ADAMSON 06 obtained this result by a two-neutrino oscillation analysis of the L/E distribution using 4.54 kton yr atmospheric neutrino data with the MINOS far detector.

[18] Supercedes ALIU 05.

[19] MICHAEL 06 best fit is for maximal mixing. See also ADAMSON 08.

[20] The best fit is for maximal mixing.

[21] ALLISON 05 result is based upon atmospheric neutrino interactions including upward-stopping muons, with an exposure of 5.9 kton yr. From a two-flavor oscillation analysis the best-fit point is $\Delta m^2 = 0.0017$ eV^2 and $\sin^2(2\theta) = 0.97$.

[22] ASHIE 05 obtained this result by a two-neutrino oscillation analysis using 92 kton yr atmospheric neutrino data from the complete Super-Kamiokande I running period.

[23] AMBROSIO 04 obtained this result, without using the absolute normalization of the neutrino flux, by combining the angular distribution of upward through-going muon tracks with $E_\mu > 1$ GeV, N_{low} and N_{high}, and the numbers of InDown + UpStop and InUp events. Here, N_{low} and N_{high} are the number of events with reconstructed neutrino energies < 30 GeV and > 130 GeV, respectively. InDown and InUp represent events with downward and upward-going tracks starting inside the detector due to neutrino interactions, while UpStop represents entering upward-going tracks which stop in the detector. The best fit is for maximal mixing.

[24] ASHIE 04 obtained this result from the L(flight length)/E(estimated neutrino energy) distribution of ν_μ disappearance probability, using the Super-Kamiokande-I 1489 live-day atmospheric neutrino data.

[25] There are several islands of allowed region from this K2K analysis, extending to high values of Δm^2. We only include the one that overlaps atmospheric neutrino analyses. The best fit is for maximal mixing.

[26] AMBROSIO 03 obtained this result on the basis of the ratio $R = N_{low}/N_{high}$, where N_{low} and N_{high} are the number of upward through-going muon events with reconstructed neutrino energy < 30 GeV and > 130 GeV, respectively. The data came from the full detector run started in 1994. The method of FELDMAN 98 is used to obtain the limits.

[27] AMBROSIO 03 obtained this result by using the ratio R and the angular distribution of the upward through-going muons. R is given in the previous note and the angular distribution is reported in AMBROSIO 01. The method of FELDMAN 98 is used to obtain the limits. The best fit is to maximal mixing.

[28] SANCHEZ 03 is based on an exposure of 5.9 kton yr. The result is obtained using a likelihood analysis of the neutrino L/E distribution for a selection μ flavor sample while the e-flavor sample provides flux normalization. The method of FELDMAN 98 is used to obtain the allowed region. The best fit is $\sin^2(2\theta) = 0.97$.

[29] AMBROSIO 01 result is based on the angular distribution of upward through-going muon tracks with $E_\mu > 1$ GeV. The data came from three different detector configurations, but the statistics is largely dominated by the full detector run, from May 1994 to December 2000. The total live time, normalized to the full detector configuration is 6.17 years. The best fit is obtained outside the physical region. The method of FELDMAN 98 is used to obtain the limits. The best fit is for maximal mixing.

[30] AMBROSIO 01 result is based on the angular distribution and normalization of upward through-going muon tracks with $E_\mu > 1$ GeV. See the previous footnote.

[31] FUKUDA 99C obtained this result from a total of 537 live days of upward through-going muon data in Super-Kamiokande between April 1996 to January 1998. With a threshold of $E_\mu > 1.6$ GeV, the observed flux is $(1.74 \pm 0.07 \pm 0.02) \times 10^{-13}$ cm^{-2}s^{-1}sr^{-1}. The best fit is $\sin^2(2\theta) = 0.95$.

[32] FUKUDA 99D obtained this result from a simultaneous fitting to zenith angle distributions of upward-stopping and through-going muons. The flux of upward-stopping muons of minimum energy of 1.6 GeV measured between April 1996 and January 1998 is $(0.39 \pm 0.04 \pm 0.02) \times 10^{-13}$ cm^{-2}s^{-1}sr^{-1}. This is compared to the expected flux of $(0.73 \pm 0.16$ (theoretical error)$) \times 10^{-13}$ cm^{-2}s^{-1}sr^{-1}. The best fit is to maximal mixing.

[33] FUKUDA 99D obtained this result from the zenith dependence of the upward-stopping/through-going flux ratio. The best fit is to maximal mixing.

[34] FUKUDA 98C obtained this result by an analysis of 33.0 kton yr atmospheric neutrino data. The best fit is for maximal mixing.

[35] HATAKEYAMA 98 obtained this result from a total of 2456 live days of upward-going muon data in Kamiokande between December 1985 and May 1995. With a threshold of $E_\mu > 1.6$ GeV, the observed flux of upward through-going muons is $(1.94 \pm 0.10\ ^{+0.07}_{-0.06}) \times 10^{-13}$ cm^{-2}s^{-1}sr^{-1}. This is compared to the expected flux of $(2.46 \pm 0.54$ (theoretical error)$) \times 10^{-13}$ cm^{-2}s^{-1}sr^{-1}. The best fit is for maximal mixing.

[36] HATAKEYAMA 98 obtained this result from a combined analysis of Kamiokande contained events (FUKUDA 94) and upward going muon events. The best fit is $\sin^2(2\theta) = 0.95$.

[37] FUKUDA 94 obtained the result by a combined analysis of sub- and multi-GeV atmospheric neutrino events in Kamiokande. The best fit is for maximal mixing.

Δm^2_{32}

The sign of Δm^2_{32} is not known at this time. Only the absolute value is quoted below. Unless otherwise specified, the ranges below correspond to the projection onto the Δm^2_{32} axis of the 90% CL contours in the $\sin^2(2\theta_{23}) - \Delta m^2_{32}$ plane presented by the authors. If uncertainties are reported with the value, they correspond to one standard deviation uncertainty.

VALUE (10^{-3} eV^2)	DOCUMENT ID		TECN	COMMENT
2.52±0.07 OUR FIT	Assuming inverted mass hierarchy			
2.44±0.06 OUR FIT	Assuming normal mass hierarchy			
2.51±0.10	[1] ABE	14	T2K	3ν osc.; normal mass hierarchy
2.56±0.10	[1] ABE	14	T2K	3ν osc.; inverted mass hierarchy
2.37±0.09	[2] ADAMSON	14	MINS	3ν osc., accel. and atmspheric; normal mass hierarchy
$2.41\ ^{+0.12}_{-0.09}$	[2] ADAMSON	14	MINS	3ν osc., accel. and atmspheric; inverted mass hierarchy
$2.54\ ^{+0.19}_{-0.20}$	[3] AN	14	DAYA	3ν osc.; normal mass hierarchy
$2.64\ ^{+0.19}_{-0.20}$	[3] AN	14	DAYA	3ν osc.; inverted mass hierarchy

• • • We do not use the following data for averages, fits, limits, etc. • • •

$2.3\ ^{+0.6}_{-0.5}$	[4] AARTSEN	13B	ICCB	DeepCore, 2ν oscillation
$2.44^{+0.17}_{-0.15}$	[5] ABE	13G	T2K	3ν osc.; normal mass hierarchy
$2.41^{+0.09}_{-0.10}$	[6] ADAMSON	13B	MINS	2ν osc.; beam + atmospheric; identical ν & $\overline{\nu}$
2.2–3.1	[7] ABE	12A	T2K	off-axis beam
$2.62^{+0.31}_{-0.28}\pm0.09$	[8] ADAMSON	12	MINS	$\overline{\nu}$ beam
1.35–2.55	[9,10] ADAMSON	12B	MINS	MINOS atmospheric
1.4–5.6	[9,11] ADAMSON	12B	MINS	MINOS pure atmospheric ν
0.9–2.5	[9,11] ADAMSON	12B	MINS	MINOS pure atmospheric $\overline{\nu}$
1.8–5.0	[12] ADRIAN-MAR..12		ANTR	atm. ν with deep see telescope
1.3–4.0	[13] ABE	11C	SKAM	atmospheric $\overline{\nu}$
$2.32^{+0.12}_{-0.08}$	ADAMSON	11	MINS	2ν oscillation; maximal mixing
$3.36^{+0.46}_{-0.40}$	[14] ADAMSON	11B	MINS	$\overline{\nu}$ beam
<3.37	[15] ADAMSON	11C	MINS	MINOS
1.9–2.6	[16] WENDELL	10	SKAM	3ν osc.; normal mass hierarchy
1.7–2.7	[16] WENDELL	10	SKAM	3ν osc.; inverted mass hierarchy
2.43 ± 0.13	ADAMSON	08A	MINS	MINOS
0.07–50	[17] ADAMSON	06	MINS	atmospheric ν with far detector
1.9–4.0	[18,19] AHN	06A	K2K	KEK to Super-K
2.2–3.8	[20] MICHAEL	06	MINS	MINOS
1.9–3.6	[18] ALIU	05	K2K	KEK to Super-K
0.3–12	[21] ALLISON	05	SOU2	
1.5–3.4	[22] ASHIE	05	SKAM	atmospheric neutrino
0.6–8.0	[23] AMBROSIO	04	MCRO	MACRO
1.9 to 3.0	[24] ASHIE	04	SKAM	L/E distribution
1.5–3.9	[25] AHN	03	K2K	KEK to Super-K
0.25–9.0	[26] AMBROSIO	03	MCRO	MACRO
0.6–7.0	[27] AMBROSIO	03	MCRO	MACRO
0.15–15	[28] SANCHEZ	03	SOU2	Soudan-2 Atmospheric
0.6–15	[29] AMBROSIO	01	MCRO	upward μ
1.0–6.0	[30] AMBROSIO	01	MCRO	upward μ
1.0–50	[31] FUKUDA	99C	SKAM	upward μ
1.5–15.0	[32] FUKUDA	99D	SKAM	upward μ
0.7–18	[33] FUKUDA	99D	SKAM	stop μ / through
0.5–6.0	[34] FUKUDA	98C	SKAM	Super-Kamiokande
0.55–50	[35] HATAKEYAMA	98	KAMI	Kamiokande
4–23	[36] HATAKEYAMA	98	KAMI	Kamiokande
5–25	[37] FUKUDA	94	KAMI	Kamiokande

[1] ABE 14 results are based on ν_μ disappearance using three-neutrino oscillation fit. The confidence intervals are derived from one dimensional profiled likelihoods. In ABE 14 the inverted mass hierarchy result is reported as $\Delta m^2_{13} = (2.48 \pm 0.10) \times 10^{-3}$ eV^2 which we converted to Δm^2_{32} by adding PDG 14 value of $\Delta m^2_{21} = (7.53 \pm 0.18) \times 10^{-5}$ eV^2.

[2] ADAMSON 14 uses a complete set of accelerator and atmospheric data. The analysis combines The analysis combines the ν_μ disappearance and ν_e appearance data using three-neutrino oscillation fit. The fit results are obtained for normal and inverted mass hierarchy assumptions.

[3] AN 14 uses six identical detectors, with three placed near the reactor cores (flux-weighted baselines of 512 and 561 m) and the remaining three at the far hall (at the flux averaged distance of 1579 m from all six reactor cores) to determine prompt energy spectra and derive $\Delta m^2_{ee} = (2.59^{+0.19}_{-0.20}) \times 10^{-3}$ eV^2. Assuming the normal (inverted) hierarchy, the fitted $\Delta m^2_{32} = (2.54^{+0.19}_{-0.20}) \times 10^{-3}$ ($(2.64^{+0.19}_{-0.20}) \times 10^{-3}$) eV^2.

[4] AARTSEN 13B obtained this result by a two-neutrino oscillation analysis using 20–100 GeV muon neutrino sample from a total of 318.9 days of live-time measurement with the low-energy subdetector DeepCore of the IceCube neutrino telescope.

[5] Based on the observation of 58 ν_μ events with 205 ± 17(syst) expected in the absence of neutrino oscillations. Superseded by ABE 14.

[6] ADAMSON 13B obtained this result from ν_μ and $\overline{\nu}_\mu$ disappearance using ν_μ (10.71×10^{20} POT) and $\overline{\nu}_\mu$ (3.36×10^{20} POT) beams, and atmospheric (37.88 kton-years) data from MINOS. The fit assumed two-flavor neutrino hypothesis and identical ν_μ and $\overline{\nu}_\mu$ oscillation parameters.

[7] ABE 12A obtained this result by a two-neutrino oscillation analysis. The best-fit point is $\Delta m^2_{32} = 2.65 \times 10^{-3}$ eV^2.

[8] ADAMSON 12 is a two-neutrino oscillation analysis using antineutrinos.

[9] ADAMSON 12B obtained this result by a two-neutrino oscillation analysis of the L/E distribution using 37.9 kton-yr atmospheric neutrino data with the MINOS far detector.

[10] The 90% single-parameter confidence interval at the best fit point is $\Delta m^2 = 0.0019 \pm 0.0004$ eV^2.

[11] The data are separated into pure samples of νs and $\overline{\nu}$s, and separate oscillation parameters for νs and $\overline{\nu}$s are fit to the data. The best fit point is (Δm^2, $\sin^2 2\theta$) = (0.0022 eV^2, 0.99) and ($\Delta\overline{m}^2$, $\sin^2 2\overline{\theta}$) = (0.0016 eV^2, 1.00). The quoted result is taken from the 90% C.L. contour in the (Δm^2, $\sin^2 2\theta$) plane obtained by minimizing the four parameter log-likelihood function with respect to the other oscillation parameters.

[12] ADRIAN-MARTINEZ 12 measured the oscillation parameters of atmospheric neutrinos with the ANTARES deep sea neutrino telescope using the data taken from 2007 to 2010 (863 days of total live time).

[13] ABE 11C obtained this result by a two-neutrino oscillation analysis with separate mixing parameters between neutrinos and antineutrinos, using the Super-Kamiokande-I+II+III atmospheric neutrino data. The corresponding 90% CL neutrino oscillation parameter range obtained from this analysis is $\Delta m^2 = 1.7$–3.0×10^{-3} eV^2.

[14] ADAMSON 11B obtained this result by a two-neutrino oscillation analysis of antineutrinos in an antineutrino enhanced beam with 1.71×10^{20} protons on target. This results is consistent with the neutrino measurements of ADAMSON 11 at 2% C.L.

[15] ADAMSON 11C obtains this result based on a study of antineutrinos in a neutrino beam and assumes maximal mixing in the two-flavor approximation.

[16] WENDELL 10 obtained this result by a three-neutrino oscillation analysis with one mass scale dominance ($\Delta m^2_{21} = 0$) using the Super-Kamiokande-I+II+III atmospheric neutrino data, and updates the HOSAKA 06A result.

[17] ADAMSON 06 obtained this result by a two-neutrino oscillation analysis of the L/E distribution using 4.54 kton yr atmospheric neutrino data with the MINOS far detector.

[18] The best fit in the physical region is for $\Delta m^2 = 2.8 \times 10^{-3}$ eV^2.

[19] Supercedes ALIU 05.

[20] MICHAEL 06 best fit is 2.74×10^{-3} eV^2. See also ADAMSON 08.

[21] ALLISON 05 result is based on an atmospheric neutrino observation with an exposure of 5.9 kton yr. From a two-flavor oscillation analysis the best-fit point is $\Delta m^2 = 0.0017$ eV^2 and $\sin^2 2\,\theta = 0.97$.

[22] ASHIE 05 obtained this result by a two-neutrino oscillation analysis using 92 kton yr atmospheric neutrino data from the complete Super-Kamiokande I running period. The best fit is for $\Delta m^2 = 2.1 \times 10^{-3}$ eV^2.

[23] AMBROSIO 04 obtained this result, without using the absolute normalization of the neutrino flux, by combining the angular distribution of upward through-going muon tracks with $E_\mu > 1$ GeV, N_{low} and N_{high}, and the numbers of InDown + UpStop and InUp events. Here, N_{low} and N_{high} are the number of events with reconstructed neutrino energies < 30 GeV and > 130 GeV, respectively. InDown and InUp represent events with downward and upward-going tracks starting inside the detector due to neutrino interactions, while UpStop represents entering upward-going tracks which stop in the detector. The best fit is for $\Delta m^2 = 2.3 \times 10^{-3}$ eV^2.

[24] ASHIE 04 obtained this result from the L(flight length)/E(estimated neutrino energy) distribution of ν_μ disappearance probability, using the Super-Kamiokande-I 1489 live-day atmospheric neutrino data. The best fit is for $\Delta m^2 = 2.4 \times 10^{-3}$ eV^2.

[25] There are several islands of allowed region from this K2K analysis, extending to high values of Δm^2. We only include the one that overlaps atmospheric neutrino analyses. The best fit is for $\Delta m^2 = 2.8 \times 10^{-3}$ eV^2.

[26] AMBROSIO 03 obtained this result on the basis of the ratio R = N_{low}/N_{high}, where N_{low} and N_{high} are the number of upward through-going muon events with reconstructed neutrino energy < 30 GeV and > 130 GeV, respectively. The data came from the full detector run started in 1994. The method of FELDMAN 98 is used to obtain the limits. The best fit is for $\Delta m^2 = 2.5 \times 10^{-3}$ eV^2.

[27] AMBROSIO 03 obtained this result by using the ratio R and the angular distribution of the upward through-going muons. R is given in the previous note and the angular distribution is reported in AMBROSIO 01. The method of FELDMAN 98 is used to obtain the limits. The best fit is for $\Delta m^2 = 2.5 \times 10^{-3}$ eV^2.

[28] SANCHEZ 03 is based on an exposure of 5.9 kton yr. The result is obtained using a likelihood analysis of the neutrino L/E distribution for a selection μ flavor sample while the e-flavor sample provides flux normalization. The method of FELDMAN 98 is used to obtain the allowed region. The best fit is for $\Delta m^2 = 5.2 \times 10^{-3}$ eV^2.

[29] AMBROSIO 01 result is based on the angular distribution of upward through-going muon tracks with $E_\mu > 1$ GeV. The data came from three different detector configurations, but the statistics is largely dominated by the full detector run, from May 1994 to December 2000. The total live time, normalized to the full detector configuration is 6.17 years. The best fit is obtained outside the physical region. The method of FELDMAN 98 is used to obtain the limits.

[30] AMBROSIO 01 result is based on the angular distribution and normalization of upward through-going muon tracks with $E_\mu > 1$ GeV. See the previous footnote.

[31] FUKUDA 99C obtained this result from a total of 537 live days of upward through-going muon data in Super-Kamiokande between April 1996 to January 1998. With a threshold of $E_\mu > 1.6$ GeV, the observed flux is $(1.74 \pm 0.07 \pm 0.02) \times 10^{-13}$ cm^{-2}s^{-1}sr^{-1}. The best fit is for $\Delta m^2 = 5.9 \times 10^{-3}$ eV^2.

[32] FUKUDA 99D obtained this result from a simultaneous fitting to zenith angle distributions of upward-stopping and through-going muons. The flux of upward-stopping muons of minimum energy of 1.6 GeV measured between April 1996 and January 1998 is $(0.39 \pm 0.04 \pm 0.02) \times 10^{-13}$ cm^{-2}s^{-1}sr^{-1}. This is compared to the expected flux of $(0.73 \pm 0.16$ (theoretical error)$) \times 10^{-13}$ cm^{-2}s^{-1}sr^{-1}. The best fit is for $\Delta m^2 = 3.9 \times 10^{-3}$ eV^2.

[33] FUKUDA 99D obtained this result from the zenith dependence of the upward-stopping/through-going flux ratio. The best fit is for $\Delta m^2 = 3.1 \times 10^{-3}$ eV^2.

[34] FUKUDA 98C obtained this result by an analysis of 33.0 kton yr atmospheric neutrino data. The best fit is for $\Delta m^2 = 2.2 \times 10^{-3}$ eV^2.

[35] HATAKEYAMA 98 obtained this result from a total of 2456 live days of upward-going muon data in Kamiokande between December 1985 and May 1995. With a threshold of $E_\mu > 1.6$ GeV, the observed flux of upward through-going muons is $(1.94 \pm 0.10^{+0.07}_{-0.06}) \times 10^{-13}$ cm^{-2}s^{-1}sr^{-1}. This is compared to the expected flux of $(2.46 \pm 0.54$ (theoretical error)$) \times 10^{-13}$ cm^{-2}s^{-1}sr^{-1}. The best fit is for $\Delta m^2 = 2.2 \times 10^{-3}$ eV^2.

[36] HATAKEYAMA 98 obtained this result from a combined analysis of Kamiokande contained events (FUKUDA 94) and upward going muon events. The best fit is for $\Delta m^2 = 13 \times 10^{-3}$ eV^2.

[37] FUKUDA 94 obtained the result by a combined analysis of sub- and multi-GeV atmospheric neutrino events in Kamiokande. The best fit is for $\Delta m^2 = 16 \times 10^{-3}$ eV^2.

$\sin^2(2\theta_{13})$

At present time direct measurements of $\sin^2(2\theta_{13})$ are derived from the reactor $\overline{\nu}_e$ disappearance at distances corresponding to the Δm^2_{32} value, i.e. L $\sim$ 1km. Alternatively, limits can also be obtained from the analysis of the solar neutrino data and accelerator-based $\nu_\mu \to \nu_e$ experiments.

VALUE (units 10^{-2})	CL%	DOCUMENT ID		TECN	COMMENT
9.3± 0.8 OUR AVERAGE					
$9.0^{+0.8}_{-0.9}$		[1] AN	14	DAYA	DayaBay, Ling Ao/Ao II reactors
10.9± 3.0±2.5		[2] ABE	12B	DCHZ	Chooz reactors
11.3± 1.3±1.9		[3] AHN	12	RENO	Yonggwang reactors
• • • We do not use the following data for averages, fits, limits, etc. • • •					
9.7± 3.4±3.4		[4] ABE	13C	DCHZ	Neutron capture on hydrogen
$8.8^{+4.9}_{-3.9}$		[5] ABE	13E	T2K	Normal mass hierarchy
$10.8^{+5.9}_{-4.6}$		[5] ABE	13E	T2K	Inverted mass hierarchy
$6.4^{+4.8}_{-3.7}$		[6] ADAMSON	13A	MINS	Normal mass hierarchy
$11.7^{+6.8}_{-6.2}$		[6] ADAMSON	13A	MINS	Inverted mass hierarchy
<44	90	AGAFONOVA	13	OPER	OPERA: 3ν
<13.9	95	[7] AHARMIM	13	FIT	global solar: 3ν
8.9± 1.0±0.5		[8] AN	13	DAYA	DayaBay, LIng Ao/Ao II reactors
8.6± 4.1±3.0		[9] ABE	12	DCHZ	Chooz reactors
9.2± 1.6±0.5		[10] AN	12	DAYA	DayaBay, Ling Ao/Ao II reactors
$9.8^{+6.7}_{-6.2}$	68	[11] ABE	11	FIT	KamLAND + global solar
< 23	95	[12] ABE	11	FIT	Global solar
5 to 21	68	[13] ABE	11A	T2K	Normal mass hierarchy
6 to 25	68	[14] ABE	11A	T2K	Inverted mass hierarchy
1 to 9	68	[15] ADAMSON	11D	MINS	Normal mass hierarchy
3 to 15	68	[16] ADAMSON	11D	MINS	Inverted mass hierarchy
8 ± 3	68	[17] FOGLI	11	FIT	Global neutrino data
7.8± 6.2	68	[18] GANDO	11	FIT	KamLAND + solar: 3ν
12.4±13.3	68	[19] GANDO	11	FIT	KamLAND: 3ν
3^{+9}_{-7}	90	[20] ADAMSON	10A	MINS	Normal mass hierarchy
6^{+14}_{-6}	90	[21] ADAMSON	10A	MINS	Inverted mass hierarchy
8^{+8}_{-7}	22,23	AHARMIM	10	FIT	KamLAND + global solar: 3ν
< 30	95	[22,24] AHARMIM	10	FIT	global solar: 3ν
< 15	90	[25] WENDELL	10	SKAM	3ν osc.; normal m hierarchy
< 33	90	[25] WENDELL	10	SKAM	3ν osc.; inverted m hierarchy
11^{+11}_{-8}		[26] ADAMSON	09	MINS	Normal mass hierarchy
18^{+15}_{-11}		[27] ADAMSON	09	MINS	Inverted mass hierarchy
6 ± 4		[28] FOGLI	08	FIT	Global neutrino data
8 ± 7		[29] FOGLI	08	FIT	Solar + KamLAND data
5 ± 5		[30] FOGLI	08	FIT	Atmospheric+LBL+CHOOZ
< 36	90	[31] YAMAMOTO	06	K2K	Accelerator experiment
< 48	90	[32] AHN	04	K2K	Accelerator experiment
< 36	90	[33] BOEHM	01		Palo Verde react.
< 45	90	[34] BOEHM	00		Palo Verde react.
< 15	90	[35] APOLLONIO	99	CHOZ	Reactor Experiment

[1] AN 14 uses six identical detectors, with three placed near the reactor cores (flux-weighted baselines of 512 and 561 m) and the remaining three at the far hall (at the flux averaged distance of 1579 m from all six reactor cores) to determine the mixing angle θ_{13} using the $\overline{\nu}_e$ observed interaction rates and energy spectra and three neutrino mixing analysis. Supersedes AN 13.

[2] ABE 12B determines the neutrino mixing angle θ_{13} using a single detector, located 1050 m from the cores of two reactors. This result is based on a spectral shape and rate analysis.

[3] AHN 12 uses two identical detectors, placed at flux weighted distances of 408.56 m and 1433.99 m from six reactor cores, to determine the mixing angle θ_{13}. This rate-only analysis excludes the no-oscillation hypothesis at 4.9 standard deviations. The value of $\Delta m^2_{31} = (2.32^{+0.12}_{-0.08}) \times 10^{-3}$ eV^2 was assumed in the analysis.

[4] ABE 13C uses delayed neutron capture on hydrogen instead of on Gd used previously. The fiducial volume is thus three times larger. The fit is based on the rate and shape analysis as in ABE 12B.

[5] ABE 13E assumes maximal θ_{23} mixing and CP phase $\delta = 0$.

[6] ADAMSON 13A results obtained from ν_e appearance, assuming $\delta = 0$, and $\sin^2(2\,\theta_{23}) = 0.957$.

[7] AHARMIM 13 obtained this result by a three-neutrino oscillation analysis with the value of Δm^2_{32} fixed to 2.45×10^{-3} eV^2, using global solar neutrino data. AHARMIM 13 global solar neutrino data include SNO's all-phases-combined analysis results on the total active ^{8}B neutrino flux and energy-dependent ν_e survival probability parameters, measurements of Cl (CLEVELAND 98), Ga (ABDURASHITOV 09 which contains combined analysis with GNO (ALTMANN 05 and Ph.D. thesis of F. Kaether)), and ^{7}Be (BELLINI 11A) rates, and ^{8}B solar-neutrino recoil electron measurements of SK-I (HOSAKA 06) zenith, SK-II (CRAVENS 08) and SK-III (ABE 11) day/night spectra, and Borexino (BELLINI 10A) spectra. AHARMIM 13 also reported a result combining global solar and KamLAND data, which is $\sin^2(2\,\theta_{13}) = (9.1^{+2.9}_{-3.1}) \times 10^{-2}$.

[8] AN 13 uses six identical detectors, with three placed near the reactor cores (flux-weighted baselines of 498 and 555 m) and the remaining three at the far hall (at the flux averaged distance of 1628 m from all six reactor cores) to determine the $\overline{\nu}_e$ interaction rate ratios. Superseded by AN 14.

[9] ABE 12 determines the $\overline{\nu}_e$ interaction rate in a single detector, located 1050 m from the cores of two reactors. The rate normalization is fixed by the results of the Bugey4 reactor experiment, thus avoiding any dependence on possible very short baseline oscillations. The value of $\Delta m^2_{31} = 2.4 \times 10^{-3}$ eV^2 is used in the analysis. Superseded by ABE 12B.

[10] AN 12 uses six identical detectors with three placed near the reactor cores (flux-weighted baselines of 470 m and 576 m) and the remaining three at the far hall (at the flux averaged distance of 1648 m from all six reactor cores) to determine the mixing angle θ_{13} using the $\overline{\nu}_e$ observed interaction rate ratios. This rate-only analysis excludes the no-oscillation hypothesis at 5.2 standard deviations. The value of $\Delta m^2_{31} = (2.32^{+0.12}_{-0.08}) \times 10^{-3}$ eV^2 was assumed in the analysis. Superseded by AN 13.

[11] ABE 11 obtained this result by a three-neutrino oscillation analysis with the value of Δm^2_{32} fixed to 2.4×10^{-3} eV^2, using solar neutrino data including Super-Kamiokande, SNO, Borexino (ARPESELLA 08A), Homestake, GALLEX/GNO, SAGE, and KamLAND data. This result implies an upper bound of $\sin^2\theta_{13} < 0.059$ (95% CL) or $\sin^2 2\theta_{13} < 0.22$ (95% CL). The normal neutrino mass hierarchy and CPT invariance are assumed.

[12] ABE 11 obtained this result by a three-neutrino oscillation analysis with the value of Δm^2_{32} fixed to 2.4×10^{-3} eV^2, using solar neutrino data including Super-Kamiokande, SNO, Borexino (ARPESELLA 08A), Homestake, and GALLEX/GNO data. The normal neutrino mass hierarchy is assumed.

[13] The quoted limit is for $\Delta m^2_{32} = 2.4 \times 10^{-3}$ eV^2, $\theta_{23} = \pi/2$, $\delta = 0$, and the normal mass hierarchy. For other values of δ, the 68% region spans from 0.03 to 0.25, and the 90% region from 0.02 to 0.32.

[14] The quoted limit is for $\Delta m^2_{32} = 2.4 \times 10^{-3}$ eV^2, $\theta_{23} = \pi/2$, $\delta = 0$, and the inverted mass hierarchy. For other values of δ, the 68% region spans from 0.04 to 0.30, and the 90% region from 0.02 to 0.39.

[15] The quoted limit is for $\Delta m^2_{32} = 2.32 \times 10^{-3}$ eV^2, $\theta_{23} = \pi/2$, $\delta = 0$, and the normal mass hierarchy. For other values of δ, the 68% region spans from 0.02 to 0.12, and the 90% region from 0 to 0.16.

[16] The quoted limit is for $\Delta m^2_{32} = 2.32 \times 10^{-3}$ eV^2, $\theta_{23} = \pi/2$, $\delta = 0$, and the inverted mass hierarchy. For other values of δ, the 68% region spans from 0.02 to 0.16, and the 90% region from 0 to 0.21.

[17] FOGLI 11 obtained this result from an analysis using the atmospheric, accelerator long baseline, CHOOZ, solar, and KamLAND data. Recently, MUELLER 11 suggested an average increase of about 3.5% in normalization of the reactor $\overline{\nu}_e$ fluxess, and using these fluxes, the fitted result becomes 0.10 ± 0.03.

[18] GANDO 11 report $\sin^2\theta_{13} = 0.020 \pm 0.016$. This result was obtained with three-neutrino fit using the KamLAND + solar data.

[19] GANDO 11 report $\sin^2\theta_{13} = 0.032 \pm 0.037$. This result was obtained with three-neutrino fit using the KamLAND data only.

[20] This result corresponds to the limit of <0.12 at 90% CL for $\Delta m^2_{32} = 2.43 \times 10^{-3}$ eV^2, $\theta_{23} = \pi/2$, and $\delta = 0$. For other values of δ, the 90% CL region spans from 0 to 0.16.

[21] This result corresponds to the limit of <0.20 at 90% CL for $\Delta m^2_{32} = 2.43 \times 10^{-3}$ eV^2, $\theta_{23} = \pi/2$, and $\delta = 0$. For other values of δ, the 90% CL region spans from 0 to 0.21.

[22] AHARMIM 10 global solar neutrino data include SNO's low-energy-threshold analysis survival probability day/night curves, SNO Phase III integral rates (AHARMIM 08), Cl (CLEVELAND 98), SAGE (ABDURASHITOV 09), Gallex/GNO (HAMPEL 99, ALTMANN 05), Borexino (ARPESELLA 08A), SK-I zenith (HOSAKA 06), and SK-II day/night spectra (CRAVENS 08).

[23] AHARMIM 10 obtained this result by a three-neutrino oscillation analysis with the value of Δm^2_{31} fixed to 2.3×10^{-3} eV^2, using global solar neutrino data and KamLAND data (ABE 08A). CPT invariance is assumed. This result implies an upper bound of $\sin^2\theta_{13} < 0.057$ (95% CL) or $\sin^2 2\theta_{13} < 0.22$ (95% CL).

[24] AHARMIM 10 obtained this result by a three-neutrino oscillation analysis with the value of Δm^2_{31} fixed to 2.3×10^{-3} eV^2, using global solar neutrino data.

[25] WENDELL 10 obtained this result by a three-neutrino oscillation analysis with one mass scale dominance ($\Delta m^2_{21} = 0$) using the Super-Kamiokande-I+II+III atmospheric neutrino data, and updates the HOSAKA 06A result.

[26] The quoted limit is for $\Delta m^2_{32} = 2.43 \times 10^{-3}$ eV^2, $\theta_{23} = \pi/2$, and $\delta = 0$. For other values of δ, the 68% CL region spans from 0.02 to 0.26.

[27] The quoted limit is for $\Delta m^2_{32} = 2.43 \times 10^{-3}$ eV^2, $\theta_{23} = \pi/2$, and $\delta = 0$. For other values of δ, the 68% CL region spans from 0.04 to 0.34.

[28] FOGLI 08 obtained this result from a global analysis of all neutrino oscillation data, that is, solar + KamLAND + atmospheric + accelerator long baseline + CHOOZ.

[29] FOGLI 08 obtained this result from an analysis using the solar and KamLAND neutrino oscillation data.

[30] FOGLI 08 obtained this result from an analysis using the atmospheric, accelerator long baseline, and CHOOZ neutrino oscillation data.

[31] YAMAMOTO 06 searched for $\nu_\mu \to \nu_e$ appearance. Assumes $2\sin^2(2\theta_{\mu e}) = \sin^2(2\theta_{13})$. The quoted limit is for $\Delta m^2_{32} = 1.9 \times 10^{-3}$ eV^2. That value of Δm^2_{32} is the one-σ low value for AHN 06A. For the AHN 06A best fit value of 2.8×10^{-3} eV^2, the $\sin^2(2\theta_{13})$ limit is < 0.26. Supersedes AHN 04.

[32] AHN 04 searched for $\nu_\mu \to \nu_e$ appearance. Assuming $2\sin^2(2\,\theta_{\mu_e}) = \sin^2(2\,\theta_{13})$, a limit on $\sin^2(2\,\theta_{\mu_e})$ is converted to a limit on $\sin^2(2\,\theta_{13})$.The quoted limit is for $\Delta m^2_{32} = 1.9 \times 10^{-3}$ eV^2. That value of Δm^2_{32} is the one-σ low value for ALIU 05. For the ALIU 05 best fit value of 2.8×10^{-3} eV^2, the $\sin^2(2\,\theta_{13})$ limit is < 0.30.

[33] The quoted limit is for $\Delta m^2_{32} = 1.9 \times 10^{-3}$ eV^2. That value of Δm^2_{32} is the 1-σ low value for ALIU 05. For the ALIU 05 best fit value of 2.8×10^{-3} eV^2, the $\sin^2 2\,\theta_{13}$ limit

is < 0.19. In this range, the θ_{13} limit is larger for lower values of Δm^2_{32}, and smaller for higher values of Δm^2_{32}.

[34] The quoted limit is for $\Delta m^2_{32} = 1.9 \times 10^{-3}$ eV^2. That value of Δm^2_{32} is the 1-σ low value for ALIU 05. For the ALIU 05 best fit value of 2.8×10^{-3} eV^2, the $\sin^2 2\,\theta_{13}$ limit is < 0.23.

[35] The quoted limit is for $\Delta m^2_{32} = 2.43 \times 10^{-3}$ eV^2. That value of Δm^2_{32} is the central value for ADAMSON 08. For the ADAMSON 08 1-σ low value of 2.30×10^{-3} eV^2, the $\sin^2 2\,\theta_{13}$ limit is < 0.16. See also APOLLONIO 03 for a detailed description of the experiment.

(C) Other neutrino mixing results

The LSND collaboration reported in AGUILAR 01 a signal which is consistent with $\overline{\nu}_\mu \to \overline{\nu}_e$ oscillations. In a three neutrino framework, this would be a measurement of θ_{12} and Δm^2_{21}. This does not appear to be consistent with most of the other neutrino data. The MiniBooNE experiment, reported in AGUILAR-AREVALO 07, does a two-neutrino analysis which, assuming *CP* conservation, rules out AGUILAR 01. However, the MiniBooNE antineutrino data reported in AGUILAR-AREVALO 13A are consistent with the signal reported in AGUILAR 01. The following listings include results which might be relevant towards understanding these observations. They include searches for $\nu_\mu \to \nu_e$, $\overline{\nu}_\mu \to \overline{\nu}_e$, sterile neutrino oscillations, and *CPT* violation.

$\Delta(m^2)$ for $\sin^2(2\theta) = 1$ ($\nu_\mu \to \nu_e$)

VALUE (eV^2)	CL%	DOCUMENT ID		TECN	COMMENT
• • • We do not use the following data for averages, fits, limits, etc. • • •					
0.015 to 0.050	90	[1] AGUILAR-AR...	13A	MBOO	MiniBooNE
<0.34	90	[2] MAHN	12	MBOO	MiniBooNE/SciBooNE
<0.034	90	AGUILAR-AR...	07	MBOO	MiniBooNE
<0.0008	90	AHN	04	K2K	Water Cherenkov
<0.4	90	ASTIER	03	NOMD	CERN SPS
<2.4	90	AVVAKUMOV	02	NTEV	NUTEV FNAL
		[3] AGUILAR	01	LSND	$\nu\mu \to \nu_e$ osc.prob.
0.03 to 0.3	95	[4] ATHANASSO...	98	LSND	$\nu_\mu \to \nu_e$
<2.3	90	[5] LOVERRE	96		CHARM/CDHS
<0.9	90	VILAIN	94C	CHM2	CERN SPS
<0.09	90	ANGELINI	86	HLBC	BEBC CERN PS

[1] Based on $\nu_\mu \to \nu_e$ appearance of 162.0 ± 47.8 events; marginally compatible with two neutrino oscillations. The best fit value is $\Delta m^2 = 3.14$ eV^2.

[2] MAHN 12 is a combined spectral fit of MiniBooNE and SciBooNE neutrino data with the range of Δm^2 up to 25 eV^2. The best limit is 0.04 at 7 eV^2.

[3] AGUILAR 01 is the final analysis of the LSND full data set. Search is made for the $\nu_\mu \to \nu_e$ oscillations using ν_μ from π^+ decay in flight by observing beam-on electron events from $\nu_e C \to e^- X$. Present analysis results in $8.1 \pm 12.2 \pm 1.7$ excess events in the $60 < E_e < 200$ MeV energy range, corresponding to oscillation probability of $0.10 \pm 0.16 \pm 0.04\%$. This is consistent, though less significant, with the previous result of ATHANASSOPOULOS 98, which it supersedes. The present analysis uses selection criteria developed for the decay at rest region, and is less effective in removing the background above 60 MeV than ATHANASSOPOULOS 98.

[4] ATHANASSOPOULOS 98 is a search for the $\nu_\mu \to \nu_e$ oscillations using ν_μ from π^+ decay in flight. The 40 observed beam-on electron events are consistent with $\nu_e C \to e^- X$; the expected background is 21.9 ± 2.1. Authors interpret this excess as evidence for an oscillation signal corresponding to oscillations with probability $(0.26 \pm 0.10 \pm 0.05)\%$. Although the significance is only 2.3 σ, this measurement is an important and consistent cross check of ATHANASSOPOULOS 96 who reported evidence for $\overline{\nu}_\mu \to \overline{\nu}_e$ oscillations from μ^+ decay at rest. See also ATHANASSOPOULOS 98B.

[5] LOVERRE 96 uses the charged-current to neutral-current ratio from the combined CHARM (ALLABY 86) and CDHS (ABRAMOWICZ 86) data from 1986.

$\sin^2(2\theta)$ for "Large" $\Delta(m^2)$ ($\nu_\mu \to \nu_e$)

VALUE (units 10^{-3})	CL%	DOCUMENT ID		TECN	COMMENT
• • • We do not use the following data for averages, fits, limits, etc. • • •					
< 7.2	90	AGAFONOVA	13	OPER	$\Delta(m^2) > 0.1$ eV^2
0.8 to 3	90	[1] AGUILAR-AR...	13A	MBOO	MiniBooNE
< 11	90	[2] ANTONELLO	13	ICAR	$\nu_\mu \to \nu_e$
< 6.8	90	[3] ANTONELLO	13A	ICAR	$\nu_\mu \to \nu_e$
<100	90	[4] MAHN	12	MBOO	MiniBooNE/SciBooNE
< 1.8	90	[5] AGUILAR-AR...	07	MBOO	MiniBooNE
<110	90	[6] AHN	04	K2K	Water Cherenkov
< 1.4	90	ASTIER	03	NOMD	CERN SPS
< 1.6	90	AVVAKUMOV	02	NTEV	NUTEV FNAL
		[7] AGUILAR	01	LSND	$\nu_\mu \to \nu_e$ osc.prob.
0.5 to 30	95	[8] ATHANASSO...	98	LSND	$\nu_\mu \to \nu_e$
< 3.0	90	[9] LOVERRE	96		CHARM/CDHS
< 9.4	90	VILAIN	94C	CHM2	CERN SPS
< 5.6	90	[10] VILAIN	94C	CHM2	CERN SPS

[1] Based on $\nu_\mu \to \nu_e$ appearance of 162.0 ± 47.8 events; marginally compatible with two neutrino oscillations. The best fit value is $\sin^2 2\theta = 0.002$.

[2] ANTONELLO 13 use the ICARUS T600 detector at LNGS and ~ 20 GeV beam of ν_μ from CERN 730 km away to search for an excess of ν_e events. Two events are found with 3.7 ± 0.6 expected from conventional sources. This result excludes some parts of the parameter space expected by LSND. Superseded by ANTONELLO 13A.

[3] Based on four events with a background of 6.4 ± 0.9 from conventional sources with an average energy of 20 GeV and 730 km from the source of ν_μ.

[4] MAHN 12 is a combined fit of MiniBooNE and SciBooNE neutrino data.

[5] The limit is $\sin^2 2\theta < 0.9 \times 10^{-3}$ at $\Delta m^2 = 2$ eV^2. That value of Δm^2 corresponds to the smallest mixing angle consistent with the reported signal from LSND in AGUILAR 01.

[6] The limit becomes $\sin^2 2\theta < 0.15$ at $\Delta m^2 = 2.8 \times 10^{-3}$ eV^2, the bets-fit value of the ν_μ disappearance analysis in K2K.

[7] AGUILAR 01 is the final analysis of the LSND full data set of the search for the $\nu_\mu \to \nu_e$ oscillations. See footnote in preceding table for further details.

[8] ATHANASSOPOULOS 98 report $(0.26 \pm 0.10 \pm 0.05)\%$ for the oscillation probability; the value of $\sin^2 2\theta$ for large Δm^2 is deduced from this probability. See footnote in preceding table for further details, and see the paper for a plot showing allowed regions. If effect is due to oscillation, it is most likely to be intermediate $\sin^2 2\theta$ and Δm^2. See also ATHANASSOPOULOS 98B.

[9] LOVERRE 96 uses the charged-current to neutral-current ratio from the combined CHARM (ALLABY 86) and CDHS (ABRAMOWICZ 86) data from 1986.

[10] VILAIN 94C limit derived by combining the ν_μ and $\overline{\nu}_\mu$ data assuming *CP* conservation.

$\Delta(m^2)$ for $\sin^2(2\theta) = 1$ ($\overline{\nu}_\mu \to \overline{\nu}_e$)

VALUE (eV^2)	CL%	DOCUMENT ID		TECN	COMMENT
• • • We do not use the following data for averages, fits, limits, etc. • • •					
0.023 to 0.060	90	[1] AGUILAR-AR...	13A	MBOO	MiniBooNE
<0.16	90	[2] CHENG	12	MBOO	MiniBooNE/SciBooNE
0.03–0.09	90	[3] AGUILAR-AR...	10	MBOO	$E_\nu > 475$ MeV
0.03–0.07	90	[4] AGUILAR-AR...	10	MBOO	$E_\nu > 200$ MeV
<0.06	90	AGUILAR-AR...	09B	MBOO	MiniBooNE
<0.055	90	[5] ARMBRUSTER	02	KAR2	Liquid Sci. calor.
<2.6	90	AVVAKUMOV	02	NTEV	NUTEV FNAL
0.03–0.05		[6] AGUILAR	01	LSND	LAMPF
0.05–0.08	90	[7] ATHANASSO...	96	LSND	LAMPF
0.048–0.090	80	[8] ATHANASSO...	95		
<0.07	90	[9] HILL	95		
<0.9	90	VILAIN	94C	CHM2	CERN SPS
<0.14	90	[10] FREEDMAN	93	CNTR	LAMPF

[1] Based on $\overline{\nu}_\mu \to \overline{\nu}_e$ appearance of 78.4 ± 28.5 events. The best fit values are $\Delta m^2 = 0.043$ eV^2 and $\sin^2 2\theta = 0.88$.

[2] CHENG 12 is a combined fit of MiniBooNE and SciBooNE antineutrino data.

[3] This value is for a two neutrino oscillation analysis for excess antineutrino events with $E_\nu > 475$ MeV. The best fit is at 0.07. The allowed region is consistent with LSND reported by AGUILAR 01. Supercedes AGUILAR-AREVALO 09B.

[4] This value is for a two neutrino oscillation analysis for excess antineutrino events with $E_\nu > 200$ MeV with subtraction of the expected 12 events low energy excess seen in the neutrino component of the beam. The best fit value is 0.007 for $\Delta(m^2) = 4.4$ eV^2.

[5] ARMBRUSTER 02 is the final analysis of the KARMEN 2 data for 17.7 m distance from the ISIS stopped pion and muon neutrino source. It is a search for $\overline{\nu}_e$, detected by the inverse β-decay reaction on protons and ^{12}C. 15 candidate events are observed, and 15.8 ± 0.5 background events are expected, hence no oscillation signal is detected. The results exclude large regions of the parameter area favored by the LSND experiment.

[6] AGUILAR 01 is the final analysis of the LSND full data set. It is a search for $\overline{\nu}_e$ 30 m from LAMPF beam stop. Neutrinos originate mainly for π^+ decay at rest. $\overline{\nu}_e$ are detected through $\overline{\nu}_e p \to e^+ n$ ($20 < E_{e^+} < 60$ MeV) in delayed coincidence with $np \to d\gamma$. Authors observe $87.9 \pm 22.4 \pm 6.0$ total excess events. The observation is attributed to $\overline{\nu}_\mu \to \overline{\nu}_e$ oscillations with the oscillation probability of $0.264 \pm 0.067 \pm 0.045\%$, consistent with the previously published result. Taking into account all constraints, the most favored allowed region of oscillation parameters is a band of $\Delta(m^2)$ from 0.2–2.0 eV^2. Supersedes ATHANASSOPOULOS 95, ATHANASSOPOULOS 96, and ATHANASSOPOULOS 98.

[7] ATHANASSOPOULOS 96 is a search for $\overline{\nu}_e$ 30 m from LAMPF beam stop. Neutrinos originate mainly from π^+ decay at rest. $\overline{\nu}_e$ could come from either $\overline{\nu}_\mu \to \overline{\nu}_e$ or $\nu_e \to \overline{\nu}_e$; our entry assumes the first interpretation. They are detected through $\overline{\nu}_e p \to e^+ n$ (20 MeV $< E_{e^+} <$60 MeV) in delayed coincidence with $np \to d\gamma$. Authors observe $51 \pm 20 \pm 8$ total excess events over an estimated background 12.5 ± 2.9. ATHANASSOPOULOS 96B is a shorter version of this paper.

[8] ATHANASSOPOULOS 95 error corresponds to the 1.6σ band in the plot. The expected background is 2.7 ± 0.4 events. Corresponds to an oscillation probability of $(0.34^{+0.20}_{-0.18} \pm 0.07)\%$. For a different interpretation, see HILL 95. Replaced by ATHANASSOPOULOS 96.

[9] HILL 95 is a report by one member of the LSND Collaboration, reporting a different conclusion from the analysis of the data of this experiment (see ATHANASSOPOULOS 95). Contrary to the rest of the LSND Collaboration, Hill finds no evidence for the neutrino oscillation $\overline{\nu}_\mu \to \overline{\nu}_e$ and obtains only upper limits.

[10] FREEDMAN 93 is a search at LAMPF for $\overline{\nu}_e$ generated from any of the three neutrino types ν_μ, $\overline{\nu}_\mu$, and ν_e which come from the beam stop. The $\overline{\nu}_e$'s would be detected by the reaction $\overline{\nu}_e p \to e^+ n$. FREEDMAN 93 replaces DURKIN 88.

$\sin^2(2\theta)$ for "Large" $\Delta(m^2)$ $(\overline{\nu}_\mu \to \overline{\nu}_e)$

VALUE (units 10^{-3})	CL%	DOCUMENT ID		TECN	COMMENT
• • • We do not use the following data for averages, fits, limits, etc. • • •					
<640	90	[1] ANTONELLO	13A	ICAR	$\overline{\nu}_e$ appearance
<150	90	[2] CHENG	12	MBOO	MiniBooNE/SciBooNE
0.4–9.0	99	[3] AGUILAR-AR...	10	MBOO	$E_\nu > 475$ MeV
0.4–9.0	99	[4] AGUILAR-AR...	10	MBOO	$E_\nu > 200$ MeV
< 3.3	90	[5] AGUILAR-AR...	09B	MBOO	MiniBooNE
< 1.7	90	[6] ARMBRUSTER	02	KAR2	Liquid Sci. calor.
< 1.1	90	AVVAKUMOV	02	NTEV	NUTEV FNAL
5.3±1.3±9.0		[7] AGUILAR	01	LSND	LAMPF
6.2±2.4±1.0		[8] ATHANASSO...	96	LSND	LAMPF
3–12	80	[9] ATHANASSO...	95		
< 6	90	[10] HILL	95		

[1] ANTONELLO 13A obtained the limit by assuming $\overline{\nu}_\mu \to \overline{\nu}_e$ oscillation from the $\sim 2\%$ of $\overline{\nu}_\mu$ evnets contamination in the CNGS beam.

[2] CHENG 12 is a combined fit of MiniBooNE and SciBooNE antineutrino data.

[3] This value is for a two neutrino oscillation analysis for excess antineutrino events with $E_\nu > 475$ MeV. At 90% CL there is no solution at high $\Delta(m^2)$. The best fit is at maximal mixing. The allowed region is consistent with LSND reported by AGUILAR 01. Supercedes AGUILAR-AREVALO 09B.

[4] This value is for a two neutrino oscillation analysis for excess antineutrino events with $E_\nu > 200$ MeV with subtraction of the expected 12 events low energy excess seen in the neutrino component of the beam. At 90% CL there is no solution at high $\Delta(m^2)$. The best fit value is 0.007 for $\Delta(m^2) = 4.4$ eV^2.

[5] This result is inconclusive with respect to small amplitude mixing suggested by LSND.

[6] ARMBRUSTER 02 is the final analysis of the KARMEN2 data. See footnote in the preceding table for further details, and the paper for the exclusion plot.

[7] AGUILAR 01 is the final analysis of the LSND full data set. The deduced oscillation probability is $0.264 \pm 0.067 \pm 0.045\%$; the value of $\sin^2 2\theta$ for large $\Delta(m^2)$ is twice this probability (although these values are excluded by other constraints). See footnote in preceding table for further details, and the paper for a plot showing allowed regions. Supersedes ATHANASSOPOULOS 95, ATHANASSOPOULOS 96, and ATHANASSOPOULOS 98.

[8] ATHANASSOPOULOS 96 reports $(0.31 \pm 0.12 \pm 0.05)\%$ for the oscillation probability; the value of $\sin^2 2\theta$ for large $\Delta(m^2)$ should be twice this probability. See footnote in preceding table for further details, and see the paper for a plot showing allowed regions.

[9] ATHANASSOPOULOS 95 error corresponds to the 1.6σ band in the plot. The expected background is 2.7 ± 0.4 events. Corresponds to an oscillation probability of $(0.34^{+0.20}_{-0.18} \pm 0.07)\%$. For a different interpretation, see HILL 95. Replaced by ATHANASSOPOULOS 96.

[10] HILL 95 is a report by one member of the LSND Collaboration, reporting a different conclusion from the analysis of the data of this experiment (see ATHANASSOPOULOS 95). Contrary to the rest of the LSND Collaboration, Hill finds no evidence for the neutrino oscillation $\overline{\nu}_\mu \to \overline{\nu}_e$ and obtains only upper limits.

$\Delta(m^2)$ for $\sin^2(2\theta) = 1$ $(\nu_\mu(\overline{\nu}_\mu) \to \nu_e(\overline{\nu}_e))$

VALUE (eV^2)	CL%	DOCUMENT ID		TECN	COMMENT
<0.075	90	BORODOV...	92	CNTR	BNL E776
• • • We do not use the following data for averages, fits, limits, etc. • • •					
<1.6	90	[1] ROMOSAN	97	CCFR	FNAL

[1] ROMOSAN 97 uses wideband beam with a 0.5 km decay region.

$\sin^2(2\theta)$ for "Large" $\Delta(m^2)$ $(\nu_\mu(\overline{\nu}_\mu) \to \nu_e(\overline{\nu}_e))$

VALUE (units 10^{-3})	CL%	DOCUMENT ID		TECN	COMMENT
<1.8	90	[1] ROMOSAN	97	CCFR	FNAL
• • • We do not use the following data for averages, fits, limits, etc. • • •					
<3.8	90	[2] MCFARLAND	95	CCFR	FNAL
<3	90	BORODOV...	92	CNTR	BNL E776

[1] ROMOSAN 97 uses wideband beam with a 0.5 km decay region.

[2] MCFARLAND 95 state that "This result is the most stringent to date for $250 < \Delta(m^2) < 450$ eV^2 and also excludes at 90%CL much of the high $\Delta(m^2)$ region favored by the recent LSND observation." See ATHANASSOPOULOS 95 and ATHANASSOPOULOS 96.

$\Delta(m^2)$ for $\sin^2(2\theta) = 1$ $(\overline{\nu}_e \not\to \overline{\nu}_e)$

VALUE (eV^2)	CL%	DOCUMENT ID	TECN	COMMENT
• • • We do not use the following data for averages, fits, limits, etc. • • •				
<0.01	90	[1] ACHKAR	95	CNTR Bugey reactor

[1] ACHKAR 95 bound is for L=15, 40, and 95 m.

$\sin^2(2\theta)$ for "Large" $\Delta(m^2)$ $(\overline{\nu}_e \not\to \overline{\nu}_e)$

VALUE	CL%	DOCUMENT ID	TECN	COMMENT
• • • We do not use the following data for averages, fits, limits, etc. • • •				
<0.02	90	[1] ACHKAR	95	CNTR For $\Delta(m^2) = 0.6$ eV^2

[1] ACHKAR 95 bound is from data for L=15, 40, and 95 m distance from the Bugey reactor.

Sterile neutrino limits from atmospheric neutrino studies

$\Delta(m^2)$ for $\sin^2(2\theta) = 1$ $(\nu_\mu \to \nu_s)$

ν_s means ν_τ or any sterile (noninteracting) ν.

VALUE (10^{-5} eV^2)	CL%	DOCUMENT ID		TECN	COMMENT
• • • We do not use the following data for averages, fits, limits, etc. • • •					
<3000 (or <550)	90	[1] OYAMA	89	KAMI	Water Cherenkov
< 4.2 or > 54.	90	BIONTA	88	IMB	Flux has ν_μ, $\overline{\nu}_\mu$, ν_e, and $\overline{\nu}_e$

[1] OYAMA 89 gives a range of limits, depending on assumptions in their analysis. They argue that the region $\Delta(m^2) = (100\text{–}1000) \times 10^{-5}$ eV^2 is not ruled out by any data for large mixing.

Search for $\nu_\mu \to \nu_s$

VALUE	DOCUMENT ID		TECN	COMMENT
• • • We do not use the following data for averages, fits, limits, etc. • • •				
	[1] AMBROSIO	01	MCRO	matter effects
	[2] FUKUDA	00	SKAM	neutral currents + matter effects

[1] AMBROSIO 01 tested the pure 2-flavor $\nu_\mu \to \nu_s$ hypothesis using matter effects which change the shape of the zenith-angle distribution of upward through-going muons. With maximum mixing and $\Delta(m^2)$ around 0.0024 eV^2, the $\nu_\mu \to \nu_s$ oscillation is disfavored with 99% confidence level with respect to the $\nu_\mu \to \nu_\tau$ hypothesis.

[2] FUKUDA 00 tested the pure 2-flavor $\nu_\mu \to \nu_s$ hypothesis using three complementary atmospheric-neutrino data samples. With this hypothesis, zenith-angle distributions are expected to show characteristic behavior due to neutral currents and matter effects. In the $\Delta(m^2)$ and $\sin^2 2\theta$ region preferred by the Super-Kamiokande data, the $\nu_\mu \to \nu_s$ hypothesis is rejected at the 99% confidence level, while the $\nu_\mu \to \nu_\tau$ hypothesis consistently fits all of the data sample.

CP violating phase

δ, *CP* violating phase

Measurements of δ come from atmospheric and accelarator experiments looking at ν_e appearance. We encode values between 0 and 2π, though it is equivalent to use $-\pi$ to π.

VALUE (rad)	CL%	DOCUMENT ID		TECN	COMMENT
• • • We do not use the following data for averages, fits, limits, etc. • • •					
$(0.05 \text{ to } 1.2)\pi$	90	[1] ADAMSON	14	MINS	normal mass hierarchy, $\theta_{23} > \pi/4$
$(0 \text{ to } 1.5)\pi$, $(1.9 \text{ to } 2)\pi$	90	[2] ADAMSON	13A	MINS	normal mass hierarchy, $\theta_{23} > \pi/4$

[1] Based on three-flavor formalism. Likelihood as a function of δ is also shown for the other three combinations of hierarchy and θ_{23} quadrant; all values of δ are allowed at 90% C.L.

[2] Based on ν_e appearance in MINOS and the calculated $\sin^2(2\theta_{23}) = 0.957$, $\theta_{23} > \pi/4$, and normal mass hierarchy. Likelihood as a function of δ is also shown for the other three combinations of hierarchy and θ_{23} quadrant; all values of δ are allowed at 90% C.L.

CPT tests

$\langle \Delta m^2_{21} - \Delta\overline{m}^2_{21} \rangle$

VALUE (10^{-4} eV^2)	CL%	DOCUMENT ID		TECN	COMMENT
• • • We do not use the following data for averages, fits, limits, etc. • • •					
<1.1	99.7	[1] DEGOUVEA	05	FIT	solar vs. reactor

[1] DEGOUVEA 05 obtained this bound at the 3σ CL from the KamLAND (ARAKI 05) and solar neutrino data.

$\langle \Delta m^2_{32} - \Delta\overline{m}^2_{32} \rangle$

VALUE (10^{-3} eV^2)	CL%	DOCUMENT ID		TECN	COMMENT
• • • We do not use the following data for averages, fits, limits, etc. • • •					
$0.6^{+2.4}_{-0.8}$	90	[1] ADAMSON	12B	MINS	MINOS atmospheric

[1] The quoted result is the single-parameter 90% C.L. interval determined from the 90% C.L. contour in the $(\Delta m^2, \Delta\overline{m}^2)$ plane, which is obtained by minimizing the four parameter log-likelihood function with respect to the other oscillation parameters.

REFERENCES FOR Neutrino Mixing

ABE	14	PRL 112 181801	K. Abe *et al.*	(T2K Collab.)
ADAMSON	14	PRL 112 191801	P. Adamson *et al.*	(MINOS Collab.)
AN	14	PRL 112 061801	F.P. An *et al.*	(Daya Bay Collab.)
PDG	14	CP C38 070001	K. Olive *et al.*	(PDG Collab.)
AARTSEN	13B	PRL 111 081801	M.G. Aartsen *et al.*	(IceCube Collab.)
ABE	13C	PL B723 66	Y. Abe *et al.*	(Double Chooz Collab.)
ABE	13E	PR D88 032002	K. Abe *et al.*	(T2K Collab.)
ABE	13G	PRL 111 211803	K. Abe *et al.*	(T2K Collab.)
ADAMSON	13A	PRL 110 171801	P. Adamson *et al.*	(MINOS Collab.)
ADAMSON	13B	PRL 110 251801	P. Adamson *et al.*	(MINOS Collab.)
AGAFONOVA	13	JHEP 1307 004	N. Agafonova *et al.*	(OPERA Collab.)
AGUILAR-AR...	13A	PRL 110 161801	A.A. Aguilar-Arevalo *et al.*	(MiniBooNE Collab.)
AHARMIM	13	PR C88 025501	B. Aharmim *et al.*	(SNO Collab.)

AN	13	CP C37 011001	F.P. An *et al.*	(Daya Bay Collab.)
Also		CP C37 011001 (errat.)	F.P. An *et al.*	(Daya Bay Collab.)
ANTONELLO	13	EPJ C73 2345	M. Antonello *et al.*	(ICARUS Collab.)
ANTONELLO	13A	EPJ C73 2599	M. Antonello *et al.*	(ICARUS Collab.)
GANDO	13	PR D88 033001	A. Gando *et al.*	(KamLAND Collab.)
ABE	12	PRL 108 131801	Y. Abe *et al.*	(Double Chooz Collab.)
ABE	12A	PR D85 031103	K. Abe *et al.*	(T2K Collab.)
ABE	12B	PR D86 052008	Y. Abe *et al.*	(Double Chooz Collab.)
ADAMSON	12	PRL 108 191801	P. Adamson *et al.*	(MINOS Collab.)
ADAMSON	12B	PR D86 052007	P. Adamson *et al.*	(MINOS Collab.)
ADRIAN-MAR...	12	PL B714 224	S. Adrian-Martinez *et al.*	(ANTARES Collab.)
AHN	12	PRL 108 191802	J.K. Ahn *et al.*	(RENO Collab.)
AN	12	PRL 108 171803	F.P. An *et al.*	(Daya Bay Collab.)
Also		CP C37 011001 (errat.)	F.P. An *et al.*	(Daya Bay Collab.)
BELLINI	12A	PRL 108 051302	G. Bellini *et al.*	(Borexino Collab.)
CHENG	12	PR D86 052009	G. Cheng *et al.*	(MiniBooNE/SciBooNE Collab.)
MAHN	12	PR D85 032007	K.B.M. Mahn *et al.*	(MiniBooNE/SciBooNE Collab.)
ABE	11	PR D83 052010	K. Abe *et al.*	(Super-Kamiokande Collab.)
ABE	11A	PRL 107 041801	K. Abe *et al.*	(T2K Collab.)
ABE	11B	PR C84 035804	S. Abe *et al.*	(KamLAND Collab.)
ABE	11C	PRL 107 241801	K. Abe *et al.*	(Super-Kamiokande Collab.)
ADAMSON	11	PRL 106 181801	P. Adamson *et al.*	(MINOS Collab.)
ADAMSON	11B	PRL 107 021801	P. Adamson *et al.*	(MINOS Collab.)
ADAMSON	11C	PR D84 071103	P. Adamson *et al.*	(MINOS Collab.)
ADAMSON	11D	PRL 107 181802	P. Adamson *et al.*	(MINOS Collab.)
BELLINI	11	PL B696 191	G. Bellini *et al.*	(Borexino Collab.)
BELLINI	11A	PRL 107 141302	G. Bellini *et al.*	(Borexino Collab.)
FOGLI	11	PR D84 053007	G.L. Fogli *et al.*	
GANDO	11	PR D83 052002	A. Gando *et al.*	(KamLAND Collab.)
MUELLER	11	PR C83 054615	Th.A Mueller *et al.*	
SERENELLI	11	APJ 743 24	A.M. Serenelli, W.C. Haxton, C. Pena-Garay	
ADAMSON	10A	PR D82 051102	P. Adamson *et al.*	(MINOS Collab.)
AGUILAR-AR...	10	PRL 105 181801	A.A. Aguilar-Arevalo *et al.*	(MiniBooNE Collab.)
AHARMIM	10	PR C81 055504	B. Aharmim *et al.*	(SNO Collab.)
BELLINI	10A	PR D82 033006	G. Bellini *et al.*	(Borexino Collab.)
DENIZ	10	PR D81 072001	M. Deniz *et al.*	(TEXONO Collab.)
KAETHER	10	PL B685 47	F. Kaether *et al.*	
WENDELL	10	PR D81 092004	R. Wendell *et al.*	(Super-Kamiokande Collab.)
ABDURASHI...	09	PR C80 015807	J.N. Abdurashitov *et al.*	(SAGE Collab.)
ADAMSON	09	PRL 103 261802	P. Adamson *et al.*	(MINOS Collab.)
AGUILAR-AR...	09B	PRL 103 111801	A.A. Aguilar-arevalo *et al.*	(MiniBooNE Collab.)
ABE	08A	PRL 100 221803	S. Abe *et al.*	(KamLAND Collab.)
Also		PRL 101 119904(E	S. Abe *et al.*	(KamLAND Collab.)
ADAMSON	08	PR D77 072002	P. Adamson *et al.*	(MINOS Collab.)
ADAMSON	08A	PRL 101 131802	P. Adamson *et al.*	(MINOS Collab.)
AHARMIM	08	PRL 101 111301	B. Aharmim *et al.*	(SNO Collab.)
Also		PR C87 015502	B. Aharmim *et al.*	(SNO Collab.)
ARPESELLA	08A	PRL 101 091302	C. Arpesella *et al.*	(Borexino Collab.)
CRAVENS	08	PR D78 032002	J.P. Cravens *et al.*	(Super-Kamiokande Collab.)
FOGLI	08	PRL 101 141801	G.L. Fogli, et al	
ADAMSON	07	PR D75 092003	P. Adamson *et al.*	(MINOS Collab.)
AGUILAR-AR...	07	PRL 98 231801	A.A. Aguilar-Arevalo *et al.*	(MiniBooNE Collab.)
AHARMIM	07	PR C75 045502	B. Aharmim *et al.*	(SNO Collab.)
ADAMSON	06	PR D73 072002	P. Adamson *et al.*	(MINOS Collab.)
AHN	06A	PR D74 072003	M.H. Ahn *et al.*	(K2K Collab.)
BALATA	06	EPJ C47 21	M. Balata *et al.*	(Borexino Collab.)
HOSAKA	06	PR D73 112001	J. Hosaka *et al.*	(Super-Kamiokande Collab.)
HOSAKA	06A	PR D74 032002	J. Hosaka *et al.*	(Super-Kamiokande Collab.)
MICHAEL	06	PRL 97 191801	D. Michael *et al.*	(MINOS Collab.)
WINTER	06A	PR C73 025503	W.T. Winter *et al.*	
YAMAMOTO	06	PRL 96 181801	S. Yamamoto *et al.*	(K2K Collab.)
AHARMIM	05A	PR C72 055502	B. Aharmim *et al.*	(SNO Collab.)
ALIU	05	PRL 94 081802	E. Aliu *et al.*	(K2K Collab.)
ALLISON	05	PR D72 052005	W.W.M. Allison *et al.*	(SOUDAN-2 Collab.)
ALTMANN	05	PL B616 174	M. Altmann *et al.*	(GNO Collab.)
ARAKI	05	PRL 94 081801	T. Araki *et al.*	(KamLAND Collab.)
ASHIE	05	PR D71 112005	Y. Ashie *et al.*	(Super-Kamiokande Collab.)
DEGOUVEA	05	PR D71 093002	A. de Gouvea, C. Pena-Garay	
AHARMIM	04	PR D70 093014	B. Aharmim *et al.*	(SNO Collab.)
AHMED	04A	PRL 92 181301	S.N. Ahmed *et al.*	(SNO Collab.)
AHN	04	PRL 93 051801	M.H. Ahn *et al.*	(K2K Collab.)
AMBROSIO	04	EPJ C36 323	M. Ambrosio *et al.*	(MACRO Collab.)
ASHIE	04	PRL 93 101801	Y. Ashie *et al.*	(Super-Kamiokande Collab.)
EGUCHI	04	PRL 92 071301	K. Eguchi *et al.*	(KamLAND Collab.)
SMY	04	PR D69 011104	M.B. Smy *et al.*	(Super-Kamiokande Collab.)
AHN	03	PRL 90 041801	M.H. Ahn *et al.*	(K2K Collab.)
AMBROSIO	03	PL B566 35	M. Ambrosio *et al.*	(MACRO Collab.)
APOLLONIO	03	EPJ C27 331	M. Apollonio *et al.*	(CHOOZ Collab.)
ASTIER	03	PL B570 19	P. Astier *et al.*	(NOMAD Collab.)
EGUCHI	03	PRL 90 021802	K. Eguchi *et al.*	(KamLAND Collab.)
GANDO	03	PRL 90 171302	Y. Gando *et al.*	(Super-Kamiokande Collab.)
IANNI	03	JP G29 2107	A. Ianni	(INFN Gran Sasso)
SANCHEZ	03	PR D68 113004	M. Sanchez *et al.*	(Soudan 2 Collab.)
ABDURASHI...	02	JETP 95 181	J.N. Abdurashitov *et al.*	(SAGE Collab.)
		Translated from ZETF 122 211.		
AHMAD	02	PRL 89 011301	Q.R. Ahmad *et al.*	(SNO Collab.)
AHMAD	02B	PRL 89 011302	Q.R. Ahmad *et al.*	(SNO Collab.)
ARMBRUSTER	02	PR D65 112001	B. Armbruster *et al.*	(KARMEN 2 Collab.)
AVVAKUMOV	02	PRL 89 011804	S. Avvakumov *et al.*	(NuTeV Collab.)
FUKUDA	02	PL B539 179	S. Fukuda *et al.*	(Super-Kamiokande Collab.)
AGUILAR	01	PR D64 112007	A. Aguilar *et al.*	(LSND Collab.)
AHMAD	01	PRL 87 071301	Q.R. Ahmad *et al.*	(SNO Collab.)
AMBROSIO	01	PL B517 59	M. Ambrosio *et al.*	(MACRO Collab.)
BOEHM	01	PR D64 112001	F. Boehm *et al.*	
FUKUDA	01	PRL 86 5651	S. Fukuda *et al.*	(Super-Kamiokande Collab.)
AMBROSIO	00	PL B478 5	M. Ambrosio *et al.*	(MACRO Collab.)
BOEHM	00	PR D62 072002	F. Boehm *et al.*	
FUKUDA	00	PRL 85 3999	S. Fukuda *et al.*	(Super-Kamiokande Collab.)
ALLISON	99	PL B449 137	W.W.M. Allison *et al.*	(Soudan 2 Collab.)
APOLLONIO	99	PL B466 415	M. Apollonio *et al.*	(CHOOZ Collab.)
Also		PL B472 434 (errat)	M. Apollonio *et al.*	(CHOOZ Collab.)
FUKUDA	99C	PRL 82 2644	Y. Fukuda *et al.*	(Super-Kamiokande Collab.)
FUKUDA	99D	PL B467 185	Y. Fukuda *et al.*	(Super-Kamiokande Collab.)
HAMPEL	99	PL B447 127	W. Hampel *et al.*	(GALLEX Collab.)
AMBROSIO	98	PL B434 451	M. Ambrosio *et al.*	(MACRO Collab.)
APOLLONIO	98	PL B420 397	M. Apollonio *et al.*	(CHOOZ Collab.)
ATHANASSO...	98	PRL 81 1774	C. Athanassopoulos *et al.*	(LSND Collab.)
ATHANASSO...	98B	PR C58 2489	C. Athanassopoulos *et al.*	(LSND Collab.)
CLEVELAND	98	APJ 496 505	B.T. Cleveland *et al.*	(Homestake Collab.)
FELDMAN	98	PR D57 3873	G.J. Feldman, R.D. Cousins	
FUKUDA	98C	PRL 81 1562	Y. Fukuda *et al.*	(Super-Kamiokande Collab.)
HATAKEYAMA	98	PRL 81 2016	S. Hatakeyama *et al.*	(Kamiokande Collab.)
CLARK	97	PRL 79 345	R. Clark *et al.*	(IMB Collab.)
ROMOSAN	97	PRL 78 2912	A. Romosan *et al.*	(CCFR Collab.)
AGLIETTA	96	JETPL 63 791	M. Aglietta *et al.*	(LSD Collab.)
		Translated from ZETFP 63 753.		
ATHANASSO...	96	PR C54 2685	C. Athanassopoulos *et al.*	(LSND Collab.)
ATHANASSO...	96B	PRL 77 3082	C. Athanassopoulos *et al.*	(LSND Collab.)
FUKUDA	96	PRL 77 1683	Y. Fukuda *et al.*	(Kamiokande Collab.)
FUKUDA	96B	PL B388 397	Y. Fukuda *et al.*	(Kamiokande Collab.)
GREENWOOD	96	PR D53 6054	Z.D. Greenwood *et al.*	(UCI, SVR, SCUC)
HAMPEL	96	PL B388 384	W. Hampel *et al.*	(GALLEX Collab.)
LOVERRE	96	PL B370 156	P.F. Loverre	
ACHKAR	95	NP B434 503	B. Achkar *et al.*	(SING, SACLD, CPPM, CDEF+)
AHLEN	95	PL B357 481	S.P. Ahlen *et al.*	(MACRO Collab.)
ATHANASSO...	95	PRL 75 2650	C. Athanassopoulos *et al.*	(LSND Collab.)
DAUM	95	ZPHY C66 417	K. Daum *et al.*	(FREJUS Collab.)
HILL	95	PRL 75 2654	J.E. Hill	(PENN)
MCFARLAND	95	PRL 75 3993	K.S. McFarland *et al.*	(CCFR Collab.)
DECLAIS	94	PL B338 383	Y. Declais *et al.*	
FUKUDA	94	PL B335 237	Y. Fukuda *et al.*	(Kamiokande Collab.)
VILAIN	94C	ZPHY C64 539	P. Vilain *et al.*	(CHARM II Collab.)
FREEDMAN	93	PR D47 811	S.J. Freedman *et al.*	(LAMPF E645 Collab.)
BECKER-SZ...	92B	PR D46 3720	R.A. Becker-Szendy *et al.*	(IMB Collab.)
BEIER	92	PL B283 446	E.W. Beier *et al.*	(KAM2 Collab.)
Also		PTRSL A346 63	E.W. Beier, E.D. Frank	(PENN)
BORODOV...	92	PRL 68 274	L. Borodovsky *et al.*	(COLU, JHU, ILL)
HIRATA	92	PL B280 146	K.S. Hirata *et al.*	(Kamiokande II Collab.)
CASPER	91	PRL 66 2561	D. Casper *et al.*	(IMB Collab.)
HIRATA	91	PRL 66 9	K.S. Hirata *et al.*	(Kamiokande II Collab.)
KUVSHINN...	91	JETPL 54 253	A.A. Kuvshinnikov *et al.*	(KIAE)
BERGER	90B	PL B245 305	C. Berger *et al.*	(FREJUS Collab.)
HIRATA	90	PRL 65 1297	K.S. Hirata *et al.*	(Kamiokande II Collab.)
AGLIETTA	89	EPL 8 611	M. Aglietta *et al.*	(FREJUS Collab.)
DAVIS	89	ARNPS 39 467	R. Davis, A.K. Mann, L. Wolfenstein	(BNL, PENN+)
OYAMA	89	PR D39 1481	Y. Oyama *et al.*	(Kamiokande II Collab.)
BIONTA	88	PR D38 768	R.M. Bionta *et al.*	(IMB Collab.)
DURKIN	88	PRL 61 1811	L.S. Durkin *et al.*	(OSU, ANL, CIT+)
ABRAMOWICZ	86	PRL 57 298	H. Abramowicz *et al.*	(CDHS Collab.)
ALLABY	86	PL B177 446	J.V. Allaby *et al.*	(CHARM Collab.)
ANGELINI	86	PL B179 307	C. Angelini *et al.*	(PISA, ATHU, PADO+)
VUILLEUMIER	82	PL 114B 298	J.L. Vuilleumier *et al.*	(CIT, SIN, MUNI)
BOLIEV	81	SJNP 34 787	M.M. Boliev *et al.*	(INRM)
		Translated from YAF 34 1418.		
KWON	81	PR D24 1097	H. Kwon *et al.*	(CIT, ISNG, MUNI)
BOEHM	80	PL 97B 310	F. Boehm *et al.*	(ILLG, CIT, ISNG, MUNI)
CROUCH	78	PR D18 2239	M.F. Crouch *et al.*	(CASE, UCI, WITW)

Heavy Neutral Leptons, Searches for

(A) Heavy Neutral Leptons

Stable Neutral Heavy Lepton MASS LIMITS

Note that LEP results in combination with REUSSER 91 exclude a fourth stable neutrino with $m < 2400$ GeV.

VALUE (GeV)	*CL%*	*DOCUMENT ID*		*TECN*	*COMMENT*
>45.0	95	ABREU	92B	DLPH	Dirac
>39.5	95	ABREU	92B	DLPH	Majorana
>44.1	95	ALEXANDER	91F	OPAL	Dirac
>37.2	95	ALEXANDER	91F	OPAL	Majorana
none 3–100	90	SATO	91	KAM2	Kamiokande II
>42.8	95	[1] ADEVA	90S	L3	Dirac
>34.8	95	[1] ADEVA	90S	L3	Majorana
>42.7	95	DECAMP	90F	ALEP	Dirac

[1] ADEVA 90S limits for the heavy neutrino apply if the mixing with the charged leptons satisfies $|U_{1j}|^2 + |U_{2j}|^2 + |U_{3j}|^2 > 6.2\times10^{-8}$ at $m_{L^0} = 20$ GeV and $> 5.1\times10^{-10}$ for $m_{L^0} = 40$ GeV.

Heavy Neutral Lepton MASS LIMITS

Limits apply only to heavy lepton type given in comment at right of data Listings.

See the "Quark and Lepton Compositeness, Searches for" Listings for limits on radiatively decaying excited neutral leptons, *i.e.* $\nu^* \to \nu\gamma$.

VALUE (GeV)	*CL%*	*DOCUMENT ID*		*TECN*	*COMMENT*
>101.3	95	ACHARD	01B	L3	Dirac coupling to e
>101.5	95	ACHARD	01B	L3	Dirac coupling to μ
> 90.3	95	ACHARD	01B	L3	Dirac coupling to τ
> 89.5	95	ACHARD	01B	L3	Majorana coupling to e
> 90.7	95	ACHARD	01B	L3	Majorana coupling to μ
> 80.5	95	ACHARD	01B	L3	Majorana coupling to τ
• • • We do not use the following data for averages, fits, limits, etc. • • •					
> 76.0	95	ABBIENDI	00I	OPAL	Majorana, coupling to e
> 88.0	95	ABBIENDI	00I	OPAL	Dirac, coupling to e
> 76.0	95	ABBIENDI	00I	OPAL	Majorana, coupling to μ
> 88.1	95	ABBIENDI	00I	OPAL	Dirac, coupling to μ
> 53.8	95	ABBIENDI	00I	OPAL	Majorana, coupling to τ
> 71.1	95	ABBIENDI	00I	OPAL	Dirac, coupling to τ
> 76.5	95	ABREU	99O	DLPH	Dirac coupling to e
> 79.5	95	ABREU	99O	DLPH	Dirac coupling to μ
> 60.5	95	ABREU	99O	DLPH	Dirac coupling to τ
> 63	95	[2,3] BUSKULIC	96S	ALEP	Dirac
> 54.3	95	[2,4] BUSKULIC	96S	ALEP	Majorana

[2] BUSKULIC 96S requires the decay length of the heavy lepton to be < 1 cm, limiting the square of the mixing angle $|U_{\ell j}|^2$ to 10^{-10}.

[3] BUSKULIC 96S limit for mixing with τ. Mass is > 63.6 GeV for mixing with e or μ.

[4] BUSKULIC 96S limit for mixing with τ. Mass is > 55.2 GeV for mixing with e or μ.

Astrophysical Limits on Neutrino MASS for $m_\nu > 1$ GeV

VALUE (GeV)	CL%	DOCUMENT ID		TECN	COMMENT
• • • We do not use the following data for averages, fits, limits, etc. • • •					
none 60–115		[5] FARGION	95	ASTR	Dirac
none 9.2–2000		[6] GARCIA	95	COSM	Nucleosynthesis
none 26–4700		[6] BECK	94	COSM	Dirac
none 6 – hundreds		[7,8] MORI	92B	KAM2	Dirac neutrino
none 24 – hundreds		[7,8] MORI	92B	KAM2	Majorana neutrino
none 10–2400	90	[9] REUSSER	91	CNTR	HPGe search
none 3–100	90	SATO	91	KAM2	Kamiokande II
		[10] ENQVIST	89	COSM	
none 12–1400		[6] CALDWELL	88	COSM	Dirac ν
none 4–16	90	[6,7] OLIVE	88	COSM	Dirac ν
none 4–35	90	OLIVE	88	COSM	Majorana ν
>4.2 to 4.7		SREDNICKI	88	COSM	Dirac ν
>5.3 to 7.4		SREDNICKI	88	COSM	Majorana ν
none 20–1000	95	[6] AHLEN	87	COSM	Dirac ν
>4.1		GRIEST	87	COSM	Dirac ν

[5] FARGION 95 bound is sensitive to assumed ν concentration in the Galaxy. See also KONOPLICH 94.

[6] These results assume that neutrinos make up dark matter in the galactic halo.

[7] Limits based on annihilations in the sun and are due to an absence of high energy neutrinos detected in underground experiments.

[8] MORI 92B results assume that neutrinos make up dark matter in the galactic halo. Limits based on annihilations in earth are also given.

[9] REUSSER 91 uses existing $\beta\beta$ detector (see FISHER 89) to search for CDM Dirac neutrinos.

[10] ENQVIST 89 argue that there is no cosmological upper bound on heavy neutrinos.

(B) Other Bounds from Nuclear and Particle Decays

Limits on $|U_{ex}|^2$ as Function of m_{ν_x}

Peak and kink search tests

Limits on $|U_{ex}|^2$ as function of m_{ν_j}

VALUE	CL%	DOCUMENT ID		TECN	COMMENT
<1 $\times 10^{-7}$	90	[11] BRITTON	92B	CNTR	50 MeV < m_{ν_x} < 130 MeV
• • • We do not use the following data for averages, fits, limits, etc. • • •					
$<5 \times 10^{-6}$	90	DELEENER-...	91		m_{ν_x}=20 MeV
$<5 \times 10^{-7}$	90	DELEENER-...	91		m_{ν_x}=40 MeV
$<3 \times 10^{-7}$	90	DELEENER-...	91		m_{ν_x}=60 MeV
$<1 \times 10^{-6}$	90	DELEENER-...	91		m_{ν_x}=80 MeV
$<1 \times 10^{-6}$	90	DELEENER-...	91		m_{ν_x}=100 MeV
$<5 \times 10^{-7}$	90	AZUELOS	86	CNTR	m_{ν_x}=60 MeV
$<2 \times 10^{-7}$	90	AZUELOS	86	CNTR	m_{ν_x}=80 MeV
$<3 \times 10^{-7}$	90	AZUELOS	86	CNTR	m_{ν_x}=100 MeV
$<1 \times 10^{-6}$	90	AZUELOS	86	CNTR	m_{ν_x}=120 MeV
$<2 \times 10^{-7}$	90	AZUELOS	86	CNTR	m_{ν_x}=130 MeV
$<1 \times 10^{-4}$	90	[12] BRYMAN	83B	CNTR	m_{ν_x}=5 MeV
$<1.5 \times 10^{-6}$	90	BRYMAN	83B	CNTR	m_{ν_x}=53 MeV
$<1 \times 10^{-5}$	90	BRYMAN	83B	CNTR	m_{ν_x}=70 MeV
$<1 \times 10^{-4}$	90	BRYMAN	83B	CNTR	m_{ν_x}=130 MeV
$<1 \times 10^{-4}$	68	[13] SHROCK	81	THEO	m_{ν_x}=10 MeV
$<5 \times 10^{-6}$	68	[13] SHROCK	81	THEO	m_{ν_x}=60 MeV
$<1 \times 10^{-5}$	68	[14] SHROCK	80	THEO	m_{ν_x}=80 MeV
$<3 \times 10^{-6}$	68	[14] SHROCK	80	THEO	m_{ν_x}=160 MeV

[11] BRITTON 92B is from a search for additional peaks in the e^+ spectrum from $\pi^+ \to e^+\nu_e$ decay at TRIUMF. See also BRITTON 92.

[12] BRYMAN 83B obtain upper limits from both direct peak search and analysis of $B(\pi \to e\nu)/B(\pi \to \mu\nu)$. Latter limits are not listed, except for this entry (i.e. — we list the most stringent limits for given mass).

[13] Analysis of $(\pi^+ \to e^+\nu_e)/(\pi^+ \to \mu^+\nu_\mu)$ and $(K^+ \to e^+\nu_e)/(K^+ \to \mu^+\nu_\mu)$ decay ratios.

[14] Analysis of $(K^+ \to e^+\nu_e)$ spectrum.

Kink search in nuclear β decay

High-sensitivity follow-up experiments show that indications for a neutrino with mass 17 keV (Simpson, Hime, and others) were not valid. Accordingly, we no longer list the experiments by these authors and some others which made positive claims of 17 keV neutrino emission. Complete listings are given in the 1994 edition (Physical Review **D50** 1173 (1994)) and in the 1998 edition (The European Physical Journal **C3** 1 (1998)). We list below only the best limits on $|U_{ex}|^2$ for each m_{ν_x}. See WIETFELDT 96 for a comprehensive review.

VALUE (units 10^{-3})	CL%	m_{ν_j} (keV)	ISOTOPE	METHOD	DOCUMENT ID	
• • • We do not use the following data for averages, fits, limits, etc. • • •						
< 4–20	90	700–3500	^{38m}K	Trap	[15] TRINCZEK	03
< 9–116	95	1–0.1	^{187}Re	cryog.	[16] GALEAZZI	01
< 1	95	10–90	^{35}S	Mag spect	[17] HOLZSCHUH	00
< 4	95	14–17	^{241}Pu	Electrostatic spec	[18] DRAGOUN	99
< 1	95	4–30	^{63}Ni	Mag spect	[19] HOLZSCHUH	99
< 10–40	90	370–640	^{37}Ar	EC ion recoil	[20] HINDI	98
< 10	95	1	^{3}H	SPEC	[21] HIDDEMANN	95
< 6	95	2	^{3}H	SPEC	[21] HIDDEMANN	95
< 2	95	3	^{3}H	SPEC	[21] HIDDEMANN	95
< 0.7	99	16.3–16.6	^{3}H	Prop chamber	[22] KALBFLEISCH	93
< 2	95	13–40	^{35}S	Si(Li)	[23] MORTARA	93
< 0.73	95	17	^{63}Ni	Mag spect	OHSHIMA	93
< 1.0	95	10–24	^{63}Ni	Mag spect	KAWAKAMI	92
< 0.9–2.5	90	1200–6800	^{20}F	beta spectrum	[24] DEUTSCH	90
< 8	90	80	^{35}S	Mag spect	[25] APALIKOV	85
< 1.5	90	60	^{35}S	Mag spect	APALIKOV	85
< 3.0	90	5–50		Mag spect	MARKEY	85
< 0.62	90	48	^{35}S	Si(Li)	OHI	85
< 0.90	90	30	^{35}S	Si(Li)	OHI	85
< 4	90	140	^{64}Cu	Mag spect	[26] SCHRECK...	83
< 8	90	440	^{64}Cu	Mag spect	[26] SCHRECK...	83
<100	90	0.1–3000		THEO	[27] SHROCK	80
< 0.1	68	80		THEO	[28] SHROCK	80

[15] TRINCZEK 03 is a search for admixture of heavy neutrino to ν_e, in contrast to $\overline{\nu}_e$ used in many other searches. Full kinematic reconstruction of the neutrino momentum by use of a magneto optical trap.

[16] GALEAZZI 01 use an cryogenic microcalorimeter to search for mass 50–1000 eV neutrino admixtures using the ^{187}Re beta spectrum with 2.4 keV endpoint. They derive limits for the admixture of heavy neutrinos, ranging from 9×10^{-3} for mass 1 keV to 0.116 for mass 100 eV. This is a significant improvement with respect to HIDDEMANN 95, especially for masses below $\sim$ 500 MeV, where the limit is about a factor of $\sim$ 2 higher.

[17] HOLZSCHUH 00 use an iron-free β spectrometer to measure the ^{35}S β decay spectrum. An analysis of the spectrum in the energy range 56–173 keV is used to derive limits for the admixture of heavy neutrinos. This extends the range of neutrino masses explored in HOLZSCHUH 99.

[18] DRAGOUN 99 analyze the β decay spectrum of ^{241}Pu in the energy range 0.2–9.2 keV to derive limits for the admixture of heavy neutrinos. It is not competitive with HOLZSCHUH 99.

[19] HOLZSCHUH 99 use an iron-free β spectrometer to measure the ^{63}Ni β decay spectrum. An analysis of the spectrum in the energy rage 33–67.8 keV is used to derive limits for the admixture of heavy neutrinos.

[20] HINDI 98 obtain a limit on heavy neutrino admixture from EC decay of ^{37}Ar by measuring the time-of-flight distribution of the recoiling ions in coincidence with x-rays or Auger electrons. The authors report upper limit for $|U_{ex}|^2$ of $\approx$ 3% for m_{ν_x}=500 keV, 1% for m_{ν_x}=550 keV, 2% for m_{ν_x}=600 keV, and 4% for m_X=650 keV. Their reported limits for $m_{\nu_x} \leq$ 450 keV are inferior to the limits of SCHRECKENBACH 83.

[21] In the beta spectrum from tritium β decay nonvanishing or mixed $m_{\overline{\nu}_1}$ state in the mass region 0.01–4 keV. For m_{ν_x} <1 keV, their upper limit on $|U_{ex}|^2$ becomes less

[22] KALBFLEISCH 93 extends the 17 keV neutrino search of BAHRAN 92, using an improved proportional chamber to which a small amount of ^{3}H is added. Systematics are significantly reduced, allowing for an improved upper limit. The authors give a 99% confidence limit on $|U_{ex}|^2$ as a function of m_{ν_x} in the range from 13.5 keV to 17.5 keV. See also the related papers BAHRAN 93, BAHRAN 93B, and BAHRAN 95 on theoretical aspects of beta spectra and fitting methods for heavy neutrinos.

[23] MORTARA 93 limit is from study using a high-resolution solid-state detector with a superconducting solenoid. The authors note that "The sensitivity to neutrino mass is verified by measurement with a mixed source of ^{35}S and ^{14}C, which artificially produces a distortion in the beta spectrum similar to that expected from the massive neutrino."

[24] DEUTSCH 90 search for emission of heavy $\overline{\nu}_e$ in super-allowed beta decay of ^{20}F by spectral analysis of the electrons.

[25] This limit was taken from the figure 3 of APALIKOV 85; the text gives a more restrictive limit of 1.7×10^{-3} at CL = 90%.

[26] SCHRECKENBACH 83 is a combined measurement of the β^+ and β^- spectrum.

[27] SHROCK 80 was a retroactive analysis of data on several superallowed β decays to search for kinks in the Kurie plot.

[28] Application of test to search for kinks in β decay Kurie plots.

Searches for Decays of Massive ν

Limits on $|U_{ex}|^2$ as function of m_{ν_x}

VALUE	CL%	DOCUMENT ID		TECN	COMMENT
• • • We do not use the following data for averages, fits, limits, etc. • • •					
$<1.6 \times 10^{-4}$	90	[29] BACK	03A	CNTR	m_{ν_x} = 4 MeV
$<4.5 \times 10^{-5}$	90	[29] BACK	03A	CNTR	m_{ν_x} = 7 MeV
$<3.8 \times 10^{-5}$	90	[29] BACK	03A	CNTR	m_{ν_x} = 10 MeV
$<1.5 \times 10^{-3}$	95	ACHARD	01	L3	m_{ν_x}=80 GeV

$<2 \times 10^{-2}$	95		ACHARD	01	L3	m_{ν_x}=175 GeV
<0.3	95		ACHARD	01	L3	m_{ν_x}=200 GeV
$<4 \times 10^{-3}$	95		ACCIARRI	99K	L3	m_{ν_x}=80 GeV
$<5 \times 10^{-2}$	95		ACCIARRI	99K	L3	m_{ν_x}= 175 GeV
$<2 \times 10^{-5}$	95	[30]	ABREU	97I	DLPH	m_{ν_x}=6 GeV
$<3 \times 10^{-5}$	95	[30]	ABREU	97I	DLPH	m_{ν_x}=50 GeV
$<1.8 \times 10^{-3}$	90	[31]	HAGNER	95	MWPC	m_{ν_h} = 1.5 MeV
$<2.5 \times 10^{-4}$	90	[31]	HAGNER	95	MWPC	m_{ν_h} = 4 MeV
$<4.2 \times 10^{-3}$	90	[31]	HAGNER	95	MWPC	m_{ν_h} = 9 MeV
$<1 \times 10^{-5}$	90	[32]	BARANOV	93		m_{ν_x}=100 MeV
$<1 \times 10^{-6}$	90	[32]	BARANOV	93		m_{ν_x}= 200 MeV
$<3 \times 10^{-7}$	90	[32]	BARANOV	93		m_{ν_x}= 300 MeV
$<2 \times 10^{-7}$	90	[32]	BARANOV	93		m_{ν_x}=400 MeV
$<6.2 \times 10^{-8}$	95		ADEVA	90S	L3	m_{ν_x}=20 GeV
$<5.1 \times 10^{-10}$	95		ADEVA	90S	L3	m_{ν_x}=40 GeV
all values ruled out	95	[33]	BURCHAT	90	MRK2	m_{ν_x} < 19.6 GeV
$<1 \times 10^{-10}$	95	[33]	BURCHAT	90	MRK2	m_{ν_x}= 22 GeV
$<1 \times 10^{-11}$	95	[33]	BURCHAT	90	MRK2	m_{ν_x}= 41 GeV
all values ruled out	95		DECAMP	90F	ALEP	m_{ν_x}= 25.0–42.7 GeV
$<1 \times 10^{-13}$	95		DECAMP	90F	ALEP	m_{ν_x}= 42.7–45.7 GeV
$<5 \times 10^{-3}$	90		AKERLOF	88	HRS	m_{ν_x}=1.8 GeV
$<2 \times 10^{-5}$	90		AKERLOF	88	HRS	m_{ν_x}=4 GeV
$<3 \times 10^{-6}$	90		AKERLOF	88	HRS	m_{ν_x}=6 GeV
$<1.2 \times 10^{-7}$	90		BERNARDI	88	CNTR	m_{ν_x}=100 MeV
$<1 \times 10^{-8}$	90		BERNARDI	88	CNTR	m_{ν_x}=200 MeV
$<2.4 \times 10^{-9}$	90		BERNARDI	88	CNTR	m_{ν_x}=300 MeV
$<2.1 \times 10^{-9}$	90		BERNARDI	88	CNTR	m_{ν_x}=400 MeV
$<2 \times 10^{-2}$	68	[34]	OBERAUER	87		m_{ν_x}=1.5 MeV
$<8 \times 10^{-4}$	68	[34]	OBERAUER	87		m_{ν_x}=4.0 MeV
$<8 \times 10^{-3}$	90		BADIER	86	CNTR	m_{ν_x}=400 MeV
$<8 \times 10^{-5}$	90		BADIER	86	CNTR	m_{ν_x}=1.7 GeV
$<8 \times 10^{-8}$	90		BERNARDI	86	CNTR	m_{ν_x}=100 MeV
$<4 \times 10^{-8}$	90		BERNARDI	86	CNTR	m_{ν_x}=200 MeV
$<6 \times 10^{-9}$	90		BERNARDI	86	CNTR	m_{ν_x}=400 MeV
$<3 \times 10^{-5}$	90		DORENBOS...	86	CNTR	m_{ν_x}=150 MeV
$<1 \times 10^{-6}$	90		DORENBOS...	86	CNTR	m_{ν_x}=500 MeV
$<1 \times 10^{-7}$	90		DORENBOS...	86	CNTR	m_{ν_x}=1.6 GeV
$<7 \times 10^{-7}$	90	[35]	COOPER-...	85	HLBC	m_{ν_x}=0.4 GeV
$<8 \times 10^{-8}$	90	[35]	COOPER-...	85	HLBC	m_{ν_x}=1.5 GeV
$<1 \times 10^{-2}$	90	[36]	BERGSMA	83B	CNTR	m_{ν_x}=10 MeV
$<1 \times 10^{-5}$	90	[36]	BERGSMA	83B	CNTR	m_{ν_x}=110 MeV
$<6 \times 10^{-7}$	90	[36]	BERGSMA	83B	CNTR	m_{ν_x}=410 MeV
$<1 \times 10^{-5}$	90		GRONAU	83		m_{ν_x}=160 MeV
$<1 \times 10^{-6}$	90		GRONAU	83		m_{ν_x}=480 MeV

[29] BACK 03A searched for heavy neutrinos emitted from ^{8}B decay in the Sun using the decay $\nu_h \rightarrow \nu_e e^+ e^-$ in the Counting Test Facility (the prototype of the Borexino detector) and obtained limits on heavy neutrino admixture for the ν_h mass range 1.1–12 MeV.

[30] ABREU 97I long-lived ν_x analysis. Short-lived analysis extends limit to lower masses with decreasing sensitivity except at 3.5 GeV, where the limit is the same as at 6 GeV.

[31] HAGNER 95 obtain limits on heavy neutrino admixture from the decay $\nu_h \rightarrow \nu_e e^+ e^-$ at a nuclear reactor for the ν_h mass range 2–9 MeV.

[32] BARANOV 93 is a search for neutrino decays into $e^+ e^- \nu_e$ using a beam dump experiment at the 70 GeV Serpukhov proton synchrotron. The limits are not as good as those achieved earlier by BERGSMA 83 and BERNARDI 86, BERNARDI 88.

[33] BURCHAT 90 includes the analyses reported in JUNG 90, ABRAMS 89C, and WENDT 87.

[34] OBERAUER 87 bounds from search for $\nu \rightarrow \nu' e e$ decay mode using reactor (anti)neutrinos.

[35] COOPER-SARKAR 85 also give limits based on model-dependent assumptions for ν_τ flux. We do not list these. Note that for this bound to be nontrivial, x is not equal to 3, i.e. ν_x cannot be the dominant mass eigenstate in ν_τ since m_{ν_3} <70 MeV (ALBRECHT 85I). Also, of course, x is not equal to 1 or 2, so a fourth generation would be required for this bound to be nontrivial.

[36] BERGSMA 83B also quote limits on $|U_{e3}|^2$ where the index 3 refers to the mass eigenstate dominantly coupled to the τ. Those limits were based on assumptions about the D_s mass and $D_s \rightarrow \tau \nu_\tau$ branching ratio which are no longer valid. See COOPER-SARKAR 85.

Limits on Coupling of μ to ν_x as Function of m_{ν_x}

Peak search test

Limits on B(π (or K) $\rightarrow \mu \nu_x$).

VALUE	CL%		DOCUMENT ID		TECN	COMMENT
• • • We do not use the following data for averages, fits, limits, etc. • • •						
		[37]	ASTIER	02	NOMD	$\pi \rightarrow \mu X$ for m_X=33.9 MeV
$<6.0 \times 10^{-10}$	95	[38]	DAUM	00	CNTR	$\pi \rightarrow \mu X$ for m_X=33.9 MeV
		[39]	FORMAGGIO	00	CNTR	$\pi \rightarrow \mu X$ for m_X=33.9 MeV
<0.22	90	[40]	ASSAMAGAN	98	SILI	m_{ν_x}= 0.53 MeV
<0.029	90	[40]	ASSAMAGAN	98	SILI	m_{ν_x}= 0.75 MeV
<0.016	90	[40]	ASSAMAGAN	98	SILI	m_{ν_x}= 1.0 MeV
$< 4\text{–}6 \times 10^{-5}$		[41]	BRYMAN	96	CNTR	m_{ν_x} = 30–33.91 MeV
$\sim 1 \times 10^{-16}$		[42]	ARMBRUSTER	95	KARM	m_{ν_x} = 33.9 MeV
$<4 \times 10^{-7}$	95	[43]	BILGER	95	LEPS	$m_{\overline{\nu}_x}$ = 33.9 MeV
$<7 \times 10^{-8}$	95	[43]	BILGER	95	LEPS	m_{ν_x} = 33.9 MeV
$<2.6 \times 10^{-8}$	95	[43]	DAUM	95B	TOF	m_{ν_x} = 33.9 MeV
$<2 \times 10^{-2}$	90		DAUM	87		m_{ν_x}=1 MeV
$<1 \times 10^{-3}$	90		DAUM	87		m_{ν_x}=2 MeV
$<6 \times 10^{-5}$	90		DAUM	87		3 MeV < m_{ν_x} < 19.5 MeV
$<3 \times 10^{-2}$	90	[44]	MINEHART	84		m_{ν_x}=2 MeV
$<1 \times 10^{-3}$	90	[44]	MINEHART	84		m_{ν_x}=4 MeV
$<3 \times 10^{-4}$	90	[44]	MINEHART	84		m_{ν_x}=10 GeV
$<5 \times 10^{-6}$	90	[45]	HAYANO	82		m_{ν_x}=330 MeV
$<1 \times 10^{-4}$	90	[45]	HAYANO	82		m_{ν_x}=70 MeV
$<9 \times 10^{-7}$	90	[45]	HAYANO	82		m_{ν_x}=250 MeV
$<1 \times 10^{-1}$	90	[44]	ABELA	81		m_{ν_x}=4 MeV
$<7 \times 10^{-5}$	90	[44]	ABELA	81		m_{ν_x}=10.5 MeV
$<2 \times 10^{-4}$	90	[44]	ABELA	81		m_{ν_x}=11.5 MeV
$<2 \times 10^{-5}$	90	[44]	ABELA	81		m_{ν_x}=16–30 MeV

[37] ASTIER 02 search for anomalous pion decay into a 33.9 MeV neutral particle. No evidence was found and the sensitivity to the branching ratio B($\pi \rightarrow \mu X$)·B($X \rightarrow \nu e^+ e^-$) is as low as 3.7×10^{-15}, depending on the X lifetime.

[38] DAUM 00 search for anomalous pion decay into a 33.9 MeV neutral particle that might be responsible for the time-distribution anomaly observed by the KARMEN Collaboration.

[39] FORMAGGIO 00 search for anomalous pion decay into a 33.9 MeV neutral particle Q^0 that might be responsible for the time-distribution anomaly observed by the KARMEN Collaboration. In the E815 (NuTeV) experiment at Fermilab no evidence was found, with sensitivity for the pion branching ratio B($\pi \rightarrow \mu Q^0$)·B($Q^0 \rightarrow$ visible) as low as 10^{-13}.

[40] ASSAMAGAN 98 obtain a limit on heavy neutrino admixture from π^+ decay essentially at rest, by measuring with good resolution the momentum distribution of the muons. However, the search uses an ad hoc shape correction. The authors report upper limit for $|U_{\mu x}|^2$ of 0.22 for m_ν = 0.53 MeV, 0.029 for m_ν = 0.75 MeV, and 0.016 for m_ν = 1.0 MeV at 90%CL.

[41] BRYMAN 96 search for massive unconventional neutrinos of mass m_{ν_x} in π^+ decay.

[42] ARMBRUSTER 95 study the reactions ^{12}C(ν_e,e^-) ^{12}N and ^{12}C(ν,ν') ^{12}C* induced by neutrinos from π^+ and μ^+ decay at the ISIS neutron spallation source at the Rutherford-Appleton laboratory. An anomaly in the time distribution can be interpreted as the decay $\pi^+ \rightarrow \mu^+ \nu_x$, where ν_x is a neutral weakly interacting particle with mass $\approx$ 33.9 MeV and spin 1/2. The lower limit to the branching ratio is a function of the lifetime of the new massive neutral particle, and reaches a minimum of a few $\times 10^{-16}$ for $\tau_x \sim 5$ s.

[43] From experiments of π^+ and π^- decay in flight at PSI, to check the claim of the KARMEN Collaboration quoted above (ARMBRUSTER 95).

[44] $\pi^+ \rightarrow \mu^+ \nu_\mu$ peak search experiment.

[45] $K^+ \rightarrow \mu^+ \nu_\mu$ peak search experiment.

Peak search test

Limits on $|U_{\mu x}|^2$ as function of m_{ν_x}

VALUE	CL%		DOCUMENT ID		TECN	COMMENT
• • • We do not use the following data for averages, fits, limits, etc. • • •						
$< 1\text{–}10 \times 10^{-4}$		[46]	BRYMAN	96	CNTR	m_{ν_x} = 30–33.91 MeV
$<2 \times 10^{-5}$	95	[47]	ASANO	81		m_{ν_x}=70 MeV
$<3 \times 10^{-6}$	95	[47]	ASANO	81		m_{ν_x}=210 MeV
$<3 \times 10^{-6}$	95	[47]	ASANO	81		m_{ν_x}=230 MeV
$<6 \times 10^{-6}$	95	[48]	ASANO	81		m_{ν_x}=240 MeV
$<5 \times 10^{-7}$	95	[48]	ASANO	81		m_{ν_x}=280 MeV
$<6 \times 10^{-6}$	95	[48]	ASANO	81		m_{ν_x}=300 MeV
$<1 \times 10^{-2}$	95		CALAPRICE	81		m_{ν_x}=7 MeV
$<3 \times 10^{-3}$	95	[49]	CALAPRICE	81		m_{ν_x}=33 MeV
$<1 \times 10^{-4}$	68	[50]	SHROCK	81	THEO	m_{ν_x}=13 MeV

$<3\times10^{-5}$	68	[50] SHROCK	81	THEO	m_{ν_x}=33 MeV
$<6\times10^{-3}$	68	[51] SHROCK	81	THEO	m_{ν_x}=80 MeV
$<5\times10^{-3}$	68	[51] SHROCK	81	THEO	m_{ν_x}=120 MeV

[46] BRYMAN 96 search for massive unconventional neutrinos of mass m_{ν_x} in π^+ decay. They interpret the result as an upper limit for the admixture of a heavy sterile or otherwise

[47] $K^+ \to \mu^+\nu_\mu$ peak search experiment.

[48] Analysis of experiment on $K^+ \to \mu^+\nu_\mu\nu_x\overline{\nu}_x$ decay.

[49] $\pi^+ \to \mu^+\nu_\mu$ peak search experiment.

[50] Analysis of magnetic spectrometer experiment, bubble chamber experiment, and emulsion experiment on $\pi^+ \to \mu^+\nu_\mu$ decay.

[51] Analysis of magnetic spectrometer experiment on $K \to \mu, \nu_\mu$ decay.

Peak Search in Muon Capture

Limits on $|U_{\mu x}|^2$ as function of m_{ν_x}

VALUE	DOCUMENT ID		COMMENT
• • • We do not use the following data for averages, fits, limits, etc. • • •			
$<1\times10^{-1}$	DEUTSCH	83	m_{ν_x}=45 MeV
$<7\times10^{-3}$	DEUTSCH	83	m_{ν_x}=70 MeV
$<1\times10^{-1}$	DEUTSCH	83	m_{ν_x}=85 MeV

Searches for Decays of Massive ν

Limits on $|U_{\mu x}|^2$ as function of m_{ν_x}

VALUE	CL%	DOCUMENT ID		TECN	COMMENT
• • • We do not use the following data for averages, fits, limits, etc. • • •					
$<5\times10^{-7}$	90	[52] VAITAITIS	99	CCFR	m_{ν_x}=0.28 GeV
$<8\times10^{-8}$	90	[52] VAITAITIS	99	CCFR	m_{ν_x}=0.37 GeV
$<5\times10^{-7}$	90	[52] VAITAITIS	99	CCFR	m_{ν_x}= 0.50 GeV
$<6\times10^{-8}$	90	[52] VAITAITIS	99	CCFR	m_{ν_x}= 1.50 GeV
$<2\times10^{-5}$	95	[53] ABREU	97I	DLPH	m_{ν_x}=6 GeV
$<3\times10^{-5}$	95	[53] ABREU	97I	DLPH	m_{ν_x}=50 GeV
$<3\times10^{-6}$	90	GALLAS	95	CNTR	m_{ν_x} = 1 GeV
$<3\times10^{-5}$	90	[54] VILAIN	95C	CHM2	m_{ν_x} = 2 GeV
$<6.2\times10^{-8}$	95	ADEVA	90S	L3	m_{ν_x}=20 GeV
$<5.1\times10^{-10}$	95	ADEVA	90S	L3	m_{ν_x}=40 GeV
all values ruled out	95	[55] BURCHAT	90	MRK2	m_{ν_x} < 19.6 GeV
$<1\times10^{-10}$	95	[55] BURCHAT	90	MRK2	m_{ν_x} = 22 GeV
$<1\times10^{-11}$	95	[55] BURCHAT	90	MRK2	m_{ν_x} = 41 GeV
all values ruled out	95	DECAMP	90F	ALEP	m_{ν_x}= 25.0–42.7 GeV
$<1\times10^{-13}$	95	DECAMP	90F	ALEP	m_{ν_x}= 42.7–45.7 GeV
$<5\times10^{-3}$	90	AKERLOF	88	HRS	m_{ν_x}=1.8 GeV
$<2\times10^{-5}$	90	AKERLOF	88	HRS	m_{ν_x}=4 GeV
$<3\times10^{-6}$	90	AKERLOF	88	HRS	m_{ν_x}=6 GeV
$<1\times10^{-7}$	90	BERNARDI	88	CNTR	m_{ν_x}=200 MeV
$<3\times10^{-9}$	90	BERNARDI	88	CNTR	m_{ν_x}=300 MeV
$<4\times10^{-4}$	90	[56] MISHRA	87	CNTR	m_{ν_x}=1.5 GeV
$<4\times10^{-3}$	90	[56] MISHRA	87	CNTR	m_{ν_x}=2.5 GeV
$<0.9\times10^{-2}$	90	[56] MISHRA	87	CNTR	m_{ν_x}=5 GeV
<0.1	90	[56] MISHRA	87	CNTR	m_{ν_x}=10 GeV
$<8\times10^{-4}$	90	BADIER	86	CNTR	m_{ν_x}=600 MeV
$<1.2\times10^{-5}$	90	BADIER	86	CNTR	m_{ν_x}=1.7 GeV
$<3\times10^{-8}$	90	BERNARDI	86	CNTR	m_{ν_x}=200 MeV
$<6\times10^{-9}$	90	BERNARDI	86	CNTR	m_{ν_x}=350 MeV
$<1\times10^{-6}$	90	DORENBOS...	86	CNTR	m_{ν_x}=500 MeV
$<1\times10^{-7}$	90	DORENBOS...	86	CNTR	m_{ν_x}=1600 MeV
$<0.8\times10^{-5}$	90	[57] COOPER-...	85	HLBC	m_{ν_x}=0.4 GeV
$<1.0\times10^{-7}$	90	[57] COOPER-...	85	HLBC	m_{ν_x}=1.5 GeV

[52] VAITAITIS 99 search for $L^0_\mu \to \mu X$. See paper for rather complicated limit as function of m_{ν_x}.

[53] ABREU 97I long-lived ν_x analysis. Short-lived analysis extends limit to lower masses with decreasing sensitivity except at 3.5 GeV, where the limit is the same as at 6 GeV.

[54] VILAIN 95C is a search for the decays of heavy isosinglet neutrinos produced by neutral current neutrino interactions. Limits were quoted for masses in the range from 0.3 to 24 GeV. The best limit is listed above.

[55] BURCHAT 90 includes the analyses reported in JUNG 90, ABRAMS 89C, and WENDT 87.

[56] See also limits on $|U_{3x}|$ from WENDT 87.

[57] COOPER-SARKAR 85 also give limits based on model-dependent assumptions for ν_τ flux. We do not list these. Note that for this bound to be nontrivial, x is not equal to 3, i.e. ν_x cannot be the dominant mass eigenstate in ν_τ since m_{ν_3} <70 MeV (ALBRECHT 85I). Also, of course, x is not equal to 1 or 2, so a fourth generation would be required for this bound to be nontrivial.

Limits on $|U_{\tau x}|^2$ as a Function of m_{ν_x}

VALUE	CL%	DOCUMENT ID		TECN	COMMENT
• • • We do not use the following data for averages, fits, limits, etc. • • •					
$<1\times10^{-2}$	90	[58] ORLOFF	02	CHRM	m_{ν_x}=45 MeV
$<1.4\times10^{-4}$	90	[58] ORLOFF	02	CHRM	m_{ν_x}=180 MeV
<0.025	90	ASTIER	01		m_{ν_x}=45 MeV
<0.002	90	ASTIER	01		m_{ν_x}=140 MeV
$<2\times10^{-5}$	95	[59] ABREU	97I	DLPH	m_{ν_x}=6 GeV
$<3\times10^{-5}$	95	[59] ABREU	97I	DLPH	m_{ν_x}=50 GeV
$<6.2\times10^{-8}$	95	ADEVA	90S	L3	m_{ν_x}=20 GeV
$<5.1\times10^{-10}$	95	ADEVA	90S	L3	m_{ν_x}=40 GeV
all values ruled out	95	[60] BURCHAT	90	MRK2	m_{ν_x} < 19.6 GeV
$<1\times10^{-10}$	95	[60] BURCHAT	90	MRK2	m_{ν_x} = 22 GeV
$<1\times10^{-11}$	95	[60] BURCHAT	90	MRK2	m_{ν_x} = 41 GeV
all values ruled out	95	DECAMP	90F	ALEP	m_{ν_x}= 25.0–42.7 GeV
$<1\times10^{-13}$	95	DECAMP	90F	ALEP	m_{ν_x}= 42.7–45.7 GeV
$<5\times10^{-2}$	80	AKERLOF	88	HRS	m_{ν_x}=2.5 GeV
$<9\times10^{-5}$	80	AKERLOF	88	HRS	m_{ν_x}=4.5 GeV

[58] ORLOFF 02 use the negative result of a search for neutral particles decaying into two electrons performed by CHARM to get these limits for a mostly isosinglet heavy neutrino.

[59] ABREU 97I long-lived ν_x analysis. Short-lived analysis extends limit to lower masses with decreasing sensitivity.

[60] BURCHAT 90 includes the analyses reported in JUNG 90, ABRAMS 89C, and WENDT 87.

Limits on $|U_{ax}|^2$

Where $a = e$, μ from ρ parameter in μ decay.

VALUE	CL%	DOCUMENT ID		TECN	COMMENT
• • • We do not use the following data for averages, fits, limits, etc. • • •					
$<1\times10^{-2}$	68	SHROCK	81B	THEO	m_{ν_x}=10 GeV
$<2\times10^{-3}$	68	SHROCK	81B	THEO	m_{ν_x}=40 MeV
$<4\times10^{-2}$	68	SHROCK	81B	THEO	m_{ν_x}=70 MeV

Limits on $|U_{1j}\times U_{2j}|$ as Function of m_{ν_j}

VALUE	CL%	DOCUMENT ID		TECN	COMMENT
• • • We do not use the following data for averages, fits, limits, etc. • • •					
$<3\times10^{-5}$	90	[61] BARANOV	93		m_{ν_j}= 80 MeV
$<3\times10^{-6}$	90	[61] BARANOV	93		m_{ν_j}= 160 MeV
$<6\times10^{-7}$	90	[61] BARANOV	93		m_{ν_j}= 240 MeV
$<2\times10^{-7}$	90	[61] BARANOV	93		m_{ν_j}= 320 MeV
$<9\times10^{-5}$	90	BERNARDI	86	CNTR	m_{ν_j}=25 MeV
$<3.6\times10^{-7}$	90	BERNARDI	86	CNTR	m_{ν_j}=100 MeV
$<3\times10^{-8}$	90	BERNARDI	86	CNTR	m_{ν_j}=200 MeV
$<6\times10^{-9}$	90	BERNARDI	86	CNTR	m_{ν_j}=350 MeV
$<1\times10^{-2}$	90	BERGSMA	83B	CNTR	m_{ν_j}=10 MeV
$<1\times10^{-5}$	90	BERGSMA	83B	CNTR	m_{ν_j}=140 MeV
$<7\times10^{-7}$	90	BERGSMA	83B	CNTR	m_{ν_j}=370 MeV

[61] BARANOV 93 is a search for neutrino decays into $e^+e^-\nu_e$ using a beam dump experiment at the 70 GeV Serpukhov proton synchrotron.

REFERENCES FOR Heavy Neutral Leptons, Searches for

BACK	03A	JETPL 78 261	H.O. Back *et al.*	(Borexino Collab.)
		Translated from ZETFP 78 707.		
TRINCZEK	03	PRL 90 012501	M. Trinczek *et al.*	
ASTIER	02	PL B527 23	P. Astier *et al.*	(NOMAD Collab.)
ORLOFF	02	PL B550 8	J. Orloff *et al.*	
ACHARD	01	PL B517 67	P. Achard *et al.*	(L3 Collab.)
ACHARD	01B	PL B517 75	P. Achard *et al.*	(L3 Collab.)
ASTIER	01	PL B506 27	P. Astier *et al.*	(NOMAD Collab.)
GALEAZZI	01	PRL 86 1978	M. Galeazzi *et al.*	
ABBIENDI	00I	EPJ C14 73	G. Abbiendi *et al.*	(OPAL Collab.)
DAUM	00	PRL 85 1815	M. Daum *et al.*	
FORMAGGIO	00	PRL 84 4043	J.A. Formaggio *et al.*	
HOLZSCHUH	00	PL B482 1	E. Holzschuh *et al.*	
ABREU	99O	EPJ C8 41	P. Abreu *et al.*	(DELPHI Collab.)
ACCIARRI	99K	PL B461 397	M. Acciarri *et al.*	(L3 Collab.)
DRAGOUN	99	JP G25 1839	O. Dragoun *et al.*	
HOLZSCHUH	99	PL B451 247	E. Holzschuh *et al.*	
VAITAITIS	99	PRL 83 4943	A. Vaitaitis *et al.*	(CCFR Collab.)
ASSAMAGAN	98	PL B434 158	K. Assamagan *et al.*	
HINDI	98	PR C58 2512	M.M. Hindi *et al.*	
PDG	98	EPJ C3 1	C. Caso *et al.*	(PDG Collab.)
ABREU	97I	ZPHY C74 57	P. Abreu *et al.*	(DELPHI Collab.)
Also		ZPHY C75 580 (erratum)	P. Abreu *et al.*	(DELPHI Collab.)
BRYMAN	96	PR D53 558	D.A. Bryman, T. Numao	(TRIU)
BUSKULIC	96S	PL B384 439	D. Buskulic *et al.*	(ALEPH Collab.)

See key on page 547

Lepton Particle Listings

Heavy Neutral Leptons, Searches for

WIETFELDT	96	PRPL 273 149	F.E. Wietfeldt, E.B. Norman	(LBL)
ARMBRUSTER	95	PL B348 19	B. Armbruster *et al.*	(KARMEN Collab.)
BAHRAN	95	PL B354 481	M.Y. Bahran, G.R. Kalbfleisch	(OKLA)
BILGER	95	PL B363 41	R. Bilger *et al.*	(TUBIN, KARLE, PSI)
DAUM	95B	PL B361 179	M. Daum *et al.*	(PSI, UVA)
FARGION	95	PR D52 1828	D. Fargion *et al.*	(ROMA, KIAM, MPEI)
GALLAS	95	PR D52 6	E. Gallas *et al.*	(MSU, FNAL, MIT, FLOR)
GARCIA	95	PR D51 1458	E. Garcia *et al.*	(ZARA, SCUC, PNL)
HAGNER	95	PR D52 1343	C. Hagner *et al.*	(MUNT, LAPP, CPPM)
HIDDEMANN	95	JP G21 639	K.H. Hiddemann, H. Daniel, O. Schwentker	(MUNT)
VILAIN	95C	PL B351 387	P. Vilain *et al.*	(CHARM II Collab.)
Also		PL B343 453	P. Vilain *et al.*	(CHARM II Collab.)
BECK	94	PL B336 141	M. Beck *et al.*	(MPIH, KIAE, SASSO)
KONOPLICH	94	PAN 57 425	R.V. Konoplich, M.Y. Khlopov	(MPEI)
PDG	94	PR D50 1173	L. Montanet *et al.*	(CERN, LBL, BOST+)
BAHRAN	93	PR D47 R754	M. Bahran, G.R. Kalbfleisch	(OKLA)
BAHRAN	93B	PR D47 R759	M. Bahran, G.R. Kalbfleisch	(OKLA)
BARANOV	93	PL B302 336	S.A. Baranov *et al.*	(JINR, SERP, BUDA)
KALBFLEISCH	93	PL B303 355	G.R. Kalbfleisch, M.Y. Bahran	(OKLA)
MORTARA	93	PRL 70 394	J.L. Mortara *et al.*	(ANL, LBL, UCB)
OHSHIMA	93	PR D47 4840	T. Ohshima *et al.*	(KEK, TUAT, RIKEN+)
ABREU	92B	PL B274 230	P. Abreu *et al.*	(DELPHI Collab.)
BAHRAN	92	PL B291 336	M.Y. Bahran, G.R. Kalbfleisch	(OKLA)
BRITTON	92	PRL 68 3000	D.I. Britton *et al.*	(TRIU, CARL)
Also		PR D49 28	D.I. Britton *et al.*	(TRIU, CARL)
BRITTON	92B	PR D46 R885	D.I. Britton *et al.*	(TRIU, CARL)
KAWAKAMI	92	PL B287 45	H. Kawakami *et al.*	(INUS, KEK, SCUC+)
MORI	92B	PL B289 463	M. Mori *et al.*	(KAM2 Collab.)
ALEXANDER	91F	ZPHY C52 175	G. Alexander *et al.*	(OPAL Collab.)
DELEENER-...	91	PR D43 3611	N. de Leener-Rosier *et al.*	(LOUV, ZURI+)
REUSSER	91	PL B255 143	D. Reusser *et al.*	(NEUC, CIT, PSI)
SATO	91	PR D44 2220	N. Sato *et al.*	(Kamiokande Collab.)
ADEVA	90S	PL B251 321	B. Adeva *et al.*	(L3 Collab.)
BURCHAT	90	PR D41 3542	P.R. Burchat *et al.*	(Mark II Collab.)
DECAMP	90F	PL B236 511	D. Decamp *et al.*	(ALEPH Collab.)
DEUTSCH	90	NP A518 149	J. Deutsch, M. Lebrun, R. Prieels	
JUNG	90	PRL 64 1091	C. Jung *et al.*	(Mark II Collab.)
ABRAMS	89C	PRL 63 2447	G.S. Abrams *et al.*	(Mark II Collab.)
ENQVIST	89	NP B317 647	K. Enqvist, K. Kainulainen, J. Maalampi	(HELS)
FISHER	89	PL B218 257	P.H. Fisher *et al.*	(CIT, NEUC, PSI)
AKERLOF	88	PR D37 577	C.W. Akerlof *et al.*	(HRS Collab.)
BERNARDI	88	PL B203 332	G. Bernardi *et al.*	(PARIN, CERN, INFN+)
CALDWELL	88	PRL 61 510	D.O. Caldwell *et al.*	(UCSB, UCB, LBL)
OLIVE	88	PL B205 553	K.A. Olive, M. Srednicki	(MINN, UCSB)
SREDNICKI	88	NP B310 693	M. Srednicki, R. Watkins, K.A. Olive	(MINN, UCSB)
AHLEN	87	PL B195 603	S.P. Ahlen *et al.*	(BOST, SCUC, HARV+)
DAUM	87	PR D36 2624	M. Daum *et al.*	(SIN, UVA)
GRIEST	87	NP B283 681	K. Griest, D. Seckel	(UCSC, CERN)
Also		NP B296 1034 (erratum)	K. Griest, D. Seckel	(UCSC, CERN)
MISHRA	87	PRL 59 1397	S.R. Mishra *et al.*	(COLU, CIT, FNAL+)
OBERAUER	87	PL B198 113	L.F. Oberauer, F. von Feilitzsch, R.L. Mossbauer	
WENDT	87	PRL 58 1810	C. Wendt *et al.*	(Mark II Collab.)
AZUELOS	86	PRL 56 2241	G. Azuelos *et al.*	(TRIU, CNRC)
BADIER	86	ZPHY C31 21	J. Badier *et al.*	(NA3 Collab.)
BERNARDI	86	PL 166B 479	G. Bernardi *et al.*	(CURIN, INFN, CDEF+)
DORENBOS...	86	PL 166B 473	J. Dorenbosch *et al.*	(CHARM Collab.)
ALBRECHT	85I	PL 163B 404	H. Albrecht *et al.*	(ARGUS Collab.)
APALIKOV	85	JETPL 42 289	A.M. Apalikov *et al.*	(ITEP)
		Translated from ZETFP 42 233.		
COOPER-...	85	PL 160B 207	A.M. Cooper-Sarkar *et al.*	(CERN, LOIC+)
MARKEY	85	PR C32 2215	J. Markey, F. Boehm	(CIT)
OHI	85	PL 160B 322	T. Ohi *et al.*	(TOKY, INUS, KEK)
MINEHART	84	PRL 52 804	R.C. Minehart *et al.*	(UVA, SIN)
BERGSMA	83	PL 122B 465	F. Bergsma *et al.*	(CHARM Collab.)
BERGSMA	83B	PL 128B 361	F. Bergsma *et al.*	(CHARM Collab.)
BRYMAN	83B	PRL 50 1546	D.A. Bryman *et al.*	(TRIU, CNRC)
DEUTSCH	83	PR D27 1644	J.P. Deutsch, M. Lebrun, R. Prieels	(LOUV)
GRONAU	83	PR D28 2762	M. Gronau	(HAIF)
SCHRECK...	83	PL 129B 265	K. Schreckenbach *et al.*	(ISNG, ILLG)
HAYANO	82	PRL 49 1305	R.S. Hayano *et al.*	(TOKY, KEK, TSUK)
ABELA	81	PL 105B 263	R. Abela *et al.*	(SIN)
ASANO	81	PL 104B 84	Y. Asano *et al.*	(KEK, TOKY, INUS, OSAK)
CALAPRICE	81	PL 106B 175	F.P. Calaprice *et al.*	(PRIN, IND)
SHROCK	81	PR D24 1232	R.E. Shrock	(STON)
SHROCK	81B	PR D24 1275	R.E. Shrock	(STON)
SHROCK	80	PL 96B 159	R.E. Shrock	(STON)

QUARKS

Notes in the Quark Listings

QUARKS

QUARK MASSES

Updated Jan 2014 by A.V. Manohar (University of California, San Diego) and C.T. Sachrajda (University of Southampton)

A. Introduction

This note discusses some of the theoretical issues relevant for the determination of quark masses, which are fundamental parameters of the Standard Model of particle physics. Unlike the leptons, quarks are confined inside hadrons and are not observed as physical particles. Quark masses therefore cannot be measured directly, but must be determined indirectly through their influence on hadronic properties. Although one often speaks loosely of quark masses as one would of the mass of the electron or muon, any quantitative statement about the value of a quark mass must make careful reference to the particular theoretical framework that is used to define it. It is important to keep this *scheme dependence* in mind when using the quark mass values tabulated in the data listings.

Historically, the first determinations of quark masses were performed using quark models. The resulting masses only make sense in the limited context of a particular quark model, and cannot be related to the quark mass parameters of the Standard Model. In order to discuss quark masses at a fundamental level, definitions based on quantum field theory be used, and the purpose of this note is to discuss these definitions and the corresponding determinations of the values of the masses.

B. Mass parameters and the QCD Lagrangian

The QCD [1] Lagrangian for N_F quark flavors is

$$\mathcal{L} = \sum_{k=1}^{N_F} \overline{q}_k \left(i \not{D} - m_k \right) q_k - \tfrac{1}{4} G_{\mu\nu} G^{\mu\nu} \,, \tag{1}$$

where $\not{D} = (\partial_\mu - i g A_\mu)\, \gamma^\mu$ is the gauge covariant derivative, A_μ is the gluon field, $G_{\mu\nu}$ is the gluon field strength, m_k is the mass parameter of the k^{th} quark, and q_k is the quark Dirac field. After renormalization, the QCD Lagrangian Eq. (1) gives finite values for physical quantities, such as scattering amplitudes. Renormalization is a procedure that invokes a subtraction scheme to render the amplitudes finite, and requires the introduction of a dimensionful scale parameter μ. The mass parameters in the QCD Lagrangian Eq. (1) depend on the renormalization scheme used to define the theory, and also on the scale parameter μ. The most commonly used renormalization scheme for QCD perturbation theory is the $\overline{\text{MS}}$ scheme.

The QCD Lagrangian has a chiral symmetry in the limit that the quark masses vanish. This symmetry is spontaneously broken by dynamical chiral symmetry breaking, and explicitly broken by the quark masses. The nonperturbative scale of dynamical chiral symmetry breaking, Λ_χ, is around 1 GeV [2]. It is conventional to call quarks heavy if $m > \Lambda_\chi$, so that explicit chiral symmetry breaking dominates (c, b, and t quarks are heavy), and light if $m < \Lambda_\chi$, so that spontaneous chiral symmetry breaking dominates (u, d and s quarks are light). The determination of light- and heavy-quark masses is considered separately in sections D and E below.

At high energies or short distances, nonperturbative effects, such as chiral symmetry breaking, become small and one can, in principle, determine quark masses by analyzing mass-dependent effects using QCD perturbation theory. Such computations are conventionally performed using the $\overline{\text{MS}}$ scheme at a scale $\mu \gg \Lambda_\chi$, and give the $\overline{\text{MS}}$ "running" mass $\overline{m}(\mu)$. We use the $\overline{\text{MS}}$ scheme when reporting quark masses; one can readily convert these values into other schemes using perturbation theory.

The μ dependence of $\overline{m}(\mu)$ at short distances can be calculated using the renormalization group equation,

$$\mu^2 \frac{\mathrm{d}\overline{m}\,(\mu)}{\mathrm{d}\mu^2} = -\gamma(\overline{\alpha}_s\,(\mu))\; \overline{m}\,(\mu)\,, \tag{2}$$

where γ is the anomalous dimension which is now known to four-loop order in perturbation theory [3,4]. $\overline{\alpha}_s$ is the coupling constant in the $\overline{\text{MS}}$ scheme. Defining the expansion coefficients γ_r by

$$\gamma\,(\overline{\alpha}_s) \equiv \sum_{r=1}^{\infty} \gamma_r \left(\frac{\overline{\alpha}_s}{4\pi} \right)^r ,$$

the first four coefficients are given by

$$\begin{aligned}
\gamma_1 &= 4, \\
\gamma_2 &= \frac{202}{3} - \frac{20 N_L}{9}, \\
\gamma_3 &= 1249 + \left(-\frac{2216}{27} - \frac{160}{3}\zeta\,(3) \right) N_L - \frac{140}{81} N_L^2, \\
\gamma_4 &= \frac{4603055}{162} + \frac{135680}{27}\zeta\,(3) - 8800\zeta\,(5) \\
&\quad + \left(-\frac{91723}{27} - \frac{34192}{9}\zeta\,(3) + 880\zeta\,(4) + \frac{18400}{9}\zeta\,(5) \right) N_L \\
&\quad + \left(\frac{5242}{243} + \frac{800}{9}\zeta\,(3) - \frac{160}{3}\zeta\,(4) \right) N_L^2 \\
&\quad + \left(-\frac{332}{243} + \frac{64}{27}\zeta\,(3) \right) N_L^3,
\end{aligned}$$

where N_L is the number of active light quark flavors at the scale μ, i.e. flavors with masses $< \mu$, and ζ is the Riemann zeta function ($\zeta(3) \simeq 1.2020569$, $\zeta(4) \simeq 1.0823232$, and $\zeta(5) \simeq 1.0369278$). In addition, as the renormalization scale crosses quark mass thresholds one needs to match the scale dependence of m below and above the threshold. There are finite threshold corrections; the necessary formulae can be found in Ref. [5].

The quark masses for light quarks discussed so far are often referred to as current quark masses. Nonrelativistic quark models use constituent quark masses, which are of order 350 MeV for the u and d quarks. Constituent quark masses

model the effects of dynamical chiral symmetry breaking, and are not related to the quark mass parameters m_k of the QCD Lagrangian Eq. (1). Constituent masses are only defined in the context of a particular hadronic model.

C. Lattice Gauge Theory

The use of the lattice simulations for *ab initio* determinations of the fundamental parameters of QCD, including the coupling constant and quark masses (except for the top-quark mass) is a very active area of research (see the review on Lattice Quantum Chromodynamics in this *Review*). Here we only briefly recall those features which are required for the determination of quark masses. In order to determine the lattice spacing (a, i.e. the distance between neighboring points of the lattice) and quark masses, one computes a convenient and appropriate set of physical quantities (frequently chosen to be a set of hadronic masses) for a variety of input values of the quark masses. The true (physical) values of the quark masses are those which correctly reproduce the set of physical quantities being used for the calibration.

The values of the quark masses obtained directly in lattice simulations are bare quark masses, corresponding to a particular discretization of QCD and with the lattice spacing as the ultraviolet cut-off. In order for these results to be useful in phenomenological applications, it is necessary to relate them to renormalized masses defined in some standard renormalization scheme such as $\overline{\rm MS}$. Provided that both the ultraviolet cut-off a^{-1} and the renormalization scale are much greater than $\Lambda_{\rm QCD}$, the bare and renormalized masses can be related in perturbation theory. However, in order to avoid uncertainties due to the unknown higher-order coefficients in lattice perturbation theory, most results obtained recently use *non-perturbative renormalization* to relate the bare masses to those defined in renormalization schemes which can be simulated directly in lattice QCD (e.g. those obtained from quark and gluon Green functions at specified momenta in the Landau gauge [51] or those defined using finite-volume techniques and the Schrödinger functional [52]) . The conversation to the $\overline{\rm MS}$ scheme (which cannot be simulated) is then performed using continuum perturbation theory.

The determination of quark masses using lattice simulations is well established and the current emphasis is on the reduction and control of the systematic uncertainties. With improved algorithms and access to more powerful computing resources, the precision of the results has improved immensely in recent years. Particularly pleasing is the observation that results obtained using different formulations of lattice QCD, with different systematic uncertainties, give results which are largely consistent with each other. This gives us broad confidence in the estimates of the systematic errors. As the precision of the results approaches the percent level, more attention will now have to be given to sources of systematic uncertainty which have only been studied in a limited way up to now. In particular most current simulations are performed with degenerate u and d quarks and without including electromagnetic effects. Vacuum polarisation effects are included with $N_f = 2 + 1$ or $N_f = 2$ flavors of sea quarks, although simulations with charm sea quarks are now beginning. In earlier *reviews*, results were presented from simulations in which vacuum polarization effects were completely neglected (this is the so-called *quenched* approximation), leading to systematic uncertainties which could not be estimated reliably. It is no longer necessary to include quenched results in compilations of quark masses.

D. Light quarks

In this section we review the determination of the masses of the light quarks u, d and s from lattice simulations and then discuss the consequences of the approximate chiral symmetry.

Lattice Gauge Theory: The most reliable determinations of the strange quark mass m_s and of the average of the up and down quark masses $m_{ud} = (m_u + m_d)/2$ are obtained from lattice simulations. As explained in section C above, the simulations are performed with degenerate up and down quarks ($m_u = m_d$) and so it is the average which is obtained directly from the computations. Below we discuss attempts to derive m_u and m_d separately using lattice results in combination with other techniques, but here we briefly present our estimate of the current status of the latest lattice results. Based largely on references [19–26], which have among the most reliable estimates of the systematic errors, our summary is

$$\overline{m}_s = (93.5 \pm 2.5)\,\text{MeV}\,, \quad \overline{m}_{ud} = (3.40 \pm 0.25)\,\text{MeV} \qquad (3)$$

and

$$\frac{\overline{m}_s}{\overline{m}_{ud}} = 27.5 \pm 0.3\,. \qquad (4)$$

The masses are given in the $\overline{\rm MS}$ scheme at a renormalization scale of 2 GeV. Because the errors are dominated by systematics, these results are not simply the combinations of all the results in quadrature, but include a judgement of the remaining uncertainties. Since the different collaborations use different formulations of lattice QCD, the (relatively small) variations of the results between the groups provides important information about the reliability of the estimates.

Current lattice simulations are performed in the isospin symmetry limit, i.e. with the masses of the up and down quarks equal, $m_u = m_d \equiv m_{ud}$ and, apart from Refs. [31,32], electromagnetic effects are not included in the simulation. It is the average of the physical up and down quark masses which is determined directly. In order to estimate m_u and m_d separately, further experimental and theoretical inputs have to be included. Recent studies which combine lattice data with studies of isospin breaking effects using chiral perturbation theory and phenomenology include those by the MILC [20,27] and BMW [22,23] collaborations and by the Flavianet Lattice Averaging Group [32]. Based on these results we summarise the current status as

$$\frac{\overline{m}_u}{\overline{m}_d} = 0.46(5)\,,\ \overline{m}_u = 2.15(15)\,\text{MeV}\,,\ \overline{m}_d = 4.70(20)\,\text{MeV}\,. \quad (5)$$

Again the masses are given in the $\overline{\rm MS}$ scheme at a renormalization scale of 2 GeV. Of particular importance is the fact that $m_u \neq 0$ since there would have been no strong CP problem had m_u been equal to zero.

The quark mass ranges for the light quarks given in the listings combine the lattice and continuum values and use the PDG method for determining errors given in the introductory notes.

Chiral Perturbation Theory: For light quarks, one can use the techniques of chiral perturbation theory [6–8] to extract quark mass ratios. The mass term for light quarks in the QCD Lagrangian is

$$\overline{\Psi} M \Psi = \overline{\Psi}_L M \Psi_R + \overline{\Psi}_R M^\dagger \Psi_L, \tag{6}$$

where M is the light quark mass matrix,

$$M = \begin{pmatrix} m_u & 0 & 0 \\ 0 & m_d & 0 \\ 0 & 0 & m_s \end{pmatrix}, \tag{7}$$

$\Psi = (u, d, s)$, and L and R are the left- and right-chiral components of Ψ given by $\Psi_{L,R} = P_{L,R}\Psi$, $P_L = (1 - \gamma_5)/2$, $P_R = (1 + \gamma_5)/2$. The mass term is the only term in the QCD Lagrangian that mixes left- and right-handed quarks. In the limit $M \to 0$, there is an independent $SU(3) \times U(1)$ flavor symmetry for the left- and right-handed quarks. The vector $U(1)$ symmetry is baryon number; the axial $U(1)$ symmetry of the classical theory is broken in the quantum theory due to the anomaly. The remaining $G_\chi = \mathrm{SU}(3)_L \times \mathrm{SU}(3)_R$ chiral symmetry of the QCD Lagrangian is spontaneously broken to $SU(3)_V$, which, in the limit $M \to 0$, leads to eight massless Goldstone bosons, the π's, K's, and η.

The symmetry G_χ is only an approximate symmetry, since it is explicitly broken by the quark mass matrix M. The Goldstone bosons acquire masses which can be computed in a systematic expansion in M, in terms of low-energy constants, which are unknown nonperturbative parameters of the effective theory, and are not fixed by the symmetries. One treats the quark mass matrix M as an external field that transforms under G_χ as $M \to LMR^\dagger$, where $\Psi_L \to L\Psi_L$ and $\Psi_R \to R\Psi_R$ are the $SU(3)_L$ and $SU(3)_R$ transformations, and writes down the most general Lagrangian invariant under G_χ. Then one sets M to its given constant value Eq. (7), which implements the symmetry breaking. To first order in M one finds that [9]

$$\begin{aligned} m^2_{\pi^0} &= B\,(m_u + m_d)\ , \\ m^2_{\pi^\pm} &= B\,(m_u + m_d) + \Delta_{\rm em}\ , \\ m^2_{K^0} = m^2_{\overline{K}^0} &= B\,(m_d + m_s)\ , \\ m^2_{K^\pm} &= B\,(m_u + m_s) + \Delta_{\rm em}\ , \\ m^2_\eta &= \frac{1}{3} B\,(m_u + m_d + 4m_s)\ , \end{aligned} \tag{8}$$

with two unknown constants B and $\Delta_{\rm em}$, the electromagnetic mass difference. From Eq. (8), one can determine the quark mass ratios [9]

$$\begin{aligned} \frac{m_u}{m_d} &= \frac{2m^2_{\pi^0} - m^2_{\pi^+} + m^2_{K^+} - m^2_{K^0}}{m^2_{K^0} - m^2_{K^+} + m^2_{\pi^+}} = 0.56\ , \\ \frac{m_s}{m_d} &= \frac{m^2_{K^0} + m^2_{K^+} - m^2_{\pi^+}}{m^2_{K^0} + m^2_{\pi^+} - m^2_{K^+}} = 20.2\ , \end{aligned} \tag{9}$$

to lowest order in chiral perturbation theory, with an error which will be estimated below. Since the mass ratios extracted using chiral perturbation theory use the symmetry transformation property of M under the chiral symmetry G_χ, it is important to use a renormalization scheme for QCD that does not change this transformation law. Any mass independent subtraction scheme such as $\overline{\rm MS}$ is suitable. The ratios of quark masses are scale independent in such a scheme, and Eq. (9) can be taken to be the ratio of $\overline{\rm MS}$ masses. Chiral perturbation theory cannot determine the overall scale of the quark masses, since it uses only the symmetry properties of M, and any multiple of M has the same G_χ transformation law as M.

Chiral perturbation theory is a systematic expansion in powers of the light quark masses. The typical expansion parameter is $m^2_K/\Lambda^2_\chi \sim 0.25$ if one uses $SU(3)$ chiral symmetry, and $m^2_\pi/\Lambda^2_\chi \sim 0.02$ if instead one uses $SU(2)$ chiral symmetry. Electromagnetic effects at the few percent level also break $SU(2)$ and $SU(3)$ symmetry. The mass formulæ Eq. (8) were derived using $SU(3)$ chiral symmetry, and are expected to have approximately a 25% uncertainty due to second order corrections. This estimate of the uncertainty is consistent with the lattice results found in Eq. (3) and Eq. (4).

There is a subtlety which arises when one tries to determine quark mass ratios at second order in chiral perturbation theory. The second order quark mass term [10]

$$\left(M^\dagger\right)^{-1} \det M^\dagger \tag{10}$$

(which can be generated by instantons) transforms in the same way under G_χ as M. Chiral perturbation theory cannot distinguish between M and $\left(M^\dagger\right)^{-1} \det M^\dagger$; one can make the replacement $M \to M(\lambda) = M + \lambda M \left(M^\dagger M\right)^{-1} \det M^\dagger$ in the chiral Lagrangian,

$$\begin{aligned} M(\lambda) &= \mathrm{diag}\,(m_u(\lambda)\,,\ m_d(\lambda)\,,\ m_s(\lambda)) \\ &= \mathrm{diag}\,(m_u + \lambda m_d m_s\,,\ m_d + \lambda m_u m_s\,,\ m_s + \lambda m_u m_d)\,, \end{aligned} \tag{11}$$

and leave all observables unchanged.

The combination

$$\left(\frac{m_u}{m_d}\right)^2 + \frac{1}{Q^2}\left(\frac{m_s}{m_d}\right)^2 = 1 \tag{12}$$

where

$$Q^2 = \frac{m^2_s - \hat{m}^2}{m^2_d - m^2_u}, \qquad \hat{m} = \frac{1}{2}\,(m_u + m_d)\,,$$

is insensitive to the transformation in Eq. (11). Eq. (12) gives an ellipse in the $m_u/m_d - m_s/m_d$ plane. The ellipse is well-determined by chiral perturbation theory, but the exact location on the ellipse, and the absolute normalization of the quark masses, has larger uncertainties. Q is determined to be in the range 21–25 from $\eta \to 3\pi$ decay and the electromagnetic contribution to the K^+–K^0 and π^+–π^0 mass differences [11].

The absolute normalization of the quark masses cannot be determined using chiral perturbation theory. Other methods, such as lattice simulations discussed above or spectral function sum rules [12,13] for hadronic correlation functions, which we review next are necessary.

Sum Rules: Sum rule methods have been used extensively to determine quark masses and for illustration we briefly discuss here their application to hadronic τ decays [14]. Other applications involve very similar techniques.

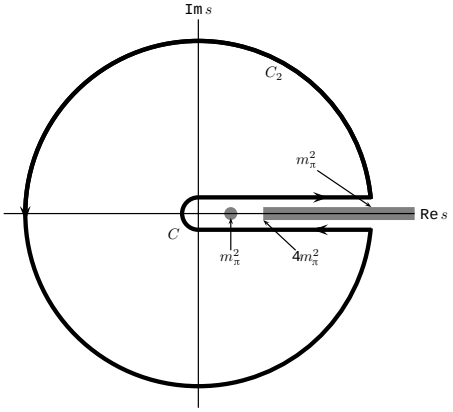

Figure 1: The analytic structure of $\Pi(s)$ in the complex s-plane. The contours C_1 and C_2 are the integration contours discussed in the text.

The experimentally measured quantity is R_τ,

$$\frac{\mathrm{d}R_\tau}{\mathrm{d}s} = \frac{\mathrm{d}\Gamma/\mathrm{d}s\left(\tau^- \to \text{hadrons} + \nu_\tau(\gamma)\right)}{\Gamma\left(\tau^- \to e^-\overline{\nu}_e\nu_\tau(\gamma)\right)} \tag{13}$$

the hadronic invariant mass spectrum in semihadronic τ decay, normalized to the leptonic τ decay rate. It is useful to define q as the total momentum of the hadronic final state, so $s = q^2$ is the hadronic invariant mass. The total hadronic τ decay rate R_τ is then given by integrating $\mathrm{d}R_\tau/\mathrm{d}s$ over the kinematically allowed range $0 \le s \le M_\tau^2$.

R_τ can be written as

$$R_\tau = 12\pi \int_0^{M_\tau^2} \frac{\mathrm{d}s}{M_\tau^2}\left(1 - \frac{s}{M_\tau^2}\right)^2 \times \left[\left(1 + 2\frac{s}{M_\tau^2}\right)\mathrm{Im}\,\Pi^T(s) + \mathrm{Im}\,\Pi^L(s)\right] \tag{14}$$

where $s = q^2$, and the hadronic spectral functions $\Pi^{L,T}$ are defined from the time-ordered correlation function of two weak currents is the time-ordered correlator of the weak interaction current ($j^\mu(x)$ and $j^\nu(0)$) by

$$\Pi^{\mu\nu}(q) = i\int \mathrm{d}^4x\; e^{iq\cdot x}\,\langle 0|\,T\left(j^\mu(x)j^\nu(0)^\dagger\right)|0\rangle\,, \tag{15}$$

$$\Pi^{\mu\nu}(q) = (-g^{\mu\nu} + q^\mu q^\nu)\,\Pi^T(s) + q^\mu q^\nu \Pi^L(s), \tag{16}$$

and the decomposition Eq. (16) is the most general possible structure consistent with Lorentz invariance.

By the optical theorem, the imaginary part of $\Pi^{\mu\nu}$ is proportional to the total cross-section for the current to produce all possible states. A detailed analysis including the phase space factors leads to Eq. (14). The spectral functions $\Pi^{L,T}(s)$ are analytic in the complex s plane, with singularities along the real axis. There is an isolated pole at $s = m_\pi^2$, and single- and multi-particle singularities for $s \ge 4m_\pi^2$, the two-particle threshold. The discontinuity along the real axis is $\Pi^{L,T}(s + i0^+) - \Pi^{L,T}(s - i0^+) = 2i\mathrm{Im}\;\Pi^{L,T}(s)$. As a result, Eq. (14) can be rewritten with the replacement $\mathrm{Im}\;\Pi^{L,T}(s) \to -i\Pi^{L,T}(s)/2$, and the integration being over the contour C_1. Finally, the contour C_1 can be deformed to C_2 without crossing any singularities, and so leaving the integral unchanged. One can derive a series of sum rules analogous to Eq. (14) by weighting the differential τ hadronic decay rate by different powers of the hadronic invariant mass,

$$R_\tau^{kl} = \int_0^{M_\tau^2} \mathrm{d}s\;\left(1 - \frac{s}{M_\tau^2}\right)^k \left(\frac{s}{M_\tau^2}\right)^l \frac{\mathrm{d}R_\tau}{\mathrm{d}s} \tag{17}$$

where $\mathrm{d}R_\tau/\mathrm{d}s$ is the hadronic invariant mass distribution in τ decay normalized to the leptonic decay rate. This leads to the final form of the sum rule(s),

$$R_\tau^{kl} = -6\pi i \int_{C_2} \frac{\mathrm{d}s}{M_\tau^2}\left(1 - \frac{s}{M_\tau^2}\right)^{2+k}\left(\frac{s}{M_\tau^2}\right)^l \times \left[\left(1 + 2\frac{s}{M_\tau^2}\right)\Pi^T(s) + \Pi^L(s)\right]. \tag{18}$$

The manipulations so far are completely rigorous and exact, relying only on the general analytic structure of quantum field theory. The left-hand side of the sum rule Eq. (18) is obtained from experiment. The right hand-side can be computed for s far away from any physical cuts using the operator product expansion (OPE) for the time-ordered product of currents in Eq. (15), and QCD perturbation theory. The OPE is an expansion for the time-ordered product Eq. (15) in a series of local operators, and is an expansion about the $q \to \infty$ limit. It gives $\Pi(s)$ as an expansion in powers of $\alpha_s(s)$ and $\Lambda^2_{\rm QCD}/s$, and is valid when s is far (in units of $\Lambda^2_{\rm QCD}$) from any singularities in the complex s-plane.

The OPE gives $\Pi(s)$ as a series in α_s, quark masses, and various non-perturbative vacuum matrix element. By computing $\Pi(s)$ theoretically, and comparing with the experimental values of R_τ^{kl}, one determines various parameters such as α_s and the quark masses. The theoretical uncertainties in using Eq. (18) arise from neglected higher order corrections (both

perturbative and non-perturbative), and because the OPE is no longer valid near the real axis, where Π has singularities. The contribution of neglected higher order corrections can be estimated as for any other perturbative computation. The error due to the failure of the OPE is more difficult to estimate. In Eq. (18), the OPE fails on the endpoints of C_2 that touch the real axis at $s = M_\tau^2$. The weight factor $(1 - s/M_\tau^2)$ in Eq. (18) vanishes at this point, so the importance of the endpoint can be reduced by choosing larger values of k.

E. Heavy quarks

For heavy-quark physics one can exploit the fact that $m_Q \gg \Lambda_{\rm QCD}$ to construct effective theories (m_Q is the mass of the heavy quark Q). The masses and decay rates of hadrons containing a single heavy quark, such as the B and D mesons can be determined using the heavy quark effective theory (HQET) [34]. The theoretical calculations involve radiative corrections computed in perturbation theory with an expansion in $\alpha_s(m_Q)$ and non-perturbative corrections with an expansion in powers of $\Lambda_{\rm QCD}/m_Q$. Due to the asymptotic nature of the QCD perturbation series, the two kinds of corrections are intimately related; an example of this are renormalon effects in the perturbative expansion which are associated with non-perturbative corrections.

Systems containing two heavy quarks such as the Υ or J/Ψ are treated using non-relativistic QCD (NRQCD) [35]. The typical momentum and energy transfers in these systems are $\alpha_s m_Q$, and $\alpha_s^2 m_Q$, respectively, so these bound states are sensitive to scales much smaller than m_Q. However, smeared observables, such as the cross-section for $e^+e^- \to \overline{b}b$ averaged over some range of s that includes several bound state energy levels, are better behaved and only sensitive to scales near m_Q. For this reason, most determinations of the c, b quark masses using perturbative calculations compare smeared observables with experiment [36–38].

There are many continuum extractions of the c and b quark masses, some with quoted errors of 10 MeV or smaller. There are systematic effects of comparable size, which are typically not included in these error estimates. Reference [30], for example, shows that even though the error estimate of m_c using the rapid convergence of the α_s perturbation series is only a few MeV, the central value of m_c can differ by a much larger amount depending on which algorithm (all of which are formally equally good) is used to determine m_c from the data. This leads to a systematic error from perturbation theory of around 20 MeV for the c quark and 25 MeV for the b quark. Electromagnetic effects, which also are important at this precision, are often not included. For this reason, we inflate the errors on the continuum extractions of m_c and m_b. The average values of m_c and m_b from continuum determinations are (see Sec. G for the 1S scheme)

$$\overline{m}_c(\overline{m}_c) = (1.275 \pm 0.025)\,\text{GeV}$$

$$\overline{m}_b(\overline{m}_b) = (4.18 \pm 0.03)\,\text{GeV}\,, \quad m_b^{\rm 1S} = (4.65 \pm 0.03)\,\text{GeV}\,.$$

Lattice simulations of QCD lead to discretization errors which are powers of $m_Q\, a$ (modulated by logarithms); the power depends on the formulation of lattice QCD being used and in most cases is quadratic. Clearly these errors can be reduced by performing simulations at smaller lattice spacings, but also by using *improved* discretizations of the theory. Recently, with more powerful computing resources, better algorithms and techniques, it has become possible to perform simulations in the charm quark region and beyond, also decreasing the extrapolation which has to be performed to reach the b-quark. A novel approach proposed in [53] has been to compare the lattice results for moments of correlation functions of $c\overline{c}$ quark-bilinear operators to perturbative calculations of the same quantities at 4-loop order. In this way both the strong coupling constant and the charm quark mass can be determined with remarkably small errors; in particular $\overline{m}_c(\overline{m}_c) = 1.273(6)\,\text{GeV}$ [26]. This lattice determination also uses the perturbative expression for the current-current correlator, and so has the perturbation theory systematic error discussed above.

Traditionally, the main approach to controlling the discretization errors in lattice studies of heavy quark physics is to perform simulations of the effective theories such as HQET and NRQCD. This remains an important technique, both in its own right and in providing additional information for extrapolations from lower masses to the bottom region. Using effective theories, m_b is obtained from what is essentially a computation of the difference of $M_{H_b} - m_b$, where M_{H_b} is the mass of a hadron H_b containing a b-quark. The relative error on m_b is therefore much smaller than that for $M_{H_b} - m_b$, and this is the reason for the small errors quoted in section G. The principal systematic errors are the matching of the effective theories to QCD and the presence of power divergences in a^{-1} in the $1/m_b$ corrections which have to be subtracted numerically. The use of HQET or NRQCD is less precise for the charm quark, but in this case, as mentioned above, direct QCD simulations have recently become possible.

F. Pole Mass

For an observable particle such as the electron, the position of the pole in the propagator is the definition of its mass. In QCD this definition of the quark mass is known as the pole mass. It is known that the on-shell quark propagator has no infrared divergences in perturbation theory [41,42], so this provides a perturbative definition of the quark mass. The pole mass cannot be used to arbitrarily high accuracy because of nonperturbative infrared effects in QCD. The full quark propagator has no pole because the quarks are confined, so that the pole mass cannot be defined outside of perturbation theory. The relation between the pole mass m_Q and the $\overline{\rm MS}$ mass $\overline{m}_Q$ is known to three loops [43,44,45,46]

$$m_Q = \overline{m}_Q(\overline{m}_Q)\left\{1 + \frac{4\overline{\alpha}_s(\overline{m}_Q)}{3\pi} + \left[-1.0414\sum_k\left(1 - \frac{4}{3}\frac{\overline{m}_{Q_k}}{\overline{m}_Q}\right) + 13.4434\right]\left[\frac{\overline{\alpha}_s(\overline{m}_Q)}{\pi}\right]^2\right.$$

$$+ \left[0.6527 N_L^2 - 26.655 N_L + 190.595\right] \left[\frac{\overline{\alpha}_s(\overline{m}_Q)}{\pi}\right]^3 \Bigg\}, \quad (19)$$

where $\overline{\alpha}_s(\mu)$ is the strong interaction coupling constants in the $\overline{\rm MS}$ scheme, and the sum over k extends over the N_L flavors Q_k lighter than Q. The complete mass dependence of the α_s^2 term can be found in [43]; the mass dependence of the α_s^3 term is not known. For the b-quark, Eq. (19) reads

$$m_b = \overline{m}_b\,(\overline{m}_b)\,[1 + 0.09 + 0.05 + 0.03]\,, \quad (20)$$

where the contributions from the different orders in α_s are shown explicitly. The two and three loop corrections are comparable in size and have the same sign as the one loop term. This is a signal of the asymptotic nature of the perturbation series [there is a renormalon in the pole mass]. Such a badly behaved perturbation expansion can be avoided by directly extracting the $\overline{\rm MS}$ mass from data without extracting the pole mass as an intermediate step.

G. Numerical values and caveats

The quark masses in the particle data listings have been obtained by using a wide variety of methods. Each method involves its own set of approximations and uncertainties. In most cases, the errors are an estimate of the size of neglected higher-order corrections or other uncertainties. The expansion parameters for some of the approximations are not very small (for example, they are $m_K^2/\Lambda_\chi^2 \sim 0.25$ for the chiral expansion and $\Lambda_{\rm QCD}/m_b \sim 0.1$ for the heavy-quark expansion), so an unexpectedly large coefficient in a neglected higher-order term could significantly alter the results. It is also important to note that the quark mass values can be significantly different in the different schemes.

The heavy quark masses obtained using HQET, QCD sum rules, or lattice gauge theory are consistent with each other if they are all converted into the same scheme and scale. We have specified all masses in the $\overline{\rm MS}$ scheme. For light quarks, the renormalization scale has been chosen to be $\mu = 2\,{\rm GeV}$. The light quark masses at 1 GeV are significantly different from those at 2 GeV, $\overline{m}(1\,{\rm GeV})/\overline{m}(2\,{\rm GeV}) \sim 1.35$. It is conventional to choose the renormalization scale equal to the quark mass for a heavy quark, so we have quoted $\overline{m}_Q(\mu)$ at $\mu = \overline{m}_Q$ for the c and b quarks. Recent analyses of inclusive B meson decays have shown that recently proposed mass definitions lead to a better behaved perturbation series than for the $\overline{\rm MS}$ mass, and hence to more accurate mass values. We have chosen to also give values for one of these, the b quark mass in the 1S-scheme [47,48]. Other schemes that have been proposed are the PS-scheme [49] and the kinetic scheme [50].

If necessary, we have converted values in the original papers to our chosen scheme using two-loop formulæ. It is important to realized that our conversions introduce significant additional errors. In converting to the $\overline{\rm MS}$ b-quark mass, for example, the three-loop conversions from the 1S and pole masses give values about 40 MeV and 135 MeV lower than the two-loop conversions. The uncertainty in $\alpha_s(M_Z) = 0.1187(20)$ gives an uncertainty of ±20 MeV and ±35 MeV respectively in the same conversions. We have not added these additional errors when we do our conversions. The α_s value in the conversion is correlated with the α_s value used in determining the quark mass, so the conversion error is not a simple additional error on the quark mass.

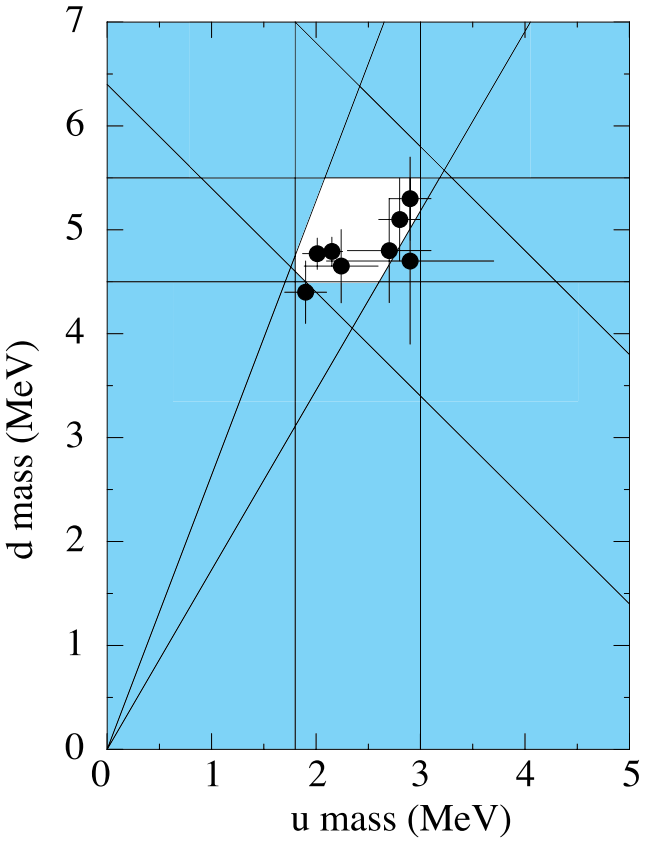

Figure 2: The allowed region (shown in white) for up quark and down quark masses. This region was determined in part from papers reporting values for m_u and m_d (data points shown) and in part from analysis of the allowed ranges of other mass parameters (see Fig. 3). The parameter $(m_u + m_d)/2$ yields the two downward-sloping lines, while m_u/m_d yields the two rising lines originating at (0,0).

See key on page 547

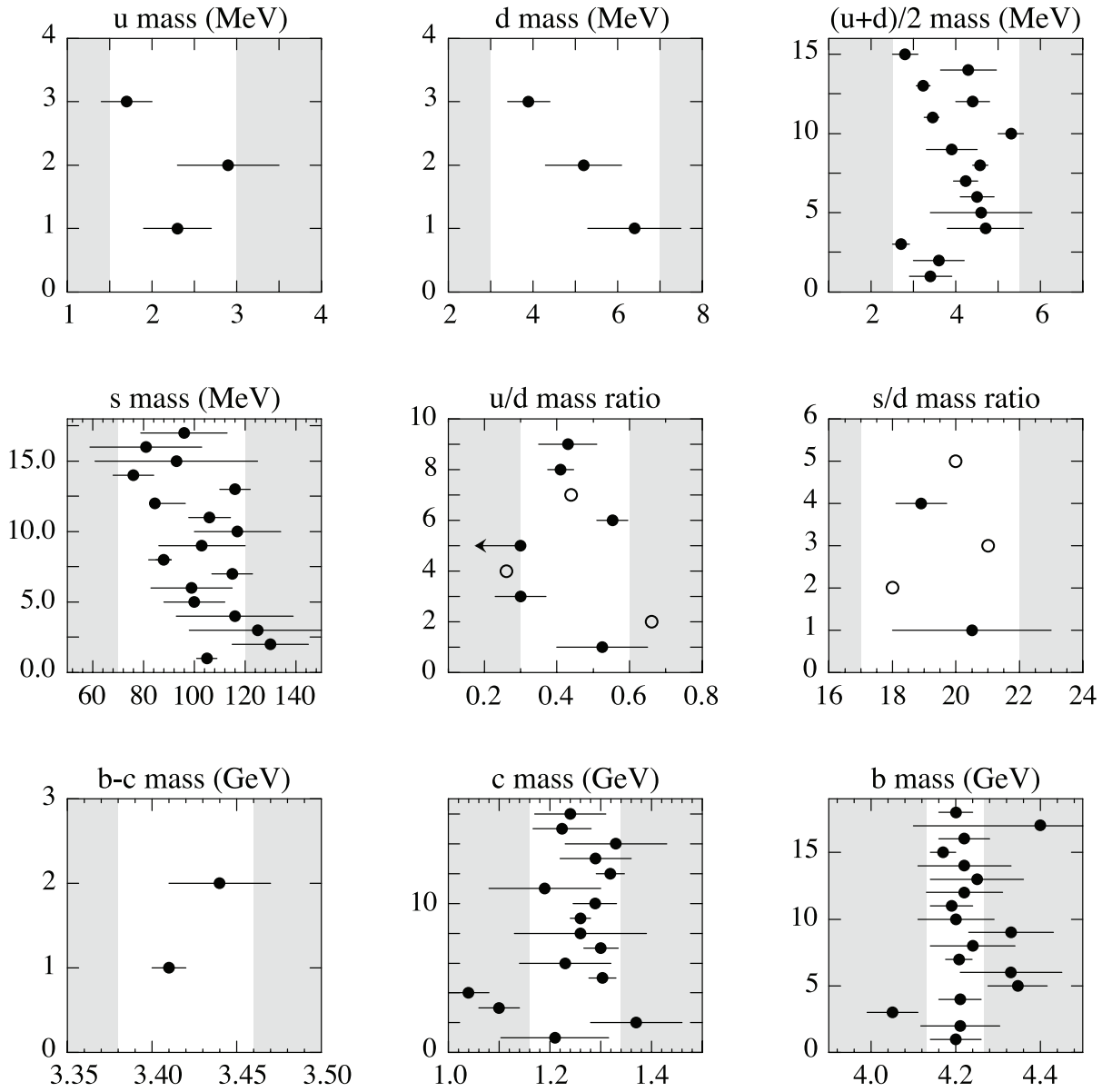

Figure 3. The values of each quark mass parameter taken from the Data Listings. The points are in chronological order with the more recent measurements at the top. Points from papers reporting no error bars are colored grey. The shaded regions indicate values excluded by our evaluations; some regions were determined in part through examination of Fig. 2.

References

1. See the review of QCD in this volume..
2. A.V. Manohar and H. Georgi, Nucl. Phys. **B234**, 189 (1984).
3. K.G. Chetyrkin, Phys. Lett. **B404**, 161 (1997).
4. J.A.M. Vermaseren, S.A. Larin, and T. van Ritbergen, Phys. Lett. **B405**, 327 (1997).
5. K.G. Chetyrkin, B.A. Kniehl, and M. Steinhauser, Nucl. Phys. **B510**, 61 (1998).
6. S. Weinberg, Physica **96A**, 327 (1979).
7. J. Gasser and H. Leutwyler, Ann. Phys. **158**, 142 (184).
8. For a review, see A. Pich, Rept. Prog. Phys. **58**, 563 (1995).
9. S. Weinberg, Trans. N.Y. Acad. Sci. **38**, 185 (1977).
10. D.B. Kaplan and A.V. Manohar, Phys. Rev. Lett. **56**, 2004 (1986).
11. H. Leutwyler, Phys. Lett. **B374**, 163 (1996).
12. S. Weinberg, Phys. Rev. Lett. **18**, 507 (1967)..
13. M.A. Shifman, A.I. Vainshtein, and V.I. Zakharov, Nucl. Phys. **B147**, 385 (1979).
14. E. Braaten, S. Narison, and A. Pich, Nucl. Phys. **B373**, 581 (1992).
15. C. Bernard *et al.*, PoS **LAT2007** (2007) 090.
16. A. Bazavov *et al.*, `arXiv:0903.3598 [hep-lat]`.
17. C. Aubin *et al.* [HPQCD Collab.], Phys. Rev. **D70**, 031504 (2004).
18. C. Aubin *et al.* [MILC Collab.], Phys. Rev. D **70** (2004) 114501.
19. B. Blossier *et al.* [ETM Collab.], Phys. Rev. **D82** (2010) 114513.
20. A. Bazavov *et al.* [MILC Collab.], PoS **CD09** (2009) 007.
21. A. Bazavov *et al.*, PoS **LATTICE2010** (2010) 083.
22. S. Durr *et al.*, Phys. Lett. **B701** (2011) 265-268.
23. S. Durr *et al.*, JHEP **1108** (2011) 148.
24. Y. Aoki *et al.* [RBC and UKQCD Collabs.], Phys. Rev. **D83** (2011) 074508.
25. C.T.H. Davies *et al.*, Phys. Rev. Lett. **104** (2010) 132003.
26. C. McNeile *et al.*, Phys. Rev. **D82** (2010) 034512.
27. C. Aubin *et al.* [MILC Collab.], Nucl. Phys. Proc. Suppl. **140** (2005) 231.
28. C. Aubin *et al.* [MILC Collab.], Phys. Rev. D **70** (2004) 114501.
29. G. Colangelo *et al.*, Eur. Phys. J. C **71** (2011) 1695.
30. B. Dehnadi *et al.*, `arXiv:1102.2264 [hep-ph]`.
31. T. Blum *et al.*, Phys. Rev. D **76** (2007) 114508.
32. G. Colangelo *et al.*, Eur. Phys. J. C **71** (2011) 1695;.
33. A. Ali Khan *et al.* [CP-PACS Collab.], Phys. Rev. D **65** (2002) 054505; [Erratum-ibid. D **67** (2003) 059901].
34. N. Isgur and M.B. Wise, Phys. Lett. **B232**, 113 (1989), *ibid*, **B237**, 527 (1990).
35. G.T. Bodwin, E. Braaten, and G.P. Lepage, Phys. Rev. **D51**, 1125 (1995).
36. A.H. Hoang, Phys. Rev. **D61**, 034005 (2000).
37. K. Melnikov and A. Yelkhovsky, Phys. Rev. **D59**, 114009 (1999).
38. M. Beneke and A. Signer, Phys. Lett. **B471**, 233 (1999).
39. A.X. El-Khadra, A.S. Kronfeld, and P.B. Mackenzie, Phys. Rev. **D55**, 3933 (1997).
40. S. Aoki, Y. Kuramashi, and S.i. Tominaga, Prog. Theor. Phys. **109**, 383 (2003).
41. R. Tarrach, Nucl. Phys. **B183**, 384 (1981).
42. A. Kronfeld, Phys. Rev. **D58**, 051501 (1998).
43. N. Gray *et al.*, Z. Phys. **C48**, 673 (1990).
44. D.J. Broadhurst, N. Gray, and K. Schilcher, Z. Phys. **C52**, 111 (1991).
45. K.G. Chetyrkin and M. Steinhauser, Phys. Rev. Lett. **83**, 4001 (1999).
46. K. Melnikov and T. van Ritbergen, Phys. Lett. **B482**, 99 (2000).
47. A.H. Hoang, Z. Ligeti, A.V. Manohar, Phys. Rev. Lett. **82**, 277 (1999).
48. A.H. Hoang, Z. Ligeti, A.V. Manohar, Phys. Rev. **D59**, 074017 (1999).
49. M. Beneke, Phys. Lett. **B434**, 115 (1998).
50. P. Gambino and N. Uraltsev, Eur. Phys. J. **C34**, 181 (2004).
51. G. Martinelli *et al.*, Nucl. Phys. B **445** (1995) 81.
52. K. Jansen *et al.*, Phys. Lett. B **372** (1996) 275.
53. I. Allison *et al.* [HPQCD Collab.], Phys. Rev. D **78** (2008) 054513.

u

$I(J^P) = \frac{1}{2}(\frac{1}{2}^+)$

Mass $m = 2.3^{+0.7}_{-0.5}$ MeV Charge $= \frac{2}{3}\ e$ $I_z = +\frac{1}{2}$

$m_u/m_d = 0.38$–0.58

d

$I(J^P) = \frac{1}{2}(\frac{1}{2}^+)$

Mass $m = 4.8^{+0.5}_{-0.3}$ MeV Charge $= -\frac{1}{3}\ e$ $I_z = -\frac{1}{2}$

$m_s/m_d = 17$–22

$\overline{m} = (m_u + m_d)/2 = 3.5^{+0.7}_{-0.2}$ MeV

s

$I(J^P) = 0(\frac{1}{2}^+)$

Mass $m = 95 \pm 5$ MeV Charge $= -\frac{1}{3}\ e$ Strangeness $= -1$

$(m_s - (m_u + m_d)/2)/(m_d - m_u) = 27.5 \pm 1.0$

LIGHT QUARKS (u, d, s)

OMITTED FROM SUMMARY TABLE

u-QUARK MASS

The u-, d-, and s-quark masses are estimates of so-called "current-quark masses," in a mass-independent subtraction scheme such as $\overline{\text{MS}}$. The ratios m_u/m_d and m_s/m_d are extracted from pion and kaon masses using chiral symmetry. The estimates of d and u masses are not without controversy and remain under active investigation. Within the literature there are even suggestions that the u quark could be essentially massless. The s-quark mass is estimated from SU(3) splittings in hadron masses.

We have normalized the $\overline{\text{MS}}$ masses at a renormalization scale of $\mu = 2$ GeV. Results quoted in the literature at $\mu = 1$ GeV have been rescaled by dividing by 1.35. The values of "Our Evaluation" were determined in part via Figures 1 and 2.

VALUE (MeV)	DOCUMENT ID		TECN	COMMENT
2.3 $^{+0.7}_{-0.5}$ OUR EVALUATION	See the ideogram below.			
$2.15 \pm 0.03 \pm 0.10$	[1] DURR	11	LATT	$\overline{\text{MS}}$ scheme
$2.24 \pm 0.10 \pm 0.34$	[2] BLUM	10	LATT	$\overline{\text{MS}}$ scheme
2.01 ± 0.14	[3] MCNEILE	10	LATT	$\overline{\text{MS}}$ scheme
2.9 ± 0.2	[4] DOMINGUEZ	09	THEO	$\overline{\text{MS}}$ scheme
2.7 ± 0.4	[5] JAMIN	06	THEO	$\overline{\text{MS}}$ scheme
1.9 ± 0.2	[6] MASON	06	LATT	$\overline{\text{MS}}$ scheme
2.8 ± 0.2	[7] NARISON	06	THEO	$\overline{\text{MS}}$ scheme

• • • We do not use the following data for averages, fits, limits, etc. • • •

2.01±0.14	[3] DAVIES	10	LATT	$\overline{\text{MS}}$ scheme
2.9 ±0.8	[8] DEANDREA	08	THEO	$\overline{\text{MS}}$ scheme
3.02±0.33	[9] BLUM	07	LATT	$\overline{\text{MS}}$ scheme
1.7 ±0.3	[10] AUBIN	04A	LATT	$\overline{\text{MS}}$ scheme

[1] DURR 11 determine quark mass from a lattice computation of the meson spectrum using $N_f = 2 + 1$ dynamical flavors. The lattice simulations were done at the physical quark mass, so that extrapolation in the quark mass was not needed. The individual m_u, m_d values are obtained using the lattice determination of the average mass m_{ud} and of the ratio m_s/m_{ud} and the value of $Q = (m_s^2 - m_{ud}^2) / (m_d^2 - m_u^2)$ as determined from $\eta \to 3\pi$ decays.

[2] BLUM 10 determines light quark masses using a QCD plus QED lattice computation of the electromagnetic mass splittings of the low-lying hadrons. The lattice simulations use 2+1 dynamical quark flavors.

[3] DAVIES 10 and MCNEILE 10 determine $\overline{m}_c(\mu)/\overline{m}_s(\mu) = 11.85 \pm 0.16$ using a lattice computation with $N_f = 2 + 1$ dynamical fermions of the pseudoscalar meson masses. Mass m_u is obtained from this using the value of m_c from ALLISON 08 or MCNEILE 10 and the BAZAVOV 10 values for the light quark mass ratios, $m_s/\overline{m}$ and m_u/m_d.

[4] DOMINGUEZ 09 use QCD finite energy sum rules for the two-point function of the divergence of the axial vector current computed to order α_s^4.

[5] JAMIN 06 determine m_u(2 GeV) by combining the value of m_s obtained from the spectral function for the scalar $K\pi$ form factor with other determinations of the quark mass ratios.

[6] MASON 06 extract light quark masses from a lattice simulation using staggered fermions with an improved action, and three dynamical light quark flavors with degenerate u and d quarks. Perturbative corrections were included at NNLO order. The quark masses m_u and m_d were determined from their $(m_u+m_d)/2$ measurement and AUBIN 04A m_u/m_d value.

[7] NARISON 06 uses sum rules for $e^+e^- \to$ hadrons to order α_s^3 to determine m_s combined with other determinations of the quark mass ratios.

[8] DEANDREA 08 determine $m_u - m_d$ from $\eta \to 3\pi^0$, and combine with the PDG 06 lattice average value of $m_u + m_d = 7.6 \pm 1.6$ to determine m_u and m_d.

[9] BLUM 07 determine quark masses from the pseudoscalar meson masses using a QED plus QCD lattice computation with two dynamical quark flavors.

[10] AUBIN 04A employ a partially quenched lattice calculation of the pseudoscalar meson masses.

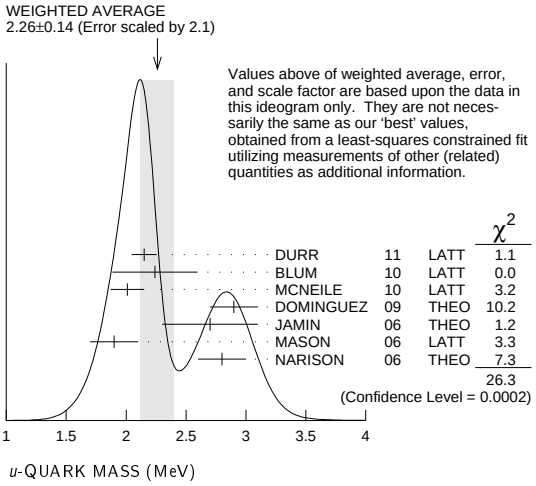

d-QUARK MASS

See the comment for the u quark above.

We have normalized the $\overline{\text{MS}}$ masses at a renormalization scale of $\mu = 2$ GeV. Results quoted in the literature at $\mu = 1$ GeV have been rescaled by dividing by 1.35. The values of "Our Evaluation" were determined in part via Figures 1 and 2.

VALUE (MeV)	DOCUMENT ID		TECN	COMMENT
4.8 $^{+0.5}_{-0.3}$ OUR EVALUATION	See the ideogram below.			
4.79±0.07±0.12	[1] DURR	11	LATT	$\overline{\text{MS}}$ scheme
4.65±0.15±0.32	[2] BLUM	10	LATT	$\overline{\text{MS}}$ scheme
4.77±0.15	[3] MCNEILE	10	LATT	$\overline{\text{MS}}$ scheme
5.3 ±0.4	[4] DOMINGUEZ	09	THEO	$\overline{\text{MS}}$ scheme
4.8 ±0.5	[5] JAMIN	06	THEO	$\overline{\text{MS}}$ scheme
4.4 ±0.3	[6] MASON	06	LATT	$\overline{\text{MS}}$ scheme
5.1 ±0.4	[7] NARISON	06	THEO	$\overline{\text{MS}}$ scheme
• • • We do not use the following data for averages, fits, limits, etc. • • •				
4.79±0.16	[3] DAVIES	10	LATT	$\overline{\text{MS}}$ scheme
4.7 ±0.8	[8] DEANDREA	08	THEO	$\overline{\text{MS}}$ scheme
5.49±0.39	[9] BLUM	07	LATT	$\overline{\text{MS}}$ scheme
3.9 ±0.5	[10] AUBIN	04A	LATT	$\overline{\text{MS}}$ scheme

[1] DURR 11 determine quark mass from a lattice computation of the meson spectrum using $N_f = 2 + 1$ dynamical flavors. The lattice simulations were done at the physical quark mass, so that extrapolation in the quark mass was not needed. The individual m_u, m_d values are obtained using the lattice determination of the average mass m_{ud} and of the ratio m_s/m_{ud} and the value of $Q = (m_s^2 - m_{ud}^2) / (m_d^2 - m_u^2)$ as determined from $\eta \to 3\pi$ decays.

[2] BLUM 10 determines light quark masses using a QCD plus QED lattice computation of the electromagnetic mass splittings of the low-lying hadrons. The lattice simulations use 2+1 dynamical quark flavors.

[3] DAVIES 10 and MCNEILE 10 determine $\overline{m}_c(\mu)/\overline{m}_s(\mu) = 11.85 \pm 0.16$ using a lattice computation with $N_f = 2 + 1$ dynamical fermions of the pseudoscalar meson masses. Mass m_d is obtained from this using the value of m_c from ALLISON 08 or MCNEILE 10 and the BAZAVOV 10 values for the light quark mass ratios, $m_s/\overline{m}$ and m_u/m_d.

[4] DOMINGUEZ 09 use QCD finite energy sum rules for the two-point function of the divergence of the axial vector current computed to order α_s^4.

[5] JAMIN 06 determine m_d(2 GeV) by combining the value of m_s obtained from the spectral function for the scalar $K\pi$ form factor with other determinations of the quark mass ratios.

[6] MASON 06 extract light quark masses from a lattice simulation using staggered fermions with an improved action, and three dynamical light quark flavors with degenerate u and d quarks. Perturbative corrections were included at NNLO order. The quark masses m_u and m_d were determined from their $(m_u+m_d)/2$ measurement and AUBIN 04A m_u/m_d value.

[7] NARISON 06 uses sum rules for $e^+e^- \to$ hadrons to order α_s^3 to determine m_s combined with other determinations of the quark mass ratios.

[8] DEANDREA 08 determine $m_u - m_d$ from $\eta \to 3\pi^0$, and combine with the PDG 06 lattice average value of $m_u + m_d = 7.6 \pm 1.6$ to determine m_u and m_d.

[9] BLUM 07 determine quark masses from the pseudoscalar meson masses using a QED plus QCD lattice computation with two dynamical quark flavors.

[10] AUBIN 04A perform three flavor dynamical lattice calculation of pseudoscalar meson masses, with continuum estimate of electromagnetic effects in the kaon masses, and one-loop perturbative renormalization constant.

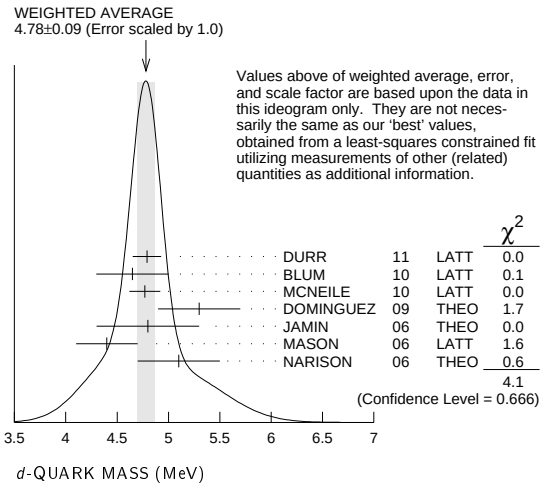

$\overline{m} = (m_u + m_d)/2$

See the comments for the u quark above.

We have normalized the $\overline{\text{MS}}$ masses at a renormalization scale of $\mu = 2$ GeV. Results quoted in the literature at $\mu = 1$ GeV have been rescaled by dividing by 1.35. The values of "Our Evaluation" were determined in part via Figures 1 and 2.

VALUE (MeV)	DOCUMENT ID		TECN	COMMENT
3.5 $^{+0.7}_{-0.2}$ OUR EVALUATION	See the ideogram below.			
3.59 ±0.21	[1] AOKI	11A	LATT	$\overline{\text{MS}}$ scheme
3.469±0.047±0.048	[2] DURR	11	LATT	$\overline{\text{MS}}$ scheme
3.6 ±0.2	[3] BLOSSIER	10	LATT	$\overline{\text{MS}}$ scheme
3.39 ±0.06	[4] MCNEILE	10	LATT	$\overline{\text{MS}}$ scheme
4.1 ±0.2	[5] DOMINGUEZ	09	THEO	$\overline{\text{MS}}$ scheme
3.72 ±0.41	[6] ALLTON	08	LATT	$\overline{\text{MS}}$ scheme
3.55 $^{+0.65}_{-0.28}$	[7] ISHIKAWA	08	LATT	$\overline{\text{MS}}$ scheme
4.25 ±0.35	[8] BLUM	07	LATT	$\overline{\text{MS}}$ scheme
4.08 ±0.25 ±0.42	[9] GOCKELER	06	LATT	$\overline{\text{MS}}$ scheme
4.7 ±0.2 ±0.3	[10] GOCKELER	06A	LATT	$\overline{\text{MS}}$ scheme
3.2 ±0.3	[11] MASON	06	LATT	$\overline{\text{MS}}$ scheme
3.95 ±0.3	[12] NARISON	06	THEO	$\overline{\text{MS}}$ scheme

Quark Particle Listings

Light Quarks (u, d, s)

• • • We do not use the following data for averages, fits, limits, etc. • • •

3.40 ±0.07	[4] DAVIES	10	LATT	$\overline{\text{MS}}$ scheme
3.85 ±0.12 ±0.4	[13] BLOSSIER	08	LATT	$\overline{\text{MS}}$ scheme
≥ 4.85 ±0.20	[14] DOMINGUEZ...	08B	THEO	$\overline{\text{MS}}$ scheme
4.026±0.048	[15] NAKAMURA	08	LATT	$\overline{\text{MS}}$ scheme
2.8 ±0.3	[16] AUBIN	04	LATT	$\overline{\text{MS}}$ scheme
4.29 ±0.14 ±0.65	[17] AOKI	03	LATT	$\overline{\text{MS}}$ scheme
3.223±0.3	[18] AOKI	03B	LATT	$\overline{\text{MS}}$ scheme
4.4 ±0.1 ±0.4	[19] BECIREVIC	03	LATT	$\overline{\text{MS}}$ scheme
4.1 ±0.3 ±1.0	[20] CHIU	03	LATT	$\overline{\text{MS}}$ scheme

[1] AOKI 11A determine quark masses from a lattice computation of the hadron spectrum using $N_f = 2 + 1$ dynamical flavors of domain wall fermions.

[2] DURR 11 determine quark mass from a lattice computation of the meson spectrum using $N_f = 2 + 1$ dynamical flavors. The lattice simulations were done at the physical quark mass, so that extrapolation in the quark mass was not needed.

[3] BLOSSIER 10 determines quark masses from a computation of the hadron spectrum using N_f=2 dynamical twisted-mass Wilson fermions.

[4] DAVIES 10 and MCNEILE 10 determine $\overline{m}_c(\mu)/\overline{m}_s(\mu) = 11.85 \pm 0.16$ using a lattice computation with $N_f = 2 + 1$ dynamical fermions of the pseudoscalar meson masses. Mass $\overline{m}$ is obtained from this using the value of m_c from ALLISON 08 or MCNEILE 10 and the BAZAVOV 10 values for the light quark mass ratio, $m_s/\overline{m}$.

[5] DOMINGUEZ 09 use QCD finite energy sum rules for the two-point function of the divergence of the axial vector current computed to order α_s^4.

[6] ALLTON 08 use a lattice computation of the π, K, and Ω masses with 2+1 dynamical flavors of domain wall quarks, and non-perturbative renormalization.

[7] ISHIKAWA 08 use a lattice computation of the light meson spectrum with 2+1 dynamical flavors of $\mathcal{O}(a)$ improved Wilson quarks, and one-loop perturbative renormalization.

[8] BLUM 07 determine quark masses from the pseudoscalar meson masses using a QED plus QCD lattice computation with two dynamical quark flavors.

[9] GOCKELER 06 use an unquenched lattice computation of the axial Ward Identity with $N_f = 2$ dynamical light quark flavors, and non-perturbative renormalization, to obtain $\overline{m}(2\text{ GeV}) = 4.08 \pm 0.25 \pm 0.19 \pm 0.23$ MeV, where the first error is statistical, the second and third are systematic due to the fit range and force scale uncertainties, respectively. We have combined the systematic errors linearly.

[10] GOCKELER 06A use an unquenched lattice computation of the pseudoscalar meson masses with $N_f = 2$ dynamical light quark flavors, and non-perturbative renormalization.

[11] MASON 06 extract light quark masses from a lattice simulation using staggered fermions with an improved action, and three dynamical light quark flavors with degenerate u and d quarks. Perturbative corrections were included at NNLO order.

[12] NARISON 06 uses sum rules for $e^+e^- \to$ hadrons to order α_s^3 to determine m_s combined with other determinations of the quark mass ratios.

[13] BLOSSIER 08 use a lattice computation of pseudoscalar meson masses and decay constants with 2 dynamical flavors and non-perturbative renormalization.

[14] DOMINGUEZ-CLARIMON 08B obtain an inequality from sum rules for the scalar two-point correlator.

[15] NAKAMURA 08 do a lattice computation using quenched domain wall fermions and non-perturbative renormalization.

[16] AUBIN 04 perform three flavor dynamical lattice calculation of pseudoscalar meson masses, with one-loop perturbative renormalization constant.

[17] AOKI 03 uses quenched lattice simulation of the meson and baryon masses with degenerate light quarks. The extrapolations are done using quenched chiral perturbation theory.

[18] The errors given in AOKI 03B were $^{+0.046}_{-0.069}$. We changed them to ±0.3 for calculating the overall best values. AOKI 03B uses lattice simulation of the meson and baryon masses with two dynamical light quarks. Simulations are performed using the $\mathcal{O}(a)$ improved Wilson action.

[19] BECIREVIC 03 perform quenched lattice computation using the vector and axial Ward identities. Uses $\mathcal{O}(a)$ improved Wilson action and nonperturbative renormalization.

[20] CHIU 03 determines quark masses from the pion and kaon masses using a lattice simulation with a chiral fermion action in quenched approximation.

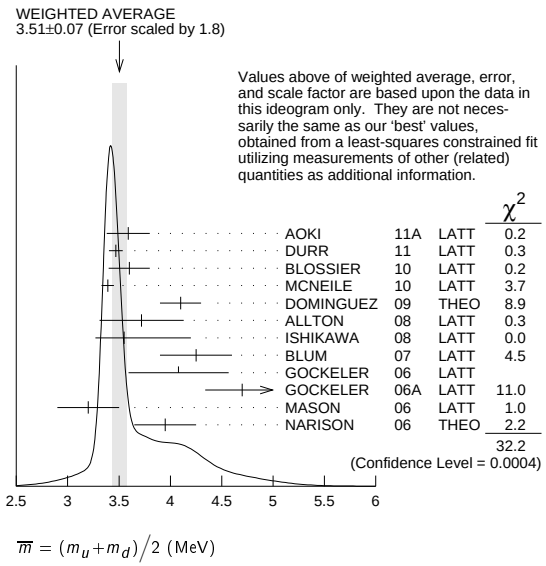

m_u/m_d MASS RATIO

VALUE	DOCUMENT ID		TECN	COMMENT
0.38–0.58 OUR EVALUATION	See the ideogram below.			
0.550±0.031	[1] BLUM	07	LATT	
0.43 ±0.08	[2] AUBIN	04A	LATT	
0.410±0.036	[3] NELSON	03	LATT	
0.553±0.043	[4] LEUTWYLER	96	THEO	Compilation

[1] BLUM 07 determine quark masses from the pseudoscalar meson masses using a QED plus QCD lattice computation with two dynamical quark flavors.

[2] AUBIN 04A perform three flavor dynamical lattice calculation of pseudoscalar meson masses, with continuum estimate of electromagnetic effects in the kaon masses.

[3] NELSON 03 computes coefficients in the order p^4 chiral Lagrangian using a lattice calculation with three dynamical flavors. The ratio m_u/m_d is obtained by combining this with the chiral perturbation theory computation of the meson masses to order p^4.

[4] LEUTWYLER 96 uses a combined fit to $\eta \to 3\pi$ and $\psi' \to J/\psi\,(\pi,\eta)$ decay rates, and the electromagnetic mass differences of the π and K.

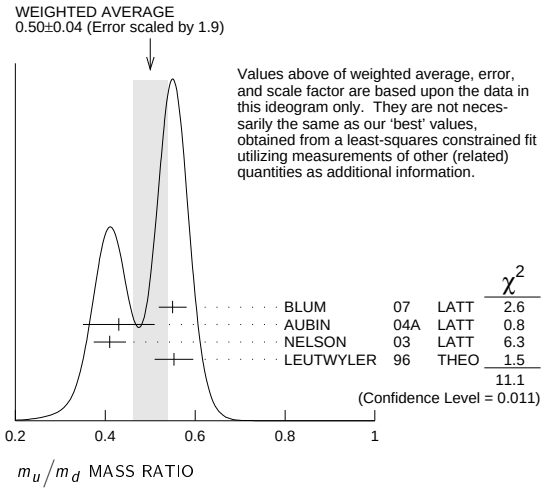

s-QUARK MASS

See the comment for the u quark above.

We have normalized the $\overline{\text{MS}}$ masses at a renormalization scale of $\mu = 2$ GeV. Results quoted in the literature at $\mu = 1$ GeV have been rescaled by dividing by 1.35.

VALUE (MeV)	DOCUMENT ID		TECN	COMMENT
95 ± 5 OUR EVALUATION	See the ideogram below.			
94 ± 9	[1] BODENSTEIN	13	THEO	$\overline{\text{MS}}$ scheme
102 ± 3 ± 1	[2] FRITZSCH	12	LATT	$\overline{\text{MS}}$ scheme
96.2± 2.7	[3] AOKI	11A	LATT	$\overline{\text{MS}}$ scheme
95.5± 1.1± 1.5	[4] DURR	11	LATT	$\overline{\text{MS}}$ scheme
95 ± 6	[5] BLOSSIER	10	LATT	$\overline{\text{MS}}$ scheme
97.6± 2.9± 5.5	[6] BLUM	10	LATT	$\overline{\text{MS}}$ scheme
92.2± 1.3	[7] MCNEILE	10	LATT	$\overline{\text{MS}}$ scheme
107.3±11.7	[8] ALLTON	08	LATT	$\overline{\text{MS}}$ scheme
102 ± 8	[9] DOMINGUEZ	08A	THEO	$\overline{\text{MS}}$ scheme
$90.1^{+17.2}_{-\ 6.1}$	[10] ISHIKAWA	08	LATT	$\overline{\text{MS}}$ scheme
105 ± 6 ± 7	[11] CHETYRKIN	06	THEO	$\overline{\text{MS}}$ scheme
111 ± 6 ±10	[12] GOCKELER	06	LATT	$\overline{\text{MS}}$ scheme
119 ± 5 ± 8	[13] GOCKELER	06A	LATT	$\overline{\text{MS}}$ scheme
92 ± 9	[14] JAMIN	06	THEO	$\overline{\text{MS}}$ scheme
87 ± 6	[15] MASON	06	LATT	$\overline{\text{MS}}$ scheme
104 ±15	[16] NARISON	06	THEO	$\overline{\text{MS}}$ scheme

• • • We do not use the following data for averages, fits, limits, etc. • • •

92.4± 1.5	[7] DAVIES	10	LATT	$\overline{\text{MS}}$ scheme
105 ± 3 ± 9	[17] BLOSSIER	08	LATT	$\overline{\text{MS}}$ scheme
105.6± 1.2	[18] NAKAMURA	08	LATT	$\overline{\text{MS}}$ scheme
119.5± 9.3	[19] BLUM	07	LATT	$\overline{\text{MS}}$ scheme
≥ 71 ± 4, ≤ 151 ± 14	[20] NARISON	06	THEO	$\overline{\text{MS}}$ scheme
$96\ ^{+\ 5}_{-\ 3}\ ^{+16}_{-18}$	[21] BAIKOV	05	THEO	$\overline{\text{MS}}$ scheme
81 ±22	[22] GAMIZ	05	THEO	$\overline{\text{MS}}$ scheme
125 ±28	[23] GORBUNOV	05	THEO	$\overline{\text{MS}}$ scheme
93 ±32	[24] NARISON	05	THEO	$\overline{\text{MS}}$ scheme
76 ± 8	[25] AUBIN	04	LATT	$\overline{\text{MS}}$ scheme
116 ± 6 ± 0.65	[26] AOKI	03	LATT	$\overline{\text{MS}}$ scheme
$84.5^{+12}_{-\ 1.7}$	[27] AOKI	03B	LATT	$\overline{\text{MS}}$ scheme
106 ± 2 ± 8	[28] BECIREVIC	03	LATT	$\overline{\text{MS}}$ scheme
92 ± 9 ±16	[29] CHIU	03	LATT	$\overline{\text{MS}}$ scheme
117 ±17	[30] GAMIZ	03	THEO	$\overline{\text{MS}}$ scheme
103 ±17	[31] GAMIZ	03	THEO	$\overline{\text{MS}}$ scheme

[1] BODENSTEIN 13 determines m_s from QCD finite energy sum rules, and the perturbative computation of the pseudoscalar correlator to five-loop order.

[2] FRITZSCH 12 determine m_s using a lattice computation with $N_f = 2$ dynamical flavors.

[3] AOKI 11A determine quark masses from a lattice computation of the hadron spectrum using $N_f = 2 + 1$ dynamical flavors of domain wall fermions.

[4] DURR 11 determine quark mass from a lattice computation of the meson spectrum using $N_f = 2 + 1$ dynamical flavors. The lattice simulations were done at the physical quark mass, so that extrapolation in the quark mass was not needed.

[5] BLOSSIER 10 determines quark masses from a computation of the hadron spectrum using N_f=2 dynamical twisted-mass Wilson fermions.

[6] BLUM 10 determines light quark masses using a QCD plus QED lattice computation of the electromagnetic mass splittings of the low-lying hadrons. The lattice simulations use 2+1 dynamical quark flavors.

[7] DAVIES 10 and MCNEILE 10 determine $\overline{m}_C(\mu)/\overline{m}_s(\mu) = 11.85 \pm 0.16$ using a lattice computation with $N_f = 2 + 1$ dynamical fermions of the pseudoscalar meson masses. Mass m_s is obtained from this using the value of m_C from ALLISON 08 or MCNEILE 10.

[8] ALLTON 08 use a lattice computation of the π, K, and Ω masses with 2+1 dynamical flavors of domain wall quarks, and non-perturbative renormalization.

[9] DOMINGUEZ 08A make determination from QCD finite energy sum rules for the pseudoscalar two-point function computed to order α_s^4.

[10] ISHIKAWA 08 use a lattice computation of the light meson spectrum with 2+1 dynamical flavors of $\mathcal{O}(a)$ improved Wilson quarks, and one-loop perturbative renormalization.

[11] CHETYRKIN 06 use QCD sum rules in the pseudoscalar channel to order α_s^4.

[12] GOCKELER 06 use an unquenched lattice computation of the axial Ward Identity with $N_f = 2$ dynamical light quark flavors, and non-perturbative renormalization, to obtain $\overline{m}_s(2\text{ GeV}) = 111 \pm 6 \pm 4 \pm 6$ MeV, where the first error is statistical, the second and third are systematic due to the fit range and force scale uncertainties, respectively. We have combined the systematic errors linearly.

[13] GOCKELER 06A use an unquenched lattice computation of the pseudoscalar meson masses with $N_f = 2$ dynamical light quark flavors, and non-perturbative renormalization.

[14] JAMIN 06 determine $\overline{m}_s(2\text{ GeV})$ from the spectral function for the scalar $K\pi$ form factor.

[15] MASON 06 extract light quark masses from a lattice simulation using staggered fermions with an improved action, and three dynamical light quark flavors with degenerate u and d quarks. Perturbative corrections were included at NNLO order.

[16] NARISON 06 uses sum rules for $e^+e^- \to$ hadrons to order α_s^3.

[17] BLOSSIER 08 use a lattice computation of pseudoscalar meson masses and decay constants with 2 dynamical flavors and non-perturbative renormalization.

[18] NAKAMURA 08 do a lattice computation using quenched domain wall fermions and non-perturbative renormalization.

[19] BLUM 07 determine quark masses from the pseudoscalar meson masses using a QED plus QCD lattice computation with two dynamical quark flavors.

[20] NARISON 06 obtains the quoted range from positivity of the spectral functions.

[21] BAIKOV 05 determines $\overline{m}_s(M_\tau) = 100^{+5+17}_{-3-19}$ from sum rules using the strange spectral function in τ decay. The computations were done to order α_s^3, with an estimate of the α_s^4 terms. We have converted the result to $\mu = 2$ GeV.

[22] GAMIZ 05 determines $\overline{m}_s(2\text{ GeV})$ from sum rules using the strange spectral function in τ decay. The computations were done to order α_s^2, with an estimate of the α_s^3 terms.

[23] GORBUNOV 05 use hadronic tau decays to N^{3}LO, including power corrections.

[24] NARISON 05 determines $\overline{m}_s(2\text{ GeV})$ from sum rules using the strange spectral function in τ decay. The computations were done to order α_s^3.

[25] AUBIN 04 perform three flavor dynamical lattice calculation of pseudoscalar meson masses, with one-loop perturbative renormalization constant.

[26] AOKI 03 uses quenched lattice simulation of the meson and baryon masses with degenerate light quarks. The extrapolations are done using quenched chiral perturbation theory. Determines m_s=113.8 $\pm$ 2.3$^{+5.8}_{-2.9}$ using K mass as input and m_s=142.3 $\pm$ 5.8$^{+22}_{-0}$ using ϕ mass as input. We have performed a weighted average of these values.

[27] AOKI 03B uses lattice simulation of the meson and baryon masses with two dynamical light quarks. Simulations are performed using the $\mathcal{O}(a)$ improved Wilson action.

[28] BECIREVIC 03 perform quenched lattice computation using the vector and axial Ward identities. Uses $\mathcal{O}(a)$ improved Wilson action and nonperturbative renormalization. They also quote $\overline{m}/m_s$=24.3 $\pm$ 0.2 $\pm$ 0.6.

[29] CHIU 03 determines quark masses from the pion and kaon masses using a lattice simulation with a chiral fermion action in quenched approximation.

[30] GAMIZ 03 determines m_s from SU(3) breaking in the τ hadronic width. The value of V_{us} is chosen to satisfy CKM unitarity.

[31] GAMIZ 03 determines m_s from SU(3) breaking in the τ hadronic width. The value of V_{us} is taken from the PDG.

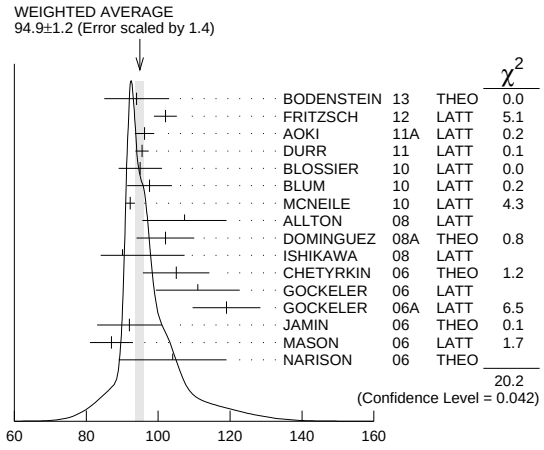

OTHER LIGHT QUARK MASS RATIOS

m_s/m_d MASS RATIO

VALUE		DOCUMENT ID		TECN	COMMENT
17–22 OUR EVALUATION					
• • • We do not use the following data for averages, fits, limits, etc. • • •					
20.0		[1] GAO	97	THEO	
18.9±0.8		[2] LEUTWYLER	96	THEO	Compilation
21		[3] DONOGHUE	92	THEO	
18		[4] GERARD	90	THEO	
18	to 23	[5] LEUTWYLER	90B	THEO	

[1] GAO 97 uses electromagnetic mass splittings of light mesons.

[2] LEUTWYLER 96 uses a combined fit to $\eta \to 3\pi$ and $\psi' \to J/\psi\,(\pi,\eta)$ decay rates, and the electromagnetic mass differences of the π and K.

[3] DONOGHUE 92 result is from a combined analysis of meson masses, $\eta \to 3\pi$ using second-order chiral perturbation theory including nonanalytic terms, and $(\psi(2S) \to J/\psi(1S)\,\pi)/(\psi(2S) \to J/\psi(1S)\,\eta)$.

[4] GERARD 90 uses large N and η-η' mixing.

[5] LEUTWYLER 90B determines quark mass ratios using second-order chiral perturbation theory for the meson and baryon masses, including nonanalytic corrections. Also uses Weinberg sum rules to determine L_7.

$m_s/\overline{m}$ MASS RATIO

$\overline{m} \equiv (m_u + m_d)/2$

VALUE	DOCUMENT ID		TECN
27.5 ±1.0 OUR EVALUATION	See the ideogram below.		
26.8 ±1.4	[1] AOKI	11A	LATT
27.53±0.20±0.08	[2] DURR	11	LATT
27.3 ±0.9	[3] BLOSSIER	10	LATT
28.8 ±1.65	[4] ALLTON	08	LATT
27.3 ±0.3 ±1.2	[5] BLOSSIER	08	LATT
23.5 ±1.5	[6] OLLER	07A	THEO
• • • We do not use the following data for averages, fits, limits, etc. • • •			
27.4 ±0.4	[7] AUBIN	04	LATT

[1] AOKI 11A determine quark masses from a lattice computation of the hadron spectrum using $N_f = 2 + 1$ dynamical flavors of domain wall fermions.

[2] DURR 11 determine quark mass from a lattice computation of the meson spectrum using $N_f = 2 + 1$ dynamical flavors. The lattice simulations were done at the physical quark mass, so that extrapolation in the quark mass was not needed.

[3] BLOSSIER 10 determines quark masses from a computation of the hadron spectrum using N_f=2 dynamical twisted-mass Wilson fermions.

[4] ALLTON 08 use a lattice computation of the π, K, and Ω masses with 2+1 dynamical flavors of domain wall quarks, and non-perturbative renormalization.

[5] BLOSSIER 08 use a lattice computation of pseudoscalar meson masses and decay constants with 2 dynamical flavors and non-perturbative renormalization.

[6] OLLER 07A use unitarized chiral perturbation theory to order p^4.

[7] Three flavor dynamical lattice calculation of pseudoscalar meson masses.

Quark Particle Listings

Light Quarks (u, d, s), c

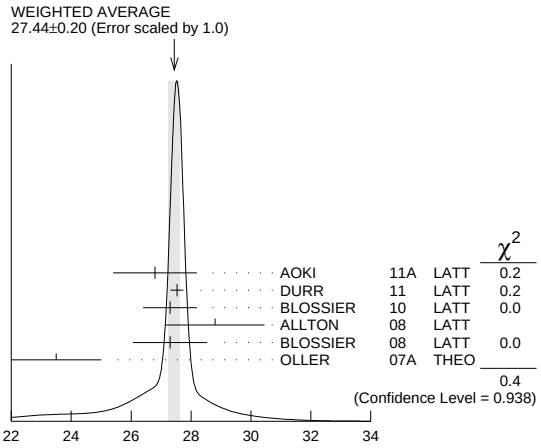

Q MASS RATIO

$Q \equiv \sqrt{(m^2_s - \overline{m}^2)/(m^2_d - m^2_u)}$; $\overline{m} \equiv (m_u + m_d)/2$

VALUE	DOCUMENT ID		TECN
• • • We do not use the following data for averages, fits, limits, etc. • • •			
22.8±0.4	[1] MARTEMYA...	05	THEO
22.7±0.8	[2] ANISOVICH	96	THEO

[1] MARTEMYANOV 05 determine Q from $\eta \to 3\pi$ decay.

[2] ANISOVICH 96 find Q from $\eta \to \pi^+\pi^-\pi^0$ decay using dispersion relations and chiral perturbation theory.

LIGHT QUARKS (u, d, s) REFERENCES

BODENSTEIN	13	JHEP 1307 138	S. Bodenstein, C.A. Dominguez, K. Schilcher	(MANZ+)
FRITZSCH	12	NP B865 397	P. Fritzsch *et al.*	(ALPHA Collab.)
AOKI	11A	PR D83 074508	Y. Aoki *et al.*	(RBC-UKQCD Collab.)
DURR	11	PL B701 265	S. Durr *et al.*	(BMW Collab.)
BAZAVOV	10	RMP 82 1349	A. Bazavov *et al.*	(MILC Collab.)
BLOSSIER	10	PR D82 114513	B. Blossier *et al.*	(ETM Collab.)
BLUM	10	PR D82 094508	T. Blum *et al.*	
DAVIES	10	PRL 104 132003	C.T.H. Davies *et al.*	(HPQCD Collab.)
MCNEILE	10	PR D82 034512	C. McNeile *et al.*	(HPQCD Collab.)
DOMINGUEZ	09	PR D79 014009	C.A. Dominguez *et al.*	
ALLISON	08	PR D78 054513	I. Allison *et al.*	(HPQCD Collab.)
ALLTON	08	PR D78 114509	C. Allton *et al.*	(RBC and UKQCD Collab.)
BLOSSIER	08	JHEP 0804 020	B. Blossier *et al.*	(ETM Collab.)
DEANDREA	08	PR D78 034032	A. Deandrea, A. Nehme, P. Talavera	
DOMINGUEZ	08A	JHEP 0805 020	C.A. Dominguez *et al.*	
DOMINGUEZ...	08B	PL B660 49	A. Dominguez-Clarimon, E. de Rafael, J. Taron	
ISHIKAWA	08	PR D78 011502	T. Ishikawa *et al.*	(CP-PACS and JLQCD Collab.)
NAKAMURA	08	PR D78 034502	Y. Nakamura *et al.*	(CP-PACS Collab.)
BLUM	07	PR D76 114508	T. Blum *et al.*	(RBC Collab.)
OLLER	07A	EPJ A34 371	J.A. Oller, L. Roca	
CHETYRKIN	06	EPJ C46 721	K.G. Chetyrkin, A. Khodjamirian	
GOCKELER	06	PR D73 054508	M. Gockeler *et al.*	(QCDSF, UKQCD Collabs)
GOCKELER	06A	PL B639 307	M. Gockeler *et al.*	(QCDSF, UKQCD Collabs)
JAMIN	06	PR D74 074009	M. Jamin, J.A. Oller, A. Pich	
MASON	06	PR D73 114501	Q. Mason *et al.*	(HPQCD Collab.)
NARISON	06	PR D74 034013	S. Narison	
PDG	06	JP G33 1	W.-M. Yao *et al.*	(PDG Collab.)
BAIKOV	05	PRL 95 012003	P.A. Baikov, K.G. Chetyrkin, J.H. Kuhn	
GAMIZ	05	PRL 94 011803	E. Gamiz *et al.*	
GORBUNOV	05	PR D71 013002	D.S. Gorbunov, A.A. Pivovarov	
MARTEMYA...	05	PR D71 017501	B.V. Martemyanov, V.S. Sopov	
NARISON	05	PL B626 101	S. Narison	
AUBIN	04	PR D70 031504	C. Aubin *et al.*	(HPQCD, MILC, UKQCD Collabs.)
AUBIN	04A	PR D70 114501	C. Aubin *et al.*	(MILC Collab.)
AOKI	03	PR D67 034503	S. Aoki *et al.*	(CP-PACS Collab.)
AOKI	03B	PR D68 054502	S. Aoki *et al.*	(CP-PACS Collab.)
BECIREVIC	03	PL B558 69	D. Becirevic, V. Lubicz, C. Tarantino	
CHIU	03	NP B673 217	T.-W. Chiu, T.-H. Hsieh	
GAMIZ	03	JHEP 0301 060	E. Gamiz *et al.*	
NELSON	03	PRL 90 021601	D. Nelson, G.T. Fleming, G.W. Kilcup	
GAO	97	PR D56 4115	D.-N. Gao, B.A. Li, M.-L. Yan	
ANISOVICH	96	PL B375 335	A.V. Anisovich, H. Leutwyler	
LEUTWYLER	96	PL B378 313	H. Leutwyler	
DONOGHUE	92	PRL 69 3444	J.F. Donoghue, B.R. Holstein, D. Wyler	(MASA+)
GERARD	90	MPL A5 391	J.M. Gerard	(MPIM)
LEUTWYLER	90B	NP B337 108	H. Leutwyler	(BERN)

C

$I(J^P) = 0(\frac{1}{2}^+)$

Charge = $\frac{2}{3}$ e Charm = +1

c-QUARK MASS

The c-quark mass corresponds to the "running" mass m_c ($\mu = m_c$) in the $\overline{\text{MS}}$ scheme. We have converted masses in other schemes to the $\overline{\text{MS}}$ scheme using two-loop QCD perturbation theory with $\alpha_s(\mu{=}m_c) = 0.38 \pm 0.03$. The value 1.275 ± 0.025 GeV for the $\overline{\text{MS}}$ mass corresponds to 1.67 ± 0.07 GeV for the pole mass (see the "Note on Quark Masses").

VALUE (GeV)	DOCUMENT ID		TECN	COMMENT
1.275±0.025 OUR EVALUATION	See the ideogram below.			
1.26 ±0.05 ±0.04	[1] ABRAMOWICZ	13C	COMB	$\overline{\text{MS}}$ scheme
1.24 $\pm 0.03\ ^{+0.03}_{-0.07}$	[2] ALEKHIN	13	THEO	$\overline{\text{MS}}$ scheme
1.282±0.011±0.022	[3] DEHNADI	13	THEO	$\overline{\text{MS}}$ scheme
1.286±0.066	[4] NARISON	13	THEO	$\overline{\text{MS}}$ scheme
1.159±0.075	[5] SAMOYLOV	13	NOMD	$\overline{\text{MS}}$ scheme
1.36 ±0.04 ±0.10	[6] ALEKHIN	12	THEO	$\overline{\text{MS}}$ scheme
1.261±0.016	[7] NARISON	12A	THEO	$\overline{\text{MS}}$ scheme
1.278±0.009	[8] BODENSTEIN	11	THEO	$\overline{\text{MS}}$ scheme
1.28 $^{+0.07}_{-0.06}$	[9] LASCHKA	11	THEO	$\overline{\text{MS}}$ scheme
1.196±0.059±0.050	[10] AUBERT	10A	BABR	$\overline{\text{MS}}$ scheme
1.28 ±0.04	[11] BLOSSIER	10	LATT	$\overline{\text{MS}}$ scheme
1.273±0.006	[12] MCNEILE	10	LATT	$\overline{\text{MS}}$ scheme
1.279±0.013	[13] CHETYRKIN	09	THEO	$\overline{\text{MS}}$ scheme
1.25 ±0.04	[14] SIGNER	09	THEO	$\overline{\text{MS}}$ scheme
1.295±0.015	[15] BOUGHEZAL	06	THEO	$\overline{\text{MS}}$ scheme
1.24 ±0.09	[16] BUCHMULLER	06	THEO	$\overline{\text{MS}}$ scheme
1.224±0.017±0.054	[17] HOANG	06	THEO	$\overline{\text{MS}}$ scheme
• • • We do not use the following data for averages, fits, limits, etc. • • •				
1.01 ±0.09 ±0.03	[18] ALEKHIN	11	THEO	$\overline{\text{MS}}$ scheme
1.299±0.026	[19] BODENSTEIN	10	THEO	$\overline{\text{MS}}$ scheme
1.261±0.018	[20] NARISON	10	THEO	$\overline{\text{MS}}$ scheme
1.268±0.009	[21] ALLISON	08	LATT	$\overline{\text{MS}}$ scheme
1.286±0.013	[22] KUHN	07	THEO	$\overline{\text{MS}}$ scheme
1.33 ±0.10	[23] AUBERT	04X	THEO	$\overline{\text{MS}}$ scheme
1.29 ±0.07	[24] HOANG	04	THEO	$\overline{\text{MS}}$ scheme
1.319±0.028	[25] DEDIVITIIS	03	LATT	$\overline{\text{MS}}$ scheme
1.19 ±0.11	[26] EIDEMULLER	03	THEO	$\overline{\text{MS}}$ scheme
1.289±0.043	[27] ERLER	03	THEO	$\overline{\text{MS}}$ scheme
1.26 ±0.02	[28] ZYABLYUK	03	THEO	$\overline{\text{MS}}$ scheme

[1] ABRAMOWICZ 13C determines m_c from charm production in deep inelastic ep scattering, using the QCD prediction at NLO order. The uncertainties from model and parameterization assumptions, and the value of α_s, of ±0.03, ±0.02, and ±0.02 respectively, have been combined in quadrature.

[2] ALEKHIN 13 determines m_c from charm production in deep inelastic scattering at HERA using approximate NNLO QCD.

[3] DEHNADI 13 determines m_c using QCD sum rules for the charmonium spectrum and charm continuum to order α_s^3 (N3LO). The statistical and systematic experimental errors of ±0.006 and ±0.009 have been combined in quadrature. The theoretical uncertainties ±0.019 from truncation of the perturbation series, ±0.010 from α_s, and ±0.002 from the gluon condensate have been combined in quadrature.

[4] NARISON 13 determines m_c using QCD spectral sum rules to order α_s^2 (NNLO) and including condensates up to dimension 6.

[5] SAMOYLOV 13 determines m_c from a study of charm dimuon production in neutrino-iron scattering using the NLO QCD result for the charm quark production cross section.

[6] ALEKHIN 12 determines m_c from heavy quark production in deep inelastic scattering at HERA using approximate NNLO QCD.

[7] NARISON 12A determines m_c using sum rules for the vector current correlator to order α_s^3, including the effect of gluon condensates up to dimension eight.

[8] BODENSTEIN 11 determine $\overline{m}_c(3\text{ GeV}) = 0.987 \pm 0.009$ GeV and $\overline{m}_c(\overline{m}_c) = 1.278 \pm 0.009$ GeV using QCD sum rules for the charm quark vector current correlator.

[9] LASCHKA 11 determine the c mass from the charmonium spectrum. The theoretical computation uses the heavy $Q\overline{Q}$ potential to order $1/m_Q$ obtained by matching the short-distance perturbative result onto lattice QCD result at larger scales.

[10] AUBERT 10A determine the b- and c-quark masses from a fit to the inclusive decay spectra in semileptonic B decays in the kinetic scheme (and convert it to the $\overline{\text{MS}}$ scheme).

[11] BLOSSIER 10 determines quark masses from a computation of the hadron spectrum using N_f=2 dynamical twisted-mass Wilson fermions.

[12] MCNEILE 10 determines m_c by comparing the order α_s^3 perturbative results for the pseudo-scalar current to lattice simulations with $N_f = 2{+}1$ sea-quarks by the HPQCD collaboration.

[13] CHETYRKIN 09 determine m_c and m_b from the $e^+e^- \to Q\overline{Q}$ cross-section and sum rules, using an order α_s^3 computation of the heavy quark vacuum polarization. They also determine $m_c(3\text{ GeV}) = 0.986 \pm 0.013$GeV.

[14] SIGNER 09 determines the c-quark mass using non-relativistic sum rules to analyze the $e^+e^- \to c\overline{c}$ cross-section near threshold. Also determine the PS mass $m_{PS}(\mu_F{=}\ 0.7$ GeV) = 1.50 ± 0.04 GeV.

[15] BOUGHEZAL 06 result comes from the first moment of the hadronic production cross-section to order α_s^3.

[16] BUCHMULLER 06 determine m_b and m_c by a global fit to inclusive B decay spectra.

[17] HOANG 06 determines $\overline{m}_c(\overline{m}_c)$ from a global fit to inclusive B decay data. The B decay distributions were computed to order $\alpha_s^2\beta_0$, and the conversion between different m_c mass schemes to order α_s^3.

[18] ALEKHIN 11 determines m_c from heavy quark production in deep inelastic scattering using fixed target and HERA data, and approximate NNLO QCD.

[19] BODENSTEIN 10 determines $\overline{m}_c(3\ \text{GeV}) = 1.008 \pm 0.026$ GeV using finite energy sum rules for the vector current correlator. The authors have converted this to $\overline{m}_c(\overline{m}_c)$ using $\alpha_s(M_Z) = 0.1189 \pm 0.0020$.

[20] NARISON 10 determines m_c from ratios of moments of vector current correlators computed to order α_s^3 and including the dimension-six gluon condensate.

[21] ALLISON 08 determine m_c by comparing four-loop perturbative results for the pseudoscalar current correlator to lattice simulations by the HPQCD collaboration. The result has been updated in MCNEILE 10.

[22] KUHN 07 determine $\overline{m}_c(\mu = 3\ \text{GeV}) = 0.986 \pm 0.013$ GeV and $\overline{m}_c(\overline{m}_c)$ from a four-loop sum-rule computation of the cross-section for $e^+e^- \to$ hadrons in the charm threshold region.

[23] AUBERT 04X obtain m_c from a fit to the hadron mass and lepton energy distributions in semileptonic B decay. The paper quotes values in the kinetic scheme. The $\overline{\text{MS}}$ value has been provided by the BABAR collaboration.

[24] HOANG 04 determines $\overline{m}_c(\overline{m}_c)$ from moments at order α_s^2 of the charm production cross-section in e^+e^- annihilation.

[25] DEDIVITIIS 03 use a quenched lattice computation of heavy-heavy and heavy-light meson masses.

[26] EIDEMULLER 03 determines m_b and m_c using QCD sum rules.

[27] ERLER 03 determines m_b and m_c using QCD sum rules. Includes recent BES data.

[28] ZYABLYUK 03 determines m_c by using QCD sum rules in the pseudoscalar channel and comparing with the η_c mass.

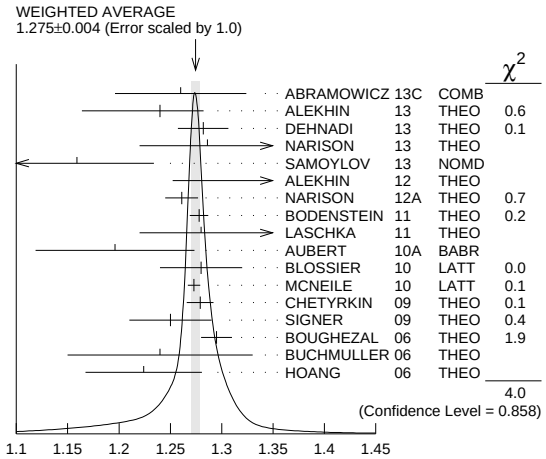

m_c/m_s MASS RATIO

VALUE		DOCUMENT ID		TECN
11.81±0.14 OUR AVERAGE	Error includes scale factor of 1.1. See the ideogram below.			
11.27±0.30±0.26	[1]	DURR	12	LATT
12.0 ±0.3	[2]	BLOSSIER	10	LATT
11.85±0.16	[3]	DAVIES	10	LATT

[1] DURR 12 determine m_c/m_s using a lattice computation with $N_f = 2$ dynamical fermions. The result is combined with other determinations of m_c to obtain $m_s(2\ \text{GeV}) = 97.0 \pm 2.6 \pm 2.5$ MeV.

[2] BLOSSIER 10 determine m_c/m_s from a computation of the hadron spectrum using $N_f = 2$ dynamical twisted-mass Wilson fermions.

[3] DAVIES 10 determine m_c/m_s from meson masses calculated on gluon fields including u, d, and s sea quarks with lattice spacing down to 0.045 fm. The Highly Improved Staggered quark formalism is used for the valence quarks.

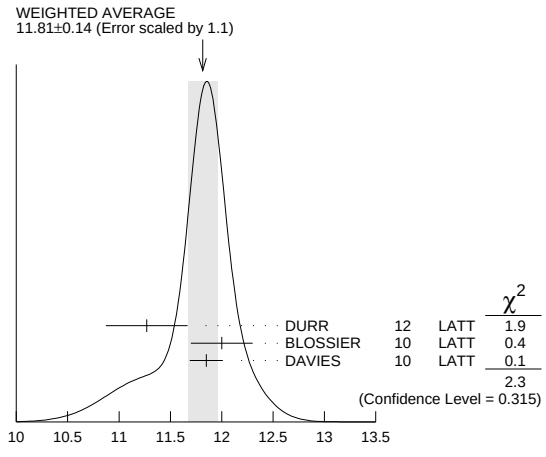

$m_b - m_c$ QUARK MASS DIFFERENCE

VALUE (GeV)		DOCUMENT ID		TECN
3.45 ±0.05 OUR EVALUATION				
• • • We do not use the following data for averages, fits, limits, etc. • • •				
3.472±0.032	[1]	AUBERT	10A	BABR
3.42 ±0.06	[2]	ABDALLAH	06B	DLPH
3.44 ±0.03	[3]	AUBERT	04X	BABR
3.41 ±0.01	[3]	BAUER	04	THEO

[1] AUBERT 10A determine the b- and c-quark masses from a fit to the inclusive decay spectra in semileptonic B decays in the kinetic scheme.

[2] ABDALLAH 06B determine $m_b - m_c$ from moments of the hadron invariant mass and lepton energy spectra in semileptonic inclusive B decays.

[3] Determine $m_b - m_c$ from a global fit to inclusive B decay spectra.

c-QUARK REFERENCES

ABRAMOWICZ	13C	EPJ C73 2311	H. Abramowicz *et al.* (H1 and Zeus Collab.)
ALEKHIN	13	PL B720 172	S. Alekhin *et al.* (SERP, DESYZ, WUPP+)
DEHNADI	13	JHEP 1309 103	B. Dehnadi *et al.* (SHRZ, VIEN, MPIM+)
NARISON	13	PL B718 1321	S. Narison (MONP)
SAMOYLOV	13	NP B876 339	O. Samoylov *et al.* (NOMAD Collab.)
ALEKHIN	12	PL B718 550	S. Alekhin *et al.* (SERP, WUPP, DESY+)
DURR	12	PRL 108 122003	S. Durr, G. Koutsou (WUPP, JULI, CYPR)
NARISON	12A	PL B706 412	S. Narison (MONP)
ALEKHIN	11	PL B699 345	S. Alekhin, S. Moch (DESY, SERP)
BODENSTEIN	11	PR D83 074014	S. Bodenstein *et al.*
LASCHKA	11	PR D83 094002	A. Laschka, N. Kaiser, W. Weise
AUBERT	10A	PR D81 032003	B. Aubert *et al.* (BABAR Collab.)
BLOSSIER	10	PR D82 114513	B. Blossier *et al.* (ETM Collab.)
BODENSTEIN	10	PR D82 114013	S. Bodenstein *et al.*
DAVIES	10	PRL 104 132003	C.T.H. Davies *et al.* (HPQCD Collab.)
MCNEILE	10	PR D82 034512	C. McNeile *et al.* (HPQCD Collab.)
NARISON	10	PL B693 559	S. Narison (MONP)
Also		PL B705 544 (errat.)	S. Narison (MONP)
CHETYRKIN	09	PR D80 074010	K.G. Chetyrkin *et al.* (KARL, BNL)
SIGNER	09	PL B672 333	A. Signer (DURH)
ALLISON	08	PR D78 054513	I. Allison *et al.* (HPQCD Collab.)
KUHN	07	NP B778 192	J.H. Kuhn, M. Steinhauser, C. Sturm
ABDALLAH	06B	EPJ C45 35	J. Abdallah *et al.* (DELPHI Collab.)
BOUGHEZAL	06	PR D74 074006	R. Boughezal, M. Czakon, T. Schutzmeier
BUCHMULLER	06	PR D73 073008	O.L. Buchmuller, H.U. Flacher (RHBL)
HOANG	06	PL B633 526	A.H. Hoang, A.V. Manohar
AUBERT	04X	PRL 93 011803	B. Aubert *et al.* (BABAR Collab.)
BAUER	04	PR D70 094017	C. Bauer *et al.*
HOANG	04	PL B594 127	A.H. Hoang, M. Jamin
DEDIVITIIS	03	NP B675 309	G.M. de Divitiis *et al.*
EIDEMULLER	03	PR D67 113002	M. Eidemuller
ERLER	03	PL B558 125	J. Erler, M. Luo
ZYABLYUK	03	JHEP 0301 081	K.N. Zyablyuk (ITEP)

b

$I(J^P) = 0(\frac{1}{2}^+)$

Charge $= -\frac{1}{3}\ e$ Bottom $= -1$

b-QUARK MASS

The first value is the "running mass" $\overline{m}_b(\mu = \overline{m}_b)$ in the $\overline{\text{MS}}$ scheme, and the second value is the $1S$ mass, which is half the mass of the $\Upsilon(1S)$ in perturbation theory. For a review of different quark mass definitions and their properties, see EL-KHADRA 02. The $1S$ mass is better suited for use in analyzing B decays than the $\overline{\text{MS}}$ mass because it gives a stable perturbative expansion. We have converted masses in other schemes to the $\overline{\text{MS}}$ mass and $1S$ mass using two-loop QCD perturbation theory with $\alpha_s(\mu = \overline{m}_b) = 0.223 \pm 0.008$. The values 4.18 ± 0.03 GeV for the $\overline{\text{MS}}$ mass and 4.66 ± 0.03 GeV for the $1S$ mass correspond to 4.78 ± 0.06 GeV for the pole mass, using the two-loop conversion formula. A discussion of masses in different schemes can be found in the "Note on Quark Masses."

$\overline{\text{MS}}$ MASS (GeV)	1S MASS (GeV)		DOCUMENT ID		TECN
4.18 ±0.03 OUR EVALUATION	of $\overline{\text{MS}}$ Mass. See the ideogram below.				
4.66 ±0.03 OUR EVALUATION	of $1S$ Mass. See the ideogram below.				
4.166±0.043	4.637 ± 0.048	[1]	LEE	13O	LATT
4.247±0.034	4.727 ± 0.039	[2]	LUCHA	13	THEO
4.236±0.069	4.715 ± 0.077	[3]	NARISON	13	THEO
4.213±0.059	4.689 ± 0.066	[4]	NARISON	13A	THEO
4.171±0.009	4.642 ± 0.010	[5]	BODENSTEIN	12	THEO
4.29 ±0.14	4.77 ± 0.16	[6]	DIMOPOUL...	12	LATT
4.235±0.003±0.055	4.755 ± 0.003 ± 0.058	[7]	HOANG	12	THEO
4.177±0.011	4.649 ± 0.012	[8]	NARISON	12	THEO
$4.18\ ^{+0.05}_{-0.04}$	$4.65\ ^{+0.06}_{-0.04}$	[9]	LASCHKA	11	THEO
4.186±0.044±0.015	4.659 ± 0.050 ± 0.017	[10]	AUBERT	10A	BABR
4.164±0.023	4.635 ± 0.026	[11]	MCNEILE	10	LATT
4.163±0.016	4.633 ± 0.018	[12]	CHETYRKIN	09	THEO
5.26 ±1.2	5.85 ± 1.3	[13]	ABDALLAH	08D	DLPH
4.243±0.049	4.723 ± 0.055	[14]	SCHWANDA	08	BELL
4.19 ±0.40	4.66 ± 0.45	[15]	ABDALLAH	06D	DLPH
4.205±0.058	4.68 ± 0.06	[16]	BOUGHEZAL	06	THEO
4.20 ±0.04	4.67 ± 0.04	[17]	BUCHMULLER	06	THEO
4.19 ±0.06	4.66 ± 0.07	[18]	PINEDA	06	THEO
4.17 ±0.03	4.68 ± 0.03	[19]	BAUER	04	THEO
4.22 ±0.11	4.72 ± 0.12	[20,21]	HOANG	04	THEO
4.19 ±0.05	4.66 ± 0.05	[22]	BORDES	03	THEO

Quark Particle Listings

b

4.20 ±0.09	4.67 ± 0.10	[23] CORCELLA	03	THEO
4.24 ±0.10	4.72 ± 0.11	[24] EIDEMULLER	03	THEO
4.207±0.031	4.682 ± 0.035	[25] ERLER	03	THEO
4.33 ±0.06 ±0.10	4.82 ± 0.07 ± 0.11	[26] MAHMOOD	03	CLEO
4.190±0.032	4.663 ± 0.036	[27] BRAMBILLA	02	THEO
4.346±0.070	4.837 ± 0.078	[28] PENIN	02	THEO
• • • We do not use the following data for averages, fits, limits, etc. • • •				
4.212±0.032	4.688 ± 0.036	[29] NARISON	12	THEO
4.171±0.014	4.642 ± 0.016	[30] NARISON	12A	THEO
4.173±0.010	4.645 ± 0.011	[31] NARISON	10	THEO
4.42 ±0.06 ±0.08	4.92 ± 0.07 ± 0.09	[32] GUAZZINI	08	LATT
4.347±0.048±0.08	4.838 ± 0.053 ± 0.09	[33] DELLA-MOR...	07	LATT
4.164±0.025	4.635 ± 0.028	[34] KUHN	07	THEO
4.4 ±0.3	4.9 ± 0.3	[20,35] GRAY	05	LATT
4.22 ±0.06	4.72 ± 0.07	[36] AUBERT	04X	THEO
4.25 ±0.11	4.76 ± 0.12	[20,37] MCNEILE	04	LATT
4.22 ±0.09	4.74 ± 0.10	[38] BAUER	03	THEO
4.33 ±0.10	4.84 ± 0.11	[20,39] DEDIVITIIS	03	LATT

[1] LEE 13O determines m_b using lattice calculations of the Υ and B_s binding energies in NRQCD, including three light dynamical quark flavors. The quark mass shift in NRQCD is determined to order α_s^2, with partial α_s^3 contributions.

[2] LUCHA 13 determines m_b from QCD sum rules for heavy-light currents using the lattice value for f_B of 191.5 ± 7.3 GeV.

[3] NARISON 13 determines m_b using QCD spectral sum rules to order α_s^2 (NNLO) and including condensates up to dimension 6. We have converted the $\overline{\text{MS}}$ value to the 1S scheme.

[4] NARISON 13A determines m_b using HQET sum rules to order α_s^2 (NNLO) and the B meson mass and decay constant.

[5] BODENSTEIN 12 determine m_b using sum rules for the vector current correlator and the $e^+e^- \to Q\overline{Q}$ total cross-section. We have converted $\overline{m}_b(\overline{m}_b)$ to the 1S scheme.

[6] DIMOPOULOS 12 determine quark masses from a lattice computation using $N_f = 2$ dynamical flavors of twisted mass fermions. We have converted $\overline{m}_b(\overline{m}_b)$ to the 1S scheme.

[7] HOANG 12 determine m_b using non-relativistic sum rules for the Υ system at order α_s^2 (NNLO) with renormalization group improvement.

[8] Determines m_b to order α_s^3 (N3LO), including the effect of gluon condensates up to dimension eight combining the methods of NARISON 12 and NARISON 12A. We have converted $\overline{m}_b(\overline{m}_b)$ to the 1S scheme.

[9] LASCHKA 11 determine the b mass from the charmonium spectrum. The theoretical computation uses the heavy $Q\overline{Q}$ potential to order $1/m_Q$ obtained by matching the short-distance perturbative result onto lattice QCD result at larger scales. We have converted $\overline{m}_b(\overline{m}_b)$ to the 1S scheme.

[10] AUBERT 10A determine the b- and c-quark masses from a fit to the inclusive decay spectra in semileptonic B decays in the kinetic scheme (and convert it to the $\overline{\text{MS}}$ scheme). We have converted this to the 1S scheme.

[11] MCNEILE 10 determines m_b by comparing order α_s^3 (N3LO) perturbative results for the pseudo-scalar current to lattice simulations with $N_f = 2{+}1$ sea-quarks by the HPQCD collaboration. We have converted $\overline{m}_b$ ($\overline{m}_b$) to the 1S scheme.

[12] CHETYRKIN 09 determine m_c and m_b from the $e^+e^- \to Q\overline{Q}$ cross-section and sum rules, using an order α_s^3 (N3LO) computation of the heavy quark vacuum polarization. We have converted their m_b to the 1S scheme.

[13] ABDALLAH 08D determine $\overline{m}_b(M_Z) = 3.76 \pm 1.0$ GeV from a leading order study of four-jet rates at LEP. We have converted this to $\overline{m}_b(\overline{m}_b)$ and m_b^{1S}.

[14] SCHWANDA 08 measure moments of the inclusive photon spectrum in $B \to X_s\gamma$ decay to determine m_b^{1S}. We have converted this to $\overline{\text{MS}}$ scheme.

[15] ABDALLAH 06D determine $m_b(M_Z) = 2.85 \pm 0.32$ GeV from Z-decay three-jet events containing a b-quark. We have converted this to $\overline{m}_b(\overline{m}_b)$ and m_b^{1S}.

[16] BOUGHEZAL 06 $\overline{\text{MS}}$ scheme result comes from the first moment of the hadronic production cross-section to order α_s^3. We have converted it to the 1S scheme.

[17] BUCHMULLER 06 determine m_b and m_c by a global fit to inclusive B decay spectra. We have converted this to the 1S scheme.

[18] PINEDA 06 $\overline{\text{MS}}$ scheme result comes from a partial NNLL evaluation (complete at order α_s^2 (NNLO)) of sum rules of the bottom production cross-section in e^+e^- annihilation. We have converted it to the 1S scheme.

[19] BAUER 04 determine m_b, m_c and $m_b - m_c$ by a global fit to inclusive B decay spectra.

[20] We have converted m_b to the 1S scheme.

[21] HOANG 04 determines $\overline{m}_b(\overline{m}_b)$ from moments at order α_s^2 of the bottom production cross-section in e^+e^- annihilation.

[22] BORDES 03 determines m_b using QCD finite energy sum rules to order α_s^2.

[23] CORCELLA 03 determines $\overline{m}_b$ using sum rules computed to order α_s^2. Includes charm quark mass effects.

[24] EIDEMULLER 03 determines $\overline{m}_b$ and $\overline{m}_c$ using QCD sum rules.

[25] ERLER 03 determines $\overline{m}_b$ and $\overline{m}_c$ using QCD sum rules. Includes recent BES data.

[26] MAHMOOD 03 determines m_b^{1S} by a fit to the lepton energy moments in $B \to X_c\ell\nu_\ell$ decay. The theoretical expressions used are of order $1/m^3$ and $\alpha_s^2\beta_0$. We have converted their result to the $\overline{\text{MS}}$ scheme.

[27] BRAMBILLA 02 determine $\overline{m}_b(\overline{m}_b)$ from a computation of the $\Upsilon(1S)$ mass to order α_s^4, including finite m_c corrections. We have converted this to the 1S scheme.

[28] PENIN 02 determines $\overline{m}_b$ from the spectrum of the Υ system.

[29] NARISON 12 determines m_b using exponential sum rules for the vector current correlator to order α_s^3, including the effect of gluon condensates up to dimension eight. We have converted $\overline{m}_b(\overline{m}_b)$ to the 1S scheme.

[30] NARISON 12A determines m_b using sum rules for the vector current correlator to order α_s^3, including the effect of gluon condensates up to dimension eight. We have converted $\overline{m}_b(\overline{m}_b)$ to the 1S scheme.

[31] NARISON 10 determines m_b from ratios of moments of vector current correlators computed to order α_s^3 and including the dimension-six gluon condensate. These values are taken from the erratum to that reference.

[32] GUAZZINI 08 determine $\overline{m}_b(\overline{m}_b)$ from a quenched lattice simulation of heavy meson masses. The ±0.08 is an estimate of the quenching error. We have converted these values to the 1S scheme.

[33] DELLA-MORTE 07 determine $\overline{m}_b(\overline{m}_b)$ from a computation of the spin-averaged B meson mass using quenched lattice HQET at order $1/m$. The ±0.08 is an estimate of the quenching error.

[34] KUHN 07 determine $\overline{m}_b(\mu = 10\text{ GeV}) = 3.609 \pm 0.025$ GeV and $\overline{m}_b(\overline{m}_b)$ from a four-loop sum-rule computation of the cross-section for $e^+e^- \to$ hadrons in the bottom threshold region. We have converted this to the 1S scheme.

[35] GRAY 05 determines $\overline{m}_b(\overline{m}_b)$ from a lattice computation of the Υ spectrum. The simulations have $2{+}1$ dynamical light flavors. The b quark is implemented using NRQCD.

[36] AUBERT 04X obtain m_b from a fit to the hadron mass and lepton energy distributions in semileptonic B decay. The paper quotes values in the kinetic scheme. The $\overline{\text{MS}}$ value has been provided by the BABAR collaboration, and we have converted this to the 1S scheme.

[37] MCNEILE 04 use lattice QCD with dynamical light quarks and a static heavy quark to compute the masses of heavy-light mesons.

[38] BAUER 03 determine the b quark mass by a global fit to B decay observables. The experimental data includes lepton energy and hadron invariant mass moments in semileptonic $B \to X_c\ell\nu_\ell$ decay, and the inclusive photon spectrum in $B \to X_s\gamma$ decay. The theoretical expressions used are of order $1/m^3$, and $\alpha_s^2\beta_0$.

[39] DEDIVITIIS 03 use a quenched lattice computation of heavy-heavy and heavy-light meson masses.

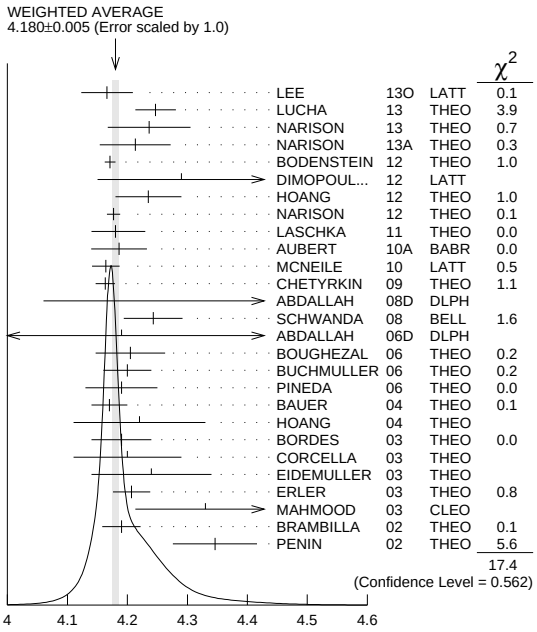

b-QUARK REFERENCES

LEE	13O	PR D87 074018	A.J. Lee *et al.*	(HPQCD Collab.)
LUCHA	13	PR D88 056011	W. Lucha, D. Melikhov, S. Simula	(VIEN, MOSU+)
NARISON	13	PL B718 1321	S. Narison	(MONP)
NARISON	13A	PL B721 269	S. Narison	(MONP)
BODENSTEIN	12	PR D85 034003	S. Bodenstein *et al.*	(CAPE, VALE, MANZ+)
DIMOPOUL...	12	JHEP 1201 046	P. Dimopoulos *et al.*	(ETM Collab.)
HOANG	12	JHEP 1210 188	A.H. Hoang, P. Ruiz-Femenia, M. Stahlhofen	(WIEN+)
NARISON	12	PL B707 259	S. Narison	(MONP)
NARISON	12A	PL B706 412	S. Narison	(MONP)
LASCHKA	11	PR D83 094002	A. Laschka, N. Kaiser, W. Weise	
AUBERT	10A	PR D81 032003	B. Aubert *et al.*	(BABAR Collab.)
MCNEILE	10	PR D82 034512	C. McNeile *et al.*	(HPQCD Collab.)
NARISON	10	PL B693 559	S. Narison	(MONP)
Also		PL B705 544 (errat.)	S. Narison	(MONP)
CHETYRKIN	09	PR D80 074010	K.G. Chetyrkin *et al.*	(KARL, BNL)
ABDALLAH	08D	EPJ C55 525	J. Abdallah *et al.*	(DELPHI Collab.)
GUAZZINI	08	JHEP 0801 076	D. Guazzini, R. Sommer, N. Tantalo	
SCHWANDA	08	PR D78 032016	C. Schwanda *et al.*	(BELLE Collab.)
DELLA-MOR...	07	JHEP 0701 007	M. Della Morte *et al.*	
KUHN	07	NP B778 192	J.H. Kuhn, M. Steinhauser, C. Sturm	
ABDALLAH	06D	EPJ C46 569	J. Abdallah *et al.*	(DELPHI Collab.)
BOUGHEZAL	06	PR D74 074006	R. Boughezal, M. Czakon, T. Schutzmeier	
BUCHMULLER	06	PR D73 073008	O.L. Buchmuller, H.U. Flacher	(RHBL)
PINEDA	06	PR D73 111501	A. Pineda, A. Signer	
GRAY	05	PR D72 094507	A. Gray *et al.*	(HPQCD, UKQCD Collab.)
AUBERT	04X	PRL 93 011803	B. Aubert *et al.*	(BABAR Collab.)
BAUER	04	PR D70 094017	C. Bauer *et al.*	
HOANG	04	PL B594 127	A.H. Hoang, M. Jamin	
MCNEILE	04	PL B600 77	C. McNeile, C. Michael, G. Thompson	(UKQCD Collab.)
BAUER	03	PR D67 054012	C.W. Bauer *et al.*	
BORDES	03	PL B562 81	J. Bordes, J. Penarrocha, K. Schilcher	
CORCELLA	03	PL B554 133	G. Corcella, A.H. Hoang	
DEDIVITIIS	03	NP B675 309	G.M. de Divitiis *et al.*	
EIDEMULLER	03	PR D67 113002	M. Eidemuller	

ERLER	03	PL B558 125	J. Erler, M. Luo	
MAHMOOD	03	PR D67 072001	A.H. Mahmood *et al.*	(CLEO Collab.)
BRAMBILLA	02	PR D65 034001	N. Brambilla, Y. Sumino, A. Vairo	
EL-KHADRA	02	ARNPS 52 201	A.X. El-Khadra, M. Luke	
PENIN	02	PL B538 335	A. Penin, M. Steinhauser	

t

$I(J^P) = 0(\frac{1}{2}^+)$

Charge = $\frac{2}{3}$ e Top = +1

THE TOP QUARK

Updated September 2013 by T.M. Liss (Univ. Illinois), F. Maltoni (Univ. Catholique de Louvain), and A. Quadt (Univ. Göttingen).

A. Introduction

The top quark is the $Q = 2/3$, $T_3 = +1/2$ member of the weak-isospin doublet containing the bottom quark (see the review on the "Electroweak Model and Constraints on New Physics" for more information). Its phenomenology is driven by its large mass. Being heavier than a W boson, it is the only quark that decays semi-weakly, i.e., into a real W boson and a b quark, before hadronization can occur. In addition, it is the only quark whose Yukawa coupling to the Higgs boson is order of unity. For these reasons the top quark plays a special role in the Standard Model (SM) and in many extensions thereof. An accurate knowledge of its properties (mass, couplings, production cross section, decay branching ratios, *etc.*) can bring key information on fundamental interactions at the electroweak breaking scale and beyond. This review provides a concise discussion of the experimental and theoretical issues involved in the determination the top-quark properties.

B. Top-quark production at the Tevatron and LHC

In hadron collisions, top quarks are produced dominantly in pairs through the processes $q\overline{q} \to t\overline{t}$ and $gg \to t\overline{t}$, at leading order in QCD. Approximately 85% of the production cross section at the Tevatron is from $q\overline{q}$ annihilation, with the remainder from gluon-gluon fusion, while at LHC energies about 90% of the production is from the latter process at $\sqrt{s} = 14$ TeV ($\approx 80\%$ at $\sqrt{s} = 7$ TeV).

Predictions for the total cross sections are now available at next-to-next-to leading order (NNLO) with next-to-next-to-leading-log (NNLL) soft gluon resummation [1]. These results supersede previous approximated ones [2]. Assuming a top-quark mass of 173.3 GeV/c^2, close to the world average [3](LHC results not yet included), the resulting theoretical prediction of the top-quark pair cross-section at NNLO+NNLL accuracy at the Tevatron at $\sqrt{s} = 1.96$ TeV is $\sigma_{t\bar{t}} = 7.164^{+0.11+0.17}_{-0.20-0.12}$ pb where the first uncertainty is from scale dependence and the second from parton distribution functions, while at the LHC at $\sqrt{s} = 7$ TeV (8 TeV) is $\sigma_{t\bar{t}} = 172.0^{+4.4+4.7}_{-5.8-4.8}$ pb ($\sigma_{t\bar{t}} = 245.8^{+6.2+6.2}_{-8.4-6.4}$ pb).

Electroweak single top-quark production mechanisms, namely from $q\overline{q}' \to t\overline{b}$ [4], $qb \to q't$ [5], mediated by virtual s-channel and t-channel W-bosons, and Wt-associated production, through $bg \to W^-t$, lead to somewhat smaller cross sections. For example, t-channel production, while suppressed by the weak coupling with respect to the strong pair production, is kinematically enhanced, resulting in a sizable cross section both at Tevatron and LHC energies. At the Tevatron, the t- and s-channel cross sections of top and antitop are identical, while at the LHC they are not. Approximate NNLO cross sections for t-channel single top-quark production ($t + \bar{t}$) are calculated for $m_t = 173.3$ GeV/c^2 to be $2.06^{+0.13}_{-0.13}$ pb in $p\overline{p}$ collisions at $\sqrt{s} = 1.96$ TeV (scale and parton distribution functions uncertainties are combined in quadrature) and $65.7^{+1.9}_{-1.9}$ ($87.1^{+0.24}_{-0.24}$) pb in pp collisions at $\sqrt{s} = 7$ (8) TeV, where 65% and 35% are the relative proportions of t and $\bar{t}$ [6]. For the s-channel, these calculations yield $1.03^{+0.05}_{-0.05}$ pb for the Tevatron, and $4.5^{+0.2}_{-0.2}(5.5^{+0.2}_{-0.2})$ pb for $\sqrt{s} = 7$ (8) TeV at the LHC, with 69% (31%) of top (anti-top) quarks [7]. While negligible at the Tevatron, at LHC energies the Wt-associated production becomes relevant. At $\sqrt{s} = 7$ (8) TeV, an approximate NNLO calculation using the MSTW2008 PDF gives $15.5^{+1.2}_{-1.2}(22.1^{+1.5}_{-1.5})$ pb ($t+\bar{t}$), with an equal proportion of top and anti-top quarks [8].

Assuming $|V_{tb}| \gg |V_{td}|, |V_{ts}|$ (see the review "The CKM Quark-Mixing Matrix" for more information), the cross sections for single top production are proportional to $|V_{tb}|^2$, and no extra hypothesis is needed on the number of quark families or on the unitarity of the CKM matrix in extracting $|V_{tb}|$. Separate measurements of the s- and t-channel processes provide sensitivity to physics beyond the Standard Model [9].

With a mass above the Wb threshold, and $|V_{tb}| \gg |V_{td}|, |V_{ts}|$, the decay width of the top quark is expected to be dominated by the two-body channel $t \to Wb$. Neglecting terms of order m_b^2/m_t^2, α_s^2, and $(\alpha_s/\pi)M_W^2/m_t^2$, the width predicted in the SM at NLO is [10]:

$$\Gamma_t = \frac{G_F m_t^3}{8\pi\sqrt{2}} \left(1 - \frac{M_W^2}{m_t^2}\right)^2 \left(1 + 2\frac{M_W^2}{m_t^2}\right) \left[1 - \frac{2\alpha_s}{3\pi}\left(\frac{2\pi^2}{3} - \frac{5}{2}\right)\right], \quad (1)$$

where m_t refers to the top-quark pole mass. The width for a value of $m_t = 173.3$ GeV/c^2 is 1.35 GeV/c^2 (we use $\alpha_s(M_Z) = 0.118$) and increases with mass. With its correspondingly short lifetime of $\approx 0.5 \times 10^{-24}$ s, the top quark is expected to decay before top-flavored hadrons or $t\bar{t}$-quarkonium-bound states can form [11]. In fact, since the decay time is close to the would-be-resonance binding time, a peak will be visible in e^+e^- scattering at the $t\bar{t}$ threshold [12] and it is in principle present (yet very difficult to measure) in hadron collisions, too [13]. The order α_s^2 QCD corrections to Γ_t are also available [14], thereby improving the overall theoretical accuracy to better than 1%.

The final states for the leading pair-production process can be divided into three classes:

A. $t\bar{t} \to W^+ b\, W^- \bar{b} \to q\,\overline{q}'\, b\, q''\,\overline{q}'''\,\bar{b}$, (45.7%)

B. $t\bar{t} \to W^+ b\, W^- \bar{b} \to q\,\overline{q}'\, b\, \ell^-\,\overline{\nu}_\ell\,\bar{b} + \ell^+\,\nu_\ell\, b\, q''\,\overline{q}'''\,\bar{b}$, (43.8%)

C. $t\bar{t} \to W^+ b\, W^- \bar{b} \to \ell\,\nu_\ell\, b\, \ell'\,\overline{\nu}_{\ell'}\,\bar{b}$. (10.5%)

The quarks in the final state evolve into jets of hadrons. A, B, and C are referred to as the all-jets, lepton+jets (ℓ+jets), and dilepton ($\ell\ell$) channels, respectively. Their relative contributions, including hadronic corrections, are given in parentheses assuming lepton universality. While ℓ in the above processes

refers to e, μ, or τ, most of the analyses distinguish the e and μ from the τ channel, which is more difficult to reconstruct. Therefore, in what follows, we will use ℓ to refer to e or μ, unless otherwise noted. Here, typically leptonic decays of τ are included. In addition to the quarks resulting from the top-quark decays, extra QCD radiation (quarks and gluons) from the colored particles in the event can lead to extra jets.

The number of jets reconstructed in the detectors depends on the decay kinematics, as well as on the algorithm for reconstructing jets used by the analysis. Information on the transverse momenta of neutrinos is obtained from the imbalance in transverse momentum measured in each event (missing p_T, which is here also called missing E_T).

The identification of top quarks in the electroweak single top channel is much more difficult than in the QCD $t\bar{t}$ channel, due to a less distinctive signature and significantly larger backgrounds, mostly due to $t\bar{t}$ and W+jets production.

Fully exclusive predictions via Monte Carlo generators for the $t\bar{t}$ and single top production processes at NLO accuracy in QCD, including top-quark decays, are available [15,16] through the MC@NLO [17] and POWHEG [18] methods.

Besides fully inclusive QCD or EW top-quark production, more exclusive final states can be accessed at hadron colliders, whose cross sections are typically much smaller, yet can provide key information on the properties of the top quark. For all relevant final states (*e.g.*, $t\bar{t}\gamma, t\bar{t}Z, t\bar{t}W, t\bar{t}H, t\bar{t}$+jets, $t\bar{t}b\bar{b}, t\bar{t}t\bar{t}$) automatic or semi-automatic predictions at NLO accuracy in QCD also in the form of event generators, *i.e.*, interfaced to parton-shower programs, are available (see the review "Monte Carlo event generators" for more information).

C. Top-quark measurements

Since the discovery of the top quark, direct measurements of $t\bar{t}$ production have been made at four center-of-mass energies, providing stringent tests of QCD. The first measurements were made in Run I at the Tevatron at $\sqrt{s} = 1.8$ TeV. In Run II at the Tevatron relatively precise measurements were made at $\sqrt{s} = 1.96$ TeV. Finally, beginning in 2010, measurements have been made at the LHC at $\sqrt{s} = 7$ TeV and $\sqrt{s} = 8$ TeV.

Production of single top quarks through electroweak interactions has now been measured with good precision at the Tevatron at $\sqrt{s} = 1.96$ TeV, and at the LHC at both $\sqrt{s} = 7$ TeV and $\sqrt{s} = 8$ TeV. Recent measurements at the Tevatron are beginning to separate the s- and t-channel production cross sections, and at the LHC, the Wt mechanism as well, though the t-channel is measured with best precision to date. The measurements allow an extraction of the CKM matrix element V_{tb}.

The top-quark mass is now measured at the 0.5% level, by far the most precisely measured quark mass. Together with the W-boson mass measurement and the newly discovered Higgs boson, this provides a stringent test of the Standard Model.

With almost 9 fb^{-1} of Tevatron data analyzed as of this writing, and almost 20 fb^{-1} of LHC data, many properties of the top quark are now being measured with precision. These include properties related to the production mechanism, such as $t\bar{t}$ spin correlations, forward-backward or charge asymmetries, and differential production cross sections, as well as properties related to the $t-W-b$ decay vertex, such as the helicity of the W-bosons from the top-quark decay. In addition, many searches for physics beyond the Standard Model are being performed with increasing reach in both production and decay channels.

In the following sections we review the current status of measurements of the characteristics of the top quark.

C.1 Top-quark production

C.1.1 $t\bar{t}$ production: Fig. 1 summarizes the $t\bar{t}$ production cross-section measurements from both the Tevatron and LHC. The most recent measurement from DØ [19], combining the measurements from the dilepton and lepton plus jets final states in 5.4 fb^{-1}, is $7.56^{+0.63}_{-0.56}$ pb. From CDF the most precise measurement made recently [20] is in 4.6 fb^{-1} and is a combination of dilepton, lepton plus jets, and all-hadronic final-state measurements, yielding 7.50 ± 0.48 pb. Both of these measurements assume a top-quark mass of 172.5 GeV/c^2. The dependence of the cross section measurements on the value chosen for the mass is less than that of the theory calculations because it only affects the determination of the acceptance. In some analyses also the shape of topological variables might be modified. Very recently, CDF updated some of their measurements with the full Run-II dataset up to 8.8 fb^{-1}. The resulting combined $t\bar{t}$ cross-section is $\sigma_{t\bar{t}} = 7.63 \pm 0.50$ pb (7.1%) for CDF, $\sigma_{t\bar{t}} = 7.56 \pm 0.59$ pb (9.3%) for DØ and $\sigma_{t\bar{t}} = 7.60 \pm 0.41$ pb (5.4%) for the Tevatron combination [21] in good agreement with the SM expectation of $7.16^{+0.20}_{-0.23}$ pb at NNLO+NNLL in perturbative QCD. The contributions to the uncertainty are 0.20 pb from statistical sources, 0.29 pb from systematic sources, and 0.21 pb from the uncertainty on the integrated luminosity.

CDF also performs measurements of the $t\bar{t}$ production cross section normalized to the Z production cross section in order to reduce the impact of the luminosity uncertainty.

The LHC experiments ATLAS and CMS use similar techniques to measure the $t\bar{t}$ cross-section in pp collisions. At $\sqrt{s} = 7$ TeV, ATLAS performs measurements in 0.7 fb^{-1} in the lepton+jets channel [22], in the dilepton channel [23], and in 1.02 fb^{-1} in the all-hadronic channel [24], which together yield a combined value of $\sigma_{t\bar{t}} = 177 \pm 3(stat.)^{+8}_{-7}(syst.) \pm 7(lumi.)$ pb (6.2%) assuming $m_t = 172.5$ GeV/c^2 [25]. Further analyses in the hadronic tau plus jets channel in 1.67 fb^{-1} [26], the hadronic tau + lepton channel in 2.05 fb^{-1} [27], and the all-hadronic channel in 4.7 fb^{-1} [28] yield consistent albeit less precise results. CMS performs $t\bar{t}$ cross-section measurements with 2.3 fb^{-1} in the e/μ+jets channel [29] and in the dilepton channel [30], with 3.5 fb^{-1} in the all-hadronic channel [31], with 2.2 fb^{-1} in the lepton+τ channel [32], and with 3.9 fb^{-1} in the τ+jets channel [33]. The most precise result is obtained in the dilepton channel, where they obtain

See key on page 547

$\sigma_{t\bar{t}} = 162 \pm 2(stat.) \pm 5(syst.) \pm 4(lumi.)$ pb, which corresponds to a 4.2% precision [30].

At $\sqrt{s} = 8$ TeV, ATLAS and CMS perform cross-section analyses as well, although only a few channels have been considered so far due to the large number of systematic uncertainties being dominant. ATLAS measures the $t\bar{t}$ cross-section in the lepton+jets channel with 5.8 fb^{-1} [34], and in the $e\mu$ dilepton channel using 20.3 fb^{-1} [35]. In the latter, they select an extremely clean sample and determine the $t\bar{t}$ cross-section simultaneously with the efficiency to reconstruct and b-tag jets, yielding $\sigma_{t\bar{t}} = 237.7 \pm 1.7(stat.) \pm 7.4(syst.) \pm 7.4(lumi.) \pm 4.0(beam\,energy)$ pb assuming $m_t = 172.5$ GeV/c^2, which corresponds to a 4.7% precision. CMS performs a template fit to the M_{lb} mass distribution using 2.7 fb^{-1} in the lepton+jets channel [36] and a cut-and-count analysis in 2.4 fb^{-1} in the dilepton channel [37]. In combination, they achieve $\sigma_{t\bar{t}} = 227 \pm 3(stat.) \pm 11(syst.) \pm 10(lumi.)$ pb for $m_t = 172.5$ GeV/c^2 [37], which corresponds to a 6.7% precision.

These experimental results should be compared to the theoretical calculations that yield $7.16^{+0.20}_{-0.23}$ pb for top-quark mass of 173.3 GeV/c^2 [1] at $\sqrt{s} = 1.96$ TeV, $\sigma_{t\bar{t}} = 172.0^{+6.4}_{-7.5}$ pb at $\sqrt{s} = 7$ TeV, and $\sigma_{t\bar{t}} = 245.8^{+8.8}_{-10.6}$ pb at $\sqrt{s} = 8$ TeV, at the LHC [1](see Section B).

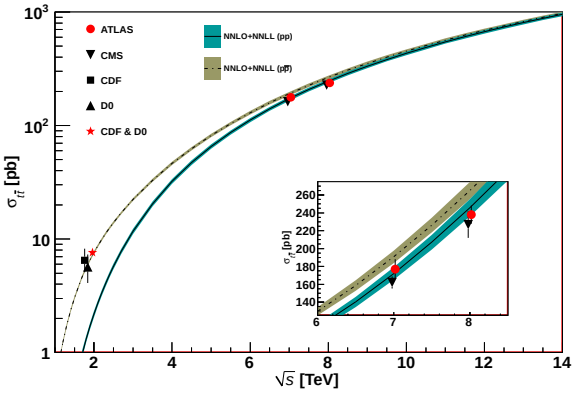

Figure 1: Measured and predicted $t\bar{t}$ production cross sections from Tevatron energies in $p\overline{p}$ collisions to LHC energies in pp collisions. Tevatron data points at $\sqrt{s} = 1.8$ TeV are from Refs. [41,42]. Those at $\sqrt{s} = 1.96$ TeV are from Refs. [19–21]. The ATLAS and CMS data points are from Refs. [25,35] and [30,36,37], respectively. Theory curves are generated using [1] for $m_t = 173.3$ GeV/c^2. Figure adapted from Ref. [40].

In Fig. 1, one sees the importance of $p\overline{p}$ at Tevatron energies where the valence antiquarks in the antiprotons contribute to the dominant $q\overline{q}$ production mechanism. At LHC energies, the dominant production mode is gluon-gluon fusion and the pp-$p\overline{p}$ difference nearly disappears. The excellent agreement of these measurements with the theory calculations is a strong validation of QCD and the soft-gluon resummation techniques employed in the calculations. The measurements reach high precision and provide stringent tests of pQCD calculations at NNLO+NNLL level including their respective PDF uncertainties.

Most of these measurements assume a $t \to Wb$ branching ratio of 100%. CDF and DØ have made direct measurements of the $t \to Wb$ branching ratio [38]. Comparing the number of events with 0, 1 and 2 tagged b jets in the lepton+jets channel, and also in the dilepton channel, using the known b-tagging efficiency, the ratio $R = B(t \to Wb)/\sum_{q=d,s,b} B(t \to Wq)$ can be extracted. In 5.4 fb^{-1} of data, DØ measures $R = 0.90 \pm 0.04$, 2.5σ from unity. A similar measurement was made by CMS in 16.7 fb^{-1} at $\sqrt{s} = 8$ TeV. They find $R = 1.023^{+0.036}_{-0.034}$ and $R > 0.945$ at 95% C.L. [39]. A significant deviation of R from unity would imply either non-SM top-quark decay (for example a flavor-changing neutral-current decay), or a fourth generation of quarks.

Thanks to the large available event samples, the Tevatron and the LHC experiments performed first differential cross-section measurements in $t\bar{t}$ production. Such measurements are crucial, as they allow even more stringent tests of perturbative QCD as description of the production mechanism, allow the extraction or the use of PDF fits, and enhance the sensitivity to possible new physics contributions. Furthermore, such measurements reduce the uncertainty in the description of $t\bar{t}$ production as background in Higgs physics and searches for rare processes or beyond Standard Model physics. Differential cross-sections are typically measured by a selection of candidate events, their kinematic reconstruction and subsequent unfolding of the obtained event counts in bins of kinematic distributions in order to correct for detector resolution effects, acceptance and migration effects. In some cases a bin-by-bin unfolding is used, other analyses use a more sophisticated technique, taking into account the known migrations effects and correlations or employing some regularization.

Using 2.7 fb^{-1}, CDF measured the differential cross-section with respect to the $t\bar{t}$ invariant mass, $d\sigma/dM_{t\bar{t}}$, in the lepton+jets channel providing sensitivity to a variety of exotic particles decaying into $t\bar{t}$ pairs [43]. In 9.7 fb^{-1} of lepton+jets data, DØ measured the differential $t\bar{t}$ production cross-section with respect to the transverse momentum and absolute rapidity of the top quarks as well as of the invariant mass of the $t\bar{t}$ pair [44], which are all found to be in good agreement with the SM predictions. Also ATLAS measured the differential $t\bar{t}$ production cross-section with respect to the top-quark transverse momentum, and of the mass, transverse momentum and rapidity of the $t\bar{t}$ system in 4.6 fb^{-1} at $\sqrt{s} = 7$ TeV in the lepton+jets channel [45]. The measured spectra are fully corrected for detector efficiency and resolution effects and are compared to several Monte Carlo simulations as well as selected theoretical calculations. The results show sensitivity to these predictions and to different sets of parton distribution functions. It is found that data is softer than all predictions in the tail of the top-quark p_T spectrum beginning at 200 GeV, particularly in the case of the `Alpgen+Herwig` generator. The $m_{t\bar{t}}$ spectrum is not well described by NLO+NNLL calculations

and there are also disagreements between the measured $y_{t\bar{t}}$ spectrum and the MC@NLO+Herwig and POWHEG+Herwig generators, both evaluated with the CT10 PDF set. All distributions show a preference for HERAPDF1.5 when used for the NLO QCD predictions. In 5.0 fb^{-1} of $\sqrt{s} = 7$ TeV data in the lepton+jets and the dilepton channels, CMS measured normalised differential $t\bar{t}$ cross-sections with respect to kinematic properties of the final-state charged leptons and jets associated to b-quarks, as well as those of the top quarks and the $t\bar{t}$ system. The data are compared with several predictions from perturbative QCD calculations and found to be consistent [46]. Recently, in 12 fb^{-1} at $\sqrt{s} = 8$ TeV, CMS repeated those measurements in the lepton+jets [47] and in the dilepton channels [48]. While the overall precision is improved, no significant deviations from the Standard Model are observed. Very recently, they also performed a normalized differential cross-section measurement in 20 fb^{-1} of lepton+jets data with respect to a number of event-level observables, including missing transverse energy, jet transverse momentum scalar sum, total event transverse momentum scalar sum, leptonic W transverse momentum, and leptonic W transverse mass. The results are consistent with the Standard Model expectations [49].

Further cross-section measurements are performed for $t\bar{t}$+heavy flavour and $t\bar{t}$+jets production [50,51].

C.1.2 Single-top production: Single-top quark production was first observed in 2009 by DØ [52] and CDF [53,54] at the Tevatron. The production cross section at the Tevatron is roughly half that of the $t\bar{t}$ cross section, but the final state with a single W-boson and typically two jets is less distinct than that for $t\bar{t}$ and much more difficult to distinguish from the background of W+jets and other sources. A recent review of the first observation and the techniques used to extract the signal from the backgrounds can be found in [55].

The dominant production at the Tevatron is through s-channel and t-channel W-boson exchange. Associated production with a W-boson (Wt production) has a cross section that is too small to observe at the Tevatron. The t-channel process is $qb \to q't$, while the s-channel process is $q\overline{q'} \to t\bar{b}$. The s- and t-channel productions can be separated kinematically. This is of particular interest because potential physics beyond the Standard Model, such as fourth-generation quarks, heavy W and Z bosons, flavor-changing-neutral-currents [9], or a charged Higgs boson, would affect the s- and t-channels differently. However, the separation is difficult and initial observations and measurements at the Tevatron by both experiments were of combined $s+t$-channel production. The two experiments combined their measurements for maximum precision with a resulting $s+t$ channel production cross section of $2.76^{+0.58}_{-0.47}$ pb [56]. The measured value assumes a top-quark mass of 170 GeV/c^2. The mass dependence of the result comes both from the acceptance dependence and from the $t\bar{t}$ background evaluation. Also the shape of discriminating topological variables is sensitive to m_t. It is therefore not necessarily a simple linear dependence but amounts to only a few tenths of picobarns over the range $170 - 175$ GeV/c^2. The measured value agrees well with the theoretical calculation at $m_t = 173$ GeV/c^2 of $\sigma_{s+t} = 3.12$ pb (including both top and anti-top production) [6,7].

Recently, CDF has updated the $s+t$-channel measurement with 7.5 fb^{-1} to $\sigma_{s+t} = 3.04^{+0.57}_{-0.53}$ pb assuming a Standard Model ratio of s- to t-channel, resulting in a lower limit of $|V_{tb}| > 0.78$ at 95% C.L. [57]. They also analyzed the full Run-II data set of 9.1 fb^{-1} in W+jets events where no electron or muon has been identified, and where the tau lepton in the $t \to Wb \to \tau\nu b$ channel is reconstructed as a jet in the calorimeters. Multivariate analysis discriminants and a profile likelihood technique are used to obtain a cross section of $\sigma_{s+t} = 3.0^{+1.5}_{-1.4}$ pb [58]. DØ has measured the combined cross section to $\sigma_{s+t} = 3.43^{+0.73}_{-0.74}$ pb for $m_t = 172.5/c^2$ GeV [59].

Both experiments have done separate measurements of the s- and t-channel cross sections by reoptimizing the analysis for one or both of the channels separately. In a simultaneous measurement of s- and t-channel cross sections, CDF measures $\sigma_s = 1.81^{+0.63}_{-0.58}$ pb and $\sigma_t = 1.49^{+0.47}_{-0.42}$ pb, respectively, in 7.5 fb^{-1} of data [57]. Using 9.4 fb^{-1}, they performed an analysis in the missing E_T plus $b\bar{b}$ channel yielding $\sigma_s = 1.10^{+0.65}_{-0.66}$ pb [58,60] and in the $l\nu b\bar{b}$ channel resulting in $\sigma_s = 1.43^{+0.44}_{-0.42}$ pb [61]. The latter also corresponds to a 3.7 standard deviations evidence. In this analysis, CDF assumes the t-channel cross-section to take the SM value. DØ performs a sophisticated multivariate analysis combining a matrix-element technique, a Bayesian neural network and boosted decision tress to form one output variable using another boosted decision tree. In 9.7 fb^{-1} of integrated luminosity, they measure $\sigma_s = 1.10^{+0.33}_{-0.31}$ pb [62], which corresponds to 3.7 standard deviations and is the first evidence for s-channel single-top production at the Tevatron. In this measurement, they also obtain $\sigma_t = 3.07^{+0.53}_{-0.49}$ pb, which corresponds to 7.7 standard deviations. In combination, the result is $\sigma_{s+t} = 4.11^{+0.60}_{-0.55}$ pb [62]. In this measurement, they do not make any assumption about the t-channel. They also set a limit on $|V_{tb}| > 0.92$ at 95% C.L. In a slightly different analysis, using 5.4 fb^{-1}, they measure the t-channel production cross section in a dedicated analysis [59,63] with a significance of 5.5 standard deviations using a variety of advanced analysis techniques similar to those described in [55]. These take advantage of kinematic differences in such things as the leading b-tagged jet p_T, centrality of jets, lepton charge times η of the jets, and the scalar sum of the energy of the final state objects. The $p\overline{p} \to tq + X$ cross section is measured to be 2.90 ± 0.59 pb, assuming a top-quark mass of 172.5 GeV/c^2. This is in good agreement with the theoretical value at this mass of 2.08 ± 0.13 pb [6]. It should be noted that the theory citations here list cross sections for t or $\overline{t}$ alone, whereas the experiments measure the sum. At the Tevatron, these cross sections are equal. The theory values quoted here already include this factor of two.

The Tevatron experiments are working on an s-channel combination, which is expected to come out very soon.

At the LHC, the t-channel cross section is expected to be more than three times as large as s-channel and Wt production, combined. Both ATLAS and CMS have measured single top production cross sections at $\sqrt{s} = 7$ TeV in pp collisions (assuming $m_t = 172.5$ GeV/c^2 unless noted otherwise), where they recently observed t-channel production [64,65]. ATLAS analyses 1.04 fb^{-1} of 7 TeV data in the lepton plus 2 or 3 jets channel with one b-tag by fitting the distribution of a multivariate discriminant constructed with a neural network, yielding $\sigma_t = 83 \pm 4(stat.)^{+20}_{-19}(syst)$ pb (this value refers to the sum of top and antitop cross-section) as well as $|V_{tb}| = 1.13^{+0.14}_{-0.13}$ and $|V_{tb}| > 0.75$ at 95% C.L. [64]. In an update with 4.7 fb^{-1} using a binned maximum likelihood fit to the output distribution of neural networks, they find $\sigma_t = 53.2 \pm 10.8$ pb and $\sigma_{\bar{t}} = 29.5^{+7.4}_{-7.5}$ pb with a cross-section charge ratio $R_t = 1.81^{+0.23}_{-0.22}$ [66] that is sensitive to the ratio of the up-quark and down-quark parton distribution functions in the proton. CMS follows two approaches in 1.6 fb^{-1} of lepton plus jets events. The first approach exploits the distributions of the pseudorapidity of the recoil jet and reconstructed top-quark mass using background estimates determined from control samples in data. The second approach is based on multivariate analysis techniques that probe the compatibility of the candidate events with the signal. They find $\sigma_t = 67.2 \pm 6.1$ pb, and $|V_{tb}| = 1.020 \pm 0.046(meas.) \pm 0.017(theor.)$ [65].

At $\sqrt{s} = 8$ TeV, both experiments repeat and refine their measurements. ATLAS uses 5.8 fb^{-1} by performing a combined binned maximum likelihood fit to the neural network output distribution. The measured t-channel cross-section is $\sigma_t = 95.1 \pm 2.4(stat.) \pm 18.0(syst.)$ pb with $|V_{tb}| = 1.04^{+0.1}_{-0.11}$ and $|V_{tb}| > 0.80$ at 95% C.L. [67]. CMS uses 5.0 fb^{-1} in the muon plus jets channel, exploiting the pseudorapidity distribution of the recoil jet. They find $\sigma_t = 80.1 \pm 5.7(stat.) \pm 11.0(syst.) \pm 4.0(lumi)$ pb [68] assuming $m_t = 173$ GeV/c^2. A combination of the two measurements yields $\sigma_t = 85 \pm 4(stat.) \pm 11(syst.) \pm 3(lumi.)$ pb [69]. Very recently, CMS has updated their measurement with the complete Run-I dataset of 20 fb^{-1} and furthermore measured the top-quark polarization in t-channel single top production to be $P_t = 0.82 \pm 0.12(stat.) \pm 0.32(syst.)$, which is consistent with the SM expectation [70]. Based on 12.2 fb^{-1}, CMS updated their results to find $\sigma_t = 49.9 \pm 9.1$ pb and $\sigma_{\bar{t}} = 28.3 \pm 5.5$ pb, which yields a cross-section charge ratio of $R_t = 1.76 \pm 0.27$ for $m_t = 173$ GeV/c^2 in agreement with the Standard Model [71].

The s-channel production cross section is expected to be only 4.6 ± 0.3 pb for $m_t = 173$ GeV/c^2 at $\sqrt{s} = 7$ TeV [7], and has not yet been observed at LHC. The Wt process has a theoretical cross section of 15.6 ± 1.2 pb [8]. This is of interest because it probes the $W - t - b$ vertex in a different kinematic region than s- and t-channel production, and because of its similarity to the associated production of a charged-Higgs boson and a top quark. The signal is difficult to extract because of its similarity to the $t\bar{t}$ signature. Furthermore, it is difficult to uniquely define because at NLO a subset of diagrams have the same final state as $t\bar{t}$ and the two interfere [72]. The cross section is calculated using the *diagram removal* technique [73] to define the signal process. In the diagram removal technique the interfering diagrams are removed, at the amplitude level, from the signal definition (an alternate technique, *diagram subtraction* removes these diagrams at the cross-section level and yields similar results). These techniques work provided the selection cuts are defined such that the interference effects are small, which is usually the case.

Both, ATLAS and CMS, also provide evidence for the associate Wt production at $\sqrt{s} = 7$ TeV [74,75]. ATLAS uses 2.05 fb^{-1} in the dilepton plus missing E_T plus jets channel, where a template fit to the final classifier distributions resulting from boosted decision trees as signal to background separation is performed. The result is incompatible with the background-only hypothesis at the 3.3σ (3.4σ expected) level, yielding $\sigma_{Wt} = 16.8 \pm 2.9(stat.) \pm 4.9(syst.)$ pb and $|V_{tb}| = 1.03^{+0.16}_{-0.19}$ [74]. CMS uses 4.9 fb^{-1} in the dilepton plus jets channel with at least one b-tag. A multivariate analysis based on kinematic properties is utilized to separate the $t\bar{t}$ background from the signal. The observed signal has a significance of 4.0σ and corresponds to a cross section of $\sigma_{Wt} = 16^{+5}_{-4}$ pb [75]. Both experiments repeated their analyses at $\sqrt{s} = 8$ TeV. ATLAS uses 20.3 fb^{-1} to select events with one electron and one oppositely-charged muon, significant missing transverse momentum and at least one b-tagged central jet. They perform a template fit to a boosted decision tree classifier distribution and obtain $\sigma_{Wt} = 27.2 \pm 5.8$ pb and $|V_{tb}| = 1.10 \pm 0.12(exp.) \pm 0.03(theory)$ [76], which corresponds to a 4.2σ significance. Assuming $|V_{tb}| \gg |V_{ts}|, |V_{td}|$ they derive $|V_{tb}| > 0.72$ at 95% C.L. CMS uses 12.2 fb^{-1} in events with two leptons and a jet originated from a b-quark. A multivariate analysis based on kinematic properties is utilized to separate the signal and background. The Wt associate production signal is observed at the level of 6.0σ, yielding $\sigma_{Wt} = 23.4^{+5.5}_{-5.4}$ pb and $|V_{tb}| = 1.03 \pm 0.12(exp.) \pm 0.04(theory)$ [77].

At ATLAS, a search for s-channel single top quark production is performed in 0.7 fb^{-1} using events containing one lepton, missing transverse energy and two b-jets. Using a cut-based analysis, an observed (expected) upper limit at 95% C.L. on the s-channel cross-section of $\sigma_s < 26.5(20.5)$ pb is obtained [78].

Fig. 2 provides a summary of all single top cross-section measurements at the Tevatron and the LHC as a function of the center-of-mass energy. All cross-section measurements are very well described by the theory calculation within their uncertainty.

C.1.3 Top-Quark Forward-Backward & Charge Asymmetry: A forward-backward asymmetry in $t\bar{t}$ production arises from an interference between the Born and box production diagrams and between diagrams with initial- and final-state gluon radiation. The asymmetry, A_{FB}, is defined by

$$A_{FB} = \frac{N(\Delta y > 0) - N(\Delta y < 0)}{N(\Delta y > 0) + N(\Delta y < 0)} \quad (2)$$

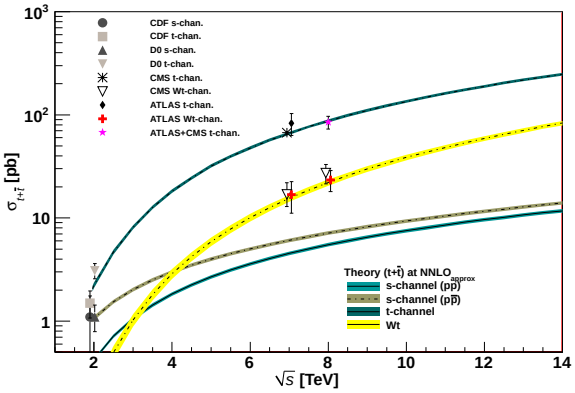

Figure 2: Measured and predicted single top production cross sections from Tevatron energies in $p\overline{p}$ collisions to LHC energies in pp collisions. Tevatron data points at $\sqrt{s} = 1.96$ TeV are from Refs. [57,60] and [62]. The ATLAS and CMS data points at $\sqrt{s} = 7$ TeV are from Refs. [64,66,74,78] and [79,65,75], respectively. The ones at $\sqrt{s} = 8$ TeV are from Refs. [67,69,76] and [68,69,77]. Theory curves are generated using [6,7,8].

where $\Delta y = y_t - y_{\bar{t}}$ is the rapidity difference between the top- and the anti-top quark. NLO calculations predict a small A_{FB} at the Tevatron. The most recent calculations at NLO, including electromagnetic and electroweak corrections, yield a predicted asymmetry of $(\approx 8.8 \pm 0.6)\%$ [80,81].

Both, CDF and DØ, have measured asymmetry values in excess of the SM prediction, fueling speculation about exotic production mechanisms (see, for example, [82] and references therein). The first measurement of this asymmetry by DØ in 0.9 fb^{-1} [83] found an asymmetry at the detector level of $(12 \pm 8)\%$. The first CDF measurement in 1.9 fb^{-1} [84] yielded $(24 \pm 14)\%$ at parton level. Both values were higher, though statistically consistent with the SM expectation. With the addition of more data, the uncertainties have been reduced, but the measured asymmetries remain in excess of the SM expectation. The most recent measurement from DØ in 5.4 fb^{-1} finds an asymmetry, corrected for detector acceptance and resolution, of $(19.6 \pm 6.5)\%$ [85]. From CDF, the most recent measurement uses 9.4 fb^{-1}, and finds $(16.4 \pm 4.7)\%$ [86]. With additional data they report further evidence for an $M_{t\bar{t}}$-dependent asymmetry first reported in [87], with a larger asymmetry at large $M_{t\bar{t}}$ and an approximately linear dependence with $M_{t\bar{t}}$. DØ does not see any significant increase at large mass [85]. The new CDF measurement also includes a differential measurement of A_{FB} in bins of $|\Delta y|$ which also shows an approximately linear dependence with a positive slope. The SM prediction is also for an approximately linear dependence with a positive slope, but these studies show that the excess above the SM prediction occurs primarily at large values of these parameters. A further study of the dependence of A_{FB} on the p_T of the $t\bar{t}$ system indicates that the asymmetry is independent of the transverse momentum of the $t\bar{t}$ system.

At the LHC, where the dominant $t\bar{t}$ production mechanism is the charge-symmetric gluon-gluon fusion, the measurement is more difficult. For the sub-dominant $q\overline{q}$ production mechanism, the symmetric pp collision does not define a forward and backward direction. Instead, the charge asymmetry, A_C, is defined in terms of a positive versus a negative $t - \bar{t}$ rapidity difference

$$A_C = \frac{N(\Delta|y| > 0) - N(\Delta|y| < 0)}{N(\Delta|y| > 0) + N(\Delta|y| < 0)} \quad (3)$$

Both CMS and ATLAS have measured A_C in the LHC dataset. Using lepton+jets events in 4.7 fb^{-1} of data at $\sqrt{s} =$ 7 TeV, ATLAS measures $A_C = (0.6 \pm 1.0)\%$ [88]. CMS, in 5.0(19.7) fb^{-1} of $\sqrt{s} = 7(8)$ TeV data uses lepton+jets events to measure $A_C = (0.4 \pm 1.5)\%$ ($A_C = (0.005 \pm 0.007(stat.) \pm 0.006(syst.))$) [89,90]. Both measurements are consistent with the SM expectation of $A_C = 1.23 \pm 0.05\%$ [81], although the uncertainties are still too large for a precision test. In their 7 and 8 TeV analyses, both, ATLAS and CMS, also provide differential measurements as a function of the $t\bar{t}$ mass, the transverse momentum p_T and the rapidity y.

Another avenue for measuring the forward-backward and charge asymmetries that has recently been exploited by the experiments is given by the measurement of the pseudorapidity distributions of the charged leptons resulting from $t\bar{t}$ decay. Although the expected asymmetry is smaller, this technique does not require the reconstruction of the top-quark direction. Single-lepton asymmetries are defined by $q \times \eta$, and dilepton asymmetries by the sign of $\Delta\eta$, where q and η are the charge and pseudorapidity of the lepton and $\Delta\eta = \eta_{\ell^+} - \eta_{\ell^-}$. DØ has recently measured the single-lepton asymmetry in 9.7 fb^{-1} of lepton+jets events, and finds a value of $(4.7 \pm 2.3^{+1.1}_{-1.4})\%$ [91], consistent with an expectation of $(3.8 \pm 0.6)\%$ [81]. A measurement by DØ using dilepton events in the same dataset [92] yields a dilepton asymmetry of $(12.3 \pm 5.4 \pm 1.5)$, less than two standard deviations away from the expectation of $(4.0 \pm 0.4)\%$ [81]. CDF, in 9.4 fb^{-1} of Tevatron data measures [93] $(9.4^{+3.2}_{-2.9})\%$. As in the DØ case, this is larger than the SM expectation, but less than two standard deviations away.

At the LHC, both ATLAS and CMS have now measured leptonic asymmetries. ATLAS, in 4.7 fb^{-1} of $\sqrt{s} = 7$ TeV data, has measured an asymmetry in dilepton events of $(2.3 \pm 1.2 \pm 0.8)\%$ [94]. CMS, in 5.0 fb^{-1} of $\sqrt{s} = 7$ TeV data, uses dilepton events to measure an asymmetry of $(1.0 \pm 1.5 \pm 0.6)\%$ [95]. Both of these are consistent, within their large uncertainties, with the SM expectation, derived by the experiments from the `MC@NLO` and `POWHEG` generators, respectively, of about 0.4%.

A model-independent comparison of the Tevatron and LHC results is made difficult by the differing $t\bar{t}$ production mechanisms at work at the two accelerators and by the symmetric nature of the pp collisions at the LHC. Given a particular model of BSM physics, a comparison can be obtained through the resulting asymmetry predicted by the model at the two machines, see Fig. 3.

See key on page 547

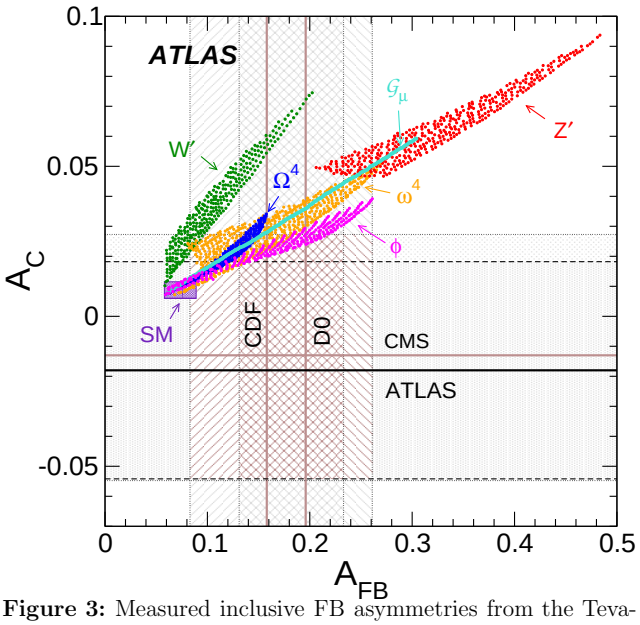

Figure 3: Measured inclusive FB asymmetries from the Tevatron and charge asymmetries from the LHC, compared to predictions from the SM as well as predictions incorporating various potential new physics contributions. The horizontal (vertical) bands and lines correspond to the ATLAS and CMS (CDF and DØ) measurements [96].

C.2 Top-Quark Properties

C.2.1 Top-Quark Mass Measurements: The most precisely studied property of the top quark is its mass. The top-quark mass has been measured in the lepton+jets, the dilepton, and the all-jets channel by all four Tevatron and LHC experiments. The latest and/or most precise results are summarized in Table 1. The lepton+jets channel still yields the most precise single measurements because of good signal to background (in particular after *b*-tagging) and the presence of only a single neutrino in the final state. The momentum of a single neutrino can be reconstructed (up to a quadratic ambiguity) via the missing E_T measurement and the constraint that the lepton and neutrino momenta reconstruct to the known W boson mass. In the large data samples available at the LHC, measurements in the dilepton channel are only slightly less precise.

A large number of techniques have now been applied to measuring the top-quark mass. The original 'template method' [97], in which Monte Carlo templates of reconstructed mass distributions are fit to data, has evolved into a precision tool in the lepton+jets channel, where the systematic uncertainty due to the jet energy scale (JES) uncertainty is controlled by a simultaneous, *in situ*, fit to the $W \to jj$ hypothesis [98]. All the latest measurements in the lepton+jets and the all-jets channels use this technique one way or the other. In 4.7 fb^{-1} of data in the lepton+jets channel, ATLAS and CMS achieve a total uncertainty of 0.9% and 0.6%, with a statistical component of 0.44% [99] and 0.25% [100], respectively. The ATLAS measurement is in fact based on a 3-dimensional template fit, determining the top-quark mass, the global jet energy scale and a *b*-to-light jet energy scale factor. The measurement from CDF with 8.7 fb^{-1} [101] achieves a precision of 0.6% in the lepton+jets channel, while DØ achieves 0.9% in 3.6 fb^{-1} [102].

The template method is complemented by the 'matrix element' method. This method was first applied by the DØ Collaboration [103], and is similar to a technique originally suggested by Kondo *et al.* [104] and Dalitz and Goldstein [105]. In the matrix element method a probability for each event is calculated as a function of the top-quark mass, using a LO matrix element for the production and decay of $t\bar{t}$ pairs. The *in situ* calibration of dijet pairs to the $W \to jj$ hypothesis is now also used with the matrix element technique to constrain the jet energy scale uncertainty. The latest measurement with this technique is from DØ in the lepton+jets channel with 3.6 fb^{-1} yielding an uncertainty of about 0.9% [102].

CMS has measured the top-quark mass at LHC using an 'ideogram' method, first used by DØ [106], in which a constrained fit is performed and an event-by-event likelihood for signal or background is calculated taking into account all jet-parton assignments. In the lepton+jets channel at CMS, with an *in situ* fit of the JES using $W \to jj$, the measurement has a precision of 1.07 GeV (0.6%) in 5 fb^{-1} [100], which is the most precise top-quark mass measurement to date.

In the dilepton channel, the signal to background is typically very good, but reconstruction of the mass is non-trivial because there are two neutrinos in the final state, yielding a kinematically unconstrained system. A variety of techniques has been developed to handle this. An analytic solution to the problem has been proposed [107], but this has not yet been used in the mass measurement. One of the two most precise measurements in the dilepton channel currently comes from using the invariant mass of the charged lepton and *b*-quark system ($M_{\ell b}$), which is sensitive to the top-quark mass and avoids the kinematic difficulties of the two-neutrino final state. In 4.7 fb^{-1} of data, ATLAS has measured the top-quark mass in the dilepton channel to a precision of 0.9% using a template fit to the $M_{\ell b}$ distribution [108]. The other dilepton-channel measurement of similar precision comes from 5.0 fb^{-1} of CMS data [109] using a so-called analytical matrix weighting technique (AMWT) in which each event is fit many times to a range of top-quark masses and each fit is assigned a weight, from the PDFs, given by the inferred kinematics of the initial state partons, and from the probability of the observed charged lepton energies for the top-quark mass in question.

Several other techniques can also yield precise measurements in the dilepton channel. In the neutrino weighting technique, similar to AMWT above, a weight is assigned by assuming a top-quark mass value and applying energy-momentum conservation to the top-quark decay, resulting in up to four possible pairs of solutions for the neutrino and anti-neutrino momenta. The missing E_T calculated in this way is then compared to the

observed missing E_T to assign a weight [110]. Another measurement in the dilepton channel uses the Dalitz and Goldstein technique [111–113].

In the all-jets channel there is no ambiguity due to neutrino momenta, but the signal to background is significantly poorer due to the severe QCD multijets background. The emphasis therefore has been on background modeling, and reduction through event selection. The most recent measurement in the all-jets channel, by CMS in 3.54 fb^{-1} [114], uses an ideogram method to extract the top-quark mass and achieves a precision of 0.8%. Here, the 1-dimensional fit for the top-mass with fixed jet energy scale is expected to be more precise than the 2-dimensional simultaneous fit for m_t and the jet energy scale. A recent measurement from ATLAS [115] uses the template method in the all-hadronic channel, also with an *in situ*, fit to the $W \to jj$ hypothesis, yielding a measurement with 2% precision in only 2.0 fb^{-1} of data. A measurement from CDF in 5.7 fb^{-1} uses a neural net to select events with a missing E_T plus jets signature [116]. A modified template method is used to extract the top-quark mass, including an *in situ* $W \to jj$ fit. A precision of 1% is achieved.

A dominant systematic uncertainty in these methods is the understanding of the jet energy scale, and so several techniques have been developed that have little sensitivity to the jet energy scale uncertainty. These include the measurement of the top-quark mass using the following techniques: Fitting of the lepton p_T spectrum of candidate events [117]; fitting of the transverse decay length of the b-jet (L_{xy}) [118]; fitting the invariant mass of a lepton from the W-decay and a muon from the semileptonic b decay [119].

Several measurements have now been made in which the top-quark mass is extracted from the measured cross section using the theoretical relationship between the mass and the production cross section, which allows the direct extraction of the $\overline{\rm MS}$ mass section [120].

Combined measurements from the Tevatron experiments and from the LHC experiments take into account the correlations between different measurements from a single experiment and between measurements from different experiments. The Tevatron average [3], using up to 8.7 fb^{-1} of data, now has a precision of 0.5%. The LHC combination, using up to 4.9 fb^{-1} of data, has a precision of just over 0.5% [121], where more work on systematic uncertainties is required. A Tevatron-LHC combination is not yet available.

The direct measurements of the top-quark mass, such as those shown in Table 1, are generally assumed to be measurements of the pole mass. Strictly speaking, the mass measured in these direct measurements is the mass used in the Monte Carlo generators. The relation between the Monte Carlo generator mass and the pole mass is uncertain at the level of 1 GeV [123], which is now comparable to the measurement uncertainty. A review of top-quark mass measurements can be found in reference [124].

Table 1: Measurements of top-quark mass from Tevatron and LHC. $\int \mathcal{L}dt$ is given in fb^{-1}. The results shown are mostly preliminary (not yet submitted for publication as of September 2013); for a complete set of published results see the Listings. Statistical uncertainties are listed first, followed by systematic uncertainties.

m_t (GeV/c^2)	Source	$\int \mathcal{L}dt$	Ref.	Channel
$174.94 \pm 1.14 \pm 0.96$	DØ Run II	3.6	[102]	ℓ+jets
$172.85 \pm 0.71 \pm 0.85$	CDF Run II	8.7	[101]	ℓ+jets
$173.93 \pm 1.64 \pm 0.87$	CDF Run II	8.7	[116]	Missing E_T+jets
$172.5 \pm 1.4 \pm 1.5$	CDF Run II	5.8	[122]	All jets
$172.31 \pm 0.75 \pm 1.35$	ATLAS	4.7	[99]	ℓ+jets
$173.09 \pm 0.64 \pm 1.50$	ATLAS	4.7	[108]	$\ell\ell$
$174.9 \pm 2.1 \pm 3.8$	ATLAS	2.04	[115]	All jets
$173.49 \pm 0.43 \pm 0.98$	CMS	5.0	[100]	ℓ+jets
$172.5 \pm 0.4 \pm 1.5$	CMS	5.0	[109]	$\ell\ell$
$173.49 \pm 0.69 \pm 1.21$	CMS	3.54	[114]	All jets
$173.20 \pm 0.51 \pm 0.71$*	CDF,DØ (I+II)	$\leq$8.7	[3]	publ. or prelim. res.
$173.29 \pm 0.23 \pm 0.92$*	ATLAS, CMS	$\leq$4.9	[121]	publ. or prelim. res.

*The Tevatron average is a combination of published Run I and preliminary or pub. Run-II meas., yielding a χ^2 of 8.5 for 11 deg. of freedom. The LHC average includes both published and preliminary results, yielding a χ^2 of 1.8 for 4 deg. of freedom.

With the discovery of a Higgs boson at the LHC with a mass of about 126 GeV [125,126], the precision measurement of the top-quark mass takes a central role in the question of the stability of the electroweak vacuum because top-quark radiative corrections tend to drive the Higgs quartic coupling, λ, negative, potentially leading to an unstable vacuum. A recent calculation at NNLO [127] leads to the conclusion of vacuum stability for a Higgs mass satisfying $M_H \geq 129.4 \pm 5.6$ GeV [128]. Given the uncertainty, a Higgs mass of 126 GeV satisfies the limit, but the central value of the Higgs and top-quark masses put the electroweak vacuum squarely in the metastable region. The uncertainty is dominated by the precision of the top-quark mass measurement and its interpretation as the pole mass. For more details, see the Higgs boson review in this volume.

As a test of the CPT-symmetry, the mass difference of top- and antitop-quarks $\Delta m_t = m_t - m_{\bar{t}}$, which is expected to be zero, can be measured. CDF measures the mass difference in 8.7 fb^{-1} of 1.96 TeV data in the lepton+jets channel using a template methode to find $\Delta m_t = -1.95 \pm 1.11(stat.) \pm 0.59(syst.)$ GeV/c^2 [129] while DØ uses 3.6 fb^{-1} of lepton+jets events and the matrix element method with at least one b-tag. They find $\Delta m_t = 0.8 \pm 1.8(stat.) \pm 0.5(syst.)$ GeV/c^2 [130]. In 4.7 fb^{-1} of 7 TeV data, ATLAS measures the mass difference in lepton+jets events with a double b-tag requirement and hence very low background to find $\Delta m_t = 0.67 \pm 0.61(stat.) \pm$

0.41(*syst.*) GeV/c^2 [131]. CMS measures the top-quark mass difference in 5 fb^{-1} of 7 TeV data in the lepton+jets channel and finds $\Delta m_t = -0.44 \pm 0.46(stat.) \pm 0.27(syst.)$ GeV/c^2 [132]. They repeat this measurement with 18.9 fb^{-1} of 8 TeV data to find $\Delta m_t = -0.27 \pm 0.20(stat.) \pm 0.12(syst.)$ GeV/c^2 [133]. All measurements are consistent with the SM expectation.

C.2.2 Top-Quark Spin Correlations and Width: One of the unique features of the top quark is that it decays before its spin can be flipped by the strong interaction. Thus the top-quark polarization is directly observable via the angular distribution of its decay products. Hence, it is possible to define and measure observables sensitive to the top-quark spin and its production mechanism. Although the top- and antitop-quarks produced by strong interactions in hadron collisions are essentially unpolarized, the spins of t and $\bar{t}$ are correlated. For QCD production at threshold, the $t\bar{t}$ system is produced in a $^3S_1$ state with parallel spins for $q\bar{q}$ annihilation or in a $^1S_0$ state with antiparallel spins for gluon-gluon fusion. Hence, the situations at the Tevatron and at the LHC are complementary. The direction of the top-quark spin is 100% correlated to the angular distributions of the down-type fermion (charged leptons or d-type quarks) in the decay. The joint angular distribution [134–136]

$$\frac{1}{\sigma}\frac{d^2\sigma}{d(\cos\theta_+)d(\cos\theta_-)} = \frac{1+\kappa\cdot\cos\theta_+\cdot\cos\theta_-}{4}, \qquad (4)$$

where θ_+ and θ_- are the angles of the daughters in the top-quark rest frame with respect to a particular spin quantization axis, is a very sensitive observable. The maximum value for κ, 0.782 at NLO at the Tevatron [137], is found in the off-diagonal basis [134], while at the LHC the value at NLO is 0.326 in the helicity basis [137]. The spin correlation could be modified by a new $t\bar{t}$ production mechanism such as through a Z' boson, Kaluza-Klein gluons, or a Higgs boson.

CDF used 5.1 fb^{-1} in the dilepton channel to measure the correlation coefficient in the beam axis [138]. The measurement was made using the expected distributions of $(\cos\theta_+, \cos\theta_-)$ and $(\cos\theta_b, \cos\theta_{\bar{b}})$ of the charged leptons or the b-quarks in the $t\bar{t}$ signal and background templates to calculate a likelihood of observed reconstructed distributions as a function of assumed κ. They determined the 68% confidence interval for the correlation coefficient κ as $-0.52 < \kappa < 0.61$ or $\kappa = 0.04 \pm 0.56$ assuming $m_t = 172.5$ GeV/c^2.

CDF also analyzed lepton+jets events in 5.3 fb^{-1} [139] assuming $m_t = 172.5$ GeV/c^2. They form three separate templates - the same-spin template, the opposite-spin template, and the background template for the 2-dimensional distributions in $\cos(\theta_l)\cos(\theta_d)$ vs. $\cos(\theta_l)\cos(\theta_b)$. The fit to the data in the helicity basis returns an opposite helicity fraction of $F_{OH} = 0.74 \pm 0.24(stat) \pm 0.11(syst)$. Converting this to the spin correlation coefficient yields $\kappa_{helicity} = 0.48 \pm 0.48(stat) \pm 0.22(syst)$. In the beamline basis, they find an opposite spin fraction of $F_{OS} = 0.86 \pm 0.32(stat) \pm 0.13(syst)$ which can be converted into a correlation coefficient of $\kappa_{beam} = 0.72 \pm 0.64(stat) \pm 0.26(syst)$.

DØ performed a measurement of the ratio f of events with correlated t and $\bar{t}$ spins to the total number of $t\bar{t}$ events in 5.3 fb^{-1} in the lepton+jets channel using a matrix element technique [140]. From 729 events, they obtain $f_{meas} = 1.15^{+0.42}_{-0.43}$ (stat + syst) and can exclude values of $f < 0.420$ at the 95% C.L. In the dilepton channel [141], they also use a matrix element method and can exclude at the 97.7% C.L. the hypothesis that the spins of the t and $\bar{t}$ are uncorrelated. The combination [140] yields $f_{meas} = 0.85 \pm 0.29$ (stat + syst) and a $t\bar{t}$ production cross section which is in good agreement with the SM prediction and previous measurements. For an expected fraction of $f = 1$, they can exclude $f < 0.481$ at the 95% C.L. For the observed value of $f_{meas} = 0.85$, they can exclude $f < 0.344(0.052)$ at the 95(99.7)% C.L. The observed fraction f_{meas} translates to a measured asymmetry value of $A_{meas} = 0.66 \pm 0.23$ (stat + syst), where the spin correlation coefficient, A, is defined as

$$A = \frac{N(\uparrow\uparrow) + N(\downarrow\downarrow) - N(\uparrow\downarrow) - N(\downarrow\uparrow)}{N(\uparrow\uparrow) + N(\downarrow\downarrow) + N(\uparrow\downarrow) + N(\downarrow\uparrow),} \qquad (5)$$

where the first arrow represents the direction of the top-quark spin along a chosen quantization axis, and the second arrow represents the same for the antitop-quark. They therefore obtain first evidence of SM spin correlation at 3.1 standard deviations.

Using 5.4 fb^{-1} of data, DØ measures the correlation in the dilepton channel also from the angles of the two leptons in the t and $\bar{t}$ rest frames, yielding a correlation strength $C = 0.10 \pm 0.45$ [142](C is equivalent to the opposite of κ in Eq. 4, in agreement with the NLO QCD prediction, but also in agreement with the no correlation hypothesis).

Spin correlations have now been conclusively measured at the LHC by both the ATLAS and CMS collaborations. In the dominant gluon fusion production mode for $t\bar{t}$ pairs at the LHC, the angular distribution between the two leptons in $t\bar{t}$ decays to dileptons is sensitive to the degree of spin correlation [143].

The ATLAS collaboration has performed a study of spin correlations in $t\bar{t}$ production at $\sqrt{s} = 7$ TeV using 2.1 fb^{-1} of data. Candidate events are selected in the dilepton topology with large missing transverse energy and at least two jets. The difference in azimuthal angle between the two charged leptons is compared to the expected distributions in the Standard Model, and to the case where the top quarks are produced with uncorrelated spin. Using the helicity basis as the quantization axis, the strength of the spin correlation between the top- and antitop-quark is measured to be $A_{helicity} = 0.40^{+0.09}_{-0.08}$ [144], which is in agreement with the NLO prediction of about 0.31 [145]. The hypothesis of no spin correlations is excluded at 5.1 standard deviations. An update of this analysis with 4.6 fb^{-1} yields results for four different variables, which have sensitivity to different properties of the production mechanism. The results can be translated to $A_{helicity} = 0.37 \pm 0.06(stat. + syst.)$ [146].

A similar analysis at CMS using dilepton events in 5.0 fb^{-1} of pp collisions at $\sqrt{s}$ = 7 TeV. The angular distribution between the two leptons is fit to extract $A_{helicity} = 0.24 \pm 0.02 \pm 0.08$ [147].

Observation of top-quark spin correlations requires a top-quark lifetime less than the spin decorrelation timescale [148]. The top-quark width, inversely proportional to its lifetime, is expected to be of order 1 GeV/c^2 (Eq. 1). The sensitivity of current experiments does not approach this level in direct measurements. Nevertheless, several measurements have been made.

CDF presents a direct measurement of the top-quark width in the lepton+jets decay channel of $t\bar{t}$ events from a data sample corresponding to 8.7 fb^{-1} of integrated luminosity. The top-quark mass and the mass of the hadronically decaying W boson that comes from the top-quark decay are reconstructed for each event and compared with templates of different top-quark widths (Γ_t) and deviations from nominal jet energy scale (ΔJES) to perform a simultaneous fit for both parameters, where ΔJES is used for the *in situ* calibration of the jet energy scale. By applying a Feldman-Cousins approach, they establish an upper limit at 95% C.L. of $\Gamma_t < 6.38$ GeV and a two-sided 68% C.L. interval of 1.10 GeV $< \Gamma_t <$ 4.05 GeV, corresponding to a lifetime interval of $1.6 \times 10^{-15} < \tau_{top} < 6.0 \times 10^{-25}$ [149], consistent with the SM prediction. For comparison, a typical hadronization timescale is an order of magnitude larger than these limits.

DØ extracts the total width of the top-quark from the partial decay width $\Gamma(t \to Wb)$ and the branching fraction $B(t \to Wb)$. $\Gamma(t \to Wb)$ is obtained from the measured t-channel cross section for single top-quark production in 5.4 fb^{-1}, and $B(t \to Wb)$ is extracted from a measurement of the ratio $R = B(t \to Wb)/B(t \to Wq)$ in $t\bar{t}$ events in lepton+jets channels with 0, 1 and 2 b-tags. Assuming $B(t \to Wq) = 1$, where q includes any kinematically accessible quark, the result is: $\Gamma_t = 2.00^{+0.47}_{-0.43}$ GeV which translates to a top-quark lifetime of $\tau_t = (3.29^{+0.90}_{-0.63}) \times 10^{-25}$ s. Assuming a high mass fourth generation b' quark and unitarity of the four-generation quark-mixing matrix, they set the first upper limit on $|V_{tb'}| < 0.59$ at 95% C.L. [150].

C.2.3 W-Boson Helicity in Top-Quark Decay: The Standard Model dictates that the top quark has the same vector-minus-axial-vector ($V - A$) charged-current weak interactions $\left(-i\frac{g}{\sqrt{2}}V_{tb}\gamma^\mu\frac{1}{2}(1-\gamma_5)\right)$ as all the other fermions. In the SM, the fraction of top-quark decays to longitudinally polarized W bosons is similar to its Yukawa coupling and hence enhanced with respect to the weak coupling. It is expected to be [151] $\mathcal{F}_0^{\rm SM} \approx x/(1+x)$, $x = m_t^2/2M_W^2$ ($\mathcal{F}_0^{\rm SM} \sim 70\%$ for $m_t = 175$ GeV/c^2). Fractions of left-handed, right-handed, or longitudinal W bosons are denoted as $\mathcal{F}_-$, $\mathcal{F}_+$, and $\mathcal{F}_0$ respectively. In the SM, $\mathcal{F}_-$ is expected to be $\approx 30\%$ and $\mathcal{F}_+ \approx 0\%$. Predictions for the W polarization fractions at NNLO in QCD are available [152].

The Tevatron and the LHC experiments use various techniques to measure the helicity of the W boson in top-quark decays, in both the lepton+jets and in dilepton channels in $t\bar{t}$ production.

The first method uses a kinematic fit, similar to that used in the lepton+jets mass analyses, but with the top-quark mass constrained to a fixed value, to improve the reconstruction of final-state observables, and render the under-constrained dilepton channel solvable. Alternatively, in the dilepton channel θ^* can also be obtained through an algebraic solution of the kinematics. The distribution of the helicity angle ($\cos\theta^*$) between the lepton and the b quark in the W rest frame provides the most direct measure of the W helicity. In a simplified version of this approach, the $\cos\theta^*$ distribution is reduced to a forward-backward asymmetry.

The second method (p_T^ℓ) uses the different lepton p_T spectra from longitudinally or transversely polarized W-decays to determine the relative contributions.

A third method uses the invariant mass of the lepton and the b-quark in top-quark decays ($M_{\ell b}^2$) as an observable, which is directly related to $\cos\theta^*$.

At the LHC, top-quark pairs in the dilepton channels are reconstructed by solving a set of six independent kinematic equations on the missing transverse energy in x- and in y-direction, two W-masses, and the two top/antitop-quark masses. In addition, the two jets with the largest p_T in the event are interpreted as b-jets. The pairing of the jets to the charged leptons is based on the minimization of the sum of invariant masses m_{min}. Simulations show that this criterion gives the correct pairing in 68% of the events.

Finally, the Matrix Element method (ME) has also been used, in which a likelihood is formed from a product of event probabilities calculated from the ME for a given set of measured kinematic variables and assumed W-helicity fractions. The results of recent CDF, DØ, ATLAS, and CMS analyses are summarized in Table 2.

The datasets are now large enough to allow for a simultaneous fit of $\mathcal{F}_0$, $\mathcal{F}_-$ and $\mathcal{F}_+$, which we denote by '3-param' or $\mathcal{F}_0$ and $\mathcal{F}_+$, which we denote by '2-param' in the table. Results with either $\mathcal{F}_0$ or $\mathcal{F}_+$ fixed at its SM value are denoted '1-param'. For the simultaneous fits, the correlation coefficient between the two values is about -0.8. A complete set of published results can be found in the Listings. All results are in agreement with the SM expectation.

CDF and DØ combined their results based on $2.7-5.4$ fb^{-1} using the BLUE method [153] for a top-quark mass of 172.5 GeV/c^2. ATLAS presents results from 1.04 fb^{-1} of $\sqrt{s}$ = 7 TeV data using a template method for the $\cos\theta^*$ distribution and angular asymmetries from the unfolded $\cos\theta^*$ distribution in the lepton+jets and the dilepton channel [155]. CMS performs a similar measurement based on template fits to the $\cos\theta^*$ distribution with 5.0 fb^{-1} of 7 TeV data in the lepton+jets final state [156]. As the polarization of the W bosons in top-quark decays is sensitive to the $W-t-b$ vertex

Lorentz structure and anomalous couplings, both experiments also derive limits on anomalous contributions to the $W-t-b$ couplings. Recently, both experiments also combined their results from 7 TeV data to obtain values on the helicity fractions as well as limits on anomalous couplings [157]. Very recently, CMS came out with a measurement of the W-helicity fractions in 19.6 fb^{-1} of muon+jets events recorded at 8 TeV [158]. Also, a first measurement of the W-boson helicity in top-quark decays was made in electroweak single top production [159], yielding consistent results.

Table 2: Measurement and 95% C.L. upper limits of the W helicity in top-quark decays. The table includes both preliminary, as of September 2013, and published results. A full set of published results is given in the Listings.

W Helicity	Source	$\int \mathcal{L}dt$ (fb^{-1})	Ref.	Method
$\mathcal{F}_0 = 0.722 \pm 0.081$	CDF+DØ Run II	2.7-5.4	[153]	$\cos\theta^*$ 2-par
$\mathcal{F}_0 = 0.682 \pm 0.057$	CDF+DØ Run II	2.7-5.4	[153]	$\cos\theta^*$ 1-par
$\mathcal{F}_0 = 0.726 \pm 0.094$	CDF Run II	8.7	[154]	ME 2-par
$\mathcal{F}_0 = 0.67 \pm 0.07$	ATLAS	1.0	[155]	$\cos\theta^*$ 3-par
$\mathcal{F}_0 = 0.682 \pm 0.045$	CMS	5.0	[156]	$\cos\theta^*$ 3-par
$\mathcal{F}_0 = 0.626 \pm 0.059$	ATLAS+CMS (7 TeV)	2.2	[157]	$\cos\theta^*$ 3-par
$\mathcal{F}_0 = 0.659 \pm 0.027$	CMS (8 TeV)	19.6	[158]	$\cos\theta^*$ 3-par
$\mathcal{F}_+ = -0.033 \pm 0.046$	CDF+DØ Run II	2.7-5.4	[153]	$\cos\theta^*$ 2-par
$\mathcal{F}_+ = -0.015 \pm 0.035$	CDF+DØ Run II	2.7-5.4	[153]	$\cos\theta^*$ 1-par
$\mathcal{F}_+ = -0.045 \pm 0.073$	CDF Run II	8.7	[154]	ME 2-par
$\mathcal{F}_+ = 0.01 \pm 0.05$	ATLAS	1.0	[155]	$\cos\theta^*$ 3-par
$\mathcal{F}_+ = 0.008 \pm 0.018$	CMS	5.0	[156]	$\cos\theta^*$ 3-par
$\mathcal{F}_+ = 0.015 \pm 0.034$	ATLAS+CMS (7 TeV)	2.2	[157]	$\cos\theta^*$ 3-par
$\mathcal{F}_+ = 0.009 \pm 0.021$	CMS (8 TeV)	19.6	[158]	$\cos\theta^*$ 3-par

C.2.4 Top-Quark Electric Charge: The top quark is the only quark whose electric charge has not been measured through production at threshold in e^+e^- collisions. Furthermore, it is the only quark whose electromagnetic coupling has not been observed and studied until recently. Since the CDF and DØ analyses on top-quark production did not associate the b, $\bar{b}$, and $W^\pm$ uniquely to the top or antitop, decays such as $t \to W^+\bar{b}, \bar{t} \to W^-b$ were not excluded. A charge 4/3 quark of this kind is consistent with current electroweak precision data. The $Z \to \ell^+\ell^-$ and $Z \to b\bar{b}$ data, in particular the discrepancy between A_{LR} from SLC at SLAC and $A_{FB}^{0,b}$ of b-quarks and $A_{FB}^{0,\ell}$ of leptons from LEP at CERN, can be fitted with a top quark of mass $m_t = 270$ GeV/c^2, provided that the right-handed b quark mixes with the isospin $+1/2$ component of an exotic doublet of charge $-1/3$ and $-4/3$ quarks, $(Q_1, Q_4)_R$ [160,161].

DØ studies the top-quark charge in double-tagged lepton+jets events, CDF does it in single tagged lepton+jets and dilepton events. Assuming the top- and antitop-quarks have equal but opposite electric charge, then reconstructing the charge of the b-quark through jet charge discrimination techniques, the $|Q_{top}| = 4/3$ and $|Q_{top}| = 2/3$ scenarios can be differentiated. For the exotic model of Chang *et al.* [161] with a top-quark charge $|Q_{top}| = 4/3$, DØ excludes the exotic model at 91.2% C.L.% [162] using 370 pb^{-1}, while CDF excludes the model at 99% C.L. [163] in 5.6 fb^{-1}. Both results indicate that the observed particle is indeed consistent with being a SM $|Q_{top}| = 2/3$ quark.

In 2.05 fb^{-1} at $\sqrt{s} = 7$ TeV, ATLAS performed a similar analysis, reconstructing the b-quark charge either via a jet-charge technique or via the lepton charge in soft muon decays in combination with a kinematic likelihood fit. They measure the top-quark charge to be $0.64 \pm 0.02(stat.) \pm 0.08(syst.)e$ from the charges of the top-quark decay products in single lepton $t\bar{t}$ events, and hence exclude the exotic scenario with charge $-4/3$ at more than 8σ [164].

In 4.6 fb^{-1} at $\sqrt{s} = 7$ TeV, CMS discriminates between the Standard Model and the exotic top-quark charge scenario in the muon+jets final states in $t\bar{t}$ events. They exploit the charge correlation between high-p_t muons from W-boson decays and soft muons from B-hadron decays in b-jets. Using an asymmetry technique, where $A = -1$ represent the exotic $q = -4/3$ scenario and $A = +1$ the Standard Model $q = +2/3$ scenario, they find $A_{meas} = 0.97 \pm 0.12(stat.) \pm 0.31(sys.)$, which agrees with the Standard Model expectation and excludes the exotics scenario at 99.9% C.L. [165].

The electromagnetic or the weak coupling of the top quark can be probed directly by investigating $t\bar{t}$ events with an additional gauge boson, like $t\bar{t}\gamma$ and $t\bar{t}Z$ events.

CDF performs a search for events containing a lepton, a photon, significant missing transverse momentum, and a jet identified as containing a b-quark and at least three jets and large total transverse energy in 6.0 fb^{-1}. They reported evidence for the observation of $t\bar{t}\gamma$ production with a cross section $\sigma_{t\bar{t}\gamma} = 0.18 \pm 0.08$ pb and a ratio of $\sigma_{t\bar{t}\gamma}/\sigma_{t\bar{t}} = 0.024 \pm 0.009$ [166].

ATLAS performed a first measurement of the $t\bar{t}\gamma$ cross section in pp collisions at $\sqrt{s} = 7$ TeV using 1.04 fb^{-1} of data. Events are selected that contain a large transverse momentum electron or muon and a large transverse momentum photon, yielding 52 and 70 events in the electron and muon samples, respectively. The resulting cross section times branching ratio into the single lepton and dilepton channels for $t\bar{t}\gamma$ production with a photon with transverse momentum above 8 GeV is $\sigma(t\bar{t}\gamma) = 2.0 \pm 0.5(stat.) \pm 0.7(syst.) \pm 0.1(lumi.)$ pb [167], which is consistent with theoretical calculations. A real test, however, of the vector and axial vector couplings in $t\bar{t}\gamma$ events or searches for possible tensor couplings of top-quarks to photons will only be feasible with an integrated luminosity of several hundred fb^{-1} in the future.

CMS also performed measurements of the $t\bar{t}W$ and $t\bar{t}Z$ production cross section at $\sqrt{s} = 7$ TeV with 5 fb^{-1}, yielding results at about 3 standard deviations significance [168]. ATLAS performed a similar analysis with 4.7 fb^{-1} in the three-lepton

channel and set an upper limit of 0.71 pb at 95% C.L. [169]. Also here, more data is expected to yield an observation.

C.3 Searches for Beyond the Standard Model Physics

The top quark plays a special role in the SM. Being the only quark with a coupling to the Higgs boson of order one, it provides the most important contributions to the quadratic radiative corrections to the Higgs mass raising the question of the naturalness of the SM. It is therefore very common for models where the naturalness problem is addressed to have new physics associated with the top quark. In SUSY, for instance, naturalness predicts the scalar top partners to be the lightest among the squarks and to be accessible at the LHC energies (see the review "Supersymmetry: Theory"). In models where the Higgs is a pseudo-Goldstone boson, such as Little Higgs models, naturalness predicts the existence of partners of the top quarks with the same spin and color, but with different electroweak couplings, the so-called vectorial t'. Stops and t''s are expected to have sizable branching ratios to top quarks. Another intriguing prediction of SUSY models with universal couplings at the unification scale is that for a top-quark mass close to the measured value, the running of the Yukawa coupling down to 1 TeV naturally leads to the radiative breaking of the electroweak symmetry [170]. In fact, the top quark plays a role in the dynamics of electroweak symmetry breaking in many models. One example is topcolor [171], where a large top-quark mass can be generated through the formation of a dynamic $t\bar{t}$ condensate, X, which is formed by a new strong gauge force coupling preferentially to the third generation. Another example is topcolor-assisted technicolor [172], predicting the existence of a heavy Z' boson that couples preferentially to the third generation of quarks. If light enough such a state might be directly accessible at the present hadron collider energies, or if too heavy, lead to four-top interactions possibly visible in the production cross section for $t\bar{t}t\bar{t}$.

Current strategies to search for new physics in top-quark events at hadron colliders are either tailored to the discovery of specific models or model independent. They can be broadly divided in two classes. In the first class new resonant states are looked for through decay processes involving the top quarks. Current searches for bosonic resonances in $t\bar{t}$ final states, or for direct stop and t' production, or for a charged Higgs in $H^+ \to t\bar{b}$ fall in the category. On the other hand, if new states are too heavy to be directly produced, they might still give rise to deviations from the SM predictions for the strength and Lorentz form of the top-quark couplings to other SM particles. Accurate predictions and measurements are therefore needed and the results be efficiently systematized in the framework of an effective field theory [173,174]. The on-going efforts to constrain the $W - t - b$ coupling and to search for flavor-changing neutral currents involving the top quark fall in this second category.

C.3.1 New Physics in Top-Quark Production: Theoretical [175–177] and experimental efforts have been devoted to the searches for new physics in $t\bar{t}$ resonances.

At the Tevatron, both the CDF and DØ collaborations have searched for resonant production of $t\bar{t}$ pairs in the lepton+jets channel [182,183]. In both analyses, the data indicate no evidence of resonant production of $t\bar{t}$ pairs. They place upper limits on the production cross section times branching fraction to $t\bar{t}$ in comparison to the prediction for a narrow ($\Gamma_{Z'} = 0.012 M_{Z'}$) leptophobic topcolor Z' boson. Within this model, they exclude Z' bosons with masses below 915 (CDF-full data set) and 835 (DØ, 5 fb^{-1}) GeV/c^2 at the 95% C.L. These limits turn out to be independent of couplings of the $t\bar{t}$ resonance (pure vector, pure axial-vector, or SM-like Z'). A similar analysis has been performed by CDF in the all-jets channel using 2.8 fb^{-1} of data [184].

At the LHC, both the CMS and ATLAS collaborations have searched for resonant production of $t\bar{t}$ pairs, employing different techniques and final-state signatures (all-jets, lepton+jets, dilepton) at $\sqrt{s} = 7$ and 8 TeV. In the low mass range, from the $t\bar{t}$ threshold to about one TeV, standard techniques based on the reconstruction of each of the decay objects (lepton, jets and b-jets, missing E_T) are used to identify the top quarks, while at higher invariant mass, the top quarks are boosted and the decay products more collimated and can appear as large-radius jets with substructure. Dedicated reconstruction techniques have been developed in recent years for boosted top quarks [185] that are currently employed at the LHC. Most of the analyses are model-independent (i.e., no assumption on the quantum numbers of the resonance is made) yet they assume a small width and no signal-background interference.

Using dilepton and lepton+jets signatures in a data set corresponding to an integrated luminosity of 5.0 fb^{-1}, the CMS collaboration finds no significant deviations from the SM background. In the dilepton analysis, upper limits are presented for the production cross section times branching fraction of top quark-antiquark resonances for masses from 750 to 3000 GeV/c^2. In particular, the existence of a leptophobic topcolor particle Z' is excluded at the 95% confidence level for resonance masses $M_{Z'} < 1.3$ (1.9) TeV/c^2 for $\Gamma_{Z'} = 0.012(0.1) M_{Z'}$ [186]. Using a lepton+jets sample, results are obtained from the combination of two dedicated searches optimized for boosted production and production at threshold. In this case, topcolor Z' bosons with narrow (wide) width are excluded at 95% confidence level for masses below 1.49 (2.04) TeV/c^2 and an upper limit of 0.3 (1.3) pb or lower is set on the production cross section times branching fraction for resonance masses above 1 TeV/c^2. Kaluza-Klein excitations of a gluon with masses below 1.82 TeV/c^2 (at 95% confidence level) in the Randall-Sundrum model are also excluded, and an upper limit of 0.7 pb or lower is set on the production cross section times branching fraction for resonance masses above 1 TeV/c^2 [187]. In 19.7 fb^{-1} of 8 TeV data, CMS recently updated their measurement in the lepton+jets and the all-jets channel to obtain an

exclusion of $M_{Z'} < 2.1(2.7)$ TeV/c^2 for $\Gamma_{Z'} = 0.013(0.1)M_{Z'}$ and gluon masses below 2.5 TeV/c^2 in Randall-Sundrum models at 95% C.L. [188].

The ATLAS collaboration has performed a search for resonant $t\bar{t}$ production in the lepton+jets channel using 4.7 fb^{-1} (14 fb^{-1}) of proton-proton (pp) collision data collected at a center-of-mass energy $\sqrt{s} = 7(8)$ TeV [189,190]. The $t\bar{t}$ system is reconstructed using both small-radius and large-radius jets, the latter being supplemented by a jet substructure analysis. A search for local excesses in the number of data events compared to the Standard Model expectation in the $t\bar{t}$ invariant mass spectrum is performed. No evidence for a $t\bar{t}$ resonance is found and 95% confidence-level limits on the production rate are determined for massive states predicted in two benchmark models. The most stringent limits come from the sample collected at 8 TeV. The upper limits on the cross section times branching ratio of a narrow Z' boson decaying to top-quark pairs range from 5.3 pb for a resonance mass of 0.5 TeV/c^2 to 0.08 pb for a mass of 3 TeV/c^2. A narrow leptophobic topcolor Z' boson with a mass below 1.8 TeV/c^2 is excluded. Upper limits are set on the cross section times branching ratio for a broad color-octet resonance with $\Gamma/m = 15.3\%$ decaying to $t\bar{t}$. These range from 9.6 pb for a mass of 0.5 TeV/c^2 to 0.152 pb for a mass of 2.5 TeV/c^2. A Kaluza-Klein excitation of the gluon in a Randall-Sundrum model (a slightly different model is used compared to CMS) is excluded for masses below 2.0 TeV/c^2.

ATLAS has also conducted a search in the all-jet final state at 7 TeV corresponding to an integrated luminosity of 4.7 fb^{-1} [191]. The $t\bar{t}$ events are reconstructed by selecting two top quarks in their fully hadronic decay modes which are reconstructed using the Cambridge/Aachen jet finder algorithm with a radius parameter of 1.5. The substructure of the jets is analysed using the HEPTopTagger algorithm [192] to separate top-quark jets from those originating from gluons and lighter quark jets. The invariant mass spectrum of the data is compared to the SM prediction, and no evidence for resonant production of top-quark pairs is found. The data are used to set upper limits on the cross section times branching ratio for resonant $t\bar{t}$ production in two models at 95% confidence level. Leptophobic Z' bosons with masses between 700 and 1000 GeV/c^2 as well as $1280 - 1320$ GeV/c^2 and Kaluza-Klein-Gluons with masses between 700 and 1620 GeV/c^2 are excluded at the 95% confidence level.

Heavy charged bosons, such as W' or H^+, can also be searched for in $t\bar{b}$ final states (for more information see the review "W'-boson searches" and "Higgs Bosons: theory and searches"). Other resonances are searched for in final states such as tZ, tj, tH, tW, bW.

For instance, ATLAS has performed a search for t-jet resonances in the lepton+jets channel of $t\bar{t}$+ jets events in 4.7 fb^{-1} at $\sqrt{s} = 7$ TeV [193]. A heavy new particle, assumed to be produced singly in association with a $t(\bar{t})$ quark, decays to a $t(\bar{t})$ quark and a light flavor quark, leading to a color singlet (triplet) resonance in the $t(\bar{t})$+jet system. The full 2011 ATLAS pp collision dataset from the LHC (4.7 fb^{-1}) is used to select $t\bar{t}$ events. The data are consistent with the SM expectation and a new particle with mass below 350 (430) GeV/c^2 for W (color triplet) models is excluded with a 95% confidence level, assuming unit right-handed coupling. ATLAS has conducted a search for the pair production of a new charge +2/3 quark (T) decaying via $T \to Zt$ in a dataset corresponding to 14.3 fb^{-1} luminosity at $\sqrt{s} = 8$ TeV [194]. Selected events contain a high transverse momentum Z-boson candidate reconstructed from a pair of oppositely charged electrons or muons. Additionally, the presence of at least two jets possessing properties consistent with the decay of a b-hadron is required, as well as large total transverse momentum of all central jets in the event. No significant excess of events above the SM expectation is observed, and upper limits are derived for vector-like quarks of various masses in a two-dimensional plane of branching ratios. Under branching ratio assumptions corresponding to a weak-isospin singlet scenario, a T quark with mass lower than 585 GeV/c^2 is excluded at the 95% confidence level. Under branching ratio assumptions corresponding to a particular weak-isospin doublet scenario, a T quark with mass lower than 680 GeV/c^2 is excluded at the 95% confidence level.

A complementary search [195] in the lepton+jets final state of the same dataset, characterized by an isolated electron or muon with moderately high transverse momentum, significant missing transverse momentum, and at least six jets is performed to look for $T \to Wb, Ht$ decays. The search exploits the high total transverse momenta of all final state objects and the high multiplicity of b-jets characteristic of signal events with at least one Higgs boson decaying into $b\bar{b}$, to discriminate against the dominant background from top-quark pair production. No significant excess of events above the SM expectation is observed, and upper limits are derived for vector-like quarks of various masses in the two-dimensional plane of $B(T \to Wb)$ versus $B(T \to Ht)$, where H is the Standard Model Higgs boson, assumed to have a mass of 125 GeV/c^2. Under the branching ratio assumptions corresponding to a weak-isospin doublet (singlet) scenario, a T quark with mass lower than 790 (640) GeV/c^2 is excluded at the 95% C.L.

Finally, a more general search is performed in the same data set [196], looking for exotic processes that result in final states containing jets including at least one b-jet, sizable missing transverse momentum, and a pair of leptons with the same electric charge. In addition to the new physics signal discussed above, this study provides limits on four top-quark production and production of two positively-charged top quarks. No significant excess of events over the background expectation is observed. This observation is interpreted as constraining the signal hypotheses, and it is found at 95% C.L. level that: the lower bound on the fourth generation B quark mass, assuming 100% branching fraction to Wt, is 0.72 TeV/c^2; the mass of a vector-like B (T) quark, assuming branching ratios to W, Z, and H decay modes consistent with the B or T being a singlet, is larger than 0.59 (0.54) TeV/c^2; the four top production cross

section must be less than 85 fb in the SM and less than 59 fb for production via a contact interaction; the mass of a sgluon must be greater than 0.80 TeV/c^2; in the context of models with two universal extra dimensions the inverse size of the extra dimensions must be larger 0.90 TeV/c^2; and the cross section for production of two positively-charged top quarks must be smaller than 210 fb.

In many models top-quark partners preferably decay to top quarks and weakly interacting neutral stable particles that are not detected. An observable especially sensitive to new physics effects in $t\bar{t}$ production is therefore the missing momentum. CMS has presented a differential cross section measurement of top-quark pair production with missing transverse energy using 5.1 fb^{-1} of data collected at 7 TeV [197]. The analysis selects events in the lepton+jets final state and the differential cross section is measured in bins of missing transverse energy. Recently, CMS has updated their analysis with 20 fb^{-1} at 8 TeV [49]. The results are consistent with the predictions of the SM. An analogous search, but more targeted to discover new physics in $t\bar{t}$ events with large missing transverse momentum in proton-proton collisions at a center-of-mass energy of 7 TeV in 1.04 fb^{-1} of data has been performed by ATLAS [198]. The search is carried out in the lepton+jets channel. The results are interpreted in terms of a model where new top-quark partners are pair-produced and each decay to an on-shell top (or antitop) quark and a long-lived undetected neutral particle. The data are found to be consistent with SM expectations. A limit at 95% C.L. is set excluding a cross-section times branching ratio of 1.1 pb for a top-partner mass of 420 GeV/c^2 and a neutral particle mass less than 10 GeV/c^2. In a model of exotic fourth generation quarks, top-partner masses are excluded up to 420 GeV/c^2 and neutral particle masses up to 140 GeV/c^2.

Flavor-changing-neutral-currents (FCNC) are hugely suppressed in the SM, and non zero only due to the large mass hierarchy between the top quark and the other quarks. Several observables are accessible at colliders to test and constrain such couplings.

CMS has performed a study of top-quark couplings through the search for a single top quark produced in association with a Z boson in 5 fb^{-1} integrated luminosity at 7 TeV [199]. The event selection requires the presence of three isolated leptons, electrons or muons, and of at least one jet. The upper limits on effective coupling strength can be translated to the 95% upper limits on the corresponding branching ratios $B(t \to gu) \leq 0.56\%$, $B(t \to gc) \leq 7.1\%$, $B(t \to Zu) \leq 0.51\%$, $B(t \to Zc) \leq 11\%$.

ATLAS has presented results on the search for single top-quark production via FCNC's in strong interactions using data collected at $\sqrt{s}$=8 TeV and corresponding to an integrated luminosity of 14.2 fb^{-1}. Flavor-changing-neutral-current events are searched for in which a light quark (u or c) interacts with a gluon to produce a single top quark, either with or without the associated production of another light quark or gluon. Candidate events of top quarks decaying into leptons and jets are selected and classified into signal- and background-like events using a neural network. The observed 95% C.L. $B(t \to ug) < 3.1 \cdot 10^{-5}$ and $B(t \to cg) < 1.6 \cdot 10^{-4}$ [200]. This result supersedes the corresponding 7 TeV analysis in 2 fb^{-1} [201].

Constraints on FCNC couplings of the top quark can also be obtained from searches for anomalous single top-quark production in e^+e^- collisions, via the process $e^+e^- \to \gamma, Z^* \to t\overline{q}$ and its charge-conjugate ($q = u, c$), or in $e^{\pm}p$ collisions, via the process $e^{\pm}u \to e^{\pm}t$. For a leptonic W decay, the topology is at least a high-p_T lepton, a high-p_T jet and missing E_T, while for a hadronic W-decay, the topology is three high-p_T jets. Limits on the cross section for this reaction have been obtained by the LEP collaborations [202] in e^+e^- collisions, and by H1 [203] and ZEUS [204] in $e^{\pm}p$ collisions. When interpreted in terms of branching ratios in top decay [205,206], the LEP limits lead to typical 95% C.L. upper bounds of $B(t \to qZ) < 0.137$. Assuming no coupling to the Z boson, the 95% C.L. limits on the anomalous FCNC coupling $\kappa_\gamma < 0.13$ and < 0.27 by ZEUS and H1, respectively, are stronger than the CDF limit of $\kappa_\gamma < 0.42$, and improve over LEP sensitivity in that domain. The H1 limit is slightly weaker than the ZEUS limit due to an observed excess of five-candidate events over an expected background of 3.2 ± 0.4. If this excess is attributed to FCNC top-quark production, this leads to a total cross section of $\sigma(ep \to e + t + X, \sqrt{s} = 319 \text{ GeV}) < 0.25$ pb [203,207].

C.3.2 New Physics in Top-Quark decays: The large sample of top quarks produced at the Tevatron and the LHC allows to measure or set stringent limits on the branching ratios of rare top-quark decays. For example, the existence of a light H^+ can be constrained by looking for $t \to H^+b$ decay, in particular with tau-leptons in the final state (for more information see the review "Higgs Bosons: theory and searches").

A first class of searches for new physics focuses on the strcuture of the $W - t - b$ vertex. Using up to 2.7 fb^{-1} of data, DØ has measured the Wtb coupling form factors by combining information from the W-boson helicity in top-quark decays in $t\bar{t}$ events and single top-quark production, allowing to place limits on the left-handed and right-handed vector and tensor couplings [225–227].

More recently, ATLAS has published the results of a search for CP violation in the decay of single top quarks produced in the t-channel where the top quarks are predicted to be highly polarized, using the lepton+jets final state [228]. The data analyzed are from pp collisions at $\sqrt{s} = 7$ TeV and correspond to an integrated luminosity of 4.7 fb^{-1}. In the Standard Model, the couplings at the Wtb vertex are left-handed, right-handed couplings being absent. A forward-backward asymmetry with respect to the normal to the plane defined by the W-momentum and the top-quark polarization has been used to probe the complex phase of a possibly non-zero value of the right-handed coupling, signaling a source of CP-violation

beyond the SM. The measured value of the asymmetry is $0.031 \pm 0.065(stat.)^{+0.029}_{-0.031}(syst.)$ in good agreement with the Standard Model.

A second class of searches focuses on FCNC's in the top-quark decays.

Both, CDF and DØ, have provided the first limits for FCNC's in Run I and II. The most recent results from CDF give $B(t \to qZ) < 3.7\%$ and $B(t \to q\gamma) < 3.2\%$ at the 95% C.L. [229] while DØ [230,231] sets $B(t \to qZ)(q = u, c$ quarks $) < 3.2\%)$ at 95% C.L., $B(t \to gu) < 2.0 \cdot 10^{-4}$, and $B(t \to gc) < 3.9 \cdot 10^{-3}$ at the 95% C.L.

At the LHC, CMS has used a sample at a center-of-mass energy of 8 TeV corresponding to 19.7 fb^{-1} of integrated luminosity to perform a search for flavor changing neutral current top-quark decay $t \to Zq$. Events with a topology compatible with the decay chain $t\bar{t} \to Wb + Zq \to \ell\nu\, b + \ell\ell q$ are searched for. There is no excess seen in the observed number of events relative to the SM prediction; thus no evidence for flavor changing neutral current in top-quark decays is found. A combination with a previous search at 7 TeV excludes a $t \to Zq$ branching fraction greater than 0.05% at the 95% confidence level [232].

The ATLAS collaboration has also searched for FCNC processes in 2.1 fb^{-1} of $t\bar{t}$ events with one top quark decaying through FCNC ($t \to qZ$) and the other through the SM dominant mode ($t \to bW$). Only the decays of the Z boson to charged leptons and leptonic W boson decays were considered as signal, leading to a final state topology characterized by the presence of three isolated leptons, at least two jets and missing transverse energy from the undetected neutrino. No evidence for an FCNC signal was found. An upper limit on the $t \to qZ$ branching ratio of $B(t \to qZ)$ <0.73% is set at the 95% confidence level [233]. Another analysis looks for FCNCs in $t \to cH$ with $H \to \gamma\gamma$ in 20 fb^{-1} of $t\bar{t}$ events at $\sqrt{s} = 9$ TeV, yielding a 95% C.L. limit of the tcH coupling of 0.17 (0.14 expected) [234].

D. Outlook

Top-quark physics at hadron colliders has developed into precision physics. Various properties of the top quark have been measured with high precision, where the LHC is about to or has already reached the precision of the Tevatron. Several $\sqrt{s}$-dependent physics quantities, such as the production cross-section, have been measured at several energies at the Tevatron and the LHC. Up to now, all measurements are consistent with the SM predictions and allow stringent tests of the underlying production mechanisms by strong and weak interactions. Given the very large event samples available at the LHC, top-quark properties will be further determined in $t\bar{t}$ as well as in electroweak single top-quark production. At the Tevatron, the $t-$ and $s-$channels for electroweak single top-quark production have been measured separately. At the LHC, significant progress has been achieved and all the three relevant channels are expected to be independently accessible in the near future. Furthermore, $t\bar{t}\gamma$, $t\bar{t}Z$ and $t\bar{t}W$ associated production will provide further information on the top-quark electroweak couplings. At the same time various models of physics beyond the SM involving top-quark production are being constrained. With the upcoming LHC Run-II with twice the center-of-mass energy and much higher luminosity, top-quark physics has the potential to shed light on new aspects of and open questions in physics at the TeV scale.

References

CDF note references can be retrieved from `www-cdf.fnal.gov/physics/new/top/top.html`, and DØ note references from `www-d0.fnal.gov/Run2Physics/WWW/documents/Run2Results.htm` and ATLAS note references from `https://twiki.cern.ch/twiki/bin/view/AtlasPublic/TopPublicResults` and CMS note references from `https://twiki.cern.ch/twiki/bin/view/CMSPublic/PhysicsResultsTOP`.

1. M. Czakon, P. Fiedler and A. Mitov, Phys. Rev. Lett. **110**, 252004 (2013).
2. M. Cacciari *et al.*, J. High Energy Phys.0809, 127 (2008); N. Kidonakis and R. Vogt, Phys. Rev. **D78**, 074005 (2008); S. Moch and P. Uwer, Nucl. Phys. (Proc. Supp.) **B183**, 75 (2008); S. Moch and P. Uwer, Phys. Rev. **D78**, 034003 (2008); U. Langenfeld, S. Moch, and P. Uwer, Phys. Rev. **D80**, 054009 (2009); M. Beneke *et al.* Phys. Lett. **B690**, 483 (2010); M. Beneke *et al.*, Nucl. Phys. **B855**, 695 (2012); V. Ahrens *et al.*, Phys. Lett. **B703**, 135 (2011); M. Cacciari *et al.*, Phys. Lett. **B710**, 612 (2012).
3. The Tevatron Electroweak Working Group, For the CDF and DØ Collabs., `arXiv:1305.3929`.
4. S. Cortese and R. Petronzio, Phys. Lett. **B253**, 494 (1991).
5. S. Willenbrock and D. Dicus, Phys. Rev. **D34**, 155 (1986).
6. N. Kidonakis, Phys. Rev. **D83**, 091503 (2011).
7. N. Kidonakis, Phys. Rev. **D81**, 054028 (2010).
8. N. Kidonakis, Phys. Rev. **D82**, 054018 (2010).
9. T. Tait and C.-P. Yuan. Phys. Rev. **D63**, 014018 (2001).
10. M. Jeżabek and J.H. Kühn, Nucl. Phys. **B314**, 1 (1989).
11. I.I.Y. Bigi *et al.*, Phys. Lett. **B181**, 157 (1986).
12. A.H. Hoang *et al.*, Phys. Rev. **D65**, 014014 (2002).
13. K. Hagiwara, Y. Sumino, and H. Yokoya, Phys. Lett. **B666**, 71 (2008).
14. A. Czarnecki and K. Melnikov, Nucl. Phys. **B544**, 520 (1999); K.G. Chetyrkin *et al.*, Phys. Rev. **D60**, 114015 (1999).
15. S. Frixione, P. Nason, and B. Webber, J. High Energy Phys.08,007 (2003); S. Frixione, P. Nason, and C. Oleari, J. High Energy Phys.07,070 (2007); S. Frixione, P. Nason, and G. Ridolfi, J. High Energy Phys.07,126 (2007).
16. S. Frixione *et al.*, J. High Energy Phys.06,092 (2006); S. Frixione *et al.*, J. High Energy Phys.08,029 (2008); S. Alioli *et al.*, J. High Energy Phys.09,111 (2009); E. Re, Eur. Phys. J. C **71**, 1547 (2011); R. Frederix, E. Re, and P. Torrielli, J. High Energy Phys.12, 130 (2012).
17. S. Frixione and B.R. Webber, J. High Energy Phys.02,029 (2002).
18. P. Nason, J. High Energy Phys.04,040 (2004).

19. V.M. Abazov *et al.* (DØ Collab.), Phys. Lett. **B704**, 403 (2011).
20. T. Aaltonen *et al.* (CDF Collab.), CDF conference note 9913 (2009).
21. T. Aaltonen *et al.* (CDF Collab. and DØ Collab.), arXiv:1309.7570, submitted to Phys. Rev. D (2013).
22. ATLAS Collab., ATLAS-CONF-2011-121.
23. G. Aad *et al.* (ATLAS Collab.), J. High Energy Phys.1205,059(2012).
24. ATLAS Collab., ATLAS-CONF-2011-140.
25. ATLAS Collab., ATLAS-CONF-2012-024.
26. G. Aad *et al.* (ATLAS Collab.), Eur. Phys. J. **C73**, 2328 (2013).
27. G. Aad *et al.* (ATLAS Collab.), Phys. Lett. **B717**, 89 (2012).
28. ATLAS Collab., ATLAS-CONF-2012-031.
29. S. Chatrchyan *et al.* (CMS Collab.), Phys. Lett. **B720**, 83 (2013).
30. S. Chatrchyan *et al.* (CMS Collab.), J. High Energy Phys.11,067(2012).
31. S. Chatrchyan *et al.* (CMS Collab.), J. High Energy Phys.1305,065(2013).
32. S. Chatrchyan *et al.* (CMS Collab.), Phys. Rev. **D85**, 112007 (2012).
33. S. Chatrchyan *et al.* (CMS Collab.), Eur. Phys. J. **C73**, 2386 (2013).
34. ATLAS Collab., ATLAS-CONF-2012-149.
35. ATLAS Collab., ATLAS-CONF-2013-097.
36. CMS Collab., CMS-PAS-TOP-12-006.
37. CMS Collab., CMS-PAS-TOP-12-007.
38. V.M. Abazov *et al.* (DØ Collab.) Phys. Rev. Lett. **107**, 121802, (2011); D. Acosta *et al.* (CDF Collab.) Phys. Rev. Lett. **95**, 102002, (2005).
39. CMS Collab., CMS-PAS-TOP-12-035.
40. ATLAS Collab., ATLAS-CONF-2011-108.
41. V.M. Abazov *et al.* (DØ Collab.), Phys. Rev. **D67**, 012004 (2003).
42. T. Affolder *et al.* (CDF Collab.), Phys. Rev. **D64**, 032002 (2001).
43. T. Affolder *et al.* (CDF Collab.), Phys. Rev. Lett. **102**, 222003 (2009).
44. DØ Collab., D0-CONF-6379 (2013).
45. ATLAS Collab., ATLAS-CONF-2013-099 (2013).
46. S. Chatrchyan *et al.* (CMS Collab.), Eur. Phys. J. **C73**, 2339 (2013).
47. CMS Collab., CMS-PAS-TOP-12-027 (2013).
48. CMS Collab., CMS-PAS-TOP-12-028 (2013).
49. CMS Collab., CMS-PAS-TOP-12-042 (2013).
50. ATLAS Collab., ATLAS-CONF-2012-16 (2012).
51. ATLAS Collab., ATLAS-CONF-2012-155 (2012).
52. V.M. Abazov *et al.* (DØ Collab.), Phys. Rev. Lett. **103**, 092001 (2009); V.M. Abazov *et al.* (DØ Collab.), Phys. Rev. **D78**, 12005 (2008); V.M. Abazov *et al.* (DØ Collab.), Phys. Rev. Lett. **98**, 181802 (2007).
53. T. Aaltonen *et al.* (CDF Collab.), Phys. Rev. Lett. **103**, 092002 (2009); T. Aaltonen *et al.* (CDF Collab.), Phys. Rev. **D81**, 072003 (2010).
54. T. Aaltonen *et al.* (CDF Collab.), Phys. Rev. **D82**, 112005 (2010).
55. A. Heinson and T. Junk, Ann. Rev. Nucl. Part. Sci. **61**, 171 (2011).
56. Tevatron Electroweak Working Group, arXiv:0908.2171v1 [hep-ex].
57. CDF Collab., CDF conference note 10793 (2012).
58. CDF Collab., CDF conference note 10979 (2013).
59. V.M. Abazov *et al.* (DØ Collab.), Phys. Rev. **D84**, 112001 (2011).
60. CDF Collab., CDF conference note 11015 (2013).
61. CDF Collab., CDF conference note 11025 (2013).
62. DØ Collab., FERMILAB-PUB-13-252-E, arXiv:1307.0731, submitted to Physics Letters B.
63. V.M. Abazov *et al.* (DØ Collab.), Phys. Lett. **B705**, 313 (2011).
64. G. Aad *et al.*, ATLAS Collab., Phys. Lett. **B717**, 330 (2012).
65. S. Chatrychan *et al.*, CMS Collab., J. High Energy Phys.12,035(2012).
66. ATLAS Collab., ATLAS-CONF-2012-056.
67. ATLAS Collab., ATLAS-CONF-2012-132.
68. CMS Collab., CMS-PAS-TOP-12-011.
69. ATLAS and CMS Collab., ATLAS-CONF-2013-098, CMS-PAS-TOP-12-002.
70. CMS Collab., CMS-PAS-TOP-13-001.
71. CMS Collab., CMS-PAS-TOP-12-038.
72. C.D. White *et al.*, J. High Energy Phys.11, 74 (2009).
73. S. Frixione *et al.*, J. High Energy Phys.07, 29 (2008).
74. G. Aad *et al.*, ATLAS Collab., Phys. Lett. **B716**, 142 (2012).
75. S. Chatrychan *et al.*, CMS Collab., Phys. Rev. Lett. **110**, 022003 (2012).
76. ATLAS Collab., ATLAS-CONF-2013-100.
77. CMS Collab., CMS-PAS-TOP-12-040.
78. ATLAS Collab., ATLAS-CONF-2011-118.
79. CMS Collab., CMS-PAS-TOP-11-003.
80. W. Hollik & D. Pagani Phys. Rev. **D84**, 093003 (2011).
81. W. Bernreuther & Z.G. Si, Phys. Rev. **D86**, 034026 (2012).
82. S. Jung, H. Murayama, A. Pierce, J.D. Wells, Phys. Rev. **D81**, 015004 (2010).
83. V.M. Abazov *et al.* (DØ Collab.), Phys. Rev. Lett. **100**, 142002 (2008).
84. T. Aaltonen *et al.* (CDF Collab.), Phys. Rev. Lett. **101**, 202001 (2008).
85. V.M. Abazov *et al.* (DØ Collab.), Phys. Rev. **D84**, 112005 (2011).
86. T. Aaltonen *et al.* (CDF Collab.), Phys. Rev. **D87**, 092002 (2013).
87. T. Aaltonen, *et al.* (CDF Collab.), Phys. Rev. **D83**, 112003 (2011).
88. ATLAS Collab., ATLAS-CONF-2013-078.
89. S. Chatrchyan *et al.* (CMS Collab.), Phys. Lett. **B717**, 129 (2012).
90. CMS Collab., CMS PAS TOP-12-033.
91. DØ Collab., DØ conference note 6381 (2013).

92. V.M. Abazov *et al.* (DØ Collab.), arXiv:1308.6690.
93. T. Aaltonen *et al.* (CDF Collab.), FERMILAB-PUB-13-309-E, arXiv:1308.1120.
94. ATLAS Collab., ATLAS-CONF-2012-057.
95. CMS Collab., CMS PAS TOP-12-010.
96. G. Aad *et al.* (ATLAS Collab.), Eur. Phys. J. **C72**, 2039 (2012).
97. F. Abe *et al.* (CDF Collab.), Phys. Rev. **D50**, 2966 (1994).
98. A. Abulencia *et al.* (CDF Collab.), Phys. Rev. **D73**, 032003 (2006).
99. ATLAS Collab., ATLAS-CONF-2013-046.
100. S. Chatrchyan *et al.* (CMS Collab.), J. High Energy Phys.12,105(2012).
101. T. Aaltonen *et al.* (CDF Collab.), Phys. Rev. Lett. **109**, 152003 (2012).
102. V.M. Abazov *et al.* (DØ Collab.), Phys. Rev. **D84**, 032004 (2011).
103. V.M. Abazov *et al.* (DØ Collab.), Nature, **429**, 638 (2004).
104. K. Kondo *et al.* J. Phys. Soc. Jpn. **G62**, 1177 (1993).
105. R.H. Dalitz and G.R. Goldstein, Phys. Rev. **D45**, 1531 (1992); Phys. Lett. **B287**, 225 (1992); Proc. Royal Soc. London **A445**, 2803 (1999).
106. V.M. Abazov *et al.* (DØ Collab.), Phys. Rev. **D75**, 092001 (2007).
107. L. Sonnenschein, Phys. Rev. **D73**, 054015 (2006).
108. ATLAS Collab., ATLAS-CONF-2013-077.
109. S. Chatrchyan *et al.* (CMS Collab.), Eur. Phys. J. **C72**, 2202 (2012).
110. B. Abbot *et al.* (DØ Collab.), Phys. Rev. **D60**, 052001 (1999); F. Abe *et al.* (CDF Collab.), Phys. Rev. Lett. **82**, 271 (1999).
111. CDF Collab., CDF conference note 10635 (2011).
112. A. Abulencia *et al.* (CDF Collab.), Phys. Rev. **D74**, 032009 (2006).
113. V.M. Abazov *et al.* (DØ Collab.), Phys. Rev. Lett. **107**, 082004 (2011).
114. CMS Collab., arXiv:1307.4617.
115. ATLAS Collab., ATLAS-CONF-2012-030.
116. T. Aaltonen *et al.* (CDF Collab.), Phys. Rev. **D88**, 011101, (2013).
117. T. Aaltonen *et al.* (CDF Collab.), Phys. Lett. **B698**, 371 (2011).
118. CMS Collab., CMS PAS TOP-12-030.
119. T. Aaltonen *et al.* (CDF Collab.), Phys. Rev. **D80**, 051104, (2009).
120. V.M. Abazov *et al.* (DØ Collab.) Phys. Rev. Lett. **100**, 192004, (2008); CMS Collab., arxiv:1307.1907;
V.M. Abazov *et al.* (DØ Collab.) Phys. Lett. **B703**, 422, (2011);
ATLAS Collab., ATLAS-CONF-2011-054;
S. Chatrchyan *et al.* (CMS Collab.), arXiv:1307.1907, submitted to Phys. Lett. B;
U. Langenfeld, S. Moch, and P. Uwer, Phys. Rev. **D80**, 054009 (2009).
121. ATLAS & CMS Collabs., ATLAS-CONF-2013-102, CMS PAS TOP-13-005.
122. CDF Collab., CDF conference note 10456 (2011), arXiv:1112.4891.
123. A.H. Hoang and J.W. Stewart, Nucl. Phys. Proc. Suppl. **185**, 220 (2008).
124. A. B. Galtieri, F. Margaroli, and I. Volobouev, Rept. on Prog. in Phys. **75**, 056201 (2012).
125. G. Aad *et al.* (ATLAS Collab.), Phys. Lett. **B716**, 1 (2012).
126. S. Chatrychyan *et al.* (CMS Collab.), Phys. Lett. **B716**, 30 (2012).
127. G. Degrassi, *et al.* arXiv:1205.6497.
128. S. Alekhin, A. Djouadi, and S. Moch., Phys. Lett. **B716**, 214, (2012).
129. T. Aaltonen *et al.* (CDF Collab.), Phys. Rev. **D87**, 052013 (2013).
130. V.M. Abazov *et al.* (DØ Collab.), Phys. Rev. **D84**, 052005 (2011).
131. G. Aad *et al.* (ATLAS Collab.), arXiv:1310.6527.
132. S. Chatrychyan *et al.* (CMS Collab.), J. High Energy Phys.06,109(2012).
133. CMS Collab., CMS-PAS-TOP-12-031.
134. G. Mahlon and S. Parke, Phys. Rev. **D53**, 4886 (1996); G. Mahlon and S. Parke, Phys. Lett. **B411**, 173 (1997).
135. G.R. Goldstein, in *Spin 96: Proceedings of the 12th International Symposium on High Energy Spin Physics,* Amsterdam, 1996, ed. C.W. Jager (World Scientific, Singapore, 1997), p. 328.
136. T. Stelzer and S. Willenbrock, Phys. Lett. **B374**, 169 (1996).
137. W. Bernreuther *et al.* Nucl. Phys. **B690**, 81 (2004).
138. CDF Collab., CDF conference note 10719 (2011).
139. CDF Collab., CDF conference note 10211 (2010).
140. V.M. Abazov *et al.* (DØ Collab.) Phys. Rev. Lett. **108**, 032004,2012.
141. V.M. Abazov *et al.* (DØ Collab.), Phys. Rev. Lett. **107**, 032001 (2011).
142. V.M. Abazov *et al.* (DØ Collab.), Phys. Lett. **B702**, 16 (2011).
143. G. Mahlon & S.J. Parke, Phys. Rev. **D81**, 074024,2010.
144. G. Aad *et al.* (ATLAS Collab.) Phys. Rev. Lett. **108**, 212001 (2012).
145. W. Bernreuther & Z.G. Si, Nucl. Phys. **B837**, 90 (2010).
146. ATLAS Collab., ATLAS-CONF-2013-101.
147. CMS Collab., CMS PAS TOP-12-004.
148. A. Falk and M. Peskin, Phys. Rev. **D49**, 3320 (1994).
149. T. Aaltonen *et al.* (CDF Collab.), arXiv:1308.4050.
150. V.M. Abazov *et al.* (DØ Collab.) Phys. Rev. **D85**, 091104R (2012).
151. G.L. Kane, G.A. Ladinsky, and C.P. Yuan, Phys. Rev. **D45**, 124 (1992).
152. A. Czarnecki, J.G. Korner, and J.H. Piclum, Phys. Rev. **D81**, 111503 (2010).
153. CDF and DØ Collab., Phys. Rev. **D85**, 071106 (2012).
154. CDF Collab., Phys. Rev. **D87**, 031103 (2013).
155. ATLAS Collab., J. High Energy Phys.1206, 088 (2012).
156. CMS Collab., CMS-PAS-TOP-11-020, CERN-PH-EP/2013-133, arXiv:1308.3879, submitted to JHEP.

157. ATLAS and CMS Collab., ATLAS-CONF-2013-033, CMS-PAS-TOP-11-025.
158. CMS Collab., CMS-PAS-TOP-13-008.
159. CMS Collab., CMS-PAS-TOP-12-020.
160. D. Choudhury, T.M.P. Tait, and C.E.M. Wagner, Phys. Rev. **D65**, 053002 (2002).
161. D. Chang, W.F. Chang, and E. Ma, Phys. Rev. **D59**, 091503 (1999), Phys. Rev. **D61**, 037301 (2000).
162. V.M. Abazov *et al.* (DØ Collab.), Phys. Rev. Lett. **98**, 041801 (2007).
163. CDF Collab., arXiv:1304.4141, submitted to Phys. Rev. D (2013).
164. ATLAS Collab., CERN-PH-EP-2013-056, arXiv:1307.4568, submitted to JHEP (2013).
165. CMS Collab., CMS-PAS-TOP-11-031.
166. T. Aaltonen *et al.* (CDF Collab.), Phys. Rev. **D84**, 031104 (2011).
167. ATLAS Collab., ATLAS-CONF-2011-153.
168. S. Chatrchyan *et al.* (CMS Collab.), Phys. Rev. Lett. **110**, 172002 (2013).
169. ATLAS Collab., ATLAS-CONF-2012-126.
170. S.P. Martin, arXiv:9709356 (1997).
171. C.T. Hill, Phys. Lett. **B266**, 419 (1991).
172. C.T. Hill, Phys. Lett. **B345**, 483 (1995).
173. C. Zhang and S. Willenbrock, Phys. Rev. **D83**, 034006 (2011).
174. J. A. Aguilar-Saavedra,Nucl. Phys. **B843**, 638 (2011).
175. V. Barger, T. Han, and D. G. E. Walker, Phys. Rev. Lett. **100**, 031801 (2008).
176. D. Choudhury *et al.*, Phys. Lett. **B657**, 69 (2007).
177. R. Frederix and F. Maltoni, J. High Energy Phys.01,047 (2009).
178. ATLAS Coll. ATLAS-CONF-2012-130.
179. ATLAS Coll. ATLAS-CONF-2012-050.
180. G. Aad *et al.* (ATLAS Coll.), J. High Energy Phys.1204, 069 (2012).
181. T. Aaltonen (CDF Collab.), Phys. Rev. **D84**, 072004 (2011).
182. T. Aaltonen (CDF Collab.), Phys. Rev. Lett. **110**, 121802 (2013).
183. DØ Collab., FERMILAB-PUB-05/9-E, submitted to Phys. Rev. Lett.
184. T. Aaltonen (CDF Collab.), Phys. Rev. **D84**, 072003 (2011).
185. A. Altheimer, *et al.* , J. Phys. G **39**, 063001 (2012).
186. S. Chatrchyan *et al.* (CMS Collab.), Phys. Rev. **D87**, 072002 (2013).
187. S. Chatrchyan *et al.* (CMS Collab.), J. High Energy Phys.1212, 015 (2012).
188. S. Chatrchyan *et al.* (CMS Collab.), arXiv:1309.2030, submitted to Phys. Rev. Lett..
189. G. Aad *et al.* (ATLAS Collab.), Phys. Rev. **D88**, 012004 (2013).
190. ATLAS Collab., ATLAS-CONF-2013-052.
191. G. Aad *et al.* (ATLAS Collab.), J. High Energy Phys.1301,116(2013).
192. T. Plehn *et al.*, J. High Energy Phys.1010, 078 (2010).
193. ATLAS Collab., ATLAS-CONF-2012-096.
194. ATLAS Collab., ATLAS-CONF-2013-056.
195. ATLAS Collab., ATLAS-CONF-2013-018.
196. ATLAS Collab., ATLAS-CONF-2013-051.
197. CMS Collab., CMS-PAS-TOP-12-019.
198. G. Aad *et al.* (ATLAS Collab.), Phys. Rev. Lett. **108**, 041805 (2012).
199. CMS Collab., CMS-PAS-TOP-12-021.
200. ATLAS Collab., ATLAS-CONF-2013-063.
201. G. Aad *et al.* (ATLAS Collab.), Phys. Lett. **B712**, 351 (2012).
202. A. Heister *et al.* (ALEPH Collab.), Phys. Lett. **B543**, 173 (2002); J. Abdallah *et al.* (DELPHI Collab.), Phys. Lett. **B590**, 21 (2004); P. Achard *et al.* (L3 Collab.), Phys. Lett. **B549**, 290 (2002); G. Abbiendi *et al.* (OPAL Collab.), Phys. Lett. **B521**, 181 (2001).
203. F.D. Aaron *et al.* (H1 Collab.), Phys. Lett. **B678**, 450 (2009).
204. H. Abramowics *et al.* (ZEUS Collab.), Phys. Lett. **B708**, 27 (2012).
205. M. Beneke *et al.*, hep-ph/0003033, in *Proceedings of 1999 CERN Workshop on Standard Model Physics (and more) at the LHC*, G. Altarelli and M.L. Mangano eds.
206. V.F. Obraztsov, S.R. Slabospitsky, and O.P. Yushchenko, Phys. Lett. **B426**, 393 (1998).
207. T. Carli, D. Dannheim, and L. Bellagamba, Mod. Phys. Lett. **A19**, 1881 (2004).
208. ATLAS Collab., ATLAS-CONF-2011-087.
209. ATLAS Collab., ATLAS-CONF-2011-123.
210. CMS Collab., CMS-PAS-TOP-10-007.
211. CMS Collab., CMS-PAS-EXO-11-055.
212. CMS Collab., CMS-PAS-EXO-11-0006.
213. F. Abe *et al.* (CDF Collab.), Phys. Rev. Lett. **79**, 357 (1997);
T. Affolder *et al.* (CDF Collab.), Phys. Rev. **D62**, 012004 (2000).
214. B. Abbott *et al.* (DØ Collab.), Phys. Rev. Lett. **82**, 4975 (1999);
V.M Abazov *et al.* (DØ Collab.), Phys. Rev. Lett. **88**, 151803 (2002).
215. A. Abulencia *et al.* (CDF Collab.), Phys. Rev. Lett. **96**, 042003 (2006).
216. T. Aaltonen *et al.* (CDF Collab.), Phys. Rev. Lett. **103**, 101803 (2009).
217. V.M. Abazov *et al.* (DØ Collab.), Phys. Rev. **D80**, 071102 (2009).
218. V.M. Abazov *et al.* (DØ Collab.), Phys. Lett. **B682**, 278 (2009).
219. V.M. Abazov *et al.* (DØ Collab.), Phys. Rev. **D80**, 051107 (2009).
220. V.M. Abazov *et al.* (DØ Collab.), Phys. Rev. **D80**, 071102 (2009).
221. ATLAS Collab., ATLAS-CONF-2011-094.
222. ATLAS Collab., ATLAS-CONF-2011-138.
223. ATLAS Collab., ATLAS-CONF-2011-151.
224. ATLAS Collab., ATLAS-CONF-2011-154.
225. V.M. Abazov *et al.* (DØ Collab.), Phys. Rev. Lett. **102**, 092002 (2009).
226. V.M. Abazov *et al.* (DØ Collab.), DØ conference note 5838 (2009).

227. V.M. Abazov *et al.* (DØ Collab.), arXiv:1110.4592, submitted to Phys.Lett.B.
228. ATLAS Collab., ATLAS-CONF-2013-032.
229. T. Aaltonen *et al.* (CDF Collab.), Phys. Rev. Lett. **101**, 192002 (2009).
230. V.M. Abazov *et al.* (DØ Collab.), Phys. Lett. **B701**, 313 (2011).
231. V.M. Abazov *et al.* (DØ Collab.), Phys. Lett. **B693**, 81 (2010).
232. CMS Collab., CMS-PAS-TOP-12-037.
233. G. Aad *et al.* (ATLAS Collab.), JHEP **1209**, 139 (2012).
234. ATLAS Collab., ATLAS-CONF-2012-081.

t-QUARK MASS

We first list the direct measurements of the top quark mass which employ the event kinematics and then list the measurements which extract a top quark mass from the measured $t\overline{t}$ cross-section using theory calculations. A discussion of the definition of the top quark mass in these measurements can be found in the review "The Top Quark."

OUR EVALUATION of $173.21 \pm 0.51 \pm 0.71$ GeV is an average of published top mass measurements from Tevatron Runs. The first combination of the top-quark mass measurements, including some unpublished data, has been performed by the CDF and D0 experiments at the Tevatron and ATLAS and CMS experiments at the LHC. The resulting combined top-quark mass is $173.34 \pm 0.27 \pm 0.71$ GeV, consistent with Tevatron average. The Tevatron average was provided by the Tevatron Electroweak Working Group (TEVEWWG). It takes correlated uncertainties into account and has a χ^2 of 8.5 for 11 degrees of freedom.

For earlier search limits see PDG 96, Physical Review **D54** 1 (1996). We no longer include a compilation of indirect top mass determinations from Standard Model Electroweak fits in the Listings (our last compilation can be found in the Listings of the 2007 partial update). For a discussion of current results see the reviews "The Top Quark" and "Electroweak Model and Constraints on New Physics."

t-Quark Mass (Direct Measurements)

The following measurements extract a *t*-quark mass from the kinematics of $t\overline{t}$ events. They are sensitive to the top quark mass used in the MC generator that is usually interpreted as the pole mass, but the theoretical uncertainty in this interpretation is hard to quantify. See the review "The Top Quark" and references therein for more information.

VALUE (GeV)		DOCUMENT ID		TECN	COMMENT
173.21± 0.51± 0.71 OUR EVALUATION					See comments in the header above.
173.93± 1.64± 0.87	[1]	AALTONEN	13H	CDF	$\not\!\!E_T$ + ≥ 4 jets (≥ 1 b)
$173.9 \pm 0.9 \,^{+1.7}_{-2.1}$	[2]	CHATRCHYAN	13S	CMS	$\ell\ell + \not\!\!E_T$ + ≥ 2*b*-tag (MT2, $MT2_T$)
174.5 ± 0.6 ± 2.3	[3]	AAD	12I	ATLS	ℓ+$\not\!\!E_T$+ ≥ 4 jets (≥ 1 *b*), MT
172.85± 0.71± 0.85	[4]	AALTONEN	12AI	CDF	ℓ+$\not\!\!E_T$+ ≥ 4j (0,1,2*b*) template
172.7 ± 9.3 ± 3.7	[5]	AALTONEN	12AL	CDF	$\tau_h + \not\!\!E_T$ +4j (≥ 1*b*)
172.5 ± 1.4 ± 1.5	[6]	AALTONEN	12G	CDF	6–8 jets with ≥ 1 *b*
173.9 ± 1.9 ± 1.6	[7]	ABAZOV	12AB	D0	$\ell\ell$+$\not\!\!E_T$+ ≥ 2j (νWT+MWT)
172.5 ± 0.4 ± 1.5	[8]	CHATRCHYAN	12BA	CMS	$\ell\ell$+$\not\!\!E_T$+ ≥ 2j (≥ 1*b*), AMWT
173.49± 0.43± 0.98	[9]	CHATRCHYAN	12BP	CMS	ℓ+$\not\!\!E_T$+ ≥ 4j (≥ 2*b*)
172.1 ± 1.1 ± 0.9	[10]	AALTONEN	11E	CDF	ℓ + jets and dilepton
174.94± 0.83± 1.24	[11]	ABAZOV	11P	D0	$\ell + \not\!\!E_T$ + 4 jets (≥ 1 *b*-tag)
173.0 ± 1.2	[12]	AALTONEN	10AE	CDF	$\ell + \not\!\!E_T$ + 4 jets (≥ 1 *b*-tag), ME method
170.7 ± 6.3 ± 2.6	[13]	AALTONEN	10D	CDF	$\ell + \not\!\!E_T$ + 4 jets (*b*-tag)
180.1 ± 3.6 ± 3.9	[14,15]	ABAZOV	04G	D0	lepton + jets
176.1 ± 5.1 ± 5.3	[16]	AFFOLDER	01	CDF	lepton + jets
167.4 ±10.3 ± 4.8	[17,18]	ABE	99B	CDF	dilepton
168.4 ±12.3 ± 3.6	[15]	ABBOTT	98D	D0	dilepton
186 ±10 ± 5.7	[17,19]	ABE	97R	CDF	6 or more jets
• • • We do not use the following data for averages, fits, limits, etc. • • •					
173.18± 0.56± 0.75	[20]	AALTONEN	12AP	TEVA	CDF, D0 combination
173.7 ± 2.8 ± 1.5	[21]	ABAZOV	12AB	D0	$\ell\ell + \not\!\!E_T$ + ≥ 2 j (νWT)
172.4 ± 1.4 ± 1.3	[22]	AALTONEN	11AC	CDF	$\ell + \not\!\!E_T$ + 4 jets (≥ 1 *b*-tag)
172.3 ± 2.4 ± 1.0	[23]	AALTONEN	11AK	CDF	Repl. by AALTONEN 13H
176.9 ± 8.0 ± 2.7	[24]	AALTONEN	11T	CDF	$\ell + \not\!\!E_T$ + 4 jets (≥ 1 *b*-tag), $p_T(\ell)$ shape
174.0 ± 1.8 ± 2.4	[25]	ABAZOV	11R	D0	dilepton + $\not\!\!E_T$ + ≥ 2 jets
175.5 ± 4.6 ± 4.6	[26]	CHATRCHYAN	11F	CMS	dilepton + $\not\!\!E_T$ + jets
169.3 ± 2.7 ± 3.2	[27]	AALTONEN	10C	CDF	dilepton + *b*-tag (MT2+NWA)
$174.8 \pm 2.4 \,^{+1.2}_{-1.0}$	[28]	AALTONEN	10E	CDF	≥ 6 jets, vtx *b*-tag
180.5 ±12.0 ± 3.6	[29]	AALTONEN	09AK	CDF	$\ell + \not\!\!E_T$ + jets (soft μ b-tag)
172.7 ± 1.8 ± 1.2	[30]	AALTONEN	09J	CDF	$\ell + \not\!\!E_T$ + 4 jets (*b*-tag)
171.1 ± 3.7 ± 2.1	[31]	AALTONEN	09K	CDF	6 jets, vtx *b*-tag
171.9 ± 1.7 ± 1.1	[32]	AALTONEN	09L	CDF	ℓ + jets, $\ell\ell$ + jets
171.2 ± 2.7 ± 2.9	[33]	AALTONEN	09O	CDF	dilepton
$165.5 \,^{+3.4}_{-3.3} \pm 3.1$	[34]	AALTONEN	09X	CDF	$\ell\ell + \not\!\!E_T$ ($\nu\phi$ weighting)
174.7 ± 4.4 ± 2.0	[35]	ABAZOV	09AH	D0	dilepton + *b*-tag (νWT+MWT)
$170.7 \,^{+4.2}_{-3.9} \pm 3.5$	[36,37]	AALTONEN	08C	CDF	dilepton, $\sigma_{t\overline{t}}$ constrained
171.5 ± 1.8 ± 1.1	[38]	ABAZOV	08AH	D0	$\ell + \not\!\!E_T$ + 4 jets
177.1 ± 4.9 ± 4.7	[39,40]	AALTONEN	07	CDF	6 jets with ≥ 1 *b* vtx
$172.3 \,^{+10.8}_{-9.6} \pm 10.8$	[41]	AALTONEN	07B	CDF	≥ 4 jets (*b*-tag)
174.0 ± 2.2 ± 4.8	[42]	AALTONEN	07D	CDF	≥ 6 jets, vtx *b*-tag
170.8 ± 2.2 ± 1.4	[43,44]	AALTONEN	07I	CDF	lepton + jets (*b*-tag)
$173.7 \pm 4.4 \,^{+2.1}_{-2.0}$	[40,45]	ABAZOV	07F	D0	lepton + jets
176.2 ± 9.2 ± 3.9	[46]	ABAZOV	07W	D0	dilepton (MWT)
179.5 ± 7.4 ± 5.6	[46]	ABAZOV	07W	D0	dilepton (νWT)
164.5 ± 3.9 ± 3.9	[44,47]	ABULENCIA	07D	CDF	dilepton
$180.7 \,^{+15.5}_{-13.4} \pm 8.6$	[48]	ABULENCIA	07J	CDF	lepton + jets
$170.3 \,^{+4.1}_{-4.5} \,^{+1.2}_{-1.8}$	[44,49]	ABAZOV	06U	D0	lepton + jets (*b*-tag)
$173.2 \,^{+2.6}_{-2.4} \pm 3.2$	[50,51]	ABULENCIA	06D	CDF	lepton + jets
$173.5 \,^{+3.7}_{-3.6} \pm 1.3$	[37,50]	ABULENCIA	06D	CDF	lepton + jets
165.2 ± 6.1 ± 3.4	[44,52]	ABULENCIA	06G	CDF	dilepton
170.1 ± 6.0 ± 4.1	[37,53]	ABULENCIA	06V	CDF	dilepton
178.5 ±13.7 ± 7.7	[54,55]	ABAZOV	05	D0	6 or more jets
176.1 ± 6.6	[56]	AFFOLDER	01	CDF	dilepton, lepton+jets, all-jets
172.1 ± 5.2 ± 4.9	[57]	ABBOTT	99G	D0	di-lepton, lepton+jets
176.0 ± 6.5	[18,58]	ABE	99B	CDF	dilepton, lepton+jets, all-jets
173.3 ± 5.6 ± 5.5	[15,59]	ABBOTT	98F	D0	lepton + jets
175.9 ± 4.8 ± 5.3	[17,60]	ABE	98E	CDF	lepton + jets
161 ±17 ±10	[17]	ABE	98F	CDF	dilepton
172.1 ± 5.2 ± 4.9	[61]	BHAT	98B	RVUE	dilepton and lepton+jets
173.8 ± 5.0	[62]	BHAT	98B	RVUE	dilepton, lepton+jets, all-jets
173.3 ± 5.6 ± 6.2	[15]	ABACHI	97E	D0	lepton + jets
$199 \,^{+19}_{-21} \pm 22$		ABACHI	95	D0	lepton + jets
176 ± 8 ±10		ABE	95F	CDF	lepton + *b*-jet
$174 \pm 10 \,^{+13}_{-12}$		ABE	94E	CDF	lepton + *b*-jet

t-Quark $\overline{\text{MS}}$ Mass from Cross-Section Measurements

The top quark $\overline{\text{MS}}$ or pole mass can be extracted from a measurement of $\sigma(t\overline{t})$ by using theory calculations. We quote below the $\overline{\text{MS}}$ mass. See the review "The Top Quark" and references therein for more information.

VALUE (GeV)	DOCUMENT ID		TECN	COMMENT
$\mathbf{160.0^{+4.8}_{-4.3}}$	[63] ABAZOV	11S	D0	$\sigma(t\overline{t})$ + theory
• • • We do not use the following data for averages, fits, limits, etc. • • •				
	[64] ABAZOV	09AG	D0	cross sects, theory + exp
	[65] ABAZOV	09R	D0	cross sects, theory + exp

t-Quark Pole Mass from Cross-Section Measurements

VALUE (GeV)	DOCUMENT ID		TECN	COMMENT
$\mathbf{176.7^{+3.8}_{-3.4}}$	[66] CHATRCHYAN	14	CMS	$\sigma(t\overline{t})$ + theory

[1] Based on 8.7 fb^{-1} in $p\overline{p}$ collisions at $\sqrt{s} = 1.96$ TeV. Events with an identified charged lepton or small $\not\!\!E_T$ are rejected from the event sample, so that the measurement is statistically independent from those in the ℓ + jets and all hadronic channels while being sensitive to those events with a τ lepton in the final state.

[2] Based on 5.0 fb^{-1} of pp data at $\sqrt{s} = 7$ TeV. CHATRCHYAN 13S studied events with di-lepton + $\not\!\!E_T$ + ≥ 2 *b*-jets, and looked for kinematical endpoints of MT2, $MT2_T$ and subsystem variables.

[3] Based on 1.04 fb^{-1} of pp data at $\sqrt{s} = 7$ TeV. Uses 2d-template analysis (MT) with m_t and jet energy scale factor (JSF) from m_W mass fit.

[4] Based on 8.7 fb^{-1} of data in $p\overline{p}$ collisions at 1.96 TeV. The JES is calibrated by using the dijet mass from the W boson decay.

[5] Use the ME method based on 2.2 fb^{-1} of data in $p\overline{p}$ collisions at 1.96 TeV.

[6] Based on 5.8 fb^{-1} of data in $p\overline{p}$ collisions at 1.96 TeV. The quoted systematic error is the sum of JES($\pm$1.0) and systematic($\pm$1.1) uncertainties. The measurement is performed with a liklihood fit technique which simultaneously determines m_t and JES.

[7] Combination with the result in 1 fb^{-1} of preceding data reported in ABAZOV 09AH as well as the MWT result of ABAZOV 11R with a statistical correlation of 60%.

[8] Based on 5.0 fb^{-1} of pp data at $\sqrt{s} = 7$ TeV. Uses an analytical matrix weighting technique (AMWT) and full kinematic analysis (KIN).

[9] Based on 5.0 fb^{-1} of pp data at $\sqrt{s} = 7$ TeV. The first error is statistical and JES combined, and the second is systematic. Ideogram method is used to obtain 2D liklihood for the kinematical fit with two parameters mtop and JES.

[10] Based on 5.6 fb^{-1} in $p\overline{p}$ collisions at $\sqrt{s} = 1.96$ TeV. Employs a multi-dimensional template likelihood technique where the lepton plus jets (one or two *b*-tags) channel gives $172.2 \pm 1.2 \pm 0.9$ GeV while the dilepton channel yields $170.3 \pm 2.0 \pm 3.1$ GeV. The results are combined. OUR EVALUATION includes the measurement in the dilepton channel only.

[11] Based on 3.6 fb^{-1} in $p\overline{p}$ collisions at $\sqrt{s} = 1.96$ TeV. ABAZOV 11P reports $174.94 \pm 0.83 \pm 0.78 \pm 0.96$ GeV, where the first uncertainty is from statistics, the second from JES, and the last from other systematic uncertainties. We combine the JES and systematic uncertainties. A matrix-element method is used where the JES uncertainty is constrained by the W mass. ABAZOV 11P describes a measurement based on 2.6 fb^{-1} that is combined with ABAZOV 08AH, which employs an independent 1 fb^{-1} of data.

[12] Based on 5.6 fb^{-1} in $p\overline{p}$ collisions at $\sqrt{s} = 1.96$ TeV. The likelihood calculated using a matrix element method gives $m_t = 173.0 \pm 0.7(\text{stat}) \pm 0.6(\text{JES}) \pm 0.9(\text{syst})$ GeV, for a total uncertainty of 1.2 GeV.

[13] Based on 1.9 fb^{-1} in $p\overline{p}$ collisions at $\sqrt{s}$ = 1.96 TeV. The result is from the measurement using the transverse decay length of b-hadrons and that using the transverse momentum of the W decay muons, which are both insensitive to the JES (jet energy scale) uncertainty. OUR EVALUATION uses only the measurement exploiting the decay length significance which yields $166.9^{+9.5}_{-8.5}$(stat)$\pm$2.9 (syst) GeV. The measurement that uses the lepton transverse momentum is excluded from the average because of a statistical correlation with other samples.

[14] Obtained by re-analysis of the lepton + jets candidate events that led to ABBOTT 98F. It is based upon the maximum likelihood method which makes use of the leading order matrix elements.

[15] Based on 125 $\pm$ 7 pb^{-1} of data at $\sqrt{s}$ = 1.8 TeV.

[16] Based on $\sim$ 106 pb^{-1} of data at $\sqrt{s}$= 1.8 TeV.

[17] Based on 109 $\pm$ 7 pb^{-1} of data at $\sqrt{s}$ = 1.8 TeV.

[18] See AFFOLDER 01 for details of systematic error re-evaluation.

[19] Based on the first observation of all hadronic decays of $t\overline{t}$ pairs. Single b-quark tagging with jet-shape variable constraints was used to select signal enriched multi-jet events. The updated systematic error is listed. See AFFOLDER 01, appendix C.

[20] Combination based on up to 5.8 fb^{-1} of data in $p\overline{p}$ collisions at 1.96 TeV.

[21] Based on 4.3 fb^{-1} of data in p-pbar collisions at 1.96 TeV. The measurement reduces the JES uncertainty by using the single lepton channel study of ABAZOV 11P.

[22] Based on 3.2 fb^{-1} in $p\overline{p}$ collisions at $\sqrt{s}$ = 1.96 TeV. The first error is from statistics and JES combined, and the latter is from the other systematic uncertainties. The result is obtained using an unbinned maximum likelihood method where the top quark mass and the JES are measured simultaneously, with Δ_{JES} = 0.3 $\pm$ 0.3(stat).

[23] Based on 5.7 fb^{-1} in $p\overline{p}$ collisions at $\sqrt{s}$ = 1.96 TeV. Events with an identified charged lepton or small $\not\!\!E_T$ are rejected from the event sample, so that the measurement is statistically independent from those in the ℓ + jets and all hadronic channels while being sensitive to those events with a τ lepton in the final state. Supersedes AALTONEN 07B.

[24] Uses a likelihood fit of the lepton p_T distribution based on 2.7 fb^{-1} in $p\overline{p}$ collisions at $\sqrt{s}$ = 1.96 TeV.

[25] Based on a matrix-element method which employs 5.4 fb^{-1} in $p\overline{p}$ collisions at $\sqrt{s}$ = 1.96 TeV. Superseded by ABAZOV 12AB.

[26] Based on 36 pb^{-1} of pp collisions at $\sqrt{s}$ = 7 TeV. A Kinematic Method using b-tagging and an analytical Matrix Weighting Technique give consistent results and are combined. Superseded by CHATRCHYAN 12BA.

[27] Based on 3.4 fb^{-1} of $p\overline{p}$ collisions at $\sqrt{s}$ = 1.96 TeV. The result is obtained by combining the MT2 variable method and the NWA (Neutrino Weighting Algorithm). The MT2 method alone gives $m_t = 168.0^{+4.8}_{-4.0}$(stat)$\pm$2.9(syst) GeV with smaller systematic error due to small JES uncertainty.

[28] Based on 2.9 fb^{-1} of $p\overline{p}$ collisions at $\sqrt{s}$ = 1.96 TeV. The first error is from statistics and JES uncertainty, and the latter is from the other systematics. Neural-network-based kinematical selection of 6 highest E_T jets with a vtx b-tag is used to distinguish signal from background. Superseded by AALTONEN 12G.

[29] Based on 2 fb^{-1} of data at $\sqrt{s}$ = 1.96 TeV. The top mass is obtained from the measurement of the invariant mass of the lepton (e or μ) from W decays and the soft μ in b-jet. The result is insensitive to jet energy scaling.

[30] Based on 1.9 fb^{-1} of data at $\sqrt{s}$ = 1.96 TeV. The first error is from statistics and jet energy scale uncertainty, and the latter is from the other systematics. Matrix element method with effective propagators.

[31] Based on 943 pb^{-1} of data at $\sqrt{s}$ = 1.96 TeV. The first error is from statistical and jet-energy-scale uncertainties, and the latter is from other systematics. AALTONEN 09K selected 6 jet events with one or more vertex b-tags and used the tree-level matrix element to construct template models of signal and background.

[32] Based on 1.9 fb^{-1} of data at $\sqrt{s}$ = 1.96 TeV. The first error is from statistical and jet-energy-scale (JES) uncertainties, and the second is from other systematics. Events with lepton + jets and those with dilepton + jets were simultaneously fit to constrain m_t and JES. Lepton + jets data only give m_t = 171.8 $\pm$ 2.2 GeV, and dilepton data only give $m_t = 171.2^{+5.3}_{-5.1}$ GeV.

[33] Based on 2 fb^{-1} of data at $\sqrt{s}$ = 1.96 TeV. Matrix Element method. Optimal selection criteria for candidate events with two high p_T leptons, high $\not\!\!E_T$, and two or more jets with and without b-tag are obtained by neural network with neuroevolution technique to minimize the statistical error of m_t.

[34] Based on 2.9 fb^{-1} of data at $\sqrt{s}$ = 1.96 TeV. Mass m_t is estimated from the likelihood for the eight-fold kinematical solutions in the plane of the azimuthal angles of the two neutrino momenta.

[35] Based on 1 fb^{-1} of data at $\sqrt{s}$ = 1.96 TeV. Events with two identified leptons, and those with one lepton plus one isolated track and a b-tag were used to constrain m_t. The result is a combination of the νWT (ν Weighting Technique) result of 176.2 $\pm$ 4.8 $\pm$ 2.1 GeV and the MWT (Matrix-element Weighting Technique) result of 173.2 $\pm$ 4.9 $\pm$ 2.0 GeV.

[36] Reports measurement of $170.7^{+4.2}_{-3.9}$ $\pm$ 2.6 $\pm$ 2.4 GeV based on 1.2 fb^{-1} of data at $\sqrt{s}$ = 1.96 TeV. The last error is due to the theoretical uncertainty on $\sigma_{t\overline{t}}$. Without the cross-section constraint a top mass of $169.7^{+5.2}_{-4.9}$ $\pm$ 3.1 GeV is obtained.

[37] Template method.

[38] Result is based on 1 fb^{-1} of data at $\sqrt{s}$ = 1.96 TeV. The first error is from statistics and jet energy scale uncertainty, and the latter is from the other systematics.

[39] Based on 310 pb^{-1} of data at $\sqrt{s}$ = 1.96 TeV.

[40] Ideogram method.

[41] Based on 311 pb^{-1} of data at $\sqrt{s}$ = 1.96 TeV. Events with 4 or more jets with $E_T >$ 15 GeV, significant missing E_T, and secondary vertex b-tag are used in the fit. About 44% of the signal acceptance is from $\tau\nu$ + 4 jets. Events with identified e or μ are vetoed to provide a statistically independent measurement.

[42] Based on 1.02 fb^{-1} of data at $\sqrt{s}$ = 1.96 TeV. Superseded by AALTONEN 12G.

[43] Based on 955 pb^{-1} of data $\sqrt{s}$ = 1.96 TeV. m_t and JES (Jet Energy Scale) are fitted simultaneously, and the first error contains the JES contribution of 1.5 GeV.

[44] Matrix element method.

[45] Based on 425 pb^{-1} of data at $\sqrt{s}$ = 1.96 TeV. The first error is a combination of statistics and JES (Jet Energy Scale) uncertainty, which has been measured simultaneously to give JES = 0.989 $\pm$ 0.029(stat).

[46] Based on 370 pb^{-1} of data at $\sqrt{s}$ = 1.96 TeV. Combined result of MWT (Matrix-element Weighting Technique) and νWT (ν Weighting Technique) analyses is 178.1 $\pm$ 6.7 $\pm$ 4.8 GeV.

[47] Based on 1.0 fb^{-1} of data at $\sqrt{s}$ = 1.96 TeV. ABULENCIA 07D improves the matrix element description by including the effects of initial-state radiation.

[48] Based on 695 pb^{-1} of data at $\sqrt{s}$ = 1.96 TeV. The transverse decay length of the b hadron is used to determine m_t, and the result is free from the JES (jet energy scale) uncertainty.

[49] Based on $\sim$ 400 pb^{-1} of data at $\sqrt{s}$ = 1.96 TeV. The first error includes statistical and systematic jet energy scale uncertainties, the second error is from the other systematics. The result is obtained with the b-tagging information. The result without b-tagging is $169.2^{+5.0}_{-7.4}{}^{+1.5}_{-1.4}$ GeV. Superseded by ABAZOV 08AH.

[50] Based on 318 pb^{-1} of data at $\sqrt{s}$ = 1.96 TeV.

[51] Dynamical likelihood method.

[52] Based on 340 pb^{-1} of data at $\sqrt{s}$ = 1.96 TeV.

[53] Based on 360 pb^{-1} of data at $\sqrt{s}$ = 1.96 TeV.

[54] Based on 110.2 $\pm$ 5.8 pb^{-1} at $\sqrt{s}$ = 1.8 TeV.

[55] Based on the all hadronic decays of $t\overline{t}$ pairs. Single b-quark tagging via the decay chain $b \to c \to \mu$ was used to select signal enriched multijet events. The result was obtained by the maximum likelihood method after bias correction.

[56] Obtained by combining the measurements in the lepton + jets [AFFOLDER 01], all-jets [ABE 97R, ABE 99B], and dilepton [ABE 99B] decay topologies.

[57] Obtained by combining the D0 result m_t (GeV) = 168.4 $\pm$ 12.3 $\pm$ 3.6 from 6 di-lepton events (see also ABBOTT 98D) and m_t (GeV) = 173.3 $\pm$ 5.6 $\pm$ 5.5 from lepton+jet events (ABBOTT 98F).

[58] Obtained by combining the CDF results of m_t (GeV)=167.4 $\pm$ 10.3 $\pm$ 4.8 from 8 dilepton events, m_t (GeV)=175.9 $\pm$ 4.8 $\pm$ 5.3 from lepton+jet events (ABE 98E), and m_t (GeV)=186.0 $\pm$ 10.0 $\pm$ 5.7 from all-jet events (ABE 97R). The systematic errors in the latter two measurements are changed in this paper.

[59] See ABAZOV 04G.

[60] The updated systematic error is listed. See AFFOLDER 01, appendix C.

[61] Obtained by combining the DØ results of m_t(GeV)=168.4 $\pm$ 12.3 $\pm$ 3.6 from 6 dilepton events and m_t(GeV)=173.3 $\pm$ 5.6 $\pm$ 5.5 from 77 lepton+jet events.

[62] Obtained by combining the DØ results from dilepton and lepton+jet events, and the CDF results (ABE 99B) from dilepton, lepton+jet events, and all-jet events.

[63] Based on 5.3 fb^{-1} in $p\overline{p}$ collisions at $\sqrt{s}$ = 1.96 TeV. ABAZOV 11S uses the measured $t\overline{t}$ production cross section of $8.13^{+1.02}_{-0.90}$ pb [ABAZOV 11E] in the lepton plus jets channel to obtain the top quark $\overline{\rm MS}$ mass by using an approximate NNLO computation (MOCH 08, LANGENFELD 09). The corresponding top quark pole mass is $167.5^{+5.4}_{-4.9}$ GeV. A different theory calculation (AHRENS 10, AHRENS 10A) is also used and yields $m_t^{\overline{\rm MS}} = 154.5^{+5.0}_{-4.3}$ GeV.

[64] Based on 1 fb^{1} of data at $\sqrt{s}$ = 1.96 TeV. Uses the ℓ + jets, $\ell\ell$, and $\ell\tau$ + jets channels. ABAZOV 09AG extract the pole mass of the top quark using two different calculations that yield $169.1^{+5.9}_{-5.2}$ GeV (MOCH 08, LANGENFELD 09) and $168.2^{+5.9}_{-5.4}$ GeV (KIDONAKIS 08).

[65] Based on 1 fb^{1} of data at $\sqrt{s}$ = 1.96 TeV. Uses the $\ell\ell$ and $\ell\tau$ + jets channels. ABAZOV 09R extract the pole mass of the top quark using two different calculations that yield $173.3^{+9.8}_{-8.6}$ GeV (MOCH 08, LANGENFELD 09) and $171.5^{+9.9}_{-8.8}$ GeV (CACCIARI 08).

[66] Used $\sigma(t\overline{t})$ from pp collisions at $\sqrt{s}$ = 7 TeV measured in CHATRCHYAN 12AX to obtain m_t(pole) for $\alpha_s(m_Z)$ = 0.1184 $\pm$ 0.0007.

$m_t - m_{\overline{t}}$

Test of CPT conservation. OUR AVERAGE assumes that the systematic uncertainties are uncorrelated.

VALUE (GeV)		DOCUMENT ID		TECN	COMMENT
-0.2 ±0.5 OUR AVERAGE		Error includes scale factor of 1.1.			
0.67$\pm$0.61$\pm$0.41	[1]	AAD	14	ATLS	ℓ + $\not\!\!E_T$ + $\geq$4j ($\geq$ 2 b-tags)
$-1.95\pm1.11\pm0.59$	[2]	AALTONEN	13E	CDF	ℓ + $\not\!\!E_T$ + $\geq$4j (0,1,2 b-tags)
$-0.44\pm0.46\pm0.27$	[3]	CHATRCHYAN	12Y	CMS	ℓ + $\not\!\!E_T$ + $\geq$4j
0.8 ±1.8 ±0.5	[4]	ABAZOV	11T	D0	ℓ + $\not\!\!E_T$ + 4 jets ($\geq$ 1 b-tag)
• • • We do not use the following data for averages, fits, limits, etc. • • •					
-3.3 ±1.4 ±1.0	[5]	AALTONEN	11K	CDF	Repl. by AALTONEN 13E
3.8 ±3.4 ±1.2	[6]	ABAZOV	09AA	D0	ℓ + $\not\!\!E_T$ + 4 jets ($\geq$ 1 b-tag)

[1] Based on 4.7 fb^{-1} of pp data at $\sqrt{s}$ = 7 TeV and an average top mass of 172.5 GeV/c^2.

[2] Based on 8.7 fb^{-1} of $p\overline{p}$ collisions at $\sqrt{s}$ = 1.96 TeV and an average top mass of 172.5 GeV/c^2.

[3] Based on 4.96 fb^{-1} of pp data at $\sqrt{s}$ = 7 TeV. Based on the fitted m_t for ℓ^+ and ℓ^- events using the Ideogram method.

[4] Based on a matrix-element method which employs 3.6 fb^{-1} in $p\overline{p}$ collisions at $\sqrt{s}$ = 1.96 TeV.

[5] Based on a template likelihood technique which employs 5.6 fb^{-1} in $p\overline{p}$ collisions at $\sqrt{s}$ = 1.96 TeV.

[6] Based on 1 fb^{-1} of data in $p\overline{p}$ collisions at $\sqrt{s}$ = 1.96 TeV.

t-quark DECAY WIDTH

VALUE (GeV)	CL%	DOCUMENT ID		TECN	COMMENT
$2.00^{+0.47}_{-0.43}$		[1] ABAZOV	12T	D0	$\Gamma(t \to bW)/\Gamma(t \to bW)$
• • • We do not use the following data for averages, fits, limits, etc. • • •					
$<$ 6.38	95	[2] AALTONEN	13Z	CDF	ℓ + $\not\!\!E_T$ + $\geq$ 4 jets ($\geq$ 0 b-tag), direct
$1.99^{+0.69}_{-0.55}$		[3] ABAZOV	11B	D0	Repl. by ABAZOV 12T
$>$ 1.21	95	[3] ABAZOV	11B	D0	$\Gamma(t \to Wb)$
$<$ 7.6	95	[4] AALTONEN	10AC	CDF	ℓ + jets, direct
$<$13.1	95	[5] AALTONEN	09M	CDF	m_t(rec) distribution

[1] Based on 5.4 fb^{-1} of data in ppbar collisions at 1.96 TeV. $\Gamma(t \to bW) = 1.87^{+0.44}_{-0.40}$ GeV is obtained from the observed t-channel sigle top quark production cross section, whereas $B(t \to bW) = 0.90 \pm 0.04$ is used assuming $\sum_q B(t \to qW) = 1$. The result is valid for $m_t = 172.5$ GeV, where as those for $m_t = 170$ and 175 GeV are given.

[2] Based on 8.7 fb^{-1} of data. The two sided 68% CL interval is $1.10 \text{ GeV} < \Gamma_t < 4.05$ GeV for $m_t = 172.5$ GeV.

[3] Based on 2.3 fb^{-1} in $p\overline{p}$ collisions at $\sqrt{s} = 1.96$ TeV. ABAZOV 11B extracted Γ_t from the partial width $\Gamma(t \to Wb) = 1.92^{+0.58}_{-0.51}$ GeV measured using the t-channel single top production cross section, and the branching fraction $\text{br}t \to Wb = 0.962^{+0.068}_{-0.066}(\text{stat})^{+0.064}_{-0.052}(\text{syst})$. The $\Gamma(t \to Wb)$ measurement gives the 95% CL lowerbound of $\Gamma(t \to Wb)$ and hence that of Γ_t.

[4] Results are based on 4.3 fb^{-1} of data in $p\overline{p}$ collisions at $\sqrt{s} = 1.96$ TeV. The top quark mass and the hadronically decaying W boson mass are reconstructed for each candidate events and compared with templates of different top quark width. The two sided 68% CL interval is $0.3 \text{ GeV} < \Gamma_t < 4.4$ GeV for $m_t = 172.5$ GeV.

[5] Based on 955 pb^{-1} of $p\overline{p}$ collision data at $\sqrt{s} = 1.96$ TeV. AALTONEN 09M selected $t\overline{t}$ candidate events for the $\ell + \not{E}_T$ + jets channel with one or two b-tags, and examine the decay width dependence of the reconstructed m_t distribution. The result is for m_t =175 GeV, whereas the upper limit is lower for smaller m_t.

t DECAY MODES

	Mode		Fraction (Γ_i/Γ)		Confidence level
Γ_1	$Wq(q = b, s, d)$				
Γ_2	Wb				
Γ_3	$\ell\nu_\ell$ anything	[a,b]	(9.4 ± 2.4) %		
Γ_4	$\tau\nu_\tau b$				
Γ_5	$\gamma q (q{=}u,c)$	[c]	< 5.9	$\times 10^{-3}$	95%
	$\Delta T = 1$ weak neutral current ($T1$) modes				
Γ_6	$Zq(q{=}u,c)$	$T1$ [d]	< 2.1	$\times 10^{-3}$	95%

[a] ℓ means e or μ decay mode, not the sum over them.

[b] Assumes lepton universality and W-decay acceptance.

[c] This limit is for $\Gamma(t \to \gamma q)/\Gamma(t \to Wb)$.

[d] This limit is for $\Gamma(t \to Zq)/\Gamma(t \to Wb)$.

t BRANCHING RATIOS

$\Gamma(Wb)/\Gamma(Wq(q=b,s,d))$ Γ_2/Γ_1

OUR AVERAGE assumes that the systematic uncertainties are uncorrelated.

VALUE	DOCUMENT ID		TECN	COMMENT
0.91±0.04 OUR AVERAGE				
0.94 ± 0.09	[1] AALTONEN	13G	CDF	$\ell + \not{E}_T +$ ≥ 3jets (≥ 1 b-tag)
0.90 ± 0.04	[2] ABAZOV	11X	D0	
• • • We do not use the following data for averages, fits, limits, etc. • • •				
$0.97^{+0.09}_{-0.08}$	[3] ABAZOV	08M	D0	ℓ + n jets with 0,1,2 b-tag
$1.03^{+0.19}_{-0.17}$	[4] ABAZOV	06K	D0	
$1.12^{+0.21+0.17}_{-0.19-0.13}$	[5] ACOSTA	05A	CDF	Repl. by AALTONEN 13G
$0.94^{+0.26+0.17}_{-0.21-0.12}$	[6] AFFOLDER	01C	CDF	

[1] Based on 8.7 fb^{-1} of $p\overline{p}$ collisions at $\sqrt{s} = 1.96$ TeV. Measure the fraction of $t \to Wb$ decays simultaneously with the $t\overline{t}$ cross section. The correlation coefficient between those two measurements is -0.434. Assume unitarity of the 3×3 CKM matrix and set $|V_{tb}| > 0.89$ at 95% CL.

[2] Based on 5.4 fb^{-1} of data. The error is statistical and systematic combined. The result is a combination of 0.95 ± 0.07 from ℓ + jets channel and 0.86 ± 0.05 from $\ell\ell$ channel. $|V^{tb}| = 0.95 \pm 0.02$ follows from the result by assuming unitarity of the 3x3 CKM matrix.

[3] Result is based on 0.9 fb^{-1} of data. The 95% CL lower bound R > 0.79 gives $|V_{tb}| > 0.89$ (95% CL).

[4] ABAZOV 06K result is from the analysis of $t\overline{t} \to \ell\nu +$ ≥ 3 jets with 230 pb^{-1} of data at $\sqrt{s} = 1.96$ TeV. It gives R > 0.61 and $|V_{tb}| > 0.78$ at 95% CL. Superseded by ABAZOV 08M.

[5] ACOSTA 05A result is from the analysis of lepton + jets and di-lepton + jets final states of $t\overline{t}$ candidate events with ∼ 162 pb^{-1} of data at $\sqrt{s} = 1.96$ TeV. The first error is statistical and the second systematic. It gives R > 0.61, or $|V_{tb}| > 0.78$ at 95% CL.

[6] AFFOLDER 01C measures the top-quark decay width ratio $R = \Gamma(Wb)/\Gamma(Wq)$, where q is a d, s, or b quark, by using the number of events with multiple b tags. The first error is statistical and the second systematic. A numerical integration of the likelihood function gives $R > 0.61$ (0.56) at 90% (95%) CL. By assuming three generation unitarity, $|V_{tb}| = 0.97^{+0.16}_{-0.12}$ or $|V_{tb}| > 0.78$ (0.75) at 90% (95%) CL is obtained. The result is based on 109 pb^{-1} of data at $\sqrt{s} = 1.8$ TeV.

$\Gamma(\ell\nu_\ell \text{anything})/\Gamma_{\text{total}}$ Γ_3/Γ

VALUE	DOCUMENT ID		TECN
0.094±0.024	[1] ABE	98X	CDF

[1] ℓ means e or μ decay mode, not the sum. Assumes lepton universality and W-decay acceptance.

$\Gamma(\tau\nu_\tau b)/\Gamma_{\text{total}}$ Γ_4/Γ

VALUE	DOCUMENT ID		TECN	COMMENT
• • • We do not use the following data for averages, fits, limits, etc. • • •				
	[1] ABULENCIA	06R	CDF	$\ell\tau$ + jets
	[2] ABE	97V	CDF	$\ell\tau$ + jets

[1] ABULENCIA 06R looked for $t\overline{t} \to (\ell\nu_\ell)(\tau\nu_\tau)b\overline{b}$ events in 194 pb^{-1} of $p\overline{p}$ collisions at $\sqrt{s} = 1.96$ TeV. 2 events are found where 1.00 ± 0.17 signal and 1.29 ± 0.25 background events are expected, giving a 95% CL upper bound for the partial width ratio $\Gamma(t \to \tau\nu q) / \Gamma_{SM}(t \to \tau\nu q) < 5.2$.

[2] ABE 97V searched for $t\overline{t} \to (\ell\nu_\ell)(\tau\nu_\tau)b\overline{b}$ events in 109 pb^{-1} of $p\overline{p}$ collisions at $\sqrt{s} = 1.8$ TeV. They observed 4 candidate events where one expects ∼ 1 signal and ∼ 2 background events. Three of the four observed events have jets identified as b candidates.

$\Gamma(\gamma q(q{=}u,c))/\Gamma_{\text{total}}$ Γ_5/Γ

VALUE	CL%	DOCUMENT ID		TECN	COMMENT
<0.0059	95	[1] CHEKANOV	03	ZEUS	$B(t \to \gamma u)$
• • • We do not use the following data for averages, fits, limits, etc. • • •					
<0.0064	95	[2] AARON	09A	H1	$t \to \gamma u$
<0.0465	95	[3] ABDALLAH	04C	DLPH	$B(\gamma c$ or $\gamma u)$
<0.0132	95	[4] AKTAS	04	H1	$B(t \to \gamma u)$
<0.041	95	[5] ACHARD	02J	L3	$B(t \to \gamma c$ or $\gamma u)$
<0.032	95	[6] ABE	98G	CDF	$t\overline{t} \to (Wb)(\gamma c$ or $\gamma u)$

[1] CHEKANOV 03 looked for single top production via FCNC in the reaction $e^\pm p \to e^\pm$ (t or $\overline{t}$) X in 130.1 pb^{-1} of data at $\sqrt{s}$=300–318 GeV. No evidence for top production and its decay into bW was found. The result is obtained for m_t=175 GeV when $B(\gamma c) = B(Zq) = 0$, where q is a u or c quark. Bounds on the effective t-u-γ and t-u-Z couplings are found in their Fig. 4. The conversion to the constraint listed is from private communication, E. Gallo, January 2004.

[2] AARON 09A looked for single top production via FCNC in $e^\pm p$ collisions at HERA with 474 pb^{-1}. The upper bound of the cross section gives the bound on the FCNC coupling $\kappa_{tu\gamma}/\Lambda < 1.03$ TeV^{-1}, which corresponds to the result for $m_t = 175$ GeV.

[3] ABDALLAH 04C looked for single top production via FCNC in the reaction $e^+e^- \to \overline{t}c$ or $\overline{t}u$ in 541 pb^{-1} of data at $\sqrt{s}$=189–208 GeV. No deviation from the SM is found, which leads to the bound on $B(t \to \gamma q)$, where q is a u or a c quark, for m_t = 175 GeV when $B(t \to Zq) = 0$ is assumed. The conversion to the listed bound is from private communication, O. Yushchenko, April 2005. The bounds on the effective t-q-γ and t-q-Z couplings are given in their Fig. 7 and Table 4, for m_t = 170–180 GeV, where most conservative bounds are found by choosing the chiral couplings to maximize the negative interference between the virtual γ and Z exchange amplitudes.

[4] AKTAS 04 looked for single top production via FCNC in $e^\pm$ collisions at HERA with 118.3 pb^{-1}, and found 5 events in the e or μ channels. By assuming that they are due to statistical fluctuation, the upper bound on the $tu\gamma$ coupling $\kappa_{tu\gamma} < 0.27$ (95% CL) is obtained. The conversion to the partial width limit, when $B(\gamma c) = B(Zu) = B(Zc) = 0$, is from private communication, E. Perez, May 2005.

[5] ACHARD 02J looked for single top production via FCNC in the reaction $e^+e^- \to \overline{t}c$ or $\overline{t}u$ in 634 pb^{-1} of data at $\sqrt{s}$= 189–209 GeV. No deviation from the SM is found, which leads to a bound on the top-quark decay branching fraction $B(\gamma q)$, where q is a u or c quark. The bound assumes $B(Zq) = 0$ and is for m_t= 175 GeV; bounds for m_t=170 GeV and 180 GeV and $B(Zq) \neq 0$ are given in Fig. 5 and Table 7.

[6] ABE 98G looked for $t\overline{t}$ events where one t decays into $q\gamma$ while the other decays into bW. The quoted bound is for $\Gamma(\gamma q)/\Gamma(Wb)$.

$\Gamma(Zq(q{=}u,c))/\Gamma_{\text{total}}$ Γ_6/Γ

Test for ΔT=1 weak neutral current. Allowed by higher-order electroweak interaction.

VALUE	CL%	DOCUMENT ID		TECN	COMMENT
<0.0021	95	[1] CHATRCHYAN	13F	CMS	$t \to Zq$ ($q = u, c$)
• • • We do not use the following data for averages, fits, limits, etc. • • •					
<0.0073	95	[2] AAD	12BT	ATLS	$t\overline{t} \to \ell^+\ell^-\ell'^\pm + \not{E}_T$ + jets
<0.032	95	[3] ABAZOV	11M	D0	$t \to Zq$ ($q = u, c$)
<0.083	95	[4] AALTONEN	09AL	CDF	$t \to Zq$ (q=c)
<0.037	95	[5] AALTONEN	08AD	CDF	$t \to Zq$ ($q = u, c$)
<0.159	95	[6] ABDALLAH	04C	DLPH	$e^+e^- \to \overline{t}c$ or $\overline{t}u$
<0.137	95	[7] ACHARD	02J	L3	$e^+e^- \to \overline{t}c$ or $\overline{t}u$
<0.14	95	[8] HEISTER	02Q	ALEP	$e^+e^- \to \overline{t}c$ or $\overline{t}u$
<0.137	95	[9] ABBIENDI	01T	OPAL	$e^+e^- \to \overline{t}c$ or $\overline{t}u$
<0.17	95	[10] BARATE	00S	ALEP	$e^+e^- \to \overline{t}c$ or $\overline{t}u$
<0.33	95	[11] ABE	98G	CDF	$t\overline{t} \to (Wb)(Zc$ or $Zu)$

[1] Based on 5.0 fb^{-1} of pp data at $\sqrt{s} = 7$ TeV. Search for FCNC decays of the top quark in $t\overline{t} \to \ell^+\ell^-\ell'^\pm\nu +$ jets (ℓ, $\ell' = e$, μ) final states found no excess of signal events.

[2] Based on 2.1 fb^{-1} of pp data at $\sqrt{s} = 7$ TeV.

[3] Based on 4.1 fb^{-1} of data. ABAZOV 11M searched for FCNC decays of the top quark in $t\overline{t} \to \ell^+\ell^-\ell'^\pm\nu +$ jets (ℓ, $\ell' = e$, μ) final states, and absence of the signal gives the bound.

[4] Based on $p\overline{p}$ data of 1.52 fb^{-1}. AALTONEN 09AL compared $t\overline{t} \to WbWb \to \ell\nu bjjb$ and $t\overline{t} \to ZcWb \to \ell\ell cjjb$ decay chains, and absence of the latter signal gives the bound. The result is for 100% longitudinally polarized Z boson and the theoretical $t\overline{t}$ production cross section The results for different Z polarizations and those without the cross section assumption are given in their Table XII.

[5] Result is based on 1.9 fb^{-1} of data at $\sqrt{s} = 1.96$ TeV. $t\overline{t} \to WbZq$ or $ZqZq$ processes have been looked for in $Z +$ ≥ 4 jet events with and without b-tag. No signal leads to the bound $B(t \to Zq) < 0.037$ (0.041) for $m_t = 175$ (170) GeV.

[6] ABDALLAH 04C looked for single top production via FCNC in the reaction $e^+e^- \to \overline{t}c$ or $\overline{t}u$ in 541 pb^{-1} of data at $\sqrt{s}$=189–208 GeV. No deviation from the SM is found, which leads to the bound on $B(t \to Zq)$, where q is a u or a c quark, for m_t = 175 GeV when $B(t \to \gamma q) = 0$ is assumed. The conversion to the listed bound is from private communication, O. Yushchenko, April 2005. The bounds on the effective t-q-γ and t-q-Z couplings are given in their Fig. 7 and Table 4, for m_t = 170–180 GeV, where

most conservative bounds are found by choosing the chiral couplings to maximize the negative interference between the virtual γ and Z exchange amplitudes.

[7] ACHARD 02J looked for single top production via FCNC in the reaction $e^+e^- \to \bar{t}c$ or $\bar{t}u$ in 634 pb^{-1} of data at $\sqrt{s}$= 189–209 GeV. No deviation from the SM is found, which leads to a bound on the top-quark decay branching fraction B(Zq), where q is a u or c quark. The bound assumes B(γq)=0 and is for m_t= 175 GeV; bounds for m_t=170 GeV and 180 GeV and B(γq) $\neq$0 are given in Fig. 5 and Table 7. Table 6 gives constraints on t-c-e-e four-fermi contact interactions.

[8] HEISTER 02Q looked for single top production via FCNC in the reaction $e^+e^- \to \bar{t}c$ or $\bar{t}u$ in 214 pb^{-1} of data at $\sqrt{s}$= 204–209 GeV. No deviation from the SM is found, which leads to a bound on the branching fraction B(Zq), where q is a u or c quark. The bound assumes B(γq)=0 and is for m_t= 174 GeV. Bounds on the effective t- (c or u)-γ and t- (c or u)- Z couplings are given in their Fig. 2.

[9] ABBIENDI 01T looked for single top production via FCNC in the reaction $e^+e^- \to \bar{t}c$ or $\bar{t}u$ in 600 pb^{-1} of data at $\sqrt{s}$= 189–209 GeV. No deviation from the SM is found, which leads to bounds on the branching fractions B(Zq) and B(γq), where q is a u or c quark. The result is obtained for m_t= 174 GeV. The upper bound becomes 9.7% (20.6%) for m_t= 169 (179) GeV. Bounds on the effective t- (c or u)-γ and t- (c or u)-Z couplings are given in their Fig. 4.

[10] BARATE 00S looked for single top production via FCNC in the reaction $e^+e^- \to \bar{t}c$ or $\bar{t}u$ in 411 pb^{-1} of data at c.m. energies between 189 and 202 GeV. No deviation from the SM is found, which leads to a bound on the branching fraction. The bound assumes B(γq)=0. Bounds on the effective t- (c or u)-γ and t- (c or u)-Z couplings are given in their Fig. 4.

[11] ABE 98G looked for $t\bar{t}$ events where one t decays into three jets and the other decays into qZ with $Z \to \ell\ell$. The quoted bound is for $\Gamma(Zq)/\Gamma(Wb)$.

t-quark EW Couplings

W helicity fractions in top decays. F_0 is the fraction of longitudinal and F_+ the fraction of right-handed W bosons. F_{V+A} is the fraction of V+A current in top decays. The effective Lagrangian (cited by ABAZOV 08AI) has terms f_1^L and f_1^R for $V-A$ and $V+A$ couplings, f_2^L and f_2^R for tensor couplings with b_R and b_L respectively.

F_0

VALUE	DOCUMENT ID		TECN	COMMENT
0.690±0.030 OUR AVERAGE				
0.726±0.066±0.067	[1] AALTONEN	13D	CDF	F_0 = B($t \to W_0 b$)
0.682±0.030±0.033	[2] CHATRCHYAN	13BH	CMS	F_0 = B($t \to W_0 b$)
0.67 ±0.07	[3] AAD	12BG	ATLS	F_0 = B($t \to W_0 b$)
0.722±0.062±0.052	[4] AALTONEN	12Z	TEVA	F_0 = B($t \to W_0 b$)
0.669±0.078±0.065	[5] ABAZOV	11C	D0	F_0 = B($t \to W_0 b$)
0.91 ±0.37 ±0.13	[6] AFFOLDER	00B	CDF	F_0 = B($t \to W_0 b$)
• • • We do not use the following data for averages, fits, limits, etc. • • •				
0.70 ±0.07 ±0.04	[7] AALTONEN	10Q	CDF	Repl. by AALTONEN 12Z
0.62 ±0.10 ±0.05	[8] AALTONEN	09Q	CDF	Repl. by AALTONEN 10Q
0.425±0.166±0.102	[9] ABAZOV	08B	D0	Repl. by ABAZOV 11C
0.85 $^{+0.15}_{-0.22}$ ±0.06	[10] ABULENCIA	07I	CDF	F_0 = B($t \to W_0 b$)
0.74 $^{+0.22}_{-0.34}$	[11] ABULENCIA	06U	CDF	F_0 = B($t \to W_0 b$)
0.56 ±0.31	[12] ABAZOV	05G	D0	F_0 = B($t \to W_0 b$)

[1] Based on 8.7 fb^{-1} of data in $p\bar{p}$ collisions at $\sqrt{s}$ = 1.96 TeV using $t\bar{t}$ events with ℓ + $\not\!\!E_T$ + $\geq$ 4 jets($\geq$ 1 b), and under the constraint $F_0 + F_+ + F_- = 1$. The statstical errors of F_0 and F_+ are correlated with correlation coefficient $\rho(F_0,F_+) = -0.69$.

[2] Based on 5.0 fb^{-1} of pp data at $\sqrt{s}$ = 7 TeV. CHATRCHYAN 13BH studied tt events with large $\not\!\!E_T$ and $\ell + \geq 4$ jets using a constrained kinematic fit.

[3] Based on 1.04 fb^{-1} of pp data at $\sqrt{s}$ = 7 TeV. AAD 12BG studied tt events with large $\not\!\!E_T$ and either $\ell + \geq 4$j or $\ell\ell + \geq 2$j. The uncertainties are not independent, $\rho(F_0,F_-) = -0.96$.

[4] Based on 2.7 and 5.1 fb^{-1} of CDF data in ℓ + jets and dilepton channels, and 5.4 fb^{-1} of D0 data in ℓ + jets and dilepton channels. F_0 = 0.682 ± 0.035 ± 0.046 if F_+ = 0.0017(1), while $F_+ = -0.015 \pm 0.018 \pm 0.030$ if F_0 = 0.688(4), where the assumed fixed values are the SM prediction for $m_t = 173.3 \pm 1.1$ GeV and $m_W = 80.399 \pm 0.023$ GeV.

[5] Results are based on 5.4 fb^{-1} of data in $p\bar{p}$ collisions at 1.96 TeV, including those of ABAZOV 08B. Under the SM constraint of f_0 = 0.698 (for m_t = 173.3 GeV, m_W = 80.399 GeV), $f_+ = 0.010 \pm 0.022 \pm 0.030$ is obtained.

[6] AFFOLDER 00B studied the angular distribution of leptonic decays of W bosons in $t \to Wb$ events. The ratio F_0 is the fraction of the helicity zero (longitudinal) W bosons in the decaying top quark rest frame. B($t \to W_+ b$) is the fraction of positive helicity (right-handed) positive charge W bosons in the top quark decays. It is obtained by assuming the Standard Model value of F_0.

[7] Results are based on 2.7 fb^{-1} of data in $p\bar{p}$ collisions at $\sqrt{s}$ = 1.96 TeV. F_0 result is obtained by assuming F_+ = 0, while F_+ result is obtained for F_0 = 0.70, the SM value. Model independent fits for the two fractions give $F_0 = 0.88 \pm 0.11 \pm 0.06$ and $F_+ = -0.15 \pm 0.07 \pm 0.06$ with correlation coefficient of -0.59. The results are for m_t = 175 GeV.

[8] Results are based on 1.9 fb^{-1} of data in $p\bar{p}$ collisions at $\sqrt{s}$ = 1.96 TeV. F_0 result is obtained assuming F_+ = 0, while F_+ result is obtained for F_0 = 0.70, the SM values. Model independent fits for the two fractions give $F_0 = 0.66 \pm 0.16 \pm 0.05$ and $F_+ = -0.03 \pm 0.06 \pm 0.03$.

[9] Based on 1 fb^{-1} at $\sqrt{s}$ = 1.96 TeV.

[10] Based on 318 pb^{-1} of data at $\sqrt{s}$ = 1.96 TeV.

[11] Based on 200 pb^{-1} of data at $\sqrt{s}$ = 1.96 TeV. $t \to Wb \to \ell\nu b$ (ℓ = e or μ). The errors are stat + syst.

[12] ABAZOV 05G studied the angular distribution of leptonic decays of W bosons in $t\bar{t}$ candidate events with lepton + jets final states, and obtained the fraction of longitudinally polarized W under the constraint of no right-handed current, F_+ = 0. Based on 125 pb^{-1} of data at $\sqrt{s}$ = 1.8 TeV.

F_-

VALUE	DOCUMENT ID		TECN	COMMENT
0.314±0.025 OUR AVERAGE				
0.310±0.022±0.022	[1] CHATRCHYAN	13BH	CMS	F_- = B($t \to W_- b$)
0.32 ±0.04	[2] AAD	12BG	ATLS	F_- = B($t \to W_- b$)

[1] Based on 5.0 fb^{-1} of pp data at $\sqrt{s}$ = 7 TeV. CHATRCHYAN 13BH studied tt events with large $\not\!\!E_T$ and $\ell + \geq 4$ jets using a constrained kinematic fit.

[2] Based on 1.04 fb^{-1} of pp data at $\sqrt{s}$ = 7 TeV. AAD 12BG studied tt events with large $\not\!\!E_T$ and either $\ell + \geq 4$j or $\ell\ell + \geq 2$j. The uncertainties are not independent, $\rho(F_0,F_-) = -0.96$.

F_+

VALUE	CL%	DOCUMENT ID		TECN	COMMENT
0.008±0.016 OUR AVERAGE					
−0.045±0.044±0.058		[1] AALTONEN	13D	CDF	F_+ = B($t \to W_+ b$)
0.008±0.012±0.014		[2] CHATRCHYAN	13BH	CMS	F_+ = B($t \to W_+ b$)
0.01 ±0.05		[3] AAD	12BG	ATLS	F_+ = B($t \to W_+ b$)
0.023±0.041±0.034		[4] ABAZOV	11C	D0	F_+ = B($t \to W_+ b$)
0.11 ±0.15		[5] AFFOLDER	00B	CDF	F_+ = B($t \to W_+ b$)
• • • We do not use the following data for averages, fits, limits, etc. • • •					
−0.033±0.034±0.031		[6] AALTONEN	12Z	TEVA	F_+ = B($t \to W_+ b$)
−0.01 ±0.02 ±0.05		[7] AALTONEN	10Q	CDF	Repl. by AALTONEN 13D
−0.04 ±0.04 ±0.03		[8] AALTONEN	09Q	CDF	Repl. by AALTONEN 10Q
0.119±0.090±0.053		[9] ABAZOV	08B	D0	Repl. by ABAZOV 11C
0.056±0.080±0.057		[10] ABAZOV	07D	D0	F_+ = B($t \to W_+ b$)
0.05 $^{+0.11}_{-0.05}$ ±0.03		[11] ABULENCIA	07I	CDF	F_+ = B($t \to W_+ b$)
< 0.26	95	[11] ABULENCIA	07I	CDF	F_+ = B($t \to W_+ b$)
< 0.27	95	[12] ABULENCIA	06U	CDF	F_+ = B($t \to W_+ b$)
0.00 ±0.13 ±0.07		[13] ABAZOV	05L	D0	F_+ = B($t \to W_+ b$)
< 0.25	95	[13] ABAZOV	05L	D0	F_+ = B($t \to W_+ b$)
< 0.24	95	[14] ACOSTA	05D	CDF	F_+ = B($t \to W_+ b$)

[1] Based on 8.7 fb^{-1} of data in $p\bar{p}$ collisions at $\sqrt{s}$ = 1.96 TeV using $t\bar{t}$ events with ℓ + $\not\!\!E_T$ + $\geq$ 4 jets($\geq$ 1 b), and under the constraint $F_0 + F_+ + F_- = 1$. The statstical errors of F_0 and F_+ are correlated with correlation coefficient $\rho(F_0,F_+) = -0.69$.

[2] Based on 5.0 fb^{-1} of pp data at $\sqrt{s}$ = 7 TeV. CHATRCHYAN 13BH studied tt events with large $\not\!\!E_T$ and $\ell + \geq 4$ jets using a constrained kinematic fit.

[3] Based on 1.04 fb^{-1} of pp data at $\sqrt{s}$ = 7 TeV. AAD 12BG studied tt events with large $\not\!\!E_T$ and either $\ell + \geq 4$j or $\ell\ell + \geq 2$j.

[4] Results are based on 5.4 fb^{-1} of data in $p\bar{p}$ collisions at 1.96 TeV, including those of ABAZOV 08B. Under the SM constraint of f_0 = 0.698 (for m_t = 173.3 GeV, m_W = 80.399 GeV), $f_+ = 0.010 \pm 0.022 \pm 0.030$ is obtained.

[5] AFFOLDER 00B studied the angular distribution of leptonic decays of W bosons in $t \to Wb$ events. The ratio F_0 is the fraction of the helicity zero (longitudinal) W bosons in the decaying top quark rest frame. B($t \to W_+ b$) is the fraction of positive helicity (right-handed) positive charge W bosons in the top quark decays. It is obtained by assuming the Standard Model value of F_0.

[6] Based on 2.7 and 5.1 fb^{-1} of CDF data in ℓ + jets and dilepton channels, and 5.4 fb^{-1} of D0 data in ℓ + jets and dilepton channels. F_0 = 0.682 ± 0.035 ± 0.046 if F_+ = 0.0017(1), while $F_+ = -0.015 \pm 0.018 \pm 0.030$ if F_0 = 0.688(4), where the assumed fixed values are the SM prediction for $m_t = 173.3 \pm 1.1$ GeV and $m_W = 80.399 \pm 0.023$ GeV.

[7] Results are based on 2.7 fb^{-1} of data in $p\bar{p}$ collisions at $\sqrt{s}$ = 1.96 TeV. F_0 result is obtained by assuming F_+ = 0, while F_+ result is obtained for F_0 = 0.70, the SM value. Model independent fits for the two fractions give $F_0 = 0.88 \pm 0.11 \pm 0.06$ and $F_+ = -0.15 \pm 0.07 \pm 0.06$ with correlation coefficient of -0.59. The results are for m_t = 175 GeV.

[8] Results are based on 1.9 fb^{-1} of data in $p\bar{p}$ collisions at $\sqrt{s}$ = 1.96 TeV. F_0 result is obtained assuming F_+ = 0, while F_+ result is obtained for F_0 = 0.70, the SM values. Model independent fits for the two fractions give $F_0 = 0.66 \pm 0.16 \pm 0.05$ and $F_+ = -0.03 \pm 0.06 \pm 0.03$.

[9] Based on 1 fb^{-1} at $\sqrt{s}$ = 1.96 TeV.

[10] Based on 370 pb^{-1} of data at $\sqrt{s}$ = 1.96 TeV, using the ℓ + jets and dilepton decay channels. The result assumes F_0 = 0.70, and it gives $F_+ < 0.23$ at 95% CL.

[11] Based on 318 pb^{-1} of data at $\sqrt{s}$ = 1.96 TeV.

[12] Based on 200 pb^{-1} of data at $\sqrt{s}$ = 1.96 TeV. $t \to Wb \to \ell\nu b$ (ℓ = e or μ). The errors are stat + syst.

[13] ABAZOV 05L studied the angular distribution of leptonic decays of W bosons in $t\bar{t}$ events, where one of the W's from t or $\bar{t}$ decays into e or μ and the other decays hadronically. The fraction of the "+" helicity W boson is obtained by assuming F_0 = 0.7, which is the generic prediction for any linear combination of V and A currents. Based on 230 ± 15 pb^{-1} of data at $\sqrt{s}$ = 1.96 TeV.

[14] ACOSTA 05D measures the $m^2_{\ell+b}$ distribution in $t\bar{t}$ production events where one or both W's decay leptonically to ℓ = e or μ, and finds a bound on the V+A coupling of the tbW vertex. By assuming the SM value of the longitudinal W fraction F_0 = B($t \to W_0 b$) = 0.70, the bound on F_+ is obtained. If the results are combined with those of AFFOLDER 00B, the bounds become $F_{V+A} < 0.61$ (95% CL) and $F_+ < 0.18$ (95 %CL), respectively. Based on 109 ± 7 pb^{-1} of data at $\sqrt{s}$ = 1.8 TeV (run I).

F_{V+A}

VALUE	CL%	DOCUMENT ID		TECN	COMMENT
< 0.29	95	[1] ABULENCIA	07G	CDF	F_{V+A} = B($t \to W b_R$)
• • • We do not use the following data for averages, fits, limits, etc. • • •					
−0.06±0.22±0.12		[1] ABULENCIA	07G	CDF	F_{V+A} = B($t \to W b_R$)
< 0.80	95	[2] ACOSTA	05D	CDF	F_{V+A} = B($t \to W b_R$)

[1] Based on 700 pb^{-1} of data at $\sqrt{s}$ = 1.96 TeV.

[2] ACOSTA 05D measures the $m^2_{\ell+b}$ distribution in $t\bar{t}$ production events where one or both W's decay leptonically to $\ell = e$ or μ, and finds a bound on the V+A coupling of the tbW vertex. By assuming the SM value of the longitudinal W fraction F_0 = B($t \to W_0 b$) = 0.70, the bound on F_+ is obtained. If the results are combined with those of AFFOLDER 00B, the bounds become $F_{V+A} < 0.61$ (95% CL) and $F_+ < 0.18$ (95 %CL), respectively. Based on 109 ± 7 pb^{-1} of data at $\sqrt{s}$ = 1.8 TeV (run I).

f_1^R

VALUE	CL%	DOCUMENT ID		TECN	COMMENT
• • • We do not use the following data for averages, fits, limits, etc. • • •					
$-0.20 < \mathrm{Re}(V_{tb}\, f_1^R) < 0.23$	95	[1] AAD	12BG	ATLS	Constr. on Wtb vtx
$(V_{tb}\, f_1^R)^2 < 0.93$	95	[2] ABAZOV	12E	D0	Single-top
$\lvert f_1^R\rvert^2 < 0.30$	95	[3] ABAZOV	12I	D0	single-t + W helicity
$\lvert f_1^R\rvert^2 < 1.01$	95	[4] ABAZOV	09J	D0	$\lvert f_1^L\rvert = 1$, $\lvert f_2^L\rvert = \lvert f_2^R\rvert = 0$
$\lvert f_1^R\rvert^2 < 2.5$	95	[5] ABAZOV	08AI	D0	$\lvert f_1^L\rvert^2 = 1.8^{+1.0}_{-1.3}$

[1] Based on 1.04 fb^{-1} of pp data at $\sqrt{s}$ = 7 TeV. AAD 12BG studied tt events with large $\not\!\!E_T$ and either $\ell + \geq 4$j or $\ell\ell + \geq 2$j.

[2] Based on 5.4 fb^{-1} of data. For each value of the form factor quoted the other two are assumed to have their SM value. Their Fig. 4 shows two-dimensional posterior probability density distributions for the anomalous couplings.

[3] Based on 5.4 fb^{-1} of data in $p\bar{p}$ collisions at 1.96 TeV. Results are obtained by combining the limits from the W helicity measurements and those from the single top quark production.

[4] Based on 1 fb^{-1} of data at $p\bar{p}$ collisions $\sqrt{s}$ = 1.96 TeV. Combined result of the W helicity measurement in $t\bar{t}$ events (ABAZOV 08B) and the search for anomalous tbW couplings in the single top production (ABAZOV 08AI). Constraints when f_1^L and one of the anomalous couplings are simultaneously allowed to vary are given in their Fig. 1 and Table 1.

[5] Result is based on 0.9 fb^{-1} of data at $\sqrt{s}$ = 1.96 TeV. Single top quark production events are used to measure the Lorentz structure of the tbW coupling. The upper bounds on the non-standard couplings are obtained when only one non-standard coupling is allowed to be present together with the SM one, $f_1^L = V_{tb}^*$.

f_2^L

VALUE	CL%	DOCUMENT ID		TECN	COMMENT
• • • We do not use the following data for averages, fits, limits, etc. • • •					
$-0.14 < \mathrm{Re}(f_2^L) < 0.11$	95	[1] AAD	12BG	ATLS	Constr. on Wtb vtx
$(V_{tb}\, f_2^L)^2 < 0.13$	95	[2] ABAZOV	12E	D0	Single-top
$\lvert f_2^L\rvert^2 < 0.05$	95	[3] ABAZOV	12I	D0	single-t + W helicity
$\lvert f_2^L\rvert^2 < 0.28$	95	[4] ABAZOV	09J	D0	$\lvert f_1^L\rvert = 1$, $\lvert f_1^R\rvert = \lvert f_2^R\rvert = 0$
$\lvert f_2^L\rvert^2 < 0.5$	95	[5] ABAZOV	08AI	D0	$\lvert f_1^L\rvert^2 = 1.4^{+0.6}_{-0.5}$

[1] Based on 1.04 fb^{-1} of pp data at $\sqrt{s}$ = 7 TeV. AAD 12BG studied tt events with large $\not\!\!E_T$ and either $\ell + \geq 4$j or $\ell\ell + \geq 2$j.

[2] Based on 5.4 fb^{-1} of data. For each value of the form factor quoted the other two are assumed to have their SM value. Their Fig. 4 shows two-dimensional posterior probability density distributions for the anomalous couplings.

[3] Based on 5.4 fb^{-1} of data in $p\bar{p}$ collisions at 1.96 TeV. Results are obtained by combining the limits from the W helicity measurements and those from the single top quark production.

[4] Based on 1 fb^{-1} of data at $p\bar{p}$ collisions $\sqrt{s}$ = 1.96 TeV. Combined result of the W helicity measurement in $t\bar{t}$ events (ABAZOV 08B) and the search for anomalous tbW couplings in the single top production (ABAZOV 08AI). Constraints when f_1^L and one of the anomalous couplings are simultaneously allowed to vary are given in their Fig. 1 and Table 1.

[5] Result is based on 0.9 fb^{-1} of data at $\sqrt{s}$ = 1.96 TeV. Single top quark production events are used to measure the Lorentz structure of the tbW coupling. The upper bounds on the non-standard couplings are obtained when only one non-standard coupling is allowed to be present together with the SM one, $f_1^L = V_{tb}^*$.

f_2^R

VALUE	CL%	DOCUMENT ID		TECN	COMMENT
• • • We do not use the following data for averages, fits, limits, etc. • • •					
$-0.08 < \mathrm{Re}(f_2^R) < 0.04$	95	[1] AAD	12BG	ATLS	Constr. on Wtb vtx
$(V_{tb}\, f_2^R)^2 < 0.06$	95	[2] ABAZOV	12E	D0	Single-top
$\lvert f_2^R\rvert^2 < 0.12$	95	[3] ABAZOV	12I	D0	single-t + W helicity
$\lvert f_2^R\rvert^2 < 0.23$	95	[4] ABAZOV	09J	D0	$\lvert f_1^L\rvert = 1$, $\lvert f_1^R\rvert = \lvert f_2^L\rvert = 0$
$\lvert f_2^R\rvert^2 < 0.3$	95	[5] ABAZOV	08AI	D0	$\lvert f_1^L\rvert^2 = 1.4^{+0.9}_{-0.8}$

[1] Based on 1.04 fb^{-1} of pp data at $\sqrt{s}$ = 7 TeV. AAD 12BG studied tt events with large $\not\!\!E_T$ and either $\ell + \geq 4$j or $\ell\ell + \geq 2$j.

[2] Based on 5.4 fb^{-1} of data. For each value of the form factor quoted the other two are assumed to have their SM value. Their Fig. 4 shows two-dimensional posterior probability density distributions for the anomalous couplings.

[3] Based on 5.4 fb^{-1} of data in $p\bar{p}$ collisions at 1.96 TeV. Results are obtained by combining the limits from the W helicity measurements and those from the single top quark production.

[4] Based on 1 fb^{-1} of data at $p\bar{p}$ collisions $\sqrt{s}$ = 1.96 TeV. Combined result of the W helicity measurement in $t\bar{t}$ events (ABAZOV 08B) and the search for anomalous tbW couplings in the single top production (ABAZOV 08AI). Constraints when f_1^L and one of the anomalous couplings are simultaneously allowed to vary are given in their Fig. 1 and Table 1.

[5] Result is based on 0.9 fb^{-1} of data at $\sqrt{s}$ = 1.96 TeV. Single top quark production events are used to measure the Lorentz structure of the tbW coupling. The upper bounds on the non-standard couplings are obtained when only one non-standard coupling is allowed to be present together with the SM one, $f_1^L = V_{tb}^*$.

Spin Correlation in $t\bar{t}$ Production

C is the correlation strength parameter, f is the ratio of events with correlated t and $\bar{t}$ spins (SM prediction: f = 1), and κ is the spin correlation coefficient. See "The Top Quark" review for more information.

VALUE	DOCUMENT ID		TECN	COMMENT
• • • We do not use the following data for averages, fits, limits, etc. • • •				
0.85 ± 0.29	[1] ABAZOV	12B	D0	f ($\ell\ell + \geq 2$ jets, $\ell + \geq 4$ jets)
$1.15^{+0.42}_{-0.43}$	[2] ABAZOV	12B	D0	f ($\ell + \not\!\!E_T + \geq 4$ jets)
$0.60^{+0.50}_{-0.16}$	[3] AALTONEN	11AR	CDF	κ ($\ell + \not\!\!E_T + \geq 4$ jets)
$0.74^{+0.40}_{-0.41}$	[4] ABAZOV	11AE	D0	f ($\ell\ell + \not\!\!E_T + \geq 2$ jets)
0.10 ± 0.45	[5] ABAZOV	11AF	D0	C ($\ell\ell + \not\!\!E_T + \geq 2$ jets)

[1] This is a combination of the lepton + jets analysis presented in ABAZOV 12B and the dilepton measurement of ABAZOV 11AE. It provides a 3.1 σ evidence for the $t\bar{t}$ spin correlation.

[2] Based on 5.3 fb^{-1} of data. The error is statistical and systematic combined. A matrix element method is used.

[3] Based on 4.3 fb^{-1} of data. The measurement is based on the angular study of the top quark decay products in the helicity basis.The theory prediction is $\kappa \approx 0.40$.

[4] Based on 5.4 fb^{-1} of data using a matrix element method. The error is statistical and systematic combined. The no-correlation hypothesis is excluded at the 97.7% CL.

[5] Based on 5.4 fb^{-1} of data. The error is statistical and systematic combined. The NLO QCD prediction is C = 0.78 ± 0.03. The neutrino weighting method is used for reconstruction of kinematics.

t-quark FCNC Couplings κ^{utg}/Λ and κ^{ctg}/Λ

VALUE (TeV^{-1})	CL%	DOCUMENT ID		TECN	COMMENT
• • • We do not use the following data for averages, fits, limits, etc. • • •					
<0.0069	95	[1] AAD	12BP	ATLS	t^{tug}/Λ ($t^{tcg} = 0$)
<0.016	95	[1] AAD	12BP	ATLS	t^{tcg}/Λ ($t^{tug} = 0$)
<0.013	95	[2] ABAZOV	10K	D0	κ^{tug}/Λ
<0.057	95	[2] ABAZOV	10K	D0	κ^{tcg}/Λ
<0.018	95	[3] AALTONEN	09N	CDF	κ^{tug}/Λ ($\kappa^{tcg} = 0$)
<0.069	95	[3] AALTONEN	09N	CDF	κ^{tcg}/Λ ($\kappa^{tug} = 0$)
<0.037	95	[4] ABAZOV	07V	D0	κ^{utg}/Λ
<0.15	95	[4] ABAZOV	07V	D0	κ^{ctg}/Λ

[1] Based on 2.05 fb^{-1} of pp data at $\sqrt{s}$ = 7 TeV. The results are obtained from the 95% CL upper limit on the single top-quark production $\sigma(qg \to t)\cdot$B($t \to bW$) < 3.9 pb, for q=u or q=c, B($t \to ug$) < 5.7×10^{-5} and B($t \to ug$) < 2.7×10^{-4}.

[2] Based on 2.3 fb^{-1} of data in $p\bar{p}$ collisions at $\sqrt{s}$ = 1.96 TeV. Upper limit of single top quark production cross section 0.20 pb and 0.27 pb via FCNC t-u-g and t-c-g couplings, respectively, lead to the bounds without assuming the absence of the other coupling. B($t \to u + g$) < 2.0×10^{-4} and B($t \to c + g$) < 3.9×10^{-3} follow.

[3] Based on 2.2 fb^{-1} of data in $p\bar{p}$ collisions at $\sqrt{s}$ = 1.96 TeV. Upper limit of single top quark production cross section $\sigma(u(c) + g \to t)$ < 1.8 pb (95% CL) via FCNC t-u-g and t-c-g couplings lead to the bounds. B($t \to u + g$) < 3.9×10^{-4} and B($t \to c + g$) < 5.7×10^{-3} follow.

[4] Result is based on 230 pb^{-1} of data at $\sqrt{s}$ = 1.96 TeV. Absence of single top quark production events via FCNC t-u-g and t-c-g couplings lead to the upper bounds on the dimensioned couplings, κ^{utg}/Λ and κ^{ctg}/Λ, respectively.

Single t-Quark Production Cross Section in $p\bar{p}$ Collisions at $\sqrt{s}$ = 1.8 TeV

Direct probe of the tbW coupling and possible new physics at $\sqrt{s}$ = 1.8 TeV.

VALUE (pb)	CL%	DOCUMENT ID		TECN	COMMENT
• • • We do not use the following data for averages, fits, limits, etc. • • •					
<24	95	[1] ACOSTA	04H	CDF	$p\bar{p} \to tb + X$, $tqb + X$
<18	95	[2] ACOSTA	02	CDF	$p\bar{p} \to tb + X$
<13	95	[3] ACOSTA	02	CDF	$p\bar{p} \to tqb + X$

[1] ACOSTA 04H bounds single top-quark production from the s-channel W-exchange process, $q'\bar{q} \to t\bar{b}$, and the t-channel W-exchange process, $q'g \to qt\bar{b}$. Based on $\sim$ 106 pb^{-1} of data.

[2] ACOSTA 02 bounds the cross section for single top-quark production via the s-channel W-exchange process, $q'\bar{q} \to t\bar{b}$. Based on $\sim$ 106 pb^{-1} of data.

[3] ACOSTA 02 bounds the cross section for single top-quark production via the t-channel W-exchange process, $q'g \to qt\bar{b}$. Based on $\sim$ 106 pb^{-1} of data.

Single t-Quark Production Cross Section in $p\bar{p}$ Collisions at $\sqrt{s}$ = 1.96 TeV

Direct probes of the tbW coupling and possible new physics at $\sqrt{s}$ = 1.96 TeV. OUR AVERAGE assumes that the systematic uncertainties are uncorrelated.

VALUE (pb)	CL%	DOCUMENT ID		TECN	COMMENT
• • • We do not use the following data for averages, fits, limits, etc. • • •					
$1.10^{+0.33}_{-0.31}$		[1] ABAZOV	13O	D0	s-channel
$3.07^{+0.54}_{-0.49}$		[1] ABAZOV	13O	D0	t-channel
$4.11^{+0.60}_{-0.55}$		[1] ABAZOV	13O	D0	s- + t-channels
0.98 ± 0.63		[2] ABAZOV	11AA	D0	s-channel
2.90 ± 0.59		[2] ABAZOV	11AA	D0	t-channel
$3.43^{+0.73}_{-0.74}$		[3] ABAZOV	11AD	D0	s- + t-channels
$1.8\ ^{+0.7}_{-0.5}$		[4] AALTONEN	10AB	CDF	s-channel
0.8 ± 0.4		[4] AALTONEN	10AB	CDF	t-channel
$4.9\ ^{+2.5}_{-2.2}$		[5] AALTONEN	10U	CDF	$\not\!\!E_T$ + jets decay
$3.14^{+0.94}_{-0.80}$		[6] ABAZOV	10	D0	t-channel

1.05 ± 0.81		[6] ABAZOV	10	D0		s-channel
< 7.3	95	[7] ABAZOV	10J	D0		τ + jets decay
$2.3\ ^{+0.6}_{-0.5}$		[8] AALTONEN	09AT	CDF		s- + t-channel
3.94 ± 0.88		[9] ABAZOV	09Z	D0		s- + t-channel
$2.2\ ^{+0.7}_{-0.6}$		[10] AALTONEN	08AH	CDF		s- + t-channel
4.7 ± 1.3		[11] ABAZOV	08I	D0		s- + t-channel
4.9 ± 1.4		[12] ABAZOV	07H	D0		s- + t-channel
< 6.4	95	[13] ABAZOV	05P	D0		$p\overline{p} \rightarrow t b + X$
< 5.0	95	[13] ABAZOV	05P	D0		$p\overline{p} \rightarrow t q b + X$
< 10.1	95	[14] ACOSTA	05N	CDF		$p\overline{p} \rightarrow t q b + X$
< 13.6	95	[14] ACOSTA	05N	CDF		$p\overline{p} \rightarrow t b + X$
< 17.8	95	[14] ACOSTA	05N	CDF		$p\overline{p} \rightarrow t b + X$, $t q b + X$

[1] Based on 9.7 fb^{-1} of data. Events with $\ell + \not{E}_T$ + 2 or 3 jets (1 or 2 b-tag) are analysed, assuming $m_t = 172.5$ GeV. The combined s- + t-channel cross section gives $|V_{tb}\, f_1^L| = 1.12^{+0.09}_{-0.08}$, or $|V_{tb}| > 0.92$ at 95% CL for $f_1^L = 1$ and a flat prior within $0 \leq |V_{tb}|^2 \leq 1$.

[2] Based on 5.4 fb^{-1} of data. The error is statistical + systematic combined. The results are for $m_t = 172.5$ GeV. Results for other m_t values are given in Table 2 of ABAZOV 11AA.

[3] Based on 5.4 fb^{-1} of data and for $m_t = 172.5$ GeV. The error is statistical + systematic combined. Results for other m_t values are given in Table III of ABAZOV 11AD. The result is obtained by assuming the SM ratio between $t b$ (s-channel) and $t q b$ (t-channel) productions, and gives $|V_{tb}\, f_1^L| = 1.02^{+0.10}_{-0.11}$, or $|V_{tb}| > 0.79$ at 95% CL for a flat prior within $0 < |V_{tb}|^2 < 1$.

[4] Based on 3.2 fb^{-1} of data. For combined s- + t-channel result see AALTONEN 09AT.

[5] Result is based on 2.1 fb^{-1} of data. Events with large missing E_T and jets with at least one b-jet without identified electron or muon are selected. Result is obtained when observed 2.1 σ excess over the background originates from the signal for $m_t = 175$ GeV, giving $|V_{tb}| = 1.24^{+0.34}_{-0.29} \pm 0.07$(theory).

[6] Result is based on 2.3 fb^{-1} of data. Events with isolated $\ell + \not{E}_T$ + 2 ,3, 4 jets with one or two b-tags are selected. The analysis assumes $m_t = 170$ GeV.

[7] Result is based on 4.8 fb^{-1} of data. Events with an isolated reconstructed tau lepton, missing E_T + 2, 3 jets with one or two b-tags are selected. When combined with ABAZOV 09Z result for $e + \mu$ channels, the s- and t-channels combined cross section is $3.84^{+0.89}_{-0.83}$ pb.

[8] Based on 3.2 fb^{-1} of data. Events with isolated $\ell + \not{E}_T$ + jets with at least one b-tag are analyzed and s- and t-channel single top events are selected by using the likelihood function, matrix element, neural-network, boosted decision tree, likelihood function optimized for s-channel process, and neural-networked based analysis of events with $\not{E}_T$ that has sensitivity for $W \rightarrow \tau\nu$ decays. The result is for $m_t = 175$ GeV, and the mean value decreases by 0.02 pb/GeV for smaller m_t. The signal has 5.0 sigma significance. The result gives $|V_{tb}| = 0.91 \pm 0.11$ (stat+syst) ± 0.07 (theory), or $|V_{tb}| > 0.71$ at 95% CL.

[9] Based on 2.3 fb^{-1} of data. Events with isolated $\ell + \not{E}_T + \geq 2$ jets with 1 or 2 b-tags are analyzed and s- and t-channel single top events are selected by using boosted decision tree, Bayesian neural networks and the matrix element method. The signal has 5.0 sigma significance. The result gives $|V_{tb}| = 1.07 \pm 0.12$, or $|V_{tb}| > 0.78$ at 95% CL. The analysis assumes $m_t = 170$ GeV.

[10] Result is based on 2.2 fb^{-1} of data. Events with isolated $\ell + \not{E}_T$ + 2, 3 jets with at least one b-tag are selected, and s- and t-channel single top events are selected by using likelihood, matrix element, and neural network discriminants. The result can be interpreted as $|V_{tb}| = 0.88^{+0.13}_{-0.12}$(stat + syst)$\pm 0.07$(theory), and $|V_{tb}| > 0.66$ (95% CL) under the $|V_{tb}| < 1$ constraint.

[11] Result is based on 0.9 fb^{-1} of data. Events with isolated $\ell + \not{E}_T$ + 2, 3, 4 jets with one or two b-vertex-tag are selected, and contributions from W + jets, $t\overline{t}$, s- and t-channel single top events are identified by using boosted decision trees, Bayesian neural networks, and matrix element analysis. The result can be interpreted as the measurement of the CKM matrix element $|V_{tb}| = 1.31^{+0.25}_{-0.21}$, or $|V_{tb}| > 0.68$ (95% CL) under the $|V_{tb}| < 1$ constraint.

[12] Result is based on 0.9 fb^{-1} of data. This result constrains V_{tb} to $0.68 < |V_{tb}| \leq 1$ at 95% CL.

[13] ABAZOV 05P bounds single top-quark production from either the s-channel W-exchange process, $q'\overline{q} \rightarrow t\overline{b}$, or the t-channel W-exchange process, $q'g \rightarrow q\, t\overline{b}$, based on ~ 230 pb^{-1} of data.

[14] ACOSTA 05N bounds single top-quark production from the t-channel W-exchange process ($q'g \rightarrow q\, t\overline{b}$), the s-channel W-exchange process ($q'\overline{q} \rightarrow t\overline{b}$), and from the combined cross section of t- and s-channel. Based on $\sim$ 162 pb^{-1} of data.

Single t-Quark Production Cross Section in pp Collisions at $\sqrt{s} = 7$ TeV

Direct probe of the $t b W$ coupling and possible new physics at $\sqrt{s} = 7$ TeV.

VALUE (pb)	DOCUMENT ID		TECN	COMMENT
• • • We do not use the following data for averages, fits, limits, etc. • • •				
$83 \pm 4\ ^{+20}_{-19}$	[1] AAD	12CH	ATLS	t-channel $\ell + \not{E}_T$+ (2,3)j (1b)
67.2 ± 6.1	[2] CHATRCHYAN	12BQ	CMS	t-channel $\ell + \not{E}_T + \geq$ 2j (1b)
$83.6 \pm 29.8 \pm 3.3$	[3] CHATRCHYAN	11R	CMS	t-channel

[1] Based on 1.04 fb^{-1} of data. The result gives $|V_{tb}| = 1.13^{+0.14}_{-0.13}$ from the ratio σ(exp)/σ(th), where σ(th) is the SM prediction for $|V_{tb}| = 1$. The 95% CL lower bound of $|V_{tb}| > 0.75$ is found if $|V_{tb}| < 1$ is assumed. $\sigma(t) = 59^{+18}_{-16}$ pb and $\sigma(\overline{t}) = 33^{+13}_{-12}$ pb are found for the separate single t and $\overline{t}$ production cross sections, respectively. The results assume $m_t = 172.5$ GeV for the acceptance.

[2] Based on 1.17 fb^{-1} of data for $\ell = \mu$, 1.56 fb^{-1} of data for $\ell = e$ at 7 TeV collected during 2011. The result gives $|V_{tb}| = 1.020 \pm 0.046$(meas)$\pm 0.017$(th). The 95% CL lower bound of $|V_{tb}| > 0.92$ is found if $|V_{tb}| < 1$ is assumed. The results assume $m_t = 172.5$ GeV for the acceptance.

[3] Based on 36 pb^{-1} of data. The first error is statistical + systematic combined, the second is luminosity. The result gives $|V_{tb}| = 1.114 \pm 0.22(exp)\pm 0.02$(th) from the ratio σ(exp)/σ(th), where σ(th) is the SM prediction for $|V_{tb}| = 1$. The 95% CL lower bound of $|V_{tb}| > 0.62$ (0.68) is found from the 2D (BDT) analysis under the constraint $0 < |V_{tb}|^2 < 1$.

Wt Production Cross Section in pp Collisions at $\sqrt{s} = 7$ TeV

VALUE (pb)	DOCUMENT ID		TECN	COMMENT
• • • We do not use the following data for averages, fits, limits, etc. • • •				
16^{+5}_{-4}	[1] CHATRCHYAN	13C	CMS	t+W channel, 2ℓ+$\not{E}_T$+1b

[1] Based on 4.9 fb^{-1} of data. The result gives $V_{tb} = 1.01^{+0.16}_{-0.13}(exp)^{+0.03}_{-0.04}$(th). $V_{tb} > 0.79$ (95% CL) if $V_{tb} < 1$ is assumed. The results assume $m_t = 172.5$ GeV for the acceptance.

Single t-Quark Production Cross Section in ep Collisions

VALUE (pb)	CL%	DOCUMENT ID		TECN	COMMENT
• • • We do not use the following data for averages, fits, limits, etc. • • •					
< 0.25	95	[1] AARON	09A	H1	$e^{\pm}p \rightarrow e^{\pm}tX$
< 0.55	95	[2] AKTAS	04	H1	$e^{\pm}p \rightarrow e^{\pm}tX$
< 0.225	95	[3] CHEKANOV	03	ZEUS	$e^{\pm}p \rightarrow e^{\pm}tX$

[1] AARON 09A looked for single top production via FCNC in $e^{\pm}p$ collisions at HERA with 474 pb^{-1} of data at $\sqrt{s} = 301$–319 GeV. The result supersedes that of AKTAS 04.

[2] AKTAS 04 looked for single top production via FCNC in $e^{\pm}$ collisions at HERA with 118.3 pb^{-1}, and found 5 events in the e or μ channels while 1.31 ± 0.22 events are expected from the Standard Model background. No excess was found for the hadronic channel. The observed cross section of $\sigma(ep \rightarrow e\, tX) = 0.29^{+0.15}_{-0.14}$ pb at $\sqrt{s} =$ 319 GeV gives the quoted upper bound if the observed events are due to statistical fluctuation.

[3] CHEKANOV 03 looked in 130.1 pb^{-1} of data at $\sqrt{s} = 301$ and 318 GeV. The limit is for $\sqrt{s} = 318$ GeV and assumes $m_t = 175$ GeV.

$t\overline{t}$ Production Cross Section in $p\overline{p}$ Collisions at $\sqrt{s} = 1.8$ TeV

Only the final combined $t\overline{t}$ production cross sections obtained from Tevatron Run I by the CDF and D0 experiments are quoted below.

VALUE (pb)	DOCUMENT ID		TECN	COMMENT
• • • We do not use the following data for averages, fits, limits, etc. • • •				
$5.69 \pm 1.21 \pm 1.04$	[1] ABAZOV	03A	D0	Combined Run I data
$6.5\ ^{+1.7}_{-1.4}$	[2] AFFOLDER	01A	CDF	Combined Run I data

[1] Combined result from 110 pb^{-1} of Tevatron Run I data. Assume $m_t = 172.1$ GeV.

[2] Combined result from 105 pb^{-1} of Tevatron Run I data. Assume $m_t = 175$ GeV.

$t\overline{t}$ Production Cross Section in $p\overline{p}$ Collisions at $\sqrt{s} = 1.96$ TeV

Unless otherwise noted the first quoted error is from statistics, the second from systematic uncertainties, and the third from luminosity. If only two errors are quoted the luminosity is included in the systematic uncertainties.

VALUE (pb)	DOCUMENT ID		TECN	COMMENT
• • • We do not use the following data for averages, fits, limits, etc. • • •				
7.09 ± 0.84	[1] AALTONEN	13AB	CDF	$\ell\ell + \not{E}_T + \geq 2$ jets
7.5 ± 1.0	[2] AALTONEN	13G	CDF	$\ell + \not{E}_T + \geq$ 3jets ($\geq 1b$-tag)
$8.8 \pm 3.3 \pm 2.2$	[3] AALTONEN	12AL	CDF	$\tau_h + \not{E}_T$ +4j ($\geq 1b$)
$8.5 \pm 0.6 \pm 0.7$	[4] AALTONEN	11D	CDF	$\ell + \not{E}_T$ + jets ($\geq 1b$-tag)
$7.64 \pm 0.57 \pm 0.45$	[5] AALTONEN	11W	CDF	$\ell + \not{E}_T$ + jets ($\geq 1b$-tag)
$7.99 \pm 0.55 \pm 0.76 \pm 0.46$	[6] AALTONEN	11Y	CDF	$\not{E}_T + \geq$ 4jets (0,1,2 b-tag)
$7.78^{+0.77}_{-0.64}$	[7] ABAZOV	11E	D0	$\ell + \not{E}_T + \geq 2$ jets
$7.56^{+0.63}_{-0.56}$	[8] ABAZOV	11Z	D0	Combination
$6.27 \pm 0.73 \pm 0.63 \pm 0.39$	[9] AALTONEN	10AA	CDF	Repl. by AALTONEN 13AB
$7.2 \pm 0.5 \pm 1.0 \pm 0.4$	[10] AALTONEN	10E	CDF	≥ 6 jets, vtx b-tag
$7.8 \pm 2.4 \pm 1.6 \pm 0.5$	[11] AALTONEN	10V	CDF	$\ell + \geq 3$ jets, soft-e b-tag
7.70 ± 0.52	[12] AALTONEN	10W	CDF	$\ell + \not{E}_T + \geq 3$ jets + b-tag, norm. to $\sigma(Z \rightarrow \ell\ell)_{TH}$
6.9 ± 2.0	[13] ABAZOV	10I	D0	≥ 6 jets with 2 b-tags
$6.9 \pm 1.2\ ^{+0.8}_{-0.7} \pm 0.4$	[14] ABAZOV	10Q	D0	τ_h + jets
$9.6 \pm 1.2\ ^{+0.6}_{-0.5} \pm 0.6$	[15] AALTONEN	09AD	CDF	$\ell\ell + \not{E}_T$ / vtx b-tag
$9.1 \pm 1.1\ ^{+1.0}_{-0.9} \pm 0.6$	[16] AALTONEN	09H	CDF	$\ell + \geq 3$ jets+$\not{E}_T$/soft μ b-tag
$8.18^{+0.98}_{-0.87}$	[17] ABAZOV	09AG	D0	ℓ + jets, $\ell\ell$ and $\ell\tau$ + jets
$7.5 \pm 1.0\ ^{+0.7}_{-0.6}\ ^{+0.6}_{-0.5}$	[18] ABAZOV	09R	D0	$\ell\ell$ and $\ell\tau$ + jets
$8.18^{+0.90}_{-0.84} \pm 0.50$	[19] ABAZOV	08M	D0	ℓ + n jets with 0,1,2 b-tag
7.62 ± 0.85	[20] ABAZOV	08N	D0	ℓ + n jets + b-tag or kinematics
$8.5\ ^{+2.7}_{-2.2}$	[21] ABULENCIA	08	CDF	$\ell^+\ell^-$ ($\ell = e, \mu$)
$8.3 \pm 1.0\ ^{+2.0}_{-1.5} \pm 0.5$	[22] AALTONEN	07D	CDF	≥ 6 jets, vtx b-tag
$7.4 \pm 1.4 \pm 1.0$	[23] ABAZOV	07O	D0	$\ell\ell$ + jets, vtx b-tag
$4.5\ ^{+2.0}_{-1.9}\ ^{+1.4}_{-1.1} \pm 0.3$	[24] ABAZOV	07P	D0	≥ 6 jets, vtx b-tag
$6.4\ ^{+1.3}_{-1.2} \pm 0.7 \pm 0.4$	[25] ABAZOV	07R	D0	$\ell + \geq 4$ jets
$6.6 \pm 0.9 \pm 0.4$	[26] ABAZOV	06X	D0	ℓ + jets, vtx b-tag

8.7 ± 0.9 $^{+1.1}_{-0.9}$	[27] ABULENCIA	06Z	CDF	ℓ + jets, vtx b-tag
5.8 ± 1.2 $^{+0.9}_{-0.7}$	[28] ABULENCIA,A	06C	CDF	missing E_T + jets, vtx b-tag
7.5 ± 2.1 $^{+3.3}_{-2.2}$ $^{+0.5}_{-0.4}$	[29] ABULENCIA,A	06E	CDF	6–8 jets, b-tag
8.9 ± 1.0 $^{+1.1}_{-1.0}$	[30] ABULENCIA,A	06F	CDF	$\ell \geq 3$ jets, b-tag
8.6 $^{+1.6}_{-1.5}$ ± 0.6	[31] ABAZOV	05Q	D0	ℓ + n jets
$8.6^{+3.2}_{-2.7} \pm 1.1 \pm 0.6$	[32] ABAZOV	05R	D0	di-lepton + n jets
6.7 $^{+1.4}_{-1.3}$ $^{+1.6}_{-1.1}$ ± 0.4	[33] ABAZOV	05X	D0	ℓ + jets / kinematics
5.3 ± 3.3 $^{+1.3}_{-1.0}$	[34] ACOSTA	05S	CDF	ℓ + jets / soft μ b-tag
6.6 ± 1.1 ± 1.5	[35] ACOSTA	05T	CDF	ℓ + jets / kinematics
6.0 $^{+1.5}_{-1.6}$ $^{+1.2}_{-1.3}$	[36] ACOSTA	05U	CDF	ℓ + jets/kinematics + vtx b-tag
5.6 $^{+1.2}_{-1.1}$ $^{+0.9}_{-0.6}$	[37] ACOSTA	05V	CDF	ℓ + n jets
7.0 $^{+2.4}_{-2.1}$ $^{+1.6}_{-1.1}$ ± 0.4	[38] ACOSTA	04I	CDF	di-lepton + jets + missing ET

[1] Based on 8.8 fb^{-1} of $p\overline{p}$ collisions at $\sqrt{s} = 1.96$ TeV.

[2] Based on 8.7 fb^{-1} of $p\overline{p}$ collisions at $\sqrt{s} = 1.96$ TeV. Measure the $t\overline{t}$ cross section simultaneously with the fraction of $t \to Wb$ decays. The correlation coefficient between those two measurements is -0.434. Assume unitarity of the 3×3 CKM matrix and set $|V_{tb}| > 0.89$ at 95% CL.

[3] Based on 2.2 fb^{-1} of data in $p\overline{p}$ collisions at 1.96 TeV. The result assumes the acceptance for $m_t = 172.5$ GeV.

[4] Based on 1.12 fb^{-1} and assumes $m_t = 175$ GeV, where the cross section changes by ± 0.1 pb for every ∓ 1 GeV shift in m_t. AALTONEN 11D fits simultaneously the $t\overline{t}$ production cross section and the b-tagging efficiency and find improvements in both measurements.

[5] Based on 2.7 fb^{-1}. The first error is from statistics and systematics, the second is from luminosity. The result is for $m_t = 175$ GeV. AALTONEN 11W fits simultaneously a jet flavor discriminator between b-, c-, and light-quarks, and find significant reduction in the systematic error.

[6] Based on 2.2 fb^{-1}. The result is for $m_t = 172.5$ GeV. AALTONEN 11Y selects multi-jet events with large $\not\!\!E_T$, and vetoes identified electrons and muons.

[7] Based on 5.3 fb^{-1}. The error is statistical + systematic + luminosity combined. The result is for $m_t = 172.5$ GeV. The results for other m_t values are given in Table XII and eq.(10) of ABAZOV 11E.

[8] Combination of a dilepton measurement presented in ABAZOV 11Z (based on 5.4 fb^{-1}), which yields $7.36^{+0.90}_{-0.79}$ (stat+syst) pb, and the lepton + jets measurement of ABAZOV 11E. The result is for $m_t = 172.5$ GeV. The results for other m_t values is given by eq.(5) of ABAZOV 11A.

[9] Based on 2.8 fb^{-1}. The result is for $m_t = 175$ GeV.

[10] Based on 2.9 fb^{-1}. Result is obtained from the fraction of signal events in the top quark mass measurement in the all hadronic decay channel.

[11] Based on 1.7 fb^{-1}. The result is for $m_t = 175$ GeV. AALTONEN 10V uses soft electrons from b-hadron decays to suppress W+jets background events.

[12] Based on 4.6 fb^{-1}. The result is for $m_t = 172.5$ GeV. The ratio $\sigma(t\overline{t} \to \ell$+jets) / $\sigma(Z/\gamma^* \to \ell\ell)$ is measured and then multiplied by the theoretical $Z/\gamma^* \to \ell\ell$ cross section of $\sigma(Z/\gamma^* \to \ell\ell) = 251.3 \pm 5.0$ pb, which is free from the luminosity error.

[13] Based on 1 fb^{-1}. The result is for $m_t = 175$ GeV. 7.9 ± 2.3 pb is found for $m_t = 170$ GeV. ABAZOV 10I uses a likelihood discriminant to separate signal from background, where the background model was created from lower jet-multiplicity data.

[14] Based on 1 fb^{-1}. The result is for $m_t = 170$ GeV. For $m_t = 175$ GeV, the result is $6.3^{+1.2}_{-1.1}$(stat)$\pm$0.7(syst)$\pm$0.4(lumi) pb. Cross section of $t\overline{t}$ production has been measured in the $t\overline{t} \to \tau_h +$ jets topology, where τ_h denotes hadronically decaying τ leptons. The result for the cross section times the branching ratio is $\sigma(t\overline{t}) \cdot$ B($t\overline{t} \to \tau_h +$ jets) $= 0.60^{+0.23+0.15}_{-0.22-0.14} \pm 0.04$ pb for $m_t = 170$ GeV.

[15] Based on 1.1 fb^{-1}. The result is for B($W \to \ell\nu$) = 10.8% and $m_t = 175$ GeV; the mean value is 9.8 for $m_t = 172.5$ GeV and 10.1 for $m_t = 170$ GeV. AALTONEN 09AD used high p_T e or μ with an isolated track to select $t\overline{t}$ decays into dileptons including $\ell = \tau$. The result is based on the candidate event samples with and without vertex b-tag.

[16] Based on 2 fb^{-1}. The result is for $m_t = 175$ GeV; the mean value is 3% higher for $m_t = 170$ GeV and 4% lower for $m_t = 180$ GeV.

[17] Result is based on 1 fb^{-1} of data. The result is for $m_t = 170$ GeV, and the mean value decreases with increasing m_t; see their Fig. 2. The result is obtained after combining ℓ + jets, $\ell\ell$, and $\ell\tau$ final states, and the ratios of the extracted cross sections are $R^{\ell\ell/\ell j} = 0.86^{+0.19}_{-0.17}$ and $R^{\ell\tau/\ell\ell-\ell j} = 0.97^{+0.32}_{-0.29}$, consistent with the SM expectation of R = 1. This leads to the upper bound of B($t \to bH^+$) as a function of m_{H^+}. Results are shown in their Fig. 1 for B($H^+ \to \tau\nu$) = 1 and B($H^+ \to c\overline{s}$) = 1 cases. Comparison of the m_t dependence of the extracted cross section and a partial NNLO prediction gives $m_t = 169.1^{+5.9}_{-5.2}$ GeV.

[18] Result is based on 1 fb^{-1} of data. The result is for $m_t = 170$ GeV, and the mean value changes by -0.07 [m_t(GeV)$-$170] pb near the reference m_t value. Comparison of the m_t dependence of the extracted cross section and a partial NNLO QCD prediction gives $m_t = 171.5^{+9.9}_{-8.8}$ GeV. The $\ell\tau$ channel alone gives $7.6^{+4.9+3.5+1.4}_{-4.3-3.4-0.9}$ pb and the $\ell\ell$ channel gives $7.5^{+1.2+0.7+0.7}_{-1.1-0.6-0.5}$ pb.

[19] Result is based on 0.9 fb^{-1} of data. The first error is from stat + syst, while the latter error is from luminosity. The result is for m_t=175 GeV, and the mean value changes by -0.09 pb·[m_t(GeV)$-$175].

[20] Result is based on 0.9 fb^{-1} of data. The cross section is obtained from the $\ell + \geq 3$ jet event rates with 1 or 2 b-tag, and also from the kinematical likelihood analysis of the $\ell + 3$, 4 jet events. The result is for m_t= 172.6 GeV, and its m_t dependence shown in Fig. 3 leads to the constraint $m_t = 170 \pm 7$ GeV when compared to the SM prediction.

[21] Result is based on 360 pb^{-1} of data. Events with high p_T oppositely charged dileptons $\ell^+\ell^-$ ($\ell = e, \mu$) are used to obtain cross sections for $t\overline{t}$, W^+W^-, and $Z \to \tau^+\tau^-$ production processes simultaneously. The other cross sections are given in Table IV.

[22] Based on 1.02 fb^{-1} of data. Result is for $m_t = 175$ GeV. Secondary vertex b-tag and neural network selections are used to achieve a signal-to-background ratio of about 1/2.

[23] Based on 425 pb^{-1} of data. Result is for $m_t = 175$ GeV. For $m_t = 170.9$ GeV, 7.8 ± 1.8(stat + syst) pb is obtained.

[24] Based on 405 $\pm$ 25 pb^{-1} of data. Result is for $m_t = 175$ GeV. The last error is for luminosity. Secondary vertex b-tag and neural network are used to separate the signal events from the background.

[25] Based on 425 pb^{-1} of data. Assumes $m_t = 175$ GeV.

[26] Based on $\sim$ 425 pb^{-1}. Assuming $m_t = 175$ GeV. The first error is combined statistical and systematic, the second one is luminosity.

[27] Based on $\sim$ 318 pb^{-1}. Assuming $m_t = 178$ GeV. The cross section changes by ± 0.08 pb for each ∓ 1 GeV change in the assumed m_t. Result is for at least one b-tag. For at least two b-tagged jets, $t\overline{t}$ signal of significance greater than 5σ is found, and the cross section is $10.1^{+1.6+2.0}_{-1.4-1.3}$ pb for $m_t = 178$ GeV.

[28] Based on $\sim$ 311 pb^{-1}. Assuming $m_t = 178$ GeV. For $m_t = 175$ GeV, the result is $6.0 \pm 1.2^{+0.9}_{-0.7}$. This is the first CDF measurement without lepton identification, and hence it has sensitivity to the $W \to \tau\nu$ mode.

[29] ABULENCIA,A 06E measures the $t\overline{t}$ production cross section in the all hadronic decay mode by selecting events with 6 to 8 jets and at least one b-jet. S/B = 1/5 has been achieved. Based on 311 pb^{-1}. Assuming $m_t = 178$ GeV.

[30] Based on $\sim$ 318 pb^{-1}. Assuming $m_t = 178$ GeV. Result is for at least one b-tag. For at least two b-tagged jets, the cross section is $11.1^{+2.3+2.5}_{-1.9-1.9}$ pb.

[31] ABAZOV 05Q measures the top-quark pair production cross section with $\sim$ 230 pb^{-1} of data, based on the analysis of W plus n-jet events where W decays into e or μ plus neutrino, and at least one of the jets is b-jet like. The first error is statistical and systematic, and the second accounts for the luminosity uncertainty. The result assumes $m_t = 175$ GeV; the mean value changes by (175$-m_t$(GeV)) $\times$ 0.06 pb in the mass range 160 to 190 GeV.

[32] ABAZOV 05R measures the top-quark pair production cross section with 224–243 pb^{-1} of data, based on the analysis of events with two charged leptons in the final state. The result assumes $m_t = 175$ GeV; the mean value changes by (175$-m_t$(GeV)) $\times$ 0.08 pb in the mass range 160 to 190 GeV.

[33] Based on 230 pb^{-1}. Assuming $m_t = 175$ GeV.

[34] Based on 194 pb^{-1}. Assuming $m_t = 175$ GeV.

[35] Based on 194 $\pm$ 11 pb^{-1}. Assuming $m_t = 175$ GeV.

[36] Based on 162 $\pm$ 10 pb^{-1}. Assuming $m_t = 175$ GeV.

[37] ACOSTA 05V measures the top-quark pair production cross section with $\sim$ 162 pb^{-1} data, based on the analysis of W plus n-jet events where W decays into e or μ plus neutrino, and at least one of the jets is b-jet like. Assumes $m_t = 175$ GeV.

[38] ACOSTA 04I measures the top-quark pair production cross section with 197 $\pm$ 12 pb^{-1} data, based on the analysis of events with two charged leptons in the final state. Assumes $m_t = 175$ GeV.

Ratio of the Production Cross Sections of $t\overline{t}\gamma$ to $t\overline{t}$ at $\sqrt{s} = 1.96$ TeV

VALUE	DOCUMENT ID		TECN	COMMENT
• • • We do not use the following data for averages, fits, limits, etc. • • •				
0.024 ± 0.009	[1] AALTONEN	11Z	CDF	$E_T(\gamma) > 10$ GeV, $\lvert\eta(\gamma)\rvert < 1.0$

[1] Based on 6.0 fb^{-1} of data. The error is statistical and systematic combined. Events with lepton + $\not\!\!E_T$ + ≥ 3 jets($\geq 1b$) with and without central, high E_T photon are measured. The result is consistent with the SM prediction of 0.024 ± 0.005. The absolute production cross section is measured to be 0.18 ± 0.08 fb. The statistical significance is 3.0 standard deviations.

$t\overline{t}$ Production Cross Section in pp Collisions at $\sqrt{s} = 7$ TeV

Unless otherwise noted the first quoted error is from statistics, the second from systematic uncertainties, and the third from luminosity. If only two errors are quoted the luminosity is included in the systematic uncertainties.

VALUE (pb)	DOCUMENT ID		TECN	COMMENT
• • • We do not use the following data for averages, fits, limits, etc. • • •				
194 ± 18 ± 46	[1] AAD	13X	ATLS	$\tau_h + \not\!\!E_T + \geq 5$j ($\geq 2b$)
139 ± 10 ± 26	[2] CHATRCHYAN	13AY	CMS	≥ 6 jets with 2 b-tags
$158.1 \pm 2.1 \pm 10.8$	[3] CHATRCHYAN	13BB	CMS	$\ell + \not\!\!E_T$ + jets(≥ 1 b-tag)
152 ± 12 ± 32	[4] CHATRCHYAN	13BE	CMS	τ_h+ $\not\!\!E_T$+ ≥ 4 jets (≥ 1 b)
177 ± 20 ± 14 ± 7	[5] AAD	12B	ATLS	Repl. by AAD 12BF
176 ± 5 $^{+14}_{-11}$ ± 8	[6] AAD	12BF	ATLS	$\ell\ell$+$\not\!\!E_T$+ ≥ 2j
187 ± 11 $^{+18}_{-17}$ ± 6	[7] AAD	12BO	ATLS	$\ell + \not\!\!E_T + \geq 3$j with b-tag
186 ± 13 ± 20 ± 7	[8] AAD	12CG	ATLS	$\ell + \tau_h$+ $\not\!\!E_T$+ ≥ 2j ($\geq 1b$)
143 ± 14 ± 22 ± 3	[9] CHATRCHYAN	12AC	CMS	$\ell + \tau_h$+ $\not\!\!E_T$+ ≥ 2j ($\geq 1b$)
$161.9 \pm 2.5^{+5.1}_{-5.0} \pm 3.6$	[10] CHATRCHYAN	12AX	CMS	$\ell\ell + \not\!\!E_T + \geq 2b$
145 ± 31 $^{+42}_{-27}$	[11] AAD	11A	ATLS	ℓ+$\not\!\!E_T$+ ≥ 4j, $\ell\ell$+$\not\!\!E_T$+ ≥ 2j
173 $^{+39}_{-32}$ ± 7	[12] CHATRCHYAN	11AA	CMS	$\ell + \not\!\!E_T + \geq 3$ jets
168 ± 18 ± 14 ± 7	[13] CHATRCHYAN	11F	CMS	$\ell\ell + \not\!\!E_T$ + jets
154 ± 17 ± 6	[14] CHATRCHYAN	11Z	CMS	Combination
194 ± 72 ± 24 ± 21	[15] KHACHATRY...	11A	CMS	$\ell\ell + \not\!\!E_T + \geq 2$ jets

[1] Based on 1.67 fb^{-1} of data. The result uses the acceptance for m_t = 172.5 GeV.
[2] Based on 3.54 fb^{-1} of data.
[3] Based on 2.3 fb^{-1} of data.
[4] Based on 3.9 fb^{-1} of data.
[5] Based on 35 pb^{-1} of data for an assumed top quark mass of m_t = 172.5 GeV.
[6] Based on 0.70 fb^{-1} of data. The 3 errors are from statistics, systematics, and luminosity. The result uses the acceptance for m_t = 172.5 GeV.
[7] Based on 35 pb^{-1} of data. The 3 errors are from statistics, systematics, and luminosity. The result uses the acceptance for m_t = 172.5 GeV and 173 $\pm$ 17$^{+18}_{-16}$ $\pm$ 6 pb is found without the b-tag.
[8] Based on 2.05 fb^{-1} of data. The hadronic τ candidates are selected using a BDT technique. The 3 errors are from statistics, systematics, and luminosity. The result uses the acceptance for m_t = 172.5 GeV.
[9] Based on 2.0 fb^{-1} and 2.2 fb^{-1} of data for $\ell = e$ and $\ell = \mu$, respectively. The 3 errors are from statistics, systematics, and luminosity. The result uses the acceptance for m_t = 172.5 GeV.
[10] Based on 2.3 fb^{-1} of data. The 3 errors are from statistics, systematics, and luminosity. The result uses the profile likelihood-ratio (PLB) method and an assumed m_t of 172.5 GeV.
[11] Based on 2.9 pb^{-1} of data. The result for single lepton channels is 142 $\pm$ 34$^{+50}_{-31}$ pb, while for the dilepton channels is 151$^{+78}_{-62}$ $\pm$ 37$^{+37}_{-24}$ pb.
[12] Result is based on 36 pb^{-1} of data. The first uncertainty corresponds to the statistical and systematic uncertainties, and the second corresponds to the luminosity.
[13] Based on 36 pb^{-1} of data. The ratio of $t\overline{t}$ and Z/γ^* cross sections is measured as $\sigma(pp \to t\overline{t})/\sigma(pp \to Z/\gamma^* \to e^+e^-/\mu^+\mu^-)$ = 0.175 $\pm$ 0.018(stat) $\pm$ 0.015(syst) for 60 < $m_{\ell\ell}$ < 120 GeV, for which they use an NNLO prediction for the denominator cross section of 972 $\pm$ 42 pb.
[14] Result is based on 36 pb^{-1} of data. The first error is from statistical and systematic uncertainties, and the second from luminosity. This is a combination of a measurement in the dilepton channel (CHATRCHYAN 11F) and the measurement in the ℓ + jets channel (CHATRCHYAN 11Z) which yields 150 $\pm$ 9 $\pm$ 17 $\pm$ 6 pb.
[15] Result is based on 3.1 $\pm$ 0.3 pb^{-1} of data.

tt Production Cross Section in pp Collisions at $\sqrt{s}$ = 7 TeV

VALUE (pb)	CL%	DOCUMENT ID		TECN	COMMENT
• • • We do not use the following data for averages, fits, limits, etc. • • •					
<1.7	95	[1] AAD	12BE	ATLS	$\ell^+\ell^+ + \not{E}_T + \geq 2$j +HT

[1] Based on 1.04 fb^{-1} of pp data at $\sqrt{s}$ = 7 TeV. The upper bounds are the same for LL, LR and RR chiral components of the two top quarks.

f(Q$_0$): $t\overline{t}$ Fraction of Events with a Veto on Additional Central Jet Activity in pp Collisions at $\sqrt{s}$ = 7 TeV

VALUE (%)	DOCUMENT ID		TECN	COMMENT
• • • We do not use the following data for averages, fits, limits, etc. • • •				
56.4 $\pm$ 1.3$^{+2.6}_{-2.8}$	[1] AAD	12BL	ATLS	Q_0 = 25 GeV ($\lvert y\rvert$ <2.1)
84.7 $\pm$ 0.9 $\pm$ 1.0	[1] AAD	12BL	ATLS	Q_0 = 75 GeV ($\lvert y\rvert$ <2.1)
95.2$^{+0.5}_{-0.6}$ $\pm$ 0.4	[1] AAD	12BL	ATLS	Q_0= 150 GeV ($\lvert y\rvert$ <2.1)

[1] Based on 2.05 fb^{-1} of data. The $t\overline{t}$ events are selected in the dilepton decay channel with two identified b-jets.

$t\overline{t}$ Charge Asymmetry (A$_C$) in pp Collisions at $\sqrt{s}$ = 7 TeV

A_C = (N($\Delta|y|$ >0) − N($\Delta|y|$ <0)) / (N($\Delta|y|$ >0) + N($\Delta|y|$ <0)) where $\Delta|y| = |y_t| - |y_{\overline{t}}|$ is the difference between the absolute values of the top and antitop rapidities and N is the number of events with $\Delta|y|$ positive or negative.

VALUE (%)	DOCUMENT ID		TECN	COMMENT
• • • We do not use the following data for averages, fits, limits, etc. • • •				
−1.9 $\pm$ 2.8 $\pm$ 2.4	[1] AAD	12BK	ATLS	$\ell + \not{E}_T + \geq$ 4j ($\geq$ 1b)
0.4 $\pm$ 1.0 $\pm$ 1.1	[2] CHATRCHYAN	12BB	CMS	$\ell + \not{E}_T + \geq$ 4j ($\geq$ 1b)
−1.3 $\pm$ 2.8$^{+2.9}_{-3.1}$	[3] CHATRCHYAN	12BS	CMS	$\ell + \not{E}_T + \geq$ 4j ($\geq$ 1b)

[1] Based on 1.04 fb^{-1} of data. The result is consistent with A_C = 0.006 $\pm$ 0.002 (MC at NLO). No significant dependence of A_C on $m_{t\overline{t}}$ is observed.
[2] Based on 5.0 fb^{-1} of data at 7 TeV.
[3] Based on 1.09 fb^{-1} of data. The result is consistent with the SM predictions.

t-quark Polarization in $t\overline{t}$ Events in pp Collisions at $\sqrt{s}$ = 7 TeV

The double differential distribution in polar angles, θ_1 (θ_2) of the decay particle of the top (anti-top) decay products, is parametrized as $(1/\sigma)d\sigma/(d\cos\theta_1\ d\cos\theta_2) = (1/4)\ (1 + A_t \cos\theta_1 + A_{\overline{t}} \cos\theta_2 - C \cos\theta_1 \cos\theta_2)$. The charged lepton is used to tag t or $\overline{t}$. The coefficient A_t and $A_{\overline{t}}$ measure the average helicity of t and $\overline{t}$, respectively. A_{CPC} assumes CP conservation, whereas A_{CPV} corresponds to maximal CP violation.

VALUE	DOCUMENT ID		TECN	COMMENT
• • • We do not use the following data for averages, fits, limits, etc. • • •				
−0.035 $\pm$ 0.014 $\pm$ 0.037	[1] AAD	13BE	ATLS	$A_{CPC} = A_t = A_{\overline{t}}$
0.020 $\pm$ 0.016$^{+0.013}_{-0.017}$	[1] AAD	13BE	ATLS	$A_{CPV} = A_t = -A_{\overline{t}}$

[1] Based on 4.7 fb^{-1} of data using the final states containing one or two isolated electrons or muons and jets with at least one b-tag.

$gg \to t\overline{t}$ Fraction in $p\overline{p}$ Collisions at $\sqrt{s}$ = 1.96 TeV

VALUE	CL%	DOCUMENT ID		TECN	COMMENT
• • • We do not use the following data for averages, fits, limits, etc. • • •					
<0.33	68	[1] AALTONEN	09F	CDF	$t\overline{t}$ correlations
0.07 $\pm$ 0.14 $\pm$ 0.07		[2] AALTONEN	08AG	CDF	low p_T number of tracks

[1] Based on 955 pb^{-1}. AALTONEN 09F used differences in the $t\overline{t}$ production angular distribution and polarization correlation to descriminate between $gg \to t\overline{t}$ and $q\overline{q} \to t\overline{t}$ subprocesses. The combination with the result of AALTONEN 08AG gives 0.07$^{+0.15}_{-0.07}$.
[2] Result is based on 0.96 fb^{-1} of data. The contribution of the subprocesses $gg \to t\overline{t}$ and $q\overline{q} \to t\overline{t}$ is distinguished by using the difference between quark and gluon initiated jets in the number of small p_T (0.3 GeV < p_T < 3 GeV) charged particles in the central region ($|\eta|$ < 1.1).

A_{FB} of $t\overline{t}$ in $p\overline{p}$ Collisions at $\sqrt{s}$ = 1.96 TeV

VALUE (%)	DOCUMENT ID		TECN	COMMENT
• • • We do not use the following data for averages, fits, limits, etc. • • •				
20.1 $\pm$ 6.7	[1] AALTONEN	13AD	CDF	a_1/a_0 in ℓ+$\not{E}_T$+ $\geq$ 4j ($\geq$ 1b)
− 0.2 $\pm$ 3.1	[1] AALTONEN	13AD	CDF	a_3,a_5,a_7 in ℓ+$\not{E}_T$+ $\geq$ 4j ($\geq$ 1b)
16.4 $\pm$ 4.7	[2] AALTONEN	13S	CDF	$\ell + \not{E}_T + \geq$ 4 jets($\geq$ 1b-tag)
9.4$^{+\ 3.2}_{-\ 2.9}$	[3] AALTONEN	13X	CDF	$\ell + \not{E}_T + \geq$ 4 jets ($\geq$ 1 b-tag)
11.8 $\pm$ 3.2	[4] ABAZOV	13A	D0	$\ell\ell$ & ℓ+ jets comb.
−11.6 $\pm$ 15.3	[5] AALTONEN	11F	CDF	$m_{t\overline{t}}$ < 450 GeV
47.5 $\pm$ 11.4	[5] AALTONEN	11F	CDF	$m_{t\overline{t}}$ > 450 GeV
19.6 $\pm$ 6.5	[6] ABAZOV	11AH	D0	$\ell + \not{E}_T + \geq$ 4 jets($\geq$ 1b-tag)
17 $\pm$ 8	[7] AALTONEN	08AB	CDF	$p\overline{p}$ frame
24 $\pm$ 14	[7] AALTONEN	08AB	CDF	$t\overline{t}$ frame
12 $\pm$ 8 $\pm$ 1	[8] ABAZOV	08L	D0	$\ell + \not{E}_T + \geq$ 4 jets

[1] Based on 9.4 fb^{-1} of data. Reported A_{FB} values come from the determination of a_i coefficients of $d\sigma/d(\cos\theta_t) = \Sigma_i\ a_i P_i(\cos(\theta_t))$ measurement. The result of a_1/a_0 = (40 $\pm$ 12)% seems higher than the NLO SM prediction of (15$^{+\ 7}_{-\ 3}$)%.
[2] Based on 9.4 fb^{-1} of data. The quoted result is the asymmetry at the parton level.
[3] Based on 9.4 fb^{-1} of data. The observed asymmetry is to be compared with the SM prediction of A^{ℓ}_{FB} = 0.038 $\pm$ 0.003.
[4] Based on 5.4 fb^{-1} of data. ABAZOV 13A studied the dilepton channel of the $t\overline{t}$ events and measured the leptonic forward-backward asymmetry to be A^{ℓ}_{FB} = 5.8 $\pm$ 5.1 $\pm$ 1.3%, which is consistent with the SM (QCD+EW) prediction of 4.7 $\pm$ 0.1%. The result is obtained after combining the measurement (15.2 $\pm$ 4.0%) in the ℓ + jets channel ABAZOV 11AH. The top quark helicity is measured by using the neutrino weighting method to be consistent with zero in both dilepton and ℓ + jets channels.
[5] Based on 5.3 fb^{-1} of data. The error is statistical and systematic combined. Events with lepton + $\not{E}_T$ + $\geq$ 4jets($\geq$ 1b) are used. AALTONEN 11F also measures the asymmetry as a function of the rapidity difference $|y_t - y_{\overline{t}}|$. The NLO QCD predictions [MCFM] are (4.0 $\pm$ 0.6)% and (8.8 $\pm$ 1.3)% for $m_{t\overline{t}}$ < 450 and > 450 GeV, respectively.
[6] Based on 5.4 fb^{-1} of data. The error is statistical and systematic combined. The quoted asymmetry is obtained after unfolding to be compared with the MC@NLO prediction of (5.0 $\pm$ 0.1)%. No significant difference between the $m_{t\overline{t}}$ < 450 and > 450 GeV data samples is found. A corrected asymmetry based on the lepton from a top quark decay of (15.2 $\pm$ 4.0)% is measured to be compared to the MC@NLO prediction of (2.1 $\pm$ 0.1)%.
[7] Result is based on 1.9 fb^{-1} of data. The FB asymmetry in the $t\overline{t}$ events has been measured in the ℓ + jets mode, where the lepton charge is used as the flavor tag. The asymmetry in the $p\overline{p}$ frame is defined in terms of cos(θ) of hadronically decaying t-quark momentum, whereas that in the $t\overline{t}$ frame is defined in terms of the t and $\overline{t}$ rapidity difference. The results are consistent ($\leq$ 2 σ) with the SM predictions.
[8] Result is based on 0.9 fb^{-1} of data. The asymmetry in the number of $t\overline{t}$ events with $y_t > y_{\overline{t}}$ and those with $y_t < y_{\overline{t}}$ has been measured in the lepton + jets final state. The observed value is consistent with the SM prediction of 0.8% by MC@NLO, and an upper bound on the $Z' \to t\overline{t}$ contribution for the SM Z-like couplings is given in in Fig. 2 for 350 GeV < $m_{Z'}$ < 1 TeV.

t-Quark Electric Charge

VALUE	DOCUMENT ID		TECN	COMMENT
0.64 $\pm$ 0.02 $\pm$ 0.08	[1] AAD	13AY	ATLS	ℓ+$\not{E}_T$+ $\geq$ 4 jets ($\geq$ 1 b)
• • • We do not use the following data for averages, fits, limits, etc. • • •				
	[2] AALTONEN	13J	CDF	$p\overline{p}$ at 1.96 TeV
	[3] AALTONEN	10S	CDF	Repl. by AALTONEN 13J
	[4] ABAZOV	07C	D0	fraction of |q|=4e/3 pair

[1] Based on 2.05 fb^{-1} of pp data at $\sqrt{s}$ = 7 TeV, the result is obtained by reconstructing $t\overline{t}$ events in the lepton + jets final state, where b-jet charges are tagged by the jet-charge algorithm. This measurement excludes the charge −4/3 assignment to the top quark at more than 8 standard deviations.
[2] AALTONEN 13J excludes the charge −4/3 assignment to the top quark at 99% CL, using 5.6 fb^{-1} of data in $p\overline{p}$ collisions at $\sqrt{s}$ = 1.96 TeV. Result is obtained by reconstructing $t\overline{t}$ events in the lepton + jets final state, where b-jet charges are tagged by the jet-charge algorithm.
[3] AALTONEN 10S excludes the charge −4/3 assignment for the top quark [CHANG 99] at 95%CL, using 2.7 fb^{-1} of data in $p\overline{p}$ collisions at $\sqrt{s}$ = 1.96 TeV. Result is obtained by reconstructing $t\overline{t}$ events in the lepton + jets final state, where b-jet charges are tagged by the SLT (soft lepton tag) algorithm.
[4] ABAZOV 07C reports an upper limit ρ < 0.80 (90% CL) on the fraction ρ of exotic quark pairs $Q\overline{Q}$ with electric charge $|q|$ = 4e/3 in $t\overline{t}$ candidate events with high p_T lepton, missing E_T and $\geq$ 4 jets. The result is obtained by measuring the fraction of events in which the quark pair decays into $W^- + b$ and $W^+ + \overline{b}$, where b and $\overline{b}$ jets are discriminated by using the charge and momenta of tracks within the jet cones. The maximum CL at which the model of CHANG 99 can be excluded is 92%. Based on 370 pb^{-1} of data at $\sqrt{s}$ = 1.96 TeV.

See key on page 547

t-Quark REFERENCES

AAD	14	PL B728 363	G. Aad *et al.*	(ATLAS Collab.)
CHATRCHYAN	14	PL B728 496	S. Chatrchyan *et al.*	(CMS Collab.)
AAD	13AY	JHEP 1311 031	G. Aad *et al.*	(ATLAS Collab.)
AAD	13BE	PRL 111 232002	G. Aad *et al.*	(ATLAS Collab.)
AAD	13X	EPJ C73 2328	G. Aad *et al.*	(ATLAS Collab.)
AALTONEN	13AB	PR D88 091103	T. Aaltonen *et al.*	(CDF Collab.)
AALTONEN	13AD	PRL 111 182002	T. Aaltonen *et al.*	(CDF Collab.)
AALTONEN	13D	PR D87 031104	T. Aaltonen *et al.*	(CDF Collab.)
AALTONEN	13E	PR D87 052013	T. Aaltonen *et al.*	(CDF Collab.)
AALTONEN	13G	PR D87 111101	T. Aaltonen *et al.*	(CDF Collab.)
AALTONEN	13H	PR D88 011101	T. Aaltonen *et al.*	(CDF Collab.)
AALTONEN	13J	PR D88 032003	T. Aaltonen *et al.*	(CDF Collab.)
AALTONEN	13S	PR D87 092002	T. Aaltonen *et al.*	(CDF Collab.)
AALTONEN	13X	PR D88 072003	T. Aaltonen *et al.*	(CDF Collab.)
AALTONEN	13Z	PRL 111 202001	T. Aaltonen *et al.*	(CDF Collab.)
ABAZOV	13A	PR D87 011103	V.M. Abazov *et al.*	(D0 Collab.)
ABAZOV	13O	PL B726 656	V.M. Abazov *et al.*	(D0 Collab.)
CHATRCHYAN	13AY	JHEP 1305 065	S. Chatrchyan *et al.*	(CMS Collab.)
CHATRCHYAN	13BB	PL B720 83	S. Chatrchyan *et al.*	(CMS Collab.)
CHATRCHYAN	13BE	EPJ C73 2386	S. Chatrchyan *et al.*	(CMS Collab.)
CHATRCHYAN	13BH	JHEP 1310 167	S. Chatrchyan *et al.*	(CMS Collab.)
CHATRCHYAN	13C	PRL 110 022003	S. Chatrchyan *et al.*	(CMS Collab.)
CHATRCHYAN	13F	PL B718 1252	S. Chatrchyan *et al.*	(CMS Collab.)
CHATRCHYAN	13S	EPJ C73 2494	S. Chatrchyan *et al.*	(CMS Collab.)
AAD	12B	PL B707 459	G. Aad *et al.*	(ATLAS Collab.)
AAD	12BE	JHEP 1204 069	G. Aad *et al.*	(ATLAS Collab.)
AAD	12BF	JHEP 1205 059	G. Aad *et al.*	(ATLAS Collab.)
AAD	12BG	JHEP 1206 088	G. Aad *et al.*	(ATLAS Collab.)
AAD	12BK	EPJ C72 2039	G. Aad *et al.*	(ATLAS Collab.)
AAD	12BL	EPJ C72 2043	G. Aad *et al.*	(ATLAS Collab.)
AAD	12BO	PL B711 244	G. Aad *et al.*	(ATLAS Collab.)
AAD	12BP	PL B712 351	G. Aad *et al.*	(ATLAS Collab.)
AAD	12BT	JHEP 1209 139	G. Aad *et al.*	(ATLAS Collab.)
AAD	12CG	PL B717 89	G. Aad *et al.*	(ATLAS Collab.)
AAD	12CH	PL B717 330	G. Aad *et al.*	(ATLAS Collab.)
AAD	12I	EPJ C72 2046	G. Aad *et al.*	(ATLAS Collab.)
AALTONEN	12AI	PRL 109 152003	T. Aaltonen *et al.*	(CDF Collab.)
AALTONEN	12AL	PRL 109 192001	T. Aaltonen *et al.*	(CDF Collab.)
AALTONEN	12AP	PR D86 092003	T. Aaltonen *et al.*	(CDF, D0 Collab.)
AALTONEN	12G	PL B714 24	T. Aaltonen *et al.*	(CDF Collab.)
AALTONEN	12Z	PR D85 071106	T. Aaltonen *et al.*	(CDF, D0 Collab.)
ABAZOV	12AB	PR D86 051103	V.M. Abazov *et al.*	(D0 Collab.)
ABAZOV	12B	PRL 108 032004	V.M. Abazov *et al.*	(D0 Collab.)
ABAZOV	12E	PL B708 21	V.M. Abazov *et al.*	(D0 Collab.)
ABAZOV	12I	PL B713 165	V.M. Abazov *et al.*	(D0 Collab.)
ABAZOV	12T	PR D85 091104	V.M. Abazov *et al.*	(D0 Collab.)
CHATRCHYAN	12AC	PR D85 112007	S. Chatrchyan *et al.*	(CMS Collab.)
CHATRCHYAN	12AX	JHEP 1211 067	S. Chatrchyan *et al.*	(CMS Collab.)
CHATRCHYAN	12BA	EPJ C72 2202	S. Chatrchyan *et al.*	(CMS Collab.)
CHATRCHYAN	12BB	PL B717 129	S. Chatrchyan *et al.*	(CMS Collab.)
CHATRCHYAN	12BP	JHEP 1212 105	S. Chatrchyan *et al.*	(CMS Collab.)
CHATRCHYAN	12BQ	JHEP 1212 035	S. Chatrchyan *et al.*	(CMS Collab.)
CHATRCHYAN	12BS	PL B709 28	S. Chatrchyan *et al.*	(CMS Collab.)
CHATRCHYAN	12Y	JHEP 1206 109	S. Chatrchyan *et al.*	(CMS Collab.)
AAD	11A	EPJ C71 1577	G. Aad *et al.*	(ATLAS Collab.)
AALTONEN	11AC	PR D84 071105	T. Aaltonen *et al.*	(CDF Collab.)
AALTONEN	11AK	PRL 107 232002	T. Aaltonen *et al.*	(CDF Collab.)
AALTONEN	11AR	PR D83 031104	T. Aaltonen *et al.*	(CDF Collab.)
AALTONEN	11D	PR D83 071102	T. Aaltonen *et al.*	(CDF Collab.)
AALTONEN	11E	PR D83 111101	T. Aaltonen *et al.*	(CDF Collab.)
AALTONEN	11F	PR D83 112003	T. Aaltonen *et al.*	(CDF Collab.)
AALTONEN	11K	PRL 106 152001	T. Aaltonen *et al.*	(CDF Collab.)
AALTONEN	11T	PL B698 371	T. Aaltonen *et al.*	(CDF Collab.)
AALTONEN	11W	PR D84 031101	T. Aaltonen *et al.*	(CDF Collab.)
AALTONEN	11Y	PR D84 032003	T. Aaltonen *et al.*	(CDF Collab.)
AALTONEN	11Z	PR D84 031104	T. Aaltonen *et al.*	(CDF Collab.)
ABAZOV	11A	PL B695 88	V.M. Abazov *et al.*	(D0 Collab.)
ABAZOV	11AA	PL B705 313	V.M. Abazov *et al.*	(D0 Collab.)
ABAZOV	11AD	PR D84 112001	V.M. Abazov *et al.*	(D0 Collab.)
ABAZOV	11AE	PRL 107 032001	V.M. Abazov *et al.*	(D0 Collab.)
ABAZOV	11AF	PL B702 16	V.M. Abazov *et al.*	(D0 Collab.)
ABAZOV	11AH	PR D84 112005	V.M. Abazov *et al.*	(D0 Collab.)
ABAZOV	11B	PRL 106 022001	V.M. Abazov *et al.*	(D0 Collab.)
ABAZOV	11C	PR D83 032009	V.M. Abazov *et al.*	(D0 Collab.)
ABAZOV	11E	PR D84 012008	V.M. Abazov *et al.*	(D0 Collab.)
ABAZOV	11M	PL B701 313	V.M. Abazov *et al.*	(D0 Collab.)
ABAZOV	11P	PR D84 032004	V.M. Abazov *et al.*	(D0 Collab.)
ABAZOV	11R	PRL 107 082004	V.M. Abazov *et al.*	(D0 Collab.)
ABAZOV	11S	PL B703 422	V.M. Abazov *et al.*	(D0 Collab.)
ABAZOV	11T	PR D84 052005	V.M. Abazov *et al.*	(D0 Collab.)
ABAZOV	11X	PRL 107 121802	V.M. Abazov *et al.*	(D0 Collab.)
ABAZOV	11Z	PL B704 403	V.M. Abazov *et al.*	(D0 Collab.)
CHATRCHYAN	11AA	EPJ C71 1721	S. Chatrchyan *et al.*	(CMS Collab.)
CHATRCHYAN	11F	JHEP 1107 049	S. Chatrchyan *et al.*	(CMS Collab.)
CHATRCHYAN	11R	PRL 107 091802	S. Chatrchyan *et al.*	(CMS Collab.)
CHATRCHYAN	11Z	PR D84 092004	S. Chatrchyan *et al.*	(CMS Collab.)
KHACHATRY...	11A	PL B695 424	V. Khachatryan *et al.*	(CMS Collab.)
AALTONEN	10AA	PR D82 052002	T. Aaltonen *et al.*	(CDF Collab.)
AALTONEN	10AB	PR D82 112005	T. Aaltonen *et al.*	(CDF Collab.)
AALTONEN	10AC	PRL 105 232003	T. Aaltonen *et al.*	(CDF Collab.)
AALTONEN	10AE	PRL 105 252001	T. Aaltonen *et al.*	(CDF Collab.)
AALTONEN	10C	PR D81 031102	T. Aaltonen *et al.*	(CDF Collab.)
AALTONEN	10D	PR D81 032002	T. Aaltonen *et al.*	(CDF Collab.)
AALTONEN	10E	PR D81 052011	T. Aaltonen *et al.*	(CDF Collab.)
AALTONEN	10Q	PRL 105 042002	T. Aaltonen *et al.*	(CDF Collab.)
AALTONEN	10S	PRL 105 101801	T. Aaltonen *et al.*	(CDF Collab.)
AALTONEN	10U	PR D81 072003	T. Aaltonen *et al.*	(CDF Collab.)
AALTONEN	10V	PR D81 092002	T. Aaltonen *et al.*	(CDF Collab.)
AALTONEN	10W	PRL 105 012001	T. Aaltonen *et al.*	(CDF Collab.)
ABAZOV	10	PL B682 363	V.M. Abazov *et al.*	(D0 Collab.)
ABAZOV	10I	PR D82 032002	V.M. Abazov *et al.*	(D0 Collab.)
ABAZOV	10J	PL B690 5	V.M. Abazov *et al.*	(D0 Collab.)
ABAZOV	10K	PL B693 81	V.M. Abazov *et al.*	(D0 Collab.)
ABAZOV	10Q	PR D82 071102	V.M. Abazov *et al.*	(D0 Collab.)
AHRENS	10	JHEP 1009 097	V. Ahrens *et al.*	(MANZ, HEIDH)
AHRENS	10A	NPBPS 205-206 48	V. Ahrens *et al.*	(MANZ, HEIDH)
AALTONEN	09AD	PR D79 112007	T. Aaltonen *et al.*	(CDF Collab.)
AALTONEN	09AK	PR D80 051104	T. Aaltonen *et al.*	(CDF Collab.)
AALTONEN	09AL	PR D80 052001	T. Aaltonen *et al.*	(CDF Collab.)
AALTONEN	09AT	PRL 103 092002	T. Aaltonen *et al.*	(CDF Collab.)
AALTONEN	09F	PR D79 031101	T. Aaltonen *et al.*	(CDF Collab.)
AALTONEN	09H	PR D79 052007	T. Aaltonen *et al.*	(CDF Collab.)
AALTONEN	09J	PR D79 072001	T. Aaltonen *et al.*	(CDF Collab.)
AALTONEN	09K	PR D79 072010	T. Aaltonen *et al.*	(CDF Collab.)
AALTONEN	09L	PR D79 092005	T. Aaltonen *et al.*	(CDF Collab.)
AALTONEN	09M	PRL 102 042001	T. Aaltonen *et al.*	(CDF Collab.)
AALTONEN	09N	PRL 102 151801	T. Aaltonen *et al.*	(CDF Collab.)
AALTONEN	09O	PRL 102 152001	T. Aaltonen *et al.*	(CDF Collab.)
AALTONEN	09Q	PL B674 160	T. Aaltonen *et al.*	(CDF Collab.)
AALTONEN	09X	PR D79 072005	T. Aaltonen *et al.*	(CDF Collab.)
AARON	09A	PL B678 450	F.D. Aaron *et al.*	(H1 Collab.)
ABAZOV	09AA	PRL 103 132001	V.M. Abazov *et al.*	(D0 Collab.)
ABAZOV	09AG	PR D80 071102	V.M. Abazov *et al.*	(D0 Collab.)
ABAZOV	09AH	PR D80 092006	V.M. Abazov *et al.*	(D0 Collab.)
ABAZOV	09J	PRL 102 092002	V.M. Abazov *et al.*	(D0 Collab.)
ABAZOV	09R	PL B679 177	V.M. Abazov *et al.*	(D0 Collab.)
ABAZOV	09Z	PRL 103 092001	V.M. Abazov *et al.*	(D0 Collab.)
LANGENFELD	09	PR D80 054009	U. Langenfeld, S. Moch, P. Uwer	
AALTONEN	08AB	PRL 101 202001	T. Aaltonen *et al.*	(CDF Collab.)
AALTONEN	08AD	PRL 101 192002	T. Aaltonen *et al.*	(CDF Collab.)
AALTONEN	08AG	PR D78 111101	T. Aaltonen *et al.*	(CDF Collab.)
AALTONEN	08AH	PRL 101 252001	T. Aaltonen *et al.*	(CDF Collab.)
AALTONEN	08C	PRL 100 062005	T. Aaltonen *et al.*	(CDF Collab.)
ABAZOV	08AH	PRL 101 182001	V.M. Abazov *et al.*	(D0 Collab.)
ABAZOV	08AI	PRL 101 221801	V.M. Abazov *et al.*	(D0 Collab.)
ABAZOV	08B	PRL 100 062004	V.M. Abazov *et al.*	(D0 Collab.)
ABAZOV	08I	PR D78 012005	V.M. Abazov *et al.*	(D0 Collab.)
ABAZOV	08L	PRL 100 142002	V.M. Abazov *et al.*	(D0 Collab.)
ABAZOV	08M	PRL 100 192003	V.M. Abazov *et al.*	(D0 Collab.)
ABAZOV	08N	PRL 100 192004	V.M. Abazov *et al.*	(D0 Collab.)
ABULENCIA	08	PR D78 012003	A. Abulencia *et al.*	(CDF Collab.)
CACCIARI	08	JHEP 0809 127	M. Cacciari *et al.*	
KIDONAKIS	08	PR D78 074005	N. Kidonakis, R. Vogt	
MOCH	08	PR D78 034003	S. Moch, P. Uwer	(BERL, KARLE)
AALTONEN	07	PRL 98 142001	T. Aaltonen *et al.*	(CDF Collab.)
AALTONEN	07B	PR D75 111103	T. Aaltonen *et al.*	(CDF Collab.)
AALTONEN	07D	PR D76 072009	T. Aaltonen *et al.*	(CDF Collab.)
AALTONEN	07I	PRL 99 182002	T. Aaltonen *et al.*	(CDF Collab.)
ABAZOV	07C	PRL 98 041801	V.M. Abazov *et al.*	(D0 Collab.)
ABAZOV	07D	PR D75 031102	V.M. Abazov *et al.*	(D0 Collab.)
ABAZOV	07F	PR D75 092001	V.M. Abazov *et al.*	(D0 Collab.)
ABAZOV	07H	PRL 98 181802	V.M. Abazov *et al.*	(D0 Collab.)
ABAZOV	07O	PR D76 052006	V.M. Abazov *et al.*	(D0 Collab.)
ABAZOV	07P	PR D76 072007	V.M. Abazov *et al.*	(D0 Collab.)
ABAZOV	07R	PR D76 092007	V.M. Abazov *et al.*	(D0 Collab.)
ABAZOV	07V	PRL 99 191802	V.M. Abazov *et al.*	(D0 Collab.)
ABAZOV	07W	PL B655 7	V.M. Abazov *et al.*	(D0 Collab.)
ABULENCIA	07D	PR D75 031105	A. Abulencia *et al.*	(CDF Collab.)
ABULENCIA	07G	PRL 98 072001	A. Abulencia *et al.*	(CDF Collab.)
ABULENCIA	07I	PR D75 052001	A. Abulencia *et al.*	(CDF Collab.)
ABULENCIA	07J	PR D75 071102	A. Abulencia *et al.*	(CDF Collab.)
ABAZOV	06K	PL B639 616	V.M. Abazov *et al.*	(D0 Collab.)
ABAZOV	06U	PR D74 092005	V.M. Abazov *et al.*	(D0 Collab.)
ABAZOV	06X	PR D74 112004	V.M. Abazov *et al.*	(D0 Collab.)
ABULENCIA	06D	PRL 96 022004	A. Abulencia *et al.*	(CDF Collab.)
Also		PR D73 032003	A. Abulencia *et al.*	(CDF Collab.)
Also		PR D73 092002	A. Abulencia *et al.*	(CDF Collab.)
ABULENCIA	06G	PRL 96 152002	A. Abulencia *et al.*	(CDF Collab.)
Also		PR D74 032009	A. Abulencia *et al.*	(CDF Collab.)
ABULENCIA	06R	PL B639 172	A. Abulencia *et al.*	(CDF Collab.)
ABULENCIA	06U	PR D73 111103	A. Abulencia *et al.*	(CDF Collab.)
ABULENCIA	06V	PR D73 112006	A. Abulencia *et al.*	(CDF Collab.)
ABULENCIA	06Z	PRL 97 082004	A. Abulencia *et al.*	(CDF Collab.)
ABULENCIA,A	06C	PRL 96 202002	A. Abulencia *et al.*	(CDF Collab.)
ABULENCIA,A	06E	PR D74 072005	A. Abulencia *et al.*	(CDF Collab.)
ABULENCIA,A	06F	PR D74 072006	A. Abulencia *et al.*	(CDF Collab.)
ABAZOV	05	PL B606 25	V.M. Abazov *et al.*	(D0 Collab.)
ABAZOV	05G	PL B617 1	V.M. Abazov *et al.*	(D0 Collab.)
ABAZOV	05L	PR D72 011104	V.M. Abazov *et al.*	(D0 Collab.)
ABAZOV	05P	PL B622 265	V.M. Abazov *et al.*	(D0 Collab.)
Also		PL B517 282	V.M. Abazov *et al.*	(D0 Collab.)
Also		PR D63 031101	B. Abbott *et al.*	(D0 Collab.)
Also		PR D75 092007	V.M. Abazov *et al.*	(D0 Collab.)
ABAZOV	05Q	PL B626 35	V.M. Abazov *et al.*	(D0 Collab.)
ABAZOV	05R	PL B626 55	V.M. Abazov *et al.*	(D0 Collab.)
ABAZOV	05X	PL B626 45	V.M. Abazov *et al.*	(D0 Collab.)
ACOSTA	05A	PRL 95 102002	D. Acosta *et al.*	(CDF Collab.)
ACOSTA	05D	PR D71 031101	D. Acosta *et al.*	(CDF Collab.)
ACOSTA	05N	PR D71 012005	D. Acosta *et al.*	(CDF Collab.)
ACOSTA	05S	PR D72 032002	D. Acosta *et al.*	(CDF Collab.)
ACOSTA	05T	PR D72 052003	D. Acosta *et al.*	(CDF Collab.)
ACOSTA	05U	PR D71 072005	D. Acosta *et al.*	(CDF Collab.)
ACOSTA	05V	PR D71 052003	D. Acosta *et al.*	(CDF Collab.)
ABAZOV	04G	NAT 429 638	V.M. Abazov *et al.*	(D0 Collab.)
ABDALLAH	04C	PL B590 21	J. Abdallah *et al.*	(DELPHI Collab.)
ACOSTA	04H	PR D69 052003	D. Acosta *et al.*	(CDF Collab.)
ACOSTA	04I	PRL 93 142001	D. Acosta *et al.*	(CDF Collab.)
AKTAS	04	EPJ C33 9	A. Aktas *et al.*	(H1 Collab.)
ABAZOV	03A	PR D67 012004	V.M. Abazov *et al.*	(D0 Collab.)
CHEKANOV	03	PL B559 153	S. Chekanov *et al.*	(ZEUS Collab.)
ACHARD	02J	PL B549 290	P. Achard *et al.*	(L3 Collab.)
ACOSTA	02	PR D65 091102	D. Acosta *et al.*	(CDF Collab.)
HEISTER	02Q	PL B543 173	A. Heister *et al.*	(ALEPH Collab.)
ABBIENDI	01T	PL B521 181	G. Abbiendi *et al.*	(OPAL Collab.)
AFFOLDER	01	PR D63 032003	T. Affolder *et al.*	(CDF Collab.)
AFFOLDER	01A	PR D64 032002	T. Affolder *et al.*	(CDF Collab.)
AFFOLDER	01C	PRL 86 3233	T. Affolder *et al.*	(CDF Collab.)
AFFOLDER	00B	PRL 84 216	T. Affolder *et al.*	(CDF Collab.)
BARATE	00S	PL B494 33	S. Barate *et al.*	(ALEPH Collab.)
ABBOTT	99G	PR D60 052001	B. Abbott *et al.*	(D0 Collab.)
ABE	99B	PRL 82 271	F. Abe *et al.*	(CDF Collab.)
Also		PRL 82 2808 (erratum)	F. Abe *et al.*	(CDF Collab.)
CHANG	99	PR D59 091503	D. Chang, W. Chang, E. Ma	
ABBOTT	98D	PRL 80 2063	B. Abbott *et al.*	(D0 Collab.)
ABBOTT	98F	PR D58 052001	B. Abbott *et al.*	(D0 Collab.)
ABE	98E	PRL 80 2767	F. Abe *et al.*	(CDF Collab.)
ABE	98F	PRL 80 2779	F. Abe *et al.*	(CDF Collab.)
ABE	98G	PRL 80 2525	F. Abe *et al.*	(CDF Collab.)
ABE	98X	PRL 80 2773	F. Abe *et al.*	(CDF Collab.)
BHAT	98B	IJMP A13 5113	P.C. Bhat, H.B. Prosper, S.S. Snyder	
ABACHI	97E	PRL 79 1197	S. Abachi *et al.*	(D0 Collab.)
ABE	97R	PRL 79 1992	F. Abe *et al.*	(CDF Collab.)
ABE	97V	PRL 79 3585	F. Abe *et al.*	(CDF Collab.)
PDG	96	PR D54 1	R. M. Barnett *et al.*	(PDG Collab.)
ABACHI	95	PRL 74 2632	S. Abachi *et al.*	(D0 Collab.)
ABE	95F	PRL 74 2626	F. Abe *et al.*	(CDF Collab.)
ABE	94E	PR D50 2966	F. Abe *et al.*	(CDF Collab.)
Also		PRL 73 225	F. Abe *et al.*	(CDF Collab.)

Quark Particle Listings

b' (Fourth Generation) Quark

b' (4^{th} Generation) Quark, Searches for

b'-quark/hadron mass limits in $p\overline{p}$ and pp collisions

VALUE (GeV)	CL%	DOCUMENT ID		TECN	COMMENT
>675	95	[1] CHATRCHYAN	13I	CMS	B($b' \to Wt$) = 1
>400	95	[2] AAD	12AU	ATLS	B($b' \to Zb$) = 1
>350	95	[3] AAD	12BC	ATLS	B($b' \to Wq$) = 1 (q=u,c)
>685	95	[4] CHATRCHYAN	12BH	CMS	$m_{t'} = m_{b'}$
>190	95	[5] ABAZOV	08X	D0	$c\tau$= 200mm
>190	95	[6] ACOSTA	03	CDF	quasi-stable b'
• • • We do not use the following data for averages, fits, limits, etc. • • •					
>480	95	[7] AAD	12AT	ATLS	B($b' \to Wt$) = 1
>450	95	[8] AAD	12BE	ATLS	B($b' \to Wt$) = 1
>611	95	[9] CHATRCHYAN	12X	CMS	B($b' \to Wt$) = 1
>372	95	[10] AALTONEN	11J	CDF	$b' \to Wt$
>361	95	[11] CHATRCHYAN	11L	CMS	Repl. by CHATRCHYAN 12X
>338	95	[12] AALTONEN	10H	CDF	$b' \to Wt$
> 380–430	95	[13] FLACCO	10	RVUE	$m_{b'} > m_{t'}$
>268	95	[14,15] AALTONEN	07C	CDF	B($b' \to Zb$) = 1 assumed
>199	95	[16] AFFOLDER	00	CDF	NC: $b' \to Zb$
>148	95	[17] ABE	98N	CDF	NC: $b' \to Zb$ +decay vertex
> 96	95	[18] ABACHI	97D	D0	NC: $b' \to b\gamma$
>128	95	[19] ABACHI	95F	D0	$\ell\ell$ + jets, ℓ + jets
> 75	95	[20] MUKHOPAD...	93	RVUE	NC: $b' \to b\ell\ell$
> 85	95	[21] ABE	92	CDF	CC: $\ell\ell$
> 72	95	[22] ABE	90B	CDF	CC: $e + \mu$
> 54	95	[23] AKESSON	90	UA2	CC: e + jets + missing E_T
> 43	95	[24] ALBAJAR	90B	UA1	CC: μ + jets
> 34	95	[25] ALBAJAR	88	UA1	CC: e or μ + jets

[1] Based on 5.0 fb^{-1} of pp data at $\sqrt{s}$ = 7 TeV. CHATRCHYAN 13I looked for events with one isolated electron or muon, large $\not\!\!E_T$, and at least four jets with large transverse momenta, where one jet is likely to originate from the decay of a bottom quark.

[2] Based on 2.0 fb^{-1} of pp data at $\sqrt{s}$ = 7 TeV. No $b' \to Zb$ invariant mass peak is found in the search of heavy quark pair production that decay into Z and a b quark in events with $Z \to e^+e^-$ and at least one b-jet. The lower mass limit is 358 GeV for a vector-like singlet b' mixing solely with the third SM generation.

[3] Based on 1.04 fb^{-1} of pp data at $\sqrt{s}$ = 7 TeV. No signal is found for the search of heavy quark pair production that decay into W and a quark in the events with dileptons, large $\not\!\!E_T$, and $\geq$ 2 jets.

[4] Based on 5 fb^{-1} of pp data at $\sqrt{s}$ = 7 TeV. CHATRCHYAN 12BH searched for QCD and EW production of single and pair of degenerate 4'th generation quarks that decay to bW or tW. Absence of signal in events with one lepton, same-sign dileptons or trileptons gives the bound. With a mass difference of 25 GeV/c^2 between $m_{t'}$ and $m_{b'}$, the corresponding limit shifts by about $\pm$20 GeV/c^2.

[5] Result is based on 1.1 fb^{-1} of data. No signal is found for the search of long-lived particles which decay into final states with two electrons or photons, and upper bound on the cross section times branching fraction is obtained for 2 < cτ< 7000 mm; see Fig. 3. 95% CL excluded region of b' lifetime and mass is shown in Fig. 4.

[6] ACOSTA 03 looked for long-lived fourth generation quarks in the data sample of 90 pb^{-1} of $\sqrt{s}$=1.8 TeV $p\overline{p}$ collisions by using the muon-like penetration and anomalously high ionization energy loss signature. The corresponding lower mass bound for the charge (2/3)e quark (t') is 220 GeV. The t' bound is higher than the b' bound because t' is more likely to produce charged hadrons than b'. The 95% CL upper bounds for the production cross sections are given in their Fig. 3.

[7] Based on 1.04 fb^{-1} of pp data at $\sqrt{s}$ = 7 TeV. No signal is found for the search of heavy quark pair production that decay into W and a t quark in the events with a high p_T isolated lepton, large $\not\!\!E_T$, and at least 6 jets in which one, two or more dijets are from W.

[8] Based on 1.04 fb^{-1} of pp data at $\sqrt{s}$ = 7 TeV. AAD 12BE looked for events with two isolated like-sign leptons and at least 2 jets, large $\not\!\!E_T$ and H_T > 350 GeV.

[9] Based on 4.9 fb^{-1} of pp data at $\sqrt{s}$ = 7 TeV. CHATRCHYAN 12X looked for events with trileptons or same-sign dileptons and at least one b jet.

[10] Based on 4.8 fb^{-1} of data in $p\overline{p}$ collisions at 1.96 TeV. AALTONEN 11J looked for events with $\ell + \not\!\!E_T + \geq$5j ($\geq$ 1 b or c). No signal is observed and the bound $\sigma(b'\overline{b}')$ < 30 fb for $m_{b'}$ > 375 GeV is found for B($b' \to Wt$) = 1.

[11] Based on 34 pb^{-1} of data in pp collisions at 7 TeV. CHATRCHYAN 11L looked for multi-jet events with trileptons or same-sign dileptons. No excess above the SM background excludes $m_{b'}$ between 255 and 361 GeV at 95% CL for B($b' \to Wt$) = 1.

[12] Based on 2.7 fb^{-1} of data in $p\overline{p}$ collisions at $\sqrt{s}$ = 1.96 TeV. AALTONEN 10H looked for pair production of heavy quarks which decay into tW^- or tW^+, in events with same sign dileptons (e or μ), several jets and large missing E_T. The result is obtained for b' which decays into tW^-. For the charge 5/3 quark ($T_{5/3}$) which decays into tW^+, $m_{T_{5/3}}$ > 365 GeV (95% CL) is found when it has the charge $-1/3$ partner B of the same mass.

[13] FLACCO 10 result is obtained from AALTONEN 10H result of $m_{b'}$ > 338 GeV, by relaxing the condition B($b' \to Wt$) = 100% when $m_{b'} > m_{t'}$.

[14] Result is based on 1.06 fb^{-1} of data. No excess from the SM Z+jet events is found when Z decays into ee or $\mu\mu$. The $m_{b'}$ bound is found by comparing the resulting upper bound on $\sigma(b'\overline{b}')$ [1-(1-B($b' \to Zb$))^2] and the LO estimate of the b' pair production cross section shown in Fig. 38 of the article.

[15] HUANG 08 reexamined the b' mass lower bound of 268 GeV obtained in AALTONEN 07C that assumes B($b' \to Zb$) = 1, which does not hold for $m_{b'}$ > 255 GeV. The lower mass bound is given in the plane of $\sin^2(\theta_{tb'})$ and $m_{b'}$.

[16] AFFOLDER 00 looked for b' that decays in to b+Z. The signal searched for is $bbZZ$ events where one Z decays into e^+e^- or $\mu^+\mu^-$ and the other Z decays hadronically. The bound assumes B($b' \to Zb$)= 100%. Between 100 GeV and 199 GeV, the 95%CL upper bound on $\sigma(b' \to \overline{b}')\times$B$^2(b' \to Zb)$ is also given (see their Fig. 2).

[17] ABE 98N looked for $Z \to e^+e^-$ decays with displaced vertices. Quoted limit assumes B($b' \to Zb$)=1 and $c\tau_{b'}$=1 cm. The limit is lower than m_Z+m_b ($\sim$ 96 GeV) if $c\tau$> 22 cm or $c\tau$< 0.009 cm. See their Fig. 4.

[18] ABACHI 97D searched for b' that decays mainly via FCNC. They obtained 95%CL upper bounds on B($b'\overline{b}' \to \gamma$+ 3 jets) and B($b'\overline{b}' \to 2\gamma$+ 2 jets), which can be interpreted as the lower mass bound $m_{b'} > m_Z+m_b$.

[19] ABACHI 95F bound on the top-quark also applies to b' and t' quarks that decay predominantly into W. See FROGGATT 97.

[20] MUKHOPADHYAYA 93 analyze CDF dilepton data of ABE 92G in terms of a new quark decaying via flavor-changing neutral current. The above limit assumes B($b' \to b\ell^+\ell^-$)=1%. For an exotic quark decaying only via virtual Z [B($b\ell^+\ell^-$) = 3%], the limit is 85 GeV.

[21] ABE 92 dilepton analysis limit of >85 GeV at CL=95% also applies to b' quarks, as discussed in ABE 90B.

[22] ABE 90B exclude the region 28–72 GeV.

[23] AKESSON 90 searched for events having an electron with p_T > 12 GeV, missing momentum > 15 GeV, and a jet with E_T > 10 GeV, $|\eta|$ < 2.2, and excluded $m_{b'}$ between 30 and 69 GeV.

[24] For the reduction of the limit due to non-charged-current decay modes, see Fig. 19 of ALBAJAR 90B.

[25] ALBAJAR 88 study events at E_{cm} = 546 and 630 GeV with a muon or isolated electron, accompanied by one or more jets and find agreement with Monte Carlo predictions for the production of charm and bottom, without the need for a new quark. The lower mass limit is obtained by using a conservative estimate for the $b'\overline{b}'$ production cross section and by assuming that it cannot be produced in W decays. The value quoted here is revised using the full $O(\alpha_s^3)$ cross section of ALTARELLI 88.

b' mass limits from single production in $p\overline{p}$ and pp collisions

VALUE (GeV)	CL%	DOCUMENT ID		TECN	COMMENT
>693	95	[26] ABAZOV	11F	D0	$qu \to q'b' \to q'(Wu)$ $\tilde{\kappa}_{ub'}$=1, B($b' \to Wu$)=1
>430	95	[26] ABAZOV	11F	D0	$qd \to qb' \to q(Zd)$ $\tilde{\kappa}_{db'}$=$\sqrt{2}$, B($b' \to Zd$)=1

[26] Based on 5.4 fb^{-1} of data in ppbar collisions at 1.96 TeV. ABAZOV 11F looked for single production of b' via the W or Z coupling to the first generation up or down quarks, respectively. Model independent cross section limits for the single production processes $p\overline{p} \to b'q \to Wuq$, and $p\overline{p} \to b'q \to Zdq$ are given in Figs. 3 and 4, respectively, and the mass limits are obtained for the model of ATRE 09 with degenerate bi-doublets of vector-like quarks.

MASS LIMITS for b' (4^{th} Generation) Quark or Hadron in e^+e^- Collisions

Search for hadrons containing a fourth-generation $-1/3$ quark denoted b'.

The last column specifies the assumption for the decay mode ($C\,C$ denotes the conventional charged-current decay) and the event signature which is looked for.

VALUE (GeV)	CL%	DOCUMENT ID		TECN	COMMENT
>46.0	95	[27] DECAMP	90F	ALEP	any decay
• • • We do not use the following data for averages, fits, limits, etc. • • •					
none 96–103	95	[28] ABDALLAH	07	DLPH	$b' \to bZ$, cW
		[29] ADRIANI	93G	L3	Quarkonium
>44.7	95	ADRIANI	93M	L3	$\Gamma(Z)$
>45	95	ABREU	91F	DLPH	$\Gamma(Z)$
none 19.4–28.2	95	ABE	90D	VNS	Any decay; event shape
>45.0	95	ABREU	90D	DLPH	B($C\,C$) = 1; event shape
>44.5	95	[30] ABREU	90D	DLPH	$b' \to cH^-$, $H^- \to \overline{c}s$, $\tau^-\nu$
>40.5	95	[31] ABREU	90D	DLPH	$\Gamma(Z \to$ hadrons)
>28.3	95	ADACHI	90	TOPZ	B(FCNC)=100%; isol. γ or 4 jets
>41.4	95	[32] AKRAWY	90B	OPAL	Any decay; acoplanarity
>45.2	95	[32] AKRAWY	90B	OPAL	B($C\,C$) = 1; acoplanarity
>46	95	[33] AKRAWY	90J	OPAL	$b' \to \gamma$ + any
>27.5	95	[34] ABE	89E	VNS	B($C\,C$) =1; μ, e
none 11.4–27.3	95	[35] ABE	89G	VNS	B($b' \to b\gamma$) > 10%; isolated γ
>44.7	95	[36] ABRAMS	89C	MRK2	B($C\,C$)= 100%; isol. track
>42.7	95	[36] ABRAMS	89C	MRK2	B(bg)= 100%; event shape
>42.0	95	[36] ABRAMS	89C	MRK2	Any decay; event shape
>28.4	95	[37,38] ADACHI	89C	TOPZ	B($C\,C$) =1; μ
>28.8	95	[39] ENO	89	AMY	B($C\,C$) $\gtrsim$ 90%; μ, e
>27.2	95	[39,40] ENO	89	AMY	any decay; event shape
>29.0	95	[39] ENO	89	AMY	B($b' \to bg$) $\gtrsim$ 85%; event shape
>24.4	95	[41] IGARASHI	88	AMY	μ,e
>23.8	95	[42] SAGAWA	88	AMY	event shape
>22.7	95	[43] ADEVA	86	MRKJ	μ
>21		[44] ALTHOFF	84C	TASS	R, event shape
>19		[45] ALTHOFF	84I	TASS	Aplanarity

[27] DECAMP 90F looked for isolated charged particles, for isolated photons, and for four-jet final states. The modes $b' \to bg$ for $B(b' \to bg) > 65\%$ $b' \to b\gamma$ for $B(b' \to b\gamma) > 5\%$ are excluded. Charged Higgs decay were not discussed.

[28] ABDALLAH 07 searched for b' pair production at E_{cm}=196–209 GeV, with 420 pb^{-1}. No signal leads to the 95% CL upper limits on $B(b' \to bZ)$ and $B(b' \to cW)$ for $m_{b'}$ = 96 to 103 GeV.

[29] ADRIANI 93G search for vector quarkonium states near Z and give limit on quarkonium-Z mixing parameter δm^2 <(10–30) GeV^2 (95%CL) for the mass 88–94.5 GeV. Using Richardson potential, a 1S $(b'\overline{b}')$ state is excluded for the mass range 87.7–94.7 GeV. This range depends on the potential choice.

[30] ABREU 90D assumed $m_{H^-} < m_{b'} - 3$ GeV.

[31] Superseded by ABREU 91F.

[32] AKRAWY 90B search was restricted to data near the Z peak at E_{cm} = 91.26 GeV at LEP. The excluded region is between 23.6 and 41.4 GeV if no H^+ decays exist. For charged Higgs decays the excluded regions are between (m_{H^+} + 1.5 GeV) and 45.5 GeV.

[33] AKRAWY 90J search for isolated photons in hadronic Z decay and derive $B(Z \to b'\overline{b}')\cdot B(b' \to \gamma X)/B(Z \to \text{hadrons}) < 2.2 \times 10^{-3}$. Mass limit assumes $B(b' \to \gamma X) > 10\%$.

[34] ABE 89E search at E_{cm} = 56–57 GeV at TRISTAN for multihadron events with a spherical shape (using thrust and acoplanarity) or containing isolated leptons.

[35] ABE 89G search was at E_{cm} = 55–60.8 GeV at TRISTAN.

[36] If the photonic decay mode is large ($B(b' \to b\gamma) > 25\%$), the ABRAMS 89C limit is 45.4 GeV. The limit for for Higgs decay ($b' \to cH^-$, $H^- \to \overline{c}s$) is 45.2 GeV.

[37] ADACHI 89C search was at E_{cm} = 56.5–60.8 GeV at TRISTAN using multi-hadron events accompanying muons.

[38] ADACHI 89C also gives limits for any mixture of CC and bg decays.

[39] ENO 89 search at E_{cm} = 50–60.8 at TRISTAN.

[40] ENO 89 considers arbitrary mixture of the charged current, bg, and $b\gamma$ decays.

[41] IGARASHI 88 searches for leptons in low-thrust events and gives $\Delta R(b') < 0.26$ (95% CL) assuming charged current decay, which translates to $m_{b'} > 24.4$ GeV.

[42] SAGAWA 88 set limit σ(top) < 6.1 pb at CL=95% for top-flavored hadron production from event shape analyses at E_{cm} = 52 GeV. By using the quark parton model cross-section formula near threshold, the above limit leads to lower mass bounds of 23.8 GeV for charge $-1/3$ quarks.

[43] ADEVA 86 give 95%CL upper bound on an excess of the normalized cross section, ΔR, as a function of the minimum c.m. energy (see their figure 3). Production of a pair of 1/3 charge quarks is excluded up to E_{cm} = 45.4 GeV.

[44] ALTHOFF 84C narrow state search sets limit $\Gamma(e^+e^-)B(\text{hadrons})$ <2.4 keV CL = 95% and heavy charge 1/3 quark pair production m >21 GeV, CL = 95%.

[45] ALTHOFF 84I exclude heavy quark pair production for 7 <m <19 GeV (1/3 charge) using aplanarity distributions (CL = 95%).

REFERENCES FOR Searches for (Fourth Generation) b' Quark

CHATRCHYAN	13I	JHEP 1301 154	S. Chatrchyan *et al.*	(CMS Collab.)
AAD	12AT	PRL 109 032001	G. Aad *et al.*	(ATLAS Collab.)
AAD	12AU	PRL 109 071801	G. Aad *et al.*	(ATLAS Collab.)
AAD	12BC	PR D86 012007	G. Aad *et al.*	(ATLAS Collab.)
AAD	12BE	JHEP 1204 069	G. Aad *et al.*	(ATLAS Collab.)
CHATRCHYAN	12BH	PR D86 112003	S. Chatrchyan *et al.*	(CMS Collab.)
CHATRCHYAN	12X	JHEP 1205 123	S. Chatrchyan *et al.*	(CMS Collab.)
AALTONEN	11J	PRL 106 141803	T. Aaltonen *et al.*	(CDF Collab.)
ABAZOV	11F	PRL 106 081801	V.M. Abazov *et al.*	(D0 Collab.)
CHATRCHYAN	11L	PL B701 204	S. Chatrchyan *et al.*	(CMS Collab.)
AALTONEN	10H	PRL 104 091801	T. Aaltonen *et al.*	(CDF Collab.)
FLACCO	10	PRL 105 111801	C.J. Flacco *et al.*	(UCI, HAIF)
ATRE	09	PR D79 054018	A. Atre *et al.*	
ABAZOV	08X	PRL 101 111802	V.M. Abazov *et al.*	(D0 Collab.)
HUANG	08	PR D77 037302	P.Q. Hung, M. Sher	(UVA, WILL)
AALTONEN	07C	PR D76 072006	T. Aaltonen *et al.*	(CDF Collab.)
ABDALLAH	07	EPJ C50 507	J. Abdallah *et al.*	(DELPHI Collab.)
ACOSTA	03	PRL 90 131801	D. Acosta *et al.*	(CDF Collab.)
AFFOLDER	00	PRL 84 835	A. Affolder *et al.*	(CDF Collab.)
ABE	98N	PR D58 051102	F. Abe *et al.*	(CDF Collab.)
ABACHI	97D	PRL 78 3818	S. Abachi *et al.*	(D0 Collab.)
FROGGATT	97	ZPHY C73 333	C.D. Froggatt, D.J. Smith, H.B. Nielsen	(GLAS+)
ABACHI	95F	PR D52 4877	S. Abachi *et al.*	(D0 Collab.)
ADRIANI	93G	PL B313 326	O. Adriani *et al.*	(L3 Collab.)
ADRIANI	93M	PRPL 236 1	O. Adriani *et al.*	(L3 Collab.)
MUKHOPAD...	93	PR D48 2105	B. Mukhopadhyaya, D.P. Roy	(TATA)
ABE	92	PRL 68 447	F. Abe *et al.*	(CDF Collab.)
Also		PR D45 3921	F. Abe *et al.*	(CDF Collab.)
ABE	92G	PR D45 3921	F. Abe *et al.*	(CDF Collab.)
ABREU	91F	NP B367 511	P. Abreu *et al.*	(DELPHI Collab.)
ABE	90B	PRL 64 147	F. Abe *et al.*	(CDF Collab.)
ABE	90D	PL B234 382	K. Abe *et al.*	(VENUS Collab.)
ABREU	90D	PL B242 536	P. Abreu *et al.*	(DELPHI Collab.)
ADACHI	90	PL B234 197	I. Adachi *et al.*	(TOPAZ Collab.)
AKESSON	90	ZPHY C46 179	T. Akesson *et al.*	(UA2 Collab.)
AKRAWY	90B	PL B236 364	M.Z. Akrawy *et al.*	(OPAL Collab.)
AKRAWY	90J	PL B246 285	M.Z. Akrawy *et al.*	(OPAL Collab.)
ALBAJAR	90B	ZPHY C48 1	C. Albajar *et al.*	(UA1 Collab.)
DECAMP	90F	PL B236 511	D. Decamp *et al.*	(ALEPH Collab.)
ABE	89E	PR D39 3524	K. Abe *et al.*	(VENUS Collab.)
ABE	89G	PRL 63 1776	K. Abe *et al.*	(VENUS Collab.)
ABRAMS	89C	PRL 63 2447	G.S. Abrams *et al.*	(Mark II Collab.)
ADACHI	89C	PL B229 427	I. Adachi *et al.*	(TOPAZ Collab.)
ENO	89	PRL 63 1910	S. Eno *et al.*	(AMY Collab.)
ALBAJAR	88	ZPHY C37 505	C. Albajar *et al.*	(UA1 Collab.)
ALTARELLI	88	NP B308 724	G. Altarelli *et al.*	(CERN, ROMA, ETH)
IGARASHI	88	PRL 60 2359	S. Igarashi *et al.*	(AMY Collab.)
SAGAWA	88	PRL 60 93	H. Sagawa *et al.*	(AMY Collab.)
ADEVA	86	PR D34 681	B. Adeva *et al.*	(Mark-J Collab.)
ALTHOFF	84C	PL 138B 441	M. Althoff *et al.*	(TASSO Collab.)
ALTHOFF	84I	ZPHY C22 307	M. Althoff *et al.*	(TASSO Collab.)

t' (4^{th} Generation) Quark, Searches for

t'-quark/hadron mass limits in $p\overline{p}$ and pp collisions

VALUE (GeV)	CL%	DOCUMENT ID		TECN	COMMENT
>700	95	[1] CHATRCHYAN	14A	CMS	$B(t' \to Wb) = 1$
>706	95	[1] CHATRCHYAN	14A	CMS	$B(t' \to Zt) = 1$
>782	95	[1] CHATRCHYAN	14A	CMS	$B(t' \to ht) = 1$
>350	95	[2] AAD	12BC	ATLS	$B(t' \to Wq)$=1 (q=d,s,b)
>420	95	[3] AAD	12C	ATLS	$t' \to Xt$ ($m_X < 140$ GeV)
>685	95	[4] CHATRCHYAN	12BH	CMS	$m_{b'} = m_{t'}$
>557	95	[5] CHATRCHYAN	12P	CMS	$t'\overline{t}' \to W^+bW^-\overline{b} \to b\ell^+\nu\overline{b}\ell^-\overline{\nu}$
• • • We do not use the following data for averages, fits, limits, etc. • • •					
>656	95	[6] AAD	13F	ATLS	$B(t' \to Wb) = 1$
>625	95	[7] CHATRCHYAN	13I	CMS	$B(t' \to Zt) = 1$
>404	95	[8] AAD	12AR	ATLS	$B(t' \to Wb) = 1$
>570	95	[9] CHATRCHYAN	12BC	CMS	$t'\overline{t}' \to W^+bW^-\overline{b}$
>400	95	[10] AALTONEN	11AH	CDF	$t' \to Xt$ ($m_X < 70$ GeV)
>358	95	[11] AALTONEN	11AL	CDF	$t' \to Wb$
>340	95	[11] AALTONEN	11AL	CDF	$t' \to Wq$ (q=d,s,b)
>360	95	[12] AALTONEN	11O	CDF	$t' \to Xt$ ($m_X < 100$ GeV)
>285	95	[13] ABAZOV	11Q	D0	$t' \to Wq$ (q=d,s,b)
>256	95	[14,15] AALTONEN	08H	CDF	$t' \to Wq$

[1] Based on 19.5 fb^{-1} of pp data at $\sqrt{s}$ = 8TeV. The t' quark is pair produced and is assumed to decay into three different final states of bW, tZ, and th. The search is carried out using events with at least one isolated lepton.

[2] Based on 1.04 fb^{-1} of pp data at $\sqrt{s}$ = 7 TeV. No signal is found for the search of heavy quark pair production that decay into W and a quark in the events with dileptons, large $\not{E}_T$, and ≥ 2 jets.

[3] Based on 1.04 fb^{-1} of data in pp collisions at 7 TeV. AAD 12C looked for $t'\overline{t}'$ production followed by t' decaying into a top quark and X, an invisible particle, in a final state with an isolated high-P_T lepton, four or more jets, and a large missing transverse energy. No excess over the SM $t\overline{t}$ production gives the upper limit on $t'\overline{t}'$ production cross section as a function of $m_{t'}$ and m_X. The result is obtained for $B(t' \to Wt) = 1$.

[4] Based on 5 fb^{-1} of pp data at $\sqrt{s}$ = 7 TeV. CHATRCHYAN 12BH searched for QCD and EW production of single and pair of degenerate 4'th generation quarks that decay to Wb or Wt. Absence of signal in events with one lepton, same-sign dileptons or tri-leptons gives the bound. With a mass difference of 25 GeV/c^2 between $m_{t'}$ and $m_{b''}$, the corresponding limit shifts by about ± 20 GeV/c^2.

[5] Based on 5.0 fb^{-1} of pp data at $\sqrt{s}$ = 7 TeV. CHATRCHYAN 12P looked for $t'\overline{t}'$ production events with two isolated high p_T leptons, large $\not{E}_T$, and 2 high p_T jets with b-tag. The absence of signal above the SM background gives the limit for $B(t' \to Wb) = 1$.

[6] Based on 4.7 fb^{-1} of pp data at $\sqrt{s}$ = 7 TeV. No signal is found for the search of heavy quark pair production that decay into W and a b quark in the events with a high p_T isolated lepton, large $\not{E}_T$ and at least 3 jets ($\geq$ 1 b-tag). Vector-like quark of charge 2/3 with $400 < m_{t'} < 550$ GeV and $B(t' \to Wb) > 0.63$ is excluded at 95% CL.

[7] Based on 5.0 fb^{-1} of pp data at $\sqrt{s}$ = 7 TeV. CHATRCHYAN 13I looked for events with one isolated electron or muon, large $\not{E}_T$, and at least four jets with large transverse momenta, where one jet is likely to originate from the decay of a bottom quark.

[8] Based on 1.04 fb^{-1} of pp data at $\sqrt{s}$ = 7 TeV. No signal is found in the search for pair produced heavy quarks that decay into W boson and a b quark in the events with a high p_T isolated lepton, large $\not{E}_T$ and at least 3 jets (≥ 1 b-tag).

[9] Based on 5.0 fb^{-1} of pp data at $\sqrt{s}$ = 7 TeV. CHATRCHYAN 12BC looked for $t'\overline{t}'$ production events with a single isolated high p_T lepton, large $\not{E}_T$ and at least 4 high p_T jets with a b-tag. The absence of signal above the SM background gives the limit for $B(t' \to Wb) = 1$.

[10] Based on 5.7 fb^{-1} of data in $p\overline{p}$ collisions at 1.96 TeV. AALTONEN 11AH looked for $t'\overline{t}'$ production followed by t' decaying into a top quark and X, an invisible particle, in the all hadronic decay mode of $t\overline{t}$. No excess over the SM $t\overline{t}$ production gives the upper limit on $t'\overline{t}'$ production cross section as a function of $m_{t'}$ and m_X. The result is obtained for $B(t' \to Xt) = 1$.

[11] Based on 5.6 fb^{-1} of data in ppbar collisions at 1.96 TeV. AALTONEN 11AL looked for $\ell + \geq 4$j events and set upper limits on $\sigma(t'\overline{t}')$ as functions of $m_{t'}$.

[12] Based on 4.8 fb^{-1} of data in $p\overline{p}$ collisions at 1.96 TeV. AALTONEN 11O looked for $t'\overline{t}'$ production signal when t' decays into a top quark and X, an invisible particle, in $\ell + \not{E}_T$ + jets channel. No excess over the SM $t\overline{t}$ production gives the upper limit on $t'\overline{t}'$ production cross section as a function of $m_{t'}$ and m_X. The result is obtained for $B(t' \to Xt) = 1$.

[13] Based on 5.3 fb^{-1} of data in $p\overline{p}$ collisions at 1.96 TeV. ABAZOV 11Q looked for $\ell + \not{E}_T + \geq 4$j events and set upper limits on $\sigma(t'\overline{t}')$ as functions of $m_{t'}$.

[14] Searches for pair production of a new heavy top-like quark t' decaying to a W boson and another quark by fitting the observed spectrum of total transverse energy and reconstructed t' mass in the lepton + jets events.

[15] HUANG 08 reexamined the t' mass lower bound of 256 GeV obtained in AALTONEN 08H that assumes $B(b' \to qZ) = 1$ for $q = u, c$ which does not hold when $m_{b'} < m_{t'} - m_W$ or the mixing $\sin^2(\theta_{bt'})$ is so tiny that the decay occurs outside of the vertex detector. Fig. 1 gives that lower bound on $m_{t'}$ in the plane of $\sin^2(\theta_{bt'})$ and $m_{b'}$.

Quark Particle Listings

t' (Fourth Generation) Quark, Free Quark Searches

t' mass limits from single production in $p\overline{p}$ and pp collisions

VALUE (GeV)	CL%	DOCUMENT ID		TECN	COMMENT
>403	95	[16] ABAZOV	11F	D0	$qd \to q't' \to q'(Wd)$ $\tilde{\kappa}_{dt'}=1$, B($t' \to Wd$)=1
>551	95	[16] ABAZOV	11F	D0	$qu \to qt' \to q(Zu)$ $\tilde{\kappa}_{ut'}=\sqrt{2}$, B($t' \to Zu$)=1

[16] Based on 5.4 fb^{-1} of data in ppbar collisions at 1.96 TeV. ABAZOV 11F looked for single production of t' via the Z or E coupling to the first generation up or down quarks, respectively. Model independent cross section limits for the single production processes $p\overline{p} \to t'q \to (Wd)q$, and $p\overline{p} \to t'q \to (Zd)q$ are given in Figs. 3 and 4, respectively, and the mass limits are obtained for the model of ATRE 09 with degenerate bi-doublets of vector-like quarks.

REFERENCES FOR Searches for (Fourth Generation) t' Quark

CHATRCHYAN	14A	PL B729 149	S. Chatrchyan *et al.*	(CMS Collab.)
AAD	13F	PL B718 1284	G. Aad *et al.*	(ATLAS Collab.)
CHATRCHYAN	13I	JHEP 1301 154	S. Chatrchyan *et al.*	(CMS Collab.)
AAD	12AR	PRL 108 261802	G. Aad *et al.*	(ATLAS Collab.)
AAD	12BC	PR D86 012007	G. Aad *et al.*	(ATLAS Collab.)
AAD	12C	PRL 108 041805	G. Aad *et al.*	(ATLAS Collab.)
CHATRCHYAN	12BC	PL B718 307	S. Chatrchyan *et al.*	(CMS Collab.)
CHATRCHYAN	12BH	PR D86 112003	S. Chatrchyan *et al.*	(CMS Collab.)
CHATRCHYAN	12P	PL B716 103	S. Chatrchyan *et al.*	(CMS Collab.)
AALTONEN	11AH	PRL 107 191803	T. Aaltonen *et al.*	(CDF Collab.)
AALTONEN	11AL	PRL 107 261801	T. Aaltonen *et al.*	(CDF Collab.)
AALTONEN	11O	PRL 106 191801	T. Aaltonen *et al.*	(CDF Collab.)
ABAZOV	11F	PRL 106 081801	V.M. Abazov *et al.*	(D0 Collab.)
ABAZOV	11Q	PRL 107 082001	V.M. Abazov *et al.*	(D0 Collab.)
ATRE	09	PR D79 054018	A. Atre *et al.*	
AALTONEN	08H	PRL 100 161803	T. Aaltonen *et al.*	(CDF Collab.)
HUANG	08	PR D77 037302	P.Q. Hung, M. Sher	(UVA, WILL)

Free Quark Searches

FREE QUARK SEARCHES

The basis for much of the theory of particle scattering and hadron spectroscopy is the construction of the hadrons from a set of fractionally charged constituents (quarks). A central but unproven hypothesis of this theory, Quantum Chromodynamics, is that quarks cannot be observed as free particles but are confined to mesons and baryons.

Experiments show that it is at best difficult to "unglue" quarks. Accelerator searches at increasing energies have produced no evidence for free quarks, while only a few cosmic-ray and matter searches have produced uncorroborated events.

This compilation is only a guide to the literature, since the quoted experimental limits are often only indicative. Reviews can be found in Refs. 1–4.

References

1. M.L. Perl, E.R. Lee, and D. Lomba, Mod. Phys. Lett. **A19**, 2595 (2004).
2. P.F. Smith, Ann. Rev. Nucl. and Part. Sci. **39**, 73 (1989).
3. L. Lyons, Phys. Reports **129**, 225 (1985).
4. M. Marinelli and G. Morpurgo, Phys. Reports **85**, 161 (1982).

Quark Production Cross Section — Accelerator Searches

X-SECT (cm^2)	CHG (e/3)	MASS (GeV)	ENERGY (GeV)	BEAM	EVTS	DOCUMENT ID		TECN
<1.7-2.3E−39	±2	100–600	7000	pp	0	[1] CHATRCHYAN	13AR	CMS
<14-5.4E−39	±1	100–600	7000	pp	0	[1] CHATRCHYAN	13AR	CMS
<1.3E−36	±2	45–84	130–172	e^+e^-	0	ABREU	97D	DLPH
<2.E−35	+2	250	1800	$p\overline{p}$	0	[2] ABE	92J	CDF
<1.E−35	+4	250	1800	$p\overline{p}$	0	[2] ABE	92J	CDF
<3.8E−28			14.5A	[28]Si–Pb	0	[3] HE	91	PLAS
<3.2E−28			14.5A	[28]Si–Cu	0	[3] HE	91	PLAS
<1.E−40	±1,2	<10		$p,\nu,\overline{\nu}$	0	BERGSMA	84B	CHRM
<1.E−36	±1,2	<9	200	μ	0	AUBERT	83C	SPEC
<2.E−10	±2,4	1–3	200	p	0	[4] BUSSIERE	80	CNTR
<5.E−38	+1,2	>5	300	p	0	[5,6] STEVENSON	79	CNTR
<1.E−33	±1	<20	52	pp	0	BASILE	78	SPEC
<9.E−39	±1,2	<6	400	p	0	[5] ANTREASYAN	77	SPEC
<8.E−35	+1,2	<20	52	pp	0	[7] FABJAN	75	CNTR
<5.E−38	−1,2	4–9	200	p	0	NASH	74	CNTR
<1.E−32	+2,4	4–24	52	pp	0	ALPER	73	SPEC
<5.E−31	+1,2,4	<12	300	p	0	LEIPUNER	73	CNTR
<6.E−34	±1,2	<13	52	pp	0	BOTT	72	CNTR
<1.E−36	−4	4	70	p	0	ANTIPOV	71	CNTR
<1.E−35	±1,2	2	28	p	0	[8] ALLABY	69B	CNTR
<4.E−37	−2	<5	70	p	0	[4] ANTIPOV	69	CNTR
<3.E−37	−1,2	2–5	70	p	0	[8] ANTIPOV	69B	CNTR
<1.E−35	+1,2	<7	30	p	0	DORFAN	65	CNTR
<2.E−35	−2	< 2.5–5	30	p	0	[9] FRANZINI	65B	CNTR
<5.E−35	+1,2	<2.2	21	p	0	BINGHAM	64	HLBC
<1.E−32	+1,2	<4.0	28	p	0	BLUM	64	HBC
<1.E−35	+1,2	<2.5	31	p	0	[9] HAGOPIAN	64	HBC
<1.E−34	+1	<2	28	p	0	LEIPUNER	64	CNTR
<1.E−33	+1,2	<2.4	24	p	0	MORRISON	64	HBC

[1] CHATRCHYAN 13AR limits assume pair-produced long-lived spin-1/2 particles neutral under SU(3)$_C$ and SU(2)$_L$.
[2] ABE 92J flux limits decrease as the mass increases from 50 to 500 GeV.
[3] HE 91 limits are for charges of the form $N\pm1/3$ from 23/3 to 38/3.
[4] Hadronic or leptonic quarks.
[5] Cross section cm^2/GeV^2.
[6] 3×10^{-5} <lifetime $< 1\times10^{-3}$ s.
[7] Includes BOTT 72 results.
[8] Assumes isotropic cm production.
[9] Cross section inferred from flux.

Quark Differential Production Cross Section — Accelerator Searches

X-SECT (cm^{2}sr^{-1}GeV^{-1})	CHG e/3	MASS (GeV)	ENERGY (GeV)	BEAM	EVTS	DOCUMENT ID		TECN
<4.E−36	−2,4	1.5–6	70	p	0	BALDIN	76	CNTR
<2.E−33	±4	5–20	52	pp	0	ALBROW	75	SPEC
<5.E−34	<7	7–15	44	pp	0	JOVANOV...	75	CNTR
<5.E−35			20	γ	0	[10] GALIK	74	CNTR
<9.E−35	−1,2		200	p	0	NASH	74	CNTR
<4.E−36	−4	2.3–2.7	70	p	0	ANTIPOV	71	CNTR
<3.E−35	±1,2	<2.7	27	p	0	ALLABY	69B	CNTR
<7.E−38	−1,2	<2.5	70	p	0	ANTIPOV	69B	CNTR

[10] Cross section in cm^2/sr/equivalent quanta.

Quark Flux — Accelerator Searches

The definition of FLUX depends on the experiment

(a) is the ratio of measured free quarks to predicted free quarks if there is no "confinement."
(b) is the probability of fractional charge on nuclear fragments. Energy is in GeV/nucleon.
(c) is the 90%CL upper limit on fractionally-charged particles produced per interaction.
(d) is quarks per collision.
(e) is inclusive quark-production cross-section ratio to $\sigma(e^+e^- \to \mu^+\mu^-)$.
(f) is quark flux per charged particle.
(g) is the flux per ν-event.
(h) is quark yield per π^- yield.
(i) is 2-body exclusive quark-production cross-section ratio to $\sigma(e^+e^- \to \mu^+\mu^-)$.

FLUX		CHG (e/3)	MASS (GeV)	ENERGY (GeV)	BEAM	EVTS	DOCUMENT ID		TECN
<1.6E−3	b	see note		200	[32]S–Pb	0	[11] HUENTRUP	96	PLAS
<6.2E−4	b	see note		10.6	[32]S–Pb	0	[11] HUENTRUP	96	PLAS
<0.94E−4	e	±2	2–30	88–94	e^+e^-	0	AKERS	95R	OPAL
<1.7E−4	e	±2	30–40	88–94	e^+e^-	0	AKERS	95R	OPAL
<3.6E−4	e	±4	5–30	88–94	e^+e^-	0	AKERS	95R	OPAL
<1.9E−4	e	±4	30–45	88–94	e^+e^-	0	AKERS	95R	OPAL
<2.E−3	e	+1	5–40	88–94	e^+e^-	0	[12] BUSKULIC	93C	ALEP
<6.E−4	e	+2	5–30	88–94	e^+e^-	0	[12] BUSKULIC	93C	ALEP
<1.2E−3	e	+4	15–40	88–94	e^+e^-	0	[12] BUSKULIC	93C	ALEP
<3.6E−4	i	+4	5.0–10.2	88–94	e^+e^-	0	BUSKULIC	93C	ALEP
<3.6E−4	i	+4	16.5–26.0	88–94	e^+e^-	0	BUSKULIC	93C	ALEP
<6.9E−4	i	+4	26.0–33.3	88–94	e^+e^-	0	BUSKULIC	93C	ALEP
<9.1E−4	i	+4	33.3–38.6	88–94	e^+e^-	0	BUSKULIC	93C	ALEP
<1.1E−3	i	+4	38.6–44.9	88–94	e^+e^-	0	BUSKULIC	93C	ALEP
<1.6E−4	b	see note		see note		0	[13] CECCHINI	93	PLAS
	b	4,5,7,8		2.1A	[16]O	0,2,0,6	[14] GHOSH	92	EMUL
<6.4E−5	g	1			$\nu,\overline{\nu}$	1	[15] BASILE	91	CNTR
<3.7E−5	g	2			$\nu,\overline{\nu}$	0	[15] BASILE	91	CNTR
<3.9E−5	g	1			$\nu,\overline{\nu}$	1	[16] BASILE	91	CNTR
<2.8E−5	g	2			$\nu,\overline{\nu}$	0	[16] BASILE	91	CNTR
<1.9E−4	c			14.5A	[28]Si–Pb	0	[17] HE	91	PLAS
<3.9E−4	c			14.5A	[28]Si–Cu	0	[17] HE	91	PLAS
<1.E−9	c	±1,2,4		14.5A	[16]O–Ar	0	MATIS	91	MDRP
<5.1E−10	c	±1,2,4		14.5A	[16]O–Hg	0	MATIS	91	MDRP
<8.1E−9	c	±1,2,4		14.5A	Si–Hg	0	MATIS	91	MDRP
<1.7E−6	c	±1,2,4		60A	[16]O–Hg	0	MATIS	91	MDRP
<3.5E−7	c	±1,2,4		200A	[16]O–Hg	0	MATIS	91	MDRP
<1.3E−6	c	±1,2,4		200A	S–Hg	0	MATIS	91	MDRP
<5E−2	e	2	19–27	52–60	e^+e^-	0	ADACHI	90C	TOPZ

<5E−2	e	4	<24	52–60	e^+e^-	0	ADACHI	90C	TOPZ
<1.E−4	e	+2	<3.5	10	e^+e^-	0	BOWCOCK	89B	CLEO
<1.E−6	d	±1,2		60	^{16}O–Hg	0	CALLOWAY	89	MDRP
<3.5E−7	d	±1,2		200	^{16}O–Hg	0	CALLOWAY	89	MDRP
<1.3E−6	d	±1,2		200	S–Hg	0	CALLOWAY	89	MDRP
<1.2E−10	d	±1	1	800	p–Hg	0	MATIS	89	MDRP
<1.1E−10	d	±2	1	800	p–Hg	0	MATIS	89	MDRP
<1.2E−10	d	±1	1	800	p–N_2	0	MATIS	89	MDRP
<7.7E−11	d	±2	1	800	p–N_2	0	MATIS	89	MDRP
<6.E−9	h	−5	0.9–2.3	12	p	0	NAKAMURA	89	SPEC
<5.E−5	g	1,2	<0.5		$\nu,\overline{\nu}d$	0	ALLASIA	88	BEBC
<3.E−4	b	See note		14.5	^{16}O–Pb	0	[18] HOFFMANN	88	PLAS
<2.E−4	b	See note		200	^{16}O–Pb	0	[19] HOFFMANN	88	PLAS
<8E−5	b	19,20,22,23		200*A*			GERBIER	87	PLAS
<2.E−4	a	±1,2	<300	320	$\overline{p}p$	0	LYONS	87	MLEV
<1.E−9	c	±1,2,4,5		14.5	^{16}O–Hg	0	SHAW	87	MDRP
<3.E−3	d	−1,2,3,4,6	<5	2	Si–Si	0	[20] ABACHI	86C	CNTR
<1.E−4	e	±1,2,4	<4	10	e^+e^-	0	ALBRECHT	85G	ARG
<6.E−5	b	±1,2	1	540	$p\overline{p}$	0	BANNER	85	UA2
<5.E−3	e	−4	1–8	29	e^+e^-	0	AIHARA	84	TPC
<1.E−2	e	±1,2	1–13	29	e^+e^-	0	AIHARA	84B	TPC
<2.E−4	b	±1		72	^{40}Ar	0	[21] BARWICK	84	CNTR
<1.E−4	e	±2	<0.4	1.4	e^+e^-	0	BONDAR	84	OLYA
<5.E−1	e	±1,2	<13	29	e^+e^-	0	GURYN	84	CNTR
<3.E−3	b	±1,2	<2	540	$p\overline{p}$	0	BANNER	83	CNTR
<1.E−4	b	±1,2		106	^{56}Fe	0	LINDGREN	83	CNTR
<3.E−3	b	$>\lvert\pm 0.1\rvert$		74	^{40}Ar	0	[21] PRICE	83	PLAS
<1.E−2	e	±1,2	<14	29	e^+e^-	0	MARINI	82B	CNTR
<8.E−2	e	±1,2	<12	29	e^+e^-	0	ROSS	82	CNTR
<3.E−4	e	±2	1.8–2	7	e^+e^-	0	WEISS	81	MRK2
<5.E−2	e	+1,2,4,5	2–12	27	e^+e^-	0	BARTEL	80	JADE
<2.E−5	g	1,2			ν	0	[15,16] BASILE	80	CNTR
<3.E−10	f	±2,4	1–3	200	p	0	[22] BOZZOLI	79	CNTR
<6.E−11	f	±1	<21	52	pp	0	BASILE	78	SPEC
<5.E−3	g				ν_μ	0	BASILE	78B	CNTR
<2.E−9	f	±1	<26	62	pp	0	BASILE	77	SPEC
<7.E−10	f	+1,2	<20	52	p	0	[23] FABJAN	75	CNTR
		+1,2	>4.5		γ	0	[15,16] GALIK	74	CNTR
		+1,2	>1.5	12	e^-	0	[15,16] BELLAMY	68	CNTR
		+1,2	>0.9		γ	0	[16] BATHOW	67	CNTR
		+1,2	>0.9	6	γ	0	[16] FOSS	67	CNTR

[11] HUENTRUP 96 quote 95% CL limits for production of fragments with charge differing by as much as ±1/3 (in units of e) for charge $6 \le Z \le 10$.

[12] BUSKULIC 93C limits for inclusive quark production are more conservative if the ALEPH hadronic fragmentation function is assumed.

[13] CECCHINI 93 limit at 90%CL for $23/3 \le Z \le 40/3$, for 16*A* GeV O, 14.5*A* Si, and 200*A* S incident on Cu target. Other limits are 2.3×10^{-4} for $17/3 \le Z \le 20/3$ and 1.2×10^{-4} for $20/3 \le Z \le 23/3$.

[14] GHOSH 92 reports measurement of spallation fragment charge based on ionization in emulsion. Out of 650 measured tracks, 2 were consistent with charge $5e/3$, and 4 with $7e/3$.

[15] Hadronic quark.

[16] Leptonic quark.

[17] HE 91 limits are for charges of the form $N \pm 1/3$ from 23/3 to 38/3, and correspond to cross-section limits of 380μb (Pb) and 320μb (Cu).

[18] The limits apply to projectile fragment charges of 17, 19, 20, 22, 23 in units of $e/3$.

[19] The limits apply to projectile fragment charges of 16, 17, 19, 20, 22, 23 in units of $e/3$.

[20] Flux limits and mass range depend on charge.

[21] Bound to nuclei.

[22] Quark lifetimes $> 1 \times 10^{-8}$ s.

[23] One candidate m <0.17 GeV.

Quark Flux — Cosmic Ray Searches

Shielding values followed with an asterisk indicate altitude in km. Shielding values not followed with an asterisk indicate sea level in kg/cm^2.

FLUX ($cm^{-2}sr^{-1}s^{-1}$)	CHG ($e/3$)	MASS (GeV)	SHIELDING	EVTS	DOCUMENT ID		TECN
< 9.2E−15	±1		3800	0	[24] AMBROSIO	00C	MCRO
<2.1E−15	±1			0	MORI	91	KAM2
<2.3E−15	±2			0	MORI	91	KAM2
<2.E−10	±1, 2		0.3	0	WADA	88	CNTR
	±4		0.3	12	[25] WADA	88	CNTR
	±4		0.3	9	[26] WADA	86	CNTR
<1.E−12	±2,3/2		−70.	0	[27] KAWAGOE	84B	PLAS
<9.E−10	±1,2		0.3	0	WADA	84B	CNTR
<4.E−9	±4		0.3	7	WADA	84B	CNTR
<2.E−12	±1,2,3		−0.3 *	0	MASHIMO	83	CNTR
<3.E−10	±1,2		0.3	0	MARINI	82	CNTR
<2.E−11	±1,2			0	MASHIMO	82	CNTR
<8.E−10	±1,2		0.3	0	[27] NAPOLITANO	82	CNTR
				3	[28] YOCK	78	CNTR
<1.E−9				0	[29] BRIATORE	76	ELEC
<2.E−11	+1			0	[30] HAZEN	75	CC
<2.E−10	+1,2			0	KRISOR	75	CNTR
<1.E−7	+1,2			0	[30,31] CLARK	74B	CC
<3.E−10	+1	>20		0	KIFUNE	74	CNTR
<8.E−11	+1			0	[30] ASHTON	73	CNTR
<2.E−8	+1,2			0	HICKS	73B	CNTR
<5.E−10	+4		2.8 *	0	BEAUCHAMP	72	CNTR
<1.E−10	+1,2			0	[30] BOHM	72B	CNTR
<1.E−10	+1,2		2.8 *	0	COX	72	ELEC
<3.E−10	+2			0	CROUCH	72	CNTR
<3.E−8			7	0	[29] DARDO	72	CNTR
<4.E−9	+1			0	[30] EVANS	72	CC
<2.E−9		>10		0	[29] TONWAR	72	CNTR
<2.E−10	+1		2.8 *	0	CHIN	71	CNTR
<3.E−10	+1,2			0	[30] CLARK	71B	CC
<1.E−10	+1,2			0	[30] HAZEN	71	CC
<5.E−10	+1,2		3.5 *	0	BOSIA	70	CNTR
	+1,2	<6.5		1	[30] CHU	70	HLBC
<2.E−9	+1			0	FAISSNER	70B	CNTR
<2.E−10	+1,2		0.8 *	0	KRIDER	70	CNTR
<5.E−11	+2			4	CAIRNS	69	CC
<8.E−10	+1,2	<10		0	FUKUSHIMA	69	CNTR
	+2			1	[30,32] MCCUSKER	69	CC
<1.E−10		>5	1.7,3.6	0	[29] BJORNBOE	68	CNTR
<1.E−8	±1,2,4		6.3,.2 *	0	[27] BRIATORE	68	CNTR
<3.E−8		>2		0	FRANZINI	68	CNTR
<9.E−11	±1,2			0	GARMIRE	68	CNTR
<4.E−10	±1			0	HANAYAMA	68	CNTR
<3.E−8		>15		0	KASHA	68	OSPK
<2.E−10	+2			0	KASHA	68B	CNTR
<2.E−10	+4			0	KASHA	68C	CNTR
<2.E−10	+2		6	0	BARTON	67	CNTR
<2.E−7	+4		0.008,0.5 *	0	BUHLER	67	CNTR
<5.E−10	1,2		0.008,0.5 *	0	BUHLER	67B	CNTR
<4.E−10	+1,2			0	GOMEZ	67	CNTR
<2.E−9	+2			0	KASHA	67	CNTR
<2.E−10	+2		220	0	BARTON	66	CNTR
<2.E−9	+1,2		0.5 *	0	BUHLER	66	CNTR
<3.E−9	+1,2			0	KASHA	66	CNTR
<2.E−9	+1,2			0	LAMB	66	CNTR
<2.E−8	+1,2	>7	2.8 *	0	DELISE	65	CNTR
<5.E−8	+2	>2.5	0.5 *	0	MASSAM	65	CNTR
<2.E−8	+1		2.5 *	0	BOWEN	64	CNTR
<2.E−7	+1		0.8	0	SUNYAR	64	CNTR

[24] AMBROSIO 00C limit is below 11×10^{-15} for $0.25 < q/e < 0.5$, and is changing rapidly near q/e=2/3, where it is 2×10^{-14}.

[25] Distribution in celestial sphere was described as anisotropic.

[26] With telescope axis at zenith angle 40° to the south.

[27] Leptonic quarks.

[28] Lifetime $> 10^{-8}$ s; charge ±0.70, 0.68, 0.42; and mass >4.4, 4.8, and 20 GeV, respectively.

[29] Time delayed air shower search.

[30] Prompt air shower search.

[31] Also $e/4$ and $e/6$ charges.

[32] No events in subsequent experiments.

Quark Density — Matter Searches

QUARKS/ NUCLEON	CHG ($e/3$)	MASS (GeV)	MATERIAL/METHOD	EVTS	DOCUMENT ID	
<1.17E−22			silicone oil drops	0	[33] LEE	02
<4.71E−22			silicone oil drops	1	[34] HALYO	00
<4.7E−21	±1,2		silicone oil drops	0	MAR	96
<8.E−22	+2		Si/infrared photoionization	0	PERERA	93
<5.E−27	±1,2		sea water/levitation	0	HOMER	92
<4.E−20	±1,2		meteorites/mag. levitation	0	JONES	89
<1.E−19	±1,2		various/spectrometer	0	MILNER	87
<5.E−22	±1,2		W/levitation	0	SMITH	87
<3.E−20	+1,2		org liq/droplet tower	0	VANPOLEN	87
<6.E−20	−1,2		org liq/droplet tower	0	VANPOLEN	87
<3.E−21	±1		Hg drops-untreated	0	SAVAGE	86
<3.E−22	±1,2		levitated niobium	0	SMITH	86
<2.E−26	±1,2		^{4}He/levitation	0	SMITH	86B
<2.E−20	>±1	0.2–250	niobium+tungs/ion	0	MILNER	85
<1.E−21	±1		levitated niobium	0	SMITH	85
	+1,2	<100	niobium/mass spec	0	KUTSCHERA	84
<5.E−22			levitated steel	0	MARINELLI	84
<9.E−20	± <13		water/oil drop	0	JOYCE	83
<2.E−21	$>\lvert\pm 1/2\rvert$		levitated steel	0	LIEBOWITZ	83
<1.E−19	±1,2		photo ion spec	0	VANDESTEEG	83
<2.E−20			mercury/oil drop	0	[35] HODGES	81
1.E−20	+1		levitated niobium	4	[36] LARUE	81
1.E−20	−1		levitated niobium	4	[36] LARUE	81
<1.E−21			levitated steel	0	MARINELLI	80B
<6.E−16			helium/mass spec	0	BOYD	79
1.E−20	+1		levitated niobium	2	[36] LARUE	79
<4.E−28			earth+/ion beam	0	OGOROD...	79
<5.E−15	+1		tungs./mass spec	0	BOYD	78
<5.E−16	+3	<1.7	hydrogen/mass spec	0	BOYD	78B
<1.E−21	±2,4		water/ion beam	0	LUND	78
<6.E−15	>1/2		levitated tungsten	0	PUTT	78
<1.E−22			metals/mass spec	0	SCHIFFER	78

Quark Particle Listings

Free Quark Searches

<5.E−15			levitated tungsten ox	0	BLAND	77
<3.E−21			levitated iron	0	GALLINARO	77
2.E−21	−1		levitated niobium	1	[36] LARUE	77
4.E−21	+1		levitated niobium	2	[36] LARUE	77
<1.E−13	+3	<7.7	hydrogen/mass spec	0	MULLER	77
<5.E−27			water+/ion beam	0	OGOROD...	77
<1.E−21			lunar+/ion spec	0	STEVENS	76
<1.E−15	+1	<60	oxygen+/ion spec	0	ELBERT	70
<5.E−19			levitated graphite	0	MORPURGO	70
<5.E−23			water+/atom beam	0	COOK	69
<1.E−17	±1,2		levitated graphite	0	BRAGINSK	68
<1.E−17			water+/uv spec	0	RANK	68
<3.E−19	±1		levitated iron	0	STOVER	67
<1.E−10			sun/uv spec	0	[37] BENNETT	66
<1.E−17	+1,2		meteorites+/ion beam	0	CHUPKA	66
<1.E−16	±1		levitated graphite	0	GALLINARO	66
<1.E−22			argon/electrometer	0	HILLAS	59
	−2		levitated oil	0	MILLIKAN	10

[33] 95% CL limit for fractional charge particles with $0.18e \leq |Q_{residual}| \leq 0.82e$ in total of 70.1 mg of silicone oil.

[34] 95% CL limit for particles with fractional charge $|Q_{residual}| > 0.16e$ in total of 17.4 mg of silicone oil.

[35] Also set limits for $Q = \pm e/6$.

[36] Note that in PHILLIPS 88 these authors report a subtle magnetic effect which could account for the apparent fractional charges.

[37] Limit inferred by JONES 77B.

REFERENCES FOR Free Quark Searches

CHATRCHYAN 13AR PR D87 092008 S. Chatrchyan *et al.* (CMS Collab.)
LEE 02 PR D66 012002 I.T. Lee *et al.*
AMBROSIO 00C PR D62 052003 M. Ambrosio *et al.* (MACRO Collab.)
HALYO 00 PRL 84 2576 V. Halyo *et al.*
ABREU 97D PL B396 315 P. Abreu *et al.* (DELPHI Collab.)
HUENTRUP 96 PR C53 358 G. Huentrup *et al.* (SIEG)
MAR 96 PR D53 6017 N.M. Mar *et al.* (SLAC, SCHAF, LANL, UCI)
AKERS 95R ZPHY C67 203 R. Akers *et al.* (OPAL Collab.)
BUSKULIC 93C PL B303 198 D. Buskulic *et al.* (ALEPH Collab.)
CECCHINI 93 ASP 1 369 S. Cecchini *et al.*
PERERA 93 PRL 70 1053 A.G.U. Perera *et al.* (PITT)
ABE 92J PR D46 R1889 F. Abe *et al.* (CDF Collab.)
GHOSH 92 NC 105A 99 D. Ghosh *et al.* (JADA, BANGB)
HOMER 92 ZPHY C55 549 G.J. Homer *et al.* (RAL, SHMP, LOQM)
BASILE 91 NC 104A 405 M. Basile *et al.* (BGNA, INFN, CERN, PLRM+)
HE 91 PR C44 1672 Y.B. He, P.B. Price (UCB)
MATIS 91 NP A525 513c H.S. Matis *et al.* (LBL, SFSU, UCI+)
MORI 91 PR D43 2843 M. Mori *et al.* (Kamiokande II Collab.)
ADACHI 90C PL B244 352 I. Adachi *et al.* (TOPAZ Collab.)
BOWCOCK 89B PR D40 263 T.J.V. Bowcock *et al.* (CLEO Collab.)
CALLOWAY 89 PL B232 549 D. Calloway *et al.* (SFSU, UCI, LBL+)
JONES 89 ZPHY C43 349 W.G. Jones *et al.* (LOIC, RAL)
MATIS 89 PR D39 1851 H.S. Matis *et al.* (LBL, SFSU, UCI+)
NAKAMURA 89 PR D39 1261 T.T. Nakamura *et al.* (KYOT, TMTC)
ALLASIA 88 PR D37 219 D. Allasia *et al.* (WA25 Collab.)
HOFFMANN 88 PL B200 583 A. Hofmann *et al.* (SIEG, USF)
PHILLIPS 88 NIM A264 125 J.D. Phillips, W.M. Fairbank, J. Navarro (STAN)
WADA 88 NC 11C 229 T. Wada, Y. Yamashita, I. Yamamoto (OKAY)
GERBIER 87 PRL 59 2535 G. Gerbier *et al.* (UCB, CERN)
LYONS 87 ZPHY C36 363 L. Lyons *et al.* (OXF, RAL, LOIC)
MILNER 87 PR D36 37 R.E. Milner *et al.* (CIT)
SHAW 87 PR D36 3533 G.L. Shaw *et al.* (UCI, LBL, LANL, SFSU)
SMITH 87 PL B197 447 P.F. Smith *et al.* (RAL, LOIC)
VANPOLEN 87 PR D36 1983 J. van Polen, R.T. Hagstrom, G. Hirsch (ANL+)
ABACHI 86C PR D33 2733 S. Abachi *et al.* (UCLA, LBL, UCD)
SAVAGE 86 PL 167B 481 M.L. Savage *et al.* (SFSU)
SMITH 86 PL B171 129 P.F. Smith *et al.* (RAL, LOIC)
SMITH 86B PL B181 407 P.F. Smith *et al.* (RAL, LOIC)
WADA 86 NC 9C 358 T. Wada (OKAY)
ALBRECHT 85G PL 156B 134 H. Albrecht *et al.* (ARGUS Collab.)
BANNER 85 PL 156B 129 M. Banner *et al.* (UA2 Collab.)
MILNER 85 PRL 54 1472 R.E. Milner *et al.* (CIT)
SMITH 85 PL 153B 188 P.F. Smith *et al.* (RAL, LOIC)
AIHARA 84 PRL 52 168 H. Aihara *et al.* (TPC Collab.)
AIHARA 84B PRL 52 2332 H. Aihara *et al.* (TPC Collab.)
BARWICK 84 PR D30 691 S.W. Barwick, J.A. Musser, J.D. Stevenson (UCB)
BERGSMA 84B ZPHY C24 217 F. Bergsma *et al.* (CHARM Collab.)
BONDAR 84 JETPL 40 1265 A.E. Bondar *et al.* (NOVO)
Translated from ZETFP 40 440.
GURYN 84 PL 139B 313 W. Guryn *et al.* (FRAS, LBL, NWES, STAN+)
KAWAGOE 84B LNC 41 604 K. Kawagoe *et al.* (TOKY)
KUTSCHERA 84 PR D29 791 W. Kutschera *et al.* (ANL, FNAL)
MARINELLI 84 PL 137B 439 M. Marinelli, G. Morpurgo (GENO)
WADA 84B LNC 40 329 T. Wada, Y. Yamashita, I. Yamamoto (OKAY)
AUBERT 83C PL 133B 461 J.J. Aubert *et al.* (EMC Collab.)
BANNER 83 PL 121B 187 M. Banner *et al.* (UA2 Collab.)
JOYCE 83 PRL 51 731 D.C. Joyce *et al.* (SFSU)
LIEBOWITZ 83 PRL 50 1640 D. Liebowitz, M. Binder, K.O.H. Ziock (UVA)
LINDGREN 83 PRL 51 1621 M.A. Lindgren *et al.* (SFSU, UCR, UCI+)
MASHIMO 83 PL 128B 327 T. Mashimo *et al.* (ICEPP)
PRICE 83 PRL 50 566 P.B. Price *et al.* (UCB)
VANDESTEEG 83 PRL 50 1234 M.J.H. van de Steeg, H.W.H.M. Jongbloets, P. Wyder
MARINI 82 PR D26 1777 A. Marini *et al.* (FRAS, LBL, NWES, STAN+)
MARINI 82B PRL 48 1649 A. Marini *et al.* (FRAS, LBL, NWES, STAN+)
MASHIMO 82 JPSJ 51 3067 T. Mashimo, K. Kawagoe, M. Koshiba (INUS)
NAPOLITANO 82 PR D25 2837 J. Napolitano *et al.* (STAN, FRAS, LBL+)
ROSS 82 PL 118B 199 M.C. Ross *et al.* (FRAS, LBL, NWES, STAN+)
HODGES 81 PRL 47 1651 C.L. Hodges *et al.* (UCR, SFSU)
LARUE 81 PRL 46 967 G.S. Larue, J.D. Phillips, W.M. Fairbank (STAN)
WEISS 81 PL 101B 439 J.M. Weiss *et al.* (SLAC, LBL, UCB)
BARTEL 80 ZPHY C6 295 W. Bartel *et al.* (JADE Collab.)
BASILE 80 LNC 29 251 M. Basile *et al.* (BGNA, CERN, FRAS, ROMA+)
BUSSIERE 80 NP B174 1 A. Bussiere *et al.* (BGNA, SACL, LAPP)
MARINELLI 80B PL 94B 433 M. Marinelli, G. Morpurgo (GENO)
Also PL 94B 427 M. Marinelli, G. Morpurgo (GENO)
BOYD 79 PRL 43 1288 R.N. Boyd *et al.* (OSU)
BOZZOLI 79 NP B159 363 W. Bozzoli *et al.* (BGNA, LAPP, SACL+)
LARUE 79 PRL 42 142 G.S. Larue, W.M. Fairbank, J.D. Phillips (STAN)
Also PRL 42 1019 G.S. Larue, W.M. Fairbank, J.D. Phillips
OGOROD... 79 JETP 49 953 D.D. Ogorodnikov, I.M. Samoilov, A.M. Solntsev
Translated from ZETF 76 1881.
STEVENSON 79 PR D20 82 M.L. Stevenson (LBL)
BASILE 78 NC 45A 171 M. Basile *et al.* (CERN, BGNA)
BASILE 78B NC 45A 281 M. Basile *et al.* (CERN, BGNA)
BOYD 78 PRL 40 216 R.N. Boyd *et al.* (ROCH)
BOYD 78B PL 72B 484 R.N. Boyd *et al.* (ROCH)
LUND 78 RA 25 75 T. Lund, R. Brandt, Y. Fares (MARB)
PUTT 78 PR D17 1466 G.D. Putt, P.C.M. Yock (AUCK)
SCHIFFER 78 PR D17 2241 J.P. Schiffer *et al.* (CHIC, ANL)
YOCK 78 PR D18 641 P.C.M. Yock (AUCK)
ANTREASYAN 77 PRL 39 513 D. Antreasyan *et al.* (EFI, PRIN)
BASILE 77 NC 40A 41 M. Basile *et al.* (CERN, BGNA)
BLAND 77 PRL 39 369 R.W. Bland *et al.* (SFSU)
GALLINARO 77 PRL 38 1255 G. Gallinaro, M. Marinelli, G. Morpurgo (GENO)
JONES 77B RMP 49 717 L.W. Jones
LARUE 77 PRL 38 1011 G.S. Larue, W.M. Fairbank, A.F. Hebard (STAN)
MULLER 77 SCI 196 521 R.A. Muller *et al.* (LBL)
OGOROD... 77 JETP 45 857 D.D. Ogorodnikov, I.M. Samoilov, A.M. Solntsev
Translated from ZETF 72 1633.
BALDIN 76 SJNP 22 264 B.Y. Baldin *et al.* (JINR)
Translated from YAF 22 512.
BRIATORE 76 NC 31A 553 L. Briatore *et al.* (LCGT, FRAS, FREIB)
STEVENS 76 PR D14 716 C.M. Stevens, J.P. Schiffer, W. Chupka (ANL)
ALBROW 75 NP B97 189 M.G. Albrow *et al.* (CERN, DARE, FOM+)
FABJAN 75 NP B101 349 C.W. Fabjan *et al.* (CERN, MPIM)
HAZEN 75 NP B95 189 W.E. Hazen *et al.* (MICH, LEED)
JOVANOV... 75 PL 56B 105 J.V. Jovanovich *et al.* (MANI, AACH, CERN+)
KRISOR 75 NC 27A 132 K. Krisor (AACH3)
CLARK 74B PR D10 2721 A.F. Clark *et al.* (LLL)
GALIK 74 PR D9 1856 R.S. Galik *et al.* (SLAC, FNAL)
KIFUNE 74 JPSJ 36 629 T. Kifune *et al.* (TOKY, KEK)
NASH 74 PRL 32 858 T. Nash *et al.* (FNAL, CORN, NYU)
ALPER 73 PL 46B 265 B. Alper *et al.* (CERN, LIVP, LUND, BOHR+)
ASHTON 73 JP A6 577 F. Ashton *et al.* (DURH)
HICKS 73B NC 14A 65 R.B. Hicks, R.W. Flint, S. Standil (MANI)
LEIPUNER 73 PRL 31 1226 L.B. Leipuner *et al.* (BNL, YALE)
BEAUCHAMP 72 PR D6 1211 W.T. Beauchamp *et al.* (ARIZ)
BOHM 72B PR 28 326 A. Bohm *et al.* (AACH)
BOTT 72 PL 40B 693 M. Bott-Bodenhausen *et al.* (CERN, MPIM)
COX 72 PR D6 1203 A.J. Cox *et al.* (ARIZ)
CROUCH 72 PR D5 2667 M.F. Crouch, K. Mori, G.R. Smith (CASE)
DARDO 72 NC 9A 319 M. Dardo *et al.* (TORI)
EVANS 72 PRSE A70 143 G.R. Evans *et al.* (EDIN, LEED)
TONWAR 72 JP A5 569 S.C. Tonwar, S. Naranan, B.V. Sreekantan (TATA)
ANTIPOV 71 NP B29 374 Y.M. Antipov *et al.* (SERP)
CHIN 71 NC 2A 419 S. Chin *et al.* (OSAK)
CLARK 71B PRL 27 51 A.F. Clark *et al.* (LLL, LBL)
HAZEN 71 PRL 26 582 W.E. Hazen (MICH)
BOSIA 70 NC 66A 167 G.F. Bosia, L. Briatore (TORI)
CHU 70 PRL 24 917 W.T. Chu *et al.* (OSU, ROSE, KANS)
Also PRL 25 550 W.W.M. Allison *et al.* (ANL)
ELBERT 70 NP B20 217 J.W. Elbert *et al.* (WISC)
FAISSNER 70B PRL 24 1357 H. Faissner *et al.* (AACH3)
KRIDER 70 PR D1 835 E.P. Krider, T. Bowen, R.M. Kalbach (ARIZ)
MORPURGO 70 NIM 79 95 G. Morpurgo, G. Gallinaro, G. Palmieri (GENO)
ALLABY 69B NC 64A 75 J.V. Allaby *et al.* (CERN)
ANTIPOV 69 PL 29B 245 Y.M. Antipov *et al.* (SERP)
ANTIPOV 69B PL 30B 576 Y.M. Antipov *et al.* (SERP)
CAIRNS 69 PR 186 1394 I. Cairns *et al.* (SYDN)
COOK 69 PR 188 2092 D.D. Cook *et al.* (ILL)
FUKUSHIMA 69 PR 178 2058 Y. Fukushima *et al.* (TOKY)
MCCUSKER 69 PRL 23 658 C.B.A. McCusker, I. Cairns (SYDN)
BELLAMY 68 PR 166 1391 E.H. Bellamy *et al.* (STAN, SLAC)
BJORNBOE 68 NC B53 241 J. Bjornboe *et al.* (BOHR, TATA, BERN+)
BRAGINSK 68 JETP 27 51 V.B. Braginsky *et al.* (MOSU)
Translated from ZETF 54 91.
BRIATORE 68 NC 57A 850 L. Briatore *et al.* (TORI, CERN, BGNA)
FRANZINI 68 PRL 21 1013 P. Franzini, S. Shulman (COLU)
GARMIRE 68 PR 166 1280 G. Garmire, C. Leong, V. Sreekantan (MIT)
HANAYAMA 68 CJP 46 S734 Y. Hanayama *et al.* (OSAK)
KASHA 68 PR 172 1297 H. Kasha, R.J. Stefanski (BNL, YALE)
KASHA 68B PRL 20 217 H. Kasha *et al.* (BNL, YALE)
KASHA 68C CJP 46 S730 H. Kasha *et al.* (BNL, YALE)
RANK 68 PR 176 1635 D. Rank (MICH)
BARTON 67 PRSL 90 87 J.C. Barton (NPOL)
BATHOW 67 PL 25B 163 G. Bathow *et al.* (DESY)
BUHLER 67 NC 49A 209 A. Buhler-Broglin *et al.* (CERN, BGNA)
BUHLER 67B NC 51A 837 A. Buhler-Broglin *et al.* (CERN, BGNA+)
FOSS 67 PL 25B 166 J. Foss *et al.* (MIT)
GOMEZ 67 PRL 18 1022 R. Gomez *et al.* (CIT)
KASHA 67 PR 154 1263 H. Kasha *et al.* (BNL, YALE)
STOVER 67 PR 164 1599 R.W. Stover, T.I. Moran, J.W. Trischka (SYRA)
BARTON 66 PL 21 360 J.C. Barton, C.T. Stockel (NPOL)
BENNETT 66 PRL 17 1196 W.R. Bennett (YALE)
BUHLER 66 NC 45A 520 A. Buhler-Broglin *et al.* (CERN, BGNA+)
CHUPKA 66 PRL 17 60 W.A. Chupka, J.P. Schiffer, C.M. Stevens (ANL)
GALLINARO 66 PL 23 609 G. Gallinaro, G. Morpurgo (GENO)
KASHA 66 PR 150 1140 H. Kasha, L.B. Leipuner, R.K. Adair (BNL, YALE)
LAMB 66 PRL 17 1068 R.C. Lamb *et al.* (ANL)
DELISE 65 PR 140B 458 D.A. de Lise, T. Bowen (ARIZ)
DORFAN 65 PRL 14 999 D.E. Dorfan *et al.* (COLU)
FRANZINI 65B PRL 14 196 P. Franzini *et al.* (BNL, COLU)
MASSAM 65 NC 40A 589 T. Massam, T. Muller, A. Zichichi (CERN)
BINGHAM 64 PL 9 201 H.H. Bingham *et al.* (CERN, EPOL)
BLUM 64 PRL 13 353A W. Blum *et al.* (CERN)
BOWEN 64 PRL 13 728 T. Bowen *et al.* (ARIZ)
HAGOPIAN 64 PRL 13 280 V. Hagopian *et al.* (PENN, BNL)
LEIPUNER 64 PRL 12 423 L.B. Leipuner *et al.* (BNL, YALE)
MORRISON 64 PL 9 199 D.R.O. Morrison (CERN)
SUNYAR 64 PR 136 B1157 A.W. Sunyar, A.Z. Schwarzschild, P.I. Connors (BNL)
HILLAS 59 NAT 184 B92 A.M. Hillas, T.E. Cranshaw (AERE)
MILLIKAN 10 Phil Mag 19 209 R.A. Millikan (CHIC)

OTHER RELATED PAPERS

LYONS 85 PRPL C129 225 L. Lyons (OXF)
Review
MARINELLI 82 PRPL 85 161 M. Marinelli, G. Morpurgo (GENO)
Review

• Indicates the particle is in the Meson Summary Table

(continued on the next page)

• Indicates the particle is in the Meson Summary Table

Notes in the Meson Listings

LIGHT UNFLAVORED MESONS
($S = C = B = 0$)

For $I = 1$ (π, b, ρ, a): $u\overline{d}$, $(u\overline{u}-d\overline{d})/\sqrt{2}$, $d\overline{u}$;
for $I = 0$ (η, η', h, h', ω, ϕ, f, f'): $c_1(u\overline{u}+d\overline{d}) + c_2(s\overline{s})$

$\pi^{\pm}$

$I^G(J^P) = 1^-(0^-)$

We have omitted some results that have been superseded by later experiments. The omitted results may be found in our 1988 edition Physics Letters **B204** 1 (1988).

$\pi^{\pm}$ MASS

The most accurate charged pion mass measurements are based upon x-ray wavelength measurements for transitions in π^--mesonic atoms. The observed line is the blend of three components, corresponding to different K-shell occupancies. JECKELMANN 94 revisits the occupancy question, with the conclusion that two sets of occupancy ratios, resulting in two different pion masses (Solutions A and B), are equally probable. We choose the higher Solution B since only this solution is consistent with a positive mass-squared for the muon neutrino, given the precise muon momentum measurements now available (DAUM 91, ASSAMAGAN 94, and ASSAMAGAN 96) for the decay of pions at rest. Earlier mass determinations with pi-mesonic atoms may have used incorrect K-shell screening corrections.

Measurements with an error of > 0.005 MeV have been omitted from this Listing.

VALUE (MeV)		DOCUMENT ID		TECN	CHG	COMMENT
139.57018±0.00035 OUR FIT	Error includes scale factor of 1.2.					
139.57018±0.00035 OUR AVERAGE	Error includes scale factor of 1.2.					
139.57071±0.00053		[1] LENZ	98	CNTR	−	pionic N2-atoms gas target
139.56995±0.00035		[2] JECKELMANN	94	CNTR	−	π^- atom, Soln. B
• • • We do not use the following data for averages, fits, limits, etc. • • •						
139.57022±0.00014		[3] ASSAMAGAN	96	SPEC	+	$\pi^+ \to \mu^+\nu_\mu$
139.56782±0.00037		[4] JECKELMANN	94	CNTR	−	π^- atom, Soln. A
139.56996±0.00067		[5] DAUM	91	SPEC	+	$\pi^+ \to \mu^+\nu$
139.56752±0.00037		[6] JECKELMANN	86B	CNTR	−	Mesonic atoms
139.5704 ±0.0011		[5] ABELA	84	SPEC	+	See DAUM 91
139.5664 ±0.0009		[7] LU	80	CNTR	−	Mesonic atoms
139.5686 ±0.0020		CARTER	76	CNTR	−	Mesonic atoms
139.5660 ±0.0024		[7,8] MARUSHEN...	76	CNTR	−	Mesonic atoms

[1] LENZ 98 result does not suffer K-electron configuration uncertainties as does JECKELMANN 94.

[2] JECKELMANN 94 Solution B (dominant 2-electron K-shell occupancy), chosen for consistency with positive $m^2_{\nu_\mu}$.

[3] ASSAMAGAN 96 measures the μ^+ momentum p_μ in $\pi^+ \to \mu^+\nu_\mu$ decay at rest to be 29.79200 ± 0.00011 MeV/c. Combined with the μ^+ mass and the assumption $m_{\nu_\mu} = 0$, this gives the π^+ mass above; if $m_{\nu_\mu} > 0$, m_{π^+} given above is a lower limit. Combined instead with m_μ and (assuming CPT) the π^- mass of JECKELMANN 94, p_μ gives an upper limit on m_{ν_μ} (see the ν_μ).

[4] JECKELMANN 94 Solution A (small 2-electron K-shell occupancy) in combination with either the DAUM 91 or ASSAMAGAN 94 pion decay muon momentum measurement yields a significantly negative $m^2_{\nu_\mu}$. It is accordingly not used in our fits.

[5] The DAUM 91 value includes the ABELA 84 result. The value is based on a measurement of the μ^+ momentum for π^+ decay at rest, $p_\mu = 29.79179 \pm 0.00053$ MeV, uses $m_\mu = 105.658389 \pm 0.000034$ MeV, and assumes that $m_{\nu_\mu} = 0$. The last assumption means that in fact the value is a lower limit.

[6] JECKELMANN 86B gives $m_\pi/m_e = 273.12677(71)$. We use $m_e = 0.51099906(15)$ MeV from COHEN 87. The authors note that two solutions for the probability distribution of K-shell occupancy fit equally well, and use other data to choose the lower of the two possible $\pi^\pm$ masses.

[7] These values are scaled with a new wavelength-energy conversion factor $V\lambda = 1.23984244(37) \times 10^{-6}$ eV m from COHEN 87. The LU 80 screening correction relies upon a theoretical calculation of inner-shell refilling rates.

[8] This MARUSHENKO 76 value used at the authors' request to use the accepted set of calibration γ energies. Error increased from 0.0017 MeV to include QED calculation error of 0.0017 MeV (12 ppm).

$m_{\pi^+} - m_{\mu^+}$

Measurements with an error > 0.05 MeV have been omitted from this Listing.

VALUE (MeV)	EVTS	DOCUMENT ID		TECN	CHG	COMMENT
• • • We do not use the following data for averages, fits, limits, etc. • • •						
33.91157±0.00067		[9] DAUM	91	SPEC	+	$\pi^+ \to \mu^+\nu$
33.9111 ±0.0011		ABELA	84	SPEC		See DAUM 91
33.925 ±0.025		BOOTH	70	CNTR	+	Magnetic spect.
33.881 ±0.035	145	HYMAN	67	HEBC	+	K^- He

[9] The DAUM 91 value assumes that $m_{\nu_\mu} = 0$ and uses our $m_\mu = 105.658389 \pm 0.000034$ MeV.

$(m_{\pi^+} - m_{\pi^-})$ / m_{average}

A test of CPT invariance.

VALUE (units 10^{-4})	DOCUMENT ID		TECN
2±5	AYRES	71	CNTR

$\pi^{\pm}$ MEAN LIFE

Measurements with an error $> 0.02 \times 10^{-8}$ s have been omitted.

VALUE (10^{-8} s)	DOCUMENT ID		TECN	CHG	COMMENT
2.6033 ±0.0005 OUR AVERAGE	Error includes scale factor of 1.2.				
2.60361±0.00052	[10] KOPTEV	95	SPEC	+	Surface μ^+'s
2.60231±0.00050±0.00084	NUMAO	95	SPEC	+	Surface μ^+'s
2.609 ±0.008	DUNAITSEV	73	CNTR	+	
2.602 ±0.004	AYRES	71	CNTR	±	
2.604 ±0.005	NORDBERG	67	CNTR	+	
2.602 ±0.004	ECKHAUSE	65	CNTR	+	
• • • We do not use the following data for averages, fits, limits, etc. • • •					
2.640 ±0.008	[11] KINSEY	66	CNTR	+	

[10] KOPTEV 95 combines the statistical and systematic errors; the statistical error dominates.

[11] Systematic errors in the calibration of this experiment are discussed by NORDBERG 67.

$(\tau_{\pi^+} - \tau_{\pi^-})$ / τ_{average}

A test of CPT invariance.

VALUE (units 10^{-4})	DOCUMENT ID		TECN
5.5± 7.1	AYRES	71	CNTR
• • • We do not use the following data for averages, fits, limits, etc. • • •			
−14 ±29	PETRUKHIN	68	CNTR
40 ±70	BARDON	66	CNTR
23 ±40	[12] LOBKOWICZ	66	CNTR

[12] This is the most conservative value given by LOBKOWICZ 66.

π^+ DECAY MODES

π^- modes are charge conjugates of the modes below.

For decay limits to particles which are not established, see the section on Searches for Axions and Other Very Light Bosons.

	Mode		Fraction (Γ_i/Γ)			Confidence level
Γ_1	$\mu^+\nu_\mu$	[a]	(99.98770±0.00004) %			
Γ_2	$\mu^+\nu_\mu\gamma$	[b]	(2.00	±0.25	) $\times 10^{-4}$	
Γ_3	$e^+\nu_e$	[a]	(1.230	±0.004	) $\times 10^{-4}$	
Γ_4	$e^+\nu_e\gamma$	[b]	(7.39	±0.05	) $\times 10^{-7}$	
Γ_5	$e^+\nu_e\pi^0$		(1.036	±0.006	) $\times 10^{-8}$	
Γ_6	$e^+\nu_e e^+e^-$		(3.2	±0.5	) $\times 10^{-9}$	
Γ_7	$e^+\nu_e\nu\overline{\nu}$		< 5		$\times 10^{-6}$	90%
Lepton Family number (LF) or Lepton number (L) violating modes						
Γ_8	$\mu^+\overline{\nu}_e$	L	[c] < 1.5		$\times 10^{-3}$	90%
Γ_9	$\mu^+\nu_e$	LF	[c] < 8.0		$\times 10^{-3}$	90%
Γ_{10}	$\mu^-e^+e^+\nu$	LF	< 1.6		$\times 10^{-6}$	90%

[a] Measurements of $\Gamma(e^+\nu_e)/\Gamma(\mu^+\nu_\mu)$ always include decays with γ's, and measurements of $\Gamma(e^+\nu_e\gamma)$ and $\Gamma(\mu^+\nu_\mu\gamma)$ never include low-energy γ's. Therefore, since no clean separation is possible, we consider the modes with γ's to be subreactions of the modes without them, and let $[\Gamma(e^+\nu_e) + \Gamma(\mu^+\nu_\mu)]/\Gamma_{\text{total}} = 100\%$.

[b] See the Particle Listings below for the energy limits used in this measurement; low-energy γ's are not included.

[c] Derived from an analysis of neutrino-oscillation experiments.

π^+ BRANCHING RATIOS

$\Gamma(e^+\nu_e)/\Gamma_{\text{total}}$ **Γ_3/Γ**

See note [a] in the list of π^+ decay modes just above, and see also the next block of data. See also the note on "Decay Constants of Charged Pseudoscalar Mesons" in the D_s^+ Listings.

VALUE (units 10^{-4})	DOCUMENT ID
1.230±0.004 OUR EVALUATION	

$[\Gamma(e^+\nu_e)+\Gamma(e^+\nu_e\gamma)]/[\Gamma(\mu^+\nu_\mu)+\Gamma(\mu^+\nu_\mu\gamma)]$ $(\Gamma_3+\Gamma_4)/(\Gamma_1+\Gamma_2)$

See note [a] in the list of π^+ decay modes above. See NUMAO 92 for a discussion of e-μ universality. See also the note on "Decay Constants of Charged Pseudoscalar Mesons" in the D_s^+ Listings.

VALUE (units 10^{-4})	EVTS	DOCUMENT ID		TECN	COMMENT
1.230 ±0.004 OUR AVERAGE					
1.2346±0.0035±0.0036	120k	CZAPEK	93	CALO	Stopping π^+
1.2265±0.0034±0.0044	190k	BRITTON	92	CNTR	Stopping π^+
1.218 ±0.014	32k	BRYMAN	86	CNTR	Stopping π^+
• • • We do not use the following data for averages, fits, limits, etc. • • •					
1.273 ±0.028	11k	[13] DICAPUA	64	CNTR	
1.21 ±0.07		ANDERSON	60	SPEC	

[13] DICAPUA 64 has been updated using the current mean life.

$\Gamma(\mu^+\nu_\mu\gamma)/\Gamma_{\text{total}}$ Γ_2/Γ

Note that measurements here do not cover the full kinematic range.

VALUE (units 10^{-4})	EVTS	DOCUMENT ID		TECN	CHG	COMMENT
2.0 ±0.24±0.08		[14] BRESSI	98	CALO	+	Stopping π^+
• • • We do not use the following data for averages, fits, limits, etc. • • •						
1.24±0.25	26	CASTAGNOLI	58	EMUL		KE_μ < 3.38 MeV

[14] BRESSI 98 result is given for $E_\gamma > 1$ MeV only. Result agrees with QED expectation, 2.283×10^{-4} and does not confirm discrepancy of earlier experiment CASTAGNOLI 58.

$\Gamma(e^+\nu_e\gamma)/\Gamma_{\text{total}}$ Γ_4/Γ

The very different values reflect the very different kinematic ranges covered (bigger range, bigger value). And none of them covers the whole kinematic range.

VALUE (units 10^{-8})	EVTS	DOCUMENT ID		TECN	COMMENT
73.86±0.54	65k	[15] BYCHKOV	09	PIBE	$e^+\nu\gamma$ at rest
• • • We do not use the following data for averages, fits, limits, etc. • • •					
16.1 ±2.3		[16] BOLOTOV	90B	SPEC	17 GeV $\pi^-\to e^-\overline{\nu}_e\gamma$
5.6 ±0.7	226	[17] STETZ	78	SPEC	$P_e > 56$ MeV/c
3.0	143	DEPOMMIER	63B	CNTR	$(KE)_{e^+\gamma} > 48$ MeV

[15] This BYCHKOV 09 value is for $E_\gamma > 10$ MeV and $\Theta_{e^+\gamma} > 40^\circ$.

[16] BOLOTOV 90B is for $E_\gamma > 21$ MeV, $E_e > 70 - 0.8\,E_\gamma$.

[17] STETZ 78 is for an $e^-\gamma$ opening angle $> 132^\circ$. Obtains 3.7 when using same cutoffs as DEPOMMIER 63B.

$\Gamma(e^+\nu_e\pi^0)/\Gamma_{\text{total}}$ Γ_5/Γ

VALUE (units 10^{-8})	EVTS	DOCUMENT ID		TECN	CHG	COMMENT
1.036±0.006 OUR AVERAGE						
1.036±0.006	64k	[18,19] POCANIC	04	PIBE	+	π decay at rest
1.026±0.039	1224	[20] MCFARLANE	85	CNTR	+	Decay in flight
1.00 $^{+0.08}_{-0.10}$	332	DEPOMMIER	68	CNTR	+	
1.07 ±0.21	38	[21] BACASTOW	65	OSPK	+	
1.10 ±0.26		[21] BERTRAM	65	OSPK	+	
1.1 ±0.2	43	[21] DUNAITSEV	65	CNTR	+	
0.97 ±0.20	36	[21] BARTLETT	64	OSPK	+	
• • • We do not use the following data for averages, fits, limits, etc. • • •						
1.15 ±0.22	52	[21] DEPOMMIER	63	CNTR	+	See DEPOMMIER 68

[18] POCANIC 04 normalizes to $e^+\nu_e$ decays, using the PDG 2004 value $B(\pi^+\to e^+\nu_e) = (1.230\pm0.004)\times10^{-4}$. We add their statistical (0.004×10^{-8}), systematic (0.004×10^{-8}) and systematic error due to the uncertainty of $B(\pi^+\to e^+\nu_e)$ (0.003×10^{-8}) in quadrature.

[19] This result can be used to calculate V_{ud} from pion beta decay: $V_{ud}^{PIBETA} = 0.9728\pm0.0030$.

[20] MCFARLANE 85 combines a measured rate (0.394 ± 0.015)/s with 1982 PDG mean life.

[21] DEPOMMIER 68 says the result of DEPOMMIER 63 is at least 10% too large because of a systematic error in the π^0 detection efficiency, and that this may be true of all the previous measurements (also V. Soergel, private communication, 1972).

$\Gamma(e^+\nu_e e^+e^-)/\Gamma(\mu^+\nu_\mu)$ Γ_6/Γ_1

VALUE (units 10^{-9})	CL%	EVTS	DOCUMENT ID		TECN	COMMENT
3.2 ±0.5 ±0.2		98	EGLI	89	SPEC	Uses $R_{PCAC}=0.068\pm0.004$
• • • We do not use the following data for averages, fits, limits, etc. • • •						
0.46±0.16±0.07		7	[22] BARANOV	92	SPEC	Stopped π^+
< 4.8	90		KORENCHE...	76B	SPEC	
<34	90		KORENCHE...	71	OSPK	

[22] This measurement by BARANOV 92 is of the structure-dependent part of the decay. The value depends on values assumed for ratios of form factors.

$\Gamma(e^+\nu_e\nu\overline{\nu})/\Gamma_{\text{total}}$ Γ_7/Γ

VALUE (units 10^{-6})	CL%	DOCUMENT ID		TECN
<5	90	PICCIOTTO	88	SPEC

$\Gamma(\mu^+\overline{\nu}_e)/\Gamma_{\text{total}}$ Γ_8/Γ

Forbidden by total lepton number conservation. See the note on "Decay Constants of Charged Pseudoscalar Mesons" in the D_s^+ Listings.

VALUE (units 10^{-3})	CL%	DOCUMENT ID		TECN	COMMENT
<1.5	90	[23] COOPER	82	HLBC	Wideband ν beam

[23] COOPER 82 limit on $\overline{\nu}_e$ observation is here interpreted as a limit on lepton number violation.

$\Gamma(\mu^+\nu_e)/\Gamma_{\text{total}}$ Γ_9/Γ

Forbidden by lepton family number conservation.

VALUE (units 10^{-3})	CL%	DOCUMENT ID		TECN	COMMENT
<8.0	90	[24] COOPER	82	HLBC	Wideband ν beam

[24] COOPER 82 limit on ν_e observation is here interpreted as a limit on lepton family number violation.

$\Gamma(\mu^-e^+e^+\nu)/\Gamma_{\text{total}}$ Γ_{10}/Γ

Forbidden by lepton family number conservation.

VALUE (units 10^{-6})	CL%	DOCUMENT ID		TECN	CHG
<1.6	90	BARANOV	91B	SPEC	+
• • • We do not use the following data for averages, fits, limits, etc. • • •					
<7.7	90	KORENCHE...	87	SPEC	+

π^+ — POLARIZATION OF EMITTED μ^+

$\pi^+\to\mu^+\nu$

Tests the Lorentz structure of leptonic charged weak interactions.

VALUE	CL%	DOCUMENT ID		TECN	CHG	COMMENT
• • • We do not use the following data for averages, fits, limits, etc. • • •						
<(−0.9959)	90	[25] FETSCHER	84	RVUE	+	
−0.99±0.16		[26] ABELA	83	SPEC	−	μ X-rays

[25] FETSCHER 84 uses only the measurement of CARR 83.

[26] Sign of measurement reversed in ABELA 83 to compare with μ^+ measurements.

FORM FACTORS FOR RADIATIVE PION AND KAON DECAYS

Updated September 2013 by M. Bychkov (University of Virginia) and G. D'Ambrosio (INFN Sezione di Napoli)

The radiative decays, $\pi^\pm\to l^\pm\nu\gamma$ and $K^\pm\to l^\pm\nu\gamma$, with l standing for an e or a μ, and γ for a real or virtual photon (e^+e^- pair), provide a powerful tool to investigate the hadronic structure of pions and kaons. The structure-dependent part SD_i of the amplitude describes the emission of photons from virtual hadronic states, and is parametrized in terms of form factors V, A, (vector, axial vector), in the standard description [1,2,3,4]. Exotic, non-standard contributions like $i = T, S$ (tensor, scalar) have also been considered. Apart from the SD terms, there is also the Inner Bremsstrahlung amplitude, IB, corresponding to photon radiation from external charged particles and described by Low theorem in terms of the physical decay $\pi^\pm(K^\pm)\to l^\pm\nu$. Experiments try to optimize their kinematics so as to minimize the IB part of the amplitude.

The SD amplitude in its standard form is given as

$$M(\mathrm{SD}_V) = \frac{-eG_FU_{qq'}}{\sqrt{2}m_P}\epsilon^\mu l^\nu V^P\epsilon_{\mu\nu\sigma\tau}k^\sigma q^\tau \qquad (1)$$

$$M(\mathrm{SD}_A) = \frac{-ieG_FU_{qq'}}{\sqrt{2}m_P}\epsilon^\mu l^\nu\{A^P[(qk-k^2)g_{\mu\nu}-q_\mu k_\nu] + R^Pk^2g_{\mu\nu}\}\,, \qquad (2)$$

which contains an additional axial form factor R^P which only can be accessed if the photon remains virtual. $U_{qq'}$ is the Cabibbo-Kobayashi-Maskawa mixing-matrix element; ϵ^μ is the polarization vector of the photon (or the effective vertex, $\epsilon^\mu = (e/k^2)\overline{u}(p_-)\gamma^\mu v(p_+)$, of the e^+e^- pair); $\ell^\nu = \overline{u}(p_\nu)\gamma^\nu(1-\gamma_5)v(p_\ell)$ is the lepton-neutrino current; q and k are the meson

See key on page 547

and photon four-momenta ($k = p_+ + p_-$ for virtual photons); and P stands for π or K.

The pion vector form factor, V^π, is related via CVC (Conserved Vector Current) to the $\pi^0 \to \gamma\gamma$ decay width. The constant term is given by $|V^\pi(0)| = (1/\alpha)\sqrt{2\Gamma_{\pi^0\to\gamma\gamma}/\pi m_{\pi^0}}$ [3]. The resulting value, $V^\pi(0) = 0.0259(9)$, has been confirmed by calculations based on chiral perturbation theory (χPT) [4], and by two experiments given in the Listings below. A recent experiment by the PIBETA collaboration [5] obtained a $V^\pi(0)$ that is in excellent agreement with the CVC hypothesis. It also measured the slope parameter a in $V^\pi(s) = V^\pi(0)(1 + a \cdot s)$, where $s = (1 - 2E_\gamma/m_\pi)$, and E_γ is the gamma energy in the pion rest frame: $a = 0.095 \pm 0.058$. A functional dependence on s is expected for all form factors. It becomes non-negligible in the case of $V^\pi(s)$ when a wide range of photon momenta is recorded; proper treatment in the analysis of K decays is mandatory.

The form factor, R^P, can be related to the electromagnetic radius, r_P, of the meson [2]: $R^P = \frac{1}{3} m_P f_P \langle r_P^2 \rangle$ using PCAC (Partial Conserved Axial vector Current; f_P is the meson decay constant). In lowest order χPT, the ratio A^π/V^π is related to the pion electric polarizability $\alpha_E = [\alpha/(8\pi^2 m_\pi f_\pi^2)] \times A^\pi/V^\pi$ [6]. The first non-trivial χPT contributions to A^K and V^K appear at $\mathcal{O}(p^4)$ [4], respectively from Gasser-Leutwyler coefficients, L_i's, and the anomalous lagrangian:

$$A^K = \frac{4\sqrt{2}M_K}{F_\pi}(L_9^r + L_{10}^r) = 0.042, \quad V^K = \frac{\sqrt{2}M_K}{8\pi^2 F_\pi} = 0.096. \tag{3}$$

$\mathcal{O}(p^6)$ contributions to A^K can be predicted accurately: they are flat in the momentum dependence and shift the $\mathcal{O}(p^4)$ value to 0.034. $\mathcal{O}(p^6)$ contributions to V^K are model dependent and can be approximated by a form factor linearly dependent on momentum. For example, when looking at the spread of results obtained within two different models, the constant piece of this linear form factor is shifted to 0.078 ± 0.005 [1,2,4].

For decay processes where the photon is real, the partial decay width can be written in analytical form as a sum of IB, SD, and IB/SD interference terms INT [1,4]:

$$\begin{aligned}\frac{d^2\Gamma_{P\to\ell\nu\gamma}}{dxdy} &= \frac{d^2\left(\Gamma_{\rm IB} + \Gamma_{\rm SD} + \Gamma_{\rm INT}\right)}{dxdy} \\ &= \frac{\alpha}{2\pi}\Gamma_{P\to\ell\nu}\frac{1}{(1-r)^2}\Bigg\{\mathrm{IB}(x,y) \\ &+\frac{1}{r}\left(\frac{m_P}{2f_P}\right)^2\Big[(V+A)^2\mathrm{SD}^+(x,y) + (V-A)^2\mathrm{SD}^-(x,y)\Big] \\ &+\frac{m_P}{f_P}\Big[(V+A)\mathrm{S}^+_{\rm INT}(x,y) + (V-A)\mathrm{S}^-_{\rm INT}(x,y)\Big]\Bigg\}. \end{aligned} \tag{4}$$

Here

$$\begin{aligned}\mathrm{IB}(x,y) &= \left[\frac{1-y+r}{x^2(x+y-1-r)}\right] \\ &\left[x^2 + 2(1-x)(1-r) - \frac{2xr(1-r)}{x+y-1-r}\right]\end{aligned}$$

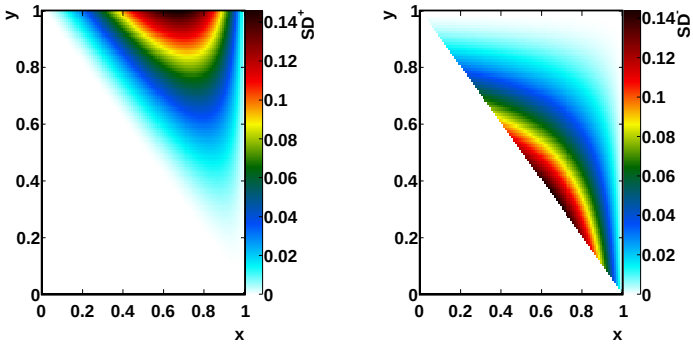

Figure 1: Components of the structure dependent terms of the decay width. Left: SD^+, right: SD^-

$$\begin{aligned}\mathrm{SD}^+(x,y) &= (x+y-1-r)\Big[(x+y-1)(1-x) - r\Big] \\ \mathrm{SD}^-(x,y) &= (1-y+r)\Big[(1-x)(1-y) + r\Big] \\ \mathrm{S}^+_{\rm INT}(x,y) &= \left[\frac{1-y+r}{x(x+y-1-r)}\right]\Big[(1-x)(1-x-y) + r\Big] \\ \mathrm{S}^-_{\rm INT}(x,y) &= \left[\frac{1-y+r}{x(x+y-1-r)}\right]\Big[x^2 - (1-x)(1-x-y) - r\Big]\end{aligned} \tag{5}$$

where $x = 2E_\gamma/m_P$, $y = 2E_\ell/m_P$, and $r = (m_\ell/m_P)^2$. The structure dependent terms SD^+ and SD^- are shown in Fig. 1. The SD^- term is maximized in the same kinematic region where overwhelming IB term dominates (along $x + y = 1$ diagonal). Thus experimental yields with less background are dominated by SD^+ contribution and proportional to $A^P + V^P$ making simultaneous precise determination of the form factors difficult.

Recently, formulas (4) and (5) have been extended to describe polarized distributions in radiative meson and muon decays [7].

The "helicity" factor r is responsible for the enhancement of the SD over the IB amplitude in the decays $\pi^\pm \to e^\pm\nu\gamma$, while $\pi^\pm \to \mu^\pm\nu\gamma$ is dominated by IB. Interference terms are important for the decay $K^\pm \to \mu^\pm\nu\gamma$ [8], but contribute only a few percent correction to pion decays. However, they provide the basis for determining the signs of V and A. Radiative corrections to the decay $\pi^+ \to e^+\nu\gamma$ have to be taken into account in the analysis of the precision experiments. They make up to 4% corrections in the total decay rate [9]. In $\pi^\pm \to e^\pm\nu e^+e^-$ and $K^\pm \to \ell^\pm\nu e^+e^-$ decays, all three form factors, V^P, A^P, and R^P, can be determined [10,11].

We give the experimental $\pi^\pm$ form factors V^π, A^π, and R^π in the Listings below. In the $K^\pm$ Listings, we give the extracted sum $A^K + V^K$ and difference $A^K - V^K$, as well as V^K, A^K and R^K. In particular KLOE has measured for the constant piece

of the form factor $A^K + V^K = 0.125 \pm 0.007 \pm 0.001$ [13] while Istra+, $V^K - A^K = 0.21 \pm 0.04 \pm 0.04$ [14].

Several searches for the exotic form factors F_T^π, F_T^K (tensor), and F_S^K (scalar) have been pursued in the past. In particular, F_T^π has been brought into focus by experimental as well as theoretical work [12]. New high-statistics data from the PIBETA collaboration have been re-analyzed together with an additional data set optimized for low backgrounds in the radiative pion decay. In particular, lower beam rates have been used in order to reduce the accidental background, thereby making the treatment of systematic uncertainties easier and more reliable. The PIBETA analysis now restricts F_T^π to the range $-5.2 \times 10^{-4} < F_T^\pi < 4.0 \times 10^{-4}$ at a 90% confidence limit [5]. This result is in excellent agreement with the most recent theoretical work [4].

Precision measurements of radiative pion and kaon decays are effective tools to study QCD in the non-perturbative region and are of interest beyond the scope of radiative decays. Meanwhile other processes such as $\pi^+ \to e^+\nu$ that seem to be better suited to search for new physics at the precision frontier are currently studied. The advantages of such process are the very accurate and reliable theoretical predictions and the more straightforward experimental analysis.

References

1. D.A. Bryman *et al.*, Phys. Reports **88**, 151 (1982). See our note on "Decay Constants of Charged Pseudoscalar Mesons" elsewhere in this *Review*;
   S.G. Brown and S.A. Bludman, Phys. Rev. **136**, B1160 (1964);
   P. DeBaenst and J. Pestieau, Nuovo Cim. **A53**, 137 (1968).
2. W.T. Chu *et al.*, Phys. Rev. **166**, 1577 (1968);
   D.Yu. Bardin and E.A. Ivanov, Sov. J. Part. Nucl. **7**, 286 (1976);
   A. Kersch and F. Scheck, Nucl. Phys. **B263**, 475 (1986).
3. V.G. Vaks and B.L. Ioffe, Nuovo Cim. **10**, 342 (1958);
   V.F. Muller, Z. Phys. **173**, 438 (1963).
4. C.Q. Geng, I-Lin Ho, and T.H. Wu, Nucl. Phys. **B684**, 281 (2004);
   J. Bijnens and P. Talavera, Nucl. Phys. **B489**, 387 (1997);
   V. Mateu and J. Portoles, Eur. Phys. J. **C52**, 325 (2007);
   R. Unterdorfer, H. Pichl, Eur. Phys. J. **C55**, 273 (2008);
   V. Cirigliano *et al.*, Rev. Mod. Phys. **84**, 399 (2012).
5. D. Počanić *et al.*, Phys. Rev. Lett. **93**, 181803 (2004);
   E. Frlež *et al.*, Phys. Rev. Lett. **93**, 181804 (2004);
   M. Bychkov *et al.*, Phys. Rev. Lett. **103**, 051802 (2009).
6. J.F. Donoghue and B.R. Holstein, Phys. Rev. **D40**, 2378 (1989).
7. E. Gabrielli and L. Trentadue, Nucl. Phys. **B792**, 48 (2008).
8. S. Adler *et al.*, Phys. Rev. Lett. **85**, 2256 (2000).
9. Yu.M. Bystritsky, E.A. Kuraev, and E.P. Velicheva, Phys. Rev. **D69**, 114004 (2004);
   R. Unterdorfer and H. Pichl have treated radiative corrections of the structure terms to lowest order within χPT for the first time. See the reference under [4].
10. S. Egli *et al.*, Phys. Lett. **B175**, 97 (1986).
11. A.A. Poblaguev *et al.*, Phys. Rev. Lett. **89**, 061803 (2002).
12. A.A. Poblaguev, Phys. Lett. **B238**, 108 (1990);
    V.N. Bolotov *et al.*, Phys. Lett. **B243**, 308 (1990);
    V.M. Belyaev and I.I. Kogan, Phys. Lett. **B280**, 238 (1992);
    A.V. Chernyshev *et al.*, Mod. Phys. Lett. **A12**, 1669 (1997);
    A.A. Poblaguev, Phys. Rev. **D68**, 054020 (2003);
    M.V. Chizhov, Phys. Part. Nucl. Lett. **2**, 193 (2005).
13. F. Ambrosino *et al.*, Eur. Phys. J. **C64**, 627 (2009).
14. V. A. Duk *et al.*, Phys. Lett. **B695**, 59 (2011).

$\pi^{\pm}$ FORM FACTORS

F_V, VECTOR FORM FACTOR

VALUE	EVTS	DOCUMENT ID		TECN	COMMENT
0.0254±0.0017 OUR AVERAGE					
0.0258±0.0017	65k	[27] BYCHKOV	09	PIBE	$e^+\nu\gamma$ at rest
0.014 ±0.009		[28] BOLOTOV	90B	SPEC	17 GeV $\pi^- \to e^-\overline{\nu}_e\gamma$
0.023 $^{+0.015}_{-0.013}$	98	EGLI	89	SPEC	$\pi^+ \to e^+\nu_e e^+e^-$

[27] The BYCHKOV 09 F_A and F_V results are highly (anti-)correlated: $F_A + 1.0286\ F_V = 0.03853 \pm 0.00014$.
[28] BOLOTOV 90B only determines the absolute value.

F_A, AXIAL-VECTOR FORM FACTOR

VALUE	EVTS	DOCUMENT ID		TECN	COMMENT
0.0119±0.0001	65k	[29,30] BYCHKOV	09	PIBE	$e^+\nu\gamma$ at rest
• • • We do not use the following data for averages, fits, limits, etc. • • •					
0.0115±0.0004	41k	[29,31] FRLEZ	04	PIBE	$\pi^+ \to e^+\nu\gamma$ at rest
0.0106±0.0060		[29,32] BOLOTOV	90B	SPEC	17 GeV $\pi^- \to e^-\overline{\nu}_e\gamma$
0.021 $^{+0.011}_{-0.013}$	98	EGLI	89	SPEC	$\pi^+ \to e^+\nu_e e^+e^-$
0.0135±0.0016		[29,32] BAY	86	SPEC	$\pi^+ \to e^+\nu\gamma$
0.006 ±0.003		[29,32] PIILONEN	86	SPEC	$\pi^+ \to e^+\nu\gamma$
0.011 ±0.003		[29,32,33] STETZ	78	SPEC	$\pi^+ \to e^+\nu\gamma$

[29] These values come from fixing the vector form factor at the CVC prediction, $F_V = 0.0259 \pm 0.0005$.
[30] When F_V is released, the BYCHKOV 09 F_A is 0.0117 ± 0.0017, and F_A and F_V results are highly (anti-)correlated: $F_A + 1.0286\ F_V = 0.03853 \pm 0.00014$.
[31] The sign of $\gamma = F_A/F_V$ is determined to be positive.
[32] Only the absolute value of F_A is determined.
[33] The result of STETZ 78 has a two-fold ambiguity. We take the solution compatible with later determinations.

VECTOR FORM FACTOR SLOPE PARAMETER a

This is a in $F_V(q^2) = F_V(0)\ (1 + a\ q^2)$

VALUE	EVTS	DOCUMENT ID		TECN	COMMENT
0.10±0.06	65k	BYCHKOV	09	PIBE	$e^+\nu\gamma$ at rest

R, SECOND AXIAL-VECTOR FORM FACTOR

VALUE	EVTS	DOCUMENT ID		TECN	COMMENT
0.059 $^{+0.009}_{-0.008}$	98	EGLI	89	SPEC	$\pi^+ \to e^+\nu_e e^+e^-$

$\pi^{\pm}$ CHARGE RADIUS

VALUE (fm)	DOCUMENT ID		TECN	COMMENT
0.672±0.008 OUR AVERAGE	Error includes scale factor of 1.7. See the ideogram below.			
0.65 ±0.05 ±0.06	ESCHRICH	01	CNTR	$\pi e \to \pi e$
0.740±0.031	LIESENFELD	99	CNTR	$ep \to e\pi^+ n$
0.663±0.006	AMENDOLIA	86	CNTR	$\pi e \to \pi e$
0.663±0.023	DALLY	82	CNTR	$\pi e \to \pi e$
0.711±0.009±0.016	BEBEK	78	CNTR	$eN \to e\pi N$
0.678±0.004±0.008	QUENZER	78	CNTR	$e^+e^- \to \pi^+\pi^-$
• • • We do not use the following data for averages, fits, limits, etc. • • •				
0.661±0.012	[34] BIJNENS	98	CNTR	χPT extraction
0.660±0.024	AMENDOLIA	84	CNTR	$\pi e \to \pi e$
0.78 $^{+0.09}_{-0.10}$	ADYLOV	77	CNTR	$\pi e \to \pi e$
0.74 $^{+0.11}_{-0.13}$	BARDIN	77	CNTR	$ep \to e\pi^+ n$
0.56 ±0.04	DALLY	77	CNTR	$\pi e \to \pi e$

[34] BIJNENS 98 fits existing data.

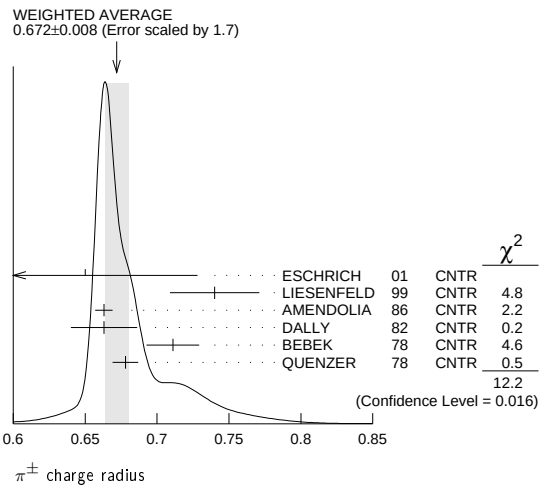

$\pi^{\pm}$ REFERENCES

We have omitted some papers that have been superseded by later experiments. The omitted papers may be found in our 1988 edition Physics Letters **B204** 1 (1988).

BYCHKOV	09	PRL 103 051802	M. Bychkov *et al.*	(PSI PIBETA Collab.)
FRLEZ	04	PRL 93 181804	E. Frlez *et al.*	(PSI PIBETA Collab.)
POCANIC	04	PRL 93 181803	D. Pocanic *et al.*	(PSI PIBETA Collab.)
ESCHRICH	01	PL B522 233	I. Eschrich *et al.*	(FNAL SELEX Collab.)
LIESENFELD	99	PL B468 20	A. Liesenfeld *et al.*	
BIJNENS	98	JHEP 9805 014	J. Bijnens *et al.*	
BRESSI	98	NP B513 555	G. Bressi *et al.*	
LENZ	98	PL B416 50	S. Lenz *et al.*	
ASSAMAGAN	96	PR D53 6065	K.A. Assamagan *et al.*	(PSI, ZURI, VILL+)
KOPTEV	95	JETPL 61 877 Translated from ZETFP 61 865.	V.P. Koptev *et al.*	(PNPI)
NUMAO	95	PR D52 4855	T. Numao *et al.*	(TRIU, BRCO)
ASSAMAGAN	94	PL B335 231	K.A. Assamagan *et al.*	(PSI, ZURI, VILL+)
JECKELMANN	94	PL B335 326	B. Jeckelmann, P.F.A. Goudsmit, H.J. Leisi	(WABRN+)
CZAPEK	93	PRL 70 17	G. Czapek *et al.*	(BERN, VILL)
BARANOV	92	SJNP 55 1644 Translated from YAF 55 2940.	V.A. Baranov *et al.*	(JINR)
BRITTON	92	PRL 68 3000	D.I. Britton *et al.*	(TRIU, CARL)
Also		PR D49 28	D.I. Britton *et al.*	(TRIU, CARL)
NUMAO	92	MPL A7 3357	T. Numao	(TRIU)
BARANOV	91B	SJNP 54 790 Translated from YAF 54 1298.	V.A. Baranov *et al.*	(JINR)
DAUM	91	PL B265 425	M. Daum *et al.*	(VILL)
BOLOTOV	90B	PL B243 308	V.N. Bolotov *et al.*	(INRM)
EGLI	89	PL B222 533	S. Egli *et al.*	(SINDRUM Collab.)
Also		PL B175 97	S. Egli *et al.*	(AACH3, ETH, SIN, ZURI)
PDG	88	PL B204 1	G.P. Yost *et al.*	(LBL+)
PICCIOTTO	88	PR D37 1131	C.E. Picciotto *et al.*	(TRIU, CNRC)
COHEN	87	RMP 59 1121	E.R. Cohen, B.N. Taylor	(RISC, NBS)
KORENCHE...	87	SJNP 46 192 Translated from YAF 46 313.	S.M. Korenchenko *et al.*	(JINR)
AMENDOLIA	86	NP B277 168	S.R. Amendolia *et al.*	(CERN NA7 Collab.)
BAY	86	PL B174 445	A. Bay *et al.*	(LAUS, ZURI)
BRYMAN	86	PR D33 1211	D.A. Bryman *et al.*	(TRIU, CNRC)
Also		PRL 50 7	D.A. Bryman *et al.*	(TRIU, CNRC)
JECKELMANN	86B	NP A457 709	B. Jeckelmann *et al.*	(ETH, FRIB)
Also		PRL 56 1444	B. Jeckelmann *et al.*	(ETH, FRIB)
PIILONEN	86	PRL 57 1402	L.E. Piilonen *et al.*	(LANL, TEMP, CHIC)
MCFARLANE	85	PR D32 547	W.K. McFarlane *et al.*	(TEMP, LANL)
ABELA	84	PL 146B 431	R. Abela *et al.*	(SIN)
Also		PL 74B 126	M. Daum *et al.*	(SIN)
Also		PR D20 2692	M. Daum *et al.*	(SIN)
AMENDOLIA	84	PL 146B 116	S.R. Amendolia *et al.*	(CERN NA7 Collab.)
FETSCHER	84	PL 140B 117	W. Fetscher	(ETH)
ABELA	83	NP A395 413	R. Abela *et al.*	(BASL, KARLK, KARLE)
CARR	83	PRL 51 627	J. Carr *et al.*	(LBL, NWES, TRIU)
COOPER	82	PL 112B 97	A.M. Cooper *et al.*	(RL)
DALLY	82	PRL 48 375	E.B. Dally *et al.*	
LU	80	PRL 45 1066	D.C. Lu *et al.*	(YALE, COLU, JHU)
BEBEK	78	PR D17 1693	C.J. Bebek *et al.*	
QUENZER	78	PL 76B 512	A. Quenzer *et al.*	(LALO)
STETZ	78	NP B138 285	A.W. Stetz *et al.*	(LBL, UCLA)
ADYLOV	77	NP B128 461	G.T. Adylov *et al.*	
BARDIN	77	NP B120 45	G. Bardin *et al.*	
DALLY	77	PRL 39 1176	E.B. Dally *et al.*	
CARTER	76	PRL 37 1380	A.L. Carter *et al.*	(CARL, CNRC, CHIC+)
KORENCHE...	76B	JETP 44 35 Translated from ZETF 71 69.	S.M. Korenchenko *et al.*	(JINR)
MARUSHEN...	76	JETPL 23 72 Translated from ZETFP 23 80.	V.I. Marushenko *et al.*	(PNPI)
Also		Private Comm.	R.E. Shafer	(FNAL)
Also		Private Comm.	A. Smirnov	(PNPI)
DUNAITSEV	73	SJNP 16 292 Translated from YAF 16 524.	A.F. Dunaitsev *et al.*	(SERP)
AYRES	71	PR D3 1051	D.S. Ayres *et al.*	(LRL, UCSB)
Also		PR 157 1288	D.S. Ayres *et al.*	(LRL)
Also		PRL 21 261	D.S. Ayres *et al.*	(LRL, UCSB)
Also		Thesis UCRL 18369	D.S. Ayres	(LRL)
Also		PRL 23 1267	A.J. Greenberg *et al.*	(LRL, UCSB)
KORENCHE...	71	SJNP 13 189 Translated from YAF 13 339.	S.M. Korenchenko *et al.*	(JINR)
BOOTH	70	PL 32B 723	P.S.L. Booth *et al.*	(LIVP)
DEPOMMIER	68	NP B4 189	P. Depommier *et al.*	(CERN)
PETRUKHIN	68	JINR P1 3862	V.I. Petrukhin *et al.*	(JINR)
HYMAN	67	PL 25B 376	L.G. Hyman *et al.*	(ANL, CMU, NWES)
NORDBERG	67	PL 24B 594	M.E. Nordberg, F. Lobkowicz, R.L. Burman	(ROCH)
BARDON	66	PRL 16 775	M. Bardon *et al.*	(COLU)
KINSEY	66	PR 144 1132	K.F. Kinsey, F. Lobkowicz, M.E. Nordberg	(ROCH)
LOBKOWICZ	66	PRL 17 548	F. Lobkowicz *et al.*	(ROCH, BNL)
BACASTOW	65	PR 139 B407	R.B. Bacastow *et al.*	(LRL, SLAC)
BERTRAM	65	PR 139 B617	W.K. Bertram *et al.*	(MICH, CMU)
DUNAITSEV	65	JETP 20 58 Translated from ZETF 47 84.	A.F. Dunaitsev *et al.*	(JINR)
ECKHAUSE	65	PL 19 348	M. Eckhause *et al.*	(WILL)
BARTLETT	64	PR 136 B1452	D. Bartlett *et al.*	(COLU)
DICAPUA	64	PR 133 B1333	M. di Capua *et al.*	(COLU)
Also		Private Comm.	L. Pondrom	(WISC)
DEPOMMIER	63	PL 5 61	P. Depommier *et al.*	(CERN)
DEPOMMIER	63B	PL 7 285	P. Depommier *et al.*	(CERN)
ANDERSON	60	PR 119 2050	H.L. Anderson *et al.*	(EFI)
CASTAGNOLI	58	PR 112 1779	C. Castagnoli, M. Muchnik	(ROMA)

π^0

$I^G(J^{PC}) = 1^-(0^{-+})$

We have omitted some results that have been superseded by later experiments. The omitted results may be found in our 1988 edition Physics Letters **B204** 1 (1988).

π^0 MASS

The value is calculated from $m_{\pi^\pm}$ and $(m_{\pi^\pm} - m_{\pi^0})$. See also the notes under the $\pi^\pm$ Mass Listings.

VALUE (MeV)	*DOCUMENT ID*	
134.9766±0.0006 OUR FIT	Error includes scale factor of 1.1.	

$m_{\pi^\pm} - m_{\pi^0}$

Measurements with an error > 0.01 MeV have been omitted.

VALUE (MeV)	*DOCUMENT ID*		*TECN*	*COMMENT*
4.5936 ±0.0005 OUR FIT				
4.5936 ±0.0005 OUR AVERAGE				
4.59364±0.00048	CRAWFORD	91	CNTR	$\pi^- p \to \pi^0 n$, n TOF
4.5930 ±0.0013	CRAWFORD	86	CNTR	$\pi^- p \to \pi^0 n$, n TOF
• • • We do not use the following data for averages, fits, limits, etc. • • •				
4.59366±0.00048	CRAWFORD	88B	CNTR	See CRAWFORD 91
4.6034 ±0.0052	VASILEVSKY	66	CNTR	
4.6056 ±0.0055	CZIRR	63	CNTR	

π^0 MEAN LIFE

Most experiments measure the π^0 width which we convert to a lifetime. ATHERTON 85 is the only direct measurement of the π^0 lifetime. Our average based only on indirect measurement yields $(8.30 \pm 0.19) \times 10^{-17}$ s. The two Primakoff measurements from 1970 have been excluded from our average because they suffered model-related systematics unknown at the time. More information on the π^0 lifetime can be found in BERNSTEIN 13.

VALUE (10^{-17} s)	*EVTS*	*DOCUMENT ID*		*TECN*	*COMMENT*
8.52±0.18 OUR AVERAGE		Error includes scale factor of 1.2.			
8.32±0.15±0.18		[1] LARIN	11	PRMX	Primakoff effect
8.5 ±1.1		[2] BYCHKOV	09	PIBE	$\pi^+ \to e^+ \nu\gamma$ at rest
8.4 ±0.5 ±0.5	1182	[3] WILLIAMS	88	CBAL	$e^+ e^- \to e^+ e^- \pi^0$
8.97±0.22±0.17		ATHERTON	85	CNTR	Direct measurement
8.2 ±0.4		[4] BROWMAN	74	CNTR	Primakoff effect
• • • We do not use the following data for averages, fits, limits, etc. • • •					
5.6 ±0.6		BELLETTINI	70	CNTR	Primakoff effect
9 ±0.68		KRYSHKIN	70	CNTR	Primakoff effect
7.3 ±1.1		BELLETTINI	65B	CNTR	Primakoff effect

[1] LARIN 11 reported $\Gamma(\pi^0 \to \gamma\gamma) = 7.82 \pm 0.14 \pm 0.17$ eV which we converted to mean life $\tau = \hbar/\Gamma$(total).
[2] BYCHKOV 09 obtains this using the conserved-vector-current relation between the vector form factor F_V and the π^0 lifetime.
[3] WILLIAMS 88 gives $\Gamma(\gamma\gamma) = 7.7 \pm 0.5 \pm 0.5$ eV. We give here $\tau = \hbar/\Gamma$(total).
[4] BROWMAN 74 gives a π^0 width $\Gamma = 8.02 \pm 0.42$ eV. The mean life is $\hbar/\Gamma$.

π^0 DECAY MODES

For decay limits to particles which are not established, see the appropriate Search sections (A^0 (axion) and Other Light Boson (X^0) Searches, etc.).

	Mode	Fraction (Γ_i/Γ)	Scale factor/ Confidence level
Γ_1	2γ	(98.823±0.034) %	S=1.5
Γ_2	$e^+ e^- \gamma$	(1.174±0.035) %	S=1.5
Γ_3	γpositronium	(1.82 ±0.29) $\times 10^{-9}$	
Γ_4	$e^+ e^+ e^- e^-$	(3.34 ±0.16) $\times 10^{-5}$	
Γ_5	$e^+ e^-$	(6.46 ±0.33) $\times 10^{-8}$	
Γ_6	4γ	< 2 $\times 10^{-8}$	CL=90%
Γ_7	$\nu\overline{\nu}$	[a] < 2.7 $\times 10^{-7}$	CL=90%
Γ_8	$\nu_e \overline{\nu}_e$	< 1.7 $\times 10^{-6}$	CL=90%
Γ_9	$\nu_\mu \overline{\nu}_\mu$	< 1.6 $\times 10^{-6}$	CL=90%
Γ_{10}	$\nu_\tau \overline{\nu}_\tau$	< 2.1 $\times 10^{-6}$	CL=90%
Γ_{11}	$\gamma\nu\overline{\nu}$	< 6 $\times 10^{-4}$	CL=90%

Meson Particle Listings

π^0

Charge conjugation (C) or Lepton Family number (LF) violating modes

Γ_{12}	3γ	C	< 3.1	$\times 10^{-8}$	CL=90%
Γ_{13}	$\mu^+ e^-$	LF	< 3.8	$\times 10^{-10}$	CL=90%
Γ_{14}	$\mu^- e^+$	LF	< 3.4	$\times 10^{-9}$	CL=90%
Γ_{15}	$\mu^+ e^- + \mu^- e^+$	LF	< 3.6	$\times 10^{-10}$	CL=90%

[a] Astrophysical and cosmological arguments give limits of order 10^{-13}; see the Particle Listings below.

CONSTRAINED FIT INFORMATION

An overall fit to 2 branching ratios uses 6 measurements and one constraint to determine 3 parameters. The overall fit has a $\chi^2 = 4.6$ for 4 degrees of freedom.

The following *off-diagonal* array elements are the correlation coefficients $\langle \delta x_i \delta x_j \rangle / (\delta x_i \cdot \delta x_j)$, in percent, from the fit to the branching fractions, $x_i \equiv \Gamma_i/\Gamma_{\text{total}}$. The fit constrains the x_i whose labels appear in this array to sum to one.

	x_1	x_2
x_2	−100	
x_4	0	−1

π^0 BRANCHING RATIOS

$\Gamma(e^+e^-\gamma)/\Gamma(2\gamma)$ Γ_2/Γ_1

VALUE (%)	EVTS	DOCUMENT ID		TECN	COMMENT
1.188±0.035 OUR FIT	Error includes scale factor of 1.5.				
1.188±0.034 OUR AVERAGE	Error includes scale factor of 1.4. See the ideogram below.				
1.140±0.024±0.033	12.5k	[5] BEDDALL	08	ALEP	$e^+e^- \to Z \to$ hadrons
1.25 ±0.04		SCHARDT	81	SPEC	$\pi^- p \to n\pi^0$
1.166±0.047	3071	[6] SAMIOS	61	HBC	$\pi^- p \to n\pi^0$
1.17 ±0.15	27	BUDAGOV	60	HBC	
• • • We do not use the following data for averages, fits, limits, etc. • • •					
1.196		JOSEPH	60	THEO	QED calculation

[5] This BEDDALL 08 value is obtained from ALEPH archived data.
[6] SAMIOS 61 value uses a Panofsky ratio = 1.62.

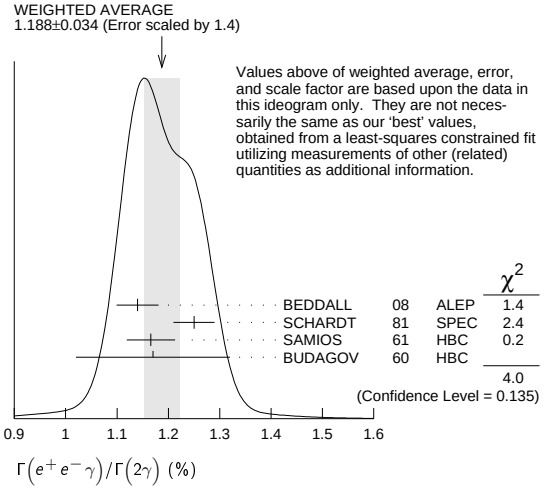

$\Gamma(\gamma\text{positronium})/\Gamma(2\gamma)$ Γ_3/Γ_1

VALUE (units 10^{-9})	EVTS	DOCUMENT ID		TECN	COMMENT
1.84±0.29	277	AFANASYEV	90	CNTR	pC 70 GeV

$\Gamma(e^+e^+e^-e^-)/\Gamma(2\gamma)$ Γ_4/Γ_1

VALUE (units 10^{-5})	EVTS	DOCUMENT ID		TECN	COMMENT
3.38±0.16 OUR FIT					
3.38±0.16 OUR AVERAGE					
3.46±0.19	30.5k	[7] ABOUZAID	08D	KTEV	$K_L^0 \to \pi^0\pi^0\pi^0_{DD}$
3.18±0.30	146	[8] SAMIOS	62B	HBC	

[7] This ABOUZAID 08D value includes all radiative final states. The error includes both statistical and systematic errors. The correlation between the Dalitz-pair planes gives a direct measurement of the π^0 parity. The $\pi^0 2\gamma^*$ form factor is measured and limits are placed on a scalar contribution to the decay.
[8] SAMIOS 62B value uses a Panofsky ratio = 1.62.

$\Gamma(e^+e^-)/\Gamma_{\text{total}}$ Γ_5/Γ

Experimental results are listed; branching ratios corrected for radiative effects are given in the footnotes. BERMAN 60 found $B(\pi^0 \to e^+e^-) \geq 4.69 \times 10^{-8}$ via an exact QED calculation.

VALUE (units 10^{-8})	EVTS	DOCUMENT ID		TECN	CHG	COMMENT
6.46±0.33 OUR AVERAGE						
6.44±0.25±0.22	794	[9] ABOUZAID	07	KTEV		$K_L^0 \to 3\pi^0$ in flight
6.9 ±2.3 ±0.6	21	[10] DESHPANDE	93	SPEC		$K^+ \to \pi^+\pi^0$
7.6 $^{+2.9}_{-2.8}$ ±0.5	8	[11] MCFARLAND	93	SPEC		$K_L^0 \to 3\pi^0$ in flight
• • • We do not use the following data for averages, fits, limits, etc. • • •						
6.09±0.40±0.24	275	[12] ALAVI-HARATI	99C	SPEC	0	Repl. by ABOUZAID 07

[9] ABOUZAID 07 result is for $m_{e^+e^-}/m_{\pi^0} > 0.95$. With radiative corrections the result becomes $(7.48 \pm 0.29 \pm 0.25) \times 10^{-8}$.
[10] The DESHPANDE 93 result with bremsstrahlung radiative corrections is $(8.0 \pm 2.6 \pm 0.6) \times 10^{-8}$.
[11] The MCFARLAND 93 result is for $B[\pi^0 \to e^+e^-, (m_{e^+e^-}/m_{\pi^0})^2 > 0.95]$. With radiative corrections it becomes $(8.8^{+4.5}_{-3.2} \pm 0.6) \times 10^{-8}$.
[12] ALAVI-HARATI 99C quote result for $B[\pi^0 \to e^+e^-, (m_{e^+e^-}/m_{\pi^0})^2 > 0.95]$ to minimize radiative contributions from $\pi^0 \to e^+e^-\gamma$. After radiative corrections they obtain $(7.04 \pm 0.46 \pm 0.28) \times 10^{-8}$.

$\Gamma(e^+e^-)/\Gamma(2\gamma)$ Γ_5/Γ_1

VALUE (units 10^{-7})	CL%	EVTS	DOCUMENT ID		TECN	COMMENT
• • • We do not use the following data for averages, fits, limits, etc. • • •						
<1.3	90		NIEBUHR	89	SPEC	$\pi^- p \to \pi^0 n$ at rest
<5.3	90		ZEPHAT	87	SPEC	$\pi^- p \to \pi^0 n$ 0.3 GeV/c
1.7 ±0.6 ±0.3		59	FRANK	83	SPEC	$\pi^- p \to n\pi^0$
1.8 ±0.6		58	MISCHKE	82	SPEC	See FRANK 83
2.23 $^{+2.40}_{-1.10}$	90	8	FISCHER	78B	SPRK	$K^+ \to \pi^+\pi^0$

$\Gamma(4\gamma)/\Gamma_{\text{total}}$ Γ_6/Γ

VALUE (units 10^{-8})	CL%	EVTS	DOCUMENT ID		TECN	COMMENT
< 2	90		MCDONOUGH	88	CBOX	$\pi^- p$ at rest
• • • We do not use the following data for averages, fits, limits, etc. • • •						
<160	90		BOLOTOV	86C	CALO	
<440	90	0	AUERBACH	80	CNTR	

$\Gamma(\nu\overline{\nu})/\Gamma_{\text{total}}$ Γ_7/Γ

The astrophysical and cosmological limits are many orders of magnitude lower, but we use the best laboratory limit for the Summary Tables.

VALUE (units 10^{-6})	CL%	EVTS	DOCUMENT ID		TECN	COMMENT
< 0.27	90		[13] ARTAMONOV	05A	B949	$K^+ \to \pi^+\pi^0$
• • • We do not use the following data for averages, fits, limits, etc. • • •						
< 0.83	90		[13] ATIYA	91	B787	$K^+ \to \pi^+\nu\nu'$
< 2.9 $\times 10^{-7}$			[14] LAM	91		Cosmological limit
< 3.2 $\times 10^{-7}$			[15] NATALE	91		SN 1987A
< 6.5	90		DORENBOS...	88	CHRM	Beam dump, prompt ν
<24	90	0	[13] HERCZEG	81	RVUE	$K^+ \to \pi^+\nu\nu'$

[13] This limit applies to all possible $\nu\nu'$ states as well as to other massless, weakly interacting states.
[14] LAM 91 considers the production of right-handed neutrinos produced from the cosmic thermal background at the temperature of about the pion mass through the reaction $\gamma\gamma \to \pi^0 \to \nu\overline{\nu}$.
[15] NATALE 91 considers the excess energy-loss rate from SN 1987A if the process $\gamma\gamma \to \pi^0 \to \nu\overline{\nu}$ occurs, permitted if the neutrinos have a right-handed component. As pointed out in LAM 91 (and confirmed by Natale), there is a factor 4 error in the NATALE 91 published result (0.8×10^{-7}).

$\Gamma(\nu_e\overline{\nu}_e)/\Gamma_{\text{total}}$ Γ_8/Γ

VALUE (units 10^{-6})	CL%	DOCUMENT ID		TECN	COMMENT
<1.7	90	DORENBOS...	88	CHRM	Beam dump, prompt ν
• • • We do not use the following data for averages, fits, limits, etc. • • •					
<3.1	90	[16] HOFFMAN	88	RVUE	Beam dump, prompt ν

[16] HOFFMAN 88 analyzes data from a 400-GeV BEBC beam-dump experiment.

$\Gamma(\nu_\mu\overline{\nu}_\mu)/\Gamma_{\text{total}}$ Γ_9/Γ

VALUE (units 10^{-6})	CL%	EVTS	DOCUMENT ID		TECN	COMMENT
<1.6	90	8.7	AUERBACH	04	LSND	800 MeV p on Cu
<3.1	90		[17] HOFFMAN	88	RVUE	Beam dump, prompt ν
• • • We do not use the following data for averages, fits, limits, etc. • • •						
<7.8	90		DORENBOS...	88	CHRM	Beam dump, prompt ν

[17] HOFFMAN 88 analyzes data from a 400-GeV BEBC beam-dump experiment.

$\Gamma(\nu_\tau\overline{\nu}_\tau)/\Gamma_{\text{total}}$ Γ_{10}/Γ

VALUE (units 10^{-6})	CL%	DOCUMENT ID		TECN	COMMENT
<2.1	90	[18] HOFFMAN	88	RVUE	Beam dump, prompt ν
• • • We do not use the following data for averages, fits, limits, etc. • • •					
<4.1	90	DORENBOS...	88	CHRM	Beam dump, prompt ν

[18] HOFFMAN 88 analyzes data from a 400-GeV BEBC beam-dump experiment.

$\Gamma(\gamma\nu\overline{\nu})/\Gamma_{total}$ Γ_{11}/Γ

Standard Model prediction is 6×10^{-18}.

VALUE	CL%	DOCUMENT ID		TECN	COMMENT
$< 6 \times 10^{-4}$	90	ATIYA	92	CNTR	$K^+ \to \gamma\nu\overline{\nu}\pi^+$

$\Gamma(3\gamma)/\Gamma_{total}$ Γ_{12}/Γ

Forbidden by C invariance.

VALUE (units 10^{-8})	CL%	EVTS	DOCUMENT ID		TECN	COMMENT
< 3.1	90		MCDONOUGH	88	CBOX	$\pi^- p$ at rest
• • • We do not use the following data for averages, fits, limits, etc. • • •						
< 38	90	0	HIGHLAND	80	CNTR	
<150	90	0	AUERBACH	78	CNTR	
<490	90	0	[19] DUCLOS	65	CNTR	
<490	90		[19] KUTIN	65	CNTR	

[19] These experiments give $B(3\gamma/2\gamma) < 5.0 \times 10^{-6}$.

$\Gamma(\mu^+ e^-)/\Gamma_{total}$ Γ_{13}/Γ

Forbidden by lepton family number conservation.

VALUE (units 10^{-9})	CL%	EVTS	DOCUMENT ID		TECN	COMMENT
< 0.38	90	0	APPEL	00	SPEC	$K^+ \to \pi^+ \mu^+ e^-$
• • • We do not use the following data for averages, fits, limits, etc. • • •						
<16	90		LEE	90	SPEC	$K^+ \to \pi^+ \mu^+ e^-$
<78	90		CAMPAGNARI	88	SPEC	See LEE 90

$\Gamma(\mu^- e^+)/\Gamma_{total}$ Γ_{14}/Γ

Forbidden by lepton family number conservation.

VALUE (units 10^{-9})	CL%	EVTS	DOCUMENT ID		TECN	COMMENT
<3.4	90	0	APPEL	00B	B865	$K^+ \to \pi^+ e^+ \mu^-$

$[\Gamma(\mu^+ e^-) + \Gamma(\mu^- e^+)]/\Gamma_{total}$ Γ_{15}/Γ

Forbidden by lepton family number conservation.

VALUE (units 10^{-9})	CL%	DOCUMENT ID		TECN	COMMENT
< 0.36	90	ABOUZAID	08C	KTEV	$K_L^0 \to 2\pi^0 \mu^\pm e^\mp$
• • • We do not use the following data for averages, fits, limits, etc. • • •					
< 17.2	90	KROLAK	94	E799	In $K_L^0 \to 3\pi^0$
<140		HERCZEG	84	RVUE	$K^+ \to \pi^+ \mu e$
< 2 $\times 10^{-6}$		HERCZEG	84	THEO	$\mu^- \to e^-$ conversion
< 70	90	BRYMAN	82	RVUE	$K^+ \to \pi^+ \mu e$

π^0 ELECTROMAGNETIC FORM FACTOR

The amplitude for the process $\pi^0 \to e^+ e^- \gamma$ contains a form factor $F(x)$ at the $\pi^0 \gamma\gamma$ vertex, where $x = [m_{e^+e^-}/m_{\pi^0}]^2$. The parameter a in the linear expansion $F(x) = 1 + ax$ is listed below.

All the measurements except that of BEHREND 91 are in the time-like region of momentum transfer.

LINEAR COEFFICIENT OF π^0 ELECTROMAGNETIC FORM FACTOR

VALUE			EVTS	DOCUMENT ID		TECN	COMMENT
0.032	**±0.004**	**OUR AVERAGE**					
+0.026	±0.024	±0.048	7548	FARZANPAY	92	SPEC	$\pi^- p \to \pi^0 n$ at rest
+0.025	±0.014	±0.026	54k	MEIJERDREES	92B	SPEC	$\pi^- p \to \pi^0 n$ at rest
+0.0326	±0.0026	±0.0026	127	[20] BEHREND	91	CELL	$e^+ e^- \to e^+ e^- \pi^0$
−0.11	±0.03	±0.08	32k	FONVIEILLE	89	SPEC	Radiation corr.
• • • We do not use the following data for averages, fits, limits, etc. • • •							
0.12	$^{+0.05}_{-0.04}$			[21] TUPPER	83	THEO	FISCHER 78 data
+0.10	±0.03		31k	[22] FISCHER	78	SPEC	Radiation corr.
+0.01	±0.11		2200	DEVONS	69	OSPK	No radiation corr.
−0.15	±0.10		7676	KOBRAK	61	HBC	No radiation corr.
−0.24	±0.16		3071	SAMIOS	61	HBC	No radiation corr.

[20] BEHREND 91 estimates that their systematic error is of the same order of magnitude as their statistical error, and so we have included a systematic error of this magnitude. The value of a is obtained by extrapolation from the region of large space-like momentum transfer assuming vector dominance.

[21] TUPPER 83 is a theoretical analysis of FISCHER 78 including 2-photon exchange in the corrections.

[22] The FISCHER 78 error is statistical only. The result without radiation corrections is $+0.05 \pm 0.03$.

π^0 REFERENCES

We have omitted some papers that have been superseded by later experiments. The omitted papers may be found in our 1988 edition Physics Letters **B204** 1 (1988).

BERNSTEIN	13	RMP 85 49	A. M. Bernstein, B. R. Holstein	(AMHT, MIT)
LARIN	11	PRL 106 162303	I. Larin *et al.*	(PrimEx Collab.)
BYCHKOV	09	PRL 103 051802	M. Bychkov *et al.*	(PSI PIBETA Collab.)
ABOUZAID	08C	PRL 100 131803	E. Abouzaid *et al.*	(FNAL KTeV Collab.)
ABOUZAID	08D	PRL 100 182001	E. Abouzaid *et al.*	(FNAL KTeV Collab.)
BEDDALL	08	EPJ C54 365	A. Beddall, A. Beddall	(UGAZ)
ABOUZAID	07	PR D75 012004	E. Abouzaid *et al.*	(KTeV Collab.)
ARTAMONOV	05A	PR D72 091102	A.V. Artamonov *et al.*	(BNL E949 Collab.)
AUERBACH	04	PRL 92 091801	L.B. Auerbach *et al.*	(LSND Collab.)
APPEL	00	PRL 85 2450	R. Appel *et al.*	(BNL 865 Collab.)
Also		Thesis, Yale Univ.	D.R. Bergman	
Also		Thesis, Univ. Zurich	S. Pislak	
APPEL	00B	PRL 85 2877	R. Appel *et al.*	(BNL 865 Collab.)
ALAVI-HARATI	99C	PRL 83 922	A. Alavi-Harati *et al.*	(FNAL KTeV Collab.)
KROLAK	94	PL B320 407	P. Krolak *et al.*	(EFI, UCLA, COLO, ELMT+)
DESHPANDE	93	PRL 71 27	A. Deshpande *et al.*	(BNL E851 Collab.)
MCFARLAND	93	PRL 71 31	K.S. McFarland *et al.*	(EFI, UCLA, COLO+)
ATIYA	92	PRL 69 733	M.S. Atiya *et al.*	(BNL, LANL, PRIN+)
FARZANPAY	92	PL B278 413	F. Farzanpay *et al.*	(ORST, TRIU, BRCO+)
MEIJERDREES	92B	PR D45 1439	R. Meijer Drees *et al.*	(PSI SINDRUM-I Collab.)
ATIYA	91	PRL 66 2189	M.S. Atiya *et al.*	(BNL, LANL, PRIN+)
BEHREND	91	ZPHY C49 401	H.J. Behrend *et al.*	(CELLO Collab.)
CRAWFORD	91	PR D43 46	J.F. Crawford *et al.*	(VILL, UVA)
LAM	91	PR D44 3345	W.P. Lam, K.W. Ng	(AST)
NATALE	91	PL B258 227	A.A. Natale	(SPIFT)
AFANASYEV	90	PL B236 116	L.G. Afanasyev *et al.*	(JINR, MOSU, SERP)
Also		SJNP 51 664	L.G. Afanasyev *et al.*	(JINR)
		Translated from YAF 51 1040.		
LEE	90	PRL 64 165	A.M. Lee *et al.*	(BNL, FNAL, VILL, WASH+)
FONVIEILLE	89	PL B233 65	H. Fonvieille *et al.*	(CLER, LYON, SACL)
NIEBUHR	89	PR D40 2796	C. Niebuhr *et al.*	(SINDRUM Collab.)
CAMPAGNARI	88	PRL 61 2062	C. Campagnari *et al.*	(BNL, FNAL, PSI+)
CRAWFORD	88B	PL B213 391	J.F. Crawford *et al.*	(PSI, UVA)
DORENBOS...	88	ZPHY C40 497	J. Dorenbosch *et al.*	(CHARM Collab.)
HOFFMAN	88	PL B208 149	C.M. Hoffman	(LANL)
MCDONOUGH	88	PR D38 2121	J.M. McDonough *et al.*	(TEMP, LANL, CHIC)
PDG	88	PL B204 1	G.P. Yost *et al.*	(LBL+)
WILLIAMS	88	PR D38 1365	D.A. Williams *et al.*	(Crystal Ball Collab.)
ZEPHAT	87	JP G13 1375	A.G. Zephat *et al.*	(OMICRON Collab.)
BOLOTOV	86C	JETPL 43 520	V.N. Bolotov *et al.*	(INRM)
		Translated from ZETFP 43 405.		
CRAWFORD	86	PRL 56 1043	J.F. Crawford *et al.*	(SIN, UVA)
ATHERTON	85	PL 158B 81	H.W. Atherton *et al.*	(CERN, ISU, LUND+)
HERCZEG	84	PR D29 1954	P. Herczeg, C.M. Hoffman	(LANL)
FRANK	83	PR D28 423	J.S. Frank *et al.*	(LANL, ARZS)
TUPPER	83	PR D28 2905	G.B. Tupper, T.R. Grose, M.A. Samuel	(OKSU)
BRYMAN	82	PR D26 2538	D.A. Bryman	(TRIU)
MISCHKE	82	PRL 48 1153	R.E. Mischke *et al.*	(LANL, ARZS)
HERCZEG	81	PL 100B 347	P. Herczeg, C.M. Hoffman	(LANL)
SCHARDT	81	PR D23 639	M.A. Schardt *et al.*	(ARZS, LANL)
AUERBACH	80	PL 90B 317	L.B. Auerbach *et al.*	(TEMP, LASL)
HIGHLAND	80	PRL 44 628	V.L. Highland *et al.*	(TEMP, LASL)
AUERBACH	78	PRL 41 275	L.B. Auerbach *et al.*	(TEMP, LASL)
FISCHER	78	PL 73B 359	J. Fischer *et al.*	(GEVA, SACL)
FISCHER	78B	PL 73B 364	J. Fischer *et al.*	(GEVA, SACL)
BROWMAN	74	PRL 33 1400	A. Browman *et al.*	(CORN, BING)
BELLETTINI	70	NC 66A 243	G. Bellettini *et al.*	(PISA, BONN)
KRYSHKIN	70	JETP 30 1037	V.I. Kryshkin, A.G. Sterligov, Y.P. Usov	(TMSK)
		Translated from ZETF 57 1917.		
DEVONS	69	PR 184 1356	S. Devons *et al.*	(COLU, ROMA)
VASILEVSKY	66	PL 23 281	I.M. Vasilevsky *et al.*	(JINR)
BELLETTINI	65B	NC 40A 1139	G. Bellettini *et al.*	(PISA, FIRZ)
DUCLOS	65	PL 19 253	J. Duclos *et al.*	(CERN, HEID)
KUTIN	65	JETPL 2 243	V.M. Kutjin, V.I. Petrukhin, Y.D. Prokoshkin	(JINR)
		Translated from ZETFP 2 387.		
CZIRR	63	PR 130 341	J.B. Czirr	(LRL)
SAMIOS	62B	PR 126 1844	N.P. Samios *et al.*	(COLU, BNL)
KOBRAK	61	NC 20 1115	H. Kobrak	(EFI)
SAMIOS	61	PR 121 275	N.P. Samios	(COLU, BNL)
BERMAN	60	NC XVIII 1192	S. Berman, D. Geffen	
BUDAGOV	60	JETP 11 755	Y.A. Budagov *et al.*	(JINR)
		Translated from ZETF 38 1047.		
JOSEPH	60	NC 16 997	D.W. Joseph	(EFI)

η

$I^G(J^{PC}) = 0^+(0^{-+})$

We have omitted some results that have been superseded by later experiments. The omitted results may be found in our 1988 edition Physics Letters **B204** (1988).

η MASS

Recent measurements resolve the obvious inconsistency in previous η mass measurements in favor of the higher value first reported by NA48 (LAI 02). We use only precise measurements consistent with this higher mass value for our η mass average.

VALUE (MeV)	EVTS	DOCUMENT ID		TECN	COMMENT
547.862±0.018 OUR AVERAGE					
547.873±0.005±0.027	1M	GOSLAWSKI	12	SPEC	$dp \to {}^3\mathrm{He}\,\eta$
547.874±0.007±0.029		AMBROSINO	07B	KLOE	$e^+e^- \to \phi \to \eta\gamma$
547.785±0.017±0.057	16k	MILLER	07	CLEO	$\psi(2S) \to J/\psi\eta$
547.843±0.030±0.041	1134	LAI	02	NA48	$\eta \to 3\pi^0$
• • • We do not use the following data for averages, fits, limits, etc. • • •					
547.311±0.028±0.032		[1] ABDEL-BARY	05	SPEC	$dp \to {}^3\mathrm{He}\,\eta$
547.12 ±0.06 ±0.25		KRUSCHE	95D	SPEC	$\gamma p \to \eta p$, threshold
547.30 ±0.15		PLOUIN	92	SPEC	$dp \to {}^3\mathrm{He}\,\eta$
547.45 ±0.25		DUANE	74	SPEC	$\pi^- p \to n$ neutrals
548.2 ±0.65		FOSTER	65C	HBC	
549.0 ±0.7	148	FOELSCHE	64	HBC	
548.0 ±1.0	91	ALFF-...	62	HBC	
549.0 ±1.2	53	BASTIEN	62	HBC	

[1] ABDEL-BARY 05 disagrees significantly with recent measurements of similar or better precision. See comment in the header.

η WIDTH

This is the partial decay rate $\Gamma(\eta \to \gamma\gamma)$ divided by the fitted branching fraction for that mode. See the note at the start of the $\Gamma(2\gamma)$ data block, next below.

VALUE (keV)	DOCUMENT ID
1.31±0.05 OUR FIT	

Meson Particle Listings

η

η DECAY MODES

	Mode	Fraction (Γ_i/Γ)	Scale factor/ Confidence level
	Neutral modes		
Γ_1	neutral modes	(72.12±0.34) %	S=1.2
Γ_2	2γ	(39.41±0.20) %	S=1.1
Γ_3	$3\pi^0$	(32.68±0.23) %	S=1.1
Γ_4	$\pi^0 2\gamma$	(2.7 ±0.5) $\times 10^{-4}$	S=1.1
Γ_5	$2\pi^0 2\gamma$	< 1.2 $\times 10^{-3}$	CL=90%
Γ_6	4γ	< 2.8 $\times 10^{-4}$	CL=90%
Γ_7	invisible	< 1.0 $\times 10^{-4}$	CL=90%
	Charged modes		
Γ_8	charged modes	(28.10±0.34) %	S=1.2
Γ_9	$\pi^+\pi^-\pi^0$	(22.92±0.28) %	S=1.2
Γ_{10}	$\pi^+\pi^-\gamma$	(4.22±0.08) %	S=1.1
Γ_{11}	$e^+e^-\gamma$	(6.9 ±0.4) $\times 10^{-3}$	S=1.3
Γ_{12}	$\mu^+\mu^-\gamma$	(3.1 ±0.4) $\times 10^{-4}$	
Γ_{13}	e^+e^-	< 5.6 $\times 10^{-6}$	CL=90%
Γ_{14}	$\mu^+\mu^-$	(5.8 ±0.8) $\times 10^{-6}$	
Γ_{15}	$2e^+2e^-$	(2.40±0.22) $\times 10^{-5}$	
Γ_{16}	$\pi^+\pi^-e^+e^-(\gamma)$	(2.68±0.11) $\times 10^{-4}$	
Γ_{17}	$e^+e^-\mu^+\mu^-$	< 1.6 $\times 10^{-4}$	CL=90%
Γ_{18}	$2\mu^+2\mu^-$	< 3.6 $\times 10^{-4}$	CL=90%
Γ_{19}	$\mu^+\mu^-\pi^+\pi^-$	< 3.6 $\times 10^{-4}$	CL=90%
Γ_{20}	$\pi^+e^-\overline{\nu}_e$ + c.c.	< 1.7 $\times 10^{-4}$	CL=90%
Γ_{21}	$\pi^+\pi^-2\gamma$	< 2.1 $\times 10^{-3}$	
Γ_{22}	$\pi^+\pi^-\pi^0\gamma$	< 5 $\times 10^{-4}$	CL=90%
Γ_{23}	$\pi^0\mu^+\mu^-\gamma$	< 3 $\times 10^{-6}$	CL=90%
	Charge conjugation (C), Parity (P), Charge conjugation × Parity (CP), or Lepton Family number (LF) violating modes		
Γ_{24}	$\pi^0\gamma$	C < 9 $\times 10^{-5}$	CL=90%
Γ_{25}	$\pi^+\pi^-$	P,CP < 1.3 $\times 10^{-5}$	CL=90%
Γ_{26}	$2\pi^0$	P,CP < 3.5 $\times 10^{-4}$	CL=90%
Γ_{27}	$2\pi^0\gamma$	C < 5 $\times 10^{-4}$	CL=90%
Γ_{28}	$3\pi^0\gamma$	C < 6 $\times 10^{-5}$	CL=90%
Γ_{29}	3γ	C < 1.6 $\times 10^{-5}$	CL=90%
Γ_{30}	$4\pi^0$	P,CP < 6.9 $\times 10^{-7}$	CL=90%
Γ_{31}	$\pi^0e^+e^-$	C [a] < 4 $\times 10^{-5}$	CL=90%
Γ_{32}	$\pi^0\mu^+\mu^-$	C [a] < 5 $\times 10^{-6}$	CL=90%
Γ_{33}	$\mu^+e^- + \mu^-e^+$	LF < 6 $\times 10^{-6}$	CL=90%

[a] C parity forbids this to occur as a single-photon process.

CONSTRAINED FIT INFORMATION

An overall fit to a decay rate and 19 branching ratios uses 49 measurements and one constraint to determine 9 parameters. The overall fit has a $\chi^2 = 43.7$ for 41 degrees of freedom.

The following *off-diagonal* array elements are the correlation coefficients $\langle \delta x_i \delta x_j \rangle / (\delta x_i \cdot \delta x_j)$, in percent, from the fit to the branching fractions, $x_i \equiv \Gamma_i/\Gamma_{\rm total}$. The fit constrains the x_i whose labels appear in this array to sum to one.

x_3	24							
x_4	−1	−1						
x_9	−73	−80	−1					
x_{10}	−56	−60	0	61				
x_{11}	−5	−5	0	−6	−4			
x_{12}	−1	0	0	−1	0	0		
x_{16}	0	0	0	0	0	0	0	
Γ	−14	−3	0	11	8	1	0	0
	x_2	x_3	x_4	x_9	x_{10}	x_{11}	x_{12}	x_{16}

	Mode	Rate (keV)	Scale factor
Γ_2	2γ	0.516 ±0.018	
Γ_3	$3\pi^0$	0.428 ±0.015	
Γ_4	$\pi^0 2\gamma$	(3.5 ±0.7) $\times 10^{-4}$	
Γ_9	$\pi^+\pi^-\pi^0$	0.300 ±0.011	
Γ_{10}	$\pi^+\pi^-\gamma$	0.0552±0.0022	
Γ_{11}	$e^+e^-\gamma$	0.0090±0.0006	1.2
Γ_{12}	$\mu^+\mu^-\gamma$	(4.1 ±0.5) $\times 10^{-4}$	
Γ_{16}	$\pi^+\pi^-e^+e^-(\gamma)$	(3.51 ±0.19) $\times 10^{-4}$	

η DECAY RATES

$\Gamma(2\gamma)$ Γ_2

See the table immediately above giving the fitted decay rates. Following the advice of NEFKENS 02, we have removed the Primakoff-effect measurement from the average. See also the "Note on the Decay Width $\Gamma(\eta \to \gamma\gamma)$," in our 1994 edition, Phys. Rev. **D50**, 1 August 1994, Part I, p. 1451, for a discussion of the various measurements.

VALUE (keV)	EVTS	DOCUMENT ID		TECN	COMMENT
0.516±0.018 OUR FIT					
0.516±0.018 OUR AVERAGE					
0.520±0.020±0.013		BABUSCI	13A	KLOE	$e^+e^- \to e^+e^-\eta$
0.51 ±0.12 ±0.05	36	BARU	90	MD1	$e^+e^- \to e^+e^-\eta$
0.490±0.010±0.048	2287	ROE	90	ASP	$e^+e^- \to e^+e^-\eta$
0.514±0.017±0.035	1295	WILLIAMS	88	CBAL	$e^+e^- \to e^+e^-\eta$
0.53 ±0.04 ±0.04		BARTEL	85E	JADE	$e^+e^- \to e^+e^-\eta$
• • • We do not use the following data for averages, fits, limits, etc. • • •					
0.476±0.062		[2] RODRIGUES	08	CNTR	Reanalysis
0.64 ±0.14 ±0.13		AIHARA	86	TPC	$e^+e^- \to e^+e^-\eta$
0.56 ±0.16	56	WEINSTEIN	83	CBAL	$e^+e^- \to e^+e^-\eta$
0.324±0.046		BROWMAN	74B	CNTR	Primakoff effect
1.00 ±0.22		[3] BEMPORAD	67	CNTR	Primakoff effect

[2] RODRIGUES 08 uses a more sophisticated calculation for the inelastic background due to incoherent photoproduction to reanalyze the η photoproduction data on Be and Cu at 9 GeV from BROWMAN 74B. This brings the value of $\Gamma(\eta \to 2\gamma)$ in line with direct measurements of the width. The error here is only statistical.

[3] BEMPORAD 67 gives $\Gamma(2\gamma) = 1.21 \pm 0.26$ keV assuming $\Gamma(2\gamma)/\Gamma(\text{total}) = 0.314$. Bemporad private communication gives $\Gamma(2\gamma)^2/\Gamma(\text{total}) = 0.380 \pm 0.083$. We evaluate this using $\Gamma(2\gamma)/\Gamma(\text{total}) = 0.38 \pm 0.01$. Not included in average because the uncertainty resulting from the separation of the coulomb and nuclear amplitudes has apparently been underestimated.

η BRANCHING RATIOS

Neutral modes

$\Gamma(\text{neutral modes})/\Gamma_{\rm total}$ $\Gamma_1/\Gamma = (\Gamma_2+\Gamma_3+\Gamma_4)/\Gamma$

VALUE	EVTS	DOCUMENT ID		TECN	COMMENT
0.7212±0.0034 OUR FIT Error includes scale factor of 1.2.					
0.705 ±0.008	16k	BASILE	71D	CNTR	MM spectrometer
• • • We do not use the following data for averages, fits, limits, etc. • • •					
0.79 ±0.08		BUNIATOV	67	OSPK	

$\Gamma(2\gamma)/\Gamma_{\rm total}$ Γ_2/Γ

VALUE (units 10^{-2})	EVTS	DOCUMENT ID		TECN	COMMENT
39.41±0.20 OUR FIT Error includes scale factor of 1.1.					
39.49±0.17±0.30	65k	ABEGG	96	SPEC	$pd \to {}^3\text{He}\eta$
• • • We do not use the following data for averages, fits, limits, etc. • • •					
38.45±0.40±0.36	14k	[4] LOPEZ	07	CLEO	$\psi(2S) \to J/\psi\eta$

[4] Not independent of other results listed for LOPEZ 07. Assuming decays of $\eta \to \gamma\gamma$, $3\pi^0$, $\pi^+\pi^-\pi^0$, $\pi^+\pi^-\gamma$, and $e^+e^-\gamma$ account for all η decays within a contribution of 0.3% to the systematic error.

$\Gamma(2\gamma)/\Gamma(\text{neutral modes})$ $\Gamma_2/\Gamma_1 = \Gamma_2/(\Gamma_2+\Gamma_3+\Gamma_4)$

VALUE	EVTS	DOCUMENT ID		TECN	COMMENT
0.5465±0.0019 OUR FIT					
0.548 ±0.023 OUR AVERAGE Error includes scale factor of 1.5.					
0.535 ±0.018		BUTTRAM	70	OSPK	
0.59 ±0.033		BUNIATOV	67	OSPK	
• • • We do not use the following data for averages, fits, limits, etc. • • •					
0.52 ±0.09	88	ABROSIMOV	80	HLBC	
0.60 ±0.14	113	KENDALL	74	OSPK	
0.57 ±0.09		STRUGALSKI	71	HLBC	
0.579 ±0.052		FELDMAN	67	OSPK	
0.416 ±0.044		DIGIUGNO	66	CNTR	Error doubled
0.44 ±0.07		GRUNHAUS	66	OSPK	
0.39 ±0.06		[5] JONES	66	CNTR	

[5] This result from combining cross sections from two different experiments.

$\Gamma(3\pi^0)/\Gamma_{\rm total}$ Γ_3/Γ

VALUE (units 10^{-2})	EVTS	DOCUMENT ID		TECN	COMMENT
32.68±0.23 OUR FIT Error includes scale factor of 1.1.					
• • • We do not use the following data for averages, fits, limits, etc. • • •					
34.03±0.56±0.49	1821	[6] LOPEZ	07	CLEO	$\psi(2S) \to J/\psi\eta$

[6] Not independent of other results listed for LOPEZ 07. Assuming decays of $\eta \to \gamma\gamma$, $3\pi^0$, $\pi^+\pi^-\pi^0$, $\pi^+\pi^-\gamma$, and $e^+e^-\gamma$ account for all η decays within a contribution of 0.3% to the systematic error.

$\Gamma(3\pi^0)/\Gamma(\text{neutral modes})$ $\Gamma_3/\Gamma_1 = \Gamma_3/(\Gamma_2+\Gamma_3+\Gamma_4)$

VALUE	EVTS	DOCUMENT ID		TECN	COMMENT
0.4531±0.0019 OUR FIT					
0.439 ±0.024		BUTTRAM	70	OSPK	
• • • We do not use the following data for averages, fits, limits, etc. • • •					
0.44 ±0.08	75	ABROSIMOV	80	HLBC	
0.32 ±0.09		STRUGALSKI	71	HLBC	
0.41 ±0.033		BUNIATOV	67	OSPK	Not indep. of $\Gamma(2\gamma)/\Gamma(\text{neutral modes})$
0.177 ±0.035		FELDMAN	67	OSPK	
0.209 ±0.054		DIGIUGNO	66	CNTR	Error doubled
0.29 ±0.10		GRUNHAUS	66	OSPK	

$\Gamma(3\pi^0)/\Gamma(2\gamma)$ Γ_3/Γ_2

VALUE	EVTS	DOCUMENT ID		TECN	COMMENT
0.829±0.006 OUR FIT					
0.829±0.007 OUR AVERAGE					
0.884±0.022±0.019	1821	LOPEZ	07	CLEO	$\psi(2S) \to J/\psi\eta$
0.817±0.012±0.032	17.4k	[7] AKHMETSHIN	05	CMD2	$e^+e^- \to \phi \to \eta\gamma$
0.826±0.024		ACHASOV	00D	SND	$e^+e^- \to \phi \to \eta\gamma$
0.832±0.005±0.012		KRUSCHE	95D	SPEC	$\gamma p \to \eta p$, threshold
0.841±0.034		AMSLER	93	CBAR	$\overline{p}p \to \pi^+\pi^-\eta$ at rest
0.822±0.009		ALDE	84	GAM2	
• • • We do not use the following data for averages, fits, limits, etc. • • •					
0.796±0.016±0.016		ACHASOV	00	SND	See ACHASOV 00D
0.91 ±0.14		COX	70B	HBC	
0.75 ±0.09		DEVONS	70	OSPK	
0.88 ±0.16		BALTAY	67D	DBC	
1.1 ±0.2		CENCE	67	OSPK	
1.25 ±0.39		BACCI	63	CNTR	Inverse BR reported

[7] Uses result from AKHMETSHIN 01B.

$\Gamma(\pi^0 2\gamma)/\Gamma_{\text{total}}$ Γ_4/Γ

Early results are summarized in the review by LANDSBERG 85.

VALUE (units 10^{-4})	CL%	EVTS	DOCUMENT ID		TECN	COMMENT
2.7 ±0.5 OUR FIT			Error includes scale factor of 1.1.			
2.21±0.24±0.47		≈ 500	[8] PRAKHOV	08	CRYB	$\pi^- p \to \eta n \approx$ threshold
• • • We do not use the following data for averages, fits, limits, etc. • • •						
3.5 ±0.7 ±0.6		1.6k	[9,10] PRAKHOV	05	CRYB	See PRAKHOV 08
<8.4	90	7	ACHASOV	01D	SND	$e^+e^- \to \phi \to \eta\gamma$
<30	90	0	DAVYDOV	81	GAM2	$\pi^- p \to \eta n$

[8] PRAKHOV 08 is a reanalysis of the data of PRAKHOV 05, using for the first time the invariant-mass spectrum of the two photons.

[9] Normalized using $\Gamma(\eta \to 2\gamma)/\Gamma = 0.3943 \pm 0.0026$.

[10] This measurement and the independent analysis of the same data by KNECHT 04 both imply a lower value of $\Gamma(\pi^0 2\gamma)$ than the one obtained by ALDE 84 from $\Gamma(\pi^0 2\gamma)/\Gamma(2\gamma)$.

$\Gamma(\pi^0 2\gamma)/\Gamma(2\gamma)$ Γ_4/Γ_2

VALUE (units 10^{-3})	EVTS	DOCUMENT ID		TECN	CHG	COMMENT
0.69±0.13 OUR FIT	Error includes scale factor of 1.1.					
1.8 ±0.4		ALDE	84	GAM2	0	
• • • We do not use the following data for averages, fits, limits, etc. • • •						
2.5 ±0.6	70	BINON	82	GAM2		See ALDE 84

$\Gamma(\pi^0 2\gamma)/\Gamma(3\pi^0)$ Γ_4/Γ_3

VALUE (units 10^{-4})	DOCUMENT ID		TECN	COMMENT
8.3±1.6 OUR FIT	Error includes scale factor of 1.1.			
• • • We do not use the following data for averages, fits, limits, etc. • • •				
8.3±2.8±1.4	[11] KNECHT	04	CRYB	$\pi^- p \to n\eta$

[11] Independent analysis of same data as PRAKHOV 05.

$\Gamma(2\pi^0 2\gamma)/\Gamma_{\text{total}}$ Γ_5/Γ

VALUE	CL%	DOCUMENT ID		TECN	COMMENT
<1.2 × 10^{-3}	90	[12] NEFKENS	05A	CRYB	p(720 MeV/c) $\pi^- \to n\eta$
• • • We do not use the following data for averages, fits, limits, etc. • • •					
<4.0 × 10^{-3}	90	BLIK	07	GAM4	$\pi^- p \to \eta n$

[12] Measurement is done in limited $\gamma\gamma$ energy range.

$\Gamma(4\gamma)/\Gamma_{\text{total}}$ Γ_6/Γ

VALUE	CL%	DOCUMENT ID		TECN	COMMENT
<2.8 × 10^{-4}	90	BLIK	07	GAM4	$\pi^- p \to \eta n$

$\Gamma(\text{invisible})/\Gamma(2\gamma)$ Γ_7/Γ_2

VALUE	CL%	DOCUMENT ID		TECN	COMMENT
<2.6 × 10^{-4}	90	[13] ABLIKIM	13	BES3	$J/\psi \to \phi\eta$
• • • We do not use the following data for averages, fits, limits, etc. • • •					
<1.65 × 10^{-3}	90	[14] ABLIKIM	06Q	BES2	$J/\psi \to \phi\eta$

[13] Based on 225M J/ψ decays.

[14] Based on 58M J/ψ decays.

Charged modes

$\Gamma(\pi^+\pi^-\pi^0)/\Gamma_{\text{total}}$ Γ_9/Γ

VALUE (units 10^{-2})	EVTS	DOCUMENT ID		TECN	COMMENT
22.92±0.28 OUR FIT	Error includes scale factor of 1.2.				
• • • We do not use the following data for averages, fits, limits, etc. • • •					
22.60±0.35±0.29	3915	[15] LOPEZ	07	CLEO	$\psi(2S) \to J/\psi\eta$

[15] Not independent of other results listed for LOPEZ 07. Assuming decays of $\eta \to \gamma\gamma$, $3\pi^0$, $\pi^+\pi^-\pi^0$, $\pi^+\pi^-\gamma$, and $e^+e^-\gamma$ account for all η decays within a contribution of 0.3% to the systematic error.

$\Gamma(\text{neutral modes})/\Gamma(\pi^+\pi^-\pi^0)$ $\Gamma_1/\Gamma_9 = (\Gamma_2+\Gamma_3+\Gamma_4)/\Gamma_9$

VALUE	EVTS	DOCUMENT ID		TECN
3.15±0.05 OUR FIT	Error includes scale factor of 1.2.			
3.26±0.30 OUR AVERAGE				
2.54±1.89	74	KENDALL	74	OSPK
3.4 ±1.1	29	AGUILAR-...	72B	HBC
2.83±0.80	70	[16] BLOODWO...	72B	HBC
3.6 ±0.6	244	FLATTE	67B	HBC
2.89±0.56		ALFF-...	66	HBC
3.6 ±0.8	50	KRAEMER	64	DBC
3.8 ±1.1		PAULI	64	DBC

[16] Error increased from published value 0.5 by Bloodworth (private communication).

$\Gamma(2\gamma)/\Gamma(\pi^+\pi^-\pi^0)$ Γ_2/Γ_9

VALUE	EVTS	DOCUMENT ID		TECN	COMMENT
1.720±0.028 OUR FIT	Error includes scale factor of 1.2.				
1.70 ±0.04 OUR AVERAGE					
1.704±0.032±0.026	3915	[17] LOPEZ	07	CLEO	$\psi(2S) \to J/\psi\eta$
1.61 ±0.14		ABLIKIM	06E	BES2	$e^+e^- \to J/\psi \to \eta\gamma$
1.78 ±0.10 ±0.13	1077	AMSLER	95	CBAR	$\overline{p}p \to \pi^+\pi^-\eta$ at rest
1.72 ±0.25	401	BAGLIN	69	HLBC	
1.61 ±0.39		FOSTER	65	HBC	

[17] LOPEZ 07 reports $\Gamma(\eta \to \pi^+\pi^-\pi^0) / \Gamma(\eta \to 2\gamma) = \Gamma_9/\Gamma_2 = 0.587 \pm 0.011 \pm 0.009$.

$\Gamma(3\pi^0)/\Gamma(\pi^+\pi^-\pi^0)$ Γ_3/Γ_9

VALUE	EVTS	DOCUMENT ID		TECN	COMMENT
1.426±0.026 OUR FIT	Error includes scale factor of 1.2.				
1.48 ±0.05 OUR AVERAGE					
1.46 ±0.03 ±0.09		ACHASOV	06A	SND	$e^+e^- \to \eta\gamma$
1.52 ±0.04 ±0.08	23k	[18] AKHMETSHIN	01B	CMD2	$e^+e^- \to \phi \to \eta\gamma$
1.44 ±0.09 ±0.10	1627	AMSLER	95	CBAR	$\overline{p}p \to \pi^+\pi^-\eta$ at rest
$1.50\ ^{+0.15}_{-0.29}$	199	BAGLIN	69	HLBC	
$1.47\ ^{+0.20}_{-0.17}$		BULLOCK	68	HLBC	
• • • We do not use the following data for averages, fits, limits, etc. • • •					
1.3 ±0.4		BAGLIN	67B	HLBC	
0.90 ±0.24		FOSTER	65	HBC	
2.0 ±1.0		FOELSCHE	64	HBC	
0.83 ±0.32		CRAWFORD	63	HBC	

[18] AKHMETSHIN 01B uses results from AKHMETSHIN 99F.

$\Gamma(\pi^+\pi^-\pi^0)/[\Gamma(2\gamma)+\Gamma(3\pi^0)]$ $\Gamma_9/(\Gamma_2+\Gamma_3)$

VALUE	DOCUMENT ID		TECN	COMMENT
0.318 ±0.005 OUR FIT	Error includes scale factor of 1.2.			
0.304 ±0.012	ACHASOV	00D	SND	$e^+e^- \to \phi \to \eta\gamma$
• • • We do not use the following data for averages, fits, limits, etc. • • •				
0.3141±0.0081±0.0058	ACHASOV	00B	SND	See ACHASOV 00D

$\Gamma(\pi^+\pi^-\gamma)/\Gamma_{\text{total}}$ Γ_{10}/Γ

VALUE (units 10^{-2})	EVTS	DOCUMENT ID		TECN	COMMENT
4.22±0.08 OUR FIT	Error includes scale factor of 1.1.				
• • • We do not use the following data for averages, fits, limits, etc. • • •					
3.96±0.14±0.14	859	[19] LOPEZ	07	CLEO	$\psi(2S) \to J/\psi\eta$

[19] Not independent of other results listed for LOPEZ 07. Assuming decays of $\eta \to \gamma\gamma$, $3\pi^0$, $\pi^+\pi^-\pi^0$, $\pi^+\pi^-\gamma$, and $e^+e^-\gamma$ account for all η decays within a contribution of 0.3% to the systematic error.

$\Gamma(\pi^+\pi^-\gamma)/\Gamma(\pi^+\pi^-\pi^0)$ Γ_{10}/Γ_9

VALUE	EVTS	DOCUMENT ID		TECN	COMMENT
0.1842±0.0027 OUR FIT					
0.1847±0.0030 OUR AVERAGE	Error includes scale factor of 1.1.				
0.1856±0.0005±0.0028	200k	BABUSCI	13	KLOE	$e^+e^- \to \phi \to \eta\gamma$
0.175 ±0.007 ±0.006	859	LOPEZ	07	CLEO	$\psi(2S) \to J/\psi\eta$
• • • We do not use the following data for averages, fits, limits, etc. • • •					
0.209 ±0.004	18k	THALER	73	ASPK	
0.201 ±0.006	7250	GORMLEY	70	ASPK	
0.28 ±0.04		BALTAY	67B	DBC	
0.25 ±0.035		LITCHFIELD	67	DBC	
0.30 ±0.06		CRAWFORD	66	HBC	
0.196 ±0.041		FOSTER	65C	HBC	

$\Gamma(e^+e^-\gamma)/\Gamma_{\text{total}}$ Γ_{11}/Γ

VALUE (units 10^{-3})	EVTS	DOCUMENT ID		TECN	COMMENT
6.9 ±0.4 OUR FIT	Error includes scale factor of 1.3.				
6.7 ±0.5 OUR AVERAGE	Error includes scale factor of 1.2.				
6.6 ±0.4 ±0.4	1345	BERGHAUSER	11	SPEC	$\gamma p \to p\eta$
7.8 ±0.5 ±0.8	435 ± 31	BERLOWSKI	08	WASA	$pd \to {}^3\text{He}\,\eta$
5.15±0.62±0.74	283	ACHASOV	01B	SND	$e^+e^- \to \phi \to \eta\gamma$
7.10±0.64±0.46	323	AKHMETSHIN	01	CMD2	$e^+e^- \to \phi \to \eta\gamma$
• • • We do not use the following data for averages, fits, limits, etc. • • •					
9.4 ±0.7 ±0.5	172	[20] LOPEZ	07	CLEO	$\psi(2S) \to J/\psi\eta$

[20] Not independent of other results listed for LOPEZ 07. Assuming decays of $\eta \to \gamma\gamma$, $3\pi^0$, $\pi^+\pi^-\pi^0$, $\pi^+\pi^-\gamma$, and $e^+e^-\gamma$ account for all η decays within a contribution of 0.3% to the systematic error.

$\Gamma(e^+e^-\gamma)/\Gamma(\pi^+\pi^-\gamma)$ Γ_{11}/Γ_{10}

VALUE	EVTS	DOCUMENT ID		TECN	COMMENT
0.163±0.011 OUR FIT	Error includes scale factor of 1.2.				
0.237±0.021±0.015	172	LOPEZ	07	CLEO	$\psi(2S) \to J/\psi\eta$

$\Gamma(e^+e^-\gamma)/\Gamma(\pi^+\pi^-\pi^0)$ Γ_{11}/Γ_9

VALUE (units 10^{-2})	EVTS	DOCUMENT ID		TECN	COMMENT
3.00±0.19 OUR FIT	Error includes scale factor of 1.3.				
2.1 ±0.5	80	JANE	75B	OSPK	See the erratum

$\Gamma(\text{neutral modes})/[\Gamma(\pi^+\pi^-\pi^0)+\Gamma(\pi^+\pi^-\gamma)+\Gamma(e^+e^-\gamma)]$ $\Gamma_1/(\Gamma_9+\Gamma_{10}+\Gamma_{11}) = (\Gamma_2+\Gamma_3+\Gamma_4)/(\Gamma_9+\Gamma_{10}+\Gamma_{11})$

VALUE	EVTS	DOCUMENT ID		TECN
2.59±0.04 OUR FIT	Error includes scale factor of 1.2.			
2.64±0.23		BALTAY	67B	DBC
• • • We do not use the following data for averages, fits, limits, etc. • • •				
4.5 ±1.0	280	[21] JAMES	66	HBC
3.20±1.26	53	[21] BASTIEN	62	HBC
2.5 ±1.0	10	[21] PICKUP	62	HBC

[21] These experiments are not used in the averages as they do not separate clearly $\eta \to \pi^+\pi^-\pi^0$ and $\eta \to \pi^+\pi^-\gamma$ from each other. The reported values thus probably contain some unknown fraction of $\eta \to \pi^+\pi^-\gamma$.

$\Gamma(2\gamma)/[\Gamma(\pi^+\pi^-\pi^0)+\Gamma(\pi^+\pi^-\gamma)+\Gamma(e^+e^-\gamma)]$ $\Gamma_2/(\Gamma_9+\Gamma_{10}+\Gamma_{11})$

VALUE	EVTS	DOCUMENT ID		TECN
1.416±0.023 OUR FIT	Error includes scale factor of 1.2.			
1.1 ±0.4 OUR AVERAGE				
1.51 ±0.93	75	KENDALL	74	OSPK
0.99 ±0.48		CRAWFORD	63	HBC

$\Gamma(\mu^+\mu^-\gamma)/\Gamma_{\text{total}}$ Γ_{12}/Γ

VALUE (units 10^{-4})	EVTS	DOCUMENT ID		TECN	COMMENT
3.1±0.4 OUR FIT					
3.1±0.4	600	DZHELYADIN	80	SPEC	$\pi^- p \to \eta n$
• • • We do not use the following data for averages, fits, limits, etc. • • •					
1.5±0.75	100	BUSHNIN	78	SPEC	See DZHELYADIN 80

$\Gamma(e^+e^-)/\Gamma_{\text{total}}$ Γ_{13}/Γ

VALUE	CL%	DOCUMENT ID		TECN	COMMENT
<5.6 $\times 10^{-6}$	90	[22] AGAKISHIEV	12A	SPEC	$pp \to \eta + X$
• • • We do not use the following data for averages, fits, limits, etc. • • •					
<2.7 $\times 10^{-5}$	90	BERLOWSKI	08	WASA	$pd \to {}^3\text{He}\,\eta$
<0.77 $\times 10^{-4}$	90	BROWDER	97B	CLE2	$e^+e^- \simeq 10.5$ GeV
<2 $\times 10^{-4}$	90	WHITE	96	SPEC	$pd \to \eta\,{}^3\text{He}$
<3 $\times 10^{-4}$	90	DAVIES	74	RVUE	Uses ESTEN 67

[22] AGAKISHIEV 12A uses a data sample of 3.5 GeV proton beam collisions on liquid hydrogen target collected by the HADES detector.

$\Gamma(\mu^+\mu^-)/\Gamma_{\text{total}}$ Γ_{14}/Γ

VALUE (units 10^{-6})	CL%	EVTS	DOCUMENT ID		TECN	COMMENT
5.8±0.8 OUR AVERAGE						
5.7±0.7±0.5		114	ABEGG	94	SPEC	$pd \to \eta\,{}^3\text{He}$
6.5±2.1		27	DZHELYADIN	80B	SPEC	$\pi^- p \to \eta n$
• • • We do not use the following data for averages, fits, limits, etc. • • •						
$5.6^{+0.6}_{-0.7}$±0.5		100	KESSLER	93	SPEC	See ABEGG 94
< 20	95	0	WEHMANN	68	OSPK	

$\Gamma(\mu^+\mu^-)/\Gamma(2\gamma)$ Γ_{14}/Γ_2

VALUE (units 10^{-5})	DOCUMENT ID		TECN
• • • We do not use the following data for averages, fits, limits, etc. • • •			
5.9±2.2	HYAMS	69	OSPK

$\Gamma(2e^+2e^-)/\Gamma_{\text{total}}$ Γ_{15}/Γ

VALUE (units 10^{-5})	CL%	EVTS	DOCUMENT ID		TECN	COMMENT
2.4±0.2±0.1		362	[23] AMBROSINO	11B	KLOE	$e^+e^- \to \phi \to \eta\gamma$
• • • We do not use the following data for averages, fits, limits, etc. • • •						
<9.7	90		BERLOWSKI	08	WASA	$pd \to {}^3\text{He}\,\eta$
<6.9	90		AKHMETSHIN	01	CMD2	$e^+e^- \to \phi \to \eta\gamma$

[23] This measurement is fully inclusive (includes "$2e^+2e^-\gamma$" channel).

$\Gamma(\pi^+\pi^-e^+e^-(\gamma))/\Gamma_{\text{total}}$ Γ_{16}/Γ

VALUE (units 10^{-4})	EVTS	DOCUMENT ID		TECN	COMMENT
2.68±0.11 OUR FIT					
2.68±0.09±0.07	1555 ±52	[24] AMBROSINO	09B	KLOE	$e^+e^- \to \phi \to \eta\gamma$
• • • We do not use the following data for averages, fits, limits, etc. • • •					
4.3 $^{+2.0}_{-1.6}$ ±0.4	16	BERLOWSKI	08	WASA	$pd \to {}^3\text{He}\,\eta$
4.3 ±1.3 ±0.4	16	BARGHOLTZ	07	CNTR	See BERLOWSKI 08
3.7 $^{+2.5}_{-1.8}$ ±0.3	4	AKHMETSHIN	01	CMD2	$e^+e^- \to \phi \to \eta\gamma$

[24] This AMBROSINO 09B value includes radiative events.

$\Gamma(e^+e^-\mu^+\mu^-)/\Gamma_{\text{total}}$ Γ_{17}/Γ

VALUE	CL%	DOCUMENT ID		TECN	COMMENT
<1.6 $\times 10^{-4}$	90	BERLOWSKI	08	WASA	$pd \to {}^3\text{He}\,\eta$

$\Gamma(2\mu^+2\mu^-)/\Gamma_{\text{total}}$ Γ_{18}/Γ

VALUE	CL%	DOCUMENT ID		TECN	COMMENT
<3.6 $\times 10^{-4}$	90	BERLOWSKI	08	WASA	$pd \to {}^3\text{He}\,\eta$

$\Gamma(\mu^+\mu^-\pi^+\pi^-)/\Gamma_{\text{total}}$ Γ_{19}/Γ

VALUE	CL%	DOCUMENT ID		TECN	COMMENT
<3.6 $\times 10^{-4}$	90	BERLOWSKI	08	WASA	$pd \to {}^3\text{He}\,\eta$

$\Gamma(\pi^+e^-\bar{\nu}_e + \text{c.c.})/\Gamma(\pi^+\pi^-\pi^0)$ Γ_{20}/Γ_9

VALUE	CL%	DOCUMENT ID		TECN	COMMENT
<7.3 $\times 10^{-4}$	90	ABLIKIM	13G	BES3	$J/\psi \to \phi\eta$

$\Gamma(\pi^+\pi^-2\gamma)/\Gamma(\pi^+\pi^-\pi^0)$ Γ_{21}/Γ_9

VALUE	CL%	DOCUMENT ID		TECN
< 9 $\times 10^{-3}$		PRICE	67	HBC
• • • We do not use the following data for averages, fits, limits, etc. • • •				
<16 $\times 10^{-3}$	95	BALTAY	67B	DBC

$\Gamma(\pi^+\pi^-\pi^0\gamma)/\Gamma(\pi^+\pi^-\pi^0)$ Γ_{22}/Γ_9

VALUE	CL%	EVTS	DOCUMENT ID		TECN
<0.24 $\times 10^{-2}$	90	0	THALER	73	ASPK
• • • We do not use the following data for averages, fits, limits, etc. • • •					
<1.7 $\times 10^{-2}$	90		ARNOLD	68	HLBC
<1.6 $\times 10^{-2}$	95		BALTAY	67B	DBC
<7.0 $\times 10^{-2}$			FLATTE	67	HBC
<0.9 $\times 10^{-2}$			PRICE	67	HBC

$\Gamma(\pi^0\mu^+\mu^-\gamma)/\Gamma_{\text{total}}$ Γ_{23}/Γ

VALUE	CL%	DOCUMENT ID		TECN	COMMENT
<3 $\times 10^{-6}$	90	DZHELYADIN	81	SPEC	$\pi^- p \to \eta n$

Forbidden modes

$\Gamma(\pi^0\gamma)/\Gamma_{\text{total}}$ Γ_{24}/Γ

Forbidden by angular momentum conservation.

VALUE	CL%	DOCUMENT ID		TECN	COMMENT
<9 $\times 10^{-5}$	90	NEFKENS	05A	CRYB	p(720 MeV/c) $\pi^- \to n\eta$

$\Gamma(\pi^+\pi^-)/\Gamma_{\text{total}}$ Γ_{25}/Γ

Forbidden by P and CP invariance.

VALUE	CL%	EVTS	DOCUMENT ID		TECN	COMMENT
< 0.13 $\times 10^{-4}$	90	16M	AMBROSINO	05A	KLOE	$e^+e^- \to \phi \to \eta\gamma$
• • • We do not use the following data for averages, fits, limits, etc. • • •						
< 3.9 $\times 10^{-4}$	90	225M	ABLIKIM	11G	BES3	$e^+e^- \to J/\psi \to \eta\gamma$
< 3.3 $\times 10^{-4}$	90		AKHMETSHIN	99B	CMD2	$e^+e^- \to \phi \to \eta\gamma$
< 9 $\times 10^{-4}$	90		AKHMETSHIN	97C	CMD2	See AKHMETSHIN 99B
<15 $\times 10^{-4}$		0	THALER	73	ASPK	

$\Gamma(2\pi^0)/\Gamma_{\text{total}}$ Γ_{26}/Γ

Forbidden by P and CP invariance.

VALUE	CL%	EVTS	DOCUMENT ID		TECN	COMMENT
<3.5 $\times 10^{-4}$	90		BLIK	07	GAM4	$\pi^- p \to \eta n$
• • • We do not use the following data for averages, fits, limits, etc. • • •						
<6.9 $\times 10^{-4}$	90	225M	ABLIKIM	11G	BES3	$e^+e^- \to J/\psi \to \eta\gamma$
<4.3 $\times 10^{-4}$	90		AKHMETSHIN	99C	CMD2	$e^+e^- \to \phi \to \eta\gamma$
<6 $\times 10^{-4}$	90		[25] ACHASOV	98	SND	$e^+e^- \to \phi \to \eta\gamma$

[25] ACHASOV 98 observes one event in a $\pm 3\sigma$ region around the η mass, while a Monte Carlo calculation gives 10 ± 5 events. The limit here is the Poisson upper limit for one observed event and no background.

$\Gamma(2\pi^0\gamma)/\Gamma_{\text{total}}$ Γ_{27}/Γ

Forbidden by C invariance.

VALUE	CL%	DOCUMENT ID		TECN	CHG	COMMENT
< 5 $\times 10^{-4}$	90	NEFKENS	05	CRYB	0	p(720 MeV/c) $\pi^- \to n\eta$
• • • We do not use the following data for averages, fits, limits, etc. • • •						
<17 $\times 10^{-4}$	90	BLIK	07	GAM4		$\pi^- p \to \eta n$

$\Gamma(3\pi^0\gamma)/\Gamma_{\text{total}}$ Γ_{28}/Γ

Forbidden by C invariance.

VALUE	CL%	DOCUMENT ID		TECN	CHG	COMMENT
< 6 $\times 10^{-5}$	90	NEFKENS	05	CRYB	0	p(720 MeV/c) $\pi^- \to n\eta$
• • • We do not use the following data for averages, fits, limits, etc. • • •						
<24 $\times 10^{-5}$	90	BLIK	07	GAM4		$\pi^- p \to \eta n$

$\Gamma(3\gamma)/\Gamma_{\text{total}}$ Γ_{29}/Γ

Forbidden by C invariance.

VALUE	CL%	DOCUMENT ID		TECN	COMMENT
• • • We do not use the following data for averages, fits, limits, etc. • • •					
<16 $\times 10^{-5}$	90	BLIK	07	GAM4	$\pi^- p \to \eta n$
< 4 $\times 10^{-5}$	90	NEFKENS	05A	CRYB	p(720 MeV/c) $\pi^- \to n\eta$

$\Gamma(3\gamma)/\Gamma(2\gamma)$ Γ_{29}/Γ_2

VALUE	CL%	DOCUMENT ID		TECN	CHG
$<1.2\times10^{-3}$	95	ALDE	84	GAM2	0

$\Gamma(3\gamma)/\Gamma(3\pi^0)$ Γ_{29}/Γ_3

VALUE	CL%	DOCUMENT ID		TECN	COMMENT
$<4.9\times10^{-5}$	90	ALOISIO	04	KLOE	$\phi\to\eta\gamma$

$\Gamma(4\pi^0)/\Gamma_{total}$ Γ_{30}/Γ

Forbidden by P and CP invariance.

VALUE	CL%	DOCUMENT ID		TECN	COMMENT
$< 6.9\times10^{-7}$	90	PRAKHOV	00	CRYB	$\pi^- p\to n\eta$, 720 MeV/c
• • • We do not use the following data for averages, fits, limits, etc. • • •					
$<200\times10^{-7}$	90	BLIK	07	GAM4	$\pi^- p\to\eta n$

$\Gamma(\pi^0 e^+ e^-)/\Gamma_{total}$ Γ_{31}/Γ

C parity forbids this to occur as a single-photon process.

VALUE	CL%	DOCUMENT ID		TECN
• • • We do not use the following data for averages, fits, limits, etc. • • •				
$< 1.6\times10^{-4}$	90	MARTYNOV	76	HLBC
$< 8.4\times10^{-4}$	90	BAZIN	68	DBC
$<70\times10^{-4}$		RITTENBERG	65	HBC

$\Gamma(\pi^0 e^+ e^-)/\Gamma(\pi^+\pi^-\pi^0)$ Γ_{31}/Γ_9

C parity forbids this to occur as a single-photon process.

VALUE	CL%	EVTS	DOCUMENT ID		TECN
$< 1.9\times10^{-4}$	90		JANE	75	OSPK
• • • We do not use the following data for averages, fits, limits, etc. • • •					
$< 42\times10^{-4}$	90		BAGLIN	67	HLBC
$< 16\times10^{-4}$	90	0	BILLING	67	HLBC
$< 77\times10^{-4}$		0	FOSTER	65B	HBC
$<110\times10^{-4}$			PRICE	65	HBC

$\Gamma(\pi^0\mu^+\mu^-)/\Gamma_{total}$ Γ_{32}/Γ

C parity forbids this to occur as a single-photon process.

VALUE	CL%	DOCUMENT ID		TECN	COMMENT
$< 5\times10^{-6}$	90	DZHELYADIN	81	SPEC	$\pi^- p\to\eta n$
• • • We do not use the following data for averages, fits, limits, etc. • • •					
$<500\times10^{-6}$		WEHMANN	68	OSPK	

$[\Gamma(\mu^+ e^-)+\Gamma(\mu^- e^+)]/\Gamma_{total}$ Γ_{33}/Γ

Forbidden by lepton family number conservation.

VALUE	CL%	DOCUMENT ID		TECN	COMMENT
$<6\times10^{-6}$	90	WHITE	96	SPEC	$pd\to\eta\,^3$He

η C-NONCONSERVING DECAY PARAMETERS

$\pi^+\pi^-\pi^0$ LEFT-RIGHT ASYMMETRY PARAMETER

Measurements with an error $> 1.0\times10^{-2}$ have been omitted.

VALUE (units 10^{-2})	EVTS	DOCUMENT ID		TECN
$0.09^{+0.11}_{-0.12}$ OUR AVERAGE				
$+0.09\pm0.10^{+0.09}_{-0.14}$	1.34M	AMBROSINO	08D	KLOE
0.28 ± 0.26	165k	JANE	74	OSPK
-0.05 ± 0.22	220k	LAYTER	72	ASPK
• • • We do not use the following data for averages, fits, limits, etc. • • •				
1.5 ± 0.5	37k	[26] GORMLEY	68C	ASPK

[26] The GORMLEY 68C asymmetry is probably due to unmeasured ($\mathbf{E}\times\mathbf{B}$) spark chamber effects. New experiments with ($\mathbf{E}\times\mathbf{B}$) controls don't observe an asymmetry.

$\pi^+\pi^-\pi^0$ SEXTANT ASYMMETRY PARAMETER

Measurements with an error $> 2.0\times10^{-2}$ have been omitted.

VALUE (units 10^{-2})	EVTS	DOCUMENT ID		TECN
$0.12^{+0.10}_{-0.11}$ OUR AVERAGE				
$+0.08\pm0.10^{+0.08}_{-0.13}$	1.34M	AMBROSINO	08D	KLOE
0.20 ± 0.25	165k	JANE	74	OSPK
0.10 ± 0.22	220k	LAYTER	72	ASPK
0.5 ± 0.5	37k	GORMLEY	68C	WIRE

$\pi^+\pi^-\pi^0$ QUADRANT ASYMMETRY PARAMETER

VALUE (units 10^{-2})	EVTS	DOCUMENT ID		TECN
-0.09 ± 0.09 OUR AVERAGE				
$-0.05\pm0.10^{+0.03}_{-0.05}$	1.34M	AMBROSINO	08D	KLOE
-0.30 ± 0.25	165k	JANE	74	OSPK
-0.07 ± 0.22	220k	LAYTER	72	ASPK

$\pi^+\pi^-\gamma$ LEFT-RIGHT ASYMMETRY PARAMETER

Measurements with an error $> 2.0\times10^{-2}$ have been omitted.

VALUE (units 10^{-2})	EVTS	DOCUMENT ID		TECN
0.9 ± 0.4 OUR AVERAGE				
1.2 ± 0.6	35k	JANE	74B	OSPK
0.5 ± 0.6	36k	THALER	72	ASPK
1.22 ± 1.56	7257	GORMLEY	70	ASPK

$\pi^+\pi^-\gamma$ PARAMETER β (D-wave)

Sensitive to a D-wave contribution: $dN/d\cos\theta = \sin^2\theta\ (1+\beta\ \cos^2\theta)$.

VALUE	EVTS	DOCUMENT ID		TECN
-0.02 ± 0.07 OUR AVERAGE		Error includes scale factor of 1.3.		
0.11 ± 0.11	35k	JANE	74B	OSPK
-0.060 ± 0.065	7250	GORMLEY	70	WIRE
• • • We do not use the following data for averages, fits, limits, etc. • • •				
0.12 ± 0.06		[27] THALER	72	ASPK

[27] The authors don't believe this indicates D-wave because the dependence of β on the γ energy is inconsistent with the theoretical prediction. A $\cos^2\theta$ dependence can also come from P- and F-wave interference.

η CP-NONCONSERVING DECAY PARAMETER

$\pi^+\pi^- e^+ e^-$ DECAY-PLANE ASYMMETRY PARAMETER A_ϕ

In the η rest frame, the total momentum of the e^+e^- pair is equal and opposite to that of the $\pi^+\pi^-$ pair. Let $\hat{z}$ be the unit vector along the momentum of the e^+e^- pair; let $\hat{n}_{ee}$ and $\hat{n}_{\pi\pi}$ be the unit vectors normal to the e^+e^- and $\pi^+\pi^-$ planes; and let ϕ be the angle between the two normals. Then

$$\sin\phi\cos\phi = [(\hat{n}_{ee}\times\hat{n}_{\pi\pi})\cdot\hat{z}]\,(\hat{n}_{ee}\cdot\hat{n}_{\pi\pi})\ ,$$

and

$$A_\phi \equiv \frac{N_{\sin\phi\cos\phi>0} - N_{\sin\phi\cos\phi<0}}{N_{\sin\phi\cos\phi>0} + N_{\sin\phi\cos\phi<0}}\ .$$

VALUE (units 10^{-2})	EVTS	DOCUMENT ID		TECN	COMMENT
$-0.6\pm2.5\pm1.8$	1555 ± 52	AMBROSINO	09B	KLOE	$e^+e^-\to\phi\to\eta\gamma$

ENERGY DEPENDENCE OF $\eta\to3\pi$ DALITZ PLOTS

PARAMETERS FOR $\eta\to\pi^+\pi^-\pi^0$

See the "Note on η Decay Parameters" in our 1994 edition, Phys. Rev. **D50**, 1 August 1994, Part I, p. 1454. The following experiments fit to one or more of the coefficients a, b, c, d, or e for $|\text{matrix element}|^2 = 1 + ay + by^2 + cx + dx^2 + exy$.

VALUE	EVTS	DOCUMENT ID		TECN	COMMENT
• • • We do not use the following data for averages, fits, limits, etc. • • •					
	1.34M	AMBROSINO	08D	KLOE	
	3230	[28] ABELE	98D	CBAR	$\bar{p}p\to\pi^0\pi^0\eta$ at rest
	1077	[29] AMSLER	95	CBAR	$\bar{p}p\to\pi^+\pi^-\eta$ at rest
	81k	LAYTER	73	ASPK	
	220k	LAYTER	72	ASPK	
	1138	CARPENTER	70	HBC	
	349	DANBURG	70	DBC	
	7250	GORMLEY	70	WIRE	
	526	BAGLIN	69	HLBC	
	7170	CNOPS	68	OSPK	
	37k	GORMLEY	68C	WIRE	
	1300	CLPWY	66	HBC	
	705	LARRIBE	66	HBC	

[28] ABELE 98D obtains $a=-1.22\pm0.07$ and $b=0.22\pm0.11$ when c (our d) is fixed at 0.06.

[29] AMSLER 95 fits to $(1+ay+by^2)$ and obtains $a=-0.94\pm0.15$ and $b=0.11\pm0.27$.

α PARAMETER FOR $\eta\to3\pi^0$

See the "Note on η Decay Parameters" in our 1994 edition, Phys. Rev. **D50**, 1 August 1994, Part I, p. 1454. The value here is of α in $|\text{matrix element}|^2 = 1+2\alpha z$.

VALUE	EVTS	DOCUMENT ID		TECN	COMMENT
-0.0315 ± 0.0015 OUR AVERAGE					
$-0.0301\pm0.0035^{+0.0022}_{-0.0035}$	512k	AMBROSINO	10A	KLOE	$e^+e^-\to\phi\to\eta\gamma$
$-0.027\pm0.008\pm0.005$	120k	[30] ADOLPH	09	WASA	$pp\to pp\eta$
$-0.0322\pm0.0012\pm0.0022$	3M	[31] PRAKHOV	09	CRYB	$\gamma p\to p\eta$
$-0.032\pm0.002\pm0.002$	1.8M	[31] UNVERZAGT	09	CRYB	$\gamma p\to p\eta$
$-0.026\pm0.010\pm0.010$	75k	BASHKANOV	07	WASA	$pp\to pp\eta$
$-0.010\pm0.021\pm0.010$	12k	ACHASOV	01C	SND	$e^+e^-\to\phi\to\eta\gamma$
-0.031 ± 0.004	1M	TIPPENS	01	CRYB	$\pi^- p\to n\eta$, 720 MeV
$-0.052\pm0.017\pm0.010$	98k	ABELE	98C	CBAR	$\bar{p}p\to5\pi^0$
-0.022 ± 0.023	50k	ALDE	84	GAM2	
• • • We do not use the following data for averages, fits, limits, etc. • • •					
$-0.038\pm0.003^{+0.012}_{-0.008}$	1.34M	[32] AMBROSINO	08D	KLOE	
-0.32 ± 0.37	192	BAGLIN	70	HLBC	

[30] This ADOLPH 09 result is independent of the BASHKANOV 07 result.

[31] The PRAKHOV 09 and UNVERZAGT 09 results are independent.

[32] This AMBROSINO 08D value is an indirect result using $\eta\to\pi^+\pi^0\pi^-$ events and a rescattering matrix that mixes isospin decay amplitudes.

η REFERENCES

ABLIKIM	13	PR D87 012009	M. Ablikim *et al.*	(BES III Collab.)
ABLIKIM	13G	PR D87 032006	M. Ablikim *et al.*	(BES III Collab.)
BABUSCI	13	PL B718 910	D. Babusci *et al.*	(KLOE/KLOE-2 Collab.)
BABUSCI	13A	JHEP 1301 119	D. Babusci *et al.*	(KLOE-2 Collab.)
AGAKISHIEV	12A	EPJ A48 64	G. Agakishiev *et al.*	(HADES Collab.)
GOSLAWSKI	12	PR D85 112011	P. Goslawski *et al.*	(COSY-ANKE Collab.)
ABLIKIM	11G	PR D84 032006	M. Ablikim *et al.*	(BES III Collab.)
AMBROSINO	11B	PL B702 324	F. Ambrosino *et al.*	(KLOE Collab.)
BERGHAUSER	11	PL B701 562	H. Berghauser *et al.*	(GIES, UCLA, GUTE)
AMBROSINO	10A	PL B694 16	F. Ambrosino *et al.*	(KLOE Collab.)
ADOLPH	09	PL B677 24	C. Adolph *et al.*	(WASA at COSY Collab.)

AMBROSINO 09B PL B675 283 F. Ambrosino *et al.* (KLOE Collab.)
PRAKHOV 09 PR C79 035204 S. Prakhov *et al.* (MAMI-C Crystal Ball Collab.)
UNVERZAGT 09 EPJ A39 169 M. Unverzagt *et al.* (MAMI-B Crystal Ball Collab.)
AMBROSINO 08D JHEP 0805 006 F. Ambrosino *et al.* (DAPHNE KLOE Collab.)
BERLOWSKI 08 PR D77 032004 M. Berlowski *et al.* (CELSIUS/WASA Collab.)
PRAKHOV 08 PR C78 015206 S. Prakhov *et al.* (BNL Crystal Ball Collab.)
RODRIGUES 08 PRL 101 012301 T.E. Rodrigues *et al.* (USP, FESP, UNESP+)
AMBROSINO 07B JHEP 0712 073 F. Ambrosino *et al.* (KLOE Collab.)
BARGHOLTZ 07 PL B644 299 Chr. Bargholtz *et al.* (CELSIUS/WASA Collab.)
BASHKANOV 07 PR C76 048201 M. Bashkanov *et al.* (CELSIUS/WASA Collab.)
BLIK 07 PAN 70 693 A.M. Blik *et al.* (GAMS Collab.)
Translated from YAF 70 724.
LOPEZ 07 PRL 99 122001 A. Lopez *et al.* (CLEO Collab.)
MILLER 07 PRL 99 122002 D.H. Miller *et al.* (CLEO Collab.)
ABLIKIM 06E PR D73 052008 M. Ablikim *et al.* (BES Collab.)
ABLIKIM 06Q PRL 97 202002 M. Ablikim *et al.* (BES Collab.)
ACHASOV 06A PR D74 014016 M.N. Achasov *et al.* (SND Collab.)
ABDEL-BARY 05 PL B619 281 M. Abdel-Bary *et al.* (GEM Collab.)
AKHMETSHIN 05 PL B605 26 R.R. Akhmetshin *et al.* (Novosibirsk CMD-2 Collab.)
AMBROSINO 05A PL B606 276 F. Ambrosino *et al.* (KLOE Collab.)
NEFKENS 05 PRL 94 041601 B.M.K. Nefkens *et al.* (BNL Crystal Ball Collab.)
NEFKENS 05A PR C72 035212 B.M.K. Nefkens *et al.* (BNL Crystal Ball Collab.)
PRAKHOV 05 PR C72 025201 S. Prakhov *et al.* (BNL Crystal Ball Collab.)
ALOISIO 04 PL B591 49 A. Aloisio *et al.* (KLOE Collab.)
KNECHT 04 PL B589 14 N. Knecht *et al.*
LAI 02 PL B533 196 A. Lai *et al.* (CERN NA48 Collab.)
NEFKENS 02 PS T99 114 B.M.K. Nefkens, J.W. Price (UCLA)
ACHASOV 01B PL B504 275 M.N. Achasov *et al.* (Novosibirsk SND Collab.)
ACHASOV 01C JETPL 73 451 M.N. Achasov *et al.* (Novosibirsk SND Collab.)
Translated from ZETFP 73 511.
ACHASOV 01D NP B600 3 M.N. Achasov *et al.* (Novosibirsk SND Collab.)
AKHMETSHIN 01 PL B501 191 R.R. Akhmetshin *et al.* (Novosibirsk CMD-2 Collab.)
AKHMETSHIN 01B PL B509 217 R.R. Akhmetshin *et al.* (Novosibirsk CMD-2 Collab.)
TIPPENS 01 PRL 87 192001 W.B. Tippens *et al.* (BNL Crystal Ball Collab.)
ACHASOV 00 EPJ C12 25 M.N. Achasov *et al.* (Novosibirsk SND Collab.)
ACHASOV 00B JETP 90 17 M.N. Achasov *et al.* (Novosibirsk SND Collab.)
Translated from ZETF 117 22.
ACHASOV 00D JETPL 72 282 M.N. Achasov *et al.* (Novosibirsk SND Collab.)
Translated from ZETFP 72 411.
PRAKHOV 00 PRL 84 4802 S. Prakhov *et al.* (BNL Crystal Ball Collab.)
AKHMETSHIN 99B PL B462 371 R.R. Akhmetshin *et al.* (Novosibirsk CMD-2 Collab.)
AKHMETSHIN 99C PL B462 380 R.R. Akhmetshin *et al.* (Novosibirsk CMD-2 Collab.)
AKHMETSHIN 99F PL B460 242 R.R. Akhmetshin *et al.* (Novosibirsk CMD-2 Collab.)
ABELE 98C PL B417 193 A. Abele *et al.* (Crystal Barrel Collab.)
ABELE 98D PL B417 197 A. Abele *et al.* (Crystal Barrel Collab.)
ACHASOV 98 PL B425 388 M.N. Achasov *et al.* (Novosibirsk SND Collab.)
AKHMETSHIN 97C PL B415 452 R.R. Akhmetshin *et al.* (Novosibirsk CMD-2 Collab.)
BROWDER 97B PR D56 5359 T.E. Browder *et al.* (CLEO Collab.)
ABEGG 96 PR D53 11 R. Abegg *et al.* (Saturne SPES2 Collab.)
WHITE 96 PR D53 6658 D.B. White *et al.* (Saturne SPES2 Collab.)
AMSLER 95 PL B346 203 C. Amsler *et al.* (Crystal Barrel Collab.)
KRUSCHE 95D ZPHY A351 237 B. Krusche *et al.* (TAPS + A2 Collab.)
ABEGG 94 PR D50 92 R. Abegg *et al.* (Saturne SPES2 Collab.)
AMSLER 93 ZPHY C58 175 C. Amsler *et al.* (Crystal Barrel Collab.)
KESSLER 93 PRL 70 892 R.S. Kessler *et al.* (Saturne SPES2 Collab.)
PLOUIN 92 PL B276 526 F. Plouin *et al.* (Saturne SPES4 Collab.)
BARU 90 ZPHY C48 581 S.E. Baru *et al.* (MD-1 Collab.)
ROE 90 PR D41 17 N.A. Roe *et al.* (ASP Collab.)
WILLIAMS 88 PR D38 1365 D.A. Williams *et al.* (Crystal Ball Collab.)
AIHARA 86 PR D33 844 H. Aihara *et al.* (TPC-2γ Collab.)
BARTEL 85E PL 160B 421 W. Bartel *et al.* (JADE Collab.)
LANDSBERG 85 PRPL 128 301 L.G. Landsberg (SERP)
ALDE 84 ZPHY C25 225 D.M. Alde *et al.* (SERP, BELG, LAPP)
Also SJNP 40 918 D.M. Alde *et al.* (SERP, BELG, LAPP)
Translated from YAF 40 1447.
WEINSTEIN 83 PR D28 2896 A.J. Weinstein *et al.* (Crystal Ball Collab.)
BINON 82 SJNP 36 391 F.G. Binon *et al.* (SERP, BELG, LAPP+)
Translated from YAF 36 670.
Also NC 71A 497 F.G. Binon *et al.* (SERP, BELG, LAPP+)
DAVYDOV 81 LNC 32 45 V.A. Davydov *et al.* (SERP, BELG, LAPP+)
Also SJNP 33 825 V.A. Davydov *et al.* (SERP, BELG, LAPP+)
Translated from YAF 33 1534.
DZHELYADIN 81 PL 105B 239 R.I. Dzhelyadin *et al.* (SERP)
Also SJNP 33 822 R.I. Dzhelyadin *et al.* (SERP)
Translated from YAF 33 1529.
ABROSIMOV 80 SJNP 31 195 A.T. Abrosimov *et al.* (JINR)
Translated from YAF 31 371.
DZHELYADIN 80 PL 94B 548 R.I. Dzhelyadin *et al.* (SERP)
Also SJNP 32 516 R.I. Dzhelyadin *et al.* (SERP)
Translated from YAF 32 998.
DZHELYADIN 80B PL 97B 471 R.I. Dzhelyadin *et al.* (SERP)
Also SJNP 32 518 R.I. Dzhelyadin *et al.* (SERP)
Translated from YAF 32 1002.
BUSHNIN 78 PL 79B 147 Y.B. Bushnin *et al.* (SERP)
Also SJNP 28 775 Y.B. Bushnin *et al.* (SERP)
Translated from YAF 28 1507.
MARTYNOV 76 SJNP 23 48 A.S. Martynov *et al.* (JINR)
Translated from YAF 23 93.
JANE 75 PL 59B 99 M.R. Jane *et al.* (RHEL, LOWC)
JANE 75B PL 59B 103 M.R. Jane *et al.* (RHEL, LOWC)
Also PL 73B 503 M.R. Jane
Erratum in private communication.
BROWMAN 74B PRL 32 1067 A. Browman *et al.* (CORN, BING)
DAVIES 74 NC 24A 324 J.D. Davies, J.G. Guy, R.K.P. Zia (BIRM, RHEL+)
DUANE 74 PRL 32 425 A. Duane *et al.* (LOIC, SHMP)
JANE 74 PL 48B 260 M.R. Jane *et al.* (RHEL, LOWC, SUSS)
JANE 74B PL 48B 265 M.R. Jane *et al.* (RHEL, LOWC, SUSS)
KENDALL 74 NC 21A 387 B.N. Kendall *et al.* (BROW, BARI, MIT)
LAYTER 73 PR D7 2565 J.G. Layter *et al.* (COLU)
THALER 73 PR D7 2569 J.J. Thaler *et al.* (COLU)
AGUILAR-... 72B PR D6 29 M. Aguilar-Benitez *et al.* (BNL)
BLOODWO... 72B NP B39 525 I.J. Bloodworth *et al.* (TNTO)
LAYTER 72 PRL 29 316 J.G. Layter *et al.* (COLU)
THALER 72 PRL 29 313 J.J. Thaler *et al.* (COLU)
BASILE 71D NC 3A 796 M. Basile *et al.* (CERN, BGNA, STRB)
STRUGALSKI 71 NP B27 429 Z.S. Strugalski *et al.* (JINR)
BAGLIN 70 NP B22 66 C. Baglin *et al.* (EPOL, MADR, STRB)
BUTTRAM 70 PRL 25 1358 M.T. Buttram, M.N. Kreisler, R.E. Mischke (PRIN)
CARPENTER 70 PR D1 1303 D.W. Carpenter *et al.* (DUKE)
COX 70B PRL 24 534 B. Cox, L. Fortney, J.P. Golson (DUKE)
DANBURG 70 PR D2 2564 J.S. Danburg *et al.* (LRL)
DEVONS 70 PR D1 1936 S. Devons *et al.* (COLU, SYRA)
GORMLEY 70 PR D2 501 M. Gormley *et al.* (COLU, BNL)
Also Thesis Nevis 181 M. Gormley (COLU)
BAGLIN 69 PL 29B 445 C. Baglin *et al.* (EPOL, UCB, MADR, STRB)
Also NP B22 66 C. Baglin *et al.* (EPOL, MADR, STRB)
HYAMS 69 PL 29B 128 B.D. Hyams *et al.* (CERN, MPIM)
ARNOLD 68 PL 27B 466 R.G. Arnold *et al.* (STRB, MADR, EPOL+)
BAZIN 68 PRL 20 895 M.J. Bazin *et al.* (PRIN, QUKI)
BULLOCK 68 PL 27B 402 F.W. Bullock *et al.* (LOUC)
CNOPS 68 PRL 21 1609 A.M. Cnops *et al.* (BNL, ORNL, UCND+)
GORMLEY 68C PRL 21 402 M. Gormley *et al.* (COLU, BNL)
WEHMANN 68 PRL 20 748 A.W. Wehmann *et al.* (HARV, CASE, SLAC+)
BAGLIN 67 PL 24B 637 C. Baglin *et al.* (EPOL, UCB)
BAGLIN 67B BAPS 12 567 C. Baglin *et al.* (EPOL, UCB)
BALTAY 67B PRL 19 1498 C. Baltay *et al.* (COLU, STON)
BALTAY 67D PRL 19 1495 C. Baltay *et al.* (COLU, BRAN)
BEMPORAD 67 PL 25B 380 C. Bemporad *et al.* (PISA, BONN)
Also Private Comm. I. Ion
BILLING 67 PL 25B 435 K.D. Billing *et al.* (LOUC, OXF)
BUNIATOV 67 PL 25B 560 S.A. Bunyatov *et al.* (CERN, KARL)
CENCE 67 PRL 19 1393 R.J. Cence *et al.* (HAWA, LRL)
ESTEN 67 PL 24B 115 M.J. Esten *et al.* (LOUC, OXF)
FELDMAN 67 PRL 18 868 M. Feldman *et al.* (PENN)
FLATTE 67 PRL 18 976 S.M. Flatte (LRL)
FLATTE 67B PR 163 1441 S.M. Flatte, C.G. Wohl (LRL)
LITCHFIELD 67 PL 24B 486 P.J. Litchfield *et al.* (RHEL, SACL)
PRICE 67 PRL 18 1207 L.R. Price, F.S. Crawford (LRL)
ALFF-... 66 PR 145 1072 C. Alff-Steinberger *et al.* (COLU, RUTG)
CLPWY 66 PR 149 1044 C. Baltay (SCUC, LRL, PURD, WISC, YALE)
CRAWFORD 66 PRL 16 333 F.S. Crawford, L.R. Price (LRL)
DIGIUGNO 66 PRL 16 767 G. di Giugno *et al.* (NAPL, TRST, FRAS)
GRUNHAUS 66 Thesis J. Grunhaus (COLU)
JAMES 66 PR 142 896 F.E. James, H.L. Kraybill (YALE, BNL)
JONES 66 PL 23 597 W.G. Jones *et al.* (LOIC, RHEL)
LARRIBE 66 PL 23 600 A. Larribe *et al.* (SACL, RHEL)
FOSTER 65 PR 138 B652 M. Foster *et al.* (WISC, PURD)
FOSTER 65B Athens Conf. M. Foster, M. Good, M. Meer (WISC)
FOSTER 65C Thesis M. Foster (WISC)
PRICE 65 PRL 15 123 L.R. Price, F.S. Crawford (LRL)
RITTENBERG 65 PRL 15 556 A. Rittenberg, G.R. Kalbfleisch (LRL, BNL)
FOELSCHE 64 PR 134 B1138 H.W.J. Foelsche, H.L. Kraybill (YALE)
KRAEMER 64 PR 136 B496 R.W. Kraemer *et al.* (JHU, NWES, WOOD)
PAULI 64 PL 13 351 E. Pauli, A. Muller (SACL)
BACCI 63 PRL 11 37 C. Bacci *et al.* (ROMA, FRAS)
CRAWFORD 63 PRL 10 546 F.S.Jr. Crawford, L.J. Lloyd, E.C. Fowler (LRL+)
Also PRL 16 907 F.S. Crawford, L.J. Lloyd, E.C. Fowler (LRL+)
ALFF-... 62 PRL 9 322 C. Alff-Steinberger *et al.* (COLU, RUTG)
BASTIEN 62 PRL 8 114 P.L. Bastien *et al.* (LRL)
PICKUP 62 PRL 8 329 E. Pickup, D.K. Robinson, E.O. Salant (CNRC+)

$f_0(500)$ or σ was $f_0(600)$

$I^G(J^{PC}) = 0^+(0^{++})$

NOTE ON SCALAR MESONS BELOW 2 GEV

Revised September 2013 by C. Amsler (Univ of Bern), S. Eidelman (Budker Institute of Nuclear Physics, Novosibirsk), T. Gutsche (University of Tübingen), C. Hanhart (Forschungszentrum Jülich), S. Spanier (University of Tennessee), and N.A. Törnqvist (University of Helsinki).

I. Introduction: In contrast to the vector and tensor mesons, the identification of the scalar mesons is a long-standing puzzle. Scalar resonances are difficult to resolve because some of them have large decay widths which cause a strong overlap between resonances and background. In addition, several decay channels sometimes open up within a short mass interval (e.g. at the $K\bar{K}$ and $\eta\eta$ thresholds), producing cusps in the line shapes of the near-by resonances. Furthermore, one expects non-$q\bar{q}$ scalar objects, such as glueballs and multiquark states in the mass range below 2 GeV (for reviews see, *e.g.*, Refs. [1–4]) .

Scalars are produced, for example, in πN scattering on polarized/unpolarized targets, $p\bar{p}$ annihilation, central hadronic production, J/Ψ, B-, D- and K-meson decays, $\gamma\gamma$ formation, and ϕ radiative decays. Especially for the lightest scalar mesons simple parameterizations fail and more advanced theory tools are necessary to extract the resonance parameters from data. In the analyses available in the literature fundamental properties of the amplitudes such as unitarity, analyticity, Lorentz invariance, chiral and flavor symmetry are implemented at different levels of rigor. Especially, chiral symmetry implies the appearance of zeros close to the threshold in elastic S-wave scattering amplitudes involving soft pions [5,6], which may be shifted or removed in associated production processes [7]. The methods employed are the K-matrix formalism, the N/D-method, the Dalitz Tuan ansatz, unitarized quark models with coupled channels, effective chiral field theories and the linear sigma model, *etc.* Dynamics near the lowest two-body thresholds in

some analyses are described by crossed channel (t, u) meson exchange or with an effective range parameterization instead of, or in addition to, resonant features in the s-channel. Dispersion theoretical approaches are applied to pin down the location of resonance poles for the low lying states [8–11].

The mass and width of a resonance are found from the position of the nearest pole in the process amplitude (T-matrix or S-matrix) at an unphysical sheet of the complex energy plane, traditionally labeled as

$$\sqrt{s_{\rm Pole}} = M - i\,\Gamma/2\ .$$

It is important to note that the Breit-Wigner parameterization agrees with this pole position only for narrow and well–separated resonances, far away from the opening of decay channels.

In this note, we discuss the light scalars below 2 GeV organized in the listings under the entries ($I = 1/2$) $K_0^*(800)$ (or κ, currently omitted from the summary table), $K_0^*(1430)$, ($I = 1$) $a_0(980)$, $a_0(1450)$, and ($I = 0$) $f_0(500)$ (or σ), $f_0(980)$, $f_0(1370)$, $f_0(1500)$, and $f_0(1710)$. This list is minimal and does not necessarily exhaust the list of actual resonances. The ($I = 2$) $\pi\pi$ and ($I = 3/2$) $K\pi$ phase shifts do not exhibit any resonant behavior. See also our notes in previous issues for further comments on, *e.g.*, scattering lengths and older papers.

II. The I = 1/2 States: The $\boldsymbol{K_0^*(1430)}$ [12] is perhaps the least controversial of the light scalar mesons. The $K\pi$ S-wave scattering has two possible isospin channels, $I = 1/2$ and $I = 3/2$. The $I = 3/2$ wave is elastic and repulsive up to 1.7 GeV [13] and contains no known resonances. The $I = 1/2$ $K\pi$ phase shift, measured from about 100 MeV above threshold in Kp production, rises smoothly, passes 90° at 1350 MeV, and continues to rise to about 170° at 1600 MeV. The first important inelastic threshold is $K\eta'(958)$. In the inelastic region the continuation of the amplitude is uncertain since the partial-wave decomposition has several solutions. The data are extrapolated towards the $K\pi$ threshold using effective range type formulas [12,14] or chiral perturbation predictions [15,16]. From analyses using unitarized amplitudes there is agreement on the presence of a resonance pole around 1410 MeV having a width of about 300 MeV. With reduced model dependence, Ref. 17 finds a larger width of 500 MeV.

Similar to the situation for the $f_0(500)$, discussed in the next section, the presence and properties of the light $\boldsymbol{K_0^*(800)}$ **(or $\boldsymbol{\kappa}$)** meson in the 700-900 MeV region are difficult to establish since it appears to have a very large width ($\Gamma \approx 500$ MeV) and resides close to the $K\pi$ threshold. Hadronic D-meson decays provide additional data points in the vicinity of the $K\pi$ threshold - experimental results from E791, *e.g.*, Ref. [18,19], FOCUS [17,20], CLEO [21], and BaBar [22] are discussed in the *Review of Charm Dalitz Plot Analyses*. Precision information from semileptonic D decays avoiding theoretically ambiguous three-body final state interactions is not available. BES II [23] (re-analyzed in [24]) finds a $K_0^*(800)$–like structure in J/ψ decays to $\bar{K}^{*0}(892)K^+\pi^-$ where $K_0^*(800)$ recoils against the $K^*(892)$. Also clean with respect to final state interaction is the decay $\tau^- \to K_S^0\pi^-\nu_\tau$ studied by Belle [25], with $K_0^*(800)$ parameters fixed to Ref. 23.

Some authors find a $K_0^*(800)$ pole in their phenomenological analysis (see, *e.g.*, [21,26–36]), while others do not need to include it in their fits (see, *e.g.*, [16,22,37–39]). Similarly to the case of the $f_0(500)$ discussed below, all works including constraints from chiral symmetry at low energies naturally seem to find a light $K_0^*(800)$ below 800 MeV, see, *e.g.*, [40–44]. In these works the $K_0^*(800)$, $f_0(500)$, $f_0(980)$ and $a_0(980)$ appear to form a nonet [41,42]. Additional evidence for this assignment is presented in Ref. 11, where the couplings of the nine states to $\bar{q}q$ sources were compared. The same low lying scalar nonet was also found earlier in the unitarized quark model of Ref. 43. The analysis of Ref. 45 is based on the Roy-Steiner equations, which include analyticity and crossing symmetry. It establishes the existence of a light $K_0^*(800)$ pole in the $K\pi \to K\pi$ amplitude on the second sheet.

III. The I = 1 States: Two isovector states are known, the established $\boldsymbol{a_0(980)}$ and the $\boldsymbol{a_0(1450)}$. Independent of any model, the $K\bar{K}$ component in the $a_0(980)$ wave function must be large: it lies just below the opening of the $K\bar{K}$ channel to which it strongly couples [14,46]. This generates an important cusp-like behavior in the resonant amplitude. Hence, its mass and width parameters are strongly distorted. To reveal its true coupling constants, a coupled channel model with energy-dependent widths and mass shift contributions is necessary. All listed $a_0(980)$ measurements agree on a mass position value near 980 MeV, but the width takes values between 50 and 100 MeV, mostly due to the different models. For example, the analysis of the $p\bar{p}$-annihilation data [14] using a unitary K-matrix description finds a width as determined from the T-matrix pole of 92 ± 8 MeV, while the observed width of the peak in the $\pi\eta$ mass spectrum is about 45 MeV.

The relative coupling $K\bar{K}/\pi\eta$ is determined indirectly from $f_1(1285)$ [47–49] or $\eta(1410)$ decays [50–52], from the line shape observed in the $\pi\eta$ decay mode [54–57], or from the coupled-channel analysis of the $\pi\pi\eta$ and $K\bar{K}\pi$ final states of $p\bar{p}$ annihilation at rest [14].

The $a_0(1450)$ is seen in $p\bar{p}$ annihilation experiments with stopped and higher momenta antiprotons, with a mass of about 1450 MeV or close to the $a_2(1320)$ meson which is typically a dominant feature. A contribution from $a_0(1450)$ is also found in the analysis of the $D^\pm \to K^+K^-\pi^\pm$ decay [58]. The broad structure at about 1300 MeV observed in $\pi N \to K\bar{K}N$ reactions [59] needs still further confirmation in its existence and isospin assignment.

IV. The I = 0 States: The $I = 0$, $J^{PC} = 0^{++}$ sector is the most complex one, both experimentally and theoretically. The data have been obtained from $\pi\pi$, $K\bar{K}$, $\eta\eta$, 4π, and $\eta\eta'(958)$ systems produced in S-wave. Analyses based on several different production processes conclude that probably four poles are needed in the mass range from $\pi\pi$ threshold to about

1600 MeV. The claimed isoscalar resonances are found under separate entries $f_0(500)$ (or σ), $f_0(980)$, $f_0(1370)$, and $f_0(1500)$.

For discussions of the $\pi\pi$ S wave below the $K\bar{K}$ threshold and on the long history of the $f_0(500)$, which was suggested in linear sigma models more than 50 years ago, see our reviews in previous editions and the conference proceedings [60].

Information on the $\pi\pi$ S-wave phase shift $\delta^I_J = \delta^0_0$ was already extracted many years ago from πN scattering [61–63], and near threshold from the K_{e4}-decay [64]. The kaon decays were later revisited leading to consistent data, however, with very much improved statistics [65,66]. The reported $\pi\pi \to K\bar{K}$ cross sections [67–70] have large uncertainties. The πN data have been analyzed in combination with high-statistics data (see entries labeled as RVUE for re-analyses of the data). The $2\pi^0$ invariant mass spectra of the $p\bar{p}$ annihilation at rest [71–73] and the central collision [74] do not show a distinct resonance structure below 900 MeV, but these data are consistently described with the standard solution for πN data [62,75], which allows for the existence of the broad $f_0(500)$. An enhancement is observed in the $\pi^+\pi^-$ invariant mass near threshold in the decays $D^+ \to \pi^+\pi^-\pi^+$ [76–103] and $J/\psi \to \omega\pi^+\pi^-$ [79,100], and in $\psi(2S) \to J/\psi\pi^+\pi^-$ with very limited phase space [81,82].

The precise **$f_0(500)$ (or σ)** pole is difficult to establish because of its large width, and because it can certainly not be modeled by a naive Breit-Wigner resonance. For the same reason a splitting in background and resonance contributions is not possible in a model-independent way. The $\pi\pi$ scattering amplitude shows an unusual energy dependence due to the presence of a zero in the unphysical regime close to the threshold [5–6], required by chiral symmetry, and possibly due to crossed channel exchanges, the $f_0(1370)$, and other dynamical features. However, most of the analyses listed under $f_0(500)$ agree on a pole position near $(500 - i\,250$ MeV). In particular, analyses of $\pi\pi$ data that include unitarity, $\pi\pi$ threshold behavior, strongly constrained by the K_{e4} data, and the chiral symmetry constraints from Adler zeroes and/or scattering lengths find a light $f_0(500)$, see, *e.g.*, [83,84].

Precise pole positions with an uncertainty of less than 20 MeV (see our table for T-matrix pole) were extracted by use of Roy equations, which are twice subtracted dispersion relations derived from crossing symmetry and analyticity. In Ref. [9] the subtraction constants were fixed to the S-wave scattering lengths a^0_0 and a^2_0 derived from matching Roy equations and two-loop chiral perturbation theory [8]. The only additional relevant input to fix the $f_0(500)$ pole turned out to be the $\pi\pi$-wave phase shifts at 800 MeV. The analysis was improved further in Ref. 11. Alternatively, in Ref. 10 only data was used as input inside Roy equations. In that reference also once-subtracted Roy–like equations, called GKPY equations, were used, since the extrapolation into the complex plane based on the twice subtracted equations leads to larger uncertainties mainly due to the limited experimental information on the

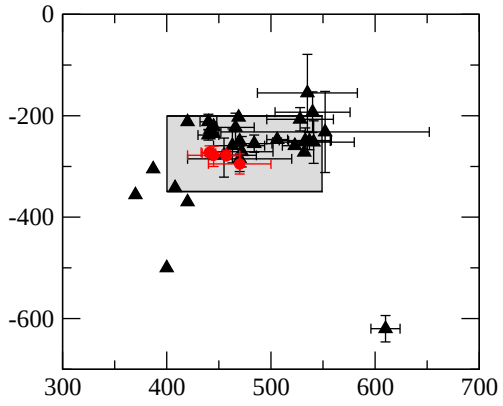

Figure 1: Location of the $f_0(500)$ (or σ) poles in the complex energy plane. Circles denote the recent analyses based on Roy(-like) dispersion relations [8–11], while all other analyses are denoted by triangles. The corresponding references are given in the listing.

isospin 2 $\pi\pi$ scattering length. All these extractions find consistent results. Using analyticity and unitarity only to describe data from $K_{2\pi}$ and K_{e4} decays, Ref. 85 finds consistent values for pole position and scattering length a^0_0. The importance of the $\pi\pi$ scattering data for fixing the $f_0(500)$ pole is nicely illustrated by comparing analyses of $\bar{p}p \to 3\pi^0$ omitting [71,86] or including [72,87] information on $\pi\pi$ scattering: while the former analyses find an extremely broad structure above 1 GeV, the latter find $f_0(500)$ masses of the order of 400 MeV.

As a result of the sensitivity of the extracted $f_0(500)$ pole position on the high accuracy low energy $\pi\pi$ scattering data [65,66], the currently quoted range of pole positions for the $f_0(500)$, namely

$$\sqrt{s^\sigma_{\rm Pole}} = (400 - 550) - i(200 - 350)\ \text{MeV}\ ,$$

in the listing was fixed including only those analyses consistent with these data, Refs. [29,32,41,43,44,53,56,72], [81–85] and [88–103] as well as the advanced dispersion analyses [8–11]. The pole positions from those references are compared to the range of poles positions quoted above in Fig. 1. Note that this range is labeled as 'our estimate' — it is not an average over the quoted analyses but is chosen to include the bulk of the analyses consistent with the mentioned criteria. An averaging procedure is not justified, since the analyses use overlapping or identical data sets.

One might also take the more radical point of view and just average the most advanced dispersive analyses, Refs. [8–11], shown as solid dots in Fig. 1, for they provide a determination of the pole positions with minimal bias. This procedure leads to the much more restricted range of $f_0(500)$ parameters

$$\sqrt{s^\sigma_{\rm Pole}} = (446 \pm 6) - i(276 \pm 5)\ \text{MeV}\ .$$

Due to the large strong width of the $f_0(500)$ an extraction of its two–photon width directly from data is not possible.

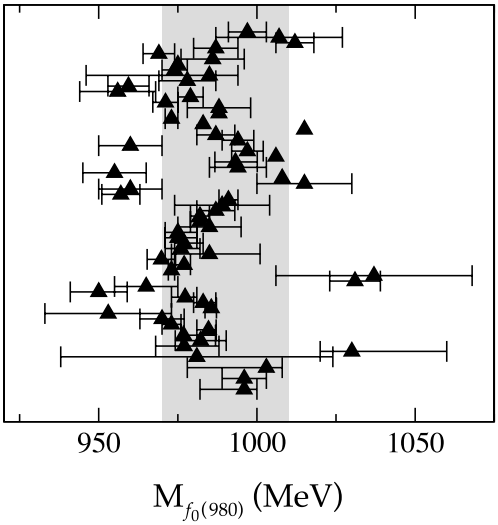

Figure 2: Values of the $f_0(980)$ masses as they appear in the listing compared to the currently quoted mass estimate. The newest references appear at the bottom, the oldest on the top. The corresponding references are given in the listing.

Thus, the values for $\Gamma(\gamma\gamma)$ quoted in the literature as well as the listing are based on the expression in the narrow width approximation [104] $\Gamma(\gamma\gamma) \simeq \alpha^2|g_\gamma|^2/(4\mathrm{Re}(\sqrt{s^\sigma_{\mathrm{Pole}}}))$ where g_γ is derived from the residue at the $f_0(500)$ pole to two photons and α denotes the electromagnetic fine structure constant. The explicit form of the expression may vary between different authors due to different definitions of the coupling constant, however, the expression given for $\Gamma(\gamma\gamma)$ is free of ambiguities. According to Refs. [105,106], the data for $f_0(500) \to \gamma\gamma$ are consistent with what is expected for a two–step process of $\gamma\gamma \to \pi^+\pi^-$ via pion exchange in the t- and u-channel, followed by a final state interaction $\pi^+\pi^- \to \pi^0\pi^0$. The same conclusion is drawn in Ref. 107 where the bulk part of the $f_0(500) \to \gamma\gamma$ decay width is dominated by re–scattering. Therefore, it might be difficult to learn anything new about the nature of the $f_0(500)$ from its $\gamma\gamma$ coupling. For the most recent work on $\gamma\gamma \to \pi\pi$, see Refs. [108,109]. There are theoretical indications (*e.g.*, [110–113]) that the $f_0(500)$ pole behaves differently from a $q\bar{q}$-state – see next section for details.

The $\boldsymbol{f_0(980)}$ overlaps strongly with the background represented mainly by the $f_0(500)$ and the $f_0(1370)$. This can lead to a dip in the $\pi\pi$ spectrum at the $K\bar{K}$ threshold. It changes from a dip into a peak structure in the $\pi^0\pi^0$ invariant mass spectrum of the reaction $\pi^- p \to \pi^0\pi^0 n$ [114], with increasing four-momentum transfer to the $\pi^0\pi^0$ system, which means increasing the a_1-exchange contribution in the amplitude, while the π-exchange decreases. The $f_0(500)$ and the $f_0(980)$ are also observed in data for radiative decays ($\phi \to f_0\gamma$) from SND [115,116], CMD2 [117], and KLOE [118,119]. A dispersive analysis was used to simultaneously pin down the pole parameters of both the $f_0(500)$ and the $f_0(980)$ [10]; the uncertainty in the pole position quoted for the latter state is of the order of 10 MeV, only (see lowest point in Fig. 2). Compared to the 2010 issue of the *Review of Particle Physics*, in this issue we extended the allowed range of $f_0(980)$ masses to include the mass value derived in Ref. 10. We now quote for the mass

$$M_{f_0(980)} = 990 \pm 20 \text{ MeV} .$$

As in case of the $f_0(500)$ (or σ), this range is not an average, but is labeled as 'our estimate'. A comparison of the mass values in the listing and the allocated range is shown in Fig. 2.

Analyses of $\gamma\gamma \to \pi\pi$ data [120–122] underline the importance of the $K\bar{K}$ coupling of $f_0(980)$, while the resulting two-photon width of the $f_0(980)$ cannot be determined precisely [123]. The prominent appearance of the $f_0(980)$ in the semi-leptonic D_S decays and decays of B and B_S-mesons implies a dominant ($\bar{s}s$) component: those decays occur via weak transitions that alternatively result in $\phi(1020)$ production. Ratios of decay rates of B and B_S mesons into J/ψ plus $f_0(980)$ or $f_0(500)$ may be used as input to extract the flavor mixing angle and to probe the tetra-quark nature of those mesons as proposed by Refs. [220,221]. The LHCb experiment finds an upper limit for the mixing angle of 31^o at 90% C.L. between $f_0(980)$ and $f_0(500)$ that corresponds to a substantial ($\bar{s}s$) content in $f_0(980)$ [222].

The $\boldsymbol{f_0}$'s above 1 GeV. A meson resonance that is very well studied experimentally, is the $\boldsymbol{f_0(1500)}$ seen by the Crystal Barrel experiment in five decay modes: $\pi\pi$, $K\bar{K}$, $\eta\eta$, $\eta\eta'(958)$, and 4π [14,72,73]. Due to its interference with the $f_0(1370)$ (and $\boldsymbol{f_0(1710)}$), the peak attributed to $f_0(1500)$ can appear shifted in invariant mass spectra. Therefore, the application of simple Breit-Wigner forms arrive at slightly different resonance masses for $f_0(1500)$. Analyses of central-production data of the likewise five decay modes Refs. [124,125] agree on the description of the S-wave with the one above. The $p\bar{p}$, $p\bar{n}/n\bar{p}$ measurements [126–128,73] show a single enhancement at 1400 MeV in the invariant 4π mass spectra, which is resolved into $f_0(1370)$ and $f_0(1500)$ [129,130]. The data on 4π from central production [131] require both resonances, too, but disagree on the relative content of $\rho\rho$ and $f_0(500)f_0(500)$ in 4π. All investigations agree that the 4π decay mode represents about half of the $f_0(1500)$ decay width and is dominant for $f_0(1370)$.

The determination of the $\pi\pi$ coupling of $\boldsymbol{f_0(1370)}$ is aggravated by the strong overlap with the broad $f_0(500)$ and $f_0(1500)$. Since it does not show up prominently in the 2π spectra, its mass and width are difficult to determine. Multichannel analyses of hadronically produced two- and three-body final states agree on a mass between 1300 MeV and 1400 MeV and a narrow $f_0(1500)$, but arrive at a somewhat smaller width for $f_0(1370)$.

V. Interpretation of the scalars below 1 GeV: In the literature, many suggestions are discussed, such as conventional

$q\bar{q}$ mesons, $q\bar{q}q\bar{q}$ or meson-meson bound states. In addition one expects a scalar glueball in this mass range. In reality, there can be superpositions of these components, and one often depends on models to determine the dominant one. Although we have seen progress in recent years, this question remains open. Here, we mention some of the present conclusions.

The $f_0(980)$ and $a_0(980)$ are often interpreted as multiquark states [140–144] or $K\bar{K}$ bound states [145]. The insight into their internal structure using two-photon widths [116,146–152] is not conclusive. The $f_0(980)$ appears as a peak structure in $J/\psi \to \phi\pi^+\pi^-$ and in D_s decays without $f_0(500)$ background, while being nearly invisible in $J/\psi \to \omega\pi^+\pi^-$. Based on that observation it is suggested that $f_0(980)$ has a large $s\bar{s}$ component, which according to Ref. 153 is surrounded by a virtual $K\bar{K}$ cloud (see also Ref. 154). Data on radiative decays ($\phi \to f_0\gamma$ and $\phi \to a_0\gamma$) from SND, CMD2, and KLOE (see above) are consistent with a prominent role of kaon loops. This observation is interpreted as evidence for a compact four-quark [155] or a molecular [160,156] nature of these states. Details of this controversy are given in the comments [157,158]; see also Ref. 159. It remains quite possible that the states $f_0(980)$ and $a_0(980)$, together with the $f_0(500)$ and the $K_0^*(800)$, form a new low-mass state nonet of predominantly four-quark states, where at larger distances the quarks recombine into a pair of pseudoscalar mesons creating a meson cloud (see *e.g.,* Ref. 161). Different QCD sum rule studies [162–166] do not agree on a tetraquark configuration for the same particle group.

Models that start directly from chiral Lagrangians, either in non-linear [44,28,83,160] or in linear [167–172] realization, predict the existence of the $f_0(500)$ meson near 500 MeV. Here the $f_0(500)$, $a_0(980)$, $f_0(980)$, and $K_0^*(800)$ (in some models the $K_0^*(1430)$) would form a nonet (not necessarily $q\bar{q}$). In the linear sigma models the lightest pseudoscalars appear as their chiral partners. In these models the light $f_0(500)$ is often referred to as the "Higgs boson of strong interactions", since here the $f_0(500)$ plays a role similar to the Higgs particle in electro-weak symmetry breaking: within the linear sigma models it is important for the mechanism of chiral symmetry breaking, which generates most of the proton mass, and what is referred to as the constituent quark mass.

In the non–linear approaches of Ref. 28 [83], the above resonances together with the low lying vector states are generated starting from chiral perturbation theory predictions near the first open channel, and then by extending the predictions to the resonance regions using unitarity and analyticity.

Ref. 167 uses a framework with explicit resonances that are unitarized and coupled to the light pseudo-scalars in a chirally invariant way. Evidence for a non-$\bar{q}q$ nature of the lightest scalar resonances is derived from their mixing scheme. To identify the nature of the resonances generated from scattering equations, in Ref. 175 the large N_c behavior of the poles was studied, with the conclusion that, while the light vector states behave consistent with what is predicted for $\bar{q}q$ states, the light scalars behave very differently. This finding provides strong support for a non-$\bar{q}q$ nature of the light scalar resonances. Note, the more refined study of Ref. 110 found, in case of the $f_0(500)$, in addition to a dominant non-$\bar{q}q$ nature, indications for a subdominant $\bar{q}q$ component located around 1 GeV. A model–independent method to identify hadronic molecules goes back to a proposal by Weinberg [176], shown to be equivalent to the pole counting arguments of Ref. 177 [178] in Ref. 179. The formalism allows one to extract the amount of molecular component in the wave function from the effective coupling constant of a physical state to a nearby continuum channel. It can be applied to near threshold states only and provided strong evidence that the $f_0(980)$ is a $\bar{K}K$ molecule, while the situation turned out to be less clear for the $a_0(980)$ (see also Refs. [152,150]) . Further insights into $a_0(980)$ and $f_0(980)$ are expected from their mixing [180]. The corresponding signal predicted in Refs. [181,182] was recently observed at BES III [183]. It turned out that in order to get a quantitative understanding of that data in addition to the mixing mechanism itself some detailed understanding of the production mechanism seems necessary [184].

In the unitarized quark model with coupled $q\bar{q}$ and meson-meson channels, the light scalars can be understood as additional manifestations of bare $q\bar{q}$ confinement states, strongly mass shifted from the 1.3 - 1.5 GeV region and very distorted due to the strong $^3P_0$ coupling to S-wave two-meson decay channels [173–185]. Thus, in these models the light scalar nonet comprising the $f_0(500)$, $f_0(980)$, $K_0^*(800)$, and $a_0(980)$, as well as the nonet consisting of the $f_0(1370)$, $f_0(1500)$ (or $f_0(1710)$), $K_0^*(1430)$, and $a_0(1450)$, respectively, are two manifestations of the same bare input states (see also Ref. 186).

Other models with different groupings of the observed resonances exist and may, *e.g.*, be found in earlier versions of this review.

VI. Interpretation of the f_0's above 1 GeV: The $f_0(1370)$ and $f_0(1500)$ decay mostly into pions (2π and 4π) while the $f_0(1710)$ decays mainly into $K\bar{K}$ final states. The $K\bar{K}$ decay branching ratio of the $f_0(1500)$ is small [124,187].

If one uses the naive quark model, it is natural to assume that the $f_0(1370)$, $a_0(1450)$, and the $K_0^*(1430)$ are in the same SU(3) flavor nonet, being the $(u\bar{u} + d\bar{d})$, $u\bar{d}$ and $u\bar{s}$ states, probably mixing with the light scalars [188], while the $f_0(1710)$ is the $s\bar{s}$ state. Indeed, the production of $f_0(1710)$ (and $f_2'(1525)$) is observed in $p\bar{p}$ annihilation [189] but the rate is suppressed compared to $f_0(1500)$ (respectively, $f_2(1270)$), as would be expected from the OZI rule for $s\bar{s}$ states. The $f_0(1500)$ would also qualify as $(u\bar{u} + d\bar{d})$ state, although it is very narrow compared to the other states and too light to be the first radial excitation.

However, in $\gamma\gamma$ collisions leading to $K_S^0K_S^0$ [190] a spin 0 signal is observed at the $f_0(1710)$ mass (together with a dominant spin 2 component), while the $f_0(1500)$ is not observed in $\gamma\gamma \to K\bar{K}$ nor $\pi^+\pi^-$ [191]. In $\gamma\gamma$ collisions leading to $\pi^0\pi^0$ Ref. 138 reports the observation of a scalar around 1470 MeV

albeit with large uncertainties on the mass and $\gamma\gamma$ couplings. This state could be the $f_0(1370)$ or the $f_0(1500)$. The upper limit from $\pi^+\pi^-$ [191] excludes a large $n\bar{n}$ (here n stands for the two lightest quarks) content for the $f_0(1500)$ and hence points to a mainly $s\bar{s}$ state [192]. This appears to contradict the small $K\bar{K}$ decay branching ratio of the $f_0(1500)$ and makes a $q\bar{q}$ assignment difficult for this state. Hence the $f_0(1500)$ could be mainly glue due the absence of a 2γ-coupling, while the $f_0(1710)$ coupling to 2γ would be compatible with an $s\bar{s}$ state. This is in accord with the recent high statistics Belle data in $\gamma\gamma \to K^0_S K^0_S$ [193] in which the $f_0(1500)$ is absent, while a prominent peak at 1710 MeV is observed with quantum numbers 0^{++}, compatible with the formation of an $s\bar{s}$ state. However, the 2γ-couplings are sensitive to glue mixing with $q\bar{q}$ [194].

Note that an isovector scalar, possibly the $a_0(1450)$ (albeit at a lower mass of 1317 MeV) is observed in $\gamma\gamma$ collisions leading to $\eta\pi^0$ [195]. The state interferes destructively with the non-resonant background, but its $\gamma\gamma$ coupling is comparable to that of the $a_2(1320)$, in accord with simple predictions (see, *e.g.*, Ref. 192).

The small width of $f_0(1500)$, and its enhanced production at low transverse momentum transfer in central collisions [199–201] also favor $f_0(1500)$ to be non-$q\bar{q}$. In the mixing scheme of Ref. 194, which uses central production data from WA102 and the recent hadronic J/ψ decay data from BES [202,203], glue is shared between $f_0(1370)$, $f_0(1500)$ and $f_0(1710)$. The $f_0(1370)$ is mainly $n\bar{n}$, the $f_0(1500)$ mainly glue and the $f_0(1710)$ dominantly $s\bar{s}$. This agrees with previous analyses [204,205].

However, alternative schemes have been proposed (*e.g.*, in Ref. 206 [207]; for a review see, *e.g.*, Ref. 1). In particular, for a scalar glueball, the two-gluon coupling to $n\bar{n}$ appears to be suppressed by chiral symmetry [208] and therefore the $K\bar{K}$ decay could be enhanced. This mechanism would imply that the $f_0(1710)$ can possibly be interpreted as an unmixed glueball [209]. In Ref. 210, a large K^+K^- scalar signal reported by Belle in B decays into $KK\bar{K}$ [211], compatible with the $f_0(1500)$, is explained as due to constructive interference with a broad glueball background. However, the Belle data are inconsistent with the BaBar measurements which show instead a broad scalar at this mass for B decays into both $K^\pm K^\pm K^\mp$ [135] and $K^+K^-\pi^0$ [212].

Whether the $f_0(1500)$ is observed in 'gluon rich' radiative J/ψ decays is debatable [213] because of the limited amount of data - more data for this and the $\gamma\gamma$ mode are needed.

In Ref. [214], further refined in Ref. [215], $f_0(1370)$ and $f_0(1710)$ (together with $f_2(1270)$ and $f_2'(1525)$) were interpreted as bound systems of two vector mesons. This picture could be tested in radiative J/ψ decays [216] as well as radiative decays of the states themselves [217]. The vector-vector component of $f_0(1710)$ might also be the origin of the enhancement seen in $J/\psi \to \gamma\phi\omega$ near threshold [218] observed at BES [219].

References

1. C. Amsler and N.A. Tornqvist, Phys. Reports **389**, 61 (2004).
2. D.V. Bugg, Phys. Reports **397**, 257 (2004).
3. F.E. Close and N.A. Tornqvist, J. Phys. **G28**, R249 (2002).
4. E. Klempt and A. Zaitsev, Phys. Reports **454**, 1 (2007).
5. J.L. Adler, Phys. Rev. **137**, B1022 (1965).
6. J.L. Adler, Phys. Rev. **139**, B1638 (1965).
7. J. A. Oller, Phys. Rev. **D71**, 054030 (2005).
8. G. Colangelo, J. Gasser, and H. Leutwyler, Nucl. Phys. **B603**, 125 (2001).
9. I. Caprini, G. Colangelo, and H. Leutwyler, Phys. Rev. Lett. **96**, 132001 (2006).
10. R. Garcia-Martin *et al.*, Phys. Rev. Lett. **107**, 072001 (2011).
11. B. Moussallam, Eur. Phys. J. **C71**, 1814 (2011).
12. D. Aston *et al.*, Nucl. Phys. **B296**, 493 (1988).
13. P.G. Estabrooks *et al.*, Nucl. Phys. **B133**, 490 (1978).
14. A. Abele *et al.*, Phys. Rev. **D57**, 3860 (1998).
15. V. Bernard, N. Kaiser, and U.-G. Meißner, Phys. Rev. **D43**, 2757 (1991).
16. S.N. Cherry and M.R. Pennington, Nucl. Phys. **A688**, 823 (2001).
17. J.M. Link *et al.*, Phys. Lett. **B648**, 156 (2007).
18. E.M. Aitala *et al.*, Phys. Rev. Lett. **89**, 121801 (2002).
19. E.M. Aitala *et al.*, Phys. Rev. **D73**, 032004 (2006).
20. J.M. Link *et al.*, Phys. Lett. **B525**, 205 (2002).
21. C. Cawlfield *et al.*, Phys. Rev. **D74**, 031108R (2006).
22. B. Aubert *et al.*, Phys. Rev. **D76**, 011102R (2007).
23. M. Ablikim *et al.*, Phys. Lett. **B633**, 681 (2006).
24. F.K. Guo *et al.*, Nucl. Phys. **A773**, 78 (2006).
25. D. Epifanov *et al.*, Phys. Lett. **B654**, 65 (2007).
26. A.V. Anisovich and A.V. Sarantsev, Phys. Lett. **B413**, 137 (1997).
27. R. Delbourgo *et al.*, Int. J. Mod. Phys. **A13**, 657 (1998).
28. J.A. Oller *et al.*, Phys. Rev. **D60**, 099906E (1999).
29. J.A. Oller and E. Oset, Phys. Rev. **D60**, 074023 (1999).
30. C.M. Shakin and H. Wang, Phys. Rev. **D63**, 014019 (2001).
31. M.D. Scadron *et al.*, Nucl. Phys. **A724**, 391 (2003).
32. D.V. Bugg, Phys. Lett. **B572**, 1 (2003).
33. M. Ishida, Prog. Theor. Phys. Supp. **149**, 190 (2003).
34. H.Q. Zheng *et al.*, Nucl. Phys. **A733**, 235 (2004).
35. Z.Y. Zhou and H.Q. Zheng, Nucl. Phys. **A775**, 212 (2006).
36. J.M. Link *et al.*, Phys. Lett. **B653**, 1 (2007).
37. S. Kopp *et al.*, Phys. Rev. **D63**, 092001 (2001).
38. J.M. Link *et al.*, Phys. Lett. **B535**, 43 (2002).
39. J.M. Link *et al.*, Phys. Lett. **B621**, 72 (2005).
40. M. Jamin *et al.*, Nucl. Phys. **B587**, 331 (2000).
41. D. Black, Phys. Rev. **D64**, 014031 (2001).
42. J. A. Oller, Nucl. Phys. **A727**, 353 (2003).
43. E. Van Beveren *et al.*, Z. Phys. **C30**, 615 (1986).
44. J.R. Pelaez, Mod. Phys. Lett. **A19**, 2879 (2004).

45. S. Descotes-Genon and B. Moussallam, Eur. Phys. J. **C48**, 553 (2006).
46. M. Bargiotti *et al.*, Eur. Phys. J. **C26**, 371 (2003).
47. D. Barberis *et al.*, Phys. Lett. **B440**, 225 (1998).
48. M.J. Corden *et al.*, Nucl. Phys. **B144**, 253 (1978).
49. C. Defoix *et al.*, Nucl. Phys. **B44**, 125 (1972).
50. Z. Bai *et al.*, Phys. Rev. Lett. **65**, 2507 (1990).
51. T. Bolton *et al.*, Phys. Rev. Lett. **69**, 1328 (1992).
52. C. Amsler *et al.*, Phys. Lett. **B353**, 571 (1995).
53. N.A. Tornqvist and M. Roos, Phys. Rev. Lett. **76**, 1575 (1996).
54. S.M. Flatte, Phys. Lett. **63B**, 224 (1976).
55. C. Amsler *et al.*, Phys. Lett. **B333**, 277 (1994).
56. G. Janssen *et al.*, Phys. Rev. **D52**, 2690 (1995).
57. D.V. Bugg, Phys. Rev. **D78**, 074023 (2008).
58. P. Rubin *et al.*, Phys. Rev. **D78**, 072003 (2008).
59. A.D. Martin and E.N. Ozmutlu, Nucl. Phys. **B158**, 520 (1979).
60. S. Ishida ed. *et al.*, *KEK-Proceedings 2000-4*.
61. S. D. Protopopescu *et al.*, Phys. Rev. **D7**, 1279 (1973).
62. G. Grayer *et al.*, Nucl. Phys. **B75**, 189 (1974).
63. H. Becker *et al.*, Nucl. Phys. **B151**, 46 (1979).
64. L. Rosselet *et al.*, Phys. Rev. **D15**, 574 (1977).
65. S. Pislak *et al.*, Phys. Rev. Lett. **87**, 221801 (2001).
66. J.R. Batley *et al.*, Eur. Phys. J. **C70**, 635 (2010).
67. W. Wetzel *et al.*, Nucl. Phys. **B115**, 208 (1976).
68. V.A. Polychronakos *et al.*, Phys. Rev. **D19**, 1317 (1979).
69. D. Cohen *et al.*, Phys. Rev. **D22**, 2595 (1980).
70. A. Etkin *et al.*, Phys. Rev. **D25**, 1786 (1982).
71. C. Amsler *et al.*, Phys. Lett. **B342**, 433 (1995).
72. C. Amsler *et al.*, Phys. Lett. **B355**, 425 (1995).
73. A. Abele *et al.*, Phys. Lett. **B380**, 453 (1996).
74. D.M. Alde *et al.*, Phys. Lett. **B397**, 250 (1997).
75. R. Kaminski, L. Lesniak, and K. Rybicki, Z. Phys. **C74**, 79 (1997).
76. E.M. Aitala *et al.*, Phys. Rev. Lett. **86**, 770 (2001).
77. J.M. Link *et al.*, Phys. Lett. **B585**, 200 (2004).
78. G. Bonvicini *et al.*, Phys. Rev. **D76**, 012001 (2007).
79. J.E. Augustin and G. Cosme, Nucl. Phys. **B320**, 1 (1989).
80. M. Ablikim *et al.*, Phys. Lett. **B598**, 149 (2004).
81. A. Gallegos *et al.*, Phys. Rev. **D69**, 074033 (2004).
82. M. Ablikim *et al.*, Phys. Lett. **B645**, 19 (2007).
83. A. Dobado and J.R. Pelaez, Phys. Rev. **D56**, 3057 (1997).
84. I. Caprini, Phys. Rev. **D77**, 114019 (2008).
85. R. Garcia-Martin, J.R. Pelaez, and F.J. Yndurain, Phys. Rev. **D76**, 074034 (2007).
86. V.V. Anisovich *et al.*, Sov. Phys. Usp. **41**, 419 (1998).
87. V.V. Anisovich, Int. Jour. of Mod. Phys. A 21, 3615 (2006).
88. B.S. Zou and D.V. Bugg, Phys. Rev. **D48**, R3948 (1993).
89. B.S. Zou and D.V. Bugg, Phys. Rev. **D50**, 3145 (1994).
90. N.N. Achasov and G.N. Shestakov, Phys. Rev. **D49**, 5779 (1994).
91. M.P. Locher *et al.*, Eur. Phys. J. **C4**, 317 (1998).
92. J.A. Oller and E. Oset, Nucl. Phys. **A652**, 407 (1999).
93. T. Hannah, Phys. Rev. **D60**, 017502 (1999).
94. R. Kaminski *et al.*, Phys. Rev. **D50**, 3145 (1994).
95. R. Kaminski *et al.*, Phys. Lett. **B413**, 130 (1997).
96. R. Kaminski *et al.*, Eur. Phys. J. **C9**, 141 (1999).
97. M. Ishida *et al.*, Prog. Theor. Phys. **104**, 203 (2000).
98. Y.S. Surovtsev *et al.*, Phys. Rev. **D61**, 054024 (2001).
99. M. Ishida *et al.*, Phys. Lett. **B518**, 47 (2001).
100. M. Ablikim *et al.*, Phys. Lett. **B598**, 149 (2004).
101. Z.Y. Zhou *et al.*, JHEP **0502**, 043 (2005).
102. D.V. Bugg *et al.*, J. Phys. **G34**, 151 (2007).
103. G. Bonvicini *et al.*, Phys. Rev. **D76**, 012001 (2007).
104. D. Morgan and M. R. Pennington, Z. Phys. **C48**, 623 (1990).
105. M.R. Pennington, Phys. Rev. Lett. **97**, 011601 (2006).
106. M.R. Pennington, Mod. Phys. Lett. **A22**, 1439 (2007).
107. G. Mennessier, S. Narison, and W. Ochs, Phys. Lett. **B665**, 205 (2008).
108. R. Garcia-Martin and B. Moussallam, Eur. Phys. J. **C70**, 155 (2010).
109. M. Hoferichter *et al.*, Eur. Phys. J. **C71**, 1743 (2011).
110. J.R. Pelaez and G. Rios, Phys. Rev. Lett. **97**, 242002 (2006).
111. H.-X. Chen, A. Hosaka, and S.-L. Zhu, Phys. Lett. **B650**, 369 (2007).
112. F. Giacosa, Phys. Rev. **D75**, 054007 (2007).
113. L. Maiani *et al.*, Eur. Phys. J. **C50**, 609 (2007).
114. N.N. Achasov and G.N. Shestakov, Phys. Rev. **D58**, 054011 (1998).
115. N.N. Achasov *et al.*, Phys. Lett. **B479**, 53 (2000).
116. N.N. Achasov *et al.*, Phys. Lett. **B485**, 349 (2000).
117. R.R. Akhmetshin *et al.*, Phys. Lett. **B462**, 371 (1999).
118. A. Aloisio *et al.*, Phys. Lett. **B536**, 209 (2002).
119. F. Ambrosino *et al.*, Eur. Phys. J. **C49**, 473 (2007).
120. M. Boglione and M.R. Pennington, Eur. Phys. J. **C9**, 11 (1999).
121. T. Mori *et al.*, Phys. Rev. **D75**, 051101R (2007).
122. N.N. Achasov and G.N. Shestakov, Phys. Rev. **D77**, 074020 (2008).
123. M.R. Pennington *et al.*, Eur. Phys. J. **C56**, 1 (2008).
124. D. Barberis *et al.*, Phys. Lett. **B462**, 462 (1999).
125. D. Barberis *et al.*, Phys. Lett. **B479**, 59 (2000).
126. M. Gaspero, Nucl. Phys. **A562**, 407 (1993).
127. A. Adamo *et al.*, Nucl. Phys. **A558**, 13C (1993).
128. C. Amsler *et al.*, Phys. Lett. **B322**, 431 (1994).
129. A. Abele *et al.*, Eur. Phys. J. **C19**, 667 (2001).
130. A. Abele *et al.*, Eur. Phys. J. **C21**, 261 (2001).
131. D. Barberis *et al.*, Phys. Lett. **B471**, 440 (2000).
132. A. Garmash *et al.*, Phys. Rev. **D65**, 092005 (2002).
133. A. Garmash *et al.*, Phys. Rev. Lett. **96**, 251803 (2006).
134. A. Garmash *et al.*, Phys. Rev. **D75**, 012006 (2007).
135. B. Aubert *et al.*, Phys. Rev. **D74**, 032003 (2006).
136. B. Aubert *et al.*, Phys. Rev. Lett. **99**, 221801 (2007).
137. E. Klempt, M. Matveev, A.V. Sarantsev, Eur. Phys. J. **C55**, 39 (2008).
138. S. Uehara *et al.*, Phys. Rev. **D78**, 052004 (2008).
139. S. Uehara *et al.*, Phys. Rev. **D80**, 032001 (2009).

140. R. Jaffe, Phys. Rev. **D15**, 267 (1977).
141. M. Alford and R.L. Jaffe, Nucl. Phys. **B578**, 367 (2000).
142. L. Maiani *et al.*, Phys. Rev. Lett. **93**, 212002 (2004).
143. L. Maiani, A.D. Polosa, and V. Riquer, Phys. Lett. **B651**, 129 (2007).
144. G. 'tHooft *et al.*, Phys. Lett. **B662**, 424 (2008).
145. J. Weinstein and N. Isgur, Phys. Rev. **D41**, 2236 (1990).
146. T. Barnes, Phys. Lett. **B165**, 434 (1985).
147. Z.P. Li *et al.*, Phys. Rev. **D43**, 2161 (1991).
148. R. Delbourgo, D. Lui, and M. Scadron, Phys. Lett. **B446**, 332 (1999).
149. J.L. Lucio and M. Napsuciale, Phys. Lett. **B454**, 365 (1999).
150. C. Hanhart *et al.*, Phys. Rev. **D75**, 074015 (2007).
151. R.H. Lemmer, Phys. Lett. **B650**, 152 (2007).
152. T. Branz, T. Gutsche, and V. Lyubovitskij, Eur. Phys. J. **A37**, 303 (2008).
153. A. Deandrea *et al.*, Phys. Lett. **B502**, 79 (2001).
154. K.M. Ecklund *et al.*, Phys. Rev. **D80**, 052009 (2010).
155. N. N. Achasov, V. N. Ivanchenko, Nucl. Phys. **B315**, 465 (1989).
156. Y. S. Kalashnikova *et al.*, Eur. Phys. J. **A24**, 437 (2005).
157. Y. S. Kalashnikova *et al.*, Phys. Rev. **D78**, 058501 (2008).
158. N. N. Achasov and A. V. Kiselev, Phys. Rev. **D78**, 058502 (2008).
159. M. Boglione and M.R. Pennington, Eur. Phys. J. **C30**, 503 (2003).
160. J.A. Oller *et al.*, Nucl. Phys. **A714**, 161 (2003).
161. F. Giacosa and G. Pagliara, Phys. Rev. **C76**, 065204 (2007).
162. S. Narison, Nucl. Phys. **B96**, 244 (2001).
163. H.J. Lee, Eur. Phys. J. **A30**, 423 (2006).
164. H.X. Chen, A. Hosaka, and S.L. Zhu, Phys. Rev. **D76**, 094025 (2007).
165. J. Sugiyama *et al.*, Phys. Rev. **D76**, 114010 (2007).
166. T. Kojo and D. Jido, Phys. Rev. **D78**, 114005 (2008).
167. D. Black *et al.*, Phys. Rev. **D59**, 074026 (1999).
168. M. Scadron, Eur. Phys. J. **C6**, 141 (1999).
169. M. Ishida, Prog. Theor. Phys. **101**, 661 (1999).
170. N. Tornqvist, Eur. Phys. J. **C11**, 359 (1999).
171. M. Napsuciale and S. Rodriguez, Phys. Lett. **B603**, 195 (2004).
172. M. Napsuciale and S. Rodriguez, Phys. Rev. **D70**, 094043 (2004).
173. N.A. Tornqvist, Z. Phys. **C68**, 647 (1995).
174. E. Van Beveren and G. Rupp, Eur. Phys. J. **C10**, 469 (1999).
175. J. R. Pelaez, Phys. Rev. Lett. **92**, 102001 (2004).
176. S. Weinberg, Phys. Rev. **130**, 776 (1963).
177. D. Morgan, Nucl. Phys. **A543**, 632 (1992).
178. N. Tornqvist, Phys. Rev. **D51**, 5312 (1995).
179. V. Baru *et al.*, Phys. Lett. **B586**, 53 (2004).
180. N. N. Achasov *et al.*, Phys. Lett. **B88**, 367 (1979).
181. J. -J. Wu *et al.*, Phys. Rev. D 75,114012(2007).
182. C. Hanhart *et al.*, Phys. Rev. **D76**, 074028 (2007).
183. M. Ablikim *et al.*, Phys. Rev. D 83,032003(2011).
184. L. Roca, Phys. Rev. D 88, 014045(2013).
185. E. Van Beveren, Eur. Phys. J. **C22**, 493 (2001).
186. M. Boglione and M.R. Pennington, Phys. Rev. **D65**, 114010 (2002).
187. A. Abele *et al.*, Phys. Lett. **B385**, 425 (1996).
188. D. Black *et al.*, Phys. Rev. **D61**, 074001 (2000).
189. C. Amsler *et al.*, Phys. Lett. **B639**, 165 (2006).
190. M. Acciarri *et al.*, Phys. Lett. **B501**, 173 (2001).
191. R. Barate *et al.*, Phys. Lett. **B472**, 189 (2000).
192. C. Amsler, Phys. Lett. **B541**, 22 (2002).
193. S. Uehara et. (Belle Collab.), prep. arXiv:1307.7457 (2013).
194. F.E. Close and Q. Zhao, Phys. Rev. **D71**, 094022 (2005).
195. S. Uehara *et al.*, Phys. Rev. **D80**, 032001 (2009).
196. H. Nakazawa *et al.*, Phys. Lett. **B615**, 39 (2005).
197. K. Abe *et al.*, Eur. Phys. J. **C32**, 323 (2004).
198. W.T. Chen *et al.*, Phys. Lett. **B651**, 15 (2007).
199. F.E. Close *et al.*, Phys. Lett. **B397**, 333 (1997).
200. F.E. Close, Phys. Lett. **B419**, 387 (1998).
201. A. Kirk, Phys. Lett. **B489**, 29 (2000).
202. M. Ablikim *et al.*, Phys. Lett. **B603**, 138 (2004).
203. M. Ablikim *et al.*, Phys. Lett. **B607**, 243 (2005).
204. C. Amsler and F.E. Close, Phys. Rev. **D53**, 295 (1996).
205. F.E. Close and A. Kirk, Eur. Phys. J. **C21**, 531 (2001).
206. P. Minkowski and W. Ochs, Eur. Phys. J. **C9**, 283 (1999).
207. W. Lee and D. Weingarten, Phys. Rev. **D61**, 014015 (2000).
208. M. Chanowitz, Phys. Rev. Lett. **95**, 172001 (2005).
209. M. Albaladejo and J.A. Oller, Phys. Rev. Lett. **101**, 252002 (2008).
210. P. Minkowski, W. Ochs, Eur. Phys. J. **C39**, 71 (2005).
211. A. Garmash *et al.*, Phys. Rev. **D71**, 092003 (2005).
212. B. Aubert *et al.*, Phys. Rev. Lett. **99**, 161802 (2007).
213. M. Ablikim *et al.*, Phys. Lett. **B642**, 441 (2006).
214. R. Molina *et al.*, Phys. Rev. **D78**, 114018 (2008).
215. C. Garcia-Recio *et al.*, Phys. Rev. **D87**, 096006 (2013).
216. L. S. Geng *et al.*, Eur. Phys. J. **A44**, 305 (2010).
217. T. Branz *et al.*, Phys. Rev. **D81**, 054037 (2010).
218. A. Martinez Torres *et al.*, Phys. Lett. **B719**, 388 (2013).
219. M. Ablikim *et al.*, Phys. Rev. Lett. **96**, 162002 (2006).
220. R. Fleischer *et al.*, Eur. Phys. J. **C71**, 1832 (2011).
221. S. Stone and L. Zhang, Phys. Rev. Lett. **111**, 062001 (2013).
222. R. Aaij *et al.*, (LHCb Collab.), Phys. Rev. **D87**, 052001 (2013).

$f_0(500)$ T-MATRIX POLE $\sqrt{s}$

Note that $\Gamma \approx 2\ \mathrm{Im}(\sqrt{s_{\mathrm{pole}}})$.

VALUE (MeV)	DOCUMENT ID		TECN	COMMENT
(400–550)−*i*(200–350) OUR ESTIMATE				
• • • We do not use the following data for averages, fits, limits, etc. • • •				
$(440 \pm 10) - i(238 \pm 10)$	[1] ALBALADEJO	12	RVUE	Compilation
$(445 \pm 25) - i(278^{+22}_{-18})$	[2,3] GARCIA-MAR.	11	RVUE	Compilation
$(457^{+14}_{-13}) - i(279^{+11}_{-7})$	[2,4] GARCIA-MAR.	11	RVUE	Compilation
$(442^{+5}_{-8}) - i(274^{+6}_{-5})$	[5] MOUSSALLAM	11	RVUE	Compilation
$(452 \pm 13) - i(259 \pm 16)$	[6] MENNESSIER	10	RVUE	Compilation
$(448 \pm 43) - i(266 \pm 43)$	[7] MENNESSIER	10	RVUE	Compilation
$(455 \pm 6^{+31}_{-13}) - i(278 \pm 6^{+34}_{-43})$	[8] CAPRINI	08	RVUE	Compilation
$(463 \pm 6^{+31}_{-17}) - i(259 \pm 6^{+33}_{-34})$	[9] CAPRINI	08	RVUE	Compilation

Meson Particle Listings

$f_0(500)$

$(552^{+84}_{-106})-i(232^{+81}_{-72})$	[10] ABLIKIM	07A	BES2	$\psi(2S) \to \pi^+\pi^- J/\psi$
$(466 \pm 18)-i(223 \pm 28)$	[11] BONVICINI	07	CLEO	$D^+ \to \pi^-\pi^+\pi^+$
$(472 \pm 30)-i(271 \pm 30)$	[12] BUGG	07A	RVUE	Compilation
$(484 \pm 17)-i(255 \pm 10)$	GARCIA-MAR..	07	RVUE	Compilation
$(430)-i(325)$	[13] ANISOVICH	06	RVUE	Compilation
$(441^{+16}_{-8})-i(272^{+9}_{-12.5})$	[14] CAPRINI	06	RVUE	$\pi\pi \to \pi\pi$
$(470 \pm 50)-i(285 \pm 25)$	[15] ZHOU	05	RVUE	
$(541 \pm 39)-i(252 \pm 42)$	[16] ABLIKIM	04A	BES2	$J/\psi \to \omega\pi^+\pi^-$
$(528 \pm 32)-i(207 \pm 23)$	[17] GALLEGOS	04	RVUE	Compilation
$(440 \pm 8)-i(212 \pm 15)$	[18] PELAEZ	04A	RVUE	$\pi\pi \to \pi\pi$
$(533 \pm 25)-i(249 \pm 25)$	[19] BUGG	03	RVUE	
$517 - i240$	BLACK	01	RVUE	$\pi^0\pi^0 \to \pi^0\pi^0$
$(470 \pm 30)-i(295 \pm 20)$	[14] COLANGELO	01	RVUE	$\pi\pi \to \pi\pi$
$(535^{+48}_{-36})-i(155^{+76}_{-53})$	[20] ISHIDA	01		$\Upsilon(3S) \to \Upsilon\pi\pi$
$610 \pm 14 - i620 \pm 26$	[21] SUROVTSEV	01	RVUE	$\pi\pi \to \pi\pi$, $K\overline{K}$
$(540^{+36}_{-29})-i(193^{+32}_{-40})$	ISHIDA	00B		$p\overline{p} \to \pi^0\pi^0\pi^0$
$445 - i235$	HANNAH	99	RVUE	π scalar form factor
$(523 \pm 12)-i(259 \pm 7)$	KAMINSKI	99	RVUE	$\pi\pi \to \pi\pi$, $K\overline{K}$, $\sigma\sigma$
$442 - i\ 227$	OLLER	99	RVUE	$\pi\pi \to \pi\pi$, $K\overline{K}$
$469 - i203$	OLLER	99B	RVUE	$\pi\pi \to \pi\pi$, $K\overline{K}$
$445 - i221$	OLLER	99C	RVUE	$\pi\pi \to \pi\pi$, $K\overline{K}$, $\eta\eta$
$(1530^{+90}_{-250})-i(560 \pm 40)$	ANISOVICH	98B	RVUE	Compilation
$420 - i\ 212$	LOCHER	98	RVUE	$\pi\pi \to \pi\pi$, $K\overline{K}$
$440 - i245$	[22] DOBADO	97	RVUE	Compilation
$(602 \pm 26)-i(196 \pm 27)$	[23] ISHIDA	97		$\pi\pi \to \pi\pi$
$(537 \pm 20)-i(250 \pm 17)$	[24] KAMINSKI	97B	RVUE	$\pi\pi \to \pi\pi$, $K\overline{K}$, 4π
$470 - i250$	[25,26] TORNQVIST	96	RVUE	$\pi\pi \to \pi\pi$, $K\overline{K}$, $K\pi$, $\eta\pi$
$387 - i305$	[26,27] JANSSEN	95	RVUE	$\pi\pi \to \pi\pi$, $K\overline{K}$
$420 - i370$	[28] ACHASOV	94	RVUE	$\pi\pi \to \pi\pi$
$(506 \pm 10)-i(247 \pm 3)$	KAMINSKI	94	RVUE	$\pi\pi \to \pi\pi$, $K\overline{K}$
$370 - i356$	[29] ZOU	94B	RVUE	$\pi\pi \to \pi\pi$, $K\overline{K}$
$408 - i342$	[26,29] ZOU	93	RVUE	$\pi\pi \to \pi\pi$, $K\overline{K}$
$470 - i208$	[30] VANBEVEREN	86	RVUE	$\pi\pi \to \pi\pi$, $K\overline{K}$, $\eta\eta$, ...
$(750 \pm 50)-i(450 \pm 50)$	[31] ESTABROOKS	79	RVUE	$\pi\pi \to \pi\pi$, $K\overline{K}$
$(660 \pm 100)-i(320 \pm 70)$	PROTOPOP...	73	HBC	$\pi\pi \to \pi\pi$, $K\overline{K}$
$650 - i370$	[32] BASDEVANT	72	RVUE	$\pi\pi \to \pi\pi$

[1] Applying the chiral unitary approach at NLO to the K_{e4} data of BATLEY 10 and $\pi N \to \pi\pi N$ data of HYAMS 73, GRAYER 74, and PROTOPOPESCU 73.
[2] Uses the K_{e4} data of BATLEY 10C and the $\pi N \to \pi\pi N$ data of HYAMS 73, GRAYER 74, and PROTOPOPESCU 73.
[3] Analytic continuation using Roy equations.
[4] Analytic continuation using GKPY equations.
[5] Using Roy equations.
[6] Average of three variants of the analytic K-matrix model. Uses the K_{e4} data of BATLEY 08A and the $\pi N \to \pi\pi N$ data of HYAMS 73 and GRAYER 74.
[7] Average of the analyses of three data sets in the K-matrix model. Uses the data of BATLEY 08A, HYAMS 73, and GRAYER 74, partially of COHEN 80 or ETKIN 82B.
[8] From the K_{e4} data of BATLEY 08A and $\pi N \to \pi\pi N$ data of HYAMS 73.
[9] From the K_{e4} data of BATLEY 08A and $\pi N \to \pi\pi N$ data of PROTOPOPESCU 73, GRAYER 74, and ESTABROOKS 74.
[10] From a mean of three different $f_0(500)$ parametrizations. Uses 40k events.
[11] From an isobar model using 2.6k events.
[12] Reanalysis of ABLIKIM 04A, PISLAK 01, and HYAMS 73 data.
[13] Using the N/D method.
[14] From the solution of the Roy equation (ROY 71) for the isoscalar S-wave and using a phase-shift analysis of HYAMS 73 and PROTOPOPESCU 73 data.
[15] Reanalysis of the data from PROTOPOPESCU 73, ESTABROOKS 74, GRAYER 74, ROSSELET 77, PISLAK 03, and AKHMETSHIN 04.
[16] From a mean of six different analyses and $f_0(500)$ parameterizations.
[17] Using data on $\psi(2S) \to J/\psi\pi\pi$ from BAI 00E and on $\Upsilon(nS) \to \Upsilon(mS)\pi\pi$ from BUTLER 94B and ALEXANDER 98.
[18] Reanalysis of data from PROTOPOPESCU 73, ESTABROOKS 74, GRAYER 74, and COHEN 80 in the unitarized ChPT model.
[19] From a combined analysis of HYAMS 73, AUGUSTIN 89, AITALA 01B, and PISLAK 01.
[20] A similar analysis (KOMADA 01) finds $(580^{+79}_{-30})-i(190^{+107}_{-49})$ MeV.
[21] Coupled channel reanalysis of BATON 70, BENSINGER 71, BAILLON 72, HYAMS 73, HYAMS 75, ROSSELET 77, COHEN 80, and ETKIN 82B using the uniformizing variable.
[22] Using the inverse amplitude method and data of ESTABROOKS 73, GRAYER 74, and PROTOPOPESCU 73.
[23] Reanalysis of data from HYAMS 73, GRAYER 74, SRINIVASAN 75, and ROSSELET 77 using the interfering amplitude method.
[24] Average and spread of 4 variants ("up" and "down") of KAMINSKI 97B 3-channel model.
[25] Uses data from BEIER 72B, OCHS 73, HYAMS 73, GRAYER 74, ROSSELET 77, CASON 83, ASTON 88, and ARMSTRONG 91B. Coupled channel analysis with flavor symmetry and all light two-pseudoscalars systems.
[26] Demonstrates explicitly that $f_0(500)$ and $f_0(1370)$ are two different poles.
[27] Analysis of data from FALVARD 88.
[28] Analysis of data from OCHS 73, ESTABROOKS 75, ROSSELET 77, and MUKHIN 80.
[29] Analysis of data from OCHS 73, GRAYER 74, and ROSSELET 77.
[30] Coupled-channel analysis using data from PROTOPOPESCU 73, HYAMS 73, HYAMS 75, GRAYER 74, ESTABROOKS 74, ESTABROOKS 75, FROGGATT 77, CORDEN 79, BISWAS 81.
[31] Analysis of data from APEL 73, GRAYER 74, CASON 76, PAWLICKI 77. Includes spread and errors of 4 solutions.
[32] Analysis of data from BATON 70, BENSINGER 71, COLTON 71, BAILLON 72,PROTOPOPESCU 73, and WALKER 67.

$f_0(500)$ BREIT-WIGNER MASS OR K-MATRIX POLE PARAMETERS

VALUE (MeV)	DOCUMENT ID		TECN	COMMENT
(400–550) OUR ESTIMATE				
• • • We do not use the following data for averages, fits, limits, etc. • • •				
513 ± 32	[33] MURAMATSU	02	CLEO	$e^+e^- \approx 10$ GeV
$478^{+24}_{-23} \pm 17$	AITALA	01B	E791	$D^+ \to \pi^-\pi^+\pi^+$
563^{+58}_{-29}	[34] ISHIDA	01		$\Upsilon(3S) \to \Upsilon\pi\pi$
555	[35] ASNER	00	CLE2	$\tau^- \to \pi^-\pi^0\pi^0\nu_\tau$
540 ± 36	ISHIDA	00B		$p\overline{p} \to \pi^0\pi^0\pi^0$
750 ± 4	ALEKSEEV	99	SPEC	$1.78\ \pi^-\ p_{\rm polar} \to \pi^-\pi^+ n$
744 ± 5	ALEKSEEV	98	SPEC	$1.78\ \pi^-\ p_{\rm polar} \to \pi^-\pi^+ n$
759 ± 5	[36] TROYAN	98		$5.2\ np \to np\pi^+\pi^-$
780 ± 30	ALDE	97	GAM2	$450\ pp \to pp\pi^0\pi^0$
585 ± 20	[37] ISHIDA	97		$\pi\pi \to \pi\pi$
761 ± 12	[38] SVEC	96	RVUE	6–$17\ \pi N_{\rm polar} \to \pi^+\pi^- N$
~ 860	[39,40] TORNQVIST	96	RVUE	$\pi\pi \to \pi\pi$, $K\overline{K}$, $K\pi$, $\eta\pi$
1165 ± 50	[41,42] ANISOVICH	95	RVUE	$\pi^-p \to \pi^0\pi^0 n$, $\overline{p}p \to \pi^0\pi^0\pi^0$, $\pi^0\pi^0\eta$, $\pi^0\eta\eta$
~ 1000	[43] ACHASOV	94	RVUE	$\pi\pi \to \pi\pi$
414 ± 20	[38] AUGUSTIN	89	DM2	

[33] Statistical uncertainty only.
[34] A similar analysis (KOMADA 01) finds 526^{+48}_{-37} MeV.
[35] From the best fit of the Dalitz plot.
[36] 6σ effect, no PWA.
[37] Reanalysis of data from HYAMS 73, GRAYER 74, SRINIVASAN 75, and ROSSELET 77 using the interfering amplitude method.
[38] Breit-Wigner fit to S-wave intensity measured in $\pi N \to \pi^-\pi^+ N$ on polarized targets. The fit does not include $f_0(980)$.
[39] Uses data from ASTON 88, OCHS 73, HYAMS 73, ARMSTRONG 91B, GRAYER 74, CASON 83, ROSSELET 77, and BEIER 72B. Coupled channel analysis with flavor symmetry and all light two-pseudoscalars systems.
[40] Also observed by ASNER 00 in $\tau^- \to \pi^-\pi^0\pi^0\nu_\tau$ decays.
[41] Uses $\pi^0\pi^0$ data from ANISOVICH 94, AMSLER 94D, and ALDE 95B, $\pi^+\pi^-$ data from OCHS 73, GRAYER 74 and ROSSELET 77, and $\eta\eta$ data from ANISOVICH 94.
[42] The pole is on Sheet III. Demonstrates explicitly that $f_0(500)$ and $f_0(1370)$ are two different poles.
[43] Analysis of data from OCHS 73, ESTABROOKS 75, ROSSELET 77, and MUKHIN 80.

$f_0(500)$ BREIT-WIGNER WIDTH

VALUE (MeV)	DOCUMENT ID		TECN	COMMENT
(400–700) OUR ESTIMATE				
• • • We do not use the following data for averages, fits, limits, etc. • • •				
335 ± 67	[44] MURAMATSU	02	CLEO	$e^+e^- \approx 10$ GeV
$324^{+42}_{-40} \pm 21$	AITALA	01B	E791	$D^+ \to \pi^-\pi^+\pi^+$
372^{+229}_{-95}	[45] ISHIDA	01		$\Upsilon(3S) \to \Upsilon\pi\pi$
540	[46] ASNER	00	CLE2	$\tau^- \to \pi^-\pi^0\pi^0\nu_\tau$
372 ± 80	ISHIDA	00B		$p\overline{p} \to \pi^0\pi^0\pi^0$
119 ± 13	ALEKSEEV	99	SPEC	$1.78\ \pi^-\ p_{\rm polar} \to \pi^-\pi^+ n$
77 ± 22	ALEKSEEV	98	SPEC	$1.78\ \pi^-\ p_{\rm polar} \to \pi^-\pi^+ n$
35 ± 12	[47] TROYAN	98		$5.2\ np \to np\pi^+\pi^-$
780 ± 60	ALDE	97	GAM2	$450\ pp \to pp\pi^0\pi^0$
385 ± 70	[48] ISHIDA	97		$\pi\pi \to \pi\pi$
290 ± 54	[49] SVEC	96	RVUE	6–$17\ \pi N_{\rm polar} \to \pi^+\pi^- N$
~ 880	[50,51] TORNQVIST	96	RVUE	$\pi\pi \to \pi\pi$, $K\overline{K}$, $K\pi$, $\eta\pi$
460 ± 40	[52,53] ANISOVICH	95	RVUE	$\pi^-p \to \pi^0\pi^0 n$, $\overline{p}p \to \pi^0\pi^0\pi^0$, $\pi^0\pi^0\eta$, $\pi^0\eta\eta$
~ 3200	[54] ACHASOV	94	RVUE	$\pi\pi \to \pi\pi$
494 ± 58	[49] AUGUSTIN	89	DM2	

[44] Statistical uncertainty only.
[45] A similar analysis (KOMADA 01) finds 301^{+145}_{-100} MeV.
[46] From the best fit of the Dalitz plot.
[47] 6σ effect, no PWA.
[48] Reanalysis of data from HYAMS 73, GRAYER 74, SRINIVASAN 75, and ROSSELET 77 using the interfering amplitude method.
[49] Breit-Wigner fit to S-wave intensity measured in $\pi N \to \pi^-\pi^+ N$ on polarized targets. The fit does not include $f_0(980)$.
[50] Uses data from ASTON 88, OCHS 73, HYAMS 73, ARMSTRONG 91B, GRAYER 74, CASON 83, ROSSELET 77, and BEIER 72B. Coupled channel analysis with flavor symmetry and all light two-pseudoscalars systems.
[51] Also observed by ASNER 00 in $\tau^- \to \pi^-\pi^0\pi^0\nu_\tau$ decays.
[52] Uses $\pi^0\pi^0$ data from ANISOVICH 94, AMSLER 94D, and ALDE 95B, $\pi^+\pi^-$ data from OCHS 73, GRAYER 74 and ROSSELET 77, and $\eta\eta$ data from ANISOVICH 94.
[53] The pole is on Sheet III. Demonstrates explicitly that $f_0(500)$ and $f_0(1370)$ are two different poles.
[54] Analysis of data from OCHS 73, ESTABROOKS 75, ROSSELET 77, and MUKHIN 80.

$f_0(500)$ DECAY MODES

	Mode	Fraction (Γ_i/Γ)
Γ_1	$\pi\pi$	dominant
Γ_2	$\gamma\gamma$	seen

$f_0(500)$ PARTIAL WIDTHS

$\Gamma(\gamma\gamma)$ Γ_2

VALUE (keV)	DOCUMENT ID		TECN	COMMENT
• • • We do not use the following data for averages, fits, limits, etc. • • •				
1.7 ±0.4	[55] HOFERICHTER	11	RVUE	Compilation
3.08±0.82	[56] MENNESSIER	11	RVUE	Compilation
$2.08\pm0.2\ ^{+0.07}_{-0.04}$	[57] MOUSSALLAM	11	RVUE	Compilation
2.08	[58] MAO	09	RVUE	Compilation
1.2 ±0.4	[59] BERNABEU	08	RVUE	
3.9 ±0.6	[56] MENNESSIER	08	RVUE	$\gamma\gamma \to \pi^+\pi^-, \pi^0\pi^0$
1.8 ±0.4	[60] OLLER	08	RVUE	Compilation
1.68±0.15	[60,61] OLLER	08A	RVUE	Compilation
3.1 ±0.5	[62,63] PENNINGTON	08	RVUE	Compilation
2.4 ±0.4	[63,64] PENNINGTON	08	RVUE	Compilation
4.1 ±0.3	[65] PENNINGTON	06	RVUE	$\gamma\gamma \to \pi^0\pi^0$
3.8 ±1.5	[66,67] BOGLIONE	99	RVUE	$\gamma\gamma \to \pi^+\pi^-, \pi^0\pi^0$
5.4 ±2.3	[66] MORGAN	90	RVUE	$\gamma\gamma \to \pi^+\pi^-, \pi^0\pi^0$
10 ±6	COURAU	86	DM1	$e^+e^- \to \pi^+\pi^-e^+e^-$

[55] Using Roy-Steiner equations with $\pi\pi$ phase shifts from an update of COLANGELO 01 and from GARCIA-MARTIN 11A.
[56] Using an analytic K-matrix model.
[57] Using dispersion integral with phase input from Roy equations and data from MARSISKE 90, BOYER 90, BEHREND 92, UEHARA 08A, and MORI 07.
[58] Used dispersion theory. The value quoted used the $f_0(500)$ pole position of $457 - i276$ MeV.
[59] Using ρ, n polarizabilities from PDG 06 and fitting to $\pi\pi$ phase motion from GARCIA-MARTIN 07 and σ-poles from GARCIA-MARTIN 07 and CAPRINI 06.
[60] Using twice-subtracted dispersion integrals.
[61] Supersedes OLLER 08.
[62] Solution A (preferred solution based on χ^2-analysis).
[63] Dispersion theory based amplitude analysis of BOYER 90, MARSISKE 90, BEHREND 92, and MORI 07.
[64] Solution B (worse than solution A; still acceptable when systematic uncertainties are included).
[65] Using unitarity and the σ pole position from CAPRINI 06.
[66] This width could equally well be assigned to the $f_0(1370)$. The authors analyse data from BOYER 90 and MARSISKE 90 and report strong correlation with $\gamma\gamma$ width of $f_2(1270)$.
[67] Supersedes MORGAN 90.

$f_0(500)$ REFERENCES

ALBALADEJO	12	PR D86 034003	M. Albaladejo, J.A. Oller	(MURC)
GARCIA-MAR...	11	PRL 107 072001	R. Garcia-Martin *et al.*	(MADR, CRAC)
GARCIA-MAR...	11A	PR D83 074004	R. Garcia-Martin *et al.*	(MADR, CRAC)
HOFERICHTER	11	EPJ C71 1743	M. Hoferichter, D.R. Phillips, C. Schat	(BONN+)
MENNESSIER	11	PL B696 40	G. Mennessier, S. Narison, X.-G. Wang	
MOUSSALLAM	11	EPJ C71 1814	B. Moussallam	
BATLEY	10	PL B686 101	J.R. Batley *et al.*	(CERN NA48/2 Collab.)
BATLEY	10C	EPJ C70 635	J.R. Batley *et al.*	(CERN NA48/2 Collab.)
MENNESSIER	10	PL B688 59	G. Mennessier, S. Narison, X.-G. Wang	
MAO	09	PR D79 116008	Y. Mao *et al.*	
BATLEY	08A	EPJ C54 411	J.R. Batley *et al.*	(CERN NA48/2 Collab.)
BERNABEU	08	PRL 100 241804	J. Bernabeu, J. Prades	(IFIC, GRAN)
CAPRINI	08	PR D77 114019	I. Caprini	
MENNESSIER	08	PL B665 205	G. Mennessier, S. Narison, W. Ochs	
OLLER	08	PL B659 201	J.A. Oller, L. Roca, C. Schat	(MURC, UBA)
OLLER	08A	EPJ A37 15	J.A. Oller, L. Roca	(MURC)
PENNINGTON	08	EPJ C56 1	M.R. Pennington *et al.*	
UEHARA	08A	PR D78 052004	S. Uehara *et al.*	(BELLE Collab.)
ABLIKIM	07A	PL B645 19	M. Ablikim *et al.*	(BES Collab.)
BONVICINI	07	PR D76 012001	G. Bonvicini *et al.*	(CLEO Collab.)
BUGG	07A	JP G34 151	D.V. Bugg *et al.*	
GARCIA-MAR...	07	PR D76 074034	R. Garcia-Martin, J.R. Pelaez, F.J. Yndurain	
MORI	07	PR D75 051101	T. Mori *et al.*	(BELLE Collab.)
ANISOVICH	06	IJMP A21 3615	V.V. Anisovich	
CAPRINI	06	PRL 96 132001	I. Caprini, G. Colangelo, H. Leutwyler	(BCIP+)
PDG	06	JP G33 1	W.-M. Yao *et al.*	(PDG Collab.)
PENNINGTON	06	PRL 97 011601	M.R. Pennington	
ZHOU	05	JHEP 0502 043	Z.Y. Zhou *et al.*	
ABLIKIM	04A	PL B598 149	M. Ablikim *et al.*	(BES Collab.)
AKHMETSHIN	04	PL B578 285	R.R. Akhmetshin *et al.*	(Novosibirsk CMD-2 Collab.)
GALLEGOS	04	PR D69 074033	A. Gallegos *et al.*	
PELAEZ	04A	MPL A19 2879	J.R. Pelaez	
BUGG	03	PL B572 1	D.V. Bugg	
PISLAK	03	PR D67 072004	S. Pislak *et al.*	(BNL E865 Collab.)
Also		PR D81 119903E	S. Pislak *et al.*	(BNL E865 Collab.)
MURAMATSU	02	PRL 89 251802	H. Muramatsu *et al.*	(CLEO Collab.)
Also		PRL 90 059901 (errat)	H. Muramatsu *et al.*	(CLEO Collab.)
AITALA	01B	PRL 86 770	E.M. Aitala *et al.*	(FNAL E791 Collab.)
BLACK	01	PR D64 014031	D. Black *et al.*	
COLANGELO	01	NP B603 125	G. Colangelo, J. Gasser, H. Leytwyler	
ISHIDA	01	PL B518 47	M. Ishida *et al.*	
KOMADA	01	PL B508 31	T. Komada *et al.*	
PISLAK	01	PRL 87 221801	S. Pislak *et al.*	(BNL E865 Collab.)
Also		PR D67 072004	S. Pislak *et al.*	(BNL E865 Collab.)
Also		PRL 105 019901E	S. Pislak *et al.*	(BNL E865 Collab.)
SUROVTSEV	01	PR D63 054024	Y.S. Surovtsev, D. Krupa, M. Nagy	
ASNER	00	PR D61 012002	D.M. Asner *et al.*	(CLEO Collab.)
BAI	00E	PR D62 032002	J. Bai *et al.*	(BES Collab.)
ISHIDA	00B	PTP 104 203	M. Ishida *et al.*	
ALEKSEEV	99	NP B541 3	I.G. Alekseev *et al.*	
BOGLIONE	99	EPJ C9 11	M. Boglione, M.R. Pennington	
HANNAH	99	PR D60 017502	T. Hannah	
KAMINSKI	99	EPJ C9 141	R. Kaminski, L. Lesniak, B. Loiseau	(CRAC, PARIN)
OLLER	99	PR D60 099906 (erratum)	J.A. Oller *et al.*	
OLLER	99B	NP A652 407 (erratum)	J.A. Oller, E. Oset	
OLLER	99C	PR D60 074023	J.A. Oller, E. Oset	
ALEKSEEV	98	PAN 61 174	I.G. Alekseev *et al.*	
ALEXANDER	98	PR D58 052004	J.P. Alexander *et al.*	(CLEO Collab.)
ANISOVICH	98B	SPU 41 419	V.V. Anisovich *et al.*	
		Translated from UFN 168 481.		
LOCHER	98	EPJ C4 317	M.P. Locher *et al.*	(PSI)
TROYAN	98	JINRRC 5-91 33	Yu. Troyan *et al.*	
ALDE	97	PL B397 350	D.M. Alde *et al.*	(GAMS Collab.)
DOBADO	97	PR D56 3057	A. Dobado, J.R. Pelaez	
ISHIDA	97	PTP 98 1005	S. Ishida *et al.*	(TOKY, MIYA, KEK)
KAMINSKI	97B	PL B413 130	R. Kaminski, L. Lesniak, B. Loiseau	(CRAC, IPN)
Also		PTP 95 745	S. Ishida *et al.*	(TOKY, MIYA, KEK)
SVEC	96	PR D53 2343	M. Svec	(MCGI)
TORNQVIST	96	PRL 76 1575	N.A. Tornqvist, M. Roos	(HELS)
ALDE	95B	ZPHY C66 375	D.M. Alde *et al.*	(GAMS Collab.)
ANISOVICH	95	PL B355 363	V.V. Anisovich *et al.*	(PNPI, SERP)
JANSSEN	95	PR D52 2690	G. Janssen *et al.*	(STON, ADLD, JULI)
ACHASOV	94	PR D49 5779	N.N. Achasov, G.N. Shestakov	(NOVM)
AMSLER	94D	PL B333 277	C. Amsler *et al.*	(Crystal Barrel Collab.)
ANISOVICH	94	PL B323 233	V.V. Anisovich *et al.*	(Crystal Barrel Collab.)
BUTLER	94B	PR D49 40	F. Butler *et al.*	(CLEO Collab.)
KAMINSKI	94	PR D50 3145	R. Kaminski, L. Lesniak, J.P. Maillet	(CRAC+)
ZOU	94B	PR D50 591	B.S. Zou, D.V. Bugg	(LOQM)
ZOU	93	PR D48 R3948	B.S. Zou, D.V. Bugg	(LOQM)
BEHREND	92	ZPHY C56 381	H.J. Behrend	(CELLO Collab.)
ARMSTRONG	91B	ZPHY C52 389	T.A. Armstrong *et al.*	(ATHU, BARI, BIRM+)
BOYER	90	PR D42 1350	J. Boyer *et al.*	(Mark II Collab.)
MARSISKE	90	PR D41 3324	H. Marsiske *et al.*	(Crystal Ball Collab.)
MORGAN	90	ZPHY C48 623	D. Morgan, M.R. Pennington	(RAL, DURH)
AUGUSTIN	89	NP B320 1	J.E. Augustin, G. Cosme	(DM2 Collab.)
ASTON	88	NP B296 493	D. Aston *et al.*	(SLAC, NAGO, CINC, INUS)
FALVARD	88	PR D38 2706	A. Falvard *et al.*	(CLER, FRAS, LALO+)
COURAU	86	NP B271 1	A. Courau *et al.*	(CLER, LALO)
VANBEVEREN	86	ZPHY C30 615	E. van Beveren *et al.*	(NIJM, BIEL)
CASON	83	PR D28 1586	N.M. Cason *et al.*	(NDAM, ANL)
ETKIN	82B	PR D25 1786	A. Etkin *et al.*	(BNL, CUNY, TUFTS, VAND)
BISWAS	81	PRL 47 1378	N.N. Biswas *et al.*	(NDAM, ANL)
COHEN	80	PR D22 2595	D. Cohen *et al.*	(ANL) IJP
MUKHIN	80	JETPL 32 601	K.N. Mukhin *et al.*	(KIAE)
		Translated from ZETFP 32 616.		
CORDEN	79	NP B157 250	M.J. Corden *et al.*	(BIRM, RHEL, TELA+) JP
ESTABROOKS	79	PR D19 2678	P. Estabrooks	(CARL)
FROGGATT	77	NP B129 89	C.D. Froggatt, J.L. Petersen	(GLAS, NORD)
PAWLICKI	77	PR D15 3196	A.J. Pawlicki *et al.*	(ANL) IJ
ROSSELET	77	PR D15 574	L. Rosselet *et al.*	(GEVA, SACL)
CASON	76	PRL 36 1485	N.M. Cason *et al.*	(NDAM, ANL) IJ
ESTABROOKS	75	NP B95 322	P.G. Estabrooks, A.D. Martin	(DURH)
HYAMS	75	NP B100 205	B.D. Hyams *et al.*	(CERN, MPIM)
SRINIVASAN	75	PR D12 681	V. Srinivasan *et al.*	(NDAM, ANL)
ESTABROOKS	74	NP B79 301	P.G. Estabrooks, A.D. Martin	(DURH)
GRAYER	74	NP B75 189	G. Grayer *et al.*	(CERN, MPIM)
APEL	73	PL 41B 542	W.D. Apel *et al.*	(KARL, PISA)
ESTABROOKS	73	Tallahassee	P.G. Estabrooks *et al.*	(CERN, MPIM)
HYAMS	73	NP B64 134	B.D. Hyams *et al.*	(CERN, MPIM)
OCHS	73	Thesis	W. Ochs	(MPIM, MUNI)
PROTOPOP...	73	PR D7 1279	S.D. Protopopescu *et al.*	(LBL)
BAILLON	72	PL 38B 555	P.H. Baillon *et al.*	(SLAC)
BASDEVANT	72	PL 41B 178	J.L. Basdevant, C.D. Froggatt, J.L. Petersen	(CERN)
BEIER	72B	PRL 29 511	E.W. Beier *et al.*	(PENN)
BENSINGER	71	PL 36B 134	J.R. Bensinger *et al.*	(WISC)
COLTON	71	PR D3 2028	E.P. Colton *et al.*	(LBL, FNAL, UCLA+)
ROY	71	PL 36B 353	S.M. Roy	
BATON	70	PL 33B 528	J.P. Baton, G. Laurens, J. Reignier	(SACL)
WALKER	67	RMP 39 695	W.D. Walker	(WISC)

$\rho(770)$

$I^G(J^{PC}) = 1^+(1^{--})$

THE $\rho(770)$

Updated May 2012 by S. Eidelman (Novosibirsk) and G. Venanzoni (Frascati).

The determination of the parameters of the $\rho(770)$ is beset with many difficulties because of its large width. In physical region fits, the line shape does not correspond to a relativistic Breit-Wigner function with a P-wave width, but requires some additional shape parameter. This dependence on parameterization was demonstrated long ago [1]. Bose-Einstein correlations are another source of shifts in the $\rho(770)$ line shape, particularly in multiparticle final state systems [2].

The same model-dependence afflicts any other source of resonance parameters, such as the energy-dependence of the phase shift δ_1^1, or the pole position. It is, therefore, not surprising that a study of $\rho(770)$ dominance in the decays of the η and η' reveals the need for specific dynamical effects, in addition to the $\rho(770)$ pole [3,4].

The cleanest determination of the $\rho(770)$ mass and width comes from e^+e^- annihilation and τ-lepton decays. Analysis of ALEPH [5] showed that the charged $\rho(770)$ parameters measured from τ-lepton decays are consistent with those of the

neutral one determined from e^+e^- data [6]. This conclusion is qualitatively supported by the later studies of CLEO [7] and Belle [8]. However, model-independent comparison of the two-pion mass spectrum in τ decays, and the $e^+e^- \to \pi^+\pi^-$ cross section, gave indications of discrepancies between the overall normalization: τ data are about 3% higher than e^+e^- data [7,9]. A detailed analysis using such two-pion mass spectra from τ decays measured by OPAL [10], CLEO [7], and ALEPH [11,12], as well as recent pion form factor measurements in e^+e^- annihilation by CMD-2 [13,14], showed that the discrepancy can be as high as 10% above the ρ meson [15,16]. This discrepancy remains after recent measurements of the two-pion cross section in e^+e^- annihilation at KLOE [17,18] and SND [19,20]. This effect is not accounted for by isospin breaking [21–24], but the accuracy of its calculation may be overestimated [25,26].

This problem seems to be solved after a recent analysis in [27] which showed that after correcting the τ data for the missing ρ - γ mixing contribution, besides the other known isospin symmetry violating corrections, the $\pi\pi$ I=1 part of the hadronic vacuum polarization contribution to the muon g - 2 is fully compatible between τ based and e^+e^- based evaluations including more recent BaBar [28] and KLOE [29] data. Further proof of the consistency of the data on τ decays to two pions and e^+e^- annihilation is given by the global fit of the whole set of the ρ, ω, and ϕ decays, taking into account mixing effects in the hidden local symmetry model [30].

References

1. J. Pisut and M. Roos, Nucl. Phys. **B6**, 325 (1968).
2. G.D. Lafferty, Z. Phys. **C60**, 659 (1993).
3. A. Abele *et al.*, Phys. Lett. **B402**, 195 (1997).
4. M. Benayoun *et al.*, Eur. Phys. J. **C31**, 525 (2003).
5. R. Barate *et al.*, Z. Phys. **C76**, 15 (1997).
6. L.M. Barkov *et al.*, Nucl. Phys. **B256**, 365 (1985).
7. S. Anderson *et al.*, Phys. Rev. **D61**, 112002 (2000).
8. M. Fujikawa *et al.*, Phys. Rev. **D78**, 072006 (2008).
9. S. Eidelman and V. Ivanchenko, Nucl. Phys. (Proc. Supp.) **B76**, 319 (1999).
10. K. Ackerstaff *et al.*, Eur. Phys. J. **C7**, 571 (1999).
11. M. Davier *et al.*, Nucl. Phys. (Proc. Supp.) **B123**, 47 (2003).
12. S. Schael *et al.*, Phys. Reports **421**, 191 (2005).
13. R.R. Akhmetshin *et al.*, Phys. Lett. **B527**, 161 (2002).
14. R.R. Akhmetshin *et al.*, Phys. Lett. **B578**, 285 (2004).
15. M. Davier *et al.*, Eur. Phys. J. **C27**, 497 (2003).
16. M. Davier *et al.*, Eur. Phys. J. **C31**, 503 (2003).
17. A. Aloisio *et al.*, Phys. Lett. **B606**, 12 (2005).
18. F. Ambrosino *et al.*, Phys. Lett. **B670**, 285 (2009).
19. M.N. Achasov *et al.*, Sov. Phys. JETP **101**, 1053 (2005).
20. M.N. Achasov *et al.*, Sov. Phys. JETP **103**, 380 (2006).
21. R. Alemany *et al.*, Eur. Phys. J. **C2**, 123 (1998).
22. H. Czyz and J.J. Kuhn, Eur. Phys. J. **C18**, 497 (2001).
23. V. Cirigliano *et al.*, Phys. Lett. **B513**, 361 (2001).
24. V. Cirigliano *et al.*, Eur. Phys. J. **C23**, 121 (2002).
25. K. Maltman and C.E. Wolfe, Phys. Rev. **D73**, 013004 (2006).
26. C.E. Wolfe and K. Maltman, Phys. Rev. **D80**, 114024 (2009).
27. F. Jegerlehner and R. Szafron, Eur. Phys. J. **C71**, 1632 (2011).
28. B. Aubert *et al.*, Phys. Rev. Lett. **103**, 231801 (2009).
29. F. Ambrosino *et al.*, Phys. Lett. **B700**, 102 (2011).
30. M. Benayoun *et al.*, Eur. Phys. J. **C72**, 1848 (2012).

$\rho(770)$ MASS

We no longer list *S*-wave Breit-Wigner fits, or data with high combinatorial background.

NEUTRAL ONLY, e^+e^-

VALUE (MeV)	EVTS	DOCUMENT ID		TECN	COMMENT
775.26±0.25 OUR AVERAGE					
775.02±0.35		[1] LEES	12G	BABR	$e^+e^- \to \pi^+\pi^-\gamma$
775.97±0.46±0.70	900k	[2] AKHMETSHIN	07		$e^+e^- \to \pi^+\pi^-$
774.6 ±0.4 ±0.5	800k	[3,4] ACHASOV	06	SND	$e^+e^- \to \pi^+\pi^-$
775.65±0.64±0.50	114k	[5,6] AKHMETSHIN	04	CMD2	$e^+e^- \to \pi^+\pi^-$
775.9 ±0.5 ±0.5	1.98M	[7] ALOISIO	03	KLOE	1.02 $e^+e^- \to \pi^+\pi^-\pi^0$
775.8 ±0.9 ±2.0	500k	[7] ACHASOV	02	SND	1.02 $e^+e^- \to \pi^+\pi^-\pi^0$
775.9 ±1.1		[8] BARKOV	85	OLYA	$e^+e^- \to \pi^+\pi^-$
• • • We do not use the following data for averages, fits, limits, etc. • • •					
775.8 ±0.5 ±0.3	1.98M	[9] ALOISIO	03	KLOE	1.02 $e^+e^- \to \pi^+\pi^-\pi^0$
775.9 ±0.6 ±0.5	1.98M	[10] ALOISIO	03	KLOE	1.02 $e^+e^- \to \pi^+\pi^-\pi^0$
775.0 ±0.6 ±1.1	500k	[11] ACHASOV	02	SND	1.02 $e^+e^- \to \pi^+\pi^-\pi^0$
775.1 ±0.7 ±5.3		[12] BENAYOUN	98	RVUE	$e^+e^- \to \pi^+\pi^-$, $\mu^+\mu^-$
770.5 ±1.9 ±5.1		[13] GARDNER	98	RVUE	0.28–0.92 $e^+e^- \to \pi^+\pi^-$
764.1 ±0.7		[14] O'CONNELL	97	RVUE	$e^+e^- \to \pi^+\pi^-$
757.5 ±1.5		[15] BERNICHA	94	RVUE	$e^+e^- \to \pi^+\pi^-$
768 ±1		[16] GESHKEN...	89	RVUE	$e^+e^- \to \pi^+\pi^-$

CHARGED ONLY, τ DECAYS and e^+e^-

VALUE (MeV)	EVTS	DOCUMENT ID		TECN	CHG	COMMENT
775.11±0.34 OUR AVERAGE						
774.6 ±0.2 ±0.5	5.4M	[17,18] FUJIKAWA	08	BELL	±	$\tau^- \to \pi^-\pi^0\nu_\tau$
775.5 ±0.7		[18,19] SCHAEL	05C	ALEP		$\tau^- \to \pi^-\pi^0\nu_\tau$
775.5 ±0.5 ±0.4	1.98M	[7] ALOISIO	03	KLOE		1.02 $e^+e^- \to \pi^+\pi^-\pi^0$
775.1 ±1.1 ±0.5	87k	[20,21] ANDERSON	00A	CLE2		$\tau^- \to \pi^-\pi^0\nu_\tau$
• • • We do not use the following data for averages, fits, limits, etc. • • •						
774.8 ±0.6 ±0.4	1.98M	[10] ALOISIO	03	KLOE	−	1.02 $e^+e^- \to \pi^+\pi^-\pi^0$
776.3 ±0.6 ±0.7	1.98M	[10] ALOISIO	03	KLOE	+	1.02 $e^+e^- \to \pi^+\pi^-\pi^0$
773.9 ±2.0 $^{+0.3}_{-1.0}$		[22] SANZ-CILLERO	03	RVUE		$\tau^- \to \pi^-\pi^0\nu_\tau$
774.5 ±0.7 ±1.5	500k	[7] ACHASOV	02	SND	±	1.02 $e^+e^- \to \pi^+\pi^-\pi^0$
775.1 ±0.5		[23] PICH	01	RVUE		$\tau^- \to \pi^-\pi^0\nu_\tau$

MIXED CHARGES, OTHER REACTIONS

VALUE (MeV)	EVTS	DOCUMENT ID		TECN	CHG	COMMENT
763.0±0.3±1.2	600k	[24] ABELE	99E	CBAR	0±	0.0 $\overline{p}p \to \pi^+\pi^-\pi^0$

CHARGED ONLY, HADROPRODUCED

VALUE (MeV)	EVTS	DOCUMENT ID		TECN	CHG	COMMENT
766.5±1.1 OUR AVERAGE						
763.7±3.2		ABELE	97	CBAR		$\overline{p}n \to \pi^-\pi^0\pi^0$
768 ±9		AGUILAR-...	91	EHS		400 pp
767 ±3	2935	[25] CAPRARO	87	SPEC	−	200 π^-Cu $\to \pi^-\pi^0$Cu
761 ±5	967	[25] CAPRARO	87	SPEC	−	200 π^-Pb $\to \pi^-\pi^0$Pb
771 ±4		HUSTON	86	SPEC	+	202 π^+A $\to \pi^+\pi^0$A
766 ±7	6500	[26] BYERLY	73	OSPK	−	5 π^-p
766.8±1.5	9650	[27] PISUT	68	RVUE	−	1.7–3.2 π^-p, t <10
767 ±6	900	[25] EISNER	67	HBC	−	4.2 π^-p, t <10

NEUTRAL ONLY, PHOTOPRODUCED

VALUE (MeV)	EVTS	DOCUMENT ID		TECN	COMMENT
769.0± 1.0 OUR AVERAGE					
771 ± 2 $^{+2}_{-1}$	63.5k	[28] ABRAMOWICZ12		ZEUS	$ep \to e\pi^+\pi^- p$
770 ± 2 ±1	79k	[29] BREITWEG	98B	ZEUS	50–100 γp
767.6± 2.7		BARTALUCCI	78	CNTR	$\gamma p \to e^+ e^- p$
775 ± 5		GLADDING	73	CNTR	2.9–4.7 γp
767 ± 4	1930	BALLAM	72	HBC	2.8 γp
770 ± 4	2430	BALLAM	72	HBC	4.7 γp
765 ±10		ALVENSLEB...	70	CNTR	γA, t <0.01
767.7± 1.9	140k	BIGGS	70	CNTR	<4.1 γC $\to \pi^+\pi^-$ C
765 ± 5	4000	ASBURY	67B	CNTR	γ + Pb
• • • We do not use the following data for averages, fits, limits, etc. • • •					
771 ± 2	79k	[30] BREITWEG	98B	ZEUS	50–100 γp

NEUTRAL ONLY, OTHER REACTIONS

VALUE (MeV)	EVTS	DOCUMENT ID		TECN	CHG	COMMENT
769.0±0.9 OUR AVERAGE		Error includes scale factor of 1.4. See the ideogram below.				
765 ±6		BERTIN	97C	OBLX		0.0 $\overline{p}p \to \pi^+\pi^-\pi^0$
773 ±1.6		WEIDENAUER	93	ASTE		$\overline{p}p \to \pi^+\pi^-\omega$
762.6±2.6		AGUILAR-...	91	EHS		400 pp
770 ±2		[31] HEYN	81	RVUE		Pion form factor
768 ±4		[32,33] BOHACIK	80	RVUE	0	
769 ±3		[26] WICKLUND	78	ASPK	0	3,4,6 $\pi^\pm N$
768 ±1	76000	DEUTSCH...	76	HBC	0	16 $\pi^+ p$
767 ±4	4100	ENGLER	74	DBC	0	6 $\pi^+ n \to \pi^+\pi^- p$
775 ±4	32000	[32] PROTOPOP...	73	HBC	0	7.1 $\pi^+ p$, t <0.4
764 ±3	6800	RATCLIFF	72	ASPK	0	15 $\pi^- p$, t <0.3
774 ±3	1700	REYNOLDS	69	HBC	0	2.26 $\pi^- p$
769.2±1.5	13300	[34] PISUT	68	RVUE	0	1.7–3.2 $\pi^- p$, t <10
• • • We do not use the following data for averages, fits, limits, etc. • • •						
773.5 ±2.5		[35] COLANGELO	01	RVUE		$\pi\pi \to \pi\pi$
762.3±0.5±1.2	600k	[36] ABELE	99E	CBAR	0	0.0 $\overline{p}p \to \pi^+\pi^-\pi^0$
777 ±2	4943	[37] ADAMS	97	E665		470 $\mu p \to \mu XB$
770 ±2		[38] BOGOLYUB...	97	MIRA		32 $\overline{p}p \to \pi^+\pi^-$X
768 ±8		[38] BOGOLYUB...	97	MIRA		32 $pp \to \pi^+\pi^-$X
761.1±2.9		DUBNICKA	89	RVUE		π form factor
777.4±2.0		[39] CHABAUD	83	ASPK	0	17 $\pi^- p$ polarized
769.5±0.7		[32,33] LANG	79	RVUE	0	
770 ±9		[33] ESTABROOKS	74	RVUE	0	17 $\pi^- p \to \pi^+\pi^- n$
773.5±1.7	11200	[25] JACOBS	72	HBC	0	2.8 $\pi^- p$
775 ±3	2250	HYAMS	68	OSPK	0	11.2 $\pi^- p$

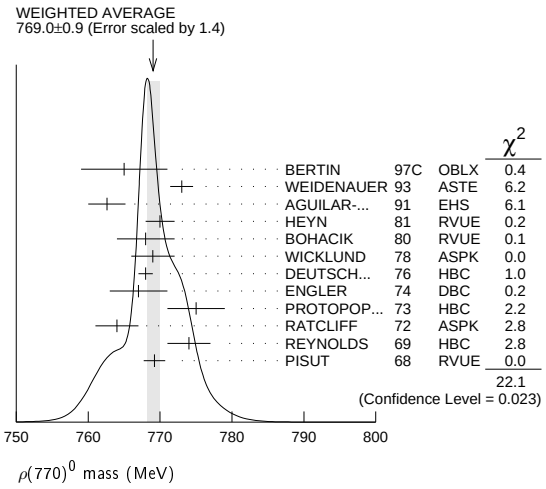

[1] Using the GOUNARIS 68 parametrization with the complex phase of the ρ–ω interference and leaving the masses and widths of the $\rho(1450)$, $\rho(1700)$, and $\rho(2150)$ resonances as free parameters of the fit.
[2] A combined fit of AKHMETSHIN 07, AULCHENKO 06, and AULCHENKO 05.
[3] Supersedes ACHASOV 05A.
[4] A fit of the SND data from 400 to 1000 MeV using parameters of the $\rho(1450)$ and $\rho(1700)$ from a fit of the data of BARKOV 85, BISELLO 89 and ANDERSON 00A.
[5] Using the GOUNARIS 68 parametrization with the complex phase of the ρ–ω interference.
[6] Update of AKHMETSHIN 02.
[7] Assuming $m_{\rho^+} = m_{\rho^-}$, $\Gamma_{\rho^+} = \Gamma_{\rho^-}$.
[8] From the GOUNARIS 68 parametrization of the pion form factor.
[9] Assuming $m_{\rho^+} = m_{\rho^-} = m_{\rho^0}$, $\Gamma_{\rho^+} = \Gamma_{\rho^-} = \Gamma_{\rho^0}$.
[10] Without limitations on masses and widths.
[11] Assuming $m_{\rho^0} = m_{\rho^\pm}$, $g_{\rho^0\pi\pi} = g_{\rho^\pm\pi\pi}$.
[12] Using the data of BARKOV 85 in the hidden local symmetry model.
[13] From the fit to $e^+e^- \to \pi^+\pi^-$ data from the compilations of HEYN 81 and BARKOV 85, including the GOUNARIS 68 parametrization of the pion form factor.
[14] A fit of BARKOV 85 data assuming the direct $\omega\pi\pi$ coupling.
[15] Applying the S-matrix formalism to the BARKOV 85 data.
[16] Includes BARKOV 85 data. Model-dependent width definition.
[17] $|F_\pi(0)|^2$ fixed to 1.
[18] From the GOUNARIS 68 parametrization of the pion form factor.
[19] The error combines statistical and systematic uncertainties. Supersedes BARATE 97M.
[20] $\rho(1700)$ mass and width fixed at 1700 MeV and 235 MeV respectively.
[21] From the GOUNARIS 68 parametrization of the pion form factor. The second error is a model error taking into account different parametrizations of the pion form factor.
[22] Using the data of BARATE 97M and the effective chiral Lagrangian.
[23] From a fit of the model-independent parameterization of the pion form factor to the data of BARATE 97M.
[24] Assuming the equality of ρ^+ and ρ^- masses and widths.
[25] Mass errors enlarged by us to $\Gamma/\sqrt{N}$; see the note with the $K^*(892)$ mass.
[26] Phase shift analysis. Systematic errors added corresponding to spread of different fits.
[27] From fit of 3-parameter relativistic P-wave Breit-Wigner to total mass distribution. Includes BATON 68, MILLER 67B, ALFF-STEINBERGER 66, HAGOPIAN 66, HAGOPIAN 66B, JACOBS 66B, JAMES 66, WEST 66, BLIEDEN 65 and CARMONY 64.
[28] Using the KUHN 90 parametrization of the pion form factor, neglecting ρ–ω interference.
[29] From the parametrization according to SOEDING 66.
[30] From the parametrization according to ROSS 66.
[31] HEYN 81 includes all spacelike and timelike F_π values until 1978.
[32] From pole extrapolation.
[33] From phase shift analysis of GRAYER 74 data.
[34] Includes MALAMUD 69, ARMENISE 68, BACON 67, HUWE 67, MILLER 67B, ALFF-STEINBERGER 66, HAGOPIAN 66, HAGOPIAN 66B, JACOBS 66B, JAMES 66, WEST 66, GOLDHABER 64, ABOLINS 63.
[35] Breit-Wigner mass from a phase-shift analysis of HYAMS 73 and PROTOPOPESCU 73 data.
[36] Using relativistic Breit-Wigner and taking into account ρ–ω interference.
[37] Systematic errors not evaluated.
[38] Systematic effects not studied.
[39] From fit of 3-parameter relativistic Breit-Wigner to helicity-zero part of P-wave intensity. CHABAUD 83 includes data of GRAYER 74.

$m_{\rho(770)^0} - m_{\rho(770)^\pm}$

VALUE (MeV)	EVTS	DOCUMENT ID		TECN	CHG	COMMENT
−0.7±0.8 OUR AVERAGE		Error includes scale factor of 1.5. See the ideogram below.				
−2.4±0.8		[40] SCHAEL	05C	ALEP		$\tau^- \to \pi^-\pi^0\nu_\tau$
0.4±0.7±0.6	1.98M	[41] ALOISIO	03	KLOE		1.02 $e^+e^- \to \pi^+\pi^-\pi^0$
1.3±1.1±2.0	500k	[41] ACHASOV	02	SND		1.02 $e^+e^- \to \pi^+\pi^-\pi^0$
1.6±0.6±1.7	600k	ABELE	99E	CBAR	0±	0.0 $\overline{p}p \to \pi^+\pi^-\pi^0$
−4 ±4	3000	[42] REYNOLDS	69	HBC	−0	2.26 $\pi^- p$
−5 ±5	3600	[42] FOSTER	68	HBC	±0	0.0 $\overline{p}p$
2.4±2.1	22950	[43] PISUT	68	RVUE		$\pi N \to \rho N$

[40] From the combined fit of the τ^- data from ANDERSON 00A and SCHAEL 05C and e^+e^- data from the compilation of BARKOV 85, AKHMETSHIN 04, and ALOISIO 05. Supersedes BARATE 97M.
[41] Assuming $m_{\rho^+} = m_{\rho^-}$, $\Gamma_{\rho^+} = \Gamma_{\rho^-}$.
[42] From quoted masses of charged and neutral modes.
[43] Includes MALAMUD 69, ARMENISE 68, BATON 68, BACON 67, HUWE 67, MILLER 67B, ALFF-STEINBERGER 66, HAGOPIAN 66, HAGOPIAN 66B, JACOBS 66B, JAMES 66, WEST 66, BLIEDEN 65, CARMONY 64, GOLDHABER 64, ABOLINS 63.

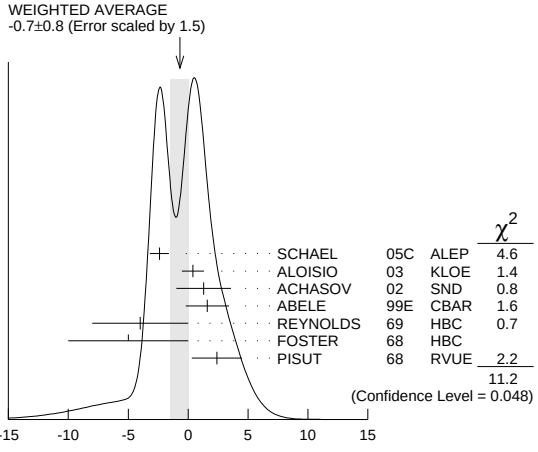

$m_{\rho(770)^+} - m_{\rho(770)^-}$

VALUE (MeV)	EVTS	DOCUMENT ID		TECN	COMMENT
• • • We do not use the following data for averages, fits, limits, etc. • • •					
1.5±0.8±0.7	1.98M	[44] ALOISIO	03	KLOE	1.02 $e^+e^- \to \pi^+\pi^-\pi^0$

[44] Without limitations on masses and widths.

Meson Particle Listings

$\rho(770)$

$\rho(770)$ RANGE PARAMETER

The range parameter R enters an energy-dependent correction to the width, of the form $(1 + q_r^2\ R^2)\ /\ (1 + q^2\ R^2)$, where q is the momentum of one of the pions in the $\pi\pi$ rest system. At resonance, $q = q_r$.

VALUE (GeV^{-1})	DOCUMENT ID		TECN	CHG	COMMENT
$5.3^{+0.9}_{-0.7}$	CHABAUD	83	ASPK	0	17 $\pi^- p$ polarized

$\rho(770)$ WIDTH

We no longer list S-wave Breit-Wigner fits, or data with high combinatorial background.

NEUTRAL ONLY, e^+e^-

VALUE (MeV)	EVTS	DOCUMENT ID		TECN	CHG	COMMENT
147.8 ±0.9 OUR AVERAGE		Error includes scale factor of 2.0. See the ideogram below.				
149.59±0.67		[45] LEES	12G	BABR		$e^+e^- \to \pi^+\pi^-\gamma$
145.98±0.75±0.50	900k	[46] AKHMETSHIN	07			$e^+e^- \to \pi^+\pi^-$
146.1 ±0.8 ±1.5	800k	[47,48] ACHASOV	06	SND		$e^+e^- \to \pi^+\pi^-$
143.85±1.33±0.80	114k	[49,50] AKHMETSHIN	04	CMD2		$e^+e^- \to \pi^+\pi^-$
147.3 ±1.5 ±0.7	1.98M	[51] ALOISIO	03	KLOE		1.02 $e^+e^- \to \pi^+\pi^-\pi^0$
151.1 ±2.6 ±3.0	500k	[51] ACHASOV	02	SND	0	1.02 $e^+e^- \to \pi^+\pi^-\pi^0$
150.5 ±3.0		[52] BARKOV	85	OLYA	0	$e^+e^- \to \pi^+\pi^-$
• • • We do not use the following data for averages, fits, limits, etc. • • •						
143.9 ±1.3 ±1.1	1.98M	[53] ALOISIO	03	KLOE		1.02 $e^+e^- \to \pi^+\pi^-\pi^0$
147.4 ±1.5 ±0.7	1.98M	[54] ALOISIO	03	KLOE		1.02 $e^+e^- \to \pi^+\pi^-\pi^0$
149.8 ±2.2 ±2.0	500k	[55] ACHASOV	02	SND		1.02 $e^+e^- \to \pi^+\pi^-\pi^0$
147.9 ±1.5 ±7.5		[56] BENAYOUN	98	RVUE		$e^+e^- \to \pi^+\pi^-$, $\mu^+\mu^-$
153.5 ±1.3 ±4.6		[57] GARDNER	98	RVUE		0.28–0.92 $e^+e^- \to \pi^+\pi^-$
145.0 ±1.7		[58] O'CONNELL	97	RVUE		$e^+e^- \to \pi^+\pi^-$
142.5 ±3.5		[59] BERNICHA	94	RVUE		$e^+e^- \to \pi^+\pi^-$
138 ±1		[60] GESHKEN...	89	RVUE		$e^+e^- \to \pi^+\pi^-$

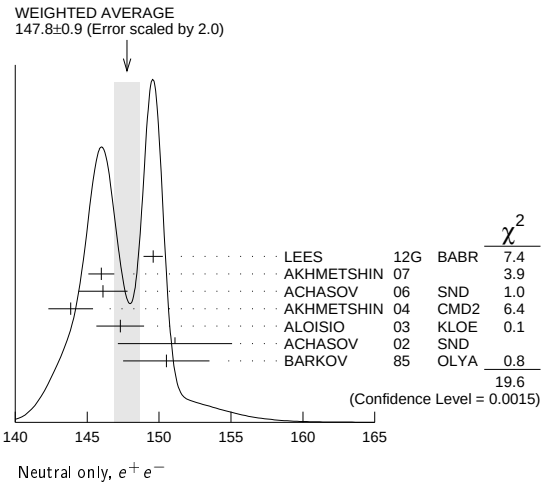

Neutral only, e^+e^-

CHARGED ONLY, τ DECAYS and e^+e^-

VALUE (MeV)	EVTS	DOCUMENT ID		TECN	CHG	COMMENT
149.1±0.8 OUR FIT						
149.1±0.8 OUR AVERAGE						
148.1±0.4±1.7	5.4M	[61,62] FUJIKAWA	08	BELL	±	$\tau^- \to \pi^-\pi^0\nu_\tau$
149.0±1.2		[62,63] SCHAEL	05C	ALEP		$\tau^- \to \pi^-\pi^0\nu_\tau$
149.9±2.3±2.0	500k	[51] ACHASOV	02	SND	±	1.02 $e^+e^- \to \pi^+\pi^-\pi^0$
150.4±1.4±1.4	87k	[64,65] ANDERSON	00A	CLE2		$\tau^- \to \pi^-\pi^0\nu_\tau$
• • • We do not use the following data for averages, fits, limits, etc. • • •						
143.7±1.3±1.2	1.98M	[51] ALOISIO	03	KLOE	±	1.02 $e^+e^- \to \pi^+\pi^-\pi^0$
142.9±1.3±1.4	1.98M	[54] ALOISIO	03	KLOE	−	1.02 $e^+e^- \to \pi^+\pi^-\pi^0$
144.7±1.4±1.2	1.98M	[54] ALOISIO	03	KLOE	+	1.02 $e^+e^- \to \pi^+\pi^-\pi^0$
$150.2\pm2.0^{+0.7}_{-1.6}$		[66] SANZ-CILLERO	03	RVUE		$\tau^- \to \pi^-\pi^0\nu_\tau$
150.9±2.2±2.0	500k	[55] ACHASOV	02	SND		1.02 $e^+e^- \to \pi^+\pi^-\pi^0$

MIXED CHARGES, OTHER REACTIONS

VALUE (MeV)	EVTS	DOCUMENT ID		TECN	CHG	COMMENT
149.5±1.3	600k	[67] ABELE	99E	CBAR	0±	0.0 $\overline{p}p \to \pi^+\pi^-\pi^0$

CHARGED ONLY, HADROPRODUCED

VALUE (MeV)	EVTS	DOCUMENT ID		TECN	CHG	COMMENT
150.2± 2.4 OUR FIT						
150.2± 2.4 OUR AVERAGE						
152.8± 4.3		ABELE	97	CBAR		$\overline{p}n \to \pi^-\pi^0\pi^0$
155 ±11	2935	[68] CAPRARO	87	SPEC	−	200 π^- Cu → $\pi^-\pi^0$ Cu
154 ±20	967	[68] CAPRARO	87	SPEC	−	200 π^- Pb → $\pi^-\pi^0$ Pb
150 ± 5		HUSTON	86	SPEC	+	202 π^+ A → $\pi^+\pi^0$ A
146 ±12	6500	[69] BYERLY	73	OSPK	−	5 $\pi^- p$
148.2± 4.1	9650	[70] PISUT	68	RVUE	−	1.7–3.2 $\pi^- p$, t <10
146 ±13	900	EISNER	67	HBC	−	4.2 $\pi^- p$, t <10

NEUTRAL ONLY, PHOTOPRODUCED

VALUE (MeV)	EVTS	DOCUMENT ID		TECN	COMMENT
151.7± 2.6 OUR AVERAGE					
155 ± 5 ± 2	63.5k	[71] ABRAMOWICZ	12	ZEUS	$ep \to e\pi^+\pi^- p$
146 ± 3 ±13	79k	[72] BREITWEG	98B	ZEUS	50–100 γp
150.9± 3.0		BARTALUCCI	78	CNTR	$\gamma p \to e^+e^- p$
• • • We do not use the following data for averages, fits, limits, etc. • • •					
138 ± 3	79k	[73] BREITWEG	98B	ZEUS	50–100 γp
147 ±11		GLADDING	73	CNTR	2.9–4.7 γp
155 ±12	2430	BALLAM	72	HBC	4.7 γp
145 ±13	1930	BALLAM	72	HBC	2.8 γp
140 ± 5		ALVENSLEB...	70	CNTR	γA, t <0.01
146.1± 2.9	140k	BIGGS	70	CNTR	<4.1 γC → $\pi^+\pi^-$ C
160 ±10		LANZEROTTI	68	CNTR	γp
130 ± 5	4000	ASBURY	67B	CNTR	γ + Pb

NEUTRAL ONLY, OTHER REACTIONS

VALUE (MeV)	EVTS	DOCUMENT ID		TECN	CHG	COMMENT
150.9± 1.7 OUR AVERAGE		Error includes scale factor of 1.1.				
122 ±20		BERTIN	97C	OBLX		0.0 $\overline{p}p \to \pi^+\pi^-\pi^0$
145.7± 5.3		WEIDENAUER	93	ASTE		$\overline{p}p \to \pi^+\pi^-\omega$
144.9± 3.7		DUBNICKA	89	RVUE		π form factor
148 ± 6		[74,75] BOHACIK	80	RVUE	0	
152 ± 9		[69] WICKLUND	78	ASPK	0	3,4,6 $\pi^\pm p$ N
154 ± 2	76000	DEUTSCH...	76	HBC	0	16 $\pi^+ p$
157 ± 8	6800	RATCLIFF	72	ASPK	0	15 $\pi^- p$, t <0.3
143 ± 8	1700	REYNOLDS	69	HBC	0	2.26 $\pi^- p$
• • • We do not use the following data for averages, fits, limits, etc. • • •						
147.0± 2.5	600k	[76] ABELE	99E	CBAR	0	0.0 $\overline{p}p \to \pi^+\pi^-\pi^0$
146 ± 3	4943	[77] ADAMS	97	E665		470 $\mu p \to \mu XB$
$160.0^{+4.1}_{-4.0}$		[78] CHABAUD	83	ASPK	0	17 $\pi^- p$ polarized
155 ± 1		[79] HEYN	81	RVUE	0	π form factor
148.0± 1.3		[74,75] LANG	79	RVUE	0	
146 ±14	4100	ENGLER	74	DBC	0	6 $\pi^+ n \to \pi^+\pi^- p$
143 ±13		[75] ESTABROOKS	74	RVUE	0	17 $\pi^- p \to \pi^+\pi^- n$
160 ±10	32000	[74] PROTOPOP...	73	HBC	0	7.1 $\pi^+ p$, t <0.4
145 ±12	2250	[68] HYAMS	68	OSPK	0	11.2 $\pi^- p$
163 ±15	13300	[80] PISUT	68	RVUE	0	1.7–3.2 $\pi^- p$, t <10

[45] Using the GOUNARIS 68 parametrization with the complex phase of the ρ–ω interference and leaving the masses and widths of the $\rho(1450)$, $\rho(1700)$, and $\rho(2150)$ resonances as free parameters of the fit.
[46] A combined fit of AKHMETSHIN 07, AULCHENKO 06, and AULCHENKO 05.
[47] Supersedes ACHASOV 05A.
[48] A fit of the SND data from 400 to 1000 MeV using parameters of the $\rho(1450)$ and $\rho(1700)$ from a fit of the data of BARKOV 85, BISELLO 89 and ANDERSON 00A.
[49] Using the GOUNARIS 68 parametrization with the complex phase of the ρ–ω interference.
[50] From a fit in the energy range 0.61 to 0.96 GeV. Update of AKHMETSHIN 02.
[51] Assuming $m_{\rho^+} = m_{\rho^-}$, $\Gamma_{\rho^+} = \Gamma_{\rho^-}$.
[52] From the GOUNARIS 68 parametrization of the pion form factor.
[53] Assuming $m_{\rho^+} = m_{\rho^-} = m_{\rho^0}$, $\Gamma_{\rho^+} = \Gamma_{\rho^-} = \Gamma_{\rho^0}$.
[54] Without limitations on masses and widths.
[55] Assuming $m_{\rho^0} = m_{\rho^\pm}$, $g_{\rho^0\pi\pi} = g_{\rho^\pm\pi\pi}$.
[56] Using the data of BARKOV 85 in the hidden local symmetry model.
[57] From the fit to $e^+e^- \to \pi^+\pi^-$ data from the compilations of HEYN 81 and BARKOV 85, including the GOUNARIS 68 parametrization of the pion form factor.
[58] A fit of BARKOV 85 data assuming the direct $\omega\pi\pi$ coupling.
[59] Applying the S-matrix formalism to the BARKOV 85 data.
[60] Includes BARKOV 85 data. Model-dependent width definition.
[61] $|F_\pi(0)|^2$ fixed to 1.
[62] From the GOUNARIS 68 parametrization of the pion form factor.
[63] The error combines statistical and systematic uncertainties. Supersedes BARATE 97M.
[64] $\rho(1700)$ mass and width fixed at 1700 MeV and 235 MeV respectively.
[65] From the GOUNARIS 68 parametrization of the pion form factor. The second error is a model error taking into account different parametrizations of the pion form factor.
[66] Using the data of BARATE 97M and the effective chiral Lagrangian.
[67] Assuming the equality of ρ^+ and ρ^- masses and widths.
[68] Width errors enlarged by us to $4\Gamma/\sqrt{N}$; see the note with the $K^*(892)$ mass.
[69] Phase shift analysis. Systematic errors added corresponding to spread of different fits.
[70] From fit of 3-parameter relativistic P-wave Breit-Wigner to total mass distribution. Includes BATON 68, MILLER 67B, ALFF-STEINBERGER 66, HAGOPIAN 66B, JACOBS 66B, JAMES 66, WEST 66, BLIEDEN 65 and CARMONY 64.
[71] Using the KUHN 90 parametrization of the pion form factor, neglecting ρ–ω interference.

[72] From the parametrization according to SOEDING 66.
[73] From the parametrization according to ROSS 66.
[74] From pole extrapolation.
[75] From phase shift analysis of GRAYER 74 data.
[76] Using relativistic Breit-Wigner and taking into account ρ-ω interference.
[77] Systematic errors not evaluated.
[78] From fit of 3-parameter relativistic Breit-Wigner to helicity-zero part of P-wave intensity. CHABAUD 83 includes data of GRAYER 74.
[79] HEYN 81 includes all spacelike and timelike F_π values until 1978.
[80] Includes MALAMUD 69, ARMENISE 68, BACON 67, HUWE 67, MILLER 67B, ALFF-STEINBERGER 66, HAGOPIAN 66, HAGOPIAN 66B, JACOBS 66B, JAMES 66, WEST 66, GOLDHABER 64, ABOLINS 63.

$\Gamma_{\rho(770)^0} - \Gamma_{\rho(770)^\pm}$

VALUE	EVTS	DOCUMENT ID		TECN	COMMENT
0.3±1.3 OUR AVERAGE		Error includes scale factor of 1.4.			
−0.2±1.0		[81] SCHAEL	05C	ALEP	$\tau^- \to \pi^-\pi^0\nu_\tau$
3.6±1.8±1.7	1.98M	[82] ALOISIO	03	KLOE	1.02 $e^+e^- \to \pi^+\pi^-\pi^0$

$\Gamma_{\rho(770)^+} - \Gamma_{\rho(770)^-}$

VALUE	EVTS	DOCUMENT ID		TECN	COMMENT
1.8±2.0±0.5	1.98M	[83] ALOISIO	03	KLOE	1.02 $e^+e^- \to \pi^+\pi^-\pi^0$

[81] From the combined fit of the τ^- data from ANDERSON 00A and SCHAEL 05C and e^+e^- data from the compilation of BARKOV 85, AKHMETSHIN 04, and ALOISIO 05. Supersedes BARATE 97M.
[82] Assuming $m_{\rho^+} = m_{\rho^-}$, $\Gamma_{\rho^+} = \Gamma_{\rho^-}$.
[83] Without limitations on masses and widths.

$\rho(770)$ DECAY MODES

	Mode	Fraction (Γ_i/Γ)	Scale factor/ Confidence level
Γ_1	$\pi\pi$	∼ 100 %	
	$\rho(770)^\pm$ decays		
Γ_2	$\pi^\pm\pi^0$	∼ 100 %	
Γ_3	$\pi^\pm\gamma$	(4.5 ±0.5) × 10^{-4}	S=2.2
Γ_4	$\pi^\pm\eta$	< 6 × 10^{-3}	CL=84%
Γ_5	$\pi^\pm\pi^+\pi^-\pi^0$	< 2.0 × 10^{-3}	CL=84%
	$\rho(770)^0$ decays		
Γ_6	$\pi^+\pi^-$	∼ 100 %	
Γ_7	$\pi^+\pi^-\gamma$	(9.9 ±1.6) × 10^{-3}	
Γ_8	$\pi^0\gamma$	(6.0 ±0.8) × 10^{-4}	
Γ_9	$\eta\gamma$	(3.00±0.20) × 10^{-4}	
Γ_{10}	$\pi^0\pi^0\gamma$	(4.5 ±0.8) × 10^{-5}	
Γ_{11}	$\mu^+\mu^-$	[a] (4.55±0.28) × 10^{-5}	
Γ_{12}	e^+e^-	[a] (4.72±0.05) × 10^{-5}	
Γ_{13}	$\pi^+\pi^-\pi^0$	($1.01^{+0.54}_{-0.36}$ ±0.34) × 10^{-4}	
Γ_{14}	$\pi^+\pi^-\pi^+\pi^-$	(1.8 ±0.9) × 10^{-5}	
Γ_{15}	$\pi^+\pi^-\pi^0\pi^0$	(1.6 ±0.8) × 10^{-5}	
Γ_{16}	$\pi^0 e^+e^-$	< 1.2 × 10^{-5}	CL=90%
Γ_{17}	ηe^+e^-		

[a] The $\omega\rho$ interference is then due to $\omega\rho$ mixing only, and is expected to be small. If $e\mu$ universality holds, $\Gamma(\rho^0 \to \mu^+\mu^-) = \Gamma(\rho^0 \to e^+e^-) \times 0.99785$.

CONSTRAINED FIT INFORMATION

An overall fit to the total width and a partial width uses 10 measurements and one constraint to determine 3 parameters. The overall fit has a $\chi^2 = 10.7$ for 8 degrees of freedom.

The following *off-diagonal* array elements are the correlation coefficients $\langle \delta p_i \delta p_j \rangle / (\delta p_i \cdot \delta p_j)$, in percent, from the fit to parameters p_i, including the branching fractions, $x_i \equiv \Gamma_i/\Gamma_{\rm total}$. The fit constrains the x_i whose labels appear in this array to sum to one.

x_3	−100	
Γ	15	−15
	x_2	x_3

	Mode	Rate (MeV)	Scale factor
Γ_2	$\pi^\pm\pi^0$	150.2 ±2.4	
Γ_3	$\pi^\pm\gamma$	0.068±0.007	2.3

CONSTRAINED FIT INFORMATION

An overall fit to the total width, a partial width, and 7 branching ratios uses 21 measurements and one constraint to determine 9 parameters. The overall fit has a $\chi^2 = 6.0$ for 13 degrees of freedom.

The following *off-diagonal* array elements are the correlation coefficients $\langle \delta p_i \delta p_j \rangle / (\delta p_i \cdot \delta p_j)$, in percent, from the fit to parameters p_i, including the branching fractions, $x_i \equiv \Gamma_i/\Gamma_{\rm total}$. The fit constrains the x_i whose labels appear in this array to sum to one.

x_7	−100							
x_8	−5	0						
x_9	−1	0	1					
x_{10}	−1	0	0	0				
x_{11}	2	−3	0	0	0			
x_{12}	0	0	−8	−9	0	0		
x_{14}	−1	0	0	0	0	0	0	
Γ	0	0	4	5	0	0	−54	0
	x_6	x_7	x_8	x_9	x_{10}	x_{11}	x_{12}	x_{14}

	Mode		Rate (MeV)	
Γ_6	$\pi^+\pi^-$		147.5	±0.9
Γ_7	$\pi^+\pi^-\gamma$		1.48	±0.24
Γ_8	$\pi^0\gamma$		0.089	±0.012
Γ_9	$\eta\gamma$		0.0447	±0.0031
Γ_{10}	$\pi^0\pi^0\gamma$		0.0066	±0.0012
Γ_{11}	$\mu^+\mu^-$	[a]	0.0068	±0.0004
Γ_{12}	e^+e^-	[a]	0.00704	±0.00006
Γ_{14}	$\pi^+\pi^-\pi^+\pi^-$		0.0027	±0.0014

$\rho(770)$ PARTIAL WIDTHS

$\Gamma(\pi^\pm\gamma)$ Γ_3

VALUE (keV)	DOCUMENT ID		TECN	CHG	COMMENT
68 ±7 OUR FIT	Error includes scale factor of 2.3.				
68 ±7 OUR AVERAGE	Error includes scale factor of 2.2. See the ideogram below.				
81 ±4 ±4	CAPRARO	87	SPEC	−	200 π^-A → $\pi^-\pi^0$A
59.8±4.0	HUSTON	86	SPEC	+	202 π^+A → $\pi^+\pi^0$A
71 ±7	JENSEN	83	SPEC	−	156–260 π^-A → $\pi^-\pi^0$A

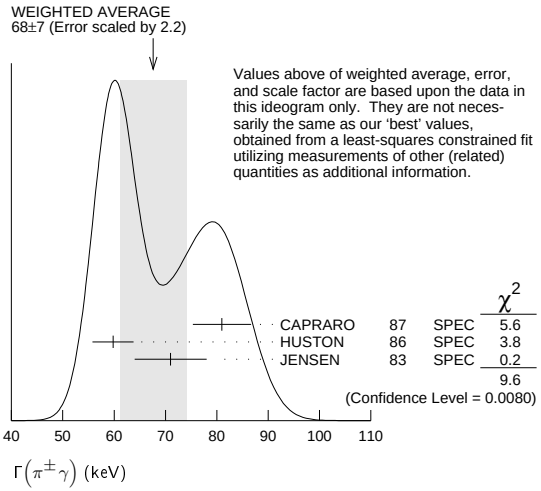

$\Gamma(e^+e^-)$ Γ_{12}

VALUE (keV)	EVTS	DOCUMENT ID		TECN	COMMENT
7.04 ±0.06 OUR FIT					
7.04 ±0.06 OUR AVERAGE					
7.048±0.057±0.050	900k	[84] AKHMETSHIN	07		$e^+e^- \to \pi^+\pi^-$
7.06 ±0.11 ±0.05	114k	[85,86] AKHMETSHIN	04	CMD2	$e^+e^- \to \pi^+\pi^-$
6.77 ±0.10 ±0.30		BARKOV	85	OLYA	$e^+e^- \to \pi^+\pi^-$
• • • We do not use the following data for averages, fits, limits, etc. • • •					
7.12 ±0.02 ±0.11	800k	[87] ACHASOV	06	SND	$e^+e^- \to \pi^+\pi^-$
6.3 ±0.1		[88] BENAYOUN	98	RVUE	$e^+e^- \to \pi^+\pi^-$, $\mu^+\mu^-$

Meson Particle Listings

$\rho(770)$

$\Gamma(\pi^0\gamma)$ Γ_8

VALUE (keV)	EVTS	DOCUMENT ID		TECN	COMMENT
• • • We do not use the following data for averages, fits, limits, etc. • • •					
77±17±11	36500	[89] ACHASOV	03	SND	0.60–0.97 $e^+e^- \to \pi^0\gamma$
121±31		DOLINSKY	89	ND	$e^+e^- \to \pi^0\gamma$

$\Gamma(\eta\gamma)$ Γ_9

VALUE (keV)	DOCUMENT ID		TECN	COMMENT
• • • We do not use the following data for averages, fits, limits, etc. • • •				
62±17	[90] DOLINSKY	89	ND	$e^+e^- \to \eta\gamma$

$\Gamma(\pi^+\pi^-\pi^+\pi^-)$ Γ_{14}

VALUE (keV)	EVTS	DOCUMENT ID		TECN	COMMENT
• • • We do not use the following data for averages, fits, limits, etc. • • •					
2.8±1.4±0.5	153	AKHMETSHIN	00	CMD2	0.6–0.97 $e^+e^- \to \pi^+\pi^-\pi^+\pi^-$

[84] A combined fit of AKHMETSHIN 07, AULCHENKO 06, and AULCHENKO 05.
[85] Using the GOUNARIS 68 parametrization with the complex phase of the ρ-ω interference.
[86] From a fit in the energy range 0.61 to 0.96 GeV. Update of AKHMETSHIN 02.
[87] Supersedes ACHASOV 05A.
[88] Using the data of BARKOV 85 in the hidden local symmetry model.
[89] Using $\Gamma_{\rm total}$= 147.9 ± 1.3 MeV and B($\rho \to \pi^0\gamma$) from ACHASOV 03.
[90] Solution corresponding to constructive ω-ρ interference.

$\rho(770)\,\Gamma(e^+e^-)\Gamma(i)/\Gamma^2(\text{total})$

$\Gamma(e^+e^-)/\Gamma_{\rm total} \times \Gamma(\pi^+\pi^-)/\Gamma_{\rm total}$ $\Gamma_{12}/\Gamma \times \Gamma_6/\Gamma$

VALUE (units 10^{-5})	EVTS	DOCUMENT ID		TECN	COMMENT
4.876±0.023±0.064	800k	[91,92] ACHASOV	06	SND	$e^+e^- \to \pi^+\pi^-$
• • • We do not use the following data for averages, fits, limits, etc. • • •					
4.72 ±0.02		[93] BENAYOUN	10	RVUE	0.4–1.05 e^+e^-

[91] Supersedes ACHASOV 05A.
[92] A fit of the SND data from 400 to 1000 MeV using parameters of the $\rho(1450)$ and $\rho(1700)$ from a fit of the data of BARKOV 85, BISELLO 89 and ANDERSON 00A.
[93] A simultaneous fit of $e^+e^- \to \pi^+\pi^-$, $\pi^+\pi^-\pi^0$, $\pi^0\gamma$, $\eta\gamma$ data.

$\Gamma(e^+e^-)/\Gamma_{\rm total} \times \Gamma(\eta\gamma)/\Gamma_{\rm total}$ $\Gamma_{12}/\Gamma \times \Gamma_9/\Gamma$

VALUE (units 10^{-8})	EVTS	DOCUMENT ID		TECN	COMMENT
1.42±0.10 OUR FIT					
1.45±0.12 OUR AVERAGE					
1.32±0.14±0.08	33k	[94] ACHASOV	07B	SND	0.6–1.38 $e^+e^- \to \eta\gamma$
1.50±0.65±0.09	17.4k	[95] AKHMETSHIN	05	CMD2	0.60-1.38 $e^+e^- \to \eta\gamma$
1.61±0.20±0.11	23k	[96,97] AKHMETSHIN	01B	CMD2	$e^+e^- \to \eta\gamma$
1.85±0.49		[98] DOLINSKY	89	ND	$e^+e^- \to \eta\gamma$
• • • We do not use the following data for averages, fits, limits, etc. • • •					
1.05±0.02		[99] BENAYOUN	10	RVUE	0.4–1.05 e^+e^-

[94] From a combined fit of $\sigma(e^+e^- \to \eta\gamma)$ with $\eta \to 3\pi^0$ and $\eta \to \pi^+\pi^-\pi^0$, and fixing B($\eta \to 3\pi^0$) / B($\eta \to \pi^+\pi^-\pi^0$) = 1.44 ± 0.04. Recalculated by us from the cross section at the peak. Supersedes ACHASOV 00D and ACHASOV 06A.
[95] From the $\eta \to 2\gamma$ decay and using B($\eta \to \gamma\gamma$)= 39.43 ± 0.26%.
[96] From the $\eta \to 3\pi^0$ decay and using B($\eta \to 3\pi^0$)= (32.24 ± 0.29) × 10^{-2}.
[97] The combined fit from 600 to 1380 MeV taking into account $\rho(770)$, $\omega(782)$, $\phi(1020)$, and $\rho(1450)$ (mass and width fixed at 1450 MeV and 310 MeV respectively).
[98] Recalculated by us from the cross section in the peak.
[99] A simultaneous fit of $e^+e^- \to \pi^+\pi^-$, $\pi^+\pi^-\pi^0$, $\pi^0\gamma$, $\eta\gamma$ data.

$\Gamma(e^+e^-)/\Gamma_{\rm total} \times \Gamma(\pi^0\gamma)/\Gamma_{\rm total}$ $\Gamma_{12}/\Gamma \times \Gamma_8/\Gamma$

VALUE (units 10^{-8})	EVTS	DOCUMENT ID		TECN	COMMENT
2.8 ±0.4 OUR FIT					
2.8 ±0.4 OUR AVERAGE					
2.90 $^{+0.60}_{-0.55}$ ±0.18	18680	AKHMETSHIN	05	CMD2	0.60-1.38 $e^+e^- \to \pi^0\gamma$
2.37 ±0.53 ±0.33	36500	[100] ACHASOV	03	SND	0.60–0.97 $e^+e^- \to \pi^0\gamma$
3.61 ±0.74 ±0.49	10625	[101] DOLINSKY	89	ND	$e^+e^- \to \pi^0\gamma$
• • • We do not use the following data for averages, fits, limits, etc. • • •					
1.875±0.026		[102] BENAYOUN	10	RVUE	0.4–1.05 e^+e^-

[100] Using $\sigma_{\phi \to \pi^0\gamma}$ from ACHASOV 00 and m_ρ= 775.97 MeV in the model with the energy-independent phase of ρ-ω interference equal to $(-10.2 \pm 7.0)^\circ$.
[101] Recalculated by us from the cross section in the peak.
[102] A simultaneous fit of $e^+e^- \to \pi^+\pi^-$, $\pi^+\pi^-\pi^0$, $\pi^0\gamma$, $\eta\gamma$ data.

$\Gamma(e^+e^-)/\Gamma_{\rm total} \times \Gamma(\pi^+\pi^-\pi^0)/\Gamma_{\rm total}$ $\Gamma_{12}/\Gamma \times \Gamma_{13}/\Gamma$

VALUE (units 10^{-9})	EVTS	DOCUMENT ID		TECN	COMMENT
• • • We do not use the following data for averages, fits, limits, etc. • • •					
0.903±0.076		[103] BENAYOUN	10	RVUE	0.4–1.05 e^+e^-
4.58 $^{+2.46}_{-1.64}$ ±1.56	1.2M	[104] ACHASOV	03D	RVUE	0.44–2.00 $e^+e^- \to \pi^+\pi^-\pi^0$

[103] A simultaneous fit of $e^+e^- \to \pi^+\pi^-$, $\pi^+\pi^-\pi^0$, $\pi^0\gamma$, $\eta\gamma$ data.
[104] Statistical significance is less than 3 σ.

$\rho(770)$ BRANCHING RATIOS

$\Gamma(\pi^\pm\eta)/\Gamma(\pi\pi)$ Γ_4/Γ_1

VALUE (units 10^{-4})	CL%	DOCUMENT ID		TECN	CHG	COMMENT
<60	84	FERBEL	66	HBC	±	$\pi^\pm p$ above 2.5

$\Gamma(\pi^\pm\pi^+\pi^-\pi^0)/\Gamma(\pi\pi)$ Γ_5/Γ_1

VALUE (units 10^{-4})	CL%	DOCUMENT ID		TECN	CHG	COMMENT
<20	84	FERBEL	66	HBC	±	$\pi^\pm p$ above 2.5
• • • We do not use the following data for averages, fits, limits, etc. • • •						
35±40		JAMES	66	HBC	+	2.1 $\pi^+ p$

$\Gamma(\mu^+\mu^-)/\Gamma(\pi^+\pi^-)$ Γ_{11}/Γ_6

VALUE (units 10^{-5})	DOCUMENT ID		TECN	COMMENT
4.60±0.28 OUR FIT				
4.6 ±0.2 ±0.2	ANTIPOV	89	SIGM	π^- Cu $\to \mu^+\mu^-\pi^-$ Cu
• • • We do not use the following data for averages, fits, limits, etc. • • •				
8.2 $^{+1.6}_{-3.6}$	[105] ROTHWELL	69	CNTR	Photoproduction
5.6 ±1.5	[106] WEHMANN	69	OSPK	12 π^- C, Fe
9.7 $^{+3.1}_{-3.3}$	[107] HYAMS	67	OSPK	11 π^- Li, H

$\Gamma(e^+e^-)/\Gamma(\pi\pi)$ Γ_{12}/Γ_1

VALUE (units 10^{-4})	DOCUMENT ID		TECN	COMMENT
• • • We do not use the following data for averages, fits, limits, etc. • • •				
0.40±0.05	[108] BENAKSAS	72	OSPK	$e^+e^- \to \pi^+\pi^-$

$\Gamma(\eta\gamma)/\Gamma_{\rm total}$ Γ_9/Γ

VALUE (units 10^{-4})	EVTS	DOCUMENT ID		TECN	CHG	COMMENT
3.00±0.21 OUR FIT						
2.90±0.32 OUR AVERAGE						
2.79±0.34±0.03	33k	[109] ACHASOV	07B	SND		0.6–1.38 $e^+e^- \to \eta\gamma$
3.6 ±0.9		[110] ANDREWS	77	CNTR	0	6.7–10 γCu
• • • We do not use the following data for averages, fits, limits, etc. • • •						
3.21±1.39±0.20	17.4k	[111,112] AKHMETSHIN	05	CMD2		0.60-1.38 $e^+e^- \to \eta\gamma$
3.39±0.42±0.23		[110,113,114] AKHMETSHIN	01B	CMD2		$e^+e^- \to \eta\gamma$
1.9 $^{+0.6}_{-0.8}$		[115] BENAYOUN	96	RVUE		0.54-1.04 $e^+e^- \to \eta\gamma$
4.0 ±1.1		[110,112] DOLINSKY	89	ND		$e^+e^- \to \eta\gamma$

$\Gamma(\pi^+\pi^-\pi^+\pi^-)/\Gamma_{\rm total}$ Γ_{14}/Γ

VALUE (units 10^{-5})	CL%	EVTS	DOCUMENT ID		TECN	COMMENT
1.8±0.9 OUR FIT						
1.8±0.9±0.3		153	AKHMETSHIN	00	CMD2	0.6–0.97 $e^+e^- \to \pi^+\pi^-\pi^+\pi^-$
• • • We do not use the following data for averages, fits, limits, etc. • • •						
<20	90		KURDADZE	88	OLYA	$e^+e^- \to \pi^+\pi^-\pi^+\pi^-$

$\Gamma(\pi^+\pi^-\pi^+\pi^-)/\Gamma(\pi\pi)$ Γ_{14}/Γ_1

VALUE (units 10^{-4})	CL%	DOCUMENT ID		TECN	CHG	COMMENT
• • • We do not use the following data for averages, fits, limits, etc. • • •						
<15	90	ERBE	69	HBC	0	2.5–5.8 γp
<20		CHUNG	68	HBC	0	3.2,4.2 $\pi^- p$
<20	90	HUSON	68	HLBC	0	16.0 $\pi^- p$
<80		JAMES	66	HBC	0	2.1 $\pi^+ p$

$\Gamma(\pi^+\pi^-\pi^0)/\Gamma_{\rm total}$ Γ_{13}/Γ

VALUE (units 10^{-4})	CL%	EVTS	DOCUMENT ID		TECN	COMMENT
• • • We do not use the following data for averages, fits, limits, etc. • • •						
1.01 $^{+0.54}_{-0.36}$ ±0.34		1.2M	[116] ACHASOV	03D	RVUE	0.44–2.00 $e^+e^- \to \pi^+\pi^-\pi^0$
<1.2	90		VASSERMAN	88B	ND	$e^+e^- \to \pi^+\pi^-\pi^0$

$\Gamma(\pi^+\pi^-\pi^0)/\Gamma(\pi\pi)$ Γ_{13}/Γ_1

VALUE	CL%	DOCUMENT ID		TECN	CHG	COMMENT
• • • We do not use the following data for averages, fits, limits, etc. • • •						
~ 0.01		BRAMON	86	RVUE	0	$J/\psi \to \omega\pi^0$
<0.01	84	[117] ABRAMS	71	HBC	0	3.7 $\pi^+ p$

$\Gamma(\pi^+\pi^-\pi^0\pi^0)/\Gamma_{\rm total}$ Γ_{15}/Γ

VALUE (units 10^{-5})	CL%	DOCUMENT ID		TECN	COMMENT
1.60±0.74±0.18		[118] ACHASOV	09A	SND	$e^+e^- \to \pi^+\pi^-\pi^0\pi^0$
• • • We do not use the following data for averages, fits, limits, etc. • • •					
< 4	90	AULCHENKO	87C	ND	$e^+e^- \to \pi^+\pi^-\pi^0\pi^0$
<20	90	KURDADZE	86	OLYA	$e^+e^- \to \pi^+\pi^-\pi^0\pi^0$

$\Gamma(\pi^+\pi^-\gamma)/\Gamma_{total}$ Γ_7/Γ

VALUE	CL%	DOCUMENT ID		TECN	COMMENT
0.0099±0.0016 OUR FIT					
0.0099±0.0016		[119] DOLINSKY	91	ND	$e^+e^- \to \pi^+\pi^-\gamma$
• • • We do not use the following data for averages, fits, limits, etc. • • •					
0.0111±0.0014		[120] VASSERMAN	88	ND	$e^+e^- \to \pi^+\pi^-\gamma$
<0.005	90	[121] VASSERMAN	88	ND	$e^+e^- \to \pi^+\pi^-\gamma$

$\Gamma(\pi^0\gamma)/\Gamma_{total}$ Γ_8/Γ

VALUE (units 10^{-4})	EVTS	DOCUMENT ID		TECN	COMMENT
• • • We do not use the following data for averages, fits, limits, etc. • • •					
$6.21^{+1.28}_{-1.18}\pm0.39$	18680	[122,123] AKHMETSHIN	05	CMD2	0.60–1.38 $e^+e^- \to \pi^0\gamma$
5.22±1.17±0.75	36500	[123,124] ACHASOV	03	SND	0.60–0.97 $e^+e^- \to \pi^0\gamma$
6.8 ±1.7		[125] BENAYOUN	96	RVUE	0.54–1.04 $e^+e^- \to \pi^0\gamma$
7.9 ±2.0		[123] DOLINSKY	89	ND	$e^+e^- \to \pi^0\gamma$

$\Gamma(\pi^0 e^+ e^-)/\Gamma_{total}$ Γ_{16}/Γ

VALUE (units 10^{-5})	CL%	DOCUMENT ID		TECN	COMMENT
<1.2	90	ACHASOV	08	SND	0.36–0.97 $e^+e^- \to \pi^0 e^+ e^-$
• • • We do not use the following data for averages, fits, limits, etc. • • •					
<1.6		AKHMETSHIN	05A	CMD2	0.72-0.84 e^+e^-

$\Gamma(\eta e^+ e^-)/\Gamma_{total}$ Γ_{17}/Γ

VALUE (units 10^{-5})	DOCUMENT ID		TECN	COMMENT
• • • We do not use the following data for averages, fits, limits, etc. • • •				
<0.7	AKHMETSHIN	05A	CMD2	0.72-0.84 e^+e^-

$\Gamma(\pi^0\pi^0\gamma)/\Gamma_{total}$ Γ_{10}/Γ

VALUE (units 10^{-5})	EVTS	DOCUMENT ID		TECN	COMMENT
4.5±0.8 OUR FIT					
$4.5^{+0.9}_{-0.8}$ OUR AVERAGE					
$5.2^{+1.5}_{-1.3}\pm0.6$	190	[126] AKHMETSHIN	04B	CMD2	0.6–0.97 $e^+e^- \to \pi^0\pi^0\gamma$
$4.1^{+1.0}_{-0.9}\pm0.3$	295	[127] ACHASOV	02F	SND	0.36–0.97 $e^+e^- \to \pi^0\pi^0\gamma$
• • • We do not use the following data for averages, fits, limits, etc. • • •					
$4.8^{+3.4}_{-1.8}\pm0.5$	63	[128] ACHASOV	00G	SND	$e^+e^- \to \pi^0\pi^0\gamma$

[105] Possibly large ρ-ω interference leads us to increase the minus error.

[106] Result contains 11 ± 11% correction using SU(3) for central value. The error on the correction takes account of possible ρ-ω interference and the upper limit agrees with the upper limit of $\omega \to \mu^+\mu^-$ from this experiment.

[107] HYAMS 67's mass resolution is 20 MeV. The ω region was excluded.

[108] The ρ' contribution is not taken into account.

[109] ACHASOV 07B reports $[\Gamma(\rho(770) \to \eta\gamma)/\Gamma_{total}] \times [B(\rho(770) \to e^+e^-)] = (1.32 \pm 0.14 \pm 0.08) \times 10^{-8}$ which we divide by our best value $B(\rho(770) \to e^+e^-) = (4.72 \pm 0.05) \times 10^{-5}$. Our first error is their experiment's error and our second error is the systematic error from using our best value. Supersedes ACHASOV 00D and ACHASOV 06A.

[110] Solution corresponding to constructive ω-ρ interference.

[111] Using $B(\rho \to e^+e^-) = (4.67 \pm 0.09) \times 10^{-5}$ and $B(\eta \to \gamma\gamma) = 39.43 \pm 0.26\%$.

[112] Not independent of the corresponding $\Gamma(e^+e^-) \times \Gamma(\eta\gamma)/\Gamma^2_{total}$.

[113] The combined fit from 600 to 1380 MeV taking into account $\rho(770)$, $\omega(782)$, $\phi(1020)$, and $\rho(1450)$ (mass and width fixed at 1450 MeV and 310 MeV respectively).

[114] Using $B(\rho \to e^+e^-) = (4.75 \pm 0.10) \times 10^{-5}$ from AKHMETSHIN 02 and $B(\eta \to 3\pi^0) = (32.24 \pm 0.29) \times 10^{-2}$.

[115] Reanalysis of DRUZHININ 84, DOLINSKY 89, and DOLINSKY 91 taking into account a triangle anomaly contribution. Constructive ρ-ω interference solution.

[116] Statistical significance is less than 3σ.

[117] Model dependent, assumes $I = 1$, 2, or 3 for the 3π system.

[118] Assuming no interference between the ρ and ω contributions.

[119] Bremsstrahlung from a decay pion and for photon energy above 50 MeV.

[120] Superseded by DOLINSKY 91.

[121] Structure radiation due to quark rearrangement in the decay.

[122] Using $B(\rho \to e^+e^-) = (4.67 \pm 0.09) \times 10^{-5}$.

[123] Not independent of the corresponding $\Gamma(e^+e^-) \times \Gamma(\pi^0\gamma)/\Gamma^2_{total}$.

[124] Using $B(\rho \to e^+e^-) = (4.54 \pm 0.10) \times 10^{-5}$.

[125] Reanalysis of DRUZHININ 84, DOLINSKY 89, and DOLINSKY 91 taking into account a triangle anomaly contribution.

[126] This branching ratio includes the conventional VMD mechanism $\rho \to \omega\pi^0$, $\omega \to \pi^0\gamma$, and the new decay mode $\rho \to f_0(500)\gamma$, $f_0(500) \to \pi^0\pi^0$ with a branching ratio $(2.0^{+1.1}_{-0.9} \pm 0.3) \times 10^{-5}$ differing from zero by 2.0 standard deviations.

[127] This branching ratio includes the conventional VMD mechanism $\rho \to \omega\pi^0$, $\omega \to \pi^0\gamma$ and the new decay mode $\rho \to f_0(500)\gamma$, $f_0(500) \to \pi^0\pi^0$ with a branching ratio $(1.9^{+0.9}_{-0.8} \pm 0.4) \times 10^{-5}$ differing from zero by 2.4 standard deviations. Supersedes ACHASOV 00G.

[128] Superseded by ACHASOV 02F.

$\rho(770)$ REFERENCES

ABRAMOWICZ 12 EPJ C72 1869 H. Abramowicz *et al.* (ZEUS Collab.)
LEES 12G PR D86 032013 J.P. Lees *et al.* (BABAR Collab.)
BENAYOUN 10 EPJ C65 211 M. Benayoun *et al.*
ACHASOV 09A JETP 109 379 M.N. Achasov *et al.* (SND Collab.)
Translated from ZETF 136 442.
ACHASOV 08 JETP 107 61 M.N. Achasov *et al.* (SND Collab.)
Translated from ZETF 134 80.
FUJIKAWA 08 PR D78 072006 M. Fujikawa *et al.* (BELLE Collab.)
ACHASOV 07B PR D76 077101 M.N. Achasov *et al.* (SND Collab.)
AKHMETSHIN 07 PL B648 28 R. Akhmetshin *et al.* (Novosibirsk CMD-2 Collab.)
ACHASOV 06 JETP 103 380 M.N. Achasov *et al.* (Novosibirsk SND Collab.)
Translated from ZETF 130 437.
ACHASOV 06A PR D74 014016 M.N. Achasov *et al.* (SND Collab.)
AULCHENKO 06 JETPL 84 413 V.M. Aulchenko *et al.* (Novosibirsk CMD-2 Collab.)
Translated from ZETFP 84 491.
ACHASOV 05A JETP 101 1053 M.N. Achasov *et al.* (Novosibirsk SND Collab.)
Translated from ZETF 128 1201.
AKHMETSHIN 05 PL B605 26 R.R. Akhmetshin *et al.* (Novosibirsk CMD-2 Collab.)
AKHMETSHIN 05A PL B613 29 R.R. Akhmetshin *et al.* (Novosibirsk CMD-2 Collab.)
ALOISIO 05 PL B606 12 A. Aloisio *et al.* (KLOE Collab.)
AULCHENKO 05 JETPL 82 743 V.M. Aulchenko *et al.* (Novosibirsk CMD-2 Collab.)
Translated from ZETFP 82 841.
SCHAEL 05C PRPL 421 191 S. Schael *et al.* (ALEPH Collab.)
AKHMETSHIN 04 PL B578 285 R.R. Akhmetshin *et al.* (Novosibirsk CMD-2 Collab.)
AKHMETSHIN 04B PL B580 119 R.R. Akhmetshin *et al.* (Novosibirsk CMD-2 Collab.)
ACHASOV 03 PL B559 171 M.N. Achasov *et al.* (Novosibirsk SND Collab.)
ACHASOV 03D PR D68 052006 M.N. Achasov *et al.* (Novosibirsk SND Collab.)
ALOISIO 03 PL B561 55 A. Aloisio *et al.* (KLOE Collab.)
SANZ-CILLERO 03 EPJ C27 587 J.J. Sanz-Cillero, A. Pich
ACHASOV 02 PR D65 032002 M.N. Achasov *et al.* (Novosibirsk SND Collab.)
ACHASOV 02F PL B537 201 M.N. Achasov *et al.* (Novosibirsk SND Collab.)
AKHMETSHIN 02 PL B527 161 R.R. Akhmetshin *et al.* (Novosibirsk CMD-2 Collab.)
AKHMETSHIN 01B PL B509 217 R.R. Akhmetshin *et al.* (Novosibirsk CMD-2 Collab.)
COLANGELO 01 NP B603 125 G. Colangelo, J. Gasser, H. Leytwyler
PICH 01 PR D63 093005 A. Pich, J. Portoles
ACHASOV 00 EPJ C12 25 M.N. Achasov *et al.* (Novosibirsk SND Collab.)
ACHASOV 00D JETPL 72 282 M.N. Achasov *et al.* (Novosibirsk SND Collab.)
Translated from ZETFP 72 411.
ACHASOV 00G JETPL 71 355 M.N. Achasov *et al.* (Novosibirsk SND Collab.)
Translated from ZETFP 71 519.
AKHMETSHIN 00 PL B475 190 R.R. Akhmetshin *et al.* (Novosibirsk CMD-2 Collab.)
ANDERSON 00A PR D61 112002 S. Anderson *et al.* (CLEO Collab.)
ABELE 99E PL B469 270 A. Abele *et al.* (Crystal Barrel Collab.)
BENAYOUN 98 EPJ C2 269 M. Benayoun *et al.* (IPNP, NOVO, ADLD+)
BREITWEG 98B EPJ C2 247 J. Breitweg *et al.* (ZEUS Collab.)
GARDNER 98 PR D57 2716 S. Gardner, H.B. O'Connell
Also PR D62 019903 (errat) S. Gardner, H.B. O'Connell
ABELE 97 PL B391 191 A. Abele *et al.* (Crystal Barrel Collab.)
ADAMS 97 ZPHY C74 237 M.R. Adams *et al.* (E665 Collab.)
BARATE 97M ZPHY C76 15 R. Barate *et al.* (ALEPH Collab.)
BERTIN 97C PL B408 476 A. Bertin *et al.* (OBELIX Collab.)
BOGOLYUB... 97 PAN 60 46 M.Y. Bogolyubsky *et al.* (MOSU, SERP)
Translated from YAF 60 53.
O'CONNELL 97 NP A623 559 H.B. O'Connell *et al.* (ADLD)
BENAYOUN 96 ZPHY C72 221 M. Benayoun *et al.* (IPNP, NOVO)
BERNICHA 94 PR D50 4454 A. Bernicha, G. Lopez Castro, J. Pestieau (LOUV+)
WEIDENAUER 93 ZPHY C59 387 P. Weidenauer *et al.* (ASTERIX Collab.)
AGUILAR-... 91 ZPHY C50 405 M. Aguilar-Benitez *et al.* (LEBC-EHS Collab.)
DOLINSKY 91 PRPL 202 99 S.I. Dolinsky *et al.* (NOVO)
KUHN 90 ZPHY C48 445 J.H. Kuhn *et al.* (MPIM)
ANTIPOV 89 ZPHY C42 185 Y.M. Antipov *et al.* (SERP, JINR, BGNA+)
BISELLO 89 PL B220 321 D. Bisello *et al.* (DM2 Collab.)
DOLINSKY 89 ZPHY C42 511 S.I. Dolinsky *et al.* (NOVO)
DUBNICKA 89 JP G15 1349 S. Dubnicka *et al.* (JINR, SLOV)
GESHKEN... 89 ZPHY C45 351 B.V. Geshkenbein (ITEP)
KURDADZE 88 JETPL 47 512 L.M. Kurdadze *et al.* (NOVO)
Translated from ZETFP 47 432.
VASSERMAN 88 SJNP 47 1035 I.B. Vasserman *et al.* (NOVO)
Translated from YAF 47 1635.
VASSERMAN 88B SJNP 48 480 I.B. Vasserman *et al.* (NOVO)
Translated from YAF 48 753.
AULCHENKO 87C IYF 87-90 Preprint V.M. Aulchenko *et al.* (NOVO)
CAPRARO 87 NP B288 659 L. Capraro *et al.* (CLER, FRAS, MILA+)
BRAMON 86 PL B173 97 A. Bramon, J. Casulleras (BARC)
HUSTON 86 PR D33 3199 J. Huston *et al.* (ROCH, FNAL, MINN)
KURDADZE 86 JETPL 43 643 L.M. Kurdadze *et al.* (NOVO)
Translated from ZETFP 43 497.
BARKOV 85 NP B256 365 L.M. Barkov *et al.* (NOVO)
DRUZHININ 84 PL 144B 136 V.P. Druzhinin *et al.* (NOVO)
CHABAUD 83 NP B223 1 V. Chabaud *et al.* (CERN, CRAC, MPIM)
JENSEN 83 PR D27 26 T. Jensen *et al.* (ROCH, FNAL, MINN)
HEYN 81 ZPHY C7 169 M.F. Heyn, C.B. Lang (GRAZ)
BOHACIK 80 PR D21 1342 J. Bohacik, H. Kuhnelt (SLOV, WIEN)
LANG 79 PR D19 956 C.B. Lang, A. Mas-Parareda (GRAZ)
BARTALUCCI 78 NC 44A 587 S. Bartalucci *et al.* (DESY, FRAS)
WICKLUND 78 PR D17 1197 A.B. Wicklund *et al.* (ANL)
ANDREWS 77 PRL 38 198 D.E. Andrews *et al.* (ROCH)
DEUTSCH... 76 NP B103 426 M. Deutschmann *et al.* (AACH3, BERL, BONN+)
ENGLER 74 PR D10 2070 A. Engler *et al.* (CMU, CASE)
ESTABROOKS 74 NP B79 301 P.G. Estabrooks, A.D. Martin (DURH)
GRAYER 74 NP B75 189 G. Grayer *et al.* (CERN, MPIM)
BYERLY 73 PR D7 637 W.L. Byerly *et al.* (MICH)
GLADDING 73 PR D8 3721 G.E. Gladding *et al.* (HARV)
HYAMS 73 NP B64 134 B.D. Hyams *et al.* (CERN, MPIM)
PROTOPOP... 73 PR D7 1279 S.D. Protopopescu *et al.* (LBL)
BALLAM 72 PR D5 545 J. Ballam *et al.* (SLAC, LBL, TUFTS)
BENAKSAS 72 PL 39B 289 D. Benaksas *et al.* (ORSAY)
JACOBS 72 PR D6 1291 L.D. Jacobs (SACL)
RATCLIFF 72 PL 38B 345 B.N. Ratcliff *et al.* (SLAC)
ABRAMS 71 PR D4 653 G.S. Abrams *et al.* (LBL)
ALVENSLEB... 70 PRL 24 786 H. Alvensleben *et al.* (DESY)
BIGGS 70 PRL 24 1197 P.J. Biggs *et al.* (DARE)
ERBE 69 PR 188 2060 R. Erbe *et al.* (German Bubble Chamber Collab.)
MALAMUD 69 Argonne Conf. 93 E.I. Malamud, P.E. Schlein (UCLA)
REYNOLDS 69 PR 184 1424 B.G. Reynolds *et al.* (FSU)
ROTHWELL 69 PRL 23 1521 P.L. Rothwell *et al.* (NEAS)
WEHMANN 69 PR 178 2095 A.A. Wehmann *et al.* (HARV, CASE, SLAC+)
ARMENISE 68 NC 54A 999 N. Armenise *et al.* (BARI, BGNA, FIRZ+)
BATON 68 PR 176 1574 J.P. Baton, G. Laurens (SACL)
CHUNG 68 PR 165 1491 S.U. Chung *et al.* (LRL)
FOSTER 68 NP B6 107 M. Foster *et al.* (CERN, CDEF)
GOUNARIS 68 PRL 21 244 G.J. Gounaris, J.J. Sakurai
HUSON 68 PL 28B 208 R. Huson *et al.* (ORSAY, MILA, UCLA)
HYAMS 68 NP B7 1 B.D. Hyams *et al.* (CERN, MPIM)
LANZEROTTI 68 PR 166 1365 L.J. Lanzerotti *et al.* (HARV)
PISUT 68 NP B6 325 J. Pisut, M. Roos (CERN)
ASBURY 67B PRL 19 865 J.G. Asbury *et al.* (DESY, COLU)
BACON 67 PR 157 1263 T.C. Bacon *et al.* (BNL)
EISNER 67 PR 164 1699 R.L. Eisner *et al.* (PURD)
HUWE 67 PL 24B 252 D.O. Huwe *et al.* (COLU)
HYAMS 67 PL 24B 634 B.D. Hyams *et al.* (CERN, MPIM)

MILLER	67B	PR 153 1423	D.H. Miller *et al.*	(PURD)
ALFF-...	66	PR 145 1072	C. Alff-Steinberger *et al.*	(COLU, RUTG)
FERBEL	66	PL 21 111	T. Ferbel	(ROCH)
HAGOPIAN	66	PR 145 1128	V. Hagopian *et al.*	(PENN, SACL)
HAGOPIAN	66B	PR 152 1183	V. Hagopian, Y.L. Pan	(PENN, LRL)
JACOBS	66B	UCRL 16877	L.D. Jacobs	(LRL)
JAMES	66	PR 142 896	F.E. James, H.L. Kraybill	(YALE, BNL)
ROSS	66	PR 149 1172	M. Ross, L. Stodolsky	
SOEDING	66	PL B19 702	P. Soeding	
WEST	66	PR 149 1089	E. West *et al.*	(WISC)
BLIEDEN	65	PL 19 444	H.R. Blieden *et al.*	(CERN MMS Collab.)
CARMONY	64	PRL 12 254	D.D. Carmony *et al.*	(UCB)
GOLDHABER	64	PRL 12 336	G. Goldhaber *et al.*	(LRL, UCB)
ABOLINS	63	PRL 11 381	M.A. Abolins *et al.*	(UCSD)

$\omega(782)$

$I^G(J^{PC}) = 0^-(1^{--})$

$\omega(782)$ MASS

VALUE (MeV)	EVTS	DOCUMENT ID		TECN	COMMENT
782.65±0.12 OUR AVERAGE		Error includes scale factor of 1.9.			See the ideogram below.
783.20±0.13±0.16	18680	AKHMETSHIN	05	CMD2	0.60–1.38 $e^+e^- \to \pi^0\gamma$
782.68±0.09±0.04	11200	[1] AKHMETSHIN	04	CMD2	$e^+e^- \to \pi^+\pi^-\pi^0$
782.79±0.08±0.09	1.2M	[2] ACHASOV	03D	RVUE	0.44–2.00 $e^+e^- \to \pi^+\pi^-\pi^0$
782.7 ±0.1 ±1.5	19500	WURZINGER	95	SPEC	1.33 $pd \to {}^3$Heω
781.96±0.17±0.80	11k	[3] AMSLER	94C	CBAR	0.0 $\overline{p}p \to \omega\eta\pi^0$
782.08±0.36±0.82	3463	[4] AMSLER	94C	CBAR	0.0 $\overline{p}p \to \omega\eta\pi^0$
781.96±0.13±0.17	15k	AMSLER	93B	CBAR	0.0 $\overline{p}p \to \omega\pi^0\pi^0$
782.4 ±0.2	270k	WEIDENAUER	93	ASTE	$\overline{p}p \to 2\pi^+2\pi^-\pi^0$
782.2 ±0.4	1488	KURDADZE	83B	OLYA	$e^+e^- \to \pi^+\pi^-\pi^0$
782.4 ±0.5	7000	[5] KEYNE	76	CNTR	$\pi^-p \to \omega n$
• • • We do not use the following data for averages, fits, limits, etc. • • •					
781.91±0.24		[6] LEES	12G	BABR	$e^+e^- \to \pi^+\pi^-\gamma$
781.78±0.10		[7] BARKOV	87	CMD	$e^+e^- \to \pi^+\pi^-\pi^0$
783.3 ±0.4	433	CORDIER	80	DM1	$e^+e^- \to \pi^+\pi^-\pi^0$
782.5 ±0.8	33260	ROOS	80	RVUE	0.0–3.6 $\overline{p}p$
782.6 ±0.8	3000	BENKHEIRI	79	OMEG	9–12 $\pi^\pm p$
781.8 ±0.6	1430	COOPER	78B	HBC	0.7–0.8 $\overline{p}p \to 5\pi$
782.7 ±0.9	535	VANAPEL...	78	HBC	7.2 $\overline{p}p \to \overline{p}p\omega$
783.5 ±0.8	2100	GESSAROLI	77	HBC	11 $\pi^-p \to \omega n$
782.5 ±0.8	418	AGUILAR-...	72B	HBC	3.9,4.6 K^-p
783.4 ±1.0	248	BIZZARRI	71	HBC	0.0 $p\overline{p} \to K^+K^-\omega$
781.0 ±0.6	510	BIZZARRI	71	HBC	0.0 $p\overline{p} \to K_1K_1\omega$
783.7 ±1.0	3583	[8] COYNE	71	HBC	3.7 $\pi^+p \to p\pi^+\pi^+\pi^-\pi^0$
784.1 ±1.2	750	ABRAMOVI...	70	HBC	3.9 π^-p
783.2 ±1.6		[9] BIGGS	70B	CNTR	$<4.1\ \gamma$C $\to \pi^+\pi^-$C
782.4 ±0.5	2400	BIZZARRI	69	HBC	0.0 $\overline{p}p$

[1] Update of AKHMETSHIN 00C.
[2] From the combined fit of ANTONELLI 92, ACHASOV 01E, ACHASOV 02E, and ACHASOV 03D data on the $\pi^+\pi^-\pi^0$ and ANTONELLI 92 on the $\omega\pi^+\pi^-$ final states. Supersedes ACHASOV 99E and ACHASOV 02E.
[3] From the $\eta \to \gamma\gamma$ decay.
[4] From the $\eta \to 3\pi^0$ decay.
[5] Observed by threshold-crossing technique. Mass resolution = 4.8 MeV FWHM.
[6] From the $\rho-\omega$ interference in the $\pi^+\pi^-$ mass spectrum using the Breit-Wigner for the ω and leaving its mass and width as free parameters of the fit.
[7] Systematic uncertainties underestimated.
[8] From best-resolution sample of COYNE 71.
[9] From ω-ρ interference in the $\pi^+\pi^-$ mass spectrum assuming ω width 12.6 MeV.

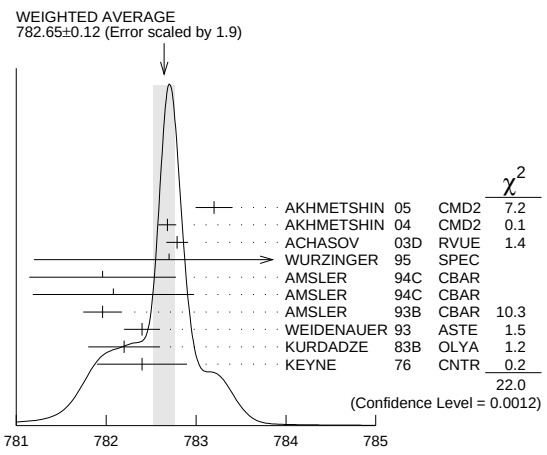

$\omega(782)$ WIDTH

VALUE (MeV)	EVTS	DOCUMENT ID		TECN	COMMENT
8.49±0.08 OUR AVERAGE					
8.68±0.23±0.10	11200	[1] AKHMETSHIN	04	CMD2	$e^+e^- \to \pi^+\pi^-\pi^0$
8.68±0.04±0.15	1.2M	[2] ACHASOV	03D	RVUE	0.44–2.00 $e^+e^- \to \pi^+\pi^-\pi^0$
8.2 ±0.3	19500	WURZINGER	95	SPEC	1.33 $pd \to {}^3$Heω
8.4 ±0.1		[3] AULCHENKO	87	ND	$e^+e^- \to \pi^+\pi^-\pi^0$
8.30±0.40		BARKOV	87	CMD	$e^+e^- \to \pi^+\pi^-\pi^0$
9.8 ±0.9	1488	KURDADZE	83B	OLYA	$e^+e^- \to \pi^+\pi^-\pi^0$
9.0 ±0.8	433	CORDIER	80	DM1	$e^+e^- \to \pi^+\pi^-\pi^0$
9.1 ±0.8	451	BENAKSAS	72B	OSPK	$e^+e^- \to \pi^+\pi^-\pi^0$
• • • We do not use the following data for averages, fits, limits, etc. • • •					
8.13±0.45		[4] LEES	12G	BABR	$e^+e^- \to \pi^+\pi^-\gamma$
12 ±2	1430	COOPER	78B	HBC	0.7–0.8 $\overline{p}p \to 5\pi$
9.4 ±2.5	2100	GESSAROLI	77	HBC	11 $\pi^-p \to \omega n$
10.22±0.43	20000	[5] KEYNE	76	CNTR	$\pi^-p \to \omega n$
13.3 ±2	418	AGUILAR-...	72B	HBC	3.9,4.6 K^-p
10.5 ±1.5		BORENSTEIN	72	HBC	2.18 K^-p
7.70±0.9 ±1.15	940	BROWN	72	MMS	2.5 $\pi^-p \to n$MM
10.3 ±1.4	510	BIZZARRI	71	HBC	0.0 $p\overline{p} \to K_1K_1\omega$
12.8 ±3.0	248	BIZZARRI	71	HBC	0.0 $p\overline{p} \to K^+K^-\omega$
9.5 ±1.0	3583	COYNE	71	HBC	3.7 $\pi^+p \to p\pi^+\pi^+\pi^-\pi^0$

[1] Update of AKHMETSHIN 00C.
[2] From the combined fit of ANTONELLI 92, ACHASOV 01E, ACHASOV 02E, and ACHASOV 03D data on the $\pi^+\pi^-\pi^0$ and ANTONELLI 92 on the $\omega\pi^+\pi^-$ final states. Supersedes ACHASOV 99E and ACHASOV 02E.
[3] Relativistic Breit-Wigner includes radiative corrections.
[4] From the $\rho-\omega$ interference in the $\pi^+\pi^-$ mass spectrum using the Breit-Wigner for the ω and leaving its mass and width as free parameters of the fit.
[5] Observed by threshold-crossing technique. Mass resolution = 4.8 MeV FWHM.

$\omega(782)$ DECAY MODES

	Mode	Fraction (Γ_i/Γ)	Scale factor/ Confidence level
Γ_1	$\pi^+\pi^-\pi^0$	(89.2 ±0.7) %	
Γ_2	$\pi^0\gamma$	(8.28±0.28) %	S=2.1
Γ_3	$\pi^+\pi^-$	($1.53^{+0.11}_{-0.13}$) %	S=1.2
Γ_4	neutrals (excluding $\pi^0\gamma$)	($8\ ^{+8}_{-5}$) $\times 10^{-3}$	S=1.1
Γ_5	$\eta\gamma$	(4.6 ±0.4) $\times 10^{-4}$	S=1.1
Γ_6	$\pi^0e^+e^-$	(7.7 ±0.6) $\times 10^{-4}$	
Γ_7	$\pi^0\mu^+\mu^-$	(1.3 ±0.4) $\times 10^{-4}$	S=2.1
Γ_8	ηe^+e^-		
Γ_9	e^+e^-	(7.28±0.14) $\times 10^{-5}$	S=1.3
Γ_{10}	$\pi^+\pi^-\pi^0\pi^0$	< 2 $\times 10^{-4}$	CL=90%
Γ_{11}	$\pi^+\pi^-\gamma$	< 3.6 $\times 10^{-3}$	CL=95%
Γ_{12}	$\pi^+\pi^-\pi^+\pi^-$	< 1 $\times 10^{-3}$	CL=90%
Γ_{13}	$\pi^0\pi^0\gamma$	(6.6 ±1.1) $\times 10^{-5}$	
Γ_{14}	$\eta\pi^0\gamma$	< 3.3 $\times 10^{-5}$	CL=90%
Γ_{15}	$\mu^+\mu^-$	(9.0 ±3.1) $\times 10^{-5}$	
Γ_{16}	3γ	< 1.9 $\times 10^{-4}$	CL=95%
	Charge conjugation (C) violating modes		
Γ_{17}	$\eta\pi^0$ C	< 2.1 $\times 10^{-4}$	CL=90%
Γ_{18}	$2\pi^0$ C	< 2.1 $\times 10^{-4}$	CL=90%
Γ_{19}	$3\pi^0$ C	< 2.3 $\times 10^{-4}$	CL=90%

CONSTRAINED FIT INFORMATION

An overall fit to 15 branching ratios uses 51 measurements and one constraint to determine 10 parameters. The overall fit has a $\chi^2 = 51.8$ for 42 degrees of freedom.

The following *off-diagonal* array elements are the correlation coefficients $\langle \delta x_i \delta x_j \rangle / (\delta x_i \cdot \delta x_j)$, in percent, from the fit to the branching fractions, $x_i \equiv \Gamma_i/\Gamma_{\rm total}$. The fit constrains the x_i whose labels appear in this array to sum to one.

	x_1	x_2	x_3	x_4	x_5	x_6	x_7	x_9	x_{13}
x_2	22								
x_3	−18	−4							
x_4	−92	−56	1						
x_5	7	7	−1	−9					
x_6	−1	0	0	0	0				
x_7	−1	0	0	0	0	0			
x_9	−38	−33	7	44	−21	0	0		
x_{13}	1	4	0	−2	0	0	0	−1	
x_{15}	0	0	0	0	0	0	0	0	0

$\omega(782)$ PARTIAL WIDTHS

$\Gamma(\pi^0\gamma)$ Γ_2

VALUE (keV)	EVTS	DOCUMENT ID		TECN	COMMENT
• • • We do not use the following data for averages, fits, limits, etc. • • •					
880±50	7815	[1] ACHASOV	13	SND	1.05–2.00 $e^+e^- \to \pi^0\pi^0\gamma$
788±12±27	36500	[2] ACHASOV	03	SND	0.60–0.97 $e^+e^- \to \pi^0\gamma$
764±51	10625	DOLINSKY	89	ND	$e^+e^- \to \pi^0\gamma$

[1] Systematic uncertainty not estimated.
[2] Using Γ_ω = 8.44 ± 0.09 MeV and B($\omega \to \pi^0\gamma$) from ACHASOV 03.

$\Gamma(\eta\gamma)$ Γ_5

VALUE (keV)	DOCUMENT ID		TECN	COMMENT
• • • We do not use the following data for averages, fits, limits, etc. • • •				
6.1±2.5	[1] DOLINSKY	89	ND	$e^+e^- \to \eta\gamma$

[1] Using Γ_ω = 8.4 ± 0.1 MeV and B($\omega \to \eta\gamma$) from DOLINSKY 89.

$\Gamma(e^+e^-)$ Γ_9

VALUE (keV)	EVTS	DOCUMENT ID		TECN	COMMENT
0.60 ±0.02 OUR EVALUATION					
• • • We do not use the following data for averages, fits, limits, etc. • • •					
0.591±0.015	11200	[1,2] AKHMETSHIN	04	CMD2	$e^+e^- \to \pi^+\pi^-\pi^0$
0.653±0.003±0.021	1.2M	[3] ACHASOV	03D	RVUE	0.44–2.00 $e^+e^- \to \pi^+\pi^-\pi^0$
0.600±0.031	10625	DOLINSKY	89	ND	$e^+e^- \to \pi^0\gamma$

[1] Using B($\omega \to \pi^+\pi^-\pi^0$) = 0.891 ± 0.007 and Γ_{total} = 8.44 ± 0.09 MeV.
[2] Update of AKHMETSHIN 00C.
[3] Using ACHASOV 03, ACHASOV 03D and B($\omega \to \pi^+\pi^-$) = (1.70 ± 0.28)%.

$\omega(782)$ $\Gamma(e^+e^-)\Gamma(i)/\Gamma^2(total)$

$\Gamma(e^+e^-)/\Gamma_{total} \times \Gamma(\pi^+\pi^-\pi^0)/\Gamma_{total}$ $\Gamma_9/\Gamma \times \Gamma_1/\Gamma$

VALUE (units 10^{-5})	EVTS	DOCUMENT ID		TECN	COMMENT
6.49±0.11 OUR FIT Error includes scale factor of 1.3.					
6.38±0.10 OUR AVERAGE Error includes scale factor of 1.1.					
6.24±0.11±0.08	11.2k	[1] AKHMETSHIN	04	CMD2	$e^+e^- \to \pi^+\pi^-\pi^0$
6.70±0.06±0.27		AUBERT,B	04N	BABR	10.6 $e^+e^- \to \pi^+\pi^-\pi^0\gamma$
6.74±0.04±0.24	1.2M	[2,3] ACHASOV	03D	RVUE	0.44–2.00 $e^+e^- \to \pi^+\pi^-\pi^0$
6.37±0.35		[2] DOLINSKY	89	ND	$e^+e^- \to \pi^+\pi^-\pi^0$
6.45±0.24		[2] BARKOV	87	CMD	$e^+e^- \to \pi^+\pi^-\pi^0$
5.79±0.42	1488	[2] KURDADZE	83B	OLYA	$e^+e^- \to \pi^+\pi^-\pi^0$
5.89±0.54	433	[2] CORDIER	80	DM1	$e^+e^- \to \pi^+\pi^-\pi^0$
7.54±0.84	451	[2] BENAKSAS	72B	OSPK	$e^+e^- \to \pi^+\pi^-\pi^0$
• • • We do not use the following data for averages, fits, limits, etc. • • •					
6.20±0.13		[4] BENAYOUN	10	RVUE	0.4–1.05 e^+e^-

[1] Update of AKHMETSHIN 00C.
[2] Recalculated by us from the cross section in the peak.
[3] From the combined fit of ANTONELLI 92, ACHASOV 01E, ACHASOV 02E, and ACHASOV 03D data on the $\pi^+\pi^-\pi^0$ and ANTONELLI 92 on the $\omega\pi^+\pi^-$ final states. Supersedes ACHASOV 99E and ACHASOV 02E.
[4] A simultaneous fit of $e^+e^- \to \pi^+\pi^-, \pi^+\pi^-\pi^0, \pi^0\gamma, \eta\gamma$ data.

$\Gamma(e^+e^-)/\Gamma_{total} \times \Gamma(\pi^0\gamma)/\Gamma_{total}$ $\Gamma_9/\Gamma \times \Gamma_2/\Gamma$

VALUE (units 10^{-6})	EVTS	DOCUMENT ID		TECN	COMMENT
6.02±0.20 OUR FIT Error includes scale factor of 1.9.					
6.45±0.17 OUR AVERAGE					
6.47±0.14±0.39	18680	AKHMETSHIN	05	CMD2	0.60-1.38 $e^+e^- \to \pi^0\gamma$
6.50±0.11±0.20	36500	[1] ACHASOV	03	SND	0.60–0.97 $e^+e^- \to \pi^0\gamma$
6.34±0.21±0.21	10625	[2] DOLINSKY	89	ND	$e^+e^- \to \pi^0\gamma$
• • • We do not use the following data for averages, fits, limits, etc. • • •					
6.80±0.13		[3] BENAYOUN	10	RVUE	0.4–1.05 e^+e^-

[1] Using $\sigma_{\phi \to \pi^0\gamma}$ from ACHASOV 00 and m_ω= 782.57 MeV in the model with the energy-independent phase of ρ-ω interference equal to $(-10.2 \pm 7.0)^\circ$.
[2] Recalculated by us from the cross section in the peak.
[3] A simultaneous fit of $e^+e^- \to \pi^+\pi^-, \pi^+\pi^-\pi^0, \pi^0\gamma, \eta\gamma$ data.

$\Gamma(e^+e^-)/\Gamma_{total} \times \Gamma(\pi^+\pi^-)/\Gamma_{total}$ $\Gamma_9/\Gamma \times \Gamma_3/\Gamma$

VALUE (units 10^{-6})	EVTS	DOCUMENT ID		TECN	COMMENT
1.225±0.058±0.041	800k	[1] ACHASOV	06	SND	$e^+e^- \to \pi^+\pi^-$
• • • We do not use the following data for averages, fits, limits, etc. • • •					
1.166±0.036		[2] BENAYOUN	13	RVUE	0.4–1.05 e^+e^-
1.05 ±0.08		[3] DAVIER	13	RVUE	$e^+e^- \to \pi^+\pi^-(\gamma)$

[1] Supersedes ACHASOV 05A.
[2] A simultaneous fit to $e^+e^- \to \pi^+\pi^-, \pi^+\pi^-\pi^0, \pi^0\gamma, \eta\gamma, K\overline{K}$, and $\tau^- \to \pi^-\pi^0\nu_\tau$ data. Supersedes BENAYOUN 10.
[3] From $e^+e^- \to \pi^+\pi^-(\gamma)$ data of LEES 12G.

$\Gamma(e^+e^-)/\Gamma_{total} \times \Gamma(\eta\gamma)/\Gamma_{total}$ $\Gamma_9/\Gamma \times \Gamma_5/\Gamma$

VALUE (units 10^{-8})	EVTS	DOCUMENT ID		TECN	COMMENT
3.32±0.28 OUR FIT Error includes scale factor of 1.1.					
3.18±0.28 OUR AVERAGE					
3.10±0.31±0.11	33k	[1] ACHASOV	07B	SND	0.6–1.38 $e^+e^- \to \eta\gamma$
$3.17^{+1.85}_{-1.31}$±0.21	17.4k	[2] AKHMETSHIN	05	CMD2	0.60-1.38 $e^+e^- \to \eta\gamma$
3.41±0.52±0.21	23k	[3,4] AKHMETSHIN	01B	CMD2	$e^+e^- \to \eta\gamma$
• • • We do not use the following data for averages, fits, limits, etc. • • •					
4.50±0.10		[5] BENAYOUN	10	RVUE	0.4–1.05 e^+e^-

[1] From a combined fit of $\sigma(e^+e^- \to \eta\gamma)$ with $\eta \to 3\pi^0$ and $\eta \to \pi^+\pi^-\pi^0$, and fixing B($\eta \to 3\pi^0$) / B($\eta \to \pi^+\pi^-\pi^0$) = 1.44 ± 0.04. Recalculated by us from the cross section at the peak. Supersedes ACHASOV 00D and ACHASOV 06A.
[2] From the $\eta \to 2\gamma$ decay and using B($\eta \to \gamma\gamma$)= 39.43 ± 0.26%.
[3] From the $\eta \to 3\pi^0$ decay and using B($\eta \to 3\pi^0$)= (32.24 ± 0.29) × 10^{-2}.
[4] The combined fit from 600 to 1380 MeV taking into account $\rho(770)$, $\omega(782)$, $\phi(1020)$, and $\rho(1450)$ (mass and width fixed at 1450 MeV and 310 MeV respectively).
[5] A simultaneous fit of $e^+e^- \to \pi^+\pi^-, \pi^+\pi^-\pi^0, \pi^0\gamma, \eta\gamma$ data.

$\omega(782)$ BRANCHING RATIOS

$\Gamma(\pi^+\pi^-\pi^0)/\Gamma_{total}$ Γ_1/Γ

NIECKNIG 12 describes final-state interactions between the three pions in a dispersive framework using data on the $\pi\pi$ P-wave scattering phase shift.

VALUE	EVTS	DOCUMENT ID		TECN	COMMENT
• • • We do not use the following data for averages, fits, limits, etc. • • •					
0.9024±0.0019		[1] AMBROSINO	08G	KLOE	1.0–1.03 $e^+e^- \to \pi^+\pi^-2\pi^0, 2\pi^0\gamma$
0.8965±0.0016±0.0048	1.2M	[2,3] ACHASOV	03D	RVUE	0.44–2.00 $e^+e^- \to \pi^+\pi^-\pi^0$
0.880 ±0.020 ±0.032	11200	[3,4] AKHMETSHIN	00C	CMD2	$e^+e^- \to \pi^+\pi^-\pi^0$
0.8942±0.0062		[3] DOLINSKY	89	ND	$e^+e^- \to \pi^+\pi^-\pi^0$

[1] Not independent of $\Gamma(\pi^0\gamma)$ / $\Gamma(\pi^+\pi^-\pi^0)$ from AMBROSINO 08G.
[2] Using ACHASOV 03, ACHASOV 03D and B($\omega \to \pi^+\pi^-$) = (1.70 ± 0.28)%.
[3] Not independent of the corresponding $\Gamma(e^+e^-) \times \Gamma(\pi^+\pi^-\pi^0)/\Gamma^2_{total}$.
[4] Using $\Gamma(e^+e^-)$=0.60 ± 0.02 keV.

$\Gamma(\pi^0\gamma)/\Gamma_{total}$ Γ_2/Γ

VALUE (units 10^{-2})	EVTS	DOCUMENT ID		TECN	COMMENT
• • • We do not use the following data for averages, fits, limits, etc. • • •					
8.09±0.14		[1] AMBROSINO	08G	KLOE	$e^+e^- \to \pi^+\pi^-2\pi^0, 2\pi^0\gamma$
9.06±0.20±0.57	18680	[2,3] AKHMETSHIN	05	CMD2	0.60-1.38 $e^+e^- \to \pi^0\gamma$
9.34±0.15±0.31	36500	[3] ACHASOV	03	SND	0.60–0.97 $e^+e^- \to \pi^0\gamma$
8.65±0.16±0.42	1.2M	[4,5] ACHASOV	03D	RVUE	0.44–2.00 $e^+e^- \to \pi^+\pi^-\pi^0$
8.39±0.24	9975	[6] BENAYOUN	96	RVUE	$e^+e^- \to \pi^0\gamma$
8.88±0.62	10625	[3] DOLINSKY	89	ND	$e^+e^- \to \pi^0\gamma$

[1] Not independent of $\Gamma(\pi^0\gamma)$ / $\Gamma(\pi^+\pi^-\pi^0)$ from AMBROSINO 08G.
[2] Using B($\omega \to e^+e^-$)= (7.14 ± 0.13) × 10^{-5}.
[3] Not independent of the corresponding $\Gamma(e^+e^-) \times \Gamma(\pi^0\gamma)/\Gamma^2_{total}$.
[4] Using ACHASOV 03, ACHASOV 03D and B($\omega \to \pi^+\pi^-$) = (1.70 ± 0.28)%.
[5] Not independent of the corresponding $\Gamma(e^+e^-) \times \Gamma(\pi^+\pi^-\pi^0)/\Gamma^2_{total}$.
[6] Reanalysis of DRUZHININ 84, DOLINSKY 89, DOLINSKY 91 taking into account the triangle anomaly contributions.

$\Gamma(\pi^0\gamma)/\Gamma(\pi^+\pi^-\pi^0)$ Γ_2/Γ_1

VALUE (units 10^{-2})	DOCUMENT ID		TECN	COMMENT
9.28±0.31 OUR FIT Error includes scale factor of 2.3.				
9.05±0.27 OUR AVERAGE Error includes scale factor of 1.8.				
8.97±0.16	AMBROSINO	08G	KLOE	$e^+e^- \to \pi^+\pi^-2\pi^0, 2\pi^0\gamma$
9.94±0.36±0.38	[1] AULCHENKO	00A	SND	$e^+e^- \to \pi^+\pi^-2\pi^0, 2\pi^0\gamma$
8.4 ±1.3	KEYNE	76	CNTR	$\pi^-p \to \omega n$
10.9 ±2.5	BENAKSAS	72C	OSPK	$e^+e^- \to \pi^0\gamma$
8.1 ±2.0	BALDIN	71	HLBC	2.9 π^+p
13 ±4	JACQUET	69B	HLBC	2.05 $\pi^+p \to \pi^+p\omega$
• • • We do not use the following data for averages, fits, limits, etc. • • •				
9.7 ±0.2 ±0.5	[2,3] ACHASOV	03D	RVUE	0.44–2.00 $e^+e^- \to \pi^+\pi^-\pi^0$
9.9 ±0.7	[2] DOLINSKY	89	ND	$e^+e^- \to \pi^0\gamma$

[1] From $\sigma^{\omega\pi^0 \to \pi^0\pi^0\gamma}_0(m_\phi)/\sigma^{\omega\pi^0 \to \pi^+\pi^-\pi^0\pi^0}_0(m_\phi)$ with a phase-space correction factor of 1/1.023.
[2] Not independent of the corresponding $\Gamma(e^+e^-) \times \Gamma(\pi^0\gamma)/\Gamma^2_{total}$.
[3] Using ACHASOV 03. Based on 1.2M events.

Meson Particle Listings

$\omega(782)$

$\Gamma(\pi^+\pi^-)/\Gamma_{total}$ Γ_3/Γ

See also $\Gamma(\pi^+\pi^-)/\Gamma(\pi^+\pi^-\pi^0)$.

VALUE (units 10^{-2})	EVTS	DOCUMENT ID		TECN	COMMENT
$1.53^{+0.11}_{-0.13}$ OUR FIT		Error includes scale factor of 1.2.			
1.49 ± 0.13 OUR AVERAGE		Error includes scale factor of 1.3. See the ideogram below.			
$1.46\pm0.12\pm0.02$	900k	[1] AKHMETSHIN	07		$e^+e^- \to \pi^+\pi^-$
$1.30\pm0.24\pm0.05$	11.2k	[2] AKHMETSHIN	04	CMD2	$e^+e^- \to \pi^+\pi^-$
$2.38^{+1.77}_{-0.90}\pm0.18$	5.4k	[3] ACHASOV	02E	SND	1.1–1.38 $e^+e^- \to \pi^+\pi^-\pi^0$
$2.3\ \pm0.5$		BARKOV	85	OLYA	$e^+e^- \to \pi^+\pi^-$
$1.6\ ^{+0.9}_{-0.7}$		QUENZER	78	DM1	$e^+e^- \to \pi^+\pi^-$
$3.6\ \pm1.9$		BENAKSAS	72	OSPK	$e^+e^- \to \pi^+\pi^-$
• • • We do not use the following data for averages, fits, limits, etc. • • •					
1.75 ± 0.11	4.5M	[4] ACHASOV	05A	SND	$e^+e^- \to \pi^+\pi^-$
2.01 ± 0.29		[5] BENAYOUN	03	RVUE	$e^+e^- \to \pi^+\pi^-$
$1.9\ \pm0.3$		[6] GARDNER	99	RVUE	$e^+e^- \to \pi^+\pi^-$
$2.3\ \pm0.4$		[7] BENAYOUN	98	RVUE	$e^+e^- \to \pi^+\pi^-, \mu^+\mu^-$
$1.0\ \pm0.11$		[8] WICKLUND	78	ASPK	3,4,6 $\pi^\pm N$
1.22 ± 0.30		ALVENSLEB...	71C	CNTR	Photoproduction
$1.3\ ^{+1.2}_{-0.9}$		MOFFEIT	71	HBC	2.8,4.7 γp
$0.80^{+0.28}_{-0.20}$		[9] BIGGS	70B	CNTR	4.2 γ C $\to \pi^+\pi^-$ C

[1] A combined fit of AKHMETSHIN 07, AULCHENKO 06, and AULCHENKO 05.
[2] Update of AKHMETSHIN 02.
[3] From the $m_{\pi^+\pi^-}$ spectrum taking into account the interference of the $\rho\pi$ and $\omega\pi$ amplitudes.
[4] Using $\Gamma(\omega \to e^+e^-)$ from the 2004 Edition of this Review (PDG 04).
[5] Using the data of AKHMETSHIN 02 in the hidden local symmetry model.
[6] Using the data of BARKOV 85.
[7] Using the data of BARKOV 85 in the hidden local symmetry model.
[8] From a model-dependent analysis assuming complete coherence.
[9] Re-evaluated under $\Gamma(\pi^+\pi^-)/\Gamma(\pi^+\pi^-\pi^0)$ by BEHREND 71 using more accurate $\omega \to \rho$ photoproduction cross-section ratio.

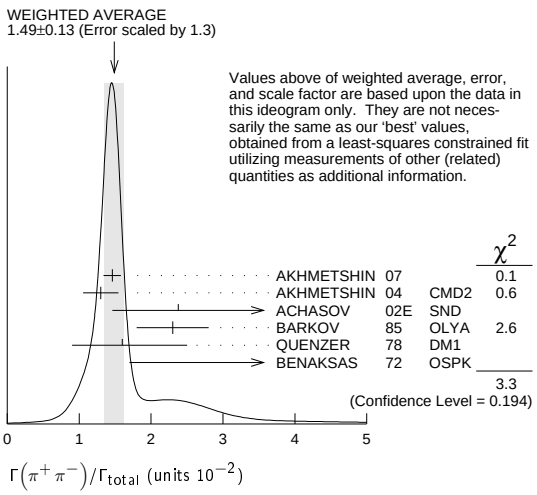

$\Gamma(\pi^+\pi^-)/\Gamma(\pi^+\pi^-\pi^0)$ Γ_3/Γ_1

See also $\Gamma(\pi^+\pi^-)/\Gamma_{total}$.

VALUE	DOCUMENT ID		TECN	COMMENT
0.0172 ± 0.0014 OUR FIT	Error includes scale factor of 1.2.			
$0.026\ \pm0.005$ OUR AVERAGE				
$0.021\ ^{+0.028}_{-0.009}$	[1,2] RATCLIFF	72	ASPK	15 $\pi^- p \to n2\pi$
$0.028\ \pm0.006$	[1] BEHREND	71	ASPK	Photoproduction
$0.022\ ^{+0.009}_{-0.01}$	[3] ROOS	70	RVUE	

[1] The fitted width of these data is 160 MeV in agreement with present average, thus the ω contribution is overestimated. Assuming ρ width 145 MeV.
[2] Significant interference effect observed. NB of $\omega \to 3\pi$ comes from an extrapolation.
[3] ROOS 70 combines ABRAMOVICH 70 and BIZZARRI 70.

$\Gamma(\pi^+\pi^-)/\Gamma(\pi^0\gamma)$ Γ_3/Γ_2

VALUE	EVTS	DOCUMENT ID		TECN	COMMENT
0.20±0.04	1.98M	[1] ALOISIO	03	KLOE	1.02 $e^+e^- \to \pi^+\pi^-\pi^0$

[1] Using the data of ALOISIO 02D.

$\Gamma(\text{neutrals})/\Gamma_{total}$ $(\Gamma_2+\Gamma_4)/\Gamma$

VALUE	EVTS	DOCUMENT ID		TECN	COMMENT
0.091 ± 0.006 OUR FIT					
0.081 ± 0.011 OUR AVERAGE					
0.075 ± 0.025		BIZZARRI	71	HBC	0.0 $p\overline{p}$
0.079 ± 0.019		DEINET	69B	OSPK	1.5 $\pi^- p$
0.084 ± 0.015		BOLLINI	68C	CNTR	2.1 $\pi^- p$
• • • We do not use the following data for averages, fits, limits, etc. • • •					
0.073 ± 0.018	42	BASILE	72B	CNTR	1.67 $\pi^- p$

$\Gamma(\text{neutrals})/\Gamma(\pi^+\pi^-\pi^0)$ $(\Gamma_2+\Gamma_4)/\Gamma_1$

VALUE	EVTS	DOCUMENT ID		TECN	COMMENT
0.102 ± 0.008 OUR FIT					
$0.103^{+0.011}_{-0.010}$ OUR AVERAGE					
$0.15\ \pm0.04$	46	AGUILAR-...	72B	HBC	3.9,4.6 $K^- p$
$0.10\ \pm0.03$	19	BARASH	67B	HBC	0.0 $\overline{p}p$
0.134 ± 0.026	850	DIGIUGNO	66B	CNTR	1.4 $\pi^- p$
0.097 ± 0.016	348	FLATTE	66	HBC	1.4 – 1.7 $K^- p \to \Lambda$MM
$0.06\ ^{+0.05}_{-0.02}$		JAMES	66	HBC	2.1 $\pi^+ p$
$0.08\ \pm0.03$	35	KRAEMER	64	DBC	1.2 $\pi^+ d$
• • • We do not use the following data for averages, fits, limits, etc. • • •					
$0.11\ \pm0.02$	20	BUSCHBECK	63	HBC	1.5 $K^- p$

$\Gamma(\pi^0\gamma)/\Gamma(\text{neutrals})$ $\Gamma_2/(\Gamma_2+\Gamma_4)$

VALUE	CL%	DOCUMENT ID		TECN	COMMENT
• • • We do not use the following data for averages, fits, limits, etc. • • •					
0.78 ± 0.07		[1] DAKIN	72	OSPK	1.4 $\pi^- p \to n$MM
>0.81	90	DEINET	69B	OSPK	

[1] Error statistical only. Authors obtain good fit also assuming $\pi^0\gamma$ as the only neutral decay.

$\Gamma(\text{neutrals})/\Gamma(\text{charged particles})$ $(\Gamma_2+\Gamma_4)/(\Gamma_1+\Gamma_3)$

VALUE	DOCUMENT ID		TECN	COMMENT
0.100 ± 0.008 OUR FIT				
0.124 ± 0.021	FELDMAN	67C	OSPK	1.2 $\pi^- p$

$\Gamma(\eta\gamma)/\Gamma_{total}$ Γ_5/Γ

VALUE (units 10^{-4})	EVTS	DOCUMENT ID		TECN	COMMENT
4.6 ±0.4 OUR FIT		Error includes scale factor of 1.1.			
6.3 ±1.3 OUR AVERAGE		Error includes scale factor of 1.2.			
6.6 ±1.7		[1] ABELE	97E	CBAR	0.0 $\overline{p}p \to 5\gamma$
8.3 ±2.1		ALDE	93	GAM2	38 $\pi^- p \to \omega n$
$3.0\ ^{+2.5}_{-1.8}$		[2] ANDREWS	77	CNTR	6.7–10 γCu
• • • We do not use the following data for averages, fits, limits, etc. • • •					
4.3 ±0.5 ±0.1	33k	[3] ACHASOV	07B	SND	0.6–1.38 $e^+e^- \to \eta\gamma$
$4.44^{+2.59}_{-1.83}\pm0.28$	17.4k	[4,5] AKHMETSHIN	05	CMD2	0.60-1.38 $e^+e^- \to \eta\gamma$
$5.10\pm0.72\pm0.34$	23k	[6] AKHMETSHIN	01B	CMD2	$e^+e^- \to \eta\gamma$
0.7 to 5.5		[7] CASE	00	CBAR	0.0 $p\overline{p} \to \eta\eta\gamma$
$6.56^{+2.41}_{-2.55}$	3525	[2,8] BENAYOUN	96	RVUE	$e^+e^- \to \eta\gamma$
7.3 ±2.9		[2,4] DOLINSKY	89	ND	$e^+e^- \to \eta\gamma$

[1] No flat $\eta\eta\gamma$ background assumed.
[2] Solution corresponding to constructive ω-ρ interference.
[3] ACHASOV 07B reports $[\Gamma(\omega(782) \to \eta\gamma)/\Gamma_{total}] \times [B(\omega(782) \to e^+e^-)] = (3.10 \pm 0.31 \pm 0.11) \times 10^{-8}$ which we divide by our best value $B(\omega(782) \to e^+e^-) = (7.28 \pm 0.14) \times 10^{-5}$. Our first error is their experiment's error and our second error is the systematic error from using our best value. Supersedes ACHASOV 00D and ACHASOV 06A.
[4] Not independent of the corresponding $\Gamma(e^+e^-) \times \Gamma(\eta\gamma)/\Gamma^2_{total}$.
[5] Using $B(\omega \to e^+e^-) = (7.14 \pm 0.13) \times 10^{-5}$ and $B(\eta \to \gamma\gamma) = 39.43 \pm 0.26\%$.
[6] Using $B(\omega \to e^+e^-) = (7.07 \pm 0.19) \times 10^{-5}$ and using $B(\eta \to 3\pi^0) = (32.24 \pm 0.29) \times 10^{-2}$. Solution corresponding to constructive ω-ρ interference. The combined fit from 600 to 1380 MeV taking into account $\rho(770)$, $\omega(782)$, $\phi(1020)$, and $\rho(1450)$ (mass and width fixed at 1450 MeV and 310 MeV respectively). Not independent of the corresponding $\Gamma(e^+e^-) \times \Gamma(\eta\gamma)/\Gamma^2_{total}$.
[7] Depending on the degree of coherence with the flat $\eta\eta\gamma$ background and using $B(\omega \to \pi^0\gamma) = (8.5 \pm 0.5) \times 10^{-2}$.
[8] Reanalysis of DRUZHININ 84, DOLINSKY 89, DOLINSKY 91 taking into account the triangle anomaly contributions.

$\Gamma(\eta\gamma)/\Gamma(\pi^0\gamma)$ Γ_5/Γ_2

VALUE	DOCUMENT ID		TECN	COMMENT
• • • We do not use the following data for averages, fits, limits, etc. • • •				
0.0098 ± 0.0024	[1] ALDE	93	GAM2	38 $\pi^- p \to \omega n$
0.0082 ± 0.0033	[2] DOLINSKY	89	ND	$e^+e^- \to \eta\gamma$
$0.010\ \pm0.045$	APEL	72B	OSPK	4–8 $\pi^- p \to n3\gamma$

[1] Model independent determination.
[2] Solution corresponding to constructive ω-ρ interference.

$\Gamma(\pi^0 e^+ e^-)/\Gamma_{\text{total}}$ Γ_6/Γ

VALUE	EVTS	DOCUMENT ID		TECN	COMMENT
7.7 ±0.6 OUR FIT					
7.7 ±0.6 OUR AVERAGE					
7.61±0.53±0.64		ACHASOV	08	SND	0.36–0.97 $e^+e^- \to \pi^0 e^+ e^-$
8.19±0.71±0.62		AKHMETSHIN	05A	CMD2	0.72–0.84 e^+e^-
5.9 ±1.9	43	DOLINSKY	88	ND	$e^+e^- \to \pi^0 e^+ e^-$

$\Gamma(\pi^0 \mu^+ \mu^-)/\Gamma_{\text{total}}$ Γ_7/Γ

VALUE	EVTS	DOCUMENT ID		TECN	COMMENT
1.3 ±0.4 OUR FIT Error includes scale factor of 2.1.					
1.3 ±0.4 OUR AVERAGE Error includes scale factor of 2.1.					
1.72±0.25±0.14	3k	ARNALDI	09	NA60	158A In–In collisions
0.96±0.23		DZHELYADIN	81B	CNTR	25–33 $\pi^- p \to \omega n$

$\Gamma(\eta e^+ e^-)/\Gamma_{\text{total}}$ Γ_8/Γ

VALUE (units 10^{-5})	DOCUMENT ID		TECN	COMMENT
• • • We do not use the following data for averages, fits, limits, etc. • • •				
<1.1	AKHMETSHIN	05A	CMD2	0.72–0.84 e^+e^-

$\Gamma(e^+ e^-)/\Gamma_{\text{total}}$ Γ_9/Γ

VALUE (units 10^{-4})	EVTS	DOCUMENT ID		TECN	COMMENT
0.728±0.014 OUR FIT Error includes scale factor of 1.3.					
• • • We do not use the following data for averages, fits, limits, etc. • • •					
0.700±0.016	11200	[1,2] AKHMETSHIN	04	CMD2	$e^+e^- \to \pi^+\pi^-\pi^0$
0.752±0.004±0.024	1.2M	[2,3] ACHASOV	03D	RVUE	0.44–2.00 $e^+e^- \to \pi^+\pi^-\pi^0$
0.714±0.036		[2] DOLINSKY	89	ND	$e^+e^- \to \pi^+\pi^-\pi^0$
0.72 ±0.03		[2] BARKOV	87	CMD	$e^+e^- \to \pi^+\pi^-\pi^0$
0.64 ±0.04	1488	[2] KURDADZE	83B	OLYA	$e^+e^- \to \pi^+\pi^-\pi^0$
0.675±0.069	433	[2] CORDIER	80	DM1	$e^+e^- \to \pi^+\pi^-\pi^0$
0.83 ±0.10	451	[2] BENAKSAS	72B	OSPK	$e^+e^- \to \pi^+\pi^-\pi^0$
0.77 ±0.06		[4] AUGUSTIN	69D	OSPK	$e^+e^- \to \pi^+\pi^-\pi^0$
0.65 ±0.13	33	[5] ASTVACAT...	68	OSPK	Assume SU(3)+mixing

[1] Using $B(\omega \to \pi^+\pi^-\pi^0) = 0.891 \pm 0.007$. Update of AKHMETSHIN 00C.
[2] Not independent of the corresponding $\Gamma(e^+e^-) \times \Gamma(\pi^+\pi^-\pi^0)/\Gamma^2_{\text{total}}$.
[3] Using ACHASOV 03, ACHASOV 03D and $B(\omega \to \pi^+\pi^-) = (1.70 \pm 0.28)\%$.
[4] Rescaled by us to correspond to ω width 8.4 MeV. Systematic errors underestimated.
[5] Not resolved from ρ decay. Error statistical only.

$\Gamma(\pi^+\pi^-\pi^0\pi^0)/\Gamma_{\text{total}}$ Γ_{10}/Γ

VALUE (units 10^{-4})	CL%	DOCUMENT ID		TECN	COMMENT
< 2	90	ACHASOV	09A	SND	$e^+e^- \to \pi^+\pi^-\pi^0\pi^0$
• • • We do not use the following data for averages, fits, limits, etc. • • •					
<200	90	KURDADZE	86	OLYA	$e^+e^- \to \pi^+\pi^-\pi^0\pi^0$

$\Gamma(\pi^+\pi^-\gamma)/\Gamma_{\text{total}}$ Γ_{11}/Γ

VALUE	CL%	DOCUMENT ID		TECN	COMMENT
<0.0036	95	WEIDENAUER	90	ASTE	$p\overline{p} \to \pi^+\pi^-\pi^+\pi^-\gamma$
• • • We do not use the following data for averages, fits, limits, etc. • • •					
<0.004	95	BITYUKOV	88B	SPEC	32 $\pi^- p \to \pi^+\pi^-\gamma$X

$\Gamma(\pi^+\pi^-\gamma)/\Gamma(\pi^+\pi^-\pi^0)$ Γ_{11}/Γ_1

VALUE	CL%	DOCUMENT ID		TECN	COMMENT
• • • We do not use the following data for averages, fits, limits, etc. • • •					
<0.066	90	KALBFLEISCH	75	HBC	2.18 $K^- p \to \Lambda\pi^+\pi^-\gamma$
<0.05	90	FLATTE	66	HBC	1.2 – 1.7 $K^- p \to \Lambda\pi^+\pi^-\gamma$

$\Gamma(\pi^+\pi^-\pi^+\pi^-)/\Gamma_{\text{total}}$ Γ_{12}/Γ

VALUE	CL%	DOCUMENT ID		TECN	COMMENT
<1 × 10^{-3}	90	KURDADZE	88	OLYA	$e^+e^- \to \pi^+\pi^-\pi^+\pi^-$

$\Gamma(\pi^0\pi^0\gamma)/\Gamma_{\text{total}}$ Γ_{13}/Γ

VALUE (units 10^{-5})	EVTS	DOCUMENT ID		TECN	COMMENT
6.6±1.1 OUR FIT					
6.5±1.2 OUR AVERAGE					
$6.4^{+2.4}_{-2.0}\pm0.8$	190	[1] AKHMETSHIN	04B	CMD2	0.6–0.97 $e^+e^- \to \pi^0\pi^0\gamma$
$6.6^{+1.4}_{-1.3}\pm0.6$	295	ACHASOV	02F	SND	0.36–0.97 $e^+e^- \to \pi^0\pi^0\gamma$
• • • We do not use the following data for averages, fits, limits, etc. • • •					
$11.8^{+2.1}_{-1.9}\pm1.4$	190	[2] AKHMETSHIN	04B	CMD2	0.6–0.97 $e^+e^- \to \pi^0\pi^0\gamma$
7.8±2.7±2.0	63	[1,3] ACHASOV	00G	SND	$e^+e^- \to \pi^0\pi^0\gamma$
12.7±2.3±2.5	63	[2,3] ACHASOV	00G	SND	$e^+e^- \to \pi^0\pi^0\gamma$

[1] In the model assuming the $\rho \to \pi^0\pi^0\gamma$ decay via the $\omega\pi$ and $f_0(500)\gamma$ mechanisms.
[2] In the model assuming the $\rho \to \pi^0\pi^0\gamma$ decay via the $\omega\pi$ mechanism only.
[3] Superseded by ACHASOV 02F.

$\Gamma(\pi^0\pi^0\gamma)/\Gamma(\pi^+\pi^-\pi^0)$ Γ_{13}/Γ_1

VALUE	CL%	DOCUMENT ID		TECN	COMMENT
<0.00045	90	DOLINSKY	89	ND	$e^+e^- \to \pi^0\pi^0\gamma$
• • • We do not use the following data for averages, fits, limits, etc. • • •					
<0.08	95	JACQUET	69B	HLBC	2.05 $\pi^+ p \to \pi^+ p\omega$

$\Gamma(\pi^0\pi^0\gamma)/\Gamma(\pi^0\gamma)$ Γ_{13}/Γ_2

VALUE (units 10^{-4})	CL%	EVTS	DOCUMENT ID		TECN	COMMENT
8.0±1.3 OUR FIT						
8.5±2.9		40 ± 14	ALDE	94B	GAM2	38$\pi^- p \to \pi^0\pi^0\gamma n$
• • • We do not use the following data for averages, fits, limits, etc. • • •						
< 50	90		DOLINSKY	89	ND	$e^+e^- \to \pi^0\pi^0\gamma$
<1800	95		KEYNE	76	CNTR	$\pi^- p \to \omega n$
<1500	90		BENAKSAS	72C	OSPK	e^+e^-
<1400			BALDIN	71	HLBC	2.9 $\pi^+ p$
<1000	90		BARMIN	64	HLBC	1.3–2.8 $\pi^- p$

$\Gamma(\pi^0\pi^0\gamma)/\Gamma(\text{neutrals})$ $\Gamma_{13}/(\Gamma_2+\Gamma_4)$

VALUE	CL%	DOCUMENT ID		TECN	COMMENT
• • • We do not use the following data for averages, fits, limits, etc. • • •					
0.22±0.07		[1] DAKIN	72	OSPK	1.4 $\pi^- p \to n$MM
<0.19	90	DEINET	69B	OSPK	

[1] See $\Gamma(\pi^0\gamma)/\Gamma(\text{neutrals})$.

$\Gamma(\eta\pi^0\gamma)/\Gamma_{\text{total}}$ Γ_{14}/Γ

VALUE (units 10^{-5})	CL%	DOCUMENT ID		TECN	COMMENT
<3.3	90	AKHMETSHIN	04B	CMD2	0.6–0.97 $e^+e^- \to \eta\pi^0\gamma$

$\Gamma(\mu^+\mu^-)/\Gamma_{\text{total}}$ Γ_{15}/Γ

VALUE (units 10^{-5})	EVTS	DOCUMENT ID		TECN	COMMENT
9.0±3.1 OUR FIT					
9.0±2.9±1.1	18	HEISTER	02C	ALEP	$Z \to \mu^+\mu^- + X$

$\Gamma(\mu^+\mu^-)/\Gamma(\pi^+\pi^-\pi^0)$ Γ_{15}/Γ_1

VALUE (units 10^{-3})	CL%	DOCUMENT ID		TECN	COMMENT
<0.2	90	WILSON	69	OSPK	12 π^-C → Fe
• • • We do not use the following data for averages, fits, limits, etc. • • •					
<1.7	74	FLATTE	66	HBC	1.2 – 1.7 $K^- p \to \Lambda\mu^+\mu^-$
<1.2		BARBARO-...	65	HBC	2.7 $K^- p$

$\Gamma(\pi^0\mu^+\mu^-)/\Gamma(\mu^+\mu^-)$ Γ_7/Γ_{15}

VALUE	EVTS	DOCUMENT ID		TECN	COMMENT
• • • We do not use the following data for averages, fits, limits, etc. • • •					
1.2±0.6	30	[1] DZHELYADIN	79	CNTR	25–33 $\pi^- p$

[1] Superseded by DZHELYADIN 81B result above.

$\Gamma(3\gamma)/\Gamma_{\text{total}}$ Γ_{16}/Γ

VALUE (units 10^{-4})	CL%	DOCUMENT ID		TECN	COMMENT
<1.9	95	[1] ABELE	97E	CBAR	0.0 $\overline{p}p \to 5\gamma$
• • • We do not use the following data for averages, fits, limits, etc. • • •					
<2	90	[1] PROKOSHKIN	95	GAM2	38 $\pi^- p \to 3\gamma n$

[1] From direct 3γ decay search.

$\Gamma(\eta\pi^0)/\Gamma_{\text{total}}$ Γ_{17}/Γ

Violates C conservation.

VALUE	CL%	DOCUMENT ID		TECN	COMMENT
• • • We do not use the following data for averages, fits, limits, etc. • • •					
<0.001	90	ALDE	94B	GAM2	38$\pi^- p \to \eta\pi^0 n$

$[\Gamma(\eta\gamma)+\Gamma(\eta\pi^0)]/\Gamma(\pi^+\pi^-\pi^0)$ $(\Gamma_5+\Gamma_{17})/\Gamma_1$

VALUE	CL%	DOCUMENT ID		TECN	COMMENT
<0.016	90	[1] FLATTE	66	HBC	1.2 – 1.7 $K^- p \to \Lambda\pi^+\pi^-$ MM
• • • We do not use the following data for averages, fits, limits, etc. • • •					
<0.045	95	JACQUET	69B	HLBC	2.05 $\pi^+ p \to \pi^+ p\omega$

[1] Restated by us using $B(\eta \to \text{charged modes}) = 29.2\%$.

$\Gamma(\eta\pi^0)/\Gamma(\pi^0\gamma)$ Γ_{17}/Γ_2

Violates C conservation.

VALUE (10^{-3})	CL%	DOCUMENT ID		TECN	COMMENT
<2.6	90	[1] STAROSTIN	09	CRYM	$\gamma p \to \eta\pi^0 p$

[1] STAROSTIN 09 reports $[\Gamma(\omega(782) \to \eta\pi^0)/\Gamma(\omega(782) \to \pi^0\gamma)] \times [B(\eta \to 2\gamma)] < 1.01 \times 10^{-3}$ which we divide by our best value $B(\eta \to 2\gamma) = 39.41 \times 10^{-2}$.

$\Gamma(2\pi^0)/\Gamma(\pi^0\gamma)$ Γ_{18}/Γ_2

Violates C conservation and Bose-Einstein statistics.

VALUE (10^{-3})	CL%	DOCUMENT ID		TECN	COMMENT
<2.59	90	STAROSTIN	09	CRYM	$\gamma p \to 2\pi^0 p$

Meson Particle Listings

$\omega(782)$, $\eta'(958)$

$\Gamma(3\pi^0)/\Gamma_{total}$ Γ_{19}/Γ

Violates C conservation.

VALUE	CL%	DOCUMENT ID	TECN	COMMENT
• • • We do not use the following data for averages, fits, limits, etc. • • •				
$<3\times10^{-4}$	90	PROKOSHKIN 95	GAM2	38 $\pi^- p \rightarrow 3\pi^0 n$

$\Gamma(3\pi^0)/\Gamma(\pi^0\gamma)$ Γ_{19}/Γ_2

Violates C conservation.

VALUE (units 10^{-3})	CL%	DOCUMENT ID	TECN	COMMENT
<2.72	90	STAROSTIN 09	CRYM	$\gamma p \rightarrow 3\pi^0 p$

$\Gamma(3\pi^0)/\Gamma(\pi^+\pi^-\pi^0)$ Γ_{19}/Γ_1

Violates C conservation.

VALUE	CL%	DOCUMENT ID	COMMENT
• • • We do not use the following data for averages, fits, limits, etc. • • •			
<0.009	90	BARBERIS 01	450 $pp \rightarrow p_f 3\pi^0 p_s$

PARAMETER Λ IN $\omega \rightarrow \pi^0\mu^+\mu^-$ DECAY

In the pole approximation the electromagnetic transition form factor for a resonance of mass M is given by the expression:

$$|F|^2 = (1 - M^2/\Lambda^2)^{-2},$$

where for the parameter Λ vector dominance predicts $\Lambda = M_\rho \approx 0.770$ GeV. The ARNALDI 09 measurement is in obvious conflict with this expectation. Note that for $\eta \rightarrow \mu^+\mu^-\gamma$ decay ARNALDI 09 and DZHELYADIN 80 obtain the value of Λ consistent with vector dominance.

VALUE (GeV)	EVTS	DOCUMENT ID	TECN	COMMENT
0.668±0.009±0.003	3k	ARNALDI 09	NA60	158A In–In collisions
• • • We do not use the following data for averages, fits, limits, etc. • • •				
0.65 ±0.03		DZHELYADIN 81B	CNTR	25–33 $\pi^- p \rightarrow \omega n$

$\omega(782)$ REFERENCES

ACHASOV 13 PR D88 054013 M.N. Achasov *et al.* (SND Collab.)
BENAYOUN 13 EPJ C73 2453 M. Benayoun, P. David, L. DelBuono (PARIN, BERLIN+)
DAVIER 13 EPJ C73 2597 M. Davier *et al.*
LEES 12G PR D86 032013 J.P. Lees *et al.* (BABAR Collab.)
NIECKNIG 12 EPJ C72 2014 F. Niecknig, B. Kubis, S.P. Schneider (BONN)
BENAYOUN 10 EPJ C65 211 M. Benayoun *et al.*
ACHASOV 09A JETP 109 379 M.N. Achasov *et al.* (SND Collab.)
Translated from ZETF 136 442.
ARNALDI 09 PL B677 260 R. Arnaldi *et al.* (NA60 Collab.)
STAROSTIN 09 PR C79 065201 A. Starostin *et al.* (Crystal Ball Collab. at MAMI)
ACHASOV 08 JETP 107 61 M.N. Achasov *et al.* (SND Collab.)
Translated from ZETF 134 80.
AMBROSINO 08G PL B669 223 F. Ambrosino *et al.* (KLOE Collab.)
ACHASOV 07B PR D76 077101 M.N. Achasov *et al.* (SND Collab.)
AKHMETSHIN 07 PL B648 28 R. Akhmetshin *et al.* (Novosibirsk CMD-2 Collab.)
ACHASOV 06 JETP 103 380 M.N. Achasov *et al.* (Novosibirsk SND Collab.)
Translated from ZETF 130 437.
ACHASOV 06A PR D74 014016 M.N. Achasov *et al.* (SND Collab.)
AULCHENKO 06 JETPL 84 413 V.M. Aulchenko *et al.* (Novosibirsk CMD-2 Collab.)
Translated from ZETFP 84 491.
ACHASOV 05A JETP 101 1053 M.N. Achasov *et al.* (Novosibirsk SND Collab.)
Translated from ZETF 128 1201.
AKHMETSHIN 05 PL B605 26 R.R. Akhmetshin *et al.* (Novosibirsk CMD-2 Collab.)
AKHMETSHIN 05A PL B613 29 R.R. Akhmetshin *et al.* (Novosibirsk CMD-2 Collab.)
AULCHENKO 05 JETPL 82 743 V.M. Aulchenko *et al.* (Novosibirsk CMD-2 Collab.)
Translated from ZETFP 82 841.
AKHMETSHIN 04 PL B578 285 R.R. Akhmetshin *et al.* (Novosibirsk CMD-2 Collab.)
AKHMETSHIN 04B PL B580 119 R.R. Akhmetshin *et al.* (Novosibirsk CMD-2 Collab.)
AUBERT,B 04N PR D70 072004 B. Aubert *et al.* (BABAR Collab.)
PDG 04 PL B592 1 S. Eidelman *et al.* (PDG Collab.)
ACHASOV 03 PL B559 171 M.N. Achasov *et al.* (Novosibirsk SND Collab.)
ACHASOV 03D PR D68 052006 M.N. Achasov *et al.* (Novosibirsk SND Collab.)
ALOISIO 03 PL B561 55 A. Aloisio *et al.* (KLOE Collab.)
BENAYOUN 03 EPJ C29 397 M. Benayoun *et al.*
ACHASOV 02E PR D66 032001 M.N. Achasov *et al.* (Novosibirsk SND Collab.)
ACHASOV 02F PL B537 201 M.N. Achasov *et al.* (Novosibirsk SND Collab.)
AKHMETSHIN 02 PL B527 161 R.R. Akhmetshin *et al.* (Novosibirsk CMD-2 Collab.)
ALOISIO 02D PL B537 21 A. Aloisio *et al.* (KLOE Collab.)
HEISTER 02C PL B528 19 A. Heister *et al.* (ALEPH Collab.)
ACHASOV 01E PR D63 072002 M.N. Achasov *et al.* (Novosibirsk SND Collab.)
AKHMETSHIN 01B PL B509 217 R.R. Akhmetshin *et al.* (Novosibirsk CMD-2 Collab.)
BARBERIS 01 PL B507 14 D. Barberis *et al.*
ACHASOV 00 EPJ C12 25 M.N. Achasov *et al.* (Novosibirsk SND Collab.)
ACHASOV 00D JETPL 72 282 M.N. Achasov *et al.* (Novosibirsk SND Collab.)
Translated from ZETFP 72 411.
ACHASOV 00G JETPL 71 355 M.N. Achasov *et al.* (Novosibirsk SND Collab.)
Translated from ZETFP 71 519.
AKHMETSHIN 00C PL B476 33 R.R. Akhmetshin *et al.* (Novosibirsk CMD-2 Collab.)
AULCHENKO 00A JETP 90 927 V.M. Aulchenko *et al.* (Novosibirsk SND Collab.)
Translated from ZETF 117 1067.
CASE 00 PR D61 032002 T. Case *et al.* (Crystal Barrel Collab.)
ACHASOV 99E PL B462 365 M.N. Achasov *et al.* (Novosibirsk SND Collab.)
GARDNER 99 PR D59 076002 S. Gardner, H.B. O'Connell
BENAYOUN 98 EPJ C2 269 M. Benayoun *et al.* (IPNP, NOVO, ADLD+)
ABELE 97E PL B411 361 A. Abele *et al.* (Crystal Barrel Collab.)
BENAYOUN 96 ZPHY C72 221 M. Benayoun *et al.* (IPNP, NOVO)
PROKOSHKIN 95 SPD 40 273 Y.D. Prokoshkin, V.D. Samoilenko (SERP)
Translated from DANS 342 610.
WURZINGER 95 PR C51 443 R. Wurzinger *et al.* (BONN, ORSAY, SACL+)
ALDE 94B PL B340 122 D.M. Alde *et al.* (SERP, BELG, LANL, LAPP+)
AMSLER 94C PL B327 425 C. Amsler *et al.* (Crystal Barrel Collab.)
ALDE 93 PAN 56 1229 D.M. Alde *et al.* (SERP, LAPP, LANL, BELG+)
Translated from YAF 56 137.
Also ZPHY C61 35 D.M. Alde *et al.* (SERP, LAPP, LANL, BELG+)
AMSLER 93B PL B311 362 C. Amsler *et al.* (Crystal Barrel Collab.)
WEIDENAUER 93 ZPHY C59 387 P. Weidenauer *et al.* (ASTERIX Collab.)
ANTONELLI 92 ZPHY C56 15 A. Antonelli *et al.* (DM2 Collab.)
DOLINSKY 91 PRPL 202 99 S.I. Dolinsky *et al.* (NOVO)
WEIDENAUER 90 ZPHY C47 353 P. Weidenauer *et al.* (ASTERIX Collab.)
DOLINSKY 89 ZPHY C42 511 S.I. Dolinsky *et al.* (NOVO)
BITYUKOV 88B SJNP 47 800 S.I. Bityukov *et al.* (SERP)
Translated from YAF 47 1258.
DOLINSKY 88 SJNP 48 277 S.I. Dolinsky *et al.* (NOVO)
Translated from YAF 48 442.
KURDADZE 88 JETPL 47 512 L.M. Kurdadze *et al.* (NOVO)
Translated from ZETFP 47 432.
AULCHENKO 87 PL B186 432 V.M. Aulchenko *et al.* (NOVO)
BARKOV 87 JETPL 46 164 L.M. Barkov *et al.* (NOVO)
Translated from ZETFP 46 132.
KURDADZE 86 JETPL 43 643 L.M. Kurdadze *et al.* (NOVO)
Translated from ZETFP 43 497.
BARKOV 85 NP B256 365 L.M. Barkov *et al.* (NOVO)
DRUZHININ 84 PL 144B 136 V.P. Druzhinin *et al.* (NOVO)
KURDADZE 83B JETPL 36 274 A.M. Kurdadze *et al.* (NOVO)
Translated from ZETFP 36 221.
DZHELYADIN 81B PL 102B 296 R.I. Dzhelyadin *et al.* (SERP)
CORDIER 80 NP B172 13 A. Cordier *et al.* (LALO)
DZHELYADIN 80 PL 94B 548 R.I. Dzhelyadin *et al.* (SERP)
ROOS 80 LNC 27 321 M. Roos, A. Pellinen (HELS)
BENKHEIRI 79 NP B150 268 P. Benkheiri *et al.* (EPOL, CERN, CDEF+)
DZHELYADIN 79 PL 84B 143 R.I. Dzhelyadin *et al.* (SERP)
COOPER 78B NP B146 1 A.M. Cooper *et al.* (TATA, CERN, CDEF+)
QUENZER 78 PL 76B 512 A. Quenzer *et al.* (LALO)
VANAPEL... 78 NP B133 245 G.W. van Apeldoorn *et al.* (ZEEM)
WICKLUND 78 PR D17 1197 A.B. Wicklund *et al.* (ANL)
ANDREWS 77 PRL 38 198 D.E. Andrews *et al.* (ROCH)
GESSAROLI 77 NP B126 382 R. Gessaroli *et al.* (BGNA, FIRZ, GENO+)
KEYNE 76 PR D14 28 J. Keyne *et al.* (LOIC, SHMP)
Also PR D8 2789 D.M. Binnie *et al.* (LOIC, SHMP)
KALBFLEISCH 75 PR D11 987 G.R. Kalbfleisch, R.C. Strand, J.W. Chapman (BNL+)
AGUILAR-... 72B PR D6 29 M. Aguilar-Benitez *et al.* (BNL)
APEL 72B PL 41B 234 W.D. Apel *et al.* (KARLK, KARLE, PISA)
BASILE 72B Phil. Conf. 153 M. Basile *et al.* (CERN)
BENAKSAS 72 PL 39B 289 D. Benaksas *et al.* (ORSAY)
BENAKSAS 72B PL 42B 507 D. Benaksas *et al.* (ORSAY)
BENAKSAS 72C PL 42B 511 D. Benaksas *et al.* (ORSAY)
BORENSTEIN 72 PR D5 1559 S.R. Borenstein *et al.* (BNL, MICH)
BROWN 72 PL 42B 117 R.M. Brown *et al.* (ILL, ILLC)
DAKIN 72 PR D6 2321 J.T. Dakin *et al.* (PRIN)
RATCLIFF 72 PL 38B 345 B.N. Ratcliff *et al.* (SLAC)
ALVENSLEB... 71C PRL 27 888 H. Alvensleben *et al.* (DESY)
BALDIN 71 SJNP 13 758 A.B. Baldin *et al.* (ITEP)
Translated from YAF 13 1318.
BEHREND 71 PRL 27 61 H.J. Behrend *et al.* (ROCH, CORN, FNAL)
BIZZARRI 71 NP B27 140 R. Bizzarri *et al.* (CERN, CDEF)
COYNE 71 NP B32 333 D.G. Coyne *et al.* (LRL)
MOFFEIT 71 NP B29 349 K.C. Moffeit *et al.* (LRL, UCB, SLAC+)
ABRAMOVI... 70 NP B20 209 M. Abramovich *et al.* (CERN)
BIGGS 70B PRL 24 1201 P.J. Biggs *et al.* (DARE)
BIZZARRI 70 PRL 25 1385 R. Bizzarri *et al.* (ROMA, SYRA)
ROOS 70 DNPL/R7 173 M. Roos (CERN)
Proc. Daresbury Study Weekend No. 1.
AUGUSTIN 69D PL 28B 513 J.E. Augustin *et al.* (ORSAY)
BIZZARRI 69 NP B14 169 R. Bizzarri *et al.* (CERN, CDEF)
DEINET 69B PL 30B 426 W. Deinet *et al.* (KARL, CERN)
JACQUET 69B NC 63A 743 F. Jacquet *et al.* (EPOL, BERG)
WILSON 69 Private Comm. R. Wilson (HARV)
Also PR 178 2095 A.A. Wehmann *et al.* (HARV, CASE, SLAC+)
ASTVACAT... 68 PL 27B 45 R.G. Astvatsaturov *et al.* (JINR, MOSU)
BOLLINI 68C NC 56A 531 D. Bollini *et al.* (CERN, BGNA, STRB)
BARASH 67B PR 156 1399 N. Barash *et al.* (COLU)
FELDMAN 67C PR 159 1219 M. Feldman *et al.* (PENN)
DIGIUGNO 66B NC 44A 1272 G. Di Giugno *et al.* (NAPL, FRAS, TRST)
FLATTE 66 PR 145 1050 S.M. Flatte *et al.* (LRL)
JAMES 66 PR 142 896 F.E. James, H.L. Kraybill (YALE, BNL)
BARBARO-... 65 PRL 14 279 A. Barbaro-Galtieri, R.D. Tripp (LRL)
BARMIN 64 JETP 18 1289 V.V. Barmin *et al.* (ITEP)
Translated from ZETF 45 1879.
KRAEMER 64 PR 136 B496 R.W. Kraemer *et al.* (JHU, NWES, WOOD)
BUSCHBECK 63 Siena Conf. 1 166 B. Buschbeck *et al.* (VIEN, CERN, ANIK)

$\eta'(958)$

$I^G(J^{PC}) = 0^+(0^{-+})$

$\eta'(958)$ MASS

VALUE (MeV)	EVTS	DOCUMENT ID		TECN	COMMENT
957.78 ±0.06 OUR AVERAGE					
957.793±0.054±0.036	3.9k	LIBBY	08	CLEO	$J/\psi \rightarrow \gamma\eta'$
957.9 ±0.2 ±0.6	4800	WURZINGER	96	SPEC	1.68 $pd \rightarrow {}^3\mathrm{He}\eta'$
957.46 ±0.33		DUANE	74	MMS	$\pi^- p \rightarrow n$MM
958.2 ±0.5	1414	DANBURG	73	HBC	2.2 $K^- p \rightarrow \Lambda\eta'$
958 ±1	400	JACOBS	73	HBC	2.9 $K^- p \rightarrow \Lambda\eta'$
956.1 ±1.1	3415	[1] BASILE	71	CNTR	1.6 $\pi^- p \rightarrow n\eta'$
• • • We do not use the following data for averages, fits, limits, etc. • • •					
957.5 ±0.2		BAI	04J	BES2	$J/\psi \rightarrow \gamma\gamma\pi^+\pi^-$
959 ±1	630	[2] BELADIDZE	92C	VES	36 π^-Be $\rightarrow \pi^-\eta'\eta$Be
958 ±1	340	[2] ARMSTRONG	91B	OMEG	300 $pp \rightarrow pp\eta\pi^+\pi^-$
958.2 ±0.4	622	[2] AUGUSTIN	90	DM2	$J/\psi \rightarrow \gamma\eta\pi^+\pi^-$
957.8 ±0.2	2420	[2] AUGUSTIN	90	DM2	$J/\psi \rightarrow \gamma\gamma\pi^+\pi^-$
956.3 ±1.0	143	[2] GIDAL	87	MRK2	$e^+e^- \rightarrow e^+e^-\eta\pi^+\pi^-$
957.4 ±1.4	535	[3] BASILE	71	CNTR	1.6 $\pi^- p \rightarrow n\eta'$
957 ±1		RITTENBERG	69	HBC	1.7–2.7 $K^- p$

[1] Using all η' decays.
[2] Systematic uncertainty not estimated.
[3] Using η' decays into neutrals. Not independent of the other listed BASILE 71 η' mass measurement.

$\eta'(958)$ WIDTH

VALUE (MeV)	EVTS	DOCUMENT ID		TECN	CHG	COMMENT
0.198±0.009 OUR FIT						
0.230±0.021 OUR AVERAGE						
0.226±0.017±0.014	2300	CZERWINSKI	10	MMS		$pp \rightarrow pp\eta'$
0.40 ±0.22	4800	WURZINGER	96	SPEC		1.68 $pd \rightarrow {}^3\mathrm{He}\eta'$
0.28 ±0.10	1000	BINNIE	79	MMS	0	$\pi^- p \rightarrow n$MM
• • • We do not use the following data for averages, fits, limits, etc. • • •						
0.20 ±0.04		BAI	04J	BES2		$J/\psi \rightarrow \gamma\gamma\pi^+\pi^-$

$\eta'(958)$ DECAY MODES

	Mode	Fraction (Γ_i/Γ)	Confidence level
Γ_1	$\pi^+\pi^-\eta$	(42.9 ±0.7) %	
Γ_2	$\rho^0\gamma$(including non-resonant $\pi^+\pi^-\gamma$)	(29.1 ±0.5) %	
Γ_3	$\pi^0\pi^0\eta$	(22.2 ±0.8) %	
Γ_4	$\omega\gamma$	(2.75±0.23) %	
Γ_5	$\gamma\gamma$	(2.20±0.08) %	
Γ_6	$3\pi^0$	(2.14±0.20) $\times10^{-3}$	
Γ_7	$\mu^+\mu^-\gamma$	(1.08±0.27) $\times10^{-4}$	
Γ_8	$\pi^+\pi^-\mu^+\mu^-$	< 2.9 $\times10^{-5}$	90%
Γ_9	$\pi^+\pi^-\pi^0$	(3.8 ±0.4) $\times10^{-3}$	
Γ_{10}	$\pi^0\rho^0$	< 4 %	90%
Γ_{11}	$2(\pi^+\pi^-)$	< 2.4 $\times10^{-4}$	90%
Γ_{12}	$\pi^+\pi^-2\pi^0$	< 2.5 $\times10^{-3}$	90%
Γ_{13}	$2(\pi^+\pi^-)$ neutrals	< 1 %	95%
Γ_{14}	$2(\pi^+\pi^-)\pi^0$	< 1.9 $\times10^{-3}$	90%
Γ_{15}	$2(\pi^+\pi^-)2\pi^0$	< 1 %	95%
Γ_{16}	$3(\pi^+\pi^-)$	< 3.1 $\times10^{-5}$	90%
Γ_{17}	$\pi^+\pi^-e^+e^-$	(2.4 $^{+1.3}_{-1.0}$) $\times10^{-3}$	
Γ_{18}	$\pi^+e^-\nu_e$ + c.c.	< 2.1 $\times10^{-4}$	90%
Γ_{19}	γe^+e^-	< 9 $\times10^{-4}$	90%
Γ_{20}	$\pi^0\gamma\gamma$	< 8 $\times10^{-4}$	90%
Γ_{21}	$4\pi^0$	< 5 $\times10^{-4}$	90%
Γ_{22}	e^+e^-	< 2.1 $\times10^{-7}$	90%
Γ_{23}	invisible	< 5 $\times10^{-4}$	90%

Charge conjugation (C), Parity (P), Lepton family number (LF) violating modes

Γ_{24}	$\pi^+\pi^-$	P,CP	< 6	$\times10^{-5}$		90%
Γ_{25}	$\pi^0\pi^0$	P,CP	< 4	$\times10^{-4}$		90%
Γ_{26}	$\pi^0e^+e^-$	C	[a] < 1.4	$\times10^{-3}$		90%
Γ_{27}	ηe^+e^-	C	[a] < 2.4	$\times10^{-3}$		90%
Γ_{28}	3γ	C	< 1.0	$\times10^{-4}$		90%
Γ_{29}	$\mu^+\mu^-\pi^0$	C	[a] < 6.0	$\times10^{-5}$		90%
Γ_{30}	$\mu^+\mu^-\eta$	C	[a] < 1.5	$\times10^{-5}$		90%
Γ_{31}	$e\mu$	LF	< 4.7	$\times10^{-4}$		90%

[a] C parity forbids this to occur as a single-photon process.

CONSTRAINED FIT INFORMATION

An overall fit to the total width, a partial width, 2 combinations of partial widths obtained from integrated cross section, and 15 branching ratios uses 43 measurements and one constraint to determine 9 parameters. The overall fit has a $\chi^2 = 48.0$ for 35 degrees of freedom.

The following *off-diagonal* array elements are the correlation coefficients $\langle\delta p_i\delta p_j\rangle/(\delta p_i\cdot\delta p_j)$, in percent, from the fit to parameters p_i, including the branching fractions, $x_i \equiv \Gamma_i/\Gamma_{total}$. The fit constrains the x_i whose labels appear in this array to sum to one.

	x_1	x_2	x_3	x_4	x_5	x_6	x_9	x_{17}
x_2	0							
x_3	−76	−58						
x_4	−19	−23	4					
x_5	−29	−25	32	−1				
x_6	−24	−18	29	1	9			
x_9	0	−2	−3	−1	−1	−1		
x_{17}	−4	−6	−5	−2	−3	−2	0	
Γ	25	5	−19	5	−71	−5	1	3

	Mode	Rate (MeV)	
Γ_1	$\pi^+\pi^-\eta$	0.085 ±0.004	
Γ_2	$\rho^0\gamma$(including non-resonant $\pi^+\pi^-\gamma$)	0.0575 ±0.0028	
Γ_3	$\pi^0\pi^0\eta$	0.0439 ±0.0023	
Γ_4	$\omega\gamma$	0.0054 ±0.0005	
Γ_5	$\gamma\gamma$	0.00435 ±0.00013	
Γ_6	$3\pi^0$	(4.2 ±0.4) $\times10^{-4}$	
Γ_9	$\pi^+\pi^-\pi^0$	(7.5 ±0.8) $\times10^{-4}$	
Γ_{17}	$\pi^+\pi^-e^+e^-$	(4.7 $^{+2.6}_{-1.9}$) $\times10^{-4}$	

$\eta'(958)$ PARTIAL WIDTHS

$\Gamma(\gamma\gamma)$ Γ_5

VALUE (keV)	EVTS	DOCUMENT ID		TECN	COMMENT
4.35±0.14 OUR FIT					
4.28±0.19 OUR AVERAGE					
4.17±0.10±0.27	2000	[4] ACCIARRI	98Q	L3	$e^+e^-\to e^+e^-\pi^+\pi^-\gamma$
4.53±0.29±0.51	266	KARCH	92	CBAL	$e^+e^-\to e^+e^-\eta\pi^0\pi^0$
3.61±0.13±0.48		[5] BEHREND	91	CELL	$e^+e^-\to e^+e^-\eta'(958)$
4.6 ±1.1 ±0.6	23	BARU	90	MD1	$e^+e^-\to e^+e^-\pi^+\pi^-\gamma$
4.57±0.25±0.44		BUTLER	90	MRK2	$e^+e^-\to e^+e^-\eta'(958)$
5.08±0.24±0.71	547	[6] ROE	90	ASP	$e^+e^-\to e^+e^-2\gamma$
3.8 ±0.7 ±0.6	34	AIHARA	88C	TPC	$e^+e^-\to e^+e^-\eta\pi^+\pi^-$
4.9 ±0.5 ±0.5	136	[7] WILLIAMS	88	CBAL	$e^+e^-\to e^+e^-2\gamma$
• • • We do not use the following data for averages, fits, limits, etc. • • •					
4.7 ±0.6 ±0.9	143	[8] GIDAL	87	MRK2	$e^+e^-\to e^+e^-\eta\pi^+\pi^-$
4.0 ±0.9		[9] BARTEL	85E	JADE	$e^+e^-\to e^+e^-2\gamma$

[4] No non-resonant $\pi^+\pi^-$ contribution found.
[5] Reevaluated by us using $B(\eta'\to\rho(770)\gamma) = (30.2\pm1.3)\%$.
[6] Reevaluated by us using $B(\eta'\to\gamma\gamma) = (2.11\pm0.13)\%$.
[7] Reevaluated by us using $B(\eta'\to\gamma\gamma) = (2.11\pm0.13)\%$.
[8] Superseded by BUTLER 90.
[9] Systematic error not evaluated.

$\eta'(958)$ Γ(i)$\Gamma(\gamma\gamma)/\Gamma$(total)

This combination of a partial width with the partial width into $\gamma\gamma$ and with the total width is obtained from the integrated cross section into channel(i) in the $\gamma\gamma$ annihilation.

$\Gamma(\gamma\gamma)\times\Gamma(\rho^0\gamma$(including non-resonant $\pi^+\pi^-\gamma))/\Gamma_{total}$ $\Gamma_5\Gamma_2/\Gamma$

VALUE (keV)	EVTS	DOCUMENT ID		TECN	COMMENT
1.27±0.04 OUR FIT					
1.26±0.07 OUR AVERAGE	Error includes scale factor of 1.2.				
1.09±0.04±0.13		BEHREND	91	CELL	$e^+e^-\to e^+e^-\rho(770)^0\gamma$
1.35±0.09±0.21		AIHARA	87	TPC	$e^+e^-\to e^+e^-\rho\gamma$
1.13±0.04±0.13	867	ALBRECHT	87B	ARG	$e^+e^-\to e^+e^-\rho\gamma$
1.53±0.09±0.21		ALTHOFF	84E	TASS	$e^+e^-\to e^+e^-\rho\gamma$
1.14±0.08±0.11	243	BERGER	84B	PLUT	$e^+e^-\to e^+e^-\rho\gamma$
1.73±0.34±0.35	95	JENNI	83	MRK2	$e^+e^-\to e^+e^-\rho\gamma$
1.49±0.13±0.027	213	BARTEL	82B	JADE	$e^+e^-\to e^+e^-\rho\gamma$
• • • We do not use the following data for averages, fits, limits, etc. • • •					
1.85±0.31±0.24	43	BEHREND	83B	CELL	$e^+e^-\to e^+e^-\rho\gamma$

$\Gamma(\gamma\gamma)\times\Gamma(\pi^0\pi^0\eta)/\Gamma_{total}$ $\Gamma_5\Gamma_3/\Gamma$

VALUE (keV)	DOCUMENT ID		TECN	COMMENT
0.97±0.05 OUR FIT				
0.92±0.06±0.11	[10] KARCH	92	CBAL	$e^+e^-\to e^+e^-\eta\pi^0\pi^0$
• • • We do not use the following data for averages, fits, limits, etc. • • •				
0.95±0.05±0.08	[11] KARCH	90	CBAL	$e^+e^-\to e^+e^-\eta\pi^0\pi^0$
1.00±0.08±0.10	[11,12] ANTREASYAN	87	CBAL	$e^+e^-\to e^+e^-\eta\pi^0\pi^0$

[10] Reevaluated by us using $B(\eta\to\gamma\gamma) = (39.21\pm0.34)\%$. Supersedes ANTREASYAN 87 and KARCH 90.
[11] Superseded by KARCH 92.
[12] Using $BR(\eta\to2\gamma)$=(38.9 ± 0.5)%.

$\eta'(958)\to\eta\pi\pi$ DECAY PARAMETERS

$$|\text{MATRIX ELEMENT}|^2 = |1+\alpha Y|^2 + CX + DX^2$$

X and Y are Dalitz variables; α is complex and C, and D are real-valued. Parameters C and D are not necessarily equal to c and d, respectively, in the generalized parameterization following this one. May be different for $\eta'(958)\to\eta\pi^+\pi^-$ and $\eta'(958)\to\eta\pi^0\pi^0$ decays. Because of different initial assumptions and strong correlations of the parameters we do not average the parameters in the section below.

$Re(\alpha)$ decay parameter

VALUE	EVTS	DOCUMENT ID		TECN	COMMENT
• • • We do not use the following data for averages, fits, limits, etc. • • •					
−0.033±0.005±0.003	44k	[13] ABLIKIM	11	BES3	$J/\psi\to\gamma\eta\pi^+\pi^-$
−0.072±0.012±0.006	7k	[14] AMELIN	05A	VES	28 $\pi^-A\to\eta\pi^+\pi^-\pi^-A^*$
−0.021±0.018±0.017	6.7k	[15] BRIERE	00	CLEO	10.6 $e^+e^-\to\eta\pi^+\pi^-X$
−0.058±0.013±0.003	5.4k	[16] ALDE	86	GAM2	38 $\pi^-p\to n\eta\pi^0\pi^0$
−0.08 ±0.03		[16,17] KALBFLEISCH	74	RVUE	$\eta'\to\eta\pi^+\pi^-$

[13] See ABLIKIM 11 for the full correlation matrix.
[14] Superseded by DOROFEEV 07, which found this parameterization unacceptable. See below.
[15] Assuming $Im(\alpha) = 0$, $C = 0$, and $D = 0$.
[16] Assuming $C = 0$.
[17] From the data of DAUBER 64, RITTENBERG 69, AGUILAR-BENITEZ 72B, JACOBS 73, and DANBURG 73.

Meson Particle Listings

$\eta'(958)$

Im(α) decay parameter

VALUE	EVTS	DOCUMENT ID		TECN	COMMENT
• • • We do not use the following data for averages, fits, limits, etc. • • •					
$0.000 \pm 0.049 \pm 0.001$	44k	[18] ABLIKIM	11	BES3	$J/\psi \to \gamma\eta\pi^+\pi^-$
$0.0 \pm 0.1 \pm 0.0$	7k	[19] AMELIN	05A	VES	28 $\pi^- A \to \eta\pi^+\pi^-\pi^- A^*$
$-0.00 \pm 0.13 \pm 0.00$	5.4k	[20] ALDE	86	GAM2	38 $\pi^- p \to n\eta\pi^0\pi^0$
0.0 ± 0.3		[20,21] KALBFLEISCH	74	RVUE	$\eta' \to \eta\pi^+\pi^-$

[18] See ABLIKIM 11 for the full correlation matrix.
[19] Superseded by DOROFEEV 07, which found this parameterization unacceptable. See below.
[20] Assuming $C = 0$.
[21] From the data of DAUBER 64, RITTENBERG 69, AGUILAR-BENITEZ 72B, JACOBS 73, and DANBURG 73.

C decay parameter

VALUE	EVTS	DOCUMENT ID		TECN	COMMENT
• • • We do not use the following data for averages, fits, limits, etc. • • •					
$+0.018 \pm 0.009 \pm 0.003$	44k	[22] ABLIKIM	11	BES3	$J/\psi \to \gamma\eta\pi^+\pi^-$
$0.020 \pm 0.018 \pm 0.004$	7k	[23] AMELIN	05A	VES	28 $\pi^- A \to \eta\pi^+\pi^-\pi^- A^*$

[22] See ABLIKIM 11 for the full correlation matrix.
[23] Superseded by DOROFEEV 07, which found this parameterization unacceptable. See below.

D decay parameter

VALUE	EVTS	DOCUMENT ID		TECN	COMMENT
• • • We do not use the following data for averages, fits, limits, etc. • • •					
$-0.059 \pm 0.012 \pm 0.004$	44k	[24] ABLIKIM	11	BES3	$J/\psi \to \gamma\eta\pi^+\pi^-$
$-0.066 \pm 0.030 \pm 0.015$	7k	[25] AMELIN	05A	VES	28 $\pi^- A \to \eta\pi^+\pi^-\pi^- A^*$
$0.00 \pm 0.03 \pm 0.00$	5.4k	[26] ALDE	86	GAM2	38 $\pi^- p \to n\eta\pi^0\pi^0$
0		[26,27] KALBFLEISCH	74	RVUE	$\eta' \to \eta\pi^+\pi^-$

[24] See ABLIKIM 11 for the full correlation matrix.
[25] Superseded by DOROFEEV 07, which found this parameterization unacceptable. See below.
[26] Assuming $C = 0$.
[27] From the data of DAUBER 64, RITTENBERG 69, AGUILAR-BENITEZ 72B, JACOBS 73, and DANBURG 73.

$\eta'(958) \to \eta\pi\pi$ DECAY PARAMETERS

$$|\text{MATRIX ELEMENT}|^2 \propto 1 + a\,Y + b\,Y^2 + c\,X + d\,X^2$$

X and Y are Dalitz variables and a, b, c, and d are real-valued parameters. May be different for $\eta'(958) \to \eta\pi^+\pi^-$ and $\eta'(958) \to \eta\pi^0\pi^0$ decays. We do not average measurements in the section below because parameter values from each experiment are strongly correlated.

a decay parameter

VALUE	EVTS	DOCUMENT ID		TECN	COMMENT
• • • We do not use the following data for averages, fits, limits, etc. • • •					
$-0.047 \pm 0.011 \pm 0.003$	44k	[28] ABLIKIM	11	BES3	$J/\psi \to \gamma\eta\pi^+\pi^-$
$-0.066 \pm 0.016 \pm 0.003$	15k	[29] BLIK	09	GAM4	32.5 $\pi^- p \to \eta' n$
$-0.127 \pm 0.016 \pm 0.008$	20k	[30] DOROFEEV	07	VES	27 $\pi^- p \to \eta' n$, $\pi^- A \to \eta'\pi^- A^*$

[28] See ABLIKIM 11 for the full correlation matrix.
[29] From $\eta' \to \eta\pi^0\pi^0$ decay.
[30] From $\eta' \to \eta\pi^+\pi^-$ decay.

b decay parameter

VALUE	EVTS	DOCUMENT ID		TECN	COMMENT
• • • We do not use the following data for averages, fits, limits, etc. • • •					
$-0.069 \pm 0.019 \pm 0.009$	44k	[31] ABLIKIM	11	BES3	$J/\psi \to \gamma\eta\pi^+\pi^-$
$-0.063 \pm 0.028 \pm 0.004$	15k	[32] BLIK	09	GAM4	32.5 $\pi^- p \to \eta' n$
$-0.106 \pm 0.028 \pm 0.014$	20k	[33] DOROFEEV	07	VES	27 $\pi^- p \to \eta' n$, $\pi^- A \to \eta'\pi^- A^*$

[31] See ABLIKIM 11 for the full correlation matrix.
[32] From $\eta' \to \eta\pi^0\pi^0$ decay.
[33] From $\eta' \to \eta\pi^+\pi^-$ decay.

c decay parameter

VALUE	EVTS	DOCUMENT ID		TECN	COMMENT
• • • We do not use the following data for averages, fits, limits, etc. • • •					
$+0.019 \pm 0.011 \pm 0.003$	44k	[34] ABLIKIM	11	BES3	$J/\psi \to \gamma\eta\pi^+\pi^-$
$-0.107 \pm 0.096 \pm 0.003$	15k	[35] BLIK	09	GAM4	32.5 $\pi^- p \to \eta' n$
$0.015 \pm 0.011 \pm 0.014$	20k	[36] DOROFEEV	07	VES	27 $\pi^- p \to \eta' n$, $\pi^- A \to \eta'\pi^- A^*$

[34] See ABLIKIM 11 for the full correlation matrix.
[35] From $\eta' \to \eta\pi^0\pi^0$ decay.
[36] From $\eta' \to \eta\pi^+\pi^-$ decay.

d decay parameter

VALUE	EVTS	DOCUMENT ID		TECN	COMMENT
• • • We do not use the following data for averages, fits, limits, etc. • • •					
$-0.073 \pm 0.012 \pm 0.003$	44k	[37] ABLIKIM	11	BES3	$J/\psi \to \gamma\eta\pi^+\pi^-$
$0.018 \pm 0.078 \pm 0.006$	15k	[38] BLIK	09	GAM4	32.5 $\pi^- p \to \eta' n$
$-0.082 \pm 0.017 \pm 0.008$	20k	[39] DOROFEEV	07	VES	27 $\pi^- p \to \eta' n$, $\pi^- A \to \eta'\pi^- A^*$

[37] See ABLIKIM 11 for the full correlation matrix.
[38] From $\eta' \to \eta\pi^0\pi^0$ decay. If $c \equiv 0$ from Bose-Einstein symmetry, $d = -0.067 \pm 0.020 \pm 0.003$.
[39] From $\eta' \to \eta\pi^+\pi^-$ decay.

$\eta'(958)$ β PARAMETER
$|\text{MATRIX ELEMENT}|^2 = (1 + 2\beta Z)$

See the "Note on η Decay Parameters" in our 1994 edition Physical Review **D50** 1173 (1994), p. 1454.

β decay parameter

VALUE	EVTS	DOCUMENT ID		TECN	COMMENT
-0.46 ± 0.22 OUR AVERAGE		Error includes scale factor of 1.4.			
-0.59 ± 0.18	235	BLIK	08	GAMS	32 $\pi^- p \to \eta' n$
-0.1 ± 0.3		ALDE	87B	GAM2	38 $\pi^- p \to n3\pi^0$

$\eta'(958)$ BRANCHING RATIOS

$\Gamma(\pi^+\pi^-\eta)/\Gamma_{\text{total}}$ Γ_1/Γ

VALUE	EVTS	DOCUMENT ID		TECN	COMMENT
0.429 ± 0.007 OUR FIT					
• • • We do not use the following data for averages, fits, limits, etc. • • •					
$0.424 \pm 0.011 \pm 0.004$	1.2k	[40] PEDLAR	09	CLEO	$J/\psi \to \gamma\eta'$

[40] Not independent of other η' branching fractions and ratios in PEDLAR 09.

$\Gamma(\pi^+\pi^-\eta(\text{charged decay}))/\Gamma_{\text{total}}$ $0.286\Gamma_1/\Gamma$

VALUE	EVTS	DOCUMENT ID		TECN	COMMENT
0.1228 ± 0.0020 OUR FIT					
• • • We do not use the following data for averages, fits, limits, etc. • • •					
0.123 ± 0.014	107	RITTENBERG	69	HBC	1.7–2.7 $K^- p$
0.10 ± 0.04	10	LONDON	66	HBC	2.24 $K^- p \to \Lambda 2\pi^+ 2\pi^- \pi^0$
0.07 ± 0.04	7	BADIER	65B	HBC	3 $K^- p$

$\Gamma(\pi^+\pi^-\eta(\text{neutral decay}))/\Gamma_{\text{total}}$ $0.714\Gamma_1/\Gamma$

VALUE	EVTS	DOCUMENT ID		TECN	COMMENT
0.307 ± 0.005 OUR FIT					
• • • We do not use the following data for averages, fits, limits, etc. • • •					
0.314 ± 0.026	281	RITTENBERG	69	HBC	1.7–2.7 $K^- p$

$\Gamma(\rho^0\gamma(\text{including non-resonant}\,\pi^+\pi^-\gamma))/\Gamma_{\text{total}}$ Γ_2/Γ

VALUE	EVTS	DOCUMENT ID		TECN	COMMENT
0.291 ± 0.006 OUR FIT					
• • • We do not use the following data for averages, fits, limits, etc. • • •					
$0.287 \pm 0.007 \pm 0.004$	0.2k	[41] PEDLAR	09	CLEO	$J/\psi \to \gamma\eta'$
0.329 ± 0.033	298	RITTENBERG	69	HBC	1.7–2.7 $K^- p$
0.2 ± 0.1	20	LONDON	66	HBC	2.24 $K^- p \to \Lambda\pi^+\pi^-\gamma$
0.34 ± 0.09	35	BADIER	65B	HBC	3 $K^- p$

[41] Not independent of other η' branching fractions and ratios in PEDLAR 09.

$\Gamma(\rho^0\gamma(\text{including non-resonant}\,\pi^+\pi^-\gamma))/\Gamma(\pi^+\pi^-\eta)$ Γ_2/Γ_1

VALUE	DOCUMENT ID		TECN	COMMENT
0.677 ± 0.017 OUR FIT				
0.683 ± 0.020 OUR AVERAGE				
$0.677 \pm 0.024 \pm 0.011$	PEDLAR	09	CLE3	$J/\psi \to \eta'\gamma$
0.69 ± 0.03	ABLIKIM	06E	BES2	$J/\psi \to \eta'\gamma$

$\Gamma(\rho^0\gamma(\text{including non-resonant}\,\pi^+\pi^-\gamma))/\Gamma(\pi^+\pi^-\eta(\text{neutral decay}))$ $\Gamma_2/0.714\Gamma_1$

VALUE	EVTS	DOCUMENT ID		TECN	COMMENT
0.949 ± 0.024 OUR FIT					
0.97 ± 0.09 OUR AVERAGE					
0.70 ± 0.22		AMSLER	04B	CBAR	0 $\bar{p}p \to \pi^+\pi^-\eta$
1.07 ± 0.17		BELADIDZE	92C	VES	36 π^-Be $\to \pi^-\eta'\eta$Be
0.92 ± 0.14	473	DANBURG	73	HBC	2.2 $K^- p \to \Lambda X^0$
1.11 ± 0.18	192	JACOBS	73	HBC	2.9 $K^- p \to \Lambda X^0$

$\Gamma(\pi^0\pi^0\eta)/\Gamma_{\text{total}}$ Γ_3/Γ

VALUE	EVTS	DOCUMENT ID		TECN	COMMENT
0.222 ± 0.008 OUR FIT					
• • • We do not use the following data for averages, fits, limits, etc. • • •					
$0.235 \pm 0.013 \pm 0.004$	3.2k	[42] PEDLAR	09	CLEO	$J/\psi \to \gamma\eta'$

[42] Not independent of other η' branching fractions and ratios in PEDLAR 09.

$\Gamma(\pi^0\pi^0\eta(3\pi^0\text{ decay}))/\Gamma_{\text{total}}$ — $0.321\Gamma_3/\Gamma$

VALUE	EVTS	DOCUMENT ID		TECN	COMMENT
0.0712±0.0026 OUR FIT					
• • • We do not use the following data for averages, fits, limits, etc. • • •					
0.11 ±0.06	4	BENSINGER	70	DBC	2.2 $\pi^+ d$

$\Gamma(\pi^0\pi^0\eta)/\Gamma(\pi^+\pi^-\eta)$ — Γ_3/Γ_1

VALUE	DOCUMENT ID		TECN	COMMENT
0.517±0.026 OUR FIT				
0.555±0.043±0.013	PEDLAR	09	CLE3	$J/\psi \to \eta'\gamma$

$\Gamma(\rho^0\gamma(\text{including non-resonant }\pi^+\pi^-\gamma))/\Gamma(\pi\pi\eta)$ — $\Gamma_2/(\Gamma_1+\Gamma_3)$

VALUE	DOCUMENT ID		TECN	COMMENT
0.447±0.012 OUR FIT				
0.43 ±0.02 ±0.02	BARBERIS	98C	OMEG	450 $pp \to p_f \eta' p_s$
• • • We do not use the following data for averages, fits, limits, etc. • • •				
0.31 ±0.15	DAVIS	68	HBC	5.5 $K^- p$

$\Gamma(\omega\gamma)/\Gamma_{\text{total}}$ — Γ_4/Γ

VALUE	EVTS	DOCUMENT ID		TECN	COMMENT
0.0275±0.0023 OUR FIT					
• • • We do not use the following data for averages, fits, limits, etc. • • •					
0.0234±0.0030±0.0004	70	[43] PEDLAR	09	CLEO	$J/\psi \to \gamma\eta'$

[43] Not independent of other η' branching fractions and ratios in PEDLAR 09.

$\Gamma(\omega\gamma)/\Gamma(\pi^+\pi^-\eta)$ — Γ_4/Γ_1

VALUE	EVTS	DOCUMENT ID		TECN	COMMENT
0.064±0.006 OUR FIT					
0.055±0.007±0.001		PEDLAR	09	CLE3	$J/\psi \to \eta'\gamma$
• • • We do not use the following data for averages, fits, limits, etc. • • •					
0.068±0.013	68	ZANFINO	77	ASPK	8.4 $\pi^- p$

$\Gamma(\omega\gamma)/\Gamma(\pi^0\pi^0\eta)$ — Γ_4/Γ_3

VALUE	DOCUMENT ID		TECN	COMMENT
0.124±0.011 OUR FIT				
0.147±0.016	ALDE	87B	GAM2	38 $\pi^- p \to n4\gamma$

$\Gamma(\rho^0\gamma(\text{including non-resonant }\pi^+\pi^-\gamma))/[\Gamma(\pi^+\pi^-\eta)+\Gamma(\pi^0\pi^0\eta)+\Gamma(\omega\gamma)]$ — $\Gamma_2/(\Gamma_1+\Gamma_3+\Gamma_4)$

VALUE	DOCUMENT ID		TECN	COMMENT
0.428±0.011 OUR FIT				
• • • We do not use the following data for averages, fits, limits, etc. • • •				
0.25 ±0.14	DAUBER	64	HBC	1.95 $K^- p$

$[\Gamma(\pi^0\pi^0\eta(\text{charged decay}))+\Gamma(\omega(\text{charged decay})\gamma)]/\Gamma_{\text{total}}$ — $(0.286\Gamma_3+0.89\Gamma_4)/\Gamma$

VALUE	EVTS	DOCUMENT ID		TECN	COMMENT
0.0880±0.0031 OUR FIT					
• • • We do not use the following data for averages, fits, limits, etc. • • •					
0.045 ±0.029	42	RITTENBERG	69	HBC	1.7–2.7 $K^- p$

$\Gamma(\pi^+\pi^-\text{neutrals})/\Gamma_{\text{total}}$ — $(0.714\Gamma_1+0.286\Gamma_3+0.89\Gamma_4)/\Gamma$

VALUE	EVTS	DOCUMENT ID		TECN	COMMENT
0.395±0.004 OUR FIT					
• • • We do not use the following data for averages, fits, limits, etc. • • •					
0.4 ±0.1	39	LONDON	66	HBC	2.24 $K^- p \to \Lambda\pi^+\pi^-$ neutrals
0.35 ±0.06	33	BADIER	65B	HBC	3 $K^- p$

$\Gamma(\gamma\gamma)/\Gamma_{\text{total}}$ — Γ_5/Γ

VALUE (units 10^{-2})	EVTS	DOCUMENT ID		TECN	COMMENT
2.20±0.08 OUR FIT					
2.00±0.15 OUR AVERAGE					
$1.98^{+0.31}_{-0.27}\pm0.07$	114	[44] WICHT	08	BELL	$B^\pm \to K^\pm\gamma\gamma$
2.00±0.18		[45] STANTON	80	SPEC	8.45 $\pi^- p \to n\pi^+\pi^- 2\gamma$
• • • We do not use the following data for averages, fits, limits, etc. • • •					
2.25±0.16±0.03	0.3k	[46] PEDLAR	09	CLEO	$J/\psi \to \gamma\eta'$
1.8 ±0.2	6000	[47] APEL	79	NICE	15–40 $\pi^- p \to n2\gamma$
2.5 ±0.7		DUANE	74	MMS	$\pi^- p \to n$MM
1.71±0.33	68	DALPIAZ	72	CNTR	1.6 $\pi^- p \to nX^0$
$2.0\ ^{+0.8}_{-0.6}$	31	HARVEY	71	OSPK	3.65 $\pi^- p \to nX^0$

[44] WICHT 08 reports $[\Gamma(\eta'(958) \to \gamma\gamma)/\Gamma_{\text{total}}] \times [B(B^+ \to \eta' K^+)] = (1.40^{+0.16+0.15}_{-0.15-0.12}) \times 10^{-6}$ which we divide by our best value $B(B^+ \to \eta' K^+) = (7.06 \pm 0.25) \times 10^{-5}$. Our first error is their experiment's error and our second error is the systematic error from using our best value.

[45] Includes APEL 79 result.

[46] Not independent of other η' branching fractions and ratios in PEDLAR 09.

[47] Data is included in STANTON 80 evaluation.

$\Gamma(\gamma\gamma)/\Gamma(\pi^+\pi^-\eta)$ — Γ_5/Γ_1

VALUE	DOCUMENT ID		TECN	COMMENT
0.0513±0.0022 OUR FIT				
0.053 ±0.004 ±0.001	PEDLAR	09	CLE3	$J/\psi \to \eta'\gamma$

$\Gamma(\gamma\gamma)/\Gamma(\rho^0\gamma(\text{including non-resonant }\pi^+\pi^-\gamma))$ — Γ_5/Γ_2

VALUE	DOCUMENT ID		TECN	COMMENT
0.0757±0.0033 OUR FIT				
0.080 ±0.008	ABLIKIM	06E	BES2	$J/\psi \to \eta'\gamma$

$\Gamma(\gamma\gamma)/\Gamma(\pi^0\pi^0\eta)$ — Γ_5/Γ_3

VALUE	DOCUMENT ID		TECN	COMMENT
0.099±0.004 OUR FIT				
0.105±0.010 OUR AVERAGE Error includes scale factor of 1.9.				
0.091±0.009	AMSLER	93	CBAR	0.0 $\bar{p}p$
0.112±0.002±0.006	ALDE	87B	GAM2	38 $\pi^- p \to n2\gamma$

$\Gamma(\gamma\gamma)/\Gamma(\pi^0\pi^0\eta(\text{neutral decay}))$ — $\Gamma_5/0.714\Gamma_3$

VALUE	EVTS	DOCUMENT ID		TECN	COMMENT
0.139±0.006 OUR FIT					
• • • We do not use the following data for averages, fits, limits, etc. • • •					
0.188±0.058	16	APEL	72	OSPK	3.8 $\pi^- p \to nX^0$

$\Gamma(\text{neutrals})/\Gamma_{\text{total}}$ — $(0.714\Gamma_3+0.09\Gamma_4+\Gamma_5)/\Gamma$

VALUE	EVTS	DOCUMENT ID		TECN	COMMENT
0.183±0.006 OUR FIT					
• • • We do not use the following data for averages, fits, limits, etc. • • •					
0.185±0.022	535	BASILE	71	CNTR	1.6 $\pi^- p \to nX^0$
0.189±0.026	123	RITTENBERG	69	HBC	1.7–2.7 $K^- p$

$\Gamma(3\pi^0)/\Gamma_{\text{total}}$ — Γ_6/Γ

VALUE (units 10^{-3})	EVTS	DOCUMENT ID		TECN	COMMENT
2.14±0.20 OUR FIT					
3.56±0.22±0.34	309	ABLIKIM	12E	BES3	$J/\psi \to \gamma(3\pi^0)$

$\Gamma(3\pi^0)/\Gamma(\pi^0\pi^0\eta)$ — Γ_6/Γ_3

VALUE (units 10^{-4})	EVTS	DOCUMENT ID		TECN	COMMENT
96± 9 OUR FIT					
78±10 OUR AVERAGE					
86±19	235	BLIK	08	GAMS	32 $\pi^- p \to \eta' n$
74±15		ALDE	87B	GAM2	38 $\pi^- p \to n6\gamma$
75±18		BINON	84	GAM2	30–40 $\pi^- p \to n6\gamma$

$\Gamma(\mu^+\mu^-\gamma)/\Gamma(\gamma\gamma)$ — Γ_7/Γ_5

VALUE (units 10^{-3})	EVTS	DOCUMENT ID		TECN	COMMENT
4.9±1.2	33	VIKTOROV	80	CNTR	25,33 $\pi^- p \to 2\mu\gamma$

$\Gamma(\pi^+\pi^-\mu^+\mu^-)/\Gamma_{\text{total}}$ — Γ_8/Γ

VALUE (units 10^{-4})	CL%	DOCUMENT ID		TECN	COMMENT
• • • We do not use the following data for averages, fits, limits, etc. • • •					
<0.29	90	[48] ABLIKIM	13O	BES3	$J/\psi \to \gamma\eta'$
<2.4	90	[49] NAIK	09	CLEO	$J/\psi \to \gamma\eta'$

[48] Using $\Gamma_2/\Gamma = (29.3 \pm 0.6)\%$ from PDG 12.

[49] Not independent of measured value of Γ_8/Γ_1 from NAIK 09.

$\Gamma(\pi^+\pi^-\mu^+\mu^-)/\Gamma(\pi^+\pi^-\eta)$ — Γ_8/Γ_1

VALUE (units 10^{-3})	CL%	DOCUMENT ID		TECN	COMMENT
<0.5	90	[50] NAIK	09	CLEO	$J/\psi \to \gamma\eta'$

[50] NAIK 09 reports $[\Gamma(\eta'(958) \to \pi^+\pi^-\mu^+\mu^-)/\Gamma(\eta'(958) \to \pi^+\pi^-\eta)]$ / $[B(\eta \to 2\gamma)] < 1.3 \times 10^{-3}$ which we multiply by our best value $B(\eta \to 2\gamma) = 39.41 \times 10^{-2}$.

$\Gamma(\pi^+\pi^-\mu^+\mu^-)/\Gamma(\rho^0\gamma(\text{including non-resonant }\pi^+\pi^-\gamma))$ — Γ_8/Γ_2

VALUE (units 10^{-4})	CL%	DOCUMENT ID		TECN	COMMENT
<1.0	90	ABLIKIM	13O	BES3	$J/\psi \to \gamma\eta'$

$\Gamma(\pi^+\pi^-\pi^0)/\Gamma_{\text{total}}$ — Γ_9/Γ

VALUE (units 10^{-3})	EVTS	DOCUMENT ID		TECN	COMMENT
3.8 ±0.4 OUR FIT					
3.8 ±0.4 OUR AVERAGE					
3.83±0.15±0.39	1014	ABLIKIM	12E	BES3	$J/\psi \to \gamma(\pi^+\pi^-\pi^0)$
$3.7\ ^{+1.1}_{-0.9}\pm0.4$		[51] NAIK	09	CLEO	$J/\psi \to \gamma\eta'$

[51] Not independent of measured value of Γ_9/Γ_1 from NAIK 09.

$\Gamma(\pi^+\pi^-\pi^0)/\Gamma(\pi^+\pi^-\eta)$ — Γ_9/Γ_1

VALUE (units 10^{-3})	EVTS	DOCUMENT ID		TECN	COMMENT
8.8 ±0.9 OUR FIT					
$\mathbf{8.28^{+2.49}_{-2.12}\pm0.04}$	20	[52] NAIK	09	CLEO	$J/\psi \to \gamma\eta'$

[52] NAIK 09 reports $[\Gamma(\eta'(958) \to \pi^+\pi^-\pi^0)/\Gamma(\eta'(958) \to \pi^+\pi^-\eta)]$ / $[B(\eta \to 2\gamma)] = (21^{+6}_{-5} \pm 2) \times 10^{-3}$ which we multiply by our best value $B(\eta \to 2\gamma) = (39.41 \pm 0.20) \times 10^{-2}$. Our first error is their experiment's error and our second error is the systematic error from using our best value.

$\Gamma(\pi^0\rho^0)/\Gamma_{\text{total}}$ — Γ_{10}/Γ

VALUE	CL%	DOCUMENT ID		TECN	COMMENT
<0.04	90	RITTENBERG	65	HBC	2.7 $K^- p$

Meson Particle Listings

$\eta'(958)$

$\Gamma(2(\pi^+\pi^-))/\Gamma_{total}$ Γ_{11}/Γ

VALUE (units 10^{-4})	CL%	DOCUMENT ID		TECN	COMMENT
• • • We do not use the following data for averages, fits, limits, etc. • • •					
< 2.4	90	[53] NAIK	09	CLEO	$J/\psi \to \gamma\eta'$
<100	90	RITTENBERG	69	HBC	1.7–2.7 K^-p

[53] Not independent of measured value of Γ_{11}/Γ_1 from NAIK 09.

$\Gamma(2(\pi^+\pi^-))/\Gamma(\pi^+\pi^-\eta)$ Γ_{11}/Γ_1

VALUE (units 10^{-3})	CL%	DOCUMENT ID		TECN	COMMENT
<0.6	90	[54] NAIK	09	CLEO	$J/\psi \to \gamma\eta'$

[54] NAIK 09 reports $[\Gamma(\eta'(958) \to 2(\pi^+\pi^-))/\Gamma(\eta'(958) \to \pi^+\pi^-\eta)]$ / $[B(\eta \to 2\gamma)]$ $< 1.4 \times 10^{-3}$ which we multiply by our best value $B(\eta \to 2\gamma) = 39.41 \times 10^{-2}$.

$\Gamma(\pi^+\pi^-2\pi^0)/\Gamma_{total}$ Γ_{12}/Γ

VALUE (units 10^{-4})	CL%	DOCUMENT ID		TECN	COMMENT
• • • We do not use the following data for averages, fits, limits, etc. • • •					
<27	90	[55] NAIK	09	CLEO	$J/\psi \to \gamma\eta'$

[55] Not independent of measured value of Γ_{12}/Γ_1 from NAIK 09.

$\Gamma(\pi^+\pi^-2\pi^0)/\Gamma(\pi^+\pi^-\eta)$ Γ_{12}/Γ_1

VALUE (units 10^{-3})	CL%	DOCUMENT ID		TECN	COMMENT
<6	90	[56] NAIK	09	CLEO	$J/\psi \to \gamma\eta'$

[56] NAIK 09 reports $[\Gamma(\eta'(958) \to \pi^+\pi^-2\pi^0)/\Gamma(\eta'(958) \to \pi^+\pi^-\eta)]$ / $[B(\eta \to 2\gamma)]$ $< 15 \times 10^{-3}$ which we multiply by our best value $B(\eta \to 2\gamma) = 39.41 \times 10^{-2}$.

$\Gamma(2(\pi^+\pi^-)\text{ neutrals})/\Gamma_{total}$ Γ_{13}/Γ

VALUE	CL%	DOCUMENT ID		TECN	COMMENT
<0.01	95	DANBURG	73	HBC	2.2 $K^-p \to \Lambda X^0$
• • • We do not use the following data for averages, fits, limits, etc. • • •					
<0.01	90	RITTENBERG	69	HBC	1.7–2.7 K^-p

$\Gamma(2(\pi^+\pi^-)\pi^0)/\Gamma_{total}$ Γ_{14}/Γ

VALUE	CL%	DOCUMENT ID		TECN	COMMENT
• • • We do not use the following data for averages, fits, limits, etc. • • •					
<0.002	90	[57] NAIK	09	CLEO	$J/\psi \to \gamma\eta'$
<0.01	90	RITTENBERG	69	HBC	1.7–2.7 K^-p

[57] Not independent of measured value of Γ_{14}/Γ_1 from NAIK 09.

$\Gamma(2(\pi^+\pi^-)\pi^0)/\Gamma(\pi^+\pi^-\eta)$ Γ_{14}/Γ_1

VALUE (units 10^{-3})	CL%	DOCUMENT ID		TECN	COMMENT
<4	90	[58] NAIK	09	CLEO	$J/\psi \to \gamma\eta'$

[58] NAIK 09 reports $[\Gamma(\eta'(958) \to 2(\pi^+\pi^-)\pi^0)/\Gamma(\eta'(958) \to \pi^+\pi^-\eta)]$ / $[B(\eta \to 2\gamma)]$ $< 11 \times 10^{-3}$ which we multiply by our best value $B(\eta \to 2\gamma) = 39.41 \times 10^{-2}$.

$\Gamma(2(\pi^+\pi^-)2\pi^0)/\Gamma_{total}$ Γ_{15}/Γ

VALUE	CL%	DOCUMENT ID		TECN	COMMENT
<0.01	95	KALBFLEISCH	64B	HBC	$K^-p \to \Lambda 2(\pi^+\pi^-)$+MM
• • • We do not use the following data for averages, fits, limits, etc. • • •					
<0.01	90	LONDON	66	HBC	Compilation

$\Gamma(3(\pi^+\pi^-))/\Gamma_{total}$ Γ_{16}/Γ

VALUE (units 10^{-5})	CL%	DOCUMENT ID		TECN	COMMENT
< 3.1	90	[59] ABLIKIM	13U	BES3	$J/\psi \to \gamma 3(\pi^+\pi^-)$
• • • We do not use the following data for averages, fits, limits, etc. • • •					
< 53	90	[60] NAIK	09	CLEO	$J/\psi \to \gamma\eta'$
<500	95	KALBFLEISCH	64B	HBC	$K^-p \to \Lambda 2(\pi^+\pi^-)$

[59] Using $B(J/\psi \to \gamma\eta'(958)) = (5.16 \pm 0.15) \times 10^{-3}$.
[60] Not independent of measured value of Γ_{16}/Γ_1 from NAIK 09.

$\Gamma(3(\pi^+\pi^-))/\Gamma(\pi^+\pi^-\eta)$ Γ_{16}/Γ_1

VALUE (units 10^{-3})	CL%	DOCUMENT ID		TECN	COMMENT
<1.2	90	[61] NAIK	09	CLEO	$J/\psi \to \gamma\eta'$

[61] NAIK 09 reports $[\Gamma(\eta'(958) \to 3(\pi^+\pi^-))/\Gamma(\eta'(958) \to \pi^+\pi^-\eta)]$ / $[B(\eta \to 2\gamma)]$ $< 3.0 \times 10^{-3}$ which we multiply by our best value $B(\eta \to 2\gamma) = 39.41 \times 10^{-2}$.

$\Gamma(\pi^+\pi^-e^+e^-)/\Gamma_{total}$ Γ_{17}/Γ

VALUE (units 10^{-3})	CL%	EVTS	DOCUMENT ID		TECN	COMMENT
2.4 $^{+1.3}_{-1.0}$ OUR FIT						
• • • We do not use the following data for averages, fits, limits, etc. • • •						
$2.11 \pm 0.12 \pm 0.14$		429	[62] ABLIKIM	13O	BES3	$J/\psi \to \gamma\eta'$
2.5 $^{+1.2}_{-0.9}$ ± 0.5			[63] NAIK	09	CLEO	$J/\psi \to \gamma\eta'$
<6	90		RITTENBERG	65	HBC	2.7 K^-p

[62] Using $\Gamma_2/\Gamma = (29.3 \pm 0.6)\%$ from PDG 12.
[63] Not independent of measured value of Γ_{17}/Γ_1 from NAIK 09.

$\Gamma(\pi^+\pi^-e^+e^-)/\Gamma(\pi^+\pi^-\eta)$ Γ_{17}/Γ_1

VALUE (units 10^{-3})	EVTS	DOCUMENT ID		TECN	COMMENT
5.6 $^{+3.0}_{-2.2}$ OUR FIT					
5.52 $^{+3.00}_{-2.30} \pm 0.03$	8	[64] NAIK	09	CLEO	$J/\psi \to \gamma\eta'$

[64] NAIK 09 reports $[\Gamma(\eta'(958) \to \pi^+\pi^-e^+e^-)/\Gamma(\eta'(958) \to \pi^+\pi^-\eta)]$ / $[B(\eta \to 2\gamma)] = (14^{+7}_{-5} \pm 3) \times 10^{-3}$ which we multiply by our best value $B(\eta \to 2\gamma) = (39.41 \pm 0.20) \times 10^{-2}$. Our first error is their experiment's error and our second error is the systematic error from using our best value.

$\Gamma(\pi^+\pi^-e^+e^-)/\Gamma(\rho^0\gamma(\text{including non-resonant }\pi^+\pi^-\gamma))$ Γ_{17}/Γ_2

VALUE (units 10^{-3})	EVTS	DOCUMENT ID		TECN	COMMENT
7.2±0.4±0.5	429	ABLIKIM	13O	BES3	$J/\psi \to \gamma\eta'$

$\Gamma(\pi^+e^-\nu_e + \text{c.c.})/\Gamma(\pi^+\pi^-\eta)$ Γ_{18}/Γ_1

VALUE (units 10^{-4})	CL%	DOCUMENT ID		TECN	COMMENT
<5.0	90	ABLIKIM	13G	BES3	$J/\psi \to \phi\eta'$

$\Gamma(\gamma e^+e^-)/\Gamma_{total}$ Γ_{19}/Γ

VALUE (units 10^{-3})	CL%	DOCUMENT ID		TECN	COMMENT
<0.9	90	BRIERE	00	CLEO	10.6 e^+e^-

$\Gamma(\pi^0\gamma\gamma)/\Gamma(\pi^0\pi^0\eta)$ Γ_{20}/Γ_3

VALUE (units 10^{-4})	CL%	DOCUMENT ID		TECN	COMMENT
<37	90	ALDE	87B	GAM2	38 $\pi^-p \to n4\gamma$

$\Gamma(4\pi^0)/\Gamma(\pi^0\pi^0\eta)$ Γ_{21}/Γ_3

VALUE (units 10^{-4})	CL%	DOCUMENT ID		TECN	COMMENT
<23	90	ALDE	87B	GAM2	38 $\pi^-p \to n8\gamma$

$\Gamma(e^+e^-)/\Gamma_{total}$ Γ_{22}/Γ

VALUE (units 10^{-7})	CL%	DOCUMENT ID		TECN	COMMENT
<2.1	90	VOROBYEV	88	ND	$e^+e^- \to \pi^+\pi^-\eta$

$\Gamma(\text{invisible})/\Gamma_{total}$ Γ_{23}/Γ

VALUE (units 10^{-4})	CL%	DOCUMENT ID		TECN	COMMENT
• • • We do not use the following data for averages, fits, limits, etc. • • •					
<9.5	90	[65] NAIK	09	CLEO	$J/\psi \to \gamma\eta'$

[65] Not independent of measured value of Γ_{23}/Γ_1 from NAIK 09.

$\Gamma(\text{invisible})/\Gamma(\gamma\gamma)$ Γ_{23}/Γ_5

VALUE (units 10^{-2})	CL%	DOCUMENT ID		TECN	COMMENT
<2.4	90	ABLIKIM	13	BES3	$J/\psi \to \phi\eta'$
• • • We do not use the following data for averages, fits, limits, etc. • • •					
<6.69	90	ABLIKIM	06Q	BES	$J/\psi \to \phi\eta'$

$\Gamma(\text{invisible})/\Gamma(\pi^+\pi^-\eta)$ Γ_{23}/Γ_1

VALUE (units 10^{-3})	CL%	DOCUMENT ID		TECN	COMMENT
• • • We do not use the following data for averages, fits, limits, etc. • • •					
<2.1	90	[66] NAIK	09	CLEO	$J/\psi \to \gamma\eta'$

[66] NAIK 09 reports $[\Gamma(\eta'(958) \to \text{invisible})/\Gamma(\eta'(958) \to \pi^+\pi^-\eta)]$ / $[B(\eta \to 2\gamma)]$ $< 5.4 \times 10^{-3}$ which we multiply by our best value $B(\eta \to 2\gamma) = 39.41 \times 10^{-2}$.

$\Gamma(\pi^+\pi^-)/\Gamma_{total}$ Γ_{24}/Γ

VALUE (units 10^{-4})	CL%	DOCUMENT ID		TECN	COMMENT
< 0.6	90	[67] ABLIKIM	11G	BES3	$J/\psi \to \gamma\pi^+\pi^-$
• • • We do not use the following data for averages, fits, limits, etc. • • •					
< 29	90	[68] MORI	07A	BELL	$\gamma\gamma \to \pi^+\pi^-$
< 3.3	90	[69] MORI	07A	BELL	$\gamma\gamma \to \pi^+\pi^-$
<800	95	DANBURG	73	HBC	2.2 $K^-p \to \Lambda X^0$
<200	90	RITTENBERG	69	HBC	1.7–2.7 K^-p

[67] ABLIKIM 11G reports $[\Gamma(\eta'(958) \to \pi^+\pi^-)/\Gamma_{total}] \times [B(J/\psi(1S) \to \gamma\eta'(958))] < 2.84 \times 10^{-7}$ which we divide by our best value $B(J/\psi(1S) \to \gamma\eta'(958)) = 5.15 \times 10^{-3}$.
[68] Taking into account interference with the $\gamma\gamma \to \pi^+\pi^-$ continuum.
[69] Without interference with the $\gamma\gamma \to \pi^+\pi^-$ continuum.

$\Gamma(\pi^0\pi^0)/\Gamma_{total}$ Γ_{25}/Γ

VALUE	CL%	DOCUMENT ID		TECN	COMMENT
<4 × 10⁻⁴	90	[70] ABLIKIM	11G	BES3	$J/\psi \to \gamma\pi^0\pi^0$

[70] ABLIKIM 11G reports $[\Gamma(\eta'(958) \to \pi^+\pi^-)/\Gamma_{total}] \times [B(J/\psi(1S) \to \gamma\eta'(958))] < 2.84 \times 10^{-7}$ which we divide by our best value $B(J/\psi(1S) \to \gamma\eta'(958)) = 5.15 \times 10^{-3}$.

$\Gamma(\pi^0\pi^0)/\Gamma(\pi^0\pi^0\eta)$ Γ_{25}/Γ_3

VALUE (units 10^{-4})	CL%	DOCUMENT ID		TECN	COMMENT
<45	90	ALDE	87B	GAM2	38 $\pi^-p \to n4\gamma$

$\Gamma(\pi^0 e^+ e^-)/\Gamma_{total}$ Γ_{26}/Γ

VALUE (units 10^{-3})	CL%	DOCUMENT ID		TECN	COMMENT
< 1.4	90	BRIERE	00	CLEO	10.6 $e^+ e^-$
• • • We do not use the following data for averages, fits, limits, etc. • • •					
<13	90	RITTENBERG	65	HBC	2.7 $K^- p$

$\Gamma(\eta e^+ e^-)/\Gamma_{total}$ Γ_{27}/Γ

VALUE (units 10^{-3})	CL%	DOCUMENT ID		TECN	COMMENT
< 2.4	90	BRIERE	00	CLEO	10.6 $e^+ e^-$
• • • We do not use the following data for averages, fits, limits, etc. • • •					
<11	90	RITTENBERG	65	HBC	2.7 $K^- p$

$\Gamma(3\gamma)/\Gamma(\pi^0\pi^0\eta)$ Γ_{28}/Γ_3

VALUE (units 10^{-4})	CL%	DOCUMENT ID		TECN	COMMENT
<4.6	90	ALDE	87B	GAM2	38 $\pi^- p \rightarrow n 3\gamma$

$\Gamma(\mu^+\mu^-\pi^0)/\Gamma_{total}$ Γ_{29}/Γ

VALUE (units 10^{-5})	CL%	DOCUMENT ID		TECN	COMMENT
<6.0	90	DZHELYADIN	81	CNTR	30 $\pi^- p \rightarrow \eta' n$

$\Gamma(\mu^+\mu^-\eta)/\Gamma_{total}$ Γ_{30}/Γ

VALUE (units 10^{-5})	CL%	DOCUMENT ID		TECN	COMMENT
<1.5	90	DZHELYADIN	81	CNTR	30 $\pi^- p \rightarrow \eta' n$

$\Gamma(e\mu)/\Gamma_{total}$ Γ_{31}/Γ

VALUE (units 10^{-4})	CL%	DOCUMENT ID		TECN	COMMENT
<4.7	90	BRIERE	00	CLEO	10.6 $e^+ e^-$

$\eta'(958)$ C-NONCONSERVING DECAY PARAMETER

See the note on η decay parameters in the Stable Particle Particle Listings for definition of this parameter.

DECAY ASYMMETRY PARAMETER FOR $\pi^+\pi^-\gamma$

VALUE	EVTS	DOCUMENT ID		TECN	COMMENT
−0.03 ±0.04 OUR AVERAGE					
-0.019 ± 0.056		AIHARA	87	TPC	$2\gamma \rightarrow \pi^+\pi^-\gamma$
-0.069 ± 0.078	295	GRIGORIAN	75	STRC	2.1 $\pi^- p$
0.00 ±0.10	103	KALBFLEISCH	75	HBC	2.18 $K^- p \rightarrow \Lambda\pi^+\pi^-\gamma$
• • • We do not use the following data for averages, fits, limits, etc. • • •					
0.07 ±0.08	152	RITTENBERG	65	HBC	2.1–2.7 $K^- p$

$\eta'(958)$ REFERENCES

ABLIKIM	13	PR D87 012009	M. Ablikim *et al.*	(BES III Collab.)
ABLIKIM	13G	PR D87 032006	M. Ablikim *et al.*	(BES III Collab.)
ABLIKIM	13O	PR D87 092011	M. Ablikim *et al.*	(BES III Collab.)
ABLIKIM	13U	PR D88 091502	M. Ablikim *et al.*	(BES III Collab.)
ABLIKIM	12E	PRL 108 182001	M. Ablikim *et al.*	(BES III Collab.)
PDG	12	PR D86 010001	J. Beringer *et al.*	(PDG Collab.)
ABLIKIM	11	PR D83 012003	M. Ablikim *et al.*	(BES III Collab.)
ABLIKIM	11G	PR D84 032006	M. Ablikim *et al.*	(BES III Collab.)
CZERWINSKI	10	PRL 105 122001	E. Czerwinski *et al.*	(COSY-11 Collab.)
BLIK	09	PAN 72 231	A.M. Blik *et al.*	(IHEP (Protvino))
		Translated from YAF 72 258.		
NAIK	09	PRL 102 061801	P. Naik *et al.*	(CLEO Collab.)
PEDLAR	09	PR D79 111101	T.K. Pedlar *et al.*	(CLEO Collab.)
BLIK	08	PAN 71 2124	A. Blik *et al.*	(GAMS-4π Collab.)
		Translated from YAF 71 2161.		
LIBBY	08	PRL 101 182002	J. Libby *et al.*	(CLEO Collab.)
WICHT	08	PL B662 323	J. Wicht *et al.*	(BELLE Collab.)
DOROFEEV	07	PL B651 22	V. Dorofeev *et al.*	(VES Collab.)
MORI	07A	JPSJ 76 074102	T. Mori *et al.*	(BELLE Collab.)
ABLIKIM	06E	PR D73 052008	M. Ablikim *et al.*	(BES Collab.)
ABLIKIM	06Q	PRL 97 202002	M. Ablikim *et al.*	(BES Collab.)
AMELIN	05A	PAN 68 372	D.V. Amelin *et al.*	(VES Collab.)
		Translated from YAF 68 401.		
AMSLER	04B	EPJ C33 23	C. Amsler *et al.*	(Crystal Barrel Collab.)
BAI	04J	PL B594 47	J.Z. Bai *et al.*	(BES Collab.)
BRIERE	00	PRL 84 26	R. Briere *et al.*	(CLEO Collab.)
ACCIARRI	98Q	PL B418 399	M. Acciarri *et al.*	(L3 Collab.)
BARBERIS	98C	PL B440 225	D. Barberis *et al.*	(WA 102 Collab.)
WURZINGER	96	PL B374 283	R. Wurzinger *et al.*	(BONN, ORSAY, SACL+)
PDG	94	PR D50 1173	L. Montanet *et al.*	(CERN, LBL, BOST+)
AMSLER	93	ZPHY C58 175	C. Amsler *et al.*	(Crystal Barrel Collab.)
BELADIDZE	92C	SJNP 55 1535	G.M. Beladidze, S.I. Bityukov, G.V. Borisov	(SERP+)
		Translated from YAF 55 2748.		
KARCH	92	ZPHY C54 33	K. Karch *et al.*	(Crystal Ball Collab.)
ARMSTRONG	91B	ZPHY C52 389	T.A. Armstrong *et al.*	(ATHU, BARI, BIRM+)
BEHREND	91	ZPHY C49 401	H.J. Behrend *et al.*	(CELLO Collab.)
AUGUSTIN	90	PR D42 10	J.E. Augustin *et al.*	(DM2 Collab.)
BARU	90	ZPHY C48 581	S.E. Baru *et al.*	(MD-1 Collab.)
BUTLER	90	PR D42 1368	F. Butler *et al.*	(Mark II Collab.)
KARCH	90	PL B249 353	K. Karch *et al.*	(Crystal Ball Collab.)
ROE	90	PR D41 17	N.A. Roe *et al.*	(ASP Collab.)
AIHARA	88C	PR D38 1	H. Aihara *et al.*	(TPC-2γ Collab.)
VOROBYEV	88	SJNP 48 273	P.V. Vorobiev *et al.*	(NOVO)
		Translated from YAF 48 436.		
WILLIAMS	88	PR D38 1365	D.A. Williams *et al.*	(Crystal Ball Collab.)
AIHARA	87	PR D35 2650	H. Aihara *et al.*	(TPC-2γ Collab.) JP
ALBRECHT	87B	PL B199 457	H. Albrecht *et al.*	(ARGUS Collab.)
ALDE	87B	ZPHY C36 603	D.M. Alde *et al.*	(LANL, BELG, SERP, LAPP)
ANTREASYAN	87	PR D36 2633	D. Antreasyan *et al.*	(Crystal Ball Collab.)
GIDAL	87	PRL 59 2012	G. Gidal *et al.*	(LBL, SLAC, HARV)
ALDE	86	PL B177 115	D.M. Alde *et al.*	(SERP, BELG, LANL, LAPP)
BARTEL	85E	PL 160B 421	W. Bartel *et al.*	(JADE Collab.)
ALTHOFF	84E	PL 147B 487	M. Althoff *et al.*	(TASSO Collab.)
BERGER	84B	PL 142B 125	C. Berger	(PLUTO Collab.)
BINON	84	PL 140B 264	F.G. Binon *et al.*	(SERP, BELG, LAPP+)
BEHREND	83B	PL 125B 518 (erratum)	H.J. Behrend *et al.*	(CELLO Collab.)
Also		PL 114B 378	H.J. Behrend *et al.*	(CELLO Collab.)
JENNI	83	PR D27 1031	P. Jenni *et al.*	(SLAC, LBL)
BARTEL	82B	PL 113B 190	W. Bartel *et al.*	(JADE Collab.)
DZHELYADIN	81	PL 105B 239	R.I. Dzhelyadin *et al.*	(SERP)
STANTON	80	PL B92 353	N.R. Stanton *et al.*	(OSU, CARL, MCGI+)
VIKTOROV	80	SJNP 32 520	V.A. Viktorov *et al.*	(SERP)
		Translated from YAF 32 1005.		
APEL	79	PL 83B 131	W.D. Apel, K.H. Augenstein, E. Bertolucci	(KARLK+)
BINNIE	79	PL 83B 141	D.M. Binnie *et al.*	(LOIC)
ZANFINO	77	PRL 38 930	C. Zanfino *et al.*	(CARL, MCGI, OHIO+)
GRIGORIAN	75	NP B91 232	A. Grigorian *et al.*	(+)
KALBFLEISCH	75	PR D11 987	G.R. Kalbfleisch, R.C. Strand, J.W. Chapman	(BNL+)
DUANE	74	PRL 32 425	A. Duane *et al.*	(LOIC, SHMP)
KALBFLEISCH	74	PR D10 916	G.R. Kalbfleisch	(BNL)
DANBURG	73	PR D8 3744	J.S. Danburg *et al.*	(BNL, MICH) JP
JACOBS	73	PR D8 18	S.M. Jacobs *et al.*	(BRAN, UMD, SYRA+) JP
AGUILAR-...	72B	PR D6 29	M. Aguilar-Benitez *et al.*	(BNL)
APEL	72	PL 40B 680	W.D. Apel *et al.*	(KARLK, KARLE, PISA)
DALPIAZ	72	PL 42B 377	P.F. Dalpiaz *et al.*	(CERN)
BASILE	71	NC 3A 371	M. Basile *et al.*	(CERN, BGNA, STRB)
HARVEY	71	PRL 27 885	E.H. Harvey *et al.*	(MINN, MICH)
BENSINGER	70	PL 33B 505	J.R. Bensinger *et al.*	(WISC)
RITTENBERG	69	Thesis UCRL 18863	A. Rittenberg	(LRL) I
DAVIS	68	PL 27B 532	R. Davis *et al.*	(NWES, ANL)
LONDON	66	PR 143 1034	G.W. London *et al.*	(BNL, SYRA) IJP
BADIER	65B	PL 17 337	J. Badier *et al.*	(EPOL, SACL, AMST)
RITTENBERG	65	PRL 15 556	A. Rittenberg, G.R. Kalbfleisch	(LRL, BNL)
DAUBER	64	PRL 13 449	P.M. Dauber *et al.*	(UCLA) JP
KALBFLEISCH	64B	PRL 13 349	G.R. Kalbfleisch, O.I. Dahl, A. Rittenberg	(LRL) JP

$f_0(980)$

$I^G(J^{PC}) = 0^+(0^{++})$

See also the minireview on scalar mesons under $f_0(500)$. (See the index for the page number.)

$f_0(980)$ MASS

VALUE (MeV)	EVTS	DOCUMENT ID		TECN	COMMENT
990 ±20 OUR ESTIMATE					
• • • We do not use the following data for averages, fits, limits, etc. • • •					
989.9± 0.4	706	ABLIKIM	12E	BES3	$J/\psi \rightarrow \gamma 3\pi$
$1003\ ^{+\ 5}_{-27}$		[1,2] GARCIA-MAR..11		RVUE	Compilation
996 ± 7		[1,3] GARCIA-MAR..11		RVUE	Compilation
$996\ ^{+\ 4}_{-14}$		[4] MOUSSALLAM11		RVUE	Compilation
981 ±43		[5] MENNESSIER	10	RVUE	Compilation
$1030\ ^{+30}_{-10}$		[6] ANISOVICH	09	RVUE	0.0 $\bar{p}p$, πN
$977\ ^{+11}_{-\ 9} \pm 1$	44	[7] ECKLUND	09	CLEO	4.17 $e^+ e^- \rightarrow D_s^- D_s^{*+}$ + c.c.
$982.2 \pm 1.0\ ^{+\ 8.1}_{-\ 8.0}$		[8] UEHARA	08A	BELL	10.6 $e^+ e^- \rightarrow e^+ e^- \pi^0\pi^0$
$976.8 \pm 0.3\ ^{+10.1}_{-\ 0.6}$	64k	[9] AMBROSINO	07	KLOE	1.02 $e^+ e^- \rightarrow \pi^0\pi^0\gamma$
$984.7 \pm 0.4\ ^{+\ 2.4}_{-\ 3.7}$	64k	[10] AMBROSINO	07	KLOE	1.02 $e^+ e^- \rightarrow \pi^0\pi^0\gamma$
973 ± 3	262 ± 30	[11] AUBERT	07AK	BABR	10.6 $e^+ e^- \rightarrow \phi\pi^+\pi^-\gamma$
970 ± 7	54 ± 9	[11] AUBERT	07AK	BABR	10.6 $e^+ e^- \rightarrow \phi\pi^0\pi^0\gamma$
953 ±20	2.6k	[12] BONVICINI	07	CLEO	$D^+ \rightarrow \pi^-\pi^+\pi^+$
$985.6\ ^{+\ 1.2}_{-\ 1.5} \pm 1.1$		[13] MORI	07	BELL	10.6 $e^+ e^- \rightarrow e^+ e^- \pi^+\pi^-$
$983.0 \pm 0.6\ ^{+\ 4.0}_{-\ 3.0}$		[14] AMBROSINO	06B	KLOE	1.02 $e^+ e^- \rightarrow \pi^+\pi^-\gamma$
$977.3 \pm 0.9\ ^{+\ 3.7}_{-\ 4.3}$		[15] AMBROSINO	06B	KLOE	1.02 $e^+ e^- \rightarrow \pi^+\pi^-\gamma$
950 ± 9	4286	[16] GARMASH	06	BELL	$B^+ \rightarrow K^+\pi^+\pi^-$
965 ±10		[17] ABLIKIM	05	BES2	$J/\psi \rightarrow \phi\pi^+\pi^-$, $\phi K^+ K^-$
1031 ± 8		[18] ANISOVICH	03	RVUE	
1037 ±31		TIKHOMIROV	03	SPEC	40.0 $\pi^- C \rightarrow K_S^0 K_S^0 K_L^0 X$
973 ± 1	2438	[19] ALOISIO	02D	KLOE	$e^+ e^- \rightarrow \pi^0\pi^0\gamma$
977 ± 3 ± 2	848	[20] AITALA	01A	E791	$D_s^+ \rightarrow \pi^-\pi^+\pi^+$
969.8± 4.5	419	[21] ACHASOV	00H	SND	$e^+ e^- \rightarrow \pi^0\pi^0\gamma$
$985\ ^{+16}_{-12}$	419	[22,23] ACHASOV	00H	SND	$e^+ e^- \rightarrow \pi^0\pi^0\gamma$
976 ± 5 ± 6		[24] AKHMETSHIN	99B	CMD2	$e^+ e^- \rightarrow \pi^+\pi^-\gamma$
977 ± 3 ± 6	268	[24] AKHMETSHIN	99C	CMD2	$e^+ e^- \rightarrow \pi^0\pi^0\gamma$
975 ± 4 ± 6		[25] AKHMETSHIN	99C	CMD2	$e^+ e^- \rightarrow \pi^0\pi^0\gamma$
975 ± 4 ± 6		[26] AKHMETSHIN	99C	CMD2	$e^+ e^- \rightarrow \pi^+\pi^-\gamma$, $\pi^0\pi^0\gamma$
985 ±10		BARBERIS	99	OMEG	450 $pp \rightarrow p_s p_f K^+ K^-$
982 ± 3		BARBERIS	99B	OMEG	450 $pp \rightarrow p_s p_f \pi^+\pi^-$
982 ± 3		BARBERIS	99C	OMEG	450 $pp \rightarrow p_s p_f \pi^0\pi^0$
987 ± 6 ± 6		[27] BARBERIS	99D	OMEG	450 $pp \rightarrow K^+ K^-$, $\pi^+\pi^-$
989 ±15		BELLAZZINI	99	GAM4	450 $pp \rightarrow pp\pi^0\pi^0$
991 ± 3		[28] KAMINSKI	99	RVUE	$\pi\pi \rightarrow \pi\pi$, $K\overline{K}$, $\sigma\sigma$

Meson Particle Listings

$f_0(980)$

~ 980			[28] OLLER	99	RVUE	$\pi\pi \to \pi\pi$, $K\overline{K}$
~ 993.5			OLLER	99B	RVUE	$\pi\pi \to \pi\pi$, $K\overline{K}$
~ 987			[28] OLLER	99C	RVUE	$\pi\pi \to \pi\pi$, $K\overline{K}$, $\eta\eta$
957	± 6		[29] ACKERSTAFF	98Q	OPAL	$Z \to f_0$ X
960	±10		ALDE	98	GAM4	
1015	±15		[28] ANISOVICH	98B	RVUE	Compilation
1008			[30] LOCHER	98	RVUE	$\pi\pi \to \pi\pi$, $K\overline{K}$
955	±10		[29] ALDE	97	GAM2	450 $pp \to pp\pi^0\pi^0$
994	± 9		[31] BERTIN	97C	OBLX	0.0 $\overline{p}p \to \pi^+\pi^-\pi^0$
993.2	± 6.5	± 6.9	[32] ISHIDA	96	RVUE	$\pi\pi \to \pi\pi$, $K\overline{K}$
1006			TORNQVIST	96	RVUE	$\pi\pi \to \pi\pi$, $K\overline{K}$, $K\pi$, $\eta\pi$
997	± 5	3k	[33] ALDE	95B	GAM2	38 $\pi^- p \to \pi^0\pi^0 n$
960	±10	10k	[34] ALDE	95B	GAM2	38 $\pi^- p \to \pi^0\pi^0 n$
994	± 5		AMSLER	95B	CBAR	0.0 $\overline{p}p \to 3\pi^0$
~ 996			[35] AMSLER	95D	CBAR	0.0 $\overline{p}p \to \pi^0\pi^0\pi^0$, $\pi^0\eta\eta$, $\pi^0\pi^0\eta$
987	± 6		[36] ANISOVICH	95	RVUE	
1015			JANSSEN	95	RVUE	$\pi\pi \to \pi\pi$, $K\overline{K}$
983			[37] BUGG	94	RVUE	$\overline{p}p \to \eta 2\pi^0$
973	± 2		[38] KAMINSKI	94	RVUE	$\pi\pi \to \pi\pi$, $K\overline{K}$
988			[39] ZOU	94B	RVUE	
988	±10		[40] MORGAN	93	RVUE	$\pi\pi(K\overline{K}) \to \pi\pi(K\overline{K})$, $J/\psi \to \phi\pi\pi(K\overline{K})$, $D_s \to \pi(\pi\pi)$
971.1	± 4.0		[29] AGUILAR-...	91	EHS	400 pp
979	± 4		[41] ARMSTRONG	91	OMEG	300 $pp \to pp\pi\pi$, $pp K\overline{K}$
956	±12		BREAKSTONE	90	SFM	$pp \to pp\pi^+\pi^-$
959.4	± 6.5		[29] AUGUSTIN	89	DM2	$J/\psi \to \omega\pi^+\pi^-$
978	± 9		[29] ABACHI	86B	HRS	$e^+e^- \to \pi^+\pi^-$ X
985.0	$^{+\ 9.0}_{-39.0}$		ETKIN	82B	MPS	23 $\pi^- p \to n 2K^0_S$
974	± 4		[41] GIDAL	81	MRK2	$J/\psi \to \pi^+\pi^-$ X
975			[42] ACHASOV	80	RVUE	
986	±10		[41] AGUILAR-...	78	HBC	0.7 $\overline{p}p \to K^0_S K^0_S$
969	± 5		[41] LEEPER	77	ASPK	2–2.4 $\pi^- p \to \pi^+\pi^- n$, $K^+K^- n$
987	± 7		[41] BINNIE	73	CNTR	$\pi^- p \to n$MM
1012	± 6		[43] GRAYER	73	ASPK	17 $\pi^- p \to \pi^+\pi^- n$
1007	±20		[43] HYAMS	73	ASPK	17 $\pi^- p \to \pi^+\pi^- n$
997	± 6		[43] PROTOPOP...	73	HBC	7 $\pi^+ p \to \pi^+ p\pi^+\pi^-$

[1] Quoted number refers to real part of pole position.
[2] Analytic continuation using Roy equations. Uses the K_{e4} data of BATLEY 10C and the $\pi N \to \pi\pi N$ data of HYAMS 73, GRAYER 74, and PROTOPOPESCU 73.
[3] Analytic continuation using GKPY equations. Uses the K_{e4} data of BATLEY 10C and the $\pi N \to \pi\pi N$ data of HYAMS 73, GRAYER 74, and PROTOPOPESCU 73.
[4] Pole position. Used Roy equations.
[5] Average of the analyses of three data sets in the K-matrix model. Uses the data of BATLEY 08A, HYAMS 73, and GRAYER 74, partially of COHEN 80 or ETKIN 82B.
[6] On sheet II in a 2-pole solution. The other pole is found on sheet III at (850−100i) MeV
[7] Using a relativistic Breit-Wigner function and taking into account the finite D_s mass.
[8] Breit-Wigner mass. Using finite width corrections according to FLATTE 76 and ACHASOV 05, and the ratio $g_{f_0 K K}/g_{f_0 \pi\pi} = 0$.
[9] In the kaon-loop fit.
[10] In the no-structure fit.
[11] Systematic errors not estimated.
[12] FLATTE 76 parameterization. $g_{f_0\pi\pi} = 329 \pm 96$ MeV/c^2 assuming $g_{f_0 K\overline{K}}/g_{f_0\pi\pi}$=2.
[13] Breit-Wigner mass. Using finite width corrections according to FLATTE 76 and ACHASOV 05, and the ratio $g_{f_0 K K}/g_{f_0\pi\pi} = 4.21 \pm 0.25 \pm 0.21$ from ABLIKIM 05.
[14] In the kaon-loop fit following formalism of ACHASOV 89.
[15] In the no-structure fit assuming a direct coupling of ϕ to $f_0\gamma$.
[16] FLATTE 76 parameterization. Supersedes GARMASH 05.
[17] FLATTE 76 parameterization, $g_{f_0 K\overline{K}}/g_{f_0\pi\pi} = 4.21 \pm 0.25 \pm 0.21$.
[18] K-matrix pole from combined analysis of $\pi^- p \to \pi^0\pi^0 n$, $\pi^- p \to K\overline{K} n$, $\pi^+\pi^- \to \pi^+\pi^-$, $\overline{p}p \to \pi^0\pi^0\pi^0$, $\pi^0\eta\eta$, $\pi^0\pi^0\eta$, $\pi^+\pi^-\pi^0$, $K^+K^-\pi^0$, $K^0_S K^0_S\pi^0$, $K^+K^0_S\pi^-$ at rest, $\overline{p}n \to \pi^-\pi^-\pi^+$, $K^0_S K^-\pi^0$, $K^0_S K^0_S\pi^-$ at rest.
[19] From the negative interference with the $f_0(500)$ meson of AITALA 01B using the ACHASOV 89 parameterization for the $f_0(980)$, a Breit-Wigner for the $f_0(500)$, and ACHASOV 01F for the $\rho\pi$ contribution.
[20] Coupled-channel Breit-Wigner, couplings g_π=0.09±0.01±0.01, g_K=0.02±0.04±0.03.
[21] Supersedes ACHASOV 98I. Using the model of ACHASOV 89.
[22] Supersedes ACHASOV 98I.
[23] In the "narrow resonance" approximation.
[24] Assuming $\Gamma(f_0)$= 40 MeV.
[25] From a narrow pole fit taking into account $f_0(980)$ and $f_0(1200)$ intermediate mechanisms.
[26] From the combined fit of the photon spectra in the reactions $e^+e^- \to \pi^+\pi^-\gamma$, $\pi^0\pi^0\gamma$.
[27] Supersedes BARBERIS 99 and BARBERIS 99B
[28] T-matrix pole.
[29] From invariant mass fit.
[30] On sheet II in a 2 pole solution. The other pole is found on sheet III at (1039−93i) MeV.
[31] On sheet II in a 2 pole solution. The other pole is found on sheet III at (963-29i) MeV.
[32] Reanalysis of data from HYAMS 73, GRAYER 74, SRINIVASAN 75, and ROSSELET 77 using the interfering amplitude method.
[33] At high $|t|$.
[34] At low $|t|$.
[35] On sheet II in a 4-pole solution, the other poles are found on sheet III at (953−55i) MeV and on sheet IV at (938−35i) MeV.
[36] Combined fit of ALDE 95B, ANISOVICH 94, AMSLER 94D.
[37] On sheet II in a 2 pole solution. The other pole is found on sheet III at (996−103i) MeV.
[38] From sheet II pole position.
[39] On sheet II in a 2 pole solution. The other pole is found on sheet III at (797−185i) MeV and can be interpreted as a shadow pole.
[40] On sheet II in a 2 pole solution. The other pole is found on sheet III at (978−28i) MeV.
[41] From coupled channel analysis.
[42] Coupled channel analysis with finite width corrections.
[43] Included in AGUILAR-BENITEZ 78 fit.

$f_0(980)$ WIDTH

Width determination very model dependent. Peak width in $\pi\pi$ is about 50 MeV, but decay width can be much larger.

VALUE (MeV)	EVTS	DOCUMENT ID		TECN	COMMENT
40 to 100 OUR ESTIMATE					
• • • We do not use the following data for averages, fits, limits, etc. • • •					
9.5 ± 1.1	706	ABLIKIM	12E	BES3	$J/\psi \to \gamma 3\pi$
42 $^{+\ 20}_{-\ 16}$		[1,2] GARCIA-MAR...	11	RVUE	Compilation
50 $^{+\ 20}_{-\ 12}$		[2,3] GARCIA-MAR...	11	RVUE	Compilation
48 $^{+\ 22}_{-\ 6}$		[4] MOUSSALLAM	11	RVUE	Compilation
36 ± 22		[5] MENNESSIER	10	RVUE	Compilation
70 $^{+\ 20}_{-\ 32}$		[6] ANISOVICH	09	RVUE	0.0 $\overline{p}p$, πN
91 $^{+\ 30}_{-\ 22}$ ± 3	44	[7] ECKLUND	09	CLEO	4.17 $e^+e^- \to D_s^- D_s^{*+}$ + c.c.
66.9 ± 2.2 $^{+17.6}_{-12.5}$		[8] UEHARA	08A	BELL	10.6 $e^+e^- \to e^+e^-\pi^0\pi^0$
65 ± 13	262 ± 30	[9] AUBERT	07AK	BABR	10.6 $e^+e^- \to \phi\pi^+\pi^-\gamma$
81 ± 21	54 ± 9	[9] AUBERT	07AK	BABR	10.6 $e^+e^- \to \phi\pi^0\pi^0\gamma$
51.3 $^{+\ 20.8}_{-\ 17.7}$ $^{+13.2}_{-\ 3.8}$		[10] MORI	07	BELL	10.6 $e^+e^- \to e^+e^-\pi^+\pi^-$
61 ± 9 $^{+14}_{-\ 8}$	2584	[11] GARMASH	05	BELL	$B^+ \to K^+\pi^+\pi^-$
64 ± 16		[12] ANISOVICH	03	RVUE	
121 ± 23		TIKHOMIROV	03	SPEC	40.0 π^-C $\to K^0_S K^0_S K^0_L$ X
~ 70		[13] BRAMON	02	RVUE	1.02 $e^+e^- \to \pi^0\pi^0\gamma$
44 ± 2 ± 2	848	[14] AITALA	01A	E791	$D_s^+ \to \pi^-\pi^+\pi^+$
201 ± 28	419	[15] ACHASOV	00H	SND	$e^+e^- \to \pi^0\pi^0\gamma$
122 ± 13	419	[16,17] ACHASOV	00H	SND	$e^+e^- \to \pi^0\pi^0\gamma$
56 ± 20		[18] AKHMETSHIN	99C	CMD2	$e^+e^- \to \pi^0\pi^0\gamma$
65 ± 20		BARBERIS	99	OMEG	450 $pp \to p_s p_f K^+K^-$
80 ± 10		BARBERIS	99B	OMEG	450 $pp \to p_s p_f \pi^+\pi^-$
80 ± 10		BARBERIS	99C	OMEG	450 $pp \to p_s p_f \pi^0\pi^0$
48 ± 12 ± 8		[19] BARBERIS	99D	OMEG	450 $pp \to K^+K^-$, $\pi^+\pi^-$
65 ± 25		BELLAZZINI	99	GAM4	450 $pp \to pp\pi^0\pi^0$
71 ± 14		[20] KAMINSKI	99	RVUE	$\pi\pi \to \pi\pi$, $K\overline{K}$, $\sigma\sigma$
~ 28		[20] OLLER	99	RVUE	$\pi\pi \to \pi\pi$, $K\overline{K}$
~ 25		OLLER	99B	RVUE	$\pi\pi \to \pi\pi$, $K\overline{K}$
~ 14		[20] OLLER	99C	RVUE	$\pi\pi \to \pi\pi$, $K\overline{K}$, $\eta\eta$
70 ± 20		ALDE	98	GAM4	
86 ± 16		[20] ANISOVICH	98B	RVUE	Compilation
54		[21] LOCHER	98	RVUE	$\pi\pi \to \pi\pi$, $K\overline{K}$
69 ± 15		[22] ALDE	97	GAM2	450 $pp \to pp\pi^0\pi^0$
38 ± 20		[23] BERTIN	97C	OBLX	0.0 $\overline{p}p \to \pi^+\pi^-\pi^0$
~ 100		[24] ISHIDA	96	RVUE	$\pi\pi \to \pi\pi$, $K\overline{K}$
34		TORNQVIST	96	RVUE	$\pi\pi \to \pi\pi$, $K\overline{K}$, $K\pi$, $\eta\pi$
48 ± 10	3k	[25] ALDE	95B	GAM2	38 $\pi^- p \to \pi^0\pi^0 n$
95 ± 20	10k	[26] ALDE	95B	GAM2	38 $\pi^- p \to \pi^0\pi^0 n$
26 ± 10		AMSLER	95B	CBAR	0.0 $\overline{p}p \to 3\pi^0$
~ 112		[27] AMSLER	95D	CBAR	0.0 $\overline{p}p \to \pi^0\pi^0\pi^0$, $\pi^0\eta\eta$, $\pi^0\pi^0\eta$
80 ± 12		[28] ANISOVICH	95	RVUE	
30		JANSSEN	95	RVUE	$\pi\pi \to \pi\pi$, $K\overline{K}$
74		[29] BUGG	94	RVUE	$\overline{p}p \to \eta 2\pi^0$
29 ± 2		[30] KAMINSKI	94	RVUE	$\pi\pi \to \pi\pi$, $K\overline{K}$
46		[31] ZOU	94B	RVUE	
48 ± 12		[32] MORGAN	93	RVUE	$\pi\pi(K\overline{K}) \to \pi\pi(K\overline{K})$, $J/\psi \to \phi\pi\pi(K\overline{K})$, $D_s \to \pi(\pi\pi)$
37.4 ± 10.6		[22] AGUILAR-...	91	EHS	400 pp
72 ± 8		[33] ARMSTRONG	91	OMEG	300 $pp \to pp\pi\pi$, $pp K\overline{K}$

110	± 30				
29	± 13				
120	±281	±20			
28	± 10				
70	to 300				
100	± 80				
30	± 8				
48	± 14				
32	± 10				
30	± 10				
54	± 16				

	BREAKSTONE 90	SFM	$pp \to pp\pi^+\pi^-$	
[22]	ABACHI 86B	HRS	$e^+e^- \to \pi^+\pi^- X$	
	ETKIN 82B	MPS	$23\ \pi^- p \to n2K_S^0$	
[33]	GIDAL 81	MRK2	$J/\psi \to \pi^+\pi^- X$	
[34]	ACHASOV 80	RVUE		
[35]	AGUILAR-... 78	HBC	$0.7\ \overline{p}p \to K_S^0 K_S^0$	
[33]	LEEPER 77	ASPK	2–$2.4\ \pi^- p \to \pi^+\pi^- n,\ K^+K^- n$	
[33]	BINNIE 73	CNTR	$\pi^- p \to n$MM	
[36]	GRAYER 73	ASPK	$17\ \pi^- p \to \pi^+\pi^- n$	
[36]	HYAMS 73	ASPK	$17\ \pi^- p \to \pi^+\pi^- n$	
[36]	PROTOPOP... 73	HBC	$7\ \pi^+ p \to \pi^+ p\pi^+\pi^-$	

[1] Analytic continuation using Roy equations. Uses the K_{e4} data of BATLEY 10C and the $\pi N \to \pi\pi N$ data of HYAMS 73, GRAYER 74, and PROTOPOPESCU 73.
[2] Quoted number refers to twice imaginary part of pole position.
[3] Analytic continuation using GKPY equations. Uses the K_{e4} data of BATLEY 10C and the $\pi N \to \pi\pi N$ data of HYAMS 73, GRAYER 74, and PROTOPOPESCU 73.
[4] Pole position. Used Roy equations.
[5] Average of the analyses of three data sets in the K-matrix model. Uses the data of BATLEY 08A, HYAMS 73, and GRAYER 74, partially of COHEN 80 or ETKIN 82B.
[6] On sheet II in a 2-pole solution. The other pole is found on sheet III at $(850-100i)$ MeV
[7] Using a relativistic Breit-Wigner function and taking into account the finite D_s mass.
[8] Breit-Wigner $\pi\pi$ width. Using finite width corrections according to FLATTE 76 and ACHASOV 05, and the ratio $g_{f_0 KK}/g_{f_0\pi\pi} = 0$.
[9] Systematic errors not estimated.
[10] Breit-Wigner $\pi\pi$ width. Using finite width corrections according to FLATTE 76 and ACHASOV 05, and the ratio $g_{f_0 KK}/g_{f_0\pi\pi} = 4.21 \pm 0.25 \pm 0.21$ from ABLIKIM 05.
[11] Breit-Wigner, solution 1, PWA ambiguous.
[12] K-matrix pole from combined analysis of $\pi^- p \to \pi^0\pi^0 n$, $\pi^- p \to K\overline{K} n$, $\pi^+\pi^- \to \pi^+\pi^-$, $\overline{p}p \to \pi^0\pi^0\pi^0$, $\pi^0\eta\eta$, $\pi^0\pi^0\eta$, $\pi^+\pi^-\pi^0$, $K^+K^-\pi^0$, $K_S^0 K_S^0\pi^0$, $K^+K_S^0\pi^-$ at rest, $\overline{p}n \to \pi^-\pi^-\pi^+$, $K_S^0 K^-\pi^0$, $K_S^0 K_S^0\pi^-$ at rest.
[13] Using the data of AKHMETSHIN 99C, ACHASOV 00H, and ALOISIO 02D.
[14] Breit-Wigner width.
[15] Supersedes ACHASOV 98I. Using the model of ACHASOV 89.
[16] Supersedes ACHASOV 98I.
[17] In the "narrow resonance" approximation.
[18] From the combined fit of the photon spectra in the reactions $e^+e^- \to \pi^+\pi^-\gamma$, $\pi^0\pi^0\gamma$.
[19] Supersedes BARBERIS 99 and BARBERIS 99B
[20] T-matrix pole.
[21] On sheet II in a 2 pole solution. The other pole is found on sheet III at $(1039-93i)$ MeV.
[22] From invariant mass fit.
[23] On sheet II in a 2 pole solution. The other pole is found on sheet III at $(963-29i)$ MeV.
[24] Reanalysis of data from HYAMS 73, GRAYER 74, SRINIVASAN 75, and ROSSELET 77 using the interfering amplitude method.
[25] At high $|t|$.
[26] At low $|t|$.
[27] On sheet II in a 4-pole solution, the other poles are found on sheet III at $(953-55i)$ MeV and on sheet IV at $(938-35i)$ MeV.
[28] Combined fit of ALDE 95B, ANISOVICH 94,
[29] On sheet II in a 2 pole solution. The other pole is found on sheet III at $(996-103i)$ MeV.
[30] From sheet II pole position.
[31] On sheet II in a 2 pole solution. The other pole is found on sheet III at $(797-185i)$ MeV and can be interpreted as a shadow pole.
[32] On sheet II in a 2 pole solution. The other pole is found on sheet III at $(978-28i)$ MeV.
[33] From coupled channel analysis.
[34] Coupled channel analysis with finite width corrections.
[35] From coupled channel fit to the HYAMS 73 and PROTOPOPESCU 73 data. With a simultaneous fit to the $\pi\pi$ phase-shifts, inelasticity and to the $K_S^0 K_S^0$ invariant mass.
[36] Included in AGUILAR-BENITEZ 78 fit.

$f_0(980)$ DECAY MODES

	Mode	Fraction (Γ_i/Γ)
Γ_1	$\pi\pi$	dominant
Γ_2	$K\overline{K}$	seen
Γ_3	$\gamma\gamma$	seen
Γ_4	e^+e^-	

$f_0(980)$ PARTIAL WIDTHS

$\Gamma(\gamma\gamma)$ Γ_3

VALUE (keV)		DOCUMENT ID		TECN	COMMENT
0.29	$^{+0.07}_{-0.06}$ **OUR AVERAGE**				
0.286±0.017	$^{+0.211}_{-0.070}$	[1] UEHARA	08A	BELL	$10.6\ e^+e^- \to e^+e^-\pi^0\pi^0$
$0.205^{+0.095}_{-0.083}$	$^{+0.147}_{-0.117}$	[2] MORI	07	BELL	$10.6\ e^+e^- \to e^+e^-\pi^+\pi^-$
$0.28^{+0.09}_{-0.13}$		[3] BOGLIONE	99	RVUE	$\gamma\gamma \to \pi^+\pi^-, \pi^0\pi^0$
0.42 ±0.06	±0.18	[4] OEST	90	JADE	$e^+e^- \to e^+e^-\pi^0\pi^0$

• • • We do not use the following data for averages, fits, limits, etc. • • •

0.16	±0.01	[5] MENNESSIER 11	RVUE		
0.29	$\pm 0.21\ ^{+0.02}_{-0.07}$	[6] MOUSSALLAM 11	RVUE	Compilation	
0.42		[7,8] PENNINGTON 08	RVUE	Compilation	
0.10		[8,9] PENNINGTON 08	RVUE	Compilation	
0.29	±0.07 ±0.12	[10,11] BOYER 90	MRK2	$e^+e^- \to e^+e^-\pi^+\pi^-$	
0.31	±0.14 ±0.09	[10,11] MARSISKE 90	CBAL	$e^+e^- \to e^+e^-\pi^0\pi^0$	
0.63	±0.14	[12] MORGAN 90	RVUE	$\gamma\gamma \to \pi^+\pi^-, \pi^0\pi^0$	

[1] Using finite width corrections according to FLATTE 76 and ACHASOV 05, and the ratio $g_{f_0 KK}/g_{f_0\pi\pi} = 0$.
[2] Using finite width corrections according to FLATTE 76 and ACHASOV 05, and the ratio $g_{f_0 KK}/g_{f_0\pi\pi} = 4.21 \pm 0.25 \pm 0.21$ from ABLIKIM 05.
[3] Supersedes MORGAN 90.
[4] OEST 90 quote systematic errors $^{+0.08}_{-0.18}$. We use ±0.18. Observed 60 events.
[5] Uses an analytic K-matrix model. Compilation.
[6] Using dispersion integral with phase input from Roy equations and data from MARSISKE 90, BOYER 90, BEHREND 92, UEHARA 08A, and MORI 07.
[7] Solution A (preferred solution based on χ^2-analysis).
[8] Dispersion theory based amplitude analysis of BOYER 90, MARSISKE 90, BEHREND 92, and MORI 07.
[9] Solution B (worse than solution A; still acceptable when systematic uncertainties are included).
[10] From analysis allowing arbitrary background unconstrained by unitarity.
[11] Data included in MORGAN 90, BOGLIONE 99 analyses.
[12] From amplitude analysis of BOYER 90 and MARSISKE 90, data corresponds to resonance parameters $m = 989$ MeV, $\Gamma = 61$ MeV.

$\Gamma(e^+e^-)$ Γ_4

VALUE (eV)	CL%	DOCUMENT ID		TECN	COMMENT
<8.4	90	VOROBYEV	88	ND	$e^+e^- \to \pi^0\pi^0$

$f_0(980)$ BRANCHING RATIOS

$\Gamma(\pi\pi)/[\Gamma(\pi\pi)+\Gamma(K\overline{K})]$ $\Gamma_1/(\Gamma_1+\Gamma_2)$

VALUE	EVTS	DOCUMENT ID		TECN	COMMENT
• • • We do not use the following data for averages, fits, limits, etc. • • •					
0.52±0.12	9.9k	[1] AUBERT	06O	BABR	$B^\pm \to K^\pm\pi^\pm\pi^\mp$
$0.75^{+0.11}_{-0.13}$		[2] ABLIKIM	05Q	BES2	$\chi_{c0} \to 2\pi^+2\pi^-, \pi^+\pi^- K^+K^-$
0.84±0.02		[3] ANISOVICH	02D	SPEC	Combined fit
~ 0.68		OLLER	99B	RVUE	$\pi\pi \to \pi\pi, K\overline{K}$
0.67±0.09		[4] LOVERRE	80	HBC	$4\ \pi^- p \to n2K_S^0$
$0.81^{+0.09}_{-0.04}$		[4] CASON	78	STRC	$7\ \pi^- p \to n2K_S^0$
0.78±0.03		[4] WETZEL	76	OSPK	$8.9\ \pi^- p \to n2K_S^0$

[1] Recalculated by us using $\Gamma(K^+K^-)\ /\ \Gamma(\pi^+\pi^-) = 0.69 \pm 0.32$ from AUBERT 06O and isospin relations.
[2] Using data from ABLIKIM 04G.
[3] From a combined K-matrix analysis of Crystal Barrel (0. $p\overline{p} \to \pi^0\pi^0\pi^0$, $\pi^0\eta\eta$, $\pi^0\pi^0\eta$), GAMS ($\pi p \to \pi^0\pi^0 n$, $\eta\eta n$, $\eta\eta' n$), and BNL ($\pi p \to K\overline{K} n$) data.
[4] Measure $\pi\pi$ elasticity assuming two resonances coupled to the $\pi\pi$ and $K\overline{K}$ channels only.

$f_0(980)$ REFERENCES

ABLIKIM	12E	PRL 108 182001	M. Ablikim *et al.* (BES III Collab.)
GARCIA-MAR...	11	PRL 107 072001	R. Garcia-Martin *et al.* (MADR, CRAC)
MENNESSIER	11	PL B696 40	G. Mennessier, S. Narison, X.-G. Wang
MOUSSALLAM	11	EPJ C71 1814	B. Moussallam
BATLEY	10C	EPJ C70 635	J.R. Batley *et al.* (CERN NA48/2 Collab.)
MENNESSIER	10	PL B688 59	G. Mennessier, S. Narison, X.-G. Wang
ANISOVICH	09	IJMP A24 2481	V.V. Anisovich, A.V. Sarantsev
ECKLUND	09	PR D80 052009	K.M. Ecklund *et al.* (CLEO Collab.)
BATLEY	08A	EPJ C54 411	J.R. Batley *et al.* (CERN NA48/2 Collab.)
PENNINGTON	08	EPJ C56 1	M.R. Pennington *et al.*
UEHARA	08A	PR D78 052004	S. Uehara *et al.* (BELLE Collab.)
AMBROSINO	07	EPJ C49 473	F. Ambrosino *et al.* (KLOE Collab.)
AUBERT	07AK	PR D76 012008	B. Aubert *et al.* (BABAR Collab.)
BONVICINI	07	PR D76 012001	G. Bonvicini *et al.* (CLEO Collab.)
MORI	07	PR D75 051101	T. Mori *et al.* (BELLE Collab.)
AMBROSINO	06B	PL B634 148	F. Ambrosino *et al.* (KLOE Collab.)
AUBERT	06O	PR D74 032003	B. Aubert *et al.* (BABAR Collab.)
GARMASH	06	PRL 96 251803	A. Garmash *et al.* (BELLE Collab.)
ABLIKIM	05	PL B607 243	M. Ablikim *et al.* (BES Collab.)
ABLIKIM	05Q	PR D72 092002	M. Ablikim *et al.* (BES Collab.)
ACHASOV	05	PR D72 013006	N.N. Achasov, G.N. Shestakov
GARMASH	05	PR D71 092003	A. Garmash *et al.* (BELLE Collab.)
ABLIKIM	04G	PR D70 092002	M. Ablikim *et al.* (BES Collab.)
ANISOVICH	03	EPJ A16 229	V.V. Anisovich *et al.*
TIKHOMIROV	03	PAN 66 828 Translated from YAF 66 860.	G.D. Tikhomirov *et al.*
ALOISIO	02D	PL B537 21	A. Aloisio *et al.* (KLOE Collab.)
ANISOVICH	02D	PAN 65 1545 Translated from YAF 65 1583.	V.V. Anisovich *et al.*
BRAMON	02	EPJ C26 253	A. Bramon *et al.*
ACHASOV	01F	PR D63 094007	N.N. Achasov, V.V. Gubin (Novosibirsk SND Collab.)
AITALA	01A	PRL 86 765	E.M. Aitala *et al.* (FNAL E791 Collab.)
AITALA	01B	PRL 86 770	E.M. Aitala *et al.* (FNAL E791 Collab.)
ACHASOV	00H	PL B485 349	M.N. Achasov *et al.* (Novosibirsk SND Collab.)
AKHMETSHIN	99B	PL B462 371	R.R. Akhmetshin *et al.* (Novosibirsk CMD-2 Collab.)
AKHMETSHIN	99C	PL B462 380	R.R. Akhmetshin *et al.* (Novosibirsk CMD-2 Collab.)
BARBERIS	99	PL B453 305	D. Barberis *et al.* (Omega Expt.)
BARBERIS	99B	PL B453 316	D. Barberis *et al.* (Omega Expt.)
BARBERIS	99C	PL B453 325	D. Barberis *et al.* (Omega Expt.)
BARBERIS	99D	PL B462 462	D. Barberis *et al.* (Omega Expt.)
BELLAZZINI	99	PL B467 296	R. Bellazzini *et al.*
BOGLIONE	99	EPJ C9 11	M. Boglione, M.R. Pennington

Meson Particle Listings

$f_0(980)$, $a_0(980)$

KAMINSKI 99 EPJ C9 141 R. Kaminski, L. Lesniak, B. Loiseau (CRAC, PARIN)
OLLER 99 PR D60 099906 (erratum) J.A. Oller *et al.*
OLLER 99B NP A652 407 (erratum) J.A. Oller, E. Oset
OLLER 99C PR D60 074023 J.A. Oller, E. Oset
ACHASOV 98I PL B440 442 M.N. Achasov *et al.*
ACKERSTAFF 98Q EPJ C4 19 K. Ackerstaff *et al.* (OPAL Collab.)
ALDE 98 EPJ A3 361 D. Alde *et al.* (GAM4 Collab.)
Also PAN 62 405 D. Alde *et al.* (GAMS Collab.)
Translated from YAF 62 446.
ANISOVICH 98B SPU 41 419 V.V. Anisovich *et al.*
Translated from UFN 168 481.
LOCHER 98 EPJ C4 317 M.P. Locher *et al.* (PSI)
ALDE 97 PL B397 350 D.M. Alde *et al.* (GAMS Collab.)
BERTIN 97C PL B408 476 A. Bertin *et al.* (OBELIX Collab.)
ISHIDA 96 PTP 95 745 S. Ishida *et al.* (TOKY, MIYA, KEK)
TORNQVIST 96 PRL 76 1575 N.A. Tornqvist, M. Roos (HELS)
ALDE 95B ZPHY C66 375 D.M. Alde *et al.* (GAMS Collab.)
AMSLER 95B PL B342 433 C. Amsler *et al.* (Crystal Barrel Collab.)
AMSLER 95D PL B355 425 C. Amsler *et al.* (Crystal Barrel Collab.)
ANISOVICH 95 PL B355 363 V.V. Anisovich *et al.* (PNPI, SERP)
JANSSEN 95 PR D52 2690 G. Janssen *et al.* (STON, ADLD, JULI)
AMSLER 94D PL B333 277 C. Amsler *et al.* (Crystal Barrel Collab.)
ANISOVICH 94 PL B323 233 V.V. Anisovich *et al.* (Crystal Barrel Collab.)
BUGG 94 PR D50 4412 D.V. Bugg *et al.* (LOQM)
KAMINSKI 94 PR D50 3145 R. Kaminski, L. Lesniak, J.P. Maillet (CRAC+)
ZOU 94B PR D50 591 B.S. Zou, D.V. Bugg (LOQM)
MORGAN 93 PR D48 1185 D. Morgan, M.R. Pennington (RAL, DURH)
BEHREND 92 ZPHY C56 381 H.J. Behrend (CELLO Collab.)
AGUILAR-... 91 ZPHY C50 405 M. Aguilar-Benitez *et al.* (LEBC-EHS Collab.)
ARMSTRONG 91 ZPHY C51 351 T.A. Armstrong *et al.* (ATHU, BARI, BIRM+)
BOYER 90 PR D42 1350 J. Boyer *et al.* (Mark II Collab.)
BREAKSTONE 90 ZPHY C48 569 A.M. Breakstone *et al.* (ISU, BGNA, CERN+)
MARSISKE 90 PR D41 3324 H. Marsiske *et al.* (Crystal Ball Collab.)
MORGAN 90 ZPHY C48 623 D. Morgan, M.R. Pennington (RAL, DURH)
OEST 90 ZPHY C47 343 T. Oest *et al.* (JADE Collab.)
ACHASOV 89 NP B315 465 N.N. Achasov, V.N. Ivanchenko
AUGUSTIN 89 NP B320 1 J.E. Augustin, G. Cosme (DM2 Collab.)
VOROBYEV 88 SJNP 48 273 P.V. Vorobiev *et al.* (NOVO)
Translated from YAF 48 436.
ABACHI 86B PRL 57 1990 S. Abachi *et al.* (PURD, ANL, IND, MICH+)
ETKIN 82B PR D25 1786 A. Etkin *et al.* (BNL, CUNY, TUFTS, VAND)
GIDAL 81 PL 107B 153 G. Gidal *et al.* (SLAC, LBL)
ACHASOV 80 SJNP 32 566 N.N. Achasov, S.A. Devyanin, G.N. Shestakov (NOVM)
Translated from YAF 32 1098.
COHEN 80 PR D22 2595 D. Cohen *et al.* (ANL) IJP
LOVERRE 80 ZPHY C6 187 P.F. Loverre *et al.* (CERN, CDEF, MADR+) IJP
AGUILAR-... 78 NP B140 73 M. Aguilar-Benitez *et al.* (MADR, BOMB+)
CASON 78 PRL 41 271 N.M. Cason *et al.* (NDAM, ANL)
LEEPER 77 PR D16 2054 R.J. Leeper *et al.* (ISU)
ROSSELET 77 PR D15 574 L. Rosselet *et al.* (GEVA, SACL)
FLATTE 76 PL 63B 224 S.M. Flatte (CERN)
WETZEL 76 NP B115 208 W. Wetzel *et al.* (ETH, CERN, LOIC)
SRINIVASAN 75 PR D12 681 V. Srinivasan *et al.* (NDAM, ANL)
GRAYER 74 NP B75 189 G. Grayer *et al.* (CERN, MPIM)
BINNIE 73 PRL 31 1534 D.M. Binnie *et al.* (LOIC, SHMP)
GRAYER 73 Tallahassee G. Grayer *et al.* (CERN, MPIM)
HYAMS 73 NP B64 134 B.D. Hyams *et al.* (CERN, MPIM)
PROTOPOP... 73 PR D7 1279 S.D. Protopopescu *et al.* (LBL)

$a_0(980)$

$I^G(J^{PC}) = 1^-(0^{++})$

See our minireview on scalar mesons under $f_0(500)$. (See the index for the page number.)

$a_0(980)$ MASS

VALUE (MeV)	DOCUMENT ID
980±20 OUR ESTIMATE	Mass determination very model dependent

$\eta\pi$ FINAL STATE ONLY

VALUE (MeV)	EVTS	DOCUMENT ID		TECN	CHG	COMMENT
• • • We do not use the following data for averages, fits, limits, etc. • • •						
982.5 ± 1.6 ±1.1	16.9k	[1] AMBROSINO	09F	KLOE		1.02 $e^+e^- \to \eta\pi^0\gamma$
986 ± 4		ANISOVICH	09	RVUE		0.0 $\overline{p}p$, πN
982.3 $^{+\ 0.6}_{-\ 0.7}$ $^{+3.1}_{-4.7}$		[2] UEHARA	09A	BELL		$\gamma\gamma \to \pi^0\eta$
987.4 ± 1.0 ±3.0		[3,4] BUGG	08A	RVUE	0	$\overline{p}p \to \pi^0\pi^0\eta$
989.1 ± 1.0 ±3.0		[4,5] BUGG	08A	RVUE	0	$\overline{p}p \to \pi^0\pi^0\eta$
985 ± 4 ±6	318	ACHARD	02B	L3		183–209 $e^+e^- \to e^+e^-\eta\pi^+\pi^-$
995 $^{+52}_{-10}$	36	[6] ACHASOV	00F	SND		$e^+e^- \to \eta\pi^0\gamma$
994 $^{+33}_{-\ 8}$	36	[7] ACHASOV	00F	SND		$e^+e^- \to \eta\pi^0\gamma$
975 ± 7		BARBERIS	00H			450 $pp \to p_f\eta\pi^0 p_s$
988 ± 8		BARBERIS	00H			450 $pp \to \Delta_f^{++}\eta\pi^- p_s$
~ 1055		[8] OLLER	99	RVUE		$\eta\pi$, $K\overline{K}$
~ 1009.2		[8] OLLER	99B	RVUE		$\pi\pi \to \pi\pi$, $K\overline{K}$
993.1 ± 2.1		[9] TEIGE	99	B852		18.3 $\pi^-p \to \eta\pi^+\pi^-n$
988 ± 6		[8] ANISOVICH	98B	RVUE		Compilation
987		TORNQVIST	96	RVUE		$\pi\pi \to \pi\pi$, $K\overline{K}$, $K\pi$, $\eta\pi$
991		JANSSEN	95	RVUE		$\eta\pi \to \eta\pi$, $K\overline{K}$, $K\pi$, $\eta\pi$
984.45± 1.23± 0.34		AMSLER	94C	CBAR		0.0 $\overline{p}p \to \omega\eta\pi^0$
982 ± 2		[10] AMSLER	92	CBAR		0.0 $\overline{p}p \to \eta\eta\pi^0$
984 ± 4	1040	[10] ARMSTRONG	91B	OMEG ±		300 $pp \to pp\eta\pi^+\pi^-$
976 ± 6		ATKINSON	84E	OMEG ±		25–55 $\gamma p \to \eta\pi n$
986 ± 3	500	[11] EVANGELIS...	81	OMEG ±		12 $\pi^-p \to \eta\pi^+\pi^-\pi^-p$
990 ± 7	145	[11] GURTU	79	HBC	±	4.2 $K^-p \to \Lambda\eta 2\pi$
980 ±11	47	CONFORTO	78	OSPK	−	4.5 $\pi^-p \to pX^-$
978 ±16	50	CORDEN	78	OMEG ±		12–15 $\pi^-p \to n\eta 2\pi$
977 ± 7		GRASSLER	77	HBC	−	16 $\pi^\mp p \to p\eta 3\pi$
989 ± 4	70	WELLS	75	HBC	−	3.1–6 $K^-p \to \Lambda\eta 2\pi$
972 ±10	150	DEFOIX	72	HBC	±	0.7 $\overline{p}p \to 7\pi$
970 ±15	20	BARNES	69C	HBC	−	4–5 $K^-p \to \Lambda\eta 2\pi$
980 ±10		CAMPBELL	69	DBC	±	2.7 π^+d
980 ±10	15	MILLER	69B	HBC	−	4.5 $K^-N \to \eta\pi\Lambda$
980 ±10	30	AMMAR	68	HBC	±	5.5 $K^-p \to \Lambda\eta 2\pi$

[1] Using the model of ACHASOV 89 and ACHASOV 03B.
[2] From a fit with the S-wave amplitude including two interfering Breit-Wigners plus a background term.
[3] Parameterizes couplings to $\overline{K}K$, $\pi\eta$, and $\pi\eta'$.
[4] Using AMSLER 94D and ABELE 98.
[5] From the T-matrix pole on sheet II.
[6] Using the model of ACHASOV 89. Supersedes ACHASOV 98B.
[7] Using the model of JAFFE 77. Supersedes ACHASOV 98B.
[8] T-matrix pole.
[9] Breit-Wigner fit, average between $a_0^\pm$ and a_0^0. The fit favors a slightly heavier $a_0^\pm$.
[10] From a single Breit-Wigner fit.
[11] From $f_1(1285)$ decay.

$K\overline{K}$ ONLY

VALUE (MeV)	EVTS	DOCUMENT ID		TECN	CHG	COMMENT
• • • We do not use the following data for averages, fits, limits, etc. • • •						
~ 1053		[12] OLLER	99C	RVUE		$\pi\pi \to \pi\pi$, $K\overline{K}$
982 ± 3		[13] ABELE	98	CBAR		0.0 $\overline{p}p \to K_L^0K^\pm\pi^\mp$
975 ±15		BERTIN	98B	OBLX	±	0.0 $\overline{p}p \to K^\pm K_s\pi^\mp$
976 ± 6	316	DEBILLY	80	HBC	±	1.2–2 $\overline{p}p \to f_1(1285)\omega$
1016 ±10	100	[14] ASTIER	67	HBC	±	0.0 $\overline{p}p$
1003.3± 7.0	143	[15] ROSENFELD	65	RVUE	±	

[12] T-matrix pole.
[13] T-matrix pole on sheet II, the pole on sheet III is at 1006-i49 MeV.
[14] ASTIER 67 includes data of BARLOW 67, CONFORTO 67, ARMENTEROS 65.
[15] Plus systematic errors.

$a_0(980)$ WIDTH

VALUE (MeV)	EVTS	DOCUMENT ID		TECN	CHG	COMMENT
50 to 100 OUR ESTIMATE		Width determination very model dependent. Peak width in $\eta\pi$ is about 60 MeV, but decay width can be much larger.				
• • • We do not use the following data for averages, fits, limits, etc. • • •						
75.6 ± 1.6 $^{+17.4}_{-10.0}$		[16] UEHARA	09A	BELL		$\gamma\gamma \to \pi^0\eta$
80.2 ± 3.8 ± 5.4		[17] BUGG	08A	RVUE	0	$\overline{p}p \to \pi^0\pi^0\eta$
50 ±13 ± 4	318	ACHARD	02B	L3		183–209 $e^+e^- \to e^+e^-\eta\pi^+\pi^-$
72 ±16		BARBERIS	00H			450 $pp \to p_f\eta\pi^0 p_s$
61 ±19		BARBERIS	00H			450 $pp \to \Delta_f^{++}\eta\pi^- p_s$
~ 42		[18] OLLER	99	RVUE		$\eta\pi$, $K\overline{K}$
~ 112		[18] OLLER	99B	RVUE		$\pi\pi \to \eta\pi$, $K\overline{K}$
71 ± 7		TEIGE	99	B852		18.3 $\pi^-p \to \eta\pi^+\pi^-n$
92 ±20		[18] ANISOVICH	98B	RVUE		Compilation
65 ±10		[19] BERTIN	98B	OBLX	±	0.0 $\overline{p}p \to K^\pm K_s\pi^\mp$
~ 100		TORNQVIST	96	RVUE		$\pi\pi \to \pi\pi$, $K\overline{K}$, $K\pi$, $\eta\pi$
202		JANSSEN	95	RVUE		$\eta\pi \to \eta\pi$, $K\overline{K}$, $K\pi$, $\eta\pi$
54.12± 0.34± 0.12		AMSLER	94C	CBAR		0.0 $\overline{p}p \to \omega\eta\pi^0$
54 ±10		[20] AMSLER	92	CBAR		0.0 $\overline{p}p \to \eta\eta\pi^0$
95 ±14	1040	[20] ARMSTRONG	91B	OMEG ±		300 $pp \to pp\eta\pi^+\pi^-$
62 ±15	500	[21] EVANGELIS...	81	OMEG ±		12 $\pi^-p \to \eta\pi^+\pi^-\pi^-p$
60 ±20	145	[21] GURTU	79	HBC	±	4.2 $K^-p \to \Lambda\eta 2\pi$
60 $^{+50}_{-30}$	47	CONFORTO	78	OSPK	−	4.5 $\pi^-p \to pX^-$
86.0 $^{+60.0}_{-50.0}$	50	CORDEN	78	OMEG ±		12–15 $\pi^-p \to n\eta 2\pi$
44 ±22		GRASSLER	77	HBC	−	16 $\pi^\mp p \to p\eta 3\pi$
80 to 300		[22] FLATTE	76	RVUE	−	4.2 $K^-p \to \Lambda\eta 2\pi$
16.0 $^{+25.0}_{-16.0}$	70	WELLS	75	HBC	−	3.1–6 $K^-p \to \Lambda\eta 2\pi$
30 ± 5	150	DEFOIX	72	HBC	±	0.7 $\overline{p}p \to 7\pi$
40 ±15		CAMPBELL	69	DBC	±	2.7 π^+d
60 ±30	15	MILLER	69B	HBC	−	4.5 $K^-N \to \eta\pi\Lambda$
80 ±30	30	AMMAR	68	HBC	±	5.5 $K^-p \to \Lambda\eta 2\pi$

[16] From a fit with the S-wave amplitude including two interfering Breit-Wigners plus a background term.
[17] From the T-matrix pole on sheet II, using AMSLER 94D and ABELE 98.
[18] T-matrix pole.
[19] The $\eta\pi$ width.
[20] From a single Breit-Wigner fit.
[21] From $f_1(1285)$ decay.
[22] Using a two-channel resonance parametrization of GAY 76B data.

$K\overline{K}$ ONLY

VALUE (MeV)	EVTS	DOCUMENT ID		TECN	CHG	COMMENT
92± 8		[23] ABELE	98	CBAR		0.0 $\overline{p}p \rightarrow K^0_L K^\pm \pi^\mp$
• • • We do not use the following data for averages, fits, limits, etc. • • •						
~ 24		[24] OLLER	99C	RVUE		$\pi\pi \rightarrow \pi\pi, K\overline{K}$
~ 25	100	[25] ASTIER	67	HBC	±	
57±13	143	[26] ROSENFELD	65	RVUE	±	

[23] T-matrix pole on sheet II, the pole on sheet III is at 1006-i49 MeV.
[24] T-matrix pole.
[25] ASTIER 67 includes data of BARLOW 67, CONFORTO 67, ARMENTEROS 65.
[26] Plus systematic errors.

$a_0(980)$ DECAY MODES

	Mode	Fraction (Γ_i/Γ)
Γ_1	$\eta\pi$	dominant
Γ_2	$K\overline{K}$	seen
Γ_3	$\rho\pi$	
Γ_4	$\gamma\gamma$	seen
Γ_5	e^+e^-	

$a_0(980)$ PARTIAL WIDTHS

$\Gamma(\gamma\gamma)$ **Γ_4**

VALUE (keV)	DOCUMENT ID		TECN	
• • • We do not use the following data for averages, fits, limits, etc. • • •				
0.30±0.10	[27] AMSLER	98	RVUE	

[27] Using $\Gamma_{\gamma\gamma}B(a0(980) \rightarrow \eta\pi) = 0.24 \pm 0.08$ keV.

$a_0(980)$ Γ(i)$\Gamma(\gamma\gamma)/\Gamma$(total)

$\Gamma(\eta\pi) \times \Gamma(\gamma\gamma)/\Gamma_{total}$ **$\Gamma_1\Gamma_4/\Gamma$**

VALUE (keV)	EVTS	DOCUMENT ID		TECN	COMMENT
0.21 $^{+0.08}_{-0.04}$ OUR AVERAGE					
$0.128^{+0.003}_{-0.002}{}^{+0.502}_{-0.043}$		[28] UEHARA	09A	BELL	$\gamma\gamma \rightarrow \pi^0\eta$
0.28 ±0.04 ±0.10	44	OEST	90	JADE	$e^+e^- \rightarrow e^+e^-\pi^0\eta$
0.19 ±0.07 $^{+0.10}_{-0.07}$		ANTREASYAN	86	CBAL	$e^+e^- \rightarrow e^+e^-\pi^0\eta$

[28] From a fit with the S-wave amplitude including two interfering Breit-Wigners plus a background term.

$\Gamma(\eta\pi) \times \Gamma(e^+e^-)/\Gamma_{total}$ **$\Gamma_1\Gamma_5/\Gamma$**

VALUE (eV)	CL%	DOCUMENT ID		TECN	COMMENT
<1.5	90	VOROBYEV	88	ND	$e^+e^- \rightarrow \pi^0\eta$

$a_0(980)$ BRANCHING RATIOS

$\Gamma(K\overline{K})/\Gamma(\eta\pi)$ **Γ_2/Γ_1**

VALUE	DOCUMENT ID		TECN	CHG	COMMENT
0.183±0.024 OUR AVERAGE Error includes scale factor of 1.2.					
0.57 ±0.16	[29] BARGIOTTI	03	OBLX		$\overline{p}p$
0.23 ±0.05	[30] ABELE	98	CBAR		0.0 $\overline{p}p \rightarrow K^0_L K^\pm \pi^\mp$
0.166±0.01 ±0.02	[31] BARBERIS	98C	OMEG		450 $pp \rightarrow p_f f_1(1285) p_s$
• • • We do not use the following data for averages, fits, limits, etc. • • •					
1.20 ±0.15	[32] ANISOVICH	09	RVUE		0.0 $\overline{p}p$, πN
1.05 ±0.07 ±0.05	[33] BUGG	08A	RVUE	0	$\overline{p}p \rightarrow \pi^0\pi^0\eta$
~ 0.60	OLLER	99B	RVUE		$\pi\pi \rightarrow \eta\pi, K\overline{K}$
0.7 ±0.3	[31] CORDEN	78	OMEG		12–15 $\pi^- p \rightarrow n\eta 2\pi$
0.25 ±0.08	[31] DEFOIX	72	HBC	±	0.7 $\overline{p} \rightarrow 7\pi$

$\Gamma(\rho\pi)/\Gamma(\eta\pi)$ **Γ_3/Γ_1**

$\rho\pi$ forbidden.

VALUE	CL%	DOCUMENT ID		TECN	CHG	COMMENT
• • • We do not use the following data for averages, fits, limits, etc. • • •						
<0.25	70	AMMAR	70	HBC	±	4.1,5.5 $K^- p \rightarrow \Lambda\eta 2\pi$

[29] Coupled channel analysis of $\pi^+\pi^-\pi^0$, $K^+K^-\pi^0$, and $K^\pm K^0_S\pi^\mp$.
[30] Using $\pi^0\pi^0\eta$ from AMSLER 94D.
[31] From the decay of $f_1(1285)$.
[32] This is a ratio of couplings.
[33] A ratio of couplings, using AMSLER 94D and ABELE 98. Supersedes BUGG 94.

$a_0(980)$ REFERENCES

AMBROSINO	09F	PL B681 5	F. Ambrosino *et al.*	(KLOE Collab.)
ANISOVICH	09	IJMP A24 2481	V.V. Anisovich, A.V. Sarantsev	
UEHARA	09A	PR D80 032001	S. Uehara *et al.*	(BELLE Collab.)
BUGG	08A	PR D78 074023	D.V. Bugg	(LOQM)
ACHASOV	03B	PR D68 014006	N.N. Achsaov, A.V. Kiselev	
BARGIOTTI	03	EPJ C26 371	M. Bargiotti *et al.*	(OBELIX Collab.)
ACHARD	02B	PL B526 269	P. Achard *et al.*	(L3 Collab.)
ACHASOV	00F	PL B479 53	M.N. Achasov *et al.*	(Novosibirsk SND Collab.)
BARBERIS	00H	PL B488 225	D. Barberis *et al.*	(WA 102 Collab.)
OLLER	99	PR D60 099906 (erratum)	J.A. Oller *et al.*	
OLLER	99B	NP A652 407 (erratum)	J.A. Oller, E. Oset	
OLLER	99C	PR D60 074023	J.A. Oller, E. Oset	
TEIGE	99	PR D59 012001	S. Teige *et al.*	(BNL E852 Collab.)
ABELE	98	PR D57 3860	A. Abele *et al.*	(Crystal Barrel Collab.)
ACHASOV	98B	PL B438 441	M.N. Achasov *et al.*	(Novosibirsk SND Collab.)
AMSLER	98	RMP 70 1293	C. Amsler	
ANISOVICH	98B	SPU 41 419	V.V. Anisovich *et al.*	
		Translated from UFN 168 481.		
BARBERIS	98C	PL B440 225	D. Barberis *et al.*	(WA 102 Collab.)
BERTIN	98B	PL B434 180	A. Bertin *et al.*	(OBELIX Collab.)
TORNQVIST	96	PRL 76 1575	N.A. Tornqvist, M. Roos	(HELS)
JANSSEN	95	PR D52 2690	G. Janssen *et al.*	(STON, ADLD, JULI)
AMSLER	94C	PL B327 425	C. Amsler *et al.*	(Crystal Barrel Collab.)
AMSLER	94D	PL B333 277	C. Amsler *et al.*	(Crystal Barrel Collab.)
BUGG	94	PR D50 4412	D.V. Bugg *et al.*	(LOQM)
AMSLER	92	PL B291 347	C. Amsler *et al.*	(Crystal Barrel Collab.)
ARMSTRONG	91B	ZPHY C52 389	T.A. Armstrong *et al.*	(ATHU, BARI, BIRM+)
OEST	90	ZPHY C47 343	T. Oest *et al.*	(JADE Collab.)
ACHASOV	89	NP B315 465	N.N. Achasov, V.N. Ivanchenko	
VOROBYEV	88	SJNP 48 273	P.V. Vorobiev *et al.*	(NOVO)
		Translated from YAF 48 436.		
ANTREASYAN	86	PR D33 1847	D. Antreasyan *et al.*	(Crystal Ball Collab.)
ATKINSON	84E	PL 138B 459	M. Atkinson *et al.*	(BONN, CERN, GLAS+)
EVANGELIS...	81	NP B178 197	C. Evangelista *et al.*	(BARI, BONN, CERN+)
DEBILLY	80	NP B176 1	L. de Billy *et al.*	(CURIN, LAUS, NEUC+)
GURTU	79	NP B151 181	A. Gurtu *et al.*	(CERN, ZEEM, NIJM, OXF)
CONFORTO	78	LNC 23 419	B. Conforto *et al.*	(RHEL, TNTO, CHIC+)
CORDEN	78	NP B144 253	M.J. Corden *et al.*	(BIRM, RHEL, TELA+)
GRASSLER	77	NP B121 189	H. Grassler *et al.*	(AACH3, BERL, BONN+)
JAFFE	77	PR D15 267,281	R. Jaffe	(MIT)
FLATTE	76	PL 63B 224	S.M. Flatte	(CERN)
GAY	76B	PL 63B 220	J.B. Gay *et al.*	(CERN, AMST, NIJM) JP
WELLS	75	NP B101 333	J. Wells *et al.*	(OXF)
DEFOIX	72	NP B44 125	C. Defoix *et al.*	(CDEF, CERN)
AMMAR	70	PR D2 430	R. Ammar *et al.*	(KANS, NWES, ANL, WISC)
BARNES	69C	PRL 23 610	V.E. Barnes *et al.*	(BNL, SYRA)
CAMPBELL	69	PRL 22 1204	J.H. Campbell *et al.*	(PURD)
MILLER	69B	PL 29B 255	D.H. Miller *et al.*	(PURD)
Also		PR 188 2011	W.L. Yen *et al.*	(PURD)
AMMAR	68	PRL 21 1832	R. Ammar *et al.*	(NWES, ANL)
ASTIER	67	PL 25B 294	A. Astier *et al.*	(CDEF, CERN, IRAD)
		Includes data of BARLOW 67, CONFORTO 67, and ARMENTEROS 65.		
BARLOW	67	NC 50A 701	J. Barlow *et al.*	(CERN, CDEF, IRAD, LIVP)
CONFORTO	67	NP B3 469	G. Conforto *et al.*	(CERN, CDEF, IPNP+)
ARMENTEROS	65	PL 17 344	R. Armenteros *et al.*	(CERN, CDEF)
ROSENFELD	65	Oxford Conf. 58	A.H. Rosenfeld	(LRL)

$\phi(1020)$

$I^G(J^{PC}) = 0^-(1^{--})$

$\phi(1020)$ MASS

VALUE (MeV)	EVTS	DOCUMENT ID		TECN	COMMENT
1019.461±0.019 OUR AVERAGE Error includes scale factor of 1.1.					
1019.51 ±0.02 ±0.05		[1] LEES	13Q	BABR	$e^+e^- \rightarrow K^+K^-\gamma$
1019.30 ±0.02 ±0.10	105k	AKHMETSHIN	06	CMD2	0.98–1.06 $e^+e^- \rightarrow \pi^+\pi^-\pi^0$
1019.52 ±0.05 ±0.05	17.4k	AKHMETSHIN	05	CMD2	0.60-1.38 $e^+e^- \rightarrow \eta\gamma$
1019.483±0.011±0.025	272k	[2] AKHMETSHIN	04	CMD2	$e^+e^- \rightarrow K^0_L K^0_S$
1019.42 ±0.05	1900k	[3] ACHASOV	01E	SND	$e^+e^- \rightarrow K^+K^-$, $K_S K_L$, $\pi^+\pi^-\pi^0$
1019.40 ±0.04 ±0.05	23k	AKHMETSHIN	01B	CMD2	$e^+e^- \rightarrow \eta\gamma$
1019.36 ±0.12		[4] ACHASOV	00B	SND	$e^+e^- \rightarrow \eta\gamma$
1019.38 ±0.07 ±0.08	2200	[5] AKHMETSHIN	99F	CMD2	$e^+e^- \rightarrow \pi^+\pi^- \geq 2\gamma$
1019.51 ±0.07 ±0.10	11169	AKHMETSHIN	98	CMD2	$e^+e^- \rightarrow \pi^+\pi^-\pi^0$
1019.5 ±0.4		BARBERIS	98	OMEG	450 $pp \rightarrow pp2K^+2K^-$
1019.42 ±0.06	55600	AKHMETSHIN	95	CMD2	$e^+e^- \rightarrow$ hadrons
1019.7 ±0.3	2012	DAVENPORT	86	MPSF	400 pA $\rightarrow 4K$X
1019.7 ±0.1 ±0.1	5079	ALBRECHT	85D	ARG	10 $e^+e^- \rightarrow K^+K^-$X
1019.3 ±0.1	1500	ARENTON	82	AEMS	11.8 polar. $pp \rightarrow K\overline{K}$
1019.67 ±0.17	25080	[6] PELLINEN	82	RVUE	
1019.52 ±0.13	3681	BUKIN	78C	OLYA	$e^+e^- \rightarrow$ hadrons
• • • We do not use the following data for averages, fits, limits, etc. • • •					
1019.441±0.008±0.080	542k	[7] AKHMETSHIN	08	CMD2	1.02 $e^+e^- \rightarrow K^+K^-$
1019.63 ±0.07	12540	[8] AUBERT,B	05J	BABR	$D^0 \rightarrow \overline{K}{}^0K^+K^-$
1019.8 ±0.7		ARMSTRONG	86	OMEG	85 $\pi^+/pp \rightarrow \pi^+/p4Kp$
1020.1 ±0.11	5526	[8] ATKINSON	86	OMEG	20–70 γp
1019.7 ±1.0		BEBEK	86	CLEO	$e^+e^- \rightarrow \Upsilon(4S)$
1019.411±0.008	642k	[9] DIJKSTRA	86	SPEC	100–200 $\pi^\pm$, $\overline{p}$, p, $K^\pm$, on Be
1020.9 ±0.2		[8] FRAME	86	OMEG	13 $K^+p \rightarrow \phi K^+p$
1021.0 ±0.2		[8] ARMSTRONG	83B	OMEG	18.5 $K^-p \rightarrow K^-K^+\Lambda$
1020.0 ±0.5		[8] ARMSTRONG	83B	OMEG	18.5 $K^-p \rightarrow K^-K^+\Lambda$

1019.7	±0.3			[8] BARATE	83	GOLI	190 π^- Be → 2μX	
1019.8	±0.2	±0.5	766	IVANOV	81	OLYA	1–1.4 e^+e^- → K^+K^-	
1019.4	±0.5		337	COOPER	78B	HBC	0.7–0.8 $\overline{p}p$ → $K^0_S K^0_L \pi^+\pi^-$	
1020	±1		383	[8] BALDI	77	CNTR	10 $\pi^- p$ → $\pi^- \phi p$	
1018.9	±0.6		800	COHEN	77	ASPK	6 $\pi^\pm N$ → K^+K^-N	
1019.7	±0.5		454	KALBFLEISCH	76	HBC	2.18 K^-p → $\Lambda K\overline{K}$	
1019.4	±0.8		984	BESCH	74	CNTR	2 γp → pK^+K^-	
1020.3	±0.4		100	BALLAM	73	HBC	2.8–9.3 γp	
1019.4	±0.7			BINNIE	73B	CNTR	$\pi^- p$ → ϕn	
1019.6	±0.5		120	[10] AGUILAR-...	72B	HBC	3.9,4.6 K^-p → ΛK^+K^-	
1019.9	±0.5		100	[10] AGUILAR-...	72B	HBC	3.9,4.6 K^-p → $K^-pK^+K^-$	
1020.4	±0.5		131	COLLEY	72	HBC	10 K^+p → $K^+p\phi$	
1019.9	±0.3		410	STOTTLE...	71	HBC	2.9 K^-p → $\Sigma/\Lambda K\overline{K}$	

[1] Using a phenomenological model based on KUHN 90 with a sum of Breit-Wigner resonances for $\rho(770)$, $\omega(782)$, $\phi(1020)$ and their higher mass excitations.
[2] Update of AKHMETSHIN 99D
[3] From the combined fit assuming that the total $\phi(1020)$ production cross section is saturated by those of K^+K^-, K_SK_L, $\pi^+\pi^-\pi^0$, and $\eta\gamma$ decays modes and using ACHASOV 00B for the $\eta\gamma$ decay mode.
[4] Using a total width of 4.43 ± 0.05 MeV. Systematic uncertainty included.
[5] Using a total width of 4.43 ± 0.05 MeV.
[6] PELLINEN 82 review includes AKERLOF 77, DAUM 81, BALDI 77, AYRES 74, DEGROOT 74.
[7] Strongly correlated with AKHMETSHIN 04.
[8] Systematic errors not evaluated.
[9] Weighted and scaled average of 12 measurements of DIJKSTRA 86.
[10] Mass errors enlarged by us to $\Gamma/\sqrt{N}$; see the note with the $K^*(892)$ mass.

$\phi(1020)$ WIDTH

VALUE (MeV)	EVTS	DOCUMENT ID		TECN	COMMENT
4.266±0.031 OUR AVERAGE		Error includes scale factor of 1.2.			
4.29 ±0.04 ±0.07		[1] LEES	13Q	BABR	$e^+e^- \to K^+K^-\gamma$
4.30 ±0.06 ±0.17	105k	AKHMETSHIN	06	CMD2	0.98–1.06 $e^+e^- \to \pi^+\pi^-\pi^0$
4.280±0.033±0.025	272k	[2] AKHMETSHIN	04	CMD2	$e^+e^- \to K^0_L K^0_S$
4.21 ±0.04	1900k	[3] ACHASOV	01E	SND	$e^+e^- \to K^+K^-$, K_SK_L, $\pi^+\pi^-\pi^0$
4.44 ±0.09	55600	AKHMETSHIN	95	CMD2	$e^+e^- \to$ hadrons
4.5 ±0.7	1500	ARENTON	82	AEMS	11.8 polar. $pp \to KK$
4.2 ±0.6	766	[4] IVANOV	81	OLYA	1–1.4 $e^+e^- \to K^+K^-$
4.3 ±0.6		[4] CORDIER	80	DM1	$e^+e^- \to \pi^+\pi^-\pi^0$
4.36 ±0.29	3681	[4] BUKIN	78C	OLYA	$e^+e^- \to$ hadrons
4.4 ±0.6	984	[4] BESCH	74	CNTR	2 $\gamma p \to pK^+K^-$
4.67 ±0.72	681	[4] BALAKIN	71	OSPK	$e^+e^- \to$ hadrons
4.09 ±0.29		BIZOT	70	OSPK	$e^+e^- \to$ hadrons
• • • We do not use the following data for averages, fits, limits, etc. • • •					
4.24 ±0.02 ±0.03	542k	[5] AKHMETSHIN	08	CMD2	1.02 $e^+e^- \to K^+K^-$
4.28 ±0.13	12540	[6] AUBERT,B	05J	BABR	$D^0 \to \overline{K}^0 K^+K^-$
4.45 ±0.06	271k	DIJKSTRA	86	SPEC	100 π^- Be
3.6 ±0.8	337	[4] COOPER	78B	HBC	0.7–0.8 $\overline{p}p$ → $K^0_S K^0_L \pi^+\pi^-$
4.5 ±0.50	1300	[4,6] AKERLOF	77	SPEC	400 pA → K^+K^-X
4.5 ±0.8	500	[4,6] AYRES	74	ASPK	3–6 $\pi^- p$ → K^+K^-n, K^-p → $K^+K^-\Lambda/\Sigma^0$
3.81 ±0.37		COSME	74B	OSPK	$e^+e^- \to K^0_L K^0_S$
3.8 ±0.7	454	[4] BORENSTEIN	72	HBC	2.18 K^-p → $K\overline{K}n$

[1] Using a phenomenological model based on KUHN 90 with a sum of Breit-Wigner resonances for $\rho(770)$, $\omega(782)$, $\phi(1020)$ and their higher mass excitations.
[2] Update of AKHMETSHIN 99D
[3] From the combined fit assuming that the total $\phi(1020)$ production cross section is saturated by those of K^+K^-, K_SK_L, $\pi^+\pi^-\pi^0$, and $\eta\gamma$ decays modes and using ACHASOV 00B for the $\eta\gamma$ decay mode.
[4] Width errors enlarged by us to $4\Gamma/\sqrt{N}$; see the note with the $K^*(892)$ mass.
[5] Strongly correlated with AKHMETSHIN 04.
[6] Systematic errors not evaluated.

$\phi(1020)$ DECAY MODES

	Mode	Fraction (Γ_i/Γ)	Scale factor/ Confidence level
Γ_1	K^+K^-	(48.9 ±0.5) %	S=1.1
Γ_2	$K^0_L K^0_S$	(34.2 ±0.4) %	S=1.1
Γ_3	$\rho\pi$ + $\pi^+\pi^-\pi^0$	(15.32 ±0.32) %	S=1.1
Γ_4	$\rho\pi$		
Γ_5	$\pi^+\pi^-\pi^0$		
Γ_6	$\eta\gamma$	(1.309±0.024) %	S=1.2
Γ_7	$\pi^0\gamma$	(1.27 ±0.06) × 10^{-3}	
Γ_8	$\ell^+\ell^-$	—	
Γ_9	e^+e^-	(2.954±0.030) × 10^{-4}	S=1.1
Γ_{10}	$\mu^+\mu^-$	(2.87 ±0.19) × 10^{-4}	
Γ_{11}	ηe^+e^-	(1.15 ±0.10) × 10^{-4}	
Γ_{12}	$\pi^+\pi^-$	(7.4 ±1.3) × 10^{-5}	
Γ_{13}	$\omega\pi^0$	(4.7 ±0.5) × 10^{-5}	
Γ_{14}	$\omega\gamma$	< 5 %	CL=84%
Γ_{15}	$\rho\gamma$	< 1.2 × 10^{-5}	CL=90%
Γ_{16}	$\pi^+\pi^-\gamma$	(4.1 ±1.3) × 10^{-5}	
Γ_{17}	$f_0(980)\gamma$	(3.22 ±0.19) × 10^{-4}	S=1.1
Γ_{18}	$\pi^0\pi^0\gamma$	(1.13 ±0.06) × 10^{-4}	
Γ_{19}	$\pi^+\pi^-\pi^+\pi^-$	(4.0 $^{+2.8}_{-2.2}$) × 10^{-6}	
Γ_{20}	$\pi^+\pi^+\pi^-\pi^-\pi^0$	< 4.6 × 10^{-6}	CL=90%
Γ_{21}	$\pi^0 e^+e^-$	(1.12 ±0.28) × 10^{-5}	
Γ_{22}	$\pi^0\eta\gamma$	(7.27 ±0.30) × 10^{-5}	S=1.5
Γ_{23}	$a_0(980)\gamma$	(7.6 ±0.6) × 10^{-5}	
Γ_{24}	$K^0\overline{K}^0\gamma$	< 1.9 × 10^{-8}	CL=90%
Γ_{25}	$\eta'(958)\gamma$	(6.25 ±0.21) × 10^{-5}	
Γ_{26}	$\eta\pi^0\pi^0\gamma$	< 2 × 10^{-5}	CL=90%
Γ_{27}	$\mu^+\mu^-\gamma$	(1.4 ±0.5) × 10^{-5}	
Γ_{28}	$\rho\gamma\gamma$	< 1.2 × 10^{-4}	CL=90%
Γ_{29}	$\eta\pi^+\pi^-$	< 1.8 × 10^{-5}	CL=90%
Γ_{30}	$\eta\mu^+\mu^-$	< 9.4 × 10^{-6}	CL=90%
Γ_{31}	$\eta U \to \eta e^+e^-$	< 1 × 10^{-6}	CL=90%
	Lepton Faminly number (LF) violating modes		
Γ_{32}	$e^\pm\mu^\mp$ *LF*	< 2 × 10^{-6}	CL=90%

CONSTRAINED FIT INFORMATION

An overall fit to 30 branching ratios uses 79 measurements and one constraint to determine 14 parameters. The overall fit has a $\chi^2 = 57.4$ for 66 degrees of freedom.

The following *off-diagonal* array elements are the correlation coefficients $\langle \delta x_i \delta x_j \rangle / (\delta x_i \cdot \delta x_j)$, in percent, from the fit to the branching fractions, $x_i \equiv \Gamma_i/\Gamma_{\rm total}$. The fit constrains the x_i whose labels appear in this array to sum to one.

	x_1	x_2	x_3	x_6	x_7	x_9	x_{10}	x_{12}	x_{13}	x_{17}
x_2	−72									
x_3	−53	−21								
x_6	−13	7	2							
x_7	−5	3	1	5						
x_9	30	−25	−10	−32	−15					
x_{10}	−4	3	1	3	2	−11				
x_{12}	−2	1	0	2	1	−5	1			
x_{13}	−2	2	1	2	1	−7	1	0		
x_{17}	0	0	0	0	0	0	0	0	0	
x_{18}	−6	4	2	17	3	−17	2	1	1	0
x_{19}	0	0	0	0	0	−1	0	0	0	0
x_{23}	0	0	0	0	0	0	0	0	0	0
x_{25}	−4	2	1	32	2	−10	1	1	1	0

	x_{18}	x_{19}	x_{23}
x_{19}	0		
x_{23}	0	0	
x_{25}	5	0	0

$\phi(1020)$ PARTIAL WIDTHS

$\Gamma(\eta\gamma)$ Γ_6

VALUE (keV)	DOCUMENT ID		TECN	COMMENT
• • • We do not use the following data for averages, fits, limits, etc. • • •				
58.9±0.5±2.4	ACHASOV	00	SND	$e^+e^- \to \eta\gamma$

$\Gamma(\pi^0\gamma)$ Γ_7

VALUE (keV)	DOCUMENT ID		TECN	COMMENT
• • • We do not use the following data for averages, fits, limits, etc. • • •				
5.40±0.16 $^{+0.43}_{-0.40}$	ACHASOV	00	SND	$e^+e^- \to \pi^0\gamma$

$\Gamma(\ell^+\ell^-)$ Γ_8

VALUE (keV)	DOCUMENT ID		TECN	COMMENT
• • • We do not use the following data for averages, fits, limits, etc. • • •				
1.320±0.017±0.015	[1] AMBROSINO	05	KLOE	1.02 $e^+e^- \to \mu^+\mu^-$

$\Gamma(e^+e^-)$ Γ_9

VALUE (keV)	DOCUMENT ID	TECN	COMMENT
1.27 ±0.04 OUR EVALUATION			
1.251±0.021 OUR AVERAGE	Error includes scale factor of 1.1.		
1.235±0.006±0.022	[2] AKHMETSHIN 11	CMD2	1.02 $e^+e^- \to \phi$
1.32 ±0.05 ±0.03	[3] AMBROSINO 05	KLOE	1.02 $e^+e^- \to e^+e^-$
1.28 ±0.05	AKHMETSHIN 95	CMD2	1.02 $e^+e^- \to \phi$

$(\Gamma(e^+e^-)\times\Gamma(\mu^+\mu^-))^{1/2}$ $(\Gamma_9\Gamma_{10})^{1/2}$

VALUE (keV)	DOCUMENT ID	TECN	COMMENT
1.320±0.018±0.017	AMBROSINO 05	KLOE	1.02 $e^+e^- \to \mu^+\mu^-$

[1] Weighted average of Γ_{ee} and $\sqrt{\Gamma_{ee}\Gamma_{\mu\mu}}$ from AMBROSINO 05 assuming lepton universality.

[2] Combined analysis of the CMD-2 data on $\phi \to K^+K^-$, $K^0_S K^0_L$, $\pi^+\pi^-\pi^0$, $\eta\gamma$ assuming that the sum of their branching fractions is 0.99741 ± 0.00007.

[3] From forward-backward asymmetry and using $\Gamma_{\rm total} = 4.26 \pm 0.05$ MeV from the 2004 edition of this Review.

$\phi(1020)$ $\Gamma(i)\Gamma(e^+e^-)/\Gamma(\text{total})$

$\Gamma(K^+K^-)\times\Gamma(e^+e^-)/\Gamma_{\rm total}$ $\Gamma_1\Gamma_9/\Gamma$

VALUE (keV)	DOCUMENT ID	TECN	COMMENT
0.6340±0.0070±0.0039	[1] LEES 13Q	BABR	$e^+e^- \to K^+K^-\gamma$

[1] Using a phenomenological model based on KUHN 90 with a sum of Breit-Wigner resonances for $\rho(770)$, $\omega(782)$, $\phi(1020)$ and their higher mass excitations. The first error combines statistical and systematic uncertainties. The second one is due to the parametrization of the charged kaon form factor and mass calibration.

$\phi(1020)$ $\Gamma(i)\Gamma(e^+e^-)/\Gamma^2(\text{total})$

$\Gamma(K^+K^-)/\Gamma_{\rm total}\times\Gamma(e^+e^-)/\Gamma_{\rm total}$ $\Gamma_1/\Gamma\times\Gamma_9/\Gamma$

VALUE (units 10^{-5})	EVTS	DOCUMENT ID	TECN	COMMENT
14.46±0.23 OUR FIT	Error includes scale factor of 1.1.			
14.24±0.30 OUR AVERAGE				
14.27±0.05±0.31	542k	AKHMETSHIN 08	CMD2	1.02 $e^+e^- \to K^+K^-$
13.93±0.14±0.99	1000k	[1] ACHASOV 01E	SND	$e^+e^- \to K^+K^-$, $K_S K_L$, $\pi^+\pi^-\pi^0$

$\Gamma(K^0_L K^0_S)/\Gamma_{\rm total}\times\Gamma(e^+e^-)/\Gamma_{\rm total}$ $\Gamma_2/\Gamma\times\Gamma_9/\Gamma$

VALUE (units 10^{-5})	EVTS	DOCUMENT ID	TECN	COMMENT
10.10±0.13 OUR FIT				
10.06±0.16 OUR AVERAGE				
10.01±0.04±0.17	272k	[2] AKHMETSHIN 04	CMD2	$e^+e^- \to K^0_L K^0_S$
10.27±0.07±0.34	500k	[1] ACHASOV 01E	SND	$e^+e^- \to K^+K^-$, $K_S K_L$, $\pi^+\pi^-\pi^0$

$[\Gamma(\rho\pi)+\Gamma(\pi^+\pi^-\pi^0)]/\Gamma_{\rm total}\times\Gamma(e^+e^-)/\Gamma_{\rm total}$ $\Gamma_3/\Gamma\times\Gamma_9/\Gamma$

VALUE (units 10^{-5})	EVTS	DOCUMENT ID	TECN	COMMENT
4.53 ±0.10 OUR FIT	Error includes scale factor of 1.1.			
4.46 ±0.12 OUR AVERAGE				
4.51 ±0.16 ±0.11	105k	AKHMETSHIN 06	CMD2	0.98–1.06 $e^+e^- \to \pi^+\pi^-\pi^0$
4.30 ±0.08 ±0.21		AUBERT,B 04N	BABR	10.6 $e^+e^- \to \pi^+\pi^-\pi^0\gamma$
4.665±0.042±0.261	400k	[1] ACHASOV 01E	SND	$e^+e^- \to K^+K^-$, $K_S K_L$, $\pi^+\pi^-\pi^0$
4.35 ±0.27 ±0.08	11169	[3] AKHMETSHIN 98	CMD2	$e^+e^- \to \pi^+\pi^-\pi^0$
• • • We do not use the following data for averages, fits, limits, etc. • • •				
4.38 ±0.12		BENAYOUN 10	RVUE	0.4–1.05 e^+e^-

$\Gamma(\eta\gamma)/\Gamma_{\rm total}\times\Gamma(e^+e^-)/\Gamma_{\rm total}$ $\Gamma_6/\Gamma\times\Gamma_9/\Gamma$

VALUE (units 10^{-6})	EVTS	DOCUMENT ID	TECN	COMMENT
3.87 ±0.07 OUR FIT	Error includes scale factor of 1.2.			
3.93 ±0.09 OUR AVERAGE	Error includes scale factor of 1.3. See the ideogram below.			
4.050±0.067±0.118	33k	[4] ACHASOV 07B	SND	0.6–1.38 $e^+e^- \to \eta\gamma$
$4.093^{+0.040}_{-0.043}$±0.247	17.4k	[5] AKHMETSHIN 05	CMD2	0.60–1.38 $e^+e^- \to \eta\gamma$
3.850±0.041±0.159	23k	[6,7] AKHMETSHIN 01B	CMD2	$e^+e^- \to \eta\gamma$
4.00 ±0.04 ±0.11		[8] ACHASOV 00	SND	$e^+e^- \to \eta\gamma$
3.53 ±0.08 ±0.17	2200	[9,10] AKHMETSHIN 99F	CMD2	$e^+e^- \to \eta\gamma$
• • • We do not use the following data for averages, fits, limits, etc. • • •				
4.19 ±0.06		[11] BENAYOUN 10	RVUE	0.4–1.05 e^+e^-

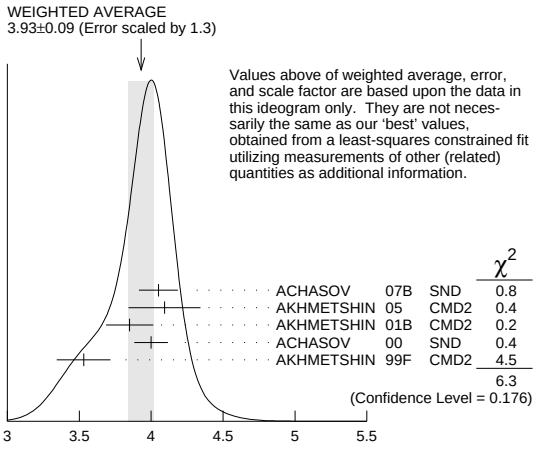

$\Gamma(\eta\gamma)/\Gamma_{\rm total}\times\Gamma(e^+e^-)/\Gamma_{\rm total}$ $\Gamma_6/\Gamma\times\Gamma_9/\Gamma$

$\Gamma(\pi^0\gamma)/\Gamma_{\rm total}\times\Gamma(e^+e^-)/\Gamma_{\rm total}$ $\Gamma_7/\Gamma\times\Gamma_9/\Gamma$

VALUE (units 10^{-7})	EVTS	DOCUMENT ID	TECN	COMMENT
3.74±0.18 OUR FIT				
3.71±0.21 OUR AVERAGE				
3.75±0.11±0.29	18680	AKHMETSHIN 05	CMD2	0.60–1.38 $e^+e^- \to \pi^0\gamma$
$3.67\pm0.10^{+0.27}_{-0.25}$		[12] ACHASOV 00	SND	$e^+e^- \to \pi^0\gamma$
• • • We do not use the following data for averages, fits, limits, etc. • • •				
4.29±0.11		[11] BENAYOUN 10	RVUE	0.4–1.05 e^+e^-

$\Gamma(\mu^+\mu^-)/\Gamma_{\rm total}\times\Gamma(e^+e^-)/\Gamma_{\rm total}$ $\Gamma_{10}/\Gamma\times\Gamma_9/\Gamma$

VALUE (units 10^{-8})	DOCUMENT ID	TECN	COMMENT
8.5 $^{+0.5}_{-0.6}$ OUR FIT			
8.8 ±0.9 OUR AVERAGE	Error includes scale factor of 1.5. See the ideogram below.		
8.36±0.59±0.37	ACHASOV 01G	SND	$e^+e^- \to \mu^+\mu^-$
9.9 ±1.4 ±0.9	[9] ACHASOV 99C	SND	$e^+e^- \to \mu^+\mu^-$
14.4 ±3.0	[3] VASSERMAN 81	OLYA	$e^+e^- \to \mu^+\mu^-$
8.6 ±5.9	[3] AUGUSTIN 73	OSPK	$e^+e^- \to \mu^+\mu^-$

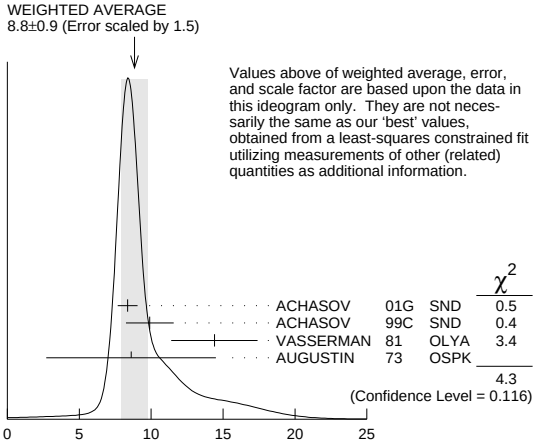

$\Gamma(\mu^+\mu^-)/\Gamma_{\rm total}\times\Gamma(e^+e^-)/\Gamma_{\rm total}$ $\Gamma_{10}/\Gamma\times\Gamma_9/\Gamma$

$\Gamma(\pi^+\pi^-)/\Gamma_{\rm total}\times\Gamma(e^+e^-)/\Gamma_{\rm total}$ $\Gamma_{12}/\Gamma\times\Gamma_9/\Gamma$

VALUE (units 10^{-8})	DOCUMENT ID	TECN	COMMENT
2.2 ±0.4 OUR FIT			
2.2 ±0.4 OUR AVERAGE			
2.1 ±0.3 ±0.3	[9] ACHASOV 00C	SND	$e^+e^- \to \pi^+\pi^-$
$1.95^{+1.15}_{-0.87}$	[3] GOLUBEV 86	ND	$e^+e^- \to \pi^+\pi^-$
$6.01^{+3.19}_{-2.51}$	[3] VASSERMAN 81	OLYA	$e^+e^- \to \pi^+\pi^-$
• • • We do not use the following data for averages, fits, limits, etc. • • •			
3.31±0.99	[13] BENAYOUN 13	RVUE	0.4–1.05 e^+e^-

$\Gamma(\omega\pi^0)/\Gamma_{\rm total}\times\Gamma(e^+e^-)/\Gamma_{\rm total}$ $\Gamma_{13}/\Gamma\times\Gamma_9/\Gamma$

VALUE (units 10^{-8})	DOCUMENT ID	TECN	COMMENT
1.40±0.15 OUR FIT			
1.37±0.17±0.01	[14,15] AMBROSINO 08G	KLOE	$e^+e^- \to \pi^+\pi^-2\pi^0$, $2\pi^0\gamma$

$\Gamma(\pi^0\pi^0\gamma)/\Gamma_{total} \times \Gamma(e^+e^-)/\Gamma_{total}$ $\Gamma_{18}/\Gamma \times \Gamma_9/\Gamma$

VALUE (units 10^{-8})	DOCUMENT ID		TECN	COMMENT
3.34±0.17 OUR FIT				
$3.33^{+0.04}_{-0.09}{}^{+0.19}_{-0.20}$	[16] AMBROSINO	07	KLOE	$e^+e^- \to \pi^0\pi^0\gamma$

$\Gamma(\pi^+\pi^-\pi^+\pi^-)/\Gamma_{total} \times \Gamma(e^+e^-)/\Gamma_{total}$ $\Gamma_{19}/\Gamma \times \Gamma_9/\Gamma$

VALUE (units 10^{-9})	EVTS	DOCUMENT ID		TECN	COMMENT
$1.2\ ^{+0.8}_{-0.7}$ **OUR FIT**					
1.17±0.52±0.64	3285	[9] AKHMETSHIN	00E	CMD2	$e^+e^- \to \pi^+\pi^-\pi^+\pi^-$

[1] From the combined fit assuming that the total $\phi(1020)$ production cross section is saturated by those of K^+K^-, K_SK_L, $\pi^+\pi^-\pi^0$, and $\eta\gamma$ decays modes and using ACHASOV 00B for the $\eta\gamma$ decay mode.
[2] Update of AKHMETSHIN 99D
[3] Recalculated by us from the cross section in the peak.
[4] From a combined fit of $\sigma(e^+e^- \to \eta\gamma)$ with $\eta \to 3\pi^0$ and $\eta \to \pi^+\pi^-\pi^0$, and fixing $B(\eta \to 3\pi^0)$ / $B(\eta \to \pi^+\pi^-\pi^0) = 1.44 \pm 0.04$. Recalculated by us from the cross section at the peak. Supersedes ACHASOV 00D and ACHASOV 06A.
[5] From the $\eta \to 2\gamma$ decay and using $B(\eta \to \gamma\gamma) = 39.43 \pm 0.26\%$.
[6] From the $\eta \to 3\pi^0$ decay and using $B(\eta \to 3\pi^0) = (32.24 \pm 0.29) \times 10^{-2}$.
[7] The combined fit from 600 to 1380 MeV taking into account $\rho(770)$, $\omega(782)$, $\phi(1020)$, and $\rho(1450)$ (mass and width fixed at 1450 MeV and 310 MeV respectively).
[8] From the $\eta \to 2\gamma$ decay and using $B(\eta \to 2\gamma) = (39.21 \pm 0.34) \times 10^{-2}$.
[9] Recalculated by the authors from the cross section in the peak.
[10] From the $\eta \to \pi^+\pi^-\pi^0$ decay and using $B(\eta \to \pi^+\pi^-\pi^0) = (23.1 \pm 0.5) \times 10^{-2}$.
[11] A simultaneous fit of $e^+e^- \to \pi^+\pi^-$, $\pi^+\pi^-\pi^0$, $\pi^0\gamma$, $\eta\gamma$ data.
[12] From the $\pi^0 \to 2\gamma$ decay and using $B(\pi^0 \to 2\gamma) = (98.798 \pm 0.032) \times 10^{-2}$.
[13] A simultaneous fit to $e^+e^- \to \pi^+\pi^-$, $\pi^+\pi^-\pi^0$, $\pi^0\gamma$, $\eta\gamma$, $K\overline{K}$, and $\tau^- \to \pi^-\pi^0\nu_\tau$ data.
[14] Recalculated by the authors from the cross section at the peak.
[15] AMBROSINO 08G reports $[\Gamma(\phi(1020) \to \omega\pi^0)/\Gamma_{total} \times \Gamma(\phi(1020) \to e^+e^-)/\Gamma_{total}] \times [B(\omega(782) \to \pi^+\pi^-\pi^0)] = (1.22 \pm 0.13 \pm 0.08) \times 10^{-8}$ which we divide by our best value $B(\omega(782) \to \pi^+\pi^-\pi^0) = (89.2 \pm 0.7) \times 10^{-2}$. Our first error is their experiment's error and our second error is the systematic error from using our best value.
[16] Calculated by the authors from the cross section at the peak.

$\phi(1020)$ BRANCHING RATIOS

$\Gamma(K^+K^-)/\Gamma_{total}$ Γ_1/Γ

VALUE	EVTS	DOCUMENT ID		TECN	COMMENT
0.489±0.005 OUR FIT Error includes scale factor of 1.1.					
0.493±0.010 OUR AVERAGE					
0.492±0.012	2913	AKHMETSHIN	95	CMD2	$e^+e^- \to K^+K^-$
0.44 ±0.05	321	KALBFLEISCH	76	HBC	2.18 $K^-p \to \Lambda K^+K^-$
0.49 ±0.06	270	DEGROOT	74	HBC	4.2 $K^-p \to \Lambda\phi$
0.540±0.034	565	BALAKIN	71	OSPK	$e^+e^- \to K^+K^-$
0.48 ±0.04	252	LINDSEY	66	HBC	2.1–2.7 $K^-p \to \Lambda K^+K^-$
• • • We do not use the following data for averages, fits, limits, etc. • • •					
0.493±0.003±0.007		[1] AKHMETSHIN	11	CMD2	1.02 $e^+e^- \to K^+K^-$
0.476±0.017	1000k	[2] ACHASOV	01E	SND	$e^+e^- \to K^+K^-, K_SK_L, \pi^+\pi^-\pi^0$

$\Gamma(K^0_LK^0_S)/\Gamma_{total}$ Γ_2/Γ

VALUE	EVTS	DOCUMENT ID		TECN	COMMENT
0.342±0.004 OUR FIT Error includes scale factor of 1.1.					
0.331±0.009 OUR AVERAGE					
0.335±0.010	40644	AKHMETSHIN	95	CMD2	$e^+e^- \to K^0_LK^0_S$
0.326±0.035		DOLINSKY	91	ND	$e^+e^- \to K^0_LK^0_S$
0.310±0.024		DRUZHININ	84	ND	$e^+e^- \to K^0_LK^0_S$
• • • We do not use the following data for averages, fits, limits, etc. • • •					
0.336±0.002±0.006		[1] AKHMETSHIN	11	CMD2	1.02 $e^+e^- \to K^0_SK^0_L$
0.351±0.013	500k	[2] ACHASOV	01E	SND	$e^+e^- \to K^+K^-, K_SK_L, \pi^+\pi^-\pi^0$
0.27 ±0.03	133	KALBFLEISCH	76	HBC	2.18 $K^-p \to \Lambda K^0_LK^0_S$
0.257±0.030	95	BALAKIN	71	OSPK	$e^+e^- \to K^0_LK^0_S$
0.40 ±0.04	167	LINDSEY	66	HBC	2.1–2.7 $K^-p \to \Lambda K^0_LK^0_S$

$\Gamma(K^0_LK^0_S)/\Gamma(K^+K^-)$ Γ_2/Γ_1

VALUE	EVTS	DOCUMENT ID		TECN	COMMENT
0.698±0.014 OUR FIT Error includes scale factor of 1.1.					
0.740±0.031 OUR AVERAGE					
0.70 ±0.06	2732	BUKIN	78C	OLYA	$e^+e^- \to K^0_LK^0_S$
0.82 ±0.08		LOSTY	78	HBC	4.2 $K^-p \to \phi$hyperon
0.71 ±0.05		LAVEN	77	HBC	10 $K^-p \to K^+K^-\Lambda$
0.71 ±0.08		LYONS	77	HBC	3–4 $K^-p \to \Lambda\phi$
0.89 ±0.10	144	AGUILAR-...	72B	HBC	3.9,4.6 K^-p
• • • We do not use the following data for averages, fits, limits, etc. • • •					
0.68 ±0.03		[3] AKHMETSHIN	95	CMD2	$e^+e^- \to K^0_LK^0_S, K^+K^-$

$\Gamma(K^0_LK^0_S)/\Gamma(K\overline{K})$ $\Gamma_2/(\Gamma_1+\Gamma_2)$

VALUE	EVTS	DOCUMENT ID		TECN	COMMENT
0.411±0.005 OUR FIT Error includes scale factor of 1.1.					
0.45 ±0.04 OUR AVERAGE					
0.44 ±0.07		LONDON	66	HBC	2.24 $K^-p \to \Lambda K\overline{K}$
0.48 ±0.07	52	BADIER	65B	HBC	3 K^-p
0.40 ±0.10	34	SCHLEIN	63	HBC	1.95 $K^-p \to \Lambda K\overline{K}$

$[\Gamma(\rho\pi) + \Gamma(\pi^+\pi^-\pi^0)]/\Gamma_{total}$ Γ_3/Γ

VALUE	EVTS	DOCUMENT ID		TECN	COMMENT
0.1532±0.0032 OUR FIT Error includes scale factor of 1.1.					
0.151 ±0.009 OUR AVERAGE Error includes scale factor of 1.7.					
0.161 ±0.008	11761	AKHMETSHIN	95	CMD2	$e^+e^- \to \pi^+\pi^-\pi^0$
0.143 ±0.007		DOLINSKY	91	ND	$e^+e^- \to \pi^+\pi^-\pi^0$
• • • We do not use the following data for averages, fits, limits, etc. • • •					
0.155 ±0.002 ±0.005		[1] AKHMETSHIN	11	CMD2	1.02 $e^+e^- \to \pi^+\pi^-\pi^0$
0.159 ±0.008	400k	[2] ACHASOV	01E	SND	$e^+e^- \to K^+K^-, K_SK_L, \pi^+\pi^-\pi^0$
0.145 ±0.009 ±0.003	11169	[4] AKHMETSHIN	98	CMD2	$e^+e^- \to \pi^+\pi^-\pi^0$
0.139 ±0.007		[5] PARROUR	76B	OSPK	e^+e^-

$[\Gamma(\rho\pi) + \Gamma(\pi^+\pi^-\pi^0)]/\Gamma(K^+K^-)$ Γ_3/Γ_1

VALUE	EVTS	DOCUMENT ID		TECN	COMMENT
0.313±0.009 OUR FIT Error includes scale factor of 1.1.					
0.28 ±0.09	34	AGUILAR-...	72B	HBC	3.9,4.6 K^-p

$[\Gamma(\rho\pi) + \Gamma(\pi^+\pi^-\pi^0)]/\Gamma(K\overline{K})$ $\Gamma_3/(\Gamma_1+\Gamma_2)$

VALUE	DOCUMENT ID		TECN	COMMENT
0.184±0.005 OUR FIT Error includes scale factor of 1.1.				
0.24 ±0.04 OUR AVERAGE				
0.237±0.039	CERRADA	77B	HBC	4.2 $K^-p \to \Lambda 3\pi$
0.30 ±0.15	LONDON	66	HBC	2.24 $K^-p \to \Lambda\pi^+\pi^-\pi^0$

$[\Gamma(\rho\pi) + \Gamma(\pi^+\pi^-\pi^0)]/\Gamma(K^0_LK^0_S)$ Γ_3/Γ_2

VALUE	EVTS	DOCUMENT ID		TECN	COMMENT
0.448±0.012 OUR FIT Error includes scale factor of 1.1.					
0.51 ±0.05 OUR AVERAGE					
0.56 ±0.07	3681	BUKIN	78C	OLYA	$e^+e^- \to K^0_LK^0_S, \pi^+\pi^-\pi^0$
0.47 ±0.06	516	COSME	74	OSPK	$e^+e^- \to \pi^+\pi^-\pi^0$

$\Gamma(\pi^+\pi^-\pi^0)/\Gamma_{total}$ Γ_5/Γ

VALUE	CL%	EVTS	DOCUMENT ID		TECN	COMMENT
• • • We do not use the following data for averages, fits, limits, etc. • • •						
$\simeq 0.0087$		1.98M	[6,7] ALOISIO	03	KLOE	1.02 $e^+e^- \to \pi^+\pi^-\pi^0$
<0.0006	90		[8] ACHASOV	02	SND	1.02 $e^+e^- \to \pi^+\pi^-\pi^0$
<0.23	90		[8] CORDIER	80	DM1	$e^+e^- \to \pi^+\pi^-\pi^0$
<0.20	90		[8] PARROUR	76B	OSPK	$e^+e^- \to \pi^+\pi^-\pi^0$

$\Gamma(\eta\gamma)/\Gamma_{total}$ Γ_6/Γ

VALUE (units 10^{-2})	EVTS	DOCUMENT ID		TECN	COMMENT
1.309±0.024 OUR FIT Error includes scale factor of 1.2.					
1.26 ±0.04 OUR AVERAGE					
1.246±0.025±0.057	10k	[9] ACHASOV	98F	SND	$e^+e^- \to 7\gamma$
1.18 ±0.11	279	[10] AKHMETSHIN	95	CMD2	$e^+e^- \to \pi^+\pi^-3\gamma$
1.30 ±0.06		[11] DRUZHININ	84	ND	$e^+e^- \to 3\gamma$
1.4 ±0.2		[12] DRUZHININ	84	ND	$e^+e^- \to 6\gamma$
0.88 ±0.20	290	KURDADZE	83C	OLYA	$e^+e^- \to 3\gamma$
1.35 ±0.29		ANDREWS	77	CNTR	6.7–10 γCu
1.5 ±0.4	54	[11] COSME	76	OSPK	e^+e^-
• • • We do not use the following data for averages, fits, limits, etc. • • •					
1.38 ±0.02 ±0.02		[1] AKHMETSHIN	11	CMD2	1.02 $e^+e^- \to \eta\gamma$
1.37 ±0.05 ±0.01	33k	[13] ACHASOV	07B	SND	0.6–1.38 $e^+e^- \to \eta\gamma$
1.373±0.014±0.085	17.4k	[14,15] AKHMETSHIN	05	CMD2	0.60–1.38 $e^+e^- \to \eta\gamma$
1.287±0.013±0.063		[16,17] AKHMETSHIN	01B	CMD2	$e^+e^- \to \eta\gamma$
1.338±0.012±0.052		[18] ACHASOV	00	SND	$e^+e^- \to \eta\gamma$
1.18 ±0.03 ±0.06	2200	[19] AKHMETSHIN	99F	CMD2	$e^+e^- \to \eta\gamma$
1.21 ±0.07		[20] BENAYOUN	96	RVUE	0.54–1.04 $e^+e^- \to \eta\gamma$

$\Gamma(\pi^0\gamma)/\Gamma_{total}$ Γ_7/Γ

VALUE (units 10^{-3})	EVTS	DOCUMENT ID		TECN	COMMENT
1.27 ±0.06 OUR FIT					
1.31 ±0.13 OUR AVERAGE					
1.30 ±0.13		DRUZHININ	84	ND	$e^+e^- \to 3\gamma$
1.4 ±0.5	32	COSME	76	OSPK	e^+e^-
• • • We do not use the following data for averages, fits, limits, etc. • • •					
1.258±0.037±0.077	18680	[21,22] AKHMETSHIN	05	CMD2	0.60–1.38 $e^+e^- \to \pi^0\gamma$
$1.226\pm0.036^{+0.096}_{-0.089}$		[23] ACHASOV	00	SND	$e^+e^- \to \pi^0\gamma$
1.26 ±0.17		[20] BENAYOUN	96	RVUE	0.54–1.04 $e^+e^- \to \pi^0\gamma$

$\Gamma(\eta\gamma)/\Gamma(\pi^0\gamma)$ Γ_6/Γ_7

VALUE	DOCUMENT ID		TECN	COMMENT
• • • We do not use the following data for averages, fits, limits, etc. • • •				
$10.9\pm0.3^{+0.7}_{-0.8}$	ACHASOV	00	SND	$e^+e^- \to \eta\gamma, \pi^0\gamma$

$\Gamma(e^+e^-)/\Gamma_{total}$ Γ_9/Γ

VALUE (units 10^{-4})	EVTS	DOCUMENT ID		TECN	COMMENT
2.954±0.030 OUR FIT		Error includes scale factor of 1.1.			
2.98 ±0.07 OUR AVERAGE		Error includes scale factor of 1.1.			
2.93 ±0.14	1900k	[24] ACHASOV	01E	SND	$e^+e^- \to K^+K^-$, K_SK_L, $\pi^+\pi^-\pi^0$
2.88 ±0.09	55600	AKHMETSHIN	95	CMD2	$e^+e^- \to$ hadrons
3.00 ±0.21	3681	BUKIN	78C	OLYA	$e^+e^- \to$ hadrons
3.10 ±0.14		[25] PARROUR	76	OSPK	e^+e^-
3.3 ±0.3		COSME	74	OSPK	$e^+e^- \to$ hadrons
2.81 ±0.25	681	BALAKIN	71	OSPK	$e^+e^- \to$ hadrons
3.50 ±0.27		CHATELUS	71	OSPK	e^+e^-

$\Gamma(\mu^+\mu^-)/\Gamma_{total}$ Γ_{10}/Γ

VALUE (units 10^{-4})	DOCUMENT ID		TECN	COMMENT
2.87±0.19 OUR FIT				
2.5 ±0.4 OUR AVERAGE				
2.69±0.46	[26] HAYES	71	CNTR	8.3,9.8 γC $\to \mu^+\mu^-$X
2.17±0.60	[26] EARLES	70	CNTR	6.0 γC $\to \mu^+\mu^-$X
• • • We do not use the following data for averages, fits, limits, etc. • • •				
2.87±0.20±0.14	[27] ACHASOV	01G	SND	$e^+e^- \to \mu^+\mu^-$
3.30±0.45±0.32	[4] ACHASOV	99C	SND	$e^+e^- \to \mu^+\mu^-$
4.83±1.02	[28] VASSERMAN	81	OLYA	$e^+e^- \to \mu^+\mu^-$
2.87±1.98	[28] AUGUSTIN	73	OSPK	$e^+e^- \to \mu^+\mu^-$

$\Gamma(\eta e^+e^-)/\Gamma_{total}$ Γ_{11}/Γ

VALUE (units 10^{-4})	EVTS	DOCUMENT ID		TECN	COMMENT
1.15±0.10 OUR AVERAGE					
1.19±0.19±0.12	213	[29] ACHASOV	01B	SND	$e^+e^- \to \gamma\gamma e^+e^-$
1.14±0.10±0.06	355	[30] AKHMETSHIN	01	CMD2	$e^+e^- \to \eta e^+e^-$
$1.3\ ^{+0.8}_{-0.6}$	7	GOLUBEV	85	ND	$e^+e^- \to \gamma\gamma e^+e^-$
• • • We do not use the following data for averages, fits, limits, etc. • • •					
1.13±0.14±0.07	183	[31] AKHMETSHIN	01	CMD2	$e^+e^- \to \eta e^+e^-$
1.21±0.14±0.09	130	[32] AKHMETSHIN	01	CMD2	$e^+e^- \to \eta e^+e^-$
1.04±0.20±0.08	42	[33] AKHMETSHIN	01	CMD2	$e^+e^- \to \eta e^+e^-$

$\Gamma(\pi^+\pi^-)/\Gamma_{total}$ Γ_{12}/Γ

VALUE (units 10^{-4})	CL%	DOCUMENT ID		TECN	COMMENT
• • • We do not use the following data for averages, fits, limits, etc. • • •					
0.71±0.11±0.09		[4] ACHASOV	00C	SND	$e^+e^- \to \pi^+\pi^-$
$0.65\ ^{+0.38}_{-0.29}$		[4] GOLUBEV	86	ND	$e^+e^- \to \pi^+\pi^-$
$2.01\ ^{+1.07}_{-0.84}$		[4] VASSERMAN	81	OLYA	$e^+e^- \to \pi^+\pi^-$
<6.6	95	BUKIN	78B	OLYA	$e^+e^- \to \pi^+\pi^-$
<2.7	95	ALVENSLEB...	72	CNTR	6.7 γC $\to$ C$\pi^+\pi^-$

$\Gamma(\omega\pi^0)/\Gamma_{total}$ Γ_{13}/Γ

VALUE (units 10^{-5})	DOCUMENT ID		TECN	COMMENT
4.7±0.5 OUR FIT				
$\mathbf{5.2^{+1.3}_{-1.1}}$	[34,35] AULCHENKO	00A	SND	$e^+e^- \to \pi^+\pi^-\pi^0\pi^0$
• • • We do not use the following data for averages, fits, limits, etc. • • •				
4.4±0.6	[36] AMBROSINO	08G	KLOE	$e^+e^- \to \pi^+\pi^-2\pi^0$, $2\pi^0\gamma$
~ 5.4	[37] ACHASOV	00E	SND	$e^+e^- \to \pi^0\pi^0\gamma$
$5.5\ ^{+1.6}_{-1.4}\pm0.3$	[35,38] AULCHENKO	00A	SND	$e^+e^- \to \pi^+\pi^-\pi^0\pi^0$
$4.8\ ^{+1.9}_{-1.7}\pm0.8$	[37] ACHASOV	99	SND	$e^+e^- \to \pi^+\pi^-\pi^0\pi^0$

$\Gamma(\omega\gamma)/\Gamma_{total}$ Γ_{14}/Γ

VALUE	CL%	DOCUMENT ID		TECN	COMMENT
<0.05	84	LINDSEY	66	HBC	2.1–2.7 $K^-p \to \Lambda\pi^+\pi^-$ neutrals

$\Gamma(\rho\gamma)/\Gamma_{total}$ Γ_{15}/Γ

VALUE (units 10^{-4})	CL%	DOCUMENT ID		TECN	COMMENT
< 0.12	90	[39] AKHMETSHIN	99B	CMD2	$e^+e^- \to \pi^+\pi^-\gamma$
• • • We do not use the following data for averages, fits, limits, etc. • • •					
< 7	90	AKHMETSHIN	97C	CMD2	$e^+e^- \to \pi^+\pi^-\gamma$
<200	84	LINDSEY	66	HBC	2.1–2.7 $K^-p \to \Lambda\pi^+\pi^-$ neutrals

$\Gamma(\pi^+\pi^-\gamma)/\Gamma_{total}$ Γ_{16}/Γ

VALUE (units 10^{-4})	CL%	EVTS	DOCUMENT ID		TECN	COMMENT
0.41±0.12±0.04		30175	[40] AKHMETSHIN	99B	CMD2	$e^+e^- \to \pi^+\pi^-\gamma$
• • • We do not use the following data for averages, fits, limits, etc. • • •						
< 0.3	90		[41] AKHMETSHIN	97C	CMD2	$e^+e^- \to \pi^+\pi^-\gamma$
<600	90		KALBFLEISCH	75	HBC	2.18 $K^-p \to \Lambda\pi^+\pi^-\gamma$
< 70	90		COSME	74	OSPK	$e^+e^- \to \pi^+\pi^-\gamma$
<400	90		LINDSEY	65	HBC	2.1–2.7 $K^-p \to \Lambda\pi^+\pi^-$ neutrals

$\Gamma(f_0(980)\gamma)/\Gamma_{total}$ Γ_{17}/Γ

VALUE (units 10^{-4})	CL%	EVTS	DOCUMENT ID		TECN	COMMENT
3.22±0.19 OUR FIT			Error includes scale factor of 1.1.			
3.21±0.19 OUR AVERAGE						
$3.21\ ^{+0.03}_{-0.09}\pm0.18$			[42] AMBROSINO	07	KLOE	$e^+e^- \to \pi^0\pi^0\gamma$
2.90±0.21±1.54			[43] AKHMETSHIN	99C	CMD2	$e^+e^- \to \pi^+\pi^-\gamma$, $\pi^0\pi^0\gamma$
• • • We do not use the following data for averages, fits, limits, etc. • • •						
4.47±0.21		2438	[44] ALOISIO	02D	KLOE	$e^+e^- \to \pi^0\pi^0\gamma$
$3.5\ \pm0.3\ ^{+1.3}_{-0.5}$		419	[45,46] ACHASOV	00H	SND	$e^+e^- \to \pi^0\pi^0\gamma$
1.93±0.46±0.50		27188	[47] AKHMETSHIN	99B	CMD2	$e^+e^- \to \pi^+\pi^-\gamma$
3.05±0.25±0.72		268	[48] AKHMETSHIN	99C	CMD2	$e^+e^- \to \pi^0\pi^0\gamma$
1.5 ±0.5		268	[49] AKHMETSHIN	99C	CMD2	$e^+e^- \to \pi^0\pi^0\gamma$
3.42±0.30±0.36		164	[45] ACHASOV	98I	SND	$e^+e^- \to 5\gamma$
< 1	90		[50] AKHMETSHIN	97C	CMD2	$e^+e^- \to \pi^+\pi^-\gamma$
< 7	90		[51] AKHMETSHIN	97C	CMD2	$e^+e^- \to \pi^+\pi^-\gamma$
< 20	90		DRUZHININ	87	ND	$e^+e^- \to \pi^0\pi^0\gamma$

$\Gamma(f_0(980)\gamma)/\Gamma(\eta\gamma)$ Γ_{17}/Γ_6

VALUE (units 10^{-2})	EVTS	DOCUMENT ID		TECN	COMMENT
2.46±0.15 OUR FIT		Error includes scale factor of 1.1.			
2.6 ±0.2 $\mathbf{\ ^{+0.8}_{-0.3}}$	419	[45] ACHASOV	00H	SND	$e^+e^- \to \pi^0\pi^0\gamma$

$\Gamma(\pi^0\pi^0\gamma)/\Gamma_{total}$ Γ_{18}/Γ

VALUE (units 10^{-4})	CL%	EVTS	DOCUMENT ID		TECN	COMMENT
1.07 ±0.06 OUR AVERAGE						
$1.07\ ^{+0.01}_{-0.03}\ ^{+0.06}_{-0.06}$			[52] AMBROSINO	07	KLOE	$e^+e^- \to \pi^0\pi^0\gamma$
1.08 ±0.17 ±0.09		268	AKHMETSHIN	99C	CMD2	$e^+e^- \to \pi^0\pi^0\gamma$
• • • We do not use the following data for averages, fits, limits, etc. • • •						
1.09 ±0.03 ±0.05		2438	ALOISIO	02D	KLOE	$e^+e^- \to \pi^0\pi^0\gamma$
1.158±0.093±0.052		419	[46,53] ACHASOV	00H	SND	$e^+e^- \to \pi^0\pi^0\gamma$
<10	90		DRUZHININ	87	ND	$e^+e^- \to 5\gamma$

$\Gamma(\pi^0\pi^0\gamma)/\Gamma(\eta\gamma)$ Γ_{18}/Γ_6

VALUE (units 10^{-2})	EVTS	DOCUMENT ID		TECN	COMMENT
0.86 ±0.04 OUR FIT					
0.865±0.070±0.017	419	[53] ACHASOV	00H	SND	$e^+e^- \to \pi^0\pi^0\gamma$
• • • We do not use the following data for averages, fits, limits, etc. • • •					
0.90 ±0.08 ±0.07	164	ACHASOV	98I	SND	$e^+e^- \to 5\gamma$

$\Gamma(\pi^+\pi^-\pi^+\pi^-)/\Gamma_{total}$ Γ_{19}/Γ

VALUE (units 10^{-6})	CL%	EVTS	DOCUMENT ID		TECN	COMMENT
• • • We do not use the following data for averages, fits, limits, etc. • • •						
3.93±1.74±2.14		3285	AKHMETSHIN	00E	CMD2	$e^+e^- \to \pi^+\pi^-\pi^+\pi^-$
< 870	90		CORDIER	79	WIRE	$e^+e^- \to \pi^+\pi^-\pi^+\pi^-$

$\Gamma(\pi^+\pi^+\pi^-\pi^-\pi^0)/\Gamma_{total}$ Γ_{20}/Γ

VALUE (units 10^{-6})	CL%	DOCUMENT ID		TECN	COMMENT
< 4.6	90	AKHMETSHIN	00E	CMD2	$e^+e^- \to \pi^+\pi^-\pi^+\pi^-\pi^0$
• • • We do not use the following data for averages, fits, limits, etc. • • •					
<150	95	BARKOV	88	CMD	$e^+e^- \to \pi^+\pi^-\pi^+\pi^-\pi^0$

$\Gamma(\pi^0e^+e^-)/\Gamma_{total}$ Γ_{21}/Γ

VALUE (units 10^{-5})	CL%	EVTS	DOCUMENT ID		TECN	COMMENT
1.12±0.28 OUR AVERAGE						
1.01±0.28±0.29		52	[54] ACHASOV	02D	SND	$e^+e^- \to \pi^0e^+e^-$
1.22±0.34±0.21		46	[55] AKHMETSHIN	01C	CMD2	$e^+e^- \to \pi^0e^+e^-$
• • • We do not use the following data for averages, fits, limits, etc. • • •						
<12	90		DOLINSKY	88	ND	$e^+e^- \to \pi^0e^+e^-$

$\Gamma(\pi^0\eta\gamma)/\Gamma_{total}$ Γ_{22}/Γ

VALUE (units 10^{-5})	CL%	EVTS	DOCUMENT ID		TECN	COMMENT
7.27±0.30 OUR AVERAGE			Error includes scale factor of 1.5. See the ideogram below.			
7.06±0.22		16.9k	[56] AMBROSINO	09F	KLOE	1.02 $e^+e^- \to \eta\pi^0\gamma$
8.51±0.51±0.57		607	[57] ALOISIO	02C	KLOE	$e^+e^- \to \eta\pi^0\gamma$
7.96±0.60±0.40		197	[58] ALOISIO	02C	KLOE	$e^+e^- \to \eta\pi^0\gamma$
8.8 ±1.4 ±0.9		36	[59] ACHASOV	00F	SND	$e^+e^- \to \eta\pi^0\gamma$
9.0 ±2.4 ±1.0		80	AKHMETSHIN	99C	CMD2	$e^+e^- \to \eta\pi^0\gamma$
• • • We do not use the following data for averages, fits, limits, etc. • • •						
7.01±0.10±0.20		13.3k	[57,60] AMBROSINO	09F	KLOE	1.02 $e^+e^- \to \eta\pi^0\gamma$
7.12±0.13±0.22		3.6k	[58,61] AMBROSINO	09F	KLOE	1.02 $e^+e^- \to \eta\pi^0\gamma$
8.3 ±2.3 ±1.2		20	ACHASOV	98B	SND	$e^+e^- \to 5\gamma$
<250	90		DOLINSKY	91	ND	$e^+e^- \to \pi^0\eta\gamma$

Meson Particle Listings

$\phi(1020)$

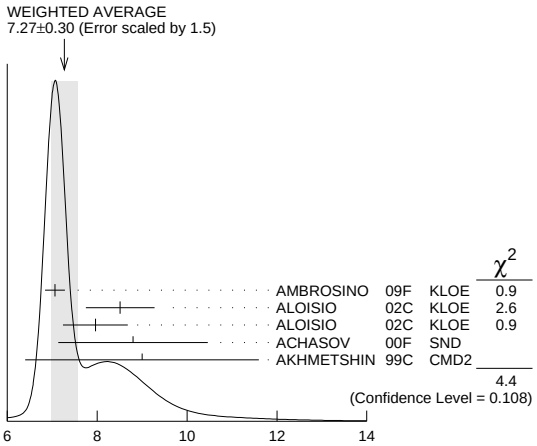

$\Gamma(a_0(980)\gamma)/\Gamma_{\text{total}}$ Γ_{23}/Γ

VALUE (units 10^{-5})	CL%	EVTS	DOCUMENT ID		TECN	COMMENT
7.6±0.6 OUR FIT						
7.6±0.6 OUR AVERAGE						
7.4±0.7			[62] ALOISIO	02C	KLOE	$e^+e^- \to \eta\pi^0\gamma$
8.8±1.7		36	[63] ACHASOV	00F	SND	$e^+e^- \to \eta\pi^0\gamma$
• • • We do not use the following data for averages, fits, limits, etc. • • •						
11 ±2			[64] GOKALP	02	RVUE	$e^+e^- \to \eta\pi^0\gamma$
<500	90		DOLINSKY	91	ND	$e^+e^- \to \pi^0\eta\gamma$

$\Gamma(f_0(980)\gamma)/\Gamma(a_0(980)\gamma)$ Γ_{17}/Γ_{23}

VALUE	DOCUMENT ID		TECN	COMMENT
6.1±0.6	[65] ALOISIO	02C	KLOE	$e^+e^- \to \eta\pi^0\gamma$

$\Gamma(K^0\overline{K}^0\gamma)/\Gamma_{\text{total}}$ Γ_{24}/Γ

VALUE	CL%	DOCUMENT ID		TECN	COMMENT
<1.9 × 10^{-8}	90	AMBROSINO	09C	KLOE	$e^+e^- \to K^0_S K^0_S\gamma$

$\Gamma(\eta'(958)\gamma)/\Gamma_{\text{total}}$ Γ_{25}/Γ

VALUE (units 10^{-5})	CL%	EVTS	DOCUMENT ID		TECN	COMMENT
6.25±0.21 OUR FIT						
6.25±0.30 OUR AVERAGE						
6.25±0.28±0.11		3407	[66] AMBROSINO	07A	KLOE	1.02 $e^+e^- \to \pi^+\pi^-7\gamma$
6.7 $^{+2.8}_{-2.4}$ ±0.8		12	[67] AULCHENKO	03B	SND	$e^+e^- \to \eta'\gamma$
• • • We do not use the following data for averages, fits, limits, etc. • • •						
6.7 $^{+5.0}_{-4.2}$ ±1.5		7	AULCHENKO	03B	SND	$e^+e^- \to 7\gamma$
6.10±0.61±0.43		120	[68] ALOISIO	02E	KLOE	1.02 $e^+e^- \to \pi^+\pi^-3\gamma$
8.2 $^{+2.1}_{-1.9}$ ±1.1		21	[69] AKHMETSHIN	00B	CMD2	$e^+e^- \to \pi^+\pi^-3\gamma$
4.9 $^{+2.2}_{-1.8}$ ±0.6		9	[70] AKHMETSHIN	00F	CMD2	$e^+e^- \to \pi^+\pi^-\pi^+\pi^- \geq 2\gamma$
6.4 ±1.6		30	[71] AKHMETSHIN	00F	CMD2	$e^+e^- \to \eta'(958)\gamma$
6.7 $^{+3.4}_{-2.9}$ ±1.0		5	[72] AULCHENKO	99	SND	$e^+e^- \to \pi^+\pi^-3\gamma$
<11	90		AULCHENKO	98	SND	$e^+e^- \to 7\gamma$
12 $^{+7}_{-5}$ ±2		6	[69] AKHMETSHIN	97B	CMD2	$e^+e^- \to \pi^+\pi^-3\gamma$
<41	90		DRUZHININ	87	ND	$e^+e^- \to \gamma\eta\pi^+\pi^-$

$\Gamma(\eta'(958)\gamma)/\Gamma(K^0_L K^0_S)$ Γ_{25}/Γ_2

VALUE (units 10^{-4})	EVTS	DOCUMENT ID		TECN	COMMENT
1.83±0.06 OUR FIT					
1.46 $^{+0.64}_{-0.54}$ ±0.18	9	[73] AKHMETSHIN	00F	CMD2	$e^+e^- \to \pi^+\pi^-\pi^+\pi^- \geq 2\gamma$

$\Gamma(\eta'(958)\gamma)/\Gamma(\eta\gamma)$ Γ_{25}/Γ_6

VALUE (units 10^{-3})	EVTS	DOCUMENT ID		TECN	COMMENT
4.77±0.15 OUR FIT					
4.78±0.20 OUR AVERAGE					
4.77±0.09±0.19	3407	AMBROSINO	07A	KLOE	1.02 $e^+e^- \to \pi^+\pi^-7\gamma$
4.70±0.47±0.31	120	[74] ALOISIO	02E	KLOE	1.02 $e^+e^- \to \pi^+\pi^-3\gamma$
6.5 $^{+1.7}_{-1.5}$ ±0.8	21	AKHMETSHIN	00B	CMD2	$e^+e^- \to \pi^+\pi^-3\gamma$
• • • We do not use the following data for averages, fits, limits, etc. • • •					
9.5 $^{+5.2}_{-4.0}$ ±1.4	6	[75] AKHMETSHIN	97B	CMD2	$e^+e^- \to \pi^+\pi^-3\gamma$

$\Gamma(\eta\pi^0\pi^0\gamma)/\Gamma_{\text{total}}$ Γ_{26}/Γ

VALUE (units 10^{-5})	CL%	DOCUMENT ID		TECN	COMMENT
<2	90	AULCHENKO	98	SND	$e^+e^- \to 7\gamma$

$\Gamma(\mu^+\mu^-\gamma)/\Gamma_{\text{total}}$ Γ_{27}/Γ

VALUE (units 10^{-5})	EVTS	DOCUMENT ID		TECN	COMMENT
1.43±0.45±0.14	27188	[47] AKHMETSHIN	99B	CMD2	$e^+e^- \to \mu^+\mu^-\gamma$
• • • We do not use the following data for averages, fits, limits, etc. • • •					
2.3 ±1.0	824 ± 33	[76] AKHMETSHIN	97C	CMD2	$e^+e^- \to \mu^+\mu^-\gamma$

$\Gamma(\rho\gamma\gamma)/\Gamma_{\text{total}}$ Γ_{28}/Γ

VALUE (units 10^{-4})	CL%	DOCUMENT ID		TECN	COMMENT
<1.2	90	AULCHENKO	08	CMD2	$\phi \to \pi^+\pi^-\gamma\gamma$
• • • We do not use the following data for averages, fits, limits, etc. • • •					
<5	90	AKHMETSHIN	98	CMD2	$e^+e^- \to \pi^+\pi^-\gamma\gamma$

$\Gamma(\eta\pi^+\pi^-)/\Gamma_{\text{total}}$ Γ_{29}/Γ

VALUE (units 10^{-5})	CL%	DOCUMENT ID		TECN	COMMENT
< 1.8	90	AKHMETSHIN	00E	CMD2	$e^+e^- \to \pi^+\pi^-\pi^+\pi^-\pi^0$
• • • We do not use the following data for averages, fits, limits, etc. • • •					
< 6.1	90	AULCHENKO	08	CMD2	$\phi \to \eta\pi^+\pi^-$
<30	90	AKHMETSHIN	98	CMD2	$e^+e^- \to \pi^+\pi^-\gamma\gamma$

$\Gamma(\eta\mu^+\mu^-)/\Gamma_{\text{total}}$ Γ_{30}/Γ

VALUE (units 10^{-6})	CL%	DOCUMENT ID		TECN	COMMENT
<9.4	90	AKHMETSHIN	01	CMD2	$e^+e^- \to \eta e^+e^-$

$\Gamma(\eta U \to \eta e^+e^-)/\Gamma_{\text{total}}$ Γ_{31}/Γ

VALUE	CL%	DOCUMENT ID		TECN	COMMENT
<1 × 10^{-6}	90	[77] BABUSCI	13B	KLOE	1.02 $e^+e^- \to \eta e^+e^-$

[1] Combined analysis of the CMD-2 data on $\phi \to K^+K^-$, $K^0_S K^0_L$, $\pi^+\pi^-\pi^0$, $\eta\gamma$ assuming that the sum of their branching fractions is 0.99741 ± 0.00007.
[2] Using B($\phi \to e^+e^-$)= (2.93 ± 0.14) × 10^{-4}.
[3] Theoretical analysis of BRAMON 00 taking into account phase-space difference, electromagnetic radiative corrections, as well as isospin breaking, predicts 0.62. FLOREZ-BAEZ 08 predicts 0.63 considering also structure-dependent radiative corrections. FISCHBACH 02 calculates additional corrections caused by the close threshold and predicts 0.68. See also BENAYOUN 01 and DUBYNSKIY 07. BENAYOUN 12 obtains 0.71±0.01 in the HLS model.
[4] Using B($\phi \to e^+e^-$)=(2.99 ± 0.08) × 10^{-4}.
[5] Using Γ(ϕ)= 4.1 MeV. If interference between the $\rho\pi$ and 3π modes is neglected, the fraction of the $\rho\pi$ is more than 80% at the 90% confidence level.
[6] From a fit without limitations on charged and neutral ρ masses and widths.
[7] Adding the direct and $\omega\pi$ contributions and considering the interference between the $\rho\pi$ and $\pi^+\pi^-\pi^0$.
[8] Neglecting the interference between the $\rho\pi$ and $\pi^+\pi^-\pi^0$.
[9] Using B($\phi \to e^+e^-$) = (2.99 ± 0.08) × 10^{-4} and B($\eta \to 3\pi^0$)= (32.2 ± 0.4) × 10^{-2}.
[10] From $\pi^+\pi^-\pi^0$ decay mode of η.
[11] From 2γ decay mode of η.
[12] From $3\pi^0$ decay mode of η.
[13] ACHASOV 07B reports [Γ($\phi(1020) \to \eta\gamma$)/$\Gamma_{\text{total}}$] × [B($\phi(1020) \to e^+e^-$)] = (4.050 ± 0.067 ± 0.118) × 10^{-6} which we divide by our best value B($\phi(1020) \to e^+e^-$) = (2.954 ± 0.030) × 10^{-4}. Our first error is their experiment's error and our second error is the systematic error from using our best value. Supersedes ACHASOV 00D and ACHASOV 06A.
[14] Using B($\phi \to e^+e^-$) = (2.98 ± 0.04) × 10^{-4} and B($\eta \to \gamma\gamma$) = 39.43 ± 0.26%.
[15] Not independent of the corresponding Γ(e^+e^-) × Γ($\eta\gamma$)/Γ^2_{total}.
[16] Using B($\phi \to e^+e^-$) = (2.99±0.08) × 10^{-4} and B($\eta \to 3\pi^0$)=(32.24±0.29) × 10^{-2}.
[17] The combined fit from 600 to 1380 MeV taking into account $\rho(770)$, $\omega(782)$, $\phi(1020)$, and $\rho(1450)$ (mass and width fixed at 1450 MeV and 310 MeV respectively).
[18] From the $\eta \to 2\gamma$ decay and using B($\phi \to e^+e^-$) =(2.99 ± 0.08) × 10^{-4}.
[19] From $\pi^+\pi^-\pi^0$ decay mode of η and using B($\phi \to e^+e^-$)= (2.99 ± 0.08) × 10^{-4}.
[20] Reanalysis of DRUZHININ 84, DOLINSKY 89, and DOLINSKY 91 taking into account a triangle anomaly contribution.
[21] Using B($\phi \to e^+e^-$) = (2.98 ± 0.04) × 10^{-4}.
[22] Not independent of the corresponding Γ(e^+e^-) × Γ($\pi^0\gamma$)/Γ^2_{total}.
[23] From the $\pi^0 \to 2\gamma$ decay and using B($\phi \to e^+e^-$) = (2.99 ± 0.08) × 10^{-4}.
[24] From the combined fit assuming that the total $\phi(1020)$ production cross section is saturated by those of K^+K^-, $K_S K_L$, $\pi^+\pi^-\pi^0$, and $\eta\gamma$ decays modes and using ACHASOV 00B for the $\eta\gamma$ decay mode.
[25] Using total width 4.2 MeV. They detect 3π mode and observe significant interference with ω tail. This is accounted for in the result quoted above.
[26] Neglecting interference between resonance and continuum.
[27] Using B($\phi \to e^+e^-$) = (2.91 ± 0.07) × 10^{-4}.
[28] Recalculated by us using B($\phi \to e^+e^-$)= (2.99 ± 0.08) × 10^{-4}.
[29] Using B($\eta \to \gamma\gamma$) = (39.25 ± 0.32)%, B($\phi \to \eta\gamma$) = (1.26 ± 0.06)%, and B($\phi \to e^+e^-$) = (3.00 ± 0.06) × 10^{-4}.
[30] The average of the branching ratios separately obtained from the $\eta \to \gamma\gamma$, $3\pi^0$, $\pi^+\pi^-\pi^0$ decays.
[31] From $\eta \to \gamma\gamma$ decays and using B($\eta \to \gamma\gamma$) = (39.33±0.25) × 10^{-2}, B($\eta \to \pi^+\pi^-\gamma$) = (4.75 ± 11) × 10^{-2}, and B($\phi \to \eta\gamma$) = (1.297 ± 0.033) × 10^{-2}.

[32] From $\eta \to 3\pi^0$ decays and using $B(\pi^0 \to \gamma\gamma) = (98.798 \pm 0.033) \times 10^{-2}$, $B(\eta \to 3\pi^0) = (32.24 \pm 0.29) \times 10^{-2}$, $B(\eta \to \pi^+\pi^-\gamma) = (4.75 \pm 0.11) \times 10^{-2}$, and $B(\phi \to \eta\gamma) = (1.297 \pm 0.033) \times 10^{-2}$.

[33] From $\eta \to \pi^+\pi^-\pi^0$ decays and using $B(\pi^0 \to \gamma\gamma) = (98.798 \pm 0.033) \times 10^{-2}$, $B(\pi^0 \to e^+e^-\gamma) = (1.198 \pm 0.032) \times 10^{-2}$, $B(\eta \to \pi^+\pi^-\pi^0) = (23.0 \pm 0.4) \times 10^{-2}$, $B(\phi \to \pi^+\pi^-\pi^0) = (15.5 \pm 0.6) \times 10^{-2}$, and $B(\phi \to \eta\gamma) = (1.297 \pm 0.033) \times 10^{-2}$.

[34] Using the 1996 and 1998 data.

[35] (2.3 ± 0.3)% correction for other decay modes of the $\omega(782)$ applied.

[36] Not independent of the corresponding $\Gamma(\omega\pi^0) \times \Gamma(e^+e^-) / \Gamma^2(\text{total})$.

[37] Using the 1996 data.

[38] Using the 1998 data.

[39] Supersedes AKHMETSHIN 97C.

[40] For $E_\gamma > 20$ MeV and assuming that $B(\phi(1020) \to f_0(980)\gamma)$ is negligible. Supersedes AKHMETSHIN 97C.

[41] For $E_\gamma > 20$ MeV and assuming that $B(\phi(1020) \to f_0(980)\gamma)$ is negligible.

[42] Obtained by the authors taking into account the $\pi^+\pi^-$ decay mode. Includes a component due to $\pi\pi$ production via the $f_0(500)$ meson. Supersedes ALOISIO 02D.

[43] From the combined fit of the photon spectra in the reactions $e^+e^- \to \pi^+\pi^-\gamma$, $\pi^0\pi^0\gamma$.

[44] From the negative interference with the $f_0(500)$ meson of AITALA 01B using the ACHASOV 89 parameterization for the $f_0(980)$, a Breit-Wigner for the $f_0(500)$, and ACHASOV 01F for the $\rho\pi$ contribution. Superseded by AMBROSINO 07.

[45] Assuming that the $\pi^0\pi^0\gamma$ final state is completely determined by the $f_0\gamma$ mechanism, neglecting the decay $B(\phi \to K\overline{K}\gamma)$ and using $B(f_0 \to \pi^+\pi^-) = 2B(f_0 \to \pi^0\pi^0)$.

[46] Using the value $B(\phi \to \eta\gamma) = (1.338 \pm 0.053) \times 10^{-2}$.

[47] For $E_\gamma > 20$ MeV. Supersedes AKHMETSHIN 97C.

[48] Neglecting other intermediate mechanisms ($\rho\pi$, $\sigma\gamma$).

[49] A narrow pole fit taking into account $f_0(980)$ and $f_0(1200)$ intermediate mechanisms.

[50] For destructive interference with the Bremsstrahlung process

[51] For constructive interference with the Bremsstrahlung process

[52] Supersedes ALOISIO 02D.

[53] Supersedes ACHASOV 98I. Excluding $\omega\pi^0$.

[54] Using various branching ratios from the 2000 Edition of this Review (PDG 00).

[55] Using $B(\pi^0 \to \gamma\gamma) = 0.98798 \pm 0.00032$, $B(\phi \to \eta\gamma) = (1.297 \pm 0.033) \times 10^{-2}$, and $B(\eta \to \pi^+\pi^-\gamma) = (4.75 \pm 0.11) \times 10^{-2}$.

[56] Combined results of $\eta \to \gamma\gamma$ and $\eta \to \pi^+\pi^-\pi^0$ decay modes measurements.

[57] From the decay mode $\eta \to \gamma\gamma$.

[58] From the decay mode $\eta \to \pi^+\pi^-\pi^0$.

[59] Supersedes ACHASOV 98B.

[60] Using $B(\phi \to \eta\gamma) = (1.304 \pm 0.025)\%$, $B(\eta \to 3\pi^0) = (32.56 \pm 0.23)\%$, and $B(\eta \to \gamma\gamma) = (39.31 \pm 0.20)\%$.

[61] Using $B(\phi \to \eta\gamma) = (1.304 \pm 0.025)\%$, $B(\eta \to 3\pi^0) = (32.56 \pm 0.23)\%$, and $B(\eta \to \pi^+\pi^-\pi^0) = (22.73 \pm 0.28)\%$.

[62] Using $M_{a_0(980)} = 984.8$ MeV and assuming $a_0(980)\gamma$ dominance.

[63] Assuming $a_0(980)\gamma$ dominance in the $\eta\pi^0\gamma$ final state.

[64] Using data of ACHASOV 00F.

[65] Using results of ALOISIO 02D and assuming that $f_0(980)$ decays into $\pi\pi$ only and $a_0(980)$ into $\eta\pi$ only.

[66] AMBROSINO 07A reports $[\Gamma(\phi(1020) \to \eta'(958)\gamma)/\Gamma_{\text{total}}] / [B(\phi(1020) \to \eta\gamma)] = (4.77 \pm 0.09 \pm 0.19) \times 10^{-3}$ which we multiply by our best value $B(\phi(1020) \to \eta\gamma) = (1.309 \pm 0.024) \times 10^{-2}$. Our first error is their experiment's error and our second error is the systematic error from using our best value.

[67] Averaging AULCHENKO 03B with AULCHENKO 99.

[68] Using $B(\phi \to \eta\gamma) = (1.297 \pm 0.033)\%$.

[69] Using the value $B(\phi \to \eta\gamma) = (1.26 \pm 0.06) \times 10^{-2}$.

[70] Using $B(\phi \to K_L^0 K_S^0) = (33.8 \pm 0.6)\%$.

[71] Averaging AKHMETSHIN 00B with AKHMETSHIN 00F.

[72] Using the value $B(\eta' \to \eta\pi^+\pi^-) = (43.7 \pm 1.5) \times 10^{-2}$ and $B(\eta \to \gamma\gamma) = (39.25 \pm 0.31) \times 10^{-2}$.

[73] Using various branching ratios of K_S^0, K_L^0, η, η' from the 2000 edition (The European Physical Journal **C15** 1 (2000)) of this Review.

[74] From the decay mode $\eta' \to \eta\pi^+\pi^-$, $\eta \to \gamma\gamma$.

[75] Superseded by AKHMETSHIN 00B.

[76] For $E_\gamma > 20$ MeV.

[77] For a narrow vector U with mass between 5 and 470 MeV, from the combined analysis of $\eta \to \pi^+\pi^-\pi^0$ and $\eta \to \pi^0\pi^0\pi^0$ from ARCHILLI 12. Measured 90% CL limits as a function of m_U range from 2.2×10^{-8} to 10^{-6}.

Lepton Faminly number (LF) violating modes

$\Gamma(e^\pm\mu^\mp)/\Gamma_{\text{total}}$ Γ_{32}/Γ

VALUE	CL%	DOCUMENT ID		TECN	COMMENT
$< 2 \times 10^{-6}$	90	ACHASOV	10A	SND	$e^+e^- \to e^\pm\mu^\mp$

$\pi^+\pi^-\pi^0$ / $\rho\pi$ AMPLITUDE RATIO a_1 IN DECAY OF $\phi \to \pi^+\pi^-\pi^0$

NIECKNIG 12 describes final-state interactions between the three pions in a dispersive framework using data on the $\pi\pi$ P-wave scattering phase shift.

VALUE (units 10^{-2})	CL%	EVTS	DOCUMENT ID		TECN	COMMENT
9.1±1.2 OUR AVERAGE						
10.1±4.4±1.7		80k	[1] AKHMETSHIN	06	CMD2	1.017–1.021 $e^+e^- \to \pi^+\pi^-\pi^0$
9.0±1.1±0.6		1.98M	[2,3] ALOISIO	03	KLOE	1.02 $e^+e^- \to \pi^+\pi^-\pi^0$
• • • We do not use the following data for averages, fits, limits, etc. • • •						
$-6 < a_1 < 6$		500k	[3] ACHASOV	02	SND	$e^+e^- \to \pi^+\pi^-\pi^0$
$-16 < a_1 < 11$	90	9.8k	[1,4] AKHMETSHIN	98	CMD2	$e^+e^- \to \pi^+\pi^-\gamma\gamma$

[1] Dalitz plot analysis taking into account interference between the contact and $\rho\pi$ amplitudes.

[2] From a fit without limitations on charged and neutral ρ masses and widths.

[3] Recalculated by us to match the notations of AKHMETSHIN 98.

[4] Assuming zero phase for the contact term.

$\phi(1020)$ REFERENCES

BABUSCI	13B	PL B720 111	D. Babusci *et al.*	(KLOE-2 Collab.)
BENAYOUN	13	EPJ C73 2453	M. Benayoun, P. David, L. DelBuono	(PARIN, BERLIN+)
LEES	13Q	PR D88 032013	J.P. Lees *et al.*	(BABAR Collab.)
ARCHILLI	12	PL B706 251	F. Archilli *et al.*	(KLOE-2 Collab.)
BENAYOUN	12	EPJ C72 1848	M. Benayoun *et al.*	
NIECKNIG	12	EPJ C72 2014	F. Niecknig, B. Kubis, S.P. Schneider	(BONN)
AKHMETSHIN	11	PL B695 412	R. Akhmetshin *et al.*	(CMD2 Collab.)
ACHASOV	10A	PR D81 057102	M.N. Achasov *et al.*	(Novosibirsk SND Collab.)
BENAYOUN	10	EPJ C65 211	M. Benayoun *et al.*	
AMBROSINO	09C	PL B679 10	F. Ambrosino *et al.*	(KLOE Collab.)
AMBROSINO	09F	PL B681 5	F. Ambrosino *et al.*	(KLOE Collab.)
AKHMETSHIN	08	PL B669 217	R.R. Akhmetshin *et al.*	(CMD-2 Collab.)
AMBROSINO	08G	PL B669 223	F. Ambrosino *et al.*	(KLOE Collab.)
AULCHENKO	08	JETPL 88 85 Translated from ZETFP 88 93.	V. Aulchenko *et al.*	(CMD-2 Collab.)
FLOREZ-BAEZ	08	PR D78 077301	F.V. Florez-Baez, G. Lopez Castro	
ACHASOV	07B	PR D76 077101	M.N. Achasov *et al.*	(SND Collab.)
AMBROSINO	07	EPJ C49 473	F. Ambrosino *et al.*	(KLOE Collab.)
AMBROSINO	07A	PL B648 267	F. Ambrosino *et al.*	(KLOE Collab.)
DUBYNSKIY	07	PR D75 113001	S. Dubynskiy *et al.*	
ACHASOV	06A	PR D74 014016	M.N. Achasov *et al.*	(SND Collab.)
AKHMETSHIN	06	PL B642 203	R.R. Akhmetshin *et al.*	(CMD-2 Collab.)
AKHMETSHIN	05	PL B605 26	R.R. Akhmetshin *et al.*	(Novosibirsk CMD-2 Collab.)
AMBROSINO	05	PL B608 199	F. Ambrosino *et al.*	(KLOE Collab.)
AUBERT,B	05J	PR D72 052008	B. Aubert *et al.*	(BABAR Collab.)
AKHMETSHIN	04	PL B578 285	R.R. Akhmetshin *et al.*	(Novosibirsk CMD-2 Collab.)
AUBERT,B	04N	PR D70 072004	B. Aubert *et al.*	(BABAR Collab.)
ALOISIO	03	PL B561 55	A. Aloisio *et al.*	(KLOE Collab.)
AULCHENKO	03B	JETP 97 24 Translated from ZETF 124 28.	V.M. Aulchenko *et al.*	(Novosibirsk SND Collab.)
ACHASOV	02	PR D65 032002	M.N. Achasov *et al.*	(Novosibirsk SND Collab.)
ACHASOV	02D	JETPL 75 449 Translated from ZETFP 75 539.	M.N. Achasov *et al.*	(Novosibirsk SND Collab.)
ALOISIO	02C	PL B536 209	A. Aloisio *et al.*	(KLOE Collab.)
ALOISIO	02D	PL B537 21	A. Aloisio *et al.*	(KLOE Collab.)
ALOISIO	02E	PL B541 45	A. Aloisio *et al.*	(KLOE Collab.)
FISCHBACH	02	PL B526 355	E. Fischbach, A.W. Overhauser, B. Woodahl	
GOKALP	02	JP G28 2783	A. Gokalp *et al.*	
ACHASOV	01B	PL B504 275	M.N. Achasov *et al.*	(Novosibirsk SND Collab.)
ACHASOV	01E	PR D63 072002	M.N. Achasov *et al.*	(Novosibirsk SND Collab.)
ACHASOV	01F	PR D63 094007	N.N. Achasov, V.V. Gubin	(Novosibirsk SND Collab.)
ACHASOV	01G	PRL 86 1698	M.N. Achasov *et al.*	(Novosibirsk SND Collab.)
AITALA	01B	PRL 86 770	E.M. Aitala *et al.*	(FNAL E791 Collab.)
AKHMETSHIN	01	PL B501 191	R.R. Akhmetshin *et al.*	(Novosibirsk CMD-2 Collab.)
AKHMETSHIN	01B	PL B509 217	R.R. Akhmetshin *et al.*	(Novosibirsk CMD-2 Collab.)
AKHMETSHIN	01C	PL B503 237	R.R. Akhmetshin *et al.*	(Novosibirsk CMD-2 Collab.)
BENAYOUN	01	EPJ C22 503	M. Benayoun, H.B. O'Connell	
ACHASOV	00	EPJ C12 25	M.N. Achasov *et al.*	(Novosibirsk SND Collab.)
ACHASOV	00B	JETP 90 17 Translated from ZETF 117 22.	M.N. Achasov *et al.*	(Novosibirsk SND Collab.)
ACHASOV	00C	PL B474 188	M.N. Achasov *et al.*	(Novosibirsk SND Collab.)
ACHASOV	00D	JETPL 72 282 Translated from ZETFP 72 411.	M.N. Achasov *et al.*	(Novosibirsk SND Collab.)
ACHASOV	00E	NP B569 158	M.N. Achasov *et al.*	(Novosibirsk SND Collab.)
ACHASOV	00F	PL B479 53	M.N. Achasov *et al.*	(Novosibirsk SND Collab.)
ACHASOV	00H	PL B485 349	M.N. Achasov *et al.*	(Novosibirsk SND Collab.)
AKHMETSHIN	00B	PL B473 337	R.R. Akhmetshin *et al.*	(Novosibirsk CMD-2 Collab.)
AKHMETSHIN	00E	PL B491 81	R.R. Akhmetshin *et al.*	(Novosibirsk CMD-2 Collab.)
AKHMETSHIN	00F	PL B494 26	R.R. Akhmetshin *et al.*	(Novosibirsk CMD-2 Collab.)
AULCHENKO	00A	JETP 90 927 Translated from ZETF 117 1067.	V.M. Aulchenko *et al.*	(Novosibirsk SND Collab.)
BRAMON	00	PL B486 406	A. Bramon *et al.*	
PDG	00	EPJ C15 1	D.E. Groom *et al.*	(PDG Collab.)
ACHASOV	99	PL B449 122	M.N. Achasov *et al.*	
ACHASOV	99C	PL B456 304	M.N. Achasov *et al.*	
AKHMETSHIN	99B	PL B462 371	R.R. Akhmetshin *et al.*	(Novosibirsk CMD-2 Collab.)
AKHMETSHIN	99C	PL B462 380	R.R. Akhmetshin *et al.*	(Novosibirsk CMD-2 Collab.)
AKHMETSHIN	99D	PL B466 385	R.R. Akhmetshin *et al.*	
Also		PL B508 217 (errat)	R.R. Akhmetshin *et al.*	(Novosibirsk CMD-2 Collab.)
AKHMETSHIN	99F	PL B460 242	R.R. Akhmetshin *et al.*	(Novosibirsk CMD-2 Collab.)
AULCHENKO	99	JETPL 69 97 Translated from ZETFP 69 87.	V.M. Aulchenko *et al.*	
ACHASOV	98B	PL B438 441	M.N. Achasov *et al.*	(Novosibirsk SND Collab.)
ACHASOV	98F	JETPL 68 573	M.N. Achasov *et al.*	(Novosibirsk SND Collab.)
ACHASOV	98I	PL B440 442	M.N. Achasov *et al.*	
AKHMETSHIN	98	PL B434 426	R.R. Akhmetshin *et al.*	(CMD-2 Collab.)
AULCHENKO	98	PL B436 199	V.M. Aulchenko *et al.*	(Novosibirsk SND Collab.)
BARBERIS	98	PL B432 436	D. Barberis *et al.*	(Omega Expt.)
AKHMETSHIN	97B	PL B415 445	R.R. Akhmetshin *et al.*	(NOVO, BOST, PITT+)
AKHMETSHIN	97C	PL B415 452	R.R. Akhmetshin *et al.*	(Novosibirsk CMD-2 Collab.)
BENAYOUN	96	ZPHY C72 221	M. Benayoun *et al.*	(IPNP, NOVO)
AKHMETSHIN	95	PL B364 199	R.R. Akhmetshin *et al.*	(Novosibirsk CMD-2 Collab.)
DOLINSKY	91	PRPL 202 99	S.I. Dolinsky *et al.*	(NOVO)
KUHN	90	ZPHY C48 445	J.H. Kuhn *et al.*	(MPIM)
ACHASOV	89	NP B315 465	N.N. Achasov, V.N. Ivanchenko	
DOLINSKY	89	ZPHY C42 511	S.I. Dolinsky *et al.*	(NOVO)
BARKOV	88	SJNP 47 248 Translated from YAF 47 393.	L.M. Barkov *et al.*	(NOVO)
DOLINSKY	88	SJNP 48 277 Translated from YAF 48 442.	S.I. Dolinsky *et al.*	(NOVO)
DRUZHININ	87	ZPHY C37 1	V.P. Druzhinin *et al.*	(NOVO)
ARMSTRONG	86	PL 166B 245	T.A. Armstrong *et al.*	(ATHU, BARI, BIRM+)
ATKINSON	86	ZPHY C30 521	M. Atkinson *et al.*	(BONN, CERN, GLAS+)
BEBEK	86	PRL 56 1893	C. Bebek *et al.*	(CLEO Collab.)
DAVENPORT	86	PR D33 2519	T.F. Davenport (TUFTS, ARIZ, FNAL, FSU, NDAM+)	
DIJKSTRA	86	ZPHY C31 375	H. Dijkstra *et al.*	(ANIK, BRIS, CERN+)
FRAME	86	NP B276 667	D. Frame *et al.*	(GLAS)
GOLUBEV	86	SJNP 44 409 Translated from YAF 44 633.	V.B. Golubev *et al.*	(NOVO)
ALBRECHT	85D	PL 153B 343	H. Albrecht *et al.*	(ARGUS Collab.)
GOLUBEV	85	SJNP 41 756 Translated from YAF 41 1183.	V.B. Golubev *et al.*	(NOVO)
DRUZHININ	84	PL 144B 136	V.P. Druzhinin *et al.*	(NOVO)
ARMSTRONG	83B	NP B224 193	T.A. Armstrong *et al.*	(BARI, BIRM, CERN+)
BARATE	83	PL 121B 449	R. Barate *et al.*	(SACL, LOIC, SHMP, IND)
KURDADZE	83C	JETPL 38 366 Translated from ZETFP 38 306.	L.M. Kurdadze *et al.*	(NOVO)
ARENTON	82	PR D25 2241	M.W. Arenton *et al.*	(ANL, ILL)
PELLINEN	82	PS 25 599	A. Pellinen, M. Roos	(HELS)
DAUM	81	PL 100B 439	C. Daum *et al.*	(AMST, BRIS, CERN, CRAC+)
IVANOV	81	PL 107B 297	P.M. Ivanov *et al.*	(NOVO)
Also		Private Comm.	S.I. Eidelman	(NOVO)
VASSERMAN	81	PL 99B 62	I.B. Vasserman *et al.*	(NOVO)
Also		SJNP 35 240 Translated from YAF 35 352.	L.M. Kurdadze *et al.*	

CORDIER	80	NP B172 13	A. Cordier *et al.*	(LALO)
CORDIER	79	PL 81B 389	A. Cordier *et al.*	(LALO)
BUKIN	78B	SJNP 27 521 Translated from YAF 27 985.	A.D. Bukin *et al.*	(NOVO)
BUKIN	78C	SJNP 27 516 Translated from YAF 27 976.	A.D. Bukin *et al.*	(NOVO)
COOPER	78B	NP B146 1	A.M. Cooper *et al.*	(TATA, CERN, CDEF+)
LOSTY	78	NP B133 38	M.J. Losty *et al.*	(CERN, AMST, NIJM+)
AKERLOF	77	PRL 39 861	C.W. Akerlof *et al.*	(FNAL, MICH, PURD)
ANDREWS	77	PRL 38 198	D.E. Andrews *et al.*	(ROCH)
BALDI	77	PL 68B 381	R. Baldi *et al.*	(GEVA)
CERRADA	77B	NP B126 241	M. Cerrada *et al.*	(AMST, CERN, NIJM+)
COHEN	77	PRL 38 269	D. Cohen *et al.*	(ANL)
LAVEN	77	NP B127 43	H. Laven *et al.*	(AACH3, BERL, CERN, LOIC+)
LYONS	77	NP B125 207	L. Lyons, A.M. Cooper, A.G. Clark	(OXF)
COSME	76	PL 63B 352	G. Cosme *et al.*	(ORSAY)
KALBFLEISCH	76	PR D13 22	G.R. Kalbfleisch, R.C. Strand, J.W. Chapman	(BNL+)
PARROUR	76	PL 63B 357	G. Parrour *et al.*	(ORSAY)
PARROUR	76B	PL 63B 362	G. Parrour *et al.*	(ORSAY)
KALBFLEISCH	75	PR D11 987	G.R. Kalbfleisch, R.C. Strand, J.W. Chapman	(BNL+)
AYRES	74	PRL 32 1463	D.S. Ayres *et al.*	(ANL)
BESCH	74	NP B70 257	H.J. Besch *et al.*	(BONN)
COSME	74	PL 48B 155	G. Cosme *et al.*	(ORSAY)
COSME	74B	PL 48B 159	G. Cosme *et al.*	(ORSAY)
DEGROOT	74	NP B74 77	A.J. de Groot *et al.*	(AMST, NIJM)
AUGUSTIN	73	PRL 30 462	J.E. Augustin *et al.*	(ORSAY)
BALLAM	73	PR D7 3150	J. Ballam *et al.*	(SLAC, LBL)
BINNIE	73B	PR D8 2789	D.M. Binnie *et al.*	(LOIC, SHMP)
AGUILAR-...	72B	PR D6 29	M. Aguilar-Benitez *et al.*	(BNL)
ALVENSLEB...	72	PRL 28 66	H. Alvensleben *et al.*	(MIT, DESY)
BORENSTEIN	72	PR D5 1559	S.R. Borenstein *et al.*	(BNL, MICH)
COLLEY	72	NP B50 1	D.C. Colley *et al.*	(BIRM, GLAS)
BALAKIN	71	PL 34B 328	V.E. Balakin *et al.*	(NOVO)
CHATELUS	71	Thesis LAL 1247	Y. Chatelus	(STRB)
Also		PL 32B 416	J.C. Bizot *et al.*	(ORSAY)
HAYES	71	PR D4 899	S. Hayes *et al.*	(CORN)
STOTTLE...	71	Thesis ORO 2504 170	A.R. Stottlemyer	(UMD)
BIZOT	70	PL 32B 416	J.C. Bizot *et al.*	(ORSAY)
Also		Liverpool Sym. 69	J.P. Perez-y-Jorba	
EARLES	70	PRL 25 1312	D.R. Earles *et al.*	(NEAS)
LINDSEY	66	PR 147 913	J.S. Lindsey, G. Smith	(LRL)
LONDON	66	PR 143 1034	G.W. London *et al.*	(BNL, SYRA) IGJPC
BADIER	65B	PL 17 337	J. Badier *et al.*	(EPOL, SACL, AMST)
LINDSEY	65	PRL 15 221	J.S. Lindsey, G.A. Smith	(LRL)
LINDSEY 65 data included in LINDSEY 66.				
SCHLEIN	63	PRL 10 368	P.E. Schlein *et al.*	(UCLA) IGJP

$h_1(1170)$

$I^G(J^{PC}) = 0^-(1^{+-})$

$h_1(1170)$ MASS

VALUE (MeV)	DOCUMENT ID		TECN	CHG	COMMENT
1170±20 OUR ESTIMATE					
• • • We do not use the following data for averages, fits, limits, etc. • • •					
1168± 4	ANDO	92	SPEC		8 $\pi^- p \rightarrow \pi^+\pi^-\pi^0 n$
1166± 5±3	[1] ANDO	92	SPEC		8 $\pi^- p \rightarrow \pi^+\pi^-\pi^0 n$
1190±60	[2] DANKOWY...	81	SPEC	0	8 $\pi p \rightarrow 3\pi n$

[1] Average and spread of values using 2 variants of the model of BOWLER 75.
[2] Uses the model of BOWLER 75.

$h_1(1170)$ WIDTH

VALUE (MeV)	DOCUMENT ID		TECN	CHG	COMMENT
360±40 OUR ESTIMATE					
• • • We do not use the following data for averages, fits, limits, etc. • • •					
345± 6	ANDO	92	SPEC		8 $\pi^- p \rightarrow \pi^+\pi^-\pi^0 n$
375± 6±34	[3] ANDO	92	SPEC		8 $\pi^- p \rightarrow \pi^+\pi^-\pi^0 n$
320±50	[4] DANKOWY...	81	SPEC	0	8 $\pi p \rightarrow 3\pi n$

[3] Average and spread of values using 2 variants of the model of BOWLER 75.
[4] Uses the model of BOWLER 75.

$h_1(1170)$ DECAY MODES

	Mode	Fraction (Γ_i/Γ)
Γ_1	$\rho\pi$	seen

$h_1(1170)$ BRANCHING RATIOS

$\Gamma(\rho\pi)/\Gamma_{total}$ **Γ_1/Γ**

VALUE	DOCUMENT ID		TECN	COMMENT
• • • We do not use the following data for averages, fits, limits, etc. • • •				
seen	ANDO	92	SPEC	8 $\pi^- p \rightarrow \pi^+\pi^-\pi^0 n$
seen	ATKINSON	84	OMEG	20–70 $\gamma p \rightarrow \pi^+\pi^-\pi^0 p$
seen	DANKOWY...	81	SPEC	8 $\pi p \rightarrow 3\pi n$

$h_1(1170)$ REFERENCES

ANDO	92	PL B291 496	A. Ando *et al.*	(KEK, KYOT, NIRS, SAGA+)
ATKINSON	84	NP B231 15	M. Atkinson *et al.*	(BONN, CERN, GLAS+)
DANKOWY...	81	PRL 46 580	J.A. Dankowych *et al.*	(TNTO, BNL, CARL+)
BOWLER	75	NP B97 227	M.G. Bowler *et al.*	(OXFTP, DARE)

$b_1(1235)$

$I^G(J^{PC}) = 1^+(1^{+-})$

$b_1(1235)$ MASS

VALUE (MeV)	EVTS	DOCUMENT ID		TECN	CHG	COMMENT
1229.5± 3.2 OUR AVERAGE Error includes scale factor of 1.6. See the ideogram below.						
1225 ± 5		WEIDENAUER	93	ASTE		$\bar{p}p \rightarrow 2\pi^+ 2\pi^- \pi^0$
1235 ±15		ALDE	92C	GAM2		38,100 $\pi^- p \rightarrow \omega\pi^0 n$
1236 ±16		FUKUI	91	SPEC		8.95 $\pi^- p \rightarrow \omega\pi^0 n$
1222 ± 6		ATKINSON	84E	OMEG	±	25–55 $\gamma p \rightarrow \omega\pi X$
1237 ± 7		ATKINSON	84E	OMEG	0	25–55 $\gamma p \rightarrow \omega\pi X$
1239 ± 5		EVANGELIS...	81	OMEG	−	12 $\pi^- p \rightarrow \omega\pi p$
1251 ± 8	450	GESSAROLI	77	HBC	−	11 $\pi^- p \rightarrow \pi^-\omega p$
1245 ±11	890	FLATTE	76C	HBC	−	4.2 $K^- p \rightarrow \pi^-\omega\Sigma^+$
1222 ± 4	1400	CHALOUPKA	74	HBC	−	3.9 $\pi^- p$
1220 ± 7	600	KARSHON	74B	HBC	+	4.9 $\pi^+ p$
• • • We do not use the following data for averages, fits, limits, etc. • • •						
1190 ±10		AUGUSTIN	89	DM2	±	$e^+e^- \rightarrow 5\pi$
1213 ± 5		ATKINSON	84C	OMEG	0	20–70 γp
1271 ±11		COLLICK	84	SPEC	+	200 $\pi^+ Z \rightarrow Z\pi\omega$

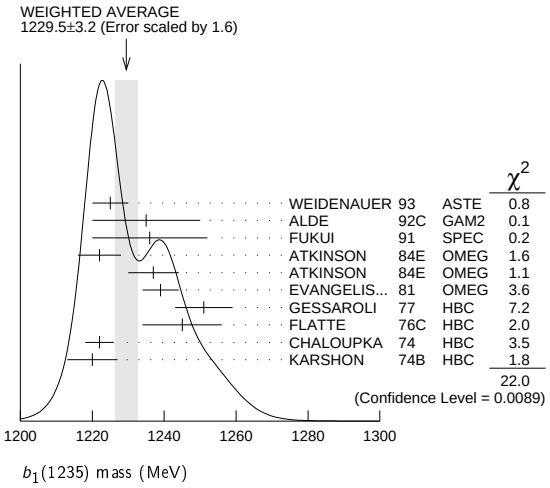

$b_1(1235)$ WIDTH

VALUE (MeV)	EVTS	DOCUMENT ID		TECN	CHG	COMMENT
142± 9 OUR AVERAGE Error includes scale factor of 1.2.						
113±12		WEIDENAUER	93	ASTE		$\bar{p}p \rightarrow 2\pi^+ 2\pi^- \pi^0$
160±30		ALDE	92C	GAM2		38,100 $\pi^- p \rightarrow \omega\pi^0 n$
151±31		FUKUI	91	SPEC		8.95 $\pi^- p \rightarrow \omega\pi^0 n$
170±15		EVANGELIS...	81	OMEG	−	12 $\pi^- p \rightarrow \omega\pi p$
170±50	225	BALTAY	78B	HBC	+	15 $\pi^+ p \rightarrow p4\pi$
155±32	450	GESSAROLI	77	HBC	−	11 $\pi^- p \rightarrow \pi^-\omega p$
182±45	890	FLATTE	76C	HBC	−	4.2 $K^- p \rightarrow \pi^-\omega\Sigma^+$
135±20	1400	CHALOUPKA	74	HBC	−	3.9 $\pi^- p$
156±22	600	KARSHON	74B	HBC	+	4.9 $\pi^+ p$
• • • We do not use the following data for averages, fits, limits, etc. • • •						
210±19		AUGUSTIN	89	DM2	±	$e^+e^- \rightarrow 5\pi$
231±14		ATKINSON	84C	OMEG	0	20–70 γp
232±29		COLLICK	84	SPEC	+	200 $\pi^+ Z \rightarrow Z\pi\omega$

$b_1(1235)$ DECAY MODES

	Mode	Fraction (Γ_i/Γ)		Confidence level
Γ_1	$\omega\pi$ [D/S amplitude ratio = 0.277 ± 0.027]	dominant		
Γ_2	$\pi^\pm\gamma$	$(1.6\pm0.4)\times10^{-3}$		
Γ_3	$\eta\rho$	seen		
Γ_4	$\pi^+\pi^+\pi^-\pi^0$	< 50	%	84%
Γ_5	$K^*(892)^\pm K^\mp$	seen		
Γ_6	$(K\overline{K})^\pm\pi^0$	< 8	%	90%
Γ_7	$K^0_S K^0_L \pi^\pm$	< 6	%	90%
Γ_8	$K^0_S K^0_S \pi^\pm$	< 2	%	90%
Γ_9	$\phi\pi$	< 1.5	%	84%

$b_1(1235)$ PARTIAL WIDTHS

$\Gamma(\pi^\pm\gamma)$ Γ_2

VALUE (keV)	DOCUMENT ID		TECN	CHG	COMMENT
230±60	COLLICK	84	SPEC	+	200 π^+Z → Z$\pi\omega$

$b_1(1235)$ D-wave/S-wave AMPLITUDE RATIO IN DECAY OF $b_1(1235) \to \omega\pi$

VALUE	EVTS	DOCUMENT ID		TECN	CHG	COMMENT
0.277±0.027 OUR AVERAGE		Error includes scale factor of 2.4. See the ideogram below.				
0.269±0.009±0.010		NOZAR	02	MPS	−	18 $\pi^- p \to \omega\pi^- p$
0.23 ±0.03		AMSLER	94C	CBAR		0.0 $\overline{p}p \to \omega\eta\pi^0$
0.45 ±0.04		AMSLER	93B	CBAR		0.0 $\overline{p}p \to \omega\pi^0\pi^0$
0.235±0.047		ATKINSON	84C	OMEG		20–70 γp
0.4 $^{+0.1}_{-0.1}$		GESSAROLI	77	HBC	−	11 $\pi^- p \to \pi^-\omega p$
0.21 ±0.08		CHUNG	75B	HBC	+	7.1 $\pi^+ p$
0.3 ±0.1		CHALOUPKA	74	HBC	−	3.9–7.5 $\pi^- p$
0.35 ±0.25	600	KARSHON	74B	HBC	+	4.9 $\pi^+ p$

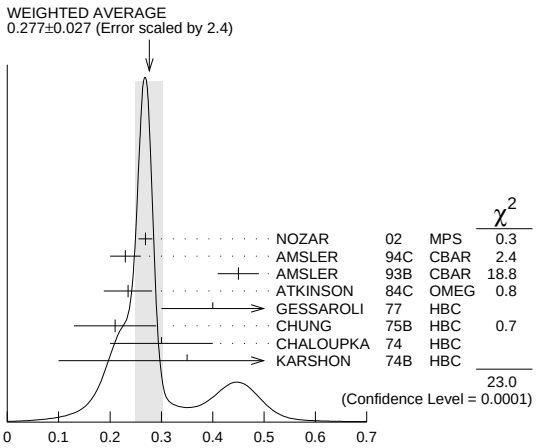

$b_1(1235)$ D-wave/S-wave amplitude ratio in decay of $b_1(1235) \to \omega\pi$

$b_1(1235)$ D-wave/S-wave AMPLITUDE PHASE DIFFERENCE IN DECAY OF $b_1(1235) \to \omega\pi$

VALUE (°)	DOCUMENT ID		TECN	CHG	COMMENT
10.5±2.4±3.9	NOZAR	02	MPS	−	18 $\pi^- p \to \omega\pi^- p$

$b_1(1235)$ BRANCHING RATIOS

$\Gamma(\eta\rho)/\Gamma(\omega\pi)$ Γ_3/Γ_1

VALUE	DOCUMENT ID		TECN	COMMENT
<0.10	ATKINSON	84D	OMEG	20–70 γp

$\Gamma(\pi^+\pi^+\pi^-\pi^0)/\Gamma(\omega\pi)$ Γ_4/Γ_1

VALUE	DOCUMENT ID		TECN	CHG	COMMENT
<0.5	ABOLINS	63	HBC	+	3.5 $\pi^+ p$

$\Gamma(K^*(892)^\pm K^\mp)/\Gamma_{total}$ Γ_5/Γ

VALUE	DOCUMENT ID		TECN	COMMENT
seen	[1] ABLIKIM	10E	BES2	$J/\psi \to K^\pm K^0_S \pi^\mp \pi^0$

[1] From a fit including ten additional resonances and energy-independent Breit-Wigner width.

$\Gamma((K\overline{K})^\pm\pi^0)/\Gamma(\omega\pi)$ Γ_6/Γ_1

VALUE	CL%	DOCUMENT ID		TECN	CHG	COMMENT
<0.08	90	BALTAY	67	HBC	±	0.0 $\overline{p}p$

$\Gamma(K^0_S K^0_L \pi^\pm)/\Gamma(\omega\pi)$ Γ_7/Γ_1

VALUE	CL%	DOCUMENT ID		TECN	CHG	COMMENT
<0.06	90	BALTAY	67	HBC	±	0.0 $\overline{p}p$

$\Gamma(K^0_S K^0_S \pi^\pm)/\Gamma(\omega\pi)$ Γ_8/Γ_1

VALUE	CL%	DOCUMENT ID		TECN	CHG	COMMENT
<0.02	90	BALTAY	67	HBC	±	0.0 $\overline{p}p$

$\Gamma(\phi\pi)/\Gamma(\omega\pi)$ Γ_9/Γ_1

VALUE	CL%	DOCUMENT ID		TECN	CHG	COMMENT
<0.004	95	VIKTOROV	96	SPEC	0	32.5 $\pi^- p \to K^+ K^- \pi^0 n$
• • • We do not use the following data for averages, fits, limits, etc. • • •						
<0.04	95	BIZZARRI	69	HBC	±	0.0 $\overline{p}p$
<0.015		DAHL	67	HBC		1.6–4.2 $\pi^- p$

$b_1(1235)$ REFERENCES

ABLIKIM	10E	PL B693 88	M. Ablikim *et al.*	(BES II Collab.)
NOZAR	02	PL B541 35	M. Nozar *et al.*	
VIKTOROV	96	PAN 59 1184 Translated from YAF 59 1239.	V.A. Viktorov *et al.*	(SERP)
AMSLER	94C	PL B327 425	C. Amsler *et al.*	(Crystal Barrel Collab.)
AMSLER	93B	PL B311 362	C. Amsler *et al.*	(Crystal Barrel Collab.)
WEIDENAUER	93	ZPHY C59 387	P. Weidenauer *et al.*	(ASTERIX Collab.)
ALDE	92C	ZPHY C54 553	D.M. Alde *et al.*	(BELG, SERP, KEK, LANL+)
FUKUI	91	PL B257 241	S. Fukui *et al.*	(SUGI, NAGO, KEK, KYOT+)
AUGUSTIN	89	NP B320 1	J.E. Augustin, G. Cosme	(DM2 Collab.)
ATKINSON	84C	NP B243 1	M. Atkinson *et al.*	(BONN, CERN, GLAS+) JP
ATKINSON	84D	NP B242 269	M. Atkinson *et al.*	(BONN, CERN, GLAS+)
ATKINSON	84E	PL 138B 459	M. Atkinson *et al.*	(BONN, CERN, GLAS+)
COLLICK	84	PRL 53 2374	B. Collick *et al.*	(MINN, ROCH, FNAL)
EVANGELIS...	81	NP B178 197	C. Evangelista *et al.*	(BARI, BONN, CERN+)
BALTAY	78B	PR D17 62	C. Baltay *et al.*	(COLU, BING)
GESSAROLI	77	NP B126 382	R. Gessaroli *et al.*	(BGNA, FIRZ, GENO+) JP
FLATTE	76C	PL 64B 225	S.M. Flatte *et al.*	(CERN, AMST, NIJM+) JP
CHUNG	75B	PR D11 2426	S.U. Chung *et al.*	(BNL, LBL, UCSC) JP
CHALOUPKA	74	PL 51B 407	V. Chaloupka *et al.*	(CERN) JP
KARSHON	74B	PR D10 3608	U. Karshon *et al.*	(REHO) JP
BIZZARRI	69	NP B14 169	R. Bizzarri *et al.*	(CERN, CDEF)
BALTAY	67	PRL 18 93	C. Baltay *et al.*	(COLU)
DAHL	67	PR 163 1377	O.I. Dahl *et al.*	(LRL)
ABOLINS	63	PRL 11 381	M.A. Abolins *et al.*	(UCSD)

$a_1(1260)$

$I^G(J^{PC}) = 1^-(1^{++})$

See also our review under the $a_1(1260)$ in PDG 06, Journal of Physics (generic for all A,B,E,G) **G33** 1 (2006).

$a_1(1260)$ MASS

VALUE (MeV)	EVTS	DOCUMENT ID		TECN	COMMENT
1230±40 OUR ESTIMATE					
1255± $^{+7}_{-17}$	420k	ALEKSEEV	10	COMP	190 $\pi^- Pb \to \pi^-\pi^-\pi^+ Pb'$
• • • We do not use the following data for averages, fits, limits, etc. • • •					
1243±12±20		[1] AUBERT	07AU	BABR	10.6 $e^+e^- \to \rho^0\rho^\pm\pi^\mp\gamma$
1230–1270	6360	[2] LINK	07A	FOCS	$D^0 \to \pi^-\pi^+\pi^-\pi^+$
1203± 3		[3] GOMEZ-DUM..	04	RVUE	$\tau^+ \to \pi^+\pi^+\pi^-\nu_\tau$
1330±24	90k	SALVINI	04	OBLX	$\overline{p}p \to 2\pi^+2\pi^-$
1331±10± 3	37k	[4] ASNER	00	CLE2	10.6 $e^+e^- \to \tau^+\tau^-$, $\tau^- \to \pi^-\pi^0\pi^0\nu_\tau$
1255± 7± 6	5904	[5] ABREU	98G	DLPH	e^+e^-
1207± 5± 8	5904	[6] ABREU	98G	DLPH	e^+e^-
1196± 4± 5	5904	[7,8] ABREU	98G	DLPH	e^+e^-
1240±10		BARBERIS	98B		450 $pp \to p_f\pi^+\pi^-\pi^0 p_s$
1262± 9± 7		[5,9] ACKERSTAFF	97R	OPAL	E^{ee}_{cm}= 88–94, $\tau \to 3\pi\nu$
1210± 7± 2		[6,9] ACKERSTAFF	97R	OPAL	E^{ee}_{cm}= 88–94, $\tau \to 3\pi\nu$
1211± $^{+50}_{-0}$ 7		[6] ALBRECHT	93C	ARG	$\tau^+ \to \pi^+\pi^+\pi^-\nu$
1121± 8		[10] ANDO	92	SPEC	8 $\pi^- p \to \pi^+\pi^-\pi^0 n$
1242±37		[11] IVANOV	91	RVUE	$\tau \to \pi^+\pi^+\pi^-\nu$
1260±14		[12] IVANOV	91	RVUE	$\tau \to \pi^+\pi^+\pi^-\nu$
1250± 9		[13] IVANOV	91	RVUE	$\tau \to \pi^+\pi^+\pi^-\nu$
1208±15		ARMSTRONG	90	OMEG	300.0$pp \to pp\pi^+\pi^-\pi^0$
1220±15		[14] ISGUR	89	RVUE	$\tau^+ \to \pi^+\pi^+\pi^-\nu$
1260±25		[15] BOWLER	88	RVUE	
1166±18±11		BAND	87	MAC	$\tau^+ \to \pi^+\pi^+\pi^-\nu$
1164±41±23		BAND	87	MAC	$\tau^+ \to \pi^+\pi^0\pi^0\nu$
1250±40		[14] TORNQVIST	87	RVUE	
1046±11		ALBRECHT	86B	ARG	$\tau^+ \to \pi^+\pi^+\pi^-\nu$
1056±20±15		RUCKSTUHL	86	DLCO	$\tau^+ \to \pi^+\pi^+\pi^-\nu$
1194±14±10		SCHMIDKE	86	MRK2	$\tau^+ \to \pi^+\pi^+\pi^-\nu$
1255±23		BELLINI	85	SPEC	40 $\pi^- A \to \pi^-\pi^+\pi^- A$
1240±80		[16] DANKOWY...	81	SPEC	8.45 $\pi^- p \to n3\pi$
1280±30		[16] DAUM	81B	CNTR	63,94 $\pi^- p \to p3\pi$
1041±13		[17] GAVILLET	77	HBC	4.2 $K^- p \to \Sigma 3\pi$

[1] The $\rho^\pm\pi^\mp$ state can be also due to the $\pi(1300)$.
[2] Using the Breit-Wigner parameterization; strong correlation between mass and width.
[3] Using the data of BARATE 98R.
[4] From a fit to the 3π mass spectrum including the $K\overline{K}^*(892)$ threshold.
[5] Uses the model of KUHN 90.
[6] Uses the model of ISGUR 89.
[7] Includes the effect of a possible a_1' state.
[8] Uses the model of FEINDT 90.
[9] Supersedes AKERS 95P.
[10] Average and spread of values using 2 variants of the model of BOWLER 75.
[11] Reanalysis of RUCKSTUHL 86.
[12] Reanalysis of SCHMIDKE 86.

[13] Reanalysis of ALBRECHT 86B.
[14] From a combined reanalysis of ALBRECHT 86B, SCHMIDKE 86, and RUCKSTUHL 86.
[15] From a combined reanalysis of ALBRECHT 86B and DAUM 81B.
[16] Uses the model of BOWLER 75.
[17] Produced in K^- backward scattering.

$a_1(1260)$ WIDTH

VALUE (MeV)	EVTS	DOCUMENT ID		TECN	COMMENT
250 to 600 OUR ESTIMATE					
$367\pm 9^{+28}_{-25}$	420k	ALEKSEEV	10	COMP	190 $\pi^- Pb \to \pi^-\pi^-\pi^+ Pb'$
• • • We do not use the following data for averages, fits, limits, etc. • • •					
$410\pm 31\pm 30$		[18] AUBERT	07AU	BABR	10.6 $e^+e^- \to \rho^0\rho^\pm\pi^\mp\gamma$
520–680	6360	[19] LINK	07A	FOCS	$D^0 \to \pi^-\pi^+\pi^-\pi^+$
480 ± 20		[20] GOMEZ-DUM..	04	RVUE	$\tau^+ \to \pi^+\pi^+\pi^-\nu_\tau$
580 ± 41	90k	SALVINI	04	OBLX	$\overline{p}p \to 2\pi^+2\pi^-$
460 ± 85	205	[21] DRUTSKOY	02	BELL	$B \to D^{(*)}K^-K^{*0}$
$814\pm 36\pm 13$	37k	[22] ASNER	00	CLE2	10.6 $e^+e^- \to \tau^+\tau^-$, $\tau^- \to \pi^-\pi^0\pi^0\nu_\tau$
450 ± 50	22k	[23] AKHMETSHIN	99E	CMD2	1.05–1.38 $e^+e^- \to \pi^+\pi^-\pi^0\pi^0$
570 ± 10		[24] BONDAR	99	RVUE	$e^+e^- \to 4\pi$, $\tau \to 3\pi\nu_\tau$
$587\pm 27\pm 21$	5904	[25] ABREU	98G	DLPH	e^+e^-
$478\pm 3\pm 15$	5904	[26] ABREU	98G	DLPH	e^+e^-
$425\pm 14\pm 8$	5904	[27,28] ABREU	98G	DLPH	e^+e^-
400 ± 35		BARBERIS	98B		450 $pp \to p_f\pi^+\pi^-\pi^0 p_s$
$621\pm 32\pm 58$		[25,29] ACKERSTAFF	97R	OPAL	$E^{ee}_{\rm cm}$= 88–94, $\tau \to 3\pi\nu$
$457\pm 15\pm 17$		[26,29] ACKERSTAFF	97R	OPAL	$E^{ee}_{\rm cm}$= 88–94, $\tau \to 3\pi\nu$
$446\pm 21^{+140}_{-0}$		[26] ALBRECHT	93C	ARG	$\tau^+ \to \pi^+\pi^+\pi^-\nu$
239 ± 11		ANDO	92	SPEC	8 $\pi^- p \to \pi^+\pi^-\pi^0 n$
$266\pm 13\pm 4$		[30] ANDO	92	SPEC	8 $\pi^- p \to \pi^+\pi^-\pi^0 n$
465^{+228}_{-143}		[31] IVANOV	91	RVUE	$\tau \to \pi^+\pi^+\pi^-\nu$
298^{+40}_{-34}		[32] IVANOV	91	RVUE	$\tau \to \pi^+\pi^+\pi^-\nu$
488 ± 32		[33] IVANOV	91	RVUE	$\tau \to \pi^+\pi^+\pi^-\nu$
430 ± 50		ARMSTRONG	90	OMEG	300.0 $pp \to pp\pi^+\pi^-\pi^0$
420 ± 40		[34] ISGUR	89	RVUE	$\tau^+ \to \pi^+\pi^+\pi^-\nu$
396 ± 43		[35] BOWLER	88	RVUE	
$405\pm 75\pm 25$		BAND	87	MAC	$\tau^+ \to \pi^+\pi^+\pi^-\nu$
$419\pm 108\pm 57$		BAND	87	MAC	$\tau^+ \to \pi^+\pi^0\pi^0\nu$
521 ± 27		ALBRECHT	86B	ARG	$\tau^+ \to \pi^+\pi^+\pi^-\nu$
$476^{+132}_{-120}\pm 54$		RUCKSTUHL	86	DLCO	$\tau^+ \to \pi^+\pi^+\pi^-\nu$
$462\pm 56\pm 30$		SCHMIDKE	86	MRK2	$\tau^+ \to \pi^+\pi^+\pi^-\nu$
292 ± 40		BELLINI	85	SPEC	40 $\pi^- A \to \pi^-\pi^+\pi^- A$
380 ± 100		[36] DANKOWY...	81	SPEC	8.45 $\pi^- p \to n3\pi$
300 ± 50		[36] DAUM	81B	CNTR	63,94 $\pi^- p \to p3\pi$
230 ± 50		[37] GAVILLET	77	HBC	4.2 $K^- p \to \Sigma 3\pi$

[18] The $\rho^\pm\pi^\mp$ state can be also due to the $\pi(1300)$.
[19] Using the Breit-Wigner parameterization; strong correlation between mass and width.
[20] Using the data of BARATE 98R.
[21] From a fit of the K^-K^{*0} distribution assuming m_{a_1} = 1230 MeV and purely resonant production of the K^-K^{*0} system.
[22] From a fit to the 3π mass spectrum including the $K\overline{K}^*(892)$ threshold.
[23] Using the $a_1(1260)$ mass of 1230 MeV.
[24] From AKHMETSHIN 99E and ASNER 00 data using the $a_1(1260)$ mass of 1230 MeV.
[25] Uses the model of KUHN 90.
[26] Uses the model of ISGUR 89.
[27] Includes the effect of a possible a_1' state.
[28] Uses the model of FEINDT 90.
[29] Supersedes AKERS 95P.
[30] Average and spread of values using 2 variants of the model of BOWLER 75.
[31] Reanalysis of RUCKSTUHL 86.
[32] Reanalysis of SCHMIDKE 86.
[33] Reanalysis of ALBRECHT 86B.
[34] From a combined reanalysis of ALBRECHT 86B, SCHMIDKE 86, and RUCKSTUHL 86.
[35] From a combined reanalysis of ALBRECHT 86B and DAUM 81B.
[36] Uses the model of BOWLER 75.
[37] Produced in K^- backward scattering.

$a_1(1260)$ DECAY MODES

	Mode	Fraction (Γ_i/Γ)
Γ_1	$\pi^+\pi^-\pi^0$	
Γ_2	$\pi^0\pi^0\pi^0$	
Γ_3	$(\rho\pi)_{S-\text{wave}}$	seen
Γ_4	$(\rho\pi)_{D-\text{wave}}$	seen
Γ_5	$(\rho(1450)\pi)_{S-\text{wave}}$	seen
Γ_6	$(\rho(1450)\pi)_{D-\text{wave}}$	seen
Γ_7	$\sigma\pi$	seen
Γ_8	$f_0(980)\pi$	not seen
Γ_9	$f_0(1370)\pi$	seen
Γ_{10}	$f_2(1270)\pi$	seen
Γ_{11}	$K\overline{K}^*(892)+$ c.c.	seen
Γ_{12}	$\pi\gamma$	seen

$a_1(1260)$ PARTIAL WIDTHS

$\Gamma(\pi\gamma)$ Γ_{12}

VALUE (keV)	DOCUMENT ID		TECN	COMMENT
640 ± 246	ZIELINSKI	84C	SPEC	200 $\pi^+ Z \to Z3\pi$

D-wave/S-wave AMPLITUDE RATIO IN DECAY OF $a_1(1260) \to \rho\pi$

VALUE	DOCUMENT ID		TECN	COMMENT
-0.062 ± 0.020 OUR AVERAGE	Error includes scale factor of 2.3. See the ideogram below.			
$-0.043\pm 0.009\pm 0.005$	LINK	07A	FOCS	$D^0 \to \pi^-\pi^+\pi^-\pi^+$
$-0.14\ \pm 0.04\ \pm 0.07$	[38] CHUNG	02	B852	18.3 $\pi^- p \to \pi^+\pi^-\pi^- p$
$-0.10\ \pm 0.02\ \pm 0.02$	[39,40] ACKERSTAFF	97R	OPAL	$E^{ee}_{\rm cm}$= 88–94, $\tau \to 3\pi\nu$
$-0.11\ \pm 0.02$	[39] ALBRECHT	93C	ARG	$\tau^+ \to \pi^+\pi^+\pi^-\nu$

[38] Deck-type background not subtracted.
[39] Uses the model of ISGUR 89.
[40] Supersedes AKERS 95P.

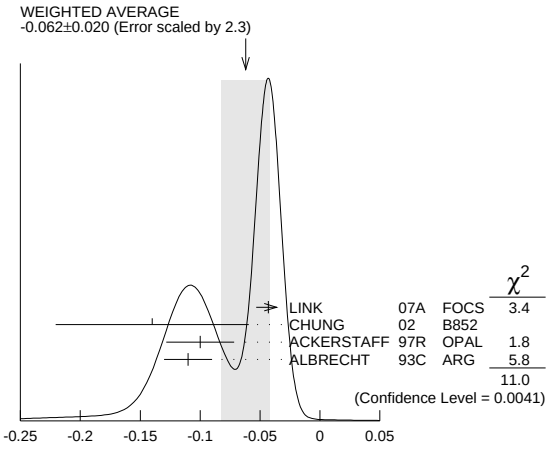

D-wave/S-wave AMPLITUDE RATIO IN DECAY OF $a_1(1260) \to \rho\pi$

$a_1(1260)$ BRANCHING RATIOS

$\Gamma((\rho\pi)_{S-\text{wave}})/\Gamma_{\text{total}}$ Γ_3/Γ

VALUE (units 10^{-2})	EVTS	DOCUMENT ID		TECN	COMMENT
• • • We do not use the following data for averages, fits, limits, etc. • • •					
60.19	37k	[41] ASNER	00	CLE2	10.6 $e^+e^- \to \tau^+\tau^-$, $\tau^- \to \pi^-\pi^0\pi^0\nu_\tau$

$\Gamma((\rho\pi)_{D-\text{wave}})/\Gamma_{\text{total}}$ Γ_4/Γ

VALUE (units 10^{-2})	EVTS	DOCUMENT ID		TECN	COMMENT
• • • We do not use the following data for averages, fits, limits, etc. • • •					
$1.30\pm 0.60\pm 0.22$	37k	[41] ASNER	00	CLE2	10.6 $e^+e^- \to \tau^+\tau^-$, $\tau^- \to \pi^-\pi^0\pi^0\nu_\tau$

$\Gamma((\rho(1450)\pi)_{S-\text{wave}})/\Gamma_{\text{total}}$ Γ_5/Γ

VALUE (units 10^{-2})	EVTS	DOCUMENT ID		TECN	COMMENT
• • • We do not use the following data for averages, fits, limits, etc. • • •					
$0.56\pm 0.84\pm 0.32$	37k	[41,42] ASNER	00	CLE2	10.6 $e^+e^- \to \tau^+\tau^-$, $\tau^- \to \pi^-\pi^0\pi^0\nu_\tau$

$\Gamma((\rho(1450)\pi)_{D-\text{wave}})/\Gamma_{\text{total}}$ Γ_6/Γ

VALUE (units 10^{-2})	EVTS	DOCUMENT ID		TECN	COMMENT
• • • We do not use the following data for averages, fits, limits, etc. • • •					
$2.04\pm 1.20\pm 0.28$	37k	[41,42] ASNER	00	CLE2	10.6 $e^+e^- \to \tau^+\tau^-$, $\tau^- \to \pi^-\pi^0\pi^0\nu_\tau$

$\Gamma(\sigma\pi)/\Gamma_{\text{total}}$ Γ_7/Γ

VALUE (units 10^{-2})	EVTS	DOCUMENT ID		TECN	COMMENT
• • • We do not use the following data for averages, fits, limits, etc. • • •					
seen		CHUNG	02	B852	18.3 $\pi^- p \to \pi^+\pi^-\pi^- p$
$18.76\pm 4.29\pm 1.48$	37k	[41,43] ASNER	00	CLE2	10.6 $e^+e^- \to \tau^+\tau^-$, $\tau^- \to \pi^-\pi^0\pi^0\nu_\tau$

$\Gamma(f_0(980)\pi)/\Gamma_{total}$ Γ_8/Γ

VALUE (units 10^{-2})	EVTS	DOCUMENT ID		TECN	COMMENT
• • • We do not use the following data for averages, fits, limits, etc. • • •					
not seen	37k	ASNER	00	CLE2	10.6 $e^+e^- \to \tau^+\tau^-$, $\tau^- \to \pi^-\pi^0\pi^0\nu_\tau$

$\Gamma(f_0(1370)\pi)/\Gamma_{total}$ Γ_9/Γ

VALUE (units 10^{-2})	EVTS	DOCUMENT ID		TECN	COMMENT
• • • We do not use the following data for averages, fits, limits, etc. • • •					
$7.40 \pm 2.71 \pm 1.26$	37k	[41,44] ASNER	00	CLE2	10.6 $e^+e^- \to \tau^+\tau^-$, $\tau^- \to \pi^-\pi^0\pi^0\nu_\tau$

$\Gamma(f_2(1270)\pi)/\Gamma_{total}$ Γ_{10}/Γ

VALUE (units 10^{-2})	EVTS	DOCUMENT ID		TECN	COMMENT
• • • We do not use the following data for averages, fits, limits, etc. • • •					
$1.19 \pm 0.49 \pm 0.17$	37k	[41,45] ASNER	00	CLE2	10.6 $e^+e^- \to \tau^+\tau^-$, $\tau^- \to \pi^-\pi^0\pi^0\nu_\tau$

$\Gamma(K\overline{K}^*(892)+\text{c.c.})/\Gamma_{total}$ Γ_{11}/Γ

VALUE (units 10^{-2})	EVTS	DOCUMENT ID		TECN	COMMENT
• • • We do not use the following data for averages, fits, limits, etc. • • •					
2.2 ± 0.5	2255	[46] COAN	04	CLEO	$\tau^- \to K^-\pi^-K^+\nu_\tau$
8 to 15	205	[47] DRUTSKOY	02	BELL	$B \to D^{(*)}K^-K^{*0}$
$3.3 \pm 0.5 \pm 0.1$	37k	[48] ASNER	00	CLE2	10.6 $e^+e^- \to \tau^+\tau^-$, $\tau^- \to \pi^-\pi^0\pi^0\nu_\tau$
2.6 ± 0.3		[49] BARATE	99R	ALEP	$\tau \to K\overline{K}\pi\nu_\tau$

$\Gamma(\sigma\pi)/\Gamma((\rho\pi)_{S-wave})$ Γ_7/Γ_3

VALUE	EVTS	DOCUMENT ID		TECN	COMMENT
• • • We do not use the following data for averages, fits, limits, etc. • • •					
0.06 ± 0.05	90k	SALVINI	04	OBLX	$\overline{p}p \to 2\pi^+2\pi^-$
~ 0.3	28k	AKHMETSHIN	99E	CMD2	1.05–1.38 $e^+e^- \to \pi^+\pi^-\pi^+\pi^-$
0.003 ± 0.003		[50] LONGACRE	82	RVUE	

$\Gamma(\pi^0\pi^0\pi^0)/\Gamma(\pi^+\pi^-\pi^0)$ Γ_2/Γ_1

VALUE	CL%	DOCUMENT ID		COMMENT
• • • We do not use the following data for averages, fits, limits, etc. • • •				
<0.008	90	[51] BARBERIS	01	450 $pp \to p_f 3\pi^0 p_s$

[41] From a fit to the Dalitz plot.
[42] Assuming for $\rho(1450)$ mass and width of 1370 and 386 MeV respectively.
[43] Assuming for σ mass and width of 860 and 880 MeV respectively.
[44] Assuming for $f_0(1370)$ mass and width of 1186 and 350 MeV respectively.
[45] Assuming for $f_2(1270)$ mass and width of 1275 and 185 MeV respectively.
[46] Using structure functions from KUHN 92 and DECKER 93A and $B(\tau^- \to K^-\pi^-K^+\nu_\tau) = (0.155 \pm 0.006 \pm 0.009)\%$ from BRIERE 03.
[47] From a comparison to ALAM 94 assuming purely resonant production of the K^-K^{*0} system.
[48] From a fit to the 3π mass spectrum including the $K\overline{K}^*(892)$ threshold.
[49] Assuming $a_1(1260)$ dominance and taking $B(\tau \to a_1(1260)\nu_\tau)$ from BUSKULIC 96.
[50] Uses multichannel Aitchison-Bowler model (BOWLER 75). Uses data from GAVILLET 77, DAUM 80, and DANKOWYCH 81.
[51] Inconsistent with observations of $\sigma\pi$, $f_0(1370)\pi$, and $f_2(1270)\pi$ decay modes.

$a_1(1260)$ REFERENCES

ALEKSEEV	10	PRL 104 241803	M.G. Alekseev *et al.*	(COMPASS Collab.)
AUBERT	07AU	PR D76 092005	B. Aubert *et al.*	(BABAR Collab.)
LINK	07A	PR D75 052003	J.M. Link *et al.*	(FNAL FOCUS Collab.)
PDG	06	JP G33 1	W.-M. Yao *et al.*	(PDG Collab.)
COAN	04	PRL 92 232001	T.E. Coan *et al.*	(CLEO Collab.)
GOMEZ-DUM...	04	PR D69 073002	D. Gomez Dumm, A. Pich, J. Portoles	
SALVINI	04	EPJ C35 21	P. Salvini *et al.*	(OBELIX Collab.)
BRIERE	03	PRL 90 181802	R. A. Briere *et al.*	(CLEO Collab.)
CHUNG	02	PR D65 072001	S.U. Chung *et al.*	(BNL E852 Collab.)
DRUTSKOY	02	PL B542 171	A. Drutskoy *et al.*	(BELLE Collab.)
BARBERIS	01	PL B507 14	D. Barberis *et al.*	
ASNER	00	PR D61 012002	D.M. Asner *et al.*	(CLEO Collab.)
AKHMETSHIN	99E	PL B466 392	R.R. Akhmetshin *et al.*	(Novosibirsk CMD-2 Collab.)
BARATE	99R	EPJ C11 599	R. Barate *et al.*	(ALEPH Collab.)
BONDAR	99	PL B466 403	A.E. Bondar *et al.*	(Novosibirsk CMD-2 Collab.)
ABREU	98G	PL B426 411	P. Abreu *et al.*	(DELPHI Collab.)
BARATE	98R	EPJ C4 409	R. Barate *et al.*	(ALEPH Collab.)
BARBERIS	98B	PL B422 399	D. Barberis *et al.*	(WA 102 Collab.)
ACKERSTAFF	97R	ZPHY C75 593	K. Ackerstaff *et al.*	(OPAL Collab.)
BUSKULIC	96	ZPHY C70 579	D. Buskulic *et al.*	(ALEPH Collab.)
AKERS	95P	ZPHY C67 45	R. Akers *et al.*	(OPAL Collab.)
ALAM	94	PR D50 43	M.S. Alam *et al.*	(CLEO Collab.)
ALBRECHT	93C	ZPHY C58 61	H. Albrecht *et al.*	(ARGUS Collab.)
DECKER	93A	ZPHY C58 445	R. Decker *et al.*	
ANDO	92	PL B291 496	A. Ando *et al.*	(KEK, KYOT, NIRS, SAGA+)
KUHN	92	ZPHY C56 661	J.H. Kuhn, E. Mirkes	
IVANOV	91	ZPHY C49 563	Y.P. Ivanov, A.A. Osipov, M.K. Volkov	(JINR)
ARMSTRONG	90	ZPHY C48 213	T.A. Armstrong, M. Benayoun, W. Beusch	(WA76 Coll.)
FEINDT	90	ZPHY C48 681	M. Feindt	(HAMB)
KUHN	90	ZPHY C48 445	J.H. Kuhn *et al.*	(MPIM)
ISGUR	89	PR D39 1357	N. Isgur, C. Morningstar, C. Reader	(TNTO)
BOWLER	88	PL B209 99	M.G. Bowler	(OXF)
BAND	87	PL B198 297	H.R. Band *et al.*	(MAC Collab.)
TORNQVIST	87	ZPHY C36 695	N.A. Tornqvist	(HELS)
ALBRECHT	86B	ZPHY C33 7	H. Albrecht *et al.*	(ARGUS Collab.)
RUCKSTUHL	86	PRL 56 2132	W. Ruckstuhl *et al.*	(DELCO Collab.)
SCHMIDKE	86	PRL 57 527	W.B. Schmidke *et al.*	(Mark II Collab.)
BELLINI	85	SJNP 41 781	D. Bellini *et al.*	
		Translated from YAF 41 1223.		
ZIELINSKI	84C	PRL 52 1195	M. Zielinski *et al.*	(ROCH, MINN, FNAL)
LONGACRE	82	PR D26 82	R.S. Longacre	(BNL)
DANKOWY...	81	PRL 46 580	J.A. Dankowych *et al.*	(TNTO, BNL, CARL+)
DAUM	81B	NP B182 269	C. Daum *et al.*	(AMST, CERN, CRAC, MPIM+)
DAUM	80	PL 89B 281	C. Daum *et al.*	(AMST, CERN, CRAC, MPIM+) JP
GAVILLET	77	PL 69B 119	P. Gavillet *et al.*	(AMST, CERN, NIJM+) JP
BOWLER	75	NP B97 227	M.G. Bowler *et al.*	(OXFTP, DARE)

$f_2(1270)$

$I^G(J^{PC}) = 0^+(2^{++})$

$f_2(1270)$ MASS

VALUE (MeV)	EVTS	DOCUMENT ID		TECN	COMMENT
1275.1± 1.2 OUR AVERAGE		Error includes scale factor of 1.1.			
$1262 \pm {}^{1}_{2} \pm 8$		ABLIKIM	06V	BES2	$e^+e^- \to J/\psi \to \gamma\pi^+\pi^-$
1275 ± 15		ABLIKIM	05	BES2	$J/\psi \to \phi\pi^+\pi^-$
1283 ± 5		ALDE	98	GAM4	100 $\pi^-p \to \pi^0\pi^0 n$
1278 ± 5		[1] BERTIN	97C	OBLX	0.0 $\overline{p}p \to \pi^+\pi^-\pi^0$
1272 ± 8	200k	PROKOSHKIN	94	GAM2	38 $\pi^-p \to \pi^0\pi^0 n$
1269.7 ± 5.2	5730	AUGUSTIN	89	DM2	$e^+e^- \to 5\pi$
1283 ± 8	400	[2] ALDE	87	GAM4	100 $\pi^-p \to 4\pi^0 n$
1274 ± 5		[2] AUGUSTIN	87	DM2	$J/\psi \to \gamma\pi^+\pi^-$
1283 ± 6		[3] LONGACRE	86	MPS	22 $\pi^-p \to n2K^0_S$
1276 ± 7		COURAU	84	DLCO	$e^+e^- \to e^+e^-\pi^+\pi^-$
1273.3 ± 2.3		[4] CHABAUD	83	ASPK	17 π^-p polarized
1280 ± 4		[5] CASON	82	STRC	8 $\pi^+p \to \Delta^{++}\pi^0\pi^0$
1281 ± 7	11600	GIDAL	81	MRK2	J/ψ decay
1282 ± 5		[6] CORDEN	79	OMEG	12–15 $\pi^-p \to n2\pi$
1269 ± 4	10k	APEL	75	NICE	40 $\pi^-p \to n2\pi^0$
1272 ± 4	4600	ENGLER	74	DBC	6 $\pi^+n \to \pi^+\pi^-p$
1277 ± 4	5300	FLATTE	71	HBC	7.0 π^+p
1273 ± 8		[2] STUNTEBECK	70	HBC	8 π^-p, 5.4 π^+d
1265 ± 8		BOESEBECK	68	HBC	8 π^+p
• • • We do not use the following data for averages, fits, limits, etc. • • •					
1270 ± 8		[7] ANISOVICH	09	RVUE	0.0 $\overline{p}p$, πN
1277 ± 6	870	[8] SCHEGELSKY	06A	RVUE	$\gamma\gamma \to K^0_S K^0_S$
1251 ± 10		TIKHOMIROV	03	SPEC	40.0 $\pi^-C \to K^0_S K^0_S K^0_L X$
1260 ± 10		[9] ALDE	97	GAM2	450 $pp \to pp\pi^0\pi^0$
1278 ± 6		[9] GRYGOREV	96	SPEC	40 $\pi^-N \to K^0_S K^0_S X$
1262 ± 11		AGUILAR-...	91	EHS	400 pp
1275 ± 10		AKER	91	CBAR	0.0 $\overline{p}p \to 3\pi^0$
1220 ± 10		BREAKSTONE	90	SFM	$pp \to pp\pi^+\pi^-$
1288 ± 12		ABACHI	86B	HRS	$e^+e^- \to \pi^+\pi^-X$
1284 ± 30	3k	BINON	83	GAM2	38 $\pi^-p \to n2\eta$
1280 ± 20	3k	APEL	82	CNTR	25 $\pi^-p \to n2\pi^0$
1284 ± 10	16000	DEUTSCH...	76	HBC	16 π^+p
1258 ± 10	600	TAKAHASHI	72	HBC	8 $\pi^-p \to n2\pi$
1275 ± 13		ARMENISE	70	HBC	9 $\pi^+n \to p\pi^+\pi^-$
1261 ± 5	1960	[2] ARMENISE	68	DBC	5.1 $\pi^+n \to p\pi^+$ MM$^-$
1270 ± 10	360	[2] ARMENISE	68	DBC	5.1 $\pi^+n \to p\pi^0$ MM
1268 ± 6		[10] JOHNSON	68	HBC	3.7–4.2 π^-p

[1] T-matrix pole.
[2] Mass errors enlarged by us to $\Gamma/\sqrt{N}$; see the note with the $K^*(892)$ mass.
[3] From a partial-wave analysis of data using a K-matrix formalism with 5 poles.
[4] From an energy-independent partial-wave analysis.
[5] From an amplitude analysis of the reaction $\pi^+\pi^- \to 2\pi^0$.
[6] From an amplitude analysis of $\pi^+\pi^- \to \pi^+\pi^-$ scattering data.
[7] 4-poles, 5-channel K matrix fit.
[8] From analysis of L3 data at 91 and 183–209 GeV.
[9] Systematic uncertainties not estimated.
[10] JOHNSON 68 includes BONDAR 63, LEE 64, DERADO 65, EISNER 67.

$f_2(1270)$ WIDTH

VALUE (MeV)	EVTS	DOCUMENT ID		TECN	COMMENT
$185.1^{+2.9}_{-2.4}$ OUR FIT		Error includes scale factor of 1.5.			
$184.2^{+4.0}_{-2.4}$ OUR AVERAGE		Error includes scale factor of 1.5. See the ideogram below.			
$175 \pm {}^{6}_{4} \pm 10$		ABLIKIM	06V	BES2	$e^+e^- \to J/\psi \to \gamma\pi^+\pi^-$
190 ± 20		ABLIKIM	05	BES2	$J/\psi \to \phi\pi^+\pi^-$
171 ± 10		ALDE	98	GAM4	100 $\pi^-p \to \pi^0\pi^0 n$
204 ± 20		[11] BERTIN	97C	OBLX	0.0 $\overline{p}p \to \pi^+\pi^-\pi^0$
192 ± 5	200k	PROKOSHKIN	94	GAM2	38 $\pi^-p \to \pi^0\pi^0 n$
180 ± 24		AGUILAR-...	91	EHS	400 pp
169 ± 9	5730	[12] AUGUSTIN	89	DM2	$e^+e^- \to 5\pi$
150 ± 30	400	[12] ALDE	87	GAM4	100 $\pi^-p \to 4\pi^0 n$
$186 \pm {}^{9}_{2}$		[13] LONGACRE	86	MPS	22 $\pi^-p \to n2K^0_S$
$179.2 \pm {}^{6.9}_{6.6}$		[14] CHABAUD	83	ASPK	17 π^-p polarized
160 ± 11		DENNEY	83	LASS	10 π^+N

Meson Particle Listings

$f_2(1270)$

196	±10	3k	APEL	82	CNTR	25 $\pi^- p \to n2\pi^0$
152	± 9		[15] CASON	82	STRC	8 $\pi^+ p \to \Delta^{++}\pi^0\pi^0$
186	±27	11600	GIDAL	81	MRK2	J/ψ decay
216	±13		[16] CORDEN	79	OMEG	12–15 $\pi^- p \to n2\pi$
190	±10	10k	APEL	75	NICE	40 $\pi^- p \to n2\pi^0$
192	±16	4600	ENGLER	74	DBC	6 $\pi^+ n \to \pi^+\pi^- p$
183	±15	5300	FLATTE	71	HBC	7 $\pi^+ p \to \Delta^{++} f_2$
196	±30		[12] STUNTEBECK	70	HBC	8 $\pi^- p$, 5.4 $\pi^+ d$
216	±20	1960	[12] ARMENISE	68	DBC	5.1 $\pi^+ n \to p\pi^+$ MM$^-$
128	±27		[12] BOESEBECK	68	HBC	8 $\pi^+ p$
176	±21		[12,17] JOHNSON	68	HBC	3.7–4.2 $\pi^- p$

• • • We do not use the following data for averages, fits, limits, etc. • • •

194	±36		[18] ANISOVICH	09	RVUE	0.0 $\overline{p}p$, πN
195	±15	870	[19] SCHEGELSKY	06A	RVUE	$\gamma\gamma \to K^0_S K^0_S$
121	±26		TIKHOMIROV	03	SPEC	40.0 π^- C $\to K^0_S K^0_S K^0_L$ X
187	±20		[20] ALDE	97	GAM2	450 $pp \to pp\pi^0\pi^0$
184	±10		[20] GRYGOREV	96	SPEC	40 $\pi^- N \to K^0_S K^0_S$ X
200	±10		AKER	91	CBAR	0.0 $\overline{p}p \to 3\pi^0$
240	±40	3k	BINON	83	GAM2	38 $\pi^- p \to n2\eta$
187	±30	650	[12] ANTIPOV	77	CIBS	25 $\pi^- p \to p3\pi$
225	±38	16000	DEUTSCH...	76	HBC	16 $\pi^+ p$
166	±28	600	[12] TAKAHASHI	72	HBC	8 $\pi^- p \to n2\pi$
173	±53		[12] ARMENISE	70	HBC	9 $\pi^+ n \to p\pi^+\pi^-$

[11] T-matrix pole.
[12] Width errors enlarged by us to $4\Gamma/\sqrt{N}$; see the note with the $K^*(892)$ mass.
[13] From a partial-wave analysis of data using a K-matrix formalism with 5 poles.
[14] From an energy-independent partial-wave analysis.
[15] From an amplitude analysis of the reaction $\pi^+\pi^- \to 2\pi^0$.
[16] From an amplitude analysis of $\pi^+\pi^- \to \pi^+\pi^-$ scattering data.
[17] JOHNSON 68 includes BONDAR 63, LEE 64, DERADO 65, EISNER 67.
[18] 4-poles, 5-channel K matrix fit.
[19] From analysis of L3 data at 91 and 183–209 GeV.
[20] Systematic uncertainties not estimated.

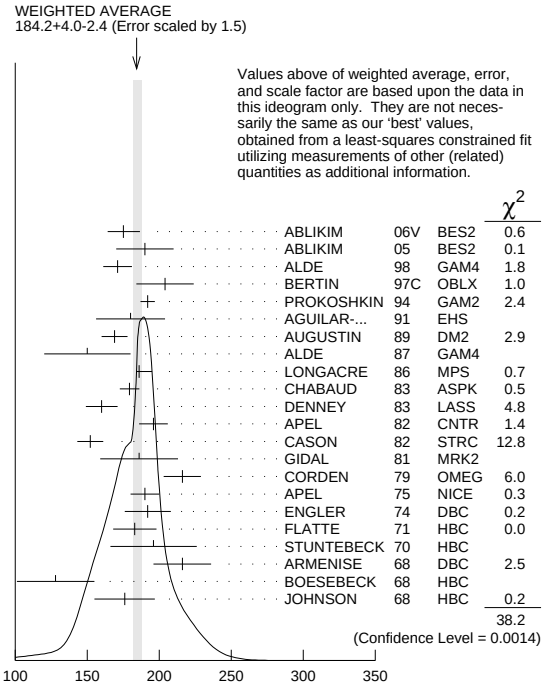

$f_2(1270)$ width (MeV)

$f_2(1270)$ DECAY MODES

	Mode	Fraction (Γ_i/Γ)	Scale factor / Confidence level
Γ_1	$\pi\pi$	(84.8 $^{+2.4}_{-1.2}$) %	S=1.2
Γ_2	$\pi^+\pi^- 2\pi^0$	(7.1 $^{+1.4}_{-2.7}$) %	S=1.3
Γ_3	$K\overline{K}$	(4.6 ±0.4) %	S=2.8
Γ_4	$2\pi^+ 2\pi^-$	(2.8 ±0.4) %	S=1.2
Γ_5	$\eta\eta$	(4.0 ±0.8) $\times 10^{-3}$	S=2.1
Γ_6	$4\pi^0$	(3.0 ±1.0) $\times 10^{-3}$	
Γ_7	$\gamma\gamma$	(1.64±0.19) $\times 10^{-5}$	S=1.9
Γ_8	$\eta\pi\pi$	< 8 $\times 10^{-3}$	CL=95%
Γ_9	$K^0 K^- \pi^+$ + c.c.	< 3.4 $\times 10^{-3}$	CL=95%
Γ_{10}	$e^+ e^-$	< 6 $\times 10^{-10}$	CL=90%

CONSTRAINED FIT INFORMATION

An overall fit to the total width, 4 partial widths, a combination of partial widths obtained from integrated cross sections, and 6 branching ratios uses 44 measurements and one constraint to determine 8 parameters. The overall fit has a $\chi^2 = 81.8$ for 37 degrees of freedom.

The following *off-diagonal* array elements are the correlation coefficients $\langle \delta p_i \delta p_j \rangle / (\delta p_i \cdot \delta p_j)$, in percent, from the fit to parameters p_i, including the branching fractions, $x_i \equiv \Gamma_i/\Gamma_{\text{total}}$. The fit constrains the x_i whose labels appear in this array to sum to one.

	x_1	x_2	x_3	x_4	x_5	x_6	x_7
x_2	−91						
x_3	11	−39					
x_4	10	−37	1				
x_5	1	−6	0	0			
x_6	0	−7	0	0	0		
x_7	8	−5	−6	1	0	0	
Γ	−78	71	−11	−8	−1	0	−11

	Mode	Rate (MeV)	Scale factor
Γ_1	$\pi\pi$	156.9 $^{+4.0}_{-1.2}$	
Γ_2	$\pi^+\pi^- 2\pi^0$	13.2 $^{+2.8}_{-5.0}$	1.3
Γ_3	$K\overline{K}$	8.5 ±0.8	2.9
Γ_4	$2\pi^+ 2\pi^-$	5.2 ±0.7	1.2
Γ_5	$\eta\eta$	0.74 ±0.14	2.1
Γ_6	$4\pi^0$	0.55 ±0.18	
Γ_7	$\gamma\gamma$	0.00303±0.00035	1.9

$f_2(1270)$ PARTIAL WIDTHS

$\Gamma(\pi\pi)$ Γ_1

VALUE (MeV)	EVTS	DOCUMENT ID		TECN	COMMENT
156.9 $^{+4.0}_{-1.2}$ OUR FIT					
157.0 $^{+6.0}_{-1.0}$		[21] LONGACRE	86	MPS	22 $\pi^- p \to n2K^0_S$
• • • We do not use the following data for averages, fits, limits, etc. • • •					
152 ±8	870	[22] SCHEGELSKY	06A	RVUE	$\gamma\gamma \to K^0_S K^0_S$

$\Gamma(K\overline{K})$ Γ_3

VALUE (MeV)	EVTS	DOCUMENT ID		TECN	COMMENT
8.5±0.8 OUR FIT Error includes scale factor of 2.9.					
9.0 $^{+0.7}_{-0.3}$		[21] LONGACRE	86	MPS	22 $\pi^- p \to n2K^0_S$
• • • We do not use the following data for averages, fits, limits, etc. • • •					
7.5±2.0	870	[22] SCHEGELSKY	06A	RVUE	$\gamma\gamma \to K^0_S K^0_S$

$\Gamma(\eta\eta)$ Γ_5

VALUE (MeV)	EVTS	DOCUMENT ID		TECN	COMMENT
0.74±0.14 OUR FIT Error includes scale factor of 2.1.					
1.0 ±0.1		[21] LONGACRE	86	MPS	22 $\pi^- p \to n2K^0_S$
• • • We do not use the following data for averages, fits, limits, etc. • • •					
1.8 ±0.4	870	[22] SCHEGELSKY	06A	RVUE	$\gamma\gamma \to K^0_S K^0_S$

$\Gamma(\gamma\gamma)$ Γ_7

The value of this width depends on the theoretical model used. Unitary approaches with scalars typically (with exception of PENNINGTON 08) give values clustering around 2.6 keV; without an S-wave contribution, values are systematically higher (typically around 3 keV).

VALUE (keV)	EVTS	DOCUMENT ID		TECN	COMMENT
3.03±0.35 OUR FIT Error includes scale factor of 1.9.					
3.14±0.20		[23,24] PENNINGTON	08	RVUE	Compilation
• • • We do not use the following data for averages, fits, limits, etc. • • •					
3.82±0.30		[24,25] PENNINGTON	08	RVUE	Compilation
2.55±0.15	870	[22] SCHEGELSKY	06A	RVUE	$\gamma\gamma \to K^0_S K^0_S$
2.84±0.35		BOGLIONE	99	RVUE	$\gamma\gamma \to \pi^+\pi^-, \pi^0\pi^0$
2.93±0.23±0.32		[26] YABUKI	95	VNS	
2.58±0.13 $^{+0.36}_{-0.27}$		[27] BEHREND	92	CELL	$e^+e^- \to e^+e^-\pi^+\pi^-$
3.10±0.35±0.35		[28] BLINOV	92	MD1	$e^+e^- \to e^+e^-\pi^+\pi^-$
2.27±0.47±0.11		ADACHI	90D	TOPZ	$e^+e^- \to e^+e^-\pi^+\pi^-$

$3.15 \pm 0.04 \pm 0.39$		BOYER	90	MRK2	$e^+e^- \to e^+e^-\pi^+\pi^-$	
$3.19 \pm 0.16^{+0.29}_{-0.28}$		MARSISKE	90	CBAL	$e^+e^- \to e^+e^-\pi^0\pi^0$	
2.35 ± 0.65		[29] MORGAN	90	RVUE	$\gamma\gamma \to \pi^+\pi^-,\ \pi^0\pi^0$	
$3.19 \pm 0.09^{+0.22}_{-0.38}$	2177	OEST	90	JADE	$e^+e^- \to e^+e^-\pi^0\pi^0$	
$3.2 \pm 0.1 \pm 0.4$		[30] AIHARA	86B	TPC	$e^+e^- \to e^+e^-\pi^+\pi^-$	
$2.5 \pm 0.1 \pm 0.5$		BEHREND	84B	CELL	$e^+e^- \to e^+e^-\pi^+\pi^-$	
$2.85 \pm 0.25 \pm 0.5$		[31] BERGER	84	PLUT	$e^+e^- \to e^+e^-2\pi$	
$2.70 \pm 0.05 \pm 0.20$		COURAU	84	DLCO	$e^+e^- \to e^+e^-\pi^+\pi^-$	
$2.52 \pm 0.13 \pm 0.38$		[32] SMITH	84C	MRK2	$e^+e^- \to e^+e^-\pi^+\pi^-$	
$2.7 \pm 0.2 \pm 0.6$		EDWARDS	82F	CBAL	$e^+e^- \to e^+e^-2\pi^0$	
$2.9^{+0.6}_{-0.4} \pm 0.6$		[33] EDWARDS	82F	CBAL	$e^+e^- \to e^+e^-2\pi^0$	
$3.2 \pm 0.2 \pm 0.6$		BRANDELIK	81B	TASS	$e^+e^- \to e^+e^-\pi^+\pi^-$	
$3.6 \pm 0.3 \pm 0.5$		ROUSSARIE	81	MRK2	$e^+e^- \to e^+e^-\pi^+\pi^-$	
2.3 ± 0.8		[34] BERGER	80B	PLUT	e^+e^-	

$\Gamma(e^+e^-)$ Γ_{10}

VALUE (eV)	CL%	DOCUMENT ID		TECN	COMMENT
<0.11	90	ACHASOV	00K	SND	$e^+e^- \to \pi^0\pi^0$
• • • We do not use the following data for averages, fits, limits, etc. • • •					
<1.7	90	VOROBYEV	88	ND	$e^+e^- \to \pi^0\pi^0$

[21] From a partial-wave analysis of data using a K-matrix formalism with 5 poles.
[22] From analysis of L3 data at 91 and 183–209 GeV and using SU(3) relations.
[23] Solution A (preferred solution based on χ^2-analysis).
[24] Dispersion theory based amplitude analysis of BOYER 90, MARSISKE 90, BEHREND 92, and MORI 07.
[25] Solution B (worse than solution A; still acceptable when systematic uncertainties are included).
[26] With a narrow scalar state around 1220 MeV.
[27] Using a unitarized model with a 300 - 500 keV wide scalar at 1100 MeV.
[28] Using the unitarized model of LYTH 85.
[29] Error includes spread of different solutions. Data of MARK2 and CRYSTAL BALL used in the analysis. Authors report strong correlations with $\gamma\gamma$ width of $f_0(1370)$: $\Gamma(f_2) + 1/4\ \Gamma(f^0) = 3.6 \pm 0.3$ KeV.
[30] Radiative corrections modify the partial widths; for instance the COURAU 84 value becomes 2.66 ± 0.21 in the calculation of LANDRO 86.
[31] Using the MENNESSIER 83 model.
[32] Superseded by BOYER 90.
[33] If helicity = 2 assumption is not made.
[34] Using mass, width and B($f_2(1270) \to 2\pi$) from PDG 78.

$f_2(1270)$ Γ(i)$\Gamma(\gamma\gamma)/\Gamma$(total)

$\Gamma(K\overline{K}) \times \Gamma(\gamma\gamma)/\Gamma_{\text{total}}$ $\Gamma_3\Gamma_7/\Gamma$

VALUE (keV)	DOCUMENT ID		TECN	COMMENT
0.139±0.019 OUR FIT Error includes scale factor of 1.9.				
0.091±0.007±0.027	[35] ALBRECHT	90G	ARG	$e^+e^- \to e^+e^-K^+K^-$
• • • We do not use the following data for averages, fits, limits, etc. • • •				
$0.104 \pm 0.007 \pm 0.072$	[36] ALBRECHT	90G	ARG	$e^+e^- \to e^+e^-K^+K^-$

[35] Using an incoherent background.
[36] Using a coherent background.

$\Gamma(\eta\eta) \times \Gamma(\gamma\gamma)/\Gamma_{\text{total}}$ $\Gamma_5\Gamma_7/\Gamma$

VALUE (eV)	DOCUMENT ID		TECN	COMMENT
$\mathbf{11.5^{+1.8+4.5}_{-2.0-3.7}}$	[37] UEHARA	10A	BELL	$10.6\ e^+e^- \to e^+e^-\eta\eta$

[37] Including interference with the $f_2'(1525)$ (parameters fixed to the values from the 2008 edition of this review, PDG 08) and $f_0(Y)$.

Helicity-0/Helicity-2 RATIO IN $\gamma\gamma \to f_2(1270) \to \pi\pi$

VALUE (units 10^{-2})	DOCUMENT ID		TECN	COMMENT
$\mathbf{3.7 \pm 0.3^{+15.9}_{-2.9}}$	UEHARA	08A	BELL	$10.6\ e^+e^- \to e^+e^-\pi^0\pi^0$
• • • We do not use the following data for averages, fits, limits, etc. • • •				
13	[38,39] PENNINGTON	08	RVUE	Compilation
26	[39,40] PENNINGTON	08	RVUE	Compilation

[38] Solution A (preferred solution based on χ^2-analysis).
[39] Dispersion theory based amplitude analysis of BOYER 90, MARSISKE 90, BEHREND 92, and MORI 07.
[40] Solution B (worse than solution A; still acceptable when systematic uncertainties are included).

$f_2(1270)$ BRANCHING RATIOS

$\Gamma(\pi\pi)/\Gamma_{\text{total}}$ Γ_1/Γ

VALUE	EVTS	DOCUMENT ID		TECN	COMMENT
0.848$^{+0.024}_{-0.012}$ OUR FIT Error includes scale factor of 1.2.					
0.837±0.020 OUR AVERAGE					
0.849 ± 0.025		CHABAUD	83	ASPK	17 π^-p polarized
0.85 ± 0.05	250	BEAUPRE	71	HBC	$8\ \pi^+p \to \Delta^{++}f_2$
0.8 ± 0.04	600	OH	70	HBC	$1.26\ \pi^-p \to \pi^+\pi^-n$

$\Gamma(\pi^+\pi^-2\pi^0)/\Gamma(\pi\pi)$ Γ_2/Γ_1

Should be twice $\Gamma(2\pi^+2\pi^-)/\Gamma(\pi\pi)$ if decay is $\rho\rho$. (See ASCOLI 68D.)

VALUE	EVTS	DOCUMENT ID		TECN	COMMENT
0.084$^{+0.018}_{-0.033}$ OUR FIT Error includes scale factor of 1.3.					
0.15 ±0.06	600	EISENBERG	74	HBC	$4.9\ \pi^+p \to \Delta^{++}f_2$
• • • We do not use the following data for averages, fits, limits, etc. • • •					
0.07		EMMS	75D	DBC	$4\ \pi^+n \to pf_2$

$\Gamma(K\overline{K})/\Gamma(\pi\pi)$ Γ_3/Γ_1

We average only experiments which either take into account $f_2(1270)$-$a_2(1320)$ interference explicitly or demonstrate that $a_2(1320)$ production is negligible.

VALUE	EVTS	DOCUMENT ID		TECN	COMMENT
0.054$^{+0.005}_{-0.006}$ OUR FIT Error includes scale factor of 2.8.					
0.041$^{+0.004}_{-0.005}$ OUR AVERAGE					
0.045 ± 0.01		[41] BARGIOTTI	03	OBLX	$\bar{p}p$
$0.037^{+0.008}_{-0.021}$		ETKIN	82B	MPS	$23\ \pi^-p \to n2K^0_S$
0.045 ± 0.009		CHABAUD	81	ASPK	17 π^-p polarized
0.039 ± 0.008		LOVERRE	80	HBC	$4\ \pi^-p \to K\overline{K}N$
• • • We do not use the following data for averages, fits, limits, etc. • • •					
0.052 ± 0.025		ABLIKIM	04E	BES2	$J/\psi \to \omega K^+K^-$
0.036 ± 0.005		[42] COSTA...	80	OMEG	$1\text{–}2.2\ \pi^-p \to K^+K^-n$
0.030 ± 0.005		[43] MARTIN	79	RVUE	
0.027 ± 0.009		[44] POLYCHRO...	79	STRC	$7\ \pi^-p \to n2K^0_S$
0.025 ± 0.015		EMMS	75D	DBC	$4\ \pi^+n \to pf_2$
0.031 ± 0.012	20	ADERHOLZ	69	HBC	$8\ \pi^+p \to K^+K^-\pi^+p$

$\Gamma(2\pi^+2\pi^-)/\Gamma(\pi\pi)$ Γ_4/Γ_1

VALUE	EVTS	DOCUMENT ID		TECN	COMMENT
0.033±0.005 OUR FIT Error includes scale factor of 1.2.					
0.033±0.004 OUR AVERAGE Error includes scale factor of 1.1.					
0.024 ± 0.006	160	EMMS	75D	DBC	$4\ \pi^+n \to pf_2$
0.051 ± 0.025	70	EISENBERG	74	HBC	$4.9\ \pi^+p \to \Delta^{++}f_2$
$0.043^{+0.007}_{-0.011}$	285	LOUIE	74	HBC	$3.9\ \pi^-p \to nf_2$
0.037 ± 0.007	154	ANDERSON	73	DBC	$6\ \pi^+n \to pf_2$
0.047 ± 0.013		OH	70	HBC	$1.26\ \pi^-p \to \pi^+\pi^-n$

$\Gamma(\eta\eta)/\Gamma_{\text{total}}$ Γ_5/Γ

VALUE (units 10^{-3})	DOCUMENT ID		TECN	COMMENT
4.0±0.8 OUR FIT Error includes scale factor of 2.1.				
2.9±0.5 OUR AVERAGE				
2.7 ± 0.7	BINON	05	GAMS	$33\ \pi^-p \to \eta\eta n$
2.8 ± 0.7	ALDE	86D	GAM4	$100\ \pi^-p \to 2\eta n$
5.2 ± 1.7	BINON	83	GAM2	$38\ \pi^-p \to 2\eta n$

$\Gamma(\eta\eta)/\Gamma(\pi\pi)$ Γ_5/Γ_1

VALUE	CL%	DOCUMENT ID		TECN	COMMENT
0.003±0.001		BARBERIS	00E		$450\ pp \to p_f\eta\eta p_s$
• • • We do not use the following data for averages, fits, limits, etc. • • •					
<0.05	95	EDWARDS	82F	CBAL	$e^+e^- \to e^+e^-2\eta$
<0.016	95	EMMS	75D	DBC	$4\ \pi^+n \to pf_2$
<0.09	95	EISENBERG	74	HBC	$4.9\ \pi^+p \to \Delta^{++}f_2$

$\Gamma(4\pi^0)/\Gamma_{\text{total}}$ Γ_6/Γ

VALUE	EVTS	DOCUMENT ID		TECN	COMMENT
0.0030±0.0010 OUR FIT					
0.003 ±0.001	400 ± 50	ALDE	87	GAM4	$100\ \pi^-p \to 4\pi^0 n$

$\Gamma(\gamma\gamma)/\Gamma_{\text{total}}$ Γ_7/Γ

VALUE (units 10^{-5})	DOCUMENT ID		TECN	COMMENT
• • • We do not use the following data for averages, fits, limits, etc. • • •				
$1.57 \pm 0.01^{+1.39}_{-0.14}$	UEHARA	08A	BELL	$10.6\ e^+e^- \to e^+e^-\pi^0\pi^0$

$\Gamma(\eta\pi\pi)/\Gamma(\pi\pi)$ Γ_8/Γ_1

VALUE	CL%	DOCUMENT ID		TECN	COMMENT
<0.010	95	EMMS	75D	DBC	$4\ \pi^+n \to pf_2$

$\Gamma(K^0K^-\pi^+ + \text{c.c.})/\Gamma(\pi\pi)$ Γ_9/Γ_1

VALUE	CL%	DOCUMENT ID		TECN	COMMENT
<0.004	95	EMMS	75D	DBC	$4\ \pi^+n \to pf_2$

$\Gamma(e^+e^-)/\Gamma_{\text{total}}$ Γ_{10}/Γ

VALUE (units 10^{-10})	CL%	DOCUMENT ID		TECN	COMMENT
<6	90	ACHASOV	00K	SND	$e^+e^- \to \pi^0\pi^0$

[41] Coupled channel analysis of $\pi^+\pi^-\pi^0$, $K^+K^-\pi^0$, and $K^\pm K^0_S\pi^\mp$.
[42] Re-evaluated by CHABAUD 83.
[43] Includes PAWLICKI 77 data.
[44] Takes into account the $f_2(1270)$-$f_2'(1525)$ interference.

Meson Particle Listings

$f_2(1270)$, $f_1(1285)$

$f_2(1270)$ REFERENCES

UEHARA	10A	PR D82 114031	S. Uehara *et al.*	(BELLE Collab.)
ANISOVICH	09	IJMP A24 2481	V.V. Anisovich, A.V. Sarantsev	
PDG	08	PL B667 1	C. Amsler *et al.*	(PDG Collab.)
PENNINGTON	08	EPJ C56 1	M.R. Pennington *et al.*	
UEHARA	08A	PR D78 052004	S. Uehara *et al.*	(BELLE Collab.)
MORI	07	PR D75 051101	T. Mori *et al.*	(BELLE Collab.)
ABLIKIM	06V	PL B642 441	M. Ablikim *et al.*	(BES Collab.)
SCHEGELSKY	06A	EPJ A27 207	V.A. Schegelsky *et al.*	
ABLIKIM	05	PL B607 243	M. Ablikim *et al.*	(BES Collab.)
BINON	05	PAN 68 960	F. Binon *et al.*	
		Translated from YAF 68 998.		
ABLIKIM	04E	PL B603 138	M. Ablikim *et al.*	(BES Collab.)
BARGIOTTI	03	EPJ C26 371	M. Bargiotti *et al.*	(OBELIX Collab.)
TIKHOMIROV	03	PAN 66 828	G.D. Tikhomirov *et al.*	
		Translated from YAF 66 860.		
ACHASOV	00K	PL B492 8	M.N. Achasov *et al.*	(Novosibirsk SND Collab.)
BARBERIS	00E	PL B479 59	D. Barberis *et al.*	(WA 102 Collab.)
BOGLIONE	99	EPJ C9 11	M. Boglione, M.R. Pennington	
ALDE	98	EPJ A3 361	D. Alde *et al.*	(GAM4 Collab.)
Also		PAN 62 405	D. Alde *et al.*	(GAMS Collab.)
		Translated from YAF 62 446.		
ALDE	97	PL B397 350	D.M. Alde *et al.*	(GAMS Collab.)
BERTIN	97C	PL B408 476	A. Bertin *et al.*	(OBELIX Collab.)
GRYGOREV	96	PAN 59 2105	V.K. Grigoriev, O.N. Baloshin, B.P. Barkov	(ITEP)
		Translated from YAF 59 2187.		
YABUKI	95	JPSJ 64 435	F. Yabuki *et al.*	(VENUS Collab.)
PROKOSHKIN	94	SPD 39 420	Y.D. Prokoshkin, A.A. Kondashov	(SERP)
		Translated from DANS 336 613.		
BEHREND	92	ZPHY C56 381	H.J. Behrend	(CELLO Collab.)
BLINOV	92	ZPHY C53 33	A.E. Blinov *et al.*	(NOVO)
AGUILAR-...	91	ZPHY C50 405	M. Aguilar-Benitez *et al.*	(LEBC-EHS Collab.)
AKER	91	PL B260 249	E. Aker *et al.*	(Crystal Barrel Collab.)
ADACHI	90D	PL B234 185	I. Adachi *et al.*	(TOPAZ Collab.)
ALBRECHT	90G	ZPHY C48 183	H. Albrecht *et al.*	(ARGUS Collab.)
BOYER	90	PR D42 1350	J. Boyer *et al.*	(Mark II Collab.)
BREAKSTONE	90	ZPHY C48 569	A.M. Breakstone *et al.*	(ISU, BGNA, CERN+)
MARSISKE	90	PR D41 3324	H. Marsiske *et al.*	(Crystal Ball Collab.)
MORGAN	90	ZPHY C48 623	D. Morgan, M.R. Pennington	(RAL, DURH)
OEST	90	ZPHY C47 343	T. Oest *et al.*	(JADE Collab.)
AUGUSTIN	89	NP B320 1	J.E. Augustin, G. Cosme	(DM2 Collab.)
VOROBYEV	88	SJNP 48 273	P.V. Vorobiev *et al.*	(NOVO)
		Translated from YAF 48 436.		
ALDE	87	PL B198 286	D.M. Alde *et al.*	(LANL, BRUX, SERP, LAPP)
AUGUSTIN	87	ZPHY C36 369	J.E. Augustin *et al.*	(LALO, CLER, FRAS+)
ABACHI	86B	PRL 57 1990	S. Abachi *et al.*	(PURD, ANL, IND, MICH+)
AIHARA	86B	PRL 57 404	H. Aihara *et al.*	(TPC-2γ Collab.)
ALDE	86D	NP B269 485	D.M. Alde *et al.*	(BELG, LAPP, SERP, CERN+)
LANDRO	86	PL B172 445	M. Landro, K.J. Mork, H.A. Olsen	(UTRO)
LONGACRE	86	PL B177 223	R.S. Longacre *et al.*	(BNL, BRAN, CUNY+)
LYTH	85	JP G11 459	D.H. Lyth	
BEHREND	84B	ZPHY C23 223	H.J. Behrend *et al.*	(CELLO Collab.)
BERGER	84	ZPHY C26 199	C. Berger *et al.*	(PLUTO Collab.)
COURAU	84	PL 147B 227	A. Courau *et al.*	(CIT, SLAC)
SMITH	84C	PR D30 851	J.R. Smith *et al.*	(SLAC, LBL, HARV)
BINON	83	NC 78A 313	F.G. Binon *et al.*	(BELG, LAPP, SERP+)
Also		SJNP 38 561	F.G. Binon *et al.*	(BELG, LAPP, SERP+)
		Translated from YAF 38 934.		
CHABAUD	83	NP B223 1	V. Chabaud *et al.*	(CERN, CRAC, MPIM)
DENNEY	83	PR D28 2726	D.L. Denney *et al.*	(IOWA, MICH)
MENNESSIER	83	ZPHY C16 241	G. Mennessier	(MONP)
APEL	82	NP B201 197	W.D. Apel *et al.*	(KARLK, KARLE, PISA, SERP+)
CASON	82	PRL 48 1316	N.M. Cason *et al.*	(NDAM, ANL)
EDWARDS	82F	PL 110B 82	C. Edwards *et al.*	(CIT, HARV, PRIN+)
ETKIN	82B	PR D25 1786	A. Etkin *et al.*	(BNL, CUNY, TUFTS, VAND)
BRANDELIK	81B	ZPHY C10 117	R. Brandelik *et al.*	(TASSO Collab.)
CHABAUD	81	APP B12 575	V. Chabaud *et al.*	(CERN, CRAC, MPIM)
GIDAL	81	PL 107B 153	G. Gidal *et al.*	(SLAC, LBL)
ROUSSARIE	81	PL 105B 304	A. Roussarie *et al.*	(SLAC, LBL)
BERGER	80B	PL 94B 254	C. Berger *et al.*	(PLUTO Collab.)
COSTA...	80	NP B175 402	G. Costa de Beauregard *et al.*	(BARI, BONN+)
LOVERRE	80	ZPHY C6 187	P.F. Loverre *et al.*	(CERN, CDEF, MADR+)
CORDEN	79	NP B157 250	M.J. Corden *et al.*	(BIRM, RHEL, TELA+)
MARTIN	79	NP B158 520	A.D. Martin, E.N. Ozmutlu	(DURH)
POLYCHRO...	79	PR D19 1317	V.A. Polychronakos *et al.*	(NDAM, ANL)
PDG	78	PL 75B 1	C. Bricman *et al.*	
ANTIPOV	77	NP B119 45	Y.M. Antipov *et al.*	(SERP, GEVA)
PAWLICKI	77	PR D15 3196	A.J. Pawlicki *et al.*	(ANL)
DEUTSCH...	76	NP B103 426	M. Deutschmann *et al.*	(AACH3, BERL, BONN+)
APEL	75	PL 57B 398	W.D. Apel *et al.*	(KARLK, KARLE, PISA, SERP+)
EMMS	75D	NP B96 155	M.J. Emms *et al.*	(BIRM, DURH, RHEL)
EISENBERG	74	PL 52B 239	Y. Eisenberg *et al.*	(REHO)
ENGLER	74	PR D10 2070	A. Engler *et al.*	(CMU, CASE)
LOUIE	74	PL 48B 385	J. Louie *et al.*	(SACL, CERN)
ANDERSON	73	PRL 31 562	J.C. Anderson *et al.*	(CMU, CASE)
TAKAHASHI	72	PR D6 1266	K. Takahashi *et al.*	(TOHOK, PENN, NDAM+)
BEAUPRE	71	NP B28 77	J.V. Beaupre *et al.*	(AACH, BERL, CERN)
FLATTE	71	PL 34B 551	S.M. Flatte *et al.*	(LBL)
ARMENISE	70	LNC 4 199	N. Armenise *et al.*	(BARI, BGNA, FIRZ)
OH	70	PR D1 2494	B.Y. Oh *et al.*	(WISC, TNTO) JP
STUNTEBECK	70	PL 32B 391	P.H. Stuntebeck *et al.*	(NDAM)
ADERHOLZ	69	NP B11 259	M. Aderholz *et al.*	(AACH3, BERL, CERN+)
ARMENISE	68	NC 54A 999	N. Armenise *et al.*	(BARI, BGNA, FIRZ+)
ASCOLI	68D	PRL 21 1712	G. Ascoli *et al.*	(ILL)
BOESEBECK	68	NP B4 501	K. Boesebeck *et al.*	(AACH, BERL, CERN)
JOHNSON	68	PR 176 1651	P.B. Johnson *et al.*	(NDAM, PURD, SLAC)
EISNER	67	PR 164 1699	R.L. Eisner *et al.*	(PURD)
DERADO	65	PRL 14 872	I. Derado *et al.*	(NDAM)
LEE	64	PRL 12 342	Y.Y. Lee *et al.*	(MICH)
BONDAR	63	PL 5 153	L. Bondar *et al.*	(AACH, BIRM, BONN, DESY+)

$f_1(1285)$

$I^G(J^{PC}) = 0^+(1^{++})$

$f_1(1285)$ MASS

VALUE (MeV)	EVTS	DOCUMENT ID		TECN	COMMENT
1281.9 ± 0.5 OUR AVERAGE		Error includes scale factor of 1.8. See the ideogram below.			
1281.16 ± 0.39 ± 0.45		[1] LEES	12X	BABR	$\tau^- \to \pi^- f_1(1285)\nu_\tau$
1285.1 ± 1.0 $^{+\ 1.6}_{-\ 0.3}$		[2] ABLIKIM	11J	BES3	$J/\psi \to \omega(\eta\pi^+\pi^-)$
1281 ± 2 ± 1		AUBERT	07AU	BABR	10.6 $e^+e^- \to f_1(1285)\pi^+\pi^-\gamma$
1276.1 ± 8.1 ± 8.0	203	BAI	04J	BES2	$J/\psi \to \gamma\gamma\pi^+\pi^-$
1274 ± 6	237	ABDALLAH	03H	DLPH	91.2 $e^+e^- \to K^0_S K^\pm\pi^\mp + X$
1280 ± 4		ACCIARRI	01G	L3	
1288 ± 4 ± 5	20k	ADAMS	01B	B852	18 GeV $\pi^- p \to K^+K^-\pi^0 n$
1284 ± 6	1400	ALDE	97B	GAM4	100 $\pi^- p \to \eta\pi^0\pi^0 n$
1281 ± 1		BARBERIS	97B	OMEG	450 $pp \to pp2(\pi^+\pi^-)$
1281 ± 1		BARBERIS	97C	OMEG	450 $pp \to pp K^0_S K^\pm\pi^\mp$
1280 ± 2		[3] ANTINORI	95	OMEG	300,450 $pp \to pp2(\pi^+\pi^-)$
1282.2 ± 1.5		LEE	94	MPS2	18 $\pi^- p \to K^+\overline{K}{}^0 2\pi^- p$
1279 ± 5		FUKUI	91C	SPEC	8.95 $\pi^- p \to \eta\pi^+\pi^- n$
1278 ± 2	140	ARMSTRONG	89	OMEG	300 $pp \to K\overline{K}\pi pp$
1278 ± 2		ARMSTRONG	89G	OMEG	85 $\pi^+ p \to 4\pi\pi p$, $pp \to 4\pi pp$
1280.1 ± 2.1	60	RATH	89	MPS	21.4 $\pi^- p \to K^0_S K^0_S \pi^0 n$
1285 ± 1	4750	[4] BIRMAN	88	MPS	8 $\pi^- p \to K^+\overline{K}{}^0\pi^- n$
1280 ± 1	504	BITYUKOV	88	SPEC	32.5 $\pi^- p \to K^+K^-\pi^0 n$
1280 ± 4		ANDO	86	SPEC	8 $\pi^- p \to \eta\pi^+\pi^- n$
1277 ± 2	420	REEVES	86	SPEC	6.6 $p\overline{p} \to K K\pi X$
1285 ± 2		CHUNG	85	SPEC	8 $\pi^- p \to N K\overline{K}\pi$
1279 ± 2	604	ARMSTRONG	84	OMEG	85 $\pi^+ p \to K\overline{K}\pi\pi p$, $pp \to K\overline{K}\pi pp$
1286 ± 1		CHAUVAT	84	SPEC	ISR 31.5 pp
1278 ± 4		EVANGELIS...	81	OMEG	12 $\pi^- p \to \eta\pi^+\pi^-\pi^- p$
1283 ± 3	103	DIONISI	80	HBC	4 $\pi^- p \to K\overline{K}\pi n$
1282 ± 2	320	NACASCH	78	HBC	0.7,0.76 $\overline{p}p \to K\overline{K}3\pi$
1279 ± 5	210	GRASSLER	77	HBC	16 $\pi^\mp p$
1286 ± 3	180	DUBOC	72	HBC	1.2 $\overline{p}p \to 2K4\pi$
1283 ± 5		DAHL	67	HBC	1.6–4.2 $\pi^- p$
• • • We do not use the following data for averages, fits, limits, etc. • • •					
1281.9 ± 0.5		[5] SOSA	99	SPEC	$pp \to p_{\rm slow}(K^0_S K^+\pi^-)\,p_{\rm fast}$
1282.8 ± 0.6		[5] SOSA	99	SPEC	$pp \to p_{\rm slow}(K^0_S K^-\pi^+)\,p_{\rm fast}$
1270 ±10		AMELIN	95	VES	37 $\pi^- N \to \pi^-\pi^+\pi^-\gamma N$
1280 ± 2		ABATZIS	94	OMEG	450 $pp \to pp2(\pi^+\pi^-)$
1282 ± 4		ARMSTRONG	93C	E760	$\overline{p}p \to \pi^0\eta\eta \to 6\gamma$
1270 ± 6 ±10		ARMSTRONG	92C	OMEG	300 $pp \to pp\pi^+\pi^-\gamma$
1281 ± 1		ARMSTRONG	89E	OMEG	300 $pp \to pp2(\pi^+\pi^-)$
1279 ± 6 ±10	16	BECKER	87	MRK3	$e^+e^- \to \phi K\overline{K}\pi$
1286 ± 9		GIDAL	87	MRK2	$e^+e^- \to e^+e^-\eta\pi^+\pi^-$
1287 ± 5	353	BITYUKOV	84B	SPEC	32 $\pi^- p \to K^+K^-\pi^0 n$
~ 1279		[6] TORNQVIST	82B	RVUE	
1275 ± 6	31	BROMBERG	80	SPEC	100 $\pi^- p \to K\overline{K}\pi X$
1288 ± 9	200	GURTU	79	HBC	4.2 $K^- p \to n\eta 2\pi$
~ 1275.0	46	[7] STANTON	79	CNTR	8.5 $\pi^- p \to n2\gamma 2\pi$
1271 ±10	34	CORDEN	78	OMEG	12–15 $\pi^- p \to K^+K^-\pi n$
1295 ±12	85	CORDEN	78	OMEG	12–15 $\pi^- p \to n5\pi$
1292 ±10	150	DEFOIX	72	HBC	0.7 $\overline{p}p \to 7\pi$
1280 ± 3	500	[8] THUN	72	MMS	13.4 $\pi^- p$
1303 ± 8		BARDADIN-...	71	HBC	8 $\pi^+ p \to p6\pi$
1283 ± 6		BOESEBECK	71	HBC	16.0 $\pi p \to p5\pi$
1270 ±10		CAMPBELL	69	DBC	2.7 $\pi^+ d$
1285 ± 7		LORSTAD	69	HBC	0.7 $\overline{p}p$, 4,5-body
1290 ± 7		D'ANDLAU	68	HBC	1.2 $\overline{p}p$, 5–6 body

[1] Using the $2\pi^+2\pi^-$ and $\pi^+\pi^-\eta$ modes of $f_1(1285)$ decay.
[2] The selected process is $J/\psi \to \omega a_0(980)\pi$.
[3] Supersedes ABATZIS 94, ARMSTRONG 89E.
[4] From partial wave analysis of $K^+\overline{K}{}^0\pi^-$ system.
[5] No systematic error given.
[6] From a unitarized quark-model calculation.
[7] From phase shift analysis of $\eta\pi^+\pi^-$ system.
[8] Seen in the missing mass spectrum.

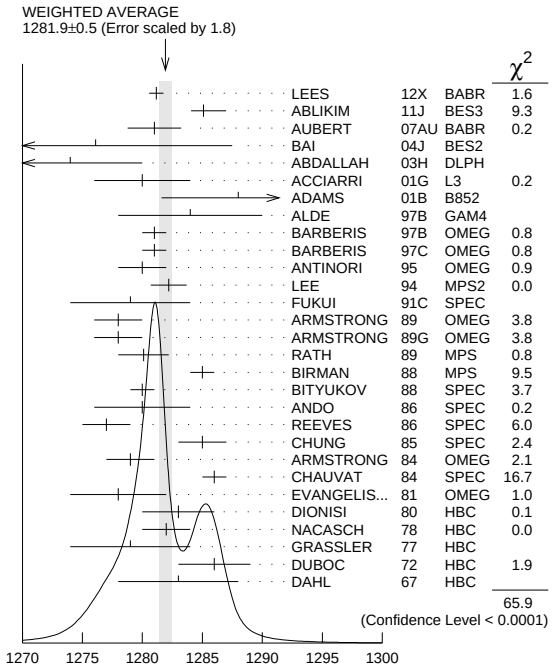

$f_1(1285)$ WIDTH

Only experiments giving width error less than 20 MeV are kept for averaging.

VALUE (MeV)	EVTS	DOCUMENT ID		TECN	COMMENT
24.2± 1.1 OUR AVERAGE		Error includes scale factor of 1.3. See the ideogram below.			
22.0± 3.1 $^{+\ 2.0}_{-\ 1.5}$		[9] ABLIKIM	11J	BES3	$J/\psi \to \omega(\eta\pi^+\pi^-)$
35 ± 6 ± 4		AUBERT	07AU	BABR	10.6 $e^+e^- \to f_1(1285)\pi^+\pi^-\gamma$
40.0± 8.6± 9.3	203	BAI	04J	BES2	$J/\psi \to \gamma\gamma\pi^+\pi^-$
29 ±12	237	ABDALLAH	03H	DLPH	91.2 $e^+e^- \to K^0_S K^\pm\pi^\mp + X$
45 ± 9 ± 7	20k	ADAMS	01B	B852	18 GeV $\pi^- p \to K^+K^-\pi^0 n$
55 ±18	1400	ALDE	97B	GAM4	100 $\pi^- p \to \eta\pi^0\pi^0 n$
24 ± 3		BARBERIS	97B	OMEG	450 $pp \to pp2(\pi^+\pi^-)$
20 ± 2		BARBERIS	97C	OMEG	450 $pp \to pp K^0_S K^\pm\pi^\mp$
36 ± 5		[10] ANTINORI	95	OMEG	300,450 $pp \to pp2(\pi^+\pi^-)$
29.0± 4.1		LEE	94	MPS2	18 $\pi^- p \to K^+\overline{K}{}^0 2\pi^- p$
25 ± 4	140	ARMSTRONG	89	OMEG	300 $pp \to K\overline{K}\pi pp$
22 ± 2	4750	[11] BIRMAN	88	MPS	8 $\pi^- p \to K^+\overline{K}{}^0\pi^- n$
25 ± 4	504	BITYUKOV	88	SPEC	32.5 $\pi^- p \to K^+K^-\pi^0 n$
19 ± 5		ANDO	86	SPEC	8 $\pi^- p \to \eta\pi^+\pi^- n$
32 ± 8	420	REEVES	86	SPEC	6.6 $p\overline{p} \to K K\pi$X
22 ± 2		CHUNG	85	SPEC	8 $\pi^- p \to N K\overline{K}\pi$
32 ± 3	604	ARMSTRONG	84	OMEG	85 $\pi^+ p \to K\overline{K}\pi\pi p$, $pp \to K\overline{K}\pi pp$
24 ± 3		CHAUVAT	84	SPEC	ISR 31.5 pp
29 ±10	103	DIONISI	80	HBC	4 $\pi^- p \to K\overline{K}\pi n$
28.3± 6.7	320	NACASCH	78	HBC	0.7,0.76 $\overline{p}p \to K\overline{K}3\pi$
• • • We do not use the following data for averages, fits, limits, etc. • • •					
18.2± 1.2		[12] SOSA	99	SPEC	$pp \to p_{\rm slow}(K^0_S K^+\pi^-)p_{\rm fast}$
19.4± 1.5		[12] SOSA	99	SPEC	$pp \to p_{\rm slow}(K^0_S K^-\pi^+)p_{\rm fast}$
40 ± 5		ABATZIS	94	OMEG	450 $pp \to pp2(\pi^+\pi^-)$
31 ± 5		ARMSTRONG	89E	OMEG	300 $pp \to pp2(\pi^+\pi^-)$
41 ±12		ARMSTRONG	89G	OMEG	85 $\pi^+ p \to 4\pi\pi p$, $pp \to 4\pi pp$
17.9±10.9	60	RATH	89	MPS	21.4 $\pi^- p \to K^0_S K^0_S \pi^0 n$
14 $^{+20}_{-14}$ ±10	16	BECKER	87	MRK3	$e^+e^- \to \phi K\overline{K}\pi$
26 ±12		EVANGELIS...	81	OMEG	12 $\pi^- p \to \eta\pi^+\pi^-\pi^- p$
25 ±15	200	GURTU	79	HBC	4.2 $K^- p \to n\eta 2\pi$
~ 10		[13] STANTON	79	CNTR	8.5 $\pi^- p \to n2\gamma 2\pi$
24 ±18	210	GRASSLER	77	HBC	16 $\pi^\mp p$
28 ± 5	150	[14] DEFOIX	72	HBC	0.7 $\overline{p}p \to 7\pi$
46 ± 9	180	[14] DUBOC	72	HBC	1.2 $\overline{p}p \to 2K4\pi$
37 ± 5	500	[15] THUN	72	MMS	13.4 $\pi^- p$
10 ±10		BOESEBECK	71	HBC	16.0 $\pi p \to p5\pi$
30 ±15		CAMPBELL	69	DBC	2.7 $\pi^+ d$
60 ±15		[14] LORSTAD	69	HBC	0.7 $\overline{p}p$, 4,5-body
35 ±10		[14] DAHL	67	HBC	1.6–4.2 $\pi^- p$

[9] The selected process is $J/\psi \to \omega a_0(980)\pi$.
[10] Supersedes ABATZIS 94, ARMSTRONG 89E.
[11] From partial wave analysis of $K^+\overline{K}{}^0\pi^-$ system.
[12] No systematic error given.
[13] From phase shift analysis of $\eta\pi^+\pi^-$ system.
[14] Resolution is not unfolded.
[15] Seen in the missing mass spectrum.

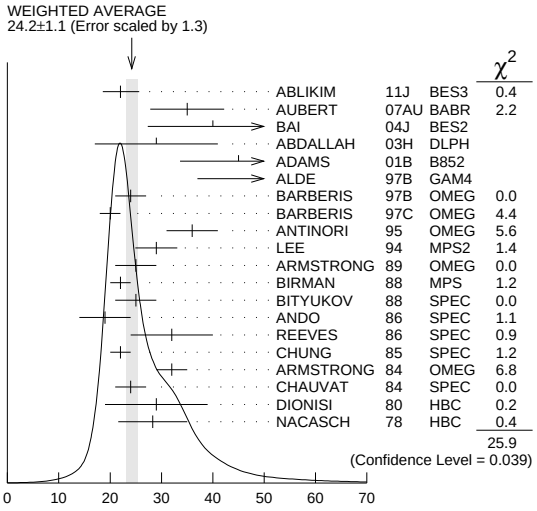

$f_1(1285)$ DECAY MODES

	Mode	Fraction (Γ_i/Γ)	Scale factor/ Confidence level
Γ_1	4π	(33.1 $^{+\ 2.1}_{-\ 1.8}$) %	S=1.3
Γ_2	$\pi^0\pi^0\pi^+\pi^-$	(22.0 $^{+\ 1.4}_{-\ 1.2}$) %	S=1.3
Γ_3	$2\pi^+2\pi^-$	(11.0 $^{+\ 0.7}_{-\ 0.6}$) %	S=1.3
Γ_4	$\rho^0\pi^+\pi^-$	(11.0 $^{+\ 0.7}_{-\ 0.6}$) %	S=1.3
Γ_5	$\rho^0\rho^0$	seen	
Γ_6	$4\pi^0$	$< 7 \times 10^{-4}$	CL=90%
Γ_7	$\eta\pi^+\pi^-$	(35 ±15) %	
Γ_8	$\eta\pi\pi$	(52.4 $^{+\ 1.9}_{-\ 2.2}$) %	S=1.2
Γ_9	$a_0(980)\pi$ [ignoring $a_0(980) \to K\overline{K}$]	(36 ± 7) %	
Γ_{10}	$\eta\pi\pi$ [excluding $a_0(980)\pi$]	(16 ± 7) %	
Γ_{11}	$K\overline{K}\pi$	(9.0± 0.4) %	S=1.1
Γ_{12}	$K\overline{K}^*(892)$	not seen	
Γ_{13}	$\pi^+\pi^-\pi^0$	(3.0± 0.9) $\times 10^{-3}$	
Γ_{14}	$\rho^\pm\pi^\mp$	$< 3.1 \times 10^{-3}$	CL=95%
Γ_{15}	$\gamma\rho^0$	(5.5± 1.3) %	S=2.8
Γ_{16}	$\phi\gamma$	(7.4± 2.6) $\times 10^{-4}$	
Γ_{17}	$\gamma\gamma^*$		
Γ_{18}	$\gamma\gamma$		

Meson Particle Listings

$f_1(1285)$

CONSTRAINED FIT INFORMATION

An overall fit to 7 branching ratios uses 16 measurements and one constraint to determine 5 parameters. The overall fit has a $\chi^2 = 24.7$ for 12 degrees of freedom.

The following *off-diagonal* array elements are the correlation coefficients $\langle \delta x_i \delta x_j \rangle / (\delta x_i \cdot \delta x_j)$, in percent, from the fit to the branching fractions, $x_i \equiv \Gamma_i/\Gamma_{\rm total}$. The fit constrains the x_i whose labels appear in this array to sum to one.

x_9	−17			
x_{10}	−8	−95		
x_{11}	46	−9	−4	
x_{15}	−36	−4	−2	−34
	x_1	x_9	x_{10}	x_{11}

$f_1(1285)$ $\Gamma(i)\Gamma(\gamma\gamma)/\Gamma(\text{total})$

$\Gamma(\eta\pi\pi) \times \Gamma(\gamma\gamma)/\Gamma_{\rm total}$ $\quad \Gamma_8\Gamma_{18}/\Gamma = (\Gamma_9+\Gamma_{10})\Gamma_{18}/\Gamma$

VALUE (keV)	CL%	DOCUMENT ID		TECN	COMMENT
<0.62	95	GIDAL	87	MRK2	$e^+e^- \to e^+e^-\eta\pi^+\pi^-$

$\Gamma(\eta\pi\pi) \times \Gamma(\gamma\gamma^*)/\Gamma_{\rm total}$ $\quad \Gamma_8\Gamma_{17}/\Gamma = (\Gamma_9+\Gamma_{10})\Gamma_{17}/\Gamma$

VALUE (keV)	EVTS	DOCUMENT ID		TECN	COMMENT
1.4 ±0.4 OUR AVERAGE		Error includes scale factor of 1.4.			
1.18±0.25±0.20	26	[16,17] AIHARA	88B	TPC	$e^+e^- \to e^+e^-\eta\pi^+\pi^-$
2.30±0.61±0.42		[16,18] GIDAL	87	MRK2	$e^+e^- \to e^+e^-\eta\pi^+\pi^-$
• • • We do not use the following data for averages, fits, limits, etc. • • •					
1.8 ±0.3 ±0.3	420	[19] ACHARD	02B	L3	183–209 $e^+e^- \to e^+e^-\eta\pi^+\pi^-$

[16] Assuming a ρ-pole form factor.
[17] Published value multiplied by $\eta\pi\pi$ branching ratio 0.49.
[18] Published value divided by 2 and multiplied by the $\eta\pi\pi$ branching ratio 0.49.
[19] Published value multiplied by the $\eta\pi\pi$ branching ratio 0.52.

$f_1(1285)$ BRANCHING RATIOS

$\Gamma(K\overline{K}\pi)/\Gamma(4\pi)$ $\quad \Gamma_{11}/\Gamma_1$

VALUE	DOCUMENT ID		TECN	COMMENT
0.271±0.016 OUR FIT	Error includes scale factor of 1.3.			
0.271±0.016 OUR AVERAGE	Error includes scale factor of 1.2.			
0.265±0.014	[20] BARBERIS	97C	OMEG	450 $pp \to pp K^0_S K^\pm\pi^\mp$
0.28 ±0.05	[21] ARMSTRONG	89E	OMEG	300 $pp \to pp f_1(1285)$
0.37 ±0.03 ±0.05	[22] ARMSTRONG	89G	OMEG	85 $\pi p \to 4\pi X$

[20] Using $2(\pi^+\pi^-)$ data from BARBERIS 97B.
[21] Assuming $\rho\pi\pi$ and $a_0(980)\pi$ intermediate states.
[22] 4π consistent with being entirely $\rho\pi\pi$.

$\Gamma(\pi^0\pi^0\pi^+\pi^-)/\Gamma_{\rm total}$ $\quad \Gamma_2/\Gamma = \frac{2}{3}\Gamma_1/\Gamma$

VALUE	DOCUMENT ID
$0.220^{+0.014}_{-0.012}$ OUR FIT	Error includes scale factor of 1.3.

$\Gamma(2\pi^+2\pi^-)/\Gamma_{\rm total}$ $\quad \Gamma_3/\Gamma = \frac{1}{3}\Gamma_1/\Gamma$

VALUE	DOCUMENT ID
$0.110^{+0.007}_{-0.006}$ OUR FIT	Error includes scale factor of 1.3.

$\Gamma(\rho^0\pi^+\pi^-)/\Gamma_{\rm total}$ $\quad \Gamma_4/\Gamma = \frac{1}{3}\Gamma_1/\Gamma$

VALUE	DOCUMENT ID
$0.110^{+0.007}_{-0.006}$ OUR FIT	Error includes scale factor of 1.3.

$\Gamma(\rho^0\pi^+\pi^-)/\Gamma(2\pi^+2\pi^-)$ $\quad \Gamma_4/\Gamma_3$

VALUE	DOCUMENT ID		TECN	COMMENT
• • • We do not use the following data for averages, fits, limits, etc. • • •				
1.0±0.4	GRASSLER	77	HBC	16 GeV $\pi^\pm p$

$\Gamma(\rho^0\rho^0)/\Gamma_{\rm total}$ $\quad \Gamma_5/\Gamma$

VALUE	DOCUMENT ID		TECN	COMMENT
• • • We do not use the following data for averages, fits, limits, etc. • • •				
seen	BARBERIS	00C		450 $pp \to p_f 4\pi p_s$

$\Gamma(4\pi^0)/\Gamma_{\rm total}$ $\quad \Gamma_6/\Gamma$

VALUE (units 10^{-4})	CL%	DOCUMENT ID		TECN	COMMENT
<7	90	ALDE	87	GAM4	100 $\pi^- p \to 4\pi^0 n$

$\Gamma(\pi^+\pi^-\pi^0)/\Gamma(\eta\pi^+\pi^-)$ $\quad \Gamma_{13}/\Gamma_7$

VALUE (%)	EVTS	DOCUMENT ID		TECN	COMMENT
0.86±0.16±0.20	2.3k	[23] DOROFEEV	11	VES	$\pi^- N \to \pi^- f_1(1285) N$

[23] Value obtained selecting the region corresponding to $f_0(980)$ in the $\pi^+\pi^-$ mass spectrum.

$\Gamma(\eta\pi\pi)/\Gamma_{\rm total}$ $\quad \Gamma_8/\Gamma = (\Gamma_9+\Gamma_{10})/\Gamma$

VALUE	DOCUMENT ID
$0.524^{+0.019}_{-0.022}$ OUR FIT	Error includes scale factor of 1.2.

$\Gamma(4\pi)/\Gamma(\eta\pi\pi)$ $\quad \Gamma_1/\Gamma_8 = \Gamma_1/(\Gamma_9+\Gamma_{10})$

VALUE	DOCUMENT ID		TECN	COMMENT
0.63±0.06 OUR FIT	Error includes scale factor of 1.2.			
0.41±0.14 OUR AVERAGE				
0.37±0.11±0.11	BOLTON	92	MRK3	$J/\psi \to \gamma f_1(1285)$
0.64±0.40	GURTU	79	HBC	4.2 $K^- p$
• • • We do not use the following data for averages, fits, limits, etc. • • •				
0.93±0.30	[24] GRASSLER	77	HBC	16 $\pi^\mp p$

[24] Assuming $\rho\pi\pi$ and $a_0(980)\pi$ intermediate states.

$\Gamma(2\pi^+2\pi^-)/\Gamma(\eta\pi\pi)$ $\quad \Gamma_3/\Gamma_8$

VALUE	DOCUMENT ID		TECN	COMMENT
0.28±0.02±0.02	[25] LEES	12X	BABR	$\tau^- \to \pi^- f_1(1285)\nu_\tau$

[25] Assuming $B(f_1(1285) \to \pi\pi\eta) = 3/2\ B(f_1(1285) \to \pi^+\pi^-\eta)$.

$\Gamma(a_0(980)\pi$ [ignoring $a_0(980) \to K\overline{K}$])$/\Gamma(\eta\pi\pi)$ $\quad \Gamma_9/\Gamma_8 = \Gamma_9/(\Gamma_9+\Gamma_{10})$

VALUE	CL%	EVTS	DOCUMENT ID		TECN	COMMENT
0.69±0.13 OUR FIT						
$0.69^{+0.13}_{-0.12}$ OUR AVERAGE						
0.72±0.15			GURTU	79	HBC	4.2 $K^- p$
0.6 $^{+0.3}_{-0.2}$			CORDEN	78	OMEG	12–15 $\pi^- p$
• • • We do not use the following data for averages, fits, limits, etc. • • •						
>0.69	95	318	ACHARD	02B	L3	183–209 $e^+e^- \to e^+e^-\eta\pi^+\pi^-$
0.28±0.07		1400	ALDE	97B	GAM4	100 $\pi^- p \to \eta\pi^0\pi^0 n$
1.0 ±0.3			GRASSLER	77	HBC	16 $\pi^\mp p$

$\Gamma(K\overline{K}\pi)/\Gamma(\eta\pi\pi)$ $\quad \Gamma_{11}/\Gamma_8 = \Gamma_{11}/(\Gamma_9+\Gamma_{10})$

VALUE	DOCUMENT ID		TECN	COMMENT
0.171±0.013 OUR FIT	Error includes scale factor of 1.1.			
0.170±0.012 OUR AVERAGE				
0.166±0.01 ±0.008	BARBERIS	98C	OMEG	450 $pp \to p_f f_1(1285) p_s$
0.42 ±0.15	GURTU	79	HBC	4.2 $K^- p$
0.5 ±0.2	[26] CORDEN	78	OMEG	12–15 $\pi^- p$
0.20 ±0.08	[27] DEFOIX	72	HBC	0.7 $\overline{p}p \to 7\pi$
0.16 ±0.08	CAMPBELL	69	DBC	2.7 $\pi^+ d$

[26] CORDEN 78 assumes low-mass $\eta\pi\pi$ region is dominantly 1^{++}. See BARBERIS 98C and MANAK 00A for discussion.
[27] $K\overline{K}$ system characterized by the $I = 1$ threshold enhancement. (See under $a_0(980)$).

$\Gamma(K\overline{K}^*(892))/\Gamma_{\rm total}$ $\quad \Gamma_{12}/\Gamma$

VALUE	DOCUMENT ID		TECN	COMMENT
not seen	NACASCH	78	HBC	0.7,0.76 $\overline{p}p \to K\overline{K}3\pi$
• • • We do not use the following data for averages, fits, limits, etc. • • •				
seen	[28] ACHARD	07	L3	183–209 $e^+e^- \to e^+e^- K^0_S K^\pm\pi^\mp$

[28] A clear signal of 19.8 ± 4.4 events observed at high Q^2.

$\Gamma(\pi^+\pi^-\pi^0)/\Gamma_{\rm total}$ $\quad \Gamma_{13}/\Gamma$

VALUE (%)	EVTS	DOCUMENT ID		TECN	COMMENT
0.30±0.055±0.074	2.3k	[29] DOROFEEV	11	VES	$\pi^- N \to \pi^- f_1(1285) N$

[29] Value obtained selecting the region corresponding to $f_0(980)$ in the $\pi^+\pi^-$ mass spectrum. The sytematic error includes the uncertainty on the partial width $f_1 \to \eta\pi\pi$ obtained from PDG 10 data.

$\Gamma(\rho^\pm\pi^\mp)/\Gamma_{\rm total}$ $\quad \Gamma_{14}/\Gamma$

VALUE (%)	CL%	DOCUMENT ID		TECN	COMMENT
<0.31	95	DOROFEEV	11	VES	$\pi^- N \to \pi^- f_1(1285) N$

$\Gamma(\gamma\rho^0)/\Gamma_{\rm total}$ $\quad \Gamma_{15}/\Gamma$

VALUE (units 10^{-2})	CL%	DOCUMENT ID		TECN	COMMENT
5.5±1.3 OUR FIT	Error includes scale factor of 2.8.				
2.8±0.7±0.6		AMELIN	95	VES	37 $\pi^- N \to \pi^-\pi^+\pi^-\gamma N$
• • • We do not use the following data for averages, fits, limits, etc. • • •					
<5	95	BITYUKOV	91B	SPEC	32 $\pi^- p \to \pi^+\pi^-\gamma n$

$\Gamma(\gamma\rho^0)/\Gamma(2\pi^+2\pi^-)$ $\quad \Gamma_{15}/\Gamma_3 = \Gamma_{15}/\frac{1}{3}\Gamma_1$

VALUE	DOCUMENT ID		TECN	COMMENT
0.50±0.13 OUR FIT	Error includes scale factor of 2.5.			
0.45±0.18	[30] COFFMAN	90	MRK3	$J/\psi \to \gamma\gamma\pi^+\pi^-$

[30] Using $B(J/\psi \to \gamma f_1(1285) \to \gamma\gamma\rho^0) = 0.25 \times 10^{-4}$ and $B(J/\psi \to \gamma f_1(1285) \to \gamma 2\pi^+2\pi^-) = 0.55 \times 10^{-4}$ given by MIR 88.

$\Gamma(\eta\pi\pi)/\Gamma(\gamma\rho^0)$ $\Gamma_8/\Gamma_{15} = (\Gamma_9+\Gamma_{10})/\Gamma_{15}$

VALUE	DOCUMENT ID	TECN	COMMENT
9.5±2.0 OUR FIT	Error includes scale factor of 2.5.		
7.9±0.9 OUR AVERAGE			
10.0±1.0±2.0	BARBERIS 98C	OMEGA	450 $pp \to p_f f_1(1285) p_s$
7.5±1.0	[31] ARMSTRONG 92C	OMEGA	300 $pp \to pp\pi^+\pi^-\gamma$, $pp\eta\pi^+\pi^-$

[31] Published value multiplied by 1.5.

$\Gamma(\gamma\rho^0)/\Gamma(K\overline{K}\pi)$ Γ_{15}/Γ_{11}

VALUE	CL%	DOCUMENT ID	TECN	COMMENT
• • • We do not use the following data for averages, fits, limits, etc. • • •				
>0.035	90	[32] COFFMAN 90	MRK3	$J/\psi \to \gamma\gamma\pi^+\pi^-$

[32] Using $B(J/\psi \to \gamma f_1(1285) \to \gamma\gamma\rho^0) = 0.25 \times 10^{-4}$ and $B(J/\psi \to \gamma f_1(1285) \to \gamma K\overline{K}\pi) = < 0.72 \times 10^{-3}$.

$\Gamma(\phi\gamma)/\Gamma(K\overline{K}\pi)$ Γ_{16}/Γ_{11}

VALUE (units 10^{-2})	CL%	EVTS	DOCUMENT ID	TECN	COMMENT
0.82±0.21±0.20		19	BITYUKOV 88	SPEC	32.5 $\pi^- p \to K^+ K^- \pi^0 n$
• • • We do not use the following data for averages, fits, limits, etc. • • •					
<0.50	95		BARBERIS 98C	OMEG	450 $pp \to p_f f_1(1285) p_s$
<0.93	95		AMELIN 95	VES	37 $\pi^- N \to \pi^-\pi^+\pi^-\gamma N$

$f_1(1285)$ REFERENCES

LEES	12X	PR D86 092010	J.P. Lees *et al.*	(BABAR Collab.)
ABLIKIM	11J	PRL 107 182001	M. Ablikim *et al.*	(BES III Collab.)
DOROFEEV	11	EPJ A47 68	V. Dorofeev *et al.*	(SERP, MIPT)
PDG	10	JP G37 075021	K. Nakamura *et al.*	(PDG Collab.)
ACHARD	07	JHEP 0703 018	P. Achard *et al.*	(L3 Collab.)
AUBERT	07AU	PR D76 092005	B. Aubert *et al.*	(BABAR Collab.)
BAI	04J	PL B594 47	J.Z. Bai *et al.*	(BES Collab.)
ABDALLAH	03H	PL B569 129	J. Abdallah *et al.*	(DELPHI Collab.)
ACHARD	02B	PL B526 269	P. Achard *et al.*	(L3 Collab.)
ACCIARRI	01G	PL B501 1	M. Acciarri *et al.*	(L3 Collab.)
ADAMS	01B	PL B516 264	G.S. Adams *et al.*	(BNL E852 Collab.)
BARBERIS	00C	PL B471 440	D. Barberis *et al.*	(WA 102 Collab.)
MANAK	00A	PR D62 012003	J.J. Manak *et al.*	(BNL E852 Collab.)
SOSA	99	PRL 83 913	M. Sosa *et al.*	
BARBERIS	98C	PL B440 225	D. Barberis *et al.*	(WA 102 Collab.)
ALDE	97B	PAN 60 386	D. Alde *et al.*	(GAMS Collab.)
		Translated from YAF 60 458.		
BARBERIS	97B	PL B413 217	D. Barberis *et al.*	(WA 102 Collab.)
BARBERIS	97C	PL B413 225	D. Barberis *et al.*	(WA 102 Collab.)
AMELIN	95	ZPHY C66 71	D.V. Amelin *et al.*	(VES Collab.)
ANTINORI	95	PL B353 589	F. Antinori *et al.*	(ATHU, BARI, BIRM+)
ABATZIS	94	PL B324 509	S. Abatzis *et al.*	(ATHU, BARI, BIRM+)
LEE	94	PL B323 227	J.H. Lee *et al.*	(BNL, IND, KYUN, MASD+)
ARMSTRONG	93C	PL B307 394	T.A. Armstrong *et al.*	(FNAL, FERR, GENO+)
ARMSTRONG	92C	ZPHY C54 371	T.A. Armstrong *et al.*	(ATHU, BARI, BIRM+)
BOLTON	92	PL B278 495	T. Bolton *et al.*	(Mark III Collab.)
BITYUKOV	91B	SJNP 54 318	S.I. Bityukov *et al.*	(SERP)
		Translated from YAF 54 529.		
FUKUI	91C	PL B267 293	S. Fukui *et al.*	(SUGI, NAGO, KEK, KYOT+)
COFFMAN	90	PR D41 1410	D.M. Coffman *et al.*	(Mark III Collab.)
ARMSTRONG	89	PL B221 216	T.A. Armstrong *et al.*	(CERN, CDEF, BIRM+) JPC
ARMSTRONG	89E	PL B228 536	T.A. Armstrong, M. Benayoun	(ATHU, BARI, BIRM+)
ARMSTRONG	89G	ZPHY C43 55	T.A. Armstrong *et al.*	(CERN, BIRM, BARI+)
RATH	89	PR D40 693	M.G. Rath *et al.*	(NDAM, BRAN, BNL, CUNY+)
AIHARA	88B	PL B209 107	H. Aihara *et al.*	(TPC-2γ Collab.)
BIRMAN	88	PRL 61 1557	A. Birman *et al.*	(BNL, FSU, IND, MASD) JP
BITYUKOV	88	PL B203 327	S.I. Bityukov *et al.*	(SERP)
MIR	88	Photon-Photon 88, 126 Conference	R. Mir	(Mark III Collab.)
ALDE	87	PL B198 286	D.M. Alde *et al.*	(LANL, BRUX, SERP, LAPP)
BECKER	87	PRL 59 186	J.J. Becker *et al.*	(Mark III Collab.)
GIDAL	87	PRL 59 2012	G. Gidal *et al.*	(LBL, SLAC, HARV)
ANDO	86	PRL 57 1296	A. Ando *et al.*	(KEK, KYOT, NIRS, SAGA+) IJP
REEVES	86	PR D34 1960	D.F. Reeves *et al.*	(FLOR, BNL, IND+) JP
CHUNG	85	PRL 55 779	S.U. Chung *et al.*	(BNL, FLOR, IND+) JP
ARMSTRONG	84	PL 146B 273	T.A. Armstrong *et al.*	(ATHU, BARI, BIRM+) JP
BITYUKOV	84B	PL 144B 133	S.I. Bityukov *et al.*	(SERP)
CHAUVAT	84	PL 148B 382	P. Chauvat *et al.*	(CERN, CLER, UCLA+)
TORNQVIST	82B	NP B203 268	N.A. Tornqvist	(HELS)
EVANGELIS...	81	NP B178 197	C. Evangelista *et al.*	(BARI, BONN, CERN+)
BROMBERG	80	PR D22 1513	C.M. Bromberg *et al.*	(CIT, FNAL, ILLC+)
DIONISI	80	NP B169 1	C. Dionisi *et al.*	(CERN, MADR, CDEF+)
GURTU	79	NP B151 181	A. Gurtu *et al.*	(CERN, ZEEM, NIJM, OXF)
STANTON	79	PRL 42 346	N.R. Stanton *et al.*	(OSU, CARL, MCGI+) JP
CORDEN	78	NP B144 253	M.J. Corden *et al.*	(BIRM, RHEL, TELA+) JP
NACASCH	78	NP B135 203	R. Nacasch *et al.*	(PARIS, MADR, CERN)
GRASSLER	77	NP B121 189	H. Grassler *et al.*	(AACH3, BERL, BONN+)
DEFOIX	72	NP B44 125	C. Defoix *et al.*	(CDEF, CERN)
DUBOC	72	NP B46 429	J. Duboc *et al.*	(PARIS, LIVP)
THUN	72	PRL 28 1733	R. Thun *et al.*	(STON, NEAS)
BARDADIN-...	71	PR D4 2711	M. Bardadin-Otwinowska *et al.*	(WARS)
BOESEBECK	71	PL 34B 659	K. Boesebeck (AACH, BERL, BONN, CERN, CRAC+)	
CAMPBELL	69	PRL 22 1204	J.H. Campbell *et al.*	(PURD)
LORSTAD	69	NP B14 63	B. Lorstad *et al.*	(CDEF, CERN) JP
D'ANDLAU	68	NP B5 693	C. d'Andlau *et al.*	(CDEF, CERN, IRAD+) IJP
DAHL	67	PR 163 1377	O.I. Dahl *et al.*	(LRL) IJP

$\eta(1295)$ $I^G(J^{PC}) = 0^+(0^{-+})$

See also the mini-review under $\eta(1405)$

$\eta(1295)$ MASS

VALUE (MeV)	EVTS	DOCUMENT ID	TECN	COMMENT
1294±4 OUR AVERAGE	Error includes scale factor of 1.6. See the ideogram below.			
1302±9±8	20k	ADAMS 01B	B852	18 GeV $\pi^- p \to K^+ K^- \pi^0 n$
1282±5	9082	MANAK 00A	MPS	18 $\pi^- p \to \eta\pi^+\pi^- n$
1299±4	2100	ALDE 97B	GAM4	100 $\pi^- p \to \eta\pi^0\pi^0 n$
1295±4		FUKUI 91C	SPEC	8.95 $\pi^- p \to \eta\pi^+\pi^- n$
• • • We do not use the following data for averages, fits, limits, etc. • • •				
1264±8		[1] AUGUSTIN 90	DM2	$J/\psi \to \gamma\eta\pi^+\pi^-$
~ 1275		STANTON 79	CNTR	8.4 $\pi^- p \to n\eta 2\pi$

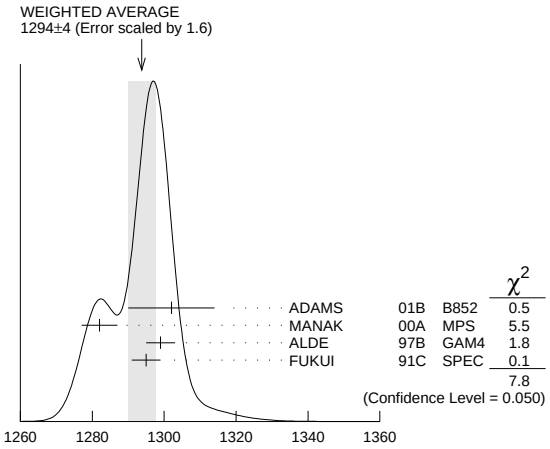

[1] PWA analysis of AUGUSTIN 92 assigns 0^{-+} quantum numbers to this state rather than 1^{++} as before.

$\eta(1295)$ WIDTH

VALUE (MeV)	EVTS	DOCUMENT ID	TECN	COMMENT
55± 5 OUR AVERAGE				
57±23±21	20k	ADAMS 01B	B852	18 GeV $\pi^- p \to K^+ K^- \pi^0 n$
66±13	9082	MANAK 00A	MPS	18 $\pi^- p \to \eta\pi^+\pi^- n$
53± 6		FUKUI 91C	SPEC	8.95 $\pi^- p \to \eta\pi^+\pi^- n$
• • • We do not use the following data for averages, fits, limits, etc. • • •				
<40	2100	ALDE 97B	GAM4	100 $\pi^- p \to \eta\pi^0\pi^0 n$
44±20		[2] AUGUSTIN 90	DM2	$J/\psi \to \gamma\eta\pi^+\pi^-$
~ 70		STANTON 79	CNTR	8.4 $\pi^- p \to n\eta 2\pi$

[2] PWA analysis of AUGUSTIN 92 assigns 0^{-+} quantum numbers to this state rather than 1^{++} as before.

$\eta(1295)$ DECAY MODES

	Mode	Fraction (Γ_i/Γ)
Γ_1	$\eta\pi^+\pi^-$	seen
Γ_2	$a_0(980)\pi$	seen
Γ_3	$\gamma\gamma$	
Γ_4	$\eta\pi^0\pi^0$	seen
Γ_5	$\eta(\pi\pi)_{S\text{-wave}}$	seen
Γ_6	$\sigma\eta$	
Γ_7	$K\overline{K}\pi$	

$\eta(1295)$ $\Gamma(i)\Gamma(\gamma\gamma)/\Gamma(total)$

$\Gamma(\eta\pi^+\pi^-) \times \Gamma(\gamma\gamma)/\Gamma_{total}$ $\Gamma_1\Gamma_3/\Gamma$

VALUE (keV)	CL%	DOCUMENT ID	TECN	COMMENT
<0.066	95	ACCIARRI 01G	L3	183–202 $e^+e^- \to e^+e^-\eta\pi^+\pi^-$
• • • We do not use the following data for averages, fits, limits, etc. • • •				
<0.6	90	AIHARA 88C	TPC	$e^+e^- \to e^+e^-\eta\pi^+\pi^-$
<0.3		ANTREASYAN 87	CBAL	$e^+e^- \to e^+e^-\eta\pi\pi$

Meson Particle Listings

$\eta(1295)$, $\pi(1300)$, $a_2(1320)$

$\Gamma(K\overline{K}\pi) \times \Gamma(\gamma\gamma)/\Gamma_{total}$ $\Gamma_7\Gamma_3/\Gamma$

VALUE (keV)	CL%	DOCUMENT ID		TECN	COMMENT
• • • We do not use the following data for averages, fits, limits, etc. • • •					
<0.014	90	[3,4] AHOHE	05	CLE2	10.6 $e^+e^- \to e^+e^- K^0_S K^\pm\pi^\mp$

[3] Using $\eta(1295)$ mass and width 1294 MeV and 55 MeV, respectively.
[4] Assuming three-body phase-space decay to $K^0_S K^\pm\pi^\mp$.

$\eta(1295)$ BRANCHING RATIOS

$\Gamma(a_0(980)\pi)/\Gamma_{total}$ Γ_2/Γ

VALUE	DOCUMENT ID		TECN	COMMENT
• • • We do not use the following data for averages, fits, limits, etc. • • •				
not seen	BERTIN	97	OBLX	0.0 $\overline{p}p \to K^\pm(K^0)\pi^\mp\pi^+\pi^-$
seen	BIRMAN	88	MPS	8 $\pi^-p \to K^+\overline{K}^0\pi^-n$
large	ANDO	86	SPEC	8 $\pi^-p \to \eta\pi^+\pi^-n$
large	STANTON	79	CNTR	8.4 $\pi^-p \to n\eta 2\pi$

$\Gamma(a_0(980)\pi)/\Gamma(\eta\pi^0\pi^0)$ Γ_2/Γ_4

VALUE	DOCUMENT ID		TECN	COMMENT
0.65±0.10	[5] ALDE	97B	GAM4	100 $\pi^-p \to \eta\pi^0\pi^0n$

[5] Assuming that $a_0(980)$ decays only to $\eta\pi$.

$\Gamma(\eta(\pi\pi)_{S\text{-wave}})/\Gamma(\eta\pi^0\pi^0)$ Γ_5/Γ_4

VALUE	DOCUMENT ID		TECN	COMMENT
0.35±0.10	ALDE	97B	GAM4	100 $\pi^-p \to \eta\pi^0\pi^0n$

$\Gamma(a_0(980)\pi)/\Gamma(\sigma\eta)$ Γ_2/Γ_6

VALUE	EVTS	DOCUMENT ID		TECN	COMMENT
0.48±0.22	9082	MANAK	00A	MPS	18 $\pi^-p \to \eta\pi^+\pi^-n$

$\eta(1295)$ REFERENCES

AHOHE	05	PR D71 072001	R. Ahohe *et al.*	(CLEO Collab.)
ACCIARRI	01G	PL B501 1	M. Acciarri *et al.*	(L3 Collab.)
ADAMS	01B	PL B516 264	G.S. Adams *et al.*	(BNL E852 Collab.)
MANAK	00A	PR D62 012003	J.J. Manak *et al.*	(BNL E852 Collab.)
ALDE	97B	PAN 60 386	D. Alde *et al.*	(GAMS Collab.)
		Translated from YAF 60 458.		
BERTIN	97	PL B400 226	A. Bertin *et al.*	(OBELIX Collab.)
AUGUSTIN	92	PR D46 1951	J.E. Augustin, G. Cosme	(DM2 Collab.)
FUKUI	91C	PL B267 293	S. Fukui *et al.*	(SUGI, NAGO, KEK, KYOT+)
AUGUSTIN	90	PR D42 10	J.E. Augustin *et al.*	(DM2 Collab.)
AIHARA	88C	PR D38 1	H. Aihara *et al.*	(TPC-2γ Collab.)
BIRMAN	88	PRL 61 1557	A. Birman *et al.*	(BNL, FSU, IND, MASD) JP
ANTREASYAN	87	PR D36 2633	D. Antreasyan *et al.*	(Crystal Ball Collab.)
ANDO	86	PRL 57 1296	A. Ando *et al.*	(KEK, KYOT, NIRS, SAGA+) IJP
STANTON	79	PRL 42 346	N.R. Stanton *et al.*	(OSU, CARL, MCGI+) JP

$\pi(1300)$

$I^G(J^{PC}) = 1^-(0^{-+})$

$\pi(1300)$ MASS

VALUE (MeV)	EVTS	DOCUMENT ID		TECN	COMMENT
1300±100 OUR ESTIMATE					
• • • We do not use the following data for averages, fits, limits, etc. • • •					
1345± 8±10	18k	[1] SCHEGELSKY	06	RVUE	$\gamma\gamma \to \pi^+\pi^-\pi^0$
1200± 40	90k	SALVINI	04	OBLX	$\overline{p}p \to 2\pi^+2\pi^-$
1343± 15±24		CHUNG	02	B852	18.3 $\pi^-p \to \pi^+\pi^-\pi^-p$
1375± 40		ABELE	01	CBAR	0.0 $\overline{p}d \to \pi^-4\pi^0p$
1275± 15		BERTIN	97D	OBLX	0.05 $\overline{p}p \to 2\pi^+2\pi^-$
~ 1114		ABELE	96	CBAR	0.0 $\overline{p}p \to 5\pi^0$
1190± 30		ZIELINSKI	84	SPEC	200 $\pi^+Z \to Z3\pi$
1240± 30		BELLINI	82	SPEC	40 $\pi^-A \to A3\pi$
1273± 50		[2] AARON	81	RVUE	
1342± 20		BONESINI	81	OMEG	12 $\pi^-p \to p3\pi$
~ 1400		DAUM	81B	SPEC	63,94 π^-p

[1] From analysis of L3 data at 183–209 GeV.
[2] Uses multichannel Aitchison-Bowler model (BOWLER 75). Uses data from DAUM 80 and DANKOWYCH 81.

$\pi(1300)$ WIDTH

VALUE (MeV)	EVTS	DOCUMENT ID		TECN	COMMENT
200 to 600 OUR ESTIMATE					
• • • We do not use the following data for averages, fits, limits, etc. • • •					
260± 20±30	18k	[3] SCHEGELSKY	06	RVUE	$\gamma\gamma \to \pi^+\pi^-\pi^0$
470±120	90k	SALVINI	04	OBLX	$\overline{p}p \to 2\pi^+2\pi^-$
449± 39±47		CHUNG	02	B852	18.3 $\pi^-p \to \pi^+\pi^-\pi^-p$
268± 50		ABELE	01	CBAR	0.0 $\overline{p}d \to \pi^-4\pi^0p$
218±100		BERTIN	97D	OBLX	0.05 $\overline{p}p \to 2\pi^+2\pi^-$
~ 340		ABELE	96	CBAR	0.0 $\overline{p}p \to 5\pi^0$
440± 80		ZIELINSKI	84	SPEC	200 $\pi^+Z \to Z3\pi$
360±120		BELLINI	82	SPEC	40 $\pi^-A \to A3\pi$
580±100		[4] AARON	81	RVUE	
220± 70		BONESINI	81	OMEG	12 $\pi^-p \to p3\pi$
~ 600		DAUM	81B	SPEC	63,94 π^-p

[3] From analysis of L3 data at 183–209 GeV.
[4] Uses multichannel Aitchison-Bowler model (BOWLER 75). Uses data from DAUM 80 and DANKOWYCH 81.

$\pi(1300)$ DECAY MODES

	Mode	Fraction (Γ_i/Γ)
Γ_1	$\rho\pi$	seen
Γ_2	$\pi(\pi\pi)_{S\text{-wave}}$	seen
Γ_3	$\gamma\gamma$	

$\pi(1300)$ $\Gamma(i)\Gamma(\gamma\gamma)/\Gamma(total)$

$\Gamma(\rho\pi) \times \Gamma(\gamma\gamma)/\Gamma_{total}$ $\Gamma_1\Gamma_3/\Gamma$

VALUE (keV)	CL%	DOCUMENT ID		TECN	COMMENT
<0.085	90	ACCIARRI	97T	L3	$e^+e^- \to e^+e^-\pi^+\pi^-\pi^0$
• • • We do not use the following data for averages, fits, limits, etc. • • •					
<0.8	95	[5] SCHEGELSKY	06	RVUE	$\gamma\gamma \to \pi^+\pi^-\pi^0$
<0.54	90	ALBRECHT	97B	ARG	$e^+e^- \to e^+e^-\pi^+\pi^-\pi^0$

[5] From analysis of L3 data at 183–209 GeV.

$\pi(1300)$ BRANCHING RATIOS

$\Gamma(\pi(\pi\pi)_{S\text{-wave}})/\Gamma(\rho\pi)$ Γ_2/Γ_1

VALUE	CL%	EVTS	DOCUMENT ID		TECN	COMMENT
• • • We do not use the following data for averages, fits, limits, etc. • • •						
2.2 ±0.4		90k	SALVINI	04	OBLX	$\overline{p}p \to 2\pi^+2\pi^-$
seen			CHUNG	02	B852	18.3 $\pi^-p \to \pi^+2\pi^-p$
<0.15	90		ABELE	01	CBAR	0.0 $\overline{p}d \to \pi^-4\pi^0p$
2.12			[6] AARON	81	RVUE	

[6] Uses multichannel Aitchison-Bowler model (BOWLER 75). Uses data from DAUM 80 and DANKOWYCH 81.

$\pi(1300)$ REFERENCES

SCHEGELSKY	06	EPJ A27 199	V.A. Schegelsky *et al.*	
SALVINI	04	EPJ C35 21	P. Salvini *et al.*	(OBELIX Collab.)
CHUNG	02	PR D65 072001	S.U. Chung *et al.*	(BNL E852 Collab.)
ABELE	01	EPJ C19 667	A. Abele *et al.*	(Crystal Barrel Collab.)
ACCIARRI	97T	PL B413 147	M. Acciarri *et al.*	(L3 Collab.)
ALBRECHT	97B	ZPHY C74 469	H. Albrecht *et al.*	(ARGUS Collab.)
BERTIN	97D	PL B414 220	A. Bertin *et al.*	(OBELIX Collab.)
ABELE	96	PL B380 453	A. Abele *et al.*	(Crystal Barrel Collab.)
ZIELINSKI	84	PR D30 1855	M. Zielinski *et al.*	(ROCH, MINN, FNAL)
BELLINI	82	PRL 48 1697	G. Bellini *et al.*	(MILA, BGNA, JINR)
AARON	81	PR D24 1207	R.A. Aaron, R.S. Longacre	(NEAS, BNL)
BONESINI	81	PL 103B 75	M. Bonesini *et al.*	(MILA, LIVP, DARE+)
DANKOWY...	81	PRL 46 580	J.A. Dankowych *et al.*	(TNTO, BNL, CARL+)
DAUM	81B	NP B182 269	C. Daum *et al.*	(AMST, CERN, CRAC, MPIM+)
DAUM	80	PL 89B 281	C. Daum *et al.*	(AMST, CERN, CRAC, MPIM+)
BOWLER	75	NP B97 227	M.G. Bowler *et al.*	(OXFTP, DARE)

$a_2(1320)$

$I^G(J^{PC}) = 1^-(2^{++})$

$a_2(1320)$ MASS

VALUE (MeV)	DOCUMENT ID
1318.3 $^{+0.5}_{-0.6}$ OUR AVERAGE Includes data from the 4 datablocks that follow this one. Error includes scale factor of 1.2.	

3π MODE

VALUE (MeV)	EVTS	DOCUMENT ID		TECN	CHG	COMMENT
The data in this block is included in the average printed for a previous datablock.						
1319.0 $^{+1.0}_{-1.3}$ OUR AVERAGE Error includes scale factor of 1.4. See the ideogram below.						
1321 ± 1 $^{+0}_{-7}$	420k	ALEKSEEV	10	COMP		190 $\pi^-Pb \to \pi^-\pi^-\pi^+Pb'$
1326 ± 2 ±2		CHUNG	02	B852		18.3 $\pi^-p \to \pi^+\pi^-\pi^-p$
1317 ± 3		BARBERIS	98B			450 $pp \to p_f\pi^+\pi^-\pi^0p_s$
1323 ± 4 ±3		ACCIARRI	97T	L3		$e^+e^- \to e^+e^-\pi^+\pi^-\pi^0$
1320 ± 7		ALBRECHT	97B	ARG		$e^+e^- \to e^+e^-\pi^+\pi^-\pi^0$
1311.3± 1.6±3.0	72.4k	AMELIN	96	VES		36 $\pi^-p \to \pi^+\pi^-\pi^0n$
1310 ± 5		ARMSTRONG	90	OMEG	0	300.0$pp \to pp\pi^+\pi^-\pi^0$

1323.8± 2.3		4022		AUGUSTIN	89	DM2	±	$J/\psi \to \rho^{\pm} a_2^{\mp}$
1320.6± 3.1		3562		AUGUSTIN	89	DM2	0	$J/\psi \to \rho^0 a_2^0$
1317	± 2	25k	[1]	DAUM	80C	SPEC	−	63,94 $\pi^- p \to 3\pi p$
1320	±10	1097	[1]	BALTAY	78B	HBC	+0	15 $\pi^+ p \to p4\pi$
1306	± 8			FERRERSORIA	78	OMEG	−	9 $\pi^- p \to p3\pi$
1318	± 7	1.6k	[1]	EMMS	75	DBC	0	4 $\pi^+ n \to p(3\pi)^0$
1315	± 5		[1]	ANTIPOV	73C	CNTR	−	25,40 $\pi^- p \to p\eta\pi^-$
1306	± 9	1580		CHALOUPKA	73	HBC	−	3.9 $\pi^- p$

• • • We do not use the following data for averages, fits, limits, etc. • • •

1300	± 2 ±4	18k	[2]	SCHEGELSKY	06	RVUE	0	$\gamma\gamma \to \pi^+\pi^-\pi^0$
1305	±14			CONDO	93	SHF		$\gamma p \to n\pi^+\pi^+\pi^-$
1310	± 2		[1]	EVANGELIS...	81	OMEG	−	12 $\pi^- p \to 3\pi p$
1343	±11	490		BALTAY	78B	HBC	0	15 $\pi^+ p \to \Delta 3\pi$
1309	± 5	5k		BINNIE	71	MMS	−	$\pi^- p$ near a_2 threshold
1299	± 6	28k		BOWEN	71	MMS	−	5 $\pi^- p$
1300	± 6	24k		BOWEN	71	MMS	+	5 $\pi^+ p$
1309	± 4	17k		BOWEN	71	MMS	−	7 $\pi^- p$
1306	± 4	941		ALSTON-...	70	HBC	+	7.0 $\pi^+ p \to 3\pi p$

[1] From a fit to $J^P = 2^+$ $\rho\pi$ partial wave.
[2] From analysis of L3 data at 183–209 GeV.

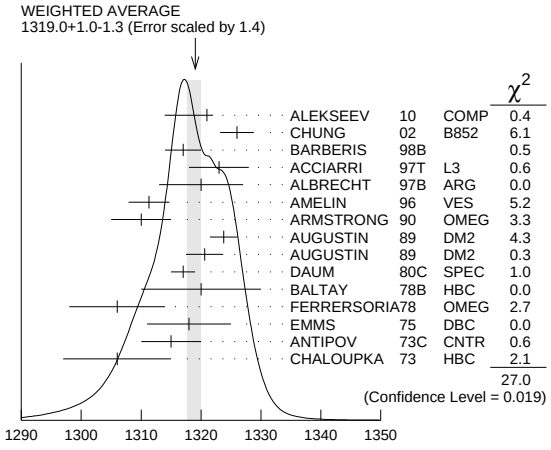

$a_2(1320)$ mass, 3π mode (MeV)

$K\overline{K}$ MODE

VALUE (MeV)	EVTS	DOCUMENT ID		TECN	CHG	COMMENT

The data in this block is included in the average printed for a previous datablock.

1318.1± 0.7 OUR AVERAGE

1319	± 5	4700	[3,4]	CLELAND	82B	SPEC	+	50 $\pi^+ p \to K^0_S K^+ p$
1324	± 6	5200	[3,4]	CLELAND	82B	SPEC	−	50 $\pi^- p \to K^0_S K^- p$
1320	± 2	4000		CHABAUD	80	SPEC	−	17 π^- A $\to K^0_S K^-$ A
1312	± 4	11000		CHABAUD	78	SPEC	−	9.8 $\pi^- p \to K^- K^0_S p$
1316	± 2	4730		CHABAUD	78	SPEC	−	18.8 $\pi^- p \to K^- K^0_S p$
1318	± 1		[3,5]	MARTIN	78D	SPEC	−	10 $\pi^- p \to K^0_S K^- p$
1320	± 2	2724		MARGULIE	76	SPEC	−	23 $\pi^- p \to K^- K^0_S p$
1313	± 4	730		FOLEY	72	CNTR	−	20.3 $\pi^- p \to K^- K^0_S p$
1319	± 3	1500	[5]	GRAYER	71	ASPK	−	17.2 $\pi^- p \to K^- K^0_S p$

• • • We do not use the following data for averages, fits, limits, etc. • • •

1304	±10	870	[6]	SCHEGELSKY	06A	RVUE	0	$\gamma\gamma \to K^0_S K^0_S$
1330	±11	1000	[3,4]	CLELAND	82B	SPEC	+	30 $\pi^+ p \to K^0_S K^+ p$
1324	± 5	350		HYAMS	78	ASPK	+	12.7 $\pi^+ p \to K^+ K^0_S p$

[3] From a fit to $J^P = 2^+$ partial wave.
[4] Number of events evaluated by us.
[5] Systematic error in mass scale subtracted.
[6] From analysis of L3 data at 91 and 183–209 GeV.

$\eta\pi$ MODE

VALUE (MeV)	EVTS	DOCUMENT ID		TECN	CHG	COMMENT

The data in this block is included in the average printed for a previous datablock.

1317.7±1.4 OUR AVERAGE

1308	±9			BARBERIS	00H			450 $pp \to p_f \eta\pi^0 p_s$
1316	±9			BARBERIS	00H			450 $pp \to \Delta^{++}_f \eta\pi^- p_s$
1317	±1 ±2			THOMPSON	97	MPS		18 $\pi^- p \to \eta\pi^- p$
1315	±5 ±2		[7]	AMSLER	94D	CBAR		0.0 $\overline{p}p \to \pi^0\pi^0\eta$
1325.1±5.1				AOYAGI	93	BKEI		$\pi^- p \to \eta\pi^- p$
1317.7±1.4±2.0				BELADIDZE	93	VES		37$\pi^- N \to \eta\pi^- N$
1323	±8	1000	[8]	KEY	73	OSPK	−	6 $\pi^- p \to p\pi^- \eta$

• • • We do not use the following data for averages, fits, limits, etc. • • •

1309	±4			ANISOVICH	09	RVUE		$\overline{p}p$, πN
1324	±5			ARMSTRONG	93C	E760	0	$\overline{p}p \to \pi^0\eta\eta \to 6\gamma$
1336.2±1.7		2561		DELFOSSE	81	SPEC	+	$\pi^{\pm} p \to p\pi^{\pm}\eta$
1330.7±2.4		1653		DELFOSSE	81	SPEC	−	$\pi^{\pm} p \to p\pi^{\pm}\eta$
1324	±8	6200	[8,9]	CONFORTO	73	OSPK	−	6 $\pi^- p \to p$MM$^-$

[7] The systematic error of 2 MeV corresponds to the spread of solutions.
[8] Error includes 5 MeV systematic mass-scale error.
[9] Missing mass with enriched MMS $= \eta\pi^-$, $\eta = 2\gamma$.

$\eta'\pi$ MODE

VALUE (MeV)	DOCUMENT ID		TECN	COMMENT

The data in this block is included in the average printed for a previous datablock.

1322 ± 7 OUR AVERAGE

1318 ± 8 $^{+3}_{-5}$	IVANOV	01	B852	18 $\pi^- p \to \eta'\pi^- p$
1327.0±10.7	BELADIDZE	93	VES	37$\pi^- N \to \eta'\pi^- N$

$a_2(1320)$ WIDTH

3π MODE

VALUE (MeV)	EVTS	DOCUMENT ID		TECN	CHG	COMMENT

105.0$^{+\ 1.6}_{-\ 1.9}$ OUR AVERAGE

110	± 2 $^{+\ 2}_{-15}$	420k		ALEKSEEV	10	COMP		190 $\pi^- Pb \to \pi^-\pi^-\pi^+ Pb'$
108	± 3 ±15			CHUNG	02	B852		18.3 $\pi^- p \to \pi^+\pi^-\pi^- p$
120	±10			BARBERIS	98B			450 $pp \to p_f \pi^+\pi^-\pi^0 p_s$
105	±10 ±11			ACCIARRI	97T	L3		$e^+e^- \to e^+e^-\pi^+\pi^-\pi^0$
120	±10			ALBRECHT	97B	ARG		$e^+e^- \to e^+e^-\pi^+\pi^-\pi^0$
103.0± 6.0± 3.3	72.4k			AMELIN	96	VES		36 $\pi^- p \to \pi^+\pi^-\pi^0 n$
120	±10			ARMSTRONG	90	OMEG	0	300.0$pp \to pp\pi^+\pi^-\pi^0$
107.0± 9.7	4022			AUGUSTIN	89	DM2	±	$J/\psi \to \rho^{\pm} a_2^{\mp}$
118.5±12.5	3562			AUGUSTIN	89	DM2	0	$J/\psi \to \rho^0 a_2^0$
97	± 5		[10]	EVANGELIS...	81	OMEG	−	12 $\pi^- p \to 3\pi p$
96	± 9	25k	[10]	DAUM	80C	SPEC	−	63,94 $\pi^- p \to 3\pi p$
110	±15	1097	[10]	BALTAY	78B	HBC	+0	15 $\pi^+ p \to p4\pi$
112	±18	1.6k	[10]	EMMS	75	DBC	0	4 $\pi^+ n \to p(3\pi)^0$
122	±14	1.2k	[10,11]	WAGNER	75	HBC	0	7 $\pi^+ p \to \Delta^{++}(3\pi)^0$
115	±15		[10]	ANTIPOV	73C	CNTR	−	25,40 $\pi^- p \to p\eta\pi^-$
99	±15	1580		CHALOUPKA	73	HBC	−	3.9 $\pi^- p$
105	± 5	28k		BOWEN	71	MMS	−	5 $\pi^- p$
99	± 5	24k		BOWEN	71	MMS	+	5 $\pi^+ p$
103	± 5	17k		BOWEN	71	MMS	−	7 $\pi^- p$

• • • We do not use the following data for averages, fits, limits, etc. • • •

117	± 6 ±20	18k	[12]	SCHEGELSKY	06	RVUE	0	$\gamma\gamma \to \pi^+\pi^-\pi^0$
120	±40			CONDO	93	SHF		$\gamma p \to n\pi^+\pi^+\pi^-$
115	±14	490		BALTAY	78B	HBC	0	15 $\pi^+ p \to \Delta 3\pi$
72	±16	5k		BINNIE	71	MMS	−	$\pi^- p$ near a_2 threshold
79	±12	941		ALSTON-...	70	HBC	+	7.0 $\pi^+ p \to 3\pi p$

[10] From a fit to $J^P = 2^+$ $\rho\pi$ partial wave.
[11] Width errors enlarged by us to $4\Gamma/\sqrt{N}$; see the note with the $K^*(892)$ mass.
[12] From analysis of L3 data at 183–209 GeV.

$K\overline{K}$ AND $\eta\pi$ MODES

VALUE (MeV)	DOCUMENT ID
107 ±5 OUR ESTIMATE	
110.4±1.7 OUR AVERAGE	Includes data from the 2 datablocks that follow this one.

$K\overline{K}$ MODE

VALUE (MeV)	EVTS	DOCUMENT ID		TECN	CHG	COMMENT

The data in this block is included in the average printed for a previous datablock.

109.8± 2.4 OUR AVERAGE

112	±20	4700	[13,14]	CLELAND	82B	SPEC	+	50 $\pi^+ p \to K^0_S K^+ p$
120	±25	5200	[13,14]	CLELAND	82B	SPEC	−	50 $\pi^- p \to K^0_S K^- p$
106	± 4	4000		CHABAUD	80	SPEC	−	17 π^- A $\to K^0_S K^-$ A
126	±11	11000		CHABAUD	78	SPEC	−	9.8 $\pi^- p \to K^- K^0_S p$
101	± 8	4730		CHABAUD	78	SPEC	−	18.8 $\pi^- p \to K^- K^0_S p$
113	± 4		[13,15]	MARTIN	78D	SPEC	−	10 $\pi^- p \to K^0_S K^- p$
105	± 8	2724	[15]	MARGULIE	76	SPEC	−	23 $\pi^- p \to K^- K^0_S p$
113	±19	730		FOLEY	72	CNTR	−	20.3 $\pi^- p \to K^- K^0_S p$
123	±13	1500	[15]	GRAYER	71	ASPK	−	17.2 $\pi^- p \to K^- K^0_S p$

Meson Particle Listings

$a_2(1320)$

• • • We do not use the following data for averages, fits, limits, etc. • • •

120	±15	870	[16] SCHEGELSKY	06A	RVUE	0	$\gamma\gamma \to K^0_S K^0_S$
121	±51	1000	[13,14] CLELAND	82B	SPEC	+	30 $\pi^+ p \to K^0_S K^+ p$
110	±18	350	HYAMS	78	ASPK	+	12.7 $\pi^+ p \to K^+ K^0_S p$

[13] From a fit to $J^P = 2^+$ partial wave.
[14] Number of events evaluated by us.
[15] Width errors enlarged by us to $4\Gamma/\sqrt{N}$; see the note with the $K^*(892)$ mass.
[16] From analysis of L3 data at 91 and 183–209 GeV.

$\eta\pi$ MODE

VALUE (MeV)	EVTS	DOCUMENT ID		TECN	CHG	COMMENT
The data in this block is included in the average printed for a previous datablock.						
111.1± 2.4 OUR AVERAGE						
115 ±20		BARBERIS	00H			450 $pp \to p_f \eta\pi^0 p_s$
112 ±14		BARBERIS	00H			450 $pp \to \Delta^{++}_f \eta\pi^- p_s$
112 ± 3 ±2		[17] AMSLER	94D	CBAR		0.0 $\overline{p}p \to \pi^0\pi^0\eta$
103 ± 6 ±3		BELADIDZE	93	VES		37$\pi^- N \to \eta\pi^- N$
112.2± 5.7	2561	DELFOSSE	81	SPEC	+	$\pi^\pm p \to p\pi^\pm\eta$
116.6± 7.7	1653	DELFOSSE	81	SPEC	−	$\pi^\pm p \to p\pi^\pm\eta$
108 ± 9	1000	KEY	73	OSPK	−	6 $\pi^- p \to p\pi^-\eta$
• • • We do not use the following data for averages, fits, limits, etc. • • •						
110 ± 4		ANISOVICH	09	RVUE		$\overline{p}p$, πN
127 ± 2 ±2		[18] THOMPSON	97	MPS		18 $\pi^- p \to \eta\pi^- p$
118 ±10		ARMSTRONG	93C	E760	0	$\overline{p}p \to \pi^0\eta\eta \to 6\gamma$
104 ± 9	6200	[19] CONFORTO	73	OSPK	−	6 $\pi^- p \to p$ MM$^-$

[17] The systematic error of 2 MeV corresponds to the spread of solutions.
[18] Resolution is not unfolded.
[19] Missing mass with enriched MMS = $\eta\pi^-$, $\eta = 2\gamma$.

$\eta'\pi$ MODE

VALUE (MeV)	DOCUMENT ID		TECN	COMMENT
119±25 OUR AVERAGE				
140±35±20	IVANOV	01	B852	18 $\pi^- p \to \eta'\pi^- p$
106±32	BELADIDZE	93	VES	37$\pi^- N \to \eta'\pi^- N$

$a_2(1320)$ DECAY MODES

	Mode	Fraction (Γ_i/Γ)	Scale factor/ Confidence level
Γ_1	3π	(70.1 ±2.7) %	S=1.2
Γ_2	$\rho(770)\pi$		
Γ_3	$f_2(1270)\pi$		
Γ_4	$\rho(1450)\pi$		
Γ_5	$\eta\pi$	(14.5 ±1.2) %	
Γ_6	$\omega\pi\pi$	(10.6 ±3.2) %	S=1.3
Γ_7	$K\overline{K}$	(4.9 ±0.8) %	
Γ_8	$\eta'(958)\pi$	(5.3 ±0.9) $\times 10^{-3}$	
Γ_9	$\pi^\pm\gamma$	(2.68±0.31) $\times 10^{-3}$	
Γ_{10}	$\gamma\gamma$	(9.4 ±0.7) $\times 10^{-6}$	
Γ_{11}	$e^+ e^-$	< 5 $\times 10^{-9}$	CL=90%

CONSTRAINED FIT INFORMATION

An overall fit to 5 branching ratios uses 18 measurements and one constraint to determine 4 parameters. The overall fit has a $\chi^2 = 9.3$ for 15 degrees of freedom.

The following *off-diagonal* array elements are the correlation coefficients $\langle \delta x_i \delta x_j \rangle / (\delta x_i \cdot \delta x_j)$, in percent, from the fit to the branching fractions, $x_i \equiv \Gamma_i/\Gamma_{\rm total}$. The fit constrains the x_i whose labels appear in this array to sum to one.

x_5	10		
x_6	−89	−46	
x_7	−1	−2	−24
	x_1	x_5	x_6

$a_2(1320)$ PARTIAL WIDTHS

$\Gamma(\eta\pi)$ Γ_5

VALUE (MeV)	EVTS	DOCUMENT ID		TECN	CHG	COMMENT
• • • We do not use the following data for averages, fits, limits, etc. • • •						
18.5±3.0	870	[20] SCHEGELSKY	06A	RVUE	0	$\gamma\gamma \to K^0_S K^0_S$

[20] From analysis of L3 data at 91 and 183–209 GeV, using $\Gamma(a_2(1320) \to \gamma\gamma) = 0.91$ keV and SU(3) relations.

$\Gamma(K\overline{K})$ Γ_7

VALUE (MeV)	EVTS	DOCUMENT ID		TECN	CHG	COMMENT
• • • We do not use the following data for averages, fits, limits, etc. • • •						
$7.0^{+2.0}_{-1.5}$	870	[21] SCHEGELSKY	06A	RVUE	0	$\gamma\gamma \to K^0_S K^0_S$

[21] From analysis of L3 data at 91 and 183–209 GeV, using $\Gamma(a_2(1320) \to \gamma\gamma) = 0.91$ keV and SU(3) relations.

$\Gamma(\pi^\pm\gamma)$ Γ_9

VALUE (keV)	EVTS	DOCUMENT ID		TECN	CHG	COMMENT
287± 30 OUR AVERAGE						
284± 25±25	7100	MOLCHANOV	01	SELX		600 $\pi^- A \to \pi^+\pi^-\pi^- A$
295± 60		CIHANGIR	82	SPEC	+	200 π^+A
• • • We do not use the following data for averages, fits, limits, etc. • • •						
461±110		[22] MAY	77	SPEC	±	9.7 γA

[22] Assuming one-pion exchange.

$\Gamma(\gamma\gamma)$ Γ_{10}

VALUE (keV)	EVTS	DOCUMENT ID		TECN	CHG	COMMENT
1.00±0.06 OUR AVERAGE						
0.98±0.05±0.09		ACCIARRI	97T	L3		$e^+e^- \to e^+e^-\pi^+\pi^-\pi^0$
0.96±0.03±0.13		ALBRECHT	97B	ARG		$e^+e^- \to e^+e^-\pi^+\pi^-\pi^0$
1.26±0.26±0.18	36	BARU	90	MD1		$e^+e^- \to e^+e^-\pi^+\pi^-\pi^0$
1.00±0.07±0.15	415	BEHREND	90C	CELL	0	$e^+e^- \to e^+e^-\pi^+\pi^-\pi^0$
1.03±0.13±0.21		BUTLER	90	MRK2		$e^+e^- \to e^+e^-\pi^+\pi^-\pi^0$
1.01±0.14±0.22	85	OEST	90	JADE		$e^+e^- \to e^+e^-\pi^0\eta$
0.90±0.27±0.15	56	[23] ALTHOFF	86	TASS	0	$e^+e^- \to e^+e^-3\pi$
1.14±0.20±0.26		[24] ANTREASYAN	86	CBAL	0	$e^+e^- \to e^+e^-\pi^0\eta$
1.06±0.18±0.19		BERGER	84C	PLUT	0	$e^+e^- \to e^+e^-3\pi$
• • • We do not use the following data for averages, fits, limits, etc. • • •						
0.81±0.19$^{+0.42}_{-0.11}$	35	[23] BEHREND	83B	CELL	0	$e^+e^- \to e^+e^-3\pi$
0.77±0.18±0.27	22	[24] EDWARDS	82F	CBAL	0	$e^+e^- \to e^+e^-\pi^0\eta$

[23] From $\rho\pi$ decay mode.
[24] From $\eta\pi^0$ decay mode.

$\Gamma(e^+e^-)$ Γ_{11}

VALUE (eV)	CL%	DOCUMENT ID		TECN	COMMENT
< 0.56	90	ACHASOV	00K	SND	$e^+e^- \to \pi^0\pi^0$
• • • We do not use the following data for averages, fits, limits, etc. • • •					
<25	90	VOROBYEV	88	ND	$e^+e^- \to \pi^0\eta$

$a_2(1320)$ $\Gamma(i)\Gamma(\gamma\gamma)/\Gamma(\text{total})$

$\Gamma(3\pi) \times \Gamma(\gamma\gamma)/\Gamma_{\rm total}$ $\Gamma_1\Gamma_{10}/\Gamma$

VALUE (keV)	EVTS	DOCUMENT ID		TECN	COMMENT
• • • We do not use the following data for averages, fits, limits, etc. • • •					
0.65±0.02±0.02	18k	[25] SCHEGELSKY	06	RVUE	$\gamma\gamma \to \pi^+\pi^-\pi^0$

[25] From analysis of L3 data at 183–209 GeV.

$\Gamma(\eta\pi) \times \Gamma(\gamma\gamma)/\Gamma_{\rm total}$ $\Gamma_5\Gamma_{10}/\Gamma$

VALUE (keV)	DOCUMENT ID		TECN	COMMENT
• • • We do not use the following data for averages, fits, limits, etc. • • •				
$0.145^{+0.097}_{-0.034}$	[26] UEHARA	09A	BELL	$e^+e^- \to e^+e^-\eta\pi^0$

[26] From the D_2-wave. The fraction of the D_0-wave is $3.4^{+2.3}_{-1.1}$%.

$\Gamma(K\overline{K}) \times \Gamma(\gamma\gamma)/\Gamma_{\rm total}$ $\Gamma_7\Gamma_{10}/\Gamma$

VALUE (keV)	DOCUMENT ID		TECN	COMMENT
0.126±0.007±0.028	[27] ALBRECHT	90G	ARG	$e^+e^- \to e^+e^-K^+K^-$
• • • We do not use the following data for averages, fits, limits, etc. • • •				
0.081±0.006±0.027	[28] ALBRECHT	90G	ARG	$e^+e^- \to e^+e^-K^+K^-$

[27] Using an incoherent background.
[28] Using a coherent background.

$a_2(1320)$ BRANCHING RATIOS

$[\Gamma(f_2(1270)\pi) + \Gamma(\rho(1450)\pi)]/\Gamma(\rho(770)\pi)$ $(\Gamma_3+\Gamma_4)/\Gamma_2$

VALUE	CL%	DOCUMENT ID		TECN	CHG	COMMENT
<0.12	90	ABRAMOVI...	70B	HBC	−	3.93 $\pi^- p$

$\Gamma(\eta\pi)/\Gamma(3\pi)$ Γ_5/Γ_1

VALUE	EVTS	DOCUMENT ID		TECN	CHG	COMMENT
0.207±0.018 OUR FIT						
0.213±0.020 OUR AVERAGE						
0.18 ±0.05		FORINO	76	HBC		11 $\pi^- p$
0.22 ±0.05	52	ANTIPOV	73	CNTR	−	40 $\pi^- p$
0.211±0.044	149	CHALOUPKA	73	HBC	−	3.9 $\pi^- p$
0.246±0.042	167	ALSTON-...	71	HBC	+	7.0 $\pi^+ p$
0.25 ±0.09	15	BOECKMANN	70	HBC	+	5.0 $\pi^+ p$
0.23 ±0.08	22	ASCOLI	68	HBC	−	5 $\pi^- p$
0.12 ±0.08		CHUNG	68	HBC	−	3.2 $\pi^- p$
0.22 ±0.09		CONTE	67	HBC	−	11.0 $\pi^- p$

$\Gamma(\omega\pi\pi)/\Gamma(3\pi)$ Γ_6/Γ_1

VALUE	EVTS	DOCUMENT ID		TECN	CHG	COMMENT
0.15±0.05 OUR FIT Error includes scale factor of 1.3.						
0.15±0.05 OUR AVERAGE Error includes scale factor of 1.3. See the ideogram below.						
0.28±0.09	60	DIAZ	74	DBC	0	6 $\pi^+ n$
0.18±0.08		[29] KARSHON	74	HBC		Avg. of above two
0.10±0.05	279	CHALOUPKA	73	HBC	−	3.9 $\pi^- p$
• • • We do not use the following data for averages, fits, limits, etc. • • •						
0.29±0.08	140	[29] KARSHON	74	HBC	0	4.9 $\pi^+ p$
0.10±0.04	60	[29] KARSHON	74	HBC	+	4.9 $\pi^+ p$
0.19±0.08		DEFOIX	73	HBC	0	0.7 $\overline{p}p$

[29] KARSHON 74 suggest an additional $I = 0$ state strongly coupled to $\omega\pi\pi$ which could explain discrepancies in branching ratios and masses. We use a central value and a systematic spread.

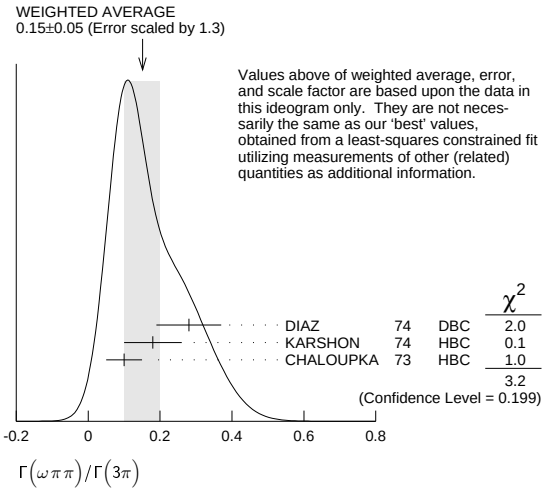

$\Gamma(K\overline{K})/\Gamma(3\pi)$ Γ_7/Γ_1

VALUE	EVTS	DOCUMENT ID		TECN	CHG	COMMENT
0.070±0.012 OUR FIT						
0.078±0.017		CHABAUD	78	RVUE		
• • • We do not use the following data for averages, fits, limits, etc. • • •						
0.011±0.003		[30] BERTIN	98B	OBLX		0.0 $\overline{p}p \rightarrow K^{\pm} K_S \pi^{\mp}$
0.056±0.014	50	[31] CHALOUPKA	73	HBC	−	3.9 $\pi^- p$
0.097±0.018	113	[31] ALSTON-...	71	HBC	+	7.0 $\pi^+ p$
0.06 ±0.03		[31] ABRAMOVI...	70B	HBC	−	3.93 $\pi^- p$
0.054±0.022		[31] CHUNG	68	HBC	−	3.2 $\pi^- p$

[30] Using 4π data from BERTIN 97D.
[31] Included in CHABAUD 78 review.

$\Gamma(K\overline{K})/\Gamma(\eta\pi)$ Γ_7/Γ_5

VALUE	DOCUMENT ID		TECN	COMMENT
• • • We do not use the following data for averages, fits, limits, etc. • • •				
0.08±0.02	[32] BERTIN	98B	OBLX	0.0 $\overline{p}p \rightarrow K^{\pm} K_S \pi^{\mp}$

[32] Using $\eta\pi\pi$ data from AMSLER 94D.

$\Gamma(\eta\pi)/[\Gamma(3\pi)+\Gamma(\eta\pi)+\Gamma(K\overline{K})]$ $\Gamma_5/(\Gamma_1+\Gamma_5+\Gamma_7)$

VALUE	EVTS	DOCUMENT ID		TECN	CHG	COMMENT
0.162±0.012 OUR FIT						
0.140±0.028 OUR AVERAGE						
0.13 ±0.04		ESPIGAT	72	HBC	±	0.0 $\overline{p}p$
0.15 ±0.04	34	BARNHAM	71	HBC	+	3.7 $\pi^+ p$

$\Gamma(K\overline{K})/[\Gamma(3\pi)+\Gamma(\eta\pi)+\Gamma(K\overline{K})]$ $\Gamma_7/(\Gamma_1+\Gamma_5+\Gamma_7)$

VALUE	EVTS	DOCUMENT ID		TECN	CHG	COMMENT
0.054±0.009 OUR FIT						
0.048±0.012 OUR AVERAGE						
0.05 ±0.02		TOET	73	HBC	+	5 $\pi^+ p$
0.09 ±0.04		TOET	73	HBC	0	5 $\pi^+ p$
0.03 ±0.02	8	DAMERI	72	HBC	−	11 $\pi^- p$
0.06 ±0.03	17	BARNHAM	71	HBC	+	3.7 $\pi^+ p$
• • • We do not use the following data for averages, fits, limits, etc. • • •						
0.020±0.004	[33] ESPIGAT		72	HBC	±	0.0 $\overline{p}p$

[33] Not averaged because of discrepancy between masses from $K\overline{K}$ and $\rho\pi$ modes.

$\Gamma(\eta'(958)\pi)/\Gamma_{total}$ Γ_8/Γ

VALUE	CL%	DOCUMENT ID		TECN	CHG	COMMENT
• • • We do not use the following data for averages, fits, limits, etc. • • •						
<0.006	95	ALDE	92B	GAM2		38,100 $\pi^- p \rightarrow \eta'\pi^0 n$
<0.02	97	BARNHAM	71	HBC	+	3.7 $\pi^+ p$
0.004±0.004		BOESEBECK	68	HBC	+	8 $\pi^+ p$

$\Gamma(\eta'(958)\pi)/\Gamma(3\pi)$ Γ_8/Γ_1

VALUE	CL%	DOCUMENT ID		TECN	CHG	COMMENT
• • • We do not use the following data for averages, fits, limits, etc. • • •						
<0.011	90	EISENSTEIN	73	HBC	−	5 $\pi^- p$
<0.04		ALSTON-...	71	HBC	+	7.0 $\pi^+ p$
$0.04\ ^{+0.03}_{-0.04}$		BOECKMANN	70	HBC	0	5.0 $\pi^+ p$

$\Gamma(\eta'(958)\pi)/\Gamma(\eta\pi)$ Γ_8/Γ_5

VALUE	DOCUMENT ID		TECN	COMMENT
0.037±0.006 OUR AVERAGE				
0.032±0.009	ABELE	97C	CBAR	0.0 $\overline{p}p \rightarrow \pi^0\pi^0\eta'$
0.047±0.010±0.004	[34] BELADIDZE	93	VES	37 $\pi^- N \rightarrow a_2^- N$
0.034±0.008±0.005	BELADIDZE	92	VES	36 π^- C $\rightarrow a_2^-$ C

[34] Using $B(\eta' \rightarrow \pi^+\pi^-\eta) = 0.441$, $B(\eta \rightarrow \gamma\gamma) = 0.389$ and $B(\eta \rightarrow \pi^+\pi^-\pi^0) = 0.236$.

$\Gamma(\pi^{\pm}\gamma)/\Gamma_{total}$ Γ_9/Γ

VALUE	DOCUMENT ID		TECN	COMMENT
• • • We do not use the following data for averages, fits, limits, etc. • • •				
$0.005\ ^{+0.005}_{-0.003}$	[35] EISENBERG	72	HBC	4.3,5.25,7.5 γp

[35] Pion-exchange model used in this estimation.

$\Gamma(e^+e^-)/\Gamma_{total}$ Γ_{11}/Γ

VALUE (units 10^{-9})	CL%	DOCUMENT ID		TECN	COMMENT
• • • We do not use the following data for averages, fits, limits, etc. • • •					
<6	90	ACHASOV	00K	SND	$e^+e^- \rightarrow \pi^0\pi^0$

$a_2(1320)$ REFERENCES

ALEKSEEV	10	PRL 104 241803	M.G. Alekseev *et al.*	(COMPASS Collab.)
ANISOVICH	09	IJMP A24 2481	V.V. Anisovich, A.V. Sarantsev	
UEHARA	09A	PR D80 032001	S. Uehara *et al.*	(BELLE Collab.)
SCHEGELSKY	06	EPJ A27 199	V.A. Schegelsky *et al.*	
SCHEGELSKY	06A	EPJ A27 207	V.A. Schegelsky *et al.*	
CHUNG	02	PR D65 072001	S.U. Chung *et al.*	(BNL E852 Collab.)
IVANOV	01	PRL 86 3977	E.I. Ivanov *et al.*	(BNL E852 Collab.)
MOLCHANOV	01	PL B521 171	V.V. Molchanov *et al.*	(FNAL SELEX Collab.)
ACHASOV	00K	PL B492 8	M.N. Achasov *et al.*	(Novosibirsk SND Collab.)
BARBERIS	00H	PL B488 225	D. Barberis *et al.*	(WA 102 Collab.)
BARBERIS	98B	PL B422 399	D. Barberis *et al.*	(WA 102 Collab.)
BERTIN	98B	PL B434 180	A. Bertin *et al.*	(OBELIX Collab.)
ABELE	97C	PL B404 179	A. Abele *et al.*	(Crystal Barrel Collab.)
ACCIARRI	97T	PL B413 147	M. Acciarri *et al.*	(L3 Collab.)
ALBRECHT	97B	ZPHY C74 469	H. Albrecht *et al.*	(ARGUS Collab.)
THOMPSON	97	PRL 79 1630	D.R. Thompson *et al.*	(BNL E852 Collab.)
AMELIN	96	ZPHY C70 71	D.V. Amelin *et al.*	(SERP, TBIL)
AMSLER	94D	PL B333 277	C. Amsler *et al.*	(Crystal Barrel Collab.)
AOYAGI	93	PL B314 246	H. Aoyagi *et al.*	(BKEI Collab.)
ARMSTRONG	93C	PL B307 394	T.A. Armstrong *et al.*	(FNAL, FERR, GENO+)
BELADIDZE	93	PL B313 276	G.M. Beladidze *et al.*	(VES Collab.)
CONDO	93	PR D48 3045	G.T. Condo *et al.*	(SLAC Hybrid Collab.)
ALDE	92B	ZPHY C54 549	D.M. Alde *et al.*	(SERP, BELG, LANL, LAPP+)
BELADIDZE	92	ZPHY C54 235	G.M. Beladidze *et al.*	(VES Collab.)
ALBRECHT	90G	ZPHY C48 183	H. Albrecht *et al.*	(ARGUS Collab.)
ARMSTRONG	90	ZPHY C48 213	T.A. Armstrong, M. Benayoun, W. Beusch (WA76 Coll.)	
BARU	90	ZPHY C48 581	S.E. Baru *et al.*	(MD-1 Collab.)
BEHREND	90C	ZPHY C46 583	H.J. Behrend *et al.*	(CELLO Collab.)
BUTLER	90	PR D42 1368	F. Butler *et al.*	(Mark II Collab.)
OEST	90	ZPHY C47 343	T. Oest *et al.*	(JADE Collab.)
AUGUSTIN	89	NP B320 1	J.E. Augustin, G. Cosme	(DM2 Collab.)
VOROBYEV	88	SJNP 48 273 Translated from YAF 48 436.	P.V. Vorobiev *et al.*	(NOVO)
ALTHOFF	86	ZPHY C31 537	M. Althoff *et al.*	(TASSO Collab.)
ANTREASYAN	86	PR D33 1847	D. Antreasyan *et al.*	(Crystal Ball Collab.)
BERGER	84C	PL 149B 427	C. Berger *et al.*	(PLUTO Collab.)
BEHREND	83B	PL 125B 518 (erratum)	H.J. Behrend *et al.*	(CELLO Collab.)
CIHANGIR	82	PL 117B 123	S. Cihangir *et al.*	(FNAL, MINN, ROCH)
CLELAND	82B	NP B208 228	W.E. Cleland *et al.*	(DURH, GEVA, LAUS+)
EDWARDS	82F	PL 110B 82	C. Edwards *et al.*	(CIT, HARV, PRIN+)
DELFOSSE	81	NP B183 349	A. Delfosse *et al.*	(GEVA, LAUS)
EVANGELIS...	81	NP B178 197	C. Evangelista *et al.*	(BARI, BONN, CERN+)
CHABAUD	80	NP B175 189	V. Chabaud *et al.*	(CERN, MPIM, AMST)
DAUM	80C	PL 89B 276	C. Daum *et al.*	(AMST, CERN, CRAC, MPIM+) JP

BALTAY	78B	PR D17 62	C. Baltay *et al.*	(COLU, BING)
CHABAUD	78	NP B145 349	V. Chabaud *et al.*	(CERN, MPIM)
FERRERSORIA	78	PL 74B 287	A. Ferrer Soria *et al.*	(ORSAY, CERN, CDEF+)
HYAMS	78	NP B146 303	B.D. Hyams *et al.*	(CERN, MPIM, ATEN)
MARTIN	78D	PL 74B 417	A.D. Martin *et al.*	(DURH, GEVA) JP
MAY	77	PR D16 1983	E.N. May *et al.*	(ROCH, CORN)
FORINO	76	NC 35A 465	A. Forino *et al.*	(BGNA, FIRZ, GENO, MILA+)
MARGULIE	76	PR D14 667	M. Margulies *et al.*	(BNL, CUNY)
EMMS	75	PL 58B 117	M.J. Emms *et al.*	(BIRM, DURH, RHEL) JP
WAGNER	75	PL 58B 201	F. Wagner, M. Tabak, D.M. Chew	(LBL) JP
DIAZ	74	PRL 32 260	J. Diaz *et al.*	(CASE, CMU)
KARSHON	74	PRL 32 852	U. Karshon *et al.*	(REHO)
ANTIPOV	73	NP B63 175	Y.M. Antipov *et al.*	(CERN, SERP) JP
ANTIPOV	73C	NP B63 153	Y.M. Antipov *et al.*	(CERN, SERP) JP
CHALOUPKA	73	PL 44B 211	V. Chaloupka *et al.*	(CERN)
CONFORTO	73	PL 45B 154	G. Conforto *et al.*	(EFI, FNAL, TNTO+)
DEFOIX	73	PL 43B 141	C. Defoix *et al.*	(CDEF)
EISENSTEIN	73	PR D7 278	L. Eisenstein *et al.*	(ILL)
KEY	73	PRL 30 503	A.W. Key *et al.*	(TNTO, EFI, FNAL, WISC)
TOET	73	NP B63 248	D.Z. Toet *et al.*	(NIJM, BONN, DURH, TORI)
DAMERI	72	NC 9A 1	M. Dameri *et al.*	(GENO, MILA, SACL)
EISENBERG	72	PR D5 15	Y. Eisenberg *et al.*	(REHO, SLAC, TELA)
ESPIGAT	72	NP B36 93	P. Espigat *et al.*	(CERN, CDEF)
FOLEY	72	PR D6 747	K.J. Foley *et al.*	(BNL, CUNY)
ALSTON-...	71	PL 34B 156	M. Alston-Garnjost *et al.*	(LRL)
BARNHAM	71	PRL 26 1494	K.W.J. Barnham *et al.*	(LBL)
BINNIE	71	PL 36B 257	D.M. Binnie *et al.*	(LOIC, SHMP)
BOWEN	71	PRL 26 1663	D.R. Bowen *et al.*	(NEAS, STON)
GRAYER	71	PL 34B 333	G. Grayer *et al.*	(CERN, MPIM)
ABRAMOVI...	70B	NP B23 466	M. Abramovich *et al.*	(CERN) JP
ALSTON-...	70	PL 33B 607	M. Alston-Garnjost *et al.*	(LRL)
BOECKMANN	70	NP B16 221	K. Boeckmann *et al.*	(BONN, DURH, NIJM+)
ASCOLI	68	PRL 20 1321	G. Ascoli *et al.*	(ILL) JP
BOESEBECK	68	NP B4 501	K. Boesebeck *et al.*	(AACH, BERL, CERN)
CHUNG	68	PR 165 1491	S.U. Chung *et al.*	(LRL)
CONTE	67	NC 51A 175	F. Conte *et al.*	(GENO, HAMB, MILA, SACL)

$f_0(1370)$

$I^G(J^{PC}) = 0^+(0^{++})$

See also the mini-reviews on scalar mesons under $f_0(500)$ (see the index for the page number) and on non-$q\overline{q}$ candidates in PDG 06, Journal of Physics (generic for all A,B,E,G) **G33** 1 (2006).

$f_0(1370)$ T-MATRIX POLE POSITION

Note that $\Gamma \approx 2\ \mathrm{Im}(\sqrt{s_{\mathrm{pole}}})$.

VALUE (MeV)	DOCUMENT ID		TECN	COMMENT
(1200–1500)−*i*(150–250) OUR ESTIMATE				
• • • We do not use the following data for averages, fits, limits, etc. • • •				
$(1290 \pm 50) - i(170^{+20}_{-40})$	[1] ANISOVICH	09	RVUE	0.0 $\overline{p}p$, πN
$(1373 \pm 15) - i(137 \pm 10)$	[2] BARGIOTTI	03	OBLX	$\overline{p}p$
$(1302 \pm 17) - i(166 \pm 18)$	[3] BARBERIS	00C		450 $pp \to p_f 4\pi p_s$
$(1312 \pm 25 \pm 10) - i(109 \pm 22 \pm 15)$	BARBERIS	99D	OMEG	450 $pp \to K^+K^-$, $\pi^+\pi^-$
$(1406 \pm 19) - i(80 \pm 6)$	[4] KAMINSKI	99	RVUE	$\pi\pi \to \pi\pi$, $K\overline{K}$, $\sigma\sigma$
$(1300 \pm 20) - i(120 \pm 20)$	ANISOVICH	98B	RVUE	Compilation
$(1290 \pm 15) - i(145 \pm 15)$	BARBERIS	97B	OMEG	450 $pp \to pp2(\pi^+\pi^-)$
$(1548 \pm 40) - i(560 \pm 40)$	BERTIN	97C	OBLX	0.0 $\overline{p}p \to \pi^+\pi^-\pi^0$
$(1380 \pm 40) - i(180 \pm 25)$	ABELE	96B	CBAR	0.0 $\overline{p}p \to \pi^0 K^0_L K^0_L$
$(1300 \pm 15) - i(115 \pm 8)$	BUGG	96	RVUE	
$(1330 \pm 50) - i(150 \pm 40)$	[5] AMSLER	95B	CBAR	$\overline{p}p \to 3\pi^0$
$(1360 \pm 35) - i(150–300)$	[5] AMSLER	95C	CBAR	$\overline{p}p \to \pi^0\eta\eta$
$(1390 \pm 30) - i(190 \pm 40)$	[6] AMSLER	95D	CBAR	$\overline{p}p \to 3\pi^0$, $\pi^0\eta\eta$, $\pi^0\pi^0\eta$
$1346 - i249$	[7,8] JANSSEN	95	RVUE	$\pi\pi \to \pi\pi$, $K\overline{K}$
$1214 - i168$	[8,9] TORNQVIST	95	RVUE	$\pi\pi \to \pi\pi$, $K\overline{K}$, $K\pi$, $\eta\pi$
$1364 - i139$	AMSLER	94D	CBAR	$\overline{p}p \to \pi^0\pi^0\eta$
$(1365^{+20}_{-55}) - i(134 \pm 35)$	ANISOVICH	94	CBAR	$\overline{p}p \to 3\pi^0, \pi^0\eta\eta$
$(1340 \pm 40) - i(127^{+30}_{-20})$	[10] BUGG	94	RVUE	$\overline{p}p \to 3\pi^0$, $\eta\eta\pi^0$, $\eta\pi^0\pi^0$
$(1430 \pm 5) - i(73 \pm 13)$	[11] KAMINSKI	94	RVUE	$\pi\pi \to \pi\pi$, $K\overline{K}$
$1420 - i220$	[12] AU	87	RVUE	$\pi\pi \to \pi\pi$, $K\overline{K}$

[1] Another pole is found at $(1510 \pm 130) - i\,(800^{+100}_{-150})$ MeV.
[2] Coupled channel analysis of $\pi^+\pi^-\pi^0$, $K^+K^-\pi^0$, and $K^\pm K^0_S\pi^\mp$.
[3] Average between $\pi^+\pi^-2\pi^0$ and $2(\pi^+\pi^-)$.
[4] T-matrix pole on sheet $---$.
[5] Supersedes ANISOVICH 94.
[6] Coupled-channel analysis of $\overline{p}p \to 3\pi^0$, $\pi^0\eta\eta$, and $\pi^0\pi^0\eta$ on sheet IV. Demonstrates explicitly that $f_0(500)$ and $f_0(1370)$ are two different poles.
[7] Analysis of data from FALVARD 88.
[8] The pole is on Sheet III. Demonstrates explicitly that $f_0(500)$ and $f_0(1370)$ are two different poles.
[9] Uses data from BEIER 72B, OCHS 73, HYAMS 73, GRAYER 74, ROSSELET 77, CASON 83, ASTON 88, and ARMSTRONG 91B. Coupled channel analysis with flavor symmetry and all light two-pseudoscalars systems.
[10] Reanalysis of ANISOVICH 94 data.
[11] T-matrix pole on sheet III.
[12] Analysis of data from OCHS 73,GRAYER 74, BECKER 79, and CASON 83.

$f_0(1370)$ BREIT-WIGNER MASS OR K-MATRIX POLE PARAMETER

VALUE (MeV)	DOCUMENT ID
1200 to 1500 OUR ESTIMATE	

$\pi\pi$ MODE

VALUE (MeV)	EVTS	DOCUMENT ID		TECN	COMMENT
• • • We do not use the following data for averages, fits, limits, etc. • • •					
1400 ± 40		[13] AUBERT	09L	BABR	$B^\pm \to \pi^\pm\pi^\pm\pi^\mp$
$1470^{+\ 6}_{-\ 7} + {}^{72}_{-255}$		[14] UEHARA	08A	BELL	10.6 $e^+e^- \to e^+e^-\pi^0\pi^0$
1259 ± 55	2.6k	BONVICINI	07	CLEO	$D^+ \to \pi^-\pi^+\pi^+$
$1309 \pm\ 1 \pm 15$		[15] BUGG	07A	RVUE	0.0 $p\overline{p} \to 3\pi^0$
1449 ± 13	4.3k	[16] GARMASH	06	BELL	$B^+ \to K^+\pi^+\pi^-$
1350 ± 50		ABLIKIM	05	BES2	$J/\psi \to \phi\pi^+\pi^-$
$1265 \pm 30^{+\ 20}_{-\ 35}$		ABLIKIM	05Q	BES2	$\psi(2S) \to \gamma\pi^+\pi^- K^+K^-$
$1434 \pm 18 \pm\ 9$	848	AITALA	01A	E791	$D^+_s \to \pi^-\pi^+\pi^+$
1308 ± 10		BARBERIS	99B	OMEG	450 $pp \to p_s p_f \pi^+\pi^-$
1315 ± 50		BELLAZZINI	99	GAM4	450 $pp \to pp\pi^0\pi^0$
1315 ± 30		ALDE	98	GAM4	100 $\pi^-p \to \pi^0\pi^0 n$
1280 ± 55		BERTIN	98	OBLX	0.05–0.405 $\overline{n}p \to \pi^+\pi^+\pi^-$
1186		[17,18] TORNQVIST	95	RVUE	$\pi\pi \to \pi\pi$, $K\overline{K}$, $K\pi$, $\eta\pi$
1472 ± 12		ARMSTRONG	91	OMEG	300 $pp \to pp\pi\pi$, $pp K\overline{K}$
1275 ± 20		BREAKSTONE	90	SFM	62 $pp \to pp\pi^+\pi^-$
1420 ± 20		AKESSON	86	SPEC	63 $pp \to pp\pi^+\pi^-$
1256		FROGGATT	77	RVUE	$\pi^+\pi^-$ channel

[13] Breit-Wigner mass.
[14] Breit-Wigner mass. May also be the $f_0(1500)$.
[15] Reanalysis of ABELE 96C data.
[16] Also observed by GARMASH 07 in $B^0 \to K^0_S\pi^+\pi^-$ decays. Supersedes GARMASH 05.
[17] Uses data from BEIER 72B, OCHS 73, HYAMS 73, GRAYER 74, ROSSELET 77, CASON 83, ASTON 88, and ARMSTRONG 91B. Coupled channel analysis with flavor symmetry and all light two-pseudoscalars systems.
[18] Also observed by ASNER 00 in $\tau^- \to \pi^-\pi^0\pi^0\nu_\tau$ decays

$K\overline{K}$ MODE

VALUE (MeV)	DOCUMENT ID		TECN	COMMENT
• • • We do not use the following data for averages, fits, limits, etc. • • •				
$1440 \pm\ 6$	VLADIMIRSK...06		SPEC	40 $\pi^-p \to K^0_S K^0_S n$
1391 ± 10	TIKHOMIROV	03	SPEC	40.0 π^-C $\to K^0_S K^0_S K^0_L$X
1440 ± 50	BOLONKIN	88	SPEC	40 $\pi^-p \to K^0_S K^0_S n$
$1463 \pm\ 9$	ETKIN	82B	MPS	23 $\pi^-p \to n2K^0_S$
1425 ± 15	WICKLUND	80	SPEC	6 $\pi N \to K^+K^-N$
~ 1300	POLYCHRO...	79	STRC	7 $\pi^-p \to n2K^0_S$

4π MODE $2(\pi\pi)_S+\rho\rho$

VALUE (MeV)	EVTS	DOCUMENT ID		TECN	COMMENT
• • • We do not use the following data for averages, fits, limits, etc. • • •					
1395 ± 40		ABELE	01	CBAR	0.0 $\overline{p}d \to \pi^- 4\pi^0 p$
1374 ± 38		AMSLER	94	CBAR	0.0 $\overline{p}p \to \pi^+\pi^- 3\pi^0$
1345 ± 12		ADAMO	93	OBLX	$\overline{n}p \to 3\pi^+ 2\pi^-$
1386 ± 30		GASPERO	93	DBC	0.0 $\overline{p}n \to 2\pi^+ 3\pi^-$
~ 1410	5751	[19] BETTINI	66	DBC	0.0 $\overline{p}n \to 2\pi^+ 3\pi^-$

[19] $\rho\rho$ dominant.

$\eta\eta$ MODE

VALUE (MeV)	DOCUMENT ID		TECN	COMMENT
• • • We do not use the following data for averages, fits, limits, etc. • • •				
$1262^{+\ 51}_{-\ 78} + {}^{82}_{-103}$	[20] UEHARA	10A	BELL	10.6 $e^+e^- \to e^+e^-\eta\eta$
1430	AMSLER	92	CBAR	0.0 $\overline{p}p \to \pi^0\eta\eta$
1220 ± 40	ALDE	86D	GAM4	100 $\pi^-p \to n2\eta$

[20] Breit-Wigner mass. May also be the $f_0(1500)$.

COUPLED CHANNEL MODE

VALUE (MeV)	DOCUMENT ID		TECN
• • • We do not use the following data for averages, fits, limits, etc. • • •			
1306 ± 20	[21] ANISOVICH	03	RVUE

[21] K-matrix pole from combined analysis of $\pi^-p \to \pi^0\pi^0 n$, $\pi^-p \to K\overline{K}n$, $\pi^+\pi^- \to \pi^+\pi^-$, $\overline{p}p \to \pi^0\pi^0\pi^0$, $\pi^0\eta\eta$, $\pi^0\pi^0\eta$, $\pi^+\pi^-\pi^0$, $K^+K^-\pi^0$, $K^0_S K^0_S\pi^0$, $K^+K^0_S\pi^-$ at rest, $\overline{p}n \to \pi^-\pi^-\pi^+$, $K^0_S K^-\pi^0$, $K^0_S K^0_S\pi^-$ at rest.

$f_0(1370)$ BREIT-WIGNER WIDTH

VALUE (MeV)	DOCUMENT ID
200 to 500 OUR ESTIMATE	

$\pi\pi$ MODE

VALUE (MeV)	EVTS	DOCUMENT ID		TECN	COMMENT
• • • We do not use the following data for averages, fits, limits, etc. • • •					
300 ± 80		[22] AUBERT	09L	BABR	$B^\pm \to \pi^\pm\pi^\pm\pi^\mp$
$90^{+\ 2+\ 50}_{-\ 1-\ 22}$		[23] UEHARA	08A	BELL	10.6 $e^+e^- \to e^+e^-\pi^0\pi^0$
298 ± 21	2.6k	BONVICINI	07	CLEO	$D^+ \to \pi^-\pi^+\pi^+$
126 ± 25	4286	[24] GARMASH	06	BELL	$B^+ \to K^+\pi^+\pi^-$
265 ± 40		ABLIKIM	05	BES2	$J/\psi \to \phi\pi^+\pi^-$
$350\pm 100^{+\ 105}_{-\ 60}$		ABLIKIM	05Q	BES2	$\psi(2S) \to \gamma\pi^+\pi^- K^+K^-$
$173\pm 32\pm 6$	848	AITALA	01A	E791	$D_s^+ \to \pi^-\pi^+\pi^+$
222 ± 20		BARBERIS	99B	OMEG	450 $pp \to p_s p_f \pi^+\pi^-$
255 ± 60		BELLAZZINI	99	GAM4	450 $pp \to pp\pi^0\pi^0$
190 ± 50		ALDE	98	GAM4	100 $\pi^- p \to \pi^0\pi^0 n$
323 ± 13		BERTIN	98	OBLX	0.05–0.405 $\overline{n}p \to \pi^+\pi^+\pi^-$
350		[25,26] TORNQVIST	95	RVUE	$\pi\pi \to \pi\pi$, $K\overline{K}$, $K\pi$, $\eta\pi$
195 ± 33		ARMSTRONG	91	OMEG	300 $pp \to pp\pi\pi$, $pp K\overline{K}$
285 ± 60		BREAKSTONE	90	SFM	62 $pp \to pp\pi^+\pi^-$
460 ± 50		AKESSON	86	SPEC	63 $pp \to pp\pi^+\pi^-$
~ 400		[27] FROGGATT	77	RVUE	$\pi^+\pi^-$ channel

[22] The systematic errors are not reported.

[23] Breit-Wigner width. May also be the $f_0(1500)$.

[24] Also observed by GARMASH 07 in $B^0 \to K^0_S\pi^+\pi^-$ decays. Supersedes GARMASH 05.

[25] Uses data from BEIER 72B, OCHS 73, HYAMS 73, GRAYER 74, ROSSELET 77, CASON 83, ASTON 88, and ARMSTRONG 91B. Coupled channel analysis with flavor symmetry and all light two-pseudoscalars systems.

[26] Also observed by ASNER 00 in $\tau^- \to \pi^-\pi^0\pi^0\nu_\tau$ decays

[27] Width defined as distance between 45 and 135° phase shift.

$K\overline{K}$ MODE

VALUE (MeV)	DOCUMENT ID		TECN	COMMENT
• • • We do not use the following data for averages, fits, limits, etc. • • •				
121 ± 15	VLADIMIRSK...06		SPEC	40 $\pi^- p \to K^0_S K^0_S n$
55 ± 26	TIKHOMIROV	03	SPEC	40.0 π^- C $\to K^0_S K^0_S K^0_L$ X
250 ± 80	BOLONKIN	88	SPEC	40 $\pi^- p \to K^0_S K^0_S n$
$118^{+138}_{-\ 16}$	ETKIN	82B	MPS	23 $\pi^- p \to n2K^0_S$
160 ± 30	WICKLUND	80	SPEC	6 $\pi N \to K^+K^- N$
~ 150	POLYCHRO...	79	STRC	7 $\pi^- p \to n2K^0_S$

4π MODE $2(\pi\pi)_S{+}\rho\rho$

VALUE (MeV)	EVTS	DOCUMENT ID		TECN	COMMENT
• • • We do not use the following data for averages, fits, limits, etc. • • •					
275 ± 55		ABELE	01	CBAR	0.0 $\overline{p}d \to \pi^- 4\pi^0 p$
375 ± 61		AMSLER	94	CBAR	0.0 $\overline{p}p \to \pi^+\pi^- 3\pi^0$
398 ± 26		ADAMO	93	OBLX	$\overline{n}p \to 3\pi^+ 2\pi^-$
310 ± 50		GASPERO	93	DBC	0.0 $\overline{p}n \to 2\pi^+ 3\pi^-$
~ 90	5751	[28] BETTINI	66	DBC	0.0 $\overline{p}n \to 2\pi^+ 3\pi^-$

[28] $\rho\rho$ dominant.

$\eta\eta$ MODE

VALUE (MeV)	DOCUMENT ID		TECN	COMMENT
• • • We do not use the following data for averages, fits, limits, etc. • • •				
$484^{+246+246}_{-170-263}$	[29] UEHARA	10A	BELL	10.6 $e^+e^- \to e^+e^-\eta\eta$
250	AMSLER	92	CBAR	0.0 $\overline{p}p \to \pi^0\eta\eta$
320 ± 40	ALDE	86D	GAM4	100 $\pi^- p \to n2\eta$

[29] Breit-Wigner width. May also be the $f_0(1500)$.

COUPLED CHANNEL MODE

VALUE (MeV)	DOCUMENT ID		TECN
• • • We do not use the following data for averages, fits, limits, etc. • • •			
147^{+30}_{-50}	[30] ANISOVICH	03	RVUE

[30] K-matrix pole from combined analysis of $\pi^- p \to \pi^0\pi^0 n$, $\pi^- p \to K\overline{K}n$, $\pi^+\pi^- \to \pi^+\pi^-$, $\overline{p}p \to \pi^0\pi^0\pi^0$, $\pi^0\eta\eta$, $\pi^0\pi^0\eta$, $\pi^+\pi^-\pi^0$, $K^+K^-\pi^0$, $K^0_S K^0_S\pi^0$, $K^+K^0_S\pi^-$ at rest, $\overline{p}n \to \pi^-\pi^-\pi^+$, $K^0_S K^-\pi^0$, $K^0_S K^0_S\pi^-$ at rest.

$f_0(1370)$ DECAY MODES

	Mode	Fraction (Γ_i/Γ)
Γ_1	$\pi\pi$	seen
Γ_2	4π	seen
Γ_3	$4\pi^0$	seen
Γ_4	$2\pi^+2\pi^-$	seen
Γ_5	$\pi^+\pi^-2\pi^0$	seen
Γ_6	$\rho\rho$	dominant
Γ_7	$2(\pi\pi)_S$-wave	seen
Γ_8	$\pi(1300)\pi$	seen
Γ_9	$a_1(1260)\pi$	seen
Γ_{10}	$\eta\eta$	seen
Γ_{11}	$K\overline{K}$	seen
Γ_{12}	$K\overline{K}n\pi$	not seen
Γ_{13}	6π	not seen
Γ_{14}	$\omega\omega$	not seen
Γ_{15}	$\gamma\gamma$	seen
Γ_{16}	e^+e^-	not seen

$f_0(1370)$ PARTIAL WIDTHS

$\Gamma(\gamma\gamma)$ Γ_{15}

See $\gamma\gamma$ widths under $f_0(500)$ and MORGAN 90.

$\Gamma(e^+e^-)$ Γ_{16}

VALUE (eV)	CL%	DOCUMENT ID		TECN	COMMENT
<20	90	VOROBYEV	88	ND	$e^+e^- \to \pi^0\pi^0$

$f_0(1370)$ Γ(i)$\Gamma(\gamma\gamma)/\Gamma$(total)

$\Gamma(\eta\eta) \times \Gamma(\gamma\gamma)/\Gamma_{\text{total}}$ $\Gamma_{10}\Gamma_{15}/\Gamma$

VALUE (eV)	DOCUMENT ID		TECN	COMMENT
• • • We do not use the following data for averages, fits, limits, etc. • • •				
$121^{+133+169}_{-\ 53-106}$	[31] UEHARA	10A	BELL	10.6 $e^+e^- \to e^+e^-\eta\eta$

[31] Including interference with the $f_2'(1525)$ (parameters fixed to the values from the 2008 edition of this review, PDG 08) and $f_2(1270)$. May also be the $f_0(1500)$.

$f_0(1370)$ BRANCHING RATIOS

$\Gamma(\pi\pi)/\Gamma_{\text{total}}$ Γ_1/Γ

VALUE	DOCUMENT ID		TECN	COMMENT
• • • We do not use the following data for averages, fits, limits, etc. • • •				
0.26 ± 0.09	BUGG	96	RVUE	
<0.15	[32] AMSLER	94	CBAR	$\overline{p}p \to \pi^+\pi^- 3\pi^0$
<0.06	GASPERO	93	DBC	0.0 $\overline{p}n \to$ hadrons

[32] Using AMSLER 95B ($3\pi^0$).

$\Gamma(4\pi)/\Gamma_{\text{total}}$ $\Gamma_2/\Gamma = (\Gamma_3{+}\Gamma_4{+}\Gamma_5)/\Gamma$

VALUE	DOCUMENT ID		TECN	COMMENT
• • • We do not use the following data for averages, fits, limits, etc. • • •				
>0.72	GASPERO	93	DBC	0.0 $\overline{p}n \to$ hadrons

$\Gamma(4\pi^0)/\Gamma(4\pi)$ Γ_3/Γ_2

VALUE	DOCUMENT ID		TECN	COMMENT
• • • We do not use the following data for averages, fits, limits, etc. • • •				
seen	ABELE	96	CBAR	0.0 $\overline{p}p \to 5\pi^0$
0.068 ± 0.005	[33] GASPERO	93	DBC	0.0 $\overline{p}n \to$ hadrons

[33] Model-dependent evaluation.

$\Gamma(2\pi^+2\pi^-)/\Gamma(4\pi)$ $\Gamma_4/\Gamma_2 = \Gamma_4/(\Gamma_3{+}\Gamma_4{+}\Gamma_5)$

VALUE	DOCUMENT ID		TECN	COMMENT
• • • We do not use the following data for averages, fits, limits, etc. • • •				
0.420 ± 0.014	[34] GASPERO	93	DBC	0.0 $\overline{p}n \to 2\pi^+ 3\pi^-$

[34] Model-dependent evaluation.

$\Gamma(\pi^+\pi^-2\pi^0)/\Gamma(4\pi)$ $\Gamma_5/\Gamma_2 = \Gamma_5/(\Gamma_3{+}\Gamma_4{+}\Gamma_5)$

VALUE	DOCUMENT ID		TECN	COMMENT
• • • We do not use the following data for averages, fits, limits, etc. • • •				
0.512 ± 0.019	[35] GASPERO	93	DBC	0.0 $\overline{p}n \to$ hadrons

[35] Model-dependent evaluation.

$\Gamma(\rho\rho)/\Gamma(4\pi)$ Γ_6/Γ_2

VALUE	DOCUMENT ID		TECN	COMMENT
• • • We do not use the following data for averages, fits, limits, etc. • • •				
0.26 ± 0.07	ABELE	01B	CBAR	0.0 $\overline{p}d \to 5\pi p$

$\Gamma(2(\pi\pi)_S\text{-wave})/\Gamma(\pi\pi)$ Γ_7/Γ_1

VALUE	DOCUMENT ID		TECN	COMMENT
• • • We do not use the following data for averages, fits, limits, etc. • • •				
5.6 ± 2.6	[36] ABELE	01	CBAR	0.0 $\overline{p}d \to \pi^- 4\pi^0 p$

[36] From the combined data of ABELE 96 and ABELE 96C.

$\Gamma(2(\pi\pi)_S\text{-wave})/\Gamma(4\pi)$ Γ_7/Γ_2

VALUE	DOCUMENT ID		TECN	COMMENT
• • • We do not use the following data for averages, fits, limits, etc. • • •				
0.51 ± 0.09	ABELE	01B	CBAR	0.0 $\overline{p}d \to 5\pi p$

Meson Particle Listings

$f_0(1370)$, $h_1(1380)$

$\Gamma(\rho\rho)/\Gamma(2(\pi\pi)_{S\text{-wave}})$ Γ_6/Γ_7

VALUE	DOCUMENT ID	TECN	COMMENT
• • • We do not use the following data for averages, fits, limits, etc. • • •			
large	BARBERIS	00C	450 $pp \to p_f 4\pi p_s$
1.6 ± 0.2	AMSLER	94	CBAR $\overline{p}p \to \pi^+\pi^- 3\pi^0$
~ 0.65	GASPERO	93	DBC 0.0 $\overline{p}n \to$ hadrons

$\Gamma(\pi(1300)\pi)/\Gamma(4\pi)$ Γ_8/Γ_2

VALUE	DOCUMENT ID	TECN	COMMENT
• • • We do not use the following data for averages, fits, limits, etc. • • •			
0.17 ± 0.06	ABELE	01B	CBAR 0.0 $\overline{p}d \to 5\pi p$

$\Gamma(a_1(1260)\pi)/\Gamma(4\pi)$ Γ_9/Γ_2

VALUE	DOCUMENT ID	TECN	COMMENT
• • • We do not use the following data for averages, fits, limits, etc. • • •			
0.06 ± 0.02	ABELE	01B	CBAR 0.0 $\overline{p}d \to 5\pi p$

$\Gamma(\eta\eta)/\Gamma(4\pi)$ $\Gamma_{10}/\Gamma_2 = \Gamma_{10}/(\Gamma_3+\Gamma_4+\Gamma_5)$

VALUE	DOCUMENT ID	TECN	COMMENT
• • • We do not use the following data for averages, fits, limits, etc. • • •			
$(28 \pm 11) \times 10^{-3}$	[37] ANISOVICH	02D	SPEC Combined fit
$(4.7 \pm 2.0) \times 10^{-3}$	BARBERIS	00E	450 $pp \to p_f \eta\eta p_s$

[37] From a combined K-matrix analysis of Crystal Barrel (0. $p\overline{p} \to \pi^0\pi^0\pi^0$, $\pi^0\eta\eta$, $\pi^0\pi^0\eta$), GAMS ($\pi p \to \pi^0\pi^0 n$, $\eta\eta n$, $\eta\eta' n$), and BNL ($\pi p \to K\overline{K}n$) data.

$\Gamma(K\overline{K})/\Gamma_{\text{total}}$ Γ_{11}/Γ

VALUE	DOCUMENT ID	TECN
• • • We do not use the following data for averages, fits, limits, etc. • • •		
0.35 ± 0.13	BUGG	96 RVUE

$\Gamma(K\overline{K})/\Gamma(\pi\pi)$ Γ_{11}/Γ_1

VALUE	DOCUMENT ID	TECN	COMMENT
• • • We do not use the following data for averages, fits, limits, etc. • • •			
0.08 ± 0.08	ABLIKIM	05	BES2 $J/\psi \to \phi\pi^+\pi^-$, ϕK^+K^-
0.91 ± 0.20	[38] BARGIOTTI	03	OBLX $\overline{p}p$
0.12 ± 0.06	[39] ANISOVICH	02D	SPEC Combined fit
$0.46 \pm 0.15 \pm 0.11$	BARBERIS	99D	OMEG 450 $pp \to K^+K^-$, $\pi^+\pi^-$

[38] Coupled channel analysis of $\pi^+\pi^-\pi^0$, $K^+K^-\pi^0$, and $K^\pm K^0_S\pi^\mp$.

[39] From a combined K-matrix analysis of Crystal Barrel (0. $p\overline{p} \to \pi^0\pi^0\pi^0$, $\pi^0\eta\eta$, $\pi^0\pi^0\eta$), GAMS ($\pi p \to \pi^0\pi^0 n$, $\eta\eta n$, $\eta\eta' n$), and BNL ($\pi p \to K\overline{K}n$) data.

$\Gamma(K\overline{K}n\pi)/\Gamma_{\text{total}}$ Γ_{12}/Γ

VALUE	DOCUMENT ID	TECN	COMMENT
• • • We do not use the following data for averages, fits, limits, etc. • • •			
<0.03	GASPERO	93	DBC 0.0 $\overline{p}n \to$ hadrons

$\Gamma(6\pi)/\Gamma_{\text{total}}$ Γ_{13}/Γ

VALUE	DOCUMENT ID	TECN	COMMENT
• • • We do not use the following data for averages, fits, limits, etc. • • •			
<0.22	GASPERO	93	DBC 0.0 $\overline{p}n \to$ hadrons

$\Gamma(\omega\omega)/\Gamma_{\text{total}}$ Γ_{14}/Γ

VALUE	DOCUMENT ID	TECN	COMMENT
• • • We do not use the following data for averages, fits, limits, etc. • • •			
<0.13	GASPERO	93	DBC 0.0 $\overline{p}n \to$ hadrons

$f_0(1370)$ REFERENCES

UEHARA	10A	PR D82 114031	S. Uehara *et al.*	(BELLE Collab.)
ANISOVICH	09	IJMP A24 2481	V.V. Anisovich, A.V. Sarantsev	
AUBERT	09L	PR D79 072006	B. Aubert *et al.*	(BABAR Collab.)
PDG	08	PL B667 1	C. Amsler *et al.*	(PDG Collab.)
UEHARA	08A	PR D78 052004	S. Uehara *et al.*	(BELLE Collab.)
BONVICINI	07	PR D76 012001	G. Bonvicini *et al.*	(CLEO Collab.)
BUGG	07A	JP G34 151	D.V. Bugg *et al.*	
GARMASH	07	PR D75 012006	A. Garmash *et al.*	(BELLE Collab.)
GARMASH	06	PRL 96 251803	A. Garmash *et al.*	(BELLE Collab.)
PDG	06	JP G33 1	W.-M. Yao *et al.*	(PDG Collab.)
VLADIMIRSK...	06	PAN 69 493	V.V. Vladimirsky *et al.*	(ITEP, Moscow)
		Translated from YAF 69 515.		
ABLIKIM	05	PL B607 243	M. Ablikim *et al.*	(BES Collab.)
ABLIKIM	05Q	PR D72 092002	M. Ablikim *et al.*	(BES Collab.)
GARMASH	05	PR D71 092003	A. Garmash *et al.*	(BELLE Collab.)
ANISOVICH	03	EPJ A16 229	V.V. Anisovich *et al.*	
BARGIOTTI	03	EPJ C26 371	M. Bargiotti *et al.*	(OBELIX Collab.)
TIKHOMIROV	03	PAN 66 828	G.D. Tikhomirov *et al.*	
		Translated from YAF 66 860.		
ANISOVICH	02D	PAN 65 1545	V.V. Anisovich *et al.*	
		Translated from YAF 65 1583.		
ABELE	01	EPJ C19 667	A. Abele *et al.*	(Crystal Barrel Collab.)
ABELE	01B	EPJ C21 261	A. Abele *et al.*	(Crystal Barrel Collab.)
AITALA	01A	PRL 86 765	E.M. Aitala *et al.*	(FNAL E791 Collab.)
ASNER	00	PR D61 012002	D.M. Asner *et al.*	(CLEO Collab.)
BARBERIS	00C	PL B471 440	D. Barberis *et al.*	(WA 102 Collab.)
BARBERIS	00E	PL B479 59	D. Barberis *et al.*	(WA 102 Collab.)
BARBERIS	99B	PL B453 316	D. Barberis *et al.*	(Omega Expt.)
BARBERIS	99D	PL B462 462	D. Barberis *et al.*	(Omega Expt.)
BELLAZZINI	99	PL B467 296	R. Bellazzini *et al.*	
KAMINSKI	99	EPJ C9 141	R. Kaminski, L. Lesniak, B. Loiseau	(CRAC, PARIN)
ALDE	98	EPJ A3 361	D. Alde *et al.*	(GAM4 Collab.)
Also		PAN 62 405	D. Alde *et al.*	(GAMS Collab.)
		Translated from YAF 62 446.		
ANISOVICH	98B	SPU 41 419	V.V. Anisovich *et al.*	
		Translated from UFN 168 481.		
BERTIN	98	PR D57 55	A. Bertin *et al.*	(OBELIX Collab.)
BARBERIS	97B	PL B413 217	D. Barberis *et al.*	(WA 102 Collab.)
BERTIN	97C	PL B408 476	A. Bertin *et al.*	(OBELIX Collab.)
ABELE	96	PL B380 453	A. Abele *et al.*	(Crystal Barrel Collab.)
ABELE	96B	PL B385 425	A. Abele *et al.*	(Crystal Barrel Collab.)
ABELE	96C	NP A609 562	A. Abele *et al.*	(Crystal Barrel Collab.)
BUGG	96	NP B471 59	D.V. Bugg, A.V. Sarantsev, B.S. Zou	(LOQM, PNPI)
AMSLER	95B	PL B342 433	C. Amsler *et al.*	(Crystal Barrel Collab.)
AMSLER	95C	PL B353 571	C. Amsler *et al.*	(Crystal Barrel Collab.)
AMSLER	95D	PL B355 425	C. Amsler *et al.*	(Crystal Barrel Collab.)
JANSSEN	95	PR D52 2690	G. Janssen *et al.*	(STON, ADLD, JULI)
TORNQVIST	95	ZPHY C68 647	N.A. Tornqvist	(HELS)
AMSLER	94	PL B322 431	C. Amsler *et al.*	(Crystal Barrel Collab.) JPC
AMSLER	94D	PL B333 277	C. Amsler *et al.*	(Crystal Barrel Collab.)
ANISOVICH	94	PL B323 233	V.V. Anisovich *et al.*	(Crystal Barrel Collab.) JPC
BUGG	94	PR D50 4412	D.V. Bugg *et al.*	(LOQM)
KAMINSKI	94	PR D50 3145	R. Kaminski, L. Lesniak, J.P. Maillet	(CRAC+)
ADAMO	93	NP A558 13C	A. Adamo *et al.*	(OBELIX Collab.) JPC
GASPERO	93	NP A562 407	M. Gaspero	(ROMAI) JPC
AMSLER	92	PL B291 347	C. Amsler *et al.*	(Crystal Barrel Collab.)
ARMSTRONG	91	ZPHY C51 351	T.A. Armstrong *et al.*	(ATHU, BARI, BIRM+)
ARMSTRONG	91B	ZPHY C52 389	T.A. Armstrong *et al.*	(ATHU, BARI, BIRM+)
BREAKSTONE	90	ZPHY C48 569	A.M. Breakstone *et al.*	(ISU, BGNA, CERN+)
MORGAN	90	ZPHY C48 623	D. Morgan, M.R. Pennington	(RAL, DURH)
ASTON	88	NP B296 493	D. Aston *et al.*	(SLAC, NAGO, CINC, INUS)
BOLONKIN	88	NP B309 426	B.V. Bolonkin *et al.*	(ITEP, SERP)
FALVARD	88	PR D38 2706	A. Falvard *et al.*	(CLER, FRAS, LALO+)
VOROBYEV	88	SJNP 48 273	P.V. Vorobiev *et al.*	(NOVO)
		Translated from YAF 48 436.		
AU	87	PR D35 1633	K.L. Au, D. Morgan, M.R. Pennington	(DURH, RAL)
AKESSON	86	NP B264 154	T. Akesson *et al.*	(Axial Field Spec. Collab.)
ALDE	86D	NP B269 485	D.M. Alde *et al.*	(BELG, LAPP, SERP, CERN+)
CASON	83	PR D28 1586	N.M. Cason *et al.*	(NDAM, ANL)
ETKIN	82B	PR D25 1786	A. Etkin *et al.*	(BNL, CUNY, TUFTS, VAND)
WICKLUND	80	PRL 45 1469	A.B. Wicklund *et al.*	(ANL)
BECKER	79	NP B151 46	H. Becker *et al.*	(MPIM, CERN, ZEEM, CRAC)
POLYCHRO...	79	PR D19 1317	V.A. Polychronakos *et al.*	(NDAM, ANL)
FROGGATT	77	NP B129 89	C.D. Froggatt, J.L. Petersen	(GLAS, NORD)
ROSSELET	77	PR D15 574	L. Rosselet *et al.*	(GEVA, SACL)
GRAYER	74	NP B75 189	G. Grayer *et al.*	(CERN, MPIM)
HYAMS	73	NP B64 134	B.D. Hyams *et al.*	(CERN, MPIM)
OCHS	73	Thesis	W. Ochs	(MPIM, MUNI)
BEIER	72B	PRL 29 511	E.W. Beier *et al.*	(PENN)
BETTINI	66	NC 42A 695	A. Bettini *et al.*	(PADO, PISA)

$h_1(1380)$ $I^G(J^{PC}) = ?^-(1^{+-})$

OMITTED FROM SUMMARY TABLE

Seen in partial-wave analysis of the $K\overline{K}\pi$ system. Needs confirmation.

$h_1(1380)$ MASS

VALUE (MeV)	DOCUMENT ID	TECN	COMMENT
1386±19 OUR AVERAGE			
1440 ± 60	ABELE	97H CBAR	$\overline{p}p \to K^0_L K^0_S \pi^0\pi^0$
1380 ± 20	ASTON	88C LASS	11 $K^- p \to K^0_S K^\pm \pi^\mp \Lambda$

$h_1(1380)$ WIDTH

VALUE (MeV)	DOCUMENT ID	TECN	COMMENT
91±30 OUR AVERAGE Error includes scale factor of 1.1.			
170 ± 80	ABELE	97H CBAR	$\overline{p}p \to K^0_L K^0_S \pi^0\pi^0$
80 ± 30	ASTON	88C LASS	11 $K^- p \to K^0_S K^\pm \pi^\mp \Lambda$

$h_1(1380)$ DECAY MODES

	Mode
Γ_1	$K\overline{K}^*(892) +$ c.c.

$h_1(1380)$ REFERENCES

ABELE	97H	PL B415 280	A. Abele *et al.*	(Crystal Barrel Collab.)
ASTON	88C	PL B201 573	D. Aston *et al.*	(SLAC, NAGO, CINC, INUS)

$\pi_1(1400)$

$I^G(J^{PC}) = 1^-(1^{-+})$

See also the mini-review under non-$q\overline{q}$ candidates in PDG 06, Journal of Physics (generic for all A,B,E,G) **G33** 1 (2006).

$\pi_1(1400)$ MASS

VALUE (MeV)			EVTS	DOCUMENT ID		TECN	CHG	COMMENT
1354	**±25**	**OUR AVERAGE**		Error includes scale factor of 1.8. See the ideogram below.				
1257	±20	±25	23.5k	ADAMS	07B	B852		18 $\pi^- p \to \eta\pi^0 n$
1384	±20	±35	90k	SALVINI	04	OBLX		$\overline{p}p \to 2\pi^+ 2\pi^-$
1360	±25			ABELE	99	CBAR		0.0 $\overline{p}p \to \pi^0\pi^0\eta$
1400	±20	±20		ABELE	98B	CBAR		0.0 $\overline{p}n \to \pi^-\pi^0\eta$
1370	±16	$^{+50}_{-30}$		[1] THOMPSON	97	MPS		18 $\pi^- p \to \eta\pi^- p$
• • • We do not use the following data for averages, fits, limits, etc. • • •								
1323.1	± 4.6			[2] AOYAGI	93	BKEI		$\pi^- p \to \eta\pi^- p$
1406	±20			[3] ALDE	88B	GAM4	0	100 $\pi^- p \to \eta\pi^0 n$

[1] Natural parity exchange, questioned by DZIERBA 03.
[2] Unnatural parity exchange.
[3] Seen in the P_0-wave intensity of the $\eta\pi^0$ system, unnatural parity exchange.

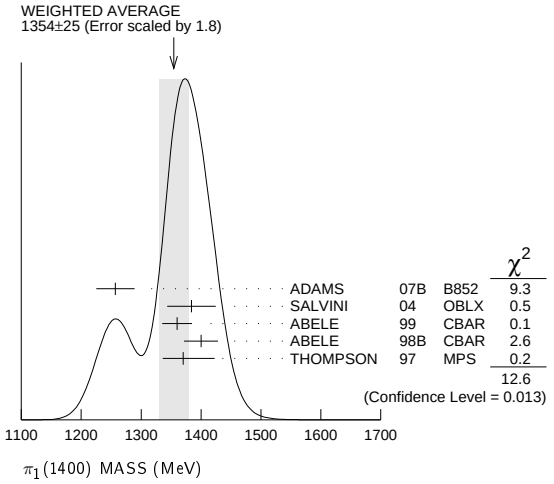

$\pi_1(1400)$ WIDTH

VALUE (MeV)			EVTS	DOCUMENT ID		TECN	CHG	COMMENT
330	**±35**	**OUR AVERAGE**						
354	±64	± 58	23.5k	ADAMS	07B	B852		18 $\pi^- p \to \eta\pi^0 n$
378	±50	± 50	90k	SALVINI	04	OBLX		$\overline{p}p \to 2\pi^+ 2\pi^-$
220	±90			ABELE	99	CBAR		0.0 $\overline{p}p \to \pi^0\pi^0\eta$
310	±50	$^{+50}_{-30}$		ABELE	98B	CBAR		0.0 $\overline{p}n \to \pi^-\pi^0\eta$
385	±40	$^{+65}_{-105}$		[4] THOMPSON	97	MPS		18 $\pi^- p \to \eta\pi^- p$
• • • We do not use the following data for averages, fits, limits, etc. • • •								
143.2	±12.5			[5] AOYAGI	93	BKEI		$\pi^- p \to \eta\pi^- p$
180	±20			[6] ALDE	88B	GAM4	0	100 $\pi^- p \to \eta\pi^0 n$

[4] Resolution is not unfolded, natural parity exchange, questioned by DZIERBA 03.
[5] Unnatural parity exchange.
[6] Seen in the P_0-wave intensity of the $\eta\pi^0$ system, unnatural parity exchange.

$\pi_1(1400)$ DECAY MODES

	Mode	Fraction (Γ_i/Γ)
Γ_1	$\eta\pi^0$	seen
Γ_2	$\eta\pi^-$	seen
Γ_3	$\eta'\pi$	

$\pi_1(1400)$ BRANCHING RATIOS

$\Gamma(\eta\pi^0)/\Gamma_{\text{total}}$ **Γ_1/Γ**

VALUE	DOCUMENT ID		TECN	CHG	COMMENT
• • • We do not use the following data for averages, fits, limits, etc. • • •					
not seen	PROKOSHKIN	95B	GAM4		100 $\pi^- p \to \eta\pi^0 n$
not seen	[7] BUGG	94	RVUE		$\overline{p}p \to \eta 2\pi^0$
not seen	[8] APEL	81	NICE	0	40 $\pi^- p \to \eta\pi^0 n$

[7] Using Crystal Barrel data.
[8] A general fit allowing S, D, and P waves (including m=0) is not done because of limited statistics.

$\Gamma(\eta\pi^-)/\Gamma_{\text{total}}$ **Γ_2/Γ**

VALUE	DOCUMENT ID		TECN	COMMENT
• • • We do not use the following data for averages, fits, limits, etc. • • •				
possibly seen	BELADIDZE	93	VES	37 $\pi^- N \to \eta\pi^- N$

$\Gamma(\eta'\pi)/\Gamma(\eta\pi^0)$ **Γ_3/Γ_1**

VALUE	CL%	DOCUMENT ID		TECN	COMMENT
• • • We do not use the following data for averages, fits, limits, etc. • • •					
<0.80	95	BOUTEMEUR	90	GAM4	100 $\pi^- p \to 4\gamma n$

$\pi_1(1400)$ REFERENCES

ADAMS	07B	PL B657 27	G.S. Adams *et al.*	(BNL E852 Collab.)
PDG	06	JP G33 1	W.-M. Yao *et al.*	(PDG Collab.)
SALVINI	04	EPJ C35 21	P. Salvini *et al.*	(OBELIX Collab.)
DZIERBA	03	PR D67 094015	A.R. Dzierba *et al.*	
ABELE	99	PL B446 349	A. Abele *et al.*	(Crystal Barrel Collab.)
ABELE	98B	PL B423 175	A. Abele *et al.*	(Crystal Barrel Collab.)
THOMPSON	97	PRL 79 1630	D.R. Thompson *et al.*	(BNL E852 Collab.)
PROKOSHKIN	95B	PAN 58 606	Y.D. Prokoshkin, S.A. Sadovsky	(SERP)
		Translated from YAF 58 662.		
BUGG	94	PR D50 4412	D.V. Bugg *et al.*	(LOQM)
AOYAGI	93	PL B314 246	H. Aoyagi *et al.*	(BKEI Collab.)
BELADIDZE	93	PL B313 276	G.M. Beladidze *et al.*	(VES Collab.)
BOUTEMEUR	90	Hadron 89 Conf. p 119	M. Boutemeur, M. Poulet	(SERP, BELG, LANL+)
ALDE	88B	PL B205 397	D.M. Alde *et al.*	(SERP, BELG, LANL, LAPP) IGJPC
APEL	81	NP B193 269	W.D. Apel *et al.*	(SERP, CERN)

$\eta(1405)$

$I^G(J^{PC}) = 0^+(0^{-+})$

THE $\eta(1405)$, $\eta(1475)$, $f_1(1420)$, AND $f_1(1510)$

Revised November 2013 by C. Amsler (Bern) and A. Masoni (INFN Cagliari).

The first observation of the $\eta(1440)$ was made in $p\overline{p}$ annihilation at rest into $\eta(1440)\pi^+\pi^-$, $\eta(1440) \to K\overline{K}\pi$ [1]. This state was reported to decay through $a_0(980)\pi$ and $K^*(892)\overline{K}$ with roughly equal contributions. The $\eta(1440)$ was also observed in radiative $J/\psi(1S)$ decay into $K\overline{K}\pi$ [2–4] and $\gamma\rho$ [5]. There is evidence for the existence of two pseudoscalars in this mass region, the $\eta(1405)$ and $\eta(1475)$. The former decays mainly through $a_0(980)\pi$ (or direct $K\overline{K}\pi$) and the latter mainly to $K^*(892)\overline{K}$.

The simultaneous observation of two pseudoscalars is reported in three production mechanisms: $\pi^- p$ [6,7]; radiative $J/\psi(1S)$ decay [8,9]; and $\overline{p}p$ annihilation at rest [10–13]. All of them give values for the masses, widths, and decay modes in reasonable agreement. However, Ref. 9 favors a state decaying into $K^*(892)\overline{K}$ at a lower mass than the state decaying into $a_0(980)\pi$. In $J/\psi(1S)$ radiative decay, the $\eta(1405)$ decays into $K\overline{K}\pi$ through $a_0(980)\pi$, and hence a signal is also expected in the $\eta\pi\pi$ mass spectrum. This was indeed observed by MARK III in $\eta\pi^+\pi^-$ [14], which reports a mass of 1400 MeV, in line with the existence of the $\eta(1405)$ decaying into $a_0(980)\pi$.

BES [15] reports an enhancement in $K^+K^-\pi^0$ around 1.44 GeV in $J/\psi(1S)$ decay, recoiling against an ω (but not a ϕ) without resolving the presence of two states nor performing a spin-parity analysis, due to low statistics. This state could also be the $f_1(1420)$ (see below). On the other hand, BES observes $\eta(1405) \to \eta\pi\pi$ in $J/\psi(1S)$ decay, recoiling against an ω [16].

The $\eta(1405)$ is also observed in $\overline{p}p$ annihilation at rest into $\eta\pi^+\pi^-\pi^0\pi^0$, where it decays into $\eta\pi\pi$ [17]. The intermediate $a_0(980)\pi$ accounts for roughly half of the $\eta\pi\pi$ signal, in agreement with MARK III [14] and DM2 [4].

However, the issue remains controversial as to whether two pseudoscalar mesons really exist. According to Ref. 18

the splitting of a single state could be due to nodes in the decay amplitudes which differ in $\eta\pi\pi$ and $K^*(892)\overline{K}$. Based on the isospin violating decay $J/\psi(1S) \to \gamma 3\pi$ observed by BES [19] the splitting could also be due to a triangular singularity mixing $\eta\pi\pi$ and $K^*(892)\overline{K}$ [20–21]. However, in a further paper [22], using the approach of [20], the authors concluded that the BES results can be reproduced either with the $\eta(1405)$ or the $\eta(1475)$or by a mixture of the two states.

The $\eta(1295)$ has been observed by four $\pi^- p$ experiments [7,23–25], and evidence is reported in $\overline{p}p$ annihilation [26–28]. In $J/\psi(1S)$ radiative decay, an $\eta(1295)$ signal is evident in the 0^{-+} $\eta\pi\pi$ wave of the DM2 data [9]. Also BaBar [29] reports evidence for a signal around 1295 MeV in B decays into $\eta\pi\pi K$. However, the existence of the $\eta(1295)$ is questioned in Refs. [18] and [30]. The authors claim a single pseudoscalar meson in the 1400 MeV region. This conclusion is based on properties of the wave functions in the $^3P_0$ model (and on an unpublished analysis of the annihilation $\bar{p}p \to 4\pi\eta$). The pseudoscalar signal around 1400 MeV is then attributed to the first radial excitation of the η.

Assuming establishment of the $\eta(1295)$, the $\eta(1475)$ could be the first radial excitation of the η', with the $\eta(1295)$ being the first radial excitation of the η. Ideal mixing, suggested by the $\eta(1295)$ and $\pi(1300)$ mass degeneracy, would then imply that the second isoscalar in the nonet is mainly $s\overline{s}$, and hence couples to $K^*\overline{K}$, in agreement with properties of the $\eta(1475)$. Also, its width matches the expected width for the radially excited $s\overline{s}$ state [31,32]. A study of radial excitations of pseudoscalar mesons [33] favors the $s\bar{s}$ interpretation of the $\eta(1475)$. However, due to the strong kinematical suppression the data are not sufficient to exclude a sizeable $s\bar{s}$ admixture also in the $\eta(1405)$.

The $K\overline{K}\pi$ and $\eta\pi\pi$ channels were studied in $\gamma\gamma$ collisions by L3 [34]. The analysis led to a clear $\eta(1475)$ signal in $K\overline{K}\pi$, decaying into $K^*\overline{K}$, very well identified in the untagged data sample, where contamination from spin 1 resonances is not allowed. At the same time, L3 [34] did not observe the $\eta(1405)$, neither in $K\overline{K}\pi$ nor in $\eta\pi\pi$. The observation of the $\eta(1475)$, combined with the absence of an $\eta(1405)$ signal, strengthens the two-resonances hypothesis. Since gluonium production is presumably suppressed in $\gamma\gamma$ collisions, the L3 results [34] suggest that $\eta(1405)$ has a large gluonic content (see also Refs. [35] and [36]) .

The L3 result is somewhat in disagreement with that of CLEO-II, which did not observe any pseudoscalar signal in $\gamma\gamma \to \eta(1475) \to K^0_S K^\pm\pi^\mp$ [37]. However, more data are required. Moreover, after the CLEO-II result, L3 performed a further analysis with full statistics [38], confirming their previous evidence for the $\eta(1475)$. The CLEO upper limit [37] for $\Gamma_{\gamma\gamma}(\eta(1475))$, and the L3 results [38], are consistent with the world average for the $\eta(1475)$ width.

BaBar [29] also reports the $\eta(1475)$ in B decays into $K\bar{K}^*$ recoiling against a K, but upper limits only are given for the $\eta(1405)$. As mentioned above, in B decays into $\eta\pi\pi K$ the $\eta(1295) \to \eta\pi\pi$ is observed while only upper limits are given for the $\eta(1405)$. The $f_1(1420)$ (and the $f_1(1285)$) are not seen.

The gluonium interpretation for the $\eta(1405)$ is not favored by lattice gauge theories which predict the 0^{-+} state above 2 GeV [39,40] (see also the article on the "Quark model" in this issue of the Review). However, the $\eta(1405)$ is an excellent candidate for the 0^{-+} glueball in the fluxtube model [41]. In this model, the 0^{++} $f_0(1500)$ glueball is also naturally related to a 0^{-+} glueball with mass degeneracy broken in QCD. Also, Ref. [42] shows that the pseudoscalar glueball could lie at a lower mass than predicted from lattice calculation. In this model the $\eta(1405)$ appears as the natural glueball candidate, see also Refs. [43–45]. A detailed review of the experimental situation is available in Ref. 46.

Let us now deal with 1^{++} isoscalars. The $f_1(1420)$, decaying into $K^*\overline{K}$, was first reported in $\pi^- p$ reactions at 4 GeV/c [47]. However, later analyses found that the 1400–1500 MeV region was far more complex [48–50]. A reanalysis of the MARK III data in radiative $J/\psi(1S)$ decay into $K\overline{K}\pi$ [8] shows the $f_1(1420)$ decaying into $K^*\overline{K}$. Also, a C=+1 state is observed in tagged $\gamma\gamma$ collisions (*e.g.*, Ref. 51).

In $\pi^- p \to \eta\pi\pi n$ charge-exchange reactions at 8–9 GeV/c the $\eta\pi\pi$ mass spectrum is dominated by the $\eta(1440)$ and $\eta(1295)$ [23,52], and at 100 GeV/c Ref. [24] reports the $\eta(1295)$ and $\eta(1440)$ decaying into $\eta\pi^0\pi^0$ with a weak $f_1(1285)$ signal, and no evidence for the $f_1(1420)$.

Axial (1^{++}) mesons are not observed in $\overline{p}p$ annihilation at rest in liquid hydrogen, which proceeds dominantly through S-wave annihilation. However, in gaseous hydrogen, P-wave annihilation is enhanced and, indeed, Ref. 11 reports $f_1(1420)$ decaying into $K^*\overline{K}$. The $f_1(1420)$, decaying into $K\overline{K}\pi$, is also seen in pp central production, together with the $f_1(1285)$. The latter decays via $a_0(980)\pi$, and the former only via $K^*\overline{K}$, while the $\eta(1440)$ is absent [53,54]. The $K^0_S K^0_S\pi^0$ decay mode of the $f_1(1420)$ establishes unambiguously C=+1. On the other hand, there is no evidence for any state decaying into $\eta\pi\pi$ around 1400 MeV, and hence the $\eta\pi\pi$ mode of the $f_1(1420)$ must be suppressed [55].

We now turn to the experimental evidence for the $f_1(1510)$. Two states, the $f_1(1420)$ and $f_1(1510)$, decaying into $K^*\overline{K}$, compete for the $s\overline{s}$ assignment in the 1^{++} nonet. The $f_1(1510)$ was seen in $K^- p \to \Lambda K\overline{K}\pi$ at 4 GeV/c [56], and at 11 GeV/c [57]. Evidence is also reported in $\pi^- p$ at 8 GeV/c, based on the phase motion of the 1^{++} $K^*\overline{K}$ wave [50]. A somewhat broader 1^{++} signal is also observed in $J/\psi(1S) \to \gamma\eta\pi^+\pi^-$ [58] as well as a small signal in $J/\psi(1S) \to \gamma\eta'\pi^+\pi^-$, attributed to the $f_1(1510)$ [59].

The absence of $f_1(1420)$ in $K^- p$ [57] argues against the $f_1(1420)$ being the $s\overline{s}$ member of the 1^{++} nonet. However, the $f_1(1420)$ was reported in $K^- p$ but not in $\pi^- p$ [60], while two experiments do not observe the $f_1(1510)$ in $K^- p$ [60,61]. The latter is also not seen in central collisions [54], or $\gamma\gamma$ collisions [62], although, surprisingly for an $s\overline{s}$ state, a

signal is reported in 4π decays [63]. These facts lead to the conclusion that $f_1(1510)$ is not well established [64].

Assigning the $f_1(1420)$ to the 1^{++} nonet, one finds a nonet mixing angle of $\sim 50^\circ$ [64]. However, arguments favoring the $f_1(1420)$ being a hybrid $q\overline{q}g$ meson, or a four-quark state, were put forward in Refs. [65] and [66], respectively, while Ref. 67 argued for a molecular state formed by the π orbiting in a P-wave around an S-wave $K\overline{K}$ state. The $f_1(1420)$ could also be an isoscalar $K^*\bar{K}$ molecule. It is interesting to note that evidence for an isovector 1^{++} partner, $a_1(1420)$ decaying into $f_0(980)\pi$, was reported recently by the COMPASS experiment in $\pi^- p \to (3\pi)^- p$ with 190 GeV/c pions [68].

Summarizing, there is convincing evidence for the $f_1(1420)$ decaying into $K^*\overline{K}$, and for two pseudoscalars in the $\eta(1440)$ region, the $\eta(1405)$ and $\eta(1475)$, decaying into $a_0(980)\pi$ and $K^*\overline{K}$, respectively. Alternatively, these two structures could originate from a single pole. Doubts have been expressed on the existence of the $\eta(1295)$. The $f_1(1510)$ is not well established.

References

1. P.H. Baillon *et al.*, Nuovo Cimento **50A**, 393 (1967).
2. D.L. Scharre *et al.*, Phys. Lett. **97B**, 329 (1980).
3. C. Edwards *et al.*, Phys. Rev. Lett. **49**, 259 (1982).
4. J.E. Augustin *et al.*, Phys. Rev. **D42**, 10 (1990).
5. J.Z. Bai *et al.*, Phys. Lett. **B594**, 47 (2004).
6. M.G. Rath *et al.*, Phys. Rev. **D40**, 693 (1989).
7. G.S. Adams *et al.*, Phys. Lett. **B516**, 264 (2001).
8. J.Z. Bai *et al.*, Phys. Rev. Lett. **65**, 2507 (1990).
9. J.E. Augustin and G. Cosme, Phys. Rev. **D46**, 1951 (1992).
10. A. Bertin *et al.*, Phys. Lett. **B361**, 187 (1995).
11. A. Bertin *et al.*, Phys. Lett. **B400**, 226 (1997).
12. C. Cicalo *et al.*, Phys. Lett. **B462**, 453 (1999).
13. F. Nichitiu *et al.*, Phys. Lett. **B545**, 261 (2002).
14. T. Bolton *et al.*, Phys. Rev. Lett. **69**, 1328 (1992).
15. M. Ablikim *et al.*, Phys. Rev. **D77**, 032005 (2008).
16. M. Ablikim *et al.*, Phys. Rev. Lett. **107**, 182001 (2011).
17. C. Amsler *et al.*, Phys. Lett. **B358**, 389 (1995).
18. E. Klempt and A. Zaitsev, Phys. Reports **454**, 1 (2007).
19. M. Ablikim *et al.*, Phys. Rev. Lett. **108**, 182001 (2012).
20. Jia-Jun Wu *et al.*, Phys. Rev. Lett. **108**, 081803 (2012).
21. Xia-Gang Wu *et al.*, prD87,014023.
22. F. Aceti *et al.*, Phys. Rev. **D86**, 1114007 (2012).
23. S. Fukui *et al.*, Phys. Lett. **B267**, 293 (1991).
24. D. Alde *et al.*, Phys. Atom. Nucl. **60**, 386 (1997).
25. J.J. Manak *et al.*, Phys. Rev. **D62**, 012003 (2000).
26. A.V. Anisovich *et al.*, Nucl. Phys. **A690**, 567 (2001).
27. A. Abele *et al.*, Phys. Rev. **D57**, 3860 (1998).
28. C. Amsler *et al.*, Eur. Phys. J. **C33**, 23 (2004).
29. B. Aubert *et al.*, Phys. Rev. Lett. **101**, 091801 (2008).
30. E. Klempt, Int. J. Mod. Phys. **A21**, 739 (2006).
31. F. Close *et al.*, Phys. Lett. **B397**, 333 (1997).
32. T. Barnes *et al.*, Phys. Rev. **D55**, 4157 (1997).
33. T. Gutsche *et al.*, Phys. Rev. **D79**, 014036 (2009).
34. M. Acciarri *et al.*, Phys. Lett. **B501**, 1 (2001).
35. F. Close *et al.*, Phys. Rev. **D55**, 5749 (1997).
36. D.M. Li *et al.*, Eur. Phys. J. **C28**, 335 (2003).
37. R. Ahohe *et al.*, Phys. Rev. **D71**, 072001 (2005).
38. P. Achard *et al.*, JHEP **0703**, 018 (2007).
39. G.S. Bali *et al.*, Phys. Lett. **B309**, 378 (1993).
40. C. Morningstar and M. Peardon, Phys. Rev. **D60**, 034509 (1999).
41. L. Faddeev *et al.*, Phys. Rev. **D70**, 114033 (2004).
42. H.-Y. Cheng *et al.*, Phys. Rev. **D79**, 014024 (2009).
43. G. Li *et al.*, J. Phys. **G35**, 055002 (2008).
44. T. Gutsche *et al.*, Phys. Rev. **D80**, 014014 (2009).
45. B. Li, Phys. Rev. **D81**, 114002 (2010).
46. A. Masoni, C. Cicalo, and G.L. Usai, J. Phys. **G32**, R293 (2006).
47. C. Dionisi *et al.*, Nucl. Phys. **B169**, 1 (1980).
48. S.U. Chung *et al.*, Phys. Rev. Lett. **55**, 779 (1985).
49. D.F. Reeves *et al.*, Phys. Rev. **D34**, 1960 (1986).
50. A. Birman *et al.*, Phys. Rev. Lett. **61**, 1557 (1988).
51. H.J. Behrend *et al.*, Z. Phys. **C42**, 367 (1989).
52. A. Ando *et al.*, Phys. Rev. Lett. **57**, 1296 (1986).
53. T.A. Armstrong *et al.*, Phys. Lett. **B221**, 216 (1989).
54. D. Barberis *et al.*, Phys. Lett. **B413**, 225 (1997).
55. T.A. Armstrong *et al.*, Z. Phys. **C52**, 389 (1991).
56. P. Gavillet *et al.*, Z. Phys. **C16**, 119 (1982).
57. D. Aston *et al.*, Phys. Lett. **B201**, 573 (1988).
58. J.Z. Bai *et al.*, Phys. Lett. **B446**, 356 (1999).
59. M. Ablikim *et al.*, Phys. Rev. Lett. **106**, 072002 (2011).
60. S. Bityukov *et al.*, Sov. J. Nucl. Phys. **39**, 738 (1984).
61. E. King *et al.*, Nucl. Phys. (Proc. Supp.) **B21**, 11 (1991).
62. H. Aihara *et al.*, Phys. Rev. **D38**, 1 (1988).
63. D.A. Bauer *et al.*, Phys. Rev. **D48**, 3976 (1993).
64. F.E. Close and A. Kirk, Z. Phys. **C76**, 469 (1997).
65. S. Ishida *et al.*, Prog. Theor. Phys. **82**, 119 (1989).
66. D.O. Caldwell, *Hadron 89 Conf., Ajaccio, Corsica*, p. 127.
67. R.S. Longacre, Phys. Rev. **D42**, 874 (1990).
68. S. Uhl, *Proc. of the Hadron 2013 Conf., Nara, Japan.*

$\eta(1405)$ MASS

VALUE (MeV) | DOCUMENT ID

1408.8±1.8 OUR AVERAGE Includes data from the 2 datablocks that follow this one. Error includes scale factor of 2.1. See the ideogram below.

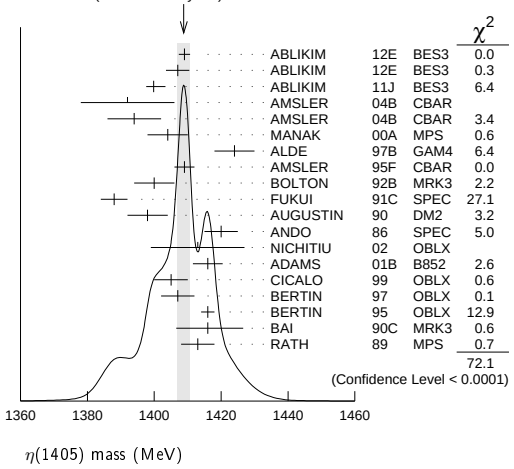

Meson Particle Listings

$\eta(1405)$

$\eta\pi\pi$ MODE

VALUE (MeV)	EVTS	DOCUMENT ID		TECN	COMMENT
The data in this block is included in the average printed for a previous datablock.					
1406.2± 2.3 OUR AVERAGE		Error includes scale factor of 2.2. See the ideogram below.			
1409.0± 1.7	743	ABLIKIM	12E	BES3	$J/\psi \to \gamma(\pi^+\pi^-\pi^0)$
1407.0± 3.5	198	ABLIKIM	12E	BES3	$J/\psi \to \gamma(\pi^0\pi^0\pi^0)$
1399.8± $2.2^{+2.8}_{-0.1}$		[1] ABLIKIM	11J	BES3	$J/\psi \to \omega(\eta\pi^+\pi^-)$
1392 ±14	900 ± 375	AMSLER	04B	CBAR	$0\,\overline{p}p \to \pi^+\pi^-\pi^+\pi^-\eta$
1394 ± 8	6.6 ± 2.0k	AMSLER	04B	CBAR	$0\,\overline{p}p \to \pi^+\pi^-\pi^0\pi^0\eta$
1404 ± 6	9082	MANAK	00A	MPS	$18\ \pi^-p \to \eta\pi^+\pi^-n$
1424 ± 6	2200	ALDE	97B	GAM4	$100\ \pi^-p \to \eta\pi^0\pi^0n$
1409 ± 3		AMSLER	95F	CBAR	$0\,\overline{p}p \to \pi^+\pi^-\pi^0\pi^0\eta$
1400 ± 6		[2] BOLTON	92B	MRK3	$J/\psi \to \gamma\eta\pi^+\pi^-$
1388 ± 4		FUKUI	91C	SPEC	$8.95\ \pi^-p \to \eta\pi^+\pi^-n$
1398 ± 6	261	[3] AUGUSTIN	90	DM2	$J/\psi \to \gamma\eta\pi^+\pi^-$
1420 ± 5		ANDO	86	SPEC	$8\ \pi^-p \to \eta\pi^+\pi^-n$
• • • We do not use the following data for averages, fits, limits, etc. • • •					
1385 ± 7		BAI	99	BES	$J/\psi \to \gamma\eta\pi^+\pi^-$

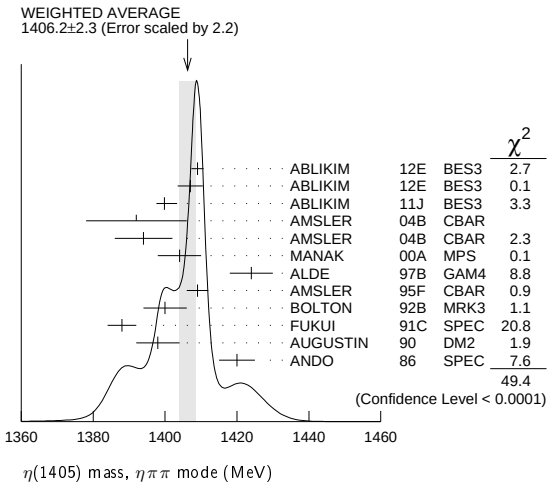

$\eta(1405)$ mass, $\eta\pi\pi$ mode (MeV)

$K\overline{K}\pi$ MODE ($a_0(980)\pi$ or direct $K\overline{K}\pi$)

VALUE (MeV)	EVTS	DOCUMENT ID		TECN	COMMENT
The data in this block is included in the average printed for a previous datablock.					
1413.9± 1.7 OUR AVERAGE		Error includes scale factor of 1.1.			
1413 ±14	3651	[4] NICHITIU	02	OBLX	
1416 ± 4 ±2	20k	ADAMS	01B	B852	18 GeV $\pi^-p \to K^+K^-\pi^0n$
1405 ± 5		[5] CICALO	99	OBLX	$0\,\overline{p}p \to K^\pm K^0_S\pi^\mp\pi^+\pi^-$
1407 ± 5		[5] BERTIN	97	OBLX	$0\,\overline{p}p \to K^\pm(K^0)\pi^\mp\pi^+\pi^-$
1416 ± 2		[5] BERTIN	95	OBLX	$0\,\overline{p}p \to K\overline{K}\pi\pi\pi$
1416 ± 8 $^{+7}_{-5}$	700	[6] BAI	90C	MRK3	$J/\psi \to \gamma K^0_S K^\pm\pi^\mp$
1413 ± 5		[6] RATH	89	MPS	$21.4\ \pi^-p \to nK^0_S K^0_S\pi^0$
• • • We do not use the following data for averages, fits, limits, etc. • • •					
1459 ± 5		[7] AUGUSTIN	92	DM2	$J/\psi \to \gamma K\overline{K}\pi$

$\pi\pi\gamma$ MODE

VALUE (MeV)	EVTS	DOCUMENT ID		TECN	COMMENT
1390±12	235 ± 91	AMSLER	04B	CBAR	$0\,\overline{p}p \to \pi^+\pi^-\pi^+\pi^-\gamma$
• • • We do not use the following data for averages, fits, limits, etc. • • •					
1424±10±11	547	BAI	04J	BES2	$J/\psi \to \gamma\gamma\pi^+\pi^-$
1401±18		[8,9] AUGUSTIN	90	DM2	$J/\psi \to \pi^+\pi^-\gamma\gamma$
1432± 8		[9] COFFMAN	90	MRK3	$J/\psi \to \pi^+\pi^-2\gamma$

4π MODE

VALUE (MeV)	EVTS	DOCUMENT ID		TECN	COMMENT
• • • We do not use the following data for averages, fits, limits, etc. • • •					
1420±20		BUGG	95	MRK3	$J/\psi \to \gamma\pi^+\pi^-\pi^+\pi^-$
1489±12	3270	[10] BISELLO	89B	DM2	$J/\psi \to 4\pi\gamma$

$K\overline{K}\pi$ MODE (unresolved)

VALUE (MeV)	EVTS	DOCUMENT ID		TECN	COMMENT
• • • We do not use the following data for averages, fits, limits, etc. • • •					
1452.7± 3.3	191	[11,12] ABLIKIM	13M	BES3	$\psi(2S) \to \omega K K\pi$
1437.6± 3.2	249 ± 35	[11,12] ABLIKIM	08E	BES2	$J/\psi \to \omega K^0_S K^+\pi^-$ + c.c.
1445.9± 5.7	62 ± 18	[11,12] ABLIKIM	08E	BES2	$J/\psi \to \omega K^+K^-\pi^0$
1442 ±10	410	[11] BAI	98C	BES	$J/\psi \to \gamma K^+K^-\pi^0$
1445 ± 8	693	[11] AUGUSTIN	90	DM2	$J/\psi \to \gamma K^0_S K^\pm\pi^\mp$
1433 ± 8	296	[11] AUGUSTIN	90	DM2	$J/\psi \to \gamma K^+K^-\pi^0$
1413 ± 8	500	[11] DUCH	89	ASTE	$\overline{p}p \to \pi^+\pi^-K^\pm\pi^\mp K^0$
1453 ± 7	170	[11] RATH	89	MPS	$21.4\ \pi^-p \to K^0_S K^0_S\pi^0n$
1419 ± 1	8800	[11] BIRMAN	88	MPS	$8\ \pi^-p \to K^+\overline{K}^0\pi^-n$
1424 ± 3	620	[11] REEVES	86	SPEC	$6.6\ p\overline{p} \to K\overline{K}\pi X$
1421 ± 2		[11] CHUNG	85	SPEC	$8\ \pi^-p \to K\overline{K}\pi n$
1440 $^{+20}_{-15}$	174	[11] EDWARDS	82E	CBAL	$J/\psi \to \gamma K^+K^-\pi^0$
1440 $^{+10}_{-15}$		[11] SCHARRE	80	MRK2	$J/\psi \to \gamma K^0_S K^\pm\pi^\mp$
1425 ± 7	800	[11,13] BAILLON	67	HBC	$0\,\overline{p}p \to K\overline{K}\pi\pi\pi$

[1] The selected process is $J/\psi \to \omega a_0(980)\pi$.
[2] From fit to the $a_0(980)\pi\ 0^{-+}$ partial wave.
[3] Best fit with a single Breit Wigner.
[4] Decaying dominantly directly to $K^+K^-\pi^0$.
[5] Decaying into $(K\overline{K})_S\pi$, $(K\pi)_S\overline{K}$, and $a_0(980)\pi$.
[6] From fit to the $a_0(980)\pi\ 0^{-+}$ partial wave. Cannot rule out a $a_0(980)\pi\ 1^{++}$ partial wave.
[7] Excluded from averaging because averaging would be meaningless.
[8] Best fit with a single Breit Wigner.
[9] This peak in the $\gamma\rho$ channel may not be related to the $\eta(1405)$.
[10] Estimated by us from various fits.
[11] These experiments identify only one pseudoscalar in the 1400–1500 range. Data could also refer to $\eta(1475)$.
[12] Systematic uncertainty not evaluated.
[13] From best fit of 0^{-+} partial wave , 50% $K^*(892)\,K$, 50% $a_0(980)\pi$.

$\eta(1405)$ WIDTH

VALUE (MeV)	DOCUMENT ID
51.0±2.9 OUR AVERAGE	Includes data from the 2 datablocks that follow this one. Error includes scale factor of 1.8. See the ideogram below.

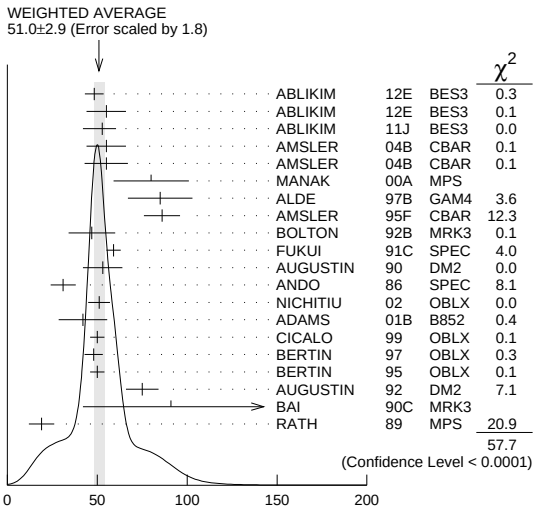

$\eta(1405)$ width (MeV)

$\eta\pi\pi$ MODE

VALUE (MeV)	EVTS	DOCUMENT ID		TECN	COMMENT
The data in this block is included in the average printed for a previous datablock.					
54 ± 4 OUR AVERAGE		Error includes scale factor of 1.6. See the ideogram below.			
48.3± 5.2	743	ABLIKIM	12E	BES3	$J/\psi \to \gamma(\pi^+\pi^-\pi^0)$
55.0±11.0	198	ABLIKIM	12E	BES3	$J/\psi \to \gamma(\pi^0\pi^0\pi^0)$
52.8± $7.6^{+0.1}_{-7.6}$		[14] ABLIKIM	11J	BES3	$J/\psi \to \omega(\eta\pi^+\pi^-)$
55 ±11	900 ± 375	AMSLER	04B	CBAR	$0\,\overline{p}p \to \pi^+\pi^-\pi^+\pi^-\eta$
55 ±12	6.6 ± 2.0k	AMSLER	04B	CBAR	$0\,\overline{p}p \to \pi^+\pi^-\pi^0\pi^0\gamma$
80 ±21	9082	MANAK	00A	MPS	$18\ \pi^-p \to \eta\pi^+\pi^-n$
85 ±18	2200	ALDE	97B	GAM4	$100\ \pi^-p \to \eta\pi^0\pi^0n$
86 ±10		AMSLER	95F	CBAR	$0\,\overline{p}p \to \pi^+\pi^-\pi^0\pi^0\eta$
47 ±13		[15] BOLTON	92B	MRK3	$J/\psi \to \gamma\eta\pi^+\pi^-$
59 ± 4		FUKUI	91C	SPEC	$8.95\ \pi^-p \to \eta\pi^+\pi^-n$
53 ±11		[16] AUGUSTIN	90	DM2	$J/\psi \to \gamma\eta\pi^+\pi^-$
31 ± 7		ANDO	86	SPEC	$8\ \pi^-p \to \eta\pi^+\pi^-n$

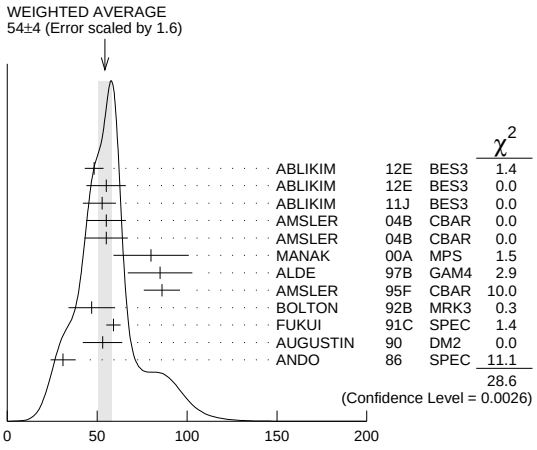

$\eta(1405)$ width $\eta\pi\pi$ mode (MeV)

$K\overline{K}\pi$ MODE ($a_0(980)\pi$ or direct $K\overline{K}\pi$)

VALUE (MeV)	EVTS	DOCUMENT ID		TECN	COMMENT
The data in this block is included in the average printed for a previous datablock.					
48± 4 OUR AVERAGE		Error includes scale factor of 2.1. See the ideogram below.			
51± 6	3651	[17] NICHITIU	02	OBLX	
42±10± 9	20k	ADAMS	01B	B852	18 GeV $\pi^- p \to K^+ K^- \pi^0 n$
50± 4		CICALO	99	OBLX	$0\ \overline{p}p \to K^\pm K^0_S \pi^\mp \pi^+ \pi^-$
48± 5		[18] BERTIN	97	OBLX	$0.0\ \overline{p}p \to K^\pm (K^0) \pi^\mp \pi^+ \pi^-$
50± 4		[18] BERTIN	95	OBLX	$0\ \overline{p}p \to K\overline{K}\pi\pi\pi$
75± 9		AUGUSTIN	92	DM2	$J/\psi \to \gamma K\overline{K}\pi$
91^{+67+15}_{-31-38}		[19] BAI	90C	MRK3	$J/\psi \to \gamma K^0_S K^\pm \pi^\mp$
19± 7		[19] RATH	89	MPS	21.4 $\pi^- p \to n K^0_S K^0_S \pi^0$

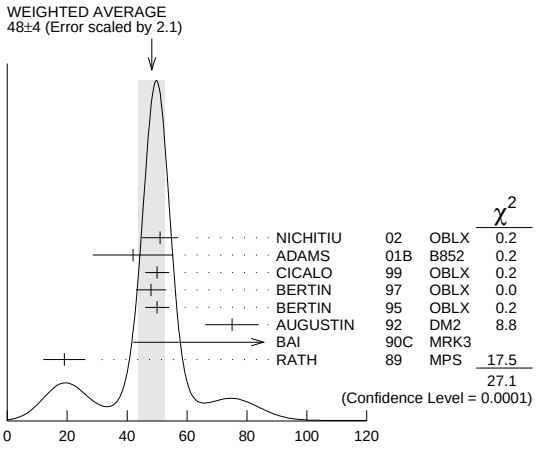

$\eta(1405)$ width $K\overline{K}\pi$ mode ($a_0(980)$ π dominant)

$\pi\pi\gamma$ MODE

VALUE (MeV)	EVTS	DOCUMENT ID		TECN	COMMENT
64 ±18	235 ± 91	AMSLER	04B	CBAR	$0\ \overline{p}p \to \pi^+\pi^-\pi^+\pi^-\gamma$
• • • We do not use the following data for averages, fits, limits, etc. • • •					
101.0± 8.8±8.8	547	BAI	04J	BES2	$J/\psi \to \gamma\gamma\pi^+\pi^-$
174 ±44		AUGUSTIN	90	DM2	$J/\psi \to \pi^+\pi^-\gamma\gamma$
90 ±26		[20] COFFMAN	90	MRK3	$J/\psi \to \pi^+\pi^- 2\gamma$

4π MODE

VALUE (MeV)	EVTS	DOCUMENT ID		TECN	COMMENT
• • • We do not use the following data for averages, fits, limits, etc. • • •					
160±30		BUGG	95	MRK3	$J/\psi \to \gamma\pi^+\pi^-\pi^+\pi^-$
144±13	3270	[21] BISELLO	89B	DM2	$J/\psi \to 4\pi\gamma$

$K\overline{K}\pi$ MODE (unresolved)

VALUE (MeV)	EVTS	DOCUMENT ID		TECN	COMMENT
• • • We do not use the following data for averages, fits, limits, etc. • • •					
45.9± 8.2	191	[22,23] ABLIKIM	13M	BES3	$\psi(2S) \to \omega K\overline{K}\pi$
48.9± 9.0	249 ± 35	[22,23] ABLIKIM	08E	BES2	$J/\psi \to \omega K^0_S K^+\pi^-$ + c.c.
34.2±18.5	62 ± 18	[22,23] ABLIKIM	08E	BES2	$J/\psi \to \omega K^+ K^-\pi^0$
93 ±14	296	[22] AUGUSTIN	90	DM2	$J/\psi \to \gamma K^+ K^-\pi^0$
105 ±10	693	[22] AUGUSTIN	90	DM2	$J/\psi \to \gamma K^0_S K^\pm \pi^\mp$
62 ±16	500	[22] DUCH	89	ASTE	$\overline{p}p \to K\overline{K}\pi\pi\pi$
100 ±11	170	[22] RATH	89	MPS	21.4 $\pi^- p \to K^0_S K^0_S \pi^0 n$
66 ± 2	8800	[22] BIRMAN	88	MPS	8 $\pi^- p \to K^+\overline{K}^0\pi^- n$
60 ±10	620	[22] REEVES	86	SPEC	6.6 $p\overline{p} \to K K\pi$X
60 ±10		[22] CHUNG	85	SPEC	8 $\pi^- p \to K\overline{K}\pi n$
$55\ ^{+20}_{-30}$	174	[22] EDWARDS	82E	CBAL	$J/\psi \to \gamma K^+ K^-\pi^0$
$50\ ^{+30}_{-20}$		[22] SCHARRE	80	MRK2	$J/\psi \to \gamma K^0_S K^\pm \pi^\mp$
80 ±10	800	[22,24] BAILLON	67	HBC	0.0 $\overline{p}p \to K\overline{K}\pi\pi\pi$

[14] The selected process is $J/\psi \to \omega a_0(980)\pi$.
[15] From fit to the $a_0(980)\pi$ 0^{-+} partial wave.
[16] From $\eta\pi^+\pi^-$ mass distribution - mainly $a_0(980)\pi$ - no spin–parity determination available.
[17] Decaying dominantly directly to $K^+K^-\pi^0$.
[18] Decaying into $(K\overline{K})_S\pi$, $(K\pi)_S\overline{K}$, and $a_0(980)\pi$.
[19] From fit to the $a_0(980)\pi$ 0^{-+} partial wave , but $a_0(980)\pi$ 1^{++} cannot be excluded.
[20] This peak in the $\gamma\rho$ channel may not be related to the $\eta(1405)$.
[21] Estimated by us from various fits.
[22] These experiments identify only one pseudoscalar in the 1400–1500 range. Data could also refer to $\eta(1475)$.
[23] Systematic uncertainty not evaluated.
[24] From best fit to 0^{-+} partial wave , 50% $K^*(892)K$, 50% $a_0(980)\pi$.

$\eta(1405)$ DECAY MODES

	Mode	Fraction (Γ_i/Γ)	Confidence level
Γ_1	$K\overline{K}\pi$	seen	
Γ_2	$\eta\pi\pi$	seen	
Γ_3	$a_0(980)\pi$	seen	
Γ_4	$\eta(\pi\pi)_S$-wave	seen	
Γ_5	$f_0(980)\eta$	seen	
Γ_6	4π	seen	
Γ_7	$\rho\rho$	<58 %	99.85%
Γ_8	$\gamma\gamma$		
Γ_9	$\rho^0\gamma$	seen	
Γ_{10}	$\phi\gamma$		
Γ_{11}	$K^*(892)K$	seen	

$\eta(1405)$ $\Gamma(i)\Gamma(\gamma\gamma)/\Gamma(\text{total})$

$\Gamma(K\overline{K}\pi) \times \Gamma(\gamma\gamma)/\Gamma_{\text{total}}$ $\Gamma_1\Gamma_8/\Gamma$

VALUE (keV)	CL%	DOCUMENT ID		TECN	COMMENT
• • • We do not use the following data for averages, fits, limits, etc. • • •					
<0.035	90	[25,26] AHOHE	05	CLE2	10.6 $e^+e^- \to e^+e^- K^0_S K^\pm\pi^\mp$

$\Gamma(\eta\pi\pi) \times \Gamma(\gamma\gamma)/\Gamma_{\text{total}}$ $\Gamma_2\Gamma_8/\Gamma$

VALUE (keV)	CL%	DOCUMENT ID		TECN	COMMENT
<0.095	95	ACCIARRI	01G	L3	183–202 $e^+e^- \to e^+e^-\eta\pi^+\pi^-$

$\Gamma(\rho^0\gamma) \times \Gamma(\gamma\gamma)/\Gamma_{\text{total}}$ $\Gamma_9\Gamma_8/\Gamma$

VALUE (keV)	CL%	DOCUMENT ID		TECN	COMMENT
• • • We do not use the following data for averages, fits, limits, etc. • • •					
<1.5	95	ALTHOFF	84E	TASS	$e^+e^- \to e^+e^-\pi^+\pi^-\gamma$

[25] Using $\eta(1405)$ mass and width 1410 MeV and 51 MeV, respectively.
[26] Assuming three-body phase-space decay to $K^0_S K^\pm\pi^\mp$.

$\eta(1405)$ BRANCHING RATIOS

$\Gamma(\eta\pi\pi)/\Gamma(K\overline{K}\pi)$ Γ_2/Γ_1

VALUE	CL%	DOCUMENT ID		TECN	COMMENT
• • • We do not use the following data for averages, fits, limits, etc. • • •					
1.09±0.48		[27] AMSLER	04B	CBAR	$0\ \overline{p}p \to \pi^+\pi^-\pi^+\pi^-\eta$
<0.5	90	EDWARDS	83B	CBAL	$J/\psi \to \eta\pi\pi\gamma$
<1.1	90	SCHARRE	80	MRK2	$J/\psi \to \eta\pi\pi\gamma$
<1.5	95	FOSTER	68B	HBC	0.0 $\overline{p}p$

$\Gamma(\rho^0\gamma)/\Gamma(\eta\pi\pi)$ Γ_9/Γ_2

VALUE	DOCUMENT ID		TECN	COMMENT
0.111±0.064	AMSLER	04B	CBAR	$0\ \overline{p}p$

$\Gamma(a_0(980)\pi)/\Gamma(K\overline{K}\pi)$ Γ_3/Γ_1

VALUE	EVTS	DOCUMENT ID		TECN	COMMENT
• • • We do not use the following data for averages, fits, limits, etc. • • •					
~ 0.15		[28] BERTIN	95	OBLX	$0\ \overline{p}p \to K\overline{K}\pi\pi\pi$
~ 0.8	500	[28] DUCH	89	ASTE	$\overline{p}p \to \pi^+\pi^- K^\pm\pi^\mp K^0$
~ 0.75		[28] REEVES	86	SPEC	6.6 $p\overline{p} \to K K\pi$X

$\Gamma(a_0(980)\pi)/\Gamma(\eta\pi\pi)$ Γ_3/Γ_2

VALUE	EVTS	DOCUMENT ID		TECN	COMMENT
• • • We do not use the following data for averages, fits, limits, etc. • • •					
0.29±0.10		ABELE	98E	CBAR	0 $p\overline{p} \to \eta\pi^0\pi^0\pi^0$
0.19±0.04	2200	[29] ALDE	97B	GAM4	100 $\pi^- p \to \eta\pi^0\pi^0 n$
0.56±0.04±0.03		[29] AMSLER	95F	CBAR	0 $\overline{p}p \to \pi^+\pi^-\pi^0\pi^0\eta$

$\Gamma(a_0(980)\pi)/\Gamma(\eta(\pi\pi)_{S\text{-wave}})$ Γ_3/Γ_4

VALUE	EVTS	DOCUMENT ID		TECN	COMMENT
• • • We do not use the following data for averages, fits, limits, etc. • • •					
0.91±0.12		ANISOVICH	01	SPEC	0.0 $\overline{p}p \to \eta\pi^+\pi^-\pi^+\pi^-$
0.15±0.04	9082	[30] MANAK	00A	MPS	18 $\pi^- p \to \eta\pi^+\pi^- n$
0.70±0.12±0.20		[31] BAI	99	BES	$J/\psi \to \gamma\eta\pi^+\pi^-$

$\Gamma(\rho^0\gamma)/\Gamma(K\overline{K}\pi)$ Γ_9/Γ_1

VALUE	DOCUMENT ID		TECN	COMMENT
0.0152±0.0038	[32] COFFMAN	90	MRK3	$J/\psi \to \gamma\gamma\pi^+\pi^-$

$\Gamma(\eta(\pi\pi)_{S\text{-wave}})/\Gamma(\eta\pi\pi)$ Γ_4/Γ_2

VALUE	EVTS	DOCUMENT ID		TECN	COMMENT
• • • We do not use the following data for averages, fits, limits, etc. • • •					
0.81±0.04	2200	ALDE	97B	GAM4	100 $\pi^- p \to \eta\pi^0\pi^0 n$

$\Gamma(f_0(980)\eta)/\Gamma(\eta\pi\pi)$ Γ_5/Γ_2

VALUE	DOCUMENT ID		TECN	COMMENT
• • • We do not use the following data for averages, fits, limits, etc. • • •				
0.32±0.07	[33] ANISOVICH	00	SPEC	0.9–1.2 $\overline{p}p \to \eta 3\pi^0$

$\Gamma(\rho\rho)/\Gamma_{\text{total}}$ Γ_7/Γ

VALUE	CL%	DOCUMENT ID		TECN	COMMENT
<0.58	99.85	[27,34] AMSLER	04B	CBAR	0 $\overline{p}p$

$\Gamma(K^*(892)K)/\Gamma(a_0(980)\pi)$ Γ_{11}/Γ_3

VALUE	DOCUMENT ID		TECN	COMMENT
• • • We do not use the following data for averages, fits, limits, etc. • • •				
0.084±0.024	[30] ADAMS	01B	B852	18 GeV $\pi^- p \to K^+K^-\pi^0 n$

$\Gamma(\phi\gamma)/\Gamma(\rho^0\gamma)$ Γ_{10}/Γ_9

VALUE	CL%	DOCUMENT ID		TECN	COMMENT
• • • We do not use the following data for averages, fits, limits, etc. • • •					
<0.77	95	[35] BAI	04J	BES2	$J/\psi \to \gamma\gamma K^+K^-$

[27] Using the data of BAILLON 67 on $\overline{p}p \to K\overline{K}\pi$.
[28] Assuming that the $a_0(980)$ decays only into $K\overline{K}$.
[29] Assuming that the $a_0(980)$ decays only into $\eta\pi$.
[30] Statistical error only.
[31] Assuming that the $a_0(980)$ decays only into $\eta\pi$.
[32] Using $B(J/\psi \to \gamma\eta(1405) \to \gamma K\overline{K}\pi)=4.2\times10^{-3}$ and $B(J/\psi \to \gamma\eta(1405) \to \gamma\gamma\rho^0)=6.4\times10^{-5}$ and assuming that the $\gamma\rho^0$ signal does not come from the $f_1(1420)$.
[33] Using preliminary Crystal Barrel data.
[34] Assuming that the $\eta(1405)$ decays are saturated by the $\pi\pi\eta$, $K\overline{K}\pi$ and $\rho\rho$ modes.
[35] Calculated by us from $B(J/\psi \to \eta(1405)\gamma \to \phi\gamma\gamma) < 0.82\times10^{-4}$ and $B(J/\psi \to \eta(1405)\gamma \to \rho^0\gamma\gamma) = (1.07\pm0.17\pm0.11)\times10^{-4}$.

$\eta(1405)$ REFERENCES

ABLIKIM	13M	PR D87 092006	M. Ablikim *et al.*	(BES III Collab.)
ABLIKIM	12E	PRL 108 182001	M. Ablikim *et al.*	(BES III Collab.)
ABLIKIM	11J	PRL 107 182001	M. Ablikim *et al.*	(BES III Collab.)
ABLIKIM	08E	PR D77 032005	M. Ablikim *et al.*	(BES Collab.)
AHOHE	05	PR D71 072001	R. Ahohe *et al.*	(CLEO Collab.)
AMSLER	04B	EPJ C33 23	C. Amsler *et al.*	(Crystal Barrel Collab.)
BAI	04J	PL B594 47	J.Z. Bai *et al.*	(BES Collab.)
NICHITIU	02	PL B545 261	F. Nichitiu *et al.*	(OBELIX Collab.)
ACCIARRI	01G	PL B501 1	M. Acciarri *et al.*	(L3 Collab.)
ADAMS	01B	PL B516 264	G.S. Adams *et al.*	(BNL E852 Collab.)
ANISOVICH	01	NP A690 567	A.V. Anisovich *et al.*	
ANISOVICH	00	PL B472 168	A.V. Anisovich *et al.*	
MANAK	00A	PR D62 012003	J.J. Manak *et al.*	(BNL E852 Collab.)
BAI	99	PL B446 356	J.Z. Bai *et al.*	(BES Collab.)
CICALO	99	PL B462 453	C. Cicalo *et al.*	(OBELIX Collab.)
ABELE	98E	NP B514 45	A. Abele *et al.*	(Crystal Barrel Collab.)
BAI	98C	PL B440 217	J.Z. Bai *et al.*	(BES Collab.)
ALDE	97B	PAN 60 386	D. Alde *et al.*	(GAMS Collab.)
		Translated from YAF 60 458.		
BERTIN	97	PL B400 226	A. Bertin *et al.*	(OBELIX Collab.)
AMSLER	95F	PL B358 389	C. Amsler *et al.*	(Crystal Barrel Collab.)
BERTIN	95	PL B361 187	A. Bertin *et al.*	(OBELIX Collab.)
BUGG	95	PL B353 378	D.V. Bugg *et al.*	(LOQM, PNPI, WASH)
AUGUSTIN	92	PR D46 1951	J.E. Augustin, G. Cosme	(DM2 Collab.)
BOLTON	92B	PRL 69 1328	T. Bolton *et al.*	(Mark III Collab.)
FUKUI	91C	PL B267 293	S. Fukui *et al.*	(SUGI, NAGO, KEK, KYOT+)
AUGUSTIN	90	PR D42 10	J.E. Augustin *et al.*	(DM2 Collab.)
BAI	90C	PRL 65 2507	Z. Bai *et al.*	(Mark III Collab.)
COFFMAN	90	PR D41 1410	D.M. Coffman *et al.*	(Mark III Collab.)
BISELLO	89B	PR D39 701	G. Busetto *et al.*	(DM2 Collab.)
DUCH	89	ZPHY C45 223	K.D. Duch *et al.*	(ASTERIX Collab.) JP
RATH	89	PR D40 693	M.G. Rath *et al.*	(NDAM, BRAN, BNL, CUNY+)
BIRMAN	88	PRL 61 1557	A. Birman *et al.*	(BNL, FSU, IND, MASD) JP
ANDO	86	PRL 57 1296	A. Ando *et al.*	(KEK, KYOT, NIRS, SAGA+) IJP
REEVES	86	PR D34 1960	D.F. Reeves *et al.*	(FLOR, BNL, IND+) JP
CHUNG	85	PRL 55 779	S.U. Chung *et al.*	(BNL, FLOR, IND+) JP
ALTHOFF	84E	PL 147B 487	M. Althoff *et al.*	(TASSO Collab.)
EDWARDS	83B	PRL 51 859	C. Edwards *et al.*	(CIT, HARV, PRIN+)
EDWARDS	82E	PRL 49 259	C. Edwards *et al.*	(CIT, HARV, PRIN+)
Also		PRL 50 219	C. Edwards *et al.*	(CIT, HARV, PRIN+)
SCHARRE	80	PL 97B 329	D.L. Scharre *et al.*	(SLAC, LBL)
FOSTER	68B	NP B8 174	M. Foster *et al.*	(CERN, CDEF)
BAILLON	67	NC 50A 393	P.H. Baillon *et al.*	(CERN, CDEF, IRAD)

$f_1(1420)$ $I^G(J^{PC}) = 0^+(1^{++})$

See the minireview under $\eta(1405)$.

$f_1(1420)$ MASS

VALUE (MeV)	EVTS	DOCUMENT ID		TECN	COMMENT
1426.4± 0.9 OUR AVERAGE		Error includes scale factor of 1.1.			
1434 ± 5 ± 5	133	[1] ACHARD	07	L3	183–209 $e^+e^- \to e^+e^- K^0_S K^\pm\pi^\mp$
1426 ± 6	711	ABDALLAH	03H	DLPH	91.2 $e^+e^- \to K^0_S K^\pm\pi^\mp + X$
1420 ±14	3651	NICHITIU	02	OBLX	
1428 ± 4 ± 2	20k	ADAMS	01B	B852	18 GeV $\pi^- p \to K^+K^-\pi^0 n$
1426 ± 1		BARBERIS	97C	OMEG	450 $pp \to pp K^0_S K^\pm\pi^\mp$
1425 ± 8		BERTIN	97	OBLX	0.0 $\overline{p}p \to K^\pm(K^0)\pi^\mp\pi^+\pi^-$
1435 ± 9		PROKOSHKIN	97B	GAM4	100 $\pi^- p \to \eta\pi^0\pi^0 n$
1430 ± 4		[2] ARMSTRONG	92E	OMEG	85,300 $\pi^+ p$, $pp \to \pi^+ p$, $pp(K\overline{K}\pi)$
1462 ±20		[3] AUGUSTIN	92	DM2	$J/\psi \to \gamma K\overline{K}\pi$
1443 $^{+\ 7}_{-\ 6}$ $^{+\ 3}_{-\ 2}$	1100	BAI	90C	MRK3	$J/\psi \to \gamma K^0_S K^\pm\pi^\mp$
1425 ±10	17	BEHREND	89	CELL	$\gamma\gamma \to K^0_S K^\pm\pi^\mp$
1442 ± 5 $^{+10}_{-17}$	111	BECKER	87	MRK3	e^+e^-, $\omega K\overline{K}\pi$
1423 ± 4		GIDAL	87B	MRK2	$e^+e^- \to e^+e^- K\overline{K}\pi$
1417 ±13	13	AIHARA	86C	TPC	$e^+e^- \to e^+e^- K\overline{K}\pi$
1422 ± 3		CHAUVAT	84	SPEC	ISR 31.5 pp
1440 ±10		[4] BROMBERG	80	SPEC	100 $\pi^- p \to K\overline{K}\pi X$
1426 ± 6	221	DIONISI	80	HBC	4 $\pi^- p \to K\overline{K}\pi n$
1420 ±20		DAHL	67	HBC	1.6–4.2 $\pi^- p$
• • • We do not use the following data for averages, fits, limits, etc. • • •					
1430.8± 0.9		[5] SOSA	99	SPEC	$pp \to p_{\text{slow}}(K^0_S K^+\pi^-)\, p_{\text{fast}}$
1433.4± 0.8		[5] SOSA	99	SPEC	$pp \to p_{\text{slow}}(K^0_S K^-\pi^+)\, p_{\text{fast}}$
1429 ± 3	389	ARMSTRONG	89	OMEG	300 $pp \to K\overline{K}\pi pp$
1425 ± 2	1520	ARMSTRONG	84	OMEG	85 $\pi^+ p$, $pp \to (\pi^+, p)(K\overline{K}\pi)p$
~ 1420		BITYUKOV	84	SPEC	32 $K^- p \to K^+K^-\pi^0 Y$

[1] From a fit with a width fixed at 55 MeV.
[2] This result supersedes ARMSTRONG 84, ARMSTRONG 89.
[3] From fit to the $K^*(892)K$ 1^{++} partial wave.
[4] Mass error increased to account for $a_0(980)$ mass cut uncertainties.
[5] No systematic error given.

$f_1(1420)$ WIDTH

VALUE (MeV)	EVTS	DOCUMENT ID		TECN	COMMENT
54.9± 2.6 OUR AVERAGE					
51 ±14	711	ABDALLAH	03H	DLPH	91.2 $e^+e^- \to K^0_S K^\pm\pi^\mp + X$
61 ± 8	3651	NICHITIU	02	OBLX	
38 ± 9 ±6	20k	ADAMS	01B	B852	18 GeV $\pi^- p \to K^+K^-\pi^0 n$
58 ± 4		BARBERIS	97C	OMEG	450 $pp \to pp K^0_S K^\pm\pi^\mp$
45 ±10		BERTIN	97	OBLX	0.0 $\overline{p}p \to K^\pm(K^0)\pi^\mp\pi^+\pi^-$
90 ±25		PROKOSHKIN	97B	GAM4	100 $\pi^- p \to \eta\pi^0\pi^0 n$
58 ±10		[6] ARMSTRONG	92E	OMEG	85,300 $\pi^+ p$, $pp \to \pi^+ p$, $pp(K\overline{K}\pi)$
129 ±41		[7] AUGUSTIN	92	DM2	$J/\psi \to \gamma K\overline{K}\pi$
68 $^{+29}_{-18}$ $^{+\ 8}_{-\ 9}$	1100	BAI	90C	MRK3	$J/\psi \to \gamma K^0_S K^\pm\pi^\mp$
42 ±22	17	BEHREND	89	CELL	$\gamma\gamma \to K^0_S K^\pm\pi^\mp$
40 $^{+17}_{-13}$ ±5	111	BECKER	87	MRK3	$e^+e^- \to \omega K\overline{K}\pi$
35 $^{+47}_{-20}$	13	AIHARA	86C	TPC	$e^+e^- \to e^+e^- K\overline{K}\pi$
47 ±10		CHAUVAT	84	SPEC	ISR 31.5 pp
62 ±14		BROMBERG	80	SPEC	100 $\pi^- p \to K\overline{K}\pi X$
40 ±15	221	DIONISI	80	HBC	4 $\pi^- p \to K\overline{K}\pi n$
60 ±20		DAHL	67	HBC	1.6–4.2 $\pi^- p$

• • • We do not use the following data for averages, fits, limits, etc. • • •

68.7± 2.9	[8] SOSA	99	SPEC	$pp \to p_{slow} (K^0_S K^+\pi^-)\, p_{fast}$
58.8± 3.3	[8] SOSA	99	SPEC	$pp \to p_{slow} (K^0_S K^-\pi^+)\, p_{fast}$
58 ± 8	389 ARMSTRONG	89	OMEG	300 $pp \to K\overline{K}\pi pp$
62 ± 5	1520 ARMSTRONG	84	OMEG	85 $\pi^+ p$, $pp \to (\pi^+, p)(K\overline{K}\pi)p$
~ 50	BITYUKOV	84	SPEC	32 $K^- p \to K^+ K^-\pi^0 Y$

[6] This result supersedes ARMSTRONG 84, ARMSTRONG 89.
[7] From fit to the $K^*(892)\,K$ 1^{++} partial wave.
[8] No systematic error given.

$f_1(1420)$ DECAY MODES

	Mode	Fraction (Γ_i/Γ)
Γ_1	$K\overline{K}\pi$	dominant
Γ_2	$K\overline{K}^*(892)+$ c.c.	dominant
Γ_3	$\eta\pi\pi$	possibly seen
Γ_4	$a_0(980)\pi$	
Γ_5	$\pi\pi\rho$	
Γ_6	4π	
Γ_7	$\rho^0\gamma$	
Γ_8	$\phi\gamma$	seen

$f_1(1420)$ Γ(i)$\Gamma(\gamma\gamma)/\Gamma$(total)

$\Gamma(K\overline{K}\pi)$ × $\Gamma(\gamma\gamma^*)/\Gamma_{total}$

VALUE (keV)	CL%	EVTS	DOCUMENT ID		TECN	COMMENT
1.9±0.4 OUR AVERAGE						
3.2±0.6±0.7		133	[9,10] ACHARD	07	L3	183–209 $e^+e^- \to e^+e^- K^0_S K^\pm\pi^\mp$
3.0±0.9±0.7			[11,12] BEHREND	89	CELL	$e^+e^- \to e^+e^- K^0_S K\pi$
$2.3^{+1.0}_{-0.9}$±0.8			HILL	89	JADE	$e^+e^- \to e^+e^- K^\pm K^0_S\pi^\mp$
1.3±0.5±0.3			AIHARA	88B	TPC	$e^+e^- \to e^+e^- K^\pm K^0_S\pi^\mp$
1.6±0.7±0.3			[11,13] GIDAL	87B	MRK2	$e^+e^- \to e^+e^- K\overline{K}\pi$
• • • We do not use the following data for averages, fits, limits, etc. • • •						
<8.0	95		JENNI	83	MRK2	$e^+e^- \to e^+e^- K\overline{K}\pi$

[9] From a fit with a width fixed at 55 MeV.
[10] The form factor parameter from the fit is 926 ± 78 MeV.
[11] Assume a ρ-pole form factor.
[12] A ϕ - pole form factor gives considerably smaller widths.
[13] Published value divided by 2.

$f_1(1420)$ BRANCHING RATIOS

$\Gamma(K\overline{K}^*(892)+$ c.c.$)/\Gamma(K\overline{K}\pi)$ Γ_2/Γ_1

VALUE	DOCUMENT ID		TECN	COMMENT
• • • We do not use the following data for averages, fits, limits, etc. • • •				
0.76±0.06	BROMBERG	80	SPEC	100 $\pi^- p \to K\overline{K}\pi X$
0.86±0.12	DIONISI	80	HBC	4 $\pi^- p \to K\overline{K}\pi n$

$\Gamma(\pi\pi\rho)/\Gamma(K\overline{K}\pi)$ Γ_5/Γ_1

VALUE	CL%	DOCUMENT ID		TECN	COMMENT
• • • We do not use the following data for averages, fits, limits, etc. • • •					
<0.3	95	CORDEN	78	OMEG	12–15 $\pi^- p$
<2.0		DAHL	67	HBC	1.6–4.2 $\pi^- p$

$\Gamma(\eta\pi\pi)/\Gamma(K\overline{K}\pi)$ Γ_3/Γ_1

VALUE	CL%	DOCUMENT ID		TECN	COMMENT
<0.1	95	ARMSTRONG	91B	OMEG	300 $pp \to pp\eta\pi^+\pi^-$
• • • We do not use the following data for averages, fits, limits, etc. • • •					
1.35±0.75		KOPKE	89	MRK3	$J/\psi \to \omega\eta\pi\pi(K\overline{K}\pi)$
<0.6	90	GIDAL	87	MRK2	$e^+e^- \to e^+e^-\eta\pi^+\pi^-$
<0.5	95	CORDEN	78	OMEG	12–15 $\pi^- p$
1.5 ±0.8		DEFOIX	72	HBC	0.7 $\overline{p}p$

$\Gamma(a_0(980)\pi)/\Gamma(\eta\pi\pi)$ Γ_4/Γ_3

VALUE	CL%	DOCUMENT ID		TECN	COMMENT
>0.1	90	PROKOSHKIN	97B	GAM4	100 $\pi^- p \to \eta\pi^0\pi^0 n$
• • • We do not use the following data for averages, fits, limits, etc. • • •					
not seen in either mode		ANDO	86	SPEC	8 $\pi^- p$
not seen in either mode		CORDEN	78	OMEG	12–15 $\pi^- p$
0.4±0.2		DEFOIX	72	HBC	0.7 $\overline{p}p \to 7\pi$

$\Gamma(4\pi)/\Gamma(K\overline{K}^*(892)+$ c.c.$)$ Γ_6/Γ_2

VALUE	CL%	DOCUMENT ID		TECN	COMMENT
• • • We do not use the following data for averages, fits, limits, etc. • • •					
<0.90	95	DIONISI	80	HBC	4 $\pi^- p$

$\Gamma(K\overline{K}\pi)/[\Gamma(K\overline{K}^*(892)+$ c.c.$)+\Gamma(a_0(980)\pi)]$ $\Gamma_1/(\Gamma_2+\Gamma_4)$

VALUE	DOCUMENT ID		TECN	COMMENT
• • • We do not use the following data for averages, fits, limits, etc. • • •				
0.65±0.27	[14] DIONISI	80	HBC	4 $\pi^- p$

[14] Calculated using $\Gamma(K\overline{K})/\Gamma(\eta\pi) = 0.24 \pm 0.07$ for $a_0(980)$ fractions.

$\Gamma(a_0(980)\pi)/\Gamma(K\overline{K}^*(892)+$ c.c.$)$ Γ_4/Γ_2

VALUE	CL%	DOCUMENT ID		TECN	COMMENT
0.04±0.01±0.01		BARBERIS	98C	OMEG	450 $pp \to p_f f_1(1420)\, p_s$
• • • We do not use the following data for averages, fits, limits, etc. • • •					
<0.04	68	ARMSTRONG	84	OMEG	85 $\pi^+ p$

$\Gamma(4\pi)/\Gamma(K\overline{K}\pi)$ Γ_6/Γ_1

VALUE	CL%	DOCUMENT ID		TECN	COMMENT
<0.62	95	ARMSTRONG	89G	OMEG	85 $\pi p \to 4\pi X$

$\Gamma(\rho^0\gamma)/\Gamma_{total}$ Γ_7/Γ

VALUE	CL%	DOCUMENT ID		TECN	COMMENT
<0.08	95	[15] ARMSTRONG	92C	SPEC	300 $pp \to pp\pi^+\pi^-\gamma$

[15] Using the data on the $\overline{K}K\pi$ mode from ARMSTRONG 89.

$\Gamma(\rho^0\gamma)/\Gamma(K\overline{K}\pi)$ Γ_7/Γ_1

VALUE	CL%	DOCUMENT ID		TECN	COMMENT
<0.02	95	BARBERIS	98C	OMEG	450 $pp \to p_f f_1(1420)\, p_s$

$\Gamma(\phi\gamma)/\Gamma(K\overline{K}\pi)$ Γ_8/Γ_1

VALUE	DOCUMENT ID		TECN	COMMENT
0.003±0.001±0.001	BARBERIS	98C	OMEG	450 $pp \to p_f f_1(1420)\, p_s$

$f_1(1420)$ REFERENCES

ACHARD	07	JHEP 0703 018	P. Achard *et al.*	(L3 Collab.)
ABDALLAH	03H	PL B569 129	J. Abdallah *et al.*	(DELPHI Collab.)
NICHITIU	02	PL B545 261	F. Nichitiu *et al.*	(OBELIX Collab.)
ADAMS	01B	PL B516 264	G.S. Adams *et al.*	(BNL E852 Collab.)
SOSA	99	PRL 83 913	M. Sosa *et al.*	
BARBERIS	98C	PL B440 225	D. Barberis *et al.*	(WA 102 Collab.)
BARBERIS	97C	PL B413 225	D. Barberis *et al.*	(WA 102 Collab.)
BERTIN	97	PL B400 226	A. Bertin *et al.*	(OBELIX Collab.)
PROKOSHKIN	97B	SPD 42 298	Yu.D. Prokoshkin, S.A. Sadovsky	
		Translated from DANS 354 751.		
ARMSTRONG	92C	ZPHY C54 371	T.A. Armstrong *et al.*	(ATHU, BARI, BIRM+)
ARMSTRONG	92E	ZPHY C56 29	T.A. Armstrong *et al.*	(ATHU, BARI, BIRM+) JPC
AUGUSTIN	92	PR D46 1951	J.E. Augustin, G. Cosme	(DM2 Collab.)
ARMSTRONG	91B	ZPHY C52 389	T.A. Armstrong *et al.*	(ATHU, BARI, BIRM+)
BAI	90C	PRL 65 2507	Z. Bai *et al.*	(Mark III Collab.)
ARMSTRONG	89	PL B221 216	T.A. Armstrong *et al.*	(CERN, CDEF, BIRM+) JPC
ARMSTRONG	89G	ZPHY C43 55	T.A. Armstrong *et al.*	(CERN, BIRM, BARI+)
BEHREND	89	ZPHY C42 367	H.J. Behrend *et al.*	(CELLO Collab.)
HILL	89	ZPHY C42 355	P. Hill *et al.*	(JADE Collab.) JP
KOPKE	89	PRPL 174 67	L. Kopke *et al.*	(CERN)
AIHARA	88B	PL B209 107	H. Aihara *et al.*	(TPC-2γ Collab.)
BECKER	87	PRL 59 186	J.J. Becker *et al.*	(Mark III Collab.) JP
GIDAL	87	PRL 59 2012	G. Gidal *et al.*	(LBL, SLAC, HARV)
GIDAL	87B	PRL 59 2016	G. Gidal *et al.*	(LBL, SLAC, HARV)
AIHARA	86C	PRL 57 2500	H. Aihara *et al.*	(TPC-2γ Collab.) JP
ANDO	86	PRL 57 1296	A. Ando *et al.*	(KEK, KYOT, NIRS, SAGA+)
ARMSTRONG	84	PL 146B 273	T.A. Armstrong *et al.*	(ATHU, BARI, BIRM+) JP
BITYUKOV	84	SJNP 39 735	S. Bityukov *et al.*	(SERP)
		Translated from YAF 39 1165.		
CHAUVAT	84	PL 148B 382	P. Chauvat *et al.*	(CERN, CLER, UCLA+)
JENNI	83	PR D27 1031	P. Jenni *et al.*	(SLAC, LBL)
BROMBERG	80	PR D22 1513	C.M. Bromberg *et al.*	(CIT, FNAL, ILLC+)
DIONISI	80	NP B169 1	C. Dionisi *et al.*	(CERN, MADR, CDEF+) IJP
CORDEN	78	NP B144 253	M.J. Corden *et al.*	(BIRM, RHEL, TELA+)
DEFOIX	72	NP B44 125	C. Defoix *et al.*	(CDEF, CERN)
DAHL	67	PR 163 1377	O.I. Dahl *et al.*	(LRL) IJP
Also		PRL 14 1074	D.H. Miller *et al.*	(LRL, UCB)

$\omega(1420)$

$I^G(J^{PC}) = 0^-(1^{--})$

$\omega(1420)$ MASS

VALUE (MeV)	EVTS	DOCUMENT ID		TECN	COMMENT
(1400–1450) OUR ESTIMATE					
• • • We do not use the following data for averages, fits, limits, etc. • • •					
1382± 23± 70		AUBERT	07AU	BABR	10.6 $e^+e^- \to \omega\pi^+\pi^-\gamma$
1350± 20± 20		AUBERT,B	04N	BABR	10.6 $e^+e^- \to \pi^+\pi^-\pi^0\gamma$
1400± 50±130	1.2M	[1] ACHASOV	03D	RVUE	0.44–2.00 $e^+e^- \to \pi^+\pi^-\pi^0$
1450± 10		[2] HENNER	02	RVUE	1.2–2.0 $e^+e^- \to \rho\pi, \omega\pi\pi$
1373± 70	177	[3] AKHMETSHIN	00D	CMD2	1.2–1.38 $e^+e^- \to \omega\pi^+\pi^-$
1370± 25	5095	ANISOVICH	00H	SPEC	0.0 $p\overline{p} \to \omega\pi^0\pi^0\pi^0$
1400^{+100}_{-200}		[4] ACHASOV	98H	RVUE	$e^+e^- \to \pi^+\pi^-\pi^0$
~ 1400		[5] ACHASOV	98H	RVUE	$e^+e^- \to \omega\pi^+\pi^-$
~ 1460		[6] ACHASOV	98H	RVUE	$e^+e^- \to K^+K^-$
1440± 70		[7] CLEGG	94	RVUE	
1419± 31	315	[8] ANTONELLI	92	DM2	1.34–2.4 $e^+e^- \to \rho\pi$

[1] From the combined fit of ANTONELLI 92, ACHASOV 01E, ACHASOV 02E, and ACHASOV 03D data on the $\pi^+\pi^-\pi^0$ and ANTONELLI 92 on the $\omega\pi^+\pi^-$ final states. Supersedes ACHASOV 99E and ACHASOV 02E.
[2] Using results of CORDIER 81 and preliminary data of DOLINSKY 91 and ANTONELLI 92.
[3] Using the data of AKHMETSHIN 00D and ANTONELLI 92. The $\rho\pi$ dominance for the energy dependence of the $\omega(1420)$ and $\omega(1650)$ width assumed.
[4] Using data from BARKOV 87, DOLINSKY 91, and ANTONELLI 92.
[5] Using the data from ANTONELLI 92.
[6] Using the data from IVANOV 81 and BISELLO 88B.
[7] From a fit to two Breit-Wigner functions and using the data of DOLINSKY 91 and ANTONELLI 92.
[8] From a fit to two Breit-Wigner functions interfering between them and with the ω,ϕ tails with fixed $(+,-,+)$ phases.

$\omega(1420)$ WIDTH

VALUE (MeV)	EVTS	DOCUMENT ID		TECN	COMMENT
(180–250) OUR ESTIMATE					
• • • We do not use the following data for averages, fits, limits, etc. • • •					
130± 50±100		AUBERT	07AU	BABR	10.6 $e^+e^- \to \omega\pi^+\pi^-\gamma$
450± 70± 70		AUBERT,B	04N	BABR	10.6 $e^+e^- \to \pi^+\pi^-\pi^0\gamma$
870^{+500}_{-300}±450	1.2M	[9] ACHASOV	03D	RVUE	0.44–2.00 $e^+e^- \to \pi^+\pi^-\pi^0$
199± 15		[10] HENNER	02	RVUE	1.2–2.0 $e^+e^- \to \rho\pi, \omega\pi\pi$
188± 45	177	[11] AKHMETSHIN	00D	CMD2	1.2–1.38 $e^+e^- \to \omega\pi^+\pi^-$
360^{+100}_{-60}	5095	ANISOVICH	00H	SPEC	0.0 $p\overline{p} \to \omega\pi^0\pi^0\pi^0$
240± 70		[12] CLEGG	94	RVUE	
174± 59	315	[13] ANTONELLI	92	DM2	1.34–2.4 $e^+e^- \to \rho\pi$

[9] From the combined fit of ANTONELLI 92, ACHASOV 01E, ACHASOV 02E, and ACHASOV 03D data on the $\pi^+\pi^-\pi^0$ and ANTONELLI 92 on the $\omega\pi^+\pi^-$ final states. Supersedes ACHASOV 99E and ACHASOV 02E.
[10] Using results of CORDIER 81 and preliminary data of DOLINSKY 91 and ANTONELLI 92.
[11] Using the data of AKHMETSHIN 00D and ANTONELLI 92. The $\rho\pi$ dominance for the energy dependence of the $\omega(1420)$ and $\omega(1650)$ width assumed.
[12] From a fit to two Breit-Wigner functions and using the data of DOLINSKY 91 and ANTONELLI 92.
[13] From a fit to two Breit-Wigner functions interfering between them and with the ω,ϕ tails with fixed $(+,-,+)$ phases.

$\omega(1420)$ DECAY MODES

	Mode	Fraction (Γ_i/Γ)
Γ_1	$\rho\pi$	dominant
Γ_2	$\omega\pi\pi$	seen
Γ_3	$b_1(1235)\pi$	seen
Γ_4	e^+e^-	seen
Γ_5	$\pi^0\gamma$	

$\omega(1420)$ $\Gamma(i)\Gamma(e^+e^-)/\Gamma^2(\text{total})$

$\Gamma(\rho\pi)/\Gamma_{\text{total}} \times \Gamma(e^+e^-)/\Gamma_{\text{total}}$ $\quad \Gamma_1/\Gamma \times \Gamma_4/\Gamma$

VALUE (units 10^{-6})	EVTS	DOCUMENT ID		TECN	COMMENT
• • • We do not use the following data for averages, fits, limits, etc. • • •					
0.82 ±0.05 ±0.06		AUBERT,B	04N	BABR	10.6 $e^+e^- \to \pi^+\pi^-\pi^0\gamma$
0.65 ±0.13 ±0.21	1.2M	[14,15] ACHASOV	03D	RVUE	0.44–2.00 $e^+e^- \to \pi^+\pi^-\pi^0$
0.625±0.160		[16,17] CLEGG	94	RVUE	
0.466±0.178		[18,19] ANTONELLI	92	DM2	1.34–2.4 $e^+e^- \to \rho\pi$

[14] Calculated by us from the cross section at the peak.
[15] From the combined fit of ANTONELLI 92, ACHASOV 01E, ACHASOV 02E, and ACHASOV 03D data on the $\pi^+\pi^-\pi^0$ and ANTONELLI 92 on the $\omega\pi^+\pi^-$ final states. Supersedes ACHASOV 99E and ACHASOV 02E.
[16] From a fit to two Breit-Wigner functions and using the data of DOLINSKY 91 and ANTONELLI 92.
[17] From the partial and leptonic width given by the authors.
[18] From a fit to two Breit-Wigner functions interfering between them and with the ω,ϕ tails with fixed $(+,-,+)$ phases.
[19] From the product of the leptonic width and partial branching ratio given by the authors.

$\Gamma(\omega\pi\pi)/\Gamma_{\text{total}} \times \Gamma(e^+e^-)/\Gamma_{\text{total}}$ $\quad \Gamma_2/\Gamma \times \Gamma_4/\Gamma$

VALUE (units 10^{-8})	DOCUMENT ID		TECN	COMMENT
• • • We do not use the following data for averages, fits, limits, etc. • • •				
19.7±5.7	AUBERT	07AU	BABR	10.6 $e^+e^- \to \omega\pi^+\pi^-\gamma$
1.9±1.9	[20] AKHMETSHIN	00D	CMD2	1.2–2.4 $e^+e^- \to \omega\pi^+\pi^-$

[20] Using the data of AKHMETSHIN 00D and ANTONELLI 92. The $\rho\pi$ dominance for the energy dependence of the $\omega(1420)$ and $\omega(1650)$ width assumed.

$\Gamma(\pi^0\gamma)/\Gamma_{\text{total}} \times \Gamma(e^+e^-)/\Gamma_{\text{total}}$ $\quad \Gamma_5/\Gamma \times \Gamma_4/\Gamma$

VALUE (units 10^{-8})	DOCUMENT ID		TECN	COMMENT
• • • We do not use the following data for averages, fits, limits, etc. • • •				
$2.03^{+0.70}_{-0.75}$	[21] AKHMETSHIN	05	CMD2	0.60-1.38 $e^+e^- \to \pi^0\gamma$

[21] Using 1420 MeV and 220 MeV for the $\omega(1420)$ mass and width.

$\omega(1420)$ BRANCHING RATIOS

$\Gamma(\omega\pi\pi)/\Gamma_{\text{total}}$ $\quad \Gamma_2/\Gamma$

VALUE	DOCUMENT ID		TECN	COMMENT
• • • We do not use the following data for averages, fits, limits, etc. • • •				
0.301±0.029	[22] HENNER	02	RVUE	1.2–2.0 $e^+e^- \to \rho\pi, \omega\pi\pi$
possibly seen	AKHMETSHIN	00D	CMD2	$e^+e^- \to \omega\pi^+\pi^-$

$\Gamma(\omega\pi\pi)/\Gamma(b_1(1235)\pi)$ $\quad \Gamma_2/\Gamma_3$

VALUE	EVTS	DOCUMENT ID		TECN	COMMENT
• • • We do not use the following data for averages, fits, limits, etc. • • •					
0.60±0.16	5095	ANISOVICH	00H	SPEC	0.0 $p\overline{p} \to \omega\pi^0\pi^0\pi^0$

$\Gamma(\rho\pi)/\Gamma_{\text{total}}$ $\quad \Gamma_1/\Gamma$

VALUE	DOCUMENT ID		TECN	COMMENT
• • • We do not use the following data for averages, fits, limits, etc. • • •				
0.699±0.029	[22] HENNER	02	RVUE	1.2–2.0 $e^+e^- \to \rho\pi, \omega\pi\pi$

$\Gamma(e^+e^-)/\Gamma_{\text{total}}$ $\quad \Gamma_4/\Gamma$

VALUE (units 10^{-7})	EVTS	DOCUMENT ID		TECN	COMMENT
• • • We do not use the following data for averages, fits, limits, etc. • • •					
~ 6.6	1.2M	[23,24] ACHASOV	03D	RVUE	0.44–2.00 $e^+e^- \to \pi^+\pi^-\pi^0$
23 ±1		[22] HENNER	02	RVUE	1.2–2.0 $e^+e^- \to \rho\pi, \omega\pi\pi$

[22] Assuming that the $\omega(1420)$ decays into $\rho\pi$ and $\omega\pi\pi$ only.
[23] Calculated by us from the cross section at the peak.
[24] Assuming that the $\omega(1420)$ decays into $\rho\pi$ only.

$\omega(1420)$ REFERENCES

AUBERT	07AU	PR D76 092005	B. Aubert *et al.*	(BABAR Collab.)
AKHMETSHIN	05	PL B605 26	R.R. Akhmetshin *et al.*	(Novosibirsk CMD-2 Collab.)
AUBERT,B	04N	PR D70 072004	B. Aubert *et al.*	(BABAR Collab.)
ACHASOV	03D	PR D68 052006	M.N. Achasov *et al.*	(Novosibirsk SND Collab.)
ACHASOV	02E	PR D66 032001	M.N. Achasov *et al.*	(Novosibirsk SND Collab.)
HENNER	02	EPJ C26 3	V.K. Henner *et al.*	
ACHASOV	01E	PR D63 072002	M.N. Achasov *et al.*	(Novosibirsk SND Collab.)
AKHMETSHIN	00D	PL B489 125	R.R. Akhmetshin *et al.*	(Novosibirsk CMD-2 Collab.)
ANISOVICH	00H	PL B485 341	A.V. Anisovich *et al.*	
ACHASOV	99E	PL B462 365	M.N. Achasov *et al.*	(Novosibirsk SND Collab.)
ACHASOV	98H	PR D57 4334	N.N. Achasov, A.A. Kozhevnikov	
CLEGG	94	ZPHY C62 455	A.B. Clegg, A. Donnachie	(LANC, MCHS)
ANTONELLI	92	ZPHY C56 15	A. Antonelli *et al.*	(DM2 Collab.)
DOLINSKY	91	PRPL 202 99	S.I. Dolinsky *et al.*	(NOVO)
BISELLO	88B	ZPHY C39 13	D. Bisello *et al.*	(PADO, CLER, FRAS+)
BARKOV	87	JETPL 46 164	L.M. Barkov *et al.*	(NOVO)
		Translated from ZETFP 46 132.		
CORDIER	81	PL 106B 155	A. Cordier *et al.*	(ORSAY)
IVANOV	81	PL 107B 297	P.M. Ivanov *et al.*	(NOVO)

$f_2(1430)$

$I^G(J^{PC}) = 0^+(2^{++})$

OMITTED FROM SUMMARY TABLE

This entry lists nearby peaks observed in the D wave of the $K\overline{K}$ and $\pi^+\pi^-$ systems. Needs confirmation.

$f_2(1430)$ MASS

VALUE (MeV)	DOCUMENT ID		TECN	COMMENT
≈ 1430 OUR ESTIMATE				
• • • We do not use the following data for averages, fits, limits, etc. • • •				
1453 ± 4	[1] VLADIMIRSK...01		SPEC	40 $\pi^- p \to K^0_S K^0_S n$
1421 ± 5	AUGUSTIN	87	DM2	$J/\psi \to \gamma\pi^+\pi^-$
1480 ± 50	AKESSON	86	SPEC	$pp \to pp\pi^+\pi^-$
1436^{+26}_{-16}	DAUM	84	CNTR	17–18 $\pi^- p \to K^+K^- n$
1412 ± 3	DAUM	84	CNTR	63 $\pi^- p \to K^0_S K^0_S n$, $K^+K^- n$
1439^{+5}_{-6}	[2] BEUSCH	67	OSPK	5,7,12 $\pi^- p \to K^0_S K^0_S n$

[1] $J^{PC} = 0^{++}$ or 2^{++}.
[2] Not seen by WETZEL 76.

$f_2(1430)$ WIDTH

VALUE (MeV)	DOCUMENT ID		TECN	COMMENT
• • • We do not use the following data for averages, fits, limits, etc. • • •				
13 ± 5	[3] VLADIMIRSK...01		SPEC	40 $\pi^- p \to K^0_S K^0_S n$
30 ± 9	AUGUSTIN	87	DM2	$J/\psi \to \gamma\pi^+\pi^-$
150 ± 50	AKESSON	86	SPEC	$pp \to pp\pi^+\pi^-$
81^{+56}_{-29}	DAUM	84	CNTR	17–18 $\pi^- p \to K^+K^- n$
14 ± 6	DAUM	84	CNTR	63 $\pi^- p \to K^0_S K^0_S n$, $K^+K^- n$
43^{+17}_{-18}	[4] BEUSCH	67	OSPK	5,7,12 $\pi^- p \to K^0_S K^0_S n$

[3] $J^{PC} = 0^{++}$ or 2^{++}.
[4] Not seen by WETZEL 76.

$f_2(1430)$ DECAY MODES

	Mode
Γ_1	$K\overline{K}$
Γ_2	$\pi\pi$

$f_2(1430)$ REFERENCES

VLADIMIRSK...	01	PAN 64 1895 Translated from YAF 64 1979.	V.V. Vladmirsky *et al.*	
AUGUSTIN	87	ZPHY C36 369	J.E. Augustin *et al.*	(LALO, CLER, FRAS+)
AKESSON	86	NP B264 154	T. Akesson *et al.*	(Axial Field Spec. Collab.)
DAUM	84	ZPHY C23 339	C. Daum *et al.*	(AMST, CERN, CRAC, MPIM+) JP
WETZEL	76	NP B115 208	W. Wetzel *et al.*	(ETH, CERN, LOIC)
BEUSCH	67	PL 25B 357	W. Beusch *et al.*	(ETH, CERN)

$a_0(1450)$

$I^G(J^{PC}) = 1^-(0^{++})$

See minireview on scalar mesons under $f_0(500)$.

$a_0(1450)$ MASS

VALUE (MeV)	EVTS	DOCUMENT ID		TECN	COMMENT
1474 ± 19 OUR AVERAGE					
1480 ± 30		ABELE	98	CBAR	0.0 $\overline{p}p \to K^0_L K^\pm \pi^\mp$
1470 ± 25		[1] AMSLER	95D	CBAR	0.0 $\overline{p}p \to \pi^0\pi^0\pi^0$, $\pi^0\eta\eta$, $\pi^0\pi^0\eta$
• • • We do not use the following data for averages, fits, limits, etc. • • •					
1515 ± 30		[2] ANISOVICH	09	RVUE	0.0 $\overline{p}p$, πN
$1316.8^{+0.7+24.7}_{-1.0-4.6}$		[3] UEHARA	09A	BELL	$\gamma\gamma \to \pi^0\eta$
1432 ± 13 ± 25		[4] BUGG	08A	RVUE	$\overline{p}p$
1477 ± 10	80k	[5] UMAN	06	E835	5.2 $\overline{p}p \to \eta\eta\pi^0$
1441^{+40}_{-15}	35280	[2] BAKER	03	SPEC	$\overline{p}p \to \omega\pi^+\pi^-\pi^0$
1303 ± 16		[6] BARGIOTTI	03	OBLX	$\overline{p}p$
1296 ± 10		[7] AMSLER	02	CBAR	0.9 $\overline{p}p \to \pi^0\pi^0\eta$
1565 ± 30		[7] ANISOVICH	98B	RVUE	Compilation
1290 ± 10		[8] BERTIN	98B	OBLX	0.0 $\overline{p}p \to K^\pm K_s \pi^\mp$
1450 ± 40		AMSLER	94D	CBAR	0.0 $\overline{p}p \to \pi^0\pi^0\eta$
1410 ± 25		ETKIN	82C	MPS	23 $\pi^- p \to n2K^0_S$
~ 1300		MARTIN	78	SPEC	10 $K^\pm p \to K^0_S \pi p$
1255 ± 5		[9] CASON	76		

[1] Coupled-channel analysis of AMSLER 95B, AMSLER 95C, and AMSLER 94D.
[2] From the pole position.
[3] May be a different state.
[4] Using data from AMSLER 94D, ABELE 98, and BAKER 03. Supersedes BUGG 94.
[5] Statistical error only.
[6] Coupled channel analysis of $\pi^+\pi^-\pi^0$, $K^+K^-\pi^0$, and $K^\pm K^0_S \pi^\mp$.
[7] T-matrix pole.
[8] Not confirmed by BUGG 08A.
[9] Isospin 0 not excluded.

$a_0(1450)$ WIDTH

VALUE (MeV)	EVTS	DOCUMENT ID		TECN	COMMENT
265 ± 13 OUR AVERAGE					
265 ± 15		ABELE	98	CBAR	0.0 $\overline{p}p \to K^0_L K^\pm \pi^\mp$
265 ± 30		[10] AMSLER	95D	CBAR	0.0 $\overline{p}p \to \pi^0\pi^0\pi^0$, $\pi^0\eta\eta$, $\pi^0\pi^0\eta$
• • • We do not use the following data for averages, fits, limits, etc. • • •					
230 ± 36		[11] ANISOVICH	09	RVUE	0.0 $\overline{p}p$, πN
$65.0^{+2.1+99.1}_{-5.4-32.6}$		[12] UEHARA	09A	BELL	$\gamma\gamma \to \pi^0\eta$
196 ± 10 ± 10		[13] BUGG	08A	RVUE	$\overline{p}p$
267 ± 11	80k	[14] UMAN	06	E835	5.2 $\overline{p}p \to \eta\eta\pi^0$
110 ± 14	35280	[11] BAKER	03	SPEC	$\overline{p}p \to \omega\pi^+\pi^-\pi^0$
92 ± 16		[15] BARGIOTTI	03	OBLX	$\overline{p}p$
81 ± 21		[16] AMSLER	02	CBAR	0.9 $\overline{p}p \to \pi^0\pi^0\eta$
292 ± 40		[16] ANISOVICH	98B	RVUE	Compilation
80 ± 5		[17] BERTIN	98B	OBLX	0.0 $\overline{p}p \to K^\pm K_s \pi^\mp$
270 ± 40		AMSLER	94D	CBAR	0.0 $\overline{p}p \to \pi^0\pi^0\eta$
230 ± 30		ETKIN	82C	MPS	23 $\pi^- p \to n2K^0_S$
~ 250		MARTIN	78	SPEC	10 $K^\pm p \to K^0_S \pi p$
79 ± 10		[18] CASON	76		

[10] Coupled-channel analysis of AMSLER 95B, AMSLER 95C, and AMSLER 94D.
[11] From the pole position.
[12] May be a different state.
[13] Using data from AMSLER 94D, ABELE 98, and BAKER 03. Supersedes BUGG 94.
[14] Statistical error only.
[15] Coupled channel analysis of $\pi^+\pi^-\pi^0$, $K^+K^-\pi^0$, and $K^\pm K^0_S \pi^\mp$.
[16] T-matrix pole.
[17] Not confirmed by BUGG 08A.
[18] Isospin 0 not excluded.

$a_0(1450)$ DECAY MODES

	Mode	Fraction (Γ_i/Γ)
Γ_1	$\pi\eta$	seen
Γ_2	$\pi\eta'(958)$	seen
Γ_3	$K\overline{K}$	seen
Γ_4	$\omega\pi\pi$	seen
Γ_5	$a_0(980)\pi\pi$	seen
Γ_6	$\gamma\gamma$	seen

$a_0(1450)$ $\Gamma(i)\Gamma(\gamma\gamma)/\Gamma(\text{total})$

$\Gamma(\pi\eta) \times \Gamma(\gamma\gamma)/\Gamma_{\text{total}}$ $\Gamma_1\Gamma_6/\Gamma$

VALUE (eV)	DOCUMENT ID		TECN	COMMENT
• • • We do not use the following data for averages, fits, limits, etc. • • •				
$432 \pm 6^{+1073}_{-256}$	[19] UEHARA	09A	BELL	$\gamma\gamma \to \pi^0\eta$

[19] May be a different state.

$a_0(1450)$ BRANCHING RATIOS

$\Gamma(\pi\eta'(958))/\Gamma(\pi\eta)$ Γ_2/Γ_1

VALUE	DOCUMENT ID		TECN	COMMENT
0.35 ± 0.16	[20] ABELE	98	CBAR	0.0 $\overline{p}p \to K^0_L K^\pm \pi^\mp$
• • • We do not use the following data for averages, fits, limits, etc. • • •				
0.43 ± 0.19	ABELE	97C	CBAR	0.0 $\overline{p}p \to \pi^0\pi^0\eta'$

[20] Using $\pi^0\eta$ from AMSLER 94D.

$\Gamma(K\overline{K})/\Gamma(\pi\eta)$ Γ_3/Γ_1

VALUE	DOCUMENT ID		TECN	COMMENT
0.88 ± 0.23	[21] ABELE	98	CBAR	0.0 $\overline{p}p \to K^0_L K^\pm \pi^\mp$

[21] Using $\pi^0\eta$ from AMSLER 94D.

$\Gamma(\omega\pi\pi)/\Gamma(\pi\eta)$ Γ_4/Γ_1

VALUE	EVTS	DOCUMENT ID		TECN	COMMENT
• • • We do not use the following data for averages, fits, limits, etc. • • •					
10.7 ± 2.3	35280	[22] BAKER	03	SPEC	$\overline{p}p \to \omega\pi^+\pi^-\pi^0$

[22] Using results on $\overline{p}p \to a_0(1450)^0\pi^0$, $a_0(1450) \to \eta\pi^0$ from ABELE 96C and assuming the $\omega\rho$ mechanism for the $\omega\pi\pi$ state.

Meson Particle Listings

$a_0(1450)$, $\rho(1450)$

$\Gamma(a_0(980)\pi\pi)/\Gamma_{total}$ Γ_5/Γ

VALUE	DOCUMENT ID		TECN	COMMENT
seen	BUGG	08A	RVUE	$\overline{p}p$

$\Gamma(a_0(980)\pi\pi)/\Gamma(\pi\eta)$ Γ_5/Γ_1

VALUE	DOCUMENT ID		TECN	CHG	COMMENT
• • • We do not use the following data for averages, fits, limits, etc. • • •					
≤ 4.3	ANISOVICH	01	RVUE	0	$\overline{p}p \rightarrow \eta 2\pi^+ 2\pi^-$

$\Gamma(\gamma\gamma)/\Gamma_{total}$ Γ_6/Γ

VALUE	DOCUMENT ID		TECN	COMMENT
seen	[23] UEHARA	09A	BELL	$\gamma\gamma \rightarrow \pi^0\eta$

[23] May be a different state.

$a_0(1450)$ REFERENCES

ANISOVICH	09	IJMP A24 2481	V.V. Anisovich, A.V. Sarantsev	
UEHARA	09A	PR D80 032001	S. Uehara *et al.*	(BELLE Collab.)
BUGG	08A	PR D78 074023	D.V. Bugg	(LOQM)
UMAN	06	PR D73 052009	I. Uman *et al.*	(FNAL E835)
BAKER	03	PL B563 140	C.A. Baker *et al.*	
BARGIOTTI	03	EPJ C26 371	M. Bargiotti *et al.*	(OBELIX Collab.)
AMSLER	02	EPJ C23 29	C. Amsler *et al.*	
ANISOVICH	01	NP A690 567	A.V. Anisovich *et al.*	
ABELE	98	PR D57 3860	A. Abele *et al.*	(Crystal Barrel Collab.)
ANISOVICH	98B	SPU 41 419	V.V. Anisovich *et al.*	
		Translated from UFN 168 481.		
BERTIN	98B	PL B434 180	A. Bertin *et al.*	(OBELIX Collab.)
ABELE	97C	PL B404 179	A. Abele *et al.*	(Crystal Barrel Collab.)
ABELE	96C	NP A609 562	A. Abele *et al.*	(Crystal Barrel Collab.)
AMSLER	95B	PL B342 433	C. Amsler *et al.*	(Crystal Barrel Collab.)
AMSLER	95C	PL B353 571	C. Amsler *et al.*	(Crystal Barrel Collab.)
AMSLER	95D	PL B355 425	C. Amsler *et al.*	(Crystal Barrel Collab.)
AMSLER	94D	PL B333 277	C. Amsler *et al.*	(Crystal Barrel Collab.) IGJPC
BUGG	94	PR D50 4412	D.V. Bugg *et al.*	(LOQM)
ETKIN	82C	PR D25 2446	A. Etkin *et al.*	(BNL, CUNY, TUFTS, VAND)
MARTIN	78	NP B134 392	A.D. Martin *et al.*	(DURH, GEVA)
CASON	76	PRL 36 1485	N.M. Cason *et al.*	(NDAM, ANL)

$\rho(1450)$

$I^G(J^{PC}) = 1^+(1^{--})$

See our mini-review under the $\rho(1700)$.

$\rho(1450)$ MASS

VALUE (MeV)	DOCUMENT ID
1465±25 OUR ESTIMATE	This is only an educated guess; the error given is larger than the error on the average of the published values.

$\eta\rho^0$ MODE

VALUE (MeV)		DOCUMENT ID		TECN	COMMENT
• • • We do not use the following data for averages, fits, limits, etc. • • •					
1497±14		[1] AKHMETSHIN	01B	CMD2	$e^+e^- \rightarrow \eta\gamma$
1421±15		[2] AKHMETSHIN	00D	CMD2	$e^+e^- \rightarrow \eta\pi^+\pi^-$
1470±20		ANTONELLI	88	DM2	$e^+e^- \rightarrow \eta\pi^+\pi^-$
1446±10		FUKUI	88	SPEC	8.95 $\pi^- p \rightarrow \eta\pi^+\pi^- n$

[1] Using the data of AKHMETSHIN 01B on $e^+e^- \rightarrow \eta\gamma$, AKHMETSHIN 00D and ANTONELLI 88 on $e^+e^- \rightarrow \eta\pi^+\pi^-$.
[2] Using the data of ANTONELLI 88, DOLINSKY 91, and AKHMETSHIN 00D. The energy-independent width of the $\rho(1450)$ and $\rho(1700)$ mesons assumed.

$\omega\pi$ MODE

VALUE (MeV)	EVTS	DOCUMENT ID		TECN	COMMENT
• • • We do not use the following data for averages, fits, limits, etc. • • •					
1491±19	7815	[1] ACHASOV	13	SND	1.05–2.00 $e^+e^- \rightarrow \pi^0\pi^0\gamma$
1582±17±25	2382	[2] AKHMETSHIN	03B	CMD2	$e^+e \rightarrow \pi^0\pi^0\gamma$
$1349\pm25^{+10}_{-5}$	341	[3] ALEXANDER	01B	CLE2	$B \rightarrow D^{(*)}\omega\pi^-$
1523±10		[4] EDWARDS	00A	CLE2	$\tau^- \rightarrow \omega\pi^-\nu_\tau$
1463±25		[5] CLEGG	94	RVUE	
1250		[6] ASTON	80C	OMEG	20–70 $\gamma p \rightarrow \omega\pi^0 p$
1290±40		[6] BARBER	80C	SPEC	3–5 $\gamma p \rightarrow \omega\pi^0 p$

[1] From a phenomenological model based on vector meson dominance with the interfering $\rho(1450)$ and $\rho(1700)$ and their widths fixed at 400 and 250 MeV, respectively. Systematic uncertainty not estimated.
[2] Using the data of AKHMETSHIN 03B and BISELLO 91B assuming the $\omega\pi^0$ and $\pi^+\pi^-$ mass dependence of the total width. $\rho(1700)$ mass and width fixed at 1700 MeV and 240 MeV, respectively.
[3] Using Breit-Wigner parameterization of the $\rho(1450)$ and assuming the $\omega\pi^-$ mass dependence for the total width.
[4] Mass-independent width parameterization. $\rho(1700)$ mass and width fixed at 1700 MeV and 235 MeV respectively.
[5] Using data from BISELLO 91B, DOLINSKY 86 and ALBRECHT 87L.
[6] Not separated from $b_1(1235)$, not pure $J^P = 1^-$ effect.

4π MODE

VALUE (MeV)	DOCUMENT ID		TECN	COMMENT
• • • We do not use the following data for averages, fits, limits, etc. • • •				
1435±40	ABELE	01B	CBAR	0.0 $\overline{p}n \rightarrow 2\pi^-2\pi^0\pi^+$
1350±50	ACHASOV	97	RVUE	$e^+e^- \rightarrow 2(\pi^+\pi^-)$
1449± 4	[1] ARMSTRONG	89E	OMEG	300 $pp \rightarrow pp2(\pi^+\pi^-)$

[1] Not clear whether this observation has I=1 or 0.

$\pi\pi$ MODE

VALUE (MeV)		EVTS	DOCUMENT ID		TECN	COMMENT
• • • We do not use the following data for averages, fits, limits, etc. • • •						
1350	$\pm20\ ^{+20}_{-30}$	63.5k	[1] ABRAMOWICZ12		ZEUS	$ep \rightarrow e\pi^+\pi^- p$
1493	±15		[2] LEES	12G	BABR	$e^+e^- \rightarrow \pi^+\pi^-\gamma$
1446	± 7 ±28	5.4M	[3,4] FUJIKAWA	08	BELL	$\tau^- \rightarrow \pi^-\pi^0\nu_\tau$
1328	±15		[5] SCHAEL	05C	ALEP	$\tau^- \rightarrow \pi^-\pi^0\nu_\tau$
1406	±15	87k	[3,6] ANDERSON	00A	CLE2	$\tau^- \rightarrow \pi^-\pi^0\nu_\tau$
~ 1368			[7] ABELE	99C	CBAR	0.0 $\overline{p}d \rightarrow \pi^+\pi^-\pi^- p$
1348	±33		BERTIN	98	OBLX	0.05–0.405 $\overline{n}p \rightarrow 2\pi^+\pi^-$
1411	±14		[8] ABELE	97	CBAR	$\overline{p}n \rightarrow \pi^-\pi^0\pi^0$
1370	$^{+90}_{-70}$		ACHASOV	97	RVUE	$e^+e^- \rightarrow \pi^+\pi^-$
1359	±40		[6] BERTIN	97C	OBLX	0.0 $\overline{p}p \rightarrow \pi^+\pi^-\pi^0$
1282	±37		BERTIN	97D	OBLX	0.05 $\overline{p}p \rightarrow 2\pi^+2\pi^-$
1424	±25		BISELLO	89	DM2	$e^+e^- \rightarrow \pi^+\pi^-$
1265.5	±75.3		DUBNICKA	89	RVUE	$e^+e^- \rightarrow \pi^+\pi^-$
1292	±17		[9] KURDADZE	83	OLYA	0.64–1.4 $e^+e^- \rightarrow \pi^+\pi^-$

[1] Using the KUHN 90 parametrization of the pion form factor, neglecting $\rho-\omega$ interference.
[2] Using the GOUNARIS 68 parametrization of the pion form factor leaving the masses and widths of the $\rho(1450)$, $\rho(1700)$, and $\rho(2150)$ resonances as free parameters of the fit.
[3] From the GOUNARIS 68 parametrization of the pion form factor.
[4] $|F_\pi(0)|^2$ fixed to 1.
[5] From the combined fit of the τ^- data from ANDERSON 00A and SCHAEL 05C and e^+e^- data from the compilation of BARKOV 85, AKHMETSHIN 04, and ALOISIO 05. $\rho(1700)$ mass and width fixed at 1713 MeV and 235 MeV, respectively. Supersedes BARATE 97M.
[6] $\rho(1700)$ mass and width fixed at 1700 MeV and 235 MeV, respectively.
[7] $\rho(1700)$ mass and width fixed at 1780 MeV and 275 MeV respectively.
[8] T-matrix pole.
[9] Using for $\rho(1700)$ mass and width 1600 ± 20 and 300 ± 10 MeV respectively.

$K\overline{K}$ MODE

VALUE (MeV)	EVTS	DOCUMENT ID		TECN	CHG	COMMENT
• • • We do not use the following data for averages, fits, limits, etc. • • •						
1422.8±6.5	27k	[1] ABELE	99D	CBAR	±	0.0 $\overline{p}p \rightarrow K^+K^-\pi^0$

[1] K-matrix pole. Isospin not determined, could be $\omega(1420)$.

$K\overline{K}^*(892)$ + c.c. MODE

VALUE (MeV)	DOCUMENT ID		TECN	COMMENT
• • • We do not use the following data for averages, fits, limits, etc. • • •				
1505±19±7	AUBERT	08S	BABR	10.6 $e^+e^- \rightarrow K\overline{K}^*(892)\gamma$

$\rho(1450)$ WIDTH

VALUE (MeV)	DOCUMENT ID
400±60 OUR ESTIMATE	This is only an educated guess; the error given is larger than the error on the average of the published values.

$\eta\rho^0$ MODE

VALUE (MeV)	DOCUMENT ID		TECN	COMMENT
• • • We do not use the following data for averages, fits, limits, etc. • • •				
226±44	[1] AKHMETSHIN	01B	CMD2	$e^+e^- \rightarrow \eta\gamma$
211±31	[2] AKHMETSHIN	00D	CMD2	$e^+e^- \rightarrow \eta\pi^+\pi^-$
230±30	ANTONELLI	88	DM2	$e^+e^- \rightarrow \eta\pi^+\pi^-$
60±15	FUKUI	88	SPEC	8.95 $\pi^- p \rightarrow \eta\pi^+\pi^- n$

[1] Using the data of AKHMETSHIN 01B on $e^+e^- \rightarrow \eta\gamma$, AKHMETSHIN 00D and ANTONELLI 88 on $e^+e^- \rightarrow \eta\pi^+\pi^-$.
[2] Using the data of ANTONELLI 88, DOLINSKY 91, and AKHMETSHIN 00D. The energy-independent width of the $\rho(1450)$ and $\rho(1700)$ mesons assumed.

$\omega\pi$ MODE

VALUE (MeV)	EVTS	DOCUMENT ID		TECN	COMMENT
• • • We do not use the following data for averages, fits, limits, etc. • • •					
429± 42±10	2382	[1] AKHMETSHIN	03B	CMD2	$e^+e \rightarrow \pi^0\pi^0\gamma$
547± 86^{+46}_{-45}	341	[2] ALEXANDER	01B	CLE2	$B \rightarrow D^{(*)}\omega\pi^-$
400± 35		[3] EDWARDS	00A	CLE2	$\tau^- \rightarrow \omega\pi^-\nu_\tau$
311± 62		[4] CLEGG	94	RVUE	
300		[5] ASTON	80C	OMEG	20–70 $\gamma p \rightarrow \omega\pi^0 p$
320±100		[5] BARBER	80C	SPEC	3–5 $\gamma p \rightarrow \omega\pi^0 p$

[1] Using the data of AKHMETSHIN 03B and BISELLO 91B assuming the $\omega\pi^0$ and $\pi^+\pi^-$ mass dependence of the total width. $\rho(1700)$ mass and width fixed at 1700 MeV and 240 MeV, respectively.
[2] Using Breit-Wigner parameterization of the $\rho(1450)$ and assuming the $\omega\pi^-$ mass dependence for the total width.
[3] Mass-independent width parameterization. $\rho(1700)$ mass and width fixed at 1700 MeV and 235 MeV respectively.
[4] Using data from BISELLO 91B, DOLINSKY 86 and ALBRECHT 87L.
[5] Not separated from $b_1(1235)$, not pure $J^P = 1^-$ effect.

4π MODE

VALUE (MeV)	DOCUMENT ID		TECN	COMMENT
• • • We do not use the following data for averages, fits, limits, etc. • • •				
325 ± 100	ABELE	01B	CBAR	$0.0\,\overline{p}n \to 2\pi^-2\pi^0\pi^+$

$\pi\pi$ MODE

VALUE (MeV)	EVTS	DOCUMENT ID		TECN	COMMENT
• • • We do not use the following data for averages, fits, limits, etc. • • •					
$460\pm30^{+40}_{-45}$	63.5k	[1] ABRAMOWICZ	12	ZEUS	$ep \to e\pi^+\pi^-p$
427 ± 31		[2] LEES	12G	BABR	$e^+e^- \to \pi^+\pi^-\gamma$
$434\pm16\pm60$	5.4M	[3,4] FUJIKAWA	08	BELL	$\tau^- \to \pi^-\pi^0\nu_\tau$
468 ± 41		[5] SCHAEL	05C	ALEP	$\tau^- \to \pi^-\pi^0\nu_\tau$
455 ± 41	87k	[3,6] ANDERSON	00A	CLE2	$\tau^- \to \pi^-\pi^0\nu_\tau$
~ 374		[7] ABELE	99C	CBAR	$0.0\,\overline{p}d \to \pi^+\pi^-\pi^-p$
275 ± 10		BERTIN	98	OBLX	0.05–$0.405\,\overline{n}p \to \pi^+\pi^+\pi^-$
343 ± 20		[8] ABELE	97	CBAR	$\overline{p}n \to \pi^-\pi^0\pi^0$
310 ± 40		[6] BERTIN	97C	OBLX	$0.0\,\overline{p}p \to \pi^+\pi^-\pi^0$
236 ± 36		BERTIN	97D	OBLX	$0.05\,\overline{p}p \to 2\pi^+2\pi^-$
269 ± 31		BISELLO	89	DM2	$e^+e^- \to \pi^+\pi^-$
391 ± 70		DUBNICKA	89	RVUE	$e^+e^- \to \pi^+\pi^-$
218 ± 46		[9] KURDADZE	83	OLYA	0.64–$1.4\ e^+e^- \to \pi^+\pi^-$

[1] Using the KUHN 90 parametrization of the pion form factor, neglecting ρ–ω interference.
[2] Using the GOUNARIS 68 parametrization of the pion form factor leaving the masses and widths of the $\rho(1450)$, $\rho(1700)$, and $\rho(2150)$ resonances as free parameters of the fit.
[3] From the GOUNARIS 68 parametrization of the pion form factor.
[4] $|F_\pi(0)|^2$ fixed to 1.
[5] From the combined fit of the τ^- data from ANDERSON 00A and SCHAEL 05C and e^+e^- data from the compilation of BARKOV 85, AKHMETSHIN 04, and ALOISIO 05. $\rho(1700)$ mass and width fixed at 1713 MeV and 235 MeV, respectively. Supersedes BARATE 97M.
[6] $\rho(1700)$ mass and width fixed at 1700 MeV and 235 MeV, respectively.
[7] $\rho(1700)$ mass and width fixed at 1780 MeV and 275 MeV respectively.
[8] T-matrix pole.
[9] Using for $\rho(1700)$ mass and width 1600 ± 20 and 300 ± 10 MeV respectively.

$K\overline{K}$ MODE

VALUE (MeV)	EVTS	DOCUMENT ID		TECN	CHG	COMMENT
• • • We do not use the following data for averages, fits, limits, etc. • • •						
146.5 ± 10.5	27k	[1] ABELE	99D	CBAR	$\pm$	$0.0\,\overline{p}p \to K^+K^-\pi^0$

[1] K-matrix pole. Isospin not determined, could be $\omega(1420)$.

$K\overline{K}^*(892)$ + c.c. MODE

VALUE (MeV)	DOCUMENT ID		TECN	COMMENT
• • • We do not use the following data for averages, fits, limits, etc. • • •				
$418\pm25\pm4$	AUBERT	08S	BABR	$10.6\ e^+e^- \to K\overline{K}^*(892)\gamma$

$\rho(1450)$ DECAY MODES

	Mode	Fraction (Γ_i/Γ)
Γ_1	$\pi\pi$	seen
Γ_2	4π	seen
Γ_3	$\omega\pi$	
Γ_4	$a_1(1260)\pi$	
Γ_5	$h_1(1170)\pi$	
Γ_6	$\pi(1300)\pi$	
Γ_7	$\rho\rho$	
Γ_8	$\rho(\pi\pi)_S$-wave	
Γ_9	e^+e^-	seen
Γ_{10}	$\eta\rho$	possibly seen
Γ_{11}	$a_2(1320)\pi$	not seen
Γ_{12}	$K\overline{K}$	not seen
Γ_{13}	$K\overline{K}^*(892)+$ c.c.	possibly seen
Γ_{14}	$\eta\gamma$	possibly seen
Γ_{15}	$f_0(500)\gamma$	not seen
Γ_{16}	$f_0(980)\gamma$	not seen
Γ_{17}	$f_0(1370)\gamma$	not seen
Γ_{18}	$f_2(1270)\gamma$	not seen

$\rho(1450)\ \Gamma(i)\Gamma(e^+e^-)/\Gamma(\text{total})$

$\Gamma(\pi\pi) \times \Gamma(e^+e^-)/\Gamma_{\text{total}}$ $\quad \Gamma_1\Gamma_9/\Gamma$

VALUE (keV)	DOCUMENT ID		TECN	COMMENT
• • • We do not use the following data for averages, fits, limits, etc. • • •				
0.12	[1] DIEKMAN	88	RVUE	$e^+e^- \to \pi^+\pi^-$
$0.027^{+0.015}_{-0.010}$	[2] KURDADZE	83	OLYA	0.64–$1.4\ e^+e^- \to \pi^+\pi^-$

$\Gamma(\eta\rho) \times \Gamma(e^+e^-)/\Gamma_{\text{total}}$ $\quad \Gamma_{10}\Gamma_9/\Gamma$

VALUE (eV)	DOCUMENT ID		TECN	COMMENT
• • • We do not use the following data for averages, fits, limits, etc. • • •				
74 ± 20	[3] AKHMETSHIN	00D	CMD2	$e^+e^- \to \eta\pi^+\pi^-$
91 ± 19	ANTONELLI	88	DM2	$e^+e^- \to \eta\pi^+\pi^-$

$\Gamma(\eta\gamma) \times \Gamma(e^+e^-)/\Gamma_{\text{total}}$ $\quad \Gamma_{14}\Gamma_9/\Gamma$

VALUE (eV)	DOCUMENT ID		TECN	COMMENT
• • • We do not use the following data for averages, fits, limits, etc. • • •				
<16.4	[4] AKHMETSHIN	05	CMD2	0.60–$1.38\ e^+e^- \to \eta\gamma$
$2.2\pm0.5\pm0.3$	[5] AKHMETSHIN	01B	CMD2	$e^+e^- \to \eta\gamma$

$\Gamma(K\overline{K}^*(892)+\text{c.c.}) \times \Gamma(e^+e^-)/\Gamma_{\text{total}}$ $\quad \Gamma_{13}\Gamma_9/\Gamma$

VALUE (eV)	DOCUMENT ID		TECN	COMMENT
• • • We do not use the following data for averages, fits, limits, etc. • • •				
$127\pm15\pm6$	AUBERT	08S	BABR	$10.6\ e^+e^- \to K\overline{K}^*(892)\gamma$

[1] Using total width = 235 MeV.
[2] Using for $\rho(1700)$ mass and width 1600 ± 20 and 300 ± 10 MeV respectively.
[3] Using the data of ANTONELLI 88, DOLINSKY 91, and AKHMETSHIN 00D. The energy-independent width of the $\rho(1450)$ and $\rho(1700)$ mesons assumed.
[4] From 2γ decay mode of η using 1465 MeV and 310 MeV for the $\rho(1450)$ mass and width. Recalculated by us.
[5] Using the data of AKHMETSHIN 01B on $e^+e^- \to \eta\gamma$, AKHMETSHIN 00D and ANTONELLI 88 on $e^+e^- \to \eta\pi^+\pi^-$. Recalculated by us using width of 226 MeV.

$\rho(1450)\ \Gamma(i)/\Gamma(\text{total}) \times \Gamma(e^+e^-)/\Gamma(\text{total})$

$\Gamma(\omega\pi)/\Gamma_{\text{total}} \times \Gamma(e^+e^-)/\Gamma_{\text{total}}$ $\quad \Gamma_3/\Gamma \times \Gamma_9/\Gamma$

VALUE ($\text{units } 10^{-6}$)	EVTS	DOCUMENT ID		TECN	COMMENT
• • • We do not use the following data for averages, fits, limits, etc. • • •					
5.3 ± 0.4	7815	[1] ACHASOV	13	SND	1.05–$2.00\ e^+e^- \to \pi^0\pi^0\gamma$

$\Gamma(f_0(500)\gamma)/\Gamma_{\text{total}} \times \Gamma(e^+e^-)/\Gamma_{\text{total}}$ $\quad \Gamma_{15}/\Gamma \times \Gamma_9/\Gamma$

VALUE ($\text{units } 10^{-9}$)	CL%	DOCUMENT ID		TECN	COMMENT
<4.0	90	ACHASOV	11	SND	$e^+e^- \to \pi^0\pi^0\gamma$

$\Gamma(f_0(980)\gamma)/\Gamma_{\text{total}} \times \Gamma(e^+e^-)/\Gamma_{\text{total}}$ $\quad \Gamma_{16}/\Gamma \times \Gamma_9/\Gamma$

VALUE ($\text{units } 10^{-9}$)	CL%	DOCUMENT ID		TECN	COMMENT
<2.6	90	ACHASOV	11	SND	$e^+e^- \to \pi^0\pi^0\gamma$

$\Gamma(f_0(1370)\gamma)/\Gamma_{\text{total}} \times \Gamma(e^+e^-)/\Gamma_{\text{total}}$ $\quad \Gamma_{17}/\Gamma \times \Gamma_9/\Gamma$

VALUE ($\text{units } 10^{-9}$)	CL%	DOCUMENT ID		TECN	COMMENT
<3.5	90	ACHASOV	11	SND	$e^+e^- \to \pi^0\pi^0\gamma$

$\Gamma(f_2(1270)\gamma)/\Gamma_{\text{total}} \times \Gamma(e^+e^-)/\Gamma_{\text{total}}$ $\quad \Gamma_{18}/\Gamma \times \Gamma_9/\Gamma$

VALUE ($\text{units } 10^{-9}$)	CL%	DOCUMENT ID		TECN	COMMENT
<0.8	90	[2] ACHASOV	11	SND	$e^+e^- \to \pi^0\pi^0\gamma$

[1] From a phenomenological model based on vector meson dominance with the interfering $\rho(1450)$ and $\rho(1700)$ and their widths fixed at 400 and 250 MeV, respectively. Systematic uncertainty not estimated.
[2] Using Breit-Wigner parametrization of the $\rho(1450)$ with mass and width of 1465 MeV and 400 MeV, respectively.

$\rho(1450)$ BRANCHING RATIOS

$\Gamma(\pi\pi)/\Gamma(4\pi)$ $\quad \Gamma_1/\Gamma_2$

VALUE	DOCUMENT ID		TECN	COMMENT
• • • We do not use the following data for averages, fits, limits, etc. • • •				
0.37 ± 0.10	[1,2] ABELE	01B	CBAR	$0.0\,\overline{p}n \to 5\pi$

$\Gamma(\omega\pi)/\Gamma_{\text{total}}$ $\quad \Gamma_3/\Gamma$

VALUE	EVTS	DOCUMENT ID		TECN	COMMENT
• • • We do not use the following data for averages, fits, limits, etc. • • •					
seen	1.6k	ACHASOV	12	SND	$e^+e^- \to \pi^0\pi^0\gamma$
~ 0.21		CLEGG	94	RVUE	

$\Gamma(\pi\pi)/\Gamma(\omega\pi)$ $\quad \Gamma_1/\Gamma_3$

VALUE	DOCUMENT ID		TECN
• • • We do not use the following data for averages, fits, limits, etc. • • •			
~ 0.32	CLEGG	94	RVUE

$\Gamma(\omega\pi)/\Gamma(4\pi)$ $\quad \Gamma_3/\Gamma_2$

VALUE	DOCUMENT ID		TECN
• • • We do not use the following data for averages, fits, limits, etc. • • •			
<0.14	CLEGG	88	RVUE

$\Gamma(a_1(1260)\pi)/\Gamma(4\pi)$ $\quad \Gamma_4/\Gamma_2$

VALUE	DOCUMENT ID		TECN	COMMENT
• • • We do not use the following data for averages, fits, limits, etc. • • •				
0.27 ± 0.08	[1] ABELE	01B	CBAR	$0.0\,\overline{p}n \to 5\pi$

Meson Particle Listings

$\rho(1450)$, $\eta(1475)$

$\Gamma(h_1(1170)\pi)/\Gamma(4\pi)$ Γ_5/Γ_2

VALUE	DOCUMENT ID	TECN	COMMENT
• • • We do not use the following data for averages, fits, limits, etc. • • •			
0.08 ± 0.04	[1] ABELE	01B CBAR	$0.0\ \overline{p}n \rightarrow 5\pi$

$\Gamma(\pi(1300)\pi)/\Gamma(4\pi)$ Γ_6/Γ_2

VALUE	DOCUMENT ID	TECN	COMMENT
• • • We do not use the following data for averages, fits, limits, etc. • • •			
0.37 ± 0.13	[1] ABELE	01B CBAR	$0.0\ \overline{p}n \rightarrow 5\pi$

$\Gamma(\rho\rho)/\Gamma(4\pi)$ Γ_7/Γ_2

VALUE	DOCUMENT ID	TECN	COMMENT
• • • We do not use the following data for averages, fits, limits, etc. • • •			
0.11 ± 0.05	[1] ABELE	01B CBAR	$0.0\ \overline{p}n \rightarrow 5\pi$

$\Gamma(\rho(\pi\pi)_{S\text{-wave}})/\Gamma(4\pi)$ Γ_8/Γ_2

VALUE	DOCUMENT ID	TECN	COMMENT
• • • We do not use the following data for averages, fits, limits, etc. • • •			
0.17 ± 0.09	[1] ABELE	01B CBAR	$0.0\ \overline{p}n \rightarrow 5\pi$

$\Gamma(\eta\rho)/\Gamma_{\text{total}}$ Γ_{10}/Γ

VALUE	DOCUMENT ID	TECN	COMMENT
• • • We do not use the following data for averages, fits, limits, etc. • • •			
<0.04	DONNACHIE 87B	RVUE	

$\Gamma(\eta\rho)/\Gamma(\omega\pi)$ Γ_{10}/Γ_3

VALUE	DOCUMENT ID	TECN	COMMENT
• • • We do not use the following data for averages, fits, limits, etc. • • •			
~ 0.24	[3] DONNACHIE 91	RVUE	
>2	FUKUI 91	SPEC	$8.95\ \pi^- p \rightarrow \omega\pi^0 n$

$\Gamma(a_2(1320)\pi)/\Gamma_{\text{total}}$ Γ_{11}/Γ

VALUE	DOCUMENT ID	TECN	COMMENT
• • • We do not use the following data for averages, fits, limits, etc. • • •			
not seen	AMELIN 00	VES	$37\ \pi^- p \rightarrow \eta\pi^+\pi^- n$

$\Gamma(K\overline{K})/\Gamma(\omega\pi)$ Γ_{12}/Γ_3

VALUE	DOCUMENT ID	TECN	COMMENT
• • • We do not use the following data for averages, fits, limits, etc. • • •			
<0.08	[3] DONNACHIE 91	RVUE	

$\Gamma(K\overline{K}^*(892)+\text{c.c.})/\Gamma_{\text{total}}$ Γ_{13}/Γ

VALUE	DOCUMENT ID	TECN	COMMENT
• • • We do not use the following data for averages, fits, limits, etc. • • •			
possibly seen	COAN 04	CLEO	$\tau^- \rightarrow K^-\pi^- K^+\nu_\tau$

[1] $\omega\pi$ not included.
[2] Using ABELE 97.
[3] Using data from BISELLO 91B, DOLINSKY 86 and ALBRECHT 87L.

$\rho(1450)$ REFERENCES

ACHASOV	13	PR D88 054013	M.N. Achasov *et al.*	(SND Collab.)
ABRAMOWICZ	12	EPJ C72 1869	H. Abramowicz *et al.*	(ZEUS Collab.)
ACHASOV	12	JETPL 94 734 Translated from ZETFP 94 796.	M.N. Achasov *et al.*	
LEES	12G	PR D86 032013	J.P. Lees *et al.*	(BABAR Collab.)
ACHASOV	11	JETP 113 75 Translated from ZETF 140 87.	M.N. Achasov *et al.*	(SND Collab.)
AUBERT	08S	PR D77 092002	B. Aubert *et al.*	(BABAR Collab.)
FUJIKAWA	08	PR D78 072006	M. Fujikawa *et al.*	(BELLE Collab.)
AKHMETSHIN	05	PL B605 26	R.R. Akhmetshin *et al.*	(Novosibirsk CMD-2 Collab.)
ALOISIO	05	PL B606 12	A. Aloisio *et al.*	(KLOE Collab.)
SCHAEL	05C	PRPL 421 191	S. Schael *et al.*	(ALEPH Collab.)
AKHMETSHIN	04	PL B578 285	R.R. Akhmetshin *et al.*	(Novosibirsk CMD-2 Collab.)
COAN	04	PRL 92 232001	T.E. Coan *et al.*	(CLEO Collab.)
AKHMETSHIN	03B	PL B562 173	R.R. Akhmetshin *et al.*	(Novosibirsk CMD-2 Collab.)
ABELE	01B	EPJ C21 261	A. Abele *et al.*	(Crystal Barrel Collab.)
AKHMETSHIN	01B	PL B509 217	R.R. Akhmetshin *et al.*	(Novosibirsk CMD-2 Collab.)
ALEXANDER	01B	PR D64 092001	J.P. Alexander *et al.*	(CLEO Collab.)
AKHMETSHIN	00D	PL B489 125	R.R. Akhmetshin *et al.*	(Novosibirsk CMD-2 Collab.)
AMELIN	00	NP A668 83	D. Amelin *et al.*	(VES Collab.)
ANDERSON	00A	PR D61 112002	S. Anderson *et al.*	(CLEO Collab.)
EDWARDS	00A	PR D61 072003	K.W. Edwards *et al.*	(CLEO Collab.)
ABELE	99C	PL B450 275	A. Abele *et al.*	(Crystal Barrel Collab.)
ABELE	99D	PL B468 178	A. Abele *et al.*	(Crystal Barrel Collab.)
BERTIN	98	PR D57 55	A. Bertin *et al.*	(OBELIX Collab.)
ABELE	97	PL B391 191	A. Abele *et al.*	(Crystal Barrel Collab.)
ACHASOV	97	PR D55 2663	N.N. Achasov *et al.*	(NOVM)
BARATE	97M	ZPHY C76 15	R. Barate *et al.*	(ALEPH Collab.)
BERTIN	97C	PL B408 476	A. Bertin *et al.*	(OBELIX Collab.)
BERTIN	97D	PL B414 220	A. Bertin *et al.*	(OBELIX Collab.)
CLEGG	94	ZPHY C62 455	A.B. Clegg, A. Donnachie	(LANC, MCHS)
BISELLO	91B	NPBPS B21 111	D. Bisello	(DM2 Collab.)
DOLINSKY	91	PRPL 202 99	S.I. Dolinsky *et al.*	(NOVO)
DONNACHIE	91	ZPHY C51 689	A. Donnachie, A.B. Clegg	(MCHS, LANC)
FUKUI	91	PL B257 241	S. Fukui *et al.*	(SUGI, NAGO, KEK, KYOT+)
KUHN	90	ZPHY C48 445	J.H. Kuhn *et al.*	(MPIM)
ARMSTRONG	89E	PL B228 536	T.A. Armstrong, M. Benayoun	(ATHU, BARI, BIRM+)
BISELLO	89	PL B220 321	D. Bisello *et al.*	(DM2 Collab.)
DUBNICKA	89	JP G15 1349	S. Dubnicka *et al.*	(JINR, SLOV)
ANTONELLI	88	PL B212 133	A. Antonelli *et al.*	(DM2 Collab.)
CLEGG	88	ZPHY C40 313	A.B. Clegg, A. Donnachie	(MCHS, LANC)
DIEKMAN	88	PRPL 159 99	B. Diekmann	(BONN)
FUKUI	88	PL B202 441	S. Fukui *et al.*	(SUGI, NAGO, KEK, KYOT+)
ALBRECHT	87L	PL B185 223	H. Albrecht *et al.*	(ARGUS Collab.)
DONNACHIE	87B	ZPHY C34 257	A. Donnachie, A.B. Clegg	(MCHS, LANC)
DOLINSKY	86	PL B174 453	S.I. Dolinsky *et al.*	(NOVO)
BARKOV	85	NP B256 365	L.M. Barkov *et al.*	(NOVO)
KURDADZE	83	JETPL 37 733 Translated from ZETFP 37 613.	L.M. Kurdadze *et al.*	(NOVO)
ASTON	80C	PL 92B 211	D. Aston	(BONN, CERN, EPOL, GLAS, LANC+)
BARBER	80C	ZPHY C4 169	D.P. Barber *et al.*	(DARE, LANC, SHEF)
GOUNARIS	68	PRL 21 244	G.J. Gounaris, J.J. Sakurai	

$\eta(1475)$

$I^G(J^{PC}) = 0^+(0^{-+})$

See also the $\eta(1405)$.

$\eta(1475)$ MASS

$K\overline{K}\pi$ MODE ($K^*(892)$ K dominant)

VALUE (MeV)	EVTS	DOCUMENT ID	TECN	COMMENT
1476± 4 OUR AVERAGE		Error includes scale factor of 1.3. See the ideogram below.		
$1469\pm14\pm13$	74	ACHARD 07	L3	$183\text{–}209\ e^+e^- \rightarrow e^+e^- K^0_S K^\pm\pi^\mp$
1460 ± 19	3651	NICHITIU 02	OBLX	
$1485\pm 8\pm 5$	20k	ADAMS 01B	B852	18 GeV $\pi^- p \rightarrow K^+K^-\pi^0 n$
1500 ± 10		CICALO 99	OBLX	$0\ \overline{p}p \rightarrow K^\pm K^0_S\pi^\mp\pi^+\pi^-$
1464 ± 10		BERTIN 97	OBLX	$0\ \overline{p}p \rightarrow K^\pm(K^0)\pi^\mp\pi^+\pi^-$
1460 ± 10		BERTIN 95	OBLX	$0\ \overline{p}p \rightarrow K\overline{K}\pi\pi\pi$
$1490^{+14+3}_{-\ 8-16}$	1100	BAI 90C	MRK3	$J/\psi \rightarrow \gamma K^0_S K^\pm\pi^\mp$
$1475\pm\ 4$		RATH 89	MPS	$21.4\ \pi^- p \rightarrow n K^0_S K^0_S\pi^0$
• • • We do not use the following data for averages, fits, limits, etc. • • •				
1421 ± 14		AUGUSTIN 92	DM2	$J/\psi \rightarrow \gamma K\overline{K}\pi$

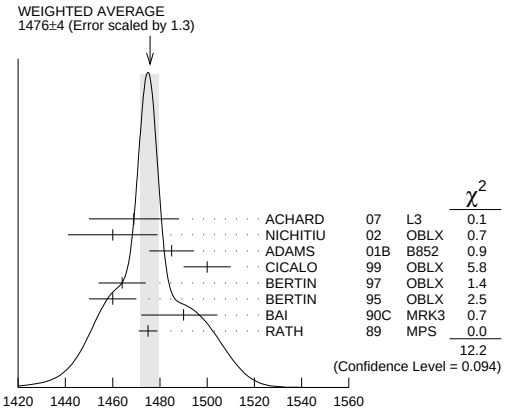

$\eta(1475)$ mass, $K\overline{K}\pi$ mode ($K^*(892)$ K dominant) (MeV)

$\eta(1475)$ WIDTH

$K\overline{K}\pi$ MODE ($K^*(892)$ K dominant)

VALUE (MeV)	EVTS	DOCUMENT ID	TECN	COMMENT
85± 9 OUR AVERAGE		Error includes scale factor of 1.5. See the ideogram below.		
$67\pm18\pm\ 7$	74	ACHARD 07	L3	$183\text{–}209\ e^+e^- \rightarrow e^+e^- K^0_S K^\pm\pi^\mp$
120 ± 19	3651	NICHITIU 02	OBLX	
$98\pm18\pm\ 3$	20k	ADAMS 01B	B852	18 GeV $\pi^- p \rightarrow K^+K^-\pi^0 n$
100 ± 20		CICALO 99	OBLX	$0\ \overline{p}p \rightarrow K^\pm K^0_S\pi^\mp\pi^+\pi^-$
105 ± 15		BERTIN 97	OBLX	$0.0\ \overline{p}p \rightarrow K^\pm(K^0)\pi^\mp\pi^+\pi^-$
105 ± 15		BERTIN 95	OBLX	$0\ \overline{p}p \rightarrow K\overline{K}\pi\pi\pi$
63 ± 18		AUGUSTIN 92	DM2	$J/\psi \rightarrow \gamma K\overline{K}\pi$
54^{+37+13}_{-21-24}		BAI 90C	MRK3	$J/\psi \rightarrow \gamma K^0_S K^\pm\pi^\mp$
51 ± 13		RATH 89	MPS	$21.4\ \pi^- p \rightarrow n K^0_S K^0_S\pi^0$

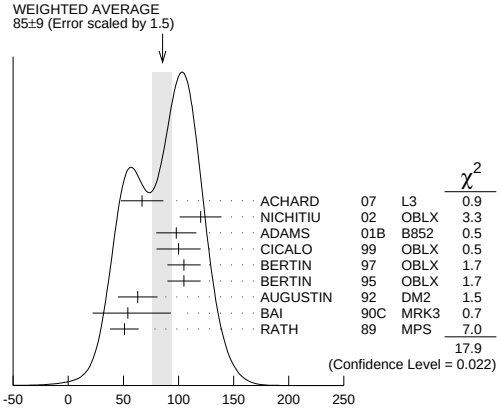

$\eta(1475)$ width $K\overline{K}\pi$ mode ($K^*(892)$ K dominant)

$\eta(1475)$ DECAY MODES

	Mode	Fraction (Γ_i/Γ)
Γ_1	$K\overline{K}\pi$	dominant
Γ_2	$K\overline{K}^*(892)+$ c.c.	seen
Γ_3	$a_0(980)\pi$	seen
Γ_4	$\gamma\gamma$	seen

$\eta(1475)$ Γ(i)$\Gamma(\gamma\gamma)/\Gamma$(total)

$\Gamma(K\overline{K}\pi) \times \Gamma(\gamma\gamma)/\Gamma_{\text{total}}$ $\Gamma_1\Gamma_4/\Gamma$

VALUE (keV)	CL%	EVTS	DOCUMENT ID		TECN	COMMENT
0.23±0.05±0.05		74	[1] ACHARD	07	L3	183–209 $e^+e^- \to e^+e^- K^0_S K^\pm\pi^\mp$
• • • We do not use the following data for averages, fits, limits, etc. • • •						
< 0.089	90		[2,3] AHOHE	05	CLE2	10.6 $e^+e^- \to e^+e^- K^0_S K^\pm\pi^\mp$

[1] Supersedes ACCIARRI 01G. Compatible with K^*K decay. Using $B(K^0_S \to \pi^+\pi^-)$= 0.6895.
[2] Using $\eta(1475)$ mass of 1481 MeV and width of 48 MeV. The upper limit increases to 0.140 keV if the world average value, 87 MeV, of the width is used.
[3] Assuming three-body phase-space decay to $K^0_S K^\pm\pi^\mp$.

$\eta(1475)$ BRANCHING RATIOS

$\Gamma(K\overline{K}^*(892)+\text{c.c.})/\Gamma(K\overline{K}\pi)$ Γ_2/Γ_1

VALUE	DOCUMENT ID		TECN	COMMENT
• • • We do not use the following data for averages, fits, limits, etc. • • •				
0.50±0.10	[4] BAILLON	67	HBC	0.0 $\overline{p}p \to K\overline{K}\pi\pi\pi$

$\Gamma(K\overline{K}^*(892)+\text{c.c.})/[\Gamma(K\overline{K}^*(892)+\text{c.c.})+\Gamma(a_0(980)\pi)]$ $\Gamma_2/(\Gamma_2+\Gamma_3)$

VALUE	CL%	DOCUMENT ID	TECN	COMMENT
• • • We do not use the following data for averages, fits, limits, etc. • • •				
<0.25	90	EDWARDS	82E CBAL	$J/\psi \to K^+K^-\pi^0\gamma$

[4] Data could also refer to $\eta(1405)$.

$\eta(1475)$ REFERENCES

ACHARD	07	JHEP 0703 018	P. Achard *et al.*	(L3 Collab.)
AHOHE	05	PR D71 072001	R. Ahohe *et al.*	(CLEO Collab.)
NICHITIU	02	PL B545 261	F. Nichitiu *et al.*	(OBELIX Collab.)
ACCIARRI	01G	PL B501 1	M. Acciarri *et al.*	(L3 Collab.)
ADAMS	01B	PL B516 264	G.S. Adams *et al.*	(BNL E852 Collab.)
CICALO	99	PL B462 453	C. Cicalo *et al.*	(OBELIX Collab.)
BERTIN	97	PL B400 226	A. Bertin *et al.*	(OBELIX Collab.)
BERTIN	95	PL B361 187	A. Bertin *et al.*	(OBELIX Collab.)
AUGUSTIN	92	PR D46 1951	J.E. Augustin, G. Cosme	(DM2 Collab.)
BAI	90C	PRL 65 2507	Z. Bai *et al.*	(Mark III Collab.)
RATH	89	PR D40 693	M.G. Rath *et al.*	(NDAM, BRAN, BNL, CUNY+)
EDWARDS	82E	PRL 49 259	C. Edwards *et al.*	(CIT, HARV, PRIN+)
BAILLON	67	NC 50A 393	P.H. Baillon *et al.*	(CERN, CDEF, IRAD)

$f_0(1500)$

$I^G(J^{PC}) = 0^+(0^{++})$

See also the mini-reviews on scalar mesons under $f_0(500)$ (see the index for the page number) and on non-$q\overline{q}$ candidates in PDG 06, Journal of Physics (generic for all A,B,E,G) **G33** 1 (2006).

$f_0(1500)$ MASS

VALUE (MeV)	EVTS	DOCUMENT ID		TECN	COMMENT
1505± 6 OUR AVERAGE		Error includes scale factor of 1.3. See the ideogram below.			
1466± 6± 20		ABLIKIM	06V	BES2	$e^+e^- \to J/\psi \to \gamma\pi^+\pi^-$
1515±12		[1] BARBERIS	00A		450 $pp \to p_f\eta\eta p_s$
1511± 9		[1,2] BARBERIS	00C		450 $pp \to p_f 4\pi p_s$
1510± 8		[1] BARBERIS	00E		450 $pp \to p_f\eta\eta p_s$
1522±25		BERTIN	98	OBLX	0.05–0.405 $\overline{n}p \to \pi^+\pi^+\pi^-$
1449±20		[1] BERTIN	97C	OBLX	0.0 $\overline{p}p \to \pi^+\pi^-\pi^0$
1515±20		ABELE	96B	CBAR	0.0 $\overline{p}p \to \pi^0 K^0_L K^0_L$
1500±15		[3] AMSLER	95B	CBAR	0.0 $\overline{p}p \to 3\pi^0$
1505±15		[4] AMSLER	95C	CBAR	0.0 $\overline{p}p \to \eta\eta\pi^0$
• • • We do not use the following data for averages, fits, limits, etc. • • •					
1486±10		[1] ANISOVICH	09	RVUE	0.0 $\overline{p}p$, πN
1470±60	568	[5] KLEMPT	08	E791	$D^+_s \to \pi^-\pi^+\pi^+$
$1470^{+\ 6+\ 72}_{-\ 7-255}$		[6] UEHARA	08A	BELL	10.6 $e^+e^- \to e^+e^-\pi^0\pi^0$
1495± 4		AMSLER	06	CBAR	0.9 $\overline{p}p \to K^+K^-\pi^0$
1539±20	9.9k	AUBERT	06O	BABR	$B^+ \to K^+K^+K^-$
1473± 5	80k	[7,8] UMAN	06	E835	5.2 $\overline{p}p \to \eta\eta\pi^0$
1478± 6		VLADIMIRSK...	06	SPEC	40 $\pi^-p \to K^0_S K^0_S n$
1493± 7		[7] BINON	05	GAMS	33 $\pi^-p \to \eta\eta n$
1524±14	1400	[9] GARMASH	05	BELL	$B^+ \to K^+K^+K^-$
$1489^{+\ 8}_{-\ 4}$		[10] ANISOVICH	03	RVUE	
1490±30		[7] ABELE	01	CBAR	0.0 $\overline{p}d \to \pi^-4\pi^0 p$
1497±10		[7] BARBERIS	99	OMEG	450 $pp \to p_s p_f K^+K^-$
1502±10		[7] BARBERIS	99B	OMEG	450 $pp \to p_s p_f \pi^+\pi^-$
1502±12± 10		[11] BARBERIS	99D	OMEG	450 $pp \to K^+K^-, \pi^+\pi^-$
1530±45		[7] BELLAZZINI	99	GAM4	450 $pp \to pp\pi^0\pi^0$
1505±18		[7] FRENCH	99		300 $pp \to p_f(K^+K^-)p_s$
1447±27		[12] KAMINSKI	99	RVUE	$\pi\pi \to \pi\pi$, $K\overline{K}$, $\sigma\sigma$
1580±80		[7] ALDE	98	GAM4	100 $\pi^-p \to \pi^0\pi^0 n$
1499± 8		[1] ANISOVICH	98B	RVUE	Compilation
~ 1520		REYES	98	SPEC	800 $pp \to p_s p_f K^0_S K^0_S$
1510±20		[1] BARBERIS	97B	OMEG	450 $pp \to pp2(\pi^+\pi^-)$
~ 1475		FRABETTI	97D	E687	$D^\pm_s \to \pi^\mp\pi^\pm\pi^\pm$
~ 1505		ABELE	96	CBAR	0.0 $\overline{p}p \to 5\pi^0$
1500± 8		[1] ABELE	96C	RVUE	Compilation
1460±20	120	[7] AMELIN	96B	VES	37 $\pi^-A \to \eta\eta\pi^-A$
1500± 8		BUGG	96	RVUE	
1500±10		[13] AMSLER	95D	CBAR	0.0 $\overline{p}p \to \pi^0\pi^0\pi^0$, $\pi^0\eta\eta$, $\pi^0\pi^0\eta$
1445± 5		[14] ANTINORI	95	OMEG	300,450 $pp \to pp2(\pi^+\pi^-)$
1497±30		[7] ANTINORI	95	OMEG	300,450 $pp \to pp\pi^+\pi^-$
~ 1505		BUGG	95	MRK3	$J/\psi \to \gamma\pi^+\pi^-\pi^+\pi^-$
1446± 5		[7] ABATZIS	94	OMEG	450 $pp \to pp2(\pi^+\pi^-)$
1545±25		[7] AMSLER	94E	CBAR	0.0 $\overline{p}p \to \pi^0\eta\eta'$
1520±25		[1,15] ANISOVICH	94	CBAR	0.0 $\overline{p}p \to 3\pi^0, \pi^0\eta\eta$
1505±20		[1,16] BUGG	94	RVUE	$\overline{p}p \to 3\pi^0$, $\eta\eta\pi^0$, $\eta\pi^0\pi^0$
1560±25		[7] AMSLER	92	CBAR	0.0 $\overline{p}p \to \pi^0\eta\eta$
1550±45± 30		[7] BELADIDZE	92C	VES	36 π^-Be $\to \pi^-\eta'\eta$Be
1449± 4		[7] ARMSTRONG	89E	OMEG	300 $pp \to pp2(\pi^+\pi^-)$
1610±20		[7] ALDE	88	GAM4	300 $\pi^-N \to \pi^-N2\eta$
~ 1525		ASTON	88D	LASS	11 $K^-p \to K^0_S K^0_S \Lambda$
1570±20	600	[7] ALDE	87	GAM4	100 $\pi^-p \to 4\pi^0 n$
1575±45		[17] ALDE	86D	GAM4	100 $\pi^-p \to 2\eta n$
1568±33		[7] BINON	84C	GAM2	38 $\pi^-p \to \eta\eta' n$
1592±25		[7] BINON	83	GAM2	38 $\pi^-p \to 2\eta n$
1525± 5		[7] GRAY	83	DBC	0.0 $\overline{p}N \to 3\pi$

[1] T-matrix pole.
[2] Average between $\pi^+\pi^-2\pi^0$ and $2(\pi^+\pi^-)$.
[3] T-matrix pole, supersedes ANISOVICH 94.
[4] T-matrix pole, supersedes ANISOVICH 94 and AMSLER 92.
[5] Reanalysis of AITALA 01A data. This state could also be $f_0(1370)$.
[6] Breit-Wigner mass. May also be the $f_0(1370)$.
[7] Breit-Wigner mass.
[8] Statistical error only.
[9] Breit-Wigner, solution 1, PWA ambiguous.
[10] K-matrix pole from combined analysis of $\pi^-p \to \pi^0\pi^0 n$, $\pi^-p \to K\overline{K}n$, $\pi^+\pi^- \to \pi^+\pi^-$, $\overline{p}p \to \pi^0\pi^0\pi^0$, $\pi^0\eta\eta$, $\pi^0\pi^0\eta$, $\pi^+\pi^-\pi^0$, $K^+K^-\pi^0$, $K^0_S K^0_S\pi^0$, $K^+K^0_S\pi^-$ at rest, $\overline{p}n \to \pi^-\pi^-\pi^+$, $K^0_S K^-\pi^0$, $K^0_S K^0_S\pi^-$ at rest.
[11] Supersedes BARBERIS 99 and BARBERIS 99B.
[12] T-matrix pole on sheet $--+$.
[13] T-matrix pole. Coupled-channel analysis of AMSLER 95B, AMSLER 95C, and AMSLER 94D.
[14] Supersedes ABATZIS 94, ARMSTRONG 89E. Breit-Wigner mass.
[15] From a simultaneous analysis of the annihilations $\overline{p}p \to 3\pi^0, \pi^0\eta\eta$.
[16] Reanalysis of ANISOVICH 94 data.
[17] From central value and spread of two solutions. Breit-Wigner mass.

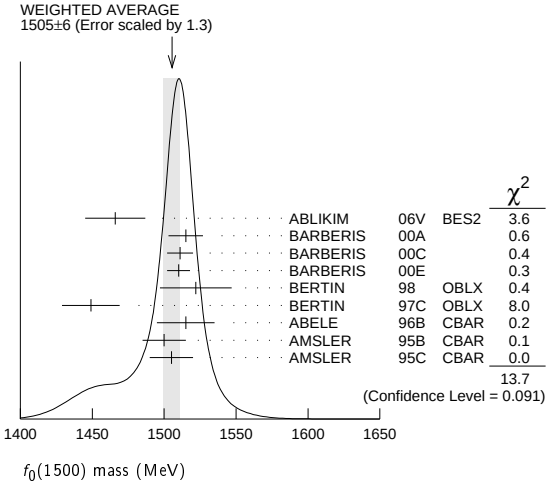

Meson Particle Listings

$f_0(1500)$

$f_0(1500)$ WIDTH

VALUE (MeV)	EVTS	DOCUMENT ID		TECN	COMMENT
109± 7 OUR AVERAGE					
$108^{+\ 14}_{-\ 11}\pm25$		ABLIKIM	06V	BES2	$e^+e^- \to J/\psi \to \gamma\pi^+\pi^-$
110± 24		[18] BARBERIS	00A		450 $pp \to p_f\eta\eta p_s$
102± 18		[18,19] BARBERIS	00C		450 $pp \to p_f 4\pi p_s$
110± 16		[18] BARBERIS	00E		450 $pp \to p_f\eta\eta p_s$
108± 33		BERTIN	98	OBLX	0.05–0.405 $\overline{n}p \to \pi^+\pi^+\pi^-$
114± 30		[18] BERTIN	97C	OBLX	0.0 $\overline{p}p \to \pi^+\pi^-\pi^0$
105± 15		ABELE	96B	CBAR	0.0 $\overline{p}p \to \pi^0 K^0_L K^0_L$
120± 25		[20] AMSLER	95B	CBAR	0.0 $\overline{p}p \to 3\pi^0$
120± 30		[21] AMSLER	95C	CBAR	0.0 $\overline{p}p \to \eta\eta\pi^0$
• • • We do not use the following data for averages, fits, limits, etc. • • •					
114± 10		[18] ANISOVICH	09	RVUE	0.0 $\overline{p}p$, πN
$90^{+\ 2+50}_{-\ 1-22}$		[22] UEHARA	08A	BELL	10.6 $e^+e^- \to e^+e^-\pi^0\pi^0$
121± 8		AMSLER	06	CBAR	0.9 $\overline{p}p \to K^+K^-\pi^0$
257± 33	9.9k	AUBERT	06O	BABR	$B^+ \to K^+K^+K^-$
108± 9	80k	[23,24] UMAN	06	E835	5.2 $\overline{p}p \to \eta\eta\pi^0$
119± 10		VLADIMIRSK...	06	SPEC	40 $\pi^-p \to K^0_S K^0_S n$
90± 15		[23] BINON	05	GAMS	33 $\pi^-p \to \eta\eta n$
136± 23	1400	[25] GARMASH	05	BELL	$B^+ \to K^+K^+K^-$
102± 10		[26] ANISOVICH	03	RVUE	
140± 40		[23] ABELE	01	CBAR	0.0 $\overline{p}d \to \pi^- 4\pi^0 p$
104± 25		[23] BARBERIS	99	OMEG	450 $pp \to p_s p_f K^+K^-$
131± 15		[23] BARBERIS	99B	OMEG	450 $pp \to p_s p_f \pi^+\pi^-$
98± 18±16		[27] BARBERIS	99D	OMEG	450 $pp \to K^+K^-, \pi^+\pi^-$
160± 50		[23] BELLAZZINI	99	GAM4	450 $pp \to pp\pi^0\pi^0$
100± 33		[23] FRENCH	99		300 $pp \to p_f(K^+K^-)p_s$
108± 46		[28] KAMINSKI	99	RVUE	$\pi\pi \to \pi\pi$, $K\overline{K}$, $\sigma\sigma$
280±100		[23] ALDE	98	GAM4	100 $\pi^-p \to \pi^0\pi^0 n$
130± 20		[18] ANISOVICH	98B	RVUE	Compilation
120± 35		[18] BARBERIS	97B	OMEG	450 $pp \to pp2(\pi^+\pi^-)$
~ 100		FRABETTI	97D	E687	$D^\pm_s \to \pi^\mp\pi^\pm\pi^\pm$
~ 169		ABELE	96	CBAR	0.0 $\overline{p}p \to 5\pi^0$
100± 30	120	[23] AMELIN	96B	VES	37 $\pi^-A \to \eta\eta\pi^-A$
132± 15		BUGG	96	RVUE	
154± 30		[29] AMSLER	95D	CBAR	0.0 $\overline{p}p \to \pi^0\pi^0\pi^0, \pi^0\eta\eta, \pi^0\pi^0\eta$
65± 10		[30] ANTINORI	95	OMEG	300,450 $pp \to pp2(\pi^+\pi^-)$
199± 30		[23] ANTINORI	95	OMEG	300,450 $pp \to pp\pi^+\pi^-$
56± 12		[23] ABATZIS	94	OMEG	450 $pp \to pp2(\pi^+\pi^-)$
100± 40		[23] AMSLER	94E	CBAR	0.0 $\overline{p}p \to \pi^0\eta\eta'$
$148^{+\ 20}_{-\ 25}$		[18,31] ANISOVICH	94	CBAR	0.0 $\overline{p}p \to 3\pi^0, \pi^0\eta\eta$
150± 20		[18,32] BUGG	94	RVUE	$\overline{p}p \to 3\pi^0, \eta\eta\pi^0, \eta\pi^0\pi^0$
245± 50		[23] AMSLER	92	CBAR	0.0 $\overline{p}p \to \pi^0\eta\eta$
153± 67±50		[23] BELADIDZE	92C	VES	36 π^-Be $\to \pi^-\eta'\eta$Be
78± 18		[23] ARMSTRONG	89E	OMEG	300 $pp \to pp2(\pi^+\pi^-)$
170± 40		[23] ALDE	88	GAM4	300 $\pi^-N \to \pi^-N2\eta$
150± 20	600	[23] ALDE	87	GAM4	100 $\pi^-p \to 4\pi^0 n$
265± 65		[33] ALDE	86D	GAM4	100 $\pi^-p \to 2\eta n$
260± 60		[23] BINON	84C	GAM2	38 $\pi^-p \to \eta\eta' n$
210± 40		[23] BINON	83	GAM2	38 $\pi^-p \to 2\eta n$
101± 13		[23] GRAY	83	DBC	0.0 $\overline{p}N \to 3\pi$

[18] T-matrix pole.
[19] Average between $\pi^+\pi^-2\pi^0$ and $2(\pi^+\pi^-)$.
[20] T-matrix pole, supersedes ANISOVICH 94.
[21] T-matrix pole, supersedes ANISOVICH 94 and AMSLER 92.
[22] Breit-Wigner width. May also be the $f_0(1370)$.
[23] Breit-Wigner width.
[24] Statistical error only.
[25] Breit-Wigner, solution 1, PWA ambiguous.
[26] K-matrix pole from combined analysis of $\pi^-p \to \pi^0\pi^0 n$, $\pi^-p \to K\overline{K}n$, $\pi^+\pi^- \to \pi^+\pi^-$, $\overline{p}p \to \pi^0\pi^0\pi^0\pi^0, \pi^0\eta\eta, \pi^0\pi^0\eta, \pi^+\pi^-\pi^0, K^+K^-\pi^0, K^0_S K^0_S\pi^0$, $K^+K^0_S\pi^-$ at rest, $\overline{p}n \to \pi^-\pi^-\pi^+, K^0_S K^-\pi^0, K^0_S K^0_S\pi^-$ at rest.
[27] Supersedes BARBERIS 99 and BARBERIS 99B.
[28] T-matrix pole on sheet $--+$.
[29] T-matrix pole. Coupled-channel analysis of AMSLER 95B, AMSLER 95C, and AMSLER 94D.
[30] Supersedes ABATZIS 94, ARMSTRONG 89E. Breit-Wigner mass.
[31] From a simultaneous analysis of the annihilations $\overline{p}p \to 3\pi^0, \pi^0\eta\eta$.
[32] Reanalysis of ANISOVICH 94 data.
[33] From central value and spread of two solutions. Breit-Wigner mass.

$f_0(1500)$ DECAY MODES

	Mode	Fraction (Γ_i/Γ)	Scale factor
Γ_1	$\pi\pi$	(34.9±2.3) %	1.2
Γ_2	$\pi^+\pi^-$	seen	
Γ_3	$2\pi^0$	seen	
Γ_4	4π	(49.5±3.3) %	1.2
Γ_5	$4\pi^0$	seen	
Γ_6	$2\pi^+2\pi^-$	seen	
Γ_7	$2(\pi\pi)$ S-wave	seen	
Γ_8	$\rho\rho$	seen	
Γ_9	$\pi(1300)\pi$	seen	
Γ_{10}	$a_1(1260)\pi$	seen	
Γ_{11}	$\eta\eta$	(5.1±0.9) %	1.4
Γ_{12}	$\eta\eta'(958)$	(1.9±0.8) %	1.7
Γ_{13}	$K\overline{K}$	(8.6±1.0) %	1.1
Γ_{14}	$\gamma\gamma$	not seen	

CONSTRAINED FIT INFORMATION

An overall fit to 6 branching ratios uses 10 measurements and one constraint to determine 5 parameters. The overall fit has a $\chi^2 = 11.4$ for 6 degrees of freedom.

The following *off-diagonal* array elements are the correlation coefficients $\langle \delta x_i \delta x_j \rangle / (\delta x_i \cdot \delta x_j)$, in percent, from the fit to the branching fractions, $x_i \equiv \Gamma_i/\Gamma_{\rm total}$. The fit constrains the x_i whose labels appear in this array to sum to one.

x_4	−83			
x_{11}	11	−52		
x_{12}	−5	−31	29	
x_{13}	39	−67	33	6
	x_1	x_4	x_{11}	x_{12}

$f_0(1500)$ Γ(i)Γ(γγ)/Γ(total)

$\Gamma(\pi\pi) \times \Gamma(\gamma\gamma)/\Gamma_{\rm total}$ **$\Gamma_1\Gamma_{14}/\Gamma$**

VALUE (eV)	CL%	DOCUMENT ID		TECN	COMMENT
• • • We do not use the following data for averages, fits, limits, etc. • • •					
$33^{+\ 12+1809}_{-\ 6-\ 21}$		[34] UEHARA	08A	BELL	10.6 $e^+e^- \to e^+e^-\pi^0\pi^0$
not seen		ACCIARRI	01H	L3	$\gamma\gamma \to K^0_S K^0_S$, $E^{ee}_{\rm cm}$= 91, 183–209 GeV
<460	95	BARATE	00E	ALEP	$\gamma\gamma \to \pi^+\pi^-$

[34] May also be the $f_0(1370)$. Multiplied by us by 3 to obtain the $\pi\pi$ value.

$f_0(1500)$ BRANCHING RATIOS

$\Gamma(\pi\pi)/\Gamma_{\rm total}$ **Γ_1/Γ**

VALUE	DOCUMENT ID		TECN	
• • • We do not use the following data for averages, fits, limits, etc. • • •				
0.454±0.104	BUGG	96	RVUE	

$\Gamma(\pi^+\pi^-)/\Gamma_{\rm total}$ **Γ_2/Γ**

VALUE	DOCUMENT ID		TECN	COMMENT
seen	BERTIN	98	OBLX	0.05–0.405 $\overline{n}p \to \pi^+\pi^+\pi^-$
• • • We do not use the following data for averages, fits, limits, etc. • • •				
possibly seen	FRABETTI	97D	E687	$D^\pm_s \to \pi^\mp\pi^\pm\pi^\pm$

$\Gamma(4\pi)/\Gamma(\pi\pi)$ **Γ_4/Γ_1**

VALUE	DOCUMENT ID		TECN	COMMENT
1.42±0.18 OUR FIT Error includes scale factor of 1.2.				
1.42±0.18 OUR AVERAGE Error includes scale factor of 1.2.				
1.37±0.16	BARBERIS	00D		450 $pp \to p_f 4\pi p_s$
2.1 ±0.6	[35] AMSLER	98	RVUE	
• • • We do not use the following data for averages, fits, limits, etc. • • •				
2.1 ±0.2	[36] ANISOVICH	02D	SPEC	Combined fit
3.4 ±0.8	[35] ABELE	96	CBAR	0.0 $\overline{p}p \to 5\pi^0$

$\Gamma(2(\pi\pi)_{S\text{-wave}})/\Gamma(\pi\pi)$ **Γ_7/Γ_1**

VALUE	DOCUMENT ID		TECN	COMMENT
• • • We do not use the following data for averages, fits, limits, etc. • • •				
0.42±0.26	[37] ABELE	01	CBAR	0.0 $\overline{p}d \to \pi^- 4\pi^0 p$

$\Gamma(2(\pi\pi)_{S\text{-wave}})/\Gamma(4\pi)$ **Γ_7/Γ_4**

VALUE	DOCUMENT ID		TECN	COMMENT
• • • We do not use the following data for averages, fits, limits, etc. • • •				
0.26±0.07	ABELE	01B	CBAR	0.0 $\overline{p}d \to 5\pi p$

$\Gamma(\rho\rho)/\Gamma(4\pi)$ Γ_8/Γ_4

VALUE	DOCUMENT ID	TECN	COMMENT
• • • We do not use the following data for averages, fits, limits, etc. • • •			
0.13±0.08	ABELE	01B CBAR	0.0 $\overline{p}d \to 5\pi p$

$\Gamma(\rho\rho)/\Gamma(2(\pi\pi)_{S\text{-wave}})$ Γ_8/Γ_7

VALUE	DOCUMENT ID	COMMENT
• • • We do not use the following data for averages, fits, limits, etc. • • •		
3.3±0.5	BARBERIS	00C 450 $pp \to p_f \pi^+\pi^- 2\pi^0 p_s$
2.6±0.4	BARBERIS	00C 450 $pp \to p_f 2(\pi^+\pi^-) p_s$

$\Gamma(\pi(1300)\pi)/\Gamma(4\pi)$ Γ_9/Γ_4

VALUE	DOCUMENT ID	TECN	COMMENT
• • • We do not use the following data for averages, fits, limits, etc. • • •			
0.50±0.25	ABELE	01B CBAR	0.0 $\overline{p}d \to 5\pi p$

$\Gamma(a_1(1260)\pi)/\Gamma(4\pi)$ Γ_{10}/Γ_4

VALUE	DOCUMENT ID	TECN	COMMENT
• • • We do not use the following data for averages, fits, limits, etc. • • •			
0.12±0.05	ABELE	01B CBAR	0.0 $\overline{p}d \to 5\pi p$

$\Gamma(\eta\eta)/\Gamma_{\text{total}}$ Γ_{11}/Γ

VALUE	DOCUMENT ID	TECN	COMMENT
• • • We do not use the following data for averages, fits, limits, etc. • • •			
large	ALDE	88 GAM4	300 $\pi^- N \to \eta\eta\pi^- N$
large	BINON	83 GAM2	38 $\pi^- p \to 2\eta n$

$\Gamma(\eta\eta)/\Gamma(\pi\pi)$ Γ_{11}/Γ_1

VALUE	DOCUMENT ID	TECN	COMMENT
0.145±0.027 OUR FIT Error includes scale factor of 1.5.			
0.14 ±0.04 OUR AVERAGE Error includes scale factor of 1.7. See the ideogram below.			
0.080±0.033	AMSLER	02 CBAR	0.9 $\overline{p}p \to \pi^0\eta\eta$, $\pi^0\pi^0\pi^0$
0.18 ±0.03	BARBERIS	00E	450 $pp \to p_f \eta\eta p_s$
0.230±0.097	[38] AMSLER	95C CBAR	0.0 $\overline{p}p \to \eta\eta\pi^0$
• • • We do not use the following data for averages, fits, limits, etc. • • •			
0.11 ±0.03	[36] ANISOVICH	02D SPEC	Combined fit
0.078±0.013	[39] ABELE	96C RVUE	Compilation
0.157±0.060	[40] AMSLER	95D CBAR	0.0 $\overline{p}p \to \pi^0\pi^0\pi^0$, $\pi^0\eta\eta$, $\pi^0\pi^0\eta$

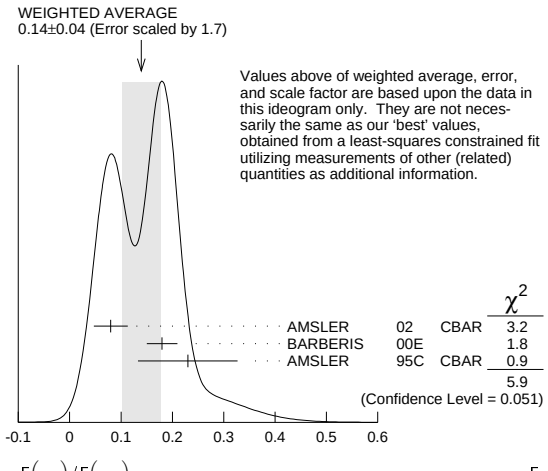

$\Gamma(4\pi^0)/\Gamma(\eta\eta)$ Γ_5/Γ_{11}

VALUE	DOCUMENT ID	TECN	COMMENT
• • • We do not use the following data for averages, fits, limits, etc. • • •			
0.8±0.3	ALDE	87 GAM4	100 $\pi^- p \to 4\pi^0 n$

$\Gamma(\eta\eta'(958))/\Gamma(\pi\pi)$ Γ_{12}/Γ_1

VALUE	DOCUMENT ID	TECN	COMMENT
0.055±0.024 OUR FIT Error includes scale factor of 1.8.			
0.095±0.026	BARBERIS	00A	450 $pp \to p_f \eta\eta p_s$
• • • We do not use the following data for averages, fits, limits, etc. • • •			
0.005±0.003	[36] ANISOVICH	02D SPEC	Combined fit

$\Gamma(\eta\eta'(958))/\Gamma(\eta\eta)$ Γ_{12}/Γ_{11}

VALUE	DOCUMENT ID	TECN	COMMENT
0.38±0.16 OUR FIT Error includes scale factor of 1.9.			
0.29±0.10	[41] AMSLER	95C CBAR	0.0 $\overline{p}p \to \eta\eta\pi^0$
• • • We do not use the following data for averages, fits, limits, etc. • • •			
0.05±0.03	[36] ANISOVICH	02D SPEC	Combined fit
0.84±0.23	ABELE	96C RVUE	Compilation
2.7 ±0.8	BINON	84C GAM2	38 $\pi^- p \to \eta\eta' n$

$\Gamma(K\overline{K})/\Gamma_{\text{total}}$ Γ_{13}/Γ

VALUE	DOCUMENT ID	TECN
• • • We do not use the following data for averages, fits, limits, etc. • • •		
0.044±0.021	BUGG 96	RVUE

$\Gamma(K\overline{K})/\Gamma(\pi\pi)$ Γ_{13}/Γ_1

VALUE	DOCUMENT ID	TECN	COMMENT
0.246±0.026 OUR FIT			
0.241±0.028 OUR AVERAGE			
0.25 ±0.03	[42] BARGIOTTI 03	OBLX	$\overline{p}p$
0.19 ±0.07	[43] ABELE 98	CBAR	0.0 $\overline{p}p \to K_L^0 K^\pm \pi^\mp$
• • • We do not use the following data for averages, fits, limits, etc. • • •			
0.16 ±0.05	[36] ANISOVICH 02D	SPEC	Combined fit
0.33 ±0.03 ±0.07	BARBERIS 99D	OMEG	450 $pp \to K^+K^-, \pi^+\pi^-$
0.20 ±0.08	[44] ABELE 96B	CBAR	0.0 $\overline{p}p \to \pi^0 K_L^0 K_L^0$

$\Gamma(K\overline{K})/\Gamma(\eta\eta)$ Γ_{13}/Γ_{11}

VALUE	CL%	DOCUMENT ID	TECN	COMMENT
1.69±0.33 OUR FIT Error includes scale factor of 1.4.				
1.85±0.41		BARBERIS 00E		450 $pp \to p_f \eta\eta p_s$
• • • We do not use the following data for averages, fits, limits, etc. • • •				
1.5 ±0.6		[36] ANISOVICH 02D	SPEC	Combined fit
<0.4	90	[45] PROKOSHKIN 91	GAM4	300 $\pi^- p \to \pi^- p\eta\eta$
<0.6		[46] BINON 83	GAM2	38 $\pi^- p \to 2\eta n$

[35] Excluding $\rho\rho$ contribution to 4π.
[36] From a combined K-matrix analysis of Crystal Barrel (0. $p\overline{p} \to \pi^0\pi^0\pi^0$, $\pi^0\eta\eta$, $\pi^0\pi^0\eta$), GAMS ($\pi p \to \pi^0\pi^0 n$, $\eta\eta n$, $\eta\eta' n$), and BNL ($\pi p \to K\overline{K}n$) data.
[37] From the combined data of ABELE 96 and ABELE 96C.
[38] Using AMSLER 95B ($3\pi^0$).
[39] 2π width determined to be 60 ± 12 MeV.
[40] Coupled-channel analysis of AMSLER 95B, AMSLER 95C, and AMSLER 94D.
[41] Using AMSLER 94E ($\eta\eta'\pi^0$).
[42] Coupled channel analysis of $\pi^+\pi^-\pi^0$, $K^+K^-\pi^0$, and $K^\pm K_S^0 \pi^\mp$.
[43] Using $\pi^0\pi^0$ from AMSLER 95B.
[44] Using AMSLER 95B ($3\pi^0$), AMSLER 94C ($2\pi^0\eta$) and SU(3).
[45] Combining results of GAM4 with those of WA76 on $K\overline{K}$ central production.
[46] Using ETKIN 82B and COHEN 80.

$f_0(1500)$ REFERENCES

ANISOVICH	09	IJMP A24 2481	V.V. Anisovich, A.V. Sarantsev	
KLEMPT	08	EPJ C55 39	E. Klempt, M. Matveev, A.V. Sarantsev	(BONN+)
UEHARA	08A	PR D78 052004	S. Uehara *et al.*	(BELLE Collab.)
ABLIKIM	06V	PL B642 441	M. Ablikim *et al.*	(BES Collab.)
AMSLER	06	PL B639 165	C. Amsler *et al.*	(CBAR Collab.)
AUBERT	06O	PR D74 032003	B. Aubert *et al.*	(BABAR Collab.)
PDG	06	JP G33 1	W.-M. Yao *et al.*	(PDG Collab.)
UMAN	06	PR D73 052009	I. Uman *et al.*	(FNAL E835)
VLADIMIRSK...	06	PAN 69 493	V.V. Vladimirsky *et al.*	(ITEP, Moscow)
		Translated from YAF 69 515.		
BINON	05	PAN 68 960	F. Binon *et al.*	
		Translated from YAF 68 998.		
GARMASH	05	PR D71 092003	A. Garmash *et al.*	(BELLE Collab.)
ANISOVICH	03	EPJ A16 229	V.V. Anisovich *et al.*	
BARGIOTTI	03	EPJ C26 371	M. Bargiotti *et al.*	(OBELIX Collab.)
AMSLER	02	EPJ C23 29	C. Amsler *et al.*	
ANISOVICH	02D	PAN 65 1545	V.V. Anisovich *et al.*	
		Translated from YAF 65 1583.		
ABELE	01	EPJ C19 667	A. Abele *et al.*	(Crystal Barrel Collab.)
ABELE	01B	EPJ C21 261	A. Abele *et al.*	(Crystal Barrel Collab.)
ACCIARRI	01H	PL B501 173	M. Acciarri *et al.*	(L3 Collab.)
AITALA	01A	PRL 86 765	E.M. Aitala *et al.*	(FNAL E791 Collab.)
BARATE	00E	PL B472 189	R. Barate *et al.*	(ALEPH Collab.)
BARBERIS	00A	PL B471 429	D. Barberis *et al.*	(WA 102 Collab.)
BARBERIS	00C	PL B471 440	D. Barberis *et al.*	(WA 102 Collab.)
BARBERIS	00D	PL B474 423	D. Barberis *et al.*	(WA 102 Collab.)
BARBERIS	00E	PL B479 59	D. Barberis *et al.*	(WA 102 Collab.)
BARBERIS	99	PL B453 305	D. Barberis *et al.*	(Omega Expt.)
BARBERIS	99B	PL B453 316	D. Barberis *et al.*	(Omega Expt.)
BARBERIS	99D	PL B462 462	D. Barberis *et al.*	(Omega Expt.)
BELLAZZINI	99	PL B467 296	R. Bellazzini *et al.*	
FRENCH	99	PL B460 213	B. French *et al.*	(WA76 Collab.)
KAMINSKI	99	EPJ C9 141	R. Kaminski, L. Lesniak, B. Loiseau	(CRAC, PARIN)
ABELE	98	PR D57 3860	A. Abele *et al.*	(Crystal Barrel Collab.)
ALDE	98	EPJ A3 361	D. Alde *et al.*	(GAM4 Collab.)
Also		PAN 62 405	D. Alde *et al.*	(GAMS Collab.)
		Translated from YAF 62 446.		
AMSLER	98	RMP 70 1293	C. Amsler	
ANISOVICH	98B	SPU 41 419	V.V. Anisovich *et al.*	
		Translated from UFN 168 481.		
BERTIN	98	PR D57 55	A. Bertin *et al.*	(OBELIX Collab.)
REYES	98	PRL 81 4079	M.A. Reyes *et al.*	
BARBERIS	97B	PL B413 217	D. Barberis *et al.*	(WA 102 Collab.)
BERTIN	97C	PL B408 476	A. Bertin *et al.*	(OBELIX Collab.)
FRABETTI	97D	PL B407 79	P.L. Frabetti *et al.*	(FNAL E687 Collab.)
ABELE	96	PL B380 453	A. Abele *et al.*	(Crystal Barrel Collab.)
ABELE	96B	PL B385 425	A. Abele *et al.*	(Crystal Barrel Collab.)
ABELE	96C	NP A609 562	A. Abele *et al.*	(Crystal Barrel Collab.)
AMELIN	96B	PAN 59 976	D.V. Amelin *et al.*	(SERP, TBIL)
		Translated from YAF 59 1021.		
BUGG	96	NP B471 59	D.V. Bugg, A.V. Sarantsev, B.S. Zou	(LOQM, PNPI)
AMSLER	95B	PL B342 433	C. Amsler *et al.*	(Crystal Barrel Collab.)
AMSLER	95C	PL B353 571	C. Amsler *et al.*	(Crystal Barrel Collab.)
AMSLER	95D	PL B355 425	C. Amsler *et al.*	(Crystal Barrel Collab.)
ANTINORI	95	PL B353 589	F. Antinori *et al.*	(ATHU, BARI, BIRM+)
BUGG	95	PL B353 378	D.V. Bugg *et al.*	(LOQM, PNPI, WASH)
ABATZIS	94	PL B324 509	S. Abatzis *et al.*	(ATHU, BARI, BIRM+)
AMSLER	94C	PL B327 425	C. Amsler *et al.*	(Crystal Barrel Collab.)
AMSLER	94D	PL B333 277	C. Amsler *et al.*	(Crystal Barrel Collab.)
AMSLER	94E	PL B340 259	C. Amsler *et al.*	(Crystal Barrel Collab.)
ANISOVICH	94	PL B323 233	V.V. Anisovich *et al.*	(Crystal Barrel Collab.)
BUGG	94	PR D50 4412	D.V. Bugg *et al.*	(LOQM)
AMSLER	92	PL B291 347	C. Amsler *et al.*	(Crystal Barrel Collab.)
BELADIDZE	92C	SJNP 55 1535	G.M. Beladidze, S.I. Bityukov, G.V. Borisov	(SERP+)
		Translated from YAF 55 2748.		

PROKOSHKIN	91	SPD 36 155 Translated from DANS 316 900.	Y.D. Prokoshkin	(GAM2, GAM4 Collab.)
ARMSTRONG	89E	PL B228 536	T.A. Armstrong, M. Benayoun	(ATHU, BARI, BIRM+)
ALDE	88	PL B201 160	D.M. Alde *et al.*	(SERP, BELG, LANL, LAPP+)
ASTON	88D	NP B301 525	D. Aston *et al.*	(SLAC, NAGO, CINC, INUS)
ALDE	87	PL B198 286	D.M. Alde *et al.*	(LANL, BRUX, SERP, LAPP)
ALDE	86D	NP B269 485	D.M. Alde *et al.*	(BELG, LAPP, SERP, CERN+)
BINON	84C	NC 80A 363	F.G. Binon *et al.*	(BELG, LAPP, SERP+)
BINON	83	NC 78A 313	F.G. Binon *et al.*	(BELG, LAPP, SERP+)
Also		SJNP 38 561 Translated from YAF 38 934.	F.G. Binon *et al.*	(BELG, LAPP, SERP+)
GRAY	83	PR D27 307	L. Gray *et al.*	(SYRA)
ETKIN	82B	PR D25 1786	A. Etkin *et al.*	(BNL, CUNY, TUFTS, VAND)
COHEN	80	PR D22 2595	D. Cohen *et al.*	(ANL)

$f_1(1510)$

$I^G(J^{PC}) = 0^+(1^{++})$

OMITTED FROM SUMMARY TABLE

See the minireview under $\eta(1405)$.

$f_1(1510)$ MASS

VALUE (MeV)	EVTS	DOCUMENT ID		TECN	COMMENT
1518± 5 OUR AVERAGE		Error includes scale factor of 1.7. See the ideogram below.			
1530±10		ASTON	88C	LASS	11 $K^- p \to K^0_S K^\pm \pi^\mp \Lambda$
1512± 4	600	[1] BIRMAN	88	MPS	8 $\pi^- p \to K^+ \overline{K}{}^0 \pi^- n$
1526± 6	271	GAVILLET	82	HBC	4.2 $K^- p \to \Lambda K K \pi$
• • • We do not use the following data for averages, fits, limits, etc. • • •					
~ 1525		[2] BAUER	93B		$\gamma\gamma^* \to \pi^+\pi^-\pi^0\pi^0$

[1] From partial wave analysis of $K^+ \overline{K}{}^0 \pi^-$ state.
[2] Not seen by AIHARA 88C in the $K^0_S K^\pm \pi^\mp$ final state.

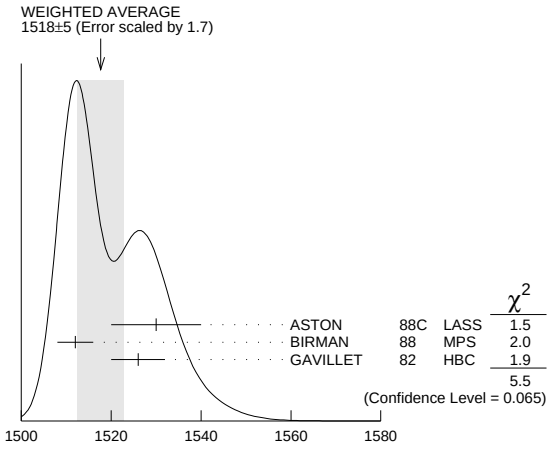

$f_1(1510)$ WIDTH

VALUE (MeV)	EVTS	DOCUMENT ID		TECN	COMMENT
73±25 OUR AVERAGE		Error includes scale factor of 2.5. See the ideogram below.			
100±40		ASTON	88C	LASS	11 $K^- p \to K^0_S K^\pm \pi^\mp \Lambda$
35±15	600	[3] BIRMAN	88	MPS	8 $\pi^- p \to K^+ \overline{K}{}^0 \pi^- n$
107±15	271	GAVILLET	82	HBC	4.2 $K^- p \to \Lambda K K \pi$

[3] From partial wave analysis of $K^+ \overline{K}{}^0 \pi^-$ state.

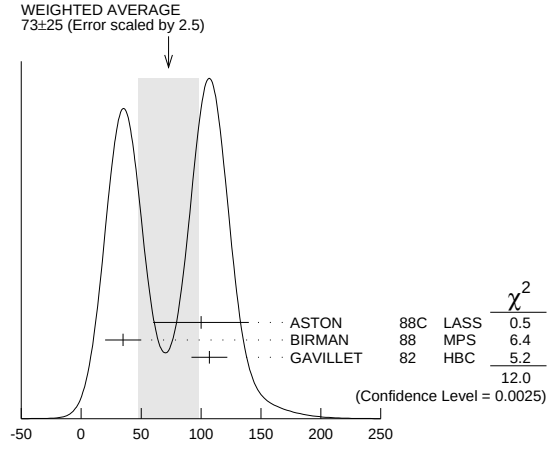

$f_1(1510)$ DECAY MODES

	Mode	Fraction (Γ_i/Γ)
Γ_1	$K\overline{K}^*(892)+$ c.c.	seen
Γ_2	$\pi^+\pi^-\eta'$	seen

$f_1(1510)$ BRANCHING RATIOS

$\Gamma(\pi^+\pi^-\eta')/\Gamma_{total}$ **Γ_2/Γ**

VALUE	EVTS	DOCUMENT ID		TECN	COMMENT
seen	230	ABLIKIM	11C	BES3	$J/\psi \to \gamma\pi^+\pi^-\eta'$

$f_1(1510)$ REFERENCES

ABLIKIM	11C	PRL 106 072002	M. Ablikim *et al.*	(BES III Collab.)
BAUER	93B	PR D48 3976	D.A. Bauer *et al.*	(SLAC)
AIHARA	88C	PR D38 1	H. Aihara *et al.*	(TPC-2γ Collab.)
ASTON	88C	PL B201 573	D. Aston *et al.*	(SLAC, NAGO, CINC, INUS) JP
BIRMAN	88	PRL 61 1557	A. Birman *et al.*	(BNL, FSU, IND, MASD) JP
GAVILLET	82	ZPHY C16 119	P. Gavillet *et al.*	(CERN, CDEF, PADO+)

$f_2'(1525)$

$I^G(J^{PC}) = 0^+(2^{++})$

$f_2'(1525)$ MASS

VALUE (MeV)	DOCUMENT ID
1525±5 OUR ESTIMATE This is only an educated guess; the error given is larger than the error on the average of the published values.	

PRODUCED BY PION BEAM

VALUE (MeV)	EVTS	DOCUMENT ID		TECN	COMMENT
• • • We do not use the following data for averages, fits, limits, etc. • • •					
1521±13		TIKHOMIROV	03	SPEC	40.0 π^- C → $K^0_S K^0_S K^0_L$ X
1547^{+10}_{-2}		[1] LONGACRE	86	MPS	22 $\pi^- p \to K^0_S K^0_S n$
1496^{+9}_{-8}		[2] CHABAUD	81	ASPK	6 $\pi^- p \to K^+ K^- n$
1497^{+8}_{-9}		CHABAUD	81	ASPK	18.4 $\pi^- p \to K^+ K^- n$
1492±29		GORLICH	80	ASPK	17 π^- p polarized → $K^+ K^- n$
1502±25		[3] CORDEN	79	OMEG	12–15 $\pi^- p \to \pi^+\pi^- n$
1480	14	CRENNELL	66	HBC	6.0 $\pi^- p \to K^0_S K^0_S n$

PRODUCED BY $K^\pm$ BEAM

VALUE (MeV)	EVTS	DOCUMENT ID		TECN	COMMENT
1523.6± 1.1 OUR AVERAGE Includes data from the datablock that follows this one. Error includes scale factor of 1.1.					
1526.8± 4.3		ASTON	88D	LASS	11 $K^- p \to K^0_S K^0_S \Lambda$
1504 ±12		BOLONKIN	86	SPEC	40 $K^- p \to K^0_S K^0_S Y$
1529 ± 3		ARMSTRONG	83B	OMEG	18.5 $K^- p \to K^- K^+ \Lambda$
1521 ± 6	650	AGUILAR-...	81B	HBC	4.2 $K^- p \to \Lambda K^+ K^-$
1521 ± 3	572	ALHARRAN	81	HBC	8.25 $K^- p \to \Lambda K \overline{K}$
1522 ± 6	123	BARREIRO	77	HBC	4.15 $K^- p \to \Lambda K^0_S K^0_S$
1528 ± 7	166	EVANGELIS...	77	OMEG	10 $K^- p \to K^+ K^- (\Lambda, \Sigma)$
1527 ± 3	120	BRANDENB...	76C	ASPK	13 $K^- p \to K^+ K^- (\Lambda, \Sigma)$
1519 ± 7	100	AGUILAR-...	72B	HBC	3.9,4.6 $K^- p \to K \overline{K} (\Lambda, \Sigma)$
• • • We do not use the following data for averages, fits, limits, etc. • • •					
1514 ± 8	61	BINON	07	GAMS	32.5 $K^- p \to \eta\eta(\Lambda/\Sigma^0)$
1513 ±10		[4] BARKOV	99	SPEC	40 $K^- p \to K^0_S K^0_S y$

PRODUCED IN e^+e^- ANNIHILATION AND PARTICLE DECAYS

VALUE (MeV)	EVTS	DOCUMENT ID		TECN	COMMENT
The data in this block is included in the average printed for a previous datablock.					
$1522.4^{+1.7}_{-1.4}$ OUR AVERAGE					
$1522.2 \pm 2.8^{+5.3}_{-2.0}$		AAIJ	13AN	LHCB	$\overline{B}{}^0_s \to J/\psi K^+ K^-$
$1525.3^{+1.2}_{-1.4} \pm 3.7 \pm 2.1$		UEHARA	13	BELL	$\gamma\gamma \to K^0_S K^0_S$
1521 ± 5		ABLIKIM	05	BES2	$J/\psi \to \phi K^+ K^-$
1518 ± 1 ± 3		ABE	04	BELL	10.6 $e^+e^- \to e^+e^- K^+ K^-$
1519 ± 2 $^{+15}_{-5}$		BAI	03G	BES	$J/\psi \to \gamma K \overline{K}$
1523 ± 6	331	[5] ACCIARRI	01H	L3	91, 183–209 $e^+e^- \to e^+e^- K^0_S K^0_S$
1535 ± 5 ± 4		ABREU	96C	DLPH	$Z^0 \to K^+ K^-$ + X
1516 ± 5 $^{+9}_{-15}$		BAI	96C	BES	$J/\psi \to \gamma K^+ K^-$
1531.6±10.0		AUGUSTIN	88	DM2	$J/\psi \to \gamma K^+ K^-$
1515 ± 5		[6] FALVARD	88	DM2	$J/\psi \to \phi K^+ K^-$
1525 ±10 ±10		BALTRUSAIT...	87	MRK3	$J/\psi \to \gamma K^+ K^-$
• • • We do not use the following data for averages, fits, limits, etc. • • •					
1523 ± 5	870	[7] SCHEGELSKY	06A	RVUE	$\gamma\gamma \to K^0_S K^0_S$
1496 ± 2		[8] FALVARD	88	DM2	$J/\psi \to \phi K^+ K^-$

PRODUCED IN $\overline{p}p$ ANNIHILATION

VALUE (MeV)		DOCUMENT ID		TECN	COMMENT
• • • We do not use the following data for averages, fits, limits, etc. • • •					
1530±12		[9] ANISOVICH	09	RVUE	0.0 $\overline{p}p$, πN
1513± 4		AMSLER	06	CBAR	0.9 $\overline{p}p \to K^+K^-\pi^0$
1508± 9		[10] AMSLER	02	CBAR	0.9 $\overline{p}p \to \pi^0\eta\eta$, $\pi^0\pi^0\pi^0$

CENTRAL PRODUCTION

VALUE (MeV)	DOCUMENT ID		TECN	COMMENT
1515±15	BARBERIS	99	OMEG	450 $pp \to p_s p_f K^+K^-$

PRODUCED IN ep COLLISIONS

VALUE (MeV)	EVTS	DOCUMENT ID		TECN	COMMENT
1512±3$^{+1.4}_{-0.5}$		[11] CHEKANOV	08	ZEUS	$ep \to K^0_S K^0_S X$
• • • We do not use the following data for averages, fits, limits, etc. • • •					
1537$^{+9}_{-8}$		84 [12] CHEKANOV	04	ZEUS	$ep \to K^0_S K^0_S X$

[1] From a partial-wave analysis of data using a K-matrix formalism with 5 poles.
[2] CHABAUD 81 is a reanalysis of PAWLICKI 77 data.
[3] From an amplitude analysis where the $f_2'(1525)$ width and elasticity are in complete disagreement with the values obtained from $K\overline{K}$ channel, making the solution dubious.
[4] Systematic errors not estimated.
[5] Supersedes ACCIARRI 95J.
[6] From an analysis ignoring interference with $f_0(1710)$.
[7] From analysis of L3 data at 91 and 183–209 GeV.
[8] From an analysis including interference with $f_0(1710)$.
[9] 4-poles, 5-channel K matrix fit.
[10] T-matrix pole.
[11] In the SU(3) based model with a specific interference pattern of the $f_2(1270)$, $a_2^0(1320)$, and $f_2'(1525)$ mesons incoherently added to the $f_0(1710)$ and non-resonant background.
[12] Systematic errors not estimated.

$f_2'(1525)$ WIDTH

VALUE (MeV)	DOCUMENT ID		COMMENT
73$^{+6}_{-5}$ OUR FIT			
76±10	PDG	90	For fitting

PRODUCED BY PION BEAM

VALUE (MeV)	DOCUMENT ID		TECN	COMMENT
• • • We do not use the following data for averages, fits, limits, etc. • • •				
102±42	TIKHOMIROV	03	SPEC	40.0 π^- C $\to K^0_S K^0_S K^0_L$ X
108$^{+5}_{-2}$	[13] LONGACRE	86	MPS	22 $\pi^- p \to K^0_S K^0_S n$
69$^{+22}_{-16}$	[14] CHABAUD	81	ASPK	6 $\pi^- p \to K^+K^- n$
137$^{+23}_{-21}$	CHABAUD	81	ASPK	18.4 $\pi^- p \to K^+K^- n$
150$^{+83}_{-50}$	GORLICH	80	ASPK	17 π^- ppolarized $\to K^+K^- n$
165±42	[15] CORDEN	79	OMEG	12–15 $\pi^- p \to \pi^+\pi^- n$
92$^{+39}_{-22}$	[16] POLYCHRO...	79	STRC	7 $\pi^- p \to n K^0_S K^0_S$

PRODUCED BY $K^\pm$ BEAM

VALUE (MeV)	EVTS	DOCUMENT ID		TECN	COMMENT
81.5$^{+2.2}_{-1.9}$ OUR AVERAGE Includes data from the datablock that follows this one.					
90 ±12		ASTON	88D	LASS	11 $K^- p \to K^0_S K^0_S \Lambda$
73 ±18		BOLONKIN	86	SPEC	40 $K^- p \to K^0_S K^0_S Y$
83 ±15		ARMSTRONG	83B	OMEG	18.5 $K^- p \to K^-K^+\Lambda$
85 ±16	650	AGUILAR-...	81B	HBC	4.2 $K^- p \to \Lambda K^+K^-$
80 $^{+14}_{-11}$	572	ALHARRAN	81	HBC	8.25 $K^- p \to \Lambda K\overline{K}$
72 ±25	166	EVANGELIS...	77	OMEG	10 $K^- p \to K^+K^-(\Lambda,\Sigma)$
69 ±22	100	AGUILAR-...	72B	HBC	3.9,4.6 $K^- p \to K\overline{K}(\Lambda,\Sigma)$
• • • We do not use the following data for averages, fits, limits, etc. • • •					
92 $^{+25}_{-16}$	61	BINON	07	GAMS	32.5 $K^- p \to \eta\eta(\Lambda/\Sigma^0)$
75 ±20		[17] BARKOV	99	SPEC	40 $K^- p \to K^0_S K^0_S y$
62 $^{+19}_{-14}$	123	BARREIRO	77	HBC	4.15 $K^- p \to \Lambda K^0_S K^0_S$
61 ± 8	120	BRANDENB...	76C	ASPK	13 $K^- p \to K^+K^-(\Lambda,\Sigma)$

PRODUCED IN e^+e^- ANNIHILATION AND PARTICLE DECAYS

VALUE (MeV)	EVTS	DOCUMENT ID		TECN	COMMENT
The data in this block is included in the average printed for a previous datablock.					
81.5$^{+2.4}_{-2.0}$ OUR AVERAGE					
84 ± 6 $^{+10}_{-5}$		AAIJ	13AN	LHCB	$\overline{B}^0_s \to J/\psi K^+K^-$
82.9$^{+2.1}_{-2.2}$ $^{+3.3}_{-2.0}$		UEHARA	13	BELL	$\gamma\gamma \to K^0_S K^0_S$
77 ±15		ABLIKIM	05	BES2	$J/\psi \to \phi K^+K^-$
82 ± 2 ± 3		ABE	04	BELL	10.6 $e^+e^- \to e^+e^-K^+K^-$
75 ± 4 $^{+15}_{-5}$		BAI	03G	BES	$J/\psi \to \gamma K\overline{K}$
100 ±15	331	[18] ACCIARRI	01H	L3	91, 183–209 $e^+e^- \to e^+e^-K^0_S K^0_S$
60 ±20 ±19		ABREU	96C	DLPH	$Z^0 \to K^+K^- + X$
60 ±23 $^{+13}_{-20}$		BAI	96C	BES	$J/\psi \to \gamma K^+K^-$
103 ±30		AUGUSTIN	88	DM2	$J/\psi \to \gamma K^+K^-$
62 ±10		[19] FALVARD	88	DM2	$J/\psi \to \phi K^+K^-$
85 ±35		BALTRUSAIT...87		MRK3	$J/\psi \to \gamma K^+K^-$
• • • We do not use the following data for averages, fits, limits, etc. • • •					
104 ±10	870	[20] SCHEGELSKY	06A	RVUE	$\gamma\gamma \to K^0_S K^0_S$
100 ± 3		[21] FALVARD	88	DM2	$J/\psi \to \phi K^+K^-$

PRODUCED IN $\overline{p}p$ ANNIHILATION

VALUE (MeV)	DOCUMENT ID		TECN	COMMENT
79± 8	[22] AMSLER	02	CBAR	0.9 $\overline{p}p \to \pi^0\eta\eta$, $\pi^0\pi^0\pi^0$
• • • We do not use the following data for averages, fits, limits, etc. • • •				
128±20	[23] ANISOVICH	09	RVUE	0.0 $\overline{p}p$, πN
76± 6	AMSLER	06	CBAR	0.9 $\overline{p}p \to K^+K^-\pi^0$

CENTRAL PRODUCTION

VALUE (MeV)	DOCUMENT ID		TECN	COMMENT
70±25	BARBERIS	99	OMEG	450 $pp \to p_s p_f K^+K^-$

PRODUCED IN ep COLLISIONS

VALUE (MeV)	EVTS	DOCUMENT ID		TECN	COMMENT
83± 9$^{+5}_{-4}$		[24] CHEKANOV	08	ZEUS	$ep \to K^0_S K^0_S X$
• • • We do not use the following data for averages, fits, limits, etc. • • •					
50$^{+34}_{-22}$	84	[25] CHEKANOV	04	ZEUS	$ep \to K^0_S K^0_S X$

[13] From a partial-wave analysis of data using a K-matrix formalism with 5 poles.
[14] CHABAUD 81 is a reanalysis of PAWLICKI 77 data.
[15] From an amplitude analysis where the $f_2'(1525)$ width and elasticity are in complete disagreement with the values obtained from $K\overline{K}$ channel, making the solution dubious.
[16] From a fit to the D with $f_2(1270)$-$f_2'(1525)$ interference. Mass fixed at 1516 MeV.
[17] Systematic errors not estimated.
[18] Supersedes ACCIARRI 95J.
[19] From an analysis ignoring interference with $f_0(1710)$.
[20] From analysis of L3 data at 91 and 183–209 GeV.
[21] From an analysis including interference with $f_0(1710)$.
[22] T-matrix pole.
[23] 4-poles, 5-channel K matrix fit.
[24] In the SU(3) based model with a specific interference pattern of the $f_2(1270)$, $a_2^0(1320)$, and $f_2'(1525)$ mesons incoherently added to the $f_0(1710)$ and non-resonant background.
[25] Systematic errors not estimated.

$f_2'(1525)$ DECAY MODES

	Mode	Fraction (Γ_i/Γ)
Γ_1	$K\overline{K}$	(88.7 ±2.2) %
Γ_2	$\eta\eta$	(10.4 ±2.2) %
Γ_3	$\pi\pi$	(8.2 ±1.5) $\times 10^{-3}$
Γ_4	$K\overline{K}^*(892)$ + c.c.	
Γ_5	$\pi K\overline{K}$	
Γ_6	$\pi\pi\eta$	
Γ_7	$\pi^+\pi^+\pi^-\pi^-$	
Γ_8	$\gamma\gamma$	(1.10±0.14) $\times 10^{-6}$

Meson Particle Listings

$f_2'(1525)$

CONSTRAINED FIT INFORMATION

An overall fit to the total width, 2 partial widths, a combination of partial widths obtained from integrated cross sections, and 3 branching ratios uses 17 measurements and one constraint to determine 5 parameters. The overall fit has a $\chi^2 = 14.3$ for 13 degrees of freedom.

The following *off-diagonal* array elements are the correlation coefficients $\langle \delta p_i \delta p_j \rangle / (\delta p_i \cdot \delta p_j)$, in percent, from the fit to parameters p_i, including the branching fractions, $x_i \equiv \Gamma_i/\Gamma_{\text{total}}$. The fit constrains the x_i whose labels appear in this array to sum to one.

x_2	−100			
x_3	−6	−1		
x_8	−6	6	1	
Γ	−23	23	−1	−56
	x_1	x_2	x_3	x_8

	Mode	Rate (MeV)
Γ_1	$K\overline{K}$	$65\ ^{+5}_{-4}$
Γ_2	$\eta\eta$	7.6 ± 1.8
Γ_3	$\pi\pi$	0.60 ± 0.12
Γ_8	$\gamma\gamma$	$(8.1 \pm 0.9) \times 10^{-5}$

$f_2'(1525)$ PARTIAL WIDTHS

$\Gamma(K\overline{K})$ Γ_1

VALUE (MeV)	DOCUMENT ID		TECN	COMMENT
$65\ ^{+5}_{-4}$ OUR FIT				
$63\ ^{+6}_{-5}$	[26] LONGACRE	86	MPS	22 $\pi^- p \rightarrow K^0_S K^0_S n$

$\Gamma(\eta\eta)$ Γ_2

VALUE (MeV)	EVTS	DOCUMENT ID		TECN	COMMENT
7.6 ± 1.8 OUR FIT					
• • • We do not use the following data for averages, fits, limits, etc. • • •					
5.0 ± 0.8	870	[27] SCHEGELSKY	06A	RVUE	$\gamma\gamma \rightarrow K^0_S K^0_S$
$24\ ^{+3}_{-1}$		[26] LONGACRE	86	MPS	22 $\pi^- p \rightarrow K^0_S K^0_S n$

$\Gamma(\pi\pi)$ Γ_3

VALUE (MeV)	EVTS	DOCUMENT ID		TECN	COMMENT
0.60 ± 0.12 OUR FIT					
$1.4\ ^{+1.0}_{-0.5}$		[26] LONGACRE	86	MPS	22 $\pi^- p \rightarrow K^0_S K^0_S n$
• • • We do not use the following data for averages, fits, limits, etc. • • •					
$0.2\ ^{+1.0}_{-0.2}$	870	[27] SCHEGELSKY	06A	RVUE	$\gamma\gamma \rightarrow K^0_S K^0_S$

$\Gamma(\gamma\gamma)$ Γ_8

VALUE (keV)	EVTS	DOCUMENT ID		TECN	COMMENT
0.081 ± 0.009 OUR FIT					
• • • We do not use the following data for averages, fits, limits, etc. • • •					
0.13 ± 0.03	870	[27] SCHEGELSKY	06A	RVUE	$\gamma\gamma \rightarrow K^0_S K^0_S$

[26] From a partial-wave analysis of data using a K-matrix formalism with 5 poles.
[27] From analysis of L3 data at 91 and 183–209 GeV, using $\Gamma(f_2'(1525) \rightarrow K\overline{K}) = 68$ MeV and SU(3) relations.

$f_2'(1525)$ Γ(i)$\Gamma(\gamma\gamma)/\Gamma$(total)

$\Gamma(K\overline{K}) \times \Gamma(\gamma\gamma)/\Gamma_{\text{total}}$ $\Gamma_1\Gamma_8/\Gamma$

VALUE (keV)	EVTS	DOCUMENT ID		TECN	COMMENT
0.072 ± 0.007 OUR FIT					
0.072 ± 0.007 OUR AVERAGE					
$0.048\ ^{+0.067}_{-0.008}\ ^{+0.108}_{-0.012}$		UEHARA	13	BELL	$\gamma\gamma \rightarrow K^0_S K^0_S$
$0.0564 \pm 0.0048 \pm 0.0116$		ABE	04	BELL	10.6 $e^+e^- \rightarrow e^+e^-K^+K^-$
$0.076 \pm 0.006 \pm 0.011$	331	[28] ACCIARRI	01H	L3	$e^+e^- \rightarrow e^+e^- K^0_S K^0_S$
$0.067 \pm 0.008 \pm 0.015$		[29] ALBRECHT	90G	ARG	$e^+e^- \rightarrow e^+e^- K^+K^-$
$0.11\ ^{+0.03}_{-0.02} \pm 0.02$		BEHREND	89C	CELL	$e^+e^- \rightarrow e^+e^- K^0_S K^0_S$
$0.10\ ^{+0.04}_{-0.03}\ ^{+0.03}_{-0.02}$		BERGER	88	PLUT	$e^+e^- \rightarrow e^+e^- K^0_S K^0_S$
$0.12 \pm 0.07 \pm 0.04$		[29] AIHARA	86B	TPC	$e^+e^- \rightarrow e^+e^- K^+K^-$
$0.11 \pm 0.02 \pm 0.04$		[29] ALTHOFF	83	TASS	$e^+e^- \rightarrow e^+e^- K\overline{K}$
• • • We do not use the following data for averages, fits, limits, etc. • • •					
$0.0314 \pm 0.0050 \pm 0.0077$		[30] ALBRECHT	90G	ARG	$e^+e^- \rightarrow e^+e^- K^+K^-$

[28] Supersedes ACCIARRI 95J. From analysis of L3 data at 91 and 183–209 GeV,
[29] Using an incoherent background.
[30] Using a coherent background.

$f_2'(1525)$ BRANCHING RATIOS

$\Gamma(\eta\eta)/\Gamma_{\text{total}}$ Γ_2/Γ

VALUE	DOCUMENT ID		TECN	COMMENT
• • • We do not use the following data for averages, fits, limits, etc. • • •				
seen	UEHARA	10A	BELL	10.6 $e^+e^- \rightarrow e^+e^-\eta\eta$
0.10 ± 0.03	[31] PROKOSHKIN	91	GAM4	300 $\pi^- p \rightarrow \pi^- p\eta\eta$

[31] Combining results of GAM4 with those of WA76 on $K\overline{K}$ central production and results of CBAL, MRK3 and DM2 on $J/\psi \rightarrow \gamma\eta\eta$.

$\Gamma(\eta\eta)/\Gamma(K\overline{K})$ Γ_2/Γ_1

VALUE	CL%	EVTS	DOCUMENT ID		TECN	COMMENT
0.118 ± 0.028 OUR FIT						
0.115 ± 0.028 OUR AVERAGE						
$0.119 \pm 0.015 \pm 0.036$	61		[32] BINON	07	GAMS	32.5 $K^- p \rightarrow \eta\eta(\Lambda/\Sigma^0)$
0.11 ± 0.04			[33] PROKOSHKIN	91	GAM4	300 $\pi^- p \rightarrow \pi^- p\eta\eta$
• • • We do not use the following data for averages, fits, limits, etc. • • •						
< 0.14	90		BARBERIS	00E		450 $pp \rightarrow p_f \eta\eta p_s$
< 0.50			BARNES	67	HBC	4.6,5.0 $K^- p$

[32] Using the compilation of the cross sections for $f_2'(1525)$ production in $K^- p$ collisions from ASTON 88D.
[33] Combining results of GAM4 with those of WA76 on $K\overline{K}$ central production and results of CBAL, MRK3 and DM2 on $J/\psi \rightarrow \gamma\eta\eta$.

$\Gamma(\pi\pi)/\Gamma_{\text{total}}$ Γ_3/Γ

VALUE	CL%	DOCUMENT ID		TECN	COMMENT
0.0082 ± 0.0016 OUR FIT					
0.0075 ± 0.0016 OUR AVERAGE					
0.007 ± 0.002		COSTA...	80	OMEG	10 $\pi^- p \rightarrow K^+K^- n$
$0.027\ ^{+0.071}_{-0.013}$		[34] GORLICH	80	ASPK	17,18 $\pi^- p$
0.0075 ± 0.0025		[34,35] MARTIN	79	RVUE	
• • • We do not use the following data for averages, fits, limits, etc. • • •					
<0.06	95	AGUILAR-...	81B	HBC	4.2 $K^- p \rightarrow \Lambda K^+ K^-$
0.19 ± 0.03		CORDEN	79	OMEG	12–15 $\pi^- p \rightarrow \pi^+\pi^- n$
<0.045	95	BARREIRO	77	HBC	4.15 $K^- p \rightarrow \Lambda K^0_S K^0_S$
0.012 ± 0.004		[34] PAWLICKI	77	SPEC	6 $\pi N \rightarrow K^+K^- N$
<0.063	90	BRANDENB...	76C	ASPK	13 $K^- p \rightarrow K^+K^-(\Lambda,\Sigma)$
<0.0086		[34] BEUSCH	75B	OSPK	8.9 $\pi^- p \rightarrow K^0\overline{K}^0 n$

[34] Assuming that the $f_2'(1525)$ is produced by an one-pion exchange production mechanism.
[35] MARTIN 79 uses the PAWLICKI 77 data with different input value of the $f_2'(1525) \rightarrow K\overline{K}$ branching ratio.

$\Gamma(\pi\pi)/\Gamma(K\overline{K})$ Γ_3/Γ_1

VALUE	DOCUMENT ID		TECN	COMMENT
0.0092 ± 0.0018 OUR FIT				
0.075 ± 0.035	AUGUSTIN	87	DM2	$J/\psi \rightarrow \gamma\pi^+\pi^-$

$[\Gamma(K\overline{K}^*(892) + \text{c.c.}) + \Gamma(\pi K\overline{K})]/\Gamma(K\overline{K})$ $(\Gamma_4+\Gamma_5)/\Gamma_1$

VALUE	CL%	DOCUMENT ID		TECN	COMMENT
• • • We do not use the following data for averages, fits, limits, etc. • • •					
<0.35	95	AGUILAR-...	72B	HBC	3.9,4.6 $K^- p$
<0.4	67	AMMAR	67	HBC	

$\Gamma(\pi\pi\eta)/\Gamma(K\overline{K})$ Γ_6/Γ_1

VALUE	CL%	DOCUMENT ID		TECN	COMMENT
• • • We do not use the following data for averages, fits, limits, etc. • • •					
<0.41	95	AGUILAR-...	72B	HBC	3.9,4.6 $K^- p$
<0.3	67	AMMAR	67	HBC	

$\Gamma(\pi^+\pi^+\pi^-\pi^-)/\Gamma(K\overline{K})$ Γ_7/Γ_1

VALUE	CL%	DOCUMENT ID		TECN	COMMENT
• • • We do not use the following data for averages, fits, limits, etc. • • •					
<0.32	95	AGUILAR-...	72B	HBC	3.9,4.6 $K^- p$

$f_2'(1525)$ REFERENCES

AAIJ	13AN	PR D87 072004	R. Aaij *et al.* (LHCb Collab.)
UEHARA	13	PTEP 2013 123C01	S. Uehara *et al.* (BELLE Collab.)
UEHARA	10A	PR D82 114031	S. Uehara *et al.* (BELLE Collab.)
ANISOVICH	09	IJMP A24 2481	V.V. Anisovich, A.V. Sarantsev
CHEKANOV	08	PRL 101 112003	S. Chekanov *et al.* (ZEUS Collab.)
BINON	07	PAN 70 1713	F. Binon *et al.* (GAMS Collab.)
		Translated from YAF 70 1758.	
AMSLER	06	PL B639 165	C. Amsler *et al.* (CBAR Collab.)
SCHEGELSKY	06A	EPJ A27 207	V.A. Schegelsky *et al.*
ABLIKIM	05	PL B607 243	M. Ablikim *et al.* (BES Collab.)
ABE	04	EPJ C32 323	K. Abe *et al.* (BELLE Collab.)
CHEKANOV	04	PL B578 33	S. Chekanov *et al.* (ZEUS Collab.)
BAI	03G	PR D68 052003	J.Z. Bai *et al.* (BES Collab.)
TIKHOMIROV	03	PAN 66 828	G.D. Tikhomirov *et al.*
		Translated from YAF 66 860.	
AMSLER	02	EPJ C23 29	C. Amsler *et al.*
ACCIARRI	01H	PL B501 173	M. Acciarri *et al.* (L3 Collab.)
BARBERIS	00E	PL B479 59	D. Barberis *et al.* (WA 102 Collab.)
BARBERIS	99	PL B453 305	D. Barberis *et al.* (Omega Expt.)
BARKOV	99	JETPL 70 248	B.P. Barkov *et al.*
		Translated from ZETFP 70 242.	

ABREU	96C	PL B379 309	P. Abreu *et al.*	(DELPHI Collab.)
BAI	96C	PRL 77 3959	J.Z. Bai *et al.*	(BES Collab.)
ACCIARRI	95J	PL B363 118	M. Acciarri *et al.*	(L3 Collab.)
PROKOSHKIN	91	SPD 36 155	Y.D. Prokoshkin	(GAM2, GAM4 Collab.)
		Translated from DANS 316 900.		
ALBRECHT	90G	ZPHY C48 183	H. Albrecht *et al.*	(ARGUS Collab.)
PDG	90	PL B239 1	J.J. Hernandez *et al.*	(IFIC, BOST, CIT+)
BEHREND	89C	ZPHY C43 91	H.J. Behrend *et al.*	(CELLO Collab.)
ASTON	88D	NP B301 525	D. Aston *et al.*	(SLAC, NAGO, CINC, INUS)
AUGUSTIN	88	PRL 60 2238	J.E. Augustin *et al.*	(DM2 Collab.)
BERGER	88	ZPHY C37 329	C. Berger *et al.*	(PLUTO Collab.)
FALVARD	88	PR D38 2706	A. Falvard *et al.*	(CLER, FRAS, LALO+)
AUGUSTIN	87	ZPHY C36 369	J.E. Augustin *et al.*	(LALO, CLER, FRAS+)
BALTRUSAIT...	87	PR D35 2077	R.M. Baltrusaitis *et al.*	(Mark III Collab.)
AIHARA	86B	PRL 57 404	H. Aihara *et al.*	(TPC-2γ Collab.)
BOLONKIN	86	SJNP 43 776	B.V. Bolonkin *et al.*	(ITEP) JP
		Translated from YAF 43 1211.		
LONGACRE	86	PL B177 223	R.S. Longacre *et al.*	(BNL, BRAN, CUNY+)
ALTHOFF	83	PL 121B 216	M. Althoff *et al.*	(TASSO Collab.)
ARMSTRONG	83B	NP B224 193	T.A. Armstrong *et al.*	(BARI, BIRM, CERN+)
AGUILAR-...	81B	ZPHY C8 313	M. Aguilar-Benitez *et al.*	(CERN, CDEF+)
ALHARRAN	81	NP B191 26	S. Al-Harran *et al.*	(BIRM, CERN, GLAS+)
CHABAUD	81	APP B12 575	V. Chabaud *et al.*	(CERN, CRAC, MPIM)
COSTA...	80	NP B175 402	G. Costa de Beauregard *et al.*	(BARI, BONN+)
GORLICH	80	NP B174 16	L. Gorlich *et al.*	(CRAC, MPIM, CERN+)
CORDEN	79	NP B157 250	M.J. Corden *et al.*	(BIRM, RHEL, TELA+) JP
MARTIN	79	NP B158 520	A.D. Martin, E.N. Ozmutlu	(DURH)
POLYCHRO...	79	PR D19 1317	V.A. Polychronakos *et al.*	(NDAM, ANL)
BARREIRO	77	NP B121 237	F. Barreiro *et al.*	(CERN, AMST, NIJM+)
EVANGELIS...	77	NP B127 384	C. Evangelista *et al.*	(BARI, BONN, CERN+)
PAWLICKI	77	PR D15 3196	A.J. Pawlicki *et al.*	(ANL) IJP
BRANDENB...	76C	NP B104 413	G.W. Brandenburg *et al.*	(SLAC)
BEUSCH	75B	PL 60B 101	W. Beusch *et al.*	(CERN, ETH)
AGUILAR-...	72B	PR D6 29	M. Aguilar-Benitez *et al.*	(BNL)
AMMAR	67	PRL 19 1071	R. Ammar *et al.*	(NWES, ANL) JP
BARNES	67	PRL 19 964	V.E. Barnes *et al.*	(BNL, SYRA) IJPC
CRENNELL	66	PRL 16 1025	D.J. Crennell *et al.*	(BNL) I

$f_2(1565)$

$I^G(J^{PC}) = 0^+(2^{++})$

OMITTED FROM SUMMARY TABLE

Seen mostly in antinucleon-nucleon annihilation. Needs confirmation in other channels.

$f_2(1565)$ MASS

VALUE (MeV)	DOCUMENT ID		TECN	COMMENT
1562±13 OUR AVERAGE	Error includes scale factor of 2.1. See the ideogram below.			
1590±10	[1] AMELIN	06	VES	36 $\pi^- p \to \omega\omega n$
1552±13	[2] AMSLER	02	CBAR	0.9 $\overline{p}p \to \pi^0\eta\eta, \pi^0\pi^0\pi^0$
1550±10±20	AMELIN	00	VES	37 $\pi^- p \to \eta\pi^+\pi^- n$
1575±18	BERTIN	98	OBLX	0.05–0.405 $\overline{n}p \to \pi^+\pi^+\pi^-$
1507±15	[2] BERTIN	97C	OBLX	0.0 $\overline{p}p \to \pi^+\pi^-\pi^0$
1565±20	MAY	90	ASTE	0.0 $\overline{p}p \to \pi^+\pi^-\pi^0$
• • • We do not use the following data for averages, fits, limits, etc. • • •				
1560±15	[3] ANISOVICH	09	RVUE	0.0 $\overline{p}p$, πN
1598±11± 9	BAKER	99B	SPEC	0 $\overline{p}p \to \omega\omega\pi^0$
1534±20	[4] ABELE	96C	RVUE	Compilation
~ 1552	[5] AMSLER	95D	CBAR	0.0 $\overline{p}p \to \pi^0\pi^0\pi^0, \pi^0\eta\eta, \pi^0\pi^0\eta$
1598±72	BALOSHIN	95	SPEC	40 π^- C $\to K^0_S K^0_S$ X
1566^{+80}_{-50}	[6] ANISOVICH	94	CBAR	0.0 $\overline{p}p \to 3\pi^0, \eta\eta\pi^0$
1502± 9	ADAMO	93	OBLX	$\overline{n}p \to \pi^+\pi^+\pi^-$
1488±10	[7] ARMSTRONG	93C	E760	$\overline{p}p \to \pi^0\eta\eta \to 6\gamma$
1508±10	[7] ARMSTRONG	93D	E760	$\overline{p}p \to 3\pi^0 \to 6\gamma$
1525±10	[7] ARMSTRONG	93D	E760	$\overline{p}p \to \eta\pi^0\pi^0 \to 6\gamma$
~ 1504	[8] WEIDENAUER	93	ASTE	0.0 $\overline{p}N \to 3\pi^-2\pi^+$
1540±15	[7] ADAMO	92	OBLX	$\overline{n}p \to \pi^+\pi^+\pi^-$
1515±10	[9] AKER	91	CBAR	0.0 $\overline{p}p \to 3\pi^0$
1477± 5	BRIDGES	86C	DBC	0.0 $\overline{p}N \to 3\pi^-2\pi^+$

[1] Supersedes the $\omega\omega$ state of BELADIDZE 92B earlier assigned to the $f_2(1640)$.
[2] T-matrix pole.
[3] On sheet II in a two-pole solution.
[4] T-matrix pole, large coupling to $\rho\rho$ and $\omega\omega$, could be $f_2(1640)$.
[5] Coupled-channel analysis of AMSLER 95B, AMSLER 95C, and AMSLER 94D.
[6] From a simultaneous analysis of the annihilations $\overline{p}p \to 3\pi^0, \pi^0\eta\eta$ including AKER 91 data.
[7] J^P not determined, could be partly $f_0(1500)$.
[8] J^P not determined.
[9] Superseded by AMSLER 95B.

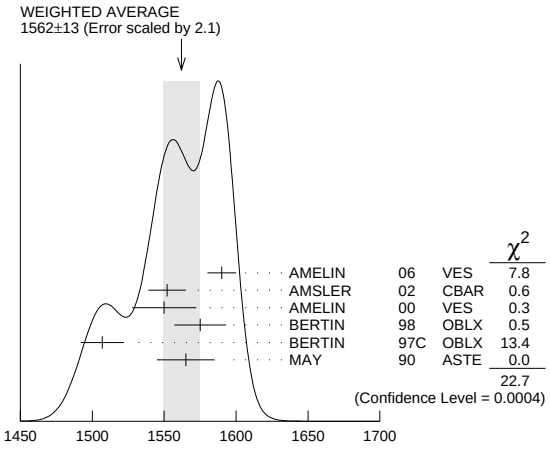

$f_2(1565)$ WIDTH

VALUE (MeV)	DOCUMENT ID		TECN	COMMENT
134± 8 OUR AVERAGE				
140± 11	[10] AMELIN	06	VES	36 $\pi^- p \to \omega\omega n$
113± 23	[11] AMSLER	02	CBAR	0.9 $\overline{p}p \to \pi^0\eta\eta, \pi^0\pi^0\pi^0$
130± 20±40	AMELIN	00	VES	37 $\pi^- p \to \eta\pi^+\pi^- n$
119± 24	BERTIN	98	OBLX	0.05–0.405 $\overline{n}p \to \pi^+\pi^+\pi^-$
130± 20	[11] BERTIN	97C	OBLX	0.0 $\overline{p}p \to \pi^+\pi^-\pi^0$
170± 40	MAY	90	ASTE	0.0 $\overline{p}p \to \pi^+\pi^-\pi^0$
• • • We do not use the following data for averages, fits, limits, etc. • • •				
280± 40	[12] ANISOVICH	09	RVUE	0.0 $\overline{p}p$, πN
180± 60	[13] ABELE	96C	RVUE	Compilation
~ 142	[14] AMSLER	95D	CBAR	0.0 $\overline{p}p \to \pi^0\pi^0\pi^0, \pi^0\eta\eta, \pi^0\pi^0\eta$
263±101	BALOSHIN	95	SPEC	40 π^- C $\to K^0_S K^0_S$ X
166^{+80}_{-20}	[15] ANISOVICH	94	CBAR	0.0 $\overline{p}p \to 3\pi^0, \eta\eta\pi^0$
130± 10	[16] ADAMO	93	OBLX	$\overline{n}p \to \pi^+\pi^+\pi^-$
148± 27	[17] ARMSTRONG	93C	E760	$\overline{p}p \to \pi^0\eta\eta \to 6\gamma$
103± 15	[17] ARMSTRONG	93D	E760	$\overline{p}p \to 3\pi^0 \to 6\gamma$
111± 10	[17] ARMSTRONG	93D	E760	$\overline{p}p \to \eta\pi^0\pi^0 \to 6\gamma$
~ 206	[18] WEIDENAUER	93	ASTE	0.0 $\overline{p}N \to 3\pi^-2\pi^+$
132± 37	[17] ADAMO	92	OBLX	$\overline{n}p \to \pi^+\pi^+\pi^-$
120± 10	[19] AKER	91	CBAR	0.0 $\overline{p}p \to 3\pi^0$
116± 9	BRIDGES	86C	DBC	0.0 $\overline{p}N \to 3\pi^-2\pi^+$

[10] Supersedes the $\omega\omega$ state of BELADIDZE 92B earlier assigned to the $f_2(1640)$.
[11] T-matrix pole.
[12] On sheet II in a two-pole solution.
[13] T-matrix pole, large coupling to $\rho\rho$ and $\omega\omega$, could be $f_2(1640)$.
[14] Coupled-channel analysis of AMSLER 95B, AMSLER 95C, and AMSLER 94D.
[15] From a simultaneous analysis of the annihilations $\overline{p}p \to 3\pi^0, \pi^0\eta\eta$ including AKER 91 data.
[16] Supersedes ADAMO 92.
[17] J^P not determined, could be partly $f_0(1500)$.
[18] J^P not determined.
[19] Superseded by AMSLER 95B.

$f_2(1565)$ DECAY MODES

	Mode	Fraction (Γ_i/Γ)
Γ_1	$\pi\pi$	seen
Γ_2	$\pi^+\pi^-$	seen
Γ_3	$\pi^0\pi^0$	seen
Γ_4	$\rho^0\rho^0$	seen
Γ_5	$2\pi^+2\pi^-$	seen
Γ_6	$\eta\eta$	seen
Γ_7	$a_2(1320)\pi$	
Γ_8	$\omega\omega$	seen
Γ_9	$K\overline{K}$	
Γ_{10}	$\gamma\gamma$	

$f_2(1565)$ PARTIAL WIDTHS

$\Gamma(\eta\eta)$ Γ_6

VALUE (MeV)	EVTS	DOCUMENT ID		TECN	COMMENT
• • • We do not use the following data for averages, fits, limits, etc. • • •					
1.2±0.3	870	[20] SCHEGELSKY	06A	RVUE	$\gamma\gamma \to K^0_S K^0_S$

Meson Particle Listings

$f_2(1565)$, $\rho(1570)$

$\Gamma(K\overline{K})$ Γ_9

VALUE (MeV)	EVTS	DOCUMENT ID		TECN	COMMENT
• • • We do not use the following data for averages, fits, limits, etc. • • •					
2.0 ± 1.0	870	[20] SCHEGELSKY	06A	RVUE	$\gamma\gamma \to K^0_S K^0_S$

$\Gamma(\gamma\gamma)$ Γ_{10}

VALUE (keV)	EVTS	DOCUMENT ID		TECN	COMMENT
• • • We do not use the following data for averages, fits, limits, etc. • • •					
0.70 ± 0.14	870	[20] SCHEGELSKY	06A	RVUE	$\gamma\gamma \to K^0_S K^0_S$

[20] From analysis of L3 data at 91 and 183–209 GeV, using $f_2(1565)$ mass of 1570 MeV, width of 160 MeV, $\Gamma(\pi\pi) = 25$ MeV, and SU(3) relations.

$f_2(1565)$ BRANCHING RATIOS

$\Gamma(\pi\pi)/\Gamma_{total}$ Γ_1/Γ

VALUE	DOCUMENT ID		TECN	COMMENT
• • • We do not use the following data for averages, fits, limits, etc. • • •				
seen	BAKER	99B	SPEC	$0\,\overline{p}p \to \omega\omega\pi^0$

$\Gamma(\pi^+\pi^-)/\Gamma_{total}$ Γ_2/Γ

VALUE	DOCUMENT ID		TECN	COMMENT
• • • We do not use the following data for averages, fits, limits, etc. • • •				
seen	BERTIN	98	OBLX	0.05–$0.405\ \overline{n}p \to \pi^+\pi^+\pi^-$
not seen	[21] ANISOVICH	94B	RVUE	$\overline{p}p \to \pi^+\pi^-\pi^0$
seen	MAY	89	ASTE	$\overline{p}p \to \pi^+\pi^-\pi^0$

[21] ANISOVICH 94B is from a reanalysis of MAY 90.

$\Gamma(\pi^0\pi^0)/\Gamma_{total}$ Γ_3/Γ

VALUE	DOCUMENT ID		TECN	COMMENT
seen	AMSLER	95B	CBAR	$0.0\,\overline{p}p \to 3\pi^0$

$\Gamma(\pi^+\pi^-)/\Gamma(\rho^0\rho^0)$ Γ_2/Γ_4

VALUE	DOCUMENT ID		TECN	COMMENT
• • • We do not use the following data for averages, fits, limits, etc. • • •				
0.042 ± 0.013	BRIDGES	86B	DBC	$\overline{p}N \to 3\pi^- 2\pi^+$

$\Gamma(\eta\eta)/\Gamma(\pi^0\pi^0)$ Γ_6/Γ_3

VALUE	DOCUMENT ID		TECN	COMMENT
• • • We do not use the following data for averages, fits, limits, etc. • • •				
$0.024\pm0.005\pm0.012$	[22] ARMSTRONG	93C	E760	$\overline{p}p \to \pi^0\eta\eta \to 6\gamma$

[22] J^P not determined, could be partly $f_0(1500)$.

$\Gamma(\omega\omega)/\Gamma_{total}$ Γ_8/Γ

VALUE	DOCUMENT ID		TECN	COMMENT
• • • We do not use the following data for averages, fits, limits, etc. • • •				
seen	BAKER	99B	SPEC	$0\,\overline{p}p \to \omega\omega\pi^0$

$f_2(1565)$ REFERENCES

ANISOVICH	09	IJMP A24 2481	V.V. Anisovich, A.V. Sarantsev	
AMELIN	06	PAN 69 690	D.V. Amelin *et al.*	(VES Collab.)
		Translated from YAF 69 715.		
SCHEGELSKY	06A	EPJ A27 207	V.A. Schegelsky *et al.*	
AMSLER	02	EPJ C23 29	C. Amsler *et al.*	
AMELIN	00	NP A668 83	D. Amelin *et al.*	(VES Collab.)
BAKER	99B	PL B467 147	C.A. Baker *et al.*	
BERTIN	98	PR D57 55	A. Bertin *et al.*	(OBELIX Collab.)
BERTIN	97C	PL B408 476	A. Bertin *et al.*	(OBELIX Collab.)
ABELE	96C	NP A609 562	A. Abele *et al.*	(Crystal Barrel Collab.)
AMSLER	95B	PL B342 433	C. Amsler *et al.*	(Crystal Barrel Collab.)
AMSLER	95C	PL B353 571	C. Amsler *et al.*	(Crystal Barrel Collab.)
AMSLER	95D	PL B355 425	C. Amsler *et al.*	(Crystal Barrel Collab.)
BALOSHIN	95	PAN 58 46	O.N. Baloshin *et al.*	(ITEP)
		Translated from YAF 58 50.		
AMSLER	94D	PL B333 277	C. Amsler *et al.*	(Crystal Barrel Collab.)
ANISOVICH	94	PL B323 233	V.V. Anisovich *et al.*	(Crystal Barrel Collab.)
ANISOVICH	94B	PR D50 1972	V.V. Anisovich *et al.*	(LOQM)
ADAMO	93	NP A558 13C	A. Adamo *et al.*	(OBELIX Collab.)
ARMSTRONG	93C	PL B307 394	T.A. Armstrong *et al.*	(FNAL, FERR, GENO+)
ARMSTRONG	93D	PL B307 399	T.A. Armstrong *et al.*	(FNAL, FERR, GENO+)
WEIDENAUER	93	ZPHY C59 387	P. Weidenauer *et al.*	(ASTERIX Collab.)
ADAMO	92	PL B287 368	A. Adamo *et al.*	(OBELIX Collab.)
BELADIDZE	92B	ZPHY C54 367	G.M. Beladidze *et al.*	(VES Collab.)
AKER	91	PL B260 249	E. Aker *et al.*	(Crystal Barrel Collab.)
MAY	90	ZPHY C46 203	B. May *et al.*	(ASTERIX Collab.)
MAY	89	PL B225 450	B. May *et al.*	(ASTERIX Collab.) IJP
BRIDGES	86B	PRL 56 215	D.L. Bridges *et al.*	(SYRA, CASE)
BRIDGES	86C	PRL 57 1534	D.L. Bridges *et al.*	(SYRA)

$\rho(1570)$ $I^G(J^{PC}) = 1^+(1^{--})$

OMITTED FROM SUMMARY TABLE

May be an OZI-violating decay mode of $\rho(1700)$. See our mini-review under the $\rho(1700)$.

$\rho(1570)$ MASS

VALUE (MeV)	EVTS	DOCUMENT ID		TECN	COMMENT
$1570\pm36\pm62$	54	[1] AUBERT	08S	BABR	$10.6\ e^+e^- \to \phi\pi^0\gamma$
• • • We do not use the following data for averages, fits, limits, etc. • • •					
1480 ± 40		[2] BITYUKOV	87	SPEC	$32.5\ \pi^-p \to \phi\pi^0 n$

[1] From the fit with two resonances.
[2] Systematic errors not estimated.

$\rho(1570)$ WIDTH

VALUE (MeV)	EVTS	DOCUMENT ID		TECN	COMMENT
$144\pm75\pm43$	54	[3] AUBERT	08S	BABR	$10.6\ e^+e^- \to \phi\pi^0\gamma$
• • • We do not use the following data for averages, fits, limits, etc. • • •					
130 ± 60		[4] BITYUKOV	87	SPEC	$32.5\ \pi^-p \to \phi\pi^0 n$

[3] From the fit with two resonances.
[4] Systematic errors not estimated.

$\rho(1570)$ DECAY MODES

	Mode	Fraction (Γ_i/Γ)
Γ_1	e^+e^-	
Γ_2	$\phi\pi$	not seen
Γ_3	$\omega\pi$	

$\rho(1570)$ $\Gamma(i)\Gamma(e^+e^-)/\Gamma(total)$

$\Gamma(\phi\pi) \times \Gamma(e^+e^-)/\Gamma_{total}$ $\Gamma_2\Gamma_1/\Gamma$

VALUE (eV)	CL%	EVTS	DOCUMENT ID		TECN	COMMENT
$3.5\pm0.9\pm0.3$		54	[5] AUBERT	08S	BABR	$10.6\ e^+e^- \to \phi\pi^0\gamma$
• • • We do not use the following data for averages, fits, limits, etc. • • •						
<70	90		[6] AULCHENKO	87B	ND	$e^+e^- \to K^0_S K^0_L \pi^0$

[5] From the fit with two resonances.
[6] Using mass and width of BITYUKOV 87.

$\rho(1570)$ BRANCHING RATIOS

$\Gamma(\phi\pi)/\Gamma_{total}$ Γ_2/Γ

VALUE	DOCUMENT ID		TECN	COMMENT
not seen	ABELE	97H	CBAR	$\overline{p}p \to K^0_L K^0_S \pi^0\pi^0$
• • • We do not use the following data for averages, fits, limits, etc. • • •				
<0.01	[7] DONNACHIE	91	RVUE	

[7] Using data from BISELLO 91B, DOLINSKY 86, and ALBRECHT 87L.

$\Gamma(\phi\pi)/\Gamma(\omega\pi)$ Γ_2/Γ_3

VALUE	CL%	DOCUMENT ID		TECN	COMMENT
• • • We do not use the following data for averages, fits, limits, etc. • • •					
>0.5	95	BITYUKOV	87	SPEC	$32.5\ \pi^-p \to \phi\pi^0 n$

$\rho(1570)$ REFERENCES

AUBERT	08S	PR D77 092002	B. Aubert *et al.*	(BABAR Collab.)
ABELE	97H	PL B415 280	A. Abele *et al.*	(Crystal Barrel Collab.)
BISELLO	91B	NPBPS B21 111	D. Bisello	(DM2 Collab.)
DONNACHIE	91	ZPHY C51 689	A. Donnachie, A.B. Clegg	(MCHS, LANC)
ALBRECHT	87L	PL B185 223	H. Albrecht *et al.*	(ARGUS Collab.)
AULCHENKO	87B	JETPL 45 145	V.M. Aulchenko *et al.*	(NOVO)
		Translated from ZETFP 45 118.		
BITYUKOV	87	PL B188 383	S.I. Bityukov *et al.*	(SERP)
DOLINSKY	86	PL B174 453	S.I. Dolinsky *et al.*	(NOVO)

$h_1(1595)$

$I^G(J^{PC}) = 0^-(1^{+-})$

OMITTED FROM SUMMARY TABLE

Seen in a partial-wave analysis of the $\omega\eta$ system produced in the reaction $\pi^- p \to \omega\eta n$ at 18 GeV/c.

$h_1(1595)$ MASS

VALUE (MeV)	DOCUMENT ID		TECN	COMMENT
$1594 \pm 15^{+10}_{-60}$	EUGENIO	01	SPEC	18 $\pi^- p \to \omega\eta n$

$h_1(1595)$ WIDTH

VALUE (MeV)	DOCUMENT ID		TECN	COMMENT
$384 \pm 60^{+70}_{-100}$	EUGENIO	01	SPEC	18 $\pi^- p \to \omega\eta n$

$h_1(1595)$ DECAY MODES

	Mode	Fraction (Γ_i/Γ)
Γ_1	$\omega\eta$	seen

$h_1(1595)$ REFERENCES

EUGENIO 01 PL B497 190 P. Eugenio *et al.*

$\pi_1(1600)$

$I^G(J^{PC}) = 1^-(1^{-+})$

$\pi_1(1600)$ MASS

VALUE (MeV)	EVTS	DOCUMENT ID		TECN	COMMENT
1662^{+8}_{-9} OUR AVERAGE					
$1660 \pm 10^{+0}_{-64}$	420k	ALEKSEEV	10	COMP	190 $\pi^- Pb \to \pi^-\pi^-\pi^+ Pb'$
$1664 \pm 8 \pm 10$	145k	[1] LU	05	B852	18 $\pi^- p \to \omega\pi^-\pi^0 p$
$1709 \pm 24 \pm 41$	69k	[2] KUHN	04	B852	18 $\pi^- p \to \eta\pi^+\pi^-\pi^- p$
$1597 \pm 10^{+45}_{-10}$		[2] IVANOV	01	B852	18 $\pi^- p \to \eta'\pi^- p$
• • • We do not use the following data for averages, fits, limits, etc. • • •					
$1593 \pm 8^{+29}_{-47}$		[2,3] ADAMS	98B	B852	18.3 $\pi^- p \to \pi^+\pi^-\pi^- p$

[1] May be a different state: natural and unnatural parity exchanges.
[2] Natural parity exchange.
[3] Superseded by DZIERBA 06 excluding this state in a more refined PWA analysis, with 2.6 M events of $\pi^- p \to \pi^-\pi^-\pi^+ p$ and 3 M events of $\pi^- p \to \pi^-\pi^0\pi^0 p$ of E852 data.

$\pi_1(1600)$ WIDTH

VALUE (MeV)	EVTS	DOCUMENT ID		TECN	COMMENT
241 ± 40 OUR AVERAGE	Error includes scale factor of 1.4. See the ideogram below.				
$269 \pm 21^{+42}_{-64}$	420k	ALEKSEEV	10	COMP	190 $\pi^- Pb \to \pi^-\pi^-\pi^+ Pb'$
$185 \pm 25 \pm 28$	145k	[4] LU	05	B852	18 $\pi^- p \to \omega\pi^-\pi^0 p$
$403 \pm 80 \pm 115$	69k	[5] KUHN	04	B852	18 $\pi^- p \to \eta\pi^+\pi^-\pi^- p$
$340 \pm 40 \pm 50$		[5] IVANOV	01	B852	18 $\pi^- p \to \eta'\pi^- p$
• • • We do not use the following data for averages, fits, limits, etc. • • •					
$168 \pm 20^{+150}_{-12}$		[5,6] ADAMS	98B	B852	18.3 $\pi^- p \to \pi^+\pi^-\pi^- p$

[4] May be a different state: natural and unnatural parity exchanges.
[5] Natural parity exchange.
[6] Superseded by DZIERBA 06 excluding this state in a more refined PWA analysis, with 2.6 M events of $\pi^- p \to \pi^-\pi^-\pi^+ p$ and 3 M events of $\pi^- p \to \pi^-\pi^0\pi^0 p$ of E852 data.

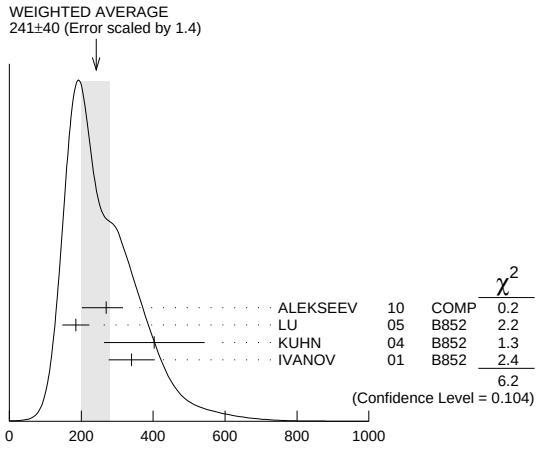

$\pi_1(1600)$ DECAY MODES

	Mode	Fraction (Γ_i/Γ)
Γ_1	$\pi\pi\pi$	not seen
Γ_2	$\rho^0\pi^-$	not seen
Γ_3	$f_2(1270)\pi^-$	not seen
Γ_4	$b_1(1235)\pi$	seen
Γ_5	$\eta'(958)\pi^-$	seen
Γ_6	$f_1(1285)\pi$	seen

$\pi_1(1600)$ BRANCHING RATIOS

$\Gamma(\rho^0\pi^-)/\Gamma_{total}$ Γ_2/Γ

VALUE	DOCUMENT ID		TECN	COMMENT
not seen	NOZAR	09	CLAS	$\gamma p \to 2\pi^+\pi^- n$
not seen	[7] DZIERBA	06	B852	18 $\pi^- p$

[7] From the PWA analysis of 2.6 M $\pi^- p \to \pi^-\pi^-\pi^+ p$ and 3 M events of $\pi^- p \to \pi^-\pi^0\pi^0 p$ of E852 data. Supersedes ADAMS 98B.

$\Gamma(f_2(1270)\pi^-)/\Gamma_{total}$ Γ_3/Γ

VALUE	DOCUMENT ID		TECN	COMMENT
not seen	[8] DZIERBA	06	B852	18 $\pi^- p$

[8] From the PWA analysis of 2.6 M $\pi^- p \to \pi^-\pi^-\pi^+ p$ and 3 M events of $\pi^- p \to \pi^-\pi^0\pi^0 p$ of E852 data. Supersedes CHUNG 02.

$\Gamma(b_1(1235)\pi)/\Gamma_{total}$ Γ_4/Γ

VALUE	EVTS	DOCUMENT ID		TECN	COMMENT
seen	35280	[9] BAKER	03	SPEC	$\bar{p}p \to \omega\pi^+\pi^-\pi^0$
• • • We do not use the following data for averages, fits, limits, etc. • • •					
seen	145k	LU	05	B852	18 $\pi^- p \to \omega\pi^-\pi^0 p$

[9] $B((b_1\pi)_{D-wave})/B((b_1\pi)_{S\text{-wave}})=0.3 \pm 0.1$.

$\Gamma(\eta'(958)\pi^-)/\Gamma_{total}$ Γ_5/Γ

VALUE	DOCUMENT ID		TECN	COMMENT
seen	IVANOV	01	B852	18 $\pi^- p \to \eta'\pi^- p$

$\Gamma(f_1(1285)\pi)/\Gamma(\eta'(958)\pi^-)$ Γ_6/Γ_5

VALUE	EVTS	DOCUMENT ID		TECN	COMMENT
3.80±0.78	69k	[10] KUHN	04	B852	18 $\pi^- p \to \eta\pi^+\pi^-\pi^- p$

[10] Using $\eta'(958)\pi$ data from IVANOV 01.

$\pi_1(1600)$ REFERENCES

ALEKSEEV	10	PRL 104 241803	M.G. Alekseev *et al.*	(COMPASS Collab.)
NOZAR	09	PRL 102 102002	M. Nozar *et al.*	(CLAS Collab.)
DZIERBA	06	PR D73 072001	A.R. Dzierba *et al.*	(BNL E852 Collab.)
LU	05	PRL 94 032002	M. Lu *et al.*	(BNL E852 Collab.)
KUHN	04	PL B595 109	J. Kuhn *et al.*	(BNL E852 Collab.)
BAKER	03	PL B563 140	C.A. Baker *et al.*	
CHUNG	02	PR D65 072001	S.U. Chung *et al.*	(BNL E852 Collab.)
IVANOV	01	PRL 86 3977	E.I. Ivanov *et al.*	(BNL E852 Collab.)
ADAMS	98B	PRL 81 5760	G.S. Adams *et al.*	(BNL E852 Collab.)

Meson Particle Listings

$a_1(1640)$, $f_2(1640)$

$a_1(1640)$

$I^G(J^{PC}) = 1^-(1^{++})$

OMITTED FROM SUMMARY TABLE

Seen in the amplitude analysis of the $3\pi^0$ system produced in $\overline{p}p \to 4\pi^0$. Possibly seen in the study of the hadronic structure in decay $\tau \to 3\pi\nu_\tau$ (ABREU 98G and ASNER 00). Needs confirmation.

$a_1(1640)$ MASS

VALUE (MeV)	EVTS	DOCUMENT ID		TECN	COMMENT
1647±22 OUR AVERAGE		Error includes scale factor of 1.4. See the ideogram below.			
1630±20	35280	[1] BAKER	03	SPEC	$\overline{p}p \to \omega\pi^+\pi^-\pi^0$
1714± 9±36		CHUNG	02	B852	18.3 $\pi^-p \to \pi^+\pi^-\pi^-p$
1640±12±30		BAKER	99	SPEC	1.94 $\overline{p}p \to 4\pi^0$
• • • We do not use the following data for averages, fits, limits, etc. • • •					
1670±90		BELLINI	85	SPEC	40 $\pi^-A \to \pi^-\pi^+\pi^-A$

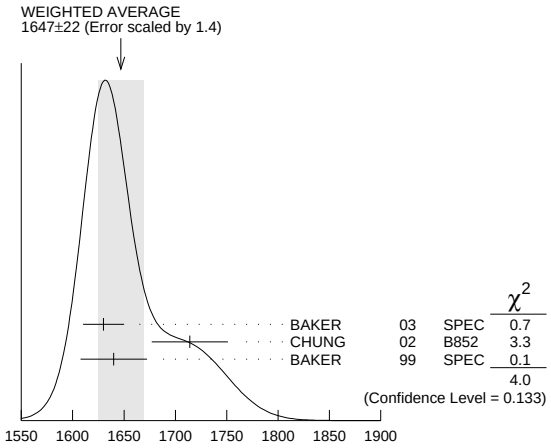

[1] Using the $a_1(1260)$ mass and width results of BOWLER 88.

$a_1(1640)$ WIDTH

VALUE (MeV)	EVTS	DOCUMENT ID		TECN	COMMENT
254± 27 OUR AVERAGE		Error includes scale factor of 1.1.			
225± 30	35280	[2] BAKER	03	SPEC	$\overline{p}p \to \omega\pi^+\pi^-\pi^0$
308± 37±62		CHUNG	02	B852	18.3 $\pi^-p \to \pi^+\pi^-\pi^-p$
300± 22±40		BAKER	99	SPEC	1.94 $\overline{p}p \to 4\pi^0$
• • • We do not use the following data for averages, fits, limits, etc. • • •					
300±100		BELLINI	85	SPEC	40 $\pi^-A \to \pi^-\pi^+\pi^-A$

[2] Using the $a_1(1260)$ mass and width results of BOWLER 88.

$a_1(1640)$ DECAY MODES

	Mode	Fraction (Γ_i/Γ)
Γ_1	$\pi\pi\pi$	seen
Γ_2	$f_2(1270)\pi$	seen
Γ_3	$\sigma\pi$	seen
Γ_4	$\rho\pi$ $S-wave$	seen
Γ_5	$\rho\pi$ $D-wave$	seen
Γ_6	$\omega\pi\pi$	seen
Γ_7	$f_1(1285)\pi$	seen
Γ_8	$a_1(1260)\eta$	not seen

$a_1(1640)$ BRANCHING RATIOS

$\Gamma(f_2(1270)\pi)/\Gamma(\sigma\pi)$ Γ_2/Γ_3

VALUE	DOCUMENT ID		TECN	COMMENT
• • • We do not use the following data for averages, fits, limits, etc. • • •				
0.24±0.07	BAKER	99	SPEC	1.94 $\overline{p}p \to 4\pi^0$

$\Gamma(\rho\pi_{D-wave})/\Gamma_{total}$ Γ_5/Γ

VALUE	DOCUMENT ID		TECN	COMMENT
• • • We do not use the following data for averages, fits, limits, etc. • • •				
seen	CHUNG	02	B852	18.3 $\pi^-p \to \pi^+\pi^-\pi^-p$
seen	AMELIN	95B	VES	36 $\pi^-A \to \pi^+\pi^-\pi^-A$

$\Gamma(\omega\pi\pi)/\Gamma_{total}$ Γ_6/Γ

VALUE	EVTS	DOCUMENT ID		TECN	COMMENT
• • • We do not use the following data for averages, fits, limits, etc. • • •					
seen	35280	[3] BAKER	03	SPEC	$\overline{p}p \to \omega\pi^+\pi^-\pi^0$

$\Gamma(f_1(1285)\pi)/\Gamma_{total}$ Γ_7/Γ

VALUE	DOCUMENT ID		TECN	COMMENT
• • • We do not use the following data for averages, fits, limits, etc. • • •				
not seen	KUHN	04	B852	18 $\pi^-p \to \eta\pi^+\pi^-\pi^-p$
seen	LEE	94	MPS2	18 $\pi^-p \to K^+\overline{K}{}^0\pi^-\pi^-p$

$\Gamma(a_1(1260)\eta)/\Gamma_{total}$ Γ_8/Γ

VALUE	DOCUMENT ID		TECN	COMMENT
not seen	KUHN	04	B852	18 $\pi^-p \to \eta\pi^+\pi^-\pi^-p$

[3] Assuming the $\omega\rho$ mechanism for the $\omega\pi\pi$ state.

$a_1(1640)$ REFERENCES

KUHN	04	PL B595 109	J. Kuhn *et al.*	(BNL E852 Collab.)
BAKER	03	PL B563 140	C.A. Baker *et al.*	
CHUNG	02	PR D65 072001	S.U. Chung *et al.*	(BNL E852 Collab.)
ASNER	00	PR D61 012002	D.M. Asner *et al.*	(CLEO Collab.)
BAKER	99	PL B449 114	C.A. Baker *et al.*	
ABREU	98G	PL B426 411	P. Abreu *et al.*	(DELPHI Collab.)
AMELIN	95B	PL B356 595	D.V. Amelin *et al.*	(SERP, TBIL)
LEE	94	PL B323 227	J.H. Lee *et al.*	(BNL, IND, KYUN, MASD+)
BOWLER	88	PL B209 99	M.G. Bowler	(OXF)
BELLINI	85	SJNP 41 781	D. Bellini *et al.*	
		Translated from YAF 41 1223.		

$f_2(1640)$

$I^G(J^{PC}) = 0^+(2^{++})$

OMITTED FROM SUMMARY TABLE

$f_2(1640)$ MASS

VALUE (MeV)	DOCUMENT ID		TECN	COMMENT
1639± 6 OUR AVERAGE	Error includes scale factor of 1.2.			
1620±16	BUGG	95	MRK3	$J/\psi \to \gamma\pi^+\pi^-\pi^+\pi^-$
1647± 7	ADAMO	92	OBLX	$\overline{n}p \to 3\pi^+2\pi^-$
1635± 7	ALDE	90	GAM2	38 $\pi^-p \to \omega\omega n$
• • • We do not use the following data for averages, fits, limits, etc. • • •				
1640± 5	AMSLER	06	CBAR	0.9 $\overline{p}p \to K^+K^-\pi^0$
1659± 6	VLADIMIRSK...	06	SPEC	40 $\pi^-p \to K^0_S K^0_S n$
1643± 7	[1] ALDE	89B	GAM2	38 $\pi^-p \to \omega\omega n$

[1] Superseded by ALDE 90.

$f_2(1640)$ WIDTH

VALUE (MeV)	CL%	DOCUMENT ID		TECN	COMMENT
$\mathbf{99^{+60}_{-40}}$ **OUR AVERAGE**		Error includes scale factor of 2.9.			
140^{+60}_{-20}		BUGG	95	MRK3	$J/\psi \to \gamma\pi^+\pi^-\pi^+\pi^-$
58±20		ADAMO	92	OBLX	$\overline{n}p \to 3\pi^+2\pi^-$
• • • We do not use the following data for averages, fits, limits, etc. • • •					
44± 9		AMSLER	06	CBAR	0.9 $\overline{p}p \to K^+K^-\pi^0$
152±18		VLADIMIRSK...	06	SPEC	40 $\pi^-p \to K^0_S K^0_S n$
< 70	90	ALDE	90	GAM2	38 $\pi^-p \to \omega\omega n$

$f_2(1640)$ DECAY MODES

	Mode	Fraction (Γ_i/Γ)
Γ_1	$\omega\omega$	seen
Γ_2	4π	seen
Γ_3	$K\overline{K}$	seen

$f_2(1640)$ BRANCHING RATIOS

$\Gamma(K\overline{K})/\Gamma_{total}$ Γ_3/Γ

VALUE	DOCUMENT ID		TECN	COMMENT
seen	AMSLER	06	CBAR	0.9 $\overline{p}p \to K^+K^-\pi^0$

$f_2(1640)$ REFERENCES

AMSLER	06	PL B639 165	C. Amsler *et al.*	(CBAR Collab.)
VLADIMIRSK...	06	PAN 69 493	V.V. Vladimirsky *et al.*	(ITEP, Moscow)
		Translated from YAF 69 515.		
BUGG	95	PL B353 378	D.V. Bugg *et al.*	(LOQM, PNPI, WASH) JP
ADAMO	92	PL B287 368	A. Adamo *et al.*	(OBELIX Collab.)
ALDE	90	PL B241 600	D.M. Alde *et al.*	(SERP, BELG, LANL, LAPP+)
ALDE	89B	PL B216 451	D.M. Alde *et al.*	(SERP, BELG, LANL, LAPP+) IGJPC

$\eta_2(1645)$

$I^G(J^{PC}) = 0^+(2^{-+})$

$\eta_2(1645)$ MASS

VALUE (MeV)	DOCUMENT ID		TECN	CHG	COMMENT
1617± 5 OUR AVERAGE					
1613± 8	BARBERIS	00B			450 $pp \to p_f \eta\pi^+\pi^- p_s$
1617± 8	BARBERIS	00C			450 $pp \to p_f 4\pi p_s$
1620±20	BARBERIS	97B	OMEG		450 $pp \to pp2(\pi^+\pi^-)$
1645±14±15	ADOMEIT	96	CBAR	0	1.94 $\overline{p}p \to \eta 3\pi^0$
• • • We do not use the following data for averages, fits, limits, etc. • • •					
1645± 6±20	ANISOVICH	00E	SPEC		0.9–1.94 $\overline{p}p \to \eta 3\pi^0$

$\eta_2(1645)$ WIDTH

VALUE (MeV)	DOCUMENT ID		TECN	CHG	COMMENT
181±11 OUR AVERAGE					
185±17	BARBERIS	00B			450 $pp \to p_f \eta\pi^+\pi^- p_s$
177±18	BARBERIS	00C			450 $pp \to p_f 4\pi p_s$
180±25	BARBERIS	97B	OMEG		450 $pp \to pp2(\pi^+\pi^-)$
180^{+40}_{-21}±25	ADOMEIT	96	CBAR	0	1.94 $\overline{p}p \to \eta 3\pi^0$
• • • We do not use the following data for averages, fits, limits, etc. • • •					
200±25	ANISOVICH	00E	SPEC		0.9–1.94 $\overline{p}p \to \eta 3\pi^0$

$\eta_2(1645)$ DECAY MODES

	Mode	Fraction (Γ_i/Γ)
Γ_1	$a_2(1320)\pi$	seen
Γ_2	$K\overline{K}\pi$	seen
Γ_3	$K^*\overline{K}$	seen
Γ_4	$\eta\pi^+\pi^-$	seen
Γ_5	$a_0(980)\pi$	seen
Γ_6	$f_2(1270)\eta$	not seen

$\eta_2(1645)$ BRANCHING RATIOS

$\Gamma(K\overline{K}\pi)/\Gamma(a_2(1320)\pi)$ Γ_2/Γ_1

VALUE	DOCUMENT ID		TECN	COMMENT
0.07±0.03	[1] BARBERIS	97C	OMEG	450 $pp \to pp K\overline{K}\pi$

[1] Using $2(\pi^+\pi^-)$ data from BARBERIS 97B.

$\Gamma(a_2(1320)\pi)/\Gamma(a_0(980)\pi)$ Γ_1/Γ_5

VALUE	DOCUMENT ID		TECN	COMMENT
13.1±2.3 OUR AVERAGE				
13.5±4.6	[2] ANISOVICH	11	SPEC	0.9–1.94 $p\overline{p}$
13.0±2.7	BARBERIS	00B		450 $pp \to p_f \eta\pi^+\pi^- p_s$

[2] Reanalysis of ADOMEIT 96 and ANISOVICH 00E.

$\Gamma(f_2(1270)\eta)/\Gamma_{total}$ Γ_6/Γ

VALUE	DOCUMENT ID		COMMENT
• • • We do not use the following data for averages, fits, limits, etc. • • •			
not seen	BARBERIS	00B	450 $pp \to p_f \eta\pi^+\pi^- p_s$

$\eta_2(1645)$ REFERENCES

ANISOVICH	11	EPJ C71 1511	A.V. Anisovich *et al.*	(LOQM, RAL, PNPI)
ANISOVICH	00E	PL B477 19	A.V. Anisovich *et al.*	
BARBERIS	00B	PL B471 435	D. Barberis *et al.*	(WA 102 Collab.)
BARBERIS	00C	PL B471 440	D. Barberis *et al.*	(WA 102 Collab.)
BARBERIS	97B	PL B413 217	D. Barberis *et al.*	(WA 102 Collab.)
BARBERIS	97C	PL B413 225	D. Barberis *et al.*	(WA 102 Collab.)
ADOMEIT	96	ZPHY C71 227	J. Adomeit *et al.*	(Crystal Barrel Collab.)

$\omega(1650)$

$I^G(J^{PC}) = 0^-(1^{--})$

$\omega(1650)$ MASS

VALUE (MeV)	EVTS	DOCUMENT ID		TECN	COMMENT
1670± 30 OUR ESTIMATE					
• • • We do not use the following data for averages, fits, limits, etc. • • •					
1667± 13± 6		AUBERT	07AU	BABR	10.6 $e^+e^- \to \omega\pi^+\pi^-\gamma$
1645± 8	13	AUBERT	06D	BABR	10.6 $e^+e^- \to \omega\eta\gamma$
1660± 10± 2		AUBERT,B	04N	BABR	10.6 $e^+e^- \to \pi^+\pi^-\pi^0\gamma$
1770± 50±60	1.2M	[1] ACHASOV	03D	RVUE	0.44–2.00 $e^+e^- \to \pi^+\pi^-\pi^0$
1619± 5		[2] HENNER	02	RVUE	1.2–2.0 $e^+e^- \to \rho\pi, \omega\pi\pi$
1700± 20		EUGENIO	01	SPEC	18 $\pi^- p \to \omega\eta n$
1705± 26	612	[3] AKHMETSHIN	00D	CMD2	$e^+e^- \to \omega\pi^+\pi^-$
1820^{+190}_{-150}		[4] ACHASOV	98H	RVUE	$e^+e^- \to \pi^+\pi^-\pi^0$
1840^{+100}_{-70}		[5] ACHASOV	98H	RVUE	$e^+e^- \to \omega\pi^+\pi^-$
1780^{+170}_{-300}		[6] ACHASOV	98H	RVUE	$e^+e^- \to K^+K^-$
~ 2100		[7] ACHASOV	98H	RVUE	$e^+e^- \to K^0_S K^\pm\pi^\mp$
1606± 9		[8] CLEGG	94	RVUE	
1662± 13	750	[9] ANTONELLI	92	DM2	1.34–2.4 $e^+e^- \to \rho\pi, \omega\pi\pi$
1670± 20		ATKINSON	83B	OMEG	20–70 $\gamma p \to 3\pi X$
1657± 13		CORDIER	81	DM1	$e^+e^- \to \omega 2\pi$
1679± 34	21	ESPOSITO	80	FRAM	$e^+e^- \to 3\pi$
1652± 17		COSME	79	OSPK	$e^+e^- \to 3\pi$

[1] From the combined fit of ANTONELLI 92, ACHASOV 01E, ACHASOV 02E, and ACHASOV 03D data on the $\pi^+\pi^-\pi^0$ and ANTONELLI 92 on the $\omega\pi^+\pi^-$ final states. Supersedes ACHASOV 99E and ACHASOV 02E.
[2] Using results of CORDIER 81 and preliminary data of DOLINSKY 91 and ANTONELLI 92.
[3] Using the data of AKHMETSHIN 00D and ANTONELLI 92. The $\rho\pi$ dominance for the energy dependence of the $\omega(1420)$ and $\omega(1650)$ width assumed.
[4] Using data from BARKOV 87, DOLINSKY 91, and ANTONELLI 92.
[5] Using the data from ANTONELLI 92.
[6] Using the data from IVANOV 81 and BISELLO 88B.
[7] Using the data from BISELLO 91C.
[8] From a fit to two Breit-Wigner functions and using the data of DOLINSKY 91 and ANTONELLI 92.
[9] From the combined fit of the $\rho\pi$ and $\omega\pi\pi$ final states.

$\omega(1650)$ WIDTH

VALUE (MeV)	EVTS	DOCUMENT ID		TECN	COMMENT
315± 35 OUR ESTIMATE					
• • • We do not use the following data for averages, fits, limits, etc. • • •					
222± 25± 20		AUBERT	07AU	BABR	10.6 $e^+e^- \to \omega\pi^+\pi^-\gamma$
114± 14	13	AUBERT	06D	BABR	10.6 $e^+e^- \to \omega\eta\gamma$
230± 30± 20		AUBERT,B	04N	BABR	10.6 $e^+e^- \to \pi^+\pi^-\pi^0\gamma$
490^{+200}_{-150}±130	1.2M	[10] ACHASOV	03D	RVUE	0.44–2.00 $e^+e^- \to \pi^+\pi^-\pi^0$
250± 14		[11] HENNER	02	RVUE	1.2–2.0 $e^+e^- \to \rho\pi, \omega\pi\pi$
250± 50		EUGENIO	01	SPEC	18 $\pi^- p \to \omega\eta n$
370± 25	612	[12] AKHMETSHIN	00D	CMD2	$e^+e^- \to \omega\pi^+\pi^-$
113± 20		[13] CLEGG	94	RVUE	
280± 24	750	[14] ANTONELLI	92	DM2	1.34–2.4 $e^+e^- \to \rho\pi, \omega\pi\pi$
160± 20		ATKINSON	83B	OMEG	20–70 $\gamma p \to 3\pi X$
136± 46		CORDIER	81	DM1	$e^+e^- \to \omega 2\pi$
99± 49	21	ESPOSITO	80	FRAM	$e^+e^- \to 3\pi$
42± 17		COSME	79	OSPK	$e^+e^- \to 3\pi$

[10] From the combined fit of ANTONELLI 92, ACHASOV 01E, ACHASOV 02E, and ACHASOV 03D data on the $\pi^+\pi^-\pi^0$ and ANTONELLI 92 on the $\omega\pi^+\pi^-$ final states. Supersedes ACHASOV 99E and ACHASOV 02E.
[11] Using results of CORDIER 81 and preliminary data of DOLINSKY 91 and ANTONELLI 92.
[12] Using the data of AKHMETSHIN 00D and ANTONELLI 92. The $\rho\pi$ dominance for the energy dependence of the $\omega(1420)$ and $\omega(1650)$ width assumed.
[13] From a fit to two Breit-Wigner functions and using the data of DOLINSKY 91 and ANTONELLI 92.
[14] From the combined fit of the $\rho\pi$ and $\omega\pi\pi$ final states.

$\omega(1650)$ DECAY MODES

	Mode	Fraction (Γ_i/Γ)
Γ_1	$\rho\pi$	seen
Γ_2	$\omega\pi\pi$	seen
Γ_3	$\omega\eta$	seen
Γ_4	e^+e^-	seen

Meson Particle Listings

$\omega(1650), \omega_3(1670)$

$\omega(1650)$ $\Gamma(i)\Gamma(e^+e^-)/\Gamma^2(\text{total})$

$\Gamma(\rho\pi)/\Gamma_{\text{total}} \times \Gamma(e^+e^-)/\Gamma_{\text{total}}$ $\quad \Gamma_1/\Gamma \times \Gamma_4/\Gamma$

VALUE (units 10^{-6})	EVTS	DOCUMENT ID		TECN	COMMENT
• • • We do not use the following data for averages, fits, limits, etc. • • •					
$1.3 \pm 0.1 \pm 0.1$		AUBERT,B	04N	BABR	$10.6\ e^+e^- \to \pi^+\pi^-\pi^0\gamma$
$1.2\ ^{+0.4}_{-0.1} \pm 0.8$	1.2M	[15,16] ACHASOV	03D	RVUE	0.44–$2.00\ e^+e^- \to \pi^+\pi^-\pi^0$
0.921 ± 0.230		[17,18] CLEGG	94	RVUE	
0.479 ± 0.050	750	[19,20] ANTONELLI	92	DM2	1.34–$2.4 e^+e^- \to \rho\pi, \omega\pi\pi$

$\Gamma(\omega\pi\pi)/\Gamma_{\text{total}} \times \Gamma(e^+e^-)/\Gamma_{\text{total}}$ $\quad \Gamma_2/\Gamma \times \Gamma_4/\Gamma$

VALUE (units 10^{-7})	EVTS	DOCUMENT ID		TECN	COMMENT
• • • We do not use the following data for averages, fits, limits, etc. • • •					
7.0 ± 0.5		AUBERT	07AU	BABR	$10.6\ e^+e^- \to \omega\pi^+\pi^-\gamma$
$4.1 \pm 0.9 \pm 1.3$	1.2M	[15,16] ACHASOV	03D	RVUE	0.44–$2.00\ e^+e^- \to \pi^+\pi^-\pi^0$
5.40 ± 0.95		[21] AKHMETSHIN	00D	CMD2	1.2–$1.38\ e^+e^- \to \omega\pi^+\pi^-$
3.18 ± 0.80		[17,18] CLEGG	94	RVUE	
6.07 ± 0.61	750	[19,20] ANTONELLI	92	DM2	1.34–$2.4\ e^+e^- \to \rho\pi, \omega\pi\pi$

$\Gamma(\omega\eta)/\Gamma_{\text{total}} \times \Gamma(e^+e^-)/\Gamma_{\text{total}}$ $\quad \Gamma_3/\Gamma \times \Gamma_4/\Gamma$

VALUE (units 10^{-6})	CL%	EVTS	DOCUMENT ID		TECN	COMMENT
• • • We do not use the following data for averages, fits, limits, etc. • • •						
0.57 ± 0.06		13	AUBERT	06D	BABR	$10.6\ e^+e^- \to \omega\eta\gamma$
<6	90		[22] AKHMETSHIN	03B	CMD2	$e^+e \to \eta\pi^0\gamma$

[15] Calculated by us from the cross section at the peak.
[16] From the combined fit of ANTONELLI 92, ACHASOV 01E, ACHASOV 02E, and ACHASOV 03D data on the $\pi^+\pi^-\pi^0$ and ANTONELLI 92 on the $\omega\pi^+\pi^-$ final states. Supersedes ACHASOV 99E and ACHASOV 02E.
[17] From a fit to two Breit-Wigner functions and using the data of DOLINSKY 91 and ANTONELLI 92.
[18] From the partial and leptonic width given by the authors.
[19] From the combined fit of the $\rho\pi$ and $\omega\pi\pi$ final states.
[20] From the product of the leptonic width and partial branching ratio given by the authors.
[21] Using the data of AKHMETSHIN 00D and ANTONELLI 92. The $\rho\pi$ dominance for the energy dependence of the $\omega(1420)$ and $\omega(1650)$ width assumed.
[22] $\omega(1650)$ mass and width fixed at 1700 MeV and 250 MeV, respectively.

$\omega(1650)$ BRANCHING RATIOS

$\Gamma(\omega\pi\pi)/\Gamma_{\text{total}}$ $\quad \Gamma_2/\Gamma$

VALUE	EVTS	DOCUMENT ID		TECN	COMMENT
• • • We do not use the following data for averages, fits, limits, etc. • • •					
~ 0.35	1.2M	[23] ACHASOV	03D	RVUE	0.44–$2.00\ e^+e^- \to \pi^+\pi^-\pi^0$
0.620 ± 0.014		[24] HENNER	02	RVUE	1.2–$2.0\ e^+e^- \to \rho\pi, \omega\pi\pi$

$\Gamma(\rho\pi)/\Gamma_{\text{total}}$ $\quad \Gamma_1/\Gamma$

VALUE	EVTS	DOCUMENT ID		TECN	COMMENT
• • • We do not use the following data for averages, fits, limits, etc. • • •					
~ 0.65	1.2M	[23] ACHASOV	03D	RVUE	0.44–$2.00\ e^+e^- \to \pi^+\pi^-\pi^0$
0.380 ± 0.014		[24] HENNER	02	RVUE	1.2–$2.0\ e^+e^- \to \rho\pi, \omega\pi\pi$

$\Gamma(e^+e^-)/\Gamma_{\text{total}}$ $\quad \Gamma_4/\Gamma$

VALUE (units 10^{-7})	EVTS	DOCUMENT ID		TECN	COMMENT
• • • We do not use the following data for averages, fits, limits, etc. • • •					
~ 18	1.2M	[24,25] ACHASOV	03D	RVUE	0.44–$2.00\ e^+e^- \to \pi^+\pi^-\pi^0$
32 ± 1		[24] HENNER	02	RVUE	1.2–$2.0\ e^+e^- \to \rho\pi, \omega\pi\pi$

[23] From the combined fit of ANTONELLI 92, ACHASOV 01E, ACHASOV 02E, and ACHASOV 03D data on the $\pi^+\pi^-\pi^0$ and ANTONELLI 92 on the $\omega\pi^+\pi^-$ final states. Supersedes ACHASOV 99E and ACHASOV 02E.
[24] Assuming that the $\omega(1650)$ decays into $\rho\pi$ and $\omega\pi\pi$ only.
[25] Calculated by us from the cross section at the peak.

$\omega(1650)$ REFERENCES

AUBERT	07AU	PR D76 092005	B. Aubert *et al.*	(BABAR Collab.)
AUBERT	06D	PR D73 052003	B. Aubert *et al.*	(BABAR Collab.)
AUBERT,B	04N	PR D70 072004	B. Aubert *et al.*	(BABAR Collab.)
ACHASOV	03D	PR D68 052006	M.N. Achasov *et al.*	(Novosibirsk SND Collab.)
AKHMETSHIN	03B	PL B562 173	R.R. Akhmetshin *et al.*	(Novosibirsk CMD-2 Collab.)
ACHASOV	02E	PR D66 032001	M.N. Achasov *et al.*	(Novosibirsk SND Collab.)
HENNER	02	EPJ C26 3	V.K. Henner *et al.*	
ACHASOV	01E	PR D63 072002	M.N. Achasov *et al.*	(Novosibirsk SND Collab.)
EUGENIO	01	PL B497 190	P. Eugenio *et al.*	
AKHMETSHIN	00D	PL B489 125	R.R. Akhmetshin *et al.*	(Novosibirsk CMD-2 Collab.)
ACHASOV	99E	PL B462 365	M.N. Achasov *et al.*	(Novosibirsk SND Collab.)
ACHASOV	98H	PR D57 4334	N.N. Achasov, A.A. Kozhevnikov	
CLEGG	94	ZPHY C62 455	A.B. Clegg, A. Donnachie	(LANC, MCHS)
ANTONELLI	92	ZPHY C56 15	A. Antonelli *et al.*	(DM2 Collab.)
BISELLO	91C	ZPHY C52 227	D. Bisello *et al.*	(DM2 Collab.)
DOLINSKY	91	PRPL 202 99	S.I. Dolinsky *et al.*	(NOVO)
BISELLO	88B	ZPHY C39 13	D. Bisello *et al.*	(PADO, CLER, FRAS+)
BARKOV	87	JETPL 46 164 Translated from ZETFP 46 132.	L.M. Barkov *et al.*	(NOVO)
ATKINSON	83B	PL 127B 132	M. Atkinson *et al.*	(BONN, CERN, GLAS+)
CORDIER	81	PL 106B 155	A. Cordier *et al.*	(ORSAY)
IVANOV	81	PL 107B 297	P.M. Ivanov *et al.*	(NOVO)
ESPOSITO	80	LNC 28 195	B. Esposito *et al.*	(FRAS, NAPL, PADO+)
COSME	79	NP B152 215	G. Cosme *et al.*	(IPN)

$\omega_3(1670)$ $\quad I^G(J^{PC}) = 0^-(3^{--})$

$\omega_3(1670)$ MASS

VALUE (MeV)	EVTS	DOCUMENT ID		TECN	COMMENT
1667 ± 4 OUR AVERAGE					
$1665.3 \pm 5.2 \pm 4.5$	23400	AMELIN	96	VES	$36\ \pi^-p \to \pi^+\pi^-\pi^0 n$
1685 ± 20	60	BAUBILLIER	79	HBC	$8.2\ K^-p$ backward
1673 ± 12	430	[1,2] BALTAY	78E	HBC	$15\ \pi^+p \to \Delta 3\pi$
1650 ± 12		CORDEN	78B	OMEG	8–$12\ \pi^-p \to N3\pi$
1669 ± 11	600	[2] WAGNER	75	HBC	$7\ \pi^+p \to \Delta^{++}3\pi$
1678 ± 14	500	DIAZ	74	DBC	$6\ \pi^+n \to p3\pi^0$
1660 ± 13	200	DIAZ	74	DBC	$6\ \pi^+n \to p\omega\pi^0\pi^0$
1679 ± 17	200	MATTHEWS	71D	DBC	$7.0\ \pi^+n \to p3\pi^0$
1670 ± 20		KENYON	69	DBC	$8\ \pi^+n \to p3\pi^0$
• • • We do not use the following data for averages, fits, limits, etc. • • •					
~ 1700	110	[1] CERRADA	77B	HBC	$4.2\ K^-p \to \Lambda 3\pi$
1695 ± 20		BARNES	69B	HBC	$4.6\ K^-p \to \omega 2\pi X$
1636 ± 20		ARMENISE	68B	DBC	$5.1\ \pi^+n \to p3\pi^0$

[1] Phase rotation seen for $J^P = 3^-$ $\rho\pi$ wave.
[2] From a fit to $I(J^P) = 0(3^-)$ $\rho\pi$ partial wave.

$\omega_3(1670)$ WIDTH

VALUE (MeV)	EVTS	DOCUMENT ID		TECN	COMMENT
168±10 OUR AVERAGE					
$149 \pm 19 \pm 7$	23400	AMELIN	96	VES	$36\ \pi^-p \to \pi^+\pi^-\pi^0 n$
160 ± 80	60	[3] BAUBILLIER	79	HBC	$8.2\ K^-p$ backward
173 ± 16	430	[4,5] BALTAY	78E	HBC	$15\ \pi^+p \to \Delta 3\pi$
253 ± 39		CORDEN	78B	OMEG	8–$12\ \pi^-p \to N3\pi$
173 ± 28	600	[3,5] WAGNER	75	HBC	$7\ \pi^+p \to \Delta^{++}3\pi$
167 ± 40	500	DIAZ	74	DBC	$6\ \pi^+n \to p3\pi^0$
122 ± 39	200	DIAZ	74	DBC	$6\ \pi^+n \to p\omega\pi^0\pi^0$
155 ± 40	200	[3] MATTHEWS	71D	DBC	$7.0\ \pi^+n \to p3\pi^0$
• • • We do not use the following data for averages, fits, limits, etc. • • •					
90 ± 20		BARNES	69B	HBC	$4.6\ K^-p \to \omega 2\pi$
100 ± 40		KENYON	69	DBC	$8\ \pi^+n \to p3\pi^0$
112 ± 60		ARMENISE	68B	DBC	$5.1\ \pi^+n \to p3\pi^0$

[3] Width errors enlarged by us to $4\Gamma/\sqrt{N}$; see the note with the $K^*(892)$ mass.
[4] Phase rotation seen for $J^P = 3^-$ $\rho\pi$ wave.
[5] From a fit to $I(J^P) = 0(3^-)$ $\rho\pi$ partial wave.

$\omega_3(1670)$ DECAY MODES

	Mode	Fraction (Γ_i/Γ)
Γ_1	$\rho\pi$	seen
Γ_2	$\omega\pi\pi$	seen
Γ_3	$b_1(1235)\pi$	possibly seen

$\omega_3(1670)$ BRANCHING RATIOS

$\Gamma(\omega\pi\pi)/\Gamma(\rho\pi)$ $\quad \Gamma_2/\Gamma_1$

VALUE	EVTS	DOCUMENT ID		TECN	COMMENT
• • • We do not use the following data for averages, fits, limits, etc. • • •					
0.71 ± 0.27	100	DIAZ	74	DBC	$6\ \pi^+n \to p5\pi^0$

$\Gamma(b_1(1235)\pi)/\Gamma(\rho\pi)$ $\quad \Gamma_3/\Gamma_1$

VALUE	DOCUMENT ID		TECN	COMMENT
possibly seen	DIAZ	74	DBC	$6\ \pi^+n \to p5\pi^0$

$\Gamma(b_1(1235)\pi)/\Gamma(\omega\pi\pi)$ $\quad \Gamma_3/\Gamma_2$

VALUE	CL%	DOCUMENT ID		TECN	COMMENT
• • • We do not use the following data for averages, fits, limits, etc. • • •					
>0.75	68	BAUBILLIER	79	HBC	$8.2\ K^-p$ backward

$\omega_3(1670)$ REFERENCES

AMELIN	96	ZPHY C70 71	D.V. Amelin *et al.*	(SERP, TBIL)
BAUBILLIER	79	PL 89B 131	M. Baubillier *et al.*	(BIRM, CERN, GLAS+)
BALTAY	78E	PRL 40 87	C. Baltay, C.V. Cautis, M. Kalelkar	(COLU) JP
CORDEN	78B	NP B138 235	M.J. Corden *et al.*	(BIRM, RHEL, TELA+)
CERRADA	77B	NP B126 241	M. Cerrada *et al.*	(AMST, CERN, NIJM+) JP
WAGNER	75	PL 58B 201	F. Wagner, M. Tabak, D.M. Chew	(LBL) JP
DIAZ	74	PRL 32 260	J. Diaz *et al.*	(CASE, CMU)
MATTHEWS	71D	PR D3 2561	J.A.J. Matthews *et al.*	(TNTO, WISC)
BARNES	69B	PRL 23 142	V.E. Barnes *et al.*	(BNL)
KENYON	69	PRL 23 146	I.R. Kenyon *et al.*	(BNL, UCND, ORNL)
ARMENISE	68B	PL 26B 336	N. Armenise *et al.*	(BARI, BGNA, FIRZ+)

$\pi_2(1670)$

$I^G(J^{PC}) = 1^-(2^{-+})$

$\pi_2(1670)$ MASS

VALUE (MeV)	EVTS	DOCUMENT ID		TECN	CHG	COMMENT
1672.2± 3.0 OUR AVERAGE		Error includes scale factor of 1.4. See the ideogram below.				
1658 ± 3 $^{+\ 24}_{-\ 8}$	420k	ALEKSEEV	10	COMP		190 $\pi^- Pb \to \pi^-\pi^-\pi^+ Pb'$
1749 ±10 ±100	145k	LU	05	B852		18 $\pi^- p \to \omega\pi^-\pi^0 p$
1676 ± 3 ± 8		[1] CHUNG	02	B852		18.3 $\pi^- p \to \pi^+\pi^-\pi^- p$
1685 ±10 ± 30		[2] BARBERIS	01			450 $pp \to p_f 3\pi^0 p_s$
1687 ± 9 ± 15		AMELIN	99	VES		37 $\pi^- A \to \omega\pi^-\pi^0 A^*$
1669 ± 4		BARBERIS	98B			450 $pp \to p_f \rho\pi p_s$
1670 ± 4		BARBERIS	98B			450 $pp \to p_f f_2(1270)\pi p_s$
1730 ±20		[3] AMELIN	95B	VES		36 $\pi^- A \to \pi^+\pi^-\pi^- A$
1690 ±14		[4] BERDNIKOV	94	VES		37 $\pi^- A \to K^+K^-\pi^- A$
1710 ±20	700	ANTIPOV	87	SIGM	−	50 π^-Cu $\to \mu^+\mu^-\pi^-$Cu
1676 ± 6		[4] EVANGELIS...	81	OMEG	−	12 $\pi^- p \to 3\pi p$
1657 ±14		[4,5] DAUM	80D	SPEC	−	63–94 $\pi p \to 3\pi$X
1662 ±10	2000	[4] BALTAY	77	HBC	+	15 $\pi^+ p \to p 3\pi$
• • • We do not use the following data for averages, fits, limits, etc. • • •						
1742 ±31 ± 49		ANTREASYAN	90	CBAL		$e^+e^- \to e^+e^-\pi^0\pi^0\pi^0$
1624 ±21		[1] BELLINI	85	SPEC		40 $\pi^- A \to \pi^-\pi^+\pi^- A$
1622 ±35		[6] BELLINI	85	SPEC		40 $\pi^- A \to \pi^-\pi^+\pi^- A$
1693 ±28		[7] BELLINI	85	SPEC		40 $\pi^- A \to \pi^-\pi^+\pi^- A$
1710 ±20		[8] DAUM	81B	SPEC	−	63,94 $\pi^- p$
1660 ±10		[4] ASCOLI	73	HBC	−	5–25 $\pi^- p \to p\pi_2$

[1] From $f_2(1270)\pi$ decay.
[2] From a fit to the invariant mass distribution.
[3] From a fit to $J^{PC} = 2^{-+}$ $f_2(1270)\pi$, $f_0(1370)\pi$ waves.
[4] From a fit to $J^P = 2^-$ S-wave $f_2(1270)\pi$ partial wave.
[5] Clear phase rotation seen in 2^-S, 2^-P, 2^-D waves. We quote central value and spread of single-resonance fits to three channels.
[6] From $\rho\pi$ decay.
[7] From $\sigma\pi$ decay.
[8] From a two-resonance fit to four 2^-0^+ waves. This should not be averaged with all the single resonance fits.

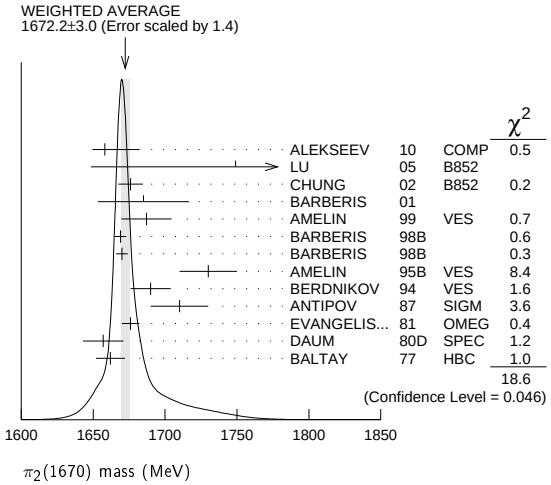

$\pi_2(1670)$ WIDTH

VALUE (MeV)	EVTS	DOCUMENT ID		TECN	CHG	COMMENT
260± 9 OUR AVERAGE		Error includes scale factor of 1.2.				
271± $^{+\ 22}_{-\ 24}$	420k	ALEKSEEV	10	COMP		190 $\pi^- Pb \to \pi^-\pi^-\pi^+ Pb'$
408± 60±250	145k	LU	05	B852		18 $\pi^- p \to \omega\pi^-\pi^0 p$
254± 3± 31		[9] CHUNG	02	B852		18.3 $\pi^- p \to \pi^+\pi^-\pi^- p$
265± 30± 40		[10] BARBERIS	01			450 $pp \to p_f 3\pi^0 p_s$
168± 43± 53		AMELIN	99	VES		37 $\pi^- A \to \omega\pi^-\pi^0 A^*$
268± 15		BARBERIS	98B			450 $pp \to p_f \rho\pi p_s$
256± 15		BARBERIS	98B			450 $pp \to p_f f_2(1270)\pi p_s$
310± 20		[11] AMELIN	95B	VES		36 $\pi^- A \to \pi^+\pi^-\pi^- A$
190± 50		[12] BERDNIKOV	94	VES		37 $\pi^- A \to K^+K^-\pi^- A$
170± 80	700	ANTIPOV	87	SIGM	−	50 π^-Cu $\to \mu^+\mu^-\pi^-$Cu
260± 20		[12] EVANGELIS...	81	OMEG	−	12 $\pi^- p \to 3\pi p$
219± 20		[12,13] DAUM	80D	SPEC	−	63–94 $\pi p \to 3\pi$X
285± 60	2000	[12] BALTAY	77	HBC	+	15 $\pi^+ p \to p 3\pi$
• • • We do not use the following data for averages, fits, limits, etc. • • •						
236± 49± 36		ANTREASYAN	90	CBAL		$e^+e^- \to e^+e^-\pi^0\pi^0\pi^0$
304± 22		[9] BELLINI	85	SPEC		40 $\pi^- A \to \pi^-\pi^+\pi^- A$
404±108		[14] BELLINI	85	SPEC		40 $\pi^- A \to \pi^-\pi^+\pi^- A$
330± 90		[15] BELLINI	85	SPEC		40 $\pi^- A \to \pi^-\pi^+\pi^- A$
312± 50		[16] DAUM	81B	SPEC	−	63,94 $\pi^- p$
270± 60		[12] ASCOLI	73	HBC	−	5–25 $\pi^- p \to p\pi_2$

[9] From $f_2(1270)\pi$ decay.
[10] From a fit to the invariant mass distribution.
[11] From a fit to $J^{PC} = 2^{-+}$ $f_2(1270)\pi$, $f_0(1370)\pi$ waves.
[12] From a fit to $J^P = 2^-$ $f_2(1270)\pi$ partial wave.
[13] Clear phase rotation seen in 2^-S, 2^-P, 2^-D waves. We quote central value and spread of single-resonance fits to three channels.
[14] From $\rho\pi$ decay.
[15] From $\sigma\pi$ decay.
[16] From a two-resonance fit to four 2^-0^+ waves. This should not be averaged with all the single resonance fits.

$\pi_2(1670)$ DECAY MODES

	Mode	Fraction (Γ_i/Γ)	Confidence level
Γ_1	3π	(95.8±1.4) %	
Γ_2	$\pi^+\pi^-\pi^0$		
Γ_3	$\pi^0\pi^0\pi^0$		
Γ_4	$f_2(1270)\pi$	(56.3±3.2) %	
Γ_5	$\rho\pi$	(31 ±4) %	
Γ_6	$\sigma\pi$	(10.9±3.4) %	
Γ_7	$(\pi\pi)_S$-wave	(8.7±3.4) %	
Γ_8	$K\overline{K}^*(892)+$ c.c.	(4.2±1.4) %	
Γ_9	$\omega\rho$	(2.7±1.1) %	
Γ_{10}	$\gamma\gamma$	$< 2.8 \times 10^{-7}$	90%
Γ_{11}	$\eta\pi$		
Γ_{12}	$\pi^\pm 2\pi^+ 2\pi^-$		
Γ_{13}	$\rho(1450)\pi$	$< 3.6 \times 10^{-3}$	97.7%
Γ_{14}	$b_1(1235)\pi$	$< 1.9 \times 10^{-3}$	97.7%
Γ_{15}	$\eta 3\pi$		
Γ_{16}	$f_1(1285)\pi$	possibly seen	
Γ_{17}	$a_2(1320)\pi$	not seen	

CONSTRAINED FIT INFORMATION

An overall fit to 4 branching ratios uses 6 measurements and one constraint to determine 4 parameters. The overall fit has a $\chi^2 = 1.9$ for 3 degrees of freedom.

The following *off-diagonal* array elements are the correlation coefficients $\langle \delta x_i \delta x_j \rangle / (\delta x_i \cdot \delta x_j)$, in percent, from the fit to the branching fractions, $x_i \equiv \Gamma_i/\Gamma_{\rm total}$. The fit constrains the x_i whose labels appear in this array to sum to one.

x_5	−53		
x_7	−29	−59	
x_8	−8	−21	−9
	x_4	x_5	x_7

$\pi_2(1670)$ PARTIAL WIDTHS

$\Gamma(\gamma\gamma)$ Γ_{10}

VALUE (keV)	CL%	DOCUMENT ID		TECN	CHG	COMMENT
<0.072	90	[17] ACCIARRI	97T	L3		$e^+e^- \to e^+e^-\pi^+\pi^-\pi^0$
• • • We do not use the following data for averages, fits, limits, etc. • • •						
<0.19	90	[17] ALBRECHT	97B	ARG		$e^+e^- \to e^+e^-\pi^+\pi^-\pi^0$
1.41 ±0.23±0.28		ANTREASYAN	90	CBAL	0	$e^+e^- \to e^+e^-\pi^0\pi^0\pi^0$
0.8 ±0.3 ±0.12		[18] BEHREND	90C	CELL	0	$e^+e^- \to e^+e^-\pi^+\pi^-\pi^0$
1.3 ±0.3 ±0.2		[19] BEHREND	90C	CELL	0	$e^+e^- \to e^+e^-\pi^+\pi^-\pi^0$

Meson Particle Listings

$\pi_2(1670)$, $\phi(1680)$

[17] Decaying into $f_2(1270)\pi$ and $\rho\pi$.
[18] Constructive interference between $f_2(1270)\pi$,$\rho\pi$ and background.
[19] Incoherent Ansatz.

$\pi_2(1670)$ $\Gamma(i)\Gamma(\gamma\gamma)/\Gamma(\text{total})$

$\Gamma(\pi^+\pi^-\pi^0) \times \Gamma(\gamma\gamma)/\Gamma_{\text{total}}$ $\Gamma_2\Gamma_{10}/\Gamma$

VALUE (keV)	CL%	DOCUMENT ID		TECN	COMMENT
<0.1	95	[20] SCHEGELSKY	06	RVUE	$\gamma\gamma \to \pi^+\pi^-\pi^0$

[20] From analysis of L3 data at 183–209 GeV.

$\pi_2(1670)$ BRANCHING RATIOS

$\Gamma(3\pi)/\Gamma_{\text{total}}$ $\Gamma_1/\Gamma = (\Gamma_4+\Gamma_5+\Gamma_7)/\Gamma$

VALUE	DOCUMENT ID
0.958±0.014 OUR FIT	

$\Gamma(\pi^0\pi^0\pi^0)/\Gamma(\pi^+\pi^-\pi^0)$ Γ_3/Γ_2

VALUE	DOCUMENT ID		COMMENT
0.29±0.03±0.05	[21] BARBERIS	01	450 $pp \to p_f 3\pi^0 p_s$

$\Gamma(\rho\pi)/0.565\Gamma(f_2(1270)\pi)$ $\Gamma_5/0.565\Gamma_4$

(With $f_2(1270) \to \pi^+\pi^-$.)

VALUE	DOCUMENT ID		TECN	COMMENT
0.97±0.09 OUR AVERAGE	Error includes scale factor of 1.9.			
0.76±0.07±0.10	CHUNG	02	B852	18.3 $\pi^- p \to \pi^+\pi^-\pi^- p$
1.01±0.05	BARBERIS	98B		450 $pp \to p_f\pi^+\pi^-\pi^0 p_s$

$\Gamma(\sigma\pi)/\Gamma(f_2(1270)\pi)$ Γ_6/Γ_4

VALUE	DOCUMENT ID		TECN	COMMENT
0.19±0.06 OUR AVERAGE				
0.17±0.02±0.07	CHUNG	02	B852	18.3 $\pi^- p \to \pi^+\pi^-\pi^- p$
0.24±0.10	[22,23] BAKER	99	SPEC	1.94 $\bar{p}p \to 4\pi^0$

$\frac{1}{2}\Gamma(\rho\pi)/\Gamma(\pi^\pm\pi^+\pi^-)$ $\frac{1}{2}\Gamma_5/(0.565\Gamma_4+\frac{1}{2}\Gamma_5+0.624\Gamma_7)$

VALUE	DOCUMENT ID		TECN	CHG	COMMENT
0.29±0.04 OUR FIT					
0.29±0.05	[24] DAUM	81B	SPEC		63,94 $\pi^- p$
• • • We do not use the following data for averages, fits, limits, etc. • • •					
<0.3	BARTSCH	68	HBC	+	8 $\pi^+ p \to 3\pi p$

$0.565\Gamma(f_2(1270)\pi)/\Gamma(\pi^\pm\pi^+\pi^-)$ $0.565\Gamma_4/(0.565\Gamma_4+\frac{1}{2}\Gamma_5+0.624\Gamma_7)$

(With $f_2(1270) \to \pi^+\pi^-$.)

VALUE	DOCUMENT ID		TECN	CHG	COMMENT
0.604±0.035 OUR FIT					
0.60 ±0.05 OUR AVERAGE	Error includes scale factor of 1.3.				
0.61 ±0.04	[24] DAUM	81B	SPEC		63,94 $\pi^- p$
0.76 $^{+0.24}_{-0.34}$	ARMENISE	69	DBC	+	5.1 $\pi^+ d \to d 3\pi$
0.35 ±0.20	BALTAY	68	HBC	+	7–8.5 $\pi^+ p$
• • • We do not use the following data for averages, fits, limits, etc. • • •					
0.59	BARTSCH	68	HBC	+	8 $\pi^+ p \to 3\pi p$

$0.624\Gamma((\pi\pi)_{S\text{-wave}})/\Gamma(\pi^\pm\pi^+\pi^-)$ $0.624\Gamma_7/(0.565\Gamma_4+\frac{1}{2}\Gamma_5+0.624\Gamma_7)$

(With $(\pi\pi)_{S\text{-wave}} \to \pi^+\pi^-$.)

VALUE	DOCUMENT ID		TECN	COMMENT
0.10±0.04 OUR FIT				
0.10±0.05	[24] DAUM	81B	SPEC	63,94 $\pi^- p$

$\Gamma(K\overline{K}^*(892)+\text{c.c.})/\Gamma(f_2(1270)\pi)$ Γ_8/Γ_4

VALUE	DOCUMENT ID		TECN	CHG	COMMENT
0.075±0.025 OUR FIT					
0.075±0.025	[25] ARMSTRONG	82B	OMEG	−	16 $\pi^- p \to K^+K^-\pi^- p$

$\Gamma(\omega\rho)/\Gamma_{\text{total}}$ Γ_9/Γ

VALUE	DOCUMENT ID		TECN	COMMENT
0.027±0.004±0.010	[26] AMELIN	99	VES	37 $\pi^- A \to \omega\pi^-\pi^0 A^*$

$\Gamma(\eta\pi)/\Gamma(\pi^\pm\pi^+\pi^-)$ $\Gamma_{11}/(0.565\Gamma_4+\frac{1}{2}\Gamma_5+0.624\Gamma_7)$

(All η decays.)

VALUE	DOCUMENT ID		TECN	CHG	COMMENT
<0.09	BALTAY	68	HBC	+	7–8.5 $\pi^+ p$
• • • We do not use the following data for averages, fits, limits, etc. • • •					
<0.10	CRENNELL	70	HBC	−	6 $\pi^- p \to f_2\pi^- N$

$\Gamma(\pi^\pm 2\pi^+ 2\pi^-)/\Gamma(\pi^\pm\pi^+\pi^-)$ $\Gamma_{12}/(0.565\Gamma_4+\frac{1}{2}\Gamma_5+0.624\Gamma_7)$

VALUE	DOCUMENT ID		TECN	CHG	COMMENT
<0.10	CRENNELL	70	HBC	−	6 $\pi^- p \to f_2\pi^- N$
<0.1	BALTAY	68	HBC	+	7,8.5 $\pi^+ p$

$\Gamma(\rho(1450)\pi)/\Gamma_{\text{total}}$ Γ_{13}/Γ

VALUE	CL%	DOCUMENT ID		TECN	COMMENT
<0.0036	97.7	AMELIN	99	VES	37 $\pi^- A \to \omega\pi^-\pi^0 A^*$

$\Gamma(b_1(1235)\pi)/\Gamma_{\text{total}}$ Γ_{14}/Γ

VALUE	CL%	DOCUMENT ID		TECN	COMMENT
<0.0019	97.7	AMELIN	99	VES	37 $\pi^- A \to \omega\pi^-\pi^0 A^*$

$\Gamma(f_1(1285)\pi)/\Gamma_{\text{total}}$ Γ_{16}/Γ

VALUE	EVTS	DOCUMENT ID		TECN	COMMENT
possibly seen	69k	KUHN	04	B852	18 $\pi^- p \to \eta\pi^+\pi^-\pi^- p$

$\Gamma(a_2(1320)\pi)/\Gamma_{\text{total}}$ Γ_{17}/Γ

VALUE	EVTS	DOCUMENT ID		TECN	COMMENT
not seen	69k	KUHN	04	B852	18 $\pi^- p \to \eta\pi^+\pi^-\pi^- p$

D-wave/S-wave RATIO FOR $\pi_2(1670) \to f_2(1270)\pi$

VALUE	DOCUMENT ID		TECN	COMMENT
−0.18±0.06	[22] BAKER	99	SPEC	1.94 $\bar{p}p \to 4\pi^0$
• • • We do not use the following data for averages, fits, limits, etc. • • •				
0.22±0.10	[24] DAUM	81B	SPEC	63,94 $\pi^- p$

F-wave/P-wave RATIO FOR $\pi_2(1670) \to \rho\pi$

VALUE	DOCUMENT ID		TECN	COMMENT
−0.72±0.07±0.14	CHUNG	02	B852	18.3 $\pi^- p \to \pi^+\pi^-\pi^- p$

[21] Using BARBERIS 98B.
[22] Using preliminary CBAR data.
[23] With the $\sigma\pi$ in L=2 and the $f_2(1270)\pi$ in L=0.
[24] From a two-resonance fit to four 2^-0^+ waves.
[25] From a partial-wave analysis of $K^+K^-\pi^-$ system.
[26] Normalized to the B($\pi_2(1670) \to f_2\pi$).

$\pi_2(1670)$ REFERENCES

ALEKSEEV	10	PRL 104 241803	M.G. Alekseev *et al.* (COMPASS Collab.)
SCHEGELSKY	06	EPJ A27 199	V.A. Schegelsky *et al.*
LU	05	PRL 94 032002	M. Lu *et al.* (BNL E852 Collab.)
KUHN	04	PL B595 109	J. Kuhn *et al.* (BNL E852 Collab.)
CHUNG	02	PR D65 072001	S.U. Chung *et al.* (BNL E852 Collab.)
BARBERIS	01	PL B507 14	D. Barberis *et al.*
AMELIN	99	PAN 62 445	D.V. Amelin *et al.* (VES Collab.)
		Translated from YAF 62 487.	
BAKER	99	PL B449 114	C.A. Baker *et al.*
BARBERIS	98B	PL B422 399	D. Barberis *et al.* (WA 102 Collab.)
ACCIARRI	97T	PL B413 147	M. Acciarri *et al.* (L3 Collab.)
ALBRECHT	97B	ZPHY C74 469	H. Albrecht *et al.* (ARGUS Collab.)
AMELIN	95B	PL B356 595	D.V. Amelin *et al.* (SERP, TBIL)
BERDNIKOV	94	PL B337 219	E.B. Berdnikov *et al.* (SERP, TBIL)
ANTREASYAN	90	ZPHY C48 561	D. Antreasyan *et al.* (Crystal Ball Collab.)
BEHREND	90C	ZPHY C46 583	H.J. Behrend *et al.* (CELLO Collab.)
ANTIPOV	87	EPL 4 403	Y.M. Antipov *et al.* (SERP, JINR, INRM+)
BELLINI	85	SJNP 41 781	D. Bellini *et al.*
		Translated from YAF 41 1223.	
ARMSTRONG	82B	NP B202 1	T.A. Armstrong, B. Baccari (AACH3, BARI, BONN+)
DAUM	81B	NP B182 269	C. Daum *et al.* (AMST, CERN, CRAC, MPIM+)
EVANGELIS...	81	NP B178 197	C. Evangelista *et al.* (BARI, BONN, CERN+)
Also		NP B186 594	C. Evangelista
DAUM	80D	PL B89 285	C. Daum *et al.* (AMST, CERN, CRAC, MPIM+) JP
BALTAY	77	PRL 39 591	C. Baltay, C.V. Cautis, M. Kalelkar (COLU) JP
ASCOLI	73	PR D7 669	G. Ascoli (ILL, TNTO, GENO, HAMB, MILA+) JP
CRENNELL	70	PRL 24 781	D.J. Crennell *et al.* (BNL)
ARMENISE	69	LNC 2 501	N. Armenise *et al.* (BARI, BGNA, FIRZ)
BALTAY	68	PRL 20 887	C. Baltay *et al.* (COLU, ROCH, RUTG, YALE) I
BARTSCH	68	NP B7 345	J. Bartsch *et al.* (AACH, BERL, CERN) JP

$\phi(1680)$

$I^G(J^{PC}) = 0^-(1^{--})$

$\phi(1680)$ MASS

e^+e^- PRODUCTION

VALUE (MeV)	EVTS	DOCUMENT ID		TECN	COMMENT
1680±20 OUR ESTIMATE					
• • • We do not use the following data for averages, fits, limits, etc. • • •					
1689± 7±10	4.8k	[1] SHEN	09	BELL	10.6 $e^+e^- \to K^+K^-\pi^+\pi^-\gamma$
1709±20±43		[2] AUBERT	08S	BABR	10.6 $e^+e^- \to$ hadrons
1623±20	948	[3] AKHMETSHIN	03	CMD2	1.05–1.38 $e^+e^- \to K^0_L K^0_S$
∼ 1500		[4] ACHASOV	98H	RVUE	$e^+e^- \to \pi^+\pi^-\pi^0$, $\omega\pi^+\pi^-$, K^+K^-
∼ 1900		[5] ACHASOV	98H	RVUE	$e^+e^- \to K^0_S K^\pm\pi^\mp$
1700±20		[6] CLEGG	94	RVUE	$e^+e^- \to K^+K^-$, $K^0_S K\pi$
1657±27	367	BISELLO	91C	DM2	$e^+e^- \to K^0_S K^\pm\pi^\mp$
1655±17		[7] BISELLO	88B	DM2	$e^+e^- \to K^+K^-$
1680±10		[8] BUON	82	DM1	$e^+e^- \to$ hadrons
1677±12		[9] MANE	82	DM1	$e^+e^- \to K^0_S K\pi$

[1] From a fit with two incoherent Breit-Wigners.
[2] From the simultaneous fit to the $K\overline{K}^*(892)+$ c.c. and $\phi\eta$ data from AUBERT 08S using the results of AUBERT 07AK.
[3] From the combined fit of AKHMETSHIN 03 and MANE 81 also including ρ, ω, and ϕ. Neither isospin nor flavor structure known.
[4] Using data from IVANOV 81, BARKOV 87, BISELLO 88B, DOLINSKY 91, and ANTONELLI 92.
[5] Using the data from BISELLO 91C.
[6] Using BISELLO 88B and MANE 82 data.

[7] From global fit including ρ, ω, ϕ and $\rho(1700)$ assume mass 1570 MeV and width 510 MeV for ρ radial excitation.
[8] From global fit of ρ, ω, ϕ and their radial excitations to channels $\omega\pi^+\pi^-$, K^+K^-, $K^0_S K^0_L$, $K^0_S K^\pm\pi^\mp$. Assume mass 1570 MeV and width 510 MeV for ρ radial excitations, mass 1570 and width 500 MeV for ω radial excitation.
[9] Fit to one channel only, neglecting interference with ω, $\rho(1700)$.

PHOTOPRODUCTION

VALUE (MeV)	DOCUMENT ID		TECN	COMMENT
• • • We do not use the following data for averages, fits, limits, etc. • • •				
1753± 3	[10] LINK	02K	FOCS	20–160 $\gamma p \to K^+K^-p$
1726±22	[10] BUSENITZ	89	TPS	$\gamma p \to K^+K^-X$
1760±20	[10] ATKINSON	85C	OMEG	20–70 $\gamma p \to K\overline{K}X$
1690±10	[10] ASTON	81F	OMEG	25–70 $\gamma p \to K^+K^-X$

[10] We list here a state decaying into K^+K^- possibly different from $\phi(1680)$.

$p\overline{p}$ ANNIHILATION

VALUE (MeV)	DOCUMENT ID		TECN	COMMENT
• • • We do not use the following data for averages, fits, limits, etc. • • •				
1700±8	[11] AMSLER	06	CBAR	0.9 $\overline{p}p \to K^+K^-\pi^0$

[11] Could also be $\rho(1700)$.

$\phi(1680)$ WIDTH

e^+e^- PRODUCTION

VALUE (MeV)	EVTS	DOCUMENT ID		TECN	COMMENT
150±50 OUR ESTIMATE This is only an educated guess; the error given is larger than the error on the average of the published values.					
• • • We do not use the following data for averages, fits, limits, etc. • • •					
211±14± 19	4.8k	[12] SHEN	09	BELL	10.6 $e^+e^- \to K^+K^-\pi^+\pi^-\gamma$
322±77±160		[13] AUBERT	08S	BABR	10.6 $e^+e^- \to$ hadrons
139±60	948	[14] AKHMETSHIN	03	CMD2	1.05–1.38 $e^+e^- \to K^0_L K^0_S$
300±60		[15] CLEGG	94	RVUE	$e^+e^- \to K^+K^-$, $K^0_S K\pi$
146±55	367	BISELLO	91C	DM2	$e^+e^- \to K^0_S K^\pm\pi^\mp$
207±45		[16] BISELLO	88B	DM2	$e^+e^- \to K^+K^-$
185±22		[17] BUON	82	DM1	$e^+e^- \to$ hadrons
102±36		[18] MANE	82	DM1	$e^+e^- \to K^0_S K\pi$

[12] From a fit with two incoherent Breit-Wigners.
[13] From the simultaneous fit to the $K\overline{K}^*(892)+$ c.c. and $\phi\eta$ data from AUBERT 08S using the results of AUBERT 07AK.
[14] From the combined fit of AKHMETSHIN 03 and MANE 81 also including ρ, ω, and ϕ. Neither isospin nor flavor structure known.
[15] Using BISELLO 88B and MANE 82 data.
[16] From global fit including ρ, ω, ϕ and $\rho(1700)$
[17] From global fit of ρ, ω, ϕ and their radial excitations to channels $\omega\pi^+\pi^-$, K^+K^-, $K^0_S K^0_L$, $K^0_S K^\pm\pi^\mp$. Assume mass 1570 MeV and width 510 MeV for ρ radial excitations, mass 1570 and width 500 MeV for ω radial excitation.
[18] Fit to one channel only, neglecting interference with ω, $\rho(1700)$.

PHOTOPRODUCTION

VALUE (MeV)	DOCUMENT ID		TECN	COMMENT
• • • We do not use the following data for averages, fits, limits, etc. • • •				
122±63	[19] LINK	02K	FOCS	20–160 $\gamma p \to K^+K^-p$
121±47	[19] BUSENITZ	89	TPS	$\gamma p \to K^+K^-X$
80±40	[19] ATKINSON	85C	OMEG	20–70 $\gamma p \to K\overline{K}X$
100±40	[19] ASTON	81F	OMEG	25–70 $\gamma p \to K^+K^-X$

[19] We list here a state decaying into K^+K^- possibly different from $\phi(1680)$.

$p\overline{p}$ ANNIHILATION

VALUE (MeV)	DOCUMENT ID		TECN	COMMENT
• • • We do not use the following data for averages, fits, limits, etc. • • •				
143±24	[20] AMSLER	06	CBAR	0.9 $\overline{p}p \to K^+K^-\pi^0$

[20] Could also be $\rho(1700)$.

$\phi(1680)$ DECAY MODES

	Mode	Fraction (Γ_i/Γ)
Γ_1	$K\overline{K}^*(892)+$ c.c.	dominant
Γ_2	$K^0_S K\pi$	seen
Γ_3	$K\overline{K}$	seen
Γ_4	$K^0_L K^0_S$	
Γ_5	e^+e^-	seen
Γ_6	$\omega\pi\pi$	not seen
Γ_7	$\phi\pi\pi$	
Γ_8	$K^+K^-\pi^+\pi^-$	seen
Γ_9	$\phi\eta$	
Γ_{10}	$K^+K^-\pi^0$	

$\phi(1680)$ $\Gamma(i)\Gamma(e^+e^-)/\Gamma^2(\text{total})$

This combination of a branching ratio into channel (i) and branching ratio into e^+e^- is directly measured and obtained from the cross section at the peak. We list only data that have not been used to determine the branching ratio into (i) or e^+e^-.

$\Gamma(K^0_L K^0_S)/\Gamma_{\text{total}} \times \Gamma(e^+e^-)/\Gamma_{\text{total}}$ $\quad \Gamma_4/\Gamma \times \Gamma_5/\Gamma$

VALUE (units 10^{-6})	EVTS	DOCUMENT ID		TECN	COMMENT
• • • We do not use the following data for averages, fits, limits, etc. • • •					
0.131±0.059	948	[21] AKHMETSHIN	03	CMD2	1.05–1.38 $e^+e^- \to K^0_L K^0_S$

[21] From the combined fit of AKHMETSHIN 03 and MANE 81 also including ρ, ω, and ϕ. Neither isospin nor flavor structure known. Recalculated by us.

$\Gamma(K\overline{K}^*(892)+\text{c.c.})/\Gamma_{\text{total}} \times \Gamma(e^+e^-)/\Gamma_{\text{total}}$ $\quad \Gamma_1/\Gamma \times \Gamma_5/\Gamma$

VALUE (units 10^{-6})	EVTS	DOCUMENT ID		TECN	COMMENT
• • • We do not use the following data for averages, fits, limits, etc. • • •					
1.15±0.16±0.01		[22] AUBERT	08S	BABR	10.6 $e^+e^- \to K\overline{K}^*(892)\gamma +$ c.c.
3.29±1.57	367	[23] BISELLO	91C	DM2	1.35–2.40 $e^+e^- \to K^0_S K^\pm\pi^\mp$

[22] From the simultaneous fit to the $K\overline{K}^*(892)+$ c.c. and $\phi\eta$ data from AUBERT 08S using the results of AUBERT 07AK.
[23] Recalculated by us with the published value of B($K\overline{K}^*(892)+$ c.c.) $\times \Gamma(e^+e^-)$.

$\Gamma(\phi\pi\pi)/\Gamma_{\text{total}} \times \Gamma(e^+e^-)/\Gamma_{\text{total}}$ $\quad \Gamma_7/\Gamma \times \Gamma_5/\Gamma$

VALUE (units 10^{-7})	EVTS	DOCUMENT ID		TECN	COMMENT
• • • We do not use the following data for averages, fits, limits, etc. • • •					
1.86±0.14±0.21	4.8k	[24] SHEN	09	BELL	10.6 $e^+e^- \to K^+K^-\pi^+\pi^-\gamma$

[24] Multiplied by 3/2 to take into account the $\phi\pi^0\pi^0$ mode. Using B($\phi \to K^+K^-$) = (49.2 ± 0.6)%.

$\Gamma(\phi\eta)/\Gamma_{\text{total}} \times \Gamma(e^+e^-)/\Gamma_{\text{total}}$ $\quad \Gamma_9/\Gamma \times \Gamma_5/\Gamma$

VALUE (units 10^{-6})	DOCUMENT ID		TECN	COMMENT
• • • We do not use the following data for averages, fits, limits, etc. • • •				
0.43±0.10±0.09	[25] AUBERT	08S	BABR	10.6 $e^+e^- \to \phi\eta\gamma$

[25] From the simultaneous fit to the $K\overline{K}^*(892)+$ c.c. and $\phi\eta$ data from AUBERT 08S using the results of AUBERT 07AK.

$\phi(1680)$ BRANCHING RATIOS

$\Gamma(K\overline{K}^*(892)+\text{c.c.})/\Gamma(K^0_S K\pi)$ $\quad \Gamma_1/\Gamma_2$

VALUE	DOCUMENT ID		TECN	COMMENT
dominant	MANE	82	DM1	$e^+e^- \to K^0_S K^\pm\pi^\mp$

$\Gamma(K\overline{K})/\Gamma(K\overline{K}^*(892)+\text{c.c.})$ $\quad \Gamma_3/\Gamma_1$

VALUE	DOCUMENT ID		TECN	COMMENT
• • • We do not use the following data for averages, fits, limits, etc. • • •				
0.07±0.01	BUON	82	DM1	e^+e^-

$\Gamma(\omega\pi\pi)/\Gamma(K\overline{K}^*(892)+\text{c.c.})$ $\quad \Gamma_6/\Gamma_1$

VALUE	DOCUMENT ID		TECN	COMMENT
<0.10	BUON	82	DM1	e^+e^-

$\Gamma(\phi\eta)/\Gamma(K\overline{K}^*(892)+\text{c.c.})$ $\quad \Gamma_9/\Gamma_1$

VALUE	DOCUMENT ID		TECN	COMMENT
• • • We do not use the following data for averages, fits, limits, etc. • • •				
≈ 0.37	[26] AUBERT	08S	BABR	10.6 $e^+e^- \to$ hadrons

[26] From the fit including data from AUBERT 07AK.

$\phi(1680)$ REFERENCES

SHEN	09	PR D80 031101	C.P. Shen *et al.* (BELLE Collab.)
AUBERT	08S	PR D77 092002	B. Aubert *et al.* (BABAR Collab.)
AUBERT	07AK	PR D76 012008	B. Aubert *et al.* (BABAR Collab.)
AMSLER	06	PL B639 165	C. Amsler *et al.* (CBAR Collab.)
AKHMETSHIN	03	PL B551 27	R.R. Akhmetshin *et al.* (Novosibirsk CMD-2 Collab.)
Also		PAN 65 1222	E.V. Anashkin, V.M. Aulchenko, R.R. Akhmetshin
		Translated from YAF 65 1255.	
LINK	02K	PL B545 50	J.M. Link *et al.* (FNAL FOCUS Collab.)
ACHASOV	98H	PR D57 4334	N.N. Achasov, A.A. Kozhevnikov
CLEGG	94	ZPHY C62 455	A.B. Clegg, A. Donnachie (LANC, MCHS)
ANTONELLI	92	ZPHY C56 15	A. Antonelli *et al.* (DM2 Collab.)
BISELLO	91C	ZPHY C52 227	D. Bisello *et al.* (DM2 Collab.)
DOLINSKY	91	PRPL 202 99	S.I. Dolinsky *et al.* (NOVO)
BUSENITZ	89	PR D40 1	J.K. Busenitz *et al.* (ILL, FNAL)
BISELLO	88B	ZPHY C39 13	D. Bisello *et al.* (PADO, CLER, FRAS+)
BARKOV	87	JETPL 46 164	L.M. Barkov *et al.* (NOVO)
		Translated from ZETFP 46 132.	
ATKINSON	85C	ZPHY C27 233	M. Atkinson *et al.* (BONN, CERN, GLAS+)
BUON	82	PL 118B 221	J. Buon *et al.* (LALO, MONP)
MANE	82	PL 112B 178	F. Mane *et al.* (LALO)
ASTON	81F	PL 104B 231	D. Aston (BONN, CERN, EPOL, GLAS, LANC+)
IVANOV	81	PL 107B 297	P.M. Ivanov *et al.* (NOVO)
MANE	81	PL 99B 261	F. Mane *et al.* (ORSAY)

Meson Particle Listings

$\rho_3(1690)$

$\rho_3(1690)$

$I^G(J^{PC}) = 1^+(3^{--})$

$\rho_3(1690)$ MASS

VALUE (MeV)	DOCUMENT ID
1688.8±2.1 OUR AVERAGE	Includes data from the 5 datablocks that follow this one.

2π MODE

VALUE (MeV)	EVTS	DOCUMENT ID		TECN	CHG	COMMENT
The data in this block is included in the average printed for a previous datablock.						
1686± 4 OUR AVERAGE						
1677±14		EVANGELIS...	81	OMEG	−	12 $\pi^- p \rightarrow 2\pi p$
1679±11	476	BALTAY	78B	HBC	0	15 $\pi^+ p \rightarrow \pi^+\pi^- n$
1678±12	175	[1] ANTIPOV	77	CIBS	0	25 $\pi^- p \rightarrow p3\pi$
1690± 7	600	[1] ENGLER	74	DBC	0	6 $\pi^+ n \rightarrow \pi^+\pi^- p$
1693± 8		[2] GRAYER	74	ASPK	0	17 $\pi^- p \rightarrow \pi^+\pi^- n$
1678±12		MATTHEWS	71C	DBC	0	7 $\pi^+ N$
• • • We do not use the following data for averages, fits, limits, etc. • • •						
1734±10		[3] CORDEN	79	OMEG		12–15 $\pi^- p \rightarrow n2\pi$
1692±12		[2,4] ESTABROOKS	75	RVUE		17 $\pi^- p \rightarrow \pi^+\pi^- n$
1737±23		ARMENISE	70	DBC	0	9 $\pi^+ N$
1650±35	122	BARTSCH	70B	HBC	+	8 $\pi^+ p \rightarrow N2\pi$
1687±21		STUNTEBECK	70	HDBC	0	8 $\pi^- p$, 5.4 $\pi^+ d$
1683±13		ARMENISE	68	DBC	0	5.1 $\pi^+ d$
1670±30		GOLDBERG	65	HBC	0	6 $\pi^+ d$, 8 $\pi^- p$

[1] Mass errors enlarged by us to $\Gamma/\sqrt{N}$; see the note with the $K^*(892)$ mass.
[2] Uses same data as HYAMS 75.
[3] From a phase shift solution containing a $f'_2(1525)$ width two times larger than the $K\overline{K}$ result.
[4] From phase-shift analysis. Error takes account of spread of different phase-shift solutions.

$K\overline{K}$ AND $K\overline{K}\pi$ MODES

VALUE (MeV)	EVTS	DOCUMENT ID		TECN	CHG	COMMENT
The data in this block is included in the average printed for a previous datablock.						
1696± 4 OUR AVERAGE						
1699± 5		ALPER	80	CNTR	0	62 $\pi^- p \rightarrow K^+ K^- n$
1698±12	6k	[5,6] MARTIN	78D	SPEC		10 $\pi p \rightarrow K^0_S K^- p$
1692± 6		BLUM	75	ASPK	0	18.4 $\pi^- p \rightarrow nK^+ K^-$
1690±16		ADERHOLZ	69	HBC	+	8 $\pi^+ p \rightarrow K\overline{K}\pi$
• • • We do not use the following data for averages, fits, limits, etc. • • •						
1694± 8		[7] COSTA...	80	OMEG		10 $\pi^- p \rightarrow K^+ K^- n$

[5] From a fit to $J^P = 3^-$ partial wave.
[6] Systematic error on mass scale subtracted.
[7] They cannot distinguish between $\rho_3(1690)$ and $\omega_3(1670)$.

$(4\pi)^\pm$ MODE

VALUE (MeV)	EVTS	DOCUMENT ID		TECN	CHG	COMMENT
The data in this block is included in the average printed for a previous datablock.						
1686± 5 OUR AVERAGE Error includes scale factor of 1.1.						
1694± 6		[8] EVANGELIS...	81	OMEG	−	12 $\pi^- p \rightarrow p4\pi$
1665±15	177	BALTAY	78B	HBC	+	15 $\pi^+ p \rightarrow p4\pi$
1670±10		THOMPSON	74	HBC	+	13 $\pi^+ p$
1687±20		CASON	73	HBC	−	8,18.5 $\pi^- p$
1685±14		[9] CASON	73	HBC	−	8,18.5 $\pi^- p$
1680±40	144	BARTSCH	70B	HBC	+	8 $\pi^+ p \rightarrow N4\pi$
1689±20	102	[9] BARTSCH	70B	HBC	+	8 $\pi^+ p \rightarrow N2\rho$
1705±21		CASO	70	HBC	−	11.2 $\pi^- p \rightarrow n\rho 2\pi$
• • • We do not use the following data for averages, fits, limits, etc. • • •						
1718±10		[10] EVANGELIS...	81	OMEG	−	12 $\pi^- p \rightarrow p4\pi$
1673± 9		[11] EVANGELIS...	81	OMEG	−	12 $\pi^- p \rightarrow p4\pi$
1733± 9	66	[9] KLIGER	74	HBC	−	4.5 $\pi^- p \rightarrow p4\pi$
1630±15		HOLMES	72	HBC	+	10–12 $K^+ p$
1720±15		BALTAY	68	HBC	+	7, 8.5 $\pi^+ p$

[8] From $\rho^-\rho^0$ mode, not independent of the other two EVANGELISTA 81 entries.
[9] From $\rho^\pm\rho^0$ mode.
[10] From $a_2(1320)^-\pi^0$ mode, not independent of the other two EVANGELISTA 81 entries.
[11] From $a_2(1320)^0\pi^-$ mode, not independent of the other two EVANGELISTA 81 entries.

$\omega\pi$ MODE

VALUE (MeV)	DOCUMENT ID		TECN	CHG	COMMENT
The data in this block is included in the average printed for a previous datablock.					
1681± 7 OUR AVERAGE					
1670±25	[12] ALDE	95	GAM2		38 $\pi^- p \rightarrow \omega\pi^0 n$
1690±15	EVANGELIS...	81	OMEG	−	12 $\pi^- p \rightarrow \omega\pi p$
1666±14	GESSAROLI	77	HBC		11 $\pi^- p \rightarrow \omega\pi p$
1686± 9	THOMPSON	74	HBC	+	13 $\pi^+ p$
• • • We do not use the following data for averages, fits, limits, etc. • • •					
1654±24	BARNHAM	70	HBC	+	10 $K^+ p \rightarrow \omega\pi X$

[12] Supersedes ALDE 92C.

$\eta\pi^+\pi^-$ MODE

(For difficulties with MMS experiments, see the $a_2(1320)$ mini-review in the 1973 edition.)

VALUE (MeV)	DOCUMENT ID		TECN	CHG	COMMENT
The data in this block is included in the average printed for a previous datablock.					
1682±12 OUR AVERAGE					
1685±10±20	AMELIN	00	VES		37 $\pi^- p \rightarrow \eta\pi^+\pi^- n$
1680±15	FUKUI	88	SPEC	0	8.95 $\pi^- p \rightarrow \eta\pi^+\pi^- n$
• • • We do not use the following data for averages, fits, limits, etc. • • •					
1700±47	[13] ANDERSON	69	MMS	−	16 $\pi^- p$ backward
1632±15	[13,14] FOCACCI	66	MMS	−	7–12 $\pi^- p \rightarrow p$MM
1700±15	[13,14] FOCACCI	66	MMS	−	7–12 $\pi^- p \rightarrow p$MM
1748±15	[13,14] FOCACCI	66	MMS	−	7–12 $\pi^- p \rightarrow p$MM

[13] Seen in 2.5–3 GeV/c $\overline{p}p$. $2\pi^+ 2\pi^-$, with 0, 1, 2 $\pi^+\pi^-$ pairs in ρ band not seen by OREN 74 (2.3 GeV/c $\overline{p}p$) with more statistics. (Jan. 1976)
[14] Not seen by BOWEN 72.

$\rho_3(1690)$ WIDTH

2π, $K\overline{K}$, AND $K\overline{K}\pi$ MODES

VALUE (MeV)	DOCUMENT ID
161±10 OUR AVERAGE	Includes data from the 5 datablocks that follow this one. Error includes scale factor of 1.5. See the ideogram below.

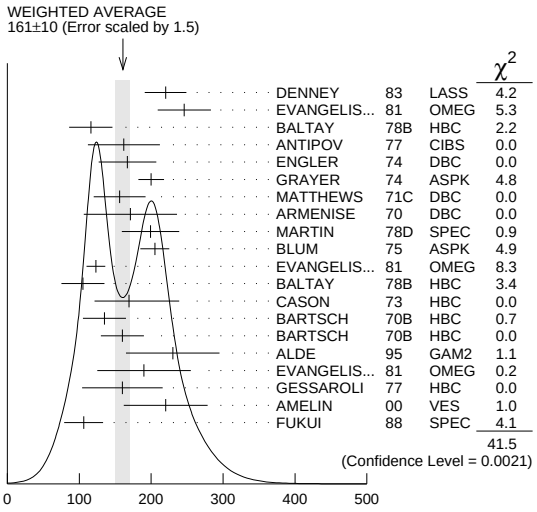

$\rho_3(1690)$ width, 2π, $K\overline{K}$, and $K\overline{K}\pi$ modes (MeV)

2π MODE

VALUE (MeV)	EVTS	DOCUMENT ID		TECN	CHG	COMMENT
The data in this block is included in the average printed for a previous datablock.						
186±14 OUR AVERAGE Error includes scale factor of 1.3. See the ideogram below.						
220±29		DENNEY	83	LASS		10 $\pi^+ N$
246±37		EVANGELIS...	81	OMEG	−	12 $\pi^- p \rightarrow 2\pi p$
116±30	476	BALTAY	78B	HBC	0	15 $\pi^+ p \rightarrow \pi^+\pi^- n$
162±50	175	[15] ANTIPOV	77	CIBS	0	25 $\pi^- p \rightarrow p3\pi$
167±40	600	ENGLER	74	DBC	0	6 $\pi^+ n \rightarrow \pi^+\pi^- p$
200±18		[16] GRAYER	74	ASPK	0	17 $\pi^- p \rightarrow \pi^+\pi^- n$
156±36		MATTHEWS	71C	DBC	0	7 $\pi^+ N$
171±65		ARMENISE	70	DBC	0	9 $\pi^+ d$

• • • We do not use the following data for averages, fits, limits, etc. • • •

322±35		[17] CORDEN	79	OMEG		12–15 $\pi^- p \to n2\pi$
240±30		[16,18] ESTABROOKS	75	RVUE		17 $\pi^- p \to \pi^+\pi^- n$
180±30	122	BARTSCH	70B	HBC	+	8 $\pi^+ p \to N2\pi$
267^{+72}_{-46}		STUNTEBECK	70	HDBC	0	8 $\pi^- p$, 5.4 $\pi^+ d$
188±49		ARMENISE	68	DBC	0	5.1 $\pi^+ d$
180±40		GOLDBERG	65	HBC	0	6 $\pi^+ d$, 8 $\pi^- p$

[15] Width errors enlarged by us to $4\Gamma/\sqrt{N}$; see the note with the $K^*(892)$ mass.
[16] Uses same data as HYAMS 75 and BECKER 79.
[17] From a phase shift solution containing a $f_2'(1525)$ width two times larger than the $K\overline{K}$ result.
[18] From phase-shift analysis. Error takes account of spread of different phase-shift solutions.

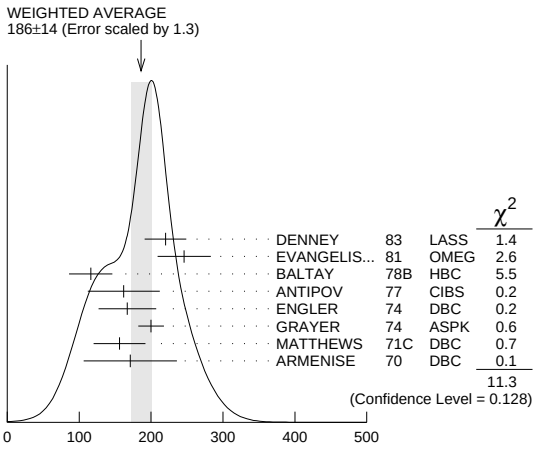

$\rho_3(1690)$ width, 2π mode (MeV)

$K\overline{K}$ AND $K\overline{K}\pi$ MODES

VALUE (MeV)	EVTS	DOCUMENT ID		TECN	CHG	COMMENT

The data in this block is included in the average printed for a previous datablock.

204±18 OUR AVERAGE

199±40	6000	[19] MARTIN	78D	SPEC		10 $\pi p \to K^0_S K^- p$
205±20		BLUM	75	ASPK	0	18.4 $\pi^- p \to nK^+ K^-$

• • • We do not use the following data for averages, fits, limits, etc. • • •

219± 4		ALPER	80	CNTR	0	62 $\pi^- p \to K^+ K^- n$
186±11		[20] COSTA...	80	OMEG		10 $\pi^- p \to K^+ K^- n$
112±60		ADERHOLZ	69	HBC	+	8 $\pi^+ p \to K\overline{K}\pi$

[19] From a fit to $J^P = 3^-$ partial wave.
[20] They cannot distinguish between $\rho_3(1690)$ and $\omega_3(1670)$.

$(4\pi)^\pm$ MODE

VALUE (MeV)	EVTS	DOCUMENT ID		TECN	CHG	COMMENT

The data in this block is included in the average printed for a previous datablock.

129±10 OUR AVERAGE

123±13		[21] EVANGELIS...	81	OMEG	−	12 $\pi^- p \to p4\pi$
105±30	177	BALTAY	78B	HBC	+	15 $\pi^+ p \to p4\pi$
169^{+70}_{-48}		CASON	73	HBC	−	8,18.5 $\pi^- p$
135±30	144	BARTSCH	70B	HBC	+	8 $\pi^+ p \to N4\pi$
160±30	102	BARTSCH	70B	HBC	+	8 $\pi^+ p \to N2\rho$

• • • We do not use the following data for averages, fits, limits, etc. • • •

230±28		[22] EVANGELIS...	81	OMEG	−	12 $\pi^- p \to p4\pi$
184±33		[23] EVANGELIS...	81	OMEG	−	12 $\pi^- p \to p4\pi$
150	66	[24] KLIGER	74	HBC	−	4.5 $\pi^- p \to p4\pi$
106±25		THOMPSON	74	HBC	+	13 $\pi^+ p$
125^{+83}_{-35}		[24] CASON	73	HBC	−	8,18.5 $\pi^- p$
130±30		HOLMES	72	HBC	+	10–12 $K^+ p$
180±30	90	[24] BARTSCH	70B	HBC	+	8 $\pi^+ p \to N a_2\pi$
100±35		BALTAY	68	HBC	+	7, 8.5 $\pi^+ p$

[21] From $\rho^-\rho^0$ mode, not independent of the other two EVANGELISTA 81 entries.
[22] From $a_2(1320)^-\pi^0$ mode, not independent of the other two EVANGELISTA 81 entries.
[23] From $a_2(1320)^0\pi^-$ mode, not independent of the other two EVANGELISTA 81 entries.
[24] From $\rho^\pm\rho^0$ mode.

$\omega\pi$ MODE

VALUE (MeV)	DOCUMENT ID		TECN	CHG	COMMENT

The data in this block is included in the average printed for a previous datablock.

190±40 OUR AVERAGE

230±65	[25] ALDE	95	GAM2			38 $\pi^- p \to \omega\pi^0 n$
190±65	EVANGELIS...	81	OMEG	−		12 $\pi^- p \to \omega\pi p$
160±56	GESSAROLI	77	HBC			11 $\pi^- p \to \omega\pi p$

• • • We do not use the following data for averages, fits, limits, etc. • • •

89±25	THOMPSON	74	HBC	+		13 $\pi^+ p$
130^{+73}_{-43}	BARNHAM	70	HBC	+		10 $K^+ p \to \omega\pi X$

[25] Supersedes ALDE 92C.

$\eta\pi^+\pi^-$ MODE

(For difficulties with MMS experiments, see the $a_2(1320)$ mini-review in the 1973 edition.)

VALUE (MeV)	DOCUMENT ID		TECN	CHG	COMMENT

The data in this block is included in the average printed for a previous datablock.

126±40 OUR AVERAGE Error includes scale factor of 1.8.

220±30±50	AMELIN	00	VES			37 $\pi^- p \to \eta\pi^+\pi^- n$
106±27	FUKUI	88	SPEC	0		8.95 $\pi^- p \to \eta\pi^+\pi^- n$

• • • We do not use the following data for averages, fits, limits, etc. • • •

195	[26] ANDERSON	69	MMS	−		16 $\pi^- p$ backward
< 21	[26,27] FOCACCI	66	MMS	−		7–12 $\pi^- p \to p$MM
< 30	[26,27] FOCACCI	66	MMS	−		7–12 $\pi^- p \to p$MM
< 38	[26,27] FOCACCI	66	MMS	−		7–12 $\pi^- p \to p$MM

[26] Seen in 2.5–3 GeV/c $\overline{p}p$. $2\pi^+2\pi^-$, with 0, 1, 2 $\pi^+\pi^-$ pairs in ρ^0 band not seen by OREN 74 (2.3 GeV/c $\overline{p}p$) with more statistics. (Jan. 1979)
[27] Not seen by BOWEN 72.

$\rho_3(1690)$ DECAY MODES

	Mode	Fraction (Γ_i/Γ)	Scale factor
Γ_1	4π	(71.1 ± 1.9) %	
Γ_2	$\pi^\pm\pi^+\pi^-\pi^0$	(67 ±22) %	
Γ_3	$\omega\pi$	(16 ± 6) %	
Γ_4	$\pi\pi$	(23.6 ± 1.3) %	
Γ_5	$K\overline{K}\pi$	(3.8 ± 1.2) %	
Γ_6	$K\overline{K}$	(1.58± 0.26) %	1.2
Γ_7	$\eta\pi^+\pi^-$	seen	
Γ_8	$\rho(770)\eta$	seen	
Γ_9	$\pi\pi\rho$	seen	
	Excluding 2ρ and $a_2(1320)\pi$.		
Γ_{10}	$a_2(1320)\pi$	seen	
Γ_{11}	$\rho\rho$	seen	
Γ_{12}	$\phi\pi$		
Γ_{13}	$\eta\pi$		
Γ_{14}	$\pi^\pm 2\pi^+ 2\pi^- \pi^0$		

CONSTRAINED FIT INFORMATION

An overall fit to 5 branching ratios uses 10 measurements and one constraint to determine 4 parameters. The overall fit has a $\chi^2 = 14.7$ for 7 degrees of freedom.

The following *off-diagonal* array elements are the correlation coefficients $\langle \delta x_i \delta x_j \rangle / (\delta x_i \cdot \delta x_j)$, in percent, from the fit to the branching fractions, $x_i \equiv \Gamma_i/\Gamma_{\text{total}}$. The fit constrains the x_i whose labels appear in this array to sum to one.

x_4	−77		
x_5	−74	17	
x_6	−15	2	0
	x_1	x_4	x_5

$\rho_3(1690)$ BRANCHING RATIOS

$\Gamma(\pi\pi)/\Gamma_{\text{total}}$ Γ_4/Γ

VALUE	DOCUMENT ID		TECN	CHG	COMMENT
0.236±0.013 OUR FIT					
0.243±0.013 OUR AVERAGE					
$0.259^{+0.018}_{-0.019}$	BECKER	79	ASPK	0	17 $\pi^- p$ polarized
0.23 ±0.02	CORDEN	79	OMEG		12–15 $\pi^- p \to n2\pi$
0.22 ±0.04	[28] MATTHEWS	71C	HDBC	0	7 $\pi^+ n \to \pi^- p$

• • • We do not use the following data for averages, fits, limits, etc. • • •

Meson Particle Listings

$\rho_3(1690)$

0.245 ± 0.006	[29] ESTABROOKS	75	RVUE		$17\ \pi^- p \rightarrow \pi^+\pi^- n$

[28] One-pion-exchange model used in this estimation.
[29] From phase-shift analysis of HYAMS 75 data.

$\Gamma(\pi\pi)/\Gamma(\pi^\pm\pi^+\pi^-\pi^0)$ Γ_4/Γ_2

VALUE	DOCUMENT ID		TECN	CHG	COMMENT
0.35 ± 0.11	CASON	73	HBC	$-$	8,18.5 $\pi^- p$
• • • We do not use the following data for averages, fits, limits, etc. • • •					
<0.2	HOLMES	72	HBC	$+$	10–12 $K^+ p$
<0.12	BALLAM	71B	HBC	$-$	16 $\pi^- p$

$\Gamma(\pi\pi)/\Gamma(4\pi)$ Γ_4/Γ_1

VALUE	DOCUMENT ID		TECN	CHG	COMMENT
0.332 ± 0.026 OUR FIT Error includes scale factor of 1.1.					
0.30 ± 0.10	BALTAY	78B	HBC	0	15 $\pi^+ p \rightarrow p 4\pi$

$\Gamma(K\overline{K})/\Gamma(\pi\pi)$ Γ_6/Γ_4

VALUE	DOCUMENT ID		TECN	CHG	COMMENT
0.067 ± 0.011 OUR FIT Error includes scale factor of 1.2.					
$0.118^{+0.040}_{-0.032}$ OUR AVERAGE Error includes scale factor of 1.7. See the ideogram below.					
$0.191^{+0.040}_{-0.037}$	GORLICH	80	ASPK	0	17,18 $\pi^- p$ polarized
0.08 ± 0.03	BARTSCH	70B	HBC	$+$	8 $\pi^+ p$
$0.08^{+0.08}_{-0.03}$	CRENNELL	68B	HBC		6.0 $\pi^- p$

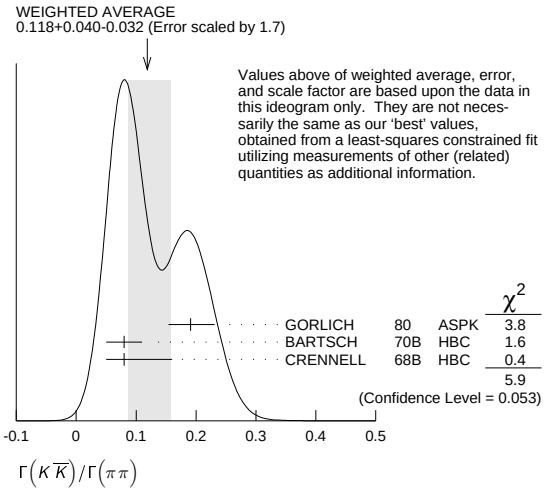

$\Gamma(K\overline{K}\pi)/\Gamma(\pi\pi)$ Γ_5/Γ_4

VALUE	DOCUMENT ID		TECN	CHG	COMMENT
0.16 ± 0.05 OUR FIT					
0.16 ± 0.05	[30] BARTSCH	70B	HBC	$+$	8 $\pi^+ p$

[30] Increased by us to correspond to $B(\rho_3(1690) \rightarrow \pi\pi)$=0.24.

$[\Gamma(\pi\pi\rho) + \Gamma(a_2(1320)\pi) + \Gamma(\rho\rho)]/\Gamma(\pi^\pm\pi^+\pi^-\pi^0)$ $(\Gamma_9+\Gamma_{10}+\Gamma_{11})/\Gamma_2$

VALUE	DOCUMENT ID		TECN	CHG	COMMENT
0.94 ± 0.09 OUR AVERAGE					
0.96 ± 0.21	BALTAY	78B	HBC	$+$	15 $\pi^+ p \rightarrow p 4\pi$
0.88 ± 0.15	BALLAM	71B	HBC	$-$	16 $\pi^- p$
1 ± 0.15	BARTSCH	70B	HBC	$+$	8 $\pi^+ p$
consistent with 1	CASO	68	HBC	$-$	11 $\pi^- p$

$\Gamma(\rho\rho)/\Gamma(\pi^\pm\pi^+\pi^-\pi^0)$ Γ_{11}/Γ_2

VALUE	EVTS	DOCUMENT ID		TECN	CHG	COMMENT
• • • We do not use the following data for averages, fits, limits, etc. • • •						
0.12 ± 0.11		BALTAY	78B	HBC	$+$	15 $\pi^+ p \rightarrow p 4\pi$
0.56	66	KLIGER	74	HBC	$-$	4.5 $\pi^- p \rightarrow p 4\pi$
0.13 ± 0.09		[31] THOMPSON	74	HBC	$+$	13 $\pi^+ p$
0.7 ± 0.15		BARTSCH	70B	HBC	$+$	8 $\pi^+ p$

[31] $\rho\rho$ and $a_2(1320)\pi$ modes are indistinguishable.

$\Gamma(\rho\rho)/[\Gamma(\pi\pi\rho) + \Gamma(a_2(1320)\pi) + \Gamma(\rho\rho)]$ $\Gamma_{11}/(\Gamma_9+\Gamma_{10}+\Gamma_{11})$

VALUE	DOCUMENT ID		TECN	CHG	COMMENT
• • • We do not use the following data for averages, fits, limits, etc. • • •					
0.48 ± 0.16	CASO	68	HBC	$-$	11 $\pi^- p$

$\Gamma(a_2(1320)\pi)/\Gamma(\pi^\pm\pi^+\pi^-\pi^0)$ Γ_{10}/Γ_2

VALUE	DOCUMENT ID		TECN	CHG	COMMENT
• • • We do not use the following data for averages, fits, limits, etc. • • •					
0.66 ± 0.08	BALTAY	78B	HBC	$+$	15 $\pi^+ p \rightarrow p 4\pi$
0.36 ± 0.14	[32] THOMPSON	74	HBC	$+$	13 $\pi^+ p$
not seen	CASON	73	HBC	$-$	8,18.5 $\pi^- p$
0.6 ± 0.15	BARTSCH	70B	HBC	$+$	8 $\pi^+ p$
0.6	BALTAY	68	HBC	$+$	7,8.5 $\pi^+ p$

[32] $\rho\rho$ and $a_2(1320)\pi$ modes are indistinguishable.

$\Gamma(\omega\pi)/\Gamma(\pi^\pm\pi^+\pi^-\pi^0)$ Γ_3/Γ_2

VALUE	CL%	DOCUMENT ID		TECN	CHG	COMMENT
0.23 ± 0.05 OUR AVERAGE Error includes scale factor of 1.2.						
0.33 ± 0.07		THOMPSON	74	HBC	$+$	13 $\pi^+ p$
0.12 ± 0.07		BALLAM	71B	HBC	$-$	16 $\pi^- p$
0.25 ± 0.10		BALTAY	68	HBC	$+$	7,8.5 $\pi^+ p$
0.25 ± 0.10		JOHNSTON	68	HBC	$-$	7.0 $\pi^- p$
• • • We do not use the following data for averages, fits, limits, etc. • • •						
<0.11	95	BALTAY	78B	HBC	$+$	15 $\pi^+ p \rightarrow p 4\pi$
<0.09		KLIGER	74	HBC	$-$	4.5 $\pi^- p \rightarrow p 4\pi$

$\Gamma(\phi\pi)/\Gamma(\pi^\pm\pi^+\pi^-\pi^0)$ Γ_{12}/Γ_2

VALUE	DOCUMENT ID		TECN	CHG	COMMENT
• • • We do not use the following data for averages, fits, limits, etc. • • •					
<0.11	BALTAY	68	HBC	$+$	7,8.5 $\pi^+ p$

$\Gamma(\pi^\pm 2\pi^+ 2\pi^- \pi^0)/\Gamma(\pi^\pm\pi^+\pi^-\pi^0)$ Γ_{14}/Γ_2

VALUE	DOCUMENT ID		TECN	CHG	COMMENT
• • • We do not use the following data for averages, fits, limits, etc. • • •					
<0.15	BALTAY	68	HBC	$+$	7,8.5 $\pi^+ p$

$\Gamma(\eta\pi)/\Gamma(\pi^\pm\pi^+\pi^-\pi^0)$ Γ_{13}/Γ_2

VALUE	DOCUMENT ID		TECN	CHG	COMMENT
• • • We do not use the following data for averages, fits, limits, etc. • • •					
<0.02	THOMPSON	74	HBC	$+$	13 $\pi^+ p$

$\Gamma(K\overline{K})/\Gamma_{\text{total}}$ Γ_6/Γ

VALUE	DOCUMENT ID		TECN	CHG	COMMENT
0.0158 ± 0.0026 OUR FIT Error includes scale factor of 1.2.					
0.0130 ± 0.0024 OUR AVERAGE					
0.013 ± 0.003	COSTA...	80	OMEG	0	10 $\pi^- p \rightarrow K^+ K^- n$
0.013 ± 0.004	[33] MARTIN	78B	SPEC	$-$	10 $\pi p \rightarrow K^0_S K^- p$

[33] From $(\Gamma_4\Gamma_6)^{1/2} = 0.056 \pm 0.034$ assuming $B(\rho_3(1690) \rightarrow \pi\pi) = 0.24$.

$\Gamma(\omega\pi)/[\Gamma(\omega\pi) + \Gamma(\rho\rho)]$ $\Gamma_3/(\Gamma_3+\Gamma_{11})$

VALUE	DOCUMENT ID		TECN	CHG	COMMENT
• • • We do not use the following data for averages, fits, limits, etc. • • •					
0.22 ± 0.08	CASON	73	HBC	$-$	8,18.5 $\pi^- p$

$\Gamma(\eta\pi^+\pi^-)/\Gamma_{\text{total}}$ Γ_7/Γ

VALUE	DOCUMENT ID		TECN	COMMENT
seen	FUKUI	88	SPEC	8.95 $\pi^- p \rightarrow \eta\pi^+\pi^- n$

$\Gamma(a_2(1320)\pi)/\Gamma(\rho(770)\eta)$ Γ_{10}/Γ_8

VALUE	DOCUMENT ID		TECN	COMMENT
5.5 ± 2.0	AMELIN	00	VES	37 $\pi^- p \rightarrow \eta\pi^+\pi^- n$

$\rho_3(1690)$ REFERENCES

AMELIN	00	NP A668 83	D. Amelin *et al.* (VES Collab.)
ALDE	95	ZPHY C66 379	D.M. Alde *et al.* (GAMS Collab.) JP
ALDE	92C	ZPHY C54 553	D.M. Alde *et al.* (BELG, SERP, KEK, LANL+)
FUKUI	88	PL B202 441	S. Fukui *et al.* (SUGI, NAGO, KEK, KYOT+)
DENNEY	83	PR D28 2726	D.L. Denney *et al.* (IOWA, MICH)
EVANGELIS...	81	NP B178 197	C. Evangelista *et al.* (BARI, BONN, CERN+)
ALPER	80	PL 94B 422	B. Alper *et al.* (AMST, CERN, CRAC, MPIM+)
COSTA...	80	NP B175 402	G. Costa de Beauregard *et al.* (BARI, BONN+)
GORLICH	80	NP B174 16	L. Gorlich *et al.* (CRAC, MPIM, CERN+)
BECKER	79	NP B151 46	H. Becker *et al.* (MPIM, CERN, ZEEM, CRAC)
CORDEN	79	NP B157 250	M.J. Corden *et al.* (BIRM, RHEL, TELA+) JP
BALTAY	78B	PR D17 62	C. Baltay *et al.* (COLU, BING)
MARTIN	78B	NP B140 158	A.D. Martin *et al.* (DURH, GEVA)
MARTIN	78D	PL 74B 417	A.D. Martin *et al.* (DURH, GEVA)
ANTIPOV	77	NP B119 45	Y.M. Antipov *et al.* (SERP, GEVA)
GESSAROLI	77	NP B126 382	R. Gessaroli *et al.* (BGNA, FIRZ, GENO+)
BLUM	75	PL 57B 403	W. Blum *et al.* (CERN, MPIM) JP
ESTABROOKS	75	NP B95 322	P.G. Estabrooks, A.D. Martin (DURH)
HYAMS	75	NP B100 205	B.D. Hyams *et al.* (CERN, MPIM)
ENGLER	74	PR D10 2070	A. Engler *et al.* (CMU, CASE)
GRAYER	74	NP B75 189	G. Grayer *et al.* (CERN, MPIM)
KLIGER	74	SJNP 19 428	G.K. Kliger *et al.* (ITEP)

Translated from YAF 19 839.

OREN	74	NP B71 189	Y. Oren *et al.*	(ANL, OXF)
THOMPSON	74	NP B69 220	G. Thompson *et al.*	(PURD)
CASON	73	PR D7 1971	N.M. Cason *et al.*	(NDAM)
BOWEN	72	PRL 29 890	D.R. Bowen *et al.*	(NEAS, STON)
HOLMES	72	PR D6 3336	R. Holmes *et al.*	(ROCH)
BALLAM	71B	PR D3 2606	J. Ballam *et al.*	(SLAC)
MATTHEWS	71C	NP B33 1	J.A.J. Matthews *et al.*	(TNTO, WISC) JP
ARMENISE	70	LNC 4 199	N. Armenise *et al.*	(BARI, BGNA, FIRZ)
BARNHAM	70	PRL 24 1083	K.W.J. Barnham *et al.*	(BIRM)
BARTSCH	70B	NP B22 109	J. Bartsch *et al.*	(AACH, BERL, CERN)
CASO	70	LNC 3 707	C. Caso *et al.*	(GENO, HAMB, MILA, SACL)
STUNTEBECK	70	PL 32B 391	P.H. Stuntebeck *et al.*	(NDAM)
ADERHOLZ	69	NP B11 259	M. Aderholz *et al.*	(AACH3, BERL, CERN+)
ANDERSON	69	PRL 22 1390	E.W. Anderson *et al.*	(BNL, CMU)
ARMENISE	68	NC 54A 999	N. Armenise *et al.*	(BARI, BGNA, FIRZ+) I
BALTAY	68	PRL 20 887	C. Baltay *et al.*	(COLU, ROCH, RUTG, YALE) I
CASO	68	NC 54A 983	C. Caso *et al.*	(GENO, HAMB, MILA, SACL)
CRENNELL	68B	PL 28B 136	D.J. Crennell *et al.*	(BNL)
JOHNSTON	68	PRL 20 1414	T.F. Johnston *et al.*	(TNTO, WISC) IJP
FOCACCI	66	PRL 17 890	M.N. Focacci *et al.*	(CERN)
GOLDBERG	65	PL 17 354	M. Goldberg *et al.*	(CERN, EPOL, ORSAY+)

$\rho(1700)$

$I^G(J^{PC}) = 1^+(1^{--})$

THE $\rho(1450)$ AND THE $\rho(1700)$

Updated May 2010 by S. Eidelman (Novosibirsk) and G. Venanzoni (Frascati).

In our 1988 edition, we replaced the $\rho(1600)$ entry with two new ones, the $\rho(1450)$ and the $\rho(1700)$, because there was emerging evidence that the 1600-MeV region actually contains two ρ-like resonances. Erkal [1] had pointed out this possibility with a theoretical analysis on the consistency of 2π and 4π electromagnetic form factors and the $\pi\pi$ scattering length. Donnachie [2], with a full analysis of data on the 2π and 4π final states in e^+e^- annihilation and photoproduction reactions, had also argued that in order to obtain a consistent picture, two resonances were necessary. The existence of $\rho(1450)$ was supported by the analysis of $\eta\rho^0$ mass spectra obtained in photoproduction and e^+e^- annihilation [3], as well as that of $e^+e^- \to \omega\pi$ [4].

The analysis of [2] was further extended by [5,6] to include new data on 4π-systems produced in e^+e^- annihilation, and in τ-decays (τ decays to 4π, and e^+e^- annihilation to 4π can be related by the Conserved Vector Current assumption). These systems were successfully analyzed using interfering contributions from two ρ-like states, and from the tail of the $\rho(770)$ decaying into two-body states. While specific conclusions on $\rho(1450) \to 4\pi$ were obtained, little could be said about the $\rho(1700)$.

Independent evidence for two 1^- states is provided by [7] in 4π electroproduction at $\langle Q^2\rangle = 1$ (GeV/c)^2, and by [8] in a high-statistics sample of the $\eta\pi\pi$ system in π^-p charge exchange.

This scenario with two overlapping resonances is supported by other data. Bisello [9] measured the pion form factor in the interval 1.35–2.4 GeV, and observed a deep minimum around 1.6 GeV. The best fit was obtained with the hypothesis of ρ-like resonances at 1420 and 1770 MeV, with widths of about 250 MeV. Antonelli [10] found that the $e^+e^- \to \eta\pi^+\pi^-$ cross section is better fitted with two fully interfering Breit-Wigners, with parameters in fair agreement with those of [2] and [9]. These results can be considered as a confirmation of the $\rho(1450)$.

Decisive evidence for the $\pi\pi$ decay mode of both $\rho(1450)$ and $\rho(1700)$ comes from $\overline{p}p$ annihilation at rest [11]. It has been shown that these resonances also possess a $K\overline{K}$ decay mode [12–14]. High-statistics studies of the decays $\tau \to \pi\pi\nu_\tau$ [15,16], and $\tau \to 4\pi\nu_\tau$ [17] also require the $\rho(1450)$, but are not sensitive to the $\rho(1700)$, because it is too close to the τ mass. A recent very-high-statistics study of the $\tau \to \pi\pi\nu_\tau$ decay performed at Belle [18] reports the first observation of both $\rho(1450)$ and $\rho(1700)$ in τ decays.

The structure of these ρ states is not yet completely clear. Barnes [19] and Close [20] claim that $\rho(1450)$ has a mass consistent with radial $2S$, but its decays show characteristics of hybrids, and suggest that this state may be a $2S$-hybrid mixture. Donnachie [21] argues that hybrid states could have a 4π decay mode dominated by the $a_1\pi$. Such behavior has been observed by [22] in $e^+e^- \to 4\pi$ in the energy range 1.05–1.38 GeV, and by [17] in $\tau \to 4\pi$ decays. Alexander [23] observes the $\rho(1450) \to \omega\pi$ decay mode in B-meson decays, however, does not find $\rho(1700) \to \omega\pi^0$. A similar conclusion is made by [24], who studied the process $e^+e^- \to \omega\pi^0$. Various decay modes of the $\rho(1450)$ and $\rho(1700)$ are observed in $\overline{p}n$ and $\overline{p}p$ annihilation [25,26], but no definite conclusions can be drawn. More data should be collected to clarify the nature of the ρ states, particularly in the energy range above 1.6 GeV.

We now list under a separate entry the $\rho(1570)$, the $\phi\pi$ state with $J^{PC} = 1^{--}$ earlier observed by [27] (referred to as $C(1480)$) and recently confirmed by [28]. While [29] shows that it may be a threshold effect, [5] and [30] suggest two independent vector states with this decay mode. The $C(1480)$ has not been seen in the $\overline{p}p$ [31] and e^+e^- [32,33] experiments. However, the sensitivity of the two latter is an order of magnitude lower than that of [28]. Note that [28] can not exclude that their observation is due to an OZI-suppressed decay mode of the $\rho(1700)$.

Several observations on the $\omega\pi$ system in the 1200-MeV region [34–40] may be interpreted in terms of either $J^P = 1^-$ $\rho(770) \to \omega\pi$ production [41], or $J^P = 1^+$ $b_1(1235)$ production [39,40]. We argue that no special entry for a $\rho(1250)$ is needed. The LASS amplitude analysis [42] showing evidence for $\rho(1270)$ is preliminary and needs confirmation. For completeness, the relevant observations are listed under the $\rho(1450)$.

Recently [43] reported a very broad 1^{--} resonance-like K^+K^- state in $J/\psi \to K^+K^-\pi^0$ decays. Its pole position corresponds to mass of 1576 MeV and width of 818 MeV. [44–46] suggest its exotic structure (molecular or multiquark), while [47] and [48] explain it by the interference between the $\rho(1450)$ and $\rho(1700)$. We quote [43] as $X(1575)$ in the section "Further States."

Evidence for ρ-like mesons decaying into 6π states was first noted by [49] in the analysis of 6π mass spectra from e^+e^- annihilation [50,51] and diffractive photoproduction [52]. Clegg [49] argued that two states at about 2.1 and 1.8 GeV exist: while the former is a candidate for the $\rho(2150)$, the latter could be a manifestation of the $\rho(1700)$ distorted by threshold effects. BaBar reported observations of the new decay modes of the $\rho(2150)$ in the channels $\eta'(958)\pi^+\pi^-$ and $f_1(1285)\pi^+\pi^-$

[53]. The relativistic quark model [54] predicts the 2^3D_1 state with $J^{PC} = 1^{--}$ at 2.15 GeV which can be identified with the $\rho(2150)$.

The E687 Collaboration at Fermilab reported an observation of a narrow-dip structure at 1.9 GeV in the $3\pi^+3\pi^-$ diffractive photoproduction [55]. A similar effect of the dip in the cross section of $e^+e^- \to 6\pi$ around 1.9 GeV has been earlier reported by DM2 [51], where 6π included both $3\pi^+3\pi^-$ and $2\pi^+2\pi^-2\pi^0$. Later the dip in the R value (the total cross section of $e^+e^- \to$ hadrons divided by the cross section of $e^+e^- \to \mu^+\mu^-$) was observed by [56], again around 1.9 GeV. This energy is close to the $N\overline{N}$ threshold, which hints at the possible relation between the dip and $N\overline{N}$, *e.g.*, the frequently discussed narrow $N\overline{N}$ resonance or just a threshold effect. Such behaviour is also characteristic of exotic objects like vector $q\overline{q}$ hybrids. Note that [57] failed to find this state in the reaction $\overline{n}p \to 3\pi^+2\pi^-\pi^0$. A reanalysis of the E687 data by [58] shows that a dip may arise due to interference of a narrow object with a broad $\rho(1700)$ independently of the nature of the former. BaBar studied the processes $e^+e^- \to 3\pi^+3\pi^-$ and $e^+e^- \to 2\pi^+2\pi^-2\pi^0$ using the radiative return, and observed a structure around 1.9 GeV in both final states [59]. The data are not well described by a single Breit-Wigner state, and a good fit is achieved while taking into account the interference of such a structure with a Jacob-Slansky amplitude for continuum. The mass of this state obtained by BaBar is consistent with [56] and [55], but the width is substantially larger. Recently [28] observed a structure at 1.9 GeV in the radiative return to the $\phi\pi$ final state, with a much smaller width of 48 ± 17 MeV consistent with that of [56,58]. We list these observations under a separate particle $\rho(1900)$, which needs confirmation.

References

1. C. Erkal, Z. Phys. **C31**, 615 (1986).
2. A. Donnachie and H. Mirzaie, Z. Phys. **C33**, 407 (1987).
3. A. Donnachie and A.B. Clegg, Z. Phys. **C34**, 257 (1987).
4. A. Donnachie and A.B. Clegg, Z. Phys. **C51**, 689 (1991).
5. A.B. Clegg and A. Donnachie, Z. Phys. **C40**, 313 (1988).
6. A.B. Clegg and A. Donnachie, Z. Phys. **C62**, 455 (1994).
7. T.J. Killian *et al.*, Phys. Rev. **D21**, 3005 (1980).
8. S. Fukui *et al.*, Phys. Lett. **B202**, 441 (1988).
9. D. Bisello *et al.*, Phys. Lett. **B220**, 321 (1989).
10. A. Antonelli *et al.*, Phys. Lett. **B212**, 133 (1988).
11. A. Abele *et al.*, Phys. Lett. **B391**, 191 (1997).
12. A. Abele *et al.*, Phys. Rev. **D57**, 3860 (1998).
13. A. Bertin *et al.*, Phys. Lett. **B434**, 180 (1998).
14. A. Abele *et al.*, Phys. Lett. **B468**, 178 (1999).
15. R. Barate *et al.*, Z. Phys. **C76**, 15 (1997).
16. S. Anderson, Phys. Rev. **D61**, 112002 (2000).
17. K.W. Edwards *et al.*, Phys. Rev. **D61**, 072003 (2000).
18. M. Fujikawa *et al.*, Phys. Rev. **D78**, 072006 (2008).
19. T. Barnes *et al.*, Phys. Rev. **D55**, 4157 (1997).
20. F.E. Close *et al.*, Phys. Rev. **D56**, 1584 (1997).
21. A. Donnachie and Yu.S. Kalashnikova, Phys. Rev. **D60**, 114011 (1999).
22. R.R. Akhmetshin *et al.*, Phys. Lett. **B466**, 392 (1999).
23. J.P. Alexander *et al.*, Phys. Rev. **D64**, 092001 (2001).
24. R.R. Akhmetshin *et al.*, Phys. Lett. **B562**, 173 (2003).
25. A. Abele *et al.*, Eur. Phys. J. **C21**, 261 (2001).
26. M. Bargiotti *et al.*, Phys. Lett. **B561**, 233 (2003).
27. S.I. Bityukov *et al.*, Phys. Lett. **B188**, 383 (1987).
28. B. Aubert *et al.*, Phys. Rev. **D77**, 092002 (2008).
29. N.N. Achasov and G.N. Shestakov, Phys. Atom. Nucl. **59**, 1262 (1996).
30. L.G. Landsberg, Sov. J. Nucl. Phys. **55**, 1051 (1992).
31. A. Abele *et al.*, Phys. Lett. **B415**, 280 (1997).
32. V.M. Aulchenko *et al.*, Sov. Phys. JETP Lett. **45**, 145 (1987).
33. D. Bisello *et al.*, Z. Phys. **C52**, 227 (1991).
34. P. Frenkiel *et al.*, Nucl. Phys. **B47**, 61 (1972).
35. G. Cosme *et al.*, Phys. Lett. **B63**, 352 (1976).
36. D.P. Barber *et al.*, Z. Phys. **C4**, 169 (1980).
37. D. Aston, Phys. Lett. **B92**, 211 (1980).
38. M. Atkinson *et al.*, Nucl. Phys. **B243**, 1 (1984).
39. J.E. Brau *et al.*, Phys. Rev. **D37**, 2379 (1988).
40. C. Amsler *et al.*, Phys. Lett. **B311**, 362 (1993).
41. J. Layssac and F.M. Renard, Nuovo Cimento **6A**, 134 (1971).
42. D. Aston *et al.*, Nucl. Phys. (Proc. Supp.) **B21**, 105 (1991).
43. M. Ablikim *et al.*, Phys. Rev. Lett. **97**, 142002 (2006).
44. G.-J. Ding and M.-L. Yan, Phys. Lett. **B643**, 33 (2006).
45. F.K. Guo *et al.*, Nucl. Phys. **A773**, 78 (2006).
46. A. Zhang *et al.*, Phys. Rev. **D76**, 036004 (2007).
47. B.A. Li, Phys. Rev. **D76**, 094016 (2007).
48. X. Liu *et al.*, Phys. Rev. **D75**, 074017 (2007).
49. A.B. Clegg and A. Donnachie, Z. Phys. **C45**, 677 (1990).
50. D. Bisello *et al.*, Phys. Lett. **107B**, 145 (1981).
51. A. Castro *et al.*, LAL-88-58(1988).
52. M. Atkinson *et al.*, Z. Phys. **C29**, 333 (1985).
53. B. Aubert *et al.*, Phys. Rev. **D76**, 092005 (2007).
54. S. Godfrey and N. Isgur, Phys. Rev. **D32**, 189 (1985).
55. P.L. Frabetti *et al.*, Phys. Lett. **B514**, 240 (2001).
56. A. Antonelli *et al.*, Phys. Lett. **B365**, 427 (1996).
57. M. Agnello *et al.*, Phys. Lett. **B527**, 39 (2002).
58. P.L. Frabetti *et al.*, Phys. Lett. **B578**, 290 (2004).
59. B. Aubert *et al.*, Phys. Rev. **D73**, 052003 (2006).

$\rho(1700)$ MASS

$\eta\rho^0$ AND $\pi^+\pi^-$ MODES

VALUE (MeV)	DOCUMENT ID
1720±20 OUR ESTIMATE	

$\eta\rho^0$ MODE

VALUE (MeV)	DOCUMENT ID		TECN	COMMENT

The data in this block is included in the average printed for a previous datablock.

• • • We do not use the following data for averages, fits, limits, etc. • • •

1740±20		ANTONELLI	88	DM2	$e^+e^- \to \eta\pi^+\pi^-$
1701±15	[1]	FUKUI	88	SPEC	8.95 $\pi^-p \to \eta\pi^+\pi^-n$

[1] Assuming $\rho^+ f_0(1370)$ decay mode interferes with $a_1(1260)^+\pi$ background. From a two Breit-Wigner fit.

$\pi\pi$ MODE

VALUE (MeV)	EVTS	DOCUMENT ID		TECN	COMMENT
The data in this block is included in the average printed for a previous datablock.					
• • • We do not use the following data for averages, fits, limits, etc. • • •					
1780 ±20 $^{+15}_{-20}$	63.5k	[2] ABRAMOWICZ12		ZEUS	$ep \to e\pi^+\pi^- p$
1861 ±17		[3] LEES	12G	BABR	$e^+e^- \to \pi^+\pi^-\gamma$
1728 ±17 ±89	5.4M	[4,5] FUJIKAWA	08	BELL	$\tau^- \to \pi^-\pi^0\nu_\tau$
1780 $^{+37}_{-29}$		[6] ABELE	97	CBAR	$\overline{p}n \to \pi^-\pi^0\pi^0$
1719 ±15		[6] BERTIN	97C	OBLX	$0.0\ \overline{p}p \to \pi^+\pi^-\pi^0$
1730 ±30		CLEGG	94	RVUE	$e^+e^- \to \pi^+\pi^-$
1768 ±21		BISELLO	89	DM2	$e^+e^- \to \pi^+\pi^-$
1745.7±91.9		DUBNICKA	89	RVUE	$e^+e^- \to \pi^+\pi^-$
1546 ±26		GESHKEN...	89	RVUE	
1650		[7] ERKAL	85	RVUE	20–$70\ \gamma p \to \gamma\pi$
1550 ±70		ABE	84B	HYBR	$20\ \gamma p \to \pi^+\pi^- p$
1590 ±20		[8] ASTON	80	OMEG	20–$70\ \gamma p \to p2\pi$
1600 ±10		[9] ATIYA	79B	SPEC	$50\ \gamma C \to C2\pi$
1598 $^{+24}_{-22}$		BECKER	79	ASPK	$17\ \pi^- p$ polarized
1659 ±25		[7] LANG	79	RVUE	
1575		[7] MARTIN	78C	RVUE	$17\ \pi^- p \to \pi^+\pi^- n$
1610 ±30		[7] FROGGATT	77	RVUE	$17\ \pi^- p \to \pi^+\pi^- n$
1590 ±20		[10] HYAMS	73	ASPK	$17\ \pi^- p \to \pi^+\pi^- n$

[2] Using the KUHN 90 parametrization of the pion form factor, neglecting ρ–ω interference.
[3] Using the GOUNARIS 68 parametrization of the pion form factor leaving the masses and widths of the $\rho(1450)$, $\rho(1700)$, and $\rho(2150)$ resonances as free parameters of the fit.
[4] $|F_\pi(0)|^2$ fixed to 1.
[5] From the GOUNARIS 68 parametrization of the pion form factor.
[6] T-matrix pole.
[7] From phase shift analysis of HYAMS 73 data.
[8] Simple relativistic Breit-Wigner fit with constant width.
[9] An additional 40 MeV uncertainty in both the mass and width is present due to the choice of the background shape.
[10] Included in BECKER 79 analysis.

$\pi\omega$ MODE

VALUE (MeV)	EVTS	DOCUMENT ID		TECN	COMMENT
• • • We do not use the following data for averages, fits, limits, etc. • • •					
1708±41	7815	[11] ACHASOV	13	SND	1.05–$2.00\ e^+e^- \to \pi^0\pi^0\gamma$
1550 to 1620		[12] ACHASOV	00I	SND	$e^+e^- \to \pi^0\pi^0\gamma$
1580 to 1710		[13] ACHASOV	00I	SND	$e^+e^- \to \pi^0\pi^0\gamma$
1710±90		ACHASOV	97	RVUE	$e^+e^- \to \omega\pi^0$

[11] From a phenomenological model based on vector meson dominance with the interfering $\rho(1450)$ and $\rho(1700)$ and their widths fixed at 400 and 250 MeV, respectively. Systematic uncertainty not estimated.
[12] Taking into account both $\rho(1450)$ and $\rho(1700)$ contributions. Using the data of ACHASOV 00I on $e^+e^- \to \omega\pi^0$ and of EDWARDS 00A on $\tau^- \to \omega\pi^-\nu_\tau$. $\rho(1450)$ mass and width fixed at 1400 MeV and 500 MeV respectively.
[13] Taking into account the $\rho(1700)$ contribution only. Using the data of ACHASOV 00I on $e^+e^- \to \omega\pi^0$ and of EDWARDS 00A on $\tau^- \to \omega\pi^-\nu_\tau$.

$K\overline{K}$ MODE

VALUE (MeV)	EVTS	DOCUMENT ID		TECN	CHG	COMMENT
• • • We do not use the following data for averages, fits, limits, etc. • • •						
1740.8±22.2	27k	[14] ABELE	99D	CBAR	±	$0.0\ \overline{p}p \to K^+K^-\pi^0$
1582 ±36	1600	CLELAND	82B	SPEC	±	$50\ \pi p \to K^0_S K^\pm p$

[14] K-matrix pole. Isospin not determined, could be $\omega(1650)$ or $\phi(1680)$.

$2\ (\pi^+\pi^-)$ MODE

VALUE (MeV)	EVTS	DOCUMENT ID		TECN	COMMENT
• • • We do not use the following data for averages, fits, limits, etc. • • •					
1851 $^{+27}_{-24}$		ACHASOV	97	RVUE	$e^+e^- \to 2(\pi^+\pi^-)$
1570± 20		[15] CORDIER	82	DM1	$e^+e^- \to 2(\pi^+\pi^-)$
1520± 30		[16] ASTON	81E	OMEG	20–$70\ \gamma p \to p4\pi$
1654± 25		[17] DIBIANCA	81	DBC	$\pi^+ d \to pp2(\pi^+\pi^-)$
1666± 39		[15] BACCI	80	FRAG	$e^+e^- \to 2(\pi^+\pi^-)$
1780	34	KILLIAN	80	SPEC	$11\ e^- p \to 2(\pi^+\pi^-)$
1500		[18] ATIYA	79B	SPEC	$50\ \gamma C \to C4\pi^\pm$
1570± 60	65	[19] ALEXANDER	75	HBC	$7.5\ \gamma p \to p4\pi$
1550± 60		[16] CONVERSI	74	OSPK	$e^+e^- \to 2(\pi^+\pi^-)$
1550± 50	160	SCHACHT	74	STRC	5.5–$9\ \gamma p \to p4\pi$
1450±100	340	SCHACHT	74	STRC	9–$18\ \gamma p \to p4\pi$
1430± 50	400	BINGHAM	72B	HBC	$9.3\ \gamma p \to p4\pi$

[15] Simple relativistic Breit-Wigner fit with model dependent width.
[16] Simple relativistic Breit-Wigner fit with constant width.
[17] One peak fit result.
[18] Parameters roughly estimated, not from a fit.
[19] Skew mass distribution compensated by Ross-Stodolsky factor.

$\pi^+\pi^-\pi^0\pi^0$ MODE

VALUE (MeV)	DOCUMENT ID		TECN	COMMENT
• • • We do not use the following data for averages, fits, limits, etc. • • •				
1660±30	ATKINSON	85B	OMEG	20–$70\ \gamma p$

$3(\pi^+\pi^-)$ AND $2(\pi^+\pi^-\pi^0)$ MODES

VALUE (MeV)	DOCUMENT ID		TECN	COMMENT
• • • We do not use the following data for averages, fits, limits, etc. • • •				
1730±34	[20] FRABETTI	04	E687	$\gamma p \to 3\pi^+ 3\pi^- p$
1783±15	CLEGG	90	RVUE	$e^+e^- \to 3(\pi^+\pi^-)2(\pi^+\pi^-\pi^0)$

[20] From a fit with two resonances with the JACOB 72 continuum.

$\rho(1700)$ WIDTH

$\eta\rho^0$ AND $\pi^+\pi^-$ MODES

VALUE (MeV)	DOCUMENT ID
250±100 OUR ESTIMATE	

$\eta\rho^0$ MODE

VALUE (MeV)	DOCUMENT ID		TECN	COMMENT
The data in this block is included in the average printed for a previous datablock.				
• • • We do not use the following data for averages, fits, limits, etc. • • •				
150±30	ANTONELLI	88	DM2	$e^+e^- \to \eta\pi^+\pi^-$
282±44	[21] FUKUI	88	SPEC	$8.95\ \pi^- p \to \eta\pi^+\pi^- n$

[21] Assuming $\rho^+ f_0(1370)$ decay mode interferes with $a_1(1260)^+\pi$ background. From a two Breit-Wigner fit.

$\pi\pi$ MODE

VALUE (MeV)	EVTS	DOCUMENT ID		TECN	COMMENT
The data in this block is included in the average printed for a previous datablock.					
• • • We do not use the following data for averages, fits, limits, etc. • • •					
310 ± 30 $^{+25}_{-35}$	63.5k	[22] ABRAMOWICZ12		ZEUS	$ep \to e\pi^+\pi^- p$
316 ± 26		[23] LEES	12G	BABR	$e^+e^- \to \pi^+\pi^-\gamma$
164 ± 21 $^{+89}_{-26}$	5.4M	[24,25] FUJIKAWA	08	BELL	$\tau^- \to \pi^-\pi^0\nu_\tau$
275 ± 45		[26] ABELE	97	CBAR	$\overline{p}n \to \pi^-\pi^0\pi^0$
310 ± 40		[26] BERTIN	97C	OBLX	$0.0\ \overline{p}p \to \pi^+\pi^-\pi^0$
400 ±100		CLEGG	94	RVUE	$e^+e^- \to \pi^+\pi^-$
224 ± 22		BISELLO	89	DM2	$e^+e^- \to \pi^+\pi^-$
242.5±163.0		DUBNICKA	89	RVUE	$e^+e^- \to \pi^+\pi^-$
620 ± 60		GESHKEN...	89	RVUE	
<315		[27] ERKAL	85	RVUE	20–$70\ \gamma p \to \gamma\pi$
280 $^{+30}_{-80}$		ABE	84B	HYBR	$20\ \gamma p \to \pi^+\pi^- p$
230 ± 80		[28] ASTON	80	OMEG	20–$70\ \gamma p \to p2\pi$
283 ± 14		[29] ATIYA	79B	SPEC	$50\ \gamma C \to C2\pi$
175 $^{+98}_{-53}$		BECKER	79	ASPK	$17\ \pi^- p$ polarized
232 ± 34		[27] LANG	79	RVUE	
340		[27] MARTIN	78C	RVUE	$17\ \pi^- p \to \pi^+\pi^- n$
300 ±100		[27] FROGGATT	77	RVUE	$17\ \pi^- p \to \pi^+\pi^- n$
180 ± 50		[30] HYAMS	73	ASPK	$17\ \pi^- p \to \pi^+\pi^- n$

[22] Using the KUHN 90 parametrization of the pion form factor, neglecting ρ–ω interference.
[23] Using the GOUNARIS 68 parametrization of the pion form factor leaving the masses and widths of the $\rho(1450)$, $\rho(1700)$, and $\rho(2150)$ resonances as free parameters of the fit.
[24] $|F_\pi(0)|^2$ fixed to 1.
[25] From the GOUNARIS 68 parametrization of the pion form factor.
[26] T-matrix pole.
[27] From phase shift analysis of HYAMS 73 data.
[28] Simple relativistic Breit-Wigner fit with constant width.
[29] An additional 40 MeV uncertainty in both the mass and width is present due to the choice of the background shape.
[30] Included in BECKER 79 analysis.

$K\overline{K}$ MODE

VALUE (MeV)	EVTS	DOCUMENT ID		TECN	CHG	COMMENT
• • • We do not use the following data for averages, fits, limits, etc. • • •						
187.2± 26.7	27k	[31] ABELE	99D	CBAR	±	$0.0\ \overline{p}p \to K^+K^-\pi^0$
265 ±120	1600	CLELAND	82B	SPEC	±	$50\ \pi p \to K^0_S K^\pm p$

[31] K-matrix pole. Isospin not determined, could be $\omega(1650)$ or $\phi(1680)$.

$2\ (\pi^+\pi^-)$ MODE

VALUE (MeV)	EVTS	DOCUMENT ID		TECN	COMMENT
• • • We do not use the following data for averages, fits, limits, etc. • • •					
510± 40		[32] CORDIER	82	DM1	$e^+e^- \to 2(\pi^+\pi^-)$
400± 50		[33] ASTON	81E	OMEG	20–$70\ \gamma p \to p4\pi$
400±146		[34] DIBIANCA	81	DBC	$\pi^+ d \to pp2(\pi^+\pi^-)$
700±160		[32] BACCI	80	FRAG	$e^+e^- \to 2(\pi^+\pi^-)$
100	34	KILLIAN	80	SPEC	$11\ e^- p \to 2(\pi^+\pi^-)$
600		[35] ATIYA	79B	SPEC	$50\ \gamma C \to C4\pi^\pm$
340±160	65	[36] ALEXANDER	75	HBC	$7.5\ \gamma p \to p4\pi$
360±100		[33] CONVERSI	74	OSPK	$e^+e^- \to 2(\pi^+\pi^-)$
400±120	160	[37] SCHACHT	74	STRC	5.5–$9\ \gamma p \to p4\pi$
850±200	340	[37] SCHACHT	74	STRC	9–$18\ \gamma p \to p4\pi$
650±100	400	BINGHAM	72B	HBC	$9.3\ \gamma p \to p4\pi$

[32] Simple relativistic Breit-Wigner fit with model-dependent width.
[33] Simple relativistic Breit-Wigner fit with constant width.
[34] One peak fit result.
[35] Parameters roughly estimated, not from a fit.
[36] Skew mass distribution compensated by Ross-Stodolsky factor.
[37] Width errors enlarged by us to $4\Gamma/\sqrt{N}$; see the note with the $K^*(892)$ mass.

Meson Particle Listings

$\rho(1700)$

$\pi^+\pi^-\pi^0\pi^0$ MODE

VALUE (MeV)	DOCUMENT ID		TECN	COMMENT
• • • We do not use the following data for averages, fits, limits, etc. • • •				
300±50	ATKINSON	85B	OMEG	20–70 γp

$\omega\pi^0$ MODE

VALUE (MeV)	DOCUMENT ID		TECN	COMMENT
• • • We do not use the following data for averages, fits, limits, etc. • • •				
350 to 580	[38] ACHASOV	00I	SND	$e^+e^- \to \pi^0\pi^0\gamma$
490 to 1040	[39] ACHASOV	00I	SND	$e^+e^- \to \pi^0\pi^0\gamma$

[38] Taking into account both $\rho(1450)$ and $\rho(1700)$ contributions. Using the data of ACHASOV 00I on $e^+e^- \to \omega\pi^0$ and of EDWARDS 00A on $\tau^- \to \omega\pi^-\nu_\tau$. $\rho(1450)$ mass and width fixed at 1400 MeV and 500 MeV respectively.

[39] Taking into account the $\rho(1700)$ contribution only. Using the data of ACHASOV 00I on $e^+e^- \to \omega\pi^0$ and of EDWARDS 00A on $\tau^- \to \omega\pi^-\nu_\tau$.

$3(\pi^+\pi^-)$ AND $2(\pi^+\pi^-\pi^0)$ MODES

VALUE (MeV)	DOCUMENT ID		TECN	COMMENT
• • • We do not use the following data for averages, fits, limits, etc. • • •				
315±100	[40] FRABETTI	04	E687	$\gamma p \to 3\pi^+ 3\pi^- p$
285± 20	CLEGG	90	RVUE	$e^+e^- \to 3(\pi^+\pi^-)2(\pi^+\pi^-\pi^0)$

[40] From a fit with two resonances with the JACOB 72 continuum.

$\rho(1700)$ DECAY MODES

	Mode	Fraction (Γ_i/Γ)
Γ_1	4π	
Γ_2	$2(\pi^+\pi^-)$	large
Γ_3	$\rho\pi\pi$	dominant
Γ_4	$\rho^0\pi^+\pi^-$	large
Γ_5	$\rho^0\pi^0\pi^0$	
Γ_6	$\rho^\pm\pi^\mp\pi^0$	large
Γ_7	$a_1(1260)\pi$	seen
Γ_8	$h_1(1170)\pi$	seen
Γ_9	$\pi(1300)\pi$	seen
Γ_{10}	$\rho\rho$	seen
Γ_{11}	$\pi^+\pi^-$	seen
Γ_{12}	$\pi\pi$	seen
Γ_{13}	$K\overline{K}^*(892)$ + c.c.	seen
Γ_{14}	$\eta\rho$	seen
Γ_{15}	$a_2(1320)\pi$	not seen
Γ_{16}	$K\overline{K}$	seen
Γ_{17}	e^+e^-	seen
Γ_{18}	$\pi^0\omega$	seen

$\rho(1700)$ $\Gamma(i)\Gamma(e^+e^-)/\Gamma(\text{total})$

This combination of a partial width with the partial width into e^+e^- and with the total width is obtained from the cross-section into channel$_i$ in e^+e^- annihilation.

$\Gamma(2(\pi^+\pi^-)) \times \Gamma(e^+e^-)/\Gamma_{\text{total}}$ $\quad \Gamma_2\Gamma_{17}/\Gamma$

VALUE (keV)	DOCUMENT ID		TECN	COMMENT
• • • We do not use the following data for averages, fits, limits, etc. • • •				
2.6 ±0.2	DELCOURT	81B	DM1	$e^+e^- \to 2(\pi^+\pi^-)$
2.83±0.42	BACCI	80	FRAG	$e^+e^- \to 2(\pi^+\pi^-)$

$\Gamma(\pi^+\pi^-) \times \Gamma(e^+e^-)/\Gamma_{\text{total}}$ $\quad \Gamma_{11}\Gamma_{17}/\Gamma$

VALUE (keV)	DOCUMENT ID		TECN	COMMENT
• • • We do not use the following data for averages, fits, limits, etc. • • •				
0.13	[41] DIEKMAN	88	RVUE	$e^+e^- \to \pi^+\pi^-$
$0.029^{+0.016}_{-0.012}$	KURDADZE	83	OLYA	0.64–1.4 $e^+e^- \to \pi^+\pi^-$

[41] Using total width = 220 MeV.

$\Gamma(K\overline{K}^*(892)+\text{c.c.}) \times \Gamma(e^+e^-)/\Gamma_{\text{total}}$ $\quad \Gamma_{13}\Gamma_{17}/\Gamma$

VALUE (keV)	DOCUMENT ID		TECN	COMMENT
• • • We do not use the following data for averages, fits, limits, etc. • • •				
0.305±0.071	[42] BIZOT	80	DM1	e^+e^-

[42] Model dependent.

$\Gamma(\eta\rho) \times \Gamma(e^+e^-)/\Gamma_{\text{total}}$ $\quad \Gamma_{14}\Gamma_{17}/\Gamma$

VALUE (eV)	DOCUMENT ID		TECN	COMMENT
• • • We do not use the following data for averages, fits, limits, etc. • • •				
7±3	ANTONELLI	88	DM2	$e^+e^- \to \eta\pi^+\pi^-$

$\Gamma(K\overline{K}) \times \Gamma(e^+e^-)/\Gamma_{\text{total}}$ $\quad \Gamma_{16}\Gamma_{17}/\Gamma$

VALUE (keV)	DOCUMENT ID		TECN	COMMENT
• • • We do not use the following data for averages, fits, limits, etc. • • •				
0.035±0.029	[43] BIZOT	80	DM1	e^+e^-

[43] Model dependent.

$\Gamma(\rho\pi\pi) \times \Gamma(e^+e^-)/\Gamma_{\text{total}}$ $\quad \Gamma_3\Gamma_{17}/\Gamma$

VALUE (keV)	DOCUMENT ID		TECN	COMMENT
• • • We do not use the following data for averages, fits, limits, etc. • • •				
3.510±0.090	[44] BIZOT	80	DM1	e^+e^-

[44] Model dependent.

$\rho(1700)$ $\Gamma(i)/\Gamma(\text{total}) \times \Gamma(e^+e^-)/\Gamma(\text{total})$

$\Gamma(\pi^0\omega)/\Gamma_{\text{total}} \times \Gamma(e^+e^-)/\Gamma_{\text{total}}$ $\quad \Gamma_{18}/\Gamma \times \Gamma_{17}/\Gamma$

VALUE (units 10^{-6})	EVTS	DOCUMENT ID		TECN	COMMENT
• • • We do not use the following data for averages, fits, limits, etc. • • •					
1.7±0.4	7815	[45] ACHASOV	13	SND	1.05–2.00 $e^+e^- \to \pi^0\pi^0\gamma$

[45] From a phenomenological model based on vector meson dominance with the interfering $\rho(1450)$ and $\rho(1700)$ and their widths fixed at 400 and 250 MeV, respectively. Systematic uncertainty not estimated.

$\rho(1700)$ BRANCHING RATIOS

$\Gamma(\rho\pi\pi)/\Gamma(4\pi)$ $\quad \Gamma_3/\Gamma_1$

VALUE	DOCUMENT ID		TECN	COMMENT
• • • We do not use the following data for averages, fits, limits, etc. • • •				
0.28±0.06	[46] ABELE	01B	CBAR	0.0 $\overline{p}n \to 5\pi$

[46] $\omega\pi$ not included.

$\Gamma(\rho^0\pi^+\pi^-)/\Gamma(2(\pi^+\pi^-))$ $\quad \Gamma_4/\Gamma_2$

VALUE	EVTS	DOCUMENT ID		TECN	COMMENT
• • • We do not use the following data for averages, fits, limits, etc. • • •					
~ 1.0		DELCOURT	81B	DM1	$e^+e^- \to 2(\pi^+\pi^-)$
0.7 ±0.1	500	SCHACHT	74	STRC	5.5–18 $\gamma p \to p4\pi$
0.80		[47] BINGHAM	72B	HBC	9.3 $\gamma p \to p4\pi$

[47] The $\pi\pi$ system is in S-wave.

$\Gamma(\rho^0\pi^0\pi^0)/\Gamma(\rho^\pm\pi^\mp\pi^0)$ $\quad \Gamma_5/\Gamma_6$

VALUE	DOCUMENT ID		TECN	CHG	COMMENT
• • • We do not use the following data for averages, fits, limits, etc. • • •					
<0.10	ATKINSON	85B	OMEG		20–70 γp
<0.15	ATKINSON	82	OMEG	0	20–70 $\gamma p \to p4\pi$

$\Gamma(a_1(1260)\pi)/\Gamma(4\pi)$ $\quad \Gamma_7/\Gamma_1$

VALUE	DOCUMENT ID		TECN	COMMENT
• • • We do not use the following data for averages, fits, limits, etc. • • •				
0.16±0.05	[48] ABELE	01B	CBAR	0.0 $\overline{p}n \to 5\pi$

[48] $\omega\pi$ not included.

$\Gamma(h_1(1170)\pi)/\Gamma(4\pi)$ $\quad \Gamma_8/\Gamma_1$

VALUE	DOCUMENT ID		TECN	COMMENT
• • • We do not use the following data for averages, fits, limits, etc. • • •				
0.17±0.06	[49] ABELE	01B	CBAR	0.0 $\overline{p}n \to 5\pi$

[49] $\omega\pi$ not included.

$\Gamma(\pi(1300)\pi)/\Gamma(4\pi)$ $\quad \Gamma_9/\Gamma_1$

VALUE	DOCUMENT ID		TECN	COMMENT
• • • We do not use the following data for averages, fits, limits, etc. • • •				
0.30±0.10	[50] ABELE	01B	CBAR	0.0 $\overline{p}n \to 5\pi$

[50] $\omega\pi$ not included.

$\Gamma(\rho\rho)/\Gamma(4\pi)$ $\quad \Gamma_{10}/\Gamma_1$

VALUE	DOCUMENT ID		TECN	COMMENT
• • • We do not use the following data for averages, fits, limits, etc. • • •				
0.09±0.03	[51] ABELE	01B	CBAR	0.0 $\overline{p}n \to 5\pi$

[51] $\omega\pi$ not included.

$\Gamma(\pi^+\pi^-)/\Gamma_{\text{total}}$ $\quad \Gamma_{11}/\Gamma$

VALUE	DOCUMENT ID		TECN	COMMENT
• • • We do not use the following data for averages, fits, limits, etc. • • •				
$0.287^{+0.043}_{-0.042}$	BECKER	79	ASPK	17 $\pi^- p$ polarized
0.15 to 0.30	[52] MARTIN	78C	RVUE	17 $\pi^- p \to \pi^+\pi^- n$
<0.20	[53] COSTA...	77B	RVUE	$e^+e^- \to 2\pi, 4\pi$
0.30 ±0.05	[52] FROGGATT	77	RVUE	17 $\pi^- p \to \pi^+\pi^- n$
<0.15	[54] EISENBERG	73	HBC	5 $\pi^+ p \to \Delta^{++}2\pi$
0.25 ±0.05	[55] HYAMS	73	ASPK	17 $\pi^- p \to \pi^+\pi^- n$

[52] From phase shift analysis of HYAMS 73 data.

[53] Estimate using unitarity, time reversal invariance, Breit-Wigner.

[54] Estimated using one-pion-exchange model.

[55] Included in BECKER 79 analysis.

$\Gamma(\pi^+\pi^-)/\Gamma(2(\pi^+\pi^-))$ Γ_{11}/Γ_2

VALUE	DOCUMENT ID		TECN	COMMENT
• • • We do not use the following data for averages, fits, limits, etc. • • •				
0.13 ± 0.05	ASTON	80	OMEG	20–70 $\gamma p \to p 2\pi$
<0.14	[56] DAVIER	73	STRC	6–18 $\gamma p \to p 4\pi$
<0.2	[57] BINGHAM	72B	HBC	9.3 $\gamma p \to p 2\pi$

[56] Upper limit is estimate.
[57] 2σ upper limit.

$\Gamma(\pi\pi)/\Gamma(4\pi)$ Γ_{12}/Γ_1

VALUE	DOCUMENT ID		TECN	COMMENT
• • • We do not use the following data for averages, fits, limits, etc. • • •				
0.16 ± 0.04	[58,59] ABELE	01B	CBAR	0.0 $\overline{p}n \to 5\pi$

[58] Using ABELE 97.
[59] $\omega\pi$ not included.

$\Gamma(K\overline{K}^*(892)+\text{c.c.})/\Gamma_{\text{total}}$ Γ_{13}/Γ

VALUE	DOCUMENT ID		TECN	COMMENT
• • • We do not use the following data for averages, fits, limits, etc. • • •				
possibly seen	COAN	04	CLEO	$\tau^- \to K^-\pi^-K^+\nu_\tau$

$\Gamma(K\overline{K}^*(892)+\text{c.c.})/\Gamma(2(\pi^+\pi^-))$ Γ_{13}/Γ_2

VALUE	DOCUMENT ID		TECN	COMMENT
• • • We do not use the following data for averages, fits, limits, etc. • • •				
0.15 ± 0.03	[60] DELCOURT	81B	DM1	$e^+e^- \to \overline{K}K\pi$

[60] Assuming $\rho(1700)$ and ω radial excitations to be degenerate in mass.

$\Gamma(\eta\rho)/\Gamma_{\text{total}}$ Γ_{14}/Γ

VALUE	CL%	DOCUMENT ID		TECN	COMMENT
• • • We do not use the following data for averages, fits, limits, etc. • • •					
possibly seen		AKHMETSHIN	00D	CMD2	$e^+e^- \to \eta\pi^+\pi^-$
<0.04		DONNACHIE	87B	RVUE	
<0.02	58	ATKINSON	86B	OMEG	20–70 γp

$\Gamma(\eta\rho)/\Gamma(2(\pi^+\pi^-))$ Γ_{14}/Γ_2

VALUE	DOCUMENT ID		TECN	COMMENT
• • • We do not use the following data for averages, fits, limits, etc. • • •				
0.123 ± 0.027	DELCOURT	82	DM1	$e^+e^- \to \pi^+\pi^-$ MM
~ 0.1	ASTON	80	OMEG	20–70 γp

$\Gamma(\pi^+\pi^-\text{neutrals})/\Gamma(2(\pi^+\pi^-))$ $(\Gamma_5+\Gamma_6+0.714\Gamma_{14})/\Gamma_2$

VALUE	DOCUMENT ID		TECN	COMMENT
• • • We do not use the following data for averages, fits, limits, etc. • • •				
2.6 ± 0.4	[61] BALLAM	74	HBC	9.3 γp

[61] Upper limit. Background not subtracted.

$\Gamma(a_2(1320)\pi)/\Gamma_{\text{total}}$ Γ_{15}/Γ

VALUE	DOCUMENT ID		TECN	COMMENT
• • • We do not use the following data for averages, fits, limits, etc. • • •				
not seen	AMELIN	00	VES	37 $\pi^-p \to \eta\pi^+\pi^-n$

$\Gamma(K\overline{K})/\Gamma(2(\pi^+\pi^-))$ Γ_{16}/Γ_2

VALUE	CL%	DOCUMENT ID		TECN	CHG	COMMENT
• • • We do not use the following data for averages, fits, limits, etc. • • •						
0.015 ± 0.010		[62] DELCOURT	81B	DM1		$e^+e^- \to \overline{K}K$
<0.04	95	BINGHAM	72B	HBC	0	9.3 γp

[62] Assuming $\rho(1700)$ and ω radial excitations to be degenerate in mass.

$\Gamma(K\overline{K})/\Gamma(K\overline{K}^*(892)+\text{c.c.})$ Γ_{16}/Γ_{13}

VALUE	DOCUMENT ID		TECN	COMMENT
• • • We do not use the following data for averages, fits, limits, etc. • • •				
0.052 ± 0.026	BUON	82	DM1	$e^+e^- \to$ hadrons

$\Gamma(\pi^0\omega)/\Gamma_{\text{total}}$ Γ_{18}/Γ

VALUE	EVTS	DOCUMENT ID		TECN	COMMENT
• • • We do not use the following data for averages, fits, limits, etc. • • •					
seen	1.6k	ACHASOV	12	SND	$e^+e^- \to \pi^0\pi^0\gamma$
not seen	2382	AKHMETSHIN	03B	CMD2	$e^+e^- \to \pi^0\pi^0\gamma$
seen		ACHASOV	97	RVUE	$e^+e^- \to \omega\pi^0$

$\rho(1700)$ REFERENCES

ACHASOV	13	PR D88 054013	M.N. Achasov *et al.*	(SND Collab.)
ABRAMOWICZ	12	EPJ C72 1869	H. Abramowicz *et al.*	(ZEUS Collab.)
ACHASOV	12	JETPL 94 734 Translated from ZETFP 94 796.	M.N. Achasov *et al.*	
LEES	12G	PR D86 032013	J.P. Lees *et al.*	(BABAR Collab.)
FUJIKAWA	08	PR D78 072006	M. Fujikawa *et al.*	(BELLE Collab.)
COAN	04	PRL 92 232001	T.E. Coan *et al.*	(CLEO Collab.)
FRABETTI	04	PL B578 290	P.L. Frabetti *et al.*	(FNAL E687 Collab.)
AKHMETSHIN	03B	PL B562 173	R.R. Akhmetshin *et al.*	(Novosibirsk CMD-2 Collab.)
ABELE	01B	EPJ C21 261	A. Abele *et al.*	(Crystal Barrel Collab.)
ACHASOV	00I	PL B486 29	M.N. Achasov *et al.*	(Novosibirsk SND Collab.)
AKHMETSHIN	00D	PL B489 125	R.R. Akhmetshin *et al.*	(Novosibirsk CMD-2 Collab.)
AMELIN	00	NP A668 83	D. Amelin *et al.*	(VES Collab.)
EDWARDS	00A	PR D61 072003	K.W. Edwards *et al.*	(CLEO Collab.)
ABELE	99D	PL B468 178	A. Abele *et al.*	(Crystal Barrel Collab.)
ABELE	97	PL B391 191	A. Abele *et al.*	(Crystal Barrel Collab.)
ACHASOV	97	PR D55 2663	N.N. Achasov *et al.*	(NOVM)
BERTIN	97C	PL B408 476	A. Bertin *et al.*	(OBELIX Collab.)
CLEGG	94	ZPHY C62 455	A.B. Clegg, A. Donnachie	(LANC, MCHS)
CLEGG	90	ZPHY C45 677	A.B. Clegg, A. Donnachie	(LANC, MCHS)
KUHN	90	ZPHY C48 445	J.H. Kuhn *et al.*	(MPIM)
BISELLO	89	PL B220 321	D. Bisello *et al.*	(DM2 Collab.)
DUBNICKA	89	JP G15 1349	S. Dubnicka *et al.*	(JINR, SLOV)
GESHKEN...	89	ZPHY C45 351	B.V. Geshkenbein	(ITEP)
ANTONELLI	88	PL B212 133	A. Antonelli *et al.*	(DM2 Collab.)
DIEKMAN	88	PRPL 159 99	B. Diekmann	(BONN)
FUKUI	88	PL B202 441	S. Fukui *et al.*	(SUGI, NAGO, KEK, KYOT+)
DONNACHIE	87B	ZPHY C34 257	A. Donnachie, A.B. Clegg	(MCHS, LANC)
ATKINSON	86B	ZPHY C30 531	M. Atkinson *et al.*	(BONN, CERN, GLAS+)
ATKINSON	85B	ZPHY C26 499	M. Atkinson *et al.*	(BONN, CERN, GLAS+)
ERKAL	85	ZPHY C29 485	C. Erkal, M.G. Olsson	(WISC)
ABE	84B	PRL 53 751	K. Abe *et al.*	(SLAC HFP Collab.)
KURDADZE	83	JETPL 37 733 Translated from ZETFP 37 613.	L.M. Kurdadze *et al.*	(NOVO)
ATKINSON	82	PL 108B 55	M. Atkinson *et al.*	(BONN, CERN, GLAS+)
BUON	82	PL 118B 221	J. Buon *et al.*	(LALO, MONP)
CLELAND	82B	NP B208 228	W.E. Cleland *et al.*	(DURH, GEVA, LAUS+)
CORDIER	82	PL 109B 129	A. Cordier *et al.*	(LALO)
DELCOURT	82	PL 113B 93	B. Delcourt *et al.*	(LALO)
ASTON	81E	NP B189 15	D. Aston	(BONN, CERN, EPOL, GLAS, LANC+)
DELCOURT	81B	Bonn Conf. 205	B. Delcourt	(ORSAY)
Also		PL 109B 129	A. Cordier *et al.*	(LALO)
DIBIANCA	81	PR D23 595	F.A. di Bianca *et al.*	(CASE, CMU)
ASTON	80	PL 92B 215	D. Aston	(BONN, CERN, EPOL, GLAS, LANC+)
BACCI	80	PL 95B 139	C. Bacci *et al.*	(ROMA, FRAS)
BIZOT	80	Madison Conf. 546	J.C. Bizot *et al.*	(LALO, MONP)
KILLIAN	80	PR D21 3005	T.J. Killian *et al.*	(CORN)
ATIYA	79B	PRL 43 1691	M.S. Atiya *et al.*	(COLU, ILL, FNAL)
BECKER	79	NP B151 46	H. Becker *et al.*	(MPIM, CERN, ZEEM, CRAC)
LANG	79	PR D19 956	C.B. Lang, A. Mas-Parareda	(GRAZ)
MARTIN	78C	ANP 114 1	A.D. Martin, M.R. Pennington	(CERN)
COSTA...	77B	PL 71B 345	B. Costa de Beauregard, B. Pire, T.N. Truong	(EPOL)
FROGGATT	77	NP B129 89	C.D. Froggatt, J.L. Petersen	(GLAS, NORD)
ALEXANDER	75	PL 57B 487	G. Alexander *et al.*	(TELA)
BALLAM	74	NP B76 375	J. Ballam *et al.*	(SLAC, LBL, MPIM)
CONVERSI	74	PL 52B 493	M. Conversi *et al.*	(ROMA, FRAS)
SCHACHT	74	NP B81 205	P. Schacht *et al.*	(MPIM)
DAVIER	73	NP B58 31	M. Davier *et al.*	(SLAC)
EISENBERG	73	PL 43B 149	Y. Eisenberg *et al.*	(REHO)
HYAMS	73	NP B64 134	B.D. Hyams *et al.*	(CERN, MPIM)
BINGHAM	72B	PL 41B 635	H.H. Bingham *et al.*	(LBL, UCB, SLAC) IGJP
JACOB	72	PR D5 1847	M. Jacob, R. Slansky	
GOUNARIS	68	PRL 21 244	G.J. Gounaris, J.J. Sakurai	

$a_2(1700)$

$I^G(J^{PC}) = 1^-(2^{++})$

OMITTED FROM SUMMARY TABLE

$a_2(1700)$ MASS

VALUE (MeV)	EVTS	DOCUMENT ID		TECN	CHG	COMMENT
1732±16 OUR AVERAGE		Error includes scale factor of 1.9.				
1737± 5± 7		ABE	04	BELL		10.6 $e^+e^- \to e^+e^-K^+K^-$
1698±44		[1] AMSLER	02	CBAR		0.9 $\overline{p}p \to \pi^0\eta\eta$
1660±40		ABELE	99B	CBAR		1.94 $\overline{p}p \to \pi^0\eta\eta$
• • • We do not use the following data for averages, fits, limits, etc. • • •						
1675±25		ANISOVICH	09	RVUE		0.0 $\overline{p}p$, πN
1722± 9±15	18k	[2] SCHEGELSKY	06	RVUE	0	$\gamma\gamma \to \pi^+\pi^-\pi^0$
1702± 7	80k	[3] UMAN	06	E835		5.2 $\overline{p}p \to \eta\eta\pi^0$
1721±13±44	145k	LU	05	B852		18 $\pi^-p \to \omega\pi^-\pi^0p$
1767±14	221	[4] ACCIARRI	01H	L3		$\gamma\gamma \to K^0_SK^0_S$, E^{ee}_{cm}= 91, 183–209 GeV
$\sim$ 1775		[5] GRYGOREV	99	SPEC		40 $\pi^-p \to K^0_SK^0_Sn$
1752±21± 4		ACCIARRI	97T	L3		$\gamma\gamma \to \pi^+\pi^-\pi^0$

[1] T-matrix pole.
[2] From analysis of L3 data at 183–209 GeV.
[3] Statistical error only.
[4] Spin 2 dominant, isospin not determined, could also be I=1.
[5] Possibly two $J^P = 2^+$ resonances with isospins 0 and 1.

$a_2(1700)$ WIDTH

VALUE (MeV)	EVTS	DOCUMENT ID		TECN	CHG	COMMENT
194± 40 OUR AVERAGE		Error includes scale factor of 1.6. See the ideogram below.				
151± 22±24		ABE	04	BELL		10.6 $e^+e^- \to e^+e^-K^+K^-$
265± 55		[6] AMSLER	02	CBAR		0.9 $\overline{p}p \to \pi^0\eta\eta$
280± 70		ABELE	99B	CBAR		1.94 $\overline{p}p \to \pi^0\eta\eta$

• • • We do not use the following data for averages, fits, limits, etc. • • •

270^{+50}_{-20}			ANISOVICH	09	RVUE	0.0 $\overline{p}p$, πN
336± 20±20	18k	[7]	SCHEGELSKY	06	RVUE	0 $\gamma\gamma \to \pi^+\pi^-\pi^0$
417± 19	80k	[8]	UMAN	06	E835	5.2 $\overline{p}p \to \eta\eta\pi^0$
279± 49±66	145k		LU	05	B852	18 $\pi^- p \to \omega\pi^-\pi^0 p$
187± 60	221	[9]	ACCIARRI	01H	L3	$\gamma\gamma \to K^0_S K^0_S$, E^{ee}_{cm}= 91, 183–209 GeV
150±110±34			ACCIARRI	97T	L3	$\gamma\gamma \to \pi^+\pi^-\pi^0$

[6] T-matrix pole.
[7] From analysis of L3 data at 183–209 GeV.
[8] Statistical error only.
[9] Spin 2 dominant, isospin not determined, could also be I=1.

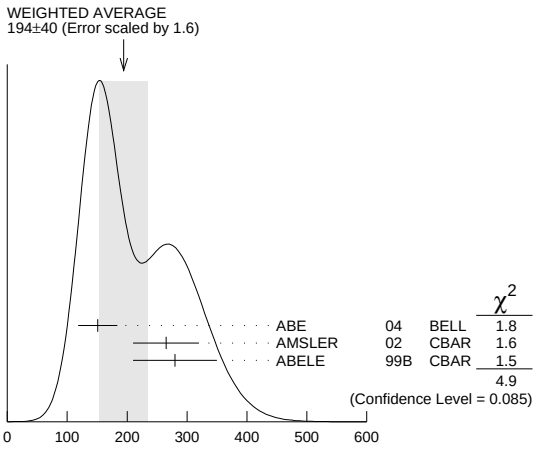

$a_2(1700)$ width

$a_2(1700)$ DECAY MODES

	Mode	Fraction (Γ_i/Γ)
Γ_1	$\eta\pi$	seen
Γ_2	$\gamma\gamma$	
Γ_3	$\rho\pi$	
Γ_4	$f_2(1270)\pi$	
Γ_5	$K\overline{K}$	seen
Γ_6	$\omega\pi^-\pi^0$	seen
Γ_7	$\omega\rho$	seen

$a_2(1700)$ PARTIAL WIDTHS

$\Gamma(\eta\pi)$ Γ_1

VALUE (MeV)	EVTS	DOCUMENT ID		TECN	COMMENT
• • • We do not use the following data for averages, fits, limits, etc. • • •					
9.5±2.0	870	[10] SCHEGELSKY	06A	RVUE	$\gamma\gamma \to K^0_S K^0_S$

$\Gamma(\gamma\gamma)$ Γ_2

VALUE (keV)	EVTS	DOCUMENT ID		TECN	COMMENT
• • • We do not use the following data for averages, fits, limits, etc. • • •					
0.30±0.05	870	[10] SCHEGELSKY	06A	RVUE	$\gamma\gamma \to K^0_S K^0_S$

$\Gamma(K\overline{K})$ Γ_5

VALUE (MeV)	EVTS	DOCUMENT ID		TECN	COMMENT
• • • We do not use the following data for averages, fits, limits, etc. • • •					
5.0±3.0	870	[10] SCHEGELSKY	06A	RVUE	$\gamma\gamma \to K^0_S K^0_S$

[10] From analysis of L3 data at 91 and 183–209 GeV, using $a_2(1700)$ mass of 1730 MeV and width of 340 MeV, and SU(3) relations.

$a_2(1700)$ Γ(i)$\Gamma(\gamma\gamma)/\Gamma$(total)

$[\Gamma(\rho\pi) + \Gamma(f_2(1270)\pi)] \times \Gamma(\gamma\gamma)/\Gamma_{total}$ $(\Gamma_3+\Gamma_4)\Gamma_2/\Gamma$

VALUE (keV)	EVTS	DOCUMENT ID		TECN	COMMENT
0.29±0.04±0.02		ACCIARRI	97T	L3	$\gamma\gamma \to \pi^+\pi^-\pi^0$
• • • We do not use the following data for averages, fits, limits, etc. • • •					
$0.37^{+0.12}_{-0.08}$±0.10	18k	[11] SCHEGELSKY	06	RVUE	$\gamma\gamma \to \pi^+\pi^-\pi^0$

$\Gamma(K\overline{K}) \times \Gamma(\gamma\gamma)/\Gamma_{total}$ $\Gamma_5\Gamma_2/\Gamma$

VALUE (eV)	DOCUMENT ID		TECN	COMMENT
• • • We do not use the following data for averages, fits, limits, etc. • • •				
20.6± 4.2± 4.6	[12] ABE	04	BELL	10.6 $e^+e^- \to e^+e^- K^+K^-$
49 ±11 ±13	[13] ACCIARRI	01H	L3	$\gamma\gamma \to K^0_S K^0_S$, E^{ee}_{cm}= 91, 183–209 GeV

[11] From analysis of L3 data at 183–209 GeV.
[12] Assuming spin 2.
[13] Spin 2 dominant, isospin not determined, could also be I=1.

$a_2(1700)$ BRANCHING RATIOS

$\Gamma(\rho\pi)/\Gamma(f_2(1270)\pi)$ Γ_3/Γ_4

VALUE	EVTS	DOCUMENT ID		TECN	COMMENT
• • • We do not use the following data for averages, fits, limits, etc. • • •					
3.4±0.4±0.1	18k	[14] SCHEGELSKY	06	RVUE	$\gamma\gamma \to \pi^+\pi^-\pi^0$

[14] From analysis of L3 data at 183–209 GeV.

$a_2(1700)$ REFERENCES

ANISOVICH	09	IJMP A24 2481	V.V. Anisovich, A.V. Sarantsev	
SCHEGELSKY	06	EPJ A27 199	V.A. Schegelsky *et al.*	
SCHEGELSKY	06A	EPJ A27 207	V.A. Schegelsky *et al.*	
UMAN	06	PR D73 052009	I. Uman *et al.*	(FNAL E835)
LU	05	PRL 94 032002	M. Lu *et al.*	(BNL E852 Collab.)
ABE	04	EPJ C32 323	K. Abe *et al.*	(BELLE Collab.)
AMSLER	02	EPJ C23 29	C. Amsler *et al.*	
ACCIARRI	01H	PL B501 173	M. Acciarri *et al.*	(L3 Collab.)
ABELE	99B	EPJ C8 67	A. Abele *et al.*	(Crystal Barrel Collab.)
GRYGOREV	99	PAN 62 470	V.K. Grygorev *et al.*	
		Translated from YAF 62 513.		
ACCIARRI	97T	PL B413 147	M. Acciarri *et al.*	(L3 Collab.)

$f_0(1710)$

$I^G(J^{PC}) = 0^+(0^{++})$

See our mini-review in the 2004 edition of this *Review*, Physics Letters **B592** 1 (2004). See also the mini-review on scalar mesons under $f_0(500)$ (see the index for the page number).

$f_0(1710)$ MASS

VALUE (MeV)	EVTS	DOCUMENT ID		TECN	COMMENT
1722^{+6}_{-5} OUR AVERAGE		Error includes scale factor of 1.6. See the ideogram below.			
1750^{+6}_{-7} $^{+29}_{-18}$		UEHARA	13	BELL	$\gamma\gamma \to K^0_S K^0_S$
1701^{+9}_{-2} ± 5	4k	[1] CHEKANOV	08	ZEUS	$ep \to K^0_S K^0_S X$
1765^{+4}_{-3} ±13		ABLIKIM	06V	BES2	$e^+e^- \to J/\psi \to \gamma\pi^+\pi^-$
1760±15 $^{+15}_{-10}$		[2] ABLIKIM	05Q	BES2	$\psi(2S) \to \gamma\pi^+\pi^- K^+K^-$
1738±30		ABLIKIM	04E	BES2	$J/\psi \to \omega K^+K^-$
1740± 4 $^{+10}_{-25}$		[3] BAI	03G	BES	$J/\psi \to \gamma K\overline{K}$
1740^{+30}_{-25}		[3] BAI	00A	BES	$J/\psi \to \gamma(\pi^+\pi^-\pi^+\pi^-)$
1698±18		[4] BARBERIS	00E		450 $pp \to p_f\eta\eta p_s$
1710±12 ±11		[5] BARBERIS	99D	OMEG	450 $pp \to K^+K^-, \pi^+\pi^-$
1710±25		[6] FRENCH	99		300 $pp \to p_f(K^+K^-)p_s$
1707±10		[7] AUGUSTIN	88	DM2	$J/\psi \to \gamma K^+K^-, K^0_S K^0_S$
1698±15		[7] AUGUSTIN	87	DM2	$J/\psi \to \gamma\pi^+\pi^-$
1720±10 ±10		[8] BALTRUSAIT...87		MRK3	$J/\psi \to \gamma K^+K^-$
1742±15		[7] WILLIAMS	84	MPSF	200 $\pi^- N \to 2K^0_S X$
1670±50		BLOOM	83	CBAL	$J/\psi \to \gamma 2\eta$
• • • We do not use the following data for averages, fits, limits, etc. • • •					
1750±13		AMSLER	06	CBAR	1.64 $\overline{p}p \to K^+K^-\pi^0$
1747± 5	80k	[9,10] UMAN	06	E835	5.2 $\overline{p}p \to \eta\eta\pi^0$
1776±15		VLADIMIRSK...06		SPEC	40 $\pi^- p \to K^0_S K^0_S n$
1790^{+40}_{-30}		[2] ABLIKIM	05	BES2	$J/\psi \to \phi\pi^+\pi^-$
1670±20		[9] BINON	05	GAMS	33 $\pi^- p \to \eta\eta n$
1726± 7	74	[10] CHEKANOV	04	ZEUS	$ep \to K^0_S K^0_S X$
1732+15		[11] ANISOVICH	03	RVUE	
1682±16		TIKHOMIROV	03	SPEC	40.0 π^- C $\to K^0_S K^0_S K^0_L X$
1670±26	3651	[3,12] NICHITIU	02	OBLX	
1770±12		[13,14] ANISOVICH	99B	SPEC	0.6–1.2 $p\overline{p} \to \eta\eta\pi^0$
1730±15		[3] BARBERIS	99	OMEG	450 $pp \to p_s p_f K^+K^-$
1750±20		[3] BARBERIS	99B	OMEG	450 $pp \to p_s p_f \pi^+\pi^-$
1750±30		[15] ANISOVICH	98B	RVUE	Compilation
1720±39		BAI	98H	BES	$J/\psi \to \gamma\pi^0\pi^0$
1775± 1.5	57	[16] BARKOV	98		$\pi^- p \to K^0_S K^0_S n$
1690±11		[17] ABREU	96C	DLPH	$Z^0 \to K^+K^- + X$
1696± 5 $^{+9}_{-34}$		[8] BAI	96C	BES	$J/\psi \to \gamma K^+K^-$
1781± 8 $^{+10}_{-31}$		[3] BAI	96C	BES	$J/\psi \to \gamma K^+K^-$

1768±14		BALOSHIN	95	SPEC	40 π^- C → $K^0_S K^0_S$ X
1750±15		[18] BUGG	95	MRK3	J/ψ → $\gamma\pi^+\pi^-\pi^+\pi^-$
1620±16		[8] BUGG	95	MRK3	J/ψ → $\gamma\pi^+\pi^-\pi^+\pi^-$
1748±10		[7] ARMSTRONG	93C	E760	$\overline{p}p$ → $\pi^0\eta\eta$ → 6γ
∼1750		BREAKSTONE	93	SFM	pp → $pp\pi^+\pi^-\pi^+\pi^-$
1744±15		[19] ALDE	92D	GAM2	38 π^-p → $\eta\eta n$
1713±10		[20] ARMSTRONG	89D	OMEG	300 pp → ppK^+K^-
1706±10		[20] ARMSTRONG	89D	OMEG	300 pp → $pp K^0_S K^0_S$
1700±15		[8] BOLONKIN	88	SPEC	40 π^-p → $K^0_S K^0_S n$
1720±60		[3] BOLONKIN	88	SPEC	40 π^-p → $K^0_S K^0_S n$
1638±10		[21] FALVARD	88	DM2	J/ψ → ϕK^+K^-, $K^0_S K^0_S$
1690± 4		[22] FALVARD	88	DM2	J/ψ → ϕK^+K^-, $K^0_S K^0_S$
1755± 8		[23] ALDE	86C	GAM2	38 π^-p → $n2\eta$
1730^{+2}_{-10}		[24] LONGACRE	86	RVUE	22 π^-p → $n2K^0_S$
1650±50		BURKE	82	MRK2	J/ψ → $\gamma2\rho$
1640±50		[25,26] EDWARDS	82D	CBAL	J/ψ → $\gamma2\eta$
1730±10	±20	[27] ETKIN	82C	MPS	23 π^-p → $n2K^0_S$

[1] In the SU(3) based model with a specific interference pattern of the $f_2(1270)$, $a_2^0(1320)$, and $f_2'(1525)$ mesons incoherently added to the $f_0(1710)$ and non-resonant background.
[2] This state may be different from $f_0(1710)$, see CLOSE 05.
[3] $J^P = 0^+$.
[4] T-matrix pole.
[5] Supersedes BARBERIS 99 and BARBERIS 99B.
[6] $J^P = 0^+$, supersedes by ARMSTRONG 89D.
[7] No J^{PC} determination.
[8] $J^P = 2^+$.
[9] Breit-Wigner mass.
[10] Systematic errors not estimated.
[11] K-matrix pole, assuming $J^P = 0^+$, from combined analysis of π^-p → $\pi^0\pi^0 n$, π^-p → $K\overline{K}n$, $\pi^+\pi^-$ → $\pi^+\pi^-$, $\overline{p}p$ → $\pi^0\pi^0\pi^0$, $\pi^0\eta\eta$, $\pi^0\pi^0\eta$, $\pi^+\pi^-\pi^0$, $K^+K^-\pi^0$, $K^0_S K^0_S\pi^0$, $K^+K^0_S\pi^-$ at rest, $\overline{p}n$ → $\pi^-\pi^-\pi^+$, $K^0_S K^-\pi^0$, $K^0_S K^0_S\pi^-$ at rest.
[12] Decaying to $f_0(1370)\pi\pi$.
[13] $J^P = 0^+$.
[14] Not seen by AMSLER 02.
[15] T-matrix pole, assuming $J^P = 0^+$
[16] No J^{PC} determination.
[17] No J^{PC} determination, width not determined.
[18] From a fit to the 0^+ partial wave.
[19] ALDE 92D combines all the GAMS-2000 data.
[20] $J^P = 2^+$, superseded by FRENCH 99.
[21] From an analysis ignoring interference with $f_2'(1525)$.
[22] From an analysis including interference with $f_2'(1525)$.
[23] Superseded by ALDE 92D.
[24] Uses MRK3 data. From a partial-wave analysis of data using a K-matrix formalism with 5 poles, but assuming spin 2. Fit with constrained inelasticity.
[25] $J^P = 2^+$ preferred.
[26] From fit neglecting nearby $f_2'(1525)$. Replaced by BLOOM 83.
[27] Superseded by LONGACRE 86.

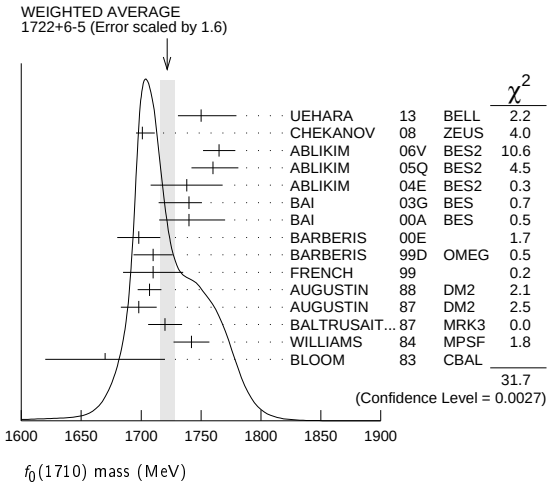

$f_0(1710)$ WIDTH

VALUE (MeV)		EVTS	DOCUMENT ID		TECN	COMMENT
135 ± 7		**OUR AVERAGE**	Error includes scale factor of 1.1.			
139	$^{+11}_{-12}$ $^{+96}_{-50}$		UEHARA	13	BELL	$\gamma\gamma$ → $K^0_S K^0_S$
100 ± 24	$^{+7}_{-22}$	4k	[28] CHEKANOV	08	ZEUS	ep → $K^0_S K^0_S X$
145 ± 8	±69		ABLIKIM	06V	BES2	e^+e^- → J/ψ → $\gamma\pi^+\pi^-$
125 ± 25	$^{+10}_{-15}$		[29] ABLIKIM	05Q	BES2	$\psi(2S)$ → $\gamma\pi^+\pi^-K^+K^-$
125 ± 20			ABLIKIM	04E	BES2	J/ψ → ωK^+K^-
166	$^{+5}_{-8}$ $^{+15}_{-10}$		[30] BAI	03G	BES	J/ψ → $\gamma K\overline{K}$
120	$^{+50}_{-40}$		[30] BAI	00A	BES	J/ψ → $\gamma(\pi^+\pi^-\pi^+\pi^-)$
120 ± 26			[31] BARBERIS	00E		450 pp → $p_f\eta\eta p_s$
126 ± 16	±18		[32] BARBERIS	99D	OMEG	450 pp → K^+K^-, $\pi^+\pi^-$
105 ± 34			[33] FRENCH	99		300 pp → $p_f(K^+K^-)p_s$
166.4 ± 33.2			[34] AUGUSTIN	88	DM2	J/ψ → γK^+K^-, $K^0_S K^0_S$
136 ± 28			[34] AUGUSTIN	87	DM2	J/ψ → $\gamma\pi^+\pi^-$
130 ± 20			[35] BALTRUSAIT...	87	MRK3	J/ψ → γK^+K^-
57 ± 38			[36] WILLIAMS	84	MPSF	200 π^-N → $2K^0_S X$
160 ± 80			BLOOM	83	CBAL	J/ψ → $\gamma2\eta$
• • • We do not use the following data for averages, fits, limits, etc. • • •						
148	$^{+40}_{-30}$		AMSLER	06	CBAR	1.64 $\overline{p}p$ → $K^+K^-\pi^0$
188 ± 13		80k	[29,37] UMAN	06	E835	5.2 $\overline{p}p$ → $\eta\eta\pi^0$
250 ± 30			VLADIMIRSK...	06	SPEC	40 π^-p → $K^0_S K^0_S n$
270	$^{+60}_{-30}$		[38] ABLIKIM	05	BES2	J/ψ → $\phi\pi^+\pi^-$
260 ± 50			[29] BINON	05	GAMS	33 π^-p → $\eta\eta n$
38	$^{+20}_{-14}$	74	[37] CHEKANOV	04	ZEUS	ep → $K^0_S K^0_S X$
144 ± 30			[39,40] ANISOVICH	03	RVUE	
320	$^{+50}_{-20}$		[40,41] ANISOVICH	03	RVUE	
102 ± 26			TIKHOMIROV	03	SPEC	40.0 π^-C → $K^0_S K^0_S K^0_L$ X
267 ± 44		3651	[30,42] NICHITIU	02	OBLX	
220 ± 40			[43,44] ANISOVICH	99B	SPEC	0.6–1.2 $p\overline{p}$ → $\eta\eta\pi^0$
100 ± 25			[30] BARBERIS	99	OMEG	450 pp → $p_s p_f K^+K^-$
160 ± 30			[30] BARBERIS	99B	OMEG	450 pp → $p_s p_f \pi^+\pi^-$
250 ±140			[45] ANISOVICH	98B	RVUE	Compilation
30 ± 7		57	[46] BARKOV	98		π^-p → $K^0_S K^0_S n$
103 ± 18	$^{+30}_{-11}$		[35] BAI	96C	BES	J/ψ → γK^+K^-
85 ± 24	$^{+22}_{-19}$		[30] BAI	96C	BES	J/ψ → γK^+K^-
56 ± 19			BALOSHIN	95	SPEC	40 π^-C → $K^0_S K^0_S$ X
160 ± 40			[47] BUGG	95	MRK3	J/ψ → $\gamma\pi^+\pi^-\pi^+\pi^-$
160	$^{+60}_{-20}$		[35] BUGG	95	MRK3	J/ψ → $\gamma\pi^+\pi^-\pi^+\pi^-$
264 ± 25			[34] ARMSTRONG	93C	E760	$\overline{p}p$ → $\pi^0\eta\eta$ → 6γ
200 to 300			BREAKSTONE	93	SFM	pp → $pp\pi^+\pi^-\pi^+\pi^-$
< 80 90% CL			[48] ALDE	92D	GAM2	38 π^-p → $\eta\eta N^*$
181 ± 30			[49] ARMSTRONG	89D	OMEG	300 pp → ppK^+K^-
104 ± 30			[49] ARMSTRONG	89D	OMEG	300 pp → $pp K^0_S K^0_S$
30 ± 20			[35] BOLONKIN	88	SPEC	40 π^-p → $K^0_S K^0_S n$
350 ±150			[30] BOLONKIN	88	SPEC	40 π^-p → $K^0_S K^0_S n$
148 ± 17			[50] FALVARD	88	DM2	J/ψ → ϕK^+K^-, $K^0_S K^0_S$
184 ± 6			[51] FALVARD	88	DM2	J/ψ → ϕK^+K^-, $K^0_S K^0_S$
122	$^{+74}_{-15}$		[52] LONGACRE	86	RVUE	22 π^-p → $n2K^0_S$
200 ±100			BURKE	82	MRK2	J/ψ → $\gamma2\rho$
220	$^{+100}_{-70}$		[53,54] EDWARDS	82D	CBAL	J/ψ → $\gamma2\eta$
200	$^{+156}_{-9}$		[55] ETKIN	82B	MPS	23 π^-p → $n2K^0_S$

[28] In the SU(3) based model with a specific interference pattern of the $f_2(1270)$, $a_2^0(1320)$, and $f_2'(1525)$ mesons incoherently added to the $f_0(1710)$ and non-resonant background.
[29] Breit-Wigner width.
[30] $J^P = 0^+$.
[31] T-matrix pole.
[32] Supersedes BARBERIS 99 and BARBERIS 99B.
[33] $J^P = 0^+$, supersedes by ARMSTRONG 89D.
[34] No J^{PC} determination.
[35] $J^P = 2^+$.
[36] No J^{PC} determination.
[37] Systematic errors not estimated.
[38] This state may be different from $f_0(1710)$, see CLOSE 05.
[39] (Solution I)
[40] K-matrix pole, assuming $J^P = 0^+$, from combined analysis of π^-p → $\pi^0\pi^0 n$, π^-p → $K\overline{K}n$, $\pi^+\pi^-$ → $\pi^+\pi^-$, $\overline{p}p$ → $\pi^0\pi^0\pi^0$, $\pi^0\eta\eta$, $\pi^0\pi^0\eta$, $\pi^+\pi^-\pi^0$, $K^+K^-\pi^0$, $K^0_S K^0_S\pi^0$, $K^+K^0_S\pi^-$ at rest, $\overline{p}n$ → $\pi^-\pi^-\pi^+$, $K^0_S K^-\pi^0$, $K^0_S K^0_S\pi^-$ at rest.
[41] (Solution I)
[42] Decaying to $f_0(1370)\pi\pi$.
[43] $J^P = 0^+$.
[44] Not seen by AMSLER 02.
[45] T-matrix pole, assuming $J^P = 0^+$
[46] No J^{PC} determination.
[47] From a fit to the 0^+ partial wave.
[48] ALDE 92D combines all the GAMS-2000 data.
[49] $J^P = 2^+$, (0^+ excluded).
[50] From an analysis ignoring interference with $f_2'(1525)$.
[51] From an analysis including interference with $f_2'(1525)$.
[52] Uses MRK3 data. From a partial-wave analysis of data using a K-matrix formalism with 5 poles, but assuming spin 2. Fit with constrained inelasticity.
[53] $J^P = 2^+$ preferred.
[54] From fit neglecting nearby $f_2'(1525)$. Replaced by BLOOM 83.
[55] From an amplitude analysis of the $K^0_S K^0_S$ system, superseded by LONGACRE 86.

Meson Particle Listings

$f_0(1710)$, $\eta(1760)$

$f_0(1710)$ DECAY MODES

	Mode	Fraction (Γ_i/Γ)
Γ_1	$K\overline{K}$	seen
Γ_2	$\eta\eta$	seen
Γ_3	$\pi\pi$	seen
Γ_4	$\gamma\gamma$	
Γ_5	$\omega\omega$	seen

$f_0(1710)$ Γ(i)$\Gamma(\gamma\gamma)/\Gamma$(total)

$\Gamma(K\overline{K}) \times \Gamma(\gamma\gamma)/\Gamma_{total}$ $\Gamma_1\Gamma_4/\Gamma$

VALUE (eV)	CL%	DOCUMENT ID		TECN	COMMENT
$12^{+3}_{-2}{}^{+227}_{-8}$		UEHARA	13	BELL	$\gamma\gamma \to K^0_S K^0_S$

• • • We do not use the following data for averages, fits, limits, etc. • • •

<480	95	ALBRECHT	90G	ARG	$\gamma\gamma \to K^+K^-$
<110	95	[56] BEHREND	89C	CELL	$\gamma\gamma \to K^0_S K^0_S$
<280	95	[56] ALTHOFF	85B	TASS	$\gamma\gamma \to K\overline{K}\pi$

[56] Assuming helicity 2.

$\Gamma(\pi\pi) \times \Gamma(\gamma\gamma)/\Gamma_{total}$ $\Gamma_3\Gamma_4/\Gamma$

VALUE (keV)	CL%	DOCUMENT ID		TECN	COMMENT
<0.82	95	[57] BARATE	00E	ALEP	$\gamma\gamma \to \pi^+\pi^-$

[57] Assuming spin 0.

$f_0(1710)$ BRANCHING RATIOS

$\Gamma(K\overline{K})/\Gamma_{total}$ Γ_1/Γ

VALUE	DOCUMENT ID		TECN	COMMENT
• • • We do not use the following data for averages, fits, limits, etc. • • •				
0.36 ± 0.12	ALBALADEJO	08	RVUE	
$0.38^{+0.09}_{-0.19}$	[58,59] LONGACRE	86	MPS	$22\ \pi^- p \to n 2K^0_S$

$\Gamma(\eta\eta)/\Gamma_{total}$ Γ_2/Γ

VALUE	DOCUMENT ID		TECN	COMMENT
• • • We do not use the following data for averages, fits, limits, etc. • • •				
0.22 ± 0.12	ALBALADEJO	08	RVUE	
$0.18^{+0.03}_{-0.13}$	[58,59] LONGACRE	86	RVUE	

$\Gamma(\pi\pi)/\Gamma_{total}$ Γ_3/Γ

VALUE	DOCUMENT ID		TECN	COMMENT
• • • We do not use the following data for averages, fits, limits, etc. • • •				
not seen	AMSLER	02	CBAR	$0.9\ \bar{p}p \to \pi^0\eta\eta, \pi^0\pi^0\pi^0$
$0.039^{+0.002}_{-0.024}$	[58,59] LONGACRE	86	RVUE	

$\Gamma(\pi\pi)/\Gamma(K\overline{K})$ Γ_3/Γ_1

VALUE	CL%	DOCUMENT ID		TECN	COMMENT
$\mathbf{0.41^{+0.11}_{-0.17}}$		ABLIKIM	06V	BES2	$e^+e^- \to J/\psi \to \gamma\pi^+\pi^-$
• • • We do not use the following data for averages, fits, limits, etc. • • •					
0.32 ± 0.14		ALBALADEJO	08	RVUE	
< 0.11	95	[60] ABLIKIM	04E	BES2	$J/\psi \to \omega K^+K^-$
$5.8\ ^{+9.1}_{-5.5}$		[61] ANISOVICH	02D	SPEC	Combined fit
$0.2\ \pm0.024\pm0.036$		BARBERIS	99D	OMEG	$450\ pp \to K^+K^-, \pi^+\pi^-$
0.39 ± 0.14		ARMSTRONG	91	OMEG	$300\ pp \to pp\pi\pi, ppK\overline{K}$

$\Gamma(\eta\eta)/\Gamma(K\overline{K})$ Γ_2/Γ_1

VALUE	CL%	DOCUMENT ID		TECN	COMMENT
$\mathbf{0.48\pm0.15}$		BARBERIS	00E		$450\ pp \to p_f\eta\eta p_s$
• • • We do not use the following data for averages, fits, limits, etc. • • •					
$0.46^{+0.70}_{-0.38}$		[61] ANISOVICH	02D	SPEC	Combined fit
<0.02	90	[62] PROKOSHKIN	91	GA24	$300\ \pi^- p \to \pi^- p\eta\eta$

$\Gamma(\omega\omega)/\Gamma_{total}$ Γ_5/Γ

VALUE	EVTS	DOCUMENT ID		TECN	COMMENT
seen	180	ABLIKIM	06H	BES	$J/\psi \to \gamma\omega\omega$

[58] From a partial-wave analysis of data using a K-matrix formalism with 5 poles, but assuming spin 2.
[59] Fit with constrained inelasticity.
[60] Using data from ABLIKIM 04A.
[61] From a combined K-matrix analysis of Crystal Barrel (0. $p\overline{p} \to \pi^0\pi^0\pi^0, \pi^0\eta\eta, \pi^0\pi^0\eta$), GAMS ($\pi p \to \pi^0\pi^0 n, \eta\eta n, \eta\eta' n$), and BNL ($\pi p \to K\overline{K}n$) data.
[62] Combining results of GAM4 with those of ARMSTRONG 89D.

$f_0(1710)$ REFERENCES

UEHARA	13	PTEP 2013 123C01	S. Uehara *et al.*	(BELLE Collab.)
ALBALADEJO	08	PRL 101 252002	M. Albaladejo, J.A. Oller	
CHEKANOV	08	PRL 101 112003	S. Chekanov *et al.*	(ZEUS Collab.)
ABLIKIM	06H	PR D73 112007	M. Ablikim *et al.*	(BES Collab.)
ABLIKIM	06V	PL B642 441	M. Ablikim *et al.*	(BES Collab.)
AMSLER	06	PL B639 165	C. Amsler *et al.*	(CBAR Collab.)
UMAN	06	PR D73 052009	I. Uman *et al.*	(FNAL E835)
VLADIMIRSK...	06	PAN 69 493 Translated from YAF 69 515.	V.V. Vladimirsky *et al.*	(ITEP, Moscow)
ABLIKIM	05	PL B607 243	M. Ablikim *et al.*	(BES Collab.)
ABLIKIM	05Q	PR D72 092002	M. Ablikim *et al.*	(BES Collab.)
BINON	05	PAN 68 960 Translated from YAF 68 998.	F. Binon *et al.*	
CLOSE	05	PR D71 094022	F.E. Close, Q. Zhao	
ABLIKIM	04A	PL B598 149	M. Ablikim *et al.*	(BES Collab.)
ABLIKIM	04E	PL B603 138	M. Ablikim *et al.*	(BES Collab.)
CHEKANOV	04	PL B578 33	S. Chekanov *et al.*	(ZEUS Collab.)
PDG	04	PL B592 1	S. Eidelman *et al.*	(PDG Collab.)
ANISOVICH	03	EPJ A16 229	V.V. Anisovich *et al.*	
BAI	03G	PR D68 052003	J.Z. Bai *et al.*	(BES Collab.)
TIKHOMIROV	03	PAN 66 828 Translated from YAF 66 860.	G.D. Tikhomirov *et al.*	
AMSLER	02	EPJ C23 29	C. Amsler *et al.*	
ANISOVICH	02D	PAN 65 1545 Translated from YAF 65 1583.	V.V. Anisovich *et al.*	
NICHITIU	02	PL B545 261	F. Nichitiu *et al.*	(OBELIX Collab.)
BAI	00A	PL B472 207	J.Z. Bai *et al.*	(BES Collab.)
BARATE	00E	PL B472 189	R. Barate *et al.*	(ALEPH Collab.)
BARBERIS	00E	PL B479 59	D. Barberis *et al.*	(WA 102 Collab.)
ANISOVICH	99B	PL B449 154	A.V. Anisovich *et al.*	
BARBERIS	99	PL B453 305	D. Barberis *et al.*	(Omega Expt.)
BARBERIS	99B	PL B453 316	D. Barberis *et al.*	(Omega Expt.)
BARBERIS	99D	PL B462 462	D. Barberis *et al.*	(Omega Expt.)
FRENCH	99	PL B460 213	B. French *et al.*	(WA76 Collab.)
ANISOVICH	98B	SPU 41 419 Translated from UFN 168 481.	V.V. Anisovich *et al.*	
BAI	98H	PRL 81 1179	J.Z. Bai *et al.*	(BES Collab.)
BARKOV	98	JETPL 68 764	B.P. Barkov *et al.*	
ABREU	96C	PL B379 309	P. Abreu *et al.*	(DELPHI Collab.)
BAI	96C	PRL 77 3959	J.Z. Bai *et al.*	(BES Collab.)
BALOSHIN	95	PAN 58 46 Translated from YAF 58 50.	O.N. Baloshin *et al.*	(ITEP)
BUGG	95	PL B353 378	D.V. Bugg *et al.*	(LOQM, PNPI, WASH)
ARMSTRONG	93C	PL B307 394	T.A. Armstrong *et al.*	(FNAL, FERR, GENO+)
BREAKSTONE	93	ZPHY C58 251	A.M. Breakstone *et al.*	(IOWA, CERN, DORT+)
ALDE	92D	PL B284 457	D.M. Alde *et al.*	(GAM2 Collab.)
Also		SJNP 54 451 Translated from YAF 54 745.	D.M. Alde *et al.*	(GAM2 Collab.)
ARMSTRONG	91	ZPHY C51 351	T.A. Armstrong *et al.*	(ATHU, BARI, BIRM+)
PROKOSHKIN	91	SPD 36 155 Translated from DANS 316 900.	Y.D. Prokoshkin	(GAM2, GAM4 Collab.)
ALBRECHT	90G	ZPHY C48 183	H. Albrecht *et al.*	(ARGUS Collab.)
ARMSTRONG	89D	PL B227 186	T.A. Armstrong, M. Benayoun	(ATHU, BARI, BIRM+)
BEHREND	89C	ZPHY C43 91	H.J. Behrend *et al.*	(CELLO Collab.)
AUGUSTIN	88	PRL 60 2238	J.E. Augustin *et al.*	(DM2 Collab.)
BOLONKIN	88	NP B309 426	B.V. Bolonkin *et al.*	(ITEP, SERP)
FALVARD	88	PR D38 2706	A. Falvard *et al.*	(CLER, FRAS, LALO+)
AUGUSTIN	87	ZPHY C36 369	J.E. Augustin *et al.*	(LALO, CLER, FRAS+)
BALTRUSAIT...	87	PR D35 2077	R.M. Baltrusaitis *et al.*	(Mark III Collab.)
ALDE	86C	PL B182 105	D.M. Alde *et al.*	(SERP, BELG, LANL, LAPP)
LONGACRE	86	PL B177 223	R.S. Longacre *et al.*	(BNL, BRAN, CUNY+)
ALTHOFF	85B	ZPHY C29 189	M. Althoff *et al.*	(TASSO Collab.)
WILLIAMS	84	PR D30 877	E.G.H. Williams *et al.*	(VAND, NDAM, TUFTS+)
BLOOM	83	ARNS 33 143	E.D. Bloom, C. Peck	(SLAC, CIT)
BURKE	82	PRL 49 632	D.L. Burke *et al.*	(LBL, SLAC)
EDWARDS	82D	PRL 48 458	C. Edwards *et al.*	(CIT, HARV, PRIN+)
ETKIN	82B	PR D25 1786	A. Etkin *et al.*	(BNL, CUNY, TUFTS, VAND)
ETKIN	82C	PR D25 2446	A. Etkin *et al.*	(BNL, CUNY, TUFTS, VAND)

$\eta(1760)$

$I^G(J^{PC}) = 0^+(0^{-+})$

OMITTED FROM SUMMARY TABLE

Seen by DM2 in the $\rho\rho$ system (BISELLO 89B). Structure in this region has been reported before in the same system (BALTRUSAITIS 86B) and in the $\omega\omega$ system (BALTRUSAITIS 85C, BISELLO 87).

$\eta(1760)$ MASS

VALUE (MeV)	EVTS	DOCUMENT ID		TECN	COMMENT
1751±15 OUR AVERAGE					
$1768^{+24}_{-25}\pm10$	465	[1] ZHANG	12A	BELL	$e^+e^- \to e^+e^-\eta'\pi^+\pi^-$
$1744\pm10\pm15$	1045	[2] ABLIKIM	06H	BES	$J/\psi \to \gamma\omega\omega$
• • • We do not use the following data for averages, fits, limits, etc. • • •					
$1703^{+12}_{-11}\pm\ 2$		[3] ZHANG	12A	BELL	$e^+e^- \to e^+e^-\eta'\pi^+\pi^-$
1760 ± 11	320	[4] BISELLO	89B	DM2	$J/\psi \to 4\pi\gamma$

[1] From a single-resonance fit.
[2] From a partial wave analysis including $\eta(1760)$, $f_0(1710)$, $f_2(1640)$, and $f_2(1910)$.
[3] From a two-resonance fit.
[4] Estimated by us from various fits. Systematic uncertainties not estimated.

$\eta(1760)$ WIDTH

VALUE (MeV)	EVTS	DOCUMENT ID		TECN	COMMENT
240±30 OUR AVERAGE					
$224^{+62}_{-56}\pm25$	465	[5] ZHANG	12A	BELL	$e^+e^- \to e^+e^-\eta'\pi^+\pi^-$
$244^{+24}_{-21}\pm25$	1045	[6] ABLIKIM	06H	BES	$J/\psi \to \gamma\omega\omega$
• • • We do not use the following data for averages, fits, limits, etc. • • •					
$42^{+36}_{-22}\pm15$		[7] ZHANG	12A	BELL	$e^+e^- \to e^+e^-\eta'\pi^+\pi^-$
60 ± 16	320	[8] BISELLO	89B	DM2	$J/\psi \to 4\pi\gamma$

[5] From a single-resonance fit.
[6] From a partial wave analysis including $\eta(1760)$, $f_0(1710)$, $f_2(1640)$, and $f_2(1910)$.
[7] From a two-resonance fit.
[8] Estimated by us from various fits. Systematic uncertainties not estimated.

$\eta(1760)$ DECAY MODES

	Mode	Fraction (Γ_i/Γ)
Γ_1	4π	
Γ_2	$2\pi^+2\pi^-$	seen
Γ_3	$\pi^+\pi^-2\pi^0$	seen
Γ_4	$\rho^0\rho^0$	seen
Γ_5	$\rho^+\rho^-$	seen
Γ_6	$2(\pi^+\pi^-\pi^0)$	
Γ_7	$\omega\omega$	seen
Γ_8	$\eta'\pi^+\pi^-$	seen
Γ_9	$\gamma\gamma$	seen

$\eta(1760)$ Γ(i)$\Gamma(\gamma\gamma)/\Gamma$(total)

$\Gamma(\eta'\pi^+\pi^-) \times \Gamma(\gamma\gamma)/\Gamma_{total}$ $\Gamma_8\Gamma_9/\Gamma$

VALUE (eV)	EVTS	DOCUMENT ID		TECN	COMMENT
$28.2^{+\ 7.9}_{-\ 7.5}\pm3.7$	465	[9] ZHANG	12A	BELL	$e^+e^- \to e^+e^-\eta'\pi^+\pi^-$
• • • We do not use the following data for averages, fits, limits, etc. • • •					
$3.0^{+\ 2.0}_{-\ 1.2}\pm0.8$	52	[10] ZHANG	12A	BELL	$e^+e^- \to e^+e^-\eta'\pi^+\pi^-$
$18\ ^{+13}_{-10}\ \pm5$	315	[11] ZHANG	12A	BELL	$e^+e^- \to e^+e^-\eta'\pi^+\pi^-$

[9] From a single-resonance fit.
[10] From a two-resonance fit. For constructive interference with the $X(1835)$.
[11] From a two-resonance fit. For destructive interference with the $X(1835)$.

$\eta(1760)$ BRANCHING RATIOS

$\Gamma(2\pi^+2\pi^-)/\Gamma_{total}$ Γ_2/Γ

VALUE	DOCUMENT ID		TECN	COMMENT
seen	BISELLO	89B	DM2	$J/\psi \to \gamma 2\pi^+2\pi^-$

$\Gamma(\pi^+\pi^-2\pi^0)/\Gamma_{total}$ Γ_3/Γ

VALUE	DOCUMENT ID		TECN	COMMENT
seen	BISELLO	89B	DM2	$J/\psi \to \gamma\pi^+\pi^-2\pi^0$

$\Gamma(\rho^0\rho^0)/\Gamma_{total}$ Γ_4/Γ

VALUE	DOCUMENT ID		TECN	COMMENT
seen	BISELLO	89B	DM2	$J/\psi \to \gamma\rho^0\rho^0$
seen	BALTRUSAIT...86		MRK3	$J/\psi \to \gamma\rho^0\rho^0$

$\Gamma(\rho^+\rho^-)/\Gamma_{total}$ Γ_5/Γ

VALUE	DOCUMENT ID		TECN	COMMENT
seen	BISELLO	89B	DM2	$J/\psi \to \gamma\rho^+\rho^-$
seen	BALTRUSAIT...86		MRK3	$J/\psi \to \gamma\rho^+\rho^-$

$\Gamma(\omega\omega)/\Gamma_{total}$ Γ_7/Γ

VALUE	DOCUMENT ID		TECN	COMMENT
seen	BISELLO	87	DM2	$J/\psi \to \omega\omega$
seen	BALTRUSAIT...85C		MRK3	$J/\psi \to \gamma\omega\omega$

$\eta(1760)$ REFERENCES

ZHANG	12A	PR D86 052002	C.C. Zhang *et al.*	(BELLE Collab.)
ABLIKIM	06H	PR D73 112007	M. Ablikim *et al.*	(BES Collab.)
BISELLO	89B	PR D39 701	G. Busetto *et al.*	(DM2 Collab.)
BISELLO	87	PL B192 239	D. Bisello *et al.*	(PADO, CLER, FRAS+)
BALTRUSAIT... 86		PR D33 629	R.M. Baltrusaitis *et al.*	(Mark III Collab.)
BALTRUSAIT... 86B		PR D33 1222	R.M. Baltrusaitis *et al.*	(Mark III Collab.)
BALTRUSAIT... 85C		PRL 55 1723	R.M. Baltrusaitis *et al.*	(CIT, UCSC+)

$\pi(1800)$ $I^G(J^{PC}) = 1^-(0^{-+})$

See also minireview under non-$q\bar{q}$ candidates in PDG 06, Journal of Physics (generic for all A,B,E,G) **G33** 1 (2006).

$\pi(1800)$ MASS

VALUE (MeV)	EVTS	DOCUMENT ID		TECN	CHG	COMMENT
1812±12 OUR AVERAGE		Error includes scale factor of 2.3. See the ideogram below.				
$1785\pm\ 9^{+12}_{-\ 6}$	420k	ALEKSEEV	10	COMP		190 $\pi^- Pb \to \pi^-\pi^-\pi^+ Pb'$
$1876\pm18\pm16$	4k	[1] EUGENIO	08	B852	–	18 $\pi^- p \to \eta\eta\pi^- p$
$1774\pm18\pm20$		[2] CHUNG	02	B852		18.3 $\pi^- p \to \pi^+\pi^-\pi^- p$
$1863\pm\ 9\pm10$		[3] CHUNG	02	B852		18.3 $\pi^- p \to \pi^+\pi^-\pi^- p$
$1840\pm10\pm10$	1200	AMELIN	96B	VES	–	37 $\pi^- A \to \eta\eta\pi^- A$
$1775\pm\ 7\pm10$		[4] AMELIN	95B	VES	–	36 $\pi^- A \to \pi^+\pi^-\pi^- A$
1790 ± 14		[5] BERDNIKOV	94	VES	–	37 $\pi^- A \to K^+K^-\pi^- A$
$1873\pm33\pm20$		BELADIDZE	92C	VES	–	36 π^-Be $\to \pi^-\eta'\eta$Be
$1814\pm10\pm23$	426 ± 57	BITYUKOV	91	VES	–	36 π^-C $\to \pi^-\eta\eta$C
1770 ± 30	1100	BELLINI	82	SPEC	–	40 $\pi^- A \to 3\pi A$
• • • We do not use the following data for averages, fits, limits, etc. • • •						
$1737\pm\ 5\pm15$		AMELIN	99	VES		37 $\pi^- A \to \omega\pi^-\pi^0 A^*$

[1] From a single-pole fit.
[2] In the $f_0(980)\pi$ wave.
[3] In the $f_0(500)\pi$ wave.
[4] From a fit to $J^{PC} = 0^{-+}$ $f_0(980)\pi$, $f_0(1370)\pi$ waves.
[5] From a fit to $J^{PC} = 0^{-+}$ $K_0^*(1430)K^-$ and $f_0(980)\pi^-$ waves.

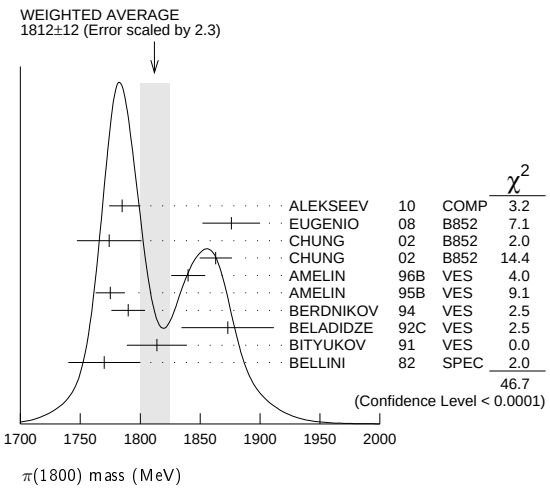

$\pi(1800)$ WIDTH

VALUE (MeV)	EVTS	DOCUMENT ID		TECN	CHG	COMMENT
208±12 OUR AVERAGE						
$208\pm22^{+21}_{-37}$	420k	ALEKSEEV	10	COMP		190 $\pi^- Pb \to \pi^-\pi^-\pi^+ Pb'$
$221\pm26\pm38$	4k	[6] EUGENIO	08	B852	–	18 $\pi^- p \to \eta\eta\pi^- p$
$223\pm48\pm50$		[7] CHUNG	02	B852		18.3 $\pi^- p \to \pi^+\pi^-\pi^- p$
$191\pm21\pm20$		[8] CHUNG	02	B852		18.3 $\pi^- p \to \pi^+\pi^-\pi^- p$
$210\pm30\pm30$	1200	AMELIN	96B	VES	–	37 $\pi^- A \to \eta\eta\pi^- A$
$190\pm15\pm15$		[9] AMELIN	95B	VES	–	36 $\pi^- A \to \pi^+\pi^-\pi^- A$
210 ± 70		[10] BERDNIKOV	94	VES	–	37 $\pi^- A \to K^+K^-\pi^- A$
$225\pm35\pm20$		BELADIDZE	92C	VES	–	36 π^-Be $\to \pi^-\eta'\eta$Be
$205\pm18\pm32$	426 ± 57	BITYUKOV	91	VES	–	36 π^-C $\to \pi^-\eta\eta$C
310 ± 50	1100	BELLINI	82	SPEC	–	40 $\pi^- A \to 3\pi A$
• • • We do not use the following data for averages, fits, limits, etc. • • •						
$259\pm19\pm\ 6$		AMELIN	99	VES		37 $\pi^- A \to \omega\pi^-\pi^0 A^*$

[6] From a single-pole fit.
[7] In the $f_0(980)\pi$ wave.
[8] In the $f_0(500)\pi$ wave.
[9] From a fit to $J^{PC} = 0^{-+}$ $f_0(980)\pi$, $f_0(1370)\pi$ waves.
[10] From a fit to $J^{PC} = 0^{-+}$ $K_0^*(1430)K^-$ and $f_0(980)\pi^-$ waves.

Meson Particle Listings

$\pi(1800)$, $f_2(1810)$

$\pi(1800)$ DECAY MODES

	Mode	Fraction (Γ_i/Γ)
Γ_1	$\pi^+\pi^-\pi^-$	seen
Γ_2	$f_0(500)\pi^-$	seen
Γ_3	$f_0(980)\pi^-$	seen
Γ_4	$f_0(1370)\pi^-$	seen
Γ_5	$f_0(1500)\pi^-$	not seen
Γ_6	$\rho\pi^-$	not seen
Γ_7	$\eta\eta\pi^-$	seen
Γ_8	$a_0(980)\eta$	seen
Γ_9	$a_2(1320)\eta$	not seen
Γ_{10}	$f_2(1270)\pi$	not seen
Γ_{11}	$f_0(1370)\pi^-$	not seen
Γ_{12}	$f_0(1500)\pi^-$	seen
Γ_{13}	$\eta\eta'(958)\pi^-$	seen
Γ_{14}	$K_0^*(1430)K^-$	seen
Γ_{15}	$K^*(892)K^-$	not seen

$\pi(1800)$ BRANCHING RATIOS

$\Gamma(f_0(980)\pi^-)/\Gamma(f_0(500)\pi^-)$ Γ_3/Γ_2

VALUE	DOCUMENT ID		TECN	COMMENT
0.44±0.08±0.38	[11] CHUNG	02	B852	18.3 $\pi^- p \to \pi^+\pi^-\pi^- p$

$\Gamma(f_0(980)\pi^-)/\Gamma(f_0(1370)\pi^-)$ Γ_3/Γ_4

VALUE	DOCUMENT ID		TECN	CHG	COMMENT
• • • We do not use the following data for averages, fits, limits, etc. • • •					
1.7±1.3	[12] AMELIN	95B	VES	–	36 $\pi^- A \to \pi^+\pi^-\pi^- A$

$\Gamma(f_0(1370)\pi^-)/\Gamma_{total}$ Γ_4/Γ

VALUE	DOCUMENT ID		TECN	CHG	COMMENT
seen	BELLINI	82	SPEC	–	40 π^-A → 3πA

$\Gamma(f_0(1500)\pi^-)/\Gamma_{total}$ Γ_5/Γ

VALUE	DOCUMENT ID		TECN	CHG	COMMENT
not seen	CHUNG	02	B852		18.3 $\pi^- p \to \pi^+\pi^-\pi^- p$

$\Gamma(\rho\pi^-)/\Gamma_{total}$ Γ_6/Γ

VALUE	DOCUMENT ID		TECN	CHG	COMMENT
not seen	BELLINI	82	SPEC	–	40 π^-A → 3πA

$\Gamma(\rho\pi^-)/\Gamma(f_0(980)\pi^-)$ Γ_6/Γ_3

VALUE	CL%	DOCUMENT ID		TECN	CHG	COMMENT
• • • We do not use the following data for averages, fits, limits, etc. • • •						
<0.25		CHUNG	02	B852		18.3 $\pi^- p \to \pi^+\pi^-\pi^- p$
<0.14	90	AMELIN	95B	VES	–	36 $\pi^- A \to \pi^+\pi^-\pi^- A$

$\Gamma(\eta\eta\pi^-)/\Gamma(\pi^+\pi^-\pi^-)$ Γ_7/Γ_1

VALUE	EVTS	DOCUMENT ID		TECN	CHG	COMMENT
• • • We do not use the following data for averages, fits, limits, etc. • • •						
0.5±0.1	1200	[12] AMELIN	96B	VES	–	37 $\pi^- A \to \eta\eta\pi^- A$

$\Gamma(a_2(1320)\eta)/\Gamma_{total}$ Γ_9/Γ

VALUE	DOCUMENT ID		TECN	COMMENT
not seen	EUGENIO	08	B852	18 $\pi^- p \to \eta\eta\pi^- p$

$\Gamma(f_2(1270)\pi)/\Gamma_{total}$ Γ_{10}/Γ

VALUE	DOCUMENT ID		TECN	COMMENT
not seen	EUGENIO	08	B852	18 $\pi^- p \to \eta\eta\pi^- p$

$\Gamma(f_0(1370)\pi^-)/\Gamma_{total}$ Γ_{11}/Γ

VALUE	DOCUMENT ID		TECN	COMMENT
not seen	EUGENIO	08	B852	18 $\pi^- p \to \eta\eta\pi^- p$

$\Gamma(f_0(1500)\pi^-)/\Gamma(a_0(980)\eta)$ Γ_{12}/Γ_8

VALUE	EVTS	DOCUMENT ID		TECN	CHG	COMMENT
• • • We do not use the following data for averages, fits, limits, etc. • • •						
0.48 ±0.17	4k	[12,13] EUGENIO	08	B852	–	18 $\pi^- p \to \eta\eta\pi^- p$
$0.030^{+0.014}_{-0.011}$		[12] ANISOVICH	01B	SPEC	0	0.6–1.94 $p\overline{p} \to \eta\eta\pi^0\pi^0$
0.08 ±0.03	1200	[12,14] AMELIN	96B	VES	–	37 $\pi^- A \to \eta\eta\pi^- A$

$\Gamma(\eta\eta'(958)\pi^-)/\Gamma(\eta\eta\pi^-)$ Γ_{13}/Γ_7

VALUE	EVTS	DOCUMENT ID		TECN	CHG	COMMENT
• • • We do not use the following data for averages, fits, limits, etc. • • •						
0.29±0.07		[12] BELADIDZE	92C	VES	–	36 π^-Be → $\pi^-\eta'\eta$Be
0.3 ±0.1	426 ± 57	[12] BITYUKOV	91	VES	–	36 π^-C → $\pi^-\eta\eta$C

$\Gamma(K_0^*(1430)K^-)/\Gamma_{total}$ Γ_{14}/Γ

VALUE	DOCUMENT ID		TECN	CHG	COMMENT
seen	BERDNIKOV	94	VES	–	37 $\pi^- A \to K^+K^-\pi^- A$

$\Gamma(K^*(892)K^-)/\Gamma_{total}$ Γ_{15}/Γ

VALUE	DOCUMENT ID		TECN	CHG	COMMENT
not seen	BERDNIKOV	94	VES	–	37 $\pi^- A \to K^+K^-\pi^- A$

[11] Assuming that $f_0(980)$ decays only to $\pi\pi$.
[12] Systematic errors not estimated.
[13] From a single-pole fit.
[14] Assuming that $f_0(1500)$ decays only to $\eta\eta$ and $a_0(980)$ decays only to $\eta\pi$.

$\pi(1800)$ REFERENCES

ALEKSEEV	10	PRL 104 241803	M.G. Alekseev *et al.*	(COMPASS Collab.)
EUGENIO	08	PL B660 466	P. Eugenio *et al.*	(BNL E852 Collab.)
PDG	06	JP G33 1	W.-M. Yao *et al.*	(PDG Collab.)
CHUNG	02	PR D65 072001	S.U. Chung *et al.*	(BNL E852 Collab.)
ANISOVICH	01B	PL B500 222	A.V. Anisovich *et al.*	
AMELIN	99	PAN 62 445 Translated from YAF 62 487.	D.V. Amelin *et al.*	(VES Collab.)
AMELIN	96B	PAN 59 976 Translated from YAF 59 1021.	D.V. Amelin *et al.*	(SERP, TBIL) IGJPC
AMELIN	95B	PL B356 595	D.V. Amelin *et al.*	(SERP, TBIL)
BERDNIKOV	94	PL B337 219	E.B. Berdnikov *et al.*	(SERP, TBIL)
BELADIDZE	92C	SJNP 55 1535 Translated from YAF 55 2748.	G.M. Beladidze, S.I. Bityukov, G.V. Borisov	(SERP+)
BITYUKOV	91	PL B268 137	S.I. Bityukov *et al.*	(SERP, TBIL)
BELLINI	82	PRL 48 1697	G. Bellini *et al.*	(MILA, BGNA, JINR)

$f_2(1810)$

$I^G(J^{PC}) = 0^+(2^{++})$

OMITTED FROM SUMMARY TABLE
Needs confirmation.

$f_2(1810)$ MASS

VALUE (MeV)	EVTS	DOCUMENT ID		TECN	COMMENT
1815±12 OUR AVERAGE		Error includes scale factor of 1.4. See the ideogram below.			
$1737\pm 9^{+198}_{-65}$		[1] UEHARA	10A	BELL	10.6 $e^+e^- \to e^+e^-\eta\eta$
1800±30	40	ALDE	88D	GAM4	300 $\pi^- p \to \pi^- p 4\pi^0$
1806±10	1600	ALDE	87	GAM4	100 $\pi^- p \to 4\pi^0 n$
1870±40		[2] ALDE	86D	GAM4	100 $\pi^- p \to \eta\eta n$
1857^{+35}_{-24}		[3] COSTA...	80	OMEG	10 $\pi^- p \to K^+K^- n$
• • • We do not use the following data for averages, fits, limits, etc. • • •					
1858^{+18}_{-71}		[4] LONGACRE	86	RVUE	Compilation
1799±15		[5] CASON	82	STRC	8 $\pi^+ p \to \Delta^{++}\pi^0\pi^0$

[1] Breit-Wigner mass.
[2] Seen in only one solution.
[3] Error increased by spread of two solutions. Included in LONGACRE 86 global analysis.
[4] From a partial-wave analysis of data using a K-matrix formalism with 5 poles. Includes compilation of several other experiments.
[5] From an amplitude analysis of the reaction $\pi^+\pi^- \to 2\pi^0$. The resonance in the $2\pi^0$ final state is not confirmed by PROKOSHKIN 97.

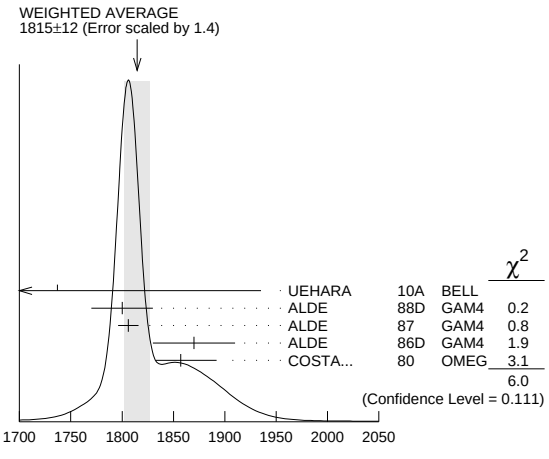

$f_2(1810)$ WIDTH

VALUE (MeV)	EVTS	DOCUMENT ID		TECN	COMMENT
197± 22 OUR AVERAGE		Error includes scale factor of 1.5.			See the ideogram below.
$228^{+\ 21+234}_{-\ 20-153}$		[6] UEHARA	10A	BELL	10.6 $e^+e^- \to e^+e^-\eta\eta$
160± 30	40	ALDE	88D	GAM4	300 $\pi^- p \to \pi^- p 4\pi^0$
190± 20	1600	ALDE	87	GAM4	100 $\pi^- p \to 4\pi^0 n$
250± 30		[7] ALDE	86D	GAM4	100 $\pi^- p \to \eta\eta n$
185^{+102}_{-139}		[8] COSTA...	80	OMEG	10 $\pi^- p \to K^+K^- n$
• • • We do not use the following data for averages, fits, limits, etc. • • •					
$388^{+\ 15}_{-\ 21}$		[9] LONGACRE	86	RVUE	Compilation
$280^{+\ 42}_{-\ 35}$		[10] CASON	82	STRC	8 $\pi^+ p \to \Delta^{++}\pi^0\pi^0$

[6] Breit-Wigner width.
[7] Seen in only one solution.
[8] Error increased by spread of two solutions. Included in LONGACRE 86 global analysis.
[9] From a partial-wave analysis of data using a K-matrix formalism with 5 poles. Includes compilation of several other experiments.
[10] From an amplitude analysis of the reaction $\pi^+\pi^- \to 2\pi^0$. The resonance in the $2\pi^0$ final state is not confirmed by PROKOSHKIN 97.

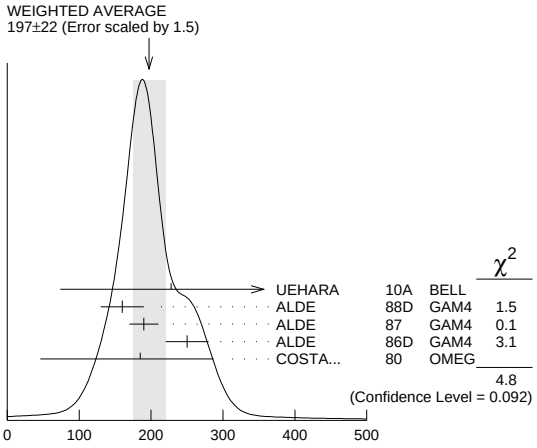

$f_2(1810)$ DECAY MODES

	Mode	Fraction (Γ_i/Γ)
Γ_1	$\pi\pi$	
Γ_2	$\eta\eta$	
Γ_3	$4\pi^0$	seen
Γ_4	K^+K^-	
Γ_5	$\gamma\gamma$	seen

$f_2(1810)\ \Gamma(i)\Gamma(\gamma\gamma)/\Gamma(\text{total})$

$\Gamma(\eta\eta) \times \Gamma(\gamma\gamma)/\Gamma_{\text{total}}$ — **$\Gamma_2\Gamma_5/\Gamma$**

VALUE (eV)	DOCUMENT ID		TECN	COMMENT
$\mathbf{5.2^{+\ 0.9+\ 37.3}_{-\ 0.8-\ \ 4.5}}$	[11] UEHARA	10A	BELL	10.6 $e^+e^- \to e^+e^-\eta\eta$

[11] Including interference with the $f_2'(1525)$ (parameters fixed to the values from the 2008 edition of this review, PDG 08) and $f_2(1270)$. May also be the $f_0(1500)$.

$f_2(1810)$ BRANCHING RATIOS

$\Gamma(\pi\pi)/\Gamma_{\text{total}}$ — **Γ_1/Γ**

VALUE	DOCUMENT ID		TECN	COMMENT
• • • We do not use the following data for averages, fits, limits, etc. • • •				
not seen	AMSLER	02	CBAR	0.9 $\bar{p}p \to \pi^0\eta\eta, \pi^0\pi^0\pi^0$
not seen	PROKOSHKIN	97	GAM2	38 $\pi^- p \to \pi^0\pi^0 n$
$0.21^{+0.02}_{-0.03}$	[12] LONGACRE	86	RVUE	Compilation
0.44±0.03	[13] CASON	82	STRC	8 $\pi^+ p \to \Delta^{++}\pi^0\pi^0$

[12] From a partial-wave analysis of data using a K-matrix formalism with 5 poles. Includes compilation of several other experiments.
[13] Included in LONGACRE 86 global analysis.

$\Gamma(\eta\eta)/\Gamma_{\text{total}}$ — **Γ_2/Γ**

VALUE	DOCUMENT ID		TECN	COMMENT
• • • We do not use the following data for averages, fits, limits, etc. • • •				
$0.008^{+0.028}_{-0.003}$	[14] LONGACRE	86	RVUE	Compilation

[14] From a partial-wave analysis of data using a K-matrix formalism with 5 poles. Includes compilation of several other experiments.

$\Gamma(\pi\pi)/\Gamma(4\pi^0)$ — **Γ_1/Γ_3**

VALUE	DOCUMENT ID		TECN	COMMENT
• • • We do not use the following data for averages, fits, limits, etc. • • •				
<0.75	ALDE	87	GAM4	100 $\pi^- p \to 4\pi^0 n$

$\Gamma(4\pi^0)/\Gamma(\eta\eta)$ — **Γ_3/Γ_2**

VALUE	DOCUMENT ID		TECN	COMMENT
• • • We do not use the following data for averages, fits, limits, etc. • • •				
0.8±0.3	ALDE	87	GAM4	100 $\pi^- p \to 4\pi^0 n$

$\Gamma(K^+K^-)/\Gamma_{\text{total}}$ — **Γ_4/Γ**

VALUE	DOCUMENT ID		TECN	COMMENT
• • • We do not use the following data for averages, fits, limits, etc. • • •				
$0.003^{+0.019}_{-0.002}$	[15] LONGACRE	86	RVUE	Compilation
seen	COSTA...	80	OMEG	10 $\pi^- p \to K^+K^- n$

[15] From a partial-wave analysis of data using a K-matrix formalism with 5 poles. Includes compilation of several other experiments.

$f_2(1810)$ REFERENCES

UEHARA	10A	PR D82 114031	S. Uehara *et al.*	(BELLE Collab.)
PDG	08	PL B667 1	C. Amsler *et al.*	(PDG Collab.)
AMSLER	02	EPJ C23 29	C. Amsler *et al.*	
PROKOSHKIN	97	SPD 42 117 Translated from DANS 353 323.	Y.D. Prokoshkin *et al.*	(SERP)
ALDE	88D	SJNP 47 810 Translated from YAF 47 1273.	D.M. Alde *et al.*	(SERP, BELG, LANL, LAPP+)
ALDE	87	PL B198 286	D.M. Alde *et al.*	(LANL, BRUX, SERP, LAPP)
ALDE	86D	NP B269 485	D.M. Alde *et al.*	(BELG, LAPP, SERP, CERN+)
LONGACRE	86	PL B177 223	R.S. Longacre *et al.*	(BNL, BRAN, CUNY+)
CASON	82	PRL 48 1316	N.M. Cason *et al.*	(NDAM, ANL)
COSTA...	80	NP B175 402	G. Costa de Beauregard *et al.*	(BARI, BONN+)

$X(1835)$

$I^G(J^{PC}) = ?^?(?^{-+})$

OMITTED FROM SUMMARY TABLE

Could be a superposition of two states, one with small width appearing as threshold enhancement in $p\bar{p}$, the other one with a larger width, decaying into $\pi^+\pi^-\eta'$. For the former ABLIKIM 12D determine $J^{PC} = 0(^{-+})$.

$X(1835)$ MASS

VALUE (MeV)	EVTS	DOCUMENT ID		TECN	COMMENT
$1835.7^{+\ 5.0}_{-\ 3.2}$ OUR AVERAGE					
$1836.5\pm\ 3.0^{+\ 5.6}_{-\ 2.1}$	4265	[1] ABLIKIM	11C	BES3	$J/\psi \to \gamma\pi^+\pi^-\eta'$
1833.7± 6.1± 2.7	264	ABLIKIM	05R	BES2	$J/\psi \to \gamma\pi^+\pi^-\eta'$
• • • We do not use the following data for averages, fits, limits, etc. • • •					
$1832\ ^{+19}_{-\ 5}\ \pm 26$		[2] ABLIKIM	12D	BES3	$J/\psi \to \gamma p\bar{p}$
$1877.3\pm\ 6.3^{+\ 3.4}_{-\ 7.4}$		[3] ABLIKIM	11J	BES3	$J/\psi \to \omega(\eta\pi^+\pi^-)$
$1837\ ^{+10}_{-12}\ ^{+\ 9}_{-\ 7}$	231	[4,5] ALEXANDER	10	CLEO	$J/\psi \to \gamma p\bar{p}$
1831 ± 7		[5,6] ABLIKIM	05R	BES2	$J/\psi \to \gamma p\bar{p}$
$1859\ ^{+\ 3}_{-10}\ ^{+\ 5}_{-25}$		[5] BAI	03F	BES2	$J/\psi \to \gamma p\bar{p}$

[1] From a fit of the $\pi^+\pi^-\eta'$ mass distribution to a combination of $\gamma f_1(1510)$, $\gamma X(1835)$, and two unconfirmed states $\gamma X(2120)$, and $\gamma X(2370)$, for $M(p\bar{p}) < 2.8$ GeV, and accounting for backgrounds from non-η' events and $J/\psi \to \pi^0\pi^+\pi^-\eta'$.
[2] From the fit including final state interaction effects in isospin 0 S-wave according to SIBIRTSEV 05A. Supersedes ABLIKIM 10G.
[3] The selected process is $J/\psi \to \omega a_0(980)\pi$. This state may be due also to $\eta_2(1870)$ or to a combination of $X(1835)$ and $\eta_2(1870)$.
[4] From a fit of the $p\bar{p}$ mass distribution to a combination of $\gamma X(1835)$, γR with $M(R) = 2100$ MeV and $\Gamma(R) = 160$ MeV, and $\gamma p\bar{p}$ phase space, for $M(p\bar{p}) < 2.85$ GeV.
[5] Evidence for a threshold enhancement in the $p\bar{p}$ mass spectrum was also reported by ABE 02K, AUBERT,B 05L, and WANG 05A in $B^+ \to p\bar{p}K^+$, WANG 05A in $B^0 \to p\bar{p}K^0_S$, ABE 02W in $\overline{B}^0 \to p\bar{p}D^0$, DEL-AMO-SANCHEZ 12 in $B \to D(D^*)p\bar{p}(\pi)$, and WEI 08 in $B^+ \to p\bar{p}\pi^+$ decays. Not seen by ATHAR 06 in $\Upsilon(1S) \to p\bar{p}\gamma$.
[6] From the fit including final state interaction effects in isospin 0 S-wave according to SIBIRTSEV 05A. Systematic errors not estimated.

$X(1835)$ WIDTH

VALUE (MeV)	CL%	EVTS	DOCUMENT ID		TECN	COMMENT
99 ±50 OUR AVERAGE			Error includes scale factor of 2.8.			
190 ± 9 $^{+38}_{-36}$		4265	[7] ABLIKIM	11C	BES3	$J/\psi \to \gamma\pi^+\pi^-\eta'$
67.7±20.3± 7.7		264	ABLIKIM	05R	BES2	$J/\psi \to \gamma\pi^+\pi^-\eta'$

Meson Particle Listings

$X(1835)$, $X(1840)$, $\phi_3(1850)$

• • • We do not use the following data for averages, fits, limits, etc. • • •

< 76		90	[8] ABLIKIM	12D	BES3	$J/\psi \to \gamma p\overline{p}$
57	± 12	$^{+19}_{-4}$	[9] ABLIKIM	11J	BES3	$J/\psi \to \omega(\eta\pi^+\pi^-)$
0	$^{+44}_{-0}$		231 [10,11] ALEXANDER	10	CLEO	$J/\psi \to \gamma p\overline{p}$
< 153		90	[11,12] ABLIKIM	05R	BES2	$J/\psi \to \gamma p\overline{p}$
< 30			[11] BAI	03F	BES2	$J/\psi \to \gamma p\overline{p}$

[7] From a fit of the $\pi^+\pi^-\eta'$ mass distribution to a combination of $\gamma f_1(1510)$, $\gamma X(1835)$, and two unconfirmed states $\gamma X(2120)$, and $\gamma X(2370)$, for $M(p\overline{p}) < 2.8$ GeV, and accounting for backgrounds from non-η' events and $J/\psi \to \pi^0\pi^+\pi^-\eta'$.

[8] From the fit including final state interaction effects in isospin 0 S-wave according to SIBIRTSEV 05A. Supersedes ABLIKIM 10G.

[9] The selected process is $J/\psi \to \omega a_0(980)\pi$. This state may be due also to $\eta_2(1870)$ or to a combination of $X(1835)$ and $\eta_2(1870)$.

[10] From a fit of the $p\overline{p}$ mass distribution to a combination of $\gamma X(1835)$, γR with $M(R) = 2100$ MeV and $\Gamma(R) = 160$ MeV, and $\gamma p\overline{p}$ phase space, for $M(p\overline{p}) < 2.85$ GeV.

[11] Evidence for a threshold enhancement in the $p\overline{p}$ mass spectrum was also reported by ABE 02K, AUBERT,B 05L, and WANG 05A in $B^+ \to p\overline{p}K^+$, WANG 05A in $B^0 \to p\overline{p}K^0_S$, ABE 02W in $\overline{B}^0 \to p\overline{p}D^0$, DEL-AMO-SANCHEZ 12 in $B \to D(D^*)p\overline{p}(\pi)$, and WEI 08 in $B^+ \to p\overline{p}\pi^+$ decays. Not seen by ATHAR 06 in $\Upsilon(1S) \to p\overline{p}\gamma$.

[12] From the fit including final state interaction effects in isospin 0 S-wave according to SIBIRTSEV 05A. Systematic errors not estimated.

$X(1835)$ DECAY MODES

	Mode	Fraction (Γ_i/Γ)
Γ_1	$p\overline{p}$	seen
Γ_2	$\eta'\pi^+\pi^-$	seen
Γ_3	$\gamma\gamma$	

$X(1835)$ $\Gamma(i)\Gamma(\gamma\gamma)/\Gamma(\text{total})$

$\Gamma(\eta'\pi^+\pi^-) \times \Gamma(\gamma\gamma)/\Gamma_{\text{total}}$ $\Gamma_2\Gamma_3/\Gamma$

VALUE (eV)	CL%	DOCUMENT ID		TECN	COMMENT
• • • We do not use the following data for averages, fits, limits, etc. • • •					
<35.6	90	[13] ZHANG	12A	BELL	$e^+e^- \to e^+e^-\eta'\pi^+\pi^-$
<83	90	[14] ZHANG	12A	BELL	$e^+e^- \to e^+e^-\eta'\pi^+\pi^-$

[13] From a two-resonance fit and constructive interference of the $\eta(1760)$ and $X(1835)$, a significance of 2.8 σ.

[14] From a two-resonance fit and destructive interference of the $\eta(1760)$ and $X(1835)$, a significance of 2.8 σ.

$X(1835)$ BRANCHING RATIOS

$\Gamma(p\overline{p})/\Gamma(\eta'\pi^+\pi^-)$ Γ_1/Γ_2

VALUE	DOCUMENT ID		TECN	COMMENT
• • • We do not use the following data for averages, fits, limits, etc. • • •				
0.333	ABLIKIM	05R	BES2	$J/\psi \to \gamma\pi^+\pi^-\eta'$

$X(1835)$ REFERENCES

ABLIKIM	12D	PRL 108 112003	M. Ablikim *et al.*	(BES III Collab.)
DEL-AMO-SA...	12	PR D85 092017	P. del Amo Sanchez *et al.*	(BABAR Collab.)
ZHANG	12A	PR D86 052002	C.C. Zhang *et al.*	(BELLE Collab.)
ABLIKIM	11C	PRL 106 072002	M. Ablikim *et al.*	(BES III Collab.)
ABLIKIM	11J	PRL 107 182001	M. Ablikim *et al.*	(BES III Collab.)
ABLIKIM	10G	CP C34 421	M. Ablikim *et al.*	(BES III Collab.)
ALEXANDER	10	PR D82 092002	J.P. Alexander *et al.*	(CLEO Collab.)
WEI	08	PL B659 80	J.-T. Wei *et al.*	(BELLE Collab.)
ATHAR	06	PR D73 032001	S.B. Athar *et al.*	(CLEO Collab.)
ABLIKIM	05R	PRL 95 262001	M. Ablikim *et al.*	(BES Collab.)
AUBERT,B	05L	PR D72 051101	B. Aubert *et al.*	(BABAR Collab.)
SIBIRTSEV	05A	PR D71 054010	A. Sibirtsev, J. Haidenbauer	
WANG	05A	PL B617 141	M.-Z. Wang *et al.*	(BELLE Collab.)
BAI	03F	PRL 91 022001	J.Z. Bai *et al.*	(BES II Collab.)
ABE	02K	PRL 88 181803	K. Abe *et al.*	(BELLE Collab.)
ABE	02W	PRL 89 151802	K. Abe *et al.*	(BELLE Collab.)

$X(1840)$

$I^G(J^{PC}) = ?^?(?^{??})$

OMITTED FROM SUMMARY TABLE

$X(1840)$ MASS

VALUE (MeV)	EVTS	DOCUMENT ID		TECN	COMMENT
$1842.2 \pm 4.2 ^{+7.1}_{-2.6}$	0.6k	ABLIKIM	13U	BES3	$J/\psi \to \gamma 3(\pi^+\pi^-)$

$X(1840)$ WIDTH

VALUE (MeV)	EVTS	DOCUMENT ID		TECN	COMMENT
$83 \pm 14 \pm 11$	0.6k	ABLIKIM	13U	BES3	$J/\psi \to \gamma 3(\pi^+\pi^-)$

$X(1840)$ DECAY MODES

	Mode	Fraction (Γ_i/Γ)
Γ_1	$3(\pi^+\pi^-)$	seen

$X(1840)$ BRANCHING RATIOS

$\Gamma(3(\pi^+\pi^-))/\Gamma_{\text{total}}$ Γ_1/Γ

VALUE	EVTS	DOCUMENT ID		TECN	COMMENT
seen	0.6k	ABLIKIM	13U	BES3	$J/\psi \to \gamma 3(\pi^+\pi^-)$

$X(1840)$ REFERENCES

ABLIKIM	13U	PR D88 091502	M. Ablikim *et al.*	(BES III Collab.)

$\phi_3(1850)$

$I^G(J^{PC}) = 0^-(3^{--})$

$\phi_3(1850)$ MASS

VALUE (MeV)	EVTS	DOCUMENT ID		TECN	COMMENT
1854 ± 7 OUR AVERAGE					
1855 ± 10		ASTON	88E	LASS	11 $K^-p \to K^-K^+\Lambda$, $K^0_S K^\pm\pi^\mp\Lambda$
$1870 ^{+30}_{-20}$	430	ARMSTRONG	82	OMEG	18.5 $K^-p \to K^-K^+\Lambda$
1850 ± 10	123	ALHARRAN	81B	HBC	8.25 $K^-p \to K\overline{K}\Lambda$

$\phi_3(1850)$ WIDTH

VALUE (MeV)	EVTS	DOCUMENT ID		TECN	COMMENT
$87 ^{+28}_{-23}$ **OUR AVERAGE** Error includes scale factor of 1.2.					
64 ± 31		ASTON	88E	LASS	11 $K^-p \to K^-K^+\Lambda$, $K^0_S K^\pm\pi^\mp\Lambda$
$160 ^{+90}_{-50}$	430	ARMSTRONG	82	OMEG	18.5 $K^-p \to K^-K^+\Lambda$
$80 ^{+40}_{-30}$	123	ALHARRAN	81B	HBC	8.25 $K^-p \to K\overline{K}\Lambda$

$\phi_3(1850)$ DECAY MODES

	Mode	Fraction (Γ_i/Γ)
Γ_1	$K\overline{K}$	seen
Γ_2	$K\overline{K}^*(892) +$ c.c.	seen

$\phi_3(1850)$ BRANCHING RATIOS

$\Gamma(K\overline{K}^*(892) + \text{c.c.})/\Gamma(K\overline{K})$ Γ_2/Γ_1

VALUE	DOCUMENT ID		TECN	COMMENT
$0.55 ^{+0.85}_{-0.45}$	ASTON	88E	LASS	11 $K^-p \to K^-K^+\Lambda$, $K^0_S K^\pm\pi^\mp\Lambda$
• • • We do not use the following data for averages, fits, limits, etc. • • •				
0.8 ± 0.4	ALHARRAN	81B	HBC	8.25 $K^-p \to K\overline{K}\pi\Lambda$

$\phi_3(1850)$ REFERENCES

ASTON	88E	PL B208 324	D. Aston *et al.*	(SLAC, NAGO, CINC, INUS) IGJPC
ARMSTRONG	82	PL 110B 77	T.A. Armstrong *et al.*	(BARI, BIRM, CERN+) JP
ALHARRAN	81B	PL 101B 357	S. Al-Harran *et al.*	(BIRM, CERN, GLAS+)

$\eta_2(1870)$

$I^G(J^{PC}) = 0^+(2^{-+})$

OMITTED FROM SUMMARY TABLE

Needs confirmation.

$\eta_2(1870)$ MASS

VALUE (MeV)	EVTS	DOCUMENT ID		TECN	COMMENT
1842± 8 OUR AVERAGE					
1835±12		BARBERIS	00B		450 $pp \to p_f \eta\pi^+\pi^- p_s$
1844±13		BARBERIS	00C		450 $pp \to p_f 4\pi p_s$
1840±25		BARBERIS	97B	OMEG	450 $pp \to pp2(\pi^+\pi^-)$
1875±20±35		ADOMEIT	96	CBAR	1.94 $\overline{p}p \to \eta 3\pi^0$
1881±32±40	26	KARCH	92	CBAL	$e^+e^- \to e^+e^-\eta\pi^0\pi^0$
• • • We do not use the following data for averages, fits, limits, etc. • • •					
1860± 5±15		ANISOVICH	00E	SPEC	0.9–1.94 $\overline{p}p \to \eta 3\pi^0$
1840±15		BAI	99	BES	$J/\psi \to \gamma\eta\pi^+\pi^-$

$\eta_2(1870)$ WIDTH

VALUE (MeV)	EVTS	DOCUMENT ID		TECN	COMMENT
225±14 OUR AVERAGE					
235±22		BARBERIS	00B		450 $pp \to p_f \eta\pi^+\pi^- p_s$
228±23		BARBERIS	00C		450 $pp \to p_f 4\pi p_s$
200±40		BARBERIS	97B	OMEG	450 $pp \to pp2(\pi^+\pi^-)$
200±25±45		ADOMEIT	96	CBAR	1.94 $\overline{p}p \to \eta 3\pi^0$
221±92±44	26	KARCH	92	CBAL	$e^+e^- \to e^+e^-\eta\pi^0\pi^0$
• • • We do not use the following data for averages, fits, limits, etc. • • •					
$250\pm25^{+50}_{-35}$		ANISOVICH	00E	SPEC	0.9–1.94 $\overline{p}p \to \eta 3\pi^0$
170±40		BAI	99	BES	$J/\psi \to \gamma\eta\pi^+\pi^-$

$\eta_2(1870)$ DECAY MODES

	Mode	Fraction (Γ_i/Γ)
Γ_1	$\eta\pi\pi$	
Γ_2	$a_2(1320)\pi$	
Γ_3	$f_2(1270)\eta$	
Γ_4	$a_0(980)\pi$	
Γ_5	$\gamma\gamma$	seen

$\eta_2(1870)$ BRANCHING RATIOS

$\Gamma(a_2(1320)\pi)/\Gamma(f_2(1270)\eta)$ Γ_2/Γ_3

VALUE	DOCUMENT ID		TECN	COMMENT
1.7 ±0.4 OUR AVERAGE				
1.60±0.40	[1] ANISOVICH	11	SPEC	0.9–1.94 $p\overline{p}$
20.4 ±6.6	BARBERIS	00B		450 $pp \to p_f \eta\pi^+\pi^- p_s$
4.1 ±2.3	ADOMEIT	96	CBAR	1.94 $\overline{p}p \to \eta 3\pi^0$

[1] Reanalysis of ADOMEIT 96 and ANISOVICH 00E.

$\Gamma(a_2(1320)\pi)/\Gamma(a_0(980)\pi)$ Γ_2/Γ_4

VALUE	DOCUMENT ID		COMMENT
32.6±12.6	BARBERIS	00B	450 $pp \to p_f \eta\pi^+\pi^- p_s$

$\Gamma(a_0(980)\pi)/\Gamma(f_2(1270)\eta)$ Γ_4/Γ_3

VALUE	DOCUMENT ID		TECN	COMMENT
0.48±0.45	[2] ANISOVICH	11	SPEC	0.9–1.94 $p\overline{p}$

[2] Reanalysis of ADOMEIT 96 and ANISOVICH 00E.

$\Gamma(\gamma\gamma)/\Gamma_{total}$ Γ_5/Γ

VALUE	DOCUMENT ID		TECN	COMMENT
seen	KARCH	92	CBAL	$e^+e^- \to e^+e^-\eta\pi^0\pi^0$

$\eta_2(1870)$ REFERENCES

ANISOVICH	11	EPJ C71 1511	A.V. Anisovich *et al.*	(LOQM, RAL, PNPI)
ANISOVICH	00E	PL B477 19	A.V. Anisovich *et al.*	
BARBERIS	00B	PL B471 435	D. Barberis *et al.*	(WA 102 Collab.)
BARBERIS	00C	PL B471 440	D. Barberis *et al.*	(WA 102 Collab.)
BAI	99	PL B446 356	J.Z. Bai *et al.*	(BES Collab.)
BARBERIS	97B	PL B413 217	D. Barberis *et al.*	(WA 102 Collab.)
ADOMEIT	96	ZPHY C71 227	J. Adomeit *et al.*	(Crystal Barrel Collab.)
KARCH	92	ZPHY C54 33	K. Karch *et al.*	(Crystal Ball Collab.)

$\pi_2(1880)$

$I^G(J^{PC}) = 1^-(2^{-+})$

$\pi(1880)$ MASS

VALUE (MeV)	EVTS	DOCUMENT ID		TECN	CHG	COMMENT
1895±16 OUR AVERAGE						
1929±24± 18	4k	EUGENIO	08	B852	–	18 $\pi^- p \to \eta\eta\pi^- p$
1876±11± 67	145k	LU	05	B852	–	18 $\pi^- p \to \omega\pi^-\pi^0 p$
2003±88±148	69k	KUHN	04	B852	–	18 $\pi^- p \to \eta\pi^+\pi^-\pi^- p$
1880±20		ANISOVICH	01B	SPEC	0	0.6–1.94 $\overline{p}p \to \eta\eta\pi^0\pi^0$

$\pi(1880)$ WIDTH

VALUE (MeV)	EVTS	DOCUMENT ID		TECN	CHG	COMMENT
235± 34 OUR AVERAGE						
323± 87± 43	4k	EUGENIO	08	B852	–	18 $\pi^- p \to \eta\eta\pi^- p$
146± 17± 62	145k	LU	05	B852	–	18 $\pi^- p \to \omega\pi^-\pi^0 p$
306±132±121	69k	KUHN	04	B852	–	18 $\pi^- p \to \eta\pi^+\pi^-\pi^- p$
255± 45		ANISOVICH	01B	SPEC	0	0.6–1.94 $\overline{p}p \to \eta\eta\pi^0\pi^0$

$\pi_2(1880)$ DECAY MODES

	Mode
Γ_1	$\eta\eta\pi^-$
Γ_2	$a_0(980)\eta$
Γ_3	$a_2(1320)\eta$
Γ_4	$f_0(1500)\pi$
Γ_5	$f_1(1285)\pi$
Γ_6	$\omega\pi^-\pi^0$

$\Gamma(a_2(1320)\eta)/\Gamma(f_1(1285)\pi)$ Γ_3/Γ_5

VALUE	EVTS	DOCUMENT ID		TECN	CHG	COMMENT
• • • We do not use the following data for averages, fits, limits, etc. • • •						
22.7±7.3	69k	KUHN	04	B852	–	18 $\pi^- p \to \eta\pi^+\pi^-\pi^- p$

$\Gamma(f_0(1500)\pi)/\Gamma(a_0(980)\eta)$ Γ_4/Γ_2

VALUE	DOCUMENT ID		TECN	CHG	COMMENT
• • • We do not use the following data for averages, fits, limits, etc. • • •					
$0.28^{+0.20}_{-0.15}$	[1] ANISOVICH	01B	SPEC	0	0.6–1.94 $\overline{p}p \to \eta\eta\pi^0\pi^0$

[1] Systematic errors not estimated.

$\pi_2(1880)$ REFERENCES

EUGENIO	08	PL B660 466	P. Eugenio *et al.*	(BNL E852 Collab.)
LU	05	PRL 94 032002	M. Lu *et al.*	(BNL E852 Collab.)
KUHN	04	PL B595 109	J. Kuhn *et al.*	(BNL E852 Collab.)
ANISOVICH	01B	PL B500 222	A.V. Anisovich *et al.*	

$\rho(1900)$

$I^G(J^{PC}) = 1^+(1^{--})$

OMITTED FROM SUMMARY TABLE

See our mini-review under the $\rho(1700)$.

$\rho(1900)$ MASS

VALUE (MeV)	EVTS	DOCUMENT ID		TECN	COMMENT
• • • We do not use the following data for averages, fits, limits, etc. • • •					
1909±17±25	54	[1] AUBERT	08S	BABR	10.6 $e^+e^- \to \phi\pi^0\gamma$
1880±30		AUBERT	06D	BABR	10.6 $e^+e^- \to 3\pi^+3\pi^-\gamma$
1860±20		AUBERT	06D	BABR	10.6 $e^+e^- \to 2(\pi^+\pi^-\pi^0)\gamma$
1910±10		[2,3] FRABETTI	04	E687	$\gamma p \to 3\pi^+3\pi^- p$
1870±10		ANTONELLI	96	SPEC	$e^+e^- \to$ hadrons

[1] From the fit with two resonances.
[2] From a fit with two resonances with the JACOB 72 continuum.
[3] Supersedes FRABETTI 01.

$\rho(1900)$ WIDTH

VALUE (MeV)	EVTS	DOCUMENT ID		TECN	COMMENT
• • • We do not use the following data for averages, fits, limits, etc. • • •					
48±17±2	54	[4] AUBERT	08S	BABR	10.6 $e^+e^- \to \phi\pi^0\gamma$
130±30		AUBERT	06D	BABR	10.6 $e^+e^- \to 3\pi^+3\pi^-\gamma$
160±20		AUBERT	06D	BABR	10.6 $e^+e^- \to 2(\pi^+\pi^-\pi^0)\gamma$
37±13		[5,6] FRABETTI	04	E687	$\gamma p \to 3\pi^+3\pi^- p$
10± 5		ANTONELLI	96	SPEC	$e^+e^- \to$ hadrons

[4] From the fit with two resonances.
[5] From a fit with two resonances with the JACOB 72 continuum.
[6] Supersedes FRABETTI 01.

Meson Particle Listings

$\rho(1900)$, $f_2(1910)$

$\rho(1900)$ $\Gamma(i)\Gamma(e^+e^-)/\Gamma^2(\text{total})$

$\Gamma(\phi\pi)/\Gamma_{\text{total}} \times \Gamma(e^+e^-)/\Gamma_{\text{total}}$ $\Gamma_4/\Gamma \times \Gamma_6/\Gamma$

VALUE (units 10^{-8})	EVTS	DOCUMENT ID		TECN	COMMENT
• • • We do not use the following data for averages, fits, limits, etc. • • •					
$4.2 \pm 1.2 \pm 0.8$	54	[7] AUBERT	08S	BABR	10.6 $e^+e^- \to \phi\pi^0\gamma$

[7] From the fit with two resonances.

$\rho(1900)$ DECAY MODES

	Mode	Fraction (Γ_i/Γ)
Γ_1	6π	seen
Γ_2	$3\pi^+3\pi^-$	seen
Γ_3	$2\pi^+2\pi^-2\pi^0$	
Γ_4	$\phi\pi$	
Γ_5	hadrons	seen
Γ_6	e^+e^-	seen
Γ_7	$\overline{N}N$	not seen

$\rho(1900)$ BRANCHING RATIOS

$\Gamma(6\pi)/\Gamma_{\text{total}}$ Γ_1/Γ

VALUE	EVTS	DOCUMENT ID		TECN	COMMENT
seen	8k	AKHMETSHIN	13	CMD3	$e^+e^- \to 3\pi^+3\pi^-$
not seen		AGNELLO	02	OBLX	$\overline{n}p \to 3\pi^+2\pi^-\pi^0$
seen		FRABETTI	01	E687	$\gamma p \to 3\pi^+3\pi^- p$
seen		ANTONELLI	96	SPEC	$e^+e^- \to$ hadrons

$\rho(1900)$ REFERENCES

AKHMETSHIN	13	PL B723 82	R.R. Akhmetshin *et al.*	(CMD-3 Collab.)
AUBERT	08S	PR D77 092002	B. Aubert *et al.*	(BABAR Collab.)
AUBERT	06D	PR D73 052003	B. Aubert *et al.*	(BABAR Collab.)
FRABETTI	04	PL B578 290	P.L. Frabetti *et al.*	(FNAL E687 Collab.)
AGNELLO	02	PL B527 39	M. Agnello *et al.*	(OBELIX Collab.)
FRABETTI	01	PL B514 240	P.L. Frabetti *et al.*	(FNAL E687 Collab.)
ANTONELLI	96	PL B365 427	A. Antonelli *et al.*	(FENICE Collab.)
JACOB	72	PR D5 1847	M. Jacob, R. Slansky	

$f_2(1910)$

$I^G(J^{PC}) = 0^+(2^{++})$

OMITTED FROM SUMMARY TABLE

We list here three different peaks with close masses and widths seen in the mass distributions of $\omega\omega$, $\eta\eta'$, and K^+K^- final states. ALDE 91B argues that they are of different nature.

$f_2(1910)$ MASS

$f_2(1910)$ $\omega\omega$ MODE

VALUE (MeV)	DOCUMENT ID		TECN	COMMENT
1903± 9 OUR AVERAGE Error includes scale factor of 1.5. See the ideogram below.				
1890 ± 10	[1] AMELIN	06	VES	36 $\pi^- p \to \omega\omega n$
1934 ± 20	ANISOVICH	00J	SPEC	
1897 ± 11	BARBERIS	00F		450 $pp \to p_f\omega\omega p_s$
1924 ± 14	ALDE	90	GAM2	38 $\pi^- p \to \omega\omega n$

[1] Supersedes BELADIDZE 92B.

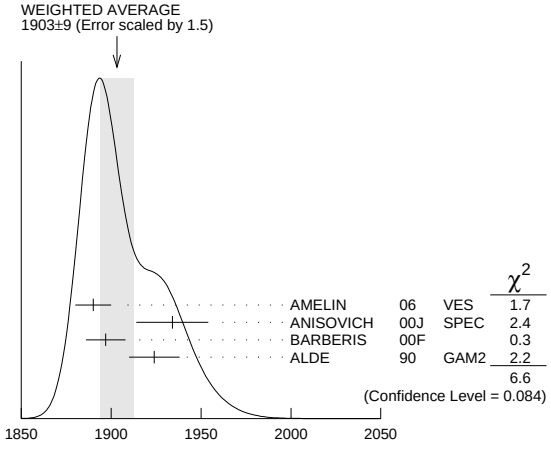

$f_2(1910)$ $\omega\omega$ MODE MASS (MeV)

$f_2(1910)$ $\eta\eta'$ MODE

VALUE (MeV)	DOCUMENT ID		TECN	COMMENT
1934±16	[2] BARBERIS	00A		450 $pp \to p_f\eta\eta' p_s$
• • • We do not use the following data for averages, fits, limits, etc. • • •				
1911 ± 10	ALDE	91B	GAM2	38 $\pi^- p \to \eta\eta' n$

[2] Also compatible with $J^{PC}=1^{-+}$.

$f_2(1910)$ K^+K^- MODE

VALUE (MeV)	DOCUMENT ID		TECN	COMMENT
• • • We do not use the following data for averages, fits, limits, etc. • • •				
1941 ± 18	AMSLER	06	CBAR	1.64 $\overline{p}p \to K^+K^-\pi^0$

$f_2(1910)$ WIDTH

$f_2(1910)$ $\omega\omega$ MODE

VALUE (MeV)	DOCUMENT ID		TECN	COMMENT
196±31 OUR AVERAGE Error includes scale factor of 2.3. See the ideogram below.				
165 ± 19	[3] AMELIN	06	VES	36 $\pi^- p \to \omega\omega n$
271 ± 25	ANISOVICH	00J	SPEC	
202 ± 32	BARBERIS	00F		450 $pp \to p_f\omega\omega p_s$
91 ± 50	ALDE	90	GAM2	38 $\pi^- p \to \omega\omega n$

[3] Supersedes BELADIDZE 92B.

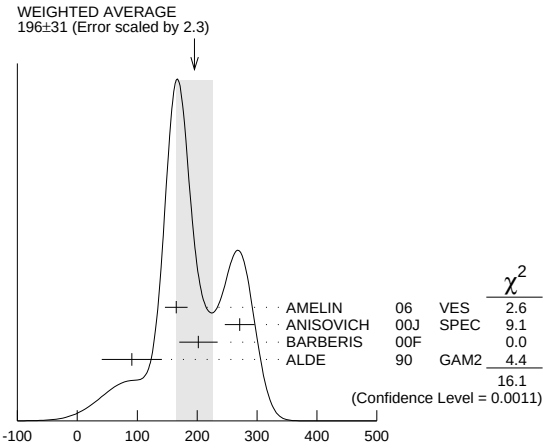

$f_2(1910)$ $\omega\omega$ MODE WIDTH(MeV)

$f_2(1910)$ $\eta\eta'$ MODE

VALUE (MeV)	DOCUMENT ID		TECN	COMMENT
141±41	[4] BARBERIS	00A		450 $pp \to p_f\eta\eta' p_s$
• • • We do not use the following data for averages, fits, limits, etc. • • •				
90 ± 35	ALDE	91B	GAM2	38 $\pi^- p \to \eta\eta' n$

[4] Also compatible with $J^{PC}=1^{-+}$.

$f_2(1910)$ K^+K^- MODE

VALUE (MeV)	DOCUMENT ID		TECN	COMMENT
• • • We do not use the following data for averages, fits, limits, etc. • • •				
120 ± 40	AMSLER	06	CBAR	1.64 $\overline{p}p \to K^+K^-\pi^0$

$f_2(1910)$ DECAY MODES

	Mode	Fraction (Γ_i/Γ)
Γ_1	$\pi^0\pi^0$	
Γ_2	K^+K^-	seen
Γ_3	$K^0_S K^0_S$	
Γ_4	$\eta\eta$	seen
Γ_5	$\omega\omega$	seen
Γ_6	$\eta\eta'$	seen
Γ_7	$\eta'\eta'$	
Γ_8	$\rho\rho$	seen
Γ_9	$a_2(1320)\pi$	seen
Γ_{10}	$f_2(1270)\eta$	seen

$f_2(1910)$ BRANCHING RATIOS

$\Gamma(K^+K^-)/\Gamma_{\text{total}}$ Γ_2/Γ

VALUE	DOCUMENT ID		TECN	COMMENT
seen	AMSLER	06	CBAR	1.64 $\overline{p}p \to K^+K^-\pi^0$

$\Gamma(\pi^0\pi^0)/\Gamma(\eta\eta')$ Γ_1/Γ_6

VALUE	DOCUMENT ID		TECN	COMMENT
• • • We do not use the following data for averages, fits, limits, etc. • • •				
<0.1	ALDE	89	GAM2	$38\pi^- p \to \eta\eta' n$

$\Gamma(K^0_S K^0_S)/\Gamma(\eta\eta')$ Γ_3/Γ_6

VALUE	CL%	DOCUMENT ID		TECN	COMMENT
• • • We do not use the following data for averages, fits, limits, etc. • • •					
<0.066	90	BALOSHIN	86	SPEC	$40\pi p \to K^0_S K^0_S n$

$\Gamma(\eta\eta)/\Gamma(\eta\eta')$ Γ_4/Γ_6

VALUE	CL%	DOCUMENT ID		TECN	COMMENT
• • • We do not use the following data for averages, fits, limits, etc. • • •					
<0.05	90	ALDE	91B	GAM2	$38\ \pi^- p \to \eta\eta' n$

$\Gamma(\omega\omega)/\Gamma(\eta\eta')$ Γ_5/Γ_6

VALUE	DOCUMENT ID		COMMENT
• • • We do not use the following data for averages, fits, limits, etc. • • •			
2.6 ± 0.6	BARBERIS	00F	$450\ pp \to p_f \omega\omega p_s$

$\Gamma(\eta'\eta')/\Gamma_{\text{total}}$ Γ_7/Γ

VALUE	DOCUMENT ID		TECN	COMMENT
• • • We do not use the following data for averages, fits, limits, etc. • • •				
probably not seen	BARBERIS	00A		$450\ pp \to p_f \eta'\eta' p_s$
possibly seen	BELADIDZE	92D	VES	$37\ \pi^- p \to \eta'\eta' n$

$\Gamma(\rho\rho)/\Gamma(\omega\omega)$ Γ_8/Γ_5

VALUE	DOCUMENT ID		COMMENT
• • • We do not use the following data for averages, fits, limits, etc. • • •			
2.6 ± 0.4	BARBERIS	00F	$450\ pp \to p_f \omega\omega p_s$

$\Gamma(f_2(1270)\eta)/\Gamma(a_2(1320)\pi)$ Γ_{10}/Γ_9

VALUE	DOCUMENT ID		TECN	COMMENT
0.09±0.05	[5] ANISOVICH	11	SPEC	0.9–1.94 $p\overline{p}$

[5] Reanalysis of ADOMEIT 96 and ANISOVICH 00E.

$f_2(1910)$ REFERENCES

ANISOVICH	11	EPJ C71 1511	A.V. Anisovich *et al.*	(LOQM, RAL, PNPI)
AMELIN	06	PAN 69 690 Translated from YAF 69 715.	D.V. Amelin *et al.*	(VES Collab.)
AMSLER	06	PL B639 165	C. Amsler *et al.*	(CBAR Collab.)
ANISOVICH	00E	PL B477 19	A.V. Anisovich *et al.*	
ANISOVICH	00J	PL B491 47	A.V. Anisovich *et al.*	
BARBERIS	00A	PL B471 429	D. Barberis *et al.*	(WA 102 Collab.)
BARBERIS	00F	PL B484 198	D. Barberis *et al.*	(WA 102 Collab.)
ADOMEIT	96	ZPHY C71 227	J. Adomeit *et al.*	(Crystal Barrel Collab.)
BELADIDZE	92B	ZPHY C54 367	G.M. Beladidze *et al.*	(VES Collab.)
BELADIDZE	92D	ZPHY C57 13	G.M. Beladidze *et al.*	(VES Collab.)
ALDE	91B	SJNP 54 455 Translated from YAF 54 751.	D.M. Alde *et al.*	(SERP, BELG, LANL, LAPP+)
Also		PL B276 375	D.M. Alde *et al.*	(BELG, SERP, KEK, LANL+)
ALDE	90	PL B241 600	D.M. Alde *et al.*	(SERP, BELG, LANL, LAPP+)
ALDE	89	PL B216 447	D.M. Alde *et al.*	(SERP, BELG, LANL, LAPP)
Also		SJNP 48 1035 Translated from YAF 48 1724.	D.M. Alde *et al.*	(BELG, SERP, LANL, LAPP)
BALOSHIN	86	SJNP 43 959 Translated from YAF 43 1487.	O.N. Baloshin *et al.*	(ITEP)

$f_2(1950)$

$I^G(J^{PC}) = 0^+(2^{++})$

$f_2(1950)$ MASS

VALUE (MeV)	DOCUMENT ID		TECN	COMMENT
1944±12 OUR AVERAGE	Error includes scale factor of 1.5. See the ideogram below.			
1930±25	[1] BINON	05	GAMS	$33\ \pi^- p \to \eta\eta n$
2010±25	ANISOVICH	00J	SPEC	
1940±50	BAI	00A	BES	$J/\psi \to \gamma(\pi^+\pi^-\pi^+\pi^-)$
1980±22	[2] BARBERIS	00C		$450\ pp \to pp4\pi$
1940±22	[3] BARBERIS	00C		$450\ pp \to pp2\pi2\pi^0$
1980±50	ANISOVICH	99B	SPEC	1.35–1.94 $p\overline{p} \to \eta\eta\pi^0$
1960±30	BARBERIS	97B	OMEG	$450\ pp \to pp2(\pi^+\pi^-)$
1918±12	ANTINORI	95	OMEG	$300,450\ pp \to pp2(\pi^+\pi^-)$
• • • We do not use the following data for averages, fits, limits, etc. • • •				
2038^{+13+12}_{-11-73}	[4] UEHARA	09	BELL	$10.6\ e^+e^- \to e^+e^-\pi^0\pi^0$
1980± 2±14	ABE	04	BELL	$10.6\ e^+e^- \to e^+e^- K^+K^-$
1867±46	[5] AMSLER	02	CBAR	$0.9\ \overline{p}p \to \pi^0\eta\eta,\ \pi^0\pi^0\pi^0$
~ 1990	[6] OAKDEN	94	RVUE	0.36–1.55 $\overline{p}p \to \pi\pi$
1950±15	[7] ASTON	91	LASS	$11\ K^- p \to \Lambda K\overline{K}\pi\pi$

[1] First solution, PWA is ambiguous.
[2] Decaying into $\pi^+\pi^-2\pi^0$.
[3] Decaying into $2(\pi^+\pi^-)$.
[4] Taking into account $f_4(2050)$.
[5] T-matrix pole.
[6] From solution B of amplitude analysis of data on $\overline{p}p \to \pi\pi$. See however KLOET 96 who fit $\pi^+\pi^-$ only and find waves only up to $J = 3$ to be important but not significantly resonant.
[7] Cannot determine spin to be 2.

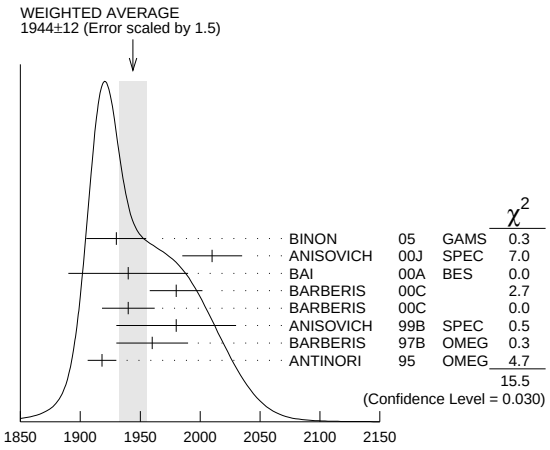

$f_2(1950)$ WIDTH

VALUE (MeV)	DOCUMENT ID		TECN	COMMENT
472± 18 OUR AVERAGE				
450± 50	[8] BINON	05	GAMS	$33\ \pi^- p \to \eta\eta n$
495± 35	ANISOVICH	00J	SPEC	
$380^{+120}_{-\ 90}$	BAI	00A	BES	$J/\psi \to \gamma(\pi^+\pi^-\pi^+\pi^-)$
520± 50	[9] BARBERIS	00C		$450\ pp \to pp4\pi$
485± 55	[10] BARBERIS	00C		$450\ pp \to pp4\pi$
500±100	ANISOVICH	99B	SPEC	1.35–1.94 $p\overline{p} \to \eta\eta\pi^0$
460± 40	BARBERIS	97B	OMEG	$450\ pp \to pp2(\pi^+\pi^-)$
390± 60	ANTINORI	95	OMEG	$300,450\ pp \to pp2(\pi^+\pi^-)$
• • • We do not use the following data for averages, fits, limits, etc. • • •				
$441^{+\ 27+\ 28}_{-\ 25-192}$	[11] UEHARA	09	BELL	$10.6\ e^+e^- \to e^+e^-\pi^0\pi^0$
297± 12± 6	ABE	04	BELL	$10.6\ e^+e^- \to e^+e^- K^+K^-$
385± 58	[12] AMSLER	02	CBAR	$0.9\ \overline{p}p \to \pi^0\eta\eta,\ \pi^0\pi^0\pi^0$
~ 100	[13] OAKDEN	94	RVUE	0.36–1.55 $\overline{p}p \to \pi\pi$
250± 50	[14] ASTON	91	LASS	$11\ K^- p \to \Lambda K\overline{K}\pi\pi$

[8] First solution, PWA is ambiguous.
[9] Decaying into $\pi^+\pi^-2\pi^0$.
[10] Decaying into $2(\pi^+\pi^-)$.
[11] Taking into account $f_4(2050)$.
[12] T-matrix pole.
[13] From solution B of amplitude analysis of data on $\overline{p}p \to \pi\pi$. See however KLOET 96 who fit $\pi^+\pi^-$ only and find waves only up to $J = 3$ to be important but not significantly resonant.
[14] Cannot determine spin to be 2.

$f_2(1950)$ DECAY MODES

	Mode	Fraction (Γ_i/Γ)
Γ_1	$K^*(892)\overline{K}^*(892)$	seen
Γ_2	$\pi\pi$	
Γ_3	$\pi^+\pi^-$	seen
Γ_4	$\pi^0\pi^0$	seen
Γ_5	4π	seen
Γ_6	$\pi^+\pi^-\pi^+\pi^-$	
Γ_7	$a_2(1320)\pi$	
Γ_8	$f_2(1270)\pi\pi$	
Γ_9	$\eta\eta$	seen
Γ_{10}	$K\overline{K}$	seen
Γ_{11}	$\gamma\gamma$	seen
Γ_{12}	$p\overline{p}$	seen

Meson Particle Listings

$f_2(1950)$, $\rho_3(1990)$, $f_2(2010)$

$f_2(1950)$ Γ(i)Γ(γγ)/Γ(total)

$\Gamma(K\overline{K}) \times \Gamma(\gamma\gamma)/\Gamma_{total}$ — **$\Gamma_{10}\Gamma_{11}/\Gamma$**

VALUE (eV)	DOCUMENT ID		TECN	COMMENT
• • • We do not use the following data for averages, fits, limits, etc. • • •				
$122 \pm 4 \pm 26$	[15] ABE	04	BELL	$10.6\ e^+e^- \to e^+e^-K^+K^-$

[15] Assuming spin 2.

$\Gamma(\pi\pi) \times \Gamma(\gamma\gamma)/\Gamma_{total}$ — **$\Gamma_2\Gamma_{11}/\Gamma$**

VALUE	DOCUMENT ID		TECN	COMMENT
• • • We do not use the following data for averages, fits, limits, etc. • • •				
$162^{+69}_{-42}{}^{+1137}_{-204}$	[16] UEHARA	09	BELL	$10.6\ e^+e^- \to e^+e^-\pi^0\pi^0$

[16] Taking into account $f_4(2050)$.

$f_2(1950)$ BRANCHING RATIOS

$\Gamma(K^*(892)\overline{K}^*(892))/\Gamma_{total}$ — **Γ_1/Γ**

VALUE	DOCUMENT ID		TECN	CHG	COMMENT
seen	ASTON	91	LASS	0	$11\ K^-p \to \Lambda K\overline{K}\pi\pi$

$\Gamma(a_2(1320)\pi)/\Gamma_{total}$ — **Γ_7/Γ**

VALUE	DOCUMENT ID		TECN	COMMENT
• • • We do not use the following data for averages, fits, limits, etc. • • •				
not seen	BARBERIS	00B		$450\ pp \to p_f\eta\pi^+\pi^-p_s$
not seen	BARBERIS	00C		$450\ pp \to p_f 4\pi p_s$
possibly seen	BARBERIS	97B	OMEG	$450\ pp \to pp2(\pi^+\pi^-)$

$\Gamma(\eta\eta)/\Gamma(4\pi)$ — **Γ_9/Γ_5**

VALUE	CL%	DOCUMENT ID		COMMENT
• • • We do not use the following data for averages, fits, limits, etc. • • •				
$<5.0 \times 10^{-3}$	90	BARBERIS	00E	$450\ pp \to p_f\eta\eta p_s$

$\Gamma(\eta\eta)/\Gamma(\pi^+\pi^-)$ — **Γ_9/Γ_3**

VALUE	DOCUMENT ID		TECN	COMMENT
0.14±0.05	AMSLER	02	CBAR	$0.9\ \overline{p}p \to \pi^0\eta\eta, \pi^0\pi^0\pi^0$

$\Gamma(p\overline{p})/\Gamma_{total}$ — **Γ_{12}/Γ**

VALUE	EVTS	DOCUMENT ID		TECN	COMMENT
seen	111	ALEXANDER	10	CLEO	$\psi(2S) \to \gamma p\overline{p}$

$f_2(1950)$ REFERENCES

ALEXANDER	10	PR D82 092002	J.P. Alexander *et al.*	(CLEO Collab.)
UEHARA	09	PR D79 052009	S. Uehara *et al.*	(BELLE Collab.)
BINON	05	PAN 68 960 Translated from YAF 68 998.	F. Binon *et al.*	
ABE	04	EPJ C32 323	K. Abe *et al.*	(BELLE Collab.)
AMSLER	02	EPJ C23 29	C. Amsler *et al.*	
ANISOVICH	00J	PL B491 47	A.V. Anisovich *et al.*	
BAI	00A	PL B472 207	J.Z. Bai *et al.*	(BES Collab.)
BARBERIS	00B	PL B471 435	D. Barberis *et al.*	(WA 102 Collab.)
BARBERIS	00C	PL B471 440	D. Barberis *et al.*	(WA 102 Collab.)
BARBERIS	00E	PL B479 59	D. Barberis *et al.*	(WA 102 Collab.)
ANISOVICH	99B	PL B449 154	A.V. Anisovich *et al.*	
BARBERIS	97B	PL B413 217	D. Barberis *et al.*	(WA 102 Collab.)
KLOET	96	PR D53 6120	W.M. Kloet, F. Myhrer	(RUTG, NORD)
ANTINORI	95	PL B353 589	F. Antinori *et al.*	(ATHU, BARI, BIRM+) JP
OAKDEN	94	NP A574 731	M.N. Oakden, M.R. Pennington	(DURH)
ASTON	91	NPBPS B21 5	D. Aston *et al.*	(LASS Collab.)

$\rho_3(1990)$

$I^G(J^{PC}) = 1^+(3^{--})$

OMITTED FROM SUMMARY TABLE

$\rho_3(1990)$ MASS

VALUE (MeV)	DOCUMENT ID		TECN	COMMENT
• • • We do not use the following data for averages, fits, limits, etc. • • •				
1982 ± 14	[1] ANISOVICH	02	SPEC	0.6–$1.9\ p\overline{p} \to \omega\pi^0, \omega\eta\pi^0, \pi^+\pi^-$
~ 2007	HASAN	94	RVUE	$\overline{p}p \to \pi\pi$

[1] From the combined analysis of ANISOVICH 00J, ANISOVICH 01D, ANISOVICH 01E, and ANISOVICH 02.

$\rho_3(1990)$ WIDTH

VALUE (MeV)	DOCUMENT ID		TECN	COMMENT
• • • We do not use the following data for averages, fits, limits, etc. • • •				
188 ± 24	[2] ANISOVICH	02	SPEC	0.6–$1.9\ p\overline{p} \to \omega\pi^0, \omega\eta\pi^0, \pi^+\pi^-$
~ 287	HASAN	94	RVUE	$\overline{p}p \to \pi\pi$

[2] From the combined analysis of ANISOVICH 00J, ANISOVICH 01D, ANISOVICH 01E, and ANISOVICH 02.

$\rho_3(1990)$ REFERENCES

ANISOVICH	02	PL B542 8	A.V. Anisovich *et al.*	
ANISOVICH	01D	PL B508 6	A.V. Anisovich *et al.*	
ANISOVICH	01E	PL B513 281	A.V. Anisovich *et al.*	
ANISOVICH	00J	PL B491 47	A.V. Anisovich *et al.*	
HASAN	94	PL B334 215	A. Hasan, D.V. Bugg	(LOQM)

$f_2(2010)$

$I^G(J^{PC}) = 0^+(2^{++})$

$f_2(2010)$ MASS

VALUE (MeV)	DOCUMENT ID		TECN	COMMENT
$\mathbf{2011^{+\ 62}_{-\ 76}}$	[1] ETKIN	88	MPS	$22\ \pi^-p \to \phi\phi n$
• • • We do not use the following data for averages, fits, limits, etc. • • •				
2005 ± 12	VLADIMIRSK...06		SPEC	$40\ \pi^-p \to K^0_S K^0_S n$
1980 ± 20	[2] BOLONKIN	88	SPEC	$40\ \pi^-p \to K^0_S K^0_S n$
$2050^{+\ 90}_{-\ 50}$	ETKIN	85	MPS	$22\ \pi^-p \to 2\phi n$
$2120^{+\ 20}_{-120}$	LINDENBAUM	84	RVUE	
2160 ± 50	ETKIN	82	MPS	$22\ \pi^-p \to 2\phi n$

[1] Includes data of ETKIN 85. The percentage of the resonance going into $\phi\phi\ 2^{++}\ S_2$, D_2, and D_0 is 98^{+1}_{-3}, 0^{+1}_{-0}, and 2^{+2}_{-1}, respectively.

[2] Statistically very weak, only 1.4 s.d.

$f_2(2010)$ WIDTH

VALUE (MeV)	DOCUMENT ID		TECN	COMMENT
$\mathbf{202^{+\ 67}_{-\ 62}}$	[3] ETKIN	88	MPS	$22\ \pi^-p \to \phi\phi n$
• • • We do not use the following data for averages, fits, limits, etc. • • •				
209 ± 32	VLADIMIRSK...06		SPEC	$40\ \pi^-p \to K^0_S K^0_S n$
145 ± 50	[4] BOLONKIN	88	SPEC	$40\ \pi^-p \to K^0_S K^0_S n$
$200^{+160}_{-\ 50}$	ETKIN	85	MPS	$22\ \pi^-p \to 2\phi n$
$300^{+150}_{-\ 50}$	LINDENBAUM	84	RVUE	
310 ± 70	ETKIN	82	MPS	$22\ \pi^-p \to 2\phi n$

[3] Includes data of ETKIN 85.

[4] Statistically very weak, only 1.4 s.d.

$f_2(2010)$ DECAY MODES

	Mode	Fraction (Γ_i/Γ)
Γ_1	$\phi\phi$	seen
Γ_2	$K\overline{K}$	seen

$f_2(2010)$ BRANCHING RATIOS

$\Gamma(K\overline{K})/\Gamma_{total}$ — **Γ_2/Γ**

VALUE	DOCUMENT ID		TECN	COMMENT
seen	VLADIMIRSK...06		SPEC	$40\ \pi^-p \to K^0_S K^0_S n$

$f_2(2010)$ REFERENCES

VLADIMIRSK...	06	PAN 69 493 Translated from YAF 69 515.	V.V. Vladimirsky *et al.*	(ITEP, Moscow)
BOLONKIN	88	NP B309 426	B.V. Bolonkin *et al.*	(ITEP, SERP)
ETKIN	88	PL B201 568	A. Etkin *et al.*	(BNL, CUNY)
ETKIN	85	PL 165B 217	A. Etkin *et al.*	(BNL, CUNY)
LINDENBAUM	84	CNPP 13 285	S.J. Lindenbaum	(CUNY)
ETKIN	82	PRL 49 1620	A. Etkin *et al.*	(BNL, CUNY)
Also		Brighton Conf. 351	S.J. Lindenbaum	(BNL, CUNY)

$f_0(2020)$

$I^G(J^{PC}) = 0^+(0^{++})$

OMITTED FROM SUMMARY TABLE

Needs confirmation.

$f_0(2020)$ MASS

VALUE (MeV)	EVTS	DOCUMENT ID		TECN	COMMENT
1992±16		[1,2] BARBERIS	00C		450 $pp \to p_f 4\pi p_s$
• • • We do not use the following data for averages, fits, limits, etc. • • •					
2037± 8	80k	[3] UMAN	06	E835	5.2 $\overline{p}p \to \eta\eta\pi^0$
2040±38		ANISOVICH	00J	SPEC	
2010±60		ALDE	98	GAM4	100 $\pi^- p \to \pi^0\pi^0 n$
2020±35		BARBERIS	97B	OMEG	450 $pp \to pp2(\pi^+\pi^-)$

[1] Average between $\pi^+\pi^- 2\pi^0$ and $2(\pi^+\pi^-)$.
[2] T-matrix pole.
[3] Statistical error only.

$f_0(2020)$ WIDTH

VALUE (MeV)	EVTS	DOCUMENT ID		TECN	COMMENT
442± 60		[4,5] BARBERIS	00C		450 $pp \to p_f 4\pi p_s$
• • • We do not use the following data for averages, fits, limits, etc. • • •					
296± 17	80k	[6] UMAN	06	E835	5.2 $\overline{p}p \to \eta\eta\pi^0$
405± 40		ANISOVICH	00J	SPEC	
240±100		ALDE	98	GAM4	100 $\pi^- p \to \pi^0\pi^0 n$
410± 50		BARBERIS	97B	OMEG	450 $pp \to pp2(\pi^+\pi^-)$

[4] Average between $\pi^+\pi^- 2\pi^0$ and $2(\pi^+\pi^-)$.
[5] T-matrix pole.
[6] Statistical error only.

$f_0(2020)$ DECAY MODES

	Mode	Fraction (Γ_i/Γ)
Γ_1	$\rho\pi\pi$	seen
Γ_2	$\pi^0\pi^0$	seen
Γ_3	$\rho\rho$	seen
Γ_4	$\omega\omega$	seen
Γ_5	$\eta\eta$	seen

$f_0(2020)$ BRANCHING RATIOS

$\Gamma(\rho\rho)/\Gamma(\omega\omega)$ **Γ_3/Γ_4**

VALUE	DOCUMENT ID		COMMENT
• • • We do not use the following data for averages, fits, limits, etc. • • •			
~ 3	BARBERIS	00F	450 $pp \to p_f\omega\omega p_s$

$\Gamma(\eta\eta)/\Gamma_{\text{total}}$ **Γ_5/Γ**

VALUE	DOCUMENT ID		TECN	COMMENT
seen	UMAN	06	E835	5.2 $\overline{p}p \to \eta\eta\pi^0$

$f_0(2020)$ REFERENCES

UMAN	06	PR D73 052009	I. Uman *et al.*	(FNAL E835)
ANISOVICH	00J	PL B491 47	A.V. Anisovich *et al.*	
BARBERIS	00C	PL B471 440	D. Barberis *et al.*	(WA 102 Collab.)
BARBERIS	00F	PL B484 198	D. Barberis *et al.*	(WA 102 Collab.)
ALDE	98	EPJ A3 361	D. Alde *et al.*	(GAM4 Collab.)
Also		PAN 62 405 Translated from YAF 62 446.	D. Alde *et al.*	(GAMS Collab.)
BARBERIS	97B	PL B413 217	D. Barberis *et al.*	(WA 102 Collab.)

$a_4(2040)$

$I^G(J^{PC}) = 1^-(4^{++})$

$a_4(2040)$ MASS

VALUE (MeV)	EVTS	DOCUMENT ID		TECN	CHG	COMMENT
1996$^{+10}_{-9}$ OUR AVERAGE	Error includes scale factor of 1.1.					
1885±13$^{+50}_{-2}$	420k	ALEKSEEV	10	COMP		190 $\pi^- Pb \to \pi^-\pi^-\pi^+ Pb'$
1985±10±13	145k	LU	05	B852		18 $\pi^- p \to \omega\pi^-\pi^0 p$
1996±25±43		CHUNG	02	B852		18.3 $\pi^- p \to 3\pi p$
2005$^{+25}_{-45}$		[1] ANISOVICH	01F	SPEC		2.0 $\overline{p}p \to 3\pi^0, \pi^0\eta, \pi^0\eta'$
2000±40$^{+60}_{-20}$		IVANOV	01	B852		18 $\pi^- p \to \eta'\pi^- p$
1944± 8±50		[2] AMELIN	99	VES		37 $\pi^- A \to \omega\pi^-\pi^0 A^*$
2010±20		[3] DONSKOV	96	GAM2	0	38 $\pi^- p \to \eta\pi^0 n$
2040±30		[4] CLELAND	82B	SPEC	±	50 $\pi p \to K^0_S K^\pm p$
2030±50		[5] CORDEN	78C	OMEG	0	15 $\pi^- p \to 3\pi n$
• • • We do not use the following data for averages, fits, limits, etc. • • •						
2004± 6	80k	[6] UMAN	06	E835		5.2 $\overline{p}p \to \eta\eta\pi^0$
1903±10		[7] BALDI	78	SPEC	−	10 $\pi^- p \to p K^0_S K^-$

[1] From the combined analysis of ANISOVICH 99C, ANISOVICH 99E, and ANISOVICH 01F.
[2] May be a different state.
[3] From a simultaneous fit to the G_+ and G_0 wave intensities.
[4] From an amplitude analysis.
[5] $J^P = 4^+$ is favored, though $J^P = 2^+$ cannot be excluded.
[6] Statistical error only.
[7] From a fit to the Y^0_8 moment. Limited by phase space.

$a_4(2040)$ WIDTH

VALUE (MeV)	EVTS	DOCUMENT ID		TECN	CHG	COMMENT
255$^{+28}_{-24}$ OUR AVERAGE	Error includes scale factor of 1.3. See the ideogram below.					
294± 25$^{+46}_{-19}$	420k	ALEKSEEV	10	COMP		190 $\pi^- Pb \to \pi^-\pi^-\pi^+ Pb'$
231± 30±46	145k	LU	05	B852		18 $\pi^- p \to \omega\pi^-\pi^0 p$
298± 81±85		CHUNG	02	B852		18.3 $\pi^- p \to 3\pi p$
180± 30		[8] ANISOVICH	01F	SPEC		2.0 $\overline{p}p \to 3\pi^0, \pi^0\eta, \pi^0\eta'$
350±100$^{+70}_{-50}$		IVANOV	01	B852		18 $\pi^- p \to \eta'\pi^- p$
324± 26±75		[9] AMELIN	99	VES		37 $\pi^- A \to \omega\pi^-\pi^0 A^*$
370± 80		[10] DONSKOV	96	GAM2	0	38 $\pi^- p \to \eta\pi^0 n$
380±150		[11] CLELAND	82B	SPEC	±	50 $\pi p \to K^0_S K^\pm p$
510±200		[12] CORDEN	78C	OMEG	0	15 $\pi^- p \to 3\pi n$
• • • We do not use the following data for averages, fits, limits, etc. • • •						
401± 16	80k	[13] UMAN	06	E835		5.2 $\overline{p}p \to \eta\eta\pi^0$
166± 43		[14] BALDI	78	SPEC	−	10 $\pi^- p \to p K^0_S K^-$

[8] From the combined analysis of ANISOVICH 99C, ANISOVICH 99E, and ANISOVICH 01F.
[9] May be a different state.
[10] From a simultaneous fit to the G_+ and G_0 wave intensities.
[11] From an amplitude analysis.
[12] $J^P = 4^+$ is favored, though $J^P = 2^+$ cannot be excluded.
[13] Statistical error only.
[14] From a fit to the Y^0_8 moment. Limited by phase space.

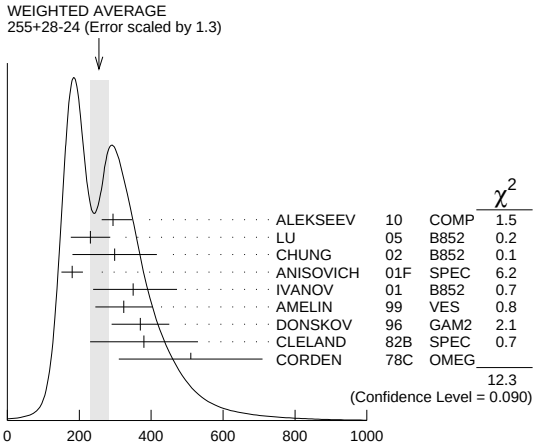

$a_4(2040)$ MASS

$a_4(2040)$ DECAY MODES

	Mode	Fraction (Γ_i/Γ)
Γ_1	$K\overline{K}$	seen
Γ_2	$\pi^+\pi^-\pi^0$	seen
Γ_3	$\rho\pi$	seen
Γ_4	$f_2(1270)\pi$	seen
Γ_5	$\omega\pi^-\pi^0$	seen
Γ_6	$\omega\rho$	seen
Γ_7	$\eta\pi^0$	seen
Γ_8	$\eta'(958)\pi$	seen

Meson Particle Listings

$a_4(2040)$, $f_4(2050)$

$a_4(2040)$ BRANCHING RATIOS

$\Gamma(K\overline{K})/\Gamma_{total}$ — **Γ_1/Γ**

VALUE	DOCUMENT ID		TECN	CHG	COMMENT
seen	BALDI	78	SPEC	±	10 $\pi^- p \rightarrow K^0_S K^- p$

$\Gamma(\pi^+\pi^-\pi^0)/\Gamma_{total}$ — **Γ_2/Γ**

VALUE	DOCUMENT ID		TECN	CHG	COMMENT
seen	CORDEN	78C	OMEG	0	15 $\pi^- p \rightarrow 3\pi n$

$\Gamma(\rho\pi)/\Gamma(f_2(1270)\pi)$ — **Γ_3/Γ_4**

VALUE	DOCUMENT ID		TECN	COMMENT
1.1±0.2±0.2	CHUNG	02	B852	18.3 $\pi^- p \rightarrow 3\pi p$

$\Gamma(\eta\pi^0)/\Gamma_{total}$ — **Γ_7/Γ**

VALUE	DOCUMENT ID		TECN	CHG	COMMENT
seen	DONSKOV	96	GAM2	0	38 $\pi^- p \rightarrow \eta\pi^0 n$

$\Gamma(\omega\rho)/\Gamma_{total}$ — **Γ_6/Γ**

VALUE	EVTS	DOCUMENT ID		TECN	COMMENT
seen	145k	LU	05	B852	18 $\pi^- p \rightarrow \omega\pi^-\pi^0 p$

$a_4(2040)$ REFERENCES

ALEKSEEV	10	PRL 104 241803	M.G. Alekseev *et al.*	(COMPASS Collab.)
UMAN	06	PR D73 052009	I. Uman *et al.*	(FNAL E835)
LU	05	PRL 94 032002	M. Lu *et al.*	(BNL E852 Collab.)
CHUNG	02	PR D65 072001	S.U. Chung *et al.*	(BNL E852 Collab.)
ANISOVICH	01F	PL B517 261	A.V. Anisovich *et al.*	
IVANOV	01	PRL 86 3977	E.I. Ivanov *et al.*	(BNL E852 Collab.)
AMELIN	99	PAN 62 445 Translated from YAF 62 487.	D.V. Amelin *et al.*	(VES Collab.)
ANISOVICH	99C	PL B452 173	A.V. Anisovich *et al.*	
ANISOVICH	99E	PL B452 187	A.V. Anisovich *et al.*	
DONSKOV	96	PAN 59 982 Translated from YAF 59 1027.	S.V. Donskov *et al.*	(GAMS Collab.) IGJPC
CLELAND	82B	NP B208 228	W.E. Cleland *et al.*	(DURH, GEVA, LAUS+)
BALDI	78	PL 74B 413	R. Baldi *et al.*	(GEVA) JP
CORDEN	78C	NP B136 77	M.J. Corden *et al.*	(BIRM, RHEL, TELA+) JP

$f_4(2050)$

$I^G(J^{PC}) = 0^+(4^{++})$

$f_4(2050)$ MASS

VALUE (MeV)	EVTS	DOCUMENT ID		TECN	COMMENT
2018±11 OUR AVERAGE		Error includes scale factor of 2.1. See the ideogram below.			
1960±15		AMELIN	06	VES	36 $\pi^- p \rightarrow \omega\omega n$
2005±10		[1] BINON	05	GAMS	33 $\pi^- p \rightarrow \eta\eta n$
1998±15		ALDE	98	GAM4	100 $\pi^- p \rightarrow \pi^0\pi^0 n$
2060±20		ALDE	90	GAM2	38 $\pi^- p \rightarrow \omega\omega n$
2038±30		AUGUSTIN	87	DM2	$J/\psi \rightarrow \gamma\pi^+\pi^-$
2086±15		BALTRUSAIT...	87	MRK3	$J/\psi \rightarrow \gamma\pi^+\pi^-$
2000±60		ALDE	86D	GAM4	100 $\pi^- p \rightarrow n2\eta$
2020±20	40k	[2] BINON	84B	GAM2	38 $\pi^- p \rightarrow n2\pi^0$
2015±28		[3] CASON	82	STRC	8 $\pi^+ p \rightarrow \Delta^{++}\pi^0\pi^0$
2031^{+25}_{-36}		ETKIN	82B	MPS	23 $\pi^- p \rightarrow n2K^0_S$
2020±30	700	APEL	75	NICE	40 $\pi^- p \rightarrow n2\pi^0$
2050±25		BLUM	75	ASPK	18.4 $\pi^- p \rightarrow nK^+K^-$
• • • We do not use the following data for averages, fits, limits, etc. • • •					
1966±25		[4] ANISOVICH	09	RVUE	0.0 $\overline{p}p$, πN
$1885^{+14+218}_{-13-25}$		[5] UEHARA	09	BELL	10.6 $e^+e^- \rightarrow e^+e^-\pi^0\pi^0$
2018± 6		ANISOVICH	00J	SPEC	2.0 $\overline{p}p \rightarrow \eta\pi^0\pi^0$, $\pi^0\pi^0$, $\eta\eta$, $\eta\eta'$, $\pi\pi$
~ 2000		[6] MARTIN	98	RVUE	$N\overline{N} \rightarrow \pi\pi$
~ 2010		[7] MARTIN	97	RVUE	$\overline{N}N \rightarrow \pi\pi$
~ 2040		[8] OAKDEN	94	RVUE	0.36–1.55 $\overline{p}p \rightarrow \pi\pi$
~ 1990		[9] OAKDEN	94	RVUE	0.36–1.55 $\overline{p}p \rightarrow \pi\pi$
1978± 5		[10] ALPER	80	CNTR	62 $\pi^- p \rightarrow K^+K^-n$
2040±10		[10] ROZANSKA	80	SPRK	18 $\pi^- p \rightarrow p\overline{p}n$
1935±13		[10] CORDEN	79	OMEG	12–15 $\pi^- p \rightarrow n2\pi$
1988± 7		EVANGELIS...	79B	OMEG	10 $\pi^- p \rightarrow K^+K^-n$
1922±14		[11] ANTIPOV	77	CIBS	25 $\pi^- p \rightarrow p3\pi$

[1] From the first PWA solution.
[2] From a partial-wave analysis of the data.
[3] From an amplitude analysis of the reaction $\pi^+\pi^- \rightarrow 2\pi^0$.
[4] K matrix pole.
[5] Taking into account the $f_2(1950)$. Helicity-2 production favored.
[6] Energy-dependent analysis.
[7] Single energy analysis.
[8] From solution A of amplitude analysis of data on $\overline{p}p \rightarrow \pi\pi$. See however KLOET 96 who fit $\pi^+\pi^-$ only and find waves only up to $J = 3$ to be important but not significantly resonant.
[9] From solution B of amplitude analysis of data on $\overline{p}p \rightarrow \pi\pi$. See however KLOET 96 who fit $\pi^+\pi^-$ only and find waves only up to $J = 3$ to be important but not significantly resonant.
[10] $I(J^P) = 0(4^+)$ from amplitude analysis assuming one-pion exchange.
[11] Width errors enlarged by us to $4\Gamma/\sqrt{N}$; see the note with the $K^*(892)$ mass.

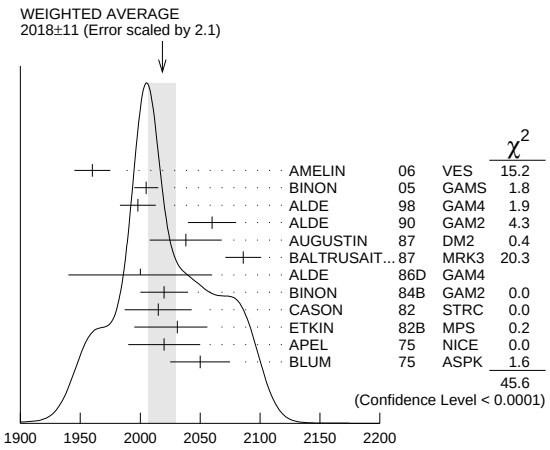

$f_4(2050)$ WIDTH

VALUE (MeV)	EVTS	DOCUMENT ID		TECN	COMMENT
237± 18 OUR AVERAGE		Error includes scale factor of 1.9. See the ideogram below.			
290± 20		AMELIN	06	VES	36 $\pi^- p \rightarrow \omega\omega n$
340± 80		[12] BINON	05	GAMS	33 $\pi^- p \rightarrow \eta\eta n$
395± 40		ALDE	98	GAM4	100 $\pi^- p \rightarrow \pi^0\pi^0 n$
170± 60		ALDE	90	GAM2	38 $\pi^- p \rightarrow \omega\omega n$
304± 60		AUGUSTIN	87	DM2	$J/\psi \rightarrow \gamma\pi^+\pi^-$
210± 63		BALTRUSAIT...	87	MRK3	$J/\psi \rightarrow \gamma\pi^+\pi^-$
400±100		ALDE	86D	GAM4	100 $\pi^- p \rightarrow n2\eta$
240± 40	40k	[13] BINON	84B	GAM2	38 $\pi^- p \rightarrow n2\pi^0$
190± 14		DENNEY	83	LASS	10 $\pi^+ n/\pi^+ p$
186^{+103}_{-58}		[14] CASON	82	STRC	8 $\pi^+ p \rightarrow \Delta^{++}\pi^0\pi^0$
305^{+36}_{-119}		ETKIN	82B	MPS	23 $\pi^- p \rightarrow n2K^0_S$
180± 60	700	APEL	75	NICE	40 $\pi^- p \rightarrow n2\pi^0$
225^{+120}_{-70}		BLUM	75	ASPK	18.4 $\pi^- p \rightarrow nK^+K^-$
• • • We do not use the following data for averages, fits, limits, etc. • • •					
260± 40		[15] ANISOVICH	09	RVUE	0.0 $\overline{p}p$, πN
$453\pm 20^{+31}_{-129}$		[16] UEHARA	09	BELL	10.6 $e^+e^- \rightarrow e^+e^-\pi^0\pi^0$
182± 7		ANISOVICH	00J	SPEC	2.0 $\overline{p}p \rightarrow \eta\pi^0\pi^0$, $\pi^0\pi^0$, $\eta\eta$, $\eta\eta'$, $\pi\pi$
~ 170		[17] MARTIN	98	RVUE	$N\overline{N} \rightarrow \pi\pi$
~ 200		[18] MARTIN	97	RVUE	$\overline{N}N \rightarrow \pi\pi$
~ 60		[19] OAKDEN	94	RVUE	0.36–1.55 $\overline{p}p \rightarrow \pi\pi$
~ 80		[20] OAKDEN	94	RVUE	0.36–1.55 $\overline{p}p \rightarrow \pi\pi$
243± 16		[21] ALPER	80	CNTR	62 $\pi^- p \rightarrow K^+K^-n$
140± 15		[21] ROZANSKA	80	SPRK	18 $\pi^- p \rightarrow p\overline{p}n$
263± 57		[21] CORDEN	79	OMEG	12–15 $\pi^- p \rightarrow n2\pi$
100± 28		EVANGELIS...	79B	OMEG	10 $\pi^- p \rightarrow K^+K^-n$
107± 56		[22] ANTIPOV	77	CIBS	25 $\pi^- p \rightarrow p3\pi$

[12] From the first PWA solution.
[13] From a partial-wave analysis of the data.
[14] From an amplitude analysis of the reaction $\pi^+\pi^- \rightarrow 2\pi^0$.
[15] K matrix pole.
[16] Taking into account the $f_2(1950)$. Helicity-2 production favored.
[17] Energy-dependent analysis.
[18] Single energy analysis.
[19] From solution A of amplitude analysis of data on $\overline{p}p \rightarrow \pi\pi$. See however KLOET 96 who fit $\pi^+\pi^-$ only and find waves only up to $J = 3$ to be important but not significantly resonant.
[20] From solution B of amplitude analysis of data on $\overline{p}p \rightarrow \pi\pi$. See however KLOET 96 who fit $\pi^+\pi^-$ only and find waves only up to $J = 3$ to be important but not significantly resonant.
[21] $I(J^P) = 0(4^+)$ from amplitude analysis assuming one-pion exchange.
[22] Width errors enlarged by us to $4\Gamma/\sqrt{N}$; see the note with the $K^*(892)$ mass.

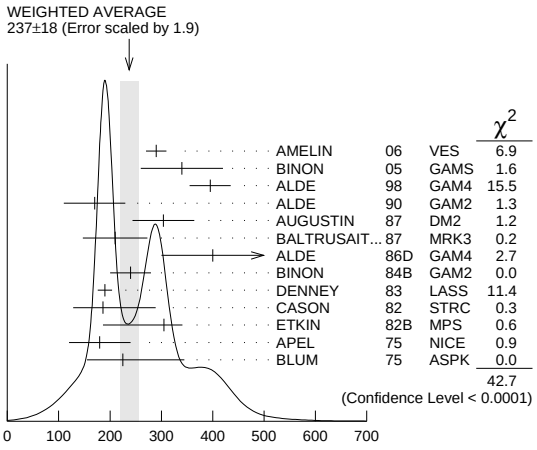

$f_4(2050)$ WIDTH

$f_4(2050)$ DECAY MODES

	Mode	Fraction (Γ_i/Γ)
Γ_1	$\omega\omega$	seen
Γ_2	$\pi\pi$	(17.0 ± 1.5) %
Γ_3	$K\overline{K}$	$(\ 6.8^{+3.4}_{-1.8}) \times 10^{-3}$
Γ_4	$\eta\eta$	$(\ 2.1\pm0.8) \times 10^{-3}$
Γ_5	$4\pi^0$	$<\ 1.2$ %
Γ_6	$\gamma\gamma$	
Γ_7	$a_2(1320)\pi$	seen

$f_4(2050)$ $\Gamma(i)\Gamma(\gamma\gamma)/\Gamma(\text{total})$

$\Gamma(K\overline{K}) \times \Gamma(\gamma\gamma)/\Gamma_{\text{total}}$ $\quad \Gamma_3\Gamma_6/\Gamma$

VALUE (keV)	CL%	DOCUMENT ID		TECN	COMMENT
• • • We do not use the following data for averages, fits, limits, etc. • • •					
<0.29	95	ALTHOFF	85B	TASS	$\gamma\gamma \to K\overline{K}\pi$

$\Gamma(\pi\pi) \times \Gamma(\gamma\gamma)/\Gamma_{\text{total}}$ $\quad \Gamma_2\Gamma_6/\Gamma$

VALUE (eV)	CL%	EVTS	DOCUMENT ID		TECN	COMMENT
• • • We do not use the following data for averages, fits, limits, etc. • • •						
$23.1^{+3.6+70.5}_{-3.3-15.6}$			[23] UEHARA	09	BELL	$10.6\ e^+e^- \to e^+e^-\pi^0\pi^0$
<1100	95	13 ± 4	OEST	90	JADE	$e^+e^- \to e^+e^-\pi^0\pi^0$

[23] Taking into account the $f_2(1950)$. Helicity-2 production favored.

$f_4(2050)$ BRANCHING RATIOS

$\Gamma(\omega\omega)/\Gamma_{\text{total}}$ $\quad \Gamma_1/\Gamma$

VALUE	DOCUMENT ID		TECN	COMMENT
seen	AMELIN	06	VES	$36\ \pi^-p \to \omega\omega n$
• • • We do not use the following data for averages, fits, limits, etc. • • •				
not seen	BARBERIS	00F		$450\ pp \to p_f\omega\omega p_s$

$\Gamma(\omega\omega)/\Gamma(\pi\pi)$ $\quad \Gamma_1/\Gamma_2$

VALUE	DOCUMENT ID		TECN	COMMENT
1.5±0.3	ALDE	90	GAM2	$38\ \pi^-p \to \omega\omega n$

$\Gamma(\pi\pi)/\Gamma_{\text{total}}$ $\quad \Gamma_2/\Gamma$

VALUE	DOCUMENT ID		TECN	COMMENT
0.170±0.015 OUR AVERAGE				
0.18 ±0.03	[24] BINON	83C	GAM2	$38\ \pi^-p \to n4\gamma$
0.16 ±0.03	[24] CASON	82	STRC	$8\ \pi^+p \to \Delta^{++}\pi^0\pi^0$
0.17 ±0.02	[24] CORDEN	79	OMEG	12–$15\ \pi^-p \to n2\pi$

[24] Assuming one pion exchange.

$\Gamma(K\overline{K})/\Gamma(\pi\pi)$ $\quad \Gamma_3/\Gamma_2$

VALUE	DOCUMENT ID		TECN	COMMENT
$\mathbf{0.04^{+0.02}_{-0.01}}$	ETKIN	82B	MPS	$23\ \pi^-p \to n2K^0_S$

$\Gamma(\eta\eta)/\Gamma_{\text{total}}$ $\quad \Gamma_4/\Gamma$

VALUE (units 10^{-3})	DOCUMENT ID		TECN	COMMENT
2.1±0.8	ALDE	86D	GAM4	$100\ \pi^-p \to n4\gamma$

$\Gamma(4\pi^0)/\Gamma_{\text{total}}$ $\quad \Gamma_5/\Gamma$

VALUE	DOCUMENT ID		TECN	COMMENT
<0.012	ALDE	87	GAM4	$100\ \pi^-p \to 4\pi^0 n$

$\Gamma(a_2(1320)\pi)/\Gamma_{\text{total}}$ $\quad \Gamma_7/\Gamma$

VALUE	DOCUMENT ID		TECN	COMMENT
seen	AMELIN	00	VES	$37\ \pi^-p \to \eta\pi^+\pi^-n$

$f_4(2050)$ REFERENCES

ANISOVICH	09	IJMP A24 2481	V.V. Anisovich, A.V. Sarantsev	
UEHARA	09	PR D79 052009	S. Uehara *et al.*	(BELLE Collab.)
AMELIN	06	PAN 69 690	D.V. Amelin *et al.*	(VES Collab.)
		Translated from YAF 69 715.		
BINON	05	PAN 68 960	F. Binon *et al.*	
		Translated from YAF 68 998.		
AMELIN	00	NP A668 83	D. Amelin *et al.*	(VES Collab.)
ANISOVICH	00J	PL B491 47	A.V. Anisovich *et al.*	
BARBERIS	00F	PL B484 198	D. Barberis *et al.*	(WA 102 Collab.)
ALDE	98	EPJ A3 361	D. Alde *et al.*	(GAM4 Collab.)
Also		PAN 62 405	D. Alde *et al.*	(GAMS Collab.)
		Translated from YAF 62 446.		
MARTIN	98	PR C57 3492	B.R. Martin *et al.*	
MARTIN	97	PR C56 1114	B.R. Martin, G.C. Oades	(LOUC, AARH)
KLOET	96	PR D53 6120	W.M. Kloet, F. Myhrer	(RUTG, NORD)
OAKDEN	94	NP A574 731	M.N. Oakden, M.R. Pennington	(DURH)
ALDE	90	PL B241 600	D.M. Alde *et al.*	(SERP, BELG, LANL, LAPP+)
OEST	90	ZPHY C47 343	T. Oest *et al.*	(JADE Collab.)
ALDE	87	PL B198 286	D.M. Alde *et al.*	(LANL, BRUX, SERP, LAPP)
AUGUSTIN	87	ZPHY C36 369	J.E. Augustin *et al.*	(LALO, CLER, FRAS+)
BALTRUSAIT...	87	PR D35 2077	R.M. Baltrusaitis *et al.*	(Mark III Collab.)
ALDE	86D	NP B269 485	D.M. Alde *et al.*	(BELG, LAPP, SERP, CERN+)
ALTHOFF	85B	ZPHY C29 189	M. Althoff *et al.*	(TASSO Collab.)
BINON	84B	LNC 39 41	F.G. Binon *et al.*	(SERP, BELG, LAPP)
BINON	83C	SJNP 38 723	F.G. Binon *et al.*	(SERP, BRUX+)
		Translated from YAF 38 1199.		
DENNEY	83	PR D28 2726	D.L. Denney *et al.*	(IOWA, MICH)
CASON	82	PRL 48 1316	N.M. Cason *et al.*	(NDAM, ANL)
ETKIN	82B	PR D25 1786	A. Etkin *et al.*	(BNL, CUNY, TUFTS, VAND)
ALPER	80	PL 94B 422	B. Alper *et al.*	(AMST, CERN, CRAC, MPIM+)
ROZANSKA	80	NP B162 505	M. Rozanska *et al.*	(MPIM, CERN)
CORDEN	79	NP B157 250	M.J. Corden *et al.*	(BIRM, RHEL, TELA+) JP
EVANGELIS...	79B	NP B154 381	C. Evangelista *et al.*	(BARI, BONN, CERN+)
ANTIPOV	77	NP B119 45	Y.M. Antipov *et al.*	(SERP, GEVA)
APEL	75	PL 57B 398	W.D. Apel *et al.*	(KARLK, KARLE, PISA, SERP+) JP
BLUM	75	PL 57B 403	W. Blum *et al.*	(CERN, MPIM) JP

$\pi_2(2100)$ $\quad I^G(J^{PC}) = 1^-(2^{-+})$

OMITTED FROM SUMMARY TABLE

Needs confirmation.

$\pi_2(2100)$ MASS

VALUE (MeV)	DOCUMENT ID		TECN	COMMENT
2090± 29 OUR AVERAGE				
2090± 30	[1] AMELIN	95B	VES	$36\ \pi^-A \to \pi^+\pi^-\pi^-A$
2100±150	[2] DAUM	81B	CNTR	$63,94\ \pi^-p \to 3\pi X$

[1] From a fit to $J^{PC} = 2^{-+}$ $f_2(1270)\pi$, $(\pi\pi)_S\pi$ waves.
[2] From a two-resonance fit to four 2^-0^+ waves.

$\pi_2(2100)$ WIDTH

VALUE (MeV)	DOCUMENT ID		TECN	COMMENT
625± 50 OUR AVERAGE Error includes scale factor of 1.2.				
520±100	[3] AMELIN	95B	VES	$36\ \pi^-A \to \pi^+\pi^-\pi^-A$
651± 50	[4] DAUM	81B	CNTR	$63,94\ \pi^-p \to 3\pi X$

[3] From a fit to $J^{PC} = 2^{-+}$ $f_2(1270)\pi$, $(\pi\pi)_S\pi$ waves.
[4] From a two-resonance fit to four 2^-0^+ waves.

$\pi_2(2100)$ DECAY MODES

	Mode	Fraction (Γ_i/Γ)
Γ_1	3π	seen
Γ_2	$\rho\pi$	seen
Γ_3	$f_2(1270)\pi$	seen
Γ_4	$(\pi\pi)_S\pi$	seen

$\pi_2(2100)$ BRANCHING RATIOS

$\Gamma(\rho\pi)/\Gamma(3\pi)$ $\quad \Gamma_2/\Gamma_1$

VALUE	DOCUMENT ID		TECN	COMMENT
0.19±0.05	[5] DAUM	81B	CNTR	$63,94\ \pi^-p$

$\Gamma(f_2(1270)\pi)/\Gamma(3\pi)$ $\quad \Gamma_3/\Gamma_1$

VALUE	DOCUMENT ID		TECN	COMMENT
0.36±0.09	[5] DAUM	81B	CNTR	$63,94\ \pi^-p$

$\Gamma((\pi\pi)_S\pi)/\Gamma(3\pi)$ $\quad \Gamma_4/\Gamma_1$

VALUE	DOCUMENT ID		TECN	COMMENT
0.45±0.07	[5] DAUM	81B	CNTR	$63,94\ \pi^-p$

Meson Particle Listings

$\pi_2(2100)$, $f_0(2100)$, $f_2(2150)$

D-wave/S-wave RATIO FOR $\pi_2(2100) \to f_2(1270)\pi$

VALUE	DOCUMENT ID		TECN	COMMENT
0.39±0.23	[5] DAUM	81B	CNTR	63,94 $\pi^- p$

[5] From a two-resonance fit to four 2^-0^+ waves.

$\pi_2(2100)$ REFERENCES

AMELIN	95B	PL B356 595	D.V. Amelin *et al.*	(SERP, TBIL)
DAUM	81B	NP B182 269	C. Daum *et al.*	(AMST, CERN, CRAC, MPIM+)

$f_0(2100)$

$I^G(J^{PC}) = 0^+(0^{++})$

OMITTED FROM SUMMARY TABLE

Needs confirmation.

$f_0(2100)$ MASS

VALUE (MeV)	EVTS	DOCUMENT ID		TECN	COMMENT
2103± 8 OUR AVERAGE					
2102±13		[1] ANISOVICH	00J	SPEC	2.0 $\overline{p}p \to \eta\pi^0\pi^0$, $\pi^0\pi^0$, $\eta\eta$, $\eta\eta'$, $\pi^+\pi^-$
2090±30		BAI	00A	BES	$J/\psi \to \gamma(\pi^+\pi^-\pi^+\pi^-)$
2105±10		ANISOVICH	99K	SPEC	0.6–1.94 $\overline{p}p \to \eta\eta$, $\eta\eta'$
• • • We do not use the following data for averages, fits, limits, etc. • • •					
2105± 8	80k	[2] UMAN	06	E835	5.2 $\overline{p}p \to \eta\eta\pi^0$
~ 2104		BUGG	95		$J/\psi \to \gamma\pi^+\pi^-\pi^+\pi^-$
~ 2122		HASAN	94	RVUE	$\overline{p}p \to \pi\pi$

[1] Includes the data of ANISOVICH 00B indicating to exotic decay pattern.
[2] Statistical error only.

$f_0(2100)$ WIDTH

VALUE (MeV)	EVTS	DOCUMENT ID		TECN	COMMENT
209± 19 OUR AVERAGE					
211± 29		[3] ANISOVICH	00J	SPEC	2.0 $\overline{p}p \to \eta\pi^0\pi^0$, $\pi^0\pi^0$, $\eta\eta$, $\eta\eta'$, $\pi^+\pi^-$
330±100		BAI	00A	BES	$J/\psi \to \gamma(\pi^+\pi^-\pi^+\pi^-)$
200± 25		ANISOVICH	99K	SPEC	0.6–1.94 $\overline{p}p \to \eta\eta$, $\eta\eta'$
• • • We do not use the following data for averages, fits, limits, etc. • • •					
236± 14	80k	[4] UMAN	06	E835	5.2 $\overline{p}p \to \eta\eta\pi^0$
~ 203		BUGG	95		$J/\psi \to \gamma\pi^+\pi^-\pi^+\pi^-$
~ 273		HASAN	94	RVUE	$\overline{p}p \to \pi\pi$

[3] Includes the data of ANISOVICH 00B indicating to exotic decay pattern.
[4] Statistical error only.

$f_0(2100)$ REFERENCES

UMAN	06	PR D73 052009	I. Uman *et al.*	(FNAL E835)
ANISOVICH	00B	NP A662 319	A.V. Anisovich *et al.*	
ANISOVICH	00J	PL B491 47	A.V. Anisovich *et al.*	
BAI	00A	PL B472 207	J.Z. Bai *et al.*	(BES Collab.)
ANISOVICH	99K	PL B468 309	A.V. Anisovich *et al.*	
BUGG	95	PL B353 378	D.V. Bugg *et al.*	(LOQM, PNPI, WASH)
HASAN	94	PL B334 215	A. Hasan, D.V. Bugg	(LOQM)

$f_2(2150)$

$I^G(J^{PC}) = 0^+(2^{++})$

OMITTED FROM SUMMARY TABLE

This entry was previously called T_0.

$f_2(2150)$ MASS

$f_2(2150)$ MASS, COMBINED MODES (MeV)

VALUE (MeV)	EVTS	DOCUMENT ID		TECN	COMMENT
2157±12 OUR AVERAGE Includes data from the 2 datablocks that follow this one.					
• • • We do not use the following data for averages, fits, limits, etc. • • •					
2170± 6	80k	[1] UMAN	06	E835	5.2 $\overline{p}p \to \eta\eta\pi^0$

[1] Statistical error only.

$\eta\eta$ MODE

VALUE (MeV)	DOCUMENT ID		TECN	COMMENT
The data in this block is included in the average printed for a previous datablock.				
2157±12 OUR AVERAGE				
2151±16	BARBERIS	00E		450 $pp \to p_f\eta\eta p_s$
2175±20	PROKOSHKIN	95D	GAM4	300 $\pi^- N \to \pi^- N 2\eta$, 450 $pp \to pp2\eta$
2130±35	SINGOVSKI	94	GAM4	450 $pp \to pp2\eta$
• • • We do not use the following data for averages, fits, limits, etc. • • •				
2140±30	[2] ABELE	99B	CBAR	
2104±20	[3] ARMSTRONG	93C	E760	$\overline{p}p \to \pi^0\eta\eta \to 6\gamma$

[2] Spin not determined.
[3] No J^{PC} determination.

$\eta\pi\pi$ MODE

VALUE (MeV)	DOCUMENT ID		TECN	CHG	COMMENT
The data in this block is included in the average printed for a previous datablock.					
• • • We do not use the following data for averages, fits, limits, etc. • • •					
2135±20±45	[4] ADOMEIT	96	CBAR	0	1.94 $\overline{p}p \to \eta 3\pi^0$

[4] ANISOVICH 00E recommends to withdraw ADOMEIT 96 that assumed a single $J^P = 2^+$ resonance.

$\overline{p}p \to \pi\pi$

VALUE (MeV)	DOCUMENT ID		TECN	COMMENT
• • • We do not use the following data for averages, fits, limits, etc. • • •				
~ 2090	[5] OAKDEN	94	RVUE	0.36–1.55 $\overline{p}p \to \pi\pi$
~ 2120	[6] OAKDEN	94	RVUE	0.36–1.55 $\overline{p}p \to \pi\pi$
~ 2170	[7] MARTIN	80B	RVUE	
~ 2150	[7] MARTIN	80C	RVUE	
~ 2150	[8] DULUDE	78B	OSPK	1–2 $\overline{p}p \to \pi^0\pi^0$

[5] OAKDEN 94 makes an amplitude analysis of LEAR data on $\overline{p}p \to \pi\pi$ using a method based on Barrelet zeros. This is solution A. The amplitude analysis of HASAN 94 includes earlier data as well, and assume that the data can be parametrized in terms of towers of nearly degenerate resonances on the leading Regge trajectory. See also KLOET 96 and MARTIN 97 who make related analyses.
[6] From solution B of amplitude analysis of data on $\overline{p}p \to \pi\pi$.
[7] $I(J^P) = 0(2^+)$ from simultaneous analysis of $p\overline{p} \to \pi^-\pi^+$ and $\pi^0\pi^0$.
[8] $I^G(J^P) = 0^+(2^+)$ from partial-wave amplitude analysis.

S-CHANNEL $\overline{p}p$, $\overline{N}N$ or $\overline{K}K$

VALUE (MeV)	DOCUMENT ID		TECN	CHG	COMMENT
• • • We do not use the following data for averages, fits, limits, etc. • • •					
$2139^{+\ 8}_{-\ 9}$	[9] EVANGELIS...	97	SPEC		0.6-2.4 $\overline{p}p \to K^0_S K^0_S$
~ 2190	[9] CUTTS	78B	CNTR		0.97–3 $\overline{p}p \to \overline{N}N$
2155±15	[9,10] COUPLAND	77	CNTR	0	0.7–2.4 $\overline{p}p \to \overline{p}p$
2193± 2	[9,11] ALSPECTOR	73	CNTR		$\overline{p}p$ S channel

[9] Isospins 0 and 1 not separated.
[10] From a fit to the total elastic cross section.
[11] Referred to as T or T region by ALSPECTOR 73.

$K\overline{K}$ MODE

VALUE (MeV)	DOCUMENT ID		TECN	COMMENT
• • • We do not use the following data for averages, fits, limits, etc. • • •				
2200±13	VLADIMIRSK...06		SPEC	40 $\pi^- p \to K^0_S K^0_S n$
2150±20	ABLIKIM	04E	BES2	$J/\psi \to \omega K^+ K^-$
2130±35	BARBERIS	99	OMEG	450 $pp \to p_s p_f K^+ K^-$

$f_2(2150)$ WIDTH

$f_2(2150)$ WIDTH, COMBINED MODES (MeV)

VALUE (MeV)	EVTS	DOCUMENT ID		TECN	COMMENT
152±30 OUR AVERAGE Includes data from the 2 datablocks that follow this one. Error includes scale factor of 1.4. See the ideogram below.					
• • • We do not use the following data for averages, fits, limits, etc. • • •					
182±11	80k	[12] UMAN	06	E835	5.2 $\overline{p}p \to \eta\eta\pi^0$

[12] Statistical error only.

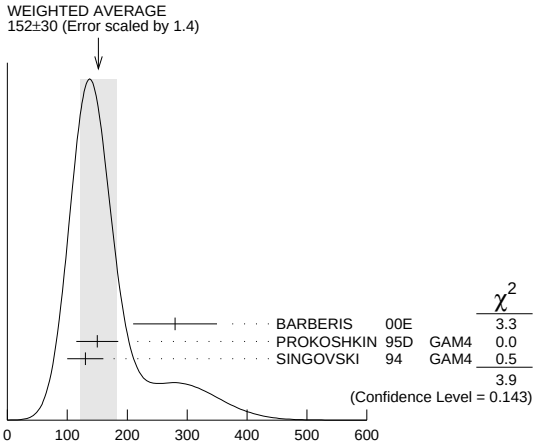

$f_2(2150)$ WIDTH, COMBINED MODES (MeV)

$\eta\eta$ MODE

VALUE (MeV)	DOCUMENT ID	TECN	COMMENT
The data in this block is included in the average printed for a previous datablock.			
152±30 OUR AVERAGE Error includes scale factor of 1.4. See the ideogram below.			
280±70	BARBERIS 00E		450 $pp \to p_f \eta\eta p_s$
150±35	PROKOSHKIN 95D	GAM4	300 $\pi^- N \to \pi^- N 2\eta$, 450 $pp \to pp2\eta$
130±30	SINGOVSKI 94	GAM4	450 $pp \to pp2\eta$
• • • We do not use the following data for averages, fits, limits, etc. • • •			
310±50	[13] ABELE 99B	CBAR	
203±10	[14] ARMSTRONG 93C	E760	$\overline{p}p \to \pi^0\eta\eta \to 6\gamma$

[13] Spin not determined.
[14] No J^{PC} determination.

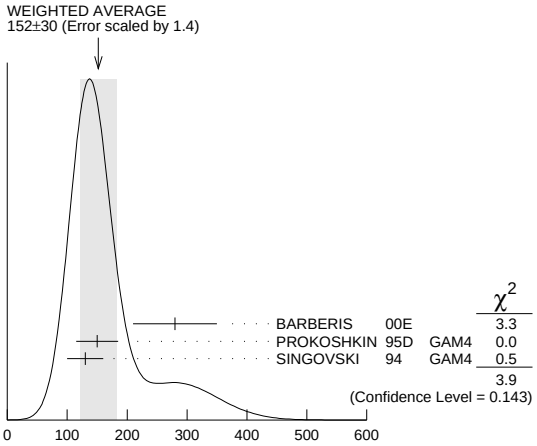

$f_2(2150)$ WIDTH, $\eta\eta$ MODE (MeV)

$\eta\pi\pi$ MODE

VALUE (MeV)	DOCUMENT ID	TECN	CHG	COMMENT
The data in this block is included in the average printed for a previous datablock.				
• • • We do not use the following data for averages, fits, limits, etc. • • •				
250±25±45	[15] ADOMEIT 96	CBAR	0	1.94 $\overline{p}p \to \eta 3\pi^0$

[15] ANISOVICH 00E recommends to withdraw ADOMEIT 96 that assumed a single $J^P = 2^+$ resonance.

$\overline{p}p \to \pi\pi$

VALUE (MeV)	DOCUMENT ID	TECN	COMMENT
250 OUR ESTIMATE			
• • • We do not use the following data for averages, fits, limits, etc. • • •			
~ 70	[16] OAKDEN 94	RVUE	0.36–1.55 $\overline{p}p \to \pi\pi$
~ 250	[17] MARTIN 80B	RVUE	
~ 250	[17] MARTIN 80C	RVUE	
~ 250	[18] DULUDE 78B	OSPK	1–2 $\overline{p}p \to \pi^0\pi^0$

[16] See however KLOET 96 who fit $\pi^+\pi^-$ only and find waves only up to $J = 3$ to be important but not significantly resonant.
[17] $I(J^P) = 0(2^+)$ from simultaneous analysis of $p\overline{p} \to \pi^-\pi^+$ and $\pi^0\pi^0$.
[18] $I^G(J^P) = 0^+(2^+)$ from partial-wave amplitude analysis.

S-CHANNEL $\overline{p}p$, $\overline{N}N$ or $\overline{K}K$

VALUE (MeV)	DOCUMENT ID	TECN	CHG	COMMENT
• • • We do not use the following data for averages, fits, limits, etc. • • •				
56^{+31}_{-16}	[19] EVANGELIS... 97	SPEC		0.6-2.4 $\overline{p}p \to K^0_S K^0_S$
135±75	[20,21] COUPLAND 77	CNTR	0	0.7–2.4 $\overline{p}p \to \overline{p}p$
98± 8	[21] ALSPECTOR 73	CNTR		$\overline{p}p$ S channel

[19] Isospin 0 and 2 not separated.
[20] From a fit to the total elastic cross section.
[21] Isospins 0 and 1 not separated.

$K\overline{K}$ MODE

VALUE (MeV)	DOCUMENT ID	TECN	COMMENT
• • • We do not use the following data for averages, fits, limits, etc. • • •			
91±62	VLADIMIRSK...06	SPEC	40 $\pi^- p \to K^0_S K^0_S n$
150±30	ABLIKIM 04E	BES2	$J/\psi \to \omega K^+ K^-$
270±50	BARBERIS 99	OMEG	450 $pp \to p_s p_f K^+ K^-$

$f_2(2150)$ DECAY MODES

	Mode	Fraction (Γ_i/Γ)
Γ_1	$\pi\pi$	
Γ_2	$\eta\eta$	seen
Γ_3	$K\overline{K}$	seen
Γ_4	$f_2(1270)\eta$	seen
Γ_5	$a_2(1320)\pi$	seen
Γ_6	$p\overline{p}$	seen

$f_2(2150)$ BRANCHING RATIOS

$\Gamma(K\overline{K})/\Gamma(\eta\eta)$ Γ_3/Γ_2

VALUE	CL%	DOCUMENT ID	TECN	COMMENT
1.28±0.23		BARBERIS 00E		450 $pp \to p_f \eta\eta p_s$
• • • We do not use the following data for averages, fits, limits, etc. • • •				
<0.1	95	[22] PROKOSHKIN 95D	GAM4	300 $\pi^- N \to \pi^- N 2\eta$, 450 $pp \to pp2\eta$

[22] Using data from ARMSTRONG 89D.

$\Gamma(\pi\pi)/\Gamma(\eta\eta)$ Γ_1/Γ_2

VALUE	CL%	DOCUMENT ID	TECN	COMMENT
• • • We do not use the following data for averages, fits, limits, etc. • • •				
<0.33	95	[23] PROKOSHKIN 95D	GAM4	300 $\pi^- N \to \pi^- N 2\eta$, 450 $pp \to pp2\eta$

[23] Derived from a $\pi^0\pi^0/\eta\eta$ limit.

$\Gamma(f_2(1270)\eta)/\Gamma(a_2(1320)\pi)$ Γ_4/Γ_5

VALUE	DOCUMENT ID	TECN	COMMENT
0.79±0.11	[24] ADOMEIT 96	CBAR	1.94 $\overline{p}p \to \eta 3\pi^0$

[24] Using B($a_2(1320) \to \eta\pi$) = 0.145

$\Gamma(p\overline{p})/\Gamma_{total}$ Γ_6/Γ

VALUE	EVTS	DOCUMENT ID	TECN	COMMENT
seen	73	ALEXANDER 10	CLEO	$\psi(2S) \to \gamma p\overline{p}$

$f_2(2150)$ REFERENCES

ALEXANDER 10	PR D82 092002	J.P. Alexander *et al.*	(CLEO Collab.)
UMAN 06	PR D73 052009	I. Uman *et al.*	(FNAL E835)
VLADIMIRSK... 06	PAN 69 493 Translated from YAF 69 515.	V.V. Vladimirsky *et al.*	(ITEP, Moscow)
ABLIKIM 04E	PL B603 138	M. Ablikim *et al.*	(BES Collab.)
ANISOVICH 00E	PL B477 19	A.V. Anisovich *et al.*	
BARBERIS 00E	PL B479 59	D. Barberis *et al.*	(WA 102 Collab.)
ABELE 99B	EPJ C8 67	A. Abele *et al.*	(Crystal Barrel Collab.)
BARBERIS 99	PL B453 305	D. Barberis *et al.*	(Omega Expt.)
EVANGELIS... 97	PR D56 3803	C. Evangelista *et al.*	(LEAR Collab.)
MARTIN 97	PR C56 1114	B.R. Martin, G.C. Oades	(LOUC, AARH)
ADOMEIT 96	ZPHY C71 227	J. Adomeit *et al.*	(Crystal Barrel Collab.)
KLOET 96	PR D53 6120	W.M. Kloet, F. Myhrer	(RUTG, NORD)
PROKOSHKIN 95D	SPD 40 495 Translated from DANS 344 469.	Y.D. Prokoshkin	(SERP) IGJPC
HASAN 94	PL B334 215	A. Hasan, D.V. Bugg	(LOQM)
OAKDEN 94	NP A574 731	M.N. Oakden, M.R. Pennington	(DURH)
SINGOVSKI 94	NC 107A 1911	A.V. Singovsky	(SERP)
ARMSTRONG 93C	PL B307 394	T.A. Armstrong *et al.*	(FNAL, FERR, GENO+)
ARMSTRONG 89D	PL B227 186	T.A. Armstrong, M. Benayoun	(ATHU, BARI, BIRM+)
MARTIN 80B	NP B176 355	B.R. Martin, D. Morgan	(LOUC, RHEL) JP
MARTIN 80C	NP B169 216	A.D. Martin, M.R. Pennington	(DURH) JP
CUTTS 78B	PR D17 16	D. Cutts *et al.*	(STON, WISC)
DULUDE 78B	PL 79B 335	R.S. Dulude *et al.*	(BROW, MIT, BARI) JP
COUPLAND 77	PL 71B 460	M. Coupland *et al.*	(LOQM, RHEL)
ALSPECTOR 73	PRL 30 511	J. Alspector *et al.*	(RUTG, UPNJ)

$\rho(2150)$

$I^G(J^{PC}) = 1^+(1^{--})$

OMITTED FROM SUMMARY TABLE

This entry was previously called $T_1(2190)$. See our mini-review under the $\rho(1700)$.

$\rho(2150)$ MASS

e^+e^- PRODUCED

VALUE (MeV)	DOCUMENT ID	TECN	COMMENT
• • • We do not use the following data for averages, fits, limits, etc. • • •			
2254±22	[1] LEES 12G	BABR	$e^+e^- \to \pi^+\pi^-\gamma$
2150±40±50	AUBERT 07AU	BABR	10.6 $e^+e^- \to f_1(1285)\pi^+\pi^-\gamma$
1990±80	AUBERT 07AU	BABR	10.6 $e^+e^- \to \eta'\pi^+\pi^-\gamma$
2153±37	BIAGINI 91	RVUE	$e^+e^- \to \pi^+\pi^-$, K^+K^-
2110±50	[2] CLEGG 90	RVUE	$e^+e^- \to 3(\pi^+\pi^-)$, $2(\pi^+\pi^-\pi^0)$

$\overline{p}p \to \pi\pi$

VALUE (MeV)	DOCUMENT ID	TECN	COMMENT
• • • We do not use the following data for averages, fits, limits, etc. • • •			
~ 2191	HASAN 94	RVUE	$\overline{p}p \to \pi\pi$
~ 2070	[3] OAKDEN 94	RVUE	0.36–1.55 $\overline{p}p \to \pi\pi$
~ 2170	[4] MARTIN 80B	RVUE	
~ 2100	[4] MARTIN 80C	RVUE	

Meson Particle Listings

$\rho(2150), \phi(2170)$

S-CHANNEL $\overline{N}N$

VALUE (MeV)	DOCUMENT ID		TECN	COMMENT
• • • We do not use the following data for averages, fits, limits, etc. • • •				
2110±35	[5] ANISOVICH	02	SPEC	0.6–1.9 $p\overline{p} \to \omega\pi^0, \omega\eta\pi^0, \pi^+\pi^-$
~ 2190	[6] CUTTS	78B	CNTR	0.97–3 $\overline{p}p \to \overline{N}N$
2155±15	[6,7] COUPLAND	77	CNTR	0.7–2.4 $\overline{p}p \to \overline{p}p$
2193± 2	[6,8] ALSPECTOR	73	CNTR	$\overline{p}p$ S channel
2190±10	[9] ABRAMS	70	CNTR	S channel $\overline{p}N$

$\pi^- p \to \omega\pi^0 n$

VALUE (MeV)	DOCUMENT ID		TECN	COMMENT
2155±21 OUR AVERAGE				
2140±30	ALDE	95	GAM2	38 $\pi^- p \to \omega\pi^0 n$
2170±30	ALDE	92C	GAM4	100 $\pi^- p \to \omega\pi^0 n$

[1] Using the GOUNARIS 68 parametrization of the pion form factor leaving the masses and widths of the $\rho(1450)$, $\rho(1700)$, and $\rho(2150)$ resonances as free parameters of the fit.
[2] Includes ATKINSON 85.
[3] See however KLOET 96 who fit $\pi^+\pi^-$ only and find waves only up to $J = 3$ to be important but not significantly resonant.
[4] $I(J^P) = 1(1^-)$ from simultaneous analysis of $p\overline{p} \to \pi^-\pi^+$ and $\pi^0\pi^0$.
[5] From the combined analysis of ANISOVICH 00J, ANISOVICH 01D, ANISOVICH 01E, and ANISOVICH 02.
[6] Isospins 0 and 1 not separated.
[7] From a fit to the total elastic cross section.
[8] Referred to as T or T region by ALSPECTOR 73.
[9] Seen as bump in $I = 1$ state. See also COOPER 68. PEASLEE 75 confirm $\overline{p}p$ results of ABRAMS 70, no narrow structure.

$\rho(2150)$ WIDTH

e^+e^- PRODUCED

VALUE (MeV)	DOCUMENT ID		TECN	COMMENT
• • • We do not use the following data for averages, fits, limits, etc. • • •				
109± 76	[10] LEES	12G	BABR	$e^+e^- \to \pi^+\pi^-\gamma$
350± 40±50	AUBERT	07AU	BABR	10.6 $e^+e^- \to f_1(1285)\pi^+\pi^-\gamma$
310±140	AUBERT	07AU	BABR	10.6 $e^+e^- \to \eta'\pi^+\pi^-\gamma$
389± 79	BIAGINI	91	RVUE	$e^+e^- \to \pi^+\pi^-$, K^+K^-
410±100	[11] CLEGG	90	RVUE	$e^+e^- \to 3(\pi^+\pi^-)$, $2(\pi^+\pi^-\pi^0)$

$\overline{p}p \to \pi\pi$

VALUE (MeV)	DOCUMENT ID		TECN	COMMENT
• • • We do not use the following data for averages, fits, limits, etc. • • •				
~ 296	HASAN	94	RVUE	$\overline{p}p \to \pi\pi$
~ 40	[12] OAKDEN	94	RVUE	0.36–1.55 $\overline{p}p \to \pi\pi$
~ 250	[13] MARTIN	80B	RVUE	
~ 200	[13] MARTIN	80C	RVUE	

S-CHANNEL $\overline{N}N$

VALUE (MeV)	DOCUMENT ID		TECN	COMMENT
• • • We do not use the following data for averages, fits, limits, etc. • • •				
230±50	[14] ANISOVICH	02	SPEC	0.6–1.9 $p\overline{p} \to \omega\pi^0, \omega\eta\pi^0, \pi^+\pi^-$
135±75	[15,16] COUPLAND	77	CNTR	0.7–2.4 $\overline{p}p \to \overline{p}p$
98± 8	[16] ALSPECTOR	73	CNTR	$\overline{p}p$ S channel
~ 85	[17] ABRAMS	70	CNTR	S channel $\overline{p}N$

$\pi^- p \to \omega\pi^0 n$

VALUE (MeV)	DOCUMENT ID		TECN	COMMENT
320±70	ALDE	95	GAM2	38 $\pi^- p \to \omega\pi^0 n$
• • • We do not use the following data for averages, fits, limits, etc. • • •				
~ 300	ALDE	92C	GAM4	100 $\pi^- p \to \omega\pi^0 n$

[10] Using the GOUNARIS 68 parametrization of the pion form factor leaving the masses and widths of the $\rho(1450)$, $\rho(1700)$, and $\rho(2150)$ resonances as free parameters of the fit.
[11] Includes ATKINSON 85.
[12] See however KLOET 96 who fit $\pi^+\pi^-$ only and find waves only up to $J = 3$ to be important but not significantly resonant.
[13] $I(J^P) = 1(1^-)$ from simultaneous analysis of $p\overline{p} \to \pi^-\pi^+$ and $\pi^0\pi^0$.
[14] From the combined analysis of ANISOVICH 00J, ANISOVICH 01D, ANISOVICH 01E, and ANISOVICH 02.
[15] From a fit to the total elastic cross section.
[16] Isospins 0 and 1 not separated.
[17] Seen as bump in $I = 1$ state. See also COOPER 68. PEASLEE 75 confirm $\overline{p}p$ results of ABRAMS 70, no narrow structure.

$\rho(2150)$ DECAY MODES

	Mode	Fraction (Γ_i/Γ)
Γ_1	e^+e^-	
Γ_2	$\pi^+\pi^-$	seen
Γ_3	K^+K^-	seen
Γ_4	$3(\pi^+\pi^-)$	seen
Γ_5	$2(\pi^+\pi^-\pi^0)$	seen
Γ_6	$\eta'\pi^+\pi^-$	seen
Γ_7	$f_1(1285)\pi^+\pi^-$	seen
Γ_8	$\omega\pi^0$	seen
Γ_9	$\omega\pi^0\eta$	seen
Γ_{10}	$p\overline{p}$	

$\rho(2150)$ $\Gamma(i)\Gamma(e^+e^-)/\Gamma^2(\text{total})$

$\Gamma(f_1(1285)\pi^+\pi^-)/\Gamma_{\text{total}} \times \Gamma(e^+e^-)/\Gamma_{\text{total}}$ $\quad \Gamma_7/\Gamma \times \Gamma_1/\Gamma$

VALUE (units 10^{-7})	DOCUMENT ID		TECN	COMMENT
3.1±0.6±0.5	[18] AUBERT	07AU	BABR	10.6 $e^+e^- \to f_1(1285)\pi^+\pi^-\gamma$

[18] Calculated by us from the reported value of cross section at the peak.

$\Gamma(\eta'\pi^+\pi^-)/\Gamma_{\text{total}} \times \Gamma(e^+e^-)/\Gamma_{\text{total}}$ $\quad \Gamma_6/\Gamma \times \Gamma_1/\Gamma$

VALUE (units 10^{-8})	DOCUMENT ID		TECN	COMMENT
• • • We do not use the following data for averages, fits, limits, etc. • • •				
4.9±1.9	[19] AUBERT	07AU	BABR	10.6 $e^+e^- \to \eta'\pi^+\pi^-\gamma$

[19] Calculated by us from the reported value of cross section at the peak.

$\rho(2150)$ REFERENCES

LEES	12G	PR D86 032013	J.P. Lees *et al.*	(BABAR Collab.)
AUBERT	07AU	PR D76 092005	B. Aubert *et al.*	(BABAR Collab.)
ANISOVICH	02	PL B542 8	A.V. Anisovich *et al.*	
ANISOVICH	01D	PL B508 6	A.V. Anisovich *et al.*	
ANISOVICH	01E	PL B513 281	A.V. Anisovich *et al.*	
ANISOVICH	00J	PL B491 47	A.V. Anisovich *et al.*	
KLOET	96	PR D53 6120	W.M. Kloet, F. Myhrer	(RUTG, NORD)
ALDE	95	ZPHY C66 379	D.M. Alde *et al.*	(GAMS Collab.) JP
HASAN	94	PL B334 215	A. Hasan, D.V. Bugg	(LOQM)
OAKDEN	94	NP A574 731	M.N. Oakden, M.R. Pennington	(DURH)
ALDE	92C	ZPHY C54 553	D.M. Alde *et al.*	(BELG, SERP, KEK, LANL+)
BIAGINI	91	NC 104A 363	M.E. Biagini *et al.*	(FRAS, PRAG)
CLEGG	90	ZPHY C45 677	A.B. Clegg, A. Donnachie	(LANC, MCHS)
ATKINSON	85	ZPHY C29 333	M. Atkinson *et al.*	(BONN, CERN, GLAS+)
MARTIN	80B	NP B176 355	B.R. Martin, D. Morgan	(LOUC, RHEL) JP
MARTIN	80C	NP B169 216	A.D. Martin, M.R. Pennington	(DURH) JP
CUTTS	78B	PR D17 16	D. Cutts *et al.*	(STON, WISC)
COUPLAND	77	PL 71B 460	M. Coupland *et al.*	(LOQM, RHEL)
PEASLEE	75	PL 57B 189	D.C. Peaslee *et al.*	(CANB, BARI, BROW+)
ALSPECTOR	73	PRL 30 511	J. Alspector *et al.*	(RUTG, UPNJ)
ABRAMS	70	PR D1 1917	R.J. Abrams *et al.*	(BNL)
COOPER	68	PRL 20 1059	W.A. Cooper *et al.*	(ANL)
GOUNARIS	68	PRL 21 244	G.J. Gounaris, J.J. Sakurai	

$\phi(2170)$ $\quad I^G(J^{PC}) = 0^-(1^{--})$

Observed by AUBERT,BE 06D in the initial-state radiation process $e^+e^- \to \phi f_0(980)\gamma$.

$\phi(2170)$ MASS

VALUE (MeV)	EVTS	DOCUMENT ID		TECN	COMMENT
2175±15 OUR AVERAGE		Error includes scale factor of 1.6. See the ideogram below.			
2186±10± 6	52	ABLIKIM	08F	BES	$J/\psi \to \eta\phi f_0(980)$
2125±22±10	483	AUBERT	08S	BABR	10.6 $e^+e^- \to \phi\eta\gamma$
2175±10±15	201	[1] AUBERT,BE	06D	BABR	10.6 $e^+e^- \to K^+K^-\pi\pi\gamma$
• • • We do not use the following data for averages, fits, limits, etc. • • •					
$2079\pm13^{+79}_{-28}$	4.8k	[2] SHEN	09	BELL	10.6 $e^+e^- \to K^+K^-\pi^+\pi^-\gamma$
2192±14	116 ± 95	[3] AUBERT	07AK	BABR	10.6 $e^+e^- \to K^+K^-\pi^+\pi^-\gamma$
2169±20	149 ± 36	[3] AUBERT	07AK	BABR	10.6 $e^+e^- \to K^+K^-\pi^0\pi^0\gamma$

[1] From the $\phi f_0(980)$ component.
[2] From a fit with two incoherent Breit-Wigners.
[3] From the $K^+K^-f_0(980)$ component.

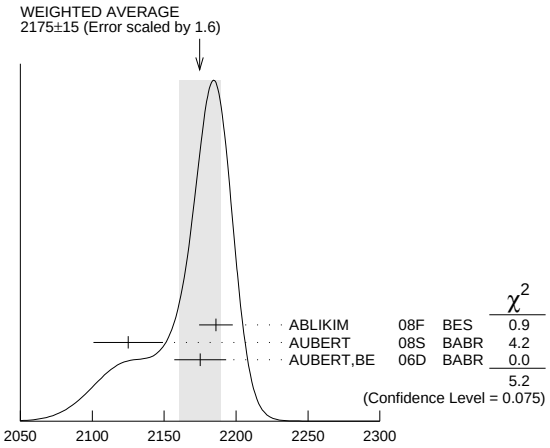

$\phi(2170)$ WIDTH

VALUE (MeV)	EVTS	DOCUMENT ID		TECN	COMMENT
61±18 OUR AVERAGE					
65±23±17	52	ABLIKIM	08F	BES	$J/\psi \to \eta\phi f_0(980)$
61±50±13	483	AUBERT	08S	BABR	10.6 $e^+e^- \to \phi\eta\gamma$
58±16±20	201	[4] AUBERT,BE	06D	BABR	10.6 $e^+e^- \to K^+K^-\pi\pi\gamma$

• • • We do not use the following data for averages, fits, limits, etc. • • •

$192 \pm 23^{+25}_{-61}$	4.8k	[5] SHEN	09	BELL	10.6	$e^+e^- \to K^+K^-\pi^+\pi^-\gamma$
71 ± 21	116 ± 95	[6] AUBERT	07AK	BABR	10.6	$e^+e^- \to K^+K^-\pi^+\pi^-\gamma$
102 ± 27	149 ± 36	[6] AUBERT	07AK	BABR	10.6	$e^+e^- \to K^+K^-\pi^0\pi^0\gamma$

[4] From the $\phi f_0(980)$ component.
[5] From a fit with two incoherent Breit-Wigners.
[6] From the $K^+K^- f_0(980)$ component.

$\phi(2170)$ DECAY MODES

	Mode	Fraction (Γ_i/Γ)
Γ_1	e^+e^-	seen
Γ_2	$\phi\eta$	
Γ_3	$\phi\pi\pi$	
Γ_4	$\phi f_0(980)$	seen
Γ_5	$K^+K^-\pi^+\pi^-$	
Γ_6	$K^+K^- f_0(980) \to K^+K^-\pi^+\pi^-$	seen
Γ_7	$K^+K^-\pi^0\pi^0$	
Γ_8	$K^+K^- f_0(980) \to K^+K^-\pi^0\pi^0$	seen
Γ_9	$K^{*0}K^\pm\pi^\mp$	not seen
Γ_{10}	$K^*(892)^0\overline{K}{}^*(892)^0$	not seen

$\phi(2170)$ Γ(i)$\Gamma(e^+e^-)/\Gamma$(total)

$\Gamma(\phi\eta) \times \Gamma(e^+e^-)/\Gamma_{\text{total}}$ $\quad \Gamma_2\Gamma_1/\Gamma$

VALUE (eV)	EVTS	DOCUMENT ID	TECN	COMMENT
• • • We do not use the following data for averages, fits, limits, etc. • • •				
$1.7 \pm 0.7 \pm 1.3$	483	AUBERT	08S BABR	10.6 $e^+e^- \to \phi\eta\gamma$

$\Gamma(\phi f_0(980)) \times \Gamma(e^+e^-)/\Gamma_{\text{total}}$ $\quad \Gamma_4\Gamma_1/\Gamma$

VALUE (eV)	EVTS	DOCUMENT ID	TECN	COMMENT
$2.5 \pm 0.8 \pm 0.4$	201	[7] AUBERT,BE	06D BABR	10.6 $e^+e^- \to K^+K^-\pi\pi\gamma$

[7] From the $\phi f_0(980)$ component.

$\phi(2170)$ Γ(i)$\Gamma(e^+e^-)/\Gamma^2$(total)

$\Gamma(\phi\pi\pi)/\Gamma_{\text{total}} \times \Gamma(e^+e^-)/\Gamma_{\text{total}}$ $\quad \Gamma_3/\Gamma \times \Gamma_1/\Gamma$

VALUE (units 10^{-7})	EVTS	DOCUMENT ID	TECN	COMMENT
• • • We do not use the following data for averages, fits, limits, etc. • • •				
$1.65 \pm 0.15 \pm 0.18$	4.8k	[8] SHEN	09 BELL	10.6 $e^+e^- \to K^+K^-\pi^+\pi^-\gamma$

[8] Multiplied by 3/2 to take into account the $\phi\pi^0\pi^0$ mode. Using B($\phi \to K^+K^-$) = $(49.2 \pm 0.6)\%$.

$\phi(2170)$ BRANCHING RATIOS

$\Gamma(K^+K^- f_0(980) \to K^+K^-\pi^+\pi^-)/\Gamma_{\text{total}}$ $\quad \Gamma_6/\Gamma$

VALUE	DOCUMENT ID	TECN	COMMENT
seen	AUBERT	07AK BABR	10.6 $e^+e^- \to K^+K^-\pi^+\pi^-\gamma$

$\Gamma(K^+K^- f_0(980) \to K^+K^-\pi^0\pi^0)/\Gamma_{\text{total}}$ $\quad \Gamma_8/\Gamma$

VALUE	DOCUMENT ID	TECN	COMMENT
seen	AUBERT	07AK BABR	10.6 $e^+e^- \to K^+K^-\pi^0\pi^0\gamma$

$\Gamma(K^{*0}K^\pm\pi^\mp)/\Gamma_{\text{total}}$ $\quad \Gamma_9/\Gamma$

VALUE	DOCUMENT ID	TECN	COMMENT
not seen	AUBERT	07AK BABR	10.6 GeV e^+e^-

$\Gamma(K^*(892)^0\overline{K}{}^*(892)^0)/\Gamma_{\text{total}}$ $\quad \Gamma_{10}/\Gamma$

VALUE	DOCUMENT ID	TECN	COMMENT
not seen	ABLIKIM	10C BES2	$J/\psi \to \eta K^+\pi^- K^-\pi^+$

$\phi(2170)$ REFERENCES

ABLIKIM	10C	PL B685 27	M. Ablikim *et al.*	(BES II Collab.)
SHEN	09	PR D80 031101	C.P. Shen *et al.*	(BELLE Collab.)
ABLIKIM	08F	PRL 100 102003	M. Ablikim *et al.*	(BES Collab.)
AUBERT	08S	PR D77 092002	B. Aubert *et al.*	(BABAR Collab.)
AUBERT	07AK	PR D76 012008	B. Aubert *et al.*	(BABAR Collab.)
AUBERT,BE	06D	PR D74 091103	B. Aubert *et al.*	(BABAR Collab.)

$f_0(2200)$ $\quad I^G(J^{PC}) = 0^+(0^{++})$

OMITTED FROM SUMMARY TABLE

Seen in $K^0_S K^0_S$ (AUGUSTIN 88), K^+K^- (ABLIKIM 05Q) and $\eta\eta$ (BINON 05) system. Not seen in $\Upsilon(1S)$ radiative decays (BARU 89).

$f_0(2200)$ MASS

VALUE (MeV)	DOCUMENT ID	TECN	COMMENT
2189 ± 13 OUR AVERAGE			
$2170 \pm 20^{+10}_{-15}$	ABLIKIM	05Q BES2	$\psi(2S) \to \gamma\pi^+\pi^- K^+K^-$
2210 ± 50	[1] BINON	05 GAMS	$33\ \pi^- p \to \eta\eta n$
2197 ± 17	[2] AUGUSTIN	88 DM2	$J/\psi \to \gamma K^0_S K^0_S$
• • • We do not use the following data for averages, fits, limits, etc. • • •			
~ 2122	HASAN	94 RVUE	$\overline{p}p \to \pi\pi$
~ 2321	HASAN	94 RVUE	$\overline{p}p \to \pi\pi$

[1] First solution, PWA is ambiguous.
[2] Cannot determine spin to be 0.

$f_0(2200)$ WIDTH

VALUE (MeV)	DOCUMENT ID	TECN	COMMENT
238 ± 50 OUR AVERAGE	Error includes scale factor of 1.2.		
$220 \pm 60^{+40}_{-45}$	ABLIKIM	05Q BES2	$\psi(2S) \to \gamma\pi^+\pi^- K^+K^-$
380 ± 90	[3] BINON	05 GAMS	$33\ \pi^- p \to \eta\eta n$
201 ± 51	[4] AUGUSTIN	88 DM2	$J/\psi \to \gamma K^0_S K^0_S$
• • • We do not use the following data for averages, fits, limits, etc. • • •			
~ 273	HASAN	94 RVUE	$\overline{p}p \to \pi\pi$
~ 223	HASAN	94 RVUE	$\overline{p}p \to \pi\pi$

[3] First solution, PWA is ambiguous.
[4] Cannot determine spin to be 0.

$f_0(2200)$ REFERENCES

ABLIKIM	05Q	PR D72 092002	M. Ablikim *et al.*	(BES Collab.)
BINON	05	PAN 68 960 Translated from YAF 68 998.	F. Binon *et al.*	
HASAN	94	PL B334 215	A. Hasan, D.V. Bugg	(LOQM)
BARU	89	ZPHY C42 505	S.E. Baru *et al.*	(NOVO)
AUGUSTIN	88	PRL 60 2238	J.E. Augustin *et al.*	(DM2 Collab.)

$f_J(2220)$ $\quad I^G(J^{PC}) = 0^+(2^{++}$ or $4^{++})$

OMITTED FROM SUMMARY TABLE

Needs confirmation. See our mini-review in the 2004 edition of this *Review*, PDG 04.

$f_J(2220)$ MASS

VALUE (MeV)	EVTS	DOCUMENT ID	TECN	COMMENT
2231.1 ± 3.5 OUR AVERAGE				
$2235 \pm 4 \pm 6$	74	BAI	96B BES	$e^+e^- \to J/\psi \to \gamma\pi^+\pi^-$
$2230 \pm 6 \pm 16$	46	BAI	96B BES	$e^+e^- \to J/\psi \to \gamma K^+K^-$
$2232 \pm 8 \pm 15$	23	BAI	96B BES	$e^+e^- \to J/\psi \to \gamma K^0_S K^0_S$
$2235 \pm 4 \pm 5$	32	BAI	96B BES	$e^+e^- \to J/\psi \to \gamma p\overline{p}$
$2209 \pm 17 \pm 10$		ASTON	88F LASS	$11\ K^- p \to K^+K^-\Lambda$
2230 ± 20		BOLONKIN	88 SPEC	$40\ \pi^- p \to K^0_S K^0_S n$
2220 ± 10	41	[1] ALDE	86B GA24	38–$100\ \pi p \to n\eta\eta'$
$2230 \pm 6 \pm 14$	93	BALTRUSAIT...86D	MRK3	$e^+e^- \to \gamma K^+K^-$
$2232 \pm 7 \pm 7$	23	BALTRUSAIT...86D	MRK3	$e^+e^- \to \gamma K^0_S K^0_S$
• • • We do not use the following data for averages, fits, limits, etc. • • •				
2223.9 ± 2.5		[2] VLADIMIRSK...08	SPEC	$40\ \pi^- p \to K^0_S K^0_S n + m\pi^0$
2246 ± 36		BAI	98H BES	$J/\psi \to \gamma\pi^0\pi^0$

[1] ALDE 86B uses data from both the GAMS-2000 and GAMS-4000 detectors.
[2] $J^{PC} = 2^{++}$. Systematic uncertainties not evaluated

$f_J(2220)$ WIDTH

VALUE (MeV)	CL%	EVTS	DOCUMENT ID	TECN	COMMENT
23^{+8}_{-7} OUR AVERAGE					
$19^{+13}_{-11} \pm 12$		74	BAI	96B BES	$e^+e^- \to J/\psi \to \gamma\pi^+\pi^-$
$20^{+20}_{-15} \pm 17$		46	BAI	96B BES	$e^+e^- \to J/\psi \to \gamma K^+K^-$
$20^{+25}_{-16} \pm 14$		23	BAI	96B BES	$e^+e^- \to J/\psi \to \gamma K^0_S K^0_S$

Meson Particle Listings

$f_J(2220)$, $\eta(2225)$

$15^{+12}_{-9}\pm 9$	32	BAI	96B	BES	$e^+e^- \to J/\psi \to \gamma p\overline{p}$
60^{+107}_{-57}		ASTON	88F	LASS	11 $K^- p \to K^+ K^- \Lambda$
80 ± 30		BOLONKIN	88	SPEC	40 $\pi^- p \to K^0_S K^0_S n$
$26^{+20}_{-16}\pm 17$	93	BALTRUSAIT...	86D	MRK3	$e^+e^- \to \gamma K^+ K^-$
$18^{+23}_{-15}\pm 10$	23	BALTRUSAIT...	86D	MRK3	$e^+e^- \to \gamma K^0_S K^0_S$

• • • We do not use the following data for averages, fits, limits, etc. • • •

8.6 ± 2.5		[3] VLADIMIRSK...	08	SPEC	40 $\pi^- p \to K^0_S K^0_S n + m\pi^0$
<80	90	ALDE	87C	GAM2	38 $\pi^- p \to \eta' \eta n$

[3] $J^{PC} = 2^{++}$. Systematic uncertainties not evaluated

$f_J(2220)$ DECAY MODES

	Mode	Fraction (Γ_i/Γ)
Γ_1	$\pi\pi$	seen
Γ_2	$\pi^+\pi^-$	seen
Γ_3	$K\overline{K}$	seen
Γ_4	$p\overline{p}$	
Γ_5	$\gamma\gamma$	not seen
Γ_6	$\eta\eta'(958)$	seen
Γ_7	$\phi\phi$	not seen
Γ_8	$\eta\eta$	not seen

$f_J(2220)$ Γ(i)$\Gamma(\gamma\gamma)/\Gamma$(total)

$\Gamma(K\overline{K}) \times \Gamma(\gamma\gamma)/\Gamma_{total}$ $\Gamma_3\Gamma_5/\Gamma$

VALUE (eV)	CL%	DOCUMENT ID		TECN	COMMENT
$<$ 1.4	95	[4] ACCIARRI	01H	L3	$\gamma\gamma \to K^0_S K^0_S$, E_{ee} = 91, 183–209 GeV

• • • We do not use the following data for averages, fits, limits, etc. • • •

$<$ 5.6	95	[4] GODANG	97	CLE2	$\gamma\gamma \to K^0_S K^0_S$
$<$ 86	95	[4] ALBRECHT	90G	ARG	$\gamma\gamma \to K^+ K^-$
$<$1000	95	[5] ALTHOFF	85B	TASS	$\gamma\gamma$, $K\overline{K}\pi$

$\Gamma(\pi\pi) \times \Gamma(\gamma\gamma)/\Gamma_{total}$ $\Gamma_1\Gamma_5/\Gamma$

VALUE (eV)	CL%	DOCUMENT ID		TECN	COMMENT
$<$2.5	95	ALAM	98C	CLE2	$\gamma\gamma \to \pi^+\pi^-$

[4] Assuming $J^P = 2^+$.
[5] True for $J^P = 0^+$ and $J^P = 2^+$.

$f_J(2220)$ Γ(i)$\Gamma(p\overline{p})/\Gamma^2$(total)

$\Gamma(p\overline{p})/\Gamma_{total} \times \Gamma(\pi\pi)/\Gamma_{total}$ $\Gamma_4/\Gamma \times \Gamma_1/\Gamma$

VALUE (units 10^{-5})	CL%	DOCUMENT ID		TECN	COMMENT
$<$18	95	[6] AMSLER	01	CBAR	1.4–1.5 $p\overline{p} \to \pi^0\pi^0$

• • • We do not use the following data for averages, fits, limits, etc. • • •

$<$(11–42)	99	[7] HASAN	96	SPEC	1.35–1.55 $p\overline{p} \to \pi^+\pi^-$

$\Gamma(p\overline{p})/\Gamma_{total} \times \Gamma(\phi\phi)/\Gamma_{total}$ $\Gamma_4/\Gamma \times \Gamma_7/\Gamma$

VALUE (units 10^{-5})	CL%	DOCUMENT ID		TECN	COMMENT
$<$6	95	[8] EVANGELIS...	98	SPEC	1.1–2.0 $p\overline{p} \to \phi\phi$

$\Gamma(p\overline{p})/\Gamma_{total} \times \Gamma(\eta\eta)/\Gamma_{total}$ $\Gamma_4/\Gamma \times \Gamma_8/\Gamma$

VALUE (units 10^{-5})	CL%	DOCUMENT ID		TECN	COMMENT
$<$4	95	[6] AMSLER	01	CBAR	1.4–1.5 $p\overline{p} \to \eta\eta$

[6] For $J^P = 2^+$ in the mass range 2222–2240 MeV and the total width between 10 and 20 MeV.
[7] For $J^P = 2^+$ and $J^P = 4^+$ in the mass range 2220–2245 MeV and the total width of 15 MeV.
[8] For $J^P = 2^+$, the mass of 2235 MeV and the total width of 15 MeV.

$f_J(2220)$ BRANCHING RATIOS

$\Gamma(p\overline{p})/\Gamma_{total}$ Γ_4/Γ

VALUE (units 10^{-4})	CL%	DOCUMENT ID		TECN	COMMENT
• • • We do not use the following data for averages, fits, limits, etc. • • •					
not seen		[9] AUBERT	07AV	BABR	$B \to p\overline{p}K^{(*)}$
not seen		WANG	05A	BELL	$B^+ \to \overline{p}pK^+$
$<$3.0	95	[10] EVANGELIS...	97	SPEC	1.96–2.40 $\overline{p}p \to K^0_S K^0_S$
$<$1.1	99.7	[11] BARNES	93	SPEC	1.3–1.57 $\overline{p}p \to K^0_S K^0_S$
$<$2.6	99.7	[11] BARDIN	87	CNTR	1.3–1.5 $\overline{p}p \to K^+ K^-$
$<$3.6	99.7	[11] SCULLI	87	CNTR	1.29–1.55 $\overline{p}p \to K^+ K^-$

[9] Assuming $\Gamma < 30$ MeV.
[10] Assuming $\Gamma \sim 20$ MeV, $J^P = 2^+$ and B($f_J(2220) \to K\overline{K}$) = 100%.
[11] Assuming Γ = 30–35 MeV, $J^P = 2^+$ and B($f_J(2220) \to K\overline{K}$) = 100%.

$\Gamma(\pi\pi)/\Gamma(K\overline{K})$ Γ_1/Γ_3

VALUE	DOCUMENT ID		TECN	COMMENT
1.0±0.5	BAI	96B	BES	$e^+e^- \to J/\psi \to \gamma 2\pi, K\overline{K}$

$\Gamma(p\overline{p})/\Gamma(K\overline{K})$ Γ_4/Γ_3

VALUE	DOCUMENT ID		TECN	COMMENT
0.17±0.09	BAI	96B	BES	$e^+e^- \to J/\psi \to \gamma p\overline{p}, K\overline{K}$

$f_J(2220)$ REFERENCES

VLADIMIRSK...	08	PAN 71 2129 Translated from YAF 71 2166.	V.V. Vladimirsky *et al.* (ITEP)
AUBERT	07AV	PR D76 092004	B. Aubert *et al.* (BABAR Collab.)
WANG	05A	PL B617 141	M.-Z. Wang *et al.* (BELLE Collab.)
PDG	04	PL B592 1	S. Eidelman *et al.* (PDG Collab.)
ACCIARRI	01H	PL B501 173	M. Acciarri *et al.* (L3 Collab.)
AMSLER	01	PL B520 175	C. Amsler *et al.* (Crystal Barrel Collab.)
ALAM	98C	PRL 81 3328	M.S. Alam *et al.* (CLEO Collab.)
BAI	98H	PRL 81 1179	J.Z. Bai *et al.* (BES Collab.)
EVANGELIS...	98	PR D57 5370	C. Evangelista *et al.* (JETSET Collab.)
EVANGELIS...	97	PR D56 3803	C. Evangelista *et al.* (LEAR Collab.)
GODANG	97	PRL 79 3829	R. Godang *et al.* (CLEO Collab.)
BAI	96B	PRL 76 3502	J.Z. Bai *et al.* (BES Collab.)
HASAN	96	PL B388 376	A. Hasan, D.V. Bugg (BRUN, LOQM)
BARNES	93	PL B309 469	P.D. Barnes *et al.* (PS185 Collab.)
ALBRECHT	90G	ZPHY C48 183	H. Albrecht *et al.* (ARGUS Collab.)
ASTON	88F	PL B215 199	D. Aston *et al.* (SLAC, NAGO, CINC, INUS) JP
BOLONKIN	88	NP B309 426	B.V. Bolonkin *et al.* (ITEP, SERP)
ALDE	87C	SJNP 45 255 Translated from YAF 45 405.	D. Alde *et al.*
BARDIN	87	PL B195 292	G. Bardin *et al.* (SACL, FERR, CERN, PADO+)
SCULLI	87	PRL 58 1715	J. Sculli *et al.* (NYU, BNL)
ALDE	86B	PL B177 120	D.M. Alde *et al.* (SERP, BELG, LANL, LAPP)
BALTRUSAIT...	86D	PRL 56 107	R.M. Baltrusaitis (CIT, UCSC, ILL, SLAC+)
ALTHOFF	85B	ZPHY C29 189	M. Althoff *et al.* (TASSO Collab.)

OTHER RELATED PAPERS

DEL-AMO-SA...	10O	PRL 105 172001	P. del Amo Sanchez *et al.* (BABAR Collab.)

$\eta(2225)$

$I^G(J^{PC}) = 0^+(0^{-+})$

OMITTED FROM SUMMARY TABLE

Seen in $J/\psi \to \gamma\phi\phi$. Possibly seen in $B \to \phi\phi K$ by LEES 11A.

$\eta(2225)$ MASS

VALUE (MeV)	EVTS	DOCUMENT ID		TECN	COMMENT
2226±16 OUR AVERAGE					
$2240^{+30}_{-20}\pm 30$	196 ± 19	ABLIKIM	08I	BES	$J/\psi \to \gamma K^+ K^- K^0_S K^0_L$
$2230\pm 25\pm 15$		BAI	90B	MRK3	$J/\psi \to \gamma K^+ K^- K^+ K^-$
$2214\pm 20\pm 13$		BAI	90B	MRK3	$J/\psi \to \gamma K^+ K^- K^0_S K^0_L$

• • • We do not use the following data for averages, fits, limits, etc. • • •

$\sim$ 2220		BISELLO	86B	DM2	$J/\psi \to \gamma K^+ K^- K^+ K^-$

$\eta(2225)$ WIDTH

VALUE (MeV)	EVTS	DOCUMENT ID		TECN	COMMENT
185^{+70}_{-40} OUR AVERAGE					
$190\pm 30^{+60}_{-40}$	196 ± 19	ABLIKIM	08I	BES	$J/\psi \to \gamma K^+ K^- K^0_S K^0_L$
$150^{+300}_{-60}\pm 60$		BAI	90B	MRK3	$J/\psi \to \gamma K^+ K^- K^+ K^-$

• • • We do not use the following data for averages, fits, limits, etc. • • •

$\sim$ 80		BISELLO	86B	DM2	$J/\psi \to \gamma K^+ K^- K^+ K^-$

$\eta(2225)$ REFERENCES

LEES	11A	PR D84 012001	J.P. Lees *et al.* (BABAR Collab.)
ABLIKIM	08I	PL B662 330	M. Ablikim *et al.* (BES Collab.)
BAI	90B	PRL 65 1309	Z. Bai *et al.* (Mark III Collab.)
BISELLO	86B	PL B179 294	D. Bisello *et al.* (DM2 Collab.)

$\rho_3(2250)$

$I^G(J^{PC}) = 1^+(3^{--})$

OMITTED FROM SUMMARY TABLE

Contains results mostly from formation experiments. For further production experiments see the Further States entry. See also $\rho(2150)$, $f_2(2150)$, $f_4(2300)$, $\rho_5(2350)$.

$\rho_3(2250)$ MASS

$\overline{p}p \to \pi\pi$ or $K\overline{K}$

VALUE (MeV)	DOCUMENT ID		TECN	CHG	COMMENT
• • • We do not use the following data for averages, fits, limits, etc. • • •					
~ 2232	HASAN	94	RVUE		$\overline{p}p \to \pi\pi$
~ 2090	[1] OAKDEN	94	RVUE		0.36–1.55 $\overline{p}p \to \pi\pi$
~ 2250	[2] MARTIN	80B	RVUE		
~ 2300	[2] MARTIN	80C	RVUE		
~ 2140	[3] CARTER	78B	CNTR	0	0.7–2.4 $\overline{p}p \to K^-K^+$
~ 2150	[4] CARTER	77	CNTR	0	0.7–2.4 $\overline{p}p \to \pi\pi$

[1] See however KLOET 96 who fit $\pi^+\pi^-$ only and find waves only up to $J = 3$ to be important but not significantly resonant.
[2] $I(J^P) = 1(3^-)$ from simultaneous analysis of $p\overline{p} \to \pi^-\pi^+$ and $\pi^0\pi^0$.
[3] $I = 0, 1$. $J^P = 3^-$ from Barrelet-zero analysis.
[4] $I(J^P) = 1(3^-)$ from amplitude analysis.

S-CHANNEL $\overline{N}N$

VALUE (MeV)	DOCUMENT ID		TECN	CHG	COMMENT
• • • We do not use the following data for averages, fits, limits, etc. • • •					
2260±20	[5] ANISOVICH	02	SPEC		0.6–1.9 $p\overline{p} \to \omega\pi^0, \omega\eta\pi^0, \pi^+\pi^-$
~ 2190	[6] CUTTS	78B	CNTR		0.97–3 $\overline{p}p \to \overline{N}N$
2155±15	[6,7] COUPLAND	77	CNTR	0	0.7–2.4 $\overline{p}p \to \overline{p}p$
2193± 2	[6,8] ALSPECTOR	73	CNTR		$\overline{p}p$ S channel
2190±10	[9] ABRAMS	70	CNTR		S channel $\overline{p}N$

[5] From the combined analysis of ANISOVICH 00J, ANISOVICH 01D, ANISOVICH 01E, and ANISOVICH 02.
[6] Isospins 0 and 1 not separated.
[7] From a fit to the total elastic cross section.
[8] Referred to as T or T region by ALSPECTOR 73.
[9] Seen as bump in $I = 1$ state. See also COOPER 68. PEASLEE 75 confirm $\overline{p}p$ results of ABRAMS 70, no narrow structure.

$\pi^-p \to \eta\pi\pi$

VALUE (MeV)	DOCUMENT ID		TECN	COMMENT
• • • We do not use the following data for averages, fits, limits, etc. • • •				
2290±20±30	AMELIN	00	VES	37 $\pi^-p \to \eta\pi^+\pi^-n$

$\rho_3(2250)$ WIDTH

$\overline{p}p \to \pi\pi$ or $K\overline{K}$

VALUE (MeV)	DOCUMENT ID		TECN	CHG	COMMENT
• • • We do not use the following data for averages, fits, limits, etc. • • •					
~ 220	HASAN	94	RVUE		$\overline{p}p \to \pi\pi$
~ 60	[10] OAKDEN	94	RVUE		0.36–1.55 $\overline{p}p \to \pi\pi$
~ 250	[11] MARTIN	80B	RVUE		
~ 200	[11] MARTIN	80C	RVUE		
~ 150	[12] CARTER	78B	CNTR	0	0.7–2.4 $\overline{p}p \to K^-K^+$
~ 200	[13] CARTER	77	CNTR	0	0.7–2.4 $\overline{p}p \to \pi\pi$

[10] See however KLOET 96 who fit $\pi^+\pi^-$ only and find waves only up to $J = 3$ to be important but not significantly resonant.
[11] $I(J^P) = 1(3^-)$ from simultaneous analysis of $p\overline{p} \to \pi^-\pi^+$ and $\pi^0\pi^0$.
[12] $I = 0, 1$. $J^P = 3^-$ from Barrelet-zero analysis.
[13] $I(J^P) = 1(3^-)$ from amplitude analysis.

S-CHANNEL $\overline{N}N$

VALUE (MeV)	DOCUMENT ID		TECN	CHG	COMMENT
• • • We do not use the following data for averages, fits, limits, etc. • • •					
160±25	[14] ANISOVICH	02	SPEC		0.6–1.9 $p\overline{p} \to \omega\pi^0, \omega\eta\pi^0, \pi^+\pi^-$
135±75	[15,16] COUPLAND	77	CNTR	0	0.7–2.4 $\overline{p}p \to \overline{p}p$
98± 8	[16] ALSPECTOR	73	CNTR		$\overline{p}p$ S channel
~ 85	[17] ABRAMS	70	CNTR		S channel $\overline{p}N$

[14] From the combined analysis of ANISOVICH 00J, ANISOVICH 01D, ANISOVICH 01E, and ANISOVICH 02.
[15] From a fit to the total elastic cross section.
[16] Isospins 0 and 1 not separated.
[17] Seen as bump in $I = 1$ state. See also COOPER 68. PEASLEE 75 confirm $\overline{p}p$ results of ABRAMS 70, no narrow structure.

$\pi^-p \to \eta\pi\pi$

VALUE (MeV)	DOCUMENT ID		TECN	COMMENT
• • • We do not use the following data for averages, fits, limits, etc. • • •				
230±50±80	AMELIN	00	VES	37 $\pi^-p \to \eta\pi^+\pi^-n$

$\rho_3(2250)$ REFERENCES

ANISOVICH	02	PL B542 8	A.V. Anisovich et al.
ANISOVICH	01D	PL B508 6	A.V. Anisovich et al.
ANISOVICH	01E	PL B513 281	A.V. Anisovich et al.
AMELIN	00	NP A668 83	D. Amelin et al. (VES Collab.)
ANISOVICH	00J	PL B491 47	A.V. Anisovich et al.
KLOET	96	PR D53 6120	W.M. Kloet, F. Myhrer (RUTG, NORD)
HASAN	94	PL B334 215	A. Hasan, D.V. Bugg (LOQM)
OAKDEN	94	NP A574 731	M.N. Oakden, M.R. Pennington (DURH)
MARTIN	80B	NP B176 355	B.R. Martin, D. Morgan (LOUC, RHEL) JP
MARTIN	80C	NP B169 216	A.D. Martin, M.R. Pennington (DURH) JP
CARTER	78B	NP B141 467	A.A. Carter (LOQM)
CUTTS	78B	PR D17 16	D. Cutts et al. (STON, WISC)
CARTER	77	PL 67B 117	A.A. Carter et al. (LOQM, RHEL) JP
COUPLAND	77	PL 71B 460	M. Coupland et al. (LOQM, RHEL)
PEASLEE	75	PL 57B 189	D.C. Peaslee et al. (CANB, BARI, BROW+)
ALSPECTOR	73	PRL 30 511	J. Alspector et al. (RUTG, UPNJ)
ABRAMS	70	PR D1 1917	R.J. Abrams et al. (BNL)
COOPER	68	PRL 20 1059	W.A. Cooper et al. (ANL)

$f_2(2300)$

$I^G(J^{PC}) = 0^+(2^{++})$

$f_2(2300)$ MASS

VALUE (MeV)	DOCUMENT ID		TECN	COMMENT
2297±28	[1] ETKIN	88	MPS	22 $\pi^-p \to \phi\phi n$
• • • We do not use the following data for averages, fits, limits, etc. • • •				
$2243^{+\ 7}_{-\ 6}{}^{+\ 3}_{-29}$	UEHARA	13	BELL	$\gamma\gamma \to K^0_S K^0_S$
2270±12	VLADIMIRSK...06		SPEC	40 $\pi^-p \to K^0_S K^0_S n$
2327± 9± 6	ABE	04	BELL	10.6 $e^+e^- \to e^+e^- K^+K^-$
2231±10	BOOTH	86	OMEG	85 π^-Be $\to 2\phi$Be
$2220^{+\ 90}_{-\ 20}$	LINDENBAUM	84	RVUE	
2320±40	ETKIN	82	MPS	22 $\pi^-p \to 2\phi n$

[1] Includes data of ETKIN 85. The percentage of the resonance going into $\phi\phi$ 2^{++} S_2, D_2, and D_0 is $6^{+15}_{-\ 5}$, 25^{+18}_{-14}, and 69^{+16}_{-27}, respectively.

$f_2(2300)$ WIDTH

VALUE (MeV)	DOCUMENT ID		TECN	COMMENT
149±41	[2] ETKIN	88	MPS	22 $\pi^-p \to \phi\phi n$
• • • We do not use the following data for averages, fits, limits, etc. • • •				
$145 \pm 12^{+27}_{-34}$	UEHARA	13	BELL	$\gamma\gamma \to K^0_S K^0_S$
90±29	VLADIMIRSK...06		SPEC	40 $\pi^-p \to K^0_S K^0_S n$
275±36±20	ABE	04	BELL	10.6 $e^+e^- \to e^+e^- K^+K^-$
133±50	BOOTH	86	OMEG	85 π^-Be $\to 2\phi$Be
200±50	LINDENBAUM	84	RVUE	
220±70	ETKIN	82	MPS	22 $\pi^-p \to 2\phi n$

[2] Includes data of ETKIN 85.

$f_2(2300)$ DECAY MODES

	Mode	Fraction (Γ_i/Γ)
Γ_1	$\phi\phi$	seen
Γ_2	$K\overline{K}$	seen
Γ_3	$\gamma\gamma$	seen

$f_2(2300)$ $\Gamma(i)\Gamma(\gamma\gamma)/\Gamma(\text{total})$

$\Gamma(K\overline{K}) \times \Gamma(\gamma\gamma)/\Gamma_{\text{total}}$ **$\Gamma_2\Gamma_3/\Gamma$**

VALUE (eV)	DOCUMENT ID		TECN	COMMENT
• • • We do not use the following data for averages, fits, limits, etc. • • •				
$3.2^{+0.5}_{-0.4} \pm 1.3 \pm 2.2$	UEHARA	13	BELL	$\gamma\gamma \to K^0_S K^0_S$
44 ±6 ±12	[3] ABE	04	BELL	10.6 $e^+e^- \to e^+e^- K^+K^-$

[3] Assuming spin 2.

$f_2(2300)$ REFERENCES

UEHARA	13	PTEP 2013 123C01	S. Uehara et al. (BELLE Collab.)
VLADIMIRSK...	06	PAN 69 493 Translated from YAF 69 515.	V.V. Vladimirsky et al. (ITEP, Moscow)
ABE	04	EPJ C32 323	K. Abe et al. (BELLE Collab.)
ETKIN	88	PL B201 568	A. Etkin et al. (BNL, CUNY)
BOOTH	86	NP B273 677	P.S.L. Booth et al. (LIVP, GLAS, CERN)
ETKIN	85	PL 165B 217	A. Etkin et al. (BNL, CUNY)
LINDENBAUM	84	CNPP 13 285	S.J. Lindenbaum (CUNY)
ETKIN	82	PRL 49 1620	A. Etkin et al. (BNL, CUNY)

Meson Particle Listings

$f_4(2300)$, $f_0(2330)$

$f_4(2300)$

$I^G(J^{PC}) = 0^+(4^{++})$

OMITTED FROM SUMMARY TABLE

This entry was previously called $U_0(2350)$. Contains results mostly from formation experiments. For further production experiments see the Further States entry. See also $\rho(2150)$, $f_2(2150)$, $\rho_3(2250)$, $\rho_5(2350)$.

$f_4(2300)$ MASS

$\overline{p}p \to \pi\pi$ or $\overline{K}K$

VALUE (MeV)	DOCUMENT ID		TECN	COMMENT
• • • We do not use the following data for averages, fits, limits, etc. • • •				
~ 2314	HASAN	94	RVUE	$\overline{p}p \to \pi\pi$
~ 2300	[1] MARTIN	80B	RVUE	
~ 2300	[1] MARTIN	80C	RVUE	
~ 2340	[2] CARTER	78B	CNTR	0.7–2.4 $\overline{p}p \to K^-K^+$
~ 2330	DULUDE	78B	OSPK	1–2 $\overline{p}p \to \pi^0\pi^0$
~ 2310	[3] CARTER	77	CNTR	0.7–2.4 $\overline{p}p \to \pi\pi$

[1] $I(J^P) = 0(4^+)$ from simultaneous analysis of $p\overline{p} \to \pi^-\pi^+$ and $\pi^0\pi^0$.
[2] $I(J^P) = 0(4^+)$ from Barrelet-zero analysis.
[3] $I(J^P) = 0(4^+)$ from amplitude analysis.

S-CHANNEL $\overline{p}p$ or $\overline{N}N$

VALUE (MeV)	DOCUMENT ID		TECN	COMMENT
• • • We do not use the following data for averages, fits, limits, etc. • • •				
2283±17	[4] ANISOVICH	00J	SPEC	
~ 2380	[5] CUTTS	78B	CNTR	0.97–3 $\overline{p}p \to \overline{N}N$
2345±15	[5,6] COUPLAND	77	CNTR	0.7–2.4 $\overline{p}p \to \overline{p}p$
2359± 2	[5,7] ALSPECTOR	73	CNTR	$\overline{p}p$ S channel
2375±10	ABRAMS	70	CNTR	S channel $\overline{N}N$

[4] From the combined analysis of ANISOVICH 99C and ANISOVICH 99F on $\overline{p}p \to \eta\pi^0\pi^0$, $\pi^0\pi^0$, $\eta\eta$, $\eta\eta'$, $\pi^+\pi^-$.
[5] Isospins 0 and 1 not separated.
[6] From a fit to the total elastic cross section.
[7] Referred to as U or U region by ALSPECTOR 73.

$\pi^-p \to \eta\pi\pi n$

VALUE (MeV)	DOCUMENT ID		TECN	COMMENT
• • • We do not use the following data for averages, fits, limits, etc. • • •				
2330±20±40	AMELIN	00	VES	37 $\pi^-p \to \eta\pi^+\pi^-n$

pp CENTRAL PRODUCTION

VALUE (MeV)	DOCUMENT ID		COMMENT
2320±60 OUR ESTIMATE			
• • • We do not use the following data for averages, fits, limits, etc. • • •			
2332±15	BARBERIS	00F	450 $pp \to p_f\omega\omega p_s$

$f_4(2300)$ WIDTH

$\overline{p}p \to \pi\pi$ or $\overline{K}K$

VALUE (MeV)	DOCUMENT ID		TECN	COMMENT
• • • We do not use the following data for averages, fits, limits, etc. • • •				
~ 278	HASAN	94	RVUE	$\overline{p}p \to \pi\pi$
~ 200	[8] MARTIN	80C	RVUE	
~ 150	[9] CARTER	78B	CNTR	0.7–2.4 $\overline{p}p \to K^-K^+$
~ 210	[10] CARTER	77	CNTR	0.7–2.4 $\overline{p}p \to \pi\pi$

[8] $I(J^P) = 0(4^+)$ from simultaneous analysis of $p\overline{p} \to \pi^-\pi^+$ and $\pi^0\pi^0$.
[9] $I(J^P) = 0(4^+)$ from Barrelet-zero analysis.
[10] $I(J^P) = 0(4^+)$ from amplitude analysis.

S-CHANNEL $\overline{p}p$ or $\overline{N}N$

VALUE (MeV)	DOCUMENT ID		TECN	COMMENT
• • • We do not use the following data for averages, fits, limits, etc. • • •				
310± 25	[11] ANISOVICH	00J	SPEC	
$135^{+150}_{-\ 65}$	[12,13] COUPLAND	77	CNTR	0.7–2.4 $\overline{p}p \to \overline{p}p$
$165^{+\ 18}_{-\ \ 8}$	[13] ALSPECTOR	73	CNTR	$\overline{p}p$ S channel
~ 190	ABRAMS	70	CNTR	S channel $\overline{N}N$

[11] From the combined analysis of ANISOVICH 99C and ANISOVICH 99F on $\overline{p}p \to \eta\pi^0\pi^0$, $\pi^0\pi^0$, $\eta\eta$, $\eta\eta'$, $\pi^+\pi^-$.
[12] From a fit to the total elastic cross section.
[13] Isospins 0 and 1 not separated.

$\pi^-p \to \eta\pi\pi n$

VALUE (MeV)	DOCUMENT ID		TECN	COMMENT
• • • We do not use the following data for averages, fits, limits, etc. • • •				
235±50±40	AMELIN	00	VES	37 $\pi^-p \to \eta\pi^+\pi^-n$

pp CENTRAL PRODUCTION

VALUE (MeV)	DOCUMENT ID		COMMENT
250±80 OUR ESTIMATE			
• • • We do not use the following data for averages, fits, limits, etc. • • •			
260±57	BARBERIS	00F	450 $pp \to p_f\omega\omega p_s$

$f_4(2300)$ DECAY MODES

	Mode	Fraction (Γ_i/Γ)
Γ_1	$\rho\rho$	seen
Γ_2	$\omega\omega$	seen
Γ_3	$\eta\pi\pi$	seen
Γ_4	$\pi\pi$	seen
Γ_5	$K\overline{K}$	seen
Γ_6	$N\overline{N}$	seen

$f_4(2300)$ BRANCHING RATIOS

$\Gamma(\rho\rho)/\Gamma(\omega\omega)$ Γ_1/Γ_2

VALUE	DOCUMENT ID		COMMENT
• • • We do not use the following data for averages, fits, limits, etc. • • •			
2.8±0.5	BARBERIS	00F	450 $pp \to p_f\omega\omega p_s$

$f_4(2300)$ REFERENCES

AMELIN	00	NP A668 83	D. Amelin *et al.*	(VES Collab.)
ANISOVICH	00J	PL B491 47	A.V. Anisovich *et al.*	
BARBERIS	00F	PL B484 198	D. Barberis *et al.*	(WA 102 Collab.)
ANISOVICH	99C	PL B452 173	A.V. Anisovich *et al.*	
ANISOVICH	99F	NP A651 253	A.V. Anisovich *et al.*	
HASAN	94	PL B334 215	A. Hasan, D.V. Bugg	(LOQM)
MARTIN	80B	NP B176 355	B.R. Martin, D. Morgan	(LOUC, RHEL) JP
MARTIN	80C	NP B169 216	A.D. Martin, M.R. Pennington	(DURH) JP
CARTER	78B	NP B141 467	A.A. Carter	(LOQM)
CUTTS	78B	PR D17 16	D. Cutts *et al.*	(STON, WISC)
DULUDE	78B	PL 79B 335	R.S. Dulude *et al.*	(BROW, MIT, BARI) JP
CARTER	77	PL 67B 117	A.A. Carter *et al.*	(LOQM, RHEL) JP
COUPLAND	77	PL 71B 460	M. Coupland *et al.*	(LOQM, RHEL)
ALSPECTOR	73	PRL 30 511	J. Alspector *et al.*	(RUTG, UPNJ)
ABRAMS	70	PR D1 1917	R.J. Abrams *et al.*	(BNL)

$f_0(2330)$

$I^G(J^{PC}) = 0^+(0^{++})$

OMITTED FROM SUMMARY TABLE

$f_0(2330)$ MASS

VALUE (MeV)	DOCUMENT ID		TECN	COMMENT
• • • We do not use the following data for averages, fits, limits, etc. • • •				
2314±25	[1] BUGG	04A	RVUE	
2337±14	ANISOVICH	00J	SPEC	2.0 $\overline{p}p \to \pi\pi, \eta\eta$
~ 2321	HASAN	94	RVUE	$\overline{p}p \to \pi\pi$

[1] Partial wave analysis of the data on $p\overline{p} \to \overline{\Lambda}\Lambda$ from BARNES 00.

$f_0(2330)$ WIDTH

VALUE (MeV)	DOCUMENT ID		TECN	COMMENT
• • • We do not use the following data for averages, fits, limits, etc. • • •				
144±20	[2] BUGG	04A	RVUE	
217±33	ANISOVICH	00J	SPEC	2.0 $\overline{p}p \to \pi\pi, \eta\eta$
~ 223	HASAN	94	RVUE	$\overline{p}p \to \pi\pi$

[2] Partial wave analysis of the data on $p\overline{p} \to \overline{\Lambda}\Lambda$ from BARNES 00.

$f_0(2330)$ REFERENCES

BUGG	04A	EPJ C36 161	D.V. Bugg	
ANISOVICH	00J	PL B491 47	A.V. Anisovich *et al.*	
BARNES	00	PR C62 055203	P.D. Barnes *et al.*	
HASAN	94	PL B334 215	A. Hasan, D.V. Bugg	(LOQM)

$f_2(2340)$

$I^G(J^{PC}) = 0^+(2^{++})$

$f_2(2340)$ MASS

VALUE (MeV)	EVTS	DOCUMENT ID		TECN	COMMENT
2339±55		[1] ETKIN	88	MPS	22 $\pi^- p \rightarrow \phi\phi n$
• • • We do not use the following data for averages, fits, limits, etc. • • •					
2350± 7	80k	[2] UMAN	06	E835	5.2 $\overline{p}p \rightarrow \eta\eta\pi^0$
2392±10		BOOTH	86	OMEG	85 π^- Be $\rightarrow 2\phi$Be
2360±20		LINDENBAUM	84	RVUE	

[1] Includes data of ETKIN 85. The percentage of the resonance going into $\phi\phi$ 2^{++} S_2, D_2, and D_0 is 37 ± 19, 4^{+12}_{-4}, and 59^{+21}_{-19}, respectively.
[2] Statistical error only.

$f_2(2340)$ WIDTH

VALUE (MeV)	EVTS	DOCUMENT ID		TECN	COMMENT
319^{+81}_{-69}		[3] ETKIN	88	MPS	22 $\pi^- p \rightarrow \phi\phi n$
• • • We do not use the following data for averages, fits, limits, etc. • • •					
218± 16	80k	[4] UMAN	06	E835	5.2 $\overline{p}p \rightarrow \eta\eta\pi^0$
198± 50		BOOTH	86	OMEG	85 π^- Be $\rightarrow 2\phi$Be
150^{+150}_{-50}		LINDENBAUM	84	RVUE	

[3] Includes data of ETKIN 85.
[4] Statistical error only.

$f_2(2340)$ DECAY MODES

	Mode	Fraction (Γ_i/Γ)
Γ_1	$\phi\phi$	seen
Γ_2	$\eta\eta$	seen

$f_2(2340)$ BRANCHING RATIOS

$\Gamma(\eta\eta)/\Gamma_{\text{total}}$ **Γ_2/Γ**

VALUE	DOCUMENT ID		TECN	COMMENT
seen	UMAN	06	E835	5.2 $\overline{p}p \rightarrow \eta\eta\pi^0$

$f_2(2340)$ REFERENCES

UMAN	06	PR D73 052009	I. Uman *et al.*	(FNAL E835)
ETKIN	88	PL B201 568	A. Etkin *et al.*	(BNL, CUNY)
BOOTH	86	NP B273 677	P.S.L. Booth *et al.*	(LIVP, GLAS, CERN)
ETKIN	85	PL 165B 217	A. Etkin *et al.*	(BNL, CUNY)
LINDENBAUM	84	CNPP 13 285	S.J. Lindenbaum	(CUNY)

$\rho_5(2350)$

$I^G(J^{PC}) = 1^+(5^{--})$

OMITTED FROM SUMMARY TABLE

This entry was previously called $U_1(2400)$. See also $\rho(2150)$, $f_2(2150)$, $\rho_3(2250)$, $f_4(2300)$.

$\rho_5(2350)$ MASS

$\pi^- p \rightarrow \omega\pi^0 n$

VALUE (MeV)	DOCUMENT ID		TECN	COMMENT
2330±35	ALDE	95	GAM2	38 $\pi^- p \rightarrow \omega\pi^0 n$

VALUE (MeV)	DOCUMENT ID		TECN	CHG	COMMENT
• • • We do not use the following data for averages, fits, limits, etc. • • •					
~ 2303	HASAN	94	RVUE		$\overline{p}p \rightarrow \pi\pi$
~ 2300	[1] MARTIN	80B	RVUE		
~ 2250	[1] MARTIN	80C	RVUE		
~ 2500	[2] CARTER	78B	CNTR	0	0.7–2.4 $\overline{p}p \rightarrow K^- K^+$
~ 2480	[3] CARTER	77	CNTR	0	0.7–2.4 $\overline{p}p \rightarrow \pi\pi$

S-CHANNEL $\overline{N}N$

VALUE (MeV)	DOCUMENT ID		TECN	CHG	COMMENT
• • • We do not use the following data for averages, fits, limits, etc. • • •					
2300±45	[4] ANISOVICH	02	SPEC		0.6–1.9 $p\overline{p} \rightarrow \omega\pi^0, \omega\eta\pi^0, \pi^+\pi^-$
2295±30	ANISOVICH	00J	SPEC		
~ 2380	[5] CUTTS	78B	CNTR		0.97–3 $\overline{p}p \rightarrow \overline{N}N$
2345±15	[5,6] COUPLAND	77	CNTR	0	0.7–2.4 $\overline{p}p \rightarrow \overline{p}p$
2359± 2	[5,7] ALSPECTOR	73	CNTR		$\overline{p}p$ S channel
2350±10	[8] ABRAMS	70	CNTR		S channel $\overline{N}N$
2360±25	[9] OH	70B	HDBC	−0	$\overline{p}(pn)$, $K^*K2\pi$

$\pi^- p \rightarrow K^+ K^- n$

VALUE (MeV)	DOCUMENT ID		TECN	CHG	COMMENT
• • • We do not use the following data for averages, fits, limits, etc. • • •					
2307±6	ALPER	80	CNTR	0	62 $\pi^- p \rightarrow K^+ K^- n$

[1] $I(J^P) = 1(5^-)$ from simultaneous analysis of $p\overline{p} \rightarrow \pi^-\pi^+$ and $\pi^0\pi^0$.
[2] $I = 0(1)$; $J^P = 5^-$ from Barrelet-zero analysis.
[3] $I(J^P) = 1(5^-)$ from amplitude analysis.
[4] From the combined analysis of ANISOVICH 00J, ANISOVICH 01D, ANISOVICH 01E, and ANISOVICH 02.
[5] Isospins 0 and 1 not separated.
[6] From a fit to the total elastic cross section.
[7] Referred to as U or U region by ALSPECTOR 73.
[8] For $I = 1$ $\overline{N}N$.
[9] No evidence for this bump seen in the $\overline{p}p$ data of CHAPMAN 71B. Narrow state not confirmed by OH 73 with more data.

$\rho_5(2350)$ WIDTH

$\pi^- p \rightarrow \omega\pi^0 n$

VALUE (MeV)	DOCUMENT ID		TECN	COMMENT
400±100	ALDE	95	GAM2	38 $\pi^- p \rightarrow \omega\pi^0 n$

$\overline{p}p \rightarrow \pi\pi$ or $\overline{K}K$

VALUE (MeV)	DOCUMENT ID		TECN	CHG	COMMENT
• • • We do not use the following data for averages, fits, limits, etc. • • •					
~ 169	HASAN	94	RVUE		$\overline{p}p \rightarrow \pi\pi$
~ 250	[10] MARTIN	80B	RVUE		
~ 300	[10] MARTIN	80C	RVUE		
~ 150	[11] CARTER	78B	CNTR	0	0.7–2.4 $\overline{p}p \rightarrow K^- K^+$
~ 210	[12] CARTER	77	CNTR	0	0.7–2.4 $\overline{p}p \rightarrow \pi\pi$

S-CHANNEL $\overline{N}N$

VALUE (MeV)	DOCUMENT ID		TECN	CHG	COMMENT
• • • We do not use the following data for averages, fits, limits, etc. • • •					
260± 75	[13] ANISOVICH	02	SPEC		0.6–1.9 $p\overline{p} \rightarrow \omega\pi^0, \omega\eta\pi^0, \pi^+\pi^-$
235^{+65}_{-40}	ANISOVICH	00J	SPEC		
135^{+150}_{-65}	[14,15] COUPLAND	77	CNTR	0	0.7–2.4 $\overline{p}p \rightarrow \overline{p}p$
165^{+18}_{-8}	[15] ALSPECTOR	73	CNTR		$\overline{p}p$ S channel
< 60	[16] OH	70B	HDBC	−0	$\overline{p}(pn)$, $K^*K2\pi$
~ 140	ABRAMS	67C	CNTR		S channel $\overline{p}N$

$\pi^- p \rightarrow K^+ K^- n$

VALUE (MeV)	DOCUMENT ID		TECN	CHG	COMMENT
• • • We do not use the following data for averages, fits, limits, etc. • • •					
245±20	ALPER	80	CNTR	0	62 $\pi^- p \rightarrow K^+ K^- n$

[10] $I(J^P) = 1(5^-)$ from simultaneous analysis of $p\overline{p} \rightarrow \pi^-\pi^+$ and $\pi^0\pi^0$.
[11] $I = 0(1)$; $J^P = 5^-$ from Barrelet-zero analysis.
[12] $I(J^P) = 1(5^-)$ from amplitude analysis.
[13] From the combined analysis of ANISOVICH 00J, ANISOVICH 01D, ANISOVICH 01E, and ANISOVICH 02.
[14] From a fit to the total elastic cross section.
[15] Isospins 0 and 1 not separated.
[16] No evidence for this bump seen in the $\overline{p}p$ data of CHAPMAN 71B. Narrow state not confirmed by OH 73 with more data.

$\rho_5(2350)$ REFERENCES

ANISOVICH	02	PL B542 8	A.V. Anisovich *et al.*	
ANISOVICH	01D	PL B508 6	A.V. Anisovich *et al.*	
ANISOVICH	01E	PL B513 281	A.V. Anisovich *et al.*	
ANISOVICH	00J	PL B491 47	A.V. Anisovich *et al.*	
ALDE	95	ZPHY C66 379	D.M. Alde *et al.*	(GAMS Collab.) JP
HASAN	94	PL B334 215	A. Hasan, D.V. Bugg	(LOQM)
ALPER	80	PL 94B 422	B. Alper *et al.*	(AMST, CERN, CRAC, MPIM+)
MARTIN	80B	NP B176 355	B.R. Martin, D. Morgan	(LOUC, RHEL) JP
MARTIN	80C	NP B169 216	A.D. Martin, M.R. Pennington	(DURH) JP
CARTER	78B	NP B141 467	A.A. Carter	(LOQM)
CUTTS	78B	PR D17 16	D. Cutts *et al.*	(STON, WISC)
CARTER	77	PL 67B 117	A.A. Carter *et al.*	(LOQM, RHEL) JP
COUPLAND	77	PL 71B 460	M. Coupland *et al.*	(LOQM, RHEL)
ALSPECTOR	73	PRL 30 511	J. Alspector *et al.*	(RUTG, UPNJ)
OH	73	NP B51 57	B.Y. Oh *et al.*	(MSU)
CHAPMAN	71B	PR D4 1275	J.W. Chapman *et al.*	(MICH)
ABRAMS	70	PR D1 1917	R.J. Abrams *et al.*	(BNL)
OH	70B	PRL 24 1257	B.Y. Oh *et al.*	(MSU)
ABRAMS	67C	PRL 18 1209	R.J. Abrams *et al.*	(BNL)

Meson Particle Listings

$a_6(2450)$, $f_6(2510)$

$a_6(2450)$

$I^G(J^{PC}) = 1^-(6^{++})$

OMITTED FROM SUMMARY TABLE

Needs confirmation.

$a_6(2450)$ MASS

VALUE (MeV)	DOCUMENT ID		TECN	CHG	COMMENT
2450±130	[1] CLELAND	82B	SPEC	±	50 $\pi p \to K^0_S K^\pm p$

[1] From an amplitude analysis.

$a_6(2450)$ WIDTH

VALUE (MeV)	DOCUMENT ID		TECN	CHG	COMMENT
400±250	[2] CLELAND	82B	SPEC	±	50 $\pi p \to K^0_S K^\pm p$

[2] From an amplitude analysis.

$a_6(2450)$ DECAY MODES

	Mode
Γ_1	$K\overline{K}$

$a_6(2450)$ REFERENCES

CLELAND	82B	NP B208 228	W.E. Cleland *et al.*	(DURH, GEVA, LAUS+)

$f_6(2510)$

$I^G(J^{PC}) = 0^+(6^{++})$

OMITTED FROM SUMMARY TABLE

Needs confirmation.

$f_6(2510)$ MASS

VALUE (MeV)	DOCUMENT ID		TECN	COMMENT
2469±29 OUR AVERAGE	Error includes scale factor of 1.5. See the ideogram below.			
2485±40	[1] ANISOVICH	00J	SPEC	1.92–2.41 $p\overline{p}$
2420±30	ALDE	98	GAM4	100 $\pi^- p \to \pi^0\pi^0 n$
2510±30	BINON	84B	GAM2	38 $\pi^- p \to n2\pi^0$

[1] From the combined analysis of ANISOVICH 99C, ANISOVICH 99F, ANISOVICH 99J, ANISOVICH 99K, and ANISOVICH 00B.

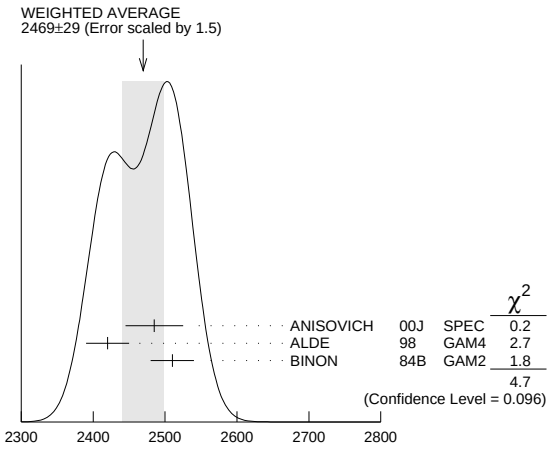

$f_6(2510)$ WIDTH

VALUE (MeV)	DOCUMENT ID		TECN	COMMENT
283±40 OUR AVERAGE	Error includes scale factor of 1.1.			
410±90	[2] ANISOVICH	00J	SPEC	1.92–2.41 $p\overline{p}$
270±60	ALDE	98	GAM4	100 $\pi^- p \to \pi^0\pi^0 n$
240±60	BINON	84B	GAM2	38 $\pi^- p \to n2\pi^0$

[2] From the combined analysis of ANISOVICH 99C, ANISOVICH 99F, ANISOVICH 99J, ANISOVICH 99K, and ANISOVICH 00B.

$f_6(2510)$ DECAY MODES

	Mode	Fraction (Γ_i/Γ)
Γ_1	$\pi\pi$	(6.0±1.0) %

$f_6(2510)$ BRANCHING RATIOS

$\Gamma(\pi\pi)/\Gamma_{total}$ Γ_1/Γ

VALUE	DOCUMENT ID		TECN	COMMENT
0.06±0.01	[3] BINON	83C	GAM2	38 $\pi^- p \to n4\gamma$

[3] Assuming one pion exchange and using data of BOLOTOV 74.

$f_6(2510)$ REFERENCES

ANISOVICH	00B	NP A662 319	A.V. Anisovich *et al.*	
ANISOVICH	00J	PL B491 47	A.V. Anisovich *et al.*	
ANISOVICH	99C	PL B452 173	A.V. Anisovich *et al.*	
ANISOVICH	99F	NP A651 253	A.V. Anisovich *et al.*	
ANISOVICH	99J	PL B471 271	A.V. Anisovich *et al.*	
ANISOVICH	99K	PL B468 309	A.V. Anisovich *et al.*	
ALDE	98	EPJ A3 361	D. Alde *et al.*	(GAM4 Collab.)
Also		PAN 62 405	D. Alde *et al.*	(GAMS Collab.)
		Translated from YAF 62 446.		
BINON	84B	LNC 39 41	F.G. Binon *et al.*	(SERP, BELG, LAPP) JP
BINON	83C	SJNP 38 723	F.G. Binon *et al.*	(SERP, BRUX+)
		Translated from YAF 38 1199.		
BOLOTOV	74	PL 52B 489	V.N. Bolotov *et al.*	(SERP)

OTHER LIGHT MESONS

Further States

OMITTED FROM SUMMARY TABLE

This section contains states observed by a single group or states poorly established that thus need confirmation.

QUANTUM NUMBERS, MASSES, WIDTHS, AND BRANCHING RATIOS

$X(360)$ $I^G(J^{PC}) = ?^?(?^{?+})$

MASS (MeV)	WIDTH (MeV)	EVTS	DOCUMENT ID	TECN	COMMENT
$360 \pm 7 \pm 9$	64 ± 18	2.3k	[1] ABRAAMYAN 09	CNTR	2.75 $dC \to \gamma\gamma X$

[1] Not seen in $pC \to \gamma\gamma X$ at 5.5 GeV/c.

$X(1070)$ $I^G(J^{PC}) = ?^?(0^{++})$

MASS (MeV)	WIDTH (MeV)	DOCUMENT ID	COMMENT
1072 ± 1	3.5 ± 0.5	[2] VLADIMIRSK...08	40 $\pi^- p \to K^0_S K^0_S n +$ mπ^0

[2] Supersedes GRIGOR'EV 05.

$X(1110)$ $I^G(J^{PC}) = 0^+(\text{even}^{++})$

MASS (MeV)	WIDTH (MeV)	DOCUMENT ID		TECN	COMMENT
1107 ± 4	$111 \pm 8 \pm 15$	DAFTARI	87	DBC	0. $\overline{p}n \to \rho^- \pi^+ \pi^-$

$f_0(1200\text{–}1600)$ $I^G(J^{PC}) = 0^+(0^{++})$

MASS (MeV)	WIDTH (MeV)	DOCUMENT ID		TECN	COMMENT
1323 ± 8	237 ± 20	VLADIMIRSK...06		SPEC	40 $\pi^- p \to K^0_S K^0_S n$
1480^{+100}_{-150}	1030^{+80}_{-170}	[3] ANISOVICH	03	SPEC	
1530^{+90}_{-250}	560 ± 40	[4] ANISOVICH	03	SPEC	

[3] K-matrix pole from combined analysis of $\pi^- p \to \pi^0\pi^0 n$, $\pi^- p \to K\overline{K} n$, $\pi^+\pi^- \to \pi^+\pi^-$, $\overline{p}p \to \pi^0\pi^0\pi^0$, $\pi^0\eta\eta$, $\pi^0\pi^0\eta$, $\pi^+\pi^-\pi^0$, $K^+K^-\pi^0$, $K^0_S K^0_S \pi^0$, $K^+K^0_S\pi^-$ at rest, $\overline{p}n \to \pi^-\pi^-\pi^+$, $K^0_S K^-\pi^0$, $K^0_S K^0_S \pi^-$ at rest.

[4] K-matrix pole from combined analysis of $\pi^- p \to \pi^0\pi^0 n$, $\pi^- p \to K\overline{K} n$, $\overline{p}p \to \pi^0\pi^0\pi^0$, $\pi^0\eta\eta$, $\pi^0\pi^0\eta$ at rest.

$X(1420)$ $I^G(J^{PC}) = 2^+(0^{++})$

MASS (MeV)	WIDTH (MeV)	DOCUMENT ID		TECN	COMMENT
1420 ± 20	160 ± 10	FILIPPI	00	OBLX	0 $\overline{n}p \to \pi^+\pi^+\pi^-$

$X(1545)$ $I^G(J^{PC}) = ?^?(?^{++})$

MASS (MeV)	WIDTH (MeV)	DOCUMENT ID	COMMENT
1545 ± 3	6.0 ± 2.5	[5] VLADIMIRSK...08	40 $\pi^- p \to K^0_S K^0_S n +$ mπ^0

[5] Supersedes VLADIMIRSKII 00.

$X(1575)$ $I^G(J^{PC}) = ?^?(1^{--})$

MASS (MeV)	WIDTH (MeV)	DOCUMENT ID		TECN	COMMENT
1576^{+49+98}_{-55-91}	$818^{+22+64}_{-23-133}$	[6] ABLIKIM	06S	BES	$J/\psi \to K^+K^-\pi^0$

[6] A broad peak observed at K^+K^- invariant mass. Mass and width above are its pole position. The observed branching ratio is $B(J/\psi \to X\pi^0)\,B(X \to K^+K^-) = (8.5 \pm 0.6^{+2.7}_{-3.6}) \times 10^{-4}$.

$X(1600)$ $I^G(J^{PC}) = 2^+(2^{++})$

MASS (MeV)	WIDTH (MeV)	DOCUMENT ID		TECN	COMMENT
1600 ± 100	400 ± 200	[7] ALBRECHT	91F	ARG	10.2 $e^+e^- \to e^+e^- 2(\pi^+\pi^-)$

[7] Our estimate.

$X(1650)$ $I^G(J^{PC}) = 0^-(?^{?-})$

MASS (MeV)	WIDTH (MeV)	EVTS	DOCUMENT ID	TECN	COMMENT
1652 ± 7	<50	100	PROKOSHKIN 96	GAM2	32,38 $\pi p \to \omega\eta n$

$X(1730)$ $I^G(J^{PC}) = ?^?(?^{?+})$

MASS (MeV)	WIDTH (MeV)	EVTS	DOCUMENT ID	TECN	COMMENT
$1731.0 \pm 1.2 \pm 2.0$	$3.2 \pm 0.8 \pm 1.3$	58	VLADIMIRSK...07	SPEC	40 $\pi^- p \to K^0_S K^0_S X$

$X(1750)$ $I^G(J^{PC}) = ?^?(1^{--})$

MASS (MeV)	WIDTH (MeV)	DOCUMENT ID		TECN	COMMENT
$1753.5 \pm 1.5 \pm 2.3$	$122.2 \pm 6.2 \pm 8.0$	LINK	02K	FOCS	20–160 $\gamma p \to K^+K^- p$

$B(X(1750) \to \overline{K}^*(892)^0 K^0 \to K^\pm\pi^\mp K^0_S)/B(X(1750) \to K^+K^-)$

VALUE	CL%	DOCUMENT ID		TECN
<0.065	90	LINK	02K	FOCS

$B(X(1750) \to \overline{K}^*(892)^\pm K^\mp \to K^\pm\pi^\mp K^0_S)/B(X(1750) \to K^+K^-)$

VALUE	CL%	DOCUMENT ID		TECN
<0.183	90	LINK	02K	FOCS

$f_2(1750)$ $I^G(J^{PC}) = 0^+(2^{++})$

MASS (MeV)	WIDTH (MeV)	EVTS	DOCUMENT ID		TECN	COMMENT
1755 ± 10	67 ± 12	870	[8] SCHEGELSKY 06A		RVUE	$\gamma\gamma \to K^0_S K^0_S$

$\Gamma(K\overline{K})$

VALUE (MeV)	EVTS	DOCUMENT ID		TECN	COMMENT
17 ± 5	870	[9] SCHEGELSKY 06A		RVUE	$\gamma\gamma \to K^0_S K^0_S$

$\Gamma(\gamma\gamma)$

VALUE (keV)	EVTS	DOCUMENT ID		TECN	COMMENT
0.13 ± 0.04	870	[9] SCHEGELSKY 06A		RVUE	$\gamma\gamma \to K^0_S K^0_S$

$\Gamma(\pi\pi)$

VALUE (MeV)	EVTS	DOCUMENT ID		TECN	COMMENT
1.3 ± 1.0	870	[9] SCHEGELSKY 06A		RVUE	$\gamma\gamma \to K^0_S K^0_S$

$\Gamma(\eta\eta)$

VALUE (MeV)	EVTS	DOCUMENT ID		TECN	COMMENT
2.0 ± 0.5	870	[9] SCHEGELSKY 06A		RVUE	$\gamma\gamma \to K^0_S K^0_S$

[8] From analysis of L3 data at 91 and 183–209 GeV.

[9] From analysis of L3 data at 91 and 183–209 GeV and using SU(3) relations.

$X(1775)$ $I^G(J^{PC}) = 1^-(?^{-+})$

MASS (MeV)	WIDTH (MeV)	DOCUMENT ID		TECN	COMMENT
1763 ± 20	192 ± 60	CONDO	91	SHF	$\gamma p \to (p\pi^+)(\pi^+\pi^-\pi^-)$
1787 ± 18	118 ± 60	CONDO	91	SHF	$\gamma p \to n\pi^+\pi^+\pi^-$

$f_0(1800)$ $I^G(J^{PC}) = 0^+(0^{++})$

MASS (MeV)	WIDTH (MeV)	DOCUMENT ID		TECN	COMMENT
$1795 \pm 7^{+23}_{-20}$	$95 \pm 10^{+78}_{-82}$	ABLIKIM	13J	BES3	$J/\psi \to \gamma\omega\phi$
$1812^{+19}_{-26} \pm 18$	$105 \pm 20 \pm 28$	[10] ABLIKIM	06J	BES2	$J/\psi \to \gamma\omega\phi$

[10] Not seen by LIU 09 in $B^\pm \to K^\pm\omega\phi$.

$X(1850 - 3100)$ $I^G(J^{PC}) = ?^?(1^{--})$

$\Gamma(e^+e^-)\cdot B(X \to \text{hadrons})$ (eV)	CL%	DOCUMENT ID		TECN	COMMENT
<120	90	[11] ANASHIN	11	KEDR	$e^+e^- \to$ hadrons

[11] This limit is center-of-mass energy dependent. We quote the most stringent one.

$X(1855)$ $I^G(J^{PC}) = ?^?(?^{??})$

MASS (MeV)	WIDTH (MeV)	DOCUMENT ID		TECN	COMMENT
1856.6 ± 5	20 ± 5	BRIDGES	86D	SPEC	0. $\overline{p}d \to \pi\pi N$

$X(1870)$ $I^G(J^{PC}) = ?^?(2^{??})$

MASS (MeV)	WIDTH (MeV)	DOCUMENT ID		TECN	COMMENT
1870 ± 40	250 ± 30	ALDE	86D	GAM4	100 $\pi^- p \to 2\eta$X

$a_3(1875)$ $I^G(J^{PC}) = 1^-(3^{++})$

MASS (MeV)	WIDTH (MeV)	DOCUMENT ID		TECN	COMMENT
$1874 \pm 43 \pm 96$	$385 \pm 121 \pm 114$	CHUNG	02	B852	18.3 $\pi^- p \to \pi^+\pi^-\pi^- p$

$B(a_3(1875) \to f_2(1270)\pi)/B(a_3(1875) \to \rho\pi)$

VALUE	DOCUMENT ID		TECN	COMMENT
0.8 ± 0.2	[12] CHUNG	02	B852	18.3 $\pi^- p \to \pi^+\pi^-\pi^- p$

[12] Using the observable fractions of 50.0% $\rho\pi$, 56.5% $f_2\pi$, and 11.8% $\rho_3\pi$.

$B(a_3(1875) \to \rho_3(1690)\pi)/B(a_3(1875) \to \rho\pi)$

VALUE	DOCUMENT ID		TECN	COMMENT
0.9 ± 0.3	[13] CHUNG	02	B852	18.3 $\pi^- p \to \pi^+\pi^-\pi^- p$

[13] Using the observable fractions of 50.0% $\rho\pi$, 56.5% $f_2\pi$, and 11.8% $\rho_3\pi$.

$a_1(1930)$ $I^G(J^{PC}) = 1^-(1^{++})$

MASS (MeV)	WIDTH (MeV)	DOCUMENT ID		TECN	COMMENT
1930^{+30}_{-70}	155 ± 45	ANISOVICH	01F	SPEC	2.0 $\overline{p}p \to 3\pi^0, \pi^0\eta, \pi^0\eta'$

Meson Particle Listings

Further States

X(1935) $I^G(J^{PC}) = 1^+(1^{-?})$

MASS (MeV)	WIDTH (MeV)	DOCUMENT ID		TECN	COMMENT
1935 ± 20	215 ± 30	EVANGELIS...	79	OMEG	10,16 $\pi^- p \to \overline{p} p n$

ρ_2(1940) $I^G(J^{PC}) = 1^+(2^{--})$

MASS (MeV)	WIDTH (MeV)	DOCUMENT ID		TECN	COMMENT
1940 ± 40	155 ± 40	[14] ANISOVICH	02	SPEC	0.6–1.9 $p\overline{p} \to \omega\pi^0$, $\omega\eta\pi^0$, $\pi^+\pi^-$

[14] From the combined analysis of ANISOVICH 00J, ANISOVICH 01D, ANISOVICH 01E, and ANISOVICH 02.

ω_3(1945) $I^G(J^{PC}) = 0^-(3^{--})$

MASS (MeV)	WIDTH (MeV)	DOCUMENT ID		TECN	COMMENT
1945 ± 20	115 ± 22	[15] ANISOVICH	02B	SPEC	0.6–1.9 $p\overline{p} \to \omega\eta$, $\omega\pi^0\pi^0$

[15] From the combined analysis of ANISOVICH 00D, ANISOVICH 01C, and ANISOVICH 02B.

a_2(1950) $I^G(J^{PC}) = 1^-(2^{++})$

MASS (MeV)	WIDTH (MeV)	DOCUMENT ID		TECN	COMMENT
1950^{+30}_{-70}	180^{+30}_{-70}	[16] ANISOVICH	01F	SPEC	1.96–2.41 $\overline{p}p$

[16] From the combined analysis of ANISOVICH 99C, ANISOVICH 99E, and ANISOVICH 01F.

ω(1960) $I^G(J^{PC}) = 0^-(1^{--})$

MASS (MeV)	WIDTH (MeV)	DOCUMENT ID		TECN	COMMENT
1960 ± 25	195 ± 60	[17] ANISOVICH	02B	SPEC	0.6–1.9 $p\overline{p} \to \omega\eta$, $\omega\pi^0\pi^0$

[17] From the combined analysis of ANISOVICH 00D, ANISOVICH 01C, and ANISOVICH 02B.

b_1(1960) $I^G(J^{PC}) = 1^+(1^{+-})$

MASS (MeV)	WIDTH (MeV)	DOCUMENT ID		TECN	COMMENT
1960 ± 35	230 ± 50	[18] ANISOVICH	02	SPEC	0.6–1.9 $p\overline{p} \to \omega\pi^0$, $\omega\eta\pi^0$, $\pi^+\pi^-$

[18] From the combined analysis of ANISOVICH 00J, ANISOVICH 01D, ANISOVICH 01E, and ANISOVICH 02.

h_1(1965) $I^G(J^{PC}) = 0^-(1^{+-})$

MASS (MeV)	WIDTH (MeV)	DOCUMENT ID		TECN	COMMENT
1965 ± 45	345 ± 75	[19] ANISOVICH	02B	SPEC	0.6–1.9 $p\overline{p} \to \omega\eta$, $\omega\pi^0\pi^0$

[19] From the combined analysis of ANISOVICH 00D, ANISOVICH 01C, and ANISOVICH 02B.

f_1(1970) $I^G(J^{PC}) = 0^+(1^{++})$

MASS (MeV)	WIDTH (MeV)	DOCUMENT ID		TECN
1971 ± 15	240 ± 45	ANISOVICH	00J	SPEC

X(1970) $I^G(J^{PC}) = ?^?(?^{??})$

MASS (MeV)	WIDTH (MeV)	DOCUMENT ID		TECN	COMMENT
1970 ± 10	40 ± 20	CHLIAPNIK...	80	HBC	32 $K^+ p \to 2K^0_S 2\pi X$

X(1975) $I^G(J^{PC}) = ?^?(?^{??})$

MASS (MeV)	WIDTH (MeV)	EVTS	DOCUMENT ID		TECN	COMMENT
1973 ± 15	80	30	CASO	70	HBC	11.2 $\pi^- p \to \rho 2\pi$

ω_2(1975) $I^G(J^{PC}) = 0^-(2^{--})$

MASS (MeV)	WIDTH (MeV)	DOCUMENT ID		TECN	COMMENT
1975 ± 20	175 ± 25	[20] ANISOVICH	02B	SPEC	0.6–1.9 $p\overline{p} \to \omega\eta$, $\omega\pi^0\pi^0$

[20] From the combined analysis of ANISOVICH 00D, ANISOVICH 01C, and ANISOVICH 02B.

a_2(1990) $I^G(J^{PC}) = 1^-(2^{++})$

MASS (MeV)	WIDTH (MeV)	EVTS	DOCUMENT ID		TECN	COMMENT
2050 ± 10 ± 40	190 ± 22 ± 100	18k	[21] SCHEGELSKY	06	RVUE	$\gamma\gamma \to \pi^+\pi^-\pi^0$
2003 ± 10 ± 19	249 ± 23 ± 32		LU	05	B852	18 $\pi^- p \to \omega\pi^-\pi^0 p$

[21] From analysis of L3 data at 183–209 GeV.

$\Gamma(\gamma\gamma)\ \Gamma(\pi^+\pi^-\pi^0)\ /\ \Gamma(\text{total})$

VALUE (keV)	EVTS	DOCUMENT ID		TECN	COMMENT
0.11 ± 0.04 ± 0.05	18k	[22] SCHEGELSKY	06	RVUE	$\gamma\gamma \to \pi^+\pi^-\pi^0$

[22] From analysis of L3 data at 183–209 GeV.

ρ(2000) $I^G(J^{PC}) = 1^+(1^{--})$

MASS (MeV)	WIDTH (MeV)	DOCUMENT ID		TECN	COMMENT
2000 ± 30	260 ± 45	[23] BUGG	04C	RVUE	Compilation
∼ 1988	∼ 244	HASAN	94	RVUE	$\overline{p}p \to \pi\pi$

[23] From the combined analysis of ANISOVICH 00J, ANISOVICH 01D, ANISOVICH 01E, and ANISOVICH 02.

f_2(2000) $I^G(J^{PC}) = 0^+(2^{++})$

MASS (MeV)	WIDTH (MeV)	DOCUMENT ID		TECN	COMMENT
2001 ± 10	312 ± 32	ANISOVICH	00J	SPEC	
∼ 1996	∼ 134	HASAN	94	RVUE	$\overline{p}p \to \pi\pi$

X(2000) $I^G(J^{PC}) = 1^-(?^{?+})$

MASS (MeV)	WIDTH (MeV)	DOCUMENT ID		TECN	CHG	COMMENT
1964 ± 35	225 ± 50	[24] ARMSTRONG	93D	E760		$\overline{p}p \to 3\pi^0 \to 6\gamma$
∼ 2100	∼ 500	[24] ANTIPOV	77	CIBS	−	25 $\pi^- p \to p\pi^-\rho_3$
2214 ± 15	355 ± 21	[25] BALTAY	77	HBC	0	15 $\pi^- p \to \Delta^{++} 3\pi$
2080 ± 40	340 ± 80	KALELKAR	75	HBC	+	15 $\pi^+ p \to p\pi^+\rho_3$

[24] Cannot determine spin to be 3.
[25] BALTAY 77 favors $J^P = ,3^+$.

X(2000) $I^G(J^{PC}) = ?^?(4^{++})$

MASS (MeV)	WIDTH (MeV)	DOCUMENT ID	TECN	COMMENT
1998 ± 3 ± 5	<15	VLADIMIRSK...03	SPEC	$\pi^- p \to K^0_S K^0_S MM$

π_2(2005) $I^G(J^{PC}) = 1^-(2^{-+})$

MASS (MeV)	WIDTH (MeV)	EVTS	DOCUMENT ID		TECN	COMMENT
1974 ± 14 ± 83	341 ± 61 ± 139	145k	LU	05	B852	18 $\pi^- p \to \omega\pi^-\pi^0 p$
2005 ± 15	200 ± 40		ANISOVICH	01F	SPEC	2.0 $\overline{p}p \to 3\pi^0$, $\pi^0\eta$, $\pi^0\eta'$

η(2010) $I^G(J^{PC}) = 0^+(0^{-+})$

MASS (MeV)	WIDTH (MeV)	DOCUMENT ID		TECN
2010^{+35}_{-60}	270 ± 60	ANISOVICH	00J	SPEC

π_1(2015) $I^G(J^{PC}) = 1^-(1^{-+})$

MASS (MeV)	WIDTH (MeV)	EVTS	DOCUMENT ID		TECN	COMMENT
2014 ± 20 ± 16	230 ± 32 ± 73	145k	LU	05	B852	18 $\pi^- p \to \omega\pi^-\pi^0 p$
2001 ± 30 ± 92	333 ± 52 ± 49	69k	KUHN	04	B852	18 $\pi^- p \to \eta\pi^+\pi^-\pi^- p$

a_0(2020) $I^G(J^{PC}) = 1^-(0^{++})$

MASS (MeV)	WIDTH (MeV)	DOCUMENT ID		TECN
2025 ± 30	330 ± 75	ANISOVICH	99C	SPEC

X(2020) $I^G(J^{PC}) = ?^?(?^{??})$

MASS (MeV)	WIDTH (MeV)	DOCUMENT ID		TECN	COMMENT
2015 ± 3	10 ± 4	FERRER	99	RVUE	$\pi p \to p p\overline{p}\pi(\pi)$

h_3(2025) $I^G(J^{PC}) = 0^-(3^{+-})$

MASS (MeV)	WIDTH (MeV)	DOCUMENT ID		TECN	COMMENT
2025 ± 20	145 ± 30	[26] ANISOVICH	02B	SPEC	0.6–1.9 $p\overline{p} \to \omega\eta$, $\omega\pi^0\pi^0$

[26] From the combined analysis of ANISOVICH 00D, ANISOVICH 01C, and ANISOVICH 02B.

b_3(2030) $I^G(J^{PC}) = 1^+(3^{+-})$

MASS (MeV)	WIDTH (MeV)	DOCUMENT ID		TECN	COMMENT
2032 ± 12	117 ± 11	[27] ANISOVICH	02	SPEC	0.6–1.9 $p\overline{p} \to \omega\pi^0$, $\omega\eta\pi^0$, $\pi^+\pi^-$

[27] From the combined analysis of ANISOVICH 00J, ANISOVICH 01D, ANISOVICH 01E, and ANISOVICH 02.

a_2(2030) $I^G(J^{PC}) = 1^-(2^{++})$

MASS (MeV)	WIDTH (MeV)	DOCUMENT ID		TECN	COMMENT
2030 ± 20	205 ± 30	[28] ANISOVICH	01F	SPEC	1.96–2.41 $\overline{p}p$

[28] From the combined analysis of ANISOVICH 99C, ANISOVICH 99E, and ANISOVICH 01F.

a_3(2030) $I^G(J^{PC}) = 1^-(3^{++})$

MASS (MeV)	WIDTH (MeV)	DOCUMENT ID		TECN	COMMENT
2031 ± 12	150 ± 18	[29] ANISOVICH	01F	SPEC	1.96–2.41 $\overline{p}p$

[29] From the combined analysis of ANISOVICH 99C, ANISOVICH 99E, and ANISOVICH 01F.

η_2(2030) $I^G(J^{PC}) = 0^+(2^{-+})$

MASS (MeV)	WIDTH (MeV)	DOCUMENT ID		TECN
2030 ± 5 ± 15	205 ± 10 ± 15	ANISOVICH	00E	SPEC

$B(a_2\pi)_{L=0}/B(a_2\pi)_{L=2}$

VALUE	DOCUMENT ID		TECN	COMMENT
0.05 ± 0.03	[30] ANISOVICH	11	SPEC	0.9–1.94 $p\overline{p}$

[30] Reanalysis of ADOMEIT 96 and ANISOVICH 00E.

B($a_0\pi$)/B($a_2\pi$)$_{L=2}$

VALUE	DOCUMENT ID		TECN	COMMENT
0.10±0.08	[31] ANISOVICH	11	SPEC	0.9–1.94 $p\overline{p}$

[31] Reanalysis of ADOMEIT 96 and ANISOVICH 00E.

B($f_2\eta$)/B($a_2\pi$)$_{L=2}$

VALUE	DOCUMENT ID		TECN	COMMENT
0.13±0.06	[32] ANISOVICH	11	SPEC	0.9–1.94 $p\overline{p}$

[32] Reanalysis of ADOMEIT 96 and ANISOVICH 00E.

$f_3(2050)$ $I^G(J^{PC}) = 0^+(3^{++})$

MASS (MeV)	WIDTH (MeV)	DOCUMENT ID		TECN	COMMENT
2048±8	213 ± 34	ANISOVICH	00J	SPEC	2.0 $p\overline{p} \to \eta\pi^0\pi^0$

$f_0(2060)$ $I^G(J^{PC}) = 0^+(0^{++})$

MASS (MeV)	WIDTH (MeV)	DOCUMENT ID		TECN	COMMENT
~ 2050	~ 120	[33] OAKDEN	94	RVUE	0.36–1.55 $\overline{p}p \to \pi\pi$
~ 2060	~ 50	[33] OAKDEN	94	RVUE	0.36–1.55 $\overline{p}p \to \pi\pi$

[33] See SEMENOV 99 and KLOET 96.

$\pi(2070)$ $I^G(J^{PC}) = 1^-(0^{-+})$

MASS (MeV)	WIDTH (MeV)	DOCUMENT ID	TECN	COMMENT
2070±35	310^{+100}_{-50}	ANISOVICH 01F	SPEC	2.0 $\overline{p}p \to 3\pi^0, \pi^0\eta, \pi^0\eta'$

$X(2075)$ $I^G(J^{PC}) = ?^?(?^{??})$

MASS (MeV)	WIDTH (MeV)	DOCUMENT ID		TECN	COMMENT
2075±12±5	90 ± 35 ± 9	[34] ABLIKIM	04J	BES2	$J/\psi \to K^- p\overline{\Lambda}$

[34] From a fit in the region $M_{p\overline{\Lambda}} - M_p - M_\Lambda < 150$ MeV. S-wave in the $p\overline{\Lambda}$ system preferred. A similar near-threshold enhancement in the $p\overline{\Lambda}$ system is observed in $B^+ \to p\overline{\Lambda}D^0$ by CHEN 11F.

$X(2080)$ $I^G(J^{PC}) = ?^?(?^{??})$

MASS (MeV)	WIDTH (MeV)	DOCUMENT ID		TECN	COMMENT
2080±10	110 ± 20	KREYMER	80	STRC	13 $\pi^- d \to p\overline{p}n(n_s)$

$X(2080)$ $I^G(J^{PC}) = ?^?(3^{-?})$

MASS (MeV)	WIDTH (MeV)	DOCUMENT ID		TECN	COMMENT
2080±10	190 ± 15	ROZANSKA	80	SPRK	18 $\pi^- p \to p\overline{p}n$

$a_1(2095)$ $I^G(J^{PC}) = 1^-(1^{++})$

MASS (MeV)	WIDTH (MeV)	EVTS	DOCUMENT ID		TECN	COMMENT
2096±17±121	451 ± 41 ± 81	69k	KUHN	04	B852	18 $\pi^- p \to \eta\pi^+\pi^-\pi^- p$

B($a_1(2095) \to f_1(1285)\pi$) / B($a_1(2095) \to a_1(1260)$)

VALUE	EVTS	DOCUMENT ID		TECN	COMMENT
3.18±0.64	69k	KUHN	04	B852	18 $\pi^- p \to \eta\pi^+\pi^-\pi^- p$

$\eta(2100)$ $I^G(J^{PC}) = 0^+(0^{-+})$

MASS (MeV)	WIDTH (MeV)	EVTS	DOCUMENT ID		TECN	COMMENT
2103±50	187 ± 75	586	[35] BISELLO	89B	DM2	$J/\psi \to 4\pi\gamma$

[35] ASTON 81B sees no peak, has 850 events in Ajinenko+Barth bins. ARESTOV 80 sees no peak.

$X(2100)$ $I^G(J^{PC}) = ?^?(0^{??})$

MASS (MeV)	WIDTH (MeV)	DOCUMENT ID		TECN	COMMENT
2100±40	250 ± 40	ALDE	86D	GAM4	100 $\pi^- p \to 2\eta X$

$X(2110)$ $I^G(J^{PC}) = 1^+(3^{-?})$

MASS (MeV)	WIDTH (MeV)	DOCUMENT ID		TECN	COMMENT
2110±10	330 ± 20	EVANGELIS...	79	OMEG	10,16 $\pi^- p \to \overline{p}pn$

$f_2(2140)$ $I^G(J^{PC}) = 0^+(2^{++})$

MASS (MeV)	WIDTH (MeV)	EVTS	DOCUMENT ID		TECN	COMMENT
2141±12	49 ± 28	389	GREEN	86	MPSF	400 $pA \to 4KX$

$X(2150)$ $I^G(J^{PC}) = ?^?(2^{+?})$

MASS (MeV)	WIDTH (MeV)	DOCUMENT ID		TECN	COMMENT
2150±10	260 ± 10	ROZANSKA	80	SPRK	18 $\pi^- p \to p\overline{p}n$

$a_2(2175)$ $I^G(J^{PC}) = 1^-(2^{++})$

MASS (MeV)	WIDTH (MeV)	DOCUMENT ID		TECN	COMMENT
2175±40	310^{+90}_{-45}	ANISOVICH	01F	SPEC	2.0 $\overline{p}p \to 3\pi^0, \pi^0\eta, \pi^0\eta'$

$\eta(2190)$ $I^G(J^{PC}) = 0^+(0^{-+})$

MASS (MeV)	WIDTH (MeV)	DOCUMENT ID		TECN
2190±50	850 ± 100	BUGG	99	BES

$\omega_2(2195)$ $I^G(J^{PC}) = 0^-(2^{--})$

MASS (MeV)	WIDTH (MeV)	DOCUMENT ID		TECN	COMMENT
2195±30	225 ± 40	[36] ANISOVICH	02B	SPEC	0.6–1.9 $p\overline{p} \to \omega\eta, \omega\pi^0\pi^0$

[36] From the combined analysis of ANISOVICH 00D, ANISOVICH 01C, and ANISOVICH 02B.

$\omega(2205)$ $I^G(J^{PC}) = 0^-(1^{--})$

MASS (MeV)	WIDTH (MeV)	DOCUMENT ID		TECN	COMMENT
2205±30	350 ± 90	[37] ANISOVICH	02B	SPEC	0.6–1.9 $p\overline{p} \to \omega\eta, \omega\pi^0\pi^0$

[37] From the combined analysis of ANISOVICH 00D, ANISOVICH 01C, and ANISOVICH 02B.

$X(2210)$ $I^G(J^{PC}) = ?^?(?^{??})$

MASS (MeV)	WIDTH (MeV)	DOCUMENT ID	TECN	COMMENT
2210^{+79}_{-21}	203^{+437}_{-87}	EVANGELIS... 79B	OMEG	10 $\pi^- p \to K^+ K^- n$

$X(2210)$ $I^G(J^{PC}) = ?^?(?^{??})$

MASS (MeV)	WIDTH (MeV)	DOCUMENT ID		TECN	COMMENT
2207±22	130	CASO	70	HBC	11.2 $\pi^- p$

$h_1(2215)$ $I^G(J^{PC}) = 0^-(1^{+-})$

MASS (MeV)	WIDTH (MeV)	DOCUMENT ID		TECN	COMMENT
2215±40	325 ± 55	[38] ANISOVICH	02B	SPEC	0.6–1.9 $p\overline{p} \to \omega\eta, \omega\pi^0\pi^0$

[38] From the combined analysis of ANISOVICH 00D, ANISOVICH 01C, and ANISOVICH 02B.

$\rho_2(2225)$ $I^G(J^{PC}) = 1^+(2^{--})$

MASS (MeV)	WIDTH (MeV)	DOCUMENT ID		TECN	COMMENT
2225±35	335^{+100}_{-50}	[39] ANISOVICH	02	SPEC	0.6–1.9 $p\overline{p} \to \omega\pi^0, \omega\eta\pi^0, \pi^+\pi^-$

[39] From the combined analysis of ANISOVICH 00J, ANISOVICH 01D, ANISOVICH 01E, and ANISOVICH 02.

$\rho_4(2230)$ $I^G(J^{PC}) = 1^+(4^{--})$

MASS (MeV)	WIDTH (MeV)	DOCUMENT ID		TECN	COMMENT
2230±25	210 ± 30	[40] ANISOVICH	02	SPEC	0.6–1.9 $p\overline{p} \to \omega\pi^0, \omega\eta\pi^0, \pi^+\pi^-$

[40] From the combined analysis of ANISOVICH 00J, ANISOVICH 01D, ANISOVICH 01E, and ANISOVICH 02.

$b_1(2240)$ $I^G(J^{PC}) = 1^+(1^{+-})$

MASS (MeV)	WIDTH (MeV)	DOCUMENT ID		TECN	COMMENT
2240±35	320 ± 85	[41] ANISOVICH	02	SPEC	0.6–1.9 $p\overline{p} \to \omega\pi^0, \omega\eta\pi^0, \pi^+\pi^-$

[41] From the combined analysis of ANISOVICH 00J, ANISOVICH 01D, ANISOVICH 01E, and ANISOVICH 02.

$f_2(2240)$ $I^G(J^{PC}) = 0^+(2^{++})$

MASS (MeV)	WIDTH (MeV)	DOCUMENT ID		TECN	COMMENT
2240±15	241 ± 30	[42] ANISOVICH	00J	SPEC	1.92–2.41 $p\overline{p}$
• • • We do not use the following data for averages, fits, limits, etc. • • •					
~ 2226	~ 226	HASAN	94	RVUE	$p\overline{p} \to \pi\pi$

[42] From the combined analysis of ANISOVICH 99C, ANISOVICH 99F, ANISOVICH 99J, ANISOVICH 99K, and ANISOVICH 00B. See also ANISOVICH 12.

$b_3(2245)$ $I^G(J^{PC}) = 1^+(3^{+-})$

MASS (MeV)	WIDTH (MeV)	DOCUMENT ID		TECN
2245±50	320 ± 70	[43] BUGG	04C	RVUE

[43] From the combined analysis of ANISOVICH 00J, ANISOVICH 01D, ANISOVICH 01E, and ANISOVICH 02.

$\eta_2(2250)$ $I^G(J^{PC}) = 0^+(2^{-+})$

MASS (MeV)	WIDTH (MeV)	DOCUMENT ID		TECN
2248±20	280 ± 20	ANISOVICH	00I	SPEC
2267±14	290 ± 50	ANISOVICH	00J	SPEC

Meson Particle Listings

Further States

$\pi_4(2250)$ $I^G(J^{PC}) = 1^-(4^{-+})$

MASS (MeV)	WIDTH (MeV)	DOCUMENT ID		TECN	COMMENT
2250 ± 15	215 ± 25	ANISOVICH	01F	SPEC	2.0 $\overline{p}p \to 3\pi^0$, $\pi^0\eta$, $\pi^0\eta'$

$\omega_4(2250)$ $I^G(J^{PC}) = 0^-(4^{--})$

MASS (MeV)	WIDTH (MeV)	DOCUMENT ID		TECN	COMMENT
2250 ± 30	150 ± 50	[44] ANISOVICH	02B	SPEC	0.6–1.9 $p\overline{p} \to \omega\eta$, $\omega\pi^0\pi^0$

[44] From the combined analysis of ANISOVICH 00D, ANISOVICH 01C, and ANISOVICH 02B.

$\omega_5(2250)$ $I^G(J^{PC}) = 0^-(5^{--})$

MASS (MeV)	WIDTH (MeV)	DOCUMENT ID		TECN
2250 ± 70	320 ± 95	[45] BUGG	04	RVUE

[45] From the combined analysis of ANISOVICH 00D, ANISOVICH 01C, and ANISOVICH 02B.

$\omega_3(2255)$ $I^G(J^{PC}) = 0^-(3^{--})$

MASS (MeV)	WIDTH (MeV)	DOCUMENT ID		TECN	COMMENT
2255 ± 15	175 ± 30	[46] ANISOVICH	02B	SPEC	0.6–1.9 $p\overline{p} \to \omega\eta$, $\omega\pi^0\pi^0$

[46] From the combined analysis of ANISOVICH 00D, ANISOVICH 01C, and ANISOVICH 02B.

$a_4(2255)$ $I^G(J^{PC}) = 1^-(4^{++})$

MASS (MeV)	WIDTH (MeV)	DOCUMENT ID		TECN	COMMENT
2237 ± 5	291 ± 12	UMAN	06	E835	5.2 $\overline{p}p \to \eta\eta\pi^0$
2255 ± 40	330^{+110}_{-50}	[47] ANISOVICH	01F	SPEC	1.96–2.41 $\overline{p}p$

[47] From the combined analysis of ANISOVICH 99C, ANISOVICH 99E, and ANISOVICH 01F.

$a_2(2255)$ $I^G(J^{PC}) = 1^-(2^{++})$

MASS (MeV)	WIDTH (MeV)	DOCUMENT ID		TECN	COMMENT
2255 ± 20	230 ± 15	[48] ANISOVICH	01G	SPEC	1.96–2.41 $\overline{p}p$

[48] From the combined analysis of ANISOVICH 99C, ANISOVICH 99E, ANISOVICH 01F, and ANISOVICH 01G.

$X(2260)$ $I^G(J^{PC}) = 0^+(4^{+?})$

MASS (MeV)	WIDTH (MeV)	DOCUMENT ID		TECN	COMMENT
2260 ± 20	400 ± 100	EVANGELIS...	79	OMEG	10,16 $\pi^- p \to \overline{p}pn$

$\rho(2270)$ $I^G(J^{PC}) = 1^+(1^{--})$

MASS (MeV)	WIDTH (MeV)	DOCUMENT ID		TECN	COMMENT
2265 ± 40	325 ± 80	[49] ANISOVICH	02	SPEC	0.6–1.9 $p\overline{p} \to \omega\pi^0$, $\omega\eta\pi^0$, $\pi^+\pi^-$
2280 ± 50	440 ± 110	ATKINSON	85	OMEG	20–70 $\gamma p \to p\omega\pi^+\pi^-\pi^0$

[49] From the combined analysis of ANISOVICH 00J, ANISOVICH 01D, ANISOVICH 01E, and ANISOVICH 02.

$a_1(2270)$ $I^G(J^{PC}) = 1^-(1^{++})$

MASS (MeV)	WIDTH (MeV)	DOCUMENT ID		TECN	COMMENT
2270^{+55}_{-40}	305^{+70}_{-40}	ANISOVICH	01F	SPEC	2.0 $\overline{p}p \to 3\pi^0$, $\pi^0\eta$, $\pi^0\eta'$

$h_3(2275)$ $I^G(J^{PC}) = 0^-(3^{+-})$

MASS (MeV)	WIDTH (MeV)	DOCUMENT ID		TECN	COMMENT
2275 ± 25	190 ± 45	[50] ANISOVICH	02B	SPEC	0.6–1.9 $p\overline{p} \to \omega\eta$, $\omega\pi^0\pi^0$

[50] From the combined analysis of ANISOVICH 00D, ANISOVICH 01C, and ANISOVICH 02B.

$a_3(2275)$ $I^G(J^{PC}) = 1^-(3^{++})$

MASS (MeV)	WIDTH (MeV)	DOCUMENT ID		TECN	COMMENT
2275 ± 35	350^{+100}_{-50}	[51] ANISOVICH	01G	SPEC	1.96–2.41 $\overline{p}p$

[51] From the combined analysis of ANISOVICH 99C, ANISOVICH 99E, ANISOVICH 01F, and ANISOVICH 01G.

$\pi_2(2285)$ $I^G(J^{PC}) = 1^-(2^{-+})$

MASS (MeV)	WIDTH (MeV)	DOCUMENT ID		TECN	COMMENT
$2285 \pm 20 \pm 25$	$250 \pm 20 \pm 25$	[52] ANISOVICH	11	SPEC	0.9–1.94 $p\overline{p}$

[52] Reanalysis of ADOMEIT 96 and ANISOVICH 00E.

$\omega_3(2285)$ $I^G(J^{PC}) = 0^-(3^{--})$

MASS (MeV)	WIDTH (MeV)	DOCUMENT ID		TECN	COMMENT
2278 ± 28	224 ± 50	[53] BUGG	04A	RVUE	
2285 ± 60	230 ± 40	[54] ANISOVICH	02B	SPEC	0.6–1.9 $p\overline{p} \to \omega\eta$, $\omega\pi^0\pi^0$

[53] Partial wave analysis of the data on $p\overline{p} \to \overline{\Lambda}\Lambda$ from BARNES 00.

[54] From the combined analysis of ANISOVICH 00D, ANISOVICH 01C, and ANISOVICH 02B.

$\omega(2290)$ $I^G(J^{PC}) = 0^-(1^{--})$

MASS (MeV)	WIDTH (MeV)	DOCUMENT ID		TECN
2290 ± 20	275 ± 35	[55] BUGG	04A	RVUE

[55] Partial wave analysis of the data on $p\overline{p} \to \overline{\Lambda}\Lambda$ from BARNES 00.

$f_2(2295)$ $I^G(J^{PC}) = 0^+(2^{++})$

MASS (MeV)	WIDTH (MeV)	DOCUMENT ID		TECN	COMMENT
2293 ± 13	216 ± 37	[56] ANISOVICH	00J	SPEC	1.92–2.41 $p\overline{p}$

[56] From the combined analysis of ANISOVICH 99C, ANISOVICH 99F, ANISOVICH 99J, ANISOVICH 99K, and ANISOVICH 00B. See also ANISOVICH 12.

$f_3(2300)$ $I^G(J^{PC}) = 0^+(3^{++})$

MASS (MeV)	WIDTH (MeV)	DOCUMENT ID		TECN
2334 ± 25	200 ± 20	[57] BUGG	04A	RVUE

[57] Partial wave analysis of the data on $p\overline{p} \to \overline{\Lambda}\Lambda$ from BARNES 00.

$f_1(2310)$ $I^G(J^{PC}) = 0^+(1^{++})$

MASS (MeV)	WIDTH (MeV)	DOCUMENT ID		TECN
2310 ± 60	255 ± 70	ANISOVICH	00J	SPEC

$\eta(2320)$ $I^G(J^{PC}) = 0^+(0^{-+})$

MASS (MeV)	WIDTH (MeV)	DOCUMENT ID		TECN
2320 ± 15	230 ± 35	[58] ANISOVICH	00M	SPEC

[58] From the combined analysis of $\overline{p}p \to \eta\eta\eta$ from ANISOVICH 00M and $\overline{p}p \to \eta\pi^0\pi^0$ from ANISOVICH 00J.

$\eta_4(2330)$ $I^G(J^{PC}) = 0^+(4^{-+})$

MASS (MeV)	WIDTH (MeV)	DOCUMENT ID		TECN	COMMENT
2328 ± 38	240 ± 90	ANISOVICH	00J	SPEC	2.0 $p\overline{p} \to \eta\pi^0\pi^0$

$\omega(2330)$ $I^G(J^{PC}) = 0^-(1^{--})$

MASS (MeV)	WIDTH (MeV)	DOCUMENT ID		TECN	COMMENT
2330 ± 30	435 ± 75	ATKINSON	88	OMEG	25–50 $\gamma p \to \rho^\pm\rho^0\pi^\mp$

$X(2340)$ $I^G(J^{PC}) = ?^?(?^{??})$

MASS (MeV)	WIDTH (MeV)	EVTS	DOCUMENT ID		TECN	COMMENT
2340 ± 20	180 ± 60	126	[59] BALTAY	75	HBC	15 $\pi^+ p \to p5\pi$

[59] Dominant decay into $\rho^0\rho^0\pi^+$. BALTAY 78 finds confirmation in $2\pi^+\pi^-2\pi^0$ events which contain $\rho^+\rho^0\pi^0$ and $2\rho^+\pi^-$.

$\pi(2360)$ $I^G(J^{PC}) = 1^-(0^{-+})$

MASS (MeV)	WIDTH (MeV)	DOCUMENT ID		TECN	COMMENT
2360 ± 25	300^{+100}_{-50}	ANISOVICH	01F	SPEC	2.0 $\overline{p}p \to 3\pi^0$, $\pi^0\eta$, $\pi^0\eta'$

$X(2360)$ $I^G(J^{PC}) = ?^?(4^{+?})$

MASS (MeV)	WIDTH (MeV)	DOCUMENT ID		TECN	COMMENT
2360 ± 10	430 ± 30	ROZANSKA	80	SPRK	18 $\pi^- p \to p\overline{p}n$

$X(2440)$ $I^G(J^{PC}) = ?^?(5^{-?})$

MASS (MeV)	WIDTH (MeV)	DOCUMENT ID		TECN	COMMENT
2440 ± 10	310 ± 20	ROZANSKA	80	SPRK	18 $\pi^- p \to p\overline{p}n$

$X(2540)$ $I^G(J^{PC}) = 0^+(0^{++})$

MASS (MeV)	WIDTH (MeV)	DOCUMENT ID		TECN	COMMENT
$2539 \pm 14^{+38}_{-14}$	$274^{+77+126}_{-61-163}$	UEHARA	13	BELL	$\gamma\gamma \to K^0_S K^0_S$

$\Gamma(\gamma\gamma) \times B(K\overline{K})$

VALUE (eV)	DOCUMENT ID		TECN	COMMENT
40^{+9+17}_{-7-40}	UEHARA	13	BELL	$\gamma\gamma \to K^0_S K^0_S$

$X(2632)$ $I^G(J^{PC}) = ?^?(?^{??})$

MASS (MeV)	WIDTH (MeV)	DOCUMENT ID		TECN	COMMENT
2635.2±3.3		[60] EVDOKIMOV	04	SELX	$X(2632) \to D_s^+ \eta$
2631.6±2.1	< 17	[61] EVDOKIMOV	04	SELX	$X(2632) \to D^0 K^+$

[60] From a mass difference to D_s^+ of 666.9 ± 3.3 MeV.

[61] From a mass difference to D^0 of 767.0 ± 2.0 MeV.

$B(X(2632) \to D^0 K^+)/B(X(2632) \to D_s^+ \eta)$

VALUE	DOCUMENT ID		TECN
0.14±0.06	[62] EVDOKIMOV	04	SELX

[62] Possible interpretation of this decay pattern is discussed by YASUI 07.

$X(2680)$ $I^G(J^{PC}) = ?^?(?^{??})$

MASS (MeV)	WIDTH (MeV)	DOCUMENT ID		TECN	COMMENT
2676±27	150	CASO	70	HBC	$11.2\ \pi^- p \to \rho^- \pi^+ \pi^- p$

$X(2710)$ $I^G(J^{PC}) = ?^?(6^{+?})$

MASS (MeV)	WIDTH (MeV)	DOCUMENT ID		TECN	COMMENT
2710±20	170 ± 40	ROZANSKA	80	SPRK	$18\ \pi^- p \to p\overline{p}n$

$X(2750)$ $I^G(J^{PC}) = ?^?(7^{-?})$

MASS (MeV)	WIDTH (MeV)	DOCUMENT ID		TECN	COMMENT
2747±32	195 ± 75	DENNEY	83	LASS	$10\ \pi^+ p \to K^+ K^- \pi^+ p$

$f_6(3100)$ $I^G(J^{PC}) = 0^+(6^{++})$

MASS (MeV)	WIDTH (MeV)	DOCUMENT ID		TECN	COMMENT
3100±100	700 ± 130	BINON	05	GAMS	$33\ \pi^- p \to \eta\eta n$

$X(3250)$ $I^G(J^{PC}) = ?^?(?^{??})$ 3-Body Decays

MASS (MeV)	WIDTH (MeV)	DOCUMENT ID		TECN	COMMENT
3250±8±20	45 ± 18	ALEEV	93	BIS2	$X(3250) \to \Lambda\overline{p}K^+$
3265±7±20	40 ± 18	ALEEV	93	BIS2	$X(3250) \to \overline{\Lambda}pK^-$

$X(3250)$ $I^G(J^{PC}) = ?^?(?^{??})$ 4-Body Decays

MASS (MeV)	WIDTH (MeV)	DOCUMENT ID		TECN	COMMENT
3245±8±20	25 ± 11	ALEEV	93	BIS2	$X(3250) \to \Lambda\overline{p}K^+\pi^\pm$
3250±9±20	50 ± 20	ALEEV	93	BIS2	$X(3250) \to \overline{\Lambda}pK^-\pi^\mp$
3270±8±20	25 ± 11	ALEEV	93	BIS2	$X(3250) \to K_S^0 p\overline{p}K^\pm$

$X(3350)$ $I^G(J^{PC}) = ?^?(?^{??})$

MASS (MeV)	WIDTH (MeV)	EVTS	DOCUMENT ID		TECN	COMMENT
$3350^{+10}_{-20}\pm20$	$70^{+40}_{-30}\pm40$	50 ± 10	[63] GABYSHEV	06A	BELL	$B^- \to \Lambda_c^+ \overline{p}\pi^-$

[63] A similar enhancement in the $\Lambda_c^+ \overline{p}$ final state is also reported by BABAR collaboration in AUBERT 10H.

REFERENCES for Further States

ABLIKIM	13J	PR D87 032008	M. Ablikim *et al.*	(BES III Collab.)
UEHARA	13	PTEP 2013 123C01	S. Uehara *et al.*	(BELLE Collab.)
ANISOVICH	12	PR D85 014001	A.V. Anisovich *et al.*	
ANASHIN	11	PL B703 543	V.V. Anashin *et al.*	(KEDR Collab.)
ANISOVICH	11	EPJ C71 1511	A.V. Anisovich *et al.*	(LOQM, RAL, PNPI)
CHEN	11F	PR D84 071501	P. Chen *et al.*	(BELLE Collab.)
AUBERT	10H	PR D82 031102	B. AUBERT *et al.*	(BABAR Collab.)
ABRAAMYAN	09	PR C80 034001	Kh.U. Abraamyan *et al.*	
LIU	09	PR D79 071102	C. Liu *et al.*	(BELLE Collab.)
VLADIMIRSK...	08	PAN 71 2129	V.V. Vladimirsky *et al.*	(ITEP)
		Translated from YAF 71 2166.		
VLADIMIRSK...	07	PAN 70 1706	V. Vladimirsky *et al.*	
		Translated from YAF 70 1751.		
YASUI	07	PR D76 034009	S. Yasui, M. Oka	
ABLIKIM	06J	PRL 96 162002	M. Ablikim *et al.*	(BES Collab.)
ABLIKIM	06S	PRL 97 142002	M. Ablikim *et al.*	(BES Collab.)
GABYSHEV	06A	PRL 97 242001	N. Gabyshev *et al.*	(BELLE Collab.)
SCHEGELSKY	06	EPJ A27 199	V.A. Schegelsky *et al.*	
SCHEGELSKY	06A	EPJ A27 207	V.A. Schegelsky *et al.*	
UMAN	06	PR D73 052009	I. Uman *et al.*	(FNAL E835)
VLADIMIRSK...	06	PAN 69 493	V.V. Vladimirsky *et al.*	(ITEP, Moscow)
		Translated from YAF 69 515.		
BINON	05	PAN 68 960	F. Binon *et al.*	
		Translated from YAF 68 998.		
GRIGOR'EV	05	PAN 68 1271	V.K. Grigor'ev *et al.*	(ITEP)
		Translated from YAF 68 1324.		
LU	05	PRL 94 032002	M. Lu *et al.*	(BNL E852 Collab.)
ABLIKIM	04J	PRL 93 112002	M. Ablikim *et al.*	(BES Collab.)
BUGG	04	PL B595 556 (errat)	D.V. Bugg	
BUGG	04A	EPJ C36 161	D.V. Bugg	
BUGG	04C	PRPL 397 257	D.V. Bugg	
EVDOKIMOV	04	PRL 93 242001	A.V. Evdokimov *et al.*	(SELEX Collab.)
KUHN	04	PL B595 109	J. Kuhn *et al.*	(BNL E852 Collab.)
ANISOVICH	03	EPJ A16 229	V.V. Anisovich *et al.*	
VLADIMIRSK...	03	PAN 66 700	V.V. Vladimirsky *et al.*	
		Translated from YAF 66 729.		
ANISOVICH	02	PL B542 8	A.V. Anisovich *et al.*	
ANISOVICH	02B	PL B542 19	A.V. Anisovich *et al.*	
CHUNG	02	PR D65 072001	S.U. Chung *et al.*	(BNL E852 Collab.)
LINK	02K	PL B545 50	J.M. Link *et al.*	(FNAL FOCUS Collab.)
ANISOVICH	01C	PL B507 23	A.V. Anisovich *et al.*	
ANISOVICH	01D	PL B508 6	A.V. Anisovich *et al.*	
ANISOVICH	01E	PL B513 281	A.V. Anisovich *et al.*	
ANISOVICH	01F	PL B517 261	A.V. Anisovich *et al.*	
ANISOVICH	01G	PL B517 273	A.V. Anisovich *et al.*	
ANISOVICH	00B	NP A662 319	A.V. Anisovich *et al.*	
ANISOVICH	00D	PL B476 15	A.V. Anisovich *et al.*	
ANISOVICH	00E	PL B477 19	A.V. Anisovich *et al.*	
ANISOVICH	00I	PL B491 40	A.V. Anisovich *et al.*	
ANISOVICH	00J	PL B491 47	A.V. Anisovich *et al.*	
ANISOVICH	00M	PL B496 145	A.V. Anisovich *et al.*	
BARNES	00	PR C62 055203	P.D. Barnes *et al.*	
FILIPPI	00	PL B495 284	A. Filippi *et al.*	(OBELIX Experiment)
VLADIMIRSKII	00	JETPL 72 486	V.V. Vladimirskii *et al.*	
		Translated from ZETFP 72 698.		
ANISOVICH	99C	PL B452 173	A.V. Anisovich *et al.*	
ANISOVICH	99E	PL B452 187	A.V. Anisovich *et al.*	
ANISOVICH	99F	NP A651 253	A.V. Anisovich *et al.*	
ANISOVICH	99J	PL B471 271	A.V. Anisovich *et al.*	
ANISOVICH	99K	PL B468 309	A.V. Anisovich *et al.*	
BUGG	99	PL B458 511	D.V. Bugg *et al.*	
FERRER	99	EPJ C10 249	A. Ferrer *et al.*	
SEMENOV	99	SPU 42 847	S.V. Semenov	
		Translated from UFN 42 937.		
ADOMEIT	96	ZPHY C71 227	J. Adomeit *et al.*	(Crystal Barrel Collab.)
KLOET	96	PR D53 6120	W.M. Kloet, F. Myhrer	(RUTG, NORD)
PROKOSHKIN	96	SPD 41 247	Y.D. Prokoshkin, V.D. Samoilenko	(SERP)
		Translated from DANS 348 481.		
HASAN	94	PL B334 215	A. Hasan, D.V. Bugg	(LOQM)
OAKDEN	94	NP A574 731	M.N. Oakden, M.R. Pennington	(DURH)
ALEEV	93	PAN 56 1358	A.N. Aleev *et al.*	(BIS-2 Collab.)
		Translated from YAF 56 100.		
ARMSTRONG	93D	PL B307 399	T.A. Armstrong *et al.*	(FNAL, FERR, GENO+)
ALBRECHT	91F	ZPHY C50 1	H. Albrecht *et al.*	(ARGUS Collab.)
CONDO	91	PR D43 2787	G.T. Condo *et al.*	(SLAC Hybrid Collab.)
BISELLO	89B	PR D39 701	G. Busetto *et al.*	(DM2 Collab.)
ATKINSON	88	ZPHY C38 535	M. Atkinson *et al.*	(BONN, CERN, GLAS+)
DAFTARI	87	PRL 58 859	I.K. Daftari *et al.*	(SYRA)
ALDE	86D	NP B269 485	D.M. Alde *et al.*	(BELG, LAPP, SERP, CERN+)
BRIDGES	86D	PL B180 313	D.L. Bridges *et al.*	(SYRA, BNL, CASE+)
GREEN	86	PRL 56 1639	D.R. Green *et al.*	(FNAL, ARIZ, FSU+)
ATKINSON	85	ZPHY C29 333	M. Atkinson *et al.*	(BONN, CERN, GLAS+)
DENNEY	83	PR D28 2726	D.L. Denney *et al.*	(IOWA, MICH)
ASTON	81B	NP B189 205	D. Aston *et al.*	(BONN, CERN, EPOL, GLAS+)
ARESTOV	80	IHEP 80-165	Y.I. Arestov *et al.*	(SERP)
CHLIAPNIK...	80	ZPHY C3 285	P.V. Chliapnikov *et al.*	(SERP, BRUX, MONS)
KREYMER	80	PR D22 36	A.E. Kreymer *et al.*	(IND, PURD, SLAC+)
ROZANSKA	80	NP B162 505	M. Rozanska *et al.*	(MPIM, CERN)
EVANGELIS...	79	NP B153 253	C. Evangelista *et al.*	(BARI, BONN, CERN+)
EVANGELIS...	79B	NP B154 381	C. Evangelista *et al.*	(BARI, BONN, CERN+)
BALTAY	78	PR D17 52	C. Baltay *et al.*	(COLU, BING)
ANTIPOV	77	NP B119 45	Y.M. Antipov *et al.*	(SERP, GEVA)
BALTAY	77	PRL 39 591	C. Baltay, C.V. Cautis, M. Kalelkar	(COLU)
BALTAY	75	PRL 35 891	C. Baltay *et al.*	(COLU, BING)
KALELKAR	75	Thesis Nevis 207	M.S. Kalelkar	(COLU)
CASO	70	LNC 3 707	C. Caso *et al.*	(GENO, HAMB, MILA, SACL)

STRANGE MESONS
($S = \pm 1$, $C = B = 0$)

$K^+ = u\overline{s}$, $K^0 = d\overline{s}$, $\overline{K}^0 = \overline{d}s$, $K^- = \overline{u}s$, similarly for K^*'s

$K^{\pm}$ $I(J^P) = \frac{1}{2}(0^-)$

THE CHARGED KAON MASS

Revised 1994 by T.G. Trippe (LBNL).

The average of the six charged kaon mass measurements which we use in the Particle Listings is

$$m_{K^\pm} = 493.677 \pm 0.013 \text{ MeV (S = 2.4)}, \quad (1)$$

where the error has been increased by the scale factor S. The large scale factor indicates a serious disagreement between different input data. The average before scaling the error is

$$m_{K^\pm} = 493.677 \pm 0.005 \text{ MeV},$$
$$\chi^2 = 22.9 \text{ for 5 D.F., Prob. } = 0.04\%, \quad (2)$$

where the high χ^2 and correspondingly low χ^2 probability further quantify the disagreement.

The main disagreement is between the two most recent and precise results,

$m_{K^\pm}$ =493.696 ± 0.007 MeV DENISOV 91

$m_{K^\pm}$ =493.636 ± 0.011 MeV (S = 1.5) GALL 88

Average =493.679 ± 0.006 MeV

$$\chi^2 = 21.2 \text{ for 1 D.F., Prob. } = 0.0004\%, \quad (3)$$

both of which are measurements of x-ray energies from kaonic atoms. Comparing the average in Eq. (3) with the overall average in Eq. (2), it is clear that DENISOV 91 and GALL 88 dominate the overall average, and that their disagreement is responsible for most of the high χ^2.

The GALL 88 measurement was made using four different kaonic atom transitions, K^- Pb (9 → 8), K^- Pb (11 → 10), K^- W (9 → 8), and K^- W (11 → 10). The $m_{K^\pm}$ values they obtain from each of these transitions is shown in the Particle Listings and in Fig. 1. Their K^- Pb (9 → 8) $m_{K^\pm}$is below and somewhat inconsistent with their other three transitions. The average of their four measurements is

$$m_{K^\pm} = 493.636 \pm 0.007,$$
$$\chi^2 = 7.0 \text{ for 3 D.F., Prob. } = 7.2\%. \quad (4)$$

This is a low but acceptable χ^2 probability so, to be conservative, GALL 88 scaled up the error on their average by S=1.5 to obtain their published error ±0.011 shown in Eq. (3) above and used in the Particle Listings average.

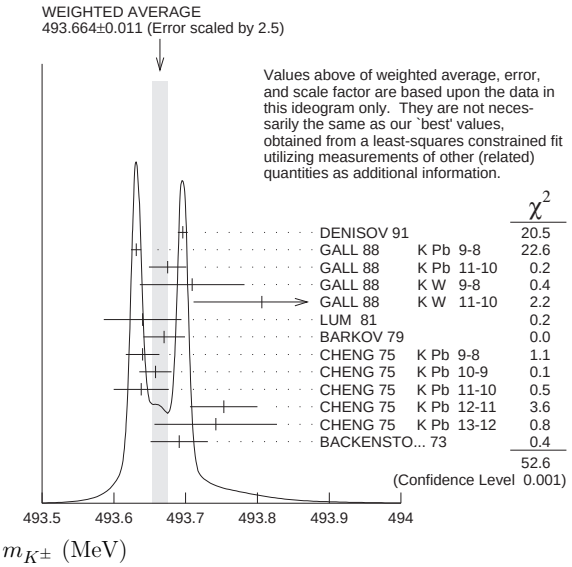

Figure 1: Ideogram of $m_{K^\pm}$ mass measurements. GALL 88 and CHENG 75 measurements are shown separately for each transition they measured.

The ideogram in Fig. 1 shows that the DENISOV 91 measurement and the GALL 88 K^- Pb (9 → 8) measurement yield two well-separated peaks. One might suspect the GALL 88 K^- Pb (9 → 8) measurement since it is responsible both for the internal inconsistency in the GALL 88 measurements and the disagreement with DENISOV 91.

To see if the disagreement could result from a systematic problem with the K^- Pb (9 → 8) transition, we have separated the CHENG 75 data, which also used K^- Pb, into its separate transitions. Figure 1 shows that the CHENG 75 and GALL 88 K^- Pb (9 → 8) values are consistent, suggesting the possibility of a common effect such as contaminant nuclear γ rays near the K^- Pb (9 → 8) transition energy, although the CHENG 75 errors are too large to make a strong conclusion. The average of all 13 measurements has a χ^2 of 52.6 as shown in Fig. 1 and the first line of Table 1, yielding an unacceptable χ^2 probability of 0.00005%. The second line of Table 1 excludes both the GALL 88 and CHENG 75 measurements of the K^- Pb (9 → 8) transition and yields a χ^2 probability of 43%. The third [fourth] line of Table 1 excludes only the GALL 88 K^- Pb (9 → 8) [DENISOV 91] measurement and yields a χ^2 probability of 20% [8.6%]. Table 1 shows that removing both measurements of the K^- Pb (9 → 8) transition produces the most consistent set of data, but that excluding only the GALL 88 K^- Pb (9 → 8) transition or DENISOV 91 also produces acceptable probabilities.

Table 1: $m_{K^{\pm}}$ averages for some combinations of Fig. 1 data.

$m_{K^{\pm}}$ (MeV)	χ^2	D.F.	Prob. (%)	Measurements used
493.664 ± 0.004	52.6	12	0.00005	all 13 measurements
493.690 ± 0.006	10.1	10	43	no K^- Pb(9→8)
493.687 ± 0.006	14.6	11	20	no GALL 88 K^- Pb(9→8)
493.642 ± 0.006	17.8	11	8.6	no DENISOV 91

Yu.M. Ivanov, representing DENISOV 91, has estimated corrections needed for the older experiments because of improved ^{192}Ir and ^{198}Au calibration γ-ray energies. He estimates that CHENG 75 and BACKENSTOSS 73 $m_{K^{\pm}}$ values could be raised by about 15 keV and 22 keV, respectively. With these estimated corrections, Table 1 becomes Table 2. The last line of Table 2 shows that if such corrections are assumed, then GALL 88 K^- Pb (9 → 8) is inconsistent with the rest of the data even when DENISOV 91 is excluded. Yu.M. Ivanov warns that these are rough estimates. Accordingly, we do not use Table 2 to reject the GALL 88 K^- Pb (9 → 8) transition, but we note that a future reanalysis of the CHENG 75 data could be useful because it might provide supporting evidence for such a rejection.

Table 2: $m_{K^{\pm}}$ averages for some combinations of Fig. 1 data after raising CHENG 75 and BACKENSTOSS 73 values by 0.015 and 0.022 MeV respectively.

$m_{K^{\pm}}$ (MeV)	χ^2	D.F.	Prob. (%)	Measurements used
493.666 ± 0.004	53.9	12	0.00003	all 13 measurements
493.693 ± 0.006	9.0	10	53	no K^- Pb(9→8)
493.690 ± 0.006	11.5	11	40	no GALL 88 K^- Pb(9→8)
493.645 ± 0.006	23.0	11	1.8	no DENISOV 91

The GALL 88 measurement uses a Ge semiconductor spectrometer which has a resolution of about 1 keV, so they run the risk of some contaminant nuclear γ rays. Studies of γ rays following stopped π^- and Σ^- absorption in nuclei (unpublished) do not show any evidence for contaminants according to GALL 88 spokesperson, B.L. Roberts. The DENISOV 91 measurement uses a crystal diffraction spectrometer with a resolution of 6.3 eV for radiation at 22.1 keV to measure the 4f-3d transition in K^- ^{12}C. The high resolution and the light nucleus reduce the probability for overlap by contaminant γ rays, compared with the measurement of GALL 88. The DENISOV 91 measurement is supported by their high-precision measurement of the 4d-2p transition energy in π^- ^{12}C, which is good agreement with the calculated energy.

While we suspect that the GALL 88 K^- Pb (9 → 8) measurements could be the problem, we are unable to find clear grounds for rejecting it. Therefore, we retain their measurement in the average and accept the large scale factor until further information can be obtained from new measurements and/or from reanalysis of GALL 88 and CHENG 75 data.

We thank B.L. Roberts (Boston Univ.) and Yu.M. Ivanov (Petersburg Nuclear Physics Inst.) for their extensive help in understanding this problem.

$K^{\pm}$ MASS

VALUE (MeV)	DOCUMENT ID		TECN	CHG	COMMENT
493.677±0.016 OUR FIT	Error includes scale factor of 2.8.				
493.677±0.013 OUR AVERAGE	Error includes scale factor of 2.4. See the ideogram below.				
493.696±0.007	[1] DENISOV	91	CNTR	–	Kaonic atoms
493.636±0.011	[2] GALL	88	CNTR	–	Kaonic atoms
493.640±0.054	LUM	81	CNTR	–	Kaonic atoms
493.670±0.029	BARKOV	79	EMUL	±	$e^+e^- \rightarrow K^+K^-$
493.657±0.020	[2] CHENG	75	CNTR	–	Kaonic atoms
493.691±0.040	BACKENSTO...73		CNTR	–	Kaonic atoms
• • • We do not use the following data for averages, fits, limits, etc. • • •					
493.631±0.007	GALL	88	CNTR	–	K^- Pb (9→ 8)
493.675±0.026	GALL	88	CNTR	–	K^- Pb (11→ 10)
493.709±0.073	GALL	88	CNTR	–	K^- W (9→ 8)
493.806±0.095	GALL	88	CNTR	–	K^- W (11→ 10)
493.640±0.022±0.008	[3] CHENG	75	CNTR	–	K^- Pb (9→ 8)
493.658±0.019±0.012	[3] CHENG	75	CNTR	–	K^- Pb (10→ 9)
493.638±0.035±0.016	[3] CHENG	75	CNTR	–	K^- Pb (11→ 10)
493.753±0.042±0.021	[3] CHENG	75	CNTR	–	K^- Pb (12→ 11)
493.742±0.081±0.027	[3] CHENG	75	CNTR	–	K^- Pb (13→ 12)

[1] Error increased from 0.0059 based on the error analysis in IVANOV 92.
[2] This value is the authors' combination of all of the separate transitions listed for this paper.
[3] The CHENG 75 values for separate transitions were calculated from their Table 7 transition energies. The first error includes a 20% systematic error in the noncircular contaminant shift. The second error is due to a ±5 eV uncertainty in the theoretical transition energies.

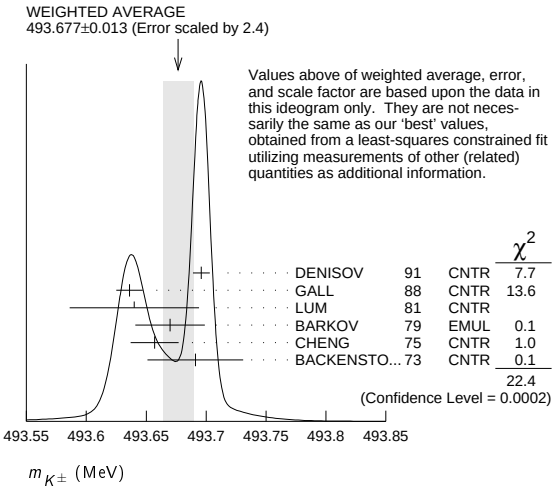

$m_{K^+} - m_{K^-}$

Test of *CPT*.

VALUE (MeV)	EVTS	DOCUMENT ID		TECN	CHG
−0.032±0.090	1.5 M	[4] FORD	72	ASPK	±

[4] FORD 72 uses $m_{\pi^+} - m_{\pi^-} = +28 \pm 70$ keV.

$K^{\pm}$ MEAN LIFE

VALUE (10^{-8} s)	EVTS	DOCUMENT ID		TECN	CHG	COMMENT
1.2380±0.0021 OUR FIT	Error includes scale factor of 1.9.					
1.2379±0.0021 OUR AVERAGE	Error includes scale factor of 1.9. See the ideogram below.					
1.2347±0.0030	15M	[5] AMBROSINO	08	KLOE	±	$\phi \rightarrow K^+K^-$
1.2451±0.0030	250k	KOPTEV	95	CNTR		K at rest, U target
1.2368±0.0041	150k	KOPTEV	95	CNTR		K at rest, Cu target
1.2380±0.0016	3M	OTT	71	CNTR	+	K at rest
1.2272±0.0036		LOBKOWICZ	69	CNTR	+	K in flight
1.2443±0.0038		FITCH	65B	CNTR	+	K at rest
• • • We do not use the following data for averages, fits, limits, etc. • • •						
1.2415±0.0024	400k	[6] KOPTEV	95	CNTR		K at rest
1.221 ±0.011		FORD	67	CNTR	±	
1.231 ±0.011		BOYARSKI	62	CNTR	+	

[5] Result obtained by averaging the decay length and decay time analyses taking correlations into account.
[6] KOPTEV 95 report this weighted average of their U-target and Cu-target results, where they have weighted by $1/\sigma$ rather than $1/\sigma^2$.

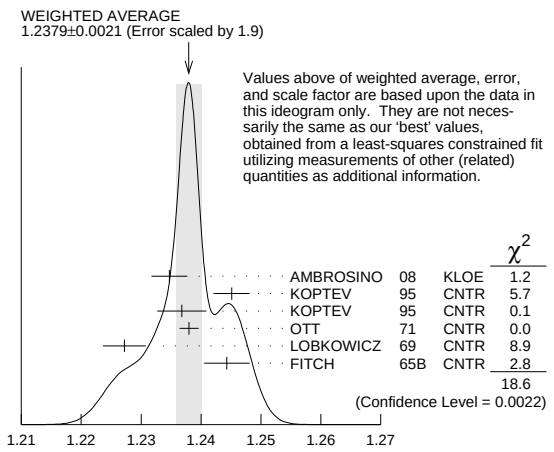

$(\tau_{K^+} - \tau_{K^-}) / \tau_{\text{average}}$

This quantity is a measure of CPT invariance in weak interactions.

VALUE (%)	DOCUMENT ID		TECN
0.10 ±0.09 OUR AVERAGE	Error includes scale factor of 1.2.		
−0.4 ±0.4	AMBROSINO	08	KLOE
0.090±0.078	LOBKOWICZ	69	CNTR
0.47 ±0.30	FORD	67	CNTR

RARE KAON DECAYS

Revised September 2013 by L. Littenberg (BNL) and G. Valencia (Iowa State University).

A. Introduction: There are several useful reviews on rare kaon decays and related topics [1–17]. Activity in rare kaon decays can be divided roughly into four categories:

1. Searches for explicit violations of the Standard Model
2. Measurements of Standard Model parameters
3. Searches for direct CP violation
4. Studies of strong interactions at low energy.

The paradigm of Category 1 is the lepton flavor violating decay $K_L \to \mu e$. Category 2 includes processes such as $K^+ \to \pi^+ \nu\overline{\nu}$, which is sensitive to $|V_{td}|$. Much of the interest in Category 3 is focused on the decays $K_L \to \pi^0 \ell\overline{\ell}$, where $\ell \equiv e, \mu, \nu$. Category 4 includes reactions like $K^+ \to \pi^+ \ell^+ \ell^-$ which constitute a testing ground for the ideas of chiral perturbation theory. Category 4 also includes $K_L \to \pi^0\gamma\gamma$ and $K_L \to \ell^+\ell^-\gamma$. The former is important in understanding a CP-conserving contribution to $K_L \to \pi^0 \ell^+ \ell^-$, whereas the latter could shed light on long distance contributions to $K_L \to \mu^+\mu^-$.

The interplay between Categories 2-4 can be illustrated in Fig. 1. The modes $K \to \pi\nu\overline{\nu}$ are the cleanest ones theoretically. They can provide accurate determinations of certain CKM parameters (shown in the figure). In combination with alternate determinations of these parameters, they also constrain new interactions. The modes $K_L \to \pi^0 e^+ e^-$, $K_L \to \pi^0 \mu^+ \mu^-$ and $K_L \to \mu^+\mu^-$ are also sensitive to CKM parameters. However, they suffer from a number of hadronic uncertainties that can be addressed, at least in part, through a systematic study of the additional modes indicated in the figure.

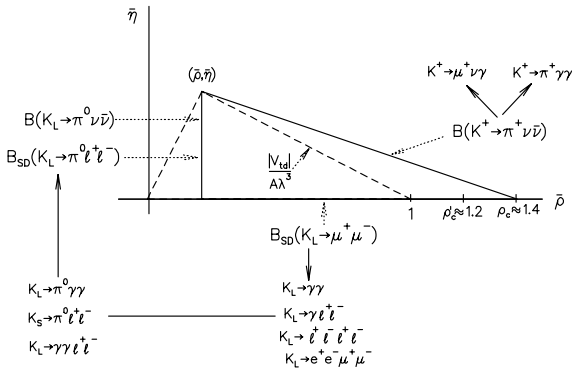

Figure 1: Role of rare kaon decays in determining the unitarity triangle. The solid arrows point to auxiliary modes needed to interpret the main results, or potential backgrounds to them.

B. Explicit violations of the Standard Model: Much activity has focussed on searches for lepton flavor violation (LFV). This is motivated by the fact that many extensions of the minimal Standard Model violate lepton flavor and by the potential to access very high energy scales. For example, the tree-level exchange of a LFV vector boson of mass M_X that couples to left-handed fermions with electroweak strength and without mixing angles yields $\mathrm{B}(K_L \to \mu e) = 4.7 \times 10^{-12} (148\ \mathrm{TeV}/M_X)^4$ [4]. This simple dimensional analysis may be used to read from Table 1 that the reaction $K_L \to \mu e$ is already probing scales of over 100 TeV. Table 1 summarizes the present experimental situation vis-à-vis LFV. The decays $K_L \to \mu^{\pm} e^{\mp}$ and $K^+ \to \pi^+ e^{\mp} \mu^{\pm}$ (or $K_L \to \pi^0 e^{\mp} \mu^{\pm}$) provide complementary information on potential family number violating interactions, since the former is sensitive to parity-odd couplings and the latter is sensitive to parity-even couplings. Limits on certain lepton-number violating kaon decays also exist, some recent ones being those of Refs. [18,19,20]. Related searches in μ and τ processes are discussed in our section "Tests of Conservation Laws."

Table 1: Searches for lepton flavor violation in K decay

Mode	90% CL upper limit	Exp't	Yr./Ref.
$K^+ \to \pi^+ e^- \mu^+$	1.2×10^{-11}	BNL-865	2005/Ref. 21
$K^+ \to \pi^+ e^+ \mu^-$	5.2×10^{-10}	BNL-865	2000/Ref. 18
$K_L \to \mu e$	4.7×10^{-12}	BNL-871	1998/Ref. 22
$K_L \to \pi^0 e\mu$	7.6×10^{-11}	KTeV	2008/Ref. 23
$K_L \to \pi^0\pi^0 e\mu$	1.7×10^{-10}	KTeV	2008/Ref. 23

Physics beyond the SM is also pursued through the search for $K^+ \to \pi^+ X^0$, where X^0 is a new light particle. The searches cover both long-lived particles (*e.g.*, hyperphoton, axion, familon, *etc.*), and short lived ones that decay to muon, electron or photon pairs. The 90% CL upper limit on $K^+ \to \pi^+ X^0$ is 7.3×10^{-11} [24] for the case of massless X^0; additional results as a function of the X^0 mass can be found in [34].

More recent bounds for a short lived pseudoscalar X^0 decaying to muons or photons are $B(K_L \to \pi^0\pi^0\mu^+\mu^-) < 1\times10^{-10}$ [25] and $B(K_L \to \pi^0\pi^0\gamma\gamma) < 2.4\times10^{-7}$ [26].

C. Measurements of Standard Model parameters:

In the SM, the decay $K^+ \to \pi^+\nu\overline{\nu}$ is dominated by one-loop diagrams with top-quark intermediate states and long-distance contributions are known to be quite small [2,27]. This permits a precise calculation of this rate in terms of SM parameters. Studies of this process are thus motivated by the possibility of detecting non-SM physics when comparing with the results of global fits [28,29].

BNL-787 observed two candidate events [30,31] in the clean high π^+ momentum and one event [32] in the low-momentum region. The successor experiment BNL-949 observed one more in the high-momentum region [24] and three more in the low-momentum region [33] yielding a branching ratio of $(1.73^{+1.15}_{-1.05})\times 10^{-10}$ [34]. A subsequent experiment, NA62, with a sensitivity goal of $\sim 10^{-12}$/event was proposed [35] at CERN in 2005. It was approved and ran with a partial detector in autumn 2012. Physics running is scheduled to start in the fall of 2014. A new experiment, ORKA [36], received Stage 1 approval from Fermilab in December 2011. It proposes to collect $O(1000)$ events in five years of running by studying kaon decays at rest. In contrast, the NA62 experiment will be performed with kaon decays in flight. In the future, this mode may provide grounds for precision tests of flavor dynamics [37]. The branching ratio can be written in a compact form that exhibits the different ingredients that go into the calculation [38],

$$\mathrm{B}(K^+ \to \pi^+\nu\overline{\nu}(\gamma)) = \kappa_+(1+\Delta_{\mathrm{EM}})\left[\left(\frac{\mathrm{Im}(V_{ts}^\star V_{td})}{\lambda^5}X_t\right)^2 + \left(\frac{\mathrm{Re}(V_{cs}^\star V_{cd})}{\lambda}(P_c+\delta P_{c,u}) + \frac{\mathrm{Re}(V_{ts}^\star V_{td})}{\lambda^5}X_t\right)^2\right]. \quad (1)$$

The parameters in Eq. (1) incorporate the *a priori* unknown hadronic matrix element in terms of the very well-measured K_{e3} rate [2] in κ_+; long distance QED corrections in Δ_{EM} [39]; the Inami-Lim function for the short distance top-quark contribution [40] including NLO QCD corrections [41] and the two-loop electroweak correction [38], all in X_t; and the charm-quark contributions due to short distance effects including NNLO QCD corrections [42] and NLO electroweak corrections via P_c [43], as well as certain long distance effects via $\delta P_{c,u}$ [44]. An interesting approximate way to cast this result in terms of the CKM parameters λ, V_{cb}, $\overline{\rho}$ and $\overline{\eta}$ (see our Section on "The Cabibbo-Kobayashi-Maskawa mixing matrix") [11] is:

$$\mathrm{B}(K^+ \to \pi^+\nu\overline{\nu}) \approx 1.6\times10^{-5}|V_{cb}|^4[\sigma\overline{\eta}^2 + (\rho_c-\overline{\rho})^2], \quad (2)$$

where $\rho_c \approx 1.45$ and $\sigma \equiv 1/(1-\frac{1}{2}\lambda^2)^2$. Thus, $\mathrm{B}(K^+ \to \pi^+\nu\overline{\nu})$ determines an ellipse in the $\overline{\rho}$, $\overline{\eta}$ plane with center $(\rho_c, 0)$ and semiaxes $\approx \frac{1}{|V_{cb}|^2}\sqrt{\frac{\mathrm{B}(K^+\to\pi^+\nu\overline{\nu})}{1.6\times10^{-5}}}$ and $\frac{1}{\sigma|V_{cb}|^2}\sqrt{\frac{\mathrm{B}(K^+\to\pi^+\nu\overline{\nu})}{1.6\times10^{-5}}}$. The latest numerical study leads to a predicted branching ratio $(7.81^{+0.80}_{-0.71}\pm0.29)\times10^{-11}$ [38], near the lower end of the measurement of BNL-787 and 949.

Modes with an extra pion, $K \to \pi\pi\nu\bar{\nu}$, could also be used in the extraction of CKM parameters as they are also dominated by short distance contributions [45]. However, they occur at much lower rates with branching rations of order 10^{-13}, and the current best bound from KEK-391a is $B(K_L \to \pi^0\pi^0\nu\bar{\nu}) < 8.1\times10^{-7}$ at 90% CL [46]. There is also an older bound of $B(K^+ \to \pi^+\pi^0\nu\bar{\nu}) < 4.3\times10^{-5}$ at 90% CL [47] from BNL-787.

The decay $K_L \to \mu^+\mu^-$ also has a short distance contribution sensitive to the CKM parameter $\overline{\rho}$, given by [11]:

$$\mathrm{B_{SD}}(K_L \to \mu^+\mu^-) \approx 2.7\times10^{-4}|V_{cb}|^4(\rho_c'-\overline{\rho})^2 \quad (3)$$

where ρ_c' depends on the charm quark mass and is approximately 1.2. This decay, however, is dominated by a long-distance contribution from a two-photon intermediate state. The absorptive (imaginary) part of the long-distance component is determined by the measured rate for $K_L \to \gamma\gamma$ to be $\mathrm{B_{abs}}(K_L \to \mu^+\mu^-) = (6.64\pm0.07)\times10^{-9}$; and it almost completely saturates the observed rate $\mathrm{B}(K_L \to \mu^+\mu^-) = (6.84\pm0.11)\times10^{-9}$ [48]. The difference between the observed rate and the absorptive component can be attributed to the (coherent) sum of the short-distance amplitude and the real part of the long-distance amplitude. The latter cannot be derived directly from experiment [49], but can be estimated with certain assumptions [50,51].

The decay $K_L \to e^+e^-$ is completely dominated by long distance physics and is easier to estimate. The result, $B(K_L \to e^+e^-) \sim 9\times10^{-12}$ [49,52], is in good agreement with the BNL-871 measurement, $(8.7^{+5.7}_{-4.1})\times10^{-12}$ [53].

The mode $K_S \to \mu^+\mu^-$ also has a short distance contribution proportional to the square of the CKM parameter $\bar{\eta}$ entering at the 10^{-13} level [15] as well as long distance contributions which arise in this case from a two photon intermediate state and result in a rate $B(K_S \to \mu^+\mu^-)_{LD} = 5.1\times10^{-12}$ [15]. A 95% (90%) c.l. limit $B(K_S \to \mu^+\mu^-) < 11(9)\times10^{-9}$ has recently been obtained by LHCb [54].

D. Searches for direct CP violation: The mode $K_L \to \pi^0\nu\overline{\nu}$ is dominantly CP-violating and free of hadronic uncertainties [2,55,56]. In the Standard Model, this mode is dominated by an intermediate top-quark state and does not suffer from the small uncertainty associated with the charm-quark intermediate state that affects the mode $K^+ \to \pi^+\nu\overline{\nu}$. The branching ratio is given by Ref. 11:

$$\mathrm{B}(K_L \to \pi^0\nu\overline{\nu}) = \kappa_L\left(\frac{\mathrm{Im}(V_{ts}^\star V_{td})}{\lambda^5}X_t\right)^2 \approx 7.6\times10^{-5}|V_{cb}|^4\overline{\eta}^2\,. \quad (4)$$

The hadronic matrix element can be related to that measured in $K_{\ell3}$ decay and is parameterized in κ_L. The latest numerical evaluation leads to a predicted branching ratio $(2.43^{+0.40}_{-0.37}\pm0.06)\times10^{-11}$ [38]. The 90% CL bound on $K^+ \to \pi^+\nu\overline{\nu}$ provides a nearly model-independent bound $B(K_L \to \pi^0\nu\overline{\nu}) < 1.46\times10^{-9}$ [57]. KEK-391a, which took data in 2004 and 2005, has published a 90% CL upper bound of $\mathrm{B}(K_L \to \pi^0\nu\overline{\nu}) \leq$

2.6×10^{-8} [58]. The KOTO experiment at J-PARC [59], whose initial goal is to reach the 10^{-11}/event level had a short physics run in the spring of 2013 and is expected to resume in 2014.

There has been much theoretical work on possible contributions to rare K decays beyond the SM. A comprehensive discussion of these can be found in Refs. [14] and [60].

The decay $K_L \to \pi^0 e^+ e^-$ also has sensitivity to the CKM parameter η through its CP-violating component. There are both direct and indirect CP-violating amplitudes that can interfere. The direct CP-violating amplitude is short distance dominated and has been calculated in detail within the SM [8]. The indirect CP-violating amplitude can be inferred from a measurement of $K_S \to \pi^0 e^+ e^-$. The complete CP-violating contribution to the rate can be written as [61,62]:

$$\mathrm{B_{CPV}} \approx 10^{-12}\left[15.7|a_S|^2 \pm 1.4\left(\frac{|V_{cb}|^2\overline{\eta}}{10^{-4}}\right)|a_S| + 0.12\left(\frac{|V_{cb}|^2\overline{\eta}}{10^{-4}}\right)^2\right] \quad (5)$$

where the three terms correspond to the indirect CP violation, the interference, and the direct CP violation respectively. The parameter a_S has been extracted by NA48 from a measurement of the decay $K_S \to \pi^0 e^+ e^-$ with the result $|a_S| = 1.06^{+0.26}_{-0.21} \pm 0.07$ [63], as well as from a measurement of the decay $K_S \to \pi^0 \mu^+ \mu^-$ with the result $|a_s| = 1.54^{+0.40}_{-0.32} \pm 0.06$ [64]. With current constraints on the CKM parameters, and assuming a positive sign for the interference term [62,65], this implies that $\mathrm{B_{CPV}}(K_L \to \pi^0 e^+ e^-) \approx (3.1 \pm 0.9)\times10^{-11}$, and that the indirect CP violation is larger than the direct CP violation. The complete CP violating amplitude for the related mode $K_L \to \pi^0 \mu^+ \mu^-$ is predicted to be $\mathrm{B_{CPV}}(K_L \to \pi^0 \mu^+ \mu^-) \approx (1.4 \pm 0.5)\times10^{-11}$ [66,15].

$K_L \to \pi^0\gamma\gamma$ also has a CP-conserving component dominated by a two-photon intermediate state. This component can be decomposed into an absorptive and a dispersive part. The absorptive part can be extracted from the measurement of the low $m_{\gamma\gamma}$ region of the $K_L \to \pi^0\gamma\gamma$ spectrum. The rate and the shape of the distribution $d\Gamma/dm_{\gamma\gamma}$ in $K_L \to \pi^0\gamma\gamma$ are well described in chiral perturbation theory in terms of three (*a priori*) unknown parameters [67,68].

Both KTeV and NA48 have studied the mode $K_L \to \pi^0\gamma\gamma$, reporting similar results. KTeV finds $B(K_L \to \pi^0\gamma\gamma) = (1.29 \pm 0.03_{\mathrm{stat}} \pm 0.05_{\mathrm{sys}}) \times 10^{-6}$ [69], while NA48 finds $B(K_L \to \pi^0\gamma\gamma) = (1.36 \pm 0.03_{\mathrm{stat}} \pm 0.03_{\mathrm{sys}} \pm 0.03_{\mathrm{norm}}) \times 10^{-6}$ [70]. Both experiments are consistent with a negligible rate in the low $m_{\gamma\gamma}$ region, suggesting a very small CP-conserving component $B_{\mathrm{CP}}(K_L \to \pi^0 e^+ e^-) \sim \mathcal{O}(10^{-13})$ [62,68,70]. There remains some model dependence in the estimate of the dispersive part of the CP-conserving $K_L \to \pi^0 e^+ e^-$ [62].

The related process, $K_L \to \pi^0\gamma e^+ e^-$, is potentially an additional background in some region of phase space [71]. This process has been observed with a branching ratio of $(1.62 \pm 0.14_{\mathrm{stat}} \pm 0.09_{\mathrm{sys}}) \times 10^{-8}$ [72].

The decay $K_L \to \gamma\gamma e^+ e^-$ constitutes the dominant background to $K_L \to \pi^0 e^+ e^-$. It was first observed by BNL-845 [73], and subsequently confirmed with a much larger sample by KTeV [74]. It has been estimated that this background will enter at about the 10^{-10} level [75,76], comparable to or larger than the signal level. Because of this, the observation of $K_L \to \pi^0 e^+ e^-$ at the SM level will depend on background subtraction with good statistics. Possible alternative strategies are discussed in Ref. 62 and references cited therein.

The 90% CL upper bound for the process $K_L \to \pi^0 e^+ e^-$ is 2.8×10^{-10} [76]. For the closely related muonic process, the published upper bound is $\mathrm{B}(K_L \to \pi^0\mu^+\mu^-) \le 3.8\times10^{-10}$ [77], compared with the SM prediction of $(1.5 \pm 0.3)\times10^{-11}$ [66] (assuming positive interference between the direct- and indirect-CP violating components).

A study of $K_L \to \pi^0\mu^+\mu^-$ has indicated that it might be possible to extract the direct CP-violating contribution by a joint study of the Dalitz plot variables and the components of the μ^+ polarization [78]. The latter tends to be quite substantial so that large statistics may not be necessary.

Combined information from the two $K_L \to \pi^0\ell^+\ell^-$ modes complements the $K \to \pi\nu\overline{\nu}$ measurements in constraining physics beyond the SM [79].

E. Other long distance dominated modes:

The decays $K^+ \to \pi^+\ell^+\ell^-$ (ℓ = e or μ) have received considerable attention. The rate and spectrum have been measured for both the electron and muon modes [80,81,20]. Ref. 61 has proposed a parametrization inspired by chiral perturbation theory, which provides a successful description of data but indicates the presence of large corrections beyond leading order. More work is needed to fully understand the origin of these large corrections. NA62 has now also observed the mode $K^+ \to \pi^+\pi^0 e^+ e^-$ [82].

The decay $K^+ \to \pi^+\gamma\gamma$ can be predicted in terms of one unknown parameter to leading order in χPT resulting in a correlation between the rate and the diphoton mass spectrum [83]. Certain important corrections at the next order are also known [84]. The rate was first measured by E787 [85] and more recently NA48/2 [86] has obtained a more precise result with 6% error along with the corresponding spectrum fits.

Much information has been recorded by KTeV and NA48 on the rates and spectrum for the Dalitz pair conversion modes $K_L \to \ell^+\ell^-\gamma$ [87,88], and $K_L \to \ell^+\ell^-\ell'^+\ell'^-$ for $\ell, \ell' =$ e or μ [19,89–91]. All these results are used to test hadronic models and could further our understanding of the long distance component in $K_L \to \mu^+\mu^-$.

References

1. D. Bryman, Int. J. Mod. Phys. **A4**, 79 (1989).
2. J. Hagelin and L. Littenberg, Prog. in Part. Nucl. Phys. **23**, 1 (1989).
3. L. Littenberg and G. Valencia, Ann. Rev. Nucl. and Part. Sci. **43**, 729 (1993).
4. J. Ritchie and S. Wojcicki, Rev. Mod. Phys. **65**, 1149 (1993).

5. B. Winstein and L. Wolfenstein, Rev. Mod. Phys. **65**, 1113 (1993).
6. G. D'Ambrosio *et al.*, *Radiative Non-Leptonic Kaon Decays*, in The DAΦNE Physics Handbook (second edition), eds. L. Maiani, G. Pancheri, and N. Paver (Frascati), Vol. I, 265 (1995).
7. A. Pich, Rept. on Prog. in Phys. **58**, 563 (1995).
8. G. Buchalla, A.J. Buras, and M.E. Lautenbacher, Rev. Mod. Phys. **68**, 1125 (1996).
9. G. D'Ambrosio and G. Isidori, Int. J. Mod. Phys. **A13**, 1 (1996).
10. P. Buchholz and B. Renk Prog. in Part. Nucl. Phys. **39**, 253 (1997).
11. A.J. Buras and R. Fleischer, TUM-HEP-275-97, hep-ph/9704376, *Heavy Flavours II*, World Scientific, eds. A.J. Buras and M. Lindner (1997), 65–238.
12. A.J. Buras, TUM-HEP-349-99, Lectures given at Lake Louise Winter Institute: Electroweak Physics, Lake Louise, Alberta, Canada, 14–20 Feb. 1999.
13. A.R. Barker and S.H. Kettell, Ann. Rev. Nucl. and Part. Sci. **50**, 249 (2000).
14. A.J. Buras, F. Schwab, and S. Uhlig, Rev. Mod. Phys. **80**, 965 (2008).
15. V. Cirigliano *et al.*, Rev. Mod. Phys. **84**, 399 (2012).
16. D. Bryman *et al.*, Ann. Rev. Nucl. and Part. Sci. **61**, 331 (2011).
17. T.K. Komatsubara, Prog. in Part. Nucl. Phys. 67, 995 (2012).
18. R. Appel *et al.*, Phys. Rev. Lett. **85**, 2877 (2000).
19. A. Alavi-Harati *et al.*, Phys. Rev. Lett. **90**, 141801 (2003).
20. J.R. Batley *et al.*, Phys. Lett. **B697**, 107 (2011).
21. A. Sher *et al.*, Phys. Rev. **D72**, 012005 (2005).
22. D. Ambrose *et al.*, Phys. Rev. Lett. **81**, 5734 (1998).
23. E. Abouzaid *et al.*, Phys. Rev. Lett. **100**, 131803 (2008).
24. V.V. Anisimovsky *et al.*, Phys. Rev. Lett. **93**, 031801 (2004).
25. E. Abouzaid *et al.*, Phys. Rev. Lett. **107**, 201803 (2011) see also, D.G. Phillips II, "Search for the Rare Decay $K_L \to \pi^0\pi^0\mu^+\mu^-$," University of Virginia thesis, May 2009.
26. Y.C. Tung *et al.*, Phys. Rev. Lett. **102**, 051802 (2009).
27. M. Lu and M.B. Wise, Phys. Lett. **B324**, 461 (1994); A.F. Falk, A. Lewandowski, and A.A. Petrov, Phys. Lett. **B505**, 107 (2001).
28. CKMfitter Group (J. Charles *et al.*), Phys. Rev. **D84**, 033005 (2011), [arXiv:1106.4041[hep-ph]], updated results and plots available at: http://ckmfitter.in2p3.fr.
29. M. Bona *et al.*, [UTfit Collab.] "Model-independent constraints on Delta F=2 operators and the scale of New Physics," arXiv:0707.0636 [hep-ph], http://www.utfit.org/UTfit/.
30. S. Adler *et al.*, Phys. Rev. Lett. **88**, 041803 (2002).
31. S. Adler *et al.*, Phys. Rev. Lett. **84**, 3768 (2000).
32. S. Adler *et al.*, Phys. Lett. **B537**, 237 (2002).
33. A.V. Artamonov *et al.*, Phys. Rev. Lett. **101**, 191802 (2008).
34. A.V. Artamonov *et al.*, Phys. Rev. **D79**, 092004 (2009).
35. G. Anelli *et al.*, CERN-SPSC-2005-013, 11 June 2005.
36. J. Comfort *et al.*, FERMILAB-PROPOSAL-1021.
37. G. D'Ambrosio and G. Isidori, Phys. Lett. **B530**, 108 (2002).
38. J. Brod, M. Gorbahn, and E. Stamou, Phys. Rev. **D83**, 034030 (2011).
39. F. Mescia and C. Smith, Phys. Rev. **D76**, 034017 (2007).
40. T. Inami and C.S. Lim, Prog. Theor. Phys. **65**, 297 (1981); Erratum Prog. Theor. Phys. **65**, 172 (1981).
41. G. Buchalla and A.J. Buras, Nucl. Phys. **B548**, 309 (1999); M. Misiak and J. Urban, Phys. Lett. **B451**, 161 (1999).
42. A.J. Buras *et al.*, Phys. Rev. Lett. **95**, 261805 (2005); A.J. Buras *et al.*, JHEP **0611**, 002 (2006).
43. J. Brod and M. Gorbahn, Phys. Rev. **D78**, 034006 (2008).
44. G. Isidori, F. Mescia, and C. Smith, Nucl. Phys. **B718**, 319 (2005); A. F. Falk, A. Lewandowski, and A. A. Petrov, Phys. Lett. **B505**, 107 (2001).
45. L. Littenberg and G. Valencia, Phys. Lett. **B385**, 379 (1996); C.-W. Chiang and F. J. Gilman, Phys. Rev. **D62**, 094026 (2000); C. Q. Geng, I. J. Hsu, and Y. C. Lin, Phys. Rev. **D50**, 5744 (1994).
46. R. Ogata, *et al.*, Phys. Rev. **D84**, 052009 (2011).
47. S. Adler, *et al.*, Phys. Rev. **D63**, 032004 (2001).
48. D. Ambrose *et al.*, Phys. Rev. Lett. **84**, 1389 (2000).
49. G. Valencia, Nucl. Phys. **B517**, 339 (1998).
50. G. D'Ambrosio, G. Isidori, and J. Portoles, Phys. Lett. **B423**, 385 (1998).
51. G. Isidori and R. Unterdorfer, JHEP **0401**, 009 (2004).
52. D. Gomez-Dumm and A. Pich, Phys. Rev. Lett. **80**, 4633 (1998).
53. D. Ambrose *et al.*, Phys. Rev. Lett. **81**, 4309 (1998).
54. R. Aaij *et al.*, JHEP **1301**, 090 (2013).
55. L. Littenberg, Phys. Rev. **D39**, 3322 (1989).
56. G. Buchalla and G. Isidori, Phys. Lett. **B440**, 170 (1998).
57. Y. Grossman and Y. Nir, Phys. Lett. **B398**, 163 (1997).
58. J.K. Ahn *et al.*, Phys. Rev. **D81**, 072004 (2010).
59. J. Comfort *et al.*, "Proposal for $K_L^0 \to \pi^0\nu\overline{\nu}$ Experiment at J-Parc," J-PARC Proposal 14 (2006).
60. D. Bryman *et al.*, Int. J. Mod. Phys. **A21**, 487 (2006).
61. G. D'Ambrosio *et al.*, JHEP **9808**, 004 (1998); C.O. Dib, I. Dunietz, and F.J. Gilman, Phys. Rev. **D39**, 2639 (1989).
62. G. Buchalla, G. D'Ambrosio, and G. Isidori, Nucl. Phys. **B672**, 387 (2003).
63. J.R. Batley *et al.*, Phys. Lett. **B576**, 43 (2003).
64. J.R. Batley *et al.*, Phys. Lett. **B599**, 197 (2004).
65. S. Friot, D. Greynat, and E. de Rafael, Phys. Lett. **B595**, 301 (2004).
66. G. Isidori, C. Smith, and R. Unterdorfer, Eur. Phys. J. **C36**, 57 (2004).
67. G. Ecker, A. Pich, and E. de Rafael, Phys. Lett. **237B**, 481 (1990); L. Cappiello, G. D'Ambrosio, and M. Miragliuolo, Phys. Lett. **B298**, 423 (1993); A. Cohen, G. Ecker, and A. Pich, Phys. Lett. **B304**, 347 (1993).

68. F. Gabbiani and G. Valencia, Phys. Rev. **D66**, 074006 (2002).
69. E. Abouzaid *et al.*, Phys. Rev. **D77**, 112004 (2008).
70. A. Lai *et al.*, Phys. Lett. **B536**, 229 (2002).
71. J. Donoghue and F. Gabbiani, Phys. Rev. **D56**, 1605 (1997).
72. E. Abouzaid *et al.*, Phys. Rev. **D76**, 052001 (2007).
73. W.M. Morse *et al.*, Phys. Rev. **D45**, 36 (1992).
74. A. Alavi-Harati *et al.*, Phys. Rev. **D64**, 012003 (2001).
75. H.B. Greenlee, Phys. Rev. **D42**, 3724 (1990).
76. A. Alavi-Harati *et al.*, Phys. Rev. Lett. **93**, 021805 (2004).
77. A. Alavi-Harati *et al.*, Phys. Rev. Lett. **84**, 5279 (2000).
78. M.V. Diwan, H. Ma, and T.L. Trueman, Phys. Rev. **D65**, 054020 (2002).
79. F. Mescia, C. Smith, and S. Trine, JHEP **0608**, 088 (2006).
80. R. Appel *et al.*, Phys. Rev. Lett. **83**, 4482 (1999); J.R. Batley *et al.*, Phys. Lett. **B677**, 246 (2009).
81. S.C. Adler *et al.*, Phys. Rev. Lett. **79**, 4756 (1997); R. Appel *et al.*, Phys. Rev. Lett. **84**, 2580 (2000); H.K. Park *et al.*, Phys. Rev. Lett. **88**, 111801 (2002).
82. R. Fantechi, Pos HQL **2012**, 014 (2012).
83. G. Ecker, A. Pich, and E. de Rafael, Nucl. Phys. **B303**, 665 (1988).
84. G. D'Ambrosio and J. Portoles, Phys. Lett. B **386**, 403 (1996) [Phys. Lett. B **389**, 770 (1996)] [Erratum-ibid. B **395**, 390 (1997)] [hep-ph/9606213].
85. P. Kitching *et al.* [E787 Collab.], Phys. Rev. Lett. **79**, 4079 (1997) [hep-ex/9708011].
86. J.R. Batley *et al.*, arXiv:1310.5499 [hep-ex](2013).
87. A. Alavi-Harati *et al.*, Phys. Rev. Lett. **87**, 071801 (2001).
88. A. Abouzaid *et al.*, Phys. Rev. Lett. **99**, 051804 (2007).
89. J.R. LaDue "Understanding Dalitz Decays of the K_L in particular the decays of $K_L \to e^+e^-\gamma$ and $K_L \to e^+e^-e^+e^-$" University of Colorado Thesis, May 2003. The preliminary result for $K_L \to e^+e^-\gamma$ in this thesis has been superseded by the final result in [88].
90. A. Alavi-Harati *et al.*, Phys. Rev. Lett. **86**, 5425 (2001).
91. V. Fanti *et al.*, Phys. Lett. **B458**, 458 (1999).

K^+ DECAY MODES

K^- modes are charge conjugates of the modes below.

	Mode	Fraction (Γ_j/Γ)	Scale factor/ Confidence level
	Leptonic and semileptonic modes		
Γ_1	$e^+\nu_e$	$(1.581\pm0.007)\times10^{-5}$	
Γ_2	$\mu^+\nu_\mu$	$(63.55\pm0.11)\%$	S=1.2
Γ_3	$\pi^0 e^+\nu_e$	$(5.07\pm0.04)\%$	S=2.1
	Called K^+_{e3}.		
Γ_4	$\pi^0\mu^+\nu_\mu$	$(3.353\pm0.034)\%$	S=1.8
	Called $K^+_{\mu3}$.		
Γ_5	$\pi^0\pi^0 e^+\nu_e$	$(2.2\pm0.4)\times10^{-5}$	
Γ_6	$\pi^+\pi^- e^+\nu_e$	$(4.254\pm0.032)\times10^{-5}$	
Γ_7	$\pi^+\pi^-\mu^+\nu_\mu$	$(1.4\pm0.9)\times10^{-5}$	
Γ_8	$\pi^0\pi^0\pi^0 e^+\nu_e$	$<3.5\times10^{-6}$	CL=90%
	Hadronic modes		
Γ_9	$\pi^+\pi^0$	$(20.66\pm0.08)\%$	S=1.2
Γ_{10}	$\pi^+\pi^0\pi^0$	$(1.761\pm0.022)\%$	S=1.1
Γ_{11}	$\pi^+\pi^+\pi^-$	$(5.59\pm0.04)\%$	S=1.3
	Leptonic and semileptonic modes with photons		
Γ_{12}	$\mu^+\nu_\mu\gamma$	[a,b] $(6.2\pm0.8)\times10^{-3}$	
Γ_{13}	$\mu^+\nu_\mu\gamma(\mathrm{SD}^+)$	[c,d] $(1.33\pm0.22)\times10^{-5}$	
Γ_{14}	$\mu^+\nu_\mu\gamma(\mathrm{SD}^+\mathrm{INT})$	[c,d] $<2.7\times10^{-5}$	CL=90%
Γ_{15}	$\mu^+\nu_\mu\gamma(\mathrm{SD}^- + \mathrm{SD}^-\mathrm{INT})$	[c,d] $<2.6\times10^{-4}$	CL=90%
Γ_{16}	$e^+\nu_e\gamma$	$(9.4\pm0.4)\times10^{-6}$	
Γ_{17}	$\pi^0 e^+\nu_e\gamma$	[a,b] $(2.56\pm0.16)\times10^{-4}$	
Γ_{18}	$\pi^0 e^+\nu_e\gamma(\mathrm{SD})$	[c,d] $<5.3\times10^{-5}$	CL=90%
Γ_{19}	$\pi^0\mu^+\nu_\mu\gamma$	[a,b] $(1.25\pm0.25)\times10^{-5}$	
Γ_{20}	$\pi^0\pi^0 e^+\nu_e\gamma$	$<5\times10^{-6}$	CL=90%
	Hadronic modes with photons or $\ell\bar{\ell}$ pairs		
Γ_{21}	$\pi^+\pi^0\gamma(\mathrm{INT})$	$(-4.2\pm0.9)\times10^{-6}$	
Γ_{22}	$\pi^+\pi^0\gamma(\mathrm{DE})$	[a,e] $(6.0\pm0.4)\times10^{-6}$	
Γ_{23}	$\pi^+\pi^0\pi^0\gamma$	[a,b] $(7.6\,^{+6.0}_{-3.0})\times10^{-6}$	
Γ_{24}	$\pi^+\pi^+\pi^-\gamma$	[a,b] $(1.04\pm0.31)\times10^{-4}$	
Γ_{25}	$\pi^+\gamma\gamma$	[a] $(9.2\pm0.7)\times10^{-7}$	
Γ_{26}	$\pi^+ 3\gamma$	[a] $<1.0\times10^{-4}$	CL=90%
Γ_{27}	$\pi^+ e^+ e^-\gamma$	$(1.19\pm0.13)\times10^{-8}$	
	Leptonic modes with $\ell\bar{\ell}$ pairs		
Γ_{28}	$e^+\nu_e\nu\overline{\nu}$	$<6\times10^{-5}$	CL=90%
Γ_{29}	$\mu^+\nu_\mu\nu\overline{\nu}$	$<6.0\times10^{-6}$	CL=90%
Γ_{30}	$e^+\nu_e e^+ e^-$	$(2.48\pm0.20)\times10^{-8}$	
Γ_{31}	$\mu^+\nu_\mu e^+ e^-$	$(7.06\pm0.31)\times10^{-8}$	
Γ_{32}	$e^+\nu_e\mu^+\mu^-$	$(1.7\pm0.5)\times10^{-8}$	
Γ_{33}	$\mu^+\nu_\mu\mu^+\mu^-$	$<4.1\times10^{-7}$	CL=90%
	Lepton Family number (LF), Lepton number (L), $\Delta S=\Delta Q$ (SQ) violating modes, or $\Delta S=1$ weak neutral current ($S1$) modes		
Γ_{34}	$\pi^+\pi^+ e^-\overline{\nu}_e$	SQ $<1.3\times10^{-8}$	CL=90%
Γ_{35}	$\pi^+\pi^+\mu^-\overline{\nu}_\mu$	SQ $<3.0\times10^{-6}$	CL=95%
Γ_{36}	$\pi^+ e^+ e^-$	$S1$ $(3.00\pm0.09)\times10^{-7}$	
Γ_{37}	$\pi^+\mu^+\mu^-$	$S1$ $(9.4\pm0.6)\times10^{-8}$	S=2.6
Γ_{38}	$\pi^+\nu\overline{\nu}$	$S1$ $(1.7\pm1.1)\times10^{-10}$	
Γ_{39}	$\pi^+\pi^0\nu\overline{\nu}$	$S1$ $<4.3\times10^{-5}$	CL=90%
Γ_{40}	$\mu^-\nu e^+ e^+$	LF $<2.1\times10^{-8}$	CL=90%
Γ_{41}	$\mu^+\nu_e$	LF [f] $<4\times10^{-3}$	CL=90%
Γ_{42}	$\pi^+\mu^+ e^-$	LF $<1.3\times10^{-11}$	CL=90%
Γ_{43}	$\pi^+\mu^- e^+$	LF $<5.2\times10^{-10}$	CL=90%
Γ_{44}	$\pi^-\mu^+ e^+$	L $<5.0\times10^{-10}$	CL=90%
Γ_{45}	$\pi^- e^+ e^+$	L $<6.4\times10^{-10}$	CL=90%
Γ_{46}	$\pi^-\mu^+\mu^+$	L [f] $<1.1\times10^{-9}$	CL=90%
Γ_{47}	$\mu^+\overline{\nu}_e$	L [f] $<3.3\times10^{-3}$	CL=90%
Γ_{48}	$\pi^0 e^+\overline{\nu}_e$	L $<3\times10^{-3}$	CL=90%
Γ_{49}	$\pi^+\gamma$	[g] $<2.3\times10^{-9}$	CL=90%

[a] See the Particle Listings below for the energy limits used in this measurement.

[b] Most of this radiative mode, the low-momentum γ part, is also included in the parent mode listed without γ's.

[c] Structure-dependent part.

[d] See the "Note on $\pi^\pm \to \ell^\pm\nu\gamma$ and $K^\pm \to \ell^\pm\nu\gamma$ Form Factors" in the $\pi^\pm$ Particle Listings for definitions and details.

[e] Direct-emission branching fraction.

[f] Derived from an analysis of neutrino-oscillation experiments.

[g] Violates angular-momentum conservation.

CONSTRAINED FIT INFORMATION

An overall fit to the mean life, a decay rate, and 13 branching ratios uses 32 measurements and one constraint to determine 8 parameters. The overall fit has a $\chi^2 = 51.8$ for 25 degrees of freedom.

The following *off-diagonal* array elements are the correlation coefficients $\langle \delta p_i \delta p_j \rangle / (\delta p_i \cdot \delta p_j)$, in percent, from the fit to parameters p_i, including the branching fractions, $x_i \equiv \Gamma_i/\Gamma_{\text{total}}$. The fit constrains the x_i whose labels appear in this array to sum to one.

x_3	−64						
x_4	−62	90					
x_5	−3	4	3				
x_9	−65	1	−1	0			
x_{10}	−13	−6	−6	0	−6		
x_{11}	−21	−9	−9	0	−10	3	
Γ	5	2	2	0	2	−1	−24
	x_2	x_3	x_4	x_5	x_9	x_{10}	x_{11}

	Mode	Rate (10^8 s^{-1})	Scale factor
Γ_2	$\mu^+ \nu_\mu$	0.5133 ±0.0013	1.5
Γ_3	$\pi^0 e^+ \nu_e$	0.0410 ±0.0004	2.1
	Called K^+_{e3}.		
Γ_4	$\pi^0 \mu^+ \nu_\mu$	0.02708±0.00028	1.9
	Called $K^+_{\mu 3}$.		
Γ_5	$\pi^0 \pi^0 e^+ \nu_e$	$(1.77\ ^{+0.35}_{-0.30}) \times 10^{-5}$	
Γ_9	$\pi^+ \pi^0$	0.1669 ±0.0007	1.3
Γ_{10}	$\pi^+ \pi^0 \pi^0$	0.01423±0.00018	1.1
Γ_{11}	$\pi^+ \pi^+ \pi^-$	0.04518±0.00029	1.2

$K^{\pm}$ DECAY RATES

$\Gamma(\mu^+ \nu_\mu)$ Γ_2

VALUE (10^6 s^{-1})	DOCUMENT ID		TECN	CHG
51.33±0.13 OUR FIT Error includes scale factor of 1.5.				
• • • We do not use the following data for averages, fits, limits, etc. • • •				
51.2 ±0.8	FORD	67	CNTR	±

$\Gamma(\pi^+ \pi^+ \pi^-)$ Γ_{11}

VALUE (10^6 s^{-1})	EVTS	DOCUMENT ID		TECN	CHG
4.518±0.029 OUR FIT Error includes scale factor of 1.2.					
4.511±0.024		[7] FORD	70	ASPK	
• • • We do not use the following data for averages, fits, limits, etc. • • •					
4.529±0.032	3.2M	[7] FORD	70	ASPK	
4.496±0.030		[7] FORD	67	CNTR	±

[7] First FORD 70 value is second FORD 70 combined with FORD 67.

$(\Gamma(K^+) - \Gamma(K^-)) / \Gamma(K)$

$K^{\pm} \to \mu^{\pm} \nu_\mu$ RATE DIFFERENCE/AVERAGE

Test of *CPT* conservation.

VALUE (%)	DOCUMENT ID		TECN
−0.54±0.41	FORD	67	CNTR

$K^{\pm} \to \pi^{\pm} \pi^+ \pi^-$ RATE DIFFERENCE/AVERAGE

Test of *CP* conservation.

VALUE (%)	EVTS	DOCUMENT ID		TECN	CHG
0.08±0.12		[8] FORD	70	ASPK	
• • • We do not use the following data for averages, fits, limits, etc. • • •					
−0.02±0.16		[9] SMITH	73	ASPK	±
0.10±0.14	3.2M	[8] FORD	70	ASPK	
−0.50±0.90		FLETCHER	67	OSPK	
−0.04±0.21		[8] FORD	67	CNTR	

[8] First FORD 70 value is second FORD 70 combined with FORD 67.
[9] SMITH 73 value of $K^{\pm} \to \pi^{\pm} \pi^+ \pi^-$ rate difference is derived from SMITH 73 value of $K^{\pm} \to \pi^{\pm} 2\pi^0$ rate difference.

$K^{\pm} \to \pi^{\pm} \pi^0 \pi^0$ RATE DIFFERENCE/AVERAGE

Test of *CP* conservation.

VALUE (%)	EVTS	DOCUMENT ID		TECN	CHG
0.0 ±0.6 OUR AVERAGE					
0.08±0.58		SMITH	73	ASPK	±
−1.1 ±1.8	1802	HERZO	69	OSPK	

$K^{\pm} \to \pi^{\pm} \pi^0$ RATE DIFFERENCE/AVERAGE

Test of *CPT* conservation.

VALUE (%)	DOCUMENT ID		TECN
0.8±1.2	HERZO	69	OSPK

$K^{\pm} \to \pi^{\pm} \pi^0 \gamma$ RATE DIFFERENCE/AVERAGE

Test of *CP* conservation.

VALUE (%)	EVTS	DOCUMENT ID		TECN	CHG	COMMENT
0.9±3.3 OUR AVERAGE						
0.8±5.8	2461	SMITH	76	WIRE	±	E_π 55–90 MeV
1.0±4.0	4000	ABRAMS	73B	ASPK	±	E_π 51–100 MeV

K^+ BRANCHING RATIOS

Leptonic and semileptonic modes

$\Gamma(e^+ \nu_e)/\Gamma(\mu^+ \nu_\mu)$ Γ_1/Γ_2

See the note on "Decay Constants of Charged Pseudoscalar Mesons" in the D_s^+ Listings.

VALUE (units 10^{-5})	EVTS	DOCUMENT ID		TECN	CHG
2.488±0.009 OUR AVERAGE					
2.488±0.007±0.007	150k	[10] LAZZERONI	13	NA62	±
2.493±0.025±0.019	13.8K	[11] AMBROSINO	09E	KLOE	±
• • • We do not use the following data for averages, fits, limits, etc. • • •					
2.487±0.011±0.007	60k	[12] LAZZERONI	11	NA62	+
2.51 ±0.15	404	HEINTZE	76	SPEC	+
2.37 ±0.17	534	HEARD	75B	SPEC	+
2.42 ±0.42	112	CLARK	72	OSPK	+

[10] LAZZERONI 13 uses full data sample collected from 2007 to 2008. This ratio is defined to be fully inclusive, including internal-bremsstrahlung.
[11] The ratio is defined to include internal-bremsstrahlung, ignoring direct-emission contributions. AMBROSINO 09E determined the ratio from the measurement of $\Gamma(K \to e\nu(\gamma))$, $E_\gamma < 10$ MeV) / $\Gamma(K \to \mu\nu(\gamma))$. 89.8% of $K \to e\nu(\gamma)$ events had $E_\gamma < 10$ MeV.
[12] This ratio is defined to be fully inclusive, including internal-bremsstrahlung.

$\Gamma(\mu^+ \nu_\mu)/\Gamma_{\text{total}}$ Γ_2/Γ

See the note on "Decay Constants of Charged Pseudoscalar Mesons" in the D_s^+ Listings.

VALUE (10^{-2})	EVTS	DOCUMENT ID		TECN	CHG	COMMENT
63.55±0.11 OUR FIT Error includes scale factor of 1.2.						
63.60±0.16 OUR AVERAGE						
63.66±0.09±0.15	865k	[13] AMBROSINO	06A	KLOE	+	
63.24±0.44	62k	CHIANG	72	OSPK	+	1.84 GeV/c K^+

[13] Fully inclusive. Used tagged kaons from ϕ decays.

$\Gamma(\pi^0 e^+ \nu_e)/\Gamma_{\text{total}}$ Γ_3/Γ

VALUE (units 10^{-2})	EVTS	DOCUMENT ID		TECN	CHG	COMMENT
5.07 ±0.04 OUR FIT Error includes scale factor of 2.1.						
4.94 ±0.05 OUR AVERAGE						
4.965±0.038±0.037		[14] AMBROSINO	08A	KLOE	±	
4.86 ±0.10	3516	CHIANG	72	OSPK	+	1.84 GeV/c K^+
• • • We do not use the following data for averages, fits, limits, etc. • • •						
4.7 ±0.3	429	SHAKLEE	64	HLBC	+	
5.0 ±0.5		ROE	61	HLBC	+	

[14] Depends on K^+ lifetime τ. AMBROSINO 08A uses PDG 06 value of $\tau = (1.2385 \pm 0.0024) \times 10^{-8}$ sec. The correlation between K^+_{e3} and $K^+_{\mu 3}$ branching fraction measurements is 62.7%.

$\Gamma(\pi^0 e^+ \nu_e)/\Gamma(\mu^+ \nu_\mu)$ Γ_3/Γ_2

VALUE	EVTS	DOCUMENT ID		TECN	CHG
0.0798±0.0008 OUR FIT Error includes scale factor of 1.9.					
• • • We do not use the following data for averages, fits, limits, etc. • • •					
0.069 ±0.006	350	ZELLER	69	ASPK	+
0.0775±0.0033	960	BOTTERILL	68C	ASPK	+
0.069 ±0.006	561	GARLAND	68	OSPK	+
0.0791±0.0054	295	[15] AUERBACH	67	OSPK	+

[15] AUERBACH 67 changed from 0.0797 ± 0.0054. See comment with ratio $\Gamma(\pi^0 \mu^+ \nu_\mu)/\Gamma(\mu^+ \nu_\mu)$. The value 0.0785 ± 0.0025 given in AUERBACH 67 is an average of AUERBACH 67 $\Gamma(\pi^0 e^+ \nu_e)/\Gamma(\mu^+ \nu_\mu)$ and CESTER 66 $\Gamma(\pi^0 e^+ \nu_e)/\left[\Gamma(\mu^+ \nu_\mu) + \Gamma(\pi^+ \pi^0)\right]$.

$\Gamma(\pi^0 e^+ \nu_e)/\left[\Gamma(\mu^+ \nu_\mu) + \Gamma(\pi^+ \pi^0)\right]$ $\Gamma_3/(\Gamma_2+\Gamma_9)$

VALUE (10^{-2})	EVTS	DOCUMENT ID		TECN	CHG
6.02±0.06 OUR FIT Error includes scale factor of 2.1.					
6.02±0.15 OUR AVERAGE					
6.16±0.22	5110	ESCHSTRUTH	68	OSPK	+
5.89±0.21	1679	CESTER	66	OSPK	+
• • • We do not use the following data for averages, fits, limits, etc. • • •					
5.92±0.65		[16] WEISSENBE...	76	SPEC	+

[16] Value calculated from WEISSENBERG 76 ($\pi^0 e\nu$), ($\mu\nu$), and ($\pi\pi^0$) values to eliminate dependence on our 1974 ($\pi 2\pi^0$) and ($\pi\pi^+\pi^-$) fractions.

$\Gamma(\pi^0 e^+ \nu_e)/\left[\Gamma(\pi^0 \mu^+ \nu_\mu) + \Gamma(\pi^+ \pi^0) + \Gamma(\pi^+ \pi^0 \pi^0)\right]$ $\Gamma_3/(\Gamma_4+\Gamma_9+\Gamma_{10})$

VALUE	EVTS	DOCUMENT ID		TECN	CHG
0.1968±0.0016 OUR FIT Error includes scale factor of 2.4.					
0.1962±0.0008±0.0035	71k	SHER	03	B865	+

Meson Particle Listings

$K^{\pm}$

$\Gamma(\pi^0 e^+ \nu_e)/\Gamma(\pi^+ \pi^0)$ Γ_3/Γ_9

VALUE	EVTS	DOCUMENT ID		TECN	CHG	COMMENT
0.2455±0.0023 OUR FIT Error includes scale factor of 2.6.						
0.2470±0.0009±0.0004	87k	BATLEY	07A	NA48	±	
• • • We do not use the following data for averages, fits, limits, etc. • • •						
0.221 ±0.012	786	[17] LUCAS	73B	HBC	−	Dalitz pairs only

[17] LUCAS 73B gives N(K_{e3}) = 786 ± 3.1%, N(2π) = 3564 ± 3.1%. We use these values to obtain quoted result.

$\Gamma(\pi^0 e^+ \nu_e)/\Gamma(\pi^+ \pi^+ \pi^-)$ Γ_3/Γ_{11}

VALUE	EVTS	DOCUMENT ID		TECN	CHG
0.907±0.010 OUR FIT Error includes scale factor of 1.6.					
• • • We do not use the following data for averages, fits, limits, etc. • • •					
0.867±0.027	2768	BARMIN	87	XEBC	+
0.856±0.040	2827	BRAUN	75	HLBC	+
0.850±0.019	4385	[18] HAIDT	71	HLBC	+
0.846±0.021	4385	[18] EICHTEN	68	HLBC	+
0.94 ±0.09	854	BELLOTTI	67B	HLBC	
0.90 ±0.06	230	BORREANI	64	HBC	+

[18] HAIDT 71 is a reanalysis of EICHTEN 68. Not included in average because of large discrepancy in $\Gamma(\pi^0 \mu^+ \nu)/\Gamma(\pi^0 e^+ \nu)$ with more precise results.

$\Gamma(\pi^0 \mu^+ \nu_\mu)/\Gamma_{\text{total}}$ Γ_4/Γ

VALUE (units 10^{-2})	EVTS	DOCUMENT ID		TECN	CHG	COMMENT
3.353±0.034 OUR FIT Error includes scale factor of 1.8.						
3.24 ±0.04 OUR AVERAGE						
3.233±0.029±0.026		[19] AMBROSINO	08A	KLOE	±	
3.33 ±0.16	2345	CHIANG	72	OSPK	+	1.84 GeV/c K^+
• • • We do not use the following data for averages, fits, limits, etc. • • •						
2.8 ±0.4		[20] TAYLOR	59	EMUL	+	

[19] Depends on K^+ lifetime τ. AMBROSINO 08A uses PDG 06 value of $\tau = (1.2385 \pm 0.0024) \times 10^{-8}$ sec. The correlation between K^+_{e3} and $K^+_{\mu 3}$ branching fraction measurements is 62.7%.

[20] Earlier experiments not averaged.

$\Gamma(\pi^0 \mu^+ \nu_\mu)/\Gamma(\mu^+ \nu_\mu)$ Γ_4/Γ_2

VALUE	EVTS	DOCUMENT ID		TECN	CHG
0.0528±0.0006 OUR FIT Error includes scale factor of 1.8.					
• • • We do not use the following data for averages, fits, limits, etc. • • •					
0.054 ±0.009	240	ZELLER	69	ASPK	+
0.0480±0.0037	424	[21] GARLAND	68	OSPK	+
0.0486±0.0040	307	[22] AUERBACH	67	OSPK	+

[21] GARLAND 68 changed from 0.055 ± 0.004 in agreement with μ-spectrum calculation of GAILLARD 70 appendix B. L.G.Pondrom, (private communication 73).

[22] AUERBACH 67 changed from 0.0602 ± 0.0046 by erratum which brings the μ-spectrum calculation into agreement with GAILLARD 70 appendix B.

$\Gamma(\pi^0 \mu^+ \nu_\mu)/\Gamma(\pi^0 e^+ \nu_e)$ Γ_4/Γ_3

VALUE	EVTS	DOCUMENT ID		TECN	CHG	COMMENT
0.6608±0.0030 OUR FIT Error includes scale factor of 1.1.						
0.6618±0.0027 OUR AVERAGE						
0.663 ±0.003 ±0.001	77k	BATLEY	07A	NA48	±	
0.671 ±0.007 ±0.008	24k	HORIE	01	SPEC		
0.670 ±0.014		[23] HEINTZE	77	SPEC	+	
0.667 ±0.017	5601	BOTTERILL	68B	ASPK	+	
• • • We use the following data for averages but not for fits. • • •						
0.6511±0.0064		[24] AMBROSINO	08A	KLOE	±	
• • • We do not use the following data for averages, fits, limits, etc. • • •						
0.608 ±0.014	1585	[25] BRAUN	75	HLBC	+	
0.705 ±0.063	554	[26] LUCAS	73B	HBC	−	Dalitz pairs only
0.698 ±0.025	3480	[27] CHIANG	72	OSPK	+	1.84 GeV/c K^+
0.596 ±0.025		[28] HAIDT	71	HLBC	+	
0.604 ±0.022	1398	[28] EICHTEN	68	HLBC		
0.703 ±0.056	1509	CALLAHAN	66B	HLBC		

[23] HEINTZE 77 value from fit to λ_0. Assumes μ-e universality.

[24] Not used in the fit. This result enters the fit via correlation of K^+_{e3} and $K^+_{\mu 3}$ branching fraction measurements of AMBROSINO 08A.

[25] BRAUN 75 value is from form factor fit. Assumes μ-e universality.

[26] LUCAS 73B gives N($K_{\mu 3}$) = 554 ± 7.6%, N(K_{e3}) = 786 ± 3.1%. We divide.

[27] CHIANG 72 $\Gamma(\pi^0 \mu^+ \nu_\mu)/\Gamma(\pi^0 e^+ \nu_e)$ is statistically independent of CHIANG 72 $\Gamma(\pi^0 \mu^+ \nu_\mu)/\Gamma_{\text{total}}$ and $\Gamma(\pi^0 e^+ \nu_e)/\Gamma_{\text{total}}$.

[28] HAIDT 71 is a reanalysis of EICHTEN 68. Not included in average because of large discrepancy with more precise results.

$[\Gamma(\pi^0 \mu^+ \nu_\mu) + \Gamma(\pi^+ \pi^0)]/\Gamma_{\text{total}}$ $(\Gamma_4+\Gamma_9)/\Gamma$

We combine these two modes for experiments measuring them in xenon bubble chamber because of difficulties of separating them there.

VALUE (units 10^{-2})	EVTS	DOCUMENT ID	TECN	CHG
24.02±0.08 OUR FIT Error includes scale factor of 1.2.				
• • • We do not use the following data for averages, fits, limits, etc. • • •				
25.4 ±0.9	886	SHAKLEE	64	HLBC +
23.4 ±1.1		ROE	61	HLBC +

$\Gamma(\pi^0 \mu^+ \nu_\mu)/\Gamma(\pi^+ \pi^0)$ Γ_4/Γ_9

VALUE	EVTS	DOCUMENT ID		TECN	CHG
0.1637±0.0006±0.0003	77k	BATLEY	07A	NA48	±

$\Gamma(\pi^0 \mu^+ \nu_\mu)/\Gamma(\pi^+ \pi^+ \pi^-)$ Γ_4/Γ_{11}

VALUE	EVTS	DOCUMENT ID		TECN	CHG	COMMENT
0.599±0.007 OUR FIT Error includes scale factor of 1.6.						
• • • We do not use the following data for averages, fits, limits, etc. • • •						
0.503±0.019	1505	[29] HAIDT	71	HLBC	+	
0.510±0.017	1505	[29] EICHTEN	68	HLBC	+	
0.63 ±0.07	2845	[30] BISI	65B	BC	+	HBC+HLBC

[29] HAIDT 71 is a reanalysis of EICHTEN 68. Not included in average because of large discrepancy in $\Gamma(\pi^0 \mu^+ \nu)/\Gamma(\pi^0 e^+ \nu)$ with more precise results.

[30] Error enlarged for background problems. See GAILLARD 70.

$\Gamma(\pi^0 \pi^0 e^+ \nu_e)/\Gamma_{\text{total}}$ Γ_5/Γ

VALUE (units 10^{-5})	EVTS	DOCUMENT ID		TECN	CHG
2.2 ±0.4 OUR FIT					
2.54±0.89	10	BARMIN	88B	HLBC	+

$\Gamma(\pi^0 \pi^0 e^+ \nu_e)/\Gamma(\pi^0 e^+ \nu_e)$ Γ_5/Γ_3

VALUE (units 10^{-4})	EVTS	DOCUMENT ID		TECN	CHG
$4.3^{+0.9}_{-0.7}$ OUR FIT					
$4.1^{+1.0}_{-0.7}$ OUR AVERAGE					
$4.2^{+1.0}_{-0.9}$	25	BOLOTOV	86B	CALO	−
$3.8^{+5.0}_{-1.2}$	2	LJUNG	73	HLBC	+

$\Gamma(\pi^+ \pi^- e^+ \nu_e)/\Gamma(\pi^+ \pi^+ \pi^-)$ Γ_6/Γ_{11}

VALUE (units 10^{-4})	EVTS	DOCUMENT ID		TECN	CHG
7.606±0.029 OUR AVERAGE					
7.615±0.008±0.028	1.1M	[31] BATLEY	12	NA48	±
7.35 ±0.01 ±0.19	388k	[32] PISLAK	01	B865	
7.21 ±0.32	30k	ROSSELET	77	SPEC	+
• • • We do not use the following data for averages, fits, limits, etc. • • •					
7.36 ±0.68	500	BOURQUIN	71	ASPK	
7.0 ±0.9	106	SCHWEINB...	71	HLBC	+
5.83 ±0.63	269	ELY	69	HLBC	+

[31] BATLEY 12 uses data collected in 2003–2004. The result is inclusive of $K^{\pm} \to \pi^+ \pi^- e^{\pm} \nu \gamma$ decays. Using PDG 12 value for $\Gamma(\pi^+ \pi^- \pi^+)/\Gamma = (5.59 \pm 0.04) \times 10^{-2}$. BATLEY 12 obtains $B(\pi^+ \pi^- e \nu) = (4.257 \pm 0.004 \pm 0.035) \times 10^{-5}$ where the syst. error is dominated by the error on the normalization mode.

[32] PISLAK 01 reports $\Gamma(\pi^+ \pi^- e^+ \nu_e)/\Gamma_{\text{total}} = (4.109 \pm 0.008 \pm 0.110) \times 10^{-5}$ using the PDG 00 value $\Gamma(\pi^+ \pi^+ \pi^-)/\Gamma_{\text{total}} = (5.59 \pm 0.05) \times 10^{-2}$. We divide by the PDG value and unfold its error from the systematic error. PISLAK 03 and PISLAK 10A give additional details on the branching ratio measurement and give improved errors on the S-wave π-π scattering length: $a_0^0 = 0.235 \pm 0.013$ and $a_0^2 = -0.0410 \pm 0.0027$.

$\Gamma(\pi^+ \pi^- \mu^+ \nu_\mu)/\Gamma_{\text{total}}$ Γ_7/Γ

VALUE (units 10^{-5})	EVTS	DOCUMENT ID		TECN	CHG
• • • We do not use the following data for averages, fits, limits, etc. • • •					
$0.77^{+0.54}_{-0.50}$	1	CLINE	65	FBC	+

$\Gamma(\pi^+ \pi^- \mu^+ \nu_\mu)/\Gamma(\pi^+ \pi^+ \pi^-)$ Γ_7/Γ_{11}

VALUE (units 10^{-4})	EVTS	DOCUMENT ID		TECN	CHG
2.57±1.55	7	BISI	67	DBC	+
• • • We do not use the following data for averages, fits, limits, etc. • • •					
~ 2.5	1	GREINER	64	EMUL	+

$\Gamma(\pi^0 \pi^0 \pi^0 e^+ \nu_e)/\Gamma_{\text{total}}$ Γ_8/Γ

VALUE (units 10^{-6})	CL%	EVTS	DOCUMENT ID		TECN	CHG
<3.5	90	0	BOLOTOV	88	SPEC	−
• • • We do not use the following data for averages, fits, limits, etc. • • •						
<9	90	0	BARMIN	92	XEBC	+

Hadronic modes

$\Gamma(\pi^+ \pi^0)/\Gamma_{\text{total}}$ Γ_9/Γ

VALUE (units 10^{-2})	EVTS	DOCUMENT ID		TECN	CHG	COMMENT
20.66±0.08 OUR FIT Error includes scale factor of 1.2.						
20.70±0.16 OUR AVERAGE Error includes scale factor of 1.8.						
20.65±0.05±0.08	1.4M	[33] AMBROSINO	08E	KLOE	+	$\phi \to K^+ K^-$
21.18±0.28	16k	CHIANG	72	OSPK	+	1.84 GeV/c K^+
• • • We do not use the following data for averages, fits, limits, etc. • • •						
21.0 ±0.6		CALLAHAN	65	HLBC		See Γ_9/Γ_{11}

[33] Fully inclusive of final-state radiation. The branching ratio is evaluated using K^+ lifetime, $\tau = 12.385$ ns.

$\Gamma(\pi^+\pi^0)/\Gamma(\pi^+\pi^+\pi^-)$ Γ_9/Γ_{11}

VALUE	EVTS	DOCUMENT ID		TECN	CHG
3.694±0.029 OUR FIT Error includes scale factor of 1.2.					
• • • We do not use the following data for averages, fits, limits, etc. • • •					
3.96 ±0.15	1045	CALLAHAN	66	FBC	+

$\Gamma(\pi^+\pi^0)/\Gamma(\mu^+\nu_\mu)$ Γ_9/Γ_2

VALUE	EVTS	DOCUMENT ID		TECN	CHG	COMMENT
0.3252±0.0016 OUR FIT Error includes scale factor of 1.2.						
0.3325±0.0032 OUR AVERAGE						
0.3329±0.0047±0.0010	45k	USHER	92	SPEC	+	$p\overline{p}$ at rest
0.3355±0.0057		[34] WEISSENBE...	76	SPEC	+	
0.3277±0.0065	4517	[35] AUERBACH	67	OSPK	+	
• • • We do not use the following data for averages, fits, limits, etc. • • •						
0.328 ±0.005	25k	[34] WEISSENBE...	74	STRC	+	
0.305 ±0.018	1600	ZELLER	69	ASPK	+	

[34] WEISSENBERG 76 revises WEISSENBERG 74.
[35] AUERBACH 67 changed from 0.3253 ± 0.0065. See comment with ratio $\Gamma(\pi^0\mu^+\nu_\mu)/\Gamma(\mu^+\nu_\mu)$.

$\Gamma(\pi^+\pi^0\pi^0)/\Gamma_{total}$ Γ_{10}/Γ

VALUE (units 10^{-2})	EVTS	DOCUMENT ID		TECN	CHG	COMMENT
1.761±0.022 OUR FIT Error includes scale factor of 1.1.						
1.775±0.028 OUR AVERAGE Error includes scale factor of 1.2.						
1.763±0.013±0.022		ALOISIO	04A	KLOE	±	
1.84 ±0.06	1307	CHIANG	72	OSPK	+	1.84 GeV/c K^+
• • • We do not use the following data for averages, fits, limits, etc. • • •						
1.53 ±0.11	198	[36] PANDOULAS	70	EMUL	+	
1.8 ±0.2	108	SHAKLEE	64	HLBC	+	
1.7 ±0.2		ROE	61	HLBC	+	
1.5 ±0.2		[37] TAYLOR	59	EMUL	+	

[36] Includes events of TAYLOR 59.
[37] Earlier experiments not averaged.

$\Gamma(\pi^+\pi^0\pi^0)/\Gamma(\pi^+\pi^0)$ Γ_{10}/Γ_9

VALUE	EVTS	DOCUMENT ID		TECN	CHG	COMMENT
0.0852±0.0011 OUR FIT Error includes scale factor of 1.1.						
• • • We do not use the following data for averages, fits, limits, etc. • • •						
0.081 ±0.005	574	[38] LUCAS	73B	HBC	−	Dalitz pairs only

[38] LUCAS 73B gives $N(\pi 2\pi^0) = 574 \pm 5.9\%$, $N(2\pi) = 3564 \pm 3.1\%$. We quote $0.5N(\pi 2\pi^0)/N(2\pi)$ where 0.5 is because only Dalitz pair π^0's were used.

$\Gamma(\pi^+\pi^0\pi^0)/\Gamma(\pi^+\pi^+\pi^-)$ Γ_{10}/Γ_{11}

VALUE	EVTS	DOCUMENT ID		TECN	CHG	COMMENT
0.315±0.004 OUR FIT Error includes scale factor of 1.1.						
0.303±0.009	2027	BISI	65	BC	+	HBC+HLBC
• • • We do not use the following data for averages, fits, limits, etc. • • •						
0.393±0.099	17	YOUNG	65	EMUL	+	

$\Gamma(\pi^+\pi^+\pi^-)/\Gamma_{total}$ Γ_{11}/Γ

VALUE (units 10^{-2})	EVTS	DOCUMENT ID		TECN	CHG	COMMENT
5.59±0.04 OUR FIT Error includes scale factor of 1.3.						
• • • We do not use the following data for averages, fits, limits, etc. • • •						
5.56±0.20	2330	[39] CHIANG	72	OSPK	+	1.84 GeV/c K^+
5.34±0.21	693	[40] PANDOULAS	70	EMUL	+	
5.71±0.15		DEMARCO	65	HBC		
6.0 ±0.4	44	YOUNG	65	EMUL	+	
5.54±0.12	2332	CALLAHAN	64	HLBC	+	
5.1 ±0.2	540	SHAKLEE	64	HLBC	+	
5.7 ±0.3		ROE	61	HLBC	+	

[39] Value is not independent of CHIANG 72 $\Gamma(\mu^+\nu_\mu)/\Gamma_{total}$, $\Gamma(\pi^+\pi^0)/\Gamma_{total}$, $\Gamma(\pi^+\pi^0\pi^0)/\Gamma_{total}$, $\Gamma(\pi^0\mu^+\nu_\mu)/\Gamma_{total}$, and $\Gamma(\pi^0 e^+\nu_e)/\Gamma_{total}$.
[40] Includes events of TAYLOR 59.

Leptonic and semileptonic modes with photons

$\Gamma(\mu^+\nu_\mu\gamma)/\Gamma_{total}$ Γ_{12}/Γ

VALUE (units 10^{-3})	EVTS	DOCUMENT ID		TECN	CHG	COMMENT
6.2±0.8 OUR AVERAGE						
6.6±1.5		[41,42] DEMIDOV	90	XEBC		$P(\mu)$ <231.5 MeV/c
6.0±0.9		BARMIN	88	HLBC	+	$P(\mu)$ <231.5 MeV/c
• • • We do not use the following data for averages, fits, limits, etc. • • •						
3.5±0.8		[42,43] DEMIDOV	90	XEBC		$E(\gamma) > 20$ MeV
3.2±0.5	57	[44] BARMIN	88	HLBC	+	$E(\gamma)$ >20 MeV
5.4±0.3		[45] AKIBA	85	SPEC		$P(\mu)$ <231.5 MeV/c

[41] $P(\mu)$ cut given in DEMIDOV 90 paper, 235.1 MeV/c, is a misprint according to authors (private communication).
[42] DEMIDOV 90 quotes only inner bremsstrahlung (IB) part.
[43] Not independent of above DEMIDOV 90 value. Cuts differ.
[44] Not independent of above BARMIN 88 value. Cuts differ.
[45] Assumes μ-e universality and uses constraints from $K \to e\nu\gamma$.

$\Gamma(\mu^+\nu_\mu\gamma(SD^+))/\Gamma_{total}$ Γ_{13}/Γ

Structure-dependent part with $+\gamma$ helicity (SD^+ term). See the "Note on $\pi^\pm \to \ell^\pm\nu\gamma$ and $K^\pm \to \ell^\pm\nu\gamma$ Form Factors" in the $\pi^\pm$ section of the Particle Data Listings above.

VALUE (units 10^{-5})	CL%	EVTS	DOCUMENT ID		TECN
1.33±0.12±0.18		2588	[46] ADLER	00B	B787
• • • We do not use the following data for averages, fits, limits, etc. • • •					
<3.0	90		AKIBA	85	SPEC

[46] ADLER 00B obtains the branching ratio by extrapolating the measurement in the kinematic region $E_\mu > 137$ MeV, $E_\gamma > 90$ MeV to the full SD^+ phase-space. Also reports $|F_V + F_A| = 0.165 \pm 0.007 \pm 0.011$ and $-0.04 < F_V - F_A < 0.24$ at 90% CL.

$\Gamma(\mu^+\nu_\mu\gamma(SD^+INT))/\Gamma_{total}$ Γ_{14}/Γ

Interference term between internal Bremsstrahlung and SD^+ term. See the "Note on $\pi^\pm \to \ell^\pm\nu\gamma$ and $K^\pm \to \ell^\pm\nu\gamma$ Form Factors" in the $\pi^\pm$ section of the Particle Data Listings above.

VALUE (units 10^{-5})	CL%	DOCUMENT ID		TECN
<2.7	90	AKIBA	85	SPEC

$\Gamma(\mu^+\nu_\mu\gamma(SD^- + SD^-INT))/\Gamma_{total}$ Γ_{15}/Γ

Sum of structure-dependent part with $-\gamma$ helicity (SD^- term) and interference term between internal Bremsstrahlung and SD^- term. See the "Note on $\pi^\pm \to \ell^\pm\nu\gamma$ and $K^\pm \to \ell^\pm\nu\gamma$ Form Factors" in the $\pi^\pm$ section of the Particle Data Listings above.

VALUE (units 10^{-4})	CL%	DOCUMENT ID		TECN
<2.6	90	[47] AKIBA	85	SPEC

[47] Assumes μ-e universality and uses constraints from $K \to e\nu\gamma$.

$\Gamma(e^+\nu_e\gamma)/\Gamma(\mu^+\nu_\mu)$ Γ_{16}/Γ_2

VALUE (units 10^{-5})	EVTS	DOCUMENT ID		TECN	CHG	COMMENT
1.483±0.066±0.013	1.4K	[48] AMBROSINO	09E	KLOE	±	E_γ in 10–250 MeV, $p_e > 200$ MeV/c

[48] AMBROSINO 09E measured the differential width $dR_\gamma/dE_\gamma = (1/\Gamma(K \to \mu\nu))(d\Gamma(K \to e\nu\gamma)/dE_\gamma)$. Result obtained by integrating the differential width over E_γ from 10 to 250 MeV.

$\Gamma(\pi^0 e^+\nu_e\gamma)/\Gamma(\pi^0 e^+\nu_e)$ Γ_{17}/Γ_3

VALUE (units 10^{-2})	EVTS	DOCUMENT ID		TECN	CHG	COMMENT
0.505±0.032 OUR AVERAGE Error includes scale factor of 1.3. See the ideogram below.						
0.47 ±0.02 ±0.03	4476	[49] AKIMENKO	07	ISTR	−	$E_\gamma > 10$ MeV, $0.6 < \cos(\theta_{e\gamma}) < 0.9$
0.46 ±0.08	82	[50] BARMIN	91	XEBC		$E_\gamma > 10$ MeV, $0.6 < \cos(\theta_{e\gamma}) < 0.9$
0.56 ±0.04	192	[51] BOLOTOV	86B	CALO	−	$E_\gamma > 10$ MeV
• • • We do not use the following data for averages, fits, limits, etc. • • •						
1.81 ±0.03 ±0.07	4476	[49] AKIMENKO	07	ISTR	−	E_γ>10 MeV, $\theta_{e\gamma}$ >10°
0.63 ±0.02 ±0.03	4476	[49] AKIMENKO	07	ISTR	−	E_γ>30 MeV, $\theta_{e\gamma}$ >20°
1.51 ±0.25	82	[50] BARMIN	91	XEBC		$E_\gamma > 10$ MeV, $\cos(\theta_{e\gamma}) < 0.98$
0.48 ±0.20	16	[52] LJUNG	73	HLBC	+	$E_\gamma > 30$ MeV
0.22 $^{+0.15}_{-0.10}$		[52] LJUNG	73	HLBC	+	$E_\gamma > 30$ MeV
0.76 ±0.28	13	[53] ROMANO	71	HLBC		$E_\gamma > 10$ MeV
0.53 ±0.22		[53] ROMANO	71	HLBC	+	$E_\gamma > 30$ MeV
1.2 ±0.8		BELLOTTI	67	HLBC		$E_\gamma > 30$ MeV

[49] AKIMENKO 07 provides values for three kinematic regions. For averaging, we use value with $E_\gamma > 10$ MeV and $0.6 < \cos(\theta_{e\gamma}) < 0.9$.
[50] BARMIN 91 quotes branching ratio $\Gamma(K \to e\pi^0\nu\gamma)/\Gamma_{all}$. The measured normalization is $[\Gamma(K \to e\pi^0\nu) + \Gamma(K \to \pi^+\pi^+\pi^-)]$. For comparison with other experiments we used $\Gamma(K \to e\pi^0\nu)/\Gamma_{all} = 0.0482$ to calculate the values quoted here.
[51] $\cos(\theta_{e\gamma})$ between 0.6 and 0.9.
[52] First LJUNG 73 value is for $\cos(\theta_{e\gamma}) < 0.9$, second value is for $\cos(\theta_{e\gamma})$ between 0.6 and 0.9 for comparison with ROMANO 71.
[53] Both ROMANO 71 values are for $\cos(\theta_{e\gamma})$ between 0.6 and 0.9. Second value is for comparison with second LJUNG 73 value. We use lowest E_γ cut for Summary Table value. See ROMANO 71 for E_γ dependence.

Meson Particle Listings

$K^{\pm}$

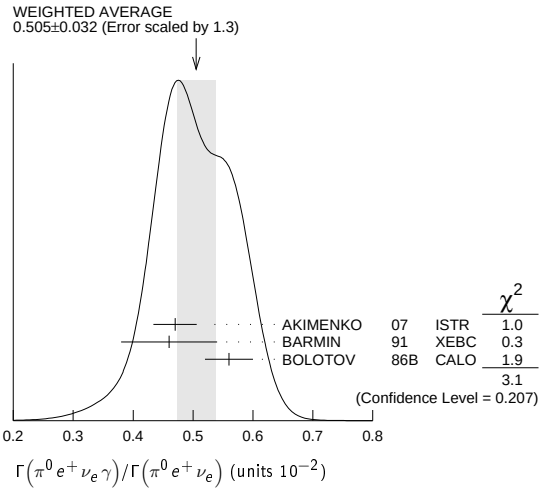

$\Gamma(\pi^0 e^+ \nu_e \gamma(\mathrm{SD}))/\Gamma_{\mathrm{total}}$ Γ_{18}/Γ

Structure-dependent part.

VALUE (units 10^{-5})	CL%	DOCUMENT ID		TECN	CHG
<5.3	90	BOLOTOV	86B	CALO	−

$\Gamma(\pi^0 \mu^+ \nu_\mu \gamma)/\Gamma_{\mathrm{total}}$ Γ_{19}/Γ

VALUE (units 10^{-5})	CL%	EVTS	DOCUMENT ID		TECN	CHG	COMMENT
1.25±0.25 OUR AVERAGE							
1.10±0.32±0.05		23	[54] ADLER	10	B787		$30 < E_\gamma < 60$ MeV
1.46±0.22±0.32		153	[55] TCHIKILEV	07	ISTR	−	$30 < E_\gamma < 60$ MeV
• • • We do not use the following data for averages, fits, limits, etc. • • •							
2.4 ±0.5 ±0.6		125	SHIMIZU	06	K470	+	$E_\gamma > 30$ MeV; $\Theta_{\mu\gamma} > 20^\circ$
<6.1	90	0	LJUNG	73	HLBC	+	$E(\gamma) > 30$ MeV

[54] Value obtained from $B(K^+ \to \pi^0 \mu^+ \nu_\mu \gamma) = (2.51 \pm 0.74 \pm 0.12) \times 10^{-5}$ obtained in the kinematic region $E_\gamma > 20$ MeV, and then theoretical $K_{\mu 3\gamma}$ spectrum has been used. Also $B(K^+ \to \pi^0 \mu^+ \nu_\mu \gamma) = (1.58 \pm 0.46 \pm 0.08) \times 10^{-5}$, for $E_\gamma > 30$ MeV and $\theta_{\mu\gamma} > 20^\circ$, was determined.

[55] Obtained from measuring $B(K_{\mu 3\gamma})$ / $B(K_{\mu 3})$ and using PDG 02 value $B(K_{\mu 3}) = 3.27\%$. $B(K_{\mu 3\gamma}) = (8.82 \pm 0.94 \pm 0.86) \times 10^{-5}$ is obtained for 5 MeV $< E_\gamma <$ 30 MeV.

$\Gamma(\pi^0 \pi^0 e^+ \nu_e \gamma)/\Gamma_{\mathrm{total}}$ Γ_{20}/Γ

VALUE (units 10^{-6})	CL%	EVTS	DOCUMENT ID		TECN	CHG	COMMENT
<5	90	0	BARMIN	92	XEBC	+	$E_\gamma > 10$ MeV

Hadronic modes with photons

$\Gamma(\pi^+ \pi^0 \gamma(\mathrm{INT}))/\Gamma_{\mathrm{total}}$ Γ_{21}/Γ

The $K^+ \to \pi^+ \pi^0 \gamma$ differential decay rate can be described in terms of T_{π^+}, the charged pion kinetic energy, and $W^2 = (P_K \cdot P_\gamma)(P_{\pi^+} \cdot P_\gamma) / (m_K m_{\pi^+})^2$; then we can write $d^2\Gamma(K^+ \to \pi^+ \pi^0 \gamma) / (dT_{\pi^+} dW^2) = d^2\Gamma(K^+ \to \pi^+ \pi^0 \gamma)_{IB} / (dT_{\pi^+} dW^2)$ [1 + 2 cos(±φ + $\delta_1^1 - \delta_0^2$) $m_\pi^2 m_K^2 W^2 X_E + m_\pi^4 m_K^4 (X_E^2 + X_M^2) W^4$]. The IB differential and total branching ratios are expressed in terms of the non-radiative experimental width $\Gamma(K^+ \to \pi^+ \pi^0)$ by Low's theorem. Using PDG 10 $B(K^+ \to \pi^+ \pi^0) = 0.2066 \pm 0.0008$, one obtains respectively $B(K^+ \to \pi^+ \pi^0 \gamma)_{IB}$ ($55 < T_{\pi^+} < 90$ MeV)$= 2.55 \times 10^{-4}$ and $B(K^+ \to \pi^+ \pi^0 \gamma)_{IB}$ ($0 < T_{\pi^+} < 80$ MeV)$= 1.80 \times 10^{-4}$. Fitting respectively the piece proportional to W^2 and the piece proportional to W^4, the interference contribution (INT), proportional to X_E, and the direct contribution (DE) proportional to $X_E^2 + X_M^2$ are extracted.

VALUE (units 10^{-6})	EVTS	DOCUMENT ID		TECN	CHG	COMMENT
−4.24±0.63±0.70	600k	[56] BATLEY	10A	NA48	±	T_{π^+} 0–80 MeV

[56] The cut on the photon energy implies $W^2 > 0.2$. BATLEY 10A obtains the INT and DE fractional branchings with respect to IB from a simultaneous kinematical fit of INT and DE and then we use the PDG 10 value for $B(K^+ \to \pi^+ \pi^0) = 20.66 \pm 0.08$ to determine the IB. The INT and DE correlation coefficients −0.83. Assuming a constant electric amplitude, X_E, this INT value implies $X_E = -24 \pm 6$ GeV^{-4}.

$\Gamma(\pi^+ \pi^0 \gamma(\mathrm{DE}))/\Gamma_{\mathrm{total}}$ Γ_{22}/Γ

Direct emission (DE) part of $\Gamma(\pi^+ \pi^0 \gamma)/\Gamma_{\mathrm{total}}$, assuming that interference (INT) component is zero.

VALUE (units 10^{-6})	EVTS	DOCUMENT ID		TECN	CHG	COMMENT
5.99±0.27±0.25	600k	[57] BATLEY	10A	NA48	±	T_{π^+} 0–80 MeV
• • • We do not use the following data for averages, fits, limits, etc. • • •						
3.8 ±0.8 ±0.7	10k	ALIEV	06	K470	+	T_{π^+} 55–90 MeV
3.7 ±3.9 ±1.0	930	UVAROV	06	ISTR	−	T_{π^-} 55–90 MeV
3.2 ±1.3 ±1.0	4k	ALIEV	03	K470	+	T_{π^+} 55–90 MeV
6.1 ±2.5 ±1.9	4k	ALIEV	03	K470	+	T_{π^+} full range
4.7 ±0.8 ±0.3	20k	[58] ADLER	00C	B787	+	T_{π^+} 55–90 MeV
20.5 ±4.6 $^{+3.9}_{-2.3}$		BOLOTOV	87	WIRE	−	T_{π^-} 55–90 MeV
15.6 ±3.5 ±5.0		ABRAMS	72	ASPK	±	$T_{\pi^\pm}$ 55–90 MeV

[57] The cut on the photon energy implies $W^2 > 0.2$. BATLEY 10A obtains the INT and DE fractional branchings with respect to IB from a simultaneous kinematical fit of INT and DE and then we use the PDG 10 value for $B(K^+ \to \pi^+ \pi^0) = 20.66 \pm 0.08$ to determine the IB. The INT and DE correlation coefficients −0.93. Assuming constant electric and magnetic amplitudes, X_E and X_M, these INTand DE values imply $X_E = -24 \pm 6$ GeV^{-4} and $X_M = -254 \pm 9$ GeV^{-4}.

[58] ADLER 00C measures the INT component to be $(-0.4 \pm 1.6)\%$ of the inner bremsstrahlung (IB) component.

$\Gamma(\pi^+ \pi^0 \pi^0 \gamma)/\Gamma(\pi^+ \pi^0 \pi^0)$ Γ_{23}/Γ_{10}

VALUE (units 10^{-4})	DOCUMENT ID		TECN	CHG	COMMENT
4.3 $^{+3.2}_{-1.7}$	BOLOTOV	85	SPEC	−	$E(\gamma) > 10$ MeV

$\Gamma(\pi^+ \pi^+ \pi^- \gamma)/\Gamma_{\mathrm{total}}$ Γ_{24}/Γ

VALUE (units 10^{-4})	EVTS	DOCUMENT ID		TECN	CHG	COMMENT
1.04±0.31 OUR AVERAGE						
1.10±0.48	7	BARMIN	89	XEBC		$E(\gamma) > 5$ MeV
1.0 ±0.4		STAMER	65	EMUL	+	$E(\gamma) > 11$ MeV

$\Gamma(\pi^+ \gamma\gamma)/\Gamma_{\mathrm{total}}$ Γ_{25}/Γ

VALUE (units 10^{-7})	CL%	EVTS	DOCUMENT ID		TECN	CHG	COMMENT
9.2 ±0.7 OUR AVERAGE							
9.10±0.72±0.22		149	[59] BATLEY	14	NA48	±	
11 ±3 ±1		31	[60] KITCHING	97	B787	+	
• • • We do not use the following data for averages, fits, limits, etc. • • •							
< 0.083	90		[61] ARTAMONOV	05	B949	+	$P_\pi > 213$ MeV/c
< 10	90	0	ATIYA	90B	B787	+	$T\pi$ 117–127 MeV
< 84	90	0	ASANO	82	CNTR	+	$T\pi$ 117–127 MeV
−420 ± 520		0	ABRAMS	77	SPEC	+	$T\pi < 92$ MeV
< 350	90	0	LJUNG	73	HLBC	+	6–102, 114–127 MeV
< 500	90	0	KLEMS	71	OSPK	+	$T\pi < 117$ MeV
−100 ± 600			CHEN	68	OSPK	+	$T\pi$ 60–90 MeV

[59] BATLEY 14 uses data collected in 2003 and 2004. Branching ratio is obtained by determining the parameter $\hat{c} = 1.41 \pm 0.38 \pm 0.11$ and integrating the $\mathcal{O}(p^6)$ chiral spectrum. A model independent value for the branching ratio is also obtained $(8.77 \pm 0.87 \pm 0.17) \times 10^{-7}$ for kinematic range $(m_{\gamma\gamma}/m_K)^2 > 0.2$.

[60] KITCHING 97 is extrapolated from their model-independent branching fraction $(6.0 \pm 1.5 \pm 0.7) \times 10^{-7}$ for 100 MeV/c<P_{π^+} < 180 MeV/c using Chiral Perturbation Theory.

[61] ARTAMONOV 05 limit assumes ChPT with $\hat{c}$= 1.8 with unitarity corrections. With $\hat{c}$= 1.6 and no unitarity corrections they obtain < 2.3×10^{-8} at 90% CL. This partial branching ratio is predicted to be 6.10×10^{-9} and 0.49×10^{-9} for the cases with and without unitarity correction.

$\Gamma(\pi^+ 3\gamma)/\Gamma_{\mathrm{total}}$ Γ_{26}/Γ

Values given here assume a phase space pion energy spectrum.

VALUE (units 10^{-4})	CL%	DOCUMENT ID		TECN	CHG	COMMENT
<1.0	90	ASANO	82	CNTR	+	$T(\pi)$ 117–127 MeV
• • • We do not use the following data for averages, fits, limits, etc. • • •						
<3.0	90	KLEMS	71	OSPK	+	$T(\pi) > 117$ MeV

$\Gamma(\pi^+ e^+ e^- \gamma)/\Gamma_{\mathrm{total}}$ Γ_{27}/Γ

VALUE (units 10^{-8})	EVTS	DOCUMENT ID		TECN	COMMENT
1.19±0.12±0.04	113	[62] BATLEY	08	NA48	$m_{ee\gamma} > 260$ MeV

[62] BATLEY 08 also reports the Chiral Perturbation Theory parameter $\hat{c} = 0.9 \pm 0.45$ obtained using the shape of the $e^+ e^- \gamma$ invariant mass spectrum. By extrapolating the theoretical amplitude to $m_{ee\gamma} < 260$ MeV, it obtains the inclusive $B(K^+ \to \pi^+ e^+ e^- \gamma) = (1.29 \pm 0.13 \pm 0.03) \times 10^{-8}$, where the first error is the combined statistical and systematic errors and the second error is from the uncertainty in $\hat{c}$.

Leptonic modes with $\ell\bar{\ell}$ pairs

$\Gamma(e^+ \nu_e \nu\bar{\nu})/\Gamma(e^+ \nu_e)$ Γ_{28}/Γ_1

VALUE	CL%	EVTS	DOCUMENT ID		TECN	CHG
<3.8	90	0	HEINTZE	79	SPEC	+

$\Gamma(\mu^+ \nu_\mu \nu\bar{\nu})/\Gamma_{\mathrm{total}}$ Γ_{29}/Γ

VALUE (units 10^{-6})	CL%	EVTS	DOCUMENT ID		TECN	CHG
<6.0	90	0	[63] PANG	73	CNTR	+

[63] PANG 73 assumes μ spectrum from ν-ν interaction of BARDIN 70.

$\Gamma(e^+\nu_e e^+ e^-)/\Gamma_{total}$ Γ_{30}/Γ

VALUE (units 10^{-8})	EVTS	DOCUMENT ID		TECN	CHG	COMMENT
2.48± 0.14±0.14	410	POBLAGUEV	02	B865	+	m_{ee} >150 MeV
• • • We do not use the following data for averages, fits, limits, etc. • • •						
20 ±20	4	DIAMANT-...	76	SPEC	+	$m_{e^+e^-}$ >140 MeV

$\Gamma(\mu^+\nu_\mu e^+ e^-)/\Gamma_{total}$ Γ_{31}/Γ

VALUE (units 10^{-8})	EVTS	DOCUMENT ID		TECN	CHG	COMMENT
7.06± 0.16±0.26	2.7k	POBLAGUEV	02	B865	+	m_{ee} >145 MeV
• • • We do not use the following data for averages, fits, limits, etc. • • •						
100 ±30	14	DIAMANT-...	76	SPEC	+	$m_{e^+e^-}$ >140 MeV

$\Gamma(e^+\nu_e\mu^+\mu^-)/\Gamma_{total}$ Γ_{32}/Γ

VALUE (units 10^{-8})	CL%	DOCUMENT ID		TECN
1.72±0.45		MA	06	B865
• • • We do not use the following data for averages, fits, limits, etc. • • •				
<50	90	ADLER	98	B787

$\Gamma(\mu^+\nu_\mu\mu^+\mu^-)/\Gamma_{total}$ Γ_{33}/Γ

VALUE (units 10^{-7})	CL%	DOCUMENT ID		TECN	CHG
<4.1	90	ATIYA	89	B787	+

Lepton Family number (LF), Lepton number (L), $\Delta S = \Delta Q$ (SQ) violating modes, or $\Delta S = 1$ weak neutral current ($S1$) modes

$\Gamma(\pi^+\pi^+ e^-\overline{\nu}_e)/\Gamma_{total}$ Γ_{34}/Γ

Test of $\Delta S = \Delta Q$ rule.

VALUE (units 10^{-7})	CL%	EVTS	DOCUMENT ID		TECN	CHG
• • • We do not use the following data for averages, fits, limits, etc. • • •						
< 9.0	95	0	SCHWEINB...	71	HLBC	+
< 6.9	95	0	ELY	69	HLBC	+
<20.	95		BIRGE	65	FBC	+

$\Gamma(\pi^+\pi^+ e^-\overline{\nu}_e)/\Gamma(\pi^+\pi^- e^+\nu_e)$ Γ_{34}/Γ_6

Test of $\Delta S = \Delta Q$ rule.

VALUE (units 10^{-4})	CL%	EVTS	DOCUMENT ID		TECN
< 3	90	3	[64] BLOCH	76	SPEC
• • • We do not use the following data for averages, fits, limits, etc. • • •					
<130.	95	0	BOURQUIN	71	ASPK

[64] BLOCH 76 quotes 3.6×10^{-4} at CL = 95%, we convert.

$\Gamma(\pi^+\pi^+\mu^-\overline{\nu}_\mu)/\Gamma_{total}$ Γ_{35}/Γ

Test of $\Delta S = \Delta Q$ rule.

VALUE (units 10^{-6})	CL%	EVTS	DOCUMENT ID	TECN	CHG
<3.0	95	0	BIRGE 65	FBC	+

$\Gamma(\pi^+ e^+ e^-)/\Gamma_{total}$ Γ_{36}/Γ

Test for $\Delta S = 1$ weak neutral current. Allowed by combined first-order weak and electromagnetic interactions.

VALUE (units 10^{-7})	EVTS	DOCUMENT ID		TECN	CHG
3.00±0.09 OUR AVERAGE					
3.11±0.04±0.12	7253	[65] BATLEY	09	NA48	±
2.94±0.05±0.14	10300	[66] APPEL	99	SPEC	+
2.75±0.23±0.13	500	[67] ALLIEGRO	92	SPEC	+
2.7 ±0.5	41	[68] BLOCH	75	SPEC	+

[65] Value extrapolated from a measurement in the region $z = (m_{ee}/m_K)^2$ >0.08. BATLEY 09 also evaluated the shape of the form factor using four different theoretical models.

[66] APPEL 99 establishes vector nature of this decay and determines form factor $f(Z) = f_0(1+\delta Z)$, $Z = M^2_{ee}/m^2_K$, $\delta = 2.14 \pm 0.13 \pm 0.15$.

[67] ALLIEGRO 92 assumes a vector interaction with a form factor given by $\lambda = 0.105 \pm 0.035 \pm 0.015$ and a correlation coefficient of -0.82.

[68] BLOCH 75 assumes a vector interaction.

$\Gamma(\pi^+\mu^+\mu^-)/\Gamma_{total}$ Γ_{37}/Γ

Test for $\Delta S = 1$ weak neutral current. Allowed by higher-order electroweak interactions.

VALUE (units 10^{-8})	CL%	EVTS	DOCUMENT ID		TECN	CHG	COMMENT
9.4 ±0.6 OUR AVERAGE Error includes scale factor of 2.6. See the ideogram below.							
9.62±0.21±0.13		3120	[69] BATLEY	11A	NA48	±	2003-04 data
9.8 ±1.0 ±0.5		110	[70] PARK	02	HYCP	±	
9.22±0.60±0.49		402	[71] MA	00	B865	+	
5.0 ±0.4 ±0.9		207	[72] ADLER	97C	B787	+	
• • • We do not use the following data for averages, fits, limits, etc. • • •							
9.7 ±1.2 ±0.4		65	PARK	02	HYCP	+	
10.0 ±1.9 ±0.7		35	PARK	02	HYCP	−	
<23	90		ATIYA	89	B787	+	

[69] BATLEY 11A also studies the form factor $f(z)$ dependence of the decay, described via single photon exchange: i) assuming a linear form factor, $f(z) = f_0(1+\delta z)$, $z = (M_{\mu\mu}/m_K)^2$, finding $f_0 = 0.470 \pm 0.040$ and $\delta = 3.11 \pm 0.57$ and ii) assuming a linear form factor including π-π rescattering , $W_{\pi\pi}$, as in DAMBROSIO 98A, finding $f(z) = G_F\, m_K^2\,(a_+ + b_+ z) + W_{\pi\pi}(z)$, $a_+ = -0.575 \pm 0.039$, $b_+ = -0.813 \pm 0.145$.

[70] PARK 02 "±" result comes from combining $K^+ \to \pi^+\mu^+\mu^-$ and $K^- \to \pi^-\mu^+\mu^-$, assuming CP is conserved.

[71] MA 00 establishes vector nature of this decay and determines form factor $f(z) = f_0(1+\delta z)$, $z = (M_{\mu\mu}/m_K)^2$, $\delta = 2.45^{+1.30}_{-0.95}$.

[72] ADLER 97C gives systematic error 0.7×10^{-8} and theoretical uncertainty 0.6×10^{-8}, which we combine in quadrature to obtain our second error.

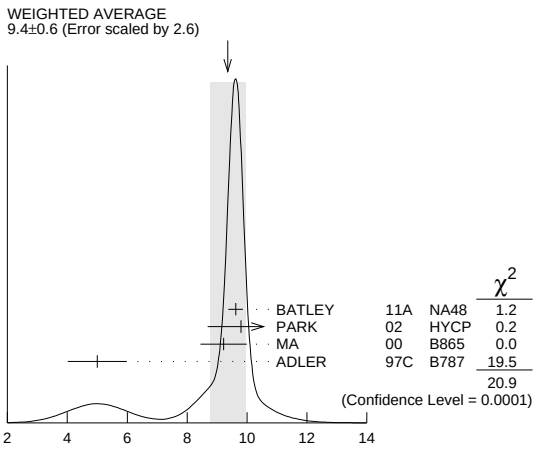

$\Gamma(\pi^+\mu^+\mu^-)/\Gamma_{total}$ Γ_{37}/Γ

$\Gamma(\pi^+\nu\overline{\nu})/\Gamma_{total}$ Γ_{38}/Γ

Test for $\Delta S = 1$ weak neutral current. Allowed by higher-order electroweak interactions. Branching ratio values are extrapolated from the momentum or energy regions shown in the comments assuming Standard Model phase space except for those labeled "Scalar" or "Tensor" to indicate the assumed non-Standard-Model interaction.

VALUE (units 10^{-9})	CL%	EVTS	DOCUMENT ID		TECN	CHG	COMMENT
$0.173^{+0.115}_{-0.105}$		7	[73] ARTAMONOV	08	B949	+	140<P_π <199 MeV, 211<P_π <229MeV
• • • We do not use the following data for averages, fits, limits, etc. • • •							
$0.789^{+0.926}_{-0.510}$		3	[74] ARTAMONOV	08	B949	+	140<P_π <199 MeV
< 2.2	90	1	[75] ADLER	04	B787	+	211<P_π <229 MeV
< 2.7	90		ADLER	04	B787	+	Scalar
< 1.8	90		ADLER	04	B787	+	Tensor
$0.147^{+0.130}_{-0.089}$		3	[76] ANISIMOVSK...	04	B949	+	211<P_π <229 MeV
$0.157^{+0.175}_{-0.082}$		2	ADLER	02	B787	+	P_π >211 MeV/c
< 4.2	90	1	ADLER	02C	B787	+	140<P_π <195 MeV
< 4.7	90		[77] ADLER	02C	B787	+	Scalar
< 2.5	90		[77] ADLER	02C	B787	+	Tensor
$0.15^{+0.34}_{-0.12}$		1	ADLER	00	B787		In ADLER 02
$0.42^{+0.97}_{-0.35}$		1	ADLER	97	B787		
< 2.4	90		ADLER	96	B787		
< 7.5	90		ATIYA	93	B787	+	$T(\pi)$ 115–127 MeV
< 5.2	90		[78] ATIYA	93	B787	+	
< 17	90	0	ATIYA	93B	B787	+	$T(\pi)$ 60–100 MeV
< 34	90		ATIYA	90	B787	+	
<140	90		ASANO	81B	CNTR	+	$T(\pi)$ 116–127 MeV

[73] Value obtained combining ANISIMOVSKY 04, ADLER 04, and the present ARTAMONOV 08 results.

[74] Observed 3 events with an estimated background of $0.93 \pm 0.17^{+0.32}_{-0.24}$. Signal-to-background ratio for each of these 3 events is 0.20, 0.42, and 0.47.

[75] Value obtained combining the previous result ADLER 02C with 1 event and the present result with 0 events to obtain an expected background 1.22 ± 0.24 events and 1 event observed.

[76] Value obtained combining the previous E787 result ADLER 02 with 2 events and the present E949 with 1 event. The additional event has a signal-to-background ratio 0.9. Superseded by ARTAMONOV 08.

[77] Superseded by ADLER 04.

[78] Combining ATIYA 93 and ATIYA 93B results. Superseded by ADLER 96.

$\Gamma(\pi^+\pi^0\nu\overline{\nu})/\Gamma_{total}$ Γ_{39}/Γ

Test for $\Delta S = 1$ weak neutral current. Allowed by higher-order electroweak interactions.

VALUE (units 10^{-5})	CL%	DOCUMENT ID		TECN
<4.3	90	[79] ADLER	01	SPEC

[79] Search region defined by 90 MeV/c<P_{π^+} <188 MeV/c and 135 MeV<E_{π^0} <180 MeV.

$\Gamma(\mu^-\nu e^+ e^+)/\Gamma(\pi^+\pi^- e^+\nu_e)$ Γ_{40}/Γ_6

Test of lepton family number conservation.

VALUE (units 10^{-3})	CL%	EVTS	DOCUMENT ID		TECN	CHG
<0.5	90	0	[80] DIAMANT-...	76	SPEC	+

[80] DIAMANT-BERGER 76 quotes this result times our 1975 $\pi^+\pi^- e\nu$ BR ratio.

$\Gamma(\mu^+\nu_e)/\Gamma_{total}$ Γ_{41}/Γ

Forbidden by lepton family number conservation.

VALUE	CL%	EVTS	DOCUMENT ID		TECN	COMMENT
<0.004	90	0	[81] LYONS	81	HLBC	200 GeV K^+ narrow band ν beam
• • • We do not use the following data for averages, fits, limits, etc. • • •						
<0.012	90		[81] COOPER	82	HLBC	Wideband ν beam

[81] COOPER 82 and LYONS 81 limits on ν_e observation are here interpreted as limits on lepton family number violation in the absence of mixing.

$\Gamma(\pi^+\mu^+ e^-)/\Gamma_{total}$ Γ_{42}/Γ

Test of lepton family number conservation.

VALUE (units 10^{-10})	CL%	DOCUMENT ID		TECN	CHG
<0.13	90	[82] SHER	05	RVUE	+
• • • We do not use the following data for averages, fits, limits, etc. • • •					
<0.21	90	SHER	05	B865	+
<0.39	90	APPEL	00	B865	+
<2.1	90	LEE	90	SPEC	+

[82] This result combines SHER 05 1998 data, APPEL 00 1996 data, and data from BERGMAN 97 and PISLAK 97 theses, all from BNL-E865, with LEE 90 BNL-E777 data.

$\Gamma(\pi^+\mu^- e^+)/\Gamma_{total}$ Γ_{43}/Γ

Test of lepton family number conservation.

VALUE (units 10^{-10})	CL%	EVTS	DOCUMENT ID		TECN	CHG
< 5.2	90	0	APPEL	00B	B865	+
• • • We do not use the following data for averages, fits, limits, etc. • • •						
<70	90	0	[83] DIAMANT-...	76	SPEC	+

[83] Measurement actually applies to the sum of the $\pi^+\mu^- e^+$ and $\pi^-\mu^+ e^+$ modes.

$\Gamma(\pi^-\mu^+ e^+)/\Gamma_{total}$ Γ_{44}/Γ

Test of total lepton number conservation.

VALUE (units 10^{-10})	CL%	EVTS	DOCUMENT ID		TECN	CHG
< 5.0	90	0	APPEL	00B	B865	+
• • • We do not use the following data for averages, fits, limits, etc. • • •						
<70	90	0	[84] DIAMANT-...	76	SPEC	+

[84] Measurement actually applies to the sum of the $\pi^+\mu^- e^+$ and $\pi^-\mu^+ e^+$ modes.

$\Gamma(\pi^- e^+ e^+)/\Gamma_{total}$ Γ_{45}/Γ

Test of total lepton number conservation.

VALUE	CL%	EVTS	DOCUMENT ID		TECN	CHG
$<6.4\times10^{-10}$	90	0	APPEL	00B	B865	+
• • • We do not use the following data for averages, fits, limits, etc. • • •						
$<9.2\times10^{-9}$	90	0	DIAMANT-...	76	SPEC	+
$<1.5\times10^{-5}$			CHANG	68	HBC	−

$\Gamma(\pi^-\mu^+\mu^+)/\Gamma_{total}$ Γ_{46}/Γ

Forbidden by total lepton number conservation.

VALUE	CL%	DOCUMENT ID		TECN	CHG
$<1.1\times10^{-9}$	90	BATLEY	11A	NA48	±
• • • We do not use the following data for averages, fits, limits, etc. • • •					
$<3.0\times10^{-9}$	90	APPEL	00B	B865	+
$<1.5\times10^{-4}$	90	[85] LITTENBERG	92	HBC	

[85] LITTENBERG 92 is from retroactive data analysis of CHANG 68 bubble chamber data.

$\Gamma(\mu^+\overline{\nu}_e)/\Gamma_{total}$ Γ_{47}/Γ

Forbidden by total lepton number conservation.

VALUE (units 10^{-3})	CL%	DOCUMENT ID		TECN	COMMENT
<3.3	90	[86] COOPER	82	HLBC	Wideband ν beam

[86] COOPER 82 limit on $\overline{\nu}_e$ observation is here interpreted as a limit on lepton number violation in the absence of mixing.

$\Gamma(\pi^0 e^+\overline{\nu}_e)/\Gamma_{total}$ Γ_{48}/Γ

Forbidden by total lepton number conservation.

VALUE	CL%	DOCUMENT ID		TECN	COMMENT
<0.003	90	[87] COOPER	82	HLBC	Wideband ν beam

[87] COOPER 82 limit on $\overline{\nu}_e$ observation is here interpreted as a limit on lepton number violation in the absence of mixing.

$\Gamma(\pi^+\gamma)/\Gamma_{total}$ Γ_{49}/Γ

Violates angular momentum conservation and gauge invariance. Current interest in this decay is as a search for non-commutative space-time effects as discussed in ARTAMONOV 05 and for exotic physics such as a vacuum expectation value of a new vector field, non-local Superstring effects, or departures from Lorentz invariance, as discussed in ADLER 02B.

VALUE (units 10^{-9})	CL%	DOCUMENT ID		TECN	CHG
< 2.3	90	ARTAMONOV	05	B949	+
• • • We do not use the following data for averages, fits, limits, etc. • • •					
< 360	90	ADLER	02B	B787	+
<1400	90	ASANO	82	CNTR	+
<4000	90	[88] KLEMS	71	OSPK	+

[88] Test of model of Selleri, Nuovo Cimento **60A** 291 (1969).

K^+ LONGITUDINAL POLARIZATION OF EMITTED μ^+

VALUE	CL%	DOCUMENT ID		TECN	CHG	COMMENT
<−0.990	90	[89] AOKI	94	SPEC	+	
• • • We do not use the following data for averages, fits, limits, etc. • • •						
<−0.990	90	IMAZATO	92	SPEC	+	Repl. by AOKI 94
−0.970 ±0.047		[90] YAMANAKA	86	SPEC	+	
−1.0 ±0.1		[90] CUTTS	69	SPRK	+	
−0.96 ±0.12		[90] COOMBES	57	CNTR	+	

[89] AOKI 94 measures $\xi P_\mu = -0.9996 \pm 0.0030 \pm 0.0048$. The above limit is obtained by summing the statistical and systematic errors in quadrature, normalizing to the physically significant region ($|\xi P_\mu| < 1$) and assuming that ξ=1, its maximum value.

[90] Assumes ξ=1.

DALITZ PLOT PARAMETERS FOR $K \to 3\pi$ DECAYS

Revised 1999 by T.G. Trippe (LBNL).

The Dalitz plot distribution for $K^\pm \to \pi^\pm\pi^\pm\pi^\mp$, $K^\pm \to \pi^0\pi^0\pi^\pm$, and $K_L^0 \to \pi^+\pi^-\pi^0$ can be parameterized by a series expansion such as that introduced by Weinberg [1]. We use the form

$$\left|M\right|^2 \propto 1 + g\frac{(s_3-s_0)}{m_{\pi^+}^2} + h\left[\frac{s_3-s_0}{m_{\pi^+}^2}\right]^2 + j\,\frac{(s_2-s_1)}{m_{\pi^+}^2} + k\left[\frac{s_2-s_1}{m_{\pi^+}^2}\right]^2 + f\,\frac{(s_2-s_1)}{m_{\pi^+}^2}\frac{(s_3-s_0)}{m_{\pi^+}^2} + \cdots , \quad (1)$$

where $m_{\pi^+}^2$ has been introduced to make the coefficients g, h, j, and k dimensionless, and

$$s_i = (P_K - P_i)^2 = (m_K - m_i)^2 - 2m_K T_i \ , \ i = 1,2,3,$$
$$s_0 = \frac{1}{3}\sum_i s_i = \frac{1}{3}(m_K^2 + m_1^2 + m_2^2 + m_3^2) \quad .$$

Here the P_i are four-vectors, m_i and T_i are the mass and kinetic energy of the i^{th} pion, and the index 3 is used for the odd pion.

The coefficient g is a measure of the slope in the variable s_3 (or T_3) of the Dalitz plot, while h and k measure the quadratic dependence on s_3 and $(s_2 - s_1)$, respectively. The coefficient j is related to the asymmetry of the plot and must be zero if CP invariance holds. Note also that if CP is good, g, h, and k must be the same for $K^+ \to \pi^+\pi^+\pi^-$ as for $K^- \to \pi^-\pi^-\pi^+$.

Since different experiments use different forms for $\left|M\right|^2$, in order to compare the experiments we have converted to g, h, j, and k whatever coefficients have been measured. Where such conversions have been done, the measured coefficient a_y, a_t, a_u, or a_v is given in the comment at the right. For definitions of these coefficients, details of this conversion, and discussion of the data, see the April 1982 version of this note [2].

References

1. S. Weinberg, Phys. Rev. Lett. **4**, 87 (1960).
2. Particle Data Group, Phys. Lett. **111B**, 69 (1982).

ENERGY DEPENDENCE OF $K^{\pm}$ DALITZ PLOT

$|\text{matrix element}|^2 = 1 + gu + hu^2 + kv^2$
where $u = (s_3 - s_0) / m_{\pi}^2$ and $v = (s_2 - s_1) / m_{\pi}^2$

LINEAR COEFFICIENT g FOR $K^{\pm} \to \pi^{\pm}\pi^+\pi^-$

Some experiments use Dalitz variables x and y. In the comments we give a_y = coefficient of y term. See note above on "Dalitz Plot Parameters for $K \to 3\pi$ Decays." For discussion of the conversion of a_y to g, see the earlier version of the same note in the *Review* published in Physics Letters **111B** 70 (1982).

VALUE	EVTS	DOCUMENT ID		TECN	CHG	COMMENT
−0.21134±0.00017	471M	[91] BATLEY	07B	NA48	±	
• • • We do not use the following data for averages, fits, limits, etc. • • •						
−0.2221 ±0.0065	225k	DEVAUX	77	SPEC	+	a_y=.2814±.0082
−0.199 ±0.008	81k	[92] LUCAS	73	HBC	−	a_y=0.252±0.011
−0.2157 ±0.0028	750k	FORD	72	ASPK	+	a_y=.2734±.0035
−0.2186 ±0.0028	750k	FORD	72	ASPK	−	a_y=.2770±.0035
−0.200 ±0.009	39819	[93] HOFFMASTER	72	HLBC	+	
−0.196 ±0.012	17898	[94] GRAUMAN	70	HLBC	+	a_y=0.228±0.030
−0.193 ±0.010	50919	MAST	69	HBC	−	a_y=0.244±0.013
−0.218 ±0.016	9994	[95] BUTLER	68	HBC	+	a_y=0.277±0.020
−0.190 ±0.023	5778	[95,96] MOSCOSO	68	HBC	−	a_y=0.242±0.029
−0.22 ±0.024	5428	[95,96] ZINCHENKO	67	HBC	+	a_y=0.28 ± 0.03
−0.220 ±0.035	1347	[97] FERRO-LUZZI	61	HBC	−	a_y=0.28 ± 0.045

[91] Final state strong interaction and radiative corrections not included in the fit.
[92] Quadratic dependence is required by K_L^0 experiments.
[93] HOFFMASTER 72 includes GRAUMAN 70 data.
[94] Emulsion data added — all events included by HOFFMASTER 72.
[95] Experiments with large errors not included in average.
[96] Also includes DBC events.
[97] No radiative corrections included.

QUADRATIC COEFFICIENT h FOR $K^{\pm} \to \pi^{\pm}\pi^+\pi^-$

VALUE (units 10^{-2})	EVTS	DOCUMENT ID		TECN	CHG
1.848±0.040	471M	[98] BATLEY	07B	NA48	±
• • • We do not use the following data for averages, fits, limits, etc. • • •					
−0.06 ±1.43	225k	DEVAUX	77	SPEC	+
1.87 ±0.62	750k	FORD	72	ASPK	+
1.25 ±0.62	750k	FORD	72	ASPK	−
−0.9 ±1.4	39819	HOFFMASTER	72	HLBC	+
−0.1 ±1.2	50919	MAST	69	HBC	−

[98] Final state strong interaction and radiative corrections not included in the fit.

QUADRATIC COEFFICIENT k FOR $K^{\pm} \to \pi^{\pm}\pi^+\pi^-$

VALUE (units 10^{-3})	EVTS	DOCUMENT ID		TECN	CHG
− 4.63± 0.14	471M	[99] BATLEY	07B	NA48	±
• • • We do not use the following data for averages, fits, limits, etc. • • •					
−20.5 ± 3.9	225k	DEVAUX	77	SPEC	+
− 7.5 ± 1.9	750k	FORD	72	ASPK	+
− 8.3 ± 1.9	750k	FORD	72	ASPK	−
−10.5 ± 4.5	39819	HOFFMASTER	72	HLBC	+
−14 ±12	50919	MAST	69	HBC	−

[99] Final state strong interaction and radiative corrections not included in the fit.

$(g_+ - g_-) / (g_+ + g_-)$ FOR $K^{\pm} \to \pi^{\pm}\pi^+\pi^-$

This is a CP violating asymmetry between linear coefficients g_+ for $K^+ \to \pi^+\pi^+\pi^-$ decay and g_- for $K^- \to \pi^-\pi^+\pi^-$ decay.

VALUE (units 10^{-4})	EVTS	DOCUMENT ID		TECN
− 1.5± 1.5±1.6	3.1G	[100] BATLEY	07E	NA48
• • • We do not use the following data for averages, fits, limits, etc. • • •				
1.7± 2.1±2.0	1.7G	[101] BATLEY	06	NA48
−70.0±53	3.2M	FORD	70	ASPK

[100] BATLEY 07E includes data from BATLEY 06. Uses quadratic parametrization and value $g_+ + g_- = 2g$ from BATLEY 07B. This measurement neglects any possible charge asymmetries in higher order slope parameters h or k.
[101] This measurement neglects any possible charge asymmetries in higher order slope parameters h or k.

LINEAR COEFFICIENT g FOR $K^{\pm} \to \pi^{\pm}\pi^0\pi^0$

Unless otherwise stated, all experiments include terms quadratic in $(s_3 - s_0) / m_{\pi^+}^2$. See note above on "Dalitz Plot Parameters for $K \to 3\pi$ Decays."

See BATUSOV 98 for a discussion of the discrepancy between their result and others, especially BOLOTOV 86. At this time we have no way to resolve the discrepancy so we depend on the large scale factor as a warning.

VALUE	EVTS	DOCUMENT ID		TECN	CHG	COMMENT
0.626 ±0.007 OUR AVERAGE						
0.6259±0.0043±0.0093	493k	AKOPDZHAN..05B		TNF	±	
0.627 ±0.004 ±0.010	252k	[102,103] AJINENKO	03B	ISTR	−	
• • • We do not use the following data for averages, fits, limits, etc. • • •						
0.736 ±0.014 ±0.012	33k	BATUSOV	98	SPEC	+	
0.582 ±0.021	43k	BOLOTOV	86	CALO	−	
0.670 ±0.054	3263	BRAUN	76B	HLBC	+	
0.630 ±0.038	5635	SHEAFF	75	HLBC	+	
0.510 ±0.060	27k	SMITH	75	WIRE	+	
0.67 ±0.06	1365	AUBERT	72	HLBC	+	
0.544 ±0.048	4048	DAVISON	69	HLBC	+	Also emulsion

[102] Measured using in-flight decays of the 25 GeV negative secondary beam.
[103] They form new world averages $g_- = (0.617 \pm 0.018)$ and $g_+ = (0.684 \pm 0.033)$ which give $\Delta g_{\tau'} = 0.051 \pm 0.028$.

QUADRATIC COEFFICIENT h FOR $K^{\pm} \to \pi^{\pm}\pi^0\pi^0$

VALUE	EVTS	DOCUMENT ID		TECN	CHG	COMMENT
0.052 ±0.008 OUR AVERAGE						
0.0551±0.0044±0.0086	493k	AKOPDZHAN..05B		TNF	±	
0.046 ±0.004 ±0.012	252k	[104] AJINENKO	03B	ISTR	−	
• • • We do not use the following data for averages, fits, limits, etc. • • •						
0.128 ±0.015 ±0.024	33k	BATUSOV	98	SPEC	+	
0.037 ±0.024	43k	BOLOTOV	86	CALO	−	
0.152 ±0.082	3263	BRAUN	76B	HLBC	+	
0.041 ±0.030	5635	SHEAFF	75	HLBC	+	
0.009 ±0.040	27k	SMITH	75	WIRE	+	
−0.01 ±0.08	1365	AUBERT	72	HLBC	+	
0.026 ±0.050	4048	DAVISON	69	HLBC	+	Also emulsion

[104] Measured using in-flight decays of the 25 GeV negative secondary beam.

QUADRATIC COEFFICIENT k FOR $K^{\pm} \to \pi^{\pm}\pi^0\pi^0$

VALUE	EVTS	DOCUMENT ID		TECN	CHG
0.0054±0.0035 OUR AVERAGE Error includes scale factor of 2.5.					
0.0082±0.0011±0.0014	493k	AKOPDZHAN..05B		TNF	±
0.001 ±0.001 ±0.002	252k	[105] AJINENKO	03B	ISTR	−
• • • We do not use the following data for averages, fits, limits, etc. • • •					
0.0197±0.0045±0.0029	33k	BATUSOV	98	SPEC	+

[105] Measured using in-flight decays of the 25 GeV negative secondary beam.

$(g_+ - g_-) / (g_+ + g_-)$ FOR $K^{\pm} \to \pi^{\pm}\pi^0\pi^0$

A nonzero value for this quantity indicates CP violation.

VALUE (units 10^{-4})	EVTS	DOCUMENT ID		TECN
1.8± 1.8 OUR AVERAGE				
1.8± 1.7±0.6	91.3M	[106] BATLEY	07E	NA48
2 ±18 ±5	619k	[107] AKOPDZHAN..05		TNF
• • • We do not use the following data for averages, fits, limits, etc. • • •				
1.8± 2.2±1.3	47M	[108] BATLEY	06A	NA48

[106] BATLEY 07E includes data from BATLEY 06A. Uses quadratic parametrization and PDG 06 value $g = 0.626 \pm 0.007$ to obtain $g_+ - g_- = (2.2 \pm 2.1 \pm 0.7) \times 10^{-4}$. Neglects any possible charge asymmetries in higher order slope parameters h or k.
[107] Asymmetry obtained assuming that $g_+ + g_- = 2 \times 0.652$ (PDG 02) and that asymmetries in h and k are zero.
[108] Linear and quadratic slopes from PDG 04 are used. Any possible charge asymmetries in higher order slope parameters h or k are neglected.

ALTERNATIVE PARAMETRIZATIONS OF $K^{\pm} \to \pi^{\pm}\pi^0\pi^0$ DALITZ PLOT

The following functional form for the matrix element suggested by $\pi\pi$ rescattering in $K^+ \to \pi^+$ "$\pi^+\pi^-$" $\to \pi^+\pi^0\pi^0$ is used for this fit (CABIBBO 04A, CABIBBO 05): Matrix element = $M_0 + M_1$ where $M_0 = 1 + (1/2)g_0\, u + (1/2)\, h'\, u^2 + (1/2)k_0\, v^2$ with $u = (s_3 - s_0)/(m_{\pi^+})^2$, $v = (s_2 - s_1)/(m_{\pi^+})^2$ and where M_1 takes into account the non-analytic piece due to pi pi rescattering amplitudes a_0 and a_2; The parameters g_0 and h' are related to the parameters g and h of the matrix element squared given in the previous section by the approximations $g_0 \sim g^{PDG}$ and $h' \sim h^{PDG} - (g/2)^2$ and $k_0 \sim k^{PDG}$.

In addition, we also consider the effective field theory framework of COLANGELO 06A and BISSEGGER 09 to extract g_{BB} and h'_{BB}.

LINEAR COEFFICIENT g_0 FOR $K^{\pm} \to \pi^{\pm}\pi^0\pi^0$

VALUE	EVTS	DOCUMENT ID		TECN	CHG
0.6525±0.0009±0.0033	60M	[109] BATLEY	09A	NA48	±
• • • We do not use the following data for averages, fits, limits, etc. • • •					
0.645 ±0.004 ±0.009	23M	[110] BATLEY	06B	NA48	±

[109] This fit is obtained with the CABIBBO 05 matrix element in the $2\pi^0$ invariant mass squared range $0.074094 < m^2_{2\pi^0} < 0.104244$ GeV^2. Electromagnetic corrections and CHPT constraints for $\pi\pi$ phase shifts (a_0 and a_2) have been used. Also measured $(a_0 - a_2)\, m_{\pi^+} = 0.2646 \pm 0.0021 \pm 0.0023$, where k_0 was kept fixed in the fit at -0.0099.
[110] Superseded by BATLEY 09A. This fit is obtained with the CABIBBO 05 matrix element in the $2\pi^0$ invariant mass squared range 0.074 GeV^2 $< m^2_{2\pi^0} <$ 0.097 GeV^2, assuming $k = 0$ (no term proportional to $(s_2 - s_1)^2$) and excluding the kinematic region around the cusp ($m^2_{2\pi^0} = (2m_{\pi^+})^2 \pm 0.000525$ GeV^2). Also π-π phase shifts a_0 and a_2 are measured: $(a_0 - a_2) m_{\pi^+} = 0.268 \pm 0.010 \pm 0.004 \pm 0.013$(external) and $a_2\, m_{\pi^+} = -0.041 \pm 0.022 \pm 0.014$.

QUADRATIC COEFFICIENT h' FOR $K^\pm \to \pi^\pm\pi^0\pi^0$

VALUE	EVTS	DOCUMENT ID		TECN	CHG
−0.0433±0.0008±0.0026	60M	[111] BATLEY	09A	NA48	±
• • • We do not use the following data for averages, fits, limits, etc. • • •					
−0.047 ±0.012 ±0.011	23M	[112] BATLEY	06B	NA48	±

[111] This fit is obtained with the CABIBBO 05 matrix element in the $2\pi^0$ invariant mass squared range $0.074094 < m^2_{2\pi^0} < 0.104244$ GeV^2. Electromagnetic corrections and CHPT constraints for $\pi\pi$ phase shifts (a_0 and a_2) have been used. Also measured $(a_0 - a_2)\, m_{\pi^+} = 0.2646 \pm 0.0021 \pm 0.0023$, where k_0 was kept fixed in the fit at -0.0099.

[112] Superseded by BATLEY 09A. This fit is obtained with the CABIBBO 05 matrix element in the $2\pi^0$ invariant mass squared range 0.074 GeV^2 $< m^2_{2\pi^0} < 0.097$ GeV^2, assuming $k = 0$ (no term proportional to $(s_2 - s_1)^2$) and excluding the kinematic region around the cusp ($m^2_{2\pi^0} = (2m_{\pi^+})^2 \pm 0.000525$ GeV^2). Also π-π phase shifts a_0 and a_2 are measured: $(a_0 - a_2) m_{\pi^+} = 0.268 \pm 0.010 \pm 0.004 \pm 0.013$(external) and $a_2\, m_{\pi^+} = -0.041 \pm 0.022 \pm 0.014$.

QUADRATIC COEFFICIENT k_0 FOR $K^\pm \to \pi^\pm\pi^0\pi^0$

VALUE	EVTS	DOCUMENT ID		TECN	CHG
0.0095±0.00017±0.00048	60M	[113] BATLEY	09A	NA48	±

[113] Assumed $a_2\, m_{\pi^+} = -0.0044$ in the fit.

LINEAR COEFFICIENT g_{BB} FOR $K^\pm \to \pi^\pm\pi^0\pi^0$

VALUE	EVTS	DOCUMENT ID		TECN	CHG
0.6219±0.0009±0.0033	60M	[114] BATLEY	09A	NA48	±

[114] This fit is obtained using parametrizations of COLANGELO 06A and BISSEGGER 09 in the $2\pi^0$ invariant mass squared range $0.074094 < m^2_{2\pi^0} < 0.104244$ GeV^2. Electromagnetic corrections and CHPT constraints for $\pi\pi$ phase shifts (a_0 and a_2) have been used. Also measured $(a_0 - a_2)\, m_{\pi^+} = 0.2633 \pm 0.0024 \pm 0.0024$, where k_0 was kept fixed in the fit at 0.0085.

QUADRATIC COEFFICIENT h'_{BB} FOR $K^\pm \to \pi^\pm\pi^0\pi^0$

VALUE	EVTS	DOCUMENT ID		TECN	CHG
−0.0520±0.0009±0.0026	60M	[115] BATLEY	09A	NA48	±

[115] This fit is obtained using parametrizations of COLANGELO 06A and BISSEGGER 09 in the $2\pi^0$ invariant mass squared range $0.074094 < m^2_{2\pi^0} < 0.104244$ GeV^2. Electromagnetic corrections and CHPT constraints for $\pi\pi$ phase shifts (a_0 and a_2) have been used. Also measured $(a_0 - a_2)\, m_{\pi^+} = 0.2633 \pm 0.0024 \pm 0.0024$, where k_0 was kept fixed in the fit at 0.0085.

$K^\pm_{\ell 3}$ AND $K^0_{\ell 3}$ FORM FACTORS

Updated September 2013 by T.G. Trippe (LBNL) and C.-J. Lin (LBNL).

Assuming that only the vector current contributes to $K \to \pi\ell\nu$ decays, we write the matrix element as

$$M \propto f_+(t)\left[(P_K + P_\pi)_\mu \overline{\ell}\gamma_\mu(1+\gamma_5)\nu\right] + f_-(t)\left[m_\ell \overline{\ell}(1+\gamma_5)\nu\right] \ , \quad (1)$$

where P_K and P_π are the four-momenta of the K and π mesons, m_ℓ is the lepton mass, and f_+ and f_- are dimensionless form factors which can depend only on $t = (P_K - P_\pi)^2$, the square of the four-momentum transfer to the leptons. If time-reversal invariance holds, f_+ and f_- are relatively real. $K_{\mu 3}$ experiments, discussed immediately below, measure f_+ and f_-, while K_{e3} experiments, discussed further below, are sensitive only to f_+ because the small electron mass makes the f_- term negligible.

$K_{\mu 3}$ Experiments. Analyses of $K_{\mu 3}$ data frequently assume a linear dependence of f_+ and f_- on t, *i.e.*,

$$f_\pm(t) = f_\pm(0)\left[1 + \lambda_\pm(t/m^2_{\pi^+})\right] \ . \quad (2)$$

Most $K_{\mu 3}$ data are adequately described by Eq. (2) for f_+ and a constant f_- (*i.e.*, $\lambda_- = 0$).

There are two equivalent parametrizations commonly used in these analyses:

(1) $\lambda_+, \xi(0)$ parametrization. Older analyses of $K_{\mu 3}$ data often introduce the ratio of the two form factors

$$\xi(t) = f_-(t)/f_+(t) \ . \quad (3)$$

The $K_{\mu 3}$ decay distribution is then described by the two parameters λ_+ and $\xi(0)$ (assuming time reversal invariance and $\lambda_- = 0$).

(2) λ_+, λ_0 parametrization. More recent $K_{\mu 3}$ analyses have parametrized in terms of the form factors f_+ and f_0, which are associated with vector and scalar exchange, respectively, to the lepton pair. f_0 is related to f_+ and f_- by

$$f_0(t) = f_+(t) + \left[t/(m_K^2 - m_\pi^2)\right] f_-(t) \ . \quad (4)$$

Here $f_0(0)$ must equal $f_+(0)$ unless $f_-(t)$ diverges at $t = 0$. The earlier assumption that f_+ is linear in t and f_- is constant leads to f_0 linear in t:

$$f_0(t) = f_0(0)\left[1 + \lambda_0(t/m^2_{\pi^+})\right] \ . \quad (5)$$

With the assumption that $f_0(0) = f_+(0)$, the two parametrizations, $(\lambda_+, \xi(0))$ and (λ_+, λ_0) are equivalent as long as correlation information is retained. (λ_+, λ_0) correlations tend to be less strong than $(\lambda_+, \xi(0))$ correlations.

Since the 2006 edition of the *Review* [4], we no longer quote results in the $(\lambda_+, \xi(0))$ parametrization. We have removed many older low statistics results from the Listings. See the 2004 version of this note [5] for these older results, and the 1982 version [6] for additional discussion of the $K^0_{\mu 3}$ parameters, correlations, and conversion between parametrizations.

Quadratic Parametrization. More recent high-statistics experiments have included a quadratic term in the expansion of $f_+(t)$,

$$f_+(t) = f_+(0)\left[1 + \lambda'_+(t/m^2_{\pi^+}) + \frac{\lambda''_+}{2}(t/m^2_{\pi^+})^2\right] \ . \quad (6)$$

If there is a non-vanishing quadratic term, then λ_+ of Eq. (2) represents the average slope, which is then different from λ'_+. Our convention is to include the factor $\frac{1}{2}$ in the quadratic term, and to use m_{π^+} even for K^+_{e3} and $K^+_{\mu 3}$ decays. We have converted other's parametrizations to match our conventions, as noted in the beginning of the "$K^\pm_{\ell 3}$ and $K^0_{\ell 3}$ Form Factors" sections of the Listings.

Pole Parametrization: The pole model describes the t-dependence of $f_+(t)$ and $f_0(t)$ in terms of the exchange of the lightest vector and scalar K^* mesons with masses M_v and M_s, respectively:

$$f_+(t) = f_+(0)\left[\frac{M_v^2}{M_v^2 - t}\right] \ , \qquad f_0(t) = f_0(0)\left[\frac{M_s^2}{M_s^2 - t}\right] \ . \quad (7)$$

Dispersive Parametrization [7,8]. This approach uses dispersive techniques and the known low-energy K-π phases to parametrize the vector and scalar form factors:

$$f_+(t) = f_+(0)\exp\left[\frac{\mathrm{t}}{\mathrm{m}^2_\pi}(\Lambda_+ + \mathrm{H(t)})\right]; \quad (8)$$

$$f_0(t) = f_+(0)\exp\left[\frac{t}{(m_K^2 - m_\pi^2)}\,(\ln[C] - G(t))\right], \qquad (9)$$

where Λ_+ is the slope of the vector form factor, and $\ln[C] = \ln[f_0(m_K^2 - m_\pi^2)]$ is the logarithm of the scalar form factor at the Callan-Treiman point. The functions H(t) and G(t) are dispersive integrals.

K_{e3} Experiments: Analysis of K_{e3} data is simpler than that of $K_{\mu 3}$ because the second term of the matrix element assuming a pure vector current [Eq. (1) above] can be neglected. Here f_+ can be assumed to be linear in t, in which case the linear coefficient λ_+ of Eq. (2) is determined, or quadratic, in which case the linear coefficient $\lambda_+^{'}$ and quadratic coefficient $\lambda_+^{''}$ of Eq. (6) are determined.

If we remove the assumption of a pure vector current, then the matrix element for the decay, in addition to the terms in Eq. (1), would contain

$$+2m_K\, f_S\, \overline{\ell}(1+\gamma_5)\nu$$
$$+(2f_T/m_K)(P_K)_\lambda(P_\pi)_\mu\, \overline{\ell}\,\sigma_{\lambda\mu}(1+\gamma_5)\nu\ , \qquad (10)$$

where f_S is the scalar form factor, and f_T is the tensor form factor. In the case of the K_{e3} decays where the f_- term can be neglected, experiments have yielded limits on $|f_S/f_+|$ and $|f_T/f_+|$.

Fits for $K_{\ell 3}$ Form Factors. For K_{e3} data, we determine best values for the three parametrizations: linear (λ_+), quadratic ($\lambda_+^{'}$, $\lambda_+^{''}$) and pole (M_v). For $K_{\mu 3}$ data, we determine best values for the three parametrizations: linear (λ_+, λ_0), quadratic ($\lambda_+^{'}, \lambda_+^{''}$, λ_0) and pole (M_v, M_s). We then assume $\mu - e$ universality so that we can combine K_{e3} and $K_{\mu 3}$ data, and again determine best values for the three parametrizations: linear (λ_+, λ_0), quadratic ($\lambda_+^{'}, \lambda_+^{''}$, λ_0), and pole (M_v, M_s). When there is more than one parameter, fits are done including input correlations. Simple averages suffice in the two K_{e3} cases where there is only one parameter: linear (λ_+) and pole (M_v).

Both KTeV and KLOE see an improvement in the quality of their fits relative to linear fits when a quadratic term is introduced, as well as when the pole parametrization is used. The quadratic parametrization has the disadvantage that the quadratic parameter $\lambda_+^{''}$ is highly correlated with the linear parameter $\lambda_+^{'}$, in the neighborhood of 95%, and that neither parameter is very well determined. The pole fit has the same number of parameters as the linear fit, but yields slightly better fit probabilities, so that it would be advisable for all experiments to include the pole parametrization as one of their choices [9].

The "Kaon Particle Listings" show the results with and without assuming μ-e universality. The "Meson Summary Tables" show all of the results assuming μ-e universality, but most results not assuming μ-e universality are given only in the Listings.

References

1. L.M. Chounet, J.M. Gaillard, and M.K. Gaillard, Phys. Reports **4C**, 199 (1972).
2. H.W. Fearing, E. Fischbach, and J. Smith, Phys. Rev. **D2**, 542 (1970).
3. N. Cabibbo and A. Maksymowicz, Phys. Lett. **9**, 352 (1964).
4. W.-M. Yao *et al.*, Particle Data Group, J. Phys. **G33**, 1 (2006).
5. S. Eidleman *et al.*, Particle Data Group, Phys. Lett. **B592**, 1 (2004).
6. M. Roos *et al.*, Particle Data Group, Phys. Lett. **111B**, 73 (1982).
7. V. Bernard *et al.*, Phys. Lett. **B638**, 48 (2006).
8. A. Lai *et al.*, Phys. Lett. **B647**, 341 (2007), and references therein.
9. We thank P. Franzini (Rome U. and Frascati) for useful discussions on this point.

$K_{\ell 3}^{\pm}$ FORM FACTORS

In the form factor comments, the following symbols are used.

f_+ and f_- are form factors for the vector matrix element.

f_S and f_T refer to the scalar and tensor term.

$f_0 = f_+ + f_-\ t/(m^2_{K^+} - m^2_{\pi^0})$.

t = momentum transfer to the π.

λ_+ and λ_0 are the linear expansion coefficients of f_+ and f_0:

$f_+(t) = f_+(0)\ (1 + \lambda_+\, t\,/m^2_{\pi^+})$

For quadratic expansion

$f_+(t) = f_+(0)\ (1 + \lambda'_+\, t\,/m^2_{\pi^+} + \frac{\lambda''_+}{2}\ t^2/m^4_{\pi^+}\ )$

as used by KTeV. If there is a non-vanishing quadratic term, then λ_+ represents an average slope, which is then different from λ'_+.

NA48 and ISTRA quadratic expansion coefficients are converted with

$\lambda'_+{}^{PDG} = \lambda_+{}^{NA48}$ and $\lambda''_+{}^{PDG} = 2\,\lambda'_+{}^{NA48}$

$\lambda'_+{}^{PDG} = (\frac{m_{\pi^+}}{m_{\pi^0}})^2\ \lambda_+{}^{ISTRA}$ and

$\lambda''_+{}^{PDG} = 2\,(\frac{m_{\pi^+}}{m_{\pi^0}})^4\ \lambda'_+{}^{ISTRA}$

ISTRA linear expansion coefficients are converted with

$\lambda_+{}^{PDG} = (\frac{m_{\pi^+}}{m_{\pi^0}})^2\ \lambda_+{}^{ISTRA}$ and $\lambda_0{}^{PDG} = (\frac{m_{\pi^+}}{m_{\pi^0}})^2\ \lambda_0{}^{ISTRA}$

The pole parametrization is

$f_+(t) = f_+(0)\ (\frac{M_V^2}{M_V^2 - t}\ )$

$f_0(t) = f_0(0)\ (\frac{M_S^2}{M_S^2 - t}\ )$

where M_V and M_S are the vector and scalar pole masses.

The following abbreviations are used:

DP = Dalitz plot analysis.

PI = π spectrum analysis.

MU = μ spectrum analysis.

POL= μ polarization analysis.

BR = $K^{\pm}_{\mu 3}/K^{\pm}_{e3}$ branching ratio analysis.

E = positron or electron spectrum analysis.

RC = radiative corrections.

λ_+ (LINEAR ENERGY DEPENDENCE OF f_+ IN $K_{e3}^{\pm}$ DECAY)

These results are for a linear expansion only. See the next section for fits including a quadratic term. For radiative correction of the $K^{\pm}_{e3}$ Dalitz plot, see GINSBERG 67, BECHERRAWY 70, CIRIGLIANO 02, CIRIGLIANO 04, and ANDRE 07. Results labeled OUR FIT are discussed in the review "$K^{\pm}_{\ell 3}$ and $K^0_{\ell 3}$ Form Factors" above. For earlier, lower statistics results, see the 2004 edition of this review, Physics Letters **B592** 1 (2004).

VALUE (units 10^{-2})	*EVTS*	*DOCUMENT ID*		*TECN*	*CHG*	*COMMENT*
2.97 ±0.05 OUR FIT Assuming μ-e universality						
2.98 ±0.05 OUR AVERAGE						
3.044±0.083±0.074	1.1M	AKOPDZANOV	09	TNF	±	
2.966±0.050±0.034	919k	[116] YUSHCHENKO	04B	ISTR	−	DP
2.78 ±0.26 ±0.30	41k	SHIMIZU	00	SPEC	+	DP
2.84 ±0.27 ±0.20	32k	[117] AKIMENKO	91	SPEC		PI, no RC
2.9 ±0.4	62k	[118] BOLOTOV	88	SPEC		PI, no RC
• • • We do not use the following data for averages, fits, limits, etc. • • •						
3.06 ±0.09 ±0.06	550k	[116,119] AJINENKO	03C	ISTR	−	DP
2.93 ±0.15 ±0.2	130k	[119] AJINENKO	02	SPEC		DP

[116] Rescaled to agree with our conventions as noted above.

[117] AKIMENKO 91 state that radiative corrections would raise λ_+ by 0.0013.

[118] BOLOTOV 88 state radiative corrections of GINSBERG 67 would raise λ_+ by 0.002.

[119] Superseded by YUSHCHENKO 04B.

Meson Particle Listings

$K^{\pm}$

λ_+ (LINEAR ENERGY DEPENDENCE OF f_+ IN $K^{\pm}_{\mu 3}$ DECAY)

Results labeled OUR FIT are discussed in the review "$K^{\pm}_{\ell 3}$ and $K^0_{\ell 3}$ Form Factors" above. For earlier, lower statistics results, see the 2004 edition of this review, Physics Letters **B592** 1 (2004).

VALUE (units 10^{-2})	EVTS	DOCUMENT ID		TECN	CHG	COMMENT
2.97±0.05 OUR FIT		Assuming μ-e universality				
2.96±0.17 OUR FIT		Not assuming μ-e universality				
2.96±0.14±0.10	540k	[120] YUSHCHENKO	04	ISTR	−	DP
• • • We do not use the following data for averages, fits, limits, etc. • • •						
3.21±0.45	112k	[121] AJINENKO	03	ISTR	−	DP

[120] Rescaled to agree with our conventions as noted above.
[121] Superseded by YUSHCHENKO 04.

λ_0 (LINEAR ENERGY DEPENDENCE OF f_0 IN $K^{\pm}_{\mu 3}$ DECAY)

Results labeled OUR FIT are discussed in the review "$K^{\pm}_{\ell 3}$ and $K^0_{\ell 3}$ Form Factors" above. For earlier, lower statistics results, see the 2004 edition of this review, Physics Letters **B592** 1 (2004).

VALUE (units 10^{-2})	$d\lambda_0/d\lambda_+$	EVTS	DOCUMENT ID		TECN	CHG	COMMENT
1.95±0.12 OUR FIT			Assuming μ-e universality				
1.96±0.13 OUR FIT			Not assuming μ-e universality				
+1.96±0.12±0.06	−0.348	540k	[122] YUSHCHENKO	04	ISTR	−	DP
• • • We do not use the following data for averages, fits, limits, etc. • • •							
+2.09±0.45	−0.46	112k	[123] AJINENKO	03	ISTR	−	DP
+1.9 ±0.64		24k	[124] HORIE	01	SPEC	+	BR
+1.9 ±1.0	+0.03	55k	[125] HEINTZE	77	SPEC	+	BR

[122] Rescaled to agree with our conventions as noted above.
[123] Superseded by YUSHCHENKO 04.
[124] HORIE 01 assumes μ-e universality in $K^{\pm}_{\ell 3}$ decay and uses SHIMIZU 00 value λ=0.0278±0.0040 from $K^{\pm}_{e3}$ decay.
[125] HEINTZE 77 uses $\lambda_+ = 0.029 \pm 0.003$. $d\lambda_0/d\lambda_+$ estimated by us.

λ'_+ (LINEAR $K^{\pm}_{e3}$ FORM FACTOR FROM QUADRATIC FIT)

VALUE (units 10^{-2})	EVTS	DOCUMENT ID		TECN	CHG	COMMENT
2.485±0.163±0.034	919k	[126,127] YUSHCHENKO	04B	ISTR	−	DP
• • • We do not use the following data for averages, fits, limits, etc. • • •						
3.07 ±0.21	550k	[126,128] AJINENKO	03C	ISTR	−	DP

[126] Rescaled to agree with our conventions as noted above.
[127] YUSHCHENKO 04B λ'_+ and λ''_+ are strongly correlated with coefficient $\rho(\lambda'_+, \lambda''_+) = -0.95$.
[128] Superseded by YUSHCHENKO 04B.

λ''_+ (QUADRATIC $K^{\pm}_{e3}$ FORM FACTOR)

VALUE (units 10^{-2})	EVTS	DOCUMENT ID		TECN	CHG	COMMENT
0.192±0.062±0.071	919k	[129,130] YUSHCHENKO	04B	ISTR	−	DP
• • • We do not use the following data for averages, fits, limits, etc. • • •						
−0.5 ±0.7 ±1.5	550k	[129,131] AJINENKO	03C	ISTR	−	DP

[129] Rescaled to agree with our conventions as noted above.
[130] YUSHCHENKO 04B λ'_+ and λ''_+ are strongly correlated with coefficient $\rho(\lambda'_+, \lambda''_+) = -0.95$.
[131] Superseded by YUSHCHENKO 04B.

$|f_S/f_+|$ FOR $K^{\pm}_{e3}$ DECAY

Ratio of scalar to f_+ couplings.

VALUE (units 10^{-2})	CL%	EVTS	DOCUMENT ID		TECN	CHG	COMMENT
−0.3 $^{+0.8}_{-0.7}$ OUR AVERAGE							
$-0.37^{+0.66}_{-0.56}\pm0.41$		919k	YUSHCHENKO	04B	ISTR	−	λ'_+, λ''_+, f_S fit
0.2 ±2.6 ±1.4		41k	SHIMIZU	00	SPEC	+	λ_+, f_S, f_T fit
• • • We do not use the following data for averages, fits, limits, etc. • • •							
$0.2\ ^{+2.0}_{-2.2}$ ±0.3		550k	[132] AJINENKO	03C	ISTR	−	λ_+, f_S, f_T fit
$-1.9\ ^{+2.5}_{-1.6}$		130k	[132] AJINENKO	02	SPEC		λ_+, f_S fit
7.0 ±1.6 ±1.6		32k	AKIMENKO	91	SPEC		λ_+, f_S, f_T, ϕ fit
0 ± 10		2827	[133] BRAUN	75	HLBC	+	
< 13	90	4017	CHIANG	72	OSPK	+	
14^{+3}_{-4}		2707	[133] STEINER	71	HLBC	+	λ_+, f_S, f_T, ϕ fit
< 23	90		BOTTERILL	68C	ASPK		
< 18	90		BELLOTTI	67B	HLBC		
< 30	95		KALMUS	67	HLBC	+	

[132] Superseded by YUSHCHENKO 04B.
[133] Statistical errors only.

$|f_T/f_+|$ FOR $K^{\pm}_{e3}$ DECAY

Ratio of tensor to f_+ couplings.

VALUE (units 10^{-2})	CL%	EVTS	DOCUMENT ID		TECN	CHG	COMMENT
− 1.2± 2.3 OUR AVERAGE							
− 1.2± 2.1± 1.1		919k	YUSHCHENKO	04B	ISTR	−	λ'_+,λ''_+,f_T fit
1 ±14 ± 9		41k	SHIMIZU	00	SPEC	+	λ_+, f_S, f_T fit
• • • We do not use the following data for averages, fits, limits, etc. • • •							
$2.1^{+6.4}_{-7.5}\pm2.6$		550k	[134] AJINENKO	03C	ISTR	−	λ_+, f_S, f_T fit
$-4.5^{+6.0}_{-5.7}$		130k	[134] AJINENKO	02	SPEC		λ_+, f_T fit
$53\ ^{+9}_{-10}$ ±10		32k	AKIMENKO	91	SPEC		λ_+, f_S, f_T, ϕ fit
7 ±37		2827	[135] BRAUN	75	HLBC	+	
< 75	90	4017	CHIANG	72	OSPK	+	
24 $^{+16}_{-14}$		2707	[135] STEINER	71	HLBC	+	λ_+, f_S, f_T, ϕ fit
< 58	90		BOTTERILL	68C	ASPK		
< 58	90		BELLOTTI	67B	HLBC		
< 110	95		KALMUS	67	HLBC	+	

[134] Superseded by YUSHCHENKO 04B.
[135] Statistical errors only.

f_S/f_+ FOR $K^{\pm}_{\mu 3}$ DECAY

Ratio of scalar to f_+ couplings.

VALUE (units 10^{-2})	EVTS	DOCUMENT ID		TECN	CHG	COMMENT
0.17±0.14±0.54	540k	[136] YUSHCHENKO	04	ISTR	−	DP
• • • We do not use the following data for averages, fits, limits, etc. • • •						
0.4 ±0.5 ±0.5	112k	[137] AJINENKO	03	ISTR	−	DP

[136] The second error is the theoretical error from the uncertainty in the chiral perturbation theory prediction for λ_0, ±0.0053, combined in quadrature with the systematic error ±0.0009.
[137] The second error is the theoretical error from the uncertainty in the chiral perturbation theory prediction for λ_0. Superseded by YUSHCHENKO 04.

f_T/f_+ FOR $K^{\pm}_{\mu 3}$ DECAY

Ratio of tensor to f_+ couplings.

VALUE (units 10^{-2})	EVTS	DOCUMENT ID		TECN	CHG	COMMENT
−0.07± 0.71±0.20	540k	YUSHCHENKO	04	ISTR	−	DP
• • • We do not use the following data for averages, fits, limits, etc. • • •						
−2.1 ± 2.8 ±1.4	112k	[138] AJINENKO	03	ISTR	−	DP
2 ±12	1585	BRAUN	75	HLBC		

[138] The second error is the theoretical error from the uncertainty in the chiral perturbation theory prediction for λ_0. Superseded by YUSHCHENKO 04.

$K^{\pm}_{\ell 4}$ FORM FACTORS

Based on the parametrizations of AMOROS 99, the $K^{\pm}_{\ell 4}$ form factors can be expressed as

$$F_s = f_s + f'_s\, q^2 + f''_s\, q^4 + f'_e\, S_e / 4m_\pi^2$$
$$F_p = f_p$$
$$G_p = g_p + g'_p\, q^2$$
$$H_p = h_p$$

where $q^2 = (S_\pi / 4m_\pi^2) - 1$, S_π is the invariant mass squared of the dipion, and S_e is the invariant mass squared of the dilepton.

f_s FOR $K^{\pm} \to \pi^+\pi^- e^{\pm}\nu$ DECAY

VALUE	EVTS	DOCUMENT ID		TECN	CHG
5.712±0.032 OUR AVERAGE					
5.705±0.003±0.035	1.1M	[139] BATLEY	12	NA48	±
5.75 ±0.02 ±0.08	400k	[140] PISLAK	03	B865	+

[139] BATLEY 12 uses data collected in 2003–2004. The result is obtained from a measurement of $\Gamma(\pi^+\pi^- e\nu)/\Gamma(\pi^+\pi^-\pi^+)$ and assumed PDG 12 value of $\Gamma(\pi^+\pi^-\pi^+)/\Gamma = (5.59 \pm 0.04) \times 10^{-2}$.
[140] Radiative corrections included. Using Roy equations and not including isospin breaking, PISLAK 03 obtains the following $\pi\pi$ scattering lengths $a_0^0 = 0.228 \pm 0.012 \pm 0.004\,^{+0.012}_{-0.016}$(theor.) and $a_0^2 = -0.0365 \pm 0.0023 \pm 0.0008\,^{+0.0031}_{-0.0026}$(theor.).

f'_s/f_s FOR $K^{\pm} \to \pi^+\pi^- e^{\pm}\nu$ DECAY

VALUE (units 10^{-2})	EVTS	DOCUMENT ID		TECN	CHG
15.2±0.7±0.5	1.13M	[141] BATLEY	10C	NA48	±
• • • We do not use the following data for averages, fits, limits, etc. • • •					
17.2±0.9±0.6	670k	[142] BATLEY	08A	NA48	±

[141] Radiative corrections included. Using Roy equations and including isospin breaking, BATLEY 10C obtains the following scattering lengths $a_0^0 = 0.2220 \pm 0.0128 \pm 0.0050 \pm 0.0037$(theor.), $a_0^2 = -0.0432 \pm 0.0086 \pm 0.0034 \pm 0.0028$(theor.). The correlation with $f''_s/f_s = -0.954$ and with $f'_e/f_s = 0.080$. Supersedes BATLEY 08A.
[142] Radiative corrections included. Using Roy equations and not including isospin breaking, BATLEY 08A obtains the following $\pi\pi$ scattering length $a_0^0 = 0.233 \pm 0.016 \pm 0.007$ $a_0^2 = -0.0471 \pm 0.011 \pm 0.004$.

f_s''/f_s FOR $K^\pm \to \pi^+\pi^- e^\pm \nu$ DECAY

VALUE (units 10^{-2})	EVTS	DOCUMENT ID		TECN	CHG
−7.3±0.7±0.6	1.13M	[143] BATLEY	10C	NA48	±
• • • We do not use the following data for averages, fits, limits, etc. • • •					
−9.0±0.9±0.7	670k	[144] BATLEY	08A	NA48	±

[143] Radiative corrections included. Using Roy equations and including isospin breaking, BATLEY 10C obtains the following scattering lengths $a_0^0 = 0.2220 \pm 0.0128 \pm 0.0050 \pm 0.0037$ (theor.), $a_0^2 = -0.0432 \pm 0.0086 \pm 0.0034 \pm 0.0028$ (theor.). The correlation with $f_s'/f_s = -0.954$ and with $f_e'/f_s = 0.019$. Supersedes BATLEY 08A.

[144] Radiative corrections included. Using Roy equations and not including isospin breaking, BATLEY 08A obtains the following $\pi\pi$ scattering length $a_0^0 = 0.233 \pm 0.016 \pm 0.007$ $a_0^2 = -0.0471 \pm 0.011 \pm 0.004$.

f_e'/f_s FOR $K^\pm \to \pi^+\pi^- e^\pm \nu$ DECAY

VALUE (units 10^{-2})	EVTS	DOCUMENT ID		TECN	CHG
6.8±0.6±0.7	1.13M	[145] BATLEY	10C	NA48	±
• • • We do not use the following data for averages, fits, limits, etc. • • •					
8.1±0.8±0.9	670k	[146] BATLEY	08A	NA48	±

[145] Radiative corrections included. Using Roy equations and including isospin breaking, BATLEY 10C obtains the following scattering lengths $a_0^0 = 0.2220 \pm 0.0128 \pm 0.0050 \pm 0.0037$ (theor.), $a_0^2 = -0.0432 \pm 0.0086 \pm 0.0034 \pm 0.0028$ (theor.). The correlation with $f_s'/f_s = 0.080$ and with $f_s''/f_s = 0.019$. Supersedes BATLEY 08A.

[146] Radiative corrections included. Using Roy equations and not including isospin breaking, BATLEY 08A obtains the following $\pi\pi$ scattering length $a_0^0 = 0.233 \pm 0.016 \pm 0.007$ $a_0^2 = -0.0471 \pm 0.011 \pm 0.004$.

f_p/f_s FOR $K^\pm \to \pi^+\pi^- e^\pm \nu$ DECAY

VALUE (units 10^{-2})	EVTS	DOCUMENT ID		TECN	CHG
−4.8±0.3±0.4	1.13M	[147] BATLEY	10C	NA48	±
• • • We do not use the following data for averages, fits, limits, etc. • • •					
−4.8±0.4±0.4	670k	[148] BATLEY	08A	NA48	±

[147] Radiative corrections included. Using Roy equations and including isospin breaking, BATLEY 10C obtains the following scattering lengths $a_0^0 = 0.2220 \pm 0.0128 \pm 0.0050 \pm 0.0037$ (theor.), $a_0^2 = -0.0432 \pm 0.0086 \pm 0.0034 \pm 0.0028$ (theor.). Supersedes BATLEY 08A.

[148] Radiative corrections included. Using Roy equations and not including isospin breaking, BATLEY 08A obtains the following $\pi\pi$ scattering length $a_0^0 = 0.233 \pm 0.016 \pm 0.007$ $a_0^2 = -0.0471 \pm 0.011 \pm 0.004$.

g_p/f_s FOR $K^\pm \to \pi^+\pi^- e^\pm \nu$ DECAY

VALUE (units 10^{-2})	EVTS	DOCUMENT ID		TECN	CHG
86.8±1.0±1.0	1.13M	[149] BATLEY	10C	NA48	±
• • • We do not use the following data for averages, fits, limits, etc. • • •					
87.3±1.3±1.2	670k	[150] BATLEY	08A	NA48	±
80.9±0.9±1.2	400k	[151] PISLAK	03	B865	±

[149] Radiative corrections included. Using Roy equations and including isospin breaking, BATLEY 10C obtains the following scattering lengths $a_0^0 = 0.2220 \pm 0.0128 \pm 0.0050 \pm 0.0037$ (theor.), $a_0^2 = -0.0432 \pm 0.0086 \pm 0.0034 \pm 0.0028$ (theor.). Supersedes BATLEY 08A. The correlation with $g_p'/f_s = -0.914$. Supersedes BATLEY 08A.

[150] Radiative corrections included. Using Roy equations and not including isospin breaking, BATLEY 08A obtains the following $\pi\pi$ scattering length $a_0^0 = 0.233 \pm 0.016 \pm 0.007$ $a_0^2 = -0.0471 \pm 0.011 \pm 0.004$.

[151] Radiative corrections included. Using Roy equations PISLAK 03 obtains the following scattering lengths $a_0^0 = 0.203 \pm 0.033 \pm 0.004$, $a_0^2 = -0.055 \pm 0.023 \pm 0.003$.

g_p'/f_s FOR $K^\pm \to \pi^+\pi^- e^\pm \nu$ DECAY

VALUE (units 10^{-2})	EVTS	DOCUMENT ID		TECN	CHG
8.9±1.7±1.3	1.13M	[152] BATLEY	10C	NA48	±
• • • We do not use the following data for averages, fits, limits, etc. • • •					
8.1±2.2±1.5	670k	[153] BATLEY	08A	NA48	±
12.0±1.9±0.7	400k	[154] PISLAK	03	B865	±

[152] Radiative corrections included. Using Roy equations and including isospin breaking, BATLEY 10C obtains the following scattering lengths $a_0^0 = 0.2220 \pm 0.0128 \pm 0.0050 \pm 0.0037$ (theor.), $a_0^2 = -0.0432 \pm 0.0086 \pm 0.0034 \pm 0.0028$ (theor.). The correlation with $g_p/f_s = -0.914$. Supersedes BATLEY 08A.

[153] Radiative corrections included. Using Roy equations and not including isospin breaking, BATLEY 08A obtains the following $\pi\pi$ scattering length $a_0^0 = 0.233 \pm 0.016 \pm 0.007$ $a_0^2 = -0.0471 \pm 0.011 \pm 0.004$.

[154] Radiative corrections included. Using Roy equations PISLAK 03 obtains the following scattering lengths $a_0^0 = 0.203 \pm 0.033 \pm 0.004$, $a_0^2 = -0.055 \pm 0.023 \pm 0.003$.

h_p/f_s FOR $K^\pm \to \pi^+\pi^- e^\pm \nu$ DECAY

VALUE (units 10^{-2})	EVTS	DOCUMENT ID		TECN	CHG
−39.8±1.5±0.8	1.13M	[155] BATLEY	10C	NA48	±
• • • We do not use the following data for averages, fits, limits, etc. • • •					
−41.1±1.9±0.8	670k	[156] BATLEY	08A	NA48	±
−51.3±3.3±3.5	400k	[157] PISLAK	03	B865	±

[155] Radiative corrections included. Using Roy equations and including isospin breaking, BATLEY 10C obtains the following scattering lengths $a_0^0 = 0.2220 \pm 0.0128 \pm 0.0050 \pm 0.0037$ (theor.), $a_0^2 = -0.0432 \pm 0.0086 \pm 0.0034 \pm 0.0028$ (theor.). Supersedes BATLEY 08A.

[156] Radiative corrections included. Using Roy equations and not including isospin breaking, BATLEY 08A obtains the following $\pi\pi$ scattering length $a_0^0 = 0.233 \pm 0.016 \pm 0.007$ $a_0^2 = -0.0471 \pm 0.011 \pm 0.004$.

[157] Radiative corrections included. Using Roy equations PISLAK 03 obtains the following scattering lengths $a_0^0 = 0.203 \pm 0.033 \pm 0.004$, $a_0^2 = -0.055 \pm 0.023 \pm 0.003$.

DECAY FORM FACTOR FOR $K^\pm \to \pi^0\pi^0 e^\pm \nu$

Given in BOLOTOV 86B, BARMIN 88B, and SHIMIZU 04.

$K^\pm \to \ell^\pm \nu\gamma$ FORM FACTORS

For definitions of the axial-vector F_A and vector F_V form factor, see the "Note on $\pi^\pm \to \ell^\pm \nu\gamma$ and $K^\pm \to \ell^\pm \nu\gamma$ Form Factors" in the $\pi^\pm$ section. In the kaon literature, often different definitions $a_K = F_A/m_K$ and $v_K = F_V/m_K$ are used.

$F_A + F_V$, SUM OF AXIAL-VECTOR AND VECTOR FORM FACTOR FOR $K \to e\nu_e\gamma$

VALUE	EVTS	DOCUMENT ID		TECN	COMMENT
0.133±0.008 OUR AVERAGE		Error includes scale factor of 1.3.			See the ideogram below.
0.125±0.007±0.001	1.4K	[158] AMBROSINO	09E	KLOE	E_γ in 10–250 MeV, $p_e > 200$ MeV/c
0.147±0.011	51	[159] HEINTZE	79	SPEC	
$0.150^{+0.018}_{-0.023}$	56	[160] HEARD	75	SPEC	

[158] Vector form factor fitted with a linear function, $V(x) = F_V(1 + \lambda(1-x))$, $x = 2E_\gamma/m_K$. The fitted value of $\lambda = 0.38 \pm 0.20 \pm 0.02$ with a correlation of −0.93 between $(F_V + F_A)$ and λ.

[159] HEINTZE 79 quotes absolute value of $|F_A + F_V| \sin\theta_C$. We use $\sin\theta_C = V_{us} = 0.2205$.

[160] HEARD 75 quotes absolute value of $|F_A + F_V| \sin\theta_C$. We use $\sin\theta_C = V_{us} = 0.2205$.

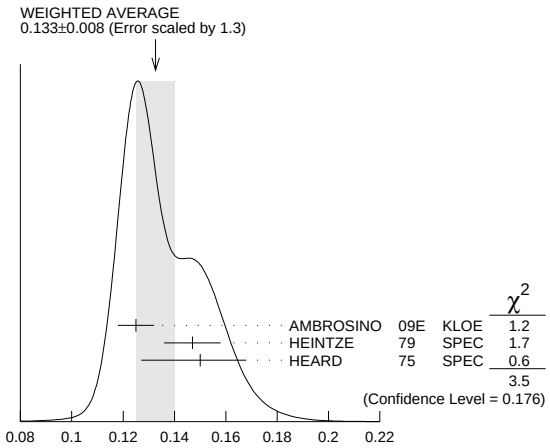

$F_A + F_V$, SUM OF AXIAL-VECTOR AND VECTOR FORM FACTOR FOR $K \to e\nu_e\gamma$

$F_A + F_V$, SUM OF AXIAL-VECTOR AND VECTOR FORM FACTOR FOR $K \to \mu\nu_\mu\gamma$

VALUE	CL%	EVTS	DOCUMENT ID		TECN	CHG
0.165±0.007±0.011		2588	[161] ADLER	00B	B787	+
• • • We do not use the following data for averages, fits, limits, etc. • • •						
−1.2 to 1.1	90		DEMIDOV	90	XEBC	
< 0.23	90		[161] AKIBA	85	SPEC	

[161] Quotes absolute value. Sign not determined.

$F_A - F_V$, DIFFERENCE OF AXIAL-VECTOR AND VECTOR FORM FACTOR FOR $K \to e\nu_e\gamma$

VALUE	EVTS	DOCUMENT ID		TECN
<0.49	90	[162] HEINTZE	79	SPEC

[162] HEINTZE 79 quotes $|F_A - F_V| < \sqrt{11}\,|F_A + F_V|$.

Meson Particle Listings

$K^{\pm}$

$F_A - F_V$, DIFFERENCE OF AXIAL-VECTOR AND VECTOR FORM FACTOR FOR $K \to \mu\nu_\mu\gamma$

VALUE	CL%	EVTS	DOCUMENT ID		TECN	CHG
−0.24 to 0.04	90	2588	ADLER	00B	B787	+
• • • We do not use the following data for averages, fits, limits, etc. • • •						
−2.2 to 0.6	90		DEMIDOV	90	XEBC	
−2.5 to 0.3	90		AKIBA	85	SPEC	

$K^{\pm}$ CHARGE RADIUS

VALUE (fm)	DOCUMENT ID		COMMENT
0.560±0.031 OUR AVERAGE			
0.580±0.040	AMENDOLIA	86B	$Ke \to Ke$
0.530±0.050	DALLY	80	$Ke \to Ke$
• • • We do not use the following data for averages, fits, limits, etc. • • •			
0.620±0.037	BLATNIK	79	VMD + dispersion relations

CP VIOLATION TESTS IN K^+ AND K^- DECAYS

$$\Delta(K^{\pm}_{\pi ee}) = \frac{\Gamma(K^+_{\pi ee})-\Gamma(K^-_{\pi ee})}{\Gamma(K^+_{\pi ee})+\Gamma(K^-_{\pi ee})}$$

VALUE (units 10^{-2})		DOCUMENT ID		TECN
−2.2±1.5±0.6	[163]	BATLEY	09	NA48

[163] This implies an upper limit of 2.1×10^{-2} at 90% CL.

$$\Delta(K^{\pm}_{\pi\mu\mu}) = \frac{\Gamma(K^+_{\pi\mu\mu})-\Gamma(K^-_{\pi\mu\mu})}{\Gamma(K^+_{\pi\mu\mu})+\Gamma(K^-_{\pi\mu\mu})}$$

VALUE		DOCUMENT ID		TECN
0.010±0.023 OUR AVERAGE				
0.011±0.023	[164]	BATLEY	11A	NA48
−0.02 ±0.11 ±0.04		PARK	02	HYCP

[164] This corresponds to the asymmetry upper limit of $< 2.9 \times 10^{-2}$ at 90% CL.

$$\Delta(K^{\pm}_{\pi\pi\gamma}) = \frac{\Gamma(K^+_{\pi\pi\gamma})-\Gamma(K^-_{\pi\pi\gamma})}{\Gamma(K^+_{\pi\pi\gamma})+\Gamma(K^-_{\pi\pi\gamma})}$$

VALUE (units 10^{-3})	EVTS		DOCUMENT ID		TECN
0.0±1.0±0.6	1M	[165]	BATLEY	10A	NA48

[165] This value implies the upper bound for this asymmetry 1.5×10^{-3} at 90% CL.

FORWARD-BACKWARD ASYMMETRY IN $K^{\pm}$ DECAYS

$$A_{FB}(K^{\pm}_{\pi\mu\mu}) = \frac{\Gamma(\cos(\theta_{K\mu})>0)-\Gamma(\cos(\theta_{K\mu})<0)}{\Gamma(\cos(\theta_{K\mu})>0)+\Gamma(\cos(\theta_{K\mu})<0)}$$

VALUE	CL%		DOCUMENT ID		TECN
$< 2.3 \times 10^{-2}$	90	[166]	BATLEY	11A	NA48

[166] BATLEY 11A gives a corresponding value of the asymmetry $A_{FB} = (-2.4 \pm 1.8) \times 10^{-2}$.

T VIOLATION TESTS IN K^+ AND K^- DECAYS

P_T in $K^+ \to \pi^0\mu^+\nu_\mu$

T-violating muon polarization. Sensitive to new sources of CP violation beyond the Standard Model.

VALUE (units 10^{-3})	EVTS		DOCUMENT ID		TECN	CHG
−1.7±2.3±1.1		[167]	ABE	04F	K246	+
• • • We do not use the following data for averages, fits, limits, etc. • • •						
−4.2±4.9±0.9	3.9M		ABE	99S	K246	+

[167] Includes three sets of data: 96-97 (ABE 99S), 98, and 99-00 totaling about three times the ABE 99S data sample. Corresponds to $P_T < 5.0 \times 10^{-3}$ at 90% CL.

P_T in $K^+ \to \mu^+\nu_\mu\gamma$

T-violating muon polarization. Sensitive to new sources of CP violation beyond the Standard Model.

VALUE (units 10^{-2})	EVTS		DOCUMENT ID		TECN	CHG
−0.64±1.85±0.10	114k	[168]	ANISIMOVSK...03		K246	+

[168] Muons stopped and polarization measured from decay to positrons.

Im(ξ) in $K^+ \to \pi^0\mu^+\nu_\mu$ DECAY (from transverse μ pol.)

Test of T reversal invariance.

VALUE	EVTS		DOCUMENT ID		TECN	CHG	COMMENT
−0.006 ±0.008 OUR AVERAGE							
−0.0053±0.0071±0.0036		[169]	ABE	04F	K246	+	
−0.016 ±0.025	20M		CAMPBELL	81	CNTR	+	Pol.
• • • We do not use the following data for averages, fits, limits, etc. • • •							
−0.013 ±0.016 ±0.003	3.9M		ABE	99S	CNTR	+	p_T K^+ at rest

[169] Includes three sets of data: 96-97 (ABE 99S), 98, and 99-00 totaling about three times the ABE 99S data sample. Corresponds to Im(ξ) < 0.016 at 90% CL.

$K^{\pm}$ REFERENCES

BATLEY	14	PL B730 141	J.R. Batley *et al.*	(CERN NA48/2 Collab.)
LAZZERONI	13	PL B719 326	C. Lazzeroni *et al.*	(CERN NA62 Collab.)
BATLEY	12	PL B715 105	J.R. Batley *et al.*	(CERN NA48/2 Collab.)
PDG	12	PR D86 010001	J. Beringer *et al.*	(PDG Collab.)
BATLEY	11A	PL B697 107	J.R. Batley *et al.*	(CERN NA48/2 Collab.)
LAZZERONI	11	PL B698 105	C. Lazzeroni *et al.*	(CERN NA62 Collab.)
ADLER	10	PR D81 092001	S. Adler *et al.*	(BNL E787 Collab.)
BATLEY	10A	EPJ C68 75	J.R. Batley *et al.*	(CERN NA48/2 Collab.)
BATLEY	10C	EPJ C70 635	J.R. Batley *et al.*	(CERN NA48/2 Collab.)
PDG	10	JP G37 075021	K. Nakamura *et al.*	(PDG Collab.)
PISLAK	10A	PRL 105 019901E	S. Pislak *et al.*	(BNL E865 Collab.)
AKOPDZANOV	09	PAN 71 2074	G.A. Akopdzanov *et al.*	(IHEP)
		Translated from YAF 71 2108.		
AMBROSINO	09E	EPJ C64 627	F. Ambrosino *et al.*	(KLOE Collab.)
Also		EPJ C65 703 (errat)	F. Ambrosino *et al.*	(KLOE Collab.)
BATLEY	09	PL B677 246	J.R. Batley *et al.*	(CERN NA48/2 Collab.)
BATLEY	09A	EPJ C64 589	J.R. Batley *et al.*	(CERN NA48/2 Collab.)
BISSEGGER	09	NP B806 178	M. Bissegger *et al.*	
AMBROSINO	08	JHEP 0801 073	F. Ambrosino *et al.*	(KLOE Collab.)
AMBROSINO	08A	JHEP 0802 098	F. Ambrosino *et al.*	(KLOE Collab.)
AMBROSINO	08E	PL B666 305	F. Ambrosino *et al.*	(KLOE Collab.)
ARTAMONOV	08	PRL 101 191802	A.V. Artamonov *et al.*	(BNL E949 Collab.)
Also		PR D79 092004	A.V. Artamonov *et al.*	(BNL E949 Collab.)
BATLEY	08	PL B659 493	J.R. Batley *et al.*	(CERN NA48/2 Collab.)
BATLEY	08A	EPJ C54 411	J.R. Batley *et al.*	(CERN NA48/2 Collab.)
AKIMENKO	07	PAN 70 702	S.A. Akimenko *et al.*	(ISTRA+ Collab.)
		Translated from YAF 70 734.		
ANDRE	07	ANP 322 2518	T. Andre	(EFI)
BATLEY	07A	EPJ C50 329	J.R. Batley *et al.*	(CERN NA48/2 Collab.)
Also		EPJ C52 1021 (errat)	J.R. Batley *et al.*	(CERN NA48/2 Collab.)
BATLEY	07B	PL B649 349	J.R. Batley *et al.*	(CERN NA48/2 Collab.)
BATLEY	07E	EPJ C52 875	J.R. Batley *et al.*	(CERN NA48/2 Collab.)
TCHIKILEV	07	PAN 70 29	O.G. Tchikilev *et al.*	(ISTRA+ Collab.)
ALIEV	06	EPJ C46 61	M.A. Aliev *et al.*	(KEK E470 Collab.)
AMBROSINO	06A	PL B632 76	F. Ambrosino *et al.*	(KLOE Collab.)
BATLEY	06	PL B634 474	J.R. Batley *et al.*	(CERN NA48/2 Collab.)
BATLEY	06A	PL B638 22	J.R. Batley *et al.*	(CERN NA48/2 Collab.)
Also		PL B640 297 (errat)	J.R. Batley *et al.*	(CERN NA48/2 Collab.)
BATLEY	06B	PL B633 173	J.R. Batley *et al.*	(CERN NA48/2 Collab.)
COLANGELO	06A	PL B638 187	G. Colangelo *et al.*	
MA	06	PR D73 037101	H. Ma *et al.*	(BNL E865 Collab.)
PDG	06	JP G33 1	W.-M. Yao *et al.*	(PDG Collab.)
SHIMIZU	06	PL B633 190	S. Shimizu *et al.*	(KEK E470 Collab.)
UVAROV	06	PAN 69 26	V.A. Uvarov *et al.*	(ISTRA+ Collab.)
AKOPDZHAN...	05	EPJ C40 343	G.A. Akopdzhanov *et al.*	(IHEP)
Also		PAN 68 948	G.A. Akopdzhanov *et al.*	(IHEP)
		Translated from YAF 68 986.		
AKOPDZHAN...	05B	JETPL 82 675	G.A. Akopdzhanov *et al.*	(IHEP)
		Translated from ZETFP 82 771.		
ARTAMONOV	05	PL B623 192	A.V. Artamonov *et al.*	(BNL E949 Collab.)
CABIBBO	05	JHEP 0503 021	N. Cabibbo, G. Isidori	(CERN, ROMAI, FRAS)
SHER	05	PR D72 012005	A. Sher *et al.*	(BNL E865 Collab.)
ABE	04F	PRL 93 131601	M. Abe *et al.*	(KEK E246 Collab.)
Also		PR D73 072005	M. Abe *et al.*	(KEK E246 Collab.)
ADLER	04	PR D70 037102	S. Adler *et al.*	(BNL E787 Collab.)
ALOISIO	04A	PL B597 139	A. Aloisio *et al.*	(KLOE Collab.)
ANISIMOVSK...	04	PRL 93 031801	V.V. Anisimovsky *et al.*	(BNL E949 Collab.)
Also		PR D77 052003	S. Adler *et al.*	(BNL E949 Collab.)
CABIBBO	04A	PRL 93 121801	N. Cabibbo	(CERN, ROMAI)
CIRIGLIANO	04	EPJ C35 53	V. Cirigliano, H. Neufeld, H. Pichl	(CIT, VALE+)
PDG	04	PL B592 1	S. Eidelman *et al.*	(PDG Collab.)
SHIMIZU	04	PR D70 037101	S. Shimizu *et al.*	(KEK E470 Collab.)
YUSHCHENKO	04	PL B581 31	O.P. Yushchenko *et al.*	(INRM, INRM)
YUSHCHENKO	04B	PL B589 111	O.P. Yushchenko *et al.*	(INRM)
AJINENKO	03	PAN 66 105	I.V. Ajinenko *et al.*	(IHEP, INRM)
		Translated from YAF 66 107.		
AJINENKO	03B	PL B567 159	I.V. Ajinenko *et al.*	(IHEP, INRM)
AJINENKO	03C	PL B574 14	I.V. Ajinenko *et al.*	(IHEP, INRM)
ALIEV	03	PL B554 7	M.A. Aliev *et al.*	(KEK E470 Collab.)
ANISIMOVSK...	03	PL B562 166	V.V. Anisimovsky *et al.*	
PISLAK	03	PR D67 072004	S. Pislak *et al.*	(BNL E865 Collab.)
Also		PR D81 119903E	S. Pislak *et al.*	(BNL E865 Collab.)
SHER	03	PRL 91 261802	A. Sher *et al.*	(BNL E865 Collab.)
ADLER	02	PRL 88 041803	S. Adler *et al.*	(BNL E787 Collab.)
ADLER	02B	PR D65 052009	S. Adler *et al.*	(BNL E787 Collab.)
ADLER	02C	PL B537 211	S. Adler *et al.*	(BNL E787 Collab.)
AJINENKO	02	PAN 65 2064	I.V. Ajinenko *et al.*	(IHEP, INRM)
		Translated from YAF 65 2125.		
CIRIGLIANO	02	EPJ C23 121	V. Cirigliano *et al.*	(VIEN, VALE, MARS)
PARK	02	PRL 88 111801	H.K. Park *et al.*	(FNAL HyperCP Collab.)
PDG	02	PR D66 010001	K. Hagiwara *et al.*	
POBLAGUEV	02	PRL 89 061803	A.A. Poblaguev *et al.*	(BNL 865 Collab.)
ADLER	01	PR D63 032004	S. Adler *et al.*	(BNL E787 Collab.)
HORIE	01	PL B513 311	K. Horie *et al.*	(KEK E426 Collab.)
PISLAK	01	PRL 87 221801	S. Pislak *et al.*	(BNL E865 Collab.)
Also		PR D67 072004	S. Pislak *et al.*	(BNL E865 Collab.)
Also		PRL 105 019901E	S. Pislak *et al.*	(BNL E865 Collab.)
ADLER	00	PRL 84 3768	S. Adler *et al.*	(BNL E787 Collab.)
ADLER	00B	PRL 85 2256	S. Adler *et al.*	(BNL E787 Collab.)
ADLER	00C	PRL 85 4856	S. Adler *et al.*	(BNL E787 Collab.)
APPEL	00	PRL 85 2450	R. Appel *et al.*	(BNL 865 Collab.)
Also		Thesis, Yale Univ.	D.R. Bergman	
Also		Thesis, Univ. Zurich	S. Pislak	
APPEL	00B	PRL 85 2877	R. Appel *et al.*	(BNL 865 Collab.)
MA	00	PRL 84 2580	H. Ma *et al.*	(BNL 865 Collab.)
PDG	00	EPJ C15 1	D.E. Groom *et al.*	(PDG Collab.)
SHIMIZU	00	PL B495 33	S. Shimizu *et al.*	(KEK E246 Collab.)
ABE	99S	PRL 83 4253	M. Abe *et al.*	(KEK E246 Collab.)
AMOROS	99	JP G25 1607	G. Amoros, J. Bijnens	(LUND, HELS)
APPEL	99	PRL 83 4482	R. Appel *et al.*	(BNL 865 Collab.)
ADLER	98	PR D58 012003	S. Adler *et al.*	(BNL E787 Collab.)
BATUSOV	98	NP B516 3	V.Y. Batusov *et al.*	
DAMBROSIO	98A	JHEP 9808 004	G. D'Ambrosio *et al.*	
ADLER	97	PRL 79 2204	S. Adler *et al.*	(BNL E787 Collab.)
ADLER	97C	PRL 79 4756	S. Adler *et al.*	(BNL E787 Collab.)
BERGMAN	97	Thesis, Yale Univ.	D.R. Bergman	
KITCHING	97	PRL 79 4079	P. Kitching *et al.*	(BNL E787 Collab.)
PISLAK	97	Thesis, Univ. Zurich	S. Pislak	
ADLER	96	PRL 76 1421	S. Adler *et al.*	(BNL E787 Collab.)
KOPTEV	95	JETPL 61 877	V.P. Koptev *et al.*	(PNPI)
		Translated from ZETFP 61 865.		
AOKI	94	PR D50 69	M. Aoki *et al.*	(INUS, KEK, TOKMS)
ATIYA	93	PRL 70 2521	M.S. Atiya *et al.*	(BNL E787 Collab.)
Also		PRL 71 305 (erratum)	M.S. Atiya *et al.*	(BNL E787 Collab.)
ATIYA	93B	PR D48 R1	M.S. Atiya *et al.*	(BNL E787 Collab.)
ALLIEGRO	92	PRL 68 278	C. Alliegro *et al.*	(BNL, FNAL, PSI+)
BARMIN	92	SJNP 55 547	V.V. Barmin *et al.*	(ITEP)
		Translated from YAF 55 976.		

IMAZATO 92 PRL 69 877 J. Imazato *et al.* (KEK, INUS, TOKY+)
IVANOV 92 THESIS Yu.M. Ivanov (PNPI)
LITTENBERG 92 PRL 68 443 L.S. Littenberg, R.E. Shrock (BNL, STON)
USHER 92 PR D45 3961 T. Usher *et al.* (UCI)
AKIMENKO 91 PL B259 225 S.A. Akimenko *et al.* (SERP, JINR, TBIL+)
BARMIN 91 SJNP 53 606 V.V. Barmin *et al.* (ITEP)
Translated from YAF 53 981.
DENISOV 91 JETPL 54 558 A.S. Denisov *et al.* (PNPI)
Translated from ZETFP 54 557.
Also THESIS Yu.M. Ivanov (PNPI)
ATIYA 90 PRL 64 21 M.S. Atiya *et al.* (BNL E787 Collab.)
ATIYA 90B PRL 65 1188 M.S. Atiya *et al.* (BNL E787 Collab.)
DEMIDOV 90 SJNP 52 1006 V.S. Demidov *et al.* (ITEP)
Translated from YAF 52 1595.
LEE 90 PRL 64 165 A.M. Lee *et al.* (BNL, FNAL, VILL, WASH+)
ATIYA 89 PRL 63 2177 M.S. Atiya *et al.* (BNL E787 Collab.)
BARMIN 89 SJNP 50 421 V.V. Barmin *et al.* (ITEP)
Translated from YAF 50 679.
BARMIN 88 SJNP 47 643 V.V. Barmin *et al.* (ITEP)
Translated from YAF 47 1011.
BARMIN 88B SJNP 48 1032 V.V. Barmin *et al.* (ITEP)
Translated from YAF 48 1719.
BOLOTOV 88 JETPL 47 7 V.N. Bolotov *et al.* (ASCI)
Translated from ZETFP 47 8.
GALL 88 PRL 60 186 K.P. Gall *et al.* (BOST, MIT, WILL, CIT+)
BARMIN 87 SJNP 45 62 V.V. Barmin *et al.* (ITEP)
Translated from YAF 45 97.
BOLOTOV 87 SJNP 45 1023 V.N. Bolotov *et al.* (INRM)
Translated from YAF 45 1652.
AMENDOLIA 86B PL B178 435 S.R. Amendolia *et al.* (CERN NA7 Collab.)
BOLOTOV 86 SJNP 44 73 V.N. Bolotov *et al.* (INRM)
Translated from YAF 44 117.
BOLOTOV 86B SJNP 44 68 V.N. Bolotov *et al.* (INRM)
Translated from YAF 44 108.
YAMANAKA 86 PR D34 85 T. Yamanaka *et al.* (KEK, TOKY)
Also PRL 52 329 R.S. Hayano *et al.* (TOKY, KEK)
AKIBA 85 PR D32 2911 Y. Akiba *et al.* (TOKY, TINT, TSUK, KEK)
BOLOTOV 85 JETPL 42 481 V.N. Bolotov *et al.* (INRM)
Translated from ZETFP 42 390.
ASANO 82 PL 113B 195 Y. Asano *et al.* (KEK, TOKY, INUS, OSAK)
COOPER 82 PL 112B 97 A.M. Cooper *et al.* (RL)
PDG 82B PL 111B 70 M. Roos *et al.* (HELS, CIT, CERN)
ASANO 81B PL 107B 159 Y. Asano *et al.* (KEK, TOKY, INUS, OSAK)
CAMPBELL 81 PRL 47 1032 M.K. Campbell *et al.* (YALE, BNL)
Also PR D27 1056 S.R. Blatt *et al.* (YALE, BNL)
LUM 81 PR D23 2522 G.K. Lum *et al.* (LBL, NBS+)
LYONS 81 ZPHY C10 215 L. Lyons, C. Albajar, G. Myatt (OXF)
DALLY 80 PRL 45 232 E.B. Dally *et al.* (UCLA+)
BARKOV 79 NP B148 53 L.M. Barkov *et al.* (NOVO, KIAE)
BLATNIK 79 LNC 24 39 S. Blatnik, J. Stahov, C.B. Lang (TUZL, GRAZ)
HEINTZE 79 NP B149 365 J. Heintze *et al.* (HEIDP, CERN)
ABRAMS 77 PR D15 22 R.J. Abrams *et al.* (BNL)
DEVAUX 77 NP B126 11 B. Devaux *et al.* (SACL, GEVA)
HEINTZE 77 PL 70B 482 J. Heintze *et al.* (HEIDP, CERN)
ROSSELET 77 PR D15 574 L. Rosselet *et al.* (GEVA, SACL)
BLOCH 76 PL 60B 393 P. Bloch *et al.* (GEVA, SACL)
BRAUN 76B LNC 17 521 H.M. Braun *et al.* (AACH3, BARI, BELG+)
DIAMANT-... 76 PL 62B 485 A.M. Diamant-Berger *et al.* (SACL, GEVA)
HEINTZE 76 PL 60B 302 J. Heintze *et al.* (HEIDP)
SMITH 76 NP B109 173 K.M. Smith *et al.* (GLAS, LIVP, OXF+)
WEISSENBE... 76 NP B115 55 A.O. Weissenberg *et al.* (ITEP, LEBD)
BLOCH 75 PL 56B 201 P. Bloch *et al.* (SACL, GEVA)
BRAUN 75 NP B89 210 H.M. Braun *et al.* (AACH3, BARI, BRUX+)
CHENG 75 NP A254 381 S.C. Cheng *et al.* (COLU, YALE)
HEARD 75 PL 55B 324 K.S. Heard *et al.* (CERN, HEIDH)
HEARD 75B PL 55B 327 K.S. Heard *et al.* (CERN, HEIDH)
SHEAFF 75 PR D12 2570 M. Sheaff (WISC)
SMITH 75 NP B91 45 K.M. Smith *et al.* (GLAS, LIVP, OXF+)
WEISSENBE... 74 PL 48B 474 A.O. Weissenberg *et al.* (ITEP, LEBD)
ABRAMS 73B PRL 30 500 R.J. Abrams *et al.* (BNL)
BACKENSTO... 73 PL 43B 431 G. Backenstoss *et al.* (CERN, KARLK, KARLE+)
LJUNG 73 PR D8 1307 D. Ljung, D. Cline (WISC)
Also PRL 28 523 D. Ljung (WISC)
Also PRL 28 1287 D. Cline, D. Ljung (WISC)
Also PRL 23 326 U. Camerini *et al.* (WISC)
LUCAS 73 PR D8 719 P.W. Lucas, H.D. Taft, W.J. Willis (YALE)
LUCAS 73B PR D8 727 P.W. Lucas, H.D. Taft, W.J. Willis (YALE)
PANG 73 PR D8 1989 C.Y. Pang *et al.* (EFI, ARIZ, LBL)
Also PL 40B 699 G.D. Cable *et al.* (EFI, LBL)
SMITH 73 NP B60 411 K.M. Smith *et al.* (GLAS, LIVP, OXF+)
ABRAMS 72 PRL 29 1118 R.J. Abrams *et al.* (BNL)
AUBERT 72 NC 12A 509 B. Aubert *et al.* (ORSAY, BRUX, EPOL)
CHIANG 72 PR D6 1254 I.H. Chiang *et al.* (ROCH, WISC)
CLARK 72 PRL 29 1274 A.R. Clark *et al.* (LBL)
FORD 72 PL 38B 335 W.T. Ford *et al.* (PRIN)
HOFFMASTER 72 NP B36 1 S. Hoffmaster *et al.* (STEV, SETO, LEHI)
BOURQUIN 71 PL 36B 615 M.H. Bourquin *et al.* (GEVA, SACL)
HAIDT 71 PR D3 10 D. Haidt (AACH, BARI, CERN, EPOL, NIJM+)
Also PL 29B 691 D. Haidt *et al.* (AACH, BARI, CERN, EPOL+)
KLEMS 71 PR D4 66 J.H. Klems, R.H. Hildebrand, R. Stiening (CHIC+)
Also PRL 24 1086 J.H. Klems, R.H. Hildebrand, R. Stiening (LRL+)
Also PRL 25 473 J.H. Klems, R.H. Hildebrand, R. Stiening (LRL+)
OTT 71 PR D3 52 R.J. Ott, T.W. Pritchard (LOQM)
ROMANO 71 PL 36B 525 F. Romano *et al.* (BARI, CERN, ORSAY)
SCHWEINB... 71 PL 36B 246 W. Schweinberger (AACH, BELG, CERN, NIJM+)
STEINER 71 PL 36B 521 H.J. Steiner (AACH, BARI, CERN, EPOL, ORSAY+)
BARDIN 70 PL 32B 121 D.Y. Bardin, S.N. Bilenky, B.M. Pontecorvo (JINR)
BECHERRAWY 70 PR D1 1452 T. Becherrawy (ROCH)
FORD 70 PRL 25 1370 W.T. Ford *et al.* (PRIN)
GAILLARD 70 CERN 70-14 J.M. Gaillard, L.M. Chounet (CERN, ORSAY)
GRAUMAN 70 PR D1 1277 J. Grauman *et al.* (STEV, SETO, LEHI)
Also PRL 23 737 J.U. Grauman *et al.* (STEV, SETO, LEHI)
PANDOULAS 70 PR D2 1205 D. Pandoulas *et al.* (STEV, SETO)
CUTTS 69 PR 184 1380 D. Cutts *et al.* (LRL, MIT)
Also PRL 20 955 D. Cutts *et al.* (LRL, MIT)
DAVISON 69 PR 180 1333 D.C. Davison *et al.* (UCR)
ELY 69 PR 180 1319 R.P.J. Ely *et al.* (LOUC, WISC, LRL)
HERZO 69 PR 186 1403 D. Herzo *et al.* (ILL)
LOBKOWICZ 69 PR 185 1676 F. Lobkowicz *et al.* (ROCH, BNL)
Also PRL 17 548 F. Lobkowicz *et al.* (ROCH, BNL)
MAST 69 PR 183 1200 T.S. Mast *et al.* (LRL)
SELLERI 69 NC 60A 291 F. Selleri
ZELLER 69 PR 182 1420 M.E. Zeller *et al.* (UCLA, LRL)
BOTTERILL 68B PRL 21 766 D.R. Botterill *et al.* (OXF)
BOTTERILL 68C PR 174 1661 D.R. Botterill *et al.* (OXF)
BUTLER 68 UCRL 18420 W.D. Butler *et al.* (LRL)
CHANG 68 PRL 20 510 C.Y. Chang *et al.* (UMD, RUTG)
CHEN 68 PRL 20 73 M. Chen *et al.* (LRL, MIT)
EICHTEN 68 PL 27B 586 T. Eichten (AACH, BARI, CERN, EPOL, ORSAY+)
ESCHSTRUTH 68 PR 165 1487 P.T. Eschstruth *et al.* (PRIN, PENN)
GARLAND 68 PR 167 1225 R. Garland *et al.* (COLU, RUTG, WISC)
MOSCOSO 68 Thesis L. Moscoso (ORSAY)
AUERBACH 67 PR 155 1505 L.B. Auerbach *et al.* (PENN, PRIN)
Also Erratum. PR D9 3216 L.B. Auerbach
BELLOTTI 67 Heidelberg Conf. E. Bellotti, A. Pullia (MILA)
BELLOTTI 67B NC 52A 1287 E. Bellotti, E. Fiorini, A. Pullia (MILA)
Also PL 20 690 E. Bellotti *et al.* (MILA)
BISI 67 PL 25B 572 V. Bisi *et al.* (TORI)
FLETCHER 67 PRL 19 98 C.R. Fletcher *et al.* (ILL)
FORD 67 PRL 18 1214 W.T. Ford *et al.* (PRIN)
GINSBERG 67 PR 162 1570 E.S. Ginsberg (MASB)
KALMUS 67 PR 159 1187 G.E. Kalmus, A. Kernan (LRL)
ZINCHENKO 67 Thesis Rutgers A.I. Zinchenko (RUTG)
CALLAHAN 66 NC 44A 90 A.C. Callahan (WISC)
CALLAHAN 66B PR 150 1153 A.C. Callahan *et al.* (WISC, LRL, UCR+)
CESTER 66 PL 21 343 R. Cester *et al.* (PPA)
See footnote 1 in AUERBACH 67.
Also PR 155 1505 L.B. Auerbach *et al.* (PENN, PRIN)
BIRGE 65 PR 139 B1600 R.W. Birge *et al.* (LRL, WISC)
BISI 65 NC 35 768 V. Bisi *et al.* (TORI)
BISI 65B PR 139 B1068 V. Bisi *et al.* (TORI)
CALLAHAN 65 PRL 15 129 A. Callahan, D. Cline (WISC)
CLINE 65 PL 15 293 D. Cline, W.F. Fry (WISC)
DEMARCO 65 PR 140B 1430 A. de Marco, C. Grosso, G. Rinaudo (TORI, CERN)
FITCH 65B PR 140B 1088 V.L. Fitch, C.A. Quarles, H.C. Wilkins (PRIN+)
STAMER 65 PR 138 B440 P. Stamer *et al.* (STEV)
YOUNG 65 Thesis UCRL 16362 P.S. Young (LRL)
Also PR 156 1464 P.S. Young, W.Z. Osborne, W.H. Barkas (LRL)
BORREANI 64 PL 12 123 G. Borreani, G. Rinaudo, A.E. Werbrouck (TORI)
CALLAHAN 64 PR 136 B1463 A. Callahan, R. March, R. Stark (WISC)
GREINER 64 PRL 13 284 D.E. Greiner, W.Z. Osborne, W.H. Barkas (LRL)
SHAKLEE 64 PR 136 B1423 F.S. Shaklee *et al.* (MICH)
BOYARSKI 62 PR 128 2398 A.M. Boyarski *et al.* (MIT)
FERRO-LUZZI 61 NC 22 1087 M. Ferro-Luzzi *et al.* (LRL)
ROE 61 PRL 7 346 B.P. Roe *et al.* (MICH, LRL)
TAYLOR 59 PR 114 359 S. Taylor *et al.* (COLU)
COOMBES 57 PR 108 1348 C.A. Coombes *et al.* (LBL)

OTHER RELATED PAPERS

LITTENBERG 93 ARNPS 43 729 L.S. Littenberg, G. Valencia (BNL, FNAL)
Rare and Radiative Kaon Decays
RITCHIE 93 RMP 65 1149 J.L. Ritchie, S.G. Wojcicki
"Rare K Decays"
BATTISTON 92 PRPL 214 293 R. Battiston *et al.* (PGIA, CERN, TRSTT)
Status and Perspectives of K Decay Physics
BRYMAN 89 IJMP A4 79 D.A. Bryman (TRIU)
"Rare Kaon Decays"
CHOUNET 72 PRPL 4C 199 L.M. Chounet, J.M. Gaillard, M.K. Gaillard (ORSAY+)
FEARING 70 PR D2 542 H.W. Fearing, E. Fischbach, J. Smith (STON, BOHR)
HAIDT 69B PL 29B 696 D. Haidt *et al.* (AACH, BARI, CERN, EPOL+)
CRONIN 68B Vienna Conf. 241 J.W. Cronin (PRIN)
Rapporteur talk.
WILLIS 67 Heidelberg Conf. 273 W.J. Willis (YALE)
Rapporteur talk.
CABIBBO 66 Berkeley Conf. 33 N. Cabibbo (CERN)
ADAIR 64 PL 12 67 R.K. Adair, L.B. Leipuner (YALE, BNL)
CABIBBO 64 PL 9 352 N. Cabibbo, A. Maksymowicz (CERN)
Also PL 11 360 N. Cabibbo, A. Maksymowicz (CERN)
Also PL 14 72 N. Cabibbo, A. Maksymowicz (CERN)
BIRGE 63 PRL 11 35 R.W. Birge *et al.* (LRL, WISC, BARI)
BLOCK 62B CERN Conf. 371 M.M. Block, L. Lendinara, L. Monari (NWES, BGNA)
BRENE 61 NP 22 553 N. Brene, L. Egardt, B. Qvist (NORD)

K^0

$I(J^P) = \frac{1}{2}(0^-)$

K^0 MASS

VALUE (MeV)	EVTS	DOCUMENT ID		TECN	COMMENT
497.614±0.024 OUR FIT Error includes scale factor of 1.6.					
497.614±0.022 OUR AVERAGE Error includes scale factor of 1.5. See the ideogram below.					
497.583±0.005±0.020	35k	AMBROSINO	07B	KLOE	$e^+e^- \to K^0_L K^0_S$
497.625±0.001±0.031	655k	LAI	02	NA48	K^0_L beam
497.661±0.033	3713	BARKOV	87B	CMD	$e^+e^- \to K^0_L K^0_S$
497.742±0.085	780	BARKOV	85B	CMD	$e^+e^- \to K^0_L K^0_S$
• • • We do not use the following data for averages, fits, limits, etc. • • •					
497.44 ±0.50		FITCH	67	OSPK	
498.9 ±0.5	4500	BALTAY	66	HBC	K^0 from $\overline{p}p$
497.44 ±0.33	2223	KIM	65B	HBC	K^0 from $\overline{p}p$
498.1 ±0.4		CHRISTENS...	64	OSPK	

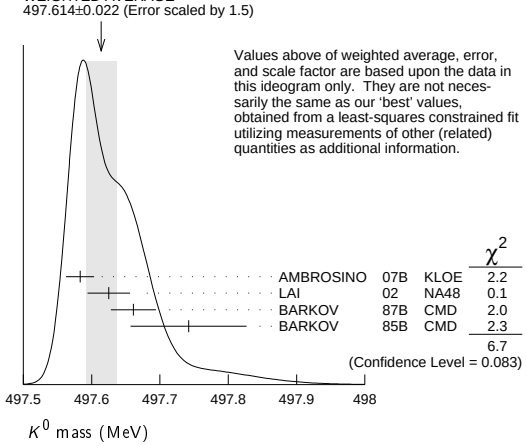

$m_{K^0} - m_{K^\pm}$

VALUE (MeV)	EVTS	DOCUMENT ID		TECN	CHG	COMMENT
3.937±0.028 OUR FIT	Error includes scale factor of 1.8.					
• • • We do not use the following data for averages, fits, limits, etc. • • •						
3.95 ±0.21	417	HILL	68B	DBC	+	$K^+ d \to K^0 p p$
3.90 ±0.25	9	BURNSTEIN	65	HBC	−	
3.71 ±0.35	7	KIM	65B	HBC	−	$K^- p \to n\overline{K}^0$
5.4 ±1.1		CRAWFORD	59	HBC	+	
3.9 ±0.6		ROSENFELD	59	HBC	−	

K^0 MEAN SQUARE CHARGE RADIUS

VALUE (fm^2)	EVTS	DOCUMENT ID		TECN	COMMENT
−0.077±0.010 OUR AVERAGE					
−0.077±0.007±0.011	5037	ABOUZAID	06	KTEV	$K_L^0 \to \pi^+\pi^- e^+ e^-$
−0.090±0.021		LAI	03C	NA48	$K_L^0 \to \pi^+\pi^- e^+ e^-$
−0.054±0.026		MOLZON	78		K_S regen. by electrons
• • • We do not use the following data for averages, fits, limits, etc. • • •					
−0.087±0.046		BLATNIK	79		VMD + dispersion relations
−0.050±0.130		FOETH	69B		K_S regen. by electrons

T-VIOLATION PARAMETER IN K^0-$\overline{K}^0$ MIXING

The asymmetry $A_T = \frac{\Gamma(\overline{K}^0 \to K^0) - \Gamma(K^0 \to \overline{K}^0)}{\Gamma(\overline{K}^0 \to K^0) + \Gamma(K^0 \to \overline{K}^0)}$ must vanish if T invariance holds.

ASYMMETRY A_T IN K^0-$\overline{K}^0$ MIXING

VALUE (units 10^{-3})	EVTS	DOCUMENT ID		TECN
6.6±1.3±1.0	640k	[1] ANGELOPO...	98E	CPLR

[1] ANGELOPOULOS 98E measures the asymmetry $A_T = [\Gamma(\overline{K}^0_{t=0} \to e^+\pi^-\nu_{t=\tau}) - \Gamma(K^0_{t=0} \to e^-\pi^+\overline{\nu}_{t=\tau})]/[\Gamma(\overline{K}^0_{t=0} \to e^+\pi^-\nu_{t=\tau}) + \Gamma(K^0_{t=0} \to e^-\pi^+\overline{\nu}_{t=\tau})]$ as a function of the neutral-kaon eigentime τ. The initial strangeness of the neutral kaon is tagged by the charge of the accompanying charged kaon in the reactions $p\overline{p} \to K^-\pi^+ K^0$ and $p\overline{p} \to K^+\pi^-\overline{K}^0$. The strangeness at the time of the decay is tagged by the lepton charge. The reported result is the average value of A_T over the interval $1\tau_S < \tau < 20\tau_S$. From this value of A_T ANGELOPOULOS 01B, assuming CPT invariance in the $e\pi\nu$ decay amplitude, determine the T-violating as $\Delta S{=}\Delta S$ conserving parameter (for its definition, see Review below) $4\mathrm{Re}(\epsilon) = (6.2 \pm 1.4 \pm 1.0) \times 10^{-3}$.

CPT INVARIANCE TESTS IN NEUTRAL KAON DECAY

Updated October 2013 by M. Antonelli (LNF-INFN, Frascati) and G. D'Ambrosio (INFN Sezione di Napoli).

CPT theorem is based on three assumptions: quantum field theory, locality, and Lorentz invariance, and thus it is a fundamental probe of our basic understanding of particle physics. Strangeness oscillation in $K^0 - \overline{K}^0$ system, described by the equation

$$i\frac{d}{dt}\begin{bmatrix} K^0 \\ \overline{K}^0 \end{bmatrix} = [M - i\Gamma/2]\begin{bmatrix} K^0 \\ \overline{K}^0 \end{bmatrix} ,$$

where M and Γ are hermitian matrices (see PDG review [1], references [2,3], and KLOE paper [5] for notations and previous literature), allows a very accurate test of CPT symmetry; indeed since CPT requires $M_{11} = M_{22}$ and $\Gamma_{11} = \Gamma_{22}$, the mass and width eigenstates, $K_{S,L}$, have a CPT-violating piece, δ, in addition to the usual CPT-conserving parameter ϵ:

$$K_{S,L} = \frac{1}{\sqrt{2\left(1+|\epsilon_{S,L}|^2\right)}}\left[\left(1+\epsilon_{S,L}\right)K^0 + \left(1-\epsilon_{S,L}\right)\overline{K}^0\right]$$

$$\epsilon_{S,L} = \frac{-i\Im\left(M_{12}\right) - \frac{1}{2}\Im\left(\Gamma_{12}\right) \mp \frac{1}{2}\left[M_{11} - M_{22} - \frac{i}{2}\left(\Gamma_{11} - \Gamma_{22}\right)\right]}{m_L - m_S + i(\Gamma_S - \Gamma_L)/2}$$
$$\equiv \epsilon \pm \delta. \qquad (1)$$

Using the phase convention $\Im(\Gamma_{12}) = 0$, we determine the phase of ϵ to be $\varphi_{SW} \equiv \arctan\frac{2(m_L - m_S)}{\Gamma_S - \Gamma_L}$. Imposing unitarity to an arbitrary combination of K^0 and $\overline{K}^0$ wave functions, we obtain the Bell-Steinberger relation [4] connecting CP and CPT violation in the mass matrix to CP and CPT violation in the decay; in fact, neglecting $\mathcal{O}(\epsilon)$ corrections to the coefficient of the CPT-violating parameter, δ, we can write [5]

$$[\frac{\Gamma_S + \Gamma_L}{\Gamma_S - \Gamma_L} + i\tan\phi_{\rm SW}][\frac{\Re(\epsilon)}{1+|\epsilon|^2} - i\Im(\delta)] = \frac{1}{\Gamma_S - \Gamma_L}\sum_f A_L(f)A_S^*(f), \qquad (2)$$

where $A_{L,S}(f) \equiv A(K_{L,S} \to f)$. We stress that this relation is phase-convention-independent. The advantage of the neutral kaon system is that only a few decay modes give significant contributions to the r.h.s. in Eq. (2); in fact, defining for the hadronic modes

$$\alpha_i \equiv \frac{1}{\Gamma_S}\langle \mathcal{A}_L(i)\mathcal{A}_S^*(i)\rangle = \eta_i \ \mathcal{B}(K_S \to i),$$
$$i = \pi^0\pi^0, \pi^+\pi^-(\gamma), 3\pi^0, \pi^0\pi^+\pi^-(\gamma), \qquad (3)$$

the recent data from CPLEAR, KLOE, KTeV, and NA48 have led to the following determinations (the analysis described in Ref. 5 has been updated by using the recent measurements of K_L branching ratios from KTeV [6,7], NA48 [8,9], and the results described in the CP violation in K_L decays minireview, and the recent KLOE result [10])

$$\alpha_{\pi^+\pi^-} = ((1.112 \pm 0.010) + i(1.061 \pm 0.010)) \times 10^{-3} ,$$
$$\alpha_{\pi^0\pi^0} = ((0.493 \pm 0.005) + i(0.471 \pm 0.005)) \times 10^{-3} ,$$
$$\alpha_{\pi^+\pi^-\pi^0} = ((0 \pm 2) + i(0 \pm 2)) \times 10^{-6},$$
$$|\alpha_{\pi^0\pi^0\pi^0}| < 1.5 \times 10^{-6} \quad \text{at } 95\% \text{ CL} . \qquad (4)$$

The semileptonic contribution to the right-handed side of Eq. (2) requires the determination of several observables: we define [2,3]

$$\mathcal{A}(K^0 \to \pi^- l^+ \nu) = \mathcal{A}_0(1-y) ,$$
$$\mathcal{A}(K^0 \to \pi^+ l^- \nu) = \mathcal{A}_0^*(1+y^*)(x_+ - x_-)^* ,$$
$$\mathcal{A}(\overline{K}^0 \to \pi^+ l^- \nu) = \mathcal{A}_0^*(1+y^*) ,$$
$$\mathcal{A}(\overline{K}^0 \to \pi^- l^+ \nu) = \mathcal{A}_0(1-y)(x_+ + x_-) , \qquad (5)$$

where x_+ (x_-) describes the violation of the $\Delta S = \Delta Q$ rule in CPT-conserving (violating) decay amplitudes, and y parametrizes CPT violation for $\Delta S = \Delta Q$ transitions. Taking advantage of their tagged $K^0(\overline{K}^0)$ beams, CPLEAR has measured $\Im(x_+)$, $\Re(x_-)$, $\Im(\delta)$, and $\Re(\delta)$ [11]. These determinations have been improved in Ref. 5 by including the information $A_S - A_L = 4[\Re(\delta) + \Re(x_-)]$, where $A_{L,S}$ are the K_L and K_S semileptonic charge asymmetries, respectively, from the PDG [12] and KLOE [13]. Here we are also including the T-violating asymmetry measurement from CPLEAR [14].

Table 1: Values, errors, and correlation coefficients for $\Re(\delta)$, $\Im(\delta)$, $\Re(x_-)$, $\Im(x_+)$, and $A_S + A_L$ obtained from a combined fit, including KLOE [5] and CPLEAR [14].

	value	Correlations coefficients				
$\Re(\delta)$	$(3.0 \pm 2.3) \times 10^{-4}$	1				
$\Im(\delta)$	$(-0.66 \pm 0.65) \times 10^{-2}$	−0.21	1			
$\Re(x_-)$	$(-0.30 \pm 0.21) \times 10^{-2}$	−0.21	−0.60	1		
$\Im(x_+)$	$(0.02 \pm 0.22) \times 10^{-2}$	−0.38	−0.14	0.47	1	
$A_S + A_L$	$(-0.40 \pm 0.83) \times 10^{-2}$	−0.10	−0.63	0.99	0.43	1

The value $A_S + A_L$ in Table 1 can be directely included in the semileptonic contributions to the Bell Steinberger relations in Eq. (2)

$$\begin{aligned}\sum_{\pi\ell\nu} &\langle \mathcal{A}_L(\pi\ell\nu)\mathcal{A}_S^*(\pi\ell\nu)\rangle \\ &= 2\Gamma(K_L \to \pi\ell\nu)(\Re(\epsilon) - \Re(y) - i(\Im(x_+) + \Im(\delta))) \\ &= 2\Gamma(K_L \to \pi\ell\nu)((A_S + A_L)/4 - i(\Im(x_+) + \Im(\delta)))\ . \quad (6)\end{aligned}$$

Defining

$$\alpha_{\pi\ell\nu} \equiv \frac{1}{\Gamma_S}\sum_{\pi\ell\nu}\langle \mathcal{A}_L(\pi\ell\nu)\mathcal{A}_S^*(\pi\ell\nu)\rangle + 2i\frac{\tau_{K_S}}{\tau_{K_L}}\mathcal{B}(K_L \to \pi\ell\nu)\Im(\delta)\ , \quad (7)$$

we find:

$$\alpha_{\pi\ell\nu} = ((-0.2 \pm 0.5) + i(0.1 \pm 0.5)) \times 10^{-5}\,.$$

Inserting the values of the α parameters into Eq. (2), we find

$$\begin{aligned}\Re(\epsilon) &= (161.1 \pm 0.5) \times 10^{-5}, \\ \Im(\delta) &= (-0.7 \pm 1.4) \times 10^{-5}\,. \quad (8)\end{aligned}$$

The complete information on Eq. (8) is given in Table 2.

Table 2: Summary of results: values, errors, and correlation coefficients for $\Re(\epsilon)$, $\Im(\delta)$, $\Re(\delta)$, and $\Re(x_-)$.

	value	Correlations coefficients			
$\Re(\epsilon)$	$(161.1 \pm 0.5) \times 10^{-5}$	+1			
$\Im(\delta)$	$(-0.7 \pm 1.4) \times 10^{-5}$	+0.09	1		
$\Re(\delta)$	$(2.4 \pm 2.3) \times 10^{-4}$	+0.08	−0.12	1	
$\Re(x_-)$	$(-4.1 \pm 1.7) \times 10^{-3}$	+0.14	0.22	−0.43	1

Now the agreement with CPT conservation, $\Im(\delta) = \Re(\delta) = \Re(x_-) = 0$, is at 18% C.L.

The allowed region in the $\Re(\epsilon) - \Im(\delta)$ plane at 68% CL and 95% C.L. is shown in the top panel of Fig. 1.

The process giving the largest contribution to the size of the allowed region is $K_L \to \pi^+\pi^-$, through the uncertainty on ϕ_{+-}.

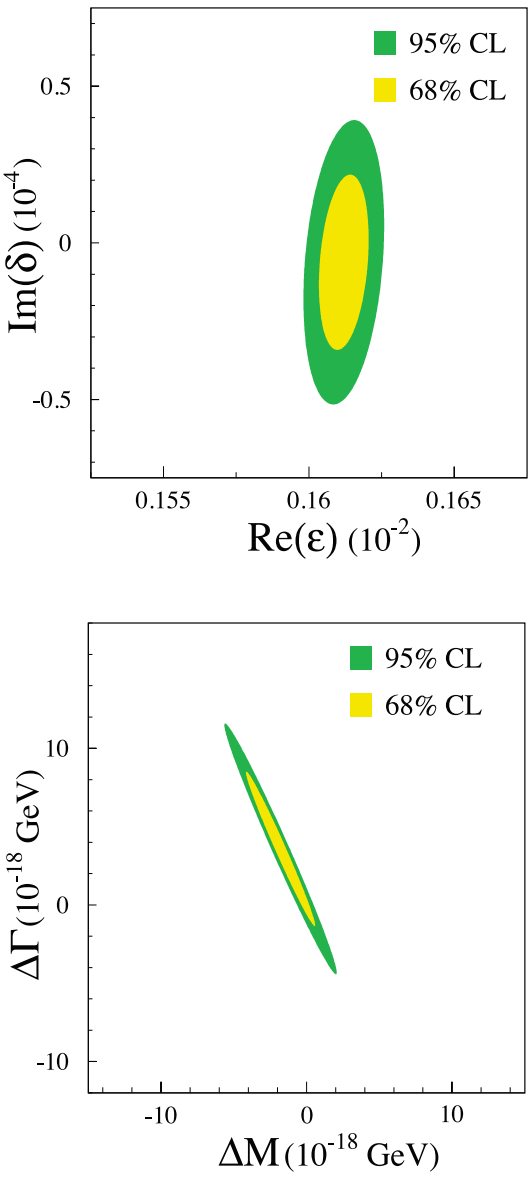

Figure 1: Top: allowed region at 68% and 95% C.L. in the $\Re(\epsilon)$, $\Im(\delta)$ plane. Bottom: allowed region at 68% and 95% C.L. in the $\Delta M, \Delta\Gamma$ plane.

The limits on $\Im(\delta)$ and $\Re(\delta)$ can be used to constrain the $K^0 - \overline{K}^0$ mass and width difference

$$\delta = \frac{i(m_{K^0} - m_{\overline{K}^0}) + \frac{1}{2}(\Gamma_{K^0} - \Gamma_{\overline{K}^0})}{\Gamma_S - \Gamma_L}\cos\phi_{SW}e^{i\phi_{SW}}[1 + \mathcal{O}(\epsilon)]\,.$$

The allowed region in the $\Delta M = (m_{K^0} - m_{\overline{K}^0}), \Delta\Gamma = (\Gamma_{K^0} - \Gamma_{\overline{K}^0})$ plane is shown in the bottom panel of Fig. 1. As a result, we improve on the previous limits (see for instance, P. Bloch in Ref. 12) and in the limit $\Gamma_{K^0} - \Gamma_{\overline{K}^0} = 0$ we obtain

$$-4.0\times10^{-19}\ \text{GeV} < m_{K^0} - m_{\overline{K}^0} < 4.0\times10^{-19}\ \text{GeV} \quad \text{at 95 \% C.L.}$$

Meson Particle Listings

K^0

References

1. See the "CP Violation in Meson Decays," in this *Review*.
2. L. Maiani, "CP And CPT Violation in Neutral Kaon Decays," L. Maiani, G. Pancheri, and N. Paver, *The Second Daphne Physics Handbook*, Vol. 1, 2.
3. G. D'Ambrosio, G. Isidori, and A. Pugliese, "CP and CPT mesurements at DAΦNE," L. Maiani, G. Pancheri, and N. Paver, *The Second Daphne Physics Handbook*, Vol. 1, 2.
4. J. S. Bell and J. Steinberger, In Wolfenstein, L. (ed.): *CP violation,* 42-57. (In *Oxford International Symposium Conference on Elementary Particles*, September 1965, 195-208, 221-222). (See Book Index).
5. F. Ambrosino *et al.*, [KLOE Collab.], JHEP **0612**, 011 (2006) [arXiv:hep-ex/0610034].
6. T. Alexopoulos *et al.*, [KTeV Collab.], Phys. Rev. **D70**, 092006 (1998).
7. E. Abouzaid *et al.* [KTeV Collab.], Phys. Rev. **D83**, 092001 (2011).
8. A. Lai *et al.*, [NA48 Collab.], Phys. Lett. **B645**, 26 (2007); A. Lai *et al.*, [NA48 Collab.], Phys. Lett. **B602**, 41 (2004).
9. We thank G. Isidori and M. Palutan for their contribution to the original analyisis [5] performed with KLOE data.
10. D. Babusci *et al.*, [KLOE Collab.], Phys. Lett. **B723**, 54 (2013).
11. A. Angelopoulos *et al.*, [CPLEAR Collab.], Phys. Lett. **B444**, 52 (1998).
12. W. M. Yao *et al.*, [Particle Data Group], J. Phys. **G33**, 1 (2006).
13. F. Ambrosino *et al.*, [KLOE Collab.], Phys. Lett. **B636**, 173 (2006) [arXiv:hep-ex/0601026].
14. P. Bloch, M. Fidecaro, private communication of the data in a finer binning format; A. Angelopoulos *et al.*, [CPLEAR Collab.], Phys. Lett. **B444**, 43 (1998).
15. We thank M. Palutan for the collaboration in this analysis.

CP-VIOLATION PARAMETERS

Re(ϵ)

VALUE (units 10^{-3})	DOCUMENT ID		TECN
1.596±0.013	[2] AMBROSINO	06H	KLOE
• • • We do not use the following data for averages, fits, limits, etc. • • •			
1.664±0.010	[3] LAI	05A	NA48

[2] AMBROSINO 06H uses Bell-Steinberger relations with the following measurements: B($K^0_L \to \pi^+\pi^-$) in AMBROSINO 06F, B($K^0_S \to \pi^0\pi^0\pi^0$) in AMBROSINO 05B, the K^0_S-semileptonic charge asymmetry in AMBROSINO 06E, and K^0-semileptonic results in ANGELOPOULOS 98F.

[3] LAI 05A values are obtained through unitarity (Bell-Steinberger relations), improving determination of η_{000} and combining other data from PDG 04 and APOSTOLAKIS 99B.

CPT-VIOLATION PARAMETERS

In K^0-$\overline{K}^0$ mixing, if CP-violating interactions include a T conserving part then

$$|K_S\rangle = [|K_1\rangle + (\epsilon+\delta)|K_2\rangle]/\sqrt{1+|\epsilon+\delta|^2}$$
$$|K_L\rangle = [|K_2\rangle + (\epsilon-\delta)|K_1\rangle]/\sqrt{1+|\epsilon-\delta|^2}$$

where

$$|K_1\rangle = [|K^0\rangle + |\overline{K}^0\rangle]/\sqrt{2}$$
$$|K_2\rangle = [|K^0\rangle - |\overline{K}^0\rangle]/\sqrt{2}$$

and

$$|\overline{K}^0\rangle = CP|K^0\rangle.$$

The parameter δ specifies the CPT-violating part.

Estimates of δ are given below assuming the validity of the $\Delta S = \Delta Q$ rule. See also THOMSON 95 for a test of CPT-symmetry conservation in K^0 decays using the Bell-Steinberger relation.

REAL PART OF δ

A nonzero value violates CPT invariance.

VALUE (units 10^{-4})	EVTS	DOCUMENT ID		TECN	COMMENT
2.51± 2.25		[4] ABOUZAID	11	KTEV	
• • • We do not use the following data for averages, fits, limits, etc. • • •					
2.3 ± 2.7		[5] AMBROSINO	06H	KLOE	
2.4 ± 2.8		[6] APOSTOLA...	99B	RVUE	
2.9 ± 2.6 ±0.6	1.3M	[7] ANGELOPO...	98F	CPLR	
180 ±200	6481	[8] DEMIDOV	95		$K_{\ell 3}$ reanalysis

[4] ABOUZAID 11 uses Bell-Steinberger relations.

[5] AMBROSINO 06H uses Bell-Steinberger relations with the following measurements: B($K^0_L \to \pi^+\pi^-$) in AMBROSINO 06F, B($K^0_S \to \pi^0\pi^0\pi^0$) in AMBROSINO 05B, the K^0_S-semileptonic charge asymmetry in AMBROSINO 06E, and K^0-semileptonic results in ANGELOPOULOS 98F.

[6] APOSTOLAKIS 99B assumes only unitarity and combines CPLEAR and other results.

[7] ANGELOPOULOS 98F use $\Delta S = \Delta Q$. If $\Delta S = \Delta Q$ is not assumed, they find $\mathrm{Re}\delta = (3.0 \pm 3.3 \pm 0.6) \times 10^{-4}$.

[8] DEMIDOV 95 reanalyzes data from HART 73 and NIEBERGALL 74.

IMAGINARY PART OF δ

A nonzero value violates CPT invariance.

VALUE (units 10^{-5})	EVTS	DOCUMENT ID		TECN	COMMENT
− 1.5± 1.6		[9] ABOUZAID	11	KTEV	
• • • We do not use the following data for averages, fits, limits, etc. • • •					
0.4± 2.1		[10] AMBROSINO	06H	KLOE	
− 0.2± 2.0		[11] LAI	05A	NA48	
2.4± 5.0		[12] APOSTOLA...	99B	RVUE	
− 90 ± 290 ±100	1.3M	[13] ANGELOPO...	98F	CPLR	
2100 ±3700	6481	[14] DEMIDOV	95		$K_{\ell 3}$ reanalysis

[9] ABOUZAID 11 uses Bell-Steinberger relations.

[10] AMBROSINO 06H uses Bell-Steinberger relations with the following measurements: B($K^0_L \to \pi^+\pi^-$) in AMBROSINO 06F, B($K^0_S \to \pi^0\pi^0\pi^0$) in AMBROSINO 05B, the K^0_S-semileptonic charge asymmetry in AMBROSINO 06E, and K^0-semileptonic results in ANGELOPOULOS 98F.

[11] LAI 05A values are obtained through unitarity (Bell-Steinberger relations), improving determination of η_{000} and combining other data from PDG 04 and APOSTOLAKIS 99B.

[12] APOSTOLAKIS 99B assumes only unitarity and combines CPLEAR and other results.

[13] If $\Delta S = \Delta Q$ is not assumed, ANGELOPOULOS 98F finds $\mathrm{Im}\delta = (-15 \pm 23 \pm 3) \times 10^{-3}$.

[14] DEMIDOV 95 reanalyzes data from HART 73 and NIEBERGALL 74.

Re(y)

A non-zero value would violate CPT invariance in $\Delta S = \Delta Q$ amplitude. Re(y) is the following combination of K_{e3} decay amplitudes:

$$\mathrm{Re(y)} = \mathrm{Re}\left(\frac{A(\overline{K}^0 \to e^-\pi^+\overline{\nu}_e)^* - A(K^0 \to e^+\pi^-\nu_e)}{A(\overline{K}^0 \to e^-\pi^+\overline{\nu}_e)^* + A(K^0 \to e^+\pi^-\nu_e)} \right)$$

VALUE (units 10^{-3})	EVTS	DOCUMENT ID		TECN
0.4±2.5	13k	[15] AMBROSINO	06E	KLOE
• • • We do not use the following data for averages, fits, limits, etc. • • •				
0.3±3.1		[16] APOSTOLA...	99B	CPLR

[15] They use the PDG 04 for the K^0_L semileptonic charge asymmetry and PDG 04 (CP review, CPT NOT ASSUMED) for Re(ϵ).

[16] Constrained by Bell-Steinberger (or unitarity) relation.

Re(x_)

A non-zero value would violate CPT invariance in decay amplitudes with $\Delta S \neq \Delta Q$. x_, used here to define Re(x_), and x_+, used below in the $\Delta S = \Delta Q$ section are the following combinations of K_{e3} decay amplitudes:

$$x_\pm = \frac{1}{2}\left(\frac{A(\overline{K}^0 \to \pi^- e^+\nu_e)}{A(K^0 \to \pi^- e^+\nu_e)} \pm \frac{A(K^0 \to \pi^+ e^-\overline{\nu}_e)^*}{A(\overline{K}^0 \to \pi^+ e^-\overline{\nu}_e)^*} \right).$$

VALUE (units 10^{-3})	EVTS	DOCUMENT ID		TECN	COMMENT
−2.9± 2.0		[17] AMBROSINO	06H	KLOE	
• • • We do not use the following data for averages, fits, limits, etc. • • •					
−0.8± 2.5	13k	[18] AMBROSINO	06E	KLOE	
−0.5± 3.0		[19] APOSTOLA...	99B	CPLR	Strangeness tagged
2 ±13 ±3	650k	ANGELOPO...	98F	CPLR	Strangeness tagged

[17] AMBROSINO 06H uses Bell-Steinberger relations with the following measurements: B($K^0_L \to \pi^+\pi^-$) in AMBROSINO 06F, B($K^0_S \to \pi^0\pi^0\pi^0$) in AMBROSINO 05B, the K^0_S-semileptonic charge asymmetry in AMBROSINO 06E, and K^0-semileptonic results in ANGELOPOULOS 98F.

[18] Uses PDG 04 for the K^0_L semileptonic charge asymmetry and Re(δ) from CPLEAR, ANGELOPOULOS 98F.

[19] Constrained by Bell-Steinberger (or unitarity) relation.

$|m_{K^0} - m_{\overline{K}^0}| / m_{\text{average}}$

A test of CPT invariance. "Our Evaluation" is described in the "Tests of Conservation Laws" section. It assumes CPT invariance in the decay and neglects some contributions from decay channels other than $\pi\pi$.

VALUE	CL%	DOCUMENT ID		TECN
$< 6 \times 10^{-19}$	90	PDG	12	
• • • We do not use the following data for averages, fits, limits, etc. • • •				
$(-3 \pm 4) \times 10^{-18}$		[20] ANGELOPO...	99B	RVUE

[20] ANGELOPOULOS 99B assumes only unitarity and combines CPLEAR and other results.

$(\Gamma_{K^0} - \Gamma_{\overline{K}^0})/m_{\text{average}}$

A test of CPT invariance.

VALUE	DOCUMENT ID		TECN
$(7.8 \pm 8.4) \times 10^{-18}$	[21] ANGELOPO...	99B	RVUE

[21] ANGELOPOULOS 99B assumes only unitarity and combines CPLEAR with other results. Correlated with $(m_{K^0} - m_{\overline{K}^0}) / m_{\text{average}}$ with a correlation coefficient of -0.95.

TESTS OF $\Delta S = \Delta Q$ RULE

Re(x_+)

A non-zero value would violate the $\Delta S = \Delta Q$ rule in CPT conserving transitions. x_+ is defined above in the Re(x_-) section.

VALUE (units 10^{-3})	EVTS	DOCUMENT ID		TECN
-0.9 ± 3.0 OUR AVERAGE				
-2 ± 10		[22] BATLEY	07D	NA48
-0.5 ± 3.6	13k	[23] AMBROSINO	06E	KLOE
-1.8 ± 6.1		[24] ANGELOPO...	98D	CPLR

[22] Result obtained from the measurement $\Gamma(K^0_S \to \pi e \nu) / \Gamma(K^0_L \to \pi e \nu) = 0.993 \pm 0.34$, neglecting possible CPT non-invariance and using PDG 06 values of $B(K^0_L \to \pi e \nu) = 0.4053 \pm 0.0015$, $\tau_L = (5.114 \pm 0.021) \times 10^{-8}$ s and $\tau_S = (0.8958 \pm 0.0005) \times 10^{-10}$ s.

[23] Re(x_+) can be shown to be equal to the following combination of rates:

$$\text{Re}(x_+) = \frac{1}{2} \frac{\Gamma(K^0_S \to \pi e \nu) - \Gamma(K^0_L \to \pi e \nu)}{\Gamma(K^0_S \to \pi e \nu) + \Gamma(K^0_L \to \pi e \nu)}$$

which is valid up to first order in terms violating CPT and/or the $\Delta S = \Delta Q$ rule.

[24] Obtained neglecting CPT violating amplitudes.

K^0 REFERENCES

PDG	12	PR D86 010001	J. Beringer *et al.*	(PDG Collab.)
ABOUZAID	11	PR D83 092001	E. Abouzaid *et al.*	(FNAL KTeV Collab.)
AMBROSINO	07B	JHEP 0712 073	F. Ambrosino *et al.*	(KLOE Collab.)
BATLEY	07D	PL B653 145	J.R. Batley *et al.*	(CERN NA48 Collab.)
ABOUZAID	06	PRL 96 101801	E. Abouzaid *et al.*	(KTeV Collab.)
AMBROSINO	06E	PL B636 173	F. Ambrosino *et al.*	(KLOE Collab.)
AMBROSINO	06F	PL B638 140	F. Ambrosino *et al.*	(KLOE Collab.)
AMBROSINO	06H	JHEP 0612 011	F. Ambrosino *et al.*	(KLOE Collab.)
PDG	06	JP G33 1	W.-M. Yao *et al.*	(PDG Collab.)
AMBROSINO	05B	PL B619 61	F. Ambrosino *et al.*	(KLOE Collab.)
LAI	05A	PL B610 165	A. Lai *et al.*	(CERN NA48 Collab.)
PDG	04	PL B592 1	S. Eidelman *et al.*	(PDG Collab.)
LAI	03C	EPJ C30 33	A. Lai *et al.*	(CERN NA48 Collab.)
LAI	02	PL B533 196	A. Lai *et al.*	(CERN NA48 Collab.)
ANGELOPO...	01B	EPJ C22 55	A. Angelopoulos *et al.*	(CPLEAR Collab.)
ANGELOPO...	99B	PL B471 332	A. Angelopoulos *et al.*	(CPLEAR Collab.)
APOSTOLA...	99B	PL B456 297	A. Apostolakis *et al.*	(CPLEAR Collab.)
ANGELOPO...	98D	PL B444 38	A. Angelopoulos *et al.*	(CPLEAR Collab.)
Also		EPJ C22 55	A. Angelopoulos *et al.*	(CPLEAR Collab.)
ANGELOPO...	98E	PL B444 43	A. Angelopoulos *et al.*	(CPLEAR Collab.)
ANGELOPO...	98F	PL B444 52	A. Angelopoulos *et al.*	(CPLEAR Collab.)
Also		EPJ C22 55	A. Angelopoulos *et al.*	(CPLEAR Collab.)
DEMIDOV	95	PAN 58 968	V. Demidov, K. Gusev, E. Shabalin	(ITEP)
From YAF 58 1041.				
THOMSON	95	PR D51 1412	G.B. Thomson, Y. Zou	(RUTG)
BARKOV	87B	SJNP 46 630	L.M. Barkov *et al.*	(NOVO)
Translated from YAF 46 1088.				
BARKOV	85B	JETPL 42 138	L.M. Barkov *et al.*	(NOVO)
Translated from ZETFP 42 113.				
BLATNIK	79	LNC 24 39	S. Blatnik, J. Stahov, C.B. Lang	(TUZL, GRAZ)
MOLZON	78	PRL 41 1213	W.R. Molzon *et al.*	(EFI+)
NIEBERGALL	74	PL 49B 103	F. Niebergall *et al.*	(CERN, ORSAY, VIEN)
HART	73	NP B66 317	J.C. Hart *et al.*	(CAVE, RHEL)
FOETH	69B	PL 30B 276	H. Foeth *et al.*	(AACH, CERN, TORI)
HILL	68B	PR 168 1534	D.G. Hill *et al.*	(BNL, CMU)
FITCH	67	PR 164 1711	V.L. Fitch *et al.*	(PRIN)
BALTAY	66	PR 142 932	C. Baltay *et al.*	(YALE, BNL)
BURNSTEIN	65	PR 138 B895	R.A. Burnstein, H.A. Rubin	(UMD)
KIM	65B	PR 140B 1334	J.K. Kim, L. Kirsch, D. Miller	(COLU)
CHRISTENS...	64	PRL 13 138	J.H. Christenson *et al.*	(PRIN)
CRAWFORD	59	PRL 2 112	F.S. Crawford *et al.*	(LRL)
ROSENFELD	59	PRL 2 110	A.H. Rosenfeld, F.T. Solmitz, R.D. Tripp	(LRL)

K^0_S

$I(J^P) = \frac{1}{2}(0^-)$

K^0_S MEAN LIFE

For earlier measurements, beginning with BOLDT 58B, see our 1986 edition, Physics Letters **170B** 130 (1986).

OUR FIT is described in the note on "CP violation in K_L decays" in the K^0_L Particle Listings. The result labeled "OUR FIT Assuming CPT" ["OUR FIT Not assuming CPT"] includes all measurements except those with the comment "Not assuming CPT" ["Assuming CPT"]. Measurements with neither comment do not assume CPT and enter both fits.

VALUE (10^{-10} s)	EVTS	DOCUMENT ID		TECN	COMMENT
0.8954 ±0.0004 OUR FIT		Error includes scale factor of 1.1. Assuming CPT			
0.89564±0.00033 OUR FIT		Not assuming CPT			
0.89589±0.00070		[1,2] ABOUZAID	11	KTEV	Not assuming CPT
0.89623±0.00047		[1,3] ABOUZAID	11	KTEV	Assuming CPT
0.89562±0.00029±0.00043	20M	[4] AMBROSINO	11	KLOE	Not assuming CPT
0.89598±0.00048±0.00051	16M	LAI	02C	NA48	
0.8971 ±0.0021		BERTANZA	97	NA31	
0.8941 ±0.0014 ±0.0009		SCHWINGEN...	95	E773	Assuming CPT
0.8929 ±0.0016		GIBBONS	93	E731	Assuming CPT
• • • We do not use the following data for averages, fits, limits, etc. • • •					
0.8965 ±0.0007		[5] ALAVI-HARATI	03	KTEV	Assuming CPT
0.8958 ±0.0013		[6] ALAVI-HARATI	03	KTEV	Not assuming CPT
0.8920 ±0.0044	214k	GROSSMAN	87	SPEC	
0.905 ±0.007		[7] ARONSON	82B	SPEC	
0.881 ±0.009	26k	ARONSON	76	SPEC	
0.8926 ±0.0032 ±0.0002		[8] CARITHERS	75	SPEC	
0.8937 ±0.0048	6M	GEWENIGER	74B	ASPK	
0.8958 ±0.0045	50k	[9] SKJEGGEST...	72	HBC	
0.856 ±0.008	19994	[10] DONALD	68B	HBC	
0.872 ±0.009	20000	[9,10] HILL	68	DBC	

[1] The two ABOUZAID 11 values use the same full KTeV dataset from 1996, 1997, and 1999. The first enters the "assuming CPT" fit and the second enters the "not assuming CPT" fit.

[2] ABOUZAID 11 fit has Δm, τ_S, ϕ_ϵ, Re(ϵ'/ϵ), and Im(ϵ'/ϵ) as free parameters. See Im(ϵ'/ϵ) in the "K^0_L CP violation" section for correlation information.

[3] ABOUZAID 11 fit has Δm and τ_S free but constrains ϕ_ϵ to the Superweak value, i.e. assumes CPT. This τ_S value is correlated with their $\Delta m = m_{K^0_L} - m_{K^0_S}$ measurement in the K^0_L listings. The correlation coefficient $\rho(\tau_S, \Delta m) = -0.670$.

[4] Fit to the proper time distribution.

[5] This ALAVI-HARATI 03 fit has Δm and τ_S free but constrains ϕ_{+-} to the Superweak value, i.e. assumes CPT. This τ_S value is correlated with their $\Delta m = m_{K^0_L} - m_{K^0_S}$ measurement in the K^0_L listings. The correlation coefficient $\rho(\tau_S, \Delta m) = -0.396$. Superseded by ABOUZAID 11.

[6] This ALAVI-HARATI 03 fit has Δm, ϕ_{+-}, and τ_{K_S} free. See ϕ_{+-} in the "K_L CP violation" section for correlation information. Superseded by ABOUZAID 11.

[7] ARONSON 82 find that K^0_S mean life may depend on the kaon energy.

[8] CARITHERS 75 measures the Δm dependence of the total decay rate (inverse mean life) to be $\Gamma(K^0_S) = [(1.122 \pm 0.004) + 0.16(\Delta m - 0.5348)/\Delta m] 10^{10}$/s, or, in terms of mean life, CARITHERS 75 measures $\tau_S = (0.8913 \pm 0.0032) - 0.238\,[\Delta m - 0.5348]$ (10^{-10} s). We have adjusted the measurement to use our best values of ($\Delta m = 0.5293 \pm 0.0009$) ($10^{10}$ $\hbar$ s^{-1}). Our first error is their experiment's error and our second error is the systematic error from using our best values.

[9] HILL 68 has been changed by the authors from the published value (0.865 ± 0.009) because of a correction in the shift due to η_{+-}. SKJEGGESTAD 72 and HILL 68 give detailed discussions of systematics encountered in this type of experiment.

[10] Pre-1971 experiments are excluded from the average because of disagreement with later more precise experiments.

K^0_S DECAY MODES

	Mode		Fraction (Γ_i/Γ)	Scale factor/ Confidence level
	Hadronic modes			
Γ_1	$\pi^0\pi^0$		(30.69±0.05) %	
Γ_2	$\pi^+\pi^-$		(69.20±0.05) %	
Γ_3	$\pi^+\pi^-\pi^0$		$(3.5 \ ^{+1.1}_{-0.9}) \times 10^{-7}$	
	Modes with photons or $\ell\bar{\ell}$ pairs			
Γ_4	$\pi^+\pi^-\gamma$	[a,b]	$(1.79 \pm 0.05) \times 10^{-3}$	
Γ_5	$\pi^+\pi^- e^+ e^-$		$(4.79 \pm 0.15) \times 10^{-5}$	
Γ_6	$\pi^0\gamma\gamma$	[a]	$(4.9 \pm 1.8) \times 10^{-8}$	
Γ_7	$\gamma\gamma$		$(2.63 \pm 0.17) \times 10^{-6}$	S=3.0
	Semileptonic modes			
Γ_8	$\pi^\pm e^\mp \nu_e$	[c]	$(7.04 \pm 0.08) \times 10^{-4}$	
Γ_9	$\pi^\pm \mu^\mp \nu_\mu$	[c,d]	$(4.69 \pm 0.05) \times 10^{-4}$	
	CP violating (CP) and $\Delta S = 1$ weak neutral current ($S1$) modes			
Γ_{10}	$3\pi^0$	CP	$< 2.6 \times 10^{-8}$	CL=90%
Γ_{11}	$\mu^+\mu^-$	$S1$	$< 9 \times 10^{-9}$	CL=90%
Γ_{12}	$e^+ e^-$	$S1$	$< 9 \times 10^{-9}$	CL=90%
Γ_{13}	$\pi^0 e^+ e^-$	$S1$ [a]	$(3.0 \ ^{+1.5}_{-1.2}) \times 10^{-9}$	
Γ_{14}	$\pi^0 \mu^+ \mu^-$	$S1$	$(2.9 \ ^{+1.5}_{-1.2}) \times 10^{-9}$	

[a] See the Particle Listings below for the energy limits used in this measurement.

[b] Most of this radiative mode, the low-momentum γ part, is also included in the parent mode listed without γ's.

[c] The value is for the sum of the charge states or particle/antiparticle states indicated.

[d] Not a measurement. Calculated as $0.666 \cdot B(\pi^\pm e^\mp \nu_e)$.

Meson Particle Listings

K^0_S

CONSTRAINED FIT INFORMATION

An overall fit to 4 branching ratios uses 5 measurements and one constraint to determine 4 parameters. The overall fit has a $\chi^2 = 0.1$ for 2 degrees of freedom.

The following *off-diagonal* array elements are the correlation coefficients $\langle \delta x_i \delta x_j \rangle / (\delta x_i \cdot \delta x_j)$, in percent, from the fit to the branching fractions, $x_i \equiv \Gamma_i / \Gamma_{\text{total}}$. The fit constrains the x_i whose labels appear in this array to sum to one.

x_2	−100		
x_8	−6	3	
x_9	−6	3	100
	x_1	x_2	x_8

K^0_S DECAY RATES

$\Gamma(\pi^\pm e^\mp \nu_e)$ Γ_8

VALUE (10^6 s^{-1})	EVTS	DOCUMENT ID		TECN	COMMENT
• • • We do not use the following data for averages, fits, limits, etc. • • •					
8.1 ±1.6	75	[11] AKHMETSHIN	99	CMD2	Tagged K^0_S using $\phi \to K^0_L K^0_S$
7.50±0.08		[12] PDG	98		
seen		BURGUN	72	HBC	$K^+ p \to K^0 p \pi^+$
9.3 ±2.5		AUBERT	65	HLBC	ΔS=ΔQ, *CP* cons. not assumed

[11] AKHMETSHIN 99 is from a measured branching ratio $B(K^0_S \to \pi e \nu_e) = (7.2 \pm 1.4) \times 10^{-4}$ and $\tau_{K^0_S} = (0.8934 \pm 0.0008) \times 10^{-10}$ s. Not independent of measured branching ratio.

[12] PDG 98 from K^0_L measurements, assuming that $\Delta S = \Delta Q$ in K^0 decay so that $\Gamma(K^0_S \to \pi^\pm e^\mp \nu_e) = \Gamma(K^0_L \to \pi^\pm e^\mp \nu_e)$.

$\Gamma(\pi^\pm \mu^\mp \nu_\mu)$ Γ_9

VALUE (10^6 s^{-1})	DOCUMENT ID		
• • • We do not use the following data for averages, fits, limits, etc. • • •			
5.25±0.07	[13] PDG	98	

[13] PDG 98 from K^0_L measurements, assuming that $\Delta S = \Delta Q$ in K^0 decay so that $\Gamma(K^0_S \to \pi^\pm \mu^\mp \nu_\mu) = \Gamma(K^0_L \to \pi^\pm \mu^\mp \nu_\mu)$.

K^0_S BRANCHING RATIOS

Hadronic modes

$\Gamma(\pi^0\pi^0)/\Gamma_{\text{total}}$ Γ_1/Γ

VALUE	EVTS	DOCUMENT ID		TECN
0.3069±0.0005 OUR FIT				
• • • We do not use the following data for averages, fits, limits, etc. • • •				
0.335 ±0.014	1066	BROWN	63	HLBC
0.288 ±0.021	198	CHRETIEN	63	HLBC
0.30 ±0.035		BROWN	61	HLBC

$\Gamma(\pi^+\pi^-)/\Gamma_{\text{total}}$ Γ_2/Γ

VALUE	EVTS	DOCUMENT ID		TECN	COMMENT
0.6920±0.0005 OUR FIT					
• • • We do not use the following data for averages, fits, limits, etc. • • •					
0.670 ±0.010	3447	DOYLE	69	HBC	$\pi^- p \to \Lambda K^0$

$\Gamma(\pi^+\pi^-)/\Gamma(\pi^0\pi^0)$ Γ_2/Γ_1

VALUE	EVTS	DOCUMENT ID		TECN	COMMENT
2.255 ±0.005 OUR FIT					
2.2549±0.0054		[14] AMBROSINO	06C	KLOE	
• • • We do not use the following data for averages, fits, limits, etc. • • •					
2.2555±0.0012±0.0054		[15] AMBROSINO	06C	KLOE	
2.236 ±0.003 ±0.015	766k	[15] ALOISIO	02B	KLOE	
2.11 ±0.09	1315	EVERHART	76	WIRE	$\pi^- p \to \Lambda K^0$
2.169 ±0.094	16k	COWELL	74	OSPK	$\pi^- p \to \Lambda K^0$
2.16 ±0.08	4799	HILL	73	DBC	$K^+ d \to K^0 pp$
2.22 ±0.10	3068	[16] ALITTI	72	HBC	$K^+ p \to \pi^+ p K^0$
2.22 ±0.08	6380	MORSE	72B	DBC	$K^+ n \to K^0 p$
2.10 ±0.11	701	[17] NAGY	72	HLBC	$K^+ n \to K^0 p$
2.22 ±0.095	6150	[18] BALTAY	71	HBC	$K p \to K^0$ neutrals
2.282 ±0.043	7944	[19] MOFFETT	70	OSPK	$K^+ n \to K^0 p$
2.12 ±0.17	267	[17] BOZOKI	69	HLBC	
2.285 ±0.055	3016	[19] GOBBI	69	OSPK	$K^+ n \to K^0 p$
2.10 ±0.06	3700	MORFIN	69	HLBC	$K^+ n \to K^0 p$

[14] This result combines AMBROSINO 06C KLOE 2001-02 data with ALOISIO 02B KLOE 2000 data. $K^0_S \to \pi^+\pi^-$ fully inclusive.

[15] Includes radiative decays $\pi^+\pi^-\gamma$.

[16] The directly measured quantity is $K^0_S \to \pi^+\pi^-/\text{all } K^0 = 0.345 \pm 0.005$.

[17] NAGY 72 is a final result which includes BOZOKI 69.

[18] The directly measured quantity is $K^0_S \to \pi^+\pi^-/\text{all } \overline{K}^0 = 0.345 \pm 0.005$.

[19] MOFFETT 70 is a final result which includes GOBBI 69.

$\Gamma(\pi^+\pi^-\pi^0)/\Gamma_{\text{total}}$ Γ_3/Γ

VALUE (units 10^{-7})	EVTS	DOCUMENT ID		TECN	COMMENT
$3.5^{+1.1}_{-0.9}$ OUR AVERAGE					
$4.7^{+2.2}_{-1.7}{}^{+1.7}_{-1.5}$		[20] BATLEY	05	NA48	
$2.5^{+1.3}_{-1.0}{}^{+0.5}_{-0.6}$	500k	[21] ADLER	97B	CPLR	
$4.8^{+2.2}_{-1.6} \pm 1.1$		[22] ZOU	96	E621	
• • • We do not use the following data for averages, fits, limits, etc. • • •					
$4.1^{+2.5}_{-1.9}{}^{+0.5}_{-0.6}$		[23] ADLER	96E	CPLR	Sup. by ADLER 97B
$3.9^{+5.4}_{-1.8}{}^{+0.9}_{-0.7}$		[24] THOMSON	94	E621	Sup. by ZOU 96

[20] BATLEY 05 is obtained by measuring the interference parameters in K_S, $K_L \to \pi^+\pi^-\pi^0$: $\text{Re}(\lambda) = 0.038 \pm 0.008 \pm 0.006$ and $\text{Im}(\lambda) = -0.013 \pm 0.005 \pm 0.004$; the correlation coeff. between $\text{Re}(\lambda)$ and $\text{Im}(\lambda)$ is 0.66 (statistical only).

[21] ADLER 97B find the *CP*-conserving parameters $\text{Re}(\lambda) = (28 \pm 7 \pm 3) \times 10^{-3}$, $\text{Im}(\lambda) = (-10 \pm 8 \pm 2) \times 10^{-3}$. They estimate $B(K^0_S \to \pi^+\pi^-\pi^0)$ from $\text{Re}(\lambda)$ and the K^0_L decay parameters. See also ANGELOPOULOS 98C.

[22] ZOU 96 is from the the measured quantities $|\rho_{+-0}| = 0.039^{+0.009}_{-0.006} \pm 0.005$ and $\phi_\rho = (-9 \pm 18)^\circ$.

[23] ADLER 96E is from the measured quantities $\text{Re}(\lambda) = 0.036 \pm 0.010^{+0.002}_{-0.003}$ and $\text{Im}(\lambda)$ consistent with zero. Note that the quantity λ is the same as ρ_{+-0} used in other footnotes.

[24] THOMSON 94 calculates this branching ratio from their measurements $|\rho_{+-0}| = 0.035^{+0.019}_{-0.011} \pm 0.004$ and $\phi_\rho = (-59 \pm 48)^\circ$ where $|\rho_{+-0}| e^{i\phi_\rho} = A(K^0_S \to \pi^+\pi^-\pi^0, I=2)/A(K^0_L \to \pi^+\pi^-\pi^0)$.

Modes with photons or $\ell\overline{\ell}$ pairs

$\Gamma(\pi^+\pi^-\gamma)/\Gamma(\pi^+\pi^-)$ Γ_4/Γ_2

VALUE (units 10^{-3})	EVTS	DOCUMENT ID		TECN	COMMENT
2.59±0.08 OUR AVERAGE					
2.56±0.09	1286	RAMBERG	93	E731	p_γ >50 MeV/c
2.68±0.15		[25] TAUREG	76	SPEC	p_γ >50 MeV/c
• • • We do not use the following data for averages, fits, limits, etc. • • •					
7.10±0.22	3723	RAMBERG	93	E731	p_γ >20 MeV/c
3.0 ±0.6	29	[26] BOBISUT	74	HLBC	p_γ >40 MeV/c
2.8 ±0.6		[27] BURGUN	73	HBC	p_γ >50 MeV/c

[25] TAUREG 76 find direct emission contribution <0.06, CL = 90%.

[26] BOBISUT 74 not included in average because p_γ cut differs. Estimates direct emission contribution to be 0.5 or less, CL = 95%.

[27] BURGUN 73 estimates that direct emission contribution is 0.3 ± 0.6.

$\Gamma(\pi^+\pi^-e^+e^-)/\Gamma_{\text{total}}$ Γ_5/Γ

VALUE (units 10^{-5})	EVTS	DOCUMENT ID		TECN	COMMENT
4.79±0.15 OUR AVERAGE					
4.83±0.11±0.14	23k	[28] BATLEY	11	NA48	2002 data
4.69±0.30	676	[29] LAI	03C	NA48	1998+1999 data
• • • We do not use the following data for averages, fits, limits, etc. • • •					
4.71±0.23±0.22	620	[29,30] LAI	03C	NA48	1999 data
4.5 ±0.7 ±0.4	56	LAI	00B	NA48	1998 data

[28] BATLEY 11 reports $[\Gamma(K^0_S \to \pi^+\pi^-e^+e^-)/\Gamma_{\text{total}}] / [B(K^0_L \to \pi^+\pi^-\pi^0)] / [B(\pi^0 \to e^+e^-\gamma)] = (3.28 \pm 0.06 \pm 0.04) \times 10^{-2}$ which we multiply by our best values $B(K^0_L \to \pi^+\pi^-\pi^0) = (12.54 \pm 0.05) \times 10^{-2}$, $B(\pi^0 \to e^+e^-\gamma) = (1.174 \pm 0.035) \times 10^{-2}$. Our first error is their experiment's error and our second error is the systematic error from using our best values. Also a limit on the absolute value of the interference between bremsstrahlung and E1 transition is given : $< 4 \times 10^{-7}$ at 90% C.L.

[29] Uses normalization $BR(K_L \to \pi^+\pi^-\pi^0) * BR(\pi^0 \to e^+e^-) = (1.505 \pm 0.047) \times 10^{-3}$ from our 2000 Edition.

[30] Second error is 0.16(syst) ±0.15(norm) combined in quadrature.

$\Gamma(\pi^0\gamma\gamma)/\Gamma_{\text{total}}$ Γ_6/Γ

VALUE (units 10^{-8})	CL%	EVTS	DOCUMENT ID		TECN	COMMENT
4.9±1.6±0.9		17	[31] LAI	04	NA48	$m^2_{\gamma\gamma}/m^2_K > 0.2$
• • • We do not use the following data for averages, fits, limits, etc. • • •						
<33	90		LAI	03B	NA48	$m^2_{\gamma\gamma}/m^2_K > 0.2$

[31] Spectrum also measured and found consistent with the one generated by a constant matrix element.

$\Gamma(\gamma\gamma)/\Gamma_{\text{total}}$ Γ_7/Γ

VALUE (units 10^{-6})	CL%	EVTS	DOCUMENT ID		TECN	COMMENT
2.63 ±0.17 OUR AVERAGE			Error includes scale factor of 3.0.			
2.26 ±0.12 ±0.06		711	[32] AMBROSINO	08C	KLOE	$\phi \to K^0_S K^0_L$
2.713±0.063±0.005		7.5k	[33] LAI	03	NA48	

• • • We do not use the following data for averages, fits, limits, etc. • • •

2.58 ±0.36 ±0.22	149		LAI	00	NA48	
2.2 ±1.1	16	[34]	BARR	95B	NA31	
2.4 ±0.9	35	[35]	BARR	95B	NA31	
< 13	90		BALATS	89	SPEC	
2.4 ±1.2	19		BURKHARDT	87	NA31	
<133	90		BARMIN	86B	XEBC	

[32] AMBROSINO 08C reports $(2.26 \pm 0.12 \pm 0.06) \times 10^{-6}$ from a measurement of $[\Gamma(K^0_S \to \gamma\gamma)/\Gamma_{total}] \times [B(K^0_S \to \pi^0\pi^0)]$ assuming $B(K^0_S \to \pi^0\pi^0) = (30.69 \pm 0.05) \times 10^{-2}$.

[33] LAI 03 reports $[\Gamma(K^0_S \to \gamma\gamma)/\Gamma_{total}] / [B(K^0_S \to \pi^0\pi^0)] = (8.84 \pm 0.18 \pm 0.10) \times 10^{-6}$ which we multiply by our best value $B(K^0_S \to \pi^0\pi^0) = (30.69 \pm 0.05) \times 10^{-2}$. Our first error is their experiment's error and our second error is the systematic error from using our best value.

[34] BARR 95B result is calculated using $B(K_L \to \gamma\gamma) = (5.86 \pm 0.17) \times 10^{-4}$.

[35] BARR 95B quotes this as the combined BARR 95B + BURKHARDT 87 result after rescaling BURKHARDT 87 to use same branching ratios and lifetimes as BARR 95B.

Semileptonic modes

$\Gamma(\pi^\pm e^\mp \nu_e)/\Gamma_{total}$ Γ_8/Γ

VALUE (units 10^{-4})	EVTS	DOCUMENT ID		TECN	COMMENT
7.04 ±0.08 OUR FIT					
7.04 ±0.08 OUR AVERAGE					
7.046±0.18±0.16		[36] BATLEY	07D	NA48	$K^0(\overline{K}^0)(t) \to \pi e \nu$
6.91 ±0.34±0.15	624	[37] ALOISIO	02	KLOE	Tagged K^0_S using $\phi \to K^0_L K^0_S$
• • • We use the following data for averages but not for fits. • • •					
7.05 ±0.09	13k	[38] AMBROSINO	06E	KLOE	Not fitted
• • • We do not use the following data for averages, fits, limits, etc. • • •					
7.2 ±1.4	75	AKHMETSHIN	99	CMD2	Tagged K^0_S using $\phi \to K^0_L K^0_S$

[36] Reconstructed from $K^0(\overline{K}^0)(t) \to \pi e \nu$ distributions using PDG values of $B(K^0_L \to \pi e \nu) = 0.4053 \pm 0.0015$, $\tau_L = (5.114 \pm 0.021) \times 10^{-8}$ s and $\tau_S = (0.8958 \pm 0.0005) \times 10^{-10}$ s.

[37] Uses the PDG 00 value for $B(K^0_S \to \pi^+\pi^-)$.

[38] Obtained by imposing $\Sigma_i B(K^0_S \to i) = 1$, where i runs over all the four branching ratios $\pi^+\pi^-$, $\pi^0\pi^0$, $\pi e \nu$, and $\pi \mu \nu$. Input value of $B(K^0_S \to \pi^+\pi^-) / B(K^0_S \to \pi^0\pi^0)$ from AMBROSINO 06C is used. To derive $\Gamma(K^0_S \to \pi^+ \mu\nu) / \Gamma(K^0_S \to \pi^+ e\nu)$, lepton universality is assumed, radiative corrections from ANDRE 07 are used, and phase space integrals are taken from KTeV, ALEXOPOULOS 04A. This branching fraction enters our fit via their $\Gamma(\pi^\pm e^\mp \nu_e) / \Gamma(\pi^+\pi^-)$ branching ratio measurement.

$\Gamma(\pi^\pm \mu^\mp \nu_\mu)/\Gamma_{total}$ Γ_9/Γ

The PDG 06 value below has not been measured but is computed to be 0.666 times the $K_S \to \pi^\pm e^\mp \nu_e$ branching fraction. It is included in the fit that constrains the four branching ratios $\pi^+\pi^-$, $\pi^0\pi^0$, $\pi e \nu$, and $\pi \mu \nu$ to sum to 1. This treatment, used by AMBROSINO 06E, is preferable to our previous practice of constraining the $\pi^+\pi^-$ and $\pi^0\pi^0$ modes to sum to 1. The 0.666 factor is obtained from AMBROSINO 06E and assumes lepton universality, radiative corrections from ANDRE 07, and phase space integrals from KTeV, ALEXOPOULOS 04A.

VALUE (units 10^{-4})	DOCUMENT ID			COMMENT
4.69 ±0.06 OUR FIT				
4.691±0.001±0.056	[39] PDG		06	calculated from $\pi^\pm e^\mp \nu_e$

[39] The PDG 06 value is computed to be $B_{PDG06}(\pi\mu\nu) = 0.666\ B_{FIT}(\pi e \nu)$. The first error specifies the arbitrarily small error, 0.001×10^{-4}, on $B_{PDG06}(\pi\mu\nu)$ for fixed $B_{FIT}(\pi e \nu)$. The second error is that due to the uncertainty in $B_{FIT}(\pi e \nu)$.

$\Gamma(\pi^\pm e^\mp \nu_e)/\Gamma(\pi^+\pi^-)$ Γ_8/Γ_2

VALUE (units 10^{-4})	EVTS	DOCUMENT ID		TECN
10.18±0.12 OUR FIT				
10.19±0.11±0.07	13k	AMBROSINO	06E	KLOE

CP violating (CP) and ΔS = 1 weak neutral current (S1) modes

$\Gamma(3\pi^0)/\Gamma_{total}$ Γ_{10}/Γ

Violates CP conservation.

VALUE (units 10^{-7})	CL%	EVTS	DOCUMENT ID		TECN	COMMENT
< 0.26	90	590M	[40] BABUSCI	13C	KLOE	$\phi \to K^0_L K^0_S$
• • • We do not use the following data for averages, fits, limits, etc. • • •						
< 1.2	90	37.8M	AMBROSINO	05B	KLOE	
< 7.4	90	4.9M	[41] LAI	05A	NA48	
<140	90	7M	ACHASOV	99D	SND	
<190	90	17300	[42] ANGELOPO...	98B	CPLR	
<370	90		BARMIN	83	HLBC	

[40] BABUSCI 13C uses 1.7 fb^{-1} of data of $\phi \to K^0_L K^0_S$ decays with K^0_L interaction in the calorimeter, collected from 2004 to 2005. No candidate events were found in the data with an expected background of $0.04^{+0.15}_{-0.03}$ events. Upper limit is obtained by normalizing to $K^0_S \to 2\pi^0$ decays.

[41] LAI 05A value is obtained from their bound on $|\eta_{000}|$ (not assuming CPT) and $B(K^0_L \to 3\pi^0) = 0.211 \pm 0.003$, and PDG 04 values for K^0_L and K^0_S lifetimes. If CPT is assumed then $B(K^0_S \to 3\pi^0)_{CPT} < 2.3 \times 10^{-7}$ at 90% CL

[42] ANGELOPOULOS 98B is from $Im(\eta_{000}) = -0.05 \pm 0.12 \pm 0.05$, assuming $Re(\eta_{000}) = Re(\epsilon) = 1.635 \times 10^{-3}$ and using the value $B(K^0_L \to \pi^0\pi^0\pi^0) = 0.2112 \pm 0.0027$.

$\Gamma(\mu^+\mu^-)/\Gamma_{total}$ Γ_{11}/Γ

Test for $\Delta S = 1$ weak neutral current. Allowed by first-order weak interaction combined with electromagnetic interaction.

VALUE (units 10^{-9})	CL%	DOCUMENT ID		TECN
<9	90	[43] AAIJ	13G	LHCB
• • • We do not use the following data for averages, fits, limits, etc. • • •				
$<3.2 \times 10^2$	90	GJESDAL	73	ASPK
$<7 \times 10^3$	90	HYAMS	69B	OSPK

[43] AAIJ 13G uses 1.0 fb^{-1} of pp collisions at $\sqrt{s} = 7$ TeV. They obtained $B(K^0_S \to \mu^+\mu^-) < 11 \times 10^{-9}$ at 95% C.L.

$\Gamma(e^+e^-)/\Gamma_{total}$ Γ_{12}/Γ

Test for $\Delta S = 1$ weak neutral current. Allowed by first-order weak interaction combined with electromagnetic interaction.

VALUE (units 10^{-7})	CL%	DOCUMENT ID		TECN	COMMENT
< 0.09	90	[44] AMBROSINO	09A	KLOE	$e^+e^- \to \phi \to K^0_S K^0_L$
• • • We do not use the following data for averages, fits, limits, etc. • • •					
< 1.4	90	ANGELOPO...	97	CPLR	
< 28	90	BLICK	94	CNTR	Hyperon facility
<100	90	BARMIN	86	XEBC	

[44] AMBROSINO 09A reports $< 0.09 \times 10^{-7}$ from a measurement of $[\Gamma(K^0_S \to e^+e^-)/\Gamma_{total}] / [B(K^0_S \to \pi^+\pi^-)]$ assuming $B(K^0_S \to \pi^+\pi^-) = (69.20 \pm 0.05) \times 10^{-2}$.

$\Gamma(\pi^0 e^+ e^-)/\Gamma_{total}$ Γ_{13}/Γ

Test for $\Delta S = 1$ weak neutral current. Allowed by first-order weak interaction combined with electromagnetic interaction.

VALUE (units 10^{-9})	CL%	EVTS	DOCUMENT ID		TECN	COMMENT
$\mathbf{3.0^{+1.5}_{-1.2} \pm 0.2}$		7	[45] BATLEY	03	NA48	m_{ee} >0.165 GeV
• • • We do not use the following data for averages, fits, limits, etc. • • •						
< 140	90		LAI	01	NA48	
< 1100	90	0	BARR	93B	NA31	
<45000	90		GIBBONS	88	E731	

[45] BATLEY 03 extrapolate also to the full kinematical region using a constant form factor and a vector matrix element. The resulting branching ratio is $(5.8^{+2.9}_{-2.4}) \times 10^{-9}$.

$\Gamma(\pi^0 \mu^+ \mu^-)/\Gamma_{total}$ Γ_{14}/Γ

Test for $\Delta S = 1$ weak neutral current. Allowed by first-order weak interaction combined with electromagnetic interaction.

VALUE (units 10^{-9})	EVTS	DOCUMENT ID		TECN	COMMENT
$\mathbf{2.9^{+1.5}_{-1.2} \pm 0.2}$	6	[46] BATLEY	04A	NA48	NA48/1 K^0_S beam

[46] Background estimate is $0.22^{+0.18}_{-0.11}$ events. Branching ratio assumes a vector matrix element and unit form factor.

K^0_S FORM FACTORS

For discussion, see note on $K_{\ell 3}$ form factors in the $K^\pm$ section of the Particle Listings above. Because the semileptonic branching fraction is smaller in K^0_S than K^0_L by the ratio of the mean lives, the K^0_S semileptonic form factor has so far been measured only in the K_{e3} mode using the linear expansion $f_+(t) = f_+(0)\ (1 + \lambda_+ t / m^2_{\pi^+})$, which gives the vector form factor $f_+(t)$ relative to its value at $t = 0$.

λ_+ (LINEAR ENERGY DEPENDENCE OF f_+ IN K^0_{e3} DECAY)

VALUE (units 10^{-2})	EVTS	DOCUMENT ID		TECN
3.39±0.41	15k	AMBROSINO	06E	KLOE

CP VIOLATION IN $K_S \to 3\pi$

Written 1996 by T. Nakada (Paul Scherrer Institute) and L. Wolfenstein (Carnegie-Mellon University).

The possible final states for the decay $K^0 \to \pi^+\pi^-\pi^0$ have isospin $I = 0$, 1, 2, and 3. The $I = 0$ and $I = 2$ states have $CP = +1$ and K_S can decay into them without violating CP symmetry, but they are expected to be strongly suppressed by centrifugal barrier effects. The $I = 1$ and $I = 3$ states, which have no centrifugal barrier, have $CP = -1$ so that the K_S decay to these requires CP violation.

In order to see CP violation in $K_S \to \pi^+\pi^-\pi^0$, it is necessary to observe the interference between K_S and K_L decay, which determines the amplitude ratio

$$\eta_{+-0} = \frac{A(K_S \to \pi^+\pi^-\pi^0)}{A(K_L \to \pi^+\pi^-\pi^0)} \ . \qquad (1)$$

If η_{+-0} is obtained from an integration over the whole Dalitz plot, there is no contribution from the $I = 0$ and $I = 2$ final states and a nonzero value of η_{+-0} is entirely due to CP violation.

Only $I = 1$ and $I = 3$ states, which are $CP = -1$, are allowed for $K^0 \to \pi^0\pi^0\pi^0$ decays and the decay of K_S into $3\pi^0$ is an unambiguous sign of CP violation. Similarly to η_{+-0}, η_{000} is defined as

$$\eta_{000} = \frac{A(K_S \to \pi^0\pi^0\pi^0)}{A(K_L \to \pi^0\pi^0\pi^0)} \ . \qquad (2)$$

If one assumes that CPT invariance holds and that there are no transitions to $I = 3$ (or to nonsymmetric $I = 1$ states), it can be shown that

$$\eta_{+-0} = \eta_{000} = \epsilon + i\frac{\text{Im } a_1}{\text{Re } a_1} \ . \qquad (3)$$

With the Wu-Yang phase convention, a_1 is the weak decay amplitude for K^0 into $I = 1$ final states; ϵ is determined from CP violation in $K_L \to 2\pi$ decays. The real parts of η_{+-0} and η_{000} are equal to Re(ϵ). Since currently-known upper limits on $|\eta_{+-0}|$ and $|\eta_{000}|$ are much larger than $|\epsilon|$, they can be interpreted as upper limits on Im(η_{+-0}) and Im(η_{000}) and so as limits on the CP-violating phase of the decay amplitude a_1.

CP-VIOLATION PARAMETERS IN K^0_S DECAY

$A_S = [\ \Gamma(K^0_S \to \pi^- e^+ \nu_e) - \Gamma(K^0_S \to \pi^+ e^- \bar{\nu}_e)\ ] \ /$ SUM

Such asymmetry violates CP. If CPT is assumed then $A_S = 2$ Re(ϵ).

VALUE (units 10^{-3})	EVTS	DOCUMENT ID		TECN
1.5 ± 9.6 ± 2.9	13k	AMBROSINO	06E	KLOE

PARAMETERS FOR $K^0_S \to 3\pi$ DECAY

Im(η_{+-0})^2 = $\Gamma(K^0_S \to \pi^+\pi^-\pi^0$, CP-violating) / $\Gamma(K^0_L \to \pi^+\pi^-\pi^0)$

CPT assumed valid (i.e. Re(η_{+-0}) $\simeq$ 0).

VALUE	CL%	EVTS	DOCUMENT ID		TECN
• • • We do not use the following data for averages, fits, limits, etc. • • •					
<0.23	90	601	[47] BARMIN	85	HLBC
<0.12	90	384	METCALF	72	ASPK

[47] BARMIN 85 find Re(η_{+-0}) = (0.05 ± 0.17) and Im(η_{+-0}) = (0.15 ± 0.33). Includes events of BALDO-CEOLIN 75.

Im(η_{+-0}) = Im(A($K^0_S \to \pi^+\pi^-\pi^0$, CP-violating) / A($K^0_L \to \pi^+\pi^-\pi^0$))

VALUE	EVTS	DOCUMENT ID		TECN	COMMENT
$\mathbf{-0.002 \pm 0.009^{+0.002}_{-0.001}}$	500k	[48] ADLER	97B	CPLR	
• • • We do not use the following data for averages, fits, limits, etc. • • •					
$-0.002 \pm 0.018 \pm 0.003$	137k	[49] ADLER	96D	CPLR	Sup. by ADLER 97B
$-0.015 \pm 0.017 \pm 0.025$	272k	[50] ZOU	94	SPEC	

[48] ADLER 97B also find Re(η_{+-0}) = $-0.002 \pm 0.007^{+0.004}_{-0.001}$. See also ANGELOPOULOS 98C.

[49] The ADLER 96D fit also yields Re(η_{+-0}) = 0.006 ± 0.013 ± 0.001 with a correlation +0.66 between real and imaginary parts. Their results correspond to $|\eta_{+-0}| < 0.037$ with 90% CL.

[50] ZOU 94 use theoretical constraint Re(η_{+-0}) = Re(ϵ) = 0.0016. Without this constraint they find Im(η_{+-0}) = 0.019 ± 0.061 and Re(η_{+-0}) = 0.019 ± 0.027.

Im(η_{000})^2 = $\Gamma(K^0_S \to 3\pi^0) \ / \ \Gamma(K^0_L \to 3\pi^0)$

CPT assumed valid (i.e. Re(η_{000}) $\simeq$ 0). This limit determines branching ratio $\Gamma(3\pi^0)/\Gamma_{\text{total}}$ above.

VALUE	CL%	EVTS	DOCUMENT ID		TECN	COMMENT
• • • We do not use the following data for averages, fits, limits, etc. • • •						
<0.1	90	632	[51] BARMIN	83	HLBC	
<0.28	90		[52] GJESDAL	74B	SPEC	Indirect meas.

[51] BARMIN 83 find Re(η_{000}) = (-0.08 ± 0.18) and Im(η_{000}) = (-0.05 ± 0.27). Assuming CPT invariance they obtain the limit quoted above.

[52] GJESDAL 74B uses $K2\pi$, $K_{\mu 3}$, and K_{e3} decay results, unitarity, and CPT. Calculates $|(\eta_{000})| = 0.26 \pm 0.20$. We convert to upper limit.

Im(η_{000}) = Im($A(K^0_S \to \pi^0\pi^0\pi^0)/A(K^0_L \to \pi^0\pi^0\pi^0)$)

$K^0_S \to \pi^0\pi^0\pi^0$ violates CP conservation, in contrast to $K^0_S \to \pi^+\pi^-\pi^0$ which has a CP-conserving part.

VALUE	EVTS	DOCUMENT ID		TECN	COMMENT
$\mathbf{(-0.1 \pm 1.6) \times 10^{-2}}$ **OUR AVERAGE**					
$0.000 \pm 0.009 \pm 0.013$	4.9M	[53] LAI	05A	NA48	Assumes CPT
$-0.05 \pm 0.12 \pm 0.05$	17300	[54] ANGELOPO...	98B	CPLR	Assumes CPT

[53] LAI 05A assumes Re(η_{000})=Re(ϵ)=1.66 × 10^{-3}. The equivalent limit is $|\eta_{000}|_{CPT} < 0.025$ at 90% CL Without assuming CPT invariance, they obtain Re(η_{000})=$-0.002 \pm 0.011 \pm 0.015$ and Im(η_{000})=$-0.003 \pm 0.013 \pm 0.017$ with a statistical correlation coefficient of 0.77 and an overall correlation coefficient of 0.57 between imaginary and real part. The equivalent limit is $|\eta_{000}| < 0.045$ at 90% CL

[54] ANGELOPOULOS 98B assumes Re(η_{000}) = Re(ϵ) = 1.635×10^{-3}. Without assuming CPT invariance, they obtain Re(η_{000}) = 0.18 ± 0.14 ± 0.06 and Im(η_{000}) = 0.15 ± 0.20 ± 0.03.

$|\eta_{000}| = |A(K^0_S \to 3\pi^0)/A(K^0_L \to 3\pi^0)|$

A non-zero value violates CP invariance.

VALUE	CL%	EVTS	DOCUMENT ID		TECN
<0.0088	90	590M	BABUSCI	13C	KLOE
• • • We do not use the following data for averages, fits, limits, etc. • • •					
<0.018	90	37.8M	AMBROSINO	05B	KLOE
<0.045	90	4.9M	LAI	05A	NA48

DECAY-PLANE ASYMMETRY IN $\pi^+\pi^- e^+ e^-$ DECAYS

This is the CP-violating asymmetry

$$A = \frac{N_{\sin\phi\cos\phi>0.0} - N_{\sin\phi\cos\phi<0.0}}{N_{\sin\phi\cos\phi>0.0} + N_{\sin\phi\cos\phi<0.0}}$$

where ϕ is the angle between the e^+e^- and $\pi^+\pi^-$ planes in the K^0_S rest frame.

CP asymmetry A in $K^0_S \to \pi^+\pi^- e^+ e^-$

VALUE (%)	DOCUMENT ID		TECN	COMMENT
$\mathbf{-0.4 \pm 0.8}$ **OUR AVERAGE**				
-0.4 ± 0.8	[55] BATLEY	11	NA48	2002 data
-1.1 ± 4.1	LAI	03C	NA48	1998+1999 data
• • • We do not use the following data for averages, fits, limits, etc. • • •				
$0.5 \pm 4.0 \pm 1.6$	LAI	03C	NA48	1999 data

[55] The result is used to set the limit $A < 1.5\%$ at 90% C.L.

K^0_S REFERENCES

AAIJ	13G	JHEP 1301 090	R. Aaij *et al.*	(LHCb Collab.)
BABUSCI	13C	PL B723 54	D. Babusci *et al.*	(KLOE-2 Collab.)
ABOUZAID	11	PR D83 092001	E. Abouzaid *et al.*	(FNAL KTeV Collab.)
AMBROSINO	11	EPJ C71 1604	F. Ambrosino *et al.*	(KLOE Collab.)
BATLEY	11	PL B694 301	J.R. Batley *et al.*	(CERN NA48/1 Collab.)
AMBROSINO	09A	PL B672 203	F. Ambrosino *et al.*	(KLOE Collab.)
AMBROSINO	08C	JHEP 0805 051	F. Ambrosino *et al.*	(KLOE Collab.)
ANDRE	07	ANP 322 2518	T. Andre	(EFI)
BATLEY	07D	PL B653 145	J.R. Batley *et al.*	(CERN NA48 Collab.)
AMBROSINO	06C	EPJ C48 767	F. Ambrosino *et al.*	(KLOE Collab.)
AMBROSINO	06E	PL B636 173	F. Ambrosino *et al.*	(KLOE Collab.)
PDG	06	JP G33 1	W.-M. Yao *et al.*	(PDG Collab.)
AMBROSINO	05B	PL B619 61	F. Ambrosino *et al.*	(KLOE Collab.)
BATLEY	05	PL B630 31	J.R. Batley *et al.*	(NA48 Collab.)
LAI	05A	PL B610 165	A. Lai *et al.*	(CERN NA48 Collab.)
ALEXOPOU...	04A	PR D70 092007	T. Alexopoulos *et al.*	(FNAL KTeV Collab.)
BATLEY	04A	PL B599 197	J.R. Batley *et al.*	(NA48 Collab.)
LAI	04	PL B578 276	A. Lai *et al.*	(CERN NA48 Collab.)
PDG	04	PL B592 1	S. Eidelman *et al.*	(PDG Collab.)
ALAVI-HARATI	03	PR D67 012005	A. Alavi-Harati *et al.*	(FNAL KTeV Collab.)
Also		PR D70 079904 (errat.)	A. Alavi-Harati *et al.*	(FNAL KTeV Collab.)
BATLEY	03	PL B576 43	J.R. Batley *et al.*	(CERN NA48 Collab.)
LAI	03	PL B551 7	A. Lai *et al.*	(CERN NA48 Collab.)
LAI	03B	PL B556 105	A. Lai *et al.*	(CERN NA48 Collab.)
LAI	03C	EPJ C30 33	A. Lai *et al.*	(CERN NA48 Collab.)
ALOISIO	02	PL B535 37	A. Aloisio *et al.*	(KLOE Collab.)
ALOISIO	02B	PL B538 21	A. Aloisio *et al.*	(KLOE Collab.)
LAI	02C	PL B537 28	A. Lai *et al.*	(CERN NA48 Collab.)
LAI	01	PL B514 253	A. Lai *et al.*	(CERN NA48 Collab.)
LAI	00	PL B493 29	A. Lai *et al.*	(CERN NA48 Collab.)
LAI	00B	PL B496 137	A. Lai *et al.*	(CERN NA48 Collab.)
PDG	00	EPJ C15 1	D.E. Groom *et al.*	(PDG Collab.)
ACHASOV	99D	PL B459 674	M.N. Achasov *et al.*	
AKHMETSHIN	99	PL B456 90	R.R. Akhmetshin *et al.*	(Novosibirsk CMD-2 Collab.)
ANGELOPO...	98B	PL B425 391	A. Angelopoulos *et al.*	(CPLEAR Collab.)
ANGELOPO...	98C	EPJ C5 389	A. Angelopoulos *et al.*	(CPLEAR Collab.)
PDG	98	EPJ C3 1	C. Caso *et al.*	(PDG Collab.)
ADLER	97B	PL B407 193	R. Adler *et al.*	(CPLEAR Collab.)
ANGELOPO...	97	PL B413 232	A. Angelopoulos *et al.*	(CPLEAR Collab.)
BERTANZA	97	ZPHY C73 629	L. Bertanza (PISA, CERN, EDIN, MANZ, ORSAY+)	
ADLER	96D	PL B370 167	R. Adler *et al.*	(CPLEAR Collab.)
ADLER	96E	PL B374 313	R. Adler *et al.*	(CPLEAR Collab.)
ZOU	96	PL B369 362	Y. Zou *et al.*	(RUTG, MINN, MICH)
BARR	95B	PL B351 579	G.D. Barr *et al.*	(CERN, EDIN, MANZ, LALO+)
SCHWINGEN...	95	PRL 74 4376	B. Schwingenheuer *et al.*	(EFI, CHIC+)
BLICK	94	PL B334 234	A.M. Blick *et al.*	(SERP, JINR)
THOMSON	94	PL B337 411	G.B. Thomson *et al.*	(RUTG, MINN, MICH)
ZOU	94	PL B329 519	Y. Zou *et al.*	(RUTG, MINN, MICH)
BARR	93B	PL B304 381	G.D. Barr *et al.*	(CERN, EDIN, MANZ, LALO+)
GIBBONS	93	PRL 70 1199	L.K. Gibbons *et al.*	(FNAL E731 Collab.)
Also		PR D55 6625	L.K. Gibbons *et al.*	(FNAL E731 Collab.)
RAMBERG	93	PRL 70 2525	E. Ramberg *et al.*	(FNAL E731 Collab.)
BALATS	89	SJNP 49 828 Translated from YAF 49 1332.	M.Y. Balats *et al.*	(ITEP)
GIBBONS	88	PRL 61 2661	L.K. Gibbons *et al.*	(FNAL E731 Collab.)
BURKHARDT	87	PL B199 139	H. Burkhardt *et al.*	(CERN, EDIN, MANZ+)
GROSSMAN	87	PRL 59 18	N. Grossman *et al.*	(MINN, MICH, RUTG)
BARMIN	86	SJNP 44 622 Translated from YAF 44 965.	V.V. Barmin *et al.*	(ITEP)

BARMIN	86B	NC 96A 159	V.V. Barmin *et al.*	(ITEP, PADO)
PDG	86B	PL 170B 130	M. Aguilar-Benitez *et al.*	(CERN, CIT+)
BARMIN	85	NC 85A 67	V.V. Barmin *et al.*	(ITEP, PADO)
Also		SJNP 41 759 Translated from YAF 41 1187.	V.V. Barmin *et al.*	(ITEP)
BARMIN	83	PL 128B 129	V.V. Barmin *et al.*	(ITEP, PADO)
Also		SJNP 39 269 Translated from YAF 39 428.	V.V. Barmin *et al.*	(ITEP, PADO)
ARONSON	82	PRL 48 1078	S.H. Aronson *et al.*	(BNL, CHIC, STAN+)
ARONSON	82B	PRL 48 1306	S.H. Aronson *et al.*	(BNL, CHIC, PURD)
Also		PL 116B 73	E. Fischbach *et al.*	(PURD, BNL, CHIC)
Also		PR D28 476	S.H. Aronson *et al.*	(BNL, CHIC, PURD)
Also		PR D28 495	S.H. Aronson *et al.*	(BNL, CHIC, PURD)
ARONSON	76	NC 32A 236	S.H. Aronson *et al.*	(WISC, EFI, UCSD+)
EVERHART	76	PR D14 661	G.C. Everhart *et al.*	(PENN)
TAUREG	76	PL 65B 92	H. Taureg *et al.*	(HEIDH, CERN, DORT)
BALDO-...	75	NC 25A 688	M. Baldo-Ceolin *et al.*	(PADO, WISC)
CARITHERS	75	PRL 34 1244	W.C.J. Carithers *et al.*	(COLU, NYU)
BOBISUT	74	LNC 11 646	F. Bobisut *et al.*	(PADO)
COWELL	74	PR D10 2083	P.L. Cowell *et al.*	(STON, COLU)
GEWENIGER	74B	PL 48B 487	C. Geweniger *et al.*	(CERN, HEIDH)
GJESDAL	74B	PL 52B 119	S. Gjesdal *et al.*	(CERN, HEIDH)
BURGUN	73	PL 46B 481	G. Burgun *et al.*	(SACL, CERN)
GJESDAL	73	PL 44B 217	S. Gjesdal *et al.*	(CERN, HEIDH)
HILL	73	PR D8 1290	D.G. Hill *et al.*	(BNL, CMU)
ALITTI	72	PL 39B 568	J. Alitti, E. Lesquoy, A. Muller	(SACL)
BURGUN	72	NP B50 194	G. Burgun *et al.*	(SACL, CERN, OSLO)
METCALF	72	PL 40B 703	M. Metcalf *et al.*	(CERN, IPN, WIEN)
MORSE	72B	PRL 28 388	R. Morse *et al.*	(COLO, PRIN, UMD)
NAGY	72	NP B47 94	E. Nagy, F. Telbisz, G. Vesztergombi	(BUDA)
Also		PL 30B 498	G. Bozoki *et al.*	(BUDA)
SKJEGGEST...	72	NP B48 343	O. Skjeggestad *et al.*	(OSLO, CERN, SACL)
BALTAY	71	PRL 27 1678	C. Baltay *et al.*	(COLU)
Also		Thesis Nevis 187	W.A. Cooper	(COLU)
MOFFETT	70	BAPS 15 512	R. Moffett *et al.*	(ROCH)
BOZOKI	69	PL 30B 498	G. Bozoki *et al.*	(BUDA)
DOYLE	69	Thesis UCRL 18139	J.C. Doyle	(LRL)
GOBBI	69	PRL 22 682	B. Gobbi *et al.*	(ROCH)
HYAMS	69B	PL 29B 521	B.D. Hyams *et al.*	(CERN, MPIM)
MORFIN	69	PRL 23 660	J.G. Morfin, D. Sinclair	(MICH)
DONALD	68B	PL 27B 58	R.A. Donald *et al.*	(LIVP, CERN, IPNP+)
HILL	68	PR 171 1418	D.G. Hill *et al.*	(BNL, CMU)
AUBERT	65	PL 17 59	B. Aubert *et al.*	(EPOL, ORSAY)
BROWN	63	PR 130 769	J.L. Brown *et al.*	(LRL, MICH)
CHRETIEN	63	PR 131 2208	M. Chretien *et al.*	(BRAN, BROW, HARV+)
BROWN	61	NC 19 1155	J.L. Brown *et al.*	(MICH)
BOLDT	58B	PRL 1 150	E. Boldt, D.O. Caldwell, Y. Pal	(MIT)

OTHER RELATED PAPERS

LITTENBERG	93	ARNPS 43 729 Rare and Radiative Kaon Decays	L.S. Littenberg, G. Valencia	(BNL, FNAL)
BATTISTON	92	PRPL 214 293 Status and Perspectives of K Decay Physics	R. Battiston *et al.*	(PGIA, CERN, TRSTT)
TRILLING	65B	UCRL 16473 Updated from 1965 Argonne Conference, page 115.	G.N. Trilling	(LRL)
CRAWFORD	62	CERN Conf. 827	F.S. Crawford	(LRL)
FITCH	61	NC 22 1160	V.L. Fitch, P.A. Piroue, R.B. Perkins	(PRIN+)
GOOD	61	PR 124 1223	R.H. Good *et al.*	(LRL)
BIRGE	60	Rochester Conf. 601	R.W. Birge *et al.*	(LRL, WISC)
MULLER	60	PRL 4 418	F. Muller *et al.*	(LRL, BNL)

K^0_L

$I(J^P) = \frac{1}{2}(0^-)$

$m_{K^0_L} - m_{K^0_S}$

For earlier measurements, beginning with GOOD 61 and FITCH 61, see our 1986 edition, Physics Letters **170B** 132 (1986).

OUR FIT is described in the note on "*CP* violation in K_L decays" in the K^0_L Particle Listings. The result labeled "OUR FIT Assuming *CPT*" ["OUR FIT Not assuming *CPT*"] includes all measurements except those with the comment "Not assuming *CPT*" ["Assuming *CPT*"]. Measurements with neither comment do not assume *CPT* and enter both fits.

VALUE ($10^{10}\ \hbar\,s^{-1}$)		*DOCUMENT ID*		*TECN*	*COMMENT*
0.5293 ±0.0009	**OUR FIT**	Error includes scale factor of 1.3. Assuming *CPT*			
0.5289 ±0.0010	**OUR FIT**	Not assuming *CPT*			
0.52797±0.00195		[1,2] ABOUZAID	11	KTEV	Not assuming *CPT*
0.52699±0.00123		[1,3] ABOUZAID	11	KTEV	Assuming *CPT*
0.5240 ±0.0044 ±0.0033		APOSTOLA...	99C	CPLR	K^0-$\overline{K}^0$ to $\pi^+\pi^-$
0.5297 ±0.0030 ±0.0022		[4] SCHWINGEN...	95	E773	20–160 GeV K beams
0.5286 ±0.0028		[5] GIBBONS	93	E731	Assuming *CPT*
0.5257 ±0.0049 ±0.0021		[4] GIBBONS	93C	E731	Not assuming *CPT*
0.5340 ±0.00255±0.0015		[6] GEWENIGER	74C	SPEC	Gap method
0.5334 ±0.0040 ±0.0015		[6,7] GJESDAL	74	SPEC	Assuming *CPT*
• • • We do not use the following data for averages, fits, limits, etc. • • •					
0.5261 ±0.0015		[8] ALAVI-HARATI	03	KTEV	Assuming *CPT*
0.5288 ±0.0043		[9] ALAVI-HARATI	03	KTEV	Not assuming *CPT*
0.5343 ±0.0063 ±0.0025		[10] ANGELOPO...	01	CPLR	
0.5295 ±0.0020 ±0.0003		[11] ANGELOPO...	98D	CPLR	Assuming *CPT*
0.5307 ±0.0013		[12] ADLER	96C	RVUE	
0.5274 ±0.0029 ±0.0005		[11] ADLER	95	CPLR	Sup. by ANGELOPOULOS 98D
0.482 ±0.014		[13] ARONSON	82B	SPEC	E=30–110 GeV
0.534 ±0.007		[14] CARNEGIE	71	ASPK	Gap method
0.542 ±0.006		[14] ARONSON	70	ASPK	Gap method
0.542 ±0.006		CULLEN	70	CNTR	

[1] The two ABOUZAID 11 values use the same data. The first enters the "assuming *CPT*" fit and the second enters the "not assuming *CPT*" fit.

[2] ABOUZAID 11 fit has Δm, τ_S, ϕ_ϵ, $\mathrm{Re}(\epsilon'/\epsilon)$, and $\mathrm{Im}(\epsilon'/\epsilon)$ as free parameters. See $\mathrm{Im}(\epsilon'/\epsilon)$ in the "K^0_L *CP* violation" section for correlation information.

[3] ABOUZAID 11 fit has Δm and τ_S free but constrains ϕ_ϵ to the Superweak value, i.e. assumes *CPT*. See "K^0_S Mean Life" section for correlation information.

[4] Fits Δm and ϕ_{+-} simultaneously. GIBBONS 93C systematic error is from B. Winstein via private communication. 20–160 GeV K beams.

[5] GIBBONS 93 value assume $\phi_{+-} = \phi_{00} = \phi_{SW} = (43.7 \pm 0.2)^\circ$, i.e. assumes *CPT*. 20–160 GeV K beams.

[6] These two experiments have a common systematic error due to the uncertainty in the momentum scale, as pointed out in WAHL 89.

[7] GJESDAL 74 uses charge asymmetry in $K^0_{\ell 3}$ decays.

[8] ALAVI-HARATI 03 fit Δm and $\tau_{K^0_S}$ simultaneously. ϕ_{+-} is constrained to the Superweak value, i.e. *CPT* is assumed. See "K^0_S Mean Life" section for correlation information. Superseded by ABOUZAID 11.

[9] ALAVI-HARATI 03 fit Δm, ϕ_{+-}, and τ_{K_S} simultaneously. See ϕ_{+-} in the "K_L *CP* violation" section for correlation information. Superseded by ABOUZAID 11.

[10] ANGELOPOULOS 01 uses strong interactions strangeness tagging at two different times.

[11] Uses $\overline{K}^0_{e3}$ and K^0_{e3} strangeness tagging at production and decay. Assumes *CPT* conservation on $\Delta S = -\Delta Q$ transitions.

[12] ADLER 96C is the result of a fit which includes nearly the same data as entered into the "OUR FIT" value above.

[13] ARONSON 82 find that Δm may depend on the kaon energy.

[14] ARONSON 70 and CARNEGIE 71 use K^0_S mean life = $(0.862 \pm 0.006) \times 10^{-10}$ s. We have not attempted to adjust these values for the subsequent change in the K^0_S mean life or in η_{+-}.

K^0_L MEAN LIFE

VALUE (10^{-8} s)	*EVTS*	*DOCUMENT ID*		*TECN*	*COMMENT*
5.116±0.021 OUR FIT	Error includes scale factor of 1.1.				
5.099±0.021 OUR AVERAGE					
5.072±0.011±0.035	13M	[1] AMBROSINO	06	KLOE	$\sum_i B_i = 1$
5.092±0.017±0.025	15M	AMBROSINO	05C	KLOE	
5.154±0.044	0.4M	VOSBURGH	72	CNTR	
• • • We do not use the following data for averages, fits, limits, etc. • • •					
5.15 ±0.14		DEVLIN	67	CNTR	

[1] AMBROSINO 06 uses $\phi \to K_L K_S$ with K_L tagged by $K_S \to \pi^+\pi^-$. The four major K_L BR's are measured, the small remainder ($\pi^+\pi^-$,$\pi^0\pi^0$,$\gamma\gamma$) is taken from PDG 04. This KLOE K_L lifetime is obtained by imposing $\sum_i B_i = 1$. The correlation matrix among the four measured K_L BR's and this K_L lifetime is

	K_{e3}	$K_{\mu 3}$	$3\pi^0$	$\pi^+\pi^-\pi^0$	τ_{K_L}
K_{e3}	1	−0.25	−0.56	−0.07	0.25
$K_{\mu 3}$		1	−0.43	−0.20	0.33
$3\pi^0$			1	−0.39	−0.21
$\pi^+\pi^-\pi^0$				1	−0.39
τ_{K_L}					1

These correlations are taken into account in our fit. The average of this KLOE mean life measurement and the independent KLOE measurement in AMBROSINO 05C is $(5.084 \pm 0.023) \times 10^{-8}$ s.

K^0_L DECAY MODES

Mode			Fraction (Γ_i/Γ)	Scale factor/ Confidence level
Semileptonic modes				
Γ_1	$\pi^\pm e^\mp \nu_e$ Called K^0_{e3}.	[a]	(40.55 ±0.11) %	S=1.7
Γ_2	$\pi^\pm \mu^\mp \nu_\mu$ Called $K^0_{\mu 3}$.	[a]	(27.04 ±0.07) %	S=1.1
Γ_3	$(\pi\mu\,\mathrm{atom})\nu$		(1.05 ±0.11) × 10^{-7}	
Γ_4	$\pi^0\pi^\pm e^\mp \nu$	[a]	(5.20 ±0.11) × 10^{-5}	
Γ_5	$\pi^\pm e^\mp \nu\, e^+ e^-$	[a]	(1.26 ±0.04) × 10^{-5}	
Hadronic modes, including Charge conjugation×Parity Violating (*CPV*) modes				
Γ_6	$3\pi^0$		(19.52 ±0.12) %	S=1.6
Γ_7	$\pi^+\pi^-\pi^0$		(12.54 ±0.05) %	
Γ_8	$\pi^+\pi^-$	*CPV* [b]	(1.967±0.010) × 10^{-3}	S=1.5
Γ_9	$\pi^0\pi^0$	*CPV*	(8.64 ±0.06) × 10^{-4}	S=1.8
Semileptonic modes with photons				
Γ_{10}	$\pi^\pm e^\mp \nu_e \gamma$	[a,c,d]	(3.79 ±0.06) × 10^{-3}	
Γ_{11}	$\pi^\pm \mu^\mp \nu_\mu \gamma$		(5.65 ±0.23) × 10^{-4}	
Hadronic modes with photons or $\ell\overline{\ell}$ pairs				
Γ_{12}	$\pi^0\pi^0\gamma$		< 2.43 × 10^{-7}	CL=90%
Γ_{13}	$\pi^+\pi^-\gamma$	[c,d]	(4.15 ±0.15) × 10^{-5}	S=2.8
Γ_{14}	$\pi^+\pi^-\gamma$(DE)		(2.84 ±0.11) × 10^{-5}	S=2.0
Γ_{15}	$\pi^0 2\gamma$	[c]	(1.273±0.033) × 10^{-6}	
Γ_{16}	$\pi^0\gamma e^+ e^-$		(1.62 ±0.17) × 10^{-8}	

Meson Particle Listings

K_L^0

Other modes with photons or $\ell\bar{\ell}$ pairs

Γ_{17}	2γ		(5.47	± 0.04)	$\times 10^{-4}$	S=1.1
Γ_{18}	3γ		$<$ 7.4		$\times 10^{-8}$	CL=90%
Γ_{19}	$e^+e^-\gamma$		(9.4	± 0.4)	$\times 10^{-6}$	S=2.0
Γ_{20}	$\mu^+\mu^-\gamma$		(3.59	± 0.11)	$\times 10^{-7}$	S=1.3
Γ_{21}	$e^+e^-\gamma\gamma$	[c]	(5.95	± 0.33)	$\times 10^{-7}$	
Γ_{22}	$\mu^+\mu^-\gamma\gamma$	[c]	(1.0	$^{+0.8}_{-0.6}$)	$\times 10^{-8}$	

Charge conjugation × Parity (*CP*) or Lepton Family number (*LF*) violating modes, or $\Delta S = 1$ weak neutral current (*S1*) modes

Γ_{23}	$\mu^+\mu^-$	*S1*		(6.84	± 0.11)	$\times 10^{-9}$	
Γ_{24}	e^+e^-	*S1*		(9	$^{+6}_{-4}$)	$\times 10^{-12}$	
Γ_{25}	$\pi^+\pi^-e^+e^-$	*S1*	[c]	(3.11	± 0.19)	$\times 10^{-7}$	
Γ_{26}	$\pi^0\pi^0e^+e^-$	*S1*	$<$	6.6		$\times 10^{-9}$	CL=90%
Γ_{27}	$\pi^0\pi^0\mu^+\mu^-$	*S1*	$<$	9.2		$\times 10^{-11}$	CL=90%
Γ_{28}	$\mu^+\mu^-e^+e^-$	*S1*		(2.69	± 0.27)	$\times 10^{-9}$	
Γ_{29}	$e^+e^-e^+e^-$	*S1*		(3.56	± 0.21)	$\times 10^{-8}$	
Γ_{30}	$\pi^0\mu^+\mu^-$	*CP,S1*	[e] $<$	3.8		$\times 10^{-10}$	CL=90%
Γ_{31}	$\pi^0e^+e^-$	*CP,S1*	[e] $<$	2.8		$\times 10^{-10}$	CL=90%
Γ_{32}	$\pi^0\nu\overline{\nu}$	*CP,S1*	[f] $<$	2.6		$\times 10^{-8}$	CL=90%
Γ_{33}	$\pi^0\pi^0\nu\overline{\nu}$	*S1*	$<$	8.1		$\times 10^{-7}$	CL=90%
Γ_{34}	$e^\pm\mu^\mp$	*LF*	[a] $<$	4.7		$\times 10^{-12}$	CL=90%
Γ_{35}	$e^\pm e^\pm\mu^\mp\mu^\mp$	*LF*	[a] $<$	4.12		$\times 10^{-11}$	CL=90%
Γ_{36}	$\pi^0\mu^\pm e^\mp$	*LF*	[a] $<$	7.6		$\times 10^{-11}$	CL=90%
Γ_{37}	$\pi^0\pi^0\mu^\pm e^\mp$	*LF*	$<$	1.7		$\times 10^{-10}$	CL=90%

[a] The value is for the sum of the charge states or particle/antiparticle states indicated.

[b] This mode includes gammas from inner bremsstrahlung but not the direct emission mode $K_L^0 \to \pi^+\pi^-\gamma$(DE).

[c] See the Particle Listings below for the energy limits used in this measurement.

[d] Most of this radiative mode, the low-momentum γ part, is also included in the parent mode listed without γ's.

[e] Allowed by higher-order electroweak interactions.

[f] Violates *CP* in leading order. Test of direct *CP* violation since the indirect *CP*-violating and *CP*-conserving contributions are expected to be suppressed.

CONSTRAINED FIT INFORMATION

An overall fit to the mean life and 15 branching ratios uses 27 measurements and one constraint to determine 11 parameters. The overall fit has a $\chi^2 = 37.4$ for 17 degrees of freedom.

The following *off-diagonal* array elements are the correlation coefficients $\langle \delta p_i \delta p_j \rangle / (\delta p_i \cdot \delta p_j)$, in percent, from the fit to parameters p_i, including the branching fractions, $x_i \equiv \Gamma_i/\Gamma_{\rm total}$. The fit constrains the x_i whose labels appear in this array to sum to one.

x_2	−21									
x_6	−77	−29								
x_7	−15	−20	−18							
x_8	53	−11	−47	4						
x_9	30	−23	−11	−12	64					
x_{13}	6	−1	−6	0	12	8				
x_{14}	6	−1	−6	0	11	7	93			
x_{17}	−46	−22	64	−14	−21	8	−3	−3		
x_{19}	−5	−2	7	−1	−3	−1	0	0	4	
Γ	−27	−9	24	15	−13	−6	−2	−2	15	2
	x_1	x_2	x_6	x_7	x_8	x_9	x_{13}	x_{14}	x_{17}	x_{19}

	Mode		Rate (10^8 s^{-1})	Scale factor
Γ_1	$\pi^\pm e^\mp \nu_e$ Called K_{e3}^0.	[a]	0.07927 ± 0.00034	1.1
Γ_2	$\pi^\pm \mu^\mp \nu_\mu$ Called $K_{\mu 3}^0$.	[a]	0.05286 ± 0.00025	1.1
Γ_6	$3\pi^0$		0.03815 ± 0.00030	1.5
Γ_7	$\pi^+\pi^-\pi^0$		0.02451 ± 0.00015	
Γ_8	$\pi^+\pi^-$	[b]	$(3.844 \pm 0.023) \times 10^{-4}$	1.2
Γ_9	$\pi^0\pi^0$		$(1.690 \pm 0.013) \times 10^{-4}$	1.4
Γ_{13}	$\pi^+\pi^-\gamma$	[c,d]	$(8.11 \pm 0.29) \times 10^{-6}$	2.7
Γ_{14}	$\pi^+\pi^-\gamma$(DE)		$(5.55 \pm 0.21) \times 10^{-6}$	2.0
Γ_{17}	2γ		$(1.069 \pm 0.010) \times 10^{-4}$	1.2
Γ_{19}	$e^+e^-\gamma$		$(1.84 \pm 0.08) \times 10^{-6}$	1.9

K_L^0 DECAY RATES

$\Gamma(\pi^+\pi^-\pi^0)$ Γ_7

VALUE (10^6 s^{-1})	EVTS	DOCUMENT ID		TECN	COMMENT
2.451±0.015 OUR FIT					
• • • We do not use the following data for averages, fits, limits, etc. • • •					
$2.32\ ^{+0.13}_{-0.15}$	192	BALDO-...	75	HLBC	Assumes *CP*
2.35 ±0.20	180	[1] JAMES	72	HBC	Assumes *CP*
2.71 ±0.28	99	CHO	71	DBC	Assumes *CP*
2.5 ±0.3	98	[1] JAMES	71	HBC	Assumes *CP*
2.12 ±0.33	50	MEISNER	71	HBC	Assumes *CP*
2.20 ±0.35	53	WEBBER	70	HBC	Assumes *CP*
$2.62\ ^{+0.28}_{-0.27}$	136	BEHR	66	HLBC	Assumes *CP*
3.26 ±0.77	18	ANDERSON	65	HBC	
1.4 ±0.4	14	FRANZINI	65	HBC	

[1] JAMES 72 is a final measurement and includes JAMES 71.

$\Gamma(\pi^\pm e^\mp \nu_e)$ Γ_1

VALUE (10^6 s^{-1})	EVTS	DOCUMENT ID		TECN	COMMENT
7.927±0.034 OUR FIT Error includes scale factor of 1.1.					
• • • We do not use the following data for averages, fits, limits, etc. • • •					
7.81 ±0.56	620	CHAN	71	HBC	
$7.52\ ^{+0.85}_{-0.72}$		AUBERT	65	HLBC	$\Delta S = \Delta Q$, *CP* assumed

$\Gamma(\pi^\pm e^\mp \nu_e) + \Gamma(\pi^\pm \mu^\mp \nu_\mu)$ $(\Gamma_1+\Gamma_2)$

VALUE (10^6 s^{-1})	EVTS	DOCUMENT ID		TECN	COMMENT
13.21±0.05 OUR FIT					
• • • We do not use the following data for averages, fits, limits, etc. • • •					
12.4 ±0.7	410	[1] BURGUN	72	HBC	$K^+p \to K^0p\pi^+$
8.47±1.69	126	[1] MANN	72	HBC	$K^-p \to n\overline{K}^0$
13.1 ±1.3	252	[1] WEBBER	71	HBC	$K^-p \to n\overline{K}^0$
11.6 ±0.9	393	[1,2] CHO	70	DBC	$K^+n \to K^0p$
10.3 ±0.8	335	[2] HILL	67	DBC	$K^+n \to K^0p$
$9.85\ ^{+1.15}_{-1.05}$	109	[1] FRANZINI	65	HBC	

[1] Assumes $\Delta S = \Delta Q$ rule.
[2] CHO 70 includes events of HILL 67.

K_L^0 BRANCHING RATIOS

Semileptonic modes

$\Gamma(\pi^\pm e^\mp \nu_e)/\Gamma_{\rm total}$ Γ_1/Γ

VALUE	EVTS	DOCUMENT ID		TECN
0.4055±0.0011 OUR FIT Error includes scale factor of 1.7.				
0.4047±0.0028 OUR AVERAGE Error includes scale factor of 3.1.				
0.4007±0.0005±0.0015	13M	[1] AMBROSINO	06	KLOE
0.4067±0.0011		[2] ALEXOPOU...	04	KTEV

[1] There are correlations between these five KLOE measurements: B($K_L \to \pi e\nu$), B($K_L \to \pi\mu\nu$), B($K_L \to 3\pi^0$), B($K_L \to \pi^+\pi^-\pi^0$), and τ_{K_L} measured in AMBROSINO 06. See the footnote for the τ_{K_L} measurement for the correlation matrix.

[2] ALEXOPOULOS 04 constrains $\sum_i B_i = 0.9993$ for the six major K_L branching fractions. The correlations among these branching fractions are taken into account in our fit. The correlation matrix is

	K_{e3}	$K_{\mu 3}$	$3\pi^0$	$\pi^+\pi^-\pi^0$	$\pi^+\pi^-$	$\pi^0\pi^0$
K_{e3}	1					
$K_{\mu 3}$	0.15	1				
$3\pi^0$	−0.77	−0.62	1			
$\pi^+\pi^-\pi^0$	0.18	0.08	−0.54	1		
$\pi^+\pi^-$	0.28	0.22	−0.48	0.49	1	
$\pi^0\pi^0$	−0.72	−0.54	0.89	−0.46	−0.39	1

$\Gamma(\pi^\pm \mu^\mp \nu_\mu)/\Gamma_{\rm total}$ Γ_2/Γ

VALUE	EVTS	DOCUMENT ID		TECN
0.2704±0.0007 OUR FIT Error includes scale factor of 1.1.				
0.2700±0.0008 OUR AVERAGE				
0.2698±0.0005±0.0015	13M	[1] AMBROSINO	06	KLOE
0.2701±0.0009		[2] ALEXOPOU...	04	KTEV

[1] There are correlations between these five KLOE measurements: B($K_L \to \pi e\nu$), B($K_L \to \pi\mu\nu$), B($K_L \to 3\pi^0$), B($K_L \to \pi^+\pi^-\pi^0$), and τ_{K_L} measured in AMBROSINO 06. See the footnote for the τ_{K_L} measurement for the correlation matrix.

[2] For correlations with other ALEXOPOULOS 04 measurements, see the footnote with their B($K_L \to \pi e\nu$) measurement.

$[\Gamma(\pi^\pm e^\mp \nu_e) + \Gamma(\pi^\pm \mu^\mp \nu_\mu)]/\Gamma_{\rm total}$ $(\Gamma_1+\Gamma_2)/\Gamma$

VALUE	DOCUMENT ID
0.6760±0.0012 OUR FIT Error includes scale factor of 1.6.	

$\Gamma(\pi^\pm\mu^\mp\nu_\mu)/\Gamma(\pi^\pm e^\mp\nu_e)$ Γ_2/Γ_1

VALUE	EVTS	DOCUMENT ID		TECN	COMMENT
0.6669±0.0027 OUR FIT	Error includes scale factor of 1.2.				
0.666 ±0.004 OUR AVERAGE	Error includes scale factor of 1.6.				
• • • We use the following data for averages but not for fits. • • •					
0.6740±0.0059	13M	[1] AMBROSINO	06	KLOE	Not in fit
0.6640±0.0014±0.0022	394K	[2] ALEXOPOU...	04	KTEV	Not in fit
• • • We do not use the following data for averages, fits, limits, etc. • • •					
0.702 ±0.011	33k	CHO	80	HBC	
0.662 ±0.037	10k	WILLIAMS	74	ASPK	
0.741 ±0.044	6700	BRANDENB...	73	HBC	
0.662 ±0.030	1309	EVANS	73	HLBC	
0.68 ±0.08	3548	BASILE	70	OSPK	
0.71 ±0.05	770	BUDAGOV	68	HLBC	

[1] AMBROSINO 06 enters the fit via their separate measurements of these two modes.
[2] ALEXOPOULOS 04 enters the fit via their separate measurements of these two modes.

$\Gamma((\pi\mu\text{atom})\nu)/\Gamma(\pi^\pm\mu^\mp\nu_\mu)$ Γ_3/Γ_2

VALUE (units 10^{-7})	EVTS	DOCUMENT ID		TECN
3.90±0.39	155	[1] ARONSON	86	SPEC
• • • We do not use the following data for averages, fits, limits, etc. • • •				
seen	18	COOMBES	76	WIRE

[1] ARONSON 86 quote theoretical value of $(4.31 \pm 0.08) \times 10^{-7}$.

$\Gamma(\pi^0\pi^\pm e^\mp\nu)/\Gamma_{\text{total}}$ Γ_4/Γ

VALUE (units 10^{-5})	CL%	EVTS	DOCUMENT ID		TECN
5.20±0.11 OUR AVERAGE					
5.21±0.07±0.09		5402	BATLEY	04	NA48
5.16±0.20±0.22		729	MAKOFF	93	E731
• • • We do not use the following data for averages, fits, limits, etc. • • •					
6.2 ±2.0		16	CARROLL	80C	SPEC
< 220	90		[1] DONALDSON	74	SPEC

[1] DONALDSON 74 uses $K_L^0 \to \pi^+\pi^-\pi^0/(\text{all } K_L^0)$ decays = 0.126.

$\Gamma(\pi^\pm e^\mp\nu e^+e^-)/\Gamma(\pi^+\pi^-\pi^0)$ Γ_5/Γ_7

VALUE (units 10^{-5})	EVTS	DOCUMENT ID		TECN	COMMENT
10.02±0.17±0.29	19k	[1] ABOUZAID	07C	KTEV	$M_{ee}^* > 5$ MeV, $E_{ee}^* > 30$ MeV

[1] E_{ee}^* is the energy of the e^+e^- pair in the kaon rest frame. ABOUZAID 07C reports $[\Gamma(K_L^0 \to \pi^\pm e^\mp\nu e^+e^-)/\Gamma(K_L^0 \to \pi^+\pi^-\pi^0)] / [B(\pi^0 \to e^+e^-\gamma)] = (8.54 \pm 0.07 \pm 0.13) \times 10^{-3}$ which we multiply by our best value $B(\pi^0 \to e^+e^-\gamma) = (1.174 \pm 0.035) \times 10^{-2}$. Our first error is their experiment's error and our second error is the systematic error from using our best value.

Hadronic modes, including Charge conjugation×Parity Violating (*CPV*) modes

$\Gamma(3\pi^0)/\Gamma_{\text{total}}$ Γ_6/Γ

VALUE	EVTS	DOCUMENT ID		TECN	COMMENT
0.1952±0.0012 OUR FIT	Error includes scale factor of 1.6.				
0.1969±0.0026 OUR AVERAGE	Error includes scale factor of 2.0.				
• • • We use the following data for averages but not for fits. • • •					
0.1997±0.0003±0.0019	13M	[1] AMBROSINO	06	KLOE	Not fitted
0.1945±0.0018		[1] ALEXOPOU...	04	KTEV	Not fitted

[1] We exclude these $B(K_L \to 3\pi^0)$ measurements from our fit because the authors have constrained K_L branching fractions to sum to one. It enters our fit via the other measurements from the experiment and their correlations, along with our constraint that the fitted branching fractions sum to one.

$\Gamma(3\pi^0)/\Gamma(\pi^\pm e^\mp\nu_e)$ Γ_6/Γ_1

VALUE	EVTS	DOCUMENT ID		TECN	COMMENT
0.481 ±0.004 OUR FIT	Error includes scale factor of 1.8.				
• • • We use the following data for averages but not for fits. • • •					
0.4782±0.0014±0.0053	209K	[1] ALEXOPOU...	04	KTEV	Not in fit
• • • We do not use the following data for averages, fits, limits, etc. • • •					
0.545 ±0.004 ±0.009	38k	KREUTZ	95	NA31	

[1] This measurement enters the fit via their separate measurements of these two modes.

$\Gamma(3\pi^0)/[\Gamma(\pi^\pm e^\mp\nu_e) + \Gamma(\pi^\pm\mu^\mp\nu_\mu) + \Gamma(\pi^+\pi^-\pi^0)]$ $\Gamma_6/(\Gamma_1+\Gamma_2+\Gamma_7)$

VALUE	EVTS	DOCUMENT ID		TECN	COMMENT
0.2436±0.0018 OUR FIT	Error includes scale factor of 1.6.				
• • • We do not use the following data for averages, fits, limits, etc. • • •					
0.251 ±0.014	549	BUDAGOV	68	HLBC	ORSAY measur.
0.277 ±0.021	444	BUDAGOV	68	HLBC	Ecole polytec.meas
$0.31 \; {}^{+0.07}_{-0.06}$	29	KULYUKINA	68	CC	
0.24 ±0.08	24	ANIKINA	64	CC	

$\Gamma(3\pi^0)/\Gamma(\pi^+\pi^-\pi^0)$ Γ_6/Γ_7

VALUE	EVTS	DOCUMENT ID		TECN	COMMENT
1.557±0.012 OUR FIT	Error includes scale factor of 1.3.				
• • • We use the following data for averages but not for fits. • • •					
1.582±0.027	13M	[1] AMBROSINO	06	KLOE	Not in fit
• • • We do not use the following data for averages, fits, limits, etc. • • •					
1.611±0.014±0.034	28k	KREUTZ	95	NA31	
1.65 ±0.07	883	BARMIN	72B	HLBC	Error statistical only
1.80 ±0.13	1010	BUDAGOV	68	HLBC	
2.0 ±0.6	188	ALEKSANYAN	64B	FBC	

[1] AMBROSINO 06 enters the fit via their separate measurements of these two modes.

$\Gamma(\pi^+\pi^-\pi^0)/\Gamma_{\text{total}}$ Γ_7/Γ

VALUE	EVTS	DOCUMENT ID		TECN
0.1254±0.0005 OUR FIT				
0.1255±0.0006 OUR AVERAGE				
0.1263±0.0004±0.0011	13M	[1] AMBROSINO	06	KLOE
0.1252±0.0007		[2] ALEXOPOU...	04	KTEV

[1] There are correlations between these five KLOE measurements: $B(K_L \to \pi e\nu)$, $B(K_L \to \pi\mu\nu)$, $B(K_L \to 3\pi^0)$, $B(K_L \to \pi^+\pi^-\pi^0)$, and τ_{K_L} measured in AMBROSINO 06. See the footnote for the τ_{K_L} measurement for the correlation matrix.
[2] For correlations with other ALEXOPOULOS 04 measurements, see the footnote with their $B(K_L \to \pi e\nu)$ measurement.

$\Gamma(\pi^+\pi^-\pi^0)/\Gamma(\pi^\pm e^\mp\nu_e)$ Γ_7/Γ_1

VALUE	EVTS	DOCUMENT ID		TECN	COMMENT
0.3092±0.0016 OUR FIT	Error includes scale factor of 1.1.				
• • • We use the following data for averages but not for fits. • • •					
0.3078±0.0005±0.0017	799K	[1] ALEXOPOU...	04	KTEV	Not in fit
• • • We do not use the following data for averages, fits, limits, etc. • • •					
0.336 ±0.003 ±0.007	28k	KREUTZ	95	NA31	

[1] This measurement enters the fit via their separate measurements for the two modes.

$\Gamma(\pi^+\pi^-\pi^0)/[\Gamma(\pi^\pm e^\mp\nu_e) + \Gamma(\pi^\pm\mu^\mp\nu_\mu) + \Gamma(\pi^+\pi^-\pi^0)]$ $\Gamma_7/(\Gamma_1+\Gamma_2+\Gamma_7)$

VALUE	EVTS	DOCUMENT ID		TECN	COMMENT
0.1565±0.0006 OUR FIT	Error includes scale factor of 1.1.				
• • • We do not use the following data for averages, fits, limits, etc. • • •					
0.163 ±0.003	6499	CHO	77	HBC	
0.1605±0.0038	1590	ALEXANDER	73B	HBC	
0.146 ±0.004	3200	BRANDENB...	73	HBC	
0.159 ±0.010	558	EVANS	73	HLBC	
0.167 ±0.016	1402	KULYUKINA	68	CC	
0.161 ±0.005		HOPKINS	67	HBC	
0.162 ±0.015	126	HAWKINS	66	HBC	
0.159 ±0.015	326	ASTBURY	65B	CC	
0.178 ±0.017	566	GUIDONI	65	HBC	
0.144 ±0.004	1729	HOPKINS	65	HBC	See HOPKINS 67

$\Gamma(\pi^+\pi^-)/\Gamma_{\text{total}}$ Γ_8/Γ

Violates *CP* conservation.

VALUE (units 10^{-3})	DOCUMENT ID		TECN
1.967±0.010 OUR FIT	Error includes scale factor of 1.5.		
1.975±0.012	[1] ALEXOPOU...	04	KTEV

[1] For correlations with other ALEXOPOULOS 04 measurements, see the footnote with their $B(K_L \to \pi e\nu)$ measurement.

$\Gamma(\pi^+\pi^-)/\Gamma(\pi^\pm e^\mp\nu_e)$ Γ_8/Γ_1

VALUE (units 10^{-3})	EVTS	DOCUMENT ID		TECN	COMMENT
4.849±0.020 OUR FIT	Error includes scale factor of 1.1.				
4.840±0.020 OUR AVERAGE					
4.826±0.022±0.016	47k	[1] LAI	07	NA48	
• • • We use the following data for averages but not for fits. • • •					
4.856±0.017±0.023	84k	[2] ALEXOPOU...	04	KTEV	Not in fit

[1] The LAI 07 central value of 4.835×10^{-3} has been reduced by 0.19% to 4.826×10^{-3} to subtract the contribution from the direct emission mode $K_L^0 \to \pi^+\pi^-\gamma(\text{DE})$.
[2] This measurement enters the fit via their separate measurements for the two modes.

$[\Gamma(\pi^+\pi^-) + \Gamma(\pi^+\pi^-\gamma(\text{DE}))]/\Gamma(\pi^\pm\mu^\mp\nu_\mu)$ $(\Gamma_8+\Gamma_{14})/\Gamma_2$

VALUE (units 10^{-3})	EVTS	DOCUMENT ID		TECN
7.38 ±0.04 OUR FIT	Error includes scale factor of 1.4.			
7.275±0.042±0.054	45k	[1] AMBROSINO	06F	KLOE

[1] Fully inclusive. Taking $B(K_L^0 \to \pi\mu\nu)$ from KLOE, AMBROSINO 06, $B(K_L^0 \to \pi^+\pi^- + \pi^+\pi^-\gamma(\text{DE})) = (1.963 \pm 0.012 \pm 0.017) \times 10^{-3}$ is obtained.

$\Gamma(\pi^+\pi^-)/[\Gamma(\pi^\pm e^\mp\nu_e) + \Gamma(\pi^\pm\mu^\mp\nu_\mu)]$ $\Gamma_8/(\Gamma_1+\Gamma_2)$

Violates *CP* conservation.

VALUE (units 10^{-3})	EVTS	DOCUMENT ID		TECN	COMMENT
2.909±0.013 OUR FIT	Error includes scale factor of 1.3.				
• • • We do not use the following data for averages, fits, limits, etc. • • •					
3.13 ±0.14	1687	COUPAL	85	SPEC	η_{+-}=2.28 ± 0.06
3.04 ±0.14	2703	DEVOE	77	SPEC	η_{+-}=2.25 ± 0.05
2.51 ±0.23	309	[1] DEBOUARD	67	OSPK	η_{+-}=2.00 ± 0.09
2.35 ±0.19	525	[1] FITCH	67	OSPK	η_{+-}=1.94 ± 0.08

[1] Old experiments excluded from fit. See subsection on η_{+-} in section on "PARAMETERS FOR $K_L^0 \to 2\pi$ DECAY" below for average η_{+-} of these experiments and for note on discrepancy.

Meson Particle Listings

K_L^0

$\Gamma(\pi^\pm e^\mp \nu_e)/\Gamma(\text{2 tracks})$ $\Gamma_1/(\Gamma_1+\Gamma_2+0.03508\Gamma_6+\Gamma_7+\Gamma_8)$

$\Gamma(2 \text{ tracks}) = \Gamma(\pi^\pm e^\mp \nu_e) + \Gamma(\pi^\pm \mu^\mp \nu_\mu) + 0.03508\ \Gamma(3\pi^0) + \Gamma(\pi^+\pi^-\pi^0) + \Gamma(\pi^+\pi^-)$ where 0.03508 is the fraction of $3\pi^0$ events with one Dalitz decay ($\pi^0 \to \gamma e^+ e^-$).

VALUE	EVTS	DOCUMENT ID		TECN
0.5006±0.0009 OUR FIT Error includes scale factor of 1.3.				
0.4978±0.0035	6.8M	LAI	04B	NA48

$\Gamma(\pi^+\pi^-)/[\Gamma(\pi^\pm e^\mp \nu_e)+\Gamma(\pi^\pm \mu^\mp \nu_\mu)+\Gamma(\pi^+\pi^-\pi^0)]$ $\Gamma_8/(\Gamma_1+\Gamma_2+\Gamma_7)$

Violates CP conservation.

VALUE (units 10^{-3})	EVTS	DOCUMENT ID		TECN	COMMENT
2.454±0.011 OUR FIT Error includes scale factor of 1.3.					
• • • We do not use the following data for averages, fits, limits, etc. • • •					
2.60 ±0.07	4200	[1] MESSNER	73	ASPK	$\eta_{+-} = 2.23 \pm 0.05$

[1] From same data as $\Gamma(\pi^+\pi^-)/\Gamma(\pi^+\pi^-\pi^0)$ MESSNER 73, but with different normalization.

$\Gamma(\pi^+\pi^-)/\Gamma(\pi^+\pi^-\pi^0)$ Γ_8/Γ_7

Violates CP conservation.

VALUE (units 10^{-2})	EVTS	DOCUMENT ID		TECN	COMMENT
1.568±0.010 OUR FIT Error includes scale factor of 1.3.					
• • • We do not use the following data for averages, fits, limits, etc. • • •					
1.64 ±0.04	4200	MESSNER	73	ASPK	$\eta_{+-} = 2.23$

$\Gamma(\pi^0\pi^0)/\Gamma_{\text{total}}$ Γ_9/Γ

Violates CP conservation.

VALUE (units 10^{-3})	DOCUMENT ID		TECN
0.864±0.006 OUR FIT Error includes scale factor of 1.8.			
0.865±0.012	[1] ALEXOPOU...	04	KTEV

[1] For correlations with other ALEXOPOULOS 04 measurements, see the footnote with their $B(K_L \to \pi e \nu)$ measurement.

$\Gamma(\pi^0\pi^0)/\Gamma(\pi^+\pi^-)$ Γ_9/Γ_8

Violates CP conservation.

VALUE	DOCUMENT ID	
0.4395±0.0023 OUR FIT Error includes scale factor of 2.0.		
0.4390±0.0012	ETAFIT	13

$\Gamma(\pi^0\pi^0)/\Gamma(3\pi^0)$ Γ_9/Γ_6

Violates CP conservation.

VALUE (units 10^{-2})	EVTS	DOCUMENT ID		TECN	COMMENT
0.443 ±0.004 OUR FIT Error includes scale factor of 2.1.					
• • • We use the following data for averages but not for fits. • • •					
0.4446±0.0016±0.0019	100K	[1] ALEXOPOU...	04	KTEV	Not in fit
• • • We do not use the following data for averages, fits, limits, etc. • • •					
0.37 ±0.08	29	BARMIN	70	HLBC	η_{00}=2.02 ± 0.23
0.32 ±0.15	30	BUDAGOV	70	HLBC	η_{00}=1.9 ± 0.5
0.46 ±0.11	57	BANNER	69	OSPK	η_{00}=2.2 ± 0.3

[1] This measurement enters the fit via their separate measurements for the two modes.

Semileptonic modes with photons

$\Gamma(\pi^\pm e^\mp \nu_e \gamma)/\Gamma(\pi^\pm e^\mp \nu_e)$ Γ_{10}/Γ_1

VALUE (units 10^{-2})	EVTS	DOCUMENT ID		TECN	COMMENT
0.935±0.015 OUR AVERAGE Error includes scale factor of 1.9. See the ideogram below.					
0.924±0.023±0.016	9k	[1] AMBROSINO	08F	KLOE	E^*_γ >30 MeV, $\theta^*_{e\gamma}$ >20°
0.916±0.017	4309	[2] ALEXOPOU...	05	KTEV	E^*_γ >30 MeV, $\theta^*_{e\gamma}$ >20°
$0.964\pm0.008^{+0.011}_{-0.009}$	19K	LAI	05	NA48	E^*_γ >30 MeV, $\theta^*_{e\gamma}$ >20°
$0.908\pm0.008^{+0.013}_{-0.012}$	15k	ALAVI-HARATI	01J	KTEV	$E^*_\gamma \geq 30$ MeV, $\theta^*_{e\gamma} \geq 20°$
$0.934\pm0.036^{+0.055}_{-0.039}$	1384	LEBER	96	NA31	$E^*_\gamma \geq 30$ MeV, $\theta^*_{e\gamma} \geq 20°$

[1] Direct emission contribution measured $\langle X \rangle = -2.3 \pm 1.3 \pm 1.4$.

[2] Also measured cut E^*_γ >10 MeV, $\theta^*_{e\gamma}$ >0° 14221 evts: $\Gamma(\pi^\pm e^\mp \nu_e \gamma)$ / $\Gamma(\pi^\pm e^\mp \nu_e)$ = (4.942 ± 0.062)%.

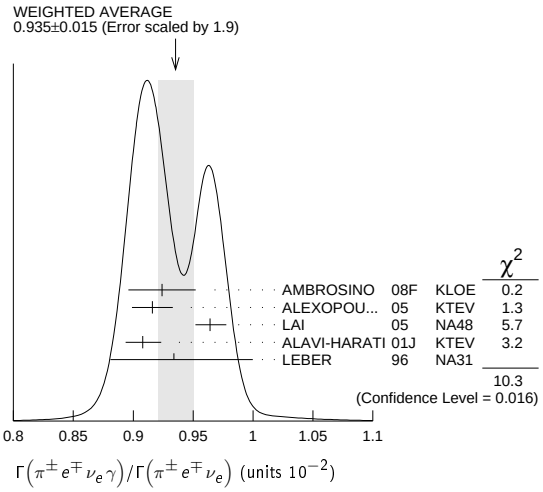

$\Gamma(\pi^\pm \mu^\mp \nu_\mu \gamma)/\Gamma(\pi^\pm \mu^\mp \nu_\mu)$ Γ_{11}/Γ_2

VALUE (units 10^{-3})	EVTS	DOCUMENT ID		TECN	COMMENT
2.09±0.08 OUR AVERAGE					
2.09±0.09		[1] ALEXOPOU...	05	KTEV	E^*_γ > 30 MeV
$2.08\pm0.17^{+0.16}_{-0.21}$	252	BENDER	98	NA48	$E^*_\gamma \geq 30$ MeV

[1] Also measured cut E^*_γ >10 MeV, 1385 evts: $\Gamma(\pi^\pm \mu^\mp \nu_\mu \gamma)$ / $\Gamma(\pi^\pm \mu^\mp \nu_\mu)$ = (0.530 ± 0.014 ± 0.012)%.

Hadronic modes with photons or $\ell\bar{\ell}$ pairs

$\Gamma(\pi^0\pi^0\gamma)/\Gamma_{\text{total}}$ Γ_{12}/Γ

VALUE (units 10^{-6})	CL%	DOCUMENT ID		TECN	COMMENT
< 0.243	90	ABOUZAID	08B	KTEV	$K_L^0 \to \pi^0\pi^0_D\gamma$, $\pi^0_D \to ee\gamma$
• • • We do not use the following data for averages, fits, limits, etc. • • •					
< 5.6	90	BARR	94	NA31	
<230	90	ROBERTS	94	E799	

$\Gamma(\pi^+\pi^-\gamma)/\Gamma(\pi^+\pi^-\pi^0)$ Γ_{13}/Γ_7

For earlier limits see our 1992 edition Physical Review **D45** S1 (1992).

VALUE (units 10^{-4})	EVTS	DOCUMENT ID		TECN	COMMENT
• • • We do not use the following data for averages, fits, limits, etc. • • •					
1.23±0.13	516	[1,2] CARROLL	80B	SPEC	E^*_γ > 20 MeV
2.33±0.23	546	[1,3] CARROLL	80B	SPEC	
3.56±0.26	1062	[1,4] CARROLL	80B	SPEC	E^*_γ > 20 MeV

[1] CARROLL 80B quotes $B(\pi^+\pi^-\gamma)$ using normalization $B(\pi^+\pi^-\pi^0) = 0.1239$. We divide by this value to obtain their measured $\Gamma(\pi^+\pi^-\gamma)$ / $\Gamma(\pi^+\pi^-\pi^0)$.

[2] Internal Bremsstrahlung component only.

[3] Direct γ emission component only.

[4] Both IB and DE components.

$\Gamma(\pi^+\pi^-\gamma)/\Gamma(\pi^+\pi^-)$ Γ_{13}/Γ_8

VALUE (units 10^{-2})	EVTS	DOCUMENT ID		TECN	COMMENT
2.11±0.08 OUR FIT Error includes scale factor of 2.9.					
2.11±0.08 OUR AVERAGE Error includes scale factor of 2.9.					
2.08±0.02±0.02	8669	[1] ALAVI-HARATI	01B	KTEV	E^*_γ > 20 MeV
2.30±0.07	3136	RAMBERG	93	E731	E^*_γ > 20 MeV

[1] ALAVI-HARATI 01B includes both Direct Emission (DE) and Inner Bremsstrahlung (IB) processes.

$\Gamma(\pi^+\pi^-\gamma(\text{DE}))/\Gamma(\pi^+\pi^-\gamma)$ Γ_{14}/Γ_{13}

These values assume that $\Gamma(K_L^0 \to \pi^+\pi^-\gamma) = \Gamma(K_L^0 \to \pi^+\pi^-\gamma(\text{DE})) + \Gamma(K_L^0 \to \pi^+\pi^-\gamma(\text{IB}))$, the sum of widths for the direct emission (DE) and inner bremsstrahlung (IE) processes, with no IB-DE interference. DE assumes a form factor as described in RAMBERG 93.

VALUE	EVTS	DOCUMENT ID		TECN	COMMENT
0.684±0.009 OUR FIT					
0.684±0.009 OUR AVERAGE					
0.689±0.021	111k	ABOUZAID	06A	KTEV	E^*_γ > 20 MeV
0.683±0.011	8669	ALAVI-HARATI	01B	KTEV	E^*_γ > 20 MeV
0.685±0.041	3136	RAMBERG	93	E731	E^*_γ > 20 MeV

$\Gamma(\pi^0 2\gamma)/\Gamma_{total}$ Γ_{15}/Γ

VALUE (units 10^{-6})	CL%	EVTS	DOCUMENT ID		TECN	COMMENT
1.273±0.033 OUR AVERAGE						
1.28 ±0.06 ±0.01		1.4k	[1] ABOUZAID	08	KTEV	
1.27 ±0.04 ±0.01		2.5k	[2] LAI	02B	NA48	
• • • We do not use the following data for averages, fits, limits, etc. • • •						
1.68 ±0.07 ±0.08		884	[3] ALAVI-HARATI	99B	KTEV	
1.7 ±0.2 ±0.2		63	[4] BARR	92	NA31	
1.86 ±0.60 ±0.60		60	PAPADIMITR...	91	E731	$m_{\gamma\gamma} > 280$ MeV
<5.1	90		PAPADIMITR...	91	E731	$m_{\gamma\gamma} < 264$ MeV
2.1 ±0.6		14	[5] BARR	90C	NA31	$m_{\gamma\gamma} > 280$ MeV

[1] ABOUZAID 08 reports $(1.29 \pm 0.03 \pm 0.05) \times 10^{-6}$ from a measurement of $[\Gamma(K^0_L \to \pi^0 2\gamma)/\Gamma_{total}]$ / $[B(K^0_L \to \pi^0\pi^0)]$ assuming $B(K^0_L \to \pi^0\pi^0) = (8.69 \pm 0.04) \times 10^{-4}$, which we rescale to our best value $B(K^0_L \to \pi^0\pi^0) = (8.64 \pm 0.06) \times 10^{-4}$. Our first error is their experiment's error and our second error is the systematic error from using our best value.

[2] LAI 02B reports $[\Gamma(K^0_L \to \pi^0 2\gamma)/\Gamma_{total}]$ / $[B(K^0_L \to \pi^0\pi^0)] = (1.467 \pm 0.032 \pm 0.032) \times 10^{-3}$ which we multiply by our best value $B(K^0_L \to \pi^0\pi^0) = (8.64 \pm 0.06) \times 10^{-4}$. Our first error is their experiment's error and our second error is the systematic error from using our best value. They also find that $B(\pi^0 2\gamma, m_{\gamma\gamma} < 110$ MeV$) < 0.6 \times 10^{-8}$(90% CL).

[3] ALAVI-HARATI 99B finds that $\Gamma(\pi^0 2\gamma, m_{\gamma\gamma} < 240$ MeV$))$ / $\Gamma(\pi^0 2\gamma) = (17.3 \pm 1.3 \pm 1.5)$%. Superseded by ABOUZAID 08.

[4] BARR 92 find that $\Gamma(\pi^0 2\gamma, m_{\gamma\gamma} < 240$ MeV$)/\Gamma(\pi^0 2\gamma) < 0.09$ (90% CL).

[5] BARR 90C superseded by BARR 92.

$\Gamma(\pi^0 \gamma e^+ e^-)/\Gamma_{total}$ Γ_{16}/Γ

VALUE (units 10^{-8})	CL%	EVTS	DOCUMENT ID		TECN
1.62±0.14±0.09		125	[1] ABOUZAID	07D	KTEV
• • • We do not use the following data for averages, fits, limits, etc. • • •					
2.34±0.35±0.13		44	ALAVI-HARATI	01E	KTEV
<71	90	0	MURAKAMI	99	SPEC

[1] ABOUZAID 07D includes 1997 (ALAVI-HARATI 01E) and 1999 data. It measures the ratio of $B(K^0_L \to \pi^0\gamma e^+ e^-)$ / $B(K^0_L \to \pi^0\pi^0_D)$, where π^0_D is the Dalitz decaying π^0, and uses PDG 06 values $B(K^0_L \to \pi^0\pi^0) = (8.69 \pm 0.04) \times 10^{-4}$, and $B(\pi^0_D \to e^+ e^- \gamma) = (1.198 \pm 0.032) \times 10^{-2}$. Supersedes ALAVI-HARATI 01E result.

Other modes with photons or $\ell\bar{\ell}$ pairs

$\Gamma(2\gamma)/\Gamma_{total}$ Γ_{17}/Γ

VALUE (units 10^{-4})	EVTS	DOCUMENT ID		TECN	COMMENT
5.47±0.04 OUR FIT Error includes scale factor of 1.1.					
• • • We do not use the following data for averages, fits, limits, etc. • • •					
4.54±0.84		[1] BANNER	72B	OSPK	
4.5 ±1.0	23	ENSTROM	71	OSPK	K^0_L 1.5–9 GeV/c
5.0 ±1.0		[2] REPELLIN	71	OSPK	
5.5 ±1.1	90	KUNZ	68	OSPK	Norm.to 3 π(C+N)

[1] This value uses $(\eta_{00}/\eta_{+-})^2 = 1.05 \pm 0.14$. In general, $\Gamma(2\gamma)/\Gamma_{total} = [(4.32 \pm 0.55) \times 10^{-4}][(\eta_{00}/\eta_{+-})^2]$.

[2] Assumes regeneration amplitude in copper at 2 GeV is 22 mb. To evaluate for a given regeneration amplitude and error, multiply by (regeneration amplitude/22mb)^2.

$\Gamma(2\gamma)/\Gamma(3\pi^0)$ Γ_{17}/Γ_6

VALUE (units 10^{-3})	EVTS	DOCUMENT ID		TECN	COMMENT
2.802±0.017 OUR FIT					
2.802±0.018 OUR AVERAGE					
2.79 ±0.02 ±0.02	27k	ADINOLFI	03	KLOE	
2.81 ±0.01 ±0.02		LAI	03	NA48	
• • • We do not use the following data for averages, fits, limits, etc. • • •					
2.13 ±0.43	28	BARMIN	71	HLBC	
2.24 ±0.28	115	BANNER	69	OSPK	
2.5 ±0.7	16	ARNOLD	68B	HLBC	Vacuum decay

$\Gamma(2\gamma)/\Gamma(\pi^0\pi^0)$ Γ_{17}/Γ_9

VALUE	EVTS	DOCUMENT ID		TECN
0.633±0.006 OUR FIT Error includes scale factor of 1.4.				
0.632±0.004±0.008	110k	BURKHARDT	87	NA31

$\Gamma(3\gamma)/\Gamma_{total}$ Γ_{18}/Γ

VALUE	CL%	DOCUMENT ID		TECN
<7.4 × 10^{-8}	90	[1] TUNG	11	K391
• • • We do not use the following data for averages, fits, limits, etc. • • •				
<2.4 × 10^{-7}	90	[2] BARR	95C	NA31

[1] TUNG 11 reports the result assuming parity violating interaction and using 2005 data (Run-II and III). Assuming parity conserving or phase space interaction, the 90% upper limits obtained are 7.5×10^{-8} and 8.6×10^{-8}, respectively.

[2] Assumes a phase-space decay distribution.

$\Gamma(e^+ e^-\gamma)/\Gamma_{total}$ Γ_{19}/Γ

VALUE (units 10^{-6})	EVTS	DOCUMENT ID		TECN
9.4±0.4 OUR FIT Error includes scale factor of 2.0.				
10.0±0.5 OUR AVERAGE Error includes scale factor of 1.5. See the ideogram below.				
10.6±0.2±0.4	6864	[1] FANTI	99B	NA48
9.2±0.5±0.5	1053	BARR	90B	NA31
$9.1 \pm 0.4^{+0.6}_{-0.5}$	919	OHL	90B	B845

[1] For FANTI 99B, the ±0.4 systematic error includes for uncertainties in the calculation, primarily uncertainties in the $\pi^0 \to e^+ e^-\gamma$ and $K^0_L \to \pi^0\pi^0$ branching ratios, evaluated using our 1999 Web edition values.

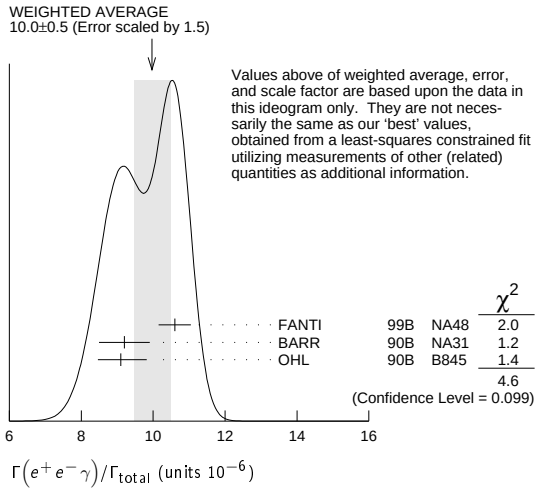

$\Gamma(e^+ e^-\gamma)/\Gamma(3\pi^0)$ Γ_{19}/Γ_6

VALUE (units 10^{-5})	EVTS	DOCUMENT ID		TECN
4.82±0.21 OUR FIT Error includes scale factor of 2.0.				
4.63±0.04±0.13	83k	[1] ABOUZAID	07B	KTEV

[1] ABOUZAID 07B reports $[\Gamma(K^0_L \to e^+ e^-\gamma)/\Gamma(K^0_L \to 3\pi^0)]$ / $[3\Gamma(\pi^0 \to 2\gamma)/\Gamma_{total} \times \Gamma(\pi^0 \to e^+ e^-\gamma)/\Gamma_{total}] = (1.3302 \pm 0.0046 \pm 0.0103) \times 10^{-3}$ which we multiply by our best value $3\Gamma(\pi^0 \to 2\gamma)/\Gamma_{total} \times \Gamma(\pi^0 \to e^+ e^-\gamma)/\Gamma_{total} = 0.0348 \pm 0.0010$. Our first error is their experiment's error and our second error is the systematic error from using our best value.

$\Gamma(\mu^+\mu^-\gamma)/\Gamma_{total}$ Γ_{20}/Γ

VALUE (units 10^{-7})	EVTS	DOCUMENT ID		TECN
3.59±0.11 OUR AVERAGE Error includes scale factor of 1.3.				
3.62±0.04±0.08	9100	ALAVI-HARATI	01G	KTEV
3.4 ±0.6 ±0.4	45	FANTI	97	NA48
3.23±0.23±0.19	197	SPENCER	95	E799

$\Gamma(e^+ e^-\gamma\gamma)/\Gamma_{total}$ Γ_{21}/Γ

VALUE (units 10^{-7})	EVTS	DOCUMENT ID		TECN	COMMENT
5.95±0.33 OUR AVERAGE					
5.84±0.15±0.32	1543	ALAVI-HARATI	01F	KTEV	$E^*_\gamma > 5$ MeV
$8.0 \pm 1.5\ ^{+1.4}_{-1.2}$	40	SETZU	98	NA31	$E^*_\gamma > 5$ MeV
6.5 ±1.2 ±0.6	58	NAKAYA	94	E799	$E^*_\gamma > 5$ MeV
6.6 ±3.2		MORSE	92	B845	$E^*_\gamma > 5$ MeV

$\Gamma(\mu^+\mu^-\gamma\gamma)/\Gamma_{total}$ Γ_{22}/Γ

VALUE (units 10^{-9})	EVTS	DOCUMENT ID		TECN	COMMENT
$\mathbf{10.4^{+7.5}_{-5.9}\pm0.7}$	4	ALAVI-HARATI	00E	KTEV	$m_{\gamma\gamma} \geq 1$ MeV/c^2

Charge conjugation × Parity (CP) or Lepton Family number (LF) violating modes, or $\Delta S = 1$ weak neutral current ($S1$) modes

$\Gamma(\mu^+\mu^-)/\Gamma(\pi^+\pi^-)$ Γ_{23}/Γ_8

Test for $\Delta S = 1$ weak neutral current. Allowed by higher-order electroweak interaction.

VALUE (units 10^{-6})	EVTS	DOCUMENT ID		TECN	COMMENT
3.48 ±0.05 OUR AVERAGE					
3.474±0.057	6210	AMBROSE	00	B871	
3.87 ±0.30	179	[1] AKAGI	95	SPEC	
3.38 ±0.17	707	HEINSON	95	B791	
• • • We do not use the following data for averages, fits, limits, etc. • • •					
3.9 ±0.3 ±0.1	178	[2] AKAGI	91B	SPEC	In AKAGI 95
3.45 ±0.18 ±0.13	368	[3] HEINSON	91	SPEC	In HEINSON 95
4.1 ±0.5	54	INAGAKI	89	SPEC	In AKAGI 91B
2.8 ±0.3 ±0.2	87	MATHIAZHA...	89B	SPEC	In HEINSON 91

[1] AKAGI 95 gives this number multiplied by the PDG 1992 average for $\Gamma(K_L^0 \to \pi^+\pi^-)/\Gamma(\text{total})$.
[2] AKAGI 91B give this number multiplied by the 1990 PDG average for $\Gamma(K_L^0 \to \pi^+\pi^-)/\Gamma(\text{total})$.
[3] HEINSON 91 give $\Gamma(K_L^0 \to \mu\mu)/\Gamma_{\text{total}}$. We divide out the $\Gamma(K_L^0 \to \pi^+\pi^-)/\Gamma_{\text{total}}$ PDG average which they used.

$\Gamma(e^+e^-)/\Gamma_{\text{total}}$ Γ_{24}/Γ

Test for $\Delta S = 1$ weak neutral current. Allowed by higher-order electroweak interaction.

VALUE (units 10^{-10})	CL%	EVTS	DOCUMENT ID		TECN
$0.087^{+0.057}_{-0.041}$		4	AMBROSE	98	B871
• • • We do not use the following data for averages, fits, limits, etc. • • •					
<1.6	90	1	AKAGI	95	SPEC
<0.41	90	0	[1] ARISAKA	93B	B791

[1] ARISAKA 93B includes all events with <6 MeV radiated energy.

$\Gamma(\pi^+\pi^-e^+e^-)/\Gamma_{\text{total}}$ Γ_{25}/Γ

Test for $\Delta S = 1$ weak neutral current. Allowed by higher-order electroweak interaction.

VALUE (units 10^{-7})	CL%	EVTS	DOCUMENT ID		TECN	COMMENT
3.11 ± 0.19 OUR AVERAGE						
$3.08 \pm 0.09 \pm 0.18$		1125	[1] LAI	03C	NA48	
$3.2 \pm 0.6 \pm 0.4$		37	ADAMS	98	KTEV	
$4.4 \pm 1.3 \pm 0.5$		13	TAKEUCHI	98	SPEC	
• • • We do not use the following data for averages, fits, limits, etc. • • •						
<4.6	90		NOMURA	97	SPEC	$m_{ee} > 4$ MeV

[1] LAI 03C second error is $0.15(\text{syst}) \pm 0.10(\text{norm})$ combined in quadrature. The normalization uses $\text{BR}(K_L \to \pi^+\pi^-\pi^0) * \text{BR}(\pi^0 \to e^+e^-) = (1.505 \pm 0.047) \times 10^{-3}$ from our 2000 Edition.

$\Gamma(\pi^0\pi^0e^+e^-)/\Gamma_{\text{total}}$ Γ_{26}/Γ

Test for $\Delta S = 1$ weak neutral current. Allowed by higher-order electroweak interaction.

VALUE (units 10^{-9})	CL%	EVTS	DOCUMENT ID		TECN
<6.6	90	1	ALAVI-HARATI	02C	E799

$\Gamma(\pi^0\pi^0\mu^+\mu^-)/\Gamma_{\text{total}}$ Γ_{27}/Γ

Test for $\Delta S = 1$ weak neutral current. Allowed by higher-order electroweak interaction.

VALUE	CL%	DOCUMENT ID		TECN
$< 9.2 \times 10^{-11}$	90	[1] ABOUZAID	11A	E799

[1] ABOUZAID 11A also reports $\text{B}(K_L^0 \to \pi^0\pi^0X^0 \to \pi^0\pi^0\mu^+\mu^-) < 1.0 \times 10^{-10}$ at 90% C.L., where the X^0 is a possible new neutral boson that was reported by PARK 05 with a mass of 214.3 ± 0.5 MeV/c^2.

$\Gamma(\mu^+\mu^-e^+e^-)/\Gamma_{\text{total}}$ Γ_{28}/Γ

Test for $\Delta S = 1$ weak neutral current. Allowed by higher-order electroweak interaction.

VALUE (units 10^{-9})	CL%	EVTS	DOCUMENT ID		TECN	COMMENT
2.69 ± 0.27 OUR AVERAGE						
$2.69 \pm 0.24 \pm 0.12$		131	[1] ALAVI-HARATI	03B	KTEV	
$2.9\ ^{+6.7}_{-2.4}$		1	GU	96	E799	
• • • We do not use the following data for averages, fits, limits, etc. • • •						
$2.62 \pm 0.40 \pm 0.17$		43	ALAVI-HARATI	01H	KTEV	Sup. by ALAVI-HARATI 03B
<4900	90		BALATS	83	SPEC	

[1] ALAVI-HARATI 03B also measures the linear slope $\alpha = -1.59 \pm 0.37$.

$\Gamma(e^+e^-e^+e^-)/\Gamma_{\text{total}}$ Γ_{29}/Γ

Test for $\Delta S = 1$ weak neutral current. Allowed by higher-order electroweak interaction.

VALUE (units 10^{-8})	EVTS	DOCUMENT ID		TECN	COMMENT
3.56 ± 0.21 OUR AVERAGE					
$3.30 \pm 0.24 \pm 0.25$	200	[1] LAI	05B	NA48	
$3.72 \pm 0.18 \pm 0.23$	441	ALAVI-HARATI	01D	KTEV	
$3.96 \pm 0.78 \pm 0.32$	27	GU	94	E799	
$3.07 \pm 1.25 \pm 0.26$	6	VAGINS	93	B845	
• • • We do not use the following data for averages, fits, limits, etc. • • •					
$6 \pm 2 \pm 1$	18	[2] AKAGI	95	SPEC	m_{ee} >470 MeV
$7 \pm 3 \pm 2$	6	[2] AKAGI	95	SPEC	m_{ee} >470 MeV
$10.4 \pm 3.7 \pm 1.1$	8	[3] BARR	95	NA31	
$6 \pm 2 \pm 1$	18	AKAGI	93	CNTR	Sup. by AKAGI 95
4 ± 3	2	BARR	91	NA31	Sup. by BARR 95

[1] LAI 05B uses 1998 and 1999 data. Data are normalized to the observed events of $K_L^0 \to \pi^+\pi^-\pi^0$ (π^0 into Dalitz pair) and PDG 04 values are used for $\text{B}(K_L^0 \to \pi^+\pi^-\pi^0)$ and $\text{B}(\pi^0 \to e^+e^-\gamma)$. The systematic error includes a normalization error of ± 0.10.
[2] Values are for the total branching fraction, acceptance-corrected for the m_{ee} cuts shown.
[3] Distribution of angles between two e^+e^- pair planes favors $CP = -1$ for K_L^0.

$\Gamma(\pi^0\mu^+\mu^-)/\Gamma_{\text{total}}$ Γ_{30}/Γ

Violates CP in leading order. Test for $\Delta S = 1$ weak neutral current. Allowed by higher-order electroweak interaction.

VALUE (units 10^{-9})	CL%	EVTS	DOCUMENT ID		TECN
<0.38	90		ALAVI-HARATI	00D	KTEV
• • • We do not use the following data for averages, fits, limits, etc. • • •					
<5.1	90	0	HARRIS	93	E799

$\Gamma(\pi^0e^+e^-)/\Gamma_{\text{total}}$ Γ_{31}/Γ

Violates CP in leading order. Direct and indirect CP-violating contributions are expected to be comparable and to dominate the CP-conserving part. LAI 02B result suggests that CP-violation effects dominate. Test for $\Delta S = 1$ weak neutral current. Allowed by higher-order electroweak interaction.

VALUE (units 10^{-10})	CL%	EVTS	DOCUMENT ID		TECN	COMMENT
< 2.8	90		[1] ALAVI-HARATI	04A	KTEV	combined result
• • • We do not use the following data for averages, fits, limits, etc. • • •						
< 3.5	90		ALAVI-HARATI	04A	KTEV	
$0.0047^{+0.0022}_{-0.0018}$			[2] LAI	02B	NA48	CP-conserving part
< 5.1	90	2	ALAVI-HARATI	01	KTEV	
0.01 to 0.02			ALAVI-HARATI	99B	KTEV	CP-conserving part
< 43	90	0	HARRIS	93B	E799	
< 75	90	0	BARKER	90	E731	
< 55	90	0	OHL	90	B845	
< 400	90		BARR	88	NA31	
<3200	90		JASTRZEM...	88	SPEC	

[1] Combined result of ALAVI-HARATI 04A 1999-2000 data set and ALAVI-HARATI 01 1997 data set.
[2] LAI 02B uses the absence of a signal in $K_L^0 \to \pi^0\gamma\gamma$ with $m(\gamma\gamma) < m(\pi^0)$ and their a_V value to predict this value.

$\Gamma(\pi^0\nu\overline{\nu})/\Gamma_{\text{total}}$ Γ_{32}/Γ

Violates CP in leading order. Test of direct CP violation since the indirect CP-violating and CP-conserving contributions are expected to be suppressed. Test of $\Delta S = 1$ weak neutral current.

VALUE (units 10^{-7})	CL%	DOCUMENT ID		TECN
< 0.26	90	[1] AHN	10	K391
• • • We do not use the following data for averages, fits, limits, etc. • • •				
< 0.67	90	[2] AHN	08	K391
< 2.1	90	[3] AHN	06	K391
< 5.9	90	ALAVI-HARATI	00	KTEV
< 16	90	ADAMS	99	KTEV
< 580	90	WEAVER	94	E799
<2200	90	GRAHAM	92	CNTR

[1] Obtained combining Run-2 (AHN 08) and Run-3 data.
[2] Value obtained using data from February to April 2005.
[3] Value obtained analyzing 10% of data of RUN 1 (performed in 2004).

$\Gamma(\pi^0\pi^0\nu\overline{\nu})/\Gamma_{\text{total}}$ Γ_{33}/Γ

VALUE	CL%	DOCUMENT ID		TECN
$< 8.1 \times 10^{-7}$	90	[1] OGATA	11	K391
• • • We do not use the following data for averages, fits, limits, etc. • • •				
$< 4.7 \times 10^{-5}$	90	[2] NIX	07	K391

[1] Using 2005 Run-I data. OGATA 11 also sets a limit on the $K_L^0 \to \pi^0\pi^0X \to$ invisible particles process: the limit on the branching fraction varied from 7.0×10^{-7} to 4.0×10^{-5} for the mass of X ranging from 50 to 200 MeV/c^2.
[2] Observed 1 event with expected background of 0.43 ± 0.35 events. NIX 07 also measured $\text{B}(K_L^0 \to \pi^0\pi^0P) < 1.2 \times 10^{-6}$ at 90% CL, where P is the pseudoscalar particle and $m_P < 100$ MeV.

$\Gamma(e^\pm\mu^\mp)/\Gamma_{\text{total}}$ Γ_{34}/Γ

Test of lepton family number conservation.

VALUE (units 10^{-11})	CL%	EVTS	DOCUMENT ID		TECN
<0.47	90		AMBROSE	98B	B871
• • • We do not use the following data for averages, fits, limits, etc. • • •					
<9.4	90	0	AKAGI	95	SPEC
<3.9	90	0	ARISAKA	93	B791
<3.3	90	0	[1] ARISAKA	93	B791

[1] This is the combined result of ARISAKA 93 and MATHIAZHAGAN 89.

$\Gamma(e^\pm e^\pm\mu^\mp\mu^\mp)/\Gamma_{\text{total}}$ Γ_{35}/Γ

Test of lepton family number conservation.

VALUE (units 10^{-11})	CL%	EVTS	DOCUMENT ID		TECN	COMMENT
< 4.12	90	0	ALAVI-HARATI	03B	KTEV	
• • • We do not use the following data for averages, fits, limits, etc. • • •						
< 12.3	90	0	[1] ALAVI-HARATI	01H	KTEV	Sup. by ALAVI-HARATI 03B
<610	90	0	[1] GU	96	E799	

[1] Assuming uniform phase space distribution.

$\Gamma(\pi^0\mu^\pm e^\mp)/\Gamma_{\text{total}}$ Γ_{36}/Γ

Test of lepton family number conservation.

VALUE (units 10^{-10})	CL%	DOCUMENT ID		TECN
< 0.76	90	ABOUZAID	08C	KTEV
• • • We do not use the following data for averages, fits, limits, etc. • • •				
<62	90	ARISAKA	98	E799

$\Gamma(\pi^0\pi^0\mu^\pm e^\mp)/\Gamma_{\text{total}}$ Γ_{37}/Γ

Test of lepton family number conservation.

VALUE (units 10^{-10})	CL%	DOCUMENT ID		TECN
<1.7	90	ABOUZAID	08C	KTEV

V_{ud}, V_{us}, THE CABIBBO ANGLE, AND CKM UNITARITY

Updated September 2013 by E. Blucher (Univ. of Chicago) and W.J. Marciano (BNL).

The Cabibbo-Kobayashi-Maskawa (CKM) [1,2] three-generation quark mixing matrix written in terms of the Wolfenstein parameters (λ, A, ρ, η) [3] nicely illustrates the orthonormality constraint of unitarity and central role played by λ.

$$V_{\rm CKM} = \begin{pmatrix} V_{ud} & V_{us} & V_{ub} \\ V_{cd} & V_{cs} & V_{cb} \\ V_{td} & V_{ts} & V_{tb} \end{pmatrix}$$

$$= \begin{pmatrix} 1-\lambda^2/2 & \lambda & A\lambda^3(\rho - i\eta) \\ -\lambda & 1-\lambda^2/2 & A\lambda^2 \\ A\lambda^3(1-\rho-i\eta) & -A\lambda^2 & 1 \end{pmatrix} + \mathcal{O}(\lambda^4)\ . \quad (1)$$

That cornerstone is a carryover from the two-generation Cabibbo angle, $\lambda = \sin(\theta_{\rm Cabibbo}) = V_{us}$. Its value is a critical ingredient in determinations of the other parameters and in tests of CKM unitarity.

Until about 10 years ago, the precise value of λ was somewhat controversial, with kaon decays suggesting [4] $\lambda \simeq 0.220$, while indirect determinations via nuclear β-decays implied a somewhat larger $\lambda \simeq 0.225 - 0.230$. This difference resulted in a 2 – 2.5 sigma deviation from the unitarity requirement

$$|V_{ud}|^2 + |V_{us}|^2 + |V_{ub}|^2 = 1, \quad (2)$$

a potential signal [6] for new physics effects. Below, we discuss the current status of V_{ud}, V_{us}, and their associated unitarity test in Eq. (2). (Since $|V_{ub}|^2 \simeq 1 \times 10^{-5}$ is negligibly small, it is ignored in this discussion.) Although current measurements show no deviation from unitarity, Eq. (2) remains the most stringent test of unitarity in the CKM matrix.

V_{ud}

The value of V_{ud} has been obtained from superallowed nuclear, neutron, and pion decays. Currently, the most precise determination of V_{ud} comes from superallowed nuclear beta-decays [6] ($0^+ \to 0^+$ transitions). Measuring their half-lives, t, and Q values that give the decay rate factor, f, leads to a precise determination of V_{ud} via the master formula [7–9]

$$|V_{ud}|^2 = \frac{2984.48(5)\,\sec}{ft(1+{\rm RC})}, \quad (3)$$

where RC denotes the entire effect of electroweak radiative corrections, nuclear structure, and isospin violating nuclear effects. RC is nucleus-dependent, ranging from about +3.0% to +3.6% for the best measured superallowed decays. The most recent analysis of Hardy and Towner [10, 11] gives a weighted average of

$$V_{ud} = 0.97425(8)_{\rm exp.}(10)_{\rm nucl.dep.}(18)_{\rm RC}\ \text{(superallowed)}\ , \quad (4)$$

which, assuming unitarity, corresponds to $\lambda = 0.2255(10)$. The average value of V_{ud} shifted upward compared to our 2007 value of 0.97418(27) primarily because of improvements in the experimental ft values and nuclear isospin breaking corrections employed. We note, however, that the possibility of additional nuclear coulombic corrections has been raised [12].

Combined measurements of the neutron lifetime, τ_n, and the ratio of axial-vector/vector couplings, $g_A \equiv G_A/G_V$, via neutron decay asymmetries can also be used to determine V_{ud}:

$$|V_{ud}|^2 = \frac{4908.7(1.9)\,\sec}{\tau_n(1+3g_A^2)}, \quad (5)$$

where the error stems from uncertainties in the electroweak radiative corrections [8] due to hadronic loop effects. Those effects were updated and their error was reduced by about a factor of 2 [9], leading to a ± 0.0002 theoretical uncertainty in V_{ud} (common to all V_{ud} extractions). Using the world averages from this *Review*

$$\tau_n^{\rm ave} = 880.0(0.9)\ \sec\ \ (\times 1.4\ \text{PDG scale factor})$$
$$g_A^{\rm ave} = 1.2701(25)\ \ (\times 1.9\ \text{PDG scale factor}) \quad (6)$$

leads to

$$V_{ud} = 0.9774(5)_{\tau_n}(16)_{g_A}(2)_{\rm RC} \quad (7)$$

with the error dominated by g_A uncertainties. The new shorter neutron lifetime average now leads to a value of V_{ud} that is inconsistent with the superallowed nuclear beta decay result in Eq. (4) by about 2 sigma. That disagreement suggests that a shift of g_A to about 1.275 (consistent with more modern day measurements [14]) or movement back to a longer neutron lifetime ($\sim$ 886 sec) is likely. Future neutron studies are expected to resolve these inconsistencies and significantly reduce the uncertainties in g_A and τ_n, potentially making them the best way to determine V_{ud}.

The PIBETA experiment at PSI measured the very small ($\mathcal{O}(10^{-8})$) branching ratio for $\pi^+ \to \pi^o e^+ \nu_e$ with about $\pm 1/2\%$ precision. Their result gives [15]

$$V_{ud} = 0.9749(26)\left[\frac{BR(\pi^+ \to e^+\nu_e(\gamma))}{1.2352 \times 10^{-4}}\right]^{\frac{1}{2}} \quad (8)$$

which is normalized using the very precisely determined theoretical prediction for $BR(\pi^+ \to e^+\nu_e(\gamma)) = 1.2352(5) \times 10^{-4}$ [7], rather than the experimental branching ratio from this *Review* of $1.230(4)\times 10^{-4}$ which would lower the value to $V_{ud} = 0.9728(30)$. Theoretical uncertainties in that determination are very small; however, much higher statistics would be required to make this approach competitive with others.

V_{us}

$|V_{us}|$ may be determined from kaon decays, hyperon decays, and tau decays. Previous determinations have most often used $K\ell 3$ decays:

$$\Gamma_{K\ell 3} = \frac{G_F^2 M_K^5}{192\pi^3} S_{EW}(1+\delta_K^\ell + \delta_{SU2})C^2\,|V_{us}|^2\,f_+^2(0) I_K^\ell. \quad (9)$$

Here, ℓ refers to either e or μ, G_F is the Fermi constant, M_K is the kaon mass, S_{EW} is the short-distance radiative correction, δ_K^ℓ is the mode-dependent long-distance radiative correction, $f_+(0)$ is the calculated form factor at zero momentum transfer

for the $\ell\nu$ system, and I_K^ℓ is the phase-space integral, which depends on measured semileptonic form factors. For charged kaon decays, δ_{SU2} is the deviation from one of the ratio of $f_+(0)$ for the charged to neutral kaon decay; it is zero for the neutral kaon. C^2 is 1 (1/2) for neutral (charged) kaon decays. Most early determinations of $|V_{us}|$ were based soley on $K \to \pi e\nu$ decays; $K \to \pi\mu\nu$ decays were not used because of large uncertainties in I_K^μ. The experimental measurements are the semileptonic decay widths (based on the semileptonic branching fractions and lifetime) and form factors (allowing calculation of the phase space integrals). Theory is needed for S_{EW}, δ_K^ℓ, δ_{SU2}, and $f_+(0)$.

Many measurements during the last decade have resulted in a significant shift in V_{us}. Most importantly, recent measurements of the $K \to \pi e\nu$ branching fractions are significantly different than earlier PDG averages, probably as a result of inadequate treatment of radiation in older experiments. This effect was first observed by BNL E865 [16] in the charged kaon system and then by KTeV [17,18] in the neutral kaon system; subsequent measurements were made by KLOE [19–22], NA48 [23–25], and ISTRA+ [26]. Current averages (*e.g.*, by the PDG [27] or Flavianet [28]) of the semileptonic branching fractions are based only on recent, high-statistics experiments where the treatment of radiation is clear. In addition to measurements of branching fractions, new measurements of lifetimes [29] and form factors [31–35], have resulted in improved precision for all of the experimental inputs to V_{us}. Precise measurements of form factors for $K_{\mu 3}$ decay make it possible to use both semileptonic decay modes to extract V_{us}.

Following the analysis of Moulson [30] and the Flavianet group [28], one finds, after including the isospin violating up-down mass difference effect, the values of $|V_{us}|f_+(0)$ in Table 1. The average of these measurements gives

$$f_+(0)|V_{us}| = 0.2163(5). \tag{10}$$

Figure 1 shows a comparison of these results with the PDG evaluation from 2002 [36], as well as $f_+(0)(1-|V_{ud}|^2-|V_{ub}|^2)^{1/2}$, the expectation for $f_+(0)|V_{us}|$ assuming unitarity, based on $|V_{ud}| = 0.9742\pm0.0003$, $|V_{ub}| = (3.6\pm0.7)\times10^{-3}$, and the lattice calculation of $f_+(0) = 0.960^{+0.005}_{-0.006}$ [37](Lattice calculations of $f_+(0)$ have improved significantly in recent years, and therefore replace the classic calculation of Leutwyler and Roos [38].) Combining the result in Eq. (10) with the above value of $f_+(0)$ gives

$$|V_{us}| = \lambda = 0.2253 \pm 0.0014. \tag{11}$$

A value of V_{us} can also be obtained from a comparison of the radiative inclusive decay rates for $K \to \mu\nu(\gamma)$ and $\pi \to \mu\nu(\gamma)$ combined with a lattice gauge theory calculation of f_K/f_π via [43]

$$\frac{|V_{us}|f_K}{|V_{ud}|f_\pi} = 0.23922(25)\left[\frac{\Gamma(K \to \mu\nu(\gamma))}{\Gamma(\pi \to \mu\nu(\gamma))}\right]^{\frac{1}{2}} \tag{12}$$

Table 1: $|V_{us}|f_+(0)$ from $K_{\ell 3}$.

Decay Mode	$\lvert V_{us}\rvert f_+(0)$
$K^\pm e3$	0.2160 ± 0.0011
$K^\pm \mu 3$	0.2158 ± 0.0013
$K_L e3$	0.2163 ± 0.0005
$K_L \mu 3$	0.2166 ± 0.0006
$K_S e3$	0.2155 ± 0.0013
Average	0.2163 ± 0.0005

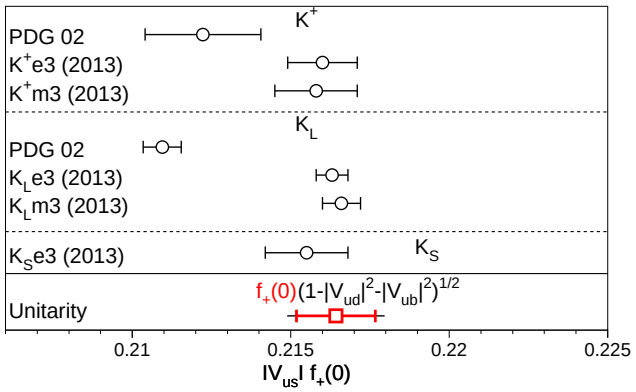

Figure 1: Comparison of determinations of $|V_{us}|f_+(0)$ from this review (labeled 2013), from the PDG 2002, and with the prediction from unitarity using $|V_{ud}|$ and the lattice calculation of $f_+(0) = 0.960^{+0.005}_{-0.006}$ [37]. For $f_+(0)(1-|V_{ud}|^2-|V_{ub}|^2)^{1/2}$, the inner error bars are from the quoted uncertainty in $f_+(0)$; the total uncertainties include the $|V_{ud}|$ and $|V_{ub}|$ errors.

with the small error coming from electroweak radiative corrections and isospin breaking effects. Employing

$$\frac{\Gamma(K \to \mu\nu(\gamma))}{\Gamma(\pi \to \mu\nu(\gamma))} = 1.3344(42), \tag{13}$$

which averages in the KLOE result [44], $B(K \to \mu\nu(\gamma)) = 63.66(9)(15)\%$ and [45]

$$f_K/f_\pi = 1.1947(45) \tag{14}$$

along with the value of V_{ud} in Eq. (4) leads to

$$|V_{us}| = 0.2253(4)(9). \tag{15}$$

It should be mentioned that hyperon decay fits suggest [5]

$$|V_{us}| = 0.2250(27) \text{ Hyperon Decays} \tag{16}$$

modulo SU(3) breaking effects that could shift that value up or down. We note that a representative effort [46] that incorporates SU(3) breaking found $V_{us} = 0.226(5)$. Strangeness changing tau

decays, averaging both inclusive and exclusive measurements, currently give [47]

$$|V_{us}| = 0.2202(15) \text{ Tau Decays}, \quad (17)$$

which differs by about 3 sigma from the kaon determination discussed above, and would, if combined with V_{ud} from super-allowed beta decays, lead to a 2.6 sigma deviation from unitarity. This discrepancy results mainly from the inclusive tau decay results that rely on Finite Energy Sum Rule techniques and assumptions. Further investigation of that approach seems to be warranted.

Employing the value of V_{ud} in Eq. (4) and $V_{us} = 0.2253(8)$, the average of the $K\ell 3$ (Eq. (11)) and $K\mu 2$ (Eq. (15) determinations of V_{us}, leads to the unitarity consistency check

$$|V_{ud}|^2 + |V_{us}|^2 + |V_{ub}|^2 = 0.9999(4)(4). \quad (18)$$

where the first error is the uncertainty from $|V_{ud}|^2$ and the second error is the uncertainty from $|V_{us}|^2$.

CKM Unitarity Constraints

The current good experimental agreement with unitarity, $|V_{ud}|^2+|V_{us}|^2+|V_{ub}|^2 = 0.9999(6)$, provides strong confirmation of Standard Model radiative corrections (which range between 3-4% depending on the nucleus used) at better than the 50 sigma level [48]. In addition, it implies constraints on "New Physics" effects at both the tree and quantum loop levels. Those effects could be in the form of contributions to nuclear beta decays, K decays and/or muon decays, with the last of these providing normalization via the muon lifetime [49], which is used to obtain the Fermi constant, $G_\mu = 1.1663787(6) \times 10^{-5}\text{GeV}^{-2}$.

In the following sections, we illustrate the implications of CKM unitarity for (1) exotic muon decays [50](beyond ordinary muon decay $\mu^+ \to e^+\nu_e\bar{\nu}_\mu$) and (2) new heavy quark mixing V_{uD} [51]. Other examples in the literature [52,53] include Z_χ boson quantum loop effects, supersymmetry, leptoquarks, compositeness etc.

Exotic Muon Decays

If additional lepton flavor violating decays such as $\mu^+ \to e^+\bar{\nu}_e\nu_\mu$ (wrong neutrinos) occur, they would cause confusion in searches for neutrino oscillations at, for example, muon storage rings/neutrino factories or other neutrino sources from muon decays. Calling the rate for all such decays Γ(exotic μ decays), they should be subtracted before the extraction of G_μ and normalization of the CKM matrix. Since that is not done and unitarity works, one has (at one-sided 95% CL)

$$|V_{ud}|^2 + |V_{us}|^2 + |V_{ub}|^2 = 1 - BR(\text{exotic } \mu \text{ decays}) \geq 0.9989 \quad (19)$$

or

$$BR(\text{exotic } \mu \text{ decays}) < 0.001 \, . \quad (20)$$

This bound is a factor of 10 better than the direct experimental bound on $\mu^+ \to e^+\bar{\nu}_e\nu_\mu$.

New Heavy Quark Mixing

Heavy D quarks naturally occur in fourth quark generation models and some heavy quark "new physics" scenarios such as E_6 grand unification. Their mixing with ordinary quarks gives rise to V_{ud} which is constrained by unitarity (one sided 95% CL)

$$|V_{ud}|^2 + |V_{us}|^2 + |V_{ub}|^2 = 1 - |V_{uD}|^2 > 0.9989$$
$$|V_{uD}| < 0.03 \, . \quad (21)$$

A similar constraint applies to heavy neutrino mixing and the couplings $V_{\mu N}$ and V_{eN}.

References

1. N. Cabibbo, Phys. Rev. Lett. **10**, 531 (1963).
2. M. Kobayashi and T. Maskawa, Prog. Theor. Phys. **49**, 652 (1973).
3. L. Wolfenstein, Phys. Rev. Lett. **51**, 1945 (1983).
4. S. Eidelman *et al.*, [Particle Data Group], Phys. Lett. **B592**, 1 (2004).
5. N. Cabibbo, E.C. Swallow, and R. Winston, Phys. Rev. Lett. **92**, 251803 (2004) [hep-ph/0307214].
6. J.C. Hardy and I.S. Towner, Phys. Rev. Lett. **94**, 092502 (2005) [nucl-th/0412050].
7. W.J. Marciano and A. Sirlin, Phys. Rev. Lett. **71**, 3629 (1993).
8. A. Czarnecki, W.J. Marciano, and A. Sirlin, Phys. Rev. **D70**, 093006 (2004) [hep-ph/0406324].
9. W.J. Marciano and A. Sirlin, Phys. Rev. Lett. **96**, 032002 (2006) [hep-ph/0510099].
10. J.C. Hardy and I.S. Towner, Phys. Rev. **C77**, 025501 (2008).
11. J.C. Hardy and I.S. Towner, Phys. Rev. **C79**, 055502 (2009).
12. G.A. Miller and A. Schwenk, Phys. Rev. **C78**, 035501 (2008); N. Auerbach, Phys. Rev. **C79**, 035502 (2009); H. Liang, N. Van Giai and J. Meng, Phys. Rev. **C79**, 064316 (2009).
13. A. Serebrov *et al.*, Phys. Lett. **B605**, 72 (2005) [nucl-ex/0408009].
14. H. Abele, Prog. in Part. Nucl. Phys. **60**, 1 (2008).
15. D. Pocanic *et al.*, Phys. Rev. Lett. **93**, 181803 (2004) [hep-ex/0312030].
16. A. Sher *et al.*, Phys. Rev. Lett. **91**, 261802 (2003).
17. T. Alexopoulos *et al.*, [KTeV Collab.], Phys. Rev. Lett. **93**, 181802 (2004) [hep-ex/0406001].
18. T. Alexopoulos *et al.*, [KTeV Collab.], Phys. Rev. **D70**, 092006 (2004) [hep-ex/0406002].
19. F. Ambrosino *et al.*, [KLOE Collab.], Phys. Lett. **B632**, 43 (2006) [hep-ex/0508027].
20. F. Ambrosino *et al.*, [KLOE Collab.], Phys. Lett. **B638**, 140 (2006) [hep-ex/0603041].
21. F. Ambrosino *et al.*, [KLOE Collab.], Phys. Lett. **B636**, 173 (2006) [hep-ex/0601026].
22. F. Ambrosino *et al.*, [KLOE Collab.], PoS **HEP2005**, 287 (2006) [Frascati Phys. Ser. **41**, 69 (2006)] [hep-ex/0510028].
23. A. Lai *et al.*, [NA48 Collab.], Phys. Lett. **B602**, 41 (2004) [hep-ex/0410059].

24. A. Lai *et al.*, [NA48 Collab.], Phys. Lett. **B645**, 26 (2007) [hep-ex/0611052].
25. J.R. Batley *et al.*, [NA48/2 Collab.], Eur. Phys. J. C **50**, 329 (2007) [hep-ex/0702015].
26. V.I. Romanovsky *et al.*, [hep-ex/0704.2052].
27. J. Beringer *et al.*, [Particle Data Group], Phys. Rev. D 86,010001(2012).
28. Flavianet Working Group on Precise SM Tests in K Decays, http://www.lnf.infn.it/wg/vus; M. Antonelli *et al.*, Eur. Phys. J. C **69**, 399 (2010). For a recent detailed review, see M. Antonelli *et al.*, [hep-ph/0907.5386].
29. F. Ambrosino *et al.*, [KLOE Collab.], Phys. Lett. **B626**, 15 (2005) [hep-ex/0507088].
30. M. Moulson, [hep-ex/1301.3046].
31. T. Alexopoulos *et al.*, [KTeV Collab.], Phys. Rev. **D70**, 092007 (2004) [hep-ex/0406003].
32. E. Abouzaid *et al.*, [KTeV Collab.], Phys. Rev. **D74**, 097101 (2006) [hep-ex/0608058].
33. F. Ambrosino *et al.*, [KLOE Collab.], Phys. Lett. **B636**, 166 (2006) [hep-ex/0601038].
34. A. Lai *et al.*, [NA48 Collab.], Phys. Lett. **B604**, 1 (2004) [hep-ex/0410065].
35. O.P. Yushchenko *et al.*, Phys. Lett. **B589**, 111 (2004) [hep-ex/0404030].
36. K. Hagiwara *et al.*, [Particle Data Group], Phys. Rev. **D66**, 1 (2002).
37. P.A. Boyle *et al.*, Eur. Phys. J. **C69**, 159 (2010); P.A. Boyle *et al.*, Phys. Rev. Lett. **100**, 141601 (2008); S. Aoki *et al.*, arXiv:1310.8555 [hep-lat].
38. H. Leutwyler and M. Roos, Z. Phys. **C25**, 91 (1984).
39. D. Becirevic *et al.*, Nucl. Phys. **B705**, 339 (2005) [hep-ph/0403217].
40. J. Bijnens and P. Talavera, Nucl. Phys. **B669**, 341 (2003).
41. V. Cirigliano *et al.*, JHEP **0504**, 006 (2005) [hep-ph/0503108].
42. M. Jamin, J.A. Oller, and A. Pich, JHEP **02**, 047 (2004).
43. V. Cirigliano and H. Neufeld, Phys. Lett. **B700**, 7 (2011); W.J. Marciano, Phys. Rev. Lett. **93**, 231803 (2004) [hep-ph/0402299].
44. F. Ambrosino *et al.*, [KLOE Collab.], Phys. Lett. **B632**, 76 (2006) [hep-ex/0509045].
45. A Bazavov *et al.*, [MILC Collab.], Phys. Rev. Lett. **110**, 172003 (2013).
46. V. Mateu and A. Pich, JHEP **0510**, 041 (2005) [hep-ph/0509045].
47. I. Nugent, arXiv:1301.0637 [hep-ex]; Y. Amhis *et al.*, [Heavy Flavor Averaging Group], arXiv:1207.1158 [hep-ex].
48. A. Sirlin, Rev. Mod. Phys. **50**, 573 (1978).
49. D. Webber *et al.*, [MuLan Collab.], Phys. Rev. Lett. **106**, 041803 (2011); V. Tishchenko *et al.*, [MuLan Collab.], Phys. Rev. **D87**, 052003 (2013).
50. K.S. Babu and S. Pakvasa, hep-ph/0204236.
51. W. Marciano and A. Sirlin, Phys. Rev. Lett. **56**, 22 (1986); P. Langacker and D. London, Phys. Rev. **D38**, 886 (1988).
52. W. Marciano and A. Sirlin, Phys. Rev. **D35**, 1672 (1987).
53. R. Barbieri *et al.*, Phys. Lett. **156B**, 348 (1985); K. Hagiwara *et al.*, Phys. Rev. Lett. **75**, 3605 (1995); A. Kurylov, M. Ramsey-Musolf, Phys. Rev. Lett. **88**, 071804 (2000).

ENERGY DEPENDENCE OF K_L^0 DALITZ PLOT

For discussion, see note on Dalitz plot parameters in the $K^\pm$ section of the Particle Listings above. For definitions of a_y, a_t, a_u, and a_y, see the earlier version of the same note in the 1982 edition of this *Review* published in Physics Letters **111B** 70 (1982).

$|\text{matrix element}|^2 = 1 + gu + hu^2 + jv + kv^2 + fuv$
where $u = (s_3 - s_0) / m_\pi^2$ and $v = (s_2 - s_1) / m_\pi^2$

LINEAR COEFFICIENT g FOR $K_L^0 \to \pi^+\pi^-\pi^0$

VALUE	EVTS	DOCUMENT ID		TECN	COMMENT
0.678 ±0.008 OUR AVERAGE		Error includes scale factor of 1.5. See the ideogram below.			
0.6823±0.0044±0.0044	500k	ANGELOPO...	98C	CPLR	
0.681 ±0.024	6499	CHO	77	HBC	
0.620 ±0.023	4709	PEACH	77	HBC	
0.677 ±0.010	509k	MESSNER	74	ASPK	$a_y = -0.917 \pm 0.013$
• • • We do not use the following data for averages, fits, limits, etc. • • •					
0.69 ±0.07	192	[1] BALDO-...	75	HLBC	
0.590 ±0.022	56k	[1] BUCHANAN	75	SPEC	$a_u = -0.277 \pm 0.010$
0.619 ±0.027	20k	[1,2] BISI	74	ASPK	$a_t = -0.282 \pm 0.011$
0.612 ±0.032		[1] ALEXANDER	73B	HBC	
0.73 ±0.04	3200	[1] BRANDENB...	73	HBC	
0.608 ±0.043	1486	[1] KRENZ	72	HLBC	$a_t = -0.277 \pm 0.018$
0.650 ±0.012	29k	[1] ALBROW	70	ASPK	$a_y = -0.858 \pm 0.015$
0.593 ±0.022	36k	[1,3] BUCHANAN	70	SPEC	$a_u = -0.278 \pm 0.010$
0.664 ±0.056	4400	[1] SMITH	70	OSPK	$a_t = -0.306 \pm 0.024$
0.400 ±0.045	2446	[1] BASILE	68B	OSPK	$a_t = -0.188 \pm 0.020$
0.649 ±0.044	1350	[1] HOPKINS	67	HBC	$a_t = -0.294 \pm 0.018$
0.428 ±0.055	1198	[1] NEFKENS	67	OSPK	$a_u = -0.204 \pm 0.025$

[1] Quadratic dependence required by some experiments. (See sections on "QUADRATIC COEFFICIENT h" and "QUADRATIC COEFFICIENT k" below.) Correlations prevent us from averaging results of fits not including g, h, and k terms.
[2] BISI 74 value comes from quadratic fit with quad. term consistent with zero. g error is thus larger than if linear fit were used.
[3] BUCHANAN 70 result revised by BUCHANAN 75 to include radiative correlations and to use more reliable K_L^0 momentum spectrum of second experiment (had same beam).

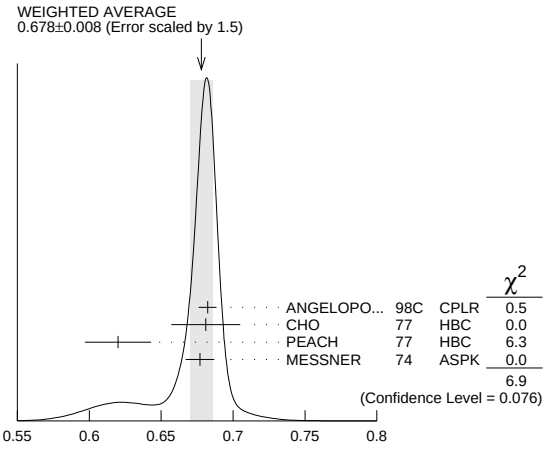

Linear coeff. g for $K_L^0 \to \pi^+\pi^-\pi^0$ matrix element squared

QUADRATIC COEFFICIENT h FOR $K_L^0 \to \pi^+\pi^-\pi^0$

VALUE	EVTS	DOCUMENT ID		TECN
0.076±0.006 OUR AVERAGE				
0.061±0.004±0.015	500k	ANGELOPO...	98C	CPLR
0.095±0.032	6499	CHO	77	HBC
0.048±0.036	4709	PEACH	77	HBC
0.079±0.007	509k	MESSNER	74	ASPK
• • • We do not use the following data for averages, fits, limits, etc. • • •				
−0.011±0.018	29k	[1] ALBROW	70	ASPK
0.043±0.052	4400	[1] SMITH	70	OSPK

See notes in section "LINEAR COEFFICIENT g FOR $K_L^0 \to \pi^+\pi^-\pi^0$ |MATRIX ELEMENT|^2" above.

[1] Quadratic coefficients h and k required by some experiments. (See section on "QUADRATIC COEFFICIENT k" below.) Correlations prevent us from averaging results of fits not including g, h, and k terms.

QUADRATIC COEFFICIENT k FOR $K_L^0 \to \pi^+\pi^-\pi^0$

VALUE	EVTS	DOCUMENT ID		TECN
0.0099±0.0015 OUR AVERAGE				
0.0104±0.0017±0.0024	500k	ANGELOPO...	98C	CPLR
0.024 ±0.010	6499	CHO	77	HBC
−0.008 ±0.012	4709	PEACH	77	HBC
0.0097±0.0018	509k	MESSNER	74	ASPK

LINEAR COEFFICIENT j FOR $K^0_L \to \pi^+\pi^-\pi^0$ (CP-VIOLATING TERM)

Listed in CP-violation section below.

QUADRATIC COEFFICIENT f FOR $K^0_L \to \pi^+\pi^-\pi^0$ (CP-VIOLATING TERM)

Listed in CP-violation section below.

QUADRATIC COEFFICIENT h FOR $K^0_L \to \pi^0\pi^0\pi^0$

No average is computed because not all measurements included the effect of final state rescattering.

VALUE (units 10^{-3})	EVTS	DOCUMENT ID		TECN
+0.59±0.20±1.16	6.8M	[1] ABOUZAID	08A	KTEV
−6.1 ±0.9 ±0.5	14.7M	[2] LAI	01B	NA48
−3.3 ±1.1 ±0.7	5M	[2,3] SOMALWAR	92	E731

[1] Result obtained using CI3pI model of CABIBBO 05 to include $\pi\pi$ rescattering effects. The systematic error includes an external error of 1.06×10^{-3} from the parametrization input of $(a_0 - a_2)\ m_{\pi^+} = 0.268 \pm 0.017$ from BATLEY 06B.

[2] LAI 01B and SOMALWAR 92 results do not include $\pi\pi$ final state rescattering effects.

[3] SOMALWAR 92 chose m_{π^+} as normalization to make it compatible with the Particle Data Group $K^0_L \to \pi^+\pi^-\pi^0$ definitions.

K^0_L FORM FACTORS

For discussion, see note on form factors in the $K^\pm$ section of the Particle Listings above.

In the form factor comments, the following symbols are used.

f_+ and f_- are form factors for the vector matrix element.

f_S and f_T refer to the scalar and tensor term.

$f_0(t) = f_+(t) + f_-(t)\ t/(m^2_{K^0} - m^2_{\pi^+})$.

t = momentum transfer to the π.

λ_+ and λ_0 are the linear expansion coefficients of f_+ and f_0:

$f_+(t) = f_+(0)\ (1 + \lambda_+ t\ /m^2_{\pi^+})$

For quadratic expansion

$f_+(t) = f_+(0)\ (1 + \lambda'_+ t\ /m^2_{\pi^+} + \frac{\lambda''_+}{2}\ t^2/m^4_{\pi^+}\ )$

as used by KTeV. If there is a non-vanishing quadratic term, then λ_+ represents an average slope, which is then different from λ'_+.

NA48 (K_{e3}) and ISTRA quadratic expansion coefficients are converted with

$\lambda'_+{}^{PDG} = \lambda_+{}^{NA48}$ and $\lambda''_+{}^{PDG} = 2\ \lambda'_+{}^{NA48}$

$\lambda'_+{}^{PDG} = (\frac{m_{\pi^+}}{m_{\pi^0}})^2\ \lambda_+{}^{ISTRA}$ and

$\lambda''_+{}^{PDG} = 2\ (\frac{m_{\pi^+}}{m_{\pi^0}})^4\ \lambda'_+{}^{ISTRA}$

ISTRA linear expansion coefficients are converted with

$\lambda_+{}^{PDG} = (\frac{m_{\pi^+}}{m_{\pi^0}})^2\ \lambda_+{}^{ISTRA}$ and $\lambda_0{}^{PDG} = (\frac{m_{\pi^+}}{m_{\pi^0}})^2\ \lambda_0{}^{ISTRA}$

The pole parametrization is

$f_+(t) = f_+(0)\ (\frac{M_V^2}{M_V^2 - t}\ )$

$f_0(t) = f_0(0)\ (\frac{M_S^2}{M_S^2 - t}\ )$

where M_V and M_S are the vector and scalar pole masses.

The dispersive parametrization is

$f_+(t) = f_+(0)\ \exp[\ \frac{t}{m^2_\pi}\ (\Lambda_+ + H(t))\ ]$;

$f_0(t) = f_+(0)\ \exp[\ \frac{t}{m^2_K - m^2_\pi}\ (\ln[C] - G(t))\ ]$,

where Λ_+ is the slope parameter and $\ln[C] = \ln[\ f_0\ (m^2_K - m^2_\pi)\ ]$ is the logarithm of the scalar form factor at the Callan-Treiman point.

$H(t)$ and $G(t)$ are dispersive integrals.

The following abbreviations are used:

DP = Dalitz plot analysis.

PI = π spectrum analysis.

MU = μ spectrum analysis.

POL= μ polarization analysis.

BR = $K^0_{\mu 3}/K^0_{e3}$ branching ratio analysis.

E = positron or electron spectrum analysis.

RC = radiative corrections.

λ_+ (LINEAR ENERGY DEPENDENCE OF f_+ IN K^0_{e3} DECAY)

For radiative correction of K^0_{e3} DP, see GINSBERG 67, BECHERRAWY 70, CIRIGLIANO 02, CIRIGLIANO 04, and ANDRE 07. Results labeled OUR FIT are discussed in the review "$K^\pm_{\ell 3}$ and $K^0_{\ell 3}$ Form Factors" in the $K^\pm$ Listings. For earlier, lower statistics results, see the 2004 edition of this review, Physics Letters **B592** 1 (2004).

VALUE (units 10^{-2})	EVTS	DOCUMENT ID		TECN	COMMENT
2.82 ±0.04	**OUR FIT**	Error includes scale factor of 1.1. Assuming μ-e universality			
2.85 ±0.04	**OUR AVERAGE**				
2.86 ±0.05 ±0.04	2M	AMBROSINO	06D	KLOE	
2.832±0.037±0.043	1.9M	ALEXOPOU...	04A	KTEV	PI, no $\mu = e$
2.88 ±0.04 ±0.11	5.6M	[1] LAI	04C	NA48	DP
• • • We do not use the following data for averages, fits, limits, etc. • • •					
2.84 ±0.07 ±0.13	5.6M	[2] LAI	04C	NA48	DP
2.45 ±0.12 ±0.22	366k	APOSTOLA...	00	CPLR	DP
3.06 ±0.34	74k	BIRULEV	81	SPEC	DP
3.12 ±0.25	500k	GJESDAL	76	SPEC	DP
2.70 ±0.28	25k	BLUMENTHAL	75	SPEC	DP

[1] Results from linear fit and assuming only vector and axial couplings.

[2] Results from linear fit with $|f_S/f_+|$ and $|f_T/f_+|$ free.

λ_+ (LINEAR ENERGY DEPENDENCE OF f_+ IN $K^0_{\mu 3}$ DECAY)

Results labeled OUR FIT are discussed in the review "$K^\pm_{\ell 3}$ and $K^0_{\ell 3}$ Form Factors" in the $K^\pm$ Listings. For earlier, lower statistics results, see the 2004 edition of this review, Physics Letters **B592** 1 (2004).

VALUE (units 10^{-2})	EVTS	DOCUMENT ID		TECN	COMMENT
2.82 ±0.04	**OUR FIT**	Error includes scale factor of 1.1. Assuming μ-e universality			
2.71 ±0.10	**OUR FIT**	Error includes scale factor of 1.4. Not assuming μ-e universality			
2.67 ±0.06 ±0.08	2.3M	[1] LAI	07A	NA48	DP
2.745±0.088±0.063	1.5M	ALEXOPOU...	04A	KTEV	DP, no $\mu = e$
2.813±0.051	3.4M	ALEXOPOU...	04A	KTEV	PI, DP, $\mu = e$
3.0 ±0.3	1.6M	DONALDSON	74B	SPEC	DP
• • • We do not use the following data for averages, fits, limits, etc. • • •					
4.27 ±0.44	150k	BIRULEV	81	SPEC	DP

[1] LAI 07A gives a correlation −0.40 between their λ_0 and λ_+ measurements.

λ_0 (LINEAR ENERGY DEPENDENCE OF f_0 IN $K^0_{\mu 3}$ DECAY)

Wherever possible, we have converted the above values of $\xi(0)$ into values of λ_0 using the associated λ^μ_+ and $d\xi(0)/d\lambda_+$. Results labeled OUR FIT are discussed in the review "$K^\pm_{\ell 3}$ and $K^0_{\ell 3}$ Form Factors" in the $K^\pm$ Listings. For earlier, lower statistics results, see the 2004 edition of this review, Physics Letters **B592** 1 (2004).

VALUE (units 10^{-2})	$d\lambda_0/d\lambda_+$	EVTS	DOCUMENT ID		TECN	COMMENT
1.38 ±0.18			**OUR FIT** Error includes scale factor of 2.2. Assuming μ-e universality			
1.42 ±0.23			**OUR FIT** Error includes scale factor of 2.8. Not assuming μ-e universality			
1.17 ±0.07 ±0.10		2.3M	[1] LAI	07A	NA48	DP
1.657±0.125	−0.44	1.5M	[2] ALEXOPOU...	04A	KTEV	DP, no $\mu = e$
1.635±0.121	−0.85	3.4M	[3] ALEXOPOU...	04A	KTEV	PI, DP, $\mu = e$
+1.9 ±0.4	−0.47	1.6M	[4] DONALDSON	74B	SPEC	DP
• • • We do not use the following data for averages, fits, limits, etc. • • •						
3.41 ±0.67	unknown	150k	[5] BIRULEV	81	SPEC	DP

[1] LAI 07A gives a correlation −0.40 between their λ_0 and λ_+ measurements.

[2] ALEXOPOULOS 04A gives a correlation −0.38 between their λ_0 and λ_+ measurements.

[3] ALEXOPOULOS 04A gives a correlation −0.36 between their λ_0 and λ_+ measurements.

[4] DONALDSON 74B $d\lambda_0/d\lambda_+$ obtained from figure 18.

[5] BIRULEV 81 gives $d\lambda_0/d\lambda_+ = -1.5$, giving an unreasonably narrow error ellipse which dominates all other results. We use $d\lambda_0/d\lambda_+ = 0$.

λ'_+(LINEAR K^0_{e3} FORM FACTOR FROM QUADRATIC FIT)

VALUE (units 10^{-2})	EVTS	DOCUMENT ID		TECN	COMMENT
2.40 ±0.12	**OUR FIT**	Error includes scale factor of 1.2. Assuming μ-e universality			
2.49 ±0.13	**OUR FIT**	Error includes scale factor of 1.1. Not assuming μ-e universality			
2.48 ±0.17	**OUR AVERAGE**	Error includes scale factor of 1.5. See the ideogram below.			
2.55 ±0.15 ±0.10	2M	[1] AMBROSINO	06D	KLOE	
2.167±0.137±0.143	1.9M	[2] ALEXOPOU...	04A	KTEV	PI, no $\mu = e$
2.80 ±0.19 ±0.15	5.6M	[3] LAI	04C	NA48	DP

[1] We use AMBROSINO 06D result in the fit not assuming μ−e universality. This result enters the fit assuming μ−e universality via AMBROSINO 07C measurement of λ'_+ in $K_{\mu 3}$ decays. AMBROSINO 06D gives a correlation −0.95 between their λ'_+ and λ''_+.

[2] ALEXOPOULOS 04A gives a correlation −0.97 between their λ'_+ and λ''_+.

[3] For LAI 04C we calculate a correlation −0.88 between their λ'_+ and λ''_+.

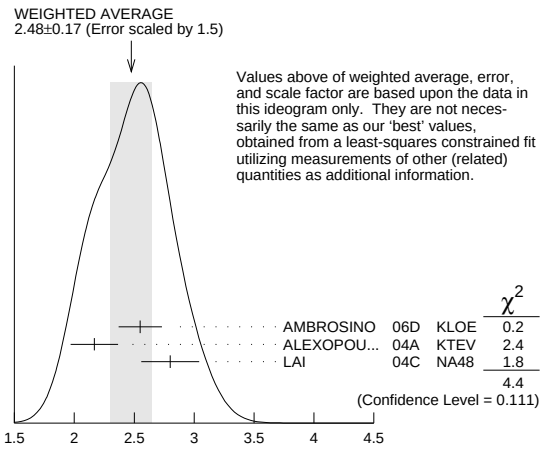

Meson Particle Listings

K^0_L

λ''_+(QUADRATIC K^0_{e3} FORM FACTOR)

VALUE (units 10^{-2})	EVTS	DOCUMENT ID		TECN	COMMENT
0.20 ±0.05 OUR FIT		Error includes scale factor of 1.2. Assuming μ-e universality			
0.16 ±0.05 OUR FIT		Error includes scale factor of 1.1. Not assuming μ-e universality			
0.17 ±0.07 OUR AVERAGE		Error includes scale factor of 1.5. See the ideogram below.			
0.14 ±0.07 ±0.04	2M	[1] AMBROSINO	06D	KLOE	
0.287±0.057±0.053	1.9M	[2] ALEXOPOU...	04A	KTEV	PI, no $\mu = e$
0.04 ±0.08 ±0.04	5.6M	[3,4] LAI	04C	NA48	DP

[1] We use AMBROSINO 06D result in the fit not assuming $\mu-e$ universality. This result enters the fit assuming $\mu-e$ universality via AMBROSINO 07C measurement of λ''_+ in $K_{\mu3}$ decays. AMBROSINO 06D gives a correlation -0.95 between their λ'_+ and λ''_+.

[2] ALEXOPOULOS 04A gives a correlation -0.97 between their λ'_+ and λ''_+.

[3] Values doubled to agree with PDG conventions described above.

[4] LAI 04C gives a correlation -0.88 between their λ'_+ and λ''_+.

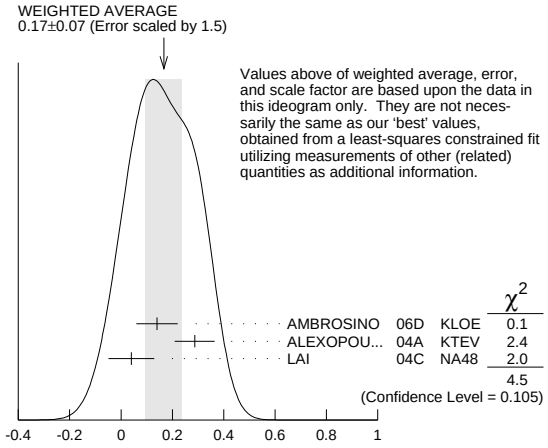

λ''_+(QUADRATIC K^0_{e3} FORM FACTOR) (units 10^{-2})

λ'_+(LINEAR $K^0_{\mu3}$ FORM FACTOR FROM QUADRATIC FIT)

VALUE (units 10^{-2})	EVTS	DOCUMENT ID		TECN	COMMENT
2.40 ±0.12 OUR FIT		Error includes scale factor of 1.2. Assuming μ-e universality			
1.89 ±0.24 OUR FIT		Not assuming μ-e universality			
2.23 ±0.98 ±0.37	1.8M	[1] AMBROSINO	07C	KLOE	no $\mu = e$
2.56 ±0.15 ±0.09	3.8M	[1] AMBROSINO	07C	KLOE	$\mu = e$
2.05 ±0.22 ±0.24	2.3M	[1] LAI	07A	NA48	DP
1.703±0.319±0.177	1.5M	[1] ALEXOPOU...	04A	KTEV	DP, no $\mu = e$
2.064±0.175	3.4M	[1] ALEXOPOU...	04A	KTEV	PI, DP, $\mu = e$

[1] See section λ_0 below for correlations.

λ''_+(QUADRATIC $K^0_{\mu3}$ FORM FACTOR)

VALUE (units 10^{-2})	EVTS	DOCUMENT ID		TECN	COMMENT
0.20 ±0.05 OUR FIT		Error includes scale factor of 1.2. Assuming μ-e universality			
0.37 ±0.12 OUR FIT		Error includes scale factor of 1.3. Not assuming μ-e universality			
0.48 ±0.49 ±0.16	1.8M	[1] AMBROSINO	07C	KLOE	no $\mu = e$
0.15 ±0.07 ±0.04	3.8M	[1] AMBROSINO	07C	KLOE	$\mu = e$
0.26 ±0.09 ±0.10	2.3M	[1] LAI	07A	NA48	DP
0.443±0.131±0.072	1.5M	[1] ALEXOPOU...	04A	KTEV	DP, no $\mu = e$
0.320±0.069	3.4M	[1] ALEXOPOU...	04A	KTEV	PI, DP, $\mu = e$

[1] See section λ_0 below for correlations.

λ_0(LINEAR f_0 $K^0_{\mu3}$ FORM FACTOR FROM QUADRATIC FIT)

VALUE (units 10^{-2})	EVTS	DOCUMENT ID		TECN	COMMENT
1.16 ±0.09 OUR FIT		Error includes scale factor of 1.2. Assuming μ-e universality			
1.07 ±0.14 OUR FIT		Error includes scale factor of 1.3. Not assuming μ-e universality			
0.91 ±0.59 ±0.26	1.8M	[1] AMBROSINO	07C	KLOE	no $\mu = e$
1.54 ±0.18 ±0.13	3.8M	[2] AMBROSINO	07C	KLOE	$\mu = e$
0.95 ±0.11 ±0.08	2.3M	[3] LAI	07A	NA48	DP
1.281±0.136±0.122	1.5M	[4] ALEXOPOU...	04A	KTEV	DP, no $\mu = e$
1.372±0.131	3.4M	[5] ALEXOPOU...	04A	KTEV	PI, DP, $\mu = e$

[1] AMBROSINO 07C, not assuming μ-e universality, gives a correlation matrix

	λ'_+	λ''_+
λ''_+	−0.97	1
λ_0	0.81	−0.91

[2] AMBROSINO 07C, assuming μ-e universality, gives a correlation matrix

	λ'_+	λ''_+
λ''_+	−0.95	1
λ_0	0.29	−0.38

[3] LAI 07A gives a correlation matrix

	λ'_+	λ''_+
λ''_+	−0.96	1
λ_0	0.63	−0.73

[4] ALEXOPOULOS 04A, not assuming μ-e universality, gives a correlation matrix

	λ'_+	λ''_+	λ_0
λ'_+	1		
λ''_+	−0.96	1	
λ_0	0.65	−0.75	1

[5] ALEXOPOULOS 04A, assuming μ-e universality, gives a correlation matrix

	λ'_+	λ''_+	λ_0
λ'_+	1		
λ''_+	−0.97	1	
λ_0	0.34	−0.44	1

M^e_V (POLE MASS FOR K^0_{e3} DECAY)

VALUE (MeV)	EVTS	DOCUMENT ID		TECN	COMMENT
878 ± 6 OUR FIT		Error includes scale factor of 1.1. Assuming μ-e universality			
875 ± 5 OUR AVERAGE					
870 ± 6 ±7	2M	AMBROSINO	06D	KLOE	
881.03± 5.12±4.94	1.9M	ALEXOPOU...	04A	KTEV	PI, no $\mu = e$
859 ±18	5.6M	LAI	04C	NA48	

M^μ_V (POLE MASS FOR $K^0_{\mu3}$ DECAY)

VALUE (MeV)	EVTS	DOCUMENT ID		TECN	COMMENT
878 ± 6 OUR FIT		Error includes scale factor of 1.1. Assuming μ-e universality			
900 ±21 OUR FIT		Error includes scale factor of 1.7. Not assuming μ-e universality			
905 ± 9 ±17	2.3M	[1] LAI	07A	NA48	DP
889.19±12.81± 9.92	1.5M	[1] ALEXOPOU...	04A	KTEV	DP, no $\mu = e$
882.32± 6.54	3.4M	[1] ALEXOPOU...	04A	KTEV	PI, DP, $\mu = e$

[1] See section M^μ_S below for correlations.

M^μ_S (POLE MASS FOR $K^0_{\mu3}$ DECAY)

VALUE (MeV)	EVTS	DOCUMENT ID		TECN	COMMENT
1252 ±90 OUR FIT		Error includes scale factor of 2.6. Assuming μ-e universality			
1222 ±80 OUR FIT		Error includes scale factor of 2.3. Not assuming μ-e universality			
1400 ±46 ±53	2.3M	[1] LAI	07A	NA48	DP
1167.14±28.30±31.04	1.5M	[2] ALEXOPOU...	04A	KTEV	PI, no $\mu = e$
1173.80±39.47	3.4M	[3] ALEXOPOU...	04A	KTEV	PI, DP, $\mu = e$

[1] LAI 07A gives a correlation -0.47 between their M^μ_S and M^μ_V measurements, not assuming μ-e universality.

[2] ALEXOPOULOS 04A gives a correlation -0.46 between their M^μ_S and M^μ_V and measurements, not assuming μ-e universality.

[3] ALEXOPOULOS 04A gives a correlation -0.40 between their M^μ_S and M^μ_V and measurements, assuming μ-e universality.

Λ_+ (DISPERSIVE VECTOR FORM FACTOR FOR $K^0_{\mu3}$ DECAY)

See the review on "$K^\pm_{\ell3}$ and $K^0_{\ell3}$ Form Factors" for details of the dispersive parametrization.

VALUE (units 10^{-1})	EVTS	DOCUMENT ID		TECN	COMMENT
0.251 ±0.006 OUR AVERAGE		Error includes scale factor of 1.5. See the ideogram below.			
0.2509±0.0035±0.0043	3.4M	[1] ABOUZAID	10	KTEV	$\mu = e$
0.257 ±0.004 ±0.004	3.8M	[2] AMBROSINO	07C	KLOE	$\mu = e$
0.233 ±0.005 ±0.008	2.3M	[3] LAI	07A	NA48	DP

[1] Obtained from a sample of 1.9 M K_{e3} and 1.5 M $K_{\mu3}$. The correlation between Λ_+ and ln(C) is -0.269.

[2] AMBROSINO 07C results include 2M K_{e3} events from AMBROSINO 06D. The correlation between Λ_+ and ln(C) is -0.26.

[3] LAI 07A gives a correlation -0.44 between their Λ_+ and ln(C) measurements.

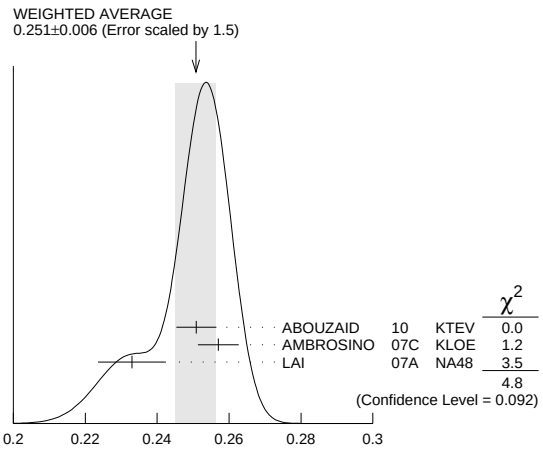

Λ_+ (DISPERSIVE VECTOR FORM FACTOR FOR $K^0_{\mu3}$ DECAY) (units 10^{-1})

ln(C) (DISPERSIVE SCALAR FORM FACTOR FOR $K^0_{\mu 3}$ DECAY)

See the review on "$K^\pm_{\ell 3}$ and $K^0_{\ell 3}$ Form Factors" for details of the dispersive parametrization.

VALUE (units 10^{-1})	EVTS	DOCUMENT ID		TECN	COMMENT
1.75 ±0.18 OUR AVERAGE		Error includes scale factor of 2.0. See the ideogram below.			
1.915±0.078±0.094	3.4M	[1] ABOUZAID	10	KTEV	$\mu = e$
2.04 ±0.19 ±0.15	3.8M	[2] AMBROSINO	07C	KLOE	$\mu = e$
1.438±0.080±0.112	2.3M	[3] LAI	07A	NA48	DP

[1] Obtained from a sample of 1.9 M K_{e3} and 1.5 M $K_{\mu 3}$. The correlation between λ_+ and ln(C) is −0.269.

[2] AMBROSINO 07C results include 2M K_{e3} events from AMBROSINO 06D. We convert (λ_+, λ_0) to $(\lambda_+, \ln(C))$ parametrization using $\ln(C) = (\lambda_0 \cdot 11.713 + 0.0398) \pm 0.0041$, where the error is due to theory parametrization of the form factor. The correlation between λ_+ and ln(C) is −0.26.

[3] LAI 07A gives a correlation −0.44 between their λ_+ and ln(C) measurements.

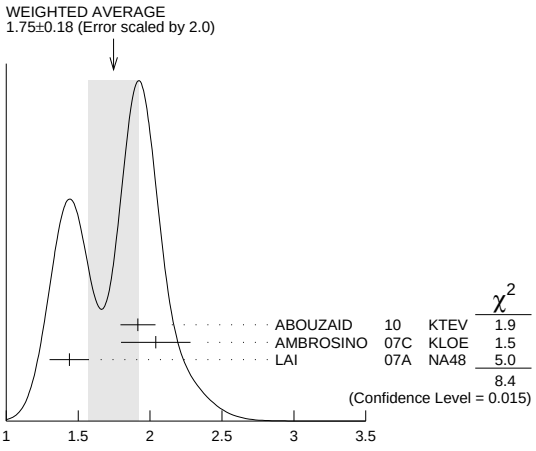

ln(C) (DISPERSIVE SCALAR FORM FACTOR FOR $K^0_{\mu 3}$ DECAY) (units 10^{-1})

$a_1(t_0, Q^2)$ FORM FACTOR PARAMETER

See HILL 06 for a definition of this parameter.

VALUE	EVTS	DOCUMENT ID		TECN
1.023±0.028±0.029	2M	[1] ABOUZAID	06C	KTEV

[1] $Q^2 = 2$ GeV^2, $t_0 = 0.49\ (m_K - m_\pi)^2$. Correlation between a_1 and a_2: $\rho_{12} = -0.064$.

$a_2(t_0, Q^2)$ FORM FACTOR PARAMETER

See HILL 06 for a definition of this parameter.

VALUE	EVTS	DOCUMENT ID		TECN
0.75±1.58±1.47	2M	[1] ABOUZAID	06C	KTEV

[1] $Q^2 = 2$ GeV^2, $t_0 = 0.49\ (m_K - m_\pi)^2$. Correlation between a_1 and a_2: $\rho_{12} = -0.064$.

$|f_S/f_+|$ FOR K^0_{e3} DECAY

Ratio of scalar to f_+ couplings.

VALUE (units 10^{-2})	CL%	EVTS	DOCUMENT ID		TECN	COMMENT
$\mathbf{1.5^{+0.7}_{-1.0} \pm 1.2}$		5.6M	[1] LAI	04C	NA48	
• • • We do not use the following data for averages, fits, limits, etc. • • •						
<9.5	95	18k	HILL	78	STRC	
<7.	68	48k	BIRULEV	76	SPEC	See also BIRULEV 81
<4.	68	25k	BLUMENTHAL	75	SPEC	

[1] Results from linear fit with $|f_S/f_+|$ and $|f_T/f_+|$ free.

$|f_T/f_+|$ FOR K^0_{e3} DECAY

Ratio of tensor to f_+ couplings.

VALUE (units 10^{-2})	CL%	EVTS	DOCUMENT ID		TECN	COMMENT
$\mathbf{5^{+3}_{-4} \pm 3}$		5.6M	[1] LAI	04C	NA48	
• • • We do not use the following data for averages, fits, limits, etc. • • •						
<40.	95	18k	HILL	78	STRC	
<34.	68	48k	BIRULEV	76	SPEC	See also BIRULEV 81
<23.	68	25k	BLUMENTHAL	75	SPEC	

[1] Results from linear fit with $|f_S/f_+|$ and $|f_T/f_+|$ free.

$|f_T/f_+|$ FOR $K^0_{\mu 3}$ DECAY

Ratio of tensor to f_+ couplings.

VALUE (units 10^{-2})	DOCUMENT ID		TECN
12.±12.	BIRULEV	81	SPEC

α_{K^*} DECAY FORM FACTOR FOR $K_L \to \ell^+\ell^-\gamma$, $K^0_L \to \ell^+\ell^-\ell'^+\ell'^-$

Average of all α_{K^*} measurements (from each of three datablocks following this one) assuming lepton universality.

VALUE	DOCUMENT ID
−0.205±0.022 OUR AVERAGE	Includes data from the 3 datablocks that follow this one. Error includes scale factor of 1.8. See the ideogram below.

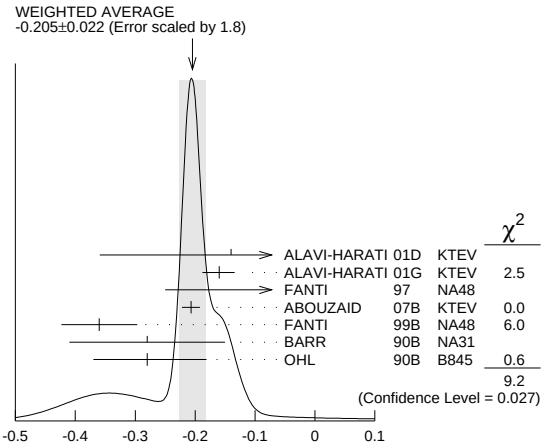

α_{K^*} DECAY FORM FACTOR FOR $K_L \to \ell^+\ell^-\gamma$, $K^0_L \to \ell^+\ell^-\ell'^+\ell'^-$

α_{K^*} DECAY FORM FACTOR FOR $K_L \to e^+e^-\gamma$

α_{K^*} is the constant in the model of BERGSTROM 83 which measures the relative strength of the vector-vector transition $K_L \to K^*\gamma$ with $K^* \to \rho, \omega, \phi \to \gamma^*$ and the pseudoscalar-pseudoscalar transition $K_L \to \pi, \eta, \eta' \to \gamma\gamma^*$.

VALUE	EVTS	DOCUMENT ID		TECN
The data in this block is included in the average printed for a previous datablock.				
−0.217±0.034 OUR AVERAGE		Error includes scale factor of 2.4.		
−0.207±0.012±0.009	83k	[1] ABOUZAID	07B	KTEV
−0.36 ±0.06 ±0.02	6864	FANTI	99B	NA48
−0.28 ±0.13		BARR	90B	NA31
$-0.280^{+0.099}_{-0.090}$		OHL	90B	B845

[1] ABOUZAID 07B measures $C \cdot \alpha_{K^*} = -0.517 \pm 0.030 \pm 0.022$. We assume $C = 2.5$, as in all other measurements.

α_{K^*} DECAY FORM FACTOR FOR $K_L \to \mu^+\mu^-\gamma$

α_{K^*} is the constant in the model of BERGSTROM 83 described in the previous section.

VALUE	EVTS	DOCUMENT ID		TECN
The data in this block is included in the average printed for a previous datablock.				
−0.158±0.027 OUR AVERAGE				
$-0.160^{+0.026}_{-0.028}$	9100	ALAVI-HARATI	01G	KTEV
$-0.04\ ^{+0.24}_{-0.21}$		FANTI	97	NA48

$\alpha^{\rm eff}_{K^*}$ DECAY FORM FACTOR FOR $K_L \to e^+e^-e^+e^-$

$\alpha^{\rm eff}_{K^*}$ is the parameter describing the relative strength of an intermediate pseudoscalar decay amplitude and a vector meson decay amplitude in the model of BERGSTROM 83. It takes into account both the radiative effects and the form factor. Since there are two e^+e^- pairs here compared with one in $e^+e^-\gamma$ decays, a factorized expression is used for the $e^+e^-e^+e^-$ decay form factor.

VALUE	EVTS	DOCUMENT ID		TECN
The data in this block is included in the average printed for a previous datablock.				
−0.14±0.16±0.15	441	ALAVI-HARATI	01D	KTEV

α_{DIP} DECAY FORM FACTOR FOR $K^0_L \to \ell^+\ell^-\gamma$, $K^0_L \to \ell^+\ell^-\ell'^+\ell'^-$

Average of all α_{DIP} measurements (from each of three datablocks following this one) assuming lepton universality.

VALUE	DOCUMENT ID
−1.69±0.08 OUR AVERAGE	Includes data from the 3 datablocks that follow this one. Error includes scale factor of 1.7.

α_{DIP} DECAY FORM FACTOR FOR $K^0_L \to e^+e^-\gamma$

α_{DIP} parameter in $K^0_L \to \gamma^*\gamma^*$ form factor by DAMBROSIO 98, motivated by vector meson dominance and a proper short distance behavior.

VALUE	EVTS	DOCUMENT ID		TECN
The data in this block is included in the average printed for a previous datablock.				
−1.729±0.043±0.028	83k	ABOUZAID	07B	KTEV

α_{DIP} DECAY FORM FACTOR FOR $K^0_L \to \mu^+\mu^-\gamma$

α_{DIP} is a constant in the model of DAMBROSIO 98 described in the previous section.

VALUE	EVTS	DOCUMENT ID		TECN
The data in this block is included in the average printed for a previous datablock.				
−1.54±0.10	9100	ALAVI-HARATI	01G	KTEV

α_{DIP} DECAY FORM FACTOR FOR $K_L^0 \to e^+e^-\mu^+\mu^-$

α_{DIP} is a constant in the model of DAMBROSIO 98 described in the previous section.

VALUE	EVTS	DOCUMENT ID		TECN
The data in this block is included in the average printed for a previous datablock.				
−1.59±0.37	131	ALAVI-HARATI	03B	KTEV

a_1/a_2 FORM FACTOR FOR M1 DIRECT EMISSION AMPLITUDE

Form factor $= \tilde{g}_{M1}\left[1+\frac{a_1/a_2}{(M_\rho^2-M_K^2)+2M_K E_\gamma^*}\right]$ as described in ALAVI-HARATI 00B.

VALUE (GeV^2)	EVTS	DOCUMENT ID		TECN	COMMENT
−0.737±0.014 OUR AVERAGE					
$-0.744\pm0.027\pm0.032$	5241	[1] ABOUZAID	06	KTEV	$\pi^+\pi^-e^+e^-$
$-0.738\pm0.007\pm0.018$	111k	[2] ABOUZAID	06A	KTEV	$\pi^+\pi^+\gamma$
$-0.81\ ^{+0.07}_{-0.13}\pm0.02$		[3] LAI	03C	NA48	$\pi^+\pi^-e^+e^-$
$-0.737\pm0.026\pm0.022$		[4] ALAVI-HARATI	01B		$\pi^+\pi^-\gamma$
$-0.720\pm0.028\pm0.009$	1766	[5] ALAVI-HARATI	00B	KTEV	$\pi^+\pi^-e^+e^-$

[1] ABOUZAID 06 also measured $|\tilde{g}_{M1}| = 1.11 \pm 0.14$.
[2] ABOUZAID 06A also measured $|\tilde{g}_{M1}| = 1.198 \pm 0.035 \pm 0.086$.
[3] LAI 03C also measured $\tilde{g}_{M1} = 0.99^{+0.28}_{-0.27} \pm 0.07$.
[4] ALAVI-HARATI 01B fit gives χ^2/DOF = 38.8/27. Linear and quadratic fits give χ^2/DOF = 43.2/27 and 37.6/26 respectively.
[5] ALAVI-HARATI 00B also measured $|\tilde{g}_{M1}| = 1.35^{+0.20}_{-0.17} \pm 0.04$.

$\overline{f}_S$ DECAY FORM FACTOR FOR $K_L^0 \to \pi^\pm\pi^0 e^\mp\nu_e$

VALUE	DOCUMENT ID		TECN
0.049±0.011 OUR AVERAGE	Error includes scale factor of 1.7.		
$0.052\pm0.006\pm0.002$	BATLEY	04	NA48
$0.010\pm0.016\pm0.017$	MAKOFF	93	E731

$\overline{f}_P$ DECAY FORM FACTOR FOR $K_L^0 \to \pi^\pm\pi^0 e^\mp\nu_e$

VALUE	DOCUMENT ID		TECN
−0.052±0.012 OUR AVERAGE			
$-0.051\pm0.011\pm0.005$	BATLEY	04	NA48
$-0.079\pm0.049\pm0.022$	MAKOFF	93	E731

λ_g DECAY FORM FACTOR FOR $K_L^0 \to \pi^\pm\pi^0 e^\mp\nu_e$

VALUE	DOCUMENT ID		TECN
0.085±0.020 OUR AVERAGE			
$0.087\pm0.019\pm0.006$	BATLEY	04	NA48
$0.014\pm0.087\pm0.070$	MAKOFF	93	E731

$\overline{h}$ DECAY FORM FACTOR FOR $K_L^0 \to \pi^\pm\pi^0 e^\mp\nu_e$

VALUE	DOCUMENT ID		TECN
−0.30±0.13 OUR AVERAGE			
$-0.32\pm0.12\pm0.07$	BATLEY	04	NA48
$-0.07\pm0.31\pm0.31$	MAKOFF	93	E731

L_3 CHIRAL PERT. THEO. PARAM. FOR $K_L^0 \to \pi^\pm\pi^0 e^\mp\nu_e$

VALUE (units 10^{-3})	DOCUMENT ID		TECN
−3.96±0.28 OUR AVERAGE	Error includes scale factor of 1.6.		
$-4.1\ \pm0.2$	BATLEY	04	NA48
$-3.4\ \pm0.4$	[1] MAKOFF	93	E731

[1] MAKOFF 93 sign has been changed to negative to agree with the sign convention used in BATLEY 04.

a_V, VECTOR MESON EXCHANGE CONTRIBUTION

VALUE	EVTS	DOCUMENT ID		TECN	COMMENT
−0.43±0.06 OUR AVERAGE		Error includes scale factor of 1.5.			
$-0.31\pm0.05\pm0.07$	1.4k	[1] ABOUZAID	08	KTEV	
$-0.46\pm0.03\pm0.04$		LAI	02B	NA48	$K_L^0 \to \pi^0 2\gamma$
$-0.67\pm0.21\pm0.12$		ALAVI-HARATI	01E	KTEV	$K_L^0 \to \pi^0 e^+e^-\gamma$
• • • We do not use the following data for averages, fits, limits, etc. • • •					
$-0.72\pm0.05\pm0.06$		[2] ALAVI-HARATI	99B	KTEV	$K_L^0 \to \pi^0 2\gamma$

[1] Using KTeV dataset collected in 1996, 1997, and 1999.
[2] Superseded by ABOUZAID 08.

CP VIOLATION IN K_L DECAYS

Updated October 2013 by L. Wolfenstein (Carnegie-Mellon University), C.-J. Lin (LBNL), and T.G. Trippe (LBNL).

The symmetries C (particle-antiparticle interchange) and P (space inversion) hold for strong and electromagnetic interactions. After the discovery of large C and P violation in the weak interactions, it appeared that the product CP was a good symmetry. In 1964 CP violation was observed in K^0 decays at a level given by the parameter $\epsilon \approx 2.3 \times 10^{-3}$.

A unified treatment of CP violation in K, D, B, and B_s mesons is given in "CP Violation in Meson Decays" by D. Kirkby and Y. Nir in this *Review*. A more detailed review including a thorough discussion of the experimental techniques used to determine CP violation parameters is given in a book by K. Kleinknecht [1]. Here we give a concise summary of the formalism needed to define the parameters of CP violation in K_L decays, and a description of our fits for the best values of these parameters.

1. Formalism for CP violation in Kaon decay:

CP violation has been observed in the semi-leptonic decays $K_L^0 \to \pi^\mp\ell^\pm\nu$, and in the nonleptonic decay $K_L^0 \to 2\pi$. The experimental numbers that have been measured are

$$A_L = \frac{\Gamma(K_L^0 \to \pi^-\ell^+\nu) - \Gamma(K_L^0 \to \pi^+\ell^-\nu)}{\Gamma(K_L^0 \to \pi^-\ell^+\nu) + \Gamma(K_L^0 \to \pi^+\ell^-\nu)} \tag{1a}$$

$$\eta_{+-} = A(K_L^0 \to \pi^+\pi^-)/A(K_S^0 \to \pi^+\pi^-) = |\eta_{+-}|\, e^{i\phi_{+-}} \tag{1b}$$

$$\eta_{00} = A(K_L^0 \to \pi^0\pi^0)/A(K_S^0 \to \pi^0\pi^0) = |\eta_{00}|\, e^{i\phi_{00}} \ . \tag{1c}$$

CP violation can occur either in the K^0–$\overline{K}^0$ mixing or in the decay amplitudes. Assuming CPT invariance, the mass eigenstates of the K^0–$\overline{K}^0$ system can be written

$$|K_S\rangle = p|K^0\rangle + q|\overline{K}^0\rangle \ , \qquad |K_L\rangle = p|K^0\rangle - q|\overline{K}^0\rangle \ . \tag{2}$$

If CP invariance held, we would have $q = p$ so that K_S would be CP-even and K_L CP-odd. (We define $|\overline{K}^0\rangle$ as CP $|K^0\rangle$). CP violation in K^0–$\overline{K}^0$ mixing is then given by the parameter $\widetilde{\epsilon}$ where

$$\frac{p}{q} = \frac{(1+\widetilde{\epsilon})}{(1-\widetilde{\epsilon})} \ . \tag{3}$$

CP violation can also occur in the decay amplitudes

$$A(K^0 \to \pi\pi(I)) = A_I e^{i\delta_I} \ , \qquad A(\overline{K}^0 \to \pi\pi(I)) = A_I^* e^{i\delta_I} \ , \tag{4}$$

where I is the isospin of $\pi\pi$, δ_I is the final-state phase shift, and A_I would be real if CP invariance held. The CP-violating observables are usually expressed in terms of ϵ and ϵ' defined by

$$\eta_{+-} = \epsilon + \epsilon' \ , \qquad \eta_{00} = \epsilon - 2\epsilon' \ . \tag{5a}$$

One can then show [2]

$$\epsilon = \widetilde{\epsilon} + i\ (\mathrm{Im}\ A_0/\mathrm{Re}\ A_0) \ , \tag{5b}$$

$$\sqrt{2}\epsilon' = ie^{i(\delta_2-\delta_0)}(\mathrm{Re}\, A_2/\mathrm{Re}\, A_0)\ (\mathrm{Im}\, A_2/\mathrm{Re}\, A_2 - \mathrm{Im}\, A_0/\mathrm{Re}\ A_0) \ , \tag{5c}$$

$$A_L = 2\mathrm{Re}\ \epsilon/(1+|\epsilon|^2) \approx 2\mathrm{Re}\ \epsilon \ . \tag{5d}$$

In Eqs. (5a), small corrections [3] of order $\epsilon' \times \mathrm{Re}\ (A_2/A_0)$ are neglected, and Eq. (5d) assumes the $\Delta S = \Delta Q$ rule.

The quantities Im A_0, Im A_2, and Im $\widetilde{\epsilon}$ depend on the choice of phase convention, since one can change the phases of K^0 and $\overline{K}^0$ by a transformation of the strange quark state $|s\rangle \to |s\rangle\ e^{i\alpha}$; of course, observables are unchanged. It is possible by a choice of phase convention to set Im A_0 or Im A_2 or Im $\widetilde{\epsilon}$ to zero, but none of these is zero with the usual phase conventions in the Standard Model. The choice Im $A_0 = 0$ is called the

Wu-Yang phase convention [4], in which case $\epsilon = \widetilde{\epsilon}$. The value of ϵ' is independent of phase convention, and a nonzero value demonstrates CP violation in the decay amplitudes, referred to as direct CP violation. The possibility that direct CP violation is essentially zero, and that CP violation occurs only in the mixing matrix, was referred to as the superweak theory [5].

By applying CPT invariance and unitarity the phase of ϵ is given approximately by

$$\phi_\epsilon \approx \tan^{-1}\frac{2(m_{K_L}-m_{K_S})}{\Gamma_{K_S}-\Gamma_{K_L}} \approx 43.52\pm0.05^\circ\ , \qquad (6a)$$

while Eq. (5c) gives the phase of ϵ' to be

$$\phi_{\epsilon'} = \delta_2 - \delta_0 + \frac{\pi}{2} \approx 42.3\pm1.5^\circ\ , \qquad (6b)$$

where the numerical value is based on an analysis of π–π scattering using chiral perturbation theory [6]. The approximation in Eq. (6a) depends on the assumption that direct CP violation is very small in all K^0 decays. This is expected to be good to a few tenths of a degree, as indicated by the small value of ϵ' and of η_{+-0} and η_{000}, the CP-violation parameters in the decays $K_S \to \pi^+\pi^-\pi^0$ [7], and $K_S \to \pi^0\pi^0\pi^0$ [8]. The relation in Eq. (6a) is exact in the superweak theory, so this is sometimes called the superweak-phase $\phi_{\rm SW}$. An important point for the analysis is that $\cos(\phi_{\epsilon'}-\phi_\epsilon) \simeq 1$. The consequence is that only two real quantities need be measured, the magnitude of ϵ and the value of (ϵ'/ϵ), including its sign. The measured quantity $|\eta_{00}/\eta_{+-}|^2$ is very close to unity so that we can write

$$|\eta_{00}/\eta_{+-}|^2 \approx 1 - 6{\rm Re}\,(\epsilon'/\epsilon) \approx 1 - 6\epsilon'/\epsilon\ , \qquad (7a)$$

$${\rm Re}(\epsilon'/\epsilon) \approx \tfrac{1}{3}(1-|\eta_{00}/\eta_{+-}|)\ . \qquad (7b)$$

From the experimental measurements in this edition of the *Review*, and the fits discussed in the next section, one finds

$$|\epsilon| = (2.228\pm0.011)\times10^{-3}\ , \qquad (8a)$$

$$\phi_\epsilon = (43.5\pm0.5)^\circ\ , \qquad (8b)$$

$${\rm Re}(\epsilon'/\epsilon) \approx \epsilon'/\epsilon = (1.66\pm0.23)\times10^{-3}\ , \qquad (8c)$$

$$\phi_{+-} = (43.4\pm0.5)^\circ\ , \qquad (8d)$$

$$\phi_{00}-\phi_{+-} = (0.34\pm0.32)^\circ\ , \qquad (8e)$$

$$A_L = (3.32\pm0.06)\times10^{-3}\ . \qquad (8f)$$

Direct CP violation, as indicated by ϵ'/ϵ, is expected in the Standard Model. However, the numerical value cannot be reliably predicted because of theoretical uncertainties [9]. The value of A_L agrees with Eq. (5d). The values of ϕ_{+-} and $\phi_{00}-\phi_{+-}$ are used to set limits on CPT violation [see "Tests of Conservation Laws"].

2. Fits for K^0_L CP-violation parameters:

In recent years, K^0_L CP-violation experiments have improved our knowledge of CP-violation parameters, and their consistency with the expectations of CPT invariance and unitarity. To determine the best values of the CP-violation parameters in $K^0_L \to \pi^+\pi^-$ and $\pi^0\pi^0$ decay, we make two types of fits, one for the phases ϕ_{+-} and ϕ_{00} jointly with Δm and τ_S, and the other for the amplitudes $|\eta_{+-}|$ and $|\eta_{00}|$ jointly with the $K^0_L \to \pi\pi$ branching fractions.

Fits to ϕ_{+-}, ϕ_{00}, $\Delta\phi$, Δm, and τ_S data: These are joint fits to the data on ϕ_{+-}, ϕ_{00}, the phase difference $\Delta\phi = \phi_{00}-\phi_{+-}$, the K^0_L–K^0_S mass difference Δm, and the K^0_S mean life τ_S, including the effects of correlations.

Measurements of ϕ_{+-} and ϕ_{00} are highly correlated with Δm and τ_S. Some measurements of τ_S are correlated with Δm. The correlations are given in the footnotes of the ϕ_{+-} and ϕ_{00} sections of the K^0_L Listings, and the τ_S section of the K^0_S Listings.

In most cases, the correlations are quoted as 100%, *i.e.*, with the value and error of ϕ_{+-} or ϕ_{00} given at a fixed value of Δm and τ_S, with additional terms specifying the dependence of the value on Δm and τ_S. These cases lead to diagonal bands in Figs. 1 and 2. The KTeV experiment [10] quotes its results as values of Δm, τ_S, ϕ_ϵ, ${\rm Re}(\epsilon'/\epsilon)$, and ${\rm Im}(\epsilon'/\epsilon)$ with correlations, leading to the ellipses labeled "b." The correlations for the KTeV measurements are given in the ${\rm Im}(\epsilon'/\epsilon)$ section of the K^0_L Listings. For small $|\epsilon'/\epsilon|$, $\phi_{+-} \approx \phi_\epsilon + {\rm Im}(\epsilon'/\epsilon)$.

Table 1: References, Document ID's, and sources corresponding to the letter labels in the figures. The data are given in the ϕ_{+-} and Δm sections of the K_L Listings, and the τ_S section of the K_S Listings.

Label	Source	PDG Document ID	Ref.
a	this *Review*	OUR FIT	
b	FNAL KTeV	ABOUZAID 11	[10]
c	CERN CPLEAR	APOSTOLAKIS 99C	[11]
d	FNAL E773	SCHWINGENHEUER 95	[12]
e	FNAL E731	GIBBONS 93,93C	[13,14]
f	CERN	GEWENIGER 74B,74C	[15,16]
g	CERN NA31	CAROSI 90	[17]
h	CERN NA48	LAI 02C	[18]
i	CERN NA31	BERTANZA 97	[19]
j	this *Review*	SUPERWEAK 13	

The data on τ_S, Δm, and ϕ_{+-} shown in Figs. 1 and 2 are combined with data on ϕ_{00} and $\phi_{00}-\phi_{+-}$ in two fits, one without assuming CPT, and the other with this assumption. The results without assuming CPT are shown as ellipses labeled "a." These ellipses are seen to be in good agreement with the superweak phase

$$\phi_{\rm SW} = \tan^{-1}\left(\frac{2\Delta m}{\Delta\Gamma}\right) = \tan^{-1}\left(\frac{2\Delta m\tau_S\tau_L}{\hbar(\tau_L-\tau_S)}\right)\ . \qquad (9)$$

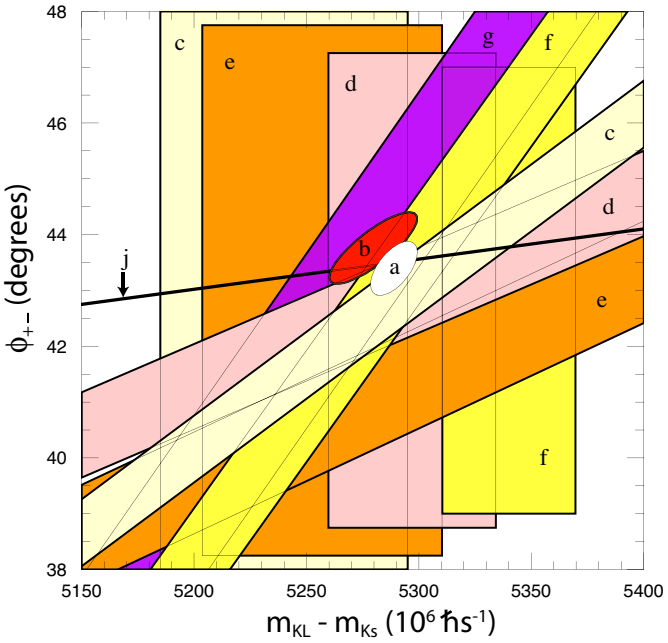

Figure 1: ϕ_{+-} vs Δm for experiments which do not assume CPT invariance. Δm measurements appear as vertical bands spanning $\Delta m \pm 1\sigma$, cut near the top and bottom to aid the eye. Most ϕ_{+-} measurements appear as diagonal bands spanning $\phi_{+-} \pm \sigma_\phi$. Data are labeled by letters: "b"–FNAL KTeV, "c"–CERN CPLEAR, "d"–FNAL E773, "e"–FNAL E731, "f"–CERN, "g"–CERN NA31, and are cited in Table 1. The narrow band "j" shows $\phi_{\rm SW}$. The ellipse "a" shows the $\chi^2 = 1$ contour of the fit result.

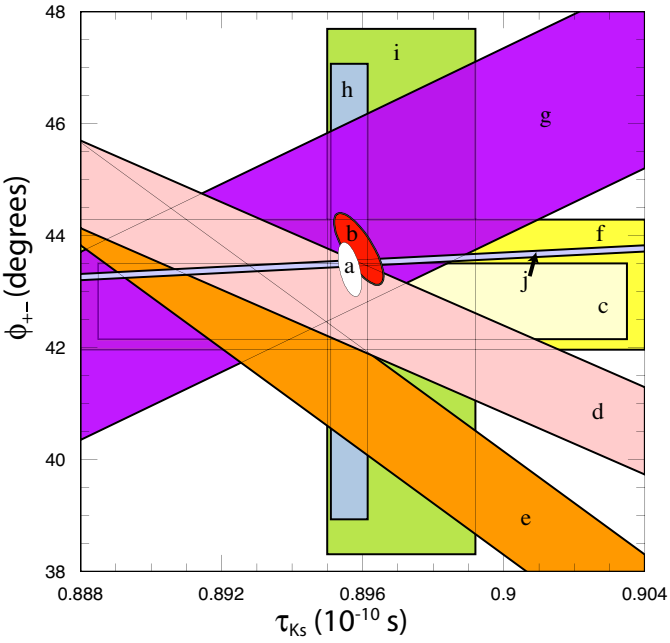

Figure 2: ϕ_{+-} vs τ_S. τ_S measurements appear as vertical bands spanning $\tau_S \pm 1\sigma$, some of which are cut near the top and bottom to aid the eye. Most ϕ_{+-} measurements appear as diagonal or horizontal bands spanning $\phi_{+-} \pm \sigma_\phi$. Data are labeled by letters: "b"–FNAL KTeV, "c"–CERN CPLEAR, "d"–FNAL E773, "e"–FNAL E731, "f"–CERN, "g"–CERN NA31, "h"–CERN NA48, "i"–CERN NA31, and are cited in Table 1. The narrow band "j" shows $\phi_{\rm SW}$. The ellipse "a" shows the fit result's $\chi^2 = 1$ contour.

In Figs. 1 and 2, $\phi_{\rm SW}$ is shown as narrow bands labeled "j."

Table 2 column 2, "Fit w/o CPT," gives the resulting fitted parameters, while Table 3 gives the correlation matrix for this fit. The white ellipses labeled "a" in Fig. 1 and Fig. 2 are the $\chi^2 = 1$ contours for this fit.

For experiments which have dependencies on unseen fit parameters, that is, parameters other than those shown on the x or y axis of the figure, their band positions are evaluated using the fit results and their band widths include the fitted uncertainty in the unseen parameters. This is also true for the $\phi_{\rm SW}$ bands.

If CPT invariance and unitarity are assumed, then by Eq. (6a), the phase of ϵ is constrained to be approximately equal to

$$\phi_{\rm SW} = (43.50258 \pm 0.00021)^\circ + 54.1(\Delta m - 0.5289)^\circ + 32.0(\tau_S - 0.89564) \quad (10)$$

where we have linearized the Δm and τ_S dependence of Eq. (9). The error ± 0.00021 is due to the uncertainty in τ_L. Here Δm has units $10^{10}\,\hbar\,{\rm s}^{-1}$ and τ_S has units 10^{-10} s.

If in addition we use the observation that $Re(\epsilon'/\epsilon) \ll 1$ and $cos(\phi_{\epsilon'} - \phi_\epsilon) \simeq 1$, as well as the numerical value of $\phi_{\epsilon'}$ given in Eq. (6b), then Eqs. (5a), which are sketched in Fig. 3, lead to the constraint

$$\begin{aligned} \phi_{00} - \phi_{+-} &\approx -3\ {\rm Im}\left(\frac{\epsilon'}{\epsilon}\right) \\ &\approx -3\ {\rm Re}\left(\frac{\epsilon'}{\epsilon}\right) \tan(\phi_{\epsilon'} - \phi_\epsilon) \\ &\approx 0.006^\circ \pm 0.008^\circ\ , \end{aligned} \quad (11)$$

so that $\phi_{+-} \approx \phi_{00} \approx \phi_\epsilon \approx \phi_{\rm SW}$.

Table 2: Fit results for ϕ_{+-}, Δm, τ_S, ϕ_{00}, $\Delta\phi = \phi_{00} - \phi_{+-}$, and ϕ_ϵ without and with the CPT assumption.

Quantity(units)	Fit w/o CPT	Fit w/ CPT
$\phi_{+-}(^\circ)$	43.4 ± 0.5 (S=1.2)	43.51 ± 0.05 (S=1.2)
$\Delta m(10^{10}\hbar\ {\rm s}^{-1})$	0.5289 ± 0.0010	0.5293 ± 0.0009 (S=1.3)
$\tau_S(10^{-10}{\rm s})$	0.89564 ± 0.00033	0.8954 ± 0.0004 (S=1.1)
$\phi_{00}(^\circ)$	43.7 ± 0.6 (S=1.2)	43.52 ± 0.05 (S=1.3)
$\Delta\phi(^\circ)$	0.34 ± 0.32	0.006 ± 0.014 (S=1.7)
$\phi_\epsilon(^\circ)$	43.5 ± 0.5 (S=1.3)	43.52 ± 0.05 (S=1.2)
χ^2	16.4	20.0
# Deg. Free.	14	16

In the fit assuming CPT, we constrain $\phi_\epsilon = \phi_{\rm SW}$ using the linear expression in Eq. (10), and constrain $\phi_{00} - \phi_{+-}$ using Eq. (11). These constraints are inserted into the Listings with the Document ID of SUPERWEAK 13. Some additional data for which the authors assumed CPT are added to this fit or substitute for other less precise data for which the authors did not make this assumption. See the Listings for details.

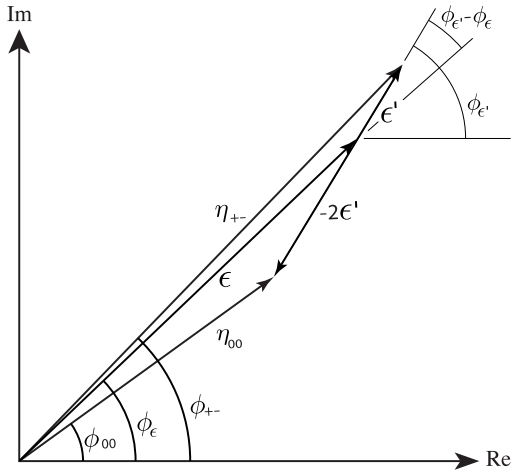

Figure 3: Sketch of Eqs. (5a). Not to scale.

The results of this fit are shown in Table 2, column 3, "Fit w/CPT," and the correlation matrix is shown in Table 4. The Δm precision is improved by the CPT assumption.

Table 3: Correlation matrix for the results of the fit without the CPT assumption

	ϕ_{+-}	Δm	τ_S	ϕ_{00}	$\Delta\phi$	ϕ_ϵ
ϕ_{+-}	1.000	0.596	−0.488	0.827	−0.040	0.976
Δm	0.596	1.000	−0.572	0.487	−0.035	0.580
τ_S	−0.488	−0.572	1.000	−0.423	−0.014	−0.484
ϕ_{00}	0.827	0.487	−0.423	1.000	0.529	0.929
$\Delta\phi$	−0.040	−0.035	−0.014	0.529	1.000	0.178
ϕ_ϵ	0.976	0.580	−0.484	0.929	0.178	1.000

Table 4: Correlation matrix for the results of the fit with the CPT assumption

	ϕ_{+-}	Δm	τ_S	ϕ_{00}	$\Delta\phi$	ϕ_ϵ
ϕ_{+-}	1.000	0.972	−0.311	0.957	−0.105	0.995
Δm	0.972	1.000	−0.509	0.958	−0.007	0.977
τ_S	−0.311	−0.509	1.000	−0.306	0.004	−0.312
ϕ_{00}	0.957	0.958	−0.306	1.000	0.189	0.981
$\Delta\phi$	−0.105	−0.007	0.004	0.189	1.000	−0.006
ϕ_ϵ	0.995	0.977	−0.312	0.981	−0.006	1.000

Fits for ϵ'/ϵ, $|\eta_{+-}|$, $|\eta_{00}|$, and B($K_L \to \pi\pi$)

We list measurements of $|\eta_{+-}|$, $|\eta_{00}|$, $|\eta_{00}/\eta_{+-}|$, and ϵ'/ϵ. Independent information on $|\eta_{+-}|$ and $|\eta_{00}|$ can be obtained from measurements of the K^0_L and K^0_S lifetimes (τ_L, τ_S), and branching ratios (B) to $\pi\pi$, using the relations

$$|\eta_{+-}| = \left[\frac{\mathrm{B}(K^0_L \to \pi^+\pi^-)}{\tau_L}\,\frac{\tau_S}{\mathrm{B}(K^0_S \to \pi^+\pi^-)}\right]^{1/2}, \quad (12a)$$

$$|\eta_{00}| = \left[\frac{\mathrm{B}(K^0_L \to \pi^0\pi^0)}{\tau_L}\,\frac{\tau_S}{\mathrm{B}(K^0_S \to \pi^0\pi^0)}\right]^{1/2}. \quad (12b)$$

For historical reasons, the branching ratio fits and the CP-violation fits are done separately, but we want to include the influence of $|\eta_{+-}|$, $|\eta_{00}|$, $|\eta_{00}/\eta_{+-}|$, and ϵ'/ϵ measurements on B($K^0_L \to \pi^+\pi^-$) and B($K^0_L \to \pi^0\pi^0$) and vice versa. We approximate a global fit to all of these measurements by first performing two independent fits: 1) BRFIT, a fit to the K^0_L branching ratios, rates, and mean life, and 2) ETAFIT, a fit to the $|\eta_{+-}|$, $|\eta_{00}|$, $|\eta_{+-}/\eta_{00}|$, and ϵ'/ϵ measurements. The results from fit 1, along with the K^0_S values from this edition, are used to compute values of $|\eta_{+-}|$ and $|\eta_{00}|$, which are included as measurements in the $|\eta_{00}|$ and $|\eta_{+-}|$ sections with a document ID of BRFIT 13. Thus, the fit values of $|\eta_{+-}|$ and $|\eta_{00}|$ given in this edition include both the direct measurements and the results from the branching ratio fit.

The process is reversed in order to include the direct $|\eta|$ measurements in the branching ratio fit. The results from fit 2 above (before including BRFIT 13 values) are used along with the K^0_L and K^0_S mean lives and the $K^0_S \to \pi\pi$ branching fractions to compute the K^0_L branching ratio $\Gamma(K^0_L \to \pi^0\pi^0)/\Gamma(K^0_L \to \pi^+\pi^-)$. This branching ratio value is included as a measurement in the branching ratio section with a document ID of ETAFIT 12. Thus, the K^0_L branching ratio fit values in this edition include the results of the direct measurement of $|\eta_{00}/\eta_{+-}|$ and ϵ'/ϵ. Most individual measurements of $|\eta_{+-}|$ and $|\eta_{00}|$ enter our fits directly via the corresponding measurements of $\Gamma(K^0_L \to \pi^+\pi^-)/\Gamma$(total) and $\Gamma(K^0_L \to \pi^0\pi^0)/\Gamma$(total), and those that do not have too large errors to have any influence on the fitted values of these branching ratios. A more detailed discussion of these fits is given in the 1990 edition of this *Review* [20].

References

1. K. Kleinknecht, "Uncovering CP violation: experimental clarification in the neutral K meson and B meson systems," *Springer Tracts in Modern Physics*, vol. 195 (Springer Verlag 2003).
2. B. Winstein and L. Wolfenstein, Rev. Mod. Phys. **65**, 1113 (1993).
3. M.S. Sozzi, Eur. Phys. J. **C36**, 37 (2004).
4. T.T. Wu and C.N. Yang, Phys. Rev. Lett. **13**, 380 (1964).
5. L. Wolfenstein, Phys. Rev. Lett. **13**, 562 (1964);
L. Wolfenstein, Comm. Nucl. Part. Phys. **21**, 275 (1994).
6. G. Colangelo, J. Gasser, and H. Leutwyler, Nucl. Phys. **B603**, 125 (2001).

7. R. Adler *et al.*, (CPLEAR Collab.), Phys. Lett. **B407**, 193 (1997);
P. Bloch, *Proceedings of Workshop on K Physics* (Orsay 1996), ed. L. Iconomidou-Fayard, Edition Frontieres, Gif-sur-Yvette, France (1997) p. 307.
8. A. Lai *et al.*, Phys. Lett. **B610**, 165 (2005).
9. G. Buchalla, A.J. Buras, and M.E. Lautenbacher, Rev. Mod. Phys. **68**, 1125 (1996);
S. Bosch *et al.*, Nucl. Phys. **B565**, 3 (2000);
S. Bertolini, M. Fabrichesi, and J.O. Egg, Rev. Mod. Phys. **72**, 65 (2000).
10. E. Abouzaid *et al.*, Phys. Rev. **D83**, 092001 (2011).
11. A. Apostolakis *et al.*, Phys. Lett. **B458**, 545 (1999).
12. B. Schwingenheuer *et al.*, Phys. Rev. Lett. **74**, 4376 (1995).
13. L.K. Gibbons *et al.*, Phys. Rev. Lett. **70**, 1199 (1993) and footnote in Ref. 12.
14. L.K. Gibbons, Thesis, RX-1487, Univ. of Chicago, 1993.
15. C. Geweniger *et al.*, Phys. Lett. **48B**, 487 (1974).
16. C. Geweniger *et al.*, Phys. Lett. **52B**, 108 (1974).
17. R. Carosi *et al.*, Phys. Lett. **B237**, 303 (1990).
18. A. Lai *et al.*, Phys. Lett. **B537**, 28 (2002).
19. L. Bertanza *et al.*, Z. Phys. **C73**, 629 (1997).
20. J.J. Hernandez *et al.*, Particle Data Group, Phys. Lett. **B239**, 1 (1990).

CP-VIOLATION PARAMETERS IN K_L^0 DECAYS

CHARGE ASYMMETRY IN $K_{\ell 3}^0$ DECAYS

Such asymmetry violates *CP*. It is related to Re(ϵ).

A_L = weighted average of $A_L(\mu)$ and $A_L(e)$

In previous editions and in the literature the symbol used for this asymmetry was δ_L or δ. We use A_L for consistency with B^0 asymmetry notation and with recent K_S^0 notation.

VALUE (%)	EVTS	DOCUMENT ID		TECN	COMMENT
0.332±0.006 OUR AVERAGE		Includes data from the 2 datablocks that follow this one.			
0.333±0.050	33M	WILLIAMS	73	ASPK	$K_{\mu 3}+K_{e3}$

$A_L(\mu) = [\Gamma(\pi^-\mu^+\nu_\mu) - \Gamma(\pi^+\mu^-\overline{\nu}_\mu)]$/SUM

Only the combined value below is put into the Meson Summary Table.

VALUE (%)	EVTS	DOCUMENT ID		TECN
The data in this block is included in the average printed for a previous datablock.				
0.304±0.025 OUR AVERAGE				
0.313±0.029	15M	GEWENIGER	74	ASPK
0.278±0.051	7.7M	PICCIONI	72	ASPK
• • • We do not use the following data for averages, fits, limits, etc. • • •				
0.60 ±0.14	4.1M	MCCARTHY	73	CNTR
0.57 ±0.17	1M	[1] PACIOTTI	69	OSPK
0.403±0.134	1M	[1] DORFAN	67	OSPK

[1] PACIOTTI 69 is a reanalysis of DORFAN 67 and is corrected for $\mu^+\mu^-$ range difference in MCCARTHY 72.

$A_L(e) = [\Gamma(\pi^-e^+\nu_e) - \Gamma(\pi^+e^-\overline{\nu}_e)]$/SUM

Only the combined value below is put into the Meson Summary Table.

VALUE (%)	EVTS	DOCUMENT ID		TECN
The data in this block is included in the average printed for a previous datablock.				
0.334 ±0.007 OUR AVERAGE				
0.3322±0.0058±0.0047	298M	ALAVI-HARATI	02	
0.341 ±0.018	34M	GEWENIGER	74	ASPK
0.318 ±0.038	40M	FITCH	73	ASPK
0.346 ±0.033	10M	MARX	70	CNTR
• • • We do not use the following data for averages, fits, limits, etc. • • •				
0.36 ±0.18	600k	ASHFORD	72	ASPK
0.246 ±0.059	10M	[1] SAAL	69	CNTR
0.224 ±0.036	10M	[1] BENNETT	67	CNTR

[1] SAAL 69 is a reanalysis of BENNETT 67.

PARAMETERS FOR $K_L^0 \to 2\pi$ DECAY

$\eta_{+-} = A(K_L^0 \to \pi^+\pi^-) / A(K_S^0 \to \pi^+\pi^-)$
$\eta_{00} = A(K_L^0 \to \pi^0\pi^0) / A(K_S^0 \to \pi^0\pi^0)$

The fitted values of $|\eta_{+-}|$ and $|\eta_{00}|$ given below are the results of a fit to $|\eta_{+-}|$, $|\eta_{00}|$, $|\eta_{00}/\eta_{+-}|$, and Re(ϵ'/ϵ). Independent information on $|\eta_{+-}|$ and $|\eta_{00}|$ can be obtained from the fitted values of the $K_L^0 \to \pi\pi$ and $K_S^0 \to \pi\pi$ branching ratios and the K_L^0 and K_S^0 lifetimes. This information is included as data in the $|\eta_{+-}|$ and $|\eta_{00}|$ sections with a Document ID "BRFIT." See the note "*CP* violation in K_L decays" above for details.

$|\eta_{00}| = |A(K_L^0 \to 2\pi^0) / A(K_S^0 \to 2\pi^0)|$

VALUE (units 10^{-3})	DOCUMENT ID		TECN	COMMENT
2.220±0.011 OUR FIT	Error includes scale factor of 1.8.			
2.243±0.014	BRFIT	13		
• • • We do not use the following data for averages, fits, limits, etc. • • •				
2.47 ±0.31 ±0.24	ANGELOPO...	98	CPLR	
2.49 ±0.40	[1] ADLER	96B	CPLR	Sup. by ANGELOPOULOS 98
2.33 ±0.18	CHRISTENS...	79	ASPK	
2.71 ±0.37	[2] WOLFF	71	OSPK	Cu reg., 4γ's
2.95 ±0.63	[2] CHOLLET	70	OSPK	Cu reg., 4γ's

[1] Error is statistical only.
[2] CHOLLET 70 gives $|\eta_{00}| = (1.23 \pm 0.24)\times$(regeneration amplitude, 2 GeV/c Cu)/10000mb. WOLFF 71 gives $|\eta_{00}| = (1.13 \pm 0.12)\times$(regeneration amplitude, 2 GeV/c Cu)/10000mb. We compute both $|\eta_{00}|$ values for (regeneration amplitude, 2 GeV/c Cu) = 24 ± 2mb. This regeneration amplitude results from averaging over FAISSNER 69, extrapolated using optical-model calculations of Bohm et al., Physics Letters **27B** 594 (1968) and the data of BALATS 71. (From H. Faissner, private communication).

$|\eta_{+-}| = |A(K_L^0 \to \pi^+\pi^-) / A(K_S^0 \to \pi^+\pi^-)|$

VALUE (units 10^{-3})	EVTS	DOCUMENT ID		TECN	COMMENT
2.232±0.011 OUR FIT	Error includes scale factor of 1.8.				
2.226±0.007	BRFIT	13			
• • • We do not use the following data for averages, fits, limits, etc. • • •					
2.223±0.012	[1] LAI	07	NA48		
2.219±0.013	[2] AMBROSINO	06F	KLOE		
2.228±0.010	[3] ALEXOPOU...	04	KTEV		
2.286±0.023±0.026	70M	[4] APOSTOLA...	99C	CPLR	K^0-$\overline{K}^0$ asymmetry
2.310±0.043±0.031		[5] ADLER	95B	CPLR	K^0-$\overline{K}^0$ asymmetry
2.32 ±0.14 ±0.03	10^5	ADLER	92B	CPLR	K^0-$\overline{K}^0$ asymmetry
2.30 ±0.035		GEWENIGER	74B	ASPK	

[1] Value obtained from the NA48 measurements of $\Gamma(K_L^0 \to \pi^+\pi^-)/\Gamma(K_L^0 \to \pi e\nu_e)$ and $\tau_{K_S^0}$ and KLOE measurements of $B(K_S^0 \to \pi^+\pi^-)$ and $\tau_{K_L^0}$. $\Gamma(K_L^0 \to \pi^+\pi^-)$ is defined to include the inner bremsstrahlung component $\Gamma(K_L^0 \to \pi^+\pi^-\gamma(\mathrm{IB}))$ but exclude the direct emission component $B(K_S^0 \to \pi^+\pi^-(\mathrm{DE}))$. Their $|\eta_{+-}|$ value is not directly used in our fit, but enters the fit via their branching ratio and lifetime measurements.
[2] AMBROSINO 06F uses KLOE branching ratios and τ_L together with τ_S from PDG 04. Their $|\eta_{+-}|$ value is not directly used in our fit, but enters the fit via their branching ratio and lifetime measurements.
[3] ALEXOPOULOS 04 $|\eta_{+-}|$ uses their $K_L^0 \to \pi\pi$ branching fractions, $\tau_S = (0.8963 \pm 0.0005)\times 10^{-10}$ s from the average of KTeV and NA48 τ_S measurements, and assumes that $\Gamma(K_S^0 \to \pi\ell\nu_\ell) = \Gamma(K_L^0 \to \pi\ell\nu_\ell)$ giving $B(K_S^0 \to \pi\ell\nu_\ell) = 0.118\%$. Their η_{+-} is not directly used in our fit, but enters our fit via their branching ratio measurements.
[4] APOSTOLAKIS 99C report $(2.264 \pm 0.023 \pm 0.026 + 9.1[\tau_S - 0.8934]) \times 10^{-3}$. We evaluate for our 2006 best value $\tau_S = (0.8958 \pm 0.0005) \times 10^{-10}$ s.
[5] ADLER 95B report $(2.312 \pm 0.043 \pm 0.030 - 1[\Delta m - 0.5274] + 9.1[\tau_S - 0.8926]) \times 10^{-3}$. We evaluate for our 1996 best values $\Delta m = (0.5304 \pm 0.0014) \times 10^{-10}\ \hbar s^{-1}$ and $\tau_S = (0.8927 \pm 0.0009) \times 10^{-10}$ s. Superseded by APOSTOLAKIS 99C.

$|\epsilon| = (2|\eta_{+-}| + |\eta_{00}|)/3$

This expression is a very good approximation, good to about one part in 10^{-4} because of the small measured value of $\phi_{00} - \phi_{+-}$ and small theoretical ambiguities.

VALUE (units 10^{-3})	DOCUMENT ID
2.228±0.011 OUR FIT	Error includes scale factor of 1.8.

$|\eta_{00}/\eta_{+-}|$

VALUE	EVTS	DOCUMENT ID		TECN
0.9950±0.0007 OUR FIT	Error includes scale factor of 1.6.			
0.9930±0.0020 OUR AVERAGE				
0.9931±0.0020		[1,2] BARR	93D	NA31
0.9904±0.0084±0.0036		[3] WOODS	88	E731
• • • We do not use the following data for averages, fits, limits, etc. • • •				
0.9939±0.0013±0.0015	1M	[1] BARR	93D	NA31
0.9899±0.0020±0.0025		[1] BURKHARDT	88	NA31

[1] This is the square root of the ratio R given by BURKHARDT 88 and BARR 93D.
[2] This is the combined results from BARR 93D and BURKHARDT 88, taking into account a common systematic uncertainty of 0.0014.
[3] We calculate $|\eta_{00}/\eta_{+-}| = 1 - 3(\epsilon'/\epsilon)$ from WOODS 88 (ϵ'/ϵ) value.

$\mathrm{Re}(\epsilon'/\epsilon) = (1-|\eta_{00}/\eta_{+-}|)/3$

We have neglected terms of order $\omega\cdot\mathrm{Re}(\epsilon'/\epsilon)$, where $\omega = \mathrm{Re}(A_2)/\mathrm{Re}(A_0) \simeq 1/22$. If included, this correction would lower $\mathrm{Re}(\epsilon'/\epsilon)$ by about 0.04×10^{-3}. See SOZZI 04.

VALUE (units 10^{-3})		DOCUMENT ID		TECN	COMMENT
1.66 ±0.23	**OUR FIT**	Error includes scale factor of 1.6.			
1.68 ±0.20	**OUR AVERAGE**	Error includes scale factor of 1.4. See the ideogram below.			
1.92 ±0.21		[1] ABOUZAID	11	KTEV	Assuming *CPT*
1.47 ±0.22		BATLEY	02	NA48	
0.74 ±0.52 ±0.29		GIBBONS	93B	E731	
• • • We use the following data for averages but not for fits. • • •					
2.3 ±0.65		[2,3] BARR	93D	NA31	
• • • We do not use the following data for averages, fits, limits, etc. • • •					
2.110±0.343		[1,4] ABOUZAID	11	KTEV	Not assuming *CPT*
2.07 ±0.28		ALAVI-HARATI	03	KTEV	In ABOUZAID 11
1.53 ±0.26		LAI	01C	NA48	Incl. in BATLEY 02
2.80 ±0.30 ±0.28		ALAVI-HARATI	99D	KTEV	In ALAVI-HARATI 03
1.85 ±0.45 ±0.58		FANTI	99C	NA48	In LAI 01C
2.0 ±0.7		[5] BARR	93D	NA31	
−0.4 ±1.4 ±0.6		PATTERSON	90	E731	in GIBBONS 93B
3.3 ±1.1		[5] BURKHARDT	88	NA31	
3.2 ±2.8 ±1.2		[2] WOODS	88	E731	

[1] The two ABOUZAID 11 values use the same data. The fits are performed with and without *CPT* invariance requirement.

[2] These values are derived from $|\eta_{00}/\eta_{+-}|$ measurements. They enter the average in this section but enter the fit via the $|\eta_{00}/\eta_{+-}|$ only.

[3] This is the combined results from BARR 93D and BURKHARDT 88, taking into account their common systematic uncertainty.

[4] We use ABOUZAID 11 $\mathrm{Re}(\epsilon'/\epsilon)$ value with *CPT* assumption in our fits for $|\eta_{+-}|$, $|\eta_{00}|$, and $\mathrm{Re}(\epsilon'/\epsilon)$.

[5] These values are derived from $|\eta_{00}/\eta_{+-}|$ measurements.

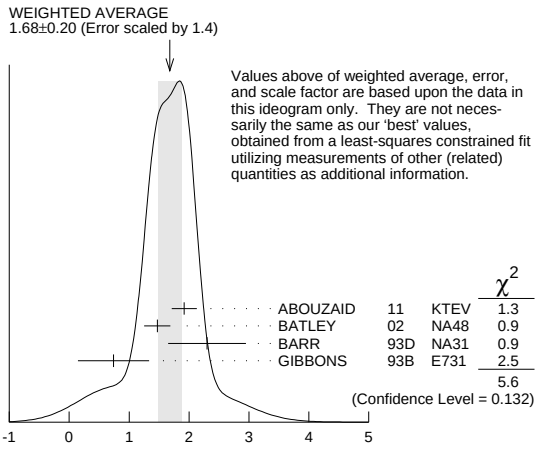

ϕ_{+-}, PHASE of η_{+-}

The dependence of the phase on Δm and τ_S is given for each experiment in the comments below, where Δm is the $K_L^0 - K_S^0$ mass difference in units $10^{10}\ \hbar s^{-1}$ and τ_S is the K_S mean life in units 10^{-10} s. We also give the regeneration phase ϕ_f in the comments below.

OUR FIT is described in the note on "*CP* violation in K_L decays" in the K_L^0 Particle Listings. Most experiments in this section are included in both the "Not Assuming *CPT*" and "Assuming *CPT*" fits. In the latter fit, they have little direct influence on ϕ_{+-} because their errors are large compared to that assuming *CPT*, but they influence Δm and τ_S through their dependencies on these parameters, which are given in the footnotes.

VALUE (°)	EVTS	DOCUMENT ID		TECN	COMMENT
43.51±0.05	**OUR FIT**	Error includes scale factor of 1.2. Assuming *CPT*			
43.4 ±0.5	**OUR FIT**	Error includes scale factor of 1.2. Not assuming *CPT*			
42.9 ±0.6 ±0.3	70M	[1] APOSTOLA...	99C	CPLR	K^0-$\overline{K}^0$ asymmetry
42.9 ±0.8 ±0.2		[2,3] SCHWINGEN...	95	E773	$CH_{1.1}$ regenerator
41.4 ±0.9 ±0.2		[3,4] GIBBONS	93	E731	B_4C regenerator
44.5 ±1.6 ±0.6		[5] CAROSI	90	NA31	Vacuum regen.
43.3 ±1.0 ±0.5		[6] GEWENIGER	74B	ASPK	Vacuum regen.
• • • We do not use the following data for averages, fits, limits, etc. • • •					
43.76±0.64		[7] ABOUZAID	11	KTEV	Not assuming *CPT*
44.12±0.72±1.20		[8] ALAVI-HARATI	03	KTEV	Not assuming *CPT*
42.5 ±0.4 ±0.3		[9,10] ADLER	96C	RVUE	
43.4 ±1.1 ±0.3		[11] ADLER	95B	CPLR	K^0-$\overline{K}^0$ asymmetry
42.3 ±4.4 ±1.4	100k	[12] ADLER	92B	CPLR	K^0-$\overline{K}^0$ asymmetry
47.7 ±2.0 ±0.9		[3,13] KARLSSON	90	E731	
44.3 ±2.8 ±0.2		[14] CARITHERS	75	SPEC	C regenerator

[1] APOSTOLAKIS 99C measures $\phi_{+-} = (43.19\pm0.53\pm0.28) + 300\,[\Delta m - 0.5301]$ (°). We have adjusted the measurement to use our best values of ($\Delta m = 0.5293 \pm 0.0009$) ($10^{10}\ \hbar\ s^{-1}$). Our first error is their experiment's error and our second error is the systematic error from using our best values.

[2] SCHWINGENHEUER 95 measures $\phi_{+-} = (43.53\pm0.76) + 173\,[\Delta m - 0.5282] - 275\,[\tau_S - 0.8926]$ (°). We have adjusted the measurement to use our best values of ($\Delta m = 0.5293 \pm 0.0009$) ($10^{10}\ \hbar\ s^{-1}$), ($\tau_S = 0.8954 \pm 0.0004$) ($10^{-10}$ s). Our first error is their experiment's error and our second error is the systematic error from using our best values.

[3] These experiments measure ϕ_{+-}–ϕ_f and calculate the regeneration phase from the power law momentum dependence of the regeneration amplitude using analyticity and dispersion relations. SCHWINGENHEUER 95 [GIBBONS 93] includes a systematic error of 0.35° [0.5°] for uncertainties in their modeling of the regeneration amplitude.

[4] GIBBONS 93 measures $\phi_{+-} = (42.21 \pm 0.9) + 189\,[\Delta m - 0.5257] - 460\,[\tau_S - 0.8922]$ (°). We have adjusted the measurement to use our best values of ($\Delta m = 0.5293 \pm 0.0009$) ($10^{10}\ \hbar\ s^{-1}$), ($\tau_S = 0.8954 \pm 0.0004$) ($10^{-10}$ s). Our first error is their experiment's error and our second error is the systematic error from using our best values. This is actually reported in SCHWINGENHEUER 95, footnote 8. GIBBONS 93 reports ϕ_{+-} (42.2 ± 1.4)°. They measure ϕ_+–ϕ_f and calculate the regeneration phase ϕ_f from the power law momentum dependence of the regeneration amplitude using analyticity. An error of 0.6° is included for possible uncertainties in the regeneration phase.

[5] CAROSI 90 measures $\phi_{+-} = (46.9 \pm 1.4 \pm 0.7) + 579\,[\Delta m - 0.5351] + 303\,[\tau_S - 0.8922]$ (°). We have adjusted the measurement to use our best values of ($\Delta m = 0.5293 \pm 0.0009$) ($10^{10}\ \hbar\ s^{-1}$), ($\tau_S = 0.8954 \pm 0.0004$) ($10^{-10}$ s). Our first error is their experiment's error and our second error is the systematic error from using our best values.

[6] GEWENIGER 74B measures $\phi_{+-} = (49.4 \pm 1.0) + 565\,[\Delta m - 0.540]$ (°). We have adjusted the measurement to use our best values of ($\Delta m = 0.5293 \pm 0.0009$) ($10^{10}\ \hbar\ s^{-1}$). Our first error is their experiment's error and our second error is the systematic error from using our best values.

[7] Not independent of other phase parameters reported in ABOUZAID 11.

[8] ALAVI-HARATI 03 ϕ_{+-} is correlated with their $\Delta m = m_{K_L^0} - m_{K_S^0}$ and τ_{K_S} measurements in the K_L^0 and K_S^0 sections respectively. The correlation coefficients are $\rho(\phi_{+-},\Delta m)=+0.955$, $\rho(\phi_{+-},\tau_S)=-0.871$, and $\rho(\tau_S,\Delta m)=-0.840$. *CPT* is not assumed. Uses scintillator Pb regenerator. Superseded by ABOUZAID 11.

[9] ADLER 96C measures $\phi_{+-} = (43.82 \pm 0.41) + 339\,[\Delta m - 0.5307] - 252\,[\tau_S - 0.8922]$ (°). We have adjusted the measurement to use our best values of ($\Delta m = 0.5293 \pm 0.0009$) ($10^{10}\ \hbar\ s^{-1}$), ($\tau_S = 0.8954 \pm 0.0004$) ($10^{-10}$ s). Our first error is their experiment's error and our second error is the systematic error from using our best values.

[10] ADLER 96C is the result of a fit which includes nearly the same data as entered into the "OUR FIT" value in the 1996 edition of this Review (Physical Review **D54** 1 (1996)).

[11] ADLER 95B measures $\phi_{+-} = (42.7 \pm 0.9 \pm 0.6) + 316\,[\Delta m - 0.5274] + 30\,[\tau_S - 0.8926]$ (°). We have adjusted the measurement to use our best values of ($\Delta m = 0.5293 \pm 0.0009$) ($10^{10}\ \hbar\ s^{-1}$), ($\tau_S = 0.8954 \pm 0.0004$) ($10^{-10}$ s). Our first error is their experiment's error and our second error is the systematic error from using our best values.

[12] ADLER 92B quote separately two systematic errors: ±0.4 from their experiment and ±1.0 degrees due to the uncertainty in the value of Δm.

[13] KARLSSON 90 systematic error does not include regeneration phase uncertainty.

[14] CARITHERS 75 measures $\phi_{+-} = (45.5 \pm 2.8) + 224\,[\Delta m - 0.5348]$ (°). We have adjusted the measurement to use our best values of ($\Delta m = 0.5293 \pm 0.0009$) ($10^{10}\ \hbar\ s^{-1}$). Our first error is their experiment's error and our second error is the systematic error from using our best values. $\phi_f = -40.9 \pm 2.6$°.

ϕ_{00}, PHASE OF η_{00}

See comment in ϕ_{+-} header above for treatment of Δm and τ_S dependence, as well as for the inclusion of data in both the "Assuming *CPT*" and "Not Assuming *CPT*" fits.

OUR FIT is described in the note on "*CP* violation in K_L decays" in the K_L^0 Particle Listings.

VALUE (°)	DOCUMENT ID		TECN	COMMENT
43.52±0.05 **OUR FIT**	Error includes scale factor of 1.3. Assuming *CPT*			
43.7 ±0.6 **OUR FIT**	Error includes scale factor of 1.2. Not assuming *CPT*			
44.5 ±2.3 ±0.5	[1] CAROSI	90	NA31	
• • • We do not use the following data for averages, fits, limits, etc. • • •				
44.06±0.68	[2] ABOUZAID	11	KTEV	Not assuming *CPT*
41.7 ±5.9 ±0.2	[3] ANGELOPO...	98	CPLR	
50.8 ±7.1 ±1.7	[4] ADLER	96B	CPLR	Sup. by ANGELOPOULOS 98
47.4 ±1.4 ±0.9	[5] KARLSSON	90	E731	

[1] CAROSI 90 measures $\phi_{00} = (47.1 \pm 2.1 \pm 1.0) + 579\,[\Delta m - 0.5351] + 252\,[\tau_S - 0.8922]$ (°). We have adjusted the measurement to use our best values of ($\Delta m = 0.5293 \pm 0.0009$) ($10^{10}\ \hbar\ s^{-1}$), ($\tau_S = 0.8954 \pm 0.0004$) ($10^{-10}$ s). Our first error is their experiment's error and our second error is the systematic error from using our best values.

[2] Not independent of other phase parameters reported in ABOUZAID 11.

[3] ANGELOPOULOS 98 measures $\phi_{00} = (42.0 \pm 5.6 \pm 1.9) + 240\,[\Delta m - 0.5307]$ (°). We have adjusted the measurement to use our best values of ($\Delta m = 0.5293 \pm 0.0009$) ($10^{10}\ \hbar\ s^{-1}$). Our first error is their experiment's error and our second error is the systematic error from using our best values. The τ_S dependence is negligible.

[4] ADLER 96B identified initial neutral kaon individually as being a K^0 or a $\overline{K}^0$. The systematic uncertainty is ±1.5° combined in quadrature with ±0.8° due to Δm.

[5] KARLSSON 90 systematic error does not include regeneration phase uncertainty.

Meson Particle Listings

K_L^0

$\phi_\epsilon = (2\phi_{+-} + \phi_{00})/3$

This expression is a very good approximation, good to about 10^{-3} degrees because of the small measured values of $\phi_{00} - \phi_{+-}$ and Re ϵ'/ϵ, and small theoretical ambiguities.

VALUE (°)			DOCUMENT ID		TECN	COMMENT
43.52	**±0.05**	**OUR FIT**	Error includes scale factor of 1.2. Assuming *CPT*			
43.5	**±0.5**	**OUR FIT**	Error includes scale factor of 1.3. Not assuming *CPT*			
43.5164	±0.0002±0.0518		[1] SUPERWEAK	13		Assuming *CPT*
43.86	±0.63		[2] ABOUZAID	11	KTEV	Not assuming *CPT*

[1] SUPERWEAK 13 is a fake measurement used to impose the *CPT* or Superweak constraint $\phi_{+-} = \phi_{SW} = \tan^{-1}[2\,\frac{\Delta m}{\hbar}\,(\frac{\tau_S\tau_L}{\tau_L-\tau_S})]$. This "measurement" is linearized using values near the PDG 04 edition values of Δm, τ_S and τ_L, and then adjusted to our current values as described in the following "measurement". SUPERWEAK 13 measures $\phi_\epsilon = (43.50258 \pm 0.00021) + 54.1\ [\Delta m - 0.5289] + 32.0\ [\tau_S - 0.89564]$ (°). We have adjusted the measurement to use our best values of ($\Delta m = 0.5293 \pm 0.0009$) ($10^{10}\ \hbar$ s^{-1}), ($\tau_S = 0.8954 \pm 0.0004$) ($10^{-10}$ s). Our first error is their experiment's error and our second error is the systematic error from using our best values.

[2] ABOUZAID 11 uses the full KTeV dataset collected in 1996, 1997, and 1999. See Im(ϵ'/ϵ) section for correlation information.

Im(ϵ'/ϵ) $= -(\phi_{00} - \phi_{+-})/3$

For small $|\epsilon'/\epsilon|$, Im(ϵ'/ϵ) is related to the phases of η_{00} and η_{+-} by the above expression.

VALUE (°)			DOCUMENT ID		TECN	COMMENT
−0.002	**±0.005**	**OUR FIT**	Error includes scale factor of 1.7. Assuming *CPT*			
−0.11	**±0.11**	**OUR FIT**	Not assuming *CPT*			
−0.0985	**±0.1157**		[1] ABOUZAID	11	KTEV	Not assuming *CPT*

[1] ABOUZAID 11 uses the full KTeV dataset collected in 1996, 1997, and 1999. The fit has Δm, τ_S, ϕ_ϵ, Re(ϵ'/ϵ), and Im(ϵ'/ϵ) as free parameters. The reported value of Im(ϵ'/ϵ) $= (-17.20 \pm 20.20) \times 10^{-4}$ rad. The correlation coefficients are $\rho(\phi_\epsilon, \Delta m) = 0.828$, $\rho(\phi_\epsilon, \tau_S) = -0.765$, $\rho(\Delta m, \tau_S) = -0.858$, $\rho(\text{Im}(\epsilon'/\epsilon), \phi_\epsilon) = -0.041$, $\rho(\text{Im}(\epsilon'/\epsilon), \Delta m) = 0.026$, $\rho(\text{Im}(\epsilon'/\epsilon), \tau_S) = -0.010$.

DECAY-PLANE ASYMMETRY IN $\pi^+\pi^- e^+ e^-$ DECAYS

This is the *CP*-violating asymmetry

$$A = \frac{N_{\sin\phi\cos\phi>0.0} - N_{\sin\phi\cos\phi<0.0}}{N_{\sin\phi\cos\phi>0.0} + N_{\sin\phi\cos\phi<0.0}}$$

where ϕ is the angle between the e^+e^- and $\pi^+\pi^-$ planes in the K_L^0 rest frame.

CP ASYMMETRY *A* in $K_L^0 \to \pi^+\pi^- e^+ e^-$

VALUE (%)		DOCUMENT ID		TECN
13.7±1.5 OUR AVERAGE				
13.6±1.4±1.5		ABOUZAID	06	KTEV
14.2±3.0±1.9		LAI	03C	NA48
13.6±2.5±1.2		ALAVI-HARATI	00B	KTEV

PARAMETERS FOR $e^+e^-e^+e^-$ DECAYS

These are the *CP*-violating parameters in the ϕ distribution, where ϕ is the angle between the planes of the two e^+e^- pairs in the kaon rest frame:

$$d\Gamma/d\phi \propto 1 + \beta_{CP}\cos(2\phi) + \gamma_{CP}\sin(2\phi)$$

β_{CP} from $K_L^0 \to e^+e^-e^+e^-$

VALUE	EVTS	DOCUMENT ID		TECN	COMMENT
−0.19±0.07 OUR AVERAGE					
−0.13±0.10±0.03	200	[1] LAI	05B	NA48	
−0.23±0.09±0.02	441	ALAVI-HARATI	01D	KTEV	$M_{ee} > 8$ MeV/c^2

[1] LAI 05B obtains $\beta_{CP} = -0.13 \pm 0.10$ (stat) if $\gamma_{CP} = 0$ is assumed.

γ_{CP} from $K_L^0 \to e^+e^-e^+e^-$

VALUE	EVTS	DOCUMENT ID		TECN	COMMENT
0.01±0.11 OUR AVERAGE		Error includes scale factor of 1.6.			
+0.13±0.10±0.03	200	LAI	05B	NA48	
−0.09±0.09±0.02	441	ALAVI-HARATI	01D	KTEV	$M_{ee} > 8$ MeV/c^2

CHARGE ASYMMETRY IN $\pi^+\pi^-\pi^0$ DECAYS

These are *CP*-violating charge-asymmetry parameters, defined at beginning of section "LINEAR COEFFICIENT *g* FOR $K_L^0 \to \pi^+\pi^-\pi^0$ above.

See also note on Dalitz plot parameters in $K^\pm$ section and note on "*CP* violation in K_L decays" above.

LINEAR COEFFICIENT *j* FOR $K_L^0 \to \pi^+\pi^-\pi^0$

VALUE	EVTS	DOCUMENT ID		TECN	
0.0012±0.0008 OUR AVERAGE					
0.0010±0.0024±0.0030	500k	ANGELOPO...	98C	CPLR	
−0.001 ±0.011	6499	CHO	77		
0.001 ±0.003	4709	PEACH	77		
0.0013±0.0009	3M	SCRIBANO	70		
0.0 ±0.017	4400	SMITH	70	OSPK	
0.001 ±0.004	238k	BLANPIED	68		

QUADRATIC COEFFICIENT *f* FOR $K_L^0 \to \pi^+\pi^-\pi^0$

VALUE	EVTS	DOCUMENT ID		TECN
0.0045±0.0024±0.0059	500k	ANGELOPO...	98C	CPLR

PARAMETERS for $K_L^0 \to \pi^+\pi^-\gamma$ DECAY

$|\eta_{+-\gamma}| = |A(K_L^0 \to \pi^+\pi^-\gamma,\ CP \text{ violating})/A(K_S^0 \to \pi^+\pi^-\gamma)|$

VALUE (units 10^{-3})	EVTS	DOCUMENT ID		TECN
2.35 ±0.07 OUR AVERAGE				
2.359±0.062±0.040	9045	MATTHEWS	95	E773
2.15 ±0.26 ±0.20	3671	RAMBERG	93B	E731

$\phi_{+-\gamma}$ = phase of $\eta_{+-\gamma}$

VALUE (°)	EVTS	DOCUMENT ID		TECN
44 ± 4 OUR AVERAGE				
43.8± 3.5± 1.9	9045	MATTHEWS	95	E773
72 ±23 ±17	3671	RAMBERG	93B	E731

$|\epsilon'_{+-\gamma}|/\epsilon$ for $K_L^0 \to \pi^+\pi^-\gamma$

VALUE	CL%	EVTS	DOCUMENT ID		TECN
<0.3	90	3671	[1] RAMBERG	93B	E731

[1] RAMBERG 93B limit on $|\epsilon'_{+-\gamma}|/\epsilon$ assumes than any difference between η_{+-} and $\eta_{+-\gamma}$ is due to direct *CP* violation.

$|g_{E1}|$ for $K_L^0 \to \pi^+\pi^-\gamma$

This parameter is the amplitude of the direct emission of a *CP* violating E1 electric dipole photon.

VALUE	CL%	EVTS	DOCUMENT ID		TECN	COMMENT
<0.21	90	111k	ABOUZAID	06A	KTEV	$E^*_\gamma > 20$ MeV

T VIOLATION TESTS IN K_L^0 DECAYS

Im(ξ) in $K^0_{\mu 3}$ DECAY (from transverse μ pol.)

Test of *T* reversal invariance.

VALUE	EVTS	DOCUMENT ID		TECN	COMMENT
−0.007±0.026 OUR AVERAGE					
0.009±0.030	12M	MORSE	80	CNTR	Polarization
0.35 ±0.30	207k	[1] CLARK	77	SPEC	POL, t=0
−0.085±0.064	2.2M	[2] SANDWEISS	73	CNTR	POL, t=0
−0.02 ±0.08		LONGO	69	CNTR	POL, t=3.3
−0.2 ±0.6		ABRAMS	68B	OSPK	Polarization
• • • We do not use the following data for averages, fits, limits, etc. • • •					
0.012±0.026		SCHMIDT	79	CNTR	Repl. by MORSE 80

[1] CLARK 77 value has additional $\xi(0)$ dependence $+0.21\text{Re}[\xi(0)]$.

[2] SANDWEISS 73 value corrected from value quoted in their paper due to new value of Re(ξ). See footnote 4 of SCHMIDT 79.

CPT-INVARIANCE TESTS IN K_L^0 DECAYS

PHASE DIFFERENCE $\phi_{00} - \phi_{+-}$

Test of *CPT*.

OUR FIT is described in the note on "*CP* violation in K_L decays" in the K_L^0 Particle Listings.

VALUE (°)		DOCUMENT ID		TECN	COMMENT
0.006±0.014 OUR FIT	Error includes scale factor of 1.7. Assuming *CPT*				
0.34 ±0.32 OUR FIT	Not assuming *CPT*				
0.006±0.008		[1] SUPERWEAK	13		Assuming *CPT*
−0.30 ±0.88		[2] SCHWINGEN...	95		Combined E731, E773
• • • We do not use the following data for averages, fits, limits, etc. • • •					
0.30 ±0.35		[3] ABOUZAID	11	KTEV	Not assuming *CPT*
0.39 ±0.22 ±0.45		[4] ALAVI-HARATI	03	KTEV	
0.62 ±0.71 ±0.75		SCHWINGEN...	95	E773	
−1.6 ±1.2		[5] GIBBONS	93	E731	
0.2 ±2.6 ±1.2		[6] CAROSI	90	NA31	
−0.3 ±2.4 ±1.2		KARLSSON	90	E731	

[1] SUPERWEAK 13 is a fake experiment to constrain $\phi_{00} - \phi_{+-}$ to a small value as described in the note "*CP* violation in K_L decays."

[2] This SCHWINGENHEUER 95 values is the combined result of SCHWINGENHEUER 95 and GIBBONS 93, accounting for correlated systematic errors.

[3] Not independent of other phase parameters reported in ABOUZAID 11.

[4] ALAVI-HARATI 03 fit Re(ϵ'/ϵ), Im(ϵ'/ϵ), Δm, τ_S, and ϕ_{+-} simultaneously, not assuming *CPT*. Phase difference is obtained from $\phi_{00} - \phi_{+-} \approx -3\text{Im}(\epsilon'/\epsilon)$ for small $|\epsilon'/\epsilon|$. Superseded by ABOUZAID 11.

[5] GIBBONS 93 give detailed dependence of systematic error on lifetime (see the section on the K_S^0 mean life) and mass difference (see the section on $m_{K_L^0} - m_{K_S^0}$).

[6] CAROSI 90 is excluded from the fit because it it is not independent of ϕ_{+-} and ϕ_{00} values.

PHASE DIFFERENCE $\phi_{+-} - \phi_{SW}$

Test of *CPT*. The Superweak phase $\phi_{SW} \equiv \tan^{-1}(2\Delta m/\Delta\Gamma)$ where $\Delta m = m_{K^0_L} - m_{K^0_S}$ and $\Delta\Gamma = \hbar(\tau_L - \tau_S)/(\tau_L\tau_S)$.

VALUE (°)	DOCUMENT ID		TECN
0.61±0.62±1.01	[1] ALAVI-HARATI 03		KTEV

[1] ALAVI-HARATI 03 fit is the same as their ϕ_{+-}, τ_{K_S}, Δm fit, except that the parameter $\phi_{+-} - \phi_{SW}$ is used in place of ϕ.

Re($\frac{2}{3}\eta_{+-} + \frac{1}{3}\eta_{00}$)$-\frac{A_L}{2}$

Test of *CPT*

VALUE (units 10^{-6})	DOCUMENT ID		TECN	COMMENT
−3±35	[1] ALAVI-HARATI 02		E799	Uses A_L from K_{e3} decays

[1] ALAVI-HARATI 02 uses PDG 00 values of η_{+-} and η_{00}.

$\Delta S = \Delta Q$ IN K^0 DECAYS

The relative amount of $\Delta S \neq \Delta Q$ component present is measured by the parameter x, defined as

$$x = A(\overline{K}^0 \to \pi^-\ell^+\nu)/A(K^0 \to \pi^-\ell^+\nu) \ .$$

We list Re{x} and Im{x} for K_{e3} and $K_{\mu3}$ combined.

$x = A(\overline{K}^0 \to \pi^-\ell^+\nu)/A(K^0 \to \pi^-\ell^+\nu) = A(\Delta S{=}-\Delta Q)/A(\Delta S{=}\Delta Q)$

REAL PART OF x

VALUE	EVTS	DOCUMENT ID		TECN	COMMENT
−0.0018±0.0041±0.0045		ANGELOPO...	98D	CPLR	K_{e3} from K^0
• • • We do not use the following data for averages, fits, limits, etc. • • •					
$0.10\ ^{+0.18}_{-0.19}$	79	SMITH	75B	WIRE	$\pi^- p \to K^0\Lambda$
0.04 ±0.03	4724	NIEBERGALL	74	ASPK	$K^+ p \to K^0 p\pi^+$
−0.008 ±0.044	1757	FACKLER	73	OSPK	K_{e3} from K^0
−0.03 ±0.07	1367	HART	73	OSPK	K_{e3} from $K^0\Lambda$
−0.070 ±0.036	1079	MALLARY	73	OSPK	K_{e3} from $K^0\Lambda$X
0.03 ±0.06	410	[1] BURGUN	72	HBC	$K^+ p \to K^0 p\pi^+$
$0.04\ ^{+0.10}_{-0.13}$	100	[2] GRAHAM	72	OSPK	$K_{\mu3}$ from $K^0\Lambda$
−0.05 ±0.09	442	[2] GRAHAM	72	OSPK	$\pi^- p \to K^0\Lambda$
$0.26\ ^{+0.10}_{-0.14}$	126	MANN	72	HBC	$K^- p \to n\overline{K}^0$
−0.13 ±0.11	342	[2] MANTSCH	72	OSPK	K_{e3} from $K^0\Lambda$
$0.04\ ^{+0.07}_{-0.08}$	222	[1] BURGUN	71	HBC	$K^+ p \to K^0 p\pi^+$
$0.25\ ^{+0.07}_{-0.09}$	252	WEBBER	71	HBC	$K^- p \to n\overline{K}^0$
0.12 ±0.09	215	[3] CHO	70	DBC	$K^+ d \to K^0 pp$
−0.020 ±0.025		[4] BENNETT	69	CNTR	Charge asym+ Cu regen.
$0.09\ ^{+0.14}_{-0.16}$	686	LITTENBERG	69	OSPK	$K^+ n \to K^0 p$
0.03 ±0.03		[4] BENNETT	68	CNTR	
$0.09\ ^{+0.07}_{-0.09}$	121	JAMES	68	HBC	$\overline{p}p$
$0.17\ ^{+0.16}_{-0.35}$	116	FELDMAN	67B	OSPK	$\pi^- p \to K^0\Lambda$
0.17 ±0.10	335	[3] HILL	67	DBC	$K^+ d \to K^0 pp$
$0.035\ ^{+0.11}_{-0.13}$	196	AUBERT	65	HLBC	K^+ charge exch.
$0.06\ ^{+0.18}_{-0.44}$	152	[5] BALDO-...	65	HLBC	K^+ charge exch.
−0.08 $^{+0.16}_{-0.28}$	109	[6] FRANZINI	65	HBC	$\overline{p}p$

[1] BURGUN 72 is a final result which includes BURGUN 71.
[2] First GRAHAM 72 value is second GRAHAM 72 value combined with MANTSCH 72.
[3] CHO 70 is analysis of unambiguous events in new data and HILL 67.
[4] BENNETT 69 is a reanalysis of BENNETT 68.
[5] BALDO-CEOLIN 65 gives x and θ converted by us to Re(x) and Im(x).
[6] FRANZINI 65 gives x and θ for Re(x) and Im(x). See SCHMIDT 67.

IMAGINARY PART OF x

Assumes $m_{K^0_L} - m_{K^0_S}$ positive. See Listings above.

VALUE	EVTS	DOCUMENT ID		TECN	COMMENT
0.0012±0.0019±0.0009	640k	ANGELOPO...	01B	CPLR	K_{e3} from K^0
• • • We do not use the following data for averages, fits, limits, etc. • • •					
0.0012±0.0019	640k	[1] ANGELOPO...	98E	CPLR	K_{e3} from K^0
$-0.10\ ^{+0.16}_{-0.19}$	79	SMITH	75B	WIRE	$\pi^- p \to K^0\Lambda$
−0.06 ±0.05	4724	NIEBERGALL	74	ASPK	$K^+ p \to K^0 p\pi^+$
−0.017 ±0.060	1757	FACKLER	73	OSPK	K_{e3} from K^0
0.09 ±0.07	1367	HART	73	OSPK	K_{e3} from $K^0\Lambda$
$0.107\ ^{+0.092}_{-0.074}$	1079	MALLARY	73	OSPK	K_{e3} from $K^0\Lambda$X
$0.07\ ^{+0.06}_{-0.07}$	410	[2] BURGUN	72	HBC	$K^+ p \to K^0 p\pi^+$
$0.12\ ^{+0.17}_{-0.16}$	100	[3] GRAHAM	72	OSPK	$K_{\mu3}$ from $K^0\Lambda$
0.05 ±0.13	442	[3] GRAHAM	72	OSPK	$\pi^- p \to K^0\Lambda$
$0.21\ ^{+0.15}_{-0.12}$	126	MANN	72	HBC	$K^- p \to n\overline{K}^0$
−0.04 ±0.16	342	[3] MANTSCH	72	OSPK	K_{e3} from $K^0\Lambda$
$0.12\ ^{+0.08}_{-0.09}$	222	[2] BURGUN	71	HBC	$K^+ p \to K^0 p\pi^+$
0.0 ±0.08	252	WEBBER	71	HBC	$K^- p \to n\overline{K}^0$
−0.08 ±0.07	215	[4] CHO	70	DBC	$K^+ d \to K^0 pp$
$-0.11\ ^{+0.10}_{-0.11}$	686	LITTENBERG	69	OSPK	$K^+ n \to K^0 p$
$+0.22\ ^{+0.37}_{-0.29}$	121	JAMES	68	HBC	$\overline{p}p$
0.0 ±0.25	116	FELDMAN	67B	OSPK	$\pi^- p \to K^0\Lambda$
−0.20 ±0.10	335	[4] HILL	67	DBC	$K^+ d \to K^0 pp$
$-0.21\ ^{+0.11}_{-0.15}$	196	AUBERT	65	HLBC	K^+ charge exch.
$-0.44\ ^{+0.32}_{-0.19}$	152	[5] BALDO-...	65	HLBC	K^+ charge exch.
$+0.24\ ^{+0.40}_{-0.30}$	109	[6] FRANZINI	65	HBC	$\overline{p}p$

[1] Superseded by ANGELOPOULOS 01B.
[2] BURGUN 72 is a final result which includes BURGUN 71.
[3] First GRAHAM 72 value is second GRAHAM 72 value combined with MANTSCH 72.
[4] Footnote 10 of HILL 67 should read +0.58, not −0.58 (private communication) CHO 70 is analysis of unambiguous events in new data and HILL 67.
[5] BALDO-CEOLIN 65 gives x and θ converted by us to Re(x) and Im(x).
[6] FRANZINI 65 gives x and θ for Re(x) and Im(x). See SCHMIDT 67.

K^0_L REFERENCES

BRFIT	13	RPP 2013 WWW edition	C.-J. Lin	(PDG Collab.)
ETAFIT	13	RPP 2013 WWW edition	C.-J. Lin	(PDG Collab.)
SUPERWEAK	13	RPP 2013 WWW edition	C.-J. Lin	(PDG Collab.)
ABOUZAID	11	PR D83 092001	E. Abouzaid *et al.*	(FNAL KTeV Collab.)
ABOUZAID	11A	PRL 107 201803	E. Abouzaid *et al.*	(KTeV Collab.)
OGATA	11	PR D84 052009	R. Ogata *et al.*	(KEK E391a Collab.)
TUNG	11	PR D83 031101	Y.C. Tung *et al.*	(KEK E391a Collab.)
ABOUZAID	10	PR D81 052001	E. Abouzaid *et al.*	(FNAL KTeV Collab.)
AHN	10	PR D81 072004	J.K. Ahn *et al.*	(KEK E391a Collab.)
ABOUZAID	08	PR D77 112004	E. Abouzaid *et al.*	(FNAL KTeV Collab.)
ABOUZAID	08A	PR D78 032009	E. Abouzaid *et al.*	(FNAL KTeV Collab.)
ABOUZAID	08B	PR D78 032014	E. Abouzaid *et al.*	(FNAL KTeV Collab.)
ABOUZAID	08C	PRL 100 131803	E. Abouzaid *et al.*	(FNAL KTeV Collab.)
AHN	08	PRL 100 201802	J.K. Ahn *et al.*	(KEK E391a Collab.)
AMBROSINO	08F	EPJ C55 539	F. Ambrosino *et al.*	(KLOE Collab.)
ABOUZAID	07B	PRL 99 051804	E. Abouzaid *et al.*	(FNAL KTeV Collab.)
ABOUZAID	07C	PRL 99 081803	E. Abouzaid *et al.*	(FNAL KTeV Collab.)
ABOUZAID	07D	PR D76 052001	E. Abouzaid *et al.*	(FNAL KTeV Collab.)
AMBROSINO	07C	JHEP 0712 105	F. Ambrosino *et al.*	(KLOE Collab.)
ANDRE	07	ANP 322 2518	T. Andre	(EFI)
LAI	07	PL B645 26	A. Lai *et al.*	(CERN NA48 Collab.)
LAI	07A	PL B647 341	A. Lai *et al.*	(CERN NA48 Collab.)
NIX	07	PR D76 011101	J. Nix *et al.*	(KEK E391a Collab.)
ABOUZAID	06	PRL 96 101801	E. Abouzaid *et al.*	(KTeV Collab.)
ABOUZAID	06A	PR D74 032004	E. Abouzaid *et al.*	(KTeV Collab.)
Also		PR D74 039905 (errat.)	E. Abouzaid *et al.*	(KTeV Collab.)
ABOUZAID	06C	PR D74 097101	E. Abouzaid *et al.*	(KTeV Collab.)
AHN	06	PR D74 051105	J.K. Ahn *et al.*	(KEK E391a Collab.)
Also		PR D74 079901 (errat.)	J.K. Ahn *et al.*	(KEK E391a Collab.)
AMBROSINO	06	PL B632 43	F. Ambrosino *et al.*	(KLOE Collab.)
AMBROSINO	06D	PL B636 166	F. Ambrosino *et al.*	(KLOE Collab.)
AMBROSINO	06F	PL B638 140	F. Ambrosino *et al.*	(KLOE Collab.)
BATLEY	06B	PL B633 173	J.R. Batley *et al.*	(CERN NA48/2 Collab.)
HILL	06	PR D74 096006	R.J. Hill	(FNAL)
PDG	06	JP G33 1	W.-M. Yao *et al.*	(PDG Collab.)
ALEXOPOU...	05	PR D71 012001	T. Alexopoulos *et al.*	(FNAL KTeV Collab.)
AMBROSINO	05C	PL B626 15	F. Ambrosino *et al.*	(KLOE Collab.)
CABIBBO	05	JHEP 0503 021	N. Cabibbo, G. Isidori	(CERN, ROMAI, FRAS)
LAI	05	PL B605 247	A. Lai *et al.*	(CERN NA48 Collab.)
LAI	05B	PL B615 31	A. Lai *et al.*	(CERN NA48 Collab.)
PARK	05	PRL 94 021801	H.K. Park *et al.*	(FNAL HyperCP Collab.)
ALAVI-HARATI	04A	PRL 93 021805	A. Alavi-Harati *et al.*	(FNAL KTeV/E799 Collab.)
ALEXOPOU...	04	PR D70 092006	T. Alexopoulos *et al.*	(FNAL KTeV Collab.)
ALEXOPOU...	04A	PR D70 092007	T. Alexopoulos *et al.*	(FNAL KTeV Collab.)
BATLEY	04	PL B595 75	J.R. Batley *et al.*	(CERN NA48 Collab.)
CIRIGLIANO	04	EPJ C35 53	V. Cirigliano, H. Neufeld, H. Pichl	(CIT, VALE+)
LAI	04B	PL B602 41	A. Lai *et al.*	(CERN NA48 Collab.)
LAI	04C	PL B604 1	A. Lai *et al.*	(CERN NA48 Collab.)
PDG	04	PL B592 1	S. Eidelman *et al.*	(PDG Collab.)
SOZZI	04	EPJ C36 37	M. Sozzi	(PISA)
ADINOLFI	03	PL B566 61	M. Adinolfi *et al.*	(KLOE Collab.)
ALAVI-HARATI	03	PR D67 012005	A. Alavi-Harati *et al.*	(FNAL KTeV Collab.)
Also		PR D70 079904 (errat.)	A. Alavi-Harati *et al.*	(FNAL KTeV Collab.)
ALAVI-HARATI	03B	PRL 90 141801	A. ALavi-Harati *et al.*	(FNAL KTeV Collab.)
LAI	03	PL B551 7	A. Lai *et al.*	(CERN NA48 Collab.)
LAI	03C	EPJ C30 33	A. Lai *et al.*	(CERN NA48 Collab.)
ALAVI-HARATI	02	PRL 88 181601	A. Alavi-Harati *et al.*	(FNAL KTeV Collab.)
ALAVI-HARATI	02C	PRL 89 211801	A. Alavi-Harati *et al.*	(FNAL KTeV Collab.)
BATLEY	02	PL B544 97	J.R. Batley *et al.*	(CERN NA48 Collab.)
CIRIGLIANO	02	EPJ C23 121	V. Cirigliano *et al.*	(VIEN, VALE, MARS)
LAI	02B	PL B536 229	A. Lai *et al.*	(CERN NA48 Collab.)
ALAVI-HARATI	01	PRL 86 397	A. Alavi-Harati *et al.*	(FNAL KTeV Collab.)
ALAVI-HARATI	01B	PRL 86 761	A. Alavi-Harati *et al.*	(FNAL KTeV Collab.)
ALAVI-HARATI	01D	PRL 86 5425	A. Alavi-Harati *et al.*	(FNAL KTeV Collab.)
ALAVI-HARATI	01E	PRL 87 021801	A. Alavi-Harati *et al.*	(FNAL KTeV Collab.)
ALAVI-HARATI	01F	PR D64 012003	A. Alavi-Harati *et al.*	(FNAL KTeV Collab.)
ALAVI-HARATI	01G	PRL 87 071801	A. Alavi-Harati *et al.*	(FNAL KTeV Collab.)
ALAVI-HARATI	01H	PRL 87 111802	A. Alavi-Harati *et al.*	(FNAL KTeV Collab.)
ALAVI-HARATI	01J	PR D64 112004	A. Alavi-Harati *et al.*	(FNAL KTeV Collab.)
ANGELOPO...	01	PL B503 49	A. Angelopoulos *et al.*	(CPLEAR Collab.)
ANGELOPO...	01B	EPJ C22 55	A. Angelopoulos *et al.*	(CPLEAR Collab.)
LAI	01B	PL B515 261	A. Lai *et al.*	(CERN NA48 Collab.)
LAI	01C	EPJ C22 231	A. Lai *et al.*	(CERN NA48 Collab.)
ALAVI-HARATI	00	PR D61 072006	A. Alavi-Harati *et al.*	(FNAL KTeV Collab.)
ALAVI-HARATI	00B	PRL 84 408	A. Alavi-Harati *et al.*	(FNAL KTeV Collab.)
ALAVI-HARATI	00D	PRL 84 5279	A. Alavi-Harati *et al.*	(FNAL KTeV Collab.)
ALAVI-HARATI	00E	PR D62 112001	A. Alavi-Harati *et al.*	(FNAL KTeV Collab.)
AMBROSE	00	PRL 84 1389	D. Ambrose *et al.*	(BNL E871 Collab.)
APOSTOLA...	00	PL B473 186	A. Apostolakis *et al.*	(CPLEAR Collab.)
PDG	00	EPJ C15 1	D.E. Groom *et al.*	(PDG Collab.)

Meson Particle Listings

K_L^0

ADAMS 99 PL B447 240 J. Adams *et al.* (FNAL KTeV Collab.)
ALAVI-HARATI 99B PRL 83 917 A. Alavi-Harati *et al.* (FNAL KTeV Collab.)
ALAVI-HARATI 99D PRL 83 22 A. Alavi-Harati *et al.* (FNAL KTeV Collab.)
APOSTOLA... 99C PL B458 545 A. Apostolakis *et al.* (CPLEAR Collab.)
Also EPJ C18 41 A. Apostolakis *et al.* (CPLEAR Collab.)
FANTI 99B PL B458 553 V. Fanti *et al.* (CERN NA48 Collab.)
FANTI 99C PL B465 335 V. Fanti *et al.* (CERN NA48 Collab.)
MURAKAMI 99 PL B463 333 K. Murakami *et al.* (KEK E162 Collab.)
ADAMS 98 PRL 80 4123 J. Adams *et al.* (FNAL KTeV Collab.)
AMBROSE 98 PRL 81 4309 D. Ambrose *et al.* (BNL E871 Collab.)
AMBROSE 98B PRL 81 5734 D. Ambrose *et al.* (BNL E871 Collab.)
ANGELOPO... 98 PL B420 191 A. Angelopoulos *et al.* (CPLEAR Collab.)
ANGELOPO... 98C EPJ C5 389 A. Angelopoulos *et al.* (CPLEAR Collab.)
ANGELOPO... 98D PL B444 38 A. Angelopoulos *et al.* (CPLEAR Collab.)
Also EPJ C22 55 A. Angelopoulos *et al.* (CPLEAR Collab.)
ANGELOPO... 98E PL B444 43 A. Angelopoulos *et al.* (CPLEAR Collab.)
ARISAKA 98 PL B432 230 K. Arisaka *et al.* (FNAL E799 Collab.)
BENDER 98 PL B418 411 M. Bender *et al.* (CERN NA48 Collab.)
DAMBROSIO 98 PL B423 385 G. D'Ambrosio, G. Isidori, J. Portoles
SETZU 98 PL B420 205 M.G. Setzu *et al.*
TAKEUCHI 98 PL B443 409 Y. Takeuchi *et al.* (KYOT, KEK, HIRO)
FANTI 97 ZPHY C76 653 V. Fanti *et al.* (CERN NA48 Collab.)
NOMURA 97 PL B408 445 T. Nomura *et al.* (KYOT, KEK, HIRO)
ADLER 96B ZPHY C70 211 R. Adler *et al.* (CPLEAR Collab.)
ADLER 96C PL B369 367 R. Adler *et al.* (CPLEAR Collab.)
GU 96 PRL 76 4312 P. Gu *et al.* (RUTG, UCLA, EFI, COLO+)
LEBER 96 PL B369 69 F. Leber *et al.* (MANZ, CERN, EDIN, ORSAY+)
PDG 96 PR D54 1 R. M. Barnett *et al.* (PDG Collab.)
ADLER 95 PL B363 237 R. Adler *et al.* (CPLEAR Collab.)
ADLER 95B PL B363 243 R. Adler *et al.* (CPLEAR Collab.)
AKAGI 95 PR D51 2061 T. Akagi *et al.* (TOHOK, TOKY, KYOT, KEK)
BARR 95 ZPHY C65 361 G.D. Barr *et al.* (CERN, EDIN, MANZ, LALO+)
BARR 95C PL B358 399 G.D. Barr *et al.* (CERN, EDIN, MANZ, LALO+)
HEINSON 95 PR D51 985 A.P. Heinson *et al.* (BNL E791 Collab.)
KREUTZ 95 ZPHY C65 67 A. Kreutz *et al.* (SIEG, EDIN, MANZ, ORSAY+)
MATTHEWS 95 PRL 75 2803 J.N. Matthews *et al.* (RUTG, EFI, ELMT+)
SCHWINGEN... 95 PRL 74 4376 B. Schwingenheuer *et al.* (EFI, CHIC+)
SPENCER 95 PRL 74 3323 M.B. Spencer *et al.* (UCLA, EFI, COLO+)
BARR 94 PL B328 528 G.D. Barr *et al.* (CERN, EDIN, MANZ, LALO+)
GU 94 PRL 72 3000 P. Gu *et al.* (RUTG, UCLA, EFI, COLO+)
NAKAYA 94 PRL 73 2169 T. Nakaya *et al.* (OSAK, UCLA, EFI, COLU+)
ROBERTS 94 PR D50 1874 D. Roberts *et al.* (UCLA, EFI, COLU+)
WEAVER 94 PRL 72 3758 M. Weaver *et al.* (UCLA, EFI, COLU, ELMT+)
AKAGI 93 PR D47 R2644 T. Akagi *et al.* (TOHOK, TOKY, KYOT, KEK)
ARISAKA 93 PRL 70 1049 K. Arisaka *et al.* (BNL E791 Collab.)
ARISAKA 93B PRL 71 3910 K. Arisaka *et al.* (BNL E791 Collab.)
BARR 93D PL B317 233 G.D. Barr *et al.* (CERN, EDIN, MANZ, LALO+)
GIBBONS 93 PRL 70 1199 L.K. Gibbons *et al.* (FNAL E731 Collab.)
Also PR D55 6625 L.K. Gibbons *et al.* (FNAL E731 Collab.)
GIBBONS 93B PRL 70 1203 L.K. Gibbons *et al.* (FNAL E731 Collab.)
GIBBONS 93C Thesis RX-1487 L.K. Gibbons (CHIC)
Also PR D55 6625 L.K. Gibbons *et al.* (FNAL E731 Collab.)
HARRIS 93 PRL 71 3914 D.A. Harris *et al.* (EFI, UCLA, COLO+)
HARRIS 93B PRL 71 3918 D.A. Harris *et al.* (EFI, UCLA, COLO+)
MAKOFF 93 PRL 70 1591 G. Makoff *et al.* (FNAL E731 Collab.)
Also PRL 75 2069 (erratum) G. Makoff *et al.*
RAMBERG 93 PRL 70 2525 E. Ramberg *et al.* (FNAL E731 Collab.)
RAMBERG 93B PRL 70 2529 E.J. Ramberg *et al.* (FNAL E731 Collab.)
VAGINS 93 PRL 71 35 M.R. Vagins *et al.* (BNL E845 Collab.)
ADLER 92B PL B286 180 R. Adler *et al.* (CPLEAR Collab.)
Also SJNP 55 840 R. Adler *et al.* (CPLEAR Collab.)
BARR 92 PL B284 440 G.D. Barr *et al.* (CERN, EDIN, MANZ, LALO+)
GRAHAM 92 PL B295 169 G.E. Graham *et al.* (FNAL E731 Collab.)
MORSE 92 PR D45 36 W.M. Morse *et al.* (BNL, YALE, VASS)
PDG 92 PR D45 S1 K. Hikasa *et al.* (KEK, LBL, BOST+)
SOMALWAR 92 PRL 68 2580 S.V. Somalwar *et al.* (FNAL E731 Collab.)
AKAGI 91B PRL 67 2618 T. Akagi *et al.* (TOHOK, TOKY, KYOT, KEK)
BARR 91 PL B259 389 G.D. Barr *et al.* (CERN, EDIN, MANZ, LALO+)
HEINSON 91 PR D44 R1 A.P. Heinson *et al.* (UCI, UCLA, LANL+)
PAPADIMITR... 91 PR D44 R573 V. Papadimitriou *et al.* (FNAL E731 Collab.)
BARKER 90 PR D41 3546 A.R. Barker *et al.* (FNAL E731 Collab.)
Also PRL 61 2661 L.K. Gibbons *et al.* (FNAL E731 Collab.)
BARR 90B PL B240 283 G.D. Barr *et al.* (CERN, EDIN, MANZ, LALO+)
BARR 90C PL B242 523 G.D. Barr *et al.* (CERN, EDIN, MANZ, LALO+)
CAROSI 90 PL B237 303 R. Carosi *et al.* (CERN, EDIN, MANZ, LALO+)
KARLSSON 90 PRL 64 2976 M. Karlsson *et al.* (FNAL E731 Collab.)
OHL 90 PRL 64 2755 K.E. Ohl *et al.* (BNL E845 Collab.)
OHL 90B PRL 65 1407 K.E. Ohl *et al.* (BNL E845 Collab.)
PATTERSON 90 PRL 64 1491 J.R. Patterson *et al.* (FNAL E731 Collab.)
INAGAKI 89 PR D40 1712 T. Inagaki *et al.* (KEK, TOKY, KYOT)
MATHIAZHA... 89 PRL 63 2181 C. Mathiazhagan *et al.* (UCI, UCLA, LANL+)
MATHIAZHA... 89B PRL 63 2185 C. Mathiazhagan *et al.* (UCI, UCLA, LANL+)
WAHL 89 CERN-EP/89-86 H. Wahl (CERN)
BARR 88 PL B214 303 G.D. Barr *et al.* (CERN, EDIN, MANZ, LALO+)
BURKHARDT 88 PL B206 169 H. Burkhardt *et al.* (CERN, EDIN, MANZ+)
JASTRZEM... 88 PRL 61 2300 E. Jastrzembski *et al.* (BNL, YALE)
WOODS 88 PRL 60 1695 M. Woods *et al.* (FNAL E731 Collab.)
BURKHARDT 87 PL B199 139 H. Burkhardt *et al.* (CERN, EDIN, MANZ+)
ARONSON 86 PR D33 3180 S.H. Aronson *et al.* (BNL, CHIC, STAN+)
Also PR 48 1078 S.H. Aronson *et al.* (BNL, CHIC, STAN+)
PDG 86C PL 170B 132 M. Aguilar-Benitez *et al.* (CERN, CIT+)
COUPAL 85 PRL 55 566 D.P. Coupal *et al.* (CHIC, SACL)
BALATS 83 SJNP 38 556 M.Y. Balats *et al.* (ITEP)
Translated from YAF 38 927.
BERGSTROM 83 PL 131B 229 L. Bergstrom, E. Masso, P. Singer (CERN)
ARONSON 82 PRL 48 1078 S.H. Aronson *et al.* (BNL, CHIC, STAN+)
ARONSON 82B PRL 48 1306 S.H. Aronson *et al.* (BNL, CHIC, PURD)
Also PL 116B 73 E. Fischbach *et al.* (PURD, BNL, CHIC)
Also PR D28 476 S.H. Aronson *et al.* (BNL, CHIC, PURD)
Also PR D28 495 S.H. Aronson *et al.* (BNL, CHIC, PURD)
PDG 82B PL 111B 70 M. Roos *et al.* (HELS, CIT, CERN)
BIRULEV 81 NP B182 1 V.K. Birulev *et al.* (JINR)
Also SJNP 31 622 V.K. Birulev *et al.* (JINR)
Translated from YAF 31 1204.
CARROLL 80B PRL 44 529 A.S. Carroll *et al.* (BNL, ROCH)
CARROLL 80C PL 96B 407 A.S. Carroll *et al.* (BNL, ROCH)
CHO 80 PR D22 2688 Y. Cho *et al.* (ANL, CMU)
MORSE 80 PR D21 1750 W.M. Morse *et al.* (BNL, YALE)
CHRISTENS... 79 PRL 43 1209 J.H. Christenson *et al.* (NYU)
SCHMIDT 79 PRL 43 556 M.P. Schmidt *et al.* (YALE, BNL)
HILL 78 PL 73B 483 D.G. Hill *et al.* (BNL, SLAC, SBER)
CHO 77 PR D15 587 Y. Cho *et al.* (ANL, CMU)
CLARK 77 PR D15 553 A.R. Clark *et al.* (LBL)
Also Thesis LBL-4275 G. Shen (LBL)
DEVOE 77 PR D16 565 R. Devoe *et al.* (EFI, ANL)
PEACH 77 NP B127 399 K.J. Peach *et al.* (BGNA, EDIN, GLAS+)
BIRULEV 76 SJNP 24 178 V.K. Birulev *et al.* (JINR)
Translated from YAF 24 340.
COOMBES 76 PRL 37 249 R.W. Coombes *et al.* (STAN, NYU)
GJESDAL 76 NP B109 118 G. Gjesdal *et al.* (CERN, HEIDH)
BALDO-... 75 NC 25A 688 M. Baldo-Ceolin *et al.* (PADO, WISC)
BLUMENTHAL 75 PRL 34 164 R.B. Blumenthal *et al.* (PENN, CHIC, TEMP)
BUCHANAN 75 PR D11 457 C.D. Buchanan *et al.* (UCLA, SLAC, JHU)
CARITHERS 75 PRL 34 1244 W.C.J. Carithers *et al.* (COLU, NYU)
SMITH 75B Thesis UCSD unpub. J.G. Smith (UCSD)
BISI 74 PL 50B 504 V. Bisi, M.I. Ferrero (TORI)
DONALDSON 74 Thesis SLAC-0184 G. Donaldson (SLAC)
Also PR D14 2839 G. Donaldson *et al.* (SLAC)
DONALDSON 74B PR D9 2960 G. Donaldson *et al.* (SLAC, UCSC)
Also PRL 31 337 G. Donaldson *et al.* (SLAC, UCSC)
GEWENIGER 74 PL 48B 483 C. Geweniger *et al.* (CERN, HEIDH)
Also Thesis CERN Int. 74-4 V. Luth (CERN)
GEWENIGER 74B PL 48B 487 C. Geweniger *et al.* (CERN, HEIDH)
Also PL 52B 119 S. Gjesdal *et al.* (CERN, HEIDH)
GEWENIGER 74C PL 52B 108 C. Geweniger *et al.* (CERN, HEIDH)
GJESDAL 74 PL 52B 113 S. Gjesdal *et al.* (CERN, HEIDH)
MESSNER 74 PRL 33 1458 R. Messner *et al.* (COLO, SLAC, UCSC)
NIEBERGALL 74 PL 49B 103 F. Niebergall *et al.* (CERN, ORSAY, VIEN)
WILLIAMS 74 PRL 33 240 H.H. Williams *et al.* (BNL, YALE)
ALEXANDER 73B NP B65 301 G. Alexander *et al.* (TELA, HEID)
BRANDENB... 73 PR D8 1978 G.W. Brandenburg *et al.* (SLAC)
EVANS 73 PR D7 36 G.R. Evans *et al.* (EDIN, CERN)
Also PRL 23 427 G.R. Evans *et al.* (EDIN, CERN)
FACKLER 73 PRL 31 847 O. Fackler *et al.* (MIT)
FITCH 73 PRL 31 1524 V.L. Fitch *et al.* (PRIN)
Also Thesis COO-3072-13 R.C. Webb (PRIN)
HART 73 NP B66 317 J.C. Hart *et al.* (CAVE, RHEL)
MALLARY 73 PR D7 1953 M.L. Mallary *et al.* (CIT)
Also PRL 25 1214 F.J. Sciulli *et al.* (CIT)
MCCARTHY 73 PR D7 687 R.L. McCarthy *et al.* (LBL)
Also PL 42B 291 R.L. McCarthy *et al.* (LBL)
Also Thesis LBL-550 R.L. McCarthy (LBL)
MESSNER 73 PRL 30 876 R. Messner *et al.* (COLO, SLAC, UCSC)
SANDWEISS 73 PRL 30 1002 J. Sandweiss *et al.* (YALE, ANL)
WILLIAMS 73 PRL 31 1521 H.H. Williams *et al.* (BNL, YALE)
ASHFORD 72 PL 38B 47 V.A. Ashford *et al.* (UCSD)
BANNER 72B PRL 29 237 M. Banner *et al.* (PRIN)
BARMIN 72B SJNP 15 638 V.V. Barmin *et al.* (ITEP)
Translated from YAF 15 1152.
BURGUN 72 NP B50 194 G. Burgun *et al.* (SACL, CERN, OSLO)
GRAHAM 72 NC 9A 166 M.F. Graham *et al.* (ILL, NEAS)
JAMES 72 NP B49 1 F. James *et al.* (CERN, SACL, OSLO)
KRENZ 72 LNC 4 213 W. Krenz *et al.* (AACH, CERN, EDIN)
MANN 72 PR D6 137 W.A. Mann *et al.* (MASA, BNL, YALE)
MANTSCH 72 NC 9A 160 P.M. Mantsch *et al.* (ILL, NEAS)
MCCARTHY 72 PL 42B 291 R.L. McCarthy *et al.* (LBL)
PICCIONI 72 PRL 29 1412 R. Piccioni *et al.* (SLAC)
Also PR D9 2939 R. Piccioni *et al.* (SLAC, UCSC, COLO)
VOSBURGH 72 PR D6 1834 K.G. Vosburgh *et al.* (RUTG, MASA)
Also PRL 26 866 K.G. Vosburgh *et al.* (RUTG, MASA)
BALATS 71 SJNP 13 53 M.Y. Balats *et al.* (ITEP)
Translated from YAF 13 93.
BARMIN 71 PL 35B 604 V.V. Barmin *et al.* (ITEP)
BURGUN 71 LNC 2 1169 G. Burgun *et al.* (SACL, CERN, OSLO)
CARNEGIE 71 PR D4 1 R.K. Carnegie *et al.* (PRIN)
CHAN 71 Thesis LBL-350 J.H.S. Chan (LBL)
CHO 71 PR D3 1557 Y. Cho *et al.* (CMU, BNL, CASE)
ENSTROM 71 PR D4 2629 J. Enstrom *et al.* (SLAC, STAN)
Also Thesis SLAC-0125 J.E. Enstrom (STAN)
JAMES 71 PL 35B 265 F. James *et al.* (CERN, SACL, OSLO)
MEISNER 71 PR D3 59 G.W. Meisner *et al.* (MASA, BNL, YALE)
REPELLIN 71 PL 36B 603 J.P. Repellin *et al.* (ORSAY, CERN)
WEBBER 71 PR D3 64 B.R. Webber *et al.* (LRL)
Also PRL 21 498 B.R. Webber *et al.* (LRL)
Also Thesis UCRL 19226 B.R. Webber (LRL)
WOLFF 71 PL 36B 517 B. Wolff *et al.* (ORSAY, CERN)
ALBROW 70 PL 33B 516 M.G. Albrow *et al.* (MCHS, DARE)
ARONSON 70 PRL 25 1057 S.H. Aronson *et al.* (EFI, ILLC, SLAC)
BARMIN 70 PL 33B 377 V.V. Barmin *et al.* (ITEP, JINR)
BASILE 70 PR D2 78 P. Basile *et al.* (SACL)
BECHERRAWY 70 PR D1 1452 T. Becherrawy (ROCH)
BUCHANAN 70 PL 33B 623 C.D. Buchanan *et al.* (SLAC, JHU, UCLA)
Also Private Comm. A.J. Cox
BUDAGOV 70 PR D2 815 I.A. Budagov *et al.* (CERN, ORSAY, EPOL)
Also PL 28B 215 I.A. Budagov *et al.* (CERN, ORSAY, EPOL)
CHO 70 PR D1 3031 Y. Cho *et al.* (CMU, BNL, CASE)
Also PRL 19 668 D.G. Hill *et al.* (BNL, CMU)
CHOLLET 70 PL 31B 658 J.C. Chollet *et al.* (CERN)
CULLEN 70 PL 32B 523 M. Cullen *et al.* (AACH, CERN, TORI)
MARX 70 PL 32B 219 J. Marx *et al.* (COLU, HARV, CERN)
Also Thesis Nevis 179 J. Marx (COLU)
SCRIBANO 70 PL 32B 224 A. Scribano *et al.* (PISA, COLU, HARV)
SMITH 70 PL 32B 133 R.C. Smith *et al.* (UMD, BNL)
WEBBER 70 PR D1 1967 B.R. Webber *et al.* (LRL)
Also Thesis UCRL 19226 B.R. Webber (LRL)
BANNER 69 PR 188 2033 M. Banner *et al.* (PRIN)
Also PRL 21 1103 M. Banner *et al.* (PRIN)
Also PRL 21 1107 J.W. Cronin, J.K. Liu, J.E. Pilcher (PRIN)
BENNETT 69 PL 29B 317 S. Bennett *et al.* (COLU, BNL)
FAISSNER 69 PL 30B 204 H. Faissner *et al.* (AACH3, CERN, TORI)
LITTENBERG 69 PRL 22 654 L.S. Littenberg *et al.* (UCSD)
LONGO 69 PR 181 1808 M.J. Longo, K.K. Young, J.A. Helland (MICH, UCLA)
PACIOTTI 69 Thesis UCRL 19446 M.A. Paciotti (LRL)
SAAL 69 Thesis H.J. Saal (COLU)
ABRAMS 68B PR 176 1603 R.J. Abrams *et al.* (ILL)
ARNOLD 68B PL 28B 56 R.G. Arnold *et al.* (CERN, ORSAY)
BASILE 68B PL 28B 58 P. Basile *et al.* (SACL)
BENNETT 68 PL 27B 244 S. Bennett *et al.* (COLU, CERN)
BLANPIED 68 PRL 21 1650 W.A. Blanpied *et al.* (CASE, HARV, MCGI)
BOHM 68B PL 27B 594 A. Bohm *et al.*
BUDAGOV 68 NC 57A 182 I.A. Budagov *et al.* (CERN, ORSAY, IPNP)
Also PL 28B 215 I.A. Budagov *et al.* (CERN, ORSAY, EPOL)
JAMES 68 NP B8 365 F. James, H. Briand (IPNP, CERN)
Also PRL 21 257 J.A. Helland, M.J. Longo, K.K. Young (UCLA, MICH)
KULYUKINA 68 JETP 26 20 L.A. Kulyukina *et al.* (JINR)
Translated from ZETF 53 29.
KUNZ 68 Thesis PU-68-46 P.F. Kunz (PRIN)
BENNETT 67 PRL 19 993 S. Bennett *et al.* (COLU)
DEBOUARD 67 NC 52A 662 X. de Bouard *et al.* (CERN)
Also PL 15 58 X. de Bouard *et al.* (CERN, ORSAY, MPIM)
DEVLIN 67 PRL 18 54 T.J. Devlin *et al.* (PRIN, UMD)
Also PR 169 1045 G.A. Sayer *et al.* (UMD, PPA, PRIN)
DORFAN 67 PRL 19 987 D.E. Dorfan *et al.* (SLAC, LRL)
FELDMAN 67B PR 155 1611 L. Feldman *et al.* (PENN)
FITCH 67 PR 164 1711 V.L. Fitch *et al.* (PRIN)
GINSBERG 67 PR 162 1570 E.S. Ginsberg (MASB)
HILL 67 PRL 19 668 D.G. Hill *et al.* (BNL, CMU)
HOPKINS 67 PRL 19 185 H.W.K. Hopkins, T.C. Bacon, F.R. Eisler (BNL)
NEFKENS 67 PR 157 1233 B.M.K. Nefkens *et al.* (ILL)
SCHMIDT 67 Thesis Nevis 160 P. Schmidt (COLU)

BEHR	66	PL 22 540	L. Behr *et al.*	(EPOL, MILA, PADO, ORSAY)
HAWKINS	66	PL 21 238	C.J.B. Hawkins	(YALE)
Also		PR 156 1444	C.J.B. Hawkins	(YALE)
ANDERSON	65	PRL 14 475	J.A. Anderson *et al.*	(LRL, WISC)
ASTBURY	65B	PL 18 175	P. Astbury *et al.*	(CERN, ZURI)
AUBERT	65	PL 17 59	B. Aubert *et al.*	(EPOL, ORSAY)
Also		PL 24B 75	J.P. Lowys *et al.*	(EPOL, ORSAY)
BALDO-...	65	NC 38 684	M. Baldo-Ceolin *et al.*	(PADO)
FRANZINI	65	PR 140B 127	P. Franzini *et al.*	(COLU, RUTG)
GUIDONI	65	Argonne Conf. 49	P. Guidoni *et al.*	(BNL, YALE)
HOPKINS	65	Argonne Conf. 67	H.W.K. Hopkins, T.C. Bacon, F. Eisler	(VAND+)
ALEKSANYAN	64B	Dubna Conf. 2 102	A.S. Aleksanyan *et al.*	(YERE)
Also		JETP 19 1019 Translated from ZETF 46 1504.	A.S. Aleksanyan *et al.*	(LEBD, MPEI, YERE)
ANIKINA	64	JETP 19 42 Translated from ZETF 46 59.	M.K. Anikina *et al.*	(GEOR, JINR)
FITCH	61	NC 22 1160	V.L. Fitch, P.A. Piroue, R.B. Perkins	(PRIN+)
GOOD	61	PR 124 1223	R.H. Good *et al.*	(LRL)

OTHER RELATED PAPERS

HAYAKAWA	93	PR D48 1150	M. Hayakawa, A.I. Sanda	(NAGO)
"Searching for *T*, *CP*, *CPT*, $\Delta S = \Delta Q$ Rule Violations in the Neutral *K* Meson System: A Guide"				
LITTENBERG	93	ARNPS 43 729	L.S. Littenberg, G. Valencia	(BNL, FNAL)
Rare and Radiative Kaon Decays				
RITCHIE	93	RMP 65 1149	J.L. Ritchie, S.G. Wojcicki	
"Rare *K* Decays"				
WINSTEIN	93	RMP 65 1113	B. Winstein, L. Wolfenstein	
"The Search for Direct *CP* Violation"				
BATTISTON	92	PRPL 214 293	R. Battiston *et al.*	(PGIA, CERN, TRSTT)
Status and Perspectives of *K* Decay Physics				
DIB	92	PR D46 2265	C.O. Dib, R.D. Peccei	(UCLA)
Tests of *CPT* conservation in the neutral kaon system.				
KLEINKNECHT	92	CNPP 20 281	K. Kleinknecht	(MANZ)
New Results on *CP* Violation in Decays of Neutral *K* Mesons.				
KLEINKNECHT	90	ZPHY C46 S57	K. Kleinknecht	(MANZ)
PEACH	90	JP G16 131	K.J. Peach	(EDIN)
BRYMAN	89	IJMP A4 79	D.A. Bryman	(TRIU)
"Rare Kaon Decays"				
KLEINKNECHT	76	ARNS 26 1	K. Kleinknecht	(DORT)
GINSBERG	73	PR D8 3887	E.S. Ginsberg, J. Smith	(MIT, STON)
GINSBERG	70	PR D1 229	E.S. Ginsberg	(HAIF)
HEUSSE	70	LNC 3 449	P. Heusse *et al.*	(ORSAY)
CRONIN	68C	Vienna Conf. 281	J.W. Cronin	(PRIN)
RUBBIA	67	PL 24B 531	C. Rubbia, J. Steinberger	(CERN, COLU)
Also		PL 23 167	C. Rubbia, J. Steinberger	(CERN, COLU)
Also		PL 20 207	C. Alff-Steinberger *et al.*	(CERN)
Also		PL 21 595	C. Alff-Steinberger *et al.*	(CERN)
AUERBACH	66	PR 149 1052	L.B. Auerbach *et al.*	(PENN)
Also		PRL 14 192	L.B. Auerbach *et al.*	(PENN)
FIRESTONE	66B	PRL 17 116	A. Firestone *et al.*	(YALE, BNL)
BEHR	65	Argonne Conf. 59	L. Behr *et al.*	(EPOL, MILA, PADO)
MESTVIRISH...	65	JINR P 2449	A.N. Mestvirishvili *et al.*	(JINR)
TRILLING	65B	UCRL 16473	G.N. Trilling	(LRL)
Updated from 1965 Argonne Conference, page 115.				
JOVANOV...	63	BNL Conf. 42	J.V. Jovanovich *et al.*	(BNL, UMD)

$K^*_0(800)$ or κ

$I(J^P) = \frac{1}{2}(0^+)$

OMITTED FROM SUMMARY TABLE

Needs confirmation. See the mini-review on scalar mesons under $f_0(500)$ (see the index for the page number).

$K^*_0(800)$ MASS

VALUE (MeV)			EVTS	DOCUMENT ID		TECN	COMMENT
682	**±29**	**OUR AVERAGE**		Error includes scale factor of 2.4. See the ideogram below.			
826	±49	$^{+49}_{-34}$	1338	[1] ABLIKIM	11B	BES2	$J/\psi \to K^0_S K^0_S \pi^+\pi^-$
849	±77	$^{+18}_{-14}$	1421	[2,3] ABLIKIM	10E	BES2	$J/\psi \to K^\pm K^0_S \pi^\mp \pi^0$
841	±30	$^{+81}_{-73}$	25k	[4,5] ABLIKIM	06C	BES2	$J/\psi \to \overline{K}^*(892)^0 K^+\pi^-$
658	±13			[6] DESCOTES-G...06		RVUE	$\pi K \to \pi K$
797	±19	±43	15k	[7,8] AITALA	02	E791	$D^+ \to K^-\pi^+\pi^+$
• • • We do not use the following data for averages, fits, limits, etc. • • •							
663	± 8	±34		[9] BUGG	10	RVUE	S-matrix pole
706.0	± 1.8	±22.8	141k	[10] BONVICINI	08A	CLEO	$D^+ \to K^-\pi^+\pi^+$
856	±17	±13	54k	[11] LINK	07B	FOCS	$D^+ \to K^-\pi^+\pi^+$
750	$^{+30}_{-55}$			[12] BUGG	06	RVUE	
855	±15		0.6k	[13] CAWLFIELD	06A	CLEO	$D^0 \to K^+K^-\pi^0$
694	±53			[3,14] ZHOU	06	RVUE	$Kp \to K^-\pi^+ n$
753	±52			[15] PELAEZ	04A	RVUE	$K\pi \to K\pi$
594	±79			[14] ZHENG	04	RVUE	$K^-p \to K^-\pi^+ n$
722	±60			[16] BUGG	03	RVUE	11 $K^-p \to K^-\pi^+ n$
905	$^{+65}_{-30}$			[17] ISHIDA	97B	RVUE	11 $K^-p \to K^-\pi^+ n$

[1] The Breit-Wigner parameters from a fit with seven intermediate resonances. The S-matrix pole position is $(764 \pm 63^{+71}_{-54}) - i\,(306 \pm 149^{+143}_{-85})$ MeV.

[2] From a fit including ten additional resonances and energy-independent Breit-Wigner width.

[3] S-matrix pole.

[4] S-matrix pole. GUO 06 in a chiral unitary approach report a mass of 757 ± 33 MeV and a width of 558 ± 82 MeV.

[5] A fit in the $K^*_0(800) + K^*(892) + K^*(1410)$ model with mass and width of the $K^*_0(800)$ from ABLIKIM 06C well describes the left slope of the $K^0_S\pi^-$ invariant mass spectrum in $\tau^- \to K^0_S\pi^-\nu_\tau$ decay studied by EPIFANOV 07.

[6] S-matrix pole. Using Roy-Steiner equations (ROY 71) as well as unitarity, analyticity and crossing symmetry constraints.

[7] Not seen by KOPP 01 using 7070 events of $D^0 \to K^-\pi^+\pi^0$. LINK 02E and LINK 05I show clear evidence for a constant non-resonant scalar amplitude rather than $K^*_0(800)$ in their high statistics analysis of $D^+ \to K^-\pi^+\mu^+\nu_\mu$.

[8] AUBERT 07T does not find evidence for the charged $K^*_0(800)$ using 11k events of $D^0 \to K^-K^+\pi^0$.

[9] S-Matrix pole. Supersedes BUGG 06. Combined analysis of ASTON 88, ABLIKIM 06C, AITALA 06, and LINK 09 using an s-dependent width with couplings to $K\pi$ and $K\eta'$, and the Adler zero near thresholds.

[10] T-matrix pole.

[11] A Breit-Wigner mass and width.

[12] S-matrix pole. Reanalysis of ASTON 88, AITALA 02, and ABLIKIM 06C using for the κ an *s*-dependent width with an Adler zero near threshold.

[13] Breit-Wigner parameters. A significant *S*-wave can be also modeled as a non-resonant contribution.

[14] Using ASTON 88.

[15] T-matrix pole. Reanalysis of data from LINGLIN 73, ESTABROOKS 78, and ASTON 88 in the unitarized ChPT model.

[16] T-matrix pole. Reanalysis of ASTON 88 data.

[17] Reanalysis of ASTON 88 using interfering Breit-Wigner amplitudes.

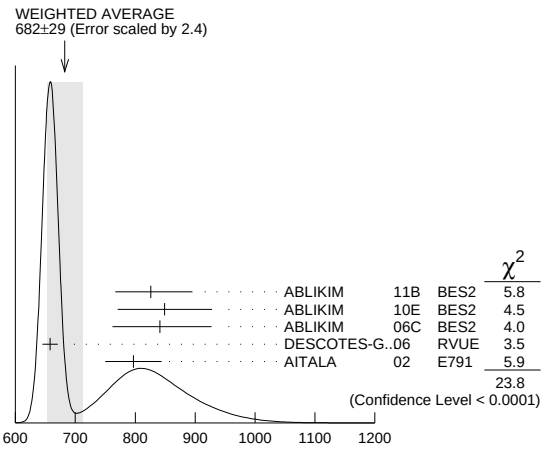

$K^*_0(800)$ WIDTH

VALUE (MeV)			EVTS	DOCUMENT ID		TECN	COMMENT
547	**± 24**	**OUR AVERAGE**		Error includes scale factor of 1.1.			
449	±156	$^{+144}_{-81}$	1338	[18] ABLIKIM	11B	BES2	$J/\psi \to K^0_S K^0_S \pi^+\pi^-$
512	± 80	$^{+92}_{-44}$	1421	[19,20] ABLIKIM	10E	BES2	$J/\psi \to K^\pm K^0_S \pi^\mp \pi^0$
618	± 90	$^{+96}_{-144}$	25k	[19,21] ABLIKIM	06C	BES2	$J/\psi \to \overline{K}^*(892)^0 K^+\pi^-$
557	± 24			[22] DESCOTES-G...06		RVUE	$\pi K \to \pi K$
410	± 43	± 87	15k	[23,24] AITALA	02	E791	$D^+ \to K^-\pi^+\pi^+$
• • • We do not use the following data for averages, fits, limits, etc. • • •							
658	± 10	± 44		[25] BUGG	10	RVUE	S-matrix pole
638.8	± 4.4	± 40.4	141k	[26] BONVICINI	08A	CLEO	$D^+ \to K^-\pi^+\pi^+$
464	± 28	± 22	54k	[27] LINK	07B	FOCS	$D^+ \to K^-\pi^+\pi^+$
684	±120			[28] BUGG	06	RVUE	
251	± 48		0.6k	[29] CAWLFIELD	06A	CLEO	$D^0 \to K^+K^-\pi^0$
606	± 59			[19,30] ZHOU	06	RVUE	$Kp \to K^-\pi^+ n$
470	± 66			[31] PELAEZ	04A	RVUE	$K\pi \to K\pi$
724	±332			[30] ZHENG	04	RVUE	$K^-p \to K^-\pi^+ n$
772	±100			[32] BUGG	03	RVUE	11 $K^-p \to K^-\pi^+ n$
545	$^{+235}_{-110}$			[33] ISHIDA	97B	RVUE	11 $K^-p \to K^-\pi^+ n$

[18] The Breit-Wigner parameters from a fit with seven intermediate resonances. The S-matrix pole position is $(764 \pm 63^{+71}_{-54}) - i\,(306 \pm 149^{+143}_{-85})$ MeV.

[19] S-matrix pole.

[20] From a fit including ten additional resonances and energy-independent Breit-Wigner width.

[21] A fit in the $K^*_0(800) + K^*(892) + K^*(1410)$ model with mass and width of the $K^*_0(800)$ from ABLIKIM 06C well describes the left slope of the $K^0_S\pi^-$ invariant mass spectrum in $\tau^- \to K^0_S\pi^-\nu_\tau$ decay studied by EPIFANOV 07.

[22] S-matrix pole. Using Roy-Steiner equations (ROY 71) as well as unitarity, analyticity and crossing symmetry constraints.

[23] Not seen by KOPP 01 using 7070 events of $D^0 \to K^-\pi^+\pi^0$. LINK 02E and LINK 05I show clear evidence for a constant non-resonant scalar amplitude rather than $K^*_0(800)$ in their high statistics analysis of $D^+ \to K^-\pi^+\mu^+\nu_\mu$.

[24] AUBERT 07T does not find evidence for the charged $K^*_0(800)$ using 11k events of $D^0 \to K^-K^+\pi^0$.

[25] S-Matrix pole. Supersedes BUGG 06. Combined analysis of ASTON 88, ABLIKIM 06C, AITALA 06, and LINK 09 using an s-dependent width with couplings to $K\pi$ and $K\eta'$, and the Adler zero near thresholds.

Meson Particle Listings

$K_0^*(800)$, $K^*(892)$

[26] T-matrix pole.
[27] A Breit-Wigner mass and width.
[28] S-matrix pole. Reanalysis of ASTON 88, AITALA 02, and ABLIKIM 06C using for the κ an s-dependent width with an Adler zero near threshold.
[29] Statistical error only. A fit to the Dalitz plot including the $K_0^*(800)^\pm$, $K^*(892)^\pm$, and ϕ resonances modeled as Breit-Wigners. A significant S-wave can be also modeled as a non-resonant contribution.
[30] Using ASTON 88.
[31] T-matrix pole. Reanalysis of data from LINGLIN 73, ESTABROOKS 78, and ASTON 88 in the unitarized ChPT model.
[32] T-matrix pole. Reanalysis of ASTON 88 data.
[33] Reanalysis of ASTON 88 using interfering Breit-Wigner amplitudes.

$K_0^*(800)$ REFERENCES

ABLIKIM	11B	PL B698 183	M. Ablikim *et al.*	(BES II Collab.)
ABLIKIM	10E	PL B693 88	M. Ablikim *et al.*	(BES II Collab.)
BUGG	10	PR D81 014002	D.V. Bugg	(LOQM)
LINK	09	PL B681 14	J.M. Link *et al.*	(FNAL FOCUS Collab.)
BONVICINI	08A	PR D78 052001	G. Bonvicini *et al.*	(CLEO Collab.)
AUBERT	07T	PR D76 011102	B. Aubert *et al.*	(BABAR Collab.)
EPIFANOV	07	PL B654 65	D. Epifanov *et al.*	(BELLE Collab.)
LINK	07B	PL B653 1	J.M. Link *et al.*	(FNAL FOCUS Collab.)
ABLIKIM	06C	PL B633 681	M. Ablikim *et al.*	(BES Collab.)
AITALA	06	PR D73 032004	E.M. Aitala *et al.*	(FNAL E791 Collab.)
Also		PR D74 059901 (errat.)	E.M. Aitala *et al.*	(FNAL E791 Collab.)
BUGG	06	PL B632 471	D.V. Bugg	(LOQM)
CAWLFIELD	06A	PR D74 031108	C. Cawlfield *et al.*	(CLEO Collab.)
DESCOTES-G...	06	EPJ C48 553	S. Descotes-Genon, B. Moussallam	
GUO	06	NP A773 78	F.K. Guo *et al.*	
ZHOU	06	NP A775 212	Z.Y. Zhou, H.Q. Zheng	
LINK	05I	PL B621 72	J.M. Link *et al.*	(FNAL FOCUS Collab.)
PELAEZ	04A	MPL A19 2879	J.R. Pelaez	
ZHENG	04	NP A733 235	H.Q. Zheng *et al.*	
BUGG	03	PL B572 1	D.V. Bugg	
AITALA	02	PRL 89 121801	E.M. Aitala *et al.*	(FNAL E791 Collab.)
LINK	02E	PL B535 43	J.M. Link *et al.*	(FNAL FOCUS Collab.)
KOPP	01	PR D63 092001	S. Kopp *et al.*	(CLEO Collab.)
ISHIDA	97B	PTP 98 621	S. Ishida *et al.*	
ASTON	88	NP B296 493	D. Aston *et al.*	(SLAC, NAGO, CINC, INUS)
ESTABROOKS	78	NP B133 490	P.G. Estabrooks *et al.*	(MCGI, CARL, DURH+)
LINGLIN	73	NP B55 408	D. Linglin	(CERN)
ROY	71	PL 36B 353	S.M. Roy	

$K^*(892)$

$I(J^P) = \frac{1}{2}(1^-)$

$K^*(892)$ MASS

CHARGED ONLY, HADROPRODUCED

VALUE (MeV)	EVTS	DOCUMENT ID		TECN	CHG	COMMENT
891.66±0.26 OUR AVERAGE						
892.6 ±0.5	5840	BAUBILLIER	84B	HBC	−	8.25 $K^- p \to \overline{K}^0 \pi^- p$
888 ±3		NAPIER	84	SPEC	+	200 $\pi^- p \to 2K^0_S X$
891 ±1		NAPIER	84	SPEC	−	200 $\pi^- p \to 2K^0_S X$
891.7 ±2.1	3700	BARTH	83	HBC	+	70 $K^+ p \to K^0 \pi^+ X$
891 ±1	4100	TOAFF	81	HBC	−	6.5 $K^- p \to \overline{K}^0 \pi^- p$
892.8 ±1.6		AJINENKO	80	HBC	+	32 $K^+ p \to K^0 \pi^+ X$
890.7 ±0.9	1800	AGUILAR-...	78B	HBC	±	0.76 $\overline{p}p \to K^\mp K^0_S \pi^\pm$
886.6 ±2.4	1225	BALAND	78	HBC	±	12 $\overline{p}p \to (K\pi)^\pm X$
891.7 ±0.6	6706	COOPER	78	HBC	±	0.76 $\overline{p}p \to (K\pi)^\pm X$
891.9 ±0.7	9000	[1] PALER	75	HBC	−	14.3 $K^- p \to (K\pi)^- X$
892.2 ±1.5	4404	AGUILAR-...	71B	HBC	−	3.9,4.6 $K^- p \to (K\pi)^- p$
891 ±2	1000	CRENNELL	69D	DBC	−	3.9 $K^- N \to K^0 \pi^- X$
890 ±3.0	720	BARLOW	67	HBC	±	1.2 $\overline{p}p \to (K^0\pi)^\pm K^\mp$
889 ±3.0	600	BARLOW	67	HBC	±	1.2 $\overline{p}p \to (K^0\pi)^\pm K\pi$
891 ±2.3	620	[2] DEBAERE	67B	HBC	+	3.5 $K^+ p \to K^0 \pi^+ p$
891.0 ±1.2	1700	[3] WOJCICKI	64	HBC	−	1.7 $K^- p \to \overline{K}^0 \pi^- p$
• • • We do not use the following data for averages, fits, limits, etc. • • •						
893.5 ±1.1	27k	[4] ABELE	99D	CBAR	±	0.0 $\overline{p}p \to K^+ K^- \pi^0$
890.4 ±0.2 ±0.5	80±0.8k	[5] BIRD	89	LASS	−	11 $K^- p \to \overline{K}^0 \pi^- p$
890.0 ±2.3	800	[2,3] CLELAND	82	SPEC	+	30 $K^+ p \to K^0_S \pi^+ p$
896.0 ±1.1	3200	[2,3] CLELAND	82	SPEC	+	50 $K^+ p \to K^0_S \pi^+ p$
893 ±1	3600	[2,3] CLELAND	82	SPEC	−	50 $K^+ p \to K^0_S \pi^- p$
896.0 ±1.9	380	DELFOSSE	81	SPEC	+	50 $K^\pm p \to K^\pm \pi^0 p$
886.0 ±2.3	187	DELFOSSE	81	SPEC	−	50 $K^\pm p \to K^\pm \pi^0 p$
894.2 ±2.0	765	[2] CLARK	73	HBC	−	3.13 $K^- p \to \overline{K}^0 \pi^- p$
894.3 ±1.5	1150	[2,3] CLARK	73	HBC	−	3.3 $K^- p \to \overline{K}^0 \pi^- p$
892.0 ±2.6	341	[2] SCHWEING...	68	HBC	−	5.5 $K^- p \to \overline{K}^0 \pi^- p$

CHARGED ONLY, PRODUCED IN τ LEPTON DECAYS

VALUE (MeV)	EVTS	DOCUMENT ID		TECN	COMMENT
895.47±0.20±0.74	53k	[6] EPIFANOV	07	BELL	$\tau^- \to K^0_S \pi^- \nu_\tau$
• • • We do not use the following data for averages, fits, limits, etc. • • •					
892.0 ±0.5		[7] BOITO	10	RVUE	$\tau^- \to K^0_S \pi^- \nu_\tau$
892.0 ±0.9		[8,9] BOITO	09	RVUE	$\tau^- \to K^0_S \pi^- \nu_\tau$
895.3 ±0.2		[8,10] JAMIN	08	RVUE	$\tau^- \to K^0_S \pi^- \nu_\tau$
896.4 ±0.9	11970	[11] BONVICINI	02	CLEO	$\tau^- \to K^- \pi^0 \nu_\tau$
895 ±2		[12] BARATE	99R	ALEP	$\tau^- \to K^- \pi^0 \nu_\tau$

NEUTRAL ONLY

VALUE (MeV)	EVTS	DOCUMENT ID		TECN	COMMENT
895.81±0.19 OUR AVERAGE		Error includes scale factor of 1.4. See the ideogram below.			
895.4 ±0.2 ±0.2	243k	[13] DEL-AMO-SA...	11I	BABR	$D^+ \to K^- \pi^+ e^+ \nu_e$
895.7 ±0.2 ±0.3	141k	[14] BONVICINI	08A	CLEO	$D^+ \to K^- \pi^+ \pi^+$
895.41±0.32$^{+0.35}_{-0.43}$	18k	[15] LINK	05I	FOCS	$D^+ \to K^- \pi^+ \mu^+ \nu_\mu$
896 ±2		BARBERIS	98E	OMEG	450 $pp \to p_f p_s K^* \overline{K}^*$
895.9 ±0.5 ±0.2		ASTON	88	LASS	11 $K^- p \to K^- \pi^+ n$
894.52±0.63	25k	[1] ATKINSON	86	OMEG	20–70 γp
894.63±0.76	20k	[1] ATKINSON	86	OMEG	20–70 γp
897 ±1	28k	EVANGELIS...	80	OMEG	10 $\pi^- p \to K^+ \pi^- (\Lambda, \Sigma)$
898.4 ±1.4	1180	AGUILAR-...	78B	HBC	0.76 $\overline{p}p \to K^\mp K^0_S \pi^\pm$
894.9 ±1.6		WICKLUND	78	ASPK	3,4,6 $K^\pm N \to (K\pi)^0 N$
897.6 ±0.9		BOWLER	77	DBC	5.4 $K^+ d \to K^+ \pi^- p p$
895.5 ±1.0	3600	MCCUBBIN	75	HBC	3.6 $K^- p \to K^- \pi^+ n$
897.1 ±0.7	22k	[1] PALER	75	HBC	14.3 $K^- p \to (K\pi)^0 X$
896.0 ±0.6	10k	FOX	74	RVUE	2 $K^- p \to K^- \pi^+ n$
896.0 ±0.6		FOX	74	RVUE	2 $K^+ n \to K^+ \pi^- p$
896 ±2		[16] MATISON	74	HBC	12 $K^+ p \to K^+ \pi^- \Delta$
896 ±1	3186	LEWIS	73	HBC	2.1–2.7 $K^+ p \to K \pi \pi p$
894.0 ±1.3		[16] LINGLIN	73	HBC	2–13 $K^+ p \to K^+ \pi^- \pi^+ p$
898.4 ±1.3	1700	[2] BUCHNER	72	DBC	4.6 $K^+ n \to K^+ \pi^- p$
897.9 ±1.1	2934	[2] AGUILAR-...	71B	HBC	3.9,4.6 $K^- p \to K^- \pi^+ n$
898.0 ±0.7	5362	[2] AGUILAR-...	71B	HBC	3.9,4.6 $K^- p \to K^- \pi^+ \pi^- p$
895 ±1	4300	[3] HABER	70	DBC	3 $K^- N \to K^- \pi^+ X$
893.7 ±2.0	10k	DAVIS	69	HBC	12 $K^+ p \to K^+ \pi^- \pi^+ p$
894.7 ±1.4	1040	[2] DAUBER	67B	HBC	2.0 $K^- p \to K^- \pi^+ \pi^- p$
• • • We do not use the following data for averages, fits, limits, etc. • • •					
894.9 ±0.5 ±0.7	14.4k	[17] MITCHELL	09A	CLEO	$D_s^+ \to K^+ K^- \pi^+$
896.2 ±0.3	20k	[8] AUBERT	07AK	BABR	10.6 $e^+ e^- \to K^{*0} K^\pm \pi^\mp \gamma$
900.7 ±1.1	5900	BARTH	83	HBC	70 $K^+ p \to K^+ \pi^- X$

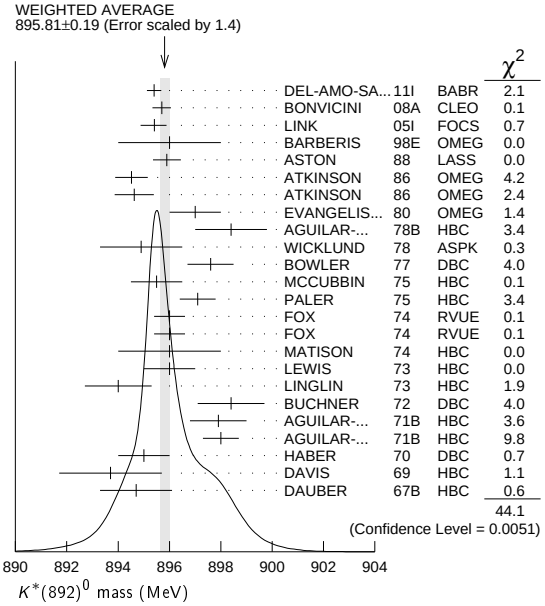

[1] Inclusive reaction. Complicated background and phase-space effects.
[2] Mass errors enlarged by us to $\Gamma/\sqrt{N}$. See note.
[3] Number of events in peak reevaluated by us.
[4] K-matrix pole.
[5] From a partial wave amplitude analysis.
[6] From a fit in the $K_0^*(800)$ + $K^*(892)$ + $K^*(1410)$ model.
[7] From the pole position of the $K\pi$ vector form factor using EPIFANOV 07 and constraints from K_{l3} decays in ANTONELLI 10.
[8] Systematic uncertainties not estimated.
[9] From the pole position of the $K\pi$ vector form factor in the complex s-plane and using EPIFANOV 07 data.
[10] Reanalysis of EPIFANOV 07 using resonance chiral theory.
[11] Calculated by us from the shift by 4.7 ± 0.9 MeV (statistical uncertainty only) reported in BONVICINI 02 with respect to the world average value from PDG 00.
[12] With mass and width of the $K^*(1410)$ fixed at 1412 MeV and 227 MeV, respectively.
[13] Taking into account the $K^*(892)^0$, S-wave and P-wave ($K^*(1410)^0$).
[14] From the isobar model with a complex pole for the κ.
[15] Fit to $K\pi$ mass spectrum includes a non-resonant scalar component.
[16] From pole extrapolation.
[17] This value comes from a fit with χ^2 of 178/117.

$K^*(892)$ MASSES AND MASS DIFFERENCES

Unrealistically small errors have been reported by some experiments. We use simple "realistic" tests for the minimum errors on the determination of a mass and width from a sample of N events:

$$\delta_{\min}(m) = \frac{\Gamma}{\sqrt{N}}, \quad \delta_{\min}(\Gamma) = 4\frac{\Gamma}{\sqrt{N}} \ . \qquad (1)$$

We consistently increase unrealistic errors before averaging. For a detailed discussion, see the 1971 edition of this Note.

$m_{K^*(892)^0} - m_{K^*(892)^\pm}$

VALUE (MeV)	EVTS	DOCUMENT ID		TECN	CHG	COMMENT
6.7±1.2 OUR AVERAGE						
7.7±1.7	2980	AGUILAR-...	78B	HBC	±0	0.76 $\overline{p}p \rightarrow K^{\mp}K^0_S\pi^{\pm}$
5.7±1.7	7338	AGUILAR-...	71B	HBC	−0	3.9,4.6 K^-p
6.3±4.1	283	[18] BARASH	67B	HBC		0.0 $\overline{p}p$

[18] Number of events in peak reevaluated by us.

$K^*(892)$ RANGE PARAMETER

All from partial wave amplitude analyses.

VALUE (GeV^{-1})	EVTS	DOCUMENT ID		TECN	CHG	COMMENT
2.1 ±0.5 ±0.5	243k	[19] DEL-AMO-SA..	11I	BABR	0	$D^+ \rightarrow K^-\pi^+e^+\nu_e$
$3.96\pm0.54^{+1.31}_{-0.90}$	18k	[20] LINK	05I	FOCS	0	$D^+ \rightarrow K^-\pi^+\mu^+\nu_\mu$
3.4 ±0.7		ASTON	88	LASS	0	11 $K^-p \rightarrow K^-\pi^+n$
• • • We do not use the following data for averages, fits, limits, etc. • • •						
12.1 ±3.2 ±3.0		BIRD	89	LASS	−	11 $K^-p \rightarrow \overline{K}^0\pi^-p$

[19] Taking into account the $K^*(892)^0$, S-wave and P-wave ($K^*(1410)^0$).
[20] Fit to $K\pi$ mass spectrum includes a non-resonant scalar component.

$K^*(892)$ WIDTH

CHARGED ONLY, HADROPRODUCED

VALUE (MeV)	EVTS	DOCUMENT ID		TECN	CHG	COMMENT
50.8±0.9 OUR FIT						
50.8±0.9 OUR AVERAGE						
49 ±2	5840	BAUBILLIER	84B	HBC	−	8.25 $K^-p \rightarrow \overline{K}^0\pi^-p$
56 ±4		NAPIER	84	SPEC	−	200 $\pi^-p \rightarrow 2K^0_S X$
51 ±2	4100	TOAFF	81	HBC	−	6.5 $K^-p \rightarrow \overline{K}^0\pi^-p$
50.5±5.6		AJINENKO	80	HBC	+	32 $K^+p \rightarrow K^0\pi^+X$
45.8±3.6	1800	AGUILAR-...	78B	HBC	±	0.76 $\overline{p}p \rightarrow K^{\mp}K^0_S\pi^{\pm}$
52.0±2.5	6706	[21] COOPER	78	HBC	±	0.76 $\overline{p}p \rightarrow (K\pi)^{\pm}X$
52.1±2.2	9000	[22] PALER	75	HBC	−	14.3 $K^-p \rightarrow (K\pi)^-X$
46.3±6.7	765	[21] CLARK	73	HBC	−	3.13 $K^-p \rightarrow \overline{K}^0\pi^-p$
48.2±5.7	1150	[21,23] CLARK	73	HBC	−	3.3 $K^-p \rightarrow \overline{K}^0\pi^-p$
54.3±3.3	4404	[21] AGUILAR-...	71B	HBC	−	3.9,4.6 $K^-p \rightarrow (K\pi)^-p$
46 ±5	1700	[21,23] WOJCICKI	64	HBC	−	1.7 $K^-p \rightarrow \overline{K}^0\pi^-p$
• • • We do not use the following data for averages, fits, limits, etc. • • •						
54.8±1.7	27k	[24] ABELE	99D	CBAR	±	0.0 $\overline{p}p \rightarrow K^+K^-\pi^0$
45.2±1 ±2	79.7±0.8k	[25] BIRD	89	LASS	−	11 $K^-p \rightarrow \overline{K}^0\pi^-p$
42.8±7.1	3700	BARTH	83	HBC	+	70 $K^+p \rightarrow K^0\pi^+X$
64.0±9.2	800	[21,23] CLELAND	82	SPEC	+	30 $K^+p \rightarrow K^0_S\pi^+p$
62.0±4.4	3200	[21,23] CLELAND	82	SPEC	+	50 $K^+p \rightarrow K^0_S\pi^+p$
55 ±4	3600	[21,23] CLELAND	82	SPEC	−	50 $K^+p \rightarrow K^0_S\pi^-p$
62.6±3.8	380	DELFOSSE	81	SPEC	+	50 $K^{\pm}p \rightarrow K^{\pm}\pi^0p$
50.5±3.9	187	DELFOSSE	81	SPEC	−	50 $K^{\pm}p \rightarrow K^{\pm}\pi^0p$

CHARGED ONLY, PRODUCED IN τ LEPTON DECAYS

VALUE (MeV)	EVTS	DOCUMENT ID		TECN	COMMENT
46.2±0.6±1.2	53k	[26] EPIFANOV	07	BELL	$\tau^- \rightarrow K^0_S\pi^-\nu_\tau$
• • • We do not use the following data for averages, fits, limits, etc. • • •					
46.5±1.1		[27] BOITO	10	RVUE	$\tau^- \rightarrow K^0_S\pi^-\nu_\tau$
46.2±0.4		[28,29] BOITO	09	RVUE	$\tau^- \rightarrow K^0_S\pi^-\nu_\tau$
47.5±0.4		[28,30] JAMIN	08	RVUE	$\tau^- \rightarrow K^0_S\pi^-\nu_\tau$
55 ±8		[31] BARATE	99R	ALEP	$\tau^- \rightarrow K^-\pi^0\nu_\tau$

NEUTRAL ONLY

VALUE (MeV)	EVTS	DOCUMENT ID		TECN	COMMENT
47.4 ±0.6 OUR FIT Error includes scale factor of 2.2.					
47.4 ±0.6 OUR AVERAGE Error includes scale factor of 2.0. See the ideogram below.					
46.5 ±0.3 ±0.2	243k	[32] DEL-AMO-SA..	11I	BABR	$D^+ \rightarrow K^-\pi^+e^+\nu_e$
45.3 ±0.5 ±0.6	141k	[33] BONVICINI	08A	CLEO	$D^+ \rightarrow K^-\pi^+\pi^+$
$47.79\pm0.86^{+1.32}_{-1.06}$	18k	[34] LINK	05I	FOCS	$D^+ \rightarrow K^-\pi^+\mu^+\nu_\mu$
54 ±3		BARBERIS	98E	OMEG	450 $pp \rightarrow p_fp_sK^*\overline{K}^*$
50.8 ±0.8 ±0.9		ASTON	88	LASS	11 $K^-p \rightarrow K^-\pi^+n$
46.5 ±4.3	5900	BARTH	83	HBC	70 $K^+p \rightarrow K^+\pi^-X$
54 ±2	28k	EVANGELIS...	80	OMEG	10 $\pi^-p \rightarrow K^+\pi^-(\Lambda,\Sigma)$
45.9 ±4.8	1180	AGUILAR-...	78B	HBC	0.76 $\overline{p}p \rightarrow K^{\mp}K^0_S\pi^{\pm}$
51.2 ±1.7		WICKLUND	78	ASPK	3,4,6 $K^{\pm}N \rightarrow (K\pi)^0N$
48.9 ±2.5		BOWLER	77	DBC	5.4 $K^+d \rightarrow K^+\pi^-pp$
$48\ ^{+3}_{-2}$	3600	MCCUBBIN	75	HBC	3.6 $K^-p \rightarrow K^-\pi^+n$
50.6 ±2.5	22k	[22] PALER	75	HBC	14.3 $K^-p \rightarrow (K\pi)^0X$
47 ±2	10k	FOX	74	RVUE	2 $K^-p \rightarrow K^-\pi^+n$
51 ±2		FOX	74	RVUE	2 $K^+n \rightarrow K^+\pi^-p$
46.0 ±3.3	3186	[21] LEWIS	73	HBC	2.1–2.7 $K^+p \rightarrow K\pi\pi p$
51.4 ±5.0	1700	[21] BUCHNER	72	DBC	4.6 $K^+n \rightarrow K^+\pi^-p$
$55.8\ ^{+4.2}_{-3.4}$	2934	[21] AGUILAR-...	71B	HBC	3.9,4.6 $K^-p \rightarrow K^-\pi^+n$
48.5 ±2.7	5362	AGUILAR-...	71B	HBC	3.9,4.6 $K^-p \rightarrow K^-\pi^+\pi^-p$
54.0 ±3.3	4300	[21,23] HABER	70	DBC	3 $K^-N \rightarrow K^-\pi^+X$
53.2 ±2.1	10k	[21] DAVIS	69	HBC	12 $K^+p \rightarrow K^+\pi^-\pi^+p$
44 ±5.5	1040	[21] DAUBER	67B	HBC	2.0 $K^-p \rightarrow K^-\pi^+\pi^-p$
• • • We do not use the following data for averages, fits, limits, etc. • • •					
45.7 ±1.1 ±0.5	14.4k	[35] MITCHELL	09A	CLEO	$D^+_s \rightarrow K^+K^-\pi^+$
50.6 ±0.9	20k	[28] AUBERT	07AK	BABR	10.6 $e^+e^- \rightarrow K^{*0}K^{\pm}\pi^{\mp}\gamma$

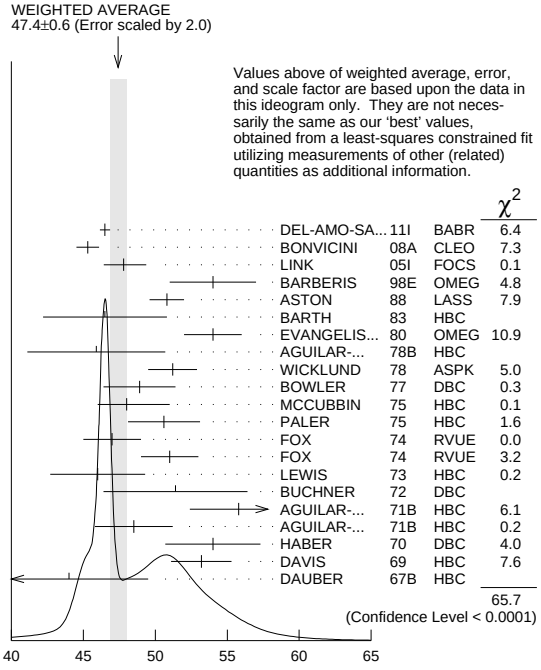

NEUTRAL ONLY (MeV)

[21] Width errors enlarged by us to $4 \times \Gamma/\sqrt{N}$; see note.
[22] Inclusive reaction. Complicated background and phase-space effects.
[23] Number of events in peak reevaluated by us.
[24] K-matrix pole.
[25] From a partial wave amplitude analysis.
[26] From a fit in the $K^*_0(800) + K^*(892) + K^*(1410)$ model.
[27] From the pole position of the $K\pi$ vector form factor using EPIFANOV 07 and constraints from K_{l3} decays in ANTONELLI 10.
[28] Systematic uncertainties not estimated.
[29] From the pole position of the $K\pi$ vector form factor in the complex s-plane and using EPIFANOV 07 data.
[30] Reanalysis of EPIFANOV 07 using resonance chiral theory.
[31] With mass and width of the $K^*(1410)$ fixed at 1412 MeV and 227 MeV, respectively.
[32] Taking into account the $K^*(892)^0$, S-wave and P-wave ($K^*(1410)^0$).
[33] From the isobar model with a complex pole for the κ.
[34] Fit to $K\pi$ mass spectrum includes a non-resonant scalar component.
[35] This value comes from a fit with χ^2 of 178/117.

Meson Particle Listings

$K^*(892)$, $K_1(1270)$

$K^*(892)$ DECAY MODES

	Mode	Fraction (Γ_i/Γ)	Confidence level
Γ_1	$K\pi$	$\sim$ 100 %	
Γ_2	$(K\pi)^\pm$	(99.901 $\pm$ 0.009) %	
Γ_3	$(K\pi)^0$	(99.754 $\pm$ 0.021) %	
Γ_4	$K^0\gamma$	(2.46 $\pm$ 0.21) $\times 10^{-3}$	
Γ_5	$K^\pm\gamma$	(9.9 $\pm$ 0.9) $\times 10^{-4}$	
Γ_6	$K\pi\pi$	< 7 $\times 10^{-4}$	95%

CONSTRAINED FIT INFORMATION

An overall fit to the total width and a partial width uses 13 measurements and one constraint to determine 3 parameters. The overall fit has a $\chi^2 = 7.8$ for 11 degrees of freedom.

The following *off-diagonal* array elements are the correlation coefficients $\langle \delta p_i \delta p_j \rangle / (\delta p_i \cdot \delta p_j)$, in percent, from the fit to parameters p_i, including the branching fractions, $x_i \equiv \Gamma_i/\Gamma_{\rm total}$. The fit constrains the x_i whose labels appear in this array to sum to one.

x_5	−100	
Γ	19	−19
	x_2	x_5

	Mode	Rate (MeV)
Γ_2	$(K\pi)^\pm$	50.7 $\pm$ 0.9
Γ_5	$K^\pm\gamma$	0.050 $\pm$ 0.005

CONSTRAINED FIT INFORMATION

An overall fit to the total width and a partial width uses 22 measurements and one constraint to determine 3 parameters. The overall fit has a $\chi^2 = 66.8$ for 20 degrees of freedom.

The following *off-diagonal* array elements are the correlation coefficients $\langle \delta p_i \delta p_j \rangle / (\delta p_i \cdot \delta p_j)$, in percent, from the fit to parameters p_i, including the branching fractions, $x_i \equiv \Gamma_i/\Gamma_{\rm total}$. The fit constrains the x_i whose labels appear in this array to sum to one.

x_4	−100	
Γ	15	−15
	x_3	x_4

	Mode	Rate (MeV)	Scale factor
Γ_3	$(K\pi)^0$	47.3 $\pm$ 0.6	2.1
Γ_4	$K^0\gamma$	0.116 $\pm$ 0.010	

$K^*(892)$ PARTIAL WIDTHS

$\Gamma(K^0\gamma)$ Γ_4

VALUE (keV)	EVTS	DOCUMENT ID		TECN	CHG	COMMENT
116 ±10 OUR FIT						
116.5± 9.9	584	CARLSMITH	86	SPEC	0	$K^0_L A \to K^0_S \pi^0 A$

$\Gamma(K^\pm\gamma)$ Γ_5

VALUE (keV)	DOCUMENT ID		TECN	CHG	COMMENT
50± 5 OUR FIT					
50± 5 OUR AVERAGE					
48±11	BERG	83	SPEC	−	156 $K^- A \to \overline{K}\pi A$
51± 5	CHANDLEE	83	SPEC	+	200 $K^+ A \to K\pi A$

$K^*(892)$ BRANCHING RATIOS

$\Gamma(K^0\gamma)/\Gamma_{\rm total}$ Γ_4/Γ

VALUE (units 10^{-3})	DOCUMENT ID		TECN	CHG	COMMENT
2.46±0.21 OUR FIT					
• • • We do not use the following data for averages, fits, limits, etc. • • •					
1.5 ±0.7	CARITHERS	75B	CNTR	0	8–16 $\overline{K}^0 A$

$\Gamma(K^\pm\gamma)/\Gamma_{\rm total}$ Γ_5/Γ

VALUE (units 10^{-3})	CL%	DOCUMENT ID		TECN	CHG	COMMENT
0.99±0.09 OUR FIT						
• • • We do not use the following data for averages, fits, limits, etc. • • •						
<1.6	95	BEMPORAD	73	CNTR	+	10–16 $K^+ A$

$\Gamma(K\pi\pi)/\Gamma((K\pi)^\pm)$ Γ_6/Γ_2

VALUE	CL%	DOCUMENT ID		TECN	CHG	COMMENT
< 7 × 10^{-4}	95	JONGEJANS	78	HBC		4 $K^- p \to p\overline{K}^0 2\pi$
• • • We do not use the following data for averages, fits, limits, etc. • • •						
<20 × 10^{-4}		WOJCICKI	64	HBC	−	1.7 $K^- p \to \overline{K}^0 \pi^- p$

$K^*(892)$ REFERENCES

DEL-AMO-SA...	11I	PR D83 072001	P. del Amo Sanchez *et al.*	(BABAR Collab.)
ANTONELLI	10	EPJ C69 399	M. Antonelli *et al.*	(FlaviaNet Working Group)
BOITO	10	JHEP 1009 031	D.R. Boito, R. Escribano, M. Jamin	(BARC)
BOITO	09	EPJ C59 821	D.R. Boito, R. Escribano, M. Jamin	
MITCHELL	09A	PR D79 072008	R.E. Mitchell *et al.*	(CLEO Collab.)
BONVICINI	08A	PR D78 052001	G. Bonvicini *et al.*	(CLEO Collab.)
JAMIN	08	PL B664 78	M. Jamin, A. Pich, J. Portoles	
AUBERT	07AK	PR D76 012008	B. Aubert *et al.*	(BABAR Collab.)
EPIFANOV	07	PL B654 65	D. Epifanov *et al.*	(BELLE Collab.)
LINK	05I	PL B621 72	J.M. Link *et al.*	(FNAL FOCUS Collab.)
BONVICINI	02	PRL 88 111803	G. Bonvicini *et al.*	(CLEO Collab.)
PDG	00	EPJ C15 1	D.E. Groom *et al.*	(PDG Collab.)
ABELE	99D	PL B468 178	A. Abele *et al.*	(Crystal Barrel Collab.)
BARATE	99R	EPJ C11 599	R. Barate *et al.*	(ALEPH Collab.)
BARBERIS	98E	PL B436 204	D. Barberis *et al.*	(Omega Expt.)
BIRD	89	SLAC-332	P.F. Bird	(SLAC)
ASTON	88	NP B296 493	D. Aston *et al.*	(SLAC, NAGO, CINC, INUS)
ATKINSON	86	ZPHY C30 521	M. Atkinson *et al.*	(BONN, CERN, GLAS+)
CARLSMITH	86	PRL 56 18	D. Carlsmith *et al.*	(EFI, SACL)
BAUBILLIER	84B	ZPHY C26 37	M. Baubillier *et al.*	(BIRM, CERN, GLAS+)
NAPIER	84	PL 149B 514	A. Napier *et al.*	(TUFTS, ARIZ, FNAL, FLOR+)
BARTH	83	NP B223 296	M. Barth *et al.*	(BRUX, CERN, GENO, MONS+)
BERG	83	Thesis UMI 83-21652	D.M. Berg	(ROCH)
CHANDLEE	83	PRL 51 168	C. Chandlee *et al.*	(ROCH, FNAL, MINN)
CLELAND	82	NP B208 189	W.E. Cleland *et al.*	(DURH, GEVA, LAUS+)
DELFOSSE	81	NP B183 349	A. Delfosse *et al.*	(GEVA, LAUS)
TOAFF	81	PR D23 1500	S. Toaff *et al.*	(ANL, KANS)
AJINENKO	80	ZPHY C5 177	I.V. Ajinenko *et al.*	(SERP, BRUX, MONS+)
EVANGELIS...	80	NP B165 383	C. Evangelista *et al.*	(BARI, BONN, CERN+)
AGUILAR-...	78B	NP B141 101	M. Aguilar-Benitez *et al.*	(MADR, TATA+)
BALAND	78	NP B140 220	J.F. Baland *et al.*	(MONS, BELG, CERN+)
COOPER	78	NP B136 365	A.M. Cooper *et al.*	(TATA, CERN, CDEF+)
JONGEJANS	78	NP B139 383	B. Jongejans *et al.*	(ZEEM, CERN, NIJM+)
WICKLUND	78	PR D17 1197	A.B. Wicklund *et al.*	(ANL)
BOWLER	77	NP B126 31	M.G. Bowler *et al.*	(OXF)
CARITHERS	75B	PRL 35 349	W.C.J. Carithers *et al.*	(ROCH, MCGI)
MCCUBBIN	75	NP B86 13	N.A. McCubbin, L. Lyons	(OXF)
PALER	75	NP B96 1	K. Paler *et al.*	(RHEL, SACL, EPOL)
FOX	74	NP B80 403	G.C. Fox, M.L. Griss	(CIT)
MATISON	74	PR D9 1872	M.J. Matison *et al.*	(LBL)
BEMPORAD	73	NP B51 1	C. Bemporad *et al.*	(CERN, ETH, LOIC)
CLARK	73	NP B54 432	A.G. Clark, L. Lyons, D. Radojicic	(OXF)
LEWIS	73	NP B60 283	P.H. Lewis *et al.*	(LOWC, LOIC, CDEF)
LINGLIN	73	NP B55 408	D. Linglin	(CERN)
BUCHNER	72	NP B45 333	K. Buchner *et al.*	(MPIM, CERN, BRUX)
AGUILAR-...	71B	PR D4 2583	M. Aguilar-Benitez, R.L. Eisner, J.B. Kinson	(BNL)
HABER	70	NP B17 289	B. Haber *et al.*	(REHO, SACL, BGNA, EPOL)
CRENNELL	69D	PRL 22 487	D.J. Crennell *et al.*	(BNL)
DAVIS	69	PRL 23 1071	P.J. Davis *et al.*	(LRL)
SCHWEING...	68	PR 166 1317	F. Schweingruber *et al.*	(ANL, NWES)
BARASH	67B	PR 156 1399	N. Barash *et al.*	(COLU)
BARLOW	67	NC 50A 701	J. Barlow *et al.*	(CERN, CDEF, IRAD, LIVP)
DAUBER	67B	PR 153 1403	P.M. Dauber *et al.*	(UCLA)
DEBAERE	67B	NC 51A 401	W. de Baere *et al.*	(BRUX, CERN)
WOJCICKI	64	PR 135 B484	S.G. Wojcicki	(LRL)

$K_1(1270)$ $I(J^P) = \frac{1}{2}(1^+)$

$K_1(1270)$ MASS

VALUE (MeV)	DOCUMENT ID
1272±7 OUR AVERAGE	Includes data from the 2 datablocks that follow this one.

PRODUCED BY K^-, BACKWARD SCATTERING, HYPERON EXCHANGE

VALUE (MeV)	EVTS	DOCUMENT ID		TECN	CHG	COMMENT
The data in this block is included in the average printed for a previous datablock.						
1275±10	700	GAVILLET	78	HBC	+	4.2 $K^- p \to \Xi^- (K\pi\pi)^+$

PRODUCED BY K BEAMS

VALUE (MeV)	DOCUMENT ID		TECN	CHG	COMMENT
The data in this block is included in the average printed for a previous datablock.					
1270±10	[1] DAUM	81C	CNTR	−	63 $K^- p \to K^- 2\pi p$
• • • We do not use the following data for averages, fits, limits, etc. • • •					
~ 1276	[2] TORNQVIST	82B	RVUE		
~ 1300	VERGEEST	79	HBC	−	4.2 $K^- p \to (\overline{K}\pi\pi)^- p$
1289±25	[3] CARNEGIE	77	ASPK	±	13 $K^\pm p \to (K\pi\pi)^\pm p$
~ 1300	BRANDENB...	76	ASPK	±	13 $K^\pm p \to (K\pi\pi)^\pm p$
~ 1270	OTTER	76	HBC	−	10,14,16 $K^- p \to (\overline{K}\pi\pi)^- p$
1260	DAVIS	72	HBC	+	12 $K^+ p$
1234±12	FIRESTONE	72B	DBC	+	12 $K^+ d$

[1] Well described in the chiral unitary approach of GENG 07 with two poles at 1195 and 1284 MeV and widths of 246 and 146 MeV, respectively.
[2] From a unitarized quark-model calculation.
[3] From a model-dependent fit with Gaussian background to BRANDENBURG 76 data.

PRODUCED BY BEAMS OTHER THAN K MESONS

VALUE (MeV)	EVTS	DOCUMENT ID		TECN	CHG	COMMENT
1248.1± 3.3±1.4		GULER	11	BELL		$B^+ \to J/\psi K^+\pi^+\pi^-$
• • • We do not use the following data for averages, fits, limits, etc. • • •						
1279 ±10	25k	[4] ABLIKIM	06C	BES2		$J/\psi \to \overline{K}^*(892)^0 K^+\pi^-$
1294 ±10	310	RODEBACK	81	HBC		$4\ \pi^- p \to \Lambda K 2\pi$
1300	40	CRENNELL	72	HBC	0	$4.5\ \pi^- p \to \Lambda K 2\pi$
1242 $^{+\ 9}_{-10}$		[5] ASTIER	69	HBC	0	$\overline{p}p$
1300	45	CRENNELL	67	HBC	0	$6\ \pi^- p \to \Lambda K 2\pi$

[4] Systematic errors not estimated.
[5] This was called the C meson.

PRODUCED IN τ LEPTON DECAYS

VALUE (MeV)	EVTS	DOCUMENT ID		TECN	CHG	COMMENT
1254±33±34	7k	ASNER	00B	CLEO	±	$\tau^- \to K^-\pi^+\pi^-\nu_\tau$

$K_1(1270)$ WIDTH

VALUE (MeV)	DOCUMENT ID
90±20 OUR ESTIMATE This is only an educated guess; the error given is larger than the error on the average of the published values.	
87± 7 OUR AVERAGE Includes data from the 2 datablocks that follow this one.	

PRODUCED BY K^-, BACKWARD SCATTERING, HYPERON EXCHANGE

VALUE (MeV)	EVTS	DOCUMENT ID		TECN	CHG	COMMENT
The data in this block is included in the average printed for a previous datablock.						
75±15	700	GAVILLET	78	HBC	+	$4.2\ K^- p \to \Xi^- K\pi\pi$

PRODUCED BY K BEAMS

VALUE (MeV)	DOCUMENT ID		TECN	CHG	COMMENT
The data in this block is included in the average printed for a previous datablock.					
90± 8	[6] DAUM	81C	CNTR	−	$63\ K^- p \to K^- 2\pi p$
• • • We do not use the following data for averages, fits, limits, etc. • • •					
∼ 150	VERGEEST	79	HBC	−	$4.2\ K^- p \to (\overline{K}\pi\pi)^- p$
150±71	[7] CARNEGIE	77	ASPK	±	$13\ K^\pm p \to (K\pi\pi)^\pm p$
∼ 200	BRANDENB...	76	ASPK	±	$13\ K^\pm p \to (K\pi\pi)^\pm p$
120	DAVIS	72	HBC	+	$12\ K^+ p$
188±21	FIRESTONE	72B	DBC	+	$12\ K^+ d$

[6] Well described in the chiral unitary approach of GENG 07 with two poles at 1195 and 1284 MeV and widths of 246 and 146 MeV, respectively.
[7] From a model-dependent fit with Gaussian background to BRANDENBURG 76 data.

PRODUCED BY BEAMS OTHER THAN K MESONS

VALUE (MeV)	EVTS	DOCUMENT ID		TECN	CHG	COMMENT
119.5± 5.2±6.7		GULER	11	BELL		$B^+ \to J/\psi K^+\pi^+\pi^-$
• • • We do not use the following data for averages, fits, limits, etc. • • •						
131 ±21	25k	[8] ABLIKIM	06C	BES2		$J/\psi \to \overline{K}^*(892)^0 K^+\pi^-$
66 ±15	310	RODEBACK	81	HBC		$4\ \pi^- p \to \Lambda K 2\pi$
60	40	CRENNELL	72	HBC	0	$4.5\ \pi^- p \to \Lambda K 2\pi$
127 $^{+\ 7}_{-25}$		ASTIER	69	HBC	0	$\overline{p}p$
60	45	CRENNELL	67	HBC	0	$6\ \pi^- p \to \Lambda K 2\pi$

[8] Systematic errors not estimated.

PRODUCED IN τ LEPTON DECAYS

VALUE (MeV)	EVTS	DOCUMENT ID		TECN	CHG	COMMENT
260$^{+90}_{-70}$±80	7k	ASNER	00B	CLEO	±	$\tau^- \to K^-\pi^+\pi^-\nu_\tau$

$K_1(1270)$ DECAY MODES

	Mode	Fraction (Γ_i/Γ)
Γ_1	$K\rho$	(42 ±6) %
Γ_2	$K_0^*(1430)\pi$	(28 ±4) %
Γ_3	$K^*(892)\pi$	(16 ±5) %
Γ_4	$K\omega$	(11.0±2.0) %
Γ_5	$Kf_0(1370)$	(3.0±2.0) %
Γ_6	γK^0	seen

$K_1(1270)$ PARTIAL WIDTHS

$\Gamma(K\rho)$ Γ_1

VALUE (MeV)	DOCUMENT ID		TECN	CHG	COMMENT
• • • We do not use the following data for averages, fits, limits, etc. • • •					
57±5	MAZZUCATO	79	HBC	+	$4.2\ K^- p \to \Xi^-(K\pi\pi)^+$
75±6	CARNEGIE	77B	ASPK	±	$13\ K^\pm p \to (K\pi\pi)^\pm p$

$\Gamma(K_0^*(1430)\pi)$ Γ_2

VALUE (MeV)	DOCUMENT ID		TECN	CHG	COMMENT
• • • We do not use the following data for averages, fits, limits, etc. • • •					
26±6	CARNEGIE	77B	ASPK	±	$13\ K^\pm p \to (K\pi\pi)^\pm p$

$\Gamma(K^*(892)\pi)$ Γ_3

VALUE (MeV)	DOCUMENT ID		TECN	CHG	COMMENT
• • • We do not use the following data for averages, fits, limits, etc. • • •					
14±11	MAZZUCATO	79	HBC	+	$4.2\ K^- p \to \Xi^-(K\pi\pi)^+$
2± 2	CARNEGIE	77B	ASPK	±	$13\ K^\pm p \to (K\pi\pi)^\pm p$

$\Gamma(K\omega)$ Γ_4

VALUE (MeV)	DOCUMENT ID		TECN	CHG	COMMENT
• • • We do not use the following data for averages, fits, limits, etc. • • •					
4±4	MAZZUCATO	79	HBC	+	$4.2\ K^- p \to \Xi^-(K\pi\pi)^+$
24±3	CARNEGIE	77B	ASPK	±	$13\ K^\pm p \to (K\pi\pi)^\pm p$

$\Gamma(Kf_0(1370))$ Γ_5

VALUE (MeV)	DOCUMENT ID		TECN	CHG	COMMENT
• • • We do not use the following data for averages, fits, limits, etc. • • •					
22±5	CARNEGIE	77B	ASPK	±	$13\ K^\pm p \to (K\pi\pi)^\pm p$

$\Gamma(\gamma K^0)$ Γ_6

VALUE (keV)	DOCUMENT ID		TECN	COMMENT
73.2±6.1±28.3	ALAVI-HARATI	02B	KTEV	$K + A \to K^* + A$

$K_1(1270)$ BRANCHING RATIOS

$\Gamma(K\rho)/\Gamma_{\text{total}}$ Γ_1/Γ

VALUE	DOCUMENT ID		TECN	COMMENT
0.42 ±0.06	[9] DAUM	81C	CNTR	$63\ K^- p \to K^- 2\pi p$
• • • We do not use the following data for averages, fits, limits, etc. • • •				
0.584±0.043	[10] GULER	11	BELL	$B^+ \to J/\psi K^+\pi^+\pi^-$
dominant	RODEBACK	81	HBC	$4\ \pi^- p \to \Lambda K 2\pi$

$\Gamma(K_0^*(1430)\pi)/\Gamma_{\text{total}}$ Γ_2/Γ

VALUE	DOCUMENT ID		TECN	COMMENT
0.28 ±0.04	[9] DAUM	81C	CNTR	$63\ K^- p \to K^- 2\pi p$
• • • We do not use the following data for averages, fits, limits, etc. • • •				
0.0201±0.0064	[10] GULER	11	BELL	$B^+ \to J/\psi K^+\pi^+\pi^-$

$\Gamma(K^*(892)\pi)/\Gamma_{\text{total}}$ Γ_3/Γ

VALUE	DOCUMENT ID		TECN	COMMENT
0.16 ±0.05	[9] DAUM	81C	CNTR	$63\ K^- p \to K^- 2\pi p$
• • • We do not use the following data for averages, fits, limits, etc. • • •				
0.171±0.023	[10] GULER	11	BELL	$B^+ \to J/\psi K^+\pi^+\pi^-$

$\Gamma(K\omega)/\Gamma_{\text{total}}$ Γ_4/Γ

VALUE	DOCUMENT ID		TECN	COMMENT
0.11 ±0.02	[9] DAUM	81C	CNTR	$63\ K^- p \to K^- 2\pi p$
• • • We do not use the following data for averages, fits, limits, etc. • • •				
0.225±0.052	[10] GULER	11	BELL	$B^+ \to J/\psi K^+\pi^+\pi^-$

$\Gamma(K\omega)/\Gamma(K\rho)$ Γ_4/Γ_1

VALUE	CL%	DOCUMENT ID		TECN	COMMENT
• • • We do not use the following data for averages, fits, limits, etc. • • •					
<0.30	95	RODEBACK	81	HBC	$4\ \pi^- p \to \Lambda K 2\pi$

$\Gamma(Kf_0(1370))/\Gamma_{\text{total}}$ Γ_5/Γ

VALUE	DOCUMENT ID		TECN	COMMENT
0.03±0.02	[9] DAUM	81C	CNTR	$63\ K^- p \to K^- 2\pi p$

D-wave/S-wave RATIO FOR $K_1(1270) \to K^*(892)\pi$

VALUE	DOCUMENT ID		TECN	COMMENT
1.0±0.7	[9] DAUM	81C	CNTR	$63\ K^- p \to K^- 2\pi p$

[9] Average from low and high t data.
[10] Assuming that decays are saturated by the $K\rho$, $K_0^*(1430)\pi$, $K^*(892)\pi$, $K\omega$ decay modes and neglecting interference between them. The values $B(\omega \to \pi^+\pi^-) = (1.53^{+0.11}_{-0.13})\%$ and $B(K_0^*(1430) \to K\pi) = (93 \pm 10)\%$ are used. Systematic uncertainties not estimated.

$K_1(1270)$ REFERENCES

GULER	11	PR D83 032005	H. Guler *et al.*	(BELLE Collab.)
GENG	07	PR D75 014017	L.S. Geng *et al.*	
ABLIKIM	06C	PL B633 681	M. Ablikim *et al.*	(BES Collab.)
ALAVI-HARATI	02B	PRL 89 072001	A. Alavi-Harati *et al.*	(FNAL KTeV Collab.)
ASNER	00B	PR D62 072006	D.M. Asner *et al.*	(CLEO Collab.)
TORNQVIST	82B	NP B203 268	N.A. Tornqvist	(HELS)
DAUM	81C	NP B187 1	C. Daum *et al.*	(AMST, CERN, CRAC, MPIM+)
RODEBACK	81	ZPHY C9 9	S. Rodeback *et al.*	(CERN, CDEF, MADR+)
MAZZUCATO	79	NP B156 532	M. Mazzucato *et al.*	(CERN, ZEEM, NIJM+)
VERGEEST	79	NP B158 265	J.S.M. Vergeest *et al.*	(NIJM, AMST, CERN+)
GAVILLET	78	PL 76B 517	P. Gavillet *et al.*	(AMST, CERN, NIJM+) JP
CARNEGIE	77	NP B127 509	R.K. Carnegie *et al.*	(SLAC)
CARNEGIE	77B	PL 68B 287	R.K. Carnegie *et al.*	(SLAC)
BRANDENB...	76	PRL 36 703	G.W. Brandenburg *et al.*	(SLAC) JP
OTTER	76	NP B106 77	G. Otter *et al.*	(AACH3, BERL, CERN, LOIC+) JP
CRENNELL	72	PR D6 1220	D.J. Crennell *et al.*	(BNL)
DAVIS	72	PR D5 2688	P.J. Davis *et al.*	(LBL)
FIRESTONE	72B	PR D5 505	A. Firestone *et al.*	(LBL)
ASTIER	69	NP B10 65	A. Astier *et al.*	(CDEF, CERN, IPNP, LIVP) JP
CRENNELL	67	PRL 19 44	D.J. Crennell *et al.*	(BNL) I

Meson Particle Listings

$K_1(1400)$, $K^*(1410)$

$K_1(1400)$

$I(J^P) = \frac{1}{2}(1^+)$

$K_1(1400)$ MASS

VALUE (MeV)	EVTS	DOCUMENT ID		TECN	CHG	COMMENT
1403± 7 OUR AVERAGE						
1463±64±68	7k	ASNER	00B	CLEO	±	$\tau^- \to K^-\pi^+\pi^-\nu_\tau$
1373±14±18		[1] ASTON	87	LASS	0	11 $K^-p \to \overline{K}^0\pi^+\pi^-n$
1392±18		BAUBILLIER	82B	HBC	0	8.25 $K^-p \to K^0_S\pi^+\pi^-n$
1410±25		DAUM	81C	CNTR	−	63 $K^-p \to K^-2\pi p$
1415±15		ETKIN	80	MPS	0	6 $K^-p \to \overline{K}^0\pi^+\pi^-n$
1404±10		[2] CARNEGIE	77	ASPK	±	13 $K^\pm p \to (K\pi\pi)^\pm p$
• • • We do not use the following data for averages, fits, limits, etc. • • •						
1418± 8	25k	[3] ABLIKIM	06C	BES2		$J/\psi \to \overline{K}^*(892)^0K^+\pi^-$
~ 1350		[4] TORNQVIST	82B	RVUE		
~ 1400		VERGEEST	79	HBC	−	4.2 $K^-p \to (\overline{K}\pi\pi)^-p$
~ 1400		BRANDENB...	76	ASPK	±	13 $K^\pm p \to (K\pi\pi)^\pm p$
1420		DAVIS	72	HBC	+	12 K^+p
1368±18		FIRESTONE	72B	DBC	+	12 K^+d

[1] From partial-wave analysis of $K^0\pi^+\pi^-$ system.
[2] From a model-dependent fit with Gaussian background to BRANDENBURG 76 data.
[3] Systematic errors not estimated.
[4] From a unitarized quark-model calculation.

$K_1(1400)$ WIDTH

VALUE (MeV)	EVTS	DOCUMENT ID		TECN	CHG	COMMENT
174± 13 OUR AVERAGE Error includes scale factor of 1.6. See the ideogram below.						
$300^{+370}_{-110}\pm140$	7k	ASNER	00B	CLEO	±	$\tau^- \to K^-\pi^+\pi^-\nu_\tau$
188± 54± 60		[5] ASTON	87	LASS	0	11 $K^-p \to \overline{K}^0\pi^+\pi^-n$
276± 65		BAUBILLIER	82B	HBC	0	8.25 $K^-p \to K^0_S\pi^+\pi^-n$
195± 25		DAUM	81C	CNTR	−	63 $K^-p \to K^-2\pi p$
180± 10		ETKIN	80	MPS	0	6 $K^-p \to \overline{K}^0\pi^+\pi^-n$
142± 16		[6] CARNEGIE	77	ASPK	±	13 $K^\pm p \to (K\pi\pi)^\pm p$
• • • We do not use the following data for averages, fits, limits, etc. • • •						
152± 16	25k	[7] ABLIKIM	06C	BES2		$J/\psi \to \overline{K}^*(892)^0K^+\pi^-$
~ 200		VERGEEST	79	HBC	−	4.2 $K^-p \to (\overline{K}\pi\pi)^-p$
~ 160		BRANDENB...	76	ASPK	±	13 $K^\pm p \to (K\pi\pi)^\pm p$
80		DAVIS	72	HBC	+	12 K^+p
241± 30		FIRESTONE	72B	DBC	+	12 K^+d

[5] From partial-wave analysis of $K^0\pi^+\pi^-$ system.
[6] From a model-dependent fit with Gaussian background to BRANDENBURG 76 data.
[7] Systematic errors not estimated.

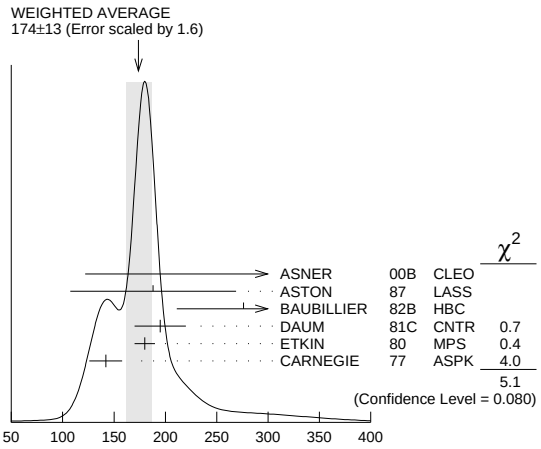

$K_1(1400)$ DECAY MODES

	Mode	Fraction (Γ_i/Γ)
Γ_1	$K^*(892)\pi$	(94 ±6) %
Γ_2	$K\rho$	(3.0±3.0) %
Γ_3	$Kf_0(1370)$	(2.0±2.0) %
Γ_4	$K\omega$	(1.0±1.0) %
Γ_5	$K_0^*(1430)\pi$	not seen
Γ_6	γK^0	seen

$K_1(1400)$ PARTIAL WIDTHS

$\Gamma(K^*(892)\pi)$ Γ_1

VALUE (MeV)	DOCUMENT ID		TECN	CHG	COMMENT
117±10	CARNEGIE	77	ASPK	±	13 $K^\pm p \to (K\pi\pi)^\pm p$

$\Gamma(K\rho)$ Γ_2

VALUE (MeV)	DOCUMENT ID		TECN	CHG	COMMENT
2±1	CARNEGIE	77	ASPK	±	13 $K^\pm p \to (K\pi\pi)^\pm p$

$\Gamma(K\omega)$ Γ_4

VALUE (MeV)	DOCUMENT ID		TECN	CHG	COMMENT
23±12	CARNEGIE	77	ASPK	±	13 $K^\pm p \to (K\pi\pi)^\pm p$

$\Gamma(\gamma K^0)$ Γ_6

VALUE (keV)	DOCUMENT ID		TECN	COMMENT
280.8±23.2±40.4	ALAVI-HARATI	02B	KTEV	$K + A \to K^* + A$

$K_1(1400)$ BRANCHING RATIOS

$\Gamma(K^*(892)\pi)/\Gamma_{total}$ Γ_1/Γ

VALUE	DOCUMENT ID		TECN	COMMENT
0.94±0.06	[8] DAUM	81C	CNTR	63 $K^-p \to K^-2\pi p$

$\Gamma(K\rho)/\Gamma_{total}$ Γ_2/Γ

VALUE	DOCUMENT ID		TECN	COMMENT
0.03±0.03	[8] DAUM	81C	CNTR	63 $K^-p \to K^-2\pi p$

$\Gamma(Kf_0(1370))/\Gamma_{total}$ Γ_3/Γ

VALUE	DOCUMENT ID		TECN	COMMENT
0.02±0.02	[8] DAUM	81C	CNTR	63 $K^-p \to K^-2\pi p$

$\Gamma(K\omega)/\Gamma_{total}$ Γ_4/Γ

VALUE	DOCUMENT ID		TECN	COMMENT
0.01±0.01	[8] DAUM	81C	CNTR	63 $K^-p \to K^-2\pi p$

$\Gamma(K_0^*(1430)\pi)/\Gamma_{total}$ Γ_5/Γ

VALUE	DOCUMENT ID		TECN	COMMENT
not seen	[8] DAUM	81C	CNTR	63 $K^-p \to K^-2\pi p$

D-wave/S-wave RATIO FOR $K_1(1400) \to K^*(892)\pi$

VALUE	DOCUMENT ID		TECN	COMMENT
0.04±0.01	[8] DAUM	81C	CNTR	63 $K^-p \to K^-2\pi p$

[8] Average from low and high t data.

$K_1(1400)$ REFERENCES

ABLIKIM	06C	PL B633 681	M. Ablikim *et al.*	(BES Collab.)
ALAVI-HARATI	02B	PRL 89 072001	A. Alavi-Harati *et al.*	(FNAL KTeV Collab.)
ASNER	00B	PR D62 072006	D.M. Asner *et al.*	(CLEO Collab.)
ASTON	87	NP B292 693	D. Aston *et al.*	(SLAC, NAGO, CINC, INUS)
BAUBILLIER	82B	NP B202 21	M. Baubillier *et al.*	(BIRM, CERN, GLAS+)
TORNQVIST	82B	NP B203 268	N.A. Tornqvist	(HELS)
DAUM	81C	NP B187 1	C. Daum *et al.*	(AMST, CERN, CRAC, MPIM+)
ETKIN	80	PR D22 42	A. Etkin *et al.*	(BNL, CUNY) JP
VERGEEST	79	NP B158 265	J.S.M. Vergeest *et al.*	(NIJM, AMST, CERN+)
CARNEGIE	77	NP B127 509	R.K. Carnegie *et al.*	(SLAC)
BRANDENB...	76	PRL 36 703	G.W. Brandenburg *et al.*	(SLAC) JP
DAVIS	72	PR D5 2688	P.J. Davis *et al.*	(LBL)
FIRESTONE	72B	PR D5 505	A. Firestone *et al.*	(LBL)

$K^*(1410)$

$I(J^P) = \frac{1}{2}(1^-)$

$K^*(1410)$ MASS

VALUE (MeV)	DOCUMENT ID		TECN	CHG	COMMENT
1414±15 OUR AVERAGE Error includes scale factor of 1.3.					
1380±21±19	ASTON	88	LASS	0	11 $K^-p \to K^-\pi^+n$
1420± 7±10	ASTON	87	LASS	0	11 $K^-p \to \overline{K}^0\pi^+\pi^-n$
• • • We do not use the following data for averages, fits, limits, etc. • • •					
1276^{+72}_{-77}	[1,2] BOITO	09	RVUE		$\tau^- \to K^0_S\pi^-\nu_\tau$
1367±54	BIRD	89	LASS	−	11 $K^-p \to \overline{K}^0\pi^-p$
1474±25	BAUBILLIER	82B	HBC	0	8.25 $K^-p \to \overline{K}^0 2\pi n$
1500±30	ETKIN	80	MPS	0	6 $K^-p \to \overline{K}^0\pi^+\pi^-n$

[1] From the pole position of the $K\pi$ vector form factor in the complex s-plane and using EPIFANOV 07 data.
[2] Systematic uncertainties not estimated.

$K^*(1410)$ WIDTH

VALUE (MeV)	DOCUMENT ID		TECN	CHG	COMMENT
232± 21 OUR AVERAGE Error includes scale factor of 1.1.					
176± 52±22	ASTON	88	LASS	0	11 $K^-p \to K^-\pi^+n$
240± 18±12	ASTON	87	LASS	0	11 $K^-p \to \overline{K}^0\pi^+\pi^-n$

• • • We do not use the following data for averages, fits, limits, etc. • • •

$198^{+\ 61}_{-\ 87}$	[3,4] BOITO	09	RVUE		$\tau^- \to K^0_S \pi^- \nu_\tau$
114±101	BIRD	89	LASS	–	11 $K^- p \to \overline{K}^0 \pi^- p$
275± 65	BAUBILLIER	82B	HBC	0	8.25 $K^- p \to \overline{K}^0 2\pi n$
500±100	ETKIN	80	MPS	0	6 $K^- p \to \overline{K}^0 \pi^+ \pi^- n$

[3] From the pole position of the $K\pi$ vector form factor in the complex s-plane and using EPIFANOV 07 data.
[4] Systematic uncertainties not estimated.

$K^*(1410)$ DECAY MODES

	Mode	Fraction (Γ_i/Γ)	Confidence level
Γ_1	$K^*(892)\pi$	> 40 %	95%
Γ_2	$K\pi$	(6.6±1.3) %	
Γ_3	$K\rho$	< 7 %	95%
Γ_4	γK^0	seen	

$K^*(1410)$ PARTIAL WIDTHS

$\Gamma(\gamma K^0)$ Γ_4

VALUE (keV)	CL%	DOCUMENT ID	TECN	COMMENT
<52.9	90	ALAVI-HARATI 02B	KTEV	$K + A \to K^* + A$

$K^*(1410)$ BRANCHING RATIOS

$\Gamma(K\rho)/\Gamma(K^*(892)\pi)$ Γ_3/Γ_1

VALUE	CL%	DOCUMENT ID		TECN	CHG	COMMENT
<0.17	95	ASTON	84	LASS	0	11 $K^- p \to \overline{K}^0 2\pi n$

$\Gamma(K\pi)/\Gamma(K^*(892)\pi)$ Γ_2/Γ_1

VALUE	CL%	DOCUMENT ID		TECN	CHG	COMMENT
<0.16	95	ASTON	84	LASS	0	11 $K^- p \to \overline{K}^0 2\pi n$

$\Gamma(K\pi)/\Gamma_{\text{total}}$ Γ_2/Γ

VALUE	DOCUMENT ID		TECN	CHG	COMMENT
0.066±0.010±0.008	ASTON	88	LASS	0	11 $K^- p \to K^- \pi^+ n$

$K^*(1410)$ REFERENCES

BOITO	09	EPJ C59 821	D.R. Boito, R. Escribano, M. Jamin	
EPIFANOV	07	PL B654 65	D. Epifanov *et al.*	(BELLE Collab.)
ALAVI-HARATI	02B	PRL 89 072001	A. Alavi-Harati *et al.*	(FNAL KTeV Collab.)
BIRD	89	SLAC-332	P.F. Bird	(SLAC)
ASTON	88	NP B296 493	D. Aston *et al.*	(SLAC, NAGO, CINC, INUS)
ASTON	87	NP B292 693	D. Aston *et al.*	(SLAC, NAGO, CINC, INUS)
ASTON	84	PL 149B 258	D. Aston *et al.*	(SLAC, CARL, OTTA) JP
BAUBILLIER	82B	NP B202 21	M. Baubillier *et al.*	(BIRM, CERN, GLAS+)
ETKIN	80	PR D22 42	A. Etkin *et al.*	(BNL, CUNY) JP

$K_0^*(1430)$

$I(J^P) = \frac{1}{2}(0^+)$

See our minireview in the 1994 edition and in this edition under the $f_0(500)$.

$K_0^*(1430)$ MASS

VALUE (MeV)	EVTS	DOCUMENT ID		TECN	CHG	COMMENT
1425 ±50 OUR ESTIMATE						

• • • We do not use the following data for averages, fits, limits, etc. • • •

1427 ± 4 ±13		[1] BUGG	10	RVUE		S-matrix pole
1466.6± 0.7± 3.4	141k	[2] BONVICINI	08A	CLEO		$D^+ \to K^- \pi^+ \pi^+$
~ 1412		[3] LINK	07	FOCS	0	$D^+ \to K^- K^+ \pi^+$
1461.0± 4.0± 2.1	54k	[4] LINK	07B	FOCS		$D^+ \to K^- \pi^+ \pi^+$
1406 ±29		[5] BUGG	06	RVUE		
1435 ± 6		[6] ZHOU	06	RVUE		$Kp \to K^- \pi^+ n$
1455 ±20 ±15		ABLIKIM	05Q	BES2		$\psi(2S) \to \gamma\pi^+\pi^- K^+ K^-$
1456 ± 8		[7] ZHENG	04	RVUE		$K^- p \to K^- \pi^+ n$
~ 1419		[8] BUGG	03	RVUE		11 $K^- p \to K^- \pi^+ n$
~ 1440		[9] LI	03	RVUE		11 $K^- p \to K^- \pi^+ n$
1459 ± 9	15k	[10] AITALA	02	E791		$D^+ \to K^- \pi^+ \pi^+$
~ 1440		[11] JAMIN	00	RVUE		$Kp \to Kp$
1436 ± 8		[12] BARBERIS	98E	OMEG		450 $pp \to p_f p_s K^+ K^- \pi^+ \pi^-$
1415 ±25		[8] ANISOVICH	97C	RVUE		11 $K^- p \to K^- \pi^+ n$
~ 1450		[13] TORNQVIST	96	RVUE		$\pi\pi \to \pi\pi$, $K\overline{K}$, $K\pi$
1412 ± 6		[14] ASTON	88	LASS	0	11 $K^- p \to K^- \pi^+ n$
~ 1430		BAUBILLIER	84B	HBC	–	8.25 $K^- p \to \overline{K}^0 \pi^- p$
~ 1425		[15,16] ESTABROOKS	78	ASPK		13 $K^\pm p \to K^\pm \pi^\pm (n, \Delta)$
~ 1450		MARTIN	78	SPEC		10 $K^\pm p \to K^0_S \pi p$

[1] S-Matrix pole. Supersedes BUGG 06. Combined analysis of ASTON 88, ABLIKIM 06C, AITALA 06, and LINK 09 using an s-dependent width with couplings to $K\pi$ and $K\eta'$, and the Adler zero near thresholds.
[2] From the isobar model with a complex pole for the κ.
[3] From a non-parametric analysis.
[4] A Breit-Wigner mass and width.
[5] S-matrix pole. Reanalysis of ASTON 88, AITALA 02, and ABLIKIM 06C including the κ with an s-dependent width and an Adler zero near threshold.
[6] S-matrix pole. Using ASTON 88 and assuming $K_0^*(800)$, $K_0^*(1950)$.
[7] Using ASTON 88 and assuming $K_0^*(800)$.
[8] T-matrix pole. Reanalysis of ASTON 88 data.
[9] Breit-Wigner fit. Using ASTON 88.
[10] Assuming a low-mass scalar $K\pi$ resonance, $\kappa(800)$.
[11] T-matrix pole. Using data from ESTABROOKS 78 and ASTON 88.
[12] J^P not determined, could be $K_2^*(1430)$.
[13] T-matrix pole.
[14] Uses a model for the background, without this background they get a mass 1340 MeV, where the phase shift passes 90°.
[15] Mass defined by pole position.
[16] From elastic $K\pi$ partial-wave analysis.

$K_0^*(1430)$ WIDTH

VALUE (MeV)	EVTS	DOCUMENT ID		TECN	CHG	COMMENT
270 ±80 OUR ESTIMATE						

• • • We do not use the following data for averages, fits, limits, etc. • • •

270 ±10 ±40		[17] BUGG	10	RVUE		S-matrix pole
174.2± 1.9± 3.2	141k	[18] BONVICINI	08A	CLEO		$D^+ \to K^- \pi^+ \pi^+$
~ 500		[19] LINK	07	FOCS	0	$D^+ \to K^- K^+ \pi^+$
177.0± 8.0± 3.4	54k	[20] LINK	07B	FOCS		$D^+ \to K^- \pi^+ \pi^+$
350 ±40		[21] BUGG	06	RVUE		
288 ±22		[22] ZHOU	06	RVUE		$Kp \to K^- \pi^+ n$
270 $\pm 45\ ^{+30}_{-35}$		ABLIKIM	05Q	BES2		$\psi(2S) \to \gamma\pi^+\pi^- K^+ K^-$
217 ±31		[23] ZHENG	04	RVUE		$K^- p \to K^- \pi^+ n$
~ 316		[24] BUGG	03	RVUE		11 $K^- p \to K^- \pi^+ n$
~ 350		[25] LI	03	RVUE		11 $K^- p \to K^- \pi^+ n$
175 ±17	15k	[26] AITALA	02	E791		$D^+ \to K^- \pi^+ \pi^+$
~ 300		[27] JAMIN	00	RVUE		$Kp \to Kp$
196 ±45		[28] BARBERIS	98E	OMEG		450 $pp \to p_f p_s K^+ K^- \pi^+ \pi^-$
330 ±50		[24] ANISOVICH	97C	RVUE		11 $K^- p \to K^- \pi^+ n$
~ 320		[29] TORNQVIST	96	RVUE		$\pi\pi \to \pi\pi$, $K\overline{K}$, $K\pi$
294 ±23		ASTON	88	LASS	0	11 $K^- p \to K^- \pi^+ n$
~ 200		BAUBILLIER	84B	HBC	–	8.25 $K^- p \to \overline{K}^0 \pi^- p$
200 to 300		[30] ESTABROOKS	78	ASPK		13 $K^\pm p \to K^\pm \pi^\pm (n, \Delta)$

[17] S-Matrix pole. Supersedes BUGG 06. Combined analysis of ASTON 88, ABLIKIM 06C, AITALA 06, and LINK 09 using an s-dependent width with couplings to $K\pi$ and $K\eta'$, and the Adler zero near thresholds.
[18] From the isobar model with a complex pole for the κ.
[19] From a non-parametric analysis.
[20] A Breit-Wigner mass and width.
[21] S-matrix pole. Reanalysis of ASTON 88, AITALA 02, and ABLIKIM 06C including the κ with an s-dependent width and an Adler zero near threshold.
[22] S-matrix pole. Using ASTON 88 and assuming $K_0^*(800)$, $K_0^*(1950)$.
[23] Using ASTON 88 and assuming $K_0^*(800)$.
[24] T-matrix pole. Reanalysis of ASTON 88 data.
[25] Breit-Wigner fit. Using ASTON 88.
[26] Assuming a low-mass scalar $K\pi$ resonance, $\kappa(800)$.
[27] T-matrix pole. Using data from ESTABROOKS 78 and ASTON 88.
[28] J^P not determined, could be $K_2^*(1430)$.
[29] T-matrix pole.
[30] From elastic $K\pi$ partial-wave analysis.

$K_0^*(1430)$ DECAY MODES

	Mode	Fraction (Γ_i/Γ)
Γ_1	$K\pi$	(93±10) %

$K_0^*(1430)$ BRANCHING RATIOS

$\Gamma(K\pi)/\Gamma_{\text{total}}$ Γ_1/Γ

VALUE	DOCUMENT ID		TECN	CHG	COMMENT
0.93±0.04±0.09	ASTON	88	LASS	0	11 $K^- p \to K^- \pi^+ n$

Meson Particle Listings

$K_0^*(1430)$, $K_2^*(1430)$

$K_0^*(1430)$ REFERENCES

BUGG	10	PR D81 014002	D.V. Bugg	(LOQM)
LINK	09	PL B681 14	J.M. Link *et al.*	(FNAL FOCUS Collab.)
BONVICINI	08A	PR D78 052001	G. Bonvicini *et al.*	(CLEO Collab.)
LINK	07	PL B648 156	J.M. Link *et al.*	(FNAL FOCUS Collab.)
LINK	07B	PL B653 1	J.M. Link *et al.*	(FNAL FOCUS Collab.)
ABLIKIM	06C	PL B633 681	M. Ablikim *et al.*	(BES Collab.)
AITALA	06	PR D73 032004	E.M. Aitala *et al.*	(FNAL E791 Collab.)
Also		PR D74 059901 (errat.)	E.M. Aitala *et al.*	(FNAL E791 Collab.)
BUGG	06	PL B632 471	D.V. Bugg	(LOQM)
ZHOU	06	NP A775 212	Z.Y. Zhou, H.Q. Zheng	
ABLIKIM	05Q	PR D72 092002	M. Ablikim *et al.*	(BES Collab.)
ZHENG	04	NP A733 235	H.Q. Zheng *et al.*	
BUGG	03	PL B572 1	D.V. Bugg	
LI	03	PR D67 034025	L. Li, B. Zou, G. Li	
AITALA	02	PRL 89 121801	E.M. Aitala *et al.*	(FNAL E791 Collab.)
JAMIN	00	NP B587 331	M. Jamin *et al.*	
BARBERIS	98E	PL B436 204	D. Barberis *et al.*	(Omega Expt.)
ANISOVICH	97C	PL B413 137	A.V. Anisovich, A.V. Sarantsev	
TORNQVIST	96	PRL 76 1575	N.A. Tornqvist, M. Roos	(HELS)
ASTON	88	NP B296 493	D. Aston *et al.*	(SLAC, NAGO, CINC, INUS)
BAUBILLIER	84B	ZPHY C26 37	M. Baubillier *et al.*	(BIRM, CERN, GLAS+)
ESTABROOKS	78	NP B133 490	P.G. Estabrooks *et al.*	(MCGI, CARL, DURH+)
MARTIN	78	NP B134 392	A.D. Martin *et al.*	(DURH, GEVA)

$K_2^*(1430)$

$I(J^P) = \frac{1}{2}(2^+)$

We consider that phase-shift analyses provide more reliable determinations of the mass and width.

$K_2^*(1430)$ MASS

CHARGED ONLY, WITH FINAL STATE $K\pi$

VALUE (MeV)	EVTS	DOCUMENT ID		TECN	CHG	COMMENT
1425.6± 1.5 OUR AVERAGE		Error includes scale factor of 1.1.				
1420 ± 4	1587	BAUBILLIER	84B	HBC	–	8.25 $K^-p \to \overline{K}^0\pi^-p$
1436 ± 5.5	400	[1,2] CLELAND	82	SPEC	+	30 $K^+p \to K^0_S\pi^+p$
1430 ± 3.2	1500	[1,2] CLELAND	82	SPEC	+	50 $K^+p \to K^0_S\pi^+p$
1430 ± 3.2	1200	[1,2] CLELAND	82	SPEC	–	50 $K^+p \to K^0_S\pi^-p$
1423 ± 5	935	TOAFF	81	HBC	–	6.5 $K^-p \to \overline{K}^0\pi^-p$
1428.0± 4.6		[3] MARTIN	78	SPEC	+	10 $K^\pm p \to K^0_S\pi p$
1423.8± 4.6		[3] MARTIN	78	SPEC	–	10 $K^\pm p \to K^0_S\pi p$
1420.0± 3.1	1400	AGUILAR-...	71B	HBC	–	3.9,4.6 K^-p
1425 ± 8.0	225	[1,2] BARNHAM	71C	HBC	+	$K^+p \to K^0\pi^+p$
1416 ±10	220	CRENNELL	69D	DBC	–	3.9 $K^-N \to \overline{K}^0\pi^-N$
1414 ±13.0	60	[1] LIND	69	HBC	+	9 $K^+p \to K^0\pi^+p$
1427 ±12	63	[1] SCHWEING...	68	HBC	–	5.5 $K^-p \to \overline{K}\pi N$
1423 ±11.0	39	[1] BASSANO	67	HBC	–	4.6–5.0 $K^-p \to \overline{K}^0\pi^-p$
• • • We do not use the following data for averages, fits, limits, etc. • • •						
1423.4± 2 ±3	24809± 820	[4] BIRD	89	LASS	–	11 $K^-p \to \overline{K}^0\pi^-p$

NEUTRAL ONLY

VALUE (MeV)	EVTS	DOCUMENT ID		TECN	COMMENT
1432.4± 1.3 OUR AVERAGE					
1431.2± 1.8± 0.7		[5] ASTON	88	LASS	11 $K^-p \to K^-\pi^+n$
1434 ± 4 ± 6		[5] ASTON	87	LASS	11 $K^-p \to \overline{K}^0\pi^+\pi^-n$
1433 ± 6 ±10		[5] ASTON	84B	LASS	11 $K^-p \to \overline{K}^0 2\pi n$
1471 ±12		[5] BAUBILLIER	82B	HBC	8.25 $K^-p \to NK^0_S\pi\pi$
1428 ± 3		[5] ASTON	81C	LASS	11 $K^-p \to K^-\pi^+n$
1434 ± 2		[5] ESTABROOKS	78	ASPK	13 $K^\pm p \to pK\pi$
1440 ±10		[5] BOWLER	77	DBC	5.5 $K^+d \to K\pi pp$
• • • We do not use the following data for averages, fits, limits, etc. • • •					
1428.5± 3.9	1786± 127	[6] AUBERT	07AK	BABR	10.6 $e^+e^- \to K^{*0}K^\pm\pi^\mp\gamma$
1420 ± 7	300	HENDRICK	76	DBC	8.25 $K^+N \to K^+\pi N$
1421.6± 4.2	800	MCCUBBIN	75	HBC	3.6 $K^-p \to K^-\pi^+n$
1420.1± 4.3		[7] LINGLIN	73	HBC	2–13 $K^+p \to K^+\pi^-X$
1419.1± 3.7	1800	AGUILAR-...	71B	HBC	3.9,4.6 K^-p
1416 ± 6	600	CORDS	71	DBC	9 $K^+n \to K^+\pi^-p$
1421.1± 2.6	2200	DAVIS	69	HBC	12 $K^+p \to K^+\pi^-X$

[1] Errors enlarged by us to $\Gamma/\sqrt{N}$; see the note with the $K^*(892)$ mass.
[2] Number of events in peak re-evaluated by us.
[3] Systematic error added by us.
[4] From a partial wave amplitude analysis.
[5] From phase shift or partial-wave analysis.
[6] Systematic errors not estimated.
[7] From pole extrapolation, using world K^+p data summary tape.

$K_2^*(1430)$ WIDTH

CHARGED ONLY, WITH FINAL STATE $K\pi$

VALUE (MeV)	EVTS	DOCUMENT ID		TECN	CHG	COMMENT
98.5± 2.7 OUR FIT		Error includes scale factor of 1.1.				
98.5± 2.9 OUR AVERAGE		Error includes scale factor of 1.1.				
109 ±22	400	[8,9] CLELAND	82	SPEC	+	30 $K^+p \to K^0_S\pi^+p$
124 ±12.8	1500	[8,9] CLELAND	82	SPEC	+	50 $K^+p \to K^0_S\pi^+p$
113 ±12.8	1200	[8,9] CLELAND	82	SPEC	–	50 $K^+p \to K^0_S\pi^-p$
85 ±16	935	TOAFF	81	HBC	–	6.5 $K^-p \to \overline{K}^0\pi^-p$
96.5± 3.8		MARTIN	78	SPEC	+	10 $K^\pm p \to K^0_S\pi p$
97.7± 4.0		MARTIN	78	SPEC	–	10 $K^\pm p \to K^0_S\pi p$
$94.7^{+15.1}_{-12.5}$	1400	AGUILAR-...	71B	HBC	–	3.9,4.6 K^-p
• • • We do not use the following data for averages, fits, limits, etc. • • •						
98 ± 4 ±4	25k	[10] BIRD	89	LASS	–	11 $K^-p \to \overline{K}^0\pi^-p$

NEUTRAL ONLY

VALUE (MeV)	EVTS	DOCUMENT ID		TECN	COMMENT
109 ± 5 OUR AVERAGE		Error includes scale factor of 1.9. See the ideogram below.			
116.5± 3.6± 1.7		[11] ASTON	88	LASS	11 $K^-p \to K^-\pi^+n$
129 ±15 ±15		[11] ASTON	87	LASS	11 $K^-p \to \overline{K}^0\pi^+\pi^-n$
131 ±24 ±20		[11] ASTON	84B	LASS	11 $K^-p \to \overline{K}^0 2\pi n$
143 ±34		[11] BAUBILLIER	82B	HBC	8.25 $K^-p \to NK^0_S\pi\pi$
98 ± 8		[11] ASTON	81C	LASS	11 $K^-p \to K^-\pi^+n$
140 ±30		[11] ETKIN	80	SPEC	6 $K^-p \to \overline{K}^0\pi^+\pi^-n$
98 ± 5		[11] ESTABROOKS	78	ASPK	13 $K^\pm p \to pK\pi$
• • • We do not use the following data for averages, fits, limits, etc. • • •					
113.7± 9.2	1786± 127	[12] AUBERT	07AK	BABR	10.6 $e^+e^- \to K^{*0}K^\pm\pi^\mp\gamma$
125 ±29	300	[8] HENDRICK	76	DBC	8.25 $K^+N \to K^+\pi N$
116 ±18	800	MCCUBBIN	75	HBC	3.6 $K^-p \to K^-\pi^+n$
61 ±14		[13] LINGLIN	73	HBC	2–13 $K^+p \to K^+\pi^-X$
$116.6^{+10.3}_{-15.5}$	1800	AGUILAR-...	71B	HBC	3.9,4.6 K^-p
144 ±24.0	600	[8] CORDS	71	DBC	9 $K^+n \to K^+\pi^-p$
101 ±10	2200	DAVIS	69	HBC	12 $K^+p \to K^+\pi^-\pi^+p$

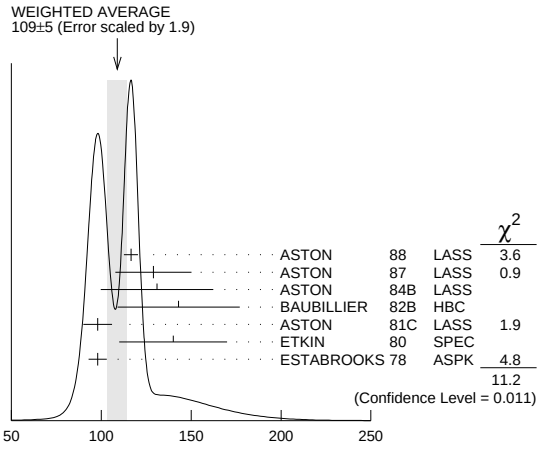

[8] Errors enlarged by us to $4\Gamma/\sqrt{N}$; see the note with the $K^*(892)$ mass.
[9] Number of events in peak re-evaluated by us.
[10] From a partial wave amplitude analysis.
[11] From phase shift or partial-wave analysis.
[12] Systematic errors not estimated.
[13] From pole extrapolation, using world K^+p data summary tape.

$K_2^*(1430)$ DECAY MODES

	Mode	Fraction (Γ_i/Γ)	Scale factor/ Confidence level
Γ_1	$K\pi$	(49.9±1.2) %	
Γ_2	$K^*(892)\pi$	(24.7±1.5) %	
Γ_3	$K^*(892)\pi\pi$	(13.4±2.2) %	
Γ_4	$K\rho$	(8.7±0.8) %	S=1.2
Γ_5	$K\omega$	(2.9±0.8) %	
Γ_6	$K^+\gamma$	(2.4±0.5) $\times 10^{-3}$	S=1.1
Γ_7	$K\eta$	($1.5^{+3.4}_{-1.0}$) $\times 10^{-3}$	S=1.3
Γ_8	$K\omega\pi$	< 7.2 $\times 10^{-4}$	CL=95%
Γ_9	$K^0\gamma$	< 9 $\times 10^{-4}$	CL=90%

CONSTRAINED FIT INFORMATION

An overall fit to the total width, a partial width, and 10 branching ratios uses 31 measurements and one constraint to determine 8 parameters. The overall fit has a $\chi^2 = 20.2$ for 24 degrees of freedom.

The following *off-diagonal* array elements are the correlation coefficients $\langle \delta p_i \delta p_j \rangle / (\delta p_i \cdot \delta p_j)$, in percent, from the fit to parameters p_i, including the branching fractions, $x_i \equiv \Gamma_i/\Gamma_{\text{total}}$. The fit constrains the x_i whose labels appear in this array to sum to one.

	x_1	x_2	x_3	x_4	x_5	x_6	x_7
x_2	−9						
x_3	−40	−73					
x_4	−8	36	−52				
x_5	−11	−3	−26	−7			
x_6	−1	−1	−1	−1	0		
x_7	−4	−7	−5	−5	−2	0	
Γ	0	0	0	0	0	−13	0

	Mode	Rate (MeV)	Scale factor
Γ_1	$K\pi$	49.1 ±1.8	
Γ_2	$K^*(892)\pi$	24.3 ±1.6	
Γ_3	$K^*(892)\pi\pi$	13.2 ±2.2	
Γ_4	$K\rho$	8.5 ±0.8	1.2
Γ_5	$K\omega$	2.9 ±0.8	
Γ_6	$K^+\gamma$	0.24±0.05	1.1
Γ_7	$K\eta$	$0.15^{+0.33}_{-0.10}$	1.3

$K_2^*(1430)$ PARTIAL WIDTHS

$\Gamma(K^+\gamma)$ Γ_6

VALUE (keV)	DOCUMENT ID		TECN	CHG	COMMENT
241±50 OUR FIT	Error includes scale factor of 1.1.				
240±45	CIHANGIR	82	SPEC	+	200 $K^+ Z \to Z K^+ \pi^0$, $Z K^0_S \pi^+$

$\Gamma(K^0\gamma)$ Γ_9

VALUE (keV)	CL%	DOCUMENT ID		TECN	CHG	COMMENT
< 5.4	90	ALAVI-HARATI	02B	KTEV		$K + A \to K^* + A$
• • • We do not use the following data for averages, fits, limits, etc. • • •						
<84	90	CARLSMITH	87	SPEC	0	60–200 $K^0_L A \to K^0_S \pi^0 A$

$K_2^*(1430)$ BRANCHING RATIOS

$\Gamma(K\pi)/\Gamma_{\text{total}}$ Γ_1/Γ

VALUE	DOCUMENT ID		TECN	CHG	COMMENT
0.499±0.012 OUR FIT					
0.488±0.014 OUR AVERAGE					
0.485±0.006±0.020	[14] ASTON	88	LASS	0	11 $K^- p \to K^- \pi^+ n$
0.49 ±0.02	[14] ESTABROOKS	78	ASPK	±	13 $K^\pm p \to p K \pi$

$\Gamma(K^*(892)\pi)/\Gamma(K\pi)$ Γ_2/Γ_1

VALUE	DOCUMENT ID		TECN	CHG	COMMENT
0.496±0.034 OUR FIT					
0.47 ±0.04 OUR AVERAGE					
0.44 ±0.09	ASTON	84B	LASS	0	11 $K^- p \to \overline{K}^0 2\pi n$
0.62 ±0.19	LAUSCHER	75	HBC	0	10,16 $K^- p \to K^- \pi^+ n$
0.54 ±0.16	DEHM	74	DBC	0	4.6 $K^+ N$
0.47 ±0.08	AGUILAR-...	71B	HBC		3.9,4.6 $K^- p$
0.47 ±0.10	BASSANO	67	HBC	−0	4.6,5.0 $K^- p$
0.45 ±0.13	BADIER	65C	HBC	−	3 $K^- p$

$\Gamma(K\omega)/\Gamma(K\pi)$ Γ_5/Γ_1

VALUE	DOCUMENT ID		TECN	CHG	COMMENT
0.059±0.017 OUR FIT					
0.070±0.035 OUR AVERAGE					
0.05 ±0.04	AGUILAR-...	71B	HBC		3.9,4.6 $K^- p$
0.13 ±0.07	BASSOMPIE...	69	HBC	0	5 $K^+ p$

$\Gamma(K\rho)/\Gamma(K\pi)$ Γ_4/Γ_1

VALUE	DOCUMENT ID		TECN	CHG	COMMENT
0.174±0.017 OUR FIT	Error includes scale factor of 1.2.				
$\mathbf{0.150^{+0.029}_{-0.017}}$ **OUR AVERAGE**					
0.18 ±0.05	ASTON	84B	LASS	0	11 $K^- p \to \overline{K}^0 2\pi n$
$0.02\ ^{+0.10}_{-0.02}$	DEHM	74	DBC	0	4.6 $K^+ N$
0.16 ±0.05	AGUILAR-...	71B	HBC		3.9,4.6 $K^- p$
0.14 ±0.10	BASSANO	67	HBC	−0	4.6,5.0 $K^- p$
0.14 ±0.07	BADIER	65C	HBC	−	3 $K^- p$

$\Gamma(K\rho)/\Gamma(K^*(892)\pi)$ Γ_4/Γ_2

VALUE	DOCUMENT ID		TECN	CHG	COMMENT
0.350±0.031 OUR FIT	Error includes scale factor of 1.4.				
0.354±0.033 OUR AVERAGE	Error includes scale factor of 1.4. See the ideogram below.				
0.293±0.032±0.020	ASTON	87	LASS	0	11 $K^- p \to \overline{K}^0 \pi^+ \pi^- n$
0.38 ±0.09	BAUBILLIER	82B	HBC	0	8.25 $K^- p \to N K^0_S \pi\pi$
0.39 ±0.03	DAUM	81C	CNTR		63 $K^- p \to K^- 2\pi p$

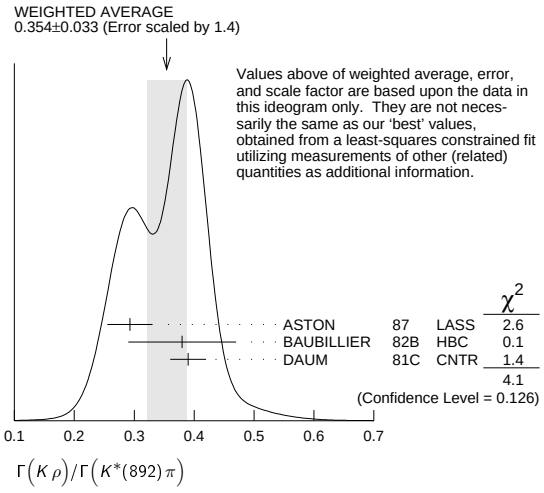

$\Gamma(K\omega)/\Gamma(K^*(892)\pi)$ Γ_5/Γ_2

VALUE	DOCUMENT ID		TECN	CHG	COMMENT
0.118±0.034 OUR FIT					
0.10 ±0.04	FIELD	67	HBC	−	3.8 $K^- p$

$\Gamma(K\eta)/\Gamma(K^*(892)\pi)$ Γ_7/Γ_2

VALUE	DOCUMENT ID		TECN	CHG	COMMENT
$\mathbf{0.006^{+0.014}_{-0.004}}$ **OUR FIT**	Error includes scale factor of 1.2.				
0.07 ±0.04	FIELD	67	HBC	−	3.8 $K^- p$

$\Gamma(K\eta)/\Gamma(K\pi)$ Γ_7/Γ_1

VALUE	CL%	DOCUMENT ID		TECN	CHG	COMMENT
$\mathbf{0.0030^{+0.0070}_{-0.0020}}$ **OUR FIT**		Error includes scale factor of 1.3.				
0 ±0.0056		[15] ASTON	88B	LASS	−	11 $K^- p \to K^- \eta p$
• • • We do not use the following data for averages, fits, limits, etc. • • •						
<0.04	95	AGUILAR-...	71B	HBC		3.9,4.6 $K^- p$
<0.065		[16] BASSOMPIE...	69	HBC		5.0 $K^+ p$
<0.02		BISHOP	69	HBC		3.5 $K^+ p$

$\Gamma(K^*(892)\pi\pi)/\Gamma_{\text{total}}$ Γ_3/Γ

VALUE	DOCUMENT ID		TECN	CHG	COMMENT
0.134±0.022 OUR FIT					
0.12 ±0.04	[17] GOLDBERG	76	HBC	−	3 $K^- p \to p \overline{K}^0 \pi\pi\pi$

$\Gamma(K^*(892)\pi\pi)/\Gamma(K\pi)$ Γ_3/Γ_1

VALUE	DOCUMENT ID		TECN	CHG	COMMENT
0.27±0.05 OUR FIT					
0.21±0.08	[16,17] JONGEJANS	78	HBC	−	4 $K^- p \to p \overline{K}^0 \pi\pi\pi$

$\Gamma(K\omega\pi)/\Gamma_{\text{total}}$ Γ_8/Γ

VALUE (units 10^{-3})	CL%	EVTS	DOCUMENT ID		TECN	COMMENT
<0.72	95	0	JONGEJANS	78	HBC	4 $K^- p \to p \overline{K}^0 4\pi$

[14] From phase shift analysis.
[15] ASTON 88B quote < 0.0092 at CL=95%. We convert this to a central value and 1 sigma error in order to be able to use it in our constrained fit.
[16] Restated by us.
[17] Assuming $\pi\pi$ system has isospin 1, which is supported by the data.

$K_2^*(1430)$ REFERENCES

AUBERT	07AK	PR D76 012008	B. Aubert *et al.*	(BABAR Collab.)
ALAVI-HARATI	02B	PRL 89 072001	A. Alavi-Harati *et al.*	(FNAL KTeV Collab.)
BIRD	89	SLAC-332	P.F. Bird	(SLAC)
ASTON	88	NP B296 493	D. Aston *et al.*	(SLAC, NAGO, CINC, INUS)
ASTON	88B	PL B201 169	D. Aston *et al.*	(SLAC, NAGO, CINC, INUS)
ASTON	87	NP B292 693	D. Aston *et al.*	(SLAC, NAGO, CINC, INUS)
CARLSMITH	87	PR D36 3502	D. Carlsmith *et al.*	(EFI, SACL)
ASTON	84B	NP B247 261	D. Aston *et al.*	(SLAC, CARL, OTTA)
BAUBILLIER	84B	ZPHY C26 37	M. Baubillier *et al.*	(BIRM, CERN, GLAS+)
BAUBILLIER	82B	NP B202 21	M. Baubillier *et al.*	(BIRM, CERN, GLAS+)
CIHANGIR	82	PL 117B 123	S. Cihangir *et al.*	(FNAL, MINN, ROCH)
CLELAND	82	NP B208 189	W.E. Cleland *et al.*	(DURH, GEVA, LAUS+)
ASTON	81C	PL 106B 235	D. Aston *et al.*	(SLAC, CARL, OTTA) JP
DAUM	81C	NP B187 1	C. Daum *et al.*	(AMST, CERN, CRAC, MPIM+)
TOAFF	81	PR D23 1500	S. Toaff *et al.*	(ANL, KANS)

Meson Particle Listings

$K_2^*(1430)$, $K(1460)$, $K_2(1580)$, $K(1630)$

ETKIN	80	PR D22 42	A. Etkin *et al.*	(BNL, CUNY) JP
ESTABROOKS	78	NP B133 490	P.G. Estabrooks *et al.*	(MCGI, CARL, DURH+)
Also		PR D17 658	P.G. Estabrooks *et al.*	(MCGI, CARL, DURH+)
JONGEJANS	78	NP B139 383	B. Jongejans *et al.*	(ZEEM, CERN, NIJM+)
MARTIN	78	NP B134 392	A.D. Martin *et al.*	(DURH, GEVA)
BOWLER	77	NP B126 31	M.G. Bowler *et al.*	(OXF)
GOLDBERG	76	LNC 17 253	J. Goldberg	(HAIF)
HENDRICK	76	NP B112 189	K. Hendrickx *et al.*	(MONS, SACL, PARIS+)
LAUSCHER	75	NP B86 189	P. Lauscher *et al.*	(ABCLV Collab.) JP
MCCUBBIN	75	NP B86 13	N.A. McCubbin, L. Lyons	(OXF)
DEHM	74	NP B75 47	G. Dehm *et al.*	(MPIM, BRUX, MONS, CERN)
LINGLIN	73	NP B55 408	D. Linglin	(CERN)
AGUILAR-...	71B	PR D4 2583	M. Aguilar-Benitez, R.L. Eisner, J.B. Kinson	(BNL)
BARNHAM	71C	NP B28 171	K.W.J. Barnham *et al.*	(BIRM, GLAS)
CORDS	71	PR D4 1974	D. Cords *et al.*	(PURD, UCD, IUPU)
BASSOMPIE...	69	NP B13 189	G. Bassompierre *et al.*	(CERN, BRUX) JP
BISHOP	69	NP B9 403	J.M. Bishop *et al.*	(WISC)
CRENNELL	69D	PRL 22 487	D.J. Crennell *et al.*	(BNL)
DAVIS	69	PRL 23 1071	P.J. Davis *et al.*	(LRL)
LIND	69	NP B14 1	V.G. Lind *et al.*	(LRL) JP
SCHWEING...	68	PR 166 1317	F. Schweingruber *et al.*	(ANL, NWES)
Also		Thesis	F.L. Schweingruber	(NWES, NWES)
BASSANO	67	PRL 19 968	D. Bassano *et al.*	(BNL, SYRA)
FIELD	67	PL 24B 638	J.H. Field *et al.*	(UCSD)
BADIER	65C	PL 19 612	J. Badier *et al.*	(EPOL, SACL, AMST)

$K(1460)$

$I(J^P) = \frac{1}{2}(0^-)$

OMITTED FROM SUMMARY TABLE

Observed in $K\pi\pi$ partial-wave analysis.

$K(1460)$ MASS

VALUE (MeV)	DOCUMENT ID		TECN	CHG	COMMENT
• • • We do not use the following data for averages, fits, limits, etc. • • •					
~ 1460	DAUM	81C	CNTR	–	63 $K^-p \to K^-2\pi p$
~ 1400	[1] BRANDENB...	76B	ASPK	±	13 $K^\pm p \to K^+2\pi p$

[1] Coupled mainly to $K f_0(1370)$. Decay into $K^*(892)\pi$ seen.

$K(1460)$ WIDTH

VALUE (MeV)	DOCUMENT ID		TECN	CHG	COMMENT
• • • We do not use the following data for averages, fits, limits, etc. • • •					
~ 260	DAUM	81C	CNTR	–	63 $K^-p \to K^-2\pi p$
~ 250	[2] BRANDENB...	76B	ASPK	±	13 $K^\pm p \to K^+2\pi p$

[2] Coupled mainly to $K f_0(1370)$. Decay into $K^*(892)\pi$ seen.

$K(1460)$ DECAY MODES

	Mode	Fraction (Γ_i/Γ)
Γ_1	$K^*(892)\pi$	seen
Γ_2	$K\rho$	seen
Γ_3	$K_0^*(1430)\pi$	seen

$K(1460)$ PARTIAL WIDTHS

$\Gamma(K^*(892)\pi)$ Γ_1

VALUE (MeV)	DOCUMENT ID		TECN	COMMENT
• • • We do not use the following data for averages, fits, limits, etc. • • •				
~ 109	DAUM	81C	CNTR	63 $K^-p \to K^-2\pi p$

$\Gamma(K\rho)$ Γ_2

VALUE (MeV)	DOCUMENT ID		TECN	COMMENT
• • • We do not use the following data for averages, fits, limits, etc. • • •				
~ 34	DAUM	81C	CNTR	63 $K^-p \to K^-2\pi p$

$\Gamma(K_0^*(1430)\pi)$ Γ_3

VALUE (MeV)	DOCUMENT ID		TECN	COMMENT
• • • We do not use the following data for averages, fits, limits, etc. • • •				
~ 117	DAUM	81C	CNTR	63 $K^-p \to K^-2\pi p$

$K(1460)$ REFERENCES

DAUM	81C	NP B187 1	C. Daum *et al.*	(AMST, CERN, CRAC, MPIM+)
BRANDENB...	76B	PRL 36 1239	G.W. Brandenburg *et al.*	(SLAC) JP

$K_2(1580)$

$I(J^P) = \frac{1}{2}(2^-)$

OMITTED FROM SUMMARY TABLE

Seen in partial-wave analysis of the $K^-\pi^+\pi^-$ system. Needs confirmation.

$K_2(1580)$ MASS

VALUE (MeV)	DOCUMENT ID		CHG	COMMENT
• • • We do not use the following data for averages, fits, limits, etc. • • •				
~ 1580	OTTER	79	–	10,14,16 K^-p

$K_2(1580)$ WIDTH

VALUE (MeV)	DOCUMENT ID		CHG	COMMENT
• • • We do not use the following data for averages, fits, limits, etc. • • •				
~ 110	OTTER	79	–	10,14,16 K^-p

$K_2(1580)$ DECAY MODES

	Mode	Fraction (Γ_i/Γ)
Γ_1	$K^*(892)\pi$	seen
Γ_2	$K_2^*(1430)\pi$	possibly seen

$K_2(1580)$ BRANCHING RATIOS

$\Gamma(K^*(892)\pi)/\Gamma_{total}$ Γ_1/Γ

VALUE	DOCUMENT ID		TECN	CHG	COMMENT
seen	OTTER	79	HBC	–	10,14,16 K^-p
• • • We do not use the following data for averages, fits, limits, etc. • • •					
possibly seen	GULER	11	BELL		$B^+ \to J/\psi K^+\pi^+\pi^-$

$\Gamma(K_2^*(1430)\pi)/\Gamma_{total}$ Γ_2/Γ

VALUE	DOCUMENT ID		TECN	CHG	COMMENT
possibly seen	OTTER	79	HBC	–	10,14,16 K^-p

$K_2(1580)$ REFERENCES

GULER	11	PR D83 032005	H. Guler *et al.*	(BELLE Collab.)
OTTER	79	NP B147 1	G. Otter *et al.*	(AACH3, BERL, CERN, LOIC+) JP

$K(1630)$

$I(J^P) = \frac{1}{2}(?^?)$

OMITTED FROM SUMMARY TABLE

Seen as a narrow peak, compatible with the experimental resolution, in the invariant mass of the $K_S^0\pi^+\pi^-$ system produced in π^-p interactions at high momentum transfers.

$K(1630)$ MASS

VALUE (MeV)	EVTS	DOCUMENT ID	TECN	COMMENT
1629±7	~ 75	KARNAUKHOV98	BC	16.0 $\pi^-p \to (K_S^0\pi^+\pi^-) X^+\pi^-X^0$

$K(1630)$ WIDTH

VALUE (MeV)	EVTS	DOCUMENT ID	TECN	COMMENT
16^{+19}_{-16}	~ 75	[1] KARNAUKHOV98	BC	16.0 $\pi^-p \to (K_S^0\pi^+\pi^-) X^+\pi^-X^0$

[1] Compatible with an experimental resolution of 14 ± 1 MeV.

$K(1630)$ DECAY MODES

	Mode
Γ_1	$K_S^0\pi^+\pi^-$

$K(1630)$ REFERENCES

KARNAUKHOV 98 PAN 61 203 V.M. Karnaukhov, C. Coca, V.I. Moroz
Translated from YAF 61 252.

$K_1(1650)$

$I(J^P) = \frac{1}{2}(1^+)$

OMITTED FROM SUMMARY TABLE

This entry contains various peaks in strange meson systems ($K^+\phi$, $K\pi\pi$) reported in partial-wave analysis in the 1600–1900 mass region.

$K_1(1650)$ MASS

VALUE (MeV)	DOCUMENT ID		TECN	CHG	COMMENT
1650±50	FRAME	86	OMEG	+	13 $K^+p \to \phi K^+p$
• • • We do not use the following data for averages, fits, limits, etc. • • •					
~ 1840	ARMSTRONG	83	OMEG	−	18.5 $K^-p \to 3Kp$
~ 1800	DAUM	81C	CNTR	−	63 $K^-p \to K^-2\pi p$

$K_1(1650)$ WIDTH

VALUE (MeV)	DOCUMENT ID		TECN	CHG	COMMENT
150±50	FRAME	86	OMEG	+	13 $K^+p \to \phi K^+p$
• • • We do not use the following data for averages, fits, limits, etc. • • •					
~ 250	DAUM	81C	CNTR	−	63 $K^-p \to K^-2\pi p$

$K_1(1650)$ DECAY MODES

	Mode
Γ_1	$K\pi\pi$
Γ_2	$K\phi$

$K_1(1650)$ REFERENCES

FRAME	86	NP B276 667	D. Frame *et al.*	(GLAS)
ARMSTRONG	83	NP B221 1	T.A. Armstrong *et al.*	(BARI, BIRM, CERN+)
DAUM	81C	NP B187 1	C. Daum *et al.*	(AMST, CERN, CRAC, MPIM+)

$K^*(1680)$

$I(J^P) = \frac{1}{2}(1^-)$

$K^*(1680)$ MASS

VALUE (MeV)	DOCUMENT ID		TECN	CHG	COMMENT
1717±27 OUR AVERAGE Error includes scale factor of 1.4.					
1677±10±32	ASTON	88	LASS	0	11 $K^-p \to K^-\pi^+n$
1735±10±20	ASTON	87	LASS	0	11 $K^-p \to \overline{K}^0\pi^+\pi^-n$
• • • We do not use the following data for averages, fits, limits, etc. • • •					
1678±64	BIRD	89	LASS	−	11 $K^-p \to \overline{K}^0\pi^-p$
1800±70	ETKIN	80	MPS	0	6 $K^-p \to \overline{K}^0\pi^+\pi^-n$
~ 1650	ESTABROOKS	78	ASPK	0	13 $K^\pm p \to K^\pm\pi^\pm n$

$K^*(1680)$ WIDTH

VALUE (MeV)	DOCUMENT ID		TECN	CHG	COMMENT
322±110 OUR AVERAGE Error includes scale factor of 4.2.					
205± 16±34	ASTON	88	LASS	0	11 $K^-p \to K^-\pi^+n$
423± 18±30	ASTON	87	LASS	0	11 $K^-p \to \overline{K}^0\pi^+\pi^-n$
• • • We do not use the following data for averages, fits, limits, etc. • • •					
454±270	BIRD	89	LASS	−	11 $K^-p \to \overline{K}^0\pi^-p$
170± 30	ETKIN	80	MPS	0	6 $K^-p \to \overline{K}^0\pi^+\pi^-n$
250 to 300	ESTABROOKS	78	ASPK	0	13 $K^\pm p \to K^\pm\pi^\pm n$

$K^*(1680)$ DECAY MODES

	Mode	Fraction (Γ_i/Γ)
Γ_1	$K\pi$	(38.7±2.5) %
Γ_2	$K\rho$	$(31.4^{+5.0}_{-2.1})$ %
Γ_3	$K^*(892)\pi$	$(29.9^{+2.2}_{-5.0})$ %

CONSTRAINED FIT INFORMATION

An overall fit to 4 branching ratios uses 4 measurements and one constraint to determine 3 parameters. The overall fit has a $\chi^2 = 2.9$ for 2 degrees of freedom.

The following *off-diagonal* array elements are the correlation coefficients $\langle \delta x_i \delta x_j \rangle / (\delta x_i \cdot \delta x_j)$, in percent, from the fit to the branching fractions, $x_i \equiv \Gamma_i/\Gamma_{\text{total}}$. The fit constrains the x_i whose labels appear in this array to sum to one.

x_2	−36		
x_3	−39	−72	
	x_1	x_2	

$K^*(1680)$ BRANCHING RATIOS

$\Gamma(K\pi)/\Gamma_{\text{total}}$ **Γ_1/Γ**

VALUE	DOCUMENT ID		TECN	CHG	COMMENT
0.387±0.026 OUR FIT					
0.388±0.014±0.022	ASTON	88	LASS	0	11 $K^-p \to K^-\pi^+n$

$\Gamma(K\pi)/\Gamma(K^*(892)\pi)$ **Γ_1/Γ_3**

VALUE	DOCUMENT ID		TECN	CHG	COMMENT
$1.30^{+0.23}_{-0.14}$ OUR FIT					
2.8 ±1.1	ASTON	84	LASS	0	11 $K^-p \to \overline{K}^0 2\pi n$

$\Gamma(K\rho)/\Gamma(K\pi)$ **Γ_2/Γ_1**

VALUE	DOCUMENT ID		TECN	CHG	COMMENT
$0.81^{+0.14}_{-0.09}$ OUR FIT					
1.2 ±0.4	ASTON	84	LASS	0	11 $K^-p \to \overline{K}^0 2\pi n$

$\Gamma(K\rho)/\Gamma(K^*(892)\pi)$ **Γ_2/Γ_3**

VALUE	DOCUMENT ID		TECN	CHG	COMMENT
$1.05^{+0.27}_{-0.11}$ OUR FIT					
$0.97\pm0.09^{+0.30}_{-0.10}$	ASTON	87	LASS	0	11 $K^-p \to \overline{K}^0\pi^+\pi^-n$

$K^*(1680)$ REFERENCES

BIRD	89	SLAC-332	P.F. Bird	(SLAC)
ASTON	88	NP B296 493	D. Aston *et al.*	(SLAC, NAGO, CINC, INUS)
ASTON	87	NP B292 693	D. Aston *et al.*	(SLAC, NAGO, CINC, INUS)
ASTON	84	PL 149B 258	D. Aston *et al.*	(SLAC, CARL, OTTA) JP
ETKIN	80	PR D22 42	A. Etkin *et al.*	(BNL, CUNY) JP
ESTABROOKS	78	NP B133 490	P.G. Estabrooks *et al.*	(MCGI, CARL, DURH+) JP

$K_2(1770)$

$I(J^P) = \frac{1}{2}(2^-)$

See our mini-review in the 2004 edition of this *Review*, PDG 04.

$K_2(1770)$ MASS

VALUE (MeV)	EVTS	DOCUMENT ID		TECN	CHG	COMMENT
1773± 8		[1] ASTON	93	LASS		11 $K^-p \to K^-\omega p$
• • • We do not use the following data for averages, fits, limits, etc. • • •						
1743±15		TIKHOMIROV	03	SPEC		40.0 π^- C → $K^0_S K^0_S K^0_L$ X
1810±20		FRAME	86	OMEG	+	13 $K^+p \to \phi K^+p$
~ 1730		ARMSTRONG	83	OMEG	−	18.5 $K^-p \to 3Kp$
~ 1780		[2] DAUM	81C	CNTR	−	63 $K^-p \to K^-2\pi p$
1710±15	60	CHUNG	74	HBC	−	7.3 $K^-p \to K^-\omega p$
1767± 6		BLIEDEN	72	MMS	−	11–16 K^-p
1730±20	306	[3] FIRESTONE	72B	DBC	+	12 K^+d
1765±40		[4] COLLEY	71	HBC	+	10 $K^+p \to K2\pi N$
1740		DENEGRI	71	DBC	−	12.6 $K^-d \to \overline{K}2\pi d$
1745±20		AGUILAR-...	70C	HBC	−	4.6 K^-p
1780±15		BARTSCH	70C	HBC	−	10.1 K^-p
1760±15		LUDLAM	70	HBC	−	12.6 K^-p

[1] From a partial wave analysis of the $K^-\omega$ system.
[2] From a partial wave analysis of the $K^-2\pi$ system.
[3] Produced in conjunction with excited deuteron.
[4] Systematic errors added correspond to spread of different fits.

$K_2(1770)$ WIDTH

VALUE (MeV)	EVTS	DOCUMENT ID		TECN	CHG	COMMENT
186±14		[5] ASTON	93	LASS		11 $K^-p \to K^-\omega p$

Meson Particle Listings

$K_2(1770)$, $K_3^*(1780)$

• • • We do not use the following data for averages, fits, limits, etc. • • •

147±70		TIKHOMIROV	03	SPEC		40.0 $\pi^- C \to K_S^0 K_S^0 K_L^0 X$
140±40		FRAME	86	OMEG	+	13 $K^+ p \to \phi K^+ p$
~ 220		ARMSTRONG	83	OMEG	−	18.5 $K^- p \to 3K p$
~ 210		[6] DAUM	81C	CNTR	−	63 $K^- p \to K^- 2\pi p$
110±50	60	CHUNG	74	HBC	−	7.3 $K^- p \to K^- \omega p$
100±26		BLIEDEN	72	MMS	−	11–16 $K^- p$
210±30	306	[7] FIRESTONE	72B	DBC	+	12 $K^+ d$
90±70		[8] COLLEY	71	HBC	+	10 $K^+ p \to K 2\pi N$
130		DENEGRI	71	DBC	−	12.6 $K^- d \to \overline{K} 2\pi d$
100±50		AGUILAR-...	70C	HBC	−	4.6 $K^- p$
138±40		BARTSCH	70C	HBC	−	10.1 $K^- p$
50^{+40}_{-20}		LUDLAM	70	HBC	−	12.6 $K^- p$

[5] From a partial wave analysis of the $K^-\omega$ system.
[6] From a partial wave analysis of the $K^- 2\pi$ system.
[7] Produced in conjunction with excited deuteron.
[8] Systematic errors added correspond to spread of different fits.

$K_2(1770)$ DECAY MODES

	Mode	Fraction (Γ_i/Γ)
Γ_1	$K\pi\pi$	
Γ_2	$K_2^*(1430)\pi$	dominant
Γ_3	$K^*(892)\pi$	seen
Γ_4	$K f_2(1270)$	seen
Γ_5	$K f_0(980)$	
Γ_6	$K\phi$	seen
Γ_7	$K\omega$	seen

$K_2(1770)$ BRANCHING RATIOS

$\Gamma(K_2^*(1430)\pi)/\Gamma(K\pi\pi)$ Γ_2/Γ_1
($K_2^*(1430) \to K\pi$)

VALUE	DOCUMENT ID		TECN	CHG	COMMENT
• • • We do not use the following data for averages, fits, limits, etc. • • •					
~ 0.03	DAUM	81C	CNTR		63 $K^- p \to K^- 2\pi p$
~ 1.0	[9] FIRESTONE	72B	DBC	+	12 $K^+ d$
<1.0	COLLEY	71	HBC		10 $K^+ p$
0.2 ±0.2	AGUILAR-...	70C	HBC	−	4.6 $K^- p$
<1.0	BARTSCH	70C	HBC	−	10.1 $K^- p$
1.0	BARBARO-...	69	HBC	+	12.0 $K^+ p$

[9] Produced in conjunction with excited deuteron.

$\Gamma(K^*(892)\pi)/\Gamma(K\pi\pi)$ Γ_3/Γ_1

VALUE	DOCUMENT ID	TECN	COMMENT
• • • We do not use the following data for averages, fits, limits, etc. • • •			
~ 0.23	DAUM	81C	CNTR 63 $K^- p \to K^- 2\pi p$

$\Gamma(K f_2(1270))/\Gamma(K\pi\pi)$ Γ_4/Γ_1
($f_2(1270) \to \pi\pi$)

VALUE	DOCUMENT ID	TECN	COMMENT
• • • We do not use the following data for averages, fits, limits, etc. • • •			
~ 0.74	DAUM	81C	CNTR 63 $K^- p \to K^- 2\pi p$

$\Gamma(K f_0(980))/\Gamma_{total}$ Γ_5/Γ

VALUE	DOCUMENT ID	TECN	COMMENT
• • • We do not use the following data for averages, fits, limits, etc. • • •			
possibly seen	TIKHOMIROV 03	SPEC	40.0 $\pi^- C \to K_S^0 K_S^0 K_L^0 X$

$\Gamma(K\phi)/\Gamma_{total}$ Γ_6/Γ

VALUE	DOCUMENT ID	TECN	CHG	COMMENT
seen	ARMSTRONG 83	OMEG	−	18.5 $K^- p \to K^- \phi N$

$\Gamma(K\omega)/\Gamma_{total}$ Γ_7/Γ

VALUE	DOCUMENT ID		TECN	CHG	COMMENT
seen	OTTER	81	HBC	±	8.25,10,16 $K^\pm p$
seen	CHUNG	74	HBC	−	7.3 $K^- p \to K^- \omega p$

$K_2(1770)$ REFERENCES

PDG	04	PL B592 1	S. Eidelman *et al.* (PDG Collab.)
TIKHOMIROV	03	PAN 66 828	G.D. Tikhomirov *et al.*
		Translated from YAF 66 860.	
ASTON	93	PL B308 186	D. Aston *et al.* (SLAC, NAGO, CINC, INUS)
FRAME	86	NP B276 667	D. Frame *et al.* (GLAS)
ARMSTRONG	83	NP B221 1	T.A. Armstrong *et al.* (BARI, BIRM, CERN+)
DAUM	81C	NP B187 1	C. Daum *et al.* (AMST, CERN, CRAC, MPIM+)
OTTER	81	NP B181 1	G. Otter (AACH3, BERL, LOIC, VIEN, BIRM+)
CHUNG	74	PL 51B 413	S.U. Chung *et al.* (BNL)
BLIEDEN	72	PL 39B 668	H.R. Blieden *et al.* (STON, NEAS)
FIRESTONE	72B	PR D5 505	A. Firestone *et al.* (LBL)
COLLEY	71	NP B26 71	D.C. Colley *et al.* (BIRM, GLAS)
DENEGRI	71	NP B28 13	D. Denegri *et al.* (JHU) JP
AGUILAR-...	70C	PRL 25 54	M. Aguilar-Benitez *et al.* (BNL)
BARTSCH	70C	PL 33B 186	J. Bartsch *et al.* (AACH, BERL, CERN+)
LUDLAM	70	PR D2 1234	T. Ludlam, J. Sandweiss, A.J. Slaughter (YALE)
BARBARO-...	69	PRL 22 1207	A. Barbaro-Galtieri *et al.* (LRL)

$K_3^*(1780)$

$I(J^P) = \frac{1}{2}(3^-)$

$K_3^*(1780)$ MASS

VALUE (MeV)	EVTS	DOCUMENT ID		TECN	CHG	COMMENT
1776± 7 OUR AVERAGE		Error includes scale factor of 1.1.				
1781± 8± 4		[1] ASTON	88	LASS	0	11 $K^- p \to K^- \pi^+ n$
1740±14±15		[1] ASTON	87	LASS	0	11 $K^- p \to \overline{K}^0 \pi^+ \pi^- n$
1779±11		[2] BALDI	76	SPEC	+	10 $K^+ p \to K^0 \pi^+ p$
1776±26		[3] BRANDENB...	76D	ASPK	0	13 $K^\pm p \to K^\pm \pi^\mp N$
• • • We do not use the following data for averages, fits, limits, etc. • • •						
1720±10±15	6111	[4] BIRD	89	LASS	−	11 $K^- p \to \overline{K}^0 \pi^- p$
1749±10		ASTON	88B	LASS	−	11 $K^- p \to K^- \eta p$
1780± 9	300	BAUBILLIER	84B	HBC	−	8.25 $K^- p \to \overline{K}^0 \pi^- p$
1790±15		BAUBILLIER	82B	HBC	0	8.25 $K^- p \to K_S^0 2\pi N$
1784± 9	2060	CLELAND	82	SPEC	±	50 $K^+ p \to K_S^0 \pi^\pm p$
1786±15		[5] ASTON	81D	LASS	0	11 $K^- p \to K^- \pi^+ n$
1762± 9	190	TOAFF	81	HBC	−	6.5 $K^- p \to \overline{K}^0 \pi^- p$
1850±50		ETKIN	80	MPS	0	6 $K^- p \to \overline{K}^0 \pi^+ \pi^-$
1812±28		BEUSCH	78	OMEG		10 $K^- p \to \overline{K}^0 \pi^+ \pi^- n$
1786± 8		CHUNG	78	MPS	0	6 $K^- p \to K^- \pi^+ n$

[1] From energy-independent partial-wave analysis.
[2] From a fit to Y_6^2 moment. $J^P = 3^-$ found.
[3] Confirmed by phase shift analysis of ESTABROOKS 78, yields $J^P = 3^-$.
[4] From a partial wave amplitude analysis.
[5] From a fit to the Y_6^0 moment.

$K_3^*(1780)$ WIDTH

VALUE (MeV)	EVTS	DOCUMENT ID		TECN	CHG	COMMENT
159±21 OUR AVERAGE		Error includes scale factor of 1.3. See the ideogram below.				
203±30± 8		[6] ASTON	88	LASS	0	11 $K^- p \to K^- \pi^+ n$
171±42±20		[6] ASTON	87	LASS	0	11 $K^- p \to \overline{K}^0 \pi^+ \pi^- n$
135±22		[7] BALDI	76	SPEC	+	10 $K^+ p \to K^0 \pi^+ p$
• • • We do not use the following data for averages, fits, limits, etc. • • •						
187±31±20	6111	[8] BIRD	89	LASS	−	11 $K^- p \to \overline{K}^0 \pi^- p$
193^{+51}_{-37}		ASTON	88B	LASS	−	11 $K^- p \to K^- \eta p$
99±30	300	BAUBILLIER	84B	HBC	−	8.25 $K^- p \to \overline{K}^0 \pi^- p$
~ 130		BAUBILLIER	82B	HBC	0	8.25 $K^- p \to K_S^0 2\pi N$
191±24	2060	CLELAND	82	SPEC	±	50 $K^+ p \to K_S^0 \pi^\pm p$
225±60		[9] ASTON	81D	LASS	0	11 $K^- p \to K^- \pi^+ n$
~ 80	190	TOAFF	81	HBC	−	6.5 $K^- p \to \overline{K}^0 \pi^- p$
240±50		ETKIN	80	MPS	0	6 $K^- p \to \overline{K}^0 \pi^+ \pi^-$
181±44		[10] BEUSCH	78	OMEG		10 $K^- p \to \overline{K}^0 \pi^+ \pi^- n$
96±31		CHUNG	78	MPS	0	6 $K^- p \to K^- \pi^+ n$
270±70		[11] BRANDENB...	76D	ASPK	0	13 $K^\pm p \to K^\pm \pi^\mp N$

[6] From energy-independent partial-wave analysis.
[7] From a fit to Y_6^2 moment. $J^P = 3^-$ found.
[8] From a partial wave amplitude analysis.
[9] From a fit to Y_6^0 moment.
[10] Errors enlarged by us to $4\Gamma/\sqrt{N}$; see the note with the $K^*(892)$ mass.
[11] ESTABROOKS 78 find that BRANDENBURG 76D data are consistent with 175 MeV width. Not averaged.

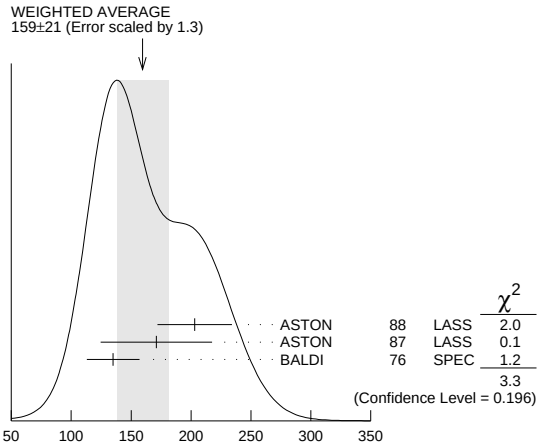

$K_3^*(1780)$ DECAY MODES

	Mode	Fraction (Γ_i/Γ)	Confidence level
Γ_1	$K\rho$	(31 ± 9) %	
Γ_2	$K^*(892)\pi$	(20 ± 5) %	
Γ_3	$K\pi$	(18.8± 1.0) %	
Γ_4	$K\eta$	(30 ±13) %	
Γ_5	$K_2^*(1430)\pi$	< 16 %	95%

CONSTRAINED FIT INFORMATION

An overall fit to 3 branching ratios uses 4 measurements and one constraint to determine 4 parameters. The overall fit has a $\chi^2 = 0.0$ for 1 degrees of freedom.

The following *off-diagonal* array elements are the correlation coefficients $\langle \delta x_i \delta x_j \rangle / (\delta x_i \cdot \delta x_j)$, in percent, from the fit to the branching fractions, $x_i \equiv \Gamma_i/\Gamma_{total}$. The fit constrains the x_i whose labels appear in this array to sum to one.

x_2	85		
x_3	18	21	
x_4	−98	−94	−27
	x_1	x_2	x_3

$K_3^*(1780)$ BRANCHING RATIOS

$\Gamma(K\rho)/\Gamma(K^*(892)\pi)$ Γ_1/Γ_2

VALUE	DOCUMENT ID		TECN	CHG	COMMENT
1.52±0.23 OUR FIT					
1.52±0.21±0.10	ASTON	87	LASS	0	11 $K^-p \to \overline{K}^0\pi^+\pi^-n$

$\Gamma(K^*(892)\pi)/\Gamma(K\pi)$ Γ_2/Γ_3

VALUE	DOCUMENT ID		TECN	CHG	COMMENT
1.09±0.26 OUR FIT					
1.09±0.26	ASTON	84B	LASS	0	11 $K^-p \to \overline{K}^0 2\pi n$

$\Gamma(K\pi)/\Gamma_{total}$ Γ_3/Γ

VALUE	DOCUMENT ID		TECN	CHG	COMMENT
0.188±0.010 OUR FIT					
0.188±0.010 OUR AVERAGE					
0.187±0.008±0.008	ASTON	88	LASS	0	11 $K^-p \to K^-\pi^+n$
0.19 ±0.02	ESTABROOKS	78	ASPK	0	13 $K^\pm p \to K\pi N$

$\Gamma(K\eta)/\Gamma(K\pi)$ Γ_4/Γ_3

VALUE	DOCUMENT ID		TECN	CHG	COMMENT
1.6 ±0.7 OUR FIT					
• • • We do not use the following data for averages, fits, limits, etc. • • •					
0.41±0.050	[12] BIRD	89	LASS	–	11 $K^-p \to \overline{K}^0\pi^-p$
0.50±0.18	ASTON	88B	LASS	–	11 $K^-p \to K^-\eta p$

[12] This result supersedes ASTON 88B.

$\Gamma(K_2^*(1430)\pi)/\Gamma(K^*(892)\pi)$ Γ_5/Γ_2

VALUE	CL%	DOCUMENT ID		TECN	CHG	COMMENT
<0.78	95	ASTON	87	LASS	0	11 $K^-p \to \overline{K}^0\pi^+\pi^-n$

$K_3^*(1780)$ REFERENCES

BIRD	89	SLAC-332	P.F. Bird	(SLAC)
ASTON	88	NP B296 493	D. Aston *et al.*	(SLAC, NAGO, CINC, INUS)
ASTON	88B	PL B201 169	D. Aston *et al.*	(SLAC, NAGO, CINC, INUS) JP
ASTON	87	NP B292 693	D. Aston *et al.*	(SLAC, NAGO, CINC, INUS)
ASTON	84B	NP B247 261	D. Aston *et al.*	(SLAC, CARL, OTTA)
BAUBILLIER	84B	ZPHY C26 37	M. Baubillier *et al.*	(BIRM, CERN, GLAS+)
BAUBILLIER	82B	NP B202 21	M. Baubillier *et al.*	(BIRM, CERN, GLAS+)
CLELAND	82	NP B208 189	W.E. Cleland *et al.*	(DURH, GEVA, LAUS+)
ASTON	81D	PL 99B 502	D. Aston *et al.*	(SLAC, CARL, OTTA) JP
TOAFF	81	PR D23 1500	S. Toaff *et al.*	(ANL, KANS)
ETKIN	80	PR D22 42	A. Etkin *et al.*	(BNL, CUNY) JP
BEUSCH	78	PL 74B 282	W. Beusch *et al.*	(CERN, AACH3, ETH) JP
CHUNG	78	PRL 40 355	S.U. Chung *et al.*	(BNL, BRAN, CUNY+) JP
ESTABROOKS	78	NP B133 490	P.G. Estabrooks *et al.*	(MCGI, CARL, DURH+) JP
Also		PR D17 658	P.G. Estabrooks *et al.*	(MCGI, CARL, DURH+)
BALDI	76	PL 63B 344	R. Baldi *et al.*	(GEVA) JP
BRANDENB...	76D	PL 60B 478	G.W. Brandenburg *et al.*	(SLAC) JP

$K_2(1820)$

$I(J^P) = \frac{1}{2}(2^-)$

See our mini-review in the 2004 edition of this *Review* (PDG 04) under $K_2(1770)$.

$K_2(1820)$ MASS

VALUE (MeV)	DOCUMENT ID		TECN	COMMENT
1816±13	[1] ASTON	93	LASS	11 $K^-p \to K^-\omega p$
• • • We do not use the following data for averages, fits, limits, etc. • • •				
~ 1840	[2] DAUM	81C	CNTR	63 $K^-p \to K^-2\pi p$

[1] From a partial wave analysis of the $K^-\omega$ system.
[2] From a partial wave analysis of the $K^-2\pi$ system.

$K_2(1820)$ WIDTH

VALUE (MeV)	DOCUMENT ID		TECN	COMMENT
276±35	[3] ASTON	93	LASS	11 $K^-p \to K^-\omega p$
• • • We do not use the following data for averages, fits, limits, etc. • • •				
~ 230	[4] DAUM	81C	CNTR	63 $K^-p \to K^-2\pi p$

[3] From a partial wave analysis of the $K^-\omega$ system.
[4] From a partial wave analysis of the $K^-2\pi$ system.

$K_2(1820)$ DECAY MODES

	Mode	Fraction (Γ_i/Γ)
Γ_1	$K\pi\pi$	
Γ_2	$K_2^*(1430)\pi$	seen
Γ_3	$K^*(892)\pi$	seen
Γ_4	$Kf_2(1270)$	seen
Γ_5	$K\omega$	seen

$K_2(1820)$ BRANCHING RATIOS

$\Gamma(K_2^*(1430)\pi)/\Gamma(K\pi\pi)$ Γ_2/Γ_1

VALUE	DOCUMENT ID	TECN	COMMENT
• • • We do not use the following data for averages, fits, limits, etc. • • •			
~ 0.77	DAUM	81C CNTR	63$K^-p \to \overline{K}2\pi p$

$\Gamma(K^*(892)\pi)/\Gamma(K\pi\pi)$ Γ_3/Γ_1

VALUE	DOCUMENT ID	TECN	COMMENT
• • • We do not use the following data for averages, fits, limits, etc. • • •			
~ 0.05	DAUM	81C CNTR	63$K^-p \to \overline{K}2\pi p$

$\Gamma(Kf_2(1270))/\Gamma(K\pi\pi)$ Γ_4/Γ_1

VALUE	DOCUMENT ID	TECN	COMMENT
• • • We do not use the following data for averages, fits, limits, etc. • • •			
~ 0.18	DAUM	81C CNTR	63$K^-p \to \overline{K}2\pi p$

$K_2(1820)$ REFERENCES

PDG	04	PL B592 1	S. Eidelman *et al.*	(PDG Collab.)
ASTON	93	PL B308 186	D. Aston *et al.*	(SLAC, NAGO, CINC, INUS)
DAUM	81C	NP B187 1	C. Daum *et al.*	(AMST, CERN, CRAC, MPIM+)

Meson Particle Listings

$K(1830)$, $K_0^*(1950)$, $K_2^*(1980)$, $K_4^*(2045)$

$K(1830)$

$I(J^P) = \frac{1}{2}(0^-)$

OMITTED FROM SUMMARY TABLE

Seen in partial-wave analysis of $K^-\phi$ system. Needs confirmation.

$K(1830)$ MASS

VALUE (MeV)	DOCUMENT ID	TECN	CHG	COMMENT
• • • We do not use the following data for averages, fits, limits, etc. • • •				
~ 1830	ARMSTRONG 83	OMEG	–	18.5 $K^-p \to 3Kp$

$K(1830)$ WIDTH

VALUE (MeV)	DOCUMENT ID	TECN	CHG	COMMENT
• • • We do not use the following data for averages, fits, limits, etc. • • •				
~ 250	ARMSTRONG 83	OMEG	–	18.5 $K^-p \to 3Kp$

$K(1830)$ DECAY MODES

	Mode
Γ_1	$K\phi$

$K(1830)$ REFERENCES

ARMSTRONG 83 NP B221 1 T.A. Armstrong *et al.* (BARI, BIRM, CERN+) JP

$K_0^*(1950)$

$I(J^P) = \frac{1}{2}(0^+)$

OMITTED FROM SUMMARY TABLE

Seen in partial-wave analysis of the $K^-\pi^+$ system. Needs confirmation.

$K_0^*(1950)$ MASS

VALUE (MeV)	DOCUMENT ID	TECN	CHG	COMMENT
1945 ± 10 ± 20	[1] ASTON 88	LASS	0	11 $K^-p \to K^-\pi^+n$
• • • We do not use the following data for averages, fits, limits, etc. • • •				
1917 ± 12	[2] ZHOU 06	RVUE		$Kp \to K^-\pi^+n$
1820 ± 40	[3] ANISOVICH 97C	RVUE		11 $K^-p \to K^-\pi^+n$

[1] We take the central value of the two solutions and the larger error given.
[2] S-matrix pole. Using ASTON 88 and assuming $K_0^*(800)$, $K_0^*(1430)$.
[3] T-matrix pole. Reanalysis of ASTON 88 data.

$K_0^*(1950)$ WIDTH

VALUE (MeV)	DOCUMENT ID	TECN	CHG	COMMENT
201 ± 34 ± 79	[4] ASTON 88	LASS	0	11 $K^-p \to K^-\pi^+n$
• • • We do not use the following data for averages, fits, limits, etc. • • •				
145 ± 38	[5] ZHOU 06	RVUE		$Kp \to K^-\pi^+n$
250 ± 100	[6] ANISOVICH 97C	RVUE		11 $K^-p \to K^-\pi^+n$

[4] We take the central value of the two solutions and the larger error given.
[5] S-matrix pole. Using ASTON 88 and assuming $K_0^*(800)$, $K_0^*(1430)$.
[6] T-matrix pole. Reanalysis of ASTON 88 data.

$K_0^*(1950)$ DECAY MODES

	Mode	Fraction (Γ_i/Γ)
Γ_1	$K\pi$	(52 ± 14) %

$K_0^*(1950)$ BRANCHING RATIOS

$\Gamma(K\pi)/\Gamma_{total}$ — **Γ_1/Γ**

VALUE	DOCUMENT ID	TECN	CHG	COMMENT
0.52 ± 0.08 ± 0.12	[7] ASTON 88	LASS	0	11 $K^-p \to K^-\pi^+n$
• • • We do not use the following data for averages, fits, limits, etc. • • •				
~ 0.60	[8] ZHOU 06	RVUE		$Kp \to K^-\pi^+n$

[7] We take the central value of the two solutions and the larger error given.
[8] S-matrix pole. Using ASTON 88 and assuming $K_0^*(800)$, $K_0^*(1430)$.

$K_0^*(1950)$ REFERENCES

ZHOU 06 NP A775 212 Z.Y. Zhou, H.Q. Zheng
ANISOVICH 97C PL B413 137 A.V. Anisovich, A.V. Sarantsev
ASTON 88 NP B296 493 D. Aston *et al.* (SLAC, NAGO, CINC, INUS)

$K_2^*(1980)$

$I(J^P) = \frac{1}{2}(2^+)$

OMITTED FROM SUMMARY TABLE

Needs confirmation.

$K_2^*(1980)$ MASS

VALUE (MeV)	EVTS	DOCUMENT ID	TECN	CHG	COMMENT
1973 ± 8 ± 25		ASTON 87	LASS	0	11 $K^-p \to \overline{K}^0\pi^+\pi^-n$
• • • We do not use the following data for averages, fits, limits, etc. • • •					
2020 ± 20		TIKHOMIROV 03	SPEC		40.0 π^-C $\to K_S^0K_S^0K_L^0$X
1978 ± 40	241 ± 47	BIRD 89	LASS	–	11 $K^-p \to \overline{K}^0\pi^-p$

$K_2^*(1980)$ WIDTH

VALUE (MeV)	EVTS	DOCUMENT ID	TECN	CHG	COMMENT
373 ± 33 ± 60		ASTON 87	LASS	0	11 $K^-p \to \overline{K}^0\pi^+\pi^-n$
• • • We do not use the following data for averages, fits, limits, etc. • • •					
180 ± 70		TIKHOMIROV 03	SPEC		40.0 π^-C $\to K_S^0K_S^0K_L^0$X
398 ± 47	241 ± 47	BIRD 89	LASS	–	11 $K^-p \to \overline{K}^0\pi^-p$

$K_2^*(1980)$ DECAY MODES

	Mode	Fraction (Γ_i/Γ)
Γ_1	$K^*(892)\pi$	possibly seen
Γ_2	$K\rho$	possibly seen
Γ_3	$Kf_2(1270)$	possibly seen

$K_2^*(1980)$ BRANCHING RATIOS

$\Gamma(K^*(892)\pi)/\Gamma_{total}$ — **Γ_1/Γ**

VALUE	DOCUMENT ID	TECN	COMMENT
possibly seen	GULER 11	BELL	$B^+ \to J/\psi K^+\pi^+\pi^-$

$\Gamma(K\rho)/\Gamma_{total}$ — **Γ_2/Γ**

VALUE	DOCUMENT ID	TECN	COMMENT
possibly seen	GULER 11	BELL	$B^+ \to J/\psi K^+\pi^+\pi^-$

$\Gamma(K\rho)/\Gamma(K^*(892)\pi)$ — **Γ_2/Γ_1**

VALUE	DOCUMENT ID	TECN	CHG	COMMENT
1.49 ± 0.24 ± 0.09	ASTON 87	LASS	0	11 $K^-p \to \overline{K}^0\pi^+\pi^-n$

$\Gamma(Kf_2(1270))/\Gamma_{total}$ — **Γ_3/Γ**

VALUE	DOCUMENT ID	TECN	COMMENT
possibly seen	TIKHOMIROV 03	SPEC	40.0 π^-C $\to K_S^0K_S^0K_L^0$X

$K_2^*(1980)$ REFERENCES

GULER 11 PR D83 032005 H. Guler *et al.* (BELLE Collab.)
TIKHOMIROV 03 PAN 66 828 G.D. Tikhomirov *et al.*
Translated from YAF 66 860.
BIRD 89 SLAC-332 P.F. Bird (SLAC)
ASTON 87 NP B292 693 D. Aston *et al.* (SLAC, NAGO, CINC, INUS)

$K_4^*(2045)$

$I(J^P) = \frac{1}{2}(4^+)$

$K_4^*(2045)$ MASS

VALUE (MeV)	EVTS	DOCUMENT ID	TECN	CHG	COMMENT
2045 ± 9 OUR AVERAGE		Error includes scale factor of 1.1.			
2062 ± 14 ± 13		[1] ASTON 86	LASS	0	11 $K^-p \to K^-\pi^+n$
2039 ± 10	400	[2,3] CLELAND 82	SPEC	±	50 $K^+p \to K_S^0\pi^\pm p$
2070^{+100}_{-40}		[4] ASTON 81C	LASS	0	11 $K^-p \to K^-\pi^+n$
• • • We do not use the following data for averages, fits, limits, etc. • • •					
2079 ± 7	431	TORRES 86	MPSF		400 $pA \to 4KX$
2088 ± 20	650	BAUBILLIER 82	HBC	–	8.25 $K^-p \to K_S^0\pi^-p$
2115 ± 46	488	CARMONY 77	HBC	0	9 $K^+d \to K^+$'s X

[1] From a fit to all moments.
[2] From a fit to 8 moments.
[3] Number of events evaluated by us.
[4] From energy-independent partial-wave analysis.

$K_4^*(2045)$ WIDTH

VALUE (MeV)	EVTS	DOCUMENT ID		TECN	CHG	COMMENT
198± 30 OUR AVERAGE						
221± 48±27		[5] ASTON	86	LASS	0	11 $K^-p \to K^-\pi^+n$
189± 35	400	[6,7] CLELAND	82	SPEC	±	50 $K^+p \to K^0_S\pi^\pm p$
• • • We do not use the following data for averages, fits, limits, etc. • • •						
61± 58	431	TORRES	86	MPSF		400 $pA \to 4KX$
$170^{+100}_{-\ 50}$	650	BAUBILLIER	82	HBC	–	8.25 $K^-p \to K^0_S\pi^-p$
240^{+500}_{-100}		[8] ASTON	81C	LASS	0	11 $K^-p \to K^-\pi^+n$
300±200		CARMONY	77	HBC	0	9 $K^+d \to K^+\pi$'s X

[5] From a fit to all moments.
[6] From a fit to 8 moments.
[7] Number of events evaluated by us.
[8] From energy-independent partial-wave analysis.

$K_4^*(2045)$ DECAY MODES

	Mode	Fraction (Γ_i/Γ)
Γ_1	$K\pi$	(9.9±1.2) %
Γ_2	$K^*(892)\pi\pi$	(9 ±5) %
Γ_3	$K^*(892)\pi\pi\pi$	(7 ±5) %
Γ_4	$\rho K\pi$	(5.7±3.2) %
Γ_5	$\omega K\pi$	(5.0±3.0) %
Γ_6	$\phi K\pi$	(2.8±1.4) %
Γ_7	$\phi K^*(892)$	(1.4±0.7) %

$K_4^*(2045)$ BRANCHING RATIOS

$\Gamma(K\pi)/\Gamma_{total}$ — **Γ_1/Γ**

VALUE	DOCUMENT ID		TECN	CHG	COMMENT
0.099±0.012	ASTON	88	LASS	0	11 $K^-p \to K^-\pi^+n$

$\Gamma(K^*(892)\pi\pi)/\Gamma(K\pi)$ — **Γ_2/Γ_1**

VALUE	DOCUMENT ID		TECN	CHG	COMMENT
0.89±0.53	BAUBILLIER	82	HBC	–	8.25 $K^-p \to pK^0_S3\pi$

$\Gamma(K^*(892)\pi\pi\pi)/\Gamma(K\pi)$ — **Γ_3/Γ_1**

VALUE	DOCUMENT ID		TECN	CHG	COMMENT
0.75±0.49	BAUBILLIER	82	HBC	–	8.25 $K^-p \to pK^0_S3\pi$

$\Gamma(\rho K\pi)/\Gamma(K\pi)$ — **Γ_4/Γ_1**

VALUE	DOCUMENT ID		TECN	CHG	COMMENT
0.58±0.32	BAUBILLIER	82	HBC	–	8.25 $K^-p \to pK^0_S3\pi$

$\Gamma(\omega K\pi)/\Gamma(K\pi)$ — **Γ_5/Γ_1**

VALUE	DOCUMENT ID		TECN	CHG	COMMENT
0.50±0.30	BAUBILLIER	82	HBC	–	8.25 $K^-p \to pK^0_S3\pi$

$\Gamma(\phi K\pi)/\Gamma_{total}$ — **Γ_6/Γ**

VALUE	DOCUMENT ID		TECN	COMMENT
0.028±0.014	[9] TORRES	86	MPSF	400 $pA \to 4KX$

$\Gamma(\phi K^*(892))/\Gamma_{total}$ — **Γ_7/Γ**

VALUE	DOCUMENT ID		TECN	COMMENT
0.014±0.007	[9] TORRES	86	MPSF	400 $pA \to 4KX$

[9] Error determination is model dependent.

$K_4^*(2045)$ REFERENCES

ASTON	88	NP B296 493	D. Aston *et al.*	(SLAC, NAGO, CINC, INUS)
ASTON	86	PL B180 308	D. Aston *et al.*	(SLAC, NAGO, CINC, INUS)
TORRES	86	PR D34 707	S. Torres *et al.*	(VPI, ARIZ, FNAL, FSU+)
BAUBILLIER	82	PL 118B 447	M. Baubillier *et al.*	(BIRM, CERN, GLAS+)
CLELAND	82	NP B208 189	W.E. Cleland *et al.*	(DURH, GEVA, LAUS+)
ASTON	81C	PL 106B 235	D. Aston *et al.*	(SLAC, CARL, OTTA) JP
CARMONY	77	PR D16 1251	D.D. Carmony *et al.*	(PURD, UCD, IUPU)

$K_2(2250)$

$I(J^P) = \frac{1}{2}(2^-)$

OMITTED FROM SUMMARY TABLE

This entry contains various peaks in strange meson systems reported in the 2150–2260 MeV region, as well as enhancements seen in the antihyperon-nucleon system, either in the mass spectra or in the $J^P = 2^-$ wave.

$K_2(2250)$ MASS

VALUE (MeV)	EVTS	DOCUMENT ID		TECN	CHG	COMMENT
2247±17 OUR AVERAGE						
2200±40		[1] ARMSTRONG	83C	OMEG	–	18 $K^-p \to \Lambda\overline{p}X$
2235±50		[1] BAUBILLIER	81	HBC	–	8 $K^-p \to \Lambda\overline{p}X$
2260±20		[1] CLELAND	81	SPEC	±	50 $K^+p \to \Lambda\overline{p}X$
• • • We do not use the following data for averages, fits, limits, etc. • • •						
2280±20		TIKHOMIROV	03	SPEC		40.0 $\pi^-C \to K^0_SK^0_SK^0_LX$
2147± 4	37	CHLIAPNIK...	79	HBC	+	32 $K^+p \to \overline{\Lambda}pX$
2240±20	20	LISSAUER	70	HBC		9 K^+p

[1] $J^P = 2^-$ from moments analysis.

$K_2(2250)$ WIDTH

VALUE (MeV)	EVTS	DOCUMENT ID		TECN	CHG	COMMENT
180±30 OUR AVERAGE		Error includes scale factor of 1.4.				
150±30		[2] ARMSTRONG	83C	OMEG	–	18 $K^-p \to \Lambda\overline{p}X$
210±30		[2] CLELAND	81	SPEC	±	50 $K^+p \to \Lambda\overline{p}X$
• • • We do not use the following data for averages, fits, limits, etc. • • •						
180±60		TIKHOMIROV	03	SPEC		40.0 $\pi^-C \to K^0_SK^0_SK^0_LX$
~ 200		[2] BAUBILLIER	81	HBC	–	8 $K^-p \to \Lambda\overline{p}X$
~ 40	37	CHLIAPNIK...	79	HBC	+	32 $K^+p \to \overline{\Lambda}pX$
80±20	20	LISSAUER	70	HBC		9 K^+p

[2] $J^P = 2^-$ from moments analysis.

$K_2(2250)$ DECAY MODES

	Mode
Γ_1	$K\pi\pi$
Γ_2	$Kf_2(1270)$
Γ_3	$K^*(892)f_0(980)$
Γ_4	$p\overline{\Lambda}$

$K_2(2250)$ REFERENCES

TIKHOMIROV	03	PAN 66 828 Translated from YAF 66 860.	G.D. Tikhomirov *et al.*	
ARMSTRONG	83C	NP B227 365	T.A. Armstrong *et al.*	(BARI, BIRM, CERN+)
BAUBILLIER	81	NP B183 1	M. Baubillier *et al.*	(BIRM, CERN, GLAS+) JP
CLELAND	81	NP B184 1	W.E. Cleland *et al.*	(PITT, GEVA, LAUS+) JP
CHLIAPNIK...	79	NP B158 253	P.V. Chliapnikov *et al.*	(CERN, BELG, MONS)
LISSAUER	70	NP B18 491	D. Lissauer *et al.*	(LBL)

$K_3(2320)$

$I(J^P) = \frac{1}{2}(3^+)$

OMITTED FROM SUMMARY TABLE

Seen in the $J^P = 3^+$ wave of the antihyperon-nucleon system. Needs confirmation.

$K_3(2320)$ MASS

VALUE (MeV)	DOCUMENT ID		TECN	CHG	COMMENT
2324±24 OUR AVERAGE					
2330±40	[1] ARMSTRONG	83C	OMEG	–	18 $K^-p \to \Lambda\overline{p}X$
2320±30	[1] CLELAND	81	SPEC	±	50 $K^+p \to \Lambda\overline{p}X$

[1] $J^P = 3^+$ from moments analysis.

$K_3(2320)$ WIDTH

VALUE (MeV)	DOCUMENT ID		TECN	CHG	COMMENT
150±30	[2] ARMSTRONG	83C	OMEG	–	18 $K^-p \to \Lambda\overline{p}X$
• • • We do not use the following data for averages, fits, limits, etc. • • •					
~ 250	[2] CLELAND	81	SPEC	±	50 $K^+p \to \Lambda\overline{p}X$

[2] $J^P = 3^+$ from moments analysis.

$K_3(2320)$ DECAY MODES

	Mode
Γ_1	$p\overline{\Lambda}$

$K_3(2320)$ REFERENCES

ARMSTRONG	83C	NP B227 365	T.A. Armstrong *et al.*	(BARI, BIRM, CERN+)
CLELAND	81	NP B184 1	W.E. Cleland *et al.*	(PITT, GEVA, LAUS+)

Meson Particle Listings

$K_5^*(2380)$, $K_4(2500)$, $K(3100)$

$K_5^*(2380)$

$I(J^P) = \frac{1}{2}(5^-)$

OMITTED FROM SUMMARY TABLE

Needs confirmation.

$K_5^*(2380)$ MASS

VALUE (MeV)	DOCUMENT ID		TECN	CHG	COMMENT
2382±14±19	[1] ASTON	86	LASS	0	11 $K^- p \rightarrow K^- \pi^+ n$

[1] From a fit to all the moments.

$K_5^*(2380)$ WIDTH

VALUE (MeV)	DOCUMENT ID		TECN	CHG	COMMENT
178±37±32	[2] ASTON	86	LASS	0	11 $K^- p \rightarrow K^- \pi^+ n$

[2] From a fit to all the moments.

$K_5^*(2380)$ DECAY MODES

	Mode	Fraction (Γ_i/Γ)
Γ_1	$K\pi$	(6.1±1.2) %

$K_5^*(2380)$ BRANCHING RATIOS

$\Gamma(K\pi)/\Gamma_{total}$ **Γ_1/Γ**

VALUE	DOCUMENT ID		TECN	CHG	COMMENT
0.061±0.012	ASTON	88	LASS	0	11 $K^- p \rightarrow K^- \pi^+ n$

$K_5^*(2380)$ REFERENCES

ASTON	88	NP B296 493	D. Aston *et al.*	(SLAC, NAGO, CINC, INUS)
ASTON	86	PL B180 308	D. Aston *et al.*	(SLAC, NAGO, CINC, INUS)

$K_4(2500)$

$I(J^P) = \frac{1}{2}(4^-)$

OMITTED FROM SUMMARY TABLE

Needs confirmation.

$K_4(2500)$ MASS

VALUE (MeV)	DOCUMENT ID		TECN	CHG	COMMENT
2490±20	[1] CLELAND	81	SPEC	±	50 $K^+ p \rightarrow \Lambda\overline{p}$

[1] $J^P = 4^-$ from moments analysis.

$K_4(2500)$ WIDTH

VALUE (MeV)	DOCUMENT ID		TECN	CHG	COMMENT
• • • We do not use the following data for averages, fits, limits, etc. • • •					
~ 250	[2] CLELAND	81	SPEC	±	50 $K^+ p \rightarrow \Lambda\overline{p}$

[2] $J^P = 4^-$ from moments analysis.

$K_4(2500)$ DECAY MODES

	Mode
Γ_1	$p\overline{\Lambda}$

$K_4(2500)$ REFERENCES

CLELAND	81	NP B184 1	W.E. Cleland *et al.*	(PITT, GEVA, LAUS+)

$K(3100)$

$I^G(J^{PC}) = ?^?(?^{??})$

OMITTED FROM SUMMARY TABLE

Narrow peak observed in several ($\Lambda\overline{p}$ + pions) and ($\overline{\Lambda}p$ + pions) states in Σ^- Be reactions by BOURQUIN 86 and in np and nA reactions by ALEEV 93. Not seen by BOEHNLEIN 91. If due to strong decays, this state has exotic quantum numbers (B=0,Q=+1,S=−1 for $\Lambda\overline{p}\pi^+\pi^+$ and $I \geq 3/2$ for $\Lambda\overline{p}\pi^-$). Needs confirmation.

$K(3100)$ MASS

VALUE (MeV)	DOCUMENT ID
≈ 3100 OUR ESTIMATE	

3-BODY DECAYS

VALUE (MeV)	DOCUMENT ID		TECN	COMMENT
3054±11 OUR AVERAGE				
3060± 7±20	[1] ALEEV	93	BIS2	$K(3100) \rightarrow \Lambda\overline{p}\pi^+$
3056± 7±20	[1] ALEEV	93	BIS2	$K(3100) \rightarrow \overline{\Lambda}p\pi^-$
3055± 8±20	[1] ALEEV	93	BIS2	$K(3100) \rightarrow \Lambda\overline{p}\pi^-$
3045± 8±20	[1] ALEEV	93	BIS2	$K(3100) \rightarrow \overline{\Lambda}p\pi^+$

4-BODY DECAYS

VALUE (MeV)	DOCUMENT ID		TECN	COMMENT
3059±11 OUR AVERAGE				
3067± 6±20	[1] ALEEV	93	BIS2	$K(3100) \rightarrow \Lambda\overline{p}\pi^+\pi^+$
3060± 8±20	[1] ALEEV	93	BIS2	$K(3100) \rightarrow \Lambda\overline{p}\pi^+\pi^-$
3055± 7±20	[1] ALEEV	93	BIS2	$K(3100) \rightarrow \overline{\Lambda}p\pi^-\pi^-$
3052± 8±20	[1] ALEEV	93	BIS2	$K(3100) \rightarrow \overline{\Lambda}p\pi^-\pi^+$
• • • We do not use the following data for averages, fits, limits, etc. • • •				
3105±30	BOURQUIN	86	SPEC	$K(3100) \rightarrow \Lambda\overline{p}\pi^+\pi^+$
3115±30	BOURQUIN	86	SPEC	$K(3100) \rightarrow \Lambda\overline{p}\pi^+\pi^-$

5-BODY DECAYS

VALUE (MeV)	DOCUMENT ID		TECN	COMMENT
• • • We do not use the following data for averages, fits, limits, etc. • • •				
3095±30	BOURQUIN	86	SPEC	$K(3100) \rightarrow \Lambda\overline{p}\pi^+\pi^+\pi^-$

[1] Supersedes ALEEV 90.

$K(3100)$ WIDTH

3-BODY DECAYS

VALUE (MeV)	DOCUMENT ID		TECN	COMMENT
• • • We do not use the following data for averages, fits, limits, etc. • • •				
42±16	[2] ALEEV	93	BIS2	$K(3100) \rightarrow \Lambda\overline{p}\pi^+$
36±15	[2] ALEEV	93	BIS2	$K(3100) \rightarrow \overline{\Lambda}p\pi^-$
50±18	[2] ALEEV	93	BIS2	$K(3100) \rightarrow \Lambda\overline{p}\pi^-$
30±15	[2] ALEEV	93	BIS2	$K(3100) \rightarrow \overline{\Lambda}p\pi^+$

4-BODY DECAYS

VALUE (MeV)	CL%	DOCUMENT ID		TECN	COMMENT
• • • We do not use the following data for averages, fits, limits, etc. • • •					
22± 8		[2] ALEEV	93	BIS2	$K(3100) \rightarrow \Lambda\overline{p}\pi^+\pi^+$
28±12		[2] ALEEV	93	BIS2	$K(3100) \rightarrow \Lambda\overline{p}\pi^+\pi^-$
32±15		[2] ALEEV	93	BIS2	$K(3100) \rightarrow \overline{\Lambda}p\pi^-\pi^-$
30±15		[2] ALEEV	93	BIS2	$K(3100) \rightarrow \overline{\Lambda}p\pi^-\pi^+$
<30	90	BOURQUIN	86	SPEC	$K(3100) \rightarrow \Lambda\overline{p}\pi^+\pi^+$
<80	90	BOURQUIN	86	SPEC	$K(3100) \rightarrow \Lambda\overline{p}\pi^+\pi^-$

5-BODY DECAYS

VALUE (MeV)	CL%	DOCUMENT ID		TECN	COMMENT
• • • We do not use the following data for averages, fits, limits, etc. • • •					
<30	90	BOURQUIN	86	SPEC	$K(3100) \rightarrow \Lambda\overline{p}\pi^+\pi^+\pi^-$

[2] Supersedes ALEEV 90.

$K(3100)$ DECAY MODES

	Mode
Γ_1	$K(3100)^0 \rightarrow \Lambda\overline{p}\pi^+$
Γ_2	$K(3100)^{--} \rightarrow \Lambda\overline{p}\pi^-$
Γ_3	$K(3100)^- \rightarrow \Lambda\overline{p}\pi^+\pi^-$
Γ_4	$K(3100)^+ \rightarrow \Lambda\overline{p}\pi^+\pi^+$
Γ_5	$K(3100)^0 \rightarrow \Lambda\overline{p}\pi^+\pi^+\pi^-$
Γ_6	$K(3100)^0 \rightarrow \Sigma(1385)^+\overline{p}$

$\Gamma(\Sigma(1385)^+\overline{p})/\Gamma(\Lambda\overline{p}\pi^+)$ **Γ_6/Γ_1**

VALUE	CL%	DOCUMENT ID		TECN	COMMENT
<0.04	90	ALEEV	93	BIS2	$K(3100)^0 \rightarrow \Sigma(1385)^+\overline{p}$

$K(3100)$ REFERENCES

ALEEV	93	PAN 56 1358 Translated from YAF 56 100.	A.N. Aleev *et al.*	(BIS-2 Collab.)
BOEHNLEIN	91	NPBPS B21 174	A. Boehnlein *et al.*	(FLOR, BNL, IND+)
ALEEV	90	ZPHY C47 533	A.N. Aleev *et al.*	(BIS-2 Collab.)
BOURQUIN	86	PL B172 113	M.H. Bourquin *et al.*	(GEVA, RAL, HEIDP+)

CHARMED MESONS ($C = \pm 1$)

$D^+ = c\overline{d}$, $D^0 = c\overline{u}$, $\overline{D}^0 = \overline{c}u$, $D^- = \overline{c}d$, similarly for D^*'s

$D^{\pm}$

$I(J^P) = \frac{1}{2}(0^-)$

$D^{\pm}$ MASS

The fit includes $D^{\pm}$, D^0, $D_s^{\pm}$, $D^{*\pm}$, D^{*0}, $D_s^{*\pm}$, $D_1(2420)^0$, $D_2^*(2460)^0$, and $D_{s1}(2536)^{\pm}$ mass and mass difference measurements.

VALUE (MeV)	EVTS	DOCUMENT ID		TECN	COMMENT
1869.61 ± 0.10 OUR FIT Error includes scale factor of 1.1.					
1869.5 ± 0.4 OUR AVERAGE					
1869.53 ± 0.49 ± 0.20	110 ± 15	ANASHIN	10A	KEDR	e^+e^- at $\psi(3770)$
1870.0 ± 0.5 ± 1.0	317	BARLAG	90C	ACCM	π^- Cu 230 GeV
1869.4 ± 0.6		[1] TRILLING	81	RVUE	e^+e^- 3.77 GeV
• • • We do not use the following data for averages, fits, limits, etc. • • •					
1875 ±10	9	ADAMOVICH	87	EMUL	Photoproduction
1860 ±16	6	ADAMOVICH	84	EMUL	Photoproduction
1863 ± 4		DERRICK	84	HRS	e^+e^- 29 GeV
1868.4 ± 0.5		[1] SCHINDLER	81	MRK2	e^+e^- 3.77 GeV
1874 ± 5		GOLDHABER	77	MRK1	D^0, D^+ recoil spectra
1868.3 ± 0.9		[1] PERUZZI	77	LGW	e^+e^- 3.77 GeV
1874 ±11		PICCOLO	77	MRK1	e^+e^- 4.03, 4.41 GeV
1876 ±15	50	PERUZZI	76	MRK1	$K^{\mp}\pi^{\pm}\pi^{\pm}$

[1] PERUZZI 77 and SCHINDLER 81 errors do not include the 0.13% uncertainty in the absolute SPEAR energy calibration. TRILLING 81 uses the high precision $J/\psi(1S)$ and $\psi(2S)$ measurements of ZHOLENTZ 80 to determine this uncertainty and combines the PERUZZI 77 and SCHINDLER 81 results to obtain the value quoted.

$D^{\pm}$ MEAN LIFE

Measurements with an error $> 100 \times 10^{-15}$ s have been omitted from the Listings.

VALUE (10^{-15} s)	EVTS	DOCUMENT ID		TECN	COMMENT
1040 ± 7 OUR AVERAGE					
1039.4 ± 4.3 ± 7.0	110k	LINK	02F	FOCS	γ nucleus, ≈ 180 GeV
$1033.6 \pm 22.1^{+9.9}_{-12.7}$	3777	BONVICINI	99	CLEO	$e^+e^- \approx \Upsilon(4S)$
1048 ±15 ±11	9k	FRABETTI	94D	E687	$D^+ \to K^-\pi^+\pi^+$
• • • We do not use the following data for averages, fits, limits, etc. • • •					
1075 ±40 ±18	2455	FRABETTI	91	E687	γ Be, $D^+ \to K^-\pi^+\pi^+$
1030 ±80 ±60	200	ALVAREZ	90	NA14	γ, $D^+ \to K^-\pi^+\pi^+$
$1050 \; {}^{+77}_{-72}$	317	[1] BARLAG	90C	ACCM	π^- Cu 230 GeV
1050 ±80 ±70	363	ALBRECHT	88I	ARG	e^+e^- 10 GeV
1090 ±30 ±25	2992	RAAB	88	E691	Photoproduction

[1] BARLAG 90C estimates the systematic error to be negligible.

D^+ DECAY MODES

Most decay modes (other than the semileptonic modes) that involve a neutral K meson are now given as K^0_S modes, not as $\overline{K}^0$ modes. Nearly always it is a K^0_S that is measured, and interference between Cabibbo-allowed and doubly Cabibbo-suppressed modes can invalidate the assumption that $2\Gamma(K^0_S) = \Gamma(\overline{K}^0)$.

	Mode	Fraction (Γ_i/Γ)		Scale factor / Confidence level
	Inclusive modes			
Γ_1	$D^+ \to e^+$ semileptonic	(16.07 ± 0.30) %		
Γ_2	$D^+ \to \mu^+$ anything	(17.6 ± 3.2) %		
Γ_3	$D^+ \to K^-$ anything	(25.7 ± 1.4) %		
Γ_4	$D^+ \to \overline{K}^0$ anything + K^0 anything	(61 ± 5) %		
Γ_5	$D^+ \to K^+$ anything	(5.9 ± 0.8) %		
Γ_6	$D^+ \to \overline{K}^*(892)^-$ anything	(6 ± 5) %		
Γ_7	$D^+ \to \overline{K}^*(892)^0$ anything	(23 ± 5) %		
Γ_8	$D^+ \to K^*(892)^0$ anything	< 6.6 %		CL=90%
Γ_9	$D^+ \to \eta$ anything	(6.3 ± 0.7) %		
Γ_{10}	$D^+ \to \eta'$ anything	(1.04 ± 0.18) %		
Γ_{11}	$D^+ \to \phi$ anything	(1.03 ± 0.12) %		
	Leptonic and semileptonic modes			
Γ_{12}	$D^+ \to e^+\nu_e$	< 8.8	$\times 10^{-6}$	CL=90%
Γ_{13}	$D^+ \to \mu^+\nu_\mu$	(3.82 ± 0.33)	$\times 10^{-4}$	
Γ_{14}	$D^+ \to \tau^+\nu_\tau$	< 1.2	$\times 10^{-3}$	CL=90%
Γ_{15}	$D^+ \to \overline{K}^0 e^+\nu_e$	(8.83 ± 0.22) %		
Γ_{16}	$D^+ \to \overline{K}^0 \mu^+\nu_\mu$	(9.2 ± 0.6) %		
Γ_{17}	$D^+ \to K^-\pi^+ e^+\nu_e$	(4.00 ± 0.10) %		
Γ_{18}	$D^+ \to \overline{K}^*(892)^0 e^+\nu_e$, $\overline{K}^*(892)^0 \to K^-\pi^+$	(3.68 ± 0.10) %		
Γ_{19}	$D^+ \to (K^-\pi^+)_{S-wave}\, e^+\nu_e$	(2.32 ± 0.10)	$\times 10^{-3}$	
Γ_{20}	$D^+ \to \overline{K}^*(1410)^0 e^+\nu_e$, $\overline{K}^*(1410)^0 \to K^-\pi^+$	< 6	$\times 10^{-3}$	CL=90%
Γ_{21}	$D^+ \to \overline{K}^*_2(1430)^0 e^+\nu_e$, $\overline{K}^*_2(1430)^0 \to K^-\pi^+$	< 5	$\times 10^{-4}$	CL=90%
Γ_{22}	$D^+ \to K^-\pi^+ e^+\nu_e$ nonresonant	< 7	$\times 10^{-3}$	CL=90%
Γ_{23}	$D^+ \to K^-\pi^+\mu^+\nu_\mu$	(3.8 ± 0.4) %		
Γ_{24}	$D^+ \to \overline{K}^*(892)^0 \mu^+\nu_\mu$, $\overline{K}^*(892)^0 \to K^-\pi^+$	(3.52 ± 0.10) %		
Γ_{25}	$D^+ \to K^-\pi^+\mu^+\nu_\mu$ nonresonant	(2.0 ± 0.5)	$\times 10^{-3}$	
Γ_{26}	$D^+ \to K^-\pi^+\pi^0\mu^+\nu_\mu$	< 1.6	$\times 10^{-3}$	CL=90%
Γ_{27}	$D^+ \to \pi^0 e^+\nu_e$	(4.05 ± 0.18)	$\times 10^{-3}$	
Γ_{28}	$D^+ \to \eta e^+\nu_e$	(1.14 ± 0.10)	$\times 10^{-3}$	
Γ_{29}	$D^+ \to \rho^0 e^+\nu_e$	$(2.18^{+0.17}_{-0.25})$	$\times 10^{-3}$	
Γ_{30}	$D^+ \to \rho^0 \mu^+\nu_\mu$	(2.4 ± 0.4)	$\times 10^{-3}$	
Γ_{31}	$D^+ \to \omega e^+\nu_e$	(1.82 ± 0.19)	$\times 10^{-3}$	
Γ_{32}	$D^+ \to \eta'(958) e^+\nu_e$	(2.2 ± 0.5)	$\times 10^{-4}$	
Γ_{33}	$D^+ \to \phi e^+\nu_e$	< 9	$\times 10^{-5}$	CL=90%
	Fractions of some of the following modes with resonances have already appeared above as submodes of particular charged-particle modes.			
Γ_{34}	$D^+ \to \overline{K}^*(892)^0 e^+\nu_e$	(5.52 ± 0.15) %		
Γ_{35}	$D^+ \to \overline{K}^*(892)^0 \mu^+\nu_\mu$	(5.28 ± 0.15) %		
Γ_{36}	$D^+ \to \overline{K}^*_0(1430)^0 \mu^+\nu_\mu$	< 2.4	$\times 10^{-4}$	CL=90%
Γ_{37}	$D^+ \to \overline{K}^*(1680)^0 \mu^+\nu_\mu$	< 1.5	$\times 10^{-3}$	CL=90%
	Hadronic modes with a $\overline{K}$ or $\overline{K}K\overline{K}$			
Γ_{38}	$D^+ \to K^0_S\pi^+$	(1.47 ± 0.07) %		S=2.0
Γ_{39}	$D^+ \to K^0_L\pi^+$	(1.46 ± 0.05) %		
Γ_{40}	$D^+ \to K^-2\pi^+$	[a] (9.13 ± 0.19) %		
Γ_{41}	$D^+ \to (K^-\pi^+)_{S-\text{wave}}\pi^+$	(7.32 ± 0.19) %		
Γ_{42}	$D^+ \to \overline{K}^*_0(800)^0\pi^+$, $\overline{K}^*_0(800) \to K^-\pi^+$			
Γ_{43}	$D^+ \to \overline{K}^*_0(1430)^0\pi^+$, $\overline{K}^*_0(1430)^0 \to K^-\pi^+$	[b] (1.21 ± 0.06) %		
Γ_{44}	$D^+ \to \overline{K}^*(892)^0\pi^+$, $\overline{K}^*(892)^0 \to K^-\pi^+$	(1.01 ± 0.11) %		
Γ_{45}	$D^+ \to \overline{K}^*(1410)^0\pi^+$, $\overline{K}^{*0} \to K^-\pi^+$	not seen		
Γ_{46}	$D^+ \to \overline{K}^*_2(1430)^0\pi^+$, $\overline{K}^*_2(1430)^0 \to K^-\pi^+$	[b] (2.2 ± 0.7)	$\times 10^{-4}$	
Γ_{47}	$D^+ \to \overline{K}^*(1680)^0\pi^+$, $\overline{K}^*(1680)^0 \to K^-\pi^+$	[b] (2.1 ± 1.1)	$\times 10^{-4}$	
Γ_{48}	$D^+ \to K^-(2\pi^+)_{I=2}$	(1.41 ± 0.26) %		
Γ_{49}	$D^+ \to K^-2\pi^+$ nonresonant			
Γ_{50}	$D^+ \to K^0_S\pi^+\pi^0$	[a] (6.99 ± 0.27) %		
Γ_{51}	$D^+ \to K^0_S\rho^+$	(4.8 ± 1.0) %		
Γ_{52}	$D^+ \to \overline{K}^*(892)^0\pi^+$, $\overline{K}^*(892)^0 \to K^0_S\pi^0$	(1.3 ± 0.6) %		
Γ_{53}	$D^+ \to K^0_S\pi^+\pi^0$ nonresonant	(9 ± 7)	$\times 10^{-3}$	
Γ_{54}	$D^+ \to K^-2\pi^+\pi^0$	[c] (5.99 ± 0.18) %		
Γ_{55}	$D^+ \to K^0_S 2\pi^+\pi^-$	[c] (3.12 ± 0.11) %		
Γ_{56}	$D^+ \to K^-3\pi^+\pi^-$	[a] (5.6 ± 0.5)	$\times 10^{-3}$	S=1.1
Γ_{57}	$D^+ \to \overline{K}^*(892)^0 2\pi^+\pi^-$, $\overline{K}^*(892)^0 \to K^-\pi^+$	(1.2 ± 0.4)	$\times 10^{-3}$	
Γ_{58}	$D^+ \to \overline{K}^*(892)^0\rho^0\pi^+$, $\overline{K}^*(892)^0 \to K^-\pi^+$	(2.2 ± 0.4)	$\times 10^{-3}$	
Γ_{59}	$D^+ \to \overline{K}^*(892)^0 a_1(1260)^+$	[d] (9.0 ± 1.8)	$\times 10^{-3}$	
Γ_{60}	$D^+ \to \overline{K}^*(892)^0 2\pi^+\pi^-$ no-ρ, $\overline{K}^*(892)^0 \to K^-\pi^+$			

Meson Particle Listings

$D^{\pm}$

Γ_{61}	$D^+ \to K^-\rho^0 2\pi^+$	$(1.68\pm0.27)\times10^{-3}$		
Γ_{62}	$D^+ \to K^-3\pi^+\pi^-$ nonresonant	$(3.9\pm2.9)\times10^{-4}$		
Γ_{63}	$D^+ \to K^+2K^0_S$	$(4.5\pm2.0)\times10^{-3}$		
Γ_{64}	$D^+ \to K^+K^-K^0_S\pi^+$	$(2.4\pm0.6)\times10^{-4}$		

Pionic modes

Γ_{65}	$D^+ \to \pi^+\pi^0$	$(1.19\pm0.06)\times10^{-3}$		
Γ_{66}	$D^+ \to 2\pi^+\pi^-$	$(3.18\pm0.18)\times10^{-3}$		
Γ_{67}	$D^+ \to \rho^0\pi^+$	$(8.1\pm1.5)\times10^{-4}$		
Γ_{68}	$D^+ \to \pi^+(\pi^+\pi^-)_{S-\text{wave}}$	$(1.78\pm0.16)\times10^{-3}$		
Γ_{69}	$D^+ \to \sigma\pi^+, \sigma \to \pi^+\pi^-$	$(1.34\pm0.12)\times10^{-3}$		
Γ_{70}	$D^+ \to f_0(980)\pi^+$, $f_0(980) \to \pi^+\pi^-$	$(1.52\pm0.33)\times10^{-4}$		
Γ_{71}	$D^+ \to f_0(1370)\pi^+$, $f_0(1370) \to \pi^+\pi^-$	$(8\pm4)\times10^{-5}$		
Γ_{72}	$D^+ \to f_2(1270)\pi^+$, $f_2(1270) \to \pi^+\pi^-$	$(4.9\pm0.9)\times10^{-4}$		
Γ_{73}	$D^+ \to \rho(1450)^0\pi^+$, $\rho(1450)^0 \to \pi^+\pi^-$	$<8\times10^{-5}$		CL=95%
Γ_{74}	$D^+ \to f_0(1500)\pi^+$, $f_0(1500) \to \pi^+\pi^-$	$(1.1\pm0.4)\times10^{-4}$		
Γ_{75}	$D^+ \to f_0(1710)\pi^+$, $f_0(1710) \to \pi^+\pi^-$	$<5\times10^{-5}$		CL=95%
Γ_{76}	$D^+ \to f_0(1790)\pi^+$, $f_0(1790) \to \pi^+\pi^-$	$<6\times10^{-5}$		CL=95%
Γ_{77}	$D^+ \to (\pi^+\pi^+)_{S-\text{wave}}\pi^-$	$<1.2\times10^{-4}$		CL=95%
Γ_{78}	$D^+ \to 2\pi^+\pi^-$ nonresonant	$<1.1\times10^{-4}$		CL=95%
Γ_{79}	$D^+ \to \pi^+2\pi^0$	$(4.6\pm0.4)\times10^{-3}$		
Γ_{80}	$D^+ \to 2\pi^+\pi^-\pi^0$	(1.13 ± 0.08) %		
Γ_{81}	$D^+ \to \eta\pi^+, \eta \to \pi^+\pi^-\pi^0$	$(8.0\pm0.5)\times10^{-4}$		
Γ_{82}	$D^+ \to \omega\pi^+, \omega \to \pi^+\pi^-\pi^0$	$<3\times10^{-4}$		CL=90%
Γ_{83}	$D^+ \to 3\pi^+2\pi^-$	$(1.61\pm0.16)\times10^{-3}$		

Fractions of some of the following modes with resonances have already appeared above as submodes of particular charged-particle modes.

Γ_{84}	$D^+ \to \eta\pi^+$	$(3.53\pm0.21)\times10^{-3}$		
Γ_{85}	$D^+ \to \eta\pi^+\pi^0$	$(1.38\pm0.35)\times10^{-3}$		
Γ_{86}	$D^+ \to \omega\pi^+$	$<3.4\times10^{-4}$		CL=90%
Γ_{87}	$D^+ \to \eta'(958)\pi^+$	$(4.67\pm0.29)\times10^{-3}$		
Γ_{88}	$D^+ \to \eta'(958)\pi^+\pi^0$	$(1.6\pm0.5)\times10^{-3}$		

Hadronic modes with a $K\overline{K}$ pair

Γ_{89}	$D^+ \to K^+K^0_S$	$(2.83\pm0.16)\times10^{-3}$		S=2.2
Γ_{90}	$D^+ \to K^+K^-\pi^+$	$(9.54\pm0.26)\times10^{-3}$	[a]	S=1.1
Γ_{91}	$D^+ \to \phi\pi^+, \phi \to K^+K^-$	$(2.65^{+0.08}_{-0.09})\times10^{-3}$		
Γ_{92}	$D^+ \to K^+\overline{K}^*(892)^0$, $\overline{K}^*(892)^0 \to K^-\pi^+$	$(2.45^{+0.09}_{-0.14})\times10^{-3}$		
Γ_{93}	$D^+ \to K^+\overline{K}^*_0(1430)^0$, $\overline{K}^*_0(1430)^0 \to K^-\pi^+$	$(1.79\pm0.34)\times10^{-3}$		
Γ_{94}	$D^+ \to K^+\overline{K}^*_2(1430)^0$, $\overline{K}^*_2 \to K^-\pi^+$	$(1.6^{+1.2}_{-0.8})\times10^{-4}$		
Γ_{95}	$D^+ \to K^+\overline{K}^*_0(800)$, $\overline{K}^*_0 \to K^-\pi^+$	$(6.7^{+3.4}_{-2.1})\times10^{-4}$		
Γ_{96}	$D^+ \to a_0(1450)^0\pi^+$, $a^0_0 \to K^+K^-$	$(4.4^{+7.0}_{-1.8})\times10^{-4}$		
Γ_{97}	$D^+ \to \phi(1680)\pi^+$, $\phi \to K^+K^-$	$(4.9^{+4.0}_{-1.9})\times10^{-5}$		
Γ_{98}	$D^+ \to K^+K^-\pi^+$ nonresonant	not seen		
Γ_{99}	$D^+ \to K^+K^0_S\pi^+\pi^-$	$(1.75\pm0.18)\times10^{-3}$		
Γ_{100}	$D^+ \to K^0_SK^-2\pi^+$	$(2.40\pm0.18)\times10^{-3}$		
Γ_{101}	$D^+ \to K^+K^-2\pi^+\pi^-$	$(2.2\pm1.2)\times10^{-4}$		

A few poorly measured branching fractions:

Γ_{102}	$D^+ \to \phi\pi^+\pi^0$	(2.3 ± 1.0) %		
Γ_{103}	$D^+ \to \phi\rho^+$	<1.5 %		CL=90%
Γ_{104}	$D^+ \to K^+K^-\pi^+\pi^0$ non-ϕ	$(1.5^{+0.7}_{-0.6})$ %		
Γ_{105}	$D^+ \to K^*(892)^+K^0_S$	(1.6 ± 0.7) %		

Doubly Cabibbo-suppressed modes

Γ_{106}	$D^+ \to K^+\pi^0$	$(1.83\pm0.26)\times10^{-4}$		S=1.4
Γ_{107}	$D^+ \to K^+\eta$	$(1.08\pm0.17)\times10^{-4}$		
Γ_{108}	$D^+ \to K^+\eta'(958)$	$(1.76\pm0.22)\times10^{-4}$		
Γ_{109}	$D^+ \to K^+\pi^+\pi^-$	$(5.27\pm0.23)\times10^{-4}$		
Γ_{110}	$D^+ \to K^+\rho^0$	$(2.0\pm0.5)\times10^{-4}$		
Γ_{111}	$D^+ \to K^*(892)^0\pi^+$, $K^*(892)^0 \to K^+\pi^-$	$(2.5\pm0.4)\times10^{-4}$		
Γ_{112}	$D^+ \to K^+f_0(980)$, $f_0(980) \to \pi^+\pi^-$	$(4.7\pm2.8)\times10^{-5}$		
Γ_{113}	$D^+ \to K^*_2(1430)^0\pi^+$, $K^*_2(1430)^0 \to K^+\pi^-$	$(4.2\pm2.9)\times10^{-5}$		
Γ_{114}	$D^+ \to K^+\pi^+\pi^-$ nonresonant	not seen		
Γ_{115}	$D^+ \to 2K^+K^-$	$(8.7\pm2.0)\times10^{-5}$		

$\Delta C = 1$ weak neutral current ($C1$) modes, or Lepton Family number (LF) or Lepton number (L) violating modes

Γ_{116}	$D^+ \to \pi^+e^+e^-$	$C1$	$<1.1\times10^{-6}$		CL=90%
Γ_{117}	$D^+ \to \pi^+\phi, \phi \to e^+e^-$		$[e]$ $(1.7^{+1.4}_{-0.9})\times10^{-6}$		
Γ_{118}	$D^+ \to \pi^+\mu^+\mu^-$	$C1$	$<7.3\times10^{-8}$		CL=90%
Γ_{119}	$D^+ \to \pi^+\phi, \phi \to \mu^+\mu^-$		$[e]$ $(1.8\pm0.8)\times10^{-6}$		
Γ_{120}	$D^+ \to \rho^+\mu^+\mu^-$	$C1$	$<5.6\times10^{-4}$		CL=90%
Γ_{121}	$D^+ \to K^+e^+e^-$		$[f]$ $<1.0\times10^{-6}$		CL=90%
Γ_{122}	$D^+ \to K^+\mu^+\mu^-$		$[f]$ $<4.3\times10^{-6}$		CL=90%
Γ_{123}	$D^+ \to \pi^+e^+\mu^-$	LF	$<2.9\times10^{-6}$		CL=90%
Γ_{124}	$D^+ \to \pi^+e^-\mu^+$	LF	$<3.6\times10^{-6}$		CL=90%
Γ_{125}	$D^+ \to K^+e^+\mu^-$	LF	$<1.2\times10^{-6}$		CL=90%
Γ_{126}	$D^+ \to K^+e^-\mu^+$	LF	$<2.8\times10^{-6}$		CL=90%
Γ_{127}	$D^+ \to \pi^-2e^+$	L	$<1.1\times10^{-6}$		CL=90%
Γ_{128}	$D^+ \to \pi^-2\mu^+$	L	$<2.2\times10^{-8}$		CL=90%
Γ_{129}	$D^+ \to \pi^-e^+\mu^+$	L	$<2.0\times10^{-6}$		CL=90%
Γ_{130}	$D^+ \to \rho^-2\mu^+$	L	$<5.6\times10^{-4}$		CL=90%
Γ_{131}	$D^+ \to K^-2e^+$	L	$<9\times10^{-7}$		CL=90%
Γ_{132}	$D^+ \to K^-2\mu^+$	L	$<1.0\times10^{-5}$		CL=90%
Γ_{133}	$D^+ \to K^-e^+\mu^+$	L	$<1.9\times10^{-6}$		CL=90%
Γ_{134}	$D^+ \to K^*(892)^-2\mu^+$	L	$<8.5\times10^{-4}$		CL=90%

Γ_{135}	Unaccounted decay modes	(51.2 ± 1.0) %	

[a] The branching fraction for this mode may differ from the sum of the submodes that contribute to it, due to interference effects. See the relevant papers.

[b] These subfractions of the $K^-2\pi^+$ mode are uncertain: see the Particle Listings.

[c] Submodes of the $D^+ \to K^-2\pi^+\pi^0$ and $K^0_S2\pi^+\pi^-$ modes were studied by ANJOS 92C and COFFMAN 92B, but with at most 142 events for the first mode and 229 for the second – not enough for precise results. With nothing new for 18 years, we refer to our 2008 edition, Physics Letters **B667** 1 (2008), for those results.

[d] The unseen decay modes of the resonances are included.

[e] This is *not* a test for the ΔC=1 weak neutral current, but leads to the $\pi^+\ell^+\ell^-$ final state.

[f] This mode is not a useful test for a ΔC=1 weak neutral current because both quarks must change flavor in this decay.

CONSTRAINED FIT INFORMATION

An overall fit to 22 branching ratios uses 31 measurements and one constraint to determine 15 parameters. The overall fit has a $\chi^2 = 32.0$ for 17 degrees of freedom.

The following *off-diagonal* array elements are the correlation coefficients $\langle \delta x_i \delta x_j \rangle / (\delta x_i \cdot \delta x_j)$, in percent, from the fit to the branching fractions, $x_i \equiv \Gamma_i/\Gamma_{\text{total}}$. The fit constrains the x_i whose labels appear in this array to sum to one.

x_{29}	0									
x_{34}	0	0								
x_{35}	22	0	0							
x_{38}	6	0	0	1						
x_{40}	15	0	0	3	44					
x_{50}	5	0	0	1	14	31				
x_{54}	6	0	0	1	18	40	56			
x_{55}	7	0	0	2	22	50	50	0		
x_{56}	3	0	0	1	10	24	7	10	12	
x_{83}	3	0	0	1	10	22	7	9	11	76
x_{89}	6	0	0	1	75	38	12	15	19	9
x_{90}	10	0	0	2	29	66	24	38	36	16
x_{106}	2	0	0	0	6	13	4	5	6	3
x_{135}	−75	−2	−15	−32	−32	−58	−54	−48	−42	−20
	x_{16}	x_{29}	x_{34}	x_{35}	x_{38}	x_{40}	x_{50}	x_{54}	x_{55}	x_{56}

x_{89}	8			
x_{90}	14	25		
x_{106}	3	5	9	
x_{135}	−18	−27	−43	−8
	x_{83}	x_{89}	x_{90}	x_{106}

D^+ BRANCHING RATIOS

Some now-obsolete measurements have been omitted from these Listings.

c-quark decays

$\Gamma(c \to e^+ \text{anything})/\Gamma(c \to \text{anything})$

For the Summary Table, we only use the average of e^+ and μ^+ measurements from $Z^0 \to c\overline{c}$ decays; see the second data block below.

VALUE	EVTS	DOCUMENT ID		TECN	COMMENT
$0.103 \pm 0.009^{+0.009}_{-0.008}$	378	[1] ABBIENDI	99K	OPAL	$Z^0 \to c\overline{c}$

[1] ABBIENDI 99K uses the excess of right-sign over wrong-sign leptons opposite reconstructed $D^*(2010)^+ \to D^0\pi^+$ decays in $Z^0 \to c\overline{c}$.

$\Gamma(c \to \mu^+ \text{anything})/\Gamma(c \to \text{anything})$

For the Summary Table, we only use the average of e^+ and μ^+ measurements from $Z^0 \to c\overline{c}$ decays; see the next data block.

VALUE	EVTS	DOCUMENT ID		TECN	COMMENT
0.082±0.005 OUR AVERAGE					
$0.073 \pm 0.008 \pm 0.002$	73	KAYIS-TOPAK...	05	CHRS	ν_μ emulsion
$0.095 \pm 0.007^{+0.014}_{-0.013}$	2829	ASTIER	00D	NOMD	$\nu_\mu \text{Fe} \to \mu^-\mu^+\text{X}$
$0.090 \pm 0.007^{+0.007}_{-0.006}$	476	[1] ABBIENDI	99K	OPAL	$Z^0 \to c\overline{c}$
$0.086 \pm 0.017^{+0.008}_{-0.007}$	69	[2] ALBRECHT	92F	ARG	$e^+e^- \approx 10$ GeV
$0.078 \pm 0.009 \pm 0.012$		ONG	88	MRK2	e^+e^- 29 GeV
$0.078 \pm 0.015 \pm 0.02$		BARTEL	87	JADE	e^+e^- 34.6 GeV
$0.082 \pm 0.012^{+0.02}_{-0.01}$		ALTHOFF	84G	TASS	e^+e^- 34.5 GeV
• • • We do not use the following data for averages, fits, limits, etc. • • •					
$0.093 \pm 0.009 \pm 0.009$	88	KAYIS-TOPAK...	02	CHRS	See KAYIS-TOPAKSU 05
$0.089 \pm 0.018 \pm 0.025$		BARTEL	85J	JADE	See BARTEL 87

[1] ABBIENDI 99K uses the excess of right-sign over wrong-sign leptons opposite reconstructed $D^*(2010)^+ \to D^0\pi^+$ decays in $Z^0 \to c\overline{c}$.
[2] ALBRECHT 92F uses the excess of right-sign over wrong-sign leptons in a sample of events tagged by fully reconstructed $D^*(2010)^+ \to D^0\pi^+$ decays.

$\Gamma(c \to \ell^+ \text{anything})/\Gamma(c \to \text{anything})$

This is an average (not a sum) of e^+ and μ^+ measurements.

VALUE	EVTS	DOCUMENT ID		TECN	COMMENT
0.096 ±0.004 OUR AVERAGE					
$0.0958 \pm 0.0042 \pm 0.0028$	1828	[1] ABREU	00O	DLPH	$Z^0 \to c\overline{c}$
$0.095 \pm 0.006\ ^{+0.007}_{-0.006}$	854	[2] ABBIENDI	99K	OPAL	$Z^0 \to c\overline{c}$

[1] ABREU 00O uses leptons opposite fully reconstructed $D^*(2010)^+$, D^+, or D^0 mesons.
[2] ABBIENDI 99K uses the excess of right-sign over wrong-sign leptons opposite reconstructed $D^*(2010)^+ \to D^0\pi^+$ decays in $Z^0 \to c\overline{c}$.

$\Gamma(c \to D^*(2010)^+ \text{anything})/\Gamma(c \to \text{anything})$

VALUE	EVTS	DOCUMENT ID		TECN	COMMENT
0.255±0.015±0.008	2371	[1] ABREU	00O	DLPH	$Z^0 \to c\overline{c}$

[1] ABREU 00O uses slow pions opposite fully reconstructed $D^*(2010)^+$, D^+, or D^0 mesons as a signal of $D^*(2010)^-$ production.

Inclusive modes

$\Gamma(e^+ \text{semileptonic})/\Gamma_{\text{total}}$ Γ_1/Γ

The sum of our $\overline{K}^0 e^+\nu_e$, $\overline{K}^*(892)^0 e^+\nu_e$, $\pi^0 e^+\nu_e$, $\eta e^+\nu_e$, $\rho^0 e^+\nu_e$, and $\omega e^+\nu_e$ branching fractions is 15.3 ± 0.4%.

VALUE (%)	EVTS	DOCUMENT ID		TECN	COMMENT
16.07±0.30 OUR AVERAGE					
$16.13 \pm 0.10 \pm 0.29$	26.2 ± 0.2k	[1] ASNER	10	CLEO	e^+e^- at 3774 MeV
$15.2 \pm 0.9 \pm 0.8$	521 ± 32	ABLIKIM	07G	BES2	$e^+e^- \approx \psi(3770)$
• • • We do not use the following data for averages, fits, limits, etc. • • •					
$16.13 \pm 0.20 \pm 0.33$	8798 ± 105	[2] ADAM	06A	CLEO	See ASNER 10
$17.0 \pm 1.9 \pm 0.7$	158	BALTRUSAIT...	85B	MRK3	e^+e^- 3.77 GeV

[1] Using the D^+ and D^0 lifetimes, ASNER 10 finds that the ratio of the D^+ and D^0 semileptonic widths is 0.985 ± 0.015 ± 0.024.
[2] Using the D^+ and D^0 lifetimes, ADAM 06A finds that the ratio of the D^+ and D^0 inclusive e^+ widths is 0.985 ± 0.028 ± 0.015, consistent with the isospin-invariance prediction of 1.

$\Gamma(\mu^+ \text{anything})/\Gamma_{\text{total}}$ Γ_2/Γ

VALUE (%)	EVTS	DOCUMENT ID		TECN	COMMENT
17.6±2.7±1.8	100 ± 12	[1] ABLIKIM	08L	BES2	$e^+e^- \approx \psi(3772)$

[1] ABLIKIM 08L finds the ratio of $D^+ \to \mu^+X$ and $D^0 \to \mu^+X$ branching fractions to be 2.59 ± 0.70 ± 0.25, in accord with the ratio of D^+ and D^0 lifetimes, 2.54 ± 0.02.

$\Gamma(K^- \text{anything})/\Gamma_{\text{total}}$ Γ_3/Γ

VALUE (%)	EVTS	DOCUMENT ID		TECN	COMMENT
25.7±1.4 OUR AVERAGE					
$24.7 \pm 1.3 \pm 1.2$	631 ± 33	ABLIKIM	07G	BES2	$e^+e^- \approx \psi(3770)$
$27.8^{+3.6}_{-3.1}$		BARLAG	92C	ACCM	π^- Cu 230 GeV
$27.1 \pm 2.3 \pm 2.4$		COFFMAN	91	MRK3	e^+e^- 3.77 GeV

$[\Gamma(\overline{K}^0 \text{anything}) + \Gamma(K^0 \text{anything})]/\Gamma_{\text{total}}$ Γ_4/Γ

VALUE (%)	EVTS	DOCUMENT ID		TECN	COMMENT
61 ±5 OUR AVERAGE					
$60.5 \pm 5.5 \pm 3.3$	244 ± 22	ABLIKIM	06U	BES2	e^+e^- at 3773 MeV
$61.2 \pm 6.5 \pm 4.3$		COFFMAN	91	MRK3	e^+e^- 3.77 GeV

$\Gamma(K^+ \text{anything})/\Gamma_{\text{total}}$ Γ_5/Γ

VALUE (%)	EVTS	DOCUMENT ID		TECN	COMMENT
5.9±0.8 OUR AVERAGE					
$6.1 \pm 0.9 \pm 0.4$	189 ± 27	ABLIKIM	07G	BES2	$e^+e^- \approx \psi(3770)$
$5.5 \pm 1.3 \pm 0.9$		COFFMAN	91	MRK3	e^+e^- 3.77 GeV

$\Gamma(K^*(892)^- \text{anything})/\Gamma_{\text{total}}$ Γ_6/Γ

VALUE (%)	EVTS	DOCUMENT ID		TECN	COMMENT
5.7±5.2±0.7	7.2 ± 6.5	ABLIKIM	06U	BES2	e^+e^- at 3773 MeV

$\Gamma(\overline{K}^*(892)^0 \text{anything})/\Gamma_{\text{total}}$ Γ_7/Γ

VALUE (%)	EVTS	DOCUMENT ID		TECN	COMMENT
23.2±4.5±3.0	189 ± 36	ABLIKIM	05P	BES	$e^+e^- \approx 3773$ MeV

$\Gamma(K^*(892)^0 \text{anything})/\Gamma_{\text{total}}$ Γ_8/Γ

VALUE (%)	CL%	DOCUMENT ID		TECN	COMMENT
<6.6	90	ABLIKIM	05P	BES	$e^+e^- \approx 3773$ MeV

$\Gamma(\eta \text{anything})/\Gamma_{\text{total}}$ Γ_9/Γ

This ratio includes η particles from η' decays.

VALUE (%)	EVTS	DOCUMENT ID		TECN	COMMENT
6.3±0.5±0.5	1972 ± 142	HUANG	06B	CLEO	e^+e^- at $\psi(3770)$

$\Gamma(\eta' \text{anything})/\Gamma_{\text{total}}$ Γ_{10}/Γ

VALUE (%)	EVTS	DOCUMENT ID		TECN	COMMENT
1.04±0.16±0.09	82 ± 13	HUANG	06B	CLEO	e^+e^- at $\psi(3770)$

$\Gamma(\phi \text{anything})/\Gamma_{\text{total}}$ Γ_{11}/Γ

VALUE (%)	EVTS	DOCUMENT ID		TECN	COMMENT
1.03±0.10±0.07	248 ± 21	HUANG	06B	CLEO	e^+e^- at $\psi(3770)$

Leptonic and semileptonic modes

$\Gamma(e^+\nu_e)/\Gamma_{\text{total}}$ Γ_{12}/Γ

VALUE	CL%	DOCUMENT ID		TECN	COMMENT
$<8.8 \times 10^{-6}$	90	EISENSTEIN	08	CLEO	e^+e^- at $\psi(3770)$
• • • We do not use the following data for averages, fits, limits, etc. • • •					
$<2.4 \times 10^{-5}$	90	ARTUSO	05A	CLEO	See EISENSTEIN 08

Meson Particle Listings

$D^{\pm}$

$\Gamma(\mu^+\nu_\mu)/\Gamma_{\text{total}}$ Γ_{13}/Γ

See the note on "Decay Constants of Charged Pseudoscalar Mesons" in the D_s^+ Listings.

VALUE (units 10^{-4})	EVTS	DOCUMENT ID		TECN	COMMENT
3.82± 0.32±0.09	150 ± 12	[1] EISENSTEIN	08	CLEO	e^+e^- at $\psi(3770)$
• • • We do not use the following data for averages, fits, limits, etc. • • •					
$12.2\ ^{+11.1}_{-\ 5.3}\ \pm1.0$	3	[2] ABLIKIM	05D	BES	$e^+e^- \approx$ 3.773 GeV
$4.40\pm\ 0.66^{+0.09}_{-0.12}$	47 ± 7	[3] ARTUSO	05A	CLEO	See EISENSTEIN 08
3.5 ± 1.4 ±0.6	7	[4] BONVICINI	04A	CLEO	Incl. in ARTUSO 05A
$8\ ^{+16}_{-\ 5}\ ^{+5}_{-2}$	1	[5] BAI	98B	BES	$e^+e^- \to D^{*+}D^-$

[1] EISENSTEIN 08, using the D^+ lifetime and assuming $|V_{cd}| = |V_{us}|$, gets f_{D^+} = (205.8 ± 8.5 ± 2.5) MeV from this measurement.

[2] ABLIKIM 05D finds a background-subtracted 2.67 ± 1.74 $D^+ \to \mu^+\nu_\mu$ events, and from this obtains $f_{D^+} = 371^{+129}_{-119} \pm 25$ MeV.

[3] ARTUSO 05A obtains $f_{D^+} = 222.6 \pm 16.7^{+2.8}_{-3.4}$ MeV from this measurement.

[4] BONVICINI 04A finds eight events with an estimated background of one, and from the branching fraction obtains $f_{D^+} = 202 \pm 41 \pm 17$ MeV.

[5] BAI 98B obtains $f_{D^+} = (300^{+180+80}_{-150-40})$ MeV from this measurement.

$\Gamma(\tau^+\nu_\tau)/\Gamma_{\text{total}}$ Γ_{14}/Γ

VALUE	CL%	DOCUMENT ID		TECN	COMMENT
$<1.2\times10^{-3}$	90	EISENSTEIN	08	CLEO	e^+e^- at $\psi(3770)$
• • • We do not use the following data for averages, fits, limits, etc. • • •					
$<2.1\times10^{-3}$	90	RUBIN	06A	CLEO	See EISENSTEIN 08

$\Gamma(\overline{K}^0 e^+\nu_e)/\Gamma_{\text{total}}$ Γ_{15}/Γ

VALUE (%)	EVTS	DOCUMENT ID		TECN	COMMENT
8.83±0.22 OUR AVERAGE					
8.83±0.10±0.20	8467	[1] BESSON	09	CLEO	e^+e^- at $\psi(3770)$
8.95±1.59±0.67	34 ± 6	[2] ABLIKIM	05A	BES	e^+e^- at $\psi(3770)$
• • • We do not use the following data for averages, fits, limits, etc. • • •					
8.53±0.13±0.23		[3] DOBBS	08	CLEO	See BESSON 09
8.71±0.38±0.37	545 ± 24	HUANG	05B	CLEO	See DOBBS 08

[1] See the form-factor parameters near the end of this D^+ Listing.

[2] The ABLIKIM 05A result together with the $D^0 \to K^-e^+\nu_e$ branching fraction of ABLIKIM 04C and Particle Data Group lifetimes gives $\Gamma(D^0 \to K^-e^+\nu_e)\ /\ \Gamma(D^+ \to \overline{K}^0 e^+\nu_e) = 1.08 \pm 0.22 \pm 0.07$; isospin invariance predicts the ratio is 1.0.

[3] DOBBS 08 establishes $\left|\frac{V_{cd}}{V_{cs}} \cdot \frac{f_+^\pi(0)}{f_+^K(0)}\right| = 0.188 \pm 0.008 \pm 0.002$ from the D^+ and D^0 decays to $\overline{K}e^+\nu_e$ and $\pi e^+\nu_e$. It also finds $\Gamma(D^0 \to K^-e^+\nu_e)\ /\ \Gamma(D^+ \to \overline{K}^0 e^+\nu_e) = 1.06 \pm 0.02 \pm 0.03$; isospin invariance predicts the ratio is 1.0.

$\Gamma(\overline{K}^0\mu^+\nu_\mu)/\Gamma_{\text{total}}$ Γ_{16}/Γ

VALUE	EVTS	DOCUMENT ID		TECN	COMMENT
0.092±0.006 OUR FIT					
0.103±0.023±0.008	29 ± 6	ABLIKIM	07	BES2	e^+e^- at 3773 MeV

$\Gamma(\overline{K}^0\mu^+\nu_\mu)/\Gamma(K^-2\pi^+)$ Γ_{16}/Γ_{40}

VALUE	EVTS	DOCUMENT ID		TECN	COMMENT
1.00 ±0.07 OUR FIT					
1.019±0.076±0.065	555 ± 39	LINK	04E	FOCS	γ nucleus, $\overline{E}_\gamma \approx$ 180 GeV

$\Gamma(K^-\pi^+e^+\nu_e)/\Gamma_{\text{total}}$ Γ_{17}/Γ

VALUE (units 10^{-2})	EVTS	DOCUMENT ID		TECN	COMMENT
• • • We do not use the following data for averages, fits, limits, etc. • • •					
3.50±0.75±0.27	29 ± 6	ABLIKIM	06O	BES2	e^+e^- at 3773 MeV
$3.5\ ^{+1.2}_{-0.7}\ \pm0.4$	14	BAI	91	MRK3	$e^+e^- \approx$ 3.77 GeV

$\Gamma(K^-\pi^+e^+\nu_e)/\Gamma(K^-2\pi^+)$ Γ_{17}/Γ_{40}

VALUE	EVTS	DOCUMENT ID		TECN	COMMENT
0.4380±0.0036±0.0042	70k±363	DEL-AMO-SA...11I		BABR	$e^+e^- \approx$ 10.6 GeV

$\Gamma(\overline{K}^*(892)^0 e^+\nu_e)/\Gamma_{\text{total}}$ Γ_{34}/Γ

Unseen decay modes of $\overline{K}^*(892)^0$ are included. See the end of the D^+ Listings for measurements of $D^+ \to \overline{K}^*(892)^0\ell^+\nu_\ell$ form-factor ratios.

VALUE (units 10^{-2})	EVTS	DOCUMENT ID		TECN	COMMENT
5.52±0.15 OUR FIT					
5.52±0.07±0.13	≈5k	BRIERE	10	CLEO	e^+e^- at $\psi(3770)$
• • • We do not use the following data for averages, fits, limits, etc. • • •					
5.06±1.21±0.40	28 ± 7	ABLIKIM	06O	BES2	e^+e^- at 3773 MeV
5.56±0.27±0.23	422 ± 21	[1] HUANG	05B	CLEO	e^+e^- at $\psi(3770)$

[1] HUANG 05B finds $\Gamma(D^0 \to K^{*-}e^+\nu_e)\ /\ \Gamma(D^+ \to \overline{K}^{*0}e^+\nu_e) = 0.98 \pm 0.08 \pm 0.04$; isospin invariance predicts the ratio is 1.0.

$\Gamma(\overline{K}^*(892)^0 e^+\nu_e)/\Gamma(K^-2\pi^+)$ Γ_{34}/Γ_{40}

Unseen decay modes of the $\overline{K}^*(892)^0$ are included. See the end of the D^+ Listings for measurements of $D^+ \to \overline{K}^*(892)^0\ell^+\nu_\ell$ form-factor ratios.

VALUE	EVTS	DOCUMENT ID		TECN	COMMENT
• • • We do not use the following data for averages, fits, limits, etc. • • •					
0.74±0.04±0.05		BRANDENB...	02	CLEO	$e^+e^- \approx \Upsilon(4S)$
0.62±0.15±0.09	35	ADAMOVICH	91	OMEG	π^- 340 GeV
0.55±0.08±0.10	880	ALBRECHT	91	ARG	$e^+e^- \approx$ 10.4 GeV
0.49±0.04±0.05		ANJOS	89B	E691	Photoproduction

$\Gamma(\overline{K}^*(892)^0 e^+\nu_e, \overline{K}^*(892)^0 \to K^-\pi^+)/\Gamma(K^-\pi^+e^+\nu_e)$ Γ_{18}/Γ_{17}

VALUE (%)	DOCUMENT ID		TECN	COMMENT
94.11±0.74±0.75	DEL-AMO-SA...11I		BABR	$e^+e^- \approx$ 10.6 GeV

$\Gamma((K^-\pi^+)_{S-wave}e^+\nu_e)/\Gamma(K^-\pi^+e^+\nu_e)$ Γ_{19}/Γ_{17}

VALUE (%)	DOCUMENT ID		TECN	COMMENT
5.79±0.16±0.15	DEL-AMO-SA...11I		BABR	$e^+e^- \approx$ 10.6 GeV

$\Gamma(\overline{K}^*(1410)^0 e^+\nu_e, \overline{K}^*(1410)^0 \to K^-\pi^+)/\Gamma_{\text{total}}$ Γ_{20}/Γ

VALUE	CL%	DOCUMENT ID		TECN	COMMENT
$<6\times10^{-3}$	90	DEL-AMO-SA...11I		BABR	$e^+e^- \approx$ 10.6 GeV

$\Gamma(\overline{K}_2^*(1430)^0 e^+\nu_e, \overline{K}_2^*(1430)^0 \to K^-\pi^+)/\Gamma_{\text{total}}$ Γ_{21}/Γ

VALUE	CL%	DOCUMENT ID		TECN	COMMENT
$<5\times10^{-4}$	90	DEL-AMO-SA...11I		BABR	$e^+e^- \approx$ 10.6 GeV

$\Gamma(K^-\pi^+e^+\nu_e \text{ nonresonant})/\Gamma_{\text{total}}$ Γ_{22}/Γ

VALUE	CL%	DOCUMENT ID		TECN	COMMENT
<0.007	90	ANJOS	89B	E691	Photoproduction

$\Gamma(K^-\pi^+\mu^+\nu_\mu)/\Gamma(\overline{K}^0\mu^+\nu_\mu)$ Γ_{23}/Γ_{16}

VALUE	EVTS	DOCUMENT ID		TECN	COMMENT
0.417±0.030±0.023	555 ± 39	LINK	04E	FOCS	γ nucleus, $\overline{E}_\gamma \approx$ 180 GeV

$\Gamma(\overline{K}^*(892)^0\mu^+\nu_\mu)/\Gamma_{\text{total}}$ Γ_{35}/Γ

VALUE (units 10^{-2})	EVTS	DOCUMENT ID		TECN	COMMENT
5.28±0.15 OUR FIT					
5.27±0.07±0.14	≈5k	BRIERE	10	CLEO	e^+e^- at $\psi(3770)$

$\Gamma(\overline{K}^*(892)^0\mu^+\nu_\mu)/\Gamma(\overline{K}^0\mu^+\nu_\mu)$ Γ_{35}/Γ_{16}

Unseen decay modes of the $\overline{K}^*(892)^0$ are included. See the end of the D^+ Listings for measurements of $D^+ \to \overline{K}^*(892)^0\ell^+\nu_\ell$ form-factor ratios.

VALUE	EVTS	DOCUMENT ID		TECN	COMMENT
0.58 ±0.04 OUR FIT					
0.594±0.043±0.033	555 ± 39	LINK	04E	FOCS	γ nucleus, $\overline{E}_\gamma \approx$ 180 GeV

$\Gamma(\overline{K}^*(892)^0\mu^+\nu_\mu)/\Gamma(K^-2\pi^+)$ Γ_{35}/Γ_{40}

Unseen decay modes of the $\overline{K}^*(892)^0$ are included. See the end of the D^+ Listings for measurements of $D^+ \to \overline{K}^*(892)^0\ell^+\nu_\ell$ form-factor ratios.

VALUE	EVTS	DOCUMENT ID		TECN	COMMENT
0.578±0.021 OUR FIT	Error includes scale factor of 1.1.				
0.57 ±0.06 OUR AVERAGE	Error includes scale factor of 1.2.				
0.72 ±0.10 ±0.05		BRANDENB...	02	CLEO	$e^+e^- \approx \Upsilon(4S)$
0.56 ±0.04 ±0.06	875	FRABETTI	93E	E687	γBe $\overline{E}_\gamma \approx$ 200 GeV
0.46 ±0.07 ±0.08	224	KODAMA	92C	E653	π^- emulsion 600 GeV
• • • We do not use the following data for averages, fits, limits, etc. • • •					
0.602±0.010±0.021	12k	[1] LINK	02J	FOCS	γ nucleus, ≈180 GeV

[1] This LINK 02J result includes the effects of an interference of a small S-wave $K^-\pi^+$ amplitude with the dominant $\overline{K}^{*0}$ amplitude. (The interference effect is reported in LINK 02E.) This result is redundant with results of LINK 04E elsewhere in these Listings.

$\Gamma(K^-\pi^+\mu^+\nu_\mu \text{ nonresonant})/\Gamma(K^-\pi^+\mu^+\nu_\mu)$ Γ_{25}/Γ_{23}

VALUE	EVTS	DOCUMENT ID		TECN	COMMENT
$0.0530\pm0.0074^{+0.0099}_{-0.0096}$	14k	LINK	05I	FOCS	γ nucleus, $\overline{E}_\gamma \approx$ 180 GeV

$\Gamma(K^-\pi^+\pi^0\mu^+\nu_\mu)/\Gamma(K^-\pi^+\mu^+\nu_\mu)$ Γ_{26}/Γ_{23}

VALUE	CL%	DOCUMENT ID		TECN	COMMENT
<0.042	90	FRABETTI	93E	E687	γBe $\overline{E}_\gamma \approx$ 200 GeV

$\Gamma(\overline{K}_0^*(1430)^0\mu^+\nu_\mu)/\Gamma(K^-\pi^+\mu^+\nu_\mu)$ Γ_{36}/Γ_{23}

Unseen decay modes of the $\overline{K}_0^*(1430)^0$ are included.

VALUE	CL%	DOCUMENT ID		TECN	COMMENT
<0.0064	90	LINK	05I	FOCS	γ A, $\overline{E}_\gamma \approx$ 180 GeV

$\Gamma(\overline{K}^*(1680)^0\mu^+\nu_\mu)/\Gamma(K^-\pi^+\mu^+\nu_\mu)$ Γ_{37}/Γ_{23}

Unseen decay modes of the $\overline{K}^*(1680)^0$ are included.

VALUE	CL%	DOCUMENT ID		TECN	COMMENT
<0.04	90	LINK	05I	FOCS	γ A, $\overline{E}_\gamma \approx$ 180 GeV

$\Gamma(\pi^0 e^+ \nu_e)/\Gamma_{total}$ Γ_{27}/Γ

VALUE (%)	EVTS	DOCUMENT ID		TECN	COMMENT
0.405±0.016±0.009	838	[1] BESSON	09	CLEO	e^+e^- at $\psi(3770)$
• • • We do not use the following data for averages, fits, limits, etc. • • •					
0.373±0.022±0.013		[2] DOBBS	08	CLEO	See BESSON 09
0.44 ±0.06 ±0.03	63 ± 9	HUANG	05B	CLEO	See DOBBS 08

[1] See the form-factor parameters near the end of this D^+ Listing.

[2] DOBBS 08 establishes $|\frac{V_{cd}}{V_{cs}} \cdot \frac{f_+^{\pi}(0)}{f_+^{K}(0)}| = 0.188 \pm 0.008 \pm 0.002$ from the D^+ and D^0 decays to $\overline{K} e^+ \nu_e$ and $\pi e^+ \nu_e$. It finds $\Gamma(D^0 \to \pi^- e^+ \nu_e) / \Gamma(D^+ \to \pi^0 e^+ \nu_e) = 2.03 \pm 0.14 \pm 0.08$; isospin invariance predicts the ratio is 2.0.

$\Gamma(\eta e^+ \nu_e)/\Gamma_{total}$ Γ_{28}/Γ

VALUE (units 10^{-4})	EVTS	DOCUMENT ID		TECN	COMMENT
11.4±0.9±0.4		YELTON	11	CLEO	e^+e^- at $\psi(3770)$
• • • We do not use the following data for averages, fits, limits, etc. • • •					
13.3±2.0±0.6	46 ± 8	MITCHELL	09B	CLEO	See YELTON 11

$\Gamma(\rho^0 e^+ \nu_e)/\Gamma_{total}$ Γ_{29}/Γ

VALUE (units 10^{-3})	EVTS	DOCUMENT ID		TECN	COMMENT
$2.18^{+0.17}_{-0.25}$ OUR FIT					
$2.17\pm0.12^{+0.12}_{-0.22}$	447 ± 25	[1] DOBBS	13	CLEO	e^+e^- at $\psi(3770)$
• • • We do not use the following data for averages, fits, limits, etc. • • •					
2.1 ±0.4 ±0.1	27 ± 6	[2] HUANG	05B	CLEO	See DOBBS 13

[1] DOBBS 13 finds $\Gamma(D^0 \to \rho^- e^+ \nu_e) / 2\,\Gamma(D^+ \to \rho^0 e^+ \nu_e) = 1.03 \pm 0.09^{+0.08}_{-0.02}$; isospin invariance predicts the ratio is 1.0.

[2] HUANG 05B finds $\Gamma(D^0 \to \rho^- e^+ \nu_e) / 2\,\Gamma(D^+ \to \rho^0 e^+ \nu_e) = 1.2^{+0.4}_{-0.3} \pm 0.1$; isospin invariance predicts the ratio is 1.0.

$\Gamma(\rho^0 e^+ \nu_e)/\Gamma(\overline{K}^*(892)^0 e^+ \nu_e)$ Γ_{29}/Γ_{34}

VALUE	EVTS	DOCUMENT ID		TECN	COMMENT
$0.0396^{+0.0033}_{-0.0050}$ OUR FIT					
0.045 ±0.014 ±0.009	49	[1] AITALA	97	E791	π^- nucleus, 500 GeV

[1] AITALA 97 explicitly subtracts $D^+ \to \eta' e^+ \nu_e$ and other backgrounds to get this result.

$\Gamma(\rho^0 \mu^+ \nu_\mu)/\Gamma(\overline{K}^*(892)^0 \mu^+ \nu_\mu)$ Γ_{30}/Γ_{35}

VALUE	EVTS	DOCUMENT ID		TECN	COMMENT
0.045±0.007 OUR AVERAGE Error includes scale factor of 1.1.					
0.041±0.006±0.004	320 ± 44	LINK	06B	FOCS	γ A, $\overline{E}_\gamma \approx$ 180 GeV
0.051±0.015±0.009	54	[1] AITALA	97	E791	π^- nucleus, 500 GeV
0.079±0.019±0.013	39	[2] FRABETTI	97	E687	γ Be, $\overline{E}_\gamma \approx$ 220 GeV

[1] AITALA 97 explicitly subtracts $D^+ \to \eta' \mu^+ \nu_\mu$ and other backgrounds to get this result.

[2] Because the reconstruction efficiency for photons is low, this FRABETTI 97 result also includes any $D^+ \to \eta' \mu^+ \nu_\mu \to \gamma\rho^0 \mu^+ \nu_\mu$ events in the numerator.

$\Gamma(\omega e^+ \nu_e)/\Gamma_{total}$ Γ_{31}/Γ

VALUE (units 10^{-3})	EVTS	DOCUMENT ID		TECN	COMMENT
1.82±0.18±0.07	129 ± 13	DOBBS	13	CLEO	e^+e^- at $\psi(3770)$
• • • We do not use the following data for averages, fits, limits, etc. • • •					
1.6 $^{+0.7}_{-0.6}$ ±0.1	$7.6^{+3.3}_{-2.7}$	HUANG	05B	CLEO	See DOBBS 13

$\Gamma(\eta'(958) e^+ \nu_e)/\Gamma_{total}$ Γ_{32}/Γ

VALUE (units 10^{-4})	CL%	DOCUMENT ID		TECN	COMMENT
2.16±0.53±0.07		YELTON	11	CLEO	e^+e^- at $\psi(3770)$
• • • We do not use the following data for averages, fits, limits, etc. • • •					
<3.5	90	MITCHELL	09B	CLEO	See YELTON 11

$\Gamma(\phi e^+ \nu_e)/\Gamma_{total}$ Γ_{33}/Γ

Unseen decay modes of the ϕ are included.

VALUE	CL%	DOCUMENT ID		TECN	COMMENT
<0.9 $\times 10^{-4}$	90	YELTON	11	CLEO	e^+e^- at $\psi(3770)$
• • • We do not use the following data for averages, fits, limits, etc. • • •					
<1.6 $\times 10^{-4}$	90	MITCHELL	09B	CLEO	See YELTON 11
<0.0201	90	ABLIKIM	06P	BES2	e^+e^- at 3773 MeV
<0.0209	90	BAI	91	MRK3	$e^+e^- \approx$ 3.77 GeV

Hadronic modes with a $\overline{K}$ or $\overline{K}K\overline{K}$

$\Gamma(K_S^0 \pi^+)/\Gamma_{total}$ Γ_{38}/Γ

VALUE (units 10^{-2})	EVTS	DOCUMENT ID		TECN	COMMENT
• • • We do not use the following data for averages, fits, limits, etc. • • •					
1.526±0.022±0.038		[1] DOBBS	07	CLEO	See MENDEZ 10
1.55 ±0.05 ±0.06	2230 ± 60	[1] HE	05	CLEO	See DOBBS 07
1.6 ±0.3 ±0.1	161	ADLER	88C	MRK3	e^+e^- 3.77 GeV

[1] DOBBS 07 and HE 05 use single- and double-tagged events in an overall fit. DOBBS 07 supersedes HE 05.

$\Gamma(K_S^0 \pi^+)/\Gamma(K^- 2\pi^+)$ Γ_{38}/Γ_{40}

VALUE	EVTS	DOCUMENT ID		TECN	COMMENT
0.161 ±0.007 OUR FIT Error includes scale factor of 3.4.					
0.158 ±0.007 OUR AVERAGE Error includes scale factor of 3.2.					
0.1682±0.0012±0.0037	30k	MENDEZ	10	CLEO	e^+e^- at 3774 MeV
0.1530±0.0023±0.0016	10.6k	LINK	02B	FOCS	γ nucleus, $\overline{E}_\gamma \approx$ 180 GeV
• • • We do not use the following data for averages, fits, limits, etc. • • •					
0.174 ±0.012 ±0.011	473	[1] BISHAI	97	CLEO	$e^+e^- \approx \Upsilon(4S)$
0.137 ±0.015 ±0.016	264	ANJOS	90C	E691	Photoproduction

[1] See BISHAI 97 for an isospin analysis of $D^+ \to \overline{K}\pi$ amplitudes.

$\Gamma(K_L^0 \pi^+)/\Gamma_{total}$ Γ_{39}/Γ

VALUE (units 10^{-2})	EVTS	DOCUMENT ID		TECN	COMMENT
1.460±0.040±0.035	2023 ± 54	[1] HE	08	CLEO	e^+e^- at $\psi(3770)$

[1] The difference of CLEO $D^+ \to K_S^0 \pi^+$ and $K_L^0 \pi^+$ branching fractions over the sum (DOBBS 07 and HE 08) is $+0.022 \pm 0.016 \pm 0.018$.

$\Gamma(K^- 2\pi^+)/\Gamma_{total}$ Γ_{40}/Γ

VALUE (units 10^{-2})	EVTS	DOCUMENT ID		TECN	COMMENT
9.13±0.19 OUR FIT					
9.14±0.10±0.17		[1] DOBBS	07	CLEO	e^+e^- at $\psi(3770)$
• • • We do not use the following data for averages, fits, limits, etc. • • •					
9.5 ±0.2 ±0.3	15.1k±130	[1] HE	05	CLEO	See DOBBS 07
9.3 ±0.6 ±0.8	1502	[2] BALEST	94	CLEO	$e^+e^- \approx \Upsilon(4S)$
6.4 $^{+1.5}_{-1.4}$		[3] BARLAG	92C	ACCM	π^- Cu 230 GeV
9.1 ±1.3 ±0.4	1164	ADLER	88C	MRK3	e^+e^- 3.77 GeV
9.1 ±1.9	239	[4] SCHINDLER	81	MRK2	e^+e^- 3.771 GeV

[1] DOBBS 07 and HE 05 use single- and double-tagged events in an overall fit. DOBBS 07 supersedes HE 05.

[2] BALEST 94 measures the ratio of $D^+ \to K^-\pi^+\pi^+$ and $D^0 \to K^-\pi^+$ branching fractions to be 2.35 ± 0.16 ± 0.16 and uses their absolute measurement of the $D^0 \to K^-\pi^+$ fraction (AKERIB 93).

[3] BARLAG 92C computes the branching fraction by topological normalization.

[4] SCHINDLER 81 (MARK-2) measures $\sigma(e^+e^- \to \psi(3770)) \times$ branching fraction to be 0.38 ± 0.05 nb. We use the MARK-3 (ADLER 88C) value of $\sigma = 4.2 \pm 0.6 \pm 0.3$ nb.

$\Gamma((K^-\pi^+)_{S-wave}\pi^+)/\Gamma(K^- 2\pi^+)$ Γ_{41}/Γ_{40}

This is the "fit fraction" from the Dalitz-plot analysis. The $K^-\pi^+$ S-wave includes a broad scalar κ ($\overline{K}_0^*(800)$), the $\overline{K}_0^*(1430)^0$, and non-resonant background.

VALUE	DOCUMENT ID		TECN	COMMENT
0.801 ±0.012 OUR AVERAGE				
0.8024±0.0138±0.0043	[1] LINK	09	FOCS	MIPWA fit, 53k evts
0.838 ±0.038	[2] BONVICINI	08A	CLEO	QMIPWA fit, 141k evts
0.786 ±0.014 ±0.018	AITALA	06	E791	Dalitz fit, 15.1k events
• • • We do not use the following data for averages, fits, limits, etc. • • •				
0.8323±0.0150±0.0008	[3] LINK	07B	FOCS	See LINK 09

[1] This LINK 09 model-independent partial-wave analysis of the $K^-\pi^+$ S-wave slices the $K^-\pi^+$ mass range into 39 bins.

[2] The BONVICINI 08A QMIPWA (quasi-model-independent partial-wave analysis) of the $K^-\pi^+$ S-wave amplitude slices the $K^-\pi^+$ mass range into 26 bins but keeps the Breit-Wigner $\overline{K}_0^*(1430)^0$.

[3] This LINK 07B fit uses a K matrix. The $K^-\pi^+$ S-wave fit fraction given above breaks down into (207.3 ± 25.5 ± 12.4)% isospin-1/2 and (40.5 ± 9.6 ± 3.2)% isospin-3/2 — with large interference between the two. The isospin-1/2 component includes the κ (or $\overline{K}_0^*(800)^0$) and $\overline{K}_0^*(1430)^0$.

$\Gamma(\overline{K}_0^*(800)^0\pi^+, \overline{K}_0^*(800) \to K^-\pi^+)/\Gamma(K^- 2\pi^+)$ Γ_{42}/Γ_{40}

This is the "fit fraction" from the Dalitz-plot analysis.

VALUE	DOCUMENT ID		TECN	COMMENT
• • • We do not use the following data for averages, fits, limits, etc. • • •				
0.478±0.121±0.053	AITALA	02	E791	See AITALA 06

$\Gamma(\overline{K}^*(892)^0\pi^+, \overline{K}^*(892)^0 \to K^-\pi^+)/\Gamma(K^- 2\pi^+)$ Γ_{44}/Γ_{40}

This is the "fit fraction" from the Dalitz-plot analysis.

VALUE	DOCUMENT ID		TECN	COMMENT
0.111 ±0.012 OUR AVERAGE Error includes scale factor of 3.7.				
0.1236±0.0034±0.0034	LINK	09	FOCS	MIPWA fit, 53k evts
0.0988±0.0046	BONVICINI	08A	CLEO	QMIPWA fit, 141k evts
0.119 ±0.002 ±0.020	AITALA	06	E791	Dalitz fit, 15.1k events
• • • We do not use the following data for averages, fits, limits, etc. • • •				
0.1361±0.0041±0.0030	[1] LINK	07B	FOCS	See LINK 09
0.123 ±0.010 ±0.009	AITALA	02	E791	See AITALA 06
0.137 ±0.006 ±0.009	FRABETTI	94G	E687	Dalitz fit, 8800 evts
0.170 ±0.009 ±0.034	ANJOS	93	E691	γBe 90–260 GeV
0.14 ±0.04 ±0.04	ALVAREZ	91B	NA14	Photoproduction
0.13 ±0.01 ±0.07	ADLER	87	MRK3	e^+e^- 3.77 GeV

[1] The statistical error on this LINK 07B value is corrected in LINK 09.

$\Gamma(\overline{K}^*(1410)^0\pi^+, \overline{K}^{*0} \to K^-\pi^+)/\Gamma(K^- 2\pi^+)$ Γ_{45}/Γ_{40}

VALUE (units 10^{-3})	DOCUMENT ID		TECN	COMMENT
not seen	LINK	09	FOCS	MIPWA fit, 53k evts
not seen	BONVICINI	08A	CLEO	QMIPWA fit, 141k evts
• • • We do not use the following data for averages, fits, limits, etc. • • •				
4.8±2.1±1.7	LINK	07B	FOCS	See LINK 09

Meson Particle Listings

$D^{\pm}$

$\Gamma(\overline{K}_0^*(1430)^0\pi^+, \overline{K}_0^*(1430)^0 \to K^-\pi^+)/\Gamma(K^-2\pi^+)$ Γ_{43}/Γ_{40}

This is the "fit fraction" from the Dalitz-plot analysis.

VALUE	DOCUMENT ID		TECN	COMMENT
0.1330±0.0062	BONVICINI	08A	CLEO	QMIPWA fit, 141k evts
• • • We do not use the following data for averages, fits, limits, etc. • • •				
0.125 ±0.014 ±0.005	AITALA	02	E791	See AITALA 06
0.284 ±0.022 ±0.059	FRABETTI	94G	E687	Dalitz fit, 8800 evts
0.248 ±0.019 ±0.017	ANJOS	93	E691	γBe 90–260 GeV

$\Gamma(\overline{K}_2^*(1430)^0\pi^+, \overline{K}_2^*(1430)^0 \to K^-\pi^+)/\Gamma(K^-2\pi^+)$ Γ_{46}/Γ_{40}

This is the "fit fraction" from the Dalitz-plot analysis.

VALUE (units 10^{-2})	DOCUMENT ID		TECN	COMMENT
0.24 ±0.08 OUR AVERAGE	Error includes scale factor of 2.2. See the ideogram below.			
0.58 ±0.10 ±0.06	LINK	09	FOCS	MIPWA fit, 53k evts
0.204±0.040	BONVICINI	08A	CLEO	QMIPWA fit, 141k evts
0.2 ±0.1 ±0.1	AITALA	06	E791	Dalitz fit, 15.1k events
• • • We do not use the following data for averages, fits, limits, etc. • • •				
0.39 ±0.09 ±0.05	LINK	07B	FOCS	See LINK 09
0.5 ±0.1 ±0.2	AITALA	02	E791	See AITALA 06

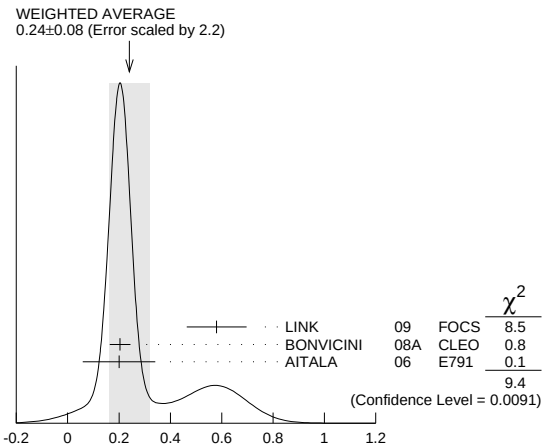

$\Gamma(\overline{K}_2^*(1430)^0\pi^+, \overline{K}_2^*(1430)^0 \to K^-\pi^+)/\Gamma(K^-2\pi^+)$ Γ_{46}/Γ_{40} (units 10^{-2})

$\Gamma(\overline{K}^*(1680)^0\pi^+, \overline{K}^*(1680)^0 \to K^-\pi^+)/\Gamma(K^-2\pi^+)$ Γ_{47}/Γ_{40}

This is the "fit fraction" from the Dalitz-plot analysis.

VALUE (units 10^{-2})	DOCUMENT ID		TECN	COMMENT
0.23 ±0.12 OUR AVERAGE				
1.75 ±0.62 ±0.54	LINK	09	FOCS	MIPWA fit, 53k evts
0.196±0.118	BONVICINI	08A	CLEO	QMIPWA fit, 141k evts
1.2 ±0.6 ±1.2	AITALA	06	E791	Dalitz fit, 15.1k events
• • • We do not use the following data for averages, fits, limits, etc. • • •				
1.90 ±0.63 ±0.43	LINK	07B	FOCS	See LINK 09
2.5 ±0.7 ±0.3	AITALA	02	E791	See AITALA 06
4.7 ±0.6 ±0.7	FRABETTI	94G	E687	Dalitz fit, 8800 evts
3.0 ±0.4 ±1.3	ANJOS	93	E691	γBe 90–260 GeV

$\Gamma(K^-(2\pi^+)_{I=2})/\Gamma(K^-2\pi^+)$ Γ_{48}/Γ_{40}

VALUE	DOCUMENT ID		TECN	COMMENT
0.155±0.028	BONVICINI	08A	CLEO	QMIPWA fit, 141k evts

$\Gamma(K^-2\pi^+ \text{ nonresonant})/\Gamma(K^-2\pi^+)$ Γ_{49}/Γ_{40}

This is the "fit fraction" from the Dalitz-plot analysis. Later analyses find little need for this decay mode.

VALUE	DOCUMENT ID		TECN	COMMENT
• • • We do not use the following data for averages, fits, limits, etc. • • •				
0.130±0.058±0.044	AITALA	02	E791	See AITALA 06
0.998±0.037±0.072	FRABETTI	94G	E687	Dalitz fit, 8800 evts
0.838±0.088±0.275	ANJOS	93	E691	γBe 90–260 GeV
0.79 ±0.07 ±0.15	ADLER	87	MRK3	e^+e^- 3.77 GeV

$\Gamma(K^0_S\pi^+\pi^0)/\Gamma_{\text{total}}$ Γ_{50}/Γ

VALUE (units 10^{-2})	EVTS	DOCUMENT ID		TECN	COMMENT
6.99±0.27 OUR FIT					
6.99±0.09±0.25		[1] DOBBS	07	CLEO	e^+e^- at $\psi(3770)$
• • • We do not use the following data for averages, fits, limits, etc. • • •					
7.2 ±0.2 ±0.4	5090±100	[1] HE	05	CLEO	See DOBBS 07
5.1 ±1.3 ±0.8	159	ADLER	88C	MRK3	e^+e^- 3.77 GeV

[1] DOBBS 07 and HE 05 use single- and double-tagged events in an overall fit. DOBBS 07 supersedes HE 05.

$\Gamma(K^0_S\rho^+)/\Gamma(K^0_S\pi^+\pi^0)$ Γ_{51}/Γ_{50}

This is the "fit fraction" from the Dalitz-plot analysis.

VALUE	DOCUMENT ID		TECN	COMMENT
0.68±0.08±0.12	ADLER	87	MRK3	e^+e^- 3.77 GeV

$\Gamma(\overline{K}^*(892)^0\pi^+, \overline{K}^*(892)^0 \to K^0_S\pi^0)/\Gamma(K^0_S\pi^+\pi^0)$ Γ_{52}/Γ_{50}

This is the "fit fraction" from the Dalitz-plot analysis.

VALUE	DOCUMENT ID		TECN	COMMENT
0.19±0.06±0.06	ADLER	87	MRK3	e^+e^- 3.77 GeV

$\Gamma(K^0_S\pi^+\pi^0 \text{ nonresonant})/\Gamma(K^0_S\pi^+\pi^0)$ Γ_{53}/Γ_{50}

This is the "fit fraction" from the Dalitz-plot analysis.

VALUE	DOCUMENT ID		TECN	COMMENT
0.13±0.07±0.08	ADLER	87	MRK3	e^+e^- 3.77 GeV

$\Gamma(K^-2\pi^+\pi^0)/\Gamma_{\text{total}}$ Γ_{54}/Γ

See our 2008 Review (Physics Letters **B667** 1 (2008)) for measurements of submodes of this mode. There is nothing new since 1992, and the two papers, ANJOS 92C, with 91 ± 12 events above background, and COFFMAN 92B, with 142 ± 20 such events, could not determine submode fractions with much accuracy.

VALUE (units 10^{-2})	EVTS	DOCUMENT ID		TECN	COMMENT
5.99±0.18 OUR FIT					
5.98±0.08±0.16		[1] DOBBS	07	CLEO	e^+e^- at $\psi(3770)$
• • • We do not use the following data for averages, fits, limits, etc. • • •					
6.0 ±0.2 ±0.2	4840±100	[1] HE	05	CLEO	See DOBBS 07
5.8 ±1.2 ±1.2	142	COFFMAN	92B	MRK3	e^+e^- 3.77 GeV
6.3 $^{+1.4}_{-1.3}$ ±1.2	175	BALTRUSAIT...86E		MRK3	See COFFMAN 92B

[1] DOBBS 07 and HE 05 use single- and double-tagged events in an overall fit. DOBBS 07 supersedes HE 05.

$\Gamma(K^0_S2\pi^+\pi^-)/\Gamma_{\text{total}}$ Γ_{55}/Γ

See our 2008 Review (Physics Letters **B667** 1 (2008)) for measurements of submodes of this mode. There is nothing new since 1992, and the two papers, ANJOS 92C, with 229 ± 17 events above background, and COFFMAN 92B, with 209 ± 20 such events, could not determine submode fractions with much accuracy.

VALUE (units 10^{-2})	EVTS	DOCUMENT ID		TECN	COMMENT
3.12 ±0.11 OUR FIT					
3.122±0.046±0.096		[1] DOBBS	07	CLEO	e^+e^- at $\psi(3770)$
• • • We do not use the following data for averages, fits, limits, etc. • • •					
3.2 ±0.1 ±0.2	3210 ± 85	[1] HE	05	CLEO	See DOBBS 07
2.1 $^{+1.0}_{-0.9}$		[2] BARLAG	92C	ACCM	π^- Cu 230 GeV
3.3 ±0.8 ±0.2	168	ADLER	88C	MRK3	e^+e^- 3.77 GeV

[1] DOBBS 07 and HE 05 use single- and double-tagged events in an overall fit. DOBBS 07 supersedes HE 05.
[2] BARLAG 92C computes the branching fraction by topological normalization.

$\Gamma(K^-3\pi^+\pi^-)/\Gamma(K^-2\pi^+)$ Γ_{56}/Γ_{40}

VALUE	EVTS	DOCUMENT ID		TECN	COMMENT
0.061±0.005 OUR FIT	Error includes scale factor of 1.1.				
0.062±0.008 OUR AVERAGE	Error includes scale factor of 1.3.				
0.058±0.002±0.006	2923	LINK	03D	FOCS	γ A, $\overline{E}_\gamma \approx$ 180 GeV
0.077±0.008±0.010	239	FRABETTI	97C	E687	γBe, $\overline{E}_\gamma \approx$ 200 GeV
• • • We do not use the following data for averages, fits, limits, etc. • • •					
0.09 ±0.01 ±0.01	113	ANJOS	90D	E691	Photoproduction

$\Gamma(\overline{K}^*(892)^0 2\pi^+\pi^-, \overline{K}^*(892)^0 \to K^-\pi^+)/\Gamma(K^-3\pi^+\pi^-)$ Γ_{57}/Γ_{56}

VALUE	DOCUMENT ID		TECN	COMMENT
0.21±0.04±0.06	LINK	03D	FOCS	γ A, $\overline{E}_\gamma \approx$ 180 GeV

$\Gamma(\overline{K}^*(892)^0\rho^0\pi^+, \overline{K}^*(892)^0 \to K^-\pi^+)/\Gamma(K^-3\pi^+\pi^-)$ Γ_{58}/Γ_{56}

VALUE	DOCUMENT ID		TECN	COMMENT
0.40±0.03±0.06	LINK	03D	FOCS	γ A, $\overline{E}_\gamma \approx$ 180 GeV

$\Gamma(\overline{K}^*(892)^0\rho^0\pi^+, \overline{K}^*(892)^0 \to K^-\pi^+)/\Gamma(K^-2\pi^+)$ Γ_{58}/Γ_{40}

VALUE	DOCUMENT ID		TECN	COMMENT
• • • We do not use the following data for averages, fits, limits, etc. • • •				
0.016±0.007±0.004	FRABETTI	97C	E687	γBe, $\overline{E}_\gamma \approx$ 200 GeV

$\Gamma(\overline{K}^*(892)^0 2\pi^+\pi^- \text{ no-}\rho, \overline{K}^*(892)^0 \to K^-\pi^+)/\Gamma(K^-2\pi^+)$ Γ_{60}/Γ_{40}

VALUE	DOCUMENT ID		TECN	COMMENT
• • • We do not use the following data for averages, fits, limits, etc. • • •				
0.032±0.010±0.008	FRABETTI	97C	E687	γBe, $\overline{E}_\gamma \approx$ 200 GeV

$\Gamma(K^-\rho^0 2\pi^+)/\Gamma(K^-3\pi^+\pi^-)$ Γ_{61}/Γ_{56}

VALUE	DOCUMENT ID		TECN	COMMENT
0.30±0.04±0.01	LINK	03D	FOCS	γ A, $\overline{E}_\gamma \approx$ 180 GeV

$\Gamma(K^-\rho^0 2\pi^+)/\Gamma(K^-2\pi^+)$ Γ_{61}/Γ_{40}

VALUE	DOCUMENT ID		TECN	COMMENT
• • • We do not use the following data for averages, fits, limits, etc. • • •				
0.034±0.009±0.005	FRABETTI	97C	E687	γBe, $\overline{E}_\gamma \approx$ 200 GeV

$\Gamma(\overline{K}^*(892)^0 a_1(1260)^+)/\Gamma(K^-2\pi^+)$ Γ_{59}/Γ_{40}

Unseen decay modes of the $\overline{K}^*(892)^0$ and $a_1(1260)^+$ are included.

VALUE	DOCUMENT ID		TECN	COMMENT
0.099±0.008±0.018	LINK	03D	FOCS	γ A, $\overline{E}_\gamma \approx$ 180 GeV

$\Gamma(K^-3\pi^+\pi^-$ nonresonant$)/\Gamma(K^-3\pi^+\pi^-)$ Γ_{62}/Γ_{56}

VALUE	CL%	DOCUMENT ID		TECN	COMMENT
0.07 ±0.05±0.01		LINK	03D	FOCS	γ A, $\overline{E}_\gamma \approx$ 180 GeV
• • • We do not use the following data for averages, fits, limits, etc. • • •					
<0.026	90	FRABETTI	97C	E687	γBe, $\overline{E}_\gamma \approx$ 200 GeV

$\Gamma(K^+2K^0_S)/\Gamma(K^-2\pi^+)$ Γ_{63}/Γ_{40}

VALUE	EVTS	DOCUMENT ID		TECN	COMMENT
0.049±0.022 OUR AVERAGE Error includes scale factor of 2.4.					
0.035±0.010±0.005	39 ± 9	ALBRECHT	94I	ARG	$e^+e^-\approx$ 10 GeV
0.085±0.018	70 ± 12	AMMAR	91	CLEO	$e^+e^-\approx$ 10.5 GeV

$\Gamma(K^+K^-K^0_S\pi^+)/\Gamma(K^0_S2\pi^+\pi^-)$ Γ_{64}/Γ_{55}

VALUE (units 10^{-3})	EVTS	DOCUMENT ID		TECN	COMMENT
7.7±1.5±0.9	35 ± 7	LINK	01C	FOCS	γ nucleus, $\overline{E}_\gamma \approx$ 180 GeV

Pionic modes

$\Gamma(\pi^+\pi^0)/\Gamma(K^-2\pi^+)$ Γ_{65}/Γ_{40}

VALUE (units 10^{-2})	EVTS	DOCUMENT ID		TECN	COMMENT
1.31±0.06 OUR AVERAGE					
1.29±0.04±0.05	2649 ± 76	MENDEZ	10	CLEO	e^+e^- at 3774 MeV
1.33±0.11±0.09	1229 ± 99	AUBERT,B	06F	BABR	$e^+e^-\approx \Upsilon(4S)$
1.44±0.19±0.10	171 ± 22	ARMS	04	CLEO	$e^+e^-\approx$ 10 GeV
• • • We do not use the following data for averages, fits, limits, etc. • • •					
1.33±0.07±0.06	914 ± 46	RUBIN	06	CLEO	See MENDEZ 10

$\Gamma(2\pi^+\pi^-)/\Gamma(K^-2\pi^+)$ Γ_{66}/Γ_{40}

VALUE (units 10^{-2})	EVTS	DOCUMENT ID		TECN	COMMENT
3.48±0.19 OUR AVERAGE Error includes scale factor of 1.4. See the ideogram below.					
3.52±0.11±0.12	3303 ± 95	RUBIN	06	CLEO	e^+e^- at $\psi(3770)$
4.1 ±1.1 ±0.3	85 ± 22	ABLIKIM	05F	BES	$e^+e^-\approx \psi(3770)$
$3.11\pm0.18^{+0.16}_{-0.26}$	1172	AITALA	01B	E791	π^- nucleus, 500 GeV
4.3 ±0.3 ±0.3	236	FRABETTI	97D	E687	γ Be $\approx$ 200 GeV
3.5 ±0.7 ±0.3	83	ANJOS	89	E691	Photoproduction

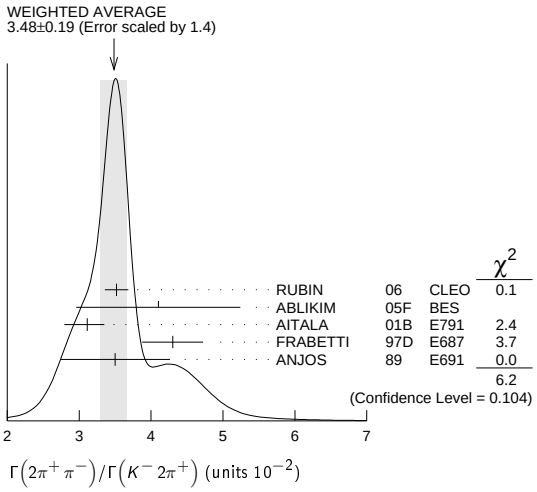

$\Gamma(\rho^0\pi^+)/\Gamma(2\pi^+\pi^-)$ Γ_{67}/Γ_{66}

This is the "fit fraction" from the Dalitz-plot analysis.

VALUE	DOCUMENT ID		TECN	COMMENT
0.25 ±0.04 OUR AVERAGE Error includes scale factor of 2.4. See the ideogram below.				
0.200 ±0.023 ±0.009	BONVICINI	07	CLEO	Dalitz fit, $\approx$ 2240 evts
0.3082±0.0314±0.0230	LINK	04	FOCS	Dalitz fit, 1527 ± 51 evts
0.336 ±0.032 ±0.022	AITALA	01B	E791	Dalitz fit, 1172 evts

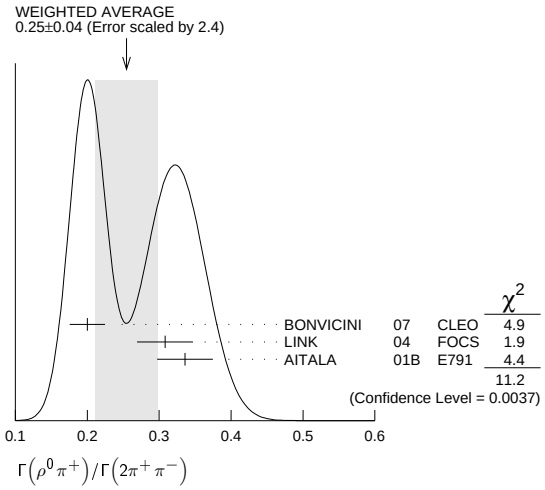

$\Gamma(\pi^+(\pi^+\pi^-)_{S-\text{wave}})/\Gamma(2\pi^+\pi^-)$ Γ_{68}/Γ_{66}

This is the "fit fraction" from the Dalitz-plot analysis. See also the next three data blocks.

VALUE	DOCUMENT ID		TECN	COMMENT
0.5600±0.0324±0.0214	[1] LINK	04	FOCS	Dalitz fit, 1527 ± 51 evts

[1] LINK 04 borrows a K-matrix parametrization from ANISOVICH 03 of the full π-π S-wave isoscalar scattering amplitude to describe the $\pi^+\pi^-$ S-wave component of the $\pi^+\pi^+\pi^-$ state. The fit fraction given above is a sum over five f_0 mesons, the $f_0(980)$, $f_0(1300)$, $f_0(1200$–$1600)$, $f_0(1500)$, and $f_0(1750)$. See LINK 04 for details and discussion.

$\Gamma(\sigma\pi^+, \sigma\to\pi^+\pi^-)/\Gamma(2\pi^+\pi^-)$ Γ_{69}/Γ_{66}

This is the "fit fraction" from the Dalitz-plot analysis.

VALUE	DOCUMENT ID		TECN	COMMENT
0.422±0.027 OUR AVERAGE				
0.418±0.014±0.025	BONVICINI	07	CLEO	Dalitz fit, $\approx$ 2240 evts
0.463±0.090±0.021	AITALA	01B	E791	Dalitz fit, 1172 evts

$\Gamma(f_0(980)\pi^+, f_0(980)\to\pi^+\pi^-)/\Gamma(2\pi^+\pi^-)$ Γ_{70}/Γ_{66}

This is the "fit fraction" from the Dalitz-plot analysis.

VALUE	DOCUMENT ID		TECN	COMMENT
0.048±0.010 OUR AVERAGE Error includes scale factor of 1.3.				
0.041±0.009±0.003	BONVICINI	07	CLEO	Dalitz fit, $\approx$ 2240 evts
0.062±0.013±0.004	AITALA	01B	E791	Dalitz fit, 1172 evts

$\Gamma(f_0(1370)\pi^+, f_0(1370)\to\pi^+\pi^-)/\Gamma(2\pi^+\pi^-)$ Γ_{71}/Γ_{66}

This is the "fit fraction" from the Dalitz-plot analysis.

VALUE	DOCUMENT ID		TECN	COMMENT
0.024±0.013 OUR AVERAGE				
0.026±0.018±0.006	BONVICINI	07	CLEO	Dalitz fit, $\approx$ 2240 evts
0.023±0.015±0.008	AITALA	01B	E791	Dalitz fit, 1172 evts

$\Gamma(f_2(1270)\pi^+, f_2(1270)\to\pi^+\pi^-)/\Gamma(2\pi^+\pi^-)$ Γ_{72}/Γ_{66}

This is the "fit fraction" from the Dalitz-plot analysis.

VALUE	DOCUMENT ID		TECN	COMMENT
0.154 ±0.025 OUR AVERAGE Error includes scale factor of 1.9. See the ideogram below.				
0.182 ±0.026 ±0.007	BONVICINI	07	CLEO	Dalitz fit, $\approx$ 2240 evts
0.1174±0.0190±0.0029	LINK	04	FOCS	Dalitz fit, 1527 ± 51 evts
0.194 ±0.025 ±0.004	AITALA	01B	E791	Dalitz fit, 1172 evts

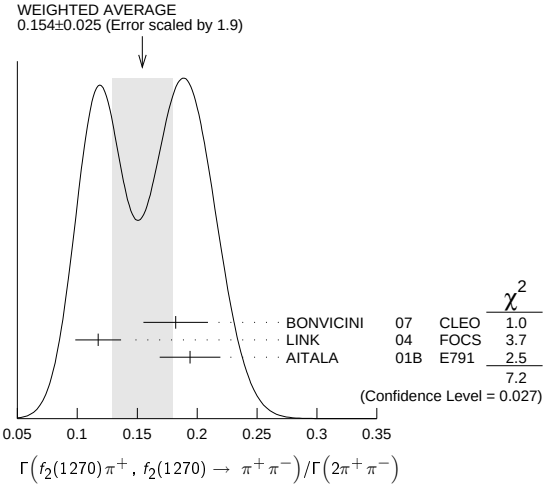

Meson Particle Listings

$D^{\pm}$

$\Gamma(\rho(1450)^0\pi^+, \rho(1450)^0 \to \pi^+\pi^-)/\Gamma(2\pi^+\pi^-)$ Γ_{73}/Γ_{66}

This is the "fit fraction" from the Dalitz-plot analysis.

VALUE	CL%	DOCUMENT ID		TECN	COMMENT
<0.024	95	BONVICINI	07	CLEO	Dalitz fit, ≈ 2240 evts
• • • We do not use the following data for averages, fits, limits, etc. • • •					
0.007±0.007±0.003		AITALA	01B	E791	Dalitz fit, 1172 evts

$\Gamma(f_0(1500)\pi^+, f_0(1500) \to \pi^+\pi^-)/\Gamma(2\pi^+\pi^-)$ Γ_{74}/Γ_{66}

This is the "fit fraction" from the Dalitz-plot analysis.

VALUE	DOCUMENT ID		TECN	COMMENT
0.034±0.010±0.008	BONVICINI	07	CLEO	Dalitz fit, ≈ 2240 evts

$\Gamma(f_0(1710)\pi^+, f_0(1710) \to \pi^+\pi^-)/\Gamma(2\pi^+\pi^-)$ Γ_{75}/Γ_{66}

This is the "fit fraction" from the Dalitz-plot analysis.

VALUE	CL%	DOCUMENT ID		TECN	COMMENT
<0.016	95	BONVICINI	07	CLEO	Dalitz fit, ≈ 2240 evts

$\Gamma(f_0(1790)\pi^+, f_0(1790) \to \pi^+\pi^-)/\Gamma(2\pi^+\pi^-)$ Γ_{76}/Γ_{66}

This is the "fit fraction" from the Dalitz-plot analysis.

VALUE	CL%	DOCUMENT ID		TECN	COMMENT
<0.02	95	BONVICINI	07	CLEO	Dalitz fit, ≈ 2240 evts

$\Gamma((\pi^+\pi^+)_{S-\text{wave}}\pi^-)/\Gamma(2\pi^+\pi^-)$ Γ_{77}/Γ_{66}

This is the "fit fraction" from the Dalitz-plot analysis.

VALUE	CL%	DOCUMENT ID		TECN	COMMENT
<0.037	95	BONVICINI	07	CLEO	Dalitz fit, ≈ 2240 evts

$\Gamma(2\pi^+\pi^-\text{ nonresonant})/\Gamma(2\pi^+\pi^-)$ Γ_{78}/Γ_{66}

This is the "fit fraction" from the Dalitz-plot analysis.

VALUE	CL%	DOCUMENT ID		TECN	COMMENT
<0.035	95	BONVICINI	07	CLEO	Dalitz fit, ≈ 2240 evts
• • • We do not use the following data for averages, fits, limits, etc. • • •					
0.078±0.060±0.027		AITALA	01B	E791	Dalitz fit, 1172 evts

$\Gamma(\pi^+2\pi^0)/\Gamma(K^-2\pi^+)$ Γ_{79}/Γ_{40}

VALUE (units 10^{-2})	EVTS	DOCUMENT ID		TECN	COMMENT
5.0±0.3±0.3	1535 ± 89	RUBIN	06	CLEO	e^+e^- at $\psi(3770)$

$\Gamma(2\pi^+\pi^-\pi^0)/\Gamma(K^-2\pi^+)$ Γ_{80}/Γ_{40}

VALUE (units 10^{-2})	EVTS	DOCUMENT ID		TECN	COMMENT
12.4±0.5±0.6	5701 ± 205	RUBIN	06	CLEO	e^+e^- at $\psi(3770)$

$\Gamma(\eta\pi^+)/\Gamma_{\text{total}}$ Γ_{84}/Γ

Unseen decay modes of the η are included.

VALUE (units 10^{-4})	EVTS	DOCUMENT ID		TECN	COMMENT
• • • We do not use the following data for averages, fits, limits, etc. • • •					
34.3±1.4±1.7	1033 ± 42	ARTUSO	08	CLEO	See MENDEZ 10

$\Gamma(\eta\pi^+)/\Gamma(K^-2\pi^+)$ Γ_{84}/Γ_{40}

Unseen decay modes of the η are included.

VALUE (units 10^{-2})	EVTS	DOCUMENT ID		TECN	COMMENT
3.87±0.09±0.19	2940 ± 68	MENDEZ	10	CLEO	e^+e^- at 3774 MeV
• • • We do not use the following data for averages, fits, limits, etc. • • •					
3.81±0.26±0.21	377 ± 26	RUBIN	06	CLEO	See ARTUSO 08

$\Gamma(\omega\pi^+)/\Gamma_{\text{total}}$ Γ_{86}/Γ

Unseen decay modes of the ω are included.

VALUE	CL%	DOCUMENT ID		TECN	COMMENT
<3.4 × 10^{-4}	90	RUBIN	06	CLEO	e^+e^- at $\psi(3770)$

$\Gamma(3\pi^+2\pi^-)/\Gamma(K^-2\pi^+)$ Γ_{83}/Γ_{40}

VALUE (units 10^{-2})	EVTS	DOCUMENT ID		TECN	COMMENT
1.77±0.17 OUR FIT					
1.73±0.20±0.17	732 ± 77	RUBIN	06	CLEO	e^+e^- at $\psi(3770)$
• • • We do not use the following data for averages, fits, limits, etc. • • •					
2.3 ±0.4 ±0.2	58	FRABETTI	97C	E687	γBe, $\overline{E}_\gamma \approx$ 200 GeV

$\Gamma(3\pi^+2\pi^-)/\Gamma(K^-3\pi^+\pi^-)$ Γ_{83}/Γ_{56}

VALUE	EVTS	DOCUMENT ID		TECN	COMMENT
0.289±0.019 OUR FIT					
0.290±0.017±0.011	835	LINK	03D	FOCS	γ A, $\overline{E}_\gamma \approx$ 180 GeV

$\Gamma(\eta\pi^+\pi^0)/\Gamma_{\text{total}}$ Γ_{85}/Γ

VALUE (units 10^{-4})	EVTS	DOCUMENT ID		TECN	COMMENT
13.8±3.1±1.6	149 ± 34	ARTUSO	08	CLEO	e^+e^- at $\psi(3770)$

$\Gamma(\eta'(958)\pi^+)/\Gamma_{\text{total}}$ Γ_{87}/Γ

Unseen decay modes of the $\eta'(958)$ are included.

VALUE (units 10^{-4})	EVTS	DOCUMENT ID		TECN	COMMENT
• • • We do not use the following data for averages, fits, limits, etc. • • •					
44.2±2.5±2.9	352 ± 20	ARTUSO	08	CLEO	See MENDEZ 10

$\Gamma(\eta'(958)\pi^+)/\Gamma(K^-2\pi^+)$ Γ_{87}/Γ_{40}

Unseen decay modes of the $\eta'(958)$ are included.

VALUE (units 10^{-2})	EVTS	DOCUMENT ID		TECN	COMMENT
5.12±0.17±0.25	1037 ± 35	MENDEZ	10	CLEO	e^+e^- at 3774 MeV

$\Gamma(\eta'(958)\pi^+\pi^0)/\Gamma_{\text{total}}$ Γ_{88}/Γ

Unseen decay modes of the $\eta'(958)$ are included.

VALUE (units 10^{-4})	EVTS	DOCUMENT ID		TECN	COMMENT
15.7±4.3±2.5	33 ± 9	ARTUSO	08	CLEO	e^+e^- at $\psi(3770)$

Hadronic modes with a $K\overline{K}$ pair

$\Gamma(K^+K^0_S)/\Gamma_{\text{total}}$ Γ_{89}/Γ

VALUE (units 10^{-3})	EVTS	DOCUMENT ID		TECN	COMMENT
• • • We do not use the following data for averages, fits, limits, etc. • • •					
3.14±0.09±0.08	1971 ±51	BONVICINI	08	CLEO	See MENDEZ 10

$\Gamma(K^+K^0_S)/\Gamma(K^0_S\pi^+)$ Γ_{89}/Γ_{38}

VALUE	EVTS	DOCUMENT ID		TECN	COMMENT
0.193 ±0.007 OUR FIT Error includes scale factor of 3.2.					
0.1901±0.0024 OUR AVERAGE					
0.1899±0.0011±0.0022	101k±561	WON	09	BELL	e^+e^- at $\Upsilon(4S)$
0.1892±0.0155±0.0073	278 ± 21	ARMS	04	CLEO	$e^+e^- \approx$ 10 GeV
0.1996±0.0119±0.0096	949	LINK	02B	FOCS	γ A, $\overline{E}_\gamma \approx$ 180 GeV
• • • We do not use the following data for averages, fits, limits, etc. • • •					
0.222 ±0.037 ±0.013	63 ± 10	ABLIKIM	05F	BES	$e^+e^- \approx \psi(3770)$
0.222 ±0.041 ±0.019	70	BISHAI	97	CLEO	See ARMS 04
0.25 ±0.04 ±0.02	129	FRABETTI	95	E687	γBe $\overline{E}_\gamma \approx$ 200 GeV
0.271 ±0.065 ±0.039	69	ANJOS	90C	E691	γBe
0.317 ±0.086 ±0.048	31	BALTRUSAIT...	85E	MRK3	e^+e^- 3.77 GeV
0.25 ±0.15	6	SCHINDLER	81	MRK2	e^+e^- 3.771 GeV

$\Gamma(K^+K^0_S)/\Gamma(K^-2\pi^+)$ Γ_{89}/Γ_{40}

VALUE (units 10^{-2})	EVTS	DOCUMENT ID		TECN	COMMENT
3.11±0.16 OUR FIT Error includes scale factor of 3.3.					
3.35±0.06±0.07	5161 ± 86	MENDEZ	10	CLEO	e^+e^- at 3774 MeV
• • • We do not use the following data for averages, fits, limits, etc. • • •					
3.02±0.18±0.15	949	[1] LINK	02B	FOCS	γ nucleus, $\overline{E}_\gamma \approx$ 180 GeV

[1] This LINK 02B result is redundant with a result in the previous datablock.

$\Gamma(K^+K^-\pi^+)/\Gamma_{\text{total}}$ Γ_{90}/Γ

VALUE (units 10^{-2})	EVTS	DOCUMENT ID		TECN	COMMENT
0.954±0.026 OUR FIT Error includes scale factor of 1.1.					
0.935±0.017±0.024		[1] DOBBS	07	CLEO	e^+e^- at $\psi(3770)$
• • • We do not use the following data for averages, fits, limits, etc. • • •					
0.97 ±0.04 ±0.04	1250 ± 40	[1] HE	05	CLEO	See DOBBS 07

[1] DOBBS 07 and HE 05 use single- and double-tagged events in an overall fit. DOBBS 07 supersedes HE 05.

$\Gamma(K^+K^-\pi^+)/\Gamma(K^-2\pi^+)$ Γ_{90}/Γ_{40}

VALUE	EVTS	DOCUMENT ID		TECN	COMMENT
0.1045±0.0022 OUR FIT Error includes scale factor of 1.3.					
0.1058±0.0029 OUR AVERAGE Error includes scale factor of 1.4.					
0.117 ±0.013 ±0.007	181 ± 20	ABLIKIM	05F	BES	$e^+e^- \approx \psi(3770)$
0.107 ±0.001 ±0.002	43k	AUBERT	05S	BABR	$e^+e^- \approx \Upsilon(4S)$
0.093 ±0.010 $^{+0.008}_{-0.006}$		JUN	00	SELX	Σ^- nucleus, 600 GeV
0.0976±0.0042±0.0046		FRABETTI	95B	E687	γ Be, $\overline{E}_\gamma \approx$ 200 GeV

$\Gamma(\phi\pi^+, \phi \to K^+K^-)/\Gamma(K^+K^-\pi^+)$ Γ_{91}/Γ_{90}

This is the "fit fraction" from the Dalitz-plot analysis.

VALUE (%)	DOCUMENT ID		TECN	COMMENT
27.8±0.4 $^{+0.2}_{-0.5}$	RUBIN	08	CLEO	Dalitz fit, 19,458±163 evts
• • • We do not use the following data for averages, fits, limits, etc. • • •				
29.2±3.1±3.0	FRABETTI	95B	E687	Dalitz fit, 915 evts

$\Gamma(K^+\overline{K}^*(892)^0, \overline{K}^*(892)^0 \to K^-\pi^+)/\Gamma(K^+K^-\pi^+)$ Γ_{92}/Γ_{90}

This is the "fit fraction" from the Dalitz-plot analysis.

VALUE (%)	DOCUMENT ID		TECN	COMMENT
25.7±0.5 $^{+0.4}_{-1.2}$	RUBIN	08	CLEO	Dalitz fit, 19,458±163 evts
• • • We do not use the following data for averages, fits, limits, etc. • • •				
30.1±2.0±2.5	FRABETTI	95B	E687	Dalitz fit, 915 evts

$\Gamma(K^+\overline{K}^*_0(1430)^0, \overline{K}^*_0(1430)^0 \to K^-\pi^+)/\Gamma(K^+K^-\pi^+)$ Γ_{93}/Γ_{90}

This is the "fit fraction" from the Dalitz-plot analysis.

VALUE (%)	DOCUMENT ID		TECN	COMMENT
18.8±1.2 $^{+3.3}_{-3.4}$	RUBIN	08	CLEO	Dalitz fit, 19,458±163 evts
• • • We do not use the following data for averages, fits, limits, etc. • • •				
37.0±3.5±1.8	FRABETTI	95B	E687	Dalitz fit, 915 evts

$\Gamma(K^+\overline{K}_2^*(1430)^0, \overline{K}_2^*\to K^-\pi^+)/\Gamma(K^+K^-\pi^+)$ Γ_{94}/Γ_{90}

This is the "fit fraction" from the Dalitz-plot analysis.

VALUE (%)	DOCUMENT ID		TECN	COMMENT
$1.7\pm0.4^{+1.2}_{-0.7}$	RUBIN	08	CLEO	Dalitz fit, 19,458±163 evts

$\Gamma(K^+\overline{K}_0^*(800), \overline{K}_0^*\to K^-\pi^+)/\Gamma(K^+K^-\pi^+)$ Γ_{95}/Γ_{90}

This is the "fit fraction" from the Dalitz-plot analysis.

VALUE (%)	DOCUMENT ID		TECN	COMMENT
$7.0\pm0.8^{+3.5}_{-2.0}$	RUBIN	08	CLEO	Dalitz fit, 19,458±163 evts

$\Gamma(a_0(1450)^0\pi^+, a_0^0\to K^+K^-)/\Gamma(K^+K^-\pi^+)$ Γ_{96}/Γ_{90}

This is the "fit fraction" from the Dalitz-plot analysis.

VALUE (%)	DOCUMENT ID		TECN	COMMENT
$4.6\pm0.6^{+7.2}_{-1.8}$	RUBIN	08	CLEO	Dalitz fit, 19,458±163 evts

$\Gamma(\phi(1680)\pi^+, \phi\to K^+K^-)/\Gamma(K^+K^-\pi^+)$ Γ_{97}/Γ_{90}

This is the "fit fraction" from the Dalitz-plot analysis.

VALUE (%)	DOCUMENT ID		TECN	COMMENT
$0.51\pm0.11^{+0.37}_{-0.16}$	RUBIN	08	CLEO	Dalitz fit, 19,458±163 evts

$\Gamma(K^*(892)^+K_S^0)/\Gamma(K_S^0\pi^+)$ Γ_{105}/Γ_{38}

Unseen decay modes of the $K^*(892)^+$ are included.

VALUE	EVTS	DOCUMENT ID		TECN	COMMENT
$1.1\pm0.3\pm0.4$	67	FRABETTI	95	E687	γBe $\overline{E}_\gamma\approx200$ GeV

$\Gamma(\phi\pi^+\pi^0)/\Gamma_{\text{total}}$ Γ_{102}/Γ

Unseen decay modes of the ϕ are included.

VALUE	DOCUMENT ID		TECN	COMMENT
0.023 ± 0.010	[1] BARLAG	92C	ACCM	π^- Cu 230 GeV

[1] BARLAG 92C computes the branching fraction using topological normalization.

$\Gamma(\phi\rho^+)/\Gamma(K^-2\pi^+)$ Γ_{103}/Γ_{40}

Unseen decay modes of the ϕ are included.

VALUE	CL%	DOCUMENT ID		TECN	COMMENT
<0.16	90	DAOUDI	92	CLEO	$e^+e^-\approx10.5$ GeV

$\Gamma(K^+K^-\pi^+\pi^0\text{non-}\phi)/\Gamma_{\text{total}}$ Γ_{104}/Γ

VALUE	DOCUMENT ID		TECN	COMMENT
$0.015^{+0.007}_{-0.006}$	[1] BARLAG	92C	ACCM	π^- Cu 230 GeV

[1] BARLAG 92C computes the branching fraction using topological normalization.

$\Gamma(K^+K^-\pi^+\pi^0\text{non-}\phi)/\Gamma(K^-2\pi^+)$ Γ_{104}/Γ_{40}

VALUE	CL%	DOCUMENT ID		TECN	COMMENT
• • • We do not use the following data for averages, fits, limits, etc. • • •					
<0.25	90	ANJOS	89E	E691	Photoproduction

$\Gamma(K^+K_S^0\pi^+\pi^-)/\Gamma(K_S^0 2\pi^+\pi^-)$ Γ_{99}/Γ_{55}

VALUE (units 10^{-2})	EVTS	DOCUMENT ID		TECN	COMMENT
$5.62\pm0.39\pm0.40$	469 ± 32	LINK	01C	FOCS	γ nucleus, $\overline{E}_\gamma\approx180$ GeV

$\Gamma(K_S^0K^-2\pi^+)/\Gamma(K_S^0 2\pi^+\pi^-)$ Γ_{100}/Γ_{55}

VALUE (units 10^{-2})	EVTS	DOCUMENT ID		TECN	COMMENT
$7.68\pm0.41\pm0.32$	670 ± 35	LINK	01C	FOCS	γ nucleus, $\overline{E}_\gamma\approx180$ GeV

$\Gamma(K^+K^-2\pi^+\pi^-)/\Gamma(K^-3\pi^+\pi^-)$ Γ_{101}/Γ_{56}

VALUE	EVTS	DOCUMENT ID		TECN	COMMENT
$0.040\pm0.009\pm0.019$	38	LINK	03D	FOCS	γ A, $\overline{E}_\gamma\approx180$ GeV

Doubly Cabibbo-suppressed modes

$\Gamma(K^+\pi^0)/\Gamma_{\text{total}}$ Γ_{106}/Γ

VALUE (units 10^{-4})	EVTS	DOCUMENT ID		TECN	COMMENT
1.83±0.26 OUR FIT	Error includes scale factor of 1.4.				
$2.52\pm0.47\pm0.26$	189 ± 37	AUBERT,B	06F	BABR	$e^+e^-\approx\Upsilon(4S)$
• • • We do not use the following data for averages, fits, limits, etc. • • •					
$2.28\pm0.36\pm0.17$	148 ± 23	DYTMAN	06	CLEO	See MENDEZ 10

$\Gamma(K^+\pi^0)/\Gamma(K^-2\pi^+)$ Γ_{106}/Γ_{40}

VALUE (units 10^{-3})	EVTS	DOCUMENT ID		TECN	COMMENT
2.01±0.29 OUR FIT	Error includes scale factor of 1.4.				
$1.9\ \pm0.2\ \pm0.1$	343 ± 37	MENDEZ	10	CLEO	e^+e^- at 3774 MeV

$\Gamma(K^+\eta)/\Gamma(\eta\pi^+)$ Γ_{107}/Γ_{84}

VALUE (%)	EVTS	DOCUMENT ID		TECN	COMMENT
$3.06\pm0.43\pm0.14$	166 ± 23	WON	11	BELL	$e^+e^-\approx\Upsilon(4S)$

$\Gamma(K^+\eta)/\Gamma(K^-2\pi^+)$ Γ_{107}/Γ_{40}

Unseen decay modes of the η are included.

VALUE (units 10^{-2})	CL%	DOCUMENT ID		TECN	COMMENT
• • • We do not use the following data for averages, fits, limits, etc. • • •					
<0.15	90	MENDEZ	10	CLEO	e^+e^- at 3774 MeV

$\Gamma(K^+\eta'(958))/\Gamma(\eta'(958)\pi^+)$ Γ_{108}/Γ_{87}

VALUE (%)	EVTS	DOCUMENT ID		TECN	COMMENT
$3.77\pm0.39\pm0.10$	180 ± 19	WON	11	BELL	$e^+e^-\approx\Upsilon(4S)$

$\Gamma(K^+\eta'(958))/\Gamma(K^-2\pi^+)$ Γ_{108}/Γ_{40}

Unseen decay modes of the $\eta'(958)$ are included.

VALUE (units 10^{-2})	CL%	DOCUMENT ID		TECN	COMMENT
• • • We do not use the following data for averages, fits, limits, etc. • • •					
<0.20	90	MENDEZ	10	CLEO	e^+e^- at 3774 MeV

$\Gamma(K^+\pi^+\pi^-)/\Gamma(K^-2\pi^+)$ Γ_{109}/Γ_{40}

VALUE (units 10^{-3})	EVTS	DOCUMENT ID		TECN	COMMENT
5.77±0.22 OUR AVERAGE					
$5.69\pm0.18\pm0.14$	2638 ± 84	KO	09	BELL	e^+e^- at $\Upsilon(4S)$
$6.5\ \pm0.8\ \pm0.4$	189 ± 24	LINK	04F	FOCS	γ A, $\overline{E}_\gamma\approx180$ GeV
$7.7\ \pm1.7\ \pm0.8$	59 ± 13	AITALA	97C	E791	π^- A, 500 GeV
$7.2\ \pm2.3\ \pm1.7$	21	FRABETTI	95E	E687	γBe, $\overline{E}_\gamma=220$ GeV

$\Gamma(K^+\rho^0)/\Gamma(K^+\pi^+\pi^-)$ $\Gamma_{110}/\Gamma_{109}$

This is the "fit fraction" from the Dalitz-plot analysis.

VALUE	DOCUMENT ID		TECN	COMMENT
0.39 ±0.09 OUR AVERAGE				
$0.3943\pm0.0787\pm0.0815$	LINK	04F	FOCS	Dalitz fit, 189 evts
$0.37\ \pm0.14\ \pm0.07$	AITALA	97C	E791	Dalitz fit, 59 evts

$\Gamma(K^+f_0(980), f_0(980)\to\pi^+\pi^-)/\Gamma(K^+\pi^+\pi^-)$ $\Gamma_{112}/\Gamma_{109}$

This is the "fit fraction" from the Dalitz-plot analysis.

VALUE	DOCUMENT ID		TECN	COMMENT
$0.0892\pm0.0333\pm0.0412$	LINK	04F	FOCS	Dalitz fit, 189 evts

$\Gamma(K^*(892)^0\pi^+, K^*(892)^0\to K^+\pi^-)/\Gamma(K^+\pi^+\pi^-)$ $\Gamma_{111}/\Gamma_{109}$

This is the "fit fraction" from the Dalitz-plot analysis.

VALUE	DOCUMENT ID		TECN	COMMENT
0.47 ±0.08 OUR AVERAGE				
$0.5220\pm0.0684\pm0.0638$	LINK	04F	FOCS	Dalitz fit, 189 evts
$0.35\ \pm0.14\ \pm0.01$	AITALA	97C	E791	Dalitz fit, 59 evts

$\Gamma(K_2^*(1430)^0\pi^+, K_2^*(1430)^0\to K^+\pi^-)/\Gamma(K^+\pi^+\pi^-)$ $\Gamma_{113}/\Gamma_{109}$

This is the "fit fraction" from the Dalitz-plot analysis.

VALUE	DOCUMENT ID		TECN	COMMENT
$0.0803\pm0.0372\pm0.0391$	LINK	04F	FOCS	Dalitz fit, 189 evts

$\Gamma(K^+\pi^+\pi^-\text{nonresonant})/\Gamma(K^+\pi^+\pi^-)$ $\Gamma_{114}/\Gamma_{109}$

This is the "fit fraction" from the Dalitz-plot analysis.

VALUE	DOCUMENT ID		TECN	COMMENT
• • • We do not use the following data for averages, fits, limits, etc. • • •				
$0.36\pm0.14\pm0.07$	[1] AITALA	97C	E791	Dalitz fit, 59 evts

[1] LINK 04F, with three times as many events, finds no need for a nonresonant amplitude.

$\Gamma(2K^+K^-)/\Gamma(K^-2\pi^+)$ Γ_{115}/Γ_{40}

VALUE (units 10^{-4})	EVTS	DOCUMENT ID		TECN	COMMENT
$9.49\pm2.17\pm0.22$	65	[1] LINK	02I	FOCS	γ nucleus, ≈180 GeV

[1] LINK 02I finds little evidence for ϕK^+ or $f_0(980)\,K^+$ submodes.

Rare or forbidden modes

$\Gamma(\pi^+e^+e^-)/\Gamma_{\text{total}}$ Γ_{116}/Γ

A test for the $\Delta C=1$ weak neutral current. Allowed by higher-order electroweak interactions.

VALUE	CL%	DOCUMENT ID		TECN	COMMENT
$<1.1\times10^{-6}$	90	LEES	11G	BABR	$e^+e^-\approx\Upsilon(4S)$
• • • We do not use the following data for averages, fits, limits, etc. • • •					
$<5.9\times10^{-6}$	90	[1] RUBIN	10	CLEO	e^+e^- at $\psi(3770)$
$<7.4\times10^{-6}$	90	HE	05A	CLEO	See RUBIN 10
$<5.2\times10^{-5}$	90	AITALA	99G	E791	π^-N 500 GeV
$<1.1\times10^{-4}$	90	FRABETTI	97B	E687	γ Be, $\overline{E}_\gamma\approx220$ GeV
$<6.6\times10^{-5}$	90	AITALA	96	E791	π^-N 500 GeV
$<2.5\times10^{-3}$	90	WEIR	90B	MRK2	e^+e^- 29 GeV
$<2.6\times10^{-3}$	90	HAAS	88	CLEO	e^+e^- 10 GeV

[1] This RUBIN 10 limit is for the e^+e^- mass in the continuum away from the $\phi(1020)$. See the next data block.

$\Gamma(\pi^+\phi, \phi\to e^+e^-)/\Gamma_{\text{total}}$ Γ_{117}/Γ

This is *not* a test for the $\Delta C=1$ weak neutral current, but leads to the $\pi^+e^+e^-$ final state.

VALUE	EVTS	DOCUMENT ID		TECN	COMMENT
$(1.7^{+1.4}_{-0.9}\pm0.1)\times10^{-6}$	4	[1] RUBIN	10	CLEO	e^+e^- at $\psi(3770)$
• • • We do not use the following data for averages, fits, limits, etc. • • •					
$(2.7^{+3.6}_{-1.8}\pm0.2)\times10^{-6}$	2	HE	05A	CLEO	See RUBIN 10

[1] This RUBIN 10 result is consistent with the known $D^+\to\phi\pi^+$ and $\phi\to e^+e^-$ fractions.

Meson Particle Listings

$D^{\pm}$

$\Gamma(\pi^+\mu^+\mu^-)/\Gamma_{\text{total}}$ Γ_{118}/Γ

A test for the $\Delta C = 1$ weak neutral current. Allowed by higher-order electroweak interactions.

VALUE	CL%	DOCUMENT ID		TECN	COMMENT
$<7.3 \times 10^{-8}$	90	AAIJ	13AF	LHCB	pp at 7 TeV
• • • We do not use the following data for averages, fits, limits, etc. • • •					
$<6.5 \times 10^{-6}$	90	LEES	11G	BABR	$e^+e^- \approx \Upsilon(4S)$
$<3.9 \times 10^{-6}$	90	[1] ABAZOV	08D	D0	$p\overline{p}$, $E_{\text{cm}} = 1.96$ TeV
$<8.8 \times 10^{-6}$	90	LINK	03F	FOCS	γ A, $\overline{E}_\gamma \approx 180$ GeV
$<1.5 \times 10^{-5}$	90	AITALA	99G	E791	π^- N 500 GeV
$<8.9 \times 10^{-5}$	90	FRABETTI	97B	E687	γ Be, $\overline{E}_\gamma \approx 220$ GeV
$<1.8 \times 10^{-5}$	90	AITALA	96	E791	π^- N 500 GeV
$<2.2 \times 10^{-4}$	90	KODAMA	95	E653	π^- emulsion 600 GeV
$<5.9 \times 10^{-3}$	90	WEIR	90B	MRK2	e^+e^- 29 GeV
$<2.9 \times 10^{-3}$	90	HAAS	88	CLEO	e^+e^- 10 GeV

[1] This ABAZOV 08D limit is for the $\mu^+\mu^-$ mass in the continuum away from the $\phi(1020)$. See the next data block.

$\Gamma(\pi^+\phi,\ \phi \to \mu^+\mu^-)/\Gamma_{\text{total}}$ Γ_{119}/Γ

This is *not* a test for the $\Delta C = 1$ weak neutral current, but leads to the $\pi^+\mu^+\mu^-$ final state.

VALUE	DOCUMENT ID		TECN	COMMENT
$(1.8 \pm 0.5 \pm 0.6) \times 10^{-6}$	[1] ABAZOV	08D	D0	$p\overline{p}$, $E_{\text{cm}} = 1.96$ TeV

[1] This ABAZOV 08D value is consistent with the known $D^+ \to \phi\pi^+$ and $\phi \to \mu^+\mu^-$ fractions.

$\Gamma(\rho^+\mu^+\mu^-)/\Gamma_{\text{total}}$ Γ_{120}/Γ

A test for the $\Delta C = 1$ weak neutral current. Allowed by higher-order electroweak interactions.

VALUE	CL%	DOCUMENT ID		TECN	COMMENT
$<5.6 \times 10^{-4}$	90	KODAMA	95	E653	π^- emulsion 600 GeV

$\Gamma(K^+e^+e^-)/\Gamma_{\text{total}}$ Γ_{121}/Γ

Both quarks would have to change flavor for this decay to occur.

VALUE	CL%	DOCUMENT ID		TECN	COMMENT
$<1.0 \times 10^{-6}$	90	LEES	11G	BABR	$e^+e^- \approx \Upsilon(4S)$
• • • We do not use the following data for averages, fits, limits, etc. • • •					
$<3.0 \times 10^{-6}$	90	RUBIN	10	CLEO	e^+e^- at $\psi(3770)$
$<6.2 \times 10^{-6}$	90	HE	05A	CLEO	See RUBIN 10
$<2.0 \times 10^{-4}$	90	AITALA	99G	E791	π^- N 500 GeV
$<2.0 \times 10^{-4}$	90	FRABETTI	97B	E687	γ Be, $\overline{E}_\gamma \approx 220$ GeV
$<4.8 \times 10^{-3}$	90	WEIR	90B	MRK2	e^+e^- 29 GeV

$\Gamma(K^+\mu^+\mu^-)/\Gamma_{\text{total}}$ Γ_{122}/Γ

Both quarks would have to change flavor for this decay to occur.

VALUE	CL%	DOCUMENT ID		TECN	COMMENT
$<4.3 \times 10^{-6}$	90	LEES	11G	BABR	$e^+e^- \approx \Upsilon(4S)$
• • • We do not use the following data for averages, fits, limits, etc. • • •					
$<9.2 \times 10^{-6}$	90	LINK	03F	FOCS	γ A, $\overline{E}_\gamma \approx 180$ GeV
$<4.4 \times 10^{-5}$	90	AITALA	99G	E791	π^- N 500 GeV
$<9.7 \times 10^{-5}$	90	FRABETTI	97B	E687	γ Be, $\overline{E}_\gamma \approx 220$ GeV
$<3.2 \times 10^{-4}$	90	KODAMA	95	E653	π^- emulsion 600 GeV
$<9.2 \times 10^{-3}$	90	WEIR	90B	MRK2	e^+e^- 29 GeV

$\Gamma(\pi^+e^+\mu^-)/\Gamma_{\text{total}}$ Γ_{123}/Γ

A test of lepton-family-number conservation.

VALUE	CL%	DOCUMENT ID		TECN	COMMENT
$<2.9 \times 10^{-6}$	90	LEES	11G	BABR	$e^+e^- \approx \Upsilon(4S)$
• • • We do not use the following data for averages, fits, limits, etc. • • •					
$<1.1 \times 10^{-4}$	90	FRABETTI	97B	E687	γ Be, $\overline{E}_\gamma \approx 220$ GeV
$<3.3 \times 10^{-3}$	90	WEIR	90B	MRK2	e^+e^- 29 GeV

$\Gamma(\pi^+e^-\mu^+)/\Gamma_{\text{total}}$ Γ_{124}/Γ

A test of lepton-family-number conservation.

VALUE	CL%	DOCUMENT ID		TECN	COMMENT
$<3.6 \times 10^{-6}$	90	LEES	11G	BABR	$e^+e^- \approx \Upsilon(4S)$
• • • We do not use the following data for averages, fits, limits, etc. • • •					
$<1.3 \times 10^{-4}$	90	FRABETTI	97B	E687	γ Be, $\overline{E}_\gamma \approx 220$ GeV
$<3.3 \times 10^{-3}$	90	WEIR	90B	MRK2	e^+e^- 29 GeV

$\Gamma(K^+e^+\mu^-)/\Gamma_{\text{total}}$ Γ_{125}/Γ

A test of lepton-family-number conservation.

VALUE	CL%	DOCUMENT ID		TECN	COMMENT
$<1.2 \times 10^{-6}$	90	LEES	11G	BABR	$e^+e^- \approx \Upsilon(4S)$
• • • We do not use the following data for averages, fits, limits, etc. • • •					
$<1.3 \times 10^{-4}$	90	FRABETTI	97B	E687	γ Be, $\overline{E}_\gamma \approx 220$ GeV
$<3.4 \times 10^{-3}$	90	WEIR	90B	MRK2	e^+e^- 29 GeV

$\Gamma(K^+e^-\mu^+)/\Gamma_{\text{total}}$ Γ_{126}/Γ

A test of lepton-family-number conservation.

VALUE	CL%	DOCUMENT ID		TECN	COMMENT
$<2.8 \times 10^{-6}$	90	LEES	11G	BABR	$e^+e^- \approx \Upsilon(4S)$
• • • We do not use the following data for averages, fits, limits, etc. • • •					
$<1.2 \times 10^{-4}$	90	FRABETTI	97B	E687	γ Be, $\overline{E}_\gamma \approx 220$ GeV
$<3.4 \times 10^{-3}$	90	WEIR	90B	MRK2	e^+e^- 29 GeV

$\Gamma(\pi^-2e^+)/\Gamma_{\text{total}}$ Γ_{127}/Γ

A test of lepton-number conservation.

VALUE	CL%	DOCUMENT ID		TECN	COMMENT
$<1.1 \times 10^{-6}$	90	RUBIN	10	CLEO	e^+e^- at $\psi(3770)$
• • • We do not use the following data for averages, fits, limits, etc. • • •					
$<1.9 \times 10^{-6}$	90	LEES	11G	BABR	$e^+e^- \approx \Upsilon(4S)$
$<3.6 \times 10^{-6}$	90	HE	05A	CLEO	See RUBIN 10
$<9.6 \times 10^{-5}$	90	AITALA	99G	E791	π^- N 500 GeV
$<1.1 \times 10^{-4}$	90	FRABETTI	97B	E687	γ Be, $\overline{E}_\gamma \approx 220$ GeV
$<4.8 \times 10^{-3}$	90	WEIR	90B	MRK2	e^+e^- 29 GeV

$\Gamma(\pi^-2\mu^+)/\Gamma_{\text{total}}$ Γ_{128}/Γ

A test of lepton-number conservation.

VALUE	CL%	DOCUMENT ID		TECN	COMMENT
$<2.2 \times 10^{-8}$	90	AAIJ	13AF	LHCB	pp at 7 TeV
• • • We do not use the following data for averages, fits, limits, etc. • • •					
$<2.0 \times 10^{-6}$	90	LEES	11G	BABR	$e^+e^- \approx \Upsilon(4S)$
$<4.8 \times 10^{-6}$	90	LINK	03F	FOCS	γ A, $\overline{E}_\gamma \approx 180$ GeV
$<1.7 \times 10^{-5}$	90	AITALA	99G	E791	π^- N 500 GeV
$<8.7 \times 10^{-5}$	90	FRABETTI	97B	E687	γ Be, $\overline{E}_\gamma \approx 220$ GeV
$<2.2 \times 10^{-4}$	90	KODAMA	95	E653	π^- emulsion 600 GeV
$<6.8 \times 10^{-3}$	90	WEIR	90B	MRK2	e^+e^- 29 GeV

$\Gamma(\pi^-e^+\mu^+)/\Gamma_{\text{total}}$ Γ_{129}/Γ

A test of lepton-number conservation.

VALUE	CL%	DOCUMENT ID		TECN	COMMENT
$<2.0 \times 10^{-6}$	90	LEES	11G	BABR	$e^+e^- \approx \Upsilon(4S)$
• • • We do not use the following data for averages, fits, limits, etc. • • •					
$<5.0 \times 10^{-5}$	90	AITALA	99G	E791	π^- N 500 GeV
$<1.1 \times 10^{-4}$	90	FRABETTI	97B	E687	γ Be, $\overline{E}_\gamma \approx 220$ GeV
$<3.7 \times 10^{-3}$	90	WEIR	90B	MRK2	e^+e^- 29 GeV

$\Gamma(\rho^-2\mu^+)/\Gamma_{\text{total}}$ Γ_{130}/Γ

A test of lepton-number conservation.

VALUE	CL%	DOCUMENT ID		TECN	COMMENT
$<5.6 \times 10^{-4}$	90	KODAMA	95	E653	π^- emulsion 600 GeV

$\Gamma(K^-2e^+)/\Gamma_{\text{total}}$ Γ_{131}/Γ

A test of lepton-number conservation.

VALUE	CL%	DOCUMENT ID		TECN	COMMENT
$<0.9 \times 10^{-6}$	90	LEES	11G	BABR	$e^+e^- \approx \Upsilon(4S)$
• • • We do not use the following data for averages, fits, limits, etc. • • •					
$<3.5 \times 10^{-6}$	90	RUBIN	10	CLEO	e^+e^- at $\psi(3770)$
$<4.5 \times 10^{-6}$	90	HE	05A	CLEO	See RUBIN 10
$<1.2 \times 10^{-4}$	90	FRABETTI	97B	E687	γ Be, $\overline{E}_\gamma \approx 220$ GeV
$<9.1 \times 10^{-3}$	90	WEIR	90B	MRK2	e^+e^- 29 GeV

$\Gamma(K^-2\mu^+)/\Gamma_{\text{total}}$ Γ_{132}/Γ

A test of lepton-number conservation.

VALUE	CL%	DOCUMENT ID		TECN	COMMENT
$<10 \times 10^{-6}$	90	LEES	11G	BABR	$e^+e^- \approx \Upsilon(4S)$
• • • We do not use the following data for averages, fits, limits, etc. • • •					
$< 1.3 \times 10^{-5}$	90	LINK	03F	FOCS	γ A, $\overline{E}_\gamma \approx 180$ GeV
$< 1.2 \times 10^{-4}$	90	FRABETTI	97B	E687	γ Be, $\overline{E}_\gamma \approx 220$ GeV
$< 3.2 \times 10^{-4}$	90	KODAMA	95	E653	π^- emulsion 600 GeV
$< 4.3 \times 10^{-3}$	90	WEIR	90B	MRK2	e^+e^- 29 GeV

$\Gamma(K^-e^+\mu^+)/\Gamma_{\text{total}}$ Γ_{133}/Γ

A test of lepton-number conservation.

VALUE	CL%	DOCUMENT ID		TECN	COMMENT
$<1.9 \times 10^{-6}$	90	LEES	11G	BABR	$e^+e^- \approx \Upsilon(4S)$
• • • We do not use the following data for averages, fits, limits, etc. • • •					
$<1.3 \times 10^{-4}$	90	FRABETTI	97B	E687	γ Be, $\overline{E}_\gamma \approx 220$ GeV
$<4.0 \times 10^{-3}$	90	WEIR	90B	MRK2	e^+e^- 29 GeV

$\Gamma(K^*(892)^-2\mu^+)/\Gamma_{\text{total}}$ Γ_{134}/Γ

A test of lepton-number conservation.

VALUE	CL%	DOCUMENT ID		TECN	COMMENT
$<8.5 \times 10^{-4}$	90	KODAMA	95	E653	π^- emulsion 600 GeV

$D^{\pm}$ CP-VIOLATING DECAY-RATE ASYMMETRIES

This is the difference between D^+ and D^- partial widths for these modes divided by the sum of the widths.

$A_{CP}(\mu^{\pm}\nu)$ in $D^+ \to \mu^+\nu_\mu$, $D^- \to \mu^-\overline{\nu}_\mu$

VALUE (%)	DOCUMENT ID		TECN	COMMENT
$+8 \pm 8$	EISENSTEIN	08	CLEO	e^+e^- at $\psi(3770)$

$A_{CP}(K^0_S\pi^{\pm})$ in $D^{\pm} \to K^0_S\pi^{\pm}$

VALUE (%)	EVTS	DOCUMENT ID		TECN	COMMENT
−0.41 ±0.09 OUR AVERAGE					
−0.363±0.094±0.067	1738k	[1] KO	12A	BELL	$e^+e^- \approx \Upsilon(nS)$
−0.44 ±0.13 ±0.10	807k	DEL-AMO-SA...	11H	BABR	$e^+e^- \approx \Upsilon(4S)$
−1.3 ±0.7 ±0.3	30k	MENDEZ	10	CLEO	e^+e^- at 3774 MeV
−1.6 ±1.5 ±0.9	10.6k	[2] LINK	02B	FOCS	γ nucleus, $\overline{E}_\gamma \approx 180$ GeV
• • • We do not use the following data for averages, fits, limits, etc. • • •					
−0.71 ±0.19 ±0.20		KO	10	BELL	See KO 12A
−0.6 ±1.0 ±0.3		DOBBS	07	CLEO	See MENDEZ 10

[1] KO 12A finds that after subtracting the contribution due to $K^0 - \overline{K}^0$ mixing, the CP asymmetry due to the change of charm is $(-0.024 \pm 0.094 \pm 0.067)\%$, consistent with zero.

[2] LINK 02B measures $N(D^+ \to K^0_S\pi^+)/N(D^+ \to K^-\pi^+\pi^+)$, the ratio of numbers of events observed, and similarly for the D^-.

$A_{CP}(K^{\mp}2\pi^{\pm})$ in $D^+ \to K^-2\pi^+$, $D^- \to K^+2\pi^-$

VALUE (%)	EVTS	DOCUMENT ID		TECN	COMMENT
−0.1±0.4±0.9	231k	MENDEZ	10	CLEO	e^+e^- at 3774 MeV
• • • We do not use the following data for averages, fits, limits, etc. • • •					
−0.5±0.4±0.9		DOBBS	07	CLEO	See MENDEZ 10

$A_{CP}(K^{\mp}\pi^{\pm}\pi^{\pm}\pi^0)$ in $D^+ \to K^-\pi^+\pi^+\pi^0$, $D^- \to K^+\pi^-\pi^-\pi^0$

VALUE (%)	DOCUMENT ID		TECN	COMMENT
+1.0±0.9±0.9	DOBBS	07	CLEO	e^+e^- at $\psi(3770)$

$A_{CP}(K^0_S\pi^{\pm}\pi^0)$ in $D^+ \to K^0_S\pi^+\pi^0$, $D^- \to K^0_S\pi^-\pi^0$

VALUE (%)	DOCUMENT ID		TECN	COMMENT
+0.3±0.9±0.3	DOBBS	07	CLEO	e^+e^- at $\psi(3770)$

$A_{CP}(K^0_S\pi^{\pm}\pi^+\pi^-)$ in $D^+ \to K^0_S\pi^+\pi^+\pi^-$, $D^- \to K^0_S\pi^-\pi^-\pi^+$

VALUE (%)	DOCUMENT ID		TECN	COMMENT
+0.1±1.1±0.6	DOBBS	07	CLEO	e^+e^- at $\psi(3770)$

$A_{CP}(\pi^{\pm}\pi^0)$ in $D^{\pm} \to \pi^{\pm}\pi^0$

VALUE (%)	EVTS	DOCUMENT ID		TECN	COMMENT
+2.9±2.9±0.3	2.6k	MENDEZ	10	CLEO	e^+e^- at 3774 MeV

$A_{CP}(\pi^{\pm}\eta)$ in $D^{\pm} \to \pi^{\pm}\eta$

VALUE (%)	EVTS	DOCUMENT ID		TECN	COMMENT
1.0 ±1.5 OUR AVERAGE		Error includes scale factor of 1.4.			
+1.74±1.13±0.19		WON	11	BELL	$e^+e^- \approx \Upsilon(4S)$
−2.0 ±2.3 ±0.3	2.9k	MENDEZ	10	CLEO	e^+e^- at 3774 MeV

$A_{CP}(\pi^{\pm}\eta'(958))$ in $D^{\pm} \to \pi^{\pm}\eta'(958)$

VALUE (%)	EVTS	DOCUMENT ID		TECN	COMMENT
−0.5 ±1.2 OUR AVERAGE		Error includes scale factor of 1.1.			
−0.12±1.12±0.17		WON	11	BELL	$e^+e^- \approx \Upsilon(4S)$
−4.0 ±3.4 ±0.3	1.0k	MENDEZ	10	CLEO	e^+e^- at 3774 MeV

$A_{CP}(K^0_S K^{\pm})$ in $D^{\pm} \to K^0_S K^{\pm}$

VALUE (%)	EVTS	DOCUMENT ID		TECN	COMMENT
−0.11±0.25 OUR AVERAGE					
−0.25±0.28±0.14	277k	[1] KO	13	BELL	e^+e^- at $\Upsilon(nS)$
0.13±0.36±0.25	159k	[2] LEES	13E	BABR	e^+e^- at $\Upsilon(4S)$
−0.2 ±1.5 ±0.9	5.2k	MENDEZ	10	CLEO	e^+e^- at 3774 MeV
7.1 ±6.1 ±1.2	949	[3] LINK	02B	FOCS	γ nucleus, $\overline{E}_\gamma \approx 180$ GeV
• • • We do not use the following data for averages, fits, limits, etc. • • •					
−0.16±0.58±0.25		KO	10	BELL	$e^+e^- \approx \Upsilon(4S)$
6.9 ±6.0 ±1.5	949	[4] LINK	02B	FOCS	γ nucleus, $\overline{E}_\gamma \approx 180$ GeV

[1] KO 13 finds that after subtracting the contribution due to $K^0 - \overline{K}^0$ mixing, the CP asymmetry is $(+0.08 \pm 0.28 \pm 0.14)\%$.

[2] LEES 13E finds that after subtracting the contribution due to $K^0 - \overline{K}^0$ mixing, the CP asymmetry is $(+0.46 \pm 0.36 \pm 0.25)\%$.

[3] LINK 02B measures $N(D^+ \to K^0_S K^+)/N(D^+ \to K^0_S\pi^+)$, the ratio of numbers of events observed, and similarly for the D^-.

[4] LINK 02B measures $N(D^+ \to K^0_S K^+)/N(D^+ \to K^-\pi^+\pi^+)$, the ratio of numbers of events observed, and similarly for the D^-.

$A_{CP}(K^+K^-\pi^{\pm})$ in $D^{\pm} \to K^+K^-\pi^{\pm}$

See also AAIJ 11G for a search for CP asymmetry in the $D^{\pm} \to K^+K^-\pi^{\pm}$ Dalitz plots using 370k decays and four different binning schemes. No evidence for CP asymmetry was found.

VALUE (%)	EVTS	DOCUMENT ID		TECN	COMMENT
0.36±0.29 OUR AVERAGE					
0.37±0.30±0.15	224k	[1] LEES	13F	BABR	e^+e^- at $\Upsilon(4S)$
−0.03±0.84±0.29		RUBIN	08	CLEO	e^+e^- at 3774 MeV
−0.1 ±1.5 ±0.8		DOBBS	07	CLEO	e^+e^- at $\psi(3770)$
+1.4 ±1.0 ±0.8	43k	[2] AUBERT	05S	BABR	e^+e^- at $\Upsilon(4S)$
+0.6 ±1.1 ±0.5	14k	[3] LINK	00B	FOCS	
−1.4 ±2.9		[3] AITALA	97B	E791	$-0.062 < A_{CP} < +0.034$ (90% CL)
−3.1 ±6.8		[3] FRABETTI	94I	E687	$-0.14 < A_{CP} < +0.081$ (90% CL)

[1] This is the integrated CP asymmetry. LEES 13F also searches for CP asymmetries in four regions of the Dalitz plots (two of which are listed below); in comparisons of binned D^+ and D^- Dalitz plots; in parametrized fits to those plots, including 2-body submodes; and in comparisons of Legendre-polynomial distributions for the K^+K^- and $K^-\pi^+$ systems.

[2] AUBERT 05S measures $N(D^+ \to K^+K^-\pi^+)/N(D^+_s \to K^+K^-\pi^+)$, the ratio of the numbers of events observed, and similarly for the D^-.

[3] FRABETTI 94I, AITALA 98C, and LINK 00B measure $N(D^+ \to K^-K^+\pi^+)/N(D^+ \to K^-\pi^+\pi^+)$, the ratio of numbers of events observed, and similarly for the D^-.

$A_{CP}(K^{\pm}K^{*0})$ in $D^+ \to K^+\overline{K}^{*0}$, $D^- \to K^-K^{*0}$

VALUE (%)	EVTS	DOCUMENT ID		TECN	COMMENT
− 0.3± 0.4 OUR AVERAGE					
− 0.3± 0.4±0.2	73k	[1] LEES	13F	BABR	e^+e^- at $\Upsilon(4S)$
− 0.4± 2.0±0.6		RUBIN	08	CLEO	Fit-fraction asymmetry
+ 0.9± 1.7±0.7	11k	[2] AUBERT	05S	BABR	e^+e^- at $\Upsilon(4S)$
− 1.0± 5.0		[3] AITALA	97B	E791	$-0.092 < A_{CP} < +0.072$ (90% CL)
−12 ±13		[3] FRABETTI	94I	E687	$-0.33 < A_{CP} < +0.094$ (90% CL)

[1] This LEES 13F result is for the $K^{\mp}\pi^{\pm}$ mass-squared between 0.4 and 1.0 GeV^2, and does not actually separate out the K^*.

[2] AUBERT 05S measures $N(D^+ \to K^+\overline{K}^{*0})/N(D^+_s \to K^+K^-\pi^+)$, the ratio of the numbers of events observed, and similarly for the D^-.

[3] FRABETTI 94I and AITALA 97B measure $N(D^+ \to K^+\overline{K}^*(892)^0)/N(D^+ \to K^-\pi^+\pi^+)$, the ratio of numbers of events observed, and similarly for the D^-.

$A_{CP}(\phi\pi^{\pm})$ in $D^{\pm} \to \phi\pi^{\pm}$

VALUE (%)	EVTS	DOCUMENT ID		TECN	COMMENT
0.09±0.19 OUR AVERAGE		Error includes scale factor of 1.2.			
−0.04±0.14±0.14	1.58M	AAIJ	13W	LHCB	pp at 7 TeV
−0.3 ±0.3 ±0.5	97k	[1] LEES	13F	BABR	e^+e^- at $\Upsilon(4S)$
+0.51±0.28±0.05	237k	STARIC	12	BELL	Mainly at $\Upsilon(4S)$
−1.8 ±1.6 $^{+0.2}_{-0.4}$		RUBIN	08	CLEO	Fit-fraction asymmetry
+0.2 ±1.5 ±0.6	10k	[2] AUBERT	05S	BABR	e^+e^- at $\Upsilon(4S)$
−2.8 ±3.6		[3] AITALA	97B	E791	$-0.087 < A_{CP} < +0.031$ (90% CL)
+6.6 ±8.6		[3] FRABETTI	94I	E687	$-0.075 < A_{CP} < +0.21$ (90% CL)

[1] This LEES 13F result is for the K^+K^- mass-squared less than 1.3 GeV^2 and the $K^{\mp}\pi^{\pm}$ mass-squared above 1.0 GeV^2, and does not actually separate out the ϕ.

[2] AUBERT 05S measures $N(D^+ \to \phi\pi^+)/N(D^+_s \to K^+K^-\pi^+)$, the ratio of the numbers of events observed, and similarly for the D^-.

[3] FRABETTI 94I and AITALA 97B measure $N(D^+ \to \phi\pi^+)/N(D^+ \to K^-\pi^+\pi^+)$, the ratio of numbers of events observed, and similarly for the D^-.

$A_{CP}(K^{\pm}K^*_0(1430)^0)$ in $D^+ \to K^+\overline{K}^*_0(1430)^0$, $D^- \to K^-K^*_0(1430)^0$

VALUE (%)	DOCUMENT ID		TECN	COMMENT
+8±6$^{+4}_{-2}$	RUBIN	08	CLEO	Fit-fraction asymmetry

$A_{CP}(K^{\pm}K^*_2(1430)^0)$ in $D^+ \to K^+\overline{K}^*_2(1430)^0$, $D^- \to K^-K^*_2(1430)^0$

VALUE (%)	DOCUMENT ID		TECN	COMMENT
+43±19$^{+5}_{-18}$	RUBIN	08	CLEO	Fit-fraction asymmetry

$A_{CP}(K^{\pm}K^*_0(800))$ in $D^+ \to K^+\overline{K}^*_0(800)$, $D^- \to K^-K^*_0(800)$

VALUE (%)	DOCUMENT ID		TECN	COMMENT
−12±11$^{+14}_{-6}$	RUBIN	08	CLEO	Fit-fraction asymmetry

$A_{CP}(a_0(1450)^0\pi^{\pm})$ in $D^{\pm} \to a_0(1450)^0\pi^{\pm}$

VALUE (%)	DOCUMENT ID		TECN	COMMENT
−19±12$^{+8}_{-11}$	RUBIN	08	CLEO	Fit-fraction asymmetry

$A_{CP}(\phi(1680)\pi^{\pm})$ in $D^{\pm} \to \phi(1680)\pi^{\pm}$

VALUE (%)	DOCUMENT ID		TECN	COMMENT
−9±22±14	RUBIN	08	CLEO	Fit-fraction asymmetry

$A_{CP}(\pi^+\pi^-\pi^{\pm})$ in $D^{\pm} \to \pi^+\pi^-\pi^{\pm}$

See also AAIJ 14C for a search for CP violation in $D^{\pm} \to \pi^+\pi^-\pi^{\pm}$ Dalitz plots using model-independent binned and unbinned methods. No evidence was found.

VALUE (%)	DOCUMENT ID		TECN	COMMENT
−1.7±4.2	[1] AITALA	97B	E791	$-0.086 < A_{CP} < +0.052$ (90% CL)

[1] AITALA 97B measure $N(D^+ \to \pi^+\pi^-\pi^+)/N(D^+ \to K^-\pi^+\pi^+)$, the ratio of numbers of events observed, and similarly for the D^-.

$A_{CP}(K^0_S K^{\pm}\pi^+\pi^-)$ in $D^{\pm} \to K^0_S K^{\pm}\pi^+\pi^-$

VALUE (%)	EVTS	DOCUMENT ID		TECN	COMMENT
−4.2±6.4±2.2	523 ± 32	LINK	05E	FOCS	γ A, $\overline{E}_\gamma \approx 180$ GeV

$A_{CP}(K^{\pm}\pi^0)$ in $D^{\pm} \to K^{\pm}\pi^0$

VALUE (%)	EVTS	DOCUMENT ID		TECN	COMMENT
−3.5±10.7±0.9	343 ± 37	MENDEZ	10	CLEO	e^+e^- at 3774 MeV

Meson Particle Listings

$D^{\pm}$

D^+-D^- T-VIOLATING DECAY-RATE ASYMMETRIES

$A_{Tviol}(K^0_S K^{\pm}\pi^+\pi^-)$ in $D^{\pm} \to K^0_S K^{\pm}\pi^+\pi^-$

$C_T \equiv \vec{p}_{K^+} \cdot (\vec{p}_{\pi^+} \times \vec{p}_{\pi^-})$ is a parity-odd correlation of the K^+, π^+, and π^- momenta for the D^+. $\overline{C}_T \equiv \vec{p}_{K^-} \cdot (\vec{p}_{\pi^-} \times \vec{p}_{\pi^+})$ is the corresponding quantity for the D^-. Then

$A_T \equiv [\Gamma(C_T > 0) - \Gamma(C_T \le 0)] \,/\, [\Gamma(C_T > 0) + \Gamma(C_T < 0)]$, and
$\overline{A}_T \equiv [\Gamma(-\overline{C}_T > 0) - \Gamma(-\overline{C}_T < 0)] \,/\, [\Gamma(-\overline{C}_T > 0) + \Gamma(-\overline{C}_T < 0)]$, and

$A_{Tviol} \equiv \frac{1}{2}(A_T - \overline{A}_T)$. C_T and $\overline{C}_T$ are commonly referred to as T-odd moments, because they are odd under T reversal. However, the T-conjugate process $K^0_S K^{\pm}\pi^+\pi^- \to D^{\pm}$ is not accessible, while the P-conjugate process is.

VALUE (units 10^{-3})	EVTS	DOCUMENT ID		TECN	COMMENT
$-12.0 \pm 10.0 \pm 4.6$	21.2 ± 0.4k	LEES	11E	BABR	$e^+e^- \approx \Upsilon(4S)$
• • • We do not use the following data for averages, fits, limits, etc. • • •					
$23 \pm 62 \pm 22$	523 ± 32	LINK	05E	FOCS	γ A, $\overline{E}_\gamma \approx 180$ GeV

$D^+ \to (\overline{K}^0/\pi^0/\eta/\rho^0/\overline{K}^{*0})\ell^+\nu_\ell$ FORM FACTORS

$f_+(0)|V_{cs}|$ in $D^+ \to \overline{K}^0\ell^+\nu_\ell$

VALUE	DOCUMENT ID		TECN	COMMENT
$0.707 \pm 0.010 \pm 0.009$	BESSON	09	CLEO	$\overline{K}^0 e^+\nu_e$ 3-parameter fit

$r_1 \equiv a_1/a_0$ in $D^+ \to \overline{K}^0\ell^+\nu_\ell$

VALUE	DOCUMENT ID		TECN	COMMENT
$-1.66 \pm 0.44 \pm 0.10$	BESSON	09	CLEO	$\overline{K}^0 e^+\nu_e$ 3-parameter fit

$r_2 \equiv a_2/a_0$ in $D^+ \to \overline{K}^0\ell^+\nu_\ell$

VALUE	DOCUMENT ID		TECN	COMMENT
$-14 \pm 11 \pm 1$	BESSON	09	CLEO	$\overline{K}^0 e^+\nu_e$ 3-parameter fit

$f_+(0)|V_{cd}|$ in $D^+ \to \pi^0\ell^+\nu_\ell$

VALUE	DOCUMENT ID		TECN	COMMENT
$0.146 \pm 0.007 \pm 0.002$	BESSON	09	CLEO	$\pi^0 e^+\nu_e$ 3-parameter fit

$r_1 \equiv a_1/a_0$ in $D^+ \to \pi^0\ell^+\nu_\ell$

VALUE	DOCUMENT ID		TECN	COMMENT
$-1.37 \pm 0.88 \pm 0.24$	BESSON	09	CLEO	$\pi^0 e^+\nu_e$ 3-parameter fit

$r_2 \equiv a_2/a_0$ in $D^+ \to \pi^0\ell^+\nu_\ell$

VALUE	DOCUMENT ID		TECN	COMMENT
$-4 \pm 5 \pm 1$	BESSON	09	CLEO	$\pi^0 e^+\nu_e$ 3-parameter fit

$f_+(0)|V_{cd}|$ in $D^+ \to \eta e^+\nu_e$

VALUE	DOCUMENT ID		TECN	COMMENT
$0.086 \pm 0.006 \pm 0.001$	YELTON	11	CLEO	z expansion

$r_1 \equiv a_1/a_0$ in $D^+ \to \eta e^+\nu_e$

VALUE	DOCUMENT ID		TECN	COMMENT
$-1.83 \pm 2.23 \pm 0.28$	YELTON	11	CLEO	z expansion

$r_V \equiv V(0)/A_1(0)$ in $D^+, D^0 \to \rho e^+\nu_e$

VALUE	DOCUMENT ID		TECN	COMMENT
$1.48 \pm 0.15 \pm 0.05$	[1] DOBBS	13	CLEO	e^+e^- at $\psi(3770)$

[1] Uses both D^+ and D^0 events. Using PDG 10 values of V_{cd} and lifetimes, DOBBS 13 gets $A_1(0) = 0.56 \pm 0.01^{+0.02}_{-0.03}$, $A_2(0) = 0.47 \pm 0.06 \pm 0.04$, and $V(0) = 0.84 \pm 0.09^{+0.05}_{-0.06}$.

$r_2 \equiv A_2(0)/A_1(0)$ in $D^+, D^0 \to \rho e^+\nu_e$

VALUE	DOCUMENT ID		TECN	COMMENT
$0.83 \pm 0.11 \pm 0.04$	[1] DOBBS	13	CLEO	e^+e^- at $\psi(3770)$

[1] Uses both D^+ and D^0 events. Using PDG 10 values of V_{cd} and lifetimes, DOBBS 13 gets $A_1(0) = 0.56 \pm 0.01^{+0.02}_{-0.03}$, $A_2(0) = 0.47 \pm 0.06 \pm 0.04$, and $V(0) = 0.84 \pm 0.09^{+0.05}_{-0.06}$.

$r_V \equiv V(0)/A_1(0)$ in $D^+ \to \overline{K}^*(892)^0\ell^+\nu_\ell$

See also BRIERE 10 for $\overline{K}^*\ell^+\nu_\ell$ helicity-basis form-factor measurements.

VALUE	EVTS	DOCUMENT ID		TECN	COMMENT
1.51 ± 0.07 OUR AVERAGE		Error includes scale factor of 2.2. See the ideogram below.			
$1.463 \pm 0.017 \pm 0.031$		[1] DEL-AMO-SA...11I		BABR	
$1.504 \pm 0.057 \pm 0.039$	15k	[2] LINK	02L	FOCS	$\overline{K}^*(892)^0\mu^+\nu_\mu$
$1.45 \pm 0.23 \pm 0.07$	763	ADAMOVICH	99	BEAT	$\overline{K}^*(892)^0\mu^+\nu_\mu$
$1.90 \pm 0.11 \pm 0.09$	3000	[3] AITALA	98B	E791	$\overline{K}^*(892)^0 e^+\nu_e$
$1.84 \pm 0.11 \pm 0.09$	3034	AITALA	98F	E791	$\overline{K}^*(892)^0\mu^+\nu_\mu$
$1.74 \pm 0.27 \pm 0.28$	874	FRABETTI	93E	E687	$\overline{K}^*(892)^0\mu^+\nu_\mu$
$2.00 \pm^{0.34}_{0.32} \pm 0.16$	305	KODAMA	92	E653	$\overline{K}^*(892)^0\mu^+\nu_\mu$
• • • We do not use the following data for averages, fits, limits, etc. • • •					
$2.0 \pm 0.6 \pm 0.3$	183	ANJOS	90E	E691	$\overline{K}^*(892)^0 e^+\nu_e$

[1] DEL-AMO-SANCHEZ 11I finds the pole mass $m_A = (2.63 \pm 0.10 \pm 0.13)$ GeV (m_V is fixed at 2 GeV).
[2] LINK 02L includes the effects of interference with an S-wave background. This much improves the goodness of fit, but does not much shift the values of the form factors.
[3] This is slightly different from the AITALA 98B value: see ref. [5] in AITALA 98F.

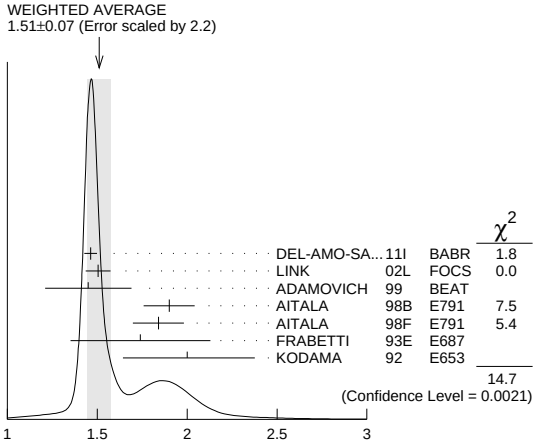

$r_V \equiv V(0)/A_1(0)$ in $D^+ \to \overline{K}^*(892)^0\ell^+\nu_\ell$

$r_2 \equiv A_2(0)/A_1(0)$ in $D^+ \to \overline{K}^*(892)^0\ell^+\nu_\ell$

See also BRIERE 10 for $\overline{K}^*\ell^+\nu_\ell$ helicity-basis form-factor measurements.

VALUE	EVTS	DOCUMENT ID		TECN	COMMENT
0.807 ± 0.025 OUR AVERAGE					
$0.801 \pm 0.020 \pm 0.020$		[1] DEL-AMO-SA...11I		BABR	
$0.875 \pm 0.049 \pm 0.064$	15k	[2] LINK	02L	FOCS	$\overline{K}^*(892)^0\mu^+\nu_\mu$
$1.00 \pm 0.15 \pm 0.03$	763	ADAMOVICH	99	BEAT	$\overline{K}^*(892)^0\mu^+\nu_\mu$
$0.71 \pm 0.08 \pm 0.09$	3000	AITALA	98B	E791	$\overline{K}^*(892)^0 e^+\nu_e$
$0.75 \pm 0.08 \pm 0.09$	3034	AITALA	98F	E791	$\overline{K}^*(892)^0\mu^+\nu_\mu$
$0.78 \pm 0.18 \pm 0.10$	874	FRABETTI	93E	E687	$\overline{K}^*(892)^0\mu^+\nu_\mu$
$0.82 \pm^{0.22}_{0.23} \pm 0.11$	305	KODAMA	92	E653	$\overline{K}^*(892)^0\mu^+\nu_\mu$
• • • We do not use the following data for averages, fits, limits, etc. • • •					
$0.0 \pm 0.5 \pm 0.2$	183	ANJOS	90E	E691	$\overline{K}^*(892)^0 e^+\nu_e$

[1] DEL-AMO-SANCHEZ 11I finds the pole mass $m_A = (2.63 \pm 0.10 \pm 0.13)$ GeV (m_V is fixed at 2 GeV).
[2] LINK 02L includes the effects of interference with an S-wave background. This much improves the goodness of fit, but does not much shift the values of the form factors.

$r_3 \equiv A_3(0)/A_1(0)$ in $D^+ \to \overline{K}^*(892)^0\ell^+\nu_\ell$

See also BRIERE 10 for $\overline{K}^*\ell^+\nu_\ell$ helicity-basis form-factor measurements.

VALUE	EVTS	DOCUMENT ID		TECN	COMMENT
$0.04 \pm 0.33 \pm 0.29$	3034	AITALA	98F	E791	$\overline{K}^*(892)^0\mu^+\nu_\mu$

Γ_L/Γ_T in $D^+ \to \overline{K}^*(892)^0\ell^+\nu_\ell$

See also BRIERE 10 for $\overline{K}^*\ell^+\nu_\ell$ helicity-basis form-factor measurements.

VALUE	EVTS	DOCUMENT ID		TECN	COMMENT
1.13 ± 0.08 OUR AVERAGE					
$1.09 \pm 0.10 \pm 0.02$	763	ADAMOVICH	99	BEAT	$\overline{K}^*(892)^0\mu^+\nu_\mu$
$1.20 \pm 0.13 \pm 0.13$	874	FRABETTI	93E	E687	$\overline{K}^*(892)^0\mu^+\nu_\mu$
$1.18 \pm 0.18 \pm 0.08$	305	KODAMA	92	E653	$\overline{K}^*(892)^0\mu^+\nu_\mu$
• • • We do not use the following data for averages, fits, limits, etc. • • •					
$1.8 \pm^{0.6}_{0.4} \pm 0.3$	183	ANJOS	90E	E691	$\overline{K}^*(892)^0 e^+\nu_e$

Γ_+/Γ_- in $D^+ \to \overline{K}^*(892)^0\ell^+\nu_\ell$

See also BRIERE 10 for $\overline{K}^*\ell^+\nu_\ell$ helicity-basis form-factor measurements.

VALUE	EVTS	DOCUMENT ID		TECN	COMMENT
0.22 ± 0.06 OUR AVERAGE		Error includes scale factor of 1.6.			
$0.28 \pm 0.05 \pm 0.02$	763	ADAMOVICH	99	BEAT	$\overline{K}^*(892)^0\mu^+\nu_\mu$
$0.16 \pm 0.05 \pm 0.02$	305	KODAMA	92	E653	$\overline{K}^*(892)^0\mu^+\nu_\mu$
• • • We do not use the following data for averages, fits, limits, etc. • • •					
$0.15 \pm^{0.07}_{0.05} \pm 0.03$	183	ANJOS	90E	E691	$\overline{K}^*(892)^0 e^+\nu_e$

$D^{\pm}$ REFERENCES

AAIJ	14C	PL B728 585	R. Aaij *et al.*	(LHCb Collab.)
AAIJ	13AF	PL B724 203	R. Aaij *et al.*	(LHCb Collab.)
AAIJ	13W	JHEP 1306 112	R. Aaij *et al.*	(LHCb Collab.)
DOBBS	13	PRL 110 131802	S. Dobbs *et al.*	(CLEO Collab.)
KO	13	JHEP 1302 098	B.R. Ko *et al.*	(BELLE Collab.)
LEES	13E	PR D87 052012	J.P. Lees *et al.*	(BABAR Collab.)
LEES	13F	PR D87 052010	J.P. Lees *et al.*	(BABAR Collab.)
KO	12A	PRL 109 119903 (errat.)	B.R. Ko *et al.*	(BELLE Collab.)
Also		PRL 109 021601	B.R. Ko *et al.*	(BELLE Collab.)
STARIC	12	PRL 108 071801	M. Staric *et al.*	(BELLE Collab.)
AAIJ	11G	PR D84 112008	R. Aaij *et al.*	(LHCb Collab.)
DEL-AMO-SA...	11H	PR D83 071103	P. del Amo Sanchez *et al.*	(BABAR Collab.)
DEL-AMO-SA...	11I	PR D83 072001	P. del Amo Sanchez *et al.*	(BABAR Collab.)
LEES	11E	PR D84 031103	J.P. Lees *et al.*	(BABAR Collab.)
LEES	11G	PR D84 072006	J.P. Lees *et al.*	(BABAR Collab.)
WON	11	PRL 107 221801	E. Won *et al.*	(BELLE Collab.)
YELTON	11	PR D84 032001	J. Yelton *et al.*	(CLEO Collab.)
ANASHIN	10A	PL B686 84	V.V. Anashin *et al.*	(VEPP-4M KEDR Collab.)
ASNER	10	PR D81 052007	D.M. Asner *et al.*	(CLEO Collab.)
BRIERE	10	PR D81 112001	R.A. Briere *et al.*	(CLEO Collab.)
KO	10	PRL 104 181602	B.R. Ko *et al.*	(BELLE Collab.)
MENDEZ	10	PR D81 052013	H. Mendez *et al.*	(CLEO Collab.)
PDG	10	JP G37 075021	K. Nakamura *et al.*	(PDG Collab.)
RUBIN	10	PR D82 092007	P. Rubin *et al.*	(CLEO Collab.)
BESSON	09	PR D80 032005	D. Besson *et al.*	(CLEO Collab.)
Also		PR D79 052010	J.Y. Ge *et al.*	(CLEO Collab.)
KO	09	PRL 102 221802	B.R. Ko *et al.*	(BELLE Collab.)
LINK	09	PL B681 14	J.M. Link *et al.*	(FNAL FOCUS Collab.)
MITCHELL	09B	PRL 102 081801	R.E. Mitchell *et al.*	(CLEO Collab.)
WON	09	PR D80 111101	E. Won *et al.*	(BELLE Collab.)
ABAZOV	08D	PRL 100 101801	V.M. Abazov *et al.*	(D0 Collab.)
ABLIKIM	08L	PL B665 16	M. Ablikim *et al.*	(BES Collab.)
ARTUSO	08	PR D77 092003	M. Artuso *et al.*	(CLEO Collab.)
BONVICINI	08	PR D77 091106	G. Bonvicini *et al.*	(CLEO Collab.)
BONVICINI	08A	PR D78 052001	G. Bonvicini *et al.*	(CLEO Collab.)
DOBBS	08	PR D77 112005	S. Dobbs *et al.*	(CLEO Collab.)
Also		PRL 100 251802	D. Cronin-Hennessy *et al.*	(CLEO Collab.)
EISENSTEIN	08	PR D78 052003	B.I. Eisenstein *et al.*	(CLEO Collab.)
HE	08	PRL 100 091801	Q. He *et al.*	(CLEO Collab.)
PDG	08	PL B667 1	C. Amsler *et al.*	(PDG Collab.)
RUBIN	08	PR D78 072003	P. Rubin *et al.*	(CLEO Collab.)
ABLIKIM	07	PL B644 20	M. Ablikim *et al.*	(BES Collab.)
ABLIKIM	07G	PL B658 1	M. Ablikim *et al.*	(BES Collab.)
BONVICINI	07	PR D76 012001	G. Bonvicini *et al.*	(CLEO Collab.)
DOBBS	07	PR D76 112001	S. Dobbs *et al.*	(CLEO Collab.)
LINK	07B	PL B653 1	J.M. Link *et al.*	(FNAL FOCUS Collab.)
ABLIKIM	06O	EPJ C47 31	M. Ablikim *et al.*	(BES Collab.)
ABLIKIM	06P	EPJ C47 39	M. Ablikim *et al.*	(BES Collab.)
ABLIKIM	06U	PL B643 246	M. Ablikim *et al.*	(BES Collab.)
ADAM	06A	PRL 97 251801	N.E. Adam *et al.*	(CLEO Collab.)
AITALA	06	PR D73 032004	E.M. Aitala *et al.*	(FNAL E791 Collab.)
Also		PR D74 059901 (errat.)	E.M. Aitala *et al.*	(FNAL E791 Collab.)
AUBERT,B	06F	PR D74 011107	B. Aubert *et al.*	(BABAR Collab.)
DYTMAN	06	PR D74 071102	S.A. Dytman *et al.*	(CLEO Collab.)
HUANG	06B	PR D74 112005	G.S. Huang *et al.*	(CLEO Collab.)
LINK	06B	PL B637 32	J.M. Link *et al.*	(FNAL FOCUS Collab.)
RUBIN	06	PRL 96 081802	P. Rubin *et al.*	(CLEO Collab.)
RUBIN	06A	PR D73 112005	P. Rubin *et al.*	(CLEO Collab.)
ABLIKIM	05A	PL B608 24	M. Ablikim *et al.*	(BES Collab.)
ABLIKIM	05D	PL B610 183	M. Ablikim *et al.*	(BES Collab.)
ABLIKIM	05F	PL B622 6	M. Ablikim *et al.*	(BES Collab.)
ABLIKIM	05P	PL B625 196	M. Ablikim *et al.*	(BES Collab.)
ARTUSO	05A	PRL 95 251801	M. Artuso *et al.*	(CLEO Collab.)
AUBERT	05S	PR D71 091101	B. Aubert *et al.*	(BABAR Collab.)
HE	05	PRL 95 121801	Q. He *et al.*	(CLEO Collab.)
Also		PRL 96 199903 (errat.)	Q. He *et al.*	(CLEO Collab.)
HE	05A	PRL 95 221802	Q. He *et al.*	(CLEO Collab.)
HUANG	05B	PRL 95 181801	G.S. Huang *et al.*	(CLEO Collab.)
KAYIS-TOPAK...	05	PL B626 24	A. Kayis-Topaksu *et al.*	(CERN CHORUS Collab.)
LINK	05E	PL B622 239	J.M. Link *et al.*	(FNAL FOCUS Collab.)
LINK	05I	PL B621 72	J.M. Link *et al.*	(FNAL FOCUS Collab.)
ABLIKIM	04C	PL B597 39	M. Ablikim *et al.*	(BEPC BES Collab.)
ARMS	04	PR D69 071102	K. Arms *et al.*	(CLEO Collab.)
BONVICINI	04A	PR D70 112004	G. Bonvicini *et al.*	(CLEO Collab.)
LINK	04	PL B585 200	J.M. Link *et al.*	(FNAL FOCUS Collab.)
LINK	04E	PL B598 33	J.M. Link *et al.*	(FNAL FOCUS Collab.)
LINK	04F	PL B601 10	J.M. Link *et al.*	(FNAL FOCUS Collab.)
ANISOVICH	03	EPJ A16 229	V.V. Anisovich *et al.*	
LINK	03D	PL B561 225	J.M. Link *et al.*	(FNAL FOCUS Collab.)
LINK	03F	PL B572 21	J.M. Link *et al.*	(FNAL FOCUS Collab.)
AITALA	02	PRL 89 121801	E.M. Aitala *et al.*	(FNAL E791 Collab.)
BRANDENB...	02	PRL 89 222001	G. Brandenburg *et al.*	(CLEO Collab.)
KAYIS-TOPAK...	02	PL B549 48	A. Kayis-Topaksu *et al.*	(CERN CHORUS Collab.)
LINK	02B	PRL 88 041602	J.M. Link *et al.*	(FNAL FOCUS Collab.)
Also		PRL 88 159903 (errat)	J.M. Link *et al.*	(FNAL FOCUS Collab.)
LINK	02E	PL B535 43	J.M. Link *et al.*	(FNAL FOCUS Collab.)
LINK	02F	PL B537 192	J.M. Link *et al.*	(FNAL FOCUS Collab.)
LINK	02I	PL B541 227	J.M. Link *et al.*	(FNAL FOCUS Collab.)
LINK	02J	PL B541 243	J.M. Link *et al.*	(FNAL FOCUS Collab.)
LINK	02L	PL B544 89	J.M. Link *et al.*	(FNAL FOCUS Collab.)
AITALA	01B	PRL 86 770	E.M. Aitala *et al.*	(FNAL E791 Collab.)
LINK	01C	PRL 87 162001	J.M. Link *et al.*	(FNAL FOCUS Collab.)
ABREU	00O	EPJ C12 209	P. Abreu *et al.*	(DELPHI Collab.)
ASTIER	00D	PL B486 35	P. Astier *et al.*	(CERN NOMAD Collab.)
JUN	00	PRL 84 1857	S.Y. Jun *et al.*	(FNAL SELEX Collab.)
LINK	00B	PL B491 232	J.M. Link *et al.*	(FNAL FOCUS Collab.)
Also		PL B495 443 (errat)	J.M. Link *et al.*	(FNAL FOCUS Collab.)
ABBIENDI	99K	EPJ C8 573	G. Abbiendi *et al.*	(OPAL Collab.)
ADAMOVICH	99	EPJ C6 35	M. Adamovich *et al.*	(CERN BEATRICE Collab.)
AITALA	99G	PL B462 401	E.M. Aitala *et al.*	(FNAL E791 Collab.)
BONVICINI	99	PRL 82 4586	G. Bonvicini *et al.*	(CLEO Collab.)
AITALA	98B	PRL 80 1393	E.M. Aitala *et al.*	(FNAL E791 Collab.)
AITALA	98C	PL B421 405	E.M. Aitala *et al.*	(FNAL E791 Collab.)
AITALA	98F	PL B440 435	E.M. Aitala *et al.*	(FNAL E791 Collab.)
BAI	98B	PL B429 188	J.Z. Bai *et al.*	(BEPC BES Collab.)
AITALA	97	PL B397 325	E.M. Aitala *et al.*	(FNAL E791 Collab.)
AITALA	97B	PL B403 377	E.M. Aitala *et al.*	(FNAL E791 Collab.)
AITALA	97C	PL B404 187	E.M. Aitala *et al.*	(FNAL E791 Collab.)
BISHAI	97	PRL 78 3261	M. Bishai *et al.*	(CLEO Collab.)
FRABETTI	97	PL B391 235	P.L. Frabetti *et al.*	(FNAL E687 Collab.)
FRABETTI	97B	PL B398 239	P.L. Frabetti *et al.*	(FNAL E687 Collab.)
FRABETTI	97C	PL B401 131	P.L. Frabetti *et al.*	(FNAL E687 Collab.)
FRABETTI	97D	PL B407 79	P.L. Frabetti *et al.*	(FNAL E687 Collab.)
AITALA	96	PRL 76 364	E.M. Aitala *et al.*	(FNAL E791 Collab.)
FRABETTI	95	PL B346 199	P.L. Frabetti *et al.*	(FNAL E687 Collab.)
FRABETTI	95B	PL B351 591	P.L. Frabetti *et al.*	(FNAL E687 Collab.)
FRABETTI	95E	PL B359 403	P.L. Frabetti *et al.*	(FNAL E687 Collab.)
KODAMA	95	PL B345 85	K. Kodama *et al.*	(FNAL E653 Collab.)
ALBRECHT	94I	ZPHY C64 375	H. Albrecht *et al.*	(ARGUS Collab.)
BALEST	94	PRL 72 2328	R. Balest *et al.*	(CLEO Collab.)
FRABETTI	94D	PL B323 459	P.L. Frabetti *et al.*	(FNAL E687 Collab.)
FRABETTI	94G	PL B331 217	P.L. Frabetti *et al.*	(FNAL E687 Collab.)
FRABETTI	94I	PR D50 R2953	P.L. Frabetti *et al.*	(FNAL E687 Collab.)
AKERIB	93	PRL 71 3070	D.S. Akerib *et al.*	(CLEO Collab.)
ANJOS	93	PR D48 56	J.C. Anjos *et al.*	(FNAL E691 Collab.)
FRABETTI	93E	PL B307 262	P.L. Frabetti *et al.*	(FNAL E687 Collab.)
ALBRECHT	92F	PL B278 202	H. Albrecht *et al.*	(ARGUS Collab.)
ANJOS	92C	PR D46 1941	J.C. Anjos *et al.*	(FNAL E691 Collab.)
BARLAG	92C	ZPHY C55 383	S. Barlag *et al.*	(ACCMOR Collab.)
Also		ZPHY C48 29	S. Barlag *et al.*	(ACCMOR Collab.)
COFFMAN	92B	PR D45 2196	D.M. Coffman *et al.*	(Mark III Collab.)
DAOUDI	92	PR D45 3965	M. Daoudi *et al.*	(CLEO Collab.)
KODAMA	92	PL B274 246	K. Kodama *et al.*	(FNAL E653 Collab.)
KODAMA	92C	PL B286 187	K. Kodama *et al.*	(FNAL E653 Collab.)
ADAMOVICH	91	PL B268 142	M.I. Adamovich *et al.*	(WA82 Collab.)
ALBRECHT	91	PL B255 634	H. Albrecht *et al.*	(ARGUS Collab.)
ALVAREZ	91B	ZPHY C50 11	M.P. Alvarez *et al.*	(CERN NA14/2 Collab.)
AMMAR	91	PR D44 3383	R. Ammar *et al.*	(CLEO Collab.)
BAI	91	PRL 66 1011	Z. Bai *et al.*	(Mark III Collab.)
COFFMAN	91	PL B263 135	D.M. Coffman *et al.*	(Mark III Collab.)
FRABETTI	91	PL B263 584	P.L. Frabetti *et al.*	(FNAL E687 Collab.)
ALVAREZ	90	ZPHY C47 539	M.P. Alvarez *et al.*	(CERN NA14/2 Collab.)
ANJOS	90C	PR D41 2705	J.C. Anjos *et al.*	(FNAL E691 Collab.)
ANJOS	90D	PR D42 2414	J.C. Anjos *et al.*	(FNAL E691 Collab.)
ANJOS	90E	PRL 65 2630	J.C. Anjos *et al.*	(FNAL E691 Collab.)
BARLAG	90C	ZPHY C46 563	S. Barlag *et al.*	(ACCMOR Collab.)
WEIR	90B	PR D41 1384	A.J. Weir *et al.*	(Mark II Collab.)
ANJOS	89	PRL 62 125	J.C. Anjos *et al.*	(FNAL E691 Collab.)
ANJOS	89B	PRL 62 722	J.C. Anjos *et al.*	(FNAL E691 Collab.)
ANJOS	89E	PL B223 267	J.C. Anjos *et al.*	(FNAL E691 Collab.)
ADLER	88C	PRL 60 89	J. Adler *et al.*	(Mark III Collab.)
ALBRECHT	88I	PL B210 267	H. Albrecht *et al.*	(ARGUS Collab.)
HAAS	88	PRL 60 1614	P. Haas *et al.*	(CLEO Collab.)
ONG	88	PRL 60 2587	R.A. Ong *et al.*	(Mark II Collab.)
RAAB	88	PR D37 2391	J.R. Raab *et al.*	(FNAL E691 Collab.)
ADAMOVICH	87	EPL 4 887	M.I. Adamovich *et al.*	(Photon Emulsion Collab.)
ADLER	87	PL B196 107	J. Adler *et al.*	(Mark III Collab.)
BARTEL	87	ZPHY C33 339	W. Bartel *et al.*	(JADE Collab.)
BALTRUSAIT...	86E	PRL 56 2140	R.M. Baltrusaitis *et al.*	(Mark III Collab.)
BALTRUSAIT...	85B	PRL 54 1976	R.M. Baltrusaitis *et al.*	(Mark III Collab.)
BALTRUSAIT...	85E	PRL 55 150	R.M. Baltrusaitis *et al.*	(Mark III Collab.)
BARTEL	85J	PL 163B 277	W. Bartel *et al.*	(JADE Collab.)
ADAMOVICH	84	PL 140B 119	M.I. Adamovich *et al.*	(CERN WA58 Collab.)
ALTHOFF	84G	ZPHY C22 219	M. Althoff *et al.*	(TASSO Collab.)
DERRICK	84	PRL 53 1971	M. Derrick *et al.*	(HRS Collab.)
SCHINDLER	81	PR D24 78	R.H. Schindler *et al.*	(Mark II Collab.)
TRILLING	81	PRPL 75 57	G.H. Trilling	(LBL, UCB) J
ZHOLENTZ	80	PL 96B 214	A.A. Zholents *et al.*	(NOVO)
Also		SJNP 34 814 Translated from YAF 34 1471.	A.A. Zholents *et al.*	(NOVO)
GOLDHABER	77	PL 69B 503	G. Goldhaber *et al.*	(Mark I Collab.)
PERUZZI	77	PRL 39 1301	I. Peruzzi *et al.*	(LGW Collab.)
PICCOLO	77	PL 70B 260	M. Piccolo *et al.*	(Mark I Collab.)
PERUZZI	76	PRL 37 569	I. Peruzzi *et al.*	(Mark I Collab.)

OTHER RELATED PAPERS

RICHMAN	95	RMP 67 893	J.D. Richman, P.R. Burchat	(UCSB, STAN)
ROSNER	95	CNPP 21 369	J. Rosner	(CHIC)

D^0

$I(J^P) = \frac{1}{2}(0^-)$

D^0 MASS

The fit includes $D^{\pm}$, D^0, $D_s^{\pm}$, $D^{*\pm}$, D^{*0}, $D_s^{*\pm}$, $D_1(2420)^0$, $D_2^*(2460)^0$, and $D_{s1}(2536)^{\pm}$ mass and mass difference measurements.

VALUE (MeV)	*EVTS*	*DOCUMENT ID*		*TECN*	*COMMENT*
1864.84 ± 0.07 OUR FIT Error includes scale factor of 1.1.					
1864.84 ± 0.07 OUR AVERAGE					
1864.75 ± 0.15 ±0.11		AAIJ	13V	LHCB	$D^0 \to K^+2K^-\pi^+$
1864.841± 0.048±0.063	4.3k	[1] LEES	13S	BABR	e^+e^- at $\Upsilon(4S)$
1865.30 ± 0.33 ±0.23	98 ± 13	ANASHIN	10A	KEDR	e^+e^- at $\psi(3770)$
1864.847± 0.150±0.095	319 ± 18	CAWLFIELD	07	CLEO	$D^0 \to K^0_S\phi$
• • • We do not use the following data for averages, fits, limits, etc. • • •					
1864.6 ± 0.3 ±1.0	641	BARLAG	90C	ACCM	π^- Cu 230 GeV
1852 ± 7	16	ADAMOVICH	87	EMUL	Photoproduction
1856 ±36	22	ADAMOVICH	84B	EMUL	Photoproduction
1861 ± 4		DERRICK	84	HRS	e^+e^- 29 GeV
1847 ± 7	1	FIORINO	81	EMUL	$\gamma N \to \overline{D}^0 +$
1863.8 ± 0.5		[2] SCHINDLER	81	MRK2	e^+e^- 3.77 GeV
1864.7 ± 0.6		[2] TRILLING	81	RVUE	e^+e^- 3.77 GeV
1863.0 ± 2.5	238	ASTON	80E	OMEG	$\gamma p \to \overline{D}^0$
1860 ± 2	143	[3] AVERY	80	SPEC	$\gamma N \to D^{*+}$
1869 ± 4	35	[3] AVERY	80	SPEC	$\gamma N \to D^{*+}$
1854 ± 6	94	[3] ATIYA	79	SPEC	$\gamma N \to D^0\overline{D}^0$
1850 ±15	64	BALTAY	78C	HBC	$\nu N \to K^0\pi\pi$
1863 ± 3		GOLDHABER	77	MRK1	D^0, D^+ recoil spectra
1863.3 ± 0.9		[2] PERUZZI	77	LGW	e^+e^- 3.77 GeV
1868 ±11		PICCOLO	77	MRK1	e^+e^- 4.03, 4.41 GeV
1865 ±15	234	GOLDHABER	76	MRK1	$K\pi$ and $K3\pi$

[1] The largest source of error in the LEES 13S value is from the uncertainty of the K^+ mass. The quoted systematic error is in fact $\pm 0.043 + 3\,(m_{K^+} - 493.677)$, in MeV.

[2] PERUZZI 77 and SCHINDLER 81 errors do not include the 0.13% uncertainty in the absolute SPEAR energy calibration. TRILLING 81 uses the high precision $J/\psi(1S)$ and $\psi(2S)$ measurements of ZHOLENTZ 80 to determine this uncertainty and combines the PERUZZI 77 and SCHINDLER 81 results to obtain the value quoted. TRILLING 81

enters the fit in the $D^\pm$ mass, and PERUZZI 77 and SCHINDLER 81 enter in the $m_{D^\pm} - m_{D^0}$, below.

[3] Error does not include possible systematic mass scale shift, estimated to be less than 5 MeV.

$m_{D^\pm} - m_{D^0}$

The fit includes $D^\pm$, D^0, $D_s^\pm$, $D^{*\pm}$, D^{*0}, $D_s^{*\pm}$, $D_1(2420)^0$, $D_2^*(2460)^0$, and $D_{s1}(2536)^\pm$ mass and mass difference measurements.

VALUE (MeV)	DOCUMENT ID		TECN	COMMENT
4.77±0.08 OUR FIT				
4.76±0.12 OUR AVERAGE				
4.76±0.12±0.07	AAIJ	13V	LHCB	$D^+ \to K^+K^-\pi^+$
4.7 ±0.3	[1] SCHINDLER	81	MRK2	e^+e^- 3.77 GeV
5.0 ±0.8	[1] PERUZZI	77	LGW	e^+e^- 3.77 GeV

[1] See the footnote on TRILLING 81 in the D^0 and $D^\pm$ sections on the mass.

D^0 MEAN LIFE

Measurements with an error $> 10 \times 10^{-15}$ s have been omitted from the average.

VALUE (10^{-15} s)	EVTS	DOCUMENT ID		TECN	COMMENT
410.1± 1.5 OUR AVERAGE					
409.6± 1.1± 1.5	210k	LINK	02F	FOCS	γ nucleus, $\approx$ 180 GeV
407.9± 6.0± 4.3	10k	KUSHNIR...	01	SELX	$K^-\pi^+$, $K^-\pi^+\pi^+\pi^-$
413 ± 3 ± 4	35k	AITALA	99E	E791	$K^-\pi^+$
408.5± 4.1$^{+\ 3.5}_{-\ 3.4}$	25k	BONVICINI	99	CLE2	$e^+e^- \approx \Upsilon(4S)$
413 ± 4 ± 3	16k	FRABETTI	94D	E687	$K^-\pi^+$, $K^-\pi^+\pi^+\pi^-$
• • • We do not use the following data for averages, fits, limits, etc. • • •					
424 ±11 ± 7	5118	FRABETTI	91	E687	$K^-\pi^+$, $K^-\pi^+\pi^+\pi^-$
417 ±18 ±15	890	ALVAREZ	90	NA14	$K^-\pi^+$, $K^-\pi^+\pi^+\pi^-$
388 $^{+23}_{-21}$	641	[1] BARLAG	90C	ACCM	π^- Cu 230 GeV
480 ±40 ±30	776	ALBRECHT	88I	ARG	e^+e^- 10 GeV
422 ± 8 ±10	4212	RAAB	88	E691	Photoproduction
420 ±50	90	BARLAG	87B	ACCM	K^- and π^- 200 GeV

[1] BARLAG 90C estimate systematic error to be negligible.

D^0–$\overline{D}^0$ MIXING

Revised May 2014 by D. M. Asner (Pacific Northwest National Laboratory)

The detailed formalism for $D^0 - \overline{D}^0$ mixing is presented in the note on "CP Violation in Meson Decays" in this *Review*. For completeness, we present an overview here. The time evolution of the D^0–$\overline{D}^0$ system is described by the Schrödinger equation

$$i\frac{\partial}{\partial t}\left(\begin{array}{c} D^0(t) \\ \overline{D}^0(t) \end{array}\right) = \left(\mathbf{M} - \tfrac{i}{2}\mathbf{\Gamma}\right)\left(\begin{array}{c} D^0(t) \\ \overline{D}^0(t) \end{array}\right), \quad (1)$$

where the $\mathbf{M}$ and $\mathbf{\Gamma}$ matrices are Hermitian, and CPT invariance requires that $M_{11} = M_{22} \equiv M$ and $\Gamma_{11} = \Gamma_{22} \equiv \Gamma$. The off-diagonal elements of these matrices describe the dispersive and absorptive parts of the mixing.

Because CP violation is expected to be quite small here, it is convenient to label the mass eigenstates by the CP quantum number in the limit of CP conservation. Thus, we write

$$|D_{1,2}\rangle = p|D^0\rangle \pm q|\overline{D}^0\rangle\,, \quad (2)$$

where

$$\left(\frac{q}{p}\right)^2 = \frac{M_{12}^* - \frac{i}{2}\Gamma_{12}^*}{M_{12} - \frac{i}{2}\Gamma_{12}}\,. \quad (3)$$

The normalization condition is $|p|^2 + |q|^2 = 1$. Our phase convention is $CP|D^0\rangle = +|\overline{D}^0\rangle$, and the sign is chosen so that D_1 has CP even, or nearly so.

The corresponding eigenvalues are

$$\omega_{1,2} \equiv m_{1,2} - \tfrac{i}{2}\Gamma_{1,2} = \left(M - \tfrac{i}{2}\Gamma\right) \pm \frac{q}{p}\left(M_{12} - \tfrac{i}{2}\Gamma_{12}\right), \quad (4)$$

where $m_{1,2}$ and $\Gamma_{1,2}$ are the masses and widths of the $D_{1,2}$.

We define dimensionless mixing parameters x and y by

$$x \equiv (m_1 - m_2)/\Gamma = \Delta m/\Gamma \quad (5)$$

and

$$y \equiv (\Gamma_1 - \Gamma_2)/2\Gamma = \Delta\Gamma/2\Gamma\,, \quad (6)$$

where $\Gamma \equiv (\Gamma_1 + \Gamma_2)/2$. If CP is conserved, then M_{12} and Γ_{12} are real, $\Delta m = 2M_{12}$, $\Delta\Gamma = 2\Gamma_{12}$, and $p = q = 1/\sqrt{2}$. The signs of Δm and $\Delta\Gamma$ are to be determined experimentally.

The parameters x and y are measured in several ways. The most precise values are obtained using the time dependence of D decays. Since D^0–$\overline{D}^0$ mixing is a small effect, the identifying tag of the initial particle as a D^0 or a $\overline{D}^0$ must be extremely accurate. The usual tag is the charge of the distinctive slow pion in the decay sequence $D^{*+} \to D^0\pi^+$ or $D^{*-} \to \overline{D}^0\pi^-$. In current experiments, the probability of mistagging is about 0.1%. The large data samples produced at the B-factories allow the production flavor to also be determined by fully reconstructing charm on the "other side" of the event—significantly reducing the mistag rate [1]. Another tag of comparable accuracy is identification of one of the D's produced from $\psi(3770) \to D^0\overline{D}^0$ decays. Although time-dependent analyses are not possible at symmetric charm-threshold facilities (the D^0 and $\overline{D}^0$ do not travel far enough), the quantum-coherent $C = -1$ $\psi(3770) \to D^0\overline{D}^0$ state provides time-integrated sensitivity [2,3].

Time-Dependent Analyses: We extend the formalism of this *Review*'s note on "CP Violation in Meson Decays." In addition to the "right-sign" instantaneous decay amplitudes $\overline{A}_f \equiv \langle f|H|\overline{D}^0\rangle$ and $A_{\overline{f}} \equiv \langle\overline{f}|H|D^0\rangle$ for final states $f = K^+\pi^-, ...$ and their CP conjugate $\overline{f} = K^-\pi^+, ...$, we include "wrong-sign" amplitudes $\overline{A}_{\overline{f}} \equiv \langle\overline{f}|H|\overline{D}^0\rangle$ and $A_f \equiv \langle f|H|D^0\rangle$.

It is conventional to normalize the wrong-sign decay distributions to the integrated rate of right-sign decays and to express time in units of the precisely measured neutral D-meson mean lifetime, $\tau_{D^0} = 1/\Gamma = 2/(\Gamma_1 + \Gamma_2)$. Starting from a pure $|D^0\rangle$ or $|\overline{D}^0\rangle$ state at $t = 0$, the time-dependent rates of decay to wrong-sign final states relative to the integrated right-sign decay rates are, to leading order:

$$r(t) \equiv \frac{\left|\langle f|H|D^0(t)\rangle\right|^2}{\left|\overline{A}_f\right|^2} = \left|\frac{q}{p}\right|^2 \left|g_+(t)\,\lambda_f^{-1} + g_-(t)\right|^2, \quad (7)$$

and

$$\overline{r}(t) \equiv \frac{\left|\langle\overline{f}|H|\overline{D}^0(t)\rangle\right|^2}{\left|A_{\overline{f}}\right|^2} = \left|\frac{p}{q}\right|^2 \left|g_+(t)\,\lambda_{\overline{f}} + g_-(t)\right|^2. \quad (8)$$

where

$$\lambda_f \equiv q\overline{A}_f/pA_f\,, \quad \lambda_{\bar{f}} \equiv q\overline{A}_{\bar{f}}/pA_{\bar{f}}\,, \quad (9)$$

and

$$g_\pm(t) = \frac{1}{2}\left(e^{-iz_1t} \pm e^{-iz_2t}\right), \quad z_{1,2} = \frac{\omega_{1,2}}{\Gamma}\,. \quad (10)$$

Note that a change in the convention for the relative phase of D^0 and $\overline{D}^0$ would cancel between q/p and $\overline{A}_f/A_f$ and leave

λ_f unchanged. We expand $r(t)$ and $\overline{r}(t)$ to second order in x and y for modes in which the ratio of decay amplitudes, $R_D = |A_f/\overline{A}_f|^2$, is very small.

Semileptonic decays: Consider the final state $f = K^+\ell^-\bar{\nu}_\ell$, where $A_f = \overline{A}_{\overline{f}} = 0$ in the Standard Model. The final state f is only accessible through mixing and $r(t)$ is

$$r(t) = |g_-(t)|^2 \left|\frac{q}{p}\right|^2 \approx \frac{e^{-t}}{4}(x^2+y^2)\,t^2 \left|\frac{q}{p}\right|^2 . \qquad (11)$$

For $\overline{r}(t)$ q/p is replaced by p/q. In the Standard Model, CP violation in charm mixing is small and $|q/p| \approx 1$. In the limit of CP conservation, $r(t) = \overline{r}(t)$, and the time-integrated mixing rate relative to the time-integrated right-sign decay rate for semileptonic decays is

$$R_M = \int_0^\infty r(t)dt = \left|\frac{q}{p}\right|^2 \frac{x^2+y^2}{2+x^2-y^2} \approx \frac{1}{2}(x^2+y^2) . \qquad (12)$$

Table 1: Results for R_M in D^0 semileptonic decays.

Year	Exper.	Final state(s)	R_M ($\times 10^{-3}$)	90% C.L.
2008	Belle [4]	$K^{(*)+}e^-\overline{\nu}_e$	$0.13\pm0.22\pm0.20$	$< 0.61 \times 10^{-3}$
2007	BaBar [1]	$K^{(*)+}e^-\overline{\nu}_e$	$0.04^{+0.70}_{-0.60}$	$(-1.3, 1.2) \times 10^{-3}$
2005*	Belle [5]	$K^{(*)+}e^-\overline{\nu}_e$	$0.02\pm0.47\pm0.14$	$< 1.0 \times 10^{-3}$
2005	CLEO [6]	$K^{(*)+}e^-\overline{\nu}_e$	$1.6\pm2.9\pm2.9$	$< 7.8 \times 10^{-3}$
2004*	BaBar [7]	$K^{(*)+}e^-\overline{\nu}_e$	$2.3\pm1.2\pm0.4$	$< 4.2 \times 10^{-3}$
2002*	FOCUS [8]	$K^+\mu^-\overline{\nu}_\mu$	$-0.76^{+0.99}_{-0.93}$	$< 1.01 \times 10^{-3}$
1996	E791 [9]	$K^+\ell^-\overline{\nu}_\ell$	$(1.1^{+3.0}_{-2.7}) \times 10^{-3}$	$< 5.0 \times 10^{-3}$
	HFAG [10]		0.13 ± 0.27	

*These measurements are excluded from the HFAG average. The FOCUS result is unpublished, the statistical correlation of the BaBar result with Ref. 1 has not been established, and the Belle result is superseded by Ref. 4.

Table 1 summarizes results for R_M from semileptonic decays; the world average from the Heavy Flavor Averaging Group (HFAG) [10] is $R_M = (1.30 \pm 2.69) \times 10^{-4}$.

Wrong-sign decays to hadronic non-CP eigenstates: Consider the final state $f = K^+\pi^-$, where A_f is doubly Cabibbo-suppressed. The ratio of decay amplitudes is

$$\frac{A_f}{\overline{A}_f} = -\sqrt{R_D}\,e^{-i\delta_f}, \quad \left|\frac{A_f}{\overline{A}_f}\right| \sim O(\tan^2\theta_c) , \qquad (13)$$

where R_D is the doubly Cabibbo-suppressed (DCS) decay rate relative to the Cabibbo-favored (CF) rate, δ_f is the strong phase difference between DCS and CF processes, and θ_c is the Cabibbo angle. The minus sign originates from the sign of V_{us} relative to V_{cd}.

We characterize the violation of CP with the real-valued parameters A_M, A_D, and ϕ. We adopt the parametrization (see Refs. 11 and 12)

$$\left|\frac{q}{p}\right|^2 = \sqrt{\frac{1+A_M}{1-A_M}}, \qquad (14)$$

$$\lambda_f^{-1} \equiv \frac{pA_f}{q\overline{A}_f} = -\sqrt{R_D}\left(\frac{(1+A_D)(1-A_M)}{(1-A_D)(1+A_M)}\right)^{1/4} e^{-i(\delta_f+\phi)} , \qquad (15)$$

$$\lambda_{\overline{f}} \equiv \frac{q\overline{A}_{\overline{f}}}{pA_{\overline{f}}} = -\sqrt{R_D}\left(\frac{(1-A_D)(1+A_M)}{(1+A_D)(1-A_M)}\right)^{1/4} e^{-i(\delta_f-\phi)} , \qquad (16)$$

and A_D is a measure of direct CP violation, while A_M is a measure of CP violation in mixing. From these relations, we obtain

$$\sqrt{\frac{1+A_D}{1-A_D}} = \frac{|A_f/\overline{A}_f|}{|\overline{A}_{\overline{f}}/A_{\overline{f}}|} , \qquad (17)$$

The angle ϕ measures CP violation in interference between mixing and decay. While A_M is independent of the decay process, A_D and ϕ, in general, depend on f.

In general, $\lambda_{\overline{f}}$ and λ_f^{-1} are independent complex numbers. More detail on CP violation in meson decays can be found in Ref. 13. To leading order, for A_D and $A_M \ll 1$,

$$r(t) = e^{-t}\left[R_D(1+A_D) + \sqrt{R_D(1+A_M)(1+A_D)}\,y'_-t + \frac{1}{2}(1+A_M)R_M\,t^2\right] \qquad (18)$$

and

$$\overline{r}(t) = e^{-t}\left[R_D(1-A_D) + \sqrt{R_D(1-A_M)(1-A_D)}\,y'_+t + \frac{1}{2}(1-A_M)R_M\,t^2\right] \qquad (19)$$

Here

$$y'_\pm \equiv y'\cos\phi \pm x'\sin\phi = y\cos(\delta_{K\pi} \mp \phi) - x\sin(\delta_{K\pi} \mp \phi) , \qquad (20)$$

where

$$x' \equiv x\cos\delta_{K\pi} + y\sin\delta_{K\pi},$$
$$y' \equiv y\cos\delta_{K\pi} - x\sin\delta_{K\pi} , \qquad (21)$$

and $R_M = \left(x^2+y^2\right)/2 = \left(x'^2+y'^2\right)/2$ is the mixing rate relative to the time-integrated Cabibbo-favored rate.

The three terms in Eq. (18) and Eq. (19) probe the three fundamental types of CP violation. In the limit of CP conservation, A_M, A_D, and ϕ are all zero. Then

$$r(t) = \overline{r}(t) = e^{-t}\left(R_D + \sqrt{R_D}\,y't + \frac{1}{2}R_M\,t^2\right) , \qquad (22)$$

and the time-integrated wrong-sign rate relative to the integrated right-sign rate is

$$R = \int_0^\infty r(t)\,dt = R_D + \sqrt{R_D}\,y' + R_M . \qquad (23)$$

The ratio R is the most readily accessible experimental quantity. In Table 2 are reported the measurements of R, R_D and A_D in $D^0 \to K^+\pi^-$, and their HFAG average [24] from a general fit; that allows for both mixing and CP violation. Typically, the fit parameters are R_D, x'^2, and y'. Table 3 summarizes the results for x'^2 and y'. Allowing for CP violation, the separate contributions to R can be extracted by fitting the $D^0 \to K^+\pi^-$ and $\overline{D}^0 \to K^-\pi^+$ decay rates.

Table 2: Results for R, R_D, and A_D in $D^0 \to K^+\pi^-$.

Year	Exper.	$R(\times 10^{-3})$	$R_D(\times 10^{-3})$	$A_D(\%)$
2014	Belle [14]	3.86±0.06	3.53±0.13	—
2013	LHCb [15]	—	3.57±0.07	−0.7±1.9
2013	CDF [16]	4.30±0.05	3.51±0.35	—
2012*	LHCb [17]	4.25±0.04	3.52±0.15	—
2007*	CDF [18]	4.15±0.10	3.04±0.55	—
2007	BaBar [19]	3.53±0.08±0.04	3.03±0.16±0.10	−2.1±5.2±1.5
2006*	Belle [20]	3.77±0.08±0.05	3.64±0.17	2.3±4.7
2005†	FOCUS [21]	$4.29^{+0.63}_{-0.61}\pm 0.28$	$5.17^{+1.47}_{-1.58}\pm 0.76$	$13^{+33}_{-25}\pm 10$
2000†	CLEO [22]	$3.32^{+0.63}_{-0.65}\pm 0.40$	4.8±1.2±0.4	$-1^{+16}_{-17}\pm 1$
1998†	E791 [23]	$6.8^{+3.4}_{-3.3}\pm 0.7$	—	—
	Average	4.13±0.03	3.49±0.04 [24]	−0.90±1.00 [24]

*These measurements are excluded from the HFAG average of R_D. The CDF result is superseded by Ref. 16 and the LHCb is superseded by Ref. 15. The LHCb result is included in the average of R. The Belle result for R and R_D is superseded by Ref. 14.

†These measurements are excluded from the HFAG average due to poor precision.

Table 3: Results on the time-dependence of $r(t)$ in $D^0 \to K^+\pi^-$ and $\overline{D}^0 \to K^-\pi^+$ decays. The Belle 2014, LHCb and CDF results assume no CP violation. The FOCUS, CLEO, and Belle 2006 results restrict x'^2 to the physical region. The confidence intervals from FOCUS, CLEO, and BaBar are obtained from the fit, whereas Belle uses a Feldman-Cousins method, and CDF uses a Bayesian method.

Year	Exper.	y' (%)	x'^2 $(\times 10^{-3})$
2014*†	Belle [14]	0.46±0.34	0.09±0.22
2013	LHCb [15]	0.48±0.10	0.055±0.049
2013	CDF [16]	0.43±0.43	0.08±0.18
2012*	LHCb [17]	0.72±0.24	−0.09±0.13
2007*	CDF [18]	0.85±0.76	−0.12±0.35
2007	BaBar [19]	0.97±0.44±0.31	−0.22±0.30±0.21
2006†	Belle [20]	$-2.8 < y' < 2.1$	< 0.72 (95% C.L.)
2005*	FOCUS [21]	$-11.2 < y' < 6.7$	< 8.0 (95% C.L.)
2000*	CLEO [22]	$-5.8 < y' < 1.0$	< 0.81 (95% C.L.)

*These measurements are excluded from the HFAG average. The CDF result is superseded by Ref. 16 and the LHCb result has been superseded by Ref. 15. The CLEO and FOCUS results are excluded due to poor precision.

† This Belle rseult allows for CP violation. HFAG uses this result for the CP-violation allowed fit. This result is not superseded by Ref. 14.

*† This Belle result does not allow for CP violation. HFAG uses this result for the CP-conserving fit. This result does not supersede Ref. 20.

Extraction of the mixing parameters x and y from the results in Table 3 requires knowledge of the relative strong phase $\delta_{K\pi}$. An interference effect that provides useful sensitivity to $\delta_{K\pi}$ arises in the decay chain $\psi(3770)\to D^0\overline{D}^0\to(f_{CP})(K^+\pi^-)$, where f_{CP} denotes a CP-even or -odd eigenstate from D^0 decay, such as K^+K^- or $K^0_S\pi^0$, respectively [27]. Here, the amplitude relation

$$\sqrt{2}\,A(D_\pm \to K^-\pi^+) = A(D^0 \to K^-\pi^+) \pm A(\overline{D}^0 \to K^-\pi^+). \quad (24)$$

where $D_\pm$ denotes a CP-even or -odd eigenstate, implies that

$$\cos\delta_{K\pi} = \frac{|A(D_+ \to K^-\pi^+)|^2 - |A(D_- \to K^-\pi^+)|^2}{2\sqrt{R_D}\,|A(D^0 \to K^-\pi^+)|^2}. \quad (25)$$

This neglects CP violation and uses $\sqrt{R_D} \ll 1$.

For multibody final states, Eqs. (13)–(23) apply separately to each point in phase-space. Although x and y do not vary across the space, knowledge of the resonant substructure is needed to extrapolate the strong phase difference δ from point to point to determine x and y.

A time-dependent analysis of the process $D^0 \to K^+\pi^-\pi^0$ from BaBar [25,26] determines the *relative* strong phase variation across the Dalitz plot and reports $x'' = (2.61^{+0.57}_{-0.68}\pm 0.39)\%$, and $y'' = (-0.06^{+0.55}_{-0.64}\pm 0.34)\%$, where x'' and y'' are defined as

$$x'' \equiv x\cos\delta_{K\pi\pi^0} + y\sin\delta_{K\pi\pi^0}\,,$$
$$y'' \equiv y\cos\delta_{K\pi\pi^0} - x\sin\delta_{K\pi\pi^0}, \quad (26)$$

in parallel to x', y', and $\delta_{K\pi}$ of Eq. (21). Here $\delta_{K\pi\pi^0}$ is the remaining strong phase difference between the DCS $D^0 \to K^+\rho^-$ and the CF $\overline{D}^0 \to K^+\rho^-$ amplitudes and does not vary across the Dalitz plot. Both strong phases, $\delta_{K\pi}$ and $\delta_{K\pi\pi^0}$, can be determined from time-integrated CP asymmetries in correlated $D^0\overline{D}^0$ produced at the $\psi(3770)$ [27,28].

Both the sign and magnitude of x and y without phase or sign ambiguity may be measured using the time-dependent resonant substructure of multibody D^0 decays [29,30]. In $D^0 \to K^0_S\pi^+\pi^-$, the DCS and CF decay amplitudes populate the same Dalitz plot, which allows direct measurement of the relative strong phases. CLEO [31], Belle [30], and BaBar [32] have measured the relative phase between $D^0 \to K^*(892)^-\pi^+$ and $D^0 \to K^*(892)^+\pi^-$ to be $(189 \pm 10 \pm 3^{+15}_{-5})^\circ$, $(171.9 \pm 1.3$ (stat. only))°, and (177.6±1.1 (stat. only))°, respectively. These results are close to the 180° expected from Cabibbo factors and a small strong phase. Table 4 summarizes the results of a time-dependent Dalitz-plot analyses.

In addition, Belle [30] has results for both the relative phase (statistical errors only) and ratio R (central values only) of the DCS fit fraction relative to the CF fit fractions for $K^*(892)^+\pi^-$, $K^*_0(1430)^+\pi^-$, $K^*_2(1430)^+\pi^-$, $K^*(1410)^+\pi^-$, and $K^*(1680)^+\pi^-$. The systematic uncertainties on R must be evaluated. The values for R in units of $\tan^4\theta_c$ are 2.94 ± 0.12, 22.0 ± 1.6, 34 ± 4, 87 ± 13, and 500 ± 500, respectively. For $K^+\pi^-$, the corresponding value for R_D is $(1.28\pm 0.02)\times\tan^4\theta_c$. Similarly, BaBar [32–35] has reported central values for R for

Table 4: Results from time-dependent Dalitz-plot analysis of $D^0 \to K^0_S\pi^+\pi^-$ (CLEO and Belle) and $D^0 \to K^0_S\pi^+\pi^-, K^0_S K^+K^-$ (BaBar). The errors are statistical, experimental systematic, and decay-model systematic, respectively.

No CP Violation			
Year	Exper.	$x\ \times 10^{-3}$	$y\ \times 10^{-3}$
2010	BaBar [32]	$1.6\pm2.3\pm1.2\pm0.8$	$5.7\pm2.0\pm1.3\pm0.7$
2007	Belle [30]	$8.0 \pm 2.9\,^{+0.9\ +1.0}_{-0.7\ -1.4}$	$3.3 \pm 2.4\,^{+0.8\ +0.6}_{-1.2\ -0.8}$
2005	CLEO [29]	$19\,^{+32}_{-33} \pm 4 \pm 4$	$-14 \pm 24 \pm 8 \pm 4$
	HFAG [33]	4.2 ± 2.1	4.6 ± 1.9
With CP Violation			
Year	Exper.	$\lvert q/p\rvert$	ϕ
2007	Belle [30]	$0.86\,^{+0.30\ +0.06}_{-0.29\ -0.03} \pm 0.08$	$(-14\,^{+16\ +5\ +2}_{-18\ -3\ -4})^\circ$

$K^*(892)^+\pi^-$, $K^*_0(1430)^+\pi^-$, and $K^*_2(1430)^+\pi^-$. The large differences in R among these final states could point to an interesting role for hadronic effects.

Decays to CP Eigenstates: When the final state f is a CP eigenstate, there is no distinction between f and $\overline{f}$, and $A_f = A_{\overline{f}}$ and $\overline{A}_{\overline{f}} = \overline{A}_f$. We denote final states with CP eigenvalues ±1 by $f_\pm$ and write $\lambda_\pm$ for $\lambda_{f_\pm}$.

The quantity y may be measured by comparing the rate for D^0 decays to non-CP eigenstates such as $K^-\pi^+$ with decays to CP eigenstates such as K^+K^- [12]. If decays to K^+K^- have a shorter effective lifetime than those to $K^-\pi^+$, y is positive.

In the limit of slow mixing ($x, y \ll 1$) and the absence of direct CP violation ($A_D = 0$), but allowing for small indirect CP violation ($|A_M|, |\phi| \ll 1$), we can write

$$\lambda_\pm = \left|\frac{q}{p}\right| e^{\pm i\phi} \ . \tag{27}$$

In this scenario, to a good approximation, the decay rates for states that are initially D^0 and $\overline{D}^0$ to a CP eigenstate have exponential time dependence:

$$r_\pm(t) \propto \exp\left(-t/\tau_\pm\right) \ , \tag{28}$$

$$\overline{r}_\pm(t) \propto \exp\left(-t/\overline{\tau}_\pm\right) \ , \tag{29}$$

where τ is measured in units of $1/\Gamma$.

The effective lifetimes are given by

$$1/\tau_\pm = 1 \pm \left|\frac{q}{p}\right| (y\cos\phi - x\sin\phi) \ , \tag{30}$$

$$1/\overline{\tau}_\pm = 1 \pm \left|\frac{p}{q}\right| (y\cos\phi + x\sin\phi) \ . \tag{31}$$

The effective decay rate to a CP eigenstate combining both D^0 and $\overline{D}^0$ decays is

$$r_\pm(t) + \overline{r}_\pm(t) \propto e^{-(1\pm y_{CP})t} \ . \tag{32}$$

Table 5: Results for y_{CP} from $D^0 \to K^+K^-$ and $\pi^+\pi^-$.

Year	Exper.	final state(s)	$y_{CP}(\%)$	$A_\Gamma(\times10^{-3})$
2013	LHCb [36]	K^+K^-	—	$-0.35\pm0.62\pm0.12$
2013	LHCb [36]	$\pi^+\pi^-$	—	$0.33\pm1.06\pm0.14$
2012*†	Belle [37]	K^+K^-,$\pi^+\pi^-$	$1.11\pm0.22\pm0.11$	$-0.3\pm2.0\pm0.8$
2012	BaBar [38]	K^+K^-,$\pi^+\pi^-$	$0.72\pm0.18\pm0.12$	$0.9\pm2.6\pm0.6$
2011	LHCb [39]	K^+K^-	$0.55\pm0.63\pm0.41$	$-5.9\pm5.9\pm2.1$
2009*	BaBar [40]	K^+K^-	$1.16\pm0.22\pm0.18$	—
2009	Belle [41]	$K^0_S K^+K^-$	$0.11\pm0.61\pm0.52$	—
2008*	BaBar [42]	K^+K^-,$\pi^+\pi^-$	$1.03\pm0.33\pm0.19$	$2.6\pm3.6\pm0.8$
2007†	Belle [43]	K^+K^-,$\pi^+\pi^-$	$1.31\pm0.32\pm0.25$	$0.1\pm3.0\pm1.5$
2003*	BaBar [44]	K^+K^-,$\pi^+\pi^-$	$0.8 \pm 0.4^{+0.5}_{-0.4}$	—
2001	CLEO [45]	K^+K^-,$\pi^+\pi^-$	$-1.2\pm2.5\pm1.4$	—
2001	Belle† [46]	K^+K^-	$-0.5\pm1.0^{+0.7}_{-0.8}$	—
2000	FOCUS [47]	K^+K^-	$3.42\pm1.39\pm0.74$	—
1999	E791 [48]	K^+K^-	$0.8\pm2.9\pm1.0$	—
	HFAG [24]		0.80 ± 0.18	-0.13 ± 0.53

*This measurement is included in the result reported by Ref. 38 and excluded from the HFAG average.

†This measurement is included in the result reported by Ref. 37.

*† This measurement is unpublished and excluded from the HFAG average.

Here

$$y_{CP} = \frac{1}{2}\left(\left|\frac{q}{p}\right| + \left|\frac{p}{q}\right|\right) y\cos\phi - \frac{1}{2}\left(\left|\frac{q}{p}\right| - \left|\frac{p}{q}\right|\right) x\sin\phi \tag{33}$$

$$\approx y\cos\phi - A_M x\sin\phi \ . \tag{34}$$

If CP is conserved, $y_{CP} = y$.

All measurements of y_{CP} are relative to the $D^0 \to K^-\pi^+$ decay rate. Table 5 summarizes the current status of measurements. Belle [37], BaBar [38], and LHCb [39] have reported y_{CP} and the decay-rate asymmetry for CP even final states (assuming $A_D = 0$)

$$A_\Gamma = \frac{\overline{\tau}_+ - \tau_+}{\overline{\tau}_+ + \tau_+} = \frac{(1/\tau_+) - (1/\overline{\tau}_+)}{(1/\tau_+) + (1/\overline{\tau}_+)} \tag{35}$$

$$= \frac{1}{2}\left(\left|\frac{q}{p}\right| - \left|\frac{p}{q}\right|\right) y\cos\phi - \frac{1}{2}\left(\left|\frac{q}{p}\right| + \left|\frac{p}{q}\right|\right) x\sin\phi \tag{36}$$

$$\approx A_M y\cos\phi - x\sin\phi \ . \tag{37}$$

Belle [41] has also reported y_{CP} for the final state $K^0_S K^+K^-$ which is dominated by the CP odd final state $K^0_S\phi$. If CP is conserved, $A_\Gamma = 0$.

Substantial work on the time-integrated CP asymmetries in decays to CP eigenstates are summarized in this *Review* [49]. Table 6 summarizes the current status of measurements of the difference in time-integrated CP asymmetry, $\Delta A_{CP} = A_K - A_\pi$, between $D^0 \to K^-K^+$ and $D^0 \to \pi^-\pi^+$. The HFAG fit is marginally consistent with no CP violation at the 0.3183% Confidence Level (2.95σ) [24].

Table 6: Results for the difference in time-integrated CP asymmetry ΔA_{CP} between $D^0 \to K^+K^-$ and $D^0 \to \pi^+\pi^-$.

Year	Exper.	$\Delta A_{CP}(\times 10^{-3})$
2014*	LHCb [50]	$1.4 \pm 1.6 \pm 0.8$
2013	LHCb [51]	$4.9 \pm 3.0 \pm 1.4$
2013*	LHCb [52]	$-3.4 \pm 1.5 \pm 1.0$
2012	LHCb [53]	$-8.2 \pm 2.1 \pm 1.1$
2013	CDF [54]	$-6.2 \pm 2.1 \pm 1.0$
2012*	Belle [37]	$-8.7 \pm 4.1 \pm 0.6$
2008	BaBar [55]	$2.4 \pm 6.2 \pm 2.6$
	HFAG [24]	-4.65 ± 1.37

*These measurements are unpublished and excluded from the HFAG average.

Coherent $D^0\overline{D}^0$ Analyses: Measurements of R_D, $\cos\delta_{K\pi}$, $\sin\delta_{K\pi}$, x, and y can be determined simultaneously from a combined fit to the time-integrated single-tag (ST) and double-tag (DT) yields in correlated $D^0\overline{D}^0$ produced at the $\psi(3770)$ [27,28].

Due to quantum correlations in the $C = -1$ and $C = +1$ $D^0\overline{D}^0$ pairs produced in the reactions $e^+e^- \to D^0\overline{D}^0(\pi^0)$ and $e^+e^- \to D^0\overline{D}^0\gamma(\pi^0)$, respectively, the time-integrated $D^0\overline{D}^0$ decay rates are sensitive to interference between amplitudes for indistinguishable final states. The size of this interference is governed by the relevant amplitude ratios and can include contributions from D^0–$\overline{D}^0$ mixing.

The following categories of final states are considered:

f or $\bar{f}$: Hadronic states accessed from either D^0 or $\overline{D}^0$ decay but that are not CP eigenstates. An example is $K^-\pi^+$, which results from Cabibbo-favored D^0 transitions or DCS $\overline{D}^0$ transitions.

ℓ^+ or ℓ^-: Semileptonic or purely leptonic final states, which, in the absence of mixing, tag unambiguously the flavor of the parent D^0.

f_+ or f_-: CP-even and CP-odd eigenstates, respectively.

The decay rates for $D^0\overline{D}^0$ pairs to all possible combinations of the above categories of final states are calculated in Ref. 2, for both $C = -1$ and $C = +1$, reproducing the work of Ref. 3. Such $D^0\overline{D}^0$ combinations, where both D final states are specified, are double tags. In addition, the rates for single tags, where either the D^0 or $\overline{D}^0$ is identified and the other neutral D decays generically are given in Ref. 2.

CLEO-c has reported results using 818 pb^{-1} of $e^+e^- \to \psi(3770)$ data [56–58], where the quantum-coherent $D^0\overline{D}^0$ pairs are in the $C = -1$ state. The values of y, R_M, $\cos\delta_{K\pi}$, and $\sin\delta_{K\pi}$ are determined from a combined fit to the ST (hadronic only) and DT yields. The hadronic final states included are $K^-\pi^+$ (f), $K^+\pi^-$ ($\bar{f}$), K^-K^+ (f_+), $\pi^+\pi^-$ (f_+), $K^0_S\pi^0\pi^0$ (f_+), $K^0_L\pi^0$ (f_+), $K^0_L\eta$ (f_+), $K^0_L\omega$ (f_+), $K^0_S\pi^0$ (f_-), $K^0_S\eta$ (f_-), $K^0_S\omega$ (f_-), and $K^0_L\pi^0\pi^0$ (f_-), and $K^0_S\pi^+\pi^-$ (mixure of f,$\bar{f}$, f_+, and f_-). The two flavored final states, $K^-\pi^+$ and $K^+\pi^-$, can be reached via CF or DCS transitions.

Semileptonic DT yields are also included, where one D is fully reconstructed in one of the hadronic modes listed above, and the other D is partially reconstructed in either $D \to Ke\nu$ or $D \to K\mu\nu$. When the lepton is accompanied by a flavor tag ($D \to K^-\pi^+$ or $K^+\pi^-$), both the "right-sign" and "wrong-sign" DT samples are used, where the electron and kaon charges are the same and opposite, respectively.

The main results of the CLEO-c analysis are the determination of $\cos\delta_{K\pi} = 0.81^{+0.22+0.07}_{-0.18-0.05}$, $\sin\delta_{K\pi} = -0.01 \pm 0.49 \pm 0.04$, and World Averages for the mixing parameters from an "extended" fit that combines the CLEO-c data with previous mixing and branching-ratio measurements [58]. These fits allow $\cos\delta_{K\pi}$, $\sin\delta_{K\pi}$ and x^2 to be unphysical. Constraining $\cos\delta_{K\pi}$ and $\sin\delta_{K\pi}$ to $[-1,+1]$—that is interpreting $\delta_{K\pi}$ as an angle—yields $\delta_{K\pi} = (18\,^{+11}_{-17} \pm 7)^\circ$. Note that measurements of y (Table 4 and Table 5) and y' (Table 3) contribute to the determination of $\delta_{K\pi}$.

Summary of Experimental Results: Several recent results indicate that charm mixing is at the upper end of the range of Standard Model estimates.

For $D^0 \to K^+\pi^-$, LHCb [15,17], CDF [16], and Belle [14] each exclude the no-mixing hypothesis by more than 5 standard deviations.

For y_{CP} in $D^0 \to K^+K^-$ and $\pi^+\pi^-$, Belle [37] and BaBar [38] find 4.5σ and 3.3σ effects. The most sensitive measurement of x and y is in $D^0 \to K^0_S\pi^+\pi^-, K^0_SK^+K^-$ from BaBar [32] and the no mixing solution is only excluded at 1.9σ. In a similar analysis, Belle [30] also finds a 2.4σ result for x.

The current situation would benefit from better knowledge of the strong phase difference $\delta_{K\pi}$ than provided by the current CLEO-c result [58]. This would allow one to unfold x and y from the $D^0 \to K^+\pi^-$ measurements of x'^2 and y', and directly compare them to the $D^0 \to K^0_S\pi^+\pi^-$ results.

The experimental data consistently indicate that the D^0 and $\overline{D}^0$ do mix. The mixing is presumably dominated by long-range processes. Under the assumption that the observed mixing is due entirely to non-Standard Model processes, significant constraints on a variety of new physics models are obtained [59]. A serious limitation to the interpretation of charm oscillations in terms of New Physics is the theoretical uncertainty of the Standard Model prediction. The evidence for time integrated CP-violation, $\Delta A_{CP} \neq 0$ is intriguing. This result is marginally consistent with Standard Model expectation [60–62].

HFAG Averaging of Charm Mixing Results:

The Heavy Flavor Averaging Group (HFAG) has made a global fit to all mixing measurements to obtain values of x, y, $\delta_{K\pi}$, $\delta_{K\pi\pi^0}$, R_D, $A_D \equiv (R^+_D - R^-_D)/(R^+_D + R^-_D)$, $|q/p|$, $\mathrm{Arg}(q/p) \equiv \phi$, and the time-integrated CP asymmetries A_K and A_π. Correlations among observables are taken into account by using the error matrices from the experiments. The measurements of $D^0 \to K^{(*)+}\ell^-\overline{\nu}$, K^+K^-, $\pi^+\pi^-$, $K^+\pi^-$, $K^+\pi^-\pi^0$, $K^+\pi^-\pi^+\pi^-$, $K^0_S\pi^+\pi^-$, and $K^0_SK^+K^-$ decays, as well as CLEO-c results for double-tagged branching fractions measured at the $\psi(3770)$ are used.

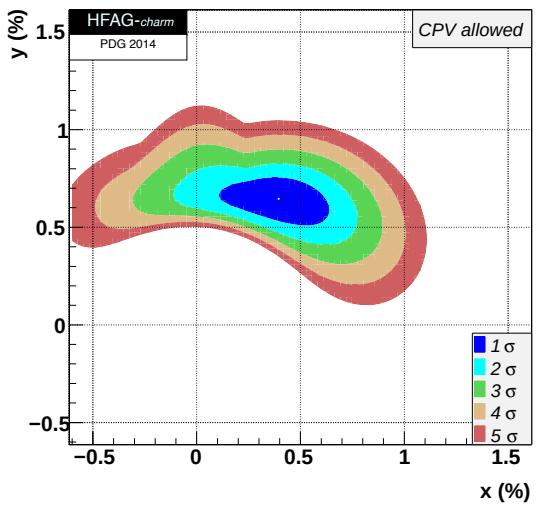

Figure 1: Two-dimensional 1σ-5σ contours for (x, y) from measurements of $D^0 \to K^{(*)+}\ell\nu$, h^+h^-, $K^+\pi^-$, $K^+\pi^-\pi^0$, $K^+\pi^-\pi^+\pi^-$, $K^0_S\pi^+\pi^-$, and $K^0_SK^+K^-$ decays, and double-tagged branching fractions measured at the $\psi(3770)$ resonance (from HFAG [24]) .

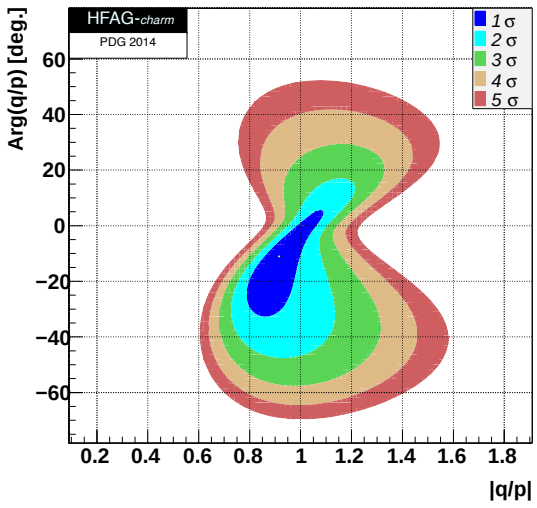

Figure 2: Two-dimensional 1σ-5σ contours for $(|q/p|$,Arg$(q/p))$ from measurements of $D^0 \to K^{(*)+}\ell\nu$, h^+h^-, $K^+\pi^-$, $K^+\pi^-\pi^0$, $K^+\pi^-\pi^+\pi^-$, $K^0_S\pi^+\pi^-$, and $K^0_SK^+K^-$ decays, and double-tagged branching fractions measured at the $\psi(3770)$ resonance (from HFAG [24]) .

Table 7: HFAG Charm Mixing Averages [24].

Parameter	No CP Violation	CP Violation Allowed	95% C.L. Interval
$x(\%)$	$0.53\,^{+0.16}_{-0.17}$	$0.39\,^{+0.17}_{-0.18}$	$[0.007, 0.803]$
$y(\%)$	0.63 ± 0.09	$0.65\,^{+0.07}_{-0.09}$	$[0.464, 0.788]$
$R_D(\%)$	0.350 ± 0.004	0.349 ± 0.004	$[0.342, 0.357]$
$\delta_{K\pi}(^\circ)$	$10.0\,^{+10.0}_{-11.3}$	$9.3\,^{+10.0}_{-12.0}$	$[-17.8, 28.2]$
$\delta_{K\pi\pi^0}(^\circ)$	$17.4\,^{+23.2}_{-23.8}$	$25.4\,^{+25.0}_{-25.1}$	$[-24.2, 75.3]$
$A_D(\%)$	—	-0.90 ± 1.00	$[-2.95, 1.02]$
$\lvert q/p\rvert$	—	$0.92\,^{+0.12}_{-0.09}$	$[0.76, 1.15]$
$\phi(^\circ)$	—	$-11.1\,^{+11.4}_{-13.5}$	$[-40.0, 10.9]$
A_K	—	-0.14 ± 0.14	$[-0.41, 0.13]$
A_π	—	0.19 ± 0.15	$[-0.11, 0.49]$

For the global fit, confidence contours in the two dimensions (x, y) and $(|q/p|, \phi)$ are obtained by letting, for any point in the two-dimensional plane, all other fit parameters take their preferred values. Figures 1 and 2 show the resulting 1-to-5 σ contours. The fits exclude the no-mixing point $(x = y = 0)$ at more than 12σ, when CP violation is allowed. The fits are consistent with no CP violation at the 50% Confidence Level. The parameters x and y differ from zero by 1.7σ and 6.1σ, respectively. One-dimensional likelihood functions for parameters are obtained by allowing, for any value of the parameter, all other fit parameters to take their preferred values. The resulting likelihood functions give central values, 68.3% C.L. intervals, and 95% C.L. intervals as listed in Table 7.

From the results of the HFAG averaging, the following can be concluded: (1) Since CP violation is small and y_{CP} is positive, the CP-even state is shorter-lived, as in the $K^0\overline{K}^0$ system; (2) However, since x appears to be positive, the CP-even state is heavier, unlike in the $K^0\overline{K}^0$ system; (3) The strong phase difference $\delta_{K\pi}$ is consistent with the SU(3) expectation of zero but large values are not excluded; (4) There is no evidence yet for CP-violation in $D^0\overline{D}^0$ mixing. Observing CP-violation in mixing ($|q/p| \neq 1$) at the current level of sensitivity would indicate new physics.

The author would like to acknowledge helpful input from Bostjan Golob, Marco Gersabeck, and especially Alan Schwartz of the Heavy Flavor Averaging Group.

References

1. B. Aubert *et al.*, Phys. Rev. **D76**, 014018 (2007).
2. D.M. Asner and W.M. Sun, Phys. Rev. **D73**, 034024 (2006); Erratum-*ibid*, **77**, 019901 (2008).
3. D. Atwood and A.A. Petrov, Phys. Rev. **D71**, 054032 (2005) Z.Z. Xing, Phys. Rev. **D55**, 196 (1997) M. Goldhaber and J.L. Rosner, Phys. Rev. **D15**, 1254 (1977).
4. U. Bitenc *et al.*, Phys. Rev. **D77**, 112003 (2008).
5. U. Bitenc *et al.*, Phys. Rev. **D72**, 071101R (2005).
6. C. Cawlfield *et al.*, Phys. Rev. **D71**, 077101 (2005).
7. B. Aubert *et al.*, Phys. Rev. **D70**, 091102R (2004).
8. K. Stenson, presented at the April Meeting of the American Physical Society (APS 03), Philadelphia, Pennsylvania, April 5-8, 2003; M. Hosack, (FOCUS Collab.), Fermilab-Thesis-2002-25.
9. E.M. Aitala *et al.*, Phys. Rev. Lett. **77**, 2384 (1996).
10. A.J. Schwartz, for the Heavy Flavor Averaging Group, `arXiv:0911.1464 [hep-ex]`.
11. Y. Nir, Lectures given at 27th SLAC Summer Institute on Particle Physics: "CP Violation in and Beyond the Standard Model (SSI 99)," Stanford, California, 7-16 Jul

1999. Published in Trieste 1999, *Particle Physics*, pp. 165-243.
12. S. Bergmann *et al.*, Phys. Lett. **B486**, 418 (2000).
13. See the Note on "CP Violation in Meson Decays" in this *Review*.
14. B.R. Ko *et al.*, Phys. Rev. Lett. **112**, 111801 (2014).
15. R. Aaij *et al.*, Phys. Rev. Lett. **111**, 251801 (2013).
16. T. Aaltonen *et al.*, Phys. Rev. Lett. **111**, 231802 (2013).
17. R. Aaij *et al.*, Phys. Rev. Lett. **110**, 101802 (2013).
18. T. Aaltonen *et al.*, Phys. Rev. Lett. **100**, 121802 (2008).
19. B. Aubert *et al.*, Phys. Rev. Lett. **98**, 211802 (2007).
20. L.M. Zhang *et al.*, Phys. Rev. Lett. **96**, 151801 (2006).
21. J.M. Link *et al.*, Phys. Lett. **B607**, 51 (2005).
22. R. Godang *et al.*, Phys. Rev. Lett. **84**, 5038 (2000).
23. E.M. Aitala *et al.*, Phys. Rev. **D57**, 13 (1998).
24. Heavy Flavor Averaging Group, `www.slac.stanford.edu/xorg/hfag/charm/PDG14/results_mix+cpv.html`.
25. B. Aubert *et al.*, Phys. Rev. Lett. **97**, 221803 (2006).
26. B. Aubert *et al.*, Phys. Rev. Lett. **103**, 211801 (2009).
27. R.A. Briere *et al.*, (CLEO Collab.), CLNS 01-1742, (2001).
28. G. Cavoto *et al.*, Prepared for *3rd Workshop on the Unitarity Triangle: CKM 2005*, San Diego, California, 15-18 Mar 2005, `hep-ph/0603019`.
29. D.M. Asner *et al.*, Phys. Rev. **D72**, 012001 (2005).
30. L.M. Zhang *et al.*, Phys. Rev. Lett. **99**, 131803 (2007).
31. H. Muramatsu *et al.*, Phys. Rev. Lett. **89**, 251802 (2002).
32. P. del Amo Sanchez *et al.*, Phys. Rev. Lett. **105**, 081803 (2010).
33. Heavy Flavor Averaging Group, `www.slac.stanford.edu/xorg/hfag/charm/March12/results_mix+cpv.html`.
34. B. Aubert *et al.*, Phys. Rev. Lett. **95**, 121802 (2005).
35. B. Aubert *et al.*, Phys. Rev. **D78**, 034023 (2008).
36. R. Aaij *et al.*, Phys. Rev. Lett. **112**, 041801 (2014).
37. M. Staric *et al.*, `arXiv:1212.3478[hep-ex]`.
38. B. Aubert *et al.*, Phys. Rev. **D87**, 012004 (2013).
39. R. Aaij *et al.*, JHEP 1204 (2012) 129.
40. B. Aubert *et al.*, Phys. Rev. **D80**, 071103R (2009).
41. A. Zupanc *et al.*, Phys. Rev. **D80**, 052006 (2009).
42. B. Aubert *et al.*, Phys. Rev. **D78**, 011105 (2008).
43. M. Staric *et al.*, Phys. Rev. Lett. **98**, 211803 (2007).
44. B. Aubert *et al.*, Phys. Rev. Lett. **91**, 121801 (2003).
45. S.E. Csorna *et al.*, Phys. Rev. **D65**, 092001 (2002).
46. K. Abe *et al.*, Phys. Rev. Lett. **88**, 162001 (2002).
47. J.M. Link *et al.*, Phys. Lett. **B485**, 62 (2000).
48. E.M. Aitala *et al.*, Phys. Rev. Lett. **83**, 32 (1999).
49. See the tabulation of A_{CP} results in the D^0 and D^+ Listings in this *Review*.
50. R. Aaij *et al.*, `arXiv:1405.2797 [hep-ex]`.
51. R. Aaij *et al.*, Phys. Lett. **B723**, 33 (2013).
52. R. Aaij *et al.*, LHCb-CONF-2013-003.
53. R. Aaij *et al.*, Phys. Rev. Lett. **108**, 111602 (2012).
54. T. Aaltonen *et al.*, Phys. Rev. Lett. **109**, 111801 (2012).
55. B. Aubert *et al.*, Phys. Rev. Lett. **100**, 061803 (2008).
56. J.L. Rosner *et al.*, Phys. Rev. Lett. **100**, 221801 (2008).
57. D.M. Asner *et al.*, Phys. Rev. **D78**, 012001 (2008).
58. D.M. Asner *et al.*, Phys. Rev. **D86**, 112001 (2012).
59. E. Golowich *et al.*, Phys. Rev. **D76**, 095009 (2007).
60. G. Isidori *et al.*, Phys. Lett. **B711**, 46 (2011).
61. E. Franco *et al.*, JHEP 1205 (2012) 140.
62. M. Gersaback *et al.*, J. Phys. **G39**, 045005 (2012).

$|m_{D_1^0} - m_{D_2^0}| = x\,\Gamma$

The D_1^0 and D_2^0 are the mass eigenstates of the D^0 meson, as described in the note on "D^0-$\overline{D}^0$ Mixing," above. The experiments usually present $x \equiv \Delta m/\Gamma$. Then $\Delta m = x\,\Gamma = x\,\hbar/\tau$.

"OUR EVALUATION" comes from CPV allowing averages provided by the Heavy Flavor Averaging Group, see the note on "D^0-$\overline{D}^0$ Mixing."

VALUE ($10^{10}\ \hbar\ s^{-1}$)	CL%	DOCUMENT ID		TECN	COMMENT
$0.95^{+0.41}_{-0.44}$ OUR EVALUATION					
1.0 ±0.8 OUR AVERAGE					Error includes scale factor of 1.5.
		[1] KO	14	BELL	$e^+e^- \to \Upsilon(nS)$
		[2] AAIJ	13CE	LHCB	pp at 7, 8 TeV
		[3] AALTONEN	13AE	CDF	$p\overline{p}$ at 1.96 TeV
$0.39 \pm 0.56 \pm 0.35$		[4] DEL-AMO-SA...	10D	BABR	e^+e^-, 10.6 GeV
$1.98 \pm 0.73^{+0.32}_{-0.41}$		[5] ZHANG	07B	BELL	$\Delta m < 3.9$, 95% CL
• • • We do not use the following data for averages, fits, limits, etc. • • •					
		[6] AAIJ	13N	LHCB	Repl. by AAIJ 13CE
$6.4\ ^{+1.4}_{-1.7} \pm 1.0$		[7] AUBERT	09AN	BABR	e^+e^- at 10.58 GeV
$-2\ ^{+7}_{-6}$		[8] LOWREY	09	CLEO	e^+e^- at $\psi(3770)$
< 7	95	[9] ZHANG	06	BELL	e^+e^-
-11 to $+22$		[5] ASNER	05	CLEO	$e^+e^- \approx 10$ GeV
< 11	90	BITENC	05	BELL	
< 30	90	CAWLFIELD	05	CLEO	
< 7	95	[9] LI	05A	BELL	See ZHANG 06
< 22	95	[10] LINK	05H	FOCS	γ nucleus
< 23	95	AUBERT	04Q	BABR	
< 11	95	[9] AUBERT	03Z	BABR	e^+e^-, 10.6 GeV
< 7	95	[11] GODANG	00	CLE2	e^+e^-
< 32	90	[12,13] AITALA	98	E791	π^- nucleus, 500 GeV
< 24	90	[14] AITALA	96C	E791	π^- nucleus, 500 GeV
< 21	90	[13,15] ANJOS	88C	E691	Photoproduction

[1] Based on 976 fb^{-1} of data collected at $\Upsilon(nS)$ resonances. Assumes no CP violation. Reported $x'^2 = (0.09 \pm 0.22) \times 10^{-3}$ and $y' = (4.6 \pm 3.4) \times 10^{-3}$, where $x' = x\cos(\delta) + y\sin(\delta)$, $y' = y\cos(\delta) - x\sin(\delta)$ and δ is the strong phase between $D^0 \to K^+\pi^-$ and $\overline{D}^0 \to K^+\pi^-$.

[2] Based on 3 fb^{-1} of data collected at $\sqrt{s} = 7$, 8 TeV. Assumes no CP violation. Reported $x'^2 = (5.5 \pm 4.9) \times 10^{-4}$ and $y' = (4.8 \pm 1.0) \times 10^{-3}$, where $x' = x\cos(\delta) + y\sin(\delta)$, $y' = y\cos(\delta) - x\sin(\delta)$ and δ is the strong phase between the $D^0 \to K^+\pi^-$ and $\overline{D}^0 \to K^+\pi^-$.

[3] Based on 9.6 fb^{-1} of data collected at the Tevatron. Assumes no CP violation. Reported $x'^2 = (0.08 \pm 0.18) \times 10^{-3}$ and $y' = (4.3 \pm 4.3) \times 10^{-3}$, where $x' = x\cos(\delta) + y\sin(\delta)$, $y' = y\cos(\delta) - x\sin(\delta)$ and δ is the strong phase between the $D^0 \to K^+\pi^-$ and $\overline{D}^0 \to K^+\pi^-$.

[4] DEL-AMO-SANCHEZ 10D uses 540,800 ± 800 $K^0_S\pi^+\pi^-$ and 79,900 ± 300 $K^0_S K^+ K^-$ events in a time-dependent amplitude analysis of the D^0 and $\overline{D}^0$ Dalitz plots. No evidence was found for CP violation, and the values here assume no such violation.

[5] The ASNER 05 and ZHANG 07B values are from the time-dependent Dalitz-plot analysis of $D^0 \to K^0_S\pi^+\pi^-$. Decay-time information and interference on the Dalitz plot are used to distinguish doubly Cabibbo-suppressed decays from mixing and to measure the relative phase between $D^0 \to K^{*+}\pi^-$ and $\overline{D}^0 \to K^{*+}\pi^-$. This value allows CP violation and is sensitive to the sign of Δm.

[6] Based on 1 fb^{-1} of data collected at $\sqrt{s} = 7$ TeV in 2011. Assumes no CP violation. Reported $x'^2 = (-0.9 \pm 1.3) \times 10^{-4}$ and $y' = (7.2 \pm 2.4) \times 10^{-3}$, where $x' = x\cos(\delta) + y\sin(\delta)$, $y' = y\cos(\delta) - x\sin(\delta)$ and δ is the strong phase between the $D^0 \to K^+\pi^-$ and $\overline{D}^0 \to K^+\pi^-$.

[7] The AUBERT 09AN values are inferred from the branching ratio $\Gamma(D^0 \to K^+\pi^-\pi^0$ via $\overline{D}^0)/\Gamma(D^0 \to K^-\pi^+\pi^0)$ given near the end of this Listings. Mixing is distinguished from DCS decays using decay-time information. Interference between mixing and DCS is allowed. The phase between $D^0 \to K^+\pi^-\pi^0$ and $\overline{D}^0 \to K^+\pi^-\pi^0$ is assumed to be small. The width difference here is y'', which is not the same as y_{CP} in the note on D^0-$\overline{D}^0$ mixing.

[8] LOWREY 09 uses quantum correlations in $e^+e^- \to D^0\overline{D}^0$ at the $\psi(3770)$. See below for coherence factors and average relative strong phases for both $D^0 \to K^-\pi^+\pi^0$ and $D^0 \to K^-\pi^-2\pi^+$. A fit that includes external measurements of charm mixing parameters gets $\Delta m = (2.34 \pm 0.61) \times 10^{10}\ \hbar\,s^{-1}$.

[9] The AUBERT 03Z, LI 05A, and ZHANG 06 limits are inferred from the D^0-$\overline{D}^0$ mixing ratio $\Gamma(K^+\pi^-$ (via $\overline{D}^0))/\Gamma(K^-\pi^+)$ given near the end of this D^0 Listings. Decay-time information is used to distinguish DCS decays from D^0-$\overline{D}^0$ mixing. The limit allows interference between the DCS and mixing ratios, and also allows CP violation. AUBERT 03Z assumes the strong phase between $D^0 \to K^+\pi^-$ and $\overline{D}^0 \to K^+\pi^-$

amplitudes is small; if an arbitrary phase is allowed, the limit degrades by 20%. The LI 05A and ZHANG 06 limits are valid for an arbitrary strong phase.

[10] This LINK 05H limit is inferred from the D^0-$\overline{D}^0$ mixing ratio $\Gamma(K^+\pi^-$ (via $\overline{D}^0$))/$\Gamma(K^-\pi^+)$ given near the end of this D^0 Listings. Decay-time information is used to distinguish DCS decays from D^0-$\overline{D}^0$ mixing. The limit allows interference between the DCS and mixing ratios, and also allows *CP* violation. The strong phase between $D^0 \to K^+\pi^-$ and $\overline{D}^0 \to K^+\pi^-$ is assumed to be small. If an arbitrary relative strong phase is allowed, the limit degrades by 25%.

[11] This GODANG 00 limit is inferred from the D^0-$\overline{D}^0$ mixing ratio $\Gamma(K^+\pi^-$ (via $\overline{D}^0$))/$\Gamma(K^-\pi^+)$ given near the end of this D^0 Listings. Decay-time information is used to distinguish DCS decays from D^0-$\overline{D}^0$ mixing. The limit allows interference between the DCS and mixing ratios, and also allows *CP* violation. The strong phase between $D^0 \to K^+\pi^-$ and $\overline{D}^0 \to K^+\pi^-$ is assumed to be small. If an arbitrary relative strong phase is allowed, the limit degrades by a factor of two.

[12] AITALA 98 allows interference between the doubly Cabibbo-suppressed and mixing amplitudes, and also allows *CP* violation in this term, but assumes that $A_D = A_R = 0$. See the note on "D^0-$\overline{D}^0$ Mixing," above.

[13] This limit is inferred from R_M for $f = K^+\pi^-$ and $f = K^+\pi^-\pi^+\pi^-$. See the note on "D^0-$\overline{D}^0$ Mixing," above. Decay-time information is used to distinguish doubly Cabibbo-suppressed decays from D^0-$\overline{D}^0$ mixing.

[14] This limit is inferred from R_M for $f = K^+\ell^-\overline{\nu}_\ell$. See the note on "$D^0$-$\overline{D}^0$ Mixing," above.

[15] ANJOS 88C assumes that $y = 0$. See the note on "D^0-$\overline{D}^0$ Mixing," above. Without this assumption, the limit degrades by about a factor of two.

$(\Gamma_{D_1^0} - \Gamma_{D_2^0})/\Gamma = 2y$

The D_1^0 and D_2^0 are the mass eigenstates of the D^0 meson, as described in the note on "D^0-$\overline{D}^0$ Mixing," above.

Due to the strong phase difference between $D^0 \to K^+\pi^-$ and $\overline{D}^0 \to K^+\pi^-$, we exclude from the average those measurements of y' that are inferred from the D^0-$\overline{D}^0$ mixing ratio $\Gamma(K^+\pi^-$ via $\overline{D}^0)$ / $\Gamma(K^+\pi^-)$ given near the end of this D^0 Listings.

Some early results have been omitted. See our 2006 *Review* (Journal of Physics (generic for all A,B,E,G) **G33** 1 (2006)).

"OUR EVALUATION" comes from CPV allowing averages provided by the Heavy Flavor Averaging Group, see the note on "D^0-$\overline{D}^0$ Mixing."

VALUE (units 10^{-2})	EVTS	DOCUMENT ID		TECN	COMMENT
$1.29^{+\ 0.14}_{-\ 0.18}$ OUR EVALUATION					
1.21 ± 0.25 OUR AVERAGE					
		[1] KO	14	BELL	$e^+e^- \to \Upsilon$(nS)
		[2] AAIJ	13CE	LHCB	pp at 7, 8 TeV
		[3] AALTONEN	13AE	CDF	$p\overline{p}$ at 1.96 TeV
$1.44 \pm 0.36 \pm 0.24$		[4] LEES	13	BABR	$e^+e^- \to \Upsilon(4S)$
$0.55 \pm 0.63 \pm 0.41$		[5] AAIJ	12K	LHCB	pp at 7 TeV
$1.14 \pm 0.40 \pm 0.30$		[6] DEL-AMO-SA..	10D	BABR	e^+e^-, 10.6 GeV
$0.22 \pm 1.22 \pm 1.04$		[7] ZUPANC	09	BELL	$e^+e^- \approx \Upsilon(4S)$
$2.62 \pm 0.64 \pm 0.50$	160k	[8] STARIC	07	BELL	$e^+e^- \approx \Upsilon(4S)$
$0.74 \pm 0.50^{+0.20}_{-0.31}$	534k	[9] ZHANG	07B	BELL	$e^+e^- \approx \Upsilon(4S)$
$-1.0 \pm 2.0\ ^{+1.4}_{-1.6}$	18k	[10] ABE	02I	BELL	$e^+e^- \approx \Upsilon(4S)$
$-2.4 \pm 5.0 \pm 2.8$	3393	[11] CSORNA	02	CLE2	$e^+e^- \approx \Upsilon(4S)$
$6.84 \pm 2.78 \pm 1.48$	10k	[10] LINK	00	FOCS	γ nucleus
$+1.6 \pm 5.8 \pm 2.1$		[10] AITALA	99E	E791	$K^-\pi^+$, K^+K^-
• • • We do not use the following data for averages, fits, limits, etc. • • •					
		[12] AAIJ	13N	LHCB	Repl. by AAIJ 13CE
$2.32 \pm 0.44 \pm 0.36$		[13] AUBERT	09AI	BABR	See LEES 13
$-0.12^{+\ 1.10}_{-\ 1.28} \pm 0.68$		[14] AUBERT	09AN	BABR	e^+e^- at 10.58 GeV
$1.4\ ^{+\ 4.8}_{-\ 5.4}$		[15] LOWREY	09	CLEO	e^+e^- at $\psi(3770)$
1.70 ± 1.52	12.7 ± 0.3k	[16] AALTONEN	08E	CDF	$p\overline{p}$, $\sqrt{s} = 1.96$ TeV
$2.06 \pm 0.66 \pm 0.38$		[17] AUBERT	08U	BABR	See AUBERT 09AI
$1.94 \pm 0.88 \pm 0.62$	4030 ± 90	[16] AUBERT	07W	BABR	$e^+e^- \approx$ 10.6 GeV
-0.7 ± 4.9	$4k \pm 88$	[16,18] ZHANG	06	BELL	e^+e^-
$-3.0\ ^{+\ 5.0}_{-\ 4.8}\ ^{+1.6}_{-0.8}$		[9] ASNER	05	CLEO	$e^+e^- \approx$ 10 GeV
-0.3 ± 5.7		[16,18] LI	05A	BELL	See ZHANG 06
$-5.2\ ^{+18.4}_{-16.8}$		[16,18] LINK	05H	FOCS	γ nucleus
$1.6 \pm 0.8\ ^{+1.0}_{-0.8}$	450k	[19] AUBERT	03P	BABR	See AUBERT 08U
$1.6\ ^{+\ 6.2}_{-12.8}$		[16,18] AUBERT	03Z	BABR	e^+e^-, 10.6 GeV
$-5.0\ ^{+\ 2.8}_{-\ 3.2} \pm 0.6$		[16] GODANG	00	CLE2	e^+e^-

[1] Based on 976 fb^{-1} of data collected at Υ(nS) resonances. Assumes no *CP* violation. Reported $x'^2 = (0.09 \pm 0.22) \times 10^{-3}$ and $y' = (4.6 \pm 3.4) \times 10^{-3}$, where $x' = x\cos(\delta) + y\sin(\delta)$, $y' = y\cos(\delta) - x\sin(\delta)$ and δ is the strong phase between $D^0 \to K^+\pi^-$ and $\overline{D}^0 \to K^+\pi^-$.

[2] Based on 3 fb^{-1} of data collected at $\sqrt{s} = 7$, 8 TeV. Assumes no *CP* violation. Reported $x'^2 = (5.5 \pm 4.9) \times 10^{-4}$ and $y' = (4.8 \pm 1.0) \times 10^{-3}$, where $x' = x\cos(\delta) + y\sin(\delta)$, $y' = y\cos(\delta) - x\sin(\delta)$ and δ is the strong phase between the $D^0 \to K^+\pi^-$ and $\overline{D}^0 \to K^+\pi^-$.

[3] Based on 9.6 fb^{-1} of data collected at the Tevatron. Assumes no *CP* violation. Reported $x'^2 = (0.08 \pm 0.18) \times 10^{-3}$ and $y' = (4.3 \pm 4.3) \times 10^{-3}$, where $x' = x\cos(\delta) + y\sin(\delta)$, $y' = y\cos(\delta) - x\sin(\delta)$ and δ is the strong phase between the $D^0 \to K^+\pi^-$ and $\overline{D}^0 \to K^+\pi^-$.

[4] Obtained $y_{CP} = (0.72 \pm 0.18 \pm 0.12)\%$ based on three effective D^0 lifetimes measured in $K^\mp\pi^\pm$, K^-K^+, and $\pi^-\pi^+$. We list $2y_{CP} = \Delta\Gamma/\Gamma$.

[5] Compared the lifetimes of D^0 decay to the *CP* eigenstate K^+K^- with D^0 decay to π^+K^-. The values here assume no *CP* violation.

[6] DEL-AMO-SANCHEZ 10D uses $540{,}800 \pm 800$ $K^0_S\pi^+\pi^-$ and $79{,}900 \pm 300$ $K^0_S K^+K^-$ events in a time-dependent amplitude analyses of the D^0 and $\overline{D}^0$ Dalitz plots. No evidence was found for *CP* violation, and the values here assume no such violation.

[7] ZUPANC 09 uses a method based on measuring the mean decay time of $D^0 \to K^0_S K^+K^-$ events for different K^+K^- mass intervals.

[8] STARIC 07 compares the lifetimes of D^0 decay to the *CP* eigenstates K^+K^- and $\pi^+\pi^-$ with D^0 decay to $K^-\pi^+$.

[9] The ASNER 05 and ZHANG 07B values are from the time-dependent Dalitz-plot analysis of $D^0 \to K^0_S\pi^+\pi^-$. Decay-time information and interference on the Dalitz plot are used to distinguish doubly Cabibbo-suppressed decays from mixing and to measure the relative phase between $D^0 \to K^{*+}\pi^-$ and $\overline{D}^0 \to K^{*+}\pi^-$. This limit allows *CP* violation.

[10] LINK 00, AITALA 99E, and ABE 02I measure the lifetime difference between $D^0 \to K^-K^+$ (*CP* even) decays and $D^0 \to K^-\pi^+$ (*CP* mixed) decays, or $y_{CP} = [\Gamma(CP+) - \Gamma(CP-)]/[\Gamma(CP+) + \Gamma(CP-)]$. We list $2y_{CP} = \Delta\Gamma/\Gamma$.

[11] CSORNA 02 measures the lifetime difference between $D^0 \to K^-K^+$ and $\pi^-\pi^+$ (*CP* even) decays and $D^0 \to K^-\pi^+$ (*CP* mixed) decays, or $y_{CP} = [\Gamma(CP+) - \Gamma(CP-)]/[\Gamma(CP+) + \Gamma(CP-)]$. We list $2y_{CP} = \Delta\Gamma/\Gamma$.

[12] Based on 1 fb^{-1} of data collected at $\sqrt{s} = 7$ TeV in 2011. Assumes no *CP* violation. Reported $x'^2 = (-0.9 \pm 1.3) \times 10^{-4}$ and $y' = (7.2 \pm 2.4) \times 10^{-3}$, where $x' = x\cos(\delta) + y\sin(\delta)$, $y' = y\cos(\delta) - x\sin(\delta)$ and δ is the strong phase between the $D^0 \to K^+\pi^-$ and $\overline{D}^0 \to K^+\pi^-$.

[13] This combines the $y_{CP} = (\tau_{K\pi}/\tau_{KK}) - 1$ using untagged $K^-\pi^+$ and K^-K^+ events of AUBERT 09AI with the disjoint y_{CP} using tagged $K^-\pi^+$, K^-K^+, and $\pi^-\pi^+$ events of AUBERT 08U.

[14] The AUBERT 09AN values are inferred from the branching ratio $\Gamma(D^0 \to K^+\pi^-\pi^0$ via $\overline{D}^0)/\Gamma(D^0 \to K^-\pi^+\pi^0)$ given near the end of this Listings. Mixing is distinguished from DCS decays using decay-time information. Interference between mixing and DCS is allowed. The phase between $D^0 \to K^+\pi^-\pi^0$ and $\overline{D}^0 \to K^+\pi^-\pi^0$ is assumed to be small. The width difference here is y'', which is not the same as y_{CP} in the note on D^0–$\overline{D}^0$ mixing.

[15] LOWREY 09 uses quantum correlations in $e^+e^- \to D^0\overline{D}^0$ at the $\psi(3770)$. See below for coherence factors and average relative strong phases for both $D^0 \to K^-\pi^+\pi^0$ and $D^0 \to K^-\pi^-2\pi^+$. A fit that includes external measurements of charm mixing parameters gets $2y = (1.62 \pm 0.32) \times 10^{-2}$.

[16] The GODANG 00, AUBERT 03Z, LINK 05H, LI 05A, ZHANG 06, AUBERT 07W, and AALTONEN 08E limits are inferred from the D^0-$\overline{D}^0$ mixing ratio $\Gamma(K^+\pi^-$ (via $\overline{D}^0$))/$\Gamma(K^-\pi^+)$ given near the end of this D^0 Listings. Decay-time information is used to distinguish DCS decays from D^0-$\overline{D}^0$ mixing. The limits allow interference between the DCS and mixing ratios, and all except AUBERT 07W and AALTONEN 08E also allow *CP* violation. The phase between $D^0 \to K^+\pi^-$ and $\overline{D}^0 \to K^+\pi^-$ is assumed to be small. This is a measurement of y' and is not the same as the y_{CP} of our note above on "D^0-$\overline{D}^0$ Mixing."

[17] This value combines the results of AUBERT 08U and AUBERT 03P.

[18] The ranges of AUBERT 03Z, LINK 05H, LI 05A, and ZHANG 06 measurements are for 95% confidence level.

[19] AUBERT 03P measures $Y \equiv 2\tau^0/(\tau^+ + \tau^-) - 1$, where τ^0 is the $D^0 \to K^-\pi^+$ (and $\overline{D}^0 \to K^+\pi^-$) lifetime, and τ^+ and τ^- are the D^0 and $\overline{D}^0$ lifetimes to *CP*-even states (here K^-K^+ and $\pi^-\pi^+$). In the limit of *CP* conservation, $Y = y \equiv \Delta\Gamma/2\Gamma$ (we list $2y = \Delta\Gamma/\Gamma$). AUBERT 03P also uses $\tau^+ - \tau^-$ to get $\Delta Y = -0.008 \pm 0.006 \pm 0.002$.

$|q/p|$

The mass eigenstates D_1^0 and D_2^0 are related to the $C = \pm 1$ states by $|D_{1,2}> = p|D^0> + q|\overline{D}^0>$. See the note on "$D^0$–$\overline{D}^0$ Mixing" above.

"OUR EVALUATION" comes from CPV allowing averages provided by the Heavy Flavor Averaging Group. This would include as-yet-unpublished results, see the note on "D^0-$\overline{D}^0$ Mixing."

VALUE	DOCUMENT ID		TECN	COMMENT
$0.92^{+0.12}_{-0.09}$ OUR EVALUATION	HFAG fit; see the note on "D^0-$\overline{D}^0$ Mixing."			
	[1] AAIJ	13CE	LHCB	pp at 7, 8 TeV
$0.86^{+0.30}_{-0.29}{}^{+0.10}_{-0.08}$	[2] ZHANG	07B	BELL	$e^+e^- \approx \Upsilon(4S)$

[1] Based on 3 fb^{-1} of data collected at $\sqrt{s} = 7$, 8 TeV. Allowing for *CP* violation, the direct *CP* violation in mixing is reported $0.75 < |q/p| < 1.24$ at the 68.3% CL for the $D^0 \to K^+\pi^-$ and $\overline{D}^0 \to K^+\pi^-$.

[2] The phase of p/q is $(-14^{+16}_{-18} \pm 5)^\circ$. The ZHANG 07B value is from the time-dependent Dalitz-plot analysis of $D^0 \to K^0_S\pi^+\pi^-$. Decay-time information and interference on the Dalitz plot are used to distinguish doubly Cabibbo-suppressed decays from mixing and to measure the relative phase between $D^0 \to K^{*+}\pi^-$ and $\overline{D}^0 \to K^{*+}\pi^-$. This value allows *CP* violation.

Meson Particle Listings

D^0

A_Γ

A_Γ is the decay-rate asymmetry for CP-even final states $A_\Gamma = (\overline{\tau}_+ - \tau_+) / (\overline{\tau}_+ + \tau_+)$. See the note on "$D^0$–$\overline{D}^0$ Mixing" above.

VALUE (units 10^{-3})			DOCUMENT ID		TECN	COMMENT
−0.125 ± 0.526		**OUR EVALUATION**				
−0.1	**± 2.1**	**OUR AVERAGE**				
0.9	± 2.6	± 0.6	LEES	13	BABR	$e^+e^- \to \Upsilon(4S)$
−5.9	± 5.9	± 2.1	AAIJ	12K	LHCB	pp at 7 TeV
0.1	± 3.0	± 2.5	STARIC	07	BELL	$e^+e^- \approx \Upsilon(4S)$
• • • We do not use the following data for averages, fits, limits, etc. • • •						
2.6	± 3.6	± 0.8	AUBERT	08U	BABR	See LEES 13
8	± 6	± 2	AUBERT	03P	BABR	$e^+e^- \approx \Upsilon(4S)$

cos δ

δ is the $D^0 \to K^+\pi^-$ relative strong phase.

VALUE		DOCUMENT ID		TECN	COMMENT
$\mathbf{0.81^{+0.22+0.07}_{-0.18-0.05}}$	[1]	ASNER	12	CLEO	$e^+e^- \to D^0\overline{D}^0$, 3.77 GeV
• • • We do not use the following data for averages, fits, limits, etc. • • •					
$1.03^{+0.31}_{-0.17} \pm 0.06$	[2]	ASNER	08	CLEO	Repl. by ASNER 12

[1] Uses quantum correlations in $e^+e^- \to D^0\overline{D}^0$ at the $\psi(3770)$, where decay rates of CP-tagged $K\pi$ final states depend on the strong phases between the decays of $D^0 \to K^+\pi^-$ and $\overline{D}^0 \to K^+\pi^-$. The measurements obtained $\sin(\delta) = -0.01 \pm 0.41 \pm 0.04$ and $|\delta| = (10^{+28+13}_{-53-00})^\circ$ as well. A fit that includes external measurements of charm mixing parameters finds $\cos(\delta) = 1.15^{+0.19+0.00}_{-0.17-0.08}$, $\sin(\delta) = 0.56^{+0.32+0.21}_{-0.31-0.20}$, and $|\delta| = (18^{+11}_{-17})^\circ$.

[2] ASNER 08 uses quantum correlations in $e^+e^- \to D^0\overline{D}^0$ at the $\psi(3770)$, where decay rates of CP-tagged $K\pi$ final states depend on $\cos\delta$ because of interfering amplitudes. The above measurement implies $|\delta| < 75^\circ$ with a confidence level of 95%. A fit that includes external measurements of charm mixing parameters finds $\cos\delta = 1.10 \pm 0.35 \pm 0.07$. See also the note on "$D^0$–$\overline{D}^0$ Mixing" p. 783 in our 2008 Review (PDG 08).

$D^0 \to K^-\pi^+\pi^0$ COHERENCE FACTOR $R_{K\pi\pi^0}$

See the note on 'D^0-$\overline{D}^0$ Mixing' for the definition. $R_{K\pi\pi^0}$ can have any value between 0 and 1. A value near 1 indicates the decay is dominated by a few intermediate states with limited interference.

VALUE		DOCUMENT ID		TECN	COMMENT
$\mathbf{0.78^{+0.11}_{-0.25}}$	[1]	LOWREY	09	CLEO	$e^+e^- \to D^0\overline{D}^0$ at $\psi(3770)$

[1] LOWREY 09 uses quantum correlations in $e^+e^- \to D^0\overline{D}^0$ at the $\psi(3770)$, where the decay rates of CP-tagged $K^-\pi^+\pi^0$ final states depend on $R_{K\pi\pi^0}$ and $\delta^{K\pi\pi^0}$. A fit that includes external measurements of charm mixing parameters gets $R_{K\pi\pi^0} = 0.84 \pm 0.07$.

$D^0 \to K^-\pi^+\pi^0$ AVERAGE RELATIVE STRONG PHASE $\delta^{K\pi\pi^0}$

VALUE (°)		DOCUMENT ID		TECN	COMMENT
$\mathbf{239^{+32}_{-28}}$	[1]	LOWREY	09	CLEO	$e^+e^- \to D^0\overline{D}^0$ at $\psi(3770)$

[1] LOWREY 09 uses quantum correlations in $e^+e^- \to D^0\overline{D}^0$ at the $\psi(3770)$, where the decay rates of CP-tagged $K^-\pi^+\pi^0$ final states depend on $R_{K\pi\pi^0}$ and $\delta^{K\pi\pi^0}$. A fit that includes external measurements of charm mixing parameters gets $\delta^{K\pi\pi^0} = (227^{+14}_{-17})^\circ$.

$D^0 \to K^-\pi^-2\pi^+$ COHERENCE FACTOR $R_{K3\pi}$

See the note on 'D^0-$\overline{D}^0$ Mixing' for the definition. $R_{K3\pi}$ can have any value between 0 and 1. A value near 1 indicates the decay is dominated by a few intermediate states with limited interference.

VALUE		DOCUMENT ID		TECN	COMMENT
$\mathbf{0.36^{+0.24}_{-0.30}}$	[1]	LOWREY	09	CLEO	$e^+e^- \to D^0\overline{D}^0$ at $\psi(3770)$

[1] LOWREY 09 uses quantum correlations in $e^+e^- \to D^0\overline{D}^0$ at the $\psi(3770)$, where the decay rates of CP-tagged $K^-\pi^-2\pi^+$ final states depend on $R_{K3\pi}$ and $\delta^{K3\pi}$. A fit that includes external measurements of charm mixing parameters gets $R_{K3\pi} = 0.33^{+0.26}_{-0.23}$.

$D^0 \to K^-\pi^-2\pi^+$ AVERAGE RELATIVE STRONG PHASE $\delta^{K3\pi}$

VALUE (°)		DOCUMENT ID		TECN	COMMENT
$\mathbf{118^{+62}_{-53}}$	[1]	LOWREY	09	CLEO	$e^+e^- \to D^0\overline{D}^0$ at $\psi(3770)$

[1] LOWREY 09 uses quantum correlations in $e^+e^- \to D^0\overline{D}^0$ at the $\psi(3770)$, where the decay rates of CP-tagged $K^-\pi^-2\pi^+$ final states depend on $R_{K3\pi}$ and $\delta^{K3\pi}$. A fit that includes external measurements of charm mixing parameters gets $\delta^{K3\pi} = (114^{+26}_{-23})^\circ$.

$D^0 \to K^0_S K^+\pi^-$ COHERENCE FACTOR $R_{K^0_S K\pi}$

VALUE	DOCUMENT ID		TECN	COMMENT
0.73 ± 0.08	[1] INSLER	12	CLEO	$e^+e^- \to D^0\overline{D}^0$ at 3.77 GeV

[1] Uses quantum correlations in $e^+e^- \to D^0\overline{D}^0$ at the $\psi(3770)$, where the signal side D decays to $K^0_S K\pi$ and the tag-side D decays to $K\pi$, $K\pi\pi\pi$, $K\pi\pi^0$.

$D^0 \to K^0_S K^+\pi^-$ AVERAGE RELATIVE STRONG PHASE $\delta^{K^0_S K\pi}$

VALUE (°)	DOCUMENT ID		TECN	COMMENT
8.3 ± 15.2	[1] INSLER	12	CLEO	$e^+e^- \to D^0\overline{D}^0$ at 3.77 GeV

[1] Uses quantum correlations in $e^+e^- \to D^0\overline{D}^0$ at the $\psi(3770)$, where the signal side D decays to $K^0_S K\pi$ and the tag-side D decays to $K\pi$, $K\pi\pi\pi$, $K\pi\pi^0$.

$D^0 \to K^*K$ COHERENCE FACTOR R_{K^*K}

VALUE	DOCUMENT ID		TECN	COMMENT
1.00 ± 0.16	[1] INSLER	12	CLEO	$e^+e^- \to D^0\overline{D}^0$ at 3.77 GeV

[1] Uses quantum correlations in $e^+e^- \to D^0\overline{D}^0$ at the $\psi(3770)$, where the signal side D decays to $K^0_S K\pi$ and the tag-side D decays to $K\pi$, $K\pi\pi\pi$, $K\pi\pi^0$.

$D^0 \to K^*K$ AVERAGE RELATIVE STRONG PHASE δ^{K^*K}

VALUE (°)	DOCUMENT ID		TECN	COMMENT
26.5 ± 15.8	[1] INSLER	12	CLEO	$e^+e^- \to D^0\overline{D}^0$ at 3.77 GeV

[1] Uses quantum correlations in $e^+e^- \to D^0\overline{D}^0$ at the $\psi(3770)$, where the signal side D decays to $K^0_S K\pi$ and the tag-side D decays to $K\pi$, $K\pi\pi\pi$, $K\pi\pi^0$.

D^0 DECAY MODES

Most decay modes (other than the semileptonic modes) that involve a neutral K meson are now given as K^0_S modes, not as $\overline{K}^0$ modes. Nearly always it is a K^0_S that is measured, and interference between Cabibbo-allowed and doubly Cabibbo-suppressed modes can invalidate the assumption that $2\,\Gamma(K^0_S) = \Gamma(\overline{K}^0)$.

	Mode		Fraction (Γ_i/Γ)	Scale factor / Confidence level
	Topological modes			
Γ_1	$D^0 \to$ 0-prongs	[a]	(15 ± 6) %	
Γ_2	$D^0 \to$ 2-prongs		(70 ± 6) %	
Γ_3	$D^0 \to$ 4-prongs	[b]	(14.5 ± 0.5) %	
Γ_4	$D^0 \to$ 6-prongs	[c]	(6.4 ± 1.3) $\times 10^{-4}$	
	Inclusive modes			
Γ_5	$D^0 \to e^+$ anything	[d]	(6.49 ± 0.11) %	
Γ_6	$D^0 \to \mu^+$ anything		(6.7 ± 0.6) %	
Γ_7	$D^0 \to K^-$ anything		(54.7 ± 2.8) %	S=1.3
Γ_8	$D^0 \to \overline{K}^0$ anything + K^0 anything		(47 ± 4) %	
Γ_9	$D^0 \to K^+$ anything		(3.4 ± 0.4) %	
Γ_{10}	$D^0 \to K^*(892)^-$ anything		(15 ± 9) %	
Γ_{11}	$D^0 \to \overline{K}^*(892)^0$ anything		(9 ± 4) %	
Γ_{12}	$D^0 \to K^*(892)^+$ anything		< 3.6 %	CL=90%
Γ_{13}	$D^0 \to K^*(892)^0$ anything		(2.8 ± 1.3) %	
Γ_{14}	$D^0 \to \eta$ anything		(9.5 ± 0.9) %	
Γ_{15}	$D^0 \to \eta'$ anything		(2.48 ± 0.27) %	
Γ_{16}	$D^0 \to \phi$ anything		(1.05 ± 0.11) %	
	Semileptonic modes			
Γ_{17}	$D^0 \to K^-\ell^+\nu_\ell$			
Γ_{18}	$D^0 \to K^- e^+\nu_e$		(3.55 ± 0.05) %	S=1.2
Γ_{19}	$D^0 \to K^-\mu^+\nu_\mu$		(3.31 ± 0.13) %	
Γ_{20}	$D^0 \to K^*(892)^- e^+\nu_e$		(2.16 ± 0.16) %	
Γ_{21}	$D^0 \to K^*(892)^-\mu^+\nu_\mu$		(1.91 ± 0.24) %	
Γ_{22}	$D^0 \to K^-\pi^0 e^+\nu_e$		(1.6 $^{+1.3}_{-0.5}$) %	
Γ_{23}	$D^0 \to \overline{K}^0\pi^- e^+\nu_e$		(2.7 $^{+0.9}_{-0.7}$) %	
Γ_{24}	$D^0 \to K^-\pi^+\pi^- e^+\nu_e$		(2.8 $^{+1.4}_{-1.1}$) $\times 10^{-4}$	
Γ_{25}	$D^0 \to K_1(1270)^- e^+\nu_e$		(7.6 $^{+4.0}_{-3.1}$) $\times 10^{-4}$	
Γ_{26}	$D^0 \to K^-\pi^+\pi^-\mu^+\nu_\mu$		< 1.2 $\times 10^{-3}$	CL=90%
Γ_{27}	$D^0 \to (\overline{K}^*(892)\pi)^-\mu^+\nu_\mu$		< 1.4 $\times 10^{-3}$	CL=90%
Γ_{28}	$D^0 \to \pi^- e^+\nu_e$		(2.89 ± 0.08) $\times 10^{-3}$	S=1.1
Γ_{29}	$D^0 \to \pi^-\mu^+\nu_\mu$		(2.37 ± 0.24) $\times 10^{-3}$	
Γ_{30}	$D^0 \to \rho^- e^+\nu_e$		(1.77 ± 0.16) $\times 10^{-3}$	
	Hadronic modes with one $\overline{K}$			
Γ_{31}	$D^0 \to K^-\pi^+$		(3.88 ± 0.05) %	S=1.1
Γ_{32}	$D^0 \to K^+\pi^-$		(1.380 ± 0.028) $\times 10^{-4}$	
Γ_{33}	$D^0 \to K^0_S\pi^0$		(1.19 ± 0.04) %	
Γ_{34}	$D^0 \to K^0_L\pi^0$		(10.0 ± 0.7) $\times 10^{-3}$	
Γ_{35}	$D^0 \to K^0_S\pi^+\pi^-$	[e]	(2.83 ± 0.20) %	S=1.1
Γ_{36}	$D^0 \to K^0_S\rho^0$		(6.3 $^{+0.7}_{-0.8}$) $\times 10^{-3}$	

Γ_{37}	$D^0 \to K^0_S\omega, \omega \to \pi^+\pi^-$		$(\ 2.1 \pm 0.6\ )\times10^{-4}$		
Γ_{38}	$D^0 \to K^0_S(\pi^+\pi^-)_{S\text{-wave}}$		$(\ 3.4 \pm 0.8\ )\times10^{-3}$		
Γ_{39}	$D^0 \to K^0_S f_0(980),$ $f_0(980) \to \pi^+\pi^-$		$(\ 1.22\ ^{+\ 0.40}_{-\ 0.24}\ )\times10^{-3}$		
Γ_{40}	$D^0 \to K^0_S f_0(1370),$ $f_0(1370) \to \pi^+\pi^-$		$(\ 2.8\ ^{+\ 0.9}_{-\ 1.3}\ )\times10^{-3}$		
Γ_{41}	$D^0 \to K^0_S f_2(1270),$ $f_2(1270) \to \pi^+\pi^-$		$(\ 9\ ^{+10}_{-\ 6}\ )\times10^{-5}$		
Γ_{42}	$D^0 \to K^*(892)^-\pi^+,$ $K^*(892)^- \to K^0_S\pi^-$		$(\ 1.66\ ^{+\ 0.15}_{-\ 0.17}\ )$ %		
Γ_{43}	$D^0 \to K^*_0(1430)^-\pi^+,$ $K^*_0(1430)^- \to K^0_S\pi^-$		$(\ 2.70\ ^{+\ 0.40}_{-\ 0.34}\ )\times10^{-3}$		
Γ_{44}	$D^0 \to K^*_2(1430)^-\pi^+,$ $K^*_2(1430)^- \to K^0_S\pi^-$		$(\ 3.4\ ^{+\ 1.9}_{-\ 1.0}\ )\times10^{-4}$		
Γ_{45}	$D^0 \to K^*(1680)^-\pi^+,$ $K^*(1680)^- \to K^0_S\pi^-$		$(\ 4 \pm 4\ )\times10^{-4}$		
Γ_{46}	$D^0 \to K^*(892)^+\pi^-,$ $K^*(892)^+ \to K^0_S\pi^+$	[f]	$(\ 1.14\ ^{+\ 0.60}_{-\ 0.34}\ )\times10^{-4}$		
Γ_{47}	$D^0 \to K^*_0(1430)^+\pi^-,$ $K^*_0(1430)^+ \to K^0_S\pi^+$	[f]	$< 1.4 \times10^{-5}$	CL=95%	
Γ_{48}	$D^0 \to K^*_2(1430)^+\pi^-,$ $K^*_2(1430)^+ \to K^0_S\pi^+$	[f]	$< 3.4 \times10^{-5}$	CL=95%	
Γ_{49}	$D^0 \to K^0_S\pi^+\pi^-$ nonresonant		$(\ 2.5\ ^{+\ 6.0}_{-\ 1.6}\ )\times10^{-4}$		
Γ_{50}	$D^0 \to K^-\pi^+\pi^0$	[e]	$(13.9 \pm 0.5\ )$ %		S=1.7
Γ_{51}	$D^0 \to K^-\rho^+$		$(10.8 \pm 0.7\ )$ %		
Γ_{52}	$D^0 \to K^-\rho(1700)^+,$ $\rho(1700)^+ \to \pi^+\pi^0$		$(\ 7.9 \pm 1.7\ )\times10^{-3}$		
Γ_{53}	$D^0 \to K^*(892)^-\pi^+,$ $K^*(892)^- \to K^-\pi^0$		$(\ 2.22\ ^{+\ 0.40}_{-\ 0.19}\ )$ %		
Γ_{54}	$D^0 \to \overline{K}^*(892)^0\pi^0,$ $\overline{K}^*(892)^0 \to K^-\pi^+$		$(\ 1.88 \pm 0.23\ )$ %		
Γ_{55}	$D^0 \to K^*_0(1430)^-\pi^+,$ $K^*_0(1430)^- \to K^-\pi^0$		$(\ 4.6 \pm 2.1\ )\times10^{-3}$		
Γ_{56}	$D^0 \to \overline{K}^*_0(1430)^0\pi^0,$ $\overline{K}^*_0(1430)^0 \to K^-\pi^+$		$(\ 5.7\ ^{+\ 5.0}_{-\ 1.5}\ )\times10^{-3}$		
Γ_{57}	$D^0 \to K^*(1680)^-\pi^+,$ $K^*(1680)^- \to K^-\pi^0$		$(\ 1.8 \pm 0.7\ )\times10^{-3}$		
Γ_{58}	$D^0 \to K^-\pi^+\pi^0$ nonresonant		$(\ 1.11\ ^{+\ 0.50}_{-\ 0.19}\ )$ %		
Γ_{59}	$D^0 \to K^0_S 2\pi^0$		$(\ 9.1 \pm 1.1\ )\times10^{-3}$		S=2.2
Γ_{60}	$D^0 \to K^0_S(2\pi^0)$-S-wave		$(\ 2.6 \pm 0.7\ )\times10^{-3}$		
Γ_{61}	$D^0 \to \overline{K}^*(892)^0\pi^0,$ $\overline{K}^*(892)^0 \to K^0_S\pi^0$		$(\ 7.8 \pm 0.7\ )\times10^{-3}$		
Γ_{62}	$D^0 \to \overline{K}^*(1430)^0\pi^0, \overline{K}^{*0} \to K^0_S\pi^0$		$(\ 4 \pm 23\ )\times10^{-5}$		
Γ_{63}	$D^0 \to \overline{K}^*(1680)^0\pi^0, \overline{K}^{*0} \to K^0_S\pi^0$		$(\ 1.0 \pm 0.4\ )\times10^{-3}$		
Γ_{64}	$D^0 \to K^0_S f_2(1270), f_2 \to 2\pi^0$		$(\ 2.3 \pm 1.1\ )\times10^{-4}$		
Γ_{65}	$D^0 \to 2K^0_S$, one $K^0_S \to 2\pi^0$		$(\ 3.2 \pm 1.1\ )\times10^{-4}$		
Γ_{66}	$D^0 \to K^0_S 2\pi^0$ nonresonant				
Γ_{67}	$D^0 \to K^-2\pi^+\pi^-$	[e]	$(\ 8.08\ ^{+\ 0.21}_{-\ 0.19}\ )$ %		S=1.3
Γ_{68}	$D^0 \to K^-\pi^+\rho^0$ total		$(\ 6.75 \pm 0.33\ )$ %		
Γ_{69}	$D^0 \to K^-\pi^+\rho^0$ 3-body		$(\ 5.1 \pm 2.3\ )\times10^{-3}$		
Γ_{70}	$D^0 \to \overline{K}^*(892)^0\rho^0,$ $\overline{K}^*(892)^0 \to K^-\pi^+$		$(\ 1.05 \pm 0.23\ )$ %		
Γ_{71}	$D^0 \to K^-a_1(1260)^+,$ $a_1(1260)^+ \to 2\pi^+\pi^-$		$(\ 3.6 \pm 0.6\ )$ %		
Γ_{72}	$D^0 \to \overline{K}^*(892)^0\pi^+\pi^-$ total, $\overline{K}^*(892)^0 \to K^-\pi^+$		$(\ 1.6 \pm 0.4\ )$ %		
Γ_{73}	$D^0 \to \overline{K}^*(892)^0\pi^+\pi^-$ 3-body, $\overline{K}^*(892)^0 \to K^-\pi^+$		$(\ 9.9 \pm 2.3\ )\times10^{-3}$		
Γ_{74}	$D^0 \to K_1(1270)^-\pi^+,$ $K_1(1270)^- \to K^-\pi^+\pi^-$	[g]	$(\ 2.9 \pm 0.3\ )\times10^{-3}$		
Γ_{75}	$D^0 \to K^-2\pi^+\pi^-$ nonresonant		$(\ 1.88 \pm 0.26\ )$ %		
Γ_{76}	$D^0 \to K^0_S\pi^+\pi^-\pi^0$	[h]	$(\ 5.2 \pm 0.6\ )$ %		
Γ_{77}	$D^0 \to K^0_S\eta, \eta \to \pi^+\pi^-\pi^0$		$(\ 1.02 \pm 0.09\ )\times10^{-3}$		
Γ_{78}	$D^0 \to K^0_S\omega, \omega \to \pi^+\pi^-\pi^0$		$(\ 9.9 \pm 0.5\ )\times10^{-3}$		
Γ_{79}	$D^0 \to K^-\pi^+2\pi^0$				
Γ_{80}	$D^0 \to K^-2\pi^+\pi^-\pi^0$		$(\ 4.2 \pm 0.4\ )$ %		
Γ_{81}	$D^0 \to \overline{K}^*(892)^0\pi^+\pi^-\pi^0,$ $\overline{K}^*(892)^0 \to K^-\pi^+$		$(\ 1.3 \pm 0.6\ )$ %		
Γ_{82}	$D^0 \to K^-\pi^+\omega, \omega \to \pi^+\pi^-\pi^0$		$(\ 2.7 \pm 0.5\ )$ %		
Γ_{83}	$D^0 \to \overline{K}^*(892)^0\omega,$ $\overline{K}^*(892)^0 \to K^-\pi^+,$ $\omega \to \pi^+\pi^-\pi^0$		$(\ 6.5 \pm 3.0\ )\times10^{-3}$		
Γ_{84}	$D^0 \to K^0_S\eta\pi^0$		$(\ 5.5 \pm 1.1\ )\times10^{-3}$		
Γ_{85}	$D^0 \to K^0_S a_0(980),$ $a_0(980) \to \eta\pi^0$		$(\ 6.5 \pm 2.0\ )\times10^{-3}$		
Γ_{86}	$D^0 \to \overline{K}^*(892)^0\eta,$ $\overline{K}^*(892)^0 \to K^0_S\pi$		$(\ 1.6 \pm 0.5\ )\times10^{-3}$		
Γ_{87}	$D^0 \to K^0_S 2\pi^+2\pi^-$		$(\ 2.69 \pm 0.31\ )\times10^{-3}$		
Γ_{88}	$D^0 \to K^0_S\rho^0\pi^+\pi^-,$ no $K^*(892)^-$		$(\ 1.1 \pm 0.7\ )\times10^{-3}$		
Γ_{89}	$D^0 \to K^*(892)^-2\pi^+\pi^-,$ $K^*(892)^- \to K^0_S\pi^-$, no ρ^0		$(\ 5 \pm 8\ )\times10^{-4}$		
Γ_{90}	$D^0 \to K^*(892)^-\rho^0\pi^+,$ $K^*(892)^- \to K^0_S\pi^-$		$(\ 1.6 \pm 0.6\ )\times10^{-3}$		
Γ_{91}	$D^0 \to K^0_S 2\pi^+2\pi^-$ nonresonant		$< 1.2 \times10^{-3}$	CL=90%	
Γ_{92}	$D^0 \to \overline{K}^0\pi^+\pi^-2\pi^0(\pi^0)$				
Γ_{93}	$D^0 \to K^-3\pi^+2\pi^-$		$(\ 2.2 \pm 0.6\ )\times10^{-4}$		

Fractions of many of the following modes with resonances have already appeared above as submodes of particular charged-particle modes. (Modes for which there are only upper limits and $\overline{K}^*(892)\rho$ submodes only appear below.)

Γ_{94}	$D^0 \to K^0_S\eta$		$(\ 4.79 \pm 0.30\ )\times10^{-3}$		
Γ_{95}	$D^0 \to K^0_S\omega$		$(\ 1.11 \pm 0.06\ )$ %		
Γ_{96}	$D^0 \to K^0_S\eta'(958)$		$(\ 9.4 \pm 0.5\ )\times10^{-3}$		
Γ_{97}	$D^0 \to K^-a_1(1260)^+$		$(\ 7.8 \pm 1.1\ )$ %		
Γ_{98}	$D^0 \to K^-a_2(1320)^+$		$< 2 \times10^{-3}$	CL=90%	
Γ_{99}	$D^0 \to \overline{K}^*(892)^0\pi^+\pi^-$ total		$(\ 2.4 \pm 0.5\ )$ %		
Γ_{100}	$D^0 \to \overline{K}^*(892)^0\pi^+\pi^-$ 3-body		$(\ 1.48 \pm 0.34\ )$ %		
Γ_{101}	$D^0 \to \overline{K}^*(892)^0\rho^0$		$(\ 1.58 \pm 0.34\ )$ %		
Γ_{102}	$D^0 \to \overline{K}^*(892)^0\rho^0$ transverse		$(\ 1.7 \pm 0.6\ )$ %		
Γ_{103}	$D^0 \to \overline{K}^*(892)^0\rho^0$ S-wave		$(\ 3.0 \pm 0.6\ )$ %		
Γ_{104}	$D^0 \to \overline{K}^*(892)^0\rho^0$ S-wave long.		$< 3 \times10^{-3}$	CL=90%	
Γ_{105}	$D^0 \to \overline{K}^*(892)^0\rho^0$ P-wave		$< 3 \times10^{-3}$	CL=90%	
Γ_{106}	$D^0 \to \overline{K}^*(892)^0\rho^0$ D-wave		$(\ 2.1 \pm 0.6\ )$ %		
Γ_{107}	$D^0 \to K^-\pi^+ f_0(980)$				
Γ_{108}	$D^0 \to \overline{K}^*(892)^0 f_0(980)$				
Γ_{109}	$D^0 \to K_1(1270)^-\pi^+$	[g]	$(\ 1.6 \pm 0.8\ )$ %		
Γ_{110}	$D^0 \to K_1(1400)^-\pi^+$		< 1.2 %	CL=90%	
Γ_{111}	$D^0 \to K^*(1410)^-\pi^+$				
Γ_{112}	$D^0 \to \overline{K}^*(892)^0\pi^+\pi^-\pi^0$		$(\ 1.9 \pm 0.9\ )$ %		
Γ_{113}	$D^0 \to \overline{K}^*(892)^0\eta$				
Γ_{114}	$D^0 \to K^-\pi^+\omega$		$(\ 3.0 \pm 0.6\ )$ %		
Γ_{115}	$D^0 \to \overline{K}^*(892)^0\omega$		$(\ 1.1 \pm 0.5\ )$ %		
Γ_{116}	$D^0 \to K^-\pi^+\eta'(958)$		$(\ 7.5 \pm 1.9\ )\times10^{-3}$		
Γ_{117}	$D^0 \to \overline{K}^*(892)^0\eta'(958)$		$< 1.1 \times10^{-3}$	CL=90%	

Hadronic modes with three K's

Γ_{118}	$D^0 \to K^0_S K^+K^-$		$(\ 4.47 \pm 0.34\ )\times10^{-3}$		
Γ_{119}	$D^0 \to K^0_S a_0(980)^0, a_0^0 \to K^+K^-$		$(\ 3.0 \pm 0.4\ )\times10^{-3}$		
Γ_{120}	$D^0 \to K^-a_0(980)^+, a_0^+ \to K^+K^0_S$		$(\ 6.0 \pm 1.8\ )\times10^{-4}$		
Γ_{121}	$D^0 \to K^+a_0(980)^-, a_0^- \to K^-K^0_S$		$< 1.1 \times10^{-4}$	CL=95%	
Γ_{122}	$D^0 \to K^0_S f_0(980), f_0 \to K^+K^-$		$< 9 \times10^{-5}$	CL=95%	
Γ_{123}	$D^0 \to K^0_S\phi, \phi \to K^+K^-$		$(\ 2.05 \pm 0.16\ )\times10^{-3}$		
Γ_{124}	$D^0 \to K^0_S f_0(1370), f_0 \to K^+K^-$		$(\ 1.7 \pm 1.1\ )\times10^{-4}$		
Γ_{125}	$D^0 \to 3K^0_S$		$(\ 9.1 \pm 1.3\ )\times10^{-4}$		
Γ_{126}	$D^0 \to K^+2K^-\pi^+$		$(\ 2.21 \pm 0.31\ )\times10^{-4}$		

Γ_{127}	$D^0 \to K^+ K^- \overline{K}^*(892)^0$, $\overline{K}^*(892)^0 \to K^- \pi^+$	$(4.4 \pm 1.7) \times 10^{-5}$		
Γ_{128}	$D^0 \to K^- \pi^+ \phi$, $\phi \to K^+ K^-$	$(4.0 \pm 1.7) \times 10^{-5}$		
Γ_{129}	$D^0 \to \phi \overline{K}^*(892)^0$, $\phi \to K^+ K^-$, $\overline{K}^*(892)^0 \to K^- \pi^+$	$(1.06 \pm 0.20) \times 10^{-4}$		
Γ_{130}	$D^0 \to K^+ 2K^- \pi^+$ nonresonant	$(3.3 \pm 1.5) \times 10^{-5}$		
Γ_{131}	$D^0 \to 2K^0_S K^\pm \pi^\mp$	$(6.0 \pm 1.3) \times 10^{-4}$		
	Pionic modes			
Γ_{132}	$D^0 \to \pi^+ \pi^-$	$(1.402 \pm 0.026) \times 10^{-3}$		S=1.1
Γ_{133}	$D^0 \to 2\pi^0$	$(8.20 \pm 0.35) \times 10^{-4}$		
Γ_{134}	$D^0 \to \pi^+ \pi^- \pi^0$	(1.43 ± 0.06) %		S=1.9
Γ_{135}	$D^0 \to \rho^+ \pi^-$	$(9.8 \pm 0.4) \times 10^{-3}$		
Γ_{136}	$D^0 \to \rho^0 \pi^0$	$(3.72 \pm 0.22) \times 10^{-3}$		
Γ_{137}	$D^0 \to \rho^- \pi^+$	$(4.96 \pm 0.24) \times 10^{-3}$		
Γ_{138}	$D^0 \to \rho(1450)^+ \pi^-$, $\rho(1450)^+ \to \pi^+ \pi^0$	$(1.6 \pm 2.0) \times 10^{-5}$		
Γ_{139}	$D^0 \to \rho(1450)^0 \pi^0$, $\rho(1450)^0 \to \pi^+ \pi^-$	$(4.3 \pm 1.9) \times 10^{-5}$		
Γ_{140}	$D^0 \to \rho(1450)^- \pi^+$, $\rho(1450)^- \to \pi^- \pi^0$	$(2.6 \pm 0.4) \times 10^{-4}$		
Γ_{141}	$D^0 \to \rho(1700)^+ \pi^-$, $\rho(1700)^+ \to \pi^+ \pi^0$	$(5.9 \pm 1.4) \times 10^{-4}$		
Γ_{142}	$D^0 \to \rho(1700)^0 \pi^0$, $\rho(1700)^0 \to \pi^+ \pi^-$	$(7.2 \pm 1.7) \times 10^{-4}$		
Γ_{143}	$D^0 \to \rho(1700)^- \pi^+$, $\rho(1700)^- \to \pi^- \pi^0$	$(4.6 \pm 1.1) \times 10^{-4}$		
Γ_{144}	$D^0 \to f_0(980) \pi^0$, $f_0(980) \to \pi^+ \pi^-$	$(3.6 \pm 0.8) \times 10^{-5}$		
Γ_{145}	$D^0 \to f_0(500) \pi^0$, $f_0(500) \to \pi^+ \pi^-$	$(1.18 \pm 0.21) \times 10^{-4}$		
Γ_{146}	$D^0 \to (\pi^+ \pi^-)_{S-\text{wave}} \pi^0$			
Γ_{147}	$D^0 \to f_0(1370) \pi^0$, $f_0(1370) \to \pi^+ \pi^-$	$(5.3 \pm 2.1) \times 10^{-5}$		
Γ_{148}	$D^0 \to f_0(1500) \pi^0$, $f_0(1500) \to \pi^+ \pi^-$	$(5.6 \pm 1.5) \times 10^{-5}$		
Γ_{149}	$D^0 \to f_0(1710) \pi^0$, $f_0(1710) \to \pi^+ \pi^-$	$(4.4 \pm 1.5) \times 10^{-5}$		
Γ_{150}	$D^0 \to f_2(1270) \pi^0$, $f_2(1270) \to \pi^+ \pi^-$	$(1.89 \pm 0.20) \times 10^{-4}$		
Γ_{151}	$D^0 \to \pi^+ \pi^- \pi^0$ nonresonant	$(1.20 \pm 0.35) \times 10^{-4}$		
Γ_{152}	$D^0 \to 3\pi^0$	$< 3.5 \times 10^{-4}$		CL=90%
Γ_{153}	$D^0 \to 2\pi^+ 2\pi^-$	$(7.42 \pm 0.21) \times 10^{-3}$		S=1.1
Γ_{154}	$D^0 \to a_1(1260)^+ \pi^-$, $a_1^+ \to 2\pi^+ \pi^-$ total	$(4.45 \pm 0.31) \times 10^{-3}$		
Γ_{155}	$D^0 \to a_1(1260)^+ \pi^-$, $a_1^+ \to \rho^0 \pi^+$ S-wave	$(3.21 \pm 0.25) \times 10^{-3}$		
Γ_{156}	$D^0 \to a_1(1260)^+ \pi^-$, $a_1^+ \to \rho^0 \pi^+$ D-wave	$(1.9 \pm 0.5) \times 10^{-4}$		
Γ_{157}	$D^0 \to a_1(1260)^+ \pi^-$, $a_1^+ \to \sigma \pi^+$	$(6.2 \pm 0.7) \times 10^{-4}$		
Γ_{158}	$D^0 \to 2\rho^0$ total	$(1.82 \pm 0.13) \times 10^{-3}$		
Γ_{159}	$D^0 \to 2\rho^0$, parallel helicities	$(8.2 \pm 3.2) \times 10^{-5}$		
Γ_{160}	$D^0 \to 2\rho^0$, perpendicular helicities	$(4.8 \pm 0.6) \times 10^{-4}$		
Γ_{161}	$D^0 \to 2\rho^0$, longitudinal helicities	$(1.25 \pm 0.10) \times 10^{-3}$		
Γ_{162}	$D^0 \to$ Resonant $(\pi^+ \pi^-) \pi^+ \pi^-$ 3-body total	$(1.48 \pm 0.12) \times 10^{-3}$		
Γ_{163}	$D^0 \to \sigma \pi^+ \pi^-$	$(6.1 \pm 0.9) \times 10^{-4}$		
Γ_{164}	$D^0 \to f_0(980) \pi^+ \pi^-$, $f_0 \to \pi^+ \pi^-$	$(1.8 \pm 0.5) \times 10^{-4}$		
Γ_{165}	$D^0 \to f_2(1270) \pi^+ \pi^-$, $f_2 \to \pi^+ \pi^-$	$(3.6 \pm 0.6) \times 10^{-4}$		
Γ_{166}	$D^0 \to \pi^+ \pi^- 2\pi^0$	(1.00 ± 0.09) %		
Γ_{167}	$D^0 \to \eta \pi^0$	$(6.8 \pm 0.7) \times 10^{-4}$	[i]	
Γ_{168}	$D^0 \to \omega \pi^0$	$< 2.6 \times 10^{-4}$	[i]	CL=90%
Γ_{169}	$D^0 \to 2\pi^+ 2\pi^- \pi^0$	$(4.1 \pm 0.5) \times 10^{-3}$		
Γ_{170}	$D^0 \to \eta \pi^+ \pi^-$	$(1.09 \pm 0.16) \times 10^{-3}$	[i]	
Γ_{171}	$D^0 \to \omega \pi^+ \pi^-$	$(1.6 \pm 0.5) \times 10^{-3}$	[i]	
Γ_{172}	$D^0 \to 3\pi^+ 3\pi^-$	$(4.2 \pm 1.2) \times 10^{-4}$		
Γ_{173}	$D^0 \to \eta'(958) \pi^0$	$(9.0 \pm 1.4) \times 10^{-4}$		
Γ_{174}	$D^0 \to \eta'(958) \pi^+ \pi^-$	$(4.5 \pm 1.7) \times 10^{-4}$		
Γ_{175}	$D^0 \to 2\eta$	$(1.67 \pm 0.20) \times 10^{-3}$		
Γ_{176}	$D^0 \to \eta \eta'(958)$	$(1.05 \pm 0.26) \times 10^{-3}$		
	Hadronic modes with a $K\overline{K}$ pair			
Γ_{177}	$D^0 \to K^+ K^-$	$(3.96 \pm 0.08) \times 10^{-3}$		S=1.4
Γ_{178}	$D^0 \to 2K^0_S$	$(1.7 \pm 0.4) \times 10^{-4}$		S=2.5
Γ_{179}	$D^0 \to K^0_S K^- \pi^+$	$(3.5 \pm 0.5) \times 10^{-3}$		S=1.2
Γ_{180}	$D^0 \to \overline{K}^*(892)^0 K^0_S$, $\overline{K}^{*0} \to K^- \pi^+$	$< 5 \times 10^{-4}$		CL=90%
Γ_{181}	$D^0 \to K^0_S K^+ \pi^-$	$(2.1 \pm 0.4) \times 10^{-3}$		S=1.3
Γ_{182}	$D^0 \to K^*(892)^0 K^0_S$, $K^{*0} \to K^+ \pi^-$	$< 1.8 \times 10^{-4}$		CL=90%
Γ_{183}	$D^0 \to K^+ K^- \pi^0$	$(3.29 \pm 0.14) \times 10^{-3}$		
Γ_{184}	$D^0 \to K^*(892)^+ K^-$, $K^*(892)^+ \to K^+ \pi^0$	$(1.46 \pm 0.07) \times 10^{-3}$		
Γ_{185}	$D^0 \to K^*(892)^- K^+$, $K^*(892)^- \to K^- \pi^0$	$(5.2 \pm 0.4) \times 10^{-4}$		
Γ_{186}	$D^0 \to (K^+ \pi^0)_{S-wave} K^-$	$(2.34 \pm 0.17) \times 10^{-3}$		
Γ_{187}	$D^0 \to (K^- \pi^0)_{S-wave} K^+$	$(1.3 \pm 0.4) \times 10^{-4}$		
Γ_{188}	$D^0 \to f_0(980) \pi^0$, $f_0 \to K^+ K^-$	$(3.5 \pm 0.6) \times 10^{-4}$		
Γ_{189}	$D^0 \to \phi \pi^0$, $\phi \to K^+ K^-$	$(6.4 \pm 0.4) \times 10^{-4}$		
Γ_{190}	$D^0 \to K^+ K^- \pi^0$ nonresonant			
Γ_{191}	$D^0 \to 2K^0_S \pi^0$	$< 5.9 \times 10^{-4}$		
Γ_{192}	$D^0 \to K^+ K^- \pi^+ \pi^-$	$(2.43 \pm 0.12) \times 10^{-3}$		
Γ_{193}	$D^0 \to \phi(\pi^+ \pi^-)_{S-wave}$, $\phi \to K^+ K^-$	$(2.50 \pm 0.33) \times 10^{-4}$		
Γ_{194}	$D^0 \to (\phi \rho^0)_{S-wave}$, $\phi \to K^+ K^-$	$(9.3 \pm 1.2) \times 10^{-4}$		
Γ_{195}	$D^0 \to (\phi \rho^0)_{D-wave}$, $\phi \to K^+ K^-$	$(8.3 \pm 2.3) \times 10^{-5}$		
Γ_{196}	$D^0 \to (K^{*0} \overline{K}^{*0})_{S-wave}$, $K^{*0} \to K^\pm \pi^\mp$	$(1.48 \pm 0.30) \times 10^{-4}$		
Γ_{197}	$D^0 \to (K^- \pi^+)_{P-wave}$, $(K^+ \pi^-)_{S-wave}$,	$(2.6 \pm 0.5) \times 10^{-4}$		
Γ_{198}	$D^0 \to K_1(1270)^+ K^-$, $K_1(1270)^+ \to K^{*0} \pi^+$	$(1.8 \pm 0.5) \times 10^{-4}$		
Γ_{199}	$D^0 \to K_1(1270)^+ K^-$, $K_1(1270)^+ \to \rho^0 K^+$	$(1.14 \pm 0.26) \times 10^{-4}$		
Γ_{200}	$D^0 \to K_1(1270)^- K^+$, $K_1(1270)^- \to \overline{K}^{*0} \pi^-$	$(2.2 \pm 1.2) \times 10^{-5}$		
Γ_{201}	$D^0 \to K_1(1270)^- K^+$, $K_1(1270)^- \to \rho^0 K^-$	$(1.46 \pm 0.25) \times 10^{-4}$		
Γ_{202}	$D^0 \to K^*(1410)^+ K^-$, $K^*(1410)^+ \to K^{*0} \pi^+$	$(1.02 \pm 0.26) \times 10^{-4}$		
Γ_{203}	$D^0 \to K^*(1410)^- K^+$, $K^*(1410)^- \to \overline{K}^{*0} \pi^-$	$(1.14 \pm 0.25) \times 10^{-4}$		
Γ_{204}	$D^0 \to K^+ K^- \rho^0$ 3-body			
Γ_{205}	$D^0 \to f_0(980) \pi^+ \pi^-$, $f_0 \to K^+ K^-$			
Γ_{206}	$D^0 \to K^*(892)^0 K^\mp \pi^\pm$ 3-body, $K^{*0} \to K^\pm \pi^\mp$			
Γ_{207}	$D^0 \to K^*(892)^0 \overline{K}^*(892)^0$, $K^{*0} \to K^\pm \pi^\mp$			
Γ_{208}	$D^0 \to K_1(1270)^\pm K^\mp$, $K_1(1270)^\pm \to K^\pm \pi^+ \pi^-$			
Γ_{209}	$D^0 \to K_1(1400)^\pm K^\mp$, $K_1(1400)^\pm \to K^\pm \pi^+ \pi^-$			
Γ_{210}	$D^0 \to 2K^0_S \pi^+ \pi^-$	$(1.23 \pm 0.24) \times 10^{-3}$		
Γ_{211}	$D^0 \to K^0_S K^- 2\pi^+ \pi^-$	$< 1.5 \times 10^{-4}$		CL=90%
Γ_{212}	$D^0 \to K^+ K^- \pi^+ \pi^- \pi^0$	$(3.1 \pm 2.0) \times 10^{-3}$		
	Other $K\overline{K}X$ modes. They include all decay modes of the ϕ, η, and ω.			
Γ_{213}	$D^0 \to \phi \pi^0$			
Γ_{214}	$D^0 \to \phi \eta$	$(1.4 \pm 0.5) \times 10^{-4}$		
Γ_{215}	$D^0 \to \phi \omega$	$< 2.1 \times 10^{-3}$		CL=90%
	Radiative modes			
Γ_{216}	$D^0 \to \rho^0 \gamma$	$< 2.4 \times 10^{-4}$		CL=90%
Γ_{217}	$D^0 \to \omega \gamma$	$< 2.4 \times 10^{-4}$		CL=90%
Γ_{218}	$D^0 \to \phi \gamma$	$(2.70 \pm 0.35) \times 10^{-5}$		
Γ_{219}	$D^0 \to \overline{K}^*(892)^0 \gamma$	$(3.27 \pm 0.34) \times 10^{-4}$		

Doubly Cabibbo suppressed (*DC*) modes or $\Delta C = 2$ forbidden via mixing (*C2M*) modes

Γ_{220}	$D^0 \to K^+ \ell^- \overline{\nu}_\ell$ via $\overline{D}^0$		$<$ 2.2	$\times 10^{-5}$	CL=90%	
Γ_{221}	$D^0 \to K^+$ or $K^*(892)^+ e^- \overline{\nu}_e$ via $\overline{D}^0$		$<$ 6	$\times 10^{-5}$	CL=90%	
Γ_{222}	$D^0 \to K^+ \pi^-$	*DC*	(1.47 $\pm$ 0.07)	$\times 10^{-4}$		S=2.8
Γ_{223}	$D^0 \to K^+ \pi^-$ via DCS		(1.31 $\pm$ 0.08)	$\times 10^{-4}$		
Γ_{224}	$D^0 \to K^+ \pi^-$ via $\overline{D}^0$		$<$ 1.6	$\times 10^{-5}$	CL=95%	
Γ_{225}	$D^0 \to K^0_S \pi^+ \pi^-$ in $D^0 \to \overline{D}^0$		$<$ 1.8	$\times 10^{-4}$	CL=95%	
Γ_{226}	$D^0 \to K^*(892)^+ \pi^-$, $K^*(892)^+ \to K^0_S \pi^+$	*DC*	($1.14 \pm {}^{0.60}_{0.34}$)	$\times 10^{-4}$		
Γ_{227}	$D^0 \to K^*_0(1430)^+ \pi^-$, $K^*_0(1430)^+ \to K^0_S \pi^+$	*DC*	$<$ 1.4	$\times 10^{-5}$		
Γ_{228}	$D^0 \to K^*_2(1430)^+ \pi^-$, $K^*_2(1430)^+ \to K^0_S \pi^+$	*DC*	$<$ 3.4	$\times 10^{-5}$		
Γ_{229}	$D^0 \to K^+ \pi^- \pi^0$	*DC*	(3.04 $\pm$ 0.17)	$\times 10^{-4}$		
Γ_{230}	$D^0 \to K^+ \pi^- \pi^0$ via $\overline{D}^0$		(7.3 $\pm$ 0.5)	$\times 10^{-4}$		
Γ_{231}	$D^0 \to K^+ \pi^+ 2\pi^-$	*DC*	(2.62 $\pm$ 0.11)	$\times 10^{-4}$		
Γ_{232}	$D^0 \to K^+ \pi^+ 2\pi^-$ via $\overline{D}^0$		$<$ 4	$\times 10^{-4}$	CL=90%	
Γ_{233}	$D^0 \to K^+ \pi^-$ or $K^+ \pi^+ 2\pi^-$ via $\overline{D}^0$					
Γ_{234}	$D^0 \to \mu^-$ anything via $\overline{D}^0$		$<$ 4	$\times 10^{-4}$	CL=90%	

$\Delta C = 1$ weak neutral current (*C1*) modes, Lepton Family number (*LF*) violating modes, Lepton (*L*) or Baryon (*B*) number violating modes

Γ_{235}	$D^0 \to \gamma\gamma$	*C1*	$<$ 2.2	$\times 10^{-6}$	CL=90%	
Γ_{236}	$D^0 \to e^+ e^-$	*C1*	$<$ 7.9	$\times 10^{-8}$	CL=90%	
Γ_{237}	$D^0 \to \mu^+ \mu^-$	*C1*	$<$ 6.2	$\times 10^{-9}$	CL=90%	
Γ_{238}	$D^0 \to \pi^0 e^+ e^-$	*C1*	$<$ 4.5	$\times 10^{-5}$	CL=90%	
Γ_{239}	$D^0 \to \pi^0 \mu^+ \mu^-$	*C1*	$<$ 1.8	$\times 10^{-4}$	CL=90%	
Γ_{240}	$D^0 \to \eta e^+ e^-$	*C1*	$<$ 1.1	$\times 10^{-4}$	CL=90%	
Γ_{241}	$D^0 \to \eta \mu^+ \mu^-$	*C1*	$<$ 5.3	$\times 10^{-4}$	CL=90%	
Γ_{242}	$D^0 \to \pi^+ \pi^- e^+ e^-$	*C1*	$<$ 3.73	$\times 10^{-4}$	CL=90%	
Γ_{243}	$D^0 \to \rho^0 e^+ e^-$	*C1*	$<$ 1.0	$\times 10^{-4}$	CL=90%	
Γ_{244}	$D^0 \to \pi^+ \pi^- \mu^+ \mu^-$	*C1*	$<$ 5.5	$\times 10^{-7}$	CL=90%	
Γ_{245}	$D^0 \to \rho^0 \mu^+ \mu^-$	*C1*	$<$ 2.2	$\times 10^{-5}$	CL=90%	
Γ_{246}	$D^0 \to \omega e^+ e^-$	*C1*	$<$ 1.8	$\times 10^{-4}$	CL=90%	
Γ_{247}	$D^0 \to \omega \mu^+ \mu^-$	*C1*	$<$ 8.3	$\times 10^{-4}$	CL=90%	
Γ_{248}	$D^0 \to K^- K^+ e^+ e^-$	*C1*	$<$ 3.15	$\times 10^{-4}$	CL=90%	
Γ_{249}	$D^0 \to \phi e^+ e^-$	*C1*	$<$ 5.2	$\times 10^{-5}$	CL=90%	
Γ_{250}	$D^0 \to K^- K^+ \mu^+ \mu^-$	*C1*	$<$ 3.3	$\times 10^{-5}$	CL=90%	
Γ_{251}	$D^0 \to \phi \mu^+ \mu^-$	*C1*	$<$ 3.1	$\times 10^{-5}$	CL=90%	
Γ_{252}	$D^0 \to \overline{K}^0 e^+ e^-$		[*j*] $<$ 1.1	$\times 10^{-4}$	CL=90%	
Γ_{253}	$D^0 \to \overline{K}^0 \mu^+ \mu^-$		[*j*] $<$ 2.6	$\times 10^{-4}$	CL=90%	
Γ_{254}	$D^0 \to K^- \pi^+ e^+ e^-$	*C1*	$<$ 3.85	$\times 10^{-4}$	CL=90%	
Γ_{255}	$D^0 \to \overline{K}^*(892)^0 e^+ e^-$		[*j*] $<$ 4.7	$\times 10^{-5}$	CL=90%	
Γ_{256}	$D^0 \to K^- \pi^+ \mu^+ \mu^-$	*C1*	$<$ 3.59	$\times 10^{-4}$	CL=90%	
Γ_{257}	$D^0 \to \overline{K}^*(892)^0 \mu^+ \mu^-$		[*j*] $<$ 2.4	$\times 10^{-5}$	CL=90%	
Γ_{258}	$D^0 \to \pi^+ \pi^- \pi^0 \mu^+ \mu^-$	*C1*	$<$ 8.1	$\times 10^{-4}$	CL=90%	
Γ_{259}	$D^0 \to \mu^\pm e^\mp$	*LF*	[*k*] $<$ 2.6	$\times 10^{-7}$	CL=90%	
Γ_{260}	$D^0 \to \pi^0 e^\pm \mu^\mp$	*LF*	[*k*] $<$ 8.6	$\times 10^{-5}$	CL=90%	
Γ_{261}	$D^0 \to \eta e^\pm \mu^\mp$	*LF*	[*k*] $<$ 1.0	$\times 10^{-4}$	CL=90%	
Γ_{262}	$D^0 \to \pi^+ \pi^- e^\pm \mu^\mp$	*LF*	[*k*] $<$ 1.5	$\times 10^{-5}$	CL=90%	
Γ_{263}	$D^0 \to \rho^0 e^\pm \mu^\mp$	*LF*	[*k*] $<$ 4.9	$\times 10^{-5}$	CL=90%	
Γ_{264}	$D^0 \to \omega e^\pm \mu^\mp$	*LF*	[*k*] $<$ 1.2	$\times 10^{-4}$	CL=90%	
Γ_{265}	$D^0 \to K^- K^+ e^\pm \mu^\mp$	*LF*	[*k*] $<$ 1.8	$\times 10^{-4}$	CL=90%	
Γ_{266}	$D^0 \to \phi e^\pm \mu^\mp$	*LF*	[*k*] $<$ 3.4	$\times 10^{-5}$	CL=90%	
Γ_{267}	$D^0 \to \overline{K}^0 e^\pm \mu^\mp$	*LF*	[*k*] $<$ 1.0	$\times 10^{-4}$	CL=90%	
Γ_{268}	$D^0 \to K^- \pi^+ e^\pm \mu^\mp$	*LF*	[*k*] $<$ 5.53	$\times 10^{-4}$	CL=90%	
Γ_{269}	$D^0 \to \overline{K}^*(892)^0 e^\pm \mu^\mp$	*LF*	[*k*] $<$ 8.3	$\times 10^{-5}$	CL=90%	
Γ_{270}	$D^0 \to 2\pi^- 2e^+ +$ c.c.	*L*	$<$ 1.12	$\times 10^{-4}$	CL=90%	
Γ_{271}	$D^0 \to 2\pi^- 2\mu^+ +$ c.c.	*L*	$<$ 2.9	$\times 10^{-5}$	CL=90%	
Γ_{272}	$D^0 \to K^- \pi^- 2e^+ +$ c.c.	*L*	$<$ 2.06	$\times 10^{-4}$	CL=90%	
Γ_{273}	$D^0 \to K^- \pi^- 2\mu^+ +$ c.c.	*L*	$<$ 3.9	$\times 10^{-4}$	CL=90%	
Γ_{274}	$D^0 \to 2K^- 2e^+ +$ c.c.	*L*	$<$ 1.52	$\times 10^{-4}$	CL=90%	
Γ_{275}	$D^0 \to 2K^- 2\mu^+ +$ c.c.	*L*	$<$ 9.4	$\times 10^{-5}$	CL=90%	
Γ_{276}	$D^0 \to \pi^- \pi^- e^+ \mu^+ +$ c.c.	*L*	$<$ 7.9	$\times 10^{-5}$	CL=90%	
Γ_{277}	$D^0 \to K^- \pi^- e^+ \mu^+ +$ c.c.	*L*	$<$ 2.18	$\times 10^{-4}$	CL=90%	
Γ_{278}	$D^0 \to 2K^- e^+ \mu^+ +$ c.c.	*L*	$<$ 5.7	$\times 10^{-5}$	CL=90%	
Γ_{279}	$D^0 \to p e^-$	*L,B*	[*l*] $<$ 1.0	$\times 10^{-5}$	CL=90%	
Γ_{280}	$D^0 \to \overline{p} e^+$	*L,B*	[*n*] $<$ 1.1	$\times 10^{-5}$	CL=90%	
Γ_{281}	Unaccounted decay modes		(38.2 $\pm$ 1.4) %			S=1.1

[*a*] This value is obtained by subtracting the branching fractions for 2-, 4- and 6-prongs from unity.

[*b*] This is the sum of our $K^- 2\pi^+ \pi^-$, $K^- 2\pi^+ \pi^- \pi^0$, $\overline{K}^0 2\pi^+ 2\pi^-$, $K^+ 2K^- \pi^+$, $2\pi^+ 2\pi^-$, $2\pi^+ 2\pi^- \pi^0$, $K^+ K^- \pi^+ \pi^-$, and $K^+ K^- \pi^+ \pi^- \pi^0$, branching fractions.

[*c*] This is the sum of our $K^- 3\pi^+ 2\pi^-$ and $3\pi^+ 3\pi^-$ branching fractions.

[*d*] The branching fractions for the $K^- e^+ \nu_e$, $K^*(892)^- e^+ \nu_e$, $\pi^- e^+ \nu_e$, and $\rho^- e^+ \nu_e$ modes add up to 6.19 $\pm$ 0.17 %.

[*e*] The branching fraction for this mode may differ from the sum of the submodes that contribute to it, due to interference effects. See the relevant papers.

[*f*] This is a doubly Cabibbo-suppressed mode.

[*g*] The two experiments measuring this fraction are in serious disagreement. See the Particle Listings.

[*h*] Submodes of the $D^0 \to K^0_S \pi^+ \pi^- \pi^0$ mode with a K^* and/or ρ were studied by COFFMAN 92B, but with only 140 events. With nothing new for 18 years, we refer to our 2008 edition, Physics Letters **B667** 1 (2008), for those results.

[*i*] This branching fraction includes all the decay modes of the resonance in the final state.

[*j*] This mode is not a useful test for a ΔC=1 weak neutral current because both quarks must change flavor in this decay.

[*k*] The value is for the sum of the charge states or particle/antiparticle states indicated.

[*l*] This limit is for either D^0 or $\overline{D}^0$ to $p e^-$.

[*n*] This limit is for either D^0 or $\overline{D}^0$ to $\overline{p} e^+$.

CONSTRAINED FIT INFORMATION

An overall fit to 54 branching ratios uses 106 measurements and one constraint to determine 31 parameters. The overall fit has a $\chi^2 = 100.3$ for 76 degrees of freedom.

The following *off-diagonal* array elements are the correlation coefficients $\langle \delta x_i \delta x_j \rangle / (\delta x_i \cdot \delta x_j)$, in percent, from the fit to the branching fractions, $x_i \equiv \Gamma_i / \Gamma_{\rm total}$. The fit constrains the x_i whose labels appear in this array to sum to one.

x_{18}	2									
x_{19}	20	9								
x_{20}	0	1	0							
x_{28}	0	0	0	0						
x_{29}	3	2	17	0	0					
x_{31}	4	49	18	2	0	3				
x_{33}	1	17	6	2	0	1	35			
x_{35}	0	7	2	15	0	0	14	16		
x_{50}	0	−2	−1	0	0	0	−3	−1	0	
x_{67}	1	10	4	0	0	1	21	8	3	54
x_{76}	0	3	1	6	0	0	5	6	40	0
x_{80}	0	4	2	0	0	0	8	3	1	8
x_{94}	1	9	3	0	0	1	18	6	2	−1
x_{95}	0	0	0	1	0	0	1	1	5	0
x_{96}	1	10	4	3	0	1	21	9	21	−1
x_{132}	2	30	11	1	0	2	62	22	8	−2
x_{133}	1	7	3	0	0	0	14	5	2	−1
x_{134}	0	−1	0	0	0	0	−1	0	0	82
x_{153}	1	13	5	1	0	1	26	9	4	29
x_{167}	0	5	2	0	0	0	11	4	1	0
x_{173}	0	4	1	0	0	0	7	3	1	0
x_{175}	0	5	2	0	0	0	10	3	1	0
x_{176}	0	2	1	0	0	0	5	2	1	0
x_{177}	2	29	11	1	0	2	60	21	8	−2
x_{178}	0	2	1	1	0	0	5	3	8	0
x_{179}	0	3	1	6	0	0	7	7	38	0
x_{181}	0	3	1	5	0	0	6	6	35	0
x_{218}	0	4	2	0	0	0	9	3	1	0
x_{222}	1	12	4	1	0	1	24	9	3	−1
x_{281}	−48	−13	−22	−18	−1	−6	−21	−14	−40	−51
	x_6	x_{18}	x_{19}	x_{20}	x_{28}	x_{29}	x_{31}	x_{33}	x_{35}	x_{50}

Meson Particle Listings

D^0

x_{76}	1									
x_{80}	15	0								
x_{94}	4	1	2							
x_{95}	0	12	0	0						
x_{96}	4	8	2	4	1					
x_{132}	13	3	5	11	0	13				
x_{133}	3	1	1	3	0	3	9			
x_{134}	45	0	6	0	0	0	−1	0		
x_{153}	57	1	10	5	0	5	16	4	24	
x_{167}	2	1	1	2	0	2	7	2	0	3
x_{173}	2	0	1	1	0	2	5	1	0	2
x_{175}	2	1	1	2	0	2	6	1	0	3
x_{176}	1	0	0	1	0	1	3	1	0	1
x_{177}	13	3	5	11	0	13	38	9	−1	16
x_{178}	1	3	0	1	0	2	3	1	0	1
x_{179}	1	15	1	1	2	8	4	1	0	2
x_{181}	1	14	0	1	2	7	4	1	0	2
x_{218}	2	0	1	2	0	2	6	1	0	2
x_{222}	5	1	2	5	0	5	15	4	0	6
x_{281}	−46	−55	−37	−6	−11	−15	−13	−3	−44	−29
	x_{67}	x_{76}	x_{80}	x_{94}	x_{95}	x_{96}	x_{132}	x_{133}	x_{134}	x_{153}

x_{173}	1								
x_{175}	1	1							
x_{176}	1	0	0						
x_{177}	7	4	6	3					
x_{178}	1	0	0	0	3				
x_{179}	1	0	1	0	4	3			
x_{181}	1	0	1	0	3	3	83		
x_{218}	1	1	1	0	8	0	1	1	
x_{222}	3	2	3	1	15	1	2	1	2
x_{281}	−3	−3	−4	−3	−13	−4	−21	−19	−2	−5
	x_{167}	x_{173}	x_{175}	x_{176}	x_{177}	x_{178}	x_{179}	x_{181}	x_{218}	x_{222}

CONSTRAINED FIT INFORMATION

An overall fit to 3 branching ratios uses 3 measurements and one constraint to determine 4 parameters. The overall fit has a $\chi^2 = 0.0$ for 0 degrees of freedom.

The following *off-diagonal* array elements are the correlation coefficients $\langle \delta x_i \delta x_j \rangle / (\delta x_i \cdot \delta x_j)$, in percent, from the fit to the branching fractions, $x_i \equiv \Gamma_i / \Gamma_{\text{total}}$. The fit constrains the x_i whose labels appear in this array to sum to one.

x_2	−100		
x_3	−46	40	
x_4	0	0	0
	x_1	x_2	x_3

D^0 BRANCHING RATIOS

Some older now obsolete results have been omitted from these Listings.

Topological modes

Γ(0-prongs)/Γ_{total} Γ_1/Γ

This value is obtained by subtracting the branching fractions for 2-, 4-, and 6-prongs from unity.

VALUE	DOCUMENT ID
0.15±0.06 OUR FIT	

Γ(4-prongs)/Γ_{total} Γ_3/Γ

This is the sum of our $K^-2\pi^+\pi^-$, $K^-2\pi^+\pi^-\pi^0$, $\overline{K}{}^0 2\pi^+2\pi^-$, $K^+2K^-\pi^+$, $2\pi^+2\pi^-$, $2\pi^+2\pi^-\pi^0$, $K^+K^-\pi^+\pi^-$, and $K^+K^-\pi^+\pi^-\pi^0$ branching fractions.

VALUE	DOCUMENT ID
0.145±0.005 OUR FIT	
0.145±0.005	PDG 12

Γ(4-prongs)/Γ(2-prongs) Γ_3/Γ_2

VALUE	EVTS	DOCUMENT ID		TECN	COMMENT
0.207±0.016 OUR FIT					
0.207±0.016±0.004	226	ONENGUT	05	CHRS	ν_μ emulsion, $\overline{E}_\nu \approx 27$ GeV

Γ(6-prongs)/Γ_{total} Γ_4/Γ

This is the sum of our $K^-3\pi^+2\pi^-$ and $3\pi^+3\pi^-$ branching fractions.

VALUE (units 10^{-4})	EVTS	DOCUMENT ID		TECN	COMMENT
6.4± 1.3 OUR FIT					
6.4± 1.3		PDG	12		
• • • We do not use the following data for averages, fits, limits, etc. • • •					
$12\ ^{+13}_{-9}\ \pm 2$	3	ONENGUT	05	CHRS	ν_μ emulsion, $\overline{E}_\nu \approx 27$ GeV

Inclusive modes

$\Gamma(e^+ \text{anything})/\Gamma_{\text{total}}$ Γ_5/Γ

The branching fractions for the $K^- e^+ \nu_e$, $K^*(892)^- e^+ \nu_e$, $\pi^- e^+ \nu_e$, and $\rho^- e^+ \nu_e$ modes add up to 6.20 ± 0.17 %.

VALUE (%)	EVTS	DOCUMENT ID		TECN	COMMENT
6.49±0.11 OUR AVERAGE					
6.46±0.09±0.11	6584 ± 96	[1] ASNER	10	CLEO	e^+e^- at 3774 MeV
6.3 ±0.7 ±0.4	290 ± 32	ABLIKIM	07G	BES2	$e^+e^- \approx \psi(3770)$
6.46±0.17±0.13	2246 ± 57	ADAM	06A	CLEO	See ASNER 10
6.9 ±0.3 ±0.5	1670	ALBRECHT	96C	ARG	$e^+e^- \approx 10$ GeV
6.64±0.18±0.29	4609	KUBOTA	96B	CLE2	$e^+e^- \approx \Upsilon(4S)$

[1] Using the D^+ and D^0 lifetimes, ASNER 10 finds that the ratio of the D^+ and D^0 semileptonic widths is 0.985 ± 0.015 ± 0.024.

$\Gamma(\mu^+ \text{anything})/\Gamma_{\text{total}}$ Γ_6/Γ

VALUE (%)	EVTS	DOCUMENT ID		TECN	COMMENT
6.7±0.6 OUR FIT					
6.4±0.8 OUR AVERAGE					
6.8±1.5±0.8	79 ± 10	[1] ABLIKIM	08L	BES2	$e^+e^- \approx \psi(3772)$
6.5±1.2±0.3	36	KAYIS-TOPAK...	05	CHRS	ν_μ emulsion
6.0±0.7±1.2	310	ALBRECHT	96C	ARG	$e^+e^- \approx 10$ GeV

[1] ABLIKIM 08L finds the ratio of $D^+ \to \mu^+ X$ and $D^0 \to \mu^+ X$ branching fractions to be 2.59 ± 0.70 ± 0.25, in accord with the ratio of D^+ and D^0 lifetimes, 2.54 ± 0.02.

$\Gamma(K^- \text{anything})/\Gamma_{\text{total}}$ Γ_7/Γ

VALUE	EVTS	DOCUMENT ID		TECN	COMMENT
0.547±0.028 OUR AVERAGE Error includes scale factor of 1.3. See the ideogram below.					
0.578±0.016±0.032	2098 ± 59	ABLIKIM	07G	BES2	$e^+e^- \approx \psi(3770)$
$0.546\ ^{+0.039}_{-0.038}$		[1] BARLAG	92C	ACCM	π^- Cu 230 GeV
0.609±0.032±0.052		COFFMAN	91	MRK3	e^+e^- 3.77 GeV
0.42 ±0.08		AGUILAR-...	87E	HYBR	πp, pp 360, 400 GeV
0.55 ±0.11	121	SCHINDLER	81	MRK2	e^+e^- 3.771 GeV
0.35 ±0.10	19	VUILLEMIN	78	LGW	e^+e^- 3.772 GeV

[1] BARLAG 92C computes the branching fraction using topological normalization.

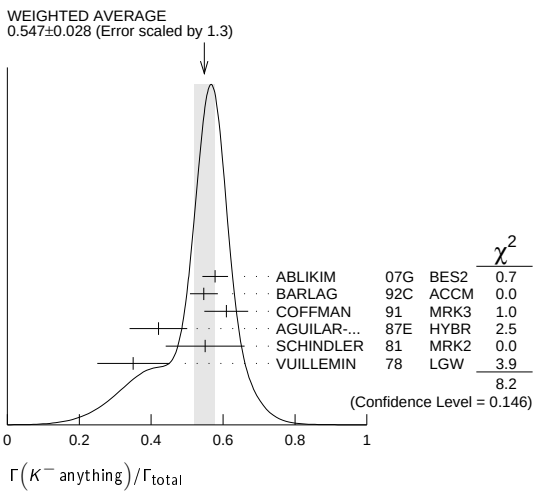

$[\Gamma(\overline{K}{}^0 \text{anything}) + \Gamma(K^0 \text{anything})]/\Gamma_{\text{total}}$ Γ_8/Γ

VALUE	EVTS	DOCUMENT ID		TECN	COMMENT
0.47 ±0.04 OUR AVERAGE					
0.476±0.048±0.030	250 ± 25	ABLIKIM	06U	BES2	e^+e^- at 3773 MeV
0.455±0.050±0.032		COFFMAN	91	MRK3	e^+e^- 3.77 GeV

$\Gamma(K^+ \text{anything})/\Gamma_{\text{total}}$ Γ_9/Γ

VALUE	EVTS	DOCUMENT ID		TECN	COMMENT
0.034±0.004 OUR AVERAGE					
0.035±0.007±0.003	119 ± 23	ABLIKIM	07G	BES2	$e^+e^- \approx \psi(3770)$
$0.034\ ^{+0.007}_{-0.005}$		[1] BARLAG	92C	ACCM	π^- Cu 230 GeV
0.028±0.009±0.004		COFFMAN	91	MRK3	e^+e^- 3.77 GeV
$0.03\ ^{+0.05}_{-0.02}$		AGUILAR-...	87E	HYBR	πp, pp 360, 400 GeV
0.08 ±0.03	25	SCHINDLER	81	MRK2	e^+e^- 3.771 GeV

[1] BARLAG 92C computes the branching fraction using topological normalization.

$\Gamma(K^*(892)^- \text{anything})/\Gamma_{\text{total}}$ Γ_{10}/Γ

VALUE	EVTS	DOCUMENT ID		TECN	COMMENT
0.153±0.083±0.019	28 ± 15	ABLIKIM	06U	BES2	e^+e^- at 3773 MeV

$\Gamma(\overline{K}^*(892)^0 \text{anything})/\Gamma_{\text{total}}$ Γ_{11}/Γ

VALUE	EVTS	DOCUMENT ID		TECN	COMMENT
0.087±0.040±0.012	96 ± 44	ABLIKIM	05P	BES	$e^+e^- \approx$ 3773 MeV

$\Gamma(K^*(892)^+ \text{anything})/\Gamma_{\text{total}}$ Γ_{12}/Γ

VALUE	CL%	DOCUMENT ID		TECN	COMMENT
<0.036	90	ABLIKIM	06U	BES2	e^+e^- at 3773 MeV

$\Gamma(K^*(892)^0 \text{anything})/\Gamma_{\text{total}}$ Γ_{13}/Γ

VALUE	EVTS	DOCUMENT ID		TECN	COMMENT
0.028±0.012±0.004	31 ± 12	ABLIKIM	05P	BES	$e^+e^- \approx$ 3773 MeV

$\Gamma(\eta \text{anything})/\Gamma_{\text{total}}$ Γ_{14}/Γ

This ratio includes η particles from η' decays.

VALUE (units 10^{-2})	EVTS	DOCUMENT ID		TECN	COMMENT
9.5±0.4±0.8	4463±197	HUANG	06B	CLEO	e^+e^- at $\psi(3770)$

$\Gamma(\eta' \text{anything})/\Gamma_{\text{total}}$ Γ_{15}/Γ

VALUE (units 10^{-2})	EVTS	DOCUMENT ID		TECN	COMMENT
2.48±0.17±0.21	299 ± 21	HUANG	06B	CLEO	e^+e^- at $\psi(3770)$

$\Gamma(\phi \text{anything})/\Gamma_{\text{total}}$ Γ_{16}/Γ

VALUE (units 10^{-2})	EVTS	DOCUMENT ID		TECN	COMMENT
1.05±0.08±0.07	368 ± 24	HUANG	06B	CLEO	e^+e^- at $\psi(3770)$
• • • We do not use the following data for averages, fits, limits, etc. • • •					
$1.71^{+0.76}_{-0.71}\pm0.17$	9	BAI	00C	BES	$e^+e^- \to D\overline{D}^*, D^*\overline{D}^*$

Semileptonic modes

$\Gamma(K^- e^+ \nu_e)/\Gamma_{\text{total}}$ Γ_{18}/Γ

VALUE (units 10^{-2})	EVTS	DOCUMENT ID		TECN	COMMENT
3.55±0.05 OUR FIT Error includes scale factor of 1.2.					
3.50±0.05 OUR AVERAGE					
3.50±0.03±0.04	14.1k	[1] BESSON	09	CLEO	e^+e^- at $\psi(3770)$
3.45±0.10±0.19	1318 ± 38	[2] WIDHALM	06	BELL	$e^+e^- \approx \Upsilon(4S)$
3.82±0.40±0.27	104 ± 11	ABLIKIM	04C	BES	e^+e^-, 3.773 GeV
3.4 ±0.5 ±0.4	55	ADLER	89	MRK3	e^+e^- 3.77 GeV
• • • We do not use the following data for averages, fits, limits, etc. • • •					
3.56±0.03±0.09		[3] DOBBS	08	CLEO	See BESSON 09
3.44±0.10±0.10	1311 ± 37	COAN	05	CLEO	See DOBBS 08

[1] See the form-factor parameters near the end of this D^0 Listing.

[2] The $\pi^- e^+ \nu_e$ and $K^- e^+ \nu_e$ results of WIDHALM 06 give $|\frac{V_{cd}}{V_{cs}} \cdot \frac{f_+^\pi(0)}{f_+^K(0)}|^2 = 0.042 \pm 0.003 \pm 0.003$.

[3] DOBBS 08 establishes $|\frac{V_{cd}}{V_{cs}} \cdot \frac{f_+^\pi(0)}{f_+^K(0)}| = 0.188 \pm 0.008 \pm 0.002$ from the D^+ and D^0 decays to $\overline{K} e^+ \nu_e$ and $\pi e^+ \nu_e$.

$\Gamma(K^- e^+ \nu_e)/\Gamma(K^- \pi^+)$ Γ_{18}/Γ_{31}

VALUE	EVTS	DOCUMENT ID		TECN	COMMENT
0.915±0.011 OUR FIT Error includes scale factor of 1.1.					
0.930±0.013 OUR AVERAGE					
0.927±0.007±0.012	76k±323	[1] AUBERT	07BG	BABR	$e^+e^- \approx \Upsilon(4S)$
0.978±0.027±0.044	2510	[2] BEAN	93C	CLE2	$e^+e^- \approx \Upsilon(4S)$
0.90 ±0.06 ±0.06	584	[3] CRAWFORD	91B	CLEO	$e^+e^- \approx$ 10.5 GeV
0.91 ±0.07 ±0.11	250	[4] ANJOS	89F	E691	Photoproduction

[1] The event samples in this AUBERT 07BG result include radiative photons. The $D^0 \to K^- e^+ \nu_e$ form factor at $q^2 = 0$ is $f_+(0) = 0.727 \pm 0.007 \pm 0.005 \pm 0.007$.

[2] BEAN 93C uses $K^- \mu^+ \nu_\mu$ as well as $K^- e^+ \nu_e$ events and makes a small phase-space adjustment to the number of the μ^+ events to use them as e^+ events. A pole mass of $2.00 \pm 0.12 \pm 0.18$ GeV/c^2 is obtained from the q^2 dependence of the decay rate.

[3] CRAWFORD 91B uses $K^- e^+ \nu_e$ and $K^- \mu^+ \nu_\mu$ candidates to measure a pole mass of $2.1^{+0.4}_{-0.2}{}^{+0.3}_{-0.2}$ GeV/c^2 from the q^2 dependence of the decay rate.

[4] ANJOS 89F measures a pole mass of $2.1^{+0.4}_{-0.2} \pm 0.2$ GeV/c^2 from the q^2 dependence of the decay rate.

$\Gamma(K^- \mu^+ \nu_\mu)/\Gamma_{\text{total}}$ Γ_{19}/Γ

VALUE (units 10^{-2})	EVTS	DOCUMENT ID		TECN	COMMENT
3.31±0.13 OUR FIT					
3.45±0.10±0.21	1249±43	WIDHALM	06	BELL	$e^+e^- \approx \Upsilon(4S)$

$\Gamma(K^- \mu^+ \nu_\mu)/\Gamma(K^- \pi^+)$ Γ_{19}/Γ_{31}

VALUE	EVTS	DOCUMENT ID		TECN	COMMENT
0.852±0.033 OUR FIT					
0.84 ±0.04 OUR AVERAGE					
0.852±0.034±0.028	1897	[1] FRABETTI	95G	E687	γBe $\overline{E}_\gamma$= 220 GeV
0.82 ±0.13 ±0.13	338	[2] FRABETTI	93I	E687	γBe $\overline{E}_\gamma$= 221 GeV
0.79 ±0.08 ±0.09	231	[3] CRAWFORD	91B	CLEO	$e^+e^- \approx$ 10.5 GeV

[1] FRABETTI 95G extracts the ratio of form factors $f_-(0)/f_+(0) = -1.3^{+3.6}_{-3.4} \pm 0.6$, and measures a pole mass of $1.87^{+0.11}_{-0.08}{}^{+0.07}_{-0.06}$ GeV/c^2 from the q^2 dependence of the decay rate.

[2] FRABETTI 93I measures a pole mass of $2.1^{+0.7}_{-0.3}{}^{+0.7}_{-0.3}$ GeV/c^2 from the q^2 dependence of the decay rate.

[3] CRAWFORD 91B measures a pole mass of $2.00 \pm 0.12 \pm 0.18$ GeV/c^2 from the q^2 dependence of the decay rate.

$\Gamma(K^- \mu^+ \nu_\mu)/\Gamma(\mu^+ \text{anything})$ Γ_{19}/Γ_6

VALUE	EVTS	DOCUMENT ID		TECN	COMMENT
0.50 ±0.05 OUR FIT					
0.472±0.051±0.040	232	KODAMA	94	E653	π^- emulsion 600 GeV
• • • We do not use the following data for averages, fits, limits, etc. • • •					
0.32 ±0.05 ±0.05	124	KODAMA	91	EMUL	pA 800 GeV

$\Gamma(K^- \pi^0 e^+ \nu_e)/\Gamma_{\text{total}}$ Γ_{22}/Γ

VALUE	EVTS	DOCUMENT ID		TECN	COMMENT
$\mathbf{0.016^{+0.013}_{-0.005}\pm0.002}$	4	[1] BAI	91	MRK3	$e^+e^- \approx$ 3.77 GeV

[1] BAI 91 finds that a fraction $0.79^{+0.15}_{-0.17}{}^{+0.09}_{-0.03}$ of combined D^+ and D^0 decays to $\overline{K}\pi e^+ \nu_e$ (24 events) are $\overline{K}^*(892) e^+ \nu_e$. BAI 91 uses 56 $K^- e^+ \nu_e$ events to measure a pole mass of $1.8 \pm 0.3 \pm 0.2$ GeV/c^2 from the q^2 dependence of the decay rate.

$\Gamma(\overline{K}^0 \pi^- e^+ \nu_e)/\Gamma_{\text{total}}$ Γ_{23}/Γ

VALUE (units 10^{-2})	EVTS	DOCUMENT ID		TECN	COMMENT
2.7 $^{+0.9}_{-0.7}$ OUR AVERAGE					
2.61±1.04±0.28	9 ± 3	ABLIKIM	06O	BES2	e^+e^- at 3773 MeV
2.8 $^{+1.7}_{-0.8}$ ±0.3	6	[1] BAI	91	MRK3	$e^+e^- \approx$ 3.77 GeV

[1] BAI 91 finds that a fraction $0.79^{+0.15}_{-0.17}{}^{+0.09}_{-0.03}$ of combined D^+ and D^0 decays to $\overline{K}\pi e^+ \nu_e$ (24 events) are $\overline{K}^*(892) e^+ \nu_e$.

$\Gamma(K^*(892)^- e^+ \nu_e)/\Gamma_{\text{total}}$ Γ_{20}/Γ

Both decay modes of the $K^*(892)^-$ are included.

VALUE (units 10^{-2})	EVTS	DOCUMENT ID		TECN	COMMENT
2.16±0.16 OUR FIT					
2.16±0.15±0.08	219 ± 16	[1] COAN	05	CLEO	e^+e^- at $\psi(3770)$

[1] COAN 05 uses both $K^- \pi^0$ and $K^0_S \pi^-$ events.

$\Gamma(K^*(892)^- e^+ \nu_e)/\Gamma(K^0_S \pi^+ \pi^-)$ Γ_{20}/Γ_{35}

Unseen decay modes of the $K^*(892)^-$ are included.

VALUE	EVTS	DOCUMENT ID		TECN	COMMENT
0.76±0.07 OUR FIT					
0.76±0.12±0.06	152	[1] BEAN	93C	CLE2	$e^+e^- \approx \Upsilon(4S)$

[1] BEAN 93C uses $K^{*-} \mu^+ \nu_\mu$ as well as $K^{*-} e^+ \nu_e$ events and makes a small phase-space adjustment to the number of the μ^+ events to use them as e^+ events.

$\Gamma(K^*(892)^- \mu^+ \nu_\mu)/\Gamma(K^0_S \pi^+ \pi^-)$ Γ_{21}/Γ_{35}

Unseen decay modes of the $K^*(892)^-$ are included.

VALUE	EVTS	DOCUMENT ID		TECN	COMMENT
0.674±0.068±0.026	175 ± 17	[1] LINK	05B	FOCS	γ A, $\overline{E}_\gamma \approx$ 180 GeV

[1] LINK 05B finds that in $D^0 \to \overline{K}^0 \pi^- \mu^+ \nu_\mu$ the $\overline{K}^0 \pi^-$ system is 6% in S-wave.

$\Gamma(K^- \pi^+ \pi^- e^+ \nu_e)/\Gamma_{\text{total}}$ Γ_{24}/Γ

VALUE (units 10^{-4})	EVTS	DOCUMENT ID		TECN	COMMENT
$\mathbf{2.8^{+1.4}_{-1.1}\pm0.3}$	8	ARTUSO	07A	CLEO	e^+e^- at $\Upsilon(3770)$

$\Gamma(K_1(1270)^- e^+ \nu_e)/\Gamma_{\text{total}}$ Γ_{25}/Γ

VALUE (units 10^{-4})	EVTS	DOCUMENT ID		TECN	COMMENT
$\mathbf{7.6^{+4.1}_{-3.0}\pm0.9}$	8	[1] ARTUSO	07A	CLEO	e^+e^- at $\Upsilon(3770)$

[1] This ARTUSO 07A result is corrected for all decay modes of the $K_1(1270)^-$.

$\Gamma(K^- \pi^+ \pi^- \mu^+ \nu_\mu)/\Gamma(K^- \mu^+ \nu_\mu)$ Γ_{26}/Γ_{19}

VALUE	CL%	DOCUMENT ID		TECN	COMMENT
<0.037	90	KODAMA	93B	E653	π^- emulsion 600 GeV

$\Gamma((\overline{K}^*(892)\pi)^- \mu^+ \nu_\mu)/\Gamma(K^- \mu^+ \nu_\mu)$ Γ_{27}/Γ_{19}

VALUE	CL%	DOCUMENT ID		TECN	COMMENT
<0.043	90	[1] KODAMA	93B	E653	π^- emulsion 600 GeV

[1] KODAMA 93B searched in $K^- \pi^+ \pi^- \mu^+ \nu_\mu$, but the limit includes other $(\overline{K}^*(892)\pi)^-$ charge states.

Meson Particle Listings

D^0

$\Gamma(\pi^- e^+ \nu_e)/\Gamma_{\text{total}}$ Γ_{28}/Γ

VALUE (units 10^{-2})	EVTS	DOCUMENT ID		TECN	COMMENT
0.289±0.008 OUR FIT Error includes scale factor of 1.1.					
0.287±0.008 OUR AVERAGE					
0.288±0.008±0.003	1374	[1] BESSON	09	CLEO	e^+e^- at $\psi(3770)$
0.279±0.027±0.016	126 ± 12	[2] WIDHALM	06	BELL	$e^+e^- \approx \Upsilon(4S)$
• • • We do not use the following data for averages, fits, limits, etc. • • •					
0.299±0.011±0.009		[3] DOBBS	08	CLEO	See BESSON 09
0.262±0.025±0.008	117 ± 11	COAN	05	CLEO	See DOBBS 08

[1] See the form-factor parameters near the end of this D^0 Listing.

[2] The $\pi^- e^+ \nu_e$ and $K^- e^+ \nu_e$ results of WIDHALM 06 give $|\frac{V_{cd}}{V_{cs}} \cdot \frac{f_+^\pi(0)}{f_+^K(0)}|^2 = 0.042 \pm 0.003 \pm 0.003$.

[3] DOBBS 08 establishes $|\frac{V_{cd}}{V_{cs}} \cdot \frac{f_+^\pi(0)}{f_+^K(0)}| = 0.188 \pm 0.008 \pm 0.002$ from the D^+ and D^0 decays to $\overline{K} e^+ \nu_e$ and $\pi e^+ \nu_e$.

$\Gamma(\pi^- e^+ \nu_e)/\Gamma(K^- e^+ \nu_e)$ Γ_{28}/Γ_{18}

VALUE	EVTS	DOCUMENT ID		TECN	COMMENT
0.0814±0.0025 OUR FIT Error includes scale factor of 1.1.					
0.085 ±0.007 OUR AVERAGE					
0.082 ±0.006 ±0.005		[1] HUANG	05	CLEO	$e^+e^- \approx \Upsilon(4S)$
0.101 ±0.020 ±0.003	91	[2] FRABETTI	96B	E687	γ Be, $\overline{E}_\gamma \approx$ 200 GeV
0.103 ±0.039 ±0.013	87	[3] BUTLER	95	CLE2	< 0.156 (90% CL)

[1] HUANG 05 uses both e and μ events, and makes a small correction to the μ events to make them effectively e events. This result gives $|\frac{V_{cd}}{V_{cs}} \cdot \frac{f_+^\pi(0)}{f_+^K(0)}|^2 = 0.038^{+0.006+0.005}_{-0.007-0.003}$.

[2] FRABETTI 96B uses both e and μ events, and makes a small correction to the μ events to make them effectively e events. This result gives $|\frac{V_{cd}}{V_{cs}} \cdot \frac{f_+^\pi(0)}{f_+^K(0)}|^2 = 0.050 \pm 0.011 \pm 0.002$.

[3] BUTLER 95 has 87 ± 33 $\pi^- e^+ \nu_e$ events. The result gives $|\frac{V_{cd}}{V_{cs}} \cdot \frac{f_+^\pi(0)}{f_+^K(0)}|^2 = 0.052 \pm 0.020 \pm 0.007$.

$\Gamma(\pi^- \mu^+ \nu_\mu)/\Gamma_{\text{total}}$ Γ_{29}/Γ

VALUE (units 10^{-2})	EVTS	DOCUMENT ID		TECN	COMMENT
0.237±0.024 OUR FIT					
0.231±0.026±0.019	106 ± 13	WIDHALM	06	BELL	$e^+e^- \approx \Upsilon(4S)$

$\Gamma(\pi^- \mu^+ \nu_\mu)/\Gamma(K^- \mu^+ \nu_\mu)$ Γ_{29}/Γ_{19}

VALUE	EVTS	DOCUMENT ID		TECN	COMMENT
0.072±0.007 OUR FIT					
0.074±0.008±0.007	288 ± 29	[1] LINK	05	FOCS	γ A, $\overline{E}_\gamma \approx$ 180 GeV

[1] LINK 05 finds the form-factor ratio $|f_0^\pi(0)/f_0^K(0)|$ to be 0.85 ± 0.04 ± 0.04 ± 0.01.

$\Gamma(\rho^- e^+ \nu_e)/\Gamma_{\text{total}}$ Γ_{30}/Γ

VALUE (units 10^{-3})	EVTS	DOCUMENT ID		TECN	COMMENT
1.77±0.12±0.10	305 ± 21	[1,2] DOBBS	13	CLEO	e^+e^- at $\psi(3770)$
• • • We do not use the following data for averages, fits, limits, etc. • • •					
1.94±0.39±0.13	31 ± 6	COAN	05	CLEO	See DOBBS 13

[1] DOBBS 13 finds $\Gamma(D^0 \to \rho^- e^+ \nu_e)$ / 2 $\Gamma(D^+ \to \rho^0 e^+ \nu_e) = 1.03 \pm 0.09^{+0.08}_{-0.02}$; isospin invariance predicts the ratio is 1.0.

[2] See the D^+ Listings for $D \to \rho e^+ \nu_e$ form factors.

Hadronic modes with a single $\overline{K}$

$\Gamma(K^- \pi^+)/\Gamma_{\text{total}}$ Γ_{31}/Γ

VALUE (units 10^{-2})	EVTS	DOCUMENT ID		TECN	COMMENT
3.88 ±0.05 OUR FIT Error includes scale factor of 1.1.					
3.91 ±0.05 OUR AVERAGE Error includes scale factor of 1.1.					
4.007±0.037±0.072	33.8 ± 0.3k	AUBERT	08L	BABR	e^+e^- at $\Upsilon(4S)$
3.891±0.035±0.069		[1] DOBBS	07	CLEO	e^+e^- at $\psi(3770)$
3.82 ±0.07 ±0.12		[2] ARTUSO	98	CLE2	CLEO average
3.90 ±0.09 ±0.12	5392	[3] BARATE	97C	ALEP	From Z decays
3.41 ±0.12 ±0.28	1173 ± 37	[3] ALBRECHT	94F	ARG	$e^+e^- \approx \Upsilon(4S)$
3.62 ±0.34 ±0.44		[3] DECAMP	91J	ALEP	From Z decays
• • • We do not use the following data for averages, fits, limits, etc. • • •					
3.91 ±0.08 ±0.09	10.3k ±100	[1] HE	05	CLEO	See DOBBS 07
3.81 ±0.15 ±0.16	1165	[4] ARTUSO	98	CLE2	e^+e^- at $\Upsilon(4S)$
3.69 ±0.11 ±0.16		[5] COAN	98	CLE2	See ARTUSO 98
4.5 ±0.6 ±0.4		[6] ALBRECHT	94	ARG	$e^+e^- \approx \Upsilon(4S)$
3.95 ±0.08 ±0.17	4208	[3,7] AKERIB	93	CLE2	See ARTUSO 98
4.5 ±0.8 ±0.5	56	[3] ABACHI	88	HRS	e^+e^- 29 GeV
4.2 ±0.4 ±0.4	930	ADLER	88C	MRK3	e^+e^- 3.77 GeV
4.1 ±0.6	263 ± 17	[8] SCHINDLER	81	MRK2	e^+e^- 3.771 GeV
4.3 ±1.0	130	[9] PERUZZI	77	LGW	e^+e^- 3.77 GeV

[1] DOBBS 07 and HE 05 use single- and double-tagged events in an overall fit. DOBBS 07 supersedes HE 05.

[2] This combines the CLEO results of ARTUSO 98, COAN 98, and AKERIB 93.

[3] ABACHI 88, DECAMP 91J, AKERIB 93, ALBRECHT 94F, and BARATE 97C use $D^*(2010)^+ \to D^0 \pi^+$ decays. The π^+ is both slow and of low p_T with respect to the event thrust axis or nearest jet ($\approx D^{*+}$ direction). The excess number of such π^+'s over background gives the number of $D^*(2010)^+ \to D^0 \pi^+$ events, and the fraction with $D^0 \to K^- \pi^+$ gives the $D^0 \to K^- \pi^+$ branching fraction.

[4] ARTUSO 98, following ALBRECHT 94, uses D^0 mesons from $\overline{B}^0 \to D^*(2010)^+ X \ell^- \overline{\nu}_\ell$ decays. Our average uses the CLEO average of this value with the values of COAN 98 and AKERIB 93.

[5] COAN 98 assumes that $\Gamma(B \to \overline{D} X \ell^+ \nu)/\Gamma(B \to X \ell^+ \nu) = 1.0 - 3|V_{ub}/V_{cb}|^2 - 0.010 \pm 0.005$, the last term accounting for $\overline{B} \to D_s^+ K X \ell^- \overline{\nu}$. COAN 98 is included in the CLEO average in ARTUSO 98.

[6] ALBRECHT 94 uses D^0 mesons from $\overline{B}^0 \to D^{*+} \ell^- \overline{\nu}_\ell$ decays. This is a different set of events than used by ALBRECHT 94F.

[7] This AKERIB 93 value includes radiative corrections; without them, the value is 0.0391 ± 0.0008 ± 0.0017. AKERIB 93 is included in the CLEO average in ARTUSO 98.

[8] SCHINDLER 81 (MARK-2) measures $\sigma(e^+e^- \to \psi(3770)) \times$ branching fraction to be 0.24 ± 0.02 nb. We use the MARK-3 (ADLER 88C) value of $\sigma = 5.8 \pm 0.5 \pm 0.6$ nb.

[9] PERUZZI 77 (MARK-1) measures $\sigma(e^+e^- \to \psi(3770)) \times$ branching fraction to be 0.25 ± 0.05 nb. We use the MARK-3 (ADLER 88C) value of $\sigma = 5.8 \pm 0.5 \pm 0.6$ nb.

$\Gamma(K^+ \pi^-)/\Gamma(K^- \pi^+)$ Γ_{32}/Γ_{31}

VALUE (units 10^{-3})	DOCUMENT ID		TECN	COMMENT
3.56 ±0.06 OUR AVERAGE				
3.53 ±0.13	[1] KO	14	BELL	$e^+e^- \to \Upsilon(nS)$
3.568±0.066	[2] AAIJ	13CE	LHCB	pp at 7, 8 TeV
3.51 ±0.35	[3] AALTONEN	13AE	CDF	$p\overline{p}$ at 1.96 TeV
• • • We do not use the following data for averages, fits, limits, etc. • • •				
3.52 ±0.15	[4] AAIJ	13N	LHCB	Repl. by AAIJ 13CE

[1] Based on 976 fb^{-1} of data collected at $\Upsilon(nS)$ resonances. Assumes no CP violation.

[2] Based on 3 fb^{-1} of data collected at $\sqrt{s} = 7$, 8 TeV. Assumes no CP violation.

[3] Based on 9.6 fb^{-1} of data collected at the Tevatron. Assumes no CP violation.

[4] Based on 1 fb^{-1} of data collected at $\sqrt{s} = 7$ TeV in 2011. Assumes no CP violation.

$\Gamma(K_S^0 \pi^0)/\Gamma_{\text{total}}$ Γ_{33}/Γ

VALUE (units 10^{-2})	EVTS	DOCUMENT ID		TECN	COMMENT
• • • We do not use the following data for averages, fits, limits, etc. • • •					
1.240±0.017±0.056	614	HE	08	CLEO	See MENDEZ 10

$\Gamma(K_S^0 \pi^0)/\Gamma(K^- \pi^+)$ Γ_{33}/Γ_{31}

VALUE	EVTS	DOCUMENT ID		TECN	COMMENT
• • • We do not use the following data for averages, fits, limits, etc. • • •					
0.68±0.12±0.11	119	ANJOS	92B	E691	γBe 80–240 GeV

$\Gamma(K_S^0 \pi^0)/[\Gamma(K^- \pi^+) + \Gamma(K^+ \pi^-)]$ $\Gamma_{33}/(\Gamma_{31}+\Gamma_{222})$

VALUE (units 10^{-2})	EVTS	DOCUMENT ID		TECN	COMMENT
30.5±0.9 OUR FIT					
30.4±0.3±0.9	20k	MENDEZ	10	CLEO	e^+e^- at 3774 MeV

$\Gamma(K_S^0 \pi^0)/\Gamma(K_S^0 \pi^+ \pi^-)$ Γ_{33}/Γ_{35}

VALUE	EVTS	DOCUMENT ID		TECN	COMMENT
0.420±0.029 OUR FIT					
0.44 ±0.02 ±0.05	1942 ± 64	PROCARIO	93B	CLE2	e^+e^- 10.36–10.7 GeV
• • • We do not use the following data for averages, fits, limits, etc. • • •					
0.34 ±0.04 ±0.02	92	[1] ALBRECHT	92P	ARG	$e^+e^- \approx$ 10 GeV
0.36 ±0.04 ±0.08	104	KINOSHITA	91	CLEO	$e^+e^- \sim$ 10.7 GeV

[1] This value is calculated from numbers in Table 1 of ALBRECHT 92P.

$\Gamma(K_L^0 \pi^0)/\Gamma_{\text{total}}$ Γ_{34}/Γ

VALUE (units 10^{-2})	EVTS	DOCUMENT ID		TECN	COMMENT
0.998±0.049±0.048	1116	[1] HE	08	CLEO	e^+e^- at $\psi(3770)$

[1] The difference of HE 08 $D^0 \to K_S^0 \pi^0$ and $K_L^0 \pi^0$ branching fractions over the sum is 0.108 ± 0.025 ± 0.024. This is consistent with U-spin symmetry and the Cabibbo angle.

$\Gamma(K_S^0 \pi^+ \pi^-)/\Gamma_{\text{total}}$ Γ_{35}/Γ

VALUE (units 10^{-2})	EVTS	DOCUMENT ID		TECN	COMMENT
• • • We do not use the following data for averages, fits, limits, etc. • • •					
2.52±0.20±0.25	284 ± 22	[1] ALBRECHT	94F	ARG	$e^+e^- \approx \Upsilon(4S)$
3.2 ±0.3 ±0.5		ADLER	87	MRK3	e^+e^- 3.77 GeV
2.6 ±0.8	32 ± 8	[2] SCHINDLER	81	MRK2	e^+e^- 3.771 GeV
4.0 ±1.2	28	[3] PERUZZI	77	LGW	e^+e^- 3.77 GeV

[1] See the footnote on the ALBRECHT 94F measurement of $\Gamma(K^- \pi^+)/\Gamma_{\text{total}}$ for the method used.

[2] SCHINDLER 81 (MARK-2) measures $\sigma(e^+e^- \to \psi(3770)) \times$ branching fraction to be 0.30 ± 0.08 nb. We use the MARK-3 (ADLER 88C) value of $\sigma = 5.8 \pm 0.5 \pm 0.6$ nb.

[3] PERUZZI 77 (MARK-1) measures $\sigma(e^+e^- \to \psi(3770)) \times$ branching fraction to be 0.46 ± 0.12 nb. We use the MARK-3 (ADLER 88C) value of $\sigma = 5.8 \pm 0.5 \pm 0.6$ nb.

$\Gamma(K^0_S\pi^+\pi^-)/\Gamma(K^-\pi^+)$ Γ_{35}/Γ_{31}

VALUE	EVTS	DOCUMENT ID		TECN	COMMENT
0.73±0.05 OUR FIT	Error includes scale factor of 1.1.				
0.81±0.05±0.08	856 ± 35	FRABETTI	94J	E687	γBe $\overline{E}_\gamma$=220 GeV
• • • We do not use the following data for averages, fits, limits, etc. • • •					
0.85±0.40	35	AVERY	80	SPEC	$\gamma N \to D^{*+}$
1.4 ±0.5	116	PICCOLO	77	MRK1	e^+e^- 4.03, 4.41 GeV

$\Gamma(K^0_S\rho^0)/\Gamma(K^0_S\pi^+\pi^-)$ Γ_{36}/Γ_{35}

This is the "fit fraction" from the Dalitz-plot analysis.

VALUE	DOCUMENT ID		TECN	COMMENT
$0.224^{+0.017}_{-0.023}$ OUR AVERAGE	Error includes scale factor of 1.7.			
0.210±0.016	[1] AUBERT	08AL	BABR	Dalitz fit, ≈ 487 k evts
$0.264\pm0.009^{+0.010}_{-0.026}$	MURAMATSU	02	CLE2	Dalitz fit, 5299 evts
• • • We do not use the following data for averages, fits, limits, etc. • • •				
$0.267\pm0.011^{+0.009}_{-0.028}$	ASNER	04A	CLEO	See MURAMATSU 02
0.350±0.028±0.067	FRABETTI	94G	E687	Dalitz fit, 597 evts
0.227±0.032±0.009	ALBRECHT	93D	ARG	Dalitz fit, 440 evts
0.215±0.051±0.037	ANJOS	93	E691	γBe 90–260 GeV
0.20 ±0.06 ±0.03	FRABETTI	92B	E687	γ Be, $\overline{E}_\gamma$= 221 GeV
0.12 ±0.01 ±0.07	ADLER	87	MRK3	e^+e^- 3.77 GeV

[1] The error on this AUBERT 08AL value includes both statistical and systematic uncertainties; the latter dominates.

$\Gamma(K^0_S\omega, \omega\to\pi^+\pi^-)/\Gamma(K^0_S\pi^+\pi^-)$ Γ_{37}/Γ_{35}

This is the "fit fraction" from the Dalitz-plot analysis.

VALUE	DOCUMENT ID		TECN	COMMENT
0.0073±0.0020 OUR AVERAGE				
0.009 ±0.010	[1] AUBERT	08AL	BABR	Dalitz fit, ≈ 487 k evts
$0.0072\pm0.0018^{+0.0010}_{-0.0009}$	MURAMATSU	02	CLE2	Dalitz fit, 5299 evts
• • • We do not use the following data for averages, fits, limits, etc. • • •				
$0.0081\pm0.0019^{+0.0018}_{-0.0010}$	ASNER	04A	CLEO	See MURAMATSU 02

[1] The error on this AUBERT 08AL value includes both statistical and systematic uncertainties; the latter dominates.

$\Gamma(K^0_S(\pi^+\pi^-)_{S-\text{wave}})/\Gamma(K^0_S\pi^+\pi^-)$ Γ_{38}/Γ_{35}

This is the "fit fraction" from the Dalitz-plot analysis. The $(\pi^+\pi^-)_{S-wave}$ includes what in isobar models are the $f_0(980)$ and $f_0(1370)$; see the following two data blocks.

VALUE	DOCUMENT ID		TECN	COMMENT
0.119±0.026	[1] AUBERT	08AL	BABR	Dalitz fit, ≈ 487 k evts

[1] The error on this AUBERT 08AL value includes both statistical and systematic uncertainties; the latter dominates.

$\Gamma(K^0_S f_0(980), f_0(980)\to\pi^+\pi^-)/\Gamma(K^0_S\pi^+\pi^-)$ Γ_{39}/Γ_{35}

This is the "fit fraction" from the Dalitz-plot analysis.

VALUE	DOCUMENT ID		TECN	COMMENT
$0.043\pm0.005^{+0.012}_{-0.006}$	MURAMATSU	02	CLE2	Dalitz fit, 5299 evts
• • • We do not use the following data for averages, fits, limits, etc. • • •				
$0.042\pm0.005^{+0.011}_{-0.005}$	ASNER	04A	CLEO	See MURAMATSU 02
0.068±0.016±0.018	FRABETTI	94G	E687	Dalitz fit, 597 evts
0.046±0.018±0.006	ALBRECHT	93D	ARG	Dalitz fit, 440 evts

$\Gamma(K^0_S f_0(1370), f_0(1370)\to\pi^+\pi^-)/\Gamma(K^0_S\pi^+\pi^-)$ Γ_{40}/Γ_{35}

This is the "fit fraction" from the Dalitz-plot analysis.

VALUE	DOCUMENT ID		TECN	COMMENT
$0.099\pm0.011^{+0.028}_{-0.044}$	MURAMATSU	02	CLE2	Dalitz fit, 5299 evts
• • • We do not use the following data for averages, fits, limits, etc. • • •				
$0.098\pm0.014^{+0.026}_{-0.036}$	ASNER	04A	CLEO	See MURAMATSU 02
0.077±0.022±0.031	FRABETTI	94G	E687	Dalitz fit, 597 evts
0.082±0.028±0.013	ALBRECHT	93D	ARG	Dalitz fit, 440 evts

$\Gamma(K^0_S f_2(1270), f_2(1270)\to\pi^+\pi^-)/\Gamma(K^0_S\pi^+\pi^-)$ Γ_{41}/Γ_{35}

This is the "fit fraction" from the Dalitz-plot analysis.

VALUE	DOCUMENT ID		TECN	COMMENT
$0.0032^{+0.0035}_{-0.0022}$ OUR AVERAGE				
0.006 ±0.007	[1] AUBERT	08AL	BABR	Dalitz fit, ≈ 487 k evts
$0.0027\pm0.0015^{+0.0037}_{-0.0017}$	MURAMATSU	02	CLE2	Dalitz fit, 5299 evts
• • • We do not use the following data for averages, fits, limits, etc. • • •				
$0.0036\pm0.0022^{+0.0032}_{-0.0019}$	ASNER	04A	CLEO	See MURAMATSU 02
0.037 ±0.014 ±0.017	FRABETTI	94G	E687	Dalitz fit, 597 evts
0.050 ±0.021 ±0.008	ALBRECHT	93D	ARG	Dalitz fit, 440 evts

[1] The error on this AUBERT 08AL value includes both statistical and systematic uncertainties; the latter dominates.

$\Gamma(K^*(892)^-\pi^+, K^*(892)^-\to K^0_S\pi^-)/\Gamma(K^0_S\pi^+\pi^-)$ Γ_{42}/Γ_{35}

This is the "fit fraction" from the Dalitz-plot analysis.

VALUE	DOCUMENT ID		TECN	COMMENT
$0.588^{+0.034}_{-0.050}$ OUR AVERAGE	Error includes scale factor of 2.0.			
0.557±0.028	[1] AUBERT	08AL	BABR	Dalitz fit, ≈ 487 k evts
$0.657\pm0.013^{+0.018}_{-0.040}$	MURAMATSU	02	CLE2	Dalitz fit, 5299 evts
• • • We do not use the following data for averages, fits, limits, etc. • • •				
$0.663\pm0.013^{+0.024}_{-0.043}$	ASNER	04A	CLEO	See MURAMATSU 02
0.625±0.036±0.026	FRABETTI	94G	E687	Dalitz fit, 597 evts
0.718±0.042±0.030	ALBRECHT	93D	ARG	Dalitz fit, 440 evts
0.480±0.097	ANJOS	93	E691	γBe 90–260 GeV
0.56 ±0.04 ±0.05	ADLER	87	MRK3	e^+e^- 3.77 GeV

[1] The error on this AUBERT 08AL value includes both statistical and systematic uncertainties; the latter dominates.

$\Gamma(K^*_0(1430)^-\pi^+, K^*_0(1430)^-\to K^0_S\pi^-)/\Gamma(K^0_S\pi^+\pi^-)$ Γ_{43}/Γ_{35}

This is the "fit fraction" from the Dalitz-plot analysis.

VALUE	DOCUMENT ID		TECN	COMMENT
$0.095^{+0.014}_{-0.010}$ OUR AVERAGE				
0.102±0.015	[1] AUBERT	08AL	BABR	Dalitz fit, ≈ 487 k evts
$0.073\pm0.007^{+0.031}_{-0.011}$	MURAMATSU	02	CLE2	Dalitz fit, 5299 evts
• • • We do not use the following data for averages, fits, limits, etc. • • •				
$0.072\pm0.007^{+0.014}_{-0.013}$	ASNER	04A	CLEO	See MURAMATSU 02
0.109±0.027±0.029	FRABETTI	94G	E687	Dalitz fit, 597 evts
0.129±0.034±0.021	ALBRECHT	93D	ARG	Dalitz fit, 440 evts

[1] The error on this AUBERT 08AL value includes both statistical and systematic uncertainties; the latter dominates.

$\Gamma(K^*_2(1430)^-\pi^+, K^*_2(1430)^-\to K^0_S\pi^-)/\Gamma(K^0_S\pi^+\pi^-)$ Γ_{44}/Γ_{35}

This is the "fit fraction" from the Dalitz-plot analysis.

VALUE	DOCUMENT ID		TECN	COMMENT
$0.0120^{+0.0070}_{-0.0035}$ OUR AVERAGE				
0.022 ±0.016	[1] AUBERT	08AL	BABR	Dalitz fit, ≈ 487 k evts
0.011 ±0.002 $^{+0.007}_{-0.003}$	MURAMATSU	02	CLE2	Dalitz fit, 5299 evts
• • • We do not use the following data for averages, fits, limits, etc. • • •				
0.011 ±0.002 $^{+0.005}_{-0.003}$	ASNER	04A	CLEO	See MURAMATSU 02

[1] The error on this AUBERT 08AL value includes both statistical and systematic uncertainties; the latter dominates.

$\Gamma(K^*(1680)^-\pi^+, K^*(1680)^-\to K^0_S\pi^-)/\Gamma(K^0_S\pi^+\pi^-)$ Γ_{45}/Γ_{35}

This is the "fit fraction" from the Dalitz-plot analysis.

VALUE	DOCUMENT ID		TECN	COMMENT
0.016±0.013 OUR AVERAGE				
0.007±0.019	[1] AUBERT	08AL	BABR	Dalitz fit, ≈ 487 k evts
$0.022\pm0.004^{+0.018}_{-0.015}$	MURAMATSU	02	CLE2	Dalitz fit, 5299 evts
• • • We do not use the following data for averages, fits, limits, etc. • • •				
$0.023\pm0.005^{+0.007}_{-0.014}$	ASNER	04A	CLEO	See MURAMATSU 02

[1] The error on this AUBERT 08AL value includes both statistical and systematic uncertainties; the latter dominates.

$\Gamma(K^*(892)^+\pi^-, K^*(892)^+\to K^0_S\pi^+)/\Gamma(K^0_S\pi^+\pi^-)$ Γ_{46}/Γ_{35}

This is the "fit fraction" from the Dalitz-plot analysis. This is a doubly Cabibbo-suppressed mode.

VALUE (units 10^{-3})	DOCUMENT ID		TECN	COMMENT
$4.0^{+2.0}_{-1.2}$ OUR AVERAGE				
4.6±2.3	[1] AUBERT	08AL	BABR	Dalitz fit, ≈ 487 k evts
$3.4\pm1.3^{+4.1}_{-0.4}$	MURAMATSU	02	CLE2	Dalitz fit, 5299 evts
• • • We do not use the following data for averages, fits, limits, etc. • • •				
$3.4\pm1.3^{+3.6}_{-0.5}$	ASNER	04A	CLEO	See MURAMATSU 02

[1] The error on this AUBERT 08AL value includes both statistical and systematic uncertainties; the latter dominates.

$\Gamma(K^*_0(1430)^+\pi^-, K^*_0(1430)^+\to K^0_S\pi^+)/\Gamma(K^0_S\pi^+\pi^-)$ Γ_{47}/Γ_{35}

This is the "fit fraction" from the Dalitz-plot analysis. This is a doubly Cabibbo-suppressed mode.

VALUE	CL%	DOCUMENT ID		TECN	COMMENT
$<5\times10^{-4}$	95	AUBERT	08AL	BABR	Dalitz fit, ≈ 487 k evts

$\Gamma(K^*_2(1430)^+\pi^-, K^*_2(1430)^+\to K^0_S\pi^+)/\Gamma(K^0_S\pi^+\pi^-)$ Γ_{48}/Γ_{35}

This is the "fit fraction" from the Dalitz-plot analysis. This is a doubly Cabibbo-suppressed mode.

VALUE	CL%	DOCUMENT ID		TECN	COMMENT
$<1.2\times10^{-3}$	95	AUBERT	08AL	BABR	Dalitz fit, ≈ 487 k evts

Meson Particle Listings

D^0

$\Gamma(K^0_S\pi^+\pi^-$ nonresonant$)/\Gamma(K^0_S\pi^+\pi^-)$ Γ_{49}/Γ_{35}

This is the "fit fraction" from the Dalitz-plot analysis. Neither FRABETTI 94G nor ALBRECHT 93D (quoted in many of the earlier submodes of $K^0_S\pi^+\pi^-$) sees evidence for a nonresonant component.

VALUE	DOCUMENT ID		TECN	COMMENT
$0.009\pm0.004^{+0.020}_{-0.004}$	MURAMATSU	02	CLE2	Dalitz fit, 5299 evts
• • • We do not use the following data for averages, fits, limits, etc. • • •				
$0.007\pm0.007^{+0.021}_{-0.006}$	ASNER	04A	CLEO	See MURAMATSU 02
$0.263\pm0.024\pm0.041$	ANJOS	93	E691	γBe 90–260 GeV
$0.26\ \pm0.08\ \pm0.05$	FRABETTI	92B	E687	γ Be, $\overline{E}_\gamma=221$ GeV
$0.33\ \pm0.05\ \pm0.10$	ADLER	87	MRK3	e^+e^- 3.77 GeV

$\Gamma(K^-\pi^+\pi^0)/\Gamma_{\rm total}$ Γ_{50}/Γ

VALUE (units 10^{-2})	EVTS	DOCUMENT ID		TECN	COMMENT
13.9 ±0.5 OUR FIT	Error includes scale factor of 1.7.				
14.57±0.12±0.38		[1] DOBBS	07	CLEO	e^+e^- at $\psi(3770)$
• • • We do not use the following data for averages, fits, limits, etc. • • •					
14.9 ±0.3 ±0.5	19k ±150	[1] HE	05	CLEO	See DOBBS 07
13.3 ±1.2 ±1.3	931	ADLER	88C	MRK3	e^+e^- 3.77 GeV
11.7 ±4.3	37	[2] SCHINDLER	81	MRK2	e^+e^- 3.771 GeV

[1] DOBBS 07 and HE 05 use single- and double-tagged events in an overall fit. DOBBS 07 supersedes HE 05.

[2] SCHINDLER 81 (MARK-2) measures $\sigma(e^+e^-\to\psi(3770))\times$ branching fraction to be 0.68 ± 0.23 nb. We use the MARK-3 (ADLER 88C) value of $\sigma=5.8\pm0.5\pm0.6$ nb.

$\Gamma(K^-\pi^+\pi^0)/\Gamma(K^-\pi^+)$ Γ_{50}/Γ_{31}

VALUE	EVTS	DOCUMENT ID		TECN	COMMENT
3.58±0.14 OUR FIT	Error includes scale factor of 1.9.				
3.44±0.30 OUR AVERAGE	Error includes scale factor of 1.5. See the ideogram below.				
$3.81\pm0.07\pm0.26$	10k	BARISH	96	CLE2	$e^+e^-\approx\Upsilon(4S)$
$3.04\pm0.16\pm0.34$	931	[1] ALBRECHT	92P	ARG	$e^+e^-\approx10$ GeV
$2.8\ \pm0.14\pm0.52$	1050	KINOSHITA	91	CLEO	$e^+e^-\sim10.7$ GeV

[1] This value is calculated from numbers in Table 1 of ALBRECHT 92P.

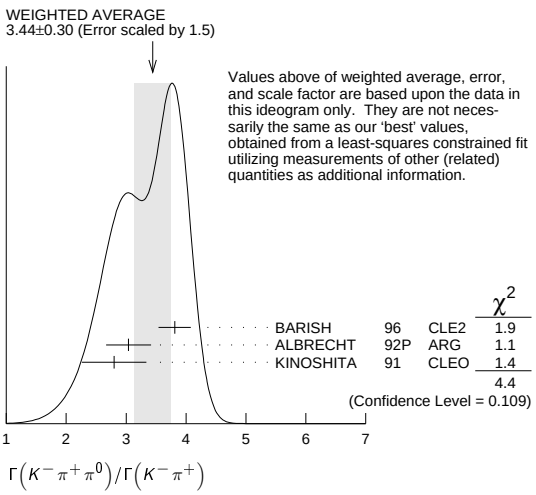

$\Gamma(K^-\rho^+)/\Gamma(K^-\pi^+\pi^0)$ Γ_{51}/Γ_{50}

This is the "fit fraction" from the Dalitz-plot analysis.

VALUE	DOCUMENT ID		TECN	COMMENT
0.78 ±0.04 OUR AVERAGE				
$0.788\pm0.019\pm0.048$	KOPP	01	CLE2	Dalitz fit, ≈ 7,000 evts
$0.765\pm0.041\pm0.054$	FRABETTI	94G	E687	Dalitz fit, 530 evts
• • • We do not use the following data for averages, fits, limits, etc. • • •				
$0.647\pm0.039\pm0.150$	ANJOS	93	E691	γBe 90–260 GeV
$0.81\ \pm0.03\ \pm0.06$	ADLER	87	MRK3	e^+e^- 3.77 GeV

$\Gamma(K^-\rho(1700)^+,\rho(1700)^+\to\pi^+\pi^0)/\Gamma(K^-\pi^+\pi^0)$ Γ_{52}/Γ_{50}

This is the "fit fraction" from the Dalitz-plot analysis.

VALUE	DOCUMENT ID		TECN	COMMENT
0.057±0.008±0.009	KOPP	01	CLE2	Dalitz fit, ≈ 7,000 evts

$\Gamma(K^*(892)^-\pi^+,K^*(892)^-\to K^-\pi^0)/\Gamma(K^-\pi^+\pi^0)$ Γ_{53}/Γ_{50}

This is the "fit fraction" from the Dalitz-plot analysis.

VALUE	DOCUMENT ID		TECN	COMMENT
$0.160^{+0.025}_{-0.013}$ OUR AVERAGE				
$0.161\pm0.007^{+0.027}_{-0.011}$	KOPP	01	CLE2	Dalitz fit, ≈ 7,000 evts
$0.148\pm0.028\pm0.049$	FRABETTI	94G	E687	Dalitz fit, 530 evts
• • • We do not use the following data for averages, fits, limits, etc. • • •				
$0.084\pm0.011\pm0.012$	ANJOS	93	E691	γBe 90–260 GeV
$0.12\ \pm0.02\ \pm0.03$	ADLER	87	MRK3	e^+e^- 3.77 GeV

$\Gamma(\overline{K}^*(892)^0\pi^0,\overline{K}^*(892)^0\to K^-\pi^+)/\Gamma(K^-\pi^+\pi^0)$ Γ_{54}/Γ_{50}

This is the "fit fraction" from the Dalitz-plot analysis.

VALUE	DOCUMENT ID		TECN	COMMENT
0.135±0.016 OUR AVERAGE				
$0.127\pm0.009\pm0.016$	KOPP	01	CLE2	Dalitz fit, ≈ 7,000 evts
$0.165\pm0.031\pm0.015$	FRABETTI	94G	E687	Dalitz fit, 530 evts
• • • We do not use the following data for averages, fits, limits, etc. • • •				
$0.142\pm0.018\pm0.024$	ANJOS	93	E691	γBe 90–260 GeV
$0.13\ \pm0.02\ \pm0.03$	ADLER	87	MRK3	e^+e^- 3.77 GeV

$\Gamma(K^*_0(1430)^-\pi^+,K^*_0(1430)^-\to K^-\pi^0)/\Gamma(K^-\pi^+\pi^0)$ Γ_{55}/Γ_{50}

This is the "fit fraction" from the Dalitz-plot analysis.

VALUE	DOCUMENT ID		TECN	COMMENT
0.033±0.006±0.014	KOPP	01	CLE2	Dalitz fit, ≈ 7,000 evts

$\Gamma(\overline{K}^*_0(1430)^0\pi^0,\overline{K}^*_0(1430)^0\to K^-\pi^+)/\Gamma(K^-\pi^+\pi^0)$ Γ_{56}/Γ_{50}

This is the "fit fraction" from the Dalitz-plot analysis.

VALUE	DOCUMENT ID		TECN	COMMENT
$0.041\pm0.006^{+0.032}_{-0.009}$	KOPP	01	CLE2	Dalitz fit, ≈ 7,000 evts

$\Gamma(K^*(1680)^-\pi^+,K^*(1680)^-\to K^-\pi^0)/\Gamma(K^-\pi^+\pi^0)$ Γ_{57}/Γ_{50}

This is the "fit fraction" from the Dalitz-plot analysis.

VALUE	DOCUMENT ID		TECN	COMMENT
0.013±0.003±0.004	KOPP	01	CLE2	Dalitz fit, ≈ 7,000 evts

$\Gamma(K^-\pi^+\pi^0$ nonresonant$)/\Gamma(K^-\pi^+\pi^0)$ Γ_{58}/Γ_{50}

This is the "fit fraction" from the Dalitz-plot analysis.

VALUE	EVTS	DOCUMENT ID		TECN	COMMENT
$0.080^{+0.040}_{-0.014}$ OUR AVERAGE					
$0.075\pm0.009^{+0.056}_{-0.011}$		KOPP	01	CLE2	Dalitz fit, ≈ 7,000 evts
$0.101\pm0.033\pm0.040$		FRABETTI	94G	E687	Dalitz fit, 530 evts
• • • We do not use the following data for averages, fits, limits, etc. • • •					
$0.036\pm0.004\pm0.018$		ANJOS	93	E691	γBe 90–260 GeV
$0.09\ \pm0.02\ \pm0.04$		ADLER	87	MRK3	e^+e^- 3.77 GeV
$0.51\ \pm0.22$	21	SUMMERS	84	E691	Photoproduction

$\Gamma(K^0_S2\pi^0)/\Gamma_{\rm total}$ Γ_{59}/Γ

VALUE (units 10^{-3})	EVTS	DOCUMENT ID		TECN	COMMENT
9.1 ±1.1 OUR AVERAGE	Error includes scale factor of 2.2.				
$10.58\pm0.38\pm0.73$	1259	LOWREY	11	CLEO	$e^+e^-\approx3.77$ GeV
$8.34\pm0.45\pm0.42$		ASNER	08	CLEO	$e^+e^-\to D^0\overline{D}^0$, 3.77 GeV

$\Gamma(K^0_S(2\pi^0)$-S-wave$)/\Gamma(K^0_S2\pi^0)$ Γ_{60}/Γ_{59}

VALUE (%)	DOCUMENT ID		TECN	COMMENT
28.9±6.3±3.1	LOWREY	11	CLEO	Dalitz analysis, 1259 evts

$\Gamma(\overline{K}^*(892)^0\pi^0,\overline{K}^*(892)^0\to K^0_S\pi^0)/\Gamma(K^0_S\pi^0)$ Γ_{61}/Γ_{33}

VALUE (%)	DOCUMENT ID		TECN	COMMENT
65.6± 5.3±2.5	LOWREY	11	CLEO	Dalitz analysis, 1259 evts
• • • We do not use the following data for averages, fits, limits, etc. • • •				
$55\ ^{+13}_{-10}\ \pm7$	PROCARIO	93B	CLE2	Dalitz plot fit, 122 evts

$\Gamma(\overline{K}^*(1430)^0\pi^0,\overline{K}^{*0}\to K^0_S\pi^0)/\Gamma(K^0_S2\pi^0)$ Γ_{62}/Γ_{59}

VALUE (%)	DOCUMENT ID		TECN	COMMENT
0.49±0.45±2.51	LOWREY	11	CLEO	Dalitz analysis, 1259 evts

$\Gamma(\overline{K}^*(1680)^0\pi^0,\overline{K}^{*0}\to K^0_S\pi^0)/\Gamma(K^0_S2\pi^0)$ Γ_{63}/Γ_{59}

VALUE (%)	DOCUMENT ID		TECN	COMMENT
11.2±2.7±2.5	LOWREY	11	CLEO	Dalitz analysis, 1259 evts

$\Gamma(K^0_Sf_2(1270),f_2\to2\pi^0)/\Gamma(K^0_S2\pi^0)$ Γ_{64}/Γ_{59}

VALUE (%)	DOCUMENT ID		TECN	COMMENT
2.48±0.91±0.78	LOWREY	11	CLEO	Dalitz analysis, 1259 evts

$\Gamma(2K^0_S,$ one $K^0_S\to2\pi^0)/\Gamma(K^0_S2\pi^0)$ Γ_{65}/Γ_{59}

VALUE (%)	DOCUMENT ID		TECN	COMMENT
3.46±0.92±0.66	LOWREY	11	CLEO	Dalitz analysis, 1259 evts

$\Gamma(K^0_S2\pi^0$ nonresonant$)/\Gamma(K^0_S\pi^0)$ Γ_{66}/Γ_{33}

VALUE	DOCUMENT ID		TECN	COMMENT
• • • We do not use the following data for averages, fits, limits, etc. • • •				
$0.37\pm0.08\pm0.04$	PROCARIO	93B	CLE2	Dalitz plot fit, 122 evts

$\Gamma(K^-2\pi^+\pi^-)/\Gamma_{total}$ Γ_{67}/Γ

VALUE (units 10^{-2})	EVTS	DOCUMENT ID		TECN	COMMENT
$8.08^{+0.21}_{-0.19}$ OUR FIT		Error includes scale factor of 1.3.			
8.17±0.33 OUR AVERAGE		Error includes scale factor of 1.7. See the ideogram below.			
8.30±0.07±0.20		[1] DOBBS	07	CLEO	e^+e^- at $\psi(3770)$
7.9 ±1.5 ±0.9		[2] ALBRECHT	94	ARG	$e^+e^- \approx \Upsilon(4S)$
6.80±0.27±0.57	1430 ± 52	[3] ALBRECHT	94F	ARG	$e^+e^- \approx \Upsilon(4S)$
9.1 ±0.8 ±0.8	992	ADLER	88C	MRK3	e^+e^- 3.77 GeV
• • • We do not use the following data for averages, fits, limits, etc. • • •					
8.3 ±0.2 ±0.3	15k ±130	[1] HE	05	CLEO	See DOBBS 07
11.7 ±2.5	185	[4] SCHINDLER	81	MRK2	e^+e^- 3.771 GeV
6.2 ±1.9	44	[5] PERUZZI	77	LGW	e^+e^- 3.77 GeV

[1] DOBBS 07 and HE 05 use single- and double-tagged events in an overall fit. DOBBS 07 supersedes HE 05.
[2] ALBRECHT 94 uses D^0 mesons from $\overline{B}^0 \to D^{*+}\ell^-\overline{\nu}_\ell$ decays. This is a different set of events than used by ALBRECHT 94F.
[3] See the footnote on the ALBRECHT 94F measurement of $\Gamma(K^-\pi^+)/\Gamma_{total}$ for the method used.
[4] SCHINDLER 81 (MARK-2) measures $\sigma(e^+e^- \to \psi(3770)) \times$ branching fraction to be 0.68 ± 0.11 nb. We use the MARK-3 (ADLER 88C) value of $\sigma = 5.8 \pm 0.5 \pm 0.6$ nb.
[5] PERUZZI 77 (MARK-1) measures $\sigma(e^+e^- \to \psi(3770)) \times$ branching fraction to be 0.36 ± 0.10 nb. We use the MARK-3 (ADLER 88C) value of $\sigma = 5.8 \pm 0.5 \pm 0.6$ nb.

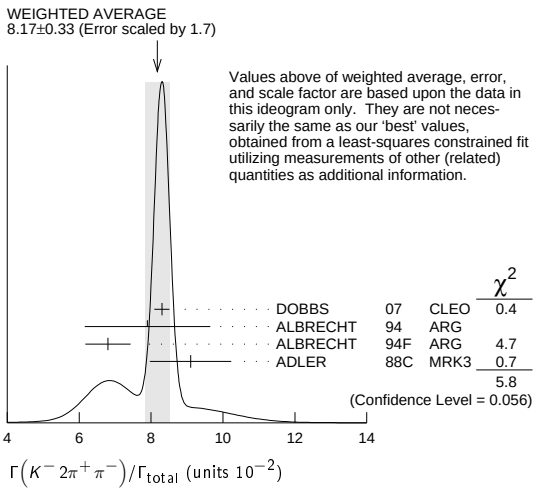

$\Gamma(K^-2\pi^+\pi^-)/\Gamma(K^-\pi^+)$ Γ_{67}/Γ_{31}

VALUE	EVTS	DOCUMENT ID		TECN	COMMENT
2.08±0.05 OUR FIT		Error includes scale factor of 1.6.			
1.97±0.09 OUR AVERAGE					
$1.94\pm0.07^{+0.09}_{-0.11}$		JUN	00	SELX	Σ^- nucleus, 600 GeV
1.7 ±0.2 ±0.2	1745	ANJOS	92C	E691	γBe 90–260 GeV
1.90±0.25±0.20	337	ALVAREZ	91B	NA14	Photoproduction
2.12±0.16±0.09		BORTOLETTO	88	CLEO	e^+e^- 10.55 GeV
2.17±0.28±0.23		ALBRECHT	85F	ARG	e^+e^- 10 GeV
• • • We do not use the following data for averages, fits, limits, etc. • • •					
2.0 ±0.9	48	BAILEY	86	ACCM	π^-Be fixed target
2.0 ±1.0	10	BAILEY	83B	SPEC	π^-Be → D^0
2.2 ±0.8	214	PICCOLO	77	MRK1	e^+e^- 4.03, 4.41 GeV

$\Gamma(K^-\pi^+\rho^0\text{total})/\Gamma(K^-2\pi^+\pi^-)$ Γ_{68}/Γ_{67}

This includes $K^-a_1(1260)^+$, $\overline{K}^*(892)^0\rho^0$, etc. The next entry gives the specifically 3-body fraction. We rely on the MARK III and E691 full amplitude analyses of the $K^-\pi^+\pi^+\pi^-$ channel for values of the resonant substructure.

VALUE	DOCUMENT ID		TECN	COMMENT
0.835±0.035 OUR AVERAGE				
0.80 ±0.03 ±0.05	ANJOS	92C	E691	1745 $K^-2\pi^+\pi^-$ evts
0.855±0.032±0.030	COFFMAN	92B	MRK3	1281 ± 45 $K^-2\pi^+\pi^-$ evts
• • • We do not use the following data for averages, fits, limits, etc. • • •				
0.98 ±0.12 ±0.10	ALVAREZ	91B	NA14	Photoproduction

$\Gamma(K^-\pi^+\rho^0\,3\text{-body})/\Gamma(K^-2\pi^+\pi^-)$ Γ_{69}/Γ_{67}

We rely on the MARK III and E691 full amplitude analyses of the $K^-\pi^+\pi^+\pi^-$ channel for values of the resonant substructure.

VALUE	EVTS	DOCUMENT ID		TECN	COMMENT
0.063±0.028 OUR AVERAGE					
0.05 ±0.03 ±0.02		ANJOS	92C	E691	1745 $K^-2\pi^+\pi^-$ evts
0.084±0.022±0.04		COFFMAN	92B	MRK3	1281 ± 45 $K^-2\pi^+\pi^-$ evts
• • • We do not use the following data for averages, fits, limits, etc. • • •					
0.77 ±0.06 ±0.06		[1] ALVAREZ	91B	NA14	Photoproduction
$0.85\ ^{+0.11}_{-0.22}$	180	PICCOLO	77	MRK1	e^+e^- 4.03, 4.41 GeV

[1] This value is for ρ^0 ($K^-\pi^+$)-nonresonant. ALVAREZ 91B cannot determine what fraction of this is $K^-a_1(1260)^+$.

$\Gamma(\overline{K}^*(892)^0\rho^0)/\Gamma(K^-2\pi^+\pi^-)$ Γ_{101}/Γ_{67}

Unseen decay modes of the $\overline{K}^*(892)^0$ are included. We rely on the MARK III and E691 full amplitude analyses of the $K^-\pi^+\pi^+\pi^-$ channel for values of the resonant substructure.

VALUE	EVTS	DOCUMENT ID		TECN	COMMENT
0.195±0.03±0.03		ANJOS	92C	E691	1745 $K^-2\pi^+\pi^-$ evts
• • • We do not use the following data for averages, fits, limits, etc. • • •					
0.34 ±0.09±0.09		ALVAREZ	91B	NA14	Photoproduction
0.75 ±0.3	5	BAILEY	83B	SPEC	πBe → D^0
$0.15\ ^{+0.16}_{-0.15}$	20	PICCOLO	77	MRK1	e^+e^- 4.03, 4.41 GeV

$\Gamma(\overline{K}^*(892)^0\rho^0\text{transverse})/\Gamma(K^-2\pi^+\pi^-)$ Γ_{102}/Γ_{67}

Unseen decay modes of the $\overline{K}^*(892)^0$ are included.

VALUE	DOCUMENT ID		TECN	COMMENT
0.213±0.024±0.075	COFFMAN	92B	MRK3	1281 ± 45 $K^-2\pi^+\pi^-$ evts

$\Gamma(\overline{K}^*(892)^0\rho^0 S\text{-wave})/\Gamma(K^-2\pi^+\pi^-)$ Γ_{103}/Γ_{67}

Unseen decay modes of the $\overline{K}^*(892)^0$ are included.

VALUE	DOCUMENT ID		TECN	COMMENT
0.375±0.045±0.06	ANJOS	92C	E691	1745 $K^-2\pi^+\pi^-$ evts

$\Gamma(\overline{K}^*(892)^0\rho^0 S\text{-wavelong.})/\Gamma_{total}$ Γ_{104}/Γ

Unseen decay modes of the $\overline{K}^*(892)^0$ are included.

VALUE	CL%	DOCUMENT ID		TECN	COMMENT
<0.003	90	COFFMAN	92B	MRK3	1281 ± 45 $K^-2\pi^+\pi^-$ evts

$\Gamma(\overline{K}^*(892)^0\rho^0 P\text{-wave})/\Gamma_{total}$ Γ_{105}/Γ

Unseen decay modes of the $\overline{K}^*(892)^0$ are included.

VALUE	CL%	DOCUMENT ID		TECN	COMMENT
<0.003	90	COFFMAN	92B	MRK3	1.3k $K^-2\pi^+\pi^-$ evts
• • • We do not use the following data for averages, fits, limits, etc. • • •					
<0.009	90	ANJOS	92C	E691	1745 $K^-2\pi^+\pi^-$ evts

$\Gamma(\overline{K}^*(892)^0\rho^0 D\text{-wave})/\Gamma(K^-2\pi^+\pi^-)$ Γ_{106}/Γ_{67}

Unseen decay modes of the $\overline{K}^*(892)^0$ are included.

VALUE	DOCUMENT ID		TECN	COMMENT
0.255±0.045±0.06	ANJOS	92C	E691	1745 $K^-2\pi^+\pi^-$ evts

$\Gamma(K^-\pi^+ f_0(980))/\Gamma_{total}$ Γ_{107}/Γ

VALUE	CL%	DOCUMENT ID		TECN	COMMENT
• • • We do not use the following data for averages, fits, limits, etc. • • •					
<0.011	90	ANJOS	92C	E691	1745 $K^-2\pi^+\pi^-$ evts

$\Gamma(\overline{K}^*(892)^0 f_0(980))/\Gamma_{total}$ Γ_{108}/Γ

VALUE	CL%	DOCUMENT ID		TECN	COMMENT
• • • We do not use the following data for averages, fits, limits, etc. • • •					
<0.007	90	ANJOS	92C	E691	1745 $K^-2\pi^+\pi^-$ evts

$\Gamma(K^-a_1(1260)^+)/\Gamma(K^-2\pi^+\pi^-)$ Γ_{97}/Γ_{67}

Unseen decay modes of the $a_1(1260)^+$ are included, assuming that the $a_1(1260)^+$ decays entirely to $\rho\pi$ [or at least to $(\pi\pi)_{I=1}\ \pi$].

VALUE	DOCUMENT ID		TECN	COMMENT
0.97 ±0.14 OUR AVERAGE				
0.94 ±0.13 ±0.20	ANJOS	92C	E691	1745 $K^-2\pi^+\pi^-$ evts
0.984±0.048±0.16	COFFMAN	92B	MRK3	1281 ± 45 $K^-2\pi^+\pi^-$ evts

$\Gamma(K^-a_2(1320)^+)/\Gamma_{total}$ Γ_{98}/Γ

Unseen decay modes of the $a_2(1320)^+$ are included.

VALUE	CL%	DOCUMENT ID		TECN	COMMENT
<0.002	90	ANJOS	92C	E691	1745 $K^-2\pi^+\pi^-$ evts
• • • We do not use the following data for averages, fits, limits, etc. • • •					
<0.006	90	COFFMAN	92B	MRK3	1281 ± 45 $K^-2\pi^+\pi^-$ evts

$\Gamma(K_1(1270)^-\pi^+)/\Gamma(K^-2\pi^+\pi^-)$ Γ_{109}/Γ_{67}

Unseen decay modes of the $K_1(1270)^-$ are included. The MARK3 and E691 experiments disagree considerably here.

VALUE	CL%	DOCUMENT ID		TECN	COMMENT
0.194±0.056±0.088		COFFMAN	92B	MRK3	1281 ± 45 $K^-2\pi^+\pi^-$ evts
• • • We do not use the following data for averages, fits, limits, etc. • • •					
<0.013	90	ANJOS	92C	E691	1745 $K^-2\pi^+\pi^-$ evts

$\Gamma(K_1(1400)^-\pi^+)/\Gamma_{total}$ Γ_{110}/Γ

VALUE	CL%	DOCUMENT ID		TECN	COMMENT
<0.012	90	COFFMAN	92B	MRK3	1281 ± 45 $K^-2\pi^+\pi^-$ evts

$\Gamma(K^*(1410)^-\pi^+)/\Gamma_{total}$ Γ_{111}/Γ

VALUE	CL%	DOCUMENT ID		TECN	COMMENT
• • • We do not use the following data for averages, fits, limits, etc. • • •					
<0.012	90	COFFMAN	92B	MRK3	1281 ± 45 $K^-2\pi^+\pi^-$ evts

$\Gamma(\overline{K}^*(892)^0\pi^+\pi^-\text{total})/\Gamma(K^-2\pi^+\pi^-)$ Γ_{99}/Γ_{67}

This includes $\overline{K}^*(892)^0\rho^0$, *etc.* The next entry gives the specifically 3-body fraction. Unseen decay modes of the $\overline{K}^*(892)^0$ are included.

VALUE	DOCUMENT ID		TECN	COMMENT
0.30±0.06±0.03	ANJOS	92C	E691	1745 $K^-2\pi^+\pi^-$ evts

$\Gamma(\overline{K}^*(892)^0\pi^+\pi^-\text{3-body})/\Gamma(K^-2\pi^+\pi^-)$ Γ_{100}/Γ_{67}

Unseen decay modes of the $\overline{K}^*(892)^0$ are included.

VALUE	DOCUMENT ID		TECN	COMMENT
0.18 ±0.04 OUR AVERAGE				
0.165±0.03 ±0.045	ANJOS	92C	E691	1745 $K^-2\pi^+\pi^-$ evts
0.210±0.027±0.06	COFFMAN	92B	MRK3	1281 ± 45 $K^-2\pi^+\pi^-$ evts

$\Gamma(K^-2\pi^+\pi^-\text{nonresonant})/\Gamma(K^-2\pi^+\pi^-)$ Γ_{75}/Γ_{67}

VALUE	DOCUMENT ID		TECN	COMMENT
0.233±0.032 OUR AVERAGE				
0.23 ±0.02 ±0.03	ANJOS	92C	E691	1745 $K^-2\pi^+\pi^-$ evts
0.242±0.025±0.06	COFFMAN	92B	MRK3	1281 ± 45 $K^-2\pi^+\pi^-$ evts

$\Gamma(K^0_S\pi^+\pi^-\pi^0)/\Gamma_{\text{total}}$ Γ_{76}/Γ

VALUE (units 10^{-2})	EVTS	DOCUMENT ID		TECN	COMMENT
5.2±0.6 OUR FIT					
5.2±1.1±1.2	140	COFFMAN	92B	MRK3	e^+e^- 3.77 GeV
• • • We do not use the following data for averages, fits, limits, etc. • • •					
$6.7^{+1.6}_{-1.7}$		[1] BARLAG	92C	ACCM	π^- Cu 230 GeV

[1] BARLAG 92C computes the branching fraction using topological normalization.

$\Gamma(K^0_S\pi^+\pi^-\pi^0)/\Gamma(K^0_S\pi^+\pi^-)$ Γ_{76}/Γ_{35}

Branching fractions for submodes of this mode with narrow resonances (the η, ω, η') are fairly well determined (see below). COFFMAN 92B gives fractions of K^* and ρ submodes, but with only 140 ± 28 events above background could not determine them with much accuracy. We omit those measurements here; they are in our 2008 Review (Physics Letters **B667** 1 (2008)).

VALUE	EVTS	DOCUMENT ID		TECN	COMMENT
1.84±0.20 OUR FIT					
1.86±0.23 OUR AVERAGE					
1.80±0.20±0.21	190	[1] ALBRECHT	92P	ARG	$e^+e^-\approx$ 10 GeV
2.8 ±0.8 ±0.8	46	ANJOS	92C	E691	γBe 90–260 GeV
1.85±0.26±0.30	158	KINOSHITA	91	CLEO	$e^+e^-\sim$ 10.7 GeV

[1] This value is calculated from numbers in Table 1 of ALBRECHT 92P.

$\Gamma(K^0_S\eta)/\Gamma_{\text{total}}$ Γ_{94}/Γ

Unseen decay modes of the η are included.

VALUE (units 10^{-3})	DOCUMENT ID		TECN	COMMENT
• • • We do not use the following data for averages, fits, limits, etc. • • •				
4.42±0.15±0.28	ASNER	08	CLEO	See MENDEZ 10

$\Gamma(K^0_S\eta)/[\Gamma(K^-\pi^+)+\Gamma(K^+\pi^-)]$ $\Gamma_{94}/(\Gamma_{31}+\Gamma_{222})$

Unseen decay modes of the η are included.

VALUE (units 10^{-2})	EVTS	DOCUMENT ID		TECN	COMMENT
12.3±0.8 OUR FIT					
12.3±0.3±0.7	2864 ± 65	MENDEZ	10	CLEO	e^+e^- at 3774 MeV

$\Gamma(K^0_S\eta)/\Gamma(K^0_S\pi^0)$ Γ_{94}/Γ_{33}

Unseen decay modes of the η are included.

VALUE	EVTS	DOCUMENT ID		TECN	COMMENT
• • • We do not use the following data for averages, fits, limits, etc. • • •					
0.32±0.04±0.03	225 ± 30	PROCARIO	93B	CLE2	$\eta\to\gamma\gamma$

$\Gamma(K^0_S\eta)/\Gamma(K^0_S\pi^+\pi^-)$ Γ_{94}/Γ_{35}

Unseen decay modes of the η are included.

VALUE	EVTS	DOCUMENT ID		TECN	COMMENT
• • • We do not use the following data for averages, fits, limits, etc. • • •					
0.14±0.02±0.02	80 ± 12	PROCARIO	93B	CLE2	$\eta\to\pi^+\pi^-\pi^0$

$\Gamma(K^0_S\omega)/\Gamma_{\text{total}}$ Γ_{95}/Γ

Unseen decay modes of the ω are included.

VALUE (%)	DOCUMENT ID		TECN	COMMENT
1.11±0.06 OUR FIT				
1.12±0.04±0.05	ASNER	08	CLEO	$e^+e^-\to D^0\overline{D}^0$, 3.77 GeV

$\Gamma(K^0_S\omega)/\Gamma(K^-\pi^+)$ Γ_{95}/Γ_{31}

Unseen decay modes of the ω are included.

VALUE	DOCUMENT ID		TECN	COMMENT
• • • We do not use the following data for averages, fits, limits, etc. • • •				
0.50±0.18±0.10	ALBRECHT	89D	ARG	e^+e^- 10 GeV

$\Gamma(K^0_S\omega)/\Gamma(K^0_S\pi^+\pi^-)$ Γ_{95}/Γ_{35}

Unseen decay modes of the ω are included.

VALUE	EVTS	DOCUMENT ID		TECN	COMMENT
0.393±0.033 OUR FIT Error includes scale factor of 1.1.					
0.33 ±0.09 OUR AVERAGE Error includes scale factor of 1.1.					
0.29 ±0.08 ±0.05	16	[1] ALBRECHT	92P	ARG	$e^+e^-\approx$ 10 GeV
0.54 ±0.14 ±0.16	40	KINOSHITA	91	CLEO	$e^+e^-\sim$ 10.7 GeV

[1] This value is calculated from numbers in Table 1 of ALBRECHT 92P.

$\Gamma(K^0_S\omega)/\Gamma(K^0_S\pi^+\pi^-\pi^0)$ Γ_{95}/Γ_{76}

Unseen decay modes of the ω are included.

VALUE	DOCUMENT ID		TECN	COMMENT
0.213±0.026 OUR FIT				
0.220±0.048±0.0116	COFFMAN	92B	MRK3	1281 ± 45 $K^-2\pi^+\pi^-$ evts

$\Gamma(K^0_S\eta'(958))/[\Gamma(K^-\pi^+)+\Gamma(K^+\pi^-)]$ $\Gamma_{96}/(\Gamma_{31}+\Gamma_{222})$

Unseen decay modes of the $\eta'(958)$ are included.

VALUE (units 10^{-2})	EVTS	DOCUMENT ID		TECN	COMMENT
24.1±1.3 OUR FIT					
24.3±0.8±1.1	1321 ± 42	MENDEZ	10	CLEO	e^+e^- at 3774 MeV

$\Gamma(K^0_S\eta'(958))/\Gamma(K^0_S\pi^+\pi^-)$ Γ_{96}/Γ_{35}

Unseen decay modes of the $\eta'(958)$ are included.

VALUE	EVTS	DOCUMENT ID		TECN	COMMENT
0.331±0.025 OUR FIT					
0.32 ±0.04 OUR AVERAGE					
0.31 ±0.02 ±0.04	594	PROCARIO	93B	CLE2	$\eta'\to\eta\pi^+\pi^-$, $\rho^0\gamma$
0.37 ±0.13 ±0.06	18	[1] ALBRECHT	92P	ARG	$e^+e^-\approx$ 10 GeV

[1] This value is calculated from numbers in Table 1 of ALBRECHT 92P.

$\Gamma(K^-\pi^+2\pi^0)/\Gamma_{\text{total}}$ Γ_{79}/Γ

VALUE	EVTS	DOCUMENT ID		TECN	COMMENT
• • • We do not use the following data for averages, fits, limits, etc. • • •					
0.177±0.029		[1] BARLAG	92C	ACCM	π^- Cu 230 GeV
0.149±0.037±0.030	24	[2] ADLER	88C	MRK3	e^+e^- 3.77 GeV
$0.209^{+0.074}_{-0.043}\pm0.012$	9	[1] AGUILAR-...	87F	HYBR	πp, pp 360, 400 GeV

[1] AGUILAR-BENITEZ 87F and BARLAG 92C compute the branching fraction using topological normalization. They do not distinguish the presence of a third π^0, and thus are not included in the average.

[2] ADLER 88C uses an absolute normalization method finding this decay channel opposite a detected $\overline{D}^0\to K^+\pi^-$ in pure $D\overline{D}$ events.

$\Gamma(K^-2\pi^+\pi^-\pi^0)/\Gamma(K^-\pi^+)$ Γ_{80}/Γ_{31}

VALUE	EVTS	DOCUMENT ID		TECN	COMMENT
1.09±0.10 OUR FIT					
0.98±0.11±0.11	225	[1] ALBRECHT	92P	ARG	$e^+e^-\approx$ 10 GeV

[1] This value is calculated from numbers in Table 1 of ALBRECHT 92P.

$\Gamma(K^-2\pi^+\pi^-\pi^0)/\Gamma(K^-2\pi^+\pi^-)$ Γ_{80}/Γ_{67}

VALUE	EVTS	DOCUMENT ID		TECN	COMMENT
0.52±0.05 OUR FIT					
0.56±0.07 OUR AVERAGE					
$0.55\pm0.07^{+0.12}_{-0.09}$	167	KINOSHITA	91	CLEO	$e^+e^-\sim$ 10.7 GeV
0.57±0.06±0.05	180	ANJOS	90D	E691	Photoproduction

$\Gamma(\overline{K}^*(892)^0\pi^+\pi^-\pi^0)/\Gamma(K^-2\pi^+\pi^-\pi^0)$ Γ_{112}/Γ_{80}

Unseen decay modes of the $\overline{K}^*(892)^0$ are included.

VALUE	DOCUMENT ID		TECN	COMMENT
0.45±0.15±0.15	ANJOS	90D	E691	Photoproduction

$\Gamma(\overline{K}^*(892)^0\eta)/\Gamma(K^-\pi^+)$ Γ_{113}/Γ_{31}

Unseen decay modes of the $\overline{K}^*(892)^0$ and η are included.

VALUE	EVTS	DOCUMENT ID		TECN	COMMENT
• • • We do not use the following data for averages, fits, limits, etc. • • •					
$0.58\pm0.19^{+0.24}_{-0.28}$	46	KINOSHITA	91	CLEO	$e^+e^-\sim$ 10.7 GeV

$\Gamma(\overline{K}^*(892)^0\eta)/\Gamma(K^-\pi^+\pi^0)$ Γ_{113}/Γ_{50}

Unseen decay modes of the $\overline{K}^*(892)^0$ and η are included.

VALUE	EVTS	DOCUMENT ID		TECN	COMMENT
• • • We do not use the following data for averages, fits, limits, etc. • • •					
0.13±0.02±0.03	214	PROCARIO	93B	CLE2	$\overline{K}^{*0}\eta\to K^-\pi^+/\gamma\gamma$

$\Gamma(K^0_S\eta\pi^0)/\Gamma(K^0_S\pi^0)$ Γ_{84}/Γ_{33}

VALUE	EVTS	DOCUMENT ID		TECN	COMMENT
0.46±0.07±0.06	155 ± 22	[1] RUBIN	04	CLEO	$e^+e^-\approx$ 10 GeV

[1] The η here is detected in its $\gamma\gamma$ mode, but other η modes are included in the value given.

$\Gamma(K^0_S a_0(980), a_0(980)\to\eta\pi^0)/\Gamma(K^0_S\eta\pi^0)$ Γ_{85}/Γ_{84}

This is the "fit fraction" from the Dalitz-plot analysis, with interference.

VALUE	DOCUMENT ID		TECN	COMMENT
1.19±0.09±0.26	[1] RUBIN	04	CLEO	Dalitz fit, 155 evts

[1] In addition to $K^0_S a_0(980)$ and $\overline{K}^*(892)^0\eta$ modes, RUBIN 04 finds a fit fraction of 0.246 ± 0.092 ± 0.091 for other, undetermined modes.

$\Gamma(\overline{K}^*(892)^0\eta, \overline{K}^*(892)^0\to K^0_S\pi^0)/\Gamma(K^0_S\eta\pi^0)$ Γ_{86}/Γ_{84}

This is the "fit fraction" from the Dalitz-plot analysis, with interference.

VALUE	DOCUMENT ID		TECN	COMMENT
0.293±0.062±0.035	[1] RUBIN	04	CLEO	Dalitz fit, 155 evts

[1] See the note on RUBIN 04 in the preceding data block.

$\Gamma(K^-\pi^+\omega)/\Gamma(K^-\pi^+)$ Γ_{114}/Γ_{31}

Unseen decay modes of the ω are included.

VALUE	EVTS	DOCUMENT ID		TECN	COMMENT
0.78±0.12±0.10	99	[1] ALBRECHT	92P	ARG	$e^+e^-\approx$ 10 GeV

[1] This value is calculated from numbers in Table 1 of ALBRECHT 92P.

$\Gamma(\overline{K}^*(892)^0\omega)/\Gamma(K^-\pi^+)$ Γ_{115}/Γ_{31}

Unseen decay modes of the $\overline{K}^*(892)^0$ and ω are included.

VALUE	EVTS	DOCUMENT ID		TECN	COMMENT
0.28±0.11±0.04	17	[1] ALBRECHT	92P	ARG	$e^+e^-\approx$ 10 GeV

[1] This value is calculated from numbers in Table 1 of ALBRECHT 92P.

$\Gamma(K^-\pi^+\eta'(958))/\Gamma(K^-2\pi^+\pi^-)$ Γ_{116}/Γ_{67}

Unseen decay modes of the $\eta'(958)$ are included.

VALUE	EVTS	DOCUMENT ID		TECN	COMMENT
0.093±0.014±0.019	286	PROCARIO	93B	CLE2	$\eta'\to\eta\pi^+\pi^-,\rho^0\gamma$

$\Gamma(\overline{K}^*(892)^0\eta'(958))/\Gamma(K^-\pi^+\eta'(958))$ $\Gamma_{117}/\Gamma_{116}$

Unseen decay modes of the $\overline{K}^*(892)^0$ are included.

VALUE	CL%	DOCUMENT ID		TECN
<0.15	90	PROCARIO	93B	CLE2

$\Gamma(K^0_S2\pi^+2\pi^-)/\Gamma(K^0_S\pi^+\pi^-)$ Γ_{87}/Γ_{35}

VALUE	EVTS	DOCUMENT ID		TECN	COMMENT
0.095±0.005±0.007	1283 ± 57	LINK	04D	FOCS	γ A, $\overline{E}_\gamma\approx$180 GeV
• • • We do not use the following data for averages, fits, limits, etc. • • •					
0.07 ±0.02 ±0.01	11	[1] ALBRECHT	92P	ARG	$e^+e^-\approx$ 10 GeV
0.149±0.026	56	AMMAR	91	CLEO	$e^+e^-\approx$ 10.5 GeV
0.18 ±0.07 ±0.04	6	ANJOS	90D	E691	Photoproduction

[1] This value is calculated from numbers in Table 1 of ALBRECHT 92P.

$\Gamma(K^0_S\rho^0\pi^+\pi^-,\text{no}\,K^*(892)^-)/\Gamma(K^0_S2\pi^+2\pi^-)$ Γ_{88}/Γ_{87}

VALUE	DOCUMENT ID		TECN	COMMENT
0.40±0.24±0.07	LINK	04D	FOCS	γ A, $\overline{E}_\gamma\approx$180 GeV

$\Gamma(K^*(892)^-2\pi^+\pi^-,K^*(892)^-\to K^0_S\pi^-,\text{no}\,\rho^0)/\Gamma(K^0_S2\pi^+2\pi^-)$ Γ_{89}/Γ_{87}

VALUE	DOCUMENT ID		TECN	COMMENT
0.17±0.28±0.02	LINK	04D	FOCS	γ A, $\overline{E}_\gamma\approx$180 GeV

$\Gamma(K^*(892)^-\rho^0\pi^+,K^*(892)^-\to K^0_S\pi^-)/\Gamma(K^0_S2\pi^+2\pi^-)$ Γ_{90}/Γ_{87}

VALUE	DOCUMENT ID		TECN	COMMENT
0.60±0.21±0.09	LINK	04D	FOCS	γ A, $\overline{E}_\gamma\approx$180 GeV

$\Gamma(K^0_S2\pi^+2\pi^-\text{nonresonant})/\Gamma(K^0_S2\pi^+2\pi^-)$ Γ_{91}/Γ_{87}

VALUE	CL%	DOCUMENT ID		TECN	COMMENT
<0.46	90	LINK	04D	FOCS	γ A, $\overline{E}_\gamma\approx$180 GeV

$\Gamma(K^-3\pi^+2\pi^-)/\Gamma(K^-2\pi^+\pi^-)$ Γ_{93}/Γ_{67}

VALUE (units 10^{-3})	EVTS	DOCUMENT ID		TECN	COMMENT
2.70±0.58±0.38	48 ± 10	LINK	04B	FOCS	γA, $\overline{E}_\gamma\approx$ 180 GeV

Hadronic modes with three K's

$\Gamma(K^0_SK^+K^-)/\Gamma(K^0_S\pi^+\pi^-)$ Γ_{118}/Γ_{35}

VALUE	EVTS	DOCUMENT ID		TECN	COMMENT
0.158±0.001±0.005	14k±116	AUBERT,B	05J	BABR	$e^+e^-\approx\ \Upsilon(4S)$
• • • We do not use the following data for averages, fits, limits, etc. • • •					
0.20 ±0.05 ±0.04	47	FRABETTI	92B	E687	γ Be, $\overline{E}_\gamma$= 221 GeV
0.170±0.022	136	AMMAR	91	CLEO	$e^+e^-\approx$ 10.5 GeV
0.24 ±0.08		BEBEK	86	CLEO	e^+e^- near $\Upsilon(4S)$
0.185±0.055	52	ALBRECHT	85B	ARG	e^+e^- 10 GeV

$\Gamma(K^0_Sa_0(980)^0,a_0^0\to K^+K^-)/\Gamma(K^0_SK^+K^-)$ $\Gamma_{119}/\Gamma_{118}$

This is the "fit fraction" from the Dalitz-plot analysis, with interference.

VALUE	DOCUMENT ID		TECN	COMMENT
0.664±0.016±0.070	AUBERT,B	05J	BABR	Dalitz fit, 12540 ± 112 evts

$\Gamma(K^-a_0(980)^+,a_0^+\to K^+K^0_S)/\Gamma(K^0_SK^+K^-)$ $\Gamma_{120}/\Gamma_{118}$

This is the "fit fraction" from the Dalitz-plot analysis, with interference.

VALUE	DOCUMENT ID		TECN	COMMENT
0.134±0.011±0.037	AUBERT,B	05J	BABR	Dalitz fit, 12540 ± 112 evts

$\Gamma(K^+a_0(980)^-,a_0^-\to K^-K^0_S)/\Gamma(K^0_SK^+K^-)$ $\Gamma_{121}/\Gamma_{118}$

This is a doubly Cabibbo-suppressed mode.

VALUE	CL%	DOCUMENT ID		TECN	COMMENT
<0.025	95	AUBERT,B	05J	BABR	Dalitz fit, 12540 ± 112 evts

$\Gamma(K^0_Sf_0(980),f_0\to K^+K^-)/\Gamma(K^0_SK^+K^-)$ $\Gamma_{122}/\Gamma_{118}$

VALUE	CL%	DOCUMENT ID		TECN	COMMENT
<0.021	95	AUBERT,B	05J	BABR	Dalitz fit, 12540 ± 112 evts

$\Gamma(K^0_S\phi,\phi\to K^+K^-)/\Gamma(K^0_SK^+K^-)$ $\Gamma_{123}/\Gamma_{118}$

This is the "fit fraction" from the Dalitz-plot analysis, with interference.

VALUE	DOCUMENT ID		TECN	COMMENT
0.459±0.007±0.007	AUBERT,B	05J	BABR	Dalitz fit, 12540 ± 112 evts

$\Gamma(K^0_Sf_0(1370),f_0\to K^+K^-)/\Gamma(K^0_SK^+K^-)$ $\Gamma_{124}/\Gamma_{118}$

This is the "fit fraction" from the Dalitz-plot analysis, with interference.

VALUE	DOCUMENT ID		TECN	COMMENT
0.038±0.007±0.023	[1] AUBERT,B	05J	BABR	Dalitz fit, 12540 ± 112 evts

[1] AUBERT,B 05J calls the mode $K^0_Sf_0(1400)$, but insofar as it is seen here at all, it is certainly the same as $f_0(1370)$.

$\Gamma(3K^0_S)/\Gamma(K^0_S\pi^+\pi^-)$ Γ_{125}/Γ_{35}

VALUE (units 10^{-2})	EVTS	DOCUMENT ID		TECN	COMMENT
3.2 ±0.4 OUR AVERAGE					
3.58±0.54±0.52	170 ± 26	LINK	05A	FOCS	γBe, $\overline{E}_\gamma\approx$180 GeV
2.78±0.38±0.48	61	ASNER	96B	CLE2	$e^+e^-\approx\ \Upsilon(4S)$
7.0 ±2.4 ±1.2	10 ± 3	FRABETTI	94J	E687	γBe, $\overline{E}_\gamma$=220 GeV
3.2 ±1.0	22	AMMAR	91	CLEO	$e^+e^-\approx$ 10.5 GeV
3.4 ±1.4 ±1.0	5	ALBRECHT	90C	ARG	$e^+e^-\approx$ 10 GeV

$\Gamma(K^+2K^-\pi^+)/\Gamma(K^-2\pi^+\pi^-)$ Γ_{126}/Γ_{67}

VALUE	EVTS	DOCUMENT ID		TECN	COMMENT
0.0027 ±0.0004 OUR AVERAGE		Error includes scale factor of 1.1.			
0.00257±0.00034±0.00024	143	LINK	03G	FOCS	γ A, $\overline{E}_\gamma\approx$180 GeV
0.0054 ±0.0016 ±0.0008	18	AITALA	01D	E791	π^- A, 500 GeV
0.0028 ±0.0007 ±0.0001	20	FRABETTI	95C	E687	γ Be, $\overline{E}_\gamma\approx$ 200 GeV

$\Gamma(\phi\overline{K}^*(892)^0,\phi\to K^+K^-,\overline{K}^*(892)^0\to K^-\pi^+)/\Gamma(K^+2K^-\pi^+)$ $\Gamma_{129}/\Gamma_{126}$

VALUE	DOCUMENT ID		TECN	COMMENT
0.48±0.06±0.01	LINK	03G	FOCS	γ A, $\overline{E}_\gamma\approx$180 GeV

$\Gamma(K^-\pi^+\phi,\phi\to K^+K^-)/\Gamma(K^+2K^-\pi^+)$ $\Gamma_{128}/\Gamma_{126}$

VALUE	DOCUMENT ID		TECN	COMMENT
0.18±0.06±0.04	LINK	03G	FOCS	γ A, $\overline{E}_\gamma\approx$180 GeV

$\Gamma(K^+K^-\overline{K}^*(892)^0,\overline{K}^*(892)^0\to K^-\pi^+)/\Gamma(K^+2K^-\pi^+)$ $\Gamma_{127}/\Gamma_{126}$

VALUE	DOCUMENT ID		TECN	COMMENT
0.20±0.07±0.02	LINK	03G	FOCS	γ A, $\overline{E}_\gamma\approx$180 GeV

$\Gamma(K^+2K^-\pi^+\text{nonresonant})/\Gamma(K^+2K^-\pi^+)$ $\Gamma_{130}/\Gamma_{126}$

VALUE	DOCUMENT ID		TECN	COMMENT
0.15±0.06±0.02	LINK	03G	FOCS	γ A, $\overline{E}_\gamma\approx$180 GeV

$\Gamma(2K^0_SK^\pm\pi^\mp)/\Gamma(K^0_S\pi^+\pi^-)$ Γ_{131}/Γ_{35}

VALUE (units 10^{-2})	EVTS	DOCUMENT ID		TECN	COMMENT
2.12±0.38±0.20	57 ± 10	LINK	05A	FOCS	γ Be, $\overline{E}_\gamma\approx$ 180 GeV

Pionic modes

$\Gamma(\pi^+\pi^-)/\Gamma(K^-\pi^+)$ Γ_{132}/Γ_{31}

VALUE (units 10^{-2})	EVTS	DOCUMENT ID		TECN	COMMENT
3.62 ±0.05 OUR FIT					
3.59 ±0.06 OUR AVERAGE					
3.594±0.054±0.040	7334 ± 97	ACOSTA	05C	CDF	$p\overline{p}$, $\sqrt{s}$ = 1.96 TeV
3.53 ±0.12 ±0.06	3453	LINK	03	FOCS	γ A, $\overline{E}_\gamma\approx$ 180 GeV
3.51 ±0.16 ±0.17	710	CSORNA	02	CLE2	$e^+e^-\approx\ \Upsilon(4S)$
4.0 ±0.2 ±0.3	2043	AITALA	98C	E791	π^- A, 500 GeV
• • • We do not use the following data for averages, fits, limits, etc. • • •					
3.62 ±0.10 ±0.08	2085 ± 54	RUBIN	06	CLEO	See MENDEZ 10
3.4 ±0.7 ±0.1	76 ± 15	ABLIKIM	05F	BES	$e^+e^-\approx\ \psi(3770)$
4.3 ±0.7 ±0.3	177	FRABETTI	94C	E687	γBe $\overline{E}_\gamma$= 220 GeV
3.48 ±0.30 ±0.23	227	SELEN	93	CLE2	$e^+e^-\approx\ \Upsilon(4S)$
5.5 ±0.8 ±0.5	120	ANJOS	91D	E691	Photoproduction
5.0 ±0.7 ±0.5	110	ALEXANDER	90	CLEO	e^+e^- 10.5–11 GeV

$\Gamma(\pi^+\pi^-)/[\Gamma(K^-\pi^+)+\Gamma(K^+\pi^-)]$ $\Gamma_{132}/(\Gamma_{31}+\Gamma_{222})$

VALUE (units 10^{-2})	EVTS	DOCUMENT ID		TECN	COMMENT
3.60±0.05 OUR FIT					
3.70±0.06±0.09	6210 ± 93	MENDEZ	10	CLEO	e^+e^- at 3774 MeV

$\Gamma(2\pi^0)/\Gamma_{\text{total}}$ Γ_{133}/Γ

VALUE (units 10^{-4})	EVTS	DOCUMENT ID		TECN	COMMENT
8.20±0.35 OUR FIT					
8.4 ±0.1 ±0.5	26k	LEES	12L	BABR	$e^+e^-\approx$ 10.58 GeV

$\Gamma(2\pi^0)/\Gamma(K^-\pi^+)$ Γ_{133}/Γ_{31}

VALUE (units 10^{-2})	EVTS	DOCUMENT ID		TECN	COMMENT
• • • We do not use the following data for averages, fits, limits, etc. • • •					
2.05±0.13±0.16	499 ± 32	RUBIN	06	CLEO	See MENDEZ 10
2.2 ±0.4 ±0.4	40	SELEN	93	CLE2	$e^+e^-\to\ \Upsilon(4S)$

Meson Particle Listings

D^0

$\Gamma(2\pi^0)/[\Gamma(K^-\pi^+)+\Gamma(K^+\pi^-)]$ $\Gamma_{133}/(\Gamma_{31}+\Gamma_{222})$

VALUE (units 10^{-2})	EVTS	DOCUMENT ID		TECN	COMMENT
2.11±0.09 OUR FIT					
2.06±0.07±0.10	1567±54	MENDEZ	10	CLEO	e^+e^- at 3774 MeV

$\Gamma(\pi^+\pi^-\pi^0)/\Gamma(K^-\pi^+)$ Γ_{134}/Γ_{31}

VALUE (units 10^{-2})	EVTS	DOCUMENT ID		TECN	COMMENT
37.0±1.6 OUR FIT Error includes scale factor of 2.1.					
34.4±0.5±1.2	11k±164	RUBIN	06	CLEO	e^+e^- at $\psi(3770)$

$\Gamma(\pi^+\pi^-\pi^0)/\Gamma(K^-\pi^+\pi^0)$ Γ_{134}/Γ_{50}

VALUE (units 10^{-2})	EVTS	DOCUMENT ID		TECN	COMMENT
10.34±0.24 OUR FIT Error includes scale factor of 2.2.					
10.41±0.23 OUR AVERAGE Error includes scale factor of 2.0.					
10.12±0.04±0.18	123k±490	ARINSTEIN	08	BELL	$e^+e^- \approx \Upsilon(4S)$
10.59±0.06±0.13	60k±343	AUBERT,B	06X	BABR	$e^+e^- \approx \Upsilon(4S)$

$\Gamma(\rho^+\pi^-)/\Gamma(\pi^+\pi^-\pi^0)$ $\Gamma_{135}/\Gamma_{134}$

This is the "fit fraction" from the Dalitz-plot analysis, with interference. See GASPERO 08 and BHATTACHARYA 10A for isospin decompositions of the $D^0 \to \pi^+\pi^0\pi^-$ Dalitz plot, both based on the amplitudes of AUBERT 07BJ. They quantify the conclusion that the final state is dominantly isospin 0.

VALUE (units 10^{-2})	DOCUMENT ID		TECN	COMMENT
68.1±0.6 OUR AVERAGE				
67.8±0.0±0.6	AUBERT	07BJ	BABR	Dalitz fit, 45k events
76.3±1.9±2.5	CRONIN-HEN..05		CLEO	$e^+e^- \approx$ 10 GeV

$\Gamma(\rho^0\pi^0)/\Gamma(\pi^+\pi^-\pi^0)$ $\Gamma_{136}/\Gamma_{134}$

This is the "fit fraction" from the Dalitz-plot analysis, with interference.

VALUE (units 10^{-2})	DOCUMENT ID		TECN	COMMENT
25.9±1.1 OUR AVERAGE				
26.2±0.5±1.1	AUBERT	07BJ	BABR	Dalitz fit, 45k events
24.4±2.0±2.1	CRONIN-HEN..05		CLEO	$e^+e^- \approx$ 10 GeV

$\Gamma(\rho^-\pi^+)/\Gamma(\pi^+\pi^-\pi^0)$ $\Gamma_{137}/\Gamma_{134}$

This is the "fit fraction" from the Dalitz-plot analysis, with interference.

VALUE (units 10^{-2})	DOCUMENT ID		TECN	COMMENT
34.6±0.8 OUR AVERAGE				
34.6±0.8±0.3	AUBERT	07BJ	BABR	Dalitz fit, 45k events
34.5±2.4±1.3	CRONIN-HEN..05		CLEO	$e^+e^- \approx$ 10 GeV

$\Gamma(\rho(1450)^+\pi^-, \rho(1450)^+ \to \pi^+\pi^0)/\Gamma(\pi^+\pi^-\pi^0)$ $\Gamma_{138}/\Gamma_{134}$

VALUE (units 10^{-2})	DOCUMENT ID		TECN	COMMENT
0.11±0.07±0.12	AUBERT	07BJ	BABR	Dalitz fit, 45k events

$\Gamma(\rho(1450)^0\pi^0, \rho(1450)^0 \to \pi^+\pi^-)/\Gamma(\pi^+\pi^-\pi^0)$ $\Gamma_{139}/\Gamma_{134}$

VALUE (units 10^{-2})	DOCUMENT ID		TECN	COMMENT
0.30±0.11±0.07	AUBERT	07BJ	BABR	Dalitz fit, 45k events

$\Gamma(\rho(1450)^-\pi^+, \rho(1450)^- \to \pi^-\pi^0)/\Gamma(\pi^+\pi^-\pi^0)$ $\Gamma_{140}/\Gamma_{134}$

VALUE (units 10^{-2})	DOCUMENT ID		TECN	COMMENT
1.79±0.22±0.12	AUBERT	07BJ	BABR	Dalitz fit, 45k events

$\Gamma(\rho(1700)^+\pi^-, \rho(1700)^+ \to \pi^+\pi^0)/\Gamma(\pi^+\pi^-\pi^0)$ $\Gamma_{141}/\Gamma_{134}$

VALUE (units 10^{-2})	DOCUMENT ID		TECN	COMMENT
4.1±0.7±0.7	AUBERT	07BJ	BABR	Dalitz fit, 45k events

$\Gamma(\rho(1700)^0\pi^0, \rho(1700)^0 \to \pi^+\pi^-)/\Gamma(\pi^+\pi^-\pi^0)$ $\Gamma_{142}/\Gamma_{134}$

VALUE (units 10^{-2})	DOCUMENT ID		TECN	COMMENT
5.0±0.6±1.0	AUBERT	07BJ	BABR	Dalitz fit, 45k events

$\Gamma(\rho(1700)^-\pi^+, \rho(1700)^- \to \pi^-\pi^0)/\Gamma(\pi^+\pi^-\pi^0)$ $\Gamma_{143}/\Gamma_{134}$

VALUE (units 10^{-2})	DOCUMENT ID		TECN	COMMENT
3.2±0.4±0.6	AUBERT	07BJ	BABR	Dalitz fit, 45k events

$\Gamma(f_0(980)\pi^0, f_0(980) \to \pi^+\pi^-)/\Gamma(\pi^+\pi^-\pi^0)$ $\Gamma_{144}/\Gamma_{134}$

VALUE (units 10^{-2})	CL%	DOCUMENT ID		TECN	COMMENT
0.25 ±0.04±0.04		AUBERT	07BJ	BABR	Dalitz fit, 45k events
• • • We do not use the following data for averages, fits, limits, etc. • • •					
<0.026	95	[1] CRONIN-HEN..05		CLEO	$e^+e^- \approx$ 10 GeV

[1] The CRONIN-HENNESSY 05 fit here includes, in addition to the three $\rho\pi$ charged states, only the $f_0(980)\pi^0$ mode. See also the next entries for limits obtained in the same way for the $f_0(500)\pi^0$ mode and for an S-wave $\pi^+\pi^-$ parametrized using a K-matrix. Our $\rho\pi$ branching ratios, given above, use the fit with the K-matrix S wave.

$\Gamma(f_0(500)\pi^0, f_0(500) \to \pi^+\pi^-)/\Gamma(\pi^+\pi^-\pi^0)$ $\Gamma_{145}/\Gamma_{134}$

The $f_0(500)$ is the σ.

VALUE (units 10^{-2})	CL%	DOCUMENT ID		TECN	COMMENT
0.82±0.10±0.10		AUBERT	07BJ	BABR	Dalitz fit, 45k events
• • • We do not use the following data for averages, fits, limits, etc. • • •					
<0.21	95	[1] CRONIN-HEN..05		CLEO	$e^+e^- \approx$ 10 GeV

[1] See the note on CRONIN-HENNESSY 05 in the proceeding data block.

$\Gamma((\pi^+\pi^-)_{S-\text{wave}}\pi^0)/\Gamma(\pi^+\pi^-\pi^0)$ $\Gamma_{146}/\Gamma_{134}$

VALUE	CL%	DOCUMENT ID		TECN	COMMENT
• • • We do not use the following data for averages, fits, limits, etc. • • •					
<0.019	95	[1] CRONIN-HEN..05		CLEO	$e^+e^- \approx$ 10 GeV

[1] See the note on CRONIN-HENNESSY 05 two data blocks up.

$\Gamma(f_0(1370)\pi^0, f_0(1370) \to \pi^+\pi^-)/\Gamma(\pi^+\pi^-\pi^0)$ $\Gamma_{147}/\Gamma_{134}$

VALUE (units 10^{-2})	DOCUMENT ID		TECN	COMMENT
0.37±0.11±0.09	AUBERT	07BJ	BABR	Dalitz fit, 45k events

$\Gamma(f_0(1500)\pi^0, f_0(1500) \to \pi^+\pi^-)/\Gamma(\pi^+\pi^-\pi^0)$ $\Gamma_{148}/\Gamma_{134}$

VALUE (units 10^{-2})	DOCUMENT ID		TECN	COMMENT
0.39±0.08±0.07	AUBERT	07BJ	BABR	Dalitz fit, 45k events

$\Gamma(f_0(1710)\pi^0, f_0(1710) \to \pi^+\pi^-)/\Gamma(\pi^+\pi^-\pi^0)$ $\Gamma_{149}/\Gamma_{134}$

VALUE (units 10^{-2})	DOCUMENT ID		TECN	COMMENT
0.31±0.07±0.08	AUBERT	07BJ	BABR	Dalitz fit, 45k events

$\Gamma(f_2(1270)\pi^0, f_2(1270) \to \pi^+\pi^-)/\Gamma(\pi^+\pi^-\pi^0)$ $\Gamma_{150}/\Gamma_{134}$

VALUE (units 10^{-2})	DOCUMENT ID		TECN	COMMENT
1.32±0.08±0.10	AUBERT	07BJ	BABR	Dalitz fit, 45k events

$\Gamma(\pi^+\pi^-\pi^0 \text{nonresonant})/\Gamma(\pi^+\pi^-\pi^0)$ $\Gamma_{151}/\Gamma_{134}$

VALUE (units 10^{-2})	DOCUMENT ID		TECN	COMMENT
0.84±0.21±0.12	AUBERT	07BJ	BABR	Dalitz fit, 45k events

$\Gamma(3\pi^0)/\Gamma_{\text{total}}$ Γ_{152}/Γ

VALUE	CL%	DOCUMENT ID		TECN	COMMENT
<3.5 × 10^{-4}	90	RUBIN	06	CLEO	e^+e^- at $\psi(3770)$

$\Gamma(2\pi^+2\pi^-)/\Gamma(K^-\pi^+)$ Γ_{153}/Γ_{31}

VALUE (units 10^{-2})	EVTS	DOCUMENT ID		TECN	COMMENT
19.1±0.5 OUR FIT Error includes scale factor of 1.1.					
19.1±0.4±0.6	7331 ± 130	RUBIN	06	CLEO	e^+e^- at $\psi(3770)$

$\Gamma(2\pi^+2\pi^-)/\Gamma(K^-2\pi^+\pi^-)$ Γ_{153}/Γ_{67}

VALUE (units 10^{-2})	EVTS	DOCUMENT ID		TECN	COMMENT
9.19±0.23 OUR FIT Error includes scale factor of 1.1.					
9.20±0.26 OUR AVERAGE					
9.14±0.18±0.22	6360±115	LINK	07A	FOCS	γBe, $\overline{E}_\gamma \approx$ 180 GeV
7.9 ±1.8 ±0.5	162	ABLIKIM	05F	BES	$e^+e^- \approx \psi(3770)$
9.5 ±0.7 ±0.2	814	FRABETTI	95C	E687	γBe, $\overline{E}_\gamma \approx$ 200 GeV
10.2 ±1.3	345	AMMAR	91	CLEO	$e^+e^- \approx$ 10.5 GeV
• • • We do not use the following data for averages, fits, limits, etc. • • •					
11.5 ±2.3 ±1.6	64	ADAMOVICH	92	OMEG	π^- 340 GeV
10.8 ±2.4 ±0.8	79	FRABETTI	92	E687	γBe
9.6 ±1.8 ±0.7	66	ANJOS	91	E691	γBe 80–240 GeV

$\Gamma(a_1(1260)^+\pi^-, a_1^+ \to 2\pi^+\pi^- \text{ total})/\Gamma(2\pi^+2\pi^-)$ $\Gamma_{154}/\Gamma_{153}$

This is the fit fraction from the coherent amplitude analysis.

VALUE (units 10^{-2})	DOCUMENT ID		TECN	COMMENT
60.0±3.0±2.4	LINK	07A	FOCS	4-body fit, ≈ 5.7k evts

$\Gamma(a_1(1260)^+\pi^-, a_1^+ \to \rho^0\pi^+ S\text{-wave})/\Gamma(2\pi^+2\pi^-)$ $\Gamma_{155}/\Gamma_{153}$

This is the fit fraction from the coherent amplitude analysis.

VALUE (units 10^{-2})	DOCUMENT ID		TECN	COMMENT
43.3±2.5±1.9	LINK	07A	FOCS	4-body fit, ≈ 5.7k evts

$\Gamma(a_1(1260)^+\pi^-, a_1^+ \to \rho^0\pi^+ D\text{-wave})/\Gamma(2\pi^+2\pi^-)$ $\Gamma_{156}/\Gamma_{153}$

This is the fit fraction from the coherent amplitude analysis.

VALUE (units 10^{-2})	DOCUMENT ID		TECN	COMMENT
2.5±0.5±0.4	LINK	07A	FOCS	4-body fit, ≈ 5.7k evts

$\Gamma(a_1(1260)^+\pi^-, a_1^+ \to \sigma\pi^+)/\Gamma(2\pi^+2\pi^-)$ $\Gamma_{157}/\Gamma_{153}$

This is the fit fraction from the coherent amplitude analysis.

VALUE (units 10^{-2})	DOCUMENT ID		TECN	COMMENT
8.3±0.7±0.6	LINK	07A	FOCS	4-body fit, ≈ 5.7k evts

$\Gamma(2\rho^0 \text{total})/\Gamma(2\pi^+2\pi^-)$ $\Gamma_{158}/\Gamma_{153}$

This is the fit fraction from the coherent amplitude analysis.

VALUE (units 10^{-2})	DOCUMENT ID		TECN	COMMENT
24.5±1.3±1.0	LINK	07A	FOCS	4-body fit, ≈ 5.7k evts

$\Gamma(2\rho^0, \text{parallel helicities})/\Gamma(2\pi^+2\pi^-)$ $\Gamma_{159}/\Gamma_{153}$

This is the fit fraction from the coherent amplitude analysis.

VALUE (units 10^{-2})	DOCUMENT ID		TECN	COMMENT
1.1±0.3±0.3	LINK	07A	FOCS	4-body fit, ≈ 5.7k evts

$\Gamma(2\rho^0, \text{perpendicular helicities})/\Gamma(2\pi^+2\pi^-)$ $\Gamma_{160}/\Gamma_{153}$

This is the fit fraction from the coherent amplitude analysis.

VALUE (units 10^{-2})	DOCUMENT ID		TECN	COMMENT
6.4±0.6±0.5	LINK	07A	FOCS	4-body fit, ≈ 5.7k evts

$\Gamma(2\rho^0, \text{longitudinal helicities})/\Gamma(2\pi^+2\pi^-)$ $\Gamma_{161}/\Gamma_{153}$

This is the fit fraction from the coherent amplitude analysis.

VALUE (units 10^{-2})	DOCUMENT ID		TECN	COMMENT
16.8±1.0±0.8	LINK	07A	FOCS	4-body fit, ≈ 5.7k evts

$\Gamma(\text{Resonant } (\pi^+\pi^-)\pi^+\pi^- \text{ 3-body total})/\Gamma(2\pi^+2\pi^-)$ $\Gamma_{162}/\Gamma_{153}$

This is the fit fraction from the coherent amplitude analysis.

VALUE (units 10^{-2})	DOCUMENT ID		TECN	COMMENT
20.0±1.2±1.0	LINK	07A	FOCS	4-body fit, ≈ 5.7k evts

$\Gamma(\sigma\pi^+\pi^-)/\Gamma(2\pi^+2\pi^-)$ $\Gamma_{163}/\Gamma_{153}$

This is the fit fraction from the coherent amplitude analysis.

VALUE (units 10^{-2})	DOCUMENT ID		TECN	COMMENT
8.2±0.9±0.7	LINK	07A	FOCS	4-body fit, ≈ 5.7k evts

$\Gamma(f_0(980)\pi^+\pi^-, f_0 \to \pi^+\pi^-)/\Gamma(2\pi^+2\pi^-)$ $\Gamma_{164}/\Gamma_{153}$

This is the fit fraction from the coherent amplitude analysis.

VALUE (units 10^{-2})	DOCUMENT ID		TECN	COMMENT
2.4±0.5±0.4	LINK	07A	FOCS	4-body fit, ≈ 5.7k evts

$\Gamma(f_2(1270)\pi^+\pi^-, f_2 \to \pi^+\pi^-)/\Gamma(2\pi^+2\pi^-)$ $\Gamma_{165}/\Gamma_{153}$

This is the fit fraction from the coherent amplitude analysis.

VALUE (units 10^{-2})	DOCUMENT ID		TECN	COMMENT
4.9±0.6±0.5	LINK	07A	FOCS	4-body fit, ≈ 5.7k evts

$\Gamma(\pi^+\pi^-2\pi^0)/\Gamma(K^-\pi^+)$ Γ_{166}/Γ_{31}

VALUE (units 10^{-2})	EVTS	DOCUMENT ID		TECN	COMMENT
25.8±1.5±1.8	2724 ± 166	RUBIN	06	CLEO	e^+e^- at $\psi(3770)$

$\Gamma(\eta\pi^0)/\Gamma_{\text{total}}$ Γ_{167}/Γ

Unseen decay modes of the η are included.

VALUE (units 10^{-4})	EVTS	DOCUMENT ID		TECN	COMMENT
• • • We do not use the following data for averages, fits, limits, etc. • • •					
6.4±1.0±0.4	156 ± 24	ARTUSO	08	CLEO	See MENDEZ 10

$\Gamma(\eta\pi^0)/\Gamma(K^-\pi^+)$ Γ_{167}/Γ_{31}

Unseen decay modes of the η are included.

VALUE (units 10^{-2})	EVTS	DOCUMENT ID		TECN	COMMENT
• • • We do not use the following data for averages, fits, limits, etc. • • •					
1.47±0.34±0.11	62 ± 14	RUBIN	06	CLEO	See ARTUSO 08

$\Gamma(\eta\pi^0)/[\Gamma(K^-\pi^+)+\Gamma(K^+\pi^-)]$ $\Gamma_{167}/(\Gamma_{31}+\Gamma_{222})$

Unseen decay modes of the η are included.

VALUE (units 10^{-2})	EVTS	DOCUMENT ID		TECN	COMMENT
1.74±0.19 OUR FIT					
1.74±0.15±0.11	481 ± 40	MENDEZ	10	CLEO	e^+e^- at 3774 MeV

$\Gamma(\omega\pi^0)/\Gamma_{\text{total}}$ Γ_{168}/Γ

Unseen decay modes of the ω are included.

VALUE	CL%	DOCUMENT ID		TECN	COMMENT
<2.6 × 10^{-4}	90	RUBIN	06	CLEO	e^+e^- at $\psi(3770)$

$\Gamma(2\pi^+2\pi^-\pi^0)/\Gamma(K^-\pi^+)$ Γ_{169}/Γ_{31}

VALUE (units 10^{-2})	EVTS	DOCUMENT ID		TECN	COMMENT
10.7±1.2±0.5	1614 ± 171	RUBIN	06	CLEO	e^+e^- at $\psi(3770)$

$\Gamma(\eta\pi^+\pi^-)/\Gamma_{\text{total}}$ Γ_{170}/Γ

Unseen decay modes of the η are included.

VALUE (units 10^{-4})	CL%	EVTS	DOCUMENT ID		TECN	COMMENT
10.9±1.3±0.9		257 ± 32	ARTUSO	08	CLEO	e^+e^- at $\psi(3770)$
• • • We do not use the following data for averages, fits, limits, etc. • • •						
<19	90		RUBIN	06	CLEO	e^+e^- at $\psi(3770)$

$\Gamma(\omega\pi^+\pi^-)/\Gamma(K^-\pi^+)$ Γ_{171}/Γ_{31}

Unseen decay modes of the ω are included.

VALUE (units 10^{-2})	EVTS	DOCUMENT ID		TECN	COMMENT
4.1±1.2±0.4	472 ± 132	RUBIN	06	CLEO	e^+e^- at $\psi(3770)$

$\Gamma(3\pi^+3\pi^-)/\Gamma(K^-2\pi^+\pi^-)$ Γ_{172}/Γ_{67}

VALUE (units 10^{-3})	EVTS	DOCUMENT ID		TECN	COMMENT
5.23±0.59±1.35	149 ± 17	LINK	04B	FOCS	γA, $\overline{E}_\gamma \approx$ 180 GeV

$\Gamma(3\pi^+3\pi^-)/\Gamma(K^-3\pi^+2\pi^-)$ Γ_{172}/Γ_{93}

VALUE	DOCUMENT ID		TECN	COMMENT
• • • We do not use the following data for averages, fits, limits, etc. • • •				
1.93±047±0.48	[1] LINK	04B	FOCS	γA, $\overline{E}_\gamma \approx$ 180 GeV

[1] This LINK 04B result is not independent of other results in these Listings.

$\Gamma(\eta'(958)\pi^0)/\Gamma_{\text{total}}$ Γ_{173}/Γ

Unseen decay modes of the $\eta'(958)$ are included.

VALUE (units 10^{-4})	EVTS	DOCUMENT ID		TECN	COMMENT
• • • We do not use the following data for averages, fits, limits, etc. • • •					
8.1±1.5±0.6	50 ± 9	ARTUSO	08	CLEO	See MENDEZ 10

$\Gamma(\eta'(958)\pi^0)/[\Gamma(K^-\pi^+)+\Gamma(K^+\pi^-)]$ $\Gamma_{173}/(\Gamma_{31}+\Gamma_{222})$

Unseen decay modes of the $\eta'(958)$ are included.

VALUE (units 10^{-2})	EVTS	DOCUMENT ID		TECN	COMMENT
2.3±0.4 OUR FIT					
2.3±0.3±0.2	159 ± 19	MENDEZ	10	CLEO	e^+e^- at 3774 MeV

$\Gamma(\eta'(958)\pi^+\pi^-)/\Gamma_{\text{total}}$ Γ_{174}/Γ

Unseen decay modes of the $\eta'(958)$ are included.

VALUE (units 10^{-4})	EVTS	DOCUMENT ID		TECN	COMMENT
4.5±1.6±0.5	21 ± 8	ARTUSO	08	CLEO	e^+e^- at $\psi(3770)$

$\Gamma(2\eta)/\Gamma_{\text{total}}$ Γ_{175}/Γ

Unseen decay modes of the η are included.

VALUE (units 10^{-4})	EVTS	DOCUMENT ID		TECN	COMMENT
• • • We do not use the following data for averages, fits, limits, etc. • • •					
16.7±1.4±1.3	255 ± 22	ARTUSO	08	CLEO	See MENDEZ 10

$\Gamma(2\eta)/[\Gamma(K^-\pi^+)+\Gamma(K^+\pi^-)]$ $\Gamma_{175}/(\Gamma_{31}+\Gamma_{222})$

Unseen decay modes of the η are included.

VALUE (units 10^{-2})	EVTS	DOCUMENT ID		TECN	COMMENT
4.3±0.5 OUR FIT					
4.3±0.3±0.4	430 ± 29	MENDEZ	10	CLEO	e^+e^- at 3774 MeV

$\Gamma(\eta\eta'(958))/\Gamma_{\text{total}}$ Γ_{176}/Γ

Unseen decay modes of the η and $\eta'(958)$ are included.

VALUE (units 10^{-4})	EVTS	DOCUMENT ID		TECN	COMMENT
• • • We do not use the following data for averages, fits, limits, etc. • • •					
12.6±2.5±1.1	46 ± 9	ARTUSO	08	CLEO	See MENDEZ 10

$\Gamma(\eta\eta'(958))/[\Gamma(K^-\pi^+)+\Gamma(K^+\pi^-)]$ $\Gamma_{176}/(\Gamma_{31}+\Gamma_{222})$

Unseen decay modes of the η and $\eta'(958)$ are included.

VALUE (units 10^{-2})	EVTS	DOCUMENT ID		TECN	COMMENT
2.7±0.7 OUR FIT					
2.7±0.6±0.3	66 ± 15	MENDEZ	10	CLEO	e^+e^- at 3774 MeV

Hadronic modes with a $K\overline{K}$ pair

$\Gamma(K^+K^-)/\Gamma_{\text{total}}$ Γ_{177}/Γ

VALUE (units 10^{-3})	EVTS	DOCUMENT ID		TECN	COMMENT
3.96±0.08 OUR FIT	Error includes scale factor of 1.4.				
• • • We do not use the following data for averages, fits, limits, etc. • • •					
4.08±0.08±0.09	4746 ± 74	BONVICINI	08	CLEO	See MENDEZ 10

$\Gamma(K^+K^-)/\Gamma(K^-\pi^+)$ Γ_{177}/Γ_{31}

VALUE	EVTS	DOCUMENT ID		TECN	COMMENT
0.1021±0.0015 OUR FIT	Error includes scale factor of 1.7.				
0.1010±0.0016 OUR AVERAGE	Error includes scale factor of 1.4. See the ideogram below.				
0.122 ±0.011 ±0.004	242 ± 20	ABLIKIM	05F	BES	$e^+e^- \approx \psi(3770)$
0.0992±0.0011±0.0012	16k±200	ACOSTA	05C	CDF	$p\overline{p}$, $\sqrt{s}$=1.96 TeV
0.0993±0.0014±0.0014	11k	LINK	03	FOCS	γ nucleus, $\overline{E}_\gamma \approx$ 180 GeV
0.1040±0.0033±0.0027	1900	CSORNA	02	CLE2	$e^+e^- \approx \Upsilon(4S)$
0.109 ±0.003 ±0.003	3317	AITALA	98C	E791	π^- nucleus, 500 GeV
0.116 ±0.007 ±0.007	1102	ASNER	96B	CLE2	$e^+e^- \approx \Upsilon(4S)$
0.109 ±0.007 ±0.009	581	FRABETTI	94C	E687	γBe $\overline{E}_\gamma$= 220 GeV
0.107 ±0.010 ±0.009	193	ANJOS	91D	E691	Photoproduction
0.117 ±0.010 ±0.007	249	ALEXANDER	90	CLEO	e^+e^- 10.5–11 GeV
• • • We do not use the following data for averages, fits, limits, etc. • • •					
0.107 ±0.029 ±0.015	103	ADAMOVICH	92	OMEG	π^- 340 GeV
0.138 ±0.027 ±0.010	155	FRABETTI	92	E687	γBe
0.16 ±0.05	34	ALVAREZ	91B	NA14	Photoproduction
0.10 ±0.02 ±0.01	131	ALBRECHT	90C	ARG	$e^+e^- \approx$ 10 GeV
0.122 ±0.018 ±0.012	118	BALTRUSAIT...	85E	MRK3	e^+e^- 3.77 GeV
0.113 ±0.030		ABRAMS	79D	MRK2	e^+e^- 3.77 GeV

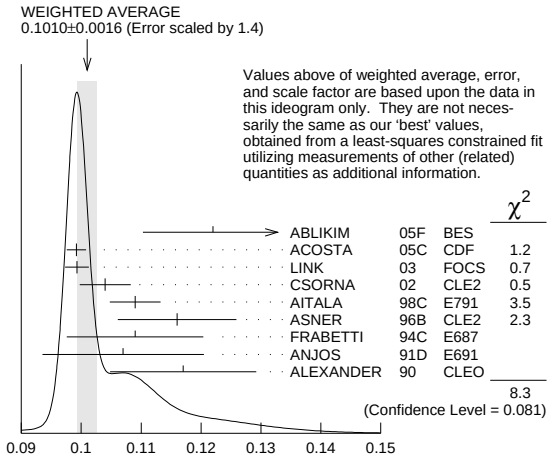

$\Gamma(K^+K^-)/\Gamma(K^-\pi^+)$

$\Gamma(K^+K^-)/[\Gamma(K^-\pi^+)+\Gamma(K^+\pi^-)]$ $\Gamma_{177}/(\Gamma_{31}+\Gamma_{222})$

VALUE (units 10^{-2})	EVTS	DOCUMENT ID		TECN	COMMENT
10.18±0.15 OUR FIT	Error includes scale factor of 1.7.				
10.41±0.11±0.12	13.8k	MENDEZ	10	CLEO	e^+e^- at 3774 MeV

$\Gamma(K^+K^-)/\Gamma(\pi^+\pi^-)$ $\Gamma_{177}/\Gamma_{132}$

The unused results here are redundant with $\Gamma(K^+K^-)/\Gamma(K^-\pi^+)$ and $\Gamma(\pi^+\pi^-)/\Gamma(K^-\pi^+)$ measurements by the same experiments.

VALUE	EVTS	DOCUMENT ID		TECN	COMMENT
• • • We do not use the following data for averages, fits, limits, etc. • • •					
2.760±0.040±0.034	7334	ACOSTA	05C	CDF	$p\overline{p}$, $\sqrt{s}$=1.96 TeV
2.81 ±0.10 ±0.06		LINK	03	FOCS	γ nucleus, $\overline{E}_\gamma \approx 180$ GeV
2.96 ±0.16 ±0.15	710	CSORNA	02	CLE2	$e^+e^- \approx \Upsilon(4S)$
2.75 ±0.15 ±0.16		AITALA	98C	E791	π^- nucleus, 500 GeV
2.53 ±0.46 ±0.19		FRABETTI	94C	E687	γBe $\overline{E}_\gamma$= 220 GeV
2.23 ±0.81 ±0.46		ADAMOVICH	92	OMEG	π^- 340 GeV
1.95 ±0.34 ±0.22		ANJOS	91D	E691	Photoproduction
2.5 ±0.7		ALBRECHT	90C	ARG	$e^+e^- \approx 10$ GeV
2.35 ±0.37 ±0.28		ALEXANDER	90	CLEO	e^+e^- 10.5–11 GeV

$\Gamma(2K^0_S)/\Gamma_{total}$ Γ_{178}/Γ

VALUE (units 10^{-4})	EVTS	DOCUMENT ID		TECN	COMMENT
• • • We do not use the following data for averages, fits, limits, etc. • • •					
1.46±0.32±0.09	68 ± 15	BONVICINI	08	CLEO	See MENDEZ 10

$\Gamma(2K^0_S)/[\Gamma(K^-\pi^+)+\Gamma(K^+\pi^-)]$ $\Gamma_{178}/(\Gamma_{31}+\Gamma_{222})$

VALUE (units 10^{-2})	EVTS	DOCUMENT ID		TECN	COMMENT
0.45±0.11 OUR FIT	Error includes scale factor of 2.5.				
0.41±0.04±0.02	215 ± 23	MENDEZ	10	CLEO	e^+e^- at 3774 MeV

$\Gamma(2K^0_S)/\Gamma(K^0_S\pi^+\pi^-)$ Γ_{178}/Γ_{35}

This is the same as $\Gamma(K^0\overline{K}^0)$ / $\Gamma(\overline{K}^0\pi^+\pi^-)$ because $D^0 \to K^0_S K^0_L$ is forbidden by CP conservation.

VALUE	EVTS	DOCUMENT ID		TECN	COMMENT
0.0061±0.0015 OUR FIT	Error includes scale factor of 2.2.				
0.0120±0.0022 OUR AVERAGE					
0.0144±0.0032±0.0016	79 ± 17	LINK	05A	FOCS	γ Be, $\overline{E}_\gamma \approx 180$ GeV
0.0101±0.0022±0.0016	26	ASNER	96B	CLE2	$e^+e^- \approx \Upsilon(4S)$
0.039 ±0.013 ±0.013	20 ± 7	FRABETTI	94J	E687	γBe $\overline{E}_\gamma$=220 GeV
• • • We do not use the following data for averages, fits, limits, etc. • • •					
0.021 $^{+0.011}_{-0.008}$ ±0.002	5	ALEXANDER	90	CLEO	e^+e^- 10.5–11 GeV

$\Gamma(K^0_S K^-\pi^+)/\Gamma(K^-\pi^+)$ Γ_{179}/Γ_{31}

VALUE	DOCUMENT ID		TECN	COMMENT
0.091±0.014 OUR FIT	Error includes scale factor of 1.2.			
0.08 ±0.03	[1] ANJOS	91	E691	γBe 80–240 GeV

[1] The factor 100 at the top of column 2 of Table I of ANJOS 91 should be omitted.

$\Gamma(K^0_S K^-\pi^+)/\Gamma(K^0_S\pi^+\pi^-)$ Γ_{179}/Γ_{35}

VALUE	EVTS	DOCUMENT ID		TECN	COMMENT
0.125±0.017 OUR FIT	Error includes scale factor of 1.2.				
0.119±0.021 OUR AVERAGE	Error includes scale factor of 1.3.				
0.108±0.019	61	AMMAR	91	CLEO	$e^+e^- \approx 10.5$ GeV
0.16 ±0.03 ±0.02	39	ALBRECHT	90C	ARG	$e^+e^- \approx 10$ GeV

$\Gamma(\overline{K}^*(892)^0 K^0_S, \overline{K}^{*0} \to K^-\pi^+)/\Gamma(K^0_S\pi^+\pi^-)$ Γ_{180}/Γ_{35}

VALUE	CL%	DOCUMENT ID		TECN	COMMENT
<0.019	90	AMMAR	91	CLEO	$e^+e^- \approx 10.5$ GeV
• • • We do not use the following data for averages, fits, limits, etc. • • •					
<0.02	90	ALBRECHT	90C	ARG	$e^+e^- \approx 10$ GeV

$\Gamma(K^0_S K^+\pi^-)/\Gamma(K^-\pi^+)$ Γ_{181}/Γ_{31}

VALUE	DOCUMENT ID		TECN	COMMENT
0.055±0.009 OUR FIT	Error includes scale factor of 1.3.			
0.05 ±0.025	[1] ANJOS	91	E691	γBe 80–240 GeV

[1] The factor 100 at the top of column 2 of Table I of ANJOS 91 should be omitted.

$\Gamma(K^0_S K^+\pi^-)/\Gamma(K^0_S\pi^+\pi^-)$ Γ_{181}/Γ_{35}

VALUE	EVTS	DOCUMENT ID		TECN	COMMENT
0.076±0.012 OUR FIT	Error includes scale factor of 1.3.				
0.098±0.020	55	AMMAR	91	CLEO	$e^+e^- \approx 10.5$ GeV

$\Gamma(K^0_S K^+\pi^-)/\Gamma(K^0_S K^-\pi^+)$ $\Gamma_{181}/\Gamma_{179}$

VALUE	DOCUMENT ID		TECN	COMMENT
0.61 ±0.06 OUR FIT	Error includes scale factor of 1.3.			
0.592±0.044±0.018	INSLER	12	CLEO	$e^+e^- \to D^0\overline{D}^0$ at 3.77 GeV

$\Gamma(K^*(892)^0 K^0_S, K^{*0} \to K^+\pi^-)/\Gamma(\overline{K}^*(892)^0 K^0_S, \overline{K}^{*0} \to K^-\pi^+)$ $\Gamma_{182}/\Gamma_{180}$

VALUE	CL%	DOCUMENT ID		TECN	COMMENT
0.356±0.034±0.007		[1] INSLER	12	CLEO	$e^+e^- \to D^0\overline{D}^0$, 3.77 GeV
• • • We do not use the following data for averages, fits, limits, etc. • • •					
<0.010	90	AMMAR	91	CLEO	$e^+e^- \approx 10.5$ GeV

[1] Uses quantum correlations in $e^+e^- \to D^0\overline{D}^0$ at the $\psi(3770)$, where the signal side D decays to $K^0_S K\pi$ and the tag-side D decays to $K\pi$, $K\pi\pi\pi$, $K\pi\pi^0$.

$\Gamma(K^+K^-\pi^0)/\Gamma(K^-\pi^+\pi^0)$ Γ_{183}/Γ_{50}

VALUE (units 10^{-2})	EVTS	DOCUMENT ID		TECN	COMMENT
2.37±0.03±0.04	11k±122	AUBERT,B	06X	BABR	$e^+e^- \approx \Upsilon(4S)$
• • • We do not use the following data for averages, fits, limits, etc. • • •					
0.95±0.26	151	ASNER	96B	CLE2	$e^+e^- \approx \Upsilon(4S)$

$\Gamma(K^*(892)^+K^-, K^*(892)^+ \to K^+\pi^0)/\Gamma(K^+K^-\pi^0)$ $\Gamma_{184}/\Gamma_{183}$

This is the "fit fraction" from the Dalitz-plot analysis with interference.

VALUE (units 10^{-2})	DOCUMENT ID		TECN	COMMENT
44.4±0.8±0.6	AUBERT	07T	BABR	Dalitz fit II, 11k evts
• • • We do not use the following data for averages, fits, limits, etc. • • •				
46.1±3.1	[1] CAWLFIELD	06A	CLEO	Dalitz fit, 627 ± 30 evts

[1] The error on this CAWLFIELD 06A result is statistical only.

$\Gamma(K^*(892)^-K^+, K^*(892)^- \to K^-\pi^0)/\Gamma(K^+K^-\pi^0)$ $\Gamma_{185}/\Gamma_{183}$

This is the "fit fraction" from the Dalitz-plot analysis with interference.

VALUE (units 10^{-2})	DOCUMENT ID		TECN	COMMENT
15.9±0.7±0.6	AUBERT	07T	BABR	Dalitz fit II, 11k evts
• • • We do not use the following data for averages, fits, limits, etc. • • •				
12.3±2.2	[1] CAWLFIELD	06A	CLEO	Dalitz fit, 627 ± 30 evts

[1] The error on this CAWLFIELD 06A result is statistical only.

$\Gamma((K^+\pi^0)_{S-wave}K^-)/\Gamma(K^+K^-\pi^0)$ $\Gamma_{186}/\Gamma_{183}$

This is the "fit fraction" from the Dalitz-plot analysis with interference.

VALUE (units 10^{-2})	DOCUMENT ID		TECN	COMMENT
71.1±3.7±1.9	[1] AUBERT	07T	BABR	Dalitz fit II, 11k evts

[1] The only major difference between fits I and II in the AUBERT 07T analysis is in this mode, where the fit-I fraction is (16.3 ± 3.4 ± 2.1)%.

$\Gamma((K^-\pi^0)_{S-wave}K^+)/\Gamma(K^+K^-\pi^0)$ $\Gamma_{187}/\Gamma_{183}$

This is the "fit fraction" from the Dalitz-plot analysis with interference.

VALUE (units 10^{-2})	DOCUMENT ID		TECN	COMMENT
3.9±0.9±1.0	AUBERT	07T	BABR	Dalitz fit II, 11k evts

$\Gamma(f_0(980)\pi^0, f_0 \to K^+K^-)/\Gamma(K^+K^-\pi^0)$ $\Gamma_{188}/\Gamma_{183}$

This is the "fit fraction" from the Dalitz-plot analysis with interference.

VALUE (units 10^{-2})	DOCUMENT ID		TECN	COMMENT
10.5±1.1±1.2	[1] AUBERT	07T	BABR	Dalitz fit II, 11k evts

[1] When AUBERT 07T replace the $f_0(980)\pi^0$ mode with $a_0(980)\pi^0$, the fit fraction is a negligibly different (11.0 ± 1.5 ± 1.2)%.

$\Gamma(\phi\pi^0, \phi \to K^+K^-)/\Gamma(K^+K^-\pi^0)$ $\Gamma_{189}/\Gamma_{183}$

This is the "fit fraction" from the Dalitz-plot analysis with interference.

VALUE (units 10^{-2})	DOCUMENT ID		TECN	COMMENT
19.4±0.6±0.5	AUBERT	07T	BABR	Dalitz fit II, 11k evts
• • • We do not use the following data for averages, fits, limits, etc. • • •				
14.9±1.6	[1] CAWLFIELD	06A	CLEO	Dalitz fit, 627 ± 30 evts

[1] The error on this CAWLFIELD 06A result is statistical only.

$\Gamma(K^+K^-\pi^0\,\text{nonresonant})/\Gamma(K^+K^-\pi^0)$ $\Gamma_{190}/\Gamma_{183}$

This is the "fit fraction" from the Dalitz-plot analysis with interference.

VALUE	DOCUMENT ID		TECN	COMMENT
• • • We do not use the following data for averages, fits, limits, etc. • • •				
0.360±0.037	[1] CAWLFIELD	06A	CLEO	Dalitz fit, 627 ± 30 evts

[1] The error is statistical only. CAWLFIELD 06A also fits the Dalitz plot replacing this flat nonresonant background with broad S–wave $\kappa^\pm \to K^\pm\pi^0$ resonances. There is no significant improvement in the fit, and $K^{*\pm}K^\mp$ and $\phi\pi^0$ results are not much changed.

$\Gamma(2K^0_S\pi^0)/\Gamma_{\text{total}}$ Γ_{191}/Γ

VALUE	DOCUMENT ID		TECN	COMMENT
<0.00059	ASNER	96B	CLE2	$e^+e^- \approx \Upsilon(4S)$

$\Gamma(\phi\pi^0)/\Gamma(K^+K^-)$ $\Gamma_{213}/\Gamma_{177}$

VALUE	EVTS	DOCUMENT ID		TECN	COMMENT
• • • We do not use the following data for averages, fits, limits, etc. • • •					
0.194±0.006±0.009	1254	TAJIMA	04	BELL	e^+e^- at $\Upsilon(4S)$

$\Gamma(\phi\eta)/\Gamma(K^+K^-)$ $\Gamma_{214}/\Gamma_{177}$

VALUE (units 10^{-2})	EVTS	DOCUMENT ID		TECN	COMMENT
3.59±1.14±0.18	31	TAJIMA	04	BELL	e^+e^- at $\Upsilon(4S)$

$\Gamma(\phi\omega)/\Gamma_{\text{total}}$ Γ_{215}/Γ

VALUE	CL%	DOCUMENT ID		TECN	COMMENT
<0.0021	90	ALBRECHT	94I	ARG	$e^+e^-\approx$ 10 GeV

$\Gamma(K^+K^-\pi^+\pi^-)/\Gamma(K^-2\pi^+\pi^-)$ Γ_{192}/Γ_{67}

VALUE (units 10^{-2})	EVTS	DOCUMENT ID		TECN	COMMENT
3.00±0.13 OUR AVERAGE					
2.95±0.11±0.08	2669 ± 101	[1] LINK	05G	FOCS	γBe, $\overline{E}_\gamma \approx$ 180 GeV
3.13±0.37±0.36	136 ± 15	AITALA	98D	E791	π^- nucleus, 500 GeV
3.5 ±0.4 ±0.2	244 ± 26	FRABETTI	95C	E687	γBe, $\overline{E}_\gamma \approx$ 200 GeV
• • • We do not use the following data for averages, fits, limits, etc. • • •					
4.4 ±1.8 ±0.5	19 ± 8	ABLIKIM	05F	BES	$e^+e^- \approx \psi(3770)$
4.1 ±0.7 ±0.5	114 ± 20	ALBRECHT	94I	ARG	$e^+e^-\approx$ 10 GeV
3.14±1.0	89 ± 29	AMMAR	91	CLEO	$e^+e^- \approx$ 10.5 GeV
$2.8\ ^{+0.8}_{-0.7}$		ANJOS	91	E691	γBe 80–240 GeV

[1] LINK 05G uses a smaller, cleaner subset of 1279 ± 48 events for the amplitude analysis that gives the results in the next data blocks.

$\Gamma(\phi(\pi^+\pi^-)_{S-wave},\ \phi\to K^+K^-)/\Gamma(K^+K^-\pi^+\pi^-)$ $\Gamma_{193}/\Gamma_{192}$

This is the fraction from a coherent amplitude analysis.

VALUE (%)	DOCUMENT ID		TECN	COMMENT
10.3±1.0±0.8	ARTUSO	12	CLEO	Fitting 2959 evts.
• • • We do not use the following data for averages, fits, limits, etc. • • •				
1 ±1	LINK	05G	FOCS	Fits 1279 ± 48 evts.

$\Gamma((\phi\rho^0)_{S-wave},\ \phi\to K^+K^-)/\Gamma(K^+K^-\pi^+\pi^-)$ $\Gamma_{194}/\Gamma_{192}$

This is the fraction from a coherent amplitude analysis.

VALUE (%)	DOCUMENT ID		TECN	COMMENT
38.3±2.5±3.8	ARTUSO	12	CLEO	Fitting 2959 evts.
• • • We do not use the following data for averages, fits, limits, etc. • • •				
29 ±2 ±1	LINK	05G	FOCS	Fits 1279 ± 48 evts.

$\Gamma((\phi\rho^0)_{D-wave},\ \phi\to K^+K^-)/\Gamma(K^+K^-\pi^+\pi^-)$ $\Gamma_{195}/\Gamma_{192}$

VALUE (%)	DOCUMENT ID		TECN	COMMENT
3.4±0.7±0.6	ARTUSO	12	CLEO	Fitting 2959 evts.

$\Gamma((K^{*0}\overline{K}^{*0})_{S-wave},\ K^{*0}\to K^\pm\pi^\mp)/\Gamma(K^+K^-\pi^+\pi^-)$ $\Gamma_{196}/\Gamma_{192}$

VALUE (%)	DOCUMENT ID		TECN	COMMENT
6.1±0.8±0.9	ARTUSO	12	CLEO	Fitting 2959 evts.

$\Gamma((K^-\pi^+)_{P-wave},\ (K^+\pi^-)_{S-wave},)/\Gamma(K^+K^-\pi^+\pi^-)$ $\Gamma_{197}/\Gamma_{192}$

VALUE (%)	DOCUMENT ID		TECN	COMMENT
10.9±1.2±1.7	ARTUSO	12	CLEO	Fitting 2959 evts.

$\Gamma(K_1(1270)^+K^-,\ K_1(1270)^+\to K^{*0}\pi^+)/\Gamma(K^+K^-\pi^+\pi^-)$ $\Gamma_{198}/\Gamma_{192}$

VALUE (%)	DOCUMENT ID		TECN	COMMENT
7.3±0.8±1.9	ARTUSO	12	CLEO	Fitting 2959 evts.

$\Gamma(K_1(1270)^+K^-,\ K_1(1270)^+\to \rho^0K^+)/\Gamma(K^+K^-\pi^+\pi^-)$ $\Gamma_{199}/\Gamma_{192}$

VALUE (%)	DOCUMENT ID		TECN	COMMENT
4.7±0.7±0.8	ARTUSO	12	CLEO	Fitting 2959 evts.

$\Gamma(K_1(1270)^-K^+,\ K_1(1270)^-\to \overline{K}^{*0}\pi^-)/\Gamma(K^+K^-\pi^+\pi^-)$ $\Gamma_{200}/\Gamma_{192}$

VALUE (%)	DOCUMENT ID		TECN	COMMENT
0.9±0.3±0.4	ARTUSO	12	CLEO	Fitting 2959 evts.

$\Gamma(K_1(1270)^-K^+,\ K_1(1270)^-\to \rho^0K^-)/\Gamma(K^+K^-\pi^+\pi^-)$ $\Gamma_{201}/\Gamma_{192}$

VALUE (%)	DOCUMENT ID		TECN	COMMENT
6.0±0.8±0.6	ARTUSO	12	CLEO	Fitting 2959 evts.

$\Gamma(K^*(1410)^+K^-,\ K^*(1410)^+\to K^{*0}\pi^+)/\Gamma(K^+K^-\pi^+\pi^-)$ $\Gamma_{202}/\Gamma_{192}$

VALUE (%)	DOCUMENT ID		TECN	COMMENT
4.2±0.7±0.8	ARTUSO	12	CLEO	Fitting 2959 evts.

$\Gamma(K^*(1410)^-K^+,\ K^*(1410)^-\to \overline{K}^{*0}\pi^-)/\Gamma(K^+K^-\pi^+\pi^-)$ $\Gamma_{203}/\Gamma_{192}$

VALUE (%)	DOCUMENT ID		TECN	COMMENT
4.7±0.7±0.7	ARTUSO	12	CLEO	Fitting 2959 evts.

$\Gamma(K^+K^-\rho^0\,\text{3-body})/\Gamma(K^+K^-\pi^+\pi^-)$ $\Gamma_{204}/\Gamma_{192}$

This is the fraction from a coherent amplitude analysis.

VALUE (%)	DOCUMENT ID		TECN	COMMENT
• • • We do not use the following data for averages, fits, limits, etc. • • •				
2±2±2	LINK	05G	FOCS	Fits 1279 ± 48 evts.

$\Gamma(f_0(980)\pi^+\pi^-,\ f_0\to K^+K^-)/\Gamma(K^+K^-\pi^+\pi^-)$ $\Gamma_{205}/\Gamma_{192}$

This is the fraction from a coherent amplitude analysis.

VALUE (%)	DOCUMENT ID		TECN	COMMENT
• • • We do not use the following data for averages, fits, limits, etc. • • •				
15±3±2	LINK	05G	FOCS	Fits 1279 ± 48 evts.

$\Gamma(K^*(892)^0K^\mp\pi^\pm\,\text{3-body},K^{*0}\to K^\pm\pi^\mp)/\Gamma(K^+K^-\pi^+\pi^-)$ $\Gamma_{206}/\Gamma_{192}$

This is the fraction from a coherent amplitude analysis.

VALUE (%)	DOCUMENT ID		TECN	COMMENT
• • • We do not use the following data for averages, fits, limits, etc. • • •				
11±2±1	LINK	05G	FOCS	Fits 1279 ± 48 evts.

$\Gamma(K^*(892)^0\overline{K}^*(892)^0,K^{*0}\to K^\pm\pi^\mp)/\Gamma(K^+K^-\pi^+\pi^-)$ $\Gamma_{207}/\Gamma_{192}$

This is the fraction from a coherent amplitude analysis.

VALUE (%)	DOCUMENT ID		TECN	COMMENT
• • • We do not use the following data for averages, fits, limits, etc. • • •				
3±2±1	LINK	05G	FOCS	Fits 1279 ± 48 evts.

$\Gamma(K_1(1270)^\pm K^\mp,K_1(1270)^\pm\to K^\pm\pi^+\pi^-)/\Gamma(K^+K^-\pi^+\pi^-)$ $\Gamma_{208}/\Gamma_{192}$

This is the fraction from a coherent amplitude analysis.

VALUE (%)	DOCUMENT ID		TECN	COMMENT
• • • We do not use the following data for averages, fits, limits, etc. • • •				
33±6±4	[1] LINK	05G	FOCS	Fits 1279 ± 48 evts.

[1] This LINK 05G value includes $K_1(1270)^\pm \to \rho^0K^\pm$, $\to K^*_0(1430)^0\pi^\pm$, and $K^*(892)^0\pi^\pm$.

$\Gamma(K_1(1400)^\pm K^\mp,K_1(1400)^\pm\to K^\pm\pi^+\pi^-)/\Gamma(K^+K^-\pi^+\pi^-)$ $\Gamma_{209}/\Gamma_{192}$

This is the fraction from a coherent amplitude analysis.

VALUE (%)	DOCUMENT ID		TECN	COMMENT
• • • We do not use the following data for averages, fits, limits, etc. • • •				
22±3±4	LINK	05G	FOCS	Fits 1279 ± 48 evts.

$\Gamma(2K^0_S\pi^+\pi^-)/\Gamma(K^0_S\pi^+\pi^-)$ Γ_{210}/Γ_{35}

VALUE (units 10^{-2})	EVTS	DOCUMENT ID		TECN	COMMENT
4.3 ±0.8 OUR AVERAGE					
4.16±0.70±0.42	113 ± 21	LINK	05A	FOCS	γ Be, $\overline{E}_\gamma \approx$ 180 GeV
6.2 ±2.0 ±1.6	25	ALBRECHT	94I	ARG	$e^+e^-\approx$ 10 GeV

$\Gamma(K^0_S K^-2\pi^+\pi^-)/\Gamma(K^0_S 2\pi^+2\pi^-)$ Γ_{211}/Γ_{87}

VALUE	CL%	DOCUMENT ID		TECN	COMMENT
<0.054	90	LINK	04D	FOCS	γ A, $\overline{E}_\gamma \approx$ 180 GeV

$\Gamma(K^+K^-\pi^+\pi^-\pi^0)/\Gamma_{\text{total}}$ Γ_{212}/Γ

VALUE	DOCUMENT ID		TECN	COMMENT
0.0031±0.0020	[1] BARLAG	92C	ACCM	π^- Cu 230 GeV

[1] BARLAG 92C computes the branching fraction using topological normalization.

Radiative modes

$\Gamma(\rho^0\gamma)/\Gamma_{\text{total}}$ Γ_{216}/Γ

VALUE	CL%	DOCUMENT ID		TECN
$<2.4\times10^{-4}$	90	ASNER	98	CLE2

$\Gamma(\omega\gamma)/\Gamma_{\text{total}}$ Γ_{217}/Γ

VALUE	CL%	DOCUMENT ID		TECN
$<2.4\times10^{-4}$	90	ASNER	98	CLE2

$\Gamma(\phi\gamma)/\Gamma(K^+K^-)$ $\Gamma_{218}/\Gamma_{177}$

VALUE (units 10^{-3})	EVTS	DOCUMENT ID		TECN	COMMENT
6.8 ±0.9 OUR FIT					
$6.31^{+1.70}_{-1.48}\pm0.30$	28	TAJIMA	04	BELL	e^+e^- at $\Upsilon(4S)$

$\Gamma(\phi\gamma)/\Gamma(K^-\pi^+)$ Γ_{218}/Γ_{31}

VALUE (units 10^{-4})	EVTS	DOCUMENT ID		TECN	COMMENT
7.0 ±0.9 OUR FIT					
7.15±0.78±0.69	243 ± 25	AUBERT	08AZ	BABR	$e^+e^-\approx$ 10.6 GeV

Meson Particle Listings

D^0

$\Gamma(\overline{K}^*(892)^0\gamma)/\Gamma(K^-\pi^+)$ Γ_{219}/Γ_{31}

VALUE (units 10^{-3})	EVTS	DOCUMENT ID		TECN	COMMENT
8.43±0.51±0.70	2286±113	AUBERT	08AZ	BABR	$e^+e^-\approx$ 10.6 GeV

Doubly Cabibbo-suppressed / Mixing modes

$\Gamma(K^+\ell^-\overline{\nu}_\ell$ via $\overline{D}^0)/\Gamma(K^-\ell^+\nu_\ell)$ Γ_{220}/Γ_{17}

This is a limit on R_M without the complications of possible doubly Cabibbo-suppressed decays that occur when using hadronic modes. For the limits on $|m_1 - m_2|$ and $(\Gamma_1 - \Gamma_2)/\Gamma$ that come from the best mixing limit, see near the beginning of these D^0 Listings.

VALUE	CL%	DOCUMENT ID		TECN	COMMENT
< 6.1 × 10^{-4}	90	[1] BITENC	08	BELL	e^+e^-, 10.58 GeV
• • • We do not use the following data for averages, fits, limits, etc. • • •					
<50 × 10^{-4}	90	[2] AITALA	96C	E791	π^- nucleus, 500 GeV

[1] The BITENC 08 right-sign sample includes about 15% of $D^0 \to K^-\pi^0\ell^+\nu_\ell$ and other decays.

[2] AITALA 96C uses $D^{*+} \to D^0\pi^+$ (and charge conjugate) decays to identify the charm at production and $D^0 \to K^-\ell^+\nu_\ell$ (and charge conjugate) decays to identify the charm at decay.

$\Gamma(K^+$ or $K^*(892)^+ e^-\overline{\nu}_e$ via $\overline{D}^0)/\left[\Gamma(K^-e^+\nu_e) + \Gamma(K^*(892)^-e^+\nu_e)\right]$ $\Gamma_{221}/(\Gamma_{18}+\Gamma_{20})$

This is a limit on R_M without the complications of possible doubly Cabibbo-suppressed decays that occur when using hadronic modes. The experiments use $D^{*+} \to D^0\pi^+$ (and charge conjugate) decays to identify the charm at production and the charge of the e to identify the charm at decay. These limits do not allow CP violation. For the limits on $|m_1 - m_2|$ and $(\Gamma_1 - \Gamma_2)/\Gamma$ that come from the best mixing limit, see near the beginning of these D^0 Listings.

VALUE	CL%	DOCUMENT ID		TECN	COMMENT
<0.001	90	BITENC	05	BELL	$e^+e^- \approx$ 10.6 GeV
• • • We do not use the following data for averages, fits, limits, etc. • • •					
$-0.0013 < R < +0.0012$	90	AUBERT	07AB	BABR	$e^+e^- \approx$ 10.58 GeV
<0.0078	90	CAWLFIELD	05	CLEO	$e^+e^- \approx$ 10.6 GeV
<0.0042	90	AUBERT,B	04Q	BABR	See AUBERT 07AB

$\Gamma(K^+\pi^-)/\Gamma(K^-\pi^+)$ Γ_{222}/Γ_{31}

This is R, the time-integrated wrong-sign rate compared to the right-sign rate. See the note on "D^0-$\overline{D}^0$ Mixing," near the start of the D^0 Listings.

The experiments here use the charge of the pion in $D^*(2010)^\pm \to (D^0$ or $\overline{D}^0)\,\pi^\pm$ decay to tell whether a D^0 or a $\overline{D}^0$ was born. The $D^0 \to K^+\pi^-$ decay can occur directly by doubly Cabibbo-suppressed (DCS) decay, or indirectly by $D^0 \to \overline{D}^0$ mixing followed by $\overline{D}^0 \to K^+\pi^-$ decay. Some of the experiments can use the decay-time information to disentangle the two mechanisms. Here, we list the experimental branching ratio, which if there is no mixing is the DCS ratio. See the next data block for values of the DCS ratio R_D, and the following data block for limits on the mixing ratio R_M. See the section on CP-violating asymmetries near the end of this D^0 Listing for values of A_D, and the note on "D^0-$\overline{D}^0$ Mixing" for limits on x' and y'.

Some early limits have been omitted from this Listing; see our 1998 edition (The European Physical Journal **C3** 1 (1998)) and our 2006 edition (Journal of Physics (generic for all A,B,E,G) **G33** 1 (2006)).

VALUE (units 10^{-3})	EVTS	DOCUMENT ID		TECN	COMMENT
3.79±0.18 OUR FIT Error includes scale factor of 3.3.					
3.79±0.18 OUR AVERAGE Error includes scale factor of 3.3. See the ideogram below.					
4.15±0.10	12.7±0.3k	[1] AALTONEN	08E	CDF	$p\overline{p}$, $\sqrt{s}$ = 1.96 TeV
3.53±0.08±0.04	4030 ± 90	[2] AUBERT	07W	BABR	$e^+e^- \approx$ 10.6 GeV
3.77±0.08±0.05	4024 ± 88	[1] ZHANG	06	BELL	e^+e^-
• • • We do not use the following data for averages, fits, limits, etc. • • •					
4.05±0.21±0.11	2.0 ± 0.1k	[3] ABULENCIA	06X	CDF	See AALTONEN 08E
$3.81 \pm 0.17^{+0.08}_{-0.16}$	845 ± 40	[2] LI	05A	BELL	See ZHANG 06
$4.29^{+0.63}_{-0.61} \pm 0.27$	234	[4] LINK	05H	FOCS	γ nucleus
3.57±0.22±0.27		[5] AUBERT	03Z	BABR	See AUBERT 07W
4.04±0.85±0.25	149	[6] LINK	01	FOCS	γ nucleus
$3.32^{+0.63}_{-0.65} \pm 0.40$	45	[1] GODANG	00	CLE2	e^+e^-
$6.8\ ^{+3.4}_{-3.3} \pm 0.7$	34	[2] AITALA	98	E791	π^- nucl., 500 GeV

[1] GODANG 00, ZHANG 06, and AALTONEN 08E allow CP violation.

[2] AITALA 98, LI 05A, and AUBERT 07W assume no CP violation.

[3] This ABULENCIA 06X result assumes no mixing.

[4] This LINK 05H result assumes no mixing but allows CP violation. If neither mixing nor CP violation is allowed, $R = (4.29 \pm 0.63 \pm 0.28) \times 10^{-3}$.

[5] This AUBERT 03Z result allows CP violation. If CP violation is not allowed, $R = 0.00359 \pm 0.00020 \pm 0.00027$.

[6] This LINK 01 result assumes no mixing or CP violation.

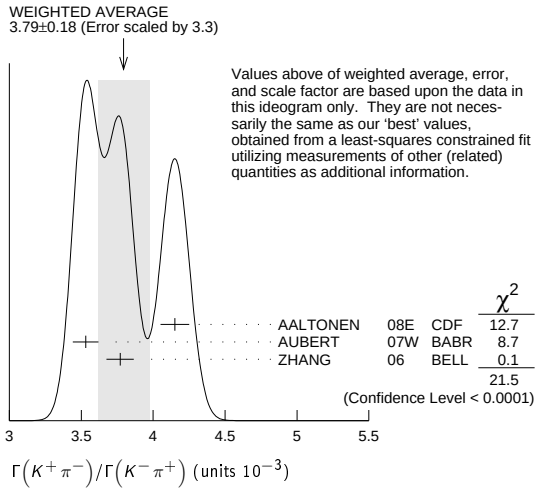

$\Gamma(K^+\pi^-$ via DCS$)/\Gamma(K^-\pi^+)$ Γ_{223}/Γ_{31}

This is R_D, the doubly Cabibbo-suppressed ratio when mixing is allowed.

VALUE (units 10^{-3})	CL%	EVTS	DOCUMENT ID		TECN	COMMENT
3.37± 0.21 OUR AVERAGE Error includes scale factor of 1.8. See the ideogram below.						
3.04± 0.55		12.7±0.3k	AALTONEN	08E	CDF	$p\overline{p}$, $\sqrt{s}$ =1.96 TeV
3.03± 0.16±0.10		4030 ± 90	[1] AUBERT	07W	BABR	$e^+e^- \approx$ 10.6 GeV
3.64± 0.17		4024 ± 88	[2] ZHANG	06	BELL	e^+e^-
$5.17^{+1.47}_{-1.58} \pm 0.76$		234	[3] LINK	05H	FOCS	γ nucleus
4.8 ± 1.2 ±0.4		45	[4] GODANG	00	CLE2	e^+e^-
• • • We do not use the following data for averages, fits, limits, etc. • • •						
2.87± 0.37		845 ± 40	LI	05A	BELL	See ZHANG 06
$2.3 < R_D < 5.2$	95		[5] AUBERT	03Z	BABR	See AUBERT 07W
$9.0\ ^{+12.0}_{-10.9} \pm 4.4$		34	[6] AITALA	98	E791	π^- nucl., 500 GeV

[1] This AUBERT 07W result is the same whether or not CP violation is allowed.

[2] This ZHANG 06 assumes no CP violation.

[3] This LINK 05H result allows CP violation. Allowing mixing but not CP violation, $R_D = (3.81\ ^{+1.67}_{-1.63} \pm 0.92) \times 10^{-3}$.

[4] This GODANG 00 result allows CP violation.

[5] This AUBERT 03Z result allows CP violation. If only mixing is allowed, the 95% confidence level interval is $(2.4 < R_D < 4.9) \times 10^{-3}$.

[6] This AITALA 98 result assumes no CP violation.

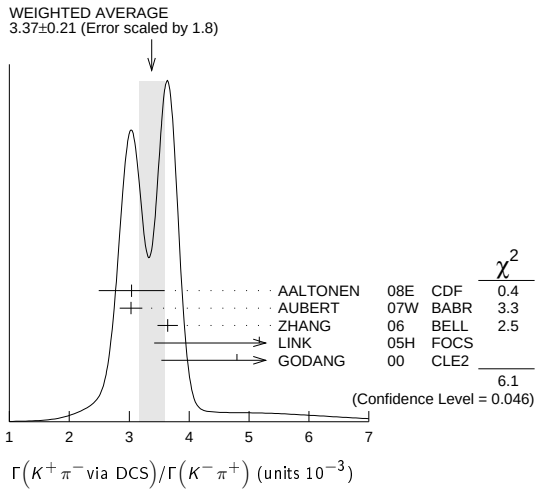

$\Gamma(K^+\pi^-$ via $\overline{D}^0)/\Gamma(K^-\pi^+)$ Γ_{224}/Γ_{31}

This is R_M in the note on "D^0-$\overline{D}^0$ Mixing" near the start of the D^0 Listings. The experiments here (1) use the charge of the pion in $D^*(2010)^\pm \to (D^0$ or $\overline{D}^0)\,\pi^\pm$ decay to tell whether a D^0 or a $\overline{D}^0$ was born; and (2) use the decay-time distribution to disentangle doubly Cabibbo-suppressed decay and mixing. For the limits on $|m_1 - m_2|$ and $(\Gamma_1 - \Gamma_2)/\Gamma$ that come from the best mixing limit, see near the beginning of these D^0 Listings.

VALUE	CL%	DOCUMENT ID		TECN	COMMENT
<0.00040	95	[1] ZHANG	06	BELL	e^+e^-

• • • We do not use the following data for averages, fits, limits, etc. • • •

<0.00046	95	[2] LI	05A	BELL	See ZHANG 06
<0.0063	95	[3] LINK	05H	FOCS	γ nucleus
<0.0013	95	[4] AUBERT	03Z	BABR	e^+e^-, 10.6 GeV
<0.00041	95	[5] GODANG	00	CLE2	e^+e^-
<0.0092	95	[6] BARATE	98W	ALEP	e^+e^- at Z^0
<0.005	90	[7] ANJOS	88C	E691	Photoproduction

[1] This ZHANG 06 result allows *CP* violation, but the result does not change if *CP* violation is not allowed.
[2] This LI 05A result allows *CP* violation. The limit becomes < 0.00042 (95% CL) if *CP* violation is not allowed.
[3] LINK 05H obtains the same result whether or not *CP* violation is allowed.
[4] This AUBERT 03Z result allows *CP* violation and assumes that the strong phase between $D^0 \to K^+\pi^-$ and $\overline{D}{}^0 \to K^+\pi^-$ is small, and limits only $D^0 \to \overline{D}{}^0$ transitions via off-shell intermediate states. The limit on transitions via on-shell intermediate states is 0.0016.
[5] This GODANG 00 result allows *CP* violation and assumes that the strong phase between $D^0 \to K^+\pi^-$ and $\overline{D}{}^0 \to K^+\pi^-$ is small, and limits only $D^0 \to \overline{D}{}^0$ transitions via off-shell intermediate states. The limit on transitions via on-shell intermediate states is 0.0017.
[6] This BARATE 98W result assumes no interference between the DCS and mixing amplitudes ($y' = 0$ in the note on "D^0-$\overline{D}{}^0$ Mixing" near the start of the D^0 Listings). When interference is allowed, the limit degrades to 0.036 (95%CL).
[7] This ANJOS 88C result assumes no interference between the DCS and mixing amplitudes ($y' = 0$ in the note on "D^0-$\overline{D}{}^0$ Mixing" near the start of the D^0 Listings). When interference is allowed, the limit degrades to 0.019.

$\Gamma(K^0_S\pi^+\pi^-$ in $D^0 \to \overline{D}{}^0)/\Gamma(K^0_S\pi^+\pi^-)$ Γ_{225}/Γ_{35}

This is R_M in the note on "D^0-$\overline{D}{}^0$ Mixing" near the start of the D^0 Listings. The experiments here (1) use the charge of the pion in $D^*(2010)^\pm \to (D^0$ or $\overline{D}{}^0)\,\pi^\pm$ decay to tell whether a D^0 or a $\overline{D}{}^0$ was born; and (2) use the decay-time distribution to disentangle doubly Cabibbo-suppressed decay and mixing. For the limits on $|m_1 - m_2|$ and $(\Gamma_1 - \Gamma_2)/\Gamma$ that come from the best mixing limit, see near the beginning of these D^0 Listings.

VALUE	CL%	DOCUMENT ID		TECN	COMMENT
<0.0063	95	[1] ASNER	05	CLEO	$e^+e^- \approx$ 10 GeV

[1] This ASNER 05 limit allows *CP* violation. If *CP* violation is not allowed, the limit is 0.0042 at 95% CL.

$\Gamma(K^+\pi^-\pi^0)/\Gamma(K^-\pi^+\pi^0)$ Γ_{229}/Γ_{50}

The experiments here use the charge of the pion in $D^*(2010)^\pm \to (D^0$ or $\overline{D}{}^0)\,\pi^\pm$ decay to tell whether a D^0 or a $\overline{D}{}^0$ was born. The $D^0 \to K^+\pi^-\pi^0$ decay can occur directly by doubly Cabibbo-suppressed (DCS) decay, or indirectly by $D^0 \to \overline{D}{}^0$ mixing followed by $\overline{D}{}^0 \to K^+\pi^-\pi^0$ decay.

VALUE (units 10^{-3})	EVTS	DOCUMENT ID		TECN	COMMENT
2.20±0.10 OUR AVERAGE					
$2.14 \pm 0.08 \pm 0.08$	763 ± 51	[1] AUBERT,B	06N	BABR	$e^+e^- \approx \Upsilon(4S)$
$2.29 \pm 0.15^{+0.13}_{-0.09}$	1978 ± 104	TIAN	05	BELL	$e^+e^- \approx \Upsilon(4S)$
$4.3\ ^{+1.1}_{-1.0} \pm 0.7$	38	BRANDENB...	01	CLE2	$e^+e^- \approx \Upsilon(4S)$

[1] This AUBERT,B 06N result assumes no mixing.

$\Gamma(K^+\pi^-\pi^0$ via $\overline{D}{}^0)/\Gamma(K^-\pi^+\pi^0)$ Γ_{230}/Γ_{50}

This is R_M in the note on "D^0-$\overline{D}{}^0$ Mixing" near the start of the D^0 Listings. The experiments here (1) use the charge of the pion in $D^*(2010)^\pm \to (D^0$ or $\overline{D}{}^0)\,\pi^\pm$ decay to tell whether a D^0 or a $\overline{D}{}^0$ was born; and (2) use the decay-time distribution to disentangle doubly Cabibbo-suppressed decay and mixing. For the limits on $|m_1 - m_2|$ and $(\Gamma_1 - \Gamma_2)/\Gamma$ that come from the best mixing limit, see near the beginning of these D^0 Listings.

VALUE (units 10^{-3})	CL%	DOCUMENT ID	TECN	COMMENT
$\mathbf{5.25^{+0.25}_{-0.31} \pm 0.12}$		AUBERT	09AN BABR	e^+e^- at 10.58 GeV

• • • We do not use the following data for averages, fits, limits, etc. • • •

<0.54	95	[1] AUBERT,B	06N	BABR	$e^+e^- \approx \Upsilon(4S)$

[1] This AUBERT,B 06N limit assumes no *CP* violation. The measured value corresponding to the limit is $(2.3^{+1.8}_{-1.4} \pm 0.4) \times 10^{-4}$. If *CP* violation is allowed, this becomes $(1.0^{+2.2}_{-0.7} \pm 0.3) \times 10^{-4}$.

$\Gamma(K^+\pi^+2\pi^-)/\Gamma(K^-2\pi^+\pi^-)$ Γ_{231}/Γ_{67}

The experiments here use the charge of the pion in $D^*(2010)^\pm \to (D^0$ or $\overline{D}{}^0)\,\pi^\pm$ decay to tell whether a D^0 or a $\overline{D}{}^0$ was born. The $D^0 \to K^+\pi^-\pi^+\pi^-$ decay can occur directly by doubly Cabibbo-suppressed (DCS) decay, or indirectly by $D^0 \to \overline{D}{}^0$ mixing followed by $\overline{D}{}^0 \to K^+\pi^-\pi^+\pi^-$ decay. Some of the experiments can use the decay-time information to disentangle the two mechanisms. Here, we list the experimental branching ratio, which if there is no mixing is the DCS ratio; in the next data block we give the limits on the mixing ratio.

Some early limits have been omitted from this Listing; see our 1998 edition (EPJ **C3** 1).

VALUE (units 10^{-3})	CL%	EVTS	DOCUMENT ID		TECN	COMMENT
3.25±0.11 OUR AVERAGE						
$3.24 \pm 0.08 \pm 0.07$		3358 ± 79	[1] WHITE	13	BELL	$e^+e^- \approx \Upsilon(4S)$
$4.4\ ^{+1.3}_{-1.2} \pm 0.4$		54	[1] DYTMAN	01	CLE2	$e^+e^- \approx \Upsilon(4S)$
$2.5\ ^{+3.6}_{-3.4} \pm 0.3$			[2] AITALA	98	E791	π^- nucl., 500 GeV

• • • We do not use the following data for averages, fits, limits, etc. • • •

$3.20 \pm 0.18^{+0.18}_{-0.13}$	1721 ± 75	[1] TIAN	05	BELL	See WHITE 13
<18	90	[1] AMMAR	91	CLEO	$e^+e^- \approx$ 10.5 GeV
<18	90	[3] ANJOS	88C	E691	Photoproduction

[1] AMMAR 91 cannot and DYTMAN 01, TIAN 05, and WHITE 13 do not distinguish between doubly Cabibbo-suppressed decay and D^0-$\overline{D}{}^0$ mixing.
[2] This AITALA 98 result assumes no D^0-$\overline{D}{}^0$ mixing (R_M in the note on "D^0-$\overline{D}{}^0$ Mixing"). It becomes $-0.0020^{+0.0117}_{-0.0106} \pm 0.0035$ when mixing is allowed and decay-time information is used to distinguish doubly Cabibbo-suppressed decays from mixing.
[3] ANJOS 88C uses decay-time information to distinguish doubly Cabibbo-suppressed (DCS) decays from D^0-$\overline{D}{}^0$ mixing. However, the result assumes no interference between the DCS and mixing amplitudes ($y' = 0$ in the note on "D^0-$\overline{D}{}^0$ Mixing" near the start of the D^0 Listings). When interference is allowed, the limit degrades to 0.033.

$\Gamma(K^+\pi^+2\pi^-$ via $\overline{D}{}^0)/\Gamma(K^-2\pi^+\pi^-)$ Γ_{232}/Γ_{67}

This is a D^0-$\overline{D}{}^0$ mixing limit. The experiments here (1) use the charge of the pion in $D^*(2010)^\pm \to (D^0$ or $\overline{D}{}^0)\,\pi^\pm$ decay to tell whether a D^0 or a $\overline{D}{}^0$ was born; and (2) use the decay-time distribution to disentangle doubly Cabibbo-suppressed decay and mixing. For the limits on $|m_{D_1^0} - m_{D_2^0}|$ and $(\Gamma_{D_1^0} - \Gamma_{D_2^0})/\Gamma_{D^0}$ that come from the best mixing limit, see near the beginning of these D^0 Listings.

VALUE	CL%	DOCUMENT ID		TECN	COMMENT
<0.005	90	[1] ANJOS	88C	E691	Photoproduction

[1] ANJOS 88C uses decay-time information to distinguish doubly Cabibbo-suppressed (DCS) decays from D^0-$\overline{D}{}^0$ mixing. However, the result assumes no interference between the DCS and mixing amplitudes ($y' = 0$ in the note on "D^0-$\overline{D}{}^0$ Mixing" near the start of the D^0 Listings). When interference is allowed, the limit degrades to 0.007.

$\Gamma(K^+\pi^-$ or $K^+\pi^+2\pi^-$ via $\overline{D}{}^0)/\Gamma(K^-\pi^+$ or $K^-2\pi^+\pi^-)$ Γ_{233}/Γ_0

This is a D^0-$\overline{D}{}^0$ mixing limit. For the limits on $|m_{D_1^0} - m_{D_2^0}|$ and $(\Gamma_{D_1^0} - \Gamma_{D_2^0})/\Gamma_{D^0}$ that come from the best mixing limit, see near the beginning of these D^0 Listings.

VALUE	CL%	DOCUMENT ID		TECN	COMMENT
• • • We do not use the following data for averages, fits, limits, etc. • • •					
<0.0085	90	[1] AITALA	98	E791	π^- nucleus, 500 GeV
<0.0037	90	[2] ANJOS	88C	E691	Photoproduction

[1] AITALA 98 uses decay-time information to distinguish doubly Cabibbo-suppressed decays from D^0-$\overline{D}{}^0$ mixing. The fit allows interference between the two amplitudes, and also allows *CP* violation in this term. The central value obtained is $0.0039^{+0.0036}_{-0.0032} \pm 0.0016$. When interference is disallowed, the result becomes $0.0021 \pm 0.0009 \pm 0.0002$.
[2] This combines results of ANJOS 88C on $K^+\pi^-$ and $K^+\pi^-\pi^+\pi^-$ (via $\overline{D}{}^0$) reported in the data block above (see footnotes there). It assumes no interference.

$\Gamma(\mu^-$ anything via $\overline{D}{}^0)/\Gamma(\mu^+$ anything) Γ_{234}/Γ_6

This is a D^0-$\overline{D}{}^0$ mixing limit. See the somewhat better limits above.

VALUE	CL%	DOCUMENT ID	TECN	COMMENT
<0.0056	90	LOUIS	86 SPEC	π^- W 225 GeV
• • • We do not use the following data for averages, fits, limits, etc. • • •				
<0.012	90	BENVENUTI	85 CNTR	μC, 200 GeV
<0.044	90	BODEK	82 SPEC	π^-, pFe $\to D^0$

Rare or forbidden modes

$\Gamma(\gamma\gamma)/\Gamma_{\text{total}}$ Γ_{235}/Γ

$D^0 \to \gamma\gamma$ is a flavor-changing neutral-current decay, forbidden in the Standard Model at the tree level.

VALUE (units 10^{-6})	CL%	DOCUMENT ID		TECN	COMMENT
< 2.2	90	LEES	12L	BABR	$e^+e^- \approx$ 10.58 GeV
• • • We do not use the following data for averages, fits, limits, etc. • • •					
<29	90	COAN	03	CLE2	$e^+e^- \approx \Upsilon(4S)$

$\Gamma(e^+e^-)/\Gamma_{\text{total}}$ Γ_{236}/Γ

A test for the $\Delta C = 1$ weak neutral current. Allowed by first-order weak interaction combined with electromagnetic interaction.

VALUE	CL%	DOCUMENT ID		TECN	COMMENT
<7.9 $\times 10^{-8}$	90	PETRIC	10	BELL	$e^+e^- \approx \Upsilon(4S)$
• • • We do not use the following data for averages, fits, limits, etc. • • •					
$<1.7 \times 10^{-7}$	90	LEES	12Q	BABR	$e^+e^- \approx$ 10.58 GeV
$<1.2 \times 10^{-6}$	90	AUBERT,B	04Y	BABR	$e^+e^- \approx \Upsilon(4S)$
$<8.19 \times 10^{-6}$	90	PRIPSTEIN	00	E789	p nucleus, 800 GeV
$<6.2 \times 10^{-6}$	90	AITALA	99G	E791	π^- N 500 GeV
$<1.3 \times 10^{-5}$	90	FREYBERGER	96	CLE2	$e^+e^- \approx \Upsilon(4S)$
$<1.3 \times 10^{-4}$	90	ADLER	88	MRK3	e^+e^- 3.77 GeV
$<1.7 \times 10^{-4}$	90	ALBRECHT	88G	ARG	e^+e^- 10 GeV
$<2.2 \times 10^{-4}$	90	HAAS	88	CLEO	e^+e^- 10 GeV

Meson Particle Listings

D^0

$\Gamma(\mu^+\mu^-)/\Gamma_{total}$ Γ_{237}/Γ

A test for the $\Delta C = 1$ weak neutral current. Allowed by first-order weak interaction combined with electromagnetic interaction.

VALUE	CL%	DOCUMENT ID		TECN	COMMENT
$<6.2 \times 10^{-9}$	90	AAIJ	13AI	LHCB	pp at 7 TeV
• • • We do not use the following data for averages, fits, limits, etc. • • •					
$0.6–8.1 \times 10^{-7}$	90	[1] LEES	12Q	BABR	$e^+e^- \approx 10.58$ GeV
$<2.1 \times 10^{-7}$	90	AALTONEN	10X	CDF	$p\overline{p}$, $\sqrt{s} = 1.96$ TeV
$<1.4 \times 10^{-7}$	90	PETRIC	10	BELL	$e^+e^- \approx \Upsilon(4S)$
$<2.0 \times 10^{-6}$	90	ABT	04	HERB	pA, 920 GeV
$<1.3 \times 10^{-6}$	90	AUBERT,B	04Y	BABR	$e^+e^- \approx \Upsilon(4S)$
$<2.5 \times 10^{-6}$	90	ACOSTA	03F	CDF	See AALTONEN 10X
$<1.56 \times 10^{-5}$	90	PRIPSTEIN	00	E789	p nucleus, 800 GeV
$<5.2 \times 10^{-6}$	90	AITALA	99G	E791	π^- N 500 GeV
$<4.1 \times 10^{-6}$	90	ADAMOVICH	97	BEAT	π^- Cu, W 350 GeV
$<4.2 \times 10^{-6}$	90	ALEXOPOU...	96	E771	p Si, 800 GeV
$<3.4 \times 10^{-5}$	90	FREYBERGER	96	CLE2	$e^+e^- \approx \Upsilon(4S)$
$<7.6 \times 10^{-6}$	90	ADAMOVICH	95	BEAT	See ADAMOVICH 97
$<4.4 \times 10^{-5}$	90	KODAMA	95	E653	π^- emulsion 600 GeV
$<3.1 \times 10^{-5}$	90	[2] MISHRA	94	E789	-4.1 ± 4.8 events
$<7.0 \times 10^{-5}$	90	ALBRECHT	88G	ARG	e^+e^- 10 GeV
$<1.1 \times 10^{-5}$	90	LOUIS	86	SPEC	π^- W 225 GeV
$<3.4 \times 10^{-4}$	90	AUBERT	85	EMC	Deep inelast. μ^- N

[1] LEES 12Q gives a 2-sided range.
[2] Here MISHRA 94 uses "the statistical approach advocated by the PDG." For an alternate approach, giving a limit of 9×10^{-6} at 90% confidence level, see the paper.

$\Gamma(\pi^0 e^+ e^-)/\Gamma_{total}$ Γ_{238}/Γ

A test for the $\Delta C = 1$ weak neutral current. Allowed by higher-order electroweak interactions.

VALUE	CL%	DOCUMENT ID		TECN	COMMENT
$<4.5 \times 10^{-5}$	90	FREYBERGER	96	CLE2	$e^+e^- \approx \Upsilon(4S)$

$\Gamma(\pi^0 \mu^+ \mu^-)/\Gamma_{total}$ Γ_{239}/Γ

A test for the ΔC=1 weak neutral current. Allowed by higher-order electroweak interactions.

VALUE	CL%	DOCUMENT ID		TECN	COMMENT
$<1.8 \times 10^{-4}$	90	KODAMA	95	E653	π^- emulsion 600 GeV
• • • We do not use the following data for averages, fits, limits, etc. • • •					
$<5.4 \times 10^{-4}$	90	FREYBERGER	96	CLE2	$e^+e^- \approx \Upsilon(4S)$

$\Gamma(\eta e^+ e^-)/\Gamma_{total}$ Γ_{240}/Γ

A test for the $\Delta C = 1$ weak neutral current. Allowed by higher-order electroweak interactions.

VALUE	CL%	DOCUMENT ID		TECN	COMMENT
$<1.1 \times 10^{-4}$	90	FREYBERGER	96	CLE2	$e^+e^- \approx \Upsilon(4S)$

$\Gamma(\eta \mu^+ \mu^-)/\Gamma_{total}$ Γ_{241}/Γ

A test for the $\Delta C = 1$ weak neutral current. Allowed by higher-order electroweak interactions.

VALUE	CL%	DOCUMENT ID		TECN	COMMENT
$<5.3 \times 10^{-4}$	90	FREYBERGER	96	CLE2	$e^+e^- \approx \Upsilon(4S)$

$\Gamma(\pi^+\pi^- e^+ e^-)/\Gamma_{total}$ Γ_{242}/Γ

A test for the $\Delta C = 1$ weak neutral current. Allowed by higher-order electroweak interactions.

VALUE	CL%	DOCUMENT ID		TECN	COMMENT
$<3.73 \times 10^{-4}$	90	AITALA	01C	E791	π^- nucleus, 500 GeV

$\Gamma(\rho^0 e^+ e^-)/\Gamma_{total}$ Γ_{243}/Γ

A test for the $\Delta C = 1$ weak neutral current. Allowed by higher-order electroweak interactions.

VALUE	CL%	DOCUMENT ID		TECN	COMMENT
$<1.0 \times 10^{-4}$	90	[1] FREYBERGER	96	CLE2	$e^+e^- \approx \Upsilon(4S)$
• • • We do not use the following data for averages, fits, limits, etc. • • •					
$<1.24 \times 10^{-4}$	90	AITALA	01C	E791	π^- nucleus, 500 GeV
$<4.5 \times 10^{-4}$	90	HAAS	88	CLEO	e^+e^- 10 GeV

[1] This FREYBERGER 96 limit is obtained using a phase-space model. The limit changes to $< 1.8 \times 10^{-4}$ using a photon pole amplitude model.

$\Gamma(\pi^+\pi^-\mu^+\mu^-)/\Gamma_{total}$ Γ_{244}/Γ

A test for the $\Delta C = 1$ weak neutral current. Allowed by higher-order electroweak interactions.

VALUE	CL%	DOCUMENT ID		TECN	COMMENT
$<5.5 \times 10^{-7}$	90	[1] AAIJ	14B	LHCB	pp at 7 TeV
• • • We do not use the following data for averages, fits, limits, etc. • • •					
$<3.0 \times 10^{-5}$	90	AITALA	01C	E791	π^- nucleus, 500 GeV

[1] AAIJ 14B measures this branching-fraction limit relative to the $\pi^+\pi^-\phi$, $\phi \to \mu^+\mu^-$ fraction. The above limit excludes the resonant ϕ, ω, and ρ regions, and then fills those gaps with a phase-space model.

$\Gamma(\rho^0\mu^+\mu^-)/\Gamma_{total}$ Γ_{245}/Γ

A test for the $\Delta C = 1$ weak neutral current. Allowed by higher-order electroweak interactions.

VALUE	CL%	DOCUMENT ID		TECN	COMMENT
$<2.2 \times 10^{-5}$	90	AITALA	01C	E791	π^- nucleus, 500 GeV
• • • We do not use the following data for averages, fits, limits, etc. • • •					
$<4.9 \times 10^{-4}$	90	[1] FREYBERGER	96	CLE2	$e^+e^- \approx \Upsilon(4S)$
$<2.3 \times 10^{-4}$	90	KODAMA	95	E653	π^- emulsion 600 GeV
$<8.1 \times 10^{-4}$	90	HAAS	88	CLEO	e^+e^- 10 GeV

[1] This FREYBERGER 96 limit is obtained using a phase-space model. The limit changes to $< 4.5 \times 10^{-4}$ using a photon pole amplitude model.

$\Gamma(\omega e^+ e^-)/\Gamma_{total}$ Γ_{246}/Γ

A test for the $\Delta C = 1$ weak neutral current. Allowed by higher-order electroweak interactions.

VALUE	CL%	DOCUMENT ID		TECN	COMMENT
$<1.8 \times 10^{-4}$	90	[1] FREYBERGER	96	CLE2	$e^+e^- \approx \Upsilon(4S)$

[1] This FREYBERGER 96 limit is obtained using a phase-space model. The limit changes to $< 2.7 \times 10^{-4}$ using a photon pole amplitude model.

$\Gamma(\omega\mu^+\mu^-)/\Gamma_{total}$ Γ_{247}/Γ

A test for the $\Delta C = 1$ weak neutral current. Allowed by higher-order electroweak interactions.

VALUE	CL%	DOCUMENT ID		TECN	COMMENT
$<8.3 \times 10^{-4}$	90	[1] FREYBERGER	96	CLE2	$e^+e^- \approx \Upsilon(4S)$

[1] This FREYBERGER 96 limit is obtained using a phase-space model. The limit changes to $< 6.5 \times 10^{-4}$ using a photon pole amplitude model.

$\Gamma(K^- K^+ e^+ e^-)/\Gamma_{total}$ Γ_{248}/Γ

A test for the $\Delta C = 1$ weak neutral current. Allowed by higher-order electroweak interactions.

VALUE	CL%	DOCUMENT ID		TECN	COMMENT
$<3.15 \times 10^{-4}$	90	AITALA	01C	E791	π^- nucleus, 500 GeV

$\Gamma(\phi e^+ e^-)/\Gamma_{total}$ Γ_{249}/Γ

A test for the $\Delta C = 1$ weak neutral current. Allowed by higher-order electroweak interactions.

VALUE	CL%	DOCUMENT ID		TECN	COMMENT
$<5.2 \times 10^{-5}$	90	[1] FREYBERGER	96	CLE2	$e^+e^- \approx \Upsilon(4S)$
• • • We do not use the following data for averages, fits, limits, etc. • • •					
$<5.9 \times 10^{-5}$	90	AITALA	01C	E791	π^- nucleus, 500 GeV

[1] This FREYBERGER 96 limit is obtained using a phase-space model. The limit changes to $< 7.6 \times 10^{-5}$ using a photon pole amplitude model.

$\Gamma(K^- K^+ \mu^+ \mu^-)/\Gamma_{total}$ Γ_{250}/Γ

A test for the $\Delta C = 1$ weak neutral current. Allowed by higher-order electroweak interactions.

VALUE	CL%	DOCUMENT ID		TECN	COMMENT
$<3.3 \times 10^{-5}$	90	AITALA	01C	E791	π^- nucleus, 500 GeV

$\Gamma(\phi\mu^+\mu^-)/\Gamma_{total}$ Γ_{251}/Γ

A test for the $\Delta C = 1$ weak neutral current. Allowed by higher-order electroweak interactions.

VALUE	CL%	DOCUMENT ID		TECN	COMMENT
$<3.1 \times 10^{-5}$	90	AITALA	01C	E791	π^- nucleus, 500 GeV
• • • We do not use the following data for averages, fits, limits, etc. • • •					
$<4.1 \times 10^{-4}$	90	[1] FREYBERGER	96	CLE2	$e^+e^- \approx \Upsilon(4S)$

[1] This FREYBERGER 96 limit is obtained using a phase-space model. The limit changes to $< 2.4 \times 10^{-4}$ using a photon pole amplitude model.

$\Gamma(\overline{K}^0 e^+ e^-)/\Gamma_{total}$ Γ_{252}/Γ

Not a useful test for $\Delta C = 1$ weak neutral current because both quarks must change flavor.

VALUE	CL%	DOCUMENT ID		TECN	COMMENT
$<1.1 \times 10^{-4}$	90	FREYBERGER	96	CLE2	$e^+e^- \approx \Upsilon(4S)$
• • • We do not use the following data for averages, fits, limits, etc. • • •					
$<1.7 \times 10^{-3}$	90	ADLER	89C	MRK3	e^+e^- 3.77 GeV

$\Gamma(\overline{K}^0\mu^+\mu^-)/\Gamma_{total}$ Γ_{253}/Γ

Not a useful test for $\Delta C = 1$ weak neutral current because both quarks must change flavor.

VALUE	CL%	DOCUMENT ID		TECN	COMMENT
$<2.6 \times 10^{-4}$	90	KODAMA	95	E653	π^- emulsion 600 GeV
• • • We do not use the following data for averages, fits, limits, etc. • • •					
$<6.7 \times 10^{-4}$	90	FREYBERGER	96	CLE2	$e^+e^- \approx \Upsilon(4S)$

$\Gamma(K^-\pi^+ e^+ e^-)/\Gamma_{total}$ Γ_{254}/Γ

A test for the $\Delta C = 1$ weak neutral current. Allowed by higher-order electroweak interactions.

VALUE	CL%	DOCUMENT ID		TECN	COMMENT
$<3.85 \times 10^{-4}$	90	AITALA	01C	E791	π^- nucleus, 500 GeV

$\Gamma(\overline{K}^*(892)^0 e^+ e^-)/\Gamma_{total}$ Γ_{255}/Γ

Not a useful test for $\Delta C = 1$ weak neutral current because both quarks must change flavor.

VALUE	CL%	DOCUMENT ID		TECN	COMMENT
$< 4.7 \times 10^{-5}$	90	AITALA	01C	E791	π^- nucleus, 500 GeV
• • • We do not use the following data for averages, fits, limits, etc. • • •					
$< 1.4 \times 10^{-4}$	90	[1] FREYBERGER	96	CLE2	$e^+ e^- \approx \Upsilon(4S)$

[1] This FREYBERGER 96 limit is obtained using a phase-space model. The limit changes to $< 2.0 \times 10^{-4}$ using a photon pole amplitude model.

$\Gamma(K^- \pi^+ \mu^+ \mu^-)/\Gamma_{total}$ Γ_{256}/Γ

A test for the $\Delta C = 1$ weak neutral current. Allowed by higher-order electroweak interactions.

VALUE	CL%	DOCUMENT ID		TECN	COMMENT
$< 3.59 \times 10^{-4}$	90	AITALA	01C	E791	π^- nucleus, 500 GeV

$\Gamma(\overline{K}^*(892)^0 \mu^+ \mu^-)/\Gamma_{total}$ Γ_{257}/Γ

Not a useful test for $\Delta C = 1$ weak neutral current because both quarks must change flavor.

VALUE	CL%	DOCUMENT ID		TECN	COMMENT
$< 2.4 \times 10^{-5}$	90	AITALA	01C	E791	π^- nucleus, 500 GeV
• • • We do not use the following data for averages, fits, limits, etc. • • •					
$< 1.18 \times 10^{-3}$	90	[1] FREYBERGER	96	CLE2	$e^+ e^- \approx \Upsilon(4S)$

[1] This FREYBERGER 96 limit is obtained using a phase-space model. The limit changes to $< 1.0 \times 10^{-3}$ using a photon pole amplitude model.

$\Gamma(\pi^+ \pi^- \pi^0 \mu^+ \mu^-)/\Gamma_{total}$ Γ_{258}/Γ

A test for the $\Delta C = 1$ weak neutral current. Allowed by higher-order electroweak interactions.

VALUE	CL%	DOCUMENT ID		TECN	COMMENT
$< 8.1 \times 10^{-4}$	90	KODAMA	95	E653	π^- emulsion 600 GeV

$\Gamma(\mu^\pm e^\mp)/\Gamma_{total}$ Γ_{259}/Γ

A test of lepton family number conservation.

VALUE	CL%	DOCUMENT ID		TECN	COMMENT
$< 2.6 \times 10^{-7}$	90	PETRIC	10	BELL	$e^+ e^- \approx \Upsilon(4S)$
• • • We do not use the following data for averages, fits, limits, etc. • • •					
$< 3.3 \times 10^{-7}$	90	LEES	12Q	BABR	$e^+ e^- \approx 10.58$ GeV
$< 8.1 \times 10^{-7}$	90	AUBERT,B	04Y	BABR	$e^+ e^- \approx \Upsilon(4S)$
$< 1.72 \times 10^{-5}$	90	PRIPSTEIN	00	E789	p nucleus, 800 GeV
$< 8.1 \times 10^{-6}$	90	AITALA	99G	E791	$\pi^- N$ 500 GeV
$< 1.9 \times 10^{-5}$	90	[1] FREYBERGER	96	CLE2	$e^+ e^- \approx \Upsilon(4S)$
$< 1.0 \times 10^{-4}$	90	ALBRECHT	88G	ARG	$e^+ e^-$ 10 GeV
$< 2.7 \times 10^{-4}$	90	HAAS	88	CLEO	$e^+ e^-$ 10 GeV
$< 1.2 \times 10^{-4}$	90	BECKER	87C	MRK3	$e^+ e^-$ 3.77 GeV
$< 9 \times 10^{-4}$	90	PALKA	87	SILI	200 GeV πp
$< 21 \times 10^{-4}$	90	[2] RILES	87	MRK2	$e^+ e^-$ 29 GeV

[1] This is the corrected result given in the erratum to FREYBERGER 96.
[2] RILES 87 assumes B($D \to K\pi$) = 3.0% and has production model dependency.

$\Gamma(\pi^0 e^\pm \mu^\mp)/\Gamma_{total}$ Γ_{260}/Γ

A test of lepton family number conservation. The value is for the sum of the two charge states.

VALUE	CL%	DOCUMENT ID		TECN	COMMENT
$< 8.6 \times 10^{-5}$	90	FREYBERGER	96	CLE2	$e^+ e^- \approx \Upsilon(4S)$

$\Gamma(\eta e^\pm \mu^\mp)/\Gamma_{total}$ Γ_{261}/Γ

A test of lepton family number conservation. The value is for the sum of the two charge states.

VALUE	CL%	DOCUMENT ID		TECN	COMMENT
$< 1.0 \times 10^{-4}$	90	FREYBERGER	96	CLE2	$e^+ e^- \approx \Upsilon(4S)$

$\Gamma(\pi^+ \pi^- e^\pm \mu^\mp)/\Gamma_{total}$ Γ_{262}/Γ

A test of lepton family-number conservation. The value is for the sum of the two charge states.

VALUE	CL%	DOCUMENT ID		TECN	COMMENT
$< 1.5 \times 10^{-5}$	90	AITALA	01C	E791	π^- nucleus, 500 GeV

$\Gamma(\rho^0 e^\pm \mu^\mp)/\Gamma_{total}$ Γ_{263}/Γ

A test of lepton family number conservation. The value is for the sum of the two charge states.

VALUE	CL%	DOCUMENT ID		TECN	COMMENT
$< 4.9 \times 10^{-5}$	90	[1] FREYBERGER	96	CLE2	$e^+ e^- \approx \Upsilon(4S)$
• • • We do not use the following data for averages, fits, limits, etc. • • •					
$< 6.6 \times 10^{-5}$	90	AITALA	01C	E791	π^- nucleus, 500 GeV

[1] This FREYBERGER 96 limit is obtained using a phase-space model. The limit changes to $< 5.0 \times 10^{-5}$ using a photon pole amplitude model.

$\Gamma(\omega e^\pm \mu^\mp)/\Gamma_{total}$ Γ_{264}/Γ

A test of lepton family number conservation. The value is for the sum of the two charge states.

VALUE	CL%	DOCUMENT ID		TECN	COMMENT
$< 1.2 \times 10^{-4}$	90	[1] FREYBERGER	96	CLE2	$e^+ e^- \approx \Upsilon(4S)$

[1] This FREYBERGER 96 limit is obtained using a phase-space model. The same limit is obtained using a photon pole amplitude model.

$\Gamma(K^- K^+ e^\pm \mu^\mp)/\Gamma_{total}$ Γ_{265}/Γ

A test of lepton family-number conservation. The value is for the sum of the two charge states.

VALUE	CL%	DOCUMENT ID		TECN	COMMENT
$< 1.8 \times 10^{-4}$	90	AITALA	01C	E791	π^- nucleus, 500 GeV

$\Gamma(\phi e^\pm \mu^\mp)/\Gamma_{total}$ Γ_{266}/Γ

A test of lepton family number conservation. The value is for the sum of the two charge states.

VALUE	CL%	DOCUMENT ID		TECN	COMMENT
$< 3.4 \times 10^{-5}$	90	[1] FREYBERGER	96	CLE2	$e^+ e^- \approx \Upsilon(4S)$
• • • We do not use the following data for averages, fits, limits, etc. • • •					
$< 4.7 \times 10^{-5}$	90	AITALA	01C	E791	π^- nucleus, 500 GeV

[1] This FREYBERGER 96 limit is obtained using a phase-space model. The limit changes to $< 3.3 \times 10^{-5}$ using a photon pole amplitude model.

$\Gamma(\overline{K}^0 e^\pm \mu^\mp)/\Gamma_{total}$ Γ_{267}/Γ

A test of lepton family number conservation. The value is for the sum of the two charge states.

VALUE	CL%	DOCUMENT ID		TECN	COMMENT
$< 1.0 \times 10^{-4}$	90	FREYBERGER	96	CLE2	$e^+ e^- \approx \Upsilon(4S)$

$\Gamma(K^- \pi^+ e^\pm \mu^\mp)/\Gamma_{total}$ Γ_{268}/Γ

A test of lepton family-number conservation. The value is for the sum of the two charge states.

VALUE	CL%	DOCUMENT ID		TECN	COMMENT
$< 5.53 \times 10^{-4}$	90	AITALA	01C	E791	π^- nucleus, 500 GeV

$\Gamma(\overline{K}^*(892)^0 e^\pm \mu^\mp)/\Gamma_{total}$ Γ_{269}/Γ

A test of lepton family number conservation. The value is for the sum of the two charge states.

VALUE	CL%	DOCUMENT ID		TECN	COMMENT
$< 8.3 \times 10^{-5}$	90	AITALA	01C	E791	π^- nucleus, 500 GeV
• • • We do not use the following data for averages, fits, limits, etc. • • •					
$< 1.0 \times 10^{-4}$	90	[1] FREYBERGER	96	CLE2	$e^+ e^- \approx \Upsilon(4S)$

[1] This FREYBERGER 96 limit is obtained using a phase-space model. The same limit is obtained using a photon pole amplitude model.

$\Gamma(2\pi^- 2e^+ + \text{c.c.})/\Gamma_{total}$ Γ_{270}/Γ

A test of lepton-number conservation. The value is for the sum of the two charge states.

VALUE	CL%	DOCUMENT ID		TECN	COMMENT
$< 1.12 \times 10^{-4}$	90	AITALA	01C	E791	π^- nucleus, 500 GeV

$\Gamma(2\pi^- 2\mu^+ + \text{c.c.})/\Gamma_{total}$ Γ_{271}/Γ

A test of lepton-number conservation. The value is for the sum of the two charge states.

VALUE	CL%	DOCUMENT ID		TECN	COMMENT
$< 2.9 \times 10^{-5}$	90	AITALA	01C	E791	π^- nucleus, 500 GeV

$\Gamma(K^- \pi^- 2e^+ + \text{c.c.})/\Gamma_{total}$ Γ_{272}/Γ

A test of lepton-number conservation. The value is for the sum of the two charge states.

VALUE	CL%	DOCUMENT ID		TECN	COMMENT
$< 2.06 \times 10^{-4}$	90	AITALA	01C	E791	π^- nucleus, 500 GeV

$\Gamma(K^- \pi^- 2\mu^+ + \text{c.c.})/\Gamma_{total}$ Γ_{273}/Γ

A test of lepton-number conservation. The value is for the sum of the two charge states.

VALUE	CL%	DOCUMENT ID		TECN	COMMENT
$< 3.9 \times 10^{-4}$	90	AITALA	01C	E791	π^- nucleus, 500 GeV

$\Gamma(2K^- 2e^+ + \text{c.c.})/\Gamma_{total}$ Γ_{274}/Γ

A test of lepton-number conservation. The value is for the sum of the two charge states.

VALUE	CL%	DOCUMENT ID		TECN	COMMENT
$< 1.52 \times 10^{-4}$	90	AITALA	01C	E791	π^- nucleus, 500 GeV

$\Gamma(2K^- 2\mu^+ + \text{c.c.})/\Gamma_{total}$ Γ_{275}/Γ

A test of lepton-number conservation. The value is for the sum of the two charge states.

VALUE	CL%	DOCUMENT ID		TECN	COMMENT
$< 9.4 \times 10^{-5}$	90	AITALA	01C	E791	π^- nucleus, 500 GeV

$\Gamma(\pi^- \pi^- e^+ \mu^+ + \text{c.c.})/\Gamma_{total}$ Γ_{276}/Γ

A test of lepton-number conservation. The value is for the sum of the two charge states.

VALUE	CL%	DOCUMENT ID		TECN	COMMENT
$< 7.9 \times 10^{-5}$	90	AITALA	01C	E791	π^- nucleus, 500 GeV

$\Gamma(K^- \pi^- e^+ \mu^+ + \text{c.c.})/\Gamma_{total}$ Γ_{277}/Γ

A test of lepton-number conservation. The value is for the sum of the two charge states.

VALUE	CL%	DOCUMENT ID		TECN	COMMENT
$< 2.18 \times 10^{-4}$	90	AITALA	01C	E791	π^- nucleus, 500 GeV

$\Gamma(2K^- e^+ \mu^+ + \text{c.c.})/\Gamma_{\text{total}}$ Γ_{278}/Γ

A test of lepton-number conservation. The value is for the sum of the two charge states.

VALUE	CL%	DOCUMENT ID		TECN	COMMENT
$<5.7 \times 10^{-5}$	90	AITALA	01C	E791	π^- nucleus, 500 GeV

$\Gamma(p e^-)/\Gamma_{\text{total}}$ Γ_{279}/Γ

A test of baryon- and lepton-number conservation.

VALUE	CL%	DOCUMENT ID		TECN	COMMENT
$<1.0 \times 10^{-5}$	90	[1] RUBIN	09	CLEO	$e^+ e^-$ at $\psi(3770)$

[1] This RUBIN 09 limit is for either $D^0 \to p e^-$ or $\overline{D}^0 \to p e^-$ decay.

$\Gamma(\overline{p} e^+)/\Gamma_{\text{total}}$ Γ_{280}/Γ

A test of baryon- and lepton-number conservation.

VALUE	CL%	DOCUMENT ID		TECN	COMMENT
$<1.1 \times 10^{-5}$	90	[1] RUBIN	09	CLEO	$e^+ e^-$ at $\psi(3770)$

[1] This RUBIN 09 limit is for either $D^0 \to \overline{p} e^+$ or $\overline{D}^0 \to \overline{p} e^+$ decay.

D^0 *CP*-VIOLATING DECAY-RATE ASYMMETRIES

This is the difference between D^0 and $\overline{D}^0$ partial widths for these modes divided by the sum of the widths. The D^0 and $\overline{D}^0$ are distinguished by the charge of the parent D^*: $D^{*+} \to D^0 \pi^+$ and $D^{*-} \to \overline{D}^0 \pi^-$.

$A_{CP}(K^+ K^-)$ in $D^0, \overline{D}^0 \to K^+ K^-$

VALUE (%)	EVTS	DOCUMENT ID		TECN	COMMENT
-0.21 ± 0.17 OUR AVERAGE					
$-0.24 \pm 0.22 \pm 0.09$	476k	[1] AALTONEN	12B	CDF	$p\overline{p}$, $\sqrt{s}$=1.96 TeV
$0.00 \pm 0.34 \pm 0.13$	129k	[2] AUBERT	08M	BABR	$e^+ e^- \approx$ 10.6 GeV
$-0.43 \pm 0.30 \pm 0.11$	120k	[3] STARIC	08	BELL	$e^+ e^- \approx \Upsilon(4S)$
$+2.0 \pm 1.2 \pm 0.6$		[4] ACOSTA	05C	CDF	$p\overline{p}$, $\sqrt{s}$=1.96 TeV
$0.0 \pm 2.2 \pm 0.8$	3023	[4] CSORNA	02	CLE2	$e^+ e^- \approx \Upsilon(4S)$
$-0.1 \pm 2.2 \pm 1.5$	3330	[4] LINK	00B	FOCS	
$-1.0 \pm 4.9 \pm 1.2$	609	[4] AITALA	98C	E791	$-0.093 < A_{CP} < +0.073$ (90% CL)

[1] See also "D^0 *CP*-violating asymmetry differences" at the end of the *CP*-violating asymmetries.
[2] AUBERT 08M uses corrected numbers of events directly, not ratios with $K^{\mp}\pi^{\pm}$ events.
[3] STARIC 08 uses $D^0 \to K^-\pi^+$ and $\overline{D}^0 \to K^+\pi^-$ decays to correct for detector-induced asymmetries.
[4] AITALA 98C, LINK 00B, CSORNA 02, and ACOSTA 05C measure $N(D^0 \to K^+K^-)/N(D^0 \to K^-\pi^+)$, the ratio of numbers of events observed, and similarly for the $\overline{D}^0$.

$A_{CP}(K^0_S K^0_S)$ in $D^0, \overline{D}^0 \to K^0_S K^0_S$

VALUE (%)	EVTS	DOCUMENT ID		TECN	COMMENT
-23 ± 19	65	BONVICINI	01	CLE2	$e^+ e^- \approx$ 10.6 GeV

$A_{CP}(\pi^+\pi^-)$ in $D^0, \overline{D}^0 \to \pi^+\pi^-$

VALUE (%)	EVTS	DOCUMENT ID		TECN	COMMENT
0.22 ± 0.21 OUR AVERAGE					
$+0.22 \pm 0.24 \pm 0.11$	215k	[1] AALTONEN	12B	CDF	$p\overline{p}$, $\sqrt{s}$=1.96 TeV
$-0.24 \pm 0.52 \pm 0.22$	63.7k	[2] AUBERT	08M	BABR	$e^+ e^- \approx$ 10.6 GeV
$+0.43 \pm 0.52 \pm 0.12$	51k	[3] STARIC	08	BELL	$e^+ e^- \approx \Upsilon(4S)$
$+1.0 \pm 1.3 \pm 0.6$		[4] ACOSTA	05C	CDF	$p\overline{p}$, $\sqrt{s}$=1.96 TeV
$+1.9 \pm 3.2 \pm 0.8$	1136	[4] CSORNA	02	CLE2	$e^+ e^- \approx \Upsilon(4S)$
$+4.8 \pm 3.9 \pm 2.5$	1177	[4] LINK	00B	FOCS	
$-4.9 \pm 7.8 \pm 3.0$	343	[4] AITALA	98C	E791	$-0.186 < A_{CP} < +0.088$ (90% CL)

[1] See also "D^0 *CP*-violating asymmetry differences" at the end of the *CP*-violating asymmetries.
[2] AUBERT 08M uses corrected numbers of events directly, not ratios with $K^{\mp}\pi^{\pm}$ events.
[3] STARIC 08 uses $D^0 \to K^-\pi^+$ and $\overline{D}^0 \to K^+\pi^-$ decays to correct for detector-induced asymmetries.
[4] AITALA 98C, LINK 00B, CSORNA 02, and ACOSTA 05C measure $N(D^0 \to \pi^+\pi^-)/N(D^0 \to K^-\pi^+)$, the ratio of numbers of events observed, and similarly for the $\overline{D}^0$.

$A_{CP}(\pi^0\pi^0)$ in $D^0, \overline{D}^0 \to \pi^0\pi^0$

VALUE (%)	EVTS	DOCUMENT ID		TECN	COMMENT
$+0.1 \pm 4.8$	810	BONVICINI	01	CLE2	$e^+ e^- \approx$ 10.6 GeV

$A_{CP}(\pi^+\pi^-\pi^0)$ in $D^0, \overline{D}^0 \to \pi^+\pi^-\pi^0$

VALUE (%)	EVTS	DOCUMENT ID		TECN	COMMENT
0.3 ± 0.4 OUR AVERAGE					
$+0.43 \pm 1.30$	123k $\pm$490	ARINSTEIN	08	BELL	$e^+ e^- \approx \Upsilon(4S)$
$+0.31 \pm 0.41 \pm 0.17$	80 $\pm$ .3k	AUBERT	08AO	BABR	$e^+ e^- \approx$ 10.6 GeV
$+1 \pm {}^{9}_{7} \pm 5$		CRONIN-HEN..05		CLEO	$e^+ e^- \approx$ 10 GeV

$A_{CP}(\rho(770)^+\pi^- \to \pi^+\pi^-\pi^0)$ in $D^0 \to \rho^+\pi^-, \overline{D}^0 \to \rho^-\pi^+$

VALUE (%)	DOCUMENT ID		TECN	COMMENT
$+1.2 \pm 0.8 \pm 0.3$	AUBERT	08AO	BABR	Table 1, $-$Col.5/2$\times$Col.2

$A_{CP}(\rho(770)^0\pi^0 \to \pi^+\pi^-\pi^0)$ in $D^0, \overline{D}^0 \to \rho^0\pi^0$

VALUE (%)	DOCUMENT ID		TECN	COMMENT
$-3.1 \pm 2.7 \pm 1.2$	AUBERT	08AO	BABR	Table 1, $-$Col.5/2$\times$Col.2

$A_{CP}(\rho(770)^-\pi^+ \to \pi^+\pi^-\pi^0)$ in $D^0 \to \rho^-\pi^+, \overline{D}^0 \to \rho^+\pi^-$

VALUE (%)	DOCUMENT ID		TECN	COMMENT
$-1.0 \pm 1.6 \pm 0.7$	AUBERT	08AO	BABR	Table 1, $-$Col.5/2$\times$Col.2

$A_{CP}(\rho(1450)^+\pi^- \to \pi^+\pi^-\pi^0)$ in $D^0 \to \rho(1450)^+\pi^-, \overline{D}^0 \to$ c.c.

VALUE (%)	DOCUMENT ID		TECN	COMMENT
$0 \pm 50 \pm 50$	AUBERT	08AO	BABR	Table 1, $-$Col.5/2$\times$Col.2

$A_{CP}(\rho(1450)^0\pi^0 \to \pi^+\pi^-\pi^0)$ in $D^0, \overline{D}^0 \to \rho(1450)^0\pi^0$

VALUE (%)	DOCUMENT ID		TECN	COMMENT
$-17 \pm 33 \pm 17$	AUBERT	08AO	BABR	Table 1, $-$Col.5/2$\times$Col.2

$A_{CP}(\rho(1450)^-\pi^+ \to \pi^+\pi^-\pi^0)$ in $D^0 \to \rho(1450)^-\pi^+, \overline{D}^0 \to$ c.c.

VALUE (%)	DOCUMENT ID		TECN	COMMENT
$+6 \pm 8 \pm 3$	AUBERT	08AO	BABR	Table 1, $-$Col.5/2$\times$Col.2

$A_{CP}(\rho(1700)^+\pi^- \to \pi^+\pi^-\pi^0)$ in $D^0 \to \rho(1700)^+\pi^-, \overline{D}^0 \to$ c.c.

VALUE (%)	DOCUMENT ID		TECN	COMMENT
$-5 \pm 13 \pm 5$	AUBERT	08AO	BABR	Table 1, $-$Col.5/2$\times$Col.2

$A_{CP}(\rho(1700)^0\pi^0 \to \pi^+\pi^-\pi^0)$ in $D^0, \overline{D}^0 \to \rho(1700)^0\pi^0$

VALUE (%)	DOCUMENT ID		TECN	COMMENT
$+13 \pm 8 \pm 3$	AUBERT	08AO	BABR	Table 1, $-$Col.5/2$\times$Col.2

$A_{CP}(\rho(1700)^-\pi^+ \to \pi^+\pi^-\pi^0)$ in $D^0 \to \rho(1700)^-\pi^+, \overline{D}^0 \to$ c.c.

VALUE (%)	DOCUMENT ID		TECN	COMMENT
$+8 \pm 10 \pm 5$	AUBERT	08AO	BABR	Table 1, $-$Col.5/2$\times$Col.2

$A_{CP}(f_0(980)\pi^0 \to \pi^+\pi^-\pi^0)$ in $D^0, \overline{D}^0 \to f_0(980)\pi^0$

VALUE (%)	DOCUMENT ID		TECN	COMMENT
$0 \pm 25 \pm 25$	AUBERT	08AO	BABR	Table 1, $-$Col.5/2$\times$Col.2

$A_{CP}(f_0(1370)\pi^0 \to \pi^+\pi^-\pi^0)$ in $D^0, \overline{D}^0 \to f_0(1370)\pi^0$

VALUE (%)	DOCUMENT ID		TECN	COMMENT
$+25 \pm 13 \pm 13$	AUBERT	08AO	BABR	Table 1, $-$Col.5/2$\times$Col.2

$A_{CP}(f_0(1500)\pi^0 \to \pi^+\pi^-\pi^0)$ in $D^0, \overline{D}^0 \to f_0(1500)\pi^0$

VALUE (%)	DOCUMENT ID		TECN	COMMENT
$0 \pm 13 \pm 13$	AUBERT	08AO	BABR	Table 1, $-$Col.5/2$\times$Col.2

$A_{CP}(f_0(1710)\pi^0 \to \pi^+\pi^-\pi^0)$ in $D^0, \overline{D}^0 \to f_0(1710)\pi^0$

VALUE (%)	DOCUMENT ID		TECN	COMMENT
$0 \pm 17 \pm 17$	AUBERT	08AO	BABR	Table 1, $-$Col.5/2$\times$Col.2

$A_{CP}(f_2(1270)\pi^0 \to \pi^+\pi^-\pi^0)$ in $D^0, \overline{D}^0 \to f_2(1270)\pi^0$

VALUE (%)	DOCUMENT ID		TECN	COMMENT
$-4 \pm 4 \pm 4$	AUBERT	08AO	BABR	Table 1, $-$Col.5/2$\times$Col.2

$A_{CP}(\sigma(400)\pi^0 \to \pi^+\pi^-\pi^0)$ in $D^0, \overline{D}^0 \to \sigma(400)\pi^0$

VALUE (%)	DOCUMENT ID		TECN	COMMENT
$+6 \pm 6 \pm 6$	AUBERT	08AO	BABR	Table 1, $-$Col.5/2$\times$Col.2

$A_{CP}(\text{nonresonant } \pi^+\pi^-\pi^0)$ in $D^0, \overline{D}^0 \to \text{nonresonant } \pi^+\pi^-\pi^0$

VALUE (%)	DOCUMENT ID		TECN	COMMENT
$-13 \pm 19 \pm 13$	AUBERT	08AO	BABR	Table 1, $-$Col.5/2$\times$Col.2

$A_{CP}(2\pi^+ 2\pi^-)$ in $D^0, \overline{D}^0 \to 2\pi^+ 2\pi^-$

VALUE	DOCUMENT ID		TECN
no evidence	[1] AAIJ	13BR	LHCB

[1] AAIJ 13BR searched for *CP* violation in binned phase space. No evidence was found.

$A_{CP}(K^+ K^-\pi^0)$ in $D^0, \overline{D}^0 \to K^+ K^-\pi^0$

VALUE (%)	EVTS	DOCUMENT ID		TECN	COMMENT
$-1.00 \pm 1.67 \pm 0.25$	11 $\pm$ 0.11k	AUBERT	08AO	BABR	$e^+ e^- \approx$ 10.6 GeV

$A_{CP}(K^*(892)^+ K^- \to K^+ K^-\pi^0)$ in $D^0 \to K^*(892)^+ K^-, \overline{D}^0 \to$ c.c.

VALUE (%)	DOCUMENT ID		TECN	COMMENT
$-0.9 \pm 1.2 \pm 0.4$	AUBERT	08AO	BABR	Table 1, $-$Col.5/2$\times$Col.2

$A_{CP}(K^*(1410)^+ K^- \to K^+ K^-\pi^0)$ in $D^0 \to K^*(1410)^+ K^-, \overline{D}^0 \to$ c.c.

VALUE (%)	DOCUMENT ID		TECN	COMMENT
$-21 \pm 23 \pm 8$	AUBERT	08AO	BABR	Table 1, $-$Col.5/2$\times$Col.2

$A_{CP}((K^+\pi^0)_{S-wave} K^- \to K^+ K^-\pi^0)$ in $D^0 \to (K^+\pi^0)_S K^-, \overline{D}^0 \to$ c.c.

VALUE (%)	DOCUMENT ID		TECN	COMMENT
$+7 \pm 15 \pm 3$	AUBERT	08AO	BABR	Table 1, $-$Col.5/2$\times$Col.2

$A_{CP}(\phi(1020)\pi^0 \to K^+ K^-\pi^0)$ in $D^0, \overline{D}^0 \to \phi(1020)\pi^0$

VALUE (%)	DOCUMENT ID		TECN	COMMENT
$+1.1 \pm 2.1 \pm 0.5$	AUBERT	08AO	BABR	Table 1, $-$Col.5/2$\times$Col.2

$A_{CP}(f_0(980)\pi^0 \to K^+ K^-\pi^0)$ in $D^0, \overline{D}^0 \to f_0(980)\pi^0$

VALUE (%)	DOCUMENT ID		TECN	COMMENT
$-3 \pm 19 \pm 1$	AUBERT	08AO	BABR	Table 1, $-$Col.5/2$\times$Col.2

See key on page 547

$A_{CP}(a_0(980)^0\pi^0 \to K^+K^-\pi^0)$ in $D^0, \overline{D}^0 \to a_0(980)^0\pi^0$

VALUE (%)	DOCUMENT ID		TECN	COMMENT
−5±16±2	[1] AUBERT	08AO	BABR	Table 1, −Col.5/2×Col.2

[1] This AUBERT 08AO value is obtained when the $a_0(980)^0$ replaces the $f_0(980)$ in the fit.

$A_{CP}(f_2'(1525)\pi^0 \to K^+K^-\pi^0)$ in $D^0, \overline{D}^0 \to f_2'(1525)\pi^0$

VALUE (%)	DOCUMENT ID		TECN	COMMENT
0±50±150	AUBERT	08AO	BABR	Table 1, −Col.5/2×Col.2

$A_{CP}(K^*(892)^-K^+ \to K^+K^-\pi^0)$ in $D^0 \to K^*(892)^-K^+, \overline{D}^0 \to$ c.c.

VALUE (%)	DOCUMENT ID		TECN	COMMENT
−5±4±1	AUBERT	08AO	BABR	Table 1, −Col.5/2×Col.2

$A_{CP}(K^*(1410)^-K^+ \to K^+K^-\pi^0)$ in $D^0 \to K^*(1410)^-K^+, \overline{D}^0 \to$ c.c.

VALUE (%)	DOCUMENT ID		TECN	COMMENT
−17±28±7	AUBERT	08AO	BABR	Table 1, −Col.5/2×Col.2

$A_{CP}((K^-\pi^0)_{S-wave}K^+ \to K^+K^-\pi^0)$ in $D^0 \to (K^-\pi^0)_S K^+, \overline{D}^0 \to$ c.c.

VALUE (%)	DOCUMENT ID		TECN	COMMENT
−7±40±8	AUBERT	08AO	BABR	Table 1, −Col.5/2×Col.2

$A_{CP}(K^0_S\pi^0)$ in $D^0, \overline{D}^0 \to K^0_S\pi^0$

VALUE (%)	EVTS	DOCUMENT ID		TECN	COMMENT
−0.27±0.21 OUR AVERAGE					
−0.28±0.19±0.10	326k	KO	11	BELL	$e^+e^- \approx \Upsilon(4S)$
+0.1 ±1.3	9099	BONVICINI	01	CLE2	$e^+e^- \approx 10.6$ GeV
• • • We do not use the following data for averages, fits, limits, etc. • • •					
−1.8 ±3.0		BARTELT	95	CLE2	See BONVICINI 01

$A_{CP}(K^0_S\eta)$ in $D^0, \overline{D}^0 \to K^0_S\eta$

VALUE (%)	EVTS	DOCUMENT ID		TECN	COMMENT
+0.54±0.51±0.16	46k	KO	11	BELL	$e^+e^- \approx \Upsilon(4S)$

$A_{CP}(K^0_S\eta')$ in $D^0, \overline{D}^0 \to K^0_S\eta'$

VALUE (%)	EVTS	DOCUMENT ID		TECN	COMMENT
+0.98±0.67±0.14	27k	KO	11	BELL	$e^+e^- \approx \Upsilon(4S)$

$A_{CP}(K^0_S\phi)$ in $D^0, \overline{D}^0 \to K^0_S\phi$

VALUE (%)	DOCUMENT ID		TECN	COMMENT
−2.8±9.4	BARTELT	95	CLE2	$-18.2 < A_{CP} < +12.6\%$ (90%CL)

$A_{CP}(K^\mp\pi^\pm)$ in $D^0 \to K^-\pi^+, \overline{D}^0 \to K^+\pi^-$

VALUE (%)	EVTS	DOCUMENT ID		TECN	COMMENT
0.1±0.7 OUR AVERAGE					
+0.5±0.4±0.9	150k	MENDEZ	10	CLEO	e^+e^- at 3774 MeV
−0.4±0.5±0.9		DOBBS	07	CLEO	e^+e^- at $\psi(3770)$

$A_{CP}(K^\pm\pi^\mp)$ in $D^0 \to K^+\pi^-, \overline{D}^0 \to K^-\pi^+$

VALUE (%)	EVTS	DOCUMENT ID		TECN	COMMENT
0.0± 1.6 OUR AVERAGE					
− 0.7± 1.9		[1] AAIJ	13CE	LHCB	pp at 7, 8 TeV
− 2.1± 5.2±1.5	4.0k	AUBERT	07W	BABR	$e^+e^- \approx 10.6$ GeV
+ 2.3± 4.7	4.0k	[2] ZHANG	06	BELL	e^+e^-
+18 ±14 ±4		[3] LINK	05H	FOCS	γ nucleus
+ 9.5± 6.1±8.3		[4] AUBERT	03Z	BABR	e^+e^-, 10.6 GeV
+ 2 $^{+19}_{-20}$ ±1	45	[5] GODANG	00	CLE2	e^+e^-
• • • We do not use the following data for averages, fits, limits, etc. • • •					
− 8.0± 7.7	0.8k	[6] LI	05A	BELL	See ZHANG 06

[1] Based on 3 fb^{-1} of data collected at $\sqrt{s} = 7$, 8 TeV. Allowing for CP violation, the direct CP-violation in mixing is reported for the $D^0 \to K^+\pi^-$ and $\overline{D}^0 \to K^+\pi^-$.
[2] This ZHANG 06 result allows mixing.
[3] This LINK 05H result assumes no mixing. If mixing is allowed, it becomes $0.13^{+0.33}_{-0.25} \pm 0.10$.
[4] This AUBERT 03Z limit assumes no mixing. If mixing is allowed, the 95% confidence-level interval is $(-2.8 < A_D < 4.9)\times10^{-3}$.
[5] This GODANG 00 result assumes no D^0-$\overline{D}^0$ mixing and becomes $-0.43 < A_{CP} < +0.34$ at 95% CL. If mixing is allowd $A_{CP} = -0.01^{+0.16}_{-0.17} \pm 0.01$.
[6] This LI 05A result allows mixing.

$A_{CP}(K^\mp\pi^\pm\pi^0)$ in $D^0 \to K^-\pi^+\pi^0, \overline{D}^0 \to K^+\pi^-\pi^0$

VALUE (%)	DOCUMENT ID		TECN	COMMENT
0.2±0.9 OUR AVERAGE				
+0.2±0.4±0.8	DOBBS	07	CLEO	e^+e^- at $\psi(3770)$
−3.1±8.6	[1] KOPP	01	CLE2	$e^+e^- \approx 10.6$ GeV

[1] KOPP 01 fits separately the D^0 and $\overline{D}^0$ Dalitz plots and then calculates the integrated difference of normalized densities divided by the integrated sum.

$A_{CP}(K^\pm\pi^\mp\pi^0)$ in $D^0 \to K^+\pi^-\pi^0, \overline{D}^0 \to K^-\pi^+\pi^0$

VALUE (%)	EVTS	DOCUMENT ID		TECN	COMMENT
0 ± 5 OUR AVERAGE					
−0.6± 5.3	1978 ± 104	TIAN	05	BELL	$e^+e^- \approx \Upsilon(4S)$
+ 9 $^{+25}_{-22}$	38	BRANDENB...	01	CLE2	$e^+e^- \approx \Upsilon(4S)$

$A_{CP}(K^0_S\pi^+\pi^-)$ in $D^0, \overline{D}^0 \to K^0_S\pi^+\pi^-$

VALUE (%)	EVTS	DOCUMENT ID		TECN	COMMENT
−0.1 ±0.8 OUR AVERAGE					
−0.05±0.57±0.54	350k	[1] AALTONEN	12AD	CDF	
−0.9 ±2.1 $^{+1.6}_{-5.7}$	4854	[2] ASNER	04A	CLEO	$e^+e^- \approx 10$ GeV

[1] This is the overall result of AALTONEN 12AD. Following are the 15 CP fit-fraction asymmetries from the amplitude analysis of the D^0 and $\overline{D}^0 \to K^0_S\pi^+\pi^-$ Dalitz plots.
[2] This is the overall result of ASNER 04A; CP-violating limits are also given below for each of the 10 resonant submodes found in an amplitude analysis of the D^0 and $\overline{D}^0 \to K^0_S\pi^+\pi^-$ Dalitz plots.

$A_{CP}(K^*(892)^\mp\pi^\pm \to K^0_S\pi^+\pi^-)$ in $D^0 \to K^{*-}\pi^+, \overline{D}^0 \to K^{*+}\pi^-$

VALUE (%)	DOCUMENT ID		TECN	COMMENT
+0.36±0.33±0.40	AALTONEN	12AD	CDF	Dalitz fit, ∼ 350k evts
• • • We do not use the following data for averages, fits, limits, etc. • • •				
+2.5 ±1.9 $^{+3.3}_{-0.8}$	ASNER	04A	CLEO	Dalitz fit, 4854 evts

$A_{CP}(K^*(892)^\pm\pi^\mp \to K^0_S\pi^+\pi^-)$ in $D^0 \to K^{*+}\pi^-, \overline{D}^0 \to K^{*-}\pi^+$

This is a doubly Cabibbo-suppressed mode.

VALUE (%)	DOCUMENT ID		TECN	COMMENT
+ 1.0± 5.7± 2.1	AALTONEN	12AD	CDF	Dalitz fit, ∼ 350k evts
• • • We do not use the following data for averages, fits, limits, etc. • • •				
−21 ±42 ±28	ASNER	04A	CLEO	Dalitz fit, 4854 evts

$A_{CP}(K^0_S\rho^0 \to K^0_S\pi^+\pi^-)$ in $D^0 \to \overline{K}^0\rho^0, \overline{D}^0 \to K^0\rho^0$

VALUE (%)	DOCUMENT ID		TECN	COMMENT
−0.05±0.50±0.08	AALTONEN	12AD	CDF	Dalitz fit, ∼ 350k evts
• • • We do not use the following data for averages, fits, limits, etc. • • •				
+3.1 ±3.8 $^{+2.7}_{-2.2}$	ASNER	04A	CLEO	Dalitz fit, 4854 evts

$A_{CP}(K^0_S\omega \to K^0_S\pi^+\pi^-)$ in $D^0 \to \overline{K}^0\omega, \overline{D}^0 \to K^0\omega$

VALUE (%)	DOCUMENT ID		TECN	COMMENT
−12.6± 6.0± 2.6	AALTONEN	12AD	CDF	Dalitz fit, ∼ 350k evts
• • • We do not use the following data for averages, fits, limits, etc. • • •				
−26 ±24 $^{+22}_{-4}$	ASNER	04A	CLEO	Dalitz fit, 4854 evts

$A_{CP}(K^0_S f_0(980) \to K^0_S\pi^+\pi^-)$ in $D^0 \to \overline{K}^0 f_0(980), \overline{D}^0 \to K^0 f_0(980)$

VALUE (%)	DOCUMENT ID		TECN	COMMENT
−0.4± 2.2± 1.6	AALTONEN	12AD	CDF	Dalitz fit, ∼ 350k evts
• • • We do not use the following data for averages, fits, limits, etc. • • •				
−4.7±11.0$^{+24.9}_{-8.8}$	ASNER	04A	CLEO	Dalitz fit, 4854 evts

$A_{CP}(K^0_S f_2(1270) \to K^0_S\pi^+\pi^-)$ in $D^0 \to \overline{K}^0 f_2(1270), \overline{D}^0 \to K^0 f_2(1270)$

VALUE (%)	DOCUMENT ID		TECN	COMMENT
− 4.0± 3.4± 3.0	AALTONEN	12AD	CDF	Dalitz fit, ∼ 350k evts
• • • We do not use the following data for averages, fits, limits, etc. • • •				
+34 ±51 $^{+33}_{-79}$	ASNER	04A	CLEO	Dalitz fit, 4854 evts

$A_{CP}(K^0_S f_0(1370) \to K^0_S\pi^+\pi^-)$ in $D^0 \to \overline{K}^0 f_0(1370), \overline{D}^0 \to K^0 f_0(1370)$

VALUE (%)	DOCUMENT ID		TECN	COMMENT
− 0.5± 4.6± 7.7	AALTONEN	12AD	CDF	Dalitz fit, ∼ 350k evts
• • • We do not use the following data for averages, fits, limits, etc. • • •				
+18 ±10 $^{+13}_{-22}$	ASNER	04A	CLEO	Dalitz fit, 4854 evts

$A_{CP}(K^0_S\rho^0(1450)) \text{ in } D^0 \to \overline{K}^0\rho^0(1450), \overline{D}^0 \to K^0\rho^0(1450)$

VALUE (%)	DOCUMENT ID		TECN	COMMENT
−4.1±5.2±8.1	AALTONEN	12AD	CDF	Dalitz fit, ∼ 350k evts

$A_{CP}(K^0_S f_0(600)) \text{ in } D^0 \to \overline{K}^0 f_0(600), \overline{D}^0 \to K^0 f_0(600)$

VALUE (%)	DOCUMENT ID		TECN	COMMENT
−2.7±2.7±3.6	AALTONEN	12AD	CDF	Dalitz fit, ∼ 350k evts

$A_{CP}(K^*(1410)^\mp\pi^\pm) \text{ in } D^0 \to K^*(1410)^-\pi^+, \overline{D}^0 \to K^*(1410)^+\pi^-$

VALUE (%)	DOCUMENT ID		TECN	COMMENT
−2.3±5.7±6.4	AALTONEN	12AD	CDF	Dalitz fit, ∼ 350k evts

$A_{CP}(K_0^*(1430)^\mp\pi^\pm \to K^0_S\pi^+\pi^-)$ in $D^0 \to K_0^*(1430)^-\pi^+, \overline{D}^0 \to$ c.c.

VALUE (%)	DOCUMENT ID		TECN	COMMENT
+4.0± 2.4±3.8	AALTONEN	12AD	CDF	Dalitz fit, ∼ 350k evts
• • • We do not use the following data for averages, fits, limits, etc. • • •				
−0.2±11.3$^{+8.8}_{-5.0}$	ASNER	04A	CLEO	Dalitz fit, 4854 evts

$A_{CP}(K_0^*(1430)^\pm\pi^\mp) \text{ in } D^0 \to K_0^*(1430)^+\pi^-, \overline{D}^0 \to K_0^*(1430)^-\pi^+$

This is a doubly Cabibbo-suppressed mode.

VALUE (%)	DOCUMENT ID		TECN	COMMENT
+12±11±10	AALTONEN	12AD	CDF	Dalitz fit, ∼ 350k evts

$A_{CP}(K_2^*(1430)^{\mp}\pi^{\pm} \to K_S^0\pi^+\pi^-)$ in $D^0 \to K_2^*(1430)^-\pi^+$, $\overline{D}^0 \to$ c.c.

VALUE (%)	DOCUMENT ID		TECN	COMMENT
+2.9± 4.0± 4.1	AALTONEN	12AD	CDF	Dalitz fit, ∼ 350k evts
• • • We do not use the following data for averages, fits, limits, etc. • • •				
$-7 \pm 25 \pm^{13}_{26}$	ASNER	04A	CLEO	Dalitz fit, 4854 evts

$A_{CP}(K_2^*(1430)^{\pm}\pi^{\mp})$ in $D^0 \to K_2^*(1430)^+\pi^-$, $\overline{D}^0 \to K_2^*(1430)^-\pi^+$

This is a doubly Cabibbo-suppressed mode.

VALUE (%)	DOCUMENT ID		TECN	COMMENT
−10±14±29	AALTONEN	12AD	CDF	Dalitz fit, ∼ 350k evts

$A_{CP}(K^*(1680)^{\mp}\pi^{\pm} \to K_S^0\pi^+\pi^-)$ in $D^0 \to K^*(1680)^-\pi^+$, $\overline{D}^0 \to$ c.c.

VALUE (%)	DOCUMENT ID		TECN	COMMENT
• • • We do not use the following data for averages, fits, limits, etc. • • •				
$-36 \pm 19 \pm^{10}_{35}$	ASNER	04A	CLEO	Dalitz fit, 4854 evts

$A_{CP}(K^-\pi^+\pi^+\pi^-)$ in $D^0 \to K^-\pi^+\pi^+\pi^-$, $\overline{D}^0 \to K^+\pi^-\pi^-\pi^+$

VALUE (%)	DOCUMENT ID		TECN	COMMENT
+0.7±0.5±0.9	DOBBS	07	CLEO	e^+e^- at $\psi(3770)$

$A_{CP}(K^{\pm}\pi^{\mp}\pi^+\pi^-)$ in $D^0 \to K^+\pi^-\pi^+\pi^-$, $\overline{D}^0 \to K^-\pi^+\pi^+\pi^-$

VALUE (%)	EVTS	DOCUMENT ID		TECN	COMMENT
−1.8±4.4	1721 ± 75	TIAN	05	BELL	$e^+e^- \approx \Upsilon(4S)$

$A_{CP}(K^+K^-\pi^+\pi^-)$ in D^0, $\overline{D}^0 \to K^+K^-\pi^+\pi^-$

See also AAIJ 13BR for a search for *CP* violation in $D^0 \to K^+K^-\pi^+\pi^-$ in binned phase space. No evidence of *CP* violation was found.

VALUE (%)	EVTS	DOCUMENT ID		TECN	COMMENT
−8.2±5.6±4.7	828 ± 46	LINK	05E	FOCS	γ A, $\overline{E}_\gamma \approx 180$ GeV

$A_{CP}(K_1^*(1270)^+K^- \to K^{*0}\pi^+K^-)$ in $D^0 \to K_1^*(1270)^+K^-$, $\overline{D}^0 \to$ c.c.

VALUE (%)	DOCUMENT ID		TECN	COMMENT
−0.7±10.4	ARTUSO	12	CLEO	Amplitude fit, 2959 evts.

$A_{CP}(K_1^*(1270)^-K^+ \to \overline{K}^{*0}\pi^-K^+)$ in $D^0 \to K_1^*(1270)^-K^+$, $\overline{D}^0 \to$ c.c.

VALUE (%)	DOCUMENT ID		TECN	COMMENT
−10.0±31.5	ARTUSO	12	CLEO	Amplitude fit, 2959 evts.

$A_{CP}(K_1^*(1270)^+K^- \to \rho^0K^+K^-)$ in $D^0 \to K_1^*(1270)^+K^-$, $\overline{D}^0 \to$ c.c.

VALUE (%)	DOCUMENT ID		TECN	COMMENT
−6.5±16.9	ARTUSO	12	CLEO	Amplitude fit, 2959 evts.

$A_{CP}(K_1^*(1270)^-K^+ \to \rho^0K^-K^+)$ in $D^0 \to K_1^*(1270)^-K^+$, $\overline{D}^0 \to$ c.c.

VALUE (%)	DOCUMENT ID		TECN	COMMENT
+9.6±12.9	ARTUSO	12	CLEO	Amplitude fit, 2959 evts.

$A_{CP}(K^*(1410)^+K^- \to K^{*0}\pi^+K^-)$ in $D^0 \to K^*(1410)^+K^-$, $\overline{D}^0 \to$ c.c.

VALUE (%)	DOCUMENT ID		TECN	COMMENT
−20.0±16.8	ARTUSO	12	CLEO	Amplitude fit, 2959 evts.

$A_{CP}(K^*(1410)^-K^+ \to \overline{K}^{*0}\pi^-K^+)$ in $D^0 \to K^*(1410)^-K^+$, $\overline{D}^0 \to$ c.c.

VALUE (%)	DOCUMENT ID		TECN	COMMENT
−1.1±13.7	ARTUSO	12	CLEO	Amplitude fit, 2959 evts.

$A_{CP}(K^{*0}\overline{K}^{*0}$ S-wave) in D^0, $\overline{D}^0 \to K^{*0}\overline{K}^{*0}$ S-wave

VALUE (%)	DOCUMENT ID		TECN	COMMENT
+9.5±13.5	ARTUSO	12	CLEO	Amplitude fit, 2959 evts.

$A_{CP}(\phi\rho^0$ S-wave) in D^0, $\overline{D}^0 \to \phi\rho^0$ S-wave

VALUE (%)	DOCUMENT ID		TECN	COMMENT
−2.7±5.3	ARTUSO	12	CLEO	Amplitude fit, 2959 evts.

$A_{CP}(\phi\rho^0$ D-wave) in D^0, $\overline{D}^0 \to \phi\rho^0$ D-wave

VALUE (%)	DOCUMENT ID		TECN	COMMENT
−37.1±19.0	ARTUSO	12	CLEO	Amplitude fit, 2959 evts.

$A_{CP}(\phi(\pi^+\pi^-)_{S-wave})$ in D^0, $\overline{D}^0 \to \phi(\pi^+\pi^-)_{S-wave}$

VALUE (%)	DOCUMENT ID		TECN	COMMENT
−8.6±10.4	ARTUSO	12	CLEO	Amplitude fit, 2959 evts.

$A_{CP}((K^-\pi^+)_{P-wave}$ $(K^+\pi^-)_{S-wave})$ in $D^0 \to (K^-\pi^+)_{P-wave}$ $(K^+\pi^-)_{S-wave}$, $\overline{D}^0 \to$ c.c.

VALUE (%)	DOCUMENT ID		TECN	COMMENT
+2.7±10.6	ARTUSO	12	CLEO	Amplitude fit, 2959 evts.

D^0 CP-VIOLATING ASYMMETRY DIFFERENCES

$\Delta A_{CP} = A_{CP}(K^+K^-) - A_{CP}(\pi^+\pi^-)$

CP violation in these modes can come from the decay amplitudes (direct) and/or from mixing or interference of mixing and decay (indirect). The difference ΔA_{CP} is primarily sensitive to the direct component, and only retains a second-order dependence on the indirect component for measurements where the mean decay time of the K^+K^- and $\pi^+\pi^-$ samples are not identical. The results below are averaged assuming the indirect component can be neglected.

VALUE (%)	EVTS	DOCUMENT ID		TECN	COMMENT
−0.46±0.25 OUR AVERAGE	Error includes scale factor of 1.8. See the ideogram below.				
$0.49 \pm 0.30 \pm 0.14$	559/222k	AAIJ	13AD	LHCB	Time-integrated
$-0.82 \pm 0.21 \pm 0.11$		AAIJ	12G	LHCB	Time-integrated
$-0.62 \pm 0.21 \pm 0.10$		AALTONEN	12O	CDF	Time-integrated
$0.24 \pm 0.62 \pm 0.26$		[1] AUBERT	08M	BABR	Time-integrated
$-0.86 \pm 0.60 \pm 0.07$	120k	STARIC	08	BELL	Time-integrated
• • • We do not use the following data for averages, fits, limits, etc. • • •					
$-0.46 \pm 0.31 \pm 0.12$		AALTONEN	12B	CDF	See AALTONEN 12O

[1] Calculated from the AUBERT 08M values of $A_{CP}(K^+K^-)$ and $A_{CP}(\pi^+\pi^-)$. The systematic error here combines the systematic errors in quadrature, and therefore somewhat over-estimates it.

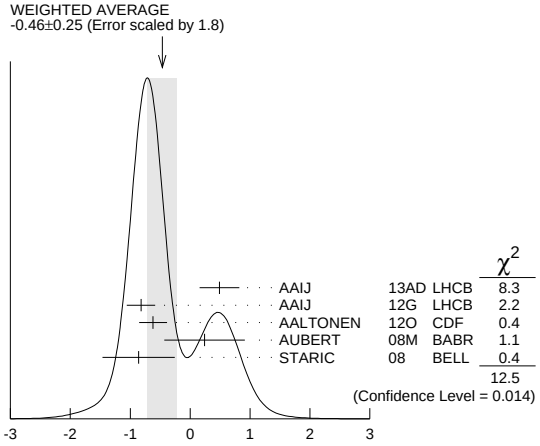

D^0-$\overline{D}^0$ T-VIOLATING DECAY-RATE ASYMMETRIES

The *CP*-sensitive *P*-odd (*T*-odd) correlation in $D^0, \overline{D}^0 \to K^+K^-\pi^+\pi^-$ decays. D^0 and $\overline{D}^0$ are distinguished by the charge of the parent D^*: $D^{*+} \to D^0\pi^+$ and $D^{*-} \to \overline{D}^0\pi^-$.

$A_{TViol}(K^+K^-\pi^+\pi^-)$ in D^0, $\overline{D}^0 \to K^+K^-\pi^+\pi^-$

$C_T \equiv \vec{p}_{K^+} \cdot (\vec{p}_{\pi^+} \times \vec{p}_{\pi^-})$ is a parity-odd correlation of the K^+, π^+, and π^- momenta (evaluated in the D^0 rest frame) for the D^0. $\overline{C}_T \equiv \vec{p}_{K^-} \cdot (\vec{p}_{\pi^-} \times \vec{p}_{\pi^+})$ is the corresponding quantity for the $\overline{D}^0$. Then
$A_T \equiv [\Gamma(C_T > 0) - \Gamma(C_T < 0)] \,/\, [\Gamma(C_T > 0) + \Gamma(C_T < 0)]$, and
$\overline{A}_T \equiv [\Gamma(-\overline{C}_T > 0) - \Gamma(-\overline{C}_T < 0)] \,/\, [\Gamma(-\overline{C}_T > 0) + \Gamma(-\overline{C}_T < 0)]$, and
$A_{Tviol} \equiv \frac{1}{2}(A_T - \overline{A}_T)$. C_T and $\overline{C}_T$ are commonly referred to as *T*-odd moments, because they are odd under *T* reversal. However, the *T*-conjugate process $K^+K^-\pi^+\pi^- \to D^0$ is not accessible, while the *P*-conjugate process is.

VALUE (units 10^{-3})	EVTS	DOCUMENT ID		TECN	COMMENT
+ 1.0± 5.1± 4.4	47k	DEL-AMO-SA...10		BABR	$e^+e^- \approx 10.6$ GeV
• • • We do not use the following data for averages, fits, limits, etc. • • •					
$+10 \pm 57 \pm 37$	828 ± 46	LINK	05E	FOCS	γ A, $\overline{E}_\gamma \approx 180$ GeV

D^0 CPT-VIOLATING DECAY-RATE ASYMMETRIES

$A_{CPT}(K^{\mp}\pi^{\pm})$ in $D^0 \to K^-\pi^+$, $\overline{D}^0 \to K^+\pi^-$

$A_{CPT}(t)$ is defined in terms of the time-dependent decay probabilities $P(D^0 \to K^-\pi^+)$ and $\overline{P}(\overline{D}^0 \to K^+\pi^-)$ by $A_{CPT}(t) = (\overline{P} - P)/(\overline{P} + P)$. For small mixing parameters $x \equiv \Delta m/\Gamma$ and $y \equiv \Delta\Gamma/2\Gamma$ (as is the case), and times t, $A_{CPT}(t)$ reduces to $[\, y\, Re\,\xi - x\, Im\,\xi\,]\,\Gamma t$, where ξ is the CPT-violating parameter.

The following is actually $y\, Re\,\xi - x\, Im\,\xi$.

VALUE	DOCUMENT ID		TECN	COMMENT
0.0083±0.0065±0.0041	LINK	03B	FOCS	γ nucleus, $\overline{E}_\gamma \approx 180$ GeV

$D^0 \to K^*(892)^-\ell^+\nu_\ell$ FORM FACTORS

$r_V \equiv V(0)/A_1(0)$ in $D^0 \to K^*(892)^-\ell^+\nu_\ell$

VALUE	DOCUMENT ID		TECN	COMMENT
1.71±0.68±0.34	LINK	05B	FOCS	$K^*(892)^-\mu^+\nu_\mu$

$r_2 \equiv A_2(0)/A_1(0)$ in $D^0 \to K^*(892)^- \ell^+ \nu_\ell$

VALUE	DOCUMENT ID		TECN	COMMENT
0.91±0.37±0.10	LINK	05B	FOCS	$K^*(892)^- \mu^+ \nu_\mu$

$D^0 \to K^-/\pi^- \ell^+ \nu_\ell$ FORM FACTORS

$f_+(0)$ in $D^0 \to K^- \ell^+ \nu_\ell$

VALUE	DOCUMENT ID		TECN	COMMENT
0.727±0.007±0.009	AUBERT	07BG	BABR	$K^- e^+ \nu_e$ 2-parameter fit

$f_+(0)\lvert V_{cs}\rvert$ in $D^0 \to K^- \ell^+ \nu_\ell$

VALUE	DOCUMENT ID		TECN	COMMENT
0.726±0.008±0.004	BESSON	09	CLEO	$K^- e^+ \nu_e$ 3-parameter fit

$r_1 \equiv a_1/a_0$ in $D^0 \to K^- \ell^+ \nu_\ell$

VALUE	DOCUMENT ID		TECN	COMMENT
−2.65±0.34±0.08	BESSON	09	CLEO	$K^- e^+ \nu_e$ 3-parameter fit

$r_2 \equiv a_1/a_0$ in $D^0 \to K^- \ell^+ \nu_\ell$

VALUE	DOCUMENT ID		TECN	COMMENT
13±9±1	BESSON	09	CLEO	$K^- e^+ \nu_e$ 3-parameter fit

$f_+(0)\lvert V_{cd}\rvert$ in $D^0 \to \pi^- \ell^+ \nu_\ell$

VALUE	DOCUMENT ID		TECN	COMMENT
0.152±0.005±0.001	BESSON	09	CLEO	$\pi^- e^+ \nu_e$ 3-parameter fit

$r_1 \equiv a_1/a_0$ in $D^0 \to \pi^- \ell^+ \nu_\ell$

VALUE	DOCUMENT ID		TECN	COMMENT
−2.80±0.49±0.04	BESSON	09	CLEO	$\pi^- e^+ \nu_e$ 3-parameter fit

$r_2 \equiv a_1/a_0$ in $D^0 \to \pi^- \ell^+ \nu_\ell$

VALUE	DOCUMENT ID		TECN	COMMENT
6±3±0	BESSON	09	CLEO	$\pi^- e^+ \nu_e$ 3-parameter fit

D^0 REFERENCES

AAIJ	14B	PL B728 234	R. Aaij *et al.*	(LHCb Collab.)
KO	14	PRL 112 111801	B.R. Ko *et al.*	(BELLE Collab.)
AAIJ	13AD	PL B723 33	R. Aaij *et al.*	(LHCb Collab.)
AAIJ	13AI	PL B725 15	R. Aaij *et al.*	(LHCb Collab.)
AAIJ	13BR	PL B726 623	R. Aaij *et al.*	(LHCb Collab.)
AAIJ	13CE	PRL 111 251801	R. Aaij *et al.*	(LHCb Collab.)
AAIJ	13N	PRL 110 101802	R. Aaij *et al.*	(LHCb Collab.)
AAIJ	13V	JHEP 1306 065	R. Aaij *et al.*	(LHCb Collab.)
AALTONEN	13AE	PRL 111 231802	T. Aaltonen *et al.*	(CDF Collab.)
DOBBS	13	PRL 110 131802	S. Dobbs *et al.*	(CLEO Collab.)
LEES	13	PR D87 012004	J.P. Lees *et al.*	(BABAR Collab.)
LEES	13S	PR D88 071104	J.P. Lees *et al.*	(BABAR Collab.)
WHITE	13	PR D88 051101	E. White *et al.*	(BELLE Collab.)
AAIJ	12G	PRL 108 111602	R. Aaij *et al.*	(LHCb Collab.)
AAIJ	12K	JHEP 1204 129	R. Aaij *et al.*	(LHCb Collab.)
AALTONEN	12AD	PR D86 032007	T. Aaltonen *et al.*	(CDF Collab.)
AALTONEN	12B	PR D85 012009	T. Aaltonen *et al.*	(CDF Collab.)
AALTONEN	12O	PRL 109 111801	T. Aaltonen *et al.*	(CDF Collab.)
ARTUSO	12	PR D85 122002	M. Artuso *et al.*	(CLEO Collab.)
ASNER	12	PR D86 112001	D.M. Asner, et al	(CLEO Collab.)
INSLER	12	PR D85 092016	J. Insler *et al.*	(CLEO Collab.)
LEES	12L	PR D85 091107	J.P. Lees *et al.*	(BABAR Collab.)
LEES	12Q	PR D86 032001	J.P. Lees *et al.*	(BABAR Collab.)
PDG	12	PR D86 010001	J. Beringer *et al.*	(PDG Collab.)
KO	11	PRL 106 211801	B.R. Ko *et al.*	(BELLE Collab.)
LOWREY	11	PR D84 092005	N. Lowrey *et al.*	(CLEO Collab.)
AALTONEN	10X	PR D82 091105	T. Aaltonen *et al.*	(CDF Collab.)
ANASHIN	10A	PL B686 84	V.V. Anashin *et al.*	(VEPP-4M KEDR Collab.)
ASNER	10	PR D81 052007	D.M. Asner *et al.*	(CLEO Collab.)
BHATTACHAR...10A		PR D81 096008	B. Bhattacharya, C.-W. Chiang, J.L. Rosner	(CHIC+)
DEL-AMO-SA...	10	PR D81 111103	P. del Amo Sanchez *et al.*	(BABAR Collab.)
DEL-AMO-SA...	10D	PRL 105 081803	P. del Amo Sanchez *et al.*	(BABAR Collab.)
MENDEZ	10	PR D81 052013	H. Mendez *et al.*	(CLEO Collab.)
PETRIC	10	PR D81 091102	M. Petric *et al.*	(BELLE Collab.)
AUBERT	09AI	PR D80 071103	B. Aubert *et al.*	(BABAR Collab.)
AUBERT	09AN	PRL 103 211801	B. Aubert *et al.*	(BABAR Collab.)
BESSON	09	PR D80 032005	D. Besson *et al.*	(CLEO Collab.)
Also		PR D79 052010	J.Y. Ge *et al.*	(CLEO Collab.)
LOWREY	09	PR D80 031105	N. Lowrey *et al.*	(CLEO Collab.)
RUBIN	09	PR D79 097101	P. Rubin *et al.*	(CLEO Collab.)
ZUPANC	09	PR D80 052006	A. Zupanc *et al.*	(BELLE Collab.)
AALTONEN	08E	PRL 100 121802	T. Aaltonen *et al.*	(CDF Collab.)
ABLIKIM	08L	PL B665 16	M. Ablikim *et al.*	(BES Collab.)
ARINSTEIN	08	PL B662 102	K. Arinstein *et al.*	(BELLE Collab.)
ARTUSO	08	PR D77 092003	M. Artuso *et al.*	(CLEO Collab.)
ASNER	08	PR D78 012001	D.M. Asner *et al.*	(CLEO Collab.)
AUBERT	08AL	PR D78 034023	B. Aubert *et al.*	(BABAR Collab.)
AUBERT	08AO	PR D78 051102	B. Aubert *et al.*	(BABAR Collab.)
AUBERT	08AZ	PR D78 071101	B. Aubert *et al.*	(BABAR Collab.)
AUBERT	08L	PRL 100 051802	B. Aubert *et al.*	(BABAR Collab.)
AUBERT	08M	PRL 100 061803	B. Aubert *et al.*	(BABAR Collab.)
AUBERT	08U	PR D78 011105	B. Aubert *et al.*	(BABAR Collab.)
BITENC	08	PR D77 112003	U. Bitenc *et al.*	(BELLE Collab.)
BONVICINI	08	PR D77 091106	G. Bonvicini *et al.*	(CLEO Collab.)
DOBBS	08	PR D77 112005	S. Dobbs *et al.*	(CLEO Collab.)
Also		PRL 100 251802	D. Cronin-Hennessy *et al.*	(CLEO Collab.)
GASPERO	08	PR D78 014015	M. Gaspero *et al.*	(ROMA, CINN, TELA)
HE	08	PRL 100 091801	Q. He *et al.*	(CLEO Collab.)
PDG	08	PL B667 1	C. Amsler *et al.*	(PDG Collab.)
STARIC	08	PL B670 190	M. Staric *et al.*	(BELLE Collab.)
ABLIKIM	07G	PL B658 1	M. Ablikim *et al.*	(BES Collab.)
ARTUSO	07A	PRL 99 191801	M. Artuso *et al.*	(CLEO Collab.)
AUBERT	07AB	PR D76 014018	B. Aubert *et al.*	(BABAR Collab.)
AUBERT	07BG	PR D76 052005	B. Aubert *et al.*	(BABAR Collab.)
AUBERT	07BJ	PRL 99 251801	B. Aubert *et al.*	(BABAR Collab.)
AUBERT	07T	PR D76 011102	B. Aubert *et al.*	(BABAR Collab.)
AUBERT	07W	PRL 98 211802	B. Aubert *et al.*	(BABAR Collab.)
CAWLFIELD	07	PRL 98 092002	C. Cawlfield *et al.*	(CLEO Collab.)
DOBBS	07	PR D76 112001	S. Dobbs *et al.*	(CLEO Collab.)
LINK	07A	PR D75 052003	J.M. Link *et al.*	(FNAL FOCUS Collab.)
STARIC	07	PRL 98 211803	M. Staric *et al.*	(BELLE Collab.)
ZHANG	07B	PRL 99 131803	L.M. Zhang *et al.*	(BELLE Collab.)
ABLIKIM	06O	EPJ C47 31	M. Ablikim *et al.*	(BES Collab.)
ABLIKIM	06U	PL B643 246	M. Ablikim *et al.*	(BES Collab.)
ABULENCIA	06X	PR D74 031109	A. Abulencia *et al.*	(CDF Collab.)
ADAM	06A	PRL 97 251801	N.E. Adam *et al.*	(CLEO Collab.)
AUBERT,B	06N	PRL 97 221803	B. Aubert *et al.*	(BABAR Collab.)
AUBERT,B	06X	PR D74 091102	B. Aubert *et al.*	(BABAR Collab.)
CAWLFIELD	06A	PR D74 031108	C. Cawlfield *et al.*	(CLEO Collab.)
HUANG	06B	PR D74 112005	G.S. Huang *et al.*	(CLEO Collab.)
PDG	06	JP G33 1	W.-M. Yao *et al.*	(PDG Collab.)
RUBIN	06	PRL 96 081802	P. Rubin *et al.*	(CLEO Collab.)
WIDHALM	06	PRL 97 061804	L. Widhalm *et al.*	(BELLE Collab.)
ZHANG	06	PRL 96 151801	L.M. Zhang *et al.*	(BELLE Collab.)
ABLIKIM	05F	PL B622 6	M. Ablikim *et al.*	(BES Collab.)
ABLIKIM	05P	PL B625 196	M. Ablikim *et al.*	(BES Collab.)
ACOSTA	05C	PRL 94 122001	D. Acosta *et al.*	(FNAL CDF Collab.)
ASNER	05	PR D72 012001	D.M. Asner *et al.*	(CLEO Collab.)
AUBERT,B	05J	PR D72 052008	B. Aubert *et al.*	(BABAR Collab.)
BITENC	05	PR D72 071101	U. Bitenc *et al.*	(BELLE Collab.)
CAWLFIELD	05	PR D71 077101	C. Cawlfield *et al.*	(CLEO Collab.)
COAN	05	PRL 95 181802	T.E. Coan *et al.*	(CLEO Collab.)
CRONIN-HEN...	05	PR D72 031102	D. Cronin-Hennessy *et al.*	(CLEO Collab.)
HE	05	PRL 95 121801	Q. He *et al.*	(CLEO Collab.)
Also		PRL 96 199903 (errat.)	Q. He *et al.*	(CLEO Collab.)
HUANG	05	PRL 94 011802	G.S. Huang *et al.*	(CLEO Collab.)
KAYIS-TOPAK...	05	PL B626 24	A. Kayis-Topaksu *et al.*	(CERN CHORUS Collab.)
LI	05A	PRL 94 071801	J. Li *et al.*	(BELLE Collab.)
LINK	05	PL B607 51	J.M. Link *et al.*	(FNAL FOCUS Collab.)
LINK	05A	PL B607 59	J.M. Link *et al.*	(FNAL FOCUS Collab.)
LINK	05B	PL B607 67	J.M. Link *et al.*	(FNAL FOCUS Collab.)
LINK	05E	PL B622 239	J.M. Link *et al.*	(FNAL FOCUS Collab.)
LINK	05G	PL B610 225	J.M. Link *et al.*	(FNAL FOCUS Collab.)
LINK	05H	PL B618 23	J.M. Link *et al.*	(FNAL FOCUS Collab.)
ONENGUT	05	PL B613 105	G. Onengut *et al.*	(CERN CHORUS Collab.)
TIAN	05	PRL 95 231801	X.C. Tian *et al.*	(BELLE Collab.)
ABLIKIM	04C	PL B597 39	M. Ablikim *et al.*	(BEPC BES Collab.)
ABT	04	PL B596 173	I. Abt *et al.*	(HERA B Collab.)
ASNER	04A	PR D70 091101	D.M. Asner *et al.*	(CLEO Collab.)
AUBERT	04Q	PR D69 051101	B. Aubert *et al.*	(BABAR Collab.)
AUBERT,B	04Q	PR D70 091102	B. Aubert *et al.*	(BABAR Collab.)
AUBERT,B	04Y	PRL 93 191801	B. Aubert *et al.*	(BaBar Collab)
LINK	04B	PL B586 21	J.M. Link *et al.*	(FNAL FOCUS Collab.)
LINK	04D	PL B586 191	J.M. Link *et al.*	(FNAL FOCUS Collab.)
RUBIN	04	PRL 93 111801	P. Rubin *et al.*	(CLEO Collab.)
TAJIMA	04	PRL 92 101803	O. Tajima *et al.*	(BELLE Collab.)
ACOSTA	03F	PR D68 091101	D. Acosta *et al.*	(CDF Collab.)
AUBERT	03P	PRL 91 121801	B. Aubert *et al.*	(BaBar Collab.)
AUBERT	03Z	PRL 91 171801	B. Aubert *et al.*	(BaBar Collab.)
COAN	03	PRL 90 101801	T.E. Coan *et al.*	(CLEO Collab.)
LINK	03	PL B555 167	J.M. Link *et al.*	(FNAL FOCUS Collab.)
LINK	03B	PL B556 7	J.M. Link *et al.*	(FNAL FOCUS Collab.)
LINK	03G	PL B575 190	J.M. Link *et al.*	(FNAL FOCUS Collab.)
ABE	02I	PR D88 162001	K. Abe *et al.*	(KEK BELLE Collab.)
CSORNA	02	PR D65 092001	S.E. Csorna *et al.*	(CLEO Collab.)
LINK	02F	PL B537 192	J.M. Link *et al.*	(FNAL FOCUS Collab.)
MURAMATSU	02	PRL 89 251802	H. Muramatsu *et al.*	(CLEO Collab.)
Also		PRL 90 059901 (errat)	H. Muramatsu *et al.*	(CLEO Collab.)
AITALA	01C	PRL 86 3969	E.M. Aitala *et al.*	(FNAL E791 Collab.)
AITALA	01D	PR D64 112003	E.M. Aitala *et al.*	(FNAL E791 Collab.)
BONVICINI	01	PR D63 071101	G. Bonvicini *et al.*	(CLEO Collab.)
BRANDENB...	01	PRL 87 071802	G. Brandenburg *et al.*	(CLEO Collab.)
DYTMAN	01	PR D64 111101	S.A. Dytman *et al.*	(CLEO Collab.)
KOPP	01	PR D63 092001	S. Kopp *et al.*	(CLEO Collab.)
KUSHNIR...	01	PRL 86 5243	A. Kushnirenko *et al.*	(FNAL SELEX Collab.)
LINK	01	PRL 86 2955	J.M. Link *et al.*	(FNAL FOCUS Collab.)
BAI	00C	PR D62 052001	J.Z. Bai *et al.*	(BEPC BES Collab.)
GODANG	00	PRL 84 5038	R. Godang *et al.*	(CLEO Collab.)
JUN	00	PRL 84 1857	S.Y. Jun *et al.*	(FNAL SELEX Collab.)
LINK	00	PL B485 62	J.M. Link *et al.*	(FNAL FOCUS Collab.)
LINK	00B	PL B491 232	J.M. Link *et al.*	(FNAL FOCUS Collab.)
Also		PL B495 443 (errat)	J.M. Link *et al.*	(FNAL FOCUS Collab.)
PRIPSTEIN	00	PR D61 032005	D. Pripstein *et al.*	(FNAL E789 Collab.)
AITALA	99E	PRL 83 32	E.M. Aitala *et al.*	(FNAL E791 Collab.)
AITALA	99G	PL B462 401	E.M. Aitala *et al.*	(FNAL E791 Collab.)
BONVICINI	99	PRL 82 4586	G. Bonvicini *et al.*	(CLEO Collab.)
AITALA	98	PR D57 13	E.M. Aitala *et al.*	(FNAL E791 Collab.)
AITALA	98C	PL B421 405	E.M. Aitala *et al.*	(FNAL E791 Collab.)
AITALA	98D	PL B423 185	E.M. Aitala *et al.*	(FNAL E791 Collab.)
ARTUSO	98	PRL 80 3193	M. Artuso *et al.*	(CLEO Collab.)
ASNER	98	PR D58 092001	D.M. Asner *et al.*	(CLEO Collab.)
BARATE	98W	PL B436 211	R. Barate *et al.*	(ALEPH Collab.)
COAN	98	PRL 80 1150	T.E. Coan *et al.*	(CLEO Collab.)
PDG	98	EPJ C3 1	C. Caso *et al.*	(PDG Collab.)
ADAMOVICH	97	PL B408 469	M.I. Adamovich *et al.*	(CERN BEATRICE Collab.)
BARATE	97C	PL B403 367	R. Barate *et al.*	(ALEPH Collab.)
AITALA	96C	PRL 77 2384	E.M. Aitala *et al.*	(FNAL E791 Collab.)
ALBRECHT	96C	PL B374 249	H. Albrecht *et al.*	(ARGUS Collab.)
ALEXOPOU...	96	PRL 77 2380	T. Alexopoulos *et al.*	(FNAL E771 Collab.)
ASNER	96B	PR D54 4211	D.M. Asner *et al.*	(CLEO Collab.)
BARISH	96	PL B373 334	B.C. Barish *et al.*	(CLEO Collab.)
FRABETTI	96B	PL B382 312	P.L. Frabetti *et al.*	(FNAL E687 Collab.)
FREYBERGER	96	PRL 76 3065	A. Freyberger *et al.*	(CLEO Collab.)
Also		PRL 77 2147 (erratum)	A. Freyberger *et al.*	(CLEO Collab.)
KUBOTA	96B	PR D54 2994	Y. Kubota *et al.*	(CLEO Collab.)
ADAMOVICH	95	PL B353 563	M.I. Adamovich *et al.*	(CERN BEATRICE Collab.)
BARTELT	95	PR D52 4860	J.E. Bartelt *et al.*	(CLEO Collab.)
BUTLER	95	PR D52 2656	F. Butler *et al.*	(CLEO Collab.)
FRABETTI	95C	PL B354 486	P.L. Frabetti *et al.*	(FNAL E687 Collab.)
FRABETTI	95G	PL B364 127	P.L. Frabetti *et al.*	(FNAL E687 Collab.)
KODAMA	95	PL B345 85	K. Kodama *et al.*	(FNAL E653 Collab.)
ALBRECHT	94	PL B324 249	H. Albrecht *et al.*	(ARGUS Collab.)
ALBRECHT	94F	PL B340 125	H. Albrecht *et al.*	(ARGUS Collab.)
ALBRECHT	94I	ZPHY C64 375	H. Albrecht *et al.*	(ARGUS Collab.)
FRABETTI	94C	PL B321 295	P.L. Frabetti *et al.*	(FNAL E687 Collab.)
FRABETTI	94D	PL B323 459	P.L. Frabetti *et al.*	(FNAL E687 Collab.)
FRABETTI	94G	PL B331 217	P.L. Frabetti *et al.*	(FNAL E687 Collab.)
FRABETTI	94J	PL B340 254	P.L. Frabetti *et al.*	(FNAL E687 Collab.)
KODAMA	94	PL B336 605	K. Kodama *et al.*	(FNAL E653 Collab.)
MISHRA	94	PR D50 R9	C.S. Mishra *et al.*	(FNAL E789 Collab.)
AKERIB	93	PRL 71 3070	D.S. Akerib *et al.*	(CLEO Collab.)
ALBRECHT	93D	PL B308 435	H. Albrecht *et al.*	(ARGUS Collab.)
ANJOS	93	PR D48 56	J.C. Anjos *et al.*	(FNAL E691 Collab.)
BEAN	93C	PL B317 647	A. Bean *et al.*	(CLEO Collab.)
FRABETTI	93I	PL B315 203	P.L. Frabetti *et al.*	(FNAL E687 Collab.)
KODAMA	93B	PL B313 260	K. Kodama *et al.*	(FNAL E653 Collab.)
PROCARIO	93B	PR D48 4007	M. Procario *et al.*	(CLEO Collab.)
SELEN	93	PRL 71 1973	M.A. Selen *et al.*	(CLEO Collab.)
ADAMOVICH	92	PL B280 163	M.I. Adamovich *et al.*	(CERN WA82 Collab.)
ALBRECHT	92P	ZPHY C56 7	H. Albrecht *et al.*	(ARGUS Collab.)
ANJOS	92B	PR D46 R1	J.C. Anjos *et al.*	(FNAL E691 Collab.)

Meson Particle Listings

D^0, $D^*(2007)^0$

ANJOS	92C	PR D46 1941	J.C. Anjos *et al.*	(FNAL E691 Collab.)
BARLAG	92C	ZPHY C55 383	S. Barlag *et al.*	(ACCMOR Collab.)
Also		ZPHY C48 29	S. Barlag *et al.*	(ACCMOR Collab.)
COFFMAN	92B	PR D45 2196	D.M. Coffman *et al.*	(Mark III Collab.)
Also		PRL 64 2615	J. Adler *et al.*	(Mark III Collab.)
FRABETTI	92	PL B281 167	P.L. Frabetti *et al.*	(FNAL E687 Collab.)
FRABETTI	92B	PL B286 195	P.L. Frabetti *et al.*	(FNAL E687 Collab.)
ALVAREZ	91B	ZPHY C50 11	M.P. Alvarez *et al.*	(CERN NA14/2 Collab.)
AMMAR	91	PR D44 3383	R. Ammar *et al.*	(CLEO Collab.)
ANJOS	91	PR D43 R635	J.C. Anjos *et al.*	(FNAL-TPS Collab.)
ANJOS	91D	PR D44 R3371	J.C. Anjos *et al.*	(FNAL-TPS Collab.)
BAI	91	PRL 66 1011	Z. Bai *et al.*	(Mark III Collab.)
COFFMAN	91	PL B263 135	D.M. Coffman *et al.*	(Mark III Collab.)
CRAWFORD	91B	PR D44 3394	G. Crawford *et al.*	(CLEO Collab.)
DECAMP	91J	PL B266 218	D. Decamp *et al.*	(ALEPH Collab.)
FRABETTI	91	PL B263 584	P.L. Frabetti *et al.*	(FNAL E687 Collab.)
KINOSHITA	91	PR D43 2836	K. Kinoshita *et al.*	(CLEO Collab.)
KODAMA	91	PRL 66 1819	K. Kodama *et al.*	(FNAL E653 Collab.)
ALBRECHT	90C	ZPHY C46 9	H. Albrecht *et al.*	(ARGUS Collab.)
ALEXANDER	90	PRL 65 1184	J. Alexander *et al.*	(CLEO Collab.)
ALVAREZ	90	ZPHY C47 539	M.P. Alvarez *et al.*	(CERN NA14/2 Collab.)
ANJOS	90D	PR D42 2414	J.C. Anjos *et al.*	(FNAL E691 Collab.)
BARLAG	90C	ZPHY C46 563	S. Barlag *et al.*	(ACCMOR Collab.)
ADLER	89	PRL 62 1821	J. Adler *et al.*	(Mark III Collab.)
ADLER	89C	PR D40 906	J. Adler *et al.*	(Mark III Collab.)
ALBRECHT	89D	ZPHY C43 181	H. Albrecht *et al.*	(ARGUS Collab.)
ANJOS	89F	PRL 62 1587	J.C. Anjos *et al.*	(FNAL E691 Collab.)
ABACHI	88	PL B205 411	S. Abachi *et al.*	(HRS Collab.)
ADLER	88	PR D37 2023	J. Adler *et al.*	(Mark III Collab.)
ADLER	88C	PRL 60 89	J. Adler *et al.*	(Mark III Collab.)
ALBRECHT	88G	PL B209 380	H. Albrecht *et al.*	(ARGUS Collab.)
ALBRECHT	88I	PL B210 267	H. Albrecht *et al.*	(ARGUS Collab.)
ANJOS	88C	PRL 60 1239	J.C. Anjos *et al.*	(FNAL E691 Collab.)
BORTOLETTO	88	PR D37 1719	D. Bortoletto *et al.*	(CLEO Collab.)
Also		PR D39 1471 (erratum)	D. Bortoletto *et al.*	(CLEO Collab.)
HAAS	88	PRL 60 1614	P. Haas *et al.*	(CLEO Collab.)
RAAB	88	PR D37 2391	J.R. Raab *et al.*	(FNAL E691 Collab.)
ADAMOVICH	87	EPL 4 887	M.I. Adamovich *et al.*	(Photon Emulsion Collab.)
ADLER	87	PL B196 107	J. Adler *et al.*	(Mark III Collab.)
AGUILAR-...	87E	ZPHY C36 551	M. Aguilar-Benitez *et al.*	(LEBC-EHS Collab.)
Also		ZPHY C40 321	M. Aguilar-Benitez *et al.*	(LEBC-EHS Collab.)
AGUILAR-...	87F	ZPHY C36 559	M. Aguilar-Benitez *et al.*	(LEBC-EHS Collab.)
Also		ZPHY C38 520 (erratum)	M. Aguilar-Benitez *et al.*	(LEBC-EHS Collab.)
BARLAG	87B	ZPHY C37 17	S. Barlag *et al.*	(ACCMOR Collab.)
BECKER	87C	PL B193 147	J.J. Becker *et al.*	(Mark III Collab.)
Also		PL B198 590 (erratum)	J.J. Becker *et al.*	(Mark III Collab.)
PALKA	87	PL B189 238	H. Palka *et al.*	(ACCMOR Collab.)
RILES	87	PR D35 2914	K. Riles *et al.*	(Mark II Collab.)
BAILEY	86	ZPHY C30 51	R. Bailey *et al.*	(ACCMOR Collab.)
BEBEK	86	PRL 56 1893	C. Bebek *et al.*	(CLEO Collab.)
LOUIS	86	PRL 56 1027	W.C. Louis *et al.*	(PRIN, CHIC, ISU)
ALBRECHT	85B	PL 158B 525	H. Albrecht *et al.*	(ARGUS Collab.)
ALBRECHT	85F	PL 150B 235	H. Albrecht *et al.*	(ARGUS Collab.)
AUBERT	85	PL 155B 461	J.J. Aubert *et al.*	(EMC Collab.)
BALTRUSAIT...	85E	PRL 55 150	R.M. Baltrusaitis *et al.*	(Mark III Collab.)
BENVENUTI	85	PL 158B 531	A.C. Benvenuti *et al.*	(BCDMS Collab.)
ADAMOVICH	84B	PL 140B 123	M.I. Adamovich *et al.*	(CERN WA58 Collab.)
DERRICK	84	PRL 53 1971	M. Derrick *et al.*	(HRS Collab.)
SUMMERS	84	PRL 52 410	D.J. Summers *et al.*	(UCSB, CARL, COLO+)
BAILEY	83B	PL 132B 237	R. Bailey *et al.*	(ACCMOR Collab.)
BODEK	82	PL 113B 82	A. Bodek *et al.*	(ROCH, CIT, CHIC, FNAL+)
FIORINO	81	LNC 30 166	A. Fiorino *et al.*	(Photon-Emul/Omega-Photon)
SCHINDLER	81	PR D24 78	R.H. Schindler *et al.*	(Mark II Collab.)
TRILLING	81	PRPL 75 57	G.H. Trilling	(LBL, UCB) J
ASTON	80E	PL 94B 113	D. Aston *et al.*	(BONN, CERN, EPOL, GLAS+)
AVERY	80	PRL 44 1309	P. Avery *et al.*	(ILL, FNAL, COLU)
ZHOLENTZ	80	PL 96B 214	A.A. Zholents *et al.*	(NOVO)
Also		SJNP 34 814	A.A. Zholents *et al.*	(NOVO)
		Translated from YAF 34 1471.		
ABRAMS	79D	PRL 43 481	G.S. Abrams *et al.*	(Mark II Collab.)
ATIYA	79	PRL 43 414	M.S. Atiya *et al.*	(COLU, ILL, FNAL)
BALTAY	78C	PRL 41 73	C. Baltay *et al.*	(COLU, BNL)
VUILLEMIN	78	PRL 41 1149	V. Vuillemin *et al.*	(LGW Collab.)
GOLDHABER	77	PL 69B 503	G. Goldhaber *et al.*	(Mark I Collab.)
PERUZZI	77	PRL 39 1301	I. Peruzzi *et al.*	(LGW Collab.)
PICCOLO	77	PL 70B 260	M. Piccolo *et al.*	(Mark I Collab.)
GOLDHABER	76	PRL 37 255	G. Goldhaber *et al.*	(Mark I Collab.)

OTHER RELATED PAPERS

RICHMAN	95	RMP 67 893	J.D. Richman, P.R. Burchat	(UCSB, STAN)
ROSNER	95	CNPP 21 369	J. Rosner	(CHIC)

$D^*(2007)^0$

$I(J^P) = \frac{1}{2}(1^-)$
I, J, P need confirmation.

J consistent with 1, value 0 ruled out (NGUYEN 77).

$D^*(2007)^0$ MASS

The fit includes $D^\pm$, D^0, $D_s^\pm$, $D^{*\pm}$, D^{*0}, $D_s^{*\pm}$, $D_1(2420)^0$, $D_2^*(2460)^0$, and $D_{s1}(2536)^\pm$ mass and mass difference measurements.

VALUE (MeV)	DOCUMENT ID	TECN	COMMENT
2006.96±0.10 OUR FIT			
• • • We do not use the following data for averages, fits, limits, etc. • • •			
2006 ±1.5	[1] GOLDHABER 77	MRK1	e^+e^-

[1] From simultaneous fit to $D^*(2010)^+$, $D^*(2007)^0$, D^+, and D^0.

$m_{D^*(2007)^0} - m_{D^0}$

The fit includes $D^\pm$, D^0, $D_s^\pm$, $D^{*\pm}$, D^{*0}, $D_s^{*\pm}$, $D_1(2420)^0$, $D_2^*(2460)^0$, and $D_{s1}(2536)^\pm$ mass and mass difference measurements.

VALUE (MeV)	EVTS	DOCUMENT ID	TECN	COMMENT
142.12±0.07 OUR FIT				
142.12±0.07 OUR AVERAGE				
142.2 ±0.3 ±0.2	145	ALBRECHT 95F	ARG	$e^+e^- \to$ hadrons
142.12±0.05±0.05	1176	BORTOLETTO 92B	CLE2	$e^+e^- \to$ hadrons
• • • We do not use the following data for averages, fits, limits, etc. • • •				
142.2 ±2.0		SADROZINSKI 80	CBAL	$D^{*0} \to D^0\pi^0$
142.7 ±1.7		[2] GOLDHABER 77	MRK1	e^+e^-

[2] From simultaneous fit to $D^*(2010)^+$, $D^*(2007)^0$, D^+, and D^0.

$D^*(2007)^0$ WIDTH

VALUE (MeV)	CL%	DOCUMENT ID	TECN	COMMENT
<2.1	90	[3] ABACHI 88B	HRS	$D^{*0} \to D^+\pi^-$

[3] Assuming $m_{D^{*0}} = 2007.2 \pm 2.1$ MeV/c^2.

$D^*(2007)^0$ DECAY MODES

$\overline{D}{}^*(2007)^0$ modes are charge conjugates of modes below.

	Mode	Fraction (Γ_i/Γ)
Γ_1	$D^0\pi^0$	(61.9±2.9) %
Γ_2	$D^0\gamma$	(38.1±2.9) %

CONSTRAINED FIT INFORMATION

An overall fit to a branching ratio uses 3 measurements and one constraint to determine 2 parameters. The overall fit has a $\chi^2 = 0.5$ for 2 degrees of freedom.

The following *off-diagonal* array elements are the correlation coefficients $\langle \delta x_i \delta x_j \rangle / (\delta x_i \cdot \delta x_j)$, in percent, from the fit to the branching fractions, $x_i \equiv \Gamma_i/\Gamma_{\rm total}$. The fit constrains the x_i whose labels appear in this array to sum to one.

x_2 | −100
x_1

$D^*(2007)^0$ BRANCHING RATIOS

$\Gamma(D^0\pi^0)/\Gamma(D^0\gamma)$ — **Γ_1/Γ_2**

VALUE	DOCUMENT ID	TECN	COMMENT
1.74±0.02±0.13	AUBERT,BE 05G	BABR	10.6 e^+e^- → hadrons

$\Gamma(D^0\pi^0)/\Gamma_{\rm total}$ — **Γ_1/Γ**

VALUE	EVTS	DOCUMENT ID	TECN	COMMENT
0.619±0.029 OUR FIT				
• • • We do not use the following data for averages, fits, limits, etc. • • •				
0.635±0.003±0.017	69k	[4] AUBERT,BE 05G	BABR	10.6 e^+e^- → hadrons
0.596±0.035±0.028	858	[5] ALBRECHT 95F	ARG	$e^+e^- \to$ hadrons
0.636±0.023±0.033	1097	[5] BUTLER 92	CLE2	$e^+e^- \to$ hadrons

$\Gamma(D^0\gamma)/\Gamma_{\rm total}$ — **Γ_2/Γ**

VALUE	EVTS	DOCUMENT ID	TECN	COMMENT
0.381±0.029 OUR FIT				
0.381±0.029 OUR AVERAGE				
0.404±0.035±0.028	456	[5] ALBRECHT 95F	ARG	$e^+e^- \to$ hadrons
0.364±0.023±0.033	621	[5] BUTLER 92	CLE2	$e^+e^- \to$ hadrons
0.37 ±0.08 ±0.08		ADLER 88D	MRK3	e^+e^-
• • • We do not use the following data for averages, fits, limits, etc. • • •				
0.365±0.003±0.017	68k	[4] AUBERT,BE 05G	BABR	10.6 e^+e^- → hadrons
0.47 ±0.23		LOW 87	HRS	29 GeV e^+e^-
0.53 ±0.13		BARTEL 85G	JADE	e^+e^-, hadrons
0.47 ±0.12		COLES 82	MRK2	e^+e^-
0.45 ±0.15		GOLDHABER 77	MRK1	e^+e^-

[4] Derived from the ratio $\Gamma(D^0\pi^0)$ / $\Gamma(D^0\gamma)$ assuming that the branching fractions of $D^{*0} \to D^0\pi^0$ and $D^{*0} \to D^0\gamma$ decays sum to 100%

[5] The BUTLER 92 and ALBRECHT 95F branching ratios are not independent, they have been constrained by the authors to sum to 100%.

$D^*(2007)^0$ REFERENCES

AUBERT,BE	05G	PR D72 091101	B. Aubert *et al.*	(BABAR Collab.)
ALBRECHT	95F	ZPHY C66 63	H. Albrecht *et al.*	(ARGUS Collab.)
BORTOLETTO	92B	PRL 69 2046	D. Bortoletto *et al.*	(CLEO Collab.)
BUTLER	92	PRL 69 2041	F. Butler *et al.*	(CLEO Collab.)
ABACHI	88B	PL B212 533	S. Abachi *et al.*	(ANL, IND, MICH, PURD+)
ADLER	88D	PL B208 152	J. Adler *et al.*	(Mark III Collab.)
LOW	87	PL B183 232	E.H. Low *et al.*	(HRS Collab.)
BARTEL	85G	PL 161B 197	W. Bartel *et al.*	(JADE Collab.)
COLES	82	PR D26 2190	M.W. Coles *et al.*	(LBL, SLAC)
SADROZINSKI	80	Madison Conf. 681	H.F.W. Sadrozinski *et al.*	(PRIN, CIT+)
GOLDHABER	77	PL 69B 503	G. Goldhaber *et al.*	(Mark I Collab.)
NGUYEN	77	PRL 39 262	H.K. Nguyen *et al.*	(LBL, SLAC) J

$D^*(2010)^\pm$

$I(J^P) = \frac{1}{2}(1^-)$
I, J, P need confirmation.

$D^*(2010)^\pm$ MASS

The fit includes $D^\pm$, D^0, $D_s^\pm$, $D^{*\pm}$, D^{*0}, $D_s^{*\pm}$, $D_1(2420)^0$, $D_2^*(2460)^0$, and $D_{s1}(2536)^\pm$ mass and mass difference measurements.

VALUE (MeV)	DOCUMENT ID	TECN	CHG	COMMENT
2010.26±0.07 OUR FIT	Error includes scale factor of 1.1.			
• • • We do not use the following data for averages, fits, limits, etc. • • •				
2008 ±3	[1] GOLDHABER 77	MRK1	±	e^+e^-
2008.6 ±1.0	[2] PERUZZI 77	LGW	±	e^+e^-

[1] From simultaneous fit to $D^*(2010)^+$, $D^*(2007)^0$, D^+, and D^0; not independent of FELDMAN 77B mass difference below.
[2] PERUZZI 77 mass not independent of FELDMAN 77B mass difference below and PERUZZI 77 D^0 mass value.

$m_{D^*(2010)^+} - m_{D^+}$

The fit includes $D^\pm$, D^0, $D_s^\pm$, $D^{*\pm}$, D^{*0}, $D_s^{*\pm}$, $D_1(2420)^0$, $D_2^*(2460)^0$, and $D_{s1}(2536)^\pm$ mass and mass difference measurements.

VALUE (MeV)	EVTS	DOCUMENT ID	TECN	COMMENT
140.66±0.08 OUR FIT				
140.64±0.08±0.06	620	BORTOLETTO92B	CLE2	$e^+e^- \to$ hadrons

$m_{D^*(2010)^+} - m_{D^0}$

The fit includes $D^\pm$, D^0, $D_s^\pm$, $D^{*\pm}$, D^{*0}, $D_s^{*\pm}$, $D_1(2420)^0$, $D_2^*(2460)^0$, and $D_{s1}(2536)^\pm$ mass and mass difference measurements.

VALUE (MeV)	EVTS	DOCUMENT ID	TECN	COMMENT
145.4257±0.0017 OUR FIT				
145.4258±0.0020 OUR AVERAGE		Error includes scale factor of 1.2.		
145.4259±0.0004±0.0017	312.8k	LEES 13X	BABR	$D^{*\pm} \to D^0\pi^\pm \to (K\pi,K3\pi)\pi^\pm$
145.412 ±0.002 ±0.012		ANASTASSOV 02	CLE2	$D^{*\pm} \to D^0\pi^\pm \to (K\pi)\pi^\pm$
145.54 ±0.08	611	[3] ADINOLFI 99	BEAT	$D^{*\pm} \to D^0\pi^\pm$
145.45 ±0.02		[3] BREITWEG 99	ZEUS	$D^{*\pm} \to D^0\pi^\pm \to (K\pi)\pi^\pm$
145.42 ±0.05		[3] BREITWEG 99	ZEUS	$D^{*\pm} \to D^0\pi^\pm \to (K^-3\pi)\pi^\pm$
145.5 ±0.15	103	[4] ADLOFF 97B	H1	$D^{*\pm} \to D^0\pi^\pm$
145.44 ±0.08	152	[4] BREITWEG 97	ZEUS	$D^{*\pm} \to D^0\pi^\pm$, $D^0 \to K^-3\pi$
145.42 ±0.11	199	[4] BREITWEG 97	ZEUS	$D^{*\pm} \to D^0\pi^\pm$, $D^0 \to K^-\pi^+$
145.4 ±0.2	48	[4] DERRICK 95	ZEUS	$D^{*\pm} \to D^0\pi^\pm$
145.39 ±0.06 ±0.03		BARLAG 92B	ACCM	π^- 230 GeV
145.5 ±0.2	115	[4] ALEXANDER 91B	OPAL	$D^{*\pm} \to D^0\pi^\pm$
145.30 ±0.06		[4] DECAMP 91J	ALEP	$D^{*\pm} \to D^0\pi^\pm$
145.40 ±0.05 ±0.10		ABACHI 88B	HRS	$D^{*\pm} \to D^0\pi^\pm$
145.46 ±0.07 ±0.03		ALBRECHT 85F	ARG	$D^{*\pm} \to D^0\pi^+$
145.5 ±0.3	28	BAILEY 83	SPEC	$D^{*\pm} \to D^0\pi^\pm$
145.5 ±0.3	60	FITCH 81	SPEC	π^- A
145.3 ±0.5	30	FELDMAN 77B	MRK1	$D^{*+} \to D^0\pi^+$
• • • We do not use the following data for averages, fits, limits, etc. • • •				
145.4256±0.0006±0.0017	138.5k	LEES 13X	BABR	$D^{*\pm} \to D^0\pi^\pm \to (K^-\pi^+)\pi^\pm$
145.4266±0.0005±0.0019	174.3k	LEES 13X	BABR	$D^{*\pm} \to D^0\pi^\pm \to (K^-2\pi^+\pi^-)\pi^\pm$
145.44 ±0.09	122	[4] BREITWEG 97B	ZEUS	$D^{*\pm} \to D^0\pi^\pm$, $D^0 \to K^-\pi^+$
145.8 ±1.5	16	AHLEN 83	HRS	$D^{*+} \to D^0\pi^+$
145.1 ±1.8	12	BAILEY 83	SPEC	$D^{*\pm} \to D^0\pi^\pm$
145.1 ±0.5	14	BAILEY 83	SPEC	$D^{*\pm} \to D^0\pi^\pm$
145.5 ±0.5	14	YELTON 82	MRK2	29 $e^+e^- \to K^-\pi^+$
~ 145.5		AVERY 80	SPEC	γA
145.2 ±0.6	2	BLIETSCHAU 79	BEBC	νp

[3] Statistical errors only.
[4] Systematic error not evaluated.

$m_{D^*(2010)^+} - m_{D^*(2007)^0}$

VALUE (MeV)	DOCUMENT ID	TECN	COMMENT
• • • We do not use the following data for averages, fits, limits, etc. • • •			
2.6±1.8	[5] PERUZZI 77	LGW	e^+e^-

[5] Not independent of FELDMAN 77B mass difference above, PERUZZI 77 D^0 mass, and GOLDHABER 77 $D^*(2007)^0$ mass.

$D^*(2010)^\pm$ WIDTH

VALUE (keV)	CL%	EVTS	DOCUMENT ID	TECN	COMMENT
83.4±1.8 OUR AVERAGE					
83.3±1.2± 1.4		312.8k	[6] LEES 13X	BABR	$D^{*\pm} \to D^0\pi^\pm \to (K\pi,K3\pi)\pi^\pm$
96 ±4 ±22			[6] ANASTASSOV 02	CLE2	$D^{*\pm} \to D^0\pi^\pm \to (K\pi)\pi^\pm$
• • • We do not use the following data for averages, fits, limits, etc. • • •					
83.4±1.7± 1.5		138.5k	[6] LEES 13X	BABR	$D^{*\pm} \to D^0\pi^\pm \to (K^-\pi^+)\pi^\pm$
83.2±1.5± 2.6		174.3k	[6] LEES 13X	BABR	$D^{*\pm} \to D^0\pi^\pm \to (K^-2\pi^+\pi^-)\pi^\pm$
<131	90	110	BARLAG 92B	ACCM	π^- 230 GeV

[6] Ignoring the electromagnetic contribution from $D^{*\pm} \to D^\pm\gamma$.

$D^*(2010)^\pm$ DECAY MODES

$D^*(2010)^-$ modes are charge conjugates of the modes below.

	Mode	Fraction (Γ_j/Γ)
Γ_1	$D^0\pi^+$	(67.7±0.5) %
Γ_2	$D^+\pi^0$	(30.7±0.5) %
Γ_3	$D^+\gamma$	(1.6±0.4) %

CONSTRAINED FIT INFORMATION

An overall fit to 3 branching ratios uses 6 measurements and one constraint to determine 3 parameters. The overall fit has a $\chi^2 = 0.3$ for 4 degrees of freedom.

The following *off-diagonal* array elements are the correlation coefficients $\langle \delta x_i \delta x_j \rangle / (\delta x_i \cdot \delta x_j)$, in percent, from the fit to the branching fractions, $x_i \equiv \Gamma_i/\Gamma_{total}$. The fit constrains the x_i whose labels appear in this array to sum to one.

x_2	−62		
x_3	−43	−44	
	x_1	x_2	

$D^*(2010)^+$ BRANCHING RATIOS

$\Gamma(D^0\pi^+)/\Gamma_{total}$ Γ_1/Γ

VALUE	DOCUMENT ID	TECN	COMMENT
0.677 ±0.005 OUR FIT			
0.677 ±0.006 OUR AVERAGE			
0.6759±0.0029±0.0064	[7,8,9] BARTELT 98	CLE2	e^+e^-
0.688 ±0.024 ±0.013	ALBRECHT 95F	ARG	$e^+e^- \to$ hadrons
0.681 ±0.010 ±0.013	[7] BUTLER 92	CLE2	$e^+e^- \to$ hadrons
• • • We do not use the following data for averages, fits, limits, etc. • • •			
0.57 ±0.04 ±0.04	ADLER 88D	MRK3	e^+e^-
0.44 ±0.10	COLES 82	MRK2	e^+e^-
0.6 ±0.15	[9] GOLDHABER 77	MRK1	e^+e^-

$\Gamma(D^+\pi^0)/\Gamma_{total}$ Γ_2/Γ

VALUE	EVTS	DOCUMENT ID	TECN	COMMENT
0.307 ±0.005 OUR FIT				
0.3073±0.0013±0.0062		[7,8,9] BARTELT 98	CLE2	e^+e^-
• • • We do not use the following data for averages, fits, limits, etc. • • •				
0.312 ±0.011 ±0.008	1404	ALBRECHT 95F	ARG	$e^+e^- \to$ hadrons
0.308 ±0.004 ±0.008	410	[7] BUTLER 92	CLE2	$e^+e^- \to$ hadrons
0.26 ±0.02 ±0.02		ADLER 88D	MRK3	e^+e^-
0.34 ±0.07		COLES 82	MRK2	e^+e^-

Meson Particle Listings

$D^*(2010)^\pm$, $D_0^*(2400)^0$, $D_0^*(2400)^\pm$, $D_1(2420)^0$

$\Gamma(D^+\gamma)/\Gamma_{\text{total}}$ Γ_3/Γ

VALUE	CL%	EVTS	DOCUMENT ID		TECN	COMMENT
0.016 ±0.004 OUR FIT						
0.016 ±0.005 OUR AVERAGE						
0.0168±0.0042±0.0029			[7,8] BARTELT	98	CLE2	e^+e^-
0.011 ±0.014 ±0.016		12	[7] BUTLER	92	CLE2	$e^+e^- \to$ hadrons
• • • We do not use the following data for averages, fits, limits, etc. • • •						
<0.052	90		ALBRECHT	95F	ARG	$e^+e^- \to$ hadrons
0.17 ±0.05 ±0.05			ADLER	88D	MRK3	e^+e^-
0.22 ±0.12			[10] COLES	82	MRK2	e^+e^-

[7] The branching ratios are not independent, they have been constrained by the authors to sum to 100%.
[8] Systematic error includes theoretical error on the prediction of the ratio of hadronic modes.
[9] Assuming that isospin is conserved in the decay.
[10] Not independent of $\Gamma(D^0\pi^+)/\Gamma_{\text{total}}$ and $\Gamma(D^+\pi^0)/\Gamma_{\text{total}}$ measurement.

$D^*(2010)^\pm$ REFERENCES

LEES	13X	PRL 111 111801	J.P. Lees *et al.*	(BABAR Collab.)
Also		PR D88 052003	J.P. Lees *et al.*	(BABAR Collab.)
Also		PR D88 079902 (errat.)	J.P. Lees *et al.*	(BABAR Collab.)
ANASTASSOV	02	PR D65 032003	A. Anastassov *et al.*	(CLEO Collab.)
ADINOLFI	99	NP B547 3	M. Adinolfi *et al.*	(Beatrice Collab.)
BREITWEG	99	EPJ C6 67	J. Breitweg *et al.*	(ZEUS Collab.)
BARTELT	98	PRL 80 3919	J. Bartelt *et al.*	(CLEO Collab.)
ADLOFF	97B	ZPHY C72 593	C. Adloff *et al.*	(H1 Collab.)
BREITWEG	97	PL B401 192	J. Breitweg *et al.*	(ZEUS Collab.)
BREITWEG	97B	PL B407 402	J. Breitweg *et al.*	(ZEUS Collab.)
ALBRECHT	95F	ZPHY C66 63	H. Albrecht *et al.*	(ARGUS Collab.)
DERRICK	95	PL B349 225	M. Derrick *et al.*	(ZEUS Collab.)
BARLAG	92B	PL B278 480	S. Barlag *et al.*	(ACCMOR Collab.)
BORTOLETTO	92B	PRL 69 2046	D. Bortoletto *et al.*	(CLEO Collab.)
BUTLER	92	PRL 69 2041	F. Butler *et al.*	(CLEO Collab.)
ALEXANDER	91B	PL B262 341	G. Alexander *et al.*	(OPAL Collab.)
DECAMP	91J	PL B266 218	D. Decamp *et al.*	(ALEPH Collab.)
ABACHI	88B	PL B212 533	S. Abachi *et al.*	(ANL, IND, MICH, PURD+)
ADLER	88D	PL B208 152	J. Adler *et al.*	(Mark III Collab.)
ALBRECHT	85F	PL 150B 235	H. Albrecht *et al.*	(ARGUS Collab.)
AHLEN	83	PRL 51 1147	S.P. Ahlen *et al.*	(ANL, IND, LBL+)
BAILEY	83	PL 132B 230	R. Bailey *et al.*	(AMST, BRIS, CERN, CRAC+)
COLES	82	PR D26 2190	M.W. Coles *et al.*	(LBL, SLAC)
YELTON	82	PRL 49 430	J.M. Yelton *et al.*	(SLAC, LBL, UCB+)
FITCH	81	PRL 46 761	V.L. Fitch *et al.*	(PRIN, SACL, TORI+)
AVERY	80	PRL 44 1309	P. Avery *et al.*	(ILL, FNAL, COLU)
BLIETSCHAU	79	PL 86B 108	J. Blietschau *et al.*	(AACH3, BONN, CERN+)
FELDMAN	77B	PRL 38 1313	G.J. Feldman *et al.*	(Mark I Collab.)
GOLDHABER	77	PL 69B 503	G. Goldhaber *et al.*	(Mark I Collab.)
PERUZZI	77	PRL 39 1301	I. Peruzzi *et al.*	(LGW Collab.)

$D_0^*(2400)^0$

$I(J^P) = \frac{1}{2}(0^+)$

$J^P = 0^+$ assignment favored (ABE 04D).

$D_0^*(2400)^0$ MASS

VALUE (MeV)	EVTS	DOCUMENT ID		TECN	COMMENT
2318±29 OUR AVERAGE Error includes scale factor of 1.7. See the ideogram below.					
2297± 8±20	3.4k	AUBERT	09AB	BABR	$B^- \to D^+\pi^-\pi^-$
2308±17±32		ABE	04D	BELL	$B^- \to D^+\pi^-\pi^-$
2407±21±35	9.8k	LINK	04A	FOCS	γ A

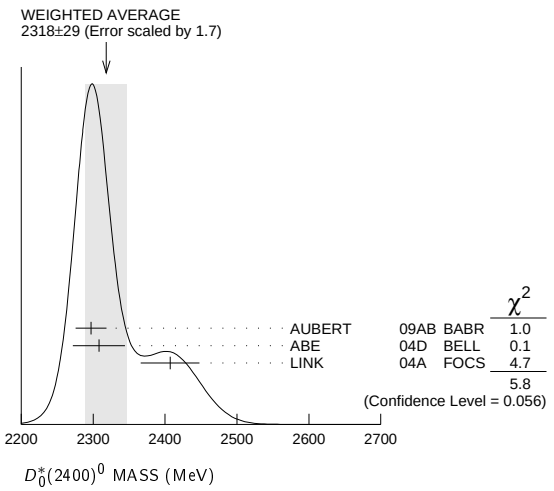

$D_0^*(2400)^0$ WIDTH

VALUE (MeV)	EVTS	DOCUMENT ID		TECN	COMMENT
267±40 OUR AVERAGE					
273±12±48	3.4k	AUBERT	09AB	BABR	$B^- \to D^+\pi^-\pi^-$
276±21±63		ABE	04D	BELL	$B^- \to D^+\pi^-\pi^-$
240±55±59	9.8k	LINK	04A	FOCS	γ A

$D_0^*(2400)^0$ DECAY MODES

	Mode	Fraction (Γ_i/Γ)
Γ_1	$D^+\pi^-$	seen

$D_0^*(2400)^0$ REFERENCES

AUBERT	09AB	PR D79 112004	B. Aubert *et al.*	(BABAR Collab.)
ABE	04D	PR D69 112002	K. Abe *et al.*	(BELLE Collab.)
LINK	04A	PL B586 11	J.M. Link *et al.*	(FOCUS Collab.)

$D_0^*(2400)^\pm$

$I(J^P) = \frac{1}{2}(0^+)$

OMITTED FROM SUMMARY TABLE
J, *P* need confirmation.

$D_0^*(2400)^\pm$ MASS

VALUE (MeV)	EVTS	DOCUMENT ID		TECN	COMMENT
2403±14±35	18.8k	LINK	04A	FOCS	γ A

$D_0^*(2400)^\pm$ WIDTH

VALUE (MeV)	EVTS	DOCUMENT ID		TECN	COMMENT
283±24±34	18.8k	LINK	04A	FOCS	γ A

$D_0^*(2400)^\pm$ DECAY MODES

	Mode	Fraction (Γ_i/Γ)
Γ_1	$D^0\pi^+$	seen

$D_0^*(2400)^\pm$ REFERENCES

LINK	04A	PL B586 11	J.M. Link *et al.*	(FOCUS Collab.)

$D_1(2420)^0$

$I(J^P) = \frac{1}{2}(1^+)$
I needs confirmation.

$D_1(2420)^0$ MASS

The fit includes $D^\pm$, D^0, $D_s^\pm$, $D^{*\pm}$, D^{*0}, $D_s^{*\pm}$, $D_1(2420)^0$, $D_2^*(2460)^0$, and $D_{s1}(2536)^\pm$ mass and mass difference measurements.

VALUE (MeV)	EVTS	DOCUMENT ID		TECN	COMMENT
2421.4±0.6 OUR FIT Error includes scale factor of 1.2.					
2421.1±0.7 OUR AVERAGE Error includes scale factor of 1.2.					
$2423.1 \pm 1.5 \pm^{0.4}_{1.0}$	2.7k	[1] ABRAMOWICZ13		ZEUS	$e^\pm p \to D^{(*)+}\pi^- X$
2420.1±0.1±0.8	103k	DEL-AMO-SA...10P		BABR	$e^+e^- \to D^{*+}\pi^- X$
2426 ±3 ±1	151	ABE	05A	BELL	$B^- \to D^0\pi^+\pi^-\pi^-$
2421.4±1.5±0.9		[2] ABE	04D	BELL	$B^- \to D^{*+}\pi^-\pi^-$
$2421\ ^{+1}_{-2}$ ±2	286	AVERY	94C	CLE2	$e^+e^- \to D^{*+}\pi^- X$
2422 ±2 ±2	51	FRABETTI	94B	E687	γBe $\to D^{*+}\pi^- X$
2428 ±3 ±2	279	AVERY	90	CLEO	$e^+e^- \to D^{*+}\pi^- X$
2414 ±2 ±5	171	ALBRECHT	89H	ARG	$e^+e^- \to D^{*+}\pi^- X$
2428 ±8 ±5	171	ANJOS	89C	TPS	$\gamma N \to D^{*+}\pi^- X$
• • • We do not use the following data for averages, fits, limits, etc. • • •					
2420.5±2.1±0.9	3110±340	[3] CHEKANOV	09	ZEUS	$e^\pm p \to D^{*+}\pi^- X$
2421.7±0.7±0.6	7.5k	ABULENCIA	06A	CDF	1900 $p\overline{p} \to D^{*+}\pi^- X$
2425 ±3	235	[4] ABREU	98M	DLPH	e^+e^-

[1] From the combined fit of the $M(D^+\pi^-)$ and $M(D^{*+}\pi^-)$ distributions. and A_{D_2} fixed to the theoretical prediction of -1.
[2] Fit includes the contribution from $D_1^*(2430)^0$.
[3] Calculated using the mass difference $m(D_1^0) - m(D^{*+})_{PDG}$ reported below and $m(D^{*+})_{PDG}$ = 2010.27 ± 0.17 MeV. The 0.17 MeV uncertainty of the PDG mass value should be added to the experimental uncertainty of 0.9 MeV.
[4] No systematic error given.

$m_{D_1^0} - m_{D^{*+}}$

The fit includes $D^\pm$, D^0, $D_s^\pm$, $D^{*\pm}$, D^{*0}, $D_s^{*\pm}$, $D_1(2420)^0$, $D_2^*(2460)^0$, and $D_{s1}(2536)^\pm$ mass and mass difference measurements.

VALUE	EVTS	DOCUMENT ID		TECN	COMMENT
411.1±0.6 OUR FIT Error includes scale factor of 1.2.					
411.5±0.8 OUR AVERAGE					
410.2±2.1±0.9	3110±340	CHEKANOV	09	ZEUS	$e^\pm p \to D^{*+}\pi^- X$
411.7±0.7±0.4	7.5k	ABULENCIA	06A	CDF	1900 $p\overline{p} \to D^{*+}\pi^- X$

$D_1(2420)^0$ WIDTH

VALUE (MeV)	EVTS	DOCUMENT ID		TECN	COMMENT
27.4± 2.5 OUR AVERAGE Error includes scale factor of 2.3. See the ideogram below.					
$38.8\pm 5.0^{+1.9}_{-5.4}$	2.7k	[5] ABRAMOWICZ13		ZEUS	$e^\pm p \to D^{(*)+}\pi^- X$
31.4± 0.5± 1.3	103k	DEL-AMO-SA...10P		BABR	$e^+e^- \to D^{*+}\pi^- X$
20.0± 1.7± 1.3	7.5k	ABULENCIA	06A	CDF	1900 $p\overline{p} \to D^{*+}\pi^- X$
24 ± 7 ± 8	151	ABE	05A	BELL	$B^- \to D^0\pi^+\pi^-\pi^-$
23.7± 2.7± 4.0		[6] ABE	04D	BELL	$B^- \to D^{*+}\pi^-\pi^-$
$20\ ^{+6}_{-5}\ \pm 3$	286	AVERY	94C	CLE2	$e^+e^- \to D^{*+}\pi^- X$
15 ± 8 ± 4	51	FRABETTI	94B	E687	γBe $\to D^{*+}\pi^- X$
$23\ ^{+8}_{-6}\ ^{+10}_{-3}$	279	AVERY	90	CLEO	$e^+e^- \to D^{*+}\pi^- X$
13 ± 6 $^{+10}_{-5}$	171	ALBRECHT	89H	ARG	$e^+e^- \to D^{*+}\pi^- X$
• • • We do not use the following data for averages, fits, limits, etc. • • •					
$53.2\pm 7.2^{+3.3}_{-4.9}$	3110±340	CHEKANOV	09	ZEUS	$e^\pm p \to D^{*+}\pi^- X$
58 ±14 ±10	171	ANJOS	89C	TPS	$\gamma N \to D^{*+}\pi^- X$

[5] From the combined fit of the $M(D^+\pi^-)$ and $M(D^{*+}\pi^-)$ distributions. and A_{D_2} fixed to the theoretical prediction of -1.
[6] Fit includes the contribution from $D_1^*(2430)^0$.

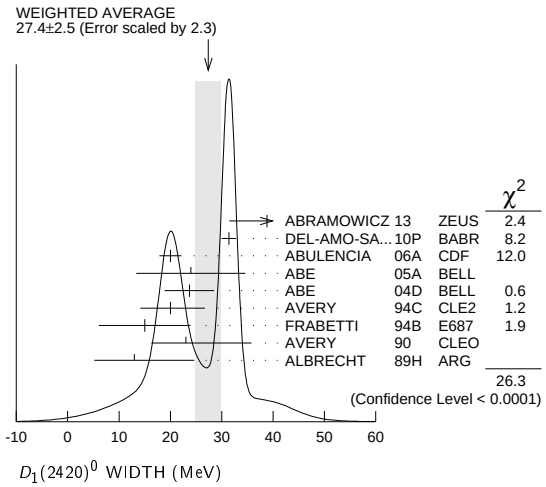

$D_1(2420)^0$ DECAY MODES

$\overline{D}_1(2420)^0$ modes are charge conjugates of modes below.

	Mode	Fraction (Γ_i/Γ)
Γ_1	$D^*(2010)^+\pi^-$	seen
Γ_2	$D^0\pi^+\pi^-$	seen
Γ_3	$D^0\rho^0$	
Γ_4	$D^0 f_0(500)$	
Γ_5	$D_0^*(2400)^+\pi^-$	
Γ_6	$D^+\pi^-$	not seen
Γ_7	$D^{*0}\pi^+\pi^-$	not seen

$D_1(2420)^0$ BRANCHING RATIOS

$\Gamma(D^*(2010)^+\pi^-)/\Gamma_{total}$ Γ_1/Γ

VALUE	DOCUMENT ID		TECN	COMMENT
seen	ACKERSTAFF	97W	OPAL	$e^+e^- \to D^{*+}\pi^- X$
seen	AVERY	90	CLEO	$e^+e^- \to D^{*+}\pi^- X$
seen	ALBRECHT	89H	ARG	$e^+e^- \to D^{*+}\pi^- X$
seen	ANJOS	89C	TPS	$\gamma N \to D^{*+}\pi^- X$

$\Gamma(D^+\pi^-)/\Gamma(D^*(2010)^+\pi^-)$ Γ_6/Γ_1

VALUE	CL%	DOCUMENT ID		TECN	COMMENT
<0.24	90	AVERY	90	CLEO	$e^+e^- \to D^+\pi^- X$

$D_1(2420)^0$ POLARIZATION AMPLITUDE A_{D_1}

A polarization amplitude A_{D_1} is a parameter that depends on the initial polarization of the D_1 and is sensitive to a possible S-wave contribution to its decay. For D_1 decays the helicity angle, θ_h, distribution varies like $1 + A_{D_1}\cos^2\theta_h$, where θ_h is the angle in the D^* rest frame between the two pions emitted by the $D_1 \to D^*\pi$ and the $D^* \to D\pi$.

Unpolarized D_1 decaying purely via D-wave is predicted to give $A_{D_1} = 3$.

VALUE	EVTS	DOCUMENT ID		TECN	COMMENT
5.73±0.25 OUR AVERAGE					
$7.8\ ^{+6.7}_{-2.7}\ ^{+4.6}_{-1.8}$	2.7k	[7] ABRAMOWICZ13		ZEUS	$e^\pm p \to D^{(*)+}\pi^- X$
5.72±0.25	103k	DEL-AMO-SA...10P		BABR	$e^+e^- \to D^{*+}\pi^- X$
$5.9\ ^{+3.0}_{-1.7}\ ^{+2.4}_{-1.0}$		CHEKANOV	09	ZEUS	$e^\pm p \to D^{*+}\pi^- X$
• • • We do not use the following data for averages, fits, limits, etc. • • •					
3.8 ±0.6 ±0.8		[8] AUBERT	09Y	BABR	$B^+ \to D_1^0\ell^+\nu_\ell$
$2.74^{+1.40}_{-0.93}$		[9] AVERY	94C	CLE2	$e^+e^- \to D^{*+}\pi^- X$

[7] From the combined fit of the $M(D^+\pi^-)$ and $M(D^{*+}\pi^-)$ distributions. and A_{D_2} fixed to the theoretical prediction of -1. A pure D-wave not excluded although some S-wave mixing possible.
[8] Assuming $\Gamma(\Upsilon(4S) \to B^+B^-)\ /\ \Gamma(\Upsilon(4S) \to B^0\overline{B}^0) = 1.065 \pm 0.026$ and equal partial widths and helicity angle distributions for charged and neutral D_1 mesons.
[9] Systematic uncertainties not estimated.

$D_1(2420)^0$ REFERENCES

ABRAMOWICZ 13	NP B866 229	H. Abramowicz *et al.*	(ZEUS Collab.)
DEL-AMO-SA... 10P	PR D82 111101	P. del Amo Sanchez *et al.*	(BABAR Collab.)
AUBERT 09Y	PRL 103 051803	B. Aubert *et al.*	(BABAR Collab.)
CHEKANOV 09	EPJ C60 25	S. Chekanov *et al.*	(ZEUS Collab.)
ABULENCIA 06A	PR D73 051104	A. Abulencia *et al.*	(CDF Collab.)
ABE 05A	PRL 94 221805	K. Abe *et al.*	(BELLE Collab.)
ABE 04D	PR D69 112002	K. Abe *et al.*	(BELLE Collab.)
ABREU 98M	PL B426 231	P. Abreu *et al.*	(DELPHI Collab.)
ACKERSTAFF 97W	ZPHY C76 425	K. Ackerstaff *et al.*	(OPAL Collab.)
AVERY 94C	PL B331 236	P. Avery *et al.*	(CLEO Collab.)
FRABETTI 94B	PRL 72 324	P.L. Frabetti *et al.*	(FNAL E687 Collab.)
AVERY 90	PR D41 774	P. Avery, D. Besson	(CLEO Collab.)
ALBRECHT 89H	PL B232 398	H. Albrecht *et al.*	(ARGUS Collab.) JP
ANJOS 89C	PRL 62 1717	J.C. Anjos *et al.*	(FNAL E691 Collab.)

$D_1(2420)^\pm$

$I(J^P) = \frac{1}{2}(?^?)$
I needs confirmation.

OMITTED FROM SUMMARY TABLE
Seen in $D^*(2007)^0\pi^+$. $J^P = 0^+$ ruled out.

$D_1(2420)^\pm$ MASS

VALUE (MeV)	EVTS	DOCUMENT ID		TECN	COMMENT
2423.2±2.4 OUR AVERAGE Error includes scale factor of 1.5. See the ideogram below.					
$2421.9\pm 4.7^{+3.4}_{-1.2}$	759	[1] ABRAMOWICZ13		ZEUS	$e^\pm p \to D^{(*)0}\pi^+ X$
2421 ±2 ±1	124	ABE	05A	BELL	$\overline{B}^0 \to D^+\pi^+\pi^-\pi^-$
2425 ±2 ±2	146	BERGFELD	94B	CLE2	$e^+e^- \to D^{*0}\pi^+ X$
2443 ±7 ±5	190	ANJOS	89C	TPS	$\gamma N \to D^0\pi^+ X^0$

[1] From the fit of the $M(D^0\pi^+)$ distribution. The widths of the D_1^+ and D_2^{*+} are fixed to 25 MeV and 37 MeV, and A_{D_1} and A_{D_2} are fixed to the theoretical predictions of 3 and -1, respectively.

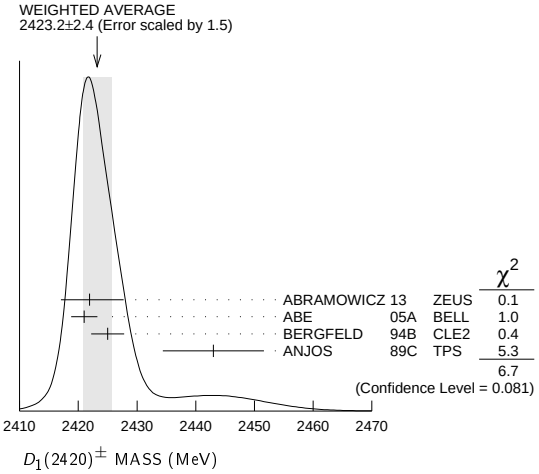

Meson Particle Listings

$D_1(2420)^{\pm}$, $D_1(2430)^0$, $D_2^*(2460)^0$

$m_{D_1^*(2420)^{\pm}} - m_{D_1^*(2420)^0}$

VALUE (MeV)	DOCUMENT ID		TECN	COMMENT
$4^{+2}_{-3} \pm 3$	BERGFELD	94B	CLE2	$e^+e^- \to$ hadrons

$D_1(2420)^{\pm}$ WIDTH

VALUE (MeV)	EVTS	DOCUMENT ID		TECN	COMMENT
25 ± 6 OUR AVERAGE					
$21 \pm 5 \pm 8$	124	ABE	05A	BELL	$\overline{B}^0 \to D^+\pi^+\pi^-\pi^-$
$26^{+8}_{-7} \pm 4$	146	BERGFELD	94B	CLE2	$e^+e^- \to D^{*0}\pi^+ X$
$41 \pm 19 \pm 8$	190	ANJOS	89C	TPS	$\gamma N \to D^0\pi^+ X^0$

$D_1(2420)^{\pm}$ DECAY MODES

$D_1^*(2420)^-$ modes are charge conjugates of modes below.

	Mode	Fraction (Γ_i/Γ)
Γ_1	$D^*(2007)^0\pi^+$	seen
Γ_2	$D^+\pi^+\pi^-$	seen
Γ_3	$D^+\rho^0$	
Γ_4	$D^+ f_0(500)$	
Γ_5	$D_0^*(2400)^0\pi^+$	
Γ_6	$D^0\pi^+$	not seen
Γ_7	$D^{*+}\pi^+\pi^-$	not seen

$D_1(2420)^{\pm}$ BRANCHING RATIOS

$\Gamma(D^*(2007)^0\pi^+)/\Gamma_{total}$ **Γ_1/Γ**

VALUE	DOCUMENT ID		TECN	COMMENT
seen	ANJOS	89C	TPS	$\gamma N \to D^0\pi^+ X^0$

$\Gamma(D^0\pi^+)/\Gamma(D^*(2007)^0\pi^+)$ **Γ_6/Γ_1**

VALUE	CL%	DOCUMENT ID		TECN	COMMENT
• • • We do not use the following data for averages, fits, limits, etc. • • •					
<0.18	90	BERGFELD	94B	CLE2	$e^+e^- \to$ hadrons

$D_1(2420)^{\pm}$ POLARIZATION AMPLITUDE A_{D_1}

A polarization amplitude A_{D_1} is a parameter that depends on the initial polarization of the D_1 and is sensitive to a possible S-wave contribution to its decay. For D_1 decays the helicity angle, θ_h, distribution varies like $1 + A_{D_1}\cos^2\theta_h$, where θ_h is the angle in the D^* rest frame between the two pions emitted by the $D_1 \to D^*\pi$ and the $D^* \to D\pi$.

Unpolarized D_1 decaying purely via D-wave is predicted to give $A_{D_1} = 3$.

VALUE	DOCUMENT ID		TECN	COMMENT
• • • We do not use the following data for averages, fits, limits, etc. • • •				
$3.8 \pm 0.6 \pm 0.8$	[2] AUBERT	09Y	BABR	$B^0 \to D_1^-\ell^+\nu_\ell$

[2] Assuming $\Gamma(\Upsilon(4S) \to B^+B^-) / \Gamma(\Upsilon(4S) \to B^0\overline{B}^0) = 1.065 \pm 0.026$ and equal partial widths and helicity angle distributions for charged and neutral D_1 mesons.

$D_1(2420)^{\pm}$ REFERENCES

ABRAMOWICZ 13	NP B866 229	H. Abramowicz *et al.*	(ZEUS Collab.)
AUBERT 09Y	PRL 103 051803	B. Aubert *et al.*	(BABAR Collab.)
ABE 05A	PRL 94 221805	K. Abe *et al.*	(BELLE Collab.)
BERGFELD 94B	PL B340 194	T. Bergfeld *et al.*	(CLEO Collab.)
ANJOS 89C	PRL 62 1717	J.C. Anjos *et al.*	(FNAL E691 Collab.)

$D_1(2430)^0$

$I(J^P) = \frac{1}{2}(1^+)$

OMITTED FROM SUMMARY TABLE

$J = 1^+$ assignment favored (ABE 04D).

$D_1(2430)^0$ MASS

VALUE (MeV)	DOCUMENT ID		TECN	COMMENT
$2427 \pm 26 \pm 25$	ABE	04D	BELL	$B^- \to D^{*+}\pi^-\pi^-$
• • • We do not use the following data for averages, fits, limits, etc. • • •				
2477 ± 28	[1] AUBERT	06L	BABR	$\overline{B}^0 \to D^{*+}\omega\pi^-$

[1] Systematic errors not estimated.

$D_1(2430)^0$ WIDTH

VALUE (MeV)	DOCUMENT ID		TECN	COMMENT
$384^{+107}_{-75} \pm 74$	ABE	04D	BELL	$B^- \to D^{*+}\pi^-\pi^-$
• • • We do not use the following data for averages, fits, limits, etc. • • •				
266 ± 97	[2] AUBERT	06L	BABR	$\overline{B}^0 \to D^{*+}\omega\pi^-$

[2] Systematic errors not estimated.

$D_1(2430)^0$ DECAY MODES

	Mode	Fraction (Γ_i/Γ)
Γ_1	$D^*(2010)^+\pi^-$	seen

$D_1(2430)^0$ REFERENCES

AUBERT 06L	PR D74 012001	B. Aubert *et al.*	(BABAR Collab.)
ABE 04D	PR D69 112002	K. Abe *et al.*	(BELLE Collab.)

$D_2^*(2460)^0$

$I(J^P) = \frac{1}{2}(2^+)$

$J^P = 2^+$ assignment strongly favored(ALBRECHT 89B, ALBRECHT 89H), natural parity confirmed by the helicity analysis(DEL-AMO-SANCHEZ 10P),

$D_2^*(2460)0$ MASS

The fit includes $D^{\pm}$, D^0, $D_s^{\pm}$, $D^{*\pm}$, D^{*0}, $D_s^{*\pm}$, $D_1(2420)^0$, $D_2^*(2460)^0$, and $D_{s1}(2536)^{\pm}$ mass and mass difference measurements.

VALUE (MeV)	EVTS	DOCUMENT ID		TECN	COMMENT
2462.6 ± 0.6 OUR FIT Error includes scale factor of 1.2.					
2461.8 ± 0.7 OUR AVERAGE Error includes scale factor of 1.1.					
$2462.5 \pm 2.4^{+1.3}_{-1.1}$	2.3k	[1] ABRAMOWICZ13		ZEUS	$e^{\pm}p \to D^{(*)+}\pi^- X$
$2462.2 \pm 0.1 \pm 0.8$	243k	DEL-AMO-SA...10P		BABR	$e^+e^- \to D^+\pi^- X$
$2460.4 \pm 1.2 \pm 2.2$	3.4k	AUBERT	09AB	BABR	$B^- \to D^+\pi^-\pi^-$
$2461.6 \pm 2.1 \pm 3.3$		[2] ABE	04D	BELL	$B^- \to D^+\pi^-\pi^-$
$2464.5 \pm 1.1 \pm 1.9$	5.8k	[2] LINK	04A	FOCS	γ A
$2465 \pm 3 \pm 3$	486	AVERY	94C	CLE2	$e^+e^- \to D^+\pi^- X$
$2453 \pm 3 \pm 2$	128	FRABETTI	94B	E687	γBe $\to D^+\pi^- X$
$2461 \pm 3 \pm 1$	440	AVERY	90	CLEO	$e^+e^- \to D^{*+}\pi^- X$
$2455 \pm 3 \pm 5$	337	ALBRECHT	89B	ARG	$e^+e^- \to D^+\pi^- X$
$2459 \pm 3 \pm 2$	153	ANJOS	89C	TPS	$\gamma N \to D^+\pi^- X$
• • • We do not use the following data for averages, fits, limits, etc. • • •					
$2469.1 \pm 3.7^{+1.2}_{-1.3}$	1560 ± 230	[3] CHEKANOV	09	ZEUS	$e^{\pm}p \to D^{(*)+}\pi^- X$
$2463.3 \pm 0.6 \pm 0.8$	20k	ABULENCIA	06A	CDF	1900 $p\overline{p} \to D^+\pi^- X$
2461 ± 6	126	[4] ABREU	98M	DLPH	e^+e^-
2466 ± 7	1	ASRATYAN	95	BEBC	53,40 $\nu(\overline{\nu}) \to pX,dX$

[1] From the combined fit of the $M(D^+\pi^-)$ and $M(D^{*+}\pi^-)$ distributions. and A_{D_2} fixed to the theoretical prediction of -1.

[2] Fit includes the contribution from $D_0^*(2400)^0$.

[3] Calculated using the mass difference $m(D_2^{*0}) - m(D^{*+})_{PDG}$ reported below and $m(D^{*+})_{PDG} = 2010.27 \pm 0.17$ MeV. The 0.17 MeV uncertainty of the PDG mass value should be added to the experimental uncertainty of $^{+1.2}_{-1.3}$ MeV.

[4] No systematic error given.

$m_{D_2^{*0}} - m_{D^+}$

The fit includes $D^{\pm}$, D^0, $D_s^{\pm}$, $D^{*\pm}$, D^{*0}, $D_s^{*\pm}$, $D_1(2420)^0$, $D_2^*(2460)^0$, and $D_{s1}(2536)^{\pm}$ mass and mass difference measurements.

VALUE (MeV)	EVTS	DOCUMENT ID	TECN	COMMENT
593.0 ± 0.6 OUR FIT Error includes scale factor of 1.2.				
$593.9 \pm 0.6 \pm 0.5$	20k	ABULENCIA 06A	CDF	1900 $p\overline{p} \to D^+\pi^- X$

$m_{D_2^{*0}} - m_{D^{*+}}$

The fit includes $D^{\pm}$, D^0, $D_s^{\pm}$, $D^{*\pm}$, D^{*0}, $D_s^{*\pm}$, $D_1(2420)^0$, $D_2^*(2460)^0$, and $D_{s1}(2536)^{\pm}$ mass and mass difference measurements.

VALUE (MeV)	EVTS	DOCUMENT ID	TECN	COMMENT
452.3 ± 0.6 OUR FIT Error includes scale factor of 1.2.				
$458.8 \pm 3.7^{+1.2}_{-1.3}$	1560 ± 230	CHEKANOV 09	ZEUS	$e^{\pm}p \to D^{(*)+}\pi^- X$

$D_2^*(2460)^0$ WIDTH

VALUE (MeV)	EVTS	DOCUMENT ID		TECN	COMMENT
49.0± 1.3 OUR AVERAGE		Error includes scale factor of 1.5. See the ideogram below.			
$46.6 \pm 8.1^{+5.9}_{-3.8}$	2.3k	[5] ABRAMOWICZ13	ZEUS		$e^\pm p \to D^{(*)+}\pi^- X$
50.5± 0.6± 0.7	243k	DEL-AMO-SA...10P	BABR		$e^+e^- \to D^+\pi^- X$
41.8± 2.5± 2.9	3.4k	AUBERT	09AB	BABR	$B^- \to D^+\pi^-\pi^-$
49.2± 2.3± 1.3	20k	ABULENCIA	06A	CDF	1900 $p\overline{p} \to D^+\pi^- X$
45.6± 4.4± 6.7		[6] ABE	04D	BELL	$B^- \to D^+\pi^-\pi^-$
38.7± 5.3± 2.9	5.8k	[6] LINK	04A	FOCS	γ A
$28 \pm {}^{8}_{7} \pm 6$	486	AVERY	94C	CLE2	$e^+e^- \to D^+\pi^- X$
25 ±10 ± 5	128	FRABETTI	94B	E687	γBe $\to D^+\pi^- X$
$20 \pm {}^{9}_{12} \pm {}^{9}_{10}$	440	AVERY	90	CLEO	$e^+e^- \to D^{*+}\pi^- X$
$15 \pm {}^{13}_{10} \pm {}^{5}_{10}$	337	ALBRECHT	89B	ARG	$e^+e^- \to D^+\pi^- X$
20 ±10 ± 5	153	ANJOS	89C	TPS	$\gamma N \to D^+\pi^- X$

[5] From the combined fit of the $M(D^+\pi^-)$ and $M(D^{*+}\pi^-)$ distributions. and A_{D_2} fixed to the theoretical prediction of -1.
[6] Fit includes the contribution from $D_0^*(2400)^0$.

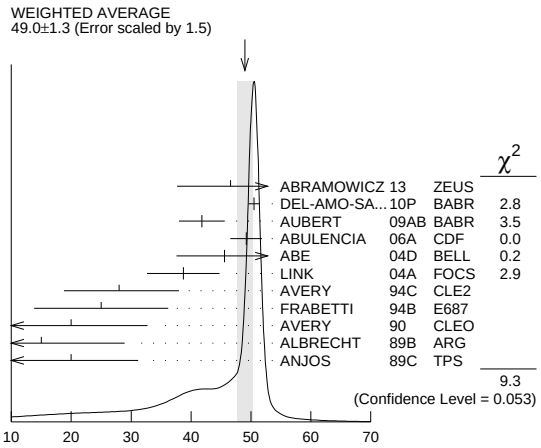

$D_2^*(2460)^0$ DECAY MODES

$\overline{D}_2^*(2460)^0$ modes are charge conjugates of modes below.

	Mode	Fraction (Γ_i/Γ)
Γ_1	$D^+\pi^-$	seen
Γ_2	$D^*(2010)^+\pi^-$	seen
Γ_3	$D^0\pi^+\pi^-$	not seen
Γ_4	$D^{*0}\pi^+\pi^-$	not seen

$D_2^*(2460)^0$ BRANCHING RATIOS

$\Gamma(D^+\pi^-)/\Gamma_{total}$ Γ_1/Γ

VALUE	EVTS	DOCUMENT ID		TECN	COMMENT
seen	3.4k	AUBERT	09AB	BABR	$B^- \to D^+\pi^-\pi^-$
seen	337	ALBRECHT	89B	ARG	$e^+e^- \to D^+\pi^- X$
seen		ANJOS	89C	TPS	$\gamma N \to D^+\pi^- X$

$\Gamma(D^*(2010)^+\pi^-)/\Gamma_{total}$ Γ_2/Γ

VALUE	DOCUMENT ID		TECN	COMMENT
seen	ACKERSTAFF	97W	OPAL	$e^+e^- \to D^{*+}\pi^- X$
seen	AVERY	90	CLEO	$e^+e^- \to D^{*+}\pi^- X$
seen	ALBRECHT	89H	ARG	$e^+e^- \to D^*\pi^- X$

$\Gamma(D^+\pi^-)/\Gamma(D^*(2010)^+\pi^-)$ Γ_1/Γ_2

VALUE	EVTS	DOCUMENT ID		TECN	COMMENT
1.54±0.15 OUR AVERAGE					
1.4 ±0.3 ±0.3	2.3k	[7] ABRAMOWICZ13	ZEUS		$e^\pm p \to D^{(*)+}\pi^- X$
1.47±0.03±0.16	379k	DEL-AMO-SA...10P	BABR		$e^+e^- \to D^{(*)+}\pi^- X$
$2.8 \pm 0.8 \pm {}^{0.5}_{0.6}$	1560±230	CHEKANOV	09	ZEUS	$e^\pm p \to D^{(*)+}\pi^- X$
2.2 ±0.7 ±0.6		AVERY	94C	CLE2	$e^+e^- \to D^{*+}\pi^- X$
2.3 ±0.8		AVERY	90	CLEO	e^+e^-
3.0 ±1.1 ±1.5		ALBRECHT	89H	ARG	$e^+e^- \to D^*\pi^- X$
• • • We do not use the following data for averages, fits, limits, etc. • • •					
1.9 ±0.5		ABE	04D	BELL	$B^- \to D^{(*)+}\pi^-\pi^-$

[7] From the combined fit of the $M(D^+\pi^-)$ and $M(D^{*+}\pi^-)$ distributions. and A_{D_2} fixed to the theoretical prediction of -1.

$\Gamma(D^+\pi^-)/[\Gamma(D^+\pi^-)+\Gamma(D^*(2010)^+\pi^-)]$ $\Gamma_1/(\Gamma_1+\Gamma_2)$

VALUE	EVTS	DOCUMENT ID		TECN	COMMENT
• • • We do not use the following data for averages, fits, limits, etc. • • •					
0.62±0.03±0.02	8414	[8] AUBERT	09Y	BABR	$B^+ \to D_2^{*0}\ell^+\nu_\ell$

[8] Assuming $\Gamma(\Upsilon(4S) \to B^+B^-)\ /\ \Gamma(\Upsilon(4S) \to B^0\overline{B}^0) = 1.065 \pm 0.026$ and equal partial widths for charged and neutral D_2^* mesons.

$D_2^*(2460)^0$ POLARIZATION AMPLITUDE A_{D_2}

A polarization amplitude A_{D_2} is a parameter that depends on the initial polarization of the D_2. For D_2 decays the helicity angle, θ_H, distribution varies like $1 + A_{D_2}\cos^2(\theta_H)$, where θ_H is the angle in the D^* rest frame between the two pions emitted by the $D_2 \to D^*\pi$ and $D^* \to D\pi$.

VALUE	EVTS	DOCUMENT ID		TECN	COMMENT
• • • We do not use the following data for averages, fits, limits, etc. • • •					
−1.16±0.35	2.3k	[9] ABRAMOWICZ13	ZEUS		$e^\pm p \to D^{(*)+}\pi^- X$
consistent with −1	243k	DEL-AMO-SA...10P	BABR		$e^+e^- \to D^+\pi^- X$
$-0.74 \pm {}^{0.49}_{0.38}$		[10] AVERY	94C	CLE2	$e^+e^- \to D^{*+}\pi^- X$

[9] From the combined fit of the $M(D^+\pi^-)$ and $M(D^{*+}\pi^-)$ distributions.
[10] Systematic uncertainties not estimated.

$D_2^*(2460)^0$ REFERENCES

ABRAMOWICZ 13	NP B866 229	H. Abramowicz *et al.*	(ZEUS Collab.)
DEL-AMO-SA... 10P	PR D82 111101	P. del Amo Sanchez *et al.*	(BABAR Collab.)
AUBERT 09AB	PR D79 112004	B. Aubert *et al.*	(BABAR Collab.)
AUBERT 09Y	PRL 103 051803	B. Aubert *et al.*	(BABAR Collab.)
CHEKANOV 09	EPJ C60 25	S. Chekanov *et al.*	(ZEUS Collab.)
ABULENCIA 06A	PR D73 051104	A. Abulencia *et al.*	(CDF Collab.)
ABE 04D	PR D69 112002	K. Abe *et al.*	(BELLE Collab.)
LINK 04A	PL B586 11	J.M. Link *et al.*	(FOCUS Collab.)
ABREU 98M	PL B426 231	P. Abreu *et al.*	(DELPHI Collab.)
ACKERSTAFF 97W	ZPHY C76 425	K. Ackerstaff *et al.*	(OPAL Collab.)
ASRATYAN 95	ZPHY C68 43	A.E. Asratyan *et al.*	(BIRM, BELG, CERN+)
AVERY 94C	PL B331 236	P. Avery *et al.*	(CLEO Collab.)
FRABETTI 94B	PRL 72 324	P.L. Frabetti *et al.*	(FNAL E687 Collab.)
AVERY 90	PR D41 774	P. Avery, D. Besson	(CLEO Collab.)
ALBRECHT 89B	PL B221 422	H. Albrecht *et al.*	(ARGUS Collab.) JP
ALBRECHT 89H	PL B232 398	H. Albrecht *et al.*	(ARGUS Collab.) JP
ANJOS 89C	PRL 62 1717	J.C. Anjos *et al.*	(FNAL E691 Collab.)

$D_2^*(2460)^\pm$ $I(J^P) = \frac{1}{2}(2^+)$

$J^P = 2^+$ assignment strongly favored(ALBRECHT 89B).

$D_2^*(2460)^\pm$ MASS

VALUE (MeV)	EVTS	DOCUMENT ID		TECN	COMMENT
2464.3±1.6 OUR AVERAGE		Error includes scale factor of 1.7. See the ideogram below.			
$2460.6 \pm 4.4^{+3.6}_{-0.8}$	1371	[1] ABRAMOWICZ13	ZEUS		$e^\pm p \to D^{(*)0}\pi^+ X$
2465.4±0.2±1.1	111k	[2] DEL-AMO-SA...10P	BABR		$e^+e^- \to D^0\pi^+ X$
$2465.7 \pm 1.8^{+1.4}_{-4.8}$	2909	KUZMIN	07	BELL	e^+e^- → hadrons
2463 ±3 ±3	310	BERGFELD	94B	CLE2	$e^+e^- \to D^0\pi^+ X$
2453 ±3 ±2	185	FRABETTI	94B	E687	γBe $\to D^0\pi^+ X$
2469 ±4 ±6		ALBRECHT	89F	ARG	$e^+e^- \to D^0\pi^+ X$
• • • We do not use the following data for averages, fits, limits, etc. • • •					
2467.6±1.5±0.8	3.5k	[3] LINK	04A	FOCS	γ A

[1] From the fit of the $M(D^0\pi^+)$ distribution. The widths of the D_1^+ and D_2^{*+} are fixed to 25 MeV and 37 MeV, and A_{D_1} and A_{D_2} are fixed to the theoretical predictions of 3 and -1, respectively.
[2] At a fixed width of 50.5 MeV.
[3] Fit includes the contribution from $D_0^*(2400)^\pm$. Not independent of the corresponding mass difference measurement, $(m_{D_2^*(2460)^\pm}) - (m_{D_2^*(2460)^0})$.

Meson Particle Listings

$D_2^*(2460)^\pm$, $D(2550)^0$, $D(2600)$

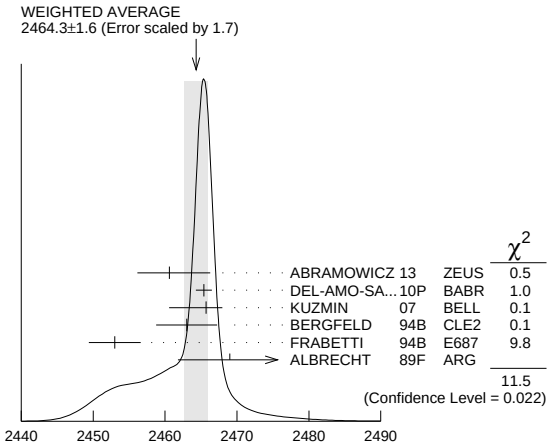

$m_{D_2^*(2460)^\pm} - m_{D_2^*(2460)^0}$

VALUE (MeV)	DOCUMENT ID		TECN	COMMENT
2.4±1.7 OUR AVERAGE				
3.1±1.9±0.9	LINK	04A	FOCS	γ A
− 2 ±4 ±4	BERGFELD	94B	CLE2	$e^+e^- \to$ hadrons
0 ±4	FRABETTI	94B	E687	γBe $\to D\pi$X
14 ±5 ±8	ALBRECHT	89F	ARG	$e^+e^- \to D^0\pi^+$X

$D_2^*(2460)^\pm$WIDTH

VALUE (MeV)	EVTS	DOCUMENT ID		TECN	COMMENT
37 ± 6 OUR AVERAGE Error includes scale factor of 1.4. See the ideogram below.					
49.7± 3.8±6.4	2909	KUZMIN	07	BELL	$e^+e^- \to$ hadrons
34.1± 6.5±4.2	3.5k	[4] LINK	04A	FOCS	γ A
27 $^{+11}_{-8}$ ±5	310	BERGFELD	94B	CLE2	$e^+e^- \to D^0\pi^+$X
23 ± 9 ±5	185	FRABETTI	94B	E687	γBe $\to D^0\pi^+$X

[4] Fit includes the contribution from $D_0^*(2400)^\pm$.

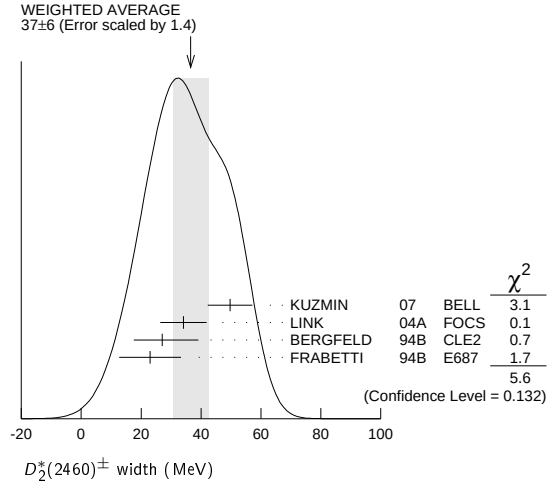

$D_2^*(2460)^\pm$ DECAY MODES

$D_2^*(2460)^-$ modes are charge conjugates of modes below.

	Mode	Fraction (Γ_i/Γ)
Γ_1	$D^0\pi^+$	seen
Γ_2	$D^{*0}\pi^+$	seen
Γ_3	$D^+\pi^+\pi^-$	not seen
Γ_4	$D^{*+}\pi^+\pi^-$	not seen

$D_2^*(2460)^\pm$ BRANCHING RATIOS

$\Gamma(D^0\pi^+)/\Gamma_{total}$ Γ_1/Γ

VALUE	DOCUMENT ID		TECN	COMMENT
seen	ALBRECHT	89F	ARG	$e^+e^- \to D^0\pi^+$X

$\Gamma(D^0\pi^+)/\Gamma(D^{*0}\pi^+)$ Γ_1/Γ_2

VALUE	EVTS	DOCUMENT ID		TECN	COMMENT
1.2±0.4 OUR AVERAGE					
1.1±0.4 $^{+0.3}_{-0.2}$	1371	[5] ABRAMOWICZ13		ZEUS	$e^\pm p \to D^{(*)0}\pi^+X$
1.9±1.1±0.3		BERGFELD	94B	CLE2	$e^+e^- \to$ hadrons

[5] From the fit of the $M(D^0\pi^+)$ distribution. The widths of the D_1^+ and D_2^{*+} are fixed to 25 MeV and 37 MeV, and A_{D_1} and A_{D_2} are fixed to the theoretical predictions of 3 and −1, respectively.

$\Gamma(D^0\pi^+)/[\Gamma(D^0\pi^+)+\Gamma(D^{*0}\pi^+)]$ $\Gamma_1/(\Gamma_1+\Gamma_2)$

VALUE	EVTS	DOCUMENT ID		TECN	COMMENT
• • • We do not use the following data for averages, fits, limits, etc. • • •					
0.62±0.03±0.02	3361	[6] AUBERT	09Y	BABR	$\overline{B}^0 \to D_2^{*+}\ell^-\nu_\ell$

[6] Assuming $\Gamma(\Upsilon(4S) \to B^+B^-) / \Gamma(\Upsilon(4S) \to B^0\overline{B}^0) = 1.065 \pm 0.026$ and equal partial widths for charged and neutral D_2^* mesons.

$D_2^*(2460)^\pm$ REFERENCES

ABRAMOWICZ 13	NP B866 229	H. Abramowicz *et al.*	(ZEUS Collab.)
DEL-AMO-SA... 10P	PR D82 111101	P. del Amo Sanchez *et al.*	(BABAR Collab.)
AUBERT 09Y	PRL 103 051803	B. Aubert *et al.*	(BABAR Collab.)
KUZMIN 07	PR D76 012006	A. Kuzmin *et al.*	(BELLE Collab.)
LINK 04A	PL B586 11	J.M. Link *et al.*	(FOCUS Collab.)
BERGFELD 94B	PL B340 194	T. Bergfeld *et al.*	(CLEO Collab.)
FRABETTI 94B	PRL 72 324	P.L. Frabetti *et al.*	(FNAL E687 Collab.)
ALBRECHT 89B	PL B221 422	H. Albrecht *et al.*	(ARGUS Collab.)
ALBRECHT 89F	PL B231 208	H. Albrecht *et al.*	(ARGUS Collab.)

$D(2550)^0$

$I(J^P) = \frac{1}{2}(0^-)$

OMITTED FROM SUMMARY TABLE

$J^P = 0^-$ assignment based on the helicity analysis (DEL-AMO-SANCHEZ 10P).

$D(2550)^0$ MASS

VALUE (MeV)	EVTS	DOCUMENT ID		TECN	COMMENT
2539.4±4.5±6.8	34k	DEL-AMO-SA...10P		BABR	$e^+e^- \to D^{*+}\pi^-X$

$D(2550)^0$ WIDTH

VALUE (MeV)	EVTS	DOCUMENT ID		TECN	COMMENT
130±12±13	34k	DEL-AMO-SA...10P		BABR	$e^+e^- \to D^{*+}\pi^-X$

$D(2550)^0$ DECAY MODES

	Mode	Fraction (Γ_i/Γ)
Γ_1	$D^{*+}\pi^-$	seen

$D(2550)^0$ REFERENCES

DEL-AMO-SA... 10P	PR D82 111101	P. del Amo Sanchez *et al.*	(BABAR Collab.)

$D(2600)$

$I(J^P) = \frac{1}{2}(?^?)$

OMITTED FROM SUMMARY TABLE

J^P consistent with natural parity (DEL-AMO-SANCHEZ 10P).

$D(2600)$ MASS

VALUE (MeV)	EVTS	DOCUMENT ID		TECN	CHG	COMMENT
2612 ±6 OUR AVERAGE Error includes scale factor of 1.9.						
2608.7±2.4±2.5	26k	DEL-AMO-SA...10P		BABR	0	$e^+e^- \to D^+\pi^-X$
2621.3±3.7±4.2	13k	[1] DEL-AMO-SA...10P		BABR	+	$e^+e^- \to D^0\pi^+X$

[1] At a fixed width of 93 MeV.

$D(2600)$ WIDTH

VALUE (MeV)	EVTS	DOCUMENT ID		TECN	COMMENT
93±6±13	26k	DEL-AMO-SA...10P		BABR	$e^+e^- \to D^+\pi^-X$

$D(2600)$ DECAY MODES

	Mode	Fraction (Γ_i/Γ)
Γ_1	$D\pi$	seen
Γ_2	$D^+\pi^-$	seen
Γ_3	$D^0\pi^\pm$	seen
Γ_4	$D^*\pi$	seen
Γ_5	$D^{*+}\pi^-$	seen

$D(2600)$ BRANCHING RATIOS

$\Gamma(D^+\pi^-)/\Gamma(D^{*+}\pi^-)$ Γ_2/Γ_5

VALUE	EVTS	DOCUMENT ID	TECN	COMMENT
0.32±0.02±0.09	76k	DEL-AMO-SA...10P	BABR	$e^+e^- \to D^{(*)+}\pi^- X$

$D(2600)$ REFERENCES

DEL-AMO-SA...10P PR D82 111101 P. del Amo Sanchez *et al.* (BABAR Collab.)

$D^*(2640)^\pm$

$I(J^P) = \frac{1}{2}(?^?)$

OMITTED FROM SUMMARY TABLE

Seen in Z decays by ABREU 98M. Not seen by ABBIENDI 01N and CHEKANOV 09. Needs confirmation.

$D^*(2640)^\pm$ MASS

VALUE (MeV)	EVTS	DOCUMENT ID		TECN	COMMENT
2637±2±6	66 ± 14	ABREU	98M	DLPH	$e^+e^- \to D^{*+}\pi^+\pi^- X$

$D^*(2640)^\pm$ WIDTH

VALUE (MeV)	CL%	DOCUMENT ID		TECN	COMMENT
<15	95	ABREU	98M	DLPH	$e^+e^- \to D^{*+}\pi^+\pi^- X$

$D^*(2640)^+$ DECAY MODES

$D^*(2640)^-$ modes are charge conjugates of modes below.

	Mode	Fraction (Γ_i/Γ)
Γ_1	$D^*(2010)^+\pi^+\pi^-$	seen

$D^*(2640)^\pm$ REFERENCES

CHEKANOV 09 EPJ C60 25 S. Chekanov *et al.* (ZEUS Collab.)
ABBIENDI 01N EPJ C20 445 G. Abbiendi *et al.* (OPAL Collab.)
ABREU 98M PL B426 231 P. Abreu *et al.* (DELPHI Collab.)

$D(2750)$

$I(J^P) = \frac{1}{2}(?^?)$

OMITTED FROM SUMMARY TABLE

$D(2750)$ MASS

VALUE (MeV)	EVTS	DOCUMENT ID		TECN	CHG	COMMENT
2761 ±5 OUR AVERAGE		Error includes scale factor of 2.5. See the ideogram below.				
2752.4±1.7±2.7	23.5k	[1] DEL-AMO-SA...10P		BABR	0	$e^+e^- \to D^{*+}\pi^- X$
2763.3±2.3±2.3	11.3k	[1] DEL-AMO-SA...10P		BABR	0	$e^+e^- \to D^+\pi^- X$
2769.7±3.8±1.5	5.7k	[1,2] DEL-AMO-SA...10P		BABR	+	$e^+e^- \to D^0\pi^+ X$

[1] The states observed in the $D^*\pi$ and $D\pi$ final states are not necessarily the same.
[2] At a fixed width of 60.9 MeV.

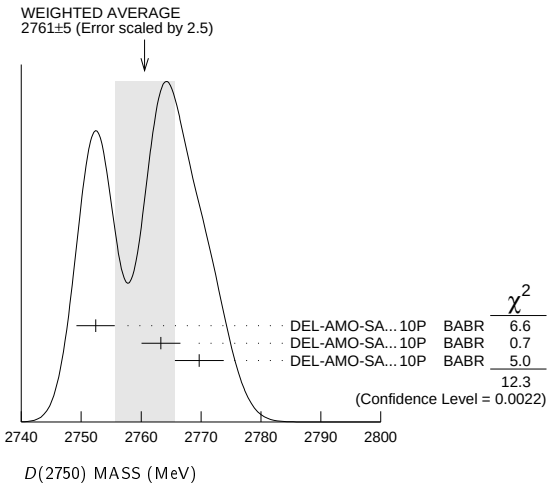

$D(2750)$ WIDTH

VALUE (MeV)	EVTS	DOCUMENT ID		TECN	COMMENT
63 ±6 OUR AVERAGE					
71 ±6 ±11	23.5k	[3] DEL-AMO-SA...10P		BABR	$e^+e^- \to D^{*+}\pi^- X$
60.9±5.1± 3.6	11.3k	[3] DEL-AMO-SA...10P		BABR	$e^+e^- \to D^+\pi^- X$

[3] The states observed in the $D^*\pi$ and $D\pi$ final states are not necessarily the same.

$D(2750)$ DECAY MODES

	Mode	Fraction (Γ_i/Γ)
Γ_1	$D\pi$	seen
Γ_2	$D^+\pi^-$	seen
Γ_3	$D^0\pi^\pm$	seen
Γ_4	$D^*\pi$	seen
Γ_5	$D^{*+}\pi^-$	seen

$D(2750)$ BRANCHING RATIOS

$\Gamma(D^+\pi^-)/\Gamma(D^{*+}\pi^-)$ Γ_2/Γ_5

VALUE	EVTS	DOCUMENT ID		TECN	COMMENT
0.42±0.05±0.11	34.8k	[4] DEL-AMO-SA...10P		BABR	$e^+e^- \to D^{(*)+}\pi^- X$

[4] The states observed in the $D^*\pi$ and $D\pi$ final states are not necessarily the same.

$D(2750)$ POLARIZATION AMPLITUDE A_D

A polarization amplitude A_D is a parameter that depends on the initial polarization of the $D(2750)$. For $D(2750)$ decays the helicity angle, θ_H, distribution varies like $1 + A_D \cos(\theta_H)$, where θ_H is the angle in the D^* rest frame between the two pions emitted by the $D(2750) \to D^*\pi$ and $D^* \to D\pi$.

VALUE	EVTS	DOCUMENT ID		TECN	COMMENT
• • • We do not use the following data for averages, fits, limits, etc. • • •					
−0.33±0.28	23.5k	[5] DEL-AMO-SA...10P		BABR	$e^+e^- \to D^{*+}\pi^- X$

[5] Systematic uncertainties not estimated. The states observed in the $D^*\pi$ and $D\pi$ final states are not necessarily the same.

$D(2750)$ REFERENCES

DEL-AMO-SA...10P PR D82 111101 P. del Amo Sanchez *et al.* (BABAR Collab.)

CHARMED, STRANGE MESONS ($C = S = \pm 1$)

$D_s^+ = c\overline{s}$, $D_s^- = \overline{c}s$, similarly for D_s^*'s

$D_s^{\pm}$

$I(J^P) = 0(0^-)$

The angular distributions of the decays of the ϕ and $\overline{K}^*(892)^0$ in the $\phi\pi^+$ and $K^+\overline{K}^*(892)^0$ modes strongly indicate that the spin is zero. The parity given is that expected of a $c\overline{s}$ ground state.

$D_s^{\pm}$ MASS

The fit includes $D^{\pm}$, D^0, $D_s^{\pm}$, $D^{*\pm}$, D^{*0}, $D_s^{*\pm}$, $D_1(2420)^0$, $D_2^*(2460)^0$, and $D_{s1}(2536)^{\pm}$ mass and mass difference measurements. Measurements of the $D_s^{\pm}$ mass with an error greater than 10 MeV are omitted from the fit and average. A number of early measurements have been omitted altogether.

VALUE (MeV)	EVTS	DOCUMENT ID		TECN	COMMENT
1968.30± 0.11 OUR FIT Error includes scale factor of 1.1.					
1969.0 ± 1.4 OUR AVERAGE Error includes scale factor of 1.5. See the ideogram below.					
1967.0 ± 1.0 ± 1.0	54	BARLAG	90C	ACCM	π^- Cu 230 GeV
1969.3 ± 1.4 ± 1.4		ALBRECHT	88	ARG	e^+e^- 9.4–10.6 GeV
1972.7 ± 1.5 ± 1.0	21	BECKER	87B	SILI	200 GeV π, K, p
1972.4 ± 3.7 ± 3.7	27	BLAYLOCK	87	MRK3	e^+e^- 4.14 GeV
1963 ± 3 ± 3	30	DERRICK	85B	HRS	e^+e^- 29 GeV
1970 ± 5 ± 5	104	CHEN	83C	CLEO	e^+e^- 10.5 GeV
• • • We do not use the following data for averages, fits, limits, etc. • • •					
1968.3 ± 0.7 ± 0.7	290	[1] ANJOS	88	E691	Photoproduction
1980 ±15	6	USHIDA	86	EMUL	ν wideband
1973.6 ± 2.6 ± 3.0	163	ALBRECHT	85D	ARG	e^+e^- 10 GeV
1948 ±28 ±10	65	AIHARA	84D	TPC	e^+e^- 29 GeV
1975 ± 9 ±10	49	ALTHOFF	84	TASS	e^+e^- 14–25 GeV
1975 ± 4	3	BAILEY	84	ACCM	hadron$^+$ Be $\rightarrow \phi\pi^+$ X

[1] ANJOS 88 enters the fit via $m_{D_s^{\pm}} - m_{D^{\pm}}$ (see below).

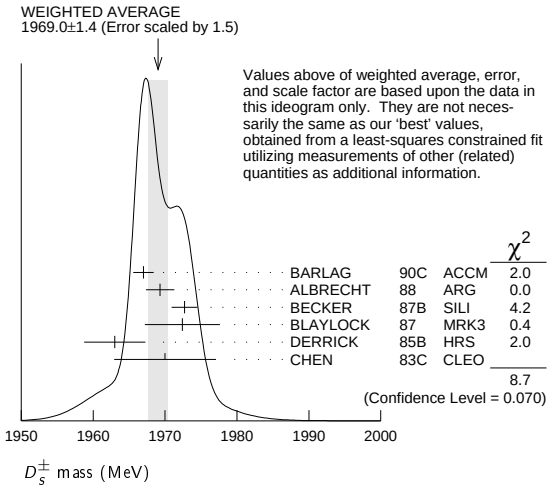

$m_{D_s^{\pm}} - m_{D^{\pm}}$

The fit includes $D^{\pm}$, D^0, $D_s^{\pm}$, $D^{*\pm}$, D^{*0}, $D_s^{*\pm}$, $D_1(2420)^0$, $D_2^*(2460)^0$, and $D_{s1}(2536)^{\pm}$ mass and mass difference measurements.

VALUE (MeV)	EVTS	DOCUMENT ID		TECN	COMMENT
98.69±0.05 OUR FIT					
98.69±0.05 OUR AVERAGE					
98.68±0.03±0.04		AAIJ	13V	LHCB	$D_s^+ \rightarrow K^+K^-\pi^+$
99.41±0.38±0.21		ACOSTA	03D	CDF2	$\overline{p}p$, $\sqrt{s}$= 1.96 TeV
98.4 ±0.1 ±0.3	48k	AUBERT	02G	BABR	$e^+e^- \approx \Upsilon(4S)$
99.5 ±0.6 ±0.3		BROWN	94	CLE2	$e^+e^- \approx \Upsilon(4S)$
98.5 ±1.5	555	CHEN	89	CLEO	e^+e^- 10.5 GeV
99.0 ±0.8	290	ANJOS	88	E691	Photoproduction

$D_s^{\pm}$ MEAN LIFE

Measurements with an error greater than 100×10^{-15} s or with fewer than 100 events have been omitted from the Listings.

VALUE (10^{-15} s)	EVTS	DOCUMENT ID		TECN	COMMENT
500 ± 7 OUR AVERAGE Error includes scale factor of 1.3. See the ideogram below.					
507.4± 5.5± 5.1	13.6k	LINK	05J	FOCS	$\Phi\pi^+$ and $\overline{K}^{*0}K^+$
472.5±17.2± 6.6	760	IORI	01	SELX	600 GeV Σ^-, π^-, p
518 ±14 ± 7	1662	AITALA	99	E791	π^- nucleus, 500 GeV
486.3±15.0$^{+\ 4.9}_{-\ 5.1}$	2167	[1] BONVICINI	99	CLE2	$e^+e^- \approx \Upsilon(4S)$
475 ±20 ± 7	900	FRABETTI	93F	E687	γBe, $\phi\pi^+$
500 ±60 ±30	104	FRABETTI	90	E687	γBe, $\phi\pi^+$
470 ±40 ±20	228	RAAB	88	E691	Photoproduction

[1] BONVICINI 99 obtains 1.19 ± 0.04 for the ratio of D_s^+ to D^0 lifetimes.

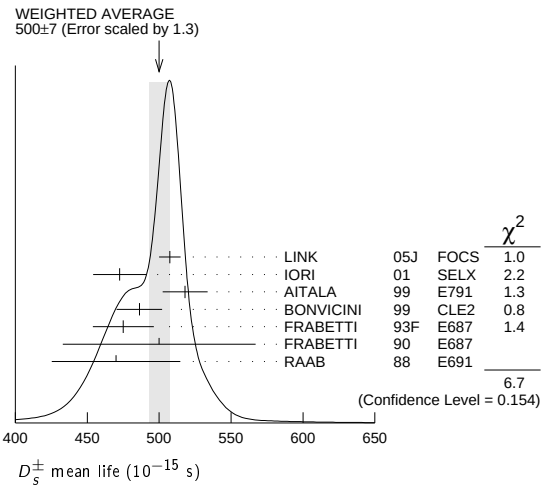

D_s^+ DECAY MODES

Unless otherwise noted, the branching fractions for modes with a resonance in the final state include all the decay modes of the resonance. D_s^- modes are charge conjugates of the modes below.

	Mode		Fraction (Γ_i/Γ)		Scale factor / Confidence level
	Inclusive modes				
Γ_1	e^+ semileptonic	[a]	(6.5 ±0.4) %		
Γ_2	π^+ anything		(119.3 ±1.4) %		
Γ_3	π^- anything		(43.2 ±0.9) %		
Γ_4	π^0 anything		(123 ±7) %		
Γ_5	K^- anything		(18.7 ±0.5) %		
Γ_6	K^+ anything		(28.9 ±0.7) %		
Γ_7	K_S^0 anything		(19.0 ±1.1) %		
Γ_8	η anything	[b]	(29.9 ±2.8) %		
Γ_9	ω anything		(6.1 ±1.4) %		
Γ_{10}	η' anything	[c]	(11.7 ±1.8) %		
Γ_{11}	$f_0(980)$ anything, $f_0 \rightarrow \pi^+\pi^-$		< 1.3	%	CL=90%
Γ_{12}	ϕ anything		(15.7 ±1.0) %		
Γ_{13}	K^+K^- anything		(15.8 ±0.7) %		
Γ_{14}	$K_S^0K^+$ anything		(5.8 ±0.5) %		
Γ_{15}	$K_S^0K^-$ anything		(1.9 ±0.4) %		
Γ_{16}	$2K_S^0$ anything		(1.70±0.32) %		
Γ_{17}	$2K^+$ anything		< 2.6	$\times 10^{-3}$	CL=90%
Γ_{18}	$2K^-$ anything		< 6	$\times 10^{-4}$	CL=90%
	Leptonic and semileptonic modes				
Γ_{19}	$e^+\nu_e$		< 8.3	$\times 10^{-5}$	CL=90%
Γ_{20}	$\mu^+\nu_\mu$		(5.56±0.25)	$\times 10^{-3}$	
Γ_{21}	$\tau^+\nu_\tau$		(5.54±0.24) %		
Γ_{22}	$K^+K^-e^+\nu_e$		—		
Γ_{23}	$\phi e^+\nu_e$	[d]	(2.49±0.14) %		
Γ_{24}	$\eta e^+\nu_e + \eta'(958)e^+\nu_e$	[d]	(3.66±0.37) %		
Γ_{25}	$\eta e^+\nu_e$	[d]	(2.67±0.29) %		S=1.1
Γ_{26}	$\eta'(958)e^+\nu_e$	[d]	(9.9 ±2.3)	$\times 10^{-3}$	
Γ_{27}	$\omega e^+\nu_e$	[e]	< 2.0	$\times 10^{-3}$	CL=90%
Γ_{28}	$K^0e^+\nu_e$		(3.7 ±1.0)	$\times 10^{-3}$	
Γ_{29}	$K^*(892)^0e^+\nu_e$	[d]	(1.8 ±0.7)	$\times 10^{-3}$	
Γ_{30}	$f_0(980)e^+\nu_e$, $f_0 \rightarrow \pi^+\pi^-$		(2.00±0.32)	$\times 10^{-3}$	

Hadronic modes with a $K\overline{K}$ pair

Γ_{31}	$K^+ K_S^0$		(1.49 ± 0.06) %		
Γ_{32}	$K^+ \overline{K}^0$		(2.95 ± 0.14) %		
Γ_{33}	$K^+ K^- \pi^+$	[f]	(5.39 ± 0.21) %		S=1.4
Γ_{34}	$\phi\pi^+$	[d,g]	(4.5 ± 0.4) %		
Γ_{35}	$\phi\pi^+$, $\phi \to K^+ K^-$	[g]	(2.24 ± 0.10) %		
Γ_{36}	$K^+ \overline{K}^*(892)^0$, $\overline{K}^{*0} \to K^- \pi^+$		(2.58 ± 0.11) %		
Γ_{37}	$f_0(980)\pi^+$, $f_0 \to K^+ K^-$		(1.14 ± 0.31) %		
Γ_{38}	$f_0(1370)\pi^+$, $f_0 \to K^+ K^-$		(7 ± 5) × 10^{-4}		
Γ_{39}	$f_0(1710)\pi^+$, $f_0 \to K^+ K^-$		(6.6 ± 2.9) × 10^{-4}		
Γ_{40}	$K^+ \overline{K}_0^*(1430)^0$, $\overline{K}_0^* \to K^- \pi^+$		(1.8 ± 0.4) × 10^{-3}		
Γ_{41}	$K^+ K_S^0 \pi^0$		(1.52 ± 0.22) %		
Γ_{42}	$2K_S^0 \pi^+$		(7.7 ± 0.6) × 10^{-3}		
Γ_{43}	$K^0 \overline{K}^0 \pi^+$		—		
Γ_{44}	$K^*(892)^+ \overline{K}^0$	[d]	(5.4 ± 1.2) %		
Γ_{45}	$K^+ K^- \pi^+ \pi^0$		(6.3 ± 0.7) %		S=1.1
Γ_{46}	$\phi\rho^+$	[d]	(8.4 $^{+1.9}_{-2.3}$) %		
Γ_{47}	$K_S^0 K^- 2\pi^+$		(1.66 ± 0.11) %		
Γ_{48}	$K^*(892)^+ \overline{K}^*(892)^0$	[d]	(7.2 ± 2.6) %		
Γ_{49}	$K^+ K_S^0 \pi^+ \pi^-$		(1.03 ± 0.10) %		
Γ_{50}	$K^+ K^- 2\pi^+ \pi^-$		(8.6 ± 1.5) × 10^{-3}		
Γ_{51}	$\phi 2\pi^+ \pi^-$	[d]	(1.21 ± 0.16) %		
Γ_{52}	$K^+ K^- \rho^0 \pi^+$ non-ϕ		< 2.6 × 10^{-4}		CL=90%
Γ_{53}	$\phi\rho^0\pi^+$, $\phi \to K^+ K^-$		(6.5 ± 1.3) × 10^{-3}		
Γ_{54}	$\phi a_1(1260)^+$, $\phi \to K^+ K^-$, $a_1^+ \to \rho^0 \pi^+$		(7.4 ± 1.2) × 10^{-3}		
Γ_{55}	$K^+ K^- 2\pi^+ \pi^-$ nonresonant		(9 ± 7) × 10^{-4}		
Γ_{56}	$2K_S^0 2\pi^+ \pi^-$		(8 ± 4) × 10^{-4}		

Hadronic modes without K's

Γ_{57}	$\pi^+ \pi^0$		< 3.4 × 10^{-4}		CL=90%
Γ_{58}	$2\pi^+ \pi^-$		(1.09 ± 0.05) %		S=1.2
Γ_{59}	$\rho^0 \pi^+$		(2.0 ± 1.2) × 10^{-4}		
Γ_{60}	$\pi^+ (\pi^+ \pi^-)_{S-\text{wave}}$	[h]	(9.0 ± 0.5) × 10^{-3}		
Γ_{61}	$f_0(980)\pi^+$, $f_0 \to \pi^+ \pi^-$				
Γ_{62}	$f_0(1370)\pi^+$, $f_0 \to \pi^+ \pi^-$				
Γ_{63}	$f_0(1500)\pi^+$, $f_0 \to \pi^+ \pi^-$				
Γ_{64}	$f_2(1270)\pi^+$, $f_2 \to \pi^+ \pi^-$		(1.09 ± 0.20) × 10^{-3}		
Γ_{65}	$\rho(1450)^0 \pi^+$, $\rho^0 \to \pi^+ \pi^-$		(3.0 ± 1.9) × 10^{-4}		
Γ_{66}	$\pi^+ 2\pi^0$		(6.5 ± 1.3) × 10^{-3}		
Γ_{67}	$2\pi^+ \pi^- \pi^0$		—		
Γ_{68}	$\eta\pi^+$	[d]	(1.69 ± 0.10) %		S=1.2
Γ_{69}	$\omega\pi^+$	[d]	(2.4 ± 0.6) × 10^{-3}		
Γ_{70}	$3\pi^+ 2\pi^-$		(7.9 ± 0.8) × 10^{-3}		
Γ_{71}	$2\pi^+ \pi^- 2\pi^0$		—		
Γ_{72}	$\eta\rho^+$	[d]	(8.9 ± 0.8) %		
Γ_{73}	$\eta\pi^+ \pi^0$		(9.2 ± 1.2) %		
Γ_{74}	$\omega\pi^+ \pi^0$	[d]	(2.8 ± 0.7) %		
Γ_{75}	$3\pi^+ 2\pi^- \pi^0$		(4.9 ± 3.2) %		
Γ_{76}	$\omega 2\pi^+ \pi^-$	[d]	(1.6 ± 0.5) %		
Γ_{77}	$\eta'(958)\pi^+$	[c,d]	(3.94 ± 0.25) %		
Γ_{78}	$3\pi^+ 2\pi^- 2\pi^0$		—		
Γ_{79}	$\omega\eta\pi^+$	[d]	< 2.13 %		CL=90%
Γ_{80}	$\eta'(958)\rho^+$	[c,d]	(12.5 ± 2.2) %		
Γ_{81}	$\eta'(958)\pi^+ \pi^0$		(5.6 ± 0.8) %		

Modes with one or three K's

Γ_{82}	$K^+ \pi^0$		(6.3 ± 2.1) × 10^{-4}		
Γ_{83}	$K_S^0 \pi^+$		(1.21 ± 0.06) × 10^{-3}		
Γ_{84}	$K^+ \eta$	[d]	(1.76 ± 0.35) × 10^{-3}		
Γ_{85}	$K^+ \omega$	[d]	< 2.4 × 10^{-3}		CL=90%
Γ_{86}	$K^+ \eta'(958)$	[d]	(1.8 ± 0.6) × 10^{-3}		
Γ_{87}	$K^+ \pi^+ \pi^-$		(6.5 ± 0.4) × 10^{-3}		
Γ_{88}	$K^+ \rho^0$		(2.5 ± 0.4) × 10^{-3}		
Γ_{89}	$K^+ \rho(1450)^0$, $\rho^0 \to \pi^+ \pi^-$		(6.9 ± 2.4) × 10^{-4}		
Γ_{90}	$K^*(892)^0 \pi^+$, $K^{*0} \to K^+ \pi^-$		(1.41 ± 0.24) × 10^{-3}		
Γ_{91}	$K^*(1410)^0 \pi^+$, $K^{*0} \to K^+ \pi^-$		(1.23 ± 0.28) × 10^{-3}		
Γ_{92}	$K^*(1430)^0 \pi^+$, $K^{*0} \to K^+ \pi^-$		(5.0 ± 3.5) × 10^{-4}		
Γ_{93}	$K^+ \pi^+ \pi^-$ nonresonant		(1.04 ± 0.34) × 10^{-3}		
Γ_{94}	$K^0 \pi^+ \pi^0$		(1.00 ± 0.18) %		
Γ_{95}	$K_S^0 2\pi^+ \pi^-$		(3.0 ± 1.1) × 10^{-3}		
Γ_{96}	$K^+ \omega\pi^0$	[d]	< 8.2 × 10^{-3}		CL=90%
Γ_{97}	$K^+ \omega\pi^+ \pi^-$	[d]	< 5.4 × 10^{-3}		CL=90%
Γ_{98}	$K^+ \omega\eta$	[d]	< 7.9 × 10^{-3}		CL=90%
Γ_{99}	$2K^+ K^-$		(2.16 ± 0.21) × 10^{-4}		
Γ_{100}	ϕK^+, $\phi \to K^+ K^-$		(8.8 ± 2.0) × 10^{-5}		

Doubly Cabibbo-suppressed modes

Γ_{101}	$2K^+ \pi^-$		(1.26 ± 0.13) × 10^{-4}		
Γ_{102}	$K^+ K^*(892)^0$, $K^{*0} \to K^+ \pi^-$		(5.9 ± 3.4) × 10^{-5}		

Baryon-antibaryon mode

Γ_{103}	$p\overline{n}$		(1.3 ± 0.4) × 10^{-3}		

$\Delta C = 1$ weak neutral current ($C1$) modes, Lepton family number (LF), or Lepton number (L) violating modes

Γ_{104}	$\pi^+ e^+ e^-$		[i] < 1.3 × 10^{-5}		CL=90%
Γ_{105}	$\pi^+\phi$, $\phi \to e^+ e^-$		[j] (6 $^{+8}_{-4}$) × 10^{-6}		
Γ_{106}	$\pi^+ \mu^+ \mu^-$		[i] < 4.1 × 10^{-7}		CL=90%
Γ_{107}	$K^+ e^+ e^-$	$C1$	< 3.7 × 10^{-6}		CL=90%
Γ_{108}	$K^+ \mu^+ \mu^-$	$C1$	< 2.1 × 10^{-5}		CL=90%
Γ_{109}	$K^*(892)^+ \mu^+ \mu^-$	$C1$	< 1.4 × 10^{-3}		CL=90%
Γ_{110}	$\pi^+ e^+ \mu^-$	LF	< 1.2 × 10^{-5}		CL=90%
Γ_{111}	$\pi^+ e^- \mu^+$	LF	< 2.0 × 10^{-5}		CL=90%
Γ_{112}	$K^+ e^+ \mu^-$	LF	< 1.4 × 10^{-5}		CL=90%
Γ_{113}	$K^+ e^- \mu^+$	LF	< 9.7 × 10^{-6}		CL=90%
Γ_{114}	$\pi^- 2e^+$	L	< 4.1 × 10^{-6}		CL=90%
Γ_{115}	$\pi^- 2\mu^+$	L	< 1.2 × 10^{-7}		CL=90%
Γ_{116}	$\pi^- e^+ \mu^+$	L	< 8.4 × 10^{-6}		CL=90%
Γ_{117}	$K^- 2e^+$	L	< 5.2 × 10^{-6}		CL=90%
Γ_{118}	$K^- 2\mu^+$	L	< 1.3 × 10^{-5}		CL=90%
Γ_{119}	$K^- e^+ \mu^+$	L	< 6.1 × 10^{-6}		CL=90%
Γ_{120}	$K^*(892)^- 2\mu^+$	L	< 1.4 × 10^{-3}		CL=90%

[a] This is the purely e^+ semileptonic branching fraction: the e^+ fraction from τ^+ decays has been subtracted off. The sum of our (non-τ) e^+ exclusive fractions — an $e^+\nu_e$ with an η, η', ϕ, K^0, K^{*0}, or $f_0(980)$ — is 7.0 ± 0.4 %

[b] This fraction includes η from η' decays.

[c] Two times (to include μ decays) the $\eta' e^+ \nu_e$ branching fraction, plus the $\eta'\pi^+$, $\eta'\rho^+$, and $\eta' K^+$ fractions, is (18.6 ± 2.3)%, which considerably exceeds the inclusive η' fraction of (11.7 ± 1.8)%. Our best guess is that the $\eta'\rho^+$ fraction, (12.5 ± 2.2)%, is too large.

[d] This branching fraction includes all the decay modes of the final-state resonance.

[e] A test for $u\overline{u}$ or $d\overline{d}$ content in the D_s^+. Neither Cabibbo-favored nor Cabibbo-suppressed decays can contribute, and ω–ϕ mixing is an unlikely explanation for any fraction above about 2×10^{-4}.

[f] The branching fraction for this mode may differ from the sum of the submodes that contribute to it, due to interference effects. See the relevant papers.

[g] We decouple the $D_s^+ \to \phi\pi^+$ branching fraction obtained from mass projections (and used to get some of the other branching fractions) from the $D_s^+ \to \phi\pi^+$, $\phi \to K^+ K^-$ branching fraction obtained from the Dalitz-plot analysis of $D_s^+ \to K^+ K^- \pi^+$. That is, the ratio of these two branching fractions is not exactly the $\phi \to K^+ K^-$ branching fraction 0.491.

[h] This is the average of a model-independent and a K-matrix parametrization of the $\pi^+ \pi^-$ S-wave and is a sum over several f_0 mesons.

[i] This mode is not a useful test for a ΔC=1 weak neutral current because both quarks must change flavor in this decay.

[j] This is *not* a test for the ΔC=1 weak neutral current, but leads to the $\pi^+ \ell^+ \ell^-$ final state.

CONSTRAINED FIT INFORMATION

An overall fit to 16 branching ratios uses 19 measurements and one constraint to determine 12 parameters. The overall fit has a $\chi^2 = 5.7$ for 8 degrees of freedom.

The following *off-diagonal* array elements are the correlation coefficients $\langle \delta x_i \delta x_j \rangle / (\delta x_i \cdot \delta x_j)$, in percent, from the fit to the branching fractions, $x_i \equiv \Gamma_i/\Gamma_{\rm total}$. The fit constrains the x_i whose labels appear in this array to sum to one.

x_{25}	16									
x_{26}	12	2								
x_{31}	0	0	0							
x_{33}	0	0	0	54						
x_{45}	0	0	0	19	45					
x_{47}	0	0	0	38	38	17				
x_{58}	0	0	0	40	69	34	28			
x_{68}	0	0	0	10	−21	−19	1	−20		
x_{69}	0	0	0	1	−2	−2	0	−2	11	
x_{87}	0	0	0	22	19	3	13	11	9	1
	x_{23}	x_{25}	x_{26}	x_{31}	x_{33}	x_{45}	x_{47}	x_{58}	x_{68}	x_{69}

D_S^+ BRANCHING FRACTIONS

Written April 2010 by J.L. Rosner (University of Chicago) and C.G. Wohl (LBNL).

More than a dozen papers on the D_s^+, most of them from the CLEO experiment, have been published since the 2008 Review. We now know enough to attempt an overview of the branching fractions. Figure 1 shows a partial breakdown of the fractions. The rest of this note is about how the figure was constructed. The values shown make heavy use of CLEO measurements of inclusive branching fractions [1] For other data and references cited in the following, see the Listings.

Modes with leptons: The bottom $(20.0 \pm 0.9)\%$ of Fig. 1 shows the fractions for the exclusive modes that include leptons. Measured $e^+\nu_e$ fractions have been doubled to get the semileptonic $\ell^+\nu$ fractions. The sum of the exclusive $e^+\nu_e$ fractions is $(6.9 \pm 0.4)\%$, consistent with an inclusive semileptonic $e^+\nu_e$ measurement of $(6.5 \pm 0.4)\%$. There seems to be little missing here.

Inclusive hadronic $K\overline{K}$ fractions: The Cabibbo-favored $c \to s$ decay in D_s^+ decay produces a final state with both an s and an $\bar{s}$; and thus decay modes with a $K\overline{K}$ pair or with an η, ω, η', or ϕ predominate (see, for example, in Fig. 1 the fractions with leptons). We consider the $K\overline{K}$ modes first. A complete picture of the exclusive $K\overline{K}$ charge modes is not yet possible, because branching fractions for more than half of those modes have yet to be measured. However, CLEO has measured the inclusive K^+, K^-, K_S^0, K^+K^-, $K^+K_S^0$, $K^-K_S^0$, and $2K_S^0$ fractions (which include modes with leptons) [1]. And each of these inclusive fractions f with a K_S^0 is equal to the corresponding fraction with a K_L^0: $f(K^+K_L^0) = f(K^+K_S^0)$, $f(2K_L^0) = f(2K_S^0)$, *etc.* Therefore, of all inclusive fractions pairing a K^+, K_S^0, or K_L^0 with a K^-, K_S^0, or K_L^0, we know all but $f(K_S^0K_L^0)$.

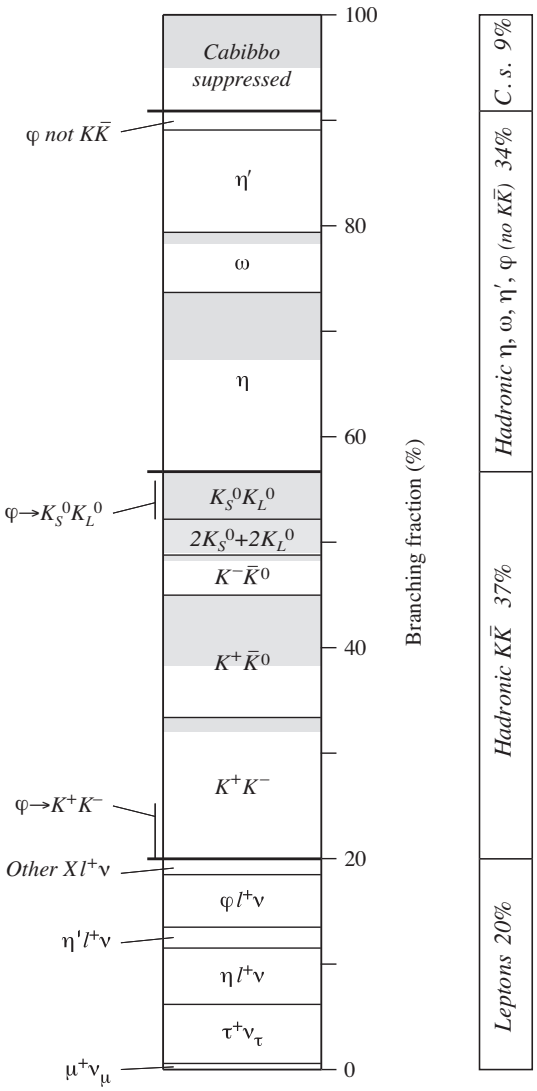

Figure 1: A partial breakdown of D_s^+ branching fractions. Shading indicates parts of bins allotted to as-yet unmeasured exclusive modes. The inclusive hadronic ϕ fraction is spread over three bins. See the text for further explanations.

We can get that fraction. The total K_S^0 fraction is

$$f(K_S^0) = f(K^+K_S^0) + f(K^-K_S^0) + 2f(2K_S^0) + f(K_S^0K_L^0) + f(\text{single } K_S^0) \ ,$$

where $f(\text{single } K_S^0)$ is the sum of the branching fractions for modes such as $K_S^0\pi^+2\pi^0$ with a K_S^0 and no second K. The $K_S^0\pi^+2\pi^0$ mode is in fact the only unmeasured single-K_S^0 mode (throughout, we shall assume that fractions for modes with a K or $K\overline{K}$ and more than three pions are negligible), and we shall take its fraction to be the same as for the $K_S^0 2\pi^+\pi^-$ mode, $(0.29 \pm 0.11)\%$. Any reasonable deviation from this value would be too small to matter much in the following. Adding the several small single-K_S^0 branching fractions, including those from semileptonic modes, we get $f(\text{single } K_S^0) = (1.67 \pm 0.26)\%$.

Using this, we have:

$$\begin{aligned} f(K^0_S K^0_L) &= f(K^0_S) - f(K^+K^0_S) - f(K^-K^0_S) - 2f(2K^0_S) \\ &\quad - f(\text{single } K^0_S) \\ &= (19.0 \pm 1.1) - (5.8 \pm 0.5) - (1.9 \pm 0.4) \\ &\quad - 2 \times (1.70 \pm 0.32) - (1.67 \pm 0.26) \\ &= (6.2 \pm 1.4)\% \ . \end{aligned}$$

Here and below we treat the errors as uncorrelated, although often they are not. However, our main aim is to get numbers for Fig. 1; errors will be secondary.

There is a check on our result: The ϕ inclusive branching fraction is $(15.7 \pm 1.0)\%$, of which 34%, or $(5.34 \pm 0.34)\%$ of D_s^+ decays, produces a $K^0_S K^0_L$. Our $f(K^0_S K^0_L) = (6.2 \pm 1.4)\%$ has to be at least this large—and it is.

We now make a table. The first column gives the various particle pairings; here we use $f(K^+\overline{K}^0) = 2\,f(K^+K^0_S)$, and likewise for $f(K^-K^0)$. The second column gives the inclusive branching fractions; the third column gives the fractions for K^+K^- and $K^0_S K^0_L$ from $\phi\ell^+\nu$ decay; the last column subtracts these off to get the purely hadronic $K\overline{K}$ inclusive fractions.

K^+K^-	15.8 (0.7)%	2.44 (0.14)%	13.4 (0.7)%
$K^+\overline{K}^0$	11.6 (1.0)		11.6 (1.0)
K^-K^0	3.8 (0.8)		3.8 (0.8)
$K^0_S K^0_S + K^0_L K^0_L$	3.4 (0.64)		3.4 (0.64)
$K^0_S K^0_L$	6.2 (1.4)	1.69 (0.10)	4.5 (1.4) .

The values in the last column are shown in Fig. 1. Their sum is $(36.7 \pm 2.1)\%$.

We can add more information to the figure by summing up measured branching fractions for exclusive modes within each bin:

K^+K^- *modes*—The sum of measured $K^+K^-\pi^+$, $K^+K^-\pi^+\pi^0$, and $K^+K^-2\pi^+\pi^-$ branching fractions is $(12.0 \pm 0.6)\%$. That leaves $(1.4 \pm 0.9)\%$ for the $K^+K^-\pi^+2\pi^0$ mode, which is the only other K^+K^- mode with three or fewer pions. In Fig. 1, this unmeasured part of the K^+K^- bin is shaded.

$K^+\overline{K}^0$ *modes*—Twice the sum of measured $K^+K^0_S$ and $K^+K^0_S\pi^+\pi^-$ branching fractions is $(4.9 \pm 0.3)\%$. This leaves $(6.7 \pm 1.0)\%$ for the unmeasured $K^+\overline{K}^0$ modes (there are four such modes with three or fewer pions). This is shaded in the figure.

K^-K^0 *modes*—Twice the $K^-K^0_S 2\pi^+$ fraction is $(3.28 \pm 0.24)\%$, which leaves about $(0.5 \pm 0.8)\%$ for $K^-K^0 2\pi^+\pi^0$, the only other K^-K^0 mode with three or fewer pions.

$K^0\overline{K}^0$ *modes*—The only measurement of $K^0\overline{K}^0$ decays is of the $2K^0_S 2\pi^+\pi^-$ fraction, $(0.084 \pm 0.035)\%$; so nearly everything is shaded here. However, most of the $K^0_S K^0_L$ fraction is accounted for by ϕ decays (see below).

Inclusive hadronic η, ω, η', and ϕ fractions: These are easier. We start with the inclusive branching fractions, and then, to avoid double counting, subtract: (1) fractions for modes with leptons; (2) η mesons that are included in the inclusive η' fraction; and (3) K^+K^- and $K^0_S K^0_L$ from ϕ decays:

$$\begin{aligned} f(\eta \text{ hadronic}) &= f(\eta \text{ inclusive}) - 0.65\, f(\eta' \text{ inclusive}) \\ &\quad - f(\eta\ell^+\nu) = (17.0 \pm 3.1)\% \\ f(\omega \text{ hadronic}) &= f(\omega \text{ inclusive}) - 0.03\, f(\eta' \text{ inclusive}) \\ &= (5.7 \pm 1.4)\% \\ f(\eta' \text{ hadronic}) &= f(\eta' \text{ inclusive}) - f(\eta'\ell^+\nu) \\ &= (9.7 \pm 1.9)\% \\ f(\phi \text{ hadronic}, \not\to K\overline{K}) &= 0.17\ [f(\phi \text{ inclusive}) \\ &\quad - f(\phi\ell^+\nu)] = (1.8 \pm 0.2)\% \ . \end{aligned}$$

The factors 0.65, 0.03, and 0.17 are the $\eta' \to \eta$, $\eta' \to \omega$, and $\phi \not\to K\overline{K}$ branching fractions. Figure 1 shows the results; the sum is $(34.2 \pm 3.9)\%$, which is about equal to the hadronic $K\overline{K}$ total.

Note that the bin marked ϕ near the top of Fig. 1 includes neither the $\phi\ell^+\nu$ decays nor the 83% of other ϕ decays that produce a $K\overline{K}$ pair. Compared to the size of that ϕ bin, there is twice as much ϕ in the $K^0_S K^0_L$ bin, and nearly three times as much in the K^+K^- bin. These contributions are indicated in those bins.

Again, we can show how much of each bin is accounted for by measured exclusive branching fractions:

η *modes*—The sum of $\eta\pi^+$, $\eta\rho^+$, and ηK^+ branching fractions is $(10.6 \pm 0.8)\%$, which leaves a good part of the inclusive hadronic η fraction, $(17.0 \pm 3.1)\%$, to be accounted for. This is shaded in the figure.

ω *modes*—The sum of $\omega\pi^+$, $\omega\pi^+\pi^0$, and $\omega 2\pi^+\pi^-$ fractions is $(4.6 \pm 0.9)\%$, which is nearly as large as the inclusive hadronic ω fraction, $(5.7 \pm 1.4)\%$.

η' *modes*—The sum of $\eta'\pi^+$, $\eta'\rho^+$, and $\eta' K^+$ fractions is $(16.5 \pm 2.2)\%$, which is much larger than the inclusive hadronic η' fraction, $(9.7 \pm 1.9)\%$. If an exclusive measurement is at fault, it almost has to be the $\eta'\rho^+$ fraction, which is $(12.5 \pm 2.2)\%$. It has been suggested that some of this signal might instead be misidentified kinematic reflections of other modes [2].

Cabibbo-suppressed modes: Remaining is $(9.1 \pm 4.5)\%$ for hadronic Cabibbo-suppressed modes having no η, ω, η', or ϕ. The contributions are:

K^0 + *pions*—Above, we found that $f(\text{single } K^0_S) = (1.67 \pm 0.26)\%$; subtracting leptonic contributions leaves $(1.20 \pm 0.24)\%$. The hadronic single-K^0 fraction is twice this, $(2.40 \pm 0.48)\%$.

K^+ + *pions*—The $K^+\pi^0$ and $K^+\pi^+\pi^-$ fractions sum to $(0.77 \pm 0.05)\%$. Much of the $K^+n\pi$ modes, where $n \geq 3$, is already in the η, ω, and η' bins, and the rest is not measured. The total K^+ fraction wanted here is probably in the 1-to-2% range.

Multi-pions—The $2\pi^+\pi^-$, $\pi^+2\pi^0$, and $3\pi^+2\pi^-$ fractions total $(2.6 \pm 0.2)\%$. Modes not measured might double this.

The sum of the three contributions is certainly not inconsistent with the Cabibbo-suppressed total of $(9.1 \pm 4.5)\%$. The sum of actually measured fractions is $(4.2 \pm 0.2)\%$.

A model: With CLEO about to publish inclusive branching fractions [1], Gronau and Rosner predicted those fractions using a "statistical isospin" model [2]. Consider, say, the $D_s^+ \to K\overline{K}\pi$ charge modes: the $K^+K^-\pi^+$ branching fraction is measured, the $K^+\overline{K}^0\pi^0$ and $K^0\overline{K}^0\pi^+$ fractions are not. The statistical isospin model assumes that all the independent isospin amplitudes for $D_s^+ \to K\overline{K}\pi$ decay are equal in magnitude and incoherent in phase—in which case, the ratio of the three fractions here is 3:3:2. (Actually, use was also made of the fact that $D_s^+ \to K\overline{K}\pi$ decay is dominated by $\phi\pi^+$, $K^+\overline{K}^{*0}$, and $K^{*+}\overline{K}^0$ submodes; but the estimated charge-mode ratios were not far from 3:3:2.) A different, quark-antiquark pair-production model was used to estimate systematic uncertainties.

In this way, unmeasured exclusive fractions were calculated from measured exclusive fractions (the latter were taken from the 2008 Review, and so did not benefit from recent results). In the hadronic sector, the measured total of 59.4% of D_s^+ decays led to an estimated total of 24.2% for unmeasured modes. Weighted counts of π^+, K_S^0, *etc.*, were then made to get the inclusive fractions.

Of interest here is that the sum of all the exclusive fractions—a way-stop in getting the inclusive values—was a nearly correct 103%. In the absence of complete measurements, the model is a way to, in effect, average over ignorance. It probably works better summed over a number of charge-mode sets than in detail. It is known to sometimes give incorrect results when there are sufficient measurements to test it.

References

1. S. Dobbs *et al.*, Phys. Rev. **D79**, 112008 (2009).
2. M. Gronau and J.L. Rosner, Phys. Rev. **D79**, 074022 (2009).

D_s^+ BRANCHING RATIOS

A number of older, now obsolete results have been omitted. They may be found in earlier editions.

Inclusive modes

$\Gamma(e^+ \text{semileptonic})/\Gamma_{total}$ Γ_1/Γ

This is the purely e^+ semileptonic branching fraction: the e^+ fraction from τ^+ decays has been subtracted off. The sum of our (non-τ) e^+ exclusive fractions — an $e^+\nu_e$ with an η, η', ϕ, K^0, K^{*0}, or $f_0(980)$ — is 6.90 ± 0.4 %

VALUE (units 10^{-2})	EVTS	DOCUMENT ID		TECN	COMMENT
6.52±0.39±0.15	536 ± 29	[1] ASNER	10	CLEO	e^+e^- at 3774 MeV

[1] Using the D_s^+ and D^0 lifetimes, ASNER 10 finds that the ratio of the D_s^+ and D^0 semileptonic widths is $0.828 \pm 0.051 \pm 0.025$.

$\Gamma(\pi^+ \text{anything})/\Gamma_{total}$ Γ_2/Γ

Events with two π^+'s count twice, etc. But π^+'s from $K_S^0 \to \pi^+\pi^-$ are not included.

VALUE (units 10^{-2})	DOCUMENT ID		TECN	COMMENT
119.3±1.2±0.7	DOBBS	09	CLEO	e^+e^- at 4170 MeV

$\Gamma(\pi^- \text{anything})/\Gamma_{total}$ Γ_3/Γ

Events with two π^-'s count twice, etc. But π^-'s from $K_S^0 \to \pi^+\pi^-$ are not included.

VALUE (units 10^{-2})	DOCUMENT ID		TECN	COMMENT
43.2±0.9±0.3	DOBBS	09	CLEO	e^+e^- at 4170 MeV

$\Gamma(\pi^0 \text{anything})/\Gamma_{total}$ Γ_4/Γ

Events with two π^0's count twice, etc. But π^0's from $K_S^0 \to 2\pi^0$ are not included.

VALUE (units 10^{-2})	DOCUMENT ID		TECN	COMMENT
123.4±3.8±5.3	DOBBS	09	CLEO	e^+e^- at 4170 MeV

$\Gamma(K^- \text{anything})/\Gamma_{total}$ Γ_5/Γ

VALUE (units 10^{-2})	DOCUMENT ID		TECN	COMMENT
18.7±0.5±0.2	DOBBS	09	CLEO	e^+e^- at 4170 MeV

$\Gamma(K^+ \text{anything})/\Gamma_{total}$ Γ_6/Γ

VALUE (units 10^{-2})	DOCUMENT ID		TECN	COMMENT
28.9±0.6±0.3	DOBBS	09	CLEO	e^+e^- at 4170 MeV

$\Gamma(K_S^0 \text{anything})/\Gamma_{total}$ Γ_7/Γ

VALUE (units 10^{-2})	DOCUMENT ID		TECN	COMMENT
19.0±1.0±0.4	DOBBS	09	CLEO	e^+e^- at 4170 MeV

$\Gamma(\eta \text{anything})/\Gamma_{total}$ Γ_8/Γ

This ratio includes η particles from η' decays.

VALUE (units 10^{-2})	EVTS	DOCUMENT ID		TECN	COMMENT
29.9±2.2±1.7		DOBBS	09	CLEO	e^+e^- at 4170 MeV
• • • We do not use the following data for averages, fits, limits, etc. • • •					
23.5±3.1±2.0	674 ± 91	HUANG	06B	CLEO	See DOBBS 09

$\Gamma(\omega \text{anything})/\Gamma_{total}$ Γ_9/Γ

VALUE (units 10^{-2})	DOCUMENT ID		TECN	COMMENT
6.1±1.4±0.3	DOBBS	09	CLEO	e^+e^- at 4170 MeV

$\Gamma(\eta' \text{anything})/\Gamma_{total}$ Γ_{10}/Γ

VALUE (units 10^{-2})	EVTS	DOCUMENT ID		TECN	COMMENT
11.7±1.7±0.7		DOBBS	09	CLEO	e^+e^- at 4170 MeV
• • • We do not use the following data for averages, fits, limits, etc. • • •					
8.7±1.9±0.8	68 ± 15	HUANG	06B	CLEO	See DOBBS 09

$\Gamma(f_0(980) \text{ anything}, f_0 \to \pi^+\pi^-)/\Gamma_{total}$ Γ_{11}/Γ

VALUE (units 10^{-2})	CL%	DOCUMENT ID		TECN	COMMENT
<1.3	90	DOBBS	09	CLEO	e^+e^- at 4170 MeV

$\Gamma(\phi \text{anything})/\Gamma_{total}$ Γ_{12}/Γ

VALUE (units 10^{-2})	EVTS	DOCUMENT ID		TECN	COMMENT
15.7±0.8±0.6		DOBBS	09	CLEO	e^+e^- at 4170 MeV
• • • We do not use the following data for averages, fits, limits, etc. • • •					
16.1±1.2±1.1	398 ± 27	HUANG	06B	CLEO	See DOBBS 09

$\Gamma(K^+K^- \text{anything})/\Gamma_{total}$ Γ_{13}/Γ

VALUE (units 10^{-2})	DOCUMENT ID		TECN	COMMENT
15.8±0.6±0.3	DOBBS	09	CLEO	e^+e^- at 4170 MeV

$\Gamma(K_S^0K^+ \text{anything})/\Gamma_{total}$ Γ_{14}/Γ

VALUE (units 10^{-2})	DOCUMENT ID		TECN	COMMENT
5.8±0.5±0.1	DOBBS	09	CLEO	e^+e^- at 4170 MeV

$\Gamma(K_S^0K^- \text{anything})/\Gamma_{total}$ Γ_{15}/Γ

VALUE (units 10^{-2})	DOCUMENT ID		TECN	COMMENT
1.9±0.4±0.1	DOBBS	09	CLEO	e^+e^- at 4170 MeV

$\Gamma(2K_S^0 \text{ anything})/\Gamma_{total}$ Γ_{16}/Γ

VALUE (units 10^{-2})	DOCUMENT ID		TECN	COMMENT
1.7±0.3±0.1	DOBBS	09	CLEO	e^+e^- at 4170 MeV

$\Gamma(2K^+ \text{anything})/\Gamma_{total}$ Γ_{17}/Γ

VALUE (units 10^{-2})	CL%	DOCUMENT ID		TECN	COMMENT
<0.26	90	DOBBS	09	CLEO	e^+e^- at 4170 MeV

$\Gamma(2K^- \text{anything})/\Gamma_{total}$ Γ_{18}/Γ

VALUE (units 10^{-2})	CL%	DOCUMENT ID		TECN	COMMENT
<0.06	90	DOBBS	09	CLEO	e^+e^- at 4170 MeV

Leptonic and semileptonic modes

LEPTONIC DECAYS OF CHARGED PSEUDOSCALAR MESONS

Revised September 2013 by J. Rosner (Univ. Chicago) and S. Stone (Syracuse Univ.)

We review the physics of purely leptonic decays of $\pi^\pm$, $K^\pm$, $D^\pm$, $D_s^\pm$, and $B^\pm$ pseudoscalar mesons. The measured decay rates are related to the product of the relevant weak-interaction-based CKM matrix element of the constituent quarks and a strong interaction parameter related to the overlap of the quark and antiquark wave-functions in the meson, called the decay constant f_P. The interplay between theory and experiment is different for each particle. Theoretical predictions of f_B that are needed in the B sector can be tested by measuring f_{D^+} and $f_{D_s^+}$ in the charm sector. The lighter $\pi^\pm$ and $K^\pm$ mesons provide stringent comparisons between experiment and theory due to the accuracy of both the measurements and the theoretical predictions [1].

Introduction: Charged mesons formed from a quark and an antiquark can decay to a charged lepton pair when these objects annihilate via a virtual W boson. Fig. 1 illustrates this process for the purely leptonic decay of a D^+ meson.

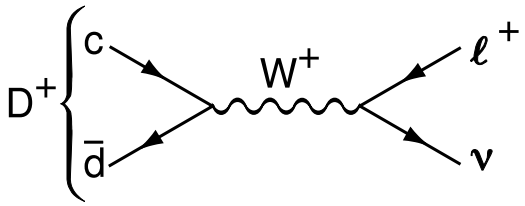

Figure 1: The annihilation process for pure D^+ leptonic decays in the Standard Model.

Similar quark-antiquark annihilations via a virtual W^+ to the $\ell^+\nu$ final states occur for the π^+, K^+, D_s^+, and B^+ mesons. (Charge-conjugate particles and decays are implied.) Let P be any of these pseudoscalar mesons. To lowest order, the decay width is

$$\Gamma(P \to \ell\nu) = \frac{G_F^2}{8\pi} f_P^2 \, m_\ell^2 M_P \left(1 - \frac{m_\ell^2}{M_P^2}\right)^2 |V_{q_1q_2}|^2 \quad . \qquad (1)$$

Here M_P is the P mass, m_ℓ is the ℓ mass, $V_{q_1q_2}$ is the Cabibbo-Kobayashi-Maskawa (CKM) matrix element between the constituent quarks $q_1\bar{q}_2$ in P, and G_F is the Fermi coupling constant. The parameter f_P is the decay constant, proportional to the matrix element of the axial current between the one-P-meson state and the vacuum, and is related to the wave-function overlap of the quark and antiquark.

The decay $P \to \ell\nu$ starts with a spin-0 meson, and ends up with a left-handed neutrino or right-handed antineutrino. By angular momentum conservation, the $\ell^\pm$ must then also be left-handed or right-handed, respectively. In the $m_\ell = 0$ limit, the decay is forbidden, and can only occur as a result of the finite ℓ mass. This helicity suppression is the origin of the m_ℓ^2 dependence of the decay width. Radiative corrections are needed when the final charged particle is an electron or muon [2].

Measurements of purely leptonic decay branching fractions and lifetimes allow an experimental determination of the product $|V_{q_1q_2}|\, f_P$. If the CKM element is well known from other measurements, then f_P can be well measured. If, on the other hand, the CKM element is not well measured, having theoretical input on f_P can allow a determination of the CKM element. The importance of measuring $\Gamma(P \to \ell\nu)$ depends on the particle being considered. For example, the measurement of $\Gamma(B^- \to \tau^-\overline{\nu})$ provides an indirect determination of $|V_{ub}|$ provided that f_B is provided by theory. In addition, f_B is crucial for using measurements of B^0-$\overline{B}^0$ mixing to extract information on the fundamental CKM parameters. Knowledge of f_{B_s} is also needed, but it cannot be directly measured as the B_s is neutral, so the violation of the SU(3) relation $f_{B_s} = f_B$ must be estimated theoretically. This difficulty does not occur for D mesons as both the D^+ and D_s^+ are charged, allowing the direct measurement of SU(3) breaking and a direct comparison with theory.

For B^- and D_s^+ decays, the existence of a charged Higgs boson (or any other charged object beyond the Standard Model) would modify the decay rates; however, this would not necessarily be true for the D^+ [3,4]. More generally, the ratio of $\tau\nu$ to $\mu\nu$ decays can serve as one probe of lepton universality [3,5].

As $|V_{ud}|$ has been quite accurately measured in super-allowed β decays [6], with a value of 0.97425(22) [7], measurements of $\Gamma(\pi^+ \to \mu^+\nu)$ yield a value for f_π. Similarly, $|V_{us}|$ has been well measured in semileptonic kaon decays, so a value for f_K from $\Gamma(K^- \to \mu^-\bar{\nu})$ can be compared to theoretical calculations. Lattice gauge theory calculations, however, have been claimed to be very accurate in determining f_K, and these have been used to predict $|V_{us}|$ [8].

Charmed mesons: Our review of current measurements starts with the charm system. Measurements have been made for $D^+ \to \mu^+\nu$, and $D_s^+ \to \mu^+\nu$ and $\tau^+\nu$. Only an upper limit has been determined for $D^+ \to \tau^+\nu$. Both CLEO-c and BES have made measurements of D^+ decay using e^+e^- collisions at the $\psi(3770)$ resonant energy where D^-D^+ pairs are copiously produced. They fully reconstruct one of the D's, say the D^-. Counting the number of these events provides the normalization for the branching fraction measurement. They then find a candidate μ^+, and then form the missing-mass squared, $MM^2 = (E_{\rm CM} - E_{D^-})^2 - \left(\overrightarrow{p}_{\rm CM} - \overrightarrow{p}_{D^-} - \overrightarrow{p}_{\mu^+}\right)^2$, taking into account their knowledge of the center-of-mass energy, $E_{\rm CM}$, and momentum, $p_{\rm CM}$, that equals zero in e^+e^- collisions. A peak at zero MM^2 infers the existence of a missing neutrino and hence the $\mu^+\nu$ decay of the D^+. CLEO-c does not explicitly identify the muon, so their data consist of a combination of $\mu^+\nu$ and $\tau^+\nu$, $\tau^+ \to \pi^+\nu$ events. This permits them to do two fits; in

one they fit for the individual components, and in the other they fix the ratio of $\tau^+\nu/\mu^+\nu$ events to be that given by the SM expectation. Thus, the latter measurement should be used for SM comparisons and the other for new physics searches. Our average uses the fixed ratio value. The measurements are shown in Table 1.

Table 1: Experimental results for $\mathcal{B}(D^+ \to \mu^+\nu)$, $\mathcal{B}(D^+ \to \tau^+\nu)$, and f_{D^+}. Numbers for f_{D^+} have been extracted using updated values for masses and $|V_{cd}|$ (see text). Radiative corrections are included. Systematic uncertainties arising from the D^+ lifetime and mass are included.

Experiment	Mode	$\mathcal{B}$	f_{D^+} (MeV)
CLEO-c [9]	$\mu^+\nu$	$(3.93 \pm 0.35 \pm 0.09) \times 10^{-4}$	$209.1 \pm 9.3 \pm 2.5$
CLEO-c [9]	$\mu^+\nu+\tau^+\nu$	$(3.82 \pm 0.32 \pm 0.09) \times 10^{-4}$	$206.2 \pm 8.6 \pm 2.6$
BES [10]	$\mu^+\nu$	$(3.74 \pm 0.21 \pm 0.06) \times 10^{-4}$	$204.0 \pm 5.7 \pm 2.0$
Average	$\mu^+\nu$	$(3.76 \pm 0.18) \times 10^{-4}$	204.6 ± 5.0
CLEO-c [13]	$\tau^+\nu$	$< 1.2 \times 10^{-3}$	

To extract the value of f_{D^+} we use the well-measured D^+ lifetime of 1.040(7) ps. The value of $|V_{cd}|$ is taken to equal to the value of $|V_{us}|$ of 0.2252(9) [7] minus higher-order correction terms [11], which results in $|V_{cd}| = 0.2251(9)$. The $\mu^+\nu$ results include a 1% correction (lowering) of the rate due to the presence of the radiative $\mu^+\nu\gamma$ final-state based on the estimate by Dobrescu and Kronfeld [12].

Before we compare this result with theoretical predictions, we discuss the D_s^+. Measurements of $f_{D_s^+}$ have been made by several groups and are listed in Table 2 [13–17]. We exclude older values obtained by normalizing to D_s^+ decay modes that are not well defined. Many measurements, for example, used the $\phi\pi^+$ mode. This decay is a subset of the $D_s^+ \to K^+K^-\pi^+$ channel which has interferences from other modes populating the K^+K^- mass region near the ϕ, the most prominent of which is the $f_0(980)$. Thus the extraction of effective $\phi\pi^+$ rate is sensitive to the mass resolution of the experiment and the cuts used to define the ϕ mass region [18,19].

To find decays in the $\mu^+\nu$ signal channels, CLEO, BaBar and Belle rely on fully reconstructing all the final-state particles except for neutrinos and using a missing-mass technique to infer the existence of the neutrino. CLEO uses $e^+e^- \to D_sD_s^*$ collisions at 4170 MeV, while Babar and Belle use $e^+e^- \to DKn\pi D_s^*$ collisions at energies near the $\Upsilon(4S)$. CLEO does a similar analysis as was done for the D^+ above. Babar and Belle do a similar MM^2 calculation by using the reconstructed hadrons, the photon from the D_s^{*+} decay and a detected μ^+. To get the normalization they do a MM^2 fit without the μ^+ and use the signal at the D_s^+ mass squared to determine the total D_s^+ yield.

When selecting the $\tau^+ \to \pi^+\bar{\nu}$ and $\tau^+ \to \rho^+\bar{\nu}$ decay modes, CLEO uses both calculation of the missing-mass and the fact that there should be no extra energy in the event beyond that deposited by the measured tagged D_s^- and the τ^+ decay products. The $\tau^+ \to e^+\nu\bar{\nu}$ mode, however, uses only extra energy. Babar and Belle also use no extra energy to discriminate signal from background in their $\tau^+\nu$ measurements.

We extract the decay constant from the measured branching ratios using the D_s^+ mass of 1.96849(32) GeV, the τ^+ mass of 1.77682(16) GeV, and a lifetime of 0.500(7) ps. We use the first-order correction $|V_{cs}| = |V_{ud}| - |V_{cb}|^2/2$ [11]; taking $|V_{ud}| = 0.97425(22)$ [6], and $|V_{cb}| = 0.04$ from an average of exclusive and inclusive semileptonic B decay results as discussed in Ref. [20], and find $|V_{cs}| = 0.97345(22)$. CLEO has included the radiative correction of 1% in the $\mu^+\nu$ rate listed in the Table [12] (the $\tau^+\nu$ rates need not be corrected). Other theoretical calculations show that the $\mu^+\nu\gamma$ rate is a factor of 40–100 below the $\mu^+\nu$ rate for charm [21]. As this is a small effect we do not attempt to correct the other measurements.

Table 2: Experimental results for $\mathcal{B}(D_s^+ \to \mu^+\nu)$, $\mathcal{B}(D_s^+ \to \tau^+\nu)$, and $f_{D_s^+}$. Numbers for $f_{D_s^+}$ have been extracted using updated values for masses and $|V_{cs}|$ (see text). Radiative corrections and systematic uncertainties for errors on the D_s^+ lifetime and mass have been included. Common systematic errors in each experiment have been taken into account.

Experiment	Mode	$\mathcal{B}(\%)$	$f_{D_s^+}$ (MeV)
CLEO-c [13]	$\mu^+\nu$	$0.565 \pm 0.045 \pm 0.017$	$257.6 \pm 10.3 \pm 4.3$
BaBar [14]	$\mu^+\nu$	$0.602 \pm 0.038 \pm 0.034$	$265.9 \pm 8.4 \pm 7.7$
Belle [15]	$\mu^+\nu$	$0.531 \pm 0.028 \pm 0.020$	$249 \pm 6.6 \pm 5.0$
Average	$\mu^+\nu$	0.556 ± 0.024	255.6 ± 5.9
CLEO-c [13]	$\tau^+\nu$ $(\pi^+\overline{\nu})$	$6.42 \pm 0.81 \pm 0.18$	$278.0 \pm 17.5 \pm 4.4$
CLEO-c [16]	$\tau^+\nu$ $(\rho^+\overline{\nu})$	$5.52 \pm 0.57 \pm 0.21$	$257.8 \pm 13.3 \pm 5.2$
CLEO-c [17]	$\tau^+\nu$ $(e^+\nu\overline{\nu})$	$5.30 \pm 0.47 \pm 0.22$	$252.6 \pm 11.2 \pm 5.6$
BaBar [14]	$\tau^+\nu$ $(e^+/\mu^+\nu\overline{\nu})$	$5.00 \pm 0.35 \pm 0.49$	$245.4 \pm 8.6 \pm 12.2$
Belle [15]	$\tau^+\nu$ $(\pi^+\overline{\nu})$	$6.04 \pm 0.43^{+0.46}_{-0.40}$	$269.6 \pm 9.6^{+10.4}_{-9.1}$
Belle [15]	$\tau^+\nu$ $(e^+\nu\overline{\nu})$	$5.37 \pm 0.33^{+0.35}_{-0.31}$	$254.2 \pm 7.8^{+8.5}_{-7.6}$
Belle [15]	$\tau^+\nu$ $(\mu^+\nu\overline{\nu})$	$5.86 \pm 0.37^{+0.34}_{-0.59}$	$265.5 \pm 8.4^{+7.9}_{-13.5}$
Average	$\tau^+\nu$	5.56 ± 0.22	258.3 ± 5.5

The average decay constant cannot simply be obtained by averaging the values in Table 2 since there are correlated errors between the $\mu^+\nu$ and $\tau^+\nu$ values. Table 3 gives the average values of f_{D_s} where the experiments have included the correlations.

Our experimental average is

$$f_{D_s^+} = (257.5 \pm 4.6) \text{ MeV}.$$

Table 3: Experimental results for $f_{D_s^+}$ taking into account the common systematic errors in the $\mu^+\nu$ and $\tau^+\nu$ measurements.

Experiment	$f_{D_s^+}$ (MeV)
CLEO-c	$259.0 \pm 6.2 \pm 3.0$
BaBar	$258.4 \pm 6.4 \pm 7.5$
Belle	$257.8 \pm 4.2 \pm 4.8$
Average of $\mu^+\nu + \tau^+\nu$	257.5 ± 4.6

Furthermore, the ratio of branching fractions is found to be

$$R \equiv \frac{\mathcal{B}(D_s^+ \to \tau^+\nu)}{\mathcal{B}(D_s^+ \to \mu^+\nu)} = 10.0 \pm 0.6,$$

where a value of 9.76 is predicted in the Standard Model. Assuming lepton universality then we can derive improved values for the leptonic decay branching fractions of

$$\mathcal{B}(D_s^+ \to \mu^+\nu) = (5.64 \pm 0.20) \times 10^{-3}, \quad \text{and}$$

$$\mathcal{B}(D_s^+ \to \tau^+\nu) = (5.51 \pm 0.20) \times 10^{-2} \ .$$

The experimentally determined ratio of decay constants is $f_{D_s^+}/f_{D^+} = 1.258 \pm 0.038$. Table 4 compares the experimental $f_{D_s^+}$ with theoretical calculations [22–27,30,31]. Most theories give values lower than the $f_{D_s^+}$ measurement. The discrepancies with the models with the smallest quoted uncertainties, both unquenched lattice calculations, are 2.0 standard deviations with HPQCD [22], and 1.9 standard deviations with the preliminary FNAL+MILC prediction [23].

Upper limits on f_{D^+} and f_{D_s} of 230 and 270 MeV, respectively, have been determined using two-point correlation functions by Khodjamirian [32]. The D^+ result is safely below this limit, while the average D_s^+ result is also, but older results [1] not used in our average are often above the limit.

Akeroyd and Chen [33] pointed out that leptonic decay widths are modified in two-Higgs-doublet models (2HDM). Specifically, for the D^+ and D_s^+, Eq. (1) is modified by a factor r_q multiplying the right-hand side [34]:

$$r_q = \left[1 + \left(\frac{1}{m_c + m_q}\right)\left(\frac{M_{D_q}}{M_{H^+}}\right)^2 \left(m_c - \frac{m_q \tan^2\beta}{1 + \epsilon_0 \tan\beta}\right)\right]^2,$$

where m_{H^+} is the charged Higgs mass, M_{D_q} is the mass of the D meson (containing the light quark q), m_c is the charm quark mass, m_q is the light-quark mass, and $\tan\beta$ is the ratio of the vacuum expectation values of the two Higgs doublets. In models where the fermion mass arises from coupling to more than one vacuum expectation value ϵ_0 can be non-zero, perhaps as large as 0.01. For the D^+, $m_d \ll m_c$, and the change due to the H^+ is very small. For the D_s^+, however, the effect can be substantial.

In order to investigate the possible presence of new physics we need to specify a SM value of $f_{D_s^+}$. We can only use a theory prediction. Our most aggressive choice is that of the unquenched lattice calculation [22], because it claims the smallest error. Since the charged Higgs would lower the rate compared to the SM, in principle, experiment gives a lower limit on the charged Higgs mass. However, the value for the

Table 4: Theoretical predictions of $f_{D_s^+}$, f_{D^+}, and $f_{D_s^+}/f_{D^+}$. Quenched lattice calculations are omitted, while PQL indicates a partially-quenched lattice calculation. (Only selected results having errors are included.)

Model	$f_{D_s^+}$(MeV)	f_{D^+}(MeV)	$f_{D_s^+}/f_{D^+}$
Experiment (our averages)	257.5 ± 4.6	204.6 ± 5.0	1.258 ± 0.038
Lattice (HPQCD) [22]	$246.0 \pm 0.7 \pm 3.5$	$208.3 \pm 1.0 \pm 3.3$	$1.187 \pm 0.004 \pm 0.012$
Lattice (FNAL+MILC) [23]	$246.4 \pm 0.5 \pm 3.6$	$209.2 \pm 3.0 \pm 3.6$	1.175 ± 0.019
PQL [24]	244 ± 8	197 ± 9	1.24 ± 0.03
QCD sum rules [25]	205 ± 22	177 ± 21	$1.16 \pm 0.01 \pm 0.03$
QCD sum rules [26]	$245.3 \pm 15.7 \pm 4.5$	$206.2 \pm 7.3 \pm 5.1$	$1.193 \pm 0.025 \pm 0.007$
QCD sum rules [27]	246 ± 6	204 ± 6	1.21 ± 0.04
QCD sum rules [28](I)	241 ± 12	208 ± 11	1.16 ± 0.07
QCD sum rules [28](II)	258 ± 13	211 ± 14	1.22 ± 0.08
QCD sum rules [29]	238^{+13}_{-23}	201^{+12}_{-13}	$1.15^{+0.04}_{-0.05}$
Field correlators [30]	260 ± 10	210 ± 10	1.24 ± 0.03
Light front [31]	268.3 ± 19.1	206 (fixed)	1.30 ± 0.04

predicted decay constant using this model is 2.0 standard deviations *below* the measurement. If this small discrepancy is to be taken seriously, either (a) the model of Ref. [22] is not representative; (b) no value of m_{H^+} in the two-Higgs doublet model will satisfy the constraint at 99% confidence level; or (c) there is new physics, different from the 2HDM, that interferes constructively with the SM amplitude such as in the R-parity-violating model of Akeroyd and Recksiegel [35].

To sum up, the standard model calculations are now consistent with the data and new physics effects are small. Limits can be placed on new particles depending on the specific model.

The B^- meson: The Belle and BaBar collaborations have found evidence for $B^- \to \tau^- \overline{\nu}$ decay in $e^+e^- \to B^-B^+$ collisions at the $\Upsilon(4S)$ energy. The analysis relies on reconstructing a hadronic or semi-leptonic B decay tag, finding a τ candidate in the remaining track and photon candidates, and examining the extra energy in the event which should be close to zero for a real τ^- decay to $e^-\nu\bar{\nu}$ or $\mu^-\nu\bar{\nu}$ opposite a B^+ tag. While the BaBar results have remained unchanged, Belle did a re-analysis of their data using the hadronic B decay sample. The branching fraction changed from $1.79^{+0.56}_{-0.49}{}^{+0.46}_{-0.51} \times 10^{-4}$ [36] to $0.72^{+0.27}_{-0.25} \pm 0.11 \times 10^{-4}$ [37]. This change demonstrates the difficulty of the analysis. It is unfortunate that other results have not been updated. The results are listed in Table 5.

Table 5: Experimental results for $\mathcal{B}(B^- \to \tau^- \overline{\nu})$.

Experiment	Tag	$\mathcal{B}$ (units of 10^{-4})
Belle [37]	Hadronic	$0.72^{+0.27}_{-0.25} \pm 0.11$
Belle [38]	Semileptonic	$1.54^{+0.38}_{-0.37}{}^{+0.29}_{-0.31}$
Belle [37]	Average	0.96 ± 0.26
BaBar [39]	Hadronic	$1.83^{+0.53}_{-0.49} \pm 0.24$
BaBar [40]	Semileptonic	$1.7 \pm 0.8 \pm 0.2$
BaBar [39]	Average	1.79 ± 0.48
	Our average	1.14 ± 0.23

There are large backgrounds under the signals in all cases. The systematic errors are also quite large. Thus, the significances are not that large. Belle quotes 3.0σ and 3.6σ for their hadronic and semileptonic tags, while BaBar quotes 3.3σ and 2.3σ for these tags. More accuracy would be useful to investigate the effects of new physics.

We extract a SM value using Eq. (1). Here theory provides a value of $f_B = (190.6 \pm 4.7)$ MeV [41]. We also need a value for $|V_{ub}|$. Here significant differences arise between using inclusive charmless semileptonic decays and the exclusive decay $B \to \pi\ell^+\nu$ [42]. The inclusive decays give rise to a value of $|V_{ub}| = (4.41 \pm 0.22) \times 10^{-3}$ while the exclusive measurements yield $|V_{ub}| = (3.23 \pm 0.31) \times 10^{-3}$, where the errors are dominantly theoretical [43]. Their average, enlarging the error in the standard manner because the results differ, is $|V_{ub}| = (4.01 \pm 0.56) \times 10^{-3}$. Using these values and the PDG values for the B^+ mass and lifetime, we arrive at the SM prediction for the $\tau^-\bar{\nu}$ branching fraction of $(1.03 \pm 0.29) \times 10^{-4}$. This value is now consistent with the average.

It is instructive to examine the correlation between the CKM angle β and $\mathcal{B}(B^- \to \tau^-\bar{\nu})$. The CKM fitter group provides a fit to a large number of measurements involving heavy quark transitions [44]. The black point in Fig. 2 shows the directly measured values from 2012, while the predictions from their fit without the direct measurements are also shown. There is about a factor of two discrepancy between the old measured average value of $\mathcal{B}(B^- \to \tau^- \overline{\nu})$ and the fit prediction. The (purple) dashed point shows the new Belle measurement only, and is consistent with the prediction, as is the new average.

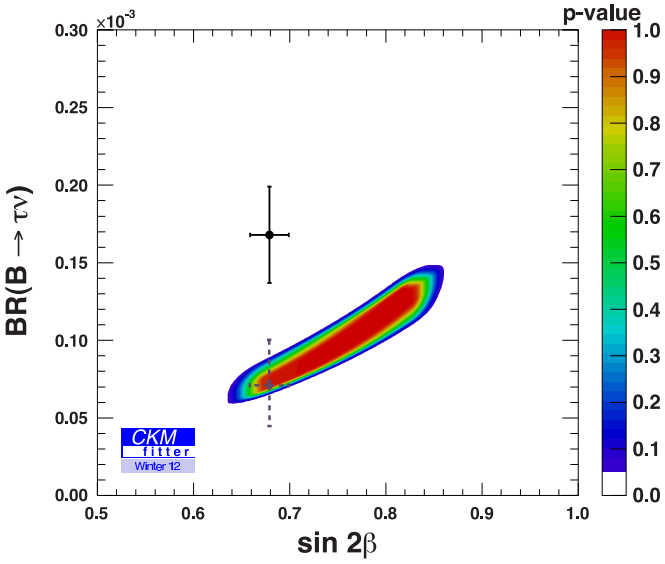

Figure 2: Measured versus predicted values of $\mathcal{B}(B^- \to \tau^- \overline{\nu})$ versus $\sin 2\beta$ from the CKM fitter group. The solid (black) point with error bars shows the old (2012) measured average value, the dashed (purple) point the new Belle measurement, while the predictions are in colors, with the color being related to the confidence level. (Adopted from the CKM Fitter group.)

Charged pions and kaons: We now discuss the determination of charged pion and kaon decay constants. The sum of branching fractions for $\pi^- \to \mu^-\bar{\nu}$ and $\pi^- \to \mu^-\bar{\nu}\gamma$ is 99.98770(4)%. The two modes are difficult to separate experimentally, so we use this sum, with Eq. (1) modified to include photon emission and radiative corrections [45]. The branching fraction together with the lifetime 26.033(5) ns gives

$$f_{\pi^-} = (130.41 \pm 0.03 \pm 0.20) \text{ MeV} .$$

The first error is due to the error on $|V_{ud}|$, 0.97425(22) [6]; the second is due to the higher-order corrections, and is much larger.

Similarly, the sum of branching fractions for $K^- \to \mu^-\bar{\nu}$ and $K^- \to \mu^-\bar{\nu}\gamma$ is 63.55(11)%, and the lifetime is 12.3840(193) ns [46]. Measurements of semileptonic kaon decays provide a value for the product $f_+(0)|V_{us}|$, where $f_+(0)$ is the form factor at zero four-momentum transfer between the initial state kaon and the final state pion. We use a value for $f_+(0)|V_{us}|$ of 0.2163(5) [46]. The $f_+(0)$ must be determined theoretically. The two most recent determinations from lattice QCD are 0.9667(23)(33) [47] and $0.9599(34)(^{+31}_{-43})$ [48], whose average is $f_+(0) = 0.9638(30)$. This is more precise than the classic Leutwyler-Roos calculation $f_+(0) = 0.961 \pm 0.008$ [49]. The result is $|V_{us}| = 0.2244(9)$, which is consistent with the hyperon decay value of 0.2250(27) [50].

Experimental branching ratios provide the ratio [52]

$$\frac{|V_{us}|f_{K^+}}{|V_{ud}|f_{\pi^-}} = 0.27598(35)(25) \ ,$$

where the first error is due to branching fractions and the second is due to electromagnetic corrections. With $|V_{ud}| = 0.97425(22)$, f_{π^-} as given above, and $|V_{us}| = 0.2244(9)$, we then find

$$f_{K^-} = (156.2 \pm 0.2 \pm 0.6 \pm 0.3) \text{ MeV} \ .$$

The first uncertainty is due to the error on Γ; the second is due to the CKM factor $|V_{us}|$, and the third is due to the higher-order corrections. The largest source of error in these corrections depends on the QCD part, which is based on one calculation in the large N_c framework. A large part of the additional uncertainty vanishes in the ratio of the K^- and π^- decay constants, which is

$$f_{K^-}/f_{\pi^-} = 1.198 \pm 0.002 \pm 0.005 \pm 0.001 \ .$$

The first uncertainty is due to the measured decay rates; the second is due to the uncertainties on the CKM factors; the third is due to the errors in the radiative correction ratio. These measurements can be used in conjunction with calculations of f_K/f_π in order to find a value for $|V_{us}|/|V_{ud}|$ [51]. Recent lattice predictions of f_K/f_π are shown in Table 6.

Table 6: Lattice calculations of f_K/f_π and extracted values of $|V_{us}|/|V_{ud}|$.

Group	f_K/f_π	$\lvert V_{us}\rvert/\lvert V_{ud}\rvert$
HPQCD [52]	1.1916 ± 0.0021	0.23160(54)
Laiho and Van de Water [53]	$1.202 \pm 0.011 \pm 0.013$	–
BMW [54]	$1.192 \pm 0.007 \pm 0.006$	0.2315(19)
MILC [55]	$1.1947 \pm 0.0026 \pm 0.0037$	0.2309(10)
RBC/UKQCD [56]	$1.204 \pm 0.007 \pm 0.025$	–

These calculations are in agreement with our experimental average. Together with the precisely measured $|V_{ud}|$, these results can be used to find an independent measure of $|V_{us}|$ [8,46].

We gratefully acknowledge support of the U. S. National Science Foundation and the U. S. Department of Energy through Grant No. DE-FG02-90ER40560. We thank A. Khodjamirian, J. Laiho, W. Marciano, S. Narison, and Z.-G. Wang for useful discussions and references.

References

1. This article is an update of the one prepared for the PDG 2012 edition; see J. L. Rosner and S. Stone in J. Beringer *et al.*, Phys. Rev. D **86**, 946 (2012).
2. Most predictions for the rate for $B^- \to \mu^-\bar{\nu}\gamma$ are in the range of 1 to 20 times the rate for $B^- \to \mu^-\bar{\nu}$. See G. Burdman, T. Goldman, and D. Wyler, Phys. Rev. **D51**, 111 (1995); P. Colangelo, F. De Fazio, and G. Nardulli, Phys. Lett. **B372**, 331 (1996); *ibid.*, **386**, 328 (1996); A. Khodjamirian, G. Stoll, and D. Wyler, Phys. Lett. **B358**, 129 (1995); G. Eilam, I. Halperin, and R. Mendel, Phys. Lett. **B361**, 137 (1995); D. Atwood, G. Eilam, and A. Soni, Mod. Phys. Lett. **A11**, 1061 (1996); C.Q. Geng and C.C. Lih, Phys. Rev. **D57**, 5697 (1998) and Mod. Phys. Lett. **A15**, 2087 (2000); G.P. Korchemsky, D. Pirjol, and T. M. Yan, Phys. Rev. **D61**, 114510 (2000); C.W. Hwang, Eur. Phys. J. **C46**, 379 (2006).
3. W.-S. Hou, Phys. Rev. **D48**, 2342 (1993).
4. See, for example, A.G. Akeroyd and S. Recksiegel, Phys. Lett. **B554**, 38 (2003); A.G. Akeroyd, Prog. Theor. Phys. **111**, 295 (2004).
5. J.L. Hewett, `hep-ph/9505246`, presented at *Lafex International School on High Energy Physics (LISHEP95)*, Rio de Janeiro, Brazil, Feb. 6-22, 1995.
6. I.S. Towner and J.C. Hardy, Phys. Rev. **C79**, 055502 (2009); *ibid.* **77**, 025501 (2008).
7. E. Blucher and W. J. Marciano, "V_{ud}, V_{us}, the Cabibbo Angle and CKM Unitarity" in J. Beringer *et al.*, (Particle Data Group), Phys. Rev. D **86**, 852 (2012).
8. G. Colangelo *et al.*, Eur. Phys. J. **C71**, 1695 (2011); W. J. Marciano, Phys. Rev. Lett. **93**, 231803 (2004); A. Jüttner, PoS LAT2007, 014 (2007) `[arXiv:0711.1239]`.
9. B. I. Eisenstein *et al.* (CLEO Collab.), Phys. Rev. **D78**, 052003 (2008). See also M. Artuso *et al.* (CLEO Collab.), Phys. Rev. Lett. **95**, 251801 (2005).
10. G. Huang (BESIII Collab.), "Recent Results from BESIII," presented at FPCP 2012, Hefei, China May, 2012, `[arXiv:1209.4813]`.
11. J. Charles *et al.*, Eur. Phys. J. **C41**, 1 (2005).
12. B. A. Dobrescu and A. S. Kronfeld, Phys. Rev. Lett. **100**, 241802 (2008).
13. J.P. Alexander *et al.* (CLEO Collab.), Phys. Rev. **D79**, 052001 (2009); M. Artuso *et al.* (CLEO Collab.), Phys. Rev. Lett. **99**, 071802 (2007).
14. P. del Amo Sanchez *et al.* (BaBar Collab.), Phys. Rev. D **82**, 091103 (2010) `[arXiv:1008.4080]`. We do not use the previous BaBar result from a subsample of data as reported in J. P. Lees *et al.* (BaBar Collab.), `[arXiv:1003.3063]`.
15. A. Zupanc *et al.*, (Belle Collab.), `[arXiv:1307.6240]`.

16. P. Naik *et al.* (CLEO Collab.), Phys. Rev. **D80**, 112004 (2009).
17. P.U.E. Onyisi *et al.* (CLEO Collab.), Phys. Rev. **D79**, 052002 (2009); K. M. Ecklund *et al.* (CLEO Collab.), Phys. Rev. Lett. **100**, 161801 (2008).
18. See J. Alexander *et al.* (CLEO Collab.), Phys. Rev. Lett. **100**, 161804 (2008).
19. We have not included a BaBar result: $\mathcal{B}(D_s^+ \to \mu^+\nu) = (6.67\pm0.83\pm0.26\pm0.66)\times10^{-3}$ and $f_{D_s^+} = (281\pm17\pm7\pm14)$ MeV based on $\mathcal{B}(D_s^+ \to \phi\pi^+) = (4.71\pm0.46)\%$. These measurements determined the ratio of the leptonic decay to a hadronic decay, usually $\Gamma(D_s^+ \to \ell^+\nu)/\Gamma(D_s^+ \to \phi\pi^+)$. See B. Aubert *et al.* (BABAR Collab.), Phys. Rev. Lett. **98**, 141801 (2007).
20. M. Artuso, E. Barberio, and S. Stone, PMC Physics A, 3:3 (2009) [arXiv:0902.3743].
21. See most papers in Ref. 2 and C.D. Lü and G.L. Song, Phys. Lett. **B562**, 75 (2003).
22. H. Na *et al.*, (HPQCD Collab.), Phys. Rev. D **86**, 054510 (2012).
23. A. Bazavov *et al.* (Fermilab/MILC Collab.), [arXiv:1112.3051], submitted to Phys. Rev. D.
24. B. Blossier *et al.*, JHEP **0907**, 043 (2009) [arXiv:0904.0954].
25. J. Bordes, J. Peñarrocha, and K. Schilcher, JHEP **0511**, 014 (2005).
26. W. Lucha, D. Melikhov, and S. Simula, Phys. Lett. **B701**, 82 (2011).
27. S. Narison, Phys. Lett. B **718**, 1321 (2013), [arXiv:1209.2023]; *ibid.*, **721**, 269 (2013).
28. Z.-G. Wang, [arXiv:1301.1399]. Cases I and II correspond to two different choices of heavy quark masses, QCD order, and renormalization scale..
29. P. Gelhausen *et al.*, Phys. Rev, D **88**, 014015 (2013) [arXiv:1305.5432]..
30. A.M. Badalian *et al.*, Phys. Rev. **D75**, 116001 (2007); see also A.M. Badalian and B.L.G. Bakker, [hep-ph/0702229].
31. C.-W. Hwang, Phys. Rev. **D81**, 054022 (2010) [arXiv:0910.0145].
32. A. Khodjamirian, Phys. Rev. **D79**, 031503 (2009).
33. A.G. Akeroyd and C.H. Chen, Phys. Rev. **D75**, 075004 (2007).
34. A.G. Akeroyd and F. Mahmoudi, JHEP **0904**, 121 (2009).
35. A.G. Akeroyd and S. Recksiegel, Phys. Lett. **B554**, 38 (2003).
36. K. Ikado *et al.* (Belle Collab.), Phys. Rev. Lett. **97**, 251802 (2006).
37. K. Ikado *et al.* (Belle Collab.), Phys. Rev. Lett. **110**, 131801 (2013)..
38. K. Hara *et al.* (Belle Collab.), Phys. Rev. **D82**, 071101R (2010).
39. J.P. Lees *et al.* (BaBar Collab.), Phys. Rev. **D88**, 031102 [arXiv:1207.0698].
40. B. Aubert *et al.* (BaBar Collab.), Phys. Rev. **D81**, 051101R (2010).
41. We have averaged the values of A. Bazavov *et al.* (Fermilab Lattice and MILC Collabs.), Phys. Rev. **D85**, 114506 (2012) ($f_B = 196.9 \pm 5.5 \pm 7.0$ MeV), and H. Na *et al.* (HPQCD Collab.), Phys. Rev. **D86**, 034506 (2012) ($f_B = 189 \pm 3.1 \pm 3.2$ MeV), assuming that 3.2 MeV of the systematic uncertainty is fully correlated. See also S. Narison [27–29], who find respective values of $f_B = 206\pm7$ MeV, 189 ± 15 MeV(I), or 190 ± 17 MeV(II), and 207^{+17}_{-9} MeV using QCD sum rules.
42. See the discussion in M. Artuso, E. Barberio, and S. Stone, Ref. 20.
43. R. Kowalewski and T. Mannel, in J. Beringer *et al.* (Particle Data Group), Phys. Rev. **D86**, 1111 (2012).
44. J. Charles *et al.* (CKMfitter Group), Phys. Rev. **D85**, 1 (2011) [arXiv:1106.4041 [hep-ph]], updated results and plots available at: http://ckmfitter.in2p3.fr.
45. W.J. Marciano and A. Sirlin, Phys. Rev. Lett. **71**, 3629 (1993); V. Cirigliano and I. Rosell, JHEP **0710**, 005 (2007).
46. Flavianet Working Group on Precise SM Tests in K Decays, M. Antonelli *et al.*, Eur. Phys. J. **C69**, 399 (2010).
47. A. Bazavov *et al.* (Fermilab Lattice and MILC Collab.), Phys. Rev. D **87**, 073012 (2013).
48. P. A. Boyle *et al.* (RBC-UKQCD Collab.), Eur. Phys. J. C **69**, 159 (2010).
49. H. Leutwyler and M. Roos, Z. Phys. **C25**, 91 (1984).
50. N. Cabibbo, E.C. Swallow, and R. Winston, Phys. Rev. Lett. **92**, 251803 (2004).
51. W. J. Marciano, Phys. Rev. Lett. **93**, 231803 (2004), [hep-ph/0402299].
52. R. J. Dowdall *et al.*, (HPQCD Collab.), [arXiv:1303.1670].
53. J. Laiho and R. Van de Water, [arXiv:1112.4861], in PoS Lattice2011, 293 (2011).
54. S. Durr *et al.*, Phys. Rev. D **81**, 054507 (2010), [arXiv:1001.4692].
55. A. Bazavov *et al.* (MILC Collab.), Phys. Rev. Lett. **110**, 172003 (2013) [arXiv:1301.5855].
56. Y. Aoki, *et al.* (RBC/UKQCD Collab.), Phys. Rev. D **83**, 074508 (2011) [arXiv:1011.0892].

$\Gamma(e^+\nu_e)/\Gamma_{\text{total}}$ Γ_{19}/Γ

VALUE	CL%	DOCUMENT ID		TECN	COMMENT
$<0.83\times10^{-4}$	90	[1] ZUPANC	13	BELL	e^+e^- at $\Upsilon(4S),\Upsilon(5S)$
• • • We do not use the following data for averages, fits, limits, etc. • • •					
$<2.3\times10^{-4}$	90	DEL-AMO-SA...10J		BABR	e^+e^-, 10.58 GeV
$<1.2\times10^{-4}$	90	ALEXANDER	09	CLEO	e^+e^- at 4170 MeV
$<1.3\times10^{-4}$	90	PEDLAR	07A	CLEO	See ALEXANDER 09

[1] ZUPANC 13 also gives the limit as $<1.0\times10^{-4}$ at 95% CL.

$\Gamma(\mu^+\nu_\mu)/\Gamma_{\text{total}}$ Γ_{20}/Γ

See the note on "Decay Constants of Charged Pseudoscalar Mesons" above.

VALUE (units 10^{-3})	EVTS	DOCUMENT ID		TECN	COMMENT
5.56±0.25 OUR AVERAGE					
$5.31\pm0.28\pm0.20$	492 ± 26	[1] ZUPANC	13	BELL	e^+e^- at $\Upsilon(4S),\Upsilon(5S)$
$6.02\pm0.38\pm0.34$	275 ± 17	[2] DEL-AMO-SA...10J		BABR	e^+e^-, 10.58 GeV
$5.65\pm0.45\pm0.17$	235 ± 14	ALEXANDER	09	CLEO	e^+e^- at 4170 MeV
• • • We do not use the following data for averages, fits, limits, etc. • • •					
$6.44\pm0.76\pm0.57$	169 ± 18	[3] WIDHALM	08	BELL	See ZUPANC 13
$5.94\pm0.66\pm0.31$	88	[4] PEDLAR	07A	CLEO	See ALEXANDER 09
$6.8\ \pm1.1\ \pm1.8$	553	[5] HEISTER	02I	ALEP	Z decays

[1] ZUPANC 13 uses both $\mu^+\nu$ and $\tau^+\nu$ events to get $f_{D_s} = (255.5 \pm 4.2 \pm 5.1)$ MeV.
[2] DEL-AMO-SANCHEZ 10J uses $\mu^+\nu_\mu$ and $\tau^+\nu_\tau$ events together to get $f_{D_s} = (258.6 \pm 6.4 \pm 7.5)$ MeV.
[3] WIDHALM 08 gets $f_{D_s} = (275 \pm 16 \pm 12)$ MeV from the branching fraction.
[4] PEDLAR 07A also fits μ^+ and τ^+ events together and gets an effective $\mu^+\nu_\mu$ branching fraction of $(6.38 \pm 0.59 \pm 0.33)\times10^{-3}$
[5] This HEISTER 02I result is not actually an independent measurement of the absolute $\mu^+\nu_\mu$ branching fraction, but is in fact based on our $\phi\pi^+$ branching fraction of $3.6 \pm 0.9\%$, so it cannot be included in our overall fit. HEISTER 02I combines its $D_s^+ \to \tau^+\nu_\tau$ and $\mu^+\nu_\mu$ branching fractions to get $f_{D_s} = (285 \pm 19 \pm 40)$ MeV.

$\Gamma(\mu^+\nu_\mu)/\Gamma(\phi\pi^+)$ Γ_{20}/Γ_{34}

See the note on "Decay Constants of Charged Pseudoscalar Mesons" above.

VALUE	EVTS	DOCUMENT ID		TECN	COMMENT
• • • We do not use the following data for averages, fits, limits, etc. • • •					
0.143±0.018±0.006	489 ± 55	[1] AUBERT	07V	BABR	$e^+e^- \approx \Upsilon(4S)$
0.23 ±0.06 ±0.04	18	[2] ALEXANDROV	00	BEAT	π^- nucleus, 350 GeV
0.173±0.023±0.035	182	[3] CHADHA	98	CLE2	$e^+e^- \approx \Upsilon(4S)$
0.245±0.052±0.074	39	[4] ACOSTA	94	CLE2	See CHADHA 98

[1] AUBERT 07V gets $f_{D_s^+}$ = (283 ± 17 ± 16) MeV, using $\Gamma(D_s^+ \to \phi\pi^+)/\Gamma$(total) = (4.71 ± 0.46)%.

[2] ALEXANDROV 00 uses $f_D^2/f_{D_s}^2 = 0.82 \pm 0.09$ from a lattice-gauge-theory calculation to get the relative numbers of $D^+ \to \mu^+\nu_\mu$ and $D_s^+ \to \mu^+\nu_\mu$ events. The present result leads to f_{D_s} = (323 ± 44 ± 36) MeV.

[3] CHADHA 98 obtains f_{D_s} = (280 ± 19 ± 28 ± 34) MeV from this measurement, using $\Gamma(D_s^+ \to \phi\pi^+)/\Gamma$(total) = 0.036 ± 0.009.

[4] ACOSTA 94 obtains f_{D_s} = (344 ± 37 ± 52 ± 42) MeV from this measurement, using $\Gamma(D_s^+ \to \phi\pi^+)/\Gamma$(total) = 0.037 ± 0.009.

$\Gamma(\tau^+\nu_\tau)/\Gamma_{\text{total}}$ Γ_{21}/Γ

See the note on "Decay Constants of Charged Pseudoscalar Mesons" above.

VALUE (units 10^{-2})	EVTS	DOCUMENT ID		TECN	COMMENT
5.54±0.24 OUR AVERAGE					
$5.70\pm0.21^{+0.31}_{-0.30}$	2.2k	[1] ZUPANC	13	BELL	e^+e^- at $\Upsilon(4S)$, $\Upsilon(5S)$
5.00±0.35±0.49	748 ± 53	[2] DEL-AMO-SA...	10J	BABR	$e^-\overline{\nu}_e\nu_\tau$, $\mu^-\overline{\nu}_\mu\nu_\tau$
6.42±0.81±0.18	126 ± 16	[3] ALEXANDER	09	CLEO	$\tau^+ \to \pi^+\overline{\nu}_\tau$
5.52±0.57±0.21	155 ± 17	[3] NAIK	09A	CLEO	$\tau^+ \to \rho^+\overline{\nu}_\tau$
5.30±0.47±0.22	181 ± 16	[3] ONYISI	09	CLEO	$\tau^+ \to e^+\nu_e\overline{\nu}_\tau$
• • • We do not use the following data for averages, fits, limits, etc. • • •					
6.17±0.71±0.34	102	[4] ECKLUND	08	CLEO	See ONYISI 09
8.0 ±1.3 ±0.4	47	[4] PEDLAR	07A	CLEO	See ALEXANDER 09
5.79±0.77±1.84	881	[5] HEISTER	02I	ALEP	Z decays
7.0 ±2.1 ±2.0	22	[6] ABBIENDI	01L	OPAL	$D_s^{*+} \to \gamma D_s^+$ from Z's
7.4 ±2.8 ±2.4	16	[7] ACCIARRI	97F	L3	$D_s^{*+} \to \gamma D_s^+$ from Z's

[1] ZUPANC 13 uses both $\mu^+\nu$ and $\tau^+\nu$ events to get f_{D_s} = (255.5 ± 4.2 ± 5.1) MeV.

[2] DEL-AMO-SANCHEZ 10J uses $\mu^+\nu_\mu$ and $\tau^+\nu_\tau$ events together to get f_{D_s} = (258.6 ± 6.4 ± 7.5) MeV.

[3] ALEXANDER 09, NAIK 09A, and ONYISI 09 use different τ decay modes and are independent. The three papers combined give f_{D_s} = (259.7 ± 7.8 ± 3.4) MeV.

[4] ECKLUND 08 and PEDLAR 07A are independent: ECKLUND 08 uses $\tau^+ \to e^+\nu_e\overline{\nu}_\tau$ events, PEDLAR 07A uses $\tau^+ \to \pi^+\overline{\nu}_\tau$ events.

[5] HEISTER 02I combines its $D_s^+ \to \tau^+\nu_\tau$ and $\mu^+\nu_\mu$ branching fractions to get f_{D_s} = (285 ± 19 ± 40) MeV.

[6] This ABBIENDI 01L value gives a decay constant f_{D_s} of (286 ± 44 ± 41) MeV.

[7] The second ACCIARRI 97F error here combines in quadrature systematic (0.016) and normalization (0.018) errors. The branching fraction gives f_{D_s} = (309 ± 58 ± 33 ± 38) MeV.

$\Gamma(\tau^+\nu_\tau)/\Gamma(\mu^+\nu_\mu)$ Γ_{21}/Γ_{20}

VALUE	EVTS	DOCUMENT ID		TECN	COMMENT
• • • We do not use the following data for averages, fits, limits, etc. • • •					
$10.73\pm0.69^{+0.56}_{-0.53}$	2.2k/492	[1] ZUPANC	13	BELL	e^+e^- at $\Upsilon(4S)$, $\Upsilon(5S)$
11.0 ±1.4 ±0.6	102	[2] ECKLUND	08	CLEO	See ONYISI 09

[1] This ZUPANC 13 ratio is not independent of the separate $\tau\nu$ and $\mu\nu$ fractions listed above.

[2] This ECKLUND 08 value also uses results from PEDLAR 07A, and it is not independent of other results in these Listings. Combined with earlier CLEO results, the decay constant f_{D_s} is 274 ± 10 ± 5 MeV.

$\Gamma(K^+K^-e^+\nu_e)/\Gamma(K^+K^-\pi^+)$ Γ_{22}/Γ_{33}

VALUE	DOCUMENT ID		TECN	COMMENT
• • • We do not use the following data for averages, fits, limits, etc. • • •				
0.558±0.007±0.016	[1] AUBERT	08AN	BABR	e^+e^- at $\Upsilon(4S)$

[1] This AUBERT 08AN ratio is only for the K^+K^- mass in the range 1.01–to–1.03 GeV in the numerator and 1.0095–to–1.0295 GeV in the denominator.

$\Gamma(\phi e^+\nu_e)/\Gamma_{\text{total}}$ Γ_{23}/Γ

See the end of the D_s^+ Listings for measurements of $D_s^+ \to \phi e^+\nu_e$ form factors. Unseen decay modes of the ϕ are included.

VALUE (units 10^{-2})	EVTS	DOCUMENT ID		TECN	COMMENT
2.49±0.14 OUR FIT					
2.54±0.14 OUR AVERAGE					
2.36±0.23±0.13	106 ± 10	ECKLUND	09	CLEO	e^+e^- at 4170 MeV
2.61±0.03±0.17	(25 ± 0.5)k	AUBERT	08AN	BABR	e^+e^- at $\Upsilon(4S)$
• • • We do not use the following data for averages, fits, limits, etc. • • •					
2.29±0.37±0.11	45	YELTON	09	CLEO	See ECKLUND 09

$\Gamma(\phi e^+\nu_e)/\Gamma(\phi\pi^+)$ Γ_{23}/Γ_{34}

As noted in the comment column, most of these measurements use $\phi\mu^+\nu_\mu$ events in addition to or instead of $\phi e^+\nu_e$ events.

VALUE	EVTS	DOCUMENT ID		TECN	COMMENT
• • • We do not use the following data for averages, fits, limits, etc. • • •					
0.540±0.033±0.048	793	LINK	02J	FOCS	Uses $\phi\mu^+\nu_\mu$
0.54 ±0.05 ±0.04	367	BUTLER	94	CLE2	Uses $\phi e^+\nu_e$ and $\phi\mu^+\nu_\mu$
0.58 ±0.17 ±0.07	97	FRABETTI	93G	E687	Uses $\phi\mu^+\nu_\mu$
0.57 ±0.15 ±0.15	104	ALBRECHT	91	ARG	Uses $\phi e^+\nu_e$
0.49 ±0.10 $^{+0.10}_{-0.14}$	54	ALEXANDER	90B	CLEO	Uses $\phi e^+\nu_e$ and $\phi\mu^+\nu_\mu$

$\Gamma(\eta e^+\nu_e)/\Gamma_{\text{total}}$ Γ_{25}/Γ

Unseen decay modes of the η are included.

VALUE (units 10^{-2})	EVTS	DOCUMENT ID		TECN	COMMENT
2.67±0.29 OUR FIT	Error includes scale factor of 1.1.				
2.48±0.29±0.13	82	YELTON	09	CLEO	e^+e^- at 4170 MeV

$\Gamma(\eta e^+\nu_e)/\Gamma(\phi e^+\nu_e)$ Γ_{25}/Γ_{23}

Unseen decay modes of the η and the ϕ are included.

VALUE	EVTS	DOCUMENT ID		TECN	COMMENT
1.07±0.12 OUR FIT	Error includes scale factor of 1.1.				
1.24±0.12±0.15	440	[1] BRANDENB...	95	CLE2	$e^+e^- \approx \Upsilon(4S)$

[1] BRANDENBURG 95 uses both e^+ and μ^+ events and makes a phase-space adjustment to use the μ^+ events as e^+ events.

$\Gamma(\eta'(958)e^+\nu_e)/\Gamma_{\text{total}}$ Γ_{26}/Γ

Unseen decay modes of the $\eta'(958)$ are included.

VALUE (units 10^{-2})	EVTS	DOCUMENT ID		TECN	COMMENT
0.99±0.23 OUR FIT					
0.91±0.33±0.05	7.5	YELTON	09	CLEO	e^+e^- at 4170 MeV

$\Gamma(\eta'(958)e^+\nu_e)/\Gamma(\phi e^+\nu_e)$ Γ_{26}/Γ_{23}

Unseen decay modes of the resonances are included.

VALUE	EVTS	DOCUMENT ID		TECN	COMMENT
0.40±0.09 OUR FIT					
0.43±0.11±0.07	29	[1] BRANDENB...	95	CLE2	$e^+e^- \approx \Upsilon(4S)$

[1] BRANDENBURG 95 uses both e^+ and μ^+ events and makes a phase-space adjustment to use the μ^+ events as e^+ events.

$\left[\Gamma(\eta e^+\nu_e) + \Gamma(\eta'(958)e^+\nu_e)\right]/\Gamma(\phi e^+\nu_e)$ $\Gamma_{24}/\Gamma_{23} = (\Gamma_{25}+\Gamma_{26})/\Gamma_{23}$

Unseen decay modes of the resonances are included.

VALUE	DOCUMENT ID		TECN	COMMENT
• • • We do not use the following data for averages, fits, limits, etc. • • •				
1.67±0.17±0.17	[1] BRANDENB...	95	CLE2	$e^+e^- \approx \Upsilon(4S)$

[1] This BRANDENBURG 95 data is redundant with data in previous blocks.

$\Gamma(\omega e^+\nu_e)/\Gamma_{\text{total}}$ Γ_{27}/Γ

A test for $u\overline{u}$ or $d\overline{d}$ content in the D_s^+. Neither Cabibbo-favored nor Cabibbo-suppressed decays can contribute, and $\omega - \phi$ mixing is an unlikely explanation for any fraction above about 2×10^{-4}.

VALUE (%)	CL%	DOCUMENT ID		TECN	COMMENT
<0.20	90	MARTIN	11	CLEO	e^+e^- at 4170 MeV

$\Gamma(K^0e^+\nu_e)/\Gamma_{\text{total}}$ Γ_{28}/Γ

VALUE (units 10^{-2})	EVTS	DOCUMENT ID		TECN	COMMENT
0.37±0.10±0.02	14	YELTON	09	CLEO	e^+e^- at 4170 MeV

$\Gamma(K^*(892)^0e^+\nu_e)/\Gamma_{\text{total}}$ Γ_{29}/Γ

Unseen decay modes of the $K^*(892)^0$ are included.

VALUE (units 10^{-2})	EVTS	DOCUMENT ID		TECN	COMMENT
0.18±0.07±0.01	7.5	YELTON	09	CLEO	e^+e^- at 4170 MeV

$\Gamma(f_0(980)e^+\nu_e, f_0 \to \pi^+\pi^-)/\Gamma_{\text{total}}$ Γ_{30}/Γ

VALUE (units 10^{-2})	EVTS	DOCUMENT ID		TECN	COMMENT
0.20±0.03±0.01	44 ± 7	ECKLUND	09	CLEO	e^+e^- at 4170 MeV
• • • We do not use the following data for averages, fits, limits, etc. • • •					
0.13±0.04±0.01	13	YELTON	09	CLEO	See ECKLUND 09

Hadronic modes with a $K\overline{K}$ pair.

$\Gamma(K^+K_S^0)/\Gamma_{\text{total}}$ Γ_{31}/Γ

VALUE (units 10^{-2})	DOCUMENT ID		TECN	COMMENT
1.49±0.06 OUR FIT				
1.52±0.05±0.03	ONYISI	13	CLEO	e^+e^- at 4.17 GeV
• • • We do not use the following data for averages, fits, limits, etc. • • •				
1.49±0.07±0.05	[1] ALEXANDER	08	CLEO	See ONYISI 13

[1] ALEXANDER 08 uses single- and double-tagged events in an overall fit. The correlation matrix for the branching fractions is used in the fit.

Meson Particle Listings

$D_s^\pm$

$\Gamma(K^+\overline{K}^0)/\Gamma_{total}$ Γ_{32}/Γ

VALUE (units 10^{-2})	EVTS	DOCUMENT ID		TECN	COMMENT
2.95±0.11±0.09	2.0k	[1] ZUPANC	13	BELL	e^+e^- at $\Upsilon(4S),\Upsilon(5S)$

[1] ZUPANC 13 finds the $\overline{K}^0$ from its missing-mass squared, not from $K^0_S \to \pi^+\pi^-$. The DCS ($D_s^+ \to K^+K^0$) contribution to this fraction is estimated to be an order of magnitude below the statistical uncertainty.

$\Gamma(K^+K^-\pi^+)/\Gamma_{total}$ Γ_{33}/Γ

VALUE (units 10^{-2})	EVTS	DOCUMENT ID		TECN	COMMENT
5.39±0.21 OUR FIT Error includes scale factor of 1.4.					
5.38±0.23 OUR AVERAGE Error includes scale factor of 1.5.					
5.55±0.14±0.13		ONYISI	13	CLEO	e^+e^- at 4.17 GeV
5.06±0.15±0.21	4.1k	ZUPANC	13	BELL	e^+e^- at $\Upsilon(4S),\Upsilon(5S)$
• • • We do not use the following data for averages, fits, limits, etc. • • •					
5.50±0.23±0.16		[1] ALEXANDER	08	CLEO	See ONYISI 13

[1] ALEXANDER 08 uses single- and double-tagged events in an overall fit. The correlation matrix for the branching fractions is used in the fit.

$\Gamma(\phi\pi^+)/\Gamma_{total}$ Γ_{34}/Γ

The results here are model-independent. For earlier, model-dependent results, see our PDG 06 edition. We decouple the $D_s^+ \to \phi\pi^+$ branching fraction obtained from mass projections (and used to get some of the other branching fractions) from the $D_s^+ \to \phi\pi^+$, $\phi \to K^+K^-$ branching fraction obtained from the Dalitz-plot analysis of $D_s^+ \to K^+K^-\pi^+$. That is, the ratio of these two branching fractions is not exactly the $\phi \to K^+K^-$ branching fraction 0.491.

VALUE (units 10^{-2})	EVTS	DOCUMENT ID		TECN	COMMENT
4.5 ±0.4 OUR AVERAGE					
4.62±0.36±0.51		[1] AUBERT	06N	BABR	e^+e^- at $\Upsilon(4S)$
4.81±0.52±0.38	212±19	[2] AUBERT	05V	BABR	$e^+e^- \approx \Upsilon(4S)$
3.59±0.77±0.48		[3] ARTUSO	96	CLE2	e^+e^- at $\Upsilon(4S)$
• • • We do not use the following data for averages, fits, limits, etc. • • •					
$3.9\ ^{+5.1}_{-1.9}\ ^{+1.8}_{-1.1}$		[4] BAI	95C	BES	e^+e^- 4.03 GeV

[1] This AUBERT 06N measurement uses $\overline{B}^0 \to D_s^{(*)-}D^{(*)+}$ and $B^- \to D_s^{(*)-}D^{(*)0}$ decays, including some from other papers. However, the result is independent of AUBERT 05V.

[2] AUBERT 05V uses the ratio of $B^0 \to D^{*-}D_s^{*+}$ events seen in two different ways, in both of which the $D^{*-} \to \overline{D}^0\pi^-$ decay is fully reconstructed: (1) The $D_s^{*+} \to D_s^+\gamma$, $D_s^+ \to \phi\pi^+$ decay is fully reconstructed. (2) The number of events in the D_s^+ peak in the missing mass spectrum against the $D^{*-}\gamma$ is measured.

[3] ARTUSO 96 uses partially reconstructed $\overline{B}^0 \to D^{*+}D_s^{*-}$ decays to get a model-independent value for $\Gamma(D_s^- \to \phi\pi^-)/\Gamma(D^0 \to K^-\pi^+)$ of 0.92 ± 0.20 ± 0.11.

[4] BAI 95C uses $e^+e^- \to D_s^+D_s^-$ events in which one or both of the $D_s^\pm$ are observed to obtain the first model-independent measurement of the $D_s^+ \to \phi\pi^+$ branching fraction, without assumptions about $\sigma(D_s^\pm)$. However, with only two "doubly-tagged" events, the statistical error is very large.

$\Gamma(\phi\pi^+,\ \phi \to K^+K^-)/\Gamma(K^+K^-\pi^+)$ Γ_{35}/Γ_{33}

This is the "fit fraction" from the Dalitz-plot analysis. We decouple the $D_s^+ \to \phi\pi^+$ branching fraction obtained from mass projections (and used to get some of the other branching fractions) from the $D_s^+ \to \phi\pi^+$, $\phi \to K^+K^-$ branching fraction obtained from the Dalitz-plot analysis of $D_s^+ \to K^+K^-\pi^+$. That is, the ratio of these two branching fractions is not exactly the $\phi \to K^+K^-$ branching fraction 0.491.

VALUE (%)	DOCUMENT ID		TECN	COMMENT
41.6±0.8 OUR AVERAGE				
41.4±0.8±0.5	DEL-AMO-SA...11G		BABR	Dalitz fit, 96k±369 evts
42.2±1.6±0.3	MITCHELL	09A	CLEO	Dalitz fit, 12k evts
• • • We do not use the following data for averages, fits, limits, etc. • • •				
39.6±3.3±4.7	FRABETTI	95B	E687	Dalitz fit, 701 evts

$\Gamma(K^+\overline{K}^*(892)^0,\overline{K}^{*0} \to K^-\pi^+)/\Gamma(K^+K^-\pi^+)$ Γ_{36}/Γ_{33}

This is the "fit fraction" from the Dalitz-plot analysis.

VALUE (%)	DOCUMENT ID		TECN	COMMENT
47.8±0.6 OUR AVERAGE				
47.9±0.5±0.5	DEL-AMO-SA...11G		BABR	Dalitz fit, 96k±369 evts
47.4±1.5±0.4	MITCHELL	09A	CLEO	Dalitz fit, 12k evts
• • • We do not use the following data for averages, fits, limits, etc. • • •				
47.8±4.6±4.0	FRABETTI	95B	E687	Dalitz fit, 701 evts

$\Gamma(f_0(980)\pi^+,\ f_0 \to K^+K^-)/\Gamma(K^+K^-\pi^+)$ Γ_{37}/Γ_{33}

This is the "fit fraction" from the Dalitz-plot analysis.

VALUE (%)	DOCUMENT ID		TECN	COMMENT
21 ±6 OUR AVERAGE Error includes scale factor of 3.5.				
16.4±0.7±2.0	DEL-AMO-SA...11G		BABR	Dalitz fit, 96k±369 evts
28.2±1.9±1.8	MITCHELL	09A	CLEO	Dalitz fit, 12k evts
• • • We do not use the following data for averages, fits, limits, etc. • • •				
11.0±3.5±2.6	FRABETTI	95B	E687	Dalitz fit, 701 evts

$\Gamma(f_0(1370)\pi^+,\ f_0 \to K^+K^-)/\Gamma(K^+K^-\pi^+)$ Γ_{38}/Γ_{33}

This is the "fit fraction" from the Dalitz-plot analysis.

VALUE (%)	DOCUMENT ID		TECN	COMMENT
1.3±0.8 OUR AVERAGE Error includes scale factor of 3.9.				
1.1±0.1±0.2	DEL-AMO-SA...11G		BABR	Dalitz fit, 96k±369 evts
4.3±0.6±0.5	MITCHELL	09A	CLEO	Dalitz fit, 12k evts

$\Gamma(f_0(1710)\pi^+,\ f_0 \to K^+K^-)/\Gamma(K^+K^-\pi^+)$ Γ_{39}/Γ_{33}

This is the "fit fraction" from the Dalitz-plot analysis.

VALUE (%)	DOCUMENT ID		TECN	COMMENT
1.2±0.5 OUR AVERAGE Error includes scale factor of 3.8.				
1.1±0.1±0.1	DEL-AMO-SA...11G		BABR	Dalitz fit, 96k±369 evts
3.4±0.5±0.3	MITCHELL	09A	CLEO	Dalitz fit, 12k evts
• • • We do not use the following data for averages, fits, limits, etc. • • •				
3.4±2.3±3.5	FRABETTI	95B	E687	Dalitz fit, 701 evts

$\Gamma(K^+\overline{K}_0^*(1430)^0,\overline{K}_0^* \to K^-\pi^+)/\Gamma(K^+K^-\pi^+)$ Γ_{40}/Γ_{33}

This is the "fit fraction" from the Dalitz-plot analysis.

VALUE (%)	DOCUMENT ID		TECN	COMMENT
3.4±0.7 OUR AVERAGE Error includes scale factor of 1.2.				
2.4±0.3±1.0	DEL-AMO-SA...11G		BABR	Dalitz fit, 96k±369 evts
3.9±0.5±0.5	MITCHELL	09A	CLEO	Dalitz fit, 12k evts
• • • We do not use the following data for averages, fits, limits, etc. • • •				
9.3±3.2±3.2	FRABETTI	95B	E687	Dalitz fit, 701 evts

$\Gamma(K^+K^0_S\pi^0)/\Gamma_{total}$ Γ_{41}/Γ

VALUE (units 10^{-2})	DOCUMENT ID		TECN	COMMENT
1.52±0.09±0.20	ONYISI	13	CLEO	e^+e^- at 4.17 GeV

$\Gamma(2K^0_S\pi^+)/\Gamma_{total}$ Γ_{42}/Γ

VALUE (units 10^{-2})	DOCUMENT ID		TECN	COMMENT
0.77±0.05±0.03	ONYISI	13	CLEO	e^+e^- at 4.17 GeV

$\Gamma(K^*(892)^+\overline{K}^0)/\Gamma(\phi\pi^+)$ Γ_{44}/Γ_{34}

Unseen decay modes of the resonances are included.

VALUE	DOCUMENT ID		TECN	COMMENT
1.20±0.21±0.13	CHEN	89	CLEO	e^+e^- 10 GeV

$\Gamma(K^+K^-\pi^+\pi^0)/\Gamma_{total}$ Γ_{45}/Γ

VALUE (units 10^{-2})	DOCUMENT ID		TECN	COMMENT
6.3 ±0.7 OUR FIT Error includes scale factor of 1.1.				
6.37±0.21±0.56	ONYISI	13	CLEO	e^+e^- at 4.17 GeV
• • • We do not use the following data for averages, fits, limits, etc. • • •				
5.65±0.29±0.40	[1] ALEXANDER	08	CLEO	See ONYISI 13

[1] ALEXANDER 08 uses single- and double-tagged events in an overall fit. The correlation matrix for the branching fractions is used in the fit.

$\Gamma(\phi\rho^+)/\Gamma(\phi\pi^+)$ Γ_{46}/Γ_{34}

VALUE	EVTS	DOCUMENT ID		TECN	COMMENT
$\mathbf{1.86\pm0.26\ ^{+0.29}_{-0.40}}$	253	AVERY	92	CLE2	$e^+e^- \simeq$ 10.5 GeV

$\Gamma(K^0_SK^-2\pi^+)/\Gamma_{total}$ Γ_{47}/Γ

VALUE (units 10^{-2})	DOCUMENT ID		TECN	COMMENT
1.66±0.11 OUR FIT				
1.69±0.07±0.08	ONYISI	13	CLEO	e^+e^- at 4.17 GeV
• • • We do not use the following data for averages, fits, limits, etc. • • •				
1.64±0.10±0.07	[1] ALEXANDER	08	CLEO	See ONYISI 13

[1] ALEXANDER 08 uses single- and double-tagged events in an overall fit. The correlation matrix for the branching fractions is used in the fit.

$\Gamma(K^*(892)^+\overline{K}^*(892)^0)/\Gamma(\phi\pi^+)$ Γ_{48}/Γ_{34}

Unseen decay modes of the resonances are included.

VALUE	DOCUMENT ID		TECN	COMMENT
1.6±0.4±0.4	ALBRECHT	92B	ARG	$e^+e^- \simeq$ 10.4 GeV

$\Gamma(K^+K^0_S\pi^+\pi^-)/\Gamma_{total}$ Γ_{49}/Γ

VALUE (units 10^{-2})	DOCUMENT ID		TECN	COMMENT
1.03±0.06±0.08	ONYISI	13	CLEO	e^+e^- at 4.17 GeV

$\Gamma(K^+K^0_S\pi^+\pi^-)/\Gamma(K^0_SK^-2\pi^+)$ Γ_{49}/Γ_{47}

VALUE	EVTS	DOCUMENT ID		TECN	COMMENT
0.586±0.052±0.043	476	LINK	01C	FOCS	γ A, $\overline{E}_\gamma \approx$ 180 GeV

$\Gamma(K^+K^-2\pi^+\pi^-)/\Gamma(K^+K^-\pi^+)$ Γ_{50}/Γ_{33}

VALUE	EVTS	DOCUMENT ID		TECN	COMMENT
0.160±0.027 OUR AVERAGE					
0.150±0.019±0.025	240	LINK	03D	FOCS	γ A, $\overline{E}_\gamma \approx$ 180 GeV
0.188±0.036±0.040	75	FRABETTI	97C	E687	γBe, $\overline{E}_\gamma \approx$ 200 GeV

$\Gamma(\phi 2\pi^+\pi^-)/\Gamma(\phi\pi^+)$ Γ_{51}/Γ_{34}

VALUE	EVTS	DOCUMENT ID		TECN	COMMENT
0.269±0.027 OUR AVERAGE					
0.249±0.024±0.021	136	LINK	03D	FOCS	γ A, $\overline{E}_\gamma \approx$ 180 GeV
0.28 ±0.06 ±0.01	40	FRABETTI	97C	E687	γBe, $\overline{E}_\gamma \approx$ 200 GeV
0.58 ±0.21 ±0.10	21	FRABETTI	92	E687	γBe
0.42 ±0.13 ±0.07	19	ANJOS	88	E691	Photoproduction
1.11 ±0.37 ±0.28	62	ALBRECHT	85D	ARG	e^+e^- 10 GeV

$\Gamma(K^+K^-\rho^0\pi^+\text{non-}\phi)/\Gamma(K^+K^-2\pi^+\pi^-)$ Γ_{52}/Γ_{50}

VALUE	CL%	DOCUMENT ID		TECN	COMMENT
<0.03	90	LINK	03D	FOCS	γ A, $\overline{E}_\gamma \approx$ 180 GeV

$\Gamma(\phi\rho^0\pi^+, \phi\to K^+K^-)/\Gamma(K^+K^-2\pi^+\pi^-)$ Γ_{53}/Γ_{50}

VALUE	DOCUMENT ID		TECN	COMMENT
0.75±0.06±0.04	LINK	03D	FOCS	γ A, $\overline{E}_\gamma \approx$ 180 GeV

$\Gamma(\phi a_1(1260)^+, \phi\to K^+K^-, a_1^+\to\rho^0\pi^+)/\Gamma(K^+K^-\pi^+)$ Γ_{54}/Γ_{33}

VALUE	DOCUMENT ID		TECN	COMMENT
0.137±0.019±0.011	LINK	03D	FOCS	γ A, $\overline{E}_\gamma \approx$ 180 GeV

$\Gamma(K^+K^-2\pi^+\pi^-\text{ nonresonant})/\Gamma(K^+K^-2\pi^+\pi^-)$ Γ_{55}/Γ_{50}

VALUE	DOCUMENT ID		TECN	COMMENT
0.10±0.06±0.05	LINK	03D	FOCS	γ A, $\overline{E}_\gamma \approx$ 180 GeV

$\Gamma(2K_S^0 2\pi^+\pi^-)/\Gamma(K_S^0 K^-2\pi^+)$ Γ_{56}/Γ_{47}

VALUE	EVTS	DOCUMENT ID		TECN	COMMENT
0.051±0.015±0.015	37 ± 10	LINK	04D	FOCS	γ A, $\overline{E}_\gamma \approx$ 180 GeV

Pionic modes

$\Gamma(\pi^+\pi^0)/\Gamma(K^+K_S^0)$ Γ_{57}/Γ_{31}

VALUE (units 10^{-2})	CL%	DOCUMENT ID		TECN	COMMENT
<2.3	90	MENDEZ	10	CLEO	e^+e^- at 4170 MeV
• • • We do not use the following data for averages, fits, limits, etc. • • •					
<4.1	90	ADAMS	07A	CLEO	See MENDEZ 10

$\Gamma(2\pi^+\pi^-)/\Gamma_{\text{total}}$ Γ_{58}/Γ

VALUE (units 10^{-2})	DOCUMENT ID		TECN	COMMENT
1.09±0.05 OUR FIT Error includes scale factor of 1.2.				
1.11±0.04±0.04	ONYISI	13	CLEO	e^+e^- at 4.17 GeV
• • • We do not use the following data for averages, fits, limits, etc. • • •				
1.11±0.07±0.04	[1] ALEXANDER	08	CLEO	See ONYISI 13

[1] ALEXANDER 08 uses single- and double-tagged events in an overall fit. The correlation matrix for the branching fractions is used in the fit.

$\Gamma(2\pi^+\pi^-)/\Gamma(K^+K^-\pi^+)$ Γ_{58}/Γ_{33}

VALUE	EVTS	DOCUMENT ID		TECN	COMMENT
0.201±0.007 OUR FIT					
0.199±0.004±0.009	≈ 10.5k	AUBERT	09O	BABR	$e^+e^-\approx$ 10.6 GeV
• • • We do not use the following data for averages, fits, limits, etc. • • •					
0.265±0.041±0.031	98	FRABETTI	97D	E687	γ Be ≈ 200 GeV

$\Gamma(\rho^0\pi^+)/\Gamma(2\pi^+\pi^-)$ Γ_{59}/Γ_{58}

VALUE	CL%	DOCUMENT ID		TECN	COMMENT
0.018±0.005±0.010		AUBERT	09O	BABR	Dalitz fit, ≈ 10.5k evts
• • • We do not use the following data for averages, fits, limits, etc. • • •					
not seen		LINK	04	FOCS	Dalitz fit, 1475 ± 50 evts
0.058±0.023±0.037		AITALA	01A	E791	Dalitz fit, 848 evts
<0.073	90	FRABETTI	97D	E687	γ Be ≈ 200 GeV

$\Gamma(\pi^+(\pi^+\pi^-)_{S-\text{wave}})/\Gamma(2\pi^+\pi^-)$ Γ_{60}/Γ_{58}

This is the "fit fraction" from the Dalitz-plot analysis. See also KLEMPT 08, which uses 568 $D_s^+\to 3\pi$ decays (over 280 background events) from FNAL E791 to study various parametrizations of the decay amplitudes. The emphasis there is more on S-wave $\pi\pi$ decay products — 20 different solutions are given — than on D_s^+ fit fractions.

VALUE	DOCUMENT ID		TECN	COMMENT
0.833 ±0.020 OUR AVERAGE				
0.830 ±0.009 ±0.019	[1] AUBERT	09O	BABR	Dalitz fit, ≈ 10.5k evts
0.8704±0.0560±0.0438	[2] LINK	04	FOCS	Dalitz fit, 1475 ± 50 evts

[1] AUBERT 09O gives the amplitude and phase of the $\pi^+\pi^-$ S-wave in 29 $\pi^+\pi^-$ invariant-mass bins.

[2] LINK 04 borrows a K-matrix parametrization from ANISOVICH 03 of the full π-π S-wave isoscalar scattering amplitude to describe the $\pi^+\pi^-$ S-wave component of the $\pi^+\pi^+\pi^-$ state. The fit fraction given above is a sum over five f_0 mesons, the $f_0(980)$, $f_0(1300)$, $f_0(1200$–$1600)$, $f_0(1500)$, and $f_0(1750)$. See LINK 04 for details and discussion.

$\Gamma(f_0(980)\pi^+, f_0\to\pi^+\pi^-)/\Gamma(2\pi^+\pi^-)$ Γ_{61}/Γ_{58}

This is the "fit fraction" from the Dalitz-plot analysis. See above for the full $\pi^+(\pi^+\pi^-)_{S-wave}$ fit fraction.

VALUE	DOCUMENT ID		TECN	COMMENT
• • • We do not use the following data for averages, fits, limits, etc. • • •				
0.565±0.043±0.047	AITALA	01A	E791	Dalitz fit, 848 evts
1.074±0.140±0.043	FRABETTI	97D	E687	γ Be ≈ 200 GeV

$\Gamma(f_0(1370)\pi^+, f_0\to\pi^+\pi^-)/\Gamma(2\pi^+\pi^-)$ Γ_{62}/Γ_{58}

This is the "fit fraction" from the Dalitz-plot analysis. See above for the full $\pi^+(\pi^+\pi^-)_{S-wave}$ fit fraction.

VALUE	DOCUMENT ID		TECN	COMMENT
• • • We do not use the following data for averages, fits, limits, etc. • • •				
0.324±0.077±0.017	AITALA	01A	E791	Dalitz fit, 848 evts

$\Gamma(f_0(1500)\pi^+, f_0\to\pi^+\pi^-)/\Gamma(2\pi^+\pi^-)$ Γ_{63}/Γ_{58}

This is the "fit fraction" from the Dalitz-plot analysis. See above for the full $\pi^+(\pi^+\pi^-)_{S-wave}$ fit fraction.

VALUE	DOCUMENT ID		TECN	COMMENT
• • • We do not use the following data for averages, fits, limits, etc. • • •				
0.274±0.014±0.019	[1] FRABETTI	97D	E687	γ Be ≈ 200 GeV

[1] FRABETTI 97D calls this mode $S(1475)\,\pi^+$, but finds the mass and width of this $S(1475)$ to be in excellent agreement with those of the $f_0(1500)$.

$\Gamma(f_2(1270)\pi^+, f_2\to\pi^+\pi^-)/\Gamma(2\pi^+\pi^-)$ Γ_{64}/Γ_{58}

This is the "fit fraction" from the Dalitz-plot analysis.

VALUE	DOCUMENT ID		TECN	COMMENT
0.101 ±0.018 OUR AVERAGE				
0.101 ±0.015 ±0.011	AUBERT	09O	BABR	Dalitz fit, ≈ 10.5k evts
0.0974±0.0449±0.0294	LINK	04	FOCS	Dalitz fit, 1475 ± 50 evts
• • • We do not use the following data for averages, fits, limits, etc. • • •				
0.197 ±0.033 ±0.006	AITALA	01A	E791	Dalitz fit, 848 evts
0.123 ±0.056 ±0.018	FRABETTI	97D	E687	γ Be ≈ 200 GeV

$\Gamma(\rho(1450)^0\pi^+, \rho^0\to\pi^+\pi^-)/\Gamma(2\pi^+\pi^-)$ Γ_{65}/Γ_{58}

This is the "fit fraction" from the Dalitz-plot analysis.

VALUE	DOCUMENT ID		TECN	COMMENT
0.027 ±0.018 OUR AVERAGE				
0.023 ±0.008 ±0.017	AUBERT	09O	BABR	Dalitz fit, ≈ 10.5k evts
0.0656±0.0343±0.0440	LINK	04	FOCS	Dalitz fit, 1475 ± 50 evts
• • • We do not use the following data for averages, fits, limits, etc. • • •				
0.044 ±0.021 ±0.002	AITALA	01A	E791	Dalitz fit, 848 evts

$\Gamma(\pi^+2\pi^0)/\Gamma_{\text{total}}$ Γ_{66}/Γ

VALUE (units 10^{-2})	EVTS	DOCUMENT ID		TECN	COMMENT
0.65±0.13±0.03	72 ± 16	NAIK	09A	CLEO	e^+e^- at 4170 MeV

$\Gamma(2\pi^+\pi^-\pi^0)/\Gamma(\phi\pi^+)$ Γ_{67}/Γ_{34}

VALUE	CL%	DOCUMENT ID		TECN	COMMENT
• • • We do not use the following data for averages, fits, limits, etc. • • •					
<3.3	90	ANJOS	89E	E691	Photoproduction

$\Gamma(\eta\pi^+)/\Gamma_{\text{total}}$ Γ_{68}/Γ

Unseen decay modes of the η are included.

VALUE (units 10^{-2})	EVTS	DOCUMENT ID		TECN	COMMENT
1.69±0.10 OUR FIT Error includes scale factor of 1.2.					
1.71±0.08 OUR AVERAGE					
1.67±0.08±0.06		ONYISI	13	CLEO	e^+e^- at 4.17 GeV
1.82±0.14±0.07	0.8k	ZUPANC	13	BELL	e^+e^- at $\Upsilon(4S), \Upsilon(5S)$
• • • We do not use the following data for averages, fits, limits, etc. • • •					
1.58±0.11±0.18	[1] ALEXANDER	08	CLEO	See ONYISI 13	

[1] ALEXANDER 08 uses single- and double-tagged events in an overall fit.

$\Gamma(\eta\pi^+)/\Gamma(K^+K_S^0)$ Γ_{68}/Γ_{31}

Unseen decay modes of the η are included.

VALUE	EVTS	DOCUMENT ID		TECN	COMMENT
1.14 ±0.07 OUR FIT Error includes scale factor of 1.2.					
• • • We do not use the following data for averages, fits, limits, etc. • • •					
1.236±0.043±0.063	2587 ± 89	MENDEZ	10	CLEO	See ONYISI 13

$\Gamma(\eta\pi^+)/\Gamma(\phi\pi^+)$ Γ_{68}/Γ_{34}

Unseen decay modes of the resonances are included.

VALUE	EVTS	DOCUMENT ID		TECN	COMMENT
• • • We do not use the following data for averages, fits, limits, etc. • • •					
0.48±0.03±0.04	920	JESSOP	98	CLE2	$e^+e^-\approx \Upsilon(4S)$
0.54±0.09±0.06	165	ALEXANDER	92	CLE2	See JESSOP 98

$\Gamma(\omega\pi^+)/\Gamma_{\text{total}}$ Γ_{69}/Γ

Unseen decay modes of the ω are included.

VALUE (units 10^{-2})	EVTS	DOCUMENT ID		TECN	COMMENT
0.24±0.06 OUR FIT					
0.21±0.09±0.01	6 ± 2.4	GE	09A	CLEO	e^+e^- at 4170 MeV

$\Gamma(\omega\pi^+)/\Gamma(\eta\pi^+)$ Γ_{69}/Γ_{68}

Unseen decay modes of the resonances are included.

VALUE	DOCUMENT ID		TECN	COMMENT
0.14±0.04 OUR FIT				
0.16±0.04±0.03	BALEST	97	CLE2	$e^+e^-\approx \Upsilon(4S)$

$\Gamma(3\pi^+2\pi^-)/\Gamma(K^+K^-\pi^+)$ Γ_{70}/Γ_{33}

VALUE	EVTS	DOCUMENT ID		TECN	COMMENT
0.146±0.014 OUR AVERAGE					
0.145±0.011±0.010	671	LINK	03D	FOCS	γ A, $\overline{E}_\gamma \approx$ 180 GeV
0.158±0.042±0.031	37	FRABETTI	97C	E687	γBe, $\overline{E}_\gamma \approx$ 200 GeV

Meson Particle Listings

$D_s^{\pm}$

$\Gamma(\eta\rho^+)/\Gamma_{total}$ Γ_{72}/Γ

Unseen decay modes of the η are included.

VALUE (units 10^{-2})	EVTS	DOCUMENT ID		TECN	COMMENT
8.9±0.6±0.5	328 ± 22	NAIK	09A	CLEO	$\eta \to 2\gamma$

$\Gamma(\eta\rho^+)/\Gamma(\phi\pi^+)$ Γ_{72}/Γ_{34}

Unseen decay modes of the resonances are included.

VALUE	EVTS	DOCUMENT ID		TECN	COMMENT
• • • We do not use the following data for averages, fits, limits, etc. • • •					
2.98±0.20±0.39	447	JESSOP	98	CLE2	$e^+e^- \approx \Upsilon(4S)$
$2.86\pm0.38^{+0.36}_{-0.38}$	217	AVERY	92	CLE2	See JESSOP 98

$\Gamma(\eta\pi^+\pi^0)/\Gamma_{total}$ Γ_{73}/Γ

VALUE (units 10^{-2})	DOCUMENT ID		TECN	COMMENT
9.2±0.4±1.1	ONYISI	13	CLEO	e^+e^- at 4.17 GeV

$\Gamma(\omega\pi^+\pi^0)/\Gamma_{total}$ Γ_{74}/Γ

Unseen decay modes of the ω are included.

VALUE (units 10^{-2})	EVTS	DOCUMENT ID		TECN	COMMENT
2.78±0.65±0.25	34 ± 7.9	GE	09A	CLEO	e^+e^- at 4170 MeV

$\Gamma(3\pi^+2\pi^-\pi^0)/\Gamma_{total}$ Γ_{75}/Γ

VALUE	DOCUMENT ID		TECN	COMMENT
$\mathbf{0.049^{+0.033}_{-0.030}}$	BARLAG	92C	ACCM	π^- 230 GeV

$\Gamma(\omega 2\pi^+\pi^-)/\Gamma_{total}$ Γ_{76}/Γ

Unseen decay modes of the ω are included.

VALUE (units 10^{-2})	EVTS	DOCUMENT ID		TECN	COMMENT
1.58±0.45±0.09	29 ± 8.2	GE	09A	CLEO	e^+e^- at 4170 MeV

$\Gamma(\eta'(958)\pi^+)/\Gamma_{total}$ Γ_{77}/Γ

Unseen decay modes of the $\eta'(958)$ are included.

VALUE (units 10^{-2})	DOCUMENT ID		TECN	COMMENT
3.94±0.15±0.20	ONYISI	13	CLEO	e^+e^- at 4.17 GeV
• • • We do not use the following data for averages, fits, limits, etc. • • •				
3.77±0.25±0.30	[1] ALEXANDER	08	CLEO	See ONYISI 13

[1] ALEXANDER 08 uses single- and double-tagged events in an overall fit.

$\Gamma(\eta'(958)\pi^+)/\Gamma(K^+K_S^0)$ Γ_{77}/Γ_{31}

Unseen decay modes of the $\eta'(958)$ are included.

VALUE	EVTS	DOCUMENT ID		TECN	COMMENT
• • • We do not use the following data for averages, fits, limits, etc. • • •					
2.654±0.088±0.139	1436 ± 47	MENDEZ	10	CLEO	See ONYISI 13

$\Gamma(\eta'(958)\pi^+)/\Gamma(\phi\pi^+)$ Γ_{77}/Γ_{34}

Unseen decay modes of the resonances are included.

VALUE	EVTS	DOCUMENT ID		TECN	COMMENT
• • • We do not use the following data for averages, fits, limits, etc. • • •					
1.03±0.06±0.07	537	JESSOP	98	CLE2	$e^+e^- \approx \Upsilon(4S)$
1.20±0.15±0.11	281	ALEXANDER	92	CLE2	See JESSOP 98
$2.5 \pm 1.0 \ ^{+1.5}_{-0.4}$	22	ALVAREZ	91	NA14	Photoproduction
2.5 ±0.5 ±0.3	215	ALBRECHT	90D	ARG	$e^+e^- \approx 10.4$ GeV

$\Gamma(\omega\eta\pi^+)/\Gamma_{total}$ Γ_{79}/Γ

Unseen decay modes of the ω and η are included.

VALUE	CL%	DOCUMENT ID		TECN	COMMENT
$\mathbf{<2.13\times10^{-2}}$	90	GE	09A	CLEO	e^+e^- at 4170 MeV

$\Gamma(\eta'(958)\rho^+)/\Gamma(\phi\pi^+)$ Γ_{80}/Γ_{34}

Unseen decay modes of the resonances are included.

VALUE	EVTS	DOCUMENT ID		TECN	COMMENT
2.78±0.28±0.30	137	JESSOP	98	CLE2	$e^+e^- \approx \Upsilon(4S)$
• • • We do not use the following data for averages, fits, limits, etc. • • •					
$3.44\pm0.62^{+0.44}_{-0.46}$	68	AVERY	92	CLE2	See JESSOP 98

$\Gamma(\eta'(958)\pi^+\pi^0)/\Gamma_{total}$ Γ_{81}/Γ

VALUE (units 10^{-2})	DOCUMENT ID		TECN	COMMENT
5.6±0.5±0.6	ONYISI	13	CLEO	e^+e^- at 4.17 GeV

Modes with one or three K's

$\Gamma(K^+\pi^0)/\Gamma(K^+K_S^0)$ Γ_{82}/Γ_{31}

VALUE (units 10^{-2})	EVTS	DOCUMENT ID		TECN	COMMENT
4.2±1.4±0.2	202 ± 70	MENDEZ	10	CLEO	e^+e^- at 4170 MeV
• • • We do not use the following data for averages, fits, limits, etc. • • •					
5.5±1.3±0.7	141 ± 34	ADAMS	07A	CLEO	See MENDEZ 10

$\Gamma(K_S^0\pi^+)/\Gamma(K^+K_S^0)$ Γ_{83}/Γ_{31}

VALUE (units 10^{-2})	EVTS	DOCUMENT ID		TECN	COMMENT
8.12±0.28 OUR AVERAGE					
8.5 ±0.7 ±0.2	393 ± 33	MENDEZ	10	CLEO	e^+e^- at 4170 MeV
8.03±0.24±0.19	17.6k±481	WON	09	BELL	e^+e^- at $\Upsilon(4S)$
10.4 ±2.4 ±1.4	113 ± 26	LINK	08	FOCS	γ A, $\overline{E}_\gamma \approx 180$ GeV
• • • We do not use the following data for averages, fits, limits, etc. • • •					
8.2 ±0.9 ±0.2	206 ± 22	ADAMS	07A	CLEO	See MENDEZ 10

$\Gamma(K^+\eta)/\Gamma(K^+K_S^0)$ Γ_{84}/Γ_{31}

Unseen decay modes of the η are included.

VALUE (units 10^{-2})	EVTS	DOCUMENT ID		TECN	COMMENT
11.8±2.2±0.6	222 ± 41	MENDEZ	10	CLEO	e^+e^- at 4170 MeV

$\Gamma(K^+\eta)/\Gamma(\eta\pi^+)$ Γ_{84}/Γ_{68}

VALUE (units 10^{-2})	EVTS	DOCUMENT ID		TECN	COMMENT
• • • We do not use the following data for averages, fits, limits, etc. • • •					
8.9±1.5±0.4	113 ± 18	ADAMS	07A	CLEO	See MENDEZ 10

$\Gamma(K^+\omega)/\Gamma_{total}$ Γ_{85}/Γ

Unseen decay modes of the ω are included.

VALUE (units 10^{-2})	CL%	DOCUMENT ID		TECN	COMMENT
<0.24	90	GE	09A	CLEO	e^+e^- at 4170 MeV

$\Gamma(K^+\eta'(958))/\Gamma(K^+K_S^0)$ Γ_{86}/Γ_{31}

Unseen decay modes of the $\eta'(958)$ are included.

VALUE (units 10^{-2})	EVTS	DOCUMENT ID		TECN	COMMENT
11.8±3.6±0.7	56 ± 17	MENDEZ	10	CLEO	e^+e^- at 4170 MeV

$\Gamma(K^+\eta'(958))/\Gamma(\eta'(958)\pi^+)$ Γ_{86}/Γ_{77}

VALUE (units 10^{-2})	EVTS	DOCUMENT ID		TECN	COMMENT
• • • We do not use the following data for averages, fits, limits, etc. • • •					
4.2±1.3±0.3	28 ± 9	ADAMS	07A	CLEO	See MENDEZ 10

$\Gamma(K^+\pi^+\pi^-)/\Gamma_{total}$ Γ_{87}/Γ

VALUE (units 10^{-2})	DOCUMENT ID		TECN	COMMENT
0.65 ±0.04 OUR FIT				
0.654±0.033±0.025	ONYISI	13	CLEO	e^+e^- at 4.17 GeV
• • • We do not use the following data for averages, fits, limits, etc. • • •				
0.69 ±0.05 ±0.03	[1] ALEXANDER	08	CLEO	See ONYISI 13

[1] ALEXANDER 08 uses single- and double-tagged events in an overall fit. The correlation matrix for the branching fractions is used in the fit.

$\Gamma(K^+\pi^+\pi^-)/\Gamma(K^+K^-\pi^+)$ Γ_{87}/Γ_{33}

VALUE	EVTS	DOCUMENT ID		TECN	COMMENT
0.121±0.008 OUR FIT	Error includes scale factor of 1.1.				
0.127±0.007±0.014	567 ± 31	LINK	04F	FOCS	γ A, $\overline{E}_\gamma \approx 180$ GeV

$\Gamma(K^+\rho^0)/\Gamma(K^+\pi^+\pi^-)$ Γ_{88}/Γ_{87}

This is the "fit fraction" from the Dalitz-plot analysis.

VALUE	DOCUMENT ID		TECN	COMMENT
0.3883±0.0531±0.0261	LINK	04F	FOCS	Dalitz fit, 567 evts

$\Gamma(K^+\rho(1450)^0, \rho^0\to\pi^+\pi^-)/\Gamma(K^+\pi^+\pi^-)$ Γ_{89}/Γ_{87}

This is the "fit fraction" from the Dalitz-plot analysis.

VALUE	DOCUMENT ID		TECN	COMMENT
0.1062±0.0351±0.0104	LINK	04F	FOCS	Dalitz fit, 567 evts

$\Gamma(K^*(892)^0\pi^+, K^{*0}\to K^+\pi^-)/\Gamma(K^+\pi^+\pi^-)$ Γ_{90}/Γ_{87}

This is the "fit fraction" from the Dalitz-plot analysis.

VALUE	DOCUMENT ID		TECN	COMMENT
0.2164±0.0321±0.0114	LINK	04F	FOCS	Dalitz fit, 567 evts

$\Gamma(K^*(1410)^0\pi^+, K^{*0}\to K^+\pi^-)/\Gamma(K^+\pi^+\pi^-)$ Γ_{91}/Γ_{87}

This is the "fit fraction" from the Dalitz-plot analysis.

VALUE	DOCUMENT ID		TECN	COMMENT
0.1882±0.0403±0.0122	LINK	04F	FOCS	Dalitz fit, 567 evts

$\Gamma(K^*(1430)^0\pi^+, K^{*0}\to K^+\pi^-)/\Gamma(K^+\pi^+\pi^-)$ Γ_{92}/Γ_{87}

This is the "fit fraction" from the Dalitz-plot analysis.

VALUE	DOCUMENT ID		TECN	COMMENT
0.0765±0.0500±0.0170	LINK	04F	FOCS	Dalitz fit, 567 evts

$\Gamma(K^+\pi^+\pi^-\text{nonresonant})/\Gamma(K^+\pi^+\pi^-)$ Γ_{93}/Γ_{87}

This is the "fit fraction" from the Dalitz-plot analysis.

VALUE	DOCUMENT ID		TECN	COMMENT
0.1588±0.0492±0.0153	LINK	04F	FOCS	Dalitz fit, 567 evts

$\Gamma(K^0\pi^+\pi^0)/\Gamma_{total}$ Γ_{94}/Γ

VALUE (units 10^{-2})	EVTS	DOCUMENT ID		TECN	COMMENT
1.00±0.18±0.04	44 ± 8	NAIK	09A	CLEO	e^+e^- at 4170 MeV

$\Gamma(K_S^0 2\pi^+\pi^-)/\Gamma(K_S^0 K^- 2\pi^+)$ Γ_{95}/Γ_{47}

VALUE	EVTS	DOCUMENT ID		TECN	COMMENT
0.18±0.04±0.05	179 ± 36	LINK	08	FOCS	γ A, $\overline{E}_\gamma \approx$ 180 GeV

$\Gamma(K^+\omega\pi^0)/\Gamma_{\text{total}}$ Γ_{96}/Γ

Unseen decay modes of the ω are included.

VALUE (units 10^{-2})	CL%	DOCUMENT ID		TECN	COMMENT
<0.82	90	GE	09A	CLEO	e^+e^- at 4170 MeV

$\Gamma(K^+\omega\pi^+\pi^-)/\Gamma_{\text{total}}$ Γ_{97}/Γ

Unseen decay modes of the ω are included.

VALUE (units 10^{-2})	CL%	DOCUMENT ID		TECN	COMMENT
<0.54	90	GE	09A	CLEO	e^+e^- at 4170 MeV

$\Gamma(K^+\omega\eta)/\Gamma_{\text{total}}$ Γ_{98}/Γ

Unseen decay modes of the ω and η are included.

VALUE (units 10^{-2})	CL%	DOCUMENT ID		TECN	COMMENT
<0.79	90	GE	09A	CLEO	e^+e^- at 4170 MeV

$\Gamma(2K^+K^-)/\Gamma(K^+K^-\pi^+)$ Γ_{99}/Γ_{33}

VALUE (units 10^{-3})	EVTS	DOCUMENT ID		TECN	COMMENT
4.0 ±0.3 ±0.2	748 ± 60	DEL-AMO-SA...11G		BABR	$e^+e^- \approx \Upsilon(4S)$
• • • We do not use the following data for averages, fits, limits, etc. • • •					
$8.95 \pm 2.12^{+2.24}_{-2.31}$	31	LINK	02I	FOCS	γ A, ≈ 180 GeV

$\Gamma(\phi K^+, \phi \to K^+K^-)/\Gamma(2K^+K^-)$ Γ_{100}/Γ_{99}

VALUE	DOCUMENT ID		TECN	COMMENT
0.41±0.08±0.03	DEL-AMO-SA...11G		BABR	$e^+e^- \approx \Upsilon(4S)$

Doubly Cabibbo-suppressed modes

$\Gamma(2K^+\pi^-)/\Gamma(K^+K^-\pi^+)$ Γ_{101}/Γ_{33}

VALUE (units 10^{-3})	EVTS	DOCUMENT ID		TECN	COMMENT
2.33±0.23 OUR AVERAGE					
2.3 ±0.3 ±0.2	356 ± 52	DEL-AMO-SA...11G		BABR	$e^+e^- \approx \Upsilon(4S)$
2.29±0.28±0.12	281 ± 34	KO	09	BELL	e^+e^- at $\Upsilon(4S)$
5.2 ±1.7 ±1.1	27 ± 9	LINK	05K	FOCS	<0.78%, CL = 90%

$\Gamma(K^+K^*(892)^0, K^{*0} \to K^+\pi^-)/\Gamma(2K^+\pi^-)$ $\Gamma_{102}/\Gamma_{101}$

VALUE	DOCUMENT ID		TECN	COMMENT
0.47±0.22±0.15	DEL-AMO-SA...11G		BABR	$e^+e^- \approx \Upsilon(4S)$

Baryon-antibaryon mode

$\Gamma(p\overline{p})/\Gamma_{\text{total}}$ Γ_{103}/Γ

This is the only baryonic mode allowed kinematically.

VALUE (units 10^{-3})	EVTS	DOCUMENT ID		TECN	COMMENT
$\mathbf{1.30 \pm 0.36^{+0.12}_{-0.16}}$	13.0 ± 3.6	ATHAR	08	CLEO	e^+e^-, $E_{\text{cm}} \approx$ 4170 MeV

Rare or forbidden modes

$\Gamma(\pi^+e^+e^-)/\Gamma_{\text{total}}$ Γ_{104}/Γ

This mode is not a useful test for a ΔC=1 weak neutral current because both quarks must change flavor in this decay.

VALUE	CL%	DOCUMENT ID		TECN	COMMENT
<13 $\times 10^{-6}$	90	LEES	11G	BABR	$e^+e^- \approx \Upsilon(4S)$
• • • We do not use the following data for averages, fits, limits, etc. • • •					
$< 2.2 \times 10^{-5}$	90	[1] RUBIN	10	CLEO	e^+e^- at 4170 MeV
$<27 \times 10^{-5}$	90	AITALA	99G	E791	$\pi^- N$ 500 GeV

[1] This RUBIN 10 limit is for the e^+e^- mass in the continuum away from the $\phi(1020)$. See the next data block.

$\Gamma(\pi^+\phi, \phi \to e^+e^-)/\Gamma_{\text{total}}$ Γ_{105}/Γ

This is *not* a test for the $\Delta C = 1$ weak neutral current, but leads to the $\pi^+e^+e^-$ final state.

VALUE	EVTS	DOCUMENT ID		TECN	COMMENT
$\mathbf{(6^{+8}_{-4} \pm 1) \times 10^{-6}}$	3	RUBIN	10	CLEO	e^+e^- at 4170 MeV

$\Gamma(\pi^+\mu^+\mu^-)/\Gamma_{\text{total}}$ Γ_{106}/Γ

This mode is not a useful test for a ΔC=1 weak neutral current because both quarks must change flavor in this decay.

VALUE	CL%	DOCUMENT ID		TECN	COMMENT
<4.1 $\times 10^{-7}$	90	AAIJ	13AF	LHCB	pp at 7 TeV
• • • We do not use the following data for averages, fits, limits, etc. • • •					
$<4.3 \times 10^{-5}$	90	LEES	11G	BABR	$e^+e^- \approx \Upsilon(4S)$
$<2.6 \times 10^{-5}$	90	LINK	03F	FOCS	γ A, $\overline{E}_\gamma \approx$ 180 GeV
$<1.4 \times 10^{-4}$	90	AITALA	99G	E791	$\pi^- N$ 500 GeV
$<4.3 \times 10^{-4}$	90	KODAMA	95	E653	π^- emulsion 600 GeV

$\Gamma(K^+e^+e^-)/\Gamma_{\text{total}}$ Γ_{107}/Γ

A test for the ΔC=1 weak neutral current. Allowed by higher-order electroweak interactions.

VALUE	CL%	DOCUMENT ID		TECN	COMMENT
<3.7 $\times 10^{-6}$	90	LEES	11G	BABR	$e^+e^- \approx \Upsilon(4S)$
• • • We do not use the following data for averages, fits, limits, etc. • • •					
$<5.2 \times 10^{-5}$	90	RUBIN	10	CLEO	e^+e^- at 4170 MeV
$<1.6 \times 10^{-3}$	90	AITALA	99G	E791	$\pi^- N$ 500 GeV

$\Gamma(K^+\mu^+\mu^-)/\Gamma_{\text{total}}$ Γ_{108}/Γ

A test for the ΔC=1 weak neutral current. Allowed by higher-order electroweak interactions.

VALUE	CL%	DOCUMENT ID		TECN	COMMENT
<21 $\times 10^{-6}$	90	LEES	11G	BABR	$e^+e^- \approx \Upsilon(4S)$
• • • We do not use the following data for averages, fits, limits, etc. • • •					
$< 3.6 \times 10^{-5}$	90	LINK	03F	FOCS	γ A, $\overline{E}_\gamma \approx$ 180 GeV
$< 1.4 \times 10^{-4}$	90	AITALA	99G	E791	$\pi^- N$ 500 GeV
$< 5.9 \times 10^{-4}$	90	KODAMA	95	E653	π^- emulsion 600 GeV

$\Gamma(K^*(892)^+\mu^+\mu^-)/\Gamma_{\text{total}}$ Γ_{109}/Γ

A test for the ΔC=1 weak neutral current. Allowed by higher-order electroweak interactions.

VALUE	CL%	DOCUMENT ID		TECN	COMMENT
<1.4 $\times 10^{-3}$	90	KODAMA	95	E653	π^- emulsion 600 GeV

$\Gamma(\pi^+e^+\mu^-)/\Gamma_{\text{total}}$ Γ_{110}/Γ

A test of lepton-family-number conservation.

VALUE	CL%	DOCUMENT ID		TECN	COMMENT
<12 $\times 10^{-6}$	90	LEES	11G	BABR	$e^+e^- \approx \Upsilon(4S)$

$\Gamma(\pi^+e^-\mu^+)/\Gamma_{\text{total}}$ Γ_{111}/Γ

A test of lepton-family-number conservation.

VALUE	CL%	DOCUMENT ID		TECN	COMMENT
<20 $\times 10^{-6}$	90	LEES	11G	BABR	$e^+e^- \approx \Upsilon(4S)$

$\Gamma(K^+e^+\mu^-)/\Gamma_{\text{total}}$ Γ_{112}/Γ

A test of lepton-family-number conservation.

VALUE	CL%	DOCUMENT ID		TECN	COMMENT
<14 $\times 10^{-6}$	90	LEES	11G	BABR	$e^+e^- \approx \Upsilon(4S)$

$\Gamma(K^+e^-\mu^+)/\Gamma_{\text{total}}$ Γ_{113}/Γ

A test of lepton-family-number conservation.

VALUE	CL%	DOCUMENT ID		TECN	COMMENT
<9.7 $\times 10^{-6}$	90	LEES	11G	BABR	$e^+e^- \approx \Upsilon(4S)$

$\Gamma(\pi^-2e^+)/\Gamma_{\text{total}}$ Γ_{114}/Γ

A test of lepton-number conservation.

VALUE	CL%	DOCUMENT ID		TECN	COMMENT
< 4.1 $\times 10^{-6}$	90	LEES	11G	BABR	$e^+e^- \approx \Upsilon(4S)$
• • • We do not use the following data for averages, fits, limits, etc. • • •					
$< 1.8 \times 10^{-5}$	90	RUBIN	10	CLEO	e^+e^- at 4170 MeV
$<69 \times 10^{-5}$	90	AITALA	99G	E791	$\pi^- N$ 500 GeV

$\Gamma(\pi^-2\mu^+)/\Gamma_{\text{total}}$ Γ_{115}/Γ

A test of lepton-number conservation.

VALUE	CL%	DOCUMENT ID		TECN	COMMENT
<1.2 $\times 10^{-7}$	90	AAIJ	13AF	LHCB	pp at 7 TeV
• • • We do not use the following data for averages, fits, limits, etc. • • •					
$<1.4 \times 10^{-5}$	90	LEES	11G	BABR	$e^+e^- \approx \Upsilon(4S)$
$<2.9 \times 10^{-5}$	90	LINK	03F	FOCS	γ A, $\overline{E}_\gamma \approx$ 180 GeV
$<8.2 \times 10^{-5}$	90	AITALA	99G	E791	$\pi^- N$ 500 GeV
$<4.3 \times 10^{-4}$	90	KODAMA	95	E653	π^- emulsion 600 GeV

$\Gamma(\pi^-e^+\mu^+)/\Gamma_{\text{total}}$ Γ_{116}/Γ

A test of lepton-number conservation.

VALUE	CL%	DOCUMENT ID		TECN	COMMENT
<8.4 $\times 10^{-6}$	90	LEES	11G	BABR	$e^+e^- \approx \Upsilon(4S)$
• • • We do not use the following data for averages, fits, limits, etc. • • •					
$<7.3 \times 10^{-4}$	90	AITALA	99G	E791	$\pi^- N$ 500 GeV

$\Gamma(K^-2e^+)/\Gamma_{\text{total}}$ Γ_{117}/Γ

A test of lepton-number conservation.

VALUE	CL%	DOCUMENT ID		TECN	COMMENT
< 5.2 $\times 10^{-6}$	90	LEES	11G	BABR	$e^+e^- \approx \Upsilon(4S)$
• • • We do not use the following data for averages, fits, limits, etc. • • •					
$< 1.7 \times 10^{-5}$	90	RUBIN	10	CLEO	e^+e^- at 4170 MeV
$<63 \times 10^{-5}$	90	AITALA	99G	E791	$\pi^- N$ 500 GeV

$\Gamma(K^-2\mu^+)/\Gamma_{\text{total}}$ Γ_{118}/Γ

A test of lepton-number conservation.

VALUE	CL%	DOCUMENT ID		TECN	COMMENT
<1.3 $\times 10^{-5}$	90	LEES	11G	BABR	$e^+e^- \approx \Upsilon(4S)$
<1.3 $\times 10^{-5}$	90	LINK	03F	FOCS	γ A, $\overline{E}_\gamma \approx$ 180 GeV
• • • We do not use the following data for averages, fits, limits, etc. • • •					
$<1.8 \times 10^{-4}$	90	AITALA	99G	E791	$\pi^- N$ 500 GeV
$<5.9 \times 10^{-4}$	90	KODAMA	95	E653	π^- emulsion 600 GeV

Meson Particle Listings

$D_s^\pm$

$\Gamma(K^- e^+ \mu^+)/\Gamma_{total}$ Γ_{119}/Γ

A test of lepton-number conservation.

VALUE	CL%	DOCUMENT ID		TECN	COMMENT
$<6.1 \times 10^{-6}$	90	LEES	11G	BABR	$e^+ e^- \approx \Upsilon(4S)$
• • • We do not use the following data for averages, fits, limits, etc. • • •					
$<6.8 \times 10^{-4}$	90	AITALA	99G	E791	π^- N 500 GeV

$\Gamma(K^*(892)^- 2\mu^+)/\Gamma_{total}$ Γ_{120}/Γ

A test of lepton-number conservation.

VALUE	CL%	DOCUMENT ID		TECN	COMMENT
$<1.4 \times 10^{-3}$	90	KODAMA	95	E653	π^- emulsion 600 GeV

$D_s^+ - D_s^-$ *CP*-VIOLATING DECAY-RATE ASYMMETRIES

This is the difference of the D_s^+ and D_s^- partial widths divided by the sum of the widths.

$A_{CP}(\mu^\pm\nu)$ in $D_s^+ \to \mu^+\nu$, $D_s^- \to \mu^-\overline{\nu}_\mu$

VALUE (%)	DOCUMENT ID		TECN	COMMENT
4.8±6.1	ALEXANDER	09	CLEO	$e^+ e^-$ at 4170 MeV

$A_{CP}(K^\pm K_S^0)$ in $D_s^\pm \to K^\pm K_S^0$

VALUE (%)	EVTS	DOCUMENT ID		TECN	COMMENT
0.08±0.26 OUR AVERAGE					
$-0.05 \pm 0.23 \pm 0.24$	288k	[1] LEES	13E	BABR	$e^+ e^-$ at $\Upsilon(4S)$
2.6 ±1.5 ±0.6		ONYISI	13	CLEO	$e^+ e^-$ at 4.17 GeV
$0.12 \pm 0.36 \pm 0.22$		KO	10	BELL	$e^+ e^- \approx \Upsilon(4S)$
• • • We do not use the following data for averages, fits, limits, etc. • • •					
4.7 ±1.8 ±0.9	4.0k	MENDEZ	10	CLEO	See ONYISI 13
4.9 ±2.1 ±0.9		ALEXANDER	08	CLEO	See MENDEZ 10

[1] LEES 13E finds that after subtracting the contribution due to $K^0 - \overline{K}^0$ mixing, the *CP* asymmetry is $(+0.28 \pm 0.23 \pm 0.24)$%.

$A_{CP}(K^+K^-\pi^\pm)$ in $D_s^\pm \to K^+K^-\pi^\pm$

VALUE (%)	DOCUMENT ID		TECN	COMMENT
−0.5±0.8±0.4	ONYISI	13	CLEO	$e^+ e^-$ at 4.17 GeV
• • • We do not use the following data for averages, fits, limits, etc. • • •				
$0.3 \pm 1.1 \pm 0.8$	ALEXANDER	08	CLEO	See ONYISI 13

$A_{CP}(K^\pm K_S^0\pi^0)$ in $D_s^\pm \to K^\pm K_S^0\pi^0$

VALUE (%)	DOCUMENT ID		TECN	COMMENT
−1.6±6.0±1.1	ONYISI	13	CLEO	$e^+ e^-$ at 4.17 GeV

$A_{CP}(2K_S^0\pi^\pm)$ in $D_s^\pm \to 2K_S^0\pi^\pm$

VALUE (%)	DOCUMENT ID		TECN	COMMENT
3.1±5.2±0.6	ONYISI	13	CLEO	$e^+ e^-$ at 4.17 GeV

$A_{CP}(K^+K^-\pi^\pm\pi^0)$ in $D_s^\pm \to K^+K^-\pi^\pm\pi^0$

VALUE (%)	DOCUMENT ID		TECN	COMMENT
0.0±2.7±1.2	ONYISI	13	CLEO	$e^+ e^-$ at 4.17 GeV
• • • We do not use the following data for averages, fits, limits, etc. • • •				
$-5.9 \pm 4.2 \pm 1.2$	ALEXANDER	08	CLEO	See ONYISI 13

$A_{CP}(K^\pm K_S^0\pi^+\pi^-)$ in $D_s^\pm \to K^\pm K_S^0\pi^+\pi^-$

VALUE (%)	DOCUMENT ID		TECN	COMMENT
−5.7±5.3±0.9	ONYISI	13	CLEO	$e^+ e^-$ at 4.17 GeV

$A_{CP}(K_S^0 K^\mp 2\pi^\pm)$ in $D_s^+ \to K_S^0 K^\mp 2\pi^\pm$

VALUE (%)	DOCUMENT ID		TECN	COMMENT
4.1±2.7±0.9	ONYISI	13	CLEO	$e^+ e^-$ at 4.17 GeV
• • • We do not use the following data for averages, fits, limits, etc. • • •				
$-0.7 \pm 3.6 \pm 1.1$	ALEXANDER	08	CLEO	See ONYISI 13

$A_{CP}(\pi^+\pi^-\pi^\pm)$ in $D_s^\pm \to \pi^+\pi^-\pi^\pm$

VALUE (%)	DOCUMENT ID		TECN	COMMENT
−0.7±3.0±0.6	ONYISI	13	CLEO	$e^+ e^-$ at 4.17 GeV
• • • We do not use the following data for averages, fits, limits, etc. • • •				
$2.0 \pm 4.6 \pm 0.7$	ALEXANDER	08	CLEO	See ONYISI 13

$A_{CP}(\pi^\pm\eta)$ in $D_s^\pm \to \pi^\pm\eta$

VALUE (%)	EVTS	DOCUMENT ID		TECN	COMMENT
1.1±3.0±0.8		ONYISI	13	CLEO	$e^+ e^-$ at 4.17 GeV
• • • We do not use the following data for averages, fits, limits, etc. • • •					
$-4.6 \pm 2.9 \pm 0.3$	2.5k	MENDEZ	10	CLEO	See ONYISI 13
$-8.2 \pm 5.2 \pm 0.8$		ALEXANDER	08	CLEO	See MENDEZ 10

$A_{CP}(\pi^\pm\eta')$ in $D_s^\pm \to \pi^\pm\eta'$

VALUE (%)	EVTS	DOCUMENT ID		TECN	COMMENT
−2.2±2.2±0.6		ONYISI	13	CLEO	$e^+ e^-$ at 4.17 GeV
• • • We do not use the following data for averages, fits, limits, etc. • • •					
$-6.1 \pm 3.0 \pm 0.3$	1.4k	MENDEZ	10	CLEO	See ONYISI 13
$-5.5 \pm 3.7 \pm 1.2$		ALEXANDER	08	CLEO	See MENDEZ 10

$A_{CP}(\eta\pi^\pm\pi^0)$ in $D_s^\pm \to \eta\pi^\pm\pi^0$

VALUE (%)	DOCUMENT ID		TECN	COMMENT
−0.5±3.9±2.0	ONYISI	13	CLEO	$e^+ e^-$ at 4.17 GeV

$A_{CP}(\eta'\pi^\pm\pi^0)$ in $D_s^\pm \to \eta'\pi^\pm\pi^0$

VALUE (%)	DOCUMENT ID		TECN	COMMENT
−0.4±7.4±1.9	ONYISI	13	CLEO	$e^+ e^-$ at 4.17 GeV

$A_{CP}(K^\pm\pi^0)$ in $D_s^\pm \to K^\pm\pi^0$

VALUE (%)	EVTS	DOCUMENT ID		TECN	COMMENT
−26.6±23.8±0.9	202 ± 70	MENDEZ	10	CLEO	$e^+ e^-$ at 4170 MeV
• • • We do not use the following data for averages, fits, limits, etc. • • •					
2 ±29		ADAMS	07A	CLEO	See MENDEZ 10

$A_{CP}(K_S^0\pi^\pm)$ in $D_s^\pm \to K_S^0\pi^\pm$

VALUE (%)	EVTS	DOCUMENT ID		TECN	COMMENT
1.2 ± 1.0 OUR AVERAGE Error includes scale factor of 1.3. See the ideogram below.					
$0.61 \pm 0.83 \pm 0.14$	25.6k	AAIJ	13W	LHCB	pp at 7 TeV
0.6 ± 2.0 ±0.3	14k	[1] LEES	13E	BABR	$e^+ e^-$ at $\Upsilon(4S)$
$5.45 \pm 2.50 \pm 0.33$		KO	10	BELL	$e^+ e^- \approx \Upsilon(4S)$
16.3 ± 7.3 ±0.3	393 ± 33	MENDEZ	10	CLEO	$e^+ e^-$ at 4170 MeV
• • • We do not use the following data for averages, fits, limits, etc. • • •					
27 ±11		ADAMS	07A	CLEO	See MENDEZ 10

[1] LEES 13E finds that after subtracting the contribution due to $K^0 - \overline{K}^0$ mixing, the *CP* asymmetry is $(+0.3 \pm 2.0 \pm 0.3)$%.

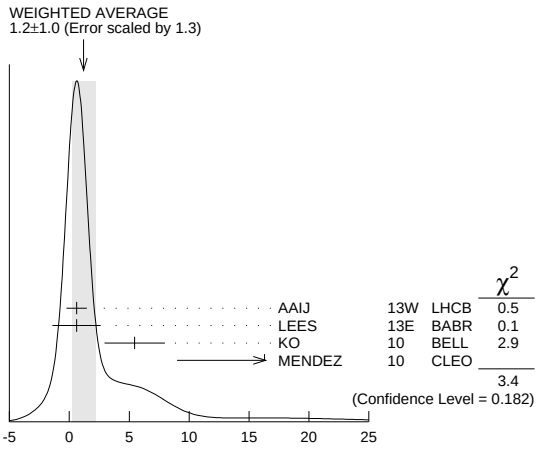

$A_{CP}(K^\pm\pi^+\pi^-)$ in $D_s^\pm \to K^\pm\pi^+\pi^-$

VALUE (%)	DOCUMENT ID		TECN	COMMENT
4.5±4.8±0.6	ONYISI	13	CLEO	$e^+ e^-$ at 4.17 GeV
• • • We do not use the following data for averages, fits, limits, etc. • • •				
$11.2 \pm 7.0 \pm 0.9$	ALEXANDER	08	CLEO	See ONYISI 13

$A_{CP}(K^\pm\eta)$ in $D_s^\pm \to K^\pm\eta$

VALUE (%)	EVTS	DOCUMENT ID		TECN	COMMENT
9.3±15.2±0.9	222 ± 41	MENDEZ	10	CLEO	$e^+ e^-$ at 4170 MeV
• • • We do not use the following data for averages, fits, limits, etc. • • •					
−20 ±18		ADAMS	07A	CLEO	See MENDEZ 10

$A_{CP}(K^\pm\eta'(958))$ in $D_s^\pm \to K^\pm\eta'(958)$

VALUE (%)	EVTS	DOCUMENT ID		TECN	COMMENT
6.0±18.9±0.9	56 ± 17	MENDEZ	10	CLEO	$e^+ e^-$ at 4170 MeV
• • • We do not use the following data for averages, fits, limits, etc. • • •					
−17 ±37		ADAMS	07A	CLEO	See MENDEZ 10

$D_s^+ - D_s^-$ *T*-VIOLATING DECAY-RATE ASYMMETRIES

$A_{Twol}(K_S^0 K^\pm\pi^+\pi^-)$ in $D_s^\pm \to K_S^0 K^\pm\pi^+\pi^-$

$C_T \equiv \vec{p}_{K^+} \cdot (\vec{p}_{\pi^+} \times \vec{p}_{\pi^-})$ is a parity-odd correlation of the K^+, π^+, and π^- momenta for the D_s^+. $\overline{C}_T \equiv \vec{p}_{K^-} \cdot (\vec{p}_{\pi^-} \times \vec{p}_{\pi^+})$ is the corresponding quantity for the D_s^-. Then

$A_T \equiv [\Gamma(C_T > 0) - \Gamma(C_T < 0)] / [\Gamma(C_T > 0) + \Gamma(C_T < 0)]$, and

$\overline{A}_T \equiv [\Gamma(-\overline{C}_T > 0) - \Gamma(-\overline{C}_T < 0)] / [\Gamma(-\overline{C}_T > 0) + \Gamma(-\overline{C}_T < 0)]$, and

$A_{T\,viol} \equiv \frac{1}{2}(A_T - \overline{A}_T)$. C_T and $\overline{C}_T$ are commonly referred to as T-odd moments, because they are odd under T reversal. However, the T-conjugate process $K^0_S K^{\pm}\pi^+\pi^- \to D_s^{\pm}$ is not accessible, while the P-conjugate process is.

VALUE (units 10^{-3})	EVTS	DOCUMENT ID		TECN	COMMENT
$-13.6\pm 7.7\pm 3.4$	29.8 ± 0.3k	LEES	11E	BABR	$e^+e^- \approx \Upsilon(4S)$
• • • We do not use the following data for averages, fits, limits, etc. • • •					
$-36\ \pm67\ \pm23$	508 ± 34	LINK	05E	FOCS	γ A, $\overline{E}_\gamma \approx 180$ GeV

$D_s^+ \to \phi\ell^+\nu_\ell$ FORM FACTORS

$r_2 \equiv A_2(0)/A_1(0)$ in $D_s^+ \to \phi\ell^+\nu_\ell$

VALUE	EVTS	DOCUMENT ID		TECN	COMMENT
0.84 ±0.11 OUR AVERAGE Error includes scale factor of 2.4.					
$0.816\pm0.036\pm0.030$	25 ± 0.5k	[1] AUBERT	08AN	BABR	$\phi e^+\nu_e$
$0.713\pm0.202\pm0.284$	793	LINK	04C	FOCS	$\phi\mu^+\nu_\mu$
$1.57\ \pm0.25\ \pm0.19$	271	AITALA	99D	E791	$\phi e^+\nu_e$, $\phi\mu^+\nu_\mu$
$1.4\ \pm0.5\ \pm0.3$	308	AVERY	94B	CLE2	$\phi e^+\nu_e$
$1.1\ \pm0.8\ \pm0.1$	90	FRABETTI	94F	E687	$\phi\mu^+\nu_\mu$
$2.1\ {}^{+0.6}_{-0.5}\ \pm0.2$	19	KODAMA	93	E653	$\phi\mu^+\nu_\mu$

[1] To compare with previous measurements, this AUBERT 08AN value is from a fit that fixes the pole masses at $m_A = 2.5$ GeV/c^2 and $m_V = 2.1$ GeV/c^2. A simultaneous fit to r_2, r_V, r_0 (a significant s-wave contribution) and m_A, gives $r_2 = 0.763 \pm 0.071 \pm 0.065$.

$r_V \equiv V(0)/A_1(0)$ in $D_s^+ \to \phi\ell^+\nu_\ell$

VALUE	EVTS	DOCUMENT ID		TECN	COMMENT
1.80 ±0.08 OUR AVERAGE					
$1.807\pm0.046\pm0.065$	25 ± 0.5k	[1] AUBERT	08AN	BABR	$\phi e^+\nu_e$
$1.549\pm0.250\pm0.148$	793	LINK	04C	FOCS	$\phi\mu^+\nu_\mu$
$2.27\ \pm0.35\ \pm0.22$	271	AITALA	99D	E791	$\phi e^+\nu_e$, $\phi\mu^+\nu_\mu$
$0.9\ \pm0.6\ \pm0.3$	308	AVERY	94B	CLE2	$\phi e^+\nu_e$
$1.8\ \pm0.9\ \pm0.2$	90	FRABETTI	94F	E687	$\phi\mu^+\nu_\mu$
$2.3\ {}^{+1.1}_{-0.9}\ \pm0.4$	19	KODAMA	93	E653	$\phi\mu^+\nu_\mu$

[1] To compare with previous measurements, this AUBERT 08AN value is from a fit that fixes the pole masses at $m_A = 2.5$ GeV/c^2 and $m_V = 2.1$ GeV/c^2. A simultaneous fit to r_2, r_V, r_0 (a significant s-wave contribution) and m_A, gives $r_V = 1.849 \pm 0.060 \pm 0.095$.

Γ_L/Γ_T in $D_s^+ \to \phi\ell^+\nu_\ell$

VALUE	EVTS	DOCUMENT ID		TECN	COMMENT
0.72±0.18 OUR AVERAGE					
$1.0\ \pm0.3\ \pm0.2$	308	AVERY	94B	CLE2	$\phi e^+\nu_e$
$1.0\ \pm0.5\ \pm0.1$	90	[1] FRABETTI	94F	E687	$\phi\mu^+\nu_\mu$
$0.54\pm0.21\pm0.10$	19	[1] KODAMA	93	E653	$\phi\mu^+\nu_\mu$

[1] FRABETTI 94F and KODAMA 93 evaluate Γ_L/Γ_T for a lepton mass of zero.

$D_s^{\pm}$ REFERENCES

AAIJ	13AF	PL B724 203	R. Aaij *et al.*	(LHCb Collab.)
AAIJ	13V	JHEP 1306 065	R. Aaij *et al.*	(LHCb Collab.)
AAIJ	13W	JHEP 1306 112	R. Aaij *et al.*	(LHCb Collab.)
LEES	13E	PR D87 052012	J.P. Lees *et al.*	(BABAR Collab.)
ONYISI	13	PR D88 032009	P.U.E. Onyisi *et al.*	(CLEO Collab.)
ZUPANC	13	JHEP 1309 139	A. Zupanc *et al.*	(BELLE Collab.)
DEL-AMO-SA...	11G	PR D83 052001	P. del Amo Sanchez *et al.*	(BABAR Collab.)
LEES	11E	PR D84 031103	J.P. Lees *et al.*	(BABAR Collab.)
LEES	11G	PR D84 072006	J.P. Lees *et al.*	(BABAR Collab.)
MARTIN	11	PR D84 012005	L. Martin *et al.*	(CLEO Collab.)
ASNER	10	PR D81 052007	D.M. Asner *et al.*	(CLEO Collab.)
DEL-AMO-SA...	10J	PR D82 091103	P. del Amo Sanchez *et al.*	(BABAR Collab.)
KO	10	PRL 104 181602	B.R. Ko *et al.*	(BELLE Collab.)
MENDEZ	10	PR D81 052013	H. Mendez *et al.*	(CLEO Collab.)
RUBIN	10	PR D82 092007	P. Rubin *et al.*	(CLEO Collab.)
ALEXANDER	09	PR D79 052001	J.P. Alexander *et al.*	(CLEO Collab.)
AUBERT	09O	PR D79 032003	B. Aubert *et al.*	(BABAR Collab.)
DOBBS	09	PR D79 112008	S. Dobbs *et al.*	(CLEO Collab.)
ECKLUND	09	PR D80 052009	K.M. Ecklund *et al.*	(CLEO Collab.)
GE	09A	PR D80 051102	J.Y. Ge *et al.*	(CLEO Collab.)
KO	09	PRL 102 221802	B.R. Ko *et al.*	(BELLE Collab.)
MITCHELL	09A	PR D79 072008	R.E. Mitchell *et al.*	(CLEO Collab.)
NAIK	09A	PR D80 112004	P. Naik *et al.*	(CLEO Collab.)
ONYISI	09	PR D79 052002	P.U.E. Onyisi *et al.*	(CLEO Collab.)
WON	09	PR D80 111101	E. Won *et al.*	(BELLE Collab.)
YELTON	09	PR D80 052007	J. Yelton *et al.*	(CLEO Collab.)
ALEXANDER	08	PRL 100 161804	J.P. Alexander *et al.*	(CLEO Collab.)
ATHAR	08	PRL 100 181802	S.B. Athar *et al.*	(CLEO Collab.)
AUBERT	08AN	PR D78 051101	B. Aubert *et al.*	(BABAR Collab.)
ECKLUND	08	PRL 100 161801	K.M. Ecklund *et al.*	(CLEO Collab.)
KLEMPT	08	EPJ C55 39	E. Klempt, M. Matveev, A.V. Sarantsev	(BONN+)
LINK	08	PL B660 147	J.M. Link *et al.*	(FNAL FOCUS Collab.)
WIDHALM	08	PRL 100 241801	L. Widhalm *et al.*	(BELLE Collab.)
ADAMS	07A	PRL 99 191805	G.S. Adams *et al.*	(CLEO Collab.)
AUBERT	07V	PRL 98 141801	B. Aubert *et al.*	(BABAR Collab.)
PEDLAR	07A	PR D76 072002	T.K. Pedlar *et al.*	(CLEO Collab.)
Also		PRL 99 071802	M. Artuso *et al.*	(CLEO Collab.)
AUBERT	06N	PR D74 031103	B. Aubert *et al.*	(BABAR Collab.)
HUANG	06B	PR D74 112005	G.S. Huang *et al.*	(CLEO Collab.)
PDG	06	JP G33 1	W.-M. Yao *et al.*	(PDG Collab.)
AUBERT	05V	PR D71 091104	B. Aubert *et al.*	(BABAR Collab.)
LINK	05E	PL B622 239	J.M. Link *et al.*	(FNAL FOCUS Collab.)
LINK	05J	PRL 95 052003	J.M. Link *et al.*	(FNAL FOCUS Collab.)
LINK	05K	PL B624 166	J.M. Link *et al.*	(FNAL FOCUS Collab.)
LINK	04	PL B585 200	J.M. Link *et al.*	(FNAL FOCUS Collab.)
LINK	04C	PL B586 183	J.M. Link *et al.*	(FNAL FOCUS Collab.)
LINK	04D	PL B586 191	J.M. Link *et al.*	(FNAL FOCUS Collab.)
LINK	04F	PL B601 10	J.M. Link *et al.*	(FNAL FOCUS Collab.)
ACOSTA	03D	PR D68 072004	D. Acosta *et al.*	(FNAL CDF-II Collab.)
ANISOVICH	03	EPJ A16 229	V.V. Anisovich *et al.*	
LINK	03D	PL B561 225	J.M. Link *et al.*	(FNAL FOCUS Collab.)
LINK	03F	PL B572 21	J.M. Link *et al.*	(FNAL FOCUS Collab.)
AUBERT	02G	PR D65 091104	B. Aubert *et al.*	(BaBar Collab.)
HEISTER	02I	PL B528 1	A. Heister *et al.*	(ALEPH Collab.)
LINK	02I	PL B541 227	J.M. Link *et al.*	(FNAL FOCUS Collab.)
LINK	02J	PL B541 243	J.M. Link *et al.*	(FNAL FOCUS Collab.)
ABBIENDI	01L	PL B516 236	G. Abbiendi *et al.*	(OPAL Collab.)
AITALA	01A	PRL 86 765	E.M. Aitala *et al.*	(FNAL E791 Collab.)
IORI	01	PL B523 22	M. Iori *et al.*	(FNAL SELEX Collab.)
LINK	01C	PRL 87 162001	J.M. Link *et al.*	(FNAL FOCUS Collab.)
ALEXANDROV	00	PL B478 31	Y. Alexandrov *et al.*	(CERN BEATRICE Collab.)
AITALA	99	PL B445 449	E.M. Aitala *et al.*	(FNAL E791 Collab.)
AITALA	99D	PL B450 294	E.M. Aitala *et al.*	(FNAL E791 Collab.)
AITALA	99G	PL B462 401	E.M. Aitala *et al.*	(FNAL E791 Collab.)
BONVICINI	99	PRL 82 4586	G. Bonvicini *et al.*	(CLEO Collab.)
CHADHA	98	PR D58 032002	M. Chada *et al.*	(CLEO Collab.)
JESSOP	98	PR D58 052002	C.P. Jessop *et al.*	(CLEO Collab.)
ACCIARRI	97F	PL B396 327	M. Acciarri *et al.*	(L3 Collab.)
BALEST	97	PRL 79 1436	R. Balest *et al.*	(CLEO Collab.)
FRABETTI	97C	PL B401 131	P.L. Frabetti *et al.*	(FNAL E687 Collab.)
FRABETTI	97D	PL B407 79	P.L. Frabetti *et al.*	(FNAL E687 Collab.)
ARTUSO	96	PL B378 364	M. Artuso *et al.*	(CLEO Collab.)
BAI	95C	PR D52 3781	J.Z. Bai *et al.*	(BES Collab.)
BRANDENB...	95	PRL 75 3804	G.W. Brandenburg *et al.*	(CLEO Collab.)
FRABETTI	95B	PL B351 591	P.L. Frabetti *et al.*	(FNAL E687 Collab.)
KODAMA	95	PL B345 85	K. Kodama *et al.*	(FNAL E653 Collab.)
ACOSTA	94	PR D49 5690	D. Acosta *et al.*	(CLEO Collab.)
AVERY	94B	PL B337 405	P. Avery *et al.*	(CLEO Collab.)
BROWN	94	PR D50 1884	D. Brown *et al.*	(CLEO Collab.)
BUTLER	94	PL B324 255	F. Butler *et al.*	(CLEO Collab.)
FRABETTI	94F	PL B328 187	P.L. Frabetti *et al.*	(FNAL E687 Collab.)
FRABETTI	93F	PRL 71 827	P.L. Frabetti *et al.*	(FNAL E687 Collab.)
FRABETTI	93G	PL B313 253	P.L. Frabetti *et al.*	(FNAL E687 Collab.)
KODAMA	93	PL B309 483	K. Kodama *et al.*	(FNAL E653 Collab.)
ALBRECHT	92B	ZPHY C53 361	H. Albrecht *et al.*	(ARGUS Collab.)
ALEXANDER	92	PRL 68 1275	J. Alexander *et al.*	(CLEO Collab.)
AVERY	92	PRL 68 1279	P. Avery *et al.*	(CLEO Collab.)
BARLAG	92C	ZPHY C55 383	S. Barlag *et al.*	(ACCMOR Collab.)
Also		ZPHY C48 29	S. Barlag *et al.*	(ACCMOR Collab.)
FRABETTI	92	PL B281 167	P.L. Frabetti *et al.*	(FNAL E687 Collab.)
ALBRECHT	91	PL B255 634	H. Albrecht *et al.*	(ARGUS Collab.)
ALVAREZ	91	PL B255 639	M.P. Alvarez *et al.*	(CERN NA14/2 Collab.)
ALBRECHT	90D	PL B245 315	H. Albrecht *et al.*	(ARGUS Collab.)
ALEXANDER	90B	PRL 65 1531	J. Alexander *et al.*	(CLEO Collab.)
BARLAG	90C	ZPHY C46 563	S. Barlag *et al.*	(ACCMOR Collab.)
FRABETTI	90	PL B251 639	P.L. Frabetti *et al.*	(FNAL E687 Collab.)
ANJOS	89E	PL B223 267	J.C. Anjos *et al.*	(FNAL E691 Collab.)
CHEN	89	PL B226 192	W.Y. Chen *et al.*	(CLEO Collab.)
ALBRECHT	88	PL B207 349	H. Albrecht *et al.*	(ARGUS Collab.)
ANJOS	88	PRL 60 897	J.C. Anjos *et al.*	(FNAL E691 Collab.)
RAAB	88	PR D37 2391	J.R. Raab *et al.*	(FNAL E691 Collab.)
BECKER	87B	PL B184 277	H. Becker *et al.*	(NA11 and NA32 Collab.)
BLAYLOCK	87	PRL 58 2171	G.T. Blaylock *et al.*	(Mark III Collab.)
USHIDA	86	PRL 56 1767	N. Ushida *et al.*	(FNAL E531 Collab.)
ALBRECHT	85D	PL 153B 343	H. Albrecht *et al.*	(ARGUS Collab.)
DERRICK	85B	PRL 54 2568	M. Derrick *et al.*	(HRS Collab.)
AIHARA	84D	PRL 53 2465	H. Aihara *et al.*	(TPC Collab.)
ALTHOFF	84	PL 136B 130	M. Althoff *et al.*	(TASSO Collab.)
BAILEY	84	PL 139B 320	R. Bailey *et al.*	(ACCMOR Collab.)
CHEN	83C	PRL 51 634	A. Chen *et al.*	(CLEO Collab.)

OTHER RELATED PAPERS

RICHMAN	95	RMP 67 893	J.D. Richman, P.R. Burchat	(UCSB, STAN)

$D_s^{*\pm}$

$I(J^P) = 0(?^?)$

J^P is natural, width and decay modes consistent with 1^-.

$D_s^{*\pm}$ MASS

The fit includes $D^{\pm}$, D^0, $D_s^{\pm}$, $D^{*\pm}$, D^{*0}, $D_s^{*\pm}$, $D_1(2420)^0$, $D_2^*(2460)^0$, and $D_{s1}(2536)^{\pm}$ mass and mass difference measurements.

VALUE (MeV)	DOCUMENT ID		TECN	COMMENT
2112.1±0.4 OUR FIT				
2106.6±2.1±2.7	[1] BLAYLOCK	87	MRK3	$e^+e^- \to D_s^{\pm}\gamma$X

[1] Assuming $D_s^{\pm}$ mass = 1968.7 ± 0.9 MeV.

$m_{D_s^{*\pm}} - m_{D_s^{\pm}}$

The fit includes $D^{\pm}$, D^0, $D_s^{\pm}$, $D^{*\pm}$, D^{*0}, $D_s^{*\pm}$, $D_1(2420)^0$, $D_2^*(2460)^0$, and $D_{s1}(2536)^{\pm}$ mass and mass difference measurements.

VALUE (MeV)	EVTS	DOCUMENT ID		TECN	COMMENT
143.8 ± 0.4 OUR FIT					
143.9 ± 0.4 OUR AVERAGE					
$143.76\pm\ 0.39\pm0.40$		GRONBERG	95	CLE2	e^+e^-
$144.22\pm\ 0.47\pm0.37$		BROWN	94	CLE2	e^+e^-
$142.5\ \pm\ 0.8\ \pm1.5$		[2] ALBRECHT	88	ARG	$e^+e^- \to D_s^{\pm}\gamma$X
$139.5\ \pm\ 8.3\ \pm9.7$	60	AIHARA	84D	TPC	$e^+e^- \to$ hadrons
• • • We do not use the following data for averages, fits, limits, etc. • • •					
$143.0\ \pm18.0$	8	ASRATYAN	85	HLBC	FNAL 15-ft, ν-^{2}H
$110\ \ \pm46$		BRANDELIK	79	DASP	$e^+e^- \to D_s^{\pm}\gamma$X

[2] Result includes data of ALBRECHT 84B.

Meson Particle Listings

$D_s^{*\pm}$, $D_{s0}^*(2317)^\pm$

$D_s^{*\pm}$ WIDTH

VALUE (MeV)	CL%	DOCUMENT ID		TECN	COMMENT
< 1.9	90	GRONBERG	95	CLE2	e^+e^-
< 4.5	90	ALBRECHT	88	ARG	$E_{\rm cm}^{ee} = 10.2$ GeV
• • • We do not use the following data for averages, fits, limits, etc. • • •					
< 4.9	90	BROWN	94	CLE2	e^+e^-
<22	90	BLAYLOCK	87	MRK3	$e^+e^- \to D_s^\pm\gamma$X

D_s^{*+} DECAY MODES

D_s^{*-} modes are charge conjugates of the modes below.

	Mode	Fraction (Γ_i/Γ)
Γ_1	$D_s^+\gamma$	(94.2±0.7) %
Γ_2	$D_s^+\pi^0$	(5.8±0.7) %

CONSTRAINED FIT INFORMATION

An overall fit to a branching ratio uses 2 measurements and one constraint to determine 2 parameters. The overall fit has a $\chi^2 =$ 0.0 for 1 degrees of freedom.

The following *off-diagonal* array elements are the correlation coefficients $\left\langle \delta x_i \delta x_j \right\rangle / (\delta x_i \cdot \delta x_j)$, in percent, from the fit to the branching fractions, $x_i \equiv \Gamma_i/\Gamma_{\rm total}$. The fit constrains the x_i whose labels appear in this array to sum to one.

x_2 | −100
x_1

D_s^{*+} BRANCHING RATIOS

$\Gamma(D_s^+\gamma)/\Gamma_{\rm total}$ Γ_1/Γ

VALUE	EVTS	DOCUMENT ID		TECN	COMMENT
0.942±0.007 OUR FIT					
• • • We do not use the following data for averages, fits, limits, etc. • • •					
0.942±0.004±0.006	16k	[3] AUBERT,BE	05G	BABR	10.6 e^+e^- → hadrons
seen		ASRATYAN	91	HLBC	$\overline{\nu}_\mu$ Ne
seen		ALBRECHT	88	ARG	$e^+e^- \to D_s^\pm\gamma$X
seen		AIHARA	84D		
seen		ALBRECHT	84B		
seen		BRANDELIK	79		

$\Gamma(D_s^+\pi^0)/\Gamma_{\rm total}$ Γ_2/Γ

VALUE	EVTS	DOCUMENT ID		TECN	COMMENT
• • • We do not use the following data for averages, fits, limits, etc. • • •					
0.059±0.004±0.006	560	[3] AUBERT,BE	05G	BABR	10.6 e^+e^- → hadrons

$\Gamma(D_s^+\pi^0)/\Gamma(D_s^+\gamma)$ Γ_2/Γ_1

VALUE	DOCUMENT ID		TECN	COMMENT
0.062±0.008 OUR FIT				
0.062±0.008 OUR AVERAGE				
0.062±0.005±0.006	AUBERT,BE	05G	BABR	10.6 e^+e^- → hadrons
$0.062^{+0.020}_{-0.018}$±0.022	GRONBERG	95	CLE2	e^+e^-

[3] Derived from the ratio $\Gamma(D_s^+\pi^0)$ / $\Gamma(D_s^+\gamma)$ assuming that the branching fractions of $D_s^{*+} \to D_s^+\pi^0$ and $D_s^{*+} \to D_s^+\gamma$ decays sum to 100%.

$D_s^{*\pm}$ REFERENCES

AUBERT,BE	05G	PR D72 091101	B. Aubert *et al.*	(BABAR Collab.)
GRONBERG	95	PRL 75 3232	J. Gronberg *et al.*	(CLEO Collab.)
BROWN	94	PR D50 1884	D. Brown *et al.*	(CLEO Collab.)
ASRATYAN	91	PL B257 525	A.E. Asratyan *et al.*	(ITEP, BELG, SACL+)
ALBRECHT	88	PL B207 349	H. Albrecht *et al.*	(ARGUS Collab.)
BLAYLOCK	87	PRL 58 2171	G.T. Blaylock *et al.*	(Mark III Collab.)
ASRATYAN	85	PL 156B 441	A.E. Asratyan *et al.*	(ITEP, SERP)
AIHARA	84D	PRL 53 2465	H. Aihara *et al.*	(TPC Collab.)
ALBRECHT	84B	PL 146B 111	H. Albrecht *et al.*	(ARGUS Collab.)
BRANDELIK	79	PL 80B 412	R. Brandelik *et al.*	(DASP Collab.)

$D_{s0}^*(2317)^\pm$

$I(J^P) = 0(0^+)$
J, P need confirmation.

AUBERT 06P does not observe neutral and doubly charged partners of the $D_{s0}^*(2317)^+$.

$D_{s0}^*(2317)^\pm$ MASS

The fit includes $D^\pm$, D^0, $D_s^\pm$, $D^{*\pm}$, D^{*0}, $D_s^{*\pm}$, $D_1(2420)^0$, $D_2^*(2460)^0$, and $D_{s1}(2536)^\pm$ mass and mass difference measurements.

VALUE (MeV)	EVTS	DOCUMENT ID		TECN	COMMENT
2317.7±0.6 OUR FIT Error includes scale factor of 1.1.					
2318.0±1.0 OUR AVERAGE Error includes scale factor of 1.4.					
2319.6±0.2±1.4	3180	AUBERT	06P	BABR	10.6 $e^+e^- \to D_s^+\pi^0 X$
2317.3±0.4±0.8	1022	[1] AUBERT	04E	BABR	10.6 e^+e^-
• • • We do not use the following data for averages, fits, limits, etc. • • •					
2317.2±1.3	88	[2] AUBERT,B	04S	BABR	$B \to D_{s0}^{(*)}(2317)^+\overline{D}^{(*)}$
2317.2±0.5±0.9	761	[3] MIKAMI	04	BELL	10.6 e^+e^-
2316.8±0.4±3.0	1267±53	[3,4] AUBERT	03G	BABR	10.6 e^+e^-
2317.6±1.3	273 ± 33	[3,5] AUBERT	03G	BABR	10.6 e^+e^-
2319.8±2.1±2.0	24	[3] KROKOVNY	03B	BELL	10.6 e^+e^-

[1] Supersedes AUBERT 03G.
[2] Systematic errors not evaluated.
[3] Not independent of the corresponding $m_{D_{s0}^*(2317)} - m_{D_s}$.
[4] From $D_s^+ \to K^+K^-\pi^+$ decay.
[5] From $D_s^+ \to K^+K^-\pi^+\pi^0$ decay.

$m_{D_{s0}^*(2317)^\pm} - m_{D_s^\pm}$

The fit includes $D^\pm$, D^0, $D_s^\pm$, $D^{*\pm}$, D^{*0}, $D_s^{*\pm}$, $D_1(2420)^0$, $D_2^*(2460)^0$, and $D_{s1}(2536)^\pm$ mass and mass difference measurements.

VALUE (MeV)	EVTS	DOCUMENT ID		TECN	COMMENT
349.4±0.6 OUR FIT Error includes scale factor of 1.1.					
349.2±0.7 OUR AVERAGE					
348.7±0.5±0.7	761	MIKAMI	04	BELL	10.6 e^+e^-
350.0±1.2±1.0	135	BESSON	03	CLE2	10.6 e^+e^-
351.3±2.1±1.9	24	[6] KROKOVNY	03B	BELL	10.6 e^+e^-
• • • We do not use the following data for averages, fits, limits, etc. • • •					
349.6±0.4±3.0	1267	[7,8] AUBERT	03G	BABR	10.6 e^+e^-
350.2±1.3	273	[9,10] AUBERT	03G	BABR	10.6 e^+e^-

[6] Recalculated by us using $m_{D_s^+} = 1968.5 \pm 0.6$ MeV.
[7] From $D_s^+ \to K^+K^-\pi^+$ decay.
[8] Recalculated by us using $m_{D_s^+} = 1967.20 \pm 0.03$ MeV.
[9] From $D_s^+ \to K^+K^-\pi^+\pi^0$ decay.
[10] Recalculated by us using $m_{D_s^+} = 1967.4 \pm 0.2$ MeV. Systematic errors not estimated.

$D_{s0}^*(2317)^\pm$ WIDTH

VALUE (MeV)	CL%	EVTS	DOCUMENT ID		TECN	COMMENT
< 3.8	95	3180	AUBERT	06P	BABR	10.6 $e^+e^- \to D_s^+\pi^0 X$
• • • We do not use the following data for averages, fits, limits, etc. • • •						
< 4.6	90	761	MIKAMI	04	BELL	10.6 e^+e^-
<10			AUBERT	03G	BABR	10.6 e^+e^-
< 7	90	135	BESSON	03	CLE2	10.6 e^+e^-

$D_{s0}^*(2317)^\pm$ DECAY MODES

$D_{s0}^*(2317)^-$ modes are charge conjugates of modes below.

	Mode	Fraction (Γ_i/Γ)
Γ_1	$D_s^+\pi^0$	seen
Γ_2	$D_s^+\gamma$	
Γ_3	$D_s^*(2112)^+\gamma$	
Γ_4	$D_s^+\gamma\gamma$	
Γ_5	$D_s^*(2112)^+\pi^0$	
Γ_6	$D_s^+\pi^+\pi^-$	
Γ_7	$D_s^+\pi^0\pi^0$	not seen

$D_{s0}^*(2317)^\pm$ BRANCHING RATIOS

$\Gamma(D_s^+\pi^0)/\Gamma_{\rm total}$ Γ_1/Γ

VALUE	EVTS	DOCUMENT ID		TECN	COMMENT
seen	1540 ± 62	AUBERT	03G	BABR	10.6 e^+e^-

$\Gamma(D_s^+\gamma)/\Gamma(D_s^+\pi^0)$ Γ_2/Γ_1

VALUE	CL%	DOCUMENT ID		TECN	COMMENT
<0.05	90	MIKAMI	04	BELL	10.6 e^+e^-
• • • We do not use the following data for averages, fits, limits, etc. • • •					
<0.14	95	AUBERT	06P	BABR	10.6 e^+e^-
<0.052	90	BESSON	03	CLE2	10.6 e^+e^-

$\Gamma(D_s^*(2112)^+\gamma)/\Gamma(D_s^+\pi^0)$ Γ_3/Γ_1

VALUE	CL%	DOCUMENT ID		TECN	COMMENT
<0.059	90	BESSON	03	CLE2	10.6 e^+e^-
• • • We do not use the following data for averages, fits, limits, etc. • • •					
<0.16	95	AUBERT	06P	BABR	10.6 e^+e^-
<0.18	90	MIKAMI	04	BELL	10.6 e^+e^-

$\Gamma(D_s^+\gamma\gamma)/\Gamma(D_s^+\pi^0)$ Γ_4/Γ_1

VALUE	CL%	DOCUMENT ID		TECN	COMMENT
<0.18	95	AUBERT	06P	BABR	10.6 e^+e^-
• • • We do not use the following data for averages, fits, limits, etc. • • •					
not seen		AUBERT	03G	BABR	10.6 e^+e^-

$\Gamma(D_s^*(2112)^+\pi^0)/\Gamma(D_s^+\pi^0)$ Γ_5/Γ_1

VALUE	CL%	DOCUMENT ID		TECN	COMMENT
<0.11	90	BESSON	03	CLE2	10.6 e^+e^-

$\Gamma(D_s^+\pi^+\pi^-)/\Gamma(D_s^+\pi^0)$ Γ_6/Γ_1

VALUE	CL%	DOCUMENT ID		TECN	COMMENT
<0.004	90	MIKAMI	04	BELL	10.6 e^+e^-
• • • We do not use the following data for averages, fits, limits, etc. • • •					
<0.005	95	AUBERT	06P	BABR	10.6 e^+e^-
<0.019	90	BESSON	03	CLE2	10.6 e^+e^-

$\Gamma(D_s^+\pi^0\pi^0)/\Gamma(D_s^+\pi^0)$ Γ_7/Γ_1

VALUE	CL%	DOCUMENT ID		TECN	COMMENT
<0.25	95	AUBERT	06P	BABR	10.6 e^+e^-

$D_{s0}^*(2317)^\pm$ REFERENCES

AUBERT	06P	PR D74 032007	B. Aubert *et al.*	(BABAR Collab.)
AUBERT	04E	PR D69 031101	B. Aubert *et al.*	(BABAR Collab.)
AUBERT,B	04S	PRL 93 181801	B. Aubert *et al.*	(BABAR Collab.)
MIKAMI	04	PRL 92 012002	Y. Mikami *et al.*	(BELLE Collab.)
AUBERT	03G	PRL 90 242001	B. Aubert *et al.*	(BaBar Collab.)
BESSON	03	PR D68 032002	D. Besson *et al.*	(CLEO Collab.)
KROKOVNY	03B	PRL 91 262002	P. Krokovny *et al.*	(BELLE Collab.)

$D_{s1}(2460)^\pm$

$I(J^P) = 0(1^+)$

$D_{s1}(2460)^\pm$ MASS

The fit includes $D^\pm$, D^0, $D_s^\pm$, $D^{*\pm}$, D^{*0}, $D_s^{*\pm}$, $D_1(2420)^0$, $D_2^*(2460)^0$, and $D_{s1}(2536)^\pm$ mass and mass difference measurements.

VALUE (MeV)	EVTS	DOCUMENT ID		TECN	COMMENT
2459.5±0.6 OUR FIT Error includes scale factor of 1.1.					
2459.6±0.9 OUR AVERAGE Error includes scale factor of 1.3.					
2460.1±0.2±0.8		[1] AUBERT	06P	BABR	10.6 e^+e^-
2458.0±1.0±1.0	195	AUBERT	04E	BABR	10.6 e^+e^-
• • • We do not use the following data for averages, fits, limits, etc. • • •					
2459.5±1.2±3.7	920	AUBERT	06P	BABR	10.6 $e^+e^- \to D_s^+\gamma X$
2458.6±1.0±2.5	560	AUBERT	06P	BABR	10.6 $e^+e^- \to D_s^+\pi^0\gamma X$
2460.2±0.2±0.8	123	AUBERT	06P	BABR	10.6 $e^+e^- \to D_s^+\pi^+\pi^- X$
2458.9±1.5	112	[2] AUBERT,B	04S	BABR	$B \to D_{s1}(2460)^+\overline{D}^{(*)}$
2461.1±1.6	139	[3] AUBERT,B	04S	BABR	$B \to D_{s1}(2460)^+\overline{D}^{(*)}$
2456.5±1.3±1.3	126	[4,5] MIKAMI	04	BELL	10.6 e^+e^-
2459.5±1.3±2.0	152	[6,7] MIKAMI	04	BELL	10.6 e^+e^-
2459.9±0.9±1.6	60	[6,7] MIKAMI	04	BELL	10.6 e^+e^-
2459.2±1.6±2.0	57	KROKOVNY	03B	BELL	10.6 e^+e^-

[1] The average of the values obtained from the $D_s^+\gamma$, $D_s^+\pi^0\gamma$,$D_s^+\pi^+\pi^-$ final state.

[2] Systematic errors not evaluated. From the decay to $D_s^{*+}\pi^0$.

[3] Systematic errors not evaluated. From the decay to $D_s^+\gamma$.

[4] Not independent of the corresponding $m_{D_{s1}(2460)^\pm} - m_{D_s^{*\pm}}$.

[5] Using $m_{D_s^{*+}} = 2112.4 \pm 0.7$ MeV.

[6] Not independent of the corresponding $m_{D_{s1}(2460)^\pm} - m_{D_s^\pm}$.

[7] Using $m_{D_s^+} = 1968.5 \pm 0.6$ MeV.

$m_{D_{s1}(2460)^\pm} - m_{D_s^{*\pm}}$

The fit includes $D^\pm$, D^0, $D_s^\pm$, $D^{*\pm}$, D^{*0}, $D_s^{*\pm}$, $D_1(2420)^0$, $D_2^*(2460)^0$, and $D_{s1}(2536)^\pm$ mass and mass difference measurements.

VALUE (MeV)	EVTS	DOCUMENT ID		TECN	COMMENT
347.3±0.7 OUR FIT Error includes scale factor of 1.2.					
347.1±2.2 OUR AVERAGE Error includes scale factor of 1.9. See the ideogram below.					
344.1±1.3±1.1	126	MIKAMI	04	BELL	10.6 e^+e^-
351.2±1.7±1.0	41	BESSON	03	CLE2	10.6 e^+e^-
346.8±1.6±1.9	57	[8] KROKOVNY	03B	BELL	10.6 e^+e^-

[8] Recalculated by us using $m_{D_s^{*+}} = 2112.4 \pm 0.7$ MeV.

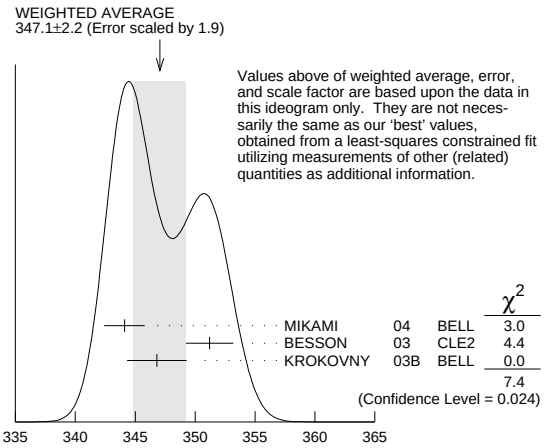

$m_{D_{s1}(2460)^\pm} - m_{D_s^\pm}$

The fit includes $D^\pm$, D^0, $D_s^\pm$, $D^{*\pm}$, D^{*0}, $D_s^{*\pm}$, $D_1(2420)^0$, $D_2^*(2460)^0$, and $D_{s1}(2536)^\pm$ mass and mass difference measurements.

VALUE (MeV)	EVTS	DOCUMENT ID		TECN	COMMENT
491.2±0.6 OUR FIT Error includes scale factor of 1.1.					
491.3±1.4 OUR AVERAGE					
491.0±1.3±1.9	152	[9] MIKAMI	04	BELL	10.6 e^+e^-
491.4±0.9±1.5	60	[10] MIKAMI	04	BELL	10.6 e^+e^-

[9] From the decay to $D_s^\pm\gamma$.

[10] From the decay to $D_s^\pm\pi^+\pi^-$.

$D_{s1}(2460)^\pm$ WIDTH

VALUE (MeV)	CL%	EVTS	DOCUMENT ID		TECN	COMMENT
< 3.5	95	123	AUBERT	06P	BABR	10.6 $e^+e^- \to D_s^+\pi^+\pi^- X$
• • • We do not use the following data for averages, fits, limits, etc. • • •						
< 6.3	95	560	AUBERT	06P	BABR	10.6 $e^+e^- \to D_s^+\pi^0\gamma X$
<10		195	AUBERT	04E	BABR	10.6 e^+e^-
< 5.5	90	126	MIKAMI	04	BELL	10.6 e^+e^-
< 7	90	41	BESSON	03	CLE2	10.6 e^+e^-

$D_{s1}(2460)^+$ DECAY MODES

$D_{s1}(2460)^-$ modes are charge conjugates of the modes below.

	Mode	Fraction (Γ_i/Γ)	Scale factor/ Confidence level
Γ_1	$D_s^{*+}\pi^0$	(48 ±11) %	
Γ_2	$D_s^+\gamma$	(18 ± 4) %	
Γ_3	$D_s^+\pi^+\pi^-$	(4.3± 1.3) %	S=1.1
Γ_4	$D_s^{*+}\gamma$	< 8 %	CL=90%
Γ_5	$D_{s0}^*(2317)^+\gamma$	($3.7^{+\ 5.0}_{-\ 2.4}$) %	
Γ_6	$D_s^+\pi^0$		
Γ_7	$D_s^+\pi^0\pi^0$		
Γ_8	$D_s^+\gamma\gamma$		

Meson Particle Listings

$D_{s1}(2460)^{\pm}$, $D_{s1}(2536)^{\pm}$

CONSTRAINED FIT INFORMATION

An overall fit to 7 branching ratios uses 8 measurements and one constraint to determine 5 parameters. The overall fit has a $\chi^2 = 3.4$ for 4 degrees of freedom.

The following *off-diagonal* array elements are the correlation coefficients $\langle \delta x_i \delta x_j \rangle / (\delta x_i \cdot \delta x_j)$, in percent, from the fit to the branching fractions, $x_i \equiv \Gamma_i / \Gamma_{\text{total}}$. The fit constrains the x_i whose labels appear in this array to sum to one.

x_2	80		
x_3	68	62	
x_5	−3	25	26
	x_1	x_2	x_3

$D_{s1}(2460)^{\pm}$ BRANCHING RATIOS

$\Gamma(D_s^{*+}\pi^0)/\Gamma_{\text{total}}$ — **Γ_1/Γ**

VALUE	EVTS	DOCUMENT ID		TECN	COMMENT
0.48±0.11 OUR FIT					
0.56±0.13±0.09		[11] AUBERT	06N	BABR	$B \to D_{s1}(2460)^- \overline{D}^{(*)}$
• • • We do not use the following data for averages, fits, limits, etc. • • •					
seen	41	BESSON	03	CLE2	10.6 e^+e^-

[11] Evaluated in AUBERT 06N including measurements from AUBERT,B 04S.

$\Gamma(D_s^+\gamma)/\Gamma_{\text{total}}$ — **Γ_2/Γ**

VALUE	DOCUMENT ID		TECN	COMMENT
0.18±0.04 OUR FIT				
0.16±0.04±0.03	[12] AUBERT	06N	BABR	$B \to D_{s1}(2460)^- \overline{D}^{(*)}$

[12] Evaluated in AUBERT 06N including measurements from AUBERT,B 04S.

$\Gamma(D_s^+\gamma)/\Gamma(D_s^{*+}\pi^0)$ — **Γ_2/Γ_1**

VALUE	CL%	EVTS	DOCUMENT ID		TECN	COMMENT
0.38 ±0.05 OUR FIT						
0.44 ±0.09 OUR AVERAGE						
0.55 ±0.13 ±0.08		152	MIKAMI	04	BELL	10.6 e^+e^-
0.38 ±0.11 ±0.04		38	KROKOVNY	03B	BELL	10.6 e^+e^-
• • • We do not use the following data for averages, fits, limits, etc. • • •						
0.274±0.045±0.020		251	[13] AUBERT,B	04S	BABR	$B \to D_{s1}(2460)^+ \overline{D}^{(*)}$
< 0.49	90		BESSON	03	CLE2	10.6 e^+e^-

[13] Used by AUBERT 06N in their measurement of $B(D_s^{*-}\pi^0)$ and $B(D_s^-\gamma)$.

$\Gamma(D_s^+\pi^+\pi^-)/\Gamma(D_s^{*+}\pi^0)$ — **Γ_3/Γ_1**

VALUE	CL%	EVTS	DOCUMENT ID		TECN	COMMENT
0.090±0.020 OUR FIT Error includes scale factor of 1.2.						
0.14 ±0.04 ±0.02		60	MIKAMI	04	BELL	10.6 e^+e^-
• • • We do not use the following data for averages, fits, limits, etc. • • •						
<0.08	90		BESSON	03	CLE2	10.6 e^+e^-

$\Gamma(D_s^{*+}\gamma)/\Gamma(D_s^{*+}\pi^0)$ — **Γ_4/Γ_1**

VALUE	CL%	DOCUMENT ID		TECN	COMMENT
<0.16	90	BESSON	03	CLE2	10.6 e^+e^-
• • • We do not use the following data for averages, fits, limits, etc. • • •					
<0.31	90	MIKAMI	04	BELL	10.6 e^+e^-

$\Gamma(D_{s0}^*(2317)^+\gamma)/\Gamma(D_s^{*+}\pi^0)$ — **Γ_5/Γ_1**

VALUE	CL%	DOCUMENT ID		TECN	COMMENT
<0.22	95	AUBERT	04E	BABR	10.6 e^+e^-
• • • We do not use the following data for averages, fits, limits, etc. • • •					
<0.58	90	BESSON	03	CLE2	10.6 e^+e^-

$\Gamma(D_s^{*+}\pi^0)/[\Gamma(D_s^{*+}\pi^0)+\Gamma(D_{s0}^*(2317)^+\gamma)]$ — **$\Gamma_1/(\Gamma_1+\Gamma_5)$**

VALUE	DOCUMENT ID		TECN	COMMENT
0.93±0.09 OUR FIT				
0.97±0.09±0.05	AUBERT	06P	BABR	10.6 e^+e^-

$\Gamma(D_s^+\gamma)/[\Gamma(D_s^{*+}\pi^0)+\Gamma(D_{s0}^*(2317)^+\gamma)]$ — **$\Gamma_2/(\Gamma_1+\Gamma_5)$**

VALUE	DOCUMENT ID		TECN	COMMENT
0.35 ±0.04 OUR FIT				
0.337±0.036±0.038	AUBERT	06P	BABR	10.6 e^+e^-

$\Gamma(D_s^+\pi^+\pi^-)/[\Gamma(D_s^{*+}\pi^0)+\Gamma(D_{s0}^*(2317)^+\gamma)]$ — **$\Gamma_3/(\Gamma_1+\Gamma_5)$**

VALUE	DOCUMENT ID		TECN	COMMENT
0.083±0.017 OUR FIT Error includes scale factor of 1.2.				
0.077±0.013±0.008	AUBERT	06P	BABR	10.6 e^+e^-

$\Gamma(D_s^{*+}\gamma)/[\Gamma(D_s^{*+}\pi^0)+\Gamma(D_{s0}^*(2317)^+\gamma)]$ — **$\Gamma_4/(\Gamma_1+\Gamma_5)$**

VALUE	CL%	DOCUMENT ID		TECN	COMMENT
<0.24	95	AUBERT	06P	BABR	10.6 e^+e^-

$\Gamma(D_{s0}^*(2317)^+\gamma)/[\Gamma(D_s^{*+}\pi^0)+\Gamma(D_{s0}^*(2317)^+\gamma)]$ — **$\Gamma_5/(\Gamma_1+\Gamma_5)$**

VALUE	CL%	DOCUMENT ID		TECN	COMMENT
<0.25	95	AUBERT	06P	BABR	10.6 e^+e^-

$\Gamma(D_s^+\pi^0)/[\Gamma(D_s^{*+}\pi^0)+\Gamma(D_{s0}^*(2317)^+\gamma)]$ — **$\Gamma_6/(\Gamma_1+\Gamma_5)$**

VALUE	CL%	DOCUMENT ID		TECN	COMMENT
<0.042	95	AUBERT	06P	BABR	10.6 e^+e^-

$\Gamma(D_s^+\pi^0\pi^0)/[\Gamma(D_s^{*+}\pi^0)+\Gamma(D_{s0}^*(2317)^+\gamma)]$ — **$\Gamma_7/(\Gamma_1+\Gamma_5)$**

VALUE	CL%	DOCUMENT ID		TECN	COMMENT
<0.68	95	AUBERT	06P	BABR	10.6 e^+e^-

$\Gamma(D_s^+\gamma\gamma)/[\Gamma(D_s^{*+}\pi^0)+\Gamma(D_{s0}^*(2317)^+\gamma)]$ — **$\Gamma_8/(\Gamma_1+\Gamma_5)$**

VALUE	CL%	DOCUMENT ID		TECN	COMMENT
<0.33	95	AUBERT	06P	BABR	10.6 e^+e^-

$D_{s1}(2460)^{\pm}$ REFERENCES

AUBERT	06N	PR D74 031103	B. Aubert *et al.*	(BABAR Collab.)
AUBERT	06P	PR D74 032007	B. Aubert *et al.*	(BABAR Collab.)
AUBERT	04E	PR D69 031101	B. Aubert *et al.*	(BABAR Collab.)
AUBERT,B	04S	PRL 93 181801	B. Aubert *et al.*	(BABAR Collab.)
MIKAMI	04	PRL 92 012002	Y. Mikami *et al.*	(BELLE Collab.)
BESSON	03	PR D68 032002	D. Besson *et al.*	(CLEO Collab.)
KROKOVNY	03B	PRL 91 262002	P. Krokovny *et al.*	(BELLE Collab.)

$D_{s1}(2536)^{\pm}$

$I(J^P) = 0(1^+)$
J, P need confirmation.

Seen in $D^*(2010)^+K^0$, $D^*(2007)^0K^+$, and $D_s^+\pi^+\pi^-$. Not seen in D^+K^0 or D^0K^+. $J^P = 1^+$ assignment strongly favored.

$D_{s1}(2536)^{\pm}$ MASS

The fit includes $D^{\pm}$, D^0, $D_s^{\pm}$, $D^{*\pm}$, D^{*0}, $D_s^{*\pm}$, $D_1(2420)^0$, $D_2^*(2460)^0$, and $D_{s1}(2536)^{\pm}$ mass and mass difference measurements.

VALUE (MeV)	EVTS	DOCUMENT ID		TECN	COMMENT
2535.10±0.08 OUR FIT Error includes scale factor of 1.1.					
2535.18±0.24 OUR AVERAGE					
2535.7 ±0.6 ±0.5	46 ± 9	[1] ABAZOV	09G	D0	$B_s^0 \to D_{s1}^- \mu^+ \nu_\mu X$
2534.78±0.31±0.40	182	AUBERT	08B	BABR	$B \to \overline{D}^{(*)} D^* K$
2534.6 ±0.3 ±0.7	193	AUBERT	06P	BABR	10.6 $e^+e^- \to D_s^+\pi^+\pi^- X$
2535.3 ±0.7	92	[2] HEISTER	02B	ALEP	$e^+e^- \to D^{*+}K^0X$, $D^{*0}K^+X$
2534.2 ±1.2	9	ASRATYAN	94	BEBC	$\nu N \to D^*K^0X, D^{*0}K^{\pm}X$
2535 ±0.6 ±1	75	FRABETTI	94B	E687	γBe $\to D^{*+}K^0X$, $D^{*0}K^+X$
2535.3 ±0.2 ±0.5	134	ALEXANDER	93	CLE2	$e^+e^- \to D^{*0}K^+X$
2534.8 ±0.6 ±0.6	44	ALEXANDER	93	CLE2	$e^+e^- \to D^{*+}K^0X$
2535.2 ±0.5 ±1.5	28	ALBRECHT	92R	ARG	10.4 $e^+e^- \to D^{*0}K^+X$
2536.6 ±0.7 ±0.4		AVERY	90	CLEO	$e^+e^- \to D^{*+}K^0X$
2535.9 ±0.6 ±2.0		ALBRECHT	89E	ARG	$D_{s1}^* \to D^*(2010)K^0$
• • • We do not use the following data for averages, fits, limits, etc. • • •					
2534.1 ±0.6	116	[3] AUSHEV	11	BELL	$B \to D_{s1}(2536)^+ D^{(*)}$
2535.08±0.01±0.15	8038	[4] LEES	11B	BABR	10.6 $e^+e^- \to D^{*+}K_S^0X$
$2535.57^{+0.44}_{-0.41}\pm0.10$	236 ± 30	[5] CHEKANOV	09	ZEUS	$e^{\pm}p \to D^{*+}K_S^0X$, $D^{*0}K^+X$
2535 ± 28		[6] ASRATYAN	88	HLBC	$\nu N \to D_s\gamma\gamma X$

[1] Using the $D^*(2010)^{\pm}$ mass of 2010.0 ± 0.4 MeV from PDG 06.
[2] Calculated using $m(D^*(2010)^{\pm}) = 2010.0 \pm 0.5$ MeV, $m(D^*(2007)^0) = 2006.7 \pm 0.5$ MeV, and the mass difference below.
[3] Systematic uncertainties not evaluated.
[4] Calculated using the mass difference $m(D_{s1}^+) - m(D^{*+})_{PDG}$ below and $m(D^{*+})_{PDG} = 2010.25 \pm 0.14$ MeV. Assuming S-wave decay of the $D_{s1}(2536)$ to $D^{*+}K_S^0$, using a Breit-Wigner line shape corresponding to L=0.
[5] Calculated using the mass difference $m(D_{s1}^+) - m(D^{*+})_{PDG}$ reported below and $m(D^{*+})_{PDG} = 2010.27 \pm 0.17$ MeV.
[6] Not seen in D^*K.

$m_{D_{s1}(2536)^{\pm}} - m_{D_s^*(2111)}$

The fit includes $D^{\pm}$, D^0, $D_s^{\pm}$, $D^{*\pm}$, D^{*0}, $D_s^{*\pm}$, $D_1(2420)^0$, $D_2^*(2460)^0$, and $D_{s1}(2536)^{\pm}$ mass and mass difference measurements.

VALUE (MeV)	DOCUMENT ID		TECN	COMMENT
423.0± 0.4 OUR FIT				
424 ±28	ASRATYAN	88	HLBC	$D_s^{*\pm}\gamma$

$m_{D_{s1}(2536)^{\pm}} - m_{D^*(2010)^{\pm}}$

The fit includes $D^{\pm}$, D^0, $D_s^{\pm}$, $D^{*\pm}$, D^{*0}, $D_s^{*\pm}$, $D_1(2420)^0$, $D_2^*(2460)^0$, and $D_{s1}(2536)^{\pm}$ mass and mass difference measurements.

VALUE (MeV)	EVTS	DOCUMENT ID		TECN	COMMENT
524.84±0.04 OUR FIT					
524.84±0.04 OUR AVERAGE					
524.83±0.01±0.04	8038	[7] LEES	11B	BABR	10.6 $e^+e^- \to D^{*+}K_S^0X$
$525.30^{+0.44}_{-0.41}$±0.10	236 ± 30	CHEKANOV	09	ZEUS	$e^{\pm}p \to D^{*+}K_S^0X$, $D^{*0}K^+X$
525.3 ±0.6 ±0.1	41	HEISTER	02B	ALEP	$e^+e^- \to D^{*+}K^0X$

[7] Assuming S-wave decay of the $D_{s1}(2536)$ to $D^{*+}K_S^0$, using a Breit-Wigner line shape corresponding to L=0.

$m_{D_{s1}(2536)^{\pm}} - m_{D^*(2007)^0}$

The fit includes $D^{\pm}$, D^0, $D_s^{\pm}$, $D^{*\pm}$, D^{*0}, $D_s^{*\pm}$, $D_1(2420)^0$, $D_2^*(2460)^0$, and $D_{s1}(2536)^{\pm}$ mass and mass difference measurements.

VALUE (MeV)	EVTS	DOCUMENT ID		TECN	COMMENT
528.14±0.08 OUR FIT					
528.1 ±1.5 OUR AVERAGE					
528.7 ±1.9 ±0.5	51	HEISTER	02B	ALEP	$e^+e^- \to D^{*0}K^+X$
527.3 ±2.2	29	ACKERSTAFF	97W	OPAL	$e^+e^- \to D^{*0}K^+X$

$D_{s1}(2536)^{\pm}$ WIDTH

VALUE (MeV)	CL%	EVTS	DOCUMENT ID		TECN	COMMENT
0.92±0.03±0.04		8038	[8] LEES	11B	BABR	10.6 $e^+e^- \to D^{*+}K_S^0X$
• • • We do not use the following data for averages, fits, limits, etc. • • •						
0.75±0.23		116	[9] AUSHEV	11	BELL	$B \to D_{s1}(2536)+D^{(*)}$
< 2.5	95	193	AUBERT	06P	BABR	10.6 $e^+e^- \to D_s^+\pi^+\pi^-X$
< 3.2	90	75	FRABETTI	94B	E687	γBe $\to D^{*+}K^0X$, $D^{*0}K^+X$
< 2.3	90		ALEXANDER	93	CLEO	$e^+e^- \to D^{*0}K^+X$
< 3.9	90		ALBRECHT	92R	ARG	10.4 $e^+e^- \to D^{*0}K^+X$
< 5.44	90		AVERY	90	CLEO	$e^+e^- \to D^{*+}K^0X$
< 4.6	90		ALBRECHT	89E	ARG	$D_{s1}^* \to D^*(2010)K^0$

[8] Assuming S-wave decay of the $D_{s1}(2536)$ to $D^{*+}K_S^0$, using a Breit-Wigner line shape corresponding to L=0.
[9] Systematic uncertainties not evaluated.

$D_{s1}(2536)^+$ DECAY MODES

$D_{s1}(2536)^-$ modes are charge conjugates of the modes below.

	Mode	Fraction (Γ_i/Γ)	Confidence level
Γ_1	$D^*(2010)^+K^0$	0.85 ±0.12	
Γ_2	$(D^*(2010)^+K^0)_{S-wave}$	0.61 ±0.09	
Γ_3	$(D^*(2010)^+K^0)_{D-wave}$		
Γ_4	$D^+\pi^-K^+$	0.028±0.005	
Γ_5	$D^*(2007)^0K^+$	**DEFINED AS 1**	
Γ_6	D^+K^0	<0.34	90%
Γ_7	D^0K^+	<0.12	90%
Γ_8	$D_s^{*+}\gamma$	possibly seen	
Γ_9	$D_s^+\pi^+\pi^-$	seen	

$D_{s1}(2536)^+$ BRANCHING RATIOS

$\Gamma(D^*(2007)^0K^+)/\Gamma(D^*(2010)^+K^0)$ Γ_5/Γ_1

VALUE	EVTS	DOCUMENT ID		TECN	COMMENT
1.18±0.16 OUR AVERAGE					
0.88±0.24±0.08	116	AUSHEV	11	BELL	$B \to D_{s1}(2536)^+D^{(*)}$
2.3 ±0.6 ±0.3	236 ± 30	CHEKANOV	09	ZEUS	$e^{\pm}p \to D^{*+}K_S^0X$, $D^{*0}K^+X$
1.32±0.47±0.23	92	[10] HEISTER	02B	ALEP	$e^+e^- \to D^{*+}K^0X$, $D^{*0}K^+X$
$1.9\ ^{+1.1}_{-0.9}$ ±0.4	35	[10] ACKERSTAFF	97W	OPAL	$e^+e^- \to D^{*0}K^+X$, $D^{*+}K^0X$
1.1 ±0.3		ALEXANDER	93	CLEO	$e^+e^- \to D^{*0}K^+X, D^{*+}K^0X$
1.4 ±0.3 ±0.2		[11] ALBRECHT	92R	ARG	10.4 $e^+e^- \to D^{*0}K^+X, D^{*+}K^0X$

[10] Ratio of the production rates measured in Z^0 decays.
[11] Evaluated by us from published inclusive cross-sections.

$\Gamma((D^*(2010)^+K^0)_{S-wave})/\Gamma(D^*(2010)^+K^0)$ Γ_2/Γ_1

VALUE	EVTS	DOCUMENT ID		TECN	COMMENT
0.72±0.05±0.01	5485	BALAGURA	08	BELL	10.6 $e^+e^- \to D^{*+}K^0X$

$\Gamma(D^+\pi^-K^+)/\Gamma(D^*(2010)^+K^0)$ Γ_4/Γ_1

VALUE (units 10^{-2})	EVTS	DOCUMENT ID		TECN	COMMENT
3.27±0.18±0.37	1264	BALAGURA	08	BELL	10.6 $e^+e^- \to D^+\pi^-K^+X$

$\Gamma(D^+K^0)/\Gamma(D^*(2010)^+K^0)$ Γ_6/Γ_1

VALUE	CL%	DOCUMENT ID		TECN	COMMENT
<0.40	90	ALEXANDER	93	CLEO	$e^+e^- \to D^{*+}K^0X$
<0.43	90	ALBRECHT	89E	ARG	$D_{s1}^* \to D^*(2010)K^0$

$\Gamma(D^0K^+)/\Gamma(D^*(2007)^0K^+)$ Γ_7/Γ_5

VALUE	CL%	DOCUMENT ID		TECN	COMMENT
<0.12	90	ALEXANDER	93	CLEO	$e^+e^- \to D^{*0}K^+X$

$\Gamma(D_s^{*+}\gamma)/\Gamma_{total}$ Γ_8/Γ

VALUE	DOCUMENT ID		TECN	COMMENT
possibly seen	ASRATYAN	88	HLBC	$\nu N \to D_s\gamma\gamma X$

$\Gamma(D_s^{*+}\gamma)/\Gamma(D^*(2007)^0K^+)$ Γ_8/Γ_5

VALUE	CL%	DOCUMENT ID		TECN	COMMENT
<0.42	90	ALEXANDER	93	CLEO	$e^+e^- \to D^{*0}K^+X$

$\Gamma(D_s^+\pi^+\pi^-)/\Gamma_{total}$ Γ_9/Γ

VALUE	DOCUMENT ID		TECN	COMMENT
seen	AUBERT	06P	BABR	10.6 $e^+e^- \to D_s^+\pi^+\pi^-X$

$D_{s1}(2536)^{\pm}$ REFERENCES

AUSHEV	11	PR D83 051102	T. Aushev *et al.*	(BELLE Collab.)
LEES	11B	PR D83 072003	J.P. Lees *et al.*	(BABAR Collab.)
ABAZOV	09G	PRL 102 051801	V.M. Abazov *et al.*	(D0 Collab.)
CHEKANOV	09	EPJ C60 25	S. Chekanov *et al.*	(ZEUS Collab.)
AUBERT	08B	PR D77 011102	B. Aubert *et al.*	(BABAR Collab.)
BALAGURA	08	PR D77 032001	V. Balagura *et al.*	(BELLE Collab.)
AUBERT	06P	PR D74 032007	B. Aubert *et al.*	(BABAR Collab.)
PDG	06	JP G33 1	W.-M. Yao *et al.*	(PDG Collab.)
HEISTER	02B	PL B526 34	A. Heister *et al.*	(ALEPH Collab.)
ACKERSTAFF	97W	ZPHY C76 425	K. Ackerstaff *et al.*	(OPAL Collab.)
ASRATYAN	94	ZPHY C61 563	A.E. Asratyan *et al.*	(BIRM, BELG, CERN+)
FRABETTI	94B	PRL 72 324	P.L. Frabetti *et al.*	(FNAL E687 Collab.)
ALEXANDER	93	PL B303 377	J. Alexander *et al.*	(CLEO Collab.)
ALBRECHT	92R	PL B297 425	H. Albrecht *et al.*	(ARGUS Collab.)
AVERY	90	PR D41 774	P. Avery, D. Besson	(CLEO Collab.)
ALBRECHT	89E	PL B230 162	H. Albrecht *et al.*	(ARGUS Collab.)
ASRATYAN	88	ZPHY C40 483	A.E. Asratyan *et al.*	(ITEP, SERP)

$D_{s2}^*(2573)$

$I(J^P) = 0(?^?)$

J^P is natural, width and decay modes consistent with 2^+.

$D_{s2}^*(2573)$ MASS

VALUE (MeV)	EVTS	DOCUMENT ID		TECN	COMMENT
2571.9±0.8 OUR AVERAGE					
2569.4±1.6±0.5	82 ± 17	AAIJ	11A	LHCB	$B_s \to D_{s2}^*(2573)\mu\overline{\nu}X$
2572.2±0.3±1.0		AUBERT,BE	06E	BABR	$e^+e^- \to DKX$
2574.5±3.3±1.6		ALBRECHT	96	ARG	$e^+e^- \to D^0K^+X$
$2573.2^{+1.7}_{-1.6}$±0.9	217	KUBOTA	94	CLE2	$e^+e^-\sim$ 10.5 GeV
• • • We do not use the following data for averages, fits, limits, etc. • • •					
2570.0±4.3	25	[1] EVDOKIMOV	04	SELX	600 $\Sigma^-A \to D^0K^+X$
2568.6±3.2	64	[2] HEISTER	02B	ALEP	$e^+e^- \to D^0K^+X$

[1] Not independent of the mass difference below.
[2] Calculated using m_{D^0}= 1864.5 ± 0.5 MeV and the mass difference below.

$m_{D_{s2}^*(2573)} - m_{D^0}$

VALUE (MeV)	EVTS	DOCUMENT ID		TECN	COMMENT
704 ±3 ±1	64	HEISTER	02B	ALEP	$e^+e^- \to D^0K^+X$
• • • We do not use the following data for averages, fits, limits, etc. • • •					
705.4±4.3	25	[3] EVDOKIMOV	04	SELX	600 $\Sigma^-A \to D^0K^+X$

[3] Systematic errors not estimated.

$D_{s2}^*(2573)$ WIDTH

VALUE (MeV)	EVTS	DOCUMENT ID		TECN	COMMENT
17 ±4 OUR AVERAGE Error includes scale factor of 1.3. See the ideogram below.					
12.1±4.5±1.6	82 ± 17	AAIJ	11A	LHCB	$B_s \to D_{s2}^*(2573)\mu\overline{\nu}X$
27.1±0.6±5.6		AUBERT,BE	06E	BABR	$e^+e^- \to DKX$
10.4±8.3±3.0		ALBRECHT	96	ARG	$e^+e^- \to D^0K^+X$
$16\ ^{+5}_{-4}$ ±3	217	KUBOTA	94	CLE2	$e^+e^-\sim$ 10.5 GeV
• • • We do not use the following data for averages, fits, limits, etc. • • •					
$14\ ^{+9}_{-6}$	25	[4] EVDOKIMOV	04	SELX	600 $\Sigma^-A \to D^0K^+X$

[4] Systematic errors not estimated.

Meson Particle Listings

$D_{s2}(2573)$, $D^*_{s1}(2700)^{\pm}$, $D^*_{sJ}(2860)^{\pm}$

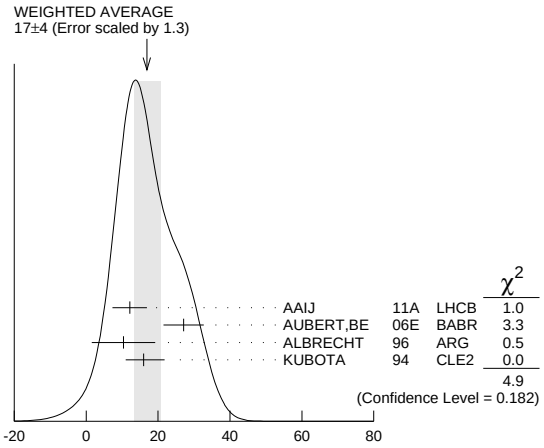

$D^*_{s2}(2573)^+$ DECAY MODES

$D^*_{s2}(2573)^-$ modes are charge conjugates of the modes below.

	Mode	Fraction (Γ_i/Γ)
Γ_1	$D^0 K^+$	seen
Γ_2	$D^*(2007)^0 K^+$	not seen

$D^*_{s2}(2573)^+$ BRANCHING RATIOS

$\Gamma(D^0 K^+)/\Gamma_{total}$ — Γ_1/Γ

VALUE	EVTS	DOCUMENT ID		TECN	CHG	COMMENT
seen	217	KUBOTA	94	CLE2	±	$e^+e^-\sim$ 10.5 GeV

$\Gamma(D^*(2007)^0 K^+)/\Gamma(D^0 K^+)$ — Γ_2/Γ_1

VALUE	CL%	DOCUMENT ID		TECN	CHG	COMMENT
<0.33	90	KUBOTA	94	CLE2	+	$e^+e^-\sim$ 10.5 GeV

$D^*_{s2}(2573)$ REFERENCES

AAIJ	11A	PL B698 14	R. Aaij *et al.*	(LHCb Collab.)
AUBERT,BE	06E	PRL 97 222001	B. Aubert *et al.*	(BABAR Collab.)
EVDOKIMOV	04	PRL 93 242001	A.V. Evdokimov *et al.*	(SELEX Collab.)
HEISTER	02B	PL B526 34	A. Heister *et al.*	(ALEPH Collab.)
ALBRECHT	96	ZPHY C69 405	H. Albrecht *et al.*	(ARGUS Collab.)
KUBOTA	94	PRL 72 1972	Y. Kubota *et al.*	(CLEO Collab.)

$D^*_{s1}(2700)^{\pm}$

$I(J^P) = 0(1^-)$

$D^*_{s1}(2700)^+$ MASS

VALUE (MeV)	EVTS	DOCUMENT ID		TECN	COMMENT
2709 ±4 OUR AVERAGE					
2709.2±1.9± 4.5	52k	[1] AAIJ	12AU	LHCB	$pp \to (DK)^+X$ at 7 TeV
2710 ±2 $^{+12}_{-7}$	10.4k	[2] AUBERT	09AR	BABR	$e^+e^- \to D^{(*)}KX$
2708 ±9 $^{+11}_{-10}$	182	BRODZICKA	08	BELL	$B^+ \to D^0\overline{D}{}^0K^+$
• • • We do not use the following data for averages, fits, limits, etc. • • •					
2688 ±4 ± 3		[3] AUBERT,BE	06E	BABR	10.6 $e^+e^- \to DKX$

[1] From the combined fit of the $D^+K^0_S$ and D^0K^+ modes in the model including the $D^*_{s2}(2573)^+$, $D^*_{s1}(2700)^+$ and spin-0 $D^*_{sJ}(2860)^+$.
[2] From simultaneous fits to the two DK mass spectra and to the total D^*K mass spectrum.
[3] Superseded by AUBERT 09AR.

$D^*_{s1}(2700)^+$ WIDTH

VALUE (MeV)	EVTS	DOCUMENT ID		TECN	COMMENT
117 ±13 OUR AVERAGE					
115.8± 7.3±12.1	52k	[4] AAIJ	12AU	LHCB	$pp \to (DK)^+X$ at 7 TeV
149 ± 7 $^{+39}_{-52}$	10.4k	[5] AUBERT	09AR	BABR	$e^+e^- \to D^{(*)}KX$
108 ±23 $^{+36}_{-31}$	182	BRODZICKA	08	BELL	$B^+ \to D^0\overline{D}{}^0K^+$
• • • We do not use the following data for averages, fits, limits, etc. • • •					
112 ± 7 ±36		[6] AUBERT,BE	06E	BABR	10.6 $e^+e^- \to DKX$

[4] From the combined fit of the $D^+K^0_S$ and D^0K^+ modes in the model including the $D^*_{s2}(2573)^+$, $D^*_{s1}(2700)^+$ and spin-0 $D^*_{sJ}(2860)^+$.
[5] From simultaneous fits to the two DK mass spectra and to the total D^*K mass spectrum.
[6] Superseded by AUBERT 09AR.

$D^*_{s1}(2700)^{\pm}$ DECAY MODES

	Mode
Γ_1	DK
Γ_2	D^0K^+
Γ_3	$D^+K^0_S$
Γ_4	D^*K
Γ_5	$D^{*0}K^+$
Γ_6	$D^{*+}K^0_S$

$D^*_{s1}(2700)^{\pm}$ BRANCHING RATIOS

$\Gamma(D^*K)/\Gamma(DK)$ — Γ_4/Γ_1

VALUE	EVTS	DOCUMENT ID		TECN	COMMENT
0.91±0.13±0.12	10.4k	[7] AUBERT	09AR	BABR	$e^+e^- \to D^{(*)}KX$

[7] From the average of the corresponding ratios with $D^{(*)0}K^+$ and $D^{(*)+}K^0_S$.

$\Gamma(D^{*0}K^+)/\Gamma(D^0K^+)$ — Γ_5/Γ_2

VALUE	EVTS	DOCUMENT ID		TECN	COMMENT
• • • We do not use the following data for averages, fits, limits, etc. • • •					
0.88±0.14±0.14	7716	[8] AUBERT	09AR	BABR	$e^+e^- \to D^{(*)}KX$

[8] From the $D^{*0}K^+$ and D^0K^+, where $D^{*0} \to D^0\pi^0$.

$\Gamma(D^{*+}K^0_S)/\Gamma(D^+K^0_S)$ — Γ_6/Γ_3

VALUE	EVTS	DOCUMENT ID		TECN	COMMENT
• • • We do not use the following data for averages, fits, limits, etc. • • •					
1.14±0.39±0.23	2700	[9] AUBERT	09AR	BABR	$e^+e^- \to D^{(*)}KX$

[9] From the $D^{*+}K^0_S$ and $D^+K^0_S$, where $D^{*+} \to D^+\pi^0$.

$D^*_{s1}(2700)^{\pm}$ REFERENCES

AAIJ	12AU	JHEP 1210 151	R. Aaij *et al.*	(LHCb Collab.)
AUBERT	09AR	PR D80 092003	B. Aubert *et al.*	(BABAR Collb.)
BRODZICKA	08	PRL 100 092001	J. Brodzicka *et al.*	(BELLE Collab.)
AUBERT,BE	06E	PRL 97 222001	B. Aubert *et al.*	(BABAR Collab.)

$D^*_{sJ}(2860)^{\pm}$

$I(J^P) = 0(?^?)$

OMITTED FROM SUMMARY TABLE

Observed by AUBERT,BE 06E and AUBERT 09AR in inclusive production of DK and D^*K in e^+e^- annihilation. J^P is natural.

$D^*_{sJ}(2860)^+$ MASS

VALUE (MeV)	EVTS	DOCUMENT ID		TECN	COMMENT
2863.2 $^{+4.0}_{-2.6}$ OUR AVERAGE					
2866.1±1.0±6.3	36k	[1] AAIJ	12AU	LHCB	$pp \to (DK)^+X$ at 7 TeV
2862 ±2 $^{+5}_{-2}$	3122	[2] AUBERT	09AR	BABR	$e^+e^- \to D^{(*)}KX$
• • • We do not use the following data for averages, fits, limits, etc. • • •					
2856.6±1.5±5.0		[3] AUBERT,BE	06E	BABR	$e^+e^- \to DKX$

[1] From the combined fit of the $D^+K^0_S$ and D^0K^+ modes in the model including the $D^*_{s2}(2573)^+$, $D^*_{s1}(2700)^+$ and spin-0 $D^*_{sJ}(2860)^+$.
[2] From simultaneous fits to the two DK mass spectra and to the total D^*K mass spectrum.
[3] Superseded by AUBERT 09AR.

$D^*_{sJ}(2860)^+$ WIDTH

VALUE (MeV)	EVTS	DOCUMENT ID		TECN	COMMENT
58 ±11 OUR AVERAGE	Error includes scale factor of 2.2.				
69.9± 3.2± 6.6	36k	[4] AAIJ	12AU	LHCB	$pp \to (DK)^+X$ at 7 TeV
48 ± 3 ± 6	3122	[5] AUBERT	09AR	BABR	$e^+e^- \to D^{(*)}KX$
• • • We do not use the following data for averages, fits, limits, etc. • • •					
47 ± 7 ±10		[6] AUBERT,BE	06E	BABR	$e^+e^- \to DKX$

[4] From the combined fit of the $D^+K^0_S$ and D^0K^+ modes in the model including the $D^*_{s2}(2573)^+$, $D^*_{s1}(2700)^+$ and spin-0 $D^*_{sJ}(2860)^+$.
[5] From simultaneous fits to the two DK mass spectra and to the total D^*K mass spectrum.
[6] Superseded by AUBERT 09AR.

$D^*_{sJ}(2860)^\pm$ DECAY MODES

	Mode
Γ_1	DK
Γ_2	D^0K^+
Γ_3	$D^+K^0_S$
Γ_4	D^*K
Γ_5	$D^{*0}K^+$
Γ_6	$D^{*+}K^0_S$

$D^*_{sJ}(2860)^\pm$ BRANCHING RATIOS

$\Gamma(D^*K)/\Gamma(DK)$ Γ_4/Γ_1

VALUE	EVTS	DOCUMENT ID		TECN	COMMENT
1.10±0.15±0.19	3122	[7] AUBERT	09AR	BABR	$e^+e^- \to D^{(*)}KX$

[7] From the average of the corresponding ratios with $D^{(*)0}K^+$ and $D^{(*)+}K^0_S$.

$\Gamma(D^{*0}K^+)/\Gamma(D^0K^+)$ Γ_5/Γ_2

VALUE	EVTS	DOCUMENT ID		TECN	COMMENT
• • • We do not use the following data for averages, fits, limits, etc. • • •					
1.04±0.17±0.20	2241	[8] AUBERT	09AR	BABR	$e^+e^- \to D^{(*)}KX$

[8] From the $D^{*0}K^+$ and D^0K^+, where $D^{*0} \to D^0\pi^0$.

$\Gamma(D^{*+}K^0_S)/\Gamma(D^+K^0_S)$ Γ_6/Γ_3

VALUE	EVTS	DOCUMENT ID		TECN	COMMENT
• • • We do not use the following data for averages, fits, limits, etc. • • •					
1.38±0.35±0.49	881	[9] AUBERT	09AR	BABR	$e^+e^- \to D^{(*)}KX$

[9] From the $D^{*+}K^0_S$ and $D^+K^0_S$, where $D^{*+} \to D^+\pi^0$.

$D^*_{sJ}(2860)^\pm$ REFERENCES

AAIJ	12AU	JHEP 1210 151	R. Aaij *et al.*	(LHCb Collab.)
AUBERT	09AR	PR D80 092003	B. Aubert *et al.*	(BABAR Collb.)
AUBERT,BE	06E	PRL 97 222001	B. Aubert *et al.*	(BABAR Collab.)

$D_{sJ}(3040)^\pm$

$I(J^P) = 0(?^?)$

OMITTED FROM SUMMARY TABLE

Observed by AUBERT 09AR in inclusive production of D^*K in e^+e^- annihilation.

$D_{sJ}(3040)^+$ MASS

VALUE (MeV)	DOCUMENT ID		TECN	COMMENT
$3044 \pm 8^{+30}_{-5}$	AUBERT	09AR	BABR	$e^+e^- \to D^*KX$

$D_{sJ}(3040)^+$ WIDTH

VALUE (MeV)	DOCUMENT ID		TECN	COMMENT
$239 \pm 35^{+46}_{-42}$	AUBERT	09AR	BABR	$e^+e^- \to D^*KX$

$D_{sJ}(3040)^\pm$ DECAY MODES

	Mode
Γ_1	D^*K
Γ_2	$D^{*0}K^+$
Γ_3	$D^{*+}K^0_S$

$D_{sJ}(3040)^\pm$ REFERENCES

AUBERT	09AR	PR D80 092003	B. Aubert *et al.*	(BABAR Collb.)

OTHER RELATED PAPERS

SUN	09	PR D80 074037	Z.-F. Sun, X. Liu	

BOTTOM MESONS ($B = \pm 1$)

$B^+ = u\overline{b}$, $B^0 = d\overline{b}$, $\overline{B}^0 = \overline{d}b$, $B^- = \overline{u}b$, similarly for B^*'s

B-particle organization

Many measurements of B decays involve admixtures of B hadrons. Previously we arbitrarily included such admixtures in the $B^\pm$ section, but because of their importance we have created two new sections: "$B^\pm/B^0$ Admixture" for $\Upsilon(4S)$ results and "$B^\pm/B^0/B_s^0$/b-baryon Admixture" for results at higher energies. Most inclusive decay branching fractions and χ_b at high energy are found in the Admixture sections. B^0-$\overline{B}^0$ mixing data are found in the B^0 section, while B_s^0-$\overline{B}_s^0$ mixing data and B-$\overline{B}$ mixing data for a B^0/B_s^0 admixture are found in the B_s^0 section. CP-violation data are found in the $B^\pm$, B^0, and $B^\pm$ B^0 Admixture sections. b-baryons are found near the end of the Baryon section. Recently, we also created a new section: "V_{cb} and V_{ub} CKM Matrix Elements."

The organization of the B sections is now as follows, where bullets indicate particle sections and brackets indicate reviews.

[Production and Decay of b-flavored Hadrons]
[A Short Note on HFAG Activities]
- $B^\pm$
  - mass, mean life
  - branching fractions
  - polarization in $B^\pm$ decay
  - CP violation
- B^0
  - mass, mean life
  - branching fractions
  - [Polarization in B decay]
  - polarization in B^0 decay
  - [B-$\overline{B}$ Mixing]
  - B^0-$\overline{B}^0$ mixing
  - CP violation
- $B^\pm$ B^0 Admixture
  - branching fractions, CP violation
  - CP violation
- $B^\pm/B^0/B_s^0$/b-baryon Admixture
  - mean life
  - production fractions
  - branching fractions
  - χ_b at high energy
  - production fractions in hadronic Z decay
- V_{cb} and V_{ub} CKM Matrix Elements
  - [Determination of V_{cb} and V_{ub}]

- B^*
  - mass
- $B_1(5721)^0$
  - mass
- $B_J^*(5732)$
  - mass, width
- $B_2(5747)^0$
  - mass
- B_s^0
  - mass, mean life
  - branching fractions
  - polarization in B_s^0 decay
  - B_s^0-$\overline{B}_s^0$ mixing
- B_s^*
  - mass
- $B_{sJ}^*(5850)$
  - mass, width
- $B_c^\pm$
  - mass, mean life
  - branching fractions

At the end of Baryon Listings:
- Λ_b
  - mass, mean life
  - branching fractions
- Σ_b, Σ_b^*
  - mass
- Ξ_b^0, Ξ_b^-
  - mean life
- Ω_b^-
  - mass, mean life
  - branching fractions
- b-baryon Admixture
  - mean life
  - branching fractions

PRODUCTION AND DECAY OF *b*-FLAVORED HADRONS

Updated March 2014 by M. Kreps (U. of Warwick, Coventry, UK) and Y. Kwon (Yonsei U., Seoul, Korea).

The b quark belongs to the third generation of quarks and is the weak–doublet partner of the t quark. The existence of the third–generation quark doublet was proposed in 1973 by Kobayashi and Maskawa [1] in their model of the quark mixing matrix ("CKM" matrix), and confirmed four years later by the first observation of a $b\overline{b}$ meson [2]. In the KM model, CP violation is explained within the Standard Model (SM) by an irreducible phase of the 3×3 unitary matrix. The regular pattern of the three lepton and quark families is one of the most intriguing puzzles in particle physics. The existence of families gives rise to many of the free parameters in the SM, including the fermion masses, and the elements of the CKM matrix.

Since the b quark is the lighter element of the third–generation quark doublet, the decays of b-flavored hadrons occur via generation-changing processes through this matrix. Because of this, and the fact that the CKM matrix is close to a 3×3 unit matrix, many interesting features such as loop and box diagrams, flavor oscillations, as well as large CP asymmetries, can be observed in the weak decays of b-flavored hadrons.

The CKM matrix is parameterized by three real parameters and one complex phase. This complex phase can become a source of CP violation in B meson decays. A crucial milestone was the first observation of CP violation in the B meson system in 2001, by the BaBar [3] and Belle [4] collaborations. They measured a large value for the parameter $\sin 2\beta$ $(= \sin 2\phi_1)$ [5], almost four decades after the discovery of a small CP asymmetry in neutral kaons. A more detailed discussion of the CKM matrix and CP violation can be found elsewhere in this *Review* [6,7].

Recent developments in the physics of b-hadrons include the significant improvement in experimental determination of the CKM angle γ, the increased information on B_s, B_c and Λ_b decays, the precise determination of Λ_b lifetime, the wealth of information in the $B^0 \to K^{*0}(892)\ell^+\ell^-$ decays and after many years of search, the observation of $B_s \to \mu^+\mu^-$ decays along with ever increasing precision on the CKM matrix parameters.

The structure of this mini-review is organized as follows. After a brief description of theory and terminology, we discuss b-quark production and current results on spectroscopy and lifetimes of b-flavored hadrons. We then discuss some basic properties of B-meson decays, followed by summaries of hadronic, rare, and electroweak penguin decays of B-mesons. There are separate mini-reviews for $B\overline{B}$ mixing [8] and the extraction of the CKM matrix elements V_{cb} and V_{ub} from B-meson decays [9] in this *Review*.

Theory and terminology: The ground states of b-flavored hadrons decay via weak interactions. In most hadrons, the b-quark is accompanied by light-partner quarks (d, u, or s), and the decay modes are well described by the decay of the b quark (spectator model) [10]. The dominant decay mode of a b quark is $b \to cW^{*-}$ (referred to as a "tree" or "spectator" decay), where the virtual W materializes either into a pair of leptons $\ell\bar{\nu}$ ("semileptonic decay"), or into a pair of quarks which then hadronizes. The decays in which the spectator quark combines with one of the quarks from W^* to form one of the final state hadrons are suppressed by a factor $\sim (1/3)^2$, because the colors of the two quarks from different sources must match ("color–suppression").

Many aspects of B decays can be understood through the Heavy Quark Effective Theory (HQET) [11]. This has been particularly successful for semileptonic decays. For further discussion of HQET, see for instance Ref. 12. For hadronic decays, one typically uses effective Hamiltonian calculations that rely on a perturbative expansion with Wilson coefficients. In addition, some form of the factorization hypothesis is commonly used, where, in analogy with semileptonic decays, two-body hadronic decays of B mesons are expressed as the product of two independent hadronic currents, one describing the formation of a charm meson (in case of the dominant $b \to cW^{*-}$ decays), and the other the hadronization of the remaining $\overline{u}d$ (or $\overline{c}s$) system from the virtual W^-. Qualitatively, for a B decay with a large energy release, the $\overline{u}d$ pair (produced as a color singlet) travels fast enough to leave the interaction region without influencing the charm meson. This is known to work well for the dominant spectator decays [13]. There are several common implementations of these ideas for hadronic B decays, the most common of which are QCD factorization (QCDF) [14], perturbative QCD (pQCD) [15], and soft collinear effective theory (SCET) [16].

The transition $b \to u$ is suppressed by $|V_{ub}/V_{cb}|^2 \sim (0.1)^2$ relative to $b \to c$ transitions. The transition $b \to s$ is a flavor-changing neutral-current (FCNC) process, and although not allowed in the SM as a tree-process, can occur via more complex loop diagrams (denoted "penguin" decays). The rates for such processes are comparable or larger than CKM-suppressed $b \to u$ processes. Penguin processes involving $b \to d$ transitions are also possible, and have been observed [17,18]. Other decay processes discussed in this *Review* include W–exchange (a W is exchanged between initial–state quarks), penguin annihilation (the gluon from a penguin loop attaches to the spectator quark, similar to an exchange diagram), and pure–annihilation (the initial quarks annihilate to a virtual W, which then decays).

Production and spectroscopy: The bound states of a $\overline{b}$ antiquark and a u, d, s, or c quark are referred to as the B_u (B^+), B_d (B^0), B_s, and B_c mesons, respectively. The B_c is the heaviest of the ground–state b-flavored mesons, and the most difficult to produce: it was observed for the first time in the semileptonic mode by CDF in 1998 [19], but its mass was accurately determined only in 2006, from the fully reconstructed mode $B_c^+ \to J/\psi\pi^+$ [20]. One of the best determination up to date uses $B_c^+ \to J\psi D_s^+$ decay and yields $M(B_c^+) = 6276.28 \pm 1.44 \pm 0.36$ MeV/c^2 [21]. As this decay has very low energy release, it allows to decrease systematic uncertainty and thus offers prospects for future increase in precision.

The first excited meson is called the B^* meson, while B^{**} is the generic name for the four orbitally excited ($L = 1$) B-meson states that correspond to the P-wave mesons in the charm system, D^{**}. Excited states of the B_s meson are similarly named B_s^* and B_s^{**}. Of the possible bound $\overline{b}b$ states, the Υ series (S-wave) and the χ_b (P-wave) are well studied. The pseudoscalar ground state η_b also has been observed by BaBar [22](and confirmed by CLEO [23]) , indirectly through the decay $\Upsilon(3S) \to \gamma\eta_b$. See Ref. 45 for classification and naming of these and other states.

Experimental studies of b decays have been performed in e^+e^- collisions at the $\Upsilon(4S)$ (ARGUS, CLEO, Belle, BaBar) and $\Upsilon(5S)$ (CLEO, Belle) resonances, as well as at higher energies, at the Z resonance (SLC, LEP), in $p\bar{p}$ (Tevatron) and pp collisions (LHC). The $e^+e^- \to b\overline{b}$ production cross-section at the Z, $\Upsilon(4S)$, and $\Upsilon(5S)$ resonances are about 6.6 nb, 1.1 nb, and 0.3 nb respectively. High-energy hadron collisions produce b-flavored hadrons of all species with much larger cross-sections: $\sigma(p\overline{p} \to bX, |\eta| < 1) \sim 30$ μb at the Tevatron ($\sqrt{s} = 1.96$ TeV), and even higher at the energies of the LHC pp collider (at $\sqrt{s} = 7$ TeV, visible b-hadron cross section at the LHCb is ~ 100 μb).

BaBar and Belle have accumulated respectively 560 fb^{-1} and 1020 fb^{-1} of data, of which 433 fb^{-1} and 710 fb^{-1} respectively are at the $\Upsilon(4S)$ resonance; CDF and D0 have accumulated by the end of their running about 10 fb^{-1} each. At the LHC, CMS and ATLAS have collected 5 fb^{-1} (20 fb^{-1}) of data at $\sqrt{s} = 7$ (8) TeV respectively and LHCb has collected about 1 fb^{-1} and 2 fb^{-1} at the two energies. These numbers indicate that the majority of b-quarks have been produced in hadron collisions, but the large backgrounds cause the hadron collider experiments to have lower selection efficiency. While traditionally only the few decay modes for which triggering and reconstruction are easiest have been studied in hadron collisions, with current experiments at hadron colliders much more is possible. This is due to triggers based on the tracking first introduced in CDF and further improved by LHCb. LHCb experiment has also reasonable capability for detection of neutral

pions and photons. While both e^+e^- and hadron colliders have their own strengths and weaknesses, in the domain of decays which involve neutrinos, e^+e^- experiments are in significant advantage.

In hadron collisions, most production happens as $b\overline{b}$ pairs, either via s-channel production or gluon–splitting, with a smaller fraction of single b-quarks produced by flavor excitation. The total b-production cross section is an interesting test of our understanding of QCD processes. For many years, experimental measurements have been several times higher than predictions. With improved measurements [24], more accurate input parameters, and more advanced calculations [25], the discrepancy between theory and data diminished and there is now good agreement between measurements and predictions.

Each quark of a $b\overline{b}$ pair produced in hadron collisions hadronizes separately and incoherently from the other, but it is still possible, although difficult, to obtain a statistical indication of the charge of a produced $b/\overline{b}$ quark ("flavor tag" or "charge tag") from the accompanying particles produced in the hadronization process, or from the decay products of the other quark. The momentum spectrum of produced b-quarks typically peaks near the b-quark mass, and extends to much higher momenta, dropping by about a decade for every ten GeV. This implies typical decay lengths of the order of a millimeter; the resolution for the decay vertex must be more precise than this to resolve the fast oscillations of B_s mesons.

In e^+e^- colliders, since the B mesons are very slow in the $\Upsilon(4S)$ rest frame, asymmetric beam energies are used to boost the decay products to improve the precision of time-dependent measurements that are crucial for the study of CP violation. At KEKB, the boost is $\beta\gamma = 0.43$, and the typical B-meson decay length is dilated from $\approx 20\ \mu m$ to $\approx 200\ \mu m$. PEP-II used a slightly larger boost, $\beta\gamma = 0.55$. The two B mesons produced in $\Upsilon(4S)$ decay are in a coherent quantum state, which makes it easier than in hadron collisions to infer the charge state of one B meson from observation of the other; however, the coherence also requires determination of the decay time of both mesons, rather than just one, in order to perform time–dependent CP–violation measurements. For B_s, which can be produced at $\Upsilon(5S)$ the situation is less favourable, as boost is not high enough to provide sufficient time resolution to resolve the fast B_s oscillations.

For the measurement of branching fractions, the initial composition of the data sample must be known. The $\Upsilon(4S)$ resonance decays predominantly to $B^0\overline{B}^0$ and B^+B^-; the current experimental upper limit for non-$B\overline{B}$ decays of the $\Upsilon(4S)$ is less than 4% at the 95% confidence level (CL) [26]. The only known modes of this category are decays to lower Υ states and a pion pair, observed with branching fractions of order 10^{-4} [27]. The ratio f_+/f_0 of the fractions of charged to neutral B productions from $\Upsilon(4S)$ decays has been measured by CLEO, BaBar, and Belle in various ways. They typically use pairs of isospin-related decays of B^+ and B^0, such that it can be assumed that $\Gamma(B^+ \to x^+) = \Gamma(B^0 \to x^0)$. In this way, the ratio of the number of events observed in these modes is proportional to $(f_+\tau_+)/(f_0\tau_0)$ [28–31]. BaBar has also performed an independent measurement of f_0 with a different method that does not require isospin symmetry or the value of the lifetime ratio, based on the number of events with one or two reconstructed $B^0 \to D^{*-}\ell^+\nu$ decays [32]. The combined result, from the current average of τ_+/τ_0, is $f_+/f_0 = 1.058 \pm 0.024$ [33]. Though the current 2.4σ discrepancy with equal production of B^+B^- and $B^0\overline{B}^0$ pairs is somewhat larger than previous averages, we still assume $f_+/f_0 = 1$ in this mini-review except where explicitly stated otherwise. This assumption is also supported by the near equality of the B^+ and B^0 masses: our fit of CLEO, ARGUS, CDF, and LHCb measurements yields $m(B^0) = 5279.58 \pm 0.17$ MeV/c^2, $m(B^+) = 5279.26 \pm 0.17$ MeV/c^2, and $m(B^0) - m(B^+) = 0.32 \pm 0.06$ MeV/c^2.

CLEO and Belle have also collected some data at the $\Upsilon(5S)$ resonance [34,35]. Belle has accumulated more than 100 fb^{-1} at this resonance. This resonance does not provide the simple final states like the $\Upsilon(4S)$: there are seven possible final states with a pair of non-strange B mesons and three with a pair of strange B mesons ($B_s^*\overline{B}_s^*$, $B_s^*\overline{B}_s$, and $B_s\overline{B}_s$). The fraction of events with a pair of B_s mesons over the total number of events with a pair of b-flavored hadrons has been measured to be $f_s[\Upsilon(5S)] = 0.201^{+0.030}_{-0.031}$, of which 90% is $B_s^*\bar{B}_s^*$ events. A few branching fractions of the B_s have been measured in this way; if the precision of f_s were improved, they would become the most accurate. Belle has observed a few new B_s modes that are difficult to reconstruct in hadron colliders and the most precise mass measurement of the B_s^* meson has been obtained [35,36]. However, the small boost of B_s mesons produced in this way prevents resolution of their fast oscillations for time-dependent measurements; these are only accessible in hadron collisions or at the Z peak.

In high-energy collisions, the produced b or $\bar{b}$ quarks can hadronize with different probabilities into the full spectrum of b-hadrons, either in their ground or excited states. Table 1 shows the measured fractions f_d, f_u, f_s, and $f_{\rm baryon}$ of B^0, B^+, B_s^0, and b baryons, respectively, in an unbiased sample of weakly decaying b hadrons produced at the Z resonance or in $p\overline{p}$ collisions [33]. The results were obtained from a fit where the sum of the fractions were constrained to equal 1.0, neglecting production of B_c mesons. The observed yields of B_c mesons at the Tevatron [19] yields $f_c = 0.2\%$, in agreement with expectations [37], and well below the current experimental uncertainties in the other fractions.

For rather long time, the average of fractions in $p\overline{p}$ collisions and in Z decay was used as it was assumed that the hadronization is identical in the two environments. It was clear that this assumption dost not have to hold in principle, because of the different momentum distributions of the b-quark in these processes; the sample used in the $p\overline{p}$ measurements has momenta close to the b mass, rather than $m_Z/2$. But in the absence of any significant evidence there was also no

strong reason against the average. Some discrepancies were observed, but as picture was also obscured by 1.8σ discrepancy in the average time-integrated mixing probability parameter $\bar{\chi} = f_d\chi_d + f_s\chi_s$ between LEP and Tevatron [8], they were not directly attributed to breakdown of the assumption that hadronization is identical. The first indication that fraction for b-baryons depends on the momentum and thus environment came from CDF [38], but available precision did not allow for firm conclusion. The final evidence for non-universality of hadronization fractions came from LHCb, where strong dependence on the transverse momentum was observed for the Λ_b fraction [39].

Table 1: Fragmentation fractions of b quarks into weakly-decaying b-hadron species in $Z \to b\overline{b}$ decay, in $p\overline{p}$ collisions at $\sqrt{s} = 1.96$ TeV.

b hadron	Fraction at Z [%]	Fraction at $\overline{p}p$[%]
B^+, B^0	40.4 ± 0.9	33.9 ± 3.9
B_s	10.3 ± 0.9	11.1 ± 1.4
b baryons	8.9 ± 1.5	21.2 ± 6.9

Excited B-meson states have been observed by CLEO, LEP, CUSB, D0, and CDF. The current world average of the B^*–B mass difference is 45.78 ± 0.35 MeV/c^2. Evidence for B^{**} (L=1) production has been initially obtained at LEP [40], as a broad resonance in the mass of an inclusively reconstructed bottom hadron candidate combined with a charged pion from the primary vertex. Detailed results from exclusive modes have been obtained at the Tevatron, allowing separation of the narrow states B_1 and B_2^* and also a measurement of the B_2^* width [41].

Also the narrow B_s^{**} states, first sighted by OPAL as a single broad enhancement in the B^+K mass spectrum [42], have now been clearly observed and separately measured at the hadron colliders [43,44]. The measured masses are $M(B_{s1}) = 5828.7 \pm 0.4$ MeV/c^2 and $M(B_{s2}^*) = 5839.96 \pm 0.2$ MeV/c^2.

Baryon states containing a b quark are labeled according to the same scheme used for non-b baryons, with the addition of a b subscript [45]. For many years, the only well-established b baryon was the Λ_b^0 (quark composition udb), with only indirect evidence for Ξ_b (dsb) production from LEP [46]. This situation has changed dramatically in the past few years due to the large samples being accumulated at the Tevatron and LHCb. Clear signals of four strongly–decaying baryon states, Σ_b^+, Σ_b^{*+} (uub), Σ_b^-, Σ_b^{*-} (ddb) have been obtained by CDF in $\Lambda_b^0\pi^\pm$ final states [47]. The strange bottom baryon $\Xi_b^\pm$ was observed in the exclusive mode $\Xi_b^\pm \to J/\psi\Xi^\pm$ by D0 [48], and CDF [49]. More recently CDF has also observed the Ξ_b in the $\Xi_c\pi$ final state [50]. The relative production of Ξ_b and Λ_b baryons has been found to be consistent with the B_s to B_d production ratio [48]. Observation of the doubly–strange bottom baryon Ω_b^- has been published by both D0 [51] and CDF [52]. However the masses measured by the two experiments show a large discrepancy. The resolution is provided by LHCb which measures the Ω_b^- mass consistent with CDF [53]. The CMS experiment added to the list also neutral spin-3/2 Ξ_b^* [54]. The masses of all these new baryons have been measured to a precision of a few MeV/c^2, and found to be in agreement with predictions from HQET.

Lifetimes: Precise lifetimes are key in extracting the weak parameters that are important for understanding the role of the CKM matrix in CP violation, such as the determination of V_{cb} and $B_s\overline{B}_s$ mixing parameters. In the naive spectator model, the heavy quark can decay only via the external spectator mechanism, and thus, the lifetimes of all mesons and baryons containing b quarks would be equal. Non–spectator effects, such as the interference between contributing amplitudes, modify this simple picture and give rise to a lifetime hierarchy for b-flavored hadrons similar to the one in the charm sector. However, since the lifetime differences are expected to scale as $1/m_Q^2$, where m_Q is the mass of the heavy quark, the variations in the b system are expected to be only 10% or less [55]. We expect:

$$\tau(B^+) \geq \tau(B^0) \approx \tau(B_s) > \tau(\Lambda_b^0) \gg \tau(B_c^+) \,. \quad (1)$$

For the B_c^+, both quarks decay weakly, so the lifetime is much shorter.

Measurements of the lifetimes of the different b-flavored hadrons thus provide a means to determine the importance of non-spectator mechanisms in the b sector. Over the past decade, the precision of silicon vertex detectors and the increasing availability of fully–reconstructed samples has resulted in much-reduced statistical and systematic uncertainties (∼1%). The averaging of precision results from different experiments is a complex task that requires careful treatment of correlated systematic uncertainties; the world averages given in Table 2 have been determined by the Heavy Flavor Averaging Group (HFAG) [33].

Table 2: Summary of inclusive and exclusive world-average b-hadron lifetime measurements. For the two B_s averages, see text below.

Particle	Lifetime [ps]
B^+	1.638 ± 0.004
B^0	1.519 ± 0.005
B_s (flavor-specific)	1.465 ± 0.031
B_s ($1/\Gamma_s$)	1.512 ± 0.007
B_c^+	0.500 ± 0.013
Λ_b^0	1.451 ± 0.013
Ξ_b^-	$1.56^{+0.27}_{-0.25}$
Ω_b^-	$1.13^{+0.53}_{-0.40}$
Ξ_b mixture	$1.49^{+0.19}_{-0.18}$
b-baryon mixture	1.449 ± 0.015
b-hadron mixture	1.568 ± 0.009

The short B_c^+ lifetime is in good agreement with predictions [56]. With large samples of B_c^+ mesons at the LHCb precision on the lifetimes should significantly improve. First measurement using semileptonic decays gives $\tau_{B_c^+} = 0.509 \pm 0.008 \pm 0.012$ [57], which is already more precise than combination of all previous experiment. For precision comparisons with theory, lifetime ratios are more sensitive. Experimentally we find:

$$\frac{\tau_{B^+}}{\tau_{B^0}} = 1.076 \pm 0.004\,, \; \frac{\tau_{B_s}}{\tau_{B^0}} = 0.995 \pm 0.006\,,$$

$$\frac{\tau_{\Lambda_b}}{\tau_{B^0}} = 0.955 \pm 0.009\,,$$

while theory makes the following predictions [55,58]

$$\frac{\tau_{B^+}}{\tau_{B^0}} = 1.06 \pm 0.02\;, \; \frac{\tau_{B_s}}{\tau_{B^0}} = 1.00 \pm 0.01\;, \; \frac{\tau_{\Lambda_b}}{\tau_{B^0}} = 0.88 \pm 0.05.$$

The ratio of B^+ to B^0 lifetimes has a precision of better than 1%, and is significantly different from 1.0, in agreement with predictions [55]. The ratio of B_s to B^0 lifetimes is expected to be very close to 1.0. While early measurements were in mild tension with theory, the high precision measurements using fully reconstructed decays and clear definition of lifetime (see below) are in good agreement with theory [59,60,61]. The Λ_b lifetime has a history of discrepancies. Predictions were higher than data before the introduction of higher-order effects lowered them. The first indication that early measurements of the Λ_b are on low side came from the CDF data [62,63]. The recent measurements from LHC experiments [64,65,66,67] significantly improve precision and favour higher lifetime, much closer to the lifetime of B^0 meson. The most precise measurement of the Λ_b lifetime performed by LHCb uses $\Lambda_b \to J/\psi p K^-$ decays and finds $\tau_{\Lambda_b} = 1.482 \pm 0.018 \pm 0.012$ ps [66]. With new results, the discrepancy between theory and experiment on the Λ_b lifetime can be considered resolved.

Neutral B mesons are two-component systems similar to neutral kaons, with a light (L) and a heavy (H) mass eigenstate, and independent decay widths Γ_L and Γ_H. The SM predicts a non-zero width difference $\Delta\Gamma = \Gamma_L - \Gamma_H > 0$ for both B_s and B_d. For B_d, $\Delta\Gamma_d/\Gamma_d$ is expected to be $\sim$0.2%. Analysis of BaBar and DELPHI data on CP-specific modes of the B^0 yield a combined result: $\Delta\Gamma_d/\Gamma_d = 0.015 \pm 0.018$ [33]. Very recently LHCb determined value of $\Delta\Gamma_d/\Gamma_d = -0.044 \pm 0.025 \pm 0.011$ [67], which is based on the comparison of lifetimes in the $B^0 \to J/\psi K^{*0}(892)$ and $B^0 \to J/\psi K_S$ decays. Average including latest LHCb measurement yields $\Delta\Gamma_d/\Gamma_d = 0.001 \pm 0.010$. The issue is much more interesting for the B_s, since the SM expectation for $\Delta\Gamma_s/\Gamma_s$ is of order 10%. This potentially non-negligible difference requires care when defining the B_s lifetime. As indicated in Table 2, two different lifetimes are defined for the B_s meson: one is defined as $1/\Gamma_s$, where Γ_s is the average width of the two mass eigenstates $(\Gamma_L + \Gamma_H)/2$; the other is obtained from "flavor-specific" (*e.g.*, semileptonic) decays and depends both on Γ_s and $\Delta\Gamma_s$. Experimentally, the quantity $\Delta\Gamma_s$ can be accessed by measuring lifetimes in decays into CP eigenstates, which in the SM are expected to be close approximations to the mass eigenstates. This has been done with the $J/\psi\phi$ mode, where the two CP eigenstates are distinguished by angular distributions, and in $B_s \to K^+K^-$ or $B_s \to J/\psi f_0(980)$ which are CP-eigenstates. The current experimental information is dominated by measurements on the $J/\psi\phi$ mode performed by CDF, D0, ATLAS and LHCb experiments. By appropriately combining all published measurements of $J/\psi\phi$ lifetimes, flavor-specific lifetimes and effective lifetimes in CP eigenstates, the HFAG group obtains a world-average $\Delta\Gamma_s/\Gamma_s = 0.138 \pm 0.012$ [33]; the latest theoretical predictions yield $\Delta\Gamma_s/\Gamma_s = 0.133 \pm 0.032$ [68], in agreement with measurements within the uncertainties. The constraint from measurements of lifetimes in CP eigenstates is based on the notion of effective lifetime introduced in Ref. [69]. In this class, measurements in decays $B_s \to J/\psi f_0(980)$ [70], $B_s \to K^+K^-$ [71] decays are used currently. From the theoretical point of view, the best quantity to use is $\Delta\Gamma_s/\Delta M_s$, which is much less affected by hadronic uncertainties [68]. Exploiting the accurate measurement of ΔM_s available [72], this can be turned into a SM prediction with an uncertainty of only 20%: $\Delta\Gamma_s/\Gamma_s = 0.137 \pm 0.027$. This is likely to be of importance in future comparisons, as the experimental precision improves with the growth of LHC samples. Historically, branching fraction of the decay $B_s \to D_s^{(*)+} D_s^{(*)-}$ was used to set an bound on $\Delta\Gamma_s/\Gamma_s$, but the method is highly model–dependent and with increased precision of direct determinations it stops to be useful.

The width difference $\Delta\Gamma_s$ is connected to the B_s mixing phase ϕ_s by $\Delta\Gamma_s = \Gamma_{12}\cos\phi_s$, where Γ_{12} is the off–diagonal element of the decay matrix [6,8,68]. The early measurements by CDF [73] and D0 [74] have produced CL contours in the $(\phi_s, \Delta\Gamma)$ plane, and both observed a mild deviation, in the same direction, from the expectation of the SM of the phase ϕ_s near $\Delta\Gamma = 0$. The possibility of a large value of ϕ_s has attracted significant interest, as it would be very clean evidence for the existence of new sources of CP violation beyond the SM. However the latest measurements from CDF [59], D0 [75], ATLAS [60] and LHCb [61], which provide significant improvements over initial measurements, show good agreement with the SM. While most experiments use up to now only $B_s \to J/\psi\phi$ decay, LHCb also exploits $B_s \to J/\psi\pi^+\pi^-$ decays, which are experimentally determined to be pure CP-odd and therefore in $B_s \to J/\psi\pi^+\pi^-$ decays no angular analysis is needed. It should be noted that in pure $B_s \to J/\psi\phi$ decay, there is an two-fold ambiguity in the sign of $\Delta\Gamma_s$ and ϕ_s. This can be resolved using the interference between the decays to $J/\psi\phi$ and $J/\psi K^+K^-$, where K^+K^- is in relative S-wave state. This has been used by LHCb experiment to determine the sign of $\Delta\Gamma_s$ to be positive [76] in accordance with SM. The world average value of the CP violating phase is $\phi_s = 0.04^{+0.10}_{-0.13}$ [33] without any tension with the SM.

***B* meson decay properties:** Semileptonic B decays $B \to X_c\ell\nu$ and $B \to X_u\ell\nu$ provide an excellent way to measure the

magnitude of the CKM elements $|V_{cb}|$ and $|V_{ub}|$ respectively, because the strong interaction effects are much simplified due to the two leptons in the final state. Both exclusive and inclusive decays can be used with dominant uncertainties being complementary. For exclusive decay analysis, knowledge of the form factors for the exclusive hadronic system $X_{c(u)}$ is required. For inclusive analysis, it is usually necessary to restrict the available phase-space of the decay products to suppress backgrounds; subsequently uncertainties are introduced in the extrapolation to the full phase-space. Moreover, restriction to a small corner of the phase-space may result in breakdown of the operator-product expansion scheme, thus making theoretical calculations unreliable. A more detailed discussion of B semileptonic decays and the extraction of $|V_{cb}|$ and $|V_{ub}|$ is given elsewhere in this *Review* [9].

On the other hand, hadronic decays of B are complicated because of strong interaction effects caused by the surrounding cloud of light quarks and gluons. While this complicates the extraction of CKM matrix elements, it also provides a great opportunity to study perturbative and non-perturbative QCD, hadronization, and Final State Interaction (FSI) effects. Pure–penguin decays were first established by the observation of $B \to K^*\gamma$ [77]. Some observed decay modes such as $B^0 \to D_s^- K^+$, may be interpreted as evidence of a W-exchange process [78]. The evidence for the decay $B^+ \to \tau^+\nu$ from Belle [79] and BaBar [80] is the first sign of a pure annihilation decay. There is growing evidence that penguin annihilation processes may be important in decays with two vector mesons in the final state [81].

Hadronic decays: Most of the hadronic B decays involve $b \to c$ transition at the quark level, resulting in a charmed hadron or charmonium in the final state. Other types of hadronic decays are very rare and will be discussed separately in the next section. The experimental results on hadronic B decays have steadily improved over the past few years, and the measurements have reached sufficient precision to challenge our understanding of the dynamics of these decays. With the good neutral particle detection and hadron identification capabilities of B-factory detectors, a substantial fraction of hadronic B decay events can be fully reconstructed. Because of the kinematic constraint of $\Upsilon(4S)$, the energy sum of the final-state particles of a B meson decay is always equal to one half of the total energy in the center of mass frame. As a result, the two variables, ΔE (energy difference) and M_B (B candidate mass with a beam-energy constraint) are very effective for suppressing combinatorial background both from $\Upsilon(4S)$ and $e^+e^- \to q\bar{q}$ continuum events. In particular, the energy-constraint in M_B improves the signal resolution by almost an order of magnitude.

The kinematically clean environment of B meson decays provides an excellent opportunity to search for new states. For instance, quark-level $b \to c\bar{c}s$ decays have been used to search for new charmonium and charm-strange mesons and study their properties in detail. In 2003, BaBar discovered a new narrow charm-strange state $D_{sJ}^*(2317)$ [82], and CLEO observed a similar state $D_{sJ}(2460)$ [83]. The properties of these new states were studied in the B meson decays, $B \to DD_{sJ}^*(2317)$ and $B \to DD_{sJ}(2460)$ by Belle [84]. Further studies of $D_{sJ}^{(*)}$ meson production in B decays have been made by Belle [85] and BaBar [86]. Now these charm-strange meson states are identified as $D_{s0}^*(2317)$ and $D_{s1}(2460)$, respectively.

More recently, Belle observed a new D_{sJ} meson produced in $B^+ \to \bar{D}^0 D_{sJ} \to \bar{D}^0 D^0 K^+$ [87]. Combined with a subsequent measurement by BaBar [88], the mass and width of this state are determined to be 2709^{+9}_{-6} MeV/c^2 and 125±30 MeV, respectively. An analysis of the helicity angle distribution determines its spin-parity to be 1^-.

A variety of exotic particles have been discovered in B decays. Belle found the $X(3872)$ state [89], which is confirmed by CDF [90] and BaBar [91]. Analyzing their full $\Upsilon(4S)$ data sample, Belle finds a new upper limit on the width of $X(3872)$ to be $\Gamma_{X(3872)} < 1.2$ MeV [92], improving on the existing limit by nearly a factor of 2. Radiative decays of $X(3872)$ can play a crucial role in understanding the nature of the particle. For example, in the molecular model the decay of $X(3872)$ to $\psi'\gamma$ is expected to be highly suppressed in comparison to the decay to $J/\psi\gamma$ [93]. BaBar has seen the evidence for the decay to $J/\psi\gamma$ [94]. The ratio $R \equiv \mathcal{B}(X(3872) \to \psi'\gamma)/\mathcal{B}(X(3872) \to J/\psi\gamma)$ is measured to be 3.4 ± 1.4 by BaBar [95], while Belle obtains $R < 2.1$ at 90% CL [96].

Belle has observed a near-threshold enhancement in the $J/\psi\omega$ invariant mass for $B \to J/\psi\omega K$ decays [97]. BaBar has studied $B \to J/\psi\pi^+\pi^- K$, finding an excess of $J/\psi\pi^+\pi^-$ events with a mass just above 4.2 GeV/c^2; this is consistent with the $Y(4260)$ that was observed by BaBar in ISR (Initial State Radiation) events [98]. A Belle study of $B \to \psi' K\pi^\pm$ [99] finds a state called $X(4430)^\pm$ that decays to $\psi'\pi^\pm$. Since it is charged, it could not be a charmonium state. This state was searched for by BaBar with similar sensitivity but was not found [100]. In a Dalitz plot analysis of $\overline{B}^0 \to \chi_{c1} K^-\pi^+$, Belle has observed two resonance-like structures in the $\chi_{c1}\pi^+$ mass distribution [101], labelled as $X(4050)^\pm$ and $X(4250)^\pm$ in this *Review*, while no evidence is found by BaBar in a search with similar sensitivity [102].

The hadronic decays $\overline{B}^0 \to D^{(*)0} h^0$, where h^0 stands for light neutral mesons such as $\pi^0, \eta^{(\prime)}, \rho^0, \omega$, proceed through color-suppressed diagrams, hence they provide useful tests on the factorization models. Both Belle and BaBar have made comprehensive measurements of such color-suppressed hadronic decays of $\overline{B}^0$ [103].

Information on B_s and Λ_b decays is limited, though improving with recent studies of large samples at the Tevatron and LHC experiments. Recent additions are decays of $B_s \to J/\psi f_0(980)$ [70,104], $B_s \to J/\psi f_2'(1525)$ [105], and $\Lambda_b \to \Lambda_c \pi^+\pi^-\pi^-$ [106]. For the later, not only the total rate is measured, but also structure involving decays through excited Λ_c and Σ_c baryons.

There have been hundreds of publications on hadronic B decays to open-charm and charmonium final states mostly from the B-factory experiments. These results are nicely summarized in a recent report by HFAG [33].

Rare B decays: All B-meson decays that do not occur through the $b \to c$ transition are usually called rare B decays. These include both semileptonic and hadronic $b \to u$ decays that are suppressed at leading order by the small CKM matrix element V_{ub}, as well as higher-order $b \to s(d)$ processes such as electroweak and gluonic penguin decays.

Charmless B meson decays into two-body hadronic final states such as $B \to \pi\pi$ and $K\pi$ are experimentally clean, and provide good opportunities to probe new physics and search for indirect and direct CP violations. Since the final state particles in these decays tend to have larger momenta than average B decay products, the event environment is cleaner than for $b \to c$ decays. Branching fractions are typically around 10^{-5}. Over the past decade, many such modes have been observed by BaBar, Belle, and CLEO. More recently, comparable samples of the modes with all charged final particles have been reconstructed in $p\bar{p}$ collisions by CDF and pp collisions by LHCb by triggering on the impact parameter of the charged tracks. This has also allowed observation of charmless decays of the B_s, in final states such as $\phi\phi$ [107], K^+K^- [108], and $K^-\pi^+$ [109], and of charmless decays of the Λ_b^0 baryon [109]. Charmless B_s modes are related to corresponding B^0 modes by U-spin symmetry, and are determined by similar amplitudes. Combining the observables from B_s and B^0 modes is a further way of eliminating hadronic uncertainties and extracting relevant CKM information [110].

Because of relatively high-momenta for final state particles, the dominant source of background in e^+e^- collisions is $q\bar{q}$ continuum events; sophisticated background suppression techniques exploiting event shape variables are essential for these analyses. In hadron collisions, the dominant background comes from QCD or partially reconstructed heavy flavors, and is similarly suppressed by a combination of kinematic and isolation requirements. The results are in general consistent among the experiments.

BaBar [111] and Belle [112] have observed the decays $B^+ \to \overline{K}^0 K^+$ and $B^0 \to K^0\overline{K}^0$. The world-average branching fractions are $\mathcal{B}(B^0 \to K^0\overline{K}^0) = (0.96^{+0.20}_{-0.18}) \times 10^{-6}$ and $\mathcal{B}(B^+ \to \overline{K}^0 K^+) = (1.36 \pm 0.27) \times 10^{-6}$. These are the first observations of hadronic $b \to d$ transitions, with significance $> 5\sigma$ for all four measurements. CP asymmetries have even been measured for these modes, though with large errors.

Most rare decay modes including $B^0 \to K^+\pi^-$ have contributions from both $b \to u$ tree and $b \to sg$ penguin processes. If the size of the two contributions are comparable, the interference between them may result in direct CP violation, seen experimentally as a charge asymmetry in the decay rate measurement. BaBar [113], Belle [114], and CDF [108] have measured the direct CP violating asymmetry in $B^0 \to K^+\pi^-$ decays. The BaBar and Belle measurements constitute observation of direct CP violation with a significance of more than 5σ. The world average for this quantity is now rather precise, -0.098 ± 0.013. There are sum rules [115] that relate the decay rates and decay-rate asymmetries between the four $K\pi$ charge states. The experimental measurements of the other three modes are not yet precise enough to test these sum rules.

There is now evidence for direct CP violation in three other decays: $B^+ \to \rho^0 K^+$ [116], $B^+ \to \eta K^+$ [117], and $B^0 \to \eta K^{*0}$ [118]. The significance is typically 3–4σ, though the significance for the $B^+ \to \eta K^+$ decay is now nearly 5σ with the recent Belle measurement [117]. In at least the first two cases, a large direct CP violation might be expected since the penguin amplitude is suppressed so the tree and penguin amplitudes may have comparable magnitudes.

The decay $B^0 \to \pi^+\pi^-$ can be used to extract the CKM angle α. This is complicated by the presence of significant contributions from penguin diagrams. An isospin analysis [119] can be used to untangle the penguin complications. The decay $B^0 \to \pi^0\pi^0$, which is now measured by both BaBar and Belle, is crucial in this analysis. Unfortunately the amount of penguin pollution in the $B \to \pi\pi$ system is rather large. In the past few years, measurements in the $B^0 \to \rho\rho$ system have produced more precise values of α, since penguin amplitudes are generally smaller for decays with vector mesons. An important ingredient in the analysis is the $B^0 \to \rho^0\rho^0$ branching fraction. The average of measurements from BaBar and Belle BaBar [120] yields a branching fraction of $(0.73 \pm 0.28) \times 10^{-6}$. This is only 3% of the $\rho^+\rho^-$ branching fraction, much smaller than the corresponding ratio in the $\pi\pi$ system.

The decay $B \to a_1\pi$ has been seen by BaBar. An analysis of the time evolution of this decay [121] together with measurements of other related decays has been used to measure the CKM angle α [122] in agreement with the more precise measurements from the $\rho\rho$ system.

Since $B \to \rho\rho$ has two vector mesons in the final state, the CP eigenvalue of the final state depends on the longitudinal polarization fraction f_L for the decay. Therefore, a measurement of f_L is needed to extract the CKM angle α. Both BaBar and Belle have measured f_L for the decays $\rho^+\rho^-$ and $\rho^+\rho^0$ and in both cases the measurements show $f_L > 0.9$, making a complete angular analysis unnecessary.

By analyzing the angular distributions of the B decays to two vector mesons, we can learn a lot about both weak- and strong-interaction dynamics in B decays. Decays that are penguin-dominated surprisingly have values of f_L near 0.5. The list of such decays has now grown to include $B \to \phi K^*$, $B \to \rho K^*$, and $B \to \omega K^*$. The reasons for this "polarization puzzle" are not fully understood. A detailed description of the angular analysis of B decays to two vector mesons can be found in a separate mini-review [123] in this *Review* .

There has been substantial progress in measurements of many other rare-B decays. The decay $B \to \eta' K$ stood out as the largest rare-B decay for many years. The reasons for

the large rate are now largely understood [14,124]. However, there are now measurements of several 3-body or quasi-3-body modes with similarly large branching fractions. States seen so far include $K\pi\pi$ (three charge states) [125], KKK (four charge states) [126], and $K^*\pi\pi$ (two charged states) [127]. Many of these analyses now include Dalitz plot treatments with many intermediate resonances. There has also been an observation of the decay $B^+ \to K^+K^-\pi^+$ by BaBar [128], noteworthy because an even number of kaons is typically indicative of suppressed $b \to d$ transitions as discussed above.

Belle [79] and BaBar [80] have found evidence for $B^+ \to \tau^+\nu$; the average branching fraction, with a significance of nearly 5σ is $(165 \pm 34) \times 10^{-6}$. This is somewhat larger than, though consistent with, the value expected in the SM. This is the first observation of a pure annihilation decay. A substantial region of parameter space of charged Higgs mass vs. $\tan\beta$ is excluded by the measurements of this mode.

Electroweak penguin decays: More than 20 years have passed since the CLEO experiment first observed an exclusive radiative $b \to s\gamma$ transition, $B \to K^*(892)\gamma$ [77], thus providing the first evidence for the one-loop FCNC electromagnetic penguin decay. Using much larger data samples, both Belle and BaBar have updated this analysis [129] with an average branching fraction $\mathcal{B}(B^0 \to K^{*0}\gamma) = (43.3 \pm 1.5) \times 10^{-6}$, and have added several new decay modes such as $B \to K_1\gamma$, $K_2^*(1430)\gamma$, *etc.* [130]. With a sample of 24 fb^{-1} at $\Upsilon(5S)$, Belle observed the radiative penguin decay of $B_s \to \phi\gamma$ [131]. The decay $B_s \to \phi\gamma$ was also seen at LHCb with higher statistics [132]. The two measurements give average branching fraction of $(36 \pm 4) \times 10^{-6}$.

Compared to $b \to s\gamma$, the $b \to d\gamma$ transitions such as $B \to \rho\gamma$, are suppressed by the small CKM element V_{td}. Both Belle and BaBar have observed these decays [17,18]. The world average $\mathcal{B}(B \to (\rho,\omega)\gamma) = (1.30 \pm 0.23) \times 10^{-6}$. This can be used to calculate $|V_{td}/V_{ts}|$ [133]; the measured values are $0.233^{+0.033}_{-0.032}$ from BaBar [18] and $0.195^{+0.025}_{-0.024}$ from Belle [17].

The observed radiative penguin branching fractions can constrain a large class of SM extensions [134]. However, due to the uncertainties in the hadronization, only the inclusive $b \to s\gamma$ rate can be reliably compared with theoretical calculations. This rate can be measured from the endpoint of the inclusive photon spectrum in B decay. By combining the measurements of $B \to X_s\gamma$ from CLEO, BaBar, and Belle experiments [135,136,137], HFAG obtains the new average: $\mathcal{B}(B \to X_s\gamma) = (3.43 \pm 0.21 \pm 0.07) \times 10^{-4}$ [33] for $E_\gamma \geq 1.6$ GeV, which averages over B^+ and B^0. Consistent but less precise results have been reported by ALEPH for inclusive b–hadrons produced at the Z, which includes also small fraction of B_s and Λ_b hadrons. The measured branching fraction can be compared to theoretical calculations. Recent calculations of $\mathcal{B}(b \to s\gamma)$ at NNLO level predict the values of $(3.15 \pm 0.23) \times 10^{-4}$ [138] and $(2.98 \pm 0.26) \times 10^{-4}$ [139], where the latter is calculated requiring $E_\gamma \geq 1.6$ GeV.

The CP asymmetry in $b \to s\gamma$ is extensively studied theoretically both in the SM and beyond [140]. According to the SM, the CP asymmetry in $b \to s\gamma$ is smaller than 1%, but some non-SM models allow significantly larger CP asymmetry ($\sim 10\%$) without altering the inclusive branching fraction. The current world average is $A_{CP} = -0.008 \pm 0.029$, again dominated by BaBar and Belle [141,136]. In addition to the CP asymmetry, BaBar also measured the isospin asymmetry $\Delta_{0-} = -0.01 \pm 0.06$ in $b \to s\gamma$ measured using sum of exclusive decays [142]. Alternative measurement using full reconstruction of the companion B in the hadronic decay modes yields consistent, but less precise result [143].

In addition, all three experiments have measured the inclusive photon energy spectrum for $b \to s\gamma$, and by analyzing the shape of the spectrum they obtain the first and second moments for photon energies. Belle has measured these moments covering the widest range in the photon energy ($1.7 < E_\gamma < 2.8$ GeV) [137]. The measurement by BaBar has slightly smaller range with lower limit at 1.8 GeV [144]. These results can be used to extract non-perturbative HQET parameters that are needed for precise determination of the CKM matrix element V_{ub}.

Additional information on FCNC processes can be obtained from $b \to s\ell^+\ell^-$ decays, which are mediated by electroweak penguin and W-box diagrams. Measurements at Belle and BaBar suffered from low statistics and therefore they typically provide average between charged and neutral B mesons as well as between e^+e^- and $\mu^+\mu^-$ finals states [145,146]. The total branching fraction measured at B-factories for $B \to K\ell^+\ell^-$ is $(0.45 \pm 0.04) \times 10^{-6}$ and for $B \to K^*(892)\ell^+\ell^-$ is $(1.05 \pm 0.10) \times 10^{-6}$. Measurements at B-factories were complemented by CDF [147], which used only muons in the final state. While precision at CDF was similar to B-factories, it had access also to $B_s \to \phi\mu^+\mu^-$ and $\Lambda_b \to \Lambda\mu^+\mu^-$ decays, which were observed for the first time [147,148] and confirmed by LHCb [149,150]. B-factory experiments also measured the branching fractions for inclusive $B \to X_s\ell^+\ell^-$ decays [151], with an average of $(3.66^{+0.76}_{-0.77}) \times 10^{-6}$ [152]. In $b \to s\ell^+\ell^-$ decays, the angular analysis provides several interesting observables, which can be studied as function of dilepton invariant mass squared, q^2. While first measurements were done by Belle, Babar and CDF, real advance of these measurements came with LHC experiments, where samples available are significantly larger than before. The best known of angular observables is forward-backward asymmetry, which was measurement in $B \to K^*(892)\ell^+\ell^-$ by several experiments having access to the decay [145,153,154,155] with most precise measurement coming from LHCb [156]. Measurements of the CP asymmetries [146,157,158], the isospin asymmetry [145,146,159] and several other angular observables [156,160] are possible in this class of decays. While most of the measurements agree with the SM, isospin asymmetry in $B \to K\mu^+\mu^-$ and one of the other angular observables measured by the LHCb exhibit small tension with the SM expectation. While the angular analysis was up to recently mainly concentrating on the decay $B \to K^*(892)\ell^+\ell^-$, with samples available at LHC, also first angular analysis of the

$B_s \to \phi\mu^+\mu^-$ decay was performed [149] with its results being consistent with the SM.

Finally the decays $B^0_{(s)} \to e^+e^-$ and $\mu^+\mu^-$ are interesting since they only proceed at second order in weak interactions in the SM, but may have large contributions from supersymmetric loops, proportional to $(\tan\beta)^6$. First limits were published 30 years ago and since then experiments at Tevatron, B-factories and LHC gradually improved those and effectively excluded whole models of new physics and significantly constrained allowed parameter space of others. For the decays to $\mu^+\mu^-$, Tevatron experiments pushed the limits down to roughly factor of 5-10 above the SM expectation [161,162]. The long journey in the search for these decays culminated in 2012, when first evidence for $B_s \to \mu^+\mu^-$ decay was seen [163]. Currently LHCb [164] and CMS [165] observe this decay with significance between 4 and 5 standard deviations. The measured branching fraction is $(2.9^{+1.1}_{-1.0})\times10^{-9}$ at LHCb and $(3.0^{+1.0}_{-0.9})\times10^{-9}$ at CMS, both in agreement with the SM expectation. The best limit for $B^0 \to \mu^+\mu^-$ is obtained by LHCb with value $< 7.4 \times 10^{-10}$ at 95% confidence level. The limits for the e^+e^- modes are: $< 2.8\times10^{-7}$ and $< 8.3\times10^{-8}$, respectively, for B_s and B^0 [166]. The searches were also performed for lepton flavour violating decays to two leptons with best limits in $e^\pm\mu^\mp$ channel, where limits are $< 3.7 \times 10^{-9}$ for B^0 and $< 1.4 \times 10^{-8}$ at 95% confidence level [167].

Summary and Outlook: The study of B mesons continues to be one of the most productive fields in particle physics. With the two asymmetric B-factory experiments Belle and BaBar, we now have a combined data sample of well over 1 ab^{-1}. CP violation has been firmly established in many decays of B mesons. Evidence for direct CP violation has been observed. Many rare decays resulting from hadronic $b \to u$ transitions and $b \to s(d)$ penguin decays have been observed, and the emerging pattern is still full of surprises. Despite the remarkable successes of the B-factory experiments, many fundamental questions in the flavor sector remain unanswered.

At Fermilab, CDF and D0 each has accumulated about 10 fb^{-1}, which is the equivalent of about 10^{12} b-hadrons produced. In spite of the low trigger efficiency of hadronic experiments, a selection of modes have been reconstructed in large quantities, giving a start to a program of studies on B_s and b-flavored baryons, in which a first major step has been the determination of the B_s oscillation frequency.

As Tevatron and B-factories stop their taking data, the new experiments at the LHC have become very active. The LHC accelerator performed very well in 2011 and 2012. The general purpose experiments ATLAS and CMS collected about 25 fb^{-1} while LHCb collected about 3 fb^{-1}. LHCb, which is almost fully dedicated to the studies of b- and c-hadrons, has a data sample that is for many decays larger than the sum of all previous experiments. Of particular note is the first evidence of the decay $B_s \to \mu^+\mu^-$ by LHCb and CMS experiments in 2013.

In addition, the preparation of the next generation high-luminosty B-factory at KEK is ongoing with first physics data taking expected in 2016. The aim to increase sample to ~ 50 ab^{-1} will make it possible to explore the indirect evidence of new physics beyond the SM in the heavy-flavor particles (b, c, and τ), in a way that is complementary to the LHC. In the same time, LHCb Collaboration is working on the upgrade of its detector, which should be installed in 2018 and 2019. Aim of the upgrade is to increase flexibility of trigger, which will allow to significantly increase instantaneous luminosity and possibly integrate about 50 fb^{-1} of data.

These experiments promise a rich spectrum of rare and precise measurements that have the potential to fundamentally affect our understanding of the SM and CP-violating phenomena.

References

1. M. Kobayashi and T. Maskawa, Prog. Theor. Phys. **49**, 652 (1973).
2. S. W. Herb *et al.*, Phys. Rev. Lett. **39**, 252 (1977).
3. B. Aubert *et al.* (BaBar Collab.), Phys. Rev. Lett. **87**, 091801 (2001).
4. K. Abe *et al.* (Belle Collab.), Phys. Rev. Lett. **87**, 091802 (2001).
5. Currently two different notations (ϕ_1, ϕ_2, ϕ_3) and (α, β, γ) are used in the literature for CKM unitarity angles. In this mini-review, we use the latter notation following the other mini-reviews in this *Review*. The two notations are related by $\phi_1 = \beta$, $\phi_2 = \alpha$ and $\phi_3 = \gamma$.
6. See the "CP Violation in Meson Decays" by D. Kirkby and Y. Nir in this *Review*.
7. See the "CKM Quark Mixing Matrix," by A. Cecucci, Z. Ligeti, and Y. Sakai, in this *Review*.
8. See the "Review on B-$\overline{B}$ Mixing," by O. Schneider in this *Review*.
9. See the "Determination of $|V_{cb}|$ and $|V_{ub}|$," by R. Kowalewski and T. Mannel in this *Review*.
10. The B_c is a special case, where a weak decay of the c quark is also possible, but the spectator model still applies.
11. B. Grinstein, Nucl. Phys. **B339**, 253 (1990); H. Georgi, Phys. Lett. **B240**, 447 (1990); A.F. Falk *et al.*, Nucl. Phys. **B343**, 1 (1990); E. Eichten and B. Hill, Phys. Lett. **B234**, 511 (1990).
12. "Heavy-Quark and Soft-Collinear Effective Theory" by C.W. Bauer and M. Neubert in this *Review*.
13. M. Neubert, "Aspects of QCD Factorization," `hep-ph/0110093`, *Proceedings of HF9*, Pasadena (2001) and references therein; Z. Ligeti *et al.*, Phys. Lett. **B507**, 142 (2001).
14. M. Beneke *et al.*, Phys. Rev. Lett. **83**, 1914 (1999); Nucl. Phys. **B591**, 313 (2000); Nucl. Phys. **B606**, 245 (2001); M. Beneke and M. Neubert, Nucl. Phys. **B675**, 333 (2003).
15. Y.Y. Keum, H-n. Li, and A.I. Sanda, Phys. Lett. **B504**, 6 (2001); Phys. Rev. **D63**, 054008 (2001); Y.Y. Keum and H-n. Li, Phys. Rev. **D63**, 074006 (2001); C.D. Lü, K. Ukai, and M.Z. Yang, Phys. Rev. **D63**, 074009 (2001); C.D. Lü and M.Z. Yang, Eur. Phys. J. **C23**, 275 (2002).

16. C.W. Bauer, S. Fleming, and M.E. Luke, Phys. Rev. **D63**, 014006 (2001); C.W. Bauer *et al.*, Phys. Rev. **D63**, 114020 (2001); C.W. Bauer and I.W. Stewart, Phys. Lett. **B516**, 134 (2001).
17. N. Taniguchi *et al.* (Belle Collab.), Phys. Rev. Lett. **101**, 111801 (2008).
18. B. Aubert *et al.* (BaBar Collab.), Phys. Rev. **D78**, 112001 (2008).
19. F. Abe *et al.* (CDF Collab.), Phys. Rev. Lett. **81**, 2432 (1998); F. Abe *et al.* (CDF Collab.), Phys. Rev. **D58**, 112004 (1998).
20. D. Acosta *et al.* (CDF Collab.), Phys. Rev. Lett. **96**, 082002 (2006).
21. R. Aaij *et al.* (LHCb Collab.), Phys. Rev. **D87**, 112012 (2013).
22. B. Aubert *et al.* (BABAR Collaboration), Phys. Rev. Lett. **101**, 071801 (2008) [Erratum-ibid. **102**, 029901 (2009)].
23. G. Bonvicini, *et al.* (CLEO Collaboration), Phys. Rev. **D81**, 031104 (2010).
24. A. Abulencia *et al.* (CDF Collab.), Phys. Rev. **D75**, 012010 (2007), and references therein; R. Aaij *et al.* (LHCb Collab.), JHEP **1308**, 117 (2013); S. Chatrchyan *et al.* (CMS Collab.), JHEP **1206**, 110 (2012), and references therein; G. Aad *et al.* (ATLAS Collab.), JHEP **1310**, 042 (2013), and references therein; B. Abelev *et al.* (ALICE Collab.), Phys. Lett. **B721**, 13 (2013).
25. M. Cacciari *et al.*, JHEP **9805**, 007 (1998); S. Frixione and B. R. Webber, JHEP **0206**, 029 (2002); M. Cacciari *et al.*, JHEP **0407**, 033 (2004); M. Cacciari *et al.*, JHEP **0604**, 006 (2006), and references therein; M. Cacciari *et al.*, JHEP **1210**, 137 (2012).
26. B. Barish *et al.* (CLEO Collab.), Phys. Rev. Lett. **76**, 1570 (1996).
27. B. Aubert *et al.* (BaBar Collab.), Phys. Rev. Lett. **96**, 232001 (2006); A. Sokolov *et al.* (Belle Collab.), Phys. Rev. **D75**, 071103 (R) (2007).
28. J.P. Alexander *et al.* (CLEO Collab.), Phys. Rev. Lett. **86**, 2737 (2001).
29. B. Aubert *et al.* (BaBar Collab.), Phys. Rev. **D65**, 032001 (2001); B. Aubert *et al.* (BaBar Collab.), Phys. Rev. **D69**, 071101 (2004).
30. S.B. Athar *et al.* (CLEO Collab.), Phys. Rev. **D66**, 052003 (2002).
31. N.C. Hastings *et al.* (Belle Collab.), Phys. Rev. **D67**, 052004 (2003).
32. B. Aubert *et al.* (BaBar Collab.), Phys. Rev. Lett. **95**, 042001 (2005).
33. Y. Amhis *et al.* (Heavy Flavor Averaging Group), arXiv:1207.1158, and online update at http://www.slac.stanford.edu/xorg/hfag/.
34. G.S. Huang *et al.* (CLEO Collab.), Phys. Rev. **D75**, 012002 (2007).
35. R. Louvot *et al.* (Belle Collab.), Phys. Rev. Lett. **102**, 021801 (2009).
36. R. Louvot [Belle Collaboration], *Proceedings of EPS09*, Krakov, Poland (2009), arXiv:0909.2160 [hep-ex].
37. M. Lusignoli, M. Masetti, and S. Petrarca, Phys. Lett. **B266**, 142 (1991); K. Cheung, Phys. Lett. **B472**, 408 (2000).
38. T. Aaltonen *et al.* (CDF Collab.), Phys. Rev. **D77**, 072003 (2008).
39. R. Aaij *et al.* (LHCb Collab.), Phys. Rev. **D85**, 032008 (2012).
40. P. Abreu *et al.* (DELPHI Collab.), Phys. Lett. **B345**, 598 (1995).
41. T. Aaltonen *et al.* (CDF Collaboration), Phys. Rev. Lett. **102**, 102003 (2009); V.M. Abazov *et al.* (D0 Collab.), Phys. Rev. Lett. **99**, 172001 (2007).
42. R. Akers *et al.* (OPAL Collab.), Z. Phys. **C66**, 19 (1995).
43. T. Aaltonen *et al.* (CDF Collab.), Phys. Rev. Lett. **100**, 082001 (2008); V.M. Abazov *et al.* (D0 Collab.), Phys. Rev. Lett. **100**, 082002 (2008).
44. R. Aaij *et al.* (LHCb Collab.), Phys. Rev. Lett. **110**, 151803 (2013).
45. See the note on "Naming scheme for hadrons," by M. Roos and C.G. Wohl in this *Review*.
46. D. Buskulic *et al.* (ALEPH Collab.), Phys. Lett. **B384**, 449 (1996); P. Abreu *et al.* (DELPHI Collab.), Z. Phys. **C68**, 541 (1995).
47. T. Aaltonen *et al.* (CDF Collab.), Phys. Rev. Lett. **99**, 202001 (2007); T. Aaltonen *et al.* (CDF Collab.), Phys. Rev. **D85**, 092011 (2012).
48. V.M. Abazov *et al.* (D0 Collab.), Phys. Rev. Lett. **99**, 052001 (2007).
49. T. Aaltonen *et al.* (CDF Collab.), Phys. Rev. Lett. **99**, 052002 (2007).
50. T. Aaltonen *et al.* (CDF Collab.), Phys. Rev. Lett. **107**, 102001 (2011).
51. V. M. Abazov *et al.* (D0 Collab.), Phys. Rev. Lett. **101**, 232002 (2008).
52. T. Aaltonen *et al.* (CDF Collab.), Phys. Rev. D **80**, 072003 (2009).
53. R. Aaij *et al.* (LHCb Collab.), Phys. Rev. Lett. **110**, 182001 (2013).
54. S. Chatrchyan *et al.* (CMS Collab.), Phys. Rev. Lett. **108**, 252002 (2012).
55. C. Tarantino, Eur. Phys. J. **C33**, S895 (2004); F. Gabbiani *et al.*, Phys. Rev. **D68**, 114006 (2003); F. Gabbiani *et al.*, Phys. Rev. **D70**, 094031 (2004).
56. C.H. Chang *et al.*, Phys. Rev. **D64**, 014003 (2001); V.V. Kiselev, A.E. Kovalsky, and A.K. Likhoded, Nucl. Phys. **B585**, 353 (2000); V.V. Kiselev, arXiv:hep-ph/0308214, and references therein.
57. R. Aaij *et al.* (LHCb Collab.), arXiv:1401.6932 [hep-ex].
58. I.I. Bigi *et al.*, in *B Decays*, 2nd ed., S. Stone (ed.), World Scientific, Singapore, 1994.
59. T. Aaltonen *et al.* (CDF Collab.), Phys. Rev. Lett. **109**, 171802 (2012).
60. G. Aad *et al.* (ATLAS Collab.), JHEP **12**, 072 (2012).
61. R. Aaij *et al.* (LHCb Collab.), Phys. Rev. D 87,112010(2013).
62. T. Aaltonen *et al.* (CDF Collab.), Phys. Rev. Lett. **104**, 102002 (2010).
63. T. Aaltonen *et al.* (CDF Collab.), Phys. Rev. Lett. **106**, 121804 (2011).
64. S. Chatrchyan *et al.* (CMS Collab.), JHEP **07**, 163 (2013).

65. G. Aad *et al.* (ATLAS Collab.), Phys. Rev. D 87,032002(2013).
66. R. Aaij *et al.* (LHCb Collab.), Phys. Rev. Lett. **111**, 102003 (2013).
67. R. Aaij *et al.* (LHCb Collab.), arXiv:1402.2554.
68. A. Lenz and U. Nierste, JHEP **0706**, 072 (2007) and numerical update in arXiv:1102.4274 [hep-ph].
69. R. Fleischer and R. Knegjens, Eur. Phys. J. **C71**, 1789 (2011).
70. A. Abulencia *et al.* (CDF Collab.), Phys. Rev. **D84**, 052012 (2012).
71. R. Aaij *et al.* (LHCb Collab.), Phys. Lett. **B707**, 349 (2012).
72. A. Abulencia *et al.* (CDF Collab.), Phys. Rev. Lett. **97**, 242003 (2006).
73. T. Aaltonen *et al.* (CDF Collab.), Phys. Rev. Lett. **100**, 121803 (2008).
74. V.M. Abazov *et al.* (D0 Collab.), Phys. Rev. **D76**, 057101 (2007).
75. V. M. Abazov *et al.* (D0 Collab.), Phys. Rev. **D85**, 032006 (2012).
76. R. Aaij *et al.* [LHCb Collaboration], arXiv:1202.4717 [hep-ex], Submitted to Phys. Rev. Lett.
77. R. Ammar *et al.* (CLEO Collab.), Phys. Rev. Lett. **71**, 674 (1993).
78. P. Krokovny *et al.* (Belle Collab.), Phys. Rev. Lett. **89**, 231804 (2002); B. Aubert *et al.* (BaBar Collab.), Phys. Rev. Lett. **98**, 081801 (2007).
79. K. Ikado *et al.* (Belle Collab.), Phys. Rev. Lett. **97**, 251802 (2006); K. Hara *et al.* (Belle Collab.), Phys. Rev. **D82**, 071101 (2010).
80. B. Aubert *et al.* (BaBar Collab.), Phys. Rev. **D77**, 011107 (2008); B. Aubert *et al.* (BaBar Collab.), Phys. Rev. **D81**, 051101 (2010).
81. M. Beneke, J. Rohrer, and D. Yang, Nucl. Phys. **B774**, 64 (2007).
82. B. Aubert *et al.* (BaBar Collab.), Phys. Rev. Lett. **90**, 242001 (2003).
83. D. Besson *et al.* (CLEO Collab.), Phys. Rev. **D68**, 032002 (2003).
84. P. Krokovny *et al.* (Belle Collab.), Phys. Rev. Lett. **91**, 262002 (2003).
85. Y. Mikami *et al.* (Belle Collab.), Phys. Rev. Lett. **92**, 012002 (2004).
86. B. Aubert *et al.* (BaBar Collab.), Phys. Rev. Lett. **93**, 181801 (2004).
87. J. Brodzicka *et al.* (Belle Collab.), Phys. Rev. Lett. **100**, 092001 (2008).
88. B. Aubert *et al.* (BaBar Collab.), Phys. Rev. **D80**, 092003 (2009).
89. S.-K. Choi *et al.* (Belle Collab.), Phys. Rev. Lett. **91**, 262001 (2003).
90. D. Acosta *et al.* (CDF II Collab.), Phys. Rev. Lett. **93**, 072001 (2004).
91. B. Aubert *et al.* (BaBar Collab.), Phys. Rev. **D71**, 071103 (2005).
92. S.-K. Choi *et al.* (Belle Collab.), Phys. Rev. **D84**, 052004 (2011).
93. E.S. Swanson, Phys. Rep. **429**, 243 (2006).
94. B. Aubert *et al.* (BaBar Collab.), Phys. Rev. **D74**, 071101 (2006).
95. B. Aubert *et al.* (BaBar Collab.), Phys. Rev. Lett. **102**, 132001 (2009).
96. V. Bhardwaj *et al.* (Belle Collab.), Phys. Rev. Lett. **107**, 091803 (2011).
97. S.-K. Choi *et al.* (Belle Collab.), Phys. Rev. Lett. **94**, 182002 (2005).
98. B. Aubert *et al.* (BaBar Collab.), Phys. Rev. Lett. **95**, 142001 (2005).
99. S.-K. Choi *et al.* (Belle Collab.), Phys. Rev. Lett. **100**, 142001 (2008); R. Mizuk *et al.* (Belle Collab.), Phys. Rev. **D80**, 031104 (2009).
100. B. Aubert *et al.* (BaBar Collab.), Phys. Rev. **D79**, 112001 (2009).
101. R. Mizuk *et al.* (Belle Collab.), Phys. Rev. **D78**, 072004 (2008).
102. J. P. Lees *et al.* (BaBar Collab.), Phys. Rev. **D85**, 052003 (2012).
103. J. P. Lees *et al.* (BaBar Collab.), Phys. Rev. **D84**, 112007 (2011); S. Blyth *et al.* (Belle Collab.), Phys. Rev. **D74**, 092002 (2006).
104. R. Aaij *et al.* (LHCb Collab.), Phys. Lett. **B698**, 115 (2011); J. Li *et al.* (Belle Collab.), Phys. Rev. Lett. **106**, 121802 (2011); V. M. Abazov *et al.* (D0 Collab.), Phys. Rev. **D85**, 011103 (2012).
105. R. Aaij *et al.* (LHCb Collab.), Phys. Rev. Lett. **707**, 497 (2012).
106. R. Aaij *et al.* (LHCb Collab.), Phys. Rev. **D84**, 092001 (2011); ibid. Phys. Rev. **D85**, 039904 (2012); T. Aaltonen *et al.* (CDF Collab.), Phys. Rev. **D85**, 032003 (2012).
107. T. Aaltonen *et al.* (CDF Collab.), Phys. Rev. Lett. **107**, 261802 (2011).
108. T. Aaltonen *et al.* (CDF Collab.), Phys. Rev. Lett. **106**, 181802 (2011).
109. T. Aaltonen *et al.* (CDF Collab.), Phys. Rev. Lett. **103**, 031801 (2009).
110. R. Fleischer, Phys. Lett. **B459**, 306 (1999); D. London and J. Matias, Phys. Rev. **D70**, 031502 (2004).
111. B. Aubert *et al.* (BaBar Collab.), Phys. Rev. Lett. **97**, 171805 (2006).
112. S.-W. Lin *et al.* (Belle Collab.), Phys. Rev. Lett. **98**, 181804 (2007).
113. B. Aubert *et al.* (BaBar Collab.), Phys. Rev. Lett. **99**, 021603 (2007).
114. S.-W. Lin *et al.* (Belle Collab.), Nature **452** 332(2008).
115. See for example M. Gronau and J.L. Rosner, Phys. Rev. **D71**, 074019 (2005); M. Gronau, Phys. Lett. **B627**, 82 (2005).
116. B. Aubert *et al.* (BaBar Collab.), Phys. Rev. **D78**, 012004 (2008); A. Garmash *et al.* (Belle Collab.), Phys. Rev. Lett. **96**, 251803 (2006).
117. C.-T. Hoi *et al.* (Belle Collab.), Phys. Rev. Lett. **108**, 031801 (2012); B. Aubert *et al.* (BaBar Collab.), Phys. Rev. **D80**, 112002 (2009).
118. B. Aubert *et al.* (BaBar Collab.), Phys. Rev. Lett. **97**, 201802 (2006); C.H. Wang *et al.* (Belle Collab.), Phys. Rev. **D75**, 092005 (2007).
119. M. Gronau and D. London, Phys. Rev. Lett. **65**, 3381 (1990).

120. B. Aubert *et al.* (BaBar Collab.), Phys. Rev. **D78**, 071104 (2008); C.C. Chiang *et al.* (Belle Collab.), Phys. Rev. **D78**, 111102 (2008).
121. B. Aubert *et al.* (BaBar Collab.), Phys. Rev. Lett. **98**, 181803 (2007).
122. B. Aubert *et al.* (BaBar Collab.), Phys. Rev. **D81**, 052009 (2010).
123. See the "Polarization in B Decays," by A. Gritsan and J.G. Smith in this *Review*.
124. A. Williamson and J. Zupan, Phys. Rev. **D74**, 014003 (2006).
125. B. Aubert *et al.* (BaBar Collab.), Phys. Rev. **D78**, 012004 (2008); A. Garmash *et al.* (Belle Collab.), Phys. Rev. Lett. **96**, 251803 (2006); P. Chang *et al.* (Belle Collab.), Phys. Lett. **B599**, 148 (2004); J.P. Lees *et al.* (BaBar Collab.), Phys. Rev. **D83**, 112010 (2011); A. Garmash *et al.* (Belle Collab.), Phys. Rev. **D75**, 012006 (2007); B. Aubert *et al.* (BaBar Collab.), Phys. Rev. **D80**, 112001 (2009).
126. A. Garmash *et al.* (Belle Collab.), Phys. Rev. **D71**, 092003 (2005); B. Aubert *et al.* (BaBar Collab.), Phys. Rev. **D74**, 032003 (2006); A. Garmash *et al.* (Belle Collab.), Phys. Rev. **D69**, 012001 (2004); B. Aubert *et al.* (BaBar Collab.), Phys. Rev. Lett. **93**, 181805 (2004); B. Aubert *et al.* (BaBar Collab.), Phys. Rev. Lett. **95**, 011801 (2005).
127. B. Aubert *et al.* (BaBar Collab.), Phys. Rev. **D74**, 051104R (2006); B. Aubert *et al.* (BaBar Collab.), Phys. Rev. **D76**, 071104R (2007).
128. B. Aubert *et al.* (BaBar Collab.), Phys. Rev. Lett. **99**, 221801 (2007).
129. M. Nakao *et al.* (Belle Collab.), Phys. Rev. **D69**, 112001 (2004); B. Aubert *et al.* (BaBar Collab.), Phys. Rev. Lett. **103**, 211802 (2009).
130. B. Aubert *et al.* (BaBar Collab.), Phys. Rev. **D70**, 091105R (2004); H. Yang *et al.* (Belle Collab.), Phys. Rev. Lett. **94**, 111802 (2005); S. Nishida *et al.* (Belle Collab.), Phys. Lett. **B610**, 23 (2005); B. Aubert *et al.* (BaBar Collab.), Phys. Rev. **D74**, 031102R (2004).
131. J. Wicht *et al.* (Belle Collab.), Phys. Rev. Lett. **100**, 121801 (2008).
132. R. Aaij *et al.* (LHCb Collab.), Nucl. Phys. **B867**, 1 (2013).
133. A. Ali *et al.*, Phys. Lett. **B595**, 323 (2004); P. Ball, G. Jones, and R. Zwicky, Phys. Rev. **D75**, 054004 (2007).
134. J.L. Hewett, Phys. Rev. Lett. **70**, 1045 (1993).
135. S. Chen *et al.* (CLEO Collab.), Phys. Rev. Lett. **87**, 251807 (2001).
136. J. P. Lees *et al.* (BaBar Collaboration), Phys. Rev. **D86**, 112008 (2012).
137. A. Limosani *et al.* (Belle Collab.), Phys. Rev. Lett. **103**, 241801 (2009).
138. M. Misiak *et al.*, Phys. Rev. Lett. **98**, 022002 (2007).
139. T. Becher and M. Neubert, Phys. Rev. Lett. **98**, 022003 (2007).
140. L. Wolfenstein and Y.L. Wu, Phys. Rev. Lett. **73**, 2809 (1994); H.M. Asatrian and A. Ioannisian, Phys. Rev. **D54**, 5642 (1996); M. Ciuchini *et al.*, Phys. Lett. **B388**, 353 (1996); S. Baek and P. Ko, Phys. Rev. Lett. **83**, 488 (1998); A.L. Kagan and M. Neubert, Phys. Rev. **D58**, 094012 (1998); K. Kiers *et al.*, Phys. Rev. **D62**, 116004 (2000).
141. S. Nishida *et al.* (Belle Collab.), Phys. Rev. Lett. **93**, 031803 (2004).
142. B. Aubert *et al.* (BaBar Collab.), Phys. Rev. **D72**, 052004 (2005).
143. B. Aubert *et al.* (BaBar Collab.), Phys. Rev. **D77**, 051103 (2008).
144. J. P. Lees *et al.* (BaBar Collab.), Phys. Rev. Lett. **109**, 191801 (2012).
145. J.-T. Wei *et al.* (Belle Collab.), Phys. Rev. Lett. **103**, 171801 (2009).
146. J. P. Lees *et al.* (BaBar Collab.), Phys. Rev. **D86**, 032012 (2012).
147. T. Aaltonen *et al.* (CDF Collab.), Phys. Rev. Lett. **107**, 201802 (2011).
148. T. Aaltonen *et al.* (CDF Collab.), Phys. Rev. Lett. **106**, 161801 (2011).
149. R. Aaij *et al.* (LHCb Collab.), JHEP **1307**, 084 (2013).
150. R. Aaij *et al.* (LHCb Collab.), Phys. Lett. **B725**, 25 (2013).
151. M. Iwasaki *et al.* (Belle Collab.), Phys. Rev. **D72**, 092005 (2005); B. Aubert *et al.* (BaBar Collab.), Phys. Rev. Lett. **93**, 081802 (2004).
152. The average is calculated by HFAG [33] including the recent unpublished value by Belle.
153. T. Aaltonen *et al.* (CDF Collab.), Phys. Rev. Lett. **108**, 081807 (2012).
154. B. Aubert *et al.* (BaBar Collab.), Phys. Rev. Lett. **102**, 091803 (2009).
155. S. Chatrchyan *et al.* (CMS Collab.), Phys. Lett. **B727**, 77 (2013).
156. R. Aaij *et al.* (LHCb Collab.), JHEP **1308**, 131 (2013).
157. R. Aaij *et al.* (LHCb Collab.), Phys. Rev. Lett. **111**, 151801 (2013).
158. R. Aaij *et al.* (LHCb Collab.), Phys. Rev. Lett. **110**, 031801 (2013).
159. R. Aaij *et al.* (LHCb Collab.), JHEP **1207**, 133 (2012).
160. R. Aaij *et al.* (LHCb Collab.), Phys. Rev. Lett. **111**, 191801 (2013).
161. T. Aaltonen *et al.* (CDF Collab.), Phys. Rev. Lett. **107**, 239903 (2011).
162. V. M. Abazov *et al.* (D0 Collab.), Phys. Rev. **D87**, 072006 (2013).
163. R. Aaij *et al.* (LHCb Collab.), Phys. Rev. Lett. **110**, 021801 (2013).
164. R. Aaij *et al.* (LHCb Collab.), Phys. Rev. Lett. **111**, 101805 (2013).
165. S. Chatrchyan *et al.* (CMS Collab.), Phys. Rev. Lett. **111**, 101804 (2013).
166. T. Aaltonen *et al.* (CDF Collab.), Phys. Rev. Lett. **102**, 201801 (2009).
167. R. Aaij *et al.* (LHCb Collab.), Phys. Rev. Lett. **111**, 141801 (2013).

Meson Particle Listings

b-flavored hadrons, $B^{\pm}$

A NOTE ON HFAG ACTIVITIES

The Heavy Flavor Averaging Group (HFAG) has been formed, continuing the activities of the LEP Heavy Flavor Steering group, to provide the averages for measurements dedicated to the b-flavor related quantities. The HFAG consists of representatives and contacts from the experimental groups: BaBar, Belle, CDF, CLEO, DØ , LEP, SLD, and LHCb.

In the averaging the input parameters used in the various analyses are adjusted (rescaled) to common values, and all known correlations are taken into account. The HFAG has seven sub-groups providing averages for b-hadron lifetimes and B-oscillation parameters, CP-violation measurements, semileptonic parameters, rare branching fractions, b-hadron decays to charm, charm mixing and decays, and τ decays. The averages provided by the HFAG are listed as "OUR EVALUATION" with a corresponding note.

The most up-to-date and complete listing of averages and more detailed information on the averaging procedures are available at:

`http://www.slac.stanford.edu/xorg/hfag` .

$B^{\pm}$ $I(J^P) = \frac{1}{2}(0^-)$

Quantum numbers not measured. Values shown are quark-model predictions.

See also the $B^{\pm}/B^0$ ADMIXTURE and $B^{\pm}/B^0/B_s^0/b$-baryon ADMIXTURE sections.

$B^{\pm}$ MASS

The fit uses m_{B^+}, $(m_{B^0} - m_{B^+})$, and m_{B^0} to determine m_{B^+}, m_{B^0}, and the mass difference.

VALUE (MeV)	EVTS	DOCUMENT ID		TECN	COMMENT
5279.26±0.17 OUR FIT					
5279.25±0.26 OUR AVERAGE					
5279.38±0.11±0.33		[1] AAIJ	12E	LHCB	pp at 7 TeV
5279.10±0.41±0.36		[2] ACOSTA	06	CDF	$p\overline{p}$ at 1.96 TeV
5279.1 ±0.4 ±0.4	526	[3] CSORNA	00	CLE2	$e^+e^- \to \Upsilon(4S)$
5279.1 ±1.7 ±1.4	147	ABE	96B	CDF	$p\overline{p}$ at 1.8 TeV
• • • We do not use the following data for averages, fits, limits, etc. • • •					
5278.8 ±0.54±2.0	362	ALAM	94	CLE2	$e^+e^- \to \Upsilon(4S)$
5278.3 ±0.4 ±2.0		BORTOLETTO	92	CLEO	$e^+e^- \to \Upsilon(4S)$
5280.5 ±1.0 ±2.0		[4] ALBRECHT	90J	ARG	$e^+e^- \to \Upsilon(4S)$
5275.8 ±1.3 ±3.0	32	ALBRECHT	87C	ARG	$e^+e^- \to \Upsilon(4S)$
5278.2 ±1.8 ±3.0	12	[5] ALBRECHT	87D	ARG	$e^+e^- \to \Upsilon(4S)$
5278.6 ±0.8 ±2.0		BEBEK	87	CLEO	$e^+e^- \to \Upsilon(4S)$

[1] Uses $B^+ \to J/\psi K^+$ fully reconstructed decays.
[2] Uses exclusively reconstructed final states containing a $J/\psi \to \mu^+\mu^-$ decays.
[3] CSORNA 00 uses fully reconstructed 526 $B^+ \to J/\psi^{(\prime)} K^+$ events and invariant masses without beam constraint.
[4] ALBRECHT 90J assumes 10580 for $\Upsilon(4S)$ mass. Supersedes ALBRECHT 87C and ALBRECHT 87D.
[5] Found using fully reconstructed decays with $J/\psi(1S)$. ALBRECHT 87D assume $m_{\Upsilon(4S)}$ = 10577 MeV.

$B^{\pm}$ MEAN LIFE

See $B^{\pm}/B^0/B_s^0/b$-baryon ADMIXTURE section for data on B-hadron mean life averaged over species of bottom particles.

"OUR EVALUATION" is an average using rescaled values of the data listed below. The average and rescaling were performed by the Heavy Flavor Averaging Group (HFAG) and are described at http://www.slac.stanford.edu/xorg/hfag/. The averaging/rescaling procedure takes into account correlations between the measurements and asymmetric lifetime errors.

VALUE (10^{-12} s)	EVTS	DOCUMENT ID		TECN	COMMENT
1.638±0.004 OUR EVALUATION					
1.637±0.004±0.003		AAIJ	14E	LHCB	pp at 7 TeV
1.639±0.009±0.009		[1] AALTONEN	11	CDF	$p\overline{p}$ at 1.96 TeV
1.663±0.023±0.015		[2] AALTONEN	11B	CDF	$p\overline{p}$ at 1.96 TeV
1.635±0.011±0.011		[3] ABE	05B	BELL	$e^+e^- \to \Upsilon(4S)$
1.624±0.014±0.018		[4] ABDALLAH	04E	DLPH	$e^+e^- \to Z$
1.636±0.058±0.025		[5] ACOSTA	02C	CDF	$p\overline{p}$ at 1.8 TeV
1.673±0.032±0.023		[6] AUBERT	01F	BABR	$e^+e^- \to \Upsilon(4S)$
1.648±0.049±0.035		[7] BARATE	00R	ALEP	$e^+e^- \to Z$
1.643±0.037±0.025		[8] ABBIENDI	99J	OPAL	$e^+e^- \to Z$
$1.637 \pm 0.058^{+0.045}_{-0.043}$		[7] ABE	98Q	CDF	$p\overline{p}$ at 1.8 TeV
1.66 ±0.06 ±0.03		[8] ACCIARRI	98S	L3	$e^+e^- \to Z$
1.66 ±0.06 ±0.05		[8] ABE	97J	SLD	$e^+e^- \to Z$
$1.58\ ^{+0.21}_{-0.18}\ ^{+0.04}_{-0.03}$	94	[5] BUSKULIC	96J	ALEP	$e^+e^- \to Z$
1.61 ±0.16 ±0.12		[7,9] ABREU	95Q	DLPH	$e^+e^- \to Z$
1.72 ±0.08 ±0.06		[10] ADAM	95	DLPH	$e^+e^- \to Z$
1.52 ±0.14 ±0.09		[7] AKERS	95T	OPAL	$e^+e^- \to Z$
• • • We do not use the following data for averages, fits, limits, etc. • • •					
1.695±0.026±0.015		[6] ABE	02H	BELL	Repl. by ABE 05B
1.68 ±0.07 ±0.02		[5] ABE	98B	CDF	Repl. by ACOSTA 02C
1.56 ±0.13 ±0.06		[7] ABE	96C	CDF	Repl. by ABE 98Q
1.58 ±0.09 ±0.03		[11] BUSKULIC	96J	ALEP	$e^+e^- \to Z$
1.58 ±0.09 ±0.04		[7] BUSKULIC	96J	ALEP	Repl. by BARATE 00R
1.70 ±0.09		[12] ADAM	95	DLPH	$e^+e^- \to Z$
1.61 ±0.16 ±0.05	148	[5] ABE	94D	CDF	Repl. by ABE 98B
$1.30\ ^{+0.33}_{-0.29}$ ±0.16	92	[7] ABREU	93D	DLPH	Sup. by ABREU 95Q
1.56 ±0.19 ±0.13	134	[10] ABREU	93G	DLPH	Sup. by ADAM 95
$1.51\ ^{+0.30}_{-0.28}\ ^{+0.12}_{-0.14}$	59	[7] ACTON	93C	OPAL	Sup. by AKERS 95T
$1.47\ ^{+0.22}_{-0.19}\ ^{+0.15}_{-0.14}$	77	[7] BUSKULIC	93D	ALEP	Sup. by BUSKULIC 96J

[1] Measured mean life using fully reconstructed decays ($J/\psi K^{(*)}$).
[2] Measured using $B^- \to D^0\pi^-$ with $D^0 \to K^-\pi^+$ events that were selected using a silicon vertex trigger.
[3] Measurement performed using a combined fit of CP-violation, mixing and lifetimes.
[4] Measurement performed using an inclusive reconstruction and B flavor identification technique.
[5] Measured mean life using fully reconstructed decays.
[6] Events are selected in which one B meson is fully reconstructed while the second B meson is reconstructed inclusively.
[7] Data analyzed using $D/D^*\ell$X event vertices.
[8] Data analyzed using charge of secondary vertex.
[9] ABREU 95Q assumes B($B^0 \to D^{**-}\ell^+\nu_\ell$) = 3.2 ± 1.7%.
[10] Data analyzed using vertex-charge technique to tag B charge.
[11] Combined result of $D/D^*\ell$X analysis and fully reconstructed B analysis.
[12] Combined ABREU 95Q and ADAM 95 result.

τ_{B^+}/τ_{B^-}

VALUE	DOCUMENT ID		TECN	COMMENT
1.002±0.004±0.002	[1] AAIJ	14E	LHCB	pp at 7 TeV

[1] Measured using $B^{\pm} \to J/\psi K^{\pm}$ decays.

B^+ DECAY MODES

B^- modes are charge conjugates of the modes below. Modes which do not identify the charge state of the B are listed in the $B^{\pm}/B^0$ ADMIXTURE section.

The branching fractions listed below assume 50% $B^0\overline{B}^0$ and 50% B^+B^- production at the $\Upsilon(4S)$. We have attempted to bring older measurements up to date by rescaling their assumed $\Upsilon(4S)$ production ratio to 50:50 and their assumed D, D_s, D^*, and ψ branching ratios to current values whenever this would affect our averages and best limits significantly.

Indentation is used to indicate a subchannel of a previous reaction. All resonant subchannels have been corrected for resonance branching fractions to the final state so the sum of the subchannel branching fractions can exceed that of the final state.

For inclusive branching fractions, *e.g.*, $B \to D^{\pm}$anything, the values usually are multiplicities, not branching fractions. They can be greater than one.

	Mode		Fraction (Γ_i/Γ)	Scale factor/ Confidence level
	Semileptonic and leptonic modes			
Γ_1	$\ell^+\nu_\ell$anything	[a]	(10.99 ±0.28) %	
Γ_2	$e^+\nu_e X_c$		(10.8 ±0.4) %	
Γ_3	$D\ell^+\nu_\ell$anything		(9.8 ±0.7) %	
Γ_4	$\overline{D}^0\ell^+\nu_\ell$	[a]	(2.27 ±0.11) %	
Γ_5	$\overline{D}^0\tau^+\nu_\tau$		(7.7 ±2.5)	$\times 10^{-3}$
Γ_6	$\overline{D}^*(2007)^0\ell^+\nu_\ell$	[a]	(5.69 ±0.19) %	
Γ_7	$\overline{D}^*(2007)^0\tau^+\nu_\tau$		(1.88 ±0.20) %	
Γ_8	$D^-\pi^+\ell^+\nu_\ell$		(4.2 ±0.5)	$\times 10^{-3}$
Γ_9	$\overline{D}_0^*(2420)^0\ell^+\nu_\ell$, $\overline{D}_0^{*0} \to D^-\pi^+$		(2.5 ±0.5)	$\times 10^{-3}$

Γ_{10}	$\overline{D}_2^*(2460)^0 \ell^+ \nu_\ell$, $\overline{D}_2^{*0} \to D^- \pi^+$		(1.53	± 0.16)	$\times 10^{-3}$		
Γ_{11}	$D^{(*)}$ n $\pi \ell^+ \nu_\ell$ (n $\geq$ 1)		(1.87	± 0.26)	%		
Γ_{12}	$D^{*-} \pi^+ \ell^+ \nu_\ell$		(6.1	± 0.6)	$\times 10^{-3}$		
Γ_{13}	$\overline{D}_1(2420)^0 \ell^+ \nu_\ell$, $\overline{D}_1^0 \to D^{*-} \pi^+$		(3.03	± 0.20)	$\times 10^{-3}$		
Γ_{14}	$\overline{D}_1'(2430)^0 \ell^+ \nu_\ell$, $\overline{D}_1'^0 \to D^{*-} \pi^+$		(2.7	± 0.6)	$\times 10^{-3}$		
Γ_{15}	$\overline{D}_2^*(2460)^0 \ell^+ \nu_\ell$, $\overline{D}_2^{*0} \to D^{*-} \pi^+$		(1.01	± 0.24)	$\times 10^{-3}$		S=2.0
Γ_{16}	$D_s^{(*)-} K^+ \ell^+ \nu_\ell$		(6.1	± 1.0)	$\times 10^{-4}$		
Γ_{17}	$D_s^- K^+ \ell^+ \nu_\ell$		(3.0	$^{+1.4}_{-1.2}$)	$\times 10^{-4}$		
Γ_{18}	$D_s^{*-} K^+ \ell^+ \nu_\ell$		(2.9	± 1.9)	$\times 10^{-4}$		
Γ_{19}	$\pi^0 \ell^+ \nu_\ell$		(7.80	± 0.27)	$\times 10^{-5}$		
Γ_{20}	$\pi^0 e^+ \nu_e$						
Γ_{21}	$\eta \ell^+ \nu_\ell$		(3.8	± 0.6)	$\times 10^{-5}$		
Γ_{22}	$\eta' \ell^+ \nu_\ell$		(2.3	± 0.8)	$\times 10^{-5}$		
Γ_{23}	$\omega \ell^+ \nu_\ell$	[a]	(1.19	± 0.09)	$\times 10^{-4}$		
Γ_{24}	$\omega \mu^+ \nu_\mu$						
Γ_{25}	$\rho^0 \ell^+ \nu_\ell$	[a]	(1.58	± 0.11)	$\times 10^{-4}$		
Γ_{26}	$p \overline{p} \ell^+ \nu_\ell$		(5.8	$^{+2.6}_{-2.3}$)	$\times 10^{-6}$		
Γ_{27}	$p \overline{p} \mu^+ \nu_\mu$		< 8.5		$\times 10^{-6}$		CL=90%
Γ_{28}	$p \overline{p} e^+ \nu_e$		(8.2	$^{+4.0}_{-3.3}$)	$\times 10^{-6}$		
Γ_{29}	$e^+ \nu_e$		< 9.8		$\times 10^{-7}$		CL=90%
Γ_{30}	$\mu^+ \nu_\mu$		< 1.0		$\times 10^{-6}$		CL=90%
Γ_{31}	$\tau^+ \nu_\tau$		(1.14	± 0.27)	$\times 10^{-4}$		S=1.3
Γ_{32}	$\ell^+ \nu_\ell \gamma$		< 1.56		$\times 10^{-5}$		CL=90%
Γ_{33}	$e^+ \nu_e \gamma$		< 1.7		$\times 10^{-5}$		CL=90%
Γ_{34}	$\mu^+ \nu_\mu \gamma$		< 2.4		$\times 10^{-5}$		CL=90%

Inclusive modes

Γ_{35}	$D^0 X$		(8.6	± 0.7)	%		
Γ_{36}	$\overline{D}^0 X$		(79	± 4)	%		
Γ_{37}	$D^+ X$		(2.5	± 0.5)	%		
Γ_{38}	$D^- X$		(9.9	± 1.2)	%		
Γ_{39}	$D_s^+ X$		(7.9	$^{+1.4}_{-1.3}$)	%		
Γ_{40}	$D_s^- X$		(1.10	$^{+0.40}_{-0.32}$)	%		
Γ_{41}	$\Lambda_c^+ X$		(2.1	$^{+0.9}_{-0.6}$)	%		
Γ_{42}	$\overline{\Lambda}_c^- X$		(2.8	$^{+1.1}_{-0.9}$)	%		
Γ_{43}	$\overline{c} X$		(97	± 4)	%		
Γ_{44}	$c X$		(23.4	$^{+2.2}_{-1.8}$)	%		
Γ_{45}	$c / \overline{c} X$		(120	± 6)	%		

***D*, *D**, or D_s modes**

Γ_{46}	$\overline{D}^0 \pi^+$		(4.81	± 0.15)	$\times 10^{-3}$		
Γ_{47}	$D_{CP(+1)} \pi^+$	[b]	(2.20	± 0.24)	$\times 10^{-3}$		
Γ_{48}	$D_{CP(-1)} \pi^+$	[b]	(2.1	± 0.4)	$\times 10^{-3}$		
Γ_{49}	$\overline{D}^0 \rho^+$		(1.34	± 0.18)	%		
Γ_{50}	$\overline{D}^0 K^+$		(3.70	± 0.17)	$\times 10^{-4}$		
Γ_{51}	$D_{CP(+1)} K^+$	[b]	(1.92	± 0.14)	$\times 10^{-4}$		
Γ_{52}	$D_{CP(-1)} K^+$	[b]	(2.00	± 0.19)	$\times 10^{-4}$		
Γ_{53}	$[K^- \pi^+]_D K^+$	[c]	< 2.8		$\times 10^{-7}$		CL=90%
Γ_{54}	$[K^+ \pi^-]_D K^+$	[c]	< 1.8		$\times 10^{-5}$		CL=90%
Γ_{55}	$[K^- \pi^+ \pi^0]_D K^+$						
Γ_{56}	$[K^+ \pi^- \pi^0]_D K^+$						
Γ_{57}	$[K^- \pi^+ \pi^+ \pi^-]_D K^+$						
Γ_{58}	$[K^+ \pi^- \pi^+ \pi^-]_D K^+$						
Γ_{59}	$[K^- \pi^+]_D K^*(892)^+$	[c]					
Γ_{60}	$[K^+ \pi^-]_D K^*(892)^+$	[c]					
Γ_{61}	$[K^- \pi^+]_D \pi^+$	[c]	(6.3	± 1.1)	$\times 10^{-7}$		
Γ_{62}	$[K^+ \pi^-]_D \pi^+$		(1.68	± 0.31)	$\times 10^{-4}$		
Γ_{63}	$[K^- \pi^+ \pi^0]_D \pi^+$						
Γ_{64}	$[K^+ \pi^- \pi^0]_D \pi^+$						
Γ_{65}	$[K^- \pi^+ \pi^+ \pi^-]_D \pi^+$						
Γ_{66}	$[K^+ \pi^- \pi^+ \pi^-]_D \pi^+$						
Γ_{67}	$[K^- \pi^+]_{(D\pi)} \pi^+$						
Γ_{68}	$[K^+ \pi^-]_{(D\pi)} \pi^+$						
Γ_{69}	$[K^- \pi^+]_{(D\gamma)} \pi^+$						
Γ_{70}	$[K^+ \pi^-]_{(D\gamma)} \pi^+$						
Γ_{71}	$[K^- \pi^+]_{(D\pi)} K^+$						
Γ_{72}	$[K^+ \pi^-]_{(D\pi)} K^+$						
Γ_{73}	$[K^- \pi^+]_{(D\gamma)} K^+$						
Γ_{74}	$[K^+ \pi^-]_{(D\gamma)} K^+$						
Γ_{75}	$[\pi^+ \pi^- \pi^0]_D K^-$		(4.6	± 0.9)	$\times 10^{-6}$		
Γ_{76}	$\overline{D}^0 K^*(892)^+$		(5.3	± 0.4)	$\times 10^{-4}$		
Γ_{77}	$D_{CP(-1)} K^*(892)^+$	[b]	(2.7	± 0.8)	$\times 10^{-4}$		
Γ_{78}	$D_{CP(+1)} K^*(892)^+$	[b]	(5.8	± 1.1)	$\times 10^{-4}$		
Γ_{79}	$\overline{D}^0 K^+ \pi^+ \pi^-$		(5.4	± 2.2)	$\times 10^{-4}$		
Γ_{80}	$\overline{D}^0 K^+ \overline{K}^0$		(5.5	± 1.6)	$\times 10^{-4}$		
Γ_{81}	$\overline{D}^0 K^+ \overline{K}^*(892)^0$		(7.5	± 1.7)	$\times 10^{-4}$		
Γ_{82}	$\overline{D}^0 \pi^+ \pi^+ \pi^-$		(5.7	± 2.2)	$\times 10^{-3}$		S=3.6
Γ_{83}	$\overline{D}^0 \pi^+ \pi^+ \pi^-$ nonresonant		(5	± 4)	$\times 10^{-3}$		
Γ_{84}	$\overline{D}^0 \pi^+ \rho^0$		(4.2	± 3.0)	$\times 10^{-3}$		
Γ_{85}	$\overline{D}^0 a_1(1260)^+$		(4	± 4)	$\times 10^{-3}$		
Γ_{86}	$\overline{D}^0 \omega \pi^+$		(4.1	± 0.9)	$\times 10^{-3}$		
Γ_{87}	$D^*(2010)^- \pi^+ \pi^+$		(1.35	± 0.22)	$\times 10^{-3}$		
Γ_{88}	$\overline{D}_1(2420)^0 \pi^+$, $\overline{D}_1^0 \to D^*(2010)^- \pi^+$		(5.3	± 2.3)	$\times 10^{-4}$		
Γ_{89}	$D^- \pi^+ \pi^+$		(1.07	± 0.05)	$\times 10^{-3}$		
Γ_{90}	$D^+ K^0$		< 2.9		$\times 10^{-6}$		CL=90%
Γ_{91}	$D^+ K^{*0}$		< 1.8		$\times 10^{-6}$		CL=90%
Γ_{92}	$D^+ \overline{K}^{*0}$		< 1.4		$\times 10^{-6}$		CL=90%
Γ_{93}	$\overline{D}^*(2007)^0 \pi^+$		(5.18	± 0.26)	$\times 10^{-3}$		
Γ_{94}	$\overline{D}^{*0}_{CP(+1)} \pi^+$	[d]	(2.9	± 0.7)	$\times 10^{-3}$		
Γ_{95}	$D^{*0}_{CP(-1)} \pi^+$	[d]	(2.6	± 1.0)	$\times 10^{-3}$		
Γ_{96}	$\overline{D}^*(2007)^0 \omega \pi^+$		(4.5	± 1.2)	$\times 10^{-3}$		
Γ_{97}	$\overline{D}^*(2007)^0 \rho^+$		(9.8	± 1.7)	$\times 10^{-3}$		
Γ_{98}	$\overline{D}^*(2007)^0 K^+$		(4.20	± 0.34)	$\times 10^{-4}$		
Γ_{99}	$\overline{D}^{*0}_{CP(+1)} K^+$	[d]	(2.8	± 0.4)	$\times 10^{-4}$		
Γ_{100}	$\overline{D}^{*0}_{CP(-1)} K^+$	[d]	(2.31	± 0.33)	$\times 10^{-4}$		
Γ_{101}	$\overline{D}^*(2007)^0 K^*(892)^+$		(8.1	± 1.4)	$\times 10^{-4}$		
Γ_{102}	$\overline{D}^*(2007)^0 K^+ \overline{K}^0$		< 1.06		$\times 10^{-3}$		CL=90%
Γ_{103}	$\overline{D}^*(2007)^0 K^+ K^*(892)^0$		(1.5	± 0.4)	$\times 10^{-3}$		
Γ_{104}	$\overline{D}^*(2007)^0 \pi^+ \pi^+ \pi^-$		(1.03	± 0.12)	%		
Γ_{105}	$\overline{D}^*(2007)^0 a_1(1260)^+$		(1.9	± 0.5)	%		
Γ_{106}	$\overline{D}^*(2007)^0 \pi^- \pi^+ \pi^+ \pi^0$		(1.8	± 0.4)	%		
Γ_{107}	$\overline{D}^{*0} 3\pi^+ 2\pi^-$		(5.7	± 1.2)	$\times 10^{-3}$		
Γ_{108}	$D^*(2010)^+ \pi^0$		< 3.6		$\times 10^{-6}$		
Γ_{109}	$D^*(2010)^+ K^0$		< 9.0		$\times 10^{-6}$		CL=90%
Γ_{110}	$D^*(2010)^- \pi^+ \pi^+ \pi^0$		(1.5	± 0.7)	%		
Γ_{111}	$D^*(2010)^- \pi^+ \pi^+ \pi^+ \pi^-$		(2.6	± 0.4)	$\times 10^{-3}$		
Γ_{112}	$\overline{D}^{**0} \pi^+$	[e]	(5.9	± 1.3)	$\times 10^{-3}$		
Γ_{113}	$\overline{D}_1^*(2420)^0 \pi^+$		(1.5	± 0.6)	$\times 10^{-3}$		S=1.3
Γ_{114}	$\overline{D}_1(2420)^0 \pi^+ \times$ B($\overline{D}_1^0 \to \overline{D}^0 \pi^+ \pi^-$)		(2.5	$^{+1.7}_{-1.4}$)	$\times 10^{-4}$		S=4.0
Γ_{115}	$\overline{D}_1(2420)^0 \pi^+ \times$ B($\overline{D}_1^0 \to \overline{D}^0 \pi^+ \pi^-$ (nonresonant))		(2.3	± 1.0)	$\times 10^{-4}$		
Γ_{116}	$\overline{D}_2^*(2462)^0 \pi^+ \times$ B($\overline{D}_2^*(2462)^0 \to D^- \pi^+$)		(3.5	± 0.4)	$\times 10^{-4}$		
Γ_{117}	$\overline{D}_2^*(2462)^0 \pi^+ \times$B($\overline{D}_2^{*0} \to \overline{D}^0 \pi^- \pi^+$)		(2.3	± 1.1)	$\times 10^{-4}$		
Γ_{118}	$\overline{D}_2^*(2462)^0 \pi^+ \times$B($\overline{D}_2^{*0} \to \overline{D}^0 \pi^- \pi^+$ (nonresonant))		< 1.7		$\times 10^{-4}$		CL=90%
Γ_{119}	$\overline{D}_2^*(2462)^0 \pi^+ \times$B($\overline{D}_2^{*0} \to D^*(2010)^- \pi^+$)		(2.2	± 1.1)	$\times 10^{-4}$		
Γ_{120}	$\overline{D}_0^*(2400)^0 \pi^+ \times$ B($\overline{D}_0^*(2400)^0 \to D^- \pi^+$)		(6.4	± 1.4)	$\times 10^{-4}$		
Γ_{121}	$\overline{D}_1(2421)^0 \pi^+ \times$ B($\overline{D}_1(2421)^0 \to D^{*-} \pi^+$)		(6.8	± 1.5)	$\times 10^{-4}$		
Γ_{122}	$\overline{D}_2^*(2462)^0 \pi^+ \times$ B($\overline{D}_2^*(2462)^0 \to D^{*-} \pi^+$)		(1.8	± 0.5)	$\times 10^{-4}$		
Γ_{123}	$\overline{D}_1'(2427)^0 \pi^+ \times$ B($\overline{D}_1'(2427)^0 \to D^{*-} \pi^+$)		(5.0	± 1.2)	$\times 10^{-4}$		
Γ_{124}	$\overline{D}_1(2420)^0 \pi^+ \times$B($\overline{D}_1^0 \to \overline{D}^{*0} \pi^+ \pi^-$)		< 6		$\times 10^{-6}$		CL=90%
Γ_{125}	$\overline{D}_1^*(2420)^0 \rho^+$		< 1.4		$\times 10^{-3}$		CL=90%
Γ_{126}	$\overline{D}_2^*(2460)^0 \pi^+$		< 1.3		$\times 10^{-3}$		CL=90%
Γ_{127}	$\overline{D}_2^*(2460)^0 \pi^+ \times$B($\overline{D}_2^{*0} \to \overline{D}^{*0} \pi^+ \pi^-$)		< 2.2		$\times 10^{-5}$		CL=90%
Γ_{128}	$\overline{D}_2^*(2460)^0 \rho^+$		< 4.7		$\times 10^{-3}$		CL=90%
Γ_{129}	$\overline{D}^0 D_s^+$		(9.0	± 0.9)	$\times 10^{-3}$		

Γ_{130}	$D_{s0}(2317)^+\overline{D}^0\times$ B($D_{s0}(2317)^+ \to D_s^+\pi^0$)	(7.3	$^{+2.2}_{-1.7}$	) $\times 10^{-4}$		
Γ_{131}	$D_{s0}(2317)^+\overline{D}^0\times$ B($D_{s0}(2317)^+ \to D_s^{*+}\gamma$)	< 7.6		$\times 10^{-4}$	CL=90%	
Γ_{132}	$D_{s0}(2317)^+\overline{D}^*(2007)^0\times$ B($D_{s0}(2317)^+ \to D_s^+\pi^0$)	(9	± 7	) $\times 10^{-4}$		
Γ_{133}	$D_{sJ}(2457)^+\overline{D}^0$	(3.1	$^{+1.0}_{-0.9}$	) $\times 10^{-3}$		
Γ_{134}	$D_{sJ}(2457)^+\overline{D}^0\times$ B($D_{sJ}(2457)^+ \to D_s^+\gamma$)	(4.6	$^{+1.3}_{-1.1}$	) $\times 10^{-4}$		
Γ_{135}	$D_{sJ}(2457)^+\overline{D}^0\times$ B($D_{sJ}(2457)^+ \to D_s^+\pi^+\pi^-$)	< 2.2		$\times 10^{-4}$	CL=90%	
Γ_{136}	$D_{sJ}(2457)^+\overline{D}^0\times$ B($D_{sJ}(2457)^+ \to D_s^+\pi^0$)	< 2.7		$\times 10^{-4}$	CL=90%	
Γ_{137}	$D_{sJ}(2457)^+\overline{D}^0\times$ B($D_{sJ}(2457)^+ \to D_s^{*+}\gamma$)	< 9.8		$\times 10^{-4}$	CL=90%	
Γ_{138}	$D_{sJ}(2457)^+\overline{D}^*(2007)^0$	(1.20	± 0.30	) %		
Γ_{139}	$D_{sJ}(2457)^+\overline{D}^*(2007)^0\times$ B($D_{sJ}(2457)^+ \to D_s^+\gamma$)	(1.4	$^{+0.7}_{-0.6}$	) $\times 10^{-3}$		
Γ_{140}	$\overline{D}^0 D_{s1}(2536)^+\times$ B($D_{s1}(2536)^+ \to D^*(2007)^0 K^+ + D^*(2010)^+ K^0$)	(4.0	± 1.0	) $\times 10^{-4}$		
Γ_{141}	$\overline{D}^0 D_{s1}(2536)^+\times$ B($D_{s1}(2536)^+ \to D^*(2007)^0 K^+$)	(2.2	± 0.7	) $\times 10^{-4}$		
Γ_{142}	$\overline{D}^*(2007)^0 D_{s1}(2536)^+\times$ B($D_{s1}(2536)^+ \to D^*(2007)^0 K^+$)	(5.5	± 1.6	) $\times 10^{-4}$		
Γ_{143}	$\overline{D}^0 D_{s1}(2536)^+\times$ B($D_{s1}(2536)^+ \to D^{*+} K^0$)	(2.3	± 1.1	) $\times 10^{-4}$		
Γ_{144}	$\overline{D}^0 D_{sJ}(2700)^+\times$ B($D_{sJ}(2700)^+ \to D^0 K^+$)	(1.13	$^{+0.26}_{-0.40}$	) $\times 10^{-3}$		
Γ_{145}	$\overline{D}^{*0} D_{s1}(2536)^+\times$ B($D_{s1}(2536)^+ \to D^{*+} K^0$)	(3.9	± 2.6	) $\times 10^{-4}$		
Γ_{146}	$\overline{D}^{*0} D_{sJ}(2573)^+\times$ B($D_{sJ}(2573)^+ \to D^0 K^+$)	< 2		$\times 10^{-4}$	CL=90%	
Γ_{147}	$\overline{D}^*(2007)^0 D_{sJ}(2573)^+\times$ B($D_{sJ}(2573)^+ \to D^0 K^+$)	< 5		$\times 10^{-4}$	CL=90%	
Γ_{148}	$\overline{D}^0 D_s^{*+}$	(7.6	± 1.6	) $\times 10^{-3}$		
Γ_{149}	$\overline{D}^*(2007)^0 D_s^+$	(8.2	± 1.7	) $\times 10^{-3}$		
Γ_{150}	$\overline{D}^*(2007)^0 D_s^{*+}$	(1.71	± 0.24	) %		
Γ_{151}	$D_s^{(*)+}\overline{D}^{**0}$	(2.7	± 1.2	) %		
Γ_{152}	$\overline{D}^*(2007)^0 D^*(2010)^+$	(8.1	± 1.7	) $\times 10^{-4}$		
Γ_{153}	$\overline{D}^0 D^*(2010)^+ + \overline{D}^*(2007)^0 D^+$	< 1.30		%	CL=90%	
Γ_{154}	$\overline{D}^0 D^*(2010)^+$	(3.9	± 0.5	) $\times 10^{-4}$		
Γ_{155}	$\overline{D}^0 D^+$	(3.8	± 0.4	) $\times 10^{-4}$		
Γ_{156}	$\overline{D}^0 D^+ K^0$	(1.55	± 0.21	) $\times 10^{-3}$		
Γ_{157}	$D^+\overline{D}^*(2007)^0$	(6.3	± 1.7	) $\times 10^{-4}$		
Γ_{158}	$\overline{D}^*(2007)^0 D^+ K^0$	(2.1	± 0.5	) $\times 10^{-3}$		
Γ_{159}	$\overline{D}^0\overline{D}^*(2010)^+ K^0$	(3.8	± 0.4	) $\times 10^{-3}$		
Γ_{160}	$\overline{D}^*(2007)^0 D^*(2010)^+ K^0$	(9.2	± 1.2	) $\times 10^{-3}$		
Γ_{161}	$\overline{D}^0 D^0 K^+$	(1.45	± 0.33	) $\times 10^{-3}$		S=2.6
Γ_{162}	$\overline{D}^*(2007)^0 D^0 K^+$	(2.26	± 0.23	) $\times 10^{-3}$		
Γ_{163}	$\overline{D}^0 D^*(2007)^0 K^+$	(6.3	± 0.5	) $\times 10^{-3}$		
Γ_{164}	$\overline{D}^*(2007)^0 D^*(2007)^0 K^+$	(1.12	± 0.13	) %		
Γ_{165}	$D^- D^+ K^+$	(2.2	± 0.7	) $\times 10^{-4}$		
Γ_{166}	$D^- D^*(2010)^+ K^+$	(6.3	± 1.1	) $\times 10^{-4}$		
Γ_{167}	$D^*(2010)^- D^+ K^+$	(6.0	± 1.3	) $\times 10^{-4}$		
Γ_{168}	$D^*(2010)^- D^*(2010)^+ K^+$	(1.32	± 0.18	) $\times 10^{-3}$		
Γ_{169}	$(\overline{D}+\overline{D}^*)(D+D^*)K$	(4.05	± 0.30	) %		
Γ_{170}	$D_s^+\pi^0$	(1.6	± 0.5	) $\times 10^{-5}$		
Γ_{171}	$D_s^{*+}\pi^0$	< 2.6		$\times 10^{-4}$	CL=90%	
Γ_{172}	$D_s^+\eta$	< 4		$\times 10^{-4}$	CL=90%	
Γ_{173}	$D_s^{*+}\eta$	< 6		$\times 10^{-4}$	CL=90%	
Γ_{174}	$D_s^+\rho^0$	< 3.0		$\times 10^{-4}$	CL=90%	
Γ_{175}	$D_s^{*+}\rho^0$	< 4		$\times 10^{-4}$	CL=90%	
Γ_{176}	$D_s^+\omega$	< 4		$\times 10^{-4}$	CL=90%	
Γ_{177}	$D_s^{*+}\omega$	< 6		$\times 10^{-4}$	CL=90%	
Γ_{178}	$D_s^+ a_1(1260)^0$	< 1.8		$\times 10^{-3}$	CL=90%	
Γ_{179}	$D_s^{*+} a_1(1260)^0$	< 1.3		$\times 10^{-3}$	CL=90%	
Γ_{180}	$D_s^+\phi$	(1.7	$^{+1.2}_{-0.7}$	) $\times 10^{-6}$		
Γ_{181}	$D_s^{*+}\phi$	< 1.2		$\times 10^{-5}$	CL=90%	
Γ_{182}	$D_s^+\overline{K}^0$	< 8		$\times 10^{-4}$	CL=90%	
Γ_{183}	$D_s^{*+}\overline{K}^0$	< 9		$\times 10^{-4}$	CL=90%	
Γ_{184}	$D_s^+\overline{K}^*(892)^0$	< 4.4		$\times 10^{-6}$	CL=90%	
Γ_{185}	$D_s^+ K^{*0}$	< 3.5		$\times 10^{-6}$	CL=90%	
Γ_{186}	$D_s^{*+}\overline{K}^*(892)^0$	< 3.5		$\times 10^{-4}$	CL=90%	
Γ_{187}	$D_s^-\pi^+ K^+$	(1.80	± 0.22	) $\times 10^{-4}$		
Γ_{188}	$D_s^{*-}\pi^+ K^+$	(1.45	± 0.24	) $\times 10^{-4}$		
Γ_{189}	$D_s^-\pi^+ K^*(892)^+$	< 5		$\times 10^{-3}$	CL=90%	
Γ_{190}	$D_s^{*-}\pi^+ K^*(892)^+$	< 7		$\times 10^{-3}$	CL=90%	
Γ_{191}	$D_s^- K^+ K^+$	(1.1	± 0.4	) $\times 10^{-5}$		
Γ_{192}	$D_s^{*-} K^+ K^+$	< 1.5		$\times 10^{-5}$	CL=90%	

Charmonium modes

Γ_{193}	$\eta_c K^+$	(9.6	± 1.1	) $\times 10^{-4}$		
Γ_{194}	$\eta_c K^+,\ \eta_c \to K_S^0 K^\mp\pi^\pm$	(2.7	± 0.6	) $\times 10^{-5}$		
Γ_{195}	$\eta_c K^*(892)^+$	(1.0	$^{+0.5}_{-0.4}$	) $\times 10^{-3}$		
Γ_{196}	$\eta_c(2S) K^+$	(3.4	± 1.8	) $\times 10^{-4}$		
Γ_{197}	$\eta_c(2S) K^+,\ \eta_c \to p\overline{p}$	< 1.06		$\times 10^{-7}$	CL=95%	
Γ_{198}	$\eta_c(2S) K^+,\ \eta_c \to K_S^0 K^\mp\pi^\pm$	(3.4	$^{+2.3}_{-1.6}$	) $\times 10^{-6}$		
Γ_{199}	$h_c(1P) K^+,\ h_c \to J/\psi\pi^+\pi^-$	< 3.4		$\times 10^{-6}$	CL=90%	
Γ_{200}	$X(3872) K^+$	< 3.2		$\times 10^{-4}$	CL=90%	
Γ_{201}	$X(3872) K^+,\ X \to p\overline{p}$	< 1.7		$\times 10^{-8}$	CL=95%	
Γ_{202}	$X(3872) K^+,\ X \to J/\psi\pi^+\pi^-$	(8.6	± 0.8	) $\times 10^{-6}$		
Γ_{203}	$X(3872) K^+,\ X \to J/\psi\gamma$	(2.1	± 0.4	) $\times 10^{-6}$		S=1.1
Γ_{204}	$X(3872) K^+,\ X \to \psi(2S)\gamma$	(4	± 4	) $\times 10^{-6}$		S=2.5
Γ_{205}	$X(3872) K^+,\ X \to J/\psi(1S)\eta$	< 7.7		$\times 10^{-6}$	CL=90%	
Γ_{206}	$X(3872) K^+,\ X \to D^0\overline{D}^0$	< 6.0		$\times 10^{-5}$	CL=90%	
Γ_{207}	$X(3872) K^+,\ X \to D^+ D^-$	< 4.0		$\times 10^{-5}$	CL=90%	
Γ_{208}	$X(3872) K^+,\ X \to D^0\overline{D}^0\pi^0$	(1.0	± 0.4	) $\times 10^{-4}$		
Γ_{209}	$X(3872) K^+,\ X \to \overline{D}^{*0} D^0$	(8.5	± 2.6	) $\times 10^{-5}$		S=1.4
Γ_{210}	$X(3872) K^*(892)^+,\ X \to J/\psi\gamma$	< 4.8		$\times 10^{-6}$	CL=90%	
Γ_{211}	$X(3872) K^*(892)^+,\ X \to \psi(2S)\gamma$	< 2.8		$\times 10^{-5}$	CL=90%	
Γ_{212}	$X(3872)^+ K^0,\ X^+ \to J/\psi(1S)\pi^+\pi^0$	[f] < 6.1		$\times 10^{-6}$	CL=90%	
Γ_{213}	$X(4430)^+ K^0,\ X^+ \to J/\psi\pi^+$	< 1.5		$\times 10^{-5}$	CL=95%	
Γ_{214}	$X(4430)^+ K^0,\ X^+ \to \psi(2S)\pi^+$	< 4.7		$\times 10^{-5}$	CL=95%	
Γ_{215}	$X(4260)^0 K^+,\ X^0 \to J/\psi\pi^+\pi^-$	< 2.9		$\times 10^{-5}$	CL=95%	
Γ_{216}	$\chi_{c0}(2P) K^+,\ X^0 \to J/\psi\gamma$	< 1.4		$\times 10^{-5}$	CL=90%	
Γ_{217}	$X(3930)^0 K^+,\ X^0 \to J/\psi\gamma$	< 2.5		$\times 10^{-6}$	CL=90%	
Γ_{218}	$J/\psi(1S) K^+$	(1.027	± 0.031	) $\times 10^{-3}$		
Γ_{219}	$J/\psi(1S) K^0\pi^+$					
Γ_{220}	$J/\psi(1S) K^+\pi^+\pi^-$	(8.1	± 1.3	) $\times 10^{-4}$		S=2.5
Γ_{221}	$\chi_{c0}(2P) K^+,\ \chi_{c0} \to p\overline{p}$	< 7.1		$\times 10^{-8}$	CL=95%	
Γ_{222}	$J/\psi(1S) K^*(892)^+$	(1.44	± 0.08	) $\times 10^{-3}$		
Γ_{223}	$J/\psi(1S) K(1270)^+$	(1.8	± 0.5	) $\times 10^{-3}$		
Γ_{224}	$J/\psi(1S) K(1400)^+$	< 5		$\times 10^{-4}$	CL=90%	
Γ_{225}	$J/\psi(1S)\eta K^+$	(1.08	± 0.33	) $\times 10^{-4}$		
Γ_{226}	$J/\psi(1S)\eta' K^+$	< 8.8		$\times 10^{-5}$	CL=90%	
Γ_{227}	$J/\psi(1S)\phi K^+$	(5.2	± 1.7	) $\times 10^{-5}$		S=1.2
Γ_{228}	$X(4140) K^+,\ X \to J/\psi(1S)\phi$	(10	± 5	) $\times 10^{-6}$		
Γ_{229}	$X(4274) K^+,\ X \to J/\psi(1S)\phi$	< 4		$\times 10^{-6}$	CL=90%	
Γ_{230}	$J/\psi(1S)\omega K^+$	(3.20	$^{+0.60}_{-0.32}$	) $\times 10^{-4}$		
Γ_{231}	$X(3872) K^+,\ X \to J/\psi\omega$	(6.0	± 2.2	) $\times 10^{-6}$		
Γ_{232}	$\chi_{c0}(2P) K^+,\ \chi_{c0} \to J/\psi\omega$	(3.0	$^{+0.9}_{-0.7}$	) $\times 10^{-5}$		
Γ_{233}	$J/\psi(1S)\pi^+$	(4.1	± 0.4	) $\times 10^{-5}$		S=2.6
Γ_{234}	$J/\psi(1S)\rho^+$	(5.0	± 0.8	) $\times 10^{-5}$		
Γ_{235}	$J/\psi(1S)\pi^+\pi^0$ nonresonant	< 7.3		$\times 10^{-6}$	CL=90%	
Γ_{236}	$J/\psi(1S) a_1(1260)^+$	< 1.2		$\times 10^{-3}$	CL=90%	
Γ_{237}	$J/\psi p\overline{p}\pi^+$	< 5.0		$\times 10^{-7}$	CL=90%	

Charmonium modes

Γ_{238}	$J/\psi(1S)\,p\overline{\Lambda}$	(	1.18	± 0.31)	$\times 10^{-5}$	
Γ_{239}	$J/\psi(1S)\,\overline{\Sigma}^0 p$	<	1.1		$\times 10^{-5}$	CL=90%
Γ_{240}	$J/\psi(1S)\,D^+$	<	1.2		$\times 10^{-4}$	CL=90%
Γ_{241}	$J/\psi(1S)\,\overline{D}^0\pi^+$	<	2.5		$\times 10^{-5}$	CL=90%
Γ_{242}	$\psi(2S)\,\pi^+$	(	2.44	± 0.30)	$\times 10^{-5}$	
Γ_{243}	$\psi(2S)\,K^+$	(	6.27	± 0.24)	$\times 10^{-4}$	
Γ_{244}	$\psi(2S)\,K^*(892)^+$	(	6.7	± 1.4)	$\times 10^{-4}$	S=1.3
Γ_{245}	$\psi(2S)\,K^0\pi^+$					
Γ_{246}	$\psi(2S)\,K^+\pi^+\pi^-$	(	4.3	± 0.5)	$\times 10^{-4}$	
Γ_{247}	$\psi(3770)\,K^+$	(	4.9	± 1.3)	$\times 10^{-4}$	
Γ_{248}	$\psi(3770)\,K+,\psi \to D^0\overline{D}^0$	(	1.6	± 0.4)	$\times 10^{-4}$	S=1.1
Γ_{249}	$\psi(3770)\,K+,\psi \to D^+D^-$	(	9.4	± 3.5)	$\times 10^{-5}$	
Γ_{250}	$\chi_{c0}\,\pi^+,\ \chi_{c0} \to \pi^+\pi^-$	<	1		$\times 10^{-7}$	CL=90%
Γ_{251}	$\chi_{c0}(1P)\,K^+$	(	1.50	$^{+0.15}_{-0.14}$)	$\times 10^{-4}$	
Γ_{252}	$\chi_{c0}\,K^*(892)^+$	<	2.1		$\times 10^{-4}$	CL=90%
Γ_{253}	$\chi_{c2}\,\pi^+,\ \chi_{c2} \to \pi^+\pi^-$	<	1		$\times 10^{-7}$	CL=90%
Γ_{254}	$\chi_{c2}\,K^+$	(	1.1	± 0.4)	$\times 10^{-5}$	
Γ_{255}	$\chi_{c2}\,K^*(892)^+$	<	1.2		$\times 10^{-4}$	CL=90%
Γ_{256}	$\chi_{c1}(1P)\,\pi^+$	(	2.2	± 0.5)	$\times 10^{-5}$	
Γ_{257}	$\chi_{c1}(1P)\,K^+$	(	4.79	± 0.23)	$\times 10^{-4}$	
Γ_{258}	$\chi_{c1}(1P)\,K^0\pi^+$					
Γ_{259}	$\chi_{c1}(1P)\,K^*(892)^+$	(	3.0	± 0.6)	$\times 10^{-4}$	S=1.1
Γ_{260}	$h_c(1P)\,K^+$	<	3.8		$\times 10^{-5}$	
Γ_{261}	$h_c(1P)\,K^+,\ h_c \to p\overline{p}$	<	6.4		$\times 10^{-8}$	CL=95%

K or K^* modes

Γ_{262}	$K^0\pi^+$	(	2.37	± 0.08)	$\times 10^{-5}$	
Γ_{263}	$K^+\pi^0$	(	1.29	± 0.05)	$\times 10^{-5}$	
Γ_{264}	$\eta' K^+$	(	7.06	± 0.25)	$\times 10^{-5}$	
Γ_{265}	$\eta' K^*(892)^+$	(	4.8	$^{+1.8}_{-1.6}$)	$\times 10^{-6}$	
Γ_{266}	$\eta' K_0^*(1430)^+$	(	5.2	± 2.1)	$\times 10^{-6}$	
Γ_{267}	$\eta' K_2^*(1430)^+$	(	2.8	± 0.5)	$\times 10^{-5}$	
Γ_{268}	ηK^+	(	2.4	± 0.4)	$\times 10^{-6}$	S=1.7
Γ_{269}	$\eta K^*(892)^+$	(	1.93	± 0.16)	$\times 10^{-5}$	
Γ_{270}	$\eta K_0^*(1430)^+$	(	1.8	± 0.4)	$\times 10^{-5}$	
Γ_{271}	$\eta K_2^*(1430)^+$	(	9.1	± 3.0)	$\times 10^{-6}$	
Γ_{272}	$\eta(1295)\,K^+ \times$ B($\eta(1295) \to \eta\pi\pi$)	(	2.9	$^{+0.8}_{-0.7}$)	$\times 10^{-6}$	
Γ_{273}	$\eta(1405)\,K^+ \times$ B($\eta(1405) \to \eta\pi\pi$)	<	1.3		$\times 10^{-6}$	CL=90%
Γ_{274}	$\eta(1405)\,K^+ \times$ B($\eta(1405) \to K^*K$)	<	1.2		$\times 10^{-6}$	CL=90%
Γ_{275}	$\eta(1475)\,K^+ \times$ B($\eta(1475) \to K^*K$)	(	1.38	$^{+0.21}_{-0.18}$)	$\times 10^{-5}$	
Γ_{276}	$f_1(1285)\,K^+$	<	2.0		$\times 10^{-6}$	CL=90%
Γ_{277}	$f_1(1420)\,K^+ \times$ B($f_1(1420) \to \eta\pi\pi$)	<	2.9		$\times 10^{-6}$	CL=90%
Γ_{278}	$f_1(1420)\,K^+ \times$ B($f_1(1420) \to K^*K$)	<	4.1		$\times 10^{-6}$	CL=90%
Γ_{279}	$\phi(1680)\,K^+ \times$ B($\phi(1680) \to K^*K$)	<	3.4		$\times 10^{-6}$	CL=90%
Γ_{280}	$f_0(1500)\,K^+$	(	3.7	± 2.2)	$\times 10^{-6}$	
Γ_{281}	ωK^+	(	6.7	± 0.8)	$\times 10^{-6}$	S=1.8
Γ_{282}	$\omega K^*(892)^+$	<	7.4		$\times 10^{-6}$	CL=90%
Γ_{283}	$\omega(K\pi)_0^{*+}$	(	2.8	± 0.4)	$\times 10^{-5}$	
Γ_{284}	$\omega K_0^*(1430)^+$	(	2.4	± 0.5)	$\times 10^{-5}$	
Γ_{285}	$\omega K_2^*(1430)^+$	(	2.1	± 0.4)	$\times 10^{-5}$	
Γ_{286}	$a_0(980)^+ K^0 \times$B($a_0(980)^+ \to \eta\pi^+$)	<	3.9		$\times 10^{-6}$	CL=90%
Γ_{287}	$a_0(980)^0 K^+ \times$B($a_0(980)^0 \to \eta\pi^0$)	<	2.5		$\times 10^{-6}$	CL=90%
Γ_{288}	$K^*(892)^0\pi^+$	(	1.01	± 0.09)	$\times 10^{-5}$	
Γ_{289}	$K^*(892)^+\pi^0$	(	8.2	± 1.9)	$\times 10^{-6}$	
Γ_{290}	$K^+\pi^-\pi^+$	(	5.10	± 0.29)	$\times 10^{-5}$	
Γ_{291}	$K^+\pi^-\pi^+$ nonresonant	(	1.63	$^{+0.21}_{-0.15}$)	$\times 10^{-5}$	
Γ_{292}	$\omega(782)\,K^+$	(	6	± 9)	$\times 10^{-6}$	
Γ_{293}	$K^+ f_0(980) \times$ B($f_0(980) \to \pi^+\pi^-$)	(	9.4	$^{+1.0}_{-1.2}$)	$\times 10^{-6}$	
Γ_{294}	$f_2(1270)^0\,K^+$	(	1.07	± 0.27)	$\times 10^{-6}$	
Γ_{295}	$f_0(1370)^0\,K^+ \times$ B($f_0(1370)^0 \to \pi^+\pi^-$)	<	1.07		$\times 10^{-5}$	CL=90%
Γ_{296}	$\rho^0(1450)\,K^+ \times$ B($\rho^0(1450) \to \pi^+\pi^-$)	<	1.17		$\times 10^{-5}$	CL=90%
Γ_{297}	$f_2'(1525)\,K^+ \times$ B($f_2'(1525) \to \pi^+\pi^-$)	<	3.4		$\times 10^{-6}$	CL=90%
Γ_{298}	$K^+\rho^0$	(	3.7	± 0.5)	$\times 10^{-6}$	
Γ_{299}	$K_0^*(1430)^0\pi^+$	(	4.5	$^{+0.9}_{-0.7}$)	$\times 10^{-5}$	S=1.5
Γ_{300}	$K_2^*(1430)^0\pi^+$	(	5.6	$^{+2.2}_{-1.5}$)	$\times 10^{-6}$	
Γ_{301}	$K^*(1410)^0\pi^+$	<	4.5		$\times 10^{-5}$	CL=90%
Γ_{302}	$K^*(1680)^0\pi^+$	<	1.2		$\times 10^{-5}$	CL=90%
Γ_{303}	$K^+\pi^0\pi^0$	(	1.62	± 0.19)	$\times 10^{-5}$	
Γ_{304}	$f_0(980)\,K^+ \times$ B($f_0 \to \pi^0\pi^0$)	(	2.8	± 0.8)	$\times 10^{-6}$	
Γ_{305}	$K^-\pi^+\pi^+$	<	9.5		$\times 10^{-7}$	CL=90%
Γ_{306}	$K^-\pi^+\pi^+$ nonresonant	<	5.6		$\times 10^{-5}$	CL=90%
Γ_{307}	$K_1(1270)^0\pi^+$	<	4.0		$\times 10^{-5}$	CL=90%
Γ_{308}	$K_1(1400)^0\pi^+$	<	3.9		$\times 10^{-5}$	CL=90%
Γ_{309}	$K^0\pi^+\pi^0$	<	6.6		$\times 10^{-5}$	CL=90%
Γ_{310}	$K^0\rho^+$	(	8.0	± 1.5)	$\times 10^{-6}$	
Γ_{311}	$K^*(892)^+\pi^+\pi^-$	(	7.5	± 1.0)	$\times 10^{-5}$	
Γ_{312}	$K^*(892)^+\rho^0$	(	4.6	± 1.1)	$\times 10^{-6}$	
Γ_{313}	$K^*(892)^+ f_0(980)$	(	4.2	± 0.7)	$\times 10^{-6}$	
Γ_{314}	$a_1^+ K^0$	(	3.5	± 0.7)	$\times 10^{-5}$	
Γ_{315}	$b_1^+ K^0 \times$ B($b_1^+ \to \omega\pi^+$)	(	9.6	± 1.9)	$\times 10^{-6}$	
Γ_{316}	$K^*(892)^0\rho^+$	(	9.2	± 1.5)	$\times 10^{-6}$	
Γ_{317}	$K_1(1400)^+\rho^0$	<	7.8		$\times 10^{-4}$	CL=90%
Γ_{318}	$K_2^*(1430)^+\rho^0$	<	1.5		$\times 10^{-3}$	CL=90%
Γ_{319}	$b_1^0 K^+ \times$ B($b_1^0 \to \omega\pi^0$)	(	9.1	± 2.0)	$\times 10^{-6}$	
Γ_{320}	$b_1^+ K^{*0} \times$ B($b_1^+ \to \omega\pi^+$)	<	5.9		$\times 10^{-6}$	CL=90%
Γ_{321}	$b_1^0 K^{*+} \times$ B($b_1^0 \to \omega\pi^0$)	<	6.7		$\times 10^{-6}$	CL=90%
Γ_{322}	$K^+\overline{K}^0$	(	1.31	± 0.17)	$\times 10^{-6}$	S=1.2
Γ_{323}	$\overline{K}^0 K^+\pi^0$	<	2.4		$\times 10^{-5}$	CL=90%
Γ_{324}	$K^+ K_S^0 K_S^0$	(	1.08	± 0.06)	$\times 10^{-5}$	
Γ_{325}	$f_0(980)\,K^+,\ f_0 \to K_S^0 K_S^0$	(	1.47	± 0.33)	$\times 10^{-5}$	
Γ_{326}	$f_0(1710)\,K^+,\ f_0 \to K_S^0 K_S^0$	(	4.8	$^{+4.0}_{-2.6}$)	$\times 10^{-7}$	
Γ_{327}	$K^+ K_S^0 K_S^0$ nonresonant	(	2.0	± 0.4)	$\times 10^{-5}$	
Γ_{328}	$K_S^0 K_S^0\pi^+$	<	5.1		$\times 10^{-7}$	CL=90%
Γ_{329}	$K^+K^-\pi^+$	(	5.0	± 0.7)	$\times 10^{-6}$	
Γ_{330}	$K^+K^-\pi^+$ nonresonant	<	7.5		$\times 10^{-5}$	CL=90%
Γ_{331}	$K^+\overline{K}^*(892)^0$	<	1.1		$\times 10^{-6}$	CL=90%
Γ_{332}	$K^+\overline{K}_0^*(1430)^0$	<	2.2		$\times 10^{-6}$	CL=90%
Γ_{333}	$K^+K^+\pi^-$	<	1.6		$\times 10^{-7}$	CL=90%
Γ_{334}	$K^+K^+\pi^-$ nonresonant	<	8.79		$\times 10^{-5}$	CL=90%
Γ_{335}	$f_2'(1525)\,K^+$	(	1.8	± 0.5)	$\times 10^{-6}$	S=1.1
Γ_{336}	$K^+ f_J(2220)$					
Γ_{337}	$K^{*+}\pi^+K^-$	<	1.18		$\times 10^{-5}$	CL=90%
Γ_{338}	$K^*(892)^+K^*(892)^0$	(	1.2	± 0.5)	$\times 10^{-6}$	
Γ_{339}	$K^{*+}K^+\pi^-$	<	6.1		$\times 10^{-6}$	CL=90%
Γ_{340}	$K^+K^-K^+$	(	3.40	± 0.14)	$\times 10^{-5}$	S=1.4
Γ_{341}	$K^+\phi$	(	8.8	$^{+0.7}_{-0.6}$)	$\times 10^{-6}$	S=1.1
Γ_{342}	$f_0(980)\,K^+ \times$ B($f_0(980) \to K^+K^-$)	(	9.4	± 3.2)	$\times 10^{-6}$	
Γ_{343}	$a_2(1320)\,K^+ \times$ B($a_2(1320) \to K^+K^-$)	<	1.1		$\times 10^{-6}$	CL=90%
Γ_{344}	$X_0(1550)\,K^+ \times$ B($X_0(1550) \to K^+K^-$)	(	4.3	± 0.7)	$\times 10^{-6}$	
Γ_{345}	$\phi(1680)\,K^+ \times$ B($\phi(1680) \to K^+K^-$)	<	8		$\times 10^{-7}$	CL=90%
Γ_{346}	$f_0(1710)\,K^+ \times$ B($f_0(1710) \to K^+K^-$)	(	1.1	± 0.6)	$\times 10^{-6}$	
Γ_{347}	$K^+K^-K^+$ nonresonant	(	2.38	$^{+0.28}_{-0.50}$)	$\times 10^{-5}$	
Γ_{348}	$K^*(892)^+K^+K^-$	(	3.6	± 0.5)	$\times 10^{-5}$	
Γ_{349}	$K^*(892)^+\phi$	(	10.0	± 2.0)	$\times 10^{-6}$	S=1.7
Γ_{350}	$\phi(K\pi)_0^{*+}$	(	8.3	± 1.6)	$\times 10^{-6}$	
Γ_{351}	$\phi K_1(1270)^+$	(	6.1	± 1.9)	$\times 10^{-6}$	
Γ_{352}	$\phi K_1(1400)^+$	<	3.2		$\times 10^{-6}$	CL=90%
Γ_{353}	$\phi K^*(1410)^+$	<	4.3		$\times 10^{-6}$	CL=90%
Γ_{354}	$\phi K_0^*(1430)^+$	(	7.0	± 1.6)	$\times 10^{-6}$	
Γ_{355}	$\phi K_2^*(1430)^+$	(	8.4	± 2.1)	$\times 10^{-6}$	
Γ_{356}	$\phi K_2^*(1770)^+$	<	1.50		$\times 10^{-5}$	CL=90%
Γ_{357}	$\phi K_2^*(1820)^+$	<	1.63		$\times 10^{-5}$	CL=90%
Γ_{358}	$a_1^+ K^{*0}$	<	3.6		$\times 10^{-6}$	CL=90%
Γ_{359}	$K^+\phi\phi$	(	5.0	± 1.2)	$\times 10^{-6}$	S=2.3

Meson Particle Listings

$B^{\pm}$

Γ_{360}	$\eta'\eta' K^+$	$<$	2.5		$\times 10^{-5}$	CL=90%	
Γ_{361}	$\omega\phi K^+$	$<$	1.9		$\times 10^{-6}$	CL=90%	
Γ_{362}	$X(1812)K^+ \times$ B($X \to \omega\phi$)	$<$	3.2		$\times 10^{-7}$	CL=90%	
Γ_{363}	$K^*(892)^+\gamma$	(	4.21	± 0.18)	$\times 10^{-5}$		
Γ_{364}	$K_1(1270)^+\gamma$	(	4.3	± 1.3)	$\times 10^{-5}$		
Γ_{365}	$\eta K^+\gamma$	(	7.9	± 0.9)	$\times 10^{-6}$		
Γ_{366}	$\eta' K^+\gamma$	(	2.9	$^{+1.0}_{-0.9}$)	$\times 10^{-6}$		
Γ_{367}	$\phi K^+\gamma$	(	2.7	± 0.4)	$\times 10^{-6}$	S=1.2	
Γ_{368}	$K^+\pi^-\pi^+\gamma$	(	2.76	± 0.22)	$\times 10^{-5}$	S=1.2	
Γ_{369}	$K^*(892)^0\pi^+\gamma$	(	2.0	$^{+0.7}_{-0.6}$)	$\times 10^{-5}$		
Γ_{370}	$K^+\rho^0\gamma$	$<$	2.0		$\times 10^{-5}$	CL=90%	
Γ_{371}	$K^+\pi^-\pi^+\gamma$ nonresonant	$<$	9.2		$\times 10^{-6}$	CL=90%	
Γ_{372}	$K^0\pi^+\pi^0\gamma$	(	4.6	± 0.5)	$\times 10^{-5}$		
Γ_{373}	$K_1(1400)^+\gamma$	$<$	1.5		$\times 10^{-5}$	CL=90%	
Γ_{374}	$K_2^*(1430)^+\gamma$	(	1.4	± 0.4)	$\times 10^{-5}$		
Γ_{375}	$K^*(1680)^+\gamma$	$<$	1.9		$\times 10^{-3}$	CL=90%	
Γ_{376}	$K_3^*(1780)^+\gamma$	$<$	3.9		$\times 10^{-5}$	CL=90%	
Γ_{377}	$K_4^*(2045)^+\gamma$	$<$	9.9		$\times 10^{-3}$	CL=90%	

Light unflavored meson modes

Γ_{378}	$\rho^+\gamma$	(	9.8	± 2.5)	$\times 10^{-7}$		
Γ_{379}	$\pi^+\pi^0$	(	5.5	± 0.4)	$\times 10^{-6}$	S=1.2	
Γ_{380}	$\pi^+\pi^+\pi^-$	(	1.52	± 0.14)	$\times 10^{-5}$		
Γ_{381}	$\rho^0\pi^+$	(	8.3	± 1.2)	$\times 10^{-6}$		
Γ_{382}	$\pi^+ f_0(980)$, $f_0 \to \pi^+\pi^-$	$<$	1.5		$\times 10^{-6}$	CL=90%	
Γ_{383}	$\pi^+ f_2(1270)$	(	1.6	$^{+0.7}_{-0.4}$)	$\times 10^{-6}$		
Γ_{384}	$\rho(1450)^0 pi+,\rho^0 \to \pi^+\pi^-$	(	1.4	$^{+0.6}_{-0.9}$)	$\times 10^{-6}$		
Γ_{385}	$f_0(1370)\pi^+$, $f_0 \to \pi^+\pi^-$	$<$	4.0		$\times 10^{-6}$	CL=90%	
Γ_{386}	$f_0(500)\pi^+$, $f_0 \to \pi^+\pi^-$	$<$	4.1		$\times 10^{-6}$	CL=90%	
Γ_{387}	$\pi^+\pi^-\pi^+$ nonresonant	(	5.3	$^{+1.5}_{-1.1}$)	$\times 10^{-6}$		
Γ_{388}	$\pi^+\pi^0\pi^0$	$<$	8.9		$\times 10^{-4}$	CL=90%	
Γ_{389}	$\rho^+\pi^0$	(	1.09	± 0.14)	$\times 10^{-5}$		
Γ_{390}	$\pi^+\pi^-\pi^+\pi^0$	$<$	4.0		$\times 10^{-3}$	CL=90%	
Γ_{391}	$\rho^+\rho^0$	(	2.40	± 0.19)	$\times 10^{-5}$		
Γ_{392}	$\rho^+ f_0(980)$, $f_0 \to \pi^+\pi^-$	$<$	2.0		$\times 10^{-6}$	CL=90%	
Γ_{393}	$a_1(1260)^+\pi^0$	(	2.6	± 0.7)	$\times 10^{-5}$		
Γ_{394}	$a_1(1260)^0\pi^+$	(	2.0	± 0.6)	$\times 10^{-5}$		
Γ_{395}	$\omega\pi^+$	(	6.9	± 0.5)	$\times 10^{-6}$		
Γ_{396}	$\omega\rho^+$	(	1.59	± 0.21)	$\times 10^{-5}$		
Γ_{397}	$\eta\pi^+$	(	4.02	± 0.27)	$\times 10^{-6}$		
Γ_{398}	$\eta\rho^+$	(	7.0	± 2.9)	$\times 10^{-6}$	S=2.8	
Γ_{399}	$\eta'\pi^+$	(	2.7	± 0.9)	$\times 10^{-6}$	S=1.9	
Γ_{400}	$\eta'\rho^+$	(	9.7	± 2.2)	$\times 10^{-6}$		
Γ_{401}	$\phi\pi^+$	$<$	1.5		$\times 10^{-7}$	CL=90%	
Γ_{402}	$\phi\rho^+$	$<$	3.0		$\times 10^{-6}$	CL=90%	
Γ_{403}	$a_0(980)^0\pi^+$, $a_0^0 \to \eta\pi^0$	$<$	5.8		$\times 10^{-6}$	CL=90%	
Γ_{404}	$a_0(980)^+\pi^0$, $a_0^+ \to \eta\pi^+$	$<$	1.4		$\times 10^{-6}$	CL=90%	
Γ_{405}	$\pi^+\pi^+\pi^+\pi^-\pi^-$	$<$	8.6		$\times 10^{-4}$	CL=90%	
Γ_{406}	$\rho^0 a_1(1260)^+$	$<$	6.2		$\times 10^{-4}$	CL=90%	
Γ_{407}	$\rho^0 a_2(1320)^+$	$<$	7.2		$\times 10^{-4}$	CL=90%	
Γ_{408}	$b_1^0\pi^+$, $b_1^0 \to \omega\pi^0$	(	6.7	± 2.0)	$\times 10^{-6}$		
Γ_{409}	$b_1^+\pi^0$, $b_1^+ \to \omega\pi^+$	$<$	3.3		$\times 10^{-6}$	CL=90%	
Γ_{410}	$\pi^+\pi^+\pi^+\pi^-\pi^-\pi^0$	$<$	6.3		$\times 10^{-3}$	CL=90%	
Γ_{411}	$b_1^+\rho^0$, $b_1^+ \to \omega\pi^+$	$<$	5.2		$\times 10^{-6}$	CL=90%	
Γ_{412}	$a_1(1260)^+ a_1(1260)^0$	$<$	1.3		%	CL=90%	
Γ_{413}	$b_1^0\rho^+$, $b_1^0 \to \omega\pi^0$	$<$	3.3		$\times 10^{-6}$	CL=90%	

Charged particle ($h^{\pm}$) modes

$h^{\pm} = K^{\pm}$ or $\pi^{\pm}$

Γ_{414}	$h^+\pi^0$	(	1.6	$^{+0.7}_{-0.6}$)	$\times 10^{-5}$		
Γ_{415}	ωh^+	(	1.38	$^{+0.27}_{-0.24}$)	$\times 10^{-5}$		
Γ_{416}	$h^+ X^0$ (Familon)	$<$	4.9		$\times 10^{-5}$	CL=90%	

Baryon modes

Γ_{417}	$p\overline{p}\pi^+$	(	1.62	± 0.20)	$\times 10^{-6}$		
Γ_{418}	$p\overline{p}\pi^+$ nonresonant	$<$	5.3		$\times 10^{-5}$	CL=90%	
Γ_{419}	$p\overline{p}\pi^+\pi^+\pi^-$						
Γ_{420}	$p\overline{p}K^+$	(	5.9	± 0.5)	$\times 10^{-6}$	S=1.5	
Γ_{421}	$\Theta(1710)^{++}\overline{p}$, $\Theta^{++} \to pK^+$	[g] $<$	9.1		$\times 10^{-8}$	CL=90%	
Γ_{422}	$f_J(2220)K^+$, $f_J \to p\overline{p}$	[g] $<$	4.1		$\times 10^{-7}$	CL=90%	
Γ_{423}	$p\overline{\Lambda}(1520)$	(	3.9	± 1.0)	$\times 10^{-7}$		
Γ_{424}	$p\overline{p}K^+$ nonresonant	$<$	8.9		$\times 10^{-5}$	CL=90%	
Γ_{425}	$p\overline{p}K^*(892)^+$	(	3.6	$^{+0.8}_{-0.7}$)	$\times 10^{-6}$		
Γ_{426}	$f_J(2220)K^{*+}$, $f_J \to p\overline{p}$	$<$	7.7		$\times 10^{-7}$	CL=90%	
Γ_{427}	$p\overline{\Lambda}$	$<$	3.2		$\times 10^{-7}$	CL=90%	
Γ_{428}	$p\overline{\Lambda}\gamma$	(	2.4	$^{+0.5}_{-0.4}$)	$\times 10^{-6}$		
Γ_{429}	$p\overline{\Lambda}\pi^0$	(	3.0	$^{+0.7}_{-0.6}$)	$\times 10^{-6}$		
Γ_{430}	$p\overline{\Sigma}(1385)^0$	$<$	4.7		$\times 10^{-7}$	CL=90%	
Γ_{431}	$\Delta^+\overline{\Lambda}$	$<$	8.2		$\times 10^{-7}$	CL=90%	
Γ_{432}	$p\overline{\Sigma}\gamma$	$<$	4.6		$\times 10^{-6}$	CL=90%	
Γ_{433}	$p\overline{\Lambda}\pi^+\pi^-$	(	5.9	± 1.1)	$\times 10^{-6}$		
Γ_{434}	$p\overline{\Lambda}\rho^0$	(	4.8	± 0.9)	$\times 10^{-6}$		
Γ_{435}	$p\overline{\Lambda}f_2(1270)$	(	2.0	± 0.8)	$\times 10^{-6}$		
Γ_{436}	$\Lambda\overline{\Lambda}\pi^+$	$<$	9.4		$\times 10^{-7}$	CL=90%	
Γ_{437}	$\Lambda\overline{\Lambda}K^+$	(	3.4	± 0.6)	$\times 10^{-6}$		
Γ_{438}	$\Lambda\overline{\Lambda}K^{*+}$	(	2.2	$^{+1.2}_{-0.9}$)	$\times 10^{-6}$		
Γ_{439}	$\overline{\Delta}^0 p$	$<$	1.38		$\times 10^{-6}$	CL=90%	
Γ_{440}	$\Delta^{++}\overline{p}$	$<$	1.4		$\times 10^{-7}$	CL=90%	
Γ_{441}	$D^+ p\overline{p}$	$<$	1.5		$\times 10^{-5}$	CL=90%	
Γ_{442}	$D^*(2010)^+ p\overline{p}$	$<$	1.5		$\times 10^{-5}$	CL=90%	
Γ_{443}	$\overline{D}^0 p\overline{p}\pi^+$	(	3.72	± 0.27)	$\times 10^{-4}$		
Γ_{444}	$\overline{D}^{*0} p\overline{p}\pi^+$	(	3.73	± 0.32)	$\times 10^{-4}$		
Γ_{445}	$D^- p\overline{p}\pi^+\pi^-$	(	1.66	± 0.30)	$\times 10^{-4}$		
Γ_{446}	$D^{*-} p\overline{p}\pi^+\pi^-$	(	1.86	± 0.25)	$\times 10^{-4}$		
Γ_{447}	$p\overline{\Lambda}^0\overline{D}^0$	(	1.43	± 0.32)	$\times 10^{-5}$		
Γ_{448}	$p\overline{\Lambda}^0\overline{D}^*(2007)^0$	$<$	5		$\times 10^{-5}$	CL=90%	
Γ_{449}	$\overline{\Lambda}_c^- p\pi^+$	(	2.8	± 0.8)	$\times 10^{-4}$		
Γ_{450}	$\overline{\Lambda}_c^- \Delta(1232)^{++}$	$<$	1.9		$\times 10^{-5}$	CL=90%	
Γ_{451}	$\overline{\Lambda}_c^- \Delta_X(1600)^{++}$	(	5.9	± 1.9)	$\times 10^{-5}$		
Γ_{452}	$\overline{\Lambda}_c^- \Delta_X(2420)^{++}$	(	4.7	± 1.6)	$\times 10^{-5}$		
Γ_{453}	$(\overline{\Lambda}_c^- p)_s\pi^+$	[h] (	3.9	± 1.3)	$\times 10^{-5}$		
Γ_{454}	$\overline{\Sigma}_c(2520)^0 p$	$<$	3		$\times 10^{-6}$	CL=90%	
Γ_{455}	$\overline{\Sigma}_c(2800)^0 p$	(	3.3	± 1.3)	$\times 10^{-5}$		
Γ_{456}	$\overline{\Lambda}_c^- p\pi^+\pi^0$	(	1.8	± 0.6)	$\times 10^{-3}$		
Γ_{457}	$\overline{\Lambda}_c^- p\pi^+\pi^+\pi^-$	(	2.2	± 0.7)	$\times 10^{-3}$		
Γ_{458}	$\overline{\Lambda}_c^- p\pi^+\pi^+\pi^-\pi^0$	$<$	1.34		%	CL=90%	
Γ_{459}	$\Lambda_c^+\Lambda_c^- K^+$	(	8.7	± 3.5)	$\times 10^{-4}$		
Γ_{460}	$\overline{\Sigma}_c(2455)^0 p$	(	3.7	± 1.3)	$\times 10^{-5}$		
Γ_{461}	$\overline{\Sigma}_c(2455)^0 p\pi^0$	(	4.4	± 1.8)	$\times 10^{-4}$		
Γ_{462}	$\overline{\Sigma}_c(2455)^0 p\pi^-\pi^+$	(	4.4	± 1.7)	$\times 10^{-4}$		
Γ_{463}	$\overline{\Sigma}_c(2455)^{--} p\pi^+\pi^+$	(	3.0	± 0.8)	$\times 10^{-4}$		
Γ_{464}	$\overline{\Lambda}_c(2593)^-/\overline{\Lambda}_c(2625)^- p\pi^+$	$<$	1.9		$\times 10^{-4}$	CL=90%	
Γ_{465}	$\overline{\Xi}^0\Lambda_c^+$, $\overline{\Xi}_c^0 \to \overline{\Xi}^+\pi^-$	(	3.0	± 1.1)	$\times 10^{-5}$		
Γ_{466}	$\overline{\Xi}_c^0\Lambda_c^+$, $\overline{\Xi}_c^0 \to \Lambda K^+\pi^-$	(	2.6	± 1.1)	$\times 10^{-5}$	S=1.1	

Lepton Family number (LF) or Lepton number (L) or Baryon number (B) violating modes, or/and $\Delta B = 1$ weak neutral current ($B1$) modes

Γ_{467}	$\pi^+\ell^+\ell^-$	$B1$	$<$	4.9		$\times 10^{-8}$	CL=90%	
Γ_{468}	$\pi^+ e^+ e^-$	$B1$	$<$	8.0		$\times 10^{-8}$	CL=90%	
Γ_{469}	$\pi^+\mu^+\mu^-$	$B1$	$<$	5.5		$\times 10^{-8}$	CL=90%	
Γ_{470}	$\pi^+\nu\overline{\nu}$	$B1$	$<$	9.8		$\times 10^{-5}$	CL=90%	
Γ_{471}	$K^+\ell^+\ell^-$	$B1$	[a] (	4.51	± 0.23)	$\times 10^{-7}$	S=1.1	
Γ_{472}	$K^+ e^+ e^-$	$B1$	(	5.5	± 0.7)	$\times 10^{-7}$		
Γ_{473}	$K^+\mu^+\mu^-$	$B1$	(	4.49	± 0.23)	$\times 10^{-7}$	S=1.1	
Γ_{474}	$\psi(4040)K^+$		$<$	1.3		$\times 10^{-4}$	CL=90%	
Γ_{475}	$\psi(4160)K^+$		(	5.1	± 2.7)	$\times 10^{-4}$		
Γ_{476}	$K^+\overline{\nu}\nu$	$B1$	$<$	1.6		$\times 10^{-5}$	CL=90%	
Γ_{477}	$\rho^+\nu\overline{\nu}$	$B1$	$<$	2.13		$\times 10^{-4}$	CL=90%	
Γ_{478}	$K^*(892)^+\ell^+\ell^-$	$B1$	[a] (	1.29	± 0.21)	$\times 10^{-6}$		
Γ_{479}	$K^*(892)^+ e^+ e^-$	$B1$	(	1.55	$^{+0.40}_{-0.31}$)	$\times 10^{-6}$		
Γ_{480}	$K^*(892)^+\mu^+\mu^-$	$B1$	(	1.12	± 0.15)	$\times 10^{-6}$		
Γ_{481}	$K^*(892)^+\nu\overline{\nu}$	$B1$	$<$	4.0		$\times 10^{-5}$	CL=90%	
Γ_{482}	$\pi^+ e^+\mu^-$	LF	$<$	6.4		$\times 10^{-3}$	CL=90%	
Γ_{483}	$\pi^+ e^-\mu^+$	LF	$<$	6.4		$\times 10^{-3}$	CL=90%	
Γ_{484}	$\pi^+ e^\pm\mu^\mp$	LF	$<$	1.7		$\times 10^{-7}$	CL=90%	
Γ_{485}	$\pi^+ e^+\tau^-$	LF	$<$	7.4		$\times 10^{-5}$	CL=90%	
Γ_{486}	$\pi^+ e^-\tau^+$	LF	$<$	2.0		$\times 10^{-5}$	CL=90%	
Γ_{487}	$\pi^+ e^\pm\tau^\mp$	LF	$<$	7.5		$\times 10^{-5}$	CL=90%	
Γ_{488}	$\pi^+\mu^+\tau^-$	LF	$<$	6.2		$\times 10^{-5}$	CL=90%	
Γ_{489}	$\pi^+\mu^-\tau^+$	LF	$<$	4.5		$\times 10^{-5}$	CL=90%	
Γ_{490}	$\pi^+\mu^\pm\tau^\mp$	LF	$<$	7.2		$\times 10^{-5}$	CL=90%	
Γ_{491}	$K^+ e^+\mu^-$	LF	$<$	9.1		$\times 10^{-8}$	CL=90%	

Γ_{492}	$K^+ e^- \mu^+$	LF	<	1.3	$\times 10^{-7}$	CL=90%
Γ_{493}	$K^+ e^\pm \mu^\mp$	LF	<	9.1	$\times 10^{-8}$	CL=90%
Γ_{494}	$K^+ e^+ \tau^-$	LF	<	4.3	$\times 10^{-5}$	CL=90%
Γ_{495}	$K^+ e^- \tau^+$	LF	<	1.5	$\times 10^{-5}$	CL=90%
Γ_{496}	$K^+ e^\pm \tau^\mp$	LF	<	3.0	$\times 10^{-5}$	CL=90%
Γ_{497}	$K^+ \mu^+ \tau^-$	LF	<	4.5	$\times 10^{-5}$	CL=90%
Γ_{498}	$K^+ \mu^- \tau^+$	LF	<	2.8	$\times 10^{-5}$	CL=90%
Γ_{499}	$K^+ \mu^\pm \tau^\mp$	LF	<	4.8	$\times 10^{-5}$	CL=90%
Γ_{500}	$K^*(892)^+ e^+ \mu^-$	LF	<	1.3	$\times 10^{-6}$	CL=90%
Γ_{501}	$K^*(892)^+ e^- \mu^+$	LF	<	9.9	$\times 10^{-7}$	CL=90%
Γ_{502}	$K^*(892)^+ e^\pm \mu^\mp$	LF	<	1.4	$\times 10^{-6}$	CL=90%
Γ_{503}	$\pi^- e^+ e^+$	L	<	2.3	$\times 10^{-8}$	CL=90%
Γ_{504}	$\pi^- \mu^+ \mu^+$	L	<	1.3	$\times 10^{-8}$	CL=95%
Γ_{505}	$\pi^- e^+ \mu^+$	L	<	1.5	$\times 10^{-7}$	CL=90%
Γ_{506}	$\rho^- e^+ e^+$	L	<	1.7	$\times 10^{-7}$	CL=90%
Γ_{507}	$\rho^- \mu^+ \mu^+$	L	<	4.2	$\times 10^{-7}$	CL=90%
Γ_{508}	$\rho^- e^+ \mu^+$	L	<	4.7	$\times 10^{-7}$	CL=90%
Γ_{509}	$K^- e^+ e^+$	L	<	3.0	$\times 10^{-8}$	CL=90%
Γ_{510}	$K^- \mu^+ \mu^+$	L	<	4.1	$\times 10^{-8}$	CL=90%
Γ_{511}	$K^- e^+ \mu^+$	L	<	1.6	$\times 10^{-7}$	CL=90%
Γ_{512}	$K^*(892)^- e^+ e^+$	L	<	4.0	$\times 10^{-7}$	CL=90%
Γ_{513}	$K^*(892)^- \mu^+ \mu^+$	L	<	5.9	$\times 10^{-7}$	CL=90%
Γ_{514}	$K^*(892)^- e^+ \mu^+$	L	<	3.0	$\times 10^{-7}$	CL=90%
Γ_{515}	$D^- e^+ e^+$	L	<	2.6	$\times 10^{-6}$	CL=90%
Γ_{516}	$D^- e^+ \mu^+$	L	<	1.8	$\times 10^{-6}$	CL=90%
Γ_{517}	$D^- \mu^+ \mu^+$	L	<	6.9	$\times 10^{-7}$	CL=95%
Γ_{518}	$D^{*-} \mu^+ \mu^+$	L	<	2.4	$\times 10^{-6}$	CL=95%
Γ_{519}	$D_s^- \mu^+ \mu^+$	L	<	5.8	$\times 10^{-7}$	CL=95%
Γ_{520}	$\overline{D}{}^0 \pi^- \mu^+ \mu^+$	L	<	1.5	$\times 10^{-6}$	CL=95%
Γ_{521}	$\Lambda^0 \mu^+$	L,B	<	6	$\times 10^{-8}$	CL=90%
Γ_{522}	$\Lambda^0 e^+$	L,B	<	3.2	$\times 10^{-8}$	CL=90%
Γ_{523}	$\overline{\Lambda}{}^0 \mu^+$	L,B	<	6	$\times 10^{-8}$	CL=90%
Γ_{524}	$\overline{\Lambda}{}^0 e^+$	L,B	<	8	$\times 10^{-8}$	CL=90%

[a] An ℓ indicates an e or a μ mode, not a sum over these modes.

[b] An $CP(\pm 1)$ indicates the $CP=+1$ and $CP=-1$ eigenstates of the D^0-$\overline{D}{}^0$ system.

[c] D denotes D^0 or $\overline{D}{}^0$.

[d] D^0_{CP+} decays into $D^0\pi^0$ with the D^0 reconstructed in CP-even eigenstates K^+K^- and $\pi^+\pi^-$.

[e] $\overline{D}{}^{**}$ represents an excited state with mass $2.2 < M < 2.8$ GeV/c^2.

[f] $X(3872)^+$ is a hypothetical charged partner of the $X(3872)$.

[g] $\Theta(1710)^{++}$ is a possible narrow pentaquark state and $G(2220)$ is a possible glueball resonance.

[h] $(\overline{\Lambda}{}_c^- p)_s$ denotes a low-mass enhancement near 3.35 GeV/c^2.

CONSTRAINED FIT INFORMATION

An overall fit to 3 branching ratios uses 6 measurements and one constraint to determine 3 parameters. The overall fit has a $\chi^2 = 3.7$ for 4 degrees of freedom.

The following *off-diagonal* array elements are the correlation coefficients $\langle \delta x_i \delta x_j \rangle / (\delta x_i \cdot \delta x_j)$, in percent, from the fit to the branching fractions, $x_i \equiv \Gamma_i/\Gamma_{\rm total}$. The fit constrains the x_i whose labels appear in this array to sum to one.

x_{322}	10	
x_{262}		

CONSTRAINED FIT INFORMATION

An overall fit to 18 branching ratios uses 53 measurements and one constraint to determine 12 parameters. The overall fit has a $\chi^2 = 48.9$ for 42 degrees of freedom.

The following *off-diagonal* array elements are the correlation coefficients $\langle \delta x_i \delta x_j \rangle / (\delta x_i \cdot \delta x_j)$, in percent, from the fit to the branching fractions, $x_i \equiv \Gamma_i/\Gamma_{\rm total}$. The fit constrains the x_i whose labels appear in this array to sum to one.

	x_6	x_7	x_{46}	x_{82}	x_{114}	x_{218}	x_{222}	x_{233}	x_{243}	x_{473}
x_7	33									
x_{46}	0	0								
x_{82}	0	0	8							
x_{114}	0	0	1	13						
x_{218}	0	0	0	0	0					
x_{222}	0	0	0	0	0	0				
x_{233}	0	0	0	0	0	28	0			
x_{243}	0	0	0	0	0	58	0	16		
x_{473}	0	0	0	0	0	14	0	4	8	
x_{480}	0	0	0	0	0	0	9	0	0	0

B^+ BRANCHING RATIOS

$\Gamma(\ell^+ \nu_\ell \text{anything})/\Gamma_{\rm total}$ Γ_1/Γ

"OUR EVALUATION" is an average using rescaled values of the data listed below. The average and rescaling were performed by the Heavy Flavor Averaging Group (HFAG) and are described at http://www.slac.stanford.edu/xorg/hfag/. The averaging/rescaling procedure takes into account correlations between the measurements.

VALUE (units 10^{-2})	DOCUMENT ID		TECN	COMMENT
10.99±0.28 OUR EVALUATION				
10.76±0.32 OUR AVERAGE Error includes scale factor of 1.1.				
11.17±0.25±0.28	[1] URQUIJO	07	BELL	$e^+e^- \to \Upsilon(4S)$
10.28±0.26±0.39	[2] AUBERT,B	06Y	BABR	$e^+e^- \to \Upsilon(4S)$
10.25±0.57±0.65	[3] ARTUSO	97	CLE2	$e^+e^- \to \Upsilon(4S)$
• • • We do not use the following data for averages, fits, limits, etc. • • •				
11.15±0.26±0.41	[4] OKABE	05	BELL	Repl. by URQUIJO 07
10.1 ±1.8 ±1.5	ATHANAS	94	CLE2	Sup. by ARTUSO 97

[1] URQUIJO 07 report a measurement of $(10.34 \pm 023 \pm 0.25)\%$ for the partial branching fraction of $B^+ \to e^+\nu_e X_c$ decay with electron energy above 0.6 GeV. We converted the result to $B^+ \to e^+\nu_e X$ branching fraction.

[2] The measurements are obtained for charged and neutral B mesons partial rates of semileptonic decay to electrons with momentum above 0.6 GeV/c in the B rest frame. The best precision on the ratio is achieved for a momentum threshold of 1.0 GeV: $B(B^+ \to e^+\nu_e X) / B(B^0 \to e^+\nu_e X) = 1.074 \pm 0.041 \pm 0.026$.

[3] ARTUSO 97 uses partial reconstruction of $B \to D^*\ell\nu_\ell$ and inclusive semileptonic branching ratio from BARISH 96B ($0.1049 \pm 0.0017 \pm 0.0043$).

[4] The measurements are obtained for charged and neutral B mesons partial rates of semileptonic decay to electrons with momentum above 0.6 GeV/c in the B rest frame, and their ratio of $B(B^+ \to e^+\nu_e X)/B(B^0 \to e^+\nu_e X) = 1.08 \pm 0.05 \pm 0.02$.

$\Gamma(e^+ \nu_e X_c)/\Gamma_{\rm total}$ Γ_2/Γ

VALUE (units 10^{-2})	DOCUMENT ID		TECN	COMMENT
10.79±0.25±0.27	[1] URQUIJO	07	BELL	$e^+e^- \to \Upsilon(4S)$

[1] Measure the independent B^+ and B^0 partial branching fractions with electron threshold energies of 0.4 GeV.

$\Gamma(\overline{D}{}^0 \ell^+ \nu_\ell)/\Gamma_{\rm total}$ Γ_4/Γ

"OUR EVALUATION" is an average using rescaled values of the data listed below. The average and rescaling were performed by the Heavy Flavor Averaging Group (HFAG) and are described at http://www.slac.stanford.edu/xorg/hfag/. The averaging/rescaling procedure takes into account correlations between the measurements. $\ell = e$ or μ, not sum over e and μ modes.

VALUE	DOCUMENT ID		TECN	COMMENT
0.0227±0.0011 OUR EVALUATION				
0.0229±0.0008 OUR AVERAGE				
0.0229±0.0008±0.0009	[1] AUBERT	10	BABR	$e^+e^- \to \Upsilon(4S)$
0.0234±0.0003±0.0013	AUBERT	09A	BABR	$e^+e^- \to \Upsilon(4S)$
0.0221±0.0013±0.0019	[2] BARTELT	99	CLE2	$e^+e^- \to \Upsilon(4S)$
0.016 ±0.006 ±0.003	[3] FULTON	91	CLEO	$e^+e^- \to \Upsilon(4S)$
• • • We do not use the following data for averages, fits, limits, etc. • • •				
0.0233±0.0009±0.0009	[1] AUBERT	08Q	BABR	Repl. by AUBERT 09A
0.0194±0.0015±0.0034	[4] ATHANAS	97	CLE2	Repl. by BARTELT 99

[1] Uses a fully reconstructed B meson as a tag on the recoil side.

[2] Assumes equal production of B^+ and B^0 at the $\Upsilon(4S)$.

[3] FULTON 91 assumes equal production of $B^0\overline{B}{}^0$ and B^+B^- at the $\Upsilon(4S)$.

[4] ATHANAS 97 uses missing energy and missing momentum to reconstruct neutrino.

$\Gamma(\overline{D}{}^0 \ell^+ \nu_\ell)/\Gamma(\ell^+ \nu_\ell \text{anything})$ Γ_4/Γ_1

VALUE	DOCUMENT ID		TECN	COMMENT
0.255±0.009±0.009	[1] AUBERT	10	BABR	$e^+e^- \to \Upsilon(4S)$

[1] Uses a fully reconstructed B meson on the recoil side.

$\Gamma(\overline{D}{}^0 \ell^+ \nu_\ell)/\Gamma(D\ell^+ \nu_\ell \text{anything})$ Γ_4/Γ_3

VALUE	DOCUMENT ID		TECN	COMMENT
0.227±0.014±0.016	[1] AUBERT	07AN	BABR	$e^+e^- \to \Upsilon(4S)$

[1] Uses a fully reconstructed B meson on the recoil side.

$\Gamma(\overline{D}^0\tau^+\nu_\tau)/\Gamma_{\text{total}}$ Γ_5/Γ

VALUE (units 10^{-2})	DOCUMENT ID		TECN	COMMENT
0.77±0.22±0.12	[1] BOZEK	10	BELL	$e^+e^- \to \Upsilon(4S)$
• • • We do not use the following data for averages, fits, limits, etc. • • •				
0.67±0.37±0.13	[2] AUBERT	08N	BABR	Repl. by AUBERT 09S

[1] Assumes equal production of B^+ and B^0 at the $\Upsilon(4S)$.
[2] Uses a fully reconstructed B meson as a tag on the recoil side.

$\Gamma(\overline{D}^0\tau^+\nu_\tau)/\Gamma(\overline{D}^0\ell^+\nu_\ell)$ Γ_5/Γ_4

VALUE	DOCUMENT ID		TECN	COMMENT
0.429±0.082±0.052	[1,2] LEES	12D	BABR	$e^+e^- \to \Upsilon(4S)$
• • • We do not use the following data for averages, fits, limits, etc. • • •				
0.314±0.170±0.049	[1] AUBERT	09S	BABR	Repl. by LEES 12D

[1] Uses a fully reconstructed B meson as a tag on the recoil side.
[2] Uses $\tau^+ \to e^+\nu_e\overline{\nu}_\tau$ and $\tau^+ \to \mu^+\nu_\mu\overline{\nu}_\tau$ and e^+ or μ^+ as ℓ^+.

$\Gamma(\overline{D}^*(2007)^0\ell^+\nu_\ell)/\Gamma_{\text{total}}$ Γ_6/Γ

"OUR EVALUATION" is an average using rescaled values of the data listed below. The average and rescaling were performed by the Heavy Flavor Averaging Group (HFAG) and are described at http://www.slac.stanford.edu/xorg/hfag/. The averaging/rescaling procedure takes into account correlations between the measurements. $\ell = e$ or μ, not sum over e and μ modes.

VALUE	EVTS	DOCUMENT ID		TECN	COMMENT
0.0569±0.0019 OUR EVALUATION					
0.0560±0.0026 OUR FIT Error includes scale factor of 1.5.					
0.0558±0.0026 OUR AVERAGE Error includes scale factor of 1.5. See the ideogram below.					
0.0540±0.0002±0.0021		AUBERT	09A	BABR	$e^+e^- \to \Upsilon(4S)$
0.0556±0.0008±0.0041		[1] AUBERT	08AT	BABR	$e^+e^- \to \Upsilon(4S)$
0.0650±0.0020±0.0043		[2] ADAM	03	CLE2	$e^+e^- \to \Upsilon(4S)$
0.066 ±0.016 ±0.015		[3] ALBRECHT	92C	ARG	$e^+e^- \to \Upsilon(4S)$
• • • We do not use the following data for averages, fits, limits, etc. • • •					
0.0583±0.0015±0.0030		[4] AUBERT	08Q	BABR	Repl. by AUBERT 09A
0.0650±0.0020±0.0043		[5] BRIERE	02	CLE2	$e^+e^- \to \Upsilon(4S)$
0.0513±0.0054±0.0064	302	[6] BARISH	95	CLE2	Repl. by ADAM 03
seen	398	[7] SANGHERA	93	CLE2	$e^+e^- \to \Upsilon(4S)$
0.041 ±0.008 $^{+0.008}_{-0.009}$		[8] FULTON	91	CLEO	$e^+e^- \to \Upsilon(4S)$
0.070 ±0.018 ±0.014		[9] ANTREASYAN	90B	CBAL	$e^+e^- \to \Upsilon(4S)$

[1] Measured using the dependence of $B^- \to D^{*0}e^-\overline{\nu}_e$ decay differential rate and the form factor description by CAPRINI 98.
[2] Simultaneous measurements of both $B^0 \to D^*(2010)^-\ell\nu$ and $B^+ \to \overline{D}(2007)^0\ell\nu$.
[3] ALBRECHT 92C reports 0.058±0.014±0.013. We rescale using the method described in STONE 94 but with the updated PDG 94 B($D^0 \to K^-\pi^+$). Assumes equal production of $B^0\overline{B}^0$ and B^+B^- at the $\Upsilon(4S)$.
[4] Uses a fully reconstructed B meson as a tag on the recoil side.
[5] The results are based on the same analysis and data sample reported in ADAM 03.
[6] BARISH 95 use B($D^0 \to K^-\pi^+$) = (3.91 ± 0.08 ± 0.17)% and B($D^{*0} \to D^0\pi^0$) = (63.6 ± 2.3 ± 3.3)%.
[7] Combining $\overline{D}^{*0}\ell^+\nu_\ell$ and $\overline{D}^{*-}\ell^+\nu_\ell$ SANGHERA 93 test $V-A$ structure and fit the decay angular distributions to obtain $A_{FB} = 3/4*(\Gamma^- - \Gamma^+)/\Gamma = 0.14 \pm 0.06 \pm 0.03$. Assuming a value of V_{cb}, they measure V, A_1, and A_2, the three form factors for the $D^*\ell\nu_\ell$ decay, where results are slightly dependent on model assumptions.
[8] Assumes equal production of $B^0\overline{B}^0$ and B^+B^- at the $\Upsilon(4S)$. Uncorrected for D and D^* branching ratio assumptions.
[9] ANTREASYAN 90B is average over B and $\overline{D}^*(2010)$ charge states.

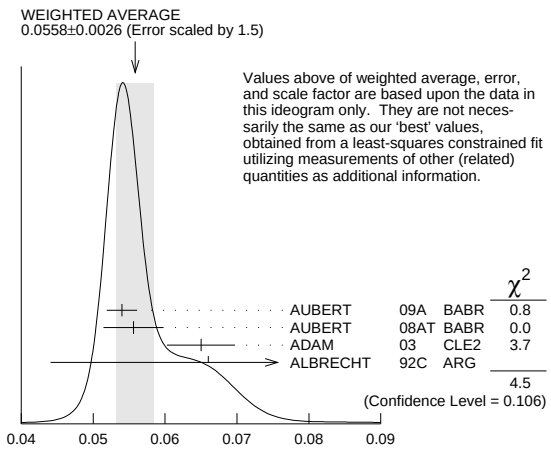

$\Gamma(\overline{D}^*(2007)^0\ell^+\nu_\ell)/\Gamma_{\text{total}}$ Γ_6/Γ

$\Gamma(\overline{D}^*(2007)^0\ell^+\nu_\ell)/\Gamma(D\ell^+\nu_\ell\,\text{anything})$ Γ_6/Γ_3

VALUE	DOCUMENT ID		TECN	COMMENT
0.582±0.018±0.030	[1] AUBERT	07AN	BABR	$e^+e^- \to \Upsilon(4S)$

[1] Uses a fully reconstructed B meson on the recoil side.

$\Gamma(\overline{D}^*(2007)^0\tau^+\nu_\tau)/\Gamma_{\text{total}}$ Γ_7/Γ

VALUE (units 10^{-2})	DOCUMENT ID		TECN	COMMENT
1.88±0.20 OUR FIT				
$2.12^{+0.28}_{-0.27}$±0.29	[1] BOZEK	10	BELL	$e^+e^- \to \Upsilon(4S)$
• • • We do not use the following data for averages, fits, limits, etc. • • •				
2.25±0.48±0.28	[2] AUBERT	08N	BABR	Repl. by AUBERT 09S

[1] Assumes equal production of B^+ and B^0 at the $\Upsilon(4S)$.
[2] Uses a fully reconstructed B meson as a tag on the recoil side.

$\Gamma(\overline{D}^*(2007)^0\tau^+\nu_\tau)/\Gamma(\overline{D}^*(2007)^0\ell^+\nu_\ell)$ Γ_7/Γ_6

VALUE	DOCUMENT ID		TECN	COMMENT
0.335±0.034 OUR FIT				
0.322±0.032±0.022	[1,2] LEES	12D	BABR	$e^+e^- \to \Upsilon(4S)$
• • • We do not use the following data for averages, fits, limits, etc. • • •				
0.346±0.073±0.034	[1] AUBERT	09S	BABR	Repl. by LEES 12D

[1] Uses a fully reconstructed B meson as a tag on the recoil side.
[2] Uses $\tau^+ \to e^+\nu_e\overline{\nu}_\tau$ and $\tau^+ \to \mu^+\nu_\mu\overline{\nu}_\tau$ and e^+ or μ^+ as ℓ^+.

$\Gamma(D^-\pi^+\ell^+\nu_\ell)/\Gamma_{\text{total}}$ Γ_8/Γ

VALUE (units 10^{-3})	DOCUMENT ID		TECN	COMMENT
4.2±0.5 OUR AVERAGE				
4.2±0.6±0.3	[1] AUBERT	08Q	BABR	$e^+e^- \to \Upsilon(4S)$
4.2±0.6±0.2	[1,2] LIVENTSEV	08	BELL	$e^+e^- \to \Upsilon(4S)$
• • • We do not use the following data for averages, fits, limits, etc. • • •				
5.5±0.9±0.3	[3] LIVENTSEV	05	BELL	Repl. by LIVENTSEV 08

[1] Uses a fully reconstructed B meson as a tag on the recoil side.
[2] LIVENTSEV 08 reports $(4.0 \pm 0.4 \pm 0.6) \times 10^{-3}$ from a measurement of $[\Gamma(B^+ \to D^-\pi^+\ell^+\nu_\ell)/\Gamma_{\text{total}}] / [\text{B}(B^+ \to \overline{D}^0\ell^+\nu_\ell)]$ assuming $\text{B}(B^+ \to \overline{D}^0\ell^+\nu_\ell) = (2.15 \pm 0.22) \times 10^{-2}$, which we rescale to our best value $\text{B}(B^+ \to \overline{D}^0\ell^+\nu_\ell) = (2.27 \pm 0.11) \times 10^{-2}$. Our first error is their experiment's error and our second error is the systematic error from using our best value.
[3] LIVENTSEV 05 reports $[\Gamma(B^+ \to D^-\pi^+\ell^+\nu_\ell)/\Gamma_{\text{total}}] / [\text{B}(B^0 \to D^-\ell^+\nu_\ell)] = 0.25 \pm 0.03 \pm 0.03$ which we multiply by our best value $\text{B}(B^0 \to D^-\ell^+\nu_\ell) = (2.19 \pm 0.12) \times 10^{-2}$. Our first error is their experiment's error and our second error is the systematic error from using our best value.

$\Gamma(\overline{D}_0^*(2420)^0\ell^+\nu_\ell,\ \overline{D}_0^{*0} \to D^-\pi^+)/\Gamma_{\text{total}}$ Γ_9/Γ

VALUE (units 10^{-3})	DOCUMENT ID		TECN	COMMENT
2.5±0.5 OUR AVERAGE				
2.6±0.5±0.4	[1] AUBERT	08BL	BABR	$e^+e^- \to \Upsilon(4S)$
2.4±0.4±0.6	[1] LIVENTSEV	08	BELL	$e^+e^- \to \Upsilon(4S)$

[1] Uses a fully reconstructed B meson as a tag on the recoil side.

$\Gamma(\overline{D}_2^*(2460)^0\ell^+\nu_\ell,\ \overline{D}_2^{*0} \to D^-\pi^+)/\Gamma_{\text{total}}$ Γ_{10}/Γ

VALUE (units 10^{-3})	DOCUMENT ID		TECN	COMMENT
1.53±0.16 OUR AVERAGE				
1.42±0.15±0.15	[1] AUBERT	09Y	BABR	$e^+e^- \to \Upsilon(4S)$
1.5 ±0.2 ±0.2	[2] AUBERT	08BL	BABR	$e^+e^- \to \Upsilon(4S)$
2.2 ±0.3 ±0.4	[2] LIVENTSEV	08	BELL	$e^+e^- \to \Upsilon(4S)$

[1] Uses a simultaneous fit of all B semileptonic decays without full reconstruction of events. AUBERT 09Y reports $\text{B}(B^+ \to \overline{D}_2^*(2460)^0\ell^+\nu_\ell) \cdot \text{B}(\overline{D}_2^*(2460)^0 \to D^{(*)-}\pi^+) = (2.29 \pm 0.23 \pm 0.21) \times 10^{-3}$ and the authors have provided us the individual measurement.
[2] Uses a fully reconstructed B meson as a tag on the recoil side.

$\Gamma(D^{(*)}n\pi\ell^+\nu_\ell(n \geq 1))/\Gamma(D\ell^+\nu_\ell\,\text{anything})$ Γ_{11}/Γ_3

VALUE	DOCUMENT ID		TECN	COMMENT
0.191±0.013±0.019	[1] AUBERT	07AN	BABR	$e^+e^- \to \Upsilon(4S)$

[1] Uses a fully reconstructed B meson on the recoil side.

$\Gamma(D^{*-}\pi^+\ell^+\nu_\ell)/\Gamma_{\text{total}}$ Γ_{12}/Γ

VALUE (units 10^{-3})	DOCUMENT ID		TECN	COMMENT
6.1±0.6 OUR AVERAGE				
5.9±0.5±0.4	[1] AUBERT	08Q	BABR	$e^+e^- \to \Upsilon(4S)$
6.8±1.1±0.3	[1,2] LIVENTSEV	08	BELL	$e^+e^- \to \Upsilon(4S)$
• • • We do not use the following data for averages, fits, limits, etc. • • •				
5.9±1.4±0.1	[3,4] LIVENTSEV	05	BELL	Repl. by LIVENTSEV 08

[1] Uses a fully reconstructed B meson as a tag on the recoil side.
[2] LIVENTSEV 08 reports $(6.4 \pm 0.8 \pm 0.9) \times 10^{-3}$ from a measurement of $[\Gamma(B^+ \to D^{*-}\pi^+\ell^+\nu_\ell)/\Gamma_{\text{total}}] / [\text{B}(B^+ \to \overline{D}^0\ell^+\nu_\ell)]$ assuming $\text{B}(B^+ \to \overline{D}^0\ell^+\nu_\ell) = (2.15 \pm 0.22) \times 10^{-2}$, which we rescale to our best value $\text{B}(B^+ \to \overline{D}^0\ell^+\nu_\ell) = (2.27 \pm 0.11) \times 10^{-2}$. Our first error is their experiment's error and our second error is the systematic error from using our best value.
[3] Excludes D^{*+} contribution to $D\pi$ modes.
[4] LIVENTSEV 05 reports $[\Gamma(B^+ \to D^{*-}\pi^+\ell^+\nu_\ell)/\Gamma_{\text{total}}] / [\text{B}(B^0 \to D^*(2010)^-\ell^+\nu_\ell)] = 0.12 \pm 0.02 \pm 0.02$ which we multiply by our best value $\text{B}(B^0 \to D^*(2010)^-\ell^+\nu_\ell) = (4.93 \pm 0.11) \times 10^{-2}$. Our first error is their experiment's error and our second error is the systematic error from using our best value.

$\Gamma(\overline{D}_1(2420)^0 \ell^+ \nu_\ell, \overline{D}_1^0 \to D^{*-}\pi^+)/\Gamma_{\text{total}}$ Γ_{13}/Γ

VALUE (units 10^{-3})	DOCUMENT ID		TECN	COMMENT
3.03±0.20 OUR AVERAGE				
2.97±0.17±0.17	[1] AUBERT	09Y	BABR	$e^+e^- \to \Upsilon(4S)$
2.9 ±0.3 ±0.3	[2] AUBERT	08BL	BABR	$e^+e^- \to \Upsilon(4S)$
4.2 ±0.7 ±0.7	[2] LIVENTSEV	08	BELL	$e^+e^- \to \Upsilon(4S)$
3.73±0.85±0.57	[3] ANASTASSOV	98	CLE2	$e^+e^- \to \Upsilon(4S)$

[1] Uses a simultaneous measurement of all B semileptonic decays without full reconstruction of events.
[2] Uses a fully reconstructed B meson as a tag on the recoil side.
[3] Assumes equal production of B^+ and B^0 at the $\Upsilon(4S)$.

$\Gamma(\overline{D}_1'(2430)^0 \ell^+ \nu_\ell, \overline{D}_1'^0 \to D^{*-}\pi^+)/\Gamma_{\text{total}}$ Γ_{14}/Γ

VALUE (units 10^{-3})	CL%	DOCUMENT ID		TECN	COMMENT
2.7±0.4±0.5		[1] AUBERT	08BL	BABR	$e^+e^- \to \Upsilon(4S)$
• • • We do not use the following data for averages, fits, limits, etc. • • •					
<0.7	90	[1] LIVENTSEV	08	BELL	$e^+e^- \to \Upsilon(4S)$

[1] Uses a fully reconstructed B meson as a tag on the recoil side.

$\Gamma(\overline{D}_2^*(2460)^0 \ell^+ \nu_\ell, \overline{D}_2^{*0} \to D^{*-}\pi^+)/\Gamma_{\text{total}}$ Γ_{15}/Γ

VALUE (units 10^{-3})	CL%	DOCUMENT ID		TECN	COMMENT
1.01±0.24 OUR AVERAGE		Error includes scale factor of 2.0.			
0.87±0.11±0.07		[1] AUBERT	09Y	BABR	$e^+e^- \to \Upsilon(4S)$
1.5 ±0.2 ±0.2		[2] AUBERT	08BL	BABR	$e^+e^- \to \Upsilon(4S)$
1.8 ±0.6 ±0.3		[2] LIVENTSEV	08	BELL	$e^+e^- \to \Upsilon(4S)$
• • • We do not use the following data for averages, fits, limits, etc. • • •					
<1.6	90	[3] ANASTASSOV	98	CLE2	$e^+e^- \to \Upsilon(4S)$

[1] Uses a simultaneous fit of all B semileptonic decays without full reconstruction of events. AUBERT 09Y reports $B(B^+ \to \overline{D}_2^*(2460)^0 \ell^+ \nu_\ell) \cdot B(\overline{D}_2^*(2460)^0 \to D^{(*)-}\pi^+) = (2.29 \pm 0.23 \pm 0.21) \times 10^{-3}$ and the authors have provided us the individual measurement.
[2] Uses a fully reconstructed B meson as a tag on the recoil side.
[3] Assumes equal production of B^+ and B^0 at the $\Upsilon(4S)$.

$\Gamma(D_s^{(*)-} K^+ \ell^+ \nu_\ell)/\Gamma_{\text{total}}$ Γ_{16}/Γ

VALUE (units 10^{-4})	DOCUMENT ID		TECN	COMMENT
6.1 ±1.0 OUR AVERAGE				
5.9 ±1.2 ±1.5	[1] STYPULA	12	BELL	$e^+e^- \to \Upsilon(4S)$
$6.13^{+1.04}_{-1.03} \pm 0.67$	[1] DEL-AMO-SA...11L		BABR	$e^+e^- \to \Upsilon(4S)$

[1] Assumes equal production of B^+ and B^0 at the $\Upsilon(4S)$.

$\Gamma(D_s^- K^+ \ell^+ \nu_\ell)/\Gamma_{\text{total}}$ Γ_{17}/Γ

VALUE (units 10^{-4})	DOCUMENT ID		TECN	COMMENT
$\mathbf{3.0 \pm 0.9^{+1.1}_{-0.8}}$	[1] STYPULA	12	BELL	$e^+e^- \to \Upsilon(4S)$

[1] Assumes equal production of B^+ and B^0 at the $\Upsilon(4S)$.

$\Gamma(D_s^{*-} K^+ \ell^+ \nu_\ell)/\Gamma_{\text{total}}$ Γ_{18}/Γ

VALUE (units 10^{-4})	DOCUMENT ID		TECN	COMMENT
$\mathbf{2.9 \pm 1.6^{+1.1}_{-1.0}}$	[1,2] STYPULA	12	BELL	$e^+e^- \to \Upsilon(4S)$

[1] Assumes equal production of B^+ and B^0 at the $\Upsilon(4S)$.
[2] STYPULA 12 provides also an upper limit of 0.56×10^{-3} at 90% CL for the same data. Also measures branching fraction of the combined modes of $D_s^- K^+ \ell^+ \nu_\ell$ and $D_s^{*-} K^+ \ell^+ \nu_\ell$ as $B(B^+ \to D_s^{(*)-} K^+ \ell^+ \nu_\ell) = (5.9 \pm 1.2 \pm 1.5) \times 10^{-4}$.

$\Gamma(\pi^0 \ell^+ \nu_\ell)/\Gamma_{\text{total}}$ Γ_{19}/Γ

"OUR EVALUATION" is an average using rescaled values of the data listed below. The average and rescaling were performed by the Heavy Flavor Averaging Group (HFAG) and are described at http://www.slac.stanford.edu/xorg/hfag/. The averaging/rescaling procedure takes into account correlations between the measurements.

VALUE (units 10^{-4})	DOCUMENT ID		TECN	COMMENT
0.780±0.027 OUR EVALUATION				
0.748±0.029 OUR AVERAGE				
0.80 ±0.08 ±0.04	[1] SIBIDANOV	13	BELL	$e^+e^- \to \Upsilon(4S)$
0.77 ±0.04 ±0.03	[2] LEES	12AA	BABR	$e^+e^- \to \Upsilon(4S)$
0.705±0.025±0.035	[3] DEL-AMO-SA...11C		BABR	$e^+e^- \to \Upsilon(4S)$
0.82 ±0.09 ±0.05	[3] AUBERT	08AV	BABR	$e^+e^- \to \Upsilon(4S)$
0.77 ±0.14 ±0.08	[4] HOKUUE	07	BELL	$e^+e^- \to \Upsilon(4S)$
• • • We do not use the following data for averages, fits, limits, etc. • • •				
0.74 ±0.05 ±0.10	[5] AUBERT,B	05O	BABR	Repl. by DEL-AMO-SANCHEZ 11C

[1] The signal events are tagged by a second B meson reconstructed in the fully hadronic decays.
[2] Uses loose neutrino reconstruction technique. Assumes $B(\Upsilon(4S) \to B^+B^-) = (51.6 \pm 0.6)\%$ and $B(\Upsilon(4S) \to B^0\overline{B}^0) = (48.4 \pm 0.6)\%$.
[3] Using the isospin symmetry relation, B^+ and B^0 branching fractions are combined.
[4] The signal events are tagged by a second B meson reconstructed in the semileptonic mode $B \to D^{(*)} \ell \nu_\ell$.
[5] B^+ and B^0 decays combined assuming isospin symmetry. Systematic errors include both experimental and form-factor uncertainties.

$\Gamma(\pi^0 e^+ \nu_e)/\Gamma_{\text{total}}$ Γ_{20}/Γ

VALUE (units 10^{-4})	CL%	DOCUMENT ID		TECN	COMMENT
• • • We do not use the following data for averages, fits, limits, etc. • • •					
0.9±0.2±0.2		[1] ALEXANDER	96T	CLE2	$e^+e^- \to \Upsilon(4S)$
<22	90	ANTREASYAN	90B	CBAL	$e^+e^- \to \Upsilon(4S)$

[1] Derived based in the reported B^0 result by assuming isospin symmetry: $\Gamma(B^0 \to \pi^- \ell^+ \nu) = 2\Gamma(B^+ \to \pi^0 \ell^+ \nu)$.

$\Gamma(\eta \ell^+ \nu_\ell)/\Gamma_{\text{total}}$ Γ_{21}/Γ

VALUE (units 10^{-4})	CL%	DOCUMENT ID		TECN	COMMENT
0.38±0.06 OUR AVERAGE					
0.38±0.05±0.05		[1] LEES	12AA	BABR	$e^+e^- \to \Upsilon(4S)$
0.31±0.06±0.08		[1] AUBERT	09Q	BABR	$e^+e^- \to \Upsilon(4S)$
0.64±0.20±0.03		[2] AUBERT	08AV	BABR	$e^+e^- \to \Upsilon(4S)$
• • • We do not use the following data for averages, fits, limits, etc. • • •					
0.36±0.05±0.04		[1] DEL-AMO-SA...11F		BABR	Repl. by LEES 12AA
<1.01	90	[3] ADAM	07	CLE2	$e^+e^- \to \Upsilon(4S)$
0.84±0.31±0.18		[4] ATHAR	03	CLE2	Repl. by ADAM 07

[1] Uses loose neutrino reconstruction technique. Assumes $B(\Upsilon(4S) \to B^+B^-) = (51.6 \pm 0.6)\%$ and $B(\Upsilon(4S) \to B^0\overline{B}^0) = (48.4 \pm 0.6)\%$.
[2] Assumes equal production of B^+ and B^0 at the $\Upsilon(4S)$.
[3] The B^0 and B^+ results are combined assuming the isospin, B lifetimes, and relative charged/neutral B production at the $\Upsilon(4S)$.
[4] ATHAR 03 reports systematic errors 0.16 ± 0.09, which are experimental systematic and systematic due to model dependence. We combine these in quadrature.

$\Gamma(\eta' \ell^+ \nu_\ell)/\Gamma_{\text{total}}$ Γ_{22}/Γ

VALUE (units 10^{-4})	DOCUMENT ID		TECN	COMMENT
0.23±0.08 OUR AVERAGE				
0.24±0.08±0.03	[1] LEES	12AA	BABR	$e^+e^- \to \Upsilon(4S)$
$0.04 \pm 0.22^{+0.05}_{-0.02}$	[2] AUBERT	08AV	BABR	$e^+e^- \to \Upsilon(4S)$
2.66±0.80±0.56	[3] ADAM	07	CLE2	$e^+e^- \to \Upsilon(4S)$
• • • We do not use the following data for averages, fits, limits, etc. • • •				
0.24±0.08±0.03	[1] DEL-AMO-SA...11F		BABR	Repl. by LEES 12AA

[1] Uses loose neutrino reconstruction technique. Assumes $B(Y(4S) \to B^+B^-) = (51.6 \pm 0.6)\%$ and $B(Y(4S) \to B^0\overline{B}^0) = (48.4 \pm 0.6)\%$.
[2] Assumes equal production of B^+ and B^0 at the $\Upsilon(4S)$.
[3] The B^0 and B^+ results are combined assuming the isospin, B lifetimes, and relative charged/neutral B production at the $\Upsilon(4S)$. Corresponds to 90% CL interval $(1.20\text{–}4.46) \times 10^{-4}$.

$\Gamma(\omega \ell^+ \nu_\ell)/\Gamma_{\text{total}}$ Γ_{23}/Γ

$\ell = e$ or μ, not sum over e and μ modes.

VALUE (units 10^{-4})	CL%	DOCUMENT ID		TECN	COMMENT
1.19±0.09 OUR AVERAGE					
1.21±0.14±0.08		[1,2] LEES	13A	BABR	$e^+e^- \to \Upsilon(4S)$
1.35±0.21±0.11		[3] LEES	13T	BABR	$e^+e^- \to \Upsilon(4S)$
1.07±0.16±0.07		[4] SIBIDANOV	13	BELL	$e^+e^- \to \Upsilon(4S)$
1.19±0.16±0.09		[2,5] LEES	12AA	BABR	$e^+e^- \to \Upsilon(4S)$
1.3 ±0.4 ±0.4		[6] SCHWANDA	04	BELL	$e^+e^- \to \Upsilon(4S)$
• • • We do not use the following data for averages, fits, limits, etc. • • •					
1.14±0.16±0.08		[2] AUBERT	09Q	BABR	Repl. by LEES 13A
<2.1	90	[7] BEAN	93B	CLE2	$e^+e^- \to \Upsilon(4S)$

[1] LEES 13A reports $(1.21 \pm 0.14 \pm 0.08) \times 10^{-4}$ from a measurement of $[\Gamma(B^+ \to \omega \ell^+ \nu_\ell)/\Gamma_{\text{total}}] \times [B(\omega(782) \to \pi^+\pi^-\pi^0)]$ assuming $B(\omega(782) \to \pi^+\pi^-\pi^0) = (89.2 \pm 0.7) \times 10^{-2}$.
[2] Uses $B(\Upsilon(4S) \to B^+B^-) = (51.6 \pm 0.6)\%$ and $B(\Upsilon(4S) \to B^0\overline{B}^0) = (48.4 \pm 0.6)\%$.
[3] Uses semileptonic tagging. Assumes $B(\omega \to \pi^+\pi^-\pi^0) = (89.2 \pm 0.7)\%$ and that the production ratio of B^+B^- to $B^0\overline{B}^0$ from $\Upsilon(4S)$ is 1.056 ± 0.028. The partial branching fractions in three bins of q^2 are also reported.
[4] The signal events are tagged by a second B meson reconstructed in the fully hadronic decays.
[5] Uses loose neutrino reconstruction technique.
[6] Assumes equal production of B^+ and B^0 at the $\Upsilon(4S)$.
[7] BEAN 93B limit set using ISGW Model. Using isospin and the quark model to combine $\Gamma(\rho^0 \ell^+ \nu_\ell)$ and $\Gamma(\rho^- \ell^+ \nu_\ell)$ with this result, they obtain a limit $<(1.6\text{–}2.7) \times 10^{-4}$ at 90% CL for $B^+ \to \omega \ell^+ \nu_\ell$. The range corresponds to the ISGW, WSB, and KS models. An upper limit on $|V_{ub}/V_{cb}| < 0.8\text{–}0.13$ at 90% CL is derived as well.

$\Gamma(\omega \mu^+ \nu_\mu)/\Gamma_{\text{total}}$ Γ_{24}/Γ

VALUE	DOCUMENT ID		TECN
• • • We do not use the following data for averages, fits, limits, etc. • • •			
seen	[1] ALBRECHT	91C	ARG

[1] In ALBRECHT 91C, one event is fully reconstructed providing evidence for the $b \to u$ transition.

$\Gamma(\rho^0 \ell^+ \nu_\ell)/\Gamma_{total}$ Γ_{25}/Γ

$\ell = e$ or μ, not sum over e and μ modes.

"OUR EVALUATION" is an average using rescaled values of the data listed below. The average and rescaling were performed by the Heavy Flavor Averaging Group (HFAG) and are described at http://www.slac.stanford.edu/xorg/hfag/. The averaging/rescaling procedure takes into account correlations between the measurements and asymmetric lifetime errors.

VALUE (units 10^{-4})	CL%	DOCUMENT ID		TECN	COMMENT
1.58±0.11 OUR EVALUATION					
1.42±0.23 OUR AVERAGE		Error includes scale factor of 2.4. See the ideogram below.			
1.83±0.10±0.10		[1] SIBIDANOV	13	BELL	$e^+e^- \to \Upsilon(4S)$
0.94±0.08±0.14		[2] DEL-AMO-SA...	11C	BABR	$e^+e^- \to \Upsilon(4S)$
1.33±0.23±0.18		[3] HOKUUE	07	BELL	$e^+e^- \to \Upsilon(4S)$
$1.34\pm0.15^{+0.28}_{-0.32}$		[4] BEHRENS	00	CLE2	$e^+e^- \to \Upsilon(4S)$
• • • We do not use the following data for averages, fits, limits, etc. • • •					
1.16±0.11±0.30		[2] AUBERT,B	05O	BABR	Repl. by DEL-AMO-SANCHEZ 11C
$1.40\pm0.21^{+0.32}_{-0.33}$		[4] BEHRENS	00	CLE2	$e^+e^- \to \Upsilon(4S)$
$1.2 \pm0.2^{+0.3}_{-0.4}$		[4] ALEXANDER	96T	CLE2	$e^+e^- \to \Upsilon(4S)$
<2.1	90	[5] BEAN	93B	CLE2	$e^+e^- \to \Upsilon(4S)$

[1] The signal events are tagged by a second B meson reconstructed in the fully hadronic decays.
[2] B^+ and B^0 decays combined assuming isospin symmetry. Systematic errors include both experimental and form-factor uncertainties.
[3] The signal events are tagged by a second B meson reconstructed in the semileptonic mode $B \to D^{(*)} \ell \nu_\ell$.
[4] Derived based in the reported B^0 result by assuming isospin symmetry: $\Gamma(B^0 \to \rho^- \ell^+ \nu) = 2\Gamma(B^+ \to \rho^0 \ell^+ \nu) \approx 2\Gamma(B^+ \to \omega \ell^+ \nu)$.
[5] BEAN 93B limit set using ISGW Model. Using isospin and the quark model to combine $\Gamma(\omega^0 \ell^+ \nu_\ell)$ and $\Gamma(\rho^- \ell^+ \nu_\ell)$ with this result, they obtain a limit $<(1.6\text{–}2.7) \times 10^{-4}$ at 90% CL for $B^+ \to \rho^0 \ell^+ \nu_\ell$. The range corresponds to the ISGW, WSB, and KS models. An upper limit on $|V_{ub}/V_{cb}| < 0.8\text{–}0.13$ at 90% CL is derived as well.

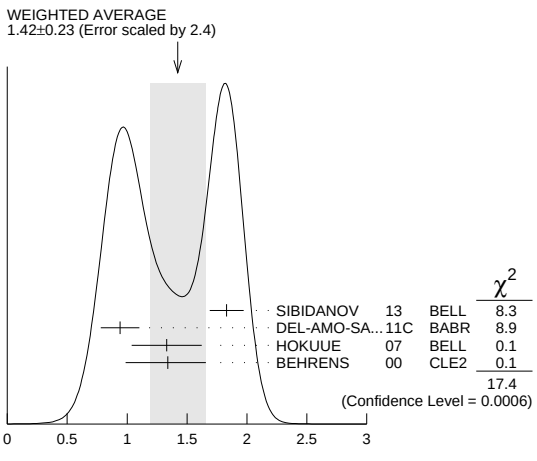

$\Gamma(p\overline{p}\ell^+\nu_\ell)/\Gamma_{total}$ Γ_{26}/Γ

VALUE (units 10^{-6})	DOCUMENT ID		TECN	COMMENT
$5.8^{+2.4}_{-2.1}\pm0.9$	[1] TIEN	14	BELL	$e^+e^- \to \Upsilon(4S)$

[1] Assumes equal production of B^+ and B^0 at the $\Upsilon(4S)$.

$\Gamma(p\overline{p}\mu^+\nu_\mu)/\Gamma_{total}$ Γ_{27}/Γ

VALUE	CL%	DOCUMENT ID		TECN	COMMENT
<8.5 × 10⁻⁶	90	[1] TIEN	14	BELL	$e^+e^- \to \Upsilon(4S)$

[1] Assumes equal production of B^+ and B^0 at the $\Upsilon(4S)$.

$\Gamma(p\overline{p}e^+\nu_e)/\Gamma_{total}$ Γ_{28}/Γ

VALUE (units 10^{-6})	CL%	DOCUMENT ID		TECN	COMMENT
$8.2^{+3.7}_{-3.2}\pm0.6$		[1] TIEN	14	BELL	$e^+e^- \to \Upsilon(4S)$
• • • We do not use the following data for averages, fits, limits, etc. • • •					
<5200	90	[2] ADAM	03B	CLE2	$e^+e^- \to \Upsilon(4S)$

[1] Assumes equal production of B^+ and B^0 at the $\Upsilon(4S)$.
[2] Based on phase-space model; if $V\text{–}A$ model is used, the 90% CL upper limit becomes $< 1.2 \times 10^{-3}$.

$\Gamma(e^+\nu_e)/\Gamma_{total}$ Γ_{29}/Γ

VALUE (units 10^{-6})	CL%	DOCUMENT ID		TECN	COMMENT
< 0.98	90	[1] SATOYAMA	07	BELL	$e^+e^- \to \Upsilon(4S)$
• • • We do not use the following data for averages, fits, limits, etc. • • •					
< 8	90	[1] AUBERT	10E	BABR	$e^+e^- \to \Upsilon(4S)$
< 1.9	90	[1] AUBERT	09V	BABR	$e^+e^- \to \Upsilon(4S)$
< 5.2	90	[1] AUBERT	08AD	BABR	$e^+e^- \to \Upsilon(4S)$
<15	90	ARTUSO	95	CLE2	$e^+e^- \to \Upsilon(4S)$

[1] Assumes equal production of B^+ and B^0 at the $\Upsilon(4S)$.

$\Gamma(\mu^+\nu_\mu)/\Gamma_{total}$ Γ_{30}/Γ

VALUE (units 10^{-6})	CL%	DOCUMENT ID		TECN	COMMENT
< 1.0	90	[1] AUBERT	09V	BABR	$e^+e^- \to \Upsilon(4S)$
• • • We do not use the following data for averages, fits, limits, etc. • • •					
<11	90	[1] AUBERT	10E	BABR	$e^+e^- \to \Upsilon(4S)$
< 5.6	90	[1] AUBERT	08AD	BABR	$e^+e^- \to \Upsilon(4S)$
< 1.7	90	[1] SATOYAMA	07	BELL	$e^+e^- \to \Upsilon(4S)$
< 6.6	90	AUBERT	04O	BABR	Repl. by AUBERT 09V
<21	90	ARTUSO	95	CLE2	$e^+e^- \to \Upsilon(4S)$

[1] Assumes equal production of B^+ and B^0 at the $\Upsilon(4S)$.

$\Gamma(\tau^+\nu_\tau)/\Gamma_{total}$ Γ_{31}/Γ

See the note on "Decay Constants of Charged Pseudoscalar Mesons" in the D_s^+ Listings.

VALUE (units 10^{-4})	CL%	DOCUMENT ID		TECN	COMMENT
1.14±0.27 OUR AVERAGE		Error includes scale factor of 1.3. See the ideogram below.			
$0.72^{+0.27}_{-0.25}\pm0.11$		[1] HARA	13	BELL	$e^+e^- \to \Upsilon(4S)$
$1.83^{+0.53}_{-0.49}\pm0.24$		[2,3] LEES	13K	BABR	$e^+e^- \to \Upsilon(4S)$
1.7 ±0.8 ±0.2		[2,4] AUBERT	10E	BABR	$e^+e^- \to \Upsilon(4S)$
$1.54^{+0.38+0.29}_{-0.37-0.31}$		[2,5] HARA	10	BELL	$e^+e^- \to \Upsilon(4S)$
• • • We do not use the following data for averages, fits, limits, etc. • • •					
$1.8^{+0.9}_{-0.8}\pm0.45$		[2,6] AUBERT	08D	BABR	Repl. by LEES 13K
0.9 ±0.6 ±0.1		[2,4] AUBERT	07AL	BABR	Repl. by AUBERT 10E
< 2.6	90	[2] AUBERT	06K	BABR	$e^+e^- \to \Upsilon(4S)$
$1.79^{+0.56+0.46}_{-0.49-0.51}$		[2,6] IKADO	06	BELL	Repl. by HARA 13
< 4.2	90	[2] AUBERT,B	05B	BABR	Repl. by AUBERT 06K
< 8.3	90	[7] BARATE	01E	ALEP	$e^+e^- \to Z$
< 8.4	90	[2] BROWDER	01	CLE2	$e^+e^- \to \Upsilon(4S)$
< 5.7	90	[8] ACCIARRI	97F	L3	$e^+e^- \to Z$
<104	90	[9] ALBRECHT	95D	ARG	$e^+e^- \to \Upsilon(4S)$
< 22	90	ARTUSO	95	CLE2	$e^+e^- \to \Upsilon(4S)$
< 18	90	[10] BUSKULIC	95	ALEP	$e^+e^- \to Z$

[1] The authors combine their result with that from HARA 10 obtaining $B(B^- \to \tau^- \overline{\nu}_\tau) = (0.96 \pm 0.26) \times 10^{-4}$ and deriving $f_B\,|V_{ub}| = (7.4 \pm 0.8 \pm 0.5) \times 10^{-4}$ GeV.
[2] Assumes equal production of B^+ and B^0 at the $\Upsilon(4S)$.
[3] Requires a fully reconstructed hadronic B-decay in the recoil. Reports that this result combined with AUBERT 10E value gives $B(B^- \to \tau^- \overline{\nu}_\tau) = (1.79 \pm 0.48) \times 10^{-4}$.
[4] Requires one reconstructed semileptonic B decay $B^- \to D^0 \ell^- \overline{\nu}_\ell X$ in the recoil.
[5] Requires one reconstructed semileptonic B decay $B^- \to D^{(*)0} \ell^- \overline{\nu}_\ell X$ in the recoil.
[6] The analysis is based on a sample of events with one fully reconstructed tag B in a hadronic decay mode $B^- \to D^{(*)0} X^-$.
[7] The energy-flow and b-tagging algorithms were used.
[8] ACCIARRI 97F uses missing-energy technique and $f(b \to B^-) = (38.2 \pm 2.5)\%$.
[9] ALBRECHT 95D uses full reconstruction of one B decay as tag.
[10] BUSKULIC 95 uses same missing-energy technique as in $\overline{b} \to \tau^+ \nu_\tau X$, but analysis is restricted to endpoint region of missing-energy distribution.

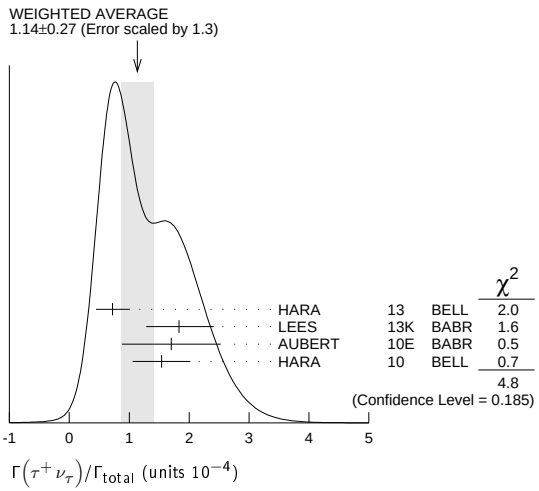

See key on page 547

$\Gamma(\ell^+\nu_\ell\gamma)/\Gamma_{total}$ Γ_{32}/Γ

VALUE	CL%	DOCUMENT ID		TECN	COMMENT
$<15.6\times10^{-6}$	90	[1] AUBERT	09AT	BABR	$e^+e^-\to\Upsilon(4S)$

[1] Assumes equal production of B^+ and B^0 at the $\Upsilon(4S)$.

$\Gamma(e^+\nu_e\gamma)/\Gamma_{total}$ Γ_{33}/Γ

VALUE	CL%	DOCUMENT ID		TECN	COMMENT
$<17\times10^{-6}$	90	[1] AUBERT	09AT	BABR	$e^+e^-\to\Upsilon(4S)$
• • • We do not use the following data for averages, fits, limits, etc. • • •					
$<200\times10^{-6}$	90	[2] BROWDER	97	CLE2	$e^+e^-\to\Upsilon(4S)$

[1] Assumes equal production of B^+ and B^0 at the $\Upsilon(4S)$.
[2] BROWDER 97 uses the hermiticity of the CLEO II detector to reconstruct the neutrino energy and momentum.

$\Gamma(\mu^+\nu_\mu\gamma)/\Gamma_{total}$ Γ_{34}/Γ

VALUE	CL%	DOCUMENT ID		TECN	COMMENT
$<24\times10^{-6}$	90	[1] AUBERT	09AT	BABR	$e^+e^-\to\Upsilon(4S)$
• • • We do not use the following data for averages, fits, limits, etc. • • •					
$<52\times10^{-6}$	90	[2] BROWDER	97	CLE2	$e^+e^-\to\Upsilon(4S)$

[1] Assumes equal production of B^+ and B^0 at the $\Upsilon(4S)$.
[2] BROWDER 97 uses the hermiticity of the CLEO II detector to reconstruct the neutrino energy and momentum.

$\Gamma(D^0X)/\Gamma_{total}$ Γ_{35}/Γ

VALUE	DOCUMENT ID		TECN	COMMENT
$0.086\pm0.006\pm0.004$	[1] AUBERT	07N	BABR	$e^+e^-\to\Upsilon(4S)$
• • • We do not use the following data for averages, fits, limits, etc. • • •				
$0.098\pm0.009\pm0.006$	[1] AUBERT,BE	04B	BABR	Repl. by AUBERT 07N

[1] Events are selected by completely reconstructing one B and searching for a reconstructed charmed particle in the rest of the event. The last error includes systematic and charm branching ratio uncertainties.

$\Gamma(\overline{D}^0X)/\Gamma_{total}$ Γ_{36}/Γ

VALUE	DOCUMENT ID		TECN	COMMENT
$0.786\pm0.016^{+0.034}_{-0.033}$	[1] AUBERT	07N	BABR	$e^+e^-\to\Upsilon(4S)$
• • • We do not use the following data for averages, fits, limits, etc. • • •				
$0.793\pm0.025^{+0.045}_{-0.044}$	[1] AUBERT,BE	04B	BABR	Repl. by AUBERT 07N

[1] Events are selected by completely reconstructing one B and searching for a reconstructed charmed particle in the rest of the event. The last error includes systematic and charm branching ratio uncertainties.

$\Gamma(D^0X)/[\Gamma(D^0X)+\Gamma(\overline{D}^0X)]$ $\Gamma_{35}/(\Gamma_{35}+\Gamma_{36})$

VALUE	DOCUMENT ID		TECN	COMMENT
$0.098\pm0.007\pm0.001$	AUBERT	07N	BABR	$e^+e^-\to\Upsilon(4S)$
• • • We do not use the following data for averages, fits, limits, etc. • • •				
$0.110\pm0.010\pm0.003$	AUBERT,BE	04B	BABR	Repl. by AUBERT 07N

$\Gamma(D^+X)/\Gamma_{total}$ Γ_{37}/Γ

VALUE	DOCUMENT ID		TECN	COMMENT
$0.025\pm0.005\pm0.002$	[1] AUBERT	07N	BABR	$e^+e^-\to\Upsilon(4S)$
• • • We do not use the following data for averages, fits, limits, etc. • • •				
$0.038\pm0.009\pm0.005$	[1] AUBERT,BE	04B	BABR	Repl. by AUBERT 07N

[1] Events are selected by completely reconstructing one B and searching for a reconstructed charmed particle in the rest of the event. The last error includes systematic and charm branching ratio uncertainties.

$\Gamma(D^-X)/\Gamma_{total}$ Γ_{38}/Γ

VALUE	DOCUMENT ID		TECN	COMMENT
$0.099\pm0.008\pm0.009$	[1] AUBERT	07N	BABR	$e^+e^-\to\Upsilon(4S)$
• • • We do not use the following data for averages, fits, limits, etc. • • •				
$0.098\pm0.012\pm0.014$	[1] AUBERT,BE	04B	BABR	Repl. by AUBERT 07N

[1] Events are selected by completely reconstructing one B and searching for a reconstructed charmed particle in the rest of the event. The last error includes systematic and charm branching ratio uncertainties.

$\Gamma(D^+X)/[\Gamma(D^+X)+\Gamma(D^-X)]$ $\Gamma_{37}/(\Gamma_{37}+\Gamma_{38})$

VALUE	DOCUMENT ID		TECN	COMMENT
$0.204\pm0.035\pm0.001$	AUBERT	07N	BABR	$e^+e^-\to\Upsilon(4S)$
• • • We do not use the following data for averages, fits, limits, etc. • • •				
$0.278\pm0.052\pm0.009$	AUBERT,BE	04B	BABR	Repl. by AUBERT 07N

$\Gamma(D_s^+X)/\Gamma_{total}$ Γ_{39}/Γ

VALUE	DOCUMENT ID		TECN	COMMENT
$0.079\pm0.006^{+0.013}_{-0.011}$	[1] AUBERT	07N	BABR	$e^+e^-\to\Upsilon(4S)$
• • • We do not use the following data for averages, fits, limits, etc. • • •				
$0.143\pm0.016^{+0.051}_{-0.034}$	[1] AUBERT,BE	04B	BABR	Repl. by AUBERT 07N

[1] Events are selected by completely reconstructing one B and searching for a reconstructed charmed particle in the rest of the event. The last error includes systematic and charm branching ratio uncertainties.

$\Gamma(D_s^-X)/\Gamma_{total}$ Γ_{40}/Γ

VALUE	CL%	DOCUMENT ID		TECN	COMMENT
$0.011^{+0.004+0.002}_{-0.003-0.001}$		[1] AUBERT	07N	BABR	$e^+e^-\to\Upsilon(4S)$
• • • We do not use the following data for averages, fits, limits, etc. • • •					
<0.022	90	[1] AUBERT,BE	04B	BABR	Repl. by AUBERT 07N

[1] Events are selected by completely reconstructing one B and searching for a reconstructed charmed particle in the rest of the event. The last error includes systematic and charm branching ratio uncertainties.

$\Gamma(D_s^+X)/[\Gamma(D_s^+X)+\Gamma(D_s^-X)]$ $\Gamma_{39}/(\Gamma_{39}+\Gamma_{40})$

VALUE	DOCUMENT ID		TECN	COMMENT
$0.884\pm0.038\pm0.002$	AUBERT	07N	BABR	$e^+e^-\to\Upsilon(4S)$
• • • We do not use the following data for averages, fits, limits, etc. • • •				
$0.966\pm0.039\pm0.012$	AUBERT,BE	04B	BABR	Repl. by AUBERT 07N

$\Gamma(D_s^-X)/[\Gamma(D_s^+X)+\Gamma(D_s^-X)]$ $\Gamma_{40}/(\Gamma_{39}+\Gamma_{40})$

VALUE	CL%	DOCUMENT ID		TECN	COMMENT
<0.126	90	AUBERT,BE	04B	BABR	$e^+e^-\to\Upsilon(4S)$

$\Gamma(\Lambda_c^+X)/\Gamma_{total}$ Γ_{41}/Γ

VALUE	DOCUMENT ID		TECN	COMMENT
$0.021\pm0.005^{+0.008}_{-0.004}$	[1] AUBERT	07N	BABR	$e^+e^-\to\Upsilon(4S)$
• • • We do not use the following data for averages, fits, limits, etc. • • •				
$0.029\pm0.008^{+0.011}_{-0.007}$	[1] AUBERT,BE	04B	BABR	Repl. by AUBERT 07N

[1] Events are selected by completely reconstructing one B and searching for a reconstructed charmed particle in the rest of the event. The last error includes systematic and charm branching ratio uncertainties.

$\Gamma(\overline{\Lambda}_c^-X)/\Gamma_{total}$ Γ_{42}/Γ

VALUE	DOCUMENT ID		TECN	COMMENT
$0.028\pm0.005^{+0.010}_{-0.007}$	[1] AUBERT	07N	BABR	$e^+e^-\to\Upsilon(4S)$
• • • We do not use the following data for averages, fits, limits, etc. • • •				
$0.035\pm0.008^{+0.013}_{-0.009}$	[1] AUBERT,BE	04B	BABR	Repl. by AUBERT 07N

[1] Events are selected by completely reconstructing one B and searching for a reconstructed charmed particle in the rest of the event. The last error includes systematic and charm branching ratio uncertainties.

$\Gamma(\Lambda_c^+X)/[\Gamma(\Lambda_c^+X)+\Gamma(\overline{\Lambda}_c^-X)]$ $\Gamma_{41}/(\Gamma_{41}+\Gamma_{42})$

VALUE	DOCUMENT ID		TECN	COMMENT
$0.427\pm0.071\pm0.001$	AUBERT	07N	BABR	$e^+e^-\to\Upsilon(4S)$
• • • We do not use the following data for averages, fits, limits, etc. • • •				
$0.452\pm0.090\pm0.003$	AUBERT,BE	04B	BABR	Repl. by AUBERT 07N

$\Gamma(\overline{c}X)/\Gamma_{total}$ Γ_{43}/Γ

VALUE	DOCUMENT ID		TECN	COMMENT
$0.968\pm0.019^{+0.041}_{-0.039}$	[1] AUBERT	07N	BABR	$e^+e^-\to\Upsilon(4S)$
• • • We do not use the following data for averages, fits, limits, etc. • • •				
$0.983\pm0.030^{+0.054}_{-0.051}$	[1] AUBERT,BE	04B	BABR	Repl. by AUBERT 07N

[1] Events are selected by completely reconstructing one B and searching for a reconstructed charmed particle in the rest of the event. The last error includes systematic and charm branching ratio uncertainties.

$\Gamma(cX)/\Gamma_{total}$ Γ_{44}/Γ

VALUE	DOCUMENT ID		TECN	COMMENT
$0.234\pm0.012^{+0.018}_{-0.014}$	[1] AUBERT	07N	BABR	$e^+e^-\to\Upsilon(4S)$
• • • We do not use the following data for averages, fits, limits, etc. • • •				
$0.330\pm0.022^{+0.055}_{-0.037}$	[1] AUBERT,BE	04B	BABR	Repl. by AUBERT 07N

[1] Events are selected by completely reconstructing one B and searching for a reconstructed charmed particle in the rest of the event. The last error includes systematic and charm branching ratio uncertainties.

$\Gamma(c/\overline{c}X)/\Gamma_{total}$ Γ_{45}/Γ

VALUE	DOCUMENT ID		TECN	COMMENT
$1.202\pm0.023^{+0.053}_{-0.049}$	[1] AUBERT	07N	BABR	$e^+e^-\to\Upsilon(4S)$
• • • We do not use the following data for averages, fits, limits, etc. • • •				
$1.313\pm0.037^{+0.088}_{-0.075}$	[1] AUBERT,BE	04B	BABR	Repl. by AUBERT 07N

[1] Events are selected by completely reconstructing one B and searching for a reconstructed charmed particle in the rest of the event. The last error includes systematic and charm branching ratio uncertainties.

Meson Particle Listings

$B^{\pm}$

$\Gamma(\overline{D}^0\pi^+)/\Gamma_{total}$ Γ_{46}/Γ

VALUE (units 10^{-3})	EVTS	DOCUMENT ID		TECN	COMMENT
4.81±0.15 OUR FIT					
4.84±0.15 OUR AVERAGE					
4.90±0.07±0.22		[1] AUBERT	07H	BABR	$e^+e^- \to \Upsilon(4S)$
5.3 ±0.6 ±0.3		[2] ABULENCIA	06J	CDF	$p\overline{p}$ at 1.96 TeV
4.49±0.21±0.23		[3] AUBERT,BE	06J	BABR	$e^+e^- \to \Upsilon(4S)$
4.97±0.12±0.29		[1,4] AHMED	02B	CLE2	$e^+e^- \to \Upsilon(4S)$
5.0 ±0.7 ±0.6	54	[5] BORTOLETTO	92	CLEO	$e^+e^- \to \Upsilon(4S)$
5.4 $^{+1.8}_{-1.5}$ $^{+1.2}_{-0.9}$	14	[6] BEBEK	87	CLEO	$e^+e^- \to \Upsilon(4S)$
• • • We do not use the following data for averages, fits, limits, etc. • • •					
4.76±0.26 $^{+0.05}_{-0.06}$		[7] AUBERT,B	04P	BABR	Repl. by AUBERT 07H
5.5 ±0.4 ±0.5	304	[8] ALAM	94	CLE2	Repl. by AHMED 02B
2.0 ±0.8 ±0.6	12	[5] ALBRECHT	90J	ARG	$e^+e^- \to \Upsilon(4S)$
1.9 ±1.0 ±0.6	7	[9] ALBRECHT	88K	ARG	$e^+e^- \to \Upsilon(4S)$

[1] Assumes equal production of B^+ and B^0 at the $\Upsilon(4S)$.

[2] ABULENCIA 06J reports $[\Gamma(B^+ \to \overline{D}^0\pi^+)/\Gamma_{total}] / [B(B^0 \to D^-\pi^+)] = 1.97 \pm 0.10 \pm 0.21$ which we multiply by our best value $B(B^0 \to D^-\pi^+) = (2.68 \pm 0.13) \times 10^{-3}$. Our first error is their experiment's error and our second error is the systematic error from using our best value.

[3] Uses a missing-mass method. Does not depend on D branching fractions or B^+/B^0 production rates.

[4] AHMED 02B reports an additional uncertainty on the branching ratios to account for 4.5% uncertainty on relative production of B^0 and B^+, which is not included here.

[5] Assumes equal production of B^+ and B^0 at the $\Upsilon(4S)$ and uses the MarkIII branching fractions for the D.

[6] BEBEK 87 value has been updated in BERKELMAN 91 to use same assumptions as noted for BORTOLETTO 92.

[7] AUBERT,B 04P reports $[\Gamma(B^+ \to \overline{D}^0\pi^+)/\Gamma_{total}] \times [B(D^0 \to K^-\pi^+)] = (1.846 \pm 0.032 \pm 0.097) \times 10^{-4}$ which we divide by our best value $B(D^0 \to K^-\pi^+) = (3.88 \pm 0.05) \times 10^{-2}$. Our first error is their experiment's error and our second error is the systematic error from using our best value.

[8] ALAM 94 assume equal production of B^+ and B^0 at the $\Upsilon(4S)$ and use the CLEOII absolute $B(D^0 \to K^-\pi^+)$ and the PDG 1992 $B(D^0 \to K^-\pi^+\pi^0)/B(D^0 \to K^-\pi^+)$ and $B(D^0 \to K^-2\pi^+\pi^-)/B(D^0 \to K^-\pi^+)$.

[9] ALBRECHT 88K assumes $B^0\overline{B}^0$:B^+B^- ratio is 45:55. Superseded by ALBRECHT 90J.

$\Gamma(\overline{D}^0\rho^+)/\Gamma_{total}$ Γ_{49}/Γ

VALUE	EVTS	DOCUMENT ID		TECN	COMMENT
0.0134±0.0018 OUR AVERAGE					
0.0135±0.0012±0.0015	212	[1] ALAM	94	CLE2	$e^+e^- \to \Upsilon(4S)$
0.013 ±0.004 ±0.004	19	[2] ALBRECHT	90J	ARG	$e^+e^- \to \Upsilon(4S)$
• • • We do not use the following data for averages, fits, limits, etc. • • •					
0.021 ±0.008 ±0.009	10	[3] ALBRECHT	88K	ARG	$e^+e^- \to \Upsilon(4S)$

[1] ALAM 94 assume equal production of B^+ and B^0 at the $\Upsilon(4S)$ and use the CLEOII absolute $B(D^0 \to K^-\pi^+)$ and the PDG 1992 $B(D^0 \to K^-\pi^+\pi^0)/B(D^0 \to K^-\pi^+)$ and $B(D^0 \to K^-2\pi^+\pi^-)/B(D^0 \to K^-\pi^+)$.

[2] Assumes equal production of B^+ and B^0 at the $\Upsilon(4S)$ and uses the MarkIII branching fractions for the D.

[3] ALBRECHT 88K assumes $B^0\overline{B}^0$:B^+B^- ratio is 45:55.

$\Gamma(\overline{D}^0K^+)/\Gamma(\overline{D}^0\pi^+)$ Γ_{50}/Γ_{46}

VALUE (units 10^{-2})	DOCUMENT ID		TECN	COMMENT
7.69±0.25 OUR AVERAGE	Error includes scale factor of 1.7. See the ideogram below.			
7.71±0.17±0.26	[1] AAIJ	13AE	LHCB	pp at 7 TeV
7.74±0.12±0.19	AAIJ	12M	LHCB	pp at 7 TeV
6.77±0.23±0.30	HORII	08	BELL	$e^+e^- \to \Upsilon(4S)$
8.31±0.35±0.20	AUBERT	04N	BABR	$e^+e^- \to \Upsilon(4S)$
9.9 $^{+1.4}_{-1.2}$ $^{+0.7}_{-0.6}$	BORNHEIM	03	CLE2	$e^+e^- \to \Upsilon(4S)$
• • • We do not use the following data for averages, fits, limits, etc. • • •				
9.4 ±0.9 ±0.7	ABE	03D	BELL	Repl. by SWAIN 03
7.7 ±0.5 ±0.6	SWAIN	03	BELL	Repl. by HORII 08
7.9 ±0.9 ±0.6	ABE	01I	BELL	Repl. by ABE 03D
5.5 ±1.4 ±0.5	ATHANAS	98	CLE2	Repl. by BORNHEIM 03

[1] Uses $B^{\pm} \to [K^{\pm}\pi^{\mp}\pi^+\pi^-]_D h^{\pm}$ mode.

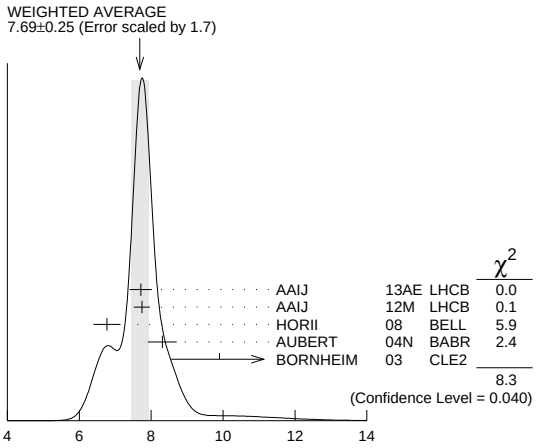

$\Gamma(D_{CP(+1)}K^+)/\Gamma(D_{CP(+1)}\pi^+)$ Γ_{51}/Γ_{47}

VALUE	DOCUMENT ID		TECN	COMMENT
0.087±0.007 OUR AVERAGE				
0.087±0.008±0.003	[1,2] ABE	06	BELL	$e^+e^- \to \Upsilon(4S)$
0.088±0.016±0.005	[3] AUBERT	04N	BABR	$e^+e^- \to \Upsilon(4S)$
• • • We do not use the following data for averages, fits, limits, etc. • • •				
0.125±0.036±0.010	[3] ABE	03D	BELL	Repl. by SWAIN 03
0.093±0.018±0.008	[3] SWAIN	03	BELL	Repl. by ABE 06

[1] Reports a double ratio of $B(B^+ \to D_{CP(+1)}K^+)/B(B^+ \to D_{CP(+1)}\pi^+)$ and $B(B^+ \to \overline{D}^0K^+)/B(B^+ \to \overline{D}^0\pi^+)$, 1.13 ± 0.16 ± 0.08. We multiply by our best value of $B(B^+ \to \overline{D}^0K^+)/B(B^+ \to \overline{D}^0\pi^+) = 0.083 \pm 0.006$. Our first error is their experiment's error and the second error is systematic error from using our best value.

[2] ABE 06 reports $[\Gamma(B^+ \to D_{CP(+1)}K^+)/\Gamma(B^+ \to D_{CP(+1)}\pi^+)] / [\Gamma(B^+ \to \overline{D}^0K^+)/\Gamma(B^+ \to \overline{D}^0\pi^+)] = 1.13 \pm 0.06 \pm 0.08$ which we multiply by our best value $\Gamma(B^+ \to \overline{D}^0K^+)/\Gamma(B^+ \to \overline{D}^0\pi^+) = 0.0769 \pm 0.0025$. Our first error is their experiment's error and our second error is the systematic error from using our best value.

[3] CP=+1 eigenstate of $D^0\overline{D}^0$ system is reconstructed via K^+K^- and $\pi^+\pi^-$.

$\Gamma(D_{CP(+1)}K^+)/\Gamma(\overline{D}^0K^+)$ Γ_{51}/Γ_{50}

VALUE	DOCUMENT ID		TECN	COMMENT
0.518±0.029 OUR AVERAGE	Error includes scale factor of 1.6.			
0.504±0.019±0.006	[1] AAIJ	12M	LHCB	pp at 7 TeV
0.65 ±0.12 ±0.06	[2] AALTONEN	10A	CDF	$p\overline{p}$ at 1.96 TeV
0.590±0.045±0.025	[3] DEL-AMO-SA..10G		BABR	$e^+e^- \to \Upsilon(4S)$
• • • We do not use the following data for averages, fits, limits, etc. • • •				
0.53 ±0.05 ±0.025	AUBERT	08AA	BABR	Repl. by DEL-AMO-SANCHEZ 10G
0.45 ±0.06 ±0.02	AUBERT	06J	BABR	Repl. by AUBERT 08AA

[1] AAIJ 12M reports $R_{CP+} = 1.007 \pm 0.038 \pm 0.012$ which we have divided by 2.

[2] Reports $R_{CP+} = 2\,(B(B^- \to D_{CP(+1)}K^-) + B(B^+ \to D_{CP(+1)}K^+)) / (B(B^- \to D^0K^-) + B(B^+ \to \overline{D}^0K^+)) = 1.30 \pm 0.24 \pm 0.12$ that we have divided by 2.

[3] Reports $R_{CP+} = 1.18 \pm 0.09 \pm 0.05$ that we have divided by 2.

$\Gamma(D_{CP(-1)}K^+)/\Gamma(D_{CP(-1)}\pi^+)$ Γ_{52}/Γ_{48}

VALUE	DOCUMENT ID		TECN	COMMENT
0.097±0.016±0.007	[1] ABE	06	BELL	$e^+e^- \to \Upsilon(4S)$
• • • We do not use the following data for averages, fits, limits, etc. • • •				
0.119±0.028±0.006	[2] ABE	03D	BELL	Repl. by SWAIN 03
0.108±0.019±0.007	[2] SWAIN	03	BELL	Repl. by ABE 06

[1] Reports a double ratio of $B(B^+ \to D_{CP(-1)}K^+)/B(B^+ \to D_{CP(-1)}\pi^+)$ and $B(B^+ \to \overline{D}^0K^+)/B(B^+ \to \overline{D}^0\pi^+)$, 1.17 ± 0.14 ± 0.14. We multiply by our best value of $B(B^+ \to \overline{D}^0K^+)/B(B^+ \to \overline{D}^0\pi^+) = 0.083 \pm 0.006$. Our first error is their experiment's error and the second error is systematic error from using our best value.

[2] CP=−1 eigenstate of $D^0\overline{D}^0$ system is reconstructed via $K^0_S\pi^0$, $K^0_S\omega$, $K^0_S\phi$, $K^0_S\eta$, and $K^0_S\eta'$.

$\Gamma(D_{CP(-1)}K^+)/\Gamma(\overline{D}^0K^+)$ Γ_{52}/Γ_{50}

VALUE	DOCUMENT ID		TECN	COMMENT
0.54 ±0.04±0.02	[1] DEL-AMO-SA..10G		BABR	$e^+e^- \to \Upsilon(4S)$
• • • We do not use the following data for averages, fits, limits, etc. • • •				
0.515±0.05±0.025	AUBERT	08AA	BABR	Repl. by DEL-AMO-SANCHEZ 10G
0.43 ±0.05±0.02	AUBERT	06J	BABR	Repl. by AUBERT 08AA

[1] Reports $R_{CP+} = 1.07 \pm 0.08 \pm 0.04$ that we have divided by 2.

See key on page 547

$\Gamma([K^-\pi^+]_D K^+)/\Gamma_{total}$ Γ_{53}/Γ

VALUE	CL%	DOCUMENT ID		TECN	COMMENT
$<2.8\times10^{-7}$	90	HORII	08	BELL	$e^+e^-\to\Upsilon(4S)$
• • • We do not use the following data for averages, fits, limits, etc. • • •					
$<6.3\times10^{-7}$	90	SAIGO	05	BELL	$e^+e^-\to\Upsilon(4S)$

$\Gamma([K^-\pi^+]_D K^+)/\Gamma([K^+\pi^-]_D K^+)$ Γ_{53}/Γ_{54}

VALUE (units 10^{-3})	CL%	DOCUMENT ID		TECN	COMMENT
15.3±1.7 OUR AVERAGE					
15.2±2.0±0.4		AAIJ	12M	LHCB	pp at 7 TeV
22.0±8.6±2.6		[1] AALTONEN	11AJ	CDF	$p\overline{p}$ at 1.96 TeV
$16.3^{+4.4}_{-4.1}{}^{+0.7}_{-1.3}$		HORII	11	BELL	$e^+e^-\to\Upsilon(4S)$
11 ±6 ±2		DEL-AMO-SA...10H		BABR	$e^+e^-\to\Upsilon(4S)$
• • • We do not use the following data for averages, fits, limits, etc. • • •					
$7.8^{+6.2}_{-5.7}{}^{+2.0}_{-2.8}$		HORII	08	BELL	Repl. by HORII 11
<29	90	[2] AUBERT	05G	BABR	Repl. by DEL-AMO-SANCHEZ 10H
<44	90	[3] SAIGO	05	BELL	$e^+e^-\to\Upsilon(4S)$
<26	90	[4] AUBERT,B	04L	BABR	Repl. by AUBERT 05G

[1] AALTONEN 11AJ also measures the ratio separately for B^+ ($R^+(K)$) and B^- ($R^-(K)$) and obtains: $R^+(K)=(42.6\pm13.7\pm2.8)\times10^{-3}$, $R^-(K)=(3.8\pm10.3\pm2.7)\times10^{-3}$.

[2] AUBERT 05G extract a constraint on the magnitude of the ratio of amplitudes $|A(B^+\to D^0K^+)\ /\ A(B^+\to\overline{D}{}^0K^+)|<0.23$ at 90% CL (Bayesian). Similar measurements from $B^+\to D^{*0}K^+$ are also reported.

[3] SAIGO 05 extract a constraint on the magnitude of the ratio of amplitudes $|A(B^+\to D^0K^+)\ /\ A(B^+\to\overline{D}{}^0K^+)|<0.27$ at 90% CL.

[4] AUBERT,B 04L extract a constraint on the magnitude of the ratio of amplitudes $|A(B^+\to D^0K^+)/A(B^+\to\overline{D}{}^0K^+)|<0.22$ at 90% CL.

$\Gamma([K^-\pi^+\pi^0]_D K^+)/\Gamma([K^+\pi^-\pi^0]_D K^+)$ Γ_{55}/Γ_{56}

VALUE (units 10^{-3})	CL%	DOCUMENT ID		TECN	COMMENT
19.8±6.2±2.4		NAYAK	13	BELL	$e^+e^-\to\Upsilon(4S)$
• • • We do not use the following data for averages, fits, limits, etc. • • •					
<21	90	[1] LEES	11D	BABR	$e^+e^-\to\Upsilon(4S)$
<39	95	[2] AUBERT	07BN	BABR	Repl. by LEES 11D

[1] Extracts a constraint on the magnitude of the ratio of amplitudes $|A(B^+\to D^0K^+)/A(B^+\to\overline{D}{}^0K^+)|<0.13$ at 95% CL.

[2] Extracts a constraint on the magnitude of the ratio of amplitudes $|A(B^+\to D^0K^+)/A(B^+\to\overline{D}{}^0K^+)|<0.19$ at 95% CL.

$\Gamma([K^-\pi^+\pi^+\pi^-]_D K^+)/\Gamma([K^+\pi^-\pi^+\pi^-]_D K^+)$ Γ_{57}/Γ_{58}

VALUE (units 10^{-2})	DOCUMENT ID		TECN	COMMENT
1.24±0.27	AAIJ	13AE	LHCB	pp at 7 TeV

$\Gamma([K^-\pi^+]_D K^*(892)^+)/\Gamma([K^+\pi^-]_D K^*(892)^+)$ Γ_{59}/Γ_{60}

VALUE	DOCUMENT ID		TECN	COMMENT
0.066±0.031±0.010	AUBERT	09AJ	BABR	$e^+e^-\to\Upsilon(4S)$
• • • We do not use the following data for averages, fits, limits, etc. • • •				
0.046±0.031±0.008	AUBERT,B	05V	BABR	Repl. by AUBERT 09AJ

$\Gamma([K^-\pi^+]_D\pi^+)/\Gamma_{total}$ Γ_{61}/Γ

VALUE (units 10^{-7})	DOCUMENT ID		TECN	COMMENT
$6.29^{+1.02}_{-0.98}{}^{+0.37}_{-0.48}$	HORII	08	BELL	$e^+e^-\to\Upsilon(4S)$
• • • We do not use the following data for averages, fits, limits, etc. • • •				
6.6 $^{+1.9}_{-1.7}$ ±0.5	SAIGO	05	BELL	Repl. by HORII 08

$\Gamma([K^-\pi^+]_D\pi^+)/\Gamma([K^+\pi^-]_D\pi^+)$ Γ_{61}/Γ_{62}

VALUE (units 10^{-3})	DOCUMENT ID		TECN	COMMENT
3.75±0.26 OUR AVERAGE Error includes scale factor of 1.3. See the ideogram below.				
4.10±0.25±0.05	AAIJ	12M	LHCB	pp at 7 TeV
2.8 ±0.7 ±0.4	[1] AALTONEN	11AJ	CDF	$p\overline{p}$ at 1.96 TeV
$3.28^{+0.38}_{-0.36}{}^{+0.12}_{-0.18}$	HORII	11	BELL	$e^+e^-\to\Upsilon(4S)$
3.3 ±0.6 ±0.4	DEL-AMO-SA...10H		BABR	$e^+e^-\to\Upsilon(4S)$
• • • We do not use the following data for averages, fits, limits, etc. • • •				
$3.40^{+0.55}_{-0.53}{}^{+0.15}_{-0.22}$	HORII	08	BELL	Repl. by HORII 11
3.5 $^{+1.0}_{-0.9}$ ±0.2	SAIGO	05	BELL	Repl. by HORII 08

[1] AALTONEN 11AJ also measures the ratio separately for B^+ ($R^+(\pi)$) and B^- ($R^-(\pi)$) and obtains: $R^+(\pi)=(2.4\pm1.0\pm0.4)\times10^{-3}$, $R^-(K)=(3.1\pm1.1\pm0.4)\times10^{-3}$.

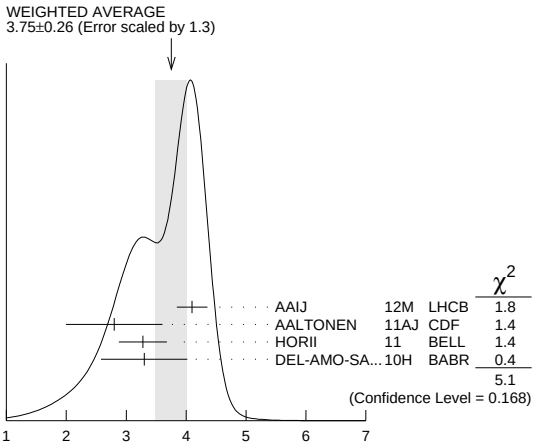

$\Gamma([K^-\pi^+\pi^0]_D\pi^+)/\Gamma([K^+\pi^-\pi^0]_D\pi^+)$ Γ_{63}/Γ_{64}

VALUE (units 10^{-3})	DOCUMENT ID		TECN	COMMENT
$1.89\pm0.54^{+0.22}_{-0.25}$	NAYAK	13	BELL	$e^+e^-\to\Upsilon(4S)$

$\Gamma([K^-\pi^+\pi^+\pi^-]_D\pi^+)/\Gamma([K^+\pi^-\pi^+\pi^-]_D\pi^+)$ Γ_{65}/Γ_{66}

VALUE (units 10^{-3})	DOCUMENT ID		TECN	COMMENT
3.7±0.4	AAIJ	13AE	LHCB	pp at 7 TeV

$\Gamma([K^-\pi^+]_{(D\pi)}\pi^+)/\Gamma([K^+\pi^-]_{(D\pi)}\pi^+)$ Γ_{67}/Γ_{68}

VALUE (units 10^{-3})	DOCUMENT ID		TECN	COMMENT
3.2±0.9±0.8	DEL-AMO-SA...10H		BABR	$e^+e^-\to\Upsilon(4S)$

$\Gamma([K^-\pi^+]_{(D\gamma)}\pi^+)/\Gamma([K^+\pi^-]_{(D\gamma)}\pi^+)$ Γ_{69}/Γ_{70}

VALUE (units 10^{-3})	DOCUMENT ID		TECN	COMMENT
2.7±1.4±2.2	DEL-AMO-SA...10H		BABR	$e^+e^-\to\Upsilon(4S)$

$\Gamma([K^-\pi^+]_{(D\pi)}K^+)/\Gamma([K^+\pi^-]_{(D\pi)}K^+)$ Γ_{71}/Γ_{72}

VALUE (units 10^{-3})	DOCUMENT ID		TECN	COMMENT
1.8±0.9±0.4	DEL-AMO-SA...10H		BABR	$e^+e^-\to\Upsilon(4S)$

$\Gamma([K^-\pi^+]_{(D\gamma)}K^+)/\Gamma([K^+\pi^-]_{(D\gamma)}K^+)$ Γ_{73}/Γ_{74}

VALUE (units 10^{-3})	DOCUMENT ID		TECN	COMMENT
1.3±1.4±0.8	DEL-AMO-SA...10H		BABR	$e^+e^-\to\Upsilon(4S)$

$\Gamma([\pi^+\pi^-\pi^0]_D K^-)/\Gamma_{total}$ Γ_{75}/Γ

VALUE (units 10^{-6})	DOCUMENT ID		TECN	COMMENT
4.6±0.8±0.4	[1] AUBERT	07BJ	BABR	$e^+e^-\to\Upsilon(4S)$
• • • We do not use the following data for averages, fits, limits, etc. • • •				
5.5±1.0±0.7	[1] AUBERT,B	05T	BABR	Repl. by AUBERT 07BJ

[1] Assumes equal production of B^+ and B^0 at the $\Upsilon(4S)$.

$\Gamma(\overline{D}{}^0K^*(892)^+)/\Gamma_{total}$ Γ_{76}/Γ

VALUE (units 10^{-4})	DOCUMENT ID		TECN	COMMENT
5.3 ±0.4 OUR AVERAGE				
5.29±0.30±0.34	[1] AUBERT	06Z	BABR	$e^+e^-\to\Upsilon(4S)$
6.1 ±1.6 ±1.7	[1] MAHAPATRA	02	CLE2	$e^+e^-\to\Upsilon(4S)$
• • • We do not use the following data for averages, fits, limits, etc. • • •				
6.3 ±0.7 ±0.5	[1] AUBERT	04Q	BABR	Repl. by AUBERT 06Z

[1] Assumes equal production of B^+ and B^0 at the $\Upsilon(4S)$.

$\Gamma(D_{CP(-1)}K^*(892)^+)/\Gamma(\overline{D}{}^0K^*(892)^+)$ Γ_{77}/Γ_{76}

VALUE	DOCUMENT ID		TECN	COMMENT
0.515±0.135±0.065	[1] AUBERT	09AJ	BABR	$e^+e^-\to\Upsilon(4S)$
• • • We do not use the following data for averages, fits, limits, etc. • • •				
0.325±0.13 ±0.04	[2] AUBERT,B	05U	BABR	Repl. by AUBERT 09AJ

[1] The authors report $R_{CP-}=1.03\pm0.27\pm0.13$ which is, assuming *CP* conservation, twice the value of the quoted above branching ratio,

[2] The authors report $R_{CP-}=0.65\pm0.26\pm0.08$ which is, assuming *CP* conservation, twice the value of the quoted above branching ratio.

$\Gamma(D_{CP(+1)}\,K^*(892)^+)/\Gamma(\overline{D}^0\,K^*(892)^+)$ Γ_{78}/Γ_{76}

VALUE	DOCUMENT ID		TECN	COMMENT
1.085 ± 0.175 ± 0.045	[1] AUBERT	09AJ	BABR	$e^+e^- \to \Upsilon(4S)$
• • • We do not use the following data for averages, fits, limits, etc. • • •				
0.98 ± 0.20 ± 0.055	[2] AUBERT,B	05U	BABR	Repl. by AUBERT 09AJ

[1] The authors report $R_{CP+} = 2.17 \pm 0.35 \pm 0.09$ which is, assuming *CP* conservation, twice the value of the quoted above branching ratio,
[2] The authors report $R_{CP+} = 1.96 \pm 0.40 \pm 0.11$ which is, assuming *CP* conservation, twice the value of the quoted above branching ratio.

$\Gamma(\overline{D}^0\,K^+\pi^+\pi^+\pi^-)/\Gamma(\overline{D}^0\pi^+\pi^+\pi^-)$ Γ_{79}/Γ_{82}

VALUE (units 10^{-2})	DOCUMENT ID		TECN	COMMENT
9.4 ± 1.3 ± 0.9	AAIJ	12T	LHCB	pp at 7 TeV

$\Gamma(\overline{D}^0\,K^+\overline{K}^0)/\Gamma_{\text{total}}$ Γ_{80}/Γ

VALUE (units 10^{-4})	DOCUMENT ID		TECN	COMMENT
5.5 ± 1.4 ± 0.8	[1] DRUTSKOY	02	BELL	$e^+e^- \to \Upsilon(4S)$

[1] Assumes equal production of B^+ and B^0 at the $\Upsilon(4S)$.

$\Gamma(\overline{D}^0\,K^+\overline{K}^*(892)^0)/\Gamma_{\text{total}}$ Γ_{81}/Γ

VALUE (units 10^{-4})	DOCUMENT ID		TECN	COMMENT
7.5 ± 1.3 ± 1.1	[1] DRUTSKOY	02	BELL	$e^+e^- \to \Upsilon(4S)$

[1] Assumes equal production of B^+ and B^0 at the $\Upsilon(4S)$.

$\Gamma(\overline{D}^0\pi^+\pi^+\pi^-)/\Gamma_{\text{total}}$ Γ_{82}/Γ

VALUE	DOCUMENT ID		TECN	COMMENT
0.0057 ± 0.0022 OUR FIT Error includes scale factor of 3.6.				
0.0115 ± 0.0029 ± 0.0021	[1] BORTOLETTO92		CLEO	$e^+e^- \to \Upsilon(4S)$

[1] BORTOLETTO 92 assumes equal production of B^+ and B^0 at the $\Upsilon(4S)$ and uses Mark III branching fractions for the D.

$\Gamma(\overline{D}^0\pi^+\pi^+\pi^-)/\Gamma(\overline{D}^0\pi^+)$ Γ_{82}/Γ_{46}

VALUE	DOCUMENT ID		TECN	COMMENT
1.2 ± 0.4 OUR FIT Error includes scale factor of 3.8.				
1.27 ± 0.06 ± 0.11	AAIJ	11E	LHCB	pp at 7 TeV

$\Gamma(\overline{D}^0\pi^+\pi^+\pi^-\,\text{nonresonant})/\Gamma_{\text{total}}$ Γ_{83}/Γ

VALUE	DOCUMENT ID		TECN	COMMENT
0.0051 ± 0.0034 ± 0.0023	[1] BORTOLETTO92		CLEO	$e^+e^- \to \Upsilon(4S)$

[1] BORTOLETTO 92 assumes equal production of B^+ and B^0 at the $\Upsilon(4S)$ and uses Mark III branching fractions for the D.

$\Gamma(\overline{D}^0\pi^+\rho^0)/\Gamma_{\text{total}}$ Γ_{84}/Γ

VALUE	DOCUMENT ID		TECN	COMMENT
0.0042 ± 0.0023 ± 0.0020	[1] BORTOLETTO92		CLEO	$e^+e^- \to \Upsilon(4S)$

[1] BORTOLETTO 92 assumes equal production of B^+ and B^0 at the $\Upsilon(4S)$ and uses Mark III branching fractions for the D.

$\Gamma(\overline{D}^0\,a_1(1260)^+)/\Gamma_{\text{total}}$ Γ_{85}/Γ

VALUE	DOCUMENT ID		TECN	COMMENT
0.0045 ± 0.0019 ± 0.0031	[1] BORTOLETTO92		CLEO	$e^+e^- \to \Upsilon(4S)$

[1] BORTOLETTO 92 assumes equal production of B^+ and B^0 at the $\Upsilon(4S)$ and uses Mark III branching fractions for the D.

$\Gamma(\overline{D}^0\omega\pi^+)/\Gamma_{\text{total}}$ Γ_{86}/Γ

VALUE	DOCUMENT ID		TECN	COMMENT
0.0041 ± 0.0007 ± 0.0006	[1] ALEXANDER	01B	CLE2	$e^+e^- \to \Upsilon(4S)$

[1] Assumes equal production of B^+ and B^0 at the $\Upsilon(4S)$. The signal is consistent with all observed $\omega\pi^+$ having proceeded through the ρ'^+ resonance at mass $1349 \pm 25^{+10}_{-5}$ MeV and width $547 \pm 86^{+46}_{-45}$ MeV.

$\Gamma(D^*(2010)^-\pi^+\pi^+)/\Gamma_{\text{total}}$ Γ_{87}/Γ

VALUE (units 10^{-3})	CL%	EVTS	DOCUMENT ID		TECN	COMMENT
1.35 ± 0.22 OUR AVERAGE						
1.25 ± 0.08 ± 0.22			[1] ABE	04D	BELL	$e^+e^- \to \Upsilon(4S)$
1.9 ± 0.7 ± 0.3		14	[2] ALAM	94	CLE2	$e^+e^- \to \Upsilon(4S)$
2.6 ± 1.4 ± 0.7		11	[3] ALBRECHT	90J	ARG	$e^+e^- \to \Upsilon(4S)$
$2.4\ ^{+1.7}_{-1.6}\ ^{+1.0}_{-0.6}$		3	[4] BEBEK	87	CLEO	$e^+e^- \to \Upsilon(4S)$
• • • We do not use the following data for averages, fits, limits, etc. • • •						
<4.	90		[5] BORTOLETTO92		CLEO	$e^+e^- \to \Upsilon(4S)$
5. ± 2. ± 3.		7	[6] ALBRECHT	87C	ARG	$e^+e^- \to \Upsilon(4S)$

[1] Assumes equal production of B^+ and B^0 at the $\Upsilon(4S)$.
[2] ALAM 94 assume equal production of B^+ and B^0 at the $\Upsilon(4S)$ and use the CLEO II $B(D^*(2010)^+ \to D^0\pi^+)$ and absolute $B(D^0 \to K^-\pi^+)$ and the PDG 1992 $B(D^0 \to K^-\pi^+\pi^0)/B(D^0 \to K^-\pi^+)$ and $B(D^0 \to K^-2\pi^+\pi^-)/B(D^0 \to K^-\pi^+)$.
[3] Assumes equal production of B^+ and B^0 at the $\Upsilon(4S)$ and uses the Mark III branching fractions for the D.
[4] BEBEK 87 value has been updated in BERKELMAN 91 to use same assumptions as noted for BORTOLETTO 92.
[5] BORTOLETTO 92 assumes equal production of B^+ and B^0 at the $\Upsilon(4S)$ and uses Mark III branching fractions for the D and $D^*(2010)$. The authors also find the product branching fraction into $D^{**}\pi$ followed by $D^{**} \to D^*(2010)\pi$ to be $0.0014\ ^{+0.0008}_{-0.0006} \pm 0.0003$ where D^{**} represents all orbitally excited D mesons.
[6] ALBRECHT 87C use PDG 86 branching ratios for D and $D^*(2010)$ and assume $B(\Upsilon(4S) \to B^+B^-) = 55\%$ and $B(\Upsilon(4S) \to B^0\overline{B}^0) = 45\%$. Superseded by ALBRECHT 90J.

$\Gamma(\overline{D}_1(2420)^0\pi^+,\ \overline{D}_1^0 \to D^*(2010)^-\pi^+)/\Gamma(\overline{D}^0\pi^+\pi^+\pi^-)$ Γ_{88}/Γ_{82}

VALUE (units 10^{-2})	DOCUMENT ID		TECN	COMMENT
9.3 ± 1.6 ± 0.9	[1] AAIJ	11E	LHCB	pp at 7 TeV

[1] AAIJ 11E reports $(9.3 \pm 1.6 \pm 0.9) \times 10^{-2}$ from a measurement of $[\Gamma(B^+ \to \overline{D}_1(2420)^0\pi^+,\ \overline{D}_1^0 \to D^*(2010)^-\pi^+)/\Gamma(B^+ \to \overline{D}^0\pi^+\pi^+\pi^-)] \times [B(D^*(2010)^+ \to D^0\pi^+)]$ assuming $B(D^*(2010)^+ \to D^0\pi^+) = (67.7 \pm 0.5) \times 10^{-2}$.

$\Gamma(D^-\pi^+\pi^+)/\Gamma_{\text{total}}$ Γ_{89}/Γ

VALUE (units 10^{-3})	CL%	EVTS	DOCUMENT ID		TECN	COMMENT
1.07 ± 0.05 OUR AVERAGE						
1.08 ± 0.03 ± 0.05			[1] AUBERT	09AB	BABR	$e^+e^- \to \Upsilon(4S)$
1.02 ± 0.04 ± 0.15			[1] ABE	04D	BELL	$e^+e^- \to \Upsilon(4S)$
• • • We do not use the following data for averages, fits, limits, etc. • • •						
<1.4	90		[2] ALAM	94	CLE2	$e^+e^- \to \Upsilon(4S)$
<7	90		[3] BORTOLETTO92		CLEO	$e^+e^- \to \Upsilon(4S)$
$2.5\ ^{+4.1}_{-2.3}\ ^{+2.4}_{-0.8}$		1	[4] BEBEK	87	CLEO	$e^+e^- \to \Upsilon(4S)$

[1] Assumes equal production of B^+ and B^0 at the $\Upsilon(4S)$.
[2] ALAM 94 assume equal production of B^+ and B^0 at the $\Upsilon(4S)$ and use the Mark III $B(D^+ \to K^-2\pi^+)$.
[3] BORTOLETTO 92 assumes equal production of B^+ and B^0 at the $\Upsilon(4S)$ and uses Mark III branching fractions for the D. The product branching fraction into $D_0^*(2340)\pi$ followed by $D_0^*(2340) \to D\pi$ is < 0.005 at 90%CL and into $D_2^*(2460)$ followed by $D_2^*(2460) \to D\pi$ is < 0.004 at 90%CL.
[4] BEBEK 87 assume the $\Upsilon(4S)$ decays 43% to $B^0\overline{B}^0$. $B(D^- \to K^+\pi^-\pi^-) = (9.1 \pm 1.3 \pm 0.4)\%$ is assumed.

$\Gamma(D^+K^0)/\Gamma_{\text{total}}$ Γ_{90}/Γ

VALUE (units 10^{-6})	CL%	DOCUMENT ID		TECN	COMMENT
<2.9	90	[1] DEL-AMO-SA...10K		BABR	$e^+e^- \to \Upsilon(4S)$
• • • We do not use the following data for averages, fits, limits, etc. • • •					
<5.0	90	[1] AUBERT,B	05E	BABR	Repl. by DEL-AMO-SANCHEZ 10K

[1] Assumes equal production of B^+ and B^0 at the $\Upsilon(4S)$.

$\Gamma(D^+K^{*0})/\Gamma_{\text{total}}$ Γ_{91}/Γ

VALUE (units 10^{-6})	CL%	DOCUMENT ID		TECN	COMMENT
<1.8	90	AAIJ	13R	LHCB	pp at 7 TeV
• • • We do not use the following data for averages, fits, limits, etc. • • •					
<3.0	90	[1] DEL-AMO-SA...10K		BABR	$e^+e^- \to \Upsilon(4S)$

[1] Assumes equal production of B^+ and B^0 at the $\Upsilon(4S)$.

$\Gamma(D^+\overline{K}^{*0})/\Gamma_{\text{total}}$ Γ_{92}/Γ

VALUE (units 10^{-6})	CL%	DOCUMENT ID		TECN	COMMENT
<1.4	90	AAIJ	13R	LHCB	pp at 7 TeV

$\Gamma(\overline{D}^*(2007)^0\pi^+)/\Gamma_{\text{total}}$ Γ_{93}/Γ

VALUE (units 10^{-3})	EVTS	DOCUMENT ID		TECN	COMMENT
5.18 ± 0.26 OUR AVERAGE					
5.52 ± 0.17 ± 0.42		[1] AUBERT	07H	BABR	$e^+e^- \to \Upsilon(4S)$
5.5 ± 0.4 ± 0.2		[2,3] AUBERT,BE	06J	BABR	$e^+e^- \to \Upsilon(4S)$
4.34 ± 0.47 ± 0.18		[4] BRANDENB...	98	CLE2	$e^+e^- \to \Upsilon(4S)$
5.2 ± 0.7 ± 0.7	71	[5] ALAM	94	CLE2	$e^+e^- \to \Upsilon(4S)$
7.2 ± 1.8 ± 1.6		[6] BORTOLETTO92		CLEO	$e^+e^- \to \Upsilon(4S)$
4.0 ± 1.4 ± 1.2	9	[6] ALBRECHT	90J	ARG	$e^+e^- \to \Upsilon(4S)$
• • • We do not use the following data for averages, fits, limits, etc. • • •					
2.7 ± 4.4		[7] BEBEK	87	CLEO	$e^+e^- \to \Upsilon(4S)$

[1] Assumes equal production of B^+ and B^0 at the $\Upsilon(4S)$.
[2] AUBERT,BE 06J reports $[\Gamma(B^+ \to \overline{D}^*(2007)^0\pi^+)/\Gamma_{\text{total}}] / [B(B^+ \to \overline{D}^0\pi^+)] = 1.14 \pm 0.07 \pm 0.04$ which we multiply by our best value $B(B^+ \to \overline{D}^0\pi^+) = (4.81 \pm 0.15) \times 10^{-3}$. Our first error is their experiment's error and our second error is the systematic error from using our best value.
[3] Uses a missing-mass method. Does not depend on D branching fractions or B^+/B^0 production rates.
[4] BRANDENBURG 98 assume equal production of B^+ and B^0 at $\Upsilon(4S)$ and use the D^* reconstruction technique. The first error is their experiment's error and the second error is the systematic error from the PDG 96 value of $B(D^* \to D\pi)$.
[5] ALAM 94 assume equal production of B^+ and B^0 at the $\Upsilon(4S)$ and use the CLEO II $B(D^*(2007)^0 \to D^0\pi^0)$ and absolute $B(D^0 \to K^-\pi^+)$ and the PDG 1992 $B(D^0 \to K^-\pi^+\pi^0)/B(D^0 \to K^-\pi^+)$ and $B(D^0 \to K^-2\pi^+\pi^-)/B(D^0 \to K^-\pi^+)$.
[6] Assumes equal production of B^+ and B^0 at the $\Upsilon(4S)$ and uses Mark III branching fractions for the D and $D^*(2010)$.
[7] This is a derived branching ratio, using the inclusive pion spectrum and other two-body B decays. BEBEK 87 assume the $\Upsilon(4S)$ decays 43% to $B^0\overline{B}^0$.

$\Gamma(\overline{D}^*(2007)^0\omega\pi^+)/\Gamma_{total}$ Γ_{96}/Γ

VALUE	DOCUMENT ID		TECN	COMMENT
$0.0045\pm0.0010\pm0.0007$	[1] ALEXANDER	01B	CLE2	$e^+e^-\to\Upsilon(4S)$

[1] Assumes equal production of B^+ and B^0 at the $\Upsilon(4S)$. The signal is consistent with all observed $\omega\pi^+$ having proceeded through the ρ'^+ resonance at mass $1349\pm25^{+10}_{-5}$ MeV and width $547\pm86^{+46}_{-45}$ MeV.

$\Gamma(\overline{D}^*(2007)^0\rho^+)/\Gamma_{total}$ Γ_{97}/Γ

VALUE	EVTS	DOCUMENT ID		TECN	COMMENT
0.0098 ± 0.0017 OUR AVERAGE					
$0.0098\pm0.0006\pm0.0017$		[1] CSORNA	03	CLE2	$e^+e^-\to\Upsilon(4S)$
$0.010\ \pm0.006\ \pm0.004$	7	[2] ALBRECHT	90J	ARG	$e^+e^-\to\Upsilon(4S)$
• • • We do not use the following data for averages, fits, limits, etc. • • •					
$0.0168\pm0.0021\pm0.0028$	86	[3] ALAM	94	CLE2	$e^+e^-\to\Upsilon(4S)$

[1] Assumes equal production of B^0 and B^+ at the $\Upsilon(4S)$ resonance. The second error combines the systematic and theoretical uncertainties in quadrature. CSORNA 03 includes data used in ALAM 94. A full angular fit to three complex helicity amplitudes is performed.

[2] Assumes equal production of B^+ and B^0 at the $\Upsilon(4S)$ and uses MarkIII branching fractions for the D and $D^*(2010)$.

[3] ALAM 94 assume equal production of B^+ and B^0 at the $\Upsilon(4S)$ and use the CLEOII $B(D^*(2007)^0\to D^0\pi^0)$ and absolute $B(D^0\to K^-\pi^+)$ and the PDG 1992 $B(D^0\to K^-\pi^+\pi^0)/B(D^0\to K^-\pi^+)$ and $B(D^0\to K^-2\pi^+\pi^-)/B(D^0\to K^-\pi^+)$. The nonresonant $\pi^+\pi^0$ contribution under the ρ^+ is negligible.

$\Gamma(\overline{D}^*(2007)^0K^+)/\Gamma_{total}$ Γ_{98}/Γ

VALUE (units 10^{-4})	DOCUMENT ID		TECN	COMMENT
4.20 ± 0.34 OUR AVERAGE				
$4.21^{+0.30}_{-0.26}\pm0.21$	[1] AUBERT	05N	BABR	$e^+e^-\to\Upsilon(4S)$
$4.0\ \pm1.1\ \pm0.2$	[2] ABE	01I	BELL	$e^+e^-\to\Upsilon(4S)$

[1] AUBERT 05N reports $[\Gamma(B^+\to\overline{D}^*(2007)^0K^+)/\Gamma_{total}]\ /\ [B(B^+\to\overline{D}^*(2007)^0\pi^+)] = 0.0813\ \pm\ 0.0040^{+0.0042}_{-0.0031}$ which we multiply by our best value $B(B^+\to\overline{D}^*(2007)^0\pi^+) = (5.18\pm0.26)\times10^{-3}$. Our first error is their experiment's error and our second error is the systematic error from using our best value.

[2] ABE 01I reports $[\Gamma(B^+\to\overline{D}^*(2007)^0K^+)/\Gamma_{total}]\ /\ [B(B^+\to\overline{D}^*(2007)^0\pi^+)] = 0.078\pm0.019\pm0.009$ which we multiply by our best value $B(B^+\to\overline{D}^*(2007)^0\pi^+) = (5.18\pm0.26)\times10^{-3}$. Our first error is their experiment's error and our second error is the systematic error from using our best value.

$\Gamma(\overline{D}^{*0}_{CP(+1)}K^+)/\Gamma_{total}$ Γ_{99}/Γ

VALUE (units 10^{-4})	DOCUMENT ID		TECN	COMMENT
$2.75\pm0.29^{+0.23}_{-0.22}$	[1] AUBERT	08BF	BABR	$e^+e^-\to\Upsilon(4S)$

[1] AUBERT 08BF reports $[\Gamma(B^+\to\overline{D}^{*0}_{CP(+1)}K^+)/\Gamma_{total}]\ /\ [B(B^+\to\overline{D}^*(2007)^0K^+)] = 0.655\pm0.065\pm0.020$ which we multiply by our best value $B(B^+\to\overline{D}^*(2007)^0K^+) = (4.20\pm0.34)\times10^{-4}$. Our first error is their experiment's error and our second error is the systematic error from using our best value.

$\Gamma(\overline{D}^{*0}_{CP(+1)}K^+)/\Gamma(\overline{D}^{*0}_{CP(+1)}\pi^+)$ Γ_{99}/Γ_{94}

VALUE	DOCUMENT ID		TECN	COMMENT
0.095 ± 0.017 OUR AVERAGE				
$0.11\ \pm0.02\ \pm0.02$	[1] ABE	06	BELL	$e^+e^-\to\Upsilon(4S)$
$0.086\pm0.021\pm0.007$	[2] AUBERT	05N	BABR	$e^+e^-\to\Upsilon(4S)$

[1] Reports a double ratio of $B(B^+\to D^{*0}_{CP(+1)}K^+)/B(B^+\to D^{*0}_{CP(+1)}\pi^+)$ and $B(B^+\to\overline{D}^{*0}K^+)/B(B^+\to\overline{D}^{*0}\pi^+)$, $1.41\pm0.25\pm0.06$. We multiply by our best value of $B(B^+\to\overline{D}^{*0}K^+)/B(B^+\to\overline{D}^{*0}\pi^+) = 0.080\pm0.011$. Our first error is their experiment's error and the second error is systematic error from using our best value.

[2] Uses $D^{*0}\to D^0\pi^0$ with D^0 reconstructed in the CP-even eigenstates K^+K^- and $\pi^+\pi^-$.

$\Gamma(\overline{D}^{*0}_{CP(-1)}K^+)/\Gamma_{total}$ Γ_{100}/Γ

VALUE (units 10^{-4})	DOCUMENT ID		TECN	COMMENT
$2.31\pm0.27^{+0.20}_{-0.18}$	[1] AUBERT	08BF	BABR	$e^+e^-\to\Upsilon(4S)$

[1] AUBERT 08BF reports $[\Gamma(B^+\to\overline{D}^{*0}_{CP(-1)}K^+)/\Gamma_{total}]\ /\ [B(B^+\to\overline{D}^*(2007)^0K^+)] = 0.55\pm0.06\pm0.02$ which we multiply by our best value $B(B^+\to\overline{D}^*(2007)^0K^+) = (4.20\pm0.34)\times10^{-4}$. Our first error is their experiment's error and our second error is the systematic error from using our best value.

$\Gamma(\overline{D}^{*0}_{CP(-1)}K^+)/\Gamma(D^{*0}_{CP(-1)}\pi^+)$ Γ_{100}/Γ_{95}

VALUE	DOCUMENT ID		TECN	COMMENT
$0.09\pm0.03\pm0.01$	[1] ABE	06	BELL	$e^+e^-\to\Upsilon(4S)$

[1] Reports a double ratio of $B(B^+\to(D^*_{CP(-1)})^0K^+)/B(B^+\to(D^*_{CP(-1)})^0\pi^+)$ and $B(B^+\to\overline{D}^{*0}K^+)/B(B^+\to\overline{D}^{*0}\pi^+)$, $1.15\pm0.31\pm0.12$. We multiply by our best value of $B(B^+\to\overline{D}^{*0}K^+)/B(B^+\to\overline{D}^{*0}\pi^+) = 0.080\pm0.011$. Our first error is their experiment's error and the second error is systematic error from using our best value.

$\Gamma(\overline{D}^*(2007)^0K^*(892)^+)/\Gamma_{total}$ Γ_{101}/Γ

VALUE (units 10^{-4})	DOCUMENT ID		TECN	COMMENT
8.1 ± 1.4 OUR AVERAGE				
$8.3\pm1.1\pm1.0$	[1] AUBERT	04K	BABR	$e^+e^-\to\Upsilon(4S)$
$7.2\pm2.2\pm2.6$	[2] MAHAPATRA	02	CLE2	$e^+e^-\to\Upsilon(4S)$

[1] Assumes equal production of B^+ and B^0 at the $\Upsilon(4S)$.

[2] Assumes equal production of B^+ and B^0 at the $\Upsilon(4S)$ and an unpolarized final state.

$\Gamma(\overline{D}^*(2007)^0K^+\overline{K}^0)/\Gamma_{total}$ Γ_{102}/Γ

VALUE (units 10^{-4})	CL%	DOCUMENT ID		TECN	COMMENT
<10.6	90	[1] DRUTSKOY	02	BELL	$e^+e^-\to\Upsilon(4S)$

[1] Assumes equal production of B^+ and B^0 at the $\Upsilon(4S)$.

$\Gamma(\overline{D}^*(2007)^0K^+K^*(892)^0)/\Gamma_{total}$ Γ_{103}/Γ

VALUE (units 10^{-4})	DOCUMENT ID		TECN	COMMENT
$15.3\pm3.1\pm2.9$	[1] DRUTSKOY	02	BELL	$e^+e^-\to\Upsilon(4S)$

[1] Assumes equal production of B^+ and B^0 at the $\Upsilon(4S)$.

$\Gamma(\overline{D}^*(2007)^0\pi^+\pi^+\pi^-)/\Gamma_{total}$ Γ_{104}/Γ

VALUE (units 10^{-2})	EVTS	DOCUMENT ID		TECN	COMMENT
$1.03\ \pm0.12$ OUR AVERAGE					
$1.055\pm0.047\pm0.129$		[1] MAJUMDER	04	BELL	$e^+e^-\to\Upsilon(4S)$
$0.94\ \pm0.20\ \pm0.17$	48	[2,3] ALAM	94	CLE2	$e^+e^-\to\Upsilon(4S)$

[1] Assumes equal production of B^+ and B^0 at the $\Upsilon(4S)$.

[2] ALAM 94 assume equal production of B^+ and B^0 at the $\Upsilon(4S)$ and use the CLEOII $B(D^*(2007)^0\to D^0\pi^0)$ and absolute $B(D^0\to K^-\pi^+)$ and the PDG 1992 $B(D^0\to K^-\pi^+\pi^0)/B(D^0\to K^-\pi^+)$ and $B(D^0\to K^-2\pi^+\pi^-)/B(D^0\to K^-\pi^+)$.

[3] The three pion mass is required to be between 1.0 and 1.6 GeV consistent with an a_1 meson. (If this channel is dominated by a_1^+, the branching ratio for $\overline{D}^{*0}a_1^+$ is twice that for $\overline{D}^{*0}\pi^+\pi^+\pi^-$.)

$\Gamma(\overline{D}^*(2007)^0a_1(1260)^+)/\Gamma_{total}$ Γ_{105}/Γ

VALUE	DOCUMENT ID		TECN	COMMENT
$0.0188\pm0.0040\pm0.0034$	[1,2] ALAM	94	CLE2	$e^+e^-\to\Upsilon(4S)$

[1] ALAM 94 value is twice their $\Gamma(\overline{D}^*(2007)^0\pi^+\pi^+\pi^-)/\Gamma_{total}$ value based on their observation that the three pions are dominantly in the $a_1(1260)$ mass range 1.0 to 1.6 GeV.

[2] ALAM 94 assume equal production of B^+ and B^0 at the $\Upsilon(4S)$ and use the CLEOII $B(D^*(2007)^0\to D^0\pi^0)$ and absolute $B(D^0\to K^-\pi^+)$ and the PDG 1992 $B(D^0\to K^-\pi^+\pi^0)/B(D^0\to K^-\pi^+)$ and $B(D^0\to K^-2\pi^+\pi^-)/B(D^0\to K^-\pi^+)$.

$\Gamma(\overline{D}^*(2007)^0\pi^-\pi^+\pi^+\pi^0)/\Gamma_{total}$ Γ_{106}/Γ

VALUE	DOCUMENT ID		TECN	COMMENT
$0.0180\pm0.0024\pm0.0027$	[1] ALEXANDER	01B	CLE2	$e^+e^-\to\Upsilon(4S)$

[1] Assumes equal production of B^+ and B^0 at the $\Upsilon(4S)$. The signal is consistent with all observed $\omega\pi^+$ having proceeded through the ρ'^+ resonance at mass $1349\pm25^{+10}_{-5}$ MeV and width $547\pm86^{+46}_{-45}$ MeV.

$\Gamma(\overline{D}^{*0}3\pi^+2\pi^-)/\Gamma_{total}$ Γ_{107}/Γ

VALUE (units 10^{-3})	DOCUMENT ID		TECN	COMMENT
$5.67\pm0.91\pm0.85$	[1] MAJUMDER	04	BELL	$e^+e^-\to\Upsilon(4S)$

[1] Assumes equal production of B^+ and B^0 at the $\Upsilon(4S)$.

$\Gamma(D^*(2010)^+\pi^0)/\Gamma_{total}$ Γ_{108}/Γ

VALUE	CL%	DOCUMENT ID		TECN	COMMENT
$<3.6\times10^{-6}$		[1] IWABUCHI	08	BELL	$e^+e^-\to\Upsilon(4S)$
• • • We do not use the following data for averages, fits, limits, etc. • • •					
$<1.7\times10^{-4}$	90	[2] BRANDENB...	98	CLE2	$e^+e^-\to\Upsilon(4S)$

[1] Assumes equal production of B^+ and B^0 at the $\Upsilon(4S)$.

[2] BRANDENBURG 98 assume equal production of B^+ and B^0 at $\Upsilon(4S)$ and use the D^* partial reconstruction technique. The first error is their experiment's error and the second error is the systematic error from the PDG 96 value of $B(D^*\to D\pi)$.

$\Gamma(D^*(2010)^+K^0)/\Gamma_{total}$ Γ_{109}/Γ

VALUE	CL%	DOCUMENT ID		TECN	COMMENT
$<9.0\times10^{-6}$	90	[1] AUBERT,B	05E	BABR	$e^+e^-\to\Upsilon(4S)$
• • • We do not use the following data for averages, fits, limits, etc. • • •					
$<9.5\times10^{-5}$	90	[1] GRITSAN	01	CLE2	$e^+e^-\to\Upsilon(4S)$

[1] Assumes equal production of B^+ and B^0 at the $\Upsilon(4S)$.

$\Gamma(D^*(2010)^-\pi^+\pi^+\pi^0)/\Gamma_{total}$ Γ_{110}/Γ

VALUE	EVTS	DOCUMENT ID		TECN	COMMENT
$0.0152\pm0.0071\pm0.0001$	26	[1] ALBRECHT	90J	ARG	$e^+e^-\to\Upsilon(4S)$
• • • We do not use the following data for averages, fits, limits, etc. • • •					
$0.043\ \pm0.013\ \pm0.026$	24	[2] ALBRECHT	87C	ARG	$e^+e^-\to\Upsilon(4S)$

[1] ALBRECHT 90J reports 0.018 ± 0.007 ± 0.005 from a measurement of $[\Gamma(B^+ \to D^*(2010)^- \pi^+ \pi^+ \pi^0)/\Gamma_{total}] \times [B(D^*(2010)^+ \to D^0 \pi^+)]$ assuming $B(D^*(2010)^+ \to D^0 \pi^+) = 0.57 \pm 0.06$, which we rescale to our best value $B(D^*(2010)^+ \to D^0 \pi^+) = (67.7 \pm 0.5) \times 10^{-2}$. Our first error is their experiment's error and our second error is the systematic error from using our best value. Assumes equal production of B^+ and B^0 at the $\Upsilon(4S)$ and uses MarkIII branching fractions for the D.
[2] ALBRECHT 87C use PDG 86 branching ratios for D and $D^*(2010)$ and assume $B(\Upsilon(4S) \to B^+ B^-) = 55\%$ and $B(\Upsilon(4S) \to B^0 \overline{B}^0) = 45\%$. Superseded by ALBRECHT 90J.

$\Gamma(D^*(2010)^- \pi^+ \pi^+ \pi^+ \pi^-)/\Gamma_{total}$ Γ_{111}/Γ

VALUE (units 10^{-3})	CL%	DOCUMENT ID		TECN	COMMENT
2.56±0.26±0.33		[1] MAJUMDER	04	BELL	$e^+e^- \to \Upsilon(4S)$
• • • We do not use the following data for averages, fits, limits, etc. • • •					
<10	90	[2] ALBRECHT	90J	ARG	$e^+e^- \to \Upsilon(4S)$

[1] Assumes equal production of B^+ and B^0 at the $\Upsilon(4S)$.
[2] Assumes equal production of B^+ and B^0 at the $\Upsilon(4S)$ and uses MarkIII branching fractions for the D and $D^*(2010)$.

$\Gamma(\overline{D}^{**0} \pi^+)/\Gamma_{total}$ Γ_{112}/Γ

D^{**0} represents an excited state with mass $2.2 < M < 2.8$ GeV/c^2.

VALUE (units 10^{-3})	DOCUMENT ID		TECN	COMMENT
5.9±1.3±0.2	[1,2] AUBERT,BE	06J	BABR	$e^+e^- \to \Upsilon(4S)$

[1] AUBERT,BE 06J reports $[\Gamma(B^+ \to \overline{D}^{**0}\pi^+)/\Gamma_{total}] / [B(B^+ \to \overline{D}^0 \pi^+)] = 1.22 \pm 0.13 \pm 0.23$ which we multiply by our best value $B(B^+ \to \overline{D}^0 \pi^+) = (4.81 \pm 0.15) \times 10^{-3}$. Our first error is their experiment's error and our second error is the systematic error from using our best value.
[2] Uses a missing-mass method. Does not depend on D branching fractions or B^+/B^0 production rates.

$\Gamma(\overline{D}_1^*(2420)^0 \pi^+)/\Gamma_{total}$ Γ_{113}/Γ

VALUE	EVTS	DOCUMENT ID		TECN	COMMENT
0.0015±0.0006 OUR AVERAGE		Error includes scale factor of 1.3.			
0.0011±0.0005±0.0002	8	[1] ALAM	94	CLE2	$e^+e^- \to \Upsilon(4S)$
0.0025±0.0007±0.0006		[2] ALBRECHT	94D	ARG	$e^+e^- \to \Upsilon(4S)$

[1] ALAM 94 assume equal production of B^+ and B^0 at the $\Upsilon(4S)$ and use the CLEO II $B(D^*(2010)^+ \to D^0\pi^+)$ and absolute $B(D^0 \to K^-\pi^+)$ and the PDG 1992 $B(D^0 \to K^-\pi^+\pi^0)/B(D^0 \to K^-\pi^+)$ and assuming $B(D_1(2420)^0 \to D^*(2010)^+\pi^-) = 67\%$.
[2] ALBRECHT 94D assume equal production of B^+ and B^0 at the $\Upsilon(4S)$ and use the CLEO II $B(D^*(2010)^+ \to D^0\pi^+)$ assuming $B(D_1(2420)^0 \to D^*(2010)^+\pi^-) = 67\%$.

$\Gamma(\overline{D}_1(2420)^0 \pi^+ \times B(\overline{D}_1^0 \to \overline{D}^0 \pi^+ \pi^-))/\Gamma_{total}$ Γ_{114}/Γ

VALUE (units 10^{-4})	DOCUMENT ID		TECN	COMMENT
2.5 $^{+1.7}_{-1.4}$ OUR FIT	Error includes scale factor of 4.0.			
1.85±0.29 $^{+0.35}_{-0.55}$	[1] ABE	05A	BELL	$e^+e^- \to \Upsilon(4S)$

[1] Assumes equal production of B^+ and B^0 at the $\Upsilon(4S)$.

$\Gamma(\overline{D}_1(2420)^0 \pi^+ \times B(\overline{D}_1^0 \to \overline{D}^0 \pi^+ \pi^-))/\Gamma(\overline{D}^0 \pi^+ \pi^+ \pi^-)$ Γ_{114}/Γ_{82}

VALUE (units 10^{-2})	DOCUMENT ID		TECN	COMMENT
4.4 $^{+3.3}_{-2.6}$ OUR FIT	Error includes scale factor of 4.0.			
10.3±1.5±0.9	AAIJ	11E	LHCB	pp at 7 TeV

$\Gamma(\overline{D}_1(2420)^0 \pi^+ \times B(\overline{D}_1^0 \to \overline{D}^0 \pi^+ \pi^- \text{(nonresonant)}))/\Gamma(\overline{D}^0 \pi^+ \pi^+ \pi^-)$ Γ_{115}/Γ_{82}

VALUE (units 10^{-2})	DOCUMENT ID		TECN	COMMENT
4.0±0.7±0.5	[1] AAIJ	11E	LHCB	pp at 7 TeV

[1] Excludes decays where $\overline{D}_1(2420)^0 \to D*(2010)^-\pi^+$.

$\Gamma(\overline{D}_2^*(2462)^0 \pi^+ \times B(\overline{D}_2^*(2462)^0 \to D^-\pi^+))/\Gamma_{total}$ Γ_{116}/Γ

VALUE (units 10^{-4})	DOCUMENT ID		TECN	COMMENT
3.5±0.4 OUR AVERAGE				
3.5±0.2±0.4	[1] AUBERT	09AB	BABR	$e^+e^- \to \Upsilon(4S)$
3.4±0.3±0.72	[1] ABE	04D	BELL	$e^+e^- \to \Upsilon(4S)$

[1] Assumes equal production of B^+ and B^0 at the $\Upsilon(4S)$.

$\Gamma(\overline{D}_2^*(2462)^0 \pi^+ \times B(\overline{D}_2^{*0} \to \overline{D}^0 \pi^- \pi^+))/\Gamma(\overline{D}^0 \pi^+ \pi^+ \pi^-)$ Γ_{117}/Γ_{82}

VALUE (units 10^{-2})	DOCUMENT ID		TECN	COMMENT
4.0±1.0±0.4	AAIJ	11E	LHCB	pp at 7 TeV

$\Gamma(\overline{D}_2^*(2462)^0 \pi^+ \times B(\overline{D}_2^{*0} \to \overline{D}^0 \pi^- \pi^+ \text{(nonresonant)}))/\Gamma(\overline{D}^0 \pi^+ \pi^+ \pi^-)$ Γ_{118}/Γ_{82}

VALUE	CL%	DOCUMENT ID		TECN	COMMENT
<3.0 × 10^{-2}	90	[1] AAIJ	11E	LHCB	pp at 7 TeV

[1] Excludes decays where $\overline{D}_2^*(2462)^0 \to D^*(2010)^-\pi^+$.

$\Gamma(\overline{D}_2^*(2462)^0 \pi^+ \times B(\overline{D}_2^{*0} \to D^*(2010)^- \pi^+))/\Gamma(\overline{D}^0 \pi^+ \pi^+ \pi^-)$ Γ_{119}/Γ_{82}

VALUE (units 10^{-2})	DOCUMENT ID		TECN	COMMENT
3.9±1.2±0.4	[1] AAIJ	11E	LHCB	pp at 7 TeV

[1] Uses $B(D^*(2010)^+ \to D^0\pi^+) = (67.7 +- 0.5)\%$.

$\Gamma(\overline{D}_0^*(2400)^0 \pi^+ \times B(\overline{D}_0^*(2400)^0 \to D^-\pi^+))/\Gamma_{total}$ Γ_{120}/Γ

VALUE (units 10^{-4})	DOCUMENT ID		TECN	COMMENT
6.4±1.4 OUR AVERAGE				
6.8±0.3±2.0	[1] AUBERT	09AB	BABR	$e^+e^- \to \Upsilon(4S)$
6.1±0.6±1.8	[1] ABE	04D	BELL	$e^+e^- \to \Upsilon(4S)$

[1] Assumes equal production of B^+ and B^0 at the $\Upsilon(4S)$.

$\Gamma(\overline{D}_1(2421)^0 \pi^+ \times B(\overline{D}_1(2421)^0 \to D^{*-}\pi^+))/\Gamma_{total}$ Γ_{121}/Γ

VALUE (units 10^{-4})	DOCUMENT ID		TECN	COMMENT
6.8±0.7±1.3	[1] ABE	04D	BELL	$e^+e^- \to \Upsilon(4S)$

[1] Assumes equal production of B^+ and B^0 at the $\Upsilon(4S)$.

$\Gamma(\overline{D}_2^*(2462)^0 \pi^+ \times B(\overline{D}_2^*(2462)^0 \to D^{*-}\pi^+))/\Gamma_{total}$ Γ_{122}/Γ

VALUE (units 10^{-4})	DOCUMENT ID		TECN	COMMENT
1.8±0.3±0.4	[1] ABE	04D	BELL	$e^+e^- \to \Upsilon(4S)$

[1] Assumes equal production of B^+ and B^0 at the $\Upsilon(4S)$.

$\Gamma(\overline{D}_1'(2427)^0 \pi^+ \times B(\overline{D}_1'(2427)^0 \to D^{*-}\pi^+))/\Gamma_{total}$ Γ_{123}/Γ

VALUE (units 10^{-4})	DOCUMENT ID		TECN	COMMENT
5.0±0.4±1.1	[1] ABE	04D	BELL	$e^+e^- \to \Upsilon(4S)$

[1] Assumes equal production of B^+ and B^0 at the $\Upsilon(4S)$.

$\Gamma(\overline{D}_1(2420)^0 \pi^+ \times B(\overline{D}_1^0 \to \overline{D}^{*0} \pi^+ \pi^-))/\Gamma_{total}$ Γ_{124}/Γ

VALUE (units 10^{-4})	CL%	DOCUMENT ID		TECN	COMMENT
<0.06	90	[1] ABE	05A	BELL	$e^+e^- \to \Upsilon(4S)$

[1] Assumes equal production of B^+ and B^0 at the $\Upsilon(4S)$.

$\Gamma(\overline{D}_1^*(2420)^0 \rho^+)/\Gamma_{total}$ Γ_{125}/Γ

VALUE	CL%	DOCUMENT ID		TECN	COMMENT
<0.0014	90	[1] ALAM	94	CLE2	$e^+e^- \to \Upsilon(4S)$

[1] ALAM 94 assume equal production of B^+ and B^0 at the $\Upsilon(4S)$ and use the CLEO II $B(D^*(2010)^+ \to D^0\pi^+)$ assuming $B(D_1(2420)^0 \to D^*(2010)^+\pi^-) = 67\%$.

$\Gamma(\overline{D}_2^*(2460)^0 \pi^+)/\Gamma_{total}$ Γ_{126}/Γ

VALUE	CL%	DOCUMENT ID		TECN	COMMENT
<0.0013	90	[1] ALAM	94	CLE2	$e^+e^- \to \Upsilon(4S)$
• • • We do not use the following data for averages, fits, limits, etc. • • •					
<0.0028	90	[2] ALAM	94	CLE2	$e^+e^- \to \Upsilon(4S)$
<0.0023	90	[3] ALBRECHT	94D	ARG	$e^+e^- \to \Upsilon(4S)$

[1] ALAM 94 assume equal production of B^+ and B^0 at the $\Upsilon(4S)$ and use the MarkIII $B(D^+ \to K^-2\pi^+)$ and $B(D_2^*(2460)^0 \to D^+\pi^-) = 30\%$.
[2] ALAM 94 assume equal production of B^+ and B^0 at the $\Upsilon(4S)$ and use the MarkIII $B(D^+ \to K^-2\pi^+)$, the CLEO II $B(D^*(2010)^+ \to D^0\pi^+)$ and $B(D_2^*(2460)^0 \to D^*(2010)^+\pi^-) = 20\%$.
[3] ALBRECHT 94D assume equal production of B^+ and B^0 at the $\Upsilon(4S)$ and use the CLEO II $B(D^*(2010)^+ \to D^0\pi^+)$ and $B(D_2^*(2460)^0 \to D^*(2010)^+\pi^-) = 30\%$.

$\Gamma(\overline{D}_2^*(2460)^0 \pi^+ \times B(\overline{D}_2^{*0} \to \overline{D}^{*0} \pi^+ \pi^-))/\Gamma_{total}$ Γ_{127}/Γ

VALUE (units 10^{-4})	CL%	DOCUMENT ID		TECN	COMMENT
<0.22	90	[1] ABE	05A	BELL	$e^+e^- \to \Upsilon(4S)$

[1] Assumes equal production of B^+ and B^0 at the $\Upsilon(4S)$.

$\Gamma(\overline{D}_2^*(2460)^0 \rho^+)/\Gamma_{total}$ Γ_{128}/Γ

VALUE	CL%	DOCUMENT ID		TECN	COMMENT
<0.0047	90	[1] ALAM	94	CLE2	$e^+e^- \to \Upsilon(4S)$
<0.005	90	[2] ALAM	94	CLE2	$e^+e^- \to \Upsilon(4S)$

[1] ALAM 94 assume equal production of B^+ and B^0 at the $\Upsilon(4S)$ and use the MarkIII $B(D^+ \to K^-2\pi^+)$ and $B(D_2^*(2460)^0 \to D^+\pi^-) = 30\%$.
[2] ALAM 94 assume equal production of B^+ and B^0 at the $\Upsilon(4S)$ and use the MarkIII $B(D^+ \to K^-2\pi^+)$, the CLEO II $B(D^*(2010)^+ \to D^0\pi^+)$ and $B(D_2^*(2460)^0 \to D^*(2010)^+\pi^-) = 20\%$.

$\Gamma(\overline{D}^0 D_s^+)/\Gamma_{total}$ Γ_{129}/Γ

VALUE (units 10^{-3})	DOCUMENT ID		TECN	COMMENT
9.0±0.9 OUR AVERAGE				
8.6±0.2±1.1	[1] AAIJ	13AP	LHCB	pp at 7 TeV
9.5±2.0±0.8	[2] AUBERT	06N	BABR	$e^+e^- \to \Upsilon(4S)$
9.8±2.6±0.9	[3] GIBAUT	96	CLE2	$e^+e^- \to \Upsilon(4S)$
14 ±8 ±1	[4] ALBRECHT	92G	ARG	$e^+e^- \to \Upsilon(4S)$
13 ±6 ±1	[5] BORTOLETTO	90	CLEO	$e^+e^- \to \Upsilon(4S)$

[1] Uses $B(B^0 \to D^- D_s^+) = (7.2 \pm 0.8) \times 10^{-3}$.

[2] AUBERT 06N reports $(0.92 \pm 0.14 \pm 0.18) \times 10^{-2}$ from a measurement of $[\Gamma(B^+ \to \overline{D}^0 D_s^+)/\Gamma_{\rm total}] \times [B(D_s^+ \to \phi\pi^+)]$ assuming $B(D_s^+ \to \phi\pi^+) = 0.0462 \pm 0.0062$, which we rescale to our best value $B(D_s^+ \to \phi\pi^+) = (4.5 \pm 0.4) \times 10^{-2}$. Our first error is their experiment's error and our second error is the systematic error from using our best value.

[3] GIBAUT 96 reports $0.0126 \pm 0.0022 \pm 0.0025$ from a measurement of $[\Gamma(B^+ \to \overline{D}^0 D_s^+)/\Gamma_{\rm total}] \times [B(D_s^+ \to \phi\pi^+)]$ assuming $B(D_s^+ \to \phi\pi^+) = 0.035$, which we rescale to our best value $B(D_s^+ \to \phi\pi^+) = (4.5 \pm 0.4) \times 10^{-2}$. Our first error is their experiment's error and our second error is the systematic error from using our best value.

[4] ALBRECHT 92G reports $0.024 \pm 0.012 \pm 0.004$ from a measurement of $[\Gamma(B^+ \to \overline{D}^0 D_s^+)/\Gamma_{\rm total}] \times [B(D_s^+ \to \phi\pi^+)]$ assuming $B(D_s^+ \to \phi\pi^+) = 0.027$, which we rescale to our best value $B(D_s^+ \to \phi\pi^+) = (4.5 \pm 0.4) \times 10^{-2}$. Our first error is their experiment's error and our second error is the systematic error from using our best value. Assumes PDG 1990 D^0 branching ratios, e.g., $B(D^0 \to K^-\pi^+) = 3.71 \pm 0.25\%$.

[5] BORTOLETTO 90 reports 0.029 ± 0.013 from a measurement of $[\Gamma(B^+ \to \overline{D}^0 D_s^+)/\Gamma_{\rm total}] \times [B(D_s^+ \to \phi\pi^+)]$ assuming $B(D_s^+ \to \phi\pi^+) = 0.02$, which we rescale to our best value $B(D_s^+ \to \phi\pi^+) = (4.5 \pm 0.4) \times 10^{-2}$. Our first error is their experiment's error and our second error is the systematic error from using our best value.

$\Gamma(D_{s0}(2317)^+ \overline{D}^0 \times B(D_{s0}(2317)^+ \to D_s^+ \pi^0))/\Gamma_{\rm total}$ Γ_{130}/Γ

VALUE (units 10^{-3})		DOCUMENT ID		TECN	COMMENT
$0.73^{+0.22}_{-0.17}$ OUR AVERAGE					
$0.80^{+0.35}_{-0.21} \pm 0.07$	[1,2]	AUBERT,B	04S	BABR	$e^+e^- \to \Upsilon(4S)$
$0.65^{+0.26}_{-0.24} \pm 0.06$	[1,3]	KROKOVNY	03B	BELL	$e^+e^- \to \Upsilon(4S)$

[1] Assumes equal production of B^+ and B^0 at the $\Upsilon(4S)$.

[2] AUBERT,B 04S reports $(1.0 \pm 0.3^{+0.4}_{-0.2}) \times 10^{-3}$ from a measurement of $[\Gamma(B^+ \to D_{s0}(2317)^+ \overline{D}^0 \times B(D_{s0}(2317)^+ \to D_s^+\pi^0))/\Gamma_{\rm total}] \times [B(D_s^+ \to \phi\pi^+)]$ assuming $B(D_s^+ \to \phi\pi^+) = 0.036 \pm 0.009$, which we rescale to our best value $B(D_s^+ \to \phi\pi^+) = (4.5 \pm 0.4) \times 10^{-2}$. Our first error is their experiment's error and our second error is the systematic error from using our best value.

[3] KROKOVNY 03B reports $(0.81^{+0.30}_{-0.27} \pm 0.24) \times 10^{-3}$ from a measurement of $[\Gamma(B^+ \to D_{s0}(2317)^+ \overline{D}^0 \times B(D_{s0}(2317)^+ \to D_s^+\pi^0))/\Gamma_{\rm total}] \times [B(D_s^+ \to \phi\pi^+)]$ assuming $B(D_s^+ \to \phi\pi^+) = 0.036 \pm 0.009$, which we rescale to our best value $B(D_s^+ \to \phi\pi^+) = (4.5 \pm 0.4) \times 10^{-2}$. Our first error is their experiment's error and our second error is the systematic error from using our best value.

$\Gamma(D_{s0}(2317)^+ \overline{D}^0 \times B(D_{s0}(2317)^+ \to D_s^{*+}\gamma))/\Gamma_{\rm total}$ Γ_{131}/Γ

VALUE (units 10^{-3})	CL%	DOCUMENT ID		TECN	COMMENT
<0.76	90	[1] KROKOVNY	03B	BELL	$e^+e^- \to \Upsilon(4S)$

[1] Assumes equal production of B^+ and B^0 at the $\Upsilon(4S)$.

$\Gamma(D_{s0}(2317)^+ \overline{D}^*(2007)^0 \times B(D_{s0}(2317)^+ \to D_s^+\pi^0))/\Gamma_{\rm total}$ Γ_{132}/Γ

VALUE (units 10^{-3})		DOCUMENT ID		TECN	COMMENT
$0.9 \pm 0.6^{+0.4}_{-0.3}$	[1]	AUBERT,B	04S	BABR	$e^+e^- \to \Upsilon(4S)$

[1] Assumes equal production of B^+ and B^0 at the $\Upsilon(4S)$.

$\Gamma(D_{sJ}(2457)^+ \overline{D}^0)/\Gamma_{\rm total}$ Γ_{133}/Γ

VALUE (units 10^{-3})		DOCUMENT ID		TECN	COMMENT
$3.1^{+1.0}_{-0.9}$ OUR AVERAGE					
$4.3 \pm 1.6 \pm 1.3$	[1]	AUBERT	06N	BABR	$e^+e^- \to \Upsilon(4S)$
$4.6^{+1.8}_{-1.6} \pm 1.0$	[2,3]	AUBERT,B	04S	BABR	$e^+e^- \to \Upsilon(4S)$
$2.1^{+1.1}_{-0.9} \pm 0.5$	[2,4]	KROKOVNY	03B	BELL	$e^+e^- \to \Upsilon(4S)$

[1] Uses a missing-mass method in the events that one of the B mesons is fully reconstructed.

[2] Assumes equal production of B^+ and B^0 at the $\Upsilon(4S)$.

[3] AUBERT,B 04S reports $[\Gamma(B^+ \to D_{sJ}(2457)^+ \overline{D}^0)/\Gamma_{\rm total}] \times [B(D_{s1}(2460)^+ \to D_s^{*+}\pi^0)] = (2.2^{+0.8}_{-0.7} \pm 0.3) \times 10^{-3}$ which we divide by our best value $B(D_{s1}(2460)^+ \to D_s^{*+}\pi^0) = (48 \pm 11) \times 10^{-2}$. Our first error is their experiment's error and our second error is the systematic error from using our best value.

[4] KROKOVNY 03B reports $[\Gamma(B^+ \to D_{sJ}(2457)^+ \overline{D}^0)/\Gamma_{\rm total}] \times [B(D_{s1}(2460)^+ \to D_s^{*+}\pi^0)] = (1.0^{+0.5}_{-0.4} \pm 0.1) \times 10^{-3}$ which we divide by our best value $B(D_{s1}(2460)^+ \to D_s^{*+}\pi^0) = (48 \pm 11) \times 10^{-2}$. Our first error is their experiment's error and our second error is the systematic error from using our best value.

$\Gamma(D_{sJ}(2457)^+ \overline{D}^0 \times B(D_{sJ}(2457)^+ \to D_s^+\gamma))/\Gamma_{\rm total}$ Γ_{134}/Γ

VALUE (units 10^{-3})		DOCUMENT ID		TECN	COMMENT
$0.46^{+0.13}_{-0.11}$ OUR AVERAGE					
$0.48^{+0.19}_{-0.13} \pm 0.04$	[1,2]	AUBERT,B	04S	BABR	$e^+e^- \to \Upsilon(4S)$
$0.45^{+0.15}_{-0.14} \pm 0.04$	[1,3]	KROKOVNY	03B	BELL	$e^+e^- \to \Upsilon(4S)$

[1] Assumes equal production of B^+ and B^0 at the $\Upsilon(4S)$.

[2] AUBERT,B 04S reports $(0.6 \pm 0.2^{+0.2}_{-0.1}) \times 10^{-3}$ from a measurement of $[\Gamma(B^+ \to D_{sJ}(2457)^+ \overline{D}^0 \times B(D_{sJ}(2457)^+ \to D_s^+\gamma))/\Gamma_{\rm total}] \times [B(D_s^+ \to \phi\pi^+)]$ assuming $B(D_s^+ \to \phi\pi^+) = 0.036 \pm 0.009$, which we rescale to our best value $B(D_s^+ \to \phi\pi^+) = (4.5 \pm 0.4) \times 10^{-2}$. Our first error is their experiment's error and our second error is the systematic error from using our best value.

[3] KROKOVNY 03B reports $(0.56^{+0.16}_{-0.15} \pm 0.17) \times 10^{-3}$ from a measurement of $[\Gamma(B^+ \to D_{sJ}(2457)^+ \overline{D}^0 \times B(D_{sJ}(2457)^+ \to D_s^+\gamma))/\Gamma_{\rm total}] \times [B(D_s^+ \to \phi\pi^+)]$ assuming $B(D_s^+ \to \phi\pi^+) = 0.036 \pm 0.009$, which we rescale to our best value $B(D_s^+ \to \phi\pi^+) = (4.5 \pm 0.4) \times 10^{-2}$. Our first error is their experiment's error and our second error is the systematic error from using our best value.

$\Gamma(D_{sJ}(2457)^+ \overline{D}^0 \times B(D_{sJ}(2457)^+ \to D_s^+\pi^+\pi^-))/\Gamma_{\rm total}$ Γ_{135}/Γ

VALUE (units 10^{-3})	CL%	DOCUMENT ID		TECN	COMMENT
<0.22	90	[1] KROKOVNY	03B	BELL	$e^+e^- \to \Upsilon(4S)$

[1] Assumes equal production of B^+ and B^0 at the $\Upsilon(4S)$.

$\Gamma(D_{sJ}(2457)^+ \overline{D}^0 \times B(D_{sJ}(2457)^+ \to D_s^+\pi^0))/\Gamma_{\rm total}$ Γ_{136}/Γ

VALUE (units 10^{-3})	CL%	DOCUMENT ID		TECN	COMMENT
<0.27	90	[1] KROKOVNY	03B	BELL	$e^+e^- \to \Upsilon(4S)$

[1] Assumes equal production of B^+ and B^0 at the $\Upsilon(4S)$.

$\Gamma(D_{sJ}(2457)^+ \overline{D}^0 \times B(D_{sJ}(2457)^+ \to D_s^{*+}\gamma))/\Gamma_{\rm total}$ Γ_{137}/Γ

VALUE (units 10^{-3})	CL%	DOCUMENT ID		TECN	COMMENT
<0.98	90	[1] KROKOVNY	03B	BELL	$e^+e^- \to \Upsilon(4S)$

[1] Assumes equal production of B^+ and B^0 at the $\Upsilon(4S)$.

$\Gamma(D_{sJ}(2457)^+ \overline{D}^*(2007)^0)/\Gamma_{\rm total}$ Γ_{138}/Γ

VALUE (units 10^{-3})		DOCUMENT ID		TECN	COMMENT
12.0 ± 3.0 OUR AVERAGE					
$11.2 \pm 2.6 \pm 2.0$	[1]	AUBERT	06N	BABR	$e^+e^- \to \Upsilon(4S)$
$16\ ^{+8}_{-6} \pm 4$	[2,3]	AUBERT,B	04S	BABR	$e^+e^- \to \Upsilon(4S)$

[1] Uses a missing-mass method in the events that one of the B mesons is fully reconstructed.

[2] AUBERT,B 04S reports $[\Gamma(B^+ \to D_{sJ}(2457)^+ \overline{D}^*(2007)^0)/\Gamma_{\rm total}] \times [B(D_{s1}(2460)^+ \to D_s^{*+}\pi^0)] = (7.6 \pm 1.7^{+3.2}_{-2.4}) \times 10^{-3}$ which we divide by our best value $B(D_{s1}(2460)^+ \to D_s^{*+}\pi^0) = (48 \pm 11) \times 10^{-2}$. Our first error is their experiment's error and our second error is the systematic error from using our best value.

[3] Assumes equal production of B^+ and B^0 at the $\Upsilon(4S)$.

$\Gamma(D_{sJ}(2457)^+ \overline{D}^*(2007)^0 \times B(D_{sJ}(2457)^+ \to D_s^+\gamma))/\Gamma_{\rm total}$ Γ_{139}/Γ

VALUE (units 10^{-3})		DOCUMENT ID		TECN	COMMENT
$1.4 \pm 0.4^{+0.6}_{-0.4}$	[1]	AUBERT,B	04S	BABR	$e^+e^- \to \Upsilon(4S)$

[1] Assumes equal production of B^+ and B^0 at the $\Upsilon(4S)$.

$\Gamma(\overline{D}^0 D_{s1}(2536)^+ \times B(D_{s1}(2536)^+ \to D^*(2007)^0 K^+))/\Gamma_{\rm total}$ Γ_{141}/Γ

VALUE (units 10^{-4})	CL%	DOCUMENT ID		TECN	COMMENT
$2.16 \pm 0.52 \pm 0.45$		[1] AUBERT	08B	BABR	$e^+e^- \to \Upsilon(4S)$
• • • We do not use the following data for averages, fits, limits, etc. • • •					
<2	90	AUBERT	03X	BABR	Repl. by AUBERT 08B

[1] Assumes equal production of B^+ and B^0 at the $\Upsilon(4S)$.

$\Gamma(\overline{D}^0 D_{s1}(2536)^+ \times B(D_{s1}(2536)^+ \to D^*(2007)^0 K^+ + D^*(2010)^+ K^0))/\Gamma_{\rm total}$ Γ_{140}/Γ

VALUE (units 10^{-4})		DOCUMENT ID		TECN	COMMENT
$3.97 \pm 0.85 \pm 0.56$	[1,2]	AUSHEV	11	BELL	$e^+e^- \to \Upsilon(4S)$

[1] Uses $\Gamma(D^*(2007)^0 \to D^0\pi^0)$ / $\Gamma(D^*(2007)^0 \to D^0\gamma) = 1.74 \pm 0.13$ and $\Gamma(D_{s1}(2536)^+ \to D^*(2007)^0 K^+)$ / $\Gamma(D_{s1}(2536)^+ \to D^*(2010)^+ K^0) = 1.36 \pm 0.2$.

[2] Assumes equal production of B^+ and B^0 at the $\Upsilon(4S)$.

$\Gamma(\overline{D}^*(2007)^0 D_{s1}(2536)^+ \times B(D_{s1}(2536)^+ \to D^*(2007)^0 K^+))/\Gamma_{\rm total}$ Γ_{142}/Γ

VALUE (units 10^{-4})	CL%	DOCUMENT ID		TECN	COMMENT
$5.46 \pm 1.17 \pm 1.04$		[1] AUBERT	08B	BABR	$e^+e^- \to \Upsilon(4S)$
• • • We do not use the following data for averages, fits, limits, etc. • • •					
<7	90	AUBERT	03X	BABR	Repl. by AUBERT 08B

[1] Assumes equal production of B^+ and B^0 at the $\Upsilon(4S)$.

$\Gamma(\overline{D}^0 D_{s1}(2536)^+ \times B(D_{s1}(2536)^+ \to D^{*+} K^0))/\Gamma_{\rm total}$ Γ_{143}/Γ

VALUE (units 10^{-4})		DOCUMENT ID		TECN	COMMENT
$2.30 \pm 0.98 \pm 0.43$	[1]	AUBERT	08B	BABR	$e^+e^- \to \Upsilon(4S)$

[1] Assumes equal production of B^+ and B^0 at the $\Upsilon(4S)$.

$\Gamma(\overline{D}^0 D_{sJ}(2700)^+ \times B(D_{sJ}(2700)^+ \to D^0 K^+))/\Gamma_{\rm total}$ Γ_{144}/Γ

VALUE (units 10^{-4})		DOCUMENT ID		TECN	COMMENT
$11.3 \pm 2.2^{+1.4}_{-2.8}$	[1]	BRODZICKA	08	BELL	$e^+e^- \to \Upsilon(4S)$

[1] Assumes equal production of B^+ and B^0 at the $\Upsilon(4S)$.

$\Gamma(\overline{D}^{*0} D_{s1}(2536)^+ \times B(D_{s1}(2536)^+ \to D^{*+} K^0))/\Gamma_{total}$ Γ_{145}/Γ

VALUE (units 10^{-4})	DOCUMENT ID		TECN	COMMENT
3.92±2.46±0.83	[1] AUBERT	08B	BABR	$e^+e^- \to \Upsilon(4S)$

[1] Assumes equal production of B^+ and B^0 at the $\Upsilon(4S)$.

$\Gamma(\overline{D}^{*0} D_{sJ}(2573)^+ \times B(D_{sJ}(2573)^+ \to D^0 K^+))/\Gamma_{total}$ Γ_{146}/Γ

VALUE (units 10^{-4})	CL%	DOCUMENT ID		TECN	COMMENT
<2	90	AUBERT	03X	BABR	$e^+e^- \to \Upsilon(4S)$

$\Gamma(\overline{D}^{*}(2007)^0 D_{sJ}(2573)^+ \times B(D_{sJ}(2573)^+ \to D^0 K^+))/\Gamma_{total}$ Γ_{147}/Γ

VALUE (units 10^{-4})	CL%	DOCUMENT ID		TECN	COMMENT
<5	90	AUBERT	03X	BABR	$e^+e^- \to \Upsilon(4S)$

$\Gamma(\overline{D}^0 D_s^{*+})/\Gamma_{total}$ Γ_{148}/Γ

VALUE	DOCUMENT ID		TECN	COMMENT
0.0076±0.0016 OUR AVERAGE				
0.0079±0.0017±0.0007	[1] AUBERT	06N	BABR	$e^+e^- \to \Upsilon(4S)$
0.0068±0.0025±0.0006	[2] GIBAUT	96	CLE2	$e^+e^- \to \Upsilon(4S)$
0.010 ±0.007 ±0.001	[3] ALBRECHT	92G	ARG	$e^+e^- \to \Upsilon(4S)$

[1] AUBERT 06N reports $(0.77 \pm 0.15 \pm 0.13) \times 10^{-2}$ from a measurement of $[\Gamma(B^+ \to \overline{D}^0 D_s^{*+})/\Gamma_{total}] \times [B(D_s^+ \to \phi\pi^+)]$ assuming $B(D_s^+ \to \phi\pi^+) = 0.0462 \pm 0.0062$, which we rescale to our best value $B(D_s^+ \to \phi\pi^+) = (4.5 \pm 0.4) \times 10^{-2}$. Our first error is their experiment's error and our second error is the systematic error from using our best value.

[2] GIBAUT 96 reports $0.0087 \pm 0.0027 \pm 0.0017$ from a measurement of $[\Gamma(B^+ \to \overline{D}^0 D_s^{*+})/\Gamma_{total}] \times [B(D_s^+ \to \phi\pi^+)]$ assuming $B(D_s^+ \to \phi\pi^+) = 0.035$, which we rescale to our best value $B(D_s^+ \to \phi\pi^+) = (4.5 \pm 0.4) \times 10^{-2}$. Our first error is their experiment's error and our second error is the systematic error from using our best value.

[3] ALBRECHT 92G reports $0.016 \pm 0.012 \pm 0.003$ from a measurement of $[\Gamma(B^+ \to \overline{D}^0 D_s^{*+})/\Gamma_{total}] \times [B(D_s^+ \to \phi\pi^+)]$ assuming $B(D_s^+ \to \phi\pi^+) = 0.027$, which we rescale to our best value $B(D_s^+ \to \phi\pi^+) = (4.5 \pm 0.4) \times 10^{-2}$. Our first error is their experiment's error and our second error is the systematic error from using our best value. Assumes PDG 1990 D^0 branching ratios, e.g., $B(D^0 \to K^-\pi^+) = 3.71 \pm 0.25\%$.

$\Gamma(\overline{D}^{*}(2007)^0 D_s^+)/\Gamma_{total}$ Γ_{149}/Γ

VALUE	DOCUMENT ID		TECN	COMMENT
0.0082±0.0017 OUR AVERAGE				
0.0078±0.0018±0.0007	[1] AUBERT	06N	BABR	$e^+e^- \to \Upsilon(4S)$
0.011 ±0.004 ±0.001	[2] GIBAUT	96	CLE2	$e^+e^- \to \Upsilon(4S)$
0.008 ±0.006 ±0.001	[3] ALBRECHT	92G	ARG	$e^+e^- \to \Upsilon(4S)$

[1] AUBERT 06N reports $(0.76 \pm 0.15 \pm 0.13) \times 10^{-2}$ from a measurement of $[\Gamma(B^+ \to \overline{D}^*(2007)^0 D_s^+)/\Gamma_{total}] \times [B(D_s^+ \to \phi\pi^+)]$ assuming $B(D_s^+ \to \phi\pi^+) = 0.0462 \pm 0.0062$, which we rescale to our best value $B(D_s^+ \to \phi\pi^+) = (4.5 \pm 0.4) \times 10^{-2}$. Our first error is their experiment's error and our second error is the systematic error from using our best value.

[2] GIBAUT 96 reports $0.0140 \pm 0.0043 \pm 0.0035$ from a measurement of $[\Gamma(B^+ \to \overline{D}^*(2007)^0 D_s^+)/\Gamma_{total}] \times [B(D_s^+ \to \phi\pi^+)]$ assuming $B(D_s^+ \to \phi\pi^+) = 0.035$, which we rescale to our best value $B(D_s^+ \to \phi\pi^+) = (4.5 \pm 0.4) \times 10^{-2}$. Our first error is their experiment's error and our second error is the systematic error from using our best value.

[3] ALBRECHT 92G reports $0.013 \pm 0.009 \pm 0.002$ from a measurement of $[\Gamma(B^+ \to \overline{D}^*(2007)^0 D_s^+)/\Gamma_{total}] \times [B(D_s^+ \to \phi\pi^+)]$ assuming $B(D_s^+ \to \phi\pi^+) = 0.027$, which we rescale to our best value $B(D_s^+ \to \phi\pi^+) = (4.5 \pm 0.4) \times 10^{-2}$. Our first error is their experiment's error and our second error is the systematic error from using our best value. Assumes PDG 1990 D^0 and $D^*(2007)^0$ branching ratios, e.g., $B(D^0 \to K^-\pi^+) = 3.71 \pm 0.25\%$ and $B(D^*(2007)^0 \to D^0\pi^0) = 55 \pm 6\%$.

$\Gamma(\overline{D}^{*}(2007)^0 D_s^{*+})/\Gamma_{total}$ Γ_{150}/Γ

VALUE	DOCUMENT ID		TECN	COMMENT
0.0171±0.0024 OUR AVERAGE				
0.0167±0.0019±0.0015	[1] AUBERT	06N	BABR	$e^+e^- \to \Upsilon(4S)$
0.024 ±0.009 ±0.002	[2] GIBAUT	96	CLE2	$e^+e^- \to \Upsilon(4S)$
0.019 ±0.010 ±0.002	[3] ALBRECHT	92G	ARG	$e^+e^- \to \Upsilon(4S)$

[1] AUBERT 06N reports $(1.62 \pm 0.22 \pm 0.18) \times 10^{-2}$ from a measurement of $[\Gamma(B^+ \to \overline{D}^*(2007)^0 D_s^{*+})/\Gamma_{total}] \times [B(D_s^+ \to \phi\pi^+)]$ assuming $B(D_s^+ \to \phi\pi^+) = 0.0462 \pm 0.0062$, which we rescale to our best value $B(D_s^+ \to \phi\pi^+) = (4.5 \pm 0.4) \times 10^{-2}$. Our first error is their experiment's error and our second error is the systematic error from using our best value.

[2] GIBAUT 96 reports $0.0310 \pm 0.0088 \pm 0.0065$ from a measurement of $[\Gamma(B^+ \to \overline{D}^*(2007)^0 D_s^{*+})/\Gamma_{total}] \times [B(D_s^+ \to \phi\pi^+)]$ assuming $B(D_s^+ \to \phi\pi^+) = 0.035$, which we rescale to our best value $B(D_s^+ \to \phi\pi^+) = (4.5 \pm 0.4) \times 10^{-2}$. Our first error is their experiment's error and our second error is the systematic error from using our best value.

[3] ALBRECHT 92G reports $0.031 \pm 0.016 \pm 0.005$ from a measurement of $[\Gamma(B^+ \to \overline{D}^*(2007)^0 D_s^{*+})/\Gamma_{total}] \times [B(D_s^+ \to \phi\pi^+)]$ assuming $B(D_s^+ \to \phi\pi^+) = 0.027$, which we rescale to our best value $B(D_s^+ \to \phi\pi^+) = (4.5 \pm 0.4) \times 10^{-2}$. Our first error is their experiment's error and our second error is the systematic error from using our best value. Assumes PDG 1990 D^0 and $D^*(2007)^0$ branching ratios, e.g., $B(D^0 \to K^-\pi^+) = 3.71 \pm 0.25\%$ and $B(D^*(2007)^0 \to D^0\pi^0) = 55 \pm 6\%$.

$\Gamma(D_s^{(*)+} \overline{D}^{**0})/\Gamma_{total}$ Γ_{151}/Γ

VALUE	DOCUMENT ID		TECN	COMMENT
(2.73±0.93±0.68) × 10^{-2}	[1] AHMED	00B	CLE2	$e^+e^- \to \Upsilon(4S)$

[1] AHMED 00B reports their experiment's uncertainties (±0.78 ± 0.48 ± 0.68)%, where the first error is statistical, the second is systematic, and the third is the uncertainty in the $D_s \to \phi\pi$ branching fraction. We combine the first two in quadrature.

$\Gamma(\overline{D}^{*}(2007)^0 D^{*}(2010)^+)/\Gamma_{total}$ Γ_{152}/Γ

VALUE (units 10^{-4})	CL%	DOCUMENT ID		TECN	COMMENT
8.1±1.2±1.2		[1] AUBERT,B	06A	BABR	$e^+e^- \to \Upsilon(4S)$
• • • We do not use the following data for averages, fits, limits, etc. • • •					
<110	90	BARATE	98Q	ALEP	$e^+e^- \to Z$

[1] Assumes equal production of B^+ and B^0 at the $\Upsilon(4S)$.

$[\Gamma(\overline{D}^0 D^{*}(2010)^+) + \Gamma(\overline{D}^{*}(2007)^0 D^{+})]/\Gamma_{total}$ Γ_{153}/Γ

VALUE (units 10^{-4})	CL%	DOCUMENT ID		TECN	COMMENT
<130	90	BARATE	98Q	ALEP	$e^+e^- \to Z$

$\Gamma(\overline{D}^0 D^{*}(2010)^+)/\Gamma_{total}$ Γ_{154}/Γ

VALUE (units 10^{-4})	DOCUMENT ID		TECN	COMMENT
3.9 ±0.5 OUR AVERAGE				
3.6 ±0.5 ±0.4	[1] AUBERT,B	06A	BABR	$e^+e^- \to \Upsilon(4S)$
4.57±0.71±0.56	[1] MAJUMDER	05	BELL	$e^+e^- \to \Upsilon(4S)$

[1] Assumes equal production of B^+ and B^0 at the $\Upsilon(4S)$.

$\Gamma(\overline{D}^0 D^{+})/\Gamma_{total}$ Γ_{155}/Γ

VALUE (units 10^{-4})	CL%	DOCUMENT ID		TECN	COMMENT
3.8 ±0.4 OUR AVERAGE					
3.85±0.31±0.38		[1] ADACHI	08	BELL	$e^+e^- \to \Upsilon(4S)$
3.8 ±0.6 ±0.5		[1] AUBERT,B	06A	BABR	$e^+e^- \to \Upsilon(4S)$
• • • We do not use the following data for averages, fits, limits, etc. • • •					
4.83±0.78±0.58		[1] MAJUMDER	05	BELL	Repl. by ADACHI 08
<67	90	BARATE	98Q	ALEP	$e^+e^- \to Z$

[1] Assumes equal production of B^+ and B^0 at the $\Upsilon(4S)$.

$\Gamma(\overline{D}^0 D^{+} K^0)/\Gamma_{total}$ Γ_{156}/Γ

VALUE (units 10^{-3})	CL%	DOCUMENT ID		TECN	COMMENT
1.55±0.17±0.13		[1] DEL-AMO-SA...11B		BABR	$e^+e^- \to \Upsilon(4S)$
• • • We do not use the following data for averages, fits, limits, etc. • • •					
<2.8	90	[1] AUBERT	03X	BABR	Repl. by DEL-AMO-SANCHEZ 11B

[1] Assumes equal production of B^+ and B^0 at the $\Upsilon(4S)$.

$\Gamma(D^{+}\overline{D}^{*}(2007)^0)/\Gamma_{total}$ Γ_{157}/Γ

VALUE (units 10^{-4})	DOCUMENT ID		TECN	COMMENT
6.3±1.4±1.0	[1] AUBERT,B	06A	BABR	$e^+e^- \to \Upsilon(4S)$

[1] Assumes equal production of B^+ and B^0 at the $\Upsilon(4S)$.

$\Gamma(\overline{D}^{*}(2007)^0 D^{+} K^0)/\Gamma_{total}$ Γ_{158}/Γ

VALUE (units 10^{-3})	CL%	DOCUMENT ID		TECN	COMMENT
2.06±0.38±0.30		[1] DEL-AMO-SA...11B		BABR	$e^+e^- \to \Upsilon(4S)$
• • • We do not use the following data for averages, fits, limits, etc. • • •					
<6.1	90	[1] AUBERT	03X	BABR	Repl. by DEL-AMO-SANCHEZ 11B

[1] Assumes equal production of B^+ and B^0 at the $\Upsilon(4S)$.

$\Gamma(\overline{D}^0 \overline{D}^{*}(2010)^+ K^0)/\Gamma_{total}$ Γ_{159}/Γ

VALUE (units 10^{-3})	DOCUMENT ID		TECN	COMMENT
3.81±0.31±0.23	[1] DEL-AMO-SA...11B		BABR	$e^+e^- \to \Upsilon(4S)$
• • • We do not use the following data for averages, fits, limits, etc. • • •				
$5.2\ ^{+1.0}_{-0.9}$ ±0.7	[1] AUBERT	03X	BABR	Repl. by DEL-AMO-SANCHEZ 11B

[1] Assumes equal production of B^+ and B^0 at the $\Upsilon(4S)$.

$\Gamma(\overline{D}^{*}(2007)^0 D^{*}(2010)^+ K^0)/\Gamma_{total}$ Γ_{160}/Γ

VALUE (units 10^{-3})	DOCUMENT ID		TECN	COMMENT
9.17±0.83±0.90	[1] DEL-AMO-SA...11B		BABR	$e^+e^- \to \Upsilon(4S)$
• • • We do not use the following data for averages, fits, limits, etc. • • •				
$7.8\ ^{+2.3}_{-2.1}$ ±1.4	[1] AUBERT	03X	BABR	Repl. by DEL-AMO-SANCHEZ 11B

[1] Assumes equal production of B^+ and B^0 at the $\Upsilon(4S)$.

$\Gamma(\overline{D}^0 D^0 K^+)/\Gamma_{total}$ Γ_{161}/Γ

VALUE (units 10^{-3})	DOCUMENT ID		TECN	COMMENT
1.45±0.33 OUR AVERAGE	Error includes scale factor of 2.6.			
1.31±0.07±0.12	[1] DEL-AMO-SA...11B		BABR	$e^+e^- \to \Upsilon(4S)$
$2.22\pm0.22^{+0.26}_{-0.24}$	[1] BRODZICKA	08	BELL	$e^+e^- \to \Upsilon(4S)$
• • • We do not use the following data for averages, fits, limits, etc. • • •				
1.17±0.21±0.15	[1] CHISTOV	04	BELL	Repl. by BRODZICKA 08
1.9 ±0.3 ±0.3	[1] AUBERT	03X	BABR	Repl. by DEL-AMO-SANCHEZ 11B

[1] Assumes equal production of B^+ and B^0 at the $\Upsilon(4S)$.

$\Gamma(\overline{D}^*(2007)^0 D^0 K^+)/\Gamma_{\text{total}}$ Γ_{162}/Γ

VALUE (units 10^{-3})	CL%	DOCUMENT ID		TECN	COMMENT
2.26±0.16±0.17		[1] DEL-AMO-SA...11B		BABR	$e^+e^- \to \Upsilon(4S)$
• • • We do not use the following data for averages, fits, limits, etc. • • •					
<3.8	90	[1] AUBERT	03X	BABR	Repl. by DEL-AMO-SANCHEZ 11B

[1] Assumes equal production of B^+ and B^0 at the $\Upsilon(4S)$.

$\Gamma(\overline{D}^0 D^*(2007)^0 K^+)/\Gamma_{\text{total}}$ Γ_{163}/Γ

VALUE (units 10^{-3})	DOCUMENT ID		TECN	COMMENT
6.32±0.19±0.45	[1] DEL-AMO-SA...11B		BABR	$e^+e^- \to \Upsilon(4S)$
• • • We do not use the following data for averages, fits, limits, etc. • • •				
4.7 ±0.7 ±0.7	[1] AUBERT	03X	BABR	Repl. by DEL-AMO-SANCHEZ 11B

[1] Assumes equal production of B^+ and B^0 at the $\Upsilon(4S)$.

$\Gamma(\overline{D}^*(2007)^0 D^*(2007)^0 K^+)/\Gamma_{\text{total}}$ Γ_{164}/Γ

VALUE (units 10^{-3})	DOCUMENT ID		TECN	COMMENT
11.23±0.36±1.26	[1] DEL-AMO-SA...11B		BABR	$e^+e^- \to \Upsilon(4S)$
• • • We do not use the following data for averages, fits, limits, etc. • • •				
$5.3\ ^{+1.1}_{-1.0}\ \pm 1.2$	[1] AUBERT	03X	BABR	Repl. by DEL-AMO-SANCHEZ 11B

[1] Assumes equal production of B^+ and B^0 at the $\Upsilon(4S)$.

$\Gamma(D^- D^+ K^+)/\Gamma_{\text{total}}$ Γ_{165}/Γ

VALUE (units 10^{-3})	CL%	DOCUMENT ID		TECN	COMMENT
0.22±0.05±0.05		[1] DEL-AMO-SA...11B		BABR	$e^+e^- \to \Upsilon(4S)$
• • • We do not use the following data for averages, fits, limits, etc. • • •					
<0.90	90	[1] CHISTOV	04	BELL	$e^+e^- \to \Upsilon(4S)$
<0.4	90	[1] AUBERT	03X	BABR	Repl. by DEL-AMO-SANCHEZ 11B

[1] Assumes equal production of B^+ and B^0 at the $\Upsilon(4S)$.

$\Gamma(D^- D^*(2010)^+ K^+)/\Gamma_{\text{total}}$ Γ_{166}/Γ

VALUE (units 10^{-3})	CL%	DOCUMENT ID		TECN	COMMENT
0.63±0.09±0.06		[1] DEL-AMO-SA...11B		BABR	$e^+e^- \to \Upsilon(4S)$
• • • We do not use the following data for averages, fits, limits, etc. • • •					
<0.7	90	[1] AUBERT	03X	BABR	Repl. by DEL-AMO-SANCHEZ 11B

[1] Assumes equal production of B^+ and B^0 at the $\Upsilon(4S)$.

$\Gamma(D^*(2010)^- D^+ K^+)/\Gamma_{\text{total}}$ Γ_{167}/Γ

VALUE (units 10^{-3})	DOCUMENT ID		TECN	COMMENT
0.60±0.10±0.08	[1] DEL-AMO-SA...11B		BABR	$e^+e^- \to \Upsilon(4S)$
• • • We do not use the following data for averages, fits, limits, etc. • • •				
1.5 ±0.3 ±0.2	[1] AUBERT	03X	BABR	Repl. by DEL-AMO-SANCHEZ 11B

[1] Assumes equal production of B^+ and B^0 at the $\Upsilon(4S)$.

$\Gamma(D^*(2010)^- D^*(2010)^+ K^+)/\Gamma_{\text{total}}$ Γ_{168}/Γ

VALUE (units 10^{-3})	CL%	DOCUMENT ID		TECN	COMMENT
1.32±0.13±0.12		[1] DEL-AMO-SA...11B		BABR	$e^+e^- \to \Upsilon(4S)$
• • • We do not use the following data for averages, fits, limits, etc. • • •					
<1.8	90	[1] AUBERT	03X	BABR	Repl. by DEL-AMO-SANCHEZ 11B

[1] Assumes equal production of B^+ and B^0 at the $\Upsilon(4S)$.

$\Gamma((\overline{D}+\overline{D}^*)(D+D^*)K)/\Gamma_{\text{total}}$ Γ_{169}/Γ

VALUE (units 10^{-2})	DOCUMENT ID		TECN	COMMENT
4.05±0.11±0.28	[1] DEL-AMO-SA...11B		BABR	$e^+e^- \to \Upsilon(4S)$
• • • We do not use the following data for averages, fits, limits, etc. • • •				
3.5 ±0.3 ±0.5	[1] AUBERT	03X	BABR	Repl. by DEL-AMO-SANCHEZ 11B

[1] Assumes equal production of B^+ and B^0 at the $\Upsilon(4S)$.

$\Gamma(D_s^+ \pi^0)/\Gamma_{\text{total}}$ Γ_{170}/Γ

VALUE (units 10^{-5})	CL%	DOCUMENT ID		TECN	COMMENT
$1.6^{+0.6}_{-0.5}\pm0.1$		[1] AUBERT	07M	BABR	$e^+e^- \to \Upsilon(4S)$
• • • We do not use the following data for averages, fits, limits, etc. • • •					
<16	90	[2] ALEXANDER	93B	CLE2	$e^+e^- \to \Upsilon(4S)$

[1] AUBERT 07M reports $[\Gamma(B^+ \to D_s^+\pi^0)/\Gamma_{\text{total}}] \times [\text{B}(D_s^+ \to \phi\pi^+)] = (7.0^{+2.4}_{-2.1}{}^{+0.6}_{-0.8}) \times 10^{-7}$ which we divide by our best value $\text{B}(D_s^+ \to \phi\pi^+) = (4.5 \pm 0.4) \times 10^{-2}$. Our first error is their experiment's error and our second error is the systematic error from using our best value.

[2] ALEXANDER 93B reports $< 2.0 \times 10^{-4}$ from a measurement of $[\Gamma(B^+ \to D_s^+\pi^0)/\Gamma_{\text{total}}] \times [\text{B}(D_s^+ \to \phi\pi^+)]$ assuming $\text{B}(D_s^+ \to \phi\pi^+) = 0.037$, which we rescale to our best value $\text{B}(D_s^+ \to \phi\pi^+) = 4.5 \times 10^{-2}$.

$[\Gamma(D_s^+\pi^0) + \Gamma(D_s^{*+}\pi^0)]/\Gamma_{\text{total}}$ $(\Gamma_{170}+\Gamma_{171})/\Gamma$

VALUE	CL%	DOCUMENT ID		TECN	COMMENT
$<5 \times 10^{-4}$	90	[1] ALBRECHT	93E	ARG	$e^+e^- \to \Upsilon(4S)$

[1] ALBRECHT 93E reports $< 0.9 \times 10^{-3}$ from a measurement of $[\left[\Gamma(B^+ \to D_s^+\pi^0) + \Gamma(B^+ \to D_s^{*+}\pi^0)\right]/\Gamma_{\text{total}}] \times [\text{B}(D_s^+ \to \phi\pi^+)]$ assuming $\text{B}(D_s^+ \to \phi\pi^+) = 0.027$, which we rescale to our best value $\text{B}(D_s^+ \to \phi\pi^+) = 4.5 \times 10^{-2}$.

$\Gamma(D_s^{*+}\pi^0)/\Gamma_{\text{total}}$ Γ_{171}/Γ

VALUE	CL%	DOCUMENT ID		TECN	COMMENT
$<2.6 \times 10^{-4}$	90	[1] ALEXANDER	93B	CLE2	$e^+e^- \to \Upsilon(4S)$

[1] ALEXANDER 93B reports $< 3.2 \times 10^{-4}$ from a measurement of $[\Gamma(B^+ \to D_s^{*+}\pi^0)/\Gamma_{\text{total}}] \times [\text{B}(D_s^+ \to \phi\pi^+)]$ assuming $\text{B}(D_s^+ \to \phi\pi^+) = 0.037$, which we rescale to our best value $\text{B}(D_s^+ \to \phi\pi^+) = 4.5 \times 10^{-2}$.

$\Gamma(D_s^+\eta)/\Gamma_{\text{total}}$ Γ_{172}/Γ

VALUE	CL%	DOCUMENT ID		TECN	COMMENT
$<4 \times 10^{-4}$	90	[1] ALEXANDER	93B	CLE2	$e^+e^- \to \Upsilon(4S)$

[1] ALEXANDER 93B reports $< 4.6 \times 10^{-4}$ from a measurement of $[\Gamma(B^+ \to D_s^+\eta)/\Gamma_{\text{total}}] \times [\text{B}(D_s^+ \to \phi\pi^+)]$ assuming $\text{B}(D_s^+ \to \phi\pi^+) = 0.037$, which we rescale to our best value $\text{B}(D_s^+ \to \phi\pi^+) = 4.5 \times 10^{-2}$.

$\Gamma(D_s^{*+}\eta)/\Gamma_{\text{total}}$ Γ_{173}/Γ

VALUE	CL%	DOCUMENT ID		TECN	COMMENT
$<6 \times 10^{-4}$	90	[1] ALEXANDER	93B	CLE2	$e^+e^- \to \Upsilon(4S)$

[1] ALEXANDER 93B reports $< 7.5 \times 10^{-4}$ from a measurement of $[\Gamma(B^+ \to D_s^{*+}\eta)/\Gamma_{\text{total}}] \times [\text{B}(D_s^+ \to \phi\pi^+)]$ assuming $\text{B}(D_s^+ \to \phi\pi^+) = 0.037$, which we rescale to our best value $\text{B}(D_s^+ \to \phi\pi^+) = 4.5 \times 10^{-2}$.

$\Gamma(D_s^+\rho^0)/\Gamma_{\text{total}}$ Γ_{174}/Γ

VALUE	CL%	DOCUMENT ID		TECN	COMMENT
$<3.0 \times 10^{-4}$	90	[1] ALEXANDER	93B	CLE2	$e^+e^- \to \Upsilon(4S)$

[1] ALEXANDER 93B reports $< 3.7 \times 10^{-4}$ from a measurement of $[\Gamma(B^+ \to D_s^+\rho^0)/\Gamma_{\text{total}}] \times [\text{B}(D_s^+ \to \phi\pi^+)]$ assuming $\text{B}(D_s^+ \to \phi\pi^+) = 0.037$, which we rescale to our best value $\text{B}(D_s^+ \to \phi\pi^+) = 4.5 \times 10^{-2}$.

$[\Gamma(D_s^+\rho^0) + \Gamma(D_s^+\overline{K}^*(892)^0)]/\Gamma_{\text{total}}$ $(\Gamma_{174}+\Gamma_{184})/\Gamma$

VALUE	CL%	DOCUMENT ID		TECN	COMMENT
$<2.0 \times 10^{-3}$	90	[1] ALBRECHT	93E	ARG	$e^+e^- \to \Upsilon(4S)$

[1] ALBRECHT 93E reports $< 3.4 \times 10^{-3}$ from a measurement of $[\left[\Gamma(B^+ \to D_s^+\rho^0) + \Gamma(B^+ \to D_s^+\overline{K}^*(892)^0)\right]/\Gamma_{\text{total}}] \times [\text{B}(D_s^+ \to \phi\pi^+)]$ assuming $\text{B}(D_s^+ \to \phi\pi^+) = 0.027$, which we rescale to our best value $\text{B}(D_s^+ \to \phi\pi^+) = 4.5 \times 10^{-2}$.

$\Gamma(D_s^{*+}\rho^0)/\Gamma_{\text{total}}$ Γ_{175}/Γ

VALUE	CL%	DOCUMENT ID		TECN	COMMENT
$<4 \times 10^{-4}$	90	[1] ALEXANDER	93B	CLE2	$e^+e^- \to \Upsilon(4S)$

[1] ALEXANDER 93B reports $< 4.8 \times 10^{-4}$ from a measurement of $[\Gamma(B^+ \to D_s^{*+}\rho^0)/\Gamma_{\text{total}}] \times [\text{B}(D_s^+ \to \phi\pi^+)]$ assuming $\text{B}(D_s^+ \to \phi\pi^+) = 0.037$, which we rescale to our best value $\text{B}(D_s^+ \to \phi\pi^+) = 4.5 \times 10^{-2}$.

$[\Gamma(D_s^{*+}\rho^0) + \Gamma(D_s^{*+}\overline{K}^*(892)^0)]/\Gamma_{\text{total}}$ $(\Gamma_{175}+\Gamma_{186})/\Gamma$

VALUE	CL%	DOCUMENT ID		TECN	COMMENT
$<1.2 \times 10^{-3}$	90	[1] ALBRECHT	93E	ARG	$e^+e^- \to \Upsilon(4S)$

[1] ALBRECHT 93E reports $< 2.0 \times 10^{-3}$ from a measurement of $[\left[\Gamma(B^+ \to D_s^{*+}\rho^0) + \Gamma(B^+ \to D_s^{*+}\overline{K}^*(892)^0)\right]/\Gamma_{\text{total}}] \times [\text{B}(D_s^+ \to \phi\pi^+)]$ assuming $\text{B}(D_s^+ \to \phi\pi^+) = 0.027$, which we rescale to our best value $\text{B}(D_s^+ \to \phi\pi^+) = 4.5 \times 10^{-2}$.

$\Gamma(D_s^+\omega)/\Gamma_{\text{total}}$ Γ_{176}/Γ

VALUE	CL%	DOCUMENT ID		TECN	COMMENT
$<4 \times 10^{-4}$	90	[1] ALEXANDER	93B	CLE2	$e^+e^- \to \Upsilon(4S)$
• • • We do not use the following data for averages, fits, limits, etc. • • •					
$<2.0 \times 10^{-3}$	90	[2] ALBRECHT	93E	ARG	$e^+e^- \to \Upsilon(4S)$

[1] ALEXANDER 93B reports $< 4.8 \times 10^{-4}$ from a measurement of $[\Gamma(B^+ \to D_s^+\omega)/\Gamma_{\text{total}}] \times [\text{B}(D_s^+ \to \phi\pi^+)]$ assuming $\text{B}(D_s^+ \to \phi\pi^+) = 0.037$, which we rescale to our best value $\text{B}(D_s^+ \to \phi\pi^+) = 4.5 \times 10^{-2}$.

[2] ALBRECHT 93E reports $< 3.4 \times 10^{-3}$ from a measurement of $[\Gamma(B^+ \to D_s^+\omega)/\Gamma_{\text{total}}] \times [\text{B}(D_s^+ \to \phi\pi^+)]$ assuming $\text{B}(D_s^+ \to \phi\pi^+) = 0.027$, which we rescale to our best value $\text{B}(D_s^+ \to \phi\pi^+) = 4.5 \times 10^{-2}$.

Meson Particle Listings

$B^{\pm}$

$\Gamma(D_s^{*+}\omega)/\Gamma_{total}$ Γ_{177}/Γ

VALUE	CL%	DOCUMENT ID		TECN	COMMENT
<6 × 10⁻⁴	90	[1] ALEXANDER	93B	CLE2	$e^+e^- \to \Upsilon(4S)$
• • • We do not use the following data for averages, fits, limits, etc. • • •					
$<1.1 \times 10^{-3}$	90	[2] ALBRECHT	93E	ARG	$e^+e^- \to \Upsilon(4S)$

[1] ALEXANDER 93B reports $< 6.8 \times 10^{-4}$ from a measurement of $[\Gamma(B^+ \to D_s^{*+}\omega)/\Gamma_{total}] \times [B(D_s^+ \to \phi\pi^+)]$ assuming $B(D_s^+ \to \phi\pi^+) = 0.037$, which we rescale to our best value $B(D_s^+ \to \phi\pi^+) = 4.5 \times 10^{-2}$.

[2] ALBRECHT 93E reports $< 1.9 \times 10^{-3}$ from a measurement of $[\Gamma(B^+ \to D_s^{*+}\omega)/\Gamma_{total}] \times [B(D_s^+ \to \phi\pi^+)]$ assuming $B(D_s^+ \to \phi\pi^+) = 0.027$, which we rescale to our best value $B(D_s^+ \to \phi\pi^+) = 4.5 \times 10^{-2}$.

$\Gamma(D_s^+ a_1(1260)^0)/\Gamma_{total}$ Γ_{178}/Γ

VALUE	CL%	DOCUMENT ID		TECN	COMMENT
<1.8 × 10⁻³	90	[1] ALBRECHT	93E	ARG	$e^+e^- \to \Upsilon(4S)$

[1] ALBRECHT 93E reports $< 3.0 \times 10^{-3}$ from a measurement of $[\Gamma(B^+ \to D_s^+ a_1(1260)^0)/\Gamma_{total}] \times [B(D_s^+ \to \phi\pi^+)]$ assuming $B(D_s^+ \to \phi\pi^+) = 0.027$, which we rescale to our best value $B(D_s^+ \to \phi\pi^+) = 4.5 \times 10^{-2}$.

$\Gamma(D_s^{*+} a_1(1260)^0)/\Gamma_{total}$ Γ_{179}/Γ

VALUE	CL%	DOCUMENT ID		TECN	COMMENT
<1.3 × 10⁻³	90	[1] ALBRECHT	93E	ARG	$e^+e^- \to \Upsilon(4S)$

[1] ALBRECHT 93E reports $< 2.2 \times 10^{-3}$ from a measurement of $[\Gamma(B^+ \to D_s^{*+} a_1(1260)^0)/\Gamma_{total}] \times [B(D_s^+ \to \phi\pi^+)]$ assuming $B(D_s^+ \to \phi\pi^+) = 0.027$, which we rescale to our best value $B(D_s^+ \to \phi\pi^+) = 4.5 \times 10^{-2}$.

$\Gamma(D_s^+\phi)/\Gamma_{total}$ Γ_{180}/Γ

VALUE (units 10^{-6})	CL%	DOCUMENT ID		TECN	COMMENT
$1.7^{+1.1}_{-0.7} \pm 0.2$		[1] AAIJ	13R	LHCB	pp at 7 TeV
• • • We do not use the following data for averages, fits, limits, etc. • • •					
< 1.9	90	[2] AUBERT	06F	BABR	$e^+e^- \to \Upsilon(4S)$
<1000	90	[3] ALBRECHT	93E	ARG	$e^+e^- \to \Upsilon(4S)$
< 260	90	[4] ALEXANDER	93B	CLE2	$e^+e^- \to \Upsilon(4S)$

[1] AAIJ 13R reports $(1.87^{+1.25}_{-0.73} \pm 0.19 \pm 0.32) \times 10^{-6}$ from a measurement of $[\Gamma(B^+ \to D_s^+\phi)/\Gamma_{total}] / [B(B^+ \to \overline{D}^0 D_s^+)]$ assuming $B(B^+ \to \overline{D}^0 D_s^+) = (10.0 \pm 1.7) \times 10^{-3}$, which we rescale to our best value $B(B^+ \to \overline{D}^0 D_s^+) = (9.0 \pm 0.9) \times 10^{-3}$. Our first error is their experiment's error and our second error is the systematic error from using our best value.

[2] Assumes equal production of B^+ and B^0 at the $\Upsilon(4S)$.

[3] ALBRECHT 93E reports $< 1.7 \times 10^{-3}$ from a measurement of $[\Gamma(B^+ \to D_s^+\phi)/\Gamma_{total}] \times [B(D_s^+ \to \phi\pi^+)]$ assuming $B(D_s^+ \to \phi\pi^+) = 0.027$, which we rescale to our best value $B(D_s^+ \to \phi\pi^+) = 4.5 \times 10^{-2}$.

[4] ALEXANDER 93B reports $< 3.1 \times 10^{-4}$ from a measurement of $[\Gamma(B^+ \to D_s^+\phi)/\Gamma_{total}] \times [B(D_s^+ \to \phi\pi^+)]$ assuming $B(D_s^+ \to \phi\pi^+) = 0.037$, which we rescale to our best value $B(D_s^+ \to \phi\pi^+) = 4.5 \times 10^{-2}$.

$\Gamma(D_s^{*+}\phi)/\Gamma_{total}$ Γ_{181}/Γ

VALUE	CL%	DOCUMENT ID		TECN	COMMENT
<1.2 × 10⁻⁵	90	[1] AUBERT	06F	BABR	$e^+e^- \to \Upsilon(4S)$
• • • We do not use the following data for averages, fits, limits, etc. • • •					
$<1.3 \times 10^{-3}$	90	[2] ALBRECHT	93E	ARG	$e^+e^- \to \Upsilon(4S)$
$<3.5 \times 10^{-4}$	90	[3] ALEXANDER	93B	CLE2	$e^+e^- \to \Upsilon(4S)$

[1] Assumes equal production of B^+ and B^0 at the $\Upsilon(4S)$.

[2] ALBRECHT 93E reports $< 2.1 \times 10^{-3}$ from a measurement of $[\Gamma(B^+ \to D_s^{*+}\phi)/\Gamma_{total}] \times [B(D_s^+ \to \phi\pi^+)]$ assuming $B(D_s^+ \to \phi\pi^+) = 0.027$, which we rescale to our best value $B(D_s^+ \to \phi\pi^+) = 4.5 \times 10^{-2}$.

[3] ALEXANDER 93B reports $< 4.2 \times 10^{-4}$ from a measurement of $[\Gamma(B^+ \to D_s^{*+}\phi)/\Gamma_{total}] \times [B(D_s^+ \to \phi\pi^+)]$ assuming $B(D_s^+ \to \phi\pi^+) = 0.037$, which we rescale to our best value $B(D_s^+ \to \phi\pi^+) = 4.5 \times 10^{-2}$.

$\Gamma(D_s^+\overline{K}^0)/\Gamma_{total}$ Γ_{182}/Γ

VALUE	CL%	DOCUMENT ID		TECN	COMMENT
<8 × 10⁻⁴	90	[1] ALEXANDER	93B	CLE2	$e^+e^- \to \Upsilon(4S)$
• • • We do not use the following data for averages, fits, limits, etc. • • •					
$<1.5 \times 10^{-3}$	90	[2] ALBRECHT	93E	ARG	$e^+e^- \to \Upsilon(4S)$

[1] ALEXANDER 93B reports $< 10.3 \times 10^{-4}$ from a measurement of $[\Gamma(B^+ \to D_s^+\overline{K}^0)/\Gamma_{total}] \times [B(D_s^+ \to \phi\pi^+)]$ assuming $B(D_s^+ \to \phi\pi^+) = 0.037$, which we rescale to our best value $B(D_s^+ \to \phi\pi^+) = 4.5 \times 10^{-2}$.

[2] ALBRECHT 93E reports $< 2.5 \times 10^{-3}$ from a measurement of $[\Gamma(B^+ \to D_s^+\overline{K}^0)/\Gamma_{total}] \times [B(D_s^+ \to \phi\pi^+)]$ assuming $B(D_s^+ \to \phi\pi^+) = 0.027$, which we rescale to our best value $B(D_s^+ \to \phi\pi^+) = 4.5 \times 10^{-2}$.

$\Gamma(D_s^{*+}\overline{K}^0)/\Gamma_{total}$ Γ_{183}/Γ

VALUE	CL%	DOCUMENT ID		TECN	COMMENT
<9 × 10⁻⁴	90	[1] ALEXANDER	93B	CLE2	$e^+e^- \to \Upsilon(4S)$
• • • We do not use the following data for averages, fits, limits, etc. • • •					
$<1.9 \times 10^{-3}$	90	[2] ALBRECHT	93E	ARG	$e^+e^- \to \Upsilon(4S)$

[1] ALEXANDER 93B reports $< 10.9 \times 10^{-4}$ from a measurement of $[\Gamma(B^+ \to D_s^{*+}\overline{K}^0)/\Gamma_{total}] \times [B(D_s^+ \to \phi\pi^+)]$ assuming $B(D_s^+ \to \phi\pi^+) = 0.037$, which we rescale to our best value $B(D_s^+ \to \phi\pi^+) = 4.5 \times 10^{-2}$.

[2] ALBRECHT 93E reports $< 3.1 \times 10^{-3}$ from a measurement of $[\Gamma(B^+ \to D_s^{*+}\overline{K}^0)/\Gamma_{total}] \times [B(D_s^+ \to \phi\pi^+)]$ assuming $B(D_s^+ \to \phi\pi^+) = 0.027$, which we rescale to our best value $B(D_s^+ \to \phi\pi^+) = 4.5 \times 10^{-2}$.

$\Gamma(D_s^+\overline{K}^*(892)^0)/\Gamma_{total}$ Γ_{184}/Γ

VALUE	CL%	DOCUMENT ID		TECN	COMMENT
<4.4 × 10⁻⁶	90	AAIJ	13R	LHCB	pp at 7 TeV
• • • We do not use the following data for averages, fits, limits, etc. • • •					
$<4 \times 10^{-4}$	90	[1] ALEXANDER	93B	CLE2	$e^+e^- \to \Upsilon(4S)$

[1] ALEXANDER 93B reports $< 4.4 \times 10^{-4}$ from a measurement of $[\Gamma(B^+ \to D_s^+\overline{K}^*(892)^0)/\Gamma_{total}] \times [B(D_s^+ \to \phi\pi^+)]$ assuming $B(D_s^+ \to \phi\pi^+) = 0.037$, which we rescale to our best value $B(D_s^+ \to \phi\pi^+) = 4.5 \times 10^{-2}$.

$\Gamma(D_s^+ K^{*0})/\Gamma_{total}$ Γ_{185}/Γ

VALUE (units 10^{-6})	CL%	DOCUMENT ID		TECN	COMMENT
<3.5	90	AAIJ	13R	LHCB	pp at 7 TeV

$\Gamma(D_s^{*+}\overline{K}^*(892)^0)/\Gamma_{total}$ Γ_{186}/Γ

VALUE	CL%	DOCUMENT ID		TECN	COMMENT
<3.5 × 10⁻⁴	90	[1] ALEXANDER	93B	CLE2	$e^+e^- \to \Upsilon(4S)$

[1] ALEXANDER 93B reports $< 4.3 \times 10^{-4}$ from a measurement of $[\Gamma(B^+ \to D_s^{*+}\overline{K}^*(892)^0)/\Gamma_{total}] \times [B(D_s^+ \to \phi\pi^+)]$ assuming $B(D_s^+ \to \phi\pi^+) = 0.037$, which we rescale to our best value $B(D_s^+ \to \phi\pi^+) = 4.5 \times 10^{-2}$.

$\Gamma(D_s^- \pi^+ K^+)/\Gamma_{total}$ Γ_{187}/Γ

VALUE (units 10^{-4})	CL%	DOCUMENT ID		TECN	COMMENT
1.80±0.22 OUR AVERAGE					
$1.71^{+0.08}_{-0.07} \pm 0.25$		[1] WIECHCZYN...	09	BELL	$e^+e^- \to \Upsilon(4S)$
$2.02 \pm 0.13 \pm 0.38$		[1] AUBERT	08G	BABR	$e^+e^- \to \Upsilon(4S)$
• • • We do not use the following data for averages, fits, limits, etc. • • •					
<7	90	[2] ALBRECHT	93E	ARG	$e^+e^- \to \Upsilon(4S)$

[1] Assumes equal production of B^+ and B^0 at the $\Upsilon(4S)$.

[2] ALBRECHT 93E reports $< 1.1 \times 10^{-3}$ from a measurement of $[\Gamma(B^+ \to D_s^- \pi^+ K^+)/\Gamma_{total}] \times [B(D_s^+ \to \phi\pi^+)]$ assuming $B(D_s^+ \to \phi\pi^+) = 0.027$, which we rescale to our best value $B(D_s^+ \to \phi\pi^+) = 4.5 \times 10^{-2}$.

$\Gamma(D_s^{*-} \pi^+ K^+)/\Gamma_{total}$ Γ_{188}/Γ

VALUE (units 10^{-4})	CL%	DOCUMENT ID		TECN	COMMENT
1.45±0.24 OUR AVERAGE					
$1.31^{+0.13}_{-0.12} \pm 0.28$		[1] WIECHCZYN...	09	BELL	$e^+e^- \to \Upsilon(4S)$
$1.67 \pm 0.16 \pm 0.35$		[1] AUBERT	08G	BABR	$e^+e^- \to \Upsilon(4S)$
• • • We do not use the following data for averages, fits, limits, etc. • • •					
<10	90	[2] ALBRECHT	93E	ARG	$e^+e^- \to \Upsilon(4S)$

[1] Assumes equal production of B^+ and B^0 at the $\Upsilon(4S)$.

[2] ALBRECHT 93E reports $< 1.6 \times 10^{-3}$ from a measurement of $[\Gamma(B^+ \to D_s^{*-} \pi^+ K^+)/\Gamma_{total}] \times [B(D_s^+ \to \phi\pi^+)]$ assuming $B(D_s^+ \to \phi\pi^+) = 0.027$, which we rescale to our best value $B(D_s^+ \to \phi\pi^+) = 4.5 \times 10^{-2}$.

$\Gamma(D_s^- \pi^+ K^*(892)^+)/\Gamma_{total}$ Γ_{189}/Γ

VALUE	CL%	DOCUMENT ID		TECN	COMMENT
<5 × 10⁻³	90	[1] ALBRECHT	93E	ARG	$e^+e^- \to \Upsilon(4S)$

[1] ALBRECHT 93E reports $< 8.6 \times 10^{-3}$ from a measurement of $[\Gamma(B^+ \to D_s^- \pi^+ K^*(892)^+)/\Gamma_{total}] \times [B(D_s^+ \to \phi\pi^+)]$ assuming $B(D_s^+ \to \phi\pi^+) = 0.027$, which we rescale to our best value $B(D_s^+ \to \phi\pi^+) = 4.5 \times 10^{-2}$.

$\Gamma(D_s^{*-} \pi^+ K^*(892)^+)/\Gamma_{total}$ Γ_{190}/Γ

VALUE	CL%	DOCUMENT ID		TECN	COMMENT
<7 × 10⁻³	90	[1] ALBRECHT	93E	ARG	$e^+e^- \to \Upsilon(4S)$

[1] ALBRECHT 93E reports $< 1.1 \times 10^{-2}$ from a measurement of $[\Gamma(B^+ \to D_s^{*-} \pi^+ K^*(892)^+)/\Gamma_{total}] \times [B(D_s^+ \to \phi\pi^+)]$ assuming $B(D_s^+ \to \phi\pi^+) = 0.027$, which we rescale to our best value $B(D_s^+ \to \phi\pi^+) = 4.5 \times 10^{-2}$.

$\Gamma(D_s^- K^+ K^+)/\Gamma_{total}$ Γ_{191}/Γ

VALUE (units 10^{-4})	DOCUMENT ID		TECN	COMMENT
$0.11 \pm 0.04 \pm 0.02$	[1] AUBERT	08G	BABR	$e^+e^- \to \Upsilon(4S)$

[1] Assumes equal production of B^+ and B^0 at the $\Upsilon(4S)$.

$\Gamma(D_s^{*-} K^+ K^+)/\Gamma_{total}$ Γ_{192}/Γ

VALUE (units 10^{-4})	CL%	DOCUMENT ID		TECN	COMMENT
<0.15	90	[1] AUBERT	08G	BABR	$e^+e^- \to \Upsilon(4S)$

[1] Assumes equal production of B^+ and B^0 at the $\Upsilon(4S)$.

$\Gamma(\eta_c K^+)/\Gamma_{total}$ Γ_{193}/Γ

VALUE (units 10^{-3})	DOCUMENT ID		TECN	COMMENT
0.96 ± 0.11 OUR AVERAGE				
0.87 ± 0.15	[1,2] AUBERT	06E	BABR	$e^+e^- \to \Upsilon(4S)$
$1.19^{+0.24}_{-0.19} \pm 0.13$	[3] AUBERT,B	05L	BABR	$e^+e^- \to \Upsilon(4S)$
$1.25 \pm 0.14^{+0.39}_{-0.40}$	[4] FANG	03	BELL	$e^+e^- \to \Upsilon(4S)$
$0.69^{+0.26}_{-0.21} \pm 0.22$	[5] EDWARDS	01	CLE2	$e^+e^- \to \Upsilon(4S)$
• • • We do not use the following data for averages, fits, limits, etc. • • •				
$1.01 \pm 0.12 \pm 0.07$	[2,6] AUBERT,B	04B	BABR	$e^+e^- \to \Upsilon(4S)$

[1] Perform measurements of absolute branching fractions using a missing mass technique.
[2] The ratio of $B(B^{\pm} \to K^{\pm}\eta_c)\, B(\eta_c \to K\overline{K}\pi) = (7.4 \pm 0.5 \pm 0.7) \times 10^{-5}$ reported in AUBERT,B 04B and $B(B^{\pm} \to K^{\pm}\eta_c) = (8.7 \pm 1.5) \times 10^{-3}$ reported in AUBERT 06E contribute to the determination of $B(\eta_c \to K\overline{K}\pi)$, which is used by others for normalization.
[3] AUBERT,B 05L reports $[\Gamma(B^+ \to \eta_c K^+)/\Gamma_{total}] \times [B(\eta_c(1S) \to p\overline{p})] = (1.8^{+0.3}_{-0.2} \pm 0.2) \times 10^{-6}$ which we divide by our best value $B(\eta_c(1S) \to p\overline{p}) = (1.52 \pm 0.16) \times 10^{-3}$. Our first error is their experiment's error and our second error is the systematic error from using our best value.
[4] Assumes equal production of B^+ and B^0 at the $\Upsilon(4S)$.
[5] EDWARDS 01 assumes equal production of B^0 and B^+ at the $\Upsilon(4S)$. The correlated uncertainties (28.3)% from $B(J/\psi(1S) \to \gamma\eta_c)$ in those modes have been accounted for.
[6] AUBERT,B 04B reports $[\Gamma(B^+ \to \eta_c K^+)/\Gamma_{total}] \times [B(\eta_c(1S) \to K\overline{K}\pi)] = (0.074 \pm 0.005 \pm 0.007) \times 10^{-3}$ which we divide by our best value $B(\eta_c(1S) \to K\overline{K}\pi) = (7.3 \pm 0.5) \times 10^{-2}$. Our first error is their experiment's error and our second error is the systematic error from using our best value.

$\Gamma(B^+ \to \eta_c K^+)/\Gamma_{total} \times \Gamma(\eta_c(1S) \to \gamma\gamma)/\Gamma_{total}$ $\Gamma_{193}/\Gamma \times \Gamma_{36}^{\eta_c(1S)}/\Gamma^{\eta_c(1S)}$

VALUE (units 10^{-6})	DOCUMENT ID		TECN	COMMENT
$0.22^{+0.09}_{-0.07} \pm 0.04$	[1] WICHT	08	BELL	$e^+e^- \to \Upsilon(4S)$

[1] Assumes equal production of B^+ and B^0 at the $\Upsilon(4S)$.

$\Gamma(\eta_c K^+,\ \eta_c \to K_S^0 K^{\mp}\pi^{\pm})/\Gamma_{total}$ Γ_{194}/Γ

VALUE (units 10^{-6})	DOCUMENT ID		TECN	COMMENT
$26.7 \pm 1.4^{+5.7}_{-5.5}$	[1,2] VINOKUROVA	11	BELL	$e^+e^- \to \Upsilon(4S)$

[1] Assumes equal production of B^0 and B^+ from Upsilon(4S) decays.
[2] VINOKUROVA 11 reports $(26.7 \pm 1.4^{+2.9}_{-2.6} \pm 4.9) \times 10^{-6}$, where the first uncertainty is statistical, the second is due to systematics, and the third comes from interference of $\eta_c(1S) \to K_S^0 K^{\pm}\pi^{\mp}$ with nonresonant $K_S^0 K^{\pm}\pi^{\mp}$. We combined both systematic uncertainties to single values.

$\Gamma(\eta_c K^*(892)^+)/\Gamma_{total}$ Γ_{195}/Γ

VALUE (units 10^{-3})	DOCUMENT ID		TECN	COMMENT
$1.0^{+0.5}_{-0.4} \pm 0.1$	[1,2] AUBERT	07AV	BABR	$e^+e^- \to \Upsilon(4S)$

[1] AUBERT 07AV reports $[\Gamma(B^+ \to \eta_c K^*(892)^+)/\Gamma_{total}] \times [B(\eta_c(1S) \to p\overline{p})] = (1.57^{+0.56+0.45}_{-0.46-0.36}) \times 10^{-6}$ which we divide by our best value $B(\eta_c(1S) \to p\overline{p}) = (1.52 \pm 0.16) \times 10^{-3}$. Our first error is their experiment's error and our second error is the systematic error from using our best value.
[2] Assumes equal production of B^+ and B^0 at the $\Upsilon(4S)$.

$\Gamma(\eta_c(2S) K^+)/\Gamma_{total}$ Γ_{196}/Γ

VALUE (units 10^{-4})	DOCUMENT ID		TECN	COMMENT
$3.4 \pm 1.8 \pm 0.3$	[1] AUBERT	06E	BABR	$e^+e^- \to \Upsilon(4S)$

[1] Perform measurements of absolute branching fractions using a missing mass technique.

$\Gamma(\eta_c(2S) K^+,\ \eta_c \to p\overline{p})/\Gamma_{total}$ Γ_{197}/Γ

VALUE	CL%	DOCUMENT ID		TECN	COMMENT
$<1.06 \times 10^{-7}$	95	[1] AAIJ	13S	LHCB	pp at 7 TeV

[1] Measured relative to $B^+ \to J/\psi K^+$ decay with charmonia reconstructed in $p\overline{p}$ final state and using $B(B^+ \to J/\psi K^+) = (1.013 \pm 0.034) \times 10^{-3}$ and $B(J/\psi \to p\overline{p}) = (2.17 \pm 0.07) \times 10^{-3}$.

$\Gamma(B^+ \to h_c(1P) K^+)/\Gamma_{total} \times \Gamma(h_c(1P) \to \eta_c(1S)\gamma)/\Gamma_{total}$ $\Gamma_{260}/\Gamma \times \Gamma_4^{h_c(1P)}/\Gamma^{h_c(1P)}$

VALUE (units 10^{-4})	CL%	DOCUMENT ID		TECN	COMMENT
<0.48	90	[1] AUBERT	08AB	BABR	$e^+e^- \to \Upsilon(4S)$

[1] Uses the production ratio of $(B^+B^-)/(B^0\overline{B}^0) = 1.026 \pm 0.032$ at $\Upsilon(4S)$.

$\Gamma(B^+ \to \eta_c(2S) K^+)/\Gamma_{total} \times \Gamma(\eta_c(2S) \to \gamma\gamma)/\Gamma_{total}$ $\Gamma_{196}/\Gamma \times \Gamma_{14}^{\eta_c(2S)}/\Gamma^{\eta_c(2S)}$

VALUE (units 10^{-6})	CL%	DOCUMENT ID		TECN	COMMENT
<0.18	90	[1] WICHT	08	BELL	$e^+e^- \to \Upsilon(4S)$

[1] Assumes equal production of B^+ and B^0 at the $\Upsilon(4S)$.

$\Gamma(\eta_c(2S) K^+,\ \eta_c \to K_S^0 K^{\mp}\pi^{\pm})/\Gamma_{total}$ Γ_{198}/Γ

VALUE (units 10^{-6})	DOCUMENT ID		TECN	COMMENT
$3.4^{+2.2+0.5}_{-1.5-0.4}$	[1,2] VINOKUROVA	11	BELL	$e^+e^- \to \Upsilon(4S)$

[1] Assumes equal production of B^0 and B^+ from Upsilon(4S) decays.
[2] The first uncertainty includes both statistical and interference effects while the second is due to systematics.

$\Gamma(J/\psi(1S) K^+)/\Gamma_{total}$ Γ_{218}/Γ

VALUE (units 10^{-4})	EVTS	DOCUMENT ID		TECN	COMMENT
10.27 ± 0.31 OUR FIT					
10.24 ± 0.35 OUR AVERAGE					
$8.1 \pm 1.3 \pm 0.7$		[1] AUBERT	06E	BABR	$e^+e^- \to \Upsilon(4S)$
$10.61 \pm 0.15 \pm 0.48$		[2] AUBERT	05J	BABR	$e^+e^- \to \Upsilon(4S)$
$10.4 \pm 1.1 \pm 0.1$		[3] AUBERT,B	05L	BABR	$e^+e^- \to \Upsilon(4S)$
$10.1 \pm 0.2 \pm 0.7$		[2] ABE	03B	BELL	$e^+e^- \to \Upsilon(4S)$
$10.2 \pm 0.8 \pm 0.7$		[2] JESSOP	97	CLE2	$e^+e^- \to \Upsilon(4S)$
$9.24 \pm 3.04 \pm 0.05$		[4] BORTOLETTO	92	CLEO	$e^+e^- \to \Upsilon(4S)$
$8.09 \pm 3.50 \pm 0.04$	6	[5] ALBRECHT	90J	ARG	$e^+e^- \to \Upsilon(4S)$
• • • We do not use the following data for averages, fits, limits, etc. • • •					
$10.1 \pm 0.3 \pm 0.5$		[2] AUBERT	02	BABR	Repl. by AUBERT 05J
$11.0 \pm 1.5 \pm 0.9$	59	[2] ALAM	94	CLE2	Repl. by JESSOP 97
$22 \pm 10 \pm 2$		BUSKULIC	92G	ALEP	$e^+e^- \to Z$
7 ± 4	3	[6] ALBRECHT	87D	ARG	$e^+e^- \to \Upsilon(4S)$
$10 \pm 7 \pm 2$	3	[7] BEBEK	87	CLEO	$e^+e^- \to \Upsilon(4S)$
9 ± 5	3	[8] ALAM	86	CLEO	$e^+e^- \to \Upsilon(4S)$

[1] Perform measurements of absolute branching fractions using a missing mass technique.
[2] Assumes equal production of B^+ and B^0 at the $\Upsilon(4S)$.
[3] AUBERT,B 05L reports $[\Gamma(B^+ \to J/\psi(1S) K^+)/\Gamma_{total}] \times [B(J/\psi(1S) \to p\overline{p})] = (2.2 \pm 0.2 \pm 0.1) \times 10^{-6}$ which we divide by our best value $B(J/\psi(1S) \to p\overline{p}) = (2.120 \pm 0.029) \times 10^{-3}$. Our first error is their experiment's error and our second error is the systematic error from using our best value.
[4] BORTOLETTO 92 reports $(8 \pm 2 \pm 2) \times 10^{-4}$ from a measurement of $[\Gamma(B^+ \to J/\psi(1S) K^+)/\Gamma_{total}] \times [B(J/\psi(1S) \to e^+e^-)]$ assuming $B(J/\psi(1S) \to e^+e^-) = 0.069 \pm 0.009$, which we rescale to our best value $B(J/\psi(1S) \to e^+e^-) = (5.971 \pm 0.032) \times 10^{-2}$. Our first error is their experiment's error and our second error is the systematic error from using our best value. Assumes equal production of B^+ and B^0 at the $\Upsilon(4S)$.
[5] ALBRECHT 90J reports $(7 \pm 3 \pm 1) \times 10^{-4}$ from a measurement of $[\Gamma(B^+ \to J/\psi(1S) K^+)/\Gamma_{total}] \times [B(J/\psi(1S) \to e^+e^-)]$ assuming $B(J/\psi(1S) \to e^+e^-) = 0.069 \pm 0.009$, which we rescale to our best value $B(J/\psi(1S) \to e^+e^-) = (5.971 \pm 0.032) \times 10^{-2}$. Our first error is their experiment's error and our second error is the systematic error from using our best value. Assumes equal production of B^+ and B^0 at the $\Upsilon(4S)$.
[6] ALBRECHT 87D assume $B^+B^-/B^0\overline{B}^0$ ratio is 55/45. Superseded by ALBRECHT 90J.
[7] BEBEK 87 value has been updated in BERKELMAN 91 to use same assumptions as noted for BORTOLETTO 92.
[8] ALAM 86 assumes $B^{\pm}/B^0$ ratio is 60/40.

$\Gamma(\eta_c K^+)/\Gamma(J/\psi(1S) K^+)$ $\Gamma_{193}/\Gamma_{218}$

VALUE	DOCUMENT ID		TECN	COMMENT
0.84 ± 0.10 OUR AVERAGE				
$0.81 \pm 0.06 \pm 0.09$	[1] AAIJ	13S	LHCB	pp at 7 TeV
$1.33 \pm 0.10 \pm 0.43$	[2] AUBERT,B	04B	BABR	$e^+e^- \to \Upsilon(4S)$

[1] AAIJ 13S reports $[\Gamma(B^+ \to \eta_c K^+)/\Gamma(B^+ \to J/\psi(1S) K^+)] \times [B(\eta_c(1S) \to p\overline{p})] / [B(J/\psi(1S) \to p\overline{p})] = 0.578 \pm 0.035 \pm 0.026$ which we multiply or divide by our best values $B(\eta_c(1S) \to p\overline{p}) = (1.52 \pm 0.16) \times 10^{-3}$, $B(J/\psi(1S) \to p\overline{p}) = (2.120 \pm 0.029) \times 10^{-3}$. Our first error is their experiment's error and our second error is the systematic error from using our best values.
[2] Uses BABAR measurement of $B(B^+ \to J/\psi K^+) = (10.1 \pm 0.3 \pm 0.5) \times 10^{-4}$.

$\Gamma(B^+ \to J/\psi(1S) K^+)/\Gamma_{total} \times \Gamma(J/\psi(1S) \to \gamma\gamma)/\Gamma_{total}$ $\Gamma_{218}/\Gamma \times \Gamma_{197}^{J/\psi(1S)}/\Gamma^{J/\psi(1S)}$

VALUE (units 10^{-6})	CL%	DOCUMENT ID		TECN	COMMENT
<0.16	90	[1] WICHT	08	BELL	$e^+e^- \to \Upsilon(4S)$

[1] Assumes equal production of B^+ and B^0 at the $\Upsilon(4S)$.

Meson Particle Listings

$B^{\pm}$

$\Gamma(J/\psi(1S)K^+\pi^+\pi^-)/\Gamma_{total}$ Γ_{220}/Γ

VALUE (units 10^{-3})	CL%	EVTS	DOCUMENT ID		TECN	COMMENT
0.81 ±0.13 OUR AVERAGE			Error includes scale factor of 2.5. See the ideogram below.			
0.716±0.010±0.060			[1] GULER	11	BELL	$e^+e^- \to \Upsilon(4S)$
1.16 ±0.07 ±0.09			[1] AUBERT	05R	BABR	$e^+e^- \to \Upsilon(4S)$
0.69 ±0.18 ±0.12			[2] ACOSTA	02F	CDF	$p\overline{p}$ 1.8 TeV
1.39 ±0.81 ±0.01			[3] BORTOLETTO	92	CLEO	$e^+e^- \to \Upsilon(4S)$
1.39 ±0.91 ±0.01		6	[4] ALBRECHT	87D	ARG	$e^+e^- \to \Upsilon(4S)$
• • • We do not use the following data for averages, fits, limits, etc. • • •						
<1.8	90		[5] ALBRECHT	90J	ARG	$e^+e^- \to \Upsilon(4S)$

[1] Assumes equal production of B^+ and B^0 at the $\Upsilon(4S)$.
[2] ACOSTA 02F uses as reference of $B(B \to J/\psi(1S)K^+) = (10.1 \pm 0.6) \times 10^{-4}$. The second error includes the systematic error and the uncertainties of the branching ratio.
[3] BORTOLETTO 92 reports $(1.2 \pm 0.6 \pm 0.4) \times 10^{-3}$ from a measurement of $[\Gamma(B^+ \to J/\psi(1S)K^+\pi^+\pi^-)/\Gamma_{total}] \times [B(J/\psi(1S) \to e^+e^-)]$ assuming $B(J/\psi(1S) \to e^+e^-) = 0.069 \pm 0.009$, which we rescale to our best value $B(J/\psi(1S) \to e^+e^-) = (5.971 \pm 0.032) \times 10^{-2}$. Our first error is their experiment's error and our second error is the systematic error from using our best value. Assumes equal production of B^+ and B^0 at the $\Upsilon(4S)$.
[4] ALBRECHT 87D reports $(1.2 \pm 0.8) \times 10^{-3}$ from a measurement of $[\Gamma(B^+ \to J/\psi(1S)K^+\pi^+\pi^-)/\Gamma_{total}] \times [B(J/\psi(1S) \to e^+e^-)]$ assuming $B(J/\psi(1S) \to e^+e^-) = 0.069 \pm 0.009$, which we rescale to our best value $B(J/\psi(1S) \to e^+e^-) = (5.971 \pm 0.032) \times 10^{-2}$. Our first error is their experiment's error and our second error is the systematic error from using our best value. They actually report 0.0011 ± 0.0007 assuming $B^+B^-/B^0\overline{B}^0$ ratio is 55/45. We rescale to 50/50. Analysis explicitly removes $B^+ \to \psi(2S)K^+$.
[5] ALBRECHT 90J reports $< 1.6 \times 10^{-3}$ from a measurement of $[\Gamma(B^+ \to J/\psi(1S)K^+\pi^+\pi^-)/\Gamma_{total}] \times [B(J/\psi(1S) \to e^+e^-)]$ assuming $B(J/\psi(1S) \to e^+e^-) = 0.069$, which we rescale to our best value $B(J/\psi(1S) \to e^+e^-) = 5.971 \times 10^{-2}$. Assumes equal production of B^+ and B^0 at the $\Upsilon(4S)$.

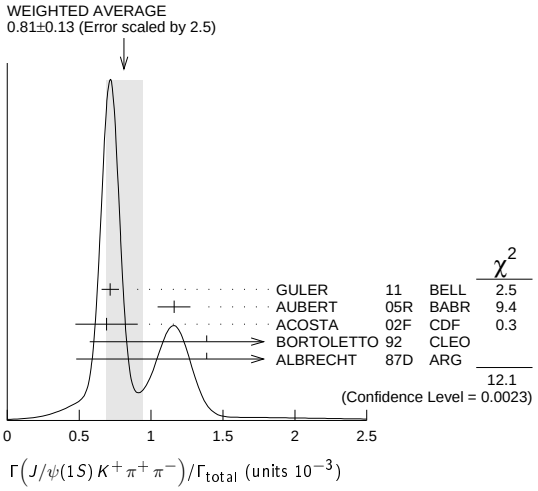

$\Gamma(h_c(1P)K^+,\ h_c \to J/\psi\pi^+\pi^-)/\Gamma_{total}$ Γ_{199}/Γ

VALUE	CL%	DOCUMENT ID		TECN	COMMENT
<3.4 × 10⁻⁶	90	[1] AUBERT	05R	BABR	$e^+e^- \to \Upsilon(4S)$

[1] Assumes equal production of B^+ and B^0 at the $\Upsilon(4S)$.

$\Gamma(X(3872)K^+)/\Gamma_{total}$ Γ_{200}/Γ

VALUE	CL%	DOCUMENT ID		TECN	COMMENT
<3.2 × 10⁻⁴	90	[1] AUBERT	06E	BABR	$e^+e^- \to \Upsilon(4S)$

[1] Perform measurements of absolute branching fractions using a missing mass technique.

$\Gamma(B^+ \to X(3872)K^+)/\Gamma_{total} \times \Gamma(X(3872) \to \gamma\gamma)/\Gamma_{total}$ $\Gamma_{200}/\Gamma \times \Gamma_7^{X(3872)}/\Gamma^{X(3872)}$

VALUE (units 10^{-6})	CL%	DOCUMENT ID		TECN	COMMENT
<0.24	90	[1] WICHT	08	BELL	$e^+e^- \to \Upsilon(4S)$

[1] Assumes equal production of B^+ and B^0 at the $\Upsilon(4S)$.

$\Gamma(X(3872)K^+,\ X \to J/\psi\pi^+\pi^-)/\Gamma_{total}$ Γ_{202}/Γ

VALUE (units 10^{-6})	DOCUMENT ID		TECN	COMMENT
8.6 ±0.8 OUR AVERAGE				
8.63±0.82±0.52	[1] CHOI	11	BELL	$e^+e^- \to \Upsilon(4S)$
8.4 ±1.5 ±0.7	[1] AUBERT	08Y	BABR	$e^+e^- \to \Upsilon(4S)$
• • • We do not use the following data for averages, fits, limits, etc. • • •				
10.1 ±2.5 ±1.0	[1] AUBERT	06	BABR	Repl. by AUBERT 08Y
12.8 ±4.1	[1] AUBERT	05R	BABR	Repl. by AUBERT 06
12.5 ±2.8 ±0.5	[2] CHOI	03	BELL	Repl. by CHOI 11

[1] Assumes equal production of B^+ and B^0 at the $\Upsilon(4S)$.
[2] CHOI 03 reports $[\Gamma(B^+ \to X(3872)K^+,\ X \to J/\psi\pi^+\pi^-)/\Gamma_{total}] / [B(B^+ \to \psi(2S)K^+)] = 0.0200 \pm 0.0038 \pm 0.0023$ which we multiply by our best value $B(B^+ \to \psi(2S)K^+) = (6.27 \pm 0.24) \times 10^{-4}$. Our first error is their experiment's error and our second error is the systematic error from using our best value.

$\Gamma(X(3872)K^+,\ X \to J/\psi\gamma)/\Gamma_{total}$ Γ_{203}/Γ

VALUE (units 10^{-6})	DOCUMENT ID		TECN	COMMENT
2.1 ±0.4 OUR AVERAGE	Error includes scale factor of 1.1.			
$1.78^{+0.48}_{-0.44} \pm 0.12$	[1] BHARDWAJ	11	BELL	$e^+e^- \to \Upsilon(4S)$
2.8 ±0.8 ±0.1	[2] AUBERT	09B	BABR	$e^+e^- \to \Upsilon(4S)$
• • • We do not use the following data for averages, fits, limits, etc. • • •				
3.3 ±1.0 ±0.3	[1] AUBERT,BE	06M	BABR	Repl. by AUBERT 09B

[1] Assumes equal production of B^+ and B^0 at the $\Upsilon(4S)$.
[2] Uses $B(\Upsilon(4S) \to B^+B^-) = (51.6 \pm 0.6)\%$ and $B(\Upsilon(4S) \to B^0\overline{B}^0) = (48.4 \pm 0.6)\%$.

$\Gamma(X(3872)K^*(892)^+,\ X \to J/\psi\gamma)/\Gamma_{total}$ Γ_{210}/Γ

VALUE (units 10^{-6})	CL%	DOCUMENT ID		TECN	COMMENT
<4.8	90	[1] AUBERT	09B	BABR	$e^+e^- \to \Upsilon(4S)$

[1] Uses $B(\Upsilon(4S) \to B^+B^-) = (51.6 \pm 0.6)\%$ and $B(\Upsilon(4S) \to B^0\overline{B}^0) = (48.4 \pm 0.6)\%$.

$\Gamma(X(3872)K^+,\ X \to \psi(2S)\gamma)/\Gamma_{total}$ Γ_{204}/Γ

VALUE (units 10^{-6})	DOCUMENT ID		TECN	COMMENT
4 ±4 OUR AVERAGE	Error includes scale factor of 2.5.			
$0.83^{+1.98}_{-1.83} \pm 0.44$	[1,2] BHARDWAJ	11	BELL	$e^+e^- \to \Upsilon(4S)$
9.5 ±2.7 ±0.6	[3] AUBERT	09B	BABR	$e^+e^- \to \Upsilon(4S)$

[1] BHARDWAJ 11 measurement is equivalent to a limit of $< 3.45 \times 10^{-6}$ at 90% CL.
[2] Assumes equal production of B^+ and B^0 at the $\Upsilon(4S)$.
[3] Uses $B(\Upsilon(4S) \to B^+B^-) = (51.6 \pm 0.6)\%$ and $B(\Upsilon(4S) \to B^0\overline{B}^0) = (48.4 \pm 0.6)\%$.

$\Gamma(X(3872)K^*(892)^+,\ X \to \psi(2S)\gamma)/\Gamma_{total}$ Γ_{211}/Γ

VALUE (units 10^{-6})	CL%	DOCUMENT ID		TECN	COMMENT
<28	90	[1] AUBERT	09B	BABR	$e^+e^- \to \Upsilon(4S)$

[1] Uses $B(\Upsilon(4S) \to B^+B^-) = (51.6 \pm 0.6)\%$ and $B(\Upsilon(4S) \to B^0\overline{B}^0) = (48.4 \pm 0.6)\%$.

$\Gamma(X(3872)K^+,\ X \to D^0\overline{D}^0)/\Gamma_{total}$ Γ_{206}/Γ

VALUE	CL%	DOCUMENT ID		TECN	COMMENT
<6.0 × 10⁻⁵	90	[1] CHISTOV	04	BELL	$e^+e^- \to \Upsilon(4S)$

[1] Assumes equal production of B^+ and B^0 at the $\Upsilon(4S)$.

$\Gamma(X(3872)K^+,\ X \to D^+D^-)/\Gamma_{total}$ Γ_{207}/Γ

VALUE	CL%	DOCUMENT ID		TECN	COMMENT
<4.0 × 10⁻⁵	90	[1] CHISTOV	04	BELL	$e^+e^- \to \Upsilon(4S)$

[1] Assumes equal production of B^+ and B^0 at the $\Upsilon(4S)$.

$\Gamma(X(3872)K^+,\ X \to D^0\overline{D}^0\pi^0)/\Gamma_{total}$ Γ_{208}/Γ

VALUE (units 10^{-4})	CL%	DOCUMENT ID		TECN	COMMENT
$1.02 \pm 0.31^{+0.21}_{-0.29}$		[1] GOKHROO	06	BELL	$e^+e^- \to \Upsilon(4S)$
• • • We do not use the following data for averages, fits, limits, etc. • • •					
<0.6	90	[2] CHISTOV	04	BELL	Repl. by GOKHROO 06

[1] Measure the near-threshold enhancements in the $(D^0\overline{D}^0\pi^0)$ system at a mass $3875.2 \pm 0.7^{+0.3}_{-1.6} \pm 0.8$ MeV/c^2.
[2] Assumes equal production of B^+ and B^0 at the $\Upsilon(4S)$.

$\Gamma(X(3872)K^+,\ X \to \overline{D}^{*0}D^0)/\Gamma_{total}$ Γ_{209}/Γ

VALUE (units 10^{-4})	DOCUMENT ID		TECN	COMMENT
0.85±0.26 OUR AVERAGE	Error includes scale factor of 1.4.			
0.77±0.16±0.10	[1] AUSHEV	10	BELL	$e^+e^- \to \Upsilon(4S)$
1.67±0.36±0.47	[1] AUBERT	08B	BABR	$e^+e^- \to \Upsilon(4S)$

[1] Assumes equal production of B^+ and B^0 at the $\Upsilon(4S)$.

$\Gamma(X(3872)K^+,\ X \to J/\psi(1S)\eta)/\Gamma_{total}$ Γ_{205}/Γ

VALUE	CL%	DOCUMENT ID		TECN	COMMENT
<7.7 × 10⁻⁶	90	[1] AUBERT	04Y	BABR	$e^+e^- \to \Upsilon(4S)$

[1] Assumes equal production of B^+ and B^0 at the $\Upsilon(4S)$.

$\Gamma(X(3872)^+K^0,\ X^+ \to J/\psi(1S)\pi^+\pi^0)/\Gamma_{total}$ Γ_{212}/Γ

VALUE (units 10^{-6})	CL%	DOCUMENT ID		TECN	COMMENT
< 6.1	90	[1,2] CHOI	11	BELL	$e^+e^- \to \Upsilon(4S)$
• • • We do not use the following data for averages, fits, limits, etc. • • •					
<22	90	[3] AUBERT	05B	BABR	$e^+e^- \to \Upsilon(4S)$

[1] Assumes $\pi^+\pi^0$ originates from ρ^+.
[2] Assumes equal production of B^+ and B^0 at the $\Upsilon(4S)$.
[3] Assumes equal production of B^+ and B^0 at the $\Upsilon(4S)$. The isovector-X hypothesis is excluded with a likelihood test at 1×10^{-4} level.

$\Gamma(X(4430)^+ K^0, X^+ \to J/\psi\pi^+)/\Gamma_{total}$ Γ_{213}/Γ

VALUE (units 10^{-5})	CL%	DOCUMENT ID		TECN	COMMENT
<1.5	95	[1] AUBERT	09AA	BABR	$e^+e^- \to \Upsilon(4S)$

[1] Assumes equal production of B^+ and B^0 at the $\Upsilon(4S)$.

$\Gamma(X(4430)^+ K^0, X^+ \to \psi(2S)\pi^+)/\Gamma_{total}$ Γ_{214}/Γ

VALUE (units 10^{-5})	CL%	DOCUMENT ID		TECN	COMMENT
<4.7	95	[1] AUBERT	09AA	BABR	$e^+e^- \to \Upsilon(4S)$

[1] Assumes equal production of B^+ and B^0 at the $\Upsilon(4S)$.

$\Gamma(X(4260)^0 K^+, X^0 \to J/\psi\pi^+\pi^-)/\Gamma_{total}$ Γ_{215}/Γ

VALUE (units 10^{-6})	CL%	DOCUMENT ID		TECN	COMMENT
<29	95	[1] AUBERT	06	BABR	$e^+e^- \to \Upsilon(4S)$

[1] Assumes equal production of B^+ and B^0 at the $\Upsilon(4S)$.

$\Gamma(\chi_{c0}(2P) K^+, X^0 \to J/\psi\gamma)/\Gamma_{total}$ Γ_{216}/Γ

VALUE (units 10^{-6})	CL%	DOCUMENT ID		TECN	COMMENT
<14	90	[1] AUBERT,BE	06M	BABR	$e^+e^- \to \Upsilon(4S)$

[1] Assumes equal production of B^+ and B^0 at the $\Upsilon(4S)$.

$\Gamma(X(3930)^0 K^+, X^0 \to J/\psi\gamma)/\Gamma_{total}$ Γ_{217}/Γ

VALUE (units 10^{-6})	CL%	DOCUMENT ID		TECN	COMMENT
<2.5	90	[1] AUBERT,BE	06M	BABR	$e^+e^- \to \Upsilon(4S)$

[1] Assumes equal production of B^+ and B^0 at the $\Upsilon(4S)$.

$\Gamma(J/\psi(1S) K^0\pi^+)/\Gamma_{total}$ Γ_{219}/Γ

VALUE (units 10^{-3})	DOCUMENT ID		TECN	COMMENT
• • • We do not use the following data for averages, fits, limits, etc. • • •				
1.101 ± 0.021	[1] AUBERT	09AA	BABR	$e^+e^- \to \Upsilon(4S)$

[1] Does not report systematic uncertainties.

$\Gamma(J/\psi(1S) K^*(892)^+)/\Gamma_{total}$ Γ_{222}/Γ

For polarization information see the Listings at the end of the "B^0 Branching Ratios" section.

VALUE (units 10^{-3})	EVTS	DOCUMENT ID		TECN	COMMENT
1.44 ±0.08 OUR FIT					
1.43 ±0.08 OUR AVERAGE					
$1.78\ ^{+0.36}_{-0.32} \pm 0.02$		[1,2] AUBERT	07AV	BABR	$e^+e^- \to \Upsilon(4S)$
$1.454 \pm 0.047 \pm 0.097$		[2] AUBERT	05J	BABR	$e^+e^- \to \Upsilon(4S)$
$1.28 \pm 0.07 \pm 0.14$		[2] ABE	02N	BELL	$e^+e^- \to \Upsilon(4S)$
$1.41 \pm 0.23 \pm 0.24$		[2] JESSOP	97	CLE2	$e^+e^- \to \Upsilon(4S)$
$1.58 \pm 0.47 \pm 0.27$		[3] ABE	96H	CDF	$p\overline{p}$ at 1.8 TeV
$1.50 \pm 1.08 \pm 0.01$		[4] BORTOLETTO	92	CLEO	$e^+e^- \to \Upsilon(4S)$
$1.85 \pm 1.30 \pm 0.01$	2	[5] ALBRECHT	90J	ARG	$e^+e^- \to \Upsilon(4S)$
• • • We do not use the following data for averages, fits, limits, etc. • • •					
$1.37 \pm 0.09 \pm 0.11$		[2] AUBERT	02	BABR	Repl. by AUBERT 05J
$1.78 \pm 0.51 \pm 0.23$	13	[2] ALAM	94	CLE2	Sup. by JESSOP 97

[1] AUBERT 07AV reports $[\Gamma(B^+ \to J/\psi(1S) K^*(892)^+)/\Gamma_{total}] \times [B(J/\psi(1S) \to p\overline{p})] = (3.78^{+0.72+0.28}_{-0.64-0.23}) \times 10^{-6}$ which we divide by our best value $B(J/\psi(1S) \to p\overline{p}) = (2.120 \pm 0.029) \times 10^{-3}$. Our first error is their experiment's error and our second error is the systematic error from using our best value.

[2] Assumes equal production of B^+ and B^0 at the $\Upsilon(4S)$.

[3] ABE 96H assumes that $B(B^+ \to J/\psi K^+) = (1.02 \pm 0.14) \times 10^{-3}$.

[4] BORTOLETTO 92 reports $(1.3 \pm 0.9 \pm 0.3) \times 10^{-3}$ from a measurement of $[\Gamma(B^+ \to J/\psi(1S) K^*(892)^+)/\Gamma_{total}] \times [B(J/\psi(1S) \to e^+e^-)]$ assuming $B(J/\psi(1S) \to e^+e^-) = 0.069 \pm 0.009$, which we rescale to our best value $B(J/\psi(1S) \to e^+e^-) = (5.971 \pm 0.032) \times 10^{-2}$. Our first error is their experiment's error and our second error is the systematic error from using our best value. Assumes equal production of B^+ and B^0 at the $\Upsilon(4S)$.

[5] ALBRECHT 90J reports $(1.6 \pm 1.1 \pm 0.3) \times 10^{-3}$ from a measurement of $[\Gamma(B^+ \to J/\psi(1S) K^*(892)^+)/\Gamma_{total}] \times [B(J/\psi(1S) \to e^+e^-)]$ assuming $B(J/\psi(1S) \to e^+e^-) = 0.069 \pm 0.009$, which we rescale to our best value $B(J/\psi(1S) \to e^+e^-) = (5.971 \pm 0.032) \times 10^{-2}$. Our first error is their experiment's error and our second error is the systematic error from using our best value. Assumes equal production of B^+ and B^0 at the $\Upsilon(4S)$.

$\Gamma(J/\psi(1S) K^*(892)^+)/\Gamma(J/\psi(1S) K^+)$ $\Gamma_{222}/\Gamma_{218}$

VALUE	DOCUMENT ID		TECN	COMMENT
1.39±0.09 OUR AVERAGE				
$1.37 \pm 0.05 \pm 0.08$	AUBERT	05J	BABR	$e^+e^- \to \Upsilon(4S)$
$1.45 \pm 0.20 \pm 0.17$	[1] JESSOP	97	CLE2	$e^+e^- \to \Upsilon(4S)$
$1.92 \pm 0.60 \pm 0.17$	ABE	96Q	CDF	$p\overline{p}$
• • • We do not use the following data for averages, fits, limits, etc. • • •				
$1.37 \pm 0.10 \pm 0.08$	[2] AUBERT	02	BABR	Repl. by AUBERT 05J

[1] JESSOP 97 assumes equal production of B^+ and B^0 at the $\Upsilon(4S)$. The measurement is actually measured as an average over kaon charged and neutral states.

[2] Assumes equal production of B^+ and B^0 at the $\Upsilon(4S)$.

$\Gamma(J/\psi(1S) K(1270)^+)/\Gamma_{total}$ Γ_{223}/Γ

VALUE (units 10^{-3})	DOCUMENT ID		TECN	COMMENT
1.80±0.34±0.39	[1] ABE	01L	BELL	$e^+e^- \to \Upsilon(4S)$

[1] Uses the PDG value of $B(B^+ \to J/\psi(1S) K^+) = (1.00 \pm 0.10) \times 10^{-3}$.

$\Gamma(J/\psi(1S) K(1400)^+)/\Gamma(J/\psi(1S) K(1270)^+)$ $\Gamma_{224}/\Gamma_{223}$

VALUE	CL%	DOCUMENT ID		TECN	COMMENT
<0.30	90	ABE	01L	BELL	$e^+e^- \to \Upsilon(4S)$

$\Gamma(J/\psi(1S)\eta K^+)/\Gamma_{total}$ Γ_{225}/Γ

VALUE (units 10^{-5})	DOCUMENT ID		TECN	COMMENT
10.8±2.3±2.4	[1] AUBERT	04Y	BABR	$e^+e^- \to \Upsilon(4S)$

[1] Assumes equal production of B^+ and B^0 at the $\Upsilon(4S)$.

$\Gamma(J/\psi(1S)\eta' K^+)/\Gamma_{total}$ Γ_{226}/Γ

VALUE (units 10^{-5})	CL%	DOCUMENT ID		TECN	COMMENT
<8.8	90	[1] XIE	07	BELL	$e^+e^- \to \Upsilon(4S)$

[1] Assumes equal production of B^+ and B^0 at the $\Upsilon(4S)$.

$\Gamma(J/\psi(1S)\phi K^+)/\Gamma_{total}$ Γ_{227}/Γ

VALUE (units 10^{-5})	DOCUMENT ID		TECN	COMMENT
5.2±1.7 OUR AVERAGE Error includes scale factor of 1.2.				
$4.4 \pm 1.4 \pm 0.5$	[1] AUBERT	03O	BABR	$e^+e^- \to \Upsilon(4S)$
$8.8^{+3.5}_{-3.0} \pm 1.3$	[2] ANASTASSOV	00	CLE2	$e^+e^- \to \Upsilon(4S)$

[1] Assumes equal production of B^+ and B^0 at the $\Upsilon(4S)$.

[2] ANASTASSOV 00 finds 10 events on a background of 0.5 ± 0.2. Assumes equal production of B^0 and B^+ at the $\Upsilon(4S)$, a uniform Dalitz plot distribution, isotropic $J/\psi(1S)$ and ϕ decays, and $B(B^+ \to J/\psi(1S)\phi K^+) = B(B^0 \to J/\psi(1S)\phi K^0)$.

$\Gamma(X(4140) K^+, X \to J/\psi(1S)\phi)/\Gamma(J/\psi(1S)\phi K^+)$ $\Gamma_{228}/\Gamma_{227}$

VALUE	CL%	DOCUMENT ID		TECN	COMMENT
0.19±0.07±0.04		[1] ABAZOV	14A	D0	$p\overline{p}$ at 1.96 TeV
• • • We do not use the following data for averages, fits, limits, etc. • • •					
<0.07	90	[2] AAIJ	12AA	LHCB	pp at 7 TeV

[1] Reported a threshold enhancement in the $J/\psi\phi$ mass distribution consistent with the $X(4140)$ state with a statistical significance of 3.1 standard deviations.

[2] Branching fractions are normalized to 382 ± 22 events of $B^+ \to J/\psi\phi K^+$.

$\Gamma(X(4274) K^+, X \to J/\psi(1S)\phi)/\Gamma(J/\psi(1S)\phi K^+)$ $\Gamma_{229}/\Gamma_{227}$

VALUE	CL%	DOCUMENT ID		TECN	COMMENT
<0.08	90	[1] AAIJ	12AA	LHCB	pp at 7 TeV

[1] Branching fractions are normalized to 382 ± 22 events of $B^+ \to J/\psi\phi K^+$.

$\Gamma(J/\psi(1S)\omega K^+)/\Gamma_{total}$ Γ_{230}/Γ

VALUE (units 10^{-4})	DOCUMENT ID		TECN	COMMENT
$3.2 \pm 0.1^{+0.6}_{-0.3}$	[1] DEL-AMO-SA...10B		BABR	$e^+e^- \to \Upsilon(4S)$
• • • We do not use the following data for averages, fits, limits, etc. • • •				
$3.5 \pm 0.2 \pm 0.4$	[1] AUBERT	08W	BABR	Repl. by DEL-AMO-SANCHEZ 10B

[1] Assumes equal production of B^+ and B^0 at the $\Upsilon(4S)$.

$\Gamma(X(3872) K^+, X \to J/\psi\omega)/\Gamma_{total}$ Γ_{231}/Γ

VALUE (units 10^{-6})	DOCUMENT ID		TECN	COMMENT
6±2±1	[1] DEL-AMO-SA...10B		BABR	$e^+e^- \to \Upsilon(4S)$

[1] Assumes equal production of B^+ and B^0 at the $\Upsilon(4S)$.

$\Gamma(X(3872) K^+, X \to p\overline{p})/\Gamma_{total}$ Γ_{201}/Γ

VALUE	CL%	DOCUMENT ID		TECN	COMMENT
$<1.7 \times 10^{-8}$	95	[1] AAIJ	13S	LHCB	pp at 7 TeV

[1] Measured relative to $B^+ \to J/\psi K^+$ decay with charmonia reconstructed in $p\overline{p}$ final state and using $B(B^+ \to J/\psi K^+) = (1.013 \pm 0.034) \times 10^{-3}$ and $B(J/\psi \to p\overline{p}) = (2.17 \pm 0.07) \times 10^{-3}$.

$\Gamma(\chi_{c0}(2P) K^+, \chi_{c0} \to J/\psi\omega)/\Gamma_{total}$ Γ_{232}/Γ

VALUE (units 10^{-5})	DOCUMENT ID		TECN	COMMENT
$3.0^{+0.7+0.5}_{-0.6-0.3}$	[1] DEL-AMO-SA...10B		BABR	$e^+e^- \to \Upsilon(4S)$
• • • We do not use the following data for averages, fits, limits, etc. • • •				
$4.9^{+1.0}_{-0.9} \pm 0.5$	[1] AUBERT	08W	BABR	Repl. by DEL-AMO-SANCHEZ 10B

[1] Assumes equal production of B^+ and B^0 at the $\Upsilon(4S)$.

$\Gamma(\chi_{c0}(2P) K^+, \chi_{c0} \to p\overline{p})/\Gamma_{total}$ Γ_{221}/Γ

VALUE	CL%	DOCUMENT ID		TECN	COMMENT
$<7.1 \times 10^{-8}$	95	[1] AAIJ	13S	LHCB	pp at 7 TeV

[1] Measured relative to $B^+ \to J/\psi K^+$ decay with charmonia reconstructed in $p\overline{p}$ final state and using $B(B^+ \to J/\psi K^+) = (1.013 \pm 0.034) \times 10^{-3}$ and $B(J/\psi \to p\overline{p}) = (2.17 \pm 0.07) \times 10^{-3}$.

Meson Particle Listings

$B^{\pm}$

$\Gamma(J/\psi(1S)\pi^+)/\Gamma_{\text{total}}$ Γ_{233}/Γ

VALUE	DOCUMENT ID		TECN	COMMENT
(4.1±0.4) × 10⁻⁵ OUR FIT	Error includes scale factor of 2.6.			
(3.8±0.6±0.3) × 10⁻⁵	[1] ABE	03B	BELL	$e^+e^- \to \Upsilon(4S)$

[1] Assumes equal production of B^+ and B^0 at the $\Upsilon(4S)$.

$\Gamma(J/\psi(1S)\pi^+)/\Gamma(J/\psi(1S)K^+)$ $\Gamma_{233}/\Gamma_{218}$

VALUE (units 10^{-2})	EVTS	DOCUMENT ID		TECN	COMMENT
4.0 ±0.4 OUR FIT	Error includes scale factor of 3.3.				
4.0 ±0.4 OUR AVERAGE	Error includes scale factor of 3.2.				
3.83±0.11±0.07		AAIJ	12AC	LHCB	pp at 7 TeV
4.86±0.82±0.15		ABULENCIA	09	CDF	$p\overline{p}$ at 1.96 TeV
5.37±0.45±0.11		AUBERT	04P	BABR	$e^+e^- \to \Upsilon(4S)$
5.0 $^{+1.9}_{-1.7}$ ±0.1		ABE	96R	CDF	$p\overline{p}$ 1.8 TeV
5.2 ±2.4		BISHAI	96	CLE2	$e^+e^- \to \Upsilon(4S)$
• • • We do not use the following data for averages, fits, limits, etc. • • •					
3.91±0.78±0.19		AUBERT	02F	BABR	Repl. by AUBERT 04P
4.3 ±2.3	5	[1] ALEXANDER	95	CLE2	Sup. by BISHAI 96

[1] Assumes equal production of B^+B^- and $B^0\overline{B}^0$ on $\Upsilon(4S)$.

$\Gamma(J/\psi(1S)\rho^+)/\Gamma_{\text{total}}$ Γ_{234}/Γ

VALUE (units 10^{-5})	CL%	DOCUMENT ID		TECN	COMMENT
5.0±0.7±0.3		[1] AUBERT	07AC	BABR	$e^+e^- \to \Upsilon(4S)$
• • • We do not use the following data for averages, fits, limits, etc. • • •					
<77	90	BISHAI	96	CLE2	$e^+e^- \to \Upsilon(4S)$

[1] Assumes equal production of B^+ and B^0 at the $\Upsilon(4S)$.

$\Gamma(J/\psi(1S)\pi^+\pi^0 \text{ nonresonant})/\Gamma_{\text{total}}$ Γ_{235}/Γ

VALUE (units 10^{-5})	CL%	DOCUMENT ID		TECN	COMMENT
<0.73	90	[1] AUBERT	07AC	BABR	$e^+e^- \to \Upsilon(4S)$

[1] Assumes equal production of B^+ and B^0 at the $\Upsilon(4S)$.

$\Gamma(J/\psi(1S)a_1(1260)^+)/\Gamma_{\text{total}}$ Γ_{236}/Γ

VALUE	CL%	DOCUMENT ID		TECN	COMMENT
<1.2 × 10⁻³	90	BISHAI	96	CLE2	$e^+e^- \to \Upsilon(4S)$

$\Gamma(J/\psi p\overline{p}\pi^+)/\Gamma_{\text{total}}$ Γ_{237}/Γ

VALUE	CL%	DOCUMENT ID		TECN	COMMENT
<5.0 × 10⁻⁷	90	[1] AAIJ	13Z	LHCB	pp at 7 TeV

[1] Uses $B(B_s^0 \to J/\psi(1S)\pi^+\pi^-) = (1.98 \pm 0.20) \times 10^{-4}$.

$\Gamma(J/\psi(1S)p\overline{\Lambda})/\Gamma_{\text{total}}$ Γ_{238}/Γ

VALUE (units 10^{-6})	CL%	DOCUMENT ID		TECN	COMMENT
11.8±3.1 OUR AVERAGE					
11.7±2.8 $^{+1.8}_{-2.3}$		[1] XIE	05	BELL	$e^+e^- \to \Upsilon(4S)$
12 $^{+9}_{-6}$		[1] AUBERT	03K	BABR	$e^+e^- \to \Upsilon(4S)$
• • • We do not use the following data for averages, fits, limits, etc. • • •					
<41	90	ZANG	04	BELL	$e^+e^- \to \Upsilon(4S)$

[1] Assumes equal production of B^+ and B^0 at the $\Upsilon(4S)$.

$\Gamma(J/\psi(1S)\overline{\Sigma}^0 p)/\Gamma_{\text{total}}$ Γ_{239}/Γ

VALUE	CL%	DOCUMENT ID		TECN	COMMENT
<1.1 × 10⁻⁵	90	[1] XIE	05	BELL	$e^+e^- \to \Upsilon(4S)$

[1] Assumes equal production of B^+ and B^0 at the $\Upsilon(4S)$.

$\Gamma(J/\psi(1S)D^+)/\Gamma_{\text{total}}$ Γ_{240}/Γ

VALUE (units 10^{-5})	CL%	DOCUMENT ID		TECN	COMMENT
<12	90	[1] AUBERT	05U	BABR	$e^+e^- \to \Upsilon(4S)$

[1] Assumes equal production of B^+ and B^0 at the $\Upsilon(4S)$.

$\Gamma(J/\psi(1S)\overline{D}^0\pi^+)/\Gamma_{\text{total}}$ Γ_{241}/Γ

VALUE (units 10^{-5})	CL%	DOCUMENT ID		TECN	COMMENT
<2.5	90	[1] ZHANG	05B	BELL	$e^+e^- \to \Upsilon(4S)$
• • • We do not use the following data for averages, fits, limits, etc. • • •					
<5.2	90	[1] AUBERT	05R	BABR	$e^+e^- \to \Upsilon(4S)$

[1] Assumes equal production of B^+ and B^0 at the $\Upsilon(4S)$.

$\Gamma(\psi(2S)\pi^+)/\Gamma_{\text{total}}$ Γ_{242}/Γ

VALUE (units 10^{-5})	DOCUMENT ID		TECN	COMMENT
2.44±0.22±0.20	[1] BHARDWAJ	08	BELL	$e^+e^- \to \Upsilon(4S)$

[1] Assumes equal production of B^+ and B^0 at the $\Upsilon(4S)$.

$\Gamma(\psi(2S)\pi^+)/\Gamma(\psi(2S)K^+)$ $\Gamma_{242}/\Gamma_{243}$

VALUE (units 10^{-2})	DOCUMENT ID		TECN	COMMENT
3.97±0.29 OUR AVERAGE				
3.95±0.40±0.12	AAIJ	12AC	LHCB	pp at 7 TeV
3.99±0.36±0.17	BHARDWAJ	08	BELL	$e^+e^- \to \Upsilon(4S)$

$\Gamma(\psi(2S)K^+)/\Gamma_{\text{total}}$ Γ_{243}/Γ

VALUE (units 10^{-4})	EVTS	DOCUMENT ID		TECN	COMMENT
6.27± 0.24 OUR FIT					
6.5 ± 0.4 OUR AVERAGE					
6.65± 0.17±0.55		[1] GULER	11	BELL	$e^+e^- \to \Upsilon(4S)$
4.9 ± 1.6 ±0.4		[2] AUBERT	06E	BABR	$e^+e^- \to \Upsilon(4S)$
6.17± 0.32±0.44		[1] AUBERT	05J	BABR	$e^+e^- \to \Upsilon(4S)$
7.8 ± 0.7 ±0.9		[1] RICHICHI	01	CLE2	$e^+e^- \to \Upsilon(4S)$
18 ± 8 ±4	5	[1] ALBRECHT	90J	ARG	$e^+e^- \to \Upsilon(4S)$
• • • We do not use the following data for averages, fits, limits, etc. • • •					
6.9 ± 0.6		[1] ABE	03B	BELL	Repl. by GULER 11
6.4 ± 0.5 ±0.8		[1] AUBERT	02	BABR	Repl. by AUBERT 05J
6.1 ± 2.3 ±0.9	7	[1] ALAM	94	CLE2	Repl. by RICHICHI 01
<5 at 90% CL		[1] BORTOLETTO	92	CLEO	$e^+e^- \to \Upsilon(4S)$
22 ±17	3	[3] ALBRECHT	87D	ARG	$e^+e^- \to \Upsilon(4S)$

[1] Assumes equal production of B^+ and B^0 at the $\Upsilon(4S)$.
[2] Perform measurements of absolute branching fractions using a missing mass technique.
[3] ALBRECHT 87D assume $B^+B^-/B^0\overline{B}^0$ ratio is 55/45. Superseded by ALBRECHT 90J.

$\Gamma(\psi(2S)K^+)/\Gamma(J/\psi(1S)K^+)$ $\Gamma_{243}/\Gamma_{218}$

VALUE	DOCUMENT ID		TECN	COMMENT
0.611±0.019 OUR FIT				
0.603±0.021 OUR AVERAGE				
0.61 ±0.11 ±0.02	[1] AAIJ	13S	LHCB	pp at 7 TeV
0.604±0.018±0.013	[2,3] AAIJ	12L	LHCB	pp at 7 TeV
0.63 ±0.05 ±0.08	ABAZOV	09Y	D0	$p\overline{p}$ at 1.96 TeV
0.558±0.082±0.056	ABE	98O	CDF	$p\overline{p}$ 1.8 TeV
• • • We do not use the following data for averages, fits, limits, etc. • • •				
0.64 ±0.06 ±0.07	[4] AUBERT	02	BABR	$e^+e^- \to \Upsilon(4S)$

[1] AAIJ 13S reports $[\Gamma(B^+ \to \psi(2S)K^+)/\Gamma(B^+ \to J/\psi(1S)K^+)] \times [B(\psi(2S) \to p\overline{p})] / [B(J/\psi(1S) \to p\overline{p})] = 0.080 \pm 0.012 \pm 0.009$ which we multiply or divide by our best values $B(\psi(2S) \to p\overline{p}) = (2.80 \pm 0.11) \times 10^{-4}$, $B(J/\psi(1S) \to p\overline{p}) = (2.120 \pm 0.029) \times 10^{-3}$. Our first error is their experiment's error and our second error is the systematic error from using our best values.
[2] AAIJ 12L reports $0.594 \pm 0.006 \pm 0.016 \pm 0.015$ from a measurement of $[\Gamma(B^+ \to \psi(2S)K^+)/\Gamma(B^+ \to J/\psi(1S)K^+)] \times [B(J/\psi(1S) \to e^+e^-)] / [B(\psi(2S) \to e^+e^-)]$ assuming $B(J/\psi(1S) \to e^+e^-) = (5.94 \pm 0.06) \times 10^{-2}$, $B(\psi(2S) \to e^+e^-) = (7.72 \pm 0.17) \times 10^{-3}$, which we rescale to our best values $B(J/\psi(1S) \to e^+e^-) = (5.971 \pm 0.032) \times 10^{-2}$, $B(\psi(2S) \to e^+e^-) = (7.89 \pm 0.17) \times 10^{-3}$. Our first error is their experiment's error and our second error is the systematic error from using our best values.
[3] Assumes $B(J/\psi \to \mu^+\mu^-) / B(\psi(2S) \to \mu^+\mu^-) = B(J/\psi \to e^+e^-) / B(\psi(2S) \to e^+e^-) = 7.69 \pm 0.19$.
[4] Assumes equal production of B^+ and B^0 at the $\Upsilon(4S)$.

$\Gamma(\psi(2S)K^*(892)^+)/\Gamma_{\text{total}}$ Γ_{244}/Γ

VALUE (units 10^{-4})	CL%	DOCUMENT ID		TECN	COMMENT
6.7 ±1.4 OUR AVERAGE	Error includes scale factor of 1.3.				
5.92±0.85±0.89		[1] AUBERT	05J	BABR	$e^+e^- \to \Upsilon(4S)$
9.2 ±1.9 ±1.2		[1] RICHICHI	01	CLE2	$e^+e^- \to \Upsilon(4S)$
• • • We do not use the following data for averages, fits, limits, etc. • • •					
<30	90	[1] ALAM	94	CLE2	Repl. by RICHICHI 01
<35	90	[1] BORTOLETTO	92	CLEO	$e^+e^- \to \Upsilon(4S)$
<49	90	[1] ALBRECHT	90J	ARG	$e^+e^- \to \Upsilon(4S)$

[1] Assumes equal production of B^+ and B^0 at the $\Upsilon(4S)$.

$\Gamma(\psi(2S)K^*(892)^+)/\Gamma(\psi(2S)K^+)$ $\Gamma_{244}/\Gamma_{243}$

VALUE	DOCUMENT ID		TECN	COMMENT
0.96±0.15±0.09	AUBERT	05J	BABR	$e^+e^- \to \Upsilon(4S)$

$\Gamma(\psi(2S)K^0\pi^+)/\Gamma_{\text{total}}$ Γ_{245}/Γ

VALUE (units 10^{-3})	DOCUMENT ID		TECN	COMMENT
• • • We do not use the following data for averages, fits, limits, etc. • • •				
0.588±0.034	[1] AUBERT	09AA	BABR	$e^+e^- \to \Upsilon(4S)$

[1] Does not report systematic uncertainties.

$\Gamma(\psi(2S)K^+\pi^+\pi^-)/\Gamma_{\text{total}}$ Γ_{246}/Γ

VALUE (units 10^{-4})	EVTS	DOCUMENT ID		TECN	COMMENT
4.3 ± 0.5 OUR AVERAGE					
4.31± 0.20±0.50		[1] GULER	11	BELL	$e^+e^- \to \Upsilon(4S)$
19 ±11 ±4	3	[1] ALBRECHT	90J	ARG	$e^+e^- \to \Upsilon(4S)$

[1] Assumes equal production of B^+ and B^0 at the $\Upsilon(4S)$.

$\Gamma(\psi(3770)K^+)/\Gamma_{\text{total}}$ Γ_{247}/Γ

VALUE (units 10^{-3})	DOCUMENT ID		TECN	COMMENT
0.49±0.13 OUR AVERAGE				
3.5 ±2.5 ±0.3	[1] AUBERT	06E	BABR	$e^+e^- \to \Upsilon(4S)$
0.48±0.11±0.07	[2] CHISTOV	04	BELL	$e^+e^- \to \Upsilon(4S)$

[1] Perform measurements of absolute branching fractions using a missing mass technique.
[2] Assumes equal production of B^+ and B^0 at the $\Upsilon(4S)$.

$\Gamma(\psi(3770)K+,\psi\to D^0\overline{D}{}^0)/\Gamma_{\rm total}$ Γ_{248}/Γ

VALUE (units 10^{-4})	DOCUMENT ID		TECN	COMMENT
1.6 ±0.4 OUR AVERAGE	Error includes scale factor of 1.1.			
1.41±0.30±0.22	[1] AUBERT	08B	BABR	$e^+e^-\to\ \Upsilon(4S)$
2.2 ±0.5 ±0.3	[1] BRODZICKA	08	BELL	$e^+e^-\to\ \Upsilon(4S)$
• • • We do not use the following data for averages, fits, limits, etc. • • •				
3.4 ±0.8 ±0.5	[1] CHISTOV	04	BELL	Repl. by BRODZICKA 08

[1] Assumes equal production of B^+ and B^0 at the $\Upsilon(4S)$.

$\Gamma(\psi(3770)K+,\psi\to D^+D^-)/\Gamma_{\rm total}$ Γ_{249}/Γ

VALUE (units 10^{-4})	DOCUMENT ID		TECN	COMMENT
0.94±0.35 OUR AVERAGE				
0.84±0.32±0.21	[1] AUBERT	08B	BABR	$e^+e^-\to\ \Upsilon(4S)$
1.4 ±0.8 ±0.2	[1] CHISTOV	04	BELL	$e^+e^-\to\ \Upsilon(4S)$

[1] Assumes equal production of B^+ and B^0 at the $\Upsilon(4S)$.

$\Gamma(\chi_{c0}\pi^+,\chi_{c0}\to\pi^+\pi^-)/\Gamma_{\rm total}$ Γ_{250}/Γ

VALUE (units 10^{-6})	CL%	DOCUMENT ID		TECN	COMMENT
<0.1	90	[1] AUBERT	09L	BABR	$e^+e^-\to\ \Upsilon(4S)$
• • • We do not use the following data for averages, fits, limits, etc. • • •					
<0.3	90	[1] AUBERT,B	05G	BABR	Repl. by AUBERT 09L

[1] Assumes equal production of B^+ and B^0 at the $\Upsilon(4S)$.

$\Gamma(\chi_{c0}(1P)K^+)/\Gamma_{\rm total}$ Γ_{251}/Γ

VALUE (units 10^{-4})	CL%	DOCUMENT ID		TECN	COMMENT
$1.50^{+0.15}_{-0.14}$ OUR AVERAGE					
1.84±0.25±0.14		[1,2] LEES	12O	BABR	$e^+e^-\to\ \Upsilon(4S)$
1.68±0.32±0.16		[1,3] LEES	12O	BABR	$e^+e^-\to\ \Upsilon(4S)$
1.8 ±0.9 ±0.1		[4] LEES	11I	BABR	$e^+e^-\to\ \Upsilon(4S)$
$1.26^{+0.28}_{-0.25}\pm0.05$		[1,5] AUBERT	08AI	BABR	$e^+e^-\to\ \Upsilon(4S)$
4.8 ±2.2 ±0.2		[6] AUBERT,BE	06M	BABR	$e^+e^-\to\ \Upsilon(4S)$
$1.12\pm0.12^{+0.30}_{-0.20}$		[1] GARMASH	06	BELL	$e^+e^-\to\ \Upsilon(4S)$
• • • We do not use the following data for averages, fits, limits, etc. • • •					
<2.7	95	[7] AAIJ	13S	LHCB	pp at 7 TeV
<5	90	[1,8] WICHT	08	BELL	$e^+e^-\to\ \Upsilon(4S)$
<1.8	90	[9] AUBERT	06E	BABR	$e^+e^-\to\ \Upsilon(4S)$
1.84±0.32±0.31		[1,10] AUBERT	06O	BABR	Repl. by LEES 12O
<8.9	90	[1] AUBERT	05K	BABR	$e^+e^-\to\ \Upsilon(4S)$
1.39±0.49±0.11		[11] AUBERT,B	05N	BABR	Repl. by AUBERT 08AI
$1.96\pm0.35^{+2.00}_{-0.42}$		[1] GARMASH	05	BELL	Repl. by GARMASH 06
2.7 ±0.7		[12] AUBERT	04T	BABR	Repl. by AUBERT,B 04P
3.0 ±0.8 ±0.3		[13] AUBERT,B	04P	BABR	Repl. by AUBERT,B 05N
$6.0\ ^{+2.1}_{-1.8}\ \pm1.1$		[14] ABE	02B	BELL	Repl. by GARMASH 05
<4.8	90	[15] EDWARDS	01	CLE2	$e^+e^-\to\ \Upsilon(4S)$

[1] Assumes equal production of B^+ and B^0 at the $\Upsilon(4S)$.

[2] Measured in the $B^+\to\ K^+K^-K^+$ decay.

[3] Measured in the $B^+\to\ K^+K^0_SK^0_S$ decay.

[4] LEES 11I reports $[\Gamma(B^+\to\ \chi_{c0}(1P)K^+)/\Gamma_{\rm total}]\times[{\rm B}(\chi_{c0}(1P)\to\ \pi\pi)]=(1.53\pm0.66\pm0.27)\times10^{-6}$ which we divide by our best value ${\rm B}(\chi_{c0}(1P)\to\ \pi\pi)=(8.33\pm0.35)\times10^{-3}$. Our first error is their experiment's error and our second error is the systematic error from using our best value.

[5] AUBERT 08AI reports $(0.70\pm0.10^{+0.12}_{-0.10})\times10^{-6}$ for ${\rm B}(B^+\to\ \chi_{c0}K^+)\times{\rm B}(\chi_{c0}\to\ \pi^+\pi^-)$. We compute ${\rm B}(B^+\to\ \chi_{c0}K^+)$ using the PDG value ${\rm B}(\chi_{c0}\to\ \pi\pi)$=(8.33±0.35)×$10^{-3}$ and 2/3 for the $\pi^+\pi^-$ fraction. Our first error is their experiment's error and the second error is systematic error from using our best value.

[6] AUBERT,BE 06M reports $[\Gamma(B^+\to\ \chi_{c0}(1P)K^+)/\Gamma_{\rm total}]\times[{\rm B}(\chi_{c0}(1P)\to\ \gamma J/\psi(1S))]=(6.1\pm2.6\pm1.1)\times10^{-6}$ which we divide by our best value ${\rm B}(\chi_{c0}(1P)\to\ \gamma J/\psi(1S))=(1.27\pm0.06)\times10^{-2}$. Our first error is their experiment's error and our second error is the systematic error from using our best value. The significance of the observed signal is 2.4 σ.

[7] AAIJ 13S reports $[\Gamma(B^+\to\ \chi_{c0}(1P)K^+)/\Gamma_{\rm total}]\times[{\rm B}(\chi_{c0}(1P)\to\ p\overline{p})]<\ 6\times10^{-8}$ which we divide by our best value ${\rm B}(\chi_{c0}(1P)\to\ p\overline{p})=2.25\times10^{-4}$.

[8] WICHT 08 reports $[\Gamma(B^+\to\ \chi_{c0}(1P)K^+)/\Gamma_{\rm total}]\times[{\rm B}(\chi_{c0}(1P)\to\ \gamma\gamma)]<\ 0.11\times10^{-6}$ which we divide by our best value ${\rm B}(\chi_{c0}(1P)\to\ \gamma\gamma)=2.23\times10^{-4}$.

[9] Perform measurements of absolute branching fractions using a missing mass technique.

[10] Measured in the $B^+\to\ K^+K^-K^+$ decay.

[11] AUBERT,B 05N reports $(0.66\pm0.22\pm0.08)\times10^{-6}$ for ${\rm B}(B^+\to\ \chi^0_cK^+)\times{\rm B}(\chi^0_c\to\ \pi^+\pi^-)$. We compute ${\rm B}(B^+\to\ \chi^0_cK^+)$ using the PDG value ${\rm B}(\chi^0_c\to\ \pi^+\pi^-)=(7.1\pm0.6)\times10^{-3}$ and 2/3 for the $\pi^+\pi^-$ fraction.

[12] The measurement performed using decay channels $\chi_{c0}\to\ \pi^+\pi^-$ and $\chi_{c0}\to\ K^+K^-$. The ratio of the branching ratios for these channels is found to be consistent with world average.

[13] AUBERT 04P reports ${\rm B}(B^+\to\ \chi_{c0}K^+)\times{\rm B}(\chi_{c0}\to\ \pi^+\pi^-)=(1.5\pm0.4\pm0.1)\times10^{-6}$ and used PDG value of ${\rm B}(\chi_{c0}\to\ \pi\pi)=(7.4\pm0.8)\times10^{-3}$ and Clebsh-Gordan coefficient to compute ${\rm B}(B^{\pm}->\chi_{c0}K^+)$.

[14] ABE 02B measures the ratio of ${\rm B}(B^+\to\ \chi_{c0}K^+)/{\rm B}(B^+\to\ J/\psi(1S)K^+)=0.60+0.21-0.18\pm0.05\pm0.08$, where the third error is due to the uncertainty in the ${\rm B}(\chi_{c0}\to\ \pi^+\pi^-)$, and uses ${\rm B}(B^+\to\ J/\psi(1S)K^+)=(10.0\pm1.0)\times10^{-4}$ to obtain the result.

[15] EDWARDS 01 assumes equal production of B^0 and B^+ at the $\Upsilon(4S)$. The correlated uncertainties (28.3)% from ${\rm B}(J/\psi(1S)\to\ \gamma\eta_c)$ in those modes have been accounted for.

$\Gamma(\chi_{c0}K^*(892)^+)/\Gamma_{\rm total}$ Γ_{252}/Γ

VALUE (units 10^{-4})	CL%	DOCUMENT ID		TECN	COMMENT
< 2.1	90	[1] AUBERT	08BD	BABR	$e^+e^-\to\ \Upsilon(4S)$
• • • We do not use the following data for averages, fits, limits, etc. • • •					
<28.6	90	[1] AUBERT	05K	BABR	Repl. by AUBERT 08BD

[1] Assumes equal production of B^+ and B^0 at the $\Upsilon(4S)$.

$\Gamma(\chi_{c2}\pi^+,\chi_{c2}\to\pi^+\pi^-)/\Gamma_{\rm total}$ Γ_{253}/Γ

VALUE (units 10^{-6})	CL%	DOCUMENT ID		TECN	COMMENT
<0.1	90	[1] AUBERT	09L	BABR	$e^+e^-\to\ \Upsilon(4S)$

[1] Assumes equal production of B^+ and B^0 at the $\Upsilon(4S)$.

$\Gamma(\chi_{c2}K^+)/\Gamma_{\rm total}$ Γ_{254}/Γ

VALUE (units 10^{-5})	CL%	DOCUMENT ID		TECN	COMMENT
$1.11^{+0.36}_{-0.34}\pm0.09$		[1] BHARDWAJ	11	BELL	$e^+e^-\to\ \Upsilon(4S)$
• • • We do not use the following data for averages, fits, limits, etc. • • •					
< 1.8	90	[2] AUBERT	09B	BABR	$e^+e^-\to\ \Upsilon(4S)$
<20	90	[3] AUBERT	06E	BABR	$e^+e^-\to\ \Upsilon(4S)$
< 2.9	90	[1] SONI	06	BELL	Repl. by BHARDWAJ 11
< 3.0	90	[1] AUBERT	05K	BABR	Repl. by AUBERT 06E

[1] Assumes equal production of B^+ and B^0 at the $\Upsilon(4S)$.

[2] Uses $\chi_{c1,2}\to\ J/\psi\gamma$. Assumes ${\rm B}(\Upsilon(4S)\to\ B^+B^-)=(51.6\pm0.6)\%$ and ${\rm B}(\Upsilon(4S)\to\ B^0\overline{B}{}^0)=(48.4\pm0.6)\%$.

[3] Perform measurements of absolute branching fractions using a missing mass technique.

$\Gamma(B^+\to\ \chi_{c2}K^+)/\Gamma_{\rm total}\times\Gamma(\chi_{c2}(1P)\to\ \gamma\gamma)/\Gamma_{\rm total}$ $\Gamma_{254}/\Gamma\times\Gamma^{\chi_{c2}(1P)}_{71}/\Gamma^{\chi_{c2}(1P)}$

VALUE (units 10^{-6})	CL%	DOCUMENT ID		TECN	COMMENT
<0.09	90	[1] WICHT	08	BELL	$e^+e^-\to\ \Upsilon(4S)$

[1] Assumes equal production of B^+ and B^0 at the $\Upsilon(4S)$.

$\Gamma(\chi_{c2}K^*(892)^+)/\Gamma_{\rm total}$ Γ_{255}/Γ

VALUE	CL%	DOCUMENT ID		TECN	COMMENT
<12 $\times10^{-5}$	90	[1] AUBERT	09B	BABR	$e^+e^-\to\ \Upsilon(4S)$
• • • We do not use the following data for averages, fits, limits, etc. • • •					
$<12.7\times10^{-5}$	90	[2] SONI	06	BELL	$e^+e^-\to\ \Upsilon(4S)$
$<\ 1.2\times10^{-5}$	90	[2] AUBERT	05K	BABR	Repl. by AUBERT 09B

[1] Uses $\chi_{c1,2}\to\ J/\psi\gamma$. Assumes ${\rm B}(\Upsilon(4S)\to\ B^+B^-)=(51.6\pm0.6)\%$ and ${\rm B}(\Upsilon(4S)\to\ B^0\overline{B}{}^0)=(48.4\pm0.6)\%$.

[2] Assumes equal production of B^+ and B^0 at the $\Upsilon(4S)$.

$\Gamma(\chi_{c1}(1P)\pi^+)/\Gamma_{\rm total}$ Γ_{256}/Γ

VALUE (units 10^{-5})	DOCUMENT ID		TECN	COMMENT
2.2±0.4±0.3	[1] KUMAR	06	BELL	$e^+e^-\to\ \Upsilon(4S)$

[1] Assumes equal production of B^+ and B^0 at the $\Upsilon(4S)$.

$\Gamma(\chi_{c1}(1P)K^+)/\Gamma_{\rm total}$ Γ_{257}/Γ

VALUE (units 10^{-4})	EVTS	DOCUMENT ID		TECN	COMMENT
4.79± 0.23 OUR AVERAGE					
4.94± 0.11±0.33		[1] BHARDWAJ	11	BELL	$e^+e^-\to\ \Upsilon(4S)$
4.5 ± 0.1 ±0.3		[2] AUBERT	09B	BABR	$e^+e^-\to\ \Upsilon(4S)$
8.1 ± 1.4 ±0.7		[3] AUBERT	06E	BABR	$e^+e^-\to\ \Upsilon(4S)$
15.5 ± 5.4 ±2.0		[4] ACOSTA	02F	CDF	$p\overline{p}$ 1.8 TeV
• • • We do not use the following data for averages, fits, limits, etc. • • •					
5.2 ± 0.4 ±0.2		[5] AUBERT,BE	06M	BABR	Repl. by AUBERT 09B
4.49± 0.19±0.53		[1] SONI	06	BELL	Repl. by BHARDWAJ 11
5.79± 0.26±0.65		[1] AUBERT	05J	BABR	Repl. by AUBERT,BE 06M
6.0 ± 0.9 ±0.2		[6] AUBERT	02	BABR	Repl. by AUBERT 05J
9.7 ± 4.0 ±0.9	6	[1] ALAM	94	CLE2	$e^+e^-\to\ \Upsilon(4S)$
19 ±13 ±6		[7] ALBRECHT	92E	ARG	$e^+e^-\to\ \Upsilon(4S)$

[1] Assumes equal production of B^+ and B^0 at the $\Upsilon(4S)$.

[2] Uses $\chi_{c1,2}\to\ J/\psi\gamma$. Assumes ${\rm B}(\Upsilon(4S)\to\ B^+B^-)=(51.6\pm0.6)\%$ and ${\rm B}(\Upsilon(4S)\to\ B^0\overline{B}{}^0)=(48.4\pm0.6)\%$.

[3] Perform measurements of absolute branching fractions using a missing mass technique.

[4] ACOSTA 02F uses as reference of ${\rm B}(B\to\ J/\psi(1S)K^+)=(10.1\pm0.6)\times10^{-4}$. The second error includes the systematic error and the uncertainties of the branching ratio.

[5] AUBERT,BE 06M reports $[\Gamma(B^+\to\ \chi_{c1}(1P)K^+)/\Gamma_{\rm total}]\times[{\rm B}(\chi_{c1}(1P)\to\ \gamma J/\psi(1S))]=(1.76\pm0.07\pm0.12)\times10^{-4}$ which we divide by our best value ${\rm B}(\chi_{c1}(1P)\to\ \gamma J/\psi(1S))=(33.9\pm1.2)\times10^{-2}$. Our first error is their experiment's error and our second error is the systematic error from using our best value.

[6] AUBERT 02 reports $(7.5\pm0.9\pm0.8)\times10^{-4}$ from a measurement of $[\Gamma(B^+\to\ \chi_{c1}(1P)K^+)/\Gamma_{\rm total}]\times[{\rm B}(\chi_{c1}(1P)\to\ \gamma J/\psi(1S))]$ assuming ${\rm B}(\chi_{c1}(1P)\to\ \gamma J/\psi(1S))=0.273\pm0.016$, which we rescale to our best value ${\rm B}(\chi_{c1}(1P)\to\ \gamma J/\psi(1S))=(33.9\pm1.2)\times10^{-2}$. Our first error is their experiment's error and our second error is the systematic error from using our best value. Assumes equal production of B^+ and B^0 at the $\Upsilon(4S)$.

[7] ALBRECHT 92E assumes no $\chi_{c2}(1P)$ production and ${\rm B}(\Upsilon(4S)\to\ B^+B^-)=50\%$.

Meson Particle Listings

$B^{\pm}$

$\Gamma(\chi_{c1}(1P)K^+)/\Gamma(J/\psi(1S)K^+)$ $\Gamma_{257}/\Gamma_{218}$

VALUE	DOCUMENT ID		TECN	COMMENT
0.60±0.07±0.02	[1] AUBERT	02	BABR	$e^+e^- \to \Upsilon(4S)$

[1] AUBERT 02 reports $0.75 \pm 0.08 \pm 0.05$ from a measurement of $[\Gamma(B^+ \to \chi_{c1}(1P)K^+)/\Gamma(B^+ \to J/\psi(1S)K^+)] \times [B(\chi_{c1}(1P) \to \gamma J/\psi(1S))] = 0.273 \pm 0.016$, which we rescale to our best value $B(\chi_{c1}(1P) \to \gamma J/\psi(1S)) = (33.9 \pm 1.2) \times 10^{-2}$. Our first error is their experiment's error and our second error is the systematic error from using our best value. Assumes equal production of B^+ and B^0 at the $\Upsilon(4S)$.

$\Gamma(\chi_{c1}(1P)\pi^+)/\Gamma(\chi_{c1}(1P)K^+)$ $\Gamma_{256}/\Gamma_{257}$

VALUE	DOCUMENT ID		TECN	COMMENT
0.043±0.008±0.003	[1] KUMAR	06	BELL	$e^+e^- \to \Upsilon(4S)$

[1] Assumes equal production of B^+ and B^0 at the $\Upsilon(4S)$.

$\Gamma(\chi_{c1}(1P)K^0\pi^+)/\Gamma(J/\psi(1S)K^0\pi^+)$ $\Gamma_{258}/\Gamma_{219}$

VALUE	DOCUMENT ID		TECN	COMMENT
0.508±0.030±0.018	[1] LEES	12B	BABR	$e^+e^- \to \Upsilon(4S)$

[1] LEES 12B reports $0.501 \pm 0.024 \pm 0.028$ from a measurement of $[\Gamma(B^+ \to \chi_{c1}(1P)K^0\pi^+)/\Gamma(B^+ \to J/\psi(1S)K^0\pi^+)] \times [B(\chi_{c1}(1P) \to \gamma J/\psi(1S))]$ assuming $B(\chi_{c1}(1P) \to \gamma J/\psi(1S)) = (34.4 \pm 1.5) \times 10^{-2}$, which we rescale to our best value $B(\chi_{c1}(1P) \to \gamma J/\psi(1S)) = (33.9 \pm 1.2) \times 10^{-2}$. Our first error is their experiment's error and our second error is the systematic error from using our best value.

$\Gamma(\chi_{c1}(1P)K^*(892)^+)/\Gamma_{\text{total}}$ Γ_{259}/Γ

VALUE (units 10^{-4})	CL%	DOCUMENT ID		TECN	COMMENT
3.0 ±0.6 OUR AVERAGE		Error includes scale factor of 1.1.			
2.6 ±0.5 ±0.4		[1] AUBERT	09B	BABR	$e^+e^- \to \Upsilon(4S)$
4.05±0.59±0.95		[2] SONI	06	BELL	$e^+e^- \to \Upsilon(4S)$
• • • We do not use the following data for averages, fits, limits, etc. • • •					
2.94±0.95±0.98		[2] AUBERT	05J	BABR	Repl. by AUBERT 09B
<21	90	[2] ALAM	94	CLE2	$e^+e^- \to \Upsilon(4S)$

[1] Uses $\chi_{c1,2} \to J/\psi\gamma$. Assumes $B(\Upsilon(4S) \to B^+B^-) = (51.6 \pm 0.6)\%$ and $B(\Upsilon(4S) \to B^0\overline{B}^0) = (48.4 \pm 0.6)\%$.

[2] Assumes equal production of B^+ and B^0 at the $\Upsilon(4S)$.

$\Gamma(\chi_{c1}(1P)K^*(892)^+)/\Gamma(\chi_{c1}(1P)K^+)$ $\Gamma_{259}/\Gamma_{257}$

VALUE	DOCUMENT ID		TECN	COMMENT
0.51±0.17±0.16	AUBERT	05J	BABR	$e^+e^- \to \Upsilon(4S)$

$\Gamma(h_c(1P)K^+)/\Gamma_{\text{total}}$ Γ_{260}/Γ

VALUE (units 10^{-5})	EVTS	DOCUMENT ID		TECN	COMMENT
<3.8	90	[1] FANG	06	BELL	$e^+e^- \to \Upsilon(4S)$

[1] Assumes equal production of B^+ and B^0 at the $\Upsilon(4S)$ and $B(h_c \to \eta_c\gamma) = 50\%$.

$\Gamma(h_c(1P)K^+,\ h_c \to p\overline{p})/\Gamma_{\text{total}}$ Γ_{261}/Γ

VALUE	CL%	DOCUMENT ID		TECN	COMMENT
<6.4 × 10^{-8}	95	[1] AAIJ	13S	LHCB	pp at 7 TeV

[1] Measured relative to $B^+ \to J/\psi K^+$ decay with charmonia reconstructed in $p\overline{p}$ final state and using $B(B^+ \to J/\psi K^+) = (1.013 \pm 0.034) \times 10^{-3}$ and $B(J/\psi \to p\overline{p}) = (2.17 \pm 0.07) \times 10^{-3}$.

$\Gamma(K^0\pi^+)/\Gamma_{\text{total}}$ Γ_{262}/Γ

VALUE (units 10^{-6})	CL%	DOCUMENT ID		TECN	COMMENT
23.7 ± 0.8 OUR FIT					
23.8 ± 0.7 OUR AVERAGE					
23.97± 0.53±0.71		[1] DUH	13	BELL	$e^+e^- \to \Upsilon(4S)$
23.9 ± 1.1 ±1.0		[1] AUBERT,BE	06C	BABR	$e^+e^- \to \Upsilon(4S)$
18.8 $^{+3.7}_{-3.3}$ $^{+2.1}_{-1.8}$		[1] BORNHEIM	03	CLE2	$e^+e^- \to \Upsilon(4S)$
• • • We do not use the following data for averages, fits, limits, etc. • • •					
22.8 $^{+0.8}_{-0.7}$ ±1.3		[1] LIN	07	BELL	Repl. by DUH 13
26.0 ± 1.3 ±1.0		[1] AUBERT,BE	05E	BABR	Repl. by AUBERT,BE 06C
22.3 ± 1.7 ±1.1		[1] AUBERT	04M	BABR	Repl. by AUBERT,BE 05E
22.0 ± 1.9 ±1.1		[1] CHAO	04	BELL	Repl. by LIN 07
19.4 $^{+3.1}_{-3.0}$ ±1.6		[1] CASEY	02	BELL	Repl. by CHAO 04
13.7 $^{+5.7}_{-4.8}$ $^{+1.9}_{-1.8}$		[1] ABE	01H	BELL	Repl. by CASEY 02
18.2 $^{+3.3}_{-3.0}$ ±2.0		[1] AUBERT	01E	BABR	Repl. by AUBERT 04M
18.2 $^{+4.6}_{-4.0}$ ±1.6		[1] CRONIN-HEN..00		CLE2	Repl. by BORNHEIM 03
23 $^{+11}_{-10}$ ±3.6		GODANG	98	CLE2	Repl. by CRONIN-HENNESSY 00
< 48	90	ASNER	96	CLE2	Repl. by GODANG 98
<190	90	ALBRECHT	91B	ARG	$e^+e^- \to \Upsilon(4S)$
<100	90	[2] AVERY	89B	CLEO	$e^+e^- \to \Upsilon(4S)$
<680	90	AVERY	87	CLEO	$e^+e^- \to \Upsilon(4S)$

[1] Assumes equal production of B^+ and B^0 at the $\Upsilon(4S)$.

[2] AVERY 89B reports $< 9 \times 10^{-5}$ assuming the $\Upsilon(4S)$ decays 43% to $B^0\overline{B}^0$. We rescale to 50%.

$\Gamma(K^+\pi^0)/\Gamma_{\text{total}}$ Γ_{263}/Γ

VALUE (units 10^{-6})	CL%	DOCUMENT ID		TECN	COMMENT
12.9 ±0.5 OUR AVERAGE					
12.62±0.31±0.56		[1] DUH	13	BELL	$e^+e^- \to \Upsilon(4S)$
13.6 ±0.6 ±0.7		[1] AUBERT	07BC	BABR	$e^+e^- \to \Upsilon(4S)$
12.9 $^{+2.4}_{-2.2}$ $^{+1.2}_{-1.1}$		[1] BORNHEIM	03	CLE2	$e^+e^- \to \Upsilon(4S)$
• • • We do not use the following data for averages, fits, limits, etc. • • •					
12.4 ±0.5 ±0.6		[1] LIN	07A	BELL	Repl. by DUH 13
12.0 ±0.7 ±0.6		[1] AUBERT	05L	BABR	Repl. by AUBERT 07BC
12.0 ±1.3 $^{+1.3}_{-0.9}$		[1] CHAO	04	BELL	Repl. by LIN 07A
12.8 $^{+1.2}_{-1.1}$ ±1.0		[1] AUBERT	03L	BABR	Repl. by AUBERT 05L
13.0 $^{+2.5}_{-2.4}$ ±1.3		[1] CASEY	02	BELL	Repl. by CHAO 04
16.3 $^{+3.5}_{-3.3}$ $^{+1.6}_{-1.8}$		[1] ABE	01H	BELL	Repl. by CASEY 02
10.8 $^{+2.1}_{-1.9}$ ±1.0		[1] AUBERT	01E	BABR	Repl. by AUBERT 03L
11.6 $^{+3.0}_{-2.7}$ $^{+1.4}_{-1.3}$		[1] CRONIN-HEN..00		CLE2	Repl. by BORNHEIM 03
<16	90	GODANG	98	CLE2	Repl. by CRONIN-HENNESSY 00
<14	90	ASNER	96	CLE2	Repl. by GODANG 98

[1] Assumes equal production of B^+ and B^0 at the $\Upsilon(4S)$.

$\Gamma(K^+\pi^0)/\Gamma(K^0\pi^+)$ $\Gamma_{263}/\Gamma_{262}$

VALUE	DOCUMENT ID		TECN	COMMENT
0.54±0.03±0.04	LIN	07A	BELL	$e^+e^- \to \Upsilon(4S)$
• • • We do not use the following data for averages, fits, limits, etc. • • •				
2.38 $^{+0.98}_{-1.10}$ $^{+0.39}_{-0.26}$	ABE	01H	BELL	Repl. by LIN 07A

$\Gamma(\eta' K^+)/\Gamma_{\text{total}}$ Γ_{264}/Γ

VALUE (units 10^{-6})	DOCUMENT ID		TECN	COMMENT
70.6± 2.5 OUR AVERAGE				
71.5± 1.3±3.2	[1] AUBERT	09AV	BABR	$e^+e^- \to \Upsilon(4S)$
64 $^{+10}_{-9}$ ±2	[1,2] WICHT	08	BELL	$e^+e^- \to \Upsilon(4S)$
69.2± 2.2±3.7	[1] SCHUEMANN	06	BELL	$e^+e^- \to \Upsilon(4S)$
80 $^{+10}_{-9}$ ±7	[1] RICHICHI	00	CLE2	$e^+e^- \to \Upsilon(4S)$
• • • We do not use the following data for averages, fits, limits, etc. • • •				
70.0± 1.5±2.8	[1] AUBERT	07AE	BABR	Repl. by AUBERT 09AV
68.9± 2.0±3.2	[1] AUBERT	05M	BABR	Repl. by AUBERT 07AE
76.9± 3.5±4.4	[1] AUBERT	03W	BABR	Repl. by AUBERT 05M
79 $^{+12}_{-11}$ ±9	[1] ABE	01M	BELL	Repl. by SCHUEMANN 06
70 ± 8 ±5	[1] AUBERT	01G	BABR	Repl. by AUBERT 03W
65 $^{+15}_{-14}$ ±9	BEHRENS	98	CLE2	Repl. by RICHICHI 00

[1] Assumes equal production of B^+ and B^0 at the $\Upsilon(4S)$.

[2] WICHT 08 reports $[\Gamma(B^+ \to \eta' K^+)/\Gamma_{\text{total}}] \times [B(\eta'(958) \to \gamma\gamma)] = (1.40^{+0.16+0.15}_{-0.15-0.12}) \times 10^{-6}$ which we divide by our best value $B(\eta'(958) \to \gamma\gamma) = (2.20 \pm 0.08) \times 10^{-2}$. Our first error is their experiment's error and our second error is the systematic error from using our best value.

$\Gamma(\eta' K^*(892)^+)/\Gamma_{\text{total}}$ Γ_{265}/Γ

VALUE (units 10^{-6})	CL%	DOCUMENT ID		TECN	COMMENT
4.8 $^{+1.6}_{-1.4}$ ±0.8		[1] DEL-AMO-SA...10A		BABR	$e^+e^- \to \Upsilon(4S)$
• • • We do not use the following data for averages, fits, limits, etc. • • •					
4.9 $^{+1.9}_{-1.7}$ ±0.8		[1] AUBERT	07E	BABR	Repl. by DEL-AMO-SANCHEZ 10A
< 2.9	90	[1] SCHUEMANN	07	BELL	$e^+e^- \to \Upsilon(4S)$
<14	90	[1] AUBERT,B	04D	BABR	Repl. by AUBERT 07E
<35	90	[1] RICHICHI	00	CLE2	$e^+e^- \to \Upsilon(4S)$
<13	90	BEHRENS	98	CLE2	Repl. by RICHICHI 00

[1] Assumes equal production of B^+ and B^0 at the $\Upsilon(4S)$.

$\Gamma(\eta' K_0^*(1430)^+)/\Gamma_{\text{total}}$ Γ_{266}/Γ

VALUE (units 10^{-6})	DOCUMENT ID		TECN	COMMENT
5.2±1.9±1.0	[1] DEL-AMO-SA...10A		BABR	$e^+e^- \to \Upsilon(4S)$

[1] Assumes equal production of B^+ and B^0 at the $\Upsilon(4S)$.

$\Gamma(\eta' K_2^*(1430)^+)/\Gamma_{\text{total}}$ Γ_{267}/Γ

VALUE (units 10^{-6})	DOCUMENT ID		TECN	COMMENT
28.0 $^{+4.6}_{-4.3}$ ±2.6	[1] DEL-AMO-SA...10A		BABR	$e^+e^- \to \Upsilon(4S)$

[1] Assumes equal production of B^+ and B^0 at the $\Upsilon(4S)$.

See key on page 547

$\Gamma(\eta K^+)/\Gamma_{total}$ Γ_{268}/Γ

VALUE (units 10^{-6})	CL%	DOCUMENT ID		TECN	COMMENT
2.4 ±0.4 OUR AVERAGE		Error includes scale factor of 1.7.			
$2.12\pm0.23\pm0.11$		[1] HOI	12	BELL	$e^+e^-\to\ \Upsilon(4S)$
$2.94^{+0.39}_{-0.34}\pm0.21$		[1] AUBERT	09AV	BABR	$e^+e^-\to\ \Upsilon(4S)$
$2.2\ ^{+2.8}_{-2.2}$		[1] RICHICHI	00	CLE2	$e^+e^-\to\ \Upsilon(4S)$
• • • We do not use the following data for averages, fits, limits, etc. • • •					
$2.21^{+0.48}_{-0.42}\pm0.01$		[1,2] WICHT	08	BELL	Repl. by HOI 12
$3.7\ \pm0.4\ \pm0.1$		[1] AUBERT	07AE	BABR	Repl. by AUBERT 09AV
$1.9\ \pm0.3\ ^{+0.2}_{-0.1}$		[1] CHANG	07B	BELL	Repl. by HOI 12
$3.3\ \pm0.6\ \pm0.3$		[1] AUBERT,B	05K	BABR	Repl. by AUBERT 07AE
$2.1\ \pm0.6\ \pm0.2$		[1] CHANG	05A	BELL	Repl. by CHANG 07B
$3.4\ \pm0.8\ \pm0.2$		[1] AUBERT	04H	BABR	Repl. by AUBERT,B 05K
<14	90	BEHRENS	98	CLE2	Repl. by RICHICHI 00

[1] Assumes equal production of B^+ and B^0 at the $\Upsilon(4S)$.
[2] WICHT 08 reports $[\Gamma(B^+\to\ \eta K^+)/\Gamma_{total}]\times[B(\eta\to\ 2\gamma)] = (0.87^{+0.16}_{-0.15}{}^{+0.10}_{-0.07})\times10^{-6}$ which we divide by our best value $B(\eta\to\ 2\gamma) = (39.41\pm0.20)\times10^{-2}$. Our first error is their experiment's error and our second error is the systematic error from using our best value.

$\Gamma(\eta K^*(892)^+)/\Gamma_{total}$ Γ_{269}/Γ

VALUE (units 10^{-6})	CL%	DOCUMENT ID		TECN	COMMENT
19.3±1.6 OUR AVERAGE					
$19.3^{+2.0}_{-1.9}\pm1.5$		[1] WANG	07B	BELL	$e^+e^-\to\ \Upsilon(4S)$
$18.9\pm1.8\pm1.3$		[1] AUBERT,B	06H	BABR	$e^+e^-\to\ \Upsilon(4S)$
$26.4^{+9.6}_{-8.2}\pm3.3$		[1] RICHICHI	00	CLE2	$e^+e^-\to\ \Upsilon(4S)$
• • • We do not use the following data for averages, fits, limits, etc. • • •					
$25.6\pm4.0\pm2.4$		[1] AUBERT,B	04D	BABR	Repl. by AUBERT,B 06H
<30	90	BEHRENS	98	CLE2	Repl. by RICHICHI 00

[1] Assumes equal production of B^+ and B^0 at the $\Upsilon(4S)$.

$\Gamma(\eta K_0^*(1430)^+)/\Gamma_{total}$ Γ_{270}/Γ

VALUE (units 10^{-6})	DOCUMENT ID		TECN	COMMENT
18.2±2.6±2.6	[1] AUBERT,B	06H	BABR	$e^+e^-\to\ \Upsilon(4S)$

[1] Assumes equal production of B^+ and B^0 at the $\Upsilon(4S)$.

$\Gamma(\eta K_2^*(1430)^+)/\Gamma_{total}$ Γ_{271}/Γ

VALUE (units 10^{-6})	DOCUMENT ID		TECN	COMMENT
9.1±2.7±1.4	[1] AUBERT,B	06H	BABR	$e^+e^-\to\ \Upsilon(4S)$

[1] Assumes equal production of B^+ and B^0 at the $\Upsilon(4S)$.

$\Gamma(\eta(1295)K^+\times B(\eta(1295)\to\ \eta\pi\pi))/\Gamma_{total}$ Γ_{272}/Γ

VALUE (units 10^{-6})	DOCUMENT ID		TECN	COMMENT
$\mathbf{2.9^{+0.8}_{-0.7}\pm0.2}$	[1] AUBERT	08X	BABR	$e^+e^-\to\ \Upsilon(4S)$

[1] Assumes equal production of B^+ and B^0 at the $\Upsilon(4S)$.

$\Gamma(\eta(1405)K^+\times B(\eta(1405)\to\ \eta\pi\pi))/\Gamma_{total}$ Γ_{273}/Γ

VALUE (units 10^{-6})	CL%	DOCUMENT ID		TECN	COMMENT
<1.3	90	[1] AUBERT	08X	BABR	$e^+e^-\to\ \Upsilon(4S)$

[1] Assumes equal production of B^+ and B^0 at the $\Upsilon(4S)$.

$\Gamma(\eta(1405)K^+\times B(\eta(1405)\to\ K^*K))/\Gamma_{total}$ Γ_{274}/Γ

VALUE (units 10^{-6})	CL%	DOCUMENT ID		TECN	COMMENT
<1.2	90	[1] AUBERT	08X	BABR	$e^+e^-\to\ \Upsilon(4S)$

[1] Assumes equal production of B^+ and B^0 at the $\Upsilon(4S)$.

$\Gamma(\eta(1475)K^+\times B(\eta(1475)\to\ K^*K))/\Gamma_{total}$ Γ_{275}/Γ

VALUE (units 10^{-6})	DOCUMENT ID		TECN	COMMENT
$\mathbf{13.8^{+1.8}_{-1.7}{}^{+1.0}_{-0.6}}$	[1] AUBERT	08X	BABR	$e^+e^-\to\ \Upsilon(4S)$

[1] Assumes equal production of B^+ and B^0 at the $\Upsilon(4S)$.

$\Gamma(f_1(1285)K^+)/\Gamma_{total}$ Γ_{276}/Γ

VALUE (units 10^{-6})	CL%	DOCUMENT ID		TECN	COMMENT
<2.0	90	[1] AUBERT	08X	BABR	$e^+e^-\to\ \Upsilon(4S)$

[1] Assumes equal production of B^+ and B^0 at the $\Upsilon(4S)$.

$\Gamma(f_1(1420)K^+\times B(f_1(1420)\to\ \eta\pi\pi))/\Gamma_{total}$ Γ_{277}/Γ

VALUE (units 10^{-6})	CL%	DOCUMENT ID		TECN	COMMENT
<2.9	90	[1] AUBERT	08X	BABR	$e^+e^-\to\ \Upsilon(4S)$

[1] Assumes equal production of B^+ and B^0 at the $\Upsilon(4S)$.

$\Gamma(f_1(1420)K^+\times B(f_1(1420)\to\ K^*K))/\Gamma_{total}$ Γ_{278}/Γ

VALUE (units 10^{-6})	CL%	DOCUMENT ID		TECN	COMMENT
<4.1	90	[1] AUBERT	08X	BABR	$e^+e^-\to\ \Upsilon(4S)$

[1] Assumes equal production of B^+ and B^0 at the $\Upsilon(4S)$.

$\Gamma(\phi(1680)K^+\times B(\phi(1680)\to\ K^*K))/\Gamma_{total}$ Γ_{279}/Γ

VALUE (units 10^{-6})	CL%	DOCUMENT ID		TECN	COMMENT
<3.4	90	[1] AUBERT	08X	BABR	$e^+e^-\to\ \Upsilon(4S)$

[1] Assumes equal production of B^+ and B^0 at the $\Upsilon(4S)$.

$\Gamma(f_0(1500)K^+)/\Gamma_{total}$ Γ_{280}/Γ

VALUE (units 10^{-6})	CL%	DOCUMENT ID		TECN	COMMENT
3.7± 2.2 OUR AVERAGE					
$17\ \pm\ 4\ \pm12$		[1] LEES	12O	BABR	$e^+e^-\to\ \Upsilon(4S)$
$20\ \pm10\ \pm27$		[2] LEES	12O	BABR	$e^+e^-\to\ \Upsilon(4S)$
$3.1^{+\ 2.2}_{-\ 2.3}\pm\ 0.2$		[3,4] AUBERT	08AI	BABR	$e^+e^-\to\ \Upsilon(4S)$
• • • We do not use the following data for averages, fits, limits, etc. • • •					
<19	90	[4,5] AUBERT,B	05N	BABR	Repl. by AUBERT 08AI

[1] Measured in the $B^+\to\ K^+K^-K^+$ decay.
[2] Measured in the $B^+\to\ K^+K_S^0K_S^0$ decay.
[3] AUBERT 08AI reports $B(B^+\to\ f_0(1500)K^+)\cdot B(f_0(1500)\to\ \pi^+\pi^-) = (0.73\pm0.21^{+0.47}_{-0.48})\times10^{-6}$. We divide this result by our best value of $B(f_0(1500)\to\ \pi\pi) = (34.9\pm2.3)\times10^{-2}$ multiplied by 2/3 to account for the $\pi^+\pi^-$ fraction. Our first quoted uncertainty is the combined experiment's uncertainty and our second is the systematic uncertainty from using out best value.
[4] Assumes equal production of B^+ and B^0 at the $\Upsilon(4S)$.
[5] AUBERT,B 05N reports $B(B^+\to\ f_0(1500)K^+)\cdot B(f_0(1500)\to\ \pi^+\pi^-)<4.4\times10^{-6}$. We divide this result by our best value of $B(f_0(1500)\to\ \pi\pi) = (34.9\pm2.3)\times10^{-2}$ multiplied by 2/3 to account for the $\pi^+\pi^-$ fraction. Our first quoted uncertainty is the combined experiment's uncertainty and our second is the systematic uncertainty from using out best value.

$\Gamma(\omega K^+)/\Gamma_{total}$ Γ_{281}/Γ

VALUE (units 10^{-6})	CL%	DOCUMENT ID		TECN	COMMENT
6.7±0.8 OUR AVERAGE		Error includes scale factor of 1.8.			
$6.3\pm0.5\pm0.3$		[1] AUBERT	07AE	BABR	$e^+e^-\to\ \Upsilon(4S)$
$8.1\pm0.6\pm0.6$		[1] JEN	06	BELL	$e^+e^-\to\ \Upsilon(4S)$
$3.2^{+2.4}_{-1.9}\pm0.8$		[1] JESSOP	00	CLE2	$e^+e^-\to\ \Upsilon(4S)$
• • • We do not use the following data for averages, fits, limits, etc. • • •					
$6.1\pm0.6\pm0.4$		[1] AUBERT,B	06E	BABR	AUBERT 07AE
$4.8\pm0.8\pm0.4$		[1] AUBERT	04H	BABR	Repl. by AUBERT,B 06E
$6.5^{+1.3}_{-1.2}\pm0.6$		[1] WANG	04A	BELL	Repl. by JEN 06
$9.2^{+2.6}_{-2.3}\pm1.0$		[1] LU	02	BELL	Repl. by WANG 04A
<4	90	[1] AUBERT	01G	BABR	$e^+e^-\to\ \Upsilon(4S)$
$1.5^{+7}_{-6}\ \pm2$		[1] BERGFELD	98	CLE2	Repl. by JESSOP 00

[1] Assumes equal production of B^+ and B^0 at the $\Upsilon(4S)$.

$\Gamma(\omega K^*(892)^+)/\Gamma_{total}$ Γ_{282}/Γ

VALUE (units 10^{-6})	CL%	DOCUMENT ID		TECN	COMMENT
< 7.4	90	[1] AUBERT	09H	BABR	$e^+e^-\to\ \Upsilon(4S)$
• • • We do not use the following data for averages, fits, limits, etc. • • •					
< 3.4	90	[1] AUBERT,B	06T	BABR	Repl. by AUBERT 09H
< 7.4	90	[1] AUBERT	05O	BABR	Repl. by AUBERT,B 06T
<87	90	[1] BERGFELD	98	CLE2	

[1] Assumes equal production of B^+ and B^0 at the $\Upsilon(4S)$.

$\Gamma(\omega(K\pi)_0^{*+})/\Gamma_{total}$ Γ_{283}/Γ

$(K\pi)_0^{*+}$ is the total S-wave composed of $K_0^*(1430)$ and nonresonant that are described using LASS shape.

VALUE (units 10^{-6})	DOCUMENT ID		TECN	COMMENT
27.5±3.0±2.6	[1] AUBERT	09H	BABR	$e^+e^-\to\ \Upsilon(4S)$

[1] Assumes equal production of B^+ and B^0 at the $\Upsilon(4S)$.

$\Gamma(\omega K_0^*(1430)^+)/\Gamma_{total}$ Γ_{284}/Γ

VALUE (units 10^{-6})	DOCUMENT ID		TECN	COMMENT
24.0±2.6±4.4	[1] AUBERT	09H	BABR	$e^+e^-\to\ \Upsilon(4S)$

[1] Assumes equal production of B^+ and B^0 at the $\Upsilon(4S)$.

$\Gamma(\omega K_2^*(1430)^+)/\Gamma_{total}$ Γ_{285}/Γ

VALUE (units 10^{-6})	DOCUMENT ID		TECN	COMMENT
21.5±3.6±2.4	[1] AUBERT	09H	BABR	$e^+e^-\to\ \Upsilon(4S)$

[1] Assumes equal production of B^+ and B^0 at the $\Upsilon(4S)$.

$\Gamma(a_0(980)^0K^+\times B(a_0(980)^0\to\ \eta\pi^0))/\Gamma_{total}$ Γ_{287}/Γ

VALUE (units 10^{-6})	CL%	DOCUMENT ID		TECN	COMMENT
<2.5	90	[1] AUBERT,BE	04	BABR	$e^+e^-\to\ \Upsilon(4S)$

[1] Assumes equal production of charged and neutral B mesons from $\Upsilon(4S)$ decays.

Meson Particle Listings

$B^{\pm}$

$\Gamma(a_0(980)^+ K^0 \times B(a_0(980)^+ \to \eta\pi^+))/\Gamma_{total}$ Γ_{286}/Γ

VALUE (units 10^{-6})	CL%	DOCUMENT ID		TECN	COMMENT
<3.9	90	[1] AUBERT,BE	04	BABR	$e^+e^- \to \Upsilon(4S)$

[1] Assumes equal production of charged and neutral B mesons from $\Upsilon(4S)$ decays.

$\Gamma(K^*(892)^0\pi^+)/\Gamma_{total}$ Γ_{288}/Γ

VALUE (units 10^{-6})	CL%	DOCUMENT ID		TECN	COMMENT
10.1 ±0.9 OUR AVERAGE					
$10.8 \pm 0.6 \,^{+1.2}_{-1.4}$		[1] AUBERT	08AI	BABR	$e^+e^- \to \Upsilon(4S)$
$9.67 \pm 0.64 \,^{+0.81}_{-0.89}$		[1] GARMASH	06	BELL	$e^+e^- \to \Upsilon(4S)$
• • • We do not use the following data for averages, fits, limits, etc. • • •					
$13.5 \pm 1.2 \,^{+0.8}_{-0.9}$		[1] AUBERT,B	05N	BABR	Repl. by AUBERT 08AI
$9.8 \pm 0.9 \,^{+1.1}_{-1.2}$		[1] GARMASH	05	BELL	Repl. by GARMASH 06
$15.5 \pm 1.8 \,^{+1.5}_{-4.0}$		[1,2] AUBERT,B	04P	BABR	Repl. by AUBERT,B 05N
$19.4 \,^{+4.2}_{-3.9} \,^{+4.1}_{-7.1}$		[3] GARMASH	02	BELL	Repl. by GARMASH 05
<119	90	[4] ABE	00C	SLD	$e^+e^- \to Z$
< 16	90	[1] JESSOP	00	CLE2	$e^+e^- \to \Upsilon(4S)$
<390	90	[5] ADAM	96D	DLPH	$e^+e^- \to Z$
< 41	90	ASNER	96	CLE2	Repl. by JESSOP 00
<480	90	[5] ABREU	95N	DLPH	Sup. by ADAM 96D
<170	90	ALBRECHT	91B	ARG	$e^+e^- \to \Upsilon(4S)$
<150	90	[6] AVERY	89B	CLEO	$e^+e^- \to \Upsilon(4S)$
<260	90	AVERY	87	CLEO	$e^+e^- \to \Upsilon(4S)$

[1] Assumes equal production of B^+ and B^0 at the $\Upsilon(4S)$.
[2] AUBERT 04P also report a branching ratio for $B^+ \to$ "higher $K*$ resonances" π^+, $K* \to K^+\pi^-$, $(25.1 \pm 2.0 \,^{+11.0}_{-5.7}) \times 10^{-6}$.
[3] Uses a reference decay mode $B^+ \to \overline{D}{}^0\pi^+$ and $\overline{D}{}^0 \to K^+\pi^-$ with $B(B^+ \to \overline{D}{}^0\pi^+)\cdot B(\overline{D}{}^0 \to K^+\pi^-) = (20.3 \pm 2.0) \times 10^{-5}$.
[4] ABE 00C assumes $B(Z \to b\overline{b}) = (21.7 \pm 0.1)\%$ and the B fractions $f_{B^0} = f_{B^+} = (39.7 \,^{+1.8}_{-2.2})\%$ and $f_{B_s} = (10.5 \,^{+1.8}_{-2.2})\%$.
[5] Assumes a B^0, B^- production fraction of 0.39 and a B_s production fraction of 0.12.
[6] AVERY 89B reports $< 1.3 \times 10^{-4}$ assuming the $\Upsilon(4S)$ decays 43% to $B^0\overline{B}{}^0$. We rescale to 50%.

$\Gamma(K^*(892)^+\pi^0)/\Gamma_{total}$ Γ_{289}/Γ

VALUE (units 10^{-6})	CL%	DOCUMENT ID		TECN	COMMENT
8.2±1.5±1.1		[1] LEES	11I	BABR	$e^+e^- \to \Upsilon(4S)$
• • • We do not use the following data for averages, fits, limits, etc. • • •					
6.9±2.0±1.3		[1] AUBERT	05X	BABR	Repl. by LEES 11I
<31	90	[1] JESSOP	00	CLE2	$e^+e^- \to \Upsilon(4S)$
<99	90	ASNER	96	CLE2	Repl. by JESSOP 00

[1] Assumes equal production of B^+ and B^0 at the $\Upsilon(4S)$.

$\Gamma(K^+\pi^-\pi^+)/\Gamma_{total}$ Γ_{290}/Γ

VALUE (units 10^{-6})	DOCUMENT ID		TECN	COMMENT
51.0±2.9 OUR AVERAGE				
54.4±1.1±4.6	[1] AUBERT	08AI	BABR	$e^+e^- \to \Upsilon(4S)$
48.8±1.1±3.6	[1] GARMASH	06	BELL	$e^+e^- \to \Upsilon(4S)$
• • • We do not use the following data for averages, fits, limits, etc. • • •				
64.1±2.4±4.0	[1] AUBERT,B	05N	BABR	Repl. by AUBERT 08AI
46.6±2.1±4.3	[1] GARMASH	05	BELL	Repl. by GARMASH 06
53.6±3.1±5.1	[1] GARMASH	04	BELL	Repl. by GARMASH 05
59.1±3.8±3.2	[2] AUBERT	03M	BABR	Repl. by AUBERT,B 05N
55.6±5.8±7.7	[3] GARMASH	02	BELL	Repl. by GARMASH 04

[1] Assumes equal production of B^+ and B^0 at the $\Upsilon(4S)$.
[2] Assumes equal production of B^0 and B^+ at the $\Upsilon(4S)$; charm and charmonium contributions are subtracted, otherwise no assumptions about intermediate resonances.
[3] Uses a reference decay mode $B^+ \to \overline{D}{}^0\pi^+$ and $\overline{D}{}^0 \to K^+\pi^-$ with $B(B^+ \to \overline{D}{}^0\pi^+)\cdot B(\overline{D}{}^0 \to K^+\pi^-) = (20.3 \pm 2.0) \times 10^{-5}$.

$\Gamma(K^+\pi^-\pi^+ \text{nonresonant})/\Gamma_{total}$ Γ_{291}/Γ

VALUE (units 10^{-6})	CL%	DOCUMENT ID		TECN	COMMENT
$16.3 \,^{+2.1}_{-1.5}$ OUR AVERAGE					
$9.3 \pm 1.0 \,^{+6.9}_{-1.7}$		[1,2] AUBERT	08AI	BABR	$e^+e^- \to \Upsilon(4S)$
$16.9 \pm 1.3 \,^{+1.7}_{-1.6}$		[1] GARMASH	06	BELL	$e^+e^- \to \Upsilon(4S)$
• • • We do not use the following data for averages, fits, limits, etc. • • •					
$2.9 \pm 0.6 \,^{+0.8}_{-0.5}$		[1] AUBERT,B	05N	BABR	Repl. by AUBERT 08AI
$17.3 \pm 1.7 \,^{+17.2}_{-8.0}$		[1] GARMASH	05	BELL	Repl. by GARMASH 06
< 17	90	[1] AUBERT,B	04P	BABR	Repl. by AUBERT,B 05N
<330	90	[3] ADAM	96D	DLPH	$e^+e^- \to Z$
< 28	90	BERGFELD	96B	CLE2	$e^+e^- \to \Upsilon(4S)$
<400	90	[3] ABREU	95N	DLPH	Sup. by ADAM 96D
<330	90	ALBRECHT	91E	ARG	$e^+e^- \to \Upsilon(4S)$
<190	90	[4] AVERY	89B	CLEO	$e^+e^- \to \Upsilon(4S)$

[1] Assumes equal production of B^+ and B^0 at the $\Upsilon(4S)$.
[2] Calculate the total nonresonant contribution by combining the S-wave composed of $K_0^*(1430)$ and nonresonant that are described using LASS shape.
[3] Assumes a B^0, B^- production fraction of 0.39 and a B_s production fraction of 0.12.
[4] AVERY 89B reports $< 1.7 \times 10^{-4}$ assuming the $\Upsilon(4S)$ decays 43% to $B^0\overline{B}{}^0$. We rescale to 50%.

$\Gamma(\omega(782)K^+)/\Gamma_{total}$ Γ_{292}/Γ

VALUE (units 10^{-6})	DOCUMENT ID		TECN	COMMENT
$\mathbf{5.9 \,^{+0.8}_{-0.9} \,^{+0.5}_{-0.4}}$	[1,2] AUBERT	08AI	BABR	$e^+e^- \to \Upsilon(4S)$

[1] Assumes equal production of B^+ and B^0 at the $\Upsilon(4S)$.
[2] AUBERT 08AI reports $[\Gamma(B^+ \to \omega(782)K^+)/\Gamma_{total}] \times [B(\omega(782) \to \pi^+\pi^-)] = (0.09 \pm 0.13 \,^{+0.036}_{-0.045}) \times 10^{-6}$ which we divide by our best value $B(\omega(782) \to \pi^+\pi^-) = (1.53 \,^{+0.11}_{-0.13}) \times 10^{-2}$. Our first error is their experiment's error and our second error is the systematic error from using our best value.

$\Gamma(K^+ f_0(980) \times B(f_0(980) \to \pi^+\pi^-))/\Gamma_{total}$ Γ_{293}/Γ

VALUE (units 10^{-6})	CL%	DOCUMENT ID		TECN	COMMENT
$9.4 \,^{+1.0}_{-1.2}$ OUR AVERAGE					
$10.3 \pm 0.5 \,^{+2.0}_{-1.4}$		[1] AUBERT	08AI	BABR	$e^+e^- \to \Upsilon(4S)$
$8.78 \pm 0.82 \,^{+0.85}_{-1.76}$		[1] GARMASH	06	BELL	$e^+e^- \to \Upsilon(4S)$
• • • We do not use the following data for averages, fits, limits, etc. • • •					
$9.47 \pm 0.97 \,^{+0.62}_{-0.88}$		[1] AUBERT,B	05N	BABR	Repl. by AUBERT 08AI
$7.55 \pm 1.24 \,^{+1.63}_{-1.18}$		[1] GARMASH	05	BELL	Repl. by GARMASH 06
$9.2 \pm 1.2 \,^{+2.1}_{-2.6}$		[2] AUBERT,B	04P	BABR	Repl. by AUBERT,B 05N
$9.6 \,^{+2.5}_{-2.3} \,^{+3.7}_{-1.7}$		[3] GARMASH	02	BELL	Repl. by GARMASH 05
<80	90	[4] AVERY	89B	CLEO	$e^+e^- \to \Upsilon(4S)$

[1] Assumes equal production of B^+ and B^0 at the $\Upsilon(4S)$.
[2] AUBERT,B 04P also reports $B(B^+ \to$ "higher f^0 resonances" $\pi^+, f(980)^0 \to \pi^+\pi^-) = (3.2 \pm 1.2 \,^{+6.0}_{-2.9}) \times 10^{-6}$.
[3] Uses a reference decay mode $B^+ \to \overline{D}{}^0\pi^+$ and $\overline{D}{}^0 \to K^+\pi^-$ with $B(B^+ \to \overline{D}{}^0\pi^+)\times B(\overline{D}{}^0 \to K^+\pi^-) = (20.3 \pm 2.0) \times 10^{-5}$. Only charged pions from the $f_0(980)$ are used.
[4] AVERY 89B reports $< 7 \times 10^{-5}$ assuming the $\Upsilon(4S)$ decays 43% to $B^0\overline{B}{}^0$. We rescale to 50%.

$\Gamma(f_2(1270)^0 K^+)/\Gamma_{total}$ Γ_{294}/Γ

VALUE (units 10^{-6})	CL%	DOCUMENT ID		TECN	COMMENT
1.07±0.27 OUR AVERAGE					
$0.88 \,^{+0.38}_{-0.33} \pm 0.01 \,^{+0.01}_{-0.03}$		[1,2] AUBERT	08AI	BABR	$e^+e^- \to \Upsilon(4S)$
$1.33 \pm 0.30 \,^{+0.23}_{-0.34}$		[1] GARMASH	06	BELL	$e^+e^- \to \Upsilon(4S)$
• • • We do not use the following data for averages, fits, limits, etc. • • •					
<16	90	[3] AUBERT,B	05N	BABR	Repl. by AUBERT 08AI
< 2.3	90	[4] GARMASH	05	BELL	Repl. by GARMASH 06

[1] Assumes equal production of B^+ and B^0 at the $\Upsilon(4S)$.
[2] AUBERT 08AI reports $(0.50 \pm 0.15 \,^{+0.15}_{-0.11}) \times 10^{-6}$ for $B(B^+ \to f_2(1270)K^+) \times B(f_2 \to \pi^+\pi^-)$. We compute $B(B^+ \to f_2(1270)K^+)$ using the PDG value $B(f_2(1270) \to \pi\pi) = (84.8 \,^{+2.4}_{-1.2})\% \times 10^{-2}$ and 2/3 for the $\pi^+\pi^-$ fraction. Our first error is their experiment's error and the second error is systematic error from using our best value.
[3] AUBERT,B 05N reports 8.9×10^{-6} at 90% CL for $B(B^+ \to f_2(1270)K^+) \times B(f_2(1270) \to \pi^+\pi^-)$. We rescaled it using the PDG value $B(f_2(1270) \to \pi\pi) = 84.7\%$ and 2/3 for the $\pi^+\pi^-$ fraction.
[4] GARMASH 05 reports 1.3×10^{-6} at 90% CL for $B(B^+ \to f_2(1270)K^+) \times B(f_2(1270) \to \pi^+\pi^-)$. We rescaled it using the PDG value $B(f_2(1270) \to \pi\pi) = 84.7\%$ and 2/3 for the $\pi^+\pi^-$ fraction.

$\Gamma(f_0(1370)^0 K^+ \times B(f_0(1370)^0 \to \pi^+\pi^-))/\Gamma_{total}$ Γ_{295}/Γ

VALUE	CL%	DOCUMENT ID		TECN	COMMENT
$\mathbf{< 10.7 \times 10^{-6}}$	90	[1] AUBERT,B	05N	BABR	$e^+e^- \to \Upsilon(4S)$

[1] Assumes equal production of B^+ and B^0 at the $\Upsilon(4S)$.

$\Gamma(\rho^0(1450)K^+ \times B(\rho^0(1450) \to \pi^+\pi^-))/\Gamma_{total}$ Γ_{296}/Γ

VALUE	CL%	DOCUMENT ID		TECN	COMMENT
$\mathbf{< 11.7 \times 10^{-6}}$	90	[1] AUBERT,B	05N	BABR	$e^+e^- \to \Upsilon(4S)$

[1] Assumes equal production of B^+ and B^0 at the $\Upsilon(4S)$.

$\Gamma(f_2'(1525)K^+ \times B(f_2'(1525) \to \pi^+\pi^-))/\Gamma_{total}$ Γ_{297}/Γ

VALUE	CL%	DOCUMENT ID		TECN	COMMENT
$\mathbf{< 3.4 \times 10^{-6}}$	90	[1] AUBERT,B	05N	BABR	$e^+e^- \to \Upsilon(4S)$

[1] Assumes equal production of B^+ and B^0 at the $\Upsilon(4S)$.

$\Gamma(K^+\rho^0)/\Gamma_{total}$ Γ_{298}/Γ

VALUE (units 10^{-6})	CL%	DOCUMENT ID		TECN	COMMENT
3.7 ±0.5 OUR AVERAGE					
$3.56\pm0.45^{+0.57}_{-0.46}$		[1] AUBERT	08AI	BABR	$e^+e^- \to \Upsilon(4S)$
$3.89\pm0.47^{+0.43}_{-0.41}$		[1] GARMASH	06	BELL	$e^+e^- \to \Upsilon(4S)$
• • • We do not use the following data for averages, fits, limits, etc. • • •					
$5.07\pm0.75^{+0.55}_{-0.88}$		[1] AUBERT,B	05N	BABR	Repl. by AUBERT 08AI
$4.78\pm0.75^{+1.01}_{-0.97}$		[1] GARMASH	05	BELL	Repl. by GARMASH 06
< 6.2	90	[2] AUBERT,B	04P	BABR	Repl. by AUBERT,B 05N
< 12	90	[3] GARMASH	02	BELL	$e^+e^- \to \Upsilon(4S)$
< 86	90	[4] ABE	00C	SLD	$e^+e^- \to Z$
< 17	90	[1] JESSOP	00	CLE2	$e^+e^- \to \Upsilon(4S)$
<120	90	[5] ADAM	96D	DLPH	$e^+e^- \to Z$
< 19	90	ASNER	96	CLE2	Repl. by JESSOP 00
<190	90	[5] ABREU	95N	DLPH	Sup. by ADAM 96D
<180	90	ALBRECHT	91B	ARG	$e^+e^- \to \Upsilon(4S)$
< 80	90	[6] AVERY	89B	CLEO	$e^+e^- \to \Upsilon(4S)$
<260	90	AVERY	87	CLEO	$e^+e^- \to \Upsilon(4S)$

[1] Assumes equal production of B^+ and B^0 at the $\Upsilon(4S)$.
[2] AUBERT 04P reports a central value of $(3.9\pm1.2^{+1.3}_{-3.5})\times10^{-6}$ for this branching ratio.
[3] Uses a reference decay mode $B^+ \to \overline{D}^0\pi^+$ and $\overline{D}^0 \to K^+\pi^-$ with $B(B^+ \to \overline{D}^0\pi^+)\cdot B(\overline{D}^0 \to K^+\pi^-) = (20.3\pm2.0)\times10^{-5}$.
[4] ABE 00C assumes $B(Z \to b\overline{b})=(21.7\pm0.1)\%$ and the B fractions $f_{B^0}=f_{B^+}=(39.7^{+1.8}_{-2.2})\%$ and $f_{B_s}=(10.5^{+1.8}_{-2.2})\%$.
[5] Assumes production fractions $f_{B^0} = f_{B^-} = 0.39$ and $f_{B_s} = 0.12$.
[6] AVERY 89B reports $< 7\times10^{-5}$ assuming the $\Upsilon(4S)$ decays 43% to $B^0\overline{B}^0$. We rescale to 50%.

$\Gamma(K_0^*(1430)^0\pi^+)/\Gamma_{total}$ Γ_{299}/Γ

VALUE (units 10^{-6})	DOCUMENT ID		TECN	COMMENT
45 $^{+9}_{-7}$ OUR AVERAGE Error includes scale factor of 1.5.				
$32.0\pm1.2^{+10.8}_{-\ 6.0}$	[1] AUBERT	08AI	BABR	$e^+e^- \to \Upsilon(4S)$
$51.6\pm1.7^{+\ 7.0}_{-\ 7.5}$	[1] GARMASH	06	BELL	$e^+e^- \to \Upsilon(4S)$
• • • We do not use the following data for averages, fits, limits, etc. • • •				
$44.4\pm2.2\pm\ 5.3$	[1,2] AUBERT,B	05N	BABR	Repl. by AUBERT 08AI
$45.0\pm2.9^{+15.0}_{-10.7}$	[1] GARMASH	05	BELL	Repl. by GARMASH 06

[1] Assumes equal production of B^+ and B^0 at the $\Upsilon(4S)$.
[2] See erratum: AUBERT,BE 06A.

$\Gamma(K_2^*(1430)^0\pi^+)/\Gamma_{total}$ Γ_{300}/Γ

VALUE (units 10^{-6})	CL%	DOCUMENT ID		TECN	COMMENT
$5.6^{+2.2}_{-1.5}\pm0.1$		[1,2] AUBERT	08AI	BABR	$e^+e^- \to \Upsilon(4S)$
• • • We do not use the following data for averages, fits, limits, etc. • • •					
< 23	90	[3] AUBERT,B	05N	BABR	Repl. by AUBERT 08AI
< 6.9	90	[4] GARMASH	05	BELL	$e^+e^- \to \Upsilon(4S)$
<680	90	ALBRECHT	91B	ARG	$e^+e^- \to \Upsilon(4S)$

[1] Assumes equal production of B^+ and B^0 at the $\Upsilon(4S)$.
[2] AUBERT 08AI reports $(1.85\pm0.41^{+0.61}_{-0.29})\times10^{-6}$ for $B(B^+ \to K_2^*(1430)^0\pi^+)\times B(K_2^*(1430)^0 \to K^+\pi^-)$. We compute $B(B^+ \to K_2^*(1430)^0\pi^+)$ using the PDG value $B(K_2^*(1430)^0 \to K\pi)=(49.9\pm1.2)\times10^{-2}$ and 2/3 for the $K^+\pi^-$ fraction. Our first error is their experiment's error and the second error is systematic error from using our best value.
[3] AUBERT,B 05N reports 7.7×10^{-6} at 90% CL for $B(B^+ \to K_2^*(1430)^0\pi^+)\times B(K_2^*(1430)^0 \to K^+\pi^-)$. We rescaled it using the PDG value $B(K_2^*(1430)^0 \to K\pi) = 49.9\%$ and 2/3 for the $K^+\pi^-$ fraction.
[4] GARMASH 05 reports 2.3×10^{-6} at 90% CL for $B(B^+ \to K_2^*(1430)^0\pi^+)\times B(K_2^*(1430)^0 \to K^+\pi^-)$. We rescaled it using the PDG value $B(K_2^*(1430)^0 \to K\pi) = 49.9\%$ and 2/3 for the $K^+\pi^-$ mode.

$\Gamma(K^*(1410)^0\pi^+)/\Gamma_{total}$ Γ_{301}/Γ

VALUE (units 10^{-6})	CL%	DOCUMENT ID		TECN	COMMENT
<45	90	[1] GARMASH	05	BELL	$e^+e^- \to \Upsilon(4S)$

[1] GARMASH 05 reports 2.0×10^{-6} at 90% CL for $B(B^+ \to K^*(1410)^0\pi^+)\times B(K^*(1410)^0 \to K^+\pi^-)$. We rescaled it using the PDG value $B(K^*(1410)^0 \to K\pi) = 6.6\%$ and 2/3 for the $K^+\pi^-$ mode.

$\Gamma(K^*(1680)^0\pi^+)/\Gamma_{total}$ Γ_{302}/Γ

VALUE (units 10^{-6})	CL%	DOCUMENT ID		TECN	COMMENT
<12	90	[1] GARMASH	05	BELL	$e^+e^- \to \Upsilon(4S)$
• • • We do not use the following data for averages, fits, limits, etc. • • •					
<15	90	[2] AUBERT,B	05N	BABR	$e^+e^- \to \Upsilon(4S)$

[1] GARMASH 05 reports 3.1×10^{-6} at 90% CL for $B(B^+ \to K^*(1680)^0\pi^+)\times B(K^*(1680)^0 \to K^+\pi^-)$. We rescaled it using the PDG value $B(K^*(1680)^0 \to K\pi) = 38.7\%$ and 2/3 for the $K^+\pi^-$ mode.
[2] AUBERT,B 05N reports 3.8×10^{-6} at 90% CL for $B(B^+ \to K^*(1680)^0\pi^+)\times B(K^*(1680)^0 \to K^+\pi^-)$. We rescaled it using the PDG value $B(K^*(1680)^0 \to K\pi) = 38.7\%$ and 2/3 for the $K^+\pi^-$ fraction.

$\Gamma(K^+\pi^0\pi^0)/\Gamma_{total}$ Γ_{303}/Γ

VALUE (units 10^{-6})	DOCUMENT ID		TECN	COMMENT
16.2±1.2±1.5	[1] LEES	11I	BABR	$e^+e^- \to \Upsilon(4S)$

[1] Assumes equal production of B^+ and B^0 at the $\Upsilon(4S)$.

$\Gamma(f_0(980)K^+\times B(f_0 \to \pi^0\pi^0))/\Gamma_{total}$ Γ_{304}/Γ

VALUE (units 10^{-6})	DOCUMENT ID		TECN	COMMENT
2.8±0.6±0.5	[1] LEES	11I	BABR	$e^+e^- \to \Upsilon(4S)$

[1] Assumes equal production of B^+ and B^0 at the $\Upsilon(4S)$.

$\Gamma(K^-\pi^+\pi^+)/\Gamma_{total}$ Γ_{305}/Γ

VALUE (units 10^{-6})	CL%	DOCUMENT ID		TECN	COMMENT
<0.95	90	[1] AUBERT	08BE	BABR	$e^+e^- \to \Upsilon(4S)$
• • • We do not use the following data for averages, fits, limits, etc. • • •					
<4.5	90	[1] GARMASH	04	BELL	$e^+e^- \to \Upsilon(4S)$
<1.8	90	[2] AUBERT	03M	BABR	Repl. by AUBERT 08BE
<7.0	90	[3] GARMASH	02	BELL	$e^+e^- \to \Upsilon(4S)$

[1] Assumes equal production of B^+ and B^0 at the $\Upsilon(4S)$.
[2] Assumes equal production of B^0 and B^+ at the $\Upsilon(4S)$; charm and charmonium contributions are subtracted, otherwise no assumptions about intermediate resonances.
[3] Uses a reference decay mode $B^+ \to \overline{D}^0\pi^+$ and $\overline{D}^0 \to K^+\pi^-$ with $B(B^+ \to \overline{D}^0\pi^+)\cdot B(\overline{D}^0 \to K^+\pi^-) = (20.3\pm2.0)\times10^{-5}$.

$\Gamma(K^-\pi^+\pi^+\text{ nonresonant})/\Gamma_{total}$ Γ_{306}/Γ

VALUE (units 10^{-6})	CL%	DOCUMENT ID		TECN	COMMENT
<56	90	BERGFELD	96B	CLE2	$e^+e^- \to \Upsilon(4S)$

$\Gamma(K_1(1270)^0\pi^+)/\Gamma_{total}$ Γ_{307}/Γ

VALUE	CL%	DOCUMENT ID		TECN	COMMENT
$<4.0\times10^{-5}$	90	[1] AUBERT	10D	BABR	$e^+e^- \to \Upsilon(4S)$

[1] Assumes equal production of B^+ and B^0 at the $\Upsilon(4S)$.

$\Gamma(K_1(1400)^0\pi^+)/\Gamma_{total}$ Γ_{308}/Γ

VALUE	CL%	DOCUMENT ID		TECN	COMMENT
$<3.9\times10^{-5}$	90	[1] AUBERT	10D	BABR	$e^+e^- \to \Upsilon(4S)$
• • • We do not use the following data for averages, fits, limits, etc. • • •					
$<2.6\times10^{-3}$	90	ALBRECHT	91B	ARG	$e^+e^- \to \Upsilon(4S)$

[1] Assumes equal production of B^+ and B^0 at the $\Upsilon(4S)$.

$\Gamma(K^0\pi^+\pi^0)/\Gamma_{total}$ Γ_{309}/Γ

VALUE	CL%	DOCUMENT ID		TECN	COMMENT
$<66\times10^{-6}$	90	[1] ECKHART	02	CLE2	$e^+e^- \to \Upsilon(4S)$

[1] Assumes equal production of B^+ and B^0 at the $\Upsilon(4S)$.

$\Gamma(K^0\rho^+)/\Gamma_{total}$ Γ_{310}/Γ

VALUE (units 10^{-6})	CL%	DOCUMENT ID		TECN	COMMENT
$8.0^{+1.4}_{-1.3}\pm0.6$		AUBERT	07Z	BABR	$e^+e^- \to \Upsilon(4S)$
• • • We do not use the following data for averages, fits, limits, etc. • • •					
<48	90	ASNER	96	CLE2	$e^+e^- \to \Upsilon(4S)$

$\Gamma(K^*(892)^+\pi^+\pi^-)/\Gamma_{total}$ Γ_{311}/Γ

VALUE (units 10^{-6})	CL%	DOCUMENT ID		TECN	COMMENT
75.3±6.0±8.1		[1] AUBERT,B	06U	BABR	$e^+e^- \to \Upsilon(4S)$
• • • We do not use the following data for averages, fits, limits, etc. • • •					
<1100	90	ALBRECHT	91E	ARG	$e^+e^- \to \Upsilon(4S)$

[1] Assumes equal production of B^+ and B^0 at the $\Upsilon(4S)$.

$\Gamma(K^*(892)^+\rho^0)/\Gamma_{total}$ Γ_{312}/Γ

VALUE (units 10^{-6})	CL%	DOCUMENT ID		TECN	COMMENT
4.6±1.0±0.4		[1] DEL-AMO-SA...11D		BABR	$e^+e^- \to \Upsilon(4S)$
• • • We do not use the following data for averages, fits, limits, etc. • • •					
< 6.1	90	[1] AUBERT,B	06G	BABR	Repl. by DEL-AMO-SANCHEZ 11D
$10.6^{+3.0}_{-2.6}\pm2.4$		[1] AUBERT	03V	BABR	Repl. by AUBERT,B 06G
< 74	90	[2] GODANG	02	CLE2	$e^+e^- \to \Upsilon(4S)$
<900	90	ALBRECHT	91B	ARG	$e^+e^- \to \Upsilon(4S)$

[1] Assumes equal production of B^+ and B^0 at the $\Upsilon(4S)$.
[2] Assumes a helicity 00 configuration. For a helicity 11 configuration, the limit decreases to 4.9×10^{-5}.

$\Gamma(K^*(892)^+ f_0(980))/\Gamma_{total}$ Γ_{313}/Γ

VALUE (units 10^{-6})	DOCUMENT ID	TECN	COMMENT
4.2±0.6±0.3	[1] DEL-AMO-SA...11D	BABR	$e^+e^- \to \Upsilon(4S)$
• • • We do not use the following data for averages, fits, limits, etc. • • •			
5.2±1.2±0.5	[1] AUBERT,B 06G	BABR	Repl. by DEL-AMO-SANCHEZ 11D

[1] Assumes equal production of B^+ and B^0 at the $\Upsilon(4S)$.

$\Gamma(a_1^+ K^0)/\Gamma_{total}$ Γ_{314}/Γ

VALUE (units 10^{-6})	DOCUMENT ID	TECN	COMMENT
34.9±5.0±4.4	[1,2] AUBERT 08F	BABR	$e^+e^- \to \Upsilon(4S)$

[1] Assumes equal production of B^+ and B^0 at the $\Upsilon(4S)$.
[2] Assumes $a_1^\pm$ decays only to 3π and $B(a_1^\pm \to \pi^\pm\pi^\mp\pi^\pm) = 0.5$.

$\Gamma(b_1^+ K^0 \times B(b_1^+ \to \omega\pi^+))/\Gamma_{total}$ Γ_{315}/Γ

VALUE (units 10^{-6})	DOCUMENT ID	TECN	COMMENT
9.6±1.7±0.9	[1] AUBERT 08AG	BABR	$e^+e^- \to \Upsilon(4S)$

[1] Assumes equal production of B^+ and B^0 at the $\Upsilon(4S)$.

$\Gamma(K^*(892)^0 \rho^+)/\Gamma_{total}$ Γ_{316}/Γ

VALUE (units 10^{-6})	DOCUMENT ID	TECN	COMMENT
9.2±1.5 OUR AVERAGE			
9.6±1.7±1.5	[1] AUBERT,B 06G	BABR	$e^+e^- \to \Upsilon(4S)$
8.9±1.7±1.2	[1] ZHANG 05D	BELL	$e^+e^- \to \Upsilon(4S)$

[1] Assumes equal production of B^+ and B^0 at the $\Upsilon(4S)$.

$\Gamma(K_1(1400)^+ \rho^0)/\Gamma_{total}$ Γ_{317}/Γ

VALUE	CL%	DOCUMENT ID	TECN	COMMENT
<7.8 × 10^{-4}	90	ALBRECHT 91B	ARG	$e^+e^- \to \Upsilon(4S)$

$\Gamma(K_2^*(1430)^+ \rho^0)/\Gamma_{total}$ Γ_{318}/Γ

VALUE	CL%	DOCUMENT ID	TECN	COMMENT
<1.5 × 10^{-3}	90	ALBRECHT 91B	ARG	$e^+e^- \to \Upsilon(4S)$

$\Gamma(b_1^0 K^+ \times B(b_1^0 \to \omega\pi^0))/\Gamma_{total}$ Γ_{319}/Γ

VALUE (units 10^{-6})	DOCUMENT ID	TECN	COMMENT
9.1±1.7±1.0	[1] AUBERT 07BI	BABR	$e^+e^- \to \Upsilon(4S)$

[1] Assumes equal production of B^+ and B^0 at the $\Upsilon(4S)$.

$\Gamma(b_1^+ K^{*0} \times B(b_1^+ \to \omega\pi^+))/\Gamma_{total}$ Γ_{320}/Γ

VALUE	CL%	DOCUMENT ID	TECN	COMMENT
<5.9 × 10^{-6}	90	[1] AUBERT 09AF	BABR	$e^+e^- \to \Upsilon(4S)$

[1] Assumes equal production of B^+ and B^0 at the $\Upsilon(4S)$.

$\Gamma(b_1^0 K^{*+} \times B(b_1^0 \to \omega\pi^0))/\Gamma_{total}$ Γ_{321}/Γ

VALUE	CL%	DOCUMENT ID	TECN	COMMENT
<6.7 × 10^{-6}	90	[1] AUBERT 09AF	BABR	$e^+e^- \to \Upsilon(4S)$

[1] Assumes equal production of B^+ and B^0 at the $\Upsilon(4S)$.

$\Gamma(K^+\overline{K}^0)/\Gamma_{total}$ Γ_{322}/Γ

VALUE (units 10^{-6})	CL%	DOCUMENT ID	TECN	COMMENT
1.31±0.17 OUR FIT Error includes scale factor of 1.2.				
1.19±0.18 OUR AVERAGE				
1.11±0.19±0.05		[1] DUH 13	BELL	$e^+e^- \to \Upsilon(4S)$
1.61±0.44±0.09		[1] AUBERT,BE 06C	BABR	$e^+e^- \to \Upsilon(4S)$
• • • We do not use the following data for averages, fits, limits, etc. • • •				
$1.22^{+0.32+0.13}_{-0.28-0.16}$		[1] LIN 07	BELL	Repl. by DUH 13
1.0 ±0.4 ±0.1		[1] ABE 05G	BELL	Repl. by LIN 07
1.5 ±0.5 ±0.1		[1] AUBERT,BE 05E	BABR	Repl. by AUBERT,BE 06C
< 2.5	90	[1] AUBERT 04M	BABR	Repl. by AUBERT,BE 05E
< 3.3	90	[1] CHAO 04	BELL	$e^+e^- \to \Upsilon(4S)$
< 3.3	90	[1] BORNHEIM 03	CLE2	$e^+e^- \to \Upsilon(4S)$
< 2.0	90	[1] CASEY 02	BELL	Repl. by CHAO 04
< 5.0	90	[1] ABE 01H	BELL	$e^+e^- \to \Upsilon(4S)$
< 2.4	90	[1] AUBERT 01E	BABR	$e^+e^- \to \Upsilon(4S)$
< 5.1	90	[1] CRONIN-HEN...00	CLE2	$e^+e^- \to \Upsilon(4S)$
<21	90	GODANG 98	CLE2	Repl. by CRONIN-HENNESSY 00

[1] Assumes equal production of B^+ and B^0 at the $\Upsilon(4S)$.

$\Gamma(K^+\overline{K}^0)/\Gamma(K^0\pi^+)$ $\Gamma_{322}/\Gamma_{262}$

VALUE	DOCUMENT ID	TECN	COMMENT
0.055±0.007 OUR FIT Error includes scale factor of 1.2.			
0.064±0.009±0.004	AAIJ 13BS	LHCB	pp at 7 TeV

$\Gamma(\overline{K}^0 K^+\pi^0)/\Gamma_{total}$ Γ_{323}/Γ

VALUE	CL%	DOCUMENT ID	TECN	COMMENT
<24 × 10^{-6}	90	[1] ECKHART 02	CLE2	$e^+e^- \to \Upsilon(4S)$

[1] Assumes equal production of B^+ and B^0 at the $\Upsilon(4S)$.

$\Gamma(K^+ K_S^0 K_S^0)/\Gamma_{total}$ Γ_{324}/Γ

VALUE (units 10^{-6})	DOCUMENT ID	TECN	COMMENT
10.8±0.6 OUR AVERAGE			
10.6±0.5±0.3	[1,2] LEES 12O	BABR	$e^+e^- \to \Upsilon(4S)$
13.4±1.9±1.5	[1] GARMASH 04	BELL	$e^+e^- \to \Upsilon(4S)$
• • • We do not use the following data for averages, fits, limits, etc. • • •			
10.7±1.2±1.0	[1] AUBERT,B 04V	BABR	Repl. by LEES 12O

[1] Assumes equal production of B^+ and B^0 at the $\Upsilon(4S)$.
[2] All intermediate charmonium and charm resonances are removed, except of χ_{c0}.

$\Gamma(f_0(980) K^+,\ f_0 \to K_S^0 K_S^0)/\Gamma_{total}$ Γ_{325}/Γ

VALUE (units 10^{-6})	DOCUMENT ID	TECN	COMMENT
14.7±2.8±1.8	[1] LEES 12O	BABR	$e^+e^- \to \Upsilon(4S)$

[1] Assumes equal production of B^+ and B^0 at the $\Upsilon(4S)$.

$\Gamma(f_0(1710) K^+,\ f_0 \to K_S^0 K_S^0)/\Gamma_{total}$ Γ_{326}/Γ

VALUE (units 10^{-6})	DOCUMENT ID	TECN	COMMENT
$0.48^{+0.40}_{-0.24}$±0.11	[1] LEES 12O	BABR	$e^+e^- \to \Upsilon(4S)$

[1] Assumes equal production of B^+ and B^0 at the $\Upsilon(4S)$.

$\Gamma(K^+ K_S^0 K_S^0 \text{ nonresonant})/\Gamma_{total}$ Γ_{327}/Γ

VALUE (units 10^{-6})	DOCUMENT ID	TECN	COMMENT
19.8±3.7±2.5	[1] LEES 12O	BABR	$e^+e^- \to \Upsilon(4S)$

[1] Assumes equal production of B^+ and B^0 at the $\Upsilon(4S)$.

$\Gamma(K_S^0 K_S^0 \pi^+)/\Gamma_{total}$ Γ_{328}/Γ

VALUE (units 10^{-6})	CL%	DOCUMENT ID	TECN	COMMENT
<0.51	90	[1] AUBERT 09J	BABR	$e^+e^- \to \Upsilon(4S)$
• • • We do not use the following data for averages, fits, limits, etc. • • •				
<3.2	90	[1] GARMASH 04	BELL	$e^+e^- \to \Upsilon(4S)$

[1] Assumes equal production of B^+ and B^0 at the $\Upsilon(4S)$.

$\Gamma(K^+ K^-\pi^+)/\Gamma_{total}$ Γ_{329}/Γ

VALUE (units 10^{-6})	CL%	DOCUMENT ID	TECN	COMMENT
5.0±0.5±0.5		[1] AUBERT 07BB	BABR	$e^+e^- \to \Upsilon(4S)$
• • • We do not use the following data for averages, fits, limits, etc. • • •				
<13	90	[1] GARMASH 04	BELL	$e^+e^- \to \Upsilon(4S)$
< 6.3	90	[1,2] AUBERT 03M	BABR	Repl. by AUBERT 07BB
<12	90	[3] GARMASH 02	BELL	$e^+e^- \to \Upsilon(4S)$

[1] Assumes equal production of B^+ and B^0 at the $\Upsilon(4S)$.
[2] Charm and charmonium contributions are subtracted, otherwise no assumptions about intermediate resonances.
[3] Uses a reference decay mode $B^+ \to \overline{D}^0\pi^+$ and $\overline{D}^0 \to K^+\pi^-$ with $B(B^+ \to \overline{D}^0\pi^+)\cdot B(\overline{D}^0 \to K^+\pi^-) = (20.3 \pm 2.0) \times 10^{-5}$.

$\Gamma(K^+ K^-\pi^+ \text{ nonresonant})/\Gamma_{total}$ Γ_{330}/Γ

VALUE (units 10^{-6})	CL%	DOCUMENT ID	TECN	COMMENT
<75	90	BERGFELD 96B	CLE2	$e^+e^- \to \Upsilon(4S)$

$\Gamma(K^+\overline{K}^*(892)^0)/\Gamma_{total}$ Γ_{331}/Γ

VALUE (units 10^{-6})	CL%	DOCUMENT ID	TECN	COMMENT
< 1.1	90	[1] AUBERT 07AR	BABR	$e^+e^- \to \Upsilon(4S)$
• • • We do not use the following data for averages, fits, limits, etc. • • •				
<129	90	ABBIENDI 00B	OPAL	$e^+e^- \to Z$
<138	90	[2] ABE 00C	SLD	$e^+e^- \to Z$
< 5.3	90	[1] JESSOP 00	CLE2	$e^+e^- \to \Upsilon(4S)$

[1] Assumes equal production of B^+ and B^0 at the $\Upsilon(4S)$.
[2] ABE 00C assumes $B(Z \to b\overline{b})$=(21.7 ± 0.1)% and the B fractions $f_{B^0}=f_{B^+}=(39.7^{+1.8}_{-2.2})\%$ and $f_{B_s}=(10.5^{+1.8}_{-2.2})\%$.

$\Gamma(K^+\overline{K}_0^*(1430)^0)/\Gamma_{total}$ Γ_{332}/Γ

VALUE (units 10^{-6})	CL%	DOCUMENT ID	TECN	COMMENT
<2.2	90	[1] AUBERT 07AR	BABR	$e^+e^- \to \Upsilon(4S)$

[1] Assumes equal production of B^+ and B^0 at the $\Upsilon(4S)$.

$\Gamma(K^+ K^+\pi^-)/\Gamma_{total}$ Γ_{333}/Γ

VALUE	CL%	DOCUMENT ID	TECN	COMMENT
<1.6 × 10^{-7}	90	[1] AUBERT 08BE	BABR	$e^+e^- \to \Upsilon(4S)$
• • • We do not use the following data for averages, fits, limits, etc. • • •				
<2.4 × 10^{-6}	90	[1] GARMASH 04	BELL	$e^+e^- \to \Upsilon(4S)$
<1.3 × 10^{-6}	90	[2] AUBERT 03M	BABR	Repl. by AUBERT 08BE
<3.2 × 10^{-6}	90	[3] GARMASH 02	BELL	$e^+e^- \to \Upsilon(4S)$

[1] Assumes equal production of B^+ and B^0 at the $\Upsilon(4S)$.
[2] Assumes equal production of B^0 and B^+ at the $\Upsilon(4S)$; charm and charmonium contributions are subtracted, otherwise no assumptions about intermediate resonances.
[3] Uses a reference decay mode $B^+ \to \overline{D}^0\pi^+$ and $\overline{D}^0 \to K^+\pi^-$ with $B(B^+ \to \overline{D}^0\pi^+)\cdot B(\overline{D}^0 \to K^+\pi^-) = (20.3 \pm 2.0) \times 10^{-5}$.

$\Gamma(K^+K^+\pi^-\text{ nonresonant})/\Gamma_{\text{total}}$ Γ_{334}/Γ

VALUE (units 10^{-6})	CL%	DOCUMENT ID		TECN	COMMENT
<87.9	90	ABBIENDI	00B	OPAL	$e^+e^- \to Z$

$\Gamma(f_2'(1525)K^+)/\Gamma_{\text{total}}$ Γ_{335}/Γ

VALUE (units 10^{-6})	CL%	DOCUMENT ID		TECN	COMMENT
1.8 ±0.5 OUR AVERAGE		Error includes scale factor of 1.1.			
$1.56\pm0.36\pm0.30$		[1,2] LEES	12O	BABR	$e^+e^- \to \Upsilon(4S)$
$2.8 \pm0.9 \,^{+0.5}_{-0.4}$		[1,3] LEES	12O	BABR	$e^+e^- \to \Upsilon(4S)$
• • • We do not use the following data for averages, fits, limits, etc. • • •					
<8	90	[1,4] GARMASH	05	BELL	$e^+e^- \to \Upsilon(4S)$

[1] Assumes equal production of B^+ and B^0 at the $\Upsilon(4S)$.
[2] Measured in the $B^+ \to K^+K^-K^+$ decay.
[3] Measured in the $B^+ \to K^+K^0_SK^0_S$ decay.
[4] GARMASH 05 reports $B(B^+ \to f_2'(1525)K^+)\cdot B(f_2'(1525) \to K^+K^-) < 4.9\times10^{-6}$ at 90% CL. We divide this result by our best value of $B(f_2'(1525) \to K\overline{K}) = 88.7\times10^{-2}$ multiplied by 2/3 to account for the K^+K^- fraction.

$\Gamma(K^+f_J(2220))/\Gamma_{\text{total}}$ Γ_{336}/Γ

VALUE (units 10^{-6})	DOCUMENT ID		TECN	COMMENT
not seen	[1] HUANG	03	BELL	$e^+e^- \to \Upsilon(4S)$

[1] No evidence is found for such decay and set a limit on $B(B^+ \to f_J(2220))\times B(f_J(2220) \to \phi\phi) < 1.2\times10^{-6}$ at 90%CL where the $f_J(2220)$ is a possible glueball state.

$\Gamma(K^{*+}\pi^+K^-)/\Gamma_{\text{total}}$ Γ_{337}/Γ

VALUE (units 10^{-6})	CL%	DOCUMENT ID		TECN	COMMENT
<11.8	90	[1] AUBERT,B	06U	BABR	$e^+e^- \to \Upsilon(4S)$

[1] Assumes equal production of B^+ and B^0 at the $\Upsilon(4S)$.

$\Gamma(K^*(892)^+K^*(892)^0)/\Gamma_{\text{total}}$ Γ_{338}/Γ

VALUE (units 10^{-6})	CL%	DOCUMENT ID		TECN	COMMENT
1.2±0.5±0.1		AUBERT	09F	BABR	$e^+e^- \to \Upsilon(4S)$
• • • We do not use the following data for averages, fits, limits, etc. • • •					
<71	90	[1] GODANG	02	CLE2	$e^+e^- \to \Upsilon(4S)$

[1] Assumes a helicity 00 configuration. For a helicity 11 configuration, the limit decreases to 4.8×10^{-5}.

$\Gamma(K^{*+}K^+\pi^-)/\Gamma_{\text{total}}$ Γ_{339}/Γ

VALUE (units 10^{-6})	CL%	DOCUMENT ID		TECN	COMMENT
<6.1	90	[1] AUBERT,B	06U	BABR	$e^+e^- \to \Upsilon(4S)$

[1] Assumes equal production of B^+ and B^0 at the $\Upsilon(4S)$.

$\Gamma(K^+K^-K^+)/\Gamma_{\text{total}}$ Γ_{340}/Γ

VALUE (units 10^{-6})	CL%	DOCUMENT ID		TECN	COMMENT
34.0±1.4 OUR AVERAGE		Error includes scale factor of 1.4.			
$34.6\pm0.6\pm0.9$		[1,2] LEES	12O	BABR	$e^+e^- \to \Upsilon(4S)$
$30.6\pm1.2\pm2.3$		[1] GARMASH	05	BELL	$e^+e^- \to \Upsilon(4S)$
• • • We do not use the following data for averages, fits, limits, etc. • • •					
$35.2\pm0.9\pm1.6$		[1] AUBERT	06O	BABR	Repl. by LEES 12O
$32.8\pm1.8\pm2.8$		[1] GARMASH	04	BELL	Repl. by GARMASH 05
$29.6\pm2.1\pm1.6$		[3] AUBERT	03M	BABR	Repl. by AUBERT 06O
$35.3\pm3.7\pm4.5$		[4] GARMASH	02	BELL	Repl. by GARMASH 04
<200	90	[5] ADAM	96D	DLPH	$e^+e^- \to Z$
<320	90	[5] ABREU	95N	DLPH	Sup. by ADAM 96D
<350	90	ALBRECHT	91E	ARG	$e^+e^- \to \Upsilon(4S)$

[1] Assumes equal production of B^+ and B^0 at the $\Upsilon(4S)$.
[2] All intermediate charmonium and charm resonances are removed, except of χ_{c0}.
[3] Assumes equal production of B^0 and B^+ at the $\Upsilon(4S)$; charm and charmonium contributions are subtracted, otherwise no assumptions about intermediate resonances.
[4] Uses a reference decay mode $B^+ \to \overline{D}^0\pi^+$ and $\overline{D}^0 \to K^+\pi^-$ with $B(B^+ \to \overline{D}^0\pi^+)\cdot B(\overline{D}^0 \to K^+\pi^-) = (20.3\pm2.0)\times10^{-5}$.
[5] Assumes B^0 and B^- production fractions of 0.39, and B_s production fraction of 0.12.

$\Gamma(K^+\phi)/\Gamma_{\text{total}}$ Γ_{341}/Γ

VALUE (units 10^{-6})	CL%	DOCUMENT ID		TECN	COMMENT
8.8 $^{+0.7}_{-0.6}$ OUR AVERAGE		Error includes scale factor of 1.1.			
$9.2 \pm0.4 \,^{+0.7}_{-0.5}$		[1] LEES	12O	BABR	$e^+e^- \to \Upsilon(4S)$
$7.6 \pm1.3 \pm0.6$		[2] ACOSTA	05J	CDF	$p\overline{p}$ at 1.96 TeV
$9.60\pm0.92 \,^{+1.05}_{-0.85}$		[1] GARMASH	05	BELL	$e^+e^- \to \Upsilon(4S)$
$5.5 \,^{+2.1}_{-1.8} \pm0.6$		[1] BRIERE	01	CLE2	$e^+e^- \to \Upsilon(4S)$
• • • We do not use the following data for averages, fits, limits, etc. • • •					
$8.4 \pm0.7 \pm0.7$		[1] AUBERT	06O	BABR	Repl. by LEES 12O
$10.0 \,^{+0.9}_{-0.8} \pm0.5$		[1] AUBERT	04A	BABR	Repl. by AUBERT 06O
$9.4 \pm1.1 \pm0.7$		[1] CHEN	03B	BELL	Repl. by GARMASH 05
$14.6 \,^{+3.0}_{-2.8} \pm2.0$		[3] GARMASH	02	BELL	Repl. by CHEN 03B
$7.7 \,^{+1.6}_{-1.4} \pm0.8$		[1] AUBERT	01D	BABR	$e^+e^- \to \Upsilon(4S)$
<144	90	[4] ABE	00C	SLD	$e^+e^- \to Z$
< 5	90	[1] BERGFELD	98	CLE2	
<280	90	[5] ADAM	96D	DLPH	$e^+e^- \to Z$
< 12	90	ASNER	96	CLE2	$e^+e^- \to \Upsilon(4S)$
<440	90	[6] ABREU	95N	DLPH	Sup. by ADAM 96D
<180	90	ALBRECHT	91B	ARG	$e^+e^- \to \Upsilon(4S)$
< 90	90	[7] AVERY	89B	CLEO	$e^+e^- \to \Upsilon(4S)$
<210	90	AVERY	87	CLEO	$e^+e^- \to \Upsilon(4S)$

[1] Assumes equal production of B^+ and B^0 at the $\Upsilon(4S)$.
[2] Uses $B(B^+ \to J/\psi K^+) = (1.00\pm0.04)\times10^{-3}$ and $B(J/\psi \to \mu^+\mu^-) = 0.0588\pm0.0010$.
[3] Uses a reference decay mode $B^+ \to \overline{D}^0\pi^+$ and $\overline{D}^0 \to K^+\pi^-$ with $B(B^+ \to \overline{D}^0\pi^+)\cdot B(\overline{D}^0 \to K^+\pi^-) = (20.3\pm2.0)\times10^{-5}$.
[4] ABE 00C assumes $B(Z \to b\overline{b}) = (21.7\pm0.1)\%$ and the B fractions $f_{B^0} = f_{B^+} = (39.7 \,^{+1.8}_{-2.2})\%$ and $f_{B_s} = (10.5 \,^{+1.8}_{-2.2})\%$.
[5] ADAM 96D assumes $f_{B^0} = f_{B^-} = 0.39$ and $f_{B_s} = 0.12$.
[6] Assumes a B^0, B^- production fraction of 0.39 and a B_s production fraction of 0.12.
[7] AVERY 89B reports $< 8\times10^{-5}$ assuming the $\Upsilon(4S)$ decays 43% to $B^0\overline{B}^0$. We rescale to 50%.

$\Gamma(f_0(980)K^+\times B(f_0(980) \to K^+K^-))/\Gamma_{\text{total}}$ Γ_{342}/Γ

VALUE (units 10^{-6})	CL%	DOCUMENT ID		TECN	COMMENT
9.4±1.6±2.8		[1] LEES	12O	BABR	$e^+e^- \to \Upsilon(4S)$
• • • We do not use the following data for averages, fits, limits, etc. • • •					
$6.5\pm2.5\pm1.6$		[1] AUBERT	06O	BABR	$e^+e^- \to \Upsilon(4S)$
<2.9	90	[1] GARMASH	05	BELL	$e^+e^- \to \Upsilon(4S)$

[1] Assumes equal production of B^+ and B^0 at the $\Upsilon(4S)$.

$\Gamma(a_2(1320)K^+\times B(a_2(1320) \to K^+K^-))/\Gamma_{\text{total}}$ Γ_{343}/Γ

VALUE	CL%	DOCUMENT ID		TECN	COMMENT
<1.1 × 10⁻⁶	90	[1] GARMASH	05	BELL	$e^+e^- \to \Upsilon(4S)$

[1] Assumes equal production of B^+ and B^0 at the $\Upsilon(4S)$.

$\Gamma(X_0(1550)K^+\times B(X_0(1550) \to K^+K^-))/\Gamma_{\text{total}}$ Γ_{344}/Γ

$X_0(1550)$ is a possible spin zero state near 1.55 GeV/c^2 invariant mass of K^+K^-.

VALUE (units 10^{-6})	DOCUMENT ID		TECN	COMMENT
4.3±0.6±0.3	[1] AUBERT	06O	BABR	$e^+e^- \to \Upsilon(4S)$

[1] Assumes equal production of B^+ and B^0 at the $\Upsilon(4S)$.

$\Gamma(\phi(1680)K^+\times B(\phi(1680) \to K^+K^-))/\Gamma_{\text{total}}$ Γ_{345}/Γ

VALUE	CL%	DOCUMENT ID		TECN	COMMENT
<0.8 × 10⁻⁶	90	[1] GARMASH	05	BELL	$e^+e^- \to \Upsilon(4S)$

[1] Assumes equal production of B^+ and B^0 at the $\Upsilon(4S)$.

$\Gamma(f_0(1710)K^+\times B(f_0(1710) \to K^+K^-))/\Gamma_{\text{total}}$ Γ_{346}/Γ

VALUE (units 10^{-6})	DOCUMENT ID		TECN	COMMENT
1.12±0.25±0.50	[1] LEES	12O	BABR	$e^+e^- \to \Upsilon(4S)$
• • • We do not use the following data for averages, fits, limits, etc. • • •				
$1.7 \pm1.0 \pm0.3$	[1] AUBERT	06O	BABR	Repl. by LEES 12O

[1] Assumes equal production of B^+ and B^0 at the $\Upsilon(4S)$.

$\Gamma(K^+K^-K^+\text{ nonresonant})/\Gamma_{\text{total}}$ Γ_{347}/Γ

VALUE (units 10^{-6})	CL%	DOCUMENT ID		TECN	COMMENT
23.8 $^{+2.8}_{-5.0}$ OUR AVERAGE					
$22.8\pm2.7\pm7.6$		[1] LEES	12O	BABR	$e^+e^- \to \Upsilon(4S)$
$24.0\pm1.5 \,^{+2.6}_{-6.0}$		[1] GARMASH	05	BELL	$e^+e^- \to \Upsilon(4S)$
• • • We do not use the following data for averages, fits, limits, etc. • • •					
$50.0\pm6.0\pm4.0$		[1] AUBERT	06O	BABR	Repl. by LEES 12O
<38	90	BERGFELD	96B	CLE2	$e^+e^- \to \Upsilon(4S)$

[1] Assumes equal production of B^+ and B^0 at the $\Upsilon(4S)$.

$\Gamma(K^*(892)^+K^+K^-)/\Gamma_{\text{total}}$ Γ_{348}/Γ

VALUE (units 10^{-6})	CL%	DOCUMENT ID		TECN	COMMENT
36.2±3.3±3.6		[1] AUBERT,B	06U	BABR	$e^+e^- \to \Upsilon(4S)$
• • • We do not use the following data for averages, fits, limits, etc. • • •					
<1600	90	ALBRECHT	91E	ARG	$e^+e^- \to \Upsilon(4S)$

[1] Assumes equal production of B^+ and B^0 at the $\Upsilon(4S)$.

Meson Particle Listings

$B^{\pm}$

$\Gamma(K^*(892)^+\phi)/\Gamma_{total}$ Γ_{349}/Γ

VALUE (units 10^{-6})	CL%	DOCUMENT ID		TECN	COMMENT
10.0±2.0 OUR AVERAGE		Error includes scale factor of 1.7.			
$11.2\pm1.0\pm0.9$		[1] AUBERT	07BA	BABR	$e^+e^- \to \Upsilon(4S)$
$6.7^{+2.1}_{-1.9}{}^{+0.7}_{-1.0}$		[1] CHEN	03B	BELL	$e^+e^- \to \Upsilon(4S)$
• • • We do not use the following data for averages, fits, limits, etc. • • •					
$12.7^{+2.2}_{-2.0}\pm1.1$		[1] AUBERT	03V	BABR	Repl. by AUBERT 07BA
$9.7^{+4.2}_{-3.4}\pm1.7$		[1] AUBERT	01D	BABR	Repl. by AUBERT 03V
< 22.5	90	[1] BRIERE	01	CLE2	$e^+e^- \to \Upsilon(4S)$
< 41	90	[1] BERGFELD	98	CLE2	
< 70	90	ASNER	96	CLE2	$e^+e^- \to \Upsilon(4S)$
<1300	90	ALBRECHT	91B	ARG	$e^+e^- \to \Upsilon(4S)$

[1] Assumes equal production of B^+ and B^0 at the $\Upsilon(4S)$.

$\Gamma(\phi(K\pi)_0^{*+})/\Gamma_{total}$ Γ_{350}/Γ

$(K\pi)_0^{*+}$ is the total S-wave composed of $K_0^*(1430)$ and nonresonant that are described using LASS shape.

VALUE (units 10^{-6})	DOCUMENT ID		TECN	COMMENT
8.3±1.4±0.8	[1] AUBERT	08BI	BABR	$e^+e^- \to \Upsilon(4S)$

[1] Assumes equal production of B^+ and B^0 at the $\Upsilon(4S)$.

$\Gamma(\phi K_1(1270)^+)/\Gamma_{total}$ Γ_{351}/Γ

VALUE (units 10^{-6})	DOCUMENT ID		TECN	COMMENT
6.1±1.6±1.1	[1] AUBERT	08BI	BABR	$e^+e^- \to \Upsilon(4S)$

[1] Assumes equal production of B^+ and B^0 at the $\Upsilon(4S)$.

$\Gamma(\phi K_1(1400)^+)/\Gamma_{total}$ Γ_{352}/Γ

VALUE (units 10^{-6})	CL%	DOCUMENT ID		TECN	COMMENT
< 3.2	90	[1] AUBERT	08BI	BABR	$e^+e^- \to \Upsilon(4S)$
• • • We do not use the following data for averages, fits, limits, etc. • • •					
<1100	90	ALBRECHT	91B	ARG	$e^+e^- \to \Upsilon(4S)$

[1] Assumes equal production of B^+ and B^0 at the $\Upsilon(4S)$.

$\Gamma(\phi K^*(1410)^+)/\Gamma_{total}$ Γ_{353}/Γ

VALUE (units 10^{-6})	CL%	DOCUMENT ID		TECN	COMMENT
<4.3	90	[1] AUBERT	08BI	BABR	$e^+e^- \to \Upsilon(4S)$

[1] Assumes equal production of B^+ and B^0 at the $\Upsilon(4S)$.

$\Gamma(\phi K_0^*(1430)^+)/\Gamma_{total}$ Γ_{354}/Γ

VALUE (units 10^{-6})	DOCUMENT ID		TECN	COMMENT
7.0±1.3±0.9	[1] AUBERT	08BI	BABR	$e^+e^- \to \Upsilon(4S)$

[1] Assumes equal production of B^+ and B^0 at the $\Upsilon(4S)$.

$\Gamma(\phi K_2^*(1430)^+)/\Gamma_{total}$ Γ_{355}/Γ

VALUE (units 10^{-6})	CL%	DOCUMENT ID		TECN	COMMENT
8.4±1.8±1.0		[1] AUBERT	08BI	BABR	$e^+e^- \to \Upsilon(4S)$
• • • We do not use the following data for averages, fits, limits, etc. • • •					
<3400	90	ALBRECHT	91B	ARG	$e^+e^- \to \Upsilon(4S)$

[1] Assumes equal production of B^+ and B^0 at the $\Upsilon(4S)$.

$\Gamma(\phi K_2^*(1770)^+)/\Gamma_{total}$ Γ_{356}/Γ

VALUE (units 10^{-6})	CL%	DOCUMENT ID		TECN	COMMENT
<15.0	90	[1] AUBERT	08BI	BABR	$e^+e^- \to \Upsilon(4S)$

[1] Assumes equal production of B^+ and B^0 at the $\Upsilon(4S)$.

$\Gamma(\phi K_2^*(1820)^+)/\Gamma_{total}$ Γ_{357}/Γ

VALUE (units 10^{-6})	CL%	DOCUMENT ID		TECN	COMMENT
<16.3	90	[1] AUBERT	08BI	BABR	$e^+e^- \to \Upsilon(4S)$

[1] Assumes equal production of B^+ and B^0 at the $\Upsilon(4S)$.

$\Gamma(a_1^+ K^{*0})/\Gamma_{total}$ Γ_{358}/Γ

VALUE (units 10^{-6})	CL%	DOCUMENT ID		TECN	COMMENT
<3.6	90	[1,2] DEL-AMO-SA...10I		BABR	$e^+e^- \to \Upsilon(4S)$

[1] Assumes $B(a_1^{\pm} \to \pi^{\pm}\pi^{\mp}\pi^{\pm}) = 0.5$

[2] Assumes equal production of B^+ and B^0 at the $\Upsilon(4S)$.

$\Gamma(K^+\phi\phi)/\Gamma_{total}$ Γ_{359}/Γ

VALUE (units 10^{-6})	DOCUMENT ID		TECN	COMMENT
5.0±1.2 OUR AVERAGE	Error includes scale factor of 2.3.			
$5.6\pm0.5\pm0.3$	[1] LEES	11A	BABR	$e^+e^- \to \Upsilon(4S)$
$2.6^{+1.1}_{-0.9}\pm0.3$	[1] HUANG	03	BELL	$e^+e^- \to \Upsilon(4S)$
• • • We do not use the following data for averages, fits, limits, etc. • • •				
$7.5\pm1.0\pm0.7$	[1] AUBERT,BE	06H	BABR	Repl. by LEES 11A

[1] Assumes equal production of B^0 and B^+ at the $\Upsilon(4S)$ and for a $\phi\phi$ invariant mass below 2.85 GeV/c^2.

$\Gamma(\eta'\eta' K^+)/\Gamma_{total}$ Γ_{360}/Γ

VALUE (units 10^{-6})	CL%	DOCUMENT ID		TECN	COMMENT
<25	90	[1] AUBERT,B	06P	BABR	$e^+e^- \to \Upsilon(4S)$

[1] Assumes equal production of B^+ and B^0 at the $\Upsilon(4S)$.

$\Gamma(\omega\phi K^+)/\Gamma_{total}$ Γ_{361}/Γ

VALUE (units 10^{-6})	CL%	DOCUMENT ID		TECN	COMMENT
<1.9	90	[1] LIU	09	BELL	$e^+e^- \to \Upsilon(4S)$

[1] Assumes equal production of B^+ and B^0 at the $\Upsilon(4S)$.

$\Gamma(X(1812)K^+ \times B(X \to \omega\phi))/\Gamma_{total}$ Γ_{362}/Γ

VALUE (units 10^{-6})	CL%	DOCUMENT ID		TECN	COMMENT
<0.32	90	[1] LIU	09	BELL	$e^+e^- \to \Upsilon(4S)$

[1] Assumes equal production of B^+ and B^0 at the $\Upsilon(4S)$.

$\Gamma(K^*(892)^+\gamma)/\Gamma_{total}$ Γ_{363}/Γ

VALUE (units 10^{-5})	CL%	DOCUMENT ID		TECN	COMMENT
4.21±0.18 OUR AVERAGE					
$4.22\pm0.14\pm0.16$		[1] AUBERT	09AO	BABR	$e^+e^- \to \Upsilon(4S)$
$4.25\pm0.31\pm0.24$		[2] NAKAO	04	BELL	$e^+e^- \to \Upsilon(4S)$
$3.76^{+0.89}_{-0.83}\pm0.28$		[2] COAN	00	CLE2	$e^+e^- \to \Upsilon(4S)$
• • • We do not use the following data for averages, fits, limits, etc. • • •					
$3.87\pm0.28\pm0.26$		[3] AUBERT,BE	04A	BABR	Repl. by AUBERT 09AO
$3.83\pm0.62\pm0.22$		[2] AUBERT	02C	BABR	Repl. by AUBERT,BE 04A
$5.7 \pm3.1 \pm1.1$		[4] AMMAR	93	CLE2	Repl. by COAN 00
< 55	90	[5] ALBRECHT	89G	ARG	$e^+e^- \to \Upsilon(4S)$
< 55	90	[5] AVERY	89B	CLEO	$e^+e^- \to \Upsilon(4S)$
<180	90	AVERY	87	CLEO	$e^+e^- \to \Upsilon(4S)$

[1] Uses $B(\Upsilon(4S) \to B^+B^-) = (51.6\pm0.6)\%$ and $B(\Upsilon(4S) \to B^0\overline{B}{}^0) = (48.4\pm0.6)\%$.

[2] Assumes equal production of B^+ and B^0 at the $\Upsilon(4S)$.

[3] Uses the production ratio of charged and neutral B from $\Upsilon(4S)$ decays $R^{+/0} = 1.006 \pm 0.048$.

[4] AMMAR 93 observed 4.1 ± 2.3 events above background.

[5] Assumes the $\Upsilon(4S)$ decays 43% to $B^0\overline{B}{}^0$.

$\Gamma(K_1(1270)^+\gamma)/\Gamma_{total}$ Γ_{364}/Γ

VALUE (units 10^{-5})	CL%	DOCUMENT ID		TECN	COMMENT
4.3±0.9±0.9		[1] YANG	05	BELL	$e^+e^- \to \Upsilon(4S)$
• • • We do not use the following data for averages, fits, limits, etc. • • •					
< 9.9	90	[1] NISHIDA	02	BELL	Repl. by YANG 05
<730	90	[2] ALBRECHT	89G	ARG	$e^+e^- \to \Upsilon(4S)$

[1] Assumes equal production of B^+ and B^0 at the $\Upsilon(4S)$.

[2] ALBRECHT 89G reports < 0.0066 assuming the $\Upsilon(4S)$ decays 45% to $B^0\overline{B}{}^0$. We rescale to 50%.

$\Gamma(\eta K^+\gamma)/\Gamma_{total}$ Γ_{365}/Γ

VALUE (units 10^{-6})	DOCUMENT ID		TECN	COMMENT
7.9±0.9 OUR AVERAGE				
$7.7\pm1.0\pm0.4$	[1,2] AUBERT	09	BABR	$e^+e^- \to \Upsilon(4S)$
$8.4\pm1.5^{+1.2}_{-0.9}$	[2,3] NISHIDA	05	BELL	$e^+e^- \to \Upsilon(4S)$
• • • We do not use the following data for averages, fits, limits, etc. • • •				
$10.0\pm1.3\pm0.5$	[1,2] AUBERT,B	06M	BABR	Repl. by AUBERT 09

[1] $m_{\eta K} < 3.25$ GeV/c^2.

[2] Assumes equal production of B^+ and B^0 at the $\Upsilon(4S)$.

[3] $m_{\eta K} < 2.4$ GeV/c^2

$\Gamma(\eta' K^+\gamma)/\Gamma_{total}$ Γ_{366}/Γ

VALUE (units 10^{-6})	DOCUMENT ID		TECN	COMMENT
$2.9^{+1.0}_{-0.9}$ OUR AVERAGE				
$3.6\pm1.2\pm0.4$	[1,2] WEDD	10	BELL	$e^+e^- \to \Upsilon(4S)$
$1.9^{+1.5}_{-1.2}\pm0.1$	[1,3] AUBERT,B	06M	BABR	$e^+e^- \to \Upsilon(4S)$

[1] Assumes equal production of B^+ and B^0 at the $\Upsilon(4S)$.

[2] $m_{\eta' K} < 3.4$ GeV/c^2.

[3] Set the upper limit of 4.2×10^{-6} at 90% CL with $m_{\eta' K} < 3.25$ GeV/c^2.

$\Gamma(\phi K^+\gamma)/\Gamma_{total}$ Γ_{367}/Γ

VALUE (units 10^{-6})	DOCUMENT ID		TECN	COMMENT
2.7 ±0.4 OUR AVERAGE	Error includes scale factor of 1.2.			
$2.48\pm0.30\pm0.24$	[1] SAHOO	11A	BELL	$e^+e^- \to \Upsilon(4S)$
$3.5 \pm0.6 \pm0.4$	[1] AUBERT	07Q	BABR	$e^+e^- \to \Upsilon(4S)$
• • • We do not use the following data for averages, fits, limits, etc. • • •				
$3.4 \pm0.9 \pm0.4$	[1] DRUTSKOY	04	BELL	Repl. by SAHOO 11A

[1] Assumes equal production of B^+ and B^0 at $\Upsilon(4S)$.

$\Gamma(K^+\pi^-\pi^+\gamma)/\Gamma_{total}$ Γ_{368}/Γ

VALUE (units 10^{-5})		DOCUMENT ID		TECN	COMMENT
2.76±0.22 OUR AVERAGE	Error includes scale factor of 1.2.				
2.95±0.13±0.20	[1,2]	AUBERT	07R	BABR	$e^+e^- \to \Upsilon(4S)$
2.50±0.18±0.22	[2,3]	YANG	05	BELL	$e^+e^- \to \Upsilon(4S)$
• • • We do not use the following data for averages, fits, limits, etc. • • •					
2.4 ±0.5 $^{+0.4}_{-0.2}$	[2,4]	NISHIDA	02	BELL	Repl. by YANG 05

[1] $M_{K\pi\pi} < 1.8$ GeV/c^2.
[2] Assumes equal production of B^+ and B^0 at the $\Upsilon(4S)$.
[3] $M_{K\pi\pi} < 2.0$ GeV/c^2.
[4] $M_{K\pi\pi} < 2.4$ GeV/c^2.

$\Gamma(K^*(892)^0\pi^+\gamma)/\Gamma_{total}$ Γ_{369}/Γ

VALUE		DOCUMENT ID		TECN	COMMENT
$(2.0^{+0.7}_{-0.6}\pm0.2)\times10^{-5}$	[1,2]	NISHIDA	02	BELL	$e^+e^- \to \Upsilon(4S)$

[1] Assumes equal production of B^+ and B^0 at the $\Upsilon(4S)$.
[2] $M_{K\pi\pi} < 2.4$ GeV/c^2.

$\Gamma(K^+\rho^0\gamma)/\Gamma_{total}$ Γ_{370}/Γ

VALUE	CL%		DOCUMENT ID		TECN	COMMENT
$<2.0\times10^{-5}$	90	[1,2]	NISHIDA	02	BELL	$e^+e^- \to \Upsilon(4S)$

[1] Assumes equal production of B^+ and B^0 at the $\Upsilon(4S)$.
[2] $M_{K\pi\pi} < 2.4$ GeV/c^2.

$\Gamma(K^+\pi^-\pi^+\gamma$ nonresonant$)/\Gamma_{total}$ Γ_{371}/Γ

VALUE	CL%		DOCUMENT ID		TECN	COMMENT
$<9.2\times10^{-6}$	90	[1,2]	NISHIDA	02	BELL	$e^+e^- \to \Upsilon(4S)$

[1] Assumes equal production of B^+ and B^0 at the $\Upsilon(4S)$.
[2] $M_{K\pi\pi} < 2.4$ GeV/c^2.

$\Gamma(K^0\pi^+\pi^0\gamma)/\Gamma_{total}$ Γ_{372}/Γ

VALUE (units 10^{-5})		DOCUMENT ID		TECN	COMMENT
4.56±0.42±0.31	[1,2]	AUBERT	07R	BABR	$e^+e^- \to \Upsilon(4S)$

[1] $M_{K\pi\pi} < 1.8$ GeV/c^2.
[2] Assumes equal production of B^+ and B^0 at the $\Upsilon(4S)$.

$\Gamma(K_1(1400)^+\gamma)/\Gamma_{total}$ Γ_{373}/Γ

VALUE (units 10^{-5})	CL%		DOCUMENT ID		TECN	COMMENT
< 1.5	90	[1]	YANG	05	BELL	$e^+e^- \to \Upsilon(4S)$
• • • We do not use the following data for averages, fits, limits, etc. • • •						
< 5.0	90	[1]	NISHIDA	02	BELL	Repl. by YANG 05
<220	90	[2]	ALBRECHT	89G	ARG	$e^+e^- \to \Upsilon(4S)$

[1] Assumes equal production of B^+ and B^0 at the $\Upsilon(4S)$.
[2] ALBRECHT 89G reports < 0.0020 assuming the $\Upsilon(4S)$ decays 45% to $B^0\overline{B}^0$. We rescale to 50%.

$\Gamma(K_2^*(1430)^+\gamma)/\Gamma_{total}$ Γ_{374}/Γ

VALUE (units 10^{-5})	CL%		DOCUMENT ID		TECN	COMMENT
1.45±0.40±0.15		[1]	AUBERT,B	04U	BABR	$e^+e^- \to \Upsilon(4S)$
• • • We do not use the following data for averages, fits, limits, etc. • • •						
<140	90	[2]	ALBRECHT	89G	ARG	$e^+e^- \to \Upsilon(4S)$

[1] Assumes equal production of B^+ and B^0 at the $\Upsilon(4S)$.
[2] ALBRECHT 89G reports < 0.0013 assuming the $\Upsilon(4S)$ decays 45% to $B^0\overline{B}^0$. We rescale to 50%.

$\Gamma(K^*(1680)^+\gamma)/\Gamma_{total}$ Γ_{375}/Γ

VALUE	CL%		DOCUMENT ID		TECN	COMMENT
<0.0019	90	[1]	ALBRECHT	89G	ARG	$e^+e^- \to \Upsilon(4S)$

[1] ALBRECHT 89G reports < 0.0017 assuming the $\Upsilon(4S)$ decays 45% to $B^0\overline{B}^0$. We rescale to 50%.

$\Gamma(K_3^*(1780)^+\gamma)/\Gamma_{total}$ Γ_{376}/Γ

VALUE (units 10^{-5})	CL%		DOCUMENT ID		TECN	COMMENT
< 39	90	[1,2]	NISHIDA	05	BELL	$e^+e^- \to \Upsilon(4S)$
• • • We do not use the following data for averages, fits, limits, etc. • • •						
<5500	90	[3]	ALBRECHT	89G	ARG	$e^+e^- \to \Upsilon(4S)$

[1] Assumes equal production of B^+ and B^0 at the $\Upsilon(4S)$.
[2] Uses $B(K_3^*(1780) \to \eta K) = 0.11^{+0.05}_{-0.04}$.
[3] ALBRECHT 89G reports < 0.005 assuming the $\Upsilon(4S)$ decays 45% to $B^0\overline{B}^0$. We rescale to 50%.

$\Gamma(K_4^*(2045)^+\gamma)/\Gamma_{total}$ Γ_{377}/Γ

VALUE	CL%		DOCUMENT ID		TECN	COMMENT
<0.0099	90	[1]	ALBRECHT	89G	ARG	$e^+e^- \to \Upsilon(4S)$

[1] ALBRECHT 89G reports < 0.0090 assuming the $\Upsilon(4S)$ decays 45% to $B^0\overline{B}^0$. We rescale to 50%.

$\Gamma(\rho^+\gamma)/\Gamma_{total}$ Γ_{378}/Γ

VALUE (units 10^{-6})	CL%		DOCUMENT ID		TECN	COMMENT
0.98±0.25 OUR AVERAGE						
$1.20^{+0.42}_{-0.37}\pm0.20$		[1]	AUBERT	08BH	BABR	$e^+e^- \to \Upsilon(4S)$
$0.87^{+0.29}_{-0.27}{}^{+0.09}_{-0.11}$		[1]	TANIGUCHI	08	BELL	$e^+e^- \to \Upsilon(4S)$
• • • We do not use the following data for averages, fits, limits, etc. • • •						
$1.10^{+0.37}_{-0.33}\pm0.09$		[1]	AUBERT	07L	BABR	Repl. by AUBERT 08BH
$0.55^{+0.42}_{-0.36}{}^{+0.09}_{-0.08}$		[1]	MOHAPATRA	06	BELL	Repl. by TANIGUCHI 08
0.9 $^{+0.6}_{-0.5}$ ±0.1	90	[1]	AUBERT	05	BABR	Repl. by AUBERT 07L
< 2.2	90	[1]	MOHAPATRA	05	BELL	$e^+e^- \to \Upsilon(4S)$
< 2.1	90	[1]	AUBERT	04C	BABR	$e^+e^- \to \Upsilon(4S)$
<13	90	[1,2]	COAN	00	CLE2	$e^+e^- \to \Upsilon(4S)$

[1] Assumes equal production of B^+ and B^0 at $\Upsilon(4S)$.
[2] No evidence for a nonresonant $K\pi\gamma$ contamination was seen; the central value assumes no contamination.

$\Gamma(\pi^+\pi^0)/\Gamma_{total}$ Γ_{379}/Γ

VALUE (units 10^{-6})	CL%		DOCUMENT ID		TECN	COMMENT
5.5 ±0.4 OUR AVERAGE		Error includes scale factor of 1.2.				
5.86±0.26±0.38		[1]	DUH	13	BELL	$e^+e^- \to \Upsilon(4S)$
5.02±0.46±0.29		[1]	AUBERT	07BC	BABR	$e^+e^- \to \Upsilon(4S)$
4.6 $^{+1.8}_{-1.6}$ $^{+0.6}_{-0.7}$		[1]	BORNHEIM	03	CLE2	$e^+e^- \to \Upsilon(4S)$
• • • We do not use the following data for averages, fits, limits, etc. • • •						
6.5 ±0.4 ±0.4		[1]	LIN	07A	BELL	Repl. by DUH 13
5.8 ±0.6 ±0.4		[1]	AUBERT	05L	BABR	Repl. by AUBERT 07BC
5.0 ±1.2 ±0.5		[1]	CHAO	04	BELL	Repl. by LIN 07A
5.5 $^{+1.0}_{-1.9}$ ±0.6		[1]	AUBERT	03L	BABR	Repl. by AUBERT 05L
7.4 $^{+2.3}_{-2.2}$ ±0.9		[1]	CASEY	02	BELL	Repl. by CHAO 04
< 13.4	90	[1]	ABE	01H	BELL	$e^+e^- \to \Upsilon(4S)$
< 9.6	90	[1]	AUBERT	01E	BABR	$e^+e^- \to \Upsilon(4S)$
< 12.7	90	[1]	CRONIN-HEN...	00	CLE2	$e^+e^- \to \Upsilon(4S)$
< 20	90		GODANG	98	CLE2	Repl. by CRONIN-HENNESSY 00
< 17	90		ASNER	96	CLE2	Repl. by GODANG 98
< 240	90	[1]	ALBRECHT	90B	ARG	$e^+e^- \to \Upsilon(4S)$
<2300	90	[2]	BEBEK	87	CLEO	$e^+e^- \to \Upsilon(4S)$

[1] Assumes equal production of B^+ and B^0 at the $\Upsilon(4S)$.
[2] BEBEK 87 assume the $\Upsilon(4S)$ decays 43% to $B^0\overline{B}^0$.

$\Gamma(\pi^+\pi^0)/\Gamma(K^0\pi^+)$ $\Gamma_{379}/\Gamma_{262}$

VALUE	DOCUMENT ID		TECN	COMMENT
0.285±0.02±0.02	LIN	07A	BELL	$e^+e^- \to \Upsilon(4S)$

$\Gamma(\pi^+\pi^+\pi^-)/\Gamma_{total}$ Γ_{380}/Γ

VALUE (units 10^{-6})	CL%		DOCUMENT ID		TECN	COMMENT
$15.2\pm0.6^{+1.3}_{-1.2}$		[1]	AUBERT	09L	BABR	$e^+e^- \to \Upsilon(4S)$
• • • We do not use the following data for averages, fits, limits, etc. • • •						
16.2±1.2±0.9		[1]	AUBERT,B	05G	BABR	Repl. by AUBERT 09L
10.9±3.3±1.6		[1]	AUBERT	03M	BABR	Repl. by AUBERT 05G
<130	90	[2]	ADAM	96D	DLPH	$e^+e^- \to Z$
<220	90	[3]	ABREU	95N	DLPH	Sup. by ADAM 96D
<450	90	[4]	ALBRECHT	90B	ARG	$e^+e^- \to \Upsilon(4S)$
<190	90	[5]	BORTOLETTO	89	CLEO	$e^+e^- \to \Upsilon(4S)$

[1] Assumes equal production of B^0 and B^+ at the $\Upsilon(4S)$; charm and charmonium contributions are subtracted, otherwise no assumptions about intermediate resonances.
[2] ADAM 96D assumes $f_{B^0} = f_{B^-} = 0.39$ and $f_{B_s} = 0.12$.
[3] Assumes a B^0, B^- production fraction of 0.39 and a B_s production fraction of 0.12.
[4] ALBRECHT 90B limit assumes equal production of $B^0\overline{B}^0$ and B^+B^- at $\Upsilon(4S)$.
[5] BORTOLETTO 89 reports $< 1.7\times10^{-4}$ assuming the $\Upsilon(4S)$ decays 43% to $B^0\overline{B}^0$. We rescale to 50%.

$\Gamma(\rho^0\pi^+)/\Gamma_{total}$ Γ_{381}/Γ

VALUE (units 10^{-6})	CL%		DOCUMENT ID		TECN	COMMENT
8.3±1.2 OUR AVERAGE						
$8.1\pm0.7^{+1.3}_{-1.6}$		[1]	AUBERT	09L	BABR	$e^+e^- \to \Upsilon(4S)$
$8.0^{+2.3}_{-2.0}\pm0.7$		[1]	GORDON	02	BELL	$e^+e^- \to \Upsilon(4S)$
$10.4^{+3.3}_{-3.4}\pm2.1$		[1]	JESSOP	00	CLE2	$e^+e^- \to \Upsilon(4S)$
• • • We do not use the following data for averages, fits, limits, etc. • • •						
$8.8\pm1.0^{+0.6}_{-0.9}$		[1]	AUBERT,B	05G	BABR	Repl. by AUBERT 09L
9.5±1.1±0.9		[1]	AUBERT	04Z	BABR	Repl. by AUBERT 05G
< 83	90	[2]	ABE	00C	SLD	$e^+e^- \to Z$
<160	90	[3]	ADAM	96D	DLPH	$e^+e^- \to Z$
< 43	90		ASNER	96	CLE2	Repl. by JESSOP 00

Meson Particle Listings

$B^{\pm}$

<260	90	[4] ABREU	95N	DLPH	Sup. by ADAM 96D
<150	90	[1] ALBRECHT	90B	ARG	$e^+e^- \to \Upsilon(4S)$
<170	90	[5] BORTOLETTO	89	CLEO	$e^+e^- \to \Upsilon(4S)$
<230	90	[5] BEBEK	87	CLEO	$e^+e^- \to \Upsilon(4S)$
<600	90	GILES	84	CLEO	Repl. by BEBEK 87

[1] Assumes equal production of B^+ and B^0 at the $\Upsilon(4S)$.
[2] ABE 00C assumes $B(Z \to b\overline{b})=(21.7 \pm 0.1)\%$ and the B fractions $f_{B^0}=f_{B^+}=(39.7^{+1.8}_{-2.2})\%$ and $f_{B_s}=(10.5^{+1.8}_{-2.2})\%$.
[3] ADAM 96D assumes $f_{B^0} = f_{B^-} = 0.39$ and $f_{B_s} = 0.12$.
[4] Assumes a B^0, B^- production fraction of 0.39 and a B_s production fraction of 0.12.
[5] Papers assume the $\Upsilon(4S)$ decays 43% to $B^0\overline{B}^0$. We rescale to 50%.

$[\Gamma(K^*(892)^0\pi^+) + \Gamma(\rho^0\pi^+)]/\Gamma_{\text{total}}$ $(\Gamma_{288}+\Gamma_{381})/\Gamma$

VALUE (units 10^{-6})	DOCUMENT ID		TECN	COMMENT
$\mathbf{170^{+120}_{-80}\pm20}$	[1] ADAM	96D	DLPH	$e^+e^- \to Z$

[1] ADAM 96D assumes $f_{B^0} = f_{B^-} = 0.39$ and $f_{B_s} = 0.12$.

$\Gamma(\pi^+ f_0(980),\ f_0 \to \pi^+\pi^-)/\Gamma_{\text{total}}$ Γ_{382}/Γ

VALUE (units 10^{-6})	CL%	DOCUMENT ID		TECN	COMMENT
< 1.5	90	[1] AUBERT	09L	BABR	$e^+e^- \to \Upsilon(4S)$
• • • We do not use the following data for averages, fits, limits, etc. • • •					
< 3.0	90	[1] AUBERT,B	05G	BABR	Repl. by AUBERT 09L
<140	90	[2] BORTOLETTO	89	CLEO	$e^+e^- \to \Upsilon(4S)$

[1] Assumes equal production of B^+ and B^0 at the $\Upsilon(4S)$.
[2] BORTOLETTO 89 reports $< 1.2 \times 10^{-4}$ assuming the $\Upsilon(4S)$ decays 43% to $B^0\overline{B}^0$. We rescale to 50%.

$\Gamma(\pi^+ f_2(1270))/\Gamma_{\text{total}}$ Γ_{383}/Γ

VALUE (units 10^{-6})	CL%	DOCUMENT ID		TECN	COMMENT
$\mathbf{1.59^{+0.66}_{-0.43}{}^{+0.02}_{-0.05}}$		[1,2] AUBERT	09L	BABR	$e^+e^- \to \Upsilon(4S)$
• • • We do not use the following data for averages, fits, limits, etc. • • •					
4.1 ±1.3 ±0.1		[2,3] AUBERT,B	05G	BABR	Repl. by AUBERT 09L
<240	90	[4] BORTOLETTO	89	CLEO	$e^+e^- \to \Upsilon(4S)$

[1] AUBERT 09L reports $[\Gamma(B^+ \to \pi^+ f_2(1270))/\Gamma_{\text{total}}] \times [B(f_2(1270) \to \pi^+\pi^-)] = (0.9 \pm 0.2 \pm 0.1^{+0.3}_{-0.1}) \times 10^{-6}$ which we divide by our best value $B(f_2(1270) \to \pi^+\pi^-) = (56.5^{+1.6}_{-0.8}) \times 10^{-2}$. Our first error is their experiment's error and our second error is the systematic error from using our best value.
[2] Assumes equal production of B^+ and B^0 at the $\Upsilon(4S)$.
[3] AUBERT,B 05G reports $[\Gamma(B^+ \to \pi^+ f_2(1270))/\Gamma_{\text{total}}] \times [B(f_2(1270) \to \pi^+\pi^-)] = (2.3 \pm 0.6 \pm 0.4) \times 10^{-6}$ which we divide by our best value $B(f_2(1270) \to \pi^+\pi^-) = (56.5^{+1.6}_{-0.8}) \times 10^{-2}$. Our first error is their experiment's error and our second error is the systematic error from using our best value.
[4] BORTOLETTO 89 reports $< 2.1 \times 10^{-4}$ assuming the $\Upsilon(4S)$ decays 43% to $B^0\overline{B}^0$. We rescale to 50%.

$\Gamma(\rho(1450)^0 pi+, \rho^0 \to \pi^+\pi^-)/\Gamma_{\text{total}}$ Γ_{384}/Γ

VALUE (units 10^{-6})	CL%	DOCUMENT ID		TECN	COMMENT
$\mathbf{1.4\pm0.4^{+0.5}_{-0.8}}$		[1] AUBERT	09L	BABR	$e^+e^- \to \Upsilon(4S)$
• • • We do not use the following data for averages, fits, limits, etc. • • •					
<2.3	90	[1] AUBERT,B	05G	BABR	Repl. by AUBERT 09L

[1] Assumes equal production of B^+ and B^0 at the $\Upsilon(4S)$.

$\Gamma(f_0(1370)\pi^+,\ f_0 \to \pi^+\pi^-)/\Gamma_{\text{total}}$ Γ_{385}/Γ

VALUE (units 10^{-6})	CL%	DOCUMENT ID		TECN	COMMENT
<4.0	90	[1] AUBERT	09L	BABR	$e^+e^- \to \Upsilon(4S)$
• • • We do not use the following data for averages, fits, limits, etc. • • •					
<3.0	90	[1] AUBERT,B	05G	BABR	Repl. by AUBERT 09L

[1] Assumes equal production of B^+ and B^0 at the $\Upsilon(4S)$.

$\Gamma(f_0(500)\pi^+,\ f_0 \to \pi^+\pi^-)/\Gamma_{\text{total}}$ Γ_{386}/Γ

VALUE (units 10^{-6})	CL%	DOCUMENT ID		TECN	COMMENT
<4.1	90	[1] AUBERT,B	05G	BABR	$e^+e^- \to \Upsilon(4S)$

[1] Assumes equal production of B^+ and B^0 at the $\Upsilon(4S)$.

$\Gamma(\pi^+\pi^-\pi^+ \text{nonresonant})/\Gamma_{\text{total}}$ Γ_{387}/Γ

VALUE (units 10^{-6})	CL%	DOCUMENT ID		TECN	COMMENT
$\mathbf{5.3\pm0.7^{+1.3}_{-0.8}}$		[1] AUBERT	09L	BABR	$e^+e^- \to \Upsilon(4S)$
• • • We do not use the following data for averages, fits, limits, etc. • • •					
< 4.6	90	[1] AUBERT,B	05G	BABR	Repl. by AUBERT 09L
<41	90	BERGFELD	96B	CLE2	$e^+e^- \to \Upsilon(4S)$

[1] Assumes equal production of B^+ and B^0 at the $\Upsilon(4S)$.

$\Gamma(\pi^+\pi^0\pi^0)/\Gamma_{\text{total}}$ Γ_{388}/Γ

VALUE	CL%	DOCUMENT ID		TECN	COMMENT
$\mathbf{<8.9 \times 10^{-4}}$	90	[1] ALBRECHT	90B	ARG	$e^+e^- \to \Upsilon(4S)$

[1] ALBRECHT 90B limit assumes equal production of $B^0\overline{B}^0$ and B^+B^- at $\Upsilon(4S)$.

$\Gamma(\rho^+\pi^0)/\Gamma_{\text{total}}$ Γ_{389}/Γ

VALUE (units 10^{-6})	CL%	DOCUMENT ID		TECN	COMMENT
10.9±1.4 OUR AVERAGE					
10.2±1.4±0.9		[1] AUBERT	07X	BABR	$e^+e^- \to \Upsilon(4S)$
$13.2\pm2.3^{+1.4}_{-1.9}$		[1] ZHANG	05A	BELL	$e^+e^- \to \Upsilon(4S)$
• • • We do not use the following data for averages, fits, limits, etc. • • •					
10.9±1.9±1.9		[1] AUBERT	04Z	BABR	Repl. by AUBERT 07X
< 43	90	[1,2] JESSOP	00	CLE2	$e^+e^- \to \Upsilon(4S)$
< 77	90	ASNER	96	CLE2	Repl. by JESSOP 00
<550	90	[1] ALBRECHT	90B	ARG	$e^+e^- \to \Upsilon(4S)$

[1] Assumes equal production of B^+ and B^0 at the $\Upsilon(4S)$.
[2] Assumes no nonresonant contributions of $B^+ \to \pi^+\pi^0\pi^0$.

$\Gamma(\pi^+\pi^-\pi^+\pi^0)/\Gamma_{\text{total}}$ Γ_{390}/Γ

VALUE	CL%	DOCUMENT ID		TECN	COMMENT
$\mathbf{<4.0 \times 10^{-3}}$	90	[1] ALBRECHT	90B	ARG	$e^+e^- \to \Upsilon(4S)$

[1] ALBRECHT 90B limit assumes equal production of $B^0\overline{B}^0$ and B^+B^- at $\Upsilon(4S)$.

$\Gamma(\rho^+\rho^0)/\Gamma_{\text{total}}$ Γ_{391}/Γ

VALUE (units 10^{-6})	CL%	DOCUMENT ID		TECN	COMMENT
24.0±1.9 OUR AVERAGE					
23.7±1.4±1.4		[1] AUBERT	09G	BABR	$e^+e^- \to \Upsilon(4S)$
$31.7\pm7.1^{+3.8}_{-6.7}$		[1,2] ZHANG	03B	BELL	$e^+e^- \to \Upsilon(4S)$
• • • We do not use the following data for averages, fits, limits, etc. • • •					
16.8±2.2±2.3		[1] AUBERT,BE	06G	BABR	Repl. by AUBERT 09G
$22.5^{+5.7}_{-5.4}\pm5.8$		[1] AUBERT	03V	BABR	Repl. by AUBERT,BE 06G
< 1000	90	[1] ALBRECHT	90B	ARG	$e^+e^- \to \Upsilon(4S)$

[1] Assumes equal production of B^+ and B^0 at the $\Upsilon(4S)$.
[2] The systematic error includes the error associated with the helicity-mix uncertainty.

$\Gamma(\rho^+ f_0(980),\ f_0 \to \pi^+\pi^-)/\Gamma_{\text{total}}$ Γ_{392}/Γ

VALUE (units 10^{-6})	CL%	DOCUMENT ID		TECN	COMMENT
<2.0	90	[1] AUBERT	09G	BABR	$e^+e^- \to \Upsilon(4S)$
• • • We do not use the following data for averages, fits, limits, etc. • • •					
<1.9	90	[1] AUBERT,BE	06G	BABR	Repl. by AUBERT 09G

[1] Assumes equal production of B^+ and B^0 at the $\Upsilon(4S)$.

$\Gamma(a_1(1260)^+\pi^0)/\Gamma_{\text{total}}$ Γ_{393}/Γ

VALUE (units 10^{-6})	CL%	DOCUMENT ID		TECN	COMMENT
26.4±5.4±4.1		[1,2] AUBERT	07BL	BABR	$e^+e^- \to \Upsilon(4S)$
• • • We do not use the following data for averages, fits, limits, etc. • • •					
<1700	90	[1] ALBRECHT	90B	ARG	$e^+e^- \to \Upsilon(4S)$

[1] Assumes equal production of B^+ and B^0 at the $\Upsilon(4S)$.
[2] Assumes a_1^+ decays only to 3π and $B(a_1^+ \to \pi^\pm\pi^\mp\pi^+) = 0.5$.

$\Gamma(a_1(1260)^0\pi^+)/\Gamma_{\text{total}}$ Γ_{394}/Γ

VALUE (units 10^{-6})	CL%	DOCUMENT ID		TECN	COMMENT
20.4±4.7±3.4		[1,2] AUBERT	07BL	BABR	$e^+e^- \to \Upsilon(4S)$
• • • We do not use the following data for averages, fits, limits, etc. • • •					
<900	90	[1] ALBRECHT	90B	ARG	$e^+e^- \to \Upsilon(4S)$

[1] Assumes equal production of B^+ and B^0 at the $\Upsilon(4S)$.
[2] Assumes a_1^0 decays only to 3π and $B(a_1^+ \to \pi^\pm\pi^\mp\pi^0) = 1.0$.

$\Gamma(\omega\pi^+)/\Gamma_{\text{total}}$ Γ_{395}/Γ

VALUE (units 10^{-6})	CL%	DOCUMENT ID		TECN	COMMENT
6.9±0.5 OUR AVERAGE					
6.7±0.5±0.4		[1] AUBERT	07AE	BABR	$e^+e^- \to \Upsilon(4S)$
6.9±0.6±0.5		[1] JEN	06	BELL	$e^+e^- \to \Upsilon(4S)$
$11.3^{+3.3}_{-2.9}\pm1.4$		[1] JESSOP	00	CLE2	$e^+e^- \to \Upsilon(4S)$
• • • We do not use the following data for averages, fits, limits, etc. • • •					
6.1±0.7±0.4		[1] AUBERT,B	06E	BABR	Repl. by AUBERT 07AE
5.5±0.9±0.5		[1] AUBERT	04H	BABR	Repl. by AUBERT,B 06E
$5.7^{+1.4}_{-1.3}\pm0.6$		[1] WANG	04A	BELL	Repl. by JEN 06
$4.2^{+2.0}_{-1.8}\pm0.5$		[1] LU	02	BELL	Repl. by WANG 04A
$6.6^{+2.1}_{-1.8}\pm0.7$		[1] AUBERT	01G	BABR	Repl. by AUBERT 04H
< 23	90	[1] BERGFELD	98	CLE2	Repl. by JESSOP 00
<400	90	[1] ALBRECHT	90B	ARG	$e^+e^- \to \Upsilon(4S)$

[1] Assumes equal production of B^+ and B^0 at the $\Upsilon(4S)$.

$\Gamma(\omega\rho^+)/\Gamma_{total}$ Γ_{396}/Γ

VALUE (units 10^{-6})	CL%	DOCUMENT ID		TECN	COMMENT
15.9±1.6±1.4		[1] AUBERT	09H	BABR	$e^+e^- \to \Upsilon(4S)$
• • • We do not use the following data for averages, fits, limits, etc. • • •					
$10.6\pm2.1^{+1.6}_{-1.0}$		[1] AUBERT,B	06T	BABR	Repl. by AUBERT 09H
$12.6^{+3.7}_{-3.3}\pm1.6$		[1] AUBERT	05O	BABR	Repl. by AUBERT,B 06T
<61	90	[1] BERGFELD	98	CLE2	

[1] Assumes equal production of B^+ and B^0 at the $\Upsilon(4S)$.

$\Gamma(\eta\pi^+)/\Gamma_{total}$ Γ_{397}/Γ

VALUE (units 10^{-6})	CL%	DOCUMENT ID		TECN	COMMENT
4.02±0.27 OUR AVERAGE					
4.07±0.26±0.21		[1] HOI	12	BELL	$e^+e^- \to \Upsilon(4S)$
4.00±0.40±0.24		[1] AUBERT	09AV	BABR	$e^+e^- \to \Upsilon(4S)$
$1.2\ ^{+2.8}_{-1.2}$		[1] RICHICHI	00	CLE2	$e^+e^- \to \Upsilon(4S)$
• • • We do not use the following data for averages, fits, limits, etc. • • •					
5.0 ±0.5 ±0.3		[1] AUBERT	07AE	BABR	Repl. by AUBERT 09AV
4.2 ±0.4 ±0.2		[1] CHANG	07B	BELL	Repl. by HOI 12
5.1 ±0.6 ±0.3		[1] AUBERT,B	05K	BABR	Repl. by AUBERT 07AE
4.8 ±0.7 ±0.3		[1] CHANG	05A	BELL	Repl. by CHANG 07B
5.3 ±1.0 ±0.3		[1] AUBERT	04H	BABR	Repl. by AUBERT,B 05K
< 15	90	BEHRENS	98	CLE2	Repl. by RICHICHI 00
<700	90	[1] ALBRECHT	90B	ARG	$e^+e^- \to \Upsilon(4S)$

[1] Assumes equal production of B^+ and B^0 at the $\Upsilon(4S)$.

$\Gamma(\eta\rho^+)/\Gamma_{total}$ Γ_{398}/Γ

VALUE (units 10^{-6})	CL%	DOCUMENT ID		TECN	COMMENT
7.0±2.9 OUR AVERAGE Error includes scale factor of 2.8.					
9.9±1.2±0.8		[1] AUBERT	08AH	BABR	$e^+e^- \to \Upsilon(4S)$
$4.1^{+1.4}_{-1.3}\pm0.4$		[1] WANG	07B	BELL	$e^+e^- \to \Upsilon(4S)$
• • • We do not use the following data for averages, fits, limits, etc. • • •					
8.4±1.9±1.1		[1] AUBERT,B	05K	BABR	Repl. by AUBERT 08AH
<14	90	[1] AUBERT,B	04D	BABR	Repl. by AUBERT,B 05K
<15	90	[1] RICHICHI	00	CLE2	$e^+e^- \to \Upsilon(4S)$
<32	90	BEHRENS	98	CLE2	Repl. by RICHICHI 00

[1] Assumes equal production of B^+ and B^0 at the $\Upsilon(4S)$.

$\Gamma(\eta'\pi^+)/\Gamma_{total}$ Γ_{399}/Γ

VALUE (units 10^{-6})	CL%	DOCUMENT ID		TECN	COMMENT
2.7 ±0.9 OUR AVERAGE Error includes scale factor of 1.9.					
3.5 ±0.6 ±0.2		[1] AUBERT	09AV	BABR	$e^+e^- \to \Upsilon(4S)$
$1.76^{+0.67}_{-0.62}{}^{+0.15}_{-0.14}$		[1] SCHUEMANN	06	BELL	$e^+e^- \to \Upsilon(4S)$
• • • We do not use the following data for averages, fits, limits, etc. • • •					
3.9 ±0.7 ±0.3		[1] AUBERT	07AE	BABR	Repl. by AUBERT 09AV
4.0 ±0.8 ±0.4		[1] AUBERT,B	05K	BABR	Repl. by AUBERT 07AE
< 4.5	90	[1] AUBERT	04H	BABR	Repl. by AUBERT,B 05K
< 7.0	90	[1] ABE	01M	BELL	$e^+e^- \to \Upsilon(4S)$
<12	90	[1] AUBERT	01G	BABR	$e^+e^- \to \Upsilon(4S)$
<12	90	[1] RICHICHI	00	CLE2	$e^+e^- \to \Upsilon(4S)$
<31	90	BEHRENS	98	CLE2	Repl. by RICHICHI 00

[1] Assumes equal production of B^+ and B^0 at the $\Upsilon(4S)$.

$\Gamma(\eta'\rho^+)/\Gamma_{total}$ Γ_{400}/Γ

VALUE (units 10^{-6})	CL%	DOCUMENT ID		TECN	COMMENT
$\mathbf{9.7^{+1.9}_{-1.8}\pm1.1}$		[1] DEL-AMO-SA...10A		BABR	$e^+e^- \to \Upsilon(4S)$
• • • We do not use the following data for averages, fits, limits, etc. • • •					
$8.7^{+3.1}_{-2.8}{}^{+2.3}_{-1.3}$		[1] AUBERT	07E	BABR	Repl. by DEL-AMO-SANCHEZ 10A
< 5.8	90	[1] SCHUEMANN	07	BELL	$e^+e^- \to \Upsilon(4S)$
<22	90	[1] AUBERT,B	04D	BABR	Repl. by AUBERT 07E
<33	90	[1] RICHICHI	00	CLE2	$e^+e^- \to \Upsilon(4S)$
<47	90	BEHRENS	98	CLE2	Repl. by RICHICHI 00

[1] Assumes equal production of B^+ and B^0 at the $\Upsilon(4S)$.

$\Gamma(\phi\pi^+)/\Gamma_{total}$ Γ_{401}/Γ

VALUE (units 10^{-7})	CL%	DOCUMENT ID		TECN	COMMENT
< 1.5	90	[1] AAIJ	14A	LHCB	pp at 7 TeV
• • • We do not use the following data for averages, fits, limits, etc. • • •					
< 3.3	90	[2] KIM	12A	BELL	$e^+e^- \to \Upsilon(4S)$
< 2.4	90	[2] AUBERT,B	06C	BABR	$e^+e^- \to \Upsilon(4S)$
< 4.1	90	[2] AUBERT	04A	BABR	Repl. by AUBERT,B 06C
< 14	90	[2] AUBERT	01D	BABR	$e^+e^- \to \Upsilon(4S)$
<1530	90	[3] ABE	00C	SLD	$e^+e^- \to Z$
< 50	90	[2] BERGFELD	98	CLE2	

[1] Measures $B(B^+ \to \phi\pi^+)/B(B^+ \to \phi K^+) < 0.018$ at 90% C.L. and assumes $B(B^+ \to \phi K^+) = (8.8^{+0.7}_{-0.6}) \times 10^{-6}$.

[2] Assumes equal production of B^+ and B^0 at the $\Upsilon(4S)$.

[3] ABE 00C assumes $B(Z \to b\overline{b}) = (21.7 \pm 0.1)\%$ and the B fractions $f_{B^0} = f_{B^+} = (39.7^{+1.8}_{-2.2})\%$ and $f_{B_s} = (10.5^{+1.8}_{-2.2})\%$.

$\Gamma(\phi\rho^+)/\Gamma_{total}$ Γ_{402}/Γ

VALUE (units 10^{-6})	CL%	DOCUMENT ID		TECN	COMMENT
< 3.0	90	[1] AUBERT	08BK	BABR	$e^+e^- \to \Upsilon(4S)$
• • • We do not use the following data for averages, fits, limits, etc. • • •					
<16		[1] BERGFELD	98	CLE2	

[1] Assumes equal production of B^+ and B^0 at the $\Upsilon(4S)$.

$\Gamma(a_0(980)^0\pi^+,\ a_0^0 \to \eta\pi^0)/\Gamma_{total}$ Γ_{403}/Γ

VALUE (units 10^{-6})	CL%	DOCUMENT ID		TECN	COMMENT
<5.8	90	[1] AUBERT,BE	04	BABR	$e^+e^- \to \Upsilon(4S)$

[1] Assumes equal production of charged and neutral B mesons from $\Upsilon(4S)$ decays.

$\Gamma(a_0(980)^+\pi^0,\ a_0^+ \to \eta\pi^+)/\Gamma_{total}$ Γ_{404}/Γ

VALUE (units 10^{-6})	CL%	DOCUMENT ID		TECN	COMMENT
<1.4	90	[1] AUBERT	08A	BABR	$e^+e^- \to \Upsilon(4S)$

[1] Assumes equal production of B^+ and B^0 at the $\Upsilon(4S)$.

$\Gamma(\pi^+\pi^+\pi^+\pi^-\pi^-)/\Gamma_{total}$ Γ_{405}/Γ

VALUE	CL%	DOCUMENT ID		TECN	COMMENT
$\mathbf{<8.6\times10^{-4}}$	90	[1] ALBRECHT	90B	ARG	$e^+e^- \to \Upsilon(4S)$

[1] ALBRECHT 90B limit assumes equal production of $B^0\overline{B}{}^0$ and B^+B^- at $\Upsilon(4S)$.

$\Gamma(\rho^0 a_1(1260)^+)/\Gamma_{total}$ Γ_{406}/Γ

VALUE	CL%	DOCUMENT ID		TECN	COMMENT
$\mathbf{<6.2\times10^{-4}}$	90	[1] BORTOLETTO89		CLEO	$e^+e^- \to \Upsilon(4S)$
• • • We do not use the following data for averages, fits, limits, etc. • • •					
$<6.0\times10^{-4}$	90	[2] ALBRECHT	90B	ARG	$e^+e^- \to \Upsilon(4S)$
$<3.2\times10^{-3}$	90	[1] BEBEK	87	CLEO	$e^+e^- \to \Upsilon(4S)$

[1] BORTOLETTO 89 reports $< 5.4\times10^{-4}$ assuming the $\Upsilon(4S)$ decays 43% to $B^0\overline{B}{}^0$. We rescale to 50%.

[2] ALBRECHT 90B limit assumes equal production of $B^0\overline{B}{}^0$ and B^+B^- at $\Upsilon(4S)$.

$\Gamma(\rho^0 a_2(1320)^+)/\Gamma_{total}$ Γ_{407}/Γ

VALUE	CL%	DOCUMENT ID		TECN	COMMENT
$\mathbf{<7.2\times10^{-4}}$	90	[1] BORTOLETTO89		CLEO	$e^+e^- \to \Upsilon(4S)$
• • • We do not use the following data for averages, fits, limits, etc. • • •					
$<2.6\times10^{-3}$	90	[2] BEBEK	87	CLEO	$e^+e^- \to \Upsilon(4S)$

[1] BORTOLETTO 89 reports $< 6.3\times10^{-4}$ assuming the $\Upsilon(4S)$ decays 43% to $B^0\overline{B}{}^0$. We rescale to 50%.

[2] BEBEK 87reports $< 2.3\times10^{-3}$ assuming the $\Upsilon(4S)$ decays 43% to $B^0\overline{B}{}^0$. We rescale to 50%.

$\Gamma(b_1^0\pi^+,\ b_1^0 \to \omega\pi^0)/\Gamma_{total}$ Γ_{408}/Γ

VALUE (units 10^{-6})	DOCUMENT ID		TECN	COMMENT
6.7±1.7±1.0	[1] AUBERT	07BI	BABR	$e^+e^- \to \Upsilon(4S)$

[1] Assumes equal production of B^+ and B^0 at the $\Upsilon(4S)$.

$\Gamma(b_1^+\pi^0,\ b_1^+ \to \omega\pi^+)/\Gamma_{total}$ Γ_{409}/Γ

VALUE (units 10^{-6})	CL%	DOCUMENT ID		TECN	COMMENT
<3.3	90	[1] AUBERT	08AG	BABR	$e^+e^- \to \Upsilon(4S)$

[1] Assumes equal production of B^+ and B^0 at the $\Upsilon(4S)$.

$\Gamma(\pi^+\pi^+\pi^+\pi^-\pi^-\pi^0)/\Gamma_{total}$ Γ_{410}/Γ

VALUE	CL%	DOCUMENT ID		TECN	COMMENT
$\mathbf{<6.3\times10^{-3}}$	90	[1] ALBRECHT	90B	ARG	$e^+e^- \to \Upsilon(4S)$

[1] ALBRECHT 90B limit assumes equal production of $B^0\overline{B}{}^0$ and B^+B^- at $\Upsilon(4S)$.

$\Gamma(b_1^+\rho^0,\ b_1^+ \to \omega\pi^+)/\Gamma_{total}$ Γ_{411}/Γ

VALUE	CL%	DOCUMENT ID		TECN	COMMENT
$\mathbf{<5.2\times10^{-6}}$	90	[1] AUBERT	09AF	BABR	$e^+e^- \to \Upsilon(4S)$

[1] Assumes equal production of B^+ and B^0 at the $\Upsilon(4S)$.

$\Gamma(b_1^0\rho^+,\ b_1^0 \to \omega\pi^0)/\Gamma_{total}$ Γ_{413}/Γ

VALUE	CL%	DOCUMENT ID		TECN	COMMENT
$\mathbf{<3.3\times10^{-6}}$	90	[1] AUBERT	09AF	BABR	$e^+e^- \to \Upsilon(4S)$

[1] Assumes equal production of B^+ and B^0 at the $\Upsilon(4S)$.

$\Gamma(a_1(1260)^+a_1(1260)^0)/\Gamma_{total}$ Γ_{412}/Γ

VALUE	CL%	DOCUMENT ID		TECN	COMMENT
$\mathbf{<1.3\times10^{-2}}$	90	[1] ALBRECHT	90B	ARG	$e^+e^- \to \Upsilon(4S)$

[1] ALBRECHT 90B limit assumes equal production of $B^0\overline{B}{}^0$ and B^+B^- at $\Upsilon(4S)$.

$\Gamma(h^+\pi^0)/\Gamma_{total}$ Γ_{414}/Γ

$h^+ = K^+$ or π^+

VALUE (units 10^{-6})	DOCUMENT ID		TECN	COMMENT
$\mathbf{16^{+6}_{-5}\pm3.6}$	GODANG	98	CLE2	$e^+e^- \to \Upsilon(4S)$

Meson Particle Listings

$B^{\pm}$

$\Gamma(\omega h^+)/\Gamma_{\text{total}}$ Γ_{415}/Γ

$h^+ = K^+$ or π^+

VALUE (units 10^{-6})	DOCUMENT ID		TECN	COMMENT
$13.8^{+2.7}_{-2.4}$ OUR AVERAGE				
$13.4^{+3.3}_{-2.9}\pm1.1$	[1] LU	02	BELL	$e^+e^- \to \Upsilon(4S)$
$14.3^{+3.6}_{-3.2}\pm2.0$	[1] JESSOP	00	CLE2	$e^+e^- \to \Upsilon(4S)$
• • • We do not use the following data for averages, fits, limits, etc. • • •				
$25\ ^{+8}_{-7}\ \pm3$	[1] BERGFELD	98	CLE2	Repl. by JESSOP 00

[1] Assumes equal production of B^+ and B^0 at the $\Upsilon(4S)$.

$\Gamma(h^+X^0(\text{Familon}))/\Gamma_{\text{total}}$ Γ_{416}/Γ

VALUE (units 10^{-6})	CL%	DOCUMENT ID		TECN	COMMENT
<49	90	[1] AMMAR	01B	CLE2	$e^+e^- \to \Upsilon(4S)$

[1] AMMAR 01B searched for the two-body decay of the B meson to a massless neutral feebly-interacting particle X^0 such as the familon, the Nambu-Goldstone boson associated with a spontaneously broken global family symmetry.

$\Gamma(p\overline{p}\pi^+)/\Gamma_{\text{total}}$ Γ_{417}/Γ

VALUE (units 10^{-6})	CL%	DOCUMENT ID		TECN	COMMENT
$1.62\pm$ 0.20 OUR AVERAGE					
$1.60^{+\ 0.22}_{-\ 0.19}\pm\ 0.12$		[1,2,3] WEI	08	BELL	$e^+e^- \to \Upsilon(4S)$
$1.69\pm\ 0.29\pm\ 0.26$		[1] AUBERT	07AV	BABR	$e^+e^- \to \Upsilon(4S)$
• • • We do not use the following data for averages, fits, limits, etc. • • •					
$3.06^{+\ 0.73}_{-\ 0.62}\pm\ 0.37$		[1,3] WANG	04	BELL	Repl. by WEI 08
< 3.7	90	[1,2] ABE	02K	BELL	Repl. by WANG 04
<500	90	[4] ABREU	95N	DLPH	Repl. by ADAM 96D
<160	90	[5] BEBEK	89	CLEO	$e^+e^- \to \Upsilon(4S)$
$570\ \pm150\ \pm210$		[6] ALBRECHT	88F	ARG	$e^+e^- \to \Upsilon(4S)$

[1] Assumes equal production of B^+ and B^0 at the $\Upsilon(4S)$.
[2] Explicitly vetoes resonant production of $p\overline{p}$ from Charmonium states.
[3] Also provides results with $m_{p\overline{p}} < 2.85$ GeV/c^2 and angular asymmetry of $p\overline{p}$ system.
[4] Assumes a B^0, B^- production fraction of 0.39 and a B_s production fraction of 0.12.
[5] BEBEK 89 reports $< 1.4\times10^{-4}$ assuming the $\Upsilon(4S)$ decays 43% to $B^0\overline{B}^0$. We rescale to 50%.
[6] ALBRECHT 88F reports $(5.2 \pm 1.4 \pm 1.9)\times10^{-4}$ assuming the $\Upsilon(4S)$ decays 45% to $B^0\overline{B}^0$. We rescale to 50%.

$\Gamma(p\overline{p}\pi^+\text{nonresonant})/\Gamma_{\text{total}}$ Γ_{418}/Γ

VALUE (units 10^{-6})	CL%	DOCUMENT ID		TECN	COMMENT
<53	90	BERGFELD	96B	CLE2	$e^+e^- \to \Upsilon(4S)$

$\Gamma(p\overline{p}\pi^+\pi^+\pi^-)/\Gamma_{\text{total}}$ Γ_{419}/Γ

VALUE	CL%	DOCUMENT ID		TECN	COMMENT
• • • We do not use the following data for averages, fits, limits, etc. • • •					
$<5.2\times10^{-4}$	90	[1] ALBRECHT	88F	ARG	$e^+e^- \to \Upsilon(4S)$

[1] ALBRECHT 88F reports $< 4.7\times10^{-4}$ assuming the $\Upsilon(4S)$ decays 45% to $B^0\overline{B}^0$. We rescale to 50%.

$\Gamma(p\overline{p}K^+)/\Gamma_{\text{total}}$ Γ_{420}/Γ

VALUE (units 10^{-6})	DOCUMENT ID		TECN	COMMENT
5.9 $\pm$0.5 OUR AVERAGE Error includes scale factor of 1.5.				
$5.54^{+0.27}_{-0.25}\pm0.36$	[1,2,3] WEI	08	BELL	$e^+e^- \to \Upsilon(4S)$
$6.7\ \pm0.5\ \pm0.4$	[1,3] AUBERT,B	05L	BABR	$e^+e^- \to \Upsilon(4S)$
• • • We do not use the following data for averages, fits, limits, etc. • • •				
$4.59^{+0.38}_{-0.34}\pm0.50$	[1,2,3] WANG	05A	BELL	Repl. by WEI 08
$5.66^{+0.67}_{-0.57}\pm0.62$	[1,2,3] WANG	04	BELL	Repl. by WANG 05A
$4.3\ ^{+1.1}_{-0.9}\ \pm0.5$	[1,2] ABE	02K	BELL	Repl. by WANG 04

[1] Assumes equal production of B^+ and B^0 at the $\Upsilon(4S)$.
[2] Explicitly vetoes resonant production of $p\overline{p}$ from Charmonium states.
[3] Provides also results with $m_{p\overline{p}} < 2.85$ GeV/c^2 and angular asymmetry of $p\overline{p}$ system.

$\Gamma(p\overline{p}K^+)/\Gamma(J/\psi(1S)K^+)$ $\Gamma_{420}/\Gamma_{218}$

VALUE	DOCUMENT ID		TECN	COMMENT
$0.0104\pm0.0005\pm0.0001$	[1,2] AAIJ	13S	LHCB	pp at 7 TeV

[1] AAIJ 13S reports $[\Gamma(B^+ \to p\overline{p}K^+)/\Gamma(B^+ \to J/\psi(1S)K^+)]$ / $[\text{B}(J/\psi(1S) \to p\overline{p})]$ $= 4.91 \pm 0.19 \pm 0.14$ which we multiply by our best value $\text{B}(J/\psi(1S) \to p\overline{p}) = (2.120 \pm 0.029)\times10^{-3}$. Our first error is their experiment's error and our second error is the systematic error from using our best value.
[2] Measurement includes contribution where $p\overline{p}$ is produced in charmonia decays.

$\Gamma(\Theta(1710)^{++}\overline{p},\ \Theta^{++} \to pK^+)/\Gamma_{\text{total}}$ Γ_{421}/Γ

VALUE (units 10^{-6})	CL%	DOCUMENT ID		TECN	COMMENT
<0.091	90	[1] WANG	05A	BELL	$e^+e^- \to \Upsilon(4S)$
• • • We do not use the following data for averages, fits, limits, etc. • • •					
<0.1	90	[1,2] AUBERT,B	05L	BABR	$e^+e^- \to \Upsilon(4S)$

[1] Assumes equal production of B^+ and B^0 at the $\Upsilon(4S)$.
[2] Provides upper limits depending on the pentaquark masses between 1.43 to 2.0 GeV/c^2.

$\Gamma(f_J(2220)K^+,\ f_J \to p\overline{p})/\Gamma_{\text{total}}$ Γ_{422}/Γ

VALUE (units 10^{-6})	CL%	DOCUMENT ID		TECN	COMMENT
<0.41	90	[1] WANG	05A	BELL	$e^+e^- \to \Upsilon(4S)$

[1] Assumes equal production of B^+ and B^0 at the $\Upsilon(4S)$.

$\Gamma(p\overline{\Lambda}(1520))/\Gamma_{\text{total}}$ Γ_{423}/Γ

VALUE (units 10^{-6})	CL%	DOCUMENT ID		TECN	COMMENT
$0.39^{+0.10}_{-0.09}\pm0.03$		[1] AAIJ	13AU	LHCB	pp at 7 TeV
• • • We do not use the following data for averages, fits, limits, etc. • • •					
<1.5	90	[2] AUBERT,B	05L	BABR	$e^+e^- \to \Upsilon(4S)$

[1] Uses $\text{B}(B^+ \to J/\psi K^+) = (1.016 \pm 0.033)\times10^{-3}$, $\text{B}(J/\psi \to p\overline{p}) = (2.17 \pm 0.07)\times10^{-3}$ and $\text{B}(\Lambda(1520) \to K^-p) = 0.234 \pm 0.016$.
[2] Assumes equal production of B^+ and B^0 at the $\Upsilon(4S)$.

$\Gamma(p\overline{p}K^+\text{nonresonant})/\Gamma_{\text{total}}$ Γ_{424}/Γ

VALUE (units 10^{-6})	CL%	DOCUMENT ID		TECN	COMMENT
<89	90	BERGFELD	96B	CLE2	$e^+e^- \to \Upsilon(4S)$

$\Gamma(p\overline{p}K^*(892)^+)/\Gamma_{\text{total}}$ Γ_{425}/Γ

VALUE (units 10^{-6})	DOCUMENT ID		TECN	COMMENT
$3.6\ ^{+0.8}_{-0.7}$ OUR AVERAGE				
$3.38^{+0.73}_{-0.60}\pm0.39$	[1,2] CHEN	08C	BELL	$e^+e^- \to \Upsilon(4S)$
$5.3\ \pm1.5\ \pm1.3$	[2] AUBERT	07AV	BABR	$e^+e^- \to \Upsilon(4S)$
• • • We do not use the following data for averages, fits, limits, etc. • • •				
$10.3\ ^{+3.6}_{-2.8}\ ^{+1.3}_{-1.7}$	[2,3] WANG	04	BELL	Repl. by CHEN 08C

[1] Explicitly vetoes resonant production of $p\overline{p}$ from charmonium states.
[2] Assumes equal production of B^+ and B^0 at the $\Upsilon(4S)$.
[3] Explicitly vetoes resonant production of $p\overline{p}$ from charmonium states. The branching fraction for $M_{p\overline{p}} < 2.85$ GeV/c^2 is also reported.

$\Gamma(f_J(2220)K^{*+},\ f_J \to p\overline{p})/\Gamma_{\text{total}}$ Γ_{426}/Γ

VALUE (units 10^{-6})	CL%	DOCUMENT ID		TECN	COMMENT
<0.77	90	[1] AUBERT	07AV	BABR	$e^+e^- \to \Upsilon(4S)$

[1] Assumes equal production of B^+ and B^0 at the $\Upsilon(4S)$.

$\Gamma(p\overline{\Lambda})/\Gamma_{\text{total}}$ Γ_{427}/Γ

VALUE (units 10^{-6})	CL%	DOCUMENT ID		TECN	COMMENT
< 0.32	90	[1] TSAI	07	BELL	$e^+e^- \to \Upsilon(4S)$
• • • We do not use the following data for averages, fits, limits, etc. • • •					
< 0.49	90	[1] CHANG	05	BELL	Repl. by TSAI 07
< 1.5	90	[1] BORNHEIM	03	CLE2	$e^+e^- \to \Upsilon(4S)$
< 2.2	90	[1] ABE	02O	BELL	$e^+e^- \to \Upsilon(4S)$
< 2.6	90	[1] COAN	99	CLE2	$e^+e^- \to \Upsilon(4S)$
<60	90	[2] AVERY	89B	CLEO	$e^+e^- \to \Upsilon(4S)$
<93	90	[3] ALBRECHT	88F	ARG	$e^+e^- \to \Upsilon(4S)$

[1] Assumes equal production of B^+ and B^0 at the $\Upsilon(4S)$.
[2] AVERY 89B reports $< 5\times10^{-5}$ assuming the $\Upsilon(4S)$ decays 43% to $B^0\overline{B}^0$. We rescale to 50%.
[3] ALBRECHT 88F reports $< 8.5\times10^{-5}$ assuming the $\Upsilon(4S)$ decays 45% to $B^0\overline{B}^0$. We rescale to 50%.

$\Gamma(p\overline{\Lambda}\gamma)/\Gamma_{\text{total}}$ Γ_{428}/Γ

VALUE (units 10^{-6})	CL%	DOCUMENT ID		TECN	COMMENT
$2.45^{+0.44}_{-0.38}\pm0.22$		[1] WANG	07C	BELL	$e^+e^- \to \Upsilon(4S)$
• • • We do not use the following data for averages, fits, limits, etc. • • •					
$2.16^{+0.58}_{-0.53}\pm0.20$		[1] LEE	05	BELL	Repl. by WANG 07C
<3.9	90	[2] EDWARDS	03	CLE2	$e^+e^- \to \Upsilon(4S)$

[1] Assumes equal production of B^+ and B^0 at the $\Upsilon(4S)$.
[2] Corresponds to $E_\gamma > 1.5$ GeV. The limit changes to 3.3×10^{-6} for $E_\gamma > 2.0$ GeV.

$\Gamma(p\overline{\Lambda}\pi^0)/\Gamma_{\text{total}}$ Γ_{429}/Γ

VALUE (units 10^{-6})	DOCUMENT ID		TECN	COMMENT
$3.00^{+0.61}_{-0.53}\pm0.33$	[1] WANG	07C	BELL	$e^+e^- \to \Upsilon(4S)$

[1] Assumes equal production of B^+ and B^0 at the $\Upsilon(4S)$.

$\Gamma(p\overline{\Sigma}(1385)^0)/\Gamma_{total}$ Γ_{430}/Γ

VALUE (units 10^{-6})	CL%	DOCUMENT ID		TECN	COMMENT
<0.47	90	[1] WANG	07C	BELL	$e^+e^- \to \Upsilon(4S)$

[1] Assumes equal production of B^+ and B^0 at the $\Upsilon(4S)$.

$\Gamma(\Delta^+\overline{\Lambda})/\Gamma_{total}$ Γ_{431}/Γ

VALUE (units 10^{-6})	CL%	DOCUMENT ID		TECN	COMMENT
<0.82	90	[1] WANG	07C	BELL	$e^+e^- \to \Upsilon(4S)$

[1] Assumes equal production of B^+ and B^0 at the $\Upsilon(4S)$.

$\Gamma(p\overline{\Sigma}\gamma)/\Gamma_{total}$ Γ_{432}/Γ

VALUE (units 10^{-6})	CL%	DOCUMENT ID		TECN	COMMENT
<4.6	90	[1] LEE	05	BELL	$e^+e^- \to \Upsilon(4S)$
• • • We do not use the following data for averages, fits, limits, etc. • • •					
<7.9	90	[2] EDWARDS	03	CLE2	$e^+e^- \to \Upsilon(4S)$

[1] Assumes equal production of B^+ and B^0 at the $\Upsilon(4S)$.
[2] Corresponds to $E_\gamma > 1.5$ GeV. The limit changes to 6.4×10^{-6} for $E_\gamma > 2.0$ GeV.

$\Gamma(p\overline{\Lambda}\pi^+\pi^-)/\Gamma_{total}$ Γ_{433}/Γ

VALUE (units 10^{-6})	CL%	DOCUMENT ID		TECN	COMMENT
$5.92^{+0.88}_{-0.84}\pm0.69$		[1] CHEN	09C	BELL	$e^+e^- \to \Upsilon(4S)$
• • • We do not use the following data for averages, fits, limits, etc. • • •					
<200	90	[2] ALBRECHT	88F	ARG	$e^+e^- \to \Upsilon(4S)$

[1] Assumes equal production of B^+ and B^0 at the $\Upsilon(4S)$.
[2] ALBRECHT 88F reports $< 1.8 \times 10^{-4}$ assuming the $\Upsilon(4S)$ decays 45% to $B^0\overline{B}^0$. We rescale to 50%.

$\Gamma(p\overline{\Lambda}\rho^0)/\Gamma_{total}$ Γ_{434}/Γ

VALUE (units 10^{-6})	DOCUMENT ID		TECN	COMMENT
$4.78^{+0.67}_{-0.64}\pm0.60$	[1] CHEN	09C	BELL	$e^+e^- \to \Upsilon(4S)$

[1] Assumes equal production of B^+ and B^0 at the $\Upsilon(4S)$.

$\Gamma(p\overline{\Lambda}f_2(1270))/\Gamma_{total}$ Γ_{435}/Γ

VALUE (units 10^{-6})	DOCUMENT ID		TECN	COMMENT
$2.03^{+0.77}_{-0.72}\pm0.27$	[1] CHEN	09C	BELL	$e^+e^- \to \Upsilon(4S)$

[1] Assumes equal production of B^+ and B^0 at the $\Upsilon(4S)$.

$\Gamma(\Lambda\overline{\Lambda}\pi^+)/\Gamma_{total}$ Γ_{436}/Γ

VALUE (units 10^{-6})	CL%	DOCUMENT ID		TECN	COMMENT
<0.94	90	[1,2] CHANG	09	BELL	Repl. by CHANG 09
• • • We do not use the following data for averages, fits, limits, etc. • • •					
<2.8	90	[2] LEE	04	BELL	$e^+e^- \to \Upsilon(4S)$

[1] For $m_{\Lambda\overline{\Lambda}} < 2.85$ GeV/c^2.
[2] Assumes equal production of B^+ and B^0 at the $\Upsilon(4S)$.

$\Gamma(\Lambda\overline{\Lambda}K^+)/\Gamma_{total}$ Γ_{437}/Γ

VALUE (units 10^{-6})	DOCUMENT ID		TECN	COMMENT
$3.38^{+0.41}_{-0.36}\pm0.41$	[1,2] CHANG	09	BELL	$e^+e^- \to \Upsilon(4S)$
• • • We do not use the following data for averages, fits, limits, etc. • • •				
$2.91^{+0.9}_{-0.70}\pm0.38$	[2] LEE	04	BELL	Repl. by CHANG 09

[1] Excluding charmonium events in $2.85 < m_{\Lambda\overline{\Lambda}} < 3.128$ GeV/c^2 and $3.315 < m_{\Lambda\overline{\Lambda}} < 3.735$ GeV/c^2. Measurements in various $m_{\Lambda\overline{\Lambda}}$ bins are also reported.
[2] Assumes equal production of B^+ and B^0 at the $\Upsilon(4S)$.

$\Gamma(\Lambda\overline{\Lambda}K^{*+})/\Gamma_{total}$ Γ_{438}/Γ

VALUE (units 10^{-6})	DOCUMENT ID		TECN	COMMENT
$2.19^{+1.13}_{-0.88}\pm0.33$	[1,2] CHANG	09	BELL	$e^+e^- \to \Upsilon(4S)$

[1] For $m_{\Lambda\overline{\Lambda}} < 2.85$ GeV/c^2.
[2] Assumes equal production of B^+ and B^0 at the $\Upsilon(4S)$.

$\Gamma(\overline{\Delta}^0 p)/\Gamma_{total}$ Γ_{439}/Γ

VALUE (units 10^{-6})	CL%	DOCUMENT ID		TECN	COMMENT
< 1.38	90	[1] WEI	08	BELL	$e^+e^- \to \Upsilon(4S)$
• • • We do not use the following data for averages, fits, limits, etc. • • •					
<380	90	[2] BORTOLETTO	89	CLEO	$e^+e^- \to \Upsilon(4S)$

[1] Assumes equal production of B^+ and B^0 at the $\Upsilon(4S)$.
[2] BORTOLETTO 89 reports $< 3.3 \times 10^{-4}$ assuming the $\Upsilon(4S)$ decays 43% to $B^0\overline{B}^0$. We rescale to 50%.

$\Gamma(\Delta^{++}\overline{p})/\Gamma_{total}$ Γ_{440}/Γ

VALUE (units 10^{-6})	CL%	DOCUMENT ID		TECN	COMMENT
< 0.14	90	[1] WEI	08	BELL	$e^+e^- \to \Upsilon(4S)$
• • • We do not use the following data for averages, fits, limits, etc. • • •					
<150	90	[2] BORTOLETTO	89	CLEO	$e^+e^- \to \Upsilon(4S)$

[1] Assumes equal production of B^+ and B^0 at the $\Upsilon(4S)$.
[2] BORTOLETTO 89 reports $< 1.3 \times 10^{-4}$ assuming the $\Upsilon(4S)$ decays 43% to $B^0\overline{B}^0$. We rescale to 50%.

$\Gamma(D^+ p\overline{p})/\Gamma_{total}$ Γ_{441}/Γ

VALUE	CL%	DOCUMENT ID		TECN	COMMENT
$<1.5 \times 10^{-5}$	90	[1] ABE	02W	BELL	$e^+e^- \to \Upsilon(4S)$

[1] Assumes equal production of B^+ and B^0 at the $\Upsilon(4S)$.

$\Gamma(D^*(2010)^+ p\overline{p})/\Gamma_{total}$ Γ_{442}/Γ

VALUE	CL%	DOCUMENT ID		TECN	COMMENT
$<1.5 \times 10^{-5}$	90	[1] ABE	02W	BELL	$e^+e^- \to \Upsilon(4S)$

[1] Assumes equal production of B^+ and B^0 at the $\Upsilon(4S)$.

$\Gamma(\overline{D}^0 p\overline{p}\pi^+)/\Gamma_{total}$ Γ_{443}/Γ

VALUE (units 10^{-4})	DOCUMENT ID		TECN	COMMENT
$3.72\pm0.11\pm0.25$	[1,2] DEL-AMO-SA...12		BABR	$e^+e^- \to \Upsilon(4S)$

[1] Uses the values of D and D^* branching fractions from PDG 08.
[2] Assumes equal production of B^+ and B^0 at the $\Upsilon(4S)$.

$\Gamma(\overline{D}^{*0} p\overline{p}\pi^+)/\Gamma_{total}$ Γ_{444}/Γ

VALUE (units 10^{-4})	DOCUMENT ID		TECN	COMMENT
$3.73\pm0.17\pm0.27$	[1,2] DEL-AMO-SA...12		BABR	$e^+e^- \to \Upsilon(4S)$

[1] Uses the values of D and D^* branching fractions from PDG 08.
[2] Assumes equal production of B^+ and B^0 at the $\Upsilon(4S)$.

$\Gamma(D^- p\overline{p}\pi^+\pi^-)/\Gamma_{total}$ Γ_{445}/Γ

VALUE (units 10^{-4})	DOCUMENT ID		TECN	COMMENT
$1.66\pm0.13\pm0.27$	[1,2] DEL-AMO-SA...12		BABR	$e^+e^- \to \Upsilon(4S)$

[1] Uses the values of D and D^* branching fractions from PDG 08.
[2] Assumes equal production of B^+ and B^0 at the $\Upsilon(4S)$.

$\Gamma(D^{*-} p\overline{p}\pi^+\pi^-)/\Gamma_{total}$ Γ_{446}/Γ

VALUE (units 10^{-4})	DOCUMENT ID		TECN	COMMENT
$1.86\pm0.16\pm0.19$	[1,2] DEL-AMO-SA...12		BABR	$e^+e^- \to \Upsilon(4S)$

[1] Uses the values of D and D^* branching fractions from PDG 08.
[2] Assumes equal production of B^+ and B^0 at the $\Upsilon(4S)$.

$\Gamma(p\overline{\Lambda}^0\overline{D}^0)/\Gamma_{total}$ Γ_{447}/Γ

VALUE (units 10^{-5})	DOCUMENT ID		TECN	COMMENT
$1.43^{+0.28}_{-0.25}\pm0.18$	[1,2] CHEN	11F	BELL	$e^+e^- \to \Upsilon(4S)$

[1] Uses $B(\Lambda \to p\pi^-) = 63.9 \pm 0.5\%$, $B(D^0 \to K^-\pi^+) = 3.89 \pm 0.05\%$, and $B(D^0 \to K^-\pi^+\pi^0) = 13.9 \pm 0.5\%$.
[2] Assumes equal production of B^0 and B^+ from Upsilon(4S) decays.

$\Gamma(p\overline{\Lambda}^0\overline{D}^*(2007)^0)/\Gamma_{total}$ Γ_{448}/Γ

VALUE (units 10^{-5})	CL%	DOCUMENT ID		TECN	COMMENT
<5	90	[1,2,3] CHEN	11F	BELL	$e^+e^- \to \Upsilon(4S)$

[1] CHEN 11F reports $< 4.8 \times 10^{-5}$ from a measurement of $[\Gamma(B^+ \to p\overline{\Lambda}^0\overline{D}^*(2007)^0)/\Gamma_{total}] / [B(D^*(2007)^0 \to D^0\pi^0)]$ assuming $B(D^*(2007)^0 \to D^0\pi^0) = (61.9 \pm 2.9) \times 10^{-2}$.
[2] Uses $B(\Lambda \to p\pi^-) = 63.9 \pm 0.5\%$ and $B(D^0 \to K^-\pi^+) = 3.89 \pm 0.05\%$.
[3] Assumes equal production of B^0 and B^+ from Upsilon(4S) decays.

$\Gamma(\overline{\Lambda}_c^- p\pi^+)/\Gamma_{total}$ Γ_{449}/Γ

VALUE (units 10^{-4})	DOCUMENT ID		TECN	COMMENT
2.8 ± 0.8 OUR AVERAGE				
$3.4\pm0.1\pm0.9$	[1,2] AUBERT	08BN	BABR	$e^+e^- \to \Upsilon(4S)$
$2.0\pm0.3\pm0.5$	[1,3] GABYSHEV	06A	BELL	$e^+e^- \to \Upsilon(4S)$
$2.4\pm0.6\pm0.6$	[1,4] DYTMAN	02	CLE2	$e^+e^- \to \Upsilon(4S)$
• • • We do not use the following data for averages, fits, limits, etc. • • •				
$1.9\pm0.5\pm0.5$	[1,5] GABYSHEV	02	BELL	Repl. by GABYSHEV 06A
$6.2^{+2.3}_{-2.0}\pm1.6$	[1,6] FU	97	CLE2	Repl. by DYTMAN 02

[1] Assumes equal production of B^+ and B^0 at the $\Upsilon(4S)$.
[2] AUBERT 08BN reports $(3.4 \pm 0.1 \pm 0.9) \times 10^{-4}$ from a measurement of $[\Gamma(B^+ \to \overline{\Lambda}_c^- p\pi^+)/\Gamma_{total}] \times [B(\Lambda_c^+ \to pK^-\pi^+)]$ assuming $B(\Lambda_c^+ \to pK^-\pi^+) = (5.0 \pm 1.3) \times 10^{-2}$.
[3] GABYSHEV 06A reports $(2.01 \pm 0.15 \pm 0.20) \times 10^{-4}$ from a measurement of $[\Gamma(B^+ \to \overline{\Lambda}_c^- p\pi^+)/\Gamma_{total}] \times [B(\Lambda_c^+ \to pK^-\pi^+)]$ assuming $B(\Lambda_c^+ \to pK^-\pi^+) = 0.05$, which we rescale to our best value $B(\Lambda_c^+ \to pK^-\pi^+) = (5.0 \pm 1.3) \times 10^{-2}$. Our first error is their experiment's error and our second error is the systematic error from using our best value.

[4] DYTMAN 02 reports $(2.4^{+0.63}_{-0.62})\times10^{-4}$ from a measurement of $[\Gamma(B^+\to\overline{\Lambda}_c^-p\pi^+)/\Gamma_{\rm total}]\times[B(\Lambda_c^+\to pK^-\pi^+)]$ assuming $B(\Lambda_c^+\to pK^-\pi^+)=0.05$, which we rescale to our best value $B(\Lambda_c^+\to pK^-\pi^+)=(5.0\pm1.3)\times10^{-2}$. Our first error is their experiment's error and our second error is the systematic error from using our best value.
[5] GABYSHEV 02 reports $(1.87^{+0.51}_{-0.49})\times10^{-4}$ from a measurement of $[\Gamma(B^+\to\overline{\Lambda}_c^-p\pi^+)/\Gamma_{\rm total}]\times[B(\Lambda_c^+\to pK^-\pi^+)]$ assuming $B(\Lambda_c^+\to pK^-\pi^+)=0.05$, which we rescale to our best value $B(\Lambda_c^+\to pK^-\pi^+)=(5.0\pm1.3)\times10^{-2}$. Our first error is their experiment's error and our second error is the systematic error from using our best value.
[6] FU 97 uses PDG 96 values of Λ_c branching fraction.

$\Gamma(\overline{\Lambda}_c^-\Delta(1232)^{++})/\Gamma_{\rm total}$ Γ_{450}/Γ

VALUE (units 10^{-5})	CL%	DOCUMENT ID		TECN	COMMENT
<1.9	90	GABYSHEV	06A	BELL	$e^+e^-\to\Upsilon(4S)$

$\Gamma(\overline{\Lambda}_c^-\Delta_X(1600)^{++})/\Gamma_{\rm total}$ Γ_{451}/Γ

VALUE (units 10^{-5})	DOCUMENT ID		TECN	COMMENT
5.9±1.2±1.5	[1] GABYSHEV	06A	BELL	$e^+e^-\to\Upsilon(4S)$

[1] GABYSHEV 06A reports $(5.9\pm1.0\pm0.6)\times10^{-5}$ from a measurement of $[\Gamma(B^+\to\overline{\Lambda}_c^-\Delta_X(1600)^{++})/\Gamma_{\rm total}]\times[B(\Lambda_c^+\to pK^-\pi^+)]$ assuming $B(\Lambda_c^+\to pK^-\pi^+)=0.05$, which we rescale to our best value $B(\Lambda_c^+\to pK^-\pi^+)=(5.0\pm1.3)\times10^{-2}$. Our first error is their experiment's error and our second error is the systematic error from using our best value.

$\Gamma(\overline{\Lambda}_c^-\Delta_X(2420)^{++})/\Gamma_{\rm total}$ Γ_{452}/Γ

VALUE (units 10^{-5})	DOCUMENT ID		TECN	COMMENT
$4.7^{+1.1}_{-1.0}\pm1.2$	[1] GABYSHEV	06A	BELL	$e^+e^-\to\Upsilon(4S)$

[1] GABYSHEV 06A reports $(4.7^{+1.0}_{-0.9}\pm0.4)\times10^{-5}$ from a measurement of $[\Gamma(B^+\to\overline{\Lambda}_c^-\Delta_X(2420)^{++})/\Gamma_{\rm total}]\times[B(\Lambda_c^+\to pK^-\pi^+)]$ assuming $B(\Lambda_c^+\to pK^-\pi^+)=0.05$, which we rescale to our best value $B(\Lambda_c^+\to pK^-\pi^+)=(5.0\pm1.3)\times10^{-2}$. Our first error is their experiment's error and our second error is the systematic error from using our best value.

$\Gamma((\overline{\Lambda}_c^-p)_s\pi^+)/\Gamma_{\rm total}$ Γ_{453}/Γ

$(\overline{\Lambda}_c^-p)_s$ denotes a low-mass enhancement near 3.35 GeV/c^2.

VALUE (units 10^{-5})	DOCUMENT ID		TECN	COMMENT
$3.9^{+0.9}_{-0.8}\pm1.0$	[1] GABYSHEV	06A	BELL	$e^+e^-\to\Upsilon(4S)$

[1] GABYSHEV 06A reports $(3.9^{+0.8}_{-0.7}\pm0.4)\times10^{-5}$ from a measurement of $[\Gamma(B^+\to(\overline{\Lambda}_c^-p)_s\pi^+)/\Gamma_{\rm total}]\times[B(\Lambda_c^+\to pK^-\pi^+)]$ assuming $B(\Lambda_c^+\to pK^-\pi^+)=0.05$, which we rescale to our best value $B(\Lambda_c^+\to pK^-\pi^+)=(5.0\pm1.3)\times10^{-2}$. Our first error is their experiment's error and our second error is the systematic error from using our best value.

$\Gamma(\overline{\Sigma}_c(2520)^0p)/\Gamma_{\rm total}$ Γ_{454}/Γ

VALUE (units 10^{-5})	CL%	DOCUMENT ID		TECN	COMMENT
<0.3	90	[1,2] AUBERT	08BN	BABR	$e^+e^-\to\Upsilon(4S)$
• • • We do not use the following data for averages, fits, limits, etc. • • •					
<2.7	90	[1,2] GABYSHEV	06A	BELL	$e^+e^-\to\Upsilon(4S)$
<4.6	90	[1,2] GABYSHEV	02	BELL	Repl. by GABYSHEV 06A

[1] Assumes equal production of B^+ and B^0 at the $\Upsilon(4S)$.
[2] Uses the value for $\Lambda_c\to pK^-\pi^+$ branching ratio (5.0 ± 1.3)%.

$\Gamma(\overline{\Sigma}_c(2520)^0p)/\Gamma(\overline{\Lambda}_c^-p\pi^+)$ $\Gamma_{454}/\Gamma_{449}$

VALUE (units 10^{-3})	CL%	DOCUMENT ID		TECN	COMMENT
<9	90	AUBERT	08BN	BABR	$e^+e^-\to\Upsilon(4S)$

$\Gamma(\overline{\Sigma}_c(2800)^0p)/\Gamma_{\rm total}$ Γ_{455}/Γ

VALUE (units 10^{-5})	DOCUMENT ID		TECN	COMMENT
3.3±0.9±0.9	[1] AUBERT	08BN	BABR	$e^+e^-\to\Upsilon(4S)$

[1] AUBERT 08BN reports $[\Gamma(B^+\to\overline{\Sigma}_c(2800)^0p)/\Gamma_{\rm total}]$ / $[B(B^+\to\overline{\Lambda}_c^-p\pi^+)]$ = 0.117 ± 0.023 ± 0.024 which we multiply by our best value $B(B^+\to\overline{\Lambda}_c^-p\pi^+)=(2.8\pm0.8)\times10^{-4}$. Our first error is their experiment's error and our second error is the systematic error from using our best value.

$\Gamma(\overline{\Lambda}_c^-p\pi^+\pi^0)/\Gamma_{\rm total}$ Γ_{456}/Γ

VALUE (units 10^{-3})	CL%	DOCUMENT ID		TECN	COMMENT
$1.81\pm0.29^{+0.52}_{-0.50}$		[1,2] DYTMAN	02	CLE2	$e^+e^-\to\Upsilon(4S)$
• • • We do not use the following data for averages, fits, limits, etc. • • •					
<3.12	90	[3] FU	97	CLE2	$e^+e^-\to\Upsilon(4S)$

[1] Assumes equal production of B^+ and B^0 at the $\Upsilon(4S)$.
[2] DYTMAN 02 measurement uses $B(\Lambda_c^-\to\overline{p}K^+\pi^-)=5.0\pm1.3\%$. The second error includes the systematic and the uncertainty of the branching ratio.
[3] FU 97 uses PDG 96 values of Λ_c branching ratio.

$\Gamma(\overline{\Lambda}_c^-p\pi^+\pi^+\pi^-)/\Gamma_{\rm total}$ Γ_{457}/Γ

VALUE (units 10^{-3})	CL%	DOCUMENT ID		TECN	COMMENT
$2.25\pm0.25^{+0.63}_{-0.61}$		[1,2] DYTMAN	02	CLE2	$e^+e^-\to\Upsilon(4S)$
• • • We do not use the following data for averages, fits, limits, etc. • • •					
<1.46	90	[3] FU	97	CLE2	$e^+e^-\to\Upsilon(4S)$

[1] Assumes equal production of B^+ and B^0 at the $\Upsilon(4S)$.
[2] DYTMAN 02 measurement uses $B(\Lambda_c^-\to\overline{p}K^+\pi^-)=5.0\pm1.3\%$. The second error includes the systematic and the uncertainty of the branching ratio.
[3] FU 97 uses PDG 96 values of Λ_c branching ratio.

$\Gamma(\overline{\Lambda}_c^-p\pi^+\pi^+\pi^-\pi^0)/\Gamma_{\rm total}$ Γ_{458}/Γ

VALUE	CL%	DOCUMENT ID		TECN	COMMENT
$<1.34\times10^{-2}$	90	[1] FU	97	CLE2	$e^+e^-\to\Upsilon(4S)$

[1] FU 97 uses PDG 96 values of Λ_c branching ratio.

$\Gamma(\Lambda_c^+\Lambda_c^-K^+)/\Gamma_{\rm total}$ Γ_{459}/Γ

VALUE (units 10^{-4})		DOCUMENT ID		TECN	COMMENT
8.7±3.5 OUR AVERAGE					
11 ±1 ±6		[1,2] AUBERT	08H	BABR	$e^+e^-\to\Upsilon(4S)$
8 ±1 ±4		[2,3] GABYSHEV	06	BELL	$e^+e^-\to\Upsilon(4S)$

[1] AUBERT 08H reports $(1.14\pm0.15\pm0.62)\times10^{-3}$ from a measurement of $[\Gamma(B^+\to\Lambda_c^+\Lambda_c^-K^+)/\Gamma_{\rm total}]\times[B(\Lambda_c^+\to pK^-\pi^+)]$ assuming $B(\Lambda_c^+\to pK^-\pi^+)=(5.0\pm1.3)\times10^{-2}$.
[2] Assumes equal production of B^+ and B^0 at the $\Upsilon(4S)$.
[3] GABYSHEV 06 reports $(7.9^{+1.0}_{-0.9}\pm3.6)\times10^{-4}$ from a measurement of $[\Gamma(B^+\to\Lambda_c^+\Lambda_c^-K^+)/\Gamma_{\rm total}]\times[B(\Lambda_c^+\to pK^-\pi^+)]$ assuming $B(\Lambda_c^+\to pK^-\pi^+)=(5.0\pm1.3)\times10^{-2}$.

$\Gamma(\overline{\Sigma}_c(2455)^0p)/\Gamma_{\rm total}$ Γ_{460}/Γ

VALUE (units 10^{-5})	CL%	DOCUMENT ID		TECN	COMMENT
3.7±0.8±1.0		[1,2] GABYSHEV	06A	BELL	$e^+e^-\to\Upsilon(4S)$
• • • We do not use the following data for averages, fits, limits, etc. • • •					
<8	90	[1,3] DYTMAN	02	CLE2	$e^+e^-\to\Upsilon(4S)$
<9.3	90	[1,4] GABYSHEV	02	BELL	Repl. by GABYSHEV 06A

[1] Assumes equal production of B^+ and B^0 at the $\Upsilon(4S)$.
[2] GABYSHEV 06A reports $(3.7\pm0.7\pm0.4)\times10^{-5}$ from a measurement of $[\Gamma(B^+\to\overline{\Sigma}_c(2455)^0p)/\Gamma_{\rm total}]\times[B(\Lambda_c^+\to pK^-\pi^+)]$ assuming $B(\Lambda_c^+\to pK^-\pi^+)=0.05$, which we rescale to our best value $B(\Lambda_c^+\to pK^-\pi^+)=(5.0\pm1.3)\times10^{-2}$. Our first error is their experiment's error and our second error is the systematic error from using our best value.
[3] DYTMAN 02 measurement uses $B(\Lambda_c^-\to\overline{p}K^+\pi^-)=5.0\pm1.3\%$. The second error includes the systematic and the uncertainty of the branching ratio.
[4] Uses the value for $\Lambda_c\to pK^-\pi^+$ branching ratio (5.0 ± 1.3)%.

$\Gamma(\overline{\Sigma}_c(2455)^0p)/\Gamma(\overline{\Lambda}_c^-p\pi^+)$ $\Gamma_{460}/\Gamma_{449}$

VALUE	DOCUMENT ID		TECN	COMMENT
0.123±0.012±0.008	[1] AUBERT	08BN	BABR	$e^+e^-\to\Upsilon(4S)$

[1] Assumes equal production of B^+ and B^0 at the $\Upsilon(4S)$.

$\Gamma(\overline{\Sigma}_c(2455)^0p\pi^0)/\Gamma_{\rm total}$ Γ_{461}/Γ

VALUE (units 10^{-4})	DOCUMENT ID		TECN	COMMENT
4.4±1.4±1.1	[1,2] DYTMAN	02	CLE2	$e^+e^-\to\Upsilon(4S)$

[1] DYTMAN 02 reports $(4.4\pm1.4)\times10^{-4}$ from a measurement of $[\Gamma(B^+\to\overline{\Sigma}_c(2455)^0p\pi^0)/\Gamma_{\rm total}]\times[B(\Lambda_c^+\to pK^-\pi^+)]$ assuming $B(\Lambda_c^+\to pK^-\pi^+)=0.05$, which we rescale to our best value $B(\Lambda_c^+\to pK^-\pi^+)=(5.0\pm1.3)\times10^{-2}$. Our first error is their experiment's error and our second error is the systematic error from using our best value.
[2] Assumes equal production of B^+ and B^0 at the $\Upsilon(4S)$.

$\Gamma(\overline{\Sigma}_c(2455)^0p\pi^-\pi^+)/\Gamma_{\rm total}$ Γ_{462}/Γ

VALUE (units 10^{-4})	DOCUMENT ID		TECN	COMMENT
4.4±1.3±1.1	[1,2] DYTMAN	02	CLE2	$e^+e^-\to\Upsilon(4S)$

[1] DYTMAN 02 reports $(4.4\pm1.3)\times10^{-4}$ from a measurement of $[\Gamma(B^+\to\overline{\Sigma}_c(2455)^0p\pi^-\pi^+)/\Gamma_{\rm total}]\times[B(\Lambda_c^+\to pK^-\pi^+)]$ assuming $B(\Lambda_c^+\to pK^-\pi^+)=0.05$, which we rescale to our best value $B(\Lambda_c^+\to pK^-\pi^+)=(5.0\pm1.3)\times10^{-2}$. Our first error is their experiment's error and our second error is the systematic error from using our best value.
[2] Assumes equal production of B^+ and B^0 at the $\Upsilon(4S)$.

$\Gamma(\overline{\Sigma}_c(2455)^{--}p\pi^+\pi^+)/\Gamma_{\rm total}$ Γ_{463}/Γ

VALUE (units 10^{-4})	DOCUMENT ID		TECN	COMMENT
3.0±0.8 OUR AVERAGE				
3.0±0.2±0.8	[1,2] LEES	12Z	BABR	$e^+e^-\to\Upsilon(4S)$
2.8±0.9±0.9	[1,3] DYTMAN	02	CLE2	$e^+e^-\to\Upsilon(4S)$

[1] Assumes equal production of B^+ and B^0 at the $\Upsilon(4S)$.

[2] LEES 12Z reports $(2.98 \pm 0.16 \pm 0.15 \pm 0.77) \times 10^{-4}$ from a measurement of $[\Gamma(B^+ \to \overline{\Sigma}_c(2455)^{--} p\pi^+\pi^+)/\Gamma_{\text{total}}] \times [B(\Lambda_c^+ \to pK^-\pi^+)]$ assuming $B(\Lambda_c^+ \to pK^-\pi^+) = (5.0 \pm 1.3) \times 10^{-2}$.

[3] DYTMAN 02 reports $(2.8 \pm 0.9 \pm 0.5 \pm 0.7) \times 10^{-4}$ from a measurement of $[\Gamma(B^+ \to \overline{\Sigma}_c(2455)^{--} p\pi^+\pi^+)/\Gamma_{\text{total}}] \times [B(\Lambda_c^+ \to pK^-\pi^+)]$ assuming $B(\Lambda_c^+ \to pK^-\pi^+) = (5.0 \pm 1.3) \times 10^{-2}$.

$\Gamma(\overline{\Lambda}_c(2593)^- / \overline{\Lambda}_c(2625)^- p\pi^+)/\Gamma_{\text{total}}$ Γ_{464}/Γ

VALUE	CL%	DOCUMENT ID		TECN	COMMENT
$<1.9 \times 10^{-4}$	90	[1,2] DYTMAN	02	CLE2	$e^+e^- \to \Upsilon(4S)$

[1] Assumes equal production of B^+ and B^0 at the $\Upsilon(4S)$.

[2] DYTMAN 02 measurement uses $B(\Lambda_c^- \to \overline{p}K^+\pi^-) = 5.0 \pm 1.3\%$. The second error includes the systematic and the uncertainty of the branching ratio.

$\Gamma(\overline{\Xi}_c^0 \Lambda_c^+, \overline{\Xi}_c^0 \to \overline{\Xi}^+\pi^-)/\Gamma_{\text{total}}$ Γ_{465}/Γ

VALUE (units 10^{-5})	DOCUMENT ID		TECN	COMMENT
3.0±1.1 OUR AVERAGE				
$2.5 \pm 0.9 \pm 0.6$	[1,2] AUBERT	08H	BABR	$e^+e^- \to \Upsilon(4S)$
$5.6^{+1.9}_{-1.5} \pm 1.9$	[2,3] CHISTOV	06A	BELL	$e^+e^- \to \Upsilon(4S)$

[1] AUBERT 08H reports $(2.51 \pm 0.89 \pm 0.61) \times 10^{-5}$ from a measurement of $[\Gamma(B^+ \to \overline{\Xi}_c^0 \Lambda_c^+, \overline{\Xi}_c^0 \to \overline{\Xi}^+\pi^-)/\Gamma_{\text{total}}] \times [B(\Lambda_c^+ \to pK^-\pi^+)]$ assuming $B(\Lambda_c^+ \to pK^-\pi^+) = (5.0 \pm 1.3) \times 10^{-2}$.

[2] Assumes equal production of B^+ and B^0 at the $\Upsilon(4S)$.

[3] CHISTOV 06A reports $(5.6^{+1.9}_{-1.5} \pm 1.9) \times 10^{-5}$ from a measurement of $[\Gamma(B^+ \to \overline{\Xi}_c^0 \Lambda_c^+, \overline{\Xi}_c^0 \to \overline{\Xi}^+\pi^-)/\Gamma_{\text{total}}] \times [B(\Lambda_c^+ \to pK^-\pi^+)]$ assuming $B(\Lambda_c^+ \to pK^-\pi^+) = (5.0 \pm 1.3) \times 10^{-2}$.

$\Gamma(\overline{\Xi}_c^0 \Lambda_c^+, \overline{\Xi}_c^0 \to \Lambda K^+\pi^-)/\Gamma_{\text{total}}$ Γ_{466}/Γ

VALUE (units 10^{-5})	DOCUMENT ID		TECN	COMMENT
2.6±1.1 OUR AVERAGE Error includes scale factor of 1.1.				
$1.7 \pm 0.9 \pm 0.5$	[1,2] AUBERT	08H	BABR	$e^+e^- \to \Upsilon(4S)$
$4.0^{+1.1}_{-0.9} \pm 1.3$	[2,3] CHISTOV	06A	BELL	$e^+e^- \to \Upsilon(4S)$

[1] AUBERT 08H reports $(1.70 \pm 0.93 \pm 0.53) \times 10^{-5}$ from a measurement of $[\Gamma(B^+ \to \overline{\Xi}_c^0 \Lambda_c^+, \overline{\Xi}_c^0 \to \Lambda K^+\pi^-)/\Gamma_{\text{total}}] \times [B(\Lambda_c^+ \to pK^-\pi^+)]$ assuming $B(\Lambda_c^+ \to pK^-\pi^+) = (5.0 \pm 1.3) \times 10^{-2}$.

[2] Assumes equal production of B^+ and B^0 at the $\Upsilon(4S)$.

[3] CHISTOV 06A reports $(4.0^{+1.1}_{-0.9} \pm 1.3) \times 10^{-5}$ from a measurement of $[\Gamma(B^+ \to \overline{\Xi}_c^0 \Lambda_c^+, \overline{\Xi}_c^0 \to \Lambda K^+\pi^-)/\Gamma_{\text{total}}] \times [B(\Lambda_c^+ \to pK^-\pi^+)]$ assuming $B(\Lambda_c^+ \to pK^-\pi^+) = (5.0 \pm 1.3) \times 10^{-2}$.

$\Gamma(\pi^+ \ell^+ \ell^-)/\Gamma_{\text{total}}$ Γ_{467}/Γ

VALUE	CL%	DOCUMENT ID		TECN	COMMENT
$<4.9 \times 10^{-8}$	90	[1] WEI	08A	BELL	$e^+e^- \to \Upsilon(4S)$
• • • We do not use the following data for averages, fits, limits, etc. • • •					
$<6.6 \times 10^{-8}$	90	[1] LEES	13M	BABR	$e^+e^- \to \Upsilon(4S)$
$<1.2 \times 10^{-7}$	90	[1] AUBERT	07AG	BABR	$e^+e^- \to \Upsilon(4S)$

[1] Assumes equal production of B^+ and B^0 at the $\Upsilon(4S)$.

$\Gamma(\pi^+ e^+ e^-)/\Gamma_{\text{total}}$ Γ_{468}/Γ

Test for ΔB=1 weak neutral current. Allowed by higher-order electroweak interactions.

VALUE	CL%	DOCUMENT ID		TECN	COMMENT
$< 8.0 \times 10^{-8}$	90	[1] WEI	08A	BELL	$e^+e^- \to \Upsilon(4S)$
• • • We do not use the following data for averages, fits, limits, etc. • • •					
$<12.5 \times 10^{-8}$	90	[1] LEES	13M	BABR	$e^+e^- \to \Upsilon(4S)$
$<18 \times 10^{-8}$	90	[1] AUBERT	07AG	BABR	$e^+e^- \to \Upsilon(4S)$
$< 3.9 \times 10^{-3}$	90	[2] WEIR	90B	MRK2	e^+e^- 29 GeV

[1] Assumes equal production of B^+ and B^0 at the $\Upsilon(4S)$.

[2] WEIR 90B assumes B^+ production cross section from LUND.

$\Gamma(\pi^+ \mu^+ \mu^-)/\Gamma_{\text{total}}$ Γ_{469}/Γ

Test for ΔB=1 weak neutral current. Allowed by higher-order electroweak interactions.

VALUE	CL%	DOCUMENT ID		TECN	COMMENT
$<5.5 \times 10^{-8}$	90	[1] LEES	13M	BABR	$e^+e^- \to \Upsilon(4S)$
• • • We do not use the following data for averages, fits, limits, etc. • • •					
$<6.9 \times 10^{-8}$	90	[1] WEI	08A	BELL	$e^+e^- \to \Upsilon(4S)$
$<2.8 \times 10^{-7}$	90	[1] AUBERT	07AG	BABR	$e^+e^- \to \Upsilon(4S)$
$<9.1 \times 10^{-3}$	90	[2] WEIR	90B	MRK2	e^+e^- 29 GeV

[1] Assumes equal production of B^+ and B^0 at the $\Upsilon(4S)$.

[2] WEIR 90B assumes B^+ production cross section from LUND.

$\Gamma(\pi^+ \mu^+ \mu^-)/\Gamma(K^+ \mu^+ \mu^-)$ $\Gamma_{469}/\Gamma_{473}$

VALUE	DOCUMENT ID		TECN	COMMENT
0.053±0.014±0.001	AAIJ	12AY	LHCB	pp at 7 TeV

$\Gamma(\pi^+ \nu\overline{\nu})/\Gamma_{\text{total}}$ Γ_{470}/Γ

Test for ΔB=1 weak neutral current. Allowed by higher-order electroweak interactions.

VALUE	CL%	DOCUMENT ID		TECN	COMMENT
$<9.8 \times 10^{-5}$	90	[1] LUTZ	13	BELL	$e^+e^- \to \Upsilon(4S)$
• • • We do not use the following data for averages, fits, limits, etc. • • •					
$<1.7 \times 10^{-4}$	90	[1] CHEN	07D	BELL	$e^+e^- \to \Upsilon(4S)$
$<1.0 \times 10^{-4}$	90	[1] AUBERT	05H	BABR	$e^+e^- \to \Upsilon(4S)$

[1] Assumes equal production of B^+ and B^0 at the $\Upsilon(4S)$.

$\Gamma(K^+ \ell^+ \ell^-)/\Gamma_{\text{total}}$ Γ_{471}/Γ

Test for ΔB=1 weak neutral current. Allowed by higher-order electroweak interactions.

VALUE (units 10^{-7})	DOCUMENT ID		TECN	COMMENT
4.51±0.23 OUR AVERAGE Error includes scale factor of 1.1.				
$4.36 \pm 0.15 \pm 0.18$	[1] AAIJ	13H	LHCB	pp at 7 TeV
$4.8 \pm 0.9 \pm 0.2$	[2] AUBERT	09T	BABR	$e^+e^- \to \Upsilon(4S)$
$5.3^{+0.6}_{-0.5} \pm 0.3$	[2] WEI	09A	BELL	$e^+e^- \to \Upsilon(4S)$
• • • We do not use the following data for averages, fits, limits, etc. • • •				
$3.8^{+0.9}_{-0.8} \pm 0.2$	[2] AUBERT,B	06J	BABR	Repl. by AUBERT 09T
$5.3^{+1.1}_{-1.0} \pm 0.3$	[2] ISHIKAWA	03	BELL	Repl. by WEI 09A

[1] Uses $B(B^+ \to J/\psi K^+ \to \mu^+\mu^- K^+) = (6.01 \pm 0.21) \times 10^{-5}$.

[2] Assumes equal production of B^+ and B^0 at the $\Upsilon(4S)$.

$\Gamma(K^+ e^+ e^-)/\Gamma_{\text{total}}$ Γ_{472}/Γ

Test for ΔB=1 weak neutral current. Allowed by higher-order electroweak interactions.

VALUE (units 10^{-7})	CL%	DOCUMENT ID		TECN	COMMENT
5.5±0.7 OUR AVERAGE					
$5.1^{+1.2}_{-1.1} \pm 0.2$		[1] AUBERT	09T	BABR	$e^+e^- \to \Upsilon(4S)$
$5.7^{+0.9}_{-0.8} \pm 0.3$		[1] WEI	09A	BELL	$e^+e^- \to \Upsilon(4S)$
• • • We do not use the following data for averages, fits, limits, etc. • • •					
$4.2^{+1.2}_{-1.1} \pm 0.2$		[1] AUBERT,B	06J	BABR	Repl. by AUBERT 09T
$10.5^{+2.5}_{-2.2} \pm 0.7$		[1] AUBERT	03U	BABR	Repl. by AUBERT,B 06J
$6.3^{+1.9}_{-1.7} \pm 0.3$		[2] ISHIKAWA	03	BELL	Repl. by WEI 09A
$<$ 14	90	[1] ABE	02	BELL	$e^+e^- \to \Upsilon(4S)$
$<$ 9	90	[1] AUBERT	02L	BABR	$e^+e^- \to \Upsilon(4S)$
$<$ 24	90	[3] ANDERSON	01B	CLE2	$e^+e^- \to \Upsilon(4S)$
$<$ 990	90	[4] ALBRECHT	91E	ARG	$e^+e^- \to \Upsilon(4S)$
$<$68000	90	[5] WEIR	90B	MRK2	e^+e^- 29 GeV
$<$ 600	90	[6] AVERY	89B	CLEO	$e^+e^- \to \Upsilon(4S)$
$<$ 2500	90	[7] AVERY	87	CLEO	$e^+e^- \to \Upsilon(4S)$

[1] Assumes equal production of B^+ and B^0 at the $\Upsilon(4S)$.

[2] Assumes equal production of B^0 and B^+ at $\Upsilon(4S)$. The second error is a total of systematic uncertainties including model dependence.

[3] The result is for di-lepton masses above 0.5 GeV.

[4] ALBRECHT 91E reports $< 9.0 \times 10^{-5}$ assuming the $\Upsilon(4S)$ decays 45% to $B^0\overline{B}^0$. We rescale to 50%.

[5] WEIR 90B assumes B^+ production cross section from LUND.

[6] AVERY 89B reports $< 5 \times 10^{-5}$ assuming the $\Upsilon(4S)$ decays 43% to $B^0\overline{B}^0$. We rescale to 50%.

[7] AVERY 87 reports $< 2.1 \times 10^{-4}$ assuming the $\Upsilon(4S)$ decays 40% to $B^0\overline{B}^0$. We rescale to 50%.

$\Gamma(K^+ \mu^+ \mu^-)/\Gamma_{\text{total}}$ Γ_{473}/Γ

Test for ΔB=1 weak neutral current. Allowed by higher-order electroweak interactions.

VALUE (units 10^{-7})	CL%	DOCUMENT ID		TECN	COMMENT
4.49±0.23 OUR FIT Error includes scale factor of 1.1.					
4.43±0.26 OUR AVERAGE Error includes scale factor of 1.2.					
$4.36 \pm 0.15 \pm 0.18$		[1] AAIJ	13H	LHCB	pp at 7 TeV
$4.1^{+1.6}_{-1.5} \pm 0.2$		[2] AUBERT	09T	BABR	$e^+e^- \to \Upsilon(4S)$
$5.3^{+0.8}_{-0.7} \pm 0.3$		[2] WEI	09A	BELL	$e^+e^- \to \Upsilon(4S)$
• • • We do not use the following data for averages, fits, limits, etc. • • •					
$3.1^{+1.5}_{-1.2} \pm 0.3$		[2] AUBERT,B	06J	BABR	Repl. by AUBERT 09T
$0.7^{+1.9}_{-1.1} \pm 0.2$		[2] AUBERT	03U	BABR	Repl. by AUBERT,B 06J
$4.5^{+1.4}_{-1.2} \pm 0.3$		[3] ISHIKAWA	03	BELL	Repl. by WEI 09A
$9.8^{+4.6}_{-3.6} \pm 1.6$		[2] ABE	02	BELL	Repl. by ISHIKAWA 03
$<$ 12	90	[2] AUBERT	02L	BABR	$e^+e^- \to \Upsilon(4S)$
$<$ 36.8	90	[4] ANDERSON	01B	CLE2	$e^+e^- \to \Upsilon(4S)$
$<$ 52	90	[5] AFFOLDER	99B	CDF	$p\overline{p}$ at 1.8 TeV
$<$ 100	90	[6] ABE	96L	CDF	Repl. by AFFOLDER 99B
$<$ 2400	90	[7] ALBRECHT	91E	ARG	$e^+e^- \to \Upsilon(4S)$
$<$64000	90	[8] WEIR	90B	MRK2	e^+e^- 29 GeV
$<$ 1700	90	[9] AVERY	89B	CLEO	$e^+e^- \to \Upsilon(4S)$
$<$ 3800	90	[10] AVERY	87	CLEO	$e^+e^- \to \Upsilon(4S)$

[1] Uses $B(B^+ \to J/\psi K^+ \to \mu^+\mu^- K^+) = (6.01 \pm 0.21) \times 10^{-5}$.
[2] Assumes equal production of B^+ and B^0 at the $\Upsilon(4S)$.
[3] Assumes equal production of B^0 and B^+ at $\Upsilon(4S)$. The second error is a total of systematic uncertainties including model dependence.
[4] The result is for di-lepton masses above 0.5 GeV.
[5] AFFOLDER 99B measured relative to $B^+ \to J/\psi(1S) K^+$.
[6] ABE 96L measured relative to $B^+ \to J/\psi(1S) K^+$ using PDG 94 branching ratios.
[7] ALBRECHT 91E reports $< 2.2 \times 10^{-4}$ assuming the $\Upsilon(4S)$ decays 45% to $B^0\overline{B}^0$. We rescale to 50%.
[8] WEIR 90B assumes B^+ production cross section from LUND.
[9] AVERY 89B reports $< 1.5 \times 10^{-4}$ assuming the $\Upsilon(4S)$ decays 43% to $B^0\overline{B}^0$. We rescale to 50%.
[10] AVERY 87 reports $< 3.2 \times 10^{-4}$ assuming the $\Upsilon(4S)$ decays 40% to $B^0\overline{B}^0$. We rescale to 50%.

$\Gamma(\psi(4040)K^+)/\Gamma_{\text{total}}$ Γ_{474}/Γ

VALUE	CL%	DOCUMENT ID	TECN	COMMENT
$<1.3 \times 10^{-4}$	90	AAIJ	13BC LHCB	pp at 7, 8 TeV

$\Gamma(\psi(4160)K^+)/\Gamma_{\text{total}}$ Γ_{475}/Γ

VALUE (units 10^{-4})	DOCUMENT ID	TECN	COMMENT
$5.1^{+1.3+2.5}_{-1.2-2.4}$	[1] AAIJ	13BC LHCB	pp at 7, 8 TeV

[1] AAIJ 13BC reports $[\Gamma(B^+ \to \psi(4160)K^+)]/\Gamma_{\text{total}}] \times B(\psi(4160) \to \mu^+\mu^-) = (3.5^{+0.9}_{-0.8}) \times 10^{-9}$ which we devide by our best value $B(\psi(4160) \to e^+e^-) = (6.9 \pm 3.3) \times 10^{-6}$ assuming lepton universality. Our first error is their experiment's error and our second error is the systematic error from using our best value.

$\Gamma(K^+\mu^+\mu^-)/\Gamma(J/\psi(1S)K^+)$ $\Gamma_{473}/\Gamma_{218}$

VALUE (units 10^{-3})	DOCUMENT ID	TECN	COMMENT
0.437±0.024 OUR FIT	Error includes scale factor of 1.1.		
0.46 ±0.04 ±0.02	AALTONEN	11AI CDF	$p\overline{p}$ at 1.96 TeV
• • • We do not use the following data for averages, fits, limits, etc. • • •			
0.38 ±0.05 ±0.02	AALTONEN	11L CDF	Repl. by AALTONEN 11AI
0.59 ±0.15 ±0.03	AALTONEN	09B CDF	Repl. by AALTONEN 11L

$\Gamma(K^+\overline{\nu}\nu)/\Gamma_{\text{total}}$ Γ_{476}/Γ

Test for ΔB=1 weak neutral current. Allowed by higher-order electroweak interactions.

VALUE	CL%	DOCUMENT ID		TECN	COMMENT
$<1.6 \times 10^{-5}$	90	[1,2] LEES	13I	BABR	$e^+e^- \to \Upsilon(4S)$
• • • We do not use the following data for averages, fits, limits, etc. • • •					
$<5.5 \times 10^{-5}$	90	[1] LUTZ	13	BELL	$e^+e^- \to \Upsilon(4S)$
$<1.3 \times 10^{-5}$	90	[1] DEL-AMO-SA	10Q	BABR	Repl. by LEES 13I
$<1.4 \times 10^{-5}$	90	[1] CHEN	07D	BELL	$e^+e^- \to \Upsilon(4S)$
$<5.2 \times 10^{-5}$	90	[1] AUBERT	05H	BABR	$e^+e^- \to \Upsilon(4S)$
$<2.4 \times 10^{-4}$	90	[1] BROWDER	01	CLE2	$e^+e^- \to \Upsilon(4S)$

[1] Assumes equal production of B^+ and B^0 at the $\Upsilon(4S)$.
[2] Also reported a limit $< 3.7 \times 10^{-5}$ at 90% CL obtained using a fully reconstructed hadronic B-tag evnets.

$\Gamma(\rho^+\nu\overline{\nu})/\Gamma_{\text{total}}$ Γ_{477}/Γ

Test for $\Delta B = 1$ weak neutral current. Allowed by higher-order electroweak interaction.

VALUE	CL%	DOCUMENT ID	TECN	COMMENT
$<2.13 \times 10^{-4}$	90	[1] LUTZ 13	BELL	$e^+e^- \to \Upsilon(4S)$
• • • We do not use the following data for averages, fits, limits, etc. • • •				
$<1.5 \times 10^{-4}$	90	[1] CHEN 07D	BELL	Repl. by LUTZ 13

[1] Assumes equal production of B^+ and B^0 at the $\Upsilon(4S)$.

$\Gamma(K^*(892)^+\ell^+\ell^-)/\Gamma_{\text{total}}$ Γ_{478}/Γ

Test for ΔB=1 weak neutral current. Allowed by higher-order electroweak interactions.

VALUE (units 10^{-7})	CL%	DOCUMENT ID		TECN	COMMENT
12.9±2.1 OUR AVERAGE					
$14.0^{+4.0}_{-3.7} \pm 0.9$		[1] AUBERT	09T	BABR	$e^+e^- \to \Upsilon(4S)$
$12.4^{+2.3}_{-2.1} \pm 1.3$		[1] WEI	09A	BELL	$e^+e^- \to \Upsilon(4S)$
• • • We do not use the following data for averages, fits, limits, etc. • • •					
$7.3^{+5.0}_{-4.2} \pm 2.1$		[1] AUBERT,B	06J	BABR	Repl. by AUBERT 09T
<22	90	[1] ISHIKAWA	03	BELL	$e^+e^- \to \Upsilon(4S)$

[1] Assumes equal production of B^+ and B^0 at the $\Upsilon(4S)$.

$\Gamma(K^*(892)^+e^+e^-)/\Gamma_{\text{total}}$ Γ_{479}/Γ

Test for ΔB=1 weak neutral current. Allowed by higher-order electroweak interactions.

VALUE (units 10^{-7})	CL%	DOCUMENT ID		TECN	COMMENT
$15.5^{+4.0}_{-3.1}$ OUR AVERAGE					
$13.8^{+4.7}_{-4.2} \pm 0.8$		[1] AUBERT	09T	BABR	$e^+e^- \to \Upsilon(4S)$
$17.3^{+5.0}_{-4.2} \pm 2.0$		[1] WEI	09A	BELL	$e^+e^- \to \Upsilon(4S)$
• • • We do not use the following data for averages, fits, limits, etc. • • •					
$7.5^{+7.6}_{-6.5} \pm 3.8$		[1] AUBERT,B	06J	BABR	Repl. by AUBERT 09T
$2.0^{+13.4}_{-8.7} \pm 2.8$		[1] AUBERT	03U	BABR	$e^+e^- \to \Upsilon(4S)$
<46	90	[2] ISHIKAWA	03	BELL	$e^+e^- \to \Upsilon(4S)$
<89	90	[1] ABE	02	BELL	Repl. by ISHIKAWA 03
<95	90	[1] AUBERT	02L	BABR	$e^+e^- \to \Upsilon(4S)$
<6900	90	[3] ALBRECHT	91E	ARG	$e^+e^- \to \Upsilon(4S)$

[1] Assumes equal production of B^+ and B^0 at the $\Upsilon(4S)$.
[2] Assumes equal production of B^0 and B^+ at $\Upsilon(4S)$. The second error is a total of systematic uncertainties including model dependence.
[3] ALBRECHT 91E reports $< 6.3 \times 10^{-4}$ assuming the $\Upsilon(4S)$ decays 45% to $B^0\overline{B}^0$. We rescale to 50%.

$\Gamma(K^*(892)^+\mu^+\mu^-)/\Gamma_{\text{total}}$ Γ_{480}/Γ

Test for ΔB=1 weak neutral current. Allowed by higher-order electroweak interactions.

VALUE (units 10^{-7})	CL%	DOCUMENT ID		TECN	COMMENT
11.2± 1.5 OUR FIT					
11.6± 1.6 OUR AVERAGE					
11.6± 1.9		AAIJ	12AH	LHCB	pp at 7 TeV
$14.6^{+7.9}_{-7.5} \pm 1.2$		[1] AUBERT	09T	BABR	$e^+e^- \to \Upsilon(4S)$
$11.1^{+3.2}_{-2.7} \pm 1.0$		[1] WEI	09A	BELL	$e^+e^- \to \Upsilon(4S)$
• • • We do not use the following data for averages, fits, limits, etc. • • •					
$9.7^{+9.4}_{-6.9} \pm 1.4$		[1] AUBERT,B	06J	BABR	Repl. by AUBERT 09T
$30.7^{+25.8}_{-17.8} \pm 4.2$		[1] AUBERT	03U	BABR	$e^+e^- \to \Upsilon(4S)$
$6.5^{+6.9+1.5}_{-5.3-1.6}$		[2] ISHIKAWA	03	BELL	Repl. by WEI 09A
<39	90	[1] ABE	02	BELL	Repl. by ISHIKAWA 03
<170	90	[1] AUBERT	02L	BABR	$e^+e^- \to \Upsilon(4S)$
<12000	90	[3] ALBRECHT	91E	ARG	$e^+e^- \to \Upsilon(4S)$

[1] Assumes equal production of B^+ and B^0 at the $\Upsilon(4S)$.
[2] Assumes equal production of B^0 and B^+ at $\Upsilon(4S)$. The second error is a total of systematic uncertainties including model dependence. The 90% C.L. upper limit is 2.2×10^{-6}.
[3] ALBRECHT 91E reports $< 1.1 \times 10^{-3}$ assuming the $\Upsilon(4S)$ decays 45% to $B^0\overline{B}^0$. We rescale to 50%.

$\Gamma(K^*(892)^+\mu^+\mu^-)/\Gamma(J/\psi(1S)K^*(892)^+)$ $\Gamma_{480}/\Gamma_{222}$

VALUE (units 10^{-3})	DOCUMENT ID	TECN	COMMENT
0.78±0.11 OUR FIT			
0.67±0.22±0.04	AALTONEN	11AI CDF	$p\overline{p}$ at 1.96 TeV

$\Gamma(K^*(892)^+\nu\overline{\nu})/\Gamma_{\text{total}}$ Γ_{481}/Γ

Test for $\Delta B = 1$ weak neutral current. Allowed by higher-order electroweak interaction.

VALUE	CL%	DOCUMENT ID		TECN	COMMENT
$<4.0 \times 10^{-5}$	90	[1] LUTZ	13	BELL	$e^+e^- \to \Upsilon(4S)$
• • • We do not use the following data for averages, fits, limits, etc. • • •					
$<6.4 \times 10^{-5}$	90	[1,2] LEES	13I	BABR	$e^+e^- \to \Upsilon(4S)$
$<8 \times 10^{-5}$	90	AUBERT	08BC	BABR	Repl. by LEES 13I
$<1.4 \times 10^{-4}$	90	[1] CHEN	07D	BELL	$e^+e^- \to \Upsilon(4S)$

[1] Assumes equal production of B^+ and B^0 at the $\Upsilon(4S)$.
[2] Also reported a limit $< 11.6 \times 10^{-5}$ at 90% CL obtained using a fully reconstructed hadronic B-tag evnets.

$\Gamma(\pi^+e^+\mu^-)/\Gamma_{\text{total}}$ Γ_{482}/Γ

Test of lepton family number conservation.

VALUE	CL%	DOCUMENT ID	TECN	COMMENT
<0.0064	90	[1] WEIR 90B	MRK2	e^+e^- 29 GeV

[1] WEIR 90B assumes B^+ production cross section from LUND.

$\Gamma(\pi^+e^-\mu^+)/\Gamma_{\text{total}}$ Γ_{483}/Γ

Test of lepton family number conservation.

VALUE	CL%	DOCUMENT ID	TECN	COMMENT
<0.0064	90	[1] WEIR 90B	MRK2	e^+e^- 29 GeV

[1] WEIR 90B assumes B^+ production cross section from LUND.

$\Gamma(\pi^+e^\pm\mu^\mp)/\Gamma_{\text{total}}$ Γ_{484}/Γ

VALUE	CL%	DOCUMENT ID	TECN	COMMENT
$<1.7 \times 10^{-7}$	90	[1] AUBERT	07AG BABR	$e^+e^- \to \Upsilon(4S)$

[1] Assumes equal production of B^+ and B^0 at the $\Upsilon(4S)$.

$\Gamma(\pi^+e^+\tau^-)/\Gamma_{\text{total}}$ Γ_{485}/Γ

Test of lepton family number conservation.

VALUE (units 10^{-6})	CL%	DOCUMENT ID	TECN	COMMENT
<74	90	[1] LEES	12P BABR	$e^+e^- \to \Upsilon(4S)$

[1] Uses a fully reconstructed hadronic B decay as a tag on the recoil side.

$\Gamma(\pi^+e^-\tau^+)/\Gamma_{\text{total}}$ Γ_{486}/Γ

Test of lepton family number conservation.

VALUE (units 10^{-6})	CL%	DOCUMENT ID	TECN	COMMENT
<20	90	[1] LEES	12P BABR	$e^+e^- \to \Upsilon(4S)$

[1] Uses a fully reconstructed hadronic B decay as a tag on the recoil side.

See key on page 547

$\Gamma(\pi^+ e^\pm \tau^\mp)/\Gamma_{total}$ Γ_{487}/Γ

Test of lepton family number conservation.

VALUE (units 10^{-6})	CL%	DOCUMENT ID		TECN	COMMENT
<75	90	[1,2] LEES	12P	BABR	$e^+e^- \to \Upsilon(4S)$

[1] Assumes $B(B^+ \to h^+\ell^+\tau^-) = B(B^+ \to h^+\ell^-\tau^+)$.
[2] Uses a fully reconstructed hadronic B decay as a tag on the recoil side.

$\Gamma(\pi^+ \mu^+ \tau^-)/\Gamma_{total}$ Γ_{488}/Γ

Test of lepton family number conservation.

VALUE (units 10^{-6})	CL%	DOCUMENT ID		TECN	COMMENT
<62	90	[1] LEES	12P	BABR	$e^+e^- \to \Upsilon(4S)$

[1] Uses a fully reconstructed hadronic B decay as a tag on the recoil side.

$\Gamma(\pi^+ \mu^- \tau^+)/\Gamma_{total}$ Γ_{489}/Γ

Test of lepton family number conservation.

VALUE (units 10^{-6})	CL%	DOCUMENT ID		TECN	COMMENT
<45	90	[1] LEES	12P	BABR	$e^+e^- \to \Upsilon(4S)$

[1] Uses a fully reconstructed hadronic B decay as a tag on the recoil side.

$\Gamma(\pi^+ \mu^\pm \tau^\mp)/\Gamma_{total}$ Γ_{490}/Γ

Test of lepton family number conservation.

VALUE (units 10^{-6})	CL%	DOCUMENT ID		TECN	COMMENT
<72	90	[1,2] LEES	12P	BABR	$e^+e^- \to \Upsilon(4S)$

[1] Assumes $B(B^+ \to h^+\ell^+\tau^-) = B(B^+ \to h^+\ell^-\tau^+)$.
[2] Uses a fully reconstructed hadronic B decay as a tag on the recoil side.

$\Gamma(K^+ e^+ \mu^-)/\Gamma_{total}$ Γ_{491}/Γ

Test of lepton family number conservation.

VALUE (units 10^{-7})	CL%	DOCUMENT ID		TECN	COMMENT
<0.91	90	[1] AUBERT,B	06J	BABR	$e^+e^- \to \Upsilon(4S)$
• • • We do not use the following data for averages, fits, limits, etc. • • •					
<8	90	[1] AUBERT	02L	BABR	Repl. by AUBERT,B 06J
$<6.4 \times 10^4$	90	[2] WEIR	90B	MRK2	e^+e^- 29 GeV

[1] Assumes equal production of B^+ and B^0 at the $\Upsilon(4S)$.
[2] WEIR 90B assumes B^+ production cross section from LUND.

$\Gamma(K^+ e^- \mu^+)/\Gamma_{total}$ Γ_{492}/Γ

Test of lepton family number conservation.

VALUE (units 10^{-7})	CL%	DOCUMENT ID		TECN	COMMENT
<1.3	90	[1] AUBERT,B	06J	BABR	$e^+e^- \to \Upsilon(4S)$
• • • We do not use the following data for averages, fits, limits, etc. • • •					
$<6.4 \times 10^4$	90	[2] WEIR	90B	MRK2	e^+e^- 29 GeV

[1] Assumes equal production of B^+ and B^0 at the $\Upsilon(4S)$.
[2] WEIR 90B assumes B^+ production cross section from LUND.

$\Gamma(K^+ e^\pm \mu^\mp)/\Gamma_{total}$ Γ_{493}/Γ

VALUE (units 10^{-7})	CL%	DOCUMENT ID		TECN	COMMENT
<0.91	90	[1] AUBERT,B	06J	BABR	$e^+e^- \to \Upsilon(4S)$

[1] Assumes equal production of B^+ and B^0 at the $\Upsilon(4S)$.

$\Gamma(K^+ e^+ \tau^-)/\Gamma_{total}$ Γ_{494}/Γ

Test of lepton family number conservation.

VALUE (units 10^{-6})	CL%	DOCUMENT ID		TECN	COMMENT
<43	90	[1] LEES	12P	BABR	$e^+e^- \to \Upsilon(4S)$

[1] Uses a fully reconstructed hadronic B decay as a tag on the recoil side.

$\Gamma(K^+ e^- \tau^+)/\Gamma_{total}$ Γ_{495}/Γ

Test of lepton family number conservation.

VALUE (units 10^{-6})	CL%	DOCUMENT ID		TECN	COMMENT
<15	90	[1] LEES	12P	BABR	$e^+e^- \to \Upsilon(4S)$

[1] Uses a fully reconstructed hadronic B decay as a tag on the recoil side.

$\Gamma(K^+ e^\pm \tau^\mp)/\Gamma_{total}$ Γ_{496}/Γ

Test of lepton family number conservation.

VALUE (units 10^{-6})	CL%	DOCUMENT ID		TECN	COMMENT
<30	90	[1,2] LEES	12P	BABR	$e^+e^- \to \Upsilon(4S)$

[1] Assumes $B(B^+ \to h^+\ell^+\tau^-) = B(B^+ \to h^+\ell^-\tau^+)$.
[2] Uses a fully reconstructed hadronic B decay as a tag on the recoil side.

$\Gamma(K^+ \mu^+ \tau^-)/\Gamma_{total}$ Γ_{497}/Γ

Test of lepton family number conservation.

VALUE (units 10^{-6})	CL%	DOCUMENT ID		TECN	COMMENT
<45	90	[1] LEES	12P	BABR	$e^+e^- \to \Upsilon(4S)$

[1] Uses a fully reconstructed hadronic B decay as a tag on the recoil side.

$\Gamma(K^+ \mu^- \tau^+)/\Gamma_{total}$ Γ_{498}/Γ

Test of lepton family number conservation.

VALUE (units 10^{-6})	CL%	DOCUMENT ID		TECN	COMMENT
<28	90	[1] LEES	12P	BABR	$e^+e^- \to \Upsilon(4S)$

[1] Uses a fully reconstructed hadronic B decay as a tag on the recoil side.

$\Gamma(K^+ \mu^\pm \tau^\mp)/\Gamma_{total}$ Γ_{499}/Γ

Test of lepton family number conservation.

VALUE (units 10^{-6})	CL%	DOCUMENT ID		TECN	COMMENT
<48	90	[1,2] LEES	12P	BABR	$e^+e^- \to \Upsilon(4S)$
• • • We do not use the following data for averages, fits, limits, etc. • • •					
<77	90	[1] AUBERT	07AZ	BABR	Repl. by LEES 12P

[1] Uses a fully reconstructed hadronic B decay as a tag on the recoil side.
[2] Assumes $B(B^+ \to h^+\ell^+\tau^-) = B(B^+ \to h^+\ell^-\tau^+)$.

$\Gamma(K^*(892)^+ e^+ \mu^-)/\Gamma_{total}$ Γ_{500}/Γ

VALUE (units 10^{-7})	CL%	DOCUMENT ID		TECN	COMMENT
<13	90	[1] AUBERT,B	06J	BABR	$e^+e^- \to \Upsilon(4S)$

[1] Assumes equal production of B^+ and B^0 at the $\Upsilon(4S)$.

$\Gamma(K^*(892)^+ e^- \mu^+)/\Gamma_{total}$ Γ_{501}/Γ

VALUE (units 10^{-7})	CL%	DOCUMENT ID		TECN	COMMENT
<9.9	90	[1] AUBERT,B	06J	BABR	$e^+e^- \to \Upsilon(4S)$

[1] Assumes equal production of B^+ and B^0 at the $\Upsilon(4S)$.

$\Gamma(K^*(892)^+ e^\pm \mu^\mp)/\Gamma_{total}$ Γ_{502}/Γ

Test of lepton family number conservation.

VALUE	CL%	DOCUMENT ID		TECN	COMMENT
$<1.4 \times 10^{-6}$	90	[1] AUBERT,B	06J	BABR	$e^+e^- \to \Upsilon(4S)$
• • • We do not use the following data for averages, fits, limits, etc. • • •					
$<7.9 \times 10^{-6}$	90	[1] AUBERT	02L	BABR	Repl. by AUBERT,B 06J

[1] Assumes equal production of B^+ and B^0 at the $\Upsilon(4S)$.

$\Gamma(\pi^- e^+ e^+)/\Gamma_{total}$ Γ_{503}/Γ

Test of total lepton number conservation.

VALUE	CL%	DOCUMENT ID		TECN	COMMENT
$<2.3 \times 10^{-8}$	90	[1] LEES	12J	BABR	$e^+e^- \to \Upsilon(4S)$
• • • We do not use the following data for averages, fits, limits, etc. • • •					
$<1.6 \times 10^{-6}$	90	[1] EDWARDS	02B	CLE2	$e^+e^- \to \Upsilon(4S)$
<0.0039	90	[2] WEIR	90B	MRK2	e^+e^- 29 GeV

[1] Assumes equal production of B^+ and B^0 at the $\Upsilon(4S)$.
[2] WEIR 90B assumes B^+ production cross section from LUND.

$\Gamma(\pi^- \mu^+ \mu^+)/\Gamma_{total}$ Γ_{504}/Γ

Test of total lepton number conservation.

VALUE	CL%	DOCUMENT ID		TECN	COMMENT
$< 1.3 \times 10^{-8}$	95	[1] AAIJ	12AD	LHCB	pp at 7 TeV
• • • We do not use the following data for averages, fits, limits, etc. • • •					
$< 4.4 \times 10^{-8}$	90	AAIJ	12C	LHCB	pp at 7 TeV
$<10.7 \times 10^{-8}$	90	[2] LEES	12J	BABR	$e^+e^- \to \Upsilon(4S)$
$< 1.4 \times 10^{-6}$	90	[2] EDWARDS	02B	CLE2	$e^+e^- \to \Upsilon(4S)$
$< 9.1 \times 10^{-3}$	90	[3] WEIR	90B	MRK2	e^+e^- 29 GeV

[1] Uses $B^+ \to J/\psi K^+$, $J/\psi \to \mu^+\mu^-$ mode for normalization. Obtains neutrino-mass-dependent upper limits in the range 0.4–1.0×10^{-8}.
[2] Assumes equal production of B^+ and B^0 at the $\Upsilon(4S)$.
[3] WEIR 90B assumes B^+ production cross section from LUND.

$\Gamma(\pi^- e^+ \mu^+)/\Gamma_{total}$ Γ_{505}/Γ

Test of total lepton number conservation.

VALUE	CL%	DOCUMENT ID		TECN	COMMENT
$<1.5 \times 10^{-7}$	90	[1] LEES	14A	BABR	$e^+e^- \to \Upsilon(4S)$
• • • We do not use the following data for averages, fits, limits, etc. • • •					
$<1.3 \times 10^{-6}$	90	[1] EDWARDS	02B	CLE2	$e^+e^- \to \Upsilon(4S)$
<0.0064	90	[2] WEIR	90B	MRK2	e^+e^- 29 GeV

[1] Assumes equal production of B^+ and B^0 at the $\Upsilon(4S)$.
[2] WEIR 90B assumes B^+ production cross section from LUND.

$\Gamma(\rho^- e^+ e^+)/\Gamma_{total}$ Γ_{506}/Γ

Test of total lepton number conservation.

VALUE (units 10^{-6})	CL%	DOCUMENT ID		TECN	COMMENT
<0.17	90	[1] LEES	14A	BABR	$e^+e^- \to \Upsilon(4S)$
• • • We do not use the following data for averages, fits, limits, etc. • • •					
<2.6	90	[1] EDWARDS	02B	CLE2	$e^+e^- \to \Upsilon(4S)$

[1] Assumes equal production of B^+ and B^0 at the $\Upsilon(4S)$.

$\Gamma(\rho^- \mu^+ \mu^+)/\Gamma_{total}$ Γ_{507}/Γ

Test of total lepton number conservation.

VALUE (units 10^{-6})	CL%	DOCUMENT ID		TECN	COMMENT
<0.42	90	LEES	14A	BABR	$e^+e^- \to \Upsilon(4S)$
• • • We do not use the following data for averages, fits, limits, etc. • • •					
<5.0	90	[1] EDWARDS	02B	CLE2	$e^+e^- \to \Upsilon(4S)$

[1] Assumes equal production of B^+ and B^0 at the $\Upsilon(4S)$.

Meson Particle Listings

$B^{\pm}$

$\Gamma(\rho^- e^+ \mu^+)/\Gamma_{total}$ Γ_{508}/Γ

Test of total lepton number conservation.

VALUE (units 10^{-6})	CL%	DOCUMENT ID		TECN	COMMENT
<0.47	90	[1] LEES	14A	BABR	$e^+e^- \to \Upsilon(4S)$
• • • We do not use the following data for averages, fits, limits, etc. • • •					
<3.3	90	[1] EDWARDS	02B	CLE2	$e^+e^- \to \Upsilon(4S)$

[1] Assumes equal production of B^+ and B^0 at the $\Upsilon(4S)$.

$\Gamma(K^- e^+ e^+)/\Gamma_{total}$ Γ_{509}/Γ

Test of total lepton number conservation.

VALUE	CL%	DOCUMENT ID		TECN	COMMENT
<3.0 $\times 10^{-8}$	90	[1] LEES	12J	BABR	$e^+e^- \to \Upsilon(4S)$
• • • We do not use the following data for averages, fits, limits, etc. • • •					
<1.0 $\times 10^{-6}$	90	[1] EDWARDS	02B	CLE2	$e^+e^- \to \Upsilon(4S)$
<0.0039	90	[2] WEIR	90B	MRK2	e^+e^- 29 GeV

[1] Assumes equal production of B^+ and B^0 at the $\Upsilon(4S)$.
[2] WEIR 90B assumes B^+ production cross section from LUND.

$\Gamma(K^- \mu^+ \mu^+)/\Gamma_{total}$ Γ_{510}/Γ

Test of total lepton number conservation.

VALUE	CL%	DOCUMENT ID		TECN	COMMENT
<4.1 $\times 10^{-8}$	90	AAIJ	12C	LHCB	pp at 7 TeV
• • • We do not use the following data for averages, fits, limits, etc. • • •					
<6.7 $\times 10^{-8}$	90	[1] LEES	12J	BABR	$e^+e^- \to \Upsilon(4S)$
<1.8 $\times 10^{-6}$	90	[1] EDWARDS	02B	CLE2	$e^+e^- \to \Upsilon(4S)$
<9.1 $\times 10^{-3}$	90	[2] WEIR	90B	MRK2	e^+e^- 29 GeV

[1] Assumes equal production of B^+ and B^0 at the $\Upsilon(4S)$.
[2] WEIR 90B assumes B^+ production cross section from LUND.

$\Gamma(K^- e^+ \mu^+)/\Gamma_{total}$ Γ_{511}/Γ

Test of total lepton number conservation.

VALUE	CL%	DOCUMENT ID		TECN	COMMENT
<1.6 $\times 10^{-7}$	90	[1] LEES	14A	BABR	$e^+e^- \to \Upsilon(4S)$
• • • We do not use the following data for averages, fits, limits, etc. • • •					
<2.0 $\times 10^{-6}$	90	[1] EDWARDS	02B	CLE2	$e^+e^- \to \Upsilon(4S)$
<0.0064	90	[2] WEIR	90B	MRK2	e^+e^- 29 GeV

[1] Assumes equal production of B^+ and B^0 at the $\Upsilon(4S)$.
[2] WEIR 90B assumes B^+ production cross section from LUND.

$\Gamma(K^*(892)^- e^+ e^+)/\Gamma_{total}$ Γ_{512}/Γ

Test of total lepton number conservation.

VALUE (units 10^{-6})	CL%	DOCUMENT ID		TECN	COMMENT
<0.40	90	[1] LEES	14A	BABR	$e^+e^- \to \Upsilon(4S)$
• • • We do not use the following data for averages, fits, limits, etc. • • •					
<2.8	90	[1] EDWARDS	02B	CLE2	$e^+e^- \to \Upsilon(4S)$

[1] Assumes equal production of B^+ and B^0 at the $\Upsilon(4S)$.

$\Gamma(K^*(892)^- \mu^+ \mu^+)/\Gamma_{total}$ Γ_{513}/Γ

Test of total lepton number conservation.

VALUE (units 10^{-6})	CL%	DOCUMENT ID		TECN	COMMENT
<0.59	90	[1] LEES	14A	BABR	$e^+e^- \to \Upsilon(4S)$
• • • We do not use the following data for averages, fits, limits, etc. • • •					
<8.3	90	[1] EDWARDS	02B	CLE2	$e^+e^- \to \Upsilon(4S)$

[1] Assumes equal production of B^+ and B^0 at the $\Upsilon(4S)$.

$\Gamma(K^*(892)^- e^+ \mu^+)/\Gamma_{total}$ Γ_{514}/Γ

Test of total lepton number conservation.

VALUE (units 10^{-6})	CL%	DOCUMENT ID		TECN	COMMENT
<0.30	90	[1] LEES	14A	BABR	$e^+e^- \to \Upsilon(4S)$
• • • We do not use the following data for averages, fits, limits, etc. • • •					
<4.4	90	[1] EDWARDS	02B	CLE2	$e^+e^- \to \Upsilon(4S)$

[1] Assumes equal production of B^+ and B^0 at the $\Upsilon(4S)$.

$\Gamma(D^- e^+ e^+)/\Gamma_{total}$ Γ_{515}/Γ

VALUE	CL%	DOCUMENT ID		TECN	COMMENT
<2.6 $\times 10^{-6}$	90	[1] LEES	14A	BABR	$e^+e^- \to \Upsilon(4S)$
<2.6 $\times 10^{-6}$	90	[1,2] SEON	11	BELL	$e^+e^- \to \Upsilon(4S)$

[1] Assumes equal production of B^0 and B^+ from Upsilon(4S) decays.
[2] Uses $D^- \to K^+\pi^-\pi^-$ mode and 3-body phase-space hypothesis for the signal decays.

$\Gamma(D^- e^+ \mu^+)/\Gamma_{total}$ Γ_{516}/Γ

VALUE	CL%	DOCUMENT ID		TECN	COMMENT
<1.8 $\times 10^{-6}$	90	[1,2] SEON	11	BELL	$e^+e^- \to \Upsilon(4S)$
• • • We do not use the following data for averages, fits, limits, etc. • • •					
<2.1 $\times 10^{-6}$	90	[1] LEES	14A	BABR	$e^+e^- \to \Upsilon(4S)$

[1] Assumes equal production of B^0 and B^+ from Upsilon(4S) decays.
[2] Uses $D^- \to K^+\pi^-\pi^-$ mode and 3-body phase-space hypothesis for the signal decays.

$\Gamma(D^- \mu^+ \mu^+)/\Gamma_{total}$ Γ_{517}/Γ

VALUE	CL%	DOCUMENT ID		TECN	COMMENT
< 6.9 $\times 10^{-7}$	95	[1] AAIJ	12AD	LHCB	pp at 7 TeV
• • • We do not use the following data for averages, fits, limits, etc. • • •					
<17 $\times 10^{-7}$	90	[2] LEES	14A	BABR	$e^+e^- \to \Upsilon(4S)$
< 1.1 $\times 10^{-6}$	90	[2,3] SEON	11	BELL	$e^+e^- \to \Upsilon(4S)$

[1] Uses $B^+ \to \psi(2S)K^+$, $\psi(2S) \to J/\psi\pi^+\pi^-$ mode for normalization.
[2] Assumes equal production of B^0 and B^+ from Upsilon(4S) decays.
[3] Uses $D^- \to K^+\pi^-\pi^-$ mode and 3-body phase-space hypothesis for the signal decays.

$\Gamma(D^{*-} \mu^+ \mu^+)/\Gamma_{total}$ Γ_{518}/Γ

VALUE	CL%	DOCUMENT ID		TECN	COMMENT
<2.4 $\times 10^{-6}$	95	[1] AAIJ	12AD	LHCB	pp at 7 TeV

[1] Uses $B^+ \to \psi(2S)K^+$, $\psi(2S) \to J/\psi\pi^+\pi^-$ mode for normalization.

$\Gamma(D_s^- \mu^+ \mu^+)/\Gamma_{total}$ Γ_{519}/Γ

VALUE	CL%	DOCUMENT ID		TECN	COMMENT
<5.8 $\times 10^{-7}$	95	[1] AAIJ	12AD	LHCB	pp at 7 TeV

[1] Uses $B^+ \to \psi(2S)K^+$, $\psi(2S) \to J/\psi\pi^+\pi^-$ mode for normalization. Obtains neutrino-mass-dependent upper limits in the range 1.5–8.0 $\times 10^{-7}$.

$\Gamma(\overline{D}^0 \pi^- \mu^+ \mu^+)/\Gamma_{total}$ Γ_{520}/Γ

VALUE	CL%	DOCUMENT ID		TECN	COMMENT
<1.5 $\times 10^{-6}$	95	[1] AAIJ	12AD	LHCB	pp at 7 TeV

[1] Uses $B^+ \to \psi(2S)K^+$, $\psi(2S) \to J/\psi\pi^+\pi^-$ mode for normalization. Obtains neutrino-mass-dependent upper limits in the range 0.3–1.5 $\times 10^{-6}$.

$\Gamma(\Lambda^0 \mu^+)/\Gamma_{total}$ Γ_{521}/Γ

VALUE	CL%	DOCUMENT ID		TECN	COMMENT
<6 $\times 10^{-8}$	90	[1,2] DEL-AMO-SA...11K		BABR	$e^+e^- \to \Upsilon(4S)$

[1] DEL-AMO-SANCHEZ 11K reports $< 6.1 \times 10^{-8}$ from a measurement of $[\Gamma(B^+ \to \Lambda^0\mu^+)/\Gamma_{total}] \times [B(\Lambda \to p\pi^-)]$ assuming $B(\Lambda \to p\pi^-) = (63.9 \pm 0.5) \times 10^{-2}$.
[2] Uses $B(\Upsilon(4S) \to B^0\overline{B}^0) = (51.6 \pm 0.6)\%$ and $B(\Upsilon(4S) \to B^+B^-) = (48.4 \pm 0.6)\%$.

$\Gamma(\Lambda^0 e^+)/\Gamma_{total}$ Γ_{522}/Γ

VALUE	CL%	DOCUMENT ID		TECN	COMMENT
<3.2 $\times 10^{-8}$	90	[1,2] DEL-AMO-SA...11K		BABR	$e^+e^- \to \Upsilon(4S)$

[1] DEL-AMO-SANCHEZ 11K reports $< 3.2 \times 10^{-8}$ from a measurement of $[\Gamma(B^+ \to \Lambda^0 e^+)/\Gamma_{total}] \times [B(\Lambda \to p\pi^-)]$ assuming $B(\Lambda \to p\pi^-) = (63.9 \pm 0.5) \times 10^{-2}$.
[2] Uses $B(\Upsilon(4S) \to B^0\overline{B}^0) = (51.6 \pm 0.6)\%$ and $B(\Upsilon(4S) \to B^+B^-) = (48.4 \pm 0.6)\%$.

$\Gamma(\overline{\Lambda}^0 \mu^+)/\Gamma_{total}$ Γ_{523}/Γ

VALUE	CL%	DOCUMENT ID		TECN	COMMENT
<6 $\times 10^{-8}$	90	[1,2] DEL-AMO-SA...11K		BABR	$e^+e^- \to \Upsilon(4S)$

[1] DEL-AMO-SANCHEZ 11K reports $< 6.2 \times 10^{-8}$ from a measurement of $[\Gamma(B^+ \to \overline{\Lambda}^0\mu^+)/\Gamma_{total}] \times [B(\Lambda \to p\pi^-)]$ assuming $B(\Lambda \to p\pi^-) = (63.9 \pm 0.5) \times 10^{-2}$.
[2] Uses $B(\Upsilon(4S) \to B^0\overline{B}^0) = (51.6 \pm 0.6)\%$ and $B(\Upsilon(4S) \to B^+B^-) = (48.4 \pm 0.6)\%$.

$\Gamma(\overline{\Lambda}^0 e^+)/\Gamma_{total}$ Γ_{524}/Γ

VALUE	CL%	DOCUMENT ID		TECN	COMMENT
<8 $\times 10^{-8}$	90	[1,2] DEL-AMO-SA...11K		BABR	$e^+e^- \to \Upsilon(4S)$

[1] DEL-AMO-SANCHEZ 11K reports $< 8.1 \times 10^{-8}$ from a measurement of $[\Gamma(B^+ \to \overline{\Lambda}^0 e^+)/\Gamma_{total}] \times [B(\Lambda \to p\pi^-)]$ assuming $B(\Lambda \to p\pi^-) = (63.9 \pm 0.5) \times 10^{-2}$.
[2] Uses $B(\Upsilon(4S) \to B^0\overline{B}^0) = (51.6 \pm 0.6)\%$ and $B(\Upsilon(4S) \to B^+B^-) = (48.4 \pm 0.6)\%$.

POLARIZATION IN B^+ DECAY

In decays involving two vector mesons, one can distinguish among the states in which meson polarizations are both longitudinal (L) or both are transverse and parallel ($\|$) or perpendicular ($\perp$) to each other with the parameters Γ_L/Γ, $\Gamma_\perp/\Gamma$, and the relative phases $\phi_\|$ and $\phi_\perp$. See the definitions in the note on "Polarization in B Decays" review in the B^0 Particle Listings.

Γ_L/Γ in $B^+ \to \overline{D}^{*0}\rho^+$

VALUE	DOCUMENT ID		TECN	COMMENT
0.892±0.018±0.016	CSORNA	03	CLE2	$e^+e^- \to \Upsilon(4S)$

Γ_L/Γ in $B^+ \to \overline{D}^{*0}K^{*+}$

VALUE	DOCUMENT ID		TECN	COMMENT
0.86±0.06±0.03	AUBERT	04K	BABR	$e^+e^- \to \Upsilon(4S)$

Γ_L/Γ in $B^+ \to J/\psi K^{*+}$

VALUE	DOCUMENT ID		TECN	COMMENT
0.604±0.015±0.018	ITOH	05	BELL	$e^+e^- \to \Upsilon(4S)$

$\Gamma_\perp/\Gamma$ in $B^+ \to J/\psi K^{*+}$

VALUE	DOCUMENT ID		TECN	COMMENT
0.180±0.014±0.010	ITOH	05	BELL	$e^+e^- \to \Upsilon(4S)$

Γ_L/Γ in $B^+ \to \omega K^{*+}$

VALUE	DOCUMENT ID		TECN	COMMENT
$0.41 \pm 0.18 \pm 0.05$	AUBERT	09H	BABR	$e^+e^- \to \Upsilon(4S)$

Γ_L/Γ in $B^+ \to \omega K_2^*(1430)^+$

VALUE	DOCUMENT ID		TECN	COMMENT
$0.56 \pm 0.10 \pm 0.04$	AUBERT	09H	BABR	$e^+e^- \to \Upsilon(4S)$

Γ_L/Γ in $B^+ \to K^{*+}\overline{K}^{*0}$

VALUE	DOCUMENT ID		TECN	COMMENT
$0.75^{+0.16}_{-0.26} \pm 0.03$	[1] AUBERT	09F	BABR	$e^+e^- \to \Upsilon(4S)$

[1] Assumes equal production of B^+ and B^0 at the $\Upsilon(4S)$.

Γ_L/Γ in $B^+ \to \phi K^*(892)^+$

VALUE	DOCUMENT ID		TECN	COMMENT
0.50 ± 0.05 OUR AVERAGE				
$0.49 \pm 0.05 \pm 0.03$	AUBERT	07BA	BABR	$e^+e^- \to \Upsilon(4S)$
$0.52 \pm 0.08 \pm 0.03$	CHEN	05A	BELL	$e^+e^- \to \Upsilon(4S)$
• • • We do not use the following data for averages, fits, limits, etc. • • •				
$0.46 \pm 0.12 \pm 0.03$	AUBERT	03V	BABR	Repl. by AUBERT 07BA

$\Gamma_\perp/\Gamma$ in $B^+ \to \phi K^{*+}$

VALUE	DOCUMENT ID		TECN	COMMENT
0.20 ± 0.05 OUR AVERAGE				
$0.21 \pm 0.05 \pm 0.02$	AUBERT	07BA	BABR	$e^+e^- \to \Upsilon(4S)$
$0.19 \pm 0.08 \pm 0.02$	CHEN	05A	BELL	$e^+e^- \to \Upsilon(4S)$

$\phi_\parallel$ in $B^+ \to \phi K^{*+}$

VALUE (°)	DOCUMENT ID		TECN	COMMENT
2.34 ± 0.18 OUR AVERAGE				
$2.47 \pm 0.20 \pm 0.07$	AUBERT	07BA	BABR	$e^+e^- \to \Upsilon(4S)$
$2.10 \pm 0.28 \pm 0.04$	CHEN	05A	BELL	$e^+e^- \to \Upsilon(4S)$

$\phi_\perp$ in $B^+ \to \phi K^{*+}$

VALUE (°)	DOCUMENT ID		TECN	COMMENT
2.58 ± 0.17 OUR AVERAGE				
$2.69 \pm 0.20 \pm 0.03$	AUBERT	07BA	BABR	$e^+e^- \to \Upsilon(4S)$
$2.31 \pm 0.30 \pm 0.07$	CHEN	05A	BELL	$e^+e^- \to \Upsilon(4S)$

$\delta_0(B^+ \to \phi K^{*+})$

VALUE (rad)	DOCUMENT ID		TECN	COMMENT
$3.07 \pm 0.18 \pm 0.06$	AUBERT	07BA	BABR	$e^+e^- \to \Upsilon(4S)$

$A_{CP}^0(B^+ \to \phi K^{*+})$

VALUE	DOCUMENT ID		TECN	COMMENT
$0.17 \pm 0.11 \pm 0.02$	AUBERT	07BA	BABR	$e^+e^- \to \Upsilon(4S)$

$A_{CP}^\perp(B^+ \to \phi K^{*+})$

VALUE	DOCUMENT ID		TECN	COMMENT
$0.22 \pm 0.24 \pm 0.08$	AUBERT	07BA	BABR	$e^+e^- \to \Upsilon(4S)$

$\Delta\phi_\parallel(B^+ \to \phi K^{*+})$

VALUE (rad)	DOCUMENT ID		TECN	COMMENT
$0.07 \pm 0.20 \pm 0.05$	AUBERT	07BA	BABR	$e^+e^- \to \Upsilon(4S)$

$\Delta\phi_\perp(B^+ \to \phi K^{*+})$

VALUE (rad)	DOCUMENT ID		TECN	COMMENT
$0.19 \pm 0.20 \pm 0.07$	AUBERT	07BA	BABR	$e^+e^- \to \Upsilon(4S)$

$\Delta\delta_0(B^+ \to \phi K^{*+})$

VALUE (rad)	DOCUMENT ID		TECN	COMMENT
$0.20 \pm 0.18 \pm 0.03$	AUBERT	07BA	BABR	$e^+e^- \to \Upsilon(4S)$

Γ_L/Γ in $B^+ \to \phi K_1(1270)^+$

VALUE	DOCUMENT ID		TECN	COMMENT
$0.46^{+0.12}_{-0.13}{}^{+0.06}_{-0.07}$	AUBERT	08BI	BABR	$e^+e^- \to \Upsilon(4S)$

Γ_L/Γ in $B^+ \to \phi K_2^*(1430)^+$

VALUE	DOCUMENT ID		TECN	COMMENT
$0.80^{+0.09}_{-0.10} \pm 0.03$	AUBERT	08BI	BABR	$e^+e^- \to \Upsilon(4S)$

$\delta_0(B^+ \to \phi K_2^*(1430)^+)$

VALUE (rad)	DOCUMENT ID		TECN	COMMENT
$3.59 \pm 0.19 \pm 0.12$	AUBERT	08BI	BABR	$e^+e^- \to \Upsilon(4S)$

$\Delta\delta_0(B^+ \to \phi K_2^*(1430)^+)$

VALUE (rad)	DOCUMENT ID		TECN	COMMENT
$-0.05 \pm 0.19 \pm 0.06$	AUBERT	08BI	BABR	$e^+e^- \to \Upsilon(4S)$

Γ_L/Γ in $B^+ \to \rho^0 K^*(892)^+$

VALUE	DOCUMENT ID		TECN	COMMENT
$0.78 \pm 0.12 \pm 0.03$	DEL-AMO-SA...11D		BABR	$e^+e^- \to \Upsilon(4S)$
• • • We do not use the following data for averages, fits, limits, etc. • • •				
$0.96^{+0.04}_{-0.15} \pm 0.04$	AUBERT	03V	BABR	Repl. by DEL-AMO-SANCHEZ 11D

$\Gamma_L/\Gamma(B^+ \to K^*(892)^0\rho^+)$

VALUE	DOCUMENT ID		TECN	COMMENT
0.48 ± 0.08 OUR AVERAGE				
$0.52 \pm 0.10 \pm 0.04$	AUBERT,B	06G	BABR	$e^+e^- \to \Upsilon(4S)$
$0.43 \pm 0.11^{+0.05}_{-0.02}$	ZHANG	05D	BELL	$e^+e^- \to \Upsilon(4S)$

Γ_L/Γ in $B^+ \to \rho^+\rho^0$

VALUE	DOCUMENT ID		TECN	COMMENT
0.950 ± 0.016 OUR AVERAGE				
$0.950 \pm 0.015 \pm 0.006$	AUBERT	09G	BABR	$e^+e^- \to \Upsilon(4S)$
$0.948 \pm 0.106 \pm 0.021$	ZHANG	03B	BELL	$e^+e^- \to \Upsilon(4S)$
• • • We do not use the following data for averages, fits, limits, etc. • • •				
$0.905 \pm 0.042^{+0.023}_{-0.027}$	AUBERT,BE	06G	BABR	Repl. by AUBERT 09G
$0.97\ ^{+0.03}_{-0.07} \pm 0.04$	AUBERT	03V	BABR	Repl. by AUBERT,BE 06G

Γ_L/Γ in $B^+ \to \omega\rho^+$

VALUE	DOCUMENT ID		TECN	COMMENT
$0.90 \pm 0.05 \pm 0.03$	AUBERT	09H	BABR	$e^+e^- \to \Upsilon(4S)$
• • • We do not use the following data for averages, fits, limits, etc. • • •				
$0.82 \pm 0.11 \pm 0.02$	AUBERT,B	06T	BABR	Repl. by AUBERT 09H
$0.88^{+0.12}_{-0.15} \pm 0.03$	AUBERT	05O	BABR	Repl. by AUBERT,B 06T

Γ_L/Γ in $B^+ \to p\overline{p}K^*(892)^+$

VALUE	DOCUMENT ID		TECN	COMMENT
$0.32 \pm 0.17 \pm 0.09$	CHEN	08C	BELL	$e^+e^- \to \Upsilon(4S)$

CP VIOLATION

A_{CP} is defined as

$$\frac{B(B^- \to \overline{f}) - B(B^+ \to f)}{B(B^- \to \overline{f}) + B(B^+ \to f)},$$

the *CP*-violation charge asymmetry of exclusive B^- and B^+ decay.

$A_{CP}(B^+ \to J/\psi(1S)K^+)$

VALUE	DOCUMENT ID		TECN	COMMENT
0.003 ± 0.006 OUR AVERAGE Error includes scale factor of 1.8. See the ideogram below.				
$0.0059 \pm 0.0036 \pm 0.0007$	ABAZOV	13M	D0	$p\overline{p}$ at 1.96 TeV
$-0.0076 \pm 0.0050 \pm 0.0022$	SAKAI	10	BELL	$e^+e^- \to \Upsilon(4S)$
$0.09 \pm 0.07 \pm 0.02$	[1] WEI	08	BELL	$e^+e^- \to \Upsilon(4S)$
$0.030 \pm 0.014 \pm 0.010$	[2] AUBERT	05J	BABR	$e^+e^- \to \Upsilon(4S)$
$0.018 \pm 0.043 \pm 0.004$	[3] BONVICINI	00	CLE2	$e^+e^- \to \Upsilon(4S)$
• • • We do not use the following data for averages, fits, limits, etc. • • •				
$0.0075 \pm 0.0061 \pm 0.0030$	[4] ABAZOV	08O	D0	Repl. by ABAZOV 13M
$0.03 \pm 0.015 \pm 0.006$	AUBERT	04P	BABR	Repl. by AUBERT 05J
$-0.026 \pm 0.022 \pm 0.017$	ABE	03B	BELL	Repl. by SAKAI 10
$0.003 \pm 0.030 \pm 0.004$	AUBERT	02F	BABR	Repl. by AUBERT 04P

[1] Uses $B^+ \to J/\psi K^+$, where $J/\psi \to p\overline{p}$.
[2] The result reported corresponds to $-A_{CP}$.
[3] A +0.3% correction is applied due to a slightly higher reconstruction efficiency for the positive kaons.
[4] Uses $J/\psi \to \mu^+\mu^-$ decay.

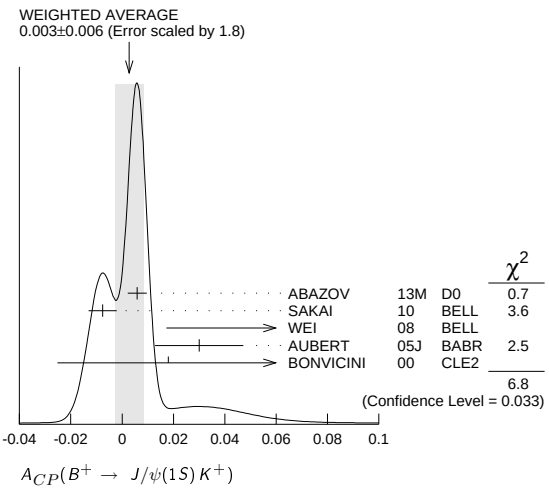

Meson Particle Listings

$B^{\pm}$

$A_{CP}(B^+ \to J/\psi(1S)\pi^+)$

VALUE (units 10^{-2})	DOCUMENT ID		TECN	COMMENT
0.1 ± 2.8 OUR AVERAGE	Error includes scale factor of 1.2.			
− 4.2 ± 4.4 ± 0.9	ABAZOV	13M	D0	$p\overline{p}$ at 1.96 TeV
0.5 ± 2.7 ± 1.1	[1] AAIJ	12AC	LHCB	pp at 7 TeV
12.3 ± 8.5 ± 0.4	AUBERT	04P	BABR	$e^+e^- \to \Upsilon(4S)$
− 2.3 ± 16.4 ± 1.5	ABE	03B	BELL	$e^+e^- \to \Upsilon(4S)$
• • • We do not use the following data for averages, fits, limits, etc. • • •				
− 9 ± 8 ± 3	[2] ABAZOV	08O	D0	Repl. by ABAZOV 13M
1 ± 22 ± 1	AUBERT	02F	BABR	Repl. by AUBERT 04P

[1] Uses $A_{CP}(B^+ \to J/\psi K^+) = 0.001 \pm 0.007$ to extract production asymmetry.
[2] Uses $J/\psi \to \mu^+\mu^-$ decay.

$A_{CP}(B^+ \to J/\psi\rho^+)$

VALUE	DOCUMENT ID		TECN	COMMENT
−0.11 ± 0.12 ± 0.08	AUBERT	07AC	BABR	$e^+e^- \to \Upsilon(4S)$

$A_{CP}(B^+ \to J/\psi K^*(892)^+)$

VALUE	DOCUMENT ID		TECN	COMMENT
−0.048 ± 0.029 ± 0.016	[1] AUBERT	05J	BABR	$e^+e^- \to \Upsilon(4S)$

[1] The result reported corresponds to $-A_{CP}$.

$A_{CP}(B^+ \to \eta_c K^+)$

VALUE	DOCUMENT ID		TECN	COMMENT
−0.02 ± 0.10 OUR AVERAGE	Error includes scale factor of 2.0.			
0.046 ± 0.057 ± 0.007	[1] AAIJ	13AU	LHCB	pp at 7 TeV
− 0.16 ± 0.08 ± 0.02	[1] WEI	08	BELL	$e^+e^- \to \Upsilon(4S)$

[1] Uses $B^+ \to \eta_c K^+$, where $\eta_c \to p\overline{p}$.

$A_{CP}(B^+ \to \psi(2S)\pi^+)$

VALUE	DOCUMENT ID		TECN	COMMENT
0.03 ± 0.06 OUR AVERAGE				
0.048 ± 0.090 ± 0.011	[1] AAIJ	12AC	LHCB	pp at 7 TeV
0.022 ± 0.085 ± 0.016	BHARDWAJ	08	BELL	$e^+e^- \to \Upsilon(4S)$

[1] Uses $A_{CP}(B^+ \to J/\psi K^+) = 0.001 \pm 0.007$ to extract production asymmetry.

$A_{CP}(B^+ \to \psi(2S)K^+)$

VALUE	DOCUMENT ID		TECN	COMMENT
−0.024 ± 0.023 OUR AVERAGE				
− 0.002 ± 0.123 ± 0.012	[1] AAIJ	13AU	LHCB	pp at 7 TeV
0.052 ± 0.059 ± 0.020	AUBERT	05J	BABR	$e^+e^- \to \Upsilon(4S)$
− 0.042 ± 0.020 ± 0.017	ABE	03B	BELL	$e^+e^- \to \Upsilon(4S)$
0.02 ± 0.091 ± 0.01	[2] BONVICINI	00	CLE2	$e^+e^- \to \Upsilon(4S)$
• • • We do not use the following data for averages, fits, limits, etc. • • •				
0.024 ± 0.014 ± 0.008	[1] AAIJ	12AC	LHCB	Repl. by AAIJ 13AU

[1] Uses $A_{CP}(B^+ \to J/\psi K^+) = 0.001 \pm 0.007$ to extract production asymmetry.
[2] A + 0.3% correction is applied due to a slightly higher reconstruction efficiency for the positive kaons.

$A_{CP}(B^+ \to \psi(2S)K^*(892)^+)$

VALUE	DOCUMENT ID		TECN	COMMENT
0.077 ± 0.207 ± 0.051	[1] AUBERT	05J	BABR	$e^+e^- \to \Upsilon(4S)$

[1] The result reported corresponds to $-A_{CP}$.

$A_{CP}(B^+ \to \chi_{c1}(1P)\pi^+)$

VALUE	DOCUMENT ID		TECN	COMMENT
0.07 ± 0.18 ± 0.02	KUMAR	06	BELL	$e^+e^- \to \Upsilon(4S)$

$A_{CP}(B^+ \to \chi_{c0}K^+)$

VALUE	DOCUMENT ID		TECN	COMMENT
−0.20 ± 0.18 OUR AVERAGE	Error includes scale factor of 1.5. See the ideogram below.			
− 0.96 ± 0.37 ± 0.04	LEES	11I	BABR	$e^+e^- \to \Upsilon(4S)$
$-0.14 \pm 0.15^{+0.03}_{-0.06}$	AUBERT	08AI	BABR	$e^+e^- \to \Upsilon(4S)$
$-0.065 \pm 0.20^{+0.035}_{-0.024}$	GARMASH	06	BELL	$e^+e^- \to \Upsilon(4S)$

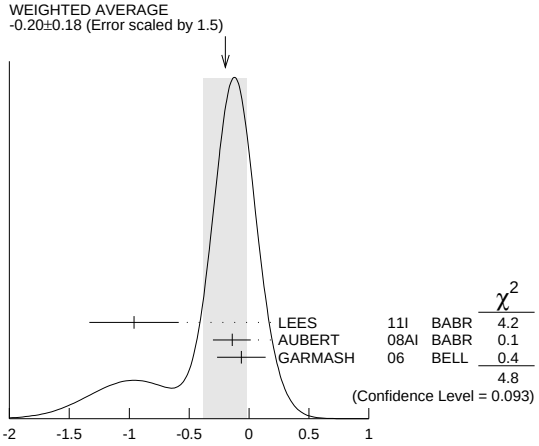

$A_{CP}(B^+ \to \chi_{c1}K^+)$

VALUE	DOCUMENT ID		TECN	COMMENT
−0.009 ± 0.033 OUR AVERAGE				
− 0.01 ± 0.03 ± 0.02	KUMAR	06	BELL	$e^+e^- \to \Upsilon(4S)$
− 0.003 ± 0.076 ± 0.017	[1] AUBERT	05J	BABR	$e^+e^- \to \Upsilon(4S)$

[1] The result reported corresponds to $-A_{CP}$.

$A_{CP}(B^+ \to \chi_{c1}K^*(892)^+)$

VALUE	DOCUMENT ID		TECN	COMMENT
0.471 ± 0.378 ± 0.268	[1] AUBERT	05J	BABR	$e^+e^- \to \Upsilon(4S)$

[1] The result reported corresponds to $-A_{CP}$.

$A_{CP}(B^+ \to \overline{D}{}^0\pi^+)$

VALUE	DOCUMENT ID		TECN	COMMENT
−0.007 ± 0.007 OUR AVERAGE				
− 0.006 ± 0.005 ± 0.010	[1] AAIJ	13AE	LHCB	pp at 7 TeV
− 0.008 ± 0.008	ABE	06	BELL	$e^+e^- \to \Upsilon(4S)$

[1] Uses $B^{\pm} \to [K^{\pm}\pi^{\mp}\pi^+\pi^-]_D h^{\pm}$ mode.

$A_{CP}(B^+ \to D_{CP(+1)}\pi^+)$

VALUE	DOCUMENT ID		TECN	COMMENT
0.035 ± 0.024	ABE	06	BELL	$e^+e^- \to \Upsilon(4S)$

$A_{CP}(B^+ \to D_{CP(-1)}\pi^+)$

VALUE	DOCUMENT ID		TECN	COMMENT
0.017 ± 0.026	ABE	06	BELL	$e^+e^- \to \Upsilon(4S)$

$A_{CP}([K^{\mp}\pi^{\pm}\pi^+\pi^-]_D\pi^+)$

VALUE	DOCUMENT ID		TECN	COMMENT
0.13 ± 0.10	AAIJ	13AE	LHCB	pp at 7 TeV

$A_{CP}(B^+ \to \overline{D}{}^0K^+)$

VALUE	DOCUMENT ID		TECN	COMMENT
0.01 ± 0.05 OUR AVERAGE	Error includes scale factor of 2.1.			
− 0.029 ± 0.020 ± 0.018	[1] AAIJ	13AE	LHCB	pp at 7 TeV
0.066 ± 0.036	ABE	06	BELL	$e^+e^- \to \Upsilon(4S)$
• • • We do not use the following data for averages, fits, limits, etc. • • •				
0.003 ± 0.080 ± 0.037	[2] ABE	03D	BELL	Repl. by SWAIN 03
0.04 ± 0.06 ± 0.03	[3] SWAIN	03	BELL	Repl. by ABE 06

[1] Uses $B^{\pm} \to [K^{\pm}\pi^{\mp}\pi^+\pi^-]_D h^{\pm}$ mode.
[2] Corresponds to 90% confidence range $-0.15 < A_{CP} < 0.16$.
[3] Corresponds to 90% confidence range $-0.07 < A_{CP} < 0.15$.

$A_{CP}([K^{\mp}\pi^{\pm}\pi^+\pi^-]_D K^+)$

VALUE	DOCUMENT ID		TECN	COMMENT
−0.42 ± 0.22	AAIJ	13AE	LHCB	pp at 7 TeV

$r_B(B^+ \to D^0K^+)$

r_B and δ_B are the amplitude ratio and relative strong phase between the amplitudes of $A(B^+ \to D^0K^+)$ and $A(B^+ \to \overline{D}{}^0K^+)$,

VALUE	CL%	DOCUMENT ID		TECN	COMMENT
0.096 ± 0.008 OUR AVERAGE					
0.097 ± 0.011		[1] AAIJ	13AE	LHCB	pp at 7 TeV
$0.092^{+0.013}_{-0.012}$		[2] LEES	13B	BABR	$e^+e^- \to \Upsilon(4S)$
0.07 ± 0.04		[3,4] AAIJ	12AQ	LHCB	pp at 7 TeV
$0.160^{+0.040+0.051}_{-0.038-0.015}$		[5] POLUEKTOV	10	BELL	$e^+e^- \to \Upsilon(4S)$

• • • We do not use the following data for averages, fits, limits, etc. • • •

$0.145 \pm 0.030 \pm 0.015$		[4,6] AIHARA	12	BELL	$e^+e^- \to \Upsilon(4S)$	
<0.13	90	[7] LEES	11D	BABR	$e^+e^- \to \Upsilon(4S)$	
$0.096 \pm 0.029 \pm 0.006$		[8] DEL-AMO-SA...	10F	BABR	Repl. by LEES 13B	
$0.095^{+0.051}_{-0.041}$		[9] DEL-AMO-SA...	10H	BABR	Repl. by LEES 13B	
$0.086 \pm 0.032 \pm 0.015$		[10] AUBERT	08AL	BABR	Repl. by DEL-AMO-SANCHEZ 10F	
<0.19	90	HORII	08	BELL	$e^+e^- \to \Upsilon(4S)$	
$0.159^{+0.054}_{-0.050} \pm 0.050$		[11] POLUEKTOV	06	BELL	Repl. by POLUEKTOV 10	
$0.12 \pm 0.08 \pm 0.05$		[12] AUBERT,B	05Y	BABR	Repl. by AUBERT 08AL	

[1] Uses $B^{\pm} \to [K^{\pm}\pi^{\mp}\pi^+\pi^-]_D h^{\pm}$ mode.
[2] Reports combination of published measurements using GGSZ, GLW, and ADS methods.
[3] Reports combined statistical and systematic uncertainties.
[4] Uses binned Dalitz plot of $\overline{D}^0 \to K^0_S\pi^+\pi^-$ decays from $B^+ \to \overline{D}^0 K^+$. Measurement of strong phases in $\overline{D}^0 \to K^0_S\pi^+\pi^-$ Dalitz plot from LIBBY 10 is used as input.
[5] Uses Dalitz plot analysis of $\overline{D}^0 \to K^0_S\pi^+\pi^-$ decays from $B^+ \to D^0 K^+$ modes. The corresponding two standard deviation interval is $0.084 < r_B < 0.239$.
[6] We combined the systematics in quadrature. The authors report separately the contribution to the systematic uncertainty due to the uncertainty on the bin-averaged strong phase difference between D^0 and $\overline{D}^0$ amplitudes.
[7] Uses decays of neutral D to $K^-\pi^+\pi^0$.
[8] Uses Dalitz plot analysis of $\overline{D}^0 \to K^0_S\pi^+\pi^-$, $K^0_S K^+K^-$ decays from $B^+ \to D^{(*)} K^{(*)+}$ modes. The corresponding two standard deviation interval is $0.037 < r_B < 0.155$.
[9] Uses the Cabibbo suppressed decay of $B^+ \to \overline{D} K^+$ followed by $\overline{D} \to K^-\pi^+$.
[10] Uses Dalitz plot analysis of $\overline{D}^0 \to K^0_S\pi^+\pi^-$ and $\overline{D}^0 \to K^0_S K^+K^-$ decays coming from $B^{\pm} \to D^{(*)} K^{(*)\pm}$ modes.
[11] Uses a Dalitz plot analysis of the $\overline{D}^0 \to K^0_S\pi^+\pi^-$ decays; Combines the DK^+, D^*K^+ and DK^{*+} modes.
[12] Uses a Dalitz analysis of neutral D decays to $K^0_S\pi^+\pi^-$ in the processes $B^{\pm} \to D^{(*)} K^{\pm}$, $D^* \to D\pi^0$, $D\gamma$.

$\delta_B(B^+ \to D^0 K^+)$

VALUE (°)	DOCUMENT ID		TECN	COMMENT
115 ±13 OR AVERAGE				
105^{+16}_{-17}	[1] LEES	13B	BABR	$e^+e^- \to \Upsilon(4S)$
137^{+35}_{-46}	[2,3] AAIJ	12AQ	LHCB	pp at 7 TeV
$136.7^{+13.0}_{-15.8} \pm 23.2$	[4] POLUEKTOV	10	BELL	$e^+e^- \to \Upsilon(4S)$
• • • We do not use the following data for averages, fits, limits, etc. • • •				
$129.9 \pm 15.0 \pm 6.0$	[3,5] AIHARA	12	BELL	$e^+e^- \to \Upsilon(4S)$
$119^{+19}_{-20} \pm 4$	[6] DEL-AMO-SA...	10F	BABR	Repl. by LEES 13B
$109^{+27}_{-30} \pm 8$	[7] AUBERT	08AL	BABR	Repl. by DEL-AMO-SANCHEZ 10F
$145.7^{+19.0}_{-19.7} \pm 23.1$	[8] POLUEKTOV	06	BELL	Repl. by POLUEKTOV 10
$104 \pm 45^{+23}_{-32}$	[9] AUBERT,B	05Y	BABR	Repl. by AUBERT 08AL

[1] Reports combination of published measurements using GGSZ, GLW, and ADS methods.
[2] Reports combined statistical and systematic uncertainties.
[3] Uses binned Dalitz plot of $\overline{D}^0 \to K^0_S\pi^+\pi^-$ decays from $B^+ \to \overline{D}^0 K^+$. Measurement of strong phases in $\overline{D}^0 \to K^0_S\pi^+\pi^-$ Dalitz plot from LIBBY 10 is used as input.
[4] Uses Dalitz plot analysis of $\overline{D}^0 \to K^0_S\pi^+\pi^-$ decays from $B^+ \to \overline{D}^0 K^+$ modes. The corresponding two standard deviation interval is $102.2° < \delta_B < 162.3°$.
[5] We combined the systematics in quadrature. The authors report separately the contribution to the systematic uncertainty due to the uncertainty on the bin-averaged strong phase difference between D^0 and $\overline{D}^0$ amplitudes.
[6] Uses Dalitz plot analysis of $\overline{D}^0 \to K^0_S\pi^+\pi^-$, $K^0_S K^+K^-$ decays from $B^+ \to D^{(*)} K^{(*)+}$ modes. The corresponding two standard deviation interval is $75° < \delta_B < 157°$.
[7] Uses Dalitz plot analysis of $\overline{D}^0 \to K^0_S\pi^+\pi^-$ and $\overline{D}^0 \to K^0_S K^+K^-$ decays coming from $B^{\pm} \to D^{(*)} K^{(*)\pm}$ modes.
[8] Uses a Dalitz plot analysis of the $\overline{D}^0 \to K^0_S\pi^+\pi^-$ decays; Combines the DK^+, D^*K^+ and DK^{*+} modes.
[9] Uses a Dalitz analysis of neutral D decays to $K^0_S\pi^+\pi^-$ in the processes $B^{\pm} \to D^{(*)} K^{\pm}$, $D^* \to D\pi^0$, $D\gamma$.

$r_B(B^+ \to \overline{D}^0 K^{*+})$

r_B and δ_B are the amplitude ratio and relative strong phase between the amplitudes of $A_{CP}(B^+ \to D^0 K^{*+})$ and $A_{CP}(B^+ \to \overline{D}^0 K^{*+})$,

VALUE	DOCUMENT ID		TECN	COMMENT
0.17 ±0.11 OR AVERAGE	Error includes scale factor of 2.3.			
$0.143^{+0.048}_{-0.049}$	[1] LEES	13B	BABR	$e^+e^- \to \Upsilon(4S)$
$0.564^{+0.216}_{-0.155} \pm 0.093$	[2] POLUEKTOV	06	BELL	$e^+e^- \to \Upsilon(4S)$
• • • We do not use the following data for averages, fits, limits, etc. • • •				
$0.166^{+0.073}_{-0.069}$	[3] DEL-AMO-SA...	10F	BABR	Repl. by LEES 13B
0.31 ± 0.07	[4] AUBERT	09AJ	BABR	Repl. by LEES 13B
$0.181^{+0.088}_{-0.108} \pm 0.042$	[5] AUBERT	08AL	BABR	Repl. by AUBERT 09AJ

[1] Reports combination of published measurements using GGSZ, GLW, and ADS methods.
[2] Uses a Dalitz plot analysis of the $\overline{D}^0 \to K^0_S\pi^+\pi^-$ decays; Combines the DK^+, D^*K^+ and DK^{*+} modes.
[3] DEL-AMO-SANCHEZ 10F reports $r_B \cdot k = 0.149^{+0.066}_{-0.062}$ for k = 0.9.
[4] Obtained by combining the GLW and ADS methods. The 2-sigma range corresponds to [0.17, 0.43].
[5] Uses Dalitz plot analysis of $\overline{D}^0 \to K^0_S\pi^+\pi^-$ and $\overline{D}^0 \to K^0_S K^+K^-$ decays coming from $B^{\pm} \to D^{(*)} K^{(*)\pm}$ modes.

$\delta_B(B^+ \to D^0 K^{*+})$

VALUE (°)	DOCUMENT ID		TECN	COMMENT
155 ±70 OR AVERAGE	Error includes scale factor of 2.0.			
101 ±43	[1] LEES	13B	BABR	$e^+e^- \to \Upsilon(4S)$
$242.6^{+20.2}_{-23.2} \pm 49.4$	[2] POLUEKTOV	06	BELL	$e^+e^- \to \Upsilon(4S)$
• • • We do not use the following data for averages, fits, limits, etc. • • •				
111 ±32	DEL-AMO-SA...	10F	BABR	Repl. by LEES 13B
$104^{+39}_{-37} \pm 18$	[3] AUBERT	08AL	BABR	Repl. by LEES 13B

[1] Reports combination of published measurements using GGSZ, GLW, and ADS methods.
[2] Uses a Dalitz plot analysis of the $\overline{D}^0 \to K^0_S\pi^+\pi^-$ decays; Combines the DK^+, D^*K^+ and DK^{*+} modes.
[3] Uses Dalitz plot analysis of $\overline{D}^0 \to K^0_S\pi^+\pi^-$ and $\overline{D}^0 \to K^0_S K^+K^-$ decays coming from $B^{\pm} \to D^{(*)} K^{(*)\pm}$ modes.

$A_{CP}(B^+ \to [K^-\pi^+]_D K^+)$

VALUE	DOCUMENT ID		TECN	COMMENT
−0.58 ±0.21 OUR AVERAGE				
$-0.82 \pm 0.44 \pm 0.09$	AALTONEN	11AJ	CDF	$p\overline{p}$ at 1.96 TeV
$-0.39^{+0.26}_{-0.28} \pm 0.04$	HORII	11	BELL	$e^+e^- \to \Upsilon(4S)$
$-0.86 \pm 0.47^{+0.12}_{-0.16}$	DEL-AMO-SA...	10H	BABR	$e^+e^- \to \Upsilon(4S)$
• • • We do not use the following data for averages, fits, limits, etc. • • •				
$-0.1^{+0.8}_{-1.0} \pm 0.4$	HORII	08	BELL	Repl. by HORII 11
$+0.88^{+0.77}_{-0.62} \pm 0.06$	SAIGO	05	BELL	Repl. by HORII 08

$A_{CP}(B^+ \to [K^-\pi^+\pi^0]_D K^+)$

VALUE	DOCUMENT ID		TECN	COMMENT
0.41 ±0.30 ±0.05	NAYAK	13	BELL	$e^+e^- \to \Upsilon(4S)$

$A_{CP}(B^+ \to [K^-\pi^+]_{\overline{D}} K^*(892)^+)$

VALUE	DOCUMENT ID		TECN	COMMENT
−0.34 ±0.43 ±0.16	AUBERT	09AJ	BABR	$e^+e^- \to \Upsilon(4S)$
• • • We do not use the following data for averages, fits, limits, etc. • • •				
$-0.22 \pm 0.61 \pm 0.17$	AUBERT,B	05V	BABR	Repl. by AUBERT 09AJ

$A_{CP}(B^+ \to [K^-\pi^+]_D \pi^+)$

VALUE	DOCUMENT ID		TECN	COMMENT
0.00 ±0.09 OUR AVERAGE				
$0.13 \pm 0.25 \pm 0.02$	AALTONEN	11AJ	CDF	$p\overline{p}$ at 1.96 TeV
$-0.04 \pm 0.11^{+0.02}_{-0.01}$	HORII	11	BELL	$e^+e^- \to \Upsilon(4S)$
$0.03 \pm 0.17 \pm 0.04$	DEL-AMO-SA...	10H	BABR	$e^+e^- \to \Upsilon(4S)$
• • • We do not use the following data for averages, fits, limits, etc. • • •				
$-0.02^{+0.15}_{-0.16} \pm 0.04$	HORII	08	BELL	Repl. by HORII 11
$+0.30^{+0.29}_{-0.25} \pm 0.06$	SAIGO	05	BELL	Repl. by HORII 08

$A_{CP}(B^+ \to [K^-\pi^+\pi^0]_D \pi^+)$

VALUE	DOCUMENT ID		TECN	COMMENT
$\mathbf{0.16 \pm 0.27^{+0.03}_{-0.04}}$	NAYAK	13	BELL	$e^+e^- \to \Upsilon(4S)$

$A_{CP}(B^+ \to [K^-\pi^+]_{(D\pi)} \pi^+)$

VALUE	DOCUMENT ID		TECN	COMMENT
−0.09 ±0.27 ±0.05	DEL-AMO-SA...	10H	BABR	$e^+e^- \to \Upsilon(4S)$

$A_{CP}(B^+ \to [K^-\pi^+]_{(D\gamma)} \pi^+)$

VALUE	DOCUMENT ID		TECN	COMMENT
−0.65 ±0.55 ±0.22	DEL-AMO-SA...	10H	BABR	$e^+e^- \to \Upsilon(4S)$

$A_{CP}(B^+ \to [K^-\pi^+]_{(D\pi)} K^+)$

VALUE	DOCUMENT ID		TECN	COMMENT
0.77 ±0.35 ±0.12	DEL-AMO-SA...	10H	BABR	$e^+e^- \to \Upsilon(4S)$

$A_{CP}(B^+ \to [K^-\pi^+]_{(D\gamma)} K^+)$

VALUE	DOCUMENT ID		TECN	COMMENT
$\mathbf{0.36 \pm 0.94^{+0.25}_{-0.41}}$	DEL-AMO-SA...	10H	BABR	$e^+e^- \to \Upsilon(4S)$

Meson Particle Listings

$B^{\pm}$

$A_{CP}(B^+ \to [\pi^+\pi^-\pi^0]_D K^+)$

VALUE	DOCUMENT ID		TECN	COMMENT
$-0.02\pm0.15\pm0.03$	[1] AUBERT	07BJ	BABR	$e^+e^- \to \Upsilon(4S)$
• • • We do not use the following data for averages, fits, limits, etc. • • •				
$-0.02\pm0.16\pm0.03$	AUBERT,B	05T	BABR	Repl. by AUBERT 07BJ

[1] Uses a Dalitz plot analysis of $D^0 \to \pi^+\pi^-\pi^0$. Also reports the one-sigma regions: $0.06 < r_B < 0.78$, $-30^\circ < \gamma < 76^\circ$, and $-27^\circ < \delta < 78^\circ$.

$A_{CP}(B^+ \to D_{CP(+1)} K^+)$

VALUE	DOCUMENT ID		TECN	COMMENT
0.170 ± 0.033 OUR AVERAGE	Error includes scale factor of 1.2.			
$0.145\pm0.032\pm0.010$	[1] AAIJ	12M	LHCB	pp at 7 TeV
$0.39 \pm0.17 \pm0.04$	AALTONEN	10A	CDF	$p\overline{p}$ at 1.96 TeV
$0.25 \pm0.06 \pm0.02$	[2] DEL-AMO-SA...	10G	BABR	$e^+e^- \to \Upsilon(4S)$
$0.06 \pm0.14 \pm0.05$	ABE	06	BELL	$e^+e^- \to \Upsilon(4S)$
• • • We do not use the following data for averages, fits, limits, etc. • • •				
$0.27 \pm0.09 \pm0.04$	AUBERT	08AA	BABR	Repl. by DEL-AMO-SANCHEZ 10G
$0.35 \pm0.13 \pm0.04$	AUBERT	06J	BABR	Repl. by AUBERT 08AA
$0.07 \pm0.17 \pm0.06$	AUBERT	04N	BABR	Repl. by AUBERT 06J
$0.29 \pm0.26 \pm0.05$	[3] ABE	03D	BELL	Repl. by SWAIN 03
$0.06 \pm0.19 \pm0.04$	[4] SWAIN	03	BELL	Repl. by ABE 06

[1] AAIJ 12M reports an evidence of direct CP violation in $B^\pm \to D K^\pm$ decays with a total significance of 5.8 σ.
[2] Reports the first evidence for direct CP violation in $B \to D K$ decays with 3.6 standard deviations.
[3] Corresponds to 90% confidence range $-0.14 < A_{CP} < 0.73$.
[4] Corresponds to 90% confidence range $-0.26 < A_{CP} < 0.38$.

$A_{ADS}(B^+ \to D K^+)$

$A_{ADS}(B^+ \to D K^+) = \frac{(R_K^- - R_K^+)}{(R_K^- + R_K^+)}$ where

$R_K^- = \Gamma(B^- \to [K^+\pi^-]_D K^-) \,/\, \Gamma(B^- \to [K^-\pi^+]_D K^-)$ and

$R_K^+ = \Gamma(B^+ \to [K^-\pi^+]_D K^+) \,/\, \Gamma(B^+ \to [K^+\pi^-]_D K^+)$

VALUE	DOCUMENT ID		TECN	COMMENT
$-0.52\pm0.15\pm0.02$	AAIJ	12M	LHCB	pp at 7 TeV

$A_{ADS}(B^+ \to D\pi^+)$

$A_{ADS}(B^+ \to D\pi^+) = \frac{(R_\pi^- - R_\pi^+)}{(R_\pi^- + R_\pi^+)}$ where

$R_\pi^- = \Gamma(B^- \to [K^+\pi^-]_D \pi^-) \,/\, \Gamma(B^- \to [K^-\pi^+]_D \pi^-)$ and

$R_\pi^+ = \Gamma(B^+ \to [K^-\pi^+]_D \pi^+) \,/\, \Gamma(B^+ \to [K^+\pi^-]_D \pi^+)$

VALUE	DOCUMENT ID		TECN	COMMENT
$0.143\pm0.062\pm0.011$	AAIJ	12M	LHCB	pp at 7 TeV

$A_{CP}(B^+ \to D_{CP(-1)} K^+)$

VALUE	DOCUMENT ID		TECN	COMMENT
-0.10 ± 0.07 OUR AVERAGE				
$-0.09\pm0.07\pm0.02$	DEL-AMO-SA...	10G	BABR	$e^+e^- \to \Upsilon(4S)$
$-0.12\pm0.14\pm0.05$	ABE	06	BELL	$e^+e^- \to \Upsilon(4S)$
• • • We do not use the following data for averages, fits, limits, etc. • • •				
$-0.09\pm0.09\pm0.02$	AUBERT	08AA	BABR	Repl. by DEL-AMO-SANCHEZ 10G
$-0.06\pm0.13\pm0.04$	AUBERT	06J	BABR	Repl. by AUBERT 08AA
$-0.22\pm0.24\pm0.04$	[1] ABE	03D	BELL	Repl. by SWAIN 03
$-0.19\pm0.17\pm0.05$	[2] SWAIN	03	BELL	Repl. by ABE 06

[1] Corresponds to 90% confidence range $-0.62 < A_{CP} < 0.18$.
[2] Corresponds to 90% confidence range $-0.47 < A_{CP} < 0.11$.

$A_{CP}(B^+ \to \overline{D}^{*0}\pi^+)$

VALUE	DOCUMENT ID		TECN	COMMENT
-0.014 ± 0.015	ABE	06	BELL	$e^+e^- \to \Upsilon(4S)$

$A_{CP}(B^+ \to (D^*_{CP(+1)})^0\pi^+)$

VALUE	DOCUMENT ID		TECN	COMMENT
-0.021 ± 0.045	ABE	06	BELL	$e^+e^- \to \Upsilon(4S)$

$A_{CP}(B^+ \to (D^*_{CP(-1)})^0\pi^+)$

VALUE	DOCUMENT ID		TECN	COMMENT
-0.090 ± 0.051	ABE	06	BELL	$e^+e^- \to \Upsilon(4S)$

$A_{CP}(B^+ \to D^{*0} K^+)$

VALUE	DOCUMENT ID		TECN	COMMENT
-0.07 ± 0.04 OUR AVERAGE				
$-0.06 \pm0.04 \pm0.01$	AUBERT	08BF	BABR	$e^+e^- \to \Upsilon(4S)$
-0.089 ± 0.086	ABE	06	BELL	$e^+e^- \to \Upsilon(4S)$

$r^*_B(B^+ \to D^{*0} K^+)$

r^*_B and δ^*_B are the amplitude ratio and relative strong phase between the amplitudes of $A(B^+ \to D^{*0} K^+)$ and $A(B^+ \to \overline{D}^{*0} K^+)$,

VALUE	DOCUMENT ID		TECN	COMMENT
$0.114^{+0.023}_{-0.040}$ OUR AVERAGE	Error includes scale factor of 1.2.			
$0.106^{+0.019}_{-0.036}$	[1] LEES	13B	BABR	$e^+e^- \to \Upsilon(4S)$
$0.196^{+0.072}_{-0.069}\pm0.064$ -0.017	[2] POLUEKTOV	10	BELL	$e^+e^- \to \Upsilon(4S)$
• • • We do not use the following data for averages, fits, limits, etc. • • •				
$0.133^{+0.042}_{-0.039}\pm0.013$	[3] DEL-AMO-SA...	10F	BABR	Repl. by LEES 13B
$0.096^{+0.035}_{-0.051}$	[4] DEL-AMO-SA...	10H	BABR	Repl. by LEES 13B
$0.135\pm0.050\pm0.012$	[5] AUBERT	08AL	BABR	Repl. by DEL-AMO-SANCHEZ 10F
$0.175^{+0.108}_{-0.099}\pm0.050$	[6] POLUEKTOV	06	BELL	Repl. by POLUEKTOV 10
$0.17 \pm0.10 \pm0.04$	[7] AUBERT,B	05Y	BABR	Repl. by AUBERT 08AL

[1] Reports combination of published measurements using GGSZ, GLW, and ADS methods.
[2] Uses Dalitz plot analysis of $\overline{D}^0 \to K^0_S\pi^+\pi^-$ decays from $B^+ \to D^{*0}K^+$ modes. The corresponding two standard deviation interval is $0.061 < r^*_B < 0.271$.
[3] Uses Dalitz plot analysis of $\overline{D}^0 \to K^0_S\pi^+\pi^-$, $K^0_S K^+ K^-$ decays from $B^+ \to D^{(*)} K^{(*)+}$ modes. The corresponding two standard deviation interval is $0.049 < r^*_B < 0.215$.
[4] Uses the Cabibbo suppressed decay of $B^+ \to \overline{D}^* K^+$ followed by $\overline{D}^* \to \overline{D}\pi^0$ or $\overline{D}\gamma$, and $\overline{D} \to K^-\pi^+$.
[5] Uses Dalitz plot analysis of $\overline{D}^0 \to K^0_S\pi^+\pi^-$ and $\overline{D}^0 \to K^0_S K^+ K^-$ decays coming from $B^\pm \to D^{(*)} K^{(*)\pm}$ modes.
[6] Uses a Dalitz plot analysis of the $\overline{D}^0 \to K^0_S\pi^+\pi^-$ decays; Combines the $D K^+$, $D^* K^+$ and $D K^{*+}$ modes.
[7] Uses a Dalitz analysis of neutral D decays to $K^0_S\pi^+\pi^-$ in the processes $B^\pm \to D^{(*)} K^\pm$, $D^* \to D\pi^0$, $D\gamma$.

$\delta^*_B(B^+ \to D^{*0} K^+)$

VALUE (°)	DOCUMENT ID		TECN	COMMENT
310^{+22}_{-28} OUR AVERAGE	Error includes scale factor of 1.3.			
$294 \pm21 \pm6$	[1] LEES	13B	BABR	$e^+e^- \to \Upsilon(4S)$
$341.9^{+18.0}_{-19.6}\pm23.1$	[2] POLUEKTOV	10	BELL	$e^+e^- \to \Upsilon(4S)$
• • • We do not use the following data for averages, fits, limits, etc. • • •				
$278 \pm21 \pm6$	[3] DEL-AMO-SA...	10F	BABR	Repl. by LEES 13B
$297 \pm27 \pm6.4$	[4] AUBERT	08AL	BABR	Repl. by DEL-AMO-SANCHEZ 10F
$302.0^{+33.8}_{-35.1}\pm23.7$	[5] POLUEKTOV	06	BELL	Repl. by POLUEKTOV 10
$296 \pm41 \pm20$	[6] AUBERT,B	05Y	BABR	Repl. by AUBERT 08AL

[1] Reports combination of published measurements using GGSZ, GLW, and ADS methods. We added 360° to the value of $(-66^{+21}_{-31})^\circ$ quoted by LEES 13B.
[2] Uses Dalitz plot analysis of $\overline{D}^0 \to K^0_S\pi^+\pi^-$ decays from $B^+ \to D^* K^+$ modes. The corresponding two standard deviation interval is $296.5^\circ < \delta^*_B < 382.7^\circ$.
[3] Uses Dalitz plot analysis of $\overline{D}^0 \to K^0_S\pi^+\pi^-$, $K^0_S K^+ K^-$ decays from $B^+ \to D^{(*)} K^{(*)+}$ modes. The corresponding two standard deviation interval is $236^\circ < \delta^*_B < 322^\circ$.
[4] Uses Dalitz plot analysis of $\overline{D}^0 \to K^0_S\pi^+\pi^-$ and $\overline{D}^0 \to K^0_S K^+ K^-$ decays coming from $B^\pm \to D^{(*)} K^{(*)\pm}$ modes.
[5] Uses a Dalitz plot analysis of the $\overline{D}^0 \to K^0_S\pi^+\pi^-$ decays; Combines the $D K^+$, $D^* K^+$ and $D K^{*+}$ modes.
[6] Uses a Dalitz analysis of neutral D decays to $K^0_S\pi^+\pi^-$ in the processes $B^\pm \to D^{(*)} K^\pm$, $D^* \to D\pi^0$, $D\gamma$.

$A_{CP}(B^+ \to D^{*0}_{CP(+1)} K^+)$

VALUE	DOCUMENT ID		TECN	COMMENT
-0.12 ± 0.08 OUR AVERAGE				
$-0.11\pm0.09\pm0.01$	AUBERT	08BF	BABR	$e^+e^- \to \Upsilon(4S)$
$-0.20\pm0.22\pm0.04$	ABE	06	BELL	$e^+e^- \to \Upsilon(4S)$
• • • We do not use the following data for averages, fits, limits, etc. • • •				
$-0.10\pm0.23^{+0.03}_{-0.04}$	AUBERT	05N	BABR	Repl. by AUBERT 08BF

$A_{CP}(B^+ \to D^*_{CP(-1)} K^+)$

VALUE	DOCUMENT ID		TECN	COMMENT
0.07 ± 0.10 OUR AVERAGE				
$+0.06\pm0.10\pm0.02$	AUBERT	08BF	BABR	$e^+e^- \to \Upsilon(4S)$
$+0.13\pm0.30\pm0.08$	ABE	06	BELL	$e^+e^- \to \Upsilon(4S)$

$A_{CP}(B^+ \to D_{CP(+1)} K^*(892)^+)$

VALUE	DOCUMENT ID		TECN	COMMENT
$+0.09\pm0.13\pm0.06$	AUBERT	09AJ	BABR	$e^+e^- \to \Upsilon(4S)$
• • • We do not use the following data for averages, fits, limits, etc. • • •				
$-0.08\pm0.19\pm0.08$	AUBERT,B	05U	BABR	Repl. by AUBERT 09AJ

$A_{CP}(B^+ \to D_{CP(-1)}K^*(892)^+)$

VALUE	DOCUMENT ID		TECN	COMMENT
$-0.23\pm0.21\pm0.07$	AUBERT	09AJ	BABR	$e^+e^- \to \Upsilon(4S)$
• • • We do not use the following data for averages, fits, limits, etc. • • •				
$-0.26\pm0.40\pm0.12$	AUBERT,B	05U	BABR	Repl. by AUBERT 09AJ

$A_{CP}(B^+ \to D_s^+\phi)$

VALUE	DOCUMENT ID		TECN	COMMENT
$-0.01\pm0.41\pm0.03$	AAIJ	13R	LHCB	pp at 7 TeV

$A_{CP}(B^+ \to D^{*+}\overline{D}^{*0})$

VALUE	DOCUMENT ID		TECN	COMMENT
$-0.15\pm0.11\pm0.02$	AUBERT,B	06A	BABR	$e^+e^- \to \Upsilon(4S)$

$A_{CP}(B^+ \to D^{*+}\overline{D}^0)$

VALUE	DOCUMENT ID		TECN	COMMENT
$-0.06\pm0.13\pm0.02$	AUBERT,B	06A	BABR	$e^+e^- \to \Upsilon(4S)$

$A_{CP}(B^+ \to D^+\overline{D}^{*0})$

VALUE	DOCUMENT ID		TECN	COMMENT
$0.13\pm0.18\pm0.04$	AUBERT,B	06A	BABR	$e^+e^- \to \Upsilon(4S)$

$A_{CP}(B^+ \to D^+\overline{D}^0)$

VALUE	DOCUMENT ID		TECN	COMMENT
-0.03 ± 0.07 OUR AVERAGE				
$0.00\pm0.08\pm0.02$	ADACHI	08	BELL	$e^+e^- \to \Upsilon(4S)$
$-0.13\pm0.14\pm0.02$	AUBERT,B	06A	BABR	$e^+e^- \to \Upsilon(4S)$

$A_{CP}(B^+ \to K_S^0\pi^+)$

VALUE	DOCUMENT ID		TECN	COMMENT
-0.017 ± 0.016 OUR AVERAGE				
$-0.022\pm0.025\pm0.010$	AAIJ	13BS	LHCB	pp at 7 TeV
$-0.011\pm0.021\pm0.006$	DUH	13	BELL	$e^+e^- \to \Upsilon(4S)$
$-0.029\pm0.039\pm0.010$	[1] AUBERT,BE	06C	BABR	$e^+e^- \to \Upsilon(4S)$
$0.18\ \pm0.24$	[2] CHEN	00	CLE2	$e^+e^- \to \Upsilon(4S)$
• • • We do not use the following data for averages, fits, limits, etc. • • •				
$0.03\ \pm0.03\ \pm0.01$	LIN	07	BELL	Repl. by DUH 13
$-0.09\ \pm0.05\ \pm0.01$	[3] AUBERT,BE	05E	BABR	Repl. by AUBERT,BE 06C
$0.05\ \pm0.05\ \pm0.01$	[4] CHAO	05A	BELL	Repl. by LIN 07
$-0.05\ \pm0.08\ \pm0.01$	[5] AUBERT	04M	BABR	Repl. by AUBERT,BE 05E
$0.07\ ^{+0.09}_{-0.08}\ ^{+0.01}_{-0.03}$	[6] UNNO	03	BELL	Repl. by CHAO 05A
$0.46\ \pm0.15\ \pm0.02$	[7] CASEY	02	BELL	Repl. by UNNO 03
$0.098^{+0.430}_{-0.343}{}^{+0.020}_{-0.063}$	[8] ABE	01K	BELL	Repl. by CASEY 02
$-0.21\ \pm0.18\ \pm0.03$	[9] AUBERT	01E	BABR	Repl. by AUBERT 04M

[1] Corresponds to 90% confidence range $-0.092 < A_{CP} < 0.036$.
[2] Corresponds to 90% confidence range $-0.22 < A_{CP} < 0.56$.
[3] Corresponds to 90% confidence range $-0.16 < A_{CP} < -0.02$.
[4] Corresponds to 90% confidence range $-0.04 < A_{CP} < 0.13$.
[5] Corresponds to 90% confidence range $-0.18 < A_{CP} < 0.08$.
[6] Corresponds to 90% confidence range $-0.10 < A_{CP} < +0.22$.
[7] Corresponds to 90% confidence range $+0.19 < A_{CP} < +0.72$.
[8] Corresponds to 90% confidence range $-0.53 < A_{CP} < 0.82$.
[9] Corresponds to 90% confidence range $-0.51 < A_{CP} < 0.09$.

$A_{CP}(B^+ \to K^+\pi^0)$

VALUE	DOCUMENT ID		TECN	COMMENT
0.037 ± 0.021 OUR AVERAGE				
$0.043\pm0.024\pm0.002$	DUH	13	BELL	$e^+e^- \to \Upsilon(4S)$
$0.030\pm0.039\pm0.010$	AUBERT	07BC	BABR	$e^+e^- \to \Upsilon(4S)$
$-0.29\ \pm0.23$	[1] CHEN	00	CLE2	$e^+e^- \to \Upsilon(4S)$
• • • We do not use the following data for averages, fits, limits, etc. • • •				
$0.07\ \pm0.03\ \pm0.01$	LIN	08	BELL	Repl. by DUH 13
$0.06\ \pm0.06\ \pm0.01$	[2] AUBERT	05L	BABR	Repl. by AUBERT 07BC
$0.06\ \pm0.06\ \pm0.02$	[2] CHAO	05A	BELL	Repl. by CHAO 04B
$0.04\ \pm0.05\ \pm0.02$	[3] CHAO	04B	BELL	Repl. by LIN 08
$-0.09\ \pm0.09\ \pm0.01$	[4] AUBERT	03L	BABR	Repl. by AUBERT 05L
$-0.02\ \pm0.19\ \pm0.02$	[5] CASEY	02	BELL	Repl. by CHAO 04B
$-0.059^{+0.222}_{-0.196}{}^{+0.055}_{-0.017}$	[6] ABE	01K	BELL	Repl. by CASEY 02
$0.00\ \pm0.18\ \pm0.04$	[7] AUBERT	01E	BABR	Repl. by AUBERT 03L

[1] Corresponds to 90% confidence range $-0.67 < A_{CP} < 0.09$.
[2] Corresponds to a 90% CL interval of $-0.06 < A_{CP} < 0.18$.
[3] Corresponds to 90% CL interval of $-0.05 < A_{CP} < 0.13$.
[4] Corresponds to 90% confidence range $-0.24 < A_{CP} < 0.06$.
[5] Corresponds to 90% confidence range $-0.35 < A_{CP} < +0.30$.
[6] Corresponds to 90% confidence range $-0.40 < A_{CP} < 0.36$.
[7] Corresponds to 90% confidence range $-0.30 < A_{CP} < +0.30$.

$A_{CP}(B^+ \to \eta' K^+)$

VALUE	DOCUMENT ID		TECN	COMMENT
0.013 ± 0.017 OUR AVERAGE				
$0.008^{+0.017}_{-0.018}\pm0.009$	AUBERT	09AV	BABR	$e^+e^- \to \Upsilon(4S)$
$0.028\pm0.028\pm0.021$	SCHUEMANN	06	BELL	$e^+e^- \to \Upsilon(4S)$
$0.03\ \pm0.12$	[1] CHEN	00	CLE2	$e^+e^- \to \Upsilon(4S)$
• • • We do not use the following data for averages, fits, limits, etc. • • •				
$0.010\pm0.022\pm0.006$	AUBERT	07AE	BABR	Repl. by AUBERT 09AV
$0.033\pm0.028\pm0.005$	[2] AUBERT	05M	BABR	Repl. by AUBERT 07AE
$0.037\pm0.045\pm0.011$	[3] AUBERT	03W	BABR	Repl. by AUBERT 05M
$-0.11\ \pm0.11\ \pm0.02$	[4] AUBERT	02E	BABR	Repl. by AUBERT 05M
$-0.015\pm0.070\pm0.009$	[5] CHEN	02B	BELL	Repl. by SCHUEMANN 06
$0.06\ \pm0.15\ \pm0.01$	[6] ABE	01M	BELL	Repl. by CHEN 02B

[1] Corresponds to 90% confidence range $-0.17 < A_{CP} < 0.23$.
[2] Corresponds to 90% confidence range $-0.012 < A_{CP} < 0.078$.
[3] Corresponds to 90% confidence range $-0.04 < A_{CP} < 0.11$.
[4] Corresponds to 90% confidence range $-0.28 < A_{CP} < 0.07$.
[5] Corresponds to 90% confidence range $-0.13 < A_{CP} < 0.10$.
[6] Corresponds to 90% confidence range $-0.20 < A_{CP} < 0.32$.

$A_{CP}(B^+ \to \eta' K^*(892)^+)$

VALUE	DOCUMENT ID		TECN	COMMENT
$-0.26\pm0.27\pm0.02$	DEL-AMO-SA...10A		BABR	$e^+e^- \to \Upsilon(4S)$
• • • We do not use the following data for averages, fits, limits, etc. • • •				
$-0.30^{+0.33}_{-0.37}\pm0.02$	[1] AUBERT	07E	BABR	Repl. by DEL-AMO-SANCHEZ 10A

[1] Reports A_{CP} with the opposite sign convention.

$A_{CP}(B^+ \to \eta' K_0^*(1430)^+)$

VALUE	DOCUMENT ID		TECN	COMMENT
$0.06\pm0.20\pm0.02$	DEL-AMO-SA...10A		BABR	$e^+e^- \to \Upsilon(4S)$

$A_{CP}(B^+ \to \eta' K_2^*(1430)^+)$

VALUE	DOCUMENT ID		TECN	COMMENT
$0.15\pm0.13\pm0.02$	DEL-AMO-SA...10A		BABR	$e^+e^- \to \Upsilon(4S)$

$A_{CP}(B^+ \to \eta K^+)$

VALUE	DOCUMENT ID		TECN	COMMENT
-0.37 ± 0.08 OUR AVERAGE				
$-0.38\pm0.11\pm0.01$	HOI	12	BELL	$e^+e^- \to \Upsilon(4S)$
$-0.36\pm0.11\pm0.03$	AUBERT	09AV	BABR	$e^+e^- \to \Upsilon(4S)$
• • • We do not use the following data for averages, fits, limits, etc. • • •				
$-0.22\pm0.11\pm0.01$	AUBERT	07AE	BABR	Repl. by AUBERT 09AV
$-0.39\pm0.16\pm0.03$	CHANG	07B	BELL	Repl. by HOI 12
$-0.20\pm0.15\pm0.01$	AUBERT,B	05K	BABR	Repl. by AUBERT 07AE
$-0.49\pm0.31\pm0.07$	CHANG	05A	BELL	Repl. by CHANG 07B
$-0.52\pm0.24\pm0.01$	AUBERT	04H	BABR	Repl. by AUBERT,B 05K

$A_{CP}(B^+ \to \eta K^*(892)^+)$

VALUE	DOCUMENT ID		TECN	COMMENT
0.02 ± 0.06 OUR AVERAGE				
$0.03\pm0.10\pm0.01$	WANG	07B	BELL	$e^+e^- \to \Upsilon(4S)$
$0.01\pm0.08\pm0.02$	AUBERT,B	06H	BABR	$e^+e^- \to \Upsilon(4S)$
• • • We do not use the following data for averages, fits, limits, etc. • • •				
$0.13\pm0.14\pm0.02$	AUBERT,B	04D	BABR	Repl. by AUBERT,B 06H

$A_{CP}(B^+ \to \eta K_0^*(1430)^+)$

VALUE	DOCUMENT ID		TECN	COMMENT
$0.05\pm0.13\pm0.02$	AUBERT,B	06H	BABR	$e^+e^- \to \Upsilon(4S)$

$A_{CP}(B^+ \to \eta K_2^*(1430)^+)$

VALUE	DOCUMENT ID		TECN	COMMENT
$-0.45\pm0.30\pm0.02$	AUBERT,B	06H	BABR	$e^+e^- \to \Upsilon(4S)$

$A_{CP}(B^+ \to \omega K^+)$

VALUE	DOCUMENT ID		TECN	COMMENT
0.02 ± 0.05 OUR AVERAGE				
$-0.01\pm0.07\pm0.01$	AUBERT	07AE	BABR	$e^+e^- \to \Upsilon(4S)$
$0.05^{+0.08}_{-0.07}\pm0.01$	JEN	06	BELL	$e^+e^- \to \Upsilon(4S)$
• • • We do not use the following data for averages, fits, limits, etc. • • •				
$0.05\pm0.09\pm0.01$	AUBERT,B	06E	BABR	Repl. by AUBERT 07AE
$-0.09\pm0.17\pm0.01$	AUBERT	04H	BABR	Repl. by AUBERT,B 06E
$0.06^{+0.21}_{-0.18}\pm0.01$	[1] WANG	04A	BELL	Repl. by JEN 06
$-0.21\pm0.28\pm0.03$	[2] LU	02	BELL	Repl. by WANG 04A

[1] Corresponds to 90% CL interval $0.15 < A_{CP} < 0.90$
[2] Corresponds to 90% confidence range $-0.70 < A_{CP} < +0.38$.

$A_{CP}(B^+ \to \omega K^{*+})$

VALUE	DOCUMENT ID		TECN	COMMENT
$+0.29\pm0.35\pm0.02$	AUBERT	09H	BABR	$e^+e^- \to \Upsilon(4S)$

Meson Particle Listings

$B^{\pm}$

$A_{CP}(B^+ \to \omega(K\pi)_0^{*+})$

VALUE	DOCUMENT ID		TECN	COMMENT
$-0.10 \pm 0.09 \pm 0.02$	AUBERT	09H	BABR	$e^+e^- \to \Upsilon(4S)$

$A_{CP}(B^+ \to \omega K_2^*(1430)^+)$

VALUE	DOCUMENT ID		TECN	COMMENT
$+0.14 \pm 0.15 \pm 0.02$	AUBERT	09H	BABR	$e^+e^- \to \Upsilon(4S)$

$A_{CP}(B^+ \to K^{*0}\pi^+)$

VALUE	DOCUMENT ID		TECN	COMMENT
-0.04 ± 0.09 OUR AVERAGE	Error includes scale factor of 2.1.			
$0.032 \pm 0.052^{+0.016}_{-0.013}$	AUBERT	08AI	BABR	$e^+e^- \to \Upsilon(4S)$
$-0.149 \pm 0.064 \pm 0.022$	GARMASH	06	BELL	$e^+e^- \to \Upsilon(4S)$
• • • We do not use the following data for averages, fits, limits, etc. • • •				
$0.068 \pm 0.078^{+0.070}_{-0.067}$	AUBERT,B	05N	BABR	Repl. by AUBERT 08AI

$A_{CP}(B^+ \to K^*(892)^+\pi^0)$

VALUE	DOCUMENT ID		TECN	COMMENT
$-0.06 \pm 0.24 \pm 0.04$	LEES	11I	BABR	$e^+e^- \to \Upsilon(4S)$
• • • We do not use the following data for averages, fits, limits, etc. • • •				
$0.04 \pm 0.29 \pm 0.05$	AUBERT	05X	BABR	Repl. by LEES 11I

$A_{CP}(B^+ \to K^+\pi^-\pi^+)$

VALUE	DOCUMENT ID		TECN	COMMENT
0.033 ± 0.010 OUR AVERAGE				
$0.032 \pm 0.008 \pm 0.008$	AAIJ	13AZ	LHCB	pp at 7 TeV
$0.028 \pm 0.020 \pm 0.023$	AUBERT	08AI	BABR	$e^+e^- \to \Upsilon(4S)$
$0.049 \pm 0.026 \pm 0.020$	GARMASH	06	BELL	$e^+e^- \to \Upsilon(4S)$
• • • We do not use the following data for averages, fits, limits, etc. • • •				
$-0.013 \pm 0.037 \pm 0.011$	AUBERT,B	05N	BABR	Repl. by AUBERT 08AI
$0.01 \pm 0.07 \pm 0.03$	AUBERT	03M	BABR	Repl. by AUBERT,B 05N

$A_{CP}(B^+ \to K^+K^-K^+ \text{nonresonant})$

VALUE	DOCUMENT ID		TECN	COMMENT
$0.060 \pm 0.044 \pm 0.019$	LEES	12O	BABR	$e^+e^- \to \Upsilon(4S)$

$A_{CP}(B^+ \to f(980)^0 K^+)$

VALUE	DOCUMENT ID		TECN	COMMENT
$-0.08 \pm 0.08 \pm 0.04$	[1] LEES	12O	BABR	$e^+e^- \to \Upsilon(4S)$

[1] Measured in the $B^+ \to K^+K^-K^+$ decay.

$A_{CP}(B^+ \to f_2(1270)K^+)$

VALUE	DOCUMENT ID		TECN	COMMENT
$-0.68^{+0.19}_{-0.17}$ OUR AVERAGE				
$-0.85 \pm 0.22^{+0.26}_{-0.13}$	AUBERT	08AI	BABR	$e^+e^- \to \Upsilon(4S)$
$-0.59 \pm 0.22 \pm 0.036$	GARMASH	06	BELL	$e^+e^- \to \Upsilon(4S)$

$A_{CP}(B^+ \to f_0(1500)K^+)$

VALUE	DOCUMENT ID		TECN	COMMENT
$0.28 \pm 0.26^{+0.15}_{-0.14}$	AUBERT	08AI	BABR	$e^+e^- \to \Upsilon(4S)$

$A_{CP}(B^+ \to f_2'(1525)^0 K^+)$

VALUE	DOCUMENT ID		TECN	COMMENT
$-0.08^{+0.05}_{-0.04}$ OUR AVERAGE				
$0.18 \pm 0.18 \pm 0.04$	[1] LEES	11I	BABR	$e^+e^- \to \Upsilon(4S)$
$-0.106 \pm 0.050^{+0.036}_{-0.015}$	AUBERT	08AI	BABR	$e^+e^- \to \Upsilon(4S)$
$-0.077 \pm 0.065^{+0.046}_{-0.026}$	GARMASH	06	BELL	$e^+e^- \to \Upsilon(4S)$
• • • We do not use the following data for averages, fits, limits, etc. • • •				
$0.14 \pm 0.10 \pm 0.04$	[2] LEES	12O	BABR	$e^+e^- \to \Upsilon(4S)$
$-0.31 \pm 0.25 \pm 0.08$	[3] AUBERT	06O	BABR	Repl. by LEES 12O
$0.088 \pm 0.095^{+0.097}_{-0.056}$	AUBERT,B	05N	BABR	Repl. by AUBERT 08AI

[1] Measured in $B^+ \to f_0 K^+$ with $f_0 \to \pi^0\pi^0$ decay.
[2] Measured in the $B^+ \to K^+K^-K^+$ decay assuming $A_{CP}(B^+ \to f_2'(1525)^0 K^+) = A_{CP}(B^+ \to f_0(1500)^0 K^+) = A_{CP}(B^+ \to f_0(1710)^0 K^+)$
[3] Measured in the $B^+ \to K^+K^-K^+$ decay.

$A_{CP}(B^+ \to \rho^0 K^+)$

VALUE	DOCUMENT ID		TECN	COMMENT
0.37 ± 0.10 OUR AVERAGE				
$0.44 \pm 0.10^{+0.06}_{-0.14}$	AUBERT	08AI	BABR	$e^+e^- \to \Upsilon(4S)$
$0.30 \pm 0.11^{+0.11}_{-0.04}$	GARMASH	06	BELL	$e^+e^- \to \Upsilon(4S)$
• • • We do not use the following data for averages, fits, limits, etc. • • •				
$0.32 \pm 0.13^{+0.10}_{-0.08}$	AUBERT,B	05N	BABR	Repl. by AUBERT 08AI

$A_{CP}(B^+ \to K_0^*(1430)^0\pi^+)$

VALUE	DOCUMENT ID		TECN	COMMENT
0.055 ± 0.033 OUR AVERAGE				
$0.032 \pm 0.035^{+0.034}_{-0.028}$	AUBERT	08AI	BABR	$e^+e^- \to \Upsilon(4S)$
$0.076 \pm 0.038^{+0.028}_{-0.022}$	GARMASH	06	BELL	$e^+e^- \to \Upsilon(4S)$
• • • We do not use the following data for averages, fits, limits, etc. • • •				
$-0.064 \pm 0.032^{+0.023}_{-0.026}$	AUBERT,B	05N	BABR	Repl. by AUBERT 08AI

$A_{CP}(B^+ \to K_2^*(1430)^0\pi^+)$

VALUE	DOCUMENT ID		TECN	COMMENT
$0.05 \pm 0.23^{+0.18}_{-0.08}$	AUBERT	08AI	BABR	$e^+e^- \to \Upsilon(4S)$

$A_{CP}(B^+ \to K^+\pi^0\pi^0)$

VALUE	DOCUMENT ID		TECN	COMMENT
$-0.06 \pm 0.06 \pm 0.04$	LEES	11I	BABR	$e^+e^- \to \Upsilon(4S)$

$A_{CP}(B^+ \to K^0\rho^+)$

VALUE	DOCUMENT ID		TECN	COMMENT
$-0.12 \pm 0.17 \pm 0.02$	AUBERT	07Z	BABR	$e^+e^- \to \Upsilon(4S)$

$A_{CP}(B^+ \to K^{*+}\pi^+\pi^-)$

VALUE	DOCUMENT ID		TECN	COMMENT
$0.07 \pm 0.07 \pm 0.04$	AUBERT,B	06U	BABR	$e^+e^- \to \Upsilon(4S)$

$A_{CP}(B^+ \to \rho^0 K^*(892)^+)$

VALUE	DOCUMENT ID		TECN	COMMENT
$0.31 \pm 0.13 \pm 0.03$	DEL-AMO-SA...11D		BABR	$e^+e^- \to \Upsilon(4S)$
• • • We do not use the following data for averages, fits, limits, etc. • • •				
$0.20^{+0.32}_{-0.29} \pm 0.04$	AUBERT	03V	BABR	Repl. by DEL-AMO-SANCHEZ 11D

$A_{CP}(B^+ \to K^*(892)^+ f_0(980))$

VALUE	DOCUMENT ID		TECN	COMMENT
$-0.15 \pm 0.12 \pm 0.03$	DEL-AMO-SA...11D		BABR	$e^+e^- \to \Upsilon(4S)$
• • • We do not use the following data for averages, fits, limits, etc. • • •				
$-0.34 \pm 0.21 \pm 0.03$	AUBERT,B	06G	BABR	Repl. by DEL-AMO-SANCHEZ 11D

$A_{CP}(B^+ \to a_1^+ K^0)$

VALUE	DOCUMENT ID		TECN	COMMENT
$+0.12 \pm 0.11 \pm 0.02$	AUBERT	08F	BABR	$e^+e^- \to \Upsilon(4S)$

$A_{CP}(B^+ \to b_1^+ K^0)$

VALUE	DOCUMENT ID		TECN	COMMENT
$-0.03 \pm 0.15 \pm 0.02$	AUBERT	08AG	BABR	$e^+e^- \to \Upsilon(4S)$

$A_{CP}(B^+ \to K^*(892)^0\rho^+)$

VALUE	DOCUMENT ID		TECN	COMMENT
$-0.01 \pm 0.16 \pm 0.02$	AUBERT,B	06G	BABR	$e^+e^- \to \Upsilon(4S)$

$A_{CP}(B^+ \to b_1^0 K^+)$

VALUE	DOCUMENT ID		TECN	COMMENT
$-0.46 \pm 0.20 \pm 0.02$	AUBERT	07BI	BABR	$e^+e^- \to \Upsilon(4S)$

$A_{CP}(B^+ \to K^0K^+)$

VALUE	DOCUMENT ID		TECN	COMMENT
0.04 ± 0.14 OUR AVERAGE				
$0.014 \pm 0.168 \pm 0.002$	DUH	13	BELL	$e^+e^- \to \Upsilon(4S)$
$0.10 \pm 0.26 \pm 0.03$	[1] AUBERT,BE	06C	BABR	$e^+e^- \to \Upsilon(4S)$
• • • We do not use the following data for averages, fits, limits, etc. • • •				
$0.13 \pm 0.23^{+0.23}_{-0.24} \pm 0.02$	LIN	07	BELL	Repl. by DUH 13
$0.15 \pm 0.33 \pm 0.03$	[2] AUBERT,BE	05E	BABR	Repl. by AUBERT,BE 06C

[1] Corresponds to 90% confidence range $-0.31 < A_{CP} < 0.54$.
[2] Corresponds to 90% confidence range $-0.43 < A_{CP} < 0.68$.

$A_{CP}(B^+ \to K_S^0K^+)$

VALUE	DOCUMENT ID		TECN	COMMENT
$-0.21 \pm 0.14 \pm 0.01$	AAIJ	13BS	LHCB	pp at 7 TeV

$A_{CP}(B^+ \to K^+K_S^0K_S^0)$

VALUE	DOCUMENT ID		TECN	COMMENT
$0.04^{+0.04}_{-0.05} \pm 0.02$	LEES	12O	BABR	$e^+e^- \to \Upsilon(4S)$
• • • We do not use the following data for averages, fits, limits, etc. • • •				
$-0.04 \pm 0.11 \pm 0.02$	[1] AUBERT,B	04V	BABR	Repl. by LEES 12O

[1] Corresponds to 90% confidence range $-0.23 < A_{CP} < 0.15$.

$A_{CP}(B^+ \to K^+K^-\pi^+)$

VALUE	DOCUMENT ID		TECN	COMMENT
−0.12 ±0.05 OUR AVERAGE	Error includes scale factor of 1.2.			
−0.141±0.040±0.019	[1] AAIJ	14	LHCB	pp at 7 TeV
0.00 ±0.10 ±0.03	AUBERT	07BB	BABR	$e^+e^- \to \Upsilon(4S)$

[1] AAIJ 14 reports $A_{CP}(B^+ \to K^+K^-\pi^+) = -0.648 \pm 0.070 \pm 0.013 \pm 0.007$ in the Dalitz plot region of $m^2_{K^+K^-} < 1.5$ GeV^2/c^4. The third uncertainty is due to the CP asymmetry of the $B^{\pm} \to J/\psi K^{\pm}$ reference mode uncertainty.

$A_{CP}(B^+ \to K^+K^-K^+)$

VALUE	DOCUMENT ID		TECN	COMMENT
−0.036±0.012 OUR AVERAGE	Error includes scale factor of 1.1.			
−0.043±0.009±0.008	AAIJ	13AZ	LHCB	pp at 7 TeV
$-0.017^{+0.019}_{-0.014}\pm0.014$	[1] LEES	12O	BABR	$e^+e^- \to \Upsilon(4S)$
• • • We do not use the following data for averages, fits, limits, etc. • • •				
−0.017±0.026±0.015	AUBERT	06O	BABR	Repl. by LEES 12O
0.02 ±0.07 ±0.03	AUBERT	03M	BABR	Repl. by AUBERT 06O

[1] All intermediate charmonium and charm resonances are removed, except of χ_{c0}.

$A_{CP}(B^+ \to \phi K^+)$

VALUE	DOCUMENT ID		TECN	COMMENT
0.04 ±0.04 OUR AVERAGE	Error includes scale factor of 2.1.			
0.022±0.021±0.009	AAIJ	14A	LHCB	pp at 7 TeV
0.128±0.044±0.013	LEES	12O	BABR	$e^+e^- \to \Upsilon(4S)$
-0.07 ±0.17 $^{+0.03}_{-0.02}$	ACOSTA	05J	CDF	$p\overline{p}$ at 1.96 TeV
0.01 ±0.12 ±0.05	[1] CHEN	03B	BELL	$e^+e^- \to \Upsilon(4S)$
• • • We do not use the following data for averages, fits, limits, etc. • • •				
0.00 ±0.08 ±0.02	AUBERT	06O	BABR	Repl. by LEES 12O
0.04 ±0.09 ±0.01	[2] AUBERT	04A	BABR	Repl. by AUBERT 06O
−0.05 ±0.20 ±0.03	[3] AUBERT	02E	BABR	$e^+e^- \to \Upsilon(4S)$

[1] Corresponds to 90% confidence range $-0.20 < A_{CP} < 0.22$.
[2] Corresponds to 90% confidence range $-0.10 < A_{CP} < 0.18$.
[3] Corresponds to 90% confidence range $-0.37 < A_{CP} < 0.28$.

$A_{CP}(B^+ \to X_0(1550)K^+)$

VALUE	DOCUMENT ID		TECN	COMMENT
−0.04±0.07±0.02	[1] AUBERT	06O	BABR	$e^+e^- \to \Upsilon(4S)$

[1] Measured in the $B^+ \to K^+K^-K^+$ decay.

$A_{CP}(B^+ \to K^{*+}K^+K^-)$

VALUE	DOCUMENT ID		TECN	COMMENT
0.11±0.08±0.03	AUBERT,B	06U	BABR	$e^+e^- \to \Upsilon(4S)$

$A_{CP}(B^+ \to \phi K^*(892)^+)$

VALUE	DOCUMENT ID		TECN	COMMENT
−0.01±0.08 OUR AVERAGE				
0.00±0.09±0.04	AUBERT	07BA	BABR	$e^+e^- \to \Upsilon(4S)$
−0.02±0.14±0.03	[1] CHEN	05A	BELL	$e^+e^- \to \Upsilon(4S)$
• • • We do not use the following data for averages, fits, limits, etc. • • •				
0.16±0.17±0.03	AUBERT	03V	BABR	Repl. by AUBERT 07BA
$-0.13\pm0.29^{+0.08}_{-0.11}$	[2] CHEN	03B	BELL	Repl. by CHEN 05A
$-0.43^{+0.36}_{-0.30}\pm0.06$	[3] AUBERT	02E	BABR	Repl. by AUBERT 03V

[1] Corresponds to 90% confidence range $-0.25 < A_{CP} < 0.22$.
[2] Corresponds to 90% confidence range $-0.64 < A_{CP} < 0.36$.
[3] Corresponds to 90% confidence range $-0.88 < A_{CP} < 0.18$.

$A_{CP}(B^+ \to \phi(K\pi)^{*+}_0)$

VALUE	DOCUMENT ID		TECN	COMMENT
0.04±0.15±0.04	AUBERT	08BI	BABR	$e^+e^- \to \Upsilon(4S)$

$A_{CP}(B^+ \to \phi K_1(1270)^+)$

VALUE	DOCUMENT ID		TECN	COMMENT
0.15±0.19±0.05	AUBERT	08BI	BABR	$e^+e^- \to \Upsilon(4S)$

$A_{CP}(B^+ \to \phi K^*_2(1430)^+)$

VALUE	DOCUMENT ID		TECN	COMMENT
−0.23±0.19±0.06	AUBERT	08BI	BABR	$e^+e^- \to \Upsilon(4S)$

$A_{CP}(B^+ \to K^+\phi\phi)$

VALUE	DOCUMENT ID		TECN	COMMENT
−0.10±0.08±0.02	[1] LEES	11A	BABR	$e^+e^- \to \Upsilon(4S)$

[1] $m_{\phi\phi} < 2.85$ GeV/c^2.

$A_{CP}(B^+ \to K^+[\phi\phi]_{\eta_c})$

VALUE	DOCUMENT ID		TECN	COMMENT
0.09±0.10±0.02	[1] LEES	11A	BABR	$e^+e^- \to \Upsilon(4S)$

[1] $m_{\phi\phi}$ is consistent with η_c mass [2.94, 3.02] GeV/c^2.

$A_{CP}(B^+ \to K^*(892)^+\gamma)$

VALUE	DOCUMENT ID		TECN	COMMENT
+0.018±0.028±0.007	AUBERT	09AO	BABR	$e^+e^- \to \Upsilon(4S)$

$A_{CP}(B^+ \to \eta K^+\gamma)$

VALUE	DOCUMENT ID		TECN	COMMENT
−0.12±0.07 OUR AVERAGE				
−0.09±0.10±0.01	[1] AUBERT	09	BABR	$e^+e^- \to \Upsilon(4S)$
−0.16±0.09±0.06	[2] NISHIDA	05	BELL	$e^+e^- \to \Upsilon(4S)$
• • • We do not use the following data for averages, fits, limits, etc. • • •				
−0.09±0.12±0.01	[1] AUBERT,B	06M	BABR	Repl. by AUBERT 09

[1] $m_{\eta K} < 3.25$ GeV/c^2.
[2] $m_{\eta K} < 2.4$ GeV/c^2

$A_{CP}(B^+ \to \phi K^+\gamma)$

VALUE	DOCUMENT ID		TECN	COMMENT
−0.13±0.11 OUR AVERAGE	Error includes scale factor of 1.1.			
−0.03±0.11±0.08	SAHOO	11A	BELL	$e^+e^- \to \Upsilon(4S)$
−0.26±0.14±0.05	AUBERT	07Q	BABR	$e^+e^- \to \Upsilon(4S)$

$A_{CP}(B^+ \to \rho^+\gamma)$

VALUE	DOCUMENT ID		TECN	COMMENT
−0.11±0.32±0.09	TANIGUCHI	08	BELL	$e^+e^- \to \Upsilon(4S)$

$A_{CP}(B^+ \to \pi^+\pi^0)$

VALUE	DOCUMENT ID		TECN	COMMENT
0.03 ±0.04 OUR AVERAGE				
0.025±0.043±0.007	DUH	13	BELL	$e^+e^- \to \Upsilon(4S)$
0.03 ±0.08 ±0.01	AUBERT	07BC	BABR	$e^+e^- \to \Upsilon(4S)$
• • • We do not use the following data for averages, fits, limits, etc. • • •				
0.07 ±0.06 ±0.01	LIN	08	BELL	Repl. by DUH 13
−0.01 ±0.10 ±0.02	[1] AUBERT	05L	BABR	Repl. by AUBERT 07BC
0.00 ±0.10 ±0.02	[2] CHAO	05A	BELL	Repl. by CHAO 04B
−0.02 ±0.10 ±0.01	[3] CHAO	04B	BELL	Repl. by LIN 08
$-0.03\ ^{+0.18}_{-0.17}$ ±0.02	[4] AUBERT	03L	BABR	Repl. by AUBERT 05L
0.30 ±0.30 $^{+0.06}_{-0.04}$	[5] CASEY	02	BELL	Repl. by CHAO 04B

[1] Corresponds to a 90% CL interval of $-0.19 < A_{CP} < 0.21$.
[2] Corresponds to a 90% CL interval of $-0.17 < A_{CP} < 0.16$.
[3] This corresponds to 90% CL interval of $-0.18 < A_{CP} < 0.14$.
[4] Corresponds to 90% confidence range $-0.32 < A_{CP} < 0.27$.
[5] Corresponds to 90% confidence range $-0.23 < A_{CP} < +0.86$.

$A_{CP}(B^+ \to \pi^+\pi^-\pi^+)$

VALUE	DOCUMENT ID		TECN	COMMENT
0.105±0.029 OUR AVERAGE	Error includes scale factor of 1.3.			
0.117±0.021±0.011	[1] AAIJ	14	LHCB	pp at 7 TeV
$0.032\pm0.044^{+0.040}_{-0.037}$	AUBERT	09L	BABR	$e^+e^- \to \Upsilon(4S)$
• • • We do not use the following data for averages, fits, limits, etc. • • •				
−0.007±0.077±0.025	AUBERT,B	05G	BABR	Repl. by AUBERT 09L
−0.39 ±0.33 ±0.12	AUBERT	03M	BABR	Repl. by AUBERT 05G

[1] AAIJ 14 reports $A_{CP}(B^+ \to \pi^+\pi^-\pi^+) = 0.584 \pm 0.082 \pm 0.027 \pm 0.007$ in the Dalitz plot region of $m^2_{\pi^+\pi^-} > 15$ GeV^2/c^4 or $m^2_{\pi^+\pi^-} < 0.4$ GeV^2/c^4. The third uncertainty is due to the CP asymmetry of the $B^{\pm} \to J/\psi K^{\pm}$ reference mode uncertainty.

$A_{CP}(B^+ \to \rho^0\pi^+)$

VALUE	DOCUMENT ID		TECN	COMMENT
0.18 ±0.07 $^{+0.05}_{-0.15}$	AUBERT	09L	BABR	$e^+e^- \to \Upsilon(4S)$
• • • We do not use the following data for averages, fits, limits, etc. • • •				
$-0.074\pm0.120^{+0.035}_{-0.055}$	AUBERT,B	05G	BABR	Repl. by AUBERT 09L
−0.19 ±0.11 ±0.02	AUBERT	04Z	BABR	Repl. by AUBERT,B 05G

$A_{CP}(B^+ \to f_2(1270)\pi^+)$

VALUE	DOCUMENT ID		TECN	COMMENT
0.41 ±0.25 $^{+0.18}_{-0.15}$	AUBERT	09L	BABR	$e^+e^- \to \Upsilon(4S)$
• • • We do not use the following data for averages, fits, limits, etc. • • •				
$-0.004\pm0.247^{+0.028}_{-0.032}$	AUBERT,B	05G	BABR	Repl. by AUBERT 09L

$A_{CP}(B^+ \to \rho^0(1450)\pi^+)$

VALUE	DOCUMENT ID		TECN	COMMENT
−0.06±0.28$^{+0.23}_{-0.40}$	AUBERT	09L	BABR	$e^+e^- \to \Upsilon(4S)$

$A_{CP}(B^+ \to f_0(1370)\pi^+)$

VALUE	DOCUMENT ID		TECN	COMMENT
0.72±0.15±0.16	AUBERT	09L	BABR	$e^+e^- \to \Upsilon(4S)$

$A_{CP}(B^+ \to \pi^+\pi^-\pi^+$ nonresonant)

VALUE	DOCUMENT ID		TECN	COMMENT
−0.14±0.14$^{+0.18}_{-0.08}$	AUBERT	09L	BABR	$e^+e^- \to \Upsilon(4S)$

Meson Particle Listings

$B^{\pm}$

$A_{CP}(B^+ \to \rho^+\pi^0)$

VALUE	DOCUMENT ID		TECN	COMMENT
0.02±0.11 OUR AVERAGE				
$-0.01\pm0.13\pm0.02$	AUBERT	07X	BABR	$e^+e^- \to \Upsilon(4S)$
$0.06\pm0.17^{+0.04}_{-0.05}$	ZHANG	05A	BELL	$e^+e^- \to \Upsilon(4S)$
• • • We do not use the following data for averages, fits, limits, etc. • • •				
$0.24\pm0.16\pm0.06$	AUBERT	04Z	BABR	Repl. by AUBERT 07X

$A_{CP}(B^+ \to \rho^+\rho^0)$

VALUE	DOCUMENT ID		TECN	COMMENT
−0.05 ±0.05 OUR AVERAGE				
$-0.054\pm0.055\pm0.010$	AUBERT	09G	BABR	$e^+e^- \to \Upsilon(4S)$
$0.00\ \pm0.22\ \pm0.03$	ZHANG	03B	BELL	$e^+e^- \to \Upsilon(4S)$
• • • We do not use the following data for averages, fits, limits, etc. • • •				
$-0.12\ \pm0.13\ \pm0.10$	AUBERT,BE	06G	BABR	Repl. by AUBERT 09G
$-0.19\ \pm0.23\ \pm0.03$	AUBERT	03V	BABR	Repl. by AUBERT,BE 06G

$A_{CP}(B^+ \to \omega\pi^+)$

VALUE	DOCUMENT ID		TECN	COMMENT
−0.04±0.06 OUR AVERAGE				
$-0.02\pm0.08\pm0.01$	AUBERT	07AE	BABR	$e^+e^- \to \Upsilon(4S)$
$-0.02\pm0.09\pm0.01$	JEN	06	BELL	$e^+e^- \to \Upsilon(4S)$
-0.34 ± 0.25	[1] CHEN	00	CLE2	$e^+e^- \to \Upsilon(4S)$
• • • We do not use the following data for averages, fits, limits, etc. • • •				
$-0.01\pm0.10\pm0.01$	AUBERT,B	06E	BABR	Repl. by AUBERT 07AE
$0.03\pm0.16\pm0.01$	AUBERT	04H	BABR	Repl. by AUBERT,B 06E
$0.50^{+0.23}_{-0.20}\pm0.02$	[2] WANG	04A	BELL	Repl. by JEN 06
$-0.01^{+0.29}_{-0.31}\pm0.03$	[3] AUBERT	02E	BABR	Repl. by AUBERT 04H

[1] Corresponds to 90% confidence range $-0.75 < A_{CP} < 0.07$.
[2] Corresponds to 90% CL interval $-0.25 < A_{CP} < 0.41$
[3] Corresponds to 90% confidence range $-0.50 < A_{CP} < 0.46$.

$A_{CP}(B^+ \to \omega\rho^+)$

VALUE	DOCUMENT ID		TECN	COMMENT
−0.20±0.09±0.02	AUBERT	09H	BABR	$e^+e^- \to \Upsilon(4S)$
• • • We do not use the following data for averages, fits, limits, etc. • • •				
$0.04\pm0.18\pm0.02$	AUBERT,B	06T	BABR	Repl. by AUBERT 09H
$0.05\pm0.26\pm0.02$	AUBERT	05O	BABR	Repl. by AUBERT,B 06T

$A_{CP}(B^+ \to \eta\pi^+)$

VALUE	DOCUMENT ID		TECN	COMMENT
−0.14±0.07 OUR AVERAGE Error includes scale factor of 1.4.				
$-0.19\pm0.06\pm0.01$	HOI	12	BELL	$e^+e^- \to \Upsilon(4S)$
$-0.03\pm0.09\pm0.03$	AUBERT	09AV	BABR	$e^+e^- \to \Upsilon(4S)$
• • • We do not use the following data for averages, fits, limits, etc. • • •				
$-0.08\pm0.10\pm0.01$	AUBERT	07AE	BABR	Repl. by AUBERT 09AV
$-0.23\pm0.09\pm0.02$	CHANG	07B	BELL	Repl. by HOI 12
$-0.13\pm0.12\pm0.01$	AUBERT,B	05K	BABR	Repl. by AUBERT 07AE
$0.07\pm0.15\pm0.03$	CHANG	05A	BELL	Repl. by CHANG 07B
$-0.44\pm0.18\pm0.01$	AUBERT	04H	BABR	Repl. by AUBERT,B 05K

$A_{CP}(B^+ \to \eta\rho^+)$

VALUE	DOCUMENT ID		TECN	COMMENT
0.11±0.11 OUR AVERAGE				
$0.13\pm0.11\pm0.02$	AUBERT	08AH	BABR	$e^+e^- \to \Upsilon(4S)$
$-0.04^{+0.34}_{-0.32}\pm0.01$	WANG	07B	BELL	$e^+e^- \to \Upsilon(4S)$
• • • We do not use the following data for averages, fits, limits, etc. • • •				
$0.02\pm0.18\pm0.02$	AUBERT,B	05K	BABR	Repl. by AUBERT 08AH

$A_{CP}(B^+ \to \eta'\pi^+)$

VALUE	DOCUMENT ID		TECN	COMMENT
0.06±0.16 OUR AVERAGE				
$0.03\pm0.17\pm0.02$	AUBERT	09AV	BABR	$e^+e^- \to \Upsilon(4S)$
$0.20^{+0.37}_{-0.36}\pm0.04$	SCHUEMANN	06	BELL	$e^+e^- \to \Upsilon(4S)$
• • • We do not use the following data for averages, fits, limits, etc. • • •				
$0.21\pm0.17\pm0.01$	AUBERT	07AE	BABR	Repl. by AUBERT 09AV
$0.14\pm0.16\pm0.01$	AUBERT,B	05K	BABR	Repl. by AUBERT 07AE

$A_{CP}(B^+ \to \eta'\rho^+)$

VALUE	DOCUMENT ID		TECN	COMMENT
0.26±0.17±0.02	DEL-AMO-SA...10A		BABR	$e^+e^- \to \Upsilon(4S)$
• • • We do not use the following data for averages, fits, limits, etc. • • •				
$0.04\pm0.28\pm0.02$	[1] AUBERT	07E	BABR	Repl. by DEL-AMO-SANCHEZ 10A

[1] Reports A_{CP} with the opposite sign convention.

$A_{CP}(B^+ \to b_1^0\pi^+)$

VALUE	DOCUMENT ID		TECN	COMMENT
+0.05±0.16±0.02	AUBERT	07BI	BABR	$e^+e^- \to \Upsilon(4S)$

$A_{CP}(B^+ \to p\bar{p}\pi^+)$

VALUE	DOCUMENT ID		TECN	COMMENT
0.00±0.04 OUR AVERAGE				
$-0.02\pm0.05\pm0.02$	[1] WEI	08	BELL	$e^+e^- \to \Upsilon(4S)$
$+0.04\pm0.07\pm0.04$	AUBERT	07AV	BABR	$e^+e^- \to \Upsilon(4S)$
• • • We do not use the following data for averages, fits, limits, etc. • • •				
$-0.16\pm0.22\pm0.01$	WANG	04	BELL	Repl. by WEI 08

[1] Requires $m_{p\bar{p}} < 2.85$ GeV/c^2.

$A_{CP}(B^+ \to p\bar{p}K^+)$

VALUE	DOCUMENT ID		TECN	COMMENT
−0.08 ±0.04 OUR AVERAGE Error includes scale factor of 1.1.				
$-0.047\pm0.036\pm0.007$	[1] AAIJ	13AU	LHCB	pp at 7 TeV
$-0.17\ \pm0.10\ \pm0.02$	[1] WEI	08	BELL	$e^+e^- \to \Upsilon(4S)$
$-0.16\ ^{+0.07}_{-0.08}\ \pm0.04$	[1] AUBERT,B	05L	BABR	$e^+e^- \to \Upsilon(4S)$
• • • We do not use the following data for averages, fits, limits, etc. • • •				
$-0.05\ \pm0.11\ \pm0.01$	WANG	04	BELL	Repl. by WEI 08

[1] Requires $m_{p\bar{p}} < 2.85$ GeV/c^2.

$A_{CP}(B^+ \to p\bar{p}K^*(892)^+)$

VALUE	DOCUMENT ID		TECN	COMMENT
0.21±0.16 OUR AVERAGE Error includes scale factor of 1.4.				
$-0.01\pm0.19\pm0.02$	CHEN	08C	BELL	$e^+e^- \to \Upsilon(4S)$
$+0.32\pm0.13\pm0.05$	AUBERT	07AV	BABR	$e^+e^- \to \Upsilon(4S)$

$A_{CP}(B^+ \to p\bar{\Lambda}\gamma)$

VALUE	DOCUMENT ID		TECN	COMMENT
+0.17±0.16±0.05	WANG	07C	BELL	$e^+e^- \to \Upsilon(4S)$

$A_{CP}(B^+ \to p\bar{\Lambda}\pi^0)$

VALUE	DOCUMENT ID		TECN	COMMENT
+0.01±0.17±0.04	WANG	07C	BELL	$e^+e^- \to \Upsilon(4S)$

$A_{CP}(B^+ \to K^+\ell^+\ell^-)$

VALUE	DOCUMENT ID		TECN	COMMENT
−0.02±0.08 OUR AVERAGE				
$-0.03\pm0.14\pm0.01$	[1] LEES	12S	BABR	$e^+e^- \to \Upsilon(4S)$
$-0.18\pm0.18\pm0.01$	AUBERT	09T	BABR	$e^+e^- \to \Upsilon(4S)$
$+0.04\pm0.10\pm0.02$	WEI	09A	BELL	$e^+e^- \to \Upsilon(4S)$
• • • We do not use the following data for averages, fits, limits, etc. • • •				
$-0.07\pm0.22\pm0.02$	AUBERT,B	06J	BABR	Repl. by AUBERT 09T

[1] Measured in the union of $0.10 < q^2 < 8.12$ GeV^2/c^4 and $q^2 > 10.11$ GeV^2/c^4. LEES 12S reports also individual measurements $A_{CP}(B^+ \to K^+\ell^+\ell^-) = 0.02 \pm 0.18 \pm 0.01$ for $0.10 < q^2 < 8.12$ GeV^2/c^4 and $A_{CP}(B^+ \to K^+\ell^+\ell^-) = -0.06^{+0.22}_{-0.21} \pm 0.01$ for $q^2 > 10.11$ GeV^2/c^4.

$A_{CP}(B^+ \to K^+e^+e^-)$

VALUE	DOCUMENT ID		TECN	COMMENT
+0.14±0.14±0.03	WEI	09A	BELL	$e^+e^- \to \Upsilon(4S)$

$A_{CP}(B^+ \to K^+\mu^+\mu^-)$

VALUE	DOCUMENT ID		TECN	COMMENT
−0.003±0.033 OUR AVERAGE				
$0.000\pm0.033\pm0.009$	AAIJ	13BN	LHCB	pp at 7 TeV
$-0.05\ \pm0.13\ \pm0.03$	WEI	09A	BELL	$e^+e^- \to \Upsilon(4S)$

$A_{CP}(B^+ \to K^{*+}\ell^+\ell^-)$

VALUE	DOCUMENT ID		TECN	COMMENT
−0.09±0.14 OUR AVERAGE				
$0.01^{+0.26}_{-0.24}\pm0.02$	AUBERT	09T	BABR	$e^+e^- \to \Upsilon(4S)$
$-0.13^{+0.17}_{-0.16}\pm0.01$	WEI	09A	BELL	$e^+e^- \to \Upsilon(4S)$
• • • We do not use the following data for averages, fits, limits, etc. • • •				
$0.03\pm0.23\pm0.03$	AUBERT,B	06J	BABR	Repl. by AUBERT 09T

$A_{CP}(B^+ \to K^*e^+e^-)$

VALUE	DOCUMENT ID		TECN	COMMENT
$\mathbf{-0.14^{+0.23}_{-0.22}\pm0.02}$	WEI	09A	BELL	$e^+e^- \to \Upsilon(4S)$

$A_{CP}(B^+ \to K^*\mu^+\mu^-)$

VALUE	DOCUMENT ID		TECN	COMMENT
−0.12±0.24±0.02	WEI	09A	BELL	$e^+e^- \to \Upsilon(4S)$

$\gamma(B^+ \to D^{(*)0}K^{(*)+})$

For angle $\gamma(\phi_3)$ of the CKM unitarity triangle, see the review on "*CP* Violation" in the Reviews section.

VALUE (°)	CL%	DOCUMENT ID		TECN	COMMENT
73 $^{+\ 7}_{-\ 9}$ OUR AVERAGE					
$72.6^{+\ 9.7}_{-17.2}$		[1,2] AAIJ	13AK	LHCB	pp at 7 TeV
$69\ ^{+17}_{-16}$		[3] LEES	13B	BABR	$e^+e^- \to \Upsilon(4S)$
$78.4^{+10.8}_{-11.6}\pm\ 9.6$		[4] POLUEKTOV	10	BELL	$e^+e^- \to \Upsilon(4S)$

• • • We do not use the following data for averages, fits, limits, etc. • • •

$44\ ^{+43}_{-38}$	[5,6] AAIJ	12AQ	LHCB	Repl. by AAIJ 13AK	
$77.3^{+15.1}_{-14.9}\pm\ 5.9$	[6,7] AIHARA	12	BELL	$e^+e^-\ \to\ \Upsilon(4S)$	
$68\ \pm14\ \pm\ 5$	[8] DEL-AMO-SA...10F		BABR	Repl. by LEES 13B	
7 to 173 95	[9] DEL-AMO-SA...10G		BABR	$e^+e^-\ \to\ \Upsilon(4S)$	
$76\ ^{+22}_{-23}\ \pm\ 7.1$	[10] AUBERT	08AL	BABR	Repl. by DEL-AMO-SANCHEZ 10F	
$53\ ^{+15}_{-18}\ \pm10$	[11] POLUEKTOV	06	BELL	Repl. by POLUEKTOV 10	
$70\ \pm31\ ^{+18}_{-15}$	[12] AUBERT,B	05Y	BABR	Repl. by AUBERT 08AL	
$77\ ^{+17}_{-19}\ \pm17$	[13] POLUEKTOV	04	BELL	Repl. by POLUEKTOV 06	

[1] The value is determined from combination of measuremets using D meson decaying to K^+K^-, $\pi^+\pi^-$, $K^\pm\pi^\mp$, $K^0_S\pi^+\pi^-$, $K^0_S K^+K^-$, and $K^\pm\pi^\mp\pi^\pm\pi^\mp$.

[2] Presents a confidence region $55.4^\circ < \gamma < 82.3^\circ$ at 68% CL with best fit value 72.6° and includes both statistical and systematic uncertainties. The corresponding 95% CL is $40.2^\circ < \gamma < 92.7^\circ$.

[3] Reports combination of published measurements using GGSZ, GLW, and ADS methods. Reports also 2σ range of 41–102° and a 5.9σ significance for $\gamma(B^+ \to D^{(*)0}K^{(*)+}) \neq 0$ hypothesis.

[4] Uses Dalitz plot analysis of $\overline{D}^0 \to K^0_S\pi^+\pi^-$ decays from $B^+ \to D^{(*)}K^+$ modes. The corresponding two standard deviation interval for γ is $54.2^\circ < \gamma < 100.5^\circ$. CP conservation in the combined result is ruled out with a significance of 3.5 standard deviations.

[5] Reports combined statistical and systematic uncertainties.

[6] Uses binned Dalitz plot of $\overline{D}^0 \to K^0_S\pi^+\pi^-$ decays from $B^+ \to \overline{D}^0K^+$. Measurement of strong phases in $\overline{D}^0 \to K^0_S\pi^+\pi^-$ Dalitz plot from LIBBY 10 is used as input.

[7] We combined the systematics in quadrature. The authors report separately the contribution to the systematic uncertainty due to the uncertainty on the bin-averaged strong phase difference between D^0 and $\overline{D}^0$ amplitudes.

[8] Uses Dalitz plot analysis of $\overline{D}^0 \to K^0_S\pi^+\pi^-$, $K^0_S K^+K^-$ decays from $B^+ \to D^{(*)}K^+$, DK^{*+} modes. The corresponding two standard deviation interval for γ is $39^\circ < \gamma < 98^\circ$. CP conservation in the combined result is ruled out with a significance of 3.5 standard deviations.

[9] Reports confidence intervals for the CKM angle γ from the measured values of the GLW parameters using $B^\pm \to DK^\pm$ decays with D mesons decaying to non-CP($K\pi$), CP-even (K^+K^-, $\pi^+\pi^-$), and CP-odd ($K^0_S\pi^0$, $K^0_S\omega$) states.

[10] Uses Dalitz plot analysis of $\overline{D}^0 \to K^0_S\pi^+\pi^-$ and $\overline{D}^0 \to K^0_S K^+K^-$ decays coming from $B^\pm \to D^{(*)}K^{(*)\pm}$ modes. The corresponding two standard deviation interval is $29^\circ < \gamma < 122^\circ$.

[11] Uses a Dalitz plot analysis of the $\overline{D}^0 \to K^0_S\pi^+\pi^-$ decays; Combines the DK^+, D^*K^+ and DK^{*+} modes. The corresponding two standard deviations interval for gamma is $8^\circ < \gamma < 111^\circ$.

[12] Uses a Dalitz plot analysis of neutral $D \to K^0_S\pi^+\pi^-$ decays coming from $B^\pm \to DK^\pm$ and $B^\pm \to D^{*0}K^\pm$ followed by $D^{*0} \to D\pi^0$, $D\gamma$. The corresponding two standard deviations interval for gamma is $12^\circ < \gamma < 137^\circ$. AUBERT,B 05Y also reports the amplitude ratios and the strong phases.

[13] Uses a Dalitz plot analysis of the 3-body $D \to K^0_S\pi^+\pi^-$ decays coming from $B^\pm \to DK^\pm$ and $B^\pm \to D^*K^\pm$ followed by $D^* \to D\pi^0$; here we use D to denote that the neutral D meson produced in the decay is an admixture of D^0 and $\overline{D}^0$. The corresponding two standard deviations interval for γ is $26^\circ < \gamma < 126^\circ$. POLUEKTOV 04 also reports the amplitude ratios and the strong phases.

PARTIAL BRANCHING FRACTIONS IN $B^+ \to K^{(*)+}\ell^+\ell^-$

B($B^+ \to K^{*+}\ell^+\ell^-$) ($q^2 < 2.0$ GeV$^2/c^4$)

VALUE (units 10^{-7})	DOCUMENT ID		TECN	COMMENT
1.4 ±0.5 OUR AVERAGE				
$1.37^{+0.60}_{-0.58}$	AAIJ	12AH	LHCB	pp at 7 TeV
$1.30\pm0.98\pm0.14$	AALTONEN	11AI	CDF	$p\overline{p}$ at 1.96 TeV

B($B^+ \to K^{*+}\ell^+\ell^-$) ($2.0 < q^2 < 4.3$ GeV$^2/c^4$)

VALUE (units 10^{-7})	DOCUMENT ID		TECN	COMMENT
1.1 ±0.5 OUR AVERAGE				
$1.24^{+0.60}_{-0.55}$	AAIJ	12AH	LHCB	pp at 7 TeV
$0.71\pm1.00\pm0.15$	AALTONEN	11AI	CDF	$p\overline{p}$ at 1.96 TeV

B($B^+ \to K^{*+}\ell^+\ell^-$) ($4.3 < q^2 < 8.68$ GeV$^2/c^4$)

VALUE (units 10^{-7})	DOCUMENT ID		TECN	COMMENT
$2.4\ ^{+0.8}_{-0.7}$ OUR AVERAGE				
$2.50^{+0.88}_{-0.74}$	AAIJ	12AH	LHCB	pp at 7 TeV
$1.71\pm1.58\pm0.49$	AALTONEN	11AI	CDF	$p\overline{p}$ at 1.96 TeV

B($B^+ \to K^{*+}\ell^+\ell^-$) ($10.09 < q^2 < 12.86$ GeV$^2/c^4$)

VALUE (units 10^{-7})	DOCUMENT ID		TECN	COMMENT
2.1 ±0.6 OUR AVERAGE				
$2.13^{+0.72}_{-0.66}$	AAIJ	12AH	LHCB	pp at 7 TeV
$1.97\pm0.99\pm0.22$	AALTONEN	11AI	CDF	$p\overline{p}$ at 1.96 TeV

B($B^+ \to K^{*+}\ell^+\ell^-$) ($14.18 < q^2 < 16.0$ GeV$^2/c^4$)

VALUE (units 10^{-7})	DOCUMENT ID		TECN	COMMENT
$0.86^{+0.40}_{-0.32}$ OUR AVERAGE				
$1.00^{+0.47}_{-0.38}$	AAIJ	12AH	LHCB	pp at 7 TeV
$0.52\pm0.61\pm0.09$	AALTONEN	11AI	CDF	$p\overline{p}$ at 1.96 TeV

B($B^+ \to K^{*+}\ell^+\ell^-$) ($q^2 > 16.0$ GeV$^2/c^4$)

VALUE (units 10^{-7})	DOCUMENT ID		TECN	COMMENT
1.3 ±0.4 OUR AVERAGE				
1.25 ± 0.46	AAIJ	12AH	LHCB	pp at 7 TeV
$1.57\pm0.96\pm0.17$	AALTONEN	11AI	CDF	$p\overline{p}$ at 1.96 TeV

B($B^+ \to K^{*+}\ell^+\ell^-$) ($1.0 < q^2 < 6.0$ GeV$^2/c^4$)

VALUE (units 10^{-7})	DOCUMENT ID		TECN	COMMENT
2.8 ±0.8 OUR AVERAGE				
$2.90^{+0.90}_{-0.85}$	AAIJ	12AH	LHCB	pp at 7 TeV
$2.57\pm1.61\pm0.40$	AALTONEN	11AI	CDF	$p\overline{p}$ at 1.96 TeV

B($B^+ \to K^{*+}\ell^+\ell^-$) ($0.0 < q^2 < 4.3$ GeV$^2/c^4$)

VALUE (units 10^{-7})	DOCUMENT ID		TECN	COMMENT
$2.01\pm1.39\pm0.27$	AALTONEN	11AI	CDF	$p\overline{p}$ at 1.96 TeV

B($B^+ \to K^+\ell^+\ell^-$) ($q^2 < 2.0$ GeV$^2/c^4$)

VALUE (units 10^{-7})	DOCUMENT ID		TECN	COMMENT
0.51 ±0.08 OUR AVERAGE	Error includes scale factor of 1.5.			
$0.556\pm0.053\pm0.027$	AAIJ	13H	LHCB	pp at 7 TeV
$0.36\ \pm0.11\ \pm0.03$	AALTONEN	11AI	CDF	$p\overline{p}$ at 1.96 TeV

B($B^+ \to K^+\ell^+\ell^-$) ($2.0 < q^2 < 4.3$ GeV$^2/c^4$)

VALUE (units 10^{-7})	DOCUMENT ID		TECN	COMMENT
0.60 ±0.07 OUR AVERAGE	Error includes scale factor of 1.3.			
$0.573\pm0.053\pm0.023$	AAIJ	13H	LHCB	pp at 7 TeV
$0.80\ \pm0.15\ \pm0.05$	AALTONEN	11AI	CDF	$p\overline{p}$ at 1.96 TeV

B($B^+ \to K^+\ell^+\ell^-$) ($4.3 < q^2 < 8.68$ GeV$^2/c^4$)

VALUE (units 10^{-7})	DOCUMENT ID		TECN	COMMENT
1.03 ±0.07 OUR AVERAGE				
$1.003\pm0.070\pm0.039$	AAIJ	13H	LHCB	pp at 7 TeV
$1.18\ \pm0.19\ \pm0.09$	AALTONEN	11AI	CDF	$p\overline{p}$ at 1.96 TeV

B($B^+ \to K^+\ell^+\ell^-$) ($10.09 < q^2 < 12.86$ GeV$^2/c^4$)

VALUE (units 10^{-7})	DOCUMENT ID		TECN	COMMENT
0.58 ±0.05 OUR AVERAGE				
$0.565\pm0.050\pm0.022$	AAIJ	13H	LHCB	pp at 7 TeV
$0.68\ \pm0.12\ \pm0.05$	AALTONEN	11AI	CDF	$p\overline{p}$ at 1.96 TeV

B($B^+ \to K^+\ell^+\ell^-$) ($14.18 < q^2 < 16.0$ GeV$^2/c^4$)

VALUE (units 10^{-7})	DOCUMENT ID		TECN	COMMENT
0.40 ±0.05 OUR AVERAGE	Error includes scale factor of 1.4.			
$0.377\pm0.036\pm0.015$	AAIJ	13H	LHCB	pp at 7 TeV
$0.53\ \pm0.10\ \pm0.03$	AALTONEN	11AI	CDF	$p\overline{p}$ at 1.96 TeV

B($B^+ \to K^+\ell^+\ell^-$) ($16.0 < q^2 < 18.0$ GeV$^2/c^4$)

VALUE (units 10^{-7})	DOCUMENT ID		TECN	COMMENT
$0.354\pm0.036\pm0.018$	AAIJ	13H	LHCB	pp at 7 TeV

B($B^+ \to K^+\ell^+\ell^-$) ($18.0 < q^2 < 22.0$ GeV$^2/c^4$)

VALUE (units 10^{-7})	DOCUMENT ID		TECN	COMMENT
$0.312\pm0.040\pm0.016$	AAIJ	13H	LHCB	pp at 7 TeV

B($B^+ \to K^+\ell^+\ell^-$) ($16.0 < q^2$ GeV$^2/c^4$)

VALUE (units 10^{-7})	DOCUMENT ID		TECN	COMMENT
$0.48\pm0.11\pm0.03$	AALTONEN	11AI	CDF	$p\overline{p}$ at 1.96 TeV

B($B^+ \to K^+\ell^+\ell^-$) ($1.0 < q^2 < 6.0$ GeV$^2/c^4$)

VALUE (units 10^{-7})	DOCUMENT ID		TECN	COMMENT
1.25 ±0.10 OUR AVERAGE				
$1.205\pm0.085\pm0.070$	AAIJ	13H	LHCB	pp at 7 TeV
$1.41\ \pm0.20\ \pm0.10$	AALTONEN	11AI	CDF	$p\overline{p}$ at 1.96 TeV

B($B^+ \to K^+\ell^+\ell^-$) ($0.0 < q^2 < 4.3$ GeV$^2/c^4$)

VALUE (units 10^{-7})	DOCUMENT ID		TECN	COMMENT
$1.13\pm0.19\pm0.08$	AALTONEN	11AI	CDF	$p\overline{p}$ at 1.96 TeV

Meson Particle Listings

$B^{\pm}$

$B^{\pm}$ REFERENCES

AAIJ 14 PRL 112 011801 R. Aaij *et al.* (LHCb Collab.)
AAIJ 14A PL B728 85 R. Aaij *et al.* (LHCb Collab.)
AAIJ 14E JHEP 1404 114 R. Aaij *et al.* (LHCb Collab.)
ABAZOV 14A PR D89 012004 V.M. Abazov *et al.* (D0 Collab.)
LEES 14A PR D89 011102 J.P. Lees *et al.* (BABAR Collab.)
TIEN 14 PR D89 011101 K.-J. Tien *et al.* (BELLE Collab.)
AAIJ 13AE PL B723 44 R. Aaij *et al.* (LHCb Collab.)
AAIJ 13AK PL B726 151 R. Aaij *et al.* (LHCb Collab.)
AAIJ 13AP PR D87 092007 R. Aaij *et al.* (LHCb Collab.)
AAIJ 13AU PR D88 052015 R. Aaij *et al.* (LHCb Collab.)
AAIJ 13AZ PRL 111 101801 R. Aaij *et al.* (LHCb Collab.)
AAIJ 13BC PRL 111 112003 R. Aaij *et al.* (LHCb Collab.)
AAIJ 13BN PRL 111 151801 R. Aaij *et al.* (LHCb Collab.)
AAIJ 13BS PL B726 646 R. Aaij *et al.* (LHCb Collab.)
AAIJ 13H JHEP 1302 105 R. Aaij *et al.* (LHCb Collab.)
AAIJ 13R JHEP 1302 043 R. Aaij *et al.* (LHCb Collab.)
AAIJ 13S EPJ C73 2462 R. Aaij *et al.* (LHCb Collab.)
AAIJ 13Z JHEP 1309 006 R. Aaij *et al.* (LHCb Collab.)
ABAZOV 13M PRL 110 241801 V.M. Abazov *et al.* (D0 Collab.)
DUH 13 PR D87 031103 Y. T. Duh *et al.* (BELLE Collab.)
HARA 13 PRL 110 131801 K. Hara *et al.* (BELLE Collab.)
LEES 13A PR D87 032004 J.P. Lees *et al.* (BABAR Collab.)
LEES 13B PR D87 052015 J.P. Lees *et al.* (BABAR Collab.)
LEES 13I PR D87 112005 J.P. Lees *et al.* (BABAR Collab.)
LEES 13K PR D88 031102 J.P. Lees *et al.* (BABAR Collab.)
LEES 13M PR D88 032012 J.P. Lees *et al.* (BABAR Collab.)
LEES 13T PR D88 072006 J.P. Lees *et al.* (BABAR Collab.)
LUTZ 13 PR D87 111103 O. Lutz *et al.* (BELLE Collab.)
NAYAK 13 PR D88 091104 M. Nayak *et al.* (BELLE Collab.)
SIBIDANOV 13 PR D88 032005 A. Sibidanov *et al.* (BELLE Collab.)
AAIJ 12AA PR D85 091103 R. Aaij *et al.* (LHCb Collab.)
AAIJ 12AC PR D85 091105 R. Aaij *et al.* (LHCb Collab.)
AAIJ 12AD PR D85 112004 R. Aaij *et al.* (LHCb Collab.)
AAIJ 12AH JHEP 1207 133 R. Aaij *et al.* (LHCb Collab.)
AAIJ 12AQ PL B718 43 R. Aaij *et al.* (LHCb Collab.)
AAIJ 12AY JHEP 1212 125 R. Aaij *et al.* (LHCb Collab.)
AAIJ 12C PRL 108 101601 R. Aaij *et al.* (LHCb Collab.)
AAIJ 12E PL B708 241 R. Aaij *et al.* (LHCb Collab.)
AAIJ 12L EPJ C72 2118 R. Aaij *et al.* (LHCb Collab.)
AAIJ 12M PL B712 203 R. Aaij *et al.* (LHCb Collab.)
Also PL B713 351 (errat) R. Aaij *et al.* (LHCb Collab.)
AAIJ 12T PRL 108 161801 R. Aaij *et al.* (LHCb Collab.)
AIHARA 12 PR D85 112014 H. Aihara *et al.* (BELLE Collab.)
DEL-AMO-SA... 12 PR D85 092017 P. del Amo Sanchez *et al.* (BABAR Collab.)
HOI 12 PRL 108 031801 C.-T. Hoi *et al.* (BELLE Collab.)
KIM 12A PR D86 031101 J.H. Kim *et al.* (BELLE Collab.)
LEES 12AA PR D86 092004 J.P. Lees *et al.* (BABAR Collab.)
LEES 12B PR D85 052003 J.P. Lees *et al.* (BABAR Collab.)
LEES 12D PRL 109 101802 J.P. Lees *et al.* (BABAR Collab.)
Also PR D88 072012 J.P. Lees *et al.* (BABAR Collab.)
LEES 12J PR D85 071103 J.P. Lees *et al.* (BABAR Collab.)
LEES 12O PR D85 112010 J.P. Lees *et al.* (BABAR Collab.)
LEES 12P PR D86 012004 J.P. Lees *et al.* (BABAR Collab.)
LEES 12S PR D86 032012 J.P. Lees *et al.* (BABAR Collab.)
LEES 12Z PR D86 091102 J.P. Lees *et al.* (BABAR Collab.)
STYPULA 12 PR D86 072007 J. Stypula *et al.* (BELLE Collab.)
AAIJ 11E PR D84 092001 R. Aaij *et al.* (LHCb Collab.)
Also PR D85 039904 (errat) R. Aaij *et al.* (LHCb Collab.)
AALTONEN 11 PRL 106 121804 T. Aaltonen *et al.* (CDF Collab.)
AALTONEN 11AI PRL 107 201802 T. Aaltonen *et al.* (CDF Collab.)
AALTONEN 11AJ PR D84 091504 T. Aaltonen *et al.* (CDF Collab.)
AALTONEN 11B PR D83 032008 T. Aaltonen *et al.* (CDF Collab.)
AALTONEN 11L PRL 106 161801 T. Aaltonen *et al.* (CDF Collab.)
AUSHEV 11 PR D83 051102 T. Aushev *et al.* (BELLE Collab.)
BHARDWAJ 11 PRL 107 091803 V. Bhardwaj *et al.* (BELLE Collab.)
CHEN 11F PR D84 071501 P. Chen *et al.* (BELLE Collab.)
CHOI 11 PR D84 052004 S.-K. Choi *et al.* (BELLE Collab.)
DEL-AMO-SA... 11B PR D83 032004 P. del Amo Sanchez *et al.* (BABAR Collab.)
DEL-AMO-SA... 11C PR D83 032007 P. del Amo Sanchez *et al.* (BABAR Collab.)
DEL-AMO-SA... 11D PR D83 051101 P. del Amo Sanchez *et al.* (BABAR Collab.)
DEL-AMO-SA... 11F PR D83 052011 P. del Amo Sanchez *et al.* (BABAR Collab.)
DEL-AMO-SA... 11K PR D83 091101 P. del Amo Sanchez *et al.* (BABAR Collab.)
DEL-AMO-SA... 11L PRL 107 041804 P. del Amo Sanchez *et al.* (BABAR Collab.)
GULER 11 PR D83 032005 H. Guler *et al.* (BELLE Collab.)
HORII 11 PRL 106 231803 Y. Horii *et al.* (BELLE Collab.)
LEES 11A PR D84 012001 J.P. Lees *et al.* (BABAR Collab.)
LEES 11D PR D84 012002 J.P. Lees *et al.* (BABAR Collab.)
LEES 11I PR D84 092007 J.P. Lees *et al.* (BABAR Collab.)
SAHOO 11A PR D84 071101 H. Sahoo *et al.* (BELLE Collab.)
SEON 11 PR D84 071106 O. Seon *et al.* (BELLE Collab.)
VINOKUROVA 11 PL B706 139 A. Vinokurova *et al.* (BELLE Collab.)
AALTONEN 10A PR D81 031105 T. Aaltonen *et al.* (CDF Collab.)
AUBERT 10 PRL 104 011802 B. Aubert *et al.* (BABAR Collab.)
AUBERT 10D PR D81 052009 B. Aubert *et al.* (BABAR Collab.)
AUBERT 10E PR D81 051101 B. Aubert *et al.* (BABAR Collab.)
AUSHEV 10 PR D81 031103 T. Aushev *et al.* (BELLE Collab.)
BOZEK 10 PR D82 072005 A. BOZEK *et al.* (BELLE Collab.)
DEL-AMO-SA... 10A PR D82 011502 P. del Amo Sanchez *et al.* (BABAR Collab.)
DEL-AMO-SA... 10B PR D82 011101 P. del Amo Sanchez *et al.* (BABAR Collab.)
DEL-AMO-SA... 10F PRL 105 121801 P. del Amo Sanchez *et al.* (BABAR Collab.)
DEL-AMO-SA... 10G PR D82 072004 P. del Amo Sanchez *et al.* (BABAR Collab.)
DEL-AMO-SA... 10H PR D82 072006 P. del Amo Sanchez *et al.* (BABAR Collab.)
DEL-AMO-SA... 10I PR D82 091101 P. del Amo Sanchez *et al.* (BABAR Collab.)
DEL-AMO-SA... 10K PR D82 092006 P. del Amo Sanchez *et al.* (BABAR Collab.)
DEL-AMO-SA... 10Q PR D82 112002 P. del Amo Sanchez *et al.* (BABAR Collab.)
HARA 10 PR D82 071101 K. Hara *et al.* (BELLE Collab.)
LIBBY 10 PR D82 112006 J. Libby *et al.* (CLEO Collab.)
POLUEKTOV 10 PR D81 112002 A. Poluektov *et al.* (BELLE Collab.)
SAKAI 10 PR D82 091104 K. Sakai *et al.* (BELLE Collab.)
WEDD 10 PR D81 111104 R. Wedd *et al.* (BELLE Collab.)
AALTONEN 09B PR D79 011104 T. Aaltonen *et al.* (CDF Collab.)
ABAZOV 09Y PR D79 111102 V.M. Abazov *et al.* (D0 Collab.)
ABULENCIA 09 PR D79 112003 A. Abulencia *et al.* (CDF Collab.)
AUBERT 09 PR D79 011102 B. Aubert *et al.* (BABAR Collab.)
AUBERT 09A PR D79 012002 B. Aubert *et al.* (BABAR Collab.)
AUBERT 09AA PR D79 112001 B. Aubert *et al.* (BABAR Collab.)
AUBERT 09AB PR D79 112004 B. Aubert *et al.* (BABAR Collab.)
AUBERT 09AF PR D80 051101 B. Aubert *et al.* (BABAR Collab.)
AUBERT 09AJ PR D80 092001 B. Aubert *et al.* (BABAR Collab.)
AUBERT 09AO PRL 103 211802 B. Aubert *et al.* (BABAR Collab.)
AUBERT 09AT PR D80 111105 B. Aubert *et al.* (BABAR Collab.)
AUBERT 09AV PR D80 112002 B. Aubert *et al.* (BABAR Collab.)
AUBERT 09B PRL 102 132001 B. Aubert *et al.* (BABAR Collab.)
AUBERT 09F PR D79 051102 B. Aubert *et al.* (BABAR Collab.)
AUBERT 09G PRL 102 141802 B. Aubert *et al.* (BABAR Collab.)
AUBERT 09H PR D79 052005 B. Aubert *et al.* (BABAR Collab.)
AUBERT 09J PR D79 051101 B. Aubert *et al.* (BABAR Collab.)
AUBERT 09L PR D79 072006 B. Aubert *et al.* (BABAR Collab.)
AUBERT 09Q PR D79 052011 B. Aubert *et al.* (BABAR Collab.)
AUBERT 09S PR D79 092002 B. Aubert *et al.* (BABAR Collab.)
AUBERT 09T PRL 102 091803 B. Aubert *et al.* (BABAR Collab.)
Also EPAPS Document No. E-PRLTAO-102-060910 (BABAR Collab.)
AUBERT 09V PR D79 091101 B. Aubert *et al.* (BABAR Collab.)
AUBERT 09Y PRL 103 051803 B. Aubert *et al.* (BABAR Collab.)
CHANG 09 PR D79 052006 Y.-W. Chang *et al.* (BELLE Collab.)
CHEN 09C PR D80 111103 P. Chen *et al.* (BELLE Collab.)
LIU 09 PR D79 071102 C. Liu *et al.* (BELLE Collab.)
WEI 09A PRL 103 171801 J.-T. Wei *et al.* (BELLE Collab.)
Also EPAPS Supplement EPAPS_appendix.pdf (BELLE Collab.)
WIECHCZYN... 09 PR D80 052005 J. Wiechczynski *et al.* (BELLE Collab.)
ABAZOV 08O PRL 100 211802 V.M. Abazov *et al.* (D0 Collab.)
ADACHI 08 PR D77 091101 I. Adachi *et al.* (BELLE Collab.)
AUBERT 08A PR D77 011101 B. Aubert *et al.* (BABAR Collab.)
AUBERT 08AA PR D77 111102 B. Aubert *et al.* (BABAR Collab.)
AUBERT 08AB PR D78 012006 B. Aubert *et al.* (BABAR Collab.)
AUBERT 08AD PR D77 091104 B. Aubert *et al.* (BABAR Collab.)
AUBERT 08AG PR D78 011104 B. Aubert *et al.* (BABAR Collab.)
AUBERT 08AH PR D78 011107 B. Aubert *et al.* (BABAR Collab.)
AUBERT 08AI PR D78 012004 B. Aubert *et al.* (BABAR Collab.)
AUBERT 08AL PR D78 034023 B. Aubert *et al.* (BABAR Collab.)
AUBERT 08AT PRL 100 231803 B. Aubert *et al.* (BABAR Collab.)
AUBERT 08AV PRL 101 081801 B. Aubert *et al.* (BABAR Collab.)
AUBERT 08B PR D77 011102 B. Aubert *et al.* (BABAR Collab.)
AUBERT 08BC PR D78 072007 B. Aubert *et al.* (BABAR Collab.)
AUBERT 08BD PR D78 091101 B. Aubert *et al.* (BABAR Collab.)
AUBERT 08BE PR D78 091102 B. Aubert *et al.* (BABAR Collab.)
AUBERT 08BF PR D78 092002 B. Aubert *et al.* (BABAR Collab.)
AUBERT 08BH PR D78 112001 B. Aubert *et al.* (BABAR Collab.)
AUBERT 08BI PRL 101 161801 B. Aubert *et al.* (BABAR Collab.)
AUBERT 08BK PRL 101 201801 B. Aubert *et al.* (BABAR Collab.)
AUBERT 08BL PRL 101 261802 B. Aubert *et al.* (BABAR Collab.)
AUBERT 08BN PR D78 112003 B. Aubert *et al.* (BABAR Collab.)
AUBERT 08D PR D77 011107 B. Aubert *et al.* (BABAR Collab.)
AUBERT 08F PRL 100 051803 B. Aubert *et al.* (BABAR Collab.)
AUBERT 08G PRL 100 171803 B. Aubert *et al.* (BABAR Collab.)
AUBERT 08H PR D77 031101 B. Aubert *et al.* (BABAR Collab.)
AUBERT 08N PRL 100 021801 B. Aubert *et al.* (BABAR Collab.)
Also PR D79 092002 B. Aubert *et al.* (BABAR Collab.)
AUBERT 08Q PRL 100 151802 B. Aubert *et al.* (BABAR Collab.)
AUBERT 08W PRL 101 082001 B. Aubert *et al.* (BABAR Collab.)
AUBERT 08X PRL 101 091801 B. Aubert *et al.* (BABAR Collab.)
AUBERT 08Y PR D77 111101 B. Aubert *et al.* (BABAR Collab.)
BHARDWAJ 08 PR D78 051104 V. Bhardwaj *et al.* (BELLE Collab.)
BRODZICKA 08 PRL 100 092001 J. Brodzicka *et al.* (BELLE Collab.)
CHEN 08C PRL 100 251801 J.-H. Chen *et al.* (BELLE Collab.)
HORII 08 PR D78 071901 Y. Horii *et al.* (BELLE Collab.)
IWABUCHI 08 PRL 101 041601 M. Iwabuchi *et al.* (BELLE Collab.)
LIN 08 NAT 452 332 S.-W. Lin *et al.* (BELLE Collab.)
LIVENTSEV 08 PR D77 091503 D. Liventsev *et al.* (BELLE Collab.)
PDG 08 PL B667 1 C. Amsler *et al.* (PDG Collab.)
TANIGUCHI 08 PRL 101 111801 N. Taniguchi *et al.* (BELLE Collab.)
WEI 08 PL B659 80 J.-T. Wei *et al.* (BELLE Collab.)
WEI 08A PR D78 011101 J.-T. Wei *et al.* (BELLE Collab.)
WICHT 08 PL B662 323 J. Wicht *et al.* (BELLE Collab.)
ADAM 07 PRL 99 041802 N.E. Adam *et al.* (CLEO Collab.)
Also PR D76 012007 D.M. Asner *et al.* (CLEO Collab.)
AUBERT 07AC PR D76 031101 B. Aubert *et al.* (BABAR Collab.)
AUBERT 07AE PR D76 031103 B. Aubert *et al.* (BABAR Collab.)
AUBERT 07AG PRL 99 051801 B. Aubert *et al.* (BABAR Collab.)
AUBERT 07AL PR D76 052002 B. Aubert *et al.* (BABAR Collab.)
AUBERT 07AN PR D76 051101 B. Aubert *et al.* (BABAR Collab.)
AUBERT 07AR PR D76 071103 B. Aubert *et al.* (BABAR Collab.)
AUBERT 07AV PR D76 092004 B. Aubert *et al.* (BABAR Collab.)
AUBERT 07AZ PRL 99 201801 B. Aubert *et al.* (BABAR Collab.)
AUBERT 07BA PRL 99 201802 B. Aubert *et al.* (BABAR Collab.)
AUBERT 07BB PRL 99 221801 B. Aubert *et al.* (BABAR Collab.)
AUBERT 07BC PR D76 091102 B. Aubert *et al.* (BABAR Collab.)
AUBERT 07BI PRL 99 241803 B. Aubert *et al.* (BABAR Collab.)
AUBERT 07BJ PRL 99 251801 B. Aubert *et al.* (BABAR Collab.)
AUBERT 07BL PRL 99 261801 B. Aubert *et al.* (BABAR Collab.)
AUBERT 07BN PR D76 111101 B. Aubert *et al.* (BABAR Collab.)
AUBERT 07E PRL 98 051802 B. Aubert *et al.* (BABAR Collab.)
AUBERT 07H PR D75 031101 B. Aubert *et al.* (BABAR Collab.)
AUBERT 07L PRL 98 151802 B. Aubert *et al.* (BABAR Collab.)
AUBERT 07M PRL 98 171801 B. Aubert *et al.* (BABAR Collab.)
AUBERT 07N PR D75 072002 B. Aubert *et al.* (BABAR Collab.)
AUBERT 07Q PR D75 051102 B. Aubert *et al.* (BABAR Collab.)
AUBERT 07R PRL 98 211804 B. Aubert *et al.* (BABAR Collab.)
Also PRL 100 189903E B. Aubert *et al.* (BABAR Collab.)
Also PRL 100 199905E B. Aubert *et al.* (BABAR Collab.)
AUBERT 07X PR D75 091103 B. Aubert *et al.* (BABAR Collab.)
AUBERT 07Z PR D76 011103 B. Aubert *et al.* (BABAR Collab.)
CHANG 07B PR D75 071104 P. Chang *et al.* (BELLE Collab.)
CHEN 07D PRL 99 221802 K.-F. Chen *et al.* (BELLE Collab.)
HOKUUE 07 PL B648 139 T. Hokuue *et al.* (BELLE Collab.)
LIN 07 PRL 98 181804 S.-W. Lin *et al.* (BELLE Collab.)
LIN 07A PRL 99 121601 S.-W. Lin *et al.* (BELLE Collab.)
SATOYAMA 07 PL B647 67 N. Satoyama *et al.* (BELLE Collab.)
SCHUEMANN 07 PR D75 092002 J. Schuemann *et al.* (BELLE Collab.)
TSAI 07 PR D75 111101 Y.-T. Tsai *et al.* (BELLE Collab.)
URQUIJO 07 PR D75 032001 P. Urquijo *et al.* (BELLE Collab.)
WANG 07B PR D75 092005 C.H. Wang *et al.* (BELLE Collab.)
WANG 07C PR D76 052004 M.-Z. Wang *et al.* (BELLE Collab.)
XIE 07 PR D75 017101 Q.L. Xie *et al.* (BELLE Collab.)
ABE 06 PR D73 051106 K. Abe *et al.* (BELLE Collab.)
ABULENCIA 06J PRL 96 191801 A. Abulencia *et al.* (CDF Collab.)
ACOSTA 06 PRL 96 202001 D. Acosta *et al.* (CDF Collab.)
AUBERT 06 PR D73 011101 B. Aubert *et al.* (BABAR Collab.)
AUBERT 06E PRL 96 052002 B. Aubert *et al.* (BABAR Collab.)
AUBERT 06F PR D73 011103 B. Aubert *et al.* (BABAR Collab.)
AUBERT 06J PR D73 051105 B. Aubert *et al.* (BABAR Collab.)
AUBERT 06K PR D73 057101 B. Aubert *et al.* (BABAR Collab.)
AUBERT 06N PR D74 031103 B. Aubert *et al.* (BABAR Collab.)
AUBERT 06O PR D74 032003 B. Aubert *et al.* (BABAR Collab.)
AUBERT 06Z PR D73 111104 B. Aubert *et al.* (BABAR Collab.)
AUBERT,B 06A PR D73 112004 B. Aubert *et al.* (BABAR Collab.)
AUBERT,B 06C PR D74 011102 B. Aubert *et al.* (BABAR Collab.)
AUBERT,B 06E PR D74 011106 B. Aubert *et al.* (BABAR Collab.)
AUBERT,B 06G PRL 97 201801 B. Aubert *et al.* (BABAR Collab.)
AUBERT,B 06H PRL 97 201802 B. Aubert *et al.* (BABAR Collab.)
AUBERT,B 06J PR D73 092001 B. Aubert *et al.* (BABAR Collab.)
AUBERT,B 06M PR D74 031102 B. Aubert *et al.* (BABAR Collab.)
AUBERT,B 06P PR D74 031105 B. Aubert *et al.* (BABAR Collab.)
AUBERT,B 06T PR D74 051102 B. Aubert *et al.* (BABAR Collab.)
AUBERT,B 06U PR D74 051104 B. Aubert *et al.* (BABAR Collab.)
AUBERT,B 06Y PR D74 091105 B. Aubert *et al.* (BABAR Collab.)
AUBERT,BE 06A PR D74 099903 (errat.) B. Aubert *et al.* (BABAR Collab.)
AUBERT,BE 06C PRL 97 171805 B. Aubert *et al.* (BABAR Collab.)
AUBERT,BE 06G PRL 97 261801 B. Aubert *et al.* (BABAR Collab.)
AUBERT,BE 06H PR D74 091101 B. Aubert *et al.* (BABAR Collab.)
AUBERT,BE 06J PR D74 111102 B. Aubert *et al.* (BABAR Collab.)
AUBERT,BE 06M PR D74 071101 B. Aubert *et al.* (BABAR Collab.)

See key on page 547

CHISTOV 06A PR D74 111105 R. Chistov *et al.* (BELLE Collab.)
FANG 06 PR D74 012007 F. Fang *et al.* (BELLE Collab.)
GABYSHEV 06 PRL 97 202003 N. Gabyshev *et al.* (BELLE Collab.)
GABYSHEV 06A PRL 97 242001 N. Gabyshev *et al.* (BELLE Collab.)
GARMASH 06 PRL 96 251803 A. Garmash *et al.* (BELLE Collab.)
GOKHROO 06 PRL 97 162002 G. Gokhroo *et al.* (BELLE Collab.)
IKADO 06 PRL 97 251802 K. Ikado *et al.* (BELLE Collab.)
JEN 06 PR D74 111101 C.-M. Jen *et al.* (BELLE Collab.)
KUMAR 06 PR D74 051103 R. Kumar *et al.* (BELLE Collab.)
MOHAPATRA 06 PRL 96 221601 D. Mohapatra *et al.* (BELLE Collab.)
POLUEKTOV 06 PR D73 112009 A. Poluektov *et al.* (BELLE Collab.)
SCHUEMANN 06 PRL 97 061802 J. Schuemann *et al.* (BELLE Collab.)
SONI 06 PL B634 155 N. Soni *et al.* (BELLE Collab.)
ABE 05A PRL 94 221805 K. Abe *et al.* (BELLE Collab.)
ABE 05B PR D71 072003 K. Abe *et al.* (BELLE Collab.)
Also PR D71 079903 (errat.) K. Abe *et al.* (BELLE Collab.)
ABE 05G PRL 95 231802 K. Abe *et al.* (BELLE Collab.)
ACOSTA 05J PRL 95 031801 D. Acosta *et al.* (CDF Collab.)
AUBERT 05 PRL 94 011801 B. Aubert *et al.* (BABAR Collab.)
AUBERT 05B PR D71 031501 B. Aubert *et al.* (BABAR Collab.)
AUBERT 05G PR D72 032004 B. Aubert *et al.* (BABAR Collab.)
AUBERT 05H PRL 94 101801 B. Aubert *et al.* (BABAR Collab.)
AUBERT 05J PRL 94 141801 B. Aubert *et al.* (BABAR Collab.)
AUBERT 05K PRL 94 171801 B. Aubert *et al.* (BABAR Collab.)
AUBERT 05L PRL 94 181802 B. Aubert *et al.* (BABAR Collab.)
AUBERT 05M PRL 94 191802 B. Aubert *et al.* (BABAR Collab.)
AUBERT 05N PR D71 031102 B. Aubert *et al.* (BABAR Collab.)
AUBERT 05O PR D71 031103 B. Aubert *et al.* (BABAR Collab.)
AUBERT 05R PR D71 071103 B. Aubert *et al.* (BABAR Collab.)
AUBERT 05U PR D71 091103 B. Aubert *et al.* (BABAR Collab.)
AUBERT 05X PR D71 111101 B. Aubert *et al.* (BABAR Collab.)
AUBERT,B 05B PRL 95 041804 B. Aubert *et al.* (BABAR Collab.)
AUBERT,B 05E PR D72 011102 B. Aubert *et al.* (BABAR Collab.)
AUBERT,B 05G PR D72 052002 B. Aubert *et al.* (BABAR Collab.)
AUBERT,B 05K PRL 95 131803 B. Aubert *et al.* (BABAR Collab.)
AUBERT,B 05L PR D72 051101 B. Aubert *et al.* (BABAR Collab.)
AUBERT,B 05N PR D72 072003 B. Aubert *et al.* (BABAR Collab.)
Also PR D74 099903 (errat.) B. Aubert *et al.* (BABAR Collab.)
AUBERT,B 05O PR D72 051102 B. Aubert *et al.* (BABAR Collab.)
AUBERT,B 05T PR D72 071102 B. Aubert *et al.* (BABAR Collab.)
AUBERT,B 05U PR D72 071103 B. Aubert *et al.* (BABAR Collab.)
AUBERT,B 05V PR D72 071104 B. Aubert *et al.* (BABAR Collab.)
AUBERT,B 05Y PRL 95 121802 B. Aubert *et al.* (BABAR Collab.)
AUBERT,BE 05E PRL 95 221801 B. Aubert *et al.* (BABAR Collab.)
CHANG 05 PR D71 072007 M.-C. Chang *et al.* (BELLE Collab.)
CHANG 05A PR D71 091106 P. Chang *et al.* (BELLE Collab.)
CHAO 05A PR D71 031502 Y. Chao *et al.* (BELLE Collab.)
CHEN 05A PRL 94 221804 K.-F. Chen *et al.* (BELLE Collab.)
GARMASH 05 PR D71 092003 A. Garmash *et al.* (BELLE Collab.)
ITOH 05 PRL 95 091601 R. Itoh *et al.* (BELLE Collab.)
LEE 05 PRL 95 061802 Y.-J. Lee *et al.* (BELLE Collab.)
LIVENTSEV 05 PR D72 051109 D. Liventsev *et al.* (BELLE Collab.)
MAJUMDER 05 PRL 95 041803 G. Majumder *et al.* (BELLE Collab.)
MOHAPATRA 05 PR D72 011101 D. Mohapatra *et al.* (BELLE Collab.)
NISHIDA 05 PL B610 23 S. Nishida *et al.* (BELLE Collab.)
OKABE 05 PL B614 27 T. Okabe *et al.* (BELLE Collab.)
SAIGO 05 PRL 94 091601 M. Saigo *et al.* (BELLE Collab.)
WANG 05A PL B617 141 M.-Z. Wang *et al.* (BELLE Collab.)
XIE 05 PR D72 051105 Q.L. Xie *et al.* (BELLE Collab.)
YANG 05 PRL 94 111802 H. Yang *et al.* (BELLE Collab.)
ZHANG 05A PRL 94 031801 J. Zhang *et al.* (BELLE Collab.)
ZHANG 05B PR D71 091107 L.M. Zhang *et al.* (BELLE Collab.)
ZHANG 05D PRL 95 141801 J. Zhang *et al.* (BELLE Collab.)
ABDALLAH 04E EPJ C33 307 J. Abdallah *et al.* (DELPHI Collab.)
ABE 04D PR D69 112002 K. Abe *et al.* (BELLE Collab.)
AUBERT 04A PR D69 011102 B. Aubert *et al.* (BABAR Collab.)
AUBERT 04C PRL 92 111801 B. Aubert *et al.* (BaBar Collab.)
AUBERT 04H PRL 92 061801 B. Aubert *et al.* (BABAR Collab.)
AUBERT 04K PRL 92 141801 B. Aubert *et al.* (BABAR Collab.)
AUBERT 04M PRL 92 201802 B. Aubert *et al.* (BABAR Collab.)
AUBERT 04N PRL 92 202002 B. Aubert *et al.* (BABAR Collab.)
AUBERT 04O PRL 92 221803 B. Aubert *et al.* (BABAR Collab.)
AUBERT 04P PRL 92 241802 B. Aubert *et al.* (BABAR Collab.)
AUBERT 04Q PR D69 051101 B. Aubert *et al.* (BABAR Collab.)
AUBERT 04T PR D69 071103 B. Aubert *et al.* (BABAR Collab.)
AUBERT 04Y PRL 93 041801 B. Aubert *et al.* (BaBar Collab.)
AUBERT 04Z PRL 93 051802 B. Aubert *et al.* (BABAR Collab.)
AUBERT,B 04B PR D70 011101 B. Aubert *et al.* (BABAR Collab.)
AUBERT,B 04D PR D70 032006 B. Aubert *et al.* (BABAR Collab.)
AUBERT,B 04L PRL 93 131804 B. Aubert *et al.* (BABAR Collab.)
AUBERT,B 04P PR D70 092001 B. Aubert *et al.* (BABAR Collab.)
AUBERT,B 04S PRL 93 181801 B. Aubert *et al.* (BABAR Collab.)
AUBERT,B 04U PR D70 091105 B. Aubert *et al.* (BABAR Collab.)
AUBERT,B 04V PRL 93 181805 B. Aubert *et al.* (BABAR Collab.)
AUBERT,BE 04 PR D70 111102 B. Aubert *et al.* (BABAR Collab.)
AUBERT,BE 04A PR D70 112006 B. Aubert *et al.* (BABAR Collab.)
AUBERT,BE 04B PR D70 091106 B. Aubert *et al.* (BABAR Collab.)
CHAO 04 PR D69 111102 Y. Chao *et al.* (BELLE Collab.)
CHAO 04B PRL 93 191802 Y. Chao *et al.* (BELLE Collab.)
CHISTOV 04 PRL 93 051803 R. Chistov *et al.* (BELLE Collab.)
DRUTSKOY 04 PRL 92 051801 A. Drutskoy *et al.* (BELLE Collab.)
GARMASH 04 PR D69 012001 A. Garmash *et al.* (BELLE Collab.)
LEE 04 PRL 93 211801 Y.-J. Lee *et al.* (BELLE Collab.)
MAJUMDER 04 PR D70 111103 G. Majumder *et al.* (BELLE Collab.)
NAKAO 04 PR D69 112001 M. Nakao *et al.* (BELLE Collab.)
POLUEKTOV 04 PR D70 072003 A. Poluektov *et al.* (BELLE Collab.)
SCHWANDA 04 PRL 93 131803 C. Schwanda *et al.* (BELLE Collab.)
WANG 04 PRL 92 131801 M.Z. Wang *et al.* (BELLE Collab.)
WANG 04A PR D70 012001 C.H. Wang *et al.* (BELLE Collab.)
ZANG 04 PR D69 017101 S.L. Zang *et al.* (BELLE Collab.)
ABE 03B PR D67 032003 K. Abe *et al.* (BELLE Collab.)
ABE 03D PRL 90 131803 K. Abe *et al.* (BELLE Collab.)
ADAM 03 PR D67 032001 N.E. Adam *et al.* (CLEO Collab.)
ADAM 03B PR D68 012004 N.E. Adam *et al.* (CLEO Collab.)
ATHAR 03 PR D68 072003 S.B. Athar *et al.* (CLEO Collab.)
AUBERT 03K PRL 90 231801 B. Aubert *et al.* (BaBar Collab.)
AUBERT 03L PRL 91 021801 B. Aubert *et al.* (BaBar Collab.)
AUBERT 03M PRL 91 051801 B. Aubert *et al.* (BaBar Collab.)
AUBERT 03O PRL 91 071801 B. Aubert *et al.* (BaBar Collab.)
AUBERT 03U PRL 91 221802 B. Aubert *et al.* (BaBar Collab.)
AUBERT 03V PRL 91 171802 B. Aubert *et al.* (BaBar Collab.)
AUBERT 03W PRL 91 161801 B. Aubert *et al.* (BaBar Collab.)
AUBERT 03X PR D68 092001 B. Aubert *et al.* (BaBar Collab.)
BORNHEIM 03 PR D68 052002 A. Bornheim *et al.* (CLEO Collab.)
CHEN 03B PRL 91 201801 K.-F. Chen *et al.* (BELLE Collab.)
CHOI 03 PRL 91 262001 S.-K. Choi *et al.* (BELLE Collab.)
CSORNA 03 PR D67 112002 S.E. Csorna *et al.* (CLEO Collab.)
EDWARDS 03 PR D68 011102 K.W. Edwards *et al.* (CLEO Collab.)
FANG 03 PRL 90 071801 F. Fang *et al.* (BELLE Collab.)
HUANG 03 PRL 91 241802 H.-C. Huang *et al.* (BELLE Collab.)
ISHIKAWA 03 PRL 91 261601 A. Ishikawa *et al.* (BELLE Collab.)
KROKOVNY 03B PRL 91 262002 P. Krokovny *et al.* (BELLE Collab.)
SWAIN 03 PR D68 051101 S.K. Swain *et al.* (BELLE Collab.)
UNNO 03 PR D68 011103 Y. Unno *et al.* (BELLE Collab.)
ZHANG 03B PRL 91 221801 J. Zhang *et al.* (BELLE Collab.)
ABE 02 PRL 88 021801 K. Abe *et al.* (BELLE Collab.)
ABE 02B PRL 88 031802 K. Abe *et al.* (BELLE Collab.)
ABE 02H PRL 88 171801 K. Abe *et al.* (BELLE Collab.)
ABE 02K PRL 88 181803 K. Abe *et al.* (BELLE Collab.)
ABE 02N PL B538 11 K. Abe *et al.* (BELLE Collab.)
ABE 02O PR D65 091103 K. Abe *et al.* (BELLE Collab.)
ABE 02W PRL 89 151802 K. Abe *et al.* (BELLE Collab.)
ACOSTA 02C PR D65 092009 D. Acosta *et al.* (CDF Collab.)
ACOSTA 02F PR D66 052005 D. Acosta *et al.* (CDF Collab.)
AHMED 02B PR D66 031101 S. Ahmed *et al.* (CLEO Collab.)
AUBERT 02 PR D65 032001 B. Aubert *et al.* (BaBar Collab.)
AUBERT 02C PRL 88 101805 B. Aubert *et al.* (BaBar Collab.)
AUBERT 02E PR D65 051101 B. Aubert *et al.* (BaBar Collab.)
AUBERT 02F PR D65 091101 B. Aubert *et al.* (BaBar Collab.)
AUBERT 02L PRL 88 241801 B. Aubert *et al.* (BaBar Collab.)
BRIERE 02 PRL 89 081803 R. Briere *et al.* (CLEO Collab.)
CASEY 02 PR D66 092002 B.C.K. Casey *et al.* (BELLE Collab.)
CHEN 02B PL B546 196 K.-F. Chen *et al.* (BELLE Collab.)
DRUTSKOY 02 PL B542 171 A. Drutskoy *et al.* (BELLE Collab.)
DYTMAN 02 PR D66 091101 S.A. Dytman *et al.* (CLEO Collab.)
ECKHART 02 PRL 89 251801 E. Eckhart *et al.* (CLEO Collab.)
EDWARDS 02B PR D65 111102 K.W. Edwards *et al.* (CLEO Collab.)
GABYSHEV 02 PR D66 091102 N. Gabyshev *et al.* (BELLE Collab.)
GARMASH 02 PR D65 092005 A. Garmash *et al.* (BELLE Collab.)
GODANG 02 PRL 88 021802 R. Godang *et al.* (CLEO Collab.)
GORDON 02 PL B542 183 A. Gordon *et al.* (BELLE Collab.)
LU 02 PRL 89 191801 R.-S. Lu *et al.* (BELLE Collab.)
MAHAPATRA 02 PRL 88 101803 R. Mahapatra *et al.* (CLEO Collab.)
NISHIDA 02 PRL 89 231801 S. Nishida *et al.* (BELLE Collab.)
ABE 01H PRL 87 101801 K. Abe *et al.* (BELLE Collab.)
ABE 01I PRL 87 111801 K. Abe *et al.* (BELLE Collab.)
ABE 01K PR D64 071101 K. Abe *et al.* (BELLE Collab.)
ABE 01L PRL 87 161601 K. Abe *et al.* (BELLE Collab.)
ABE 01M PL B517 309 K. Abe *et al.* (BELLE Collab.)
ALEXANDER 01B PR D64 092001 J.P. Alexander *et al.* (CLEO Collab.)
AMMAR 01B PRL 87 271801 R. Ammar *et al.* (CLEO Collab.)
ANDERSON 01B PRL 87 181803 S. Anderson *et al.* (CLEO Collab.)
AUBERT 01D PRL 87 151801 B. Aubert *et al.* (BaBar Collab.)
AUBERT 01E PRL 87 151802 B. Aubert *et al.* (BaBar Collab.)
AUBERT 01F PRL 87 201803 B. Aubert *et al.* (BaBar Collab.)
AUBERT 01G PRL 87 221802 B. Aubert *et al.* (BaBar Collab.)
BARATE 01E EPJ C19 213 R. Barate *et al.* (ALEPH Collab.)
BRIERE 01 PRL 86 3718 R.A. Briere *et al.* (CLEO Collab.)
BROWDER 01 PRL 86 2950 T.E. Browder *et al.* (CLEO Collab.)
EDWARDS 01 PRL 86 30 K.W. Edwards *et al.* (CLEO Collab.)
GRITSAN 01 PR D64 077501 A. Gritsan *et al.* (CLEO Collab.)
RICHICHI 01 PR D63 031103 S.J. Richichi *et al.* (CLEO Collab.)
ABBIENDI 00B PL B476 233 G. Abbiendi *et al.* (OPAL Collab.)
ABE 00C PR D62 071101 K. Abe *et al.* (SLD Collab.)
AHMED 00B PR D62 112003 S. Ahmed *et al.* (CLEO Collab.)
ANASTASSOV 00 PRL 84 1393 A. Anastassov *et al.* (CLEO Collab.)
BARATE 00R PL B492 275 R. Barate *et al.* (ALEPH Collab.)
BEHRENS 00 PR D61 052001 B.H. Behrens *et al.* (CLEO Collab.)
BONVICINI 00 PRL 84 5940 G. Bonvicini *et al.* (CLEO Collab.)
CHEN 00 PRL 85 525 S. Chen *et al.* (CLEO Collab.)
COAN 00 PRL 84 5283 T.E. Coan *et al.* (CLEO Collab.)
CRONIN-HEN... 00 PRL 85 515 D. Cronin-Hennessy *et al.* (CLEO Collab.)
CSORNA 00 PR D61 111101 S.E. Csorna *et al.* (CLEO Collab.)
JESSOP 00 PRL 85 2881 C.P. Jessop *et al.* (CLEO Collab.)
RICHICHI 00 PRL 85 520 S.J. Richichi *et al.* (CLEO Collab.)
ABBIENDI 99J EPJ C12 609 G. Abbiendi *et al.* (OPAL Collab.)
AFFOLDER 99B PRL 83 3378 T. Affolder *et al.* (CDF Collab.)
BARTELT 99 PRL 82 3746 J. Bartelt *et al.* (CLEO Collab.)
COAN 99 PR D59 111101 T.E. Coan *et al.* (CLEO Collab.)
ABE 98B PR D57 5382 F. Abe *et al.* (CDF Collab.)
ABE 98O PR D58 072001 F. Abe *et al.* (CDF Collab.)
ABE 98Q PR D58 092002 F. Abe *et al.* (CDF Collab.)
ACCIARRI 98S PL B438 417 M. Acciarri *et al.* (L3 Collab.)
ANASTASSOV 98 PRL 80 4127 A. Anastassov *et al.* (CLEO Collab.)
ATHANAS 98 PRL 80 5493 M. Athanas *et al.* (CLEO Collab.)
BARATE 98Q EPJ C4 387 R. Barate *et al.* (ALEPH Collab.)
BEHRENS 98 PRL 80 3710 B.H. Behrens *et al.* (CLEO Collab.)
BERGFELD 98 PRL 81 272 T. Bergfeld *et al.* (CLEO Collab.)
BRANDENB... 98 PRL 80 2762 G. Brandenbrug *et al.* (CLEO Collab.)
CAPRINI 98 NP B530 153 I. Caprini, L. Lellouch, M. Neubert (BCIP, CERN)
GODANG 98 PRL 80 3456 R. Godang *et al.* (CLEO Collab.)
ABE 97J PR 79 590 K. Abe *et al.* (SLD Collab.)
ACCIARRI 97F PL B396 327 M. Acciarri *et al.* (L3 Collab.)
ARTUSO 97 PL B399 321 M. Artuso *et al.* (CLEO Collab.)
ATHANAS 97 PRL 79 2208 M. Athanas *et al.* (CLEO Collab.)
BROWDER 97 PR D56 11 T. Browder *et al.* (CLEO Collab.)
FU 97 PRL 79 3125 X. Fu *et al.* (CLEO Collab.)
JESSOP 97 PRL 79 4533 C.P. Jessop *et al.* (CLEO Collab.)
ABE 96B PR D53 3496 F. Abe *et al.* (CDF Collab.)
ABE 96C PRL 76 4462 F. Abe *et al.* (CDF Collab.)
ABE 96H PRL 76 2015 F. Abe *et al.* (CDF Collab.)
ABE 96L PRL 76 4675 F. Abe *et al.* (CDF Collab.)
ABE 96Q PR D54 6596 F. Abe *et al.* (CDF Collab.)
ABE 96R PRL 77 5176 F. Abe *et al.* (CDF Collab.)
ADAM 96D ZPHY C72 207 W. Adam *et al.* (DELPHI Collab.)
ALEXANDER 96T PRL 77 5000 J.P. Alexander *et al.* (CLEO Collab.)
ASNER 96 PR D53 1039 D.M. Asner *et al.* (CLEO Collab.)
BARISH 96B PRL 76 1570 B.C. Barish *et al.* (CLEO Collab.)
BERGFELD 96B PRL 77 4503 T. Bergfeld *et al.* (CLEO Collab.)
BISHAI 96 PL B369 186 M. Bishai *et al.* (CLEO Collab.)
BUSKULIC 96J ZPHY C71 31 D. Buskulic *et al.* (ALEPH Collab.)
GIBAUT 96 PR D53 4734 D. Gibaut *et al.* (CLEO Collab.)
PDG 96 PR D54 1 R. M. Barnett *et al.* (PDG Collab.)
ABREU 95N PL B357 255 P. Abreu *et al.* (DELPHI Collab.)
ABREU 95Q ZPHY C68 13 P. Abreu *et al.* (DELPHI Collab.)
ADAM 95 ZPHY C68 363 W. Adam *et al.* (DELPHI Collab.)
AKERS 95T ZPHY C67 379 R. Akers *et al.* (OPAL Collab.)
ALBRECHT 95D PL B353 554 H. Albrecht *et al.* (ARGUS Collab.)
ALEXANDER 95 PL B341 435 J. Alexander *et al.* (CLEO Collab.)
Also PL B347 469 (erratum) J. Alexander *et al.* (CLEO Collab.)
ARTUSO 95 PRL 75 785 M. Artuso *et al.* (CLEO Collab.)
BARISH 95 PR D51 1014 B.C. Barish *et al.* (CLEO Collab.)
BUSKULIC 95 PL B343 444 D. Buskulic *et al.* (ALEPH Collab.)
ABE 94D PRL 72 3456 F. Abe *et al.* (CDF Collab.)
ALAM 94 PR D50 43 M.S. Alam *et al.* (CLEO Collab.)
ALBRECHT 94D PL B335 526 H. Albrecht *et al.* (ARGUS Collab.)
ATHANAS 94 PRL 73 3503 M. Athanas *et al.* (CLEO Collab.)
Also PRL 74 3090 (erratum) M. Athanas *et al.* (CLEO Collab.)
PDG 94 PR D50 1173 L. Montanet *et al.* (CERN, LBL, BOST+)
STONE 94 HEPSY 93-11 S. Stone
Published in B Decays, 2nd Edition, World Scientific, Singapore
ABREU 93D ZPHY C57 181 P. Abreu *et al.* (DELPHI Collab.)
ABREU 93G PL B312 253 P. Abreu *et al.* (DELPHI Collab.)
ACTON 93C PL B307 247 P.D. Acton *et al.* (OPAL Collab.)

Meson Particle Listings

$B^{\pm}$, B^0

ALBRECHT	93E	ZPHY C60 11	H. Albrecht *et al.*	(ARGUS Collab.)
ALEXANDER	93B	PL B319 365	J. Alexander *et al.*	(CLEO Collab.)
AMMAR	93	PRL 71 674	R. Ammar *et al.*	(CLEO Collab.)
BEAN	93B	PRL 70 2681	A. Bean *et al.*	(CLEO Collab.)
BUSKULIC	93D	PL B307 194	D. Buskulic *et al.*	(ALEPH Collab.)
Also		PL B325 537 (erratum)	D. Buskulic *et al.*	(ALEPH Collab.)
SANGHERA	93	PR D47 791	S. Sanghera *et al.*	(CLEO Collab.)
ALBRECHT	92C	PL B275 195	H. Albrecht *et al.*	(ARGUS Collab.)
ALBRECHT	92E	PL B277 209	H. Albrecht *et al.*	(ARGUS Collab.)
ALBRECHT	92G	ZPHY C54 1	H. Albrecht *et al.*	(ARGUS Collab.)
BORTOLETTO	92	PR D45 21	D. Bortoletto *et al.*	(CLEO Collab.)
BUSKULIC	92G	PL B295 396	D. Buskulic *et al.*	(ALEPH Collab.)
ALBRECHT	91B	PL B254 288	H. Albrecht *et al.*	(ARGUS Collab.)
ALBRECHT	91C	PL B255 297	H. Albrecht *et al.*	(ARGUS Collab.)
ALBRECHT	91E	PL B262 148	H. Albrecht *et al.*	(ARGUS Collab.)
BERKELMAN	91	ARNPS 41 1	K. Berkelman, S. Stone	(CORN, SYRA)
"Decays of B Mesons"				
FULTON	91	PR D43 651	R. Fulton *et al.*	(CLEO Collab.)
ALBRECHT	90B	PL B241 278	H. Albrecht *et al.*	(ARGUS Collab.)
ALBRECHT	90J	ZPHY C48 543	H. Albrecht *et al.*	(ARGUS Collab.)
ANTREASYAN	90B	ZPHY C48 553	D. Antreasyan *et al.*	(Crystal Ball Collab.)
BORTOLETTO	90	PRL 64 2117	D. Bortoletto *et al.*	(CLEO Collab.)
Also		PR D45 21	D. Bortoletto *et al.*	(CLEO Collab.)
WEIR	90B	PR D41 1384	A.J. Weir *et al.*	(Mark II Collab.)
ALBRECHT	89G	PL B229 304	H. Albrecht *et al.*	(ARGUS Collab.)
AVERY	89B	PL B223 470	P. Avery *et al.*	(CLEO Collab.)
BEBEK	89	PRL 62 8	C. Bebek *et al.*	(CLEO Collab.)
BORTOLETTO	89	PRL 62 2436	D. Bortoletto *et al.*	(CLEO Collab.)
ALBRECHT	88F	PL B209 119	H. Albrecht *et al.*	(ARGUS Collab.)
ALBRECHT	88K	PL B215 424	H. Albrecht *et al.*	(ARGUS Collab.)
ALBRECHT	87C	PL B185 218	H. Albrecht *et al.*	(ARGUS Collab.)
ALBRECHT	87D	PL B199 451	H. Albrecht *et al.*	(ARGUS Collab.)
AVERY	87	PL B183 429	P. Avery *et al.*	(CLEO Collab.)
BEBEK	87	PR D36 1289	C. Bebek *et al.*	(CLEO Collab.)
ALAM	86	PR D34 3279	M.S. Alam *et al.*	(CLEO Collab.)
PDG	86	PL 170B 1	M. Aguilar-Benitez *et al.*	(CERN, CIT+)
GILES	84	PR D30 2279	R. Giles *et al.*	(CLEO Collab.)

B^0

$I(J^P) = \frac{1}{2}(0^-)$

Quantum numbers not measured. Values shown are quark-model predictions.

See also the $B^{\pm}/B^0$ ADMIXTURE and $B^{\pm}/B^0/B_s^0$/b-baryon ADMIXTURE sections.

See the Note "Production and Decay of b-flavored Hadrons" at the beginning of the $B^{\pm}$ Particle Listings and the Note on "B^0-$\overline{B}^0$ Mixing" near the end of the B^0 Particle Listings.

B^0 MASS

The fit uses m_{B^+}, $(m_{B^0} - m_{B^+})$, and m_{B^0} to determine m_{B^+}, m_{B^0}, and the mass difference.

VALUE (MeV)	EVTS	DOCUMENT ID		TECN	COMMENT
5279.58±0.17 OUR FIT					
5279.55±0.26 OUR AVERAGE					
5279.6 ±0.2 ±1.0		[1] AAD	13U	ATLS	pp at 7 TeV
5279.58±0.15±0.28		[2] AAIJ	12E	LHCB	pp at 7 TeV
5279.63±0.53±0.33		[3] ACOSTA	06	CDF	$p\overline{p}$ at 1.96 TeV
5279.1 ±0.7 ±0.3	135	[4] CSORNA	00	CLE2	$e^+e^- \to \Upsilon(4S)$
5281.3 ±2.2 ±1.4	51	ABE	96B	CDF	$p\overline{p}$ at 1.8 TeV
• • • We do not use the following data for averages, fits, limits, etc. • • •					
5279.2 ±0.54±2.0	340	ALAM	94	CLE2	$e^+e^- \to \Upsilon(4S)$
5278.0 ±0.4 ±2.0		BORTOLETTO	92	CLEO	$e^+e^- \to \Upsilon(4S)$
5279.6 ±0.7 ±2.0	40	[5] ALBRECHT	90J	ARG	$e^+e^- \to \Upsilon(4S)$
5278.2 ±1.0 ±3.0	40	ALBRECHT	87C	ARG	$e^+e^- \to \Upsilon(4S)$
5279.5 ±1.6 ±3.0	7	[6] ALBRECHT	87D	ARG	$e^+e^- \to \Upsilon(4S)$
5280.6 ±0.8 ±2.0		BEBEK	87	CLEO	$e^+e^- \to \Upsilon(4S)$

[1] Measured with $B_d^0 \to J/\psi(\mu^+\mu^-)\, K_S^0(\pi^+\pi^-)$ decays.
[2] Uses $B^0 \to J/\psi K^0$ fully reconstructed decays.
[3] Uses exclusively reconstructed final states containing a $J/\psi \to \mu^+\mu^-$ decays.
[4] CSORNA 00 uses fully reconstructed 135 $B^0 \to J/\psi^{(\prime)} K_S^0$ events and invariant masses without beam constraint.
[5] ALBRECHT 90J assumes 10580 for $\Upsilon(4S)$ mass. Supersedes ALBRECHT 87C and ALBRECHT 87D.
[6] Found using fully reconstructed decays with J/ψ. ALBRECHT 87D assume $m_{\Upsilon(4S)} =$ 10577 MeV.

$m_{B^0} - m_{B^+}$

VALUE (MeV)	DOCUMENT ID		TECN	COMMENT
0.32±0.06 OUR FIT				
0.32±0.05 OUR AVERAGE				
0.20±0.17±0.11	[1] AAIJ	12E	LHCB	pp at 7 TeV
0.33±0.05±0.03	[2] AUBERT	08AF	BABR	$e^+e^- \to \Upsilon(4S)$
0.53±0.67±0.14	[3] ACOSTA	06	CDF	$p\overline{p}$ at 1.96 TeV
0.41±0.25±0.19	ALAM	94	CLE2	$e^+e^- \to \Upsilon(4S)$
−0.4 ±0.6 ±0.5	BORTOLETTO	92	CLEO	$e^+e^- \to \Upsilon(4S)$
−0.9 ±1.2 ±0.5	ALBRECHT	90J	ARG	$e^+e^- \to \Upsilon(4S)$
2.0 ±1.1 ±0.3	[4] BEBEK	87	CLEO	$e^+e^- \to \Upsilon(4S)$

[1] Uses exclusively reconstructed final states containing a $J/\psi \to \mu^+\mu^-$ decay.
[2] Uses the B-momentum distributions in the e^+e^- rest frame.
[3] Uses exclusively reconstructed final states containing a $J/\psi \to \mu^+\mu^-$ decays.
[4] BEBEK 87 actually measure the difference between half of $E_{\rm cm}$ and the $B^{\pm}$ or B^0 mass, so the $m_{B^0} - m_{B^{\pm}}$ is more accurate. Assume $m_{\Upsilon(4S)} =$ 10580 MeV.

$m_{B_H^0} - m_{B_L^0}$

See the B^0-$\overline{B}^0$ MIXING PARAMETERS section near the end of these B^0 Listings.

B^0 MEAN LIFE

See $B^{\pm}/B^0/B_s^0$/b-baryon ADMIXTURE section for data on B-hadron mean life averaged over species of bottom particles.

"OUR EVALUATION" is an average using rescaled values of the data listed below. The average and rescaling were performed by the Heavy Flavor Averaging Group (HFAG) and are described at http://www.slac.stanford.edu/xorg/hfag/. The averaging/rescaling procedure takes into account correlations between the measurements and asymmetric lifetime errors.

VALUE (10^{-12} s)	EVTS	DOCUMENT ID		TECN	COMMENT
1.519±0.005 OUR EVALUATION					
1.499±0.013±0.005		[1] AAIJ	14E	LHCB	pp at 7 TeV
1.524±0.006±0.004		[2] AAIJ	14E	LHCB	pp at 7 TeV
1.509±0.012±0.018		[3] AAD	13U	ATLS	pp at 7 TeV
1.508±0.025±0.043		[1] ABAZOV	12U	D0	$p\overline{p}$ at 1.96 TeV
1.507±0.010±0.008		[4] AALTONEN	11	CDF	$p\overline{p}$ at 1.96 TeV
1.414±0.018±0.034		[5] ABAZOV	09E	D0	$p\overline{p}$ at 1.96 TeV
$1.504 \pm 0.013 ^{+0.018}_{-0.013}$		[6] AUBERT	06G	BABR	$e^+e^- \to \Upsilon(4S)$
1.534±0.008±0.010		[7] ABE	05B	BELL	$e^+e^- \to \Upsilon(4S)$
1.531±0.021±0.031		[8] ABDALLAH	04E	DLPH	$e^+e^- \to Z$
$1.523 ^{+0.024}_{-0.023} \pm 0.022$		[9] AUBERT	03C	BABR	$e^+e^- \to \Upsilon(4S)$
1.533±0.034±0.038		[10] AUBERT	03H	BABR	$e^+e^- \to \Upsilon(4S)$
1.497±0.073±0.032		[11] ACOSTA	02C	CDF	$p\overline{p}$ at 1.8 TeV
1.529±0.012±0.029		[12] AUBERT	02H	BABR	$e^+e^- \to \Upsilon(4S)$
1.546±0.032±0.022		[13] AUBERT	01F	BABR	$e^+e^- \to \Upsilon(4S)$
1.541±0.028±0.023		[12] ABBIENDI,G	00B	OPAL	$e^+e^- \to Z$
1.518±0.053±0.034		[14] BARATE	00R	ALEP	$e^+e^- \to Z$
1.523±0.057±0.053		[15] ABBIENDI	99J	OPAL	$e^+e^- \to Z$
$1.474 \pm 0.039 ^{+0.052}_{-0.051}$		[14] ABE	98Q	CDF	$p\overline{p}$ at 1.8 TeV
1.52 ±0.06 ±0.04		[15] ACCIARRI	98S	L3	$e^+e^- \to Z$
1.64 ±0.08 ±0.08		[15] ABE	97J	SLD	$e^+e^- \to Z$
1.532±0.041±0.040		[16] ABREU	97F	DLPH	$e^+e^- \to Z$
$1.25 ^{+0.15}_{-0.13} \pm 0.05$	121	[11] BUSKULIC	96J	ALEP	$e^+e^- \to Z$
$1.49 ^{+0.17}_{-0.15} ^{+0.08}_{-0.06}$		[17] BUSKULIC	96J	ALEP	$e^+e^- \to Z$
$1.61 ^{+0.14}_{-0.13} \pm 0.08$		[14,18] ABREU	95Q	DLPH	$e^+e^- \to Z$
1.63 ±0.14 ±0.13		[19] ADAM	95	DLPH	$e^+e^- \to Z$
1.53 ±0.12 ±0.08		[14,20] AKERS	95T	OPAL	$e^+e^- \to Z$
• • • We do not use the following data for averages, fits, limits, etc. • • •					
$1.501 ^{+0.078}_{-0.074} \pm 0.050$		[1] ABAZOV	07S	D0	Repl. by ABAZOV 12U
1.524±0.030±0.016		[1] ABULENCIA	07A	CDF	Repl. by AALTONEN 11
$1.473 ^{+0.052}_{-0.050} \pm 0.023$		[5] ABAZOV	05B	D0	Repl. by ABAZOV 05W
$1.40 ^{+0.11}_{-0.10} \pm 0.03$		[1] ABAZOV	05C	D0	Repl. by ABAZOV 07S
1.530±0.043±0.023		[5] ABAZOV	05W	D0	Repl. by ABAZOV 09E
1.54 ±0.05 ±0.02		[21] ACOSTA	05	CDF	Repl. by AALTONEN 11
1.554±0.030±0.019		[13] ABE	02H	BELL	Repl. by ABE 05B
1.58 ±0.09 ±0.02		[11] ABE	98B	CDF	Repl. by ACOSTA 02C
1.54 ±0.08 ±0.06		[14] ABE	96C	CDF	Repl. by ABE 98Q
1.55 ±0.06 ±0.03		[22] BUSKULIC	96J	ALEP	$e^+e^- \to Z$
1.61 ±0.07 ±0.04		[14] BUSKULIC	96J	ALEP	Repl. by BARATE 00R
1.62 ±0.12		[23] ADAM	95	DLPH	$e^+e^- \to Z$
1.57 ±0.18 ±0.08	121	[11] ABE	94D	CDF	Repl. by ABE 98B
$1.17 ^{+0.29}_{-0.23} \pm 0.16$	96	[14] ABREU	93D	DLPH	Sup. by ABREU 95Q
1.55 ±0.25 ±0.18	76	[19] ABREU	93G	DLPH	Sup. by ADAM 95
$1.51 ^{+0.24}_{-0.23} ^{+0.12}_{-0.14}$	78	[14] ACTON	93C	OPAL	Sup. by AKERS 95T
$1.52 ^{+0.20}_{-0.18} ^{+0.07}_{-0.13}$	77	[14] BUSKULIC	93D	ALEP	Sup. by BUSKULIC 96J
$1.20 ^{+0.52}_{-0.36} ^{+0.16}_{-0.14}$	15	[24] WAGNER	90	MRK2	$E_{\rm cm}^{ee} = 29$ GeV
$0.82 ^{+0.57}_{-0.37} \pm 0.27$		[25] AVERILL	89	HRS	$E_{\rm cm}^{ee} = 29$ GeV

[1] Measured mean life using $B^0 \to J/\psi K_S^0$ decays.
[2] Measured using $B^0 \to J/\psi K^{*0}$ decays.
[3] Measured with $B_d^0 \to J/\psi(\mu^+\mu^-)\, K_S^0(\pi^+\pi^-)$ decays.
[4] Measured mean life using fully reconstructed decays ($J/\psi K^{(*)}$).
[5] Measured mean life using $B^0 \to J/\psi K^{*0}$ decays.
[6] Measured using a simultaneous fit of the B^0 lifetime and $\overline{B}^0 B^0$ oscillation frequency Δm_d in the partially reconstructed $B^0 \to D^{*-}\ell\nu$ decays.
[7] Measurement performed using a combined fit of CP-violation, mixing and lifetimes.
[8] Measurement performed using an inclusive reconstruction and B flavor identification technique.

[9] AUBERT 03C uses a sample of approximately 14,000 exclusively reconstructed $B^0 \to D^*(2010)^- \ell\nu$ and simultaneously measures the lifetime and oscillation frequency.
[10] Measurement performed with decays $B^0 \to D^{*-}\pi^+$ and $B^0 \to D^{*-}\rho^+$ using a partial reconstruction technique.
[11] Measured mean life using fully reconstructed decays.
[12] Data analyzed using partially reconstructed $\overline{B}^0 \to D^{*+}\ell^-\overline{\nu}$ decays.
[13] Events are selected in which one B meson is fully reconstructed while the second B meson is reconstructed inclusively.
[14] Data analyzed using $D/D^*\ell$X event vertices.
[15] Data analyzed using charge of secondary vertex.
[16] Data analyzed using inclusive $D/D^*\ell X$.
[17] Measured mean life using partially reconstructed $D^{*-}\pi^+$X vertices.
[18] ABREU 95Q assumes B($B^0 \to D^{**-}\ell^+\nu_\ell$) = 3.2 ± 1.7%.
[19] Data analyzed using vertex-charge technique to tag B charge.
[20] AKERS 95T assumes B($B^0 \to D_s^{(*)}D^{0(*)}$) = 5.0 ± 0.9% to find B^+/B^0 yield.
[21] Measured using the time-dependent angular analysis of $B^0_d \to J/\psi K^{*0}$ decays.
[22] Combined result of $D/D^*\ell$x analysis, fully reconstructed B analysis, and partially reconstructed $D^{*-}\pi^+$ X analysis.
[23] Combined ABREU 95Q and ADAM 95 result.
[24] WAGNER 90 tagged B^0 mesons by their decays into $D^{*-}e^+\nu$ and $D^{*-}\mu^+\nu$ where the D^{*-} is tagged by its decay into $\pi^-\overline{D}^0$.
[25] AVERILL 89 is an estimate of the B^0 mean lifetime assuming that $B^0 \to D^{*+}$ + X always.

$\tau_{B^0}/\tau_{\overline{B}^0}$

VALUE	DOCUMENT ID		TECN	COMMENT
1.000±0.008±0.009	[1] AAIJ	14E	LHCB	pp at 7 TeV

[1] Measured using $B^0 \to J/\psi K^{*0}$ decays.

MEAN LIFE RATIO τ_{B^+}/τ_{B^0}

τ_{B^+}/τ_{B^0} (direct measurements)

"OUR EVALUATION" is an average using rescaled values of the data listed below. The average and rescaling were performed by the Heavy Flavor Averaging Group (HFAG) and are described at http://www.slac.stanford.edu/xorg/hfag/. The averaging/rescaling procedure takes into account correlations between the measurements and asymmetric lifetime errors.

VALUE	EVTS	DOCUMENT ID		TECN	COMMENT
1.076±0.004 OUR EVALUATION					
1.074±0.005±0.003		[1] AAIJ	14E	LHCB	pp at 7 TeV
1.088±0.009±0.004		[2] AALTONEN	11	CDF	$p\overline{p}$ at 1.96 TeV
1.080±0.016±0.014		[3] ABAZOV	05D	D0	$p\overline{p}$ at 1.96 TeV
1.066±0.008±0.008		[4] ABE	05B	BELL	$e^+e^- \to \Upsilon(4S)$
1.060±0.021±0.024		[5] ABDALLAH	04E	DLPH	$e^+e^- \to Z$
1.093±0.066±0.028		[6] ACOSTA	02C	CDF	$p\overline{p}$ at 1.8 TeV
1.082±0.026±0.012		[7] AUBERT	01F	BABR	$e^+e^- \to \Upsilon(4S)$
1.085±0.059±0.018		[3] BARATE	00R	ALEP	$e^+e^- \to Z$
1.079±0.064±0.041		[8] ABBIENDI	99J	OPAL	$e^+e^- \to Z$
1.110±0.056 $^{+0.033}_{-0.030}$		[3] ABE	98Q	CDF	$p\overline{p}$ at 1.8 TeV
1.09 ±0.07 ±0.03		[8] ACCIARRI	98S	L3	$e^+e^- \to Z$
1.01 ±0.07 ±0.06		[8] ABE	97J	SLD	$e^+e^- \to Z$
1.27 $^{+0.23}_{-0.19}$ $^{+0.03}_{-0.02}$		[6] BUSKULIC	96J	ALEP	$e^+e^- \to Z$
1.00 $^{+0.17}_{-0.15}$ ±0.10		[3,9] ABREU	95Q	DLPH	$e^+e^- \to Z$
1.06 $^{+0.13}_{-0.11}$ ±0.10		[10] ADAM	95	DLPH	$e^+e^- \to Z$
0.99 ±0.14 $^{+0.05}_{-0.04}$		[3,11] AKERS	95T	OPAL	$e^+e^- \to Z$
• • • We do not use the following data for averages, fits, limits, etc. • • •					
1.091±0.023±0.014		[7] ABE	02H	BELL	Repl. by ABE 05B
1.06 ±0.07 ±0.02		[6] ABE	98B	CDF	Repl. by ACOSTA 02C
1.01 ±0.11 ±0.02		[3] ABE	96C	CDF	Repl. by ABE 98Q
1.03 ±0.08 ±0.02		[12] BUSKULIC	96J	ALEP	$e^+e^- \to Z$
0.98 ±0.08 ±0.03		[3] BUSKULIC	96J	ALEP	Repl. by BARATE 00R
1.02 ±0.16 ±0.05	269	[6] ABE	94D	CDF	Repl. by ABE 98B
1.11 $^{+0.51}_{-0.39}$ ±0.11	188	[3] ABREU	93D	DLPH	Sup. by ABREU 95Q
1.01 $^{+0.29}_{-0.22}$ ±0.12	253	[10] ABREU	93G	DLPH	Sup. by ADAM 95
1.0 $^{+0.33}_{-0.25}$ ±0.08	130	ACTON	93C	OPAL	Sup. by AKERS 95T
0.96 $^{+0.19}_{-0.15}$ $^{+0.18}_{-0.12}$	154	[3] BUSKULIC	93D	ALEP	Sup. by BUSKULIC 96J

[1] Measured using $B \to J/\psi K^{(*)}$ decays.
[2] Measured mean life using fully reconstructed decays ($J/\psi K^{(*)}$).
[3] Data analyzed using $D/D^*\mu$X vertices.
[4] Measurement performed using a combined fit of CP-violation, mixing and lifetimes.
[5] Measurement performed using an inclusive reconstruction and B flavor identification technique.
[6] Measured using fully reconstructed decays.
[7] Events are selected in which one B meson is fully reconstructed while the second B meson is reconstructed inclusively.
[8] Data analyzed using charge of secondary vertex.
[9] ABREU 95Q assumes B($B^0 \to D^{**-}\ell^+\nu_\ell$) = 3.2 ± 1.7%.
[10] Data analyzed using vertex-charge technique to tag B charge.
[11] AKERS 95T assumes B($B^0 \to D_s^{(*)}D^{0(*)}$) = 5.0 ± 0.9% to find B^+/B^0 yield.
[12] Combined result of $D/D^*\ell$X analysis and fully reconstructed B analysis.

τ_{B^+}/τ_{B^0} (inferred from branching fractions)

These measurements are inferred from the branching fractions for semileptonic decay or other spectator-dominated decays by assuming that the rates for such decays are equal for B^0 and B^+. We do not use measurements which assume equal production of B^0 and B^+ because of the large uncertainty in the production ratio.

"OUR EVALUATION" has been obtained by the Heavy Flavor Averaging Group (HFAG) by taking into account correlations between measurements.

VALUE	CL%	EVTS	DOCUMENT ID		TECN	COMMENT
1.076±0.034 OUR EVALUATION						
1.07 ±0.04 OUR AVERAGE						
1.07 ±0.04 ±0.03			URQUIJO	07	BELL	$e^+e^- \to \Upsilon(4S)$
1.067±0.041±0.033			AUBERT,B	06Y	BABR	$e^+e^- \to \Upsilon(4S)$
• • • We do not use the following data for averages, fits, limits, etc. • • •						
0.95 $^{+0.117}_{-0.080}$±0.091			[1] ARTUSO	97	CLE2	$e^+e^- \to \Upsilon(4S)$
1.15 ±0.17 ±0.06			[2] JESSOP	97	CLE2	$e^+e^- \to \Upsilon(4S)$
0.93 ±0.18 ±0.12			[3] ATHANAS	94	CLE2	Sup. by ARTUSO 97
0.91 ±0.27 ±0.21			[4] ALBRECHT	92C	ARG	$e^+e^- \to \Upsilon(4S)$
1.0 ±0.4		29	[4,5] ALBRECHT	92G	ARG	$e^+e^- \to \Upsilon(4S)$
0.89 ±0.19 ±0.13			[4] FULTON	91	CLEO	$e^+e^- \to \Upsilon(4S)$
1.00 ±0.23 ±0.14			[4] ALBRECHT	89L	ARG	$e^+e^- \to \Upsilon(4S)$
0.49 to 2.3	90		[6] BEAN	87B	CLEO	$e^+e^- \to \Upsilon(4S)$

[1] ARTUSO 97 uses partial reconstruction of $B \to D^*\ell\nu_\ell$ and independent of B^0 and B^+ production fraction.
[2] Assumes equal production of B^+ and B^0 at the $\Upsilon(4S)$.
[3] ATHANAS 94 uses events tagged by fully reconstructed B^- decays and partially or fully reconstructed B^0 decays.
[4] Assumes equal production of B^0 and B^+.
[5] ALBRECHT 92G data analyzed using $B \to D_s\overline{D}$, $D_s\overline{D}^*$, $D_s^*\overline{D}$, $D_s^*\overline{D}^*$ events.
[6] BEAN 87B assume the fraction of $B^0\overline{B}^0$ events at the $\Upsilon(4S)$ is 0.41.

sgn(Re(λ_{CP})) $\Delta\Gamma_{B^0_d}$ / $\Gamma_{B^0_d}$

$\Gamma_{B^0_d}$ and $\Delta\Gamma_{B^0_d}$ are the decay rate average and difference between two B^0_d CP eigenstates (light − heavy). The λ_{CP} characterizes B^0 and $\overline{B}^0$ decays to states of charmonium plus K^0_L, see the review on "CP Violation" in the reviews section.

"OUR EVALUATION" has been obtained by the Heavy Flavor Averaging Group (HFAG) by taking into account correlations between measurements.

VALUE (units 10^{-2})	DOCUMENT ID		TECN	COMMENT
0.1±1.0 OUR EVALUATION				
−0.4±2.0 OUR AVERAGE Includes data from the datablock that follows this one. Error includes scale factor of 1.3. See the ideogram below.				
−4.4±2.5±1.1	[1] AAIJ	14E	LHCB	pp at 7 TeV
1.7±1.8±1.1	[2] HIGUCHI	12	BELL	$e^+e^- \to \Upsilon(4S)$
0.8±3.7±1.8	[3] AUBERT,B	04C	BABR	$e^+e^- \to \Upsilon(4S)$

[1] Measured using the effective lifetimes of $B^0 \to J/\psi K^0_S$ and $B^0 \to J/\psi K^{*0}$ decays.
[2] Reports $-\Delta\Gamma_d/\Gamma_d$ using $B^0 \to J/\psi K^0_S$, $J/\psi K^0_L$, $D^-\pi^+$, $D^{*-}\pi^+$, $D^{*-}\rho^+$, and $D^{*-}\ell^+\nu$ decays.
[3] Corresponds to 90% confidence range [−0.084, 0.068].

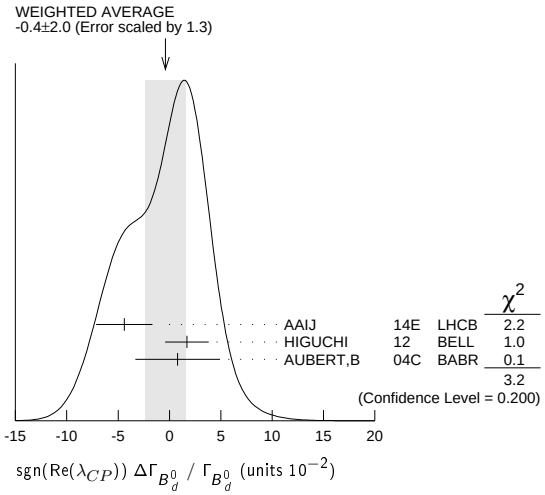

$|\Delta\Gamma_{B^0_d}|/\Gamma_{B^0_d}$

VALUE	CL%	DOCUMENT ID		TECN	COMMENT
The data in this block is included in the average printed for a previous datablock.					
<0.18	95	[1] ABDALLAH	03B	DLPH	$e^+e^- \to Z$
• • • We do not use the following data for averages, fits, limits, etc. • • •					
<0.80	95	[2,3] BEHRENS	00B	CLE2	$e^+e^- \to \Upsilon(4S)$

Meson Particle Listings

B^0

[1] Using the measured τ_{B^0}=1.55 ± 0.03 ps.

[2] BEHRENS 00B uses high-momentum lepton tags and partially reconstructed $\overline{B}^0 \to D^{*+}\pi^-$, ρ^- decays to determine the flavor of the B meson.

[3] Assumes Δ_{md}=0.478 ± 0.018 ps^{-1} and τ_{B^0}=1.548 ± 0.032 ps.

B^0 DECAY MODES

$\overline{B}^0$ modes are charge conjugates of the modes below. Reactions indicate the weak decay vertex and do not include mixing. Modes which do not identify the charge state of the B are listed in the $B^\pm/B^0$ ADMIXTURE section.

The branching fractions listed below assume 50% $B^0\overline{B}^0$ and 50% B^+B^- production at the $\Upsilon(4S)$. We have attempted to bring older measurements up to date by rescaling their assumed $\Upsilon(4S)$ production ratio to 50:50 and their assumed D, D_s, D^*, and ψ branching ratios to current values whenever this would affect our averages and best limits significantly.

Indentation is used to indicate a subchannel of a previous reaction. All resonant subchannels have been corrected for resonance branching fractions to the final state so the sum of the subchannel branching fractions can exceed that of the final state.

For inclusive branching fractions, *e.g.*, $B \to D^\pm$ anything, the values usually are multiplicities, not branching fractions. They can be greater than one.

	Mode		Fraction (Γ_i/Γ)	Scale factor/ Confidence level
Γ_1	$\ell^+\nu_\ell$ anything	[a]	(10.33 ± 0.28) %	
Γ_2	$e^+\nu_e X_c$		(10.1 ± 0.4) %	
Γ_3	$D\ell^+\nu_\ell$ anything		(9.2 ± 0.8) %	
Γ_4	$D^-\ell^+\nu_\ell$	[a]	(2.19 ± 0.12) %	
Γ_5	$D^-\tau^+\nu_\tau$		(1.03 ± 0.22) %	
Γ_6	$D^*(2010)^-\ell^+\nu_\ell$	[a]	(4.93 ± 0.11) %	
Γ_7	$D^*(2010)^-\tau^+\nu_\tau$		(1.84 ± 0.22) %	
Γ_8	$\overline{D}^0\pi^-\ell^+\nu_\ell$		(4.3 ± 0.6) × 10^{-3}	
Γ_9	$D_0^*(2400)^-\ell^+\nu_\ell$, $D_0^{*-} \to \overline{D}^0\pi^-$		(3.0 ± 1.2) × 10^{-3}	S=1.8
Γ_{10}	$D_2^*(2460)^-\ell^+\nu_\ell$, $D_2^{*-} \to \overline{D}^0\pi^-$		(1.21 ± 0.33) × 10^{-3}	S=1.8
Γ_{11}	$\overline{D}^{(*)}n\pi\ell^+\nu_\ell (n \geq 1)$		(2.3 ± 0.5) %	
Γ_{12}	$\overline{D}^{*0}\pi^-\ell^+\nu_\ell$		(4.9 ± 0.8) × 10^{-3}	
Γ_{13}	$D_1(2420)^-\ell^+\nu_\ell$, $D_1^- \to \overline{D}^{*0}\pi^-$		(2.80 ± 0.28) × 10^{-3}	
Γ_{14}	$D_1'(2430)^-\ell^+\nu_\ell$, $D_1'^- \to \overline{D}^{*0}\pi^-$		(3.1 ± 0.9) × 10^{-3}	
Γ_{15}	$D_2^*(2460)^-\ell^+\nu_\ell$, $D_2^{*-} \to \overline{D}^{*0}\pi^-$		(6.8 ± 1.2) × 10^{-4}	
Γ_{16}	$\rho^-\ell^+\nu_\ell$	[a]	(2.94 ± 0.21) × 10^{-4}	
Γ_{17}	$\pi^-\ell^+\nu_\ell$	[a]	(1.45 ± 0.05) × 10^{-4}	
Γ_{18}	$\pi^-\mu^+\nu_\mu$			
	Inclusive modes			
Γ_{19}	$K^\pm$ anything		(78 ± 8) %	
Γ_{20}	D^0X		(8.1 ± 1.5) %	
Γ_{21}	$\overline{D}^0X$		(47.4 ± 2.8) %	
Γ_{22}	D^+X		< 3.9 %	CL=90%
Γ_{23}	D^-X		(36.9 ± 3.3) %	
Γ_{24}	D_s^+X		(10.3 $^{+\ 2.1}_{-\ 1.8}$) %	
Γ_{25}	D_s^-X		< 2.6 %	CL=90%
Γ_{26}	Λ_c^+X		< 3.1 %	CL=90%
Γ_{27}	$\overline{\Lambda}_c^-X$		(5.0 $^{+\ 2.1}_{-\ 1.5}$) %	
Γ_{28}	$\overline{c}X$		(95 ± 5) %	
Γ_{29}	cX		(24.6 ± 3.1) %	
Γ_{30}	$\overline{c}cX$		(119 ± 6) %	
	D, D^*, or D_s modes			
Γ_{31}	$D^-\pi^+$		(2.68 ± 0.13) × 10^{-3}	
Γ_{32}	$D^-\rho^+$		(7.8 ± 1.3) × 10^{-3}	
Γ_{33}	$D^-K^0\pi^+$		(4.9 ± 0.9) × 10^{-4}	
Γ_{34}	$D^-K^*(892)^+$		(4.5 ± 0.7) × 10^{-4}	
Γ_{35}	$D^-\omega\pi^+$		(2.8 ± 0.6) × 10^{-3}	
Γ_{36}	D^-K^+		(1.97 ± 0.21) × 10^{-4}	
Γ_{37}	$D^-K^+\pi^+\pi^-$		(3.8 ± 0.9) × 10^{-4}	
Γ_{38}	$D^-K^+\overline{K}^0$		< 3.1 × 10^{-4}	CL=90%
Γ_{39}	$D^-K^+\overline{K}^*(892)^0$		(8.8 ± 1.9) × 10^{-4}	
Γ_{40}	$\overline{D}^0\pi^+\pi^-$		(8.4 ± 0.9) × 10^{-4}	
Γ_{41}	$D^*(2010)^-\pi^+$		(2.76 ± 0.13) × 10^{-3}	
Γ_{42}	$\overline{D}^0K^+K^-$		(4.7 ± 1.2) × 10^{-5}	
Γ_{43}	$D^-\pi^+\pi^+\pi^-$		(6.4 ± 0.7) × 10^{-3}	
Γ_{44}	($D^-\pi^+\pi^+\pi^-$) nonresonant		(3.9 ± 1.9) × 10^{-3}	
Γ_{45}	$D^-\pi^+\rho^0$		(1.1 ± 1.0) × 10^{-3}	
Γ_{46}	$D^-a_1(1260)^+$		(6.0 ± 3.3) × 10^{-3}	
Γ_{47}	$D^*(2010)^-\pi^+\pi^0$		(1.5 ± 0.5) %	
Γ_{48}	$D^*(2010)^-\rho^+$		(6.8 ± 0.9) × 10^{-3}	
Γ_{49}	$D^*(2010)^-K^+$		(2.14 ± 0.16) × 10^{-4}	
Γ_{50}	$D^*(2010)^-K^0\pi^+$		(3.0 ± 0.8) × 10^{-4}	
Γ_{51}	$D^*(2010)^-K^*(892)^+$		(3.3 ± 0.6) × 10^{-4}	
Γ_{52}	$D^*(2010)^-K^+\overline{K}^0$		< 4.7 × 10^{-4}	CL=90%
Γ_{53}	$D^*(2010)^-K^+\overline{K}^*(892)^0$		(1.29 ± 0.33) × 10^{-3}	
Γ_{54}	$D^*(2010)^-\pi^+\pi^+\pi^-$		(7.0 ± 0.8) × 10^{-3}	S=1.3
Γ_{55}	($D^*(2010)^-\pi^+\pi^+\pi^-$) nonresonant		(0.0 ± 2.5) × 10^{-3}	
Γ_{56}	$D^*(2010)^-\pi^+\rho^0$		(5.7 ± 3.2) × 10^{-3}	
Γ_{57}	$D^*(2010)^-a_1(1260)^+$		(1.30 ± 0.27) %	
Γ_{58}	$\overline{D}_1(2420)^0\pi^-\pi^+$, $\overline{D}_1^0 \to D^{*-}\pi^+$		(1.4 ± 0.4) × 10^{-4}	
Γ_{59}	$D^*(2010)^-K^+\pi^-\pi^+$		(4.5 ± 0.7) × 10^{-4}	
Γ_{60}	$D^*(2010)^-\pi^+\pi^+\pi^-\pi^0$		(1.76 ± 0.27) %	
Γ_{61}	$D^{*-}3\pi^+2\pi^-$		(4.7 ± 0.9) × 10^{-3}	
Γ_{62}	$\overline{D}^*(2010)^-\omega\pi^+$		(2.89 ± 0.30) × 10^{-3}	
Γ_{63}	$D_1(2430)^0\omega\times$ B($D_1(2430)^0 \to D^{*-}\pi^+$)		(4.1 ± 1.6) × 10^{-4}	
Γ_{64}	$\overline{D}^{**-}\pi^+$	[b]	(2.1 ± 1.0) × 10^{-3}	
Γ_{65}	$D_1(2420)^-\pi^+\times$ B($D_1^- \to D^-\pi^+\pi^-$)		(1.00 $^{+\ 0.21}_{-\ 0.25}$) × 10^{-4}	
Γ_{66}	$D_1(2420)^-\pi^+\times$ B($D_1^- \to D^{*-}\pi^+\pi^-$)		< 3.3 × 10^{-5}	CL=90%
Γ_{67}	$\overline{D}_2^*(2460)^-\pi^+\times$ B($D_2^*(2460)^- \to D^0\pi^-$)		(2.15 ± 0.35) × 10^{-4}	
Γ_{68}	$\overline{D}_0^*(2400)^-\pi^+\times$ B($D_0^*(2400)^- \to D^0\pi^-$)		(6.0 ± 3.0) × 10^{-5}	
Γ_{69}	$D_2^*(2460)^-\pi^+\times$ B($(D_2^*)^- \to D^{*-}\pi^+\pi^-$)		< 2.4 × 10^{-5}	CL=90%
Γ_{70}	$\overline{D}_2^*(2460)^-\rho^+$		< 4.9 × 10^{-3}	CL=90%
Γ_{71}	$D^0\overline{D}^0$		(1.4 ± 0.7) × 10^{-5}	
Γ_{72}	$D^{*0}\overline{D}^0$		< 2.9 × 10^{-4}	CL=90%
Γ_{73}	D^-D^+		(2.11 ± 0.18) × 10^{-4}	
Γ_{74}	$D^\pm D^{*\mp}$ (CP-averaged)		(6.1 ± 0.6) × 10^{-4}	
Γ_{75}	$D^-D_s^+$		(7.2 ± 0.8) × 10^{-3}	
Γ_{76}	$D^*(2010)^-D_s^+$		(8.0 ± 1.1) × 10^{-3}	
Γ_{77}	$D^-D_s^{*+}$		(7.4 ± 1.6) × 10^{-3}	
Γ_{78}	$D^*(2010)^-D_s^{*+}$		(1.77 ± 0.14) %	
Γ_{79}	$D_{s0}(2317)^-K^+\times$ B($D_{s0}(2317)^- \to D_s^-\pi^0$)		(4.2 ± 1.4) × 10^{-5}	
Γ_{80}	$D_{s0}(2317)^-\pi^+\times$ B($D_{s0}(2317)^- \to D_s^-\pi^0$)		< 2.5 × 10^{-5}	CL=90%
Γ_{81}	$D_{sJ}(2457)^-K^+\times$ B($D_{sJ}(2457)^- \to D_s^-\pi^0$)		< 9.4 × 10^{-6}	CL=90%
Γ_{82}	$D_{sJ}(2457)^-\pi^+\times$ B($D_{sJ}(2457)^- \to D_s^-\pi^0$)		< 4.0 × 10^{-6}	CL=90%
Γ_{83}	$D_s^-D_s^+$		< 3.6 × 10^{-5}	CL=90%
Γ_{84}	$D_s^{*-}D_s^+$		< 1.3 × 10^{-4}	CL=90%
Γ_{85}	$D_s^{*-}D_s^{*+}$		< 2.4 × 10^{-4}	CL=90%
Γ_{86}	$D_{s0}(2317)^+D^-\times$ B($D_{s0}(2317)^+ \to D_s^+\pi^0$)		(9.7 $^{+\ 4.0}_{-\ 3.3}$) × 10^{-4}	S=1.5
Γ_{87}	$D_{s0}(2317)^+D^-\times$ B($D_{s0}(2317)^+ \to D_s^{*+}\gamma$)		< 9.5 × 10^{-4}	CL=90%
Γ_{88}	$D_{s0}(2317)^+D^*(2010)^-\times$ B($D_{s0}(2317)^+ \to D_s^+\pi^0$)		(1.5 ± 0.6) × 10^{-3}	
Γ_{89}	$D_{sJ}(2457)^+D^-$		(3.5 ± 1.1) × 10^{-3}	
Γ_{90}	$D_{sJ}(2457)^+D^-\times$ B($D_{sJ}(2457)^+ \to D_s^+\gamma$)		(6.5 $^{+\ 1.7}_{-\ 1.4}$) × 10^{-4}	
Γ_{91}	$D_{sJ}(2457)^+D^-\times$ B($D_{sJ}(2457)^+ \to D_s^{*+}\gamma$)		< 6.0 × 10^{-4}	CL=90%
Γ_{92}	$D_{sJ}(2457)^+D^-\times$ B($D_{sJ}(2457)^+ \to D_s^+\pi^+\pi^-$)		< 2.0 × 10^{-4}	CL=90%

Γ_{93}	$D_{sJ}(2457)^+ D^-\times$ B($D_{sJ}(2457)^+ \to D_s^+\pi^0$)	<	3.6	$\times 10^{-4}$	CL=90%
Γ_{94}	$D^*(2010)^- D_{sJ}(2457)^+$	(	9.3 ± 2.2)	$\times 10^{-3}$	
Γ_{95}	$D_{sJ}(2457)^+ D^*(2010)\times$ B($D_{sJ}(2457)^+ \to D_s^+\gamma$)	(	$2.3\ ^{+\ 0.9}_{-\ 0.7}$)	$\times 10^{-3}$	
Γ_{96}	$D^- D_{s1}(2536)^+\times$ B($D_{s1}(2536)^+ \to D^{*0}K^+ + D^{*+}K^0$)	(	2.8 ± 0.7)	$\times 10^{-4}$	
Γ_{97}	$D^- D_{s1}(2536)^+\times$ B($D_{s1}(2536)^+ \to D^{*0}K^+$)	(	1.7 ± 0.6)	$\times 10^{-4}$	
Γ_{98}	$D^- D_{s1}(2536)^+\times$ B($D_{s1}(2536)^+ \to D^{*+}K^0$)	(	2.6 ± 1.1)	$\times 10^{-4}$	
Γ_{99}	$D^*(2010)^- D_{s1}(2536)^+\times$ B($D_{s1}(2536)^+ \to D^{*0}K^+ + D^{*+}K^0$)	(	5.0 ± 1.4)	$\times 10^{-4}$	
Γ_{100}	$D^*(2010)^- D_{s1}(2536)^+\times$ B($D_{s1}(2536)^+ \to D^{*0}K^+$)	(	3.3 ± 1.1)	$\times 10^{-4}$	
Γ_{101}	$D^{*-} D_{s1}(2536)^+\times$ B($D_{s1}(2536)^+ \to D^{*+}K^0$)	(	5.0 ± 1.7)	$\times 10^{-4}$	
Γ_{102}	$D^- D_{sJ}(2573)^+\times$ B($D_{sJ}(2573)^+ \to D^0K^+$)	<	1	$\times 10^{-4}$	CL=90%
Γ_{103}	$D^*(2010)^- D_{sJ}(2573)^+\times$ B($D_{sJ}(2573)^+ \to D^0K^+$)	<	2	$\times 10^{-4}$	CL=90%
Γ_{104}	$D^+\pi^-$	(	7.8 ± 1.4)	$\times 10^{-7}$	
Γ_{105}	$D_s^+\pi^-$	(	2.16± 0.26)	$\times 10^{-5}$	
Γ_{106}	$D_s^{*+}\pi^-$	(	2.1 ± 0.4)	$\times 10^{-5}$	S=1.4
Γ_{107}	$D_s^+\rho^-$	<	2.4	$\times 10^{-5}$	CL=90%
Γ_{108}	$D_s^{*+}\rho^-$	(	4.1 ± 1.3)	$\times 10^{-5}$	
Γ_{109}	$D_s^+ a_0^-$	<	1.9	$\times 10^{-5}$	CL=90%
Γ_{110}	$D_s^{*+} a_0^-$	<	3.6	$\times 10^{-5}$	CL=90%
Γ_{111}	$D_s^+ a_1(1260)^-$	<	2.1	$\times 10^{-3}$	CL=90%
Γ_{112}	$D_s^{*+} a_1(1260)^-$	<	1.7	$\times 10^{-3}$	CL=90%
Γ_{113}	$D_s^+ a_2^-$	<	1.9	$\times 10^{-4}$	CL=90%
Γ_{114}	$D_s^{*+} a_2^-$	<	2.0	$\times 10^{-4}$	CL=90%
Γ_{115}	$D_s^- K^+$	(	2.2 ± 0.5)	$\times 10^{-5}$	S=1.8
Γ_{116}	$D_s^{*-} K^+$	(	2.19± 0.30)	$\times 10^{-5}$	
Γ_{117}	$D_s^- K^*(892)^+$	(	3.5 ± 1.0)	$\times 10^{-5}$	
Γ_{118}	$D_s^{*-} K^*(892)^+$	(	$3.2\ ^{+\ 1.5}_{-\ 1.3}$)	$\times 10^{-5}$	
Γ_{119}	$D_s^-\pi^+ K^0$	(	1.10± 0.33)	$\times 10^{-4}$	
Γ_{120}	$D_s^{*-}\pi^+ K^0$	<	1.10	$\times 10^{-4}$	CL=90%
Γ_{121}	$D_s^- K^+\pi^+\pi^-$	(	1.8 ± 0.5)	$\times 10^{-4}$	
Γ_{122}	$D_s^-\pi^+ K^*(892)^0$	<	3.0	$\times 10^{-3}$	CL=90%
Γ_{123}	$D_s^{*-}\pi^+ K^*(892)^0$	<	1.6	$\times 10^{-3}$	CL=90%
Γ_{124}	$\overline{D}^0 K^0$	(	5.2 ± 0.7)	$\times 10^{-5}$	
Γ_{125}	$\overline{D}^0 K^+\pi^-$	(	8.8 ± 1.7)	$\times 10^{-5}$	
Γ_{126}	$\overline{D}^0 K^*(892)^0$	(	4.2 ± 0.6)	$\times 10^{-5}$	
Γ_{127}	$D_2^*(2460)^- K^+\times$ B($D_2^*(2460)^- \to \overline{D}^0\pi^-$)	(	1.8 ± 0.5)	$\times 10^{-5}$	
Γ_{128}	$\overline{D}^0 K^+\pi^-$ non-resonant	<	3.7	$\times 10^{-5}$	CL=90%
Γ_{129}	$[K^+K^-]_D K^*(892)^0$	(	$5.8\ ^{+\ 1.8}_{-\ 1.6}$)	$\times 10^{-5}$	
Γ_{130}	$\overline{D}^0\pi^0$	(	2.63± 0.14)	$\times 10^{-4}$	
Γ_{131}	$\overline{D}^0\rho^0$	(	3.2 ± 0.5)	$\times 10^{-4}$	
Γ_{132}	$\overline{D}^0 f_2$	(	1.2 ± 0.4)	$\times 10^{-4}$	
Γ_{133}	$\overline{D}^0\eta$	(	2.36± 0.32)	$\times 10^{-4}$	S=2.5
Γ_{134}	$\overline{D}^0\eta'$	(	1.38± 0.16)	$\times 10^{-4}$	S=1.3
Γ_{135}	$\overline{D}^0\omega$	(	2.53± 0.16)	$\times 10^{-4}$	
Γ_{136}	$D^0\phi$	<	1.16	$\times 10^{-5}$	CL=90%
Γ_{137}	$D^0 K^+\pi^-$	(	5.3 ± 3.2)	$\times 10^{-6}$	
Γ_{138}	$D^0 K^*(892)^0$	<	1.1	$\times 10^{-5}$	CL=90%
Γ_{139}	$\overline{D}^{*0}\gamma$	<	2.5	$\times 10^{-5}$	CL=90%
Γ_{140}	$\overline{D}^*(2007)^0\pi^0$	(	2.2 ± 0.6)	$\times 10^{-4}$	S=2.6
Γ_{141}	$\overline{D}^*(2007)^0\rho^0$	<	5.1	$\times 10^{-4}$	CL=90%
Γ_{142}	$\overline{D}^*(2007)^0\eta$	(	2.3 ± 0.6)	$\times 10^{-4}$	S=2.8
Γ_{143}	$\overline{D}^*(2007)^0\eta'$	(	1.40± 0.22)	$\times 10^{-4}$	
Γ_{144}	$\overline{D}^*(2007)^0\pi^+\pi^-$	(	6.2 ± 2.2)	$\times 10^{-4}$	
Γ_{145}	$\overline{D}^*(2007)^0 K^0$	(	3.6 ± 1.2)	$\times 10^{-5}$	
Γ_{146}	$\overline{D}^*(2007)^0 K^*(892)^0$	<	6.9	$\times 10^{-5}$	CL=90%
Γ_{147}	$D^*(2007)^0 K^*(892)^0$	<	4.0	$\times 10^{-5}$	CL=90%
Γ_{148}	$D^*(2007)^0\pi^+\pi^+\pi^-\pi^-$	(	2.7 ± 0.5)	$\times 10^{-3}$	
Γ_{149}	$D^*(2010)^+ D^*(2010)^-$	(	8.0 ± 0.6)	$\times 10^{-4}$	
Γ_{150}	$\overline{D}^*(2007)^0\omega$	(	3.6 ± 1.1)	$\times 10^{-4}$	S=3.1
Γ_{151}	$D^*(2010)^+ D^-$	(	6.1 ± 1.5)	$\times 10^{-4}$	S=1.6
Γ_{152}	$D^*(2007)^0\overline{D}^*(2007)^0$	<	9	$\times 10^{-5}$	CL=90%
Γ_{153}	$D^- D^0 K^+$	(	1.07± 0.11)	$\times 10^{-3}$	
Γ_{154}	$D^- D^*(2007)^0 K^+$	(	3.5 ± 0.4)	$\times 10^{-3}$	
Γ_{155}	$D^*(2010)^- D^0 K^+$	(	2.47± 0.21)	$\times 10^{-3}$	
Γ_{156}	$D^*(2010)^- D^*(2007)^0 K^+$	(	1.06± 0.09)	%	
Γ_{157}	$D^- D^+ K^0$	(	7.5 ± 1.7)	$\times 10^{-4}$	
Γ_{158}	$D^*(2010)^- D^+ K^0 + D^- D^*(2010)^+ K^0$	(	6.4 ± 0.5)	$\times 10^{-3}$	
Γ_{159}	$D^*(2010)^- D^*(2010)^+ K^0$	(	8.1 ± 0.7)	$\times 10^{-3}$	
Γ_{160}	$D^{*-} D_{s1}(2536)^+\times$ B($D_{s1}(2536)^+ \to D^{*+}K^0$)	(	8.0 ± 2.4)	$\times 10^{-4}$	
Γ_{161}	$\overline{D}^0 D^0 K^0$	(	2.7 ± 1.1)	$\times 10^{-4}$	
Γ_{162}	$\overline{D}^0 D^*(2007)^0 K^0 + \overline{D}^*(2007)^0 D^0 K^0$	(	1.1 ± 0.5)	$\times 10^{-3}$	
Γ_{163}	$\overline{D}^*(2007)^0 D^*(2007)^0 K^0$	(	2.4 ± 0.9)	$\times 10^{-3}$	
Γ_{164}	$(\overline{D}+\overline{D}^*)(D+D^*)K$	(	3.68± 0.26)	%	

Charmonium modes

Γ_{165}	$\eta_c K^0$	(	7.9 ± 1.2)	$\times 10^{-4}$	
Γ_{166}	$\eta_c K^*(892)^0$	(	6.3 ± 0.9)	$\times 10^{-4}$	
Γ_{167}	$\eta_c(2S) K^{*0}$	<	3.9	$\times 10^{-4}$	CL=90%
Γ_{168}	$h_c(1P) K^{*0}$	<	4	$\times 10^{-4}$	CL=90%
Γ_{169}	$J/\psi(1S) K^0$	(	8.73± 0.32)	$\times 10^{-4}$	
Γ_{170}	$J/\psi(1S) K^+\pi^-$	(	1.2 ± 0.6)	$\times 10^{-3}$	
Γ_{171}	$J/\psi(1S) K^*(892)^0$	(	1.32± 0.06)	$\times 10^{-3}$	
Γ_{172}	$J/\psi(1S)\eta K_S^0$	(	8 ± 4)	$\times 10^{-5}$	
Γ_{173}	$J/\psi(1S)\eta' K_S^0$	<	2.5	$\times 10^{-5}$	CL=90%
Γ_{174}	$J/\psi(1S)\phi K^0$	(	9.4 ± 2.6)	$\times 10^{-5}$	
Γ_{175}	$J/\psi(1S)\omega K^0$	(	2.3 ± 0.4)	$\times 10^{-4}$	
Γ_{176}	$X(3872) K^0\times$ B($X \to J/\psi\omega$)	(	6.0 ± 3.2)	$\times 10^{-6}$	
Γ_{177}	$\chi_{c0}(2P)$, $\chi_{c0} \to J/\psi\omega$	(	2.1 ± 0.9)	$\times 10^{-5}$	
Γ_{178}	$J/\psi(1S) K(1270)^0$	(	1.3 ± 0.5)	$\times 10^{-3}$	
Γ_{179}	$J/\psi(1S)\pi^0$	(	1.76± 0.16)	$\times 10^{-5}$	S=1.1
Γ_{180}	$J/\psi(1S)\eta$	(	1.23± 0.19)	$\times 10^{-5}$	
Γ_{181}	$J/\psi(1S)\pi^+\pi^-$	(	4.03± 0.18)	$\times 10^{-5}$	
Γ_{182}	$J/\psi(1S)\pi^+\pi^-$ nonresonant	<	1.2	$\times 10^{-5}$	CL=90%
Γ_{183}	$J/\psi(1S) f_0(500)$, $f_0 \to \pi\pi$	(	$6.5\ ^{+\ 2.6}_{-\ 1.1}$)	$\times 10^{-6}$	
Γ_{184}	$J/\psi(1S) f_2$	(	4.2 ± 0.7)	$\times 10^{-6}$	
Γ_{185}	$J/\psi(1S)\rho^0$	(	2.58± 0.21)	$\times 10^{-5}$	
Γ_{186}	$J/\psi(1S) f_0(980)$, $f_0 \to \pi^+\pi^-$	<	1.1	$\times 10^{-6}$	CL=90%
Γ_{187}	$J/\psi(1S)\rho(1450)^0$, $\rho^0 \to \pi\pi$	(	$2.1\ ^{+\ 2.5}_{-\ 0.7}$)	$\times 10^{-6}$	
Γ_{188}	$J/\psi(1S)\omega$	(	2.3 ± 0.6)	$\times 10^{-5}$	
Γ_{189}	$J/\psi(1S) K^+ K^-$	(	2.6 ± 0.4)	$\times 10^{-6}$	
Γ_{190}	$J/\psi(1S) a_0(980)$, $a_0 \to K^+K^-$	(	4.7 ± 3.4)	$\times 10^{-7}$	
Γ_{191}	$J/\psi(1S)\phi$	<	1.9	$\times 10^{-7}$	CL=90%
Γ_{192}	$J/\psi(1S)\eta'(958)$	<	7.4	$\times 10^{-6}$	CL=90%
Γ_{193}	$J/\psi(1S) K^0\pi^+\pi^-$	(	1.0 ± 0.4)	$\times 10^{-3}$	
Γ_{194}	$J/\psi(1S) K^0\rho^0$	(	5.4 ± 3.0)	$\times 10^{-4}$	
Γ_{195}	$J/\psi(1S) K^*(892)^+\pi^-$	(	8 ± 4)	$\times 10^{-4}$	
Γ_{196}	$J/\psi(1S) K^*(892)^0\pi^+\pi^-$	(	6.6 ± 2.2)	$\times 10^{-4}$	
Γ_{197}	$X(3872)^- K^+$	<	5	$\times 10^{-4}$	CL=90%
Γ_{198}	$X(3872)^- K^+\times$ B($X(3872)^- \to J/\psi(1S)\pi^-\pi^0$) [c]	<	4.2	$\times 10^{-6}$	CL=90%
Γ_{199}	$X(3872) K^0\times$ B($X \to J/\psi\pi^+\pi^-$)	(	4.3 ± 1.3)	$\times 10^{-6}$	
Γ_{200}	$X(3872) K^0\times$ B($X \to J/\psi\gamma$)	<	2.4	$\times 10^{-6}$	CL=90%
Γ_{201}	$X(3872) K^*(892)^0\times$ B($X \to J/\psi\gamma$)	<	2.8	$\times 10^{-6}$	CL=90%
Γ_{202}	$X(3872) K^0\times$ B($X \to \psi(2S)\gamma$)	<	6.62	$\times 10^{-6}$	CL=90%
Γ_{203}	$X(3872) K^*(892)^0\times$ B($X \to \psi(2S)\gamma$)	<	4.4	$\times 10^{-6}$	CL=90%
Γ_{204}	$X(3872) K^0\times$ B($X \to D^0\overline{D}^0\pi^0$)	(	1.7 ± 0.8)	$\times 10^{-4}$	
Γ_{205}	$X(3872) K^0\times$ B($X \to \overline{D}^{*0} D^0$)	(	1.2 ± 0.4)	$\times 10^{-4}$	
Γ_{206}	$X(4430)^\pm K^\mp\times$ B($X^\pm \to \psi(2S)\pi^\pm$)	(	$6.0\ ^{+\ 3.0}_{-\ 2.4}$)	$\times 10^{-5}$	

Γ_{207}	$X(4430)^{\pm}K^{\mp}\times$ B($X^{\pm}\to J/\psi\pi^{\pm}$)		$<$	4	$\times10^{-6}$	CL=95%
Γ_{208}	$J/\psi(1S)\,p\overline{p}$		$<$	5.2	$\times10^{-7}$	CL=90%
Γ_{209}	$J/\psi(1S)\,\gamma$		$<$	1.6	$\times10^{-6}$	CL=90%
Γ_{210}	$J/\psi(1S)\,\overline{D}^0$		$<$	1.3	$\times10^{-5}$	CL=90%
Γ_{211}	$\psi(2S)\,K^0$		(	6.2 ± 0.5)	$\times10^{-4}$	
Γ_{212}	$\psi(3770)\,K^0\times$ B($\psi\to\overline{D}^0D^0$)		$<$	1.23	$\times10^{-4}$	CL=90%
Γ_{213}	$\psi(3770)\,K^0\times$ B($\psi\to D^-D^+$)		$<$	1.88	$\times10^{-4}$	CL=90%
Γ_{214}	$\psi(2S)\pi^+\pi^-$		(	2.3 ± 0.4)	$\times10^{-5}$	
Γ_{215}	$\psi(2S)\,K^+\pi^-$		(	5.8 ± 0.4)	$\times10^{-4}$	
Γ_{216}	$\psi(2S)\,K^*(892)^0$		(	6.0 ± 0.4)	$\times10^{-4}$	S=1.1
Γ_{217}	$\chi_{c0}\,K^0$		(	1.47± 0.27)	$\times10^{-4}$	
Γ_{218}	$\chi_{c0}\,K^*(892)^0$		(	1.7 ± 0.4)	$\times10^{-4}$	
Γ_{219}	$\chi_{c2}\,K^0$		$<$	1.5	$\times10^{-5}$	CL=90%
Γ_{220}	$\chi_{c2}\,K^*(892)^0$		(	5.0 ± 1.2)	$\times10^{-5}$	S=1.1
Γ_{221}	$\chi_{c1}\,\pi^0$		(	1.12± 0.28)	$\times10^{-5}$	
Γ_{222}	$\chi_{c1}\,K^0$		(	3.93± 0.27)	$\times10^{-4}$	
Γ_{223}	$\chi_{c1}\,K^-\pi^+$		(	3.8 ± 0.4)	$\times10^{-4}$	
Γ_{224}	$\chi_{c1}\,K^*(892)^0$		(	2.42± 0.21)	$\times10^{-4}$	S=1.3
Γ_{225}	$X(4051)^+K^-\times$B($X^+\to\chi_{c1}\pi^+$)		(	$3.0\ ^{+\ 4.0}_{-\ 1.8}$)	$\times10^{-5}$	
Γ_{226}	$X(4248)^+K^-\times$B($X^+\to\chi_{c1}\pi^+$)		(	$4.0\ ^{+20.0}_{-\ 1.0}$)	$\times10^{-5}$	

K* or *K* modes

Γ_{227}	$K^+\pi^-$		(	1.96± 0.05)	$\times10^{-5}$	
Γ_{228}	$K^0\pi^0$		(	9.9 ± 0.5)	$\times10^{-6}$	
Γ_{229}	$\eta' K^0$		(	6.6 ± 0.4)	$\times10^{-5}$	S=1.4
Γ_{230}	$\eta' K^*(892)^0$		(	3.1 ± 0.9)	$\times10^{-6}$	
Γ_{231}	$\eta' K_0^*(1430)^0$		(	6.3 ± 1.6)	$\times10^{-6}$	
Γ_{232}	$\eta' K_2^*(1430)^0$		(	1.37± 0.32)	$\times10^{-5}$	
Γ_{233}	ηK^0		(	$1.23^{+\ 0.27}_{-\ 0.24}$)	$\times10^{-6}$	
Γ_{234}	$\eta K^*(892)^0$		(	1.59± 0.10)	$\times10^{-5}$	
Γ_{235}	$\eta K_0^*(1430)^0$		(	1.10± 0.22)	$\times10^{-5}$	
Γ_{236}	$\eta K_2^*(1430)^0$		(	9.6 ± 2.1)	$\times10^{-6}$	
Γ_{237}	ωK^0		(	5.0 ± 0.6)	$\times10^{-6}$	
Γ_{238}	$a_0(980)^0\,K^0\times$ B($a_0(980)^0\to\eta\pi^0$)		$<$	7.8	$\times10^{-6}$	CL=90%
Γ_{239}	$b_1^0K^0\times$ B($b_1^0\to\omega\pi^0$)		$<$	7.8	$\times10^{-6}$	CL=90%
Γ_{240}	$a_0(980)^{\pm}K^{\mp}\times$ B($a_0(980)^{\pm}\to\eta\pi^{\pm}$)		$<$	1.9	$\times10^{-6}$	CL=90%
Γ_{241}	$b_1^-K^+\times$ B($b_1^-\to\omega\pi^-$)		(	7.4 ± 1.4)	$\times10^{-6}$	
Γ_{242}	$b_1^0K^{*0}\times$ B($b_1^0\to\omega\pi^0$)		$<$	8.0	$\times10^{-6}$	CL=90%
Γ_{243}	$b_1^-K^{*+}\times$ B($b_1^-\to\omega\pi^-$)		$<$	5.0	$\times10^{-6}$	CL=90%
Γ_{244}	$a_0(1450)^{\pm}K^{\mp}\times$ B($a_0(1450)^{\pm}\to\eta\pi^{\pm}$)		$<$	3.1	$\times10^{-6}$	CL=90%
Γ_{245}	$K_S^0X^0$(Familon)		$<$	5.3	$\times10^{-5}$	CL=90%
Γ_{246}	$\omega K^*(892)^0$		(	2.0 ± 0.5)	$\times10^{-6}$	
Γ_{247}	$\omega(K\pi)_0^{*0}$		(	1.84± 0.25)	$\times10^{-5}$	
Γ_{248}	$\omega K_0^*(1430)^0$		(	1.60± 0.34)	$\times10^{-5}$	
Γ_{249}	$\omega K_2^*(1430)^0$		(	1.01± 0.23)	$\times10^{-5}$	
Γ_{250}	$\omega K^+\pi^-$ nonresonant		(	5.1 ± 1.0)	$\times10^{-6}$	
Γ_{251}	$K^+\pi^-\pi^0$		(	3.78± 0.32)	$\times10^{-5}$	
Γ_{252}	$K^+\rho^-$		(	7.0 ± 0.9)	$\times10^{-6}$	
Γ_{253}	$K^+\rho(1450)^-$		(	2.4 ± 1.2)	$\times10^{-6}$	
Γ_{254}	$K^+\rho(1700)^-$		(	6 ± 7)	$\times10^{-7}$	
Γ_{255}	$(K^+\pi^-\pi^0)$ non-resonant		(	2.8 ± 0.6)	$\times10^{-6}$	
Γ_{256}	$(K\pi)_0^{*+}\pi^-\times$ B($(K\pi)_0^{*+}\to K^+\pi^0$)		(	3.4 ± 0.5)	$\times10^{-5}$	
Γ_{257}	$(K\pi)_0^{*0}\pi^0\times$B($(K\pi)_0^{*0}\to K^+\pi^-$)		(	8.6 ± 1.7)	$\times10^{-6}$	
Γ_{258}	$K_2^*(1430)^0\pi^0$		$<$	4.0	$\times10^{-6}$	CL=90%
Γ_{259}	$K^*(1680)^0\pi^0$		$<$	7.5	$\times10^{-6}$	CL=90%
Γ_{260}	$K_x^{*0}\pi^0$	[d]	(	6.1 ± 1.6)	$\times10^{-6}$	
Γ_{261}	$K^0\pi^+\pi^-$		(	6.5 ± 0.8)	$\times10^{-5}$	S=1.2
Γ_{262}	$K^0\pi^+\pi^-$ non-resonant		(	$1.47^{+\ 0.40}_{-\ 0.26}$)	$\times10^{-5}$	S=2.1
Γ_{263}	$K^0\rho^0$		(	4.7 ± 0.6)	$\times10^{-6}$	
Γ_{264}	$K^*(892)^+\pi^-$		(	8.4 ± 0.8)	$\times10^{-6}$	
Γ_{265}	$K_0^*(1430)^+\pi^-$		(	3.3 ± 0.7)	$\times10^{-5}$	S=2.0
Γ_{266}	$K_x^{*+}\pi^-$	[d]	(	5.1 ± 1.6)	$\times10^{-6}$	
Γ_{267}	$K^*(1410)^+\pi^-\times$ B($K^*(1410)^+\to K^0\pi^+$)		$<$	3.8	$\times10^{-6}$	CL=90%
Γ_{268}	$f_0(980)\,K^0\times$ B($f_0(980)\to\pi^+\pi^-$)		(	7.0 ± 0.9)	$\times10^{-6}$	
Γ_{269}	$f_2(1270)\,K^0$		(	$2.7\ ^{+\ 1.3}_{-\ 1.2}$)	$\times10^{-6}$	
Γ_{270}	$f_x(1300)\,K^0\times$ B($f_x\to\pi^+\pi^-$)		(	1.8 ± 0.7)	$\times10^{-6}$	
Γ_{271}	$K^*(892)^0\pi^0$		(	3.3 ± 0.6)	$\times10^{-6}$	
Γ_{272}	$K_2^*(1430)^+\pi^-$		$<$	6	$\times10^{-6}$	CL=90%
Γ_{273}	$K^*(1680)^+\pi^-$		$<$	1.0	$\times10^{-5}$	CL=90%
Γ_{274}	$K^+\pi^-\pi^+\pi^-$	[e]	$<$	2.3	$\times10^{-4}$	CL=90%
Γ_{275}	$\rho^0K^+\pi^-$		(	2.8 ± 0.7)	$\times10^{-6}$	
Γ_{276}	$f_0(980)\,K^+\pi^-$, $f_0\to\pi\pi$		(	$1.4\ ^{+\ 0.5}_{-\ 0.6}$)	$\times10^{-6}$	
Γ_{277}	$K^+\pi^-\pi^+\pi^-$ nonresonant		$<$	2.1	$\times10^{-6}$	CL=90%
Γ_{278}	$K^*(892)^0\pi^+\pi^-$		(	5.5 ± 0.5)	$\times10^{-5}$	
Γ_{279}	$K^*(892)^0\rho^0$		(	3.9 ± 1.3)	$\times10^{-6}$	S=1.9
Γ_{280}	$K^*(892)^0\,f_0(980)$, $f_0\to\pi\pi$		(	$3.9\ ^{+\ 2.1}_{-\ 1.8}$)	$\times10^{-6}$	S=3.9
Γ_{281}	$K_1(1270)^+\pi^-$		$<$	3.0	$\times10^{-5}$	CL=90%
Γ_{282}	$K_1(1400)^+\pi^-$		$<$	2.7	$\times10^{-5}$	CL=90%
Γ_{283}	$a_1(1260)^-K^+$	[e]	(	1.6 ± 0.4)	$\times10^{-5}$	
Γ_{284}	$K^*(892)^+\rho^-$		(	1.03± 0.26)	$\times10^{-5}$	
Γ_{285}	$K_0^*(1430)^+\rho^-$		(	2.8 ± 1.2)	$\times10^{-5}$	
Γ_{286}	$K_1(1400)^0\rho^0$		$<$	3.0	$\times10^{-3}$	CL=90%
Γ_{287}	$K_0^*(1430)^0\rho^0$		(	2.7 ± 0.6)	$\times10^{-5}$	
Γ_{288}	$K_0^*(1430)^0\,f_0(980)$, $f_0\to\pi\pi$		(	2.7 ± 0.9)	$\times10^{-6}$	
Γ_{289}	$K_2^*(1430)^0\,f_0(980)$, $f_0\to\pi\pi$		(	8.6 ± 2.0)	$\times10^{-6}$	
Γ_{290}	K^+K^-		(	1.3 ± 0.5)	$\times10^{-7}$	
Γ_{291}	$K^0\overline{K}^0$		(	1.21± 0.16)	$\times10^{-6}$	
Γ_{292}	$K^0K^-\pi^+$		(	7.3 ± 1.1)	$\times10^{-6}$	S=1.2
Γ_{293}	$\overline{K}^{*0}K^0+K^{*0}\overline{K}^0$		$<$	1.9	$\times10^{-6}$	
Γ_{294}	$K^+K^-\pi^0$		(	2.2 ± 0.6)	$\times10^{-6}$	
Γ_{295}	$K_S^0K_S^0\pi^0$		$<$	9	$\times10^{-7}$	CL=90%
Γ_{296}	$K_S^0K_S^0\eta$		$<$	1.0	$\times10^{-6}$	CL=90%
Γ_{297}	$K_S^0K_S^0\eta'$		$<$	2.0	$\times10^{-6}$	CL=90%
Γ_{298}	$K^0K^+K^-$		(	2.63± 0.15)	$\times10^{-5}$	S=1.3
Γ_{299}	$K^0\phi$		(	7.3 ± 0.7)	$\times10^{-6}$	
Γ_{300}	$f_0(980)\,K^0$, $f_0\to K^+K^-$		(	$7.0\ ^{+\ 3.5}_{-\ 3.0}$)	$\times10^{-6}$	
Γ_{301}	$f_0(1500)\,K^0$		(	$1.3\ ^{+\ 0.7}_{-\ 0.5}$)	$\times10^{-5}$	
Γ_{302}	$f_2'(1525)^0\,K^0$		(	$3\ ^{+\ 5}_{-\ 4}$)	$\times10^{-7}$	
Γ_{303}	$f_0(1710)\,K^0$, $f_0\to K^+K^-$		(	4.4 ± 0.9)	$\times10^{-6}$	
Γ_{304}	$K^0K^+K^-$ nonresonant		(	3.3 ± 1.0)	$\times10^{-5}$	
Γ_{305}	$K_S^0K_S^0K_S^0$		(	6.0 ± 0.5)	$\times10^{-6}$	S=1.1
Γ_{306}	$f_0(980)\,K^0$, $f_0\to K_S^0K_S^0$		(	2.7 ± 1.8)	$\times10^{-6}$	
Γ_{307}	$f_0(1710)\,K^0$, $f_0\to K_S^0K_S^0$		(	$5.0\ ^{+\ 5.0}_{-\ 2.6}$)	$\times10^{-7}$	
Γ_{308}	$f_0(2010)\,K^0$, $f_0\to K_S^0K_S^0$		(	5 ± 6)	$\times10^{-7}$	
Γ_{309}	$K_S^0K_S^0K_S^0$ nonresonant		(	1.33± 0.31)	$\times10^{-5}$	
Γ_{310}	$K_S^0K_S^0K_L^0$		$<$	1.6	$\times10^{-5}$	CL=90%
Γ_{311}	$K^*(892)^0K^+K^-$		(	2.75± 0.26)	$\times10^{-5}$	
Γ_{312}	$K^*(892)^0\phi$		(	1.00± 0.05)	$\times10^{-5}$	
Γ_{313}	$K^+K^-\pi^+\pi^-$ nonresonant		$<$	7.17	$\times10^{-5}$	CL=90%
Γ_{314}	$K^*(892)^0K^-\pi^+$		(	4.5 ± 1.3)	$\times10^{-6}$	
Γ_{315}	$K^*(892)^0\overline{K}^*(892)^0$		(	8 ± 5)	$\times10^{-7}$	S=2.2
Γ_{316}	$K^+K^+\pi^-\pi^-$ nonresonant		$<$	6.0	$\times10^{-6}$	CL=90%
Γ_{317}	$K^*(892)^0K^+\pi^-$		$<$	2.2	$\times10^{-6}$	CL=90%
Γ_{318}	$K^*(892)^0K^*(892)^0$		$<$	2	$\times10^{-7}$	CL=90%
Γ_{319}	$K^*(892)^+K^*(892)^-$		$<$	2.0	$\times10^{-6}$	CL=90%
Γ_{320}	$K_1(1400)^0\phi$		$<$	5.0	$\times10^{-3}$	CL=90%
Γ_{321}	$\phi(K\pi)_0^{*0}$		(	4.3 ± 0.4)	$\times10^{-6}$	
Γ_{322}	$\phi(K\pi)_0^{*0}$ $(1.60<m_{K\pi}<2.15)$	[f]	$<$	1.7	$\times10^{-6}$	CL=90%
Γ_{323}	$K_0^*(1430)^0K^-\pi^+$		$<$	3.18	$\times10^{-5}$	CL=90%
Γ_{324}	$K_0^*(1430)^0\overline{K}^*(892)^0$		$<$	3.3	$\times10^{-6}$	CL=90%
Γ_{325}	$K_0^*(1430)^0\overline{K}_0^*(1430)^0$		$<$	8.4	$\times10^{-6}$	CL=90%
Γ_{326}	$K_0^*(1430)^0\phi$		(	3.9 ± 0.8)	$\times10^{-6}$	
Γ_{327}	$K_0^*(1430)^0K^*(892)^0$		$<$	1.7	$\times10^{-6}$	CL=90%
Γ_{328}	$K_0^*(1430)^0K_0^*(1430)^0$		$<$	4.7	$\times10^{-6}$	CL=90%
Γ_{329}	$K^*(1680)^0\phi$		$<$	3.5	$\times10^{-6}$	CL=90%
Γ_{330}	$K^*(1780)^0\phi$		$<$	2.7	$\times10^{-6}$	CL=90%
Γ_{331}	$K^*(2045)^0\phi$		$<$	1.53	$\times10^{-5}$	CL=90%
Γ_{332}	$K_2^*(1430)^0\rho^0$		$<$	1.1	$\times10^{-3}$	CL=90%
Γ_{333}	$K_2^*(1430)^0\phi$		(	6.8 ± 0.9)	$\times10^{-6}$	S=1.2
Γ_{334}	$K^0\phi\phi$		(	4.5 ± 0.9)	$\times10^{-6}$	

Γ_{335}	$\eta'\eta' K^0$		<	3.1	$\times 10^{-5}$	CL=90%
Γ_{336}	$\eta K^0\gamma$		(	7.6 ± 1.8)	$\times 10^{-6}$	
Γ_{337}	$\eta' K^0\gamma$		<	6.4	$\times 10^{-6}$	CL=90%
Γ_{338}	$K^0\phi\gamma$		(	2.7 ± 0.7)	$\times 10^{-6}$	
Γ_{339}	$K^+\pi^-\gamma$		(	4.6 ± 1.4)	$\times 10^{-6}$	
Γ_{340}	$K^*(892)^0\gamma$		(	4.33± 0.15)	$\times 10^{-5}$	
Γ_{341}	$K^*(1410)\gamma$		<	1.3	$\times 10^{-4}$	CL=90%
Γ_{342}	$K^+\pi^-\gamma$ nonresonant		<	2.6	$\times 10^{-6}$	CL=90%
Γ_{343}	$K^*(892)^0 X(214)\times$ B($X\to\mu^+\mu^-$)	[g]	<	2.26	$\times 10^{-8}$	CL=90%
Γ_{344}	$K^0\pi^+\pi^-\gamma$		(	1.95± 0.22)	$\times 10^{-5}$	
Γ_{345}	$K^+\pi^-\pi^0\gamma$		(	4.1 ± 0.4)	$\times 10^{-5}$	
Γ_{346}	$K_1(1270)^0\gamma$		<	5.8	$\times 10^{-5}$	CL=90%
Γ_{347}	$K_1(1400)^0\gamma$		<	1.2	$\times 10^{-5}$	CL=90%
Γ_{348}	$K_2^*(1430)^0\gamma$		(	1.24± 0.24)	$\times 10^{-5}$	
Γ_{349}	$K^*(1680)^0\gamma$		<	2.0	$\times 10^{-3}$	CL=90%
Γ_{350}	$K_3^*(1780)^0\gamma$		<	8.3	$\times 10^{-5}$	CL=90%
Γ_{351}	$K_4^*(2045)^0\gamma$		<	4.3	$\times 10^{-3}$	CL=90%

Light unflavored meson modes

Γ_{352}	$\rho^0\gamma$		(	8.6 ± 1.5)	$\times 10^{-7}$	
Γ_{353}	$\rho^0 X(214)\times$ B($X\to\mu^+\mu^-$)	[g]	<	1.73	$\times 10^{-8}$	CL=90%
Γ_{354}	$\omega\gamma$		(	$4.4\ ^{+\ 1.8}_{-\ 1.6}$)	$\times 10^{-7}$	
Γ_{355}	$\phi\gamma$		<	8.5	$\times 10^{-7}$	CL=90%
Γ_{356}	$\pi^+\pi^-$		(	5.12± 0.19)	$\times 10^{-6}$	
Γ_{357}	$\pi^0\pi^0$		(	1.91± 0.22)	$\times 10^{-6}$	
Γ_{358}	$\eta\pi^0$		<	1.5	$\times 10^{-6}$	CL=90%
Γ_{359}	$\eta\eta$		<	1.0	$\times 10^{-6}$	CL=90%
Γ_{360}	$\eta'\pi^0$		(	1.2 ± 0.6)	$\times 10^{-6}$	S=1.7
Γ_{361}	$\eta'\eta'$		<	1.7	$\times 10^{-6}$	CL=90%
Γ_{362}	$\eta'\eta$		<	1.2	$\times 10^{-6}$	CL=90%
Γ_{363}	$\eta'\rho^0$		<	1.3	$\times 10^{-6}$	CL=90%
Γ_{364}	$\eta' f_0(980)\times$ B($f_0(980)\to\pi^+\pi^-$)		<	9	$\times 10^{-7}$	CL=90%
Γ_{365}	$\eta\rho^0$		<	1.5	$\times 10^{-6}$	CL=90%
Γ_{366}	$\eta f_0(980)\times$ B($f_0(980)\to\pi^+\pi^-$)		<	4	$\times 10^{-7}$	CL=90%
Γ_{367}	$\omega\eta$		(	$9.4\ ^{+\ 4.0}_{-\ 3.1}$)	$\times 10^{-7}$	
Γ_{368}	$\omega\eta'$		(	$1.0\ ^{+\ 0.5}_{-\ 0.4}$)	$\times 10^{-6}$	
Γ_{369}	$\omega\rho^0$		<	1.6	$\times 10^{-6}$	CL=90%
Γ_{370}	$\omega f_0(980)\times$ B($f_0(980)\to\pi^+\pi^-$)		<	1.5	$\times 10^{-6}$	CL=90%
Γ_{371}	$\omega\omega$		(	1.2 ± 0.4)	$\times 10^{-6}$	
Γ_{372}	$\phi\pi^0$		<	1.5	$\times 10^{-7}$	CL=90%
Γ_{373}	$\phi\eta$		<	5	$\times 10^{-7}$	CL=90%
Γ_{374}	$\phi\eta'$		<	5	$\times 10^{-7}$	CL=90%
Γ_{375}	$\phi\rho^0$		<	3.3	$\times 10^{-7}$	CL=90%
Γ_{376}	$\phi f_0(980)\times$ B($f_0\to\pi^+\pi^-$)		<	3.8	$\times 10^{-7}$	CL=90%
Γ_{377}	$\phi\omega$		<	7	$\times 10^{-7}$	CL=90%
Γ_{378}	$\phi\phi$		<	2	$\times 10^{-7}$	CL=90%
Γ_{379}	$a_0(980)^\pm\pi^\mp\times$ B($a_0(980)^\pm\to\eta\pi^\pm$)		<	3.1	$\times 10^{-6}$	CL=90%
Γ_{380}	$a_0(1450)^\pm\pi^\mp\times$ B($a_0(1450)^\pm\to\eta\pi^\pm$)		<	2.3	$\times 10^{-6}$	CL=90%
Γ_{381}	$\pi^+\pi^-\pi^0$		<	7.2	$\times 10^{-4}$	CL=90%
Γ_{382}	$\rho^0\pi^0$		(	2.0 ± 0.5)	$\times 10^{-6}$	
Γ_{383}	$\rho^\mp\pi^\pm$	[h]	(	2.30± 0.23)	$\times 10^{-5}$	
Γ_{384}	$\pi^+\pi^-\pi^+\pi^-$		<	1.93	$\times 10^{-5}$	CL=90%
Γ_{385}	$\rho^0\pi^+\pi^-$		<	8.8	$\times 10^{-6}$	CL=90%
Γ_{386}	$\rho^0\rho^0$		(	7.3 ± 2.8)	$\times 10^{-7}$	
Γ_{387}	$f_0(980)\pi^+\pi^-$		<	3.8	$\times 10^{-6}$	CL=90%
Γ_{388}	$\rho^0 f_0(980)\times$ B($f_0(980)\to\pi^+\pi^-$)		<	3	$\times 10^{-7}$	CL=90%
Γ_{389}	$f_0(980) f_0(980)\times$ B$^2(f_0(980)\to\pi^+\pi^-)$		<	1	$\times 10^{-7}$	CL=90%
Γ_{390}	$f_0(980) f_0(980)\times$ B($f_0\to\pi^+\pi^-$) $\times$ B($f_0\to K^+K^-$)		<	2.3	$\times 10^{-7}$	CL=90%
Γ_{391}	$a_1(1260)^\mp\pi^\pm$	[h]	(	2.6 ± 0.5)	$\times 10^{-5}$	S=1.9
Γ_{392}	$a_2(1320)^\mp\pi^\pm$	[h]	<	6.3	$\times 10^{-6}$	CL=90%
Γ_{393}	$\pi^+\pi^-\pi^0\pi^0$		<	3.1	$\times 10^{-3}$	CL=90%
Γ_{394}	$\rho^+\rho^-$		(	2.42± 0.31)	$\times 10^{-5}$	
Γ_{395}	$a_1(1260)^0\pi^0$		<	1.1	$\times 10^{-3}$	CL=90%
Γ_{396}	$\omega\pi^0$		<	5	$\times 10^{-7}$	CL=90%
Γ_{397}	$\pi^+\pi^+\pi^-\pi^-\pi^0$		<	9.0	$\times 10^{-3}$	CL=90%
Γ_{398}	$a_1(1260)^+\rho^-$		<	6.1	$\times 10^{-5}$	CL=90%
Γ_{399}	$a_1(1260)^0\rho^0$		<	2.4	$\times 10^{-3}$	CL=90%
Γ_{400}	$b_1^\mp\pi^\pm\times$ B($b_1^\mp\to\omega\pi^\mp$)		(	1.09± 0.15)	$\times 10^{-5}$	
Γ_{401}	$b_1^0\pi^0\times$ B($b_1^0\to\omega\pi^0$)		<	1.9	$\times 10^{-6}$	CL=90%
Γ_{402}	$b_1^-\rho^+\times$ B($b_1^-\to\omega\pi^-$)		<	1.4	$\times 10^{-6}$	CL=90%
Γ_{403}	$b_1^0\rho^0\times$ B($b_1^0\to\omega\pi^0$)		<	3.4	$\times 10^{-6}$	CL=90%
Γ_{404}	$\pi^+\pi^+\pi^+\pi^-\pi^-\pi^-$		<	3.0	$\times 10^{-3}$	CL=90%
Γ_{405}	$a_1(1260)^+ a_1(1260)^-\times$ B$^2(a_1^+\to 2\pi^+\pi^-)$		(	1.18± 0.31)	$\times 10^{-5}$	
Γ_{406}	$\pi^+\pi^+\pi^+\pi^-\pi^-\pi^-\pi^0$		<	1.1	%	CL=90%

Baryon modes

Γ_{407}	$p\overline{p}$		(	$1.5\ ^{+\ 0.7}_{-\ 0.5}$)	$\times 10^{-8}$	
Γ_{408}	$p\overline{p}\pi^+\pi^-$		<	2.5	$\times 10^{-4}$	CL=90%
Γ_{409}	$p\overline{p}K^0$		(	2.66± 0.32)	$\times 10^{-6}$	
Γ_{410}	$\Theta(1540)^+\overline{p}$, $\Theta^+\to pK_S^0$	[i]	<	5	$\times 10^{-8}$	CL=90%
Γ_{411}	$f_J(2220)K^0$, $f_J\to p\overline{p}$		<	4.5	$\times 10^{-7}$	CL=90%
Γ_{412}	$p\overline{p}K^*(892)^0$		(	$1.24^{+\ 0.28}_{-\ 0.25}$)	$\times 10^{-6}$	
Γ_{413}	$f_J(2220)K_0^*$, $f_J\to p\overline{p}$		<	1.5	$\times 10^{-7}$	CL=90%
Γ_{414}	$p\overline{\Lambda}\pi^-$		(	3.14± 0.29)	$\times 10^{-6}$	
Γ_{415}	$p\overline{\Sigma}(1385)^-$		<	2.6	$\times 10^{-7}$	CL=90%
Γ_{416}	$\Delta^0\overline{\Lambda}$		<	9.3	$\times 10^{-7}$	CL=90%
Γ_{417}	$p\overline{\Lambda}K^-$		<	8.2	$\times 10^{-7}$	CL=90%
Γ_{418}	$p\overline{\Sigma}^0\pi^-$		<	3.8	$\times 10^{-6}$	CL=90%
Γ_{419}	$\overline{\Lambda}\Lambda$		<	3.2	$\times 10^{-7}$	CL=90%
Γ_{420}	$\overline{\Lambda}\Lambda K^0$		(	$4.8\ ^{+\ 1.0}_{-\ 0.9}$)	$\times 10^{-6}$	
Γ_{421}	$\overline{\Lambda}\Lambda K^{*0}$		(	$2.5\ ^{+\ 0.9}_{-\ 0.8}$)	$\times 10^{-6}$	
Γ_{422}	$\overline{\Lambda}\Lambda D^0$		(	$1.1\ ^{+\ 0.6}_{-\ 0.5}$)	$\times 10^{-5}$	
Γ_{423}	$\Delta^0\overline{\Delta}^0$		<	1.5	$\times 10^{-3}$	CL=90%
Γ_{424}	$\Delta^{++}\overline{\Delta}^{--}$		<	1.1	$\times 10^{-4}$	CL=90%
Γ_{425}	$\overline{D}^0 p\overline{p}$		(	1.04± 0.07)	$\times 10^{-4}$	
Γ_{426}	$D_s^-\overline{\Lambda}p$		(	2.8 ± 0.9)	$\times 10^{-5}$	
Γ_{427}	$\overline{D}^*(2007)^0 p\overline{p}$		(	9.9 ± 1.1)	$\times 10^{-5}$	
Γ_{428}	$D^*(2010)^- p\overline{n}$		(	1.4 ± 0.4)	$\times 10^{-3}$	
Γ_{429}	$D^- p\overline{p}\pi^+$		(	3.32± 0.31)	$\times 10^{-4}$	
Γ_{430}	$D^*(2010)^- p\overline{p}\pi^+$		(	4.7 ± 0.5)	$\times 10^{-4}$	S=1.2
Γ_{431}	$\overline{D}^0 p\overline{p}\pi^+\pi^-$		(	3.0 ± 0.5)	$\times 10^{-4}$	
Γ_{432}	$\overline{D}^{*0} p\overline{p}\pi^+\pi^-$		(	1.9 ± 0.5)	$\times 10^{-4}$	
Γ_{433}	$\Theta_c\overline{p}\pi^+$, $\Theta_c\to D^- p$		<	9	$\times 10^{-6}$	CL=90%
Γ_{434}	$\Theta_c\overline{p}\pi^+$, $\Theta_c\to D^{*-} p$		<	1.4	$\times 10^{-5}$	CL=90%
Γ_{435}	$\overline{\Sigma}_c^{--}\Delta^{++}$		<	1.0	$\times 10^{-3}$	CL=90%
Γ_{436}	$\overline{\Lambda}_c^- p\pi^+\pi^-$		(	1.3 ± 0.4)	$\times 10^{-3}$	
Γ_{437}	$\overline{\Lambda}_c^- p$		(	2.0 ± 0.4)	$\times 10^{-5}$	
Γ_{438}	$\overline{\Lambda}_c^- p\pi^0$		(	1.9 ± 0.5)	$\times 10^{-4}$	
Γ_{439}	$\Sigma_c(2455)^- p$		<	3.0	$\times 10^{-5}$	
Γ_{440}	$\overline{\Lambda}_c^- p\pi^+\pi^-\pi^0$		<	5.07	$\times 10^{-3}$	CL=90%
Γ_{441}	$\overline{\Lambda}_c^- p\pi^+\pi^-\pi^+\pi^-$		<	2.74	$\times 10^{-3}$	CL=90%
Γ_{442}	$\overline{\Lambda}_c^- p\pi^+\pi^-$		(	1.17± 0.23)	$\times 10^{-3}$	
Γ_{443}	$\overline{\Lambda}_c^- p\pi^+\pi^-$ (nonresonant)		(	7.1 ± 1.4)	$\times 10^{-4}$	
Γ_{444}	$\overline{\Sigma}_c(2520)^{--} p\pi^+$		(	1.17± 0.25)	$\times 10^{-4}$	
Γ_{445}	$\overline{\Sigma}_c(2520)^0 p\pi^-$		<	3.1	$\times 10^{-5}$	CL=90%
Γ_{446}	$\overline{\Sigma}_c(2455)^0 p\pi^-$		(	1.04± 0.22)	$\times 10^{-4}$	
Γ_{447}	$\overline{\Sigma}_c(2455)^0 N^0$, $N^0\to p\pi^-$		(	8.0 ± 2.9)	$\times 10^{-5}$	
Γ_{448}	$\overline{\Sigma}_c(2455)^{--} p\pi^+$		(	2.2 ± 0.4)	$\times 10^{-4}$	
Γ_{449}	$\Lambda_c^- p K^+\pi^-$		(	4.3 ± 1.4)	$\times 10^{-5}$	
Γ_{450}	$\overline{\Sigma}_c(2455)^{--} p K^+$, $\overline{\Sigma}_c^{--}\to\overline{\Lambda}_c^-\pi^-$		(	1.1 ± 0.4)	$\times 10^{-5}$	
Γ_{451}	$\Lambda_c^- p K^*(892)^0$		<	2.42	$\times 10^{-5}$	CL=90%
Γ_{452}	$\overline{\Lambda}_c^- \Lambda K^+$		(	3.8 ± 1.3)	$\times 10^{-5}$	
Γ_{453}	$\overline{\Lambda}_c^- \Lambda_c^+$		<	6.2	$\times 10^{-5}$	CL=90%
Γ_{454}	$\overline{\Lambda}_c(2593)^-$ / $\overline{\Lambda}_c(2625)^- p$		<	1.1	$\times 10^{-4}$	CL=90%
Γ_{455}	$\overline{\Xi}_c^-\Lambda_c^+$, $\overline{\Xi}_c^-\to\overline{\Xi}^+\pi^-\pi^-$		(	2.2 ± 2.3)	$\times 10^{-5}$	S=1.9
Γ_{456}	$\Lambda_c^+\Lambda_c^- K^0$		(	5.4 ± 3.2)	$\times 10^{-4}$	

Lepton Family number (LF) or Lepton number (L) or Baryon number (B) violating modes, or/and $\Delta B = 1$ weak neutral current ($B1$) modes

Γ_{457}	$\gamma\gamma$	$B1$	<	3.2	$\times 10^{-7}$	CL=90%
Γ_{458}	e^+e^-	$B1$	<	8.3	$\times 10^{-8}$	CL=90%
Γ_{459}	$e^+e^-\gamma$	$B1$	<	1.2	$\times 10^{-7}$	CL=90%

Γ_{460}	$\mu^+\mu^-$	$B1$	$<$	6.3	$\times 10^{-10}$	CL=90%	
Γ_{461}	$\mu^+\mu^-\gamma$	$B1$	$<$	1.6	$\times 10^{-7}$	CL=90%	
Γ_{462}	$\mu^+\mu^-\mu^+\mu^-$		$<$	5.3	$\times 10^{-9}$	CL=90%	
Γ_{463}	$SP,\ S\to\mu^+\mu^-,\ P\to\mu^+\mu^-$		[j] $<$	5.1	$\times 10^{-9}$	CL=90%	
Γ_{464}	$\tau^+\tau^-$	$B1$	$<$	4.1	$\times 10^{-3}$	CL=90%	
Γ_{465}	$\pi^0\ell^+\ell^-$	$B1$	$<$	5.3	$\times 10^{-8}$	CL=90%	
Γ_{466}	$\pi^0 e^+ e^-$	$B1$	$<$	8.4	$\times 10^{-8}$	CL=90%	
Γ_{467}	$\pi^0\mu^+\mu^-$	$B1$	$<$	6.9	$\times 10^{-8}$	CL=90%	
Γ_{468}	$\eta\ell^+\ell^-$		$<$	6.4	$\times 10^{-8}$	CL=90%	
Γ_{469}	$\eta e^+ e^-$		$<$	1.08	$\times 10^{-7}$	CL=90%	
Γ_{470}	$\eta\mu^+\mu^-$		$<$	1.12	$\times 10^{-7}$	CL=90%	
Γ_{471}	$\pi^0\nu\overline{\nu}$	$B1$	$<$	6.9	$\times 10^{-5}$	CL=90%	
Γ_{472}	$K^0\ell^+\ell^-$	$B1$	[a]	$3.1\ ^{+\ 0.8}_{-\ 0.7}$	$\times 10^{-7}$		
Γ_{473}	$K^0 e^+ e^-$	$B1$		$1.6\ ^{+\ 1.0}_{-\ 0.8}$	$\times 10^{-7}$		
Γ_{474}	$K^0\mu^+\mu^-$	$B1$		$3.4\ \pm\ 0.5$	$\times 10^{-7}$		
Γ_{475}	$K^0\nu\overline{\nu}$	$B1$	$<$	4.9	$\times 10^{-5}$	CL=90%	
Γ_{476}	$\rho^0\nu\overline{\nu}$	$B1$	$<$	2.08	$\times 10^{-4}$	CL=90%	
Γ_{477}	$K^*(892)^0\ell^+\ell^-$	$B1$	[a]	$9.9\ ^{+\ 1.2}_{-\ 1.1}$	$\times 10^{-7}$		
Γ_{478}	$K^*(892)^0 e^+ e^-$	$B1$		$1.03^{+\ 0.19}_{-\ 0.17}$	$\times 10^{-6}$		
Γ_{479}	$K^*(892)^0\mu^+\mu^-$	$B1$		$1.05\pm\ 0.10$	$\times 10^{-6}$		
Γ_{480}	$K^*(892)^0\nu\overline{\nu}$	$B1$	$<$	5.5	$\times 10^{-5}$	CL=90%	
Γ_{481}	$\phi\nu\overline{\nu}$	$B1$	$<$	1.27	$\times 10^{-4}$	CL=90%	
Γ_{482}	$e^\pm\mu^\mp$	LF	[h] $<$	2.8	$\times 10^{-9}$	CL=90%	
Γ_{483}	$\pi^0 e^\pm\mu^\mp$	LF	$<$	1.4	$\times 10^{-7}$	CL=90%	
Γ_{484}	$K^0 e^\pm\mu^\mp$	LF	$<$	2.7	$\times 10^{-7}$	CL=90%	
Γ_{485}	$K^*(892)^0 e^+\mu^-$	LF	$<$	5.3	$\times 10^{-7}$	CL=90%	
Γ_{486}	$K^*(892)^0 e^-\mu^+$	LF	$<$	3.4	$\times 10^{-7}$	CL=90%	
Γ_{487}	$K^*(892)^0 e^\pm\mu^\mp$	LF	$<$	5.8	$\times 10^{-7}$	CL=90%	
Γ_{488}	$e^\pm\tau^\mp$	LF	[h] $<$	2.8	$\times 10^{-5}$	CL=90%	
Γ_{489}	$\mu^\pm\tau^\mp$	LF	[h] $<$	2.2	$\times 10^{-5}$	CL=90%	
Γ_{490}	invisible	$B1$	$<$	2.4	$\times 10^{-5}$	CL=90%	
Γ_{491}	$\nu\overline{\nu}\gamma$	$B1$	$<$	1.7	$\times 10^{-5}$	CL=90%	
Γ_{492}	$\Lambda_c^+\mu^-$	L,B	$<$	1.8	$\times 10^{-6}$	CL=90%	
Γ_{493}	$\Lambda_c^+ e^-$	L,B	$<$	5	$\times 10^{-6}$	CL=90%	

[a] An ℓ indicates an e or a μ mode, not a sum over these modes.

[b] $\overline{D}^{**}$ represents an excited state with mass $2.2 < M < 2.8$ GeV/c^2.

[c] $X(3872)^+$ is a hypothetical charged partner of the $X(3872)$.

[d] Stands for the possible candidates of $K^*(1410)$, $K_0^*(1430)$ and $K_2^*(1430)$.

[e] B^0 and B_s^0 contributions not separated. Limit is on weighted average of the two decay rates.

[f] This decay refers to the coherent sum of resonant and nonresonant $J^P = 0^+$ $K\pi$ components with $1.60 < m_{K\pi} < 2.15$ GeV/c^2.

[g] $X(214)$ is a hypothetical particle of mass 214 MeV/c^2 reported by the HyperCP experiment, Physical Review Letters **94** 021801 (2005)

[h] The value is for the sum of the charge states or particle/antiparticle states indicated.

[i] $\Theta(1540)^+$ denotes a possible narrow pentaquark state.

[j] Here S and P are the hypothetical scalar and pseudoscalar particles with masses of 2.5 GeV/c^2 and 214.3 MeV/c^2, respectively.

CONSTRAINED FIT INFORMATION

An overall fit to 28 branching ratios uses 68 measurements and one constraint to determine 19 parameters. The overall fit has a $\chi^2 = 44.0$ for 50 degrees of freedom.

The following *off-diagonal* array elements are the correlation coefficients $\langle \delta x_i \delta x_j \rangle / (\delta x_i \cdot \delta x_j)$, in percent, from the fit to the branching fractions, $x_i \equiv \Gamma_i/\Gamma_{\rm total}$. The fit constrains the x_i whose labels appear in this array to sum to one.

	x_6	x_7	x_{31}	x_{43}	x_{65}	x_{169}	x_{171}	x_{211}	x_{216}	x_{220}
x_7	32									
x_{31}	0	0								
x_{43}	0	0	43							
x_{65}	0	0	6	13						
x_{169}	0	0	0	0	0					
x_{171}	0	0	0	0	0	0				
x_{211}	0	0	0	0	0	0	0			
x_{216}	0	0	0	0	0	0	0	20		
x_{220}	0	0	0	0	0	0	7	0	0	
x_{224}	0	0	0	0	0	0	31	0	0	23
x_{227}	0	0	0	0	0	0	0	0	0	0
x_{261}	0	0	0	0	0	0	0	0	0	0
x_{292}	0	0	0	0	0	0	0	0	0	0
x_{298}	0	0	0	0	0	0	0	0	0	0
x_{356}	0	0	0	0	0	0	0	0	0	0
x_{474}	0	0	0	0	0	0	6	0	0	0
x_{479}	0	0	0	0	0	0	32	0	0	2

	x_{224}	x_{227}	x_{261}	x_{292}	x_{298}	x_{356}	x_{474}
x_{227}	0						
x_{261}	0	0					
x_{292}	0	0	36				
x_{298}	0	0	40	14			
x_{356}	0	27	0	0	0		
x_{474}	0	0	0	0	0	0	
x_{479}	10	0	0	0	0	0	0

B^0 BRANCHING RATIOS

For branching ratios in which the charge of the decaying B is not determined, see the $B^\pm$ section.

$\Gamma(\ell^+\nu_\ell\text{anything})/\Gamma_{\rm total}$ Γ_1/Γ

"OUR EVALUATION" is an average using rescaled values of the data listed below. The average and rescaling were performed by the Heavy Flavor Averaging Group (HFAG) and are described at http://www.slac.stanford.edu/xorg/hfag/. The averaging/rescaling procedure takes into account correlations between the measurements.

VALUE (units 10^{-2})	DOCUMENT ID		TECN	COMMENT
10.33±0.28 OUR EVALUATION				
10.14±0.30 OUR AVERAGE	Error includes scale factor of 1.1.			
10.46±0.30±0.23	[1] URQUIJO	07	BELL	$e^+e^-\to\Upsilon(4S)$
9.64±0.27±0.33	[2] AUBERT,B	06Y	BABR	$e^+e^-\to\Upsilon(4S)$
10.78±0.60±0.69	[3] ARTUSO	97	CLE2	$e^+e^-\to\Upsilon(4S)$
9.3 ±1.1 ±1.5	ALBRECHT	94	ARG	$e^+e^-\to\Upsilon(4S)$
9.9 ±3.0 ±0.9	HENDERSON	92	CLEO	$e^+e^-\to\Upsilon(4S)$
• • • We do not use the following data for averages, fits, limits, etc. • • •				
10.32±0.36±0.35	[4] OKABE	05	BELL	Repl. by URQUIJO 07
10.9 ±0.7 ±1.1	ATHANAS	94	CLE2	Sup. by ARTUSO 97

[1] URQUIJO 07 report a measurement of (9.80 ± 0.29 ± 0.21)% for the partial branching fraction of $B\to e\nu_e X_c$ decay with electron energy above 0.6 GeV. We converted the result to $B\to e\nu_e X$ branching fraction.

[2] The measurements are obtained for charged and neutral B mesons partial rates of semileptonic decay to electrons with momentum above 0.6 GeV/c in the B rest frame. The best precision on the ratio is achieved for a momentum threshold of 1.0 GeV: $B(B^+\to e^+\nu_e X)$ / $B(B^0\to e^+\nu_e X) = 1.074 \pm 0.041 \pm 0.026$.

[3] ARTUSO 97 uses partial reconstruction of $B\to D^*\ell\nu_\ell$ and inclusive semileptonic branching ratio from BARISH 96B (0.1049 ± 0.0017 ± 0.0043).

[4] The measurements are obtained for charged and neutral B mesons partial rates of semileptonic decay to electrons with momentum above 0.6 GeV/c in the B rest frame, and their ratio of $B(B^+\to e^+\nu_e X)/B(B^0\to e^+\nu_e X) = 1.08 \pm 0.05 \pm 0.02$.

$\Gamma(e^+\nu_e X_c)/\Gamma_{\rm total}$ Γ_2/Γ

VALUE (units 10^{-2})	DOCUMENT ID		TECN	COMMENT
10.08±0.30±0.22	[1] URQUIJO	07	BELL	$e^+e^-\to\Upsilon(4S)$

[1] Measure the independent B^+ and B^0 partial branching fractions with electron threshold energies of 0.4 GeV.

$\Gamma(D^-\ell^+\nu_\ell)/\Gamma_{\rm total}$ Γ_4/Γ

ℓ denotes e or μ, not the sum.

"OUR EVALUATION" is an average using rescaled values of the data listed below. The average and rescaling were performed by the Heavy Flavor Averaging Group (HFAG) and are described at http://www.slac.stanford.edu/xorg/hfag/. The averaging/rescaling procedure takes into account correlations between the measurements.

VALUE	DOCUMENT ID		TECN	COMMENT
0.0219±0.0012 OUR EVALUATION				
0.0218±0.0012 OUR AVERAGE				
0.0221±0.0011±0.0011	[1] AUBERT	10	BABR	$e^+e^- \to \Upsilon(4S)$
0.0213±0.0012±0.0039	ABE	02E	BELL	$e^+e^- \to \Upsilon(4S)$
0.0209±0.0013±0.0018	[2] BARTELT	99	CLE2	$e^+e^- \to \Upsilon(4S)$
0.0235±0.0020±0.0044	[3] BUSKULIC	97	ALEP	$e^+e^- \to Z$
• • • We do not use the following data for averages, fits, limits, etc. • • •				
0.0221±0.0011±0.0012	[1] AUBERT	08Q	BABR	Repl. by AUBERT 10
0.0187±0.0015±0.0032	[4] ATHANAS	97	CLE2	Repl. by BARTELT 99
0.018 ±0.006 ±0.003	[5] FULTON	91	CLEO	$e^+e^- \to \Upsilon(4S)$
0.020 ±0.007 ±0.006	[6] ALBRECHT	89J	ARG	$e^+e^- \to \Upsilon(4S)$

[1] Uses a fully reconstructed B meson as a tag on the recoil side.
[2] Assumes equal production of B^+ and B^0 at the $\Upsilon(4S)$.
[3] BUSKULIC 97 assumes fraction (B^+) = fraction (B^0) = (37.8 ± 2.2)% and PDG 96 values for B lifetime and branching ratio of D^* and D decays.
[4] ATHANAS 97 uses missing energy and missing momentum to reconstruct neutrino.
[5] FULTON 91 assumes assuming equal production of B^0 and B^+ at the $\Upsilon(4S)$ and uses Mark III D and D^* branching ratios.
[6] ALBRECHT 89J reports 0.018 ± 0.006 ± 0.005. We rescale using the method described in STONE 94 but with the updated PDG 94 B($D^0 \to K^-\pi^+$).

$\Gamma(D^-\ell^+\nu_\ell)/\Gamma(\ell^+\nu_\ell \text{anything})$ Γ_4/Γ_1

VALUE	DOCUMENT ID		TECN	COMMENT
0.230±0.011±0.011	[1] AUBERT	10	BABR	$e^+e^- \to \Upsilon(4S)$

[1] Uses a fully reconstructed B meson on the recoil side.

$\Gamma(D^-\ell^+\nu_\ell)/\Gamma(D\ell^+\nu_\ell \text{anything})$ Γ_4/Γ_3

VALUE	DOCUMENT ID		TECN	COMMENT
0.215±0.016±0.013	[1] AUBERT	07AN	BABR	$e^+e^- \to \Upsilon(4S)$

[1] Uses a fully reconstructed B meson on the recoil side.

$\Gamma(D^-\tau^+\nu_\tau)/\Gamma_{\text{total}}$ Γ_5/Γ

VALUE (units 10^{-2})	DOCUMENT ID		TECN	COMMENT
• • • We do not use the following data for averages, fits, limits, etc. • • •				
1.04±0.35±0.18	[1] AUBERT	08N	BABR	Repl. by AUBERT 09S

[1] Uses a fully reconstructed B meson as a tag on the recoil side.

$\Gamma(D^-\tau^+\nu_\tau)/\Gamma(D^-\ell^+\nu_\ell)$ Γ_5/Γ_4

VALUE	DOCUMENT ID		TECN	COMMENT
0.469±0.084±0.053	[1,2] LEES	12D	BABR	$e^+e^- \to \Upsilon(4S)$
• • • We do not use the following data for averages, fits, limits, etc. • • •				
0.489±0.165±0.069	[1] AUBERT	09S	BABR	Repl. by LEES 12D

[1] Uses a fully reconstructed B meson as a tag on the recoil side.
[2] Uses $\tau^+ \to e^+\nu_e\overline{\nu}_\tau$ and $\tau^+ \to \mu^+\nu_\mu\overline{\nu}_\tau$ and e^+ or μ^+ as ℓ^+.

$\Gamma(D^*(2010)^-\ell^+\nu_\ell)/\Gamma_{\text{total}}$ Γ_6/Γ

"OUR EVALUATION" is an average using rescaled values of the data listed below. The average and rescaling were performed by the Heavy Flavor Averaging Group (HFAG) and are described at http://www.slac.stanford.edu/xorg/hfag/. The averaging/rescaling procedure takes into account correlations between the measurements.

VALUE	EVTS	DOCUMENT ID		TECN	COMMENT
0.0493±0.0011 OUR EVALUATION					
0.0510±0.0023 OUR FIT Error includes scale factor of 1.6.					
0.0509±0.0022 OUR AVERAGE Error includes scale factor of 1.6. See the ideogram below.					
0.0458±0.0003±0.0026		[1] DUNGEL	10	BELL	$e^+e^- \to \Upsilon(4S)$
0.0549±0.0016±0.0025		[2] AUBERT	08Q	BABR	$e^+e^- \to \Upsilon(4S)$
0.0469±0.0004±0.0034		[3] AUBERT	08R	BABR	$e^+e^- \to \Upsilon(4S)$
0.0590±0.0022±0.0050		[4] ABDALLAH	04D	DLPH	$e^+e^- \to Z^0$
0.0609±0.0019±0.0040		[5] ADAM	03	CLE2	$e^+e^- \to \Upsilon(4S)$
$0.0470\pm0.0013^{+0.0036}_{-0.0031}$		[6] ABREU	01H	DLPH	$e^+e^- \to Z$
0.0526±0.0020±0.0046		[7] ABBIENDI	00Q	OPAL	$e^+e^- \to Z$
0.0553±0.0026±0.0052		[8] BUSKULIC	97	ALEP	$e^+e^- \to Z$
• • • We do not use the following data for averages, fits, limits, etc. • • •					
$0.0490\pm0.0007^{+0.0036}_{-0.0035}$		[4] AUBERT	05E	BABR	Repl. by AUBERT 08R
0.0539±0.0011±0.0034		[9] ABDALLAH	04D	DLPH	$e^+e^- \to Z^0$
0.0459±0.0023±0.0040		[10] ABE	02F	BELL	Repl. by DUNGEL 10
0.0609±0.0019±0.0040		[11] BRIERE	02	CLE2	$e^+e^- \to \Upsilon(4S)$
0.0508±0.0021±0.0066		[12] ACKERSTAFF	97G	OPAL	Repl. by ABBIENDI 00Q
0.0552±0.0017±0.0068		[13] ABREU	96P	DLPH	Repl. by ABREU 01H
0.0449±0.0032±0.0039	376	[14] BARISH	95	CLE2	Repl. by ADAM 03
0.0518±0.0030±0.0062	410	[15] BUSKULIC	95N	ALEP	Sup. by BUSKULIC 97
0.045 ±0.003 ±0.004		[16] ALBRECHT	94	ARG	$e^+e^- \to \Upsilon(4S)$
0.047 ±0.005 ±0.005	235	[17] ALBRECHT	93	ARG	$e^+e^- \to \Upsilon(4S)$
seen	398	[18] SANGHERA	93	CLE2	$e^+e^- \to \Upsilon(4S)$
0.070 ±0.018 ±0.014		[19] ANTREASYAN	90B	CBAL	$e^+e^- \to \Upsilon(4S)$
		[20] ALBRECHT	89C	ARG	$e^+e^- \to \Upsilon(4S)$
0.060 ±0.010 ±0.014		[21] ALBRECHT	89J	ARG	$e^+e^- \to \Upsilon(4S)$
0.040 ±0.004 ±0.006		[22] BORTOLETTO	89B	CLEO	$e^+e^- \to \Upsilon(4S)$
0.070 ±0.012 ±0.019	47	[23] ALBRECHT	87J	ARG	$e^+e^- \to \Upsilon(4S)$

[1] Uses fully reconstructed $D^{*-}\ell^+\nu$ events ($\ell = e$ or μ).
[2] Uses a fully reconstructed B meson as a tag on the recoil side.
[3] Measured using fully reconstructed D^* sample and a simultaneous fit to the Caprini-Lellouch-Neubert form factor parameters: $\rho^2 = 1.191 \pm 0.048 \pm 0.028$, $R_1(1) = 1.429 \pm 0.061 \pm 0.044$, and $R_2(1) = 0.827 \pm 0.038 \pm 0.022$.
[4] Measured using fully reconstructed D^* sample.
[5] Uses the combined fit of both $B^0 \to D^*(2010)^-\ell\nu$ and $B^+ \to \overline{D}(2007)^0\ell\nu$ samples.
[6] ABREU 01H measured using about 5000 partial reconstructed D^* sample.
[7] ABBIENDI 00Q assumes the fraction B($b \to B^0$)= $(39.7^{+1.8}_{-2.2})$%. This result is an average of two methods using exclusive and partial D^* reconstruction.
[8] BUSKULIC 97 assumes fraction (B^+) = fraction (B^0) = (37.8 ± 2.2)% and PDG 96 values for B lifetime and D^* and D branching fractions.
[9] Combines with previous partial reconstructed D^* measurement.
[10] Assumes equal production of B^+ and B^0 at the $\Upsilon(4S)$.
[11] The results are based on the same analysis and data sample reported in ADAM 03.
[12] ACKERSTAFF 97G assumes fraction (B^+) = fraction (B^0) = (37.8±2.2)% and PDG 96 values for B lifetime and branching ratio of D^* and D decays.
[13] ABREU 96P result is the average of two methods using exclusive and partial D^* reconstruction.
[14] BARISH 95 use B($D^0 \to K^-\pi^+$) = (3.91 ± 0.08 ± 0.17)% and B($D^{*+} \to D^0\pi^+$) = (68.1 ± 1.0 ± 1.3)%.
[15] BUSKULIC 95N assumes fraction (B^+) = fraction (B^0) = 38.2 ± 1.3 ± 2.2% and τ_{B^0} = 1.58 ± 0.06 ps. $\Gamma(D^{*-}\ell^+\nu_\ell)$/total = [5.18 − 0.13(fraction(B^0)−38.2)−1.5(τ_{B^0} − 1.58)]%.
[16] ALBRECHT 94 assumes B($D^{*+} \to D^0\pi^+$) = 68.1 ± 1.0 ± 1.3%. Uses partial reconstruction of D^{*+} and is independent of D^0 branching ratios.
[17] ALBRECHT 93 reports 0.052 ± 0.005 ± 0.006. We rescale using the method described in STONE 94 but with the updated PDG 94 B($D^0 \to K^-\pi^+$). We have taken their average e and μ value. They also obtain $\alpha = 2*\Gamma^0/(\Gamma^- + \Gamma^+) - 1 = 1.1 \pm 0.4 \pm 0.2$, $A_{AF} = 3/4*(\Gamma^- - \Gamma^+)/\Gamma = 0.2 \pm 0.08 \pm 0.06$ and a value of $|V_{cb}|$ = 0.036–0.045 depending on model assumptions.
[18] Combining $\overline{D}^{*0}\ell^+\nu_\ell$ and $\overline{D}^{*-}\ell^+\nu_\ell$ SANGHERA 93 test $V-A$ structure and fit the decay angular distributions to obtain $A_{FB} = 3/4*(\Gamma^- - \Gamma^+)/\Gamma = 0.14 \pm 0.06 \pm 0.03$. Assuming a value of V_{cb}, they measure V, A_1, and A_2, the three form factors for the $D^*\ell\nu_\ell$ decay, where results are slightly dependent on model assumptions.
[19] ANTREASYAN 90B is average over B and $\overline{D}^*(2010)$ charge states.
[20] The measurement of ALBRECHT 89C suggests a D^* polarization γ_L/γ_T of 0.85 ± 0.45. or $\alpha = 0.7 \pm 0.9$.
[21] ALBRECHT 89J is ALBRECHT 87J value rescaled using B($D^*(2010)^- \to D^0\pi^-$) = 0.57 ± 0.04 ± 0.04. Superseded by ALBRECHT 93.
[22] We have taken average of the the BORTOLETTO 89B values for electrons and muons, 0.046 ± 0.005 ± 0.007. We rescale using the method described in STONE 94 but with the updated PDG 94 B($D^0 \to K^-\pi^+$). The measurement suggests a D^* polarization parameter value $\alpha = 0.65 \pm 0.66 \pm 0.25$.
[23] ALBRECHT 87J assume μ-e universality, the B($\Upsilon(4S) \to B^0\overline{B}^0$) = 0.45, the B($D^0 \to K^-\pi^+$) = (0.042 ± 0.004 ± 0.004), and the B($D^*(2010)^- \to D^0\pi^-$) = 0.49 ± 0.08. Superseded by ALBRECHT 89J.

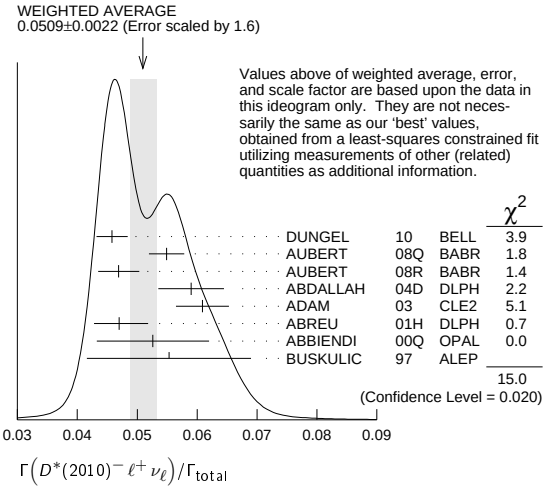

$\Gamma(D^*(2010)^-\ell^+\nu_\ell)/\Gamma(D\ell^+\nu_\ell \text{anything})$ Γ_6/Γ_3

VALUE	DOCUMENT ID		TECN	COMMENT
0.537±0.031±0.036	[1] AUBERT	07AN	BABR	$e^+e^- \to \Upsilon(4S)$

[1] Uses a fully reconstructed B meson on the recoil side.

$\Gamma(D^*(2010)^-\tau^+\nu_\tau)/\Gamma_{\text{total}}$ Γ_7/Γ

VALUE (units 10^{-2})	DOCUMENT ID		TECN	COMMENT
1.84±0.22 OUR FIT				
$\mathbf{2.02^{+0.40}_{-0.37}\pm0.37}$	[1] MATYJA	07	BELL	$e^+e^- \to \Upsilon(4S)$
• • • We do not use the following data for averages, fits, limits, etc. • • •				
1.11±0.51±0.06	[2] AUBERT	08N	BABR	Repl. by AUBERT 09S

[1] Observed in the recoil of the accompanying B meson.
[2] Uses a fully reconstructed B meson as a tag on the recoil side.

Meson Particle Listings

B^0

$\Gamma(D^*(2010)^-\tau^+\nu_\tau)/\Gamma(D^*(2010)^-\ell^+\nu_\ell)$ Γ_7/Γ_6

VALUE	DOCUMENT ID		TECN	COMMENT
0.36 ±0.04 OUR FIT				
0.355±0.039±0.021	[1,2] LEES	12D	BABR	$e^+e^- \to \Upsilon(4S)$
• • • We do not use the following data for averages, fits, limits, etc. • • •				
0.207±0.095±0.008	[1] AUBERT	09S	BABR	Repl. by LEES 12D

[1] Uses a fully reconstructed B meson as a tag on the recoil side.
[2] Uses $\tau^+ \to e^+\nu_e\overline{\nu}_\tau$ and $\tau^+ \to \mu^+\nu_\mu\overline{\nu}_\tau$ and e^+ or μ^+ as ℓ^+.

$\Gamma(\overline{D}^0\pi^-\ell^+\nu_\ell)/\Gamma_{\text{total}}$ Γ_8/Γ

VALUE (units 10^{-3})	DOCUMENT ID		TECN	COMMENT
4.3±0.6 OUR AVERAGE				
4.3±0.8±0.3	[1] AUBERT	08Q	BABR	$e^+e^- \to \Upsilon(4S)$
4.3±0.9±0.2	[1,2] LIVENTSEV	08	BELL	$e^+e^- \to \Upsilon(4S)$
• • • We do not use the following data for averages, fits, limits, etc. • • •				
3.4±1.0±0.2	[3] LIVENTSEV	05	BELL	Repl. by LIVENTSEV 08

[1] Uses a fully reconstructed B meson as a tag on the recoil side.
[2] LIVENTSEV 08 reports $(4.2 \pm 0.7 \pm 0.6) \times 10^{-3}$ from a measurement of $[\Gamma(B^0 \to \overline{D}^0\pi^-\ell^+\nu_\ell)/\Gamma_{\text{total}}] / [\mathrm{B}(B^0 \to D^-\ell^+\nu_\ell)]$ assuming $\mathrm{B}(B^0 \to D^-\ell^+\nu_\ell) = (2.12 \pm 0.20) \times 10^{-2}$, which we rescale to our best value $\mathrm{B}(B^0 \to D^-\ell^+\nu_\ell) = (2.19 \pm 0.12) \times 10^{-2}$. Our first error is their experiment's error and our second error is the systematic error from using our best value.
[3] LIVENTSEV 05 reports $[\Gamma(B^0 \to \overline{D}^0\pi^-\ell^+\nu_\ell)/\Gamma_{\text{total}}] / [\mathrm{B}(B^+ \to \overline{D}^0\ell^+\nu_\ell)] = 0.15 \pm 0.03 \pm 0.03$ which we multiply by our best value $\mathrm{B}(B^+ \to \overline{D}^0\ell^+\nu_\ell) = (2.27 \pm 0.11) \times 10^{-2}$. Our first error is their experiment's error and our second error is the systematic error from using our best value.

$\Gamma(D_0^*(2400)^-\ell^+\nu_\ell,\ D_0^{*-} \to \overline{D}^0\pi^-)/\Gamma_{\text{total}}$ Γ_9/Γ

VALUE (units 10^{-3})	DOCUMENT ID		TECN	COMMENT
3.0±1.2 OUR AVERAGE Error includes scale factor of 1.8.				
4.4±0.8±0.6	[1] AUBERT	08BL	BABR	$e^+e^- \to \Upsilon(4S)$
2.0±0.7±0.5	[1] LIVENTSEV	08	BELL	$e^+e^- \to \Upsilon(4S)$

[1] Uses a fully reconstructed B meson as a tag on the recoil side.

$\Gamma(D_2^*(2460)^-\ell^+\nu_\ell,\ D_2^{*-} \to \overline{D}^0\pi^-)/\Gamma_{\text{total}}$ Γ_{10}/Γ

VALUE (units 10^{-3})	DOCUMENT ID		TECN	COMMENT
1.21±0.33 OUR AVERAGE Error includes scale factor of 1.8.				
1.10±0.17±0.08	[1] AUBERT	09Y	BABR	$e^+e^- \to \Upsilon(4S)$
2.2 ±0.4 ±0.4	[2] LIVENTSEV	08	BELL	$e^+e^- \to \Upsilon(4S)$

[1] Uses a simultaneous fit of all B semileptonic decays without full reconstruction of events. AUBERT 09Y reports $\mathrm{B}(B^0 \to \overline{D}_2^*(2460)^-\ell^+\nu_\ell) \cdot \mathrm{B}(\overline{D}_2^*(2460)^- \to \overline{D}^{(*)0}\pi^-) = (1.77 \pm 0.26 \pm 0.11) \times 10^{-3}$ and the authors have provided us the individual measurement.
[2] Uses a fully reconstructed B meson as a tag on the recoil side.

$\Gamma(\overline{D}^{(*)}\,n\pi\ell^+\nu_\ell(n \geq 1))/\Gamma(D\ell^+\nu_\ell\,\text{anything})$ Γ_{11}/Γ_3

VALUE	DOCUMENT ID		TECN	COMMENT
0.248±0.032±0.030	[1] AUBERT	07AN	BABR	$e^+e^- \to \Upsilon(4S)$

[1] Uses a fully reconstructed B meson on the recoil side.

$\Gamma(\overline{D}^{*0}\pi^-\ell^+\nu_\ell)/\Gamma_{\text{total}}$ Γ_{12}/Γ

VALUE (units 10^{-3})	DOCUMENT ID		TECN	COMMENT
4.9±0.8 OUR AVERAGE				
4.8±0.8±0.4	[1] AUBERT	08Q	BABR	$e^+e^- \to \Upsilon(4S)$
5.8±2.3±0.3	[1,2] LIVENTSEV	08	BELL	$e^+e^- \to \Upsilon(4S)$
• • • We do not use the following data for averages, fits, limits, etc. • • •				
5.7±1.3±0.2	[3,4] LIVENTSEV	05	BELL	Repl. by LIVENTSEV 08

[1] Uses a fully reconstructed B meson as a tag on the recoil side.
[2] LIVENTSEV 08 reports $(5.6 \pm 2.1 \pm 0.8) \times 10^{-3}$ from a measurement of $[\Gamma(B^0 \to \overline{D}^{*0}\pi^-\ell^+\nu_\ell)/\Gamma_{\text{total}}] / [\mathrm{B}(B^0 \to D^-\ell^+\nu_\ell)]$ assuming $\mathrm{B}(B^0 \to D^-\ell^+\nu_\ell) = (2.12 \pm 0.20) \times 10^{-2}$, which we rescale to our best value $\mathrm{B}(B^0 \to D^-\ell^+\nu_\ell) = (2.19 \pm 0.12) \times 10^{-2}$. Our first error is their experiment's error and our second error is the systematic error from using our best value.
[3] Excludes D^{*+} contribution to $D\pi$ modes.
[4] LIVENTSEV 05 reports $[\Gamma(B^0 \to \overline{D}^{*0}\pi^-\ell^+\nu_\ell)/\Gamma_{\text{total}}] / [\mathrm{B}(B^+ \to \overline{D}^*(2007)^0\ell^+\nu_\ell)] = 0.10 \pm 0.02 \pm 0.01$ which we multiply by our best value $\mathrm{B}(B^+ \to \overline{D}^*(2007)^0\ell^+\nu_\ell) = (5.69 \pm 0.19) \times 10^{-2}$. Our first error is their experiment's error and our second error is the systematic error from using our best value.

$\Gamma(D_1(2420)^-\ell^+\nu_\ell,\ D_1^- \to \overline{D}^{*0}\pi^-)/\Gamma_{\text{total}}$ Γ_{13}/Γ

VALUE (units 10^{-3})	DOCUMENT ID		TECN	COMMENT
2.80±0.28 OUR AVERAGE				
2.78±0.24±0.25	[1] AUBERT	09Y	BABR	$e^+e^- \to \Upsilon(4S)$
2.7 ±0.4 ±0.3	[2] AUBERT	08BL	BABR	$e^+e^- \to \Upsilon(4S)$
5.4 ±1.9 ±0.9	[2] LIVENTSEV	08	BELL	$e^+e^- \to \Upsilon(4S)$

[1] Uses a simultaneous measurement of all B semileptonic decays without full reconstruction of events.
[2] Uses a fully reconstructed B meson as a tag on the recoil side.

$\Gamma(D_1'(2430)^-\ell^+\nu_\ell,\ D_1'^- \to \overline{D}^{*0}\pi^-)/\Gamma_{\text{total}}$ Γ_{14}/Γ

VALUE (units 10^{-3})	CL%	DOCUMENT ID		TECN	COMMENT
3.1±0.7±0.5		[1] AUBERT	08BL	BABR	$e^+e^- \to \Upsilon(4S)$
• • • We do not use the following data for averages, fits, limits, etc. • • •					
<5.0	90	[1] LIVENTSEV	08	BELL	$e^+e^- \to \Upsilon(4S)$

[1] Uses a fully reconstructed B meson as a tag on the recoil side.

$\Gamma(D_2^*(2460)^-\ell^+\nu_\ell,\ D_2^{*-} \to \overline{D}^{*0}\pi^-)/\Gamma_{\text{total}}$ Γ_{15}/Γ

VALUE (units 10^{-3})	CL%	DOCUMENT ID		TECN	COMMENT
0.68±0.12 OUR AVERAGE					
0.67±0.12±0.05		[1] AUBERT	09Y	BABR	$e^+e^- \to \Upsilon(4S)$
0.7 ±0.2 ±0.2		[2] AUBERT	08BL	BABR	$e^+e^- \to \Upsilon(4S)$
• • • We do not use the following data for averages, fits, limits, etc. • • •					
<3.0	90	[2] LIVENTSEV	08	BELL	$e^+e^- \to \Upsilon(4S)$

[1] Uses a simultaneous fit of all B semileptonic decays without full reconstruction of events. AUBERT 09Y reports $\mathrm{B}(B^0 \to \overline{D}_2^*(2460)^-\ell^+\nu_\ell) \cdot \mathrm{B}(\overline{D}_2^*(2460)^- \to \overline{D}^{(*)0}\pi^-) = (1.77 \pm 0.26 \pm 0.11) \times 10^{-3}$ and the authors have provided us the individual measurement.
[2] Uses a fully reconstructed B meson as a tag on the recoil side.

$\Gamma(\rho^-\ell^+\nu_\ell)/\Gamma_{\text{total}}$ Γ_{16}/Γ

$\ell = e$ or μ, not sum over e and μ modes.

"OUR EVALUATION" has been obtained by the Heavy Flavor Averaging Group (HFAG) by including both B^0 and B^+ decays. The average assumes equality of the semileptonic decay width for these isospin conjugate states.

VALUE (units 10^{-4})	CL%	DOCUMENT ID		TECN	COMMENT
2.94±0.11±0.18 OUR EVALUATION					
2.45±0.32 OUR AVERAGE Error includes scale factor of 1.6. See the ideogram below.					
3.22±0.27±0.24		[1] SIBIDANOV	13	BELL	$e^+e^- \to \Upsilon(4S)$
1.75±0.15±0.27		[2] DEL-AMO-SA...11C		BABR	$e^+e^- \to \Upsilon(4S)$
2.93±0.37±0.37		[3] ADAM	07	CLE2	$e^+e^- \to \Upsilon(4S)$
2.17±0.54±0.32		[4] HOKUUE	07	BELL	$e^+e^- \to \Upsilon(4S)$
$2.57 \pm 0.29 \,^{+0.53}_{-0.62}$		[5] BEHRENS	00	CLE2	$e^+e^- \to \Upsilon(4S)$
• • • We do not use the following data for averages, fits, limits, etc. • • •					
2.14±0.21±0.56		[2] AUBERT,B	05O	BABR	Repl. by DEL-AMO-SANCHEZ 11C
$2.17 \pm 0.34 \,^{+0.62}_{-0.68}$		[6] ATHAR	03	CLE2	Repl. by ADAM 07
3.29±0.42±0.72		[7] AUBERT	03E	BABR	Repl. by AUBERT,B 05O
$2.69 \pm 0.41 \,^{+0.61}_{-0.64}$		[8] BEHRENS	00	CLE2	$e^+e^- \to \Upsilon(4S)$
$2.5 \pm 0.4 \,^{+0.7}_{-0.9}$		[9] ALEXANDER	96T	CLE2	Repl. by BEHRENS 00
<4.1	90	[10] BEAN	93B	CLE2	$e^+e^- \to \Upsilon(4S)$

[1] The signal events are tagged by a second B meson reconstructed in the fully hadronic decays.
[2] B^+ and B^0 decays combined assuming isospin symmetry. Systematic errors include both experimental and form-factor uncertainties.
[3] The B^0 and B^+ results are combined assuming the isospin, B lifetimes, and relative charged/neutral B production at the $\Upsilon(4S)$.
[4] The signal events are tagged by a second B meson reconstructed in the semileptonic mode $B \to D^{(*)}\ell\nu_\ell$.
[5] Averaging with ALEXANDER 96T results including experimental and theoretical correlations considered, BEHRENS 00 reports systematic errors $^{+0.33}_{-0.46} \pm 0.41$, where the second error is theoretical model dependence. We combine these in quadrature.
[6] ATHAR 03 reports systematic errors $^{+0.47}_{-0.50} \pm 0.41 \pm 0.01$, which are experimental systematic, systematic due to residual form-factor uncertainties in the signal, and systematic due to residual form-factor uncertainties in the cross-feed modes, respectively. We combine these in quadrature.
[7] Uses isospin constraints and extrapolation to all electron energies according to five different form-factor calculations. The second error combines the systematic and theoretical uncertainties in quadrature.
[8] BEHRENS 00 reports $^{+0.35}_{-0.40} \pm 0.50$, where the second error is the theoretical model dependence. We combine these in quadrature. B^+ and B^0 decays combined using isospin symmetry: $\Gamma(B^0 \to \rho^-\ell^+\nu) = 2\Gamma(B^+ \to \rho^0\ell^+\nu) \approx 2\Gamma(B^+ \to \omega\ell^+\nu)$. No evidence for $\omega\ell\nu$ is reported.
[9] ALEXANDER 96T reports $^{+0.5}_{-0.7} \pm 0.5$ where the second error is the theoretical model dependence. We combine these in quadrature. B^+ and B^0 decays combined using isospin symmetry: $\Gamma(B^0 \to \rho^-\ell^+\nu) = 2\Gamma(B^+ \to \rho^0\ell^+\nu) \approx 2\Gamma(B^+ \to \omega\ell^+\nu)$. No evidence for $\omega\ell\nu$ is reported.
[10] BEAN 93B limit set using ISGW Model. Using isospin and the quark model to combine $\Gamma(\rho^0\ell^+\nu_\ell)$ and $\Gamma(\omega\ell^+\nu_\ell)$ with this result, they obtain a limit $<(1.6\text{–}2.7) \times 10^{-4}$ at 90% CL for $B^+ \to (\omega \text{or } \rho^0)\ell^+\nu_\ell$. The range corresponds to the ISGW, WSB, and KS models. An upper limit on $|V_{ub}/V_{cb}| < 0.08\text{–}0.13$ at 90% CL is derived as well.

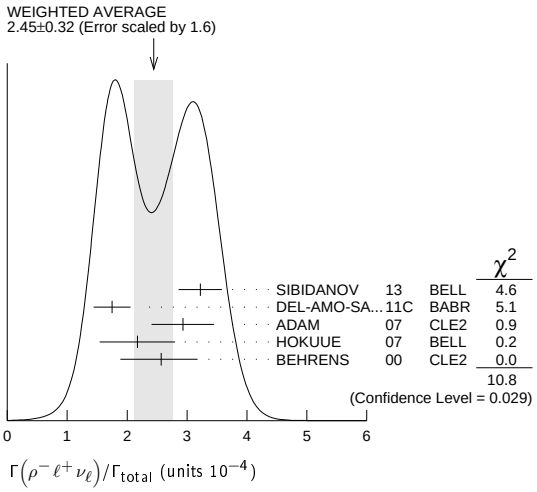

$\Gamma(\pi^-\ell^+\nu_\ell)/\Gamma_{total}$ Γ_{17}/Γ

"OUR EVALUATION" is provided by the Heavy Flavor Averaging Group (HFAG) and the procedure is described at http://www.slac.stanford.edu/xorg/hfag/.

VALUE (units 10^{-4})	DOCUMENT ID		TECN	COMMENT
1.45±0.05 OUR EVALUATION				
1.46±0.04 OUR AVERAGE				
1.49±0.09±0.07	[1] SIBIDANOV	13	BELL	$e^+e^- \to \Upsilon(4S)$
1.47±0.05±0.06	[2,3] LEES	12AA	BABR	$e^+e^- \to \Upsilon(4S)$
1.41±0.05±0.07	[4] DEL-AMO-SA...	11C	BABR	$e^+e^- \to \Upsilon(4S)$
1.49±0.04±0.07	[2] HA	11	BELL	$e^+e^- \to \Upsilon(4S)$
1.54±0.17±0.09	[4] AUBERT	08AV	BABR	$e^+e^- \to \Upsilon(4S)$
1.37±0.15±0.11	[5,6] ADAM	07	CLE2	$e^+e^- \to \Upsilon(4S)$
1.38±0.19±0.14	[7] HOKUUE	07	BELL	$e^+e^- \to \Upsilon(4S)$
• • • We do not use the following data for averages, fits, limits, etc. • • •				
1.42±0.05±0.08	[2] DEL-AMO-SA...	11F	BABR	Repl. by LEES 12AA
1.46±0.07±0.08	[8] AUBERT	07J	BABR	Repl. by DEL-AMO-SANCHEZ 11F
1.33±0.17±0.11	[9] AUBERT,B	06K	BABR	Repl. by AUBERT 08AV
1.38±0.10±0.18	[10] AUBERT,B	05O	BABR	Repl. by DEL-AMO-SANCHEZ 11C
1.33±0.18±0.13	[11] ATHAR	03	CLE2	Repl. by ADAM 07
1.8 ±0.4 ±0.4	[12] ALEXANDER	96T	CLE2	Repl. by ATHAR 03

[1] The signal events are tagged by a second B meson reconstructed in the fully hadronic decays.

[2] Uses loose neutrino reconstruction technique. Assumes $B(\Upsilon(4S) \to B^+B^-) = (51.6 \pm 0.6)\%$ and $B(\Upsilon(4S) \to B^0\overline{B}^0) = (48.4 \pm 0.6)\%$.

[3] Reports also a branching fraction value $B(B^0 \to \pi^-\ell^+\nu) = (1.45 \pm 0.04 \pm 0.06) \times 10^{-4}$ from the decays of B^+ and B^0 that are combined using the isospin symmetry relation.

[4] Using the isospin symmetry relation, B^+ and B^0 branching fractions are combined.

[5] The B^0 and B^+ results are combined assuming the isospin, B lifetimes, and relative charged/neutral B production at the $\Upsilon(4S)$.

[6] Also report the rate for $q^2 > 16$ GeV^2 of $(0.41 \pm 0.08 \pm 0.04) \times 10^{-4}$ from which they obtain $|V_{ub}| = 3.6 \pm 0.4 \pm 0.2^{+0.6}_{-0.4}$ (last error is from theory).

[7] The signal events are tagged by a second B meson reconstructed in the semileptonic mode $B \to D^{(*)}\ell\nu_\ell$.

[8] The analysis uses events in which the signal B decays are reconstructed with an innovative loose neutrino reconstruction technique.

[9] The signals are tagged by a second B meson reconstructed in a semileptonic or hadronic decay. The B^0 and B^+ results are combined assuming the isospin symmetry.

[10] B^+ and B^0 decays combined assuming isospin symmetry. Systematic errors include both experimental and form-factor uncertainties.

[11] ATHAR 03 reports systematic errors $0.11 \pm 0.01 \pm 0.07$, which are experimental systematic, systematic due to residual form-factor uncertainties in the signal, and systematic due to residual form-factor uncertainties in the cross-feed modes, respectively. We combine these in quadrature.

[12] ALEXANDER 96T gives systematic errors $\pm 0.3 \pm 0.2$ where the second error reflects the estimated model dependence. We combine these in quadrature. Assumes isospin symmetry: $\Gamma(B^0 \to \pi^-\ell^+\nu) = 2 \times \Gamma(B^+ \to \pi^0\ell^+\nu)$.

$\Gamma(\pi^-\mu^+\nu_\mu)/\Gamma_{total}$ Γ_{18}/Γ

VALUE	DOCUMENT ID		TECN	
• • • We do not use the following data for averages, fits, limits, etc. • • •				
seen	[1] ALBRECHT	91C	ARG	

[1] In ALBRECHT 91C, one event is fully reconstructed providing evidence for the $b \to u$ transition.

$\Gamma(K^\pm \text{anything})/\Gamma_{total}$ Γ_{19}/Γ

VALUE	DOCUMENT ID		TECN	COMMENT
0.78±0.08	[1] ALBRECHT	96D	ARG	$e^+e^- \to \Upsilon(4S)$

[1] Average multiplicity.

$\Gamma(D^0X)/\Gamma_{total}$ Γ_{20}/Γ

VALUE	DOCUMENT ID		TECN	COMMENT
0.081±0.014±0.005	[1] AUBERT	07N	BABR	$e^+e^- \to \Upsilon(4S)$
• • • We do not use the following data for averages, fits, limits, etc. • • •				
0.063±0.019±0.005	[1] AUBERT,BE	04B	BABR	Repl. by AUBERT 07N

[1] Events are selected by completely reconstructing one B and searching for a reconstructed charmed particle in the rest of the event. The last error includes systematic and charm branching ratio uncertainties.

$\Gamma(\overline{D}^0X)/\Gamma_{total}$ Γ_{21}/Γ

VALUE	DOCUMENT ID		TECN	COMMENT
0.474±0.020$^{+0.020}_{-0.019}$	[1] AUBERT	07N	BABR	$e^+e^- \to \Upsilon(4S)$
• • • We do not use the following data for averages, fits, limits, etc. • • •				
0.511±0.031±0.028	[1] AUBERT,BE	04B	BABR	Repl. by AUBERT 07N

[1] Events are selected by completely reconstructing one B and searching for a reconstructed charmed particle in the rest of the event. The last error includes systematic and charm branching ratio uncertainties.

$\Gamma(D^0X)/[\Gamma(D^0X)+\Gamma(\overline{D}^0X)]$ $\Gamma_{20}/(\Gamma_{20}+\Gamma_{21})$

VALUE	DOCUMENT ID		TECN	COMMENT
0.146±0.022±0.006	AUBERT	07N	BABR	$e^+e^- \to \Upsilon(4S)$
• • • We do not use the following data for averages, fits, limits, etc. • • •				
0.110±0.031±0.008	AUBERT,BE	04B	BABR	Repl. by AUBERT 07N

$\Gamma(D^+X)/\Gamma_{total}$ Γ_{22}/Γ

VALUE	CL%	DOCUMENT ID		TECN	COMMENT
<0.039	90	[1] AUBERT	07N	BABR	$e^+e^- \to \Upsilon(4S)$
• • • We do not use the following data for averages, fits, limits, etc. • • •					
<0.051	90	[1] AUBERT,BE	04B	BABR	Repl. by AUBERT 07N

[1] Events are selected by completely reconstructing one B and searching for a reconstructed charmed particle in the rest of the event. The last error includes systematic and charm branching ratio uncertainties.

$\Gamma(D^-X)/\Gamma_{total}$ Γ_{23}/Γ

VALUE	DOCUMENT ID		TECN	COMMENT
0.369±0.016$^{+0.030}_{-0.027}$	[1] AUBERT	07N	BABR	$e^+e^- \to \Upsilon(4S)$
• • • We do not use the following data for averages, fits, limits, etc. • • •				
0.397±0.030$^{+0.040}_{-0.038}$	[1] AUBERT,BE	04B	BABR	Repl. by AUBERT 07N

[1] Events are selected by completely reconstructing one B and searching for a reconstructed charmed particle in the rest of the event. The last error includes systematic and charm branching ratio uncertainties.

$\Gamma(D^+X)/[\Gamma(D^+X)+\Gamma(D^-X)]$ $\Gamma_{22}/(\Gamma_{22}+\Gamma_{23})$

VALUE	DOCUMENT ID		TECN	COMMENT
0.058±0.028±0.006	AUBERT	07N	BABR	$e^+e^- \to \Upsilon(4S)$
• • • We do not use the following data for averages, fits, limits, etc. • • •				
0.055±0.040±0.006	AUBERT,BE	04B	BABR	Repl. by AUBERT 07N

$\Gamma(D_s^+X)/\Gamma_{total}$ Γ_{24}/Γ

VALUE	DOCUMENT ID		TECN	COMMENT
0.103±0.012$^{+0.017}_{-0.014}$	[1] AUBERT	07N	BABR	$e^+e^- \to \Upsilon(4S)$
• • • We do not use the following data for averages, fits, limits, etc. • • •				
0.109±0.021$^{+0.039}_{-0.024}$	[1] AUBERT,BE	04B	BABR	Repl. by AUBERT 07N

[1] Events are selected by completely reconstructing one B and searching for a reconstructed charmed particle in the rest of the event. The last error includes systematic and charm branching ratio uncertainties.

$\Gamma(D_s^-X)/\Gamma_{total}$ Γ_{25}/Γ

VALUE	CL%	DOCUMENT ID		TECN	COMMENT
<0.026	90	[1] AUBERT	07N	BABR	$e^+e^- \to \Upsilon(4S)$
• • • We do not use the following data for averages, fits, limits, etc. • • •					
<0.087	90	[1] AUBERT,BE	04B	BABR	Repl. by AUBERT 07N

[1] Events are selected by completely reconstructing one B and searching for a reconstructed charmed particle in the rest of the event. The last error includes systematic and charm branching ratio uncertainties.

$\Gamma(D_s^+X)/[\Gamma(D_s^+X)+\Gamma(D_s^-X)]$ $\Gamma_{24}/(\Gamma_{24}+\Gamma_{25})$

VALUE	DOCUMENT ID		TECN	COMMENT
0.879±0.066±0.005	AUBERT	07N	BABR	$e^+e^- \to \Upsilon(4S)$
• • • We do not use the following data for averages, fits, limits, etc. • • •				
0.733±0.092±0.010	AUBERT,BE	04B	BABR	Repl. by AUBERT 07N

$\Gamma(\Lambda_c^+X)/\Gamma_{total}$ Γ_{26}/Γ

VALUE	CL%	DOCUMENT ID		TECN	COMMENT
<0.031	90	[1] AUBERT	07N	BABR	$e^+e^- \to \Upsilon(4S)$
• • • We do not use the following data for averages, fits, limits, etc. • • •					
<0.038	90	[1] AUBERT,BE	04B	BABR	Repl. by AUBERT 07N

[1] Events are selected by completely reconstructing one B and searching for a reconstructed charmed particle in the rest of the event. The last error includes systematic and charm branching ratio uncertainties.

Meson Particle Listings

B^0

$\Gamma(\overline{\Lambda}_c^- X)/\Gamma_{\text{total}}$ Γ_{27}/Γ

VALUE	DOCUMENT ID		TECN	COMMENT
$0.05 \pm 0.010^{+0.019}_{-0.011}$	[1] AUBERT	07N	BABR	$e^+e^- \to \Upsilon(4S)$
• • • We do not use the following data for averages, fits, limits, etc. • • •				
$0.049 \pm 0.017^{+0.018}_{-0.011}$	[1] AUBERT,BE	04B	BABR	Repl. by AUBERT 07N

[1] Events are selected by completely reconstructing one B and searching for a reconstructed charmed particle in the rest of the event. The last error includes systematic and charm branching ratio uncertainties.

$\Gamma(\Lambda_c^+ X)/[\Gamma(\Lambda_c^+ X)+\Gamma(\overline{\Lambda}_c^- X)]$ $\Gamma_{26}/(\Gamma_{26}+\Gamma_{27})$

VALUE	DOCUMENT ID		TECN	COMMENT
$0.243^{+0.119}_{-0.121} \pm 0.003$	AUBERT	07N	BABR	$e^+e^- \to \Upsilon(4S)$
• • • We do not use the following data for averages, fits, limits, etc. • • •				
$0.286 \pm 0.142 \pm 0.007$	AUBERT,BE	04B	BABR	Repl. by AUBERT 07N

$\Gamma(\overline{c}X)/\Gamma_{\text{total}}$ Γ_{28}/Γ

VALUE	DOCUMENT ID		TECN	COMMENT
$0.947 \pm 0.030^{+0.045}_{-0.040}$	[1] AUBERT	07N	BABR	$e^+e^- \to \Upsilon(4S)$
• • • We do not use the following data for averages, fits, limits, etc. • • •				
$1.039 \pm 0.051^{+0.063}_{-0.058}$	[1] AUBERT,BE	04B	BABR	Repl. by AUBERT 07N

[1] Events are selected by completely reconstructing one B and searching for a reconstructed charmed particle in the rest of the event. The last error includes systematic and charm branching ratio uncertainties.

$\Gamma(cX)/\Gamma_{\text{total}}$ Γ_{29}/Γ

VALUE	DOCUMENT ID		TECN	COMMENT
$0.246 \pm 0.024^{+0.021}_{-0.017}$	[1] AUBERT	07N	BABR	$e^+e^- \to \Upsilon(4S)$
• • • We do not use the following data for averages, fits, limits, etc. • • •				
$0.237 \pm 0.036^{+0.041}_{-0.027}$	[1] AUBERT,BE	04B	BABR	Repl. by AUBERT 07N

[1] Events are selected by completely reconstructing one B and searching for a reconstructed charmed particle in the rest of the event. The last error includes systematic and charm branching ratio uncertainties.

$\Gamma(\overline{c}cX)/\Gamma_{\text{total}}$ Γ_{30}/Γ

VALUE	DOCUMENT ID		TECN	COMMENT
$1.193 \pm 0.030^{+0.053}_{-0.049}$	[1] AUBERT	07N	BABR	$e^+e^- \to \Upsilon(4S)$
• • • We do not use the following data for averages, fits, limits, etc. • • •				
$1.276 \pm 0.062^{+0.088}_{-0.074}$	[1] AUBERT,BE	04B	BABR	Repl. by AUBERT 07N

[1] Events are selected by completely reconstructing one B and searching for a reconstructed charmed particle in the rest of the event. The last error includes systematic and charm branching ratio uncertainties.

$\Gamma(D^-\pi^+)/\Gamma_{\text{total}}$ Γ_{31}/Γ

VALUE (units 10^{-3})	EVTS	DOCUMENT ID		TECN	COMMENT
2.68 ± 0.13 OUR FIT					
2.68 ± 0.13 OUR AVERAGE					
$2.55 \pm 0.05 \pm 0.16$		[1] AUBERT	07H	BABR	$e^+e^- \to \Upsilon(4S)$
$3.03 \pm 0.23 \pm 0.23$		[2] AUBERT,BE	06J	BABR	$e^+e^- \to \Upsilon(4S)$
$2.68 \pm 0.12 \pm 0.24$		[1,3] AHMED	02B	CLE2	$e^+e^- \to \Upsilon(4S)$
$2.7 \pm 0.6 \pm 0.5$		[4] BORTOLETTO	92	CLEO	$e^+e^- \to \Upsilon(4S)$
$4.8 \pm 1.1 \pm 1.1$	22	[5] ALBRECHT	90J	ARG	$e^+e^- \to \Upsilon(4S)$
$5.1 \ ^{+2.8}_{-2.5} \ ^{+1.3}_{-1.2}$	4	[6] BEBEK	87	CLEO	$e^+e^- \to \Upsilon(4S)$
• • • We do not use the following data for averages, fits, limits, etc. • • •					
$2.90 \pm 0.21 \pm 0.14$		[1,7] AUBERT,B	04O	BABR	Repl. by AUBERT 07H
$2.9 \pm 0.4 \pm 0.1$	81	[8] ALAM	94	CLE2	Repl. by AHMED 02B
$3.1 \pm 1.3 \pm 1.0$	7	[5] ALBRECHT	88K	ARG	$e^+e^- \to \Upsilon(4S)$

[1] Assumes equal production of B^+ and B^0 at the $\Upsilon(4S)$.

[2] Uses a missing-mass method. Does not depend on D branching fractions or B^+/B^0 production rates.

[3] AHMED 02B reports an additional uncertainty on the branching ratios to account for 4.5% uncertainty on relative production of B^0 and B^+, which is not included here.

[4] BORTOLETTO 92 assumes equal production of B^+ and B^0 at the $\Upsilon(4S)$ and uses Mark III branching fractions for the D.

[5] ALBRECHT 88K assumes $B^0\overline{B}^0$:B^+B^- production ratio is 45:55. Superseded by ALBRECHT 90J which assumes 50:50.

[6] BEBEK 87 value has been updated in BERKELMAN 91 to use same assumptions as noted for BORTOLETTO 92.

[7] AUBERT,B 04O reports $[\Gamma(B^0 \to D^-\pi^+)/\Gamma_{\text{total}}] \times [B(D^+ \to K^0_S\pi^+)] = (42.7 \pm 2.1 \pm 2.2) \times 10^{-6}$ which we divide by our best value $B(D^+ \to K^0_S\pi^+) = (1.47 \pm 0.07) \times 10^{-2}$. Our first error is their experiment's error and our second error is the systematic error from using our best value.

[8] ALAM 94 reports $[\Gamma(B^0 \to D^-\pi^+)/\Gamma_{\text{total}}] \times [B(D^+ \to K^-2\pi^+)] = (0.265 \pm 0.032 \pm 0.023) \times 10^{-3}$ which we divide by our best value $B(D^+ \to K^-2\pi^+) = (9.13 \pm 0.19) \times 10^{-2}$. Our first error is their experiment's error and our second error is the systematic error from using our best value. Assumes equal production of B^+ and B^0 at the $\Upsilon(4S)$.

$\Gamma(D^-\ell^+\nu_\ell)/\Gamma(D^-\pi^+)$ Γ_4/Γ_{31}

VALUE	DOCUMENT ID		TECN	COMMENT
9.9 ± 1.0 ± 0.9	AALTONEN	09E	CDF	$p\overline{p}$ at 1.96 TeV

$\Gamma(D^-\rho^+)/\Gamma_{\text{total}}$ Γ_{32}/Γ

VALUE	EVTS	DOCUMENT ID		TECN	COMMENT
0.0078 ± 0.0013 OUR AVERAGE					
$0.0077 \pm 0.0013 \pm 0.0002$	79	[1] ALAM	94	CLE2	$e^+e^- \to \Upsilon(4S)$
$0.009 \pm 0.005 \pm 0.003$	9	[2] ALBRECHT	90J	ARG	$e^+e^- \to \Upsilon(4S)$
• • • We do not use the following data for averages, fits, limits, etc. • • •					
$0.022 \pm 0.012 \pm 0.009$	6	[2] ALBRECHT	88K	ARG	$e^+e^- \to \Upsilon(4S)$

[1] ALAM 94 reports $[\Gamma(B^0 \to D^-\rho^+)/\Gamma_{\text{total}}] \times [B(D^+ \to K^-2\pi^+)] = 0.000704 \pm 0.000096 \pm 0.000070$ which we divide by our best value $B(D^+ \to K^-2\pi^+) = (9.13 \pm 0.19) \times 10^{-2}$. Our first error is their experiment's error and our second error is the systematic error from using our best value. Assumes equal production of B^+ and B^0 at the $\Upsilon(4S)$.

[2] ALBRECHT 88K assumes $B^0\overline{B}^0$:B^+B^- production ratio is 45:55. Superseded by ALBRECHT 90J which assumes 50:50.

$\Gamma(D^-K^0\pi^+)/\Gamma_{\text{total}}$ Γ_{33}/Γ

VALUE (units 10^{-4})	DOCUMENT ID		TECN	COMMENT
4.9 ± 0.7 ± 0.5	[1] AUBERT,BE	05B	BABR	$e^+e^- \to \Upsilon(4S)$

[1] Assumes equal production of B^+ and B^0 at the $\Upsilon(4S)$.

$\Gamma(D^-K^*(892)^+)/\Gamma_{\text{total}}$ Γ_{34}/Γ

VALUE (units 10^{-4})	DOCUMENT ID		TECN	COMMENT
4.5 ± 0.7 OUR AVERAGE				
$4.6 \pm 0.6 \pm 0.5$	[1] AUBERT,BE	05B	BABR	$e^+e^- \to \Upsilon(4S)$
$3.7 \pm 1.5 \pm 1.0$	[1] MAHAPATRA	02	CLE2	$e^+e^- \to \Upsilon(4S)$

[1] Assumes equal production of B^+ and B^0 at the $\Upsilon(4S)$.

$\Gamma(D^-\omega\pi^+)/\Gamma_{\text{total}}$ Γ_{35}/Γ

VALUE	DOCUMENT ID		TECN	COMMENT
0.0028 ± 0.0005 ± 0.0004	[1] ALEXANDER	01B	CLE2	$e^+e^- \to \Upsilon(4S)$

[1] Assumes equal production of B^+ and B^0 at the $\Upsilon(4S)$. The signal is consistent with all observed $\omega\pi^+$ having proceeded through the ρ'^+ resonance at mass $1349 \pm 25^{+10}_{-5}$ MeV and width $547 \pm 86^{+46}_{-45}$ MeV.

$\Gamma(D^-K^+)/\Gamma_{\text{total}}$ Γ_{36}/Γ

VALUE (units 10^{-4})	DOCUMENT ID		TECN	COMMENT
1.97 ± 0.21 OUR AVERAGE				
$2.01 \pm 0.18 \pm 0.14$	[1] AAIJ	11F	LHCB	pp at 7 TeV
$1.8 \pm 0.4 \pm 0.1$	[2] ABE	01I	BELL	$e^+e^- \to \Upsilon(4S)$

[1] AAIJ 11F reports $(2.01 \pm 0.18 \pm 0.14) \times 10^{-4}$ from a measurement of $[\Gamma(B^0 \to D^-K^+)/\Gamma_{\text{total}}] / [B(B^0 \to D^-\pi^+)]$ assuming $B(B^0 \to D^-\pi^+) = (2.68 \pm 0.13) \times 10^{-3}$.

[2] ABE 01I reports $[\Gamma(B^0 \to D^-K^+)/\Gamma_{\text{total}}] / [B(B^0 \to D^-\pi^+)] = (6.8 \pm 1.5 \pm 0.7) \times 10^{-2}$ which we multiply by our best value $B(B^0 \to D^-\pi^+) = (2.68 \pm 0.13) \times 10^{-3}$. Our first error is their experiment's error and our second error is the systematic error from using our best value.

$\Gamma(D^-K^+)/\Gamma(D^-\pi^+)$ Γ_{36}/Γ_{31}

VALUE (units 10^{-2})	DOCUMENT ID		TECN	COMMENT
8.22 ± 0.11 ± 0.25	AAIJ	13P	LHCB	pp at 7 TeV

$\Gamma(D^-K^+\pi^+\pi^-)/\Gamma(D^-\pi^+\pi^+\pi^-)$ Γ_{37}/Γ_{43}

VALUE (units 10^{-2})	DOCUMENT ID		TECN	COMMENT
5.9 ± 1.1 ± 0.5	AAIJ	12T	LHCB	pp at 7 TeV

$\Gamma(D^-K^+\overline{K}^0)/\Gamma_{\text{total}}$ Γ_{38}/Γ

VALUE (units 10^{-4})	CL%	DOCUMENT ID		TECN	COMMENT
< 3.1	90	[1] DRUTSKOY	02	BELL	$e^+e^- \to \Upsilon(4S)$

[1] Assumes equal production of B^+ and B^0 at the $\Upsilon(4S)$.

$\Gamma(D^-K^+\overline{K}^*(892)^0)/\Gamma_{\text{total}}$ Γ_{39}/Γ

VALUE (units 10^{-4})	DOCUMENT ID		TECN	COMMENT
8.8 ± 1.1 ± 1.5	[1] DRUTSKOY	02	BELL	$e^+e^- \to \Upsilon(4S)$

[1] Assumes equal production of B^+ and B^0 at the $\Upsilon(4S)$.

$\Gamma(\overline{D}^0\pi^+\pi^-)/\Gamma_{\text{total}}$ Γ_{40}/Γ

VALUE (units 10^{-4})	CL%	EVTS	DOCUMENT ID		TECN	COMMENT
8.4 ± 0.4 ± 0.8			[1] KUZMIN	07	BELL	$e^+e^- \to \Upsilon(4S)$
• • • We do not use the following data for averages, fits, limits, etc. • • •						
$8.0 \pm 0.6 \pm 1.5$			[1,2] SATPATHY	03	BELL	Repl. by KUZMIN 07
< 16	90		[1] ALAM	94	CLE2	$e^+e^- \to \Upsilon(4S)$
< 70	90		[3] BORTOLETTO	92	CLEO	$e^+e^- \to \Upsilon(4S)$
<340	90		[4] BEBEK	87	CLEO	$e^+e^- \to \Upsilon(4S)$
700 ± 500		5	[5] BEHRENDS	83	CLEO	$e^+e^- \to \Upsilon(4S)$

[1] Assumes equal production of B^+ and B^0 at the $\Upsilon(4S)$.
[2] No assumption about the intermediate mechanism is made in the analysis.
[3] BORTOLETTO 92 assumes equal production of B^+ and B^0 at the $\Upsilon(4S)$ and uses Mark III branching fractions for the D. The product branching fraction into $D_0^*(2340)\pi$ followed by $D_0^*(2340) \to D^0\pi$ is < 0.0001 at 90% CL and into $D_2^*(2460)$ followed by $D_2^*(2460) \to D^0\pi$ is < 0.0004 at 90% CL.
[4] BEBEK 87 assume the $\Upsilon(4S)$ decays 43% to $B^0\overline{B}^0$. We rescale to 50%. $B(D^0 \to K^-\pi^+) = (4.2 \pm 0.4 \pm 0.4)\%$ and $B(D^0 \to K^-\pi^+\pi^+\pi^-) = (9.1 \pm 0.8 \pm 0.8)\%$ were used.
[5] Corrected by us using assumptions: $B(D^0 \to K^-\pi^+) = (0.042 \pm 0.006)$ and $B(\Upsilon(4S) \to B^0\overline{B}^0) = 50\%$. The product branching ratio is $B(B^0 \to \overline{D}^0\pi^+\pi^-)B(\overline{D}^0 \to K^+\pi^-) = (0.39 \pm 0.26) \times 10^{-2}$.

$\Gamma(D^*(2010)^-\pi^+)/\Gamma_{\text{total}}$ Γ_{41}/Γ

VALUE (units 10^{-3})	EVTS	DOCUMENT ID		TECN	COMMENT
2.76±0.13 OUR AVERAGE					
2.79±0.08±0.17		[1] AUBERT	07H	BABR	$e^+e^- \to \Upsilon(4S)$
2.7 ±0.4 ±0.1		[2,3] AUBERT,BE	06J	BABR	$e^+e^- \to \Upsilon(4S)$
2.81±0.24±0.05		[4] BRANDENB...	98	CLE2	$e^+e^- \to \Upsilon(4S)$
2.6 ±0.3 ±0.4	82	[5] ALAM	94	CLE2	$e^+e^- \to \Upsilon(4S)$
3.37±0.96±0.02		[6] BORTOLETTO	92	CLEO	$e^+e^- \to \Upsilon(4S)$
2.36±0.88±0.02	12	[7] ALBRECHT	90J	ARG	$e^+e^- \to \Upsilon(4S)$
$2.36^{+1.50}_{-1.10}\pm0.02$	5	[8] BEBEK	87	CLEO	$e^+e^- \to \Upsilon(4S)$
• • • We do not use the following data for averages, fits, limits, etc. • • •					
10 ±4 ±1	8	[9] AKERS	94J	OPAL	$e^+e^- \to Z$
2.7 ±1.4 ±1.0	5	[10] ALBRECHT	87C	ARG	$e^+e^- \to \Upsilon(4S)$
3.5 ±2 ±2		[11] ALBRECHT	86F	ARG	$e^+e^- \to \Upsilon(4S)$
17 ±5 ±5	41	[12] GILES	84	CLEO	$e^+e^- \to \Upsilon(4S)$

[1] Assumes equal production of B^+ and B^0 at the $\Upsilon(4S)$.
[2] AUBERT,BE 06J reports $[\Gamma(B^0 \to D^*(2010)^-\pi^+)/\Gamma_{\text{total}}] / [B(B^0 \to D^-\pi^+)] = 0.99 \pm 0.11 \pm 0.08$ which we multiply by our best value $B(B^0 \to D^-\pi^+) = (2.68 \pm 0.13) \times 10^{-3}$. Our first error is their experiment's error and our second error is the systematic error from using our best value.
[3] Uses a missing-mass method. Does not depend on D branching fractions or B^+/B^0 production rates.
[4] BRANDENBURG 98 assume equal production of B^+ and B^0 at $\Upsilon(4S)$ and use the D^* reconstruction technique. The first error is their experiment's error and the second error is the systematic error from the PDG 96 value of $B(D^* \to D\pi)$.
[5] ALAM 94 assume equal production of B^+ and B^0 at the $\Upsilon(4S)$ and use the CLEO II $B(D^*(2010)^+ \to D^0\pi^+)$ and absolute $B(D^0 \to K^-\pi^+)$ and the PDG 1992 $B(D^0 \to K^-\pi^+\pi^0)/B(D^0 \to K^-\pi^+)$ and $B(D^0 \to K^-2\pi^+\pi^-)/B(D^0 \to K^-\pi^+)$.
[6] BORTOLETTO 92 reports $(4.0 \pm 1.0 \pm 0.7) \times 10^{-3}$ from a measurement of $[\Gamma(B^0 \to D^*(2010)^-\pi^+)/\Gamma_{\text{total}}] \times [B(D^*(2010)^+ \to D^0\pi^+)]$ assuming $B(D^*(2010)^+ \to D^0\pi^+) = 0.57 \pm 0.06$, which we rescale to our best value $B(D^*(2010)^+ \to D^0\pi^+) = (67.7 \pm 0.5) \times 10^{-2}$. Our first error is their experiment's error and our second error is the systematic error from using our best value. Assumes equal production of B^+ and B^0 at the $\Upsilon(4S)$ and uses Mark III branching fractions for the D.
[7] ALBRECHT 90J reports $(2.8 \pm 0.9 \pm 0.6) \times 10^{-3}$ from a measurement of $[\Gamma(B^0 \to D^*(2010)^-\pi^+)/\Gamma_{\text{total}}] \times [B(D^*(2010)^+ \to D^0\pi^+)]$ assuming $B(D^*(2010)^+ \to D^0\pi^+) = 0.57 \pm 0.06$, which we rescale to our best value $B(D^*(2010)^+ \to D^0\pi^+) = (67.7 \pm 0.5) \times 10^{-2}$. Our first error is their experiment's error and our second error is the systematic error from using our best value. Assumes equal production of B^+ and B^0 at the $\Upsilon(4S)$ and uses Mark III branching fractions for the D.
[8] BEBEK 87 reports $(2.8^{+1.5+1.0}_{-1.2-0.6}) \times 10^{-3}$ from a measurement of $[\Gamma(B^0 \to D^*(2010)^-\pi^+)/\Gamma_{\text{total}}] \times [B(D^*(2010)^+ \to D^0\pi^+)]$ assuming $B(D^*(2010)^+ \to D^0\pi^+) = 0.57 \pm 0.06$, which we rescale to our best value $B(D^*(2010)^+ \to D^0\pi^+) = (67.7 \pm 0.5) \times 10^{-2}$. Our first error is their experiment's error and our second error is the systematic error from using our best value. Updated in BERKELMAN 91 to use same assumptions as noted for BORTOLETTO 92 and ALBRECHT 90J.
[9] Assumes $B(Z \to b\overline{b}) = 0.217$ and 38% B_d production fraction.
[10] ALBRECHT 87C use PDG 86 branching ratios for D and $D^*(2010)$ and assume $B(\Upsilon(4S) \to B^+B^-) = 55\%$ and $B(\Upsilon(4S) \to B^0\overline{B}^0) = 45\%$. Superseded by ALBRECHT 90J.
[11] ALBRECHT 86F uses pseudomass that is independent of D^0 and D^+ branching ratios.
[12] Assumes $B(D^*(2010)^+ \to D^0\pi^+) = 0.60^{+0.08}_{-0.15}$. Assumes $B(\Upsilon(4S) \to B^0\overline{B}^0) = 0.40 \pm 0.02$ Does not depend on D branching ratios.

$\Gamma(D^*(2010)^-\ell^+\nu_\ell)/\Gamma(D^*(2010)^-\pi^+)$ Γ_6/Γ_{41}

VALUE	DOCUMENT ID		TECN	COMMENT
16.5±2.3±1.1	AALTONEN	09E	CDF	$p\overline{p}$ at 1.96 TeV

$\Gamma(\overline{D}^0K^+K^-)/\Gamma(\overline{D}^0\pi^+\pi^-)$ Γ_{42}/Γ_{40}

VALUE	DOCUMENT ID		TECN	COMMENT
0.056±0.011±0.007	AAIJ	12AM	LHCB	pp at 7 TeV

$\Gamma(D^-\pi^+\pi^+\pi^-)/\Gamma_{\text{total}}$ Γ_{43}/Γ

VALUE	DOCUMENT ID		TECN	COMMENT
0.0064±0.0007 OUR FIT				
0.0080±0.0021±0.0014	[1] BORTOLETTO	92	CLEO	$e^+e^- \to \Upsilon(4S)$

[1] BORTOLETTO 92 assumes equal production of B^+ and B^0 at the $\Upsilon(4S)$ and uses Mark III branching fractions for the D.

$\Gamma(D^-\pi^+\pi^+\pi^-)/\Gamma(D^-\pi^+)$ Γ_{43}/Γ_{31}

VALUE	DOCUMENT ID		TECN	COMMENT
2.38±0.23 OUR FIT				
2.38±0.11±0.21	AAIJ	11E	LHCB	pp at 7 TeV

$\Gamma((D^-\pi^+\pi^+\pi^-)\text{ nonresonant})/\Gamma_{\text{total}}$ Γ_{44}/Γ

VALUE	DOCUMENT ID		TECN	COMMENT
0.0039±0.0014±0.0013	[1] BORTOLETTO	92	CLEO	$e^+e^- \to \Upsilon(4S)$

[1] BORTOLETTO 92 assumes equal production of B^+ and B^0 at the $\Upsilon(4S)$ and uses Mark III branching fractions for the D.

$\Gamma(D^-\pi^+\rho^0)/\Gamma_{\text{total}}$ Γ_{45}/Γ

VALUE	DOCUMENT ID		TECN	COMMENT
0.0011±0.0009±0.0004	[1] BORTOLETTO	92	CLEO	$e^+e^- \to \Upsilon(4S)$

[1] BORTOLETTO 92 assumes equal production of B^+ and B^0 at the $\Upsilon(4S)$ and uses Mark III branching fractions for the D.

$\Gamma(D^-a_1(1260)^+)/\Gamma_{\text{total}}$ Γ_{46}/Γ

VALUE	DOCUMENT ID		TECN	COMMENT
0.0060±0.0022±0.0024	[1] BORTOLETTO	92	CLEO	$e^+e^- \to \Upsilon(4S)$

[1] BORTOLETTO 92 assumes equal production of B^+ and B^0 at the $\Upsilon(4S)$ and uses Mark III branching fractions for the D.

$\Gamma(D^*(2010)^-\pi^+\pi^0)/\Gamma_{\text{total}}$ Γ_{47}/Γ

VALUE	EVTS	DOCUMENT ID		TECN	COMMENT
0.0152±0.0052±0.0001	51	[1] ALBRECHT	90J	ARG	$e^+e^- \to \Upsilon(4S)$
• • • We do not use the following data for averages, fits, limits, etc. • • •					
0.015 ±0.008 ±0.008	8	[2] ALBRECHT	87C	ARG	$e^+e^- \to \Upsilon(4S)$

[1] ALBRECHT 90J reports $0.018 \pm 0.004 \pm 0.005$ from a measurement of $[\Gamma(B^0 \to D^*(2010)^-\pi^+\pi^0)/\Gamma_{\text{total}}] \times [B(D^*(2010)^+ \to D^0\pi^+)]$ assuming $B(D^*(2010)^+ \to D^0\pi^+) = 0.57 \pm 0.06$, which we rescale to our best value $B(D^*(2010)^+ \to D^0\pi^+) = (67.7 \pm 0.5) \times 10^{-2}$. Our first error is their experiment's error and our second error is the systematic error from using our best value. Assumes equal production of B^+ and B^0 at the $\Upsilon(4S)$ and uses Mark III branching fractions for the D.
[2] ALBRECHT 87C use PDG 86 branching ratios for D and $D^*(2010)$ and assume $B(\Upsilon(4S) \to B^+B^-) = 55\%$ and $B(\Upsilon(4S) \to B^0\overline{B}^0) = 45\%$. Superseded by ALBRECHT 90J.

$\Gamma(D^*(2010)^-\rho^+)/\Gamma_{\text{total}}$ Γ_{48}/Γ

VALUE	EVTS	DOCUMENT ID		TECN	COMMENT
0.0068 ±0.0009 OUR AVERAGE					
0.0068 ±0.0003 ±0.0009		[1] CSORNA	03	CLE2	$e^+e^- \to \Upsilon(4S)$
0.0160 ±0.0113 ±0.0001		[2] BORTOLETTO	92	CLEO	$e^+e^- \to \Upsilon(4S)$
0.00589±0.00352±0.00004	19	[3] ALBRECHT	90J	ARG	$e^+e^- \to \Upsilon(4S)$
• • • We do not use the following data for averages, fits, limits, etc. • • •					
0.0074 ±0.0010 ±0.0014	76	[4,5] ALAM	94	CLE2	$e^+e^- \to \Upsilon(4S)$
0.081 ±0.029 $^{+0.059}_{-0.024}$	19	[6] CHEN	85	CLEO	$e^+e^- \to \Upsilon(4S)$

[1] Assumes equal production of B^0 and B^+ at the $\Upsilon(4S)$ resonance. The second error combines the systematic and theoretical uncertainties in quadrature. CSORNA 03 includes data used in ALAM 94. A full angular fit to three complex helicity amplitudes is performed.
[2] BORTOLETTO 92 reports $0.019 \pm 0.008 \pm 0.011$ from a measurement of $[\Gamma(B^0 \to D^*(2010)^-\rho^+)/\Gamma_{\text{total}}] \times [B(D^*(2010)^+ \to D^0\pi^+)]$ assuming $B(D^*(2010)^+ \to D^0\pi^+) = 0.57 \pm 0.06$, which we rescale to our best value $B(D^*(2010)^+ \to D^0\pi^+) = (67.7 \pm 0.5) \times 10^{-2}$. Our first error is their experiment's error and our second error is the systematic error from using our best value. Assumes equal production of B^+ and B^0 at the $\Upsilon(4S)$ and uses Mark III branching fractions for the D.
[3] ALBRECHT 90J reports $0.007 \pm 0.003 \pm 0.003$ from a measurement of $[\Gamma(B^0 \to D^*(2010)^-\rho^+)/\Gamma_{\text{total}}] \times [B(D^*(2010)^+ \to D^0\pi^+)]$ assuming $B(D^*(2010)^+ \to D^0\pi^+) = 0.57 \pm 0.06$, which we rescale to our best value $B(D^*(2010)^+ \to D^0\pi^+) = (67.7 \pm 0.5) \times 10^{-2}$. Our first error is their experiment's error and our second error is the systematic error from using our best value. Assumes equal production of B^+ and B^0 at the $\Upsilon(4S)$ and uses Mark III branching fractions for the D.
[4] ALAM 94 assume equal production of B^+ and B^0 at the $\Upsilon(4S)$ and use the CLEO II $B(D^*(2010)^+ \to D^0\pi^+)$ and absolute $B(D^0 \to K^-\pi^+)$ and the PDG 1992 $B(D^0 \to K^-\pi^+\pi^0)/B(D^0 \to K^-\pi^+)$ and $B(D^0 \to K^-2\pi^+\pi^-)/B(D^0 \to K^-\pi^+)$.
[5] This decay is nearly completely longitudinally polarized, $\Gamma_L/\Gamma = (93 \pm 5 \pm 5)\%$, as expected from the factorization hypothesis (ROSNER 90). The nonresonant $\pi^+\pi^0$ contribution under the ρ^+ is less than 9% at 90% CL.
[6] Uses $B(D^* \to D^0\pi^+) = 0.6 \pm 0.15$ and $B(\Upsilon(4S) \to B^0\overline{B}^0) = 0.4$. Does not depend on D branching ratios.

$\Gamma(D^*(2010)^-K^+)/\Gamma_{\text{total}}$ Γ_{49}/Γ

VALUE (units 10^{-4})	DOCUMENT ID		TECN	COMMENT
2.14±0.16 OUR AVERAGE				
2.14±0.12±0.10	[1] AUBERT	06A	BABR	$e^+e^- \to \Upsilon(4S)$
2.0 ±0.4 ±0.1	[2] ABE	01I	BELL	$e^+e^- \to \Upsilon(4S)$

[1] AUBERT 06A reports $[\Gamma(B^0 \to D^*(2010)^-K^+)/\Gamma_{\text{total}}] / [B(B^0 \to D^*(2010)^-\pi^+)] = 0.0776 \pm 0.0034 \pm 0.0029$ which we multiply by our best value $B(B^0 \to D^*(2010)^-\pi^+) = (2.76 \pm 0.13) \times 10^{-3}$. Our first error is their experiment's error and our second error is the systematic error from using our best value.
[2] ABE 01I reports $[\Gamma(B^0 \to D^*(2010)^-K^+)/\Gamma_{\text{total}}] / [B(B^0 \to D^*(2010)^-\pi^+)] = 0.074 \pm 0.015 \pm 0.006$ which we multiply by our best value $B(B^0 \to D^*(2010)^-\pi^+) = (2.76 \pm 0.13) \times 10^{-3}$. Our first error is their experiment's error and our second error is the systematic error from using our best value.

$\Gamma(D^*(2010)^- K^+)/\Gamma(D^*(2010)^- \pi^+)$ Γ_{49}/Γ_{41}

VALUE	DOCUMENT ID		TECN	COMMENT
$(7.76\pm0.34\pm0.26)\times10^{-2}$	AAIJ	13AO	LHCB	pp at 7 TeV

$\Gamma(D^*(2010)^- K^0\pi^+)/\Gamma_{total}$ Γ_{50}/Γ

VALUE (units 10^{-4})	DOCUMENT ID		TECN	COMMENT
$3.0\pm0.7\pm0.3$	[1] AUBERT,BE	05B	BABR	$e^+e^-\to\ \Upsilon(4S)$

[1] Assumes equal production of B^+ and B^0 at the $\Upsilon(4S)$.

$\Gamma(D^*(2010)^- K^*(892)^+)/\Gamma_{total}$ Γ_{51}/Γ

VALUE (units 10^{-4})	DOCUMENT ID		TECN	COMMENT
3.3 ± 0.6 OUR AVERAGE				
$3.2\pm0.6\pm0.3$	[1] AUBERT,BE	05B	BABR	$e^+e^-\to\ \Upsilon(4S)$
$3.8\pm1.3\pm0.8$	[2] MAHAPATRA	02	CLE2	$e^+e^-\to\ \Upsilon(4S)$

[1] Assumes equal production of B^+ and B^0 at the $\Upsilon(4S)$.
[2] Assumes equal production of B^+ and B^0 at the $\Upsilon(4S)$ and an unpolarized final state.

$\Gamma(D^*(2010)^- K^+\overline{K}^0)/\Gamma_{total}$ Γ_{52}/Γ

VALUE (units 10^{-4})	CL%	DOCUMENT ID		TECN	COMMENT
<4.7	90	[1] DRUTSKOY	02	BELL	$e^+e^-\to\ \Upsilon(4S)$

[1] Assumes equal production of B^+ and B^0 at the $\Upsilon(4S)$.

$\Gamma(D^*(2010)^- K^+\overline{K}^*(892)^0)/\Gamma_{total}$ Γ_{53}/Γ

VALUE (units 10^{-4})	DOCUMENT ID		TECN	COMMENT
$12.9\pm2.2\pm2.5$	[1] DRUTSKOY	02	BELL	$e^+e^-\to\ \Upsilon(4S)$

[1] Assumes equal production of B^+ and B^0 at the $\Upsilon(4S)$.

$\Gamma(D^*(2010)^-\pi^+\pi^+\pi^-)/\Gamma_{total}$ Γ_{54}/Γ

VALUE	CL%	DOCUMENT ID		TECN	COMMENT
$0.0070\ \pm0.0008$ OUR AVERAGE		Error includes scale factor of 1.3. See the ideogram below.			
$0.00681\pm0.00023\pm0.00072$		[1] MAJUMDER	04	BELL	$e^+e^-\to\ \Upsilon(4S)$
$0.0063\ \pm0.0010\ \pm0.0011$		[2,3] ALAM	94	CLE2	$e^+e^-\to\ \Upsilon(4S)$
$0.0134\ \pm0.0036\ \pm0.0001$		[4] BORTOLETTO	92	CLEO	$e^+e^-\to\ \Upsilon(4S)$
$0.0101\ \pm0.0041\ \pm0.0001$		[5] ALBRECHT	90J	ARG	$e^+e^-\to\ \Upsilon(4S)$
• • • We do not use the following data for averages, fits, limits, etc. • • •					
$0.033\ \ \pm0.009\ \ \pm0.016$		[6] ALBRECHT	87C	ARG	$e^+e^-\to\ \Upsilon(4S)$
<0.042	90	[7] BEBEK	87	CLEO	$e^+e^-\to\ \Upsilon(4S)$

[1] Assumes equal production of B^+ and B^0 at the $\Upsilon(4S)$.
[2] ALAM 94 assume equal production of B^+ and B^0 at the $\Upsilon(4S)$ and use the CLEO II $B(D^*(2010)^+\to D^0\pi^+)$ and absolute $B(D^0\to K^-\pi^+)$ and the PDG 1992 $B(D^0\to K^-\pi^+\pi^0)/B(D^0\to K^-\pi^+)$ and $B(D^0\to K^-2\pi^+\pi^-)/B(D^0\to K^-\pi^+)$.
[3] The three pion mass is required to be between 1.0 and 1.6 GeV consistent with an a_1 meson. (If this channel is dominated by a_1^+, the branching ratio for $\overline{D}^{*-}a_1^+$ is twice that for $\overline{D}^{*-}\pi^+\pi^+\pi^-$.)
[4] BORTOLETTO 92 reports $0.0159\pm0.0028\pm0.0037$ from a measurement of $[\Gamma(B^0\to D^*(2010)^-\pi^+\pi^+\pi^-)/\Gamma_{total}]\times[B(D^*(2010)^+\to D^0\pi^+)]$ assuming $B(D^*(2010)^+\to D^0\pi^+)=0.57\pm0.06$, which we rescale to our best value $B(D^*(2010)^+\to D^0\pi^+)=(67.7\pm0.5)\times10^{-2}$. Our first error is their experiment's error and our second error is the systematic error from using our best value. Assumes equal production of B^+ and B^0 at the $\Upsilon(4S)$ and uses Mark III branching fractions for the D.
[5] ALBRECHT 90J reports $0.012\pm0.003\pm0.004$ from a measurement of $[\Gamma(B^0\to D^*(2010)^-\pi^+\pi^+\pi^-)/\Gamma_{total}]\times[B(D^*(2010)^+\to D^0\pi^+)]$ assuming $B(D^*(2010)^+\to D^0\pi^+)=0.57\pm0.06$, which we rescale to our best value $B(D^*(2010)^+\to D^0\pi^+)=(67.7\pm0.5)\times10^{-2}$. Our first error is their experiment's error and our second error is the systematic error from using our best value. Assumes equal production of B^+ and B^0 at the $\Upsilon(4S)$ and uses Mark III branching fractions for the D.
[6] ALBRECHT 87C use PDG 86 branching ratios for D and $D^*(2010)$ and assume $B(\Upsilon(4S)\to B^+B^-)=55\%$ and $B(\Upsilon(4S)\to B^0\overline{B}^0)=45\%$. Superseded by ALBRECHT 90J.
[7] BEBEK 87 value has been updated in BERKELMAN 91 to use same assumptions as noted for BORTOLETTO 92.

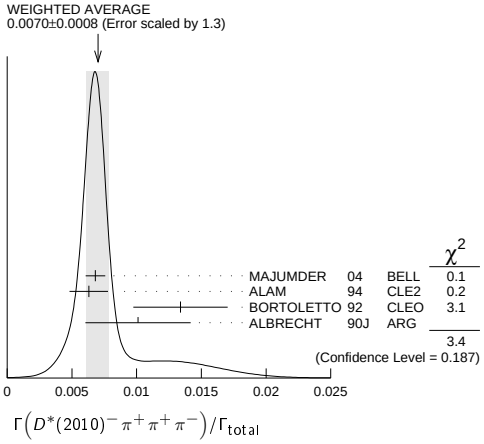

$\Gamma((D^*(2010)^-\pi^+\pi^+\pi^-)$ nonresonant$)/\Gamma_{total}$ Γ_{55}/Γ

VALUE	DOCUMENT ID		TECN	COMMENT
$0.0000\pm0.0019\pm0.0016$	[1] BORTOLETTO92		CLEO	$e^+e^-\to\ \Upsilon(4S)$

[1] BORTOLETTO 92 assumes equal production of B^+ and B^0 at the $\Upsilon(4S)$ and uses Mark III branching fractions for the D and $D^*(2010)$.

$\Gamma(D^*(2010)^-\pi^+\rho^0)/\Gamma_{total}$ Γ_{56}/Γ

VALUE	DOCUMENT ID		TECN	COMMENT
$0.00573\pm0.00317\pm0.00004$	[1] BORTOLETTO92		CLEO	$e^+e^-\to\ \Upsilon(4S)$

[1] BORTOLETTO 92 reports $0.0068\pm0.0032\pm0.0021$ from a measurement of $[\Gamma(B^0\to D^*(2010)^-\pi^+\rho^0)/\Gamma_{total}]\times[B(D^*(2010)^+\to D^0\pi^+)]$ assuming $B(D^*(2010)^+\to D^0\pi^+)=0.57\pm0.06$, which we rescale to our best value $B(D^*(2010)^+\to D^0\pi^+)=(67.7\pm0.5)\times10^{-2}$. Our first error is their experiment's error and our second error is the systematic error from using our best value. Assumes equal production of B^+ and B^0 at the $\Upsilon(4S)$ and uses Mark III branching fractions for the D.

$\Gamma(D^*(2010)^- a_1(1260)^+)/\Gamma_{total}$ Γ_{57}/Γ

VALUE	DOCUMENT ID		TECN	COMMENT
0.0130 ± 0.0027 OUR AVERAGE				
$0.0126\pm0.0020\pm0.0022$	[1,2] ALAM	94	CLE2	$e^+e^-\to\ \Upsilon(4S)$
$0.0152\pm0.0070\pm0.0001$	[3] BORTOLETTO92		CLEO	$e^+e^-\to\ \Upsilon(4S)$

[1] ALAM 94 value is twice their $\Gamma(D^*(2010)^-\pi^+\pi^+\pi^-)/\Gamma_{total}$ value based on their observation that the three pions are dominantly in the $a_1(1260)$ mass range 1.0 to 1.6 GeV.
[2] ALAM 94 assume equal production of B^+ and B^0 at the $\Upsilon(4S)$ and use the CLEO II $B(D^*(2010)^+\to D^0\pi^+)$ and absolute $B(D^0\to K^-\pi^+)$ and the PDG 1992 $B(D^0\to K^-\pi^+\pi^0)/B(D^0\to K^-\pi^+)$ and $B(D^0\to K^-2\pi^+\pi^-)/B(D^0\to K^-\pi^+)$.
[3] BORTOLETTO 92 reports $0.018\pm0.006\pm0.006$ from a measurement of $[\Gamma(B^0\to D^*(2010)^-a_1(1260)^+)/\Gamma_{total}]\times[B(D^*(2010)^+\to D^0\pi^+)]$ assuming $B(D^*(2010)^+\to D^0\pi^+)=0.57\pm0.06$, which we rescale to our best value $B(D^*(2010)^+\to D^0\pi^+)=(67.7\pm0.5)\times10^{-2}$. Our first error is their experiment's error and our second error is the systematic error from using our best value. Assumes equal production of B^+ and B^0 at the $\Upsilon(4S)$ and uses Mark III branching fractions for the D.

$\Gamma(\overline{D}_1(2420)^0\pi^-\pi^+,\ \overline{D}_1^0\to D^{*-}\pi^+)/\Gamma(D^*(2010)^-\pi^+\pi^+\pi^-)$ Γ_{58}/Γ_{54}

VALUE	DOCUMENT ID		TECN	COMMENT
$(2.04\pm0.42\pm0.22)\times10^{-2}$	AAIJ	13AO	LHCB	pp at 7 TeV

$\Gamma(D^*(2010)^- K^+\pi^-\pi^+)/\Gamma(D^*(2010)^-\pi^+\pi^+\pi^-)$ Γ_{59}/Γ_{54}

VALUE	DOCUMENT ID		TECN	COMMENT
$(6.47\pm0.37\pm0.35)\times10^{-2}$	AAIJ	13AO	LHCB	pp at 7 TeV

$\Gamma(D^*(2010)^-\pi^+\pi^+\pi^-\pi^0)/\Gamma_{total}$ Γ_{60}/Γ

VALUE	EVTS	DOCUMENT ID		TECN	COMMENT
0.0176 ± 0.0027 OUR AVERAGE					
$0.0172\pm0.0014\pm0.0024$		[1] ALEXANDER	01B	CLE2	$e^+e^-\to\ \Upsilon(4S)$
$0.0345\pm0.0181\pm0.0003$	28	[2] ALBRECHT	90J	ARG	$e^+e^-\to\ \Upsilon(4S)$

[1] Assumes equal production of B^+ and B^0 at the $\Upsilon(4S)$. The signal is consistent with all observed $\omega\pi^+$ having proceeded through the ρ'^+ resonance at mass $1349\pm25^{+10}_{-\ 5}$ MeV and width $547\pm86^{+46}_{-45}$ MeV.
[2] ALBRECHT 90J reports $0.041\pm0.015\pm0.016$ from a measurement of $[\Gamma(B^0\to D^*(2010)^-\pi^+\pi^+\pi^-\pi^0)/\Gamma_{total}]\times[B(D^*(2010)^+\to D^0\pi^+)]$ assuming $B(D^*(2010)^+\to D^0\pi^+)=0.57\pm0.06$, which we rescale to our best value $B(D^*(2010)^+\to D^0\pi^+)=(67.7\pm0.5)\times10^{-2}$. Our first error is their experiment's error and our second error is the systematic error from using our best value. Assumes equal production of B^+ and B^0 at the $\Upsilon(4S)$ and uses Mark III branching fractions for the D.

$\Gamma(D^{*-}3\pi^+2\pi^-)/\Gamma_{total}$ Γ_{61}/Γ

VALUE (units 10^{-3})	DOCUMENT ID		TECN	COMMENT
$4.72\pm0.59\pm0.71$	[1] MAJUMDER	04	BELL	$e^+e^-\to\ \Upsilon(4S)$

[1] Assumes equal production of B^+ and B^0 at the $\Upsilon(4S)$.

$\Gamma(\overline{D}^*(2010)^-\omega\pi^+)/\Gamma_{total}$ Γ_{62}/Γ

VALUE (units 10^{-3})	DOCUMENT ID		TECN	COMMENT
2.89 ± 0.30 OUR AVERAGE				
$2.88\pm0.21\pm0.31$	[1] AUBERT	06L	BABR	$e^+e^-\to\ \Upsilon(4S)$
$2.9\ \ \pm0.3\ \ \pm0.4$	[1,2] ALEXANDER	01B	CLE2	$e^+e^-\to\ \Upsilon(4S)$

[1] Assumes equal production of B^+ and B^0 at the $\Upsilon(4S)$.
[2] The signal is consistent with all observed $\omega\pi^+$ having proceeded through the ρ'^+ resonance at mass $1349\pm25^{+10}_{-\ 5}$ MeV and width $547\pm86^{+46}_{-45}$ MeV.

$\Gamma(D_1(2430)^0\omega\times B(D_1(2430)^0\to D^{*-}\pi^+))/\Gamma_{total}$ Γ_{63}/Γ

VALUE (units 10^{-4})	DOCUMENT ID		TECN	COMMENT
$4.1\pm1.2\pm1.1$	[1] AUBERT	06L	BABR	$e^+e^-\to\ \Upsilon(4S)$

[1] Obtained by fitting the events with $\cos\theta_{D^*}<0.5$ and scaling up the result by a factor of 4/3. No interference effects between $B^0\to D_1'\omega$ and $D^*\omega\pi$ are assumed.

$\Gamma(\overline{D}^{**-}\pi^+)/\Gamma_{total}$ Γ_{64}/Γ

D^{**-} represents an excited state with mass $2.2 < M < 2.8$ GeV/c^2.

VALUE (units 10^{-3})	DOCUMENT ID		TECN	COMMENT
2.1±1.0±0.1	[1,2] AUBERT,BE	06J	BABR	$e^+e^- \to \Upsilon(4S)$

[1] AUBERT,BE 06J reports $[\Gamma(B^0 \to \overline{D}^{**-}\pi^+)/\Gamma_{total}] / [B(B^0 \to D^-\pi^+)] = 0.77 \pm 0.22 \pm 0.29$ which we multiply by our best value $B(B^0 \to D^-\pi^+) = (2.68 \pm 0.13) \times 10^{-3}$. Our first error is their experiment's error and our second error is the systematic error from using our best value.

[2] Uses a missing-mass method. Does not depend on D branching fractions or B^+/B^0 production rates.

$\Gamma(D_1(2420)^-\pi^+ \times B(D_1^- \to D^-\pi^+\pi^-))/\Gamma_{total}$ Γ_{65}/Γ

VALUE (units 10^{-4})	DOCUMENT ID		TECN	COMMENT
$1.00^{+0.21}_{-0.25}$ OUR FIT				
$0.89\pm0.15^{+0.17}_{-0.32}$	[1] ABE	05A	BELL	$e^+e^- \to \Upsilon(4S)$

[1] Assumes equal production of B^+ and B^0 at the $\Upsilon(4S)$.

$\Gamma(D_1(2420)^-\pi^+ \times B(D_1^- \to D^-\pi^+\pi^-))/\Gamma(D^-\pi^+\pi^+\pi^-)$ Γ_{65}/Γ_{43}

VALUE (units 10^{-2})	DOCUMENT ID		TECN	COMMENT
$1.57^{+0.35}_{-0.40}$ OUR FIT				
2.1 ±0.5 $^{+0.3}_{-0.5}$	AAIJ	11E	LHCB	pp at 7 TeV

$\Gamma(D_1(2420)^-\pi^+ \times B(D_1^- \to D^{*-}\pi^+\pi^-))/\Gamma_{total}$ Γ_{66}/Γ

VALUE (units 10^{-4})	CL%	DOCUMENT ID		TECN	COMMENT
<0.33	90	[1] ABE	05A	BELL	$e^+e^- \to \Upsilon(4S)$

[1] Assumes equal production of B^+ and B^0 at the $\Upsilon(4S)$.

$\Gamma(D^*(2010)^-\pi^+\pi^+\pi^-)/\Gamma(D^*(2010)^-\pi^+)$ Γ_{54}/Γ_{41}

VALUE	DOCUMENT ID		TECN	COMMENT
2.64±0.04±0.13	AAIJ	13AO	LHCB	pp at 7 TeV

$\Gamma(\overline{D}_2^*(2460)^-\pi^+ \times B(D_2^*(2460)^- \to D^0\pi^-))/\Gamma_{total}$ Γ_{67}/Γ

VALUE (units 10^{-4})	CL%	DOCUMENT ID		TECN	COMMENT
2.15±0.17±0.31		[1,2] KUZMIN	07	BELL	$e^+e^- \to \Upsilon(4S)$
• • • We do not use the following data for averages, fits, limits, etc. • • •					
<14.7	90	[1] ALAM	94	CLE2	$e^+e^- \to \Upsilon(4S)$

[1] Assumes equal production of B^+ and B^0 at the $\Upsilon(4S)$.

[2] Our second uncertainty combines systematics and model errors quoted in the paper.

$\Gamma(\overline{D}_0^*(2400)^-\pi^+ \times B(D_0^*(2400)^- \to D^0\pi^-))/\Gamma_{total}$ Γ_{68}/Γ

VALUE (units 10^{-4})	DOCUMENT ID		TECN	COMMENT
0.60±0.13±0.27	[1,2] KUZMIN	07	BELL	$e^+e^- \to \Upsilon(4S)$

[1] Assumes equal production of B^+ and B^0 at the $\Upsilon(4S)$.

[2] Our second uncertainty combines systematics and model errors quoted in the paper.

$\Gamma(D_2^*(2460)^-\pi^+ \times B((D_2^*)^- \to D^{*-}\pi^+\pi^-))/\Gamma_{total}$ Γ_{69}/Γ

VALUE (units 10^{-4})	CL%	DOCUMENT ID		TECN	COMMENT
<0.24	90	[1] ABE	05A	BELL	$e^+e^- \to \Upsilon(4S)$

[1] Assumes equal production of B^+ and B^0 at the $\Upsilon(4S)$.

$\Gamma(\overline{D}_2^*(2460)^-\rho^+)/\Gamma_{total}$ Γ_{70}/Γ

VALUE	CL%	DOCUMENT ID		TECN	COMMENT
<0.0049	90	[1] ALAM	94	CLE2	$e^+e^- \to \Upsilon(4S)$

[1] ALAM 94 assumes equal production of B^+ and B^0 at the $\Upsilon(4S)$ and use the CLEO II absolute $B(D^0 \to K^-\pi^+)$ and $B(D_2^*(2460)^+ \to D^0\pi^+) = 30\%$.

$\Gamma(D^0\overline{D}^0)/\Gamma_{total}$ Γ_{71}/Γ

VALUE (units 10^{-4})	CL%	DOCUMENT ID		TECN	COMMENT
0.14±0.06±0.03		[1] AAIJ	13AP	LHCB	pp at 7 TeV
• • • We do not use the following data for averages, fits, limits, etc. • • •					
<0.43	90	[2] ADACHI	08	BELL	$e^+e^- \to \Upsilon(4S)$
<0.6	90	[2] AUBERT,B	06A	BABR	$e^+e^- \to \Upsilon(4S)$

[1] Uses $B(B^0 \to D^-D^+) = (2.11 \pm 0.31) \times 10^{-4}$ and $B(B^+ \to \overline{D}^0 D_s^+) = (10.1 \pm 1.7) \times 10^{-3}$.

[2] Assumes equal production of B^+ and B^0 at the $\Upsilon(4S)$.

$\Gamma(D^{*0}\overline{D}^0)/\Gamma_{total}$ Γ_{72}/Γ

VALUE (units 10^{-4})	CL%	DOCUMENT ID		TECN	COMMENT
<2.9	90	[1] AUBERT,B	06A	BABR	$e^+e^- \to \Upsilon(4S)$

[1] Assumes equal production of B^+ and B^0 at the $\Upsilon(4S)$.

$\Gamma(D^-D^+)/\Gamma_{total}$ Γ_{73}/Γ

VALUE (units 10^{-4})	CL%	DOCUMENT ID		TECN	COMMENT
2.11±0.18 OUR AVERAGE					
2.12±0.16±0.18		[1] ROHRKEN	12	BELL	$e^+e^- \to \Upsilon(4S)$
1.97±0.20±0.20		[1] FRATINA	07	BELL	$e^+e^- \to \Upsilon(4S)$
2.8 ±0.4 ±0.5		[1] AUBERT,B	06A	BABR	$e^+e^- \to \Upsilon(4S)$
• • • We do not use the following data for averages, fits, limits, etc. • • •					
1.91±0.51±0.30		[1] MAJUMDER	05	BELL	Repl. by FRATINA 07
< 9.4	90	[1] LIPELES	00	CLE2	$e^+e^- \to \Upsilon(4S)$
<59	90	BARATE	98Q	ALEP	$e^+e^- \to Z$
<12	90	ASNER	97	CLE2	$e^+e^- \to \Upsilon(4S)$

[1] Assumes equal production of B^+ and B^0 at the $\Upsilon(4S)$.

$\Gamma(D^\pm D^{*\mp}(CP\text{-averaged}))/\Gamma_{total}$ Γ_{74}/Γ

VALUE (units 10^{-4})	DOCUMENT ID		TECN	COMMENT
6.14±0.29±0.50	[1] ROHRKEN	12	BELL	$e^+e^- \to \Upsilon(4S)$

[1] Assumes equal production of B^+ and B^0 at the $\Upsilon(4S)$.

$\Gamma(D^-D_s^+)/\Gamma_{total}$ Γ_{75}/Γ

VALUE	EVTS	DOCUMENT ID		TECN	COMMENT
0.0072±0.0008 OUR AVERAGE					
0.0073±0.0004±0.0007		[1] ZUPANC	07	BELL	$e^+e^- \to \Upsilon(4S)$
0.0066±0.0014±0.0006		[2] AUBERT	06N	BABR	$e^+e^- \to \Upsilon(4S)$
0.0068±0.0024±0.0006		[3] GIBAUT	96	CLE2	$e^+e^- \to \Upsilon(4S)$
0.010 ±0.009 ±0.001		[4] ALBRECHT	92G	ARG	$e^+e^- \to \Upsilon(4S)$
0.0053±0.0030±0.0005		[5] BORTOLETTO	92	CLEO	$e^+e^- \to \Upsilon(4S)$
• • • We do not use the following data for averages, fits, limits, etc. • • •					
0.012 ±0.007	3	[6] BORTOLETTO	90	CLEO	$e^+e^- \to \Upsilon(4S)$

[1] ZUPANC 07 reports $(7.5 \pm 0.2 \pm 1.1) \times 10^{-3}$ from a measurement of $[\Gamma(B^0 \to D^-D_s^+)/\Gamma_{total}] \times [B(D_s^+ \to \phi\pi^+)]$ assuming $B(D_s^+ \to \phi\pi^+) = (4.4 \pm 0.6) \times 10^{-2}$, which we rescale to our best value $B(D_s^+ \to \phi\pi^+) = (4.5 \pm 0.4) \times 10^{-2}$. Our first error is their experiment's error and our second error is the systematic error from using our best value.

[2] AUBERT 06N reports $(0.64 \pm 0.13 \pm 0.10) \times 10^{-2}$ from a measurement of $[\Gamma(B^0 \to D^-D_s^+)/\Gamma_{total}] \times [B(D_s^+ \to \phi\pi^+)]$ assuming $B(D_s^+ \to \phi\pi^+) = 0.0462 \pm 0.0062$, which we rescale to our best value $B(D_s^+ \to \phi\pi^+) = (4.5 \pm 0.4) \times 10^{-2}$. Our first error is their experiment's error and our second error is the systematic error from using our best value.

[3] GIBAUT 96 reports $0.0087 \pm 0.0024 \pm 0.0020$ from a measurement of $[\Gamma(B^0 \to D^-D_s^+)/\Gamma_{total}] \times [B(D_s^+ \to \phi\pi^+)]$ assuming $B(D_s^+ \to \phi\pi^+) = 0.035$, which we rescale to our best value $B(D_s^+ \to \phi\pi^+) = (4.5 \pm 0.4) \times 10^{-2}$. Our first error is their experiment's error and our second error is the systematic error from using our best value.

[4] ALBRECHT 92G reports $0.017 \pm 0.013 \pm 0.006$ from a measurement of $[\Gamma(B^0 \to D^-D_s^+)/\Gamma_{total}] \times [B(D_s^+ \to \phi\pi^+)]$ assuming $B(D_s^+ \to \phi\pi^+) = 0.027$, which we rescale to our best value $B(D_s^+ \to \phi\pi^+) = (4.5 \pm 0.4) \times 10^{-2}$. Our first error is their experiment's error and our second error is the systematic error from using our best value. Assumes PDG 1990 D^+ branching ratios, e.g., $B(D^+ \to K^-2\pi^+) = 7.7 \pm 1.0\%$.

[5] BORTOLETTO 92 reports $0.0080 \pm 0.0045 \pm 0.0030$ from a measurement of $[\Gamma(B^0 \to D^-D_s^+)/\Gamma_{total}] \times [B(D_s^+ \to \phi\pi^+)]$ assuming $B(D_s^+ \to \phi\pi^+) = 0.030 \pm 0.011$, which we rescale to our best value $B(D_s^+ \to \phi\pi^+) = (4.5 \pm 0.4) \times 10^{-2}$. Our first error is their experiment's error and our second error is the systematic error from using our best value. Assumes equal production of B^+ and B^0 at the $\Upsilon(4S)$ and uses Mark III branching fractions for the D.

[6] BORTOLETTO 90 assume $B(D_s \to \phi\pi^+) = 2\%$. Superseded by BORTOLETTO 92.

$\Gamma(D^*(2010)^-D_s^+)/\Gamma_{total}$ Γ_{76}/Γ

VALUE	EVTS	DOCUMENT ID		TECN	COMMENT
0.0080±0.0011 OUR AVERAGE					
0.0073±0.0013±0.0007		[1] AUBERT	06N	BABR	$e^+e^- \to \Upsilon(4S)$
0.0083±0.0015±0.0007		[2] AUBERT	03I	BABR	$e^+e^- \to \Upsilon(4S)$
0.0088±0.0017±0.0008		[3] AHMED	00B	CLE2	$e^+e^- \to \Upsilon(4S)$
0.008 ±0.006 ±0.001		[4] ALBRECHT	92G	ARG	$e^+e^- \to \Upsilon(4S)$
0.011 ±0.006 ±0.001		[5] BORTOLETTO	92	CLEO	$e^+e^- \to \Upsilon(4S)$
• • • We do not use the following data for averages, fits, limits, etc. • • •					
0.0072±0.0022±0.0006		[6] GIBAUT	96	CLE2	Repl. by AHMED 00B
0.024 ±0.014	3	[7] BORTOLETTO	90	CLEO	$e^+e^- \to \Upsilon(4S)$

[1] AUBERT 06N reports $(0.71 \pm 0.13 \pm 0.09) \times 10^{-2}$ from a measurement of $[\Gamma(B^0 \to D^*(2010)^-D_s^+)/\Gamma_{total}] \times [B(D_s^+ \to \phi\pi^+)]$ assuming $B(D_s^+ \to \phi\pi^+) = 0.0462 \pm 0.0062$, which we rescale to our best value $B(D_s^+ \to \phi\pi^+) = (4.5 \pm 0.4) \times 10^{-2}$. Our first error is their experiment's error and our second error is the systematic error from using our best value.

[2] AUBERT 03I reports $0.0103 \pm 0.0014 \pm 0.0013$ from a measurement of $[\Gamma(B^0 \to D^*(2010)^-D_s^+)/\Gamma_{total}] \times [B(D_s^+ \to \phi\pi^+)]$ assuming $B(D_s^+ \to \phi\pi^+) = 0.036$, which we rescale to our best value $B(D_s^+ \to \phi\pi^+) = (4.5 \pm 0.4) \times 10^{-2}$. Our first error is their experiment's error and our second error is the systematic error from using our best value.

[3] AHMED 00B reports $0.0110 \pm 0.0018 \pm 0.0011$ from a measurement of $[\Gamma(B^0 \to D^*(2010)^-D_s^+)/\Gamma_{total}] \times [B(D_s^+ \to \phi\pi^+)]$ assuming $B(D_s^+ \to \phi\pi^+) = 0.036$,

which we rescale to our best value $B(D_s^+ \to \phi\pi^+) = (4.5 \pm 0.4) \times 10^{-2}$. Our first error is their experiment's error and our second error is the systematic error from using our best value.

[4] ALBRECHT 92G reports $0.014 \pm 0.010 \pm 0.003$ from a measurement of $[\Gamma(B^0 \to D^*(2010)^- D_s^+)/\Gamma_{total}] \times [B(D_s^+ \to \phi\pi^+)]$ assuming $B(D_s^+ \to \phi\pi^+) = 0.027$, which we rescale to our best value $B(D_s^+ \to \phi\pi^+) = (4.5 \pm 0.4) \times 10^{-2}$. Our first error is their experiment's error and our second error is the systematic error from using our best value. Assumes PDG 1990 D^+ and $D^*(2010)^+$ branching ratios, e.g., $B(D^0 \to K^-\pi^+) = 3.71 \pm 0.25\%$, $B(D^+ \to K^-2\pi^+) = 7.1 \pm 1.0\%$, and $B(D^*(2010)^+ \to D^0\pi^+) = 55 \pm 4\%$.

[5] BORTOLETTO 92 reports $0.016 \pm 0.009 \pm 0.006$ from a measurement of $[\Gamma(B^0 \to D^*(2010)^- D_s^+)/\Gamma_{total}] \times [B(D_s^+ \to \phi\pi^+)]$ assuming $B(D_s^+ \to \phi\pi^+) = 0.030 \pm 0.011$, which we rescale to our best value $B(D_s^+ \to \phi\pi^+) = (4.5 \pm 0.4) \times 10^{-2}$. Our first error is their experiment's error and our second error is the systematic error from using our best value. Assumes equal production of B^+ and B^0 at the $\Upsilon(4S)$ and uses Mark III branching fractions for the D and $D^*(2010)$.

[6] GIBAUT 96 reports $0.0093 \pm 0.0023 \pm 0.0016$ from a measurement of $[\Gamma(B^0 \to D^*(2010)^- D_s^+)/\Gamma_{total}] \times [B(D_s^+ \to \phi\pi^+)]$ assuming $B(D_s^+ \to \phi\pi^+) = 0.035$, which we rescale to our best value $B(D_s^+ \to \phi\pi^+) = (4.5 \pm 0.4) \times 10^{-2}$. Our first error is their experiment's error and our second error is the systematic error from using our best value.

[7] BORTOLETTO 90 assume $B(D_s \to \phi\pi^+) = 2\%$. Superseded by BORTOLETTO 92.

$\Gamma(D^- D_s^{*+})/\Gamma_{total}$ — Γ_{77}/Γ

VALUE	DOCUMENT ID		TECN	COMMENT
0.0074±0.0016 OUR AVERAGE				
0.0071±0.0016±0.0006	[1] AUBERT	06N	BABR	$e^+e^- \to \Upsilon(4S)$
0.0078±0.0032±0.0007	[2] GIBAUT	96	CLE2	$e^+e^- \to \Upsilon(4S)$
0.016 ±0.012 ±0.001	[3] ALBRECHT	92G	ARG	$e^+e^- \to \Upsilon(4S)$

[1] AUBERT 06N reports $(0.69 \pm 0.16 \pm 0.09) \times 10^{-2}$ from a measurement of $[\Gamma(B^0 \to D^- D_s^{*+})/\Gamma_{total}] \times [B(D_s^+ \to \phi\pi^+)]$ assuming $B(D_s^+ \to \phi\pi^+) = 0.0462 \pm 0.0062$, which we rescale to our best value $B(D_s^+ \to \phi\pi^+) = (4.5 \pm 0.4) \times 10^{-2}$. Our first error is their experiment's error and our second error is the systematic error from using our best value.

[2] GIBAUT 96 reports $0.0100 \pm 0.0035 \pm 0.0022$ from a measurement of $[\Gamma(B^0 \to D^- D_s^{*+})/\Gamma_{total}] \times [B(D_s^+ \to \phi\pi^+)]$ assuming $B(D_s^+ \to \phi\pi^+) = 0.035$, which we rescale to our best value $B(D_s^+ \to \phi\pi^+) = (4.5 \pm 0.4) \times 10^{-2}$. Our first error is their experiment's error and our second error is the systematic error from using our best value.

[3] ALBRECHT 92G reports $0.027 \pm 0.017 \pm 0.009$ from a measurement of $[\Gamma(B^0 \to D^- D_s^{*+})/\Gamma_{total}] \times [B(D_s^+ \to \phi\pi^+)]$ assuming $B(D_s^+ \to \phi\pi^+) = 0.027$, which we rescale to our best value $B(D_s^+ \to \phi\pi^+) = (4.5 \pm 0.4) \times 10^{-2}$. Our first error is their experiment's error and our second error is the systematic error from using our best value. Assumes PDG 1990 D^+ branching ratios, e.g., $B(D^+ \to K^-2\pi^+) = 7.7 \pm 1.0\%$.

$\Gamma(D^*(2010)^- D_s^{*+})/\Gamma_{total}$ — Γ_{78}/Γ

VALUE	DOCUMENT ID		TECN	COMMENT
0.0177±0.0014 OUR AVERAGE				
0.0173±0.0018±0.0015	[1] AUBERT	06N	BABR	$e^+e^- \to \Upsilon(4S)$
0.0188±0.0009±0.0017	[2] AUBERT	05V	BABR	$e^+e^- \to \Upsilon(4S)$
0.0158±0.0027±0.0014	[3] AUBERT	03I	BABR	$e^+e^- \to \Upsilon(4S)$
0.015 ±0.004 ±0.001	[4] AHMED	00B	CLE2	$e^+e^- \to \Upsilon(4S)$
0.016 ±0.009 ±0.001	[5] ALBRECHT	92G	ARG	$e^+e^- \to \Upsilon(4S)$
• • • We do not use the following data for averages, fits, limits, etc. • • •				
0.016 ±0.005 ±0.001	[6] GIBAUT	96	CLE2	Repl. by AHMED 00B

[1] AUBERT 06N reports $(1.68 \pm 0.21 \pm 0.19) \times 10^{-2}$ from a measurement of $[\Gamma(B^0 \to D^*(2010)^- D_s^{*+})/\Gamma_{total}] \times [B(D_s^+ \to \phi\pi^+)]$ assuming $B(D_s^+ \to \phi\pi^+) = 0.0462 \pm 0.0062$, which we rescale to our best value $B(D_s^+ \to \phi\pi^+) = (4.5 \pm 0.4) \times 10^{-2}$. Our first error is their experiment's error and our second error is the systematic error from using our best value.

[2] A partial reconstruction technique is used and the result is independent of the particle decay rate of D_S^+ meson. It also provides a model-independent determination of $B(D_S^+ \to \phi\pi^+) = (4.81 \pm 0.52 \pm 0.38)\%$.

[3] AUBERT 03I reports $0.0197 \pm 0.0015 \pm 0.0030$ from a measurement of $[\Gamma(B^0 \to D^*(2010)^- D_s^{*+})/\Gamma_{total}] \times [B(D_s^+ \to \phi\pi^+)]$ assuming $B(D_s^+ \to \phi\pi^+) = 0.036$, which we rescale to our best value $B(D_s^+ \to \phi\pi^+) = (4.5 \pm 0.4) \times 10^{-2}$. Our first error is their experiment's error and our second error is the systematic error from using our best value.

[4] AHMED 00B reports $0.0182 \pm 0.0037 \pm 0.0025$ from a measurement of $[\Gamma(B^0 \to D^*(2010)^- D_s^{*+})/\Gamma_{total}] \times [B(D_s^+ \to \phi\pi^+)]$ assuming $B(D_s^+ \to \phi\pi^+) = 0.036$, which we rescale to our best value $B(D_s^+ \to \phi\pi^+) = (4.5 \pm 0.4) \times 10^{-2}$. Our first error is their experiment's error and our second error is the systematic error from using our best value.

[5] ALBRECHT 92G reports $0.026 \pm 0.014 \pm 0.006$ from a measurement of $[\Gamma(B^0 \to D^*(2010)^- D_s^{*+})/\Gamma_{total}] \times [B(D_s^+ \to \phi\pi^+)]$ assuming $B(D_s^+ \to \phi\pi^+) = 0.027$, which we rescale to our best value $B(D_s^+ \to \phi\pi^+) = (4.5 \pm 0.4) \times 10^{-2}$. Our first error is their experiment's error and our second error is the systematic error from using our best value. Assumes PDG 1990 D^+ and $D^*(2010)^+$ branching ratios, e.g., $B(D^0 \to K^-\pi^+) = 3.71 \pm 0.25\%$, $B(D^+ \to K^-2\pi^+) = 7.1 \pm 1.0\%$, and $B(D^*(2010)^+ \to D^0\pi^+) = 55 \pm 4\%$.

[6] GIBAUT 96 reports $0.0203 \pm 0.0050 \pm 0.0036$ from a measurement of $[\Gamma(B^0 \to D^*(2010)^- D_s^{*+})/\Gamma_{total}] \times [B(D_s^+ \to \phi\pi^+)]$ assuming $B(D_s^+ \to \phi\pi^+) = 0.035$, which we rescale to our best value $B(D_s^+ \to \phi\pi^+) = (4.5 \pm 0.4) \times 10^{-2}$. Our first error is their experiment's error and our second error is the systematic error from using our best value.

$\left[\Gamma(D^*(2010)^- D_s^+) + \Gamma(D^*(2010)^- D_s^{*+})\right]/\Gamma_{total}$ — $(\Gamma_{76}+\Gamma_{78})/\Gamma$

VALUE (units 10^{-2})	EVTS	DOCUMENT ID		TECN	COMMENT
2.5 ±0.4 OUR AVERAGE					
2.40±0.35±0.22		[1] AUBERT	03I	BABR	$e^+e^- \to \Upsilon(4S)$
3.3 ±0.9 ±0.3	22	[2] BORTOLETTO	90	CLEO	$e^+e^- \to \Upsilon(4S)$

[1] AUBERT 03I reports $(3.00 \pm 0.19 \pm 0.39) \times 10^{-2}$ from a measurement of $\left[\Gamma(B^0 \to D^*(2010)^- D_s^+) + \Gamma(B^0 \to D^*(2010)^- D_s^{*+})\right]/\Gamma_{total}] \times [B(D_s^+ \to \phi\pi^+)]$ assuming $B(D_s^+ \to \phi\pi^+) = 0.036$, which we rescale to our best value $B(D_s^+ \to \phi\pi^+) = (4.5 \pm 0.4) \times 10^{-2}$. Our first error is their experiment's error and our second error is the systematic error from using our best value.

[2] BORTOLETTO 90 reports $(7.5 \pm 2.0) \times 10^{-2}$ from a measurement of $\left[\left[\Gamma(B^0 \to D^*(2010)^- D_s^+) + \Gamma(B^0 \to D^*(2010)^- D_s^{*+})\right]/\Gamma_{total}] \times [B(D_s^+ \to \phi\pi^+)]$ assuming $B(D_s^+ \to \phi\pi^+) = 0.02$, which we rescale to our best value $B(D_s^+ \to \phi\pi^+) = (4.5 \pm 0.4) \times 10^{-2}$. Our first error is their experiment's error and our second error is the systematic error from using our best value.

$\Gamma(D_{s0}(2317)^- K^+ \times B(D_{s0}(2317)^- \to D_s^-\pi^0))/\Gamma_{total}$ — Γ_{79}/Γ

VALUE (units 10^{-5})	DOCUMENT ID		TECN	COMMENT
$\mathbf{4.2^{+1.4}_{-1.3}\pm0.4}$	[1] DRUTSKOY	05	BELL	$e^+e^- \to \Upsilon(4S)$

[1] DRUTSKOY 05 reports $(5.3^{+1.5}_{-1.3} \pm 1.6) \times 10^{-5}$ from a measurement of $[\Gamma(B^0 \to D_{s0}(2317)^- K^+ \times B(D_{s0}(2317)^- \to D_s^-\pi^0))/\Gamma_{total}] \times [B(D_s^+ \to \phi\pi^+)]$ assuming $B(D_s^+ \to \phi\pi^+) = 0.036 \pm 0.009$, which we rescale to our best value $B(D_s^+ \to \phi\pi^+) = (4.5 \pm 0.4) \times 10^{-2}$. Our first error is their experiment's error and our second error is the systematic error from using our best value.

$\Gamma(D_{s0}(2317)^- \pi^+ \times B(D_{s0}(2317)^- \to D_s^-\pi^0))/\Gamma_{total}$ — Γ_{80}/Γ

VALUE (units 10^{-5})	CL%	DOCUMENT ID		TECN	COMMENT
<2.5	90	[1] DRUTSKOY	05	BELL	$e^+e^- \to \Upsilon(4S)$

[1] Assumes equal production of B^+ and B^0 at the $\Upsilon(4S)$.

$\Gamma(D_{sJ}(2457)^- K^+ \times B(D_{sJ}(2457)^- \to D_s^-\pi^0))/\Gamma_{total}$ — Γ_{81}/Γ

VALUE (units 10^{-5})	CL%	DOCUMENT ID		TECN	COMMENT
<0.94	90	[1] DRUTSKOY	05	BELL	$e^+e^- \to \Upsilon(4S)$

[1] Assumes equal production of B^+ and B^0 at the $\Upsilon(4S)$.

$\Gamma(D_{sJ}(2457)^- \pi^+ \times B(D_{sJ}(2457)^- \to D_s^-\pi^0))/\Gamma_{total}$ — Γ_{82}/Γ

VALUE (units 10^{-5})	CL%	DOCUMENT ID		TECN	COMMENT
<0.40	90	[1] DRUTSKOY	05	BELL	$e^+e^- \to \Upsilon(4S)$

[1] Assumes equal production of B^+ and B^0 at the $\Upsilon(4S)$.

$\Gamma(D_s^- D_s^+)/\Gamma_{total}$ — Γ_{83}/Γ

VALUE	CL%	DOCUMENT ID		TECN	COMMENT
$\mathbf{< 3.6 \times 10^{-5}}$	90	[1] ZUPANC	07	BELL	$e^+e^- \to \Upsilon(4S)$
• • • We do not use the following data for averages, fits, limits, etc. • • •					
$<10 \times 10^{-5}$	90	[1] AUBERT,BE	05F	BABR	$e^+e^- \to \Upsilon(4S)$

[1] Assumes equal production of B^+ and B^0 at the $\Upsilon(4S)$.

$\Gamma(D_s^{*-} D_s^+)/\Gamma_{total}$ — Γ_{84}/Γ

VALUE	CL%	DOCUMENT ID		TECN	COMMENT
$\mathbf{< 1.3 \times 10^{-4}}$	90	[1] AUBERT,BE	05F	BABR	$e^+e^- \to \Upsilon(4S)$

[1] Assumes equal production of B^+ and B^0 at the $\Upsilon(4S)$.

$\Gamma(D_s^{*-} D_s^{*+})/\Gamma_{total}$ — Γ_{85}/Γ

VALUE	CL%	DOCUMENT ID		TECN	COMMENT
$\mathbf{< 2.4 \times 10^{-4}}$	90	[1] AUBERT,BE	05F	BABR	$e^+e^- \to \Upsilon(4S)$

[1] Assumes equal production of B^+ and B^0 at the $\Upsilon(4S)$.

$\Gamma(D_{s0}(2317)^+ D^- \times B(D_{s0}(2317)^+ \to D_s^+\pi^0))/\Gamma_{total}$ — Γ_{86}/Γ

VALUE (units 10^{-3})	DOCUMENT ID		TECN	COMMENT
$\mathbf{0.97^{+0.40}_{-0.33}}$ **OUR AVERAGE** Error includes scale factor of 1.5.				
$1.4\ ^{+0.5}_{-0.4} \pm 0.1$	[1,2] AUBERT,B	04S	BABR	$e^+e^- \to \Upsilon(4S)$
$0.69^{+0.29}_{-0.24} \pm 0.06$	[1,3] KROKOVNY	03B	BELL	$e^+e^- \to \Upsilon(4S)$

[1] Assumes equal production of B^+ and B^0 at the $\Upsilon(4S)$.

[2] AUBERT,B 04S reports $(1.8 \pm 0.4^{+0.7}_{-0.5}) \times 10^{-3}$ from a measurement of $[\Gamma(B^0 \to D_{s0}(2317)^+ D^- \times B(D_{s0}(2317)^+ \to D_s^+ \pi^0))/\Gamma_{total}] \times [B(D_s^+ \to \phi\pi^+)]$ assuming $B(D_s^+ \to \phi\pi^+) = 0.036 \pm 0.009$, which we rescale to our best value $B(D_s^+ \to \phi\pi^+) = (4.5 \pm 0.4) \times 10^{-2}$. Our first error is their experiment's error and our second error is the systematic error from using our best value.

[3] KROKOVNY 03B reports $(0.86^{+0.33}_{-0.26} \pm 0.26) \times 10^{-3}$ from a measurement of $[\Gamma(B^0 \to D_{s0}(2317)^+ D^- \times B(D_{s0}(2317)^+ \to D_s^+ \pi^0))/\Gamma_{total}] \times [B(D_s^+ \to \phi\pi^+)]$ assuming $B(D_s^+ \to \phi\pi^+) = 0.036 \pm 0.009$, which we rescale to our best value $B(D_s^+ \to \phi\pi^+) = (4.5 \pm 0.4) \times 10^{-2}$. Our first error is their experiment's error and our second error is the systematic error from using our best value.

$\Gamma(D_{s0}(2317)^+ D^- \times B(D_{s0}(2317)^+ \to D_s^{*+}\gamma))/\Gamma_{total}$ Γ_{87}/Γ

VALUE (units 10^{-3})	CL%	DOCUMENT ID		TECN	COMMENT
<0.95	90	[1] KROKOVNY	03B	BELL	$e^+e^- \to \Upsilon(4S)$

[1] Assumes equal production of B^+ and B^0 at the $\Upsilon(4S)$.

$\Gamma(D_{s0}(2317)^+ D^*(2010)^- \times B(D_{s0}(2317)^+ \to D_s^+\pi^0))/\Gamma_{total}$ Γ_{88}/Γ

VALUE (units 10^{-3})	DOCUMENT ID		TECN	COMMENT
$1.5 \pm 0.4^{+0.5}_{-0.4}$	[1] AUBERT,B	04S	BABR	$e^+e^- \to \Upsilon(4S)$

[1] Assumes equal production of B^+ and B^0 at the $\Upsilon(4S)$.

$\Gamma(D_{sJ}(2457)^+ D^-)/\Gamma_{total}$ Γ_{89}/Γ

VALUE (units 10^{-3})	DOCUMENT ID		TECN	COMMENT
3.5 ± 1.1 OUR AVERAGE				
$2.6 \pm 1.5 \pm 0.7$	[1] AUBERT	06N	BABR	$e^+e^- \to \Upsilon(4S)$
$4.8^{+2.2}_{-1.6} \pm 1.1$	[2,3] AUBERT,B	04S	BABR	$e^+e^- \to \Upsilon(4S)$
$3.9^{+1.5}_{-1.3} \pm 0.9$	[2,4] KROKOVNY	03B	BELL	$e^+e^- \to \Upsilon(4S)$

[1] Uses a missing-mass method in the events that one of the B mesons is fully reconstructed.

[2] Assumes equal production of B^+ and B^0 at the $\Upsilon(4S)$.

[3] AUBERT,B 04S reports $[\Gamma(B^0 \to D_{sJ}(2457)^+ D^-)/\Gamma_{total}] \times [B(D_{s1}(2460)^+ \to D_s^{*+}\pi^0)] = (2.3^{+1.0}_{-0.7} \pm 0.3) \times 10^{-3}$ which we divide by our best value $B(D_{s1}(2460)^+ \to D_s^{*+}\pi^0) = (48 \pm 11) \times 10^{-2}$. Our first error is their experiment's error and our second error is the systematic error from using our best value.

[4] KROKOVNY 03B reports $[\Gamma(B^0 \to D_{sJ}(2457)^+ D^-)/\Gamma_{total}] \times [B(D_{s1}(2460)^+ \to D_s^{*+}\pi^0)] = (1.9^{+0.7}_{-0.6} \pm 0.2) \times 10^{-3}$ which we divide by our best value $B(D_{s1}(2460)^+ \to D_s^{*+}\pi^0) = (48 \pm 11) \times 10^{-2}$. Our first error is their experiment's error and our second error is the systematic error from using our best value.

$\Gamma(D_{sJ}(2457)^+ D^- \times B(D_{sJ}(2457)^+ \to D_s^+\gamma))/\Gamma_{total}$ Γ_{90}/Γ

VALUE (units 10^{-3})	DOCUMENT ID		TECN	COMMENT
$0.65^{+0.17}_{-0.14}$ OUR AVERAGE				
$0.64^{+0.24}_{-0.16} \pm 0.06$	[1,2] AUBERT,B	04S	BABR	$e^+e^- \to \Upsilon(4S)$
$0.66^{+0.21}_{-0.19} \pm 0.06$	[1,3] KROKOVNY	03B	BELL	$e^+e^- \to \Upsilon(4S)$

[1] Assumes equal production of B^+ and B^0 at the $\Upsilon(4S)$.

[2] AUBERT,B 04S reports $(0.8 \pm 0.2^{+0.3}_{-0.2}) \times 10^{-3}$ from a measurement of $[\Gamma(B^0 \to D_{sJ}(2457)^+ D^- \times B(D_{sJ}(2457)^+ \to D_s^+\gamma))/\Gamma_{total}] \times [B(D_s^+ \to \phi\pi^+)]$ assuming $B(D_s^+ \to \phi\pi^+) = 0.036 \pm 0.009$, which we rescale to our best value $B(D_s^+ \to \phi\pi^+) = (4.5 \pm 0.4) \times 10^{-2}$. Our first error is their experiment's error and our second error is the systematic error from using our best value.

[3] KROKOVNY 03B reports $(0.82^{+0.22}_{-0.19} \pm 0.25) \times 10^{-3}$ from a measurement of $[\Gamma(B^0 \to D_{sJ}(2457)^+ D^- \times B(D_{sJ}(2457)^+ \to D_s^+\gamma))/\Gamma_{total}] \times [B(D_s^+ \to \phi\pi^+)]$ assuming $B(D_s^+ \to \phi\pi^+) = 0.036 \pm 0.009$, which we rescale to our best value $B(D_s^+ \to \phi\pi^+) = (4.5 \pm 0.4) \times 10^{-2}$. Our first error is their experiment's error and our second error is the systematic error from using our best value.

$\Gamma(D_{sJ}(2457)^+ D^- \times B(D_{sJ}(2457)^+ \to D_s^{*+}\gamma))/\Gamma_{total}$ Γ_{91}/Γ

VALUE (units 10^{-3})	CL%	DOCUMENT ID		TECN	COMMENT
<0.60	90	[1] KROKOVNY	03B	BELL	$e^+e^- \to \Upsilon(4S)$

[1] Assumes equal production of B^+ and B^0 at the $\Upsilon(4S)$.

$\Gamma(D_{sJ}(2457)^+ D^- \times B(D_{sJ}(2457)^+ \to D_s^+\pi^+\pi^-))/\Gamma_{total}$ Γ_{92}/Γ

VALUE (units 10^{-3})	CL%	DOCUMENT ID		TECN	COMMENT
<0.20	90	[1] KROKOVNY	03B	BELL	$e^+e^- \to \Upsilon(4S)$

[1] Assumes equal production of B^+ and B^0 at the $\Upsilon(4S)$.

$\Gamma(D_{sJ}(2457)^+ D^- \times B(D_{sJ}(2457)^+ \to D_s^+\pi^0))/\Gamma_{total}$ Γ_{93}/Γ

VALUE (units 10^{-3})	CL%	DOCUMENT ID		TECN	COMMENT
<0.36	90	[1] KROKOVNY	03B	BELL	$e^+e^- \to \Upsilon(4S)$

[1] Assumes equal production of B^+ and B^0 at the $\Upsilon(4S)$.

$\Gamma(D^*(2010)^- D_{sJ}(2457)^+)/\Gamma_{total}$ Γ_{94}/Γ

VALUE (units 10^{-3})	DOCUMENT ID		TECN	COMMENT
9.3 ± 2.2 OUR AVERAGE				
$8.8 \pm 2.0 \pm 1.4$	[1] AUBERT	06N	BABR	$e^+e^- \to \Upsilon(4S)$
$11\ ^{+5}_{-4} \pm 3$	[2,3] AUBERT,B	04S	BABR	$e^+e^- \to \Upsilon(4S)$

[1] Uses a missing-mass method in the events that one of the B mesons is fully reconstructed.

[2] AUBERT,B 04S reports $[\Gamma(B^0 \to D^*(2010)^- D_{sJ}(2457)^+)/\Gamma_{total}] \times [B(D_{s1}(2460)^+ \to D_s^{*+}\pi^0)] = (5.5 \pm 1.2^{+2.2}_{-1.6}) \times 10^{-3}$ which we divide by our best value $B(D_{s1}(2460)^+ \to D_s^{*+}\pi^0) = (48 \pm 11) \times 10^{-2}$. Our first error is their experiment's error and our second error is the systematic error from using our best value.

[3] Assumes equal production of B^+ and B^0 at the $\Upsilon(4S)$.

$\Gamma(D_{sJ}(2457)^+ D^*(2010) \times B(D_{sJ}(2457)^+ \to D_s^+\gamma))/\Gamma_{total}$ Γ_{95}/Γ

VALUE (units 10^{-3})	DOCUMENT ID		TECN	COMMENT
$2.3 \pm 0.3^{+0.9}_{-0.6}$	[1] AUBERT,B	04S	BABR	$e^+e^- \to \Upsilon(4S)$

[1] Assumes equal production of B^+ and B^0 at the $\Upsilon(4S)$.

$\Gamma(D^- D_{s1}(2536)^+ \times B(D_{s1}(2536)^+ \to D^{*0}K^+ + D^{*+}K^0))/\Gamma_{total}$ $\Gamma_{96}/\Gamma = (\Gamma_{97}+\Gamma_{98})/\Gamma$

VALUE (units 10^{-4})	DOCUMENT ID		TECN	COMMENT
$2.75 \pm 0.62 \pm 0.36$	[1,2] AUSHEV	11	BELL	$e^+e^- \to \Upsilon(4S)$

[1] Uses $\Gamma(D^*(2007)^0 \to D^0\pi^0)\ /\ \Gamma(D^*(2007)^0 \to D^0\gamma) = 1.74 \pm 0.13$ and $\Gamma(D_{s1}(2536)^+ \to D^*(2007)^0 K^+)\ /\ \Gamma(D_{s1}(2536)^+ \to D^*(2010)^+ K^0) = 1.36 \pm 0.2$.

[2] Assumes equal production of B^+ and B^0 at the $\Upsilon(4S)$.

$\Gamma(D^- D_{s1}(2536)^+ \times B(D_{s1}(2536)^+ \to D^{*0}K^+))/\Gamma_{total}$ Γ_{97}/Γ

VALUE (units 10^{-4})	CL%	DOCUMENT ID		TECN	COMMENT
$1.71 \pm 0.48 \pm 0.32$		[1] AUBERT	08B	BABR	$e^+e^- \to \Upsilon(4S)$
• • • We do not use the following data for averages, fits, limits, etc. • • •					
<5	90	AUBERT	03X	BABR	Repl. by AUBERT 08B

[1] Assumes equal production of B^+ and B^0 at the $\Upsilon(4S)$.

$\Gamma(D^- D_{s1}(2536)^+ \times B(D_{s1}(2536)^+ \to D^{*+}K^0))/\Gamma_{total}$ Γ_{98}/Γ

VALUE (units 10^{-4})	DOCUMENT ID		TECN	COMMENT
$2.61 \pm 1.03 \pm 0.31$	[1] AUBERT	08B	BABR	$e^+e^- \to \Upsilon(4S)$

[1] Assumes equal production of B^+ and B^0 at the $\Upsilon(4S)$.

$\Gamma(D^*(2010)^- D_{s1}(2536)^+ \times B(D_{s1}(2536)^+ \to D^{*0}K^+ + D^{*+}K^0))/\Gamma_{total}$ $\Gamma_{99}/\Gamma = (\Gamma_{100}+\Gamma_{101})/\Gamma$

VALUE (units 10^{-4})	DOCUMENT ID		TECN	COMMENT
$5.01 \pm 1.21 \pm 0.70$	[1,2] AUSHEV	11	BELL	$e^+e^- \to \Upsilon(4S)$

[1] Uses $\Gamma(D^*(2007)^0 \to D^0\pi^0)\ /\ \Gamma(D^*(2007)^0 \to D^0\gamma) = 1.74 \pm 0.13$ and $\Gamma(D_{s1}(2536)^+ \to D^*(2007)^0 K^+)\ /\ \Gamma(D_{s1}(2536)^+ \to D^*(2010)^+ K^0) = 1.36 \pm 0.2$.

[2] Assumes equal production of B^+ and B^0 at the $\Upsilon(4S)$.

$\Gamma(D^*(2010)^- D_{s1}(2536)^+ \times B(D_{s1}(2536)^+ \to D^{*0}K^+))/\Gamma_{total}$ Γ_{100}/Γ

VALUE (units 10^{-4})	CL%	DOCUMENT ID		TECN	COMMENT
$3.32 \pm 0.88 \pm 0.66$		[1] AUBERT	08B	BABR	$e^+e^- \to \Upsilon(4S)$
• • • We do not use the following data for averages, fits, limits, etc. • • •					
<7	90	AUBERT	03X	BABR	Repl. by AUBERT 08B

[1] Assumes equal production of B^+ and B^0 at the $\Upsilon(4S)$.

$\Gamma(D^{*-} D_{s1}(2536)^+ \times B(D_{s1}(2536)^+ \to D^{*+}K^0))/\Gamma_{total}$ Γ_{101}/Γ

VALUE (units 10^{-4})	DOCUMENT ID		TECN	COMMENT
$5.00 \pm 1.51 \pm 0.67$	[1] AUBERT	08B	BABR	$e^+e^- \to \Upsilon(4S)$

[1] Assumes equal production of B^+ and B^0 at the $\Upsilon(4S)$.

$\Gamma(D^- D_{sJ}(2573)^+ \times B(D_{sJ}(2573)^+ \to D^0K^+))/\Gamma_{total}$ Γ_{102}/Γ

VALUE (units 10^{-4})	CL%	DOCUMENT ID		TECN	COMMENT
<1	90	AUBERT	03X	BABR	$e^+e^- \to \Upsilon(4S)$

$\Gamma(D^*(2010)^- D_{sJ}(2573)^+ \times B(D_{sJ}(2573)^+ \to D^0K^+))/\Gamma_{total}$ Γ_{103}/Γ

VALUE (units 10^{-4})	CL%	DOCUMENT ID		TECN	COMMENT
<2	90	AUBERT	03X	BABR	$e^+e^- \to \Upsilon(4S)$

$\Gamma(D^+\pi^-)/\Gamma_{total}$ Γ_{104}/Γ

VALUE (units 10^{-7})	DOCUMENT ID		TECN	COMMENT
$7.8 \pm 1.3 \pm 0.4$	[1,2] DAS	10	BELL	$e^+e^- \to \Upsilon(4S)$

[1] DAS 10 reports $[\Gamma(B^0 \to D^+\pi^-)/\Gamma_{total}]\ /\ [B(B^0 \to D^-\pi^+)] = (2.92 \pm 0.38 \pm 0.31) \times 10^{-4}$ which we multiply by our best value $B(B^0 \to D^-\pi^+) = (2.68 \pm 0.13) \times 10^{-3}$. Our first error is their experiment's error and our second error is the systematic error from using our best value.

[2] Derived using $\tan(\theta_C)\ f_D/f_{D_s}\ \sqrt{B(B^0 \to D_s^+\pi^-)/B(B^0 \to D^-\pi^+)}$ by assuming the flavor SU(3) symmetry, where θ_C is the Cabibbo angle, f_D (f_{D_s}) is the D (D_s) meson decay constant.

$\Gamma(D_s^+\pi^-)/\Gamma_{total}$ Γ_{105}/Γ

VALUE (units 10^{-6})	CL%	DOCUMENT ID		TECN	COMMENT
21.6±2.6 OUR AVERAGE					
19.9±2.6±1.8		[1] DAS	10	BELL	$e^+e^- \to \Upsilon(4S)$
25 ±4 ±2		[1] AUBERT	08AJ	BABR	$e^+e^- \to \Upsilon(4S)$
• • • We do not use the following data for averages, fits, limits, etc. • • •					
14.0±3.5±1.3		[2] AUBERT	07K	BABR	Repl. by AUBERT 08AJ
25 ±9 ±2		[3] AUBERT	03D	BABR	Repl. by AUBERT 07K
19 $^{+9}_{-7}$ ±2		[4] KROKOVNY	02	BELL	Repl. by DAS 10
< 220	90	[5] ALEXANDER	93B	CLE2	$e^+e^- \to \Upsilon(4S)$
<1300	90	[6] BORTOLETTO	90	CLEO	$e^+e^- \to \Upsilon(4S)$

[1] Assumes equal production of B^+ and B^0 at the $\Upsilon(4S)$.

[2] AUBERT 07K reports $[\Gamma(B^0 \to D_s^+\pi^-)/\Gamma_{total}] \times [B(D_s^+ \to \phi\pi^+)] = (0.63\pm0.15\pm0.05)\times10^{-6}$ which we divide by our best value $B(D_s^+ \to \phi\pi^+) = (4.5\pm0.4)\times10^{-2}$. Our first error is their experiment's error and our second error is the systematic error from using our best value.

[3] AUBERT 03D reports $[\Gamma(B^0 \to D_s^+\pi^-)/\Gamma_{total}] \times [B(D_s^+ \to \phi\pi^+)] = (1.13\pm0.33\pm0.21)\times10^{-6}$ which we divide by our best value $B(D_s^+ \to \phi\pi^+) = (4.5\pm0.4)\times10^{-2}$. Our first error is their experiment's error and our second error is the systematic error from using our best value.

[4] KROKOVNY 02 reports $[\Gamma(B^0 \to D_s^+\pi^-)/\Gamma_{total}] \times [B(D_s^+ \to \phi\pi^+)] = (0.86^{+0.37}_{-0.30} \pm 0.11)\times10^{-6}$ which we divide by our best value $B(D_s^+ \to \phi\pi^+) = (4.5\pm0.4)\times10^{-2}$. Our first error is their experiment's error and our second error is the systematic error from using our best value.

[5] ALEXANDER 93B reports $< 270\times10^{-6}$ from a measurement of $[\Gamma(B^0 \to D_s^+\pi^-)/\Gamma_{total}] \times [B(D_s^+ \to \phi\pi^+)]$ assuming $B(D_s^+ \to \phi\pi^+) = 0.037$, which we rescale to our best value $B(D_s^+ \to \phi\pi^+) = 4.5\times10^{-2}$.

[6] BORTOLETTO 90 assume $B(D_s \to \phi\pi^+) = 2\%$.

$[\Gamma(D_s^+\pi^-) + \Gamma(D_s^-K^+)]/\Gamma_{total}$ $(\Gamma_{105}+\Gamma_{115})/\Gamma$

VALUE	CL%	DOCUMENT ID		TECN	COMMENT
<1.0 × 10⁻³	90	[1] ALBRECHT	93E	ARG	$e^+e^- \to \Upsilon(4S)$

[1] ALBRECHT 93E reports $< 1.7\times10^{-3}$ from a measurement of $[\left[\Gamma(B^0 \to D_s^+\pi^-) + \Gamma(B^0 \to D_s^-K^+)\right]/\Gamma_{total}] \times [B(D_s^+ \to \phi\pi^+)]$ assuming $B(D_s^+ \to \phi\pi^+) = 0.027$, which we rescale to our best value $B(D_s^+ \to \phi\pi^+) = 4.5\times10^{-2}$.

$\Gamma(D_s^{*+}\pi^-)/\Gamma_{total}$ Γ_{106}/Γ

VALUE (units 10^{-5})	CL%	DOCUMENT ID		TECN	COMMENT
2.1 ±0.4 OUR AVERAGE		Error includes scale factor of 1.4.			
1.75±0.34±0.20		[1] JOSHI	10	BELL	$e^+e^- \to \Upsilon(4S)$
2.6 $^{+0.5}_{-0.4}$ ±0.2		[1] AUBERT	08AJ	BABR	$e^+e^- \to \Upsilon(4S)$
• • • We do not use the following data for averages, fits, limits, etc. • • •					
2.9 ±0.7 ±0.3		[2] AUBERT	07K	BABR	Repl. by AUBERT 08AJ
< 4.1	90	AUBERT	03D	BABR	Repl. by AUBERT 07K
<40	90	[3] ALEXANDER	93B	CLE2	$e^+e^- \to \Upsilon(4S)$

[1] Assumes equal production of B^+ and B^0 at the $\Upsilon(4S)$.

[2] AUBERT 07K reports $[\Gamma(B^0 \to D_s^{*+}\pi^-)/\Gamma_{total}] \times [B(D_s^+ \to \phi\pi^+)] = (1.32\pm0.27\pm0.15)\times10^{-6}$ which we divide by our best value $B(D_s^+ \to \phi\pi^+) = (4.5\pm0.4)\times10^{-2}$. Our first error is their experiment's error and our second error is the systematic error from using our best value.

[3] ALEXANDER 93B reports $< 44\times10^{-5}$ from a measurement of $[\Gamma(B^0 \to D_s^{*+}\pi^-)/\Gamma_{total}] \times [B(D_s^+ \to \phi\pi^+)]$ assuming $B(D_s^+ \to \phi\pi^+) = 0.037$, which we rescale to our best value $B(D_s^+ \to \phi\pi^+) = 4.5\times10^{-2}$.

$[\Gamma(D_s^{*+}\pi^-) + \Gamma(D_s^{*-}K^+)]/\Gamma_{total}$ $(\Gamma_{106}+\Gamma_{116})/\Gamma$

VALUE	CL%	DOCUMENT ID		TECN	COMMENT
<7 × 10⁻⁴	90	[1] ALBRECHT	93E	ARG	$e^+e^- \to \Upsilon(4S)$

[1] ALBRECHT 93E reports $< 1.2\times10^{-3}$ from a measurement of $[\left[\Gamma(B^0 \to D_s^{*+}\pi^-) + \Gamma(B^0 \to D_s^{*-}K^+)\right]/\Gamma_{total}] \times [B(D_s^+ \to \phi\pi^+)]$ assuming $B(D_s^+ \to \phi\pi^+) = 0.027$, which we rescale to our best value $B(D_s^+ \to \phi\pi^+) = 4.5\times10^{-2}$.

$\Gamma(D_s^+\rho^-)/\Gamma_{total}$ Γ_{107}/Γ

VALUE (units 10^{-5})	CL%	DOCUMENT ID		TECN	COMMENT
< 2.4	90	[1] AUBERT	08AJ	BABR	$e^+e^- \to \Upsilon(4S)$
• • • We do not use the following data for averages, fits, limits, etc. • • •					
<130	90	[2] ALBRECHT	93E	ARG	$e^+e^- \to \Upsilon(4S)$
< 50	90	[3] ALEXANDER	93B	CLE2	$e^+e^- \to \Upsilon(4S)$

[1] Assumes equal production of B^+ and B^0 at the $\Upsilon(4S)$.

[2] ALBRECHT 93E reports $< 2.2\times10^{-3}$ from a measurement of $[\Gamma(B^0 \to D_s^+\rho^-)/\Gamma_{total}] \times [B(D_s^+ \to \phi\pi^+)]$ assuming $B(D_s^+ \to \phi\pi^+) = 0.027$, which we rescale to our best value $B(D_s^+ \to \phi\pi^+) = 4.5\times10^{-2}$.

[3] ALEXANDER 93B reports $< 6.6\times10^{-4}$ from a measurement of $[\Gamma(B^0 \to D_s^+\rho^-)/\Gamma_{total}] \times [B(D_s^+ \to \phi\pi^+)]$ assuming $B(D_s^+ \to \phi\pi^+) = 0.037$, which we rescale to our best value $B(D_s^+ \to \phi\pi^+) = 4.5\times10^{-2}$.

$\Gamma(D_s^{*+}\rho^-)/\Gamma_{total}$ Γ_{108}/Γ

VALUE (units 10^{-5})	CL%	DOCUMENT ID		TECN	COMMENT
4.1 $^{+1.3}_{-1.2}$ ±0.4		[1] AUBERT	08AJ	BABR	$e^+e^- \to \Upsilon(4S)$
• • • We do not use the following data for averages, fits, limits, etc. • • •					
<150	90	[2] ALBRECHT	93E	ARG	$e^+e^- \to \Upsilon(4S)$
< 60	90	[3] ALEXANDER	93B	CLE2	$e^+e^- \to \Upsilon(4S)$

[1] Assumes equal production of B^+ and B^0 at the $\Upsilon(4S)$.

[2] ALBRECHT 93E reports $< 2.5\times10^{-3}$ from a measurement of $[\Gamma(B^0 \to D_s^{*+}\rho^-)/\Gamma_{total}] \times [B(D_s^+ \to \phi\pi^+)]$ assuming $B(D_s^+ \to \phi\pi^+) = 0.027$, which we rescale to our best value $B(D_s^+ \to \phi\pi^+) = 4.5\times10^{-2}$.

[3] ALEXANDER 93B reports $< 7.4\times10^{-4}$ from a measurement of $[\Gamma(B^0 \to D_s^{*+}\rho^-)/\Gamma_{total}] \times [B(D_s^+ \to \phi\pi^+)]$ assuming $B(D_s^+ \to \phi\pi^+) = 0.037$, which we rescale to our best value $B(D_s^+ \to \phi\pi^+) = 4.5\times10^{-2}$.

$\Gamma(D_s^+a_0^-)/\Gamma_{total}$ Γ_{109}/Γ

VALUE (units 10^{-5})	CL%	DOCUMENT ID		TECN	COMMENT
<1.9	90	[1] AUBERT	06X	BABR	$e^+e^- \to \Upsilon(4S)$

[1] Assumes equal production of B^+ and B^0 at the $\Upsilon(4S)$.

$\Gamma(D_s^{*+}a_0^-)/\Gamma_{total}$ Γ_{110}/Γ

VALUE (units 10^{-5})	CL%	DOCUMENT ID		TECN	COMMENT
<3.6	90	[1] AUBERT	06X	BABR	$e^+e^- \to \Upsilon(4S)$

[1] Assumes equal production of B^+ and B^0 at the $\Upsilon(4S)$.

$\Gamma(D_s^+a_1(1260)^-)/\Gamma_{total}$ Γ_{111}/Γ

VALUE	CL%	DOCUMENT ID		TECN	COMMENT
<2.1 × 10⁻³	90	[1] ALBRECHT	93E	ARG	$e^+e^- \to \Upsilon(4S)$

[1] ALBRECHT 93E reports $< 3.5\times10^{-3}$ from a measurement of $[\Gamma(B^0 \to D_s^+a_1(1260)^-)/\Gamma_{total}] \times [B(D_s^+ \to \phi\pi^+)]$ assuming $B(D_s^+ \to \phi\pi^+) = 0.027$, which we rescale to our best value $B(D_s^+ \to \phi\pi^+) = 4.5\times10^{-2}$.

$\Gamma(D_s^{*+}a_1(1260)^-)/\Gamma_{total}$ Γ_{112}/Γ

VALUE	CL%	DOCUMENT ID		TECN	COMMENT
<1.7 × 10⁻³	90	[1] ALBRECHT	93E	ARG	$e^+e^- \to \Upsilon(4S)$

[1] ALBRECHT 93E reports $< 2.9\times10^{-3}$ from a measurement of $[\Gamma(B^0 \to D_s^{*+}a_1(1260)^-)/\Gamma_{total}] \times [B(D_s^+ \to \phi\pi^+)]$ assuming $B(D_s^+ \to \phi\pi^+) = 0.027$, which we rescale to our best value $B(D_s^+ \to \phi\pi^+) = 4.5\times10^{-2}$.

$\Gamma(D_s^+a_2^-)/\Gamma_{total}$ Γ_{113}/Γ

VALUE (units 10^{-5})	CL%	DOCUMENT ID		TECN	COMMENT
<19	90	[1] AUBERT	06X	BABR	$e^+e^- \to \Upsilon(4S)$

[1] Assumes equal production of B^+ and B^0 at the $\Upsilon(4S)$.

$\Gamma(D_s^{*+}a_2^-)/\Gamma_{total}$ Γ_{114}/Γ

VALUE (units 10^{-5})	CL%	DOCUMENT ID		TECN	COMMENT
<20	90	[1] AUBERT	06X	BABR	$e^+e^- \to \Upsilon(4S)$

[1] Assumes equal production of B^+ and B^0 at the $\Upsilon(4S)$.

$\Gamma(D_s^-K^+)/\Gamma_{total}$ Γ_{115}/Γ

VALUE (units 10^{-6})	CL%	DOCUMENT ID		TECN	COMMENT
22 ± 5 OUR AVERAGE		Error includes scale factor of 1.8.			
19.1± 2.4±1.7		[1] DAS	10	BELL	$e^+e^- \to \Upsilon(4S)$
29 ± 4 ±2		[1] AUBERT	08AJ	BABR	$e^+e^- \to \Upsilon(4S)$
• • • We do not use the following data for averages, fits, limits, etc. • • •					
27 ± 5 ±2		[2] AUBERT	07K	BABR	Repl. by AUBERT 08AJ
26 ±10 ±2		[3] AUBERT	03D	BABR	Repl. by AUBERT 07K
36 $^{+11}_{-10}$ ±3		[4] KROKOVNY	02	BELL	Repl. by DAS 10
< 190	90	[5] ALEXANDER	93B	CLE2	$e^+e^- \to \Upsilon(4S)$
<1300	90	[6] BORTOLETTO	90	CLEO	$e^+e^- \to \Upsilon(4S)$

[1] Assumes equal production of B^+ and B^0 at the $\Upsilon(4S)$.

[2] AUBERT 07K reports $[\Gamma(B^0 \to D_s^-K^+)/\Gamma_{total}] \times [B(D_s^+ \to \phi\pi^+)] = (1.21\pm0.17\pm0.11)\times10^{-6}$ which we divide by our best value $B(D_s^+ \to \phi\pi^+) = (4.5\pm0.4)\times10^{-2}$. Our first error is their experiment's error and our second error is the systematic error from using our best value.

[3] AUBERT 03D reports $[\Gamma(B^0 \to D_s^-K^+)/\Gamma_{total}] \times [B(D_s^+ \to \phi\pi^+)] = (1.16\pm0.36\pm0.24)\times10^{-6}$ which we divide by our best value $B(D_s^+ \to \phi\pi^+) = (4.5\pm0.4)\times10^{-2}$. Our first error is their experiment's error and our second error is the systematic error from using our best value.

[4] KROKOVNY 02 reports $[\Gamma(B^0 \to D_s^-K^+)/\Gamma_{total}] \times [B(D_s^+ \to \phi\pi^+)] = (1.61^{+0.45}_{-0.38} \pm 0.21)\times10^{-6}$ which we divide by our best value $B(D_s^+ \to \phi\pi^+) = (4.5\pm0.4)\times10^{-2}$. Our first error is their experiment's error and our second error is the systematic error from using our best value.

[5] ALEXANDER 93B reports $< 230\times10^{-6}$ from a measurement of $[\Gamma(B^0 \to D_s^-K^+)/\Gamma_{total}] \times [B(D_s^+ \to \phi\pi^+)]$ assuming $B(D_s^+ \to \phi\pi^+) = 0.037$, which we rescale to our best value $B(D_s^+ \to \phi\pi^+) = 4.5\times10^{-2}$.

[6] BORTOLETTO 90 assume $B(D_s \to \phi\pi^+) = 2\%$.

$\Gamma(D_s^{*-}K^+)/\Gamma_{total}$ Γ_{116}/Γ

VALUE (units 10^{-5})	CL%	DOCUMENT ID		TECN	COMMENT
2.19±0.30 OUR AVERAGE					
2.02±0.33±0.22		[1] JOSHI	10	BELL	$e^+e^- \to \Upsilon(4S)$
2.4 ±0.4 ±0.2		[1] AUBERT	08AJ	BABR	$e^+e^- \to \Upsilon(4S)$
• • • We do not use the following data for averages, fits, limits, etc. • • •					
2.2 ±0.6 ±0.2		[2] AUBERT	07K	BABR	Repl. by AUBERT 08AJ
< 2.5	90	AUBERT	03D	BABR	Repl. by AUBERT 07K
<14	90	[3] ALEXANDER	93B	CLE2	$e^+e^- \to \Upsilon(4S)$

[1] Assumes equal production of B^+ and B^0 at the $\Upsilon(4S)$.

[2] AUBERT 07K reports $[\Gamma(B^0 \to D_s^{*-}K^+)/\Gamma_{total}] \times [B(D_s^+ \to \phi\pi^+)] = (0.97\pm0.24\pm0.12)\times10^{-6}$ which we divide by our best value $B(D_s^+ \to \phi\pi^+) = (4.5\pm0.4)\times10^{-2}$. Our first error is their experiment's error and our second error is the systematic error from using our best value.

[3] ALEXANDER 93B reports $< 17\times10^{-5}$ from a measurement of $[\Gamma(B^0 \to D_s^{*-}K^+)/\Gamma_{total}] \times [B(D_s^+ \to \phi\pi^+)]$ assuming $B(D_s^+ \to \phi\pi^+) = 0.037$, which we rescale to our best value $B(D_s^+ \to \phi\pi^+) = 4.5\times10^{-2}$.

$\Gamma(D_s^-K^*(892)^+)/\Gamma_{total}$ Γ_{117}/Γ

VALUE (units 10^{-5})	CL%	DOCUMENT ID		TECN	COMMENT
$\mathbf{3.5^{+1.0}_{-0.9}\pm0.4}$		[1] AUBERT	08AJ	BABR	$e^+e^- \to \Upsilon(4S)$
• • • We do not use the following data for averages, fits, limits, etc. • • •					
<280	90	[2] ALBRECHT	93E	ARG	$e^+e^- \to \Upsilon(4S)$
< 80	90	[3] ALEXANDER	93B	CLE2	$e^+e^- \to \Upsilon(4S)$

[1] Assumes equal production of B^+ and B^0 at the $\Upsilon(4S)$.

[2] ALBRECHT 93E reports $< 4.6\times10^{-3}$ from a measurement of $[\Gamma(B^0 \to D_s^-K^*(892)^+)/\Gamma_{total}] \times [B(D_s^+ \to \phi\pi^+)]$ assuming $B(D_s^+ \to \phi\pi^+) = 0.027$, which we rescale to our best value $B(D_s^+ \to \phi\pi^+) = 4.5\times10^{-2}$.

[3] ALEXANDER 93B reports $< 9.7\times10^{-4}$ from a measurement of $[\Gamma(B^0 \to D_s^-K^*(892)^+)/\Gamma_{total}] \times [B(D_s^+ \to \phi\pi^+)]$ assuming $B(D_s^+ \to \phi\pi^+) = 0.037$, which we rescale to our best value $B(D_s^+ \to \phi\pi^+) = 4.5\times10^{-2}$.

$\Gamma(D_s^{*-}K^*(892)^+)/\Gamma_{total}$ Γ_{118}/Γ

VALUE (units 10^{-5})	CL%	DOCUMENT ID		TECN	COMMENT
$\mathbf{3.2^{+1.4}_{-1.2}\pm0.4}$		[1] AUBERT	08AJ	BABR	$e^+e^- \to \Upsilon(4S)$
• • • We do not use the following data for averages, fits, limits, etc. • • •					
<350	90	[2] ALBRECHT	93E	ARG	$e^+e^- \to \Upsilon(4S)$
< 90	90	[3] ALEXANDER	93B	CLE2	$e^+e^- \to \Upsilon(4S)$

[1] Assumes equal production of B^+ and B^0 at the $\Upsilon(4S)$.

[2] ALBRECHT 93E reports $< 5.8\times10^{-3}$ from a measurement of $[\Gamma(B^0 \to D_s^{*-}K^*(892)^+)/\Gamma_{total}] \times [B(D_s^+ \to \phi\pi^+)]$ assuming $B(D_s^+ \to \phi\pi^+) = 0.027$, which we rescale to our best value $B(D_s^+ \to \phi\pi^+) = 4.5\times10^{-2}$.

[3] ALEXANDER 93B reports $< 11.0\times10^{-4}$ from a measurement of $[\Gamma(B^0 \to D_s^{*-}K^*(892)^+)/\Gamma_{total}] \times [B(D_s^+ \to \phi\pi^+)]$ assuming $B(D_s^+ \to \phi\pi^+) = 0.037$, which we rescale to our best value $B(D_s^+ \to \phi\pi^+) = 4.5\times10^{-2}$.

$\Gamma(D_s^-\pi^+K^0)/\Gamma_{total}$ Γ_{119}/Γ

VALUE (units 10^{-4})	CL%	DOCUMENT ID		TECN	COMMENT
1.10±0.26±0.20		[1] AUBERT	08G	BABR	$e^+e^- \to \Upsilon(4S)$
• • • We do not use the following data for averages, fits, limits, etc. • • •					
<40	90	[2] ALBRECHT	93E	ARG	$e^+e^- \to \Upsilon(4S)$

[1] Assumes equal production of B^+ and B^0 at the $\Upsilon(4S)$.

[2] ALBRECHT 93E reports $< 7.3\times10^{-3}$ from a measurement of $[\Gamma(B^0 \to D_s^-\pi^+K^0)/\Gamma_{total}] \times [B(D_s^+ \to \phi\pi^+)]$ assuming $B(D_s^+ \to \phi\pi^+) = 0.027$, which we rescale to our best value $B(D_s^+ \to \phi\pi^+) = 4.5\times10^{-2}$.

$\Gamma(D_s^{*-}\pi^+K^0)/\Gamma_{total}$ Γ_{120}/Γ

VALUE (units 10^{-4})	CL%	DOCUMENT ID		TECN	COMMENT
< 1.10	90	[1] AUBERT	08G	BABR	$e^+e^- \to \Upsilon(4S)$
• • • We do not use the following data for averages, fits, limits, etc. • • •					
<25	90	[2] ALBRECHT	93E	ARG	$e^+e^- \to \Upsilon(4S)$

[1] Assumes equal production of B^+ and B^0 at the $\Upsilon(4S)$.

[2] ALBRECHT 93E reports $< 4.2\times10^{-3}$ from a measurement of $[\Gamma(B^0 \to D_s^{*-}\pi^+K^0)/\Gamma_{total}] \times [B(D_s^+ \to \phi\pi^+)]$ assuming $B(D_s^+ \to \phi\pi^+) = 0.027$, which we rescale to our best value $B(D_s^+ \to \phi\pi^+) = 4.5\times10^{-2}$.

$\Gamma(D_s^-K^+\pi^+\pi^-)/\Gamma_{total}$ Γ_{121}/Γ

VALUE (units 10^{-4})	DOCUMENT ID		TECN	COMMENT
1.8±0.3±0.4	[1] AAIJ	12AX	LHCB	pp at 7 TeV

[1] AAIJ 12AX reports $[\Gamma(B^0 \to D_s^-K^+\pi^+\pi^-)/\Gamma_{total}] / [B(B_s^0 \to D_s^-K^+\pi^+\pi^-)] = 0.54 \pm 0.07 \pm 0.07$ which we multiply by our best value $B(B_s^0 \to D_s^-K^+\pi^+\pi^-) = (3.3 \pm 0.7)\times10^{-4}$. Our first error is their experiment's error and our second error is the systematic error from using our best value.

$\Gamma(D_s^-\pi^+K^*(892)^0)/\Gamma_{total}$ Γ_{122}/Γ

VALUE	CL%	DOCUMENT ID		TECN	COMMENT
<3.0 × 10⁻³	90	[1] ALBRECHT	93E	ARG	$e^+e^- \to \Upsilon(4S)$

[1] ALBRECHT 93E reports $< 5.0\times10^{-3}$ from a measurement of $[\Gamma(B^0 \to D_s^-\pi^+K^*(892)^0)/\Gamma_{total}] \times [B(D_s^+ \to \phi\pi^+)]$ assuming $B(D_s^+ \to \phi\pi^+) = 0.027$, which we rescale to our best value $B(D_s^+ \to \phi\pi^+) = 4.5\times10^{-2}$.

$\Gamma(D_s^{*-}\pi^+K^*(892)^0)/\Gamma_{total}$ Γ_{123}/Γ

VALUE	CL%	DOCUMENT ID		TECN	COMMENT
<1.6 × 10⁻³	90	[1] ALBRECHT	93E	ARG	$e^+e^- \to \Upsilon(4S)$

[1] ALBRECHT 93E reports $< 2.7\times10^{-3}$ from a measurement of $[\Gamma(B^0 \to D_s^{*-}\pi^+K^*(892)^0)/\Gamma_{total}] \times [B(D_s^+ \to \phi\pi^+)]$ assuming $B(D_s^+ \to \phi\pi^+) = 0.027$, which we rescale to our best value $B(D_s^+ \to \phi\pi^+) = 4.5\times10^{-2}$.

$\Gamma(\overline{D}^0K^0)/\Gamma_{total}$ Γ_{124}/Γ

VALUE (units 10^{-5})	DOCUMENT ID		TECN	COMMENT
5.2±0.7 OUR AVERAGE				
5.3±0.7±0.3	[1] AUBERT,B	06L	BABR	$e^+e^- \to \Upsilon(4S)$
$5.0^{+1.3}_{-1.2}\pm0.6$	[1] KROKOVNY	03	BELL	$e^+e^- \to \Upsilon(4S)$

[1] Assumes equal production of B^+ and B^0 at the $\Upsilon(4S)$.

$\Gamma(\overline{D}^0K^+\pi^-)/\Gamma_{total}$ Γ_{125}/Γ

VALUE (units 10^{-6})	DOCUMENT ID		TECN	COMMENT
88±15±9	[1] AUBERT	06A	BABR	$e^+e^- \to \Upsilon(4S)$

[1] Assumes equal production of B^+ and B^0 at the $\Upsilon(4S)$.

$\Gamma(\overline{D}^0K^+\pi^-)/\Gamma(\overline{D}^0\pi^+\pi^-)$ Γ_{125}/Γ_{40}

VALUE	DOCUMENT ID		TECN	COMMENT
0.106±0.007±0.008	AAIJ	13AQ	LHCB	pp at 7 TeV

$\Gamma(\overline{D}^0K^*(892)^0)/\Gamma_{total}$ Γ_{126}/Γ

VALUE (units 10^{-5})	DOCUMENT ID		TECN	COMMENT
4.2±0.6 OUR AVERAGE				
4.0±0.7±0.3	[1] AUBERT,B	06L	BABR	$e^+e^- \to \Upsilon(4S)$
$4.8^{+1.1}_{-1.0}\pm0.5$	[1] KROKOVNY	03	BELL	$e^+e^- \to \Upsilon(4S)$
• • • We do not use the following data for averages, fits, limits, etc. • • •				
5.7±0.9±0.6	[1] AUBERT	06A	BABR	Repl. by AUBERT,B 06L

[1] Assumes equal production of B^+ and B^0 at the $\Upsilon(4S)$.

$\Gamma(D_2^*(2460)^-K^+ \times B(D_2^*(2460)^- \to \overline{D}^0\pi^-))/\Gamma_{total}$ Γ_{127}/Γ

VALUE (units 10^{-6})	DOCUMENT ID		TECN	COMMENT
18.3±4.0±3.1	[1] AUBERT	06A	BABR	$e^+e^- \to \Upsilon(4S)$

[1] Assumes equal production of B^+ and B^0 at the $\Upsilon(4S)$.

$\Gamma(\overline{D}^0K^+\pi^-\text{non-resonant})/\Gamma_{total}$ Γ_{128}/Γ

VALUE (units 10^{-6})	CL%	DOCUMENT ID		TECN	COMMENT
<37	90	[1] AUBERT	06A	BABR	$e^+e^- \to \Upsilon(4S)$

[1] Assumes equal production of B^+ and B^0 at the $\Upsilon(4S)$.

$\Gamma([K^+K^-]_D K^*(892)^0)/\Gamma(\overline{D}^0K^*(892)^0)$ $\Gamma_{129}/\Gamma_{126}$

VALUE	DOCUMENT ID		TECN	COMMENT
$\mathbf{1.36^{+0.37}_{-0.32}\pm0.07}$	AAIJ	13L	LHCB	pp at 7 TeV

$\Gamma(\overline{D}^0\pi^0)/\Gamma_{total}$ Γ_{130}/Γ

VALUE (units 10^{-4})	CL%	DOCUMENT ID		TECN	COMMENT
2.63±0.14 OUR AVERAGE					
2.69±0.09±0.13		[1] LEES	11M	BABR	$e^+e^- \to \Upsilon(4S)$
2.25±0.14±0.35		[1] BLYTH	06	BELL	$e^+e^- \to \Upsilon(4S)$
$2.74^{+0.36}_{-0.32}\pm0.55$		[1] COAN	02	CLE2	$e^+e^- \to \Upsilon(4S)$
• • • We do not use the following data for averages, fits, limits, etc. • • •					
2.9 ±0.2 ±0.3		[1] AUBERT	04B	BABR	Repl. by LEES 11M
3.1 ±0.4 ±0.5		[1] ABE	02J	BELL	Repl. by BLYTH 06
<1.2	90	[2] NEMATI	98	CLE2	Repl. by COAN 02
<4.8	90	[3] ALAM	94	CLE2	Repl. by NEMATI 98

[1] Assumes equal production of B^+ and B^0 at the $\Upsilon(4S)$.

[2] NEMATI 98 assumes equal production of B^+ and B^0 at the $\Upsilon(4S)$ and use the PDG 96 values for D^0, D^{*0}, η, η', and ω branching fractions.

[3] ALAM 94 assume equal production of B^+ and B^0 at the $\Upsilon(4S)$ and use the CLEO II absolute $B(D^0 \to K^-\pi^+\pi^0)$ and the PDG 1992 $B(D^0 \to K^-\pi^+\pi^0)/B(D^0 \to K^-\pi^+)$ and $B(D^0 \to K^-2\pi^+\pi^-)/B(D^0 \to K^-\pi^+)$.

$\Gamma(\overline{D}^0\rho^0)/\Gamma_{total}$ Γ_{131}/Γ

VALUE (units 10^{-4})	CL%	DOCUMENT ID		TECN	COMMENT
3.19±0.20±0.45		[1,2] KUZMIN	07	BELL	$e^+e^- \to \Upsilon(4S)$
• • • We do not use the following data for averages, fits, limits, etc. • • •					
2.9 ±1.0 ±0.4		[1] SATPATHY	03	BELL	Repl. by KUZMIN 07
< 3.9	90	[3] NEMATI	98	CLE2	$e^+e^- \to \Upsilon(4S)$
< 5.5	90	[4] ALAM	94	CLE2	Repl. by NEMATI 98
< 6.0	90	[5] BORTOLETTO	92	CLEO	$e^+e^- \to \Upsilon(4S)$
<27.0	90	[6] ALBRECHT	88K	ARG	$e^+e^- \to \Upsilon(4S)$

[1] Assumes equal production of B^+ and B^0 at the $\Upsilon(4S)$.
[2] Our second uncertainty combines systematics and model errors quoted in the paper.
[3] NEMATI 98 assumes equal production of B^+ and B^0 at the $\Upsilon(4S)$ and use the PDG 96 values for D^0, D^{*0}, η, η', and ω branching fractions.
[4] ALAM 94 assume equal production of B^+ and B^0 at the $\Upsilon(4S)$ and use the CLEO II absolute B($D^0 \to K^-\pi^+$) and the PDG 1992 B($D^0 \to K^-\pi^+\pi^0$)/B($D^0 \to K^-\pi^+$) and B($D^0 \to K^-2\pi^+\pi^-$)/B($D^0 \to K^-\pi^+$).
[5] BORTOLETTO 92 assumes equal production of B^+ and B^0 at the $\Upsilon(4S)$ and uses Mark III branching fractions for the D.
[6] ALBRECHT 88K reports < 0.003 assuming $B^0\overline{B}^0$:B^+B^- production ratio is 45:55. We rescale to 50%.

$\Gamma(\overline{D}^0 f_2)/\Gamma_{total}$ Γ_{132}/Γ

VALUE (units 10^{-4})	DOCUMENT ID		TECN	COMMENT
1.20±0.18±0.38	[1,2] KUZMIN	07	BELL	$e^+e^- \to \Upsilon(4S)$

[1] Assumes equal production of B^+ and B^0 at the $\Upsilon(4S)$.
[2] Our second uncertainty combines systematics and model errors quoted in the paper.

$\Gamma(\overline{D}^0\eta)/\Gamma_{total}$ Γ_{133}/Γ

VALUE (units 10^{-4})	CL%	DOCUMENT ID		TECN	COMMENT
2.36±0.32 OUR AVERAGE		Error includes scale factor of 2.5.			
2.53±0.09±0.11		[1] LEES	11M	BABR	$e^+e^- \to \Upsilon(4S)$
1.77±0.16±0.21		[1] BLYTH	06	BELL	$e^+e^- \to \Upsilon(4S)$
• • • We do not use the following data for averages, fits, limits, etc. • • •					
2.5 ±0.2 ±0.3		[1] AUBERT	04B	BABR	Repl. by LEES 11M
1.4 $^{+0.5}_{-0.4}$ ±0.3		[1] ABE	02J	BELL	Repl. by BLYTH 06
<1.3	90	[2] NEMATI	98	CLE2	$e^+e^- \to \Upsilon(4S)$
<6.8	90	[3] ALAM	94	CLE2	Repl. by NEMATI 98

[1] Assumes equal production of B^+ and B^0 at the $\Upsilon(4S)$.
[2] NEMATI 98 assumes equal production of B^+ and B^0 at the $\Upsilon(4S)$ and use the PDG 96 values for D^0, D^{*0}, η, η', and ω branching fractions.
[3] ALAM 94 assume equal production of B^+ and B^0 at the $\Upsilon(4S)$ and use the CLEO II absolute B($D^0 \to K^-\pi^+$) and the PDG 1992 B($D^0 \to K^-\pi^+\pi^0$)/B($D^0 \to K^-\pi^+$) and B($D^0 \to K^-2\pi^+\pi^-$)/B($D^0 \to K^-\pi^+$).

$\Gamma(\overline{D}^0\eta')/\Gamma_{total}$ Γ_{134}/Γ

VALUE (units 10^{-4})	CL%	DOCUMENT ID		TECN	COMMENT
1.38±0.16 OUR AVERAGE		Error includes scale factor of 1.3.			
1.48±0.13±0.07		[1] LEES	11M	BABR	$e^+e^- \to \Upsilon(4S)$
1.14±0.20 $^{+0.10}_{-0.13}$		[1] SCHUMANN	05	BELL	$e^+e^- \to \Upsilon(4S)$
• • • We do not use the following data for averages, fits, limits, etc. • • •					
1.7 ±0.4 ±0.2		[1] AUBERT	04B	BABR	Repl. by LEES 11M
<9.4	90	[2] NEMATI	98	CLE2	$e^+e^- \to \Upsilon(4S)$
<8.6	90	[3] ALAM	94	CLE2	Repl. by NEMATI 98

[1] Assumes equal production of B^+ and B^0 at the $\Upsilon(4S)$.
[2] NEMATI 98 assumes equal production of B^+ and B^0 at the $\Upsilon(4S)$ and use the PDG 96 values for D^0, D^{*0}, η, η', and ω branching fractions.
[3] ALAM 94 assume equal production of B^+ and B^0 at the $\Upsilon(4S)$ and use the CLEO II absolute B($D^0 \to K^-\pi^+$) and the PDG 1992 B($D^0 \to K^-\pi^+\pi^0$)/B($D^0 \to K^-\pi^+$) and B($D^0 \to K^-2\pi^+\pi^-$)/B($D^0 \to K^-\pi^+$).

$\Gamma(\overline{D}^0\eta')/\Gamma(\overline{D}^0\eta)$ $\Gamma_{134}/\Gamma_{133}$

VALUE	DOCUMENT ID		TECN	COMMENT
0.54±0.07±0.01	LEES	11M	BABR	$e^+e^- \to \Upsilon(4S)$
• • • We do not use the following data for averages, fits, limits, etc. • • •				
0.7 ±0.2 ±0.1	AUBERT	04B	BABR	Repl. by LEES 11M

$\Gamma(\overline{D}^0\omega)/\Gamma_{total}$ Γ_{135}/Γ

VALUE (units 10^{-4})	CL%	DOCUMENT ID		TECN	COMMENT
2.53±0.16 OUR AVERAGE					
2.57±0.11±0.14		[1] LEES	11M	BABR	$e^+e^- \to \Upsilon(4S)$
2.37±0.23±0.28		[1] BLYTH	06	BELL	$e^+e^- \to \Upsilon(4S)$
• • • We do not use the following data for averages, fits, limits, etc. • • •					
3.0 ±0.3 ±0.4		[1] AUBERT	04B	BABR	Repl. by LEES 11M
1.8 ±0.5 $^{+0.4}_{-0.3}$		[1] ABE	02J	BELL	Repl. by BLYTH 06
<5.1	90	[2] NEMATI	98	CLE2	$e^+e^- \to \Upsilon(4S)$
<6.3	90	[3] ALAM	94	CLE2	Repl. by NEMATI 98

[1] Assumes equal production of B^+ and B^0 at the $\Upsilon(4S)$.
[2] NEMATI 98 assumes equal production of B^+ and B^0 at the $\Upsilon(4S)$ and use the PDG 96 values for D^0, D^{*0}, η, η', and ω branching fractions.
[3] ALAM 94 assume equal production of B^+ and B^0 at the $\Upsilon(4S)$ and use the CLEO II absolute B($D^0 \to K^-\pi^+$) and the PDG 1992 B($D^0 \to K^-\pi^+\pi^0$)/B($D^0 \to K^-\pi^+$) and B($D^0 \to K^-2\pi^+\pi^-$)/B($D^0 \to K^-\pi^+$).

$\Gamma(D^0\phi)/\Gamma_{total}$ Γ_{136}/Γ

VALUE (units 10^{-6})	CL%	DOCUMENT ID		TECN	COMMENT
<11.6	90	[1] AUBERT	07AO	BABR	$e^+e^- \to \Upsilon(4S)$

[1] Assumes equal production of B^+ and B^0 at the $\Upsilon(4S)$.

$\Gamma(D^0K^+\pi^-)/\Gamma_{total}$ Γ_{137}/Γ

VALUE (units 10^{-6})	CL%	DOCUMENT ID		TECN	COMMENT
• • • We do not use the following data for averages, fits, limits, etc. • • •					
<19	90	[1] AUBERT	06A	BABR	Repl. by AUBERT 09AE

[1] Assumes equal production of B^+ and B^0 at the $\Upsilon(4S)$.

$\Gamma(D^0K^+\pi^-)/\Gamma(\overline{D}^0K^+\pi^-)$ $\Gamma_{137}/\Gamma_{125}$

VALUE	DOCUMENT ID		TECN	COMMENT
0.060±0.034 OUR AVERAGE				
0.045 $^{+0.056}_{-0.050}$ $^{+0.028}_{-0.018}$	[1,2] NEGISHI	12	BELL	$e^+e^- \to \Upsilon(4S)$
0.068±0.042	[3] AUBERT	09AE	BABR	$e^+e^- \to \Upsilon(4S)$

[1] Assumes equal production of B^0 and B^+ from $\Upsilon(4S)$ decays.
[2] Uses $D^0 \to K^-\pi^+$ mode. Restricts $K^+\pi^-$ mass within ±50 MeV of the nominal K^{*0} mass. Corresponds to the upper limit, < 0.16 at 95% CL.
[3] Reports a signal at the level of 2.5 standard deviations after combining results from $D^0 \to K^+\pi^-$, $K^+\pi^-\pi^0$, and $K^+\pi^-\pi^+\pi^-$.

$\Gamma(D^0K^*(892)^0)/\Gamma_{total}$ Γ_{138}/Γ

VALUE (units 10^{-5})	CL%	DOCUMENT ID		TECN	COMMENT
<1.1	90	[1] AUBERT,B	06L	BABR	$e^+e^- \to \Upsilon(4S)$
• • • We do not use the following data for averages, fits, limits, etc. • • •					
<1.8	90	[1] KROKOVNY	03	BELL	$e^+e^- \to \Upsilon(4S)$

[1] Assumes equal production of B^+ and B^0 at the $\Upsilon(4S)$.

$\Gamma(\overline{D}^{*0}\gamma)/\Gamma_{total}$ Γ_{139}/Γ

VALUE	CL%	DOCUMENT ID		TECN	COMMENT
<2.5 × 10^{-5}	90	[1] AUBERT,B	05Q	BABR	$e^+e^- \to \Upsilon(4S)$
• • • We do not use the following data for averages, fits, limits, etc. • • •					
<5.0 × 10^{-5}	90	[1] ARTUSO	00	CLE2	$e^+e^- \to \Upsilon(4S)$

[1] Assumes equal production of B^+ and B^0 at the $\Upsilon(4S)$.

$\Gamma(\overline{D}^*(2007)^0\pi^0)/\Gamma_{total}$ Γ_{140}/Γ

VALUE (units 10^{-4})	CL%	DOCUMENT ID		TECN	COMMENT
2.2 ±0.6 OUR AVERAGE		Error includes scale factor of 2.6. See the ideogram below.			
3.05±0.14±0.28		[1] LEES	11M	BABR	$e^+e^- \to \Upsilon(4S)$
1.39±0.18±0.26		[1] BLYTH	06	BELL	$e^+e^- \to \Upsilon(4S)$
2.20 $^{+0.59}_{-0.52}$ ±0.79		[1] COAN	02	CLE2	$e^+e^- \to \Upsilon(4S)$
• • • We do not use the following data for averages, fits, limits, etc. • • •					
2.9 ±0.4 ±0.5		[1] AUBERT	04B	BABR	Repl. by LEES 11M
2.7 $^{+0.8}_{-0.7}$ $^{+0.5}_{-0.6}$		[1] ABE	02J	BELL	Repl. by BLYTH 06
<4.4	90	[2] NEMATI	98	CLE2	Repl. by COAN 02
<9.7	90	[3] ALAM	94	CLE2	Repl. by NEMATI 98

[1] Assumes equal production of B^+ and B^0 at the $\Upsilon(4S)$.
[2] NEMATI 98 assumes equal production of B^+ and B^0 at the $\Upsilon(4S)$ and use the PDG 96 values for D^0, D^{*0}, η, η', and ω branching fractions.
[3] ALAM 94 assume equal production of B^+ and B^0 at the $\Upsilon(4S)$ and use the CLEO II B($D^*(2007)^0 \to D^0\pi^0$) and absolute B($D^0 \to K^-\pi^+$) and the PDG 1992 B($D^0 \to K^-\pi^+\pi^0$)/B($D^0 \to K^-\pi^+$) and B($D^0 \to K^-2\pi^+\pi^-$)/B($D^0 \to K^-\pi^+$).

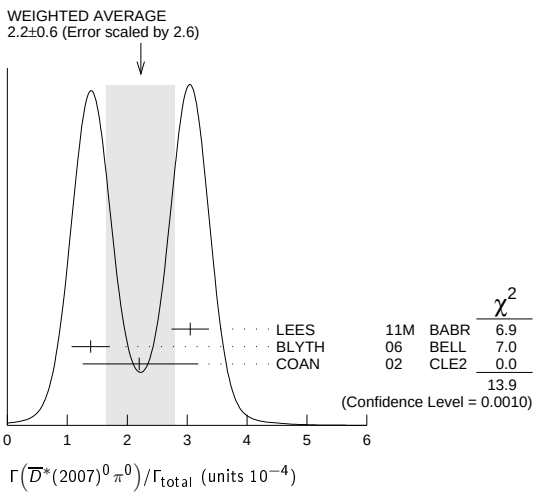

See key on page 547

$\Gamma(\overline{D}^0\pi^0)/\Gamma(\overline{D}^*(2007)^0\pi^0)$ $\Gamma_{130}/\Gamma_{140}$

VALUE	DOCUMENT ID		TECN	COMMENT
0.90±0.08 OUR AVERAGE				
0.88±0.05±0.06	LEES	11M	BABR	$e^+e^- \to \Upsilon(4S)$
1.62±0.23±0.35	BLYTH	06	BELL	$e^+e^- \to \Upsilon(4S)$
• • • We do not use the following data for averages, fits, limits, etc. • • •				
1.0 ±0.1 ±0.2	AUBERT	04B	BABR	Repl. by LEES 11M

$\Gamma(\overline{D}^*(2007)^0\rho^0)/\Gamma_{total}$ Γ_{141}/Γ

VALUE	CL%	DOCUMENT ID		TECN	COMMENT
<5.1 × 10⁻⁴	90	[1] SATPATHY	03	BELL	$e^+e^- \to \Upsilon(4S)$
• • • We do not use the following data for averages, fits, limits, etc. • • •					
<0.00056	90	[2] NEMATI	98	CLE2	$e^+e^- \to \Upsilon(4S)$
<0.00117	90	[3] ALAM	94	CLE2	Repl. by NEMATI 98

[1] Assumes equal production of B^+ and B^0 at the $\Upsilon(4S)$.
[2] NEMATI 98 assumes equal production of B^+ and B^0 at the $\Upsilon(4S)$ and use the PDG 96 values for D^0, D^{*0}, η, η', and ω branching fractions.
[3] ALAM 94 assume equal production of B^+ and B^0 at the $\Upsilon(4S)$ and use the CLEO II $B(D^*(2007)^0 \to D^0\pi^0)$ and absolute $B(D^0 \to K^-\pi^+)$ and the PDG 1992 $B(D^0 \to K^-\pi^+\pi^0)/B(D^0 \to K^-\pi^+)$ and $B(D^0 \to K^-2\pi^+\pi^-)/B(D^0 \to K^-\pi^+)$.

$\Gamma(\overline{D}^*(2007)^0\eta)/\Gamma_{total}$ Γ_{142}/Γ

VALUE (units 10^{-4})	CL%	DOCUMENT ID		TECN	COMMENT
2.3 ±0.6 OUR AVERAGE		Error includes scale factor of 2.8.			
2.69±0.14±0.23		[1] LEES	11M	BABR	$e^+e^- \to \Upsilon(4S)$
1.40±0.28±0.26		[1] BLYTH	06	BELL	$e^+e^- \to \Upsilon(4S)$
• • • We do not use the following data for averages, fits, limits, etc. • • •					
2.6 ±0.4 ±0.4		[1] AUBERT	04B	BABR	Repl. by LEES 11M
<4.6	90	[1] ABE	02J	BELL	$e^+e^- \to \Upsilon(4S)$
<2.6	90	[2] NEMATI	98	CLE2	$e^+e^- \to \Upsilon(4S)$
<6.9	90	[3] ALAM	94	CLE2	Repl. by NEMATI 98

[1] Assumes equal production of B^+ and B^0 at the $\Upsilon(4S)$.
[2] NEMATI 98 assumes equal production of B^+ and B^0 at the $\Upsilon(4S)$ and use the PDG 96 values for D^0, D^{*0}, η, η', and ω branching fractions.
[3] ALAM 94 assume equal production of B^+ and B^0 at the $\Upsilon(4S)$ and use the CLEO II $B(D^*(2007)^0 \to D^0\pi^0)$ and absolute $B(D^0 \to K^-\pi^+)$ and the PDG 1992 $B(D^0 \to K^-\pi^+\pi^0)/B(D^0 \to K^-\pi^+)$ and $B(D^0 \to K^-2\pi^+\pi^-)/B(D^0 \to K^-\pi^+)$.

$\Gamma(\overline{D}^0\eta)/\Gamma(\overline{D}^*(2007)^0\eta)$ $\Gamma_{133}/\Gamma_{142}$

VALUE	DOCUMENT ID		TECN	COMMENT
0.99±0.10 OUR AVERAGE				
0.97±0.07±0.07	LEES	11M	BABR	$e^+e^- \to \Upsilon(4S)$
1.27±0.29±0.25	BLYTH	06	BELL	$e^+e^- \to \Upsilon(4S)$
• • • We do not use the following data for averages, fits, limits, etc. • • •				
0.9 ±0.2 ±0.1	AUBERT	04B	BABR	Repl. by LEES 11M

$\Gamma(\overline{D}^*(2007)^0\eta')/\Gamma(\overline{D}^*(2007)^0\eta)$ $\Gamma_{143}/\Gamma_{142}$

VALUE	DOCUMENT ID		TECN	COMMENT
0.61±0.14±0.02	LEES	11M	BABR	$e^+e^- \to \Upsilon(4S)$
• • • We do not use the following data for averages, fits, limits, etc. • • •				
0.5 ±0.3 ±0.1	AUBERT	04B	BABR	Repl. by LEES 11M

$\Gamma(\overline{D}^*(2007)^0\eta')/\Gamma_{total}$ Γ_{143}/Γ

VALUE (units 10^{-4})	CL%	DOCUMENT ID		TECN	COMMENT
1.40±0.22 OUR AVERAGE					
1.48±0.22±0.13		[1] LEES	11M	BABR	$e^+e^- \to \Upsilon(4S)$
1.21±0.34±0.22		[1] SCHUMANN	05	BELL	$e^+e^- \to \Upsilon(4S)$
• • • We do not use the following data for averages, fits, limits, etc. • • •					
1.3 ±0.7 ±0.2		[1,2] AUBERT	04B	BABR	Repl. by LEES 11M
<14	90	BRANDENB...	98	CLE2	$e^+e^- \to \Upsilon(4S)$
<19	90	[3] NEMATI	98	CLE2	$e^+e^- \to \Upsilon(4S)$
<27	90	[4] ALAM	94	CLE2	Repl. by NEMATI 98

[1] Assumes equal production of B^+ and B^0 at the $\Upsilon(4S)$.
[2] Reports an upper limit $< 2.6 \times 10^{-4}$ at 90% CL.
[3] NEMATI 98 assumes equal production of B^+ and B^0 at the $\Upsilon(4S)$ and use the PDG 96 values for D^0, D^{*0}, η, η', and ω branching fractions.
[4] ALAM 94 assume equal production of B^+ and B^0 at the $\Upsilon(4S)$ and use the CLEO II $B(D^*(2007)^0 \to D^0\pi^0)$ and absolute $B(D^0 \to K^-\pi^+)$ and the PDG 1992 $B(D^0 \to K^-\pi^+\pi^0)/B(D^0 \to K^-\pi^+)$ and $B(D^0 \to K^-2\pi^+\pi^-)/B(D^0 \to K^-\pi^+)$.

$\Gamma(\overline{D}^0\eta')/\Gamma(\overline{D}^*(2007)^0\eta')$ $\Gamma_{134}/\Gamma_{143}$

VALUE	DOCUMENT ID		TECN	COMMENT
0.96±0.18±0.06	LEES	11M	BABR	$e^+e^- \to \Upsilon(4S)$
• • • We do not use the following data for averages, fits, limits, etc. • • •				
1.3 ±0.8 ±0.2	AUBERT	04B	BABR	Repl. by LEES 11M

$\Gamma(\overline{D}^*(2007)^0\pi^+\pi^-)/\Gamma_{total}$ Γ_{144}/Γ

VALUE	DOCUMENT ID		TECN	COMMENT
(6.2±1.2±1.8) × 10⁻⁴	[1,2] SATPATHY	03	BELL	$e^+e^- \to \Upsilon(4S)$

[1] Assumes equal production of B^+ and B^0 at the $\Upsilon(4S)$.
[2] No assumption about the intermediate mechanism is made in the analysis.

$\Gamma(\overline{D}^*(2007)^0K^0)/\Gamma_{total}$ Γ_{145}/Γ

VALUE (units 10^{-5})	CL%	DOCUMENT ID		TECN	COMMENT
3.6±1.2±0.3		[1] AUBERT,B	06L	BABR	$e^+e^- \to \Upsilon(4S)$
• • • We do not use the following data for averages, fits, limits, etc. • • •					
<6.6	90	[1] KROKOVNY	03	BELL	$e^+e^- \to \Upsilon(4S)$

[1] Assumes equal production of B^+ and B^0 at the $\Upsilon(4S)$.

$\Gamma(\overline{D}^*(2007)^0K^*(892)^0)/\Gamma_{total}$ Γ_{146}/Γ

VALUE	CL%	DOCUMENT ID		TECN	COMMENT
<6.9 × 10⁻⁵	90	[1] KROKOVNY	03	BELL	$e^+e^- \to \Upsilon(4S)$

[1] Assumes equal production of B^+ and B^0 at the $\Upsilon(4S)$.

$\Gamma(D^*(2007)^0K^*(892)^0)/\Gamma_{total}$ Γ_{147}/Γ

VALUE	CL%	DOCUMENT ID		TECN	COMMENT
<4.0 × 10⁻⁵	90	[1] KROKOVNY	03	BELL	$e^+e^- \to \Upsilon(4S)$

[1] Assumes equal production of B^+ and B^0 at the $\Upsilon(4S)$.

$\Gamma(D^*(2007)^0\pi^+\pi^+\pi^-\pi^-)/\Gamma_{total}$ Γ_{148}/Γ

VALUE (units 10^{-3})	DOCUMENT ID		TECN	COMMENT
2.7 ±0.5 OUR AVERAGE				
2.60±0.47±0.37	[1] MAJUMDER	04	BELL	$e^+e^- \to \Upsilon(4S)$
3.0 ±0.7 ±0.6	[1] EDWARDS	02	CLE2	$e^+e^- \to \Upsilon(4S)$

[1] Assumes equal production of B^+ and B^0 at the $\Upsilon(4S)$.

$\Gamma(D^*(2007)^0\pi^+\pi^+\pi^-\pi^-)/\Gamma(D^*(2010)^-\pi^+\pi^+\pi^-\pi^0)$ Γ_{148}/Γ_{60}

VALUE	DOCUMENT ID		TECN	COMMENT
0.17±0.04±0.02	[1] EDWARDS	02	CLE2	$e^+e^- \to \Upsilon(4S)$

[1] Assumes equal production of B^+ and B^0 at the $\Upsilon(4S)$.

$\Gamma(D^*(2010)^+D^*(2010)^-)/\Gamma_{total}$ Γ_{149}/Γ

VALUE (units 10^{-4})	CL%	DOCUMENT ID		TECN	COMMENT
8.0 ±0.6 OUR AVERAGE					
7.82±0.38±0.63		[1] KRONENBITT.12		BELL	$e^+e^- \to \Upsilon(4S)$
8.1 ±0.6 ±1.0		[1] AUBERT,B	06A	BABR	$e^+e^- \to \Upsilon(4S)$
9.9 $^{+4.2}_{-3.3}$ ±1.2		[1] LIPELES	00	CLE2	$e^+e^- \to \Upsilon(4S)$
• • • We do not use the following data for averages, fits, limits, etc. • • •					
8.1 ±0.8 ±1.1		[1] MIYAKE	05	BELL	Repl. by KRONENBITTER 12
8.3 ±1.6 ±1.2		[1,2] AUBERT	02M	BABR	Repl. by AUBERT,B 06B
6.2 $^{+4.0}_{-2.9}$ ±1.0		[3] ARTUSO	99	CLE2	Repl. by LIPELES 00
<61	90	[4] BARATE	98Q	ALEP	$e^+e^- \to Z$
<22	90	[5] ASNER	97	CLE2	Repl. by ARTUSO 99

[1] Assumes equal production of B^+ and B^0 at the $\Upsilon(4S)$.
[2] AUBERT 02M also assumes the measured CP-odd fraction of the final states is 0.22 ± 0.18 ± 0.03.
[3] ARTUSO 99 uses $B(\Upsilon(4S) \to B^0\overline{B}^0)$=(48 ± 4)%.
[4] BARATE 98Q (ALEPH) observes 2 events with an expected background of 0.10 ± 0.03 which corresponds to a branching ratio of $(2.3^{+1.9}_{-1.2} \pm 0.4) \times 10^{-3}$.
[5] ASNER 97 at CLEO observes 1 event with an expected background of 0.022 ± 0.011. This corresponds to a branching ratio of $(5.3^{+7.1}_{-3.7} \pm 1.0) \times 10^{-4}$.

$\Gamma(\overline{D}^*(2007)^0\omega)/\Gamma_{total}$ Γ_{150}/Γ

VALUE (units 10^{-4})	CL%	DOCUMENT ID		TECN	COMMENT
3.6 ±1.1 OUR AVERAGE		Error includes scale factor of 3.1.			
4.55±0.24±0.39		[1] LEES	11M	BABR	$e^+e^- \to \Upsilon(4S)$
2.29±0.39±0.40		[1] BLYTH	06	BELL	$e^+e^- \to \Upsilon(4S)$
• • • We do not use the following data for averages, fits, limits, etc. • • •					
4.2 ±0.7 ±0.9	90	[1] AUBERT	04B	BABR	Repl. by LEES 11M
< 7.9	90	[1] ABE	02J	BELL	$e^+e^- \to \Upsilon(4S)$
< 7.4	90	[2] NEMATI	98	CLE2	$e^+e^- \to \Upsilon(4S)$
<21	90	[3] ALAM	94	CLE2	Repl. by NEMATI 98

[1] Assumes equal production of B^+ and B^0 at the $\Upsilon(4S)$.
[2] NEMATI 98 assumes equal production of B^+ and B^0 at the $\Upsilon(4S)$ and use the PDG 96 values for D^0, D^{*0}, η, η', and ω branching fractions.
[3] ALAM 94 assume equal production of B^+ and B^0 at the $\Upsilon(4S)$ and use the CLEO II $B(D^*(2007)^0 \to D^0\pi^0)$ and absolute $B(D^0 \to K^-\pi^+)$ and the PDG 1992 $B(D^0 \to K^-\pi^+\pi^0)/B(D^0 \to K^-\pi^+)$ and $B(D^0 \to K^-2\pi^+\pi^-)/B(D^0 \to K^-\pi^+)$.

$\Gamma(\overline{D}^0\omega)/\Gamma(\overline{D}^*(2007)^0\omega)$ $\Gamma_{135}/\Gamma_{150}$

VALUE	DOCUMENT ID		TECN	COMMENT
0.58±0.06 OUR AVERAGE				
0.56±0.04±0.04	LEES	11M	BABR	$e^+e^- \to \Upsilon(4S)$
1.04±0.20±0.17	BLYTH	06	BELL	$e^+e^- \to \Upsilon(4S)$
• • • We do not use the following data for averages, fits, limits, etc. • • •				
0.7 ±0.1 ±0.1	AUBERT	04B	BABR	Repl. by LEES 11M

$\Gamma(D^*(2010)^+ D^-)/\Gamma_{total}$ Γ_{151}/Γ

VALUE (units 10^{-4})	CL%	DOCUMENT ID		TECN	COMMENT
6.1±1.5 OUR AVERAGE		Error includes scale factor of 1.6.			
5.7±0.7±0.7		[1] AUBERT,B	06A	BABR	$e^+e^- \to \Upsilon(4S)$
$11.7\pm2.6^{+2.2}_{-2.5}$		[1,2] ABE	02Q	BELL	$e^+e^- \to \Upsilon(4S)$
• • • We do not use the following data for averages, fits, limits, etc. • • •					
8.8±1.0±1.3		[1] AUBERT	03J	BABR	Repl. by AUBERT,B 06B
$14.8\pm3.8^{+2.8}_{-3.1}$		[1,3] ABE	02Q	BELL	$e^+e^- \to \Upsilon(4S)$
< 6.3	90	[1] LIPELES	00	CLE2	$e^+e^- \to \Upsilon(4S)$
<56	90	BARATE	98Q	ALEP	$e^+e^- \to Z$
<18	90	ASNER	97	CLE2	$e^+e^- \to \Upsilon(4S)$

[1] Assumes equal production of B^+ and B^0 at the $\Upsilon(4S)$.
[2] The measurement is performed using fully reconstructed D^* and D^+ decays.
[3] The measurement is performed using a partial reconstruction technique for the D^* and fully reconstructed D^+ decays as a cross check.

$\Gamma(D^*(2007)^0 \overline{D}{}^*(2007)^0)/\Gamma_{total}$ Γ_{152}/Γ

VALUE (units 10^{-4})	CL%	DOCUMENT ID		TECN	COMMENT
< 0.9	90	[1] AUBERT,B	06A	BABR	$e^+e^- \to \Upsilon(4S)$
• • • We do not use the following data for averages, fits, limits, etc. • • •					
<270	90	BARATE	98Q	ALEP	$e^+e^- \to Z$

[1] Assumes equal production of B^+ and B^0 at the $\Upsilon(4S)$.

$\Gamma(D^- D^0 K^+)/\Gamma_{total}$ Γ_{153}/Γ

VALUE (units 10^{-3})	DOCUMENT ID		TECN	COMMENT
1.07±0.07±0.09	[1] DEL-AMO-SA...11B		BABR	$e^+e^- \to \Upsilon(4S)$
• • • We do not use the following data for averages, fits, limits, etc. • • •				
1.7 ±0.3 ±0.3	[1] AUBERT	03X	BABR	Repl. by DEL-AMO-SANCHEZ 11B

[1] Assumes equal production of B^+ and B^0 at the $\Upsilon(4S)$.

$\Gamma(D^- D^*(2007)^0 K^+)/\Gamma_{total}$ Γ_{154}/Γ

VALUE (units 10^{-3})	DOCUMENT ID		TECN	COMMENT
3.46±0.18±0.37	[1] DEL-AMO-SA...11B		BABR	$e^+e^- \to \Upsilon(4S)$
• • • We do not use the following data for averages, fits, limits, etc. • • •				
4.6 ±0.7 ±0.7	[1] AUBERT	03X	BABR	Repl. by DEL-AMO-SANCHEZ 11B

[1] Assumes equal production of B^+ and B^0 at the $\Upsilon(4S)$.

$\Gamma(D^*(2010)^- D^0 K^+)/\Gamma_{total}$ Γ_{155}/Γ

VALUE (units 10^{-3})	DOCUMENT ID		TECN	COMMENT
2.47±0.10±0.18	[1] DEL-AMO-SA...11B		BABR	$e^+e^- \to \Upsilon(4S)$
• • • We do not use the following data for averages, fits, limits, etc. • • •				
$3.1\ ^{+0.4}_{-0.3}\ \pm0.4$	[1] AUBERT	03X	BABR	Repl. by DEL-AMO-SANCHEZ 11B

[1] Assumes equal production of B^+ and B^0 at the $\Upsilon(4S)$.

$\Gamma(D^*(2010)^- D^*(2007)^0 K^+)/\Gamma_{total}$ Γ_{156}/Γ

VALUE (units 10^{-3})	DOCUMENT ID		TECN	COMMENT
10.6±0.33±0.86	[1] DEL-AMO-SA...11B		BABR	$e^+e^- \to \Upsilon(4S)$
• • • We do not use the following data for averages, fits, limits, etc. • • •				
11.8±1.0 ±1.7	[1] AUBERT	03X	BABR	Repl. by DEL-AMO-SANCHEZ 11B

[1] Assumes equal production of B^+ and B^0 at the $\Upsilon(4S)$.

$\Gamma(D^- D^+ K^0)/\Gamma_{total}$ Γ_{157}/Γ

VALUE (units 10^{-3})	CL%	DOCUMENT ID		TECN	COMMENT
0.75±0.12±0.12		[1] DEL-AMO-SA...11B		BABR	$e^+e^- \to \Upsilon(4S)$
• • • We do not use the following data for averages, fits, limits, etc. • • •					
<1.7	90	[1] AUBERT	03X	BABR	Repl. by DEL-AMO-SANCHEZ 11B

[1] Assumes equal production of B^+ and B^0 at the $\Upsilon(4S)$.

$[\Gamma(D^*(2010)^- D^+ K^0) + \Gamma(D^- D^*(2010)^+ K^0)]/\Gamma_{total}$ Γ_{158}/Γ

VALUE (units 10^{-3})	DOCUMENT ID		TECN	COMMENT
6.41±0.36±0.39	[1] DEL-AMO-SA...11B		BABR	$e^+e^- \to \Upsilon(4S)$
• • • We do not use the following data for averages, fits, limits, etc. • • •				
6.5 ±1.2 ±1.0	[1] AUBERT	03X	BABR	Repl. by DEL-AMO-SANCHEZ 11B

[1] Assumes equal production of B^+ and B^0 at the $\Upsilon(4S)$.

$\Gamma(D^*(2010)^- D^*(2010)^+ K^0)/\Gamma_{total}$ Γ_{159}/Γ

VALUE (units 10^{-3})	DOCUMENT ID		TECN	COMMENT
8.1 ±0.7 OUR AVERAGE				
8.26±0.43±0.67	[1] DEL-AMO-SA...11B		BABR	$e^+e^- \to \Upsilon(4S)$
6.8 ±0.8 ±1.4	[1,2] DALSENO	07	BELL	$e^+e^- \to \Upsilon(4S)$
8.8 ±0.8 ±1.4	[1,2] AUBERT,B	06Q	BABR	$e^+e^- \to \Upsilon(4S)$
• • • We do not use the following data for averages, fits, limits, etc. • • •				
$8.8\ ^{+1.5}_{-1.4}\ \pm1.3$	[1] AUBERT	03X	BABR	Repl. by AUBERT,B 06Q

[1] Assumes equal production of B^+ and B^0 at the $\Upsilon(4S)$.
[2] The result is rescaled by a factor of 2 to convert from K^0_S to K^0.

$\Gamma(D^{*-} D_{s1}(2536)^+ \times B(D_{s1}(2536)^+ \to D^{*+} K^0))/\Gamma_{total}$ Γ_{160}/Γ

VALUE (units 10^{-4})	DOCUMENT ID		TECN	COMMENT
8.0±2.4 OUR AVERAGE				
$7.6^{+4.8}_{-4.2}{}^{+1.6}_{-1.4}$	[1,2] DALSENO	07	BELL	$e^+e^- \to \Upsilon(4S)$
8.2±2.6±1.2	[1,2] AUBERT,B	06Q	BABR	$e^+e^- \to \Upsilon(4S)$

[1] Assumes equal production of B^+ and B^0 at the $\Upsilon(4S)$.
[2] The result is rescaled by a factor of 2 to convert from K^0_S to K^0.

$\Gamma(\overline{D}{}^0 D^0 K^0)/\Gamma_{total}$ Γ_{161}/Γ

VALUE (units 10^{-3})	CL%	DOCUMENT ID		TECN	COMMENT
0.27±0.10±0.05		[1] DEL-AMO-SA...11B		BABR	$e^+e^- \to \Upsilon(4S)$
• • • We do not use the following data for averages, fits, limits, etc. • • •					
<1.4	90	[1] AUBERT	03X	BABR	Repl. by DEL-AMO-SANCHEZ 11B

[1] Assumes equal production of B^+ and B^0 at the $\Upsilon(4S)$.

$[\Gamma(\overline{D}{}^0 D^*(2007)^0 K^0) + \Gamma(\overline{D}{}^*(2007)^0 D^0 K^0)]/\Gamma_{total}$ Γ_{162}/Γ

VALUE (units 10^{-3})	CL%	DOCUMENT ID		TECN	COMMENT
1.08±0.32±0.36		[1] DEL-AMO-SA...11B		BABR	$e^+e^- \to \Upsilon(4S)$
• • • We do not use the following data for averages, fits, limits, etc. • • •					
<3.7	90	[1] AUBERT	03X	BABR	Repl. by DEL-AMO-SANCHEZ 11B

[1] Assumes equal production of B^+ and B^0 at the $\Upsilon(4S)$.

$\Gamma(\overline{D}{}^*(2007)^0 D^*(2007)^0 K^0)/\Gamma_{total}$ Γ_{163}/Γ

VALUE (units 10^{-3})	CL%	DOCUMENT ID		TECN	COMMENT
2.40±0.55±0.67		[1] DEL-AMO-SA...11B		BABR	$e^+e^- \to \Upsilon(4S)$
• • • We do not use the following data for averages, fits, limits, etc. • • •					
<6.6	90	[1] AUBERT	03X	BABR	Repl. by DEL-AMO-SANCHEZ 11B

[1] Assumes equal production of B^+ and B^0 at the $\Upsilon(4S)$.

$\Gamma((\overline{D}+\overline{D}^*)(D+D^*)K)/\Gamma_{total}$ Γ_{164}/Γ

VALUE (units 10^{-2})	DOCUMENT ID		TECN	COMMENT
3.68±0.10±0.24	[1] DEL-AMO-SA...11B		BABR	$e^+e^- \to \Upsilon(4S)$
• • • We do not use the following data for averages, fits, limits, etc. • • •				
4.3 ±0.3 ±0.6	[1] AUBERT	03X	BABR	Repl. by DEL-AMO-SANCHEZ 11B

[1] Assumes equal production of B^+ and B^0 at the $\Upsilon(4S)$.

$\Gamma(\eta_c K^0)/\Gamma_{total}$ Γ_{165}/Γ

VALUE (units 10^{-3})	DOCUMENT ID		TECN	COMMENT
0.79±0.12 OUR AVERAGE				
$0.55^{+0.19}_{-0.17}\pm0.06$	[1,2] AUBERT	07AV	BABR	$e^+e^- \to \Upsilon(4S)$
0.88±0.15±0.06	[1,3] AUBERT,B	04B	BABR	$e^+e^- \to \Upsilon(4S)$
$1.23\pm0.23^{+0.40}_{-0.41}$	[1] FANG	03	BELL	$e^+e^- \to \Upsilon(4S)$
$1.09^{+0.55}_{-0.42}\pm0.33$	[4] EDWARDS	01	CLE2	$e^+e^- \to \Upsilon(4S)$

[1] Assumes equal production of B^+ and B^0 at the $\Upsilon(4S)$.
[2] AUBERT 07AV reports $[\Gamma(B^0 \to \eta_c K^0)/\Gamma_{total}] \times [B(\eta_c(1S) \to p\overline{p})] = (0.83^{+0.28}_{-0.26} \pm 0.05)\times10^{-6}$ which we divide by our best value $B(\eta_c(1S) \to p\overline{p}) = (1.52\pm0.16)\times10^{-3}$. Our first error is their experiment's error and our second error is the systematic error from using our best value.
[3] AUBERT,B 04B reports $[\Gamma(B^0 \to \eta_c K^0)/\Gamma_{total}] \times [B(\eta_c(1S) \to K\overline{K}\pi)] = (0.0648 \pm 0.0085 \pm 0.0071) \times 10^{-3}$ which we divide by our best value $B(\eta_c(1S) \to K\overline{K}\pi) = (7.3 \pm 0.5) \times 10^{-2}$. Our first error is their experiment's error and our second error is the systematic error from using our best value.
[4] EDWARDS 01 assumes equal production of B^0 and B^+ at the $\Upsilon(4S)$. The correlated uncertainties (28.3)% from $B(J/\psi(1S) \to \gamma\eta_c)$ in those modes have been accounted for.

$\Gamma(\eta_c K^0)/\Gamma(J/\psi(1S) K^0)$ $\Gamma_{165}/\Gamma_{169}$

VALUE	DOCUMENT ID		TECN	COMMENT
1.39±0.20±0.45	[1] AUBERT,B	04B	BABR	$e^+e^- \to \Upsilon(4S)$

[1] Uses BABAR measurement of $B(B^0 \to J/\psi K^0) = (8.5 \pm 0.5 \pm 0.6) \times 10^{-4}$.

$\Gamma(\eta_c K^*(892)^0)/\Gamma_{total}$ Γ_{166}/Γ

VALUE (units 10^{-3})	DOCUMENT ID		TECN	COMMENT
0.63±0.09 OUR AVERAGE				
0.59±0.07±0.07	[1,2] AUBERT	08AB	BABR	$e^+e^- \to \Upsilon(4S)$
$0.68^{+0.21}_{-0.19}\pm0.07$	[3,4] AUBERT	07AV	BABR	$e^+e^- \to \Upsilon(4S)$
$1.62\pm0.32^{+0.55}_{-0.60}$	[4] FANG	03	BELL	$e^+e^- \to \Upsilon(4S)$

[1] AUBERT 08AB reports $[\Gamma(B^0 \to \eta_c K^*(892)^0)/\Gamma_{total}] / [B(B^+ \to \eta_c K^+)] = 0.62 \pm 0.06 \pm 0.05$ which we multiply by our best value $B(B^+ \to \eta_c K^+) = (9.6\pm1.1)\times10^{-4}$. Our first error is their experiment's error and our second error is the systematic error from using our best value.
[2] Uses the production ratio of $(B^+B^-)/(B^0\overline{B}{}^0) = 1.026 \pm 0.032$ at $\Upsilon(4S)$.
[3] AUBERT 07AV reports $[\Gamma(B^0 \to \eta_c K^*(892)^0)/\Gamma_{total}] \times [B(\eta_c(1S) \to p\overline{p})] = (1.03^{+0.27}_{-0.24} \pm 0.17) \times 10^{-6}$ which we divide by our best value $B(\eta_c(1S) \to p\overline{p}) = (1.52 \pm 0.16) \times 10^{-3}$. Our first error is their experiment's error and our second error is the systematic error from using our best value.
[4] Assumes equal production of B^+ and B^0 at the $\Upsilon(4S)$.

$\Gamma(\eta_c(2S)K^{*0})/\Gamma_{total}$ Γ_{167}/Γ

VALUE (units 10^{-4})	CL%	DOCUMENT ID		TECN	COMMENT
<3.9	90	[1] AUBERT	08AB	BABR	$e^+e^- \to \Upsilon(4S)$

[1] Uses the production ratio of $(B^+B^-)/(B^0\overline{B}^0) = 1.026 \pm 0.032$ at $\Upsilon(4S)$.

$\Gamma(B^0 \to h_c(1P)K^{*0})/\Gamma_{total} \times \Gamma(h_c(1P) \to \eta_c(1S)\gamma)/\Gamma_{total}$ $\Gamma_{168}/\Gamma \times \Gamma_4^{h_c(1P)}/\Gamma^{h_c(1P)}$

VALUE (units 10^{-4})	CL%	DOCUMENT ID		TECN	COMMENT
<2.2	90	[1] AUBERT	08AB	BABR	$e^+e^- \to \Upsilon(4S)$

[1] Uses the production ratio of $(B^+B^-)/(B^0\overline{B}^0) = 1.026 \pm 0.032$ at $\Upsilon(4S)$.

$\Gamma(\eta_c K^*(892)^0)/\Gamma(\eta_c K^0)$ $\Gamma_{166}/\Gamma_{165}$

VALUE	DOCUMENT ID		TECN	COMMENT
$1.33 \pm 0.36^{+0.24}_{-0.33}$	FANG	03	BELL	$e^+e^- \to \Upsilon(4S)$

$\Gamma(J/\psi(1S)K^0)/\Gamma_{total}$ Γ_{169}/Γ

VALUE (units 10^{-4})	CL%	EVTS	DOCUMENT ID		TECN	COMMENT
8.73±0.32 OUR FIT						
8.72±0.32 OUR AVERAGE						
$8.8\ ^{+1.4}_{-1.3} \pm 0.1$			[1,2] AUBERT	07AV	BABR	$e^+e^- \to \Upsilon(4S)$
$8.69 \pm 0.22 \pm 0.30$			[2] AUBERT	05J	BABR	$e^+e^- \to \Upsilon(4S)$
$7.9 \pm 0.4 \pm 0.9$			[2] ABE	03B	BELL	$e^+e^- \to \Upsilon(4S)$
$9.5 \pm 0.8 \pm 0.6$			[2] AVERY	00	CLE2	$e^+e^- \to \Upsilon(4S)$
$11.5 \pm 2.3 \pm 1.7$			[3] ABE	96H	CDF	$p\overline{p}$ at 1.8 TeV
$6.93 \pm 4.07 \pm 0.04$			[4] BORTOLETTO	92	CLEO	$e^+e^- \to \Upsilon(4S)$
$9.24 \pm 7.21 \pm 0.05$	2		[5] ALBRECHT	90J	ARG	$e^+e^- \to \Upsilon(4S)$
• • • We do not use the following data for averages, fits, limits, etc. • • •						
$8.3 \pm 0.4 \pm 0.5$			[2] AUBERT	02	BABR	Repl. by AUBERT 05J
$8.5\ ^{+1.4}_{-1.2} \pm 0.6$			[2] JESSOP	97	CLE2	Repl. by AVERY 00
$7.5 \pm 2.4 \pm 0.8$		10	[4] ALAM	94	CLE2	Sup. by JESSOP 97
<50	90		ALAM	86	CLEO	$e^+e^- \to \Upsilon(4S)$

[1] AUBERT 07AV reports $[\Gamma(B^0 \to J/\psi(1S)K^0)/\Gamma_{total}] \times [B(J/\psi(1S) \to p\overline{p})] = (1.87^{+0.28}_{-0.26} \pm 0.07) \times 10^{-6}$ which we divide by our best value $B(J/\psi(1S) \to p\overline{p}) = (2.120 \pm 0.029) \times 10^{-3}$. Our first error is their experiment's error and our second error is the systematic error from using our best value.

[2] Assumes equal production of B^+ and B^0 at the $\Upsilon(4S)$.

[3] ABE 96H assumes that $B(B^+ \to J/\psi K^+) = (1.02 \pm 0.14) \times 10^{-3}$.

[4] BORTOLETTO 92 reports $(6 \pm 3 \pm 2) \times 10^{-4}$ from a measurement of $[\Gamma(B^0 \to J/\psi(1S)K^0)/\Gamma_{total}] \times [B(J/\psi(1S) \to e^+e^-)]$ assuming $B(J/\psi(1S) \to e^+e^-) = 0.069 \pm 0.009$, which we rescale to our best value $B(J/\psi(1S) \to e^+e^-) = (5.971 \pm 0.032) \times 10^{-2}$. Our first error is their experiment's error and our second error is the systematic error from using our best value. Assumes equal production of B^+ and B^0 at the $\Upsilon(4S)$.

[5] ALBRECHT 90J reports $(8 \pm 6 \pm 2) \times 10^{-4}$ from a measurement of $[\Gamma(B^0 \to J/\psi(1S)K^0)/\Gamma_{total}] \times [B(J/\psi(1S) \to e^+e^-)]$ assuming $B(J/\psi(1S) \to e^+e^-) = 0.069 \pm 0.009$, which we rescale to our best value $B(J/\psi(1S) \to e^+e^-) = (5.971 \pm 0.032) \times 10^{-2}$. Our first error is their experiment's error and our second error is the systematic error from using our best value. Assumes equal production of B^+ and B^0 at the $\Upsilon(4S)$.

$\Gamma(J/\psi(1S)K^+\pi^-)/\Gamma_{total}$ Γ_{170}/Γ

VALUE (units 10^{-3})	CL%	EVTS	DOCUMENT ID		TECN	COMMENT
1.16 ±0.56 ±0.01			[1] BORTOLETTO	92	CLEO	$e^+e^- \to \Upsilon(4S)$
• • • We do not use the following data for averages, fits, limits, etc. • • •						
1.079 ± 0.011			[2] AUBERT	09AA	BABR	$e^+e^- \to \Upsilon(4S)$
<1.3	90		[3] ALBRECHT	87D	ARG	$e^+e^- \to \Upsilon(4S)$
<6.3	90	2	GILES	84	CLEO	$e^+e^- \to \Upsilon(4S)$

[1] BORTOLETTO 92 reports $(1.0 \pm 0.4 \pm 0.3) \times 10^{-3}$ from a measurement of $[\Gamma(B^0 \to J/\psi(1S)K^+\pi^-)/\Gamma_{total}] \times [B(J/\psi(1S) \to e^+e^-)]$ assuming $B(J/\psi(1S) \to e^+e^-) = 0.069 \pm 0.009$, which we rescale to our best value $B(J/\psi(1S) \to e^+e^-) = (5.971 \pm 0.032) \times 10^{-2}$. Our first error is their experiment's error and our second error is the systematic error from using our best value. Assumes equal production of B^+ and B^0 at the $\Upsilon(4S)$.

[2] Does not report systematic uncertainties.

[3] ALBRECHT 87D assume $B^+B^-/B^0\overline{B}^0$ ratio is 55/45. $K\pi$ system is specifically selected as nonresonant.

$\Gamma(J/\psi(1S)K^*(892)^0)/\Gamma_{total}$ Γ_{171}/Γ

VALUE (units 10^{-3})	EVTS	DOCUMENT ID		TECN	COMMENT
1.32 ±0.06 OUR FIT					
1.33 ±0.06 OUR AVERAGE					
$1.33\ ^{+0.22}_{-0.21} \pm 0.02$		[1,2] AUBERT	07AV	BABR	$e^+e^- \to \Upsilon(4S)$
$1.309 \pm 0.026 \pm 0.077$		[2] AUBERT	05J	BABR	$e^+e^- \to \Upsilon(4S)$
$1.29 \pm 0.05 \pm 0.13$		[2] ABE	02N	BELL	$e^+e^- \to \Upsilon(4S)$
$1.74 \pm 0.20 \pm 0.18$		[3] ABE	98O	CDF	$p\overline{p}$ 1.8 TeV
$1.32 \pm 0.17 \pm 0.17$		[4] JESSOP	97	CLE2	$e^+e^- \to \Upsilon(4S)$
$1.27 \pm 0.65 \pm 0.01$		[5] BORTOLETTO	92	CLEO	$e^+e^- \to \Upsilon(4S)$
$1.27 \pm 0.60 \pm 0.01$	6	[6] ALBRECHT	90J	ARG	$e^+e^- \to \Upsilon(4S)$
$4.04 \pm 1.81 \pm 0.02$	5	[7] BEBEK	87	CLEO	$e^+e^- \to \Upsilon(4S)$
• • • We do not use the following data for averages, fits, limits, etc. • • •					
$1.24 \pm 0.05 \pm 0.09$		[2] AUBERT	02	BABR	Repl. by AUBERT 05J
$1.36 \pm 0.27 \pm 0.22$		[8] ABE	96H	CDF	Sup. by ABE 98O
$1.69 \pm 0.31 \pm 0.18$	29	[9] ALAM	94	CLE2	Sup. by JESSOP 97
		[10] ALBRECHT	94G	ARG	$e^+e^- \to \Upsilon(4S)$
4.0 ± 0.30		[11] ALBAJAR	91E	UA1	$E_{cm}^{p\overline{p}} = 630$ GeV
3.3 ± 0.18	5	[12] ALBRECHT	87D	ARG	$e^+e^- \to \Upsilon(4S)$
4.1 ± 0.18	5	[13] ALAM	86	CLEO	Repl. by BEBEK 87

[1] AUBERT 07AV reports $[\Gamma(B^0 \to J/\psi(1S)K^*(892)^0)/\Gamma_{total}] \times [B(J/\psi(1S) \to p\overline{p})] = (2.82^{+0.30+0.36}_{-0.28-0.35}) \times 10^{-6}$ which we divide by our best value $B(J/\psi(1S) \to p\overline{p}) = (2.120 \pm 0.029) \times 10^{-3}$. Our first error is their experiment's error and our second error is the systematic error from using our best value.

[2] Assumes equal production of B^+ and B^0 at the $\Upsilon(4S)$.

[3] ABE 98O reports $[B(B^0 \to J/\psi(1S)K^*(892)^0)]/[B(B^+ \to J/\psi(1S)K^+)] = 1.76 \pm 0.14 \pm 0.15$. We multiply by our best value $B(B^+ \to J/\psi(1S)K^+) = (9.9 \pm 1.0) \times 10^{-4}$. Our first error is their experiment's error and our second error is the systematic error from using our best value.

[4] Assumes equal production of B^+ and B^0 at the $\Upsilon(4S)$.

[5] BORTOLETTO 92 reports $(1.1 \pm 0.5 \pm 0.3) \times 10^{-3}$ from a measurement of $[\Gamma(B^0 \to J/\psi(1S)K^*(892)^0)/\Gamma_{total}] \times [B(J/\psi(1S) \to e^+e^-)]$ assuming $B(J/\psi(1S) \to e^+e^-) = 0.069 \pm 0.009$, which we rescale to our best value $B(J/\psi(1S) \to e^+e^-) = (5.971 \pm 0.032) \times 10^{-2}$. Our first error is their experiment's error and our second error is the systematic error from using our best value. Assumes equal production of B^+ and B^0 at the $\Upsilon(4S)$.

[6] ALBRECHT 90J reports $(1.1 \pm 0.5 \pm 0.2) \times 10^{-3}$ from a measurement of $[\Gamma(B^0 \to J/\psi(1S)K^*(892)^0)/\Gamma_{total}] \times [B(J/\psi(1S) \to e^+e^-)]$ assuming $B(J/\psi(1S) \to e^+e^-) = 0.069 \pm 0.009$, which we rescale to our best value $B(J/\psi(1S) \to e^+e^-) = (5.971 \pm 0.032) \times 10^{-2}$. Our first error is their experiment's error and our second error is the systematic error from using our best value. Assumes equal production of B^+ and B^0 at the $\Upsilon(4S)$.

[7] BEBEK 87 reports $(3.5 \pm 1.6 \pm 0.3) \times 10^{-3}$ from a measurement of $[\Gamma(B^0 \to J/\psi(1S)K^*(892)^0)/\Gamma_{total}] \times [B(J/\psi(1S) \to e^+e^-)]$ assuming $B(J/\psi(1S) \to e^+e^-) = 0.069 \pm 0.009$, which we rescale to our best value $B(J/\psi(1S) \to e^+e^-) = (5.971 \pm 0.032) \times 10^{-2}$. Our first error is their experiment's error and our second error is the systematic error from using our best value. Updated in BORTOLETTO 92 to use the same assumptions.

[8] ABE 96H assumes that $B(B^+ \to J/\psi K^+) = (1.02 \pm 0.14) \times 10^{-3}$.

[9] The neutral and charged B events together are predominantly longitudinally polarized, $\Gamma_L/\Gamma = 0.080 \pm 0.08 \pm 0.05$. This can be compared with a prediction using HQET, 0.73 (KRAMER 92). This polarization indicates that the $B \to \psi K^*$ decay is dominated by the $CP = -1$ CP eigenstate. Assumes equal production of B^+ and B^0 at the $\Upsilon(4S)$.

[10] ALBRECHT 94G measures the polarization in the vector-vector decay to be predominantly longitudinal, $\Gamma_T/\Gamma = 0.03 \pm 0.16 \pm 0.15$ making the neutral decay a CP eigenstate when the K^{*0} decays through $K_S^0\pi^0$.

[11] ALBAJAR 91E assumes B_d^0 production fraction of 36%.

[12] ALBRECHT 87D assume $B^+B^-/B^0\overline{B}^0$ ratio is 55/45. Superseded by ALBRECHT 90J.

[13] ALAM 86 assumes $B^\pm/B^0$ ratio is 60/40. The observation of the decay $B^+ \to J/\psi K^*(892)^+$ (HAAS 85) has been retracted in this paper.

$\Gamma(J/\psi(1S)K^*(892)^0)/\Gamma(J/\psi(1S)K^0)$ $\Gamma_{171}/\Gamma_{169}$

VALUE	DOCUMENT ID		TECN	COMMENT
1.50±0.09 OUR AVERAGE				
$1.51 \pm 0.05 \pm 0.08$	AUBERT	05J	BABR	$e^+e^- \to \Upsilon(4S)$
$1.39 \pm 0.36 \pm 0.10$	ABE	96Q	CDF	$p\overline{p}$
• • • We do not use the following data for averages, fits, limits, etc. • • •				
$1.49 \pm 0.10 \pm 0.08$	[1] AUBERT	02	BABR	Repl. by AUBERT 05J

[1] Assumes equal production of B^+ and B^0 at the $\Upsilon(4S)$.

$\Gamma(J/\psi(1S)\eta K_S^0)/\Gamma_{total}$ Γ_{172}/Γ

VALUE (units 10^{-5})	DOCUMENT ID		TECN	COMMENT
8.4±2.6±2.7	[1] AUBERT	04Y	BABR	$e^+e^- \to \Upsilon(4S)$

[1] Assumes equal production of B^+ and B^0 at the $\Upsilon(4S)$.

$\Gamma(J/\psi(1S)\eta' K_S^0)/\Gamma_{total}$ Γ_{173}/Γ

VALUE (units 10^{-5})	CL%	DOCUMENT ID		TECN	COMMENT
<2.5	90	[1] XIE	07	BELL	$e^+e^- \to \Upsilon(4S)$

[1] Assumes equal production of B^+ and B^0 at the $\Upsilon(4S)$.

$\Gamma(J/\psi(1S)\omega K^0)/\Gamma_{total}$ Γ_{175}/Γ

VALUE (units 10^{-4})	DOCUMENT ID		TECN	COMMENT
2.3±0.3±0.3	[1] DEL-AMO-SA...10B		BABR	$e^+e^- \to \Upsilon(4S)$
• • • We do not use the following data for averages, fits, limits, etc. • • •				
$3.1 \pm 0.6 \pm 0.3$	[1] AUBERT	08W	BABR	Repl. by DEL-AMO-SANCHEZ 10B

[1] Assumes equal production of B^+ and B^0 at the $\Upsilon(4S)$.

$\Gamma(X(3872)K^0 \times B(X \to J/\psi\omega))/\Gamma_{total}$ Γ_{176}/Γ

VALUE (units 10^{-6})	DOCUMENT ID		TECN	COMMENT
6±3±1	[1] DEL-AMO-SA...10B		BABR	$e^+e^- \to \Upsilon(4S)$

[1] Assumes equal production of B^+ and B^0 at the $\Upsilon(4S)$.

Meson Particle Listings

B^0

$\Gamma(\chi_{c0}(2P),\ \chi_{c0} \to J/\psi\omega)/\Gamma_{total}$ Γ_{177}/Γ

VALUE (units 10^{-5})	DOCUMENT ID	TECN	COMMENT
2.1±0.9±0.3	[1] DEL-AMO-SA...10B	BABR	$e^+e^- \to \Upsilon(4S)$
• • • We do not use the following data for averages, fits, limits, etc. • • •			
$1.3^{+1.3}_{-1.1}\pm0.2$	[1,2] AUBERT	08W BABR	Repl. by DEL-AMO-SANCHEZ 10B

[1] Assumes equal production of B^+ and B^0 at the $\Upsilon(4S)$.
[2] Corresponds to upper limit of 3.9×10^{-5} at 90% CL.

$\Gamma(J/\psi(1S)\phi K^0)/\Gamma_{total}$ Γ_{174}/Γ

VALUE	DOCUMENT ID	TECN	COMMENT
(9.4±2.6) × 10^{-5} OUR AVERAGE			
$(10.2\pm3.8\pm1.0)\times10^{-5}$	[1] AUBERT	03O BABR	$e^+e^- \to \Upsilon(4S)$
$(\ 8.8^{+3.5}_{-3.0}\pm1.3)\times10^{-5}$	[2] ANASTASSOV 00	CLE2	$e^+e^- \to \Upsilon(4S)$

[1] Assumes equal production of B^+ and B^0 at the $\Upsilon(4S)$.
[2] ANASTASSOV 00 finds 10 events on a background of 0.5 ± 0.2. Assumes equal production of B^0 and B^+ at the $\Upsilon(4S)$, a uniform Dalitz plot distribution, isotropic $J/\psi(1S)$ and ϕ decays, and $B(B^+ \to J/\psi(1S)\phi K^+) = B(B^0 \to J/\psi(1S)\phi K^0)$.

$\Gamma(J/\psi(1S)K(1270)^0)/\Gamma_{total}$ Γ_{178}/Γ

VALUE (units 10^{-3})	DOCUMENT ID	TECN	COMMENT
1.30±0.34±0.32	[1] ABE	01L BELL	$e^+e^- \to \Upsilon(4S)$

[1] Assumes equal production of B^+ and B^0 at the $\Upsilon(4S)$ and uses the PDG value of $B(B^+ \to J/\psi(1S)K^+) = (1.00\pm0.10)\times10^{-3}$.

$\Gamma(J/\psi(1S)\pi^0)/\Gamma_{total}$ Γ_{179}/Γ

VALUE (units 10^{-5})	CL%	DOCUMENT ID	TECN	COMMENT
1.76±0.16 OUR AVERAGE		Error includes scale factor of 1.1.		
$1.69\pm0.14\pm0.07$		[1] AUBERT	08AU BABR	$e^+e^- \to \Upsilon(4S)$
$2.3\ \pm0.5\ \pm0.2$		[1] ABE	03B BELL	$e^+e^- \to \Upsilon(4S)$
$2.5\ ^{+1.1}_{-0.9}\ \pm0.2$		[1] AVERY	00 CLE2	$e^+e^- \to \Upsilon(4S)$
• • • We do not use the following data for averages, fits, limits, etc. • • •				
$1.94\pm0.22\pm0.17$		[1] AUBERT,B	06B BABR	Repl. by AUBERT 08AU
$2.0\ \pm0.6\ \pm0.2$		[1] AUBERT	02 BABR	Repl. by AUBERT,B 06B
<32	90	[2] ACCIARRI	97C L3	
<5.8	90	BISHAI	96 CLE2	Sup. by AVERY 00
<690	90	[1] ALEXANDER	95 CLE2	Sup. by BISHAI 96

[1] Assumes equal production of B^+ and B^0 at the $\Upsilon(4S)$.
[2] ACCIARRI 97C assumes B^0 production fraction (39.5 ± 4.0%) and B_s (12.0 ± 3.0%).

$\Gamma(J/\psi(1S)\eta)/\Gamma_{total}$ Γ_{180}/Γ

VALUE (units 10^{-6})	CL%	DOCUMENT ID	TECN	COMMENT
$12.3^{+1.8}_{-1.7}\pm0.7$		[1,2] CHANG	12 BELL	$e^+e^- \to \Upsilon(4S)$
• • • We do not use the following data for averages, fits, limits, etc. • • •				
$9.5\pm1.7\pm0.8$		[2] CHANG	07A BELL	Repl. by CHANG 12
<27	90	[2] AUBERT	03O BABR	$e^+e^- \to \Upsilon(4S)$
<1200	90	[3] ACCIARRI	97C L3	

[1] Reconstructs η in $\gamma\gamma$ and $\pi^+\pi^-\pi^0$ decays.
[2] Assumes equal production of B^+ and B^0 at the $\Upsilon(4S)$.
[3] ACCIARRI 97C assumes B^0 production fraction (39.5 ± 4.0%) and B_s (12.0 ± 3.0%).

$\Gamma(J/\psi(1S)\pi^+\pi^-)/\Gamma_{total}$ Γ_{181}/Γ

VALUE (units 10^{-5})	DOCUMENT ID	TECN	COMMENT
4.03±0.18 OUR AVERAGE			
$4.01\pm0.14\pm0.12$	[1,2] AAIJ	13M LHCB	pp at 7 TeV
$4.6\ \pm0.7\ \pm0.6$	[3] AUBERT	03B BABR	$e^+e^- \to \Upsilon(4S)$

[1] AAIJ 13M reports $(3.97\pm0.09\pm0.11\pm0.16)\times10^{-5}$ from a measurement of $[\Gamma(B^0 \to J/\psi(1S)\pi^+\pi^-)/\Gamma_{total}]$ / $[B(B^+ \to J/\psi(1S)K^+)]$ assuming $B(B^+ \to J/\psi(1S)K^+) = (1.018\pm0.042)\times10^{-3}$, which we rescale to our best value $B(B^+ \to J/\psi(1S)K^+) = (1.027\pm0.031)\times10^{-3}$. Our first error is their experiment's error and our second error is the systematic error from using our best value.
[2] AAIJ 13M does not report correlations between various measurements of the $J/\psi\pi\pi$ final state.
[3] Assumes equal production of B^+ and B^0 at the $\Upsilon(4S)$.

$\Gamma(J/\psi(1S)\pi^+\pi^-\ \text{nonresonant})/\Gamma_{total}$ Γ_{182}/Γ

VALUE (units 10^{-5})	CL%	DOCUMENT ID	TECN	COMMENT
<1.2	90	[1] AUBERT	07AC BABR	$e^+e^- \to \Upsilon(4S)$

[1] Assumes equal production of B^+ and B^0 at the $\Upsilon(4S)$.

$\Gamma(J/\psi(1S)f_0(500),\ f_0 \to \pi\pi)/\Gamma_{total}$ Γ_{183}/Γ

VALUE (units 10^{-6})	DOCUMENT ID	TECN	COMMENT
$6.5^{+2.5}_{-1.1}\pm0.3$	[1,2] AAIJ	13M LHCB	pp at 7 TeV

[1] AAIJ 13M reports $(6.4\ \pm\ 0.8^{+2.4}_{-0.8})\times10^{-6}$ from a measurement of $[\Gamma(B^0 \to J/\psi(1S)f_0(500),\ f_0 \to \pi\pi)/\Gamma_{total}]$ / $[B(B^0 \to J/\psi(1S)\pi^+\pi^-)]$ assuming $B(B^0 \to J/\psi(1S)\pi^+\pi^-) = (3.97\pm0.09\pm0.11\pm0.16)\times10^{-5}$, which we rescale to our best value $B(B^0 \to J/\psi(1S)\pi^+\pi^-) = (4.03\pm0.18)\times10^{-5}$. Our first error is their experiment's error and our second error is the systematic error from using our best value.
[2] AAIJ 13M does not report correlations between various measurements of the $J/\psi\pi\pi$ final state. Measured in Dalitz plot like analysis of $B^0 \to J/\psi\pi^+\pi^-$.

$\Gamma(J/\psi(1S)f_2)/\Gamma_{total}$ Γ_{184}/Γ

VALUE (units 10^{-5})	CL%	DOCUMENT ID	TECN	COMMENT
0.42±0.06±0.02		[1,2] AAIJ	13M LHCB	pp at 7 TeV
• • • We do not use the following data for averages, fits, limits, etc. • • •				
<0.5	90	[3,4] AUBERT	07AC BABR	$e^+e^- \to \Upsilon(4S)$

[1] AAIJ 13M reports $[\Gamma(B^0 \to J/\psi(1S)f_2)/\Gamma_{total}] \times [B(f_2(1270) \to \pi\pi)] = (3.5\pm0.4\pm0.4)\times10^{-6}$ from a measurement of $[\Gamma(B^0 \to J/\psi(1S)f_2)/\Gamma_{total}] \times [B(f_2(1270) \to \pi\pi)]$ / $[B(B^0 \to J/\psi(1S)\pi^+\pi^-)]$ assuming $B(B^0 \to J/\psi(1S)\pi^+\pi^-) = (3.97\pm0.09\pm0.11\pm0.16)\times10^{-5}$, which we rescale to our best values $B(f_2(1270) \to \pi\pi) = (84.8^{+2.4}_{-1.2})\times10^{-2}$, $B(B^0 \to J/\psi(1S)\pi^+\pi^-) = (4.03\pm0.18)\times10^{-5}$. Our first error is their experiment's error and our second error is the systematic error from using our best values.
[2] AAIJ 13M does not report correlations between various measurements of the $J/\psi\pi\pi$ final state. Measured in Dalitz plot like analysis of $B^0 \to J/\psi\pi^+\pi^-$.
[3] AUBERT 07AC reports $[\Gamma(B^0 \to J/\psi(1S)f_2)/\Gamma_{total}] \times [B(f_2(1270) \to \pi\pi)] < 0.46\times10^{-5}$ which we divide by our best value $B(f_2(1270) \to \pi\pi) = 84.8\times10^{-2}$.
[4] Assumes equal production of B^+ and B^0 at the $\Upsilon(4S)$.

$\Gamma(J/\psi(1S)\rho^0)/\Gamma_{total}$ Γ_{185}/Γ

VALUE (units 10^{-5})	CL%	DOCUMENT ID	TECN	COMMENT
2.58±0.21 OUR AVERAGE				
$2.53^{+0.22}_{-0.23}\pm0.11$		[1,2] AAIJ	13M LHCB	pp at 7 TeV
$2.7\ \pm0.3\ \pm0.2$		[3] AUBERT	07AC BABR	$e^+e^- \to \Upsilon(4S)$
• • • We do not use the following data for averages, fits, limits, etc. • • •				
$1.6\ \pm0.6\ \pm0.4$		[3] AUBERT	03B BABR	Repl. by AUBERT 07AC
<25	90	BISHAI	96 CLE2	$e^+e^- \to \Upsilon(4S)$

[1] AAIJ 13M reports $(2.49^{+0.20+0.16}_{-0.13-0.23}) \times 10^{-5}$ from a measurement of $[\Gamma(B^0 \to J/\psi(1S)\rho^0)/\Gamma_{total}]$ / $[B(B^0 \to J/\psi(1S)\pi^+\pi^-)]$ assuming $B(B^0 \to J/\psi(1S)\pi^+\pi^-) = (3.97\pm0.09\pm0.11\pm0.16)\times10^{-5}$, which we rescale to our best value $B(B^0 \to J/\psi(1S)\pi^+\pi^-) = (4.03\pm0.18)\times10^{-5}$. Our first error is their experiment's error and our second error is the systematic error from using our best value.
[2] AAIJ 13M does not report correlations between various measurements of the $J/\psi\pi\pi$ final state. Measured in Dalitz plot like analysis of $B^0 \to J/\psi\pi^+\pi^-$. Assumes $B(\rho(770)^0 \to \pi\pi) = 100\%$.
[3] Assumes equal production of B^+ and B^0 at the $\Upsilon(4S)$.

$\Gamma(J/\psi(1S)f_0(980),\ f_0 \to \pi^+\pi^-)/\Gamma_{total}$ Γ_{186}/Γ

VALUE	CL%	DOCUMENT ID	TECN	COMMENT
<1.1 × 10^{-6}	90	[1] AAIJ	13M LHCB	pp at 7 TeV

[1] AAIJ 13M does not provide correlations between various measurements of the $J/\psi\pi^+\pi^-$ final state. The measurements were obtained from a Dalitz plot like analysis of $B^0 \to J/\psi\pi^+\pi^-$. Also reports $\Gamma(J/\psi(1S)f_0(980),\ f_0 \to \pi^+\pi^-)/\Gamma_{total} = (6.1^{+3.1+1.7}_{-2.0-1.4})\times10^{-6}$.

$\Gamma(J/\psi(1S)\rho(1450)^0,\ \rho^0 \to \pi\pi)/\Gamma_{total}$ Γ_{187}/Γ

VALUE (units 10^{-6})	DOCUMENT ID	TECN	COMMENT
$2.1^{+2.4}_{-0.7}\pm0.1$	[1,2] AAIJ	13M LHCB	pp at 7 TeV

[1] AAIJ 13M reports $(2.1^{+1.0+2.2}_{-0.6-0.4}) \times 10^{-6}$ from a measurement of $[\Gamma(B^0 \to J/\psi(1S)\rho(1450)^0,\ \rho^0 \to \pi\pi)/\Gamma_{total}]$ / $[B(B^0 \to J/\psi(1S)\pi^+\pi^-)]$ assuming $B(B^0 \to J/\psi(1S)\pi^+\pi^-) = (3.97\pm0.09\pm0.11\pm0.16)\times10^{-5}$, which we rescale to our best value $B(B^0 \to J/\psi(1S)\pi^+\pi^-) = (4.03\pm0.18)\times10^{-5}$. Our first error is their experiment's error and our second error is the systematic error from using our best value.
[2] AAIJ 13M does not report correlations between various measurements of the $J/\psi\pi\pi$ final state. Measured in Dalitz plot like analysis of $B^0 \to J/\psi\pi^+\pi^-$.

$\Gamma(J/\psi(1S)\omega)/\Gamma_{total}$ Γ_{188}/Γ

VALUE	CL%	DOCUMENT ID	TECN	COMMENT
• • • We do not use the following data for averages, fits, limits, etc. • • •				
$<2.7\times10^{-4}$	90	BISHAI	96 CLE2	$e^+e^- \to \Upsilon(4S)$

$\Gamma(J/\psi(1S)\omega)/\Gamma(J/\psi(1S)\rho^0)$ $\Gamma_{188}/\Gamma_{185}$

VALUE	DOCUMENT ID	TECN	COMMENT
$0.61^{+0.24+0.31}_{-0.14-0.16}$	[1,2] AAIJ	13M LHCB	pp at 7 TeV

[1] AAIJ 13M reports $0.61^{+0.24+0.31}_{-0.14-0.16}$ from a measurement of $[\Gamma(B^0 \to J/\psi(1S)\omega)/\Gamma(B^0 \to J/\psi(1S)\rho^0)] \times [B(\omega(782) \to \pi^+\pi^-)]$ assuming $B(\omega(782) \to \pi^+\pi^-) = (1.53^{+0.11}_{-0.13})\times10^{-2}$.
[2] AAIJ 13M does not report correlations between various measurements of the $J/\psi\pi\pi$ final state. Measured in Dalitz plot like analysis of $B^0 \to J/\psi\pi^+\pi^-$. Assumes $B(\rho(770)^0 \to \pi\pi) = 100\%$.

$\Gamma(J/\psi(1S)\omega)/\Gamma(J/\psi(1S)\rho^0)$ $\Gamma_{188}/\Gamma_{185}$

VALUE	DOCUMENT ID	TECN	COMMENT
$0.89\pm0.19^{+0.07}_{-0.13}$	AAIJ	13A LHCB	pp at 7 TeV

$\Gamma(J/\psi(1S)K^+K^-)/\Gamma_{total}$ Γ_{189}/Γ

VALUE (units 10^{-6})	DOCUMENT ID		TECN	COMMENT
2.55±0.35±0.08	[1] AAIJ	13BT	LHCB	pp at 7 TeV

[1] AAIJ 13BT reports $(2.53 \pm 0.31 \pm 0.19) \times 10^{-6}$ from a measurement of $[\Gamma(B^0 \to J/\psi(1S)K^+K^-)/\Gamma_{total}]$ / $[B(B^+ \to J/\psi(1S)K^+)]$ assuming $B(B^+ \to J/\psi(1S)K^+) = (1.018 \pm 0.042) \times 10^{-3}$, which we rescale to our best value $B(B^+ \to J/\psi(1S)K^+) = (1.027 \pm 0.031) \times 10^{-3}$. Our first error is their experiment's error and our second error is the systematic error from using our best value.

$\Gamma(J/\psi(1S)a_0(980),\ a_0 \to K^+K^-)/\Gamma_{total}$ Γ_{190}/Γ

VALUE (units 10^{-6})	DOCUMENT ID		TECN	COMMENT
0.470±0.331±0.072	[1] AAIJ	13BT	LHCB	pp at 7 TeV

[1] AAIJ 13BT uses $B(\overline{B}^0 \to J/\psi K^+K^-) = (2.53 \pm 0.31 \pm 0.19) \times 10^{-6}$ to derive this result. It also reports the equivalent upper limit of $< 9.0 \times 10^{-7}$ at 90% CL.

$\Gamma(J/\psi(1S)\phi)/\Gamma_{total}$ Γ_{191}/Γ

VALUE (units 10^{-6})	CL%	DOCUMENT ID		TECN	COMMENT
<0.19	90	[1] AAIJ	13BT	LHCB	pp at 7 TeV
• • • We do not use the following data for averages, fits, limits, etc. • • •					
<0.94	90	[2] LIU	08I	BELL	$e^+e^- \to \Upsilon(4S)$
<9.2	90	[2] AUBERT	03O	BABR	$e^+e^- \to \Upsilon(4S)$

[1] AAIJ 13BT uses $B(B^0 \to J/\psi(1S)K^+K^-) = (2.53 \pm 0.31 \pm 0.19) \times 10^{-6}$ and $B(\phi \to K^+K^-) = (48.9 \pm 0.5)\%$ to obtain this result.
[2] Assumes equal production of B^+ and B^0 at the $\Upsilon(4S)$.

$\Gamma(J/\psi(1S)\eta'(958))/\Gamma_{total}$ Γ_{192}/Γ

VALUE (units 10^{-6})	CL%	DOCUMENT ID		TECN	COMMENT
< 7.4	90	[1,2] CHANG	12	BELL	$e^+e^- \to \Upsilon(4S)$
• • • We do not use the following data for averages, fits, limits, etc. • • •					
<63	90	[2] AUBERT	03O	BABR	$e^+e^- \to \Upsilon(4S)$

[1] Reconstructs $\eta'(985)$ in $\eta\pi^+\pi^-$ and $\rho(770)^0\gamma$ decays.
[2] Assumes equal production of B^+ and B^0 at the $\Upsilon(4S)$.

$\Gamma(J/\psi(1S)K^0\pi^+\pi^-)/\Gamma_{total}$ Γ_{193}/Γ

VALUE (units 10^{-4})	DOCUMENT ID		TECN	COMMENT
10.3±3.3±1.5	[1] AFFOLDER	02B	CDF	$p\overline{p}$ 1.8 TeV

[1] Uses $B^0 \to J/\psi(1S)K^0_S$ decay as a reference and $B(B^0 \to J/\psi(1S)K^0) = 8.3 \times 10^{-4}$.

$\Gamma(J/\psi(1S)K^0\rho^0)/\Gamma_{total}$ Γ_{194}/Γ

VALUE (units 10^{-4})	DOCUMENT ID		TECN	COMMENT
5.4±2.9±0.9	[1] AFFOLDER	02B	CDF	$p\overline{p}$ 1.8 TeV

[1] Uses $B^0 \to J/\psi(1S)K^0_S$ decay as a reference and $B(B^0 \to J/\psi(1S)K^0) = 8.3 \times 10^{-4}$.

$\Gamma(J/\psi(1S)K^*(892)^+\pi^-)/\Gamma_{total}$ Γ_{195}/Γ

VALUE (units 10^{-4})	DOCUMENT ID		TECN	COMMENT
7.7±4.1±1.3	[1] AFFOLDER	02B	CDF	$p\overline{p}$ 1.8 TeV

[1] Uses $B^0 \to J/\psi(1S)K^0_S$ decay as a reference and $B(B^0 \to J/\psi(1S)K^0) = 8.3 \times 10^{-4}$.

$\Gamma(J/\psi(1S)K^*(892)^0\pi^+\pi^-)/\Gamma_{total}$ Γ_{196}/Γ

VALUE (units 10^{-4})	DOCUMENT ID		TECN	COMMENT
6.6±1.9±1.1	[1] AFFOLDER	02B	CDF	$p\overline{p}$ 1.8 TeV

[1] Uses $B^0 \to J/\psi(1S)K^*(892)^0$ decay as a reference and $B(B^0 \to J/\psi(1S)K^0) = 12.4 \times 10^{-4}$.

$\Gamma(X(3872)^-K^+)/\Gamma_{total}$ Γ_{197}/Γ

VALUE	CL%	DOCUMENT ID		TECN	COMMENT
$< 5 \times 10^{-4}$	90	[1] AUBERT	06E	BABR	$e^+e^- \to \Upsilon(4S)$

[1] Perform measurements of absolute branching fractions using a missing mass technique.

$\Gamma(X(3872)^-K^+ \times B(X(3872)^- \to J/\psi(1S)\pi^-\pi^0))/\Gamma_{total}$ Γ_{198}/Γ

VALUE (units 10^{-6})	CL%	DOCUMENT ID		TECN	COMMENT
<4.2	90	[1,2] CHOI	11	BELL	$e^+e^- \to \Upsilon(4S)$
• • • We do not use the following data for averages, fits, limits, etc. • • •					
<5.4	90	[2,3] AUBERT	05B	BABR	$e^+e^- \to \Upsilon(4S)$

[1] Assumes $\pi^+\pi^0$ originates from ρ^+.
[2] Assumes equal production of B^+ and B^0 at the $\Upsilon(4S)$.
[3] The isovector-X hypothesis is excluded with a likelihood test at 1×10^{-4} level.

$\Gamma(X(3872)K^0 \times B(X \to J/\psi\pi^+\pi^-))/\Gamma_{total}$ Γ_{199}/Γ

VALUE (units 10^{-6})	CL%	DOCUMENT ID		TECN	COMMENT
4.3±1.2±0.4		[1,2] CHOI	11	BELL	$e^+e^- \to \Upsilon(4S)$
• • • We do not use the following data for averages, fits, limits, etc. • • •					
< 6.0	90	[2] AUBERT	08Y	BABR	$e^+e^- \to \Upsilon(4S)$
<10.3	90	[2,3] AUBERT	06	BABR	Repl. by AUBERT 08Y

[1] CHOI 11 reports $[\Gamma(B^0 \to X(3872)K^0 \times B(X \to J/\psi\pi^+\pi^-))/\Gamma_{total}]$ / $[B(B^+ \to X(3872)K^+,\ X \to J/\psi\pi^+\pi^-)] = 0.50 \pm 0.14 \pm 0.04$ which we multiply by our best value $B(B^+ \to X(3872)K^+,\ X \to J/\psi\pi^+\pi^-) = (8.6 \pm 0.8) \times 10^{-6}$. Our first error is their experiment's error and our second error is the systematic error from using our best value.
[2] Assumes equal production of B^+ and B^0 at the $\Upsilon(4S)$.
[3] The lower limit is also given to be 1.34×10^{-6} at 90% CL.

$\Gamma(X(3872)K^0 \times B(X \to J/\psi\gamma))/\Gamma_{total}$ Γ_{200}/Γ

VALUE (units 10^{-6})	CL%	DOCUMENT ID		TECN	COMMENT
<2.4	90	[1] BHARDWAJ	11	BELL	$e^+e^- \to \Upsilon(4S)$
• • • We do not use the following data for averages, fits, limits, etc. • • •					
<4.9	90	[2] AUBERT	09B	BABR	$e^+e^- \to \Upsilon(4S)$

[1] Assumes equal production of B^+ and B^0 at the $\Upsilon(4S)$.
[2] Uses $B(\Upsilon(4S) \to B^+B^-) = (51.6 \pm 0.6)\%$ and $B(\Upsilon(4S) \to B^0\overline{B}^0) = (48.4 \pm 0.6)\%$.

$\Gamma(X(3872)K^*(892)^0 \times B(X \to J/\psi\gamma))/\Gamma_{total}$ Γ_{201}/Γ

VALUE (units 10^{-6})	CL%	DOCUMENT ID		TECN	COMMENT
<2.8	90	[1] AUBERT	09B	BABR	$e^+e^- \to \Upsilon(4S)$

[1] Uses $B(\Upsilon(4S) \to B^+B^-) = (51.6 \pm 0.6)\%$ and $B(\Upsilon(4S) \to B^0\overline{B}^0) = (48.4 \pm 0.6)\%$.

$\Gamma(X(3872)K^0 \times B(X \to \psi(2S)\gamma))/\Gamma_{total}$ Γ_{202}/Γ

VALUE (units 10^{-6})	CL%	DOCUMENT ID		TECN	COMMENT
< 6.62	90	[1] BHARDWAJ	11	BELL	$e^+e^- \to \Upsilon(4S)$
• • • We do not use the following data for averages, fits, limits, etc. • • •					
<19	90	[2] AUBERT	09B	BABR	$e^+e^- \to \Upsilon(4S)$

[1] Assumes equal production of B^+ and B^0 at the $\Upsilon(4S)$.
[2] Uses $B(\Upsilon(4S) \to B^+B^-) = (51.6 \pm 0.6)\%$ and $B(\Upsilon(4S) \to B^0\overline{B}^0) = (48.4 \pm 0.6)\%$.

$\Gamma(X(3872)K^*(892)^0 \times B(X \to \psi(2S)\gamma))/\Gamma_{total}$ Γ_{203}/Γ

VALUE (units 10^{-6})	CL%	DOCUMENT ID		TECN	COMMENT
<4.4	90	[1] AUBERT	09B	BABR	$e^+e^- \to \Upsilon(4S)$

[1] Uses $B(\Upsilon(4S) \to B^+B^-) = (51.6 \pm 0.6)\%$ and $B(\Upsilon(4S) \to B^0\overline{B}^0) = (48.4 \pm 0.6)\%$.

$\Gamma(X(3872)K^0 \times B(X \to D^0\overline{D}^0\pi^0))/\Gamma_{total}$ Γ_{204}/Γ

VALUE (units 10^{-4})	DOCUMENT ID		TECN	COMMENT
$1.66 \pm 0.70^{+0.32}_{-0.37}$	[1] GOKHROO	06	BELL	$e^+e^- \to \Upsilon(4S)$

[1] Measure the near-threshold enhancements in the $(D^0\overline{D}^0\pi^0)$ system at a mass $3875.2 \pm 0.7^{+0.3}_{-1.6} \pm 0.8$ MeV/c^2.

$\Gamma(X(3872)K^0 \times B(X \to \overline{D}^{*0}D^0))/\Gamma_{total}$ Γ_{205}/Γ

VALUE (units 10^{-4})		DOCUMENT ID		TECN	COMMENT
1.2 ±0.4 OUR AVERAGE					
0.97±0.46±0.13	[1]	AUSHEV	10	BELL	$e^+e^- \to \Upsilon(4S)$
2.22±1.05±0.42	[1,2]	AUBERT	08B	BABR	$e^+e^- \to \Upsilon(4S)$

[1] Assumes equal production of B^+ and B^0 at the $\Upsilon(4S)$.
[2] This result is equivalent to the the 90% CL upper limit of 4.37×10^{-4}

$\Gamma(X(4430)^\pm K^\mp \times B(X^\pm \to \psi(2S)\pi^\pm))/\Gamma_{total}$ Γ_{206}/Γ

VALUE (units 10^{-5})	CL%	DOCUMENT ID		TECN	COMMENT
$6.0^{+1.7+2.5}_{-2.0-1.4}$		CHILIKIN	13	BELL	$e^+e^- \to \Upsilon(4S)$
• • • We do not use the following data for averages, fits, limits, etc. • • •					
<3.1	95	[1] AUBERT	09AA	BABR	$e^+e^- \to \Upsilon(4S)$
$3.2^{+1.8+5.3}_{-0.9-1.6}$		[1] MIZUK	09	BELL	$e^+e^- \to \Upsilon(4S)$
4.1±1.0±1.4		[1,2] CHOI	08	BELL	Repl. by MIZUK 09

[1] Assumes equal production of B^+ and B^0 at the $\Upsilon(4S)$.
[2] Establishes the $X(4430)^+$ with a significance of 6.5 sigma. Needs confirmation.

$\Gamma(X(4430)^\pm K^\mp \times B(X^\pm \to J/\psi\pi^\pm))/\Gamma_{total}$ Γ_{207}/Γ

VALUE (units 10^{-5})	CL%	DOCUMENT ID		TECN	COMMENT
<0.4	95	[1] AUBERT	09AA	BABR	$e^+e^- \to \Upsilon(4S)$

[1] Assumes equal production of B^+ and B^0 at the $\Upsilon(4S)$.

$\Gamma(J/\psi(1S)p\overline{p})/\Gamma_{total}$ Γ_{208}/Γ

VALUE	CL%	DOCUMENT ID		TECN	COMMENT
$< 5.2 \times 10^{-7}$	90	[1] AAIJ	13Z	LHCB	pp at 7 TeV
• • • We do not use the following data for averages, fits, limits, etc. • • •					
$< 8.3 \times 10^{-7}$	90	[2] XIE	05	BELL	$e^+e^- \to \Upsilon(4S)$
$< 1.9 \times 10^{-6}$	90	[2] AUBERT	03K	BABR	$e^+e^- \to \Upsilon(4S)$

[1] Uses $B(B^0_s \to J/\psi(1S)\pi^+\pi^-) = (1.98 \pm 0.20) \times 10^{-4}$.
[2] Assumes equal production of B^+ and B^0 at the $\Upsilon(4S)$.

$\Gamma(J/\psi(1S)\gamma)/\Gamma_{total}$ Γ_{209}/Γ

VALUE (units 10^{-6})	CL%	DOCUMENT ID		TECN	COMMENT
<1.6	90	[1] AUBERT,B	04T	BABR	$e^+e^- \to \Upsilon(4S)$

[1] Assumes equal production of B^+ and B^0 at the $\Upsilon(4S)$.

$\Gamma(J/\psi(1S)\overline{D}^0)/\Gamma_{total}$ Γ_{210}/Γ

VALUE (units 10^{-5})	CL%	DOCUMENT ID		TECN	COMMENT
<1.3	90	[1] AUBERT	05U	BABR	$e^+e^- \to \Upsilon(4S)$
• • • We do not use the following data for averages, fits, limits, etc. • • •					
<2.0	90	[1] ZHANG	05B	BELL	$e^+e^- \to \Upsilon(4S)$

[1] Assumes equal production of B^+ and B^0 at the $\Upsilon(4S)$.

$\Gamma(\psi(2S)K^0)/\Gamma_{total}$ Γ_{211}/Γ

VALUE (units 10^{-4})	CL%	DOCUMENT ID		TECN	COMMENT
6.2 ±0.5 OUR FIT					
6.2 ±0.6 OUR AVERAGE					
6.46±0.65±0.51		[1] AUBERT	05J	BABR	$e^+e^- \to \Upsilon(4S)$
6.7 ±1.1		[1] ABE	03B	BELL	$e^+e^- \to \Upsilon(4S)$
5.0 ±1.1 ±0.6		[1] RICHICHI	01	CLE2	$e^+e^- \to \Upsilon(4S)$
• • • We do not use the following data for averages, fits, limits, etc. • • •					
6.9 ±1.1 ±1.1		[1] AUBERT	02	BABR	Repl. by AUBERT 05J
< 8	90	[1] ALAM	94	CLE2	$e^+e^- \to \Upsilon(4S)$
<15	90	[1] BORTOLETTO	92	CLEO	$e^+e^- \to \Upsilon(4S)$
<28	90	[1] ALBRECHT	90J	ARG	$e^+e^- \to \Upsilon(4S)$

[1] Assumes equal production of B^+ and B^0 at the $\Upsilon(4S)$.

$\Gamma(\psi(2S)K^0)/\Gamma(J/\psi(1S)K^0)$ $\Gamma_{211}/\Gamma_{169}$

VALUE	DOCUMENT ID		TECN	COMMENT
0.82±0.13±0.12	[1] AUBERT	02	BABR	$e^+e^- \to \Upsilon(4S)$

[1] Assumes equal production of B^+ and B^0 at the $\Upsilon(4S)$.

$\Gamma(\psi(3770)K^0 \times B(\psi \to \overline{D}^0 D^0))/\Gamma_{total}$ Γ_{212}/Γ

VALUE (units 10^{-4})	CL%	DOCUMENT ID		TECN	COMMENT
<1.23	90	[1] AUBERT	08B	BABR	$e^+e^- \to \Upsilon(4S)$

[1] Assumes equal production of B^+ and B^0 at the $\Upsilon(4S)$.

$\Gamma(\psi(3770)K^0 \times B(\psi \to D^- D^+))/\Gamma_{total}$ Γ_{213}/Γ

VALUE (units 10^{-4})	CL%	DOCUMENT ID		TECN	COMMENT
<1.88	90	[1] AUBERT	08B	BABR	$e^+e^- \to \Upsilon(4S)$

[1] Assumes equal production of B^+ and B^0 at the $\Upsilon(4S)$.

$\Gamma(\psi(2S)\pi^+\pi^-)/\Gamma(J/\psi(1S)\pi^+\pi^-)$ $\Gamma_{214}/\Gamma_{181}$

VALUE	DOCUMENT ID		TECN	COMMENT
0.56±0.07±0.05	[1] AAIJ	13AA	LHCB	pp at 7 TeV

[1] Assuming lepton universality for dimuon decay modes of J/ψ and $\psi(2S)$ mesons, the ratio $B(J/\psi \to \mu^+\mu^-)/B(\psi(2S) \to \mu^+\mu^-) = B(J/\psi \to e^+e^-)/B(\psi(2S) \to e^+e^-) = 7.69 \pm 0.19$ was used.

$\Gamma(\psi(2S)K^+\pi^-)/\Gamma_{total}$ Γ_{215}/Γ

VALUE (units 10^{-4})	CL%	DOCUMENT ID		TECN	COMMENT
5.80±0.39		[1,2] CHILIKIN	13	BELL	$e^+e^- \to \Upsilon(4S)$
• • • We do not use the following data for averages, fits, limits, etc. • • •					
5.57±0.16		[3] AUBERT	09AA	BABR	$e^+e^- \to \Upsilon(4S)$
5.68±0.13±0.42		[2] MIZUK	09	BELL	$e^+e^- \to \Upsilon(4S)$
<10	90	[2] ALBRECHT	90J	ARG	$e^+e^- \to \Upsilon(4S)$

[1] Combines measurements with $\psi(2S) \to \ell^+\ell^-$ with measurement from MIZUK 09 which uses $\psi(2S) \to J/\psi\pi^+\pi^-$.
[2] Assumes equal production of B^+ and B^0 at the $\Upsilon(4S)$.
[3] Does not report systematic uncertainties.

$\Gamma(\psi(2S)K^*(892)^0)/\Gamma_{total}$ Γ_{216}/Γ

VALUE (units 10^{-4})	CL%	DOCUMENT ID		TECN	COMMENT
6.0 ±0.4 OUR FIT Error includes scale factor of 1.1.					
6.0 $^{+0.5}_{-0.7}$ OUR AVERAGE Error includes scale factor of 1.1.					
5.55$^{+0.22}_{-0.23}$$^{+0.41}_{-0.84}$		[1] CHILIKIN	13	BELL	$e^+e^- \to \Upsilon(4S)$
6.49±0.59±0.97		[1] AUBERT	05J	BABR	$e^+e^- \to \Upsilon(4S)$
7.6 ±1.1 ±1.0		[1] RICHICHI	01	CLE2	$e^+e^- \to \Upsilon(4S)$
9.0 ±2.2 ±0.9		[2] ABE	98O	CDF	$p\overline{p}$ 1.8 TeV
• • • We do not use the following data for averages, fits, limits, etc. • • •					
5.52$^{+0.35}_{-0.32}$$^{+0.53}_{-0.58}$		[1] MIZUK	09	BELL	$e^+e^- \to \Upsilon(4S)$
<19	90	[1] ALAM	94	CLE2	Repl. by RICHICHI 01
14 ±8 ±4		[1] BORTOLETTO	92	CLEO	$e^+e^- \to \Upsilon(4S)$
<23	90	[1] ALBRECHT	90J	ARG	$e^+e^- \to \Upsilon(4S)$

[1] Assumes equal production of B^+ and B^0 at the $\Upsilon(4S)$.
[2] ABE 98O reports $[B(B^0 \to \psi(2S)K^*(892)^0)]/[B(B^+ \to J/\psi(1S)K^+)] = 0.908 \pm 0.194 \pm 0.10$. We multiply by our best value $B(B^+ \to J/\psi(1S)K^+) = (9.9 \pm 1.0) \times 10^{-4}$. Our first error is their experiment's error and our second error is the systematic error from using our best value.

$\Gamma(\psi(2S)K^*(892)^0)/\Gamma(\psi(2S)K^0)$ $\Gamma_{216}/\Gamma_{211}$

VALUE	DOCUMENT ID		TECN	COMMENT
0.97±0.10 OUR FIT				
1.00±0.14±0.09	AUBERT	05J	BABR	$e^+e^- \to \Upsilon(4S)$

$\Gamma(\psi(2S)K^*(892)^0)/\Gamma(J/\psi(1S)K^*(892)^0)$ $\Gamma_{216}/\Gamma_{171}$

VALUE	DOCUMENT ID		TECN	COMMENT
0.484±0.018±0.011	[1,2] AAIJ	12L	LHCB	pp at 7 TeV

[1] AAIJ 12L reports $0.476 \pm 0.014 \pm 0.010 \pm 0.012$ from a measurement of $[\Gamma(B^0 \to \psi(2S)K^*(892)^0)/\Gamma(B^0 \to J/\psi(1S)K^*(892)^0)] \times [B(J/\psi(1S) \to e^+e^-)] / [B(\psi(2S) \to e^+e^-)]$ assuming $B(J/\psi(1S) \to e^+e^-) = (5.94 \pm 0.06) \times 10^{-2}$, $B(\psi(2S) \to e^+e^-) = (7.72 \pm 0.17) \times 10^{-3}$, which we rescale to our best values $B(J/\psi(1S) \to e^+e^-) = (5.971 \pm 0.032) \times 10^{-2}$, $B(\psi(2S) \to e^+e^-) = (7.89 \pm 0.17) \times 10^{-3}$. Our first error is their experiment's error and our second error is the systematic error from using our best values.
[2] Assumes $B(J/\psi \to \mu^+\mu^-) / B(\psi(2S) \to \mu^+\mu^-) = B(J/\psi \to e^+e^-) / B(\psi(2S) \to e^+e^-) = 7.69 \pm 0.19$.

$\Gamma(\chi_{c0}K^0)/\Gamma_{total}$ Γ_{217}/Γ

VALUE (units 10^{-6})	CL%	DOCUMENT ID		TECN	COMMENT
147± 27 OUR AVERAGE					
149$^{+105}_{-87}$± 8		[1,2] LEES	12I	BABR	$e^+e^- \to \Upsilon(4S)$
148± 30±13		[1,3] LEES	12O	BABR	$e^+e^- \to \Upsilon(4S)$
142$^{+55}_{-44}$±22		[1,4] AUBERT	09AU	BABR	$e^+e^- \to \Upsilon(4S)$
• • • We do not use the following data for averages, fits, limits, etc. • • •					
< 113	90	[4] GARMASH	07	BELL	$e^+e^- \to \Upsilon(4S)$
<1240	90	[1] AUBERT	05K	BABR	$e^+e^- \to \Upsilon(4S)$
< 500	90	[5] EDWARDS	01	CLE2	$e^+e^- \to \Upsilon(4S)$

[1] Assumes equal production of B^+ and B^0 at the $\Upsilon(4S)$.
[2] LEES 12I reports $[\Gamma(B^0 \to \chi_{c0}K^0)/\Gamma_{total}] \times [B(\chi_{c0}(1P) \to K^0_S K^0_S)] = (0.46^{+0.25}_{-0.17} \pm 0.21) \times 10^{-6}$ which we divide by our best value $B(\chi_{c0}(1P) \to K^0_S K^0_S) = (3.10 \pm 0.18) \times 10^{-3}$. Our first error is their experiment's error and our second error is the systematic error from using our best value.
[3] Measured in the $B^0 \to K^0_S K^+ K^-$ decay.
[4] Uses Dalitz plot analysis of the $B^0 \to K^0\pi^+\pi^-$ final state decays.
[5] EDWARDS 01 assumes equal production of B^0 and B^+ at the $\Upsilon(4S)$. The correlated uncertainties (28.3)% from $B(J/\psi(1S) \to \gamma\eta_C)$ in those modes have been accounted for.

$\Gamma(\chi_{c0}K^*(892)^0)/\Gamma_{total}$ Γ_{218}/Γ

VALUE (units 10^{-4})	CL%	DOCUMENT ID		TECN	COMMENT
1.7±0.3±0.2		[1] AUBERT	08BD	BABR	$e^+e^- \to \Upsilon(4S)$
• • • We do not use the following data for averages, fits, limits, etc. • • •					
<7.7	90	[1] AUBERT	05K	BABR	Repl. by AUBERT 08BD

[1] Assumes equal production of B^+ and B^0 at the $\Upsilon(4S)$.

$\Gamma(\chi_{c2}K^0)/\Gamma_{total}$ Γ_{219}/Γ

VALUE	CL%	DOCUMENT ID		TECN	COMMENT
<1.5 × 10^{-5}	90	[1] BHARDWAJ	11	BELL	$e^+e^- \to \Upsilon(4S)$
• • • We do not use the following data for averages, fits, limits, etc. • • •					
<2.8 × 10^{-5}	90	[2] AUBERT	09B	BABR	$e^+e^- \to \Upsilon(4S)$
<2.6 × 10^{-5}	90	[1] SONI	06	BELL	Repl. by BHARDWAJ 11
<4.1 × 10^{-5}	90	[1] AUBERT	05K	BABR	$e^+e^- \to \Upsilon(4S)$

[1] Assumes equal production of B^+ and B^0 at the $\Upsilon(4S)$.
[2] Uses $\chi_{c1,2} \to J/\psi\gamma$. Assumes $B(\Upsilon(4S) \to B^+B^-) = (51.6 \pm 0.6)\%$ and $B(\Upsilon(4S) \to B^0\overline{B}^0) = (48.4 \pm 0.6)\%$.

$\Gamma(\chi_{c2}K^*(892)^0)/\Gamma_{total}$ Γ_{220}/Γ

VALUE (units 10^{-5})	CL%	DOCUMENT ID		TECN	COMMENT
5.0±1.2 OUR FIT Error includes scale factor of 1.1.					
6.6±1.8±0.5		[1] AUBERT	09B	BABR	$e^+e^- \to \Upsilon(4S)$
• • • We do not use the following data for averages, fits, limits, etc. • • •					
<7.1	90	[2] SONI	06	BELL	$e^+e^- \to \Upsilon(4S)$
<3.6	90	[2] AUBERT	05K	BABR	Repl. by AUBERT 09B

[1] Uses $\chi_{c1,2} \to J/\psi\gamma$. Assumes $B(\Upsilon(4S) \to B^+B^-) = (51.6 \pm 0.6)\%$ and $B(\Upsilon(4S) \to B^0\overline{B}^0) = (48.4 \pm 0.6)\%$.
[2] Assumes equal production of B^+ and B^0 at the $\Upsilon(4S)$.

$\Gamma(\chi_{c2}K^*(892)^0)/\Gamma(\chi_{c1}K^*(892)^0)$ $\Gamma_{220}/\Gamma_{224}$

VALUE (units 10^{-2})	DOCUMENT ID		TECN	COMMENT
20 ±5 OUR FIT Error includes scale factor of 1.1.				
17.1±5.0±2.0	[1] AAIJ	13AC	LHCB	pp at 7 TeV

[1] Uses $B(\chi_{c1} \to J/\psi\gamma)/B(\chi_{c2} \to J/\psi\gamma) = 1.76 \pm 0.11$.

$\Gamma(\chi_{c1}\pi^0)/\Gamma_{total}$ Γ_{221}/Γ

VALUE (units 10^{-5})	DOCUMENT ID		TECN	COMMENT
1.12±0.25±0.12	[1] KUMAR	08	BELL	$e^+e^- \to \Upsilon(4S)$

[1] Assumes equal production of B^+ and B^0 at the $\Upsilon(4S)$.

$\Gamma(\chi_{c1}K^0)/\Gamma_{total}$ Γ_{222}/Γ

VALUE (units 10^{-4})	CL%	DOCUMENT ID		TECN	COMMENT
3.93±0.27 OUR AVERAGE					
$3.78^{+0.17}_{-0.16}\pm0.33$		[1] BHARDWAJ	11	BELL	$e^+e^-\to\ \Upsilon(4S)$
4.2 ±0.3 ±0.3		[2] AUBERT	09B	BABR	$e^+e^-\to\ \Upsilon(4S)$
$3.1\ ^{+1.6}_{-1.1}\pm0.1$		[3] AVERY	00	CLE2	$e^+e^-\to\ \Upsilon(4S)$
• • • We do not use the following data for averages, fits, limits, etc. • • •					
$3.51\pm0.33\pm0.45$		[1] SONI	06	BELL	Repl. by BHARDWAJ 11
$4.53\pm0.41\pm0.51$		[1] AUBERT	05J	BABR	Repl. by AUBERT 09B
4.3 ±1.4 ±0.2		[4] AUBERT	02	BABR	Repl. by AUBERT 05J
<27	90	[1] ALAM	94	CLE2	$e^+e^-\to\ \Upsilon(4S)$

[1] Assumes equal production of B^+ and B^0 at the $\Upsilon(4S)$.

[2] Uses $\chi_{c1,2}\to J/\psi\gamma$. Assumes B($\Upsilon(4S)\to B^+B^-$) = (51.6±0.6)% and B($\Upsilon(4S)\to B^0\overline{B}^0$) = (48.4 ± 0.6)%.

[3] AVERY 00 reports $(3.9^{+1.9}_{-1.3}\pm0.4)\times10^{-4}$ from a measurement of $[\Gamma(B^0\to\chi_{c1}K^0)/\Gamma_{total}]\times[B(\chi_{c1}(1P)\to\gamma J/\psi(1S))]$ assuming $B(\chi_{c1}(1P)\to\gamma J/\psi(1S))=0.273\pm0.016$, which we rescale to our best value $B(\chi_{c1}(1P)\to\gamma J/\psi(1S))=(33.9\pm1.2)\times10^{-2}$. Our first error is their experiment's error and our second error is the systematic error from using our best value. Assumes equal production of B^+ and B^0 at the $\Upsilon(4S)$.

[4] AUBERT 02 reports $(5.4\pm1.4\pm1.1)\times10^{-4}$ from a measurement of $[\Gamma(B^0\to\chi_{c1}K^0)/\Gamma_{total}]\times[B(\chi_{c1}(1P)\to\gamma J/\psi(1S))]$ assuming $B(\chi_{c1}(1P)\to\gamma J/\psi(1S))=0.273\pm0.016$, which we rescale to our best value $B(\chi_{c1}(1P)\to\gamma J/\psi(1S))=(33.9\pm1.2)\times10^{-2}$. Our first error is their experiment's error and our second error is the systematic error from using our best value. Assumes equal production of B^+ and B^0 at the $\Upsilon(4S)$.

$\Gamma(\chi_{c1}K^0)/\Gamma(J/\psi(1S)K^0)$ $\Gamma_{222}/\Gamma_{169}$

VALUE	DOCUMENT ID		TECN	COMMENT
0.53±0.16±0.02	[1] AUBERT	02	BABR	$e^+e^-\to\ \Upsilon(4S)$

[1] AUBERT 02 reports 0.66 ± 0.11 ± 0.17 from a measurement of $[\Gamma(B^0\to\chi_{c1}K^0)/\Gamma(B^0\to J/\psi(1S)K^0)]\times[B(\chi_{c1}(1P)\to\gamma J/\psi(1S))]$ assuming $B(\chi_{c1}(1P)\to\gamma J/\psi(1S))=0.273\pm0.016$, which we rescale to our best value $B(\chi_{c1}(1P)\to\gamma J/\psi(1S))=(33.9\pm1.2)\times10^{-2}$. Our first error is their experiment's error and our second error is the systematic error from using our best value. Assumes equal production of B^+ and B^0 at the $\Upsilon(4S)$.

$\Gamma(\chi_{c1}K^-\pi^+)/\Gamma_{total}$ Γ_{223}/Γ

VALUE (units 10^{-4})	DOCUMENT ID		TECN	COMMENT
3.83±0.10±0.39	[1] MIZUK	08	BELL	$e^+e^-\to\ \Upsilon(4S)$

[1] Assumes equal production of B^+ and B^0 at the $\Upsilon(4S)$.

$\Gamma(\chi_{c1}K^-\pi^+)/\Gamma(J/\psi(1S)K^+\pi^-)$ $\Gamma_{223}/\Gamma_{170}$

VALUE	DOCUMENT ID		TECN	COMMENT
0.481±0.021±0.017	[1] LEES	12B	BABR	

[1] LEES 12B reports $0.474\pm0.013\pm0.026$ from a measurement of $[\Gamma(B^0\to\chi_{c1}K^-\pi^+)/\Gamma(B^0\to J/\psi(1S)K^+\pi^-)]\times[B(\chi_{c1}(1P)\to\gamma J/\psi(1S))]$ assuming $B(\chi_{c1}(1P)\to\gamma J/\psi(1S))=(34.4\pm1.5)\times10^{-2}$, which we rescale to our best value $B(\chi_{c1}(1P)\to\gamma J/\psi(1S))=(33.9\pm1.2)\times10^{-2}$. Our first error is their experiment's error and our second error is the systematic error from using our best value.

$\Gamma(\chi_{c1}K^*(892)^0)/\Gamma_{total}$ Γ_{224}/Γ

VALUE (units 10^{-4})	CL%	DOCUMENT ID		TECN	COMMENT
2.42±0.21 OUR FIT Error includes scale factor of 1.3.					
$2.22^{+0.40}_{-0.31}$ OUR AVERAGE Error includes scale factor of 1.6.					
2.5 ±0.2 ±0.2		[1] AUBERT	09B	BABR	$e^+e^-\to\ \Upsilon(4S)$
$1.73^{+0.15+0.34}_{-0.12-0.22}$		[2] MIZUK	08	BELL	$e^+e^-\to\ \Upsilon(4S)$
• • • We do not use the following data for averages, fits, limits, etc. • • •					
$3.14\pm0.34\pm0.72$		[2] SONI	06	BELL	Repl. by MIZUK 08
$3.27\pm0.42\pm0.64$		[2] AUBERT	05J	BABR	Repl. by AUBERT 09B
3.9 ±1.3 ±0.1		[3] AUBERT	02	BABR	Repl. by AUBERT 05J
<21	90	[4] ALAM	94	CLE2	$e^+e^-\to\ \Upsilon(4S)$

[1] Uses $\chi_{c1,2}\to J/\psi\gamma$. Assumes B($\Upsilon(4S)\to B^+B^-$) = (51.6±0.6)% and B($\Upsilon(4S)\to B^0\overline{B}^0$) = (48.4 ± 0.6)%.

[2] Assumes equal production of B^+ and B^0 at the $\Upsilon(4S)$.

[3] AUBERT 02 reports $(4.8\pm1.4\pm0.9)\times10^{-4}$ from a measurement of $[\Gamma(B^0\to\chi_{c1}K^*(892)^0)/\Gamma_{total}]\times[B(\chi_{c1}(1P)\to\gamma J/\psi(1S))]$ assuming $B(\chi_{c1}(1P)\to\gamma J/\psi(1S))=0.273\pm0.016$, which we rescale to our best value $B(\chi_{c1}(1P)\to\gamma J/\psi(1S))=(33.9\pm1.2)\times10^{-2}$. Our first error is their experiment's error and our second error is the systematic error from using our best value. Assumes equal production of B^+ and B^0 at the $\Upsilon(4S)$.

[4] BORTOLETTO 92 assumes equal production of B^+ and B^0 at the $\Upsilon(4S)$.

$\Gamma(\chi_{c1}K^*(892)^0)/\Gamma(J/\psi(1S)K^*(892)^0)$ $\Gamma_{224}/\Gamma_{171}$

VALUE (units 10^{-2})	DOCUMENT ID		TECN	COMMENT
18.4±1.6 OUR FIT Error includes scale factor of 1.2.				
19.8±1.1±1.5	[1] AAIJ	13AC	LHCB	pp at 7 TeV

[1] Uses $B(\chi_{c1}\to J/\psi\gamma)$ = (34.4 ± 1.5)%.

$\Gamma(X(4051)^+K^-\times B(X^+\to\chi_{c1}\pi^+))/\Gamma_{total}$ Γ_{225}/Γ

VALUE (units 10^{-5})	CL%	DOCUMENT ID		TECN	COMMENT
$3.0^{+1.5+3.7}_{-0.8-1.6}$		[1] MIZUK	08	BELL	$e^+e^-\to\ \Upsilon(4S)$
• • • We do not use the following data for averages, fits, limits, etc. • • •					
<1.8	90	[1,2] LEES	12B	BABR	

[1] Assumes equal production of B^+ and B^0 at the $\Upsilon(4S)$.

[2] Uses $\chi_{c1}\to J/\psi\gamma$ mode. Uses $\chi_{c1}\to J/\psi\gamma$ mode. Finds a good description of the data without this $B^0\to X(4051)^+K^-$ decay mode in a fit.

$\Gamma(X(4248)^+K^-\times B(X^+\to\chi_{c1}\pi^+))/\Gamma_{total}$ Γ_{226}/Γ

VALUE (units 10^{-5})	CL%	DOCUMENT ID		TECN	COMMENT
$4.0^{+2.3+19.7}_{-0.9-0.5}$		[1] MIZUK	08	BELL	$e^+e^-\to\ \Upsilon(4S)$
• • • We do not use the following data for averages, fits, limits, etc. • • •					
<4.0	90	[1,2] LEES	12B	BABR	

[1] Assumes equal production of B^+ and B^0 at the $\Upsilon(4S)$.

[2] Uses $\chi_{c1}\to J/\psi\gamma$ mode. Finds a good description of the data without this $B^0\to X(4248)^+K^-$ decay mode in a fit.

$\Gamma(\chi_{c1}K^*(892)^0)/\Gamma(\chi_{c1}K^0)$ $\Gamma_{224}/\Gamma_{222}$

VALUE	DOCUMENT ID		TECN	COMMENT
0.72±0.11±0.12	AUBERT	05J	BABR	$e^+e^-\to\ \Upsilon(4S)$
• • • We do not use the following data for averages, fits, limits, etc. • • •				
0.89±0.34±0.17	[1] AUBERT	02	BABR	Repl. by AUBERT 05J

[1] Assumes equal production of B^+ and B^0 at the $\Upsilon(4S)$.

$\Gamma(K^+\pi^-)/\Gamma_{total}$ Γ_{227}/Γ

VALUE (units 10^{-6})	CL%	DOCUMENT ID		TECN	COMMENT
19.6 ± 0.5 OUR FIT					
19.6 ± 0.5 OUR AVERAGE					
20.00± 0.34±0.60		[1] DUH	13	BELL	$e^+e^-\to\ \Upsilon(4S)$
19.1 ± 0.6 ±0.6		[1] AUBERT	07B	BABR	$e^+e^-\to\ \Upsilon(4S)$
$18.0\ ^{+2.3}_{-2.1}\ ^{+1.2}_{-0.9}$		[1] BORNHEIM	03	CLE2	$e^+e^-\to\ \Upsilon(4S)$
• • • We do not use the following data for averages, fits, limits, etc. • • •					
19.9 ± 0.4 ±0.8		[1] LIN	07A	BELL	Repl. by DUH 13
18.5 ± 1.0 ±0.7		[1] CHAO	04	BELL	Repl. by LIN 07A
17.9 ± 0.9 ±0.7		[1] AUBERT	02Q	BABR	Repl. by AUBERT 07B
22.5 ± 1.9 ±1.8		[1] CASEY	02	BELL	Repl. by CHAO 04
$19.3\ ^{+3.4}_{-3.2}\ ^{+1.5}_{-0.6}$		[1] ABE	01H	BELL	Repl. by CASEY 02
16.7 ± 1.6 ±1.3		[1] AUBERT	01E	BABR	Repl. by AUBERT 02Q
< 66	90	[2] ABE	00C	SLD	$e^+e^-\to\ Z$
$17.2\ ^{+2.5}_{-2.4}$ ±1.2		[1] CRONIN-HEN..00		CLE2	Repl. by BORNHEIM 03
$15\ ^{+5.}_{-4}$ ±1.4		GODANG	98	CLE2	Repl. by CRONIN-HENNESSY 00
$24\ ^{+17}_{-11}$ ±2		[3] ADAM	96D	DLPH	$e^+e^-\to\ Z$
< 17	90	ASNER	96	CLE2	Sup. by ADAM 96D
< 30	90	[4] BUSKULIC	96V	ALEP	$e^+e^-\to\ Z$
< 90	90	[5] ABREU	95N	DLPH	Sup. by ADAM 96D
< 81	90	[6] AKERS	94L	OPAL	$e^+e^-\to\ Z$
< 26	90	[7] BATTLE	93	CLE2	$e^+e^-\to\ \Upsilon(4S)$
<180	90	ALBRECHT	91B	ARG	$e^+e^-\to\ \Upsilon(4S)$
< 90	90	[8] AVERY	89B	CLEO	$e^+e^-\to\ \Upsilon(4S)$
<320	90	AVERY	87	CLEO	$e^+e^-\to\ \Upsilon(4S)$

[1] Assumes equal production of B^+ and B^0 at the $\Upsilon(4S)$.

[2] ABE 00C assumes $B(Z\to b\overline{b})=(21.7\pm0.1)\%$ and the B fractions $f_{B^0}=f_{B^+}=(39.7^{+1.8}_{-2.2})\%$ and $f_{B_s}=(10.5^{+1.8}_{-2.2})\%$.

[3] ADAM 96D assumes $f_{B^0}=f_{B^-}=0.39$ and $f_{B_s}=0.12$. Contributions from B^0 and B_s decays cannot be separated. Limits are given for the weighted average of the decay rates for the two neutral B mesons.

[4] BUSKULIC 96V assumes PDG 96 production fractions for B^0, B^+, B_s, b baryons.

[5] Assumes a B^0, B^- production fraction of 0.39 and a B_s production fraction of 0.12. Contributions from B^0 and B_s^0 decays cannot be separated. Limits are given for the weighted average of the decay rates for the two neutral B mesons.

[6] Assumes $B(Z\to b\overline{b})=0.217$ and B_d^0 (B_s^0) fraction 39.5% (12%).

[7] BATTLE 93 assumes equal production of $B^0\overline{B}^0$ and B^+B^- at $\Upsilon(4S)$.

[8] Assumes the $\Upsilon(4S)$ decays 43% to $B^0\overline{B}^0$.

$\Gamma(K^+\pi^-)/\Gamma(K^0\pi^0)$ $\Gamma_{227}/\Gamma_{228}$

VALUE	DOCUMENT ID		TECN	COMMENT
2.16±0.16±0.16	LIN	07A	BELL	$e^+e^-\to\ \Upsilon(4S)$
• • • We do not use the following data for averages, fits, limits, etc. • • •				
$1.20^{+0.50}_{-0.58}\pm0.22\ -0.32$	[1] ABE	01H	BELL	Repl. by LIN 07A

[1] Assumes equal production of B^+ and B^0 at the $\Upsilon(4S)$.

Meson Particle Listings

B^0

$[\Gamma(K^+\pi^-)+\Gamma(\pi^+\pi^-)]/\Gamma_{total}$ $(\Gamma_{227}+\Gamma_{356})/\Gamma$

VALUE (units 10^{-6})	EVTS	DOCUMENT ID		TECN	COMMENT
19± 6 OUR AVERAGE					
$28^{+15}_{-10}\pm20$		[1] ADAM	96D	DLPH	$e^+e^-\to Z$
$18^{+6}_{-5}{}^{+3}_{-4}$	17.2	ASNER	96	CLE2	$e^+e^-\to\Upsilon(4S)$
• • • We do not use the following data for averages, fits, limits, etc. • • •					
$24^{+8}_{-7}\pm2$		[2] BATTLE	93	CLE2	$e^+e^-\to\Upsilon(4S)$

[1] ADAM 96D assumes $f_{B^0}=f_{B^-}=0.39$ and $f_{B_s}=0.12$. Contributions from B^0 and B_s decays cannot be separated. Limits are given for the weighted average of the decay rates for the two neutral B mesons.
[2] BATTLE 93 assumes equal production of $B^0\overline{B}{}^0$ and B^+B^- at $\Upsilon(4S)$.

$\Gamma(K^0\pi^0)/\Gamma_{total}$ Γ_{228}/Γ

VALUE (units 10^{-6})	CL%	DOCUMENT ID		TECN	COMMENT
9.9 ±0.5 OUR AVERAGE					
$9.68\pm0.46\pm0.50$		[1] DUH	13	BELL	$e^+e^-\to\Upsilon(4S)$
10.1 ±0.6 ±0.4		[1] LEES	13D	BABR	$e^+e^-\to\Upsilon(4S)$
$12.8\ ^{+4.0}_{-3.3}\ ^{+1.7}_{-1.4}$		[1] BORNHEIM	03	CLE2	$e^+e^-\to\Upsilon(4S)$
• • • We do not use the following data for averages, fits, limits, etc. • • •					
8.7 ±0.5 ±0.6		[1] FUJIKAWA	10A	BELL	Repl. by DUH 13
10.3 ±0.7 ±0.6		[1] AUBERT	08E	BABR	Repl. by LEES 13D
9.2 ±0.7 ±0.6		[1] LIN	07A	BELL	Repl. by FUJIKAWA 10A
11.4 ±0.9 ±0.6		[1] AUBERT	05Y	BABR	Repl. by AUBERT 08E
11.4 ±1.7 ±0.8		[1] AUBERT	04M	BABR	Repl. by AUBERT 05Y
$11.7\pm2.3\ ^{+1.2}_{-1.3}$		[1] CHAO	04	BELL	Repl. by LIN 07A
$8.0\ ^{+3.3}_{-3.1}\pm1.6$		[1] CASEY	02	BELL	Repl. by CHAO 04
$16.0\ ^{+7.2}_{-5.9}\ ^{+2.5}_{-2.7}$		[1] ABE	01H	BELL	Repl. by CASEY 02
$8.2\ ^{+3.1}_{-2.7}\pm1.2$		[1] AUBERT	01E	BABR	Repl. by AUBERT 04M
$14.6\ ^{+5.9}_{-5.1}\ ^{+2.4}_{-3.3}$		[1] CRONIN-HEN...00		CLE2	Repl. by BORNHEIM 03
<41	90	GODANG	98	CLE2	Repl. by CRONIN-HENNESSY 00
<40	90	ASNER	96	CLE2	Rep. by GODANG 98

[1] Assumes equal production of B^+ and B^0 at the $\Upsilon(4S)$.

$\Gamma(\eta' K^0)/\Gamma_{total}$ Γ_{229}/Γ

VALUE (units 10^{-6})	DOCUMENT ID		TECN	COMMENT
66 ± 4 OUR AVERAGE	Error includes scale factor of 1.4.			
$68.5\pm2.2\pm3.1$	[1] AUBERT	09AV	BABR	$e^+e^-\to\Upsilon(4S)$
$58.9\ ^{+3.6}_{-3.5}\pm4.3$	[1] SCHUEMANN	06	BELL	$e^+e^-\to\Upsilon(4S)$
$89\ ^{+18}_{-16}\pm9$	[1] RICHICHI	00	CLE2	$e^+e^-\to\Upsilon(4S)$
• • • We do not use the following data for averages, fits, limits, etc. • • •				
$66.6\pm2.6\pm2.8$	[1] AUBERT	07AE	BABR	Repl. by AUBERT 09AV
$67.4\pm3.3\pm3.2$	[1] AUBERT	05M	BABR	AUBERT 07AE
$60.6\pm5.6\pm4.6$	[1] AUBERT	03W	BABR	Repl. by AUBERT 05M
$55\ ^{+19}_{-16}\pm8$	[1] ABE	01M	BELL	Repl. by SCHUEMANN 06
$42\ ^{+13}_{-11}\pm4$	[1] AUBERT	01G	BABR	Repl. by AUBERT 03W
$47\ ^{+27}_{-20}\pm9$	BEHRENS	98	CLE2	Repl. by RICHICHI 00

[1] Assumes equal production of B^+ and B^0 at the $\Upsilon(4S)$.

$\Gamma(\eta' K^*(892)^0)/\Gamma_{total}$ Γ_{230}/Γ

VALUE (units 10^{-6})	CL%	DOCUMENT ID		TECN	COMMENT
$3.1\ ^{+0.9}_{-0.8}\pm0.3$		[1] DEL-AMO-SA...10A		BABR	$e^+e^-\to\Upsilon(4S)$
• • • We do not use the following data for averages, fits, limits, etc. • • •					
$3.8\pm1.1\pm0.5$		[1] AUBERT	07E	BABR	Repl. by DEL-AMO-SANCHEZ 10A
< 2.6	90	[1] SCHUEMANN	07	BELL	$e^+e^-\to\Upsilon(4S)$
< 7.6	90	[1] AUBERT,B	04D	BABR	Repl. by AUBERT 07E
<24	90	[1] RICHICHI	00	CLE2	$e^+e^-\to\Upsilon(4S)$
<39	90	BEHRENS	98	CLE2	Repl. by RICHICHI 00

[1] Assumes equal production of B^+ and B^0 at the $\Upsilon(4S)$.

$\Gamma(\eta' K_0^*(1430)^0)/\Gamma_{total}$ Γ_{231}/Γ

VALUE (units 10^{-6})	DOCUMENT ID		TECN	COMMENT
6.3±1.3±0.9	[1] DEL-AMO-SA...10A		BABR	$e^+e^-\to\Upsilon(4S)$

[1] Assumes equal production of B^+ and B^0 at the $\Upsilon(4S)$.

$\Gamma(\eta' K_2^*(1430)^0)/\Gamma_{total}$ Γ_{232}/Γ

VALUE (units 10^{-6})	DOCUMENT ID		TECN	COMMENT
$13.7\ ^{+3.0}_{-2.9}\pm1.2$	[1] DEL-AMO-SA...10A		BABR	$e^+e^-\to\Upsilon(4S)$

[1] Assumes equal production of B^+ and B^0 at the $\Upsilon(4S)$.

$\Gamma(\eta K^0)/\Gamma_{total}$ Γ_{233}/Γ

VALUE (units 10^{-6})	CL%	DOCUMENT ID		TECN	COMMENT
$1.23\ ^{+0.27}_{-0.24}$ OUR AVERAGE					
$1.27\ ^{+0.33}_{-0.29}\pm0.08$		[1] HOI	12	BELL	$e^+e^-\to\Upsilon(4S)$
$1.15\ ^{+0.43}_{-0.38}\pm0.09$		[1] AUBERT	09AV	BABR	$e^+e^-\to\Upsilon(4S)$
• • • We do not use the following data for averages, fits, limits, etc. • • •					
< 1.9	90	[1] CHANG	07B	BELL	Repl. by HOI 12
< 2.9	90	[1] AUBERT,B	06V	BABR	$e^+e^-\to\Upsilon(4S)$
< 2.5	90	[1] AUBERT,B	05K	BABR	$e^+e^-\to\Upsilon(4S)$
< 2.0	90	[1] CHANG	05A	BELL	Repl. by CHANG 07B
< 5.2	90	[1] AUBERT	04H	BABR	Repl. by AUBERT,B 05K
< 9.3	90	[1] RICHICHI	00	CLE2	$e^+e^-\to\Upsilon(4S)$
<33	90	BEHRENS	98	CLE2	Repl. by RICHICHI 00

[1] Assumes equal production of B^+ and B^0 at the $\Upsilon(4S)$.

$\Gamma(\eta K^*(892)^0)/\Gamma_{total}$ Γ_{234}/Γ

VALUE (units 10^{-6})	CL%	DOCUMENT ID		TECN	COMMENT
15.9±1.0 OUR AVERAGE					
$15.2\pm1.2\pm1.0$		[1] WANG	07B	BELL	$e^+e^-\to\Upsilon(4S)$
$16.5\pm1.1\pm0.8$		[1] AUBERT,B	06H	BABR	$e^+e^-\to\Upsilon(4S)$
$13.8\ ^{+5.5}_{-4.6}\pm1.6$		[1] RICHICHI	00	CLE2	$e^+e^-\to\Upsilon(4S)$
• • • We do not use the following data for averages, fits, limits, etc. • • •					
$18.6\pm2.3\pm1.2$		[1] AUBERT,B	04D	BABR	Repl. by AUBERT,B 06H
<30	90	BEHRENS	98	CLE2	Repl. by RICHICHI 00

[1] Assumes equal production of B^+ and B^0 at the $\Upsilon(4S)$.

$\Gamma(\eta K_0^*(1430)^0)/\Gamma_{total}$ Γ_{235}/Γ

VALUE (units 10^{-6})	DOCUMENT ID		TECN	COMMENT
11.0±1.6±1.5	[1] AUBERT,B	06H	BABR	$e^+e^-\to\Upsilon(4S)$

[1] Assumes equal production of B^+ and B^0 at the $\Upsilon(4S)$.

$\Gamma(\eta K_2^*(1430)^0)/\Gamma_{total}$ Γ_{236}/Γ

VALUE (units 10^{-6})	DOCUMENT ID		TECN	COMMENT
9.6±1.8±1.1	[1] AUBERT,B	06H	BABR	$e^+e^-\to\Upsilon(4S)$

[1] Assumes equal production of B^+ and B^0 at the $\Upsilon(4S)$.

$\Gamma(\omega K^0)/\Gamma_{total}$ Γ_{237}/Γ

VALUE (units 10^{-6})	CL%	DOCUMENT ID		TECN	COMMENT
5.0±0.6 OUR AVERAGE					
$5.4\pm0.8\pm0.3$		[1] AUBERT	07AE	BABR	$e^+e^-\to\Upsilon(4S)$
$4.4\ ^{+0.8}_{-0.7}\pm0.4$		[1] JEN	06	BELL	$e^+e^-\to\Upsilon(4S)$
$10.0\ ^{+5.4}_{-4.2}\pm1.4$		[1] JESSOP	00	CLE2	$e^+e^-\to\Upsilon(4S)$
• • • We do not use the following data for averages, fits, limits, etc. • • •					
$6.2\pm1.0\pm0.4$		[1] AUBERT,B	06E	BABR	Repl. by AUBERT 07AE
$5.9\ ^{+1.6}_{-1.3}\pm0.5$		[1] AUBERT	04H	BABR	Repl. by AUBERT,B 06E
$4.0\ ^{+1.9}_{-1.6}\pm0.5$		[1] WANG	04A	BELL	Repl. by JEN 06
<13	90	[1] AUBERT	01G	BABR	Repl. by AUBERT 04H
<57	90	[1] BERGFELD	98	CLE2	Repl. by JESSOP 00

[1] Assumes equal production of B^+ and B^0 at the $\Upsilon(4S)$.

$\Gamma(a_0(980)^0 K^0\times B(a_0(980)^0\to\eta\pi^0))/\Gamma_{total}$ Γ_{238}/Γ

VALUE (units 10^{-6})	CL%	DOCUMENT ID		TECN	COMMENT
<7.8	90	[1] AUBERT,BE	04	BABR	$e^+e^-\to\Upsilon(4S)$

[1] Assumes equal production of charged and neutral B mesons from $\Upsilon(4S)$ decays.

$\Gamma(b_1^0 K^0\times B(b_1^0\to\omega\pi^0))/\Gamma_{total}$ Γ_{239}/Γ

VALUE (units 10^{-6})	CL%	DOCUMENT ID		TECN	COMMENT
<7.8	90	[1] AUBERT	08AG	BABR	$e^+e^-\to\Upsilon(4S)$

[1] Assumes equal production of B^+ and B^0 at the $\Upsilon(4S)$.

$\Gamma(a_0(980)^\pm K^\mp\times B(a_0(980)^\pm\to\eta\pi^\pm))/\Gamma_{total}$ Γ_{240}/Γ

VALUE (units 10^{-6})	CL%	DOCUMENT ID		TECN	COMMENT
<1.9	90	[1] AUBERT	07Y	BABR	$e^+e^-\to\Upsilon(4S)$
• • • We do not use the following data for averages, fits, limits, etc. • • •					
<2.1	90	[1] AUBERT,BE	04	BABR	Repl. by AUBERT 07Y

[1] Assumes equal production of B^+ and B^0 at the $\Upsilon(4S)$.

$\Gamma(b_1^- K^+\times B(b_1^-\to\omega\pi^-))/\Gamma_{total}$ Γ_{241}/Γ

VALUE (units 10^{-6})	DOCUMENT ID		TECN	COMMENT
7.4±1.0±1.0	[1] AUBERT	07BI	BABR	$e^+e^-\to\Upsilon(4S)$

[1] Assumes equal production of B^+ and B^0 at the $\Upsilon(4S)$.

$\Gamma(b_1^0 K^{*0} \times B(b_1^0 \to \omega\pi^0))/\Gamma_{total}$ Γ_{242}/Γ

VALUE	CL%	DOCUMENT ID		TECN	COMMENT
$<8.0 \times 10^{-6}$	90	[1] AUBERT	09AF	BABR	$e^+e^- \to \Upsilon(4S)$

[1] Assumes equal production of B^+ and B^0 at the $\Upsilon(4S)$.

$\Gamma(b_1^- K^{*+} \times B(b_1^- \to \omega\pi^-))/\Gamma_{total}$ Γ_{243}/Γ

VALUE	CL%	DOCUMENT ID		TECN	COMMENT
$<5.0 \times 10^{-6}$	90	[1] AUBERT	09AF	BABR	$e^+e^- \to \Upsilon(4S)$

[1] Assumes equal production of B^+ and B^0 at the $\Upsilon(4S)$.

$\Gamma(a_0(1450)^\pm K^\mp \times B(a_0(1450)^\pm \to \eta\pi^\pm))/\Gamma_{total}$ Γ_{244}/Γ

VALUE (units 10^{-6})	CL%	DOCUMENT ID		TECN	COMMENT
<3.1	90	[1] AUBERT	07Y	BABR	$e^+e^- \to \Upsilon(4S)$

[1] Assumes equal production of B^+ and B^0 at the $\Upsilon(4S)$.

$\Gamma(K_S^0 X^0(\text{Familon}))/\Gamma_{total}$ Γ_{245}/Γ

VALUE (units 10^{-6})	CL%	DOCUMENT ID		TECN	COMMENT
<53	90	[1] AMMAR	01B	CLE2	$e^+e^- \to \Upsilon(4S)$

[1] AMMAR 01B searched for the two-body decay of the B meson to a massless neutral feebly-interacting particle X^0 such as the familon, the Nambu-Goldstone boson associated with a spontaneously broken global family symmetry.

$\Gamma(\omega K^*(892)^0)/\Gamma_{total}$ Γ_{246}/Γ

VALUE (units 10^{-6})	CL%	DOCUMENT ID		TECN	COMMENT
2.0 ± 0.5 OUR AVERAGE					
$2.2 \pm 0.6 \pm 0.2$		[1] AUBERT	09H	BABR	$e^+e^- \to \Upsilon(4S)$
$1.8 \pm 0.7 \pm 0.3$		[1] GOLDENZWE..08		BELL	$e^+e^- \to \Upsilon(4S)$
• • • We do not use the following data for averages, fits, limits, etc. • • •					
< 4.2	90	[1] AUBERT,B	06T	BABR	Repl. by AUBERT 09H
< 6.0	90	[1] AUBERT	05O	BABR	Repl. by AUBERT,B 06T
<23	90	[1] BERGFELD	98	CLE2	

[1] Assumes equal production of B^+ and B^0 at the $\Upsilon(4S)$.

$\Gamma(\omega(K\pi)_0^{*0})/\Gamma_{total}$ Γ_{247}/Γ

$(K\pi)_0^{*0}$ is the total S-wave composed of $K_0^*(1430)$ and nonresonant that are described using LASS shape.

VALUE (units 10^{-6})	DOCUMENT ID		TECN	COMMENT
$18.4 \pm 1.8 \pm 1.7$	[1] AUBERT	09H	BABR	$e^+e^- \to \Upsilon(4S)$

[1] Assumes equal production of B^+ and B^0 at the $\Upsilon(4S)$.

$\Gamma(\omega K_0^*(1430)^0)/\Gamma_{total}$ Γ_{248}/Γ

VALUE (units 10^{-6})	DOCUMENT ID		TECN	COMMENT
$16.0 \pm 1.6 \pm 3.0$	[1] AUBERT	09H	BABR	$e^+e^- \to \Upsilon(4S)$

[1] Assumes equal production of B^+ and B^0 at the $\Upsilon(4S)$.

$\Gamma(\omega K_2^*(1430)^0)/\Gamma_{total}$ Γ_{249}/Γ

VALUE (units 10^{-6})	DOCUMENT ID		TECN	COMMENT
$10.1 \pm 2.0 \pm 1.1$	[1] AUBERT	09H	BABR	$e^+e^- \to \Upsilon(4S)$

[1] Assumes equal production of B^+ and B^0 at the $\Upsilon(4S)$.

$\Gamma(\omega K^+\pi^-\text{ nonresonant})/\Gamma_{total}$ Γ_{250}/Γ

VALUE (units 10^{-6})	DOCUMENT ID		TECN	COMMENT
$5.1 \pm 0.7 \pm 0.7$	[1,2] GOLDENZWE..08		BELL	$e^+e^- \to \Upsilon(4S)$

[1] Assumes equal production of B^+ and B^0 at the $\Upsilon(4S)$.
[2] For the $K\pi$ mass range 0.755–1.250 GeV/c^2, excluding $K^*(892)$.

$\Gamma(K^+\pi^-\pi^0)/\Gamma_{total}$ Γ_{251}/Γ

VALUE (units 10^{-6})	CL%	DOCUMENT ID		TECN	COMMENT
37.8 ± 3.2 OUR AVERAGE					
$38.5 \pm 1.0 \pm 3.9$		[1,2] LEES	11	BABR	$e^+e^- \to \Upsilon(4S)$
$36.6^{+4.2}_{-4.3} \pm 3.0$		[1] CHANG	04	BELL	$e^+e^- \to \Upsilon(4S)$
• • • We do not use the following data for averages, fits, limits, etc. • • •					
$35.7^{+2.6}_{-1.5} \pm 2.2$		[1] AUBERT	08AQ	BABR	Repl. by LEES 11
<40	90	[1] ECKHART	02	CLE2	$e^+e^- \to \Upsilon(4S)$

[1] Assumes equal production of B^+ and B^0 at the $\Upsilon(4S)$.
[2] Uses Dalitz plot analysis of $B^0 \to K^+\pi^-\pi^0$ decays.

$\Gamma(K^+\rho^-)/\Gamma_{total}$ Γ_{252}/Γ

VALUE (units 10^{-6})	CL%	DOCUMENT ID		TECN	COMMENT
7.0 ± 0.9 OUR AVERAGE					
$6.6 \pm 0.5 \pm 0.8$		[1,2] LEES	11	BABR	$e^+e^- \to \Upsilon(4S)$
$15.1^{+3.4}_{-3.3}{}^{+2.4}_{-2.6}$		[1] CHANG	04	BELL	$e^+e^- \to \Upsilon(4S)$
• • • We do not use the following data for averages, fits, limits, etc. • • •					
$8.0^{+0.8}_{-1.3} \pm 0.6$		[1] AUBERT	08AQ	BABR	Repl. by LEES 11
$7.3^{+1.3}_{-1.2} \pm 1.3$		[1] AUBERT	03T	BABR	Repl. by AUBERT 08AQ
<32	90	[1] JESSOP	00	CLE2	$e^+e^- \to \Upsilon(4S)$
<35	90	ASNER	96	CLE2	Repl. by JESSOP 00

[1] Assumes equal production of B^+ and B^0 at the $\Upsilon(4S)$.
[2] Uses Dalitz plot analysis of $B^0 \to K^+\pi^-\pi^0$ decays.

$\Gamma(K^+\rho(1450)^-)/\Gamma_{total}$ Γ_{253}/Γ

VALUE (units 10^{-6})	CL%	DOCUMENT ID		TECN	COMMENT
$2.4 \pm 1.0 \pm 0.6$		[1,2] LEES	11	BABR	$e^+e^- \to \Upsilon(4S)$
• • • We do not use the following data for averages, fits, limits, etc. • • •					
<2.1	90	[1] AUBERT	08AQ	BABR	Repl. by LEES 11

[1] Assumes equal production of B^+ and B^0 at the $\Upsilon(4S)$.
[2] Uses Dalitz plot analysis of $B^0 \to K^+\pi^-\pi^0$ decays.

$\Gamma(K^+\rho(1700)^-)/\Gamma_{total}$ Γ_{254}/Γ

VALUE (units 10^{-6})	CL%	DOCUMENT ID		TECN	COMMENT
$0.6 \pm 0.6 \pm 0.4$		[1,2] LEES	11	BABR	$e^+e^- \to \Upsilon(4S)$
• • • We do not use the following data for averages, fits, limits, etc. • • •					
<1.1	90	[1] AUBERT	08AQ	BABR	Repl. by LEES 11

[1] Assumes equal production of B^+ and B^0 at the $\Upsilon(4S)$.
[2] Uses Dalitz plot analysis of $B^0 \to K^+\pi^-\pi^0$ decays.

$\Gamma((K^+\pi^-\pi^0)\text{ non-resonant})/\Gamma_{total}$ Γ_{255}/Γ

VALUE (units 10^{-6})	CL%	DOCUMENT ID		TECN	COMMENT
$2.8 \pm 0.5 \pm 0.4$		[1,2] LEES	11	BABR	$e^+e^- \to \Upsilon(4S)$
• • • We do not use the following data for averages, fits, limits, etc. • • •					
$4.4 \pm 0.9 \pm 0.5$		[1] AUBERT	08AQ	BABR	Repl. by LEES 11
<9.4	90	[1] CHANG	04	BELL	$e^+e^- \to \Upsilon(4S)$

[1] Assumes equal production of B^+ and B^0 at the $\Upsilon(4S)$.
[2] Uses Dalitz plot analysis of $B^0 \to K^+\pi^-\pi^0$ decays. The quoted value is only for the flat part of the non-resonant component.

$\Gamma((K\pi)_0^{*+}\pi^- \times B((K\pi)_0^{*+} \to K^+\pi^0))/\Gamma_{total}$ Γ_{256}/Γ

$(K\pi)_0^{*+}$ is the total S-wave composed of $K_0^*(1430)$ and nonresonant that are described using LASS shape.

VALUE (units 10^{-6})	DOCUMENT ID		TECN	COMMENT
$34.2 \pm 2.4 \pm 4.1$	[1,2] LEES	11	BABR	$e^+e^- \to \Upsilon(4S)$
• • • We do not use the following data for averages, fits, limits, etc. • • •				
$9.4^{+1.1}_{-1.3}{}^{+2.3}_{-2.1}$	[1] AUBERT	08AQ	BABR	Repl. by LEES 11

[1] Assumes equal production of B^+ and B^0 at the $\Upsilon(4S)$.
[2] Uses Dalitz plot analysis of $B^0 \to K^+\pi^-\pi^0$ decays.

$\Gamma((K\pi)_0^{*0}\pi^0 \times B((K\pi)_0^{*0} \to K^+\pi^-))/\Gamma_{total}$ Γ_{257}/Γ

$(K\pi)_0^{*0}$ is the total S-wave composed of $K_0^*(1430)$ and nonresonant that are described using LASS shape.

VALUE (units 10^{-6})	DOCUMENT ID		TECN	COMMENT
$8.6 \pm 1.1 \pm 1.3$	[1,2] LEES	11	BABR	$e^+e^- \to \Upsilon(4S)$
• • • We do not use the following data for averages, fits, limits, etc. • • •				
$8.7^{+1.1}_{-0.9}{}^{+2.8}_{-2.6}$	[1] AUBERT	08AQ	BABR	Repl. by LEES 11

[1] Assumes equal production of B^+ and B^0 at the $\Upsilon(4S)$.
[2] Uses Dalitz plot analysis of $B^0 \to K^+\pi^-\pi^0$ decays.

$\Gamma(K_2^*(1430)^0\pi^0)/\Gamma_{total}$ Γ_{258}/Γ

VALUE (units 10^{-6})	CL%	DOCUMENT ID		TECN	COMMENT
<4.0	90	[1] AUBERT	08AQ	BABR	$e^+e^- \to \Upsilon(4S)$

[1] Assumes equal production of B^+ and B^0 at the $\Upsilon(4S)$.

$\Gamma(K^*(1680)^0\pi^0)/\Gamma_{total}$ Γ_{259}/Γ

VALUE (units 10^{-6})	CL%	DOCUMENT ID		TECN	COMMENT
<7.5	90	[1] AUBERT	08AQ	BABR	$e^+e^- \to \Upsilon(4S)$

[1] Assumes equal production of B^+ and B^0 at the $\Upsilon(4S)$.

$\Gamma(K_x^{*0}\pi^0)/\Gamma_{total}$ Γ_{260}/Γ

K_x^{*0} stands for the possible candidates of $K^*(1410)$, $K_0^*(1430)$ and $K_2^*(1430)$.

VALUE (units 10^{-6})	DOCUMENT ID		TECN	COMMENT
$6.1^{+1.6}_{-1.5}{}^{+0.5}_{-0.6}$	[1] CHANG	04	BELL	$e^+e^- \to \Upsilon(4S)$

[1] Assumes equal production of B^+ and B^0 at the $\Upsilon(4S)$.

$\Gamma(K^0\pi^+\pi^-)/\Gamma_{total}$ Γ_{261}/Γ

VALUE (units 10^{-6})	CL%	DOCUMENT ID		TECN	COMMENT
49.6 ± 2.0 OUR AVERAGE					
$50.2 \pm 1.5 \pm 1.8$		[1] AUBERT	09AU	BABR	$e^+e^- \to \Upsilon(4S)$
$47.5 \pm 2.4 \pm 3.7$		[2] GARMASH	07	BELL	$e^+e^- \to \Upsilon(4S)$
$50\ ^{+10}_{-9} \pm 7$		[1] ECKHART	02	CLE2	$e^+e^- \to \Upsilon(4S)$
• • • We do not use the following data for averages, fits, limits, etc. • • •					
$43.0 \pm 2.3 \pm 2.3$		[1] AUBERT	06I	BABR	Repl. by AUBERT 09AU
$43.7 \pm 3.8 \pm 3.4$		[1] AUBERT,B	04O	BABR	Repl. by AUBERT 06I
$45.4 \pm 5.2 \pm 5.9$		[1] GARMASH	04	BELL	Repl. by GARMASH 07
<440	90	ALBRECHT	91E	ARG	$e^+e^- \to \Upsilon(4S)$

[1] Assumes equal production of B^+ and B^0 at the $\Upsilon(4S)$.
[2] Uses Dalitz plot analysis of the $B^0 \to K^0\pi^+\pi^-$ final state decays.

Meson Particle Listings

B^0

$\Gamma(K^0\pi^+\pi^-\text{ non-resonant})/\Gamma_{\text{total}}$ Γ_{262}/Γ

VALUE (units 10^{-6})	DOCUMENT ID		TECN	COMMENT
$14.7^{+4.0}_{-2.6}$ OUR AVERAGE	Error includes scale factor of 2.1.			
$11.1^{+2.5}_{-1.0}\pm0.9$	[1] AUBERT	09AU	BABR	$e^+e^-\to\Upsilon(4S)$
$19.9\pm2.5^{+1.7}_{-2.0}$	[2] GARMASH	07	BELL	$e^+e^-\to\Upsilon(4S)$

[1] Assumes equal production of B^+ and B^0 at the $\Upsilon(4S)$.
[2] Uses Dalitz plot analysis of the $B^0\to K^0\pi^+\pi^-$ final state decays.

$\Gamma(K^0\rho^0)/\Gamma_{\text{total}}$ Γ_{263}/Γ

VALUE (units 10^{-6})	CL%	DOCUMENT ID		TECN	COMMENT
4.7 ± 0.6 OUR AVERAGE					
$4.4^{+0.7}_{-0.6}\pm0.3$		[1] AUBERT	09AU	BABR	$e^+e^-\to\Upsilon(4S)$
$6.1\pm1.0^{+1.1}_{-1.2}$		[2] GARMASH	07	BELL	$e^+e^-\to\Upsilon(4S)$
• • • We do not use the following data for averages, fits, limits, etc. • • •					
$4.9\pm0.8\pm0.9$		[1] AUBERT	07F	BABR	Repl. by AUBERT 09AU
$<$ 39	90	ASNER	96	CLEO	$e^+e^-\to\Upsilon(4S)$
$<$ 320	90	ALBRECHT	91B	ARG	$e^+e^-\to\Upsilon(4S)$
$<$ 500	90	[3] AVERY	89B	CLEO	$e^+e^-\to\Upsilon(4S)$
$<$64000	90	[4] AVERY	87	CLEO	$e^+e^-\to\Upsilon(4S)$

[1] Assumes equal production of B^+ and B^0 at the $\Upsilon(4S)$.
[2] Uses Dalitz plot analysis of the $B^0\to K^0\pi^+\pi^-$ final state decays.
[3] AVERY 89B reports $< 5.8\times10^{-4}$ assuming the $\Upsilon(4S)$ decays 43% to $B^0\overline{B}^0$. We rescale to 50%.
[4] AVERY 87 reports < 0.08 assuming the $\Upsilon(4S)$ decays 40% to $B^0\overline{B}^0$. We rescale to 50%.

$\Gamma(K^*(892)^+\pi^-)/\Gamma_{\text{total}}$ Γ_{264}/Γ

VALUE (units 10^{-6})	CL%	DOCUMENT ID		TECN	COMMENT
8.4 ± 0.8 OUR AVERAGE					
$8.0\pm1.1\pm0.8$		[1,2] LEES	11	BABR	$e^+e^-\to\Upsilon(4S)$
$8.3^{+0.9}_{-0.8}\pm0.8$		[2,3] AUBERT	09AU	BABR	$e^+e^-\to\Upsilon(4S)$
$8.4\pm1.1^{+1.0}_{-0.9}$		[3] GARMASH	07	BELL	$e^+e^-\to\Upsilon(4S)$
$16\ ^{+6}_{-5}\ \pm2$		[2] ECKHART	02	CLE2	$e^+e^-\to\Upsilon(4S)$
• • • We do not use the following data for averages, fits, limits, etc. • • •					
$12.6^{+2.7}_{-1.6}\pm0.9$		[1,2] AUBERT	08AQ	BABR	Repl. by LEES 11
$11.0\pm1.5\pm0.71$		[2] AUBERT	06I	BABR	Repl. by AUBERT 09AU
$12.9\pm2.4\pm1.4$		[2] AUBERT,B	04O	BABR	Repl. by AUBERT 06I
$14.8^{+4.6+2.8}_{-4.4-1.3}$		[2] CHANG	04	BELL	Repl. by GARMASH 07
$<$ 72	90	ASNER	96	CLE2	$e^+e^-\to\Upsilon(4S)$
$<$620	90	ALBRECHT	91B	ARG	$e^+e^-\to\Upsilon(4S)$
$<$380	90	[4] AVERY	89B	CLEO	$e^+e^-\to\Upsilon(4S)$
$<$560	90	[5] AVERY	87	CLEO	$e^+e^-\to\Upsilon(4S)$

[1] Uses Dalitz plot analysis of $B^0\to K^+\pi^-\pi^0$ decays.
[2] Assumes equal production of B^+ and B^0 at the $\Upsilon(4S)$.
[3] Uses Dalitz plot analysis of the $B^0\to K^0\pi^+\pi^-$ final state decays.
[4] AVERY 89B reports $< 4.4\times10^{-4}$ assuming the $\Upsilon(4S)$ decays 43% to $B^0\overline{B}^0$. We rescale to 50%.
[5] AVERY 87 reports $< 7\times10^{-4}$ assuming the $\Upsilon(4S)$ decays 40% to $B^0\overline{B}^0$. We rescale to 50%.

$\Gamma(K_0^*(1430)^+\pi^-)/\Gamma_{\text{total}}$ Γ_{265}/Γ

VALUE (units 10^{-6})	DOCUMENT ID		TECN	COMMENT
33 ±7 OUR AVERAGE	Error includes scale factor of 2.0.			
$29.9^{+2.3}_{-1.7}\pm3.6$	[1,2] AUBERT	09AU	BABR	$e^+e^-\to\Upsilon(4S)$
$49.7\pm3.8^{+6.8}_{-8.2}$	[2] GARMASH	07	BELL	$e^+e^-\to\Upsilon(4S)$

[1] Assumes equal production of B^+ and B^0 at the $\Upsilon(4S)$.
[2] Uses Dalitz plot analysis of the $B^0\to K^0\pi^+\pi^-$ final state decays.

$\Gamma(K_x^{*+}\pi^-)/\Gamma_{\text{total}}$ Γ_{266}/Γ

K_x^{*+} stands for the possible candidates of $K^*(1410)$, $K_0^*(1430)$ and $K_2^*(1430)$.

VALUE (units 10^{-6})	DOCUMENT ID		TECN	COMMENT
$5.1\pm1.5^{+0.6}_{-0.7}$	[1] CHANG	04	BELL	$e^+e^-\to\Upsilon(4S)$

[1] Assumes equal production of B^+ and B^0 at the $\Upsilon(4S)$.

$\Gamma(K^*(1410)^+\pi^-\times B(K^*(1410)^+\to K^0\pi^+))/\Gamma_{\text{total}}$ Γ_{267}/Γ

VALUE (units 10^{-6})	CL%	DOCUMENT ID		TECN	COMMENT
<3.8	90	[1] GARMASH	07	BELL	$e^+e^-\to\Upsilon(4S)$

[1] Uses Dalitz plot analysis of the $B^0\to K^0\pi^+\pi^-$ final state decays.

$\Gamma(f_0(980)K^0\times B(f_0(980)\to\pi^+\pi^-))/\Gamma_{\text{total}}$ Γ_{268}/Γ

VALUE (units 10^{-6})	CL%	DOCUMENT ID		TECN	COMMENT
7.0 ± 0.9 OUR AVERAGE					
$6.9\pm0.8\pm0.6$		[1] AUBERT	09AU	BABR	$e^+e^-\to\Upsilon(4S)$
$7.6\pm1.7^{+0.9}_{-1.3}$		[2] GARMASH	07	BELL	$e^+e^-\to\Upsilon(4S)$
• • • We do not use the following data for averages, fits, limits, etc. • • •					
$5.5\pm0.7\pm0.6$		[1] AUBERT	06I	BABR	Repl. by AUBERT 09AU
$<$360	90	[3] AVERY	89B	CLEO	$e^+e^-\to\Upsilon(4S)$

[1] Assumes equal production of B^+ and B^0 at the $\Upsilon(4S)$.
[2] Uses Dalitz plot analysis of the $B^0\to K^0\pi^+\pi^-$ final state decays.
[3] AVERY 89B reports $< 4.2\times10^{-4}$ assuming the $\Upsilon(4S)$ decays 43% to $B^0\overline{B}^0$. We rescale to 50%.

$\Gamma(f_2(1270)K^0)/\Gamma_{\text{total}}$ Γ_{269}/Γ

VALUE (units 10^{-6})	CL%	DOCUMENT ID		TECN	COMMENT
$2.7^{+1.0}_{-0.8}\pm0.9$		[1] AUBERT	09AU	BABR	$e^+e^-\to\Upsilon(4S)$
• • • We do not use the following data for averages, fits, limits, etc. • • •					
$<$2.5	90	[2] GARMASH	07	BELL	$e^+e^-\to\Upsilon(4S)$

[1] Assumes equal production of B^+ and B^0 at the $\Upsilon(4S)$.
[2] GARMASH 07 reports $B(B^0\to f_2(1270)K^0)\times B(f_2(1270)\to\pi^+\pi^-)<1.4\times10^{-6}$ using Dalitz plot analysis. We compute $B(B^0\to f_2(1270)K^0)$ using the PDG value $B(f_2(1270)\to\pi\pi)=84.8\times10^{-2}$ and 2/3 for the $\pi^+\pi^-$ fraction.

$\Gamma(f_X(1300)K^0\times B(f_X\to\pi^+\pi^-))/\Gamma_{\text{total}}$ Γ_{270}/Γ

VALUE (units 10^{-6})	DOCUMENT ID		TECN	COMMENT
$1.81^{+0.55}_{-0.45}\pm0.48$	[1] AUBERT	09AU	BABR	$e^+e^-\to\Upsilon(4S)$

[1] Assumes equal production of B^+ and B^0 at the $\Upsilon(4S)$.

$\Gamma(K^*(892)^0\pi^0)/\Gamma_{\text{total}}$ Γ_{271}/Γ

VALUE (units 10^{-6})	CL%	DOCUMENT ID		TECN	COMMENT
$3.3\pm0.5\pm0.4$		[1,2] LEES	11	BABR	$e^+e^-\to\Upsilon(4S)$
• • • We do not use the following data for averages, fits, limits, etc. • • •					
$3.6\pm0.7\pm0.4$		[1,2] AUBERT	08AQ	BABR	Repl. by LEES 11
$<$ 3.5	90	[2] CHANG	04	BELL	$e^+e^-\to\Upsilon(4S)$
$<$ 3.6	90	JESSOP	00	CLE2	$e^+e^-\to\Upsilon(4S)$
$<$28	90	ASNER	96	CLE2	Repl. by JESSOP 00

[1] Uses Dalitz plot analysis of $B^0\to K^+\pi^-\pi^0$ decays.
[2] Assumes equal production of B^+ and B^0 at the $\Upsilon(4S)$.

$\Gamma(K_2^*(1430)^+\pi^-)/\Gamma_{\text{total}}$ Γ_{272}/Γ

VALUE (units 10^{-6})	CL%	DOCUMENT ID		TECN	COMMENT
$<$ 6	90	[1] GARMASH	07	BELL	$e^+e^-\to\Upsilon(4S)$
• • • We do not use the following data for averages, fits, limits, etc. • • •					
$<$ 16.2	90	[2,3] AUBERT	08AQ	BABR	$e^+e^-\to\Upsilon(4S)$
$<$ 18	90	[3] GARMASH	04	BELL	Repl. by GARMASH 07
$<$2600	90	ALBRECHT	91B	ARG	$e^+e^-\to\Upsilon(4S)$

[1] GARMASH 07 reports $B(B^0\to K_2^*(1430)^+\pi^-)\times B(K_2^{*+}\to K^0\pi^+)<2.1\times10^{-6}$ using Dalitz plot analysis. We compute $B(B^0\to K_2^*(1430)^+\pi^-)$ using the PDG value $B(K_2^*(1430)\to K\pi)=49.9\times10^{-2}$ and 2/3 for the $K^0\pi^+$ fraction.
[2] Uses Dalitz plot analysis of $B^0\to K^+\pi^-\pi^0$ decays.
[3] Assumes equal production of B^+ and B^0 at the $\Upsilon(4S)$.

$\Gamma(K^*(1680)^+\pi^-)/\Gamma_{\text{total}}$ Γ_{273}/Γ

VALUE (units 10^{-6})	CL%	DOCUMENT ID		TECN	COMMENT
<10	90	[1] GARMASH	07	BELL	$e^+e^-\to\Upsilon(4S)$
• • • We do not use the following data for averages, fits, limits, etc. • • •					
$<$25	90	[2,3] AUBERT	08AQ	BABR	$e^+e^-\to\Upsilon(4S)$

[1] GARMASH 07 reports $B(B^0\to K^*(1680)^+\pi^-)\times B(K^{*+}\to K^0\pi^+)<2.6\times10^{-6}$ using Dalitz plot analysis. We compute $B(B^0\to K^*(1680)^+\pi^-)$ using the PDG value $B(K^*(1680)\to K\pi)=38.7\times10^{-2}$ and 2/3 for the $K^0\pi^+$ fraction.
[2] Uses Dalitz plot analysis of $B^0\to K^+\pi^-\pi^0$ decays.
[3] Assumes equal production of B^+ and B^0 at the $\Upsilon(4S)$.

$\Gamma(K^+\pi^-\pi^+\pi^-)/\Gamma_{\text{total}}$ Γ_{274}/Γ

VALUE	CL%	DOCUMENT ID		TECN	COMMENT
$<2.3\times10^{-4}$	90	[1] ADAM	96D	DLPH	$e^+e^-\to Z$
• • • We do not use the following data for averages, fits, limits, etc. • • •					
$<2.1\times10^{-4}$	90	[2] ABREU	95N	DLPH	Sup. by ADAM 96D

[1] ADAM 96D assumes $f_{B^0}=f_{B^-}=0.39$ and $f_{B_s}=0.12$. Contributions from B^0 and B_s decays cannot be separated. Limits are given for the weighted average of the decay rates for the two neutral B mesons.
[2] Assumes a B^0, B^- production fraction of 0.39 and a B_s production fraction of 0.12. Contributions from B^0 and B_s^0 decays cannot be separated. Limits are given for the weighted average of the decay rates for the two neutral B mesons.

$\Gamma(\rho^0 K^+\pi^-)/\Gamma_{total}$ Γ_{275}/Γ

VALUE (units 10^{-6})		DOCUMENT ID		TECN	COMMENT
2.8±0.5±0.5	[1,2]	KYEONG	09	BELL	$e^+e^- \to \Upsilon(4S)$

[1] Assumes equal production of B^+ and B^0 at the $\Upsilon(4S)$.
[2] Required $0.75 < m_{K^+\pi^-} < 1.20$ GeV/c^2.

$\Gamma(f_0(980)K^+\pi^-,\ f_0 \to \pi\pi)/\Gamma_{total}$ Γ_{276}/Γ

VALUE (units 10^{-6})		DOCUMENT ID		TECN	COMMENT
$1.4\pm0.4^{+0.3}_{-0.4}$	[1,2]	KYEONG	09	BELL	$e^+e^- \to \Upsilon(4S)$

[1] Assumes equal production of B^+ and B^0 at the $\Upsilon(4S)$.
[2] Required $0.75 < m_{K^+K^-} < 1.2$ GeV/c^2.

$\Gamma(K^+\pi^-\pi^+\pi^-$ nonresonant$)/\Gamma_{total}$ Γ_{277}/Γ

VALUE	CL%	DOCUMENT ID		TECN	COMMENT
$<2.1\times10^{-6}$	90	[1,2] KYEONG	09	BELL	$e^+e^- \to \Upsilon(4S)$

[1] Assumes equal production of B^+ and B^0 at the $\Upsilon(4S)$.
[2] Required $0.55 < m_{\pi^+\pi^-} < 1.42$ and $0.75 < m_{K^+\pi^-} < 1.20$ GeV/c^2.

$\Gamma(K^*(892)^0\pi^+\pi^-)/\Gamma_{total}$ Γ_{278}/Γ

VALUE (units 10^{-6})	CL%	DOCUMENT ID		TECN	COMMENT
54.5±2.9±4.3		[1] AUBERT	07AS	BABR	$e^+e^- \to \Upsilon(4S)$
• • • We do not use the following data for averages, fits, limits, etc. • • •					
$4.5^{+1.1+0.9}_{-1.0-1.6}$		[1,2] KYEONG	09	BELL	$e^+e^- \to \Upsilon(4S)$
<1400	90	ALBRECHT	91E	ARG	$e^+e^- \to \Upsilon(4S)$

[1] Assumes equal production of B^+ and B^0 at the $\Upsilon(4S)$.
[2] Required $0.55 < m_{\pi^+\pi^-} < 1.42$ GeV/c^2.

$\Gamma(K^*(892)^0\rho^0)/\Gamma_{total}$ Γ_{279}/Γ

VALUE (units 10^{-6})	CL%	DOCUMENT ID		TECN	COMMENT
3.9±1.3 OUR AVERAGE		Error includes scale factor of 1.9.			
$5.1\pm0.6^{+0.6}_{-0.8}$		[1] LEES	12K	BABR	$e^+e^- \to \Upsilon(4S)$
$2.1^{+0.8+0.9}_{-0.7-0.5}$		[1] KYEONG	09	BELL	$e^+e^- \to \Upsilon(4S)$
• • • We do not use the following data for averages, fits, limits, etc. • • •					
$5.6\pm0.9\pm1.3$		[1] AUBERT,B	06G	BABR	Repl. by LEES 12K
< 34	90	[2] GODANG	02	CLE2	$e^+e^- \to \Upsilon(4S)$
<286	90	[3] ABE	00C	SLD	$e^+e^- \to Z$
<460	90	ALBRECHT	91B	ARG	$e^+e^- \to \Upsilon(4S)$
<580	90	[4] AVERY	89B	CLEO	$e^+e^- \to \Upsilon(4S)$
<960	90	[5] AVERY	87	CLEO	$e^+e^- \to \Upsilon(4S)$

[1] Assumes equal production of B^+ and B^0 at the $\Upsilon(4S)$.
[2] Assumes a helicity 00 configuration. For a helicity 11 configuration, the limit decreases to 2.4×10^{-5}.
[3] ABE 00C assumes $B(Z \to b\overline{b})=(21.7\pm0.1)\%$ and the B fractions $f_{B^0}=f_{B^+}=(39.7^{+1.8}_{-2.2})\%$ and $f_{B_s}=(10.5^{+1.8}_{-2.2})\%$.
[4] AVERY 89B reports $< 6.7\times10^{-4}$ assuming the $\Upsilon(4S)$ decays 43% to $B^0\overline{B}^0$. We rescale to 50%.
[5] AVERY 87 reports $< 1.2\times10^{-3}$ assuming the $\Upsilon(4S)$ decays 40% to $B^0\overline{B}^0$. We rescale to 50%.

$\Gamma(K^*(892)^0 f_0(980),\ f_0 \to \pi\pi)/\Gamma_{total}$ Γ_{280}/Γ

VALUE (units 10^{-6})	CL%	DOCUMENT ID		TECN	COMMENT
$3.9^{+2.1}_{-1.8}$ OUR AVERAGE		Error includes scale factor of 3.9.			
$5.7\pm0.6\pm0.4$		[1] LEES	12K	BABR	$e^+e^- \to \Upsilon(4S)$
$1.4^{+0.6+0.6}_{-0.5-0.4}$		[1,2] KYEONG	09	BELL	$e^+e^- \to \Upsilon(4S)$
• • • We do not use the following data for averages, fits, limits, etc. • • •					
< 4.3	90	[1] AUBERT,B	06G	BABR	$e^+e^- \to \Upsilon(4S)$
<170	90	[3] AVERY	89B	CLEO	$e^+e^- \to \Upsilon(4S)$

[1] Assumes equal production of B^+ and B^0 at the $\Upsilon(4S)$.
[2] The upper limit is 2.2×10^{-6} at 90% CL.
[3] AVERY 89B reports $< 2.0\times10^{-4}$ assuming the $\Upsilon(4S)$ decays 43% to $B^0\overline{B}^0$. We rescale to 50%.

$\Gamma(K_1(1270)^+\pi^-)/\Gamma_{total}$ Γ_{281}/Γ

VALUE	CL%	DOCUMENT ID		TECN	COMMENT
$<3.0\times10^{-5}$	90	[1] AUBERT	10D	BABR	$e^+e^- \to \Upsilon(4S)$

[1] Assumes equal production of B^+ and B^0 at the $\Upsilon(4S)$.

$\Gamma(K_1(1400)^+\pi^-)/\Gamma_{total}$ Γ_{282}/Γ

VALUE	CL%	DOCUMENT ID		TECN	COMMENT
$<2.7\times10^{-5}$	90	[1] AUBERT	10D	BABR	$e^+e^- \to \Upsilon(4S)$
• • • We do not use the following data for averages, fits, limits, etc. • • •					
$<1.1\times10^{-3}$	90	ALBRECHT	91B	ARG	$e^+e^- \to \Upsilon(4S)$

[1] Assumes equal production of B^+ and B^0 at the $\Upsilon(4S)$.

$\Gamma(a_1(1260)^- K^+)/\Gamma_{total}$ Γ_{283}/Γ

VALUE (units 10^{-6})	CL%	DOCUMENT ID		TECN	COMMENT
16.3±2.9±2.3		[1,2] AUBERT	08F	BABR	$e^+e^- \to \Upsilon(4S)$
• • • We do not use the following data for averages, fits, limits, etc. • • •					
<230	90	[3] ADAM	96D	DLPH	$e^+e^- \to Z$
<390	90	[4] ABREU	95N	DLPH	Sup. by ADAM 96D

[1] Assumes equal production of B^+ and B^0 at the $\Upsilon(4S)$.
[2] Assumes $a_1^\pm$ decays only to 3π and $B(a_1^\pm \to \pi^\pm\pi^\mp\pi^\pm) = 0.5$.
[3] ADAM 96D assumes $f_{B^0} = f_{B^-} = 0.39$ and $f_{B_s} = 0.12$. Contributions from B^0 and B_s decays cannot be separated. Limits are given for the weighted average of the decay rates for the two neutral B mesons.
[4] Assumes a B^0, B^- production fraction of 0.39 and a B_s production fraction of 0.12. Contributions from B^0 and B_s^0 decays cannot be separated. Limits are given for the weighted average of the decay rates for the two neutral B mesons.

$\Gamma(K^*(892)^+\rho^-)/\Gamma_{total}$ Γ_{284}/Γ

VALUE (units 10^{-6})	CL%	DOCUMENT ID		TECN	COMMENT
10.3±2.3±1.3		[1] LEES	12K	BABR	$e^+e^- \to \Upsilon(4S)$
• • • We do not use the following data for averages, fits, limits, etc. • • •					
<12.0	90	[1] AUBERT,B	06G	BABR	Repl. by LEES 12K

[1] Assumes equal production of B^+ and B^0 at the $\Upsilon(4S)$.

$\Gamma(K_0^*(1430)^+\rho^-)/\Gamma_{total}$ Γ_{285}/Γ

VALUE (units 10^{-6})	DOCUMENT ID		TECN	COMMENT
28±10±6	[1] LEES	12K	BABR	$e^+e^- \to \Upsilon(4S)$

[1] Assumes equal production of B^+ and B^0 at the $\Upsilon(4S)$.

$\Gamma(K_1(1400)^0\rho^0)/\Gamma_{total}$ Γ_{286}/Γ

VALUE	CL%	DOCUMENT ID		TECN	COMMENT
$<3.0\times10^{-3}$	90	ALBRECHT	91B	ARG	$e^+e^- \to \Upsilon(4S)$

$\Gamma(K_0^*(1430)^0\rho^0)/\Gamma_{total}$ Γ_{287}/Γ

VALUE (units 10^{-6})	DOCUMENT ID		TECN	COMMENT
27±4±4	[1] LEES	12K	BABR	$e^+e^- \to \Upsilon(4S)$

[1] Assumes equal production of B^+ and B^0 at the $\Upsilon(4S)$.

$\Gamma(K_0^*(1430)^0 f_0(980),\ f_0 \to \pi\pi)/\Gamma_{total}$ Γ_{288}/Γ

VALUE (units 10^{-6})	DOCUMENT ID		TECN	COMMENT
2.7±0.7±0.6	[1] LEES	12K	BABR	$e^+e^- \to \Upsilon(4S)$

[1] Assumes equal production of B^+ and B^0 at the $\Upsilon(4S)$.

$\Gamma(K_2^*(1430)^0 f_0(980),\ f_0 \to \pi\pi)/\Gamma_{total}$ Γ_{289}/Γ

VALUE (units 10^{-6})	DOCUMENT ID		TECN	COMMENT
8.6±1.7±1.0	[1] LEES	12K	BABR	$e^+e^- \to \Upsilon(4S)$

[1] Assumes equal production of B^+ and B^0 at the $\Upsilon(4S)$.

$\Gamma(K^+K^-)/\Gamma_{total}$ Γ_{290}/Γ

VALUE (units 10^{-6})	CL%	DOCUMENT ID		TECN	COMMENT
0.13±0.05 OUR AVERAGE					
$0.10\pm0.08\pm0.04$		[1,2] DUH	13	BELL	$e^+e^- \to \Upsilon(4S)$
$0.12^{+0.08}_{-0.07}\pm0.01$		[3] AAIJ	12AR	LHCB	pp at 7 TeV
$0.23\pm0.10\pm0.10$		[4] AALTONEN	12L	CDF	$p\overline{p}$ at 1.96 TeV
• • • We do not use the following data for averages, fits, limits, etc. • • •					
< 0.7	90	[5] AALTONEN	09C	CDF	Repl. by AALTONEN 12L
< 0.5	90	[2] AUBERT	07B	BABR	$e^+e^- \to \Upsilon(4S)$
< 0.41	90	[2] LIN	07	BELL	Repl. by DUH 13
< 1.8	90	[6] ABULENCIA,A	06D	CDF	Repl. by AALTONEN 09C
< 0.37	90	ABE	05G	BELL	Repl. by LIN 07
< 0.7	90	CHAO	04	BELL	$e^+e^- \to \Upsilon(4S)$
< 0.8	90	[2] BORNHEIM	03	CLE2	$e^+e^- \to \Upsilon(4S)$
< 0.6	90	[2] AUBERT	02Q	BABR	$e^+e^- \to \Upsilon(4S)$
< 0.9	90	[2] CASEY	02	BELL	$e^+e^- \to \Upsilon(4S)$
< 2.7	90	[2] ABE	01H	BELL	$e^+e^- \to \Upsilon(4S)$
< 2.5	90	[2] AUBERT	01E	BABR	$e^+e^- \to \Upsilon(4S)$
< 66	90	[7] ABE	00C	SLD	$e^+e^- \to Z$
< 1.9	90	[2] CRONIN-HEN...00		CLE2	$e^+e^- \to \Upsilon(4S)$
< 4.3	90	GODANG	98	CLE2	Repl. by CRONIN-HENNESSY 00
< 46		[8] ADAM	96D	DLPH	$e^+e^- \to Z$
< 4	90	ASNER	96	CLE2	Repl. by GODANG 98
< 18	90	[9] BUSKULIC	96V	ALEP	$e^+e^- \to Z$
<120	90	[10] ABREU	95N	DLPH	Sup. by ADAM 96D
< 7	90	[2] BATTLE	93	CLE2	$e^+e^- \to \Upsilon(4S)$

[1] DUH 13 reports also for the same data $B(B^0 \to K^+K^-) < 0.20\times10^{-6}$ at 90% CL.
[2] Assumes equal production of B^+ and B^0 at the $\Upsilon(4S)$.
[3] AAIJ 12AR reports $[\Gamma(B^0 \to K^+K^-)/\Gamma_{total}] / [B(B_s^0 \to K^+K^-)] / [\Gamma(\overline{b} \to B_s^0)/\Gamma(\overline{b} \to B^0)] = 0.018^{+0.008}_{-0.007} \pm 0.009$ which we multiply by our best values $B(B_s^0 \to K^+K^-) = (2.49 \pm 0.17)\times10^{-5}$, $\Gamma(\overline{b} \to B_s^0)/\Gamma(\overline{b} \to B^0) = 0.261 \pm 0.015$. Our first error is their experiment's error and our second error is the systematic error from using our best values.
[4] Reported a central value of $(0.23 \pm 0.10 \pm 0.10)\times10^{-6}$ using $B(B^0 \to K^+\pi^-) = (19.4 \pm 0.6)\times10^{-6}$.
[5] Obtains this result from $B(K^+K^-)/B(K^+\pi^-) = 0.020 \pm 0.008 \pm 0.006$, assuming $B(B^0 \to K^+\pi^-) = (19.4 \pm 0.6)\times10^{-6}$.
[6] ABULENCIA,A 06D obtains this from $\Gamma(K^+K^-)/\Gamma(K^+\pi^-) < 0.10$ at 90% CL, assuming $B(B^0 \to K^+\pi^-) = (18.9 \pm 0.7)\times10^{-6}$.
[7] ABE 00C assumes $B(Z \to b\overline{b})$=(21.7 ± 0.1)% and the B fractions $f_{B^0}=f_{B^+}=(39.7^{+1.8}_{-2.2})$% and $f_{B_s}=(10.5^{+1.8}_{-2.2})$%.
[8] ADAM 96D assumes $f_{B^0} = f_{B^-} = 0.39$ and $f_{B_s} = 0.12$. Contributions from B^0 and B_s decays cannot be separated. Limits are given for the weighted average of the decay rates for the two neutral B mesons.
[9] BUSKULIC 96V assumes PDG 96 production fractions for B^0, B^+, B_s, b baryons.
[10] Assumes a B^0, B^- production fraction of 0.39 and a B_s production fraction of 0.12. Contributions from B^0 and B_s^0 decays cannot be separated. Limits are given for the weighted average of the decay rates for the two neutral B mesons.

$\Gamma(K^0\overline{K}^0)/\Gamma_{total}$ Γ_{291}/Γ

VALUE (units 10^{-6})	CL%	DOCUMENT ID		TECN	COMMENT
1.21±0.16 OUR AVERAGE					
1.26±0.19±0.05		[1] DUH	13	BELL	$e^+e^- \to \Upsilon(4S)$
1.08±0.28±0.11		[1] AUBERT,BE	06C	BABR	$e^+e^- \to \Upsilon(4S)$
• • • We do not use the following data for averages, fits, limits, etc. • • •					
$0.87^{+0.25}_{-0.20}\pm0.09$		[1] LIN	07	BELL	Repl. by DUH 13
0.8 ±0.3 ±0.9		[1] ABE	05G	BELL	Repl. by LIN 07
$1.19^{+0.40}_{-0.35}\pm0.13$		[1] AUBERT,BE	05E	BABR	Repl. by AUBERT,BE 06C
< 1.8	90	[1] AUBERT	04M	BABR	$e^+e^- \to \Upsilon(4S)$
< 1.5	90	[1] CHAO	04	BELL	Repl. by ABE 05G
< 3.3	90	[1] BORNHEIM	03	CLE2	$e^+e^- \to \Upsilon(4S)$
< 4.1	90	[1] CASEY	02	BELL	$e^+e^- \to \Upsilon(4S)$
<17	90	GODANG	98	CLE2	$e^+e^- \to \Upsilon(4S)$

[1] Assumes equal production of B^+ and B^0 at the $\Upsilon(4S)$.

$\Gamma(K^0K^-\pi^+)/\Gamma_{total}$ Γ_{292}/Γ

VALUE (units 10^{-6})	CL%	DOCUMENT ID		TECN	COMMENT
7.3±1.1 OUR FIT Error includes scale factor of 1.2.					
6.4±1.0±0.6		[1] DEL-AMO-SA...10E		BABR	$e^+e^- \to \Upsilon(4S)$
• • • We do not use the following data for averages, fits, limits, etc. • • •					
<18	90	[1] GARMASH	04	BELL	$e^+e^- \to \Upsilon(4S)$
<21	90	[1] ECKHART	02	CLE2	$e^+e^- \to \Upsilon(4S)$

[1] Assumes equal production of B^+ and B^0 at the $\Upsilon(4S)$.

$\Gamma(K^0K^-\pi^+)/\Gamma(K^0\pi^+\pi^-)$ $\Gamma_{292}/\Gamma_{261}$

VALUE	DOCUMENT ID		TECN	COMMENT
0.112±0.018 OUR FIT Error includes scale factor of 1.2.				
0.128±0.017±0.009	AAIJ	13BP	LHCB	pp at 7 TeV

$[\Gamma(\overline{K}^{*0}K^0) + \Gamma(K^{*0}\overline{K}^0)]/\Gamma_{total}$ Γ_{293}/Γ

VALUE (units 10^{-6})	DOCUMENT ID		TECN	COMMENT
<1.9	[1] AUBERT,BE	06N	BABR	$e^+e^- \to \Upsilon(4S)$

[1] Assumes equal production of B^+ and B^0 at the $\Upsilon(4S)$.

$\Gamma(K^+K^-\pi^0)/\Gamma_{total}$ Γ_{294}/Γ

VALUE (units 10^{-6})	CL%	DOCUMENT ID		TECN	COMMENT
2.17±0.60±0.24		[1] GAUR	13	BELL	$e^+e^- \to \Upsilon(4S)$
• • • We do not use the following data for averages, fits, limits, etc. • • •					
<19	90	[1] ECKHART	02	CLE2	$e^+e^- \to \Upsilon(4S)$

[1] Assumes equal production of B^+ and B^0 at the $\Upsilon(4S)$.

$\Gamma(K_S^0K_S^0\pi^0)/\Gamma_{total}$ Γ_{295}/Γ

VALUE	CL%	DOCUMENT ID		TECN	COMMENT
<0.9 × 10⁻⁶	90	[1] AUBERT	09AD	BABR	$e^+e^- \to \Upsilon(4S)$

[1] Assumes equal production of B^+ and B^0 at the $\Upsilon(4S)$.

$\Gamma(K_S^0K_S^0\eta)/\Gamma_{total}$ Γ_{296}/Γ

VALUE	CL%	DOCUMENT ID		TECN	COMMENT
<1.0 × 10⁻⁶	90	[1] AUBERT	09AD	BABR	$e^+e^- \to \Upsilon(4S)$

[1] Assumes equal production of B^+ and B^0 at the $\Upsilon(4S)$.

$\Gamma(K_S^0K_S^0\eta')/\Gamma_{total}$ Γ_{297}/Γ

VALUE	CL%	DOCUMENT ID		TECN	COMMENT
<2.0 × 10⁻⁶	90	[1] AUBERT	09AD	BABR	$e^+e^- \to \Upsilon(4S)$

[1] Assumes equal production of B^+ and B^0 at the $\Upsilon(4S)$.

$\Gamma(K^0K^+K^-)/\Gamma_{total}$ Γ_{298}/Γ

VALUE (units 10^{-6})	CL%	DOCUMENT ID		TECN	COMMENT
26.3±1.5 OUR FIT Error includes scale factor of 1.3.					
26.6±1.2 OUR AVERAGE					
26.5±0.9±0.8		[1,2] LEES	12O	BABR	$e^+e^- \to \Upsilon(4S)$
28.3±3.3±4.0		[1] GARMASH	04	BELL	$e^+e^- \to \Upsilon(4S)$
• • • We do not use the following data for averages, fits, limits, etc. • • •					
23.8±2.0±1.6		[1] AUBERT,B	04V	BABR	Repl. by LEES 12O
<1300	90	ALBRECHT	91E	ARG	$e^+e^- \to \Upsilon(4S)$

[1] Assumes equal production of B^+ and B^0 at the $\Upsilon(4S)$.
[2] All intermediate charmonium and charm resonances are removed, except of χ_{c0}.

$\Gamma(K^0K^+K^-)/\Gamma(K^0\pi^+\pi^-)$ $\Gamma_{298}/\Gamma_{261}$

VALUE	DOCUMENT ID		TECN	COMMENT
0.40 ±0.04 OUR FIT Error includes scale factor of 1.2.				
0.385±0.031±0.023	AAIJ	13BP	LHCB	pp at 7 TeV

$\Gamma(K^0\phi)/\Gamma_{total}$ Γ_{299}/Γ

VALUE (units 10^{-6})	CL%	DOCUMENT ID		TECN	COMMENT
7.3±0.7 OUR AVERAGE					
$7.1\pm0.6^{+0.4}_{-0.3}$		[1] LEES	12O	BABR	$e^+e^- \to \Upsilon(4S)$
$9.0^{+2.2}_{-1.8}\pm0.7$		[1] CHEN	03B	BELL	$e^+e^- \to \Upsilon(4S)$
• • • We do not use the following data for averages, fits, limits, etc. • • •					
$8.4^{+1.5}_{-1.3}\pm0.5$		[1] AUBERT	04A	BABR	Repl. by LEES 12O
$8.1^{+3.1}_{-2.5}\pm0.8$		[1] AUBERT	01D	BABR	$e^+e^- \to \Upsilon(4S)$
< 12.3	90	[1] BRIERE	01	CLE2	$e^+e^- \to \Upsilon(4S)$
< 31	90	[1] BERGFELD	98	CLE2	
< 88	90	ASNER	96	CLE2	$e^+e^- \to \Upsilon(4S)$
< 720	90	ALBRECHT	91B	ARG	$e^+e^- \to \Upsilon(4S)$
< 420	90	[2] AVERY	89B	CLEO	$e^+e^- \to \Upsilon(4S)$
<1000	90	[3] AVERY	87	CLEO	$e^+e^- \to \Upsilon(4S)$

[1] Assumes equal production of B^+ and B^0 at the $\Upsilon(4S)$.
[2] AVERY 89B reports $< 4.9\times10^{-4}$ assuming the $\Upsilon(4S)$ decays 43% to $B^0\overline{B}^0$. We rescale to 50%.
[3] AVERY 87 reports $< 1.3\times10^{-3}$ assuming the $\Upsilon(4S)$ decays 40% to $B^0\overline{B}^0$. We rescale to 50%.

$\Gamma(f_0(980)K^0, f_0 \to K^+K^-)/\Gamma_{total}$ Γ_{300}/Γ

VALUE (units 10^{-6})	DOCUMENT ID		TECN	COMMENT
$\mathbf{7.0^{+2.6}_{-1.8}\pm2.4}$	[1] LEES	12O	BABR	$e^+e^- \to \Upsilon(4S)$

[1] Assumes equal production of B^+ and B^0 at the $\Upsilon(4S)$.

$\Gamma(f_0(1500)K^0)/\Gamma_{total}$ Γ_{301}/Γ

VALUE (units 10^{-6})	DOCUMENT ID		TECN	COMMENT
$\mathbf{13.3^{+5.8}_{-4.4}\pm3.2}$	[1] LEES	12O	BABR	$e^+e^- \to \Upsilon(4S)$

[1] Assumes equal production of B^+ and B^0 at the $\Upsilon(4S)$.

$\Gamma(f_2'(1525)^0K^0)/\Gamma_{total}$ Γ_{302}/Γ

VALUE (units 10^{-6})	DOCUMENT ID		TECN	COMMENT
$\mathbf{0.29^{+0.27}_{-0.18}\pm0.36}$	[1] LEES	12O	BABR	$e^+e^- \to \Upsilon(4S)$

[1] Assumes equal production of B^+ and B^0 at the $\Upsilon(4S)$.

$\Gamma(f_0(1710)K^0, f_0 \to K^+K^-)/\Gamma_{total}$ Γ_{303}/Γ

VALUE (units 10^{-6})	DOCUMENT ID		TECN	COMMENT
4.4±0.7±0.5	[1] LEES	12O	BABR	$e^+e^- \to \Upsilon(4S)$

[1] Assumes equal production of B^+ and B^0 at the $\Upsilon(4S)$.

$\Gamma(K^0K^+K^-\text{nonresonant})/\Gamma_{total}$ Γ_{304}/Γ

VALUE (units 10^{-6})	DOCUMENT ID		TECN	COMMENT
33±5±9	[1] LEES	12O	BABR	$e^+e^- \to \Upsilon(4S)$

[1] Assumes equal production of B^+ and B^0 at the $\Upsilon(4S)$.

$\Gamma(K_S^0K_S^0K_S^0)/\Gamma_{total}$ Γ_{305}/Γ

VALUE (units 10^{-6})	DOCUMENT ID		TECN	COMMENT
6.0 ±0.5 OUR AVERAGE Error includes scale factor of 1.1.				
6.19±0.48±0.19	[1] LEES	12I	BABR	$e^+e^- \to \Upsilon(4S)$
$4.2\ ^{+1.6}_{-1.3}\ \pm0.8$	[1] GARMASH	04	BELL	$e^+e^- \to \Upsilon(4S)$
• • • We do not use the following data for averages, fits, limits, etc. • • •				
$6.9\ ^{+0.9}_{-0.8}\ \pm0.6$	[1] AUBERT,B	05	BABR	Repl. by LEES 12I

[1] Assumes equal production of B^+ and B^0 at the $\Upsilon(4S)$.

$\Gamma(f_0(980)K^0,\ f_0\to K^0_S K^0_S)/\Gamma_{total}$ Γ_{306}/Γ

VALUE (units 10^{-6})	DOCUMENT ID		TECN	COMMENT
$2.7^{+1.3}_{-1.2}\pm1.3$	[1,2] LEES	12I	BABR	$e^+e^-\to\ \Upsilon(4S)$

[1] Assumes equal production of B^+ and B^0 at the $\Upsilon(4S)$.
[2] Uses Dalitz plot analysis of the $B^0\to\ K^0_S K^0_S K^0_S$ decay.

$\Gamma(f_0(1710)K^0,\ f_0\to K^0_S K^0_S)/\Gamma_{total}$ Γ_{307}/Γ

VALUE (units 10^{-6})	DOCUMENT ID		TECN	COMMENT
$0.50^{+0.46}_{-0.24}\pm0.11$	[1,2] LEES	12I	BABR	$e^+e^-\to\ \Upsilon(4S)$

[1] Assumes equal production of B^+ and B^0 at the $\Upsilon(4S)$.
[2] Uses Dalitz plot analysis of the $B^0\to\ K^0_S K^0_S K^0_S$ decay.

$\Gamma(f_0(2010)K^0,\ f_0\to K^0_S K^0_S)/\Gamma_{total}$ Γ_{308}/Γ

VALUE (units 10^{-6})	DOCUMENT ID		TECN	COMMENT
$0.54^{+0.21}_{-0.20}\pm0.52$	[1,2] LEES	12I	BABR	$e^+e^-\to\ \Upsilon(4S)$

[1] Assumes equal production of B^+ and B^0 at the $\Upsilon(4S)$.
[2] Uses Dalitz plot analysis of the $B^0\to\ K^0_S K^0_S K^0_S$ decay.

$\Gamma(K^0_S K^0_S K^0_S\,\text{nonresonant})/\Gamma_{total}$ Γ_{309}/Γ

VALUE (units 10^{-6})	DOCUMENT ID		TECN	COMMENT
$13.3^{+2.2}_{-2.3}\pm2.2$	[1,2] LEES	12I	BABR	$e^+e^-\to\ \Upsilon(4S)$

[1] Assumes equal production of B^+ and B^0 at the $\Upsilon(4S)$.
[2] Uses Dalitz plot analysis of the $B^0\to\ K^0_S K^0_S K^0_S$ decay.

$\Gamma(K^0_S K^0_S K^0_L)/\Gamma_{total}$ Γ_{310}/Γ

VALUE (units 10^{-6})	CL%	DOCUMENT ID		TECN	COMMENT
<16	90	[1] AUBERT,B	06R	BABR	$e^+e^-\to\ \Upsilon(4S)$

[1] Assumes equal production of B^+ and B^0 at the $\Upsilon(4S)$.

$\Gamma(K^*(892)^0K^+K^-)/\Gamma_{total}$ Γ_{311}/Γ

VALUE (units 10^{-6})	CL%	DOCUMENT ID		TECN	COMMENT
$27.5\pm1.3\pm2.2$		[1] AUBERT	07AS	BABR	$e^+e^-\to\ \Upsilon(4S)$
• • • We do not use the following data for averages, fits, limits, etc. • • •					
<610	90	ALBRECHT	91E	ARG	$e^+e^-\to\ \Upsilon(4S)$

[1] Assumes equal production of B^+ and B^0 at the $\Upsilon(4S)$.

$\Gamma(K^*(892)^0\phi)/\Gamma_{total}$ Γ_{312}/Γ

VALUE (units 10^{-6})	CL%	DOCUMENT ID		TECN	COMMENT
10.0 ± 0.5 OUR AVERAGE					
$10.4\pm0.5\pm0.6$		[1] PRIM	13	BELL	$e^+e^-\to\ \Upsilon(4S)$
$9.7\pm0.5\pm0.5$		[1] AUBERT	08BG	BABR	$e^+e^-\to\ \Upsilon(4S)$
$11.5^{+4.5+1.8}_{-3.7-1.7}$		[1] BRIERE	01	CLE2	$e^+e^-\to\ \Upsilon(4S)$
• • • We do not use the following data for averages, fits, limits, etc. • • •					
$9.2\pm0.7\pm0.6$		[1] AUBERT	07D	BABR	Repl. by AUBERT 08BG
$9.2\pm0.9\pm0.5$		[1] AUBERT,B	04W	BABR	Repl. by AUBERT 07D
$11.2\pm1.3\pm0.8$		[1] AUBERT	03V	BABR	Repl. by AUBERT,B 04W
$10.0^{+1.6+0.7}_{-1.5-0.8}$		[1] CHEN	03B	BELL	Repl. by PRIM 13
$8.7^{+2.5}_{-2.1}\pm1.1$		[1] AUBERT	01D	BABR	Repl. by AUBERT 03V
<384	90	[2] ABE	00C	SLD	$e^+e^-\to\ Z$
< 21	90	[1] BERGFELD	98	CLE2	
< 43	90	ASNER	96	CLE2	$e^+e^-\to\ \Upsilon(4S)$
<320	90	ALBRECHT	91B	ARG	$e^+e^-\to\ \Upsilon(4S)$
<380	90	[3] AVERY	89B	CLEO	$e^+e^-\to\ \Upsilon(4S)$
<380	90	[4] AVERY	87	CLEO	$e^+e^-\to\ \Upsilon(4S)$

[1] Assumes equal production of B^+ and B^0 at the $\Upsilon(4S)$.
[2] ABE 00C assumes $B(Z\to\ b\overline{b})=(21.7\pm0.1)\%$ and the B fractions $f_{B^0}=f_{B^+}=(39.7^{+1.8}_{-2.2})\%$ and $f_{B_s}=(10.5^{+1.8}_{-2.2})\%$.
[3] AVERY 89B reports $<4.4\times10^{-4}$ assuming the $\Upsilon(4S)$ decays 43% to $B^0\overline{B}^0$. We rescale to 50%.
[4] AVERY 87 reports $<4.7\times10^{-4}$ assuming the $\Upsilon(4S)$ decays 40% to $B^0\overline{B}^0$. We rescale to 50%.

$\Gamma(K^+K^-\pi^+\pi^-\,\text{nonresonant})/\Gamma_{total}$ Γ_{313}/Γ

VALUE (units 10^{-6})	CL%	DOCUMENT ID		TECN	COMMENT
<71.7	90	[1,2] CHIANG	10	BELL	$e^+e^-\to\ \Upsilon(4S)$

[1] Measured in the range $0.7<m_{K\pi}<1.7$ and corrected using PS assumption for the full $K\pi$ mass range.
[2] Assumes equal production of B^+ and B^0 at the $\Upsilon(4S)$.

$\Gamma(K^*(892)^0K^-\pi^+)/\Gamma_{total}$ Γ_{314}/Γ

VALUE (units 10^{-6})	DOCUMENT ID		TECN	COMMENT
4.5 ±1.3 OUR AVERAGE				
$2.11^{+5.63+4.85}_{-5.26-4.75}$	[1,2] CHIANG	10	BELL	$e^+e^-\to\ \Upsilon(4S)$
$4.6\ \pm1.1\ \pm0.8$	[2] AUBERT	07AS	BABR	$e^+e^-\to\ \Upsilon(4S)$

[1] Measured in the range $0.7<m_{K\pi}<1.7$ and corrected using PS assumption for the full $K\pi$ mass range. The quoted result is equivalent to the upper limit of $<13.9\times10^{-6}$ at 90% CL.
[2] Assumes equal production of B^+ and B^0 at the $\Upsilon(4S)$.

$\Gamma(K^*(892)^0\overline{K}^*(892)^0)/\Gamma_{total}$ Γ_{315}/Γ

VALUE (units 10^{-6})	CL%	DOCUMENT ID		TECN	COMMENT
0.8 ±0.5 OUR AVERAGE Error includes scale factor of 2.2.					
$0.26^{+0.33+0.10}_{-0.29-0.08}$		[1,2] CHIANG	10	BELL	$e^+e^-\to\ \Upsilon(4S)$
$1.28^{+0.35}_{-0.30}\pm0.11$		[2] AUBERT	08I	BABR	$e^+e^-\to\ \Upsilon(4S)$
• • • We do not use the following data for averages, fits, limits, etc. • • •					
< 22	90	[3] GODANG	02	CLE2	$e^+e^-\to\ \Upsilon(4S)$
<469	90	[4] ABE	00C	SLD	$e^+e^-\to\ Z$

[1] Measured in the range $0.7<m_{K\pi}<1.7$ and corrected using PS assumption for the full $K\pi$ mass range. The quoted result is equivalent to the upper limit of $<0.8\times10^{-6}$ at 90% CL.
[2] Assumes equal production of B^+ and B^0 at the $\Upsilon(4S)$.
[3] Assumes a helicity 00 configuration. For a helicity 11 configuration, the limit decreases to 1.9×10^{-5}.
[4] ABE 00C assumes $B(Z\to\ b\overline{b})=(21.7\pm0.1)\%$ and the B fractions $f_{B^0}=f_{B^+}=(39.7^{+1.8}_{-2.2})\%$ and $f_{B_s}=(10.5^{+1.8}_{-2.2})\%$.

$\Gamma(K^+K^+\pi^-\pi^-\,\text{nonresonant})/\Gamma_{total}$ Γ_{316}/Γ

VALUE (units 10^{-6})	CL%	DOCUMENT ID		TECN	COMMENT
<6.0	90	[1] CHIANG	10	BELL	$e^+e^-\to\ \Upsilon(4S)$

[1] Assumes equal production of B^+ and B^0 at the $\Upsilon(4S)$.

$\Gamma(K^*(892)^0K^+\pi^-)/\Gamma_{total}$ Γ_{317}/Γ

VALUE (units 10^{-6})	CL%	DOCUMENT ID		TECN	COMMENT
<2.2	90	[1] AUBERT	07AS	BABR	$e^+e^-\to\ \Upsilon(4S)$
• • • We do not use the following data for averages, fits, limits, etc. • • •					
<7.6	90	[1] CHIANG	10	BELL	$e^+e^-\to\ \Upsilon(4S)$

[1] Assumes equal production of B^+ and B^0 at the $\Upsilon(4S)$.

$\Gamma(K^*(892)^0K^*(892)^0)/\Gamma_{total}$ Γ_{318}/Γ

VALUE (units 10^{-6})	CL%	DOCUMENT ID		TECN	COMMENT
< 0.2	90	[1] CHIANG	10	BELL	$e^+e^-\to\ \Upsilon(4S)$
• • • We do not use the following data for averages, fits, limits, etc. • • •					
< 0.41	90	[1] AUBERT	08I	BABR	$e^+e^-\to\ \Upsilon(4S)$
<37	90	[2] GODANG	02	CLE2	$e^+e^-\to\ \Upsilon(4S)$

[1] Assumes equal production of B^+ and B^0 at the $\Upsilon(4S)$.
[2] Assumes a helicity 00 configuration. For a helicity 11 configuration, the limit decreases to 2.9×10^{-5}.

$\Gamma(K^*(892)^+K^*(892)^-)/\Gamma_{total}$ Γ_{319}/Γ

VALUE (units 10^{-6})	CL%	DOCUMENT ID		TECN	COMMENT
< 2.0	90	[1] AUBERT	08AP	BABR	$e^+e^-\to\ \Upsilon(4S)$
• • • We do not use the following data for averages, fits, limits, etc. • • •					
<141	90	[2] GODANG	02	CLE2	$e^+e^-\to\ \Upsilon(4S)$

[1] Assumes equal production of B^+ and B^0 at the $\Upsilon(4S)$.
[2] Assumes a helicity 00 configuration. For a helicity 11 configuration, the limit decreases to 8.9×10^{-5}.

$\Gamma(K_1(1400)^0\phi)/\Gamma_{total}$ Γ_{320}/Γ

VALUE	CL%	DOCUMENT ID		TECN	COMMENT
$<5.0\times10^{-3}$	90	ALBRECHT	91B	ARG	$e^+e^-\to\ \Upsilon(4S)$

$\Gamma(\phi(K\pi)_0^{*0})/\Gamma_{total}$ Γ_{321}/Γ

This decay refers to the coherent sum of resonant and nonresonant $J^P=0^+$ $K\pi$ components with $1.13<m_{K\pi}<1.53$ GeV/c^2.

VALUE (units 10^{-6})	DOCUMENT ID		TECN	COMMENT
4.3±0.4 OUR AVERAGE				
$4.3\pm0.4\pm0.4$	[1] PRIM	13	BELL	$e^+e^-\to\ \Upsilon(4S)$
$4.3\pm0.6\pm0.4$	[1] AUBERT	08BG	BABR	$e^+e^-\to\ \Upsilon(4S)$
• • • We do not use the following data for averages, fits, limits, etc. • • •				
$5.0\pm0.8\pm0.3$	[1] AUBERT	07D	BABR	Repl. by AUBERT 08BG

[1] Assumes equal production of B^+ and B^0 at the $\Upsilon(4S)$.

$\Gamma(\phi(K\pi)_0^{*0}\,(1.60<m_{K\pi}<2.15))/\Gamma_{total}$ Γ_{322}/Γ

This decay refers to the coherent sum of resonant and nonresonant $J^P=0^+$ $K\pi$ components with $1.60<m_{K\pi}<2.15$ GeV/c^2.

VALUE (units 10^{-6})	CL%	DOCUMENT ID		TECN	COMMENT
<1.7	90	[1] AUBERT	07AO	BABR	$e^+e^-\to\ \Upsilon(4S)$

[1] Assumes equal production of B^+ and B^0 at the $\Upsilon(4S)$.

$\Gamma(K_0^*(1430)^0 K^-\pi^+)/\Gamma_{total}$ Γ_{323}/Γ

VALUE (units 10^{-6})	CL%	DOCUMENT ID		TECN	COMMENT
<31.8	90	[1,2] CHIANG	10	BELL	$e^+e^- \to \Upsilon(4S)$

[1] Measured in the range $0.7 < m_{K\pi} < 1.7$ and corrected using PS assumption for the full $K\pi$ mass range.
[2] Assumes equal production of B^+ and B^0 at the $\Upsilon(4S)$.

$\Gamma(K_0^*(1430)^0 \overline{K}^*(892)^0)/\Gamma_{total}$ Γ_{324}/Γ

VALUE (units 10^{-6})	CL%	DOCUMENT ID		TECN	COMMENT
<3.3	90	[1,2] CHIANG	10	BELL	$e^+e^- \to \Upsilon(4S)$

[1] Measured in the range $0.7 < m_{K\pi} < 1.7$ and corrected using PS assumption for the full $K\pi$ mass range.
[2] Assumes equal production of B^+ and B^0 at the $\Upsilon(4S)$.

$\Gamma(K_0^*(1430)^0 \overline{K}_0^*(1430)^0)/\Gamma_{total}$ Γ_{325}/Γ

VALUE (units 10^{-6})	CL%	DOCUMENT ID		TECN	COMMENT
<8.4	90	[1,2] CHIANG	10	BELL	$e^+e^- \to \Upsilon(4S)$

[1] Measured in the range $0.7 < m_{K\pi} < 1.7$ and corrected using PS assumption for the full $K\pi$ mass range.
[2] Assumes equal production of B^+ and B^0 at the $\Upsilon(4S)$.

$\Gamma(K_0^*(1430)^0 \phi)/\Gamma_{total}$ Γ_{326}/Γ

VALUE (units 10^{-6})	DOCUMENT ID		TECN	COMMENT
3.9±0.5±0.6	[1] AUBERT	08BG	BABR	$e^+e^- \to \Upsilon(4S)$
• • • We do not use the following data for averages, fits, limits, etc. • • •				
4.6±0.7±0.6	[1] AUBERT	07D	BABR	Repl. by AUBERT 08BG
seen	[2] AUBERT,B	04W	BABR	Repl. by AUBERT 07D

[1] Assumes equal production of B^+ and B^0 at the $\Upsilon(4S)$.
[2] Observed 181 ± 17 events with statistical significance greater than 10 σ.

$\Gamma(K_0^*(1430)^0 K^*(892)^0)/\Gamma_{total}$ Γ_{327}/Γ

VALUE (units 10^{-6})	CL%	DOCUMENT ID		TECN	COMMENT
<1.7	90	[1] CHIANG	10	BELL	$e^+e^- \to \Upsilon(4S)$

[1] Assumes equal production of B^+ and B^0 at the $\Upsilon(4S)$.

$\Gamma(K_0^*(1430)^0 K_0^*(1430)^0)/\Gamma_{total}$ Γ_{328}/Γ

VALUE (units 10^{-6})	CL%	DOCUMENT ID		TECN	COMMENT
<4.7	90	[1] CHIANG	10	BELL	$e^+e^- \to \Upsilon(4S)$

[1] Assumes equal production of B^+ and B^0 at the $\Upsilon(4S)$.

$\Gamma(K^*(1680)^0 \phi)/\Gamma_{total}$ Γ_{329}/Γ

VALUE (units 10^{-6})	CL%	DOCUMENT ID		TECN	COMMENT
<3.5	90	[1] AUBERT	07AO	BABR	$e^+e^- \to \Upsilon(4S)$

[1] Assumes equal production of B^+ and B^0 at the $\Upsilon(4S)$.

$\Gamma(K^*(1780)^0 \phi)/\Gamma_{total}$ Γ_{330}/Γ

VALUE (units 10^{-6})	CL%	DOCUMENT ID		TECN	COMMENT
<2.7	90	[1] AUBERT	07AO	BABR	$e^+e^- \to \Upsilon(4S)$

[1] Assumes equal production of B^+ and B^0 at the $\Upsilon(4S)$.

$\Gamma(K^*(2045)^0 \phi)/\Gamma_{total}$ Γ_{331}/Γ

VALUE (units 10^{-6})	CL%	DOCUMENT ID		TECN	COMMENT
<15.3	90	[1] AUBERT	07AO	BABR	$e^+e^- \to \Upsilon(4S)$

[1] Assumes equal production of B^+ and B^0 at the $\Upsilon(4S)$.

$\Gamma(K_2^*(1430)^0 \rho^0)/\Gamma_{total}$ Γ_{332}/Γ

VALUE (units 10^{-6})	CL%	DOCUMENT ID		TECN	COMMENT
<1.1 × 10³	90	ALBRECHT	91B	ARG	$e^+e^- \to \Upsilon(4S)$

$\Gamma(K_2^*(1430)^0 \phi)/\Gamma_{total}$ Γ_{333}/Γ

VALUE (units 10^{-6})	CL%	DOCUMENT ID		TECN	COMMENT
6.8±0.9 OUR AVERAGE		Error includes scale factor of 1.2.			
$5.5^{+0.9}_{-0.7}\pm1.0$		[1] PRIM	13	BELL	$e^+e^- \to \Upsilon(4S)$
7.5±0.9±0.5		[1] AUBERT	08BG	BABR	$e^+e^- \to \Upsilon(4S)$
• • • We do not use the following data for averages, fits, limits, etc. • • •					
7.8±1.1±0.6		[1] AUBERT	07D	BABR	Repl. by AUBERT 08BG
seen		[2] AUBERT,B	04W	BABR	Repl. by AUBERT 07D
<1400	90	ALBRECHT	91B	ARG	$e^+e^- \to \Upsilon(4S)$

[1] Assumes equal production of B^+ and B^0 at the $\Upsilon(4S)$.
[2] The angular distribution of $B \to \phi K^*(1430)$ provides evidence with statistical significance of 3.2 σ.

$\Gamma(K^0\phi\phi)/\Gamma_{total}$ Γ_{334}/Γ

VALUE (units 10^{-6})	DOCUMENT ID		TECN	COMMENT
4.5±0.8±0.3	[1] LEES	11A	BABR	$e^+e^- \to \Upsilon(4S)$
• • • We do not use the following data for averages, fits, limits, etc. • • •				
$4.1^{+1.7}_{-1.4}\pm0.4$	[1] AUBERT,BE	06H	BABR	Repl. by LEES 11A

[1] Assumes equal production of B^0 and B^+ at the $\Upsilon(4S)$ and for a $\phi\phi$ invariant mass below 2.85 GeV/c^2.

$\Gamma(\eta'\eta' K^0)/\Gamma_{total}$ Γ_{335}/Γ

VALUE (units 10^{-6})	CL%	DOCUMENT ID		TECN	COMMENT
<31	90	[1] AUBERT,B	06P	BABR	$e^+e^- \to \Upsilon(4S)$

[1] Assumes equal production of B^+ and B^0 at the $\Upsilon(4S)$.

$\Gamma(\eta K^0\gamma)/\Gamma_{total}$ Γ_{336}/Γ

VALUE (units 10^{-6})	DOCUMENT ID		TECN	COMMENT
7.6±1.8 OUR AVERAGE				
$7.1^{+2.1}_{-2.0}\pm0.4$	[1,2] AUBERT	09	BABR	$e^+e^- \to \Upsilon(4S)$
$8.7^{+3.1}_{-2.7}{}^{+1.9}_{-1.6}$	[2,3] NISHIDA	05	BELL	$e^+e^- \to \Upsilon(4S)$
• • • We do not use the following data for averages, fits, limits, etc. • • •				
$11.3^{+2.8}_{-1.6}\pm0.6$	[1,2] AUBERT,B	06M	BABR	Repl. by AUBERT 09

[1] $m_{\eta K} < 3.25$ GeV/c^2.
[2] Assumes equal production of B^+ and B^0 at the $\Upsilon(4S)$.
[3] $m_{\eta K} < 2.4$ GeV/c^2

$\Gamma(\eta' K^0\gamma)/\Gamma_{total}$ Γ_{337}/Γ

VALUE (units 10^{-6})	CL%	DOCUMENT ID		TECN	COMMENT
<6.4	90	[1,2] WEDD	10	BELL	$e^+e^- \to \Upsilon(4S)$
• • • We do not use the following data for averages, fits, limits, etc. • • •					
<6.6	90	[1,3] AUBERT,B	06M	BABR	$e^+e^- \to \Upsilon(4S)$

[1] Assumes equal production of B^+ and B^0 at the $\Upsilon(4S)$.
[2] $m_{\eta' K} < 3.4$ GeV/c^2.
[3] $m_{\eta' K} < 3.25$ GeV/c^2.

$\Gamma(K^0\phi\gamma)/\Gamma_{total}$ Γ_{338}/Γ

VALUE (units 10^{-6})	CL%	DOCUMENT ID		TECN	COMMENT
2.74±0.60±0.32		[1] SAHOO	11A	BELL	$e^+e^- \to \Upsilon(4S)$
• • • We do not use the following data for averages, fits, limits, etc. • • •					
<2.7	90	[1] AUBERT	07Q	BABR	$e^+e^- \to \Upsilon(4S)$
<8.3	90	[1] DRUTSKOY	04	BELL	$e^+e^- \to \Upsilon(4S)$

[1] Assumes equal production of B^+ and B^0 at $\Upsilon(4S)$.

$\Gamma(K^+\pi^-\gamma)/\Gamma_{total}$ Γ_{339}/Γ

VALUE	DOCUMENT ID		TECN	COMMENT
$\mathbf{(4.6^{+1.3}_{-1.2}{}^{+0.5}_{-0.7})\times10^{-6}}$	[1,2] NISHIDA	02	BELL	$e^+e^- \to \Upsilon(4S)$

[1] Assumes equal production of B^+ and B^0 at the $\Upsilon(4S)$.
[2] 1.25 GeV/c^2 $< M_{K\pi} <$ 1.6 GeV/c^2

$\Gamma(K^*(892)^0\gamma)/\Gamma_{total}$ Γ_{340}/Γ

VALUE (units 10^{-6})	CL%	DOCUMENT ID		TECN	COMMENT
43.3± 1.5 OUR AVERAGE					
44.7± 1.0±1.6		[1] AUBERT	09AO	BABR	$e^+e^- \to \Upsilon(4S)$
40.1± 2.1±1.7		[2] NAKAO	04	BELL	$e^+e^- \to \Upsilon(4S)$
$45.5^{+7.2}_{-6.8}\pm3.4$		[3] COAN	00	CLE2	$e^+e^- \to \Upsilon(4S)$
• • • We do not use the following data for averages, fits, limits, etc. • • •					
39.2± 2.0±2.4		[4] AUBERT,BE	04A	BABR	Repl. by AUBERT 09AO
< 110	90	ACOSTA	02G	CDF	$p\overline{p}$ at 1.8 TeV
42.3± 4.0±2.2		[2] AUBERT	02C	BABR	Repl. by AUBERT,BE 04A
< 210	90	[5] ADAM	96D	DLPH	$e^+e^- \to Z$
40 ±17 ±8		[6] AMMAR	93	CLE2	Repl. by COAN 00
< 420	90	ALBRECHT	89G	ARG	$e^+e^- \to \Upsilon(4S)$
< 240	90	[7] AVERY	89B	CLEO	$e^+e^- \to \Upsilon(4S)$
<2100	90	AVERY	87	CLEO	$e^+e^- \to \Upsilon(4S)$

[1] Uses B($\Upsilon(4S) \to B^+B^-$) = (51.6 ± 0.6)% and B($\Upsilon(4S) \to B^0\overline{B}^0$) = (48.4 ± 0.6)%.
[2] Assumes equal production of B^+ and B^0 at the $\Upsilon(4S)$.
[3] Assumes equal production of B^+ and B^0 at the $\Upsilon(4S)$. No evidence for a nonresonant $K\pi\gamma$ contamination was seen; the central value assumes no contamination.
[4] Uses the production ratio of charged and neutral B from $\Upsilon(4S)$ decays $R^{+/0} = 1.006 \pm 0.048$.
[5] ADAM 96D assumes $f_{B^0} = f_{B^-} = 0.39$ and $f_{B_s} = 0.12$.
[6] AMMAR 93 observed 6.6 ± 2.8 events above background.
[7] AVERY 89B reports $< 2.8 \times 10^{-4}$ assuming the $\Upsilon(4S)$ decays 43% to $B^0\overline{B}^0$. We rescale to 50%.

$\Gamma(K^*(1410)\gamma)/\Gamma_{total}$ Γ_{341}/Γ

VALUE	CL%	DOCUMENT ID		TECN	COMMENT
<1.3 × 10⁻⁴	90	[1] NISHIDA	02	BELL	$e^+e^- \to \Upsilon(4S)$

[1] Assumes equal production of B^+ and B^0 at the $\Upsilon(4S)$.

$\Gamma(K^+\pi^-\gamma$ nonresonant$)/\Gamma_{total}$ Γ_{342}/Γ

VALUE	CL%	DOCUMENT ID		TECN	COMMENT
<2.6 × 10⁻⁶	90	[1,2] NISHIDA	02	BELL	$e^+e^- \to \Upsilon(4S)$

[1] Assumes equal production of B^+ and B^0 at the $\Upsilon(4S)$.
[2] 1.25 GeV/c^2 $< M_{K\pi} <$ 1.6 GeV/c^2

$\Gamma(K^*(892)^0X(214)\times B(X\to\mu^+\mu^-))/\Gamma_{total}$ Γ_{343}/Γ

$X(214)$ is a hypothetical particle of mass 214 MeV/c^2 reported by the HyperCP experiment (PARK 05)

VALUE (units 10^{-8})	CL%	DOCUMENT ID		TECN	COMMENT
<2.26	90	[1,2] HYUN	10	BELL	$e^+e^-\to\Upsilon(4S)$

[1] Assumes equal production of B^+ and B^0 at the $\Upsilon(4S)$.
[2] Based on scalar nature of X particle. With a vector X assumption, the upper limit is 2.27×10^{-8}.

$\Gamma(K^0\pi^+\pi^-\gamma)/\Gamma_{total}$ Γ_{344}/Γ

VALUE (units 10^{-5})		DOCUMENT ID		TECN	COMMENT
1.95±0.22 OUR AVERAGE					
1.85±0.21±0.12		[1,2] AUBERT	07R	BABR	$e^+e^-\to\Upsilon(4S)$
2.40±0.4 ±0.3		[2,3] YANG	05	BELL	$e^+e^-\to\Upsilon(4S)$

[1] $M_{K\pi\pi}<1.8$ GeV/c^2.
[2] Assumes equal production of B^+ and B^0 at the $\Upsilon(4S)$.
[3] $M_{K\pi\pi}<2.0$ GeV/c^2.

$\Gamma(K^+\pi^-\pi^0\gamma)/\Gamma_{total}$ Γ_{345}/Γ

VALUE (units 10^{-5})	DOCUMENT ID		TECN	COMMENT
4.07±0.22±0.31	[1,2] AUBERT	07R	BABR	$e^+e^-\to\Upsilon(4S)$

[1] $M_{K\pi\pi}<1.8$ GeV/c^2.
[2] Assumes equal production of B^+ and B^0 at the $\Upsilon(4S)$.

$\Gamma(K_1(1270)^0\gamma)/\Gamma_{total}$ Γ_{346}/Γ

VALUE (units 10^{-5})	CL%	DOCUMENT ID		TECN	COMMENT
< 5.8	90	[1] YANG	05	BELL	$e^+e^-\to\Upsilon(4S)$
• • • We do not use the following data for averages, fits, limits, etc. • • •					
<700	90	[2] ALBRECHT	89G	ARG	$e^+e^-\to\Upsilon(4S)$

[1] Assumes equal production of B^+ and B^0 at the $\Upsilon(4S)$.
[2] ALBRECHT 89G reports < 0.0078 assuming the $\Upsilon(4S)$ decays 45% to $B^0\overline{B}^0$. We rescale to 50%.

$\Gamma(K_1(1400)^0\gamma)/\Gamma_{total}$ Γ_{347}/Γ

VALUE (units 10^{-5})	CL%	DOCUMENT ID		TECN	COMMENT
< 1.2	90	[1] YANG	05	BELL	$e^+e^-\to\Upsilon(4S)$
• • • We do not use the following data for averages, fits, limits, etc. • • •					
<430	90	[2] ALBRECHT	89G	ARG	$e^+e^-\to\Upsilon(4S)$

[1] Assumes equal production of B^+ and B^0 at the $\Upsilon(4S)$.
[2] ALBRECHT 89G reports < 0.0048 assuming the $\Upsilon(4S)$ decays 45% to $B^0\overline{B}^0$. We rescale to 50%.

$\Gamma(K_2^*(1430)^0\gamma)/\Gamma_{total}$ Γ_{348}/Γ

VALUE (units 10^{-5})	CL%	DOCUMENT ID		TECN	COMMENT
1.24±0.24 OUR AVERAGE					
1.22±0.25±0.10		[1] AUBERT,B	04U	BABR	$e^+e^-\to\Upsilon(4S)$
1.3 ±0.5 ±0.1		[1] NISHIDA	02	BELL	$e^+e^-\to\Upsilon(4S)$
• • • We do not use the following data for averages, fits, limits, etc. • • •					
<40	90	[2] ALBRECHT	89G	ARG	$e^+e^-\to\Upsilon(4S)$

[1] Assumes equal production of B^+ and B^0 at the $\Upsilon(4S)$.
[2] ALBRECHT 89G reports $<4.4\times10^{-4}$ assuming the $\Upsilon(4S)$ decays 45% to $B^0\overline{B}^0$. We rescale to 50%.

$\Gamma(K^*(1680)^0\gamma)/\Gamma_{total}$ Γ_{349}/Γ

VALUE	CL%	DOCUMENT ID		TECN	COMMENT
<0.0020	90	[1] ALBRECHT	89G	ARG	$e^+e^-\to\Upsilon(4S)$

[1] ALBRECHT 89G reports < 0.0022 assuming the $\Upsilon(4S)$ decays 45% to $B^0\overline{B}^0$. We rescale to 50%.

$\Gamma(K_3^*(1780)^0\gamma)/\Gamma_{total}$ Γ_{350}/Γ

VALUE (units 10^{-6})	CL%	DOCUMENT ID		TECN	COMMENT
< 83	90	[1,2] NISHIDA	05	BELL	$e^+e^-\to\Upsilon(4S)$
• • • We do not use the following data for averages, fits, limits, etc. • • •					
<10000	90	[3] ALBRECHT	89G	ARG	$e^+e^-\to\Upsilon(4S)$

[1] Assumes equal production of B^+ and B^0 at the $\Upsilon(4S)$.
[2] Uses $B(K_3^*(1780)\to\eta K)=0.11^{+0.05}_{-0.04}$.
[3] ALBRECHT 89G reports < 0.011 assuming the $\Upsilon(4S)$ decays 45% to $B^0\overline{B}^0$. We rescale to 50%.

$\Gamma(K_4^*(2045)^0\gamma)/\Gamma_{total}$ Γ_{351}/Γ

VALUE	CL%	DOCUMENT ID		TECN	COMMENT
<0.0043	90	[1] ALBRECHT	89G	ARG	$e^+e^-\to\Upsilon(4S)$

[1] ALBRECHT 89G reports < 0.0048 assuming the $\Upsilon(4S)$ decays 45% to $B^0\overline{B}^0$. We rescale to 50%.

$\Gamma(\rho^0\gamma)/\Gamma_{total}$ Γ_{352}/Γ

VALUE (units 10^{-6})	CL%	DOCUMENT ID		TECN	COMMENT
0.86±0.15 OUR AVERAGE					
$0.97^{+0.24}_{-0.22}\pm0.06$		[1] AUBERT	08BH	BABR	$e^+e^-\to\Upsilon(4S)$
$0.78^{+0.17}_{-0.16}{}^{+0.09}_{-0.10}$		[1] TANIGUCHI	08	BELL	$e^+e^-\to\Upsilon(4S)$
• • • We do not use the following data for averages, fits, limits, etc. • • •					
$0.79^{+0.22}_{-0.20}\pm0.06$		[1] AUBERT	07L	BABR	Repl. by AUBERT 08BH
$1.25^{+0.37}_{-0.33}{}^{+0.07}_{-0.06}$		[1] MOHAPATRA	06	BELL	Repl. by TANIGUCHI 08
0.0 ±0.2 ±0.1	90	[1] AUBERT	05	BABR	Repl. by AUBERT 07L
< 0.8	90	[1] MOHAPATRA	05	BELL	$e^+e^-\to\Upsilon(4S)$
< 1.2	90	[1] AUBERT	04C	BABR	$e^+e^-\to\Upsilon(4S)$
<17	90	[1] COAN	00	CLE2	$e^+e^-\to\Upsilon(4S)$

[1] Assumes equal production of B^+ and B^0 at the $\Upsilon(4S)$.

$\Gamma(\rho^0X(214)\times B(X\to\mu^+\mu^-))/\Gamma_{total}$ Γ_{353}/Γ

$X(214)$ is a hypothetical particle of mass 214 MeV/c^2 reported by the HyperCP experiment (PARK 05)

VALUE (units 10^{-8})	CL%	DOCUMENT ID		TECN	COMMENT
<1.73	90	[1,2] HYUN	10	BELL	$e^+e^-\to\Upsilon(4S)$

[1] Assumes equal production of B^+ and B^0 at the $\Upsilon(4S)$.
[2] The result is the same for a scalar or vector X particle.

$\Gamma(\rho^0\gamma)/\Gamma(K^*(892)^0\gamma)$ $\Gamma_{352}/\Gamma_{340}$

VALUE (units 10^{-2})	DOCUMENT ID		TECN	COMMENT
$2.06^{+0.45}_{-0.43}{}^{+0.14}_{-0.16}$	TANIGUCHI	08	BELL	$e^+e^-\to\Upsilon(4S)$

$\Gamma(\omega\gamma)/\Gamma_{total}$ Γ_{354}/Γ

VALUE (units 10^{-6})	CL%	DOCUMENT ID		TECN	COMMENT
$0.44^{+0.18}_{-0.16}$ OUR AVERAGE					
$0.50^{+0.27}_{-0.23}\pm0.09$		[1] AUBERT	08BH	BABR	$e^+e^-\to\Upsilon(4S)$
$0.40^{+0.19}_{-0.17}\pm0.13$		[1] TANIGUCHI	08	BELL	$e^+e^-\to\Upsilon(4S)$
• • • We do not use the following data for averages, fits, limits, etc. • • •					
$0.40^{+0.24}_{-0.20}\pm0.05$		[1] AUBERT	07L	BABR	Repl. by AUBERT 08BH
$0.56^{+0.34}_{-0.27}{}^{+0.05}_{-0.10}$		[1] MOHAPATRA	06	BELL	Repl. by TANIGUCHI 08
<1.0	90	[1] AUBERT	05	BABR	Repl. by AUBERT 07L
<0.8	90	[1] MOHAPATRA	05	BELL	Repl. by MOHAPATRA 06
<1.0	90	[1] AUBERT	04C	BABR	$e^+e^-\to\Upsilon(4S)$
<9.2	90	[1] COAN	00	CLE2	$e^+e^-\to\Upsilon(4S)$

[1] Assumes equal production of B^+ and B^0 at the $\Upsilon(4S)$.

$\Gamma(\phi\gamma)/\Gamma_{total}$ Γ_{355}/Γ

VALUE	CL%	DOCUMENT ID		TECN	COMMENT
$<8.5\times10^{-7}$	90	[1] AUBERT,BE	05C	BABR	$e^+e^-\to\Upsilon(4S)$
• • • We do not use the following data for averages, fits, limits, etc. • • •					
$<0.33\times10^{-5}$	90	[1] COAN	00	CLE2	$e^+e^-\to\Upsilon(4S)$

[1] Assumes equal production of B^+ and B^0 at the $\Upsilon(4S)$.

$\Gamma(\pi^+\pi^-)/\Gamma_{total}$ Γ_{356}/Γ

VALUE (units 10^{-6})	CL%	DOCUMENT ID		TECN	COMMENT
5.12±0.19 OUR FIT					
5.13±0.24 OUR AVERAGE					
5.04±0.21±0.18		[1] DUH	13	BELL	$e^+e^-\to\Upsilon(4S)$
5.5 ±0.4 ±0.3		[1] AUBERT	07B	BABR	$e^+e^-\to\Upsilon(4S)$
$4.5\ ^{+1.4}_{-1.2}\ ^{+0.5}_{-0.4}$		[1] BORNHEIM	03	CLE2	$e^+e^-\to\Upsilon(4S)$
• • • We do not use the following data for averages, fits, limits, etc. • • •					
5.1 ±0.2 ±0.2		[1] LIN	07A	BELL	Repl. by DUH 13
4.4 ±0.6 ±0.3		[1] CHAO	04	BELL	Repl. by LIN 07A
4.7 ±0.6 ±0.2		[1] AUBERT	02Q	BABR	Repl. by AUBERT 07B
5.4 ±1.2 ±0.5		[1] CASEY	02	BELL	Repl. by CHAO 04
$5.6\ ^{+2.3}_{-2.0}\ ^{+0.4}_{-0.5}$		[1] ABE	01H	BELL	Repl. by CASEY 02
4.1 ±1.0 ±0.7		[1] AUBERT	01E	BABR	Repl. by AUBERT 02Q
< 67	90	[2] ABE	00C	SLD	$e^+e^-\to Z$
$4.3\ ^{+1.6}_{-1.4}\ \pm0.5$		[1] CRONIN-HEN..00		CLE2	Repl. by BORNHEIM 03
< 15	90	GODANG	98	CLE2	Repl. by CRONIN-HENNESSY 00
< 45	90	[3] ADAM	96D	DLPH	$e^+e^-\to Z$
< 20	90	ASNER	96	CLE2	Repl. by GODANG 98
< 41	90	[4] BUSKULIC	96V	ALEP	$e^+e^-\to Z$
< 55	90	[5] ABREU	95N	DLPH	Sup. by ADAM 96D
< 47	90	[6] AKERS	94L	OPAL	$e^+e^-\to Z$
< 29	90	[1] BATTLE	93	CLE2	$e^+e^-\to\Upsilon(4S)$
<130	90	[1] ALBRECHT	90B	ARG	$e^+e^-\to\Upsilon(4S)$
< 77	90	[7] BORTOLETTO	89	CLEO	$e^+e^-\to\Upsilon(4S)$
<260	90	[7] BEBEK	87	CLEO	$e^+e^-\to\Upsilon(4S)$
<500	90	GILES	84	CLEO	$e^+e^-\to\Upsilon(4S)$

[1] Assumes equal production of B^+ and B^0 at the $\Upsilon(4S)$.
[2] ABE 00C assumes B($Z \to b\overline{b}$)=(21.7 ± 0.1)% and the B fractions $f_{B^0}=f_{B^+}=(39.7^{+1.8}_{-2.2})$% and $f_{B_s}=(10.5^{+1.8}_{-2.2})$%.
[3] ADAM 96D assumes $f_{B^0} = f_{B^-} = 0.39$ and $f_{B_s} = 0.12$.
[4] BUSKULIC 96V assumes PDG 96 production fractions for B^0, B^+, B_s, b baryons.
[5] Assumes a B^0, B^- production fraction of 0.39 and a B_s production fraction of 0.12.
[6] Assumes B($Z \to b\overline{b}$) = 0.217 and B^0_d (B^0_s) fraction 39.5% (12%).
[7] Paper assumes the $\Upsilon(4S)$ decays 43% to $B^0\overline{B}^0$. We rescale to 50%.

$\Gamma(\pi^+\pi^-)/\Gamma(K^+\pi^-)$ $\Gamma_{356}/\Gamma_{227}$

VALUE	DOCUMENT ID		TECN	COMMENT
0.261±0.010 OUR FIT				
0.261±0.015 OUR AVERAGE				
0.262±0.009±0.017	AAIJ	12AR	LHCB	pp at 7 TeV
0.259±0.017±0.016	AALTONEN	11N	CDF	$p\overline{p}$ at 1.96 TeV
• • • We do not use the following data for averages, fits, limits, etc. • • •				
0.21 ±0.05 ±0.03	ABULENCIA,A	06D	CDF	Repl. by AALTONEN 11N

$\Gamma(\pi^0\pi^0)/\Gamma_{total}$ Γ_{357}/Γ

VALUE (units 10^{-6})	CL%	DOCUMENT ID		TECN	COMMENT
1.91±0.22 OUR AVERAGE					
1.83±0.21±0.13		[1] LEES	13D	BABR	$e^+e^- \to \Upsilon(4S)$
2.3 $^{+0.4}_{-0.5}$ $^{+0.2}_{-0.3}$		[1] CHAO	05	BELL	$e^+e^- \to \Upsilon(4S)$
• • • We do not use the following data for averages, fits, limits, etc. • • •					
1.47±0.25±0.12		[1] AUBERT	07BC	BABR	Repl. by LEES 13D
1.17±0.32±0.10		[1] AUBERT	05L	BABR	Repl. by AUBERT 07BC
< 3.6	90	[1] AUBERT	03L	BABR	$e^+e^- \to \Upsilon(4S)$
2.1 ±0.6 ±0.3		[1] AUBERT	03S	BABR	Repl. by AUBERT 05L
< 4.4	90	[1] BORNHEIM	03	CLE2	$e^+e^- \to \Upsilon(4S)$
1.7 ±0.6 ±0.2		[1] LEE	03	BELL	Repl. by CHAO 05
< 5.7	90	[1] ASNER	02	CLE2	$e^+e^- \to \Upsilon(4S)$
< 6.4	90	[1] CASEY	02	BELL	$e^+e^- \to \Upsilon(4S)$
< 9.3	90	GODANG	98	CLE2	Repl. by ASNER 02
< 9.1	90	ASNER	96	CLE2	Repl. by GODANG 98
<60	90	[2] ACCIARRI	95H	L3	$e^+e^- \to Z$

[1] Assumes equal production of B^+ and B^0 at the $\Upsilon(4S)$.
[2] ACCIARRI 95H assumes $f_{B^0} = 39.5 \pm 4.0$ and $f_{B_s} = 12.0 \pm 3.0$%.

$\Gamma(\eta\pi^0)/\Gamma_{total}$ Γ_{358}/Γ

VALUE (units 10^{-6})	CL%	DOCUMENT ID		TECN	COMMENT
< 1.5	90	[1] AUBERT	08AH	BABR	$e^+e^- \to \Upsilon(4S)$
• • • We do not use the following data for averages, fits, limits, etc. • • •					
< 1.3	90	[1] AUBERT	06W	BABR	Repl. by AUBERT 08AH
< 2.5	90	[1] CHANG	05A	BELL	$e^+e^- \to \Upsilon(4S)$
< 2.5	90	[1] AUBERT,B	04D	BABR	Repl. by AUBERT 06W
< 2.9	90	[1] RICHICHI	00	CLE2	$e^+e^- \to \Upsilon(4S)$
< 8	90	BEHRENS	98	CLE2	Repl. by RICHICHI 00
< 250	90	[2] ACCIARRI	95H	L3	$e^+e^- \to Z$
<1800	90	[1] ALBRECHT	90B	ARG	$e^+e^- \to \Upsilon(4S)$

[1] Assumes equal production of B^+ and B^0 at the $\Upsilon(4S)$.
[2] ACCIARRI 95H assumes $f_{B^0} = 39.5 \pm 4.0$ and $f_{B_s} = 12.0 \pm 3.0$%.

$\Gamma(\eta\eta)/\Gamma_{total}$ Γ_{359}/Γ

VALUE (units 10^{-6})	CL%	DOCUMENT ID		TECN	COMMENT
< 1.0	90	[1] AUBERT	09AV	BABR	$e^+e^- \to \Upsilon(4S)$
• • • We do not use the following data for averages, fits, limits, etc. • • •					
< 1.8	90	[1] AUBERT,B	06V	BABR	Repl. by AUBERT 09AV
< 2.0	90	[1] CHANG	05A	BELL	$e^+e^- \to \Upsilon(4S)$
< 2.8	90	[1] AUBERT,B	04X	BABR	$e^+e^- \to \Upsilon(4S)$
< 18	90	BEHRENS	98	CLE2	$e^+e^- \to \Upsilon(4S)$
<410	90	[2] ACCIARRI	95H	L3	$e^+e^- \to Z$

[1] Assumes equal production of B^+ and B^0 at the $\Upsilon(4S)$.
[2] ACCIARRI 95H assumes $f_{B^0} = 39.5 \pm 4.0$ and $f_{B_s} = 12.0 \pm 3.0$%.

$\Gamma(\eta'\pi^0)/\Gamma_{total}$ Γ_{360}/Γ

VALUE (units 10^{-6})	CL%	DOCUMENT ID		TECN	COMMENT
1.2±0.6 OUR AVERAGE		Error includes scale factor of 1.7.			
0.9±0.4±0.1		[1] AUBERT	08AH	BABR	$e^+e^- \to \Upsilon(4S)$
2.8±1.0±0.3		[1] SCHUEMANN	06	BELL	$e^+e^- \to \Upsilon(4S)$
• • • We do not use the following data for averages, fits, limits, etc. • • •					
$0.8^{+0.8}_{-0.6}$±0.1		[1] AUBERT	06W	BABR	Repl. by AUBERT 08AH
$1.0^{+1.4}_{-1.0}$±0.8	90	[1] AUBERT,B	04D	BABR	Repl. by AUBERT 06W
< 5.7	90	[1] RICHICHI	00	CLE2	$e^+e^- \to \Upsilon(4S)$
<11	90	BEHRENS	98	CLE2	Repl. by RICHICHI 00

[1] Assumes equal production of B^+ and B^0 at the $\Upsilon(4S)$.

$\Gamma(\eta'\eta')/\Gamma_{total}$ Γ_{361}/Γ

VALUE (units 10^{-6})	CL%	DOCUMENT ID		TECN	COMMENT
< 1.7	90	[1] AUBERT	09AV	BABR	$e^+e^- \to \Upsilon(4S)$
• • • We do not use the following data for averages, fits, limits, etc. • • •					
< 6.5	90	[1] SCHUEMANN	07	BELL	$e^+e^- \to \Upsilon(4S)$
< 2.4	90	[1] AUBERT,B	06V	BABR	Repl. by AUBERT 09AV
<10	90	[1] AUBERT,B	04X	BABR	Repl. by AUBERT,B 06V
<47	90	BEHRENS	98	CLE2	$e^+e^- \to \Upsilon(4S)$

[1] Assumes equal production of B^+ and B^0 at the $\Upsilon(4S)$.

$\Gamma(\eta'\eta)/\Gamma_{total}$ Γ_{362}/Γ

VALUE (units 10^{-6})	CL%	DOCUMENT ID		TECN	COMMENT
< 1.2	90	[1] AUBERT	08AH	BABR	$e^+e^- \to \Upsilon(4S)$
• • • We do not use the following data for averages, fits, limits, etc. • • •					
< 4.5	90	[1] SCHUEMANN	07	BELL	$e^+e^- \to \Upsilon(4S)$
< 1.7	90	[1] AUBERT	06W	BABR	Repl. by AUBERT 08AH
< 4.6	90	[1] AUBERT,B	04X	BABR	$e^+e^- \to \Upsilon(4S)$
<27	90	BEHRENS	98	CLE2	$e^+e^- \to \Upsilon(4S)$

[1] Assumes equal production of B^+ and B^0 at the $\Upsilon(4S)$.

$\Gamma(\eta'\rho^0)/\Gamma_{total}$ Γ_{363}/Γ

VALUE (units 10^{-6})	CL%	DOCUMENT ID		TECN	COMMENT
< 1.3	90	[1] SCHUEMANN	07	BELL	$e^+e^- \to \Upsilon(4S)$
• • • We do not use the following data for averages, fits, limits, etc. • • •					
< 2.8	90	[1] DEL-AMO-SA...10A		BABR	$e^+e^- \to \Upsilon(4S)$
< 3.7	90	AUBERT	07E	BABR	Repl. by DEL-AMO-SANCHEZ 10A
< 4.3	90	[1] AUBERT,B	04D	BABR	Repl. by AUBERT 07E
<12	90	[1] RICHICHI	00	CLE2	$e^+e^- \to \Upsilon(4S)$
<23	90	BEHRENS	98	CLE2	Repl. by RICHICHI 00

[1] Assumes equal production of B^+ and B^0 at the $\Upsilon(4S)$.

$\Gamma(\eta' f_0(980)\times B(f_0(980)\to\pi^+\pi^-))/\Gamma_{total}$ Γ_{364}/Γ

VALUE (units 10^{-6})	CL%	DOCUMENT ID		TECN	COMMENT
<0.9	90	[1] DEL-AMO-SA...10A		BABR	$e^+e^- \to \Upsilon(4S)$
• • • We do not use the following data for averages, fits, limits, etc. • • •					
<1.5	90	AUBERT	07E	BABR	Repl. by DEL-AMO-SANCHEZ 10A

[1] Assumes equal production of B^+ and B^0 at the $\Upsilon(4S)$.

$\Gamma(\eta\rho^0)/\Gamma_{total}$ Γ_{365}/Γ

VALUE (units 10^{-6})	CL%	DOCUMENT ID		TECN	COMMENT
< 1.5	90	[1] AUBERT	07Y	BABR	$e^+e^- \to \Upsilon(4S)$
• • • We do not use the following data for averages, fits, limits, etc. • • •					
< 1.9	90	[1] WANG	07B	BELL	$e^+e^- \to \Upsilon(4S)$
< 1.5	90	[1] AUBERT,B	04D	BABR	Repl. by AUBERT 07Y
<10	90	[1] RICHICHI	00	CLE2	$e^+e^- \to \Upsilon(4S)$
<13	90	BEHRENS	98	CLE2	Repl. by RICHICHI 00

[1] Assumes equal production of B^+ and B^0 at the $\Upsilon(4S)$.

$\Gamma(\eta f_0(980)\times B(f_0(980)\to\pi^+\pi^-))/\Gamma_{total}$ Γ_{366}/Γ

VALUE (units 10^{-6})	CL%	DOCUMENT ID		TECN	COMMENT
<0.4	90	[1] AUBERT	07Y	BABR	$e^+e^- \to \Upsilon(4S)$

[1] Assumes equal production of B^+ and B^0 at the $\Upsilon(4S)$.

$\Gamma(\omega\eta)/\Gamma_{total}$ Γ_{367}/Γ

VALUE (units 10^{-6})	CL%	DOCUMENT ID		TECN	COMMENT
$\mathbf{0.94^{+0.35}_{-0.30}\pm0.09}$		[1] AUBERT	09AV	BABR	$e^+e^- \to \Upsilon(4S)$
• • • We do not use the following data for averages, fits, limits, etc. • • •					
< 1.9	90	[1] AUBERT,B	05K	BABR	Repl. by AUBERT 09AV
4.0 $^{+1.3}_{-1.2}$ ±0.4		[1] AUBERT,B	04X	BABR	Repl. by AUBERT,B 05K
<12	90	[1] BERGFELD	98	CLE2	

[1] Assumes equal production of B^+ and B^0 at the $\Upsilon(4S)$.

$\Gamma(\omega\eta')/\Gamma_{total}$ Γ_{368}/Γ

VALUE (units 10^{-6})	CL%	DOCUMENT ID		TECN	COMMENT
$\mathbf{1.01^{+0.46}_{-0.38}\pm0.09}$		[1] AUBERT	09AV	BABR	$e^+e^- \to \Upsilon(4S)$
• • • We do not use the following data for averages, fits, limits, etc. • • •					
< 2.2	90	[1] SCHUEMANN	07	BELL	$e^+e^- \to \Upsilon(4S)$
< 2.8	90	[1] AUBERT,B	04X	BABR	$e^+e^- \to \Upsilon(4S)$
<60	90	[1] BERGFELD	98	CLE2	

[1] Assumes equal production of B^+ and B^0 at the $\Upsilon(4S)$.

$\Gamma(\omega\rho^0)/\Gamma_{total}$ Γ_{369}/Γ

VALUE (units 10^{-6})	CL%	DOCUMENT ID		TECN	COMMENT
< 1.6	90	[1] AUBERT	09H	BABR	$e^+e^- \to \Upsilon(4S)$
• • • We do not use the following data for averages, fits, limits, etc. • • •					
< 1.5	90	[1] AUBERT,B	06T	BABR	Repl. by AUBERT 09H
< 3.3	90	[1] AUBERT	05O	BABR	Repl. by AUBERT,B 06T
<11	90	[1] BERGFELD	98	CLE2	

[1] Assumes equal production of B^+ and B^0 at the $\Upsilon(4S)$.

$\Gamma(\omega f_0(980)\times B(f_0(980)\to\pi^+\pi^-))/\Gamma_{total}$ Γ_{370}/Γ

VALUE (units 10^{-6})	CL%	DOCUMENT ID		TECN	COMMENT
<1.5	90	[1] AUBERT	09H	BABR	$e^+e^- \to \Upsilon(4S)$
• • • We do not use the following data for averages, fits, limits, etc. • • •					
<1.5	90	[1] AUBERT,B	06T	BABR	Repl. by AUBERT 09H

[1] Assumes equal production of B^+ and B^0 at the $\Upsilon(4S)$.

$\Gamma(\omega\omega)/\Gamma_{total}$ Γ_{371}/Γ

VALUE (units 10^{-6})	CL%	DOCUMENT ID		TECN	COMMENT
$\mathbf{1.2\pm0.3^{+0.3}_{-0.2}}$		[1] LEES	14	BABR	$e^+e^- \to \Upsilon(4S)$
• • • We do not use the following data for averages, fits, limits, etc. • • •					
< 4.0	90	[1] AUBERT,B	06T	BABR	Repl. by LEES 14
<19	90	[1] BERGFELD	98	CLE2	

[1] Assumes equal production of B^+ and B^0 at the $\Upsilon(4S)$.

$\Gamma(\phi\pi^0)/\Gamma_{total}$ Γ_{372}/Γ

VALUE (units 10^{-6})	CL%	DOCUMENT ID		TECN	COMMENT
<0.15	90	[1] KIM	12A	BELL	$e^+e^- \to \Upsilon(4S)$
• • • We do not use the following data for averages, fits, limits, etc. • • •					
<0.28	90	[1] AUBERT,B	06C	BABR	$e^+e^- \to \Upsilon(4S)$
<1.0	90	[1] AUBERT,B	04D	BABR	Repl. by AUBERT,B 06C
<5	90	[1] BERGFELD	98	CLE2	

[1] Assumes equal production of B^+ and B^0 at the $\Upsilon(4S)$.

$\Gamma(\phi\eta)/\Gamma_{total}$ Γ_{373}/Γ

VALUE (units 10^{-6})	CL%	DOCUMENT ID		TECN	COMMENT
<0.5	90	[1] AUBERT	09AV	BABR	$e^+e^- \to \Upsilon(4S)$
• • • We do not use the following data for averages, fits, limits, etc. • • •					
<0.6	90	[1] AUBERT,B	06V	BABR	Repl. by AUBERT 09AV
<1.0	90	[1] AUBERT,B	04X	BABR	Repl. by AUBERT,B 06V
<9	90	[1] BERGFELD	98	CLE2	

[1] Assumes equal production of B^+ and B^0 at the $\Upsilon(4S)$.

$\Gamma(\phi\eta')/\Gamma_{total}$ Γ_{374}/Γ

VALUE (units 10^{-6})	CL%	DOCUMENT ID		TECN	COMMENT
< 0.5	90	[1] SCHUEMANN	07	BELL	$e^+e^- \to \Upsilon(4S)$
• • • We do not use the following data for averages, fits, limits, etc. • • •					
< 1.1	90	[1] AUBERT	09AV	BABR	$e^+e^- \to \Upsilon(4S)$
< 1.0	90	[1] AUBERT,B	06V	BABR	Repl. by AUBERT 09AV
< 4.5	90	[1] AUBERT,B	04X	BABR	Repl. by AUBERT,B 06V
<31	90	[1] BERGFELD	98	CLE2	

[1] Assumes equal production of B^+ and B^0 at the $\Upsilon(4S)$.

$\Gamma(\phi\rho^0)/\Gamma_{total}$ Γ_{375}/Γ

VALUE (units 10^{-6})	CL%	DOCUMENT ID		TECN	COMMENT
< 0.33	90	[1] AUBERT	08BK	BABR	$e^+e^- \to \Upsilon(4S)$
• • • We do not use the following data for averages, fits, limits, etc. • • •					
<156	90	[2] ABE	00C	SLD	$e^+e^- \to Z$
< 13	90	[1] BERGFELD	98	CLE2	

[1] Assumes equal production of B^+ and B^0 at the $\Upsilon(4S)$.

[2] ABE 00C assumes $B(Z \to b\overline{b})=(21.7 \pm 0.1)\%$ and the B fractions $f_{B^0}=f_{B^+}=(39.7^{+1.8}_{-2.2})\%$ and $f_{B_s}=(10.5^{+1.8}_{-2.2})\%$.

$\Gamma(\phi f_0(980)\times B(f_0\to\pi^+\pi^-))/\Gamma_{total}$ Γ_{376}/Γ

VALUE (units 10^{-6})	CL%	DOCUMENT ID		TECN	COMMENT
<0.38	90	[1] AUBERT	08BK	BABR	$e^+e^- \to \Upsilon(4S)$

[1] Assumes equal production of B^+ and B^0 at the $\Upsilon(4S)$.

$\Gamma(\phi\omega)/\Gamma_{total}$ Γ_{377}/Γ

VALUE (units 10^{-6})	CL%	DOCUMENT ID		TECN	COMMENT
< 0.7	90	[1] LEES	14	BABR	$e^+e^- \to \Upsilon(4S)$
• • • We do not use the following data for averages, fits, limits, etc. • • •					
< 1.2	90	[2] AUBERT,B	06T	BABR	Repl. by LEES 14
<21	90	[2] BERGFELD	98	CLE2	

[2] Assumes equal production of B^+ and B^0 at the $\Upsilon(4S)$.

$\Gamma(\phi\phi)/\Gamma_{total}$ Γ_{378}/Γ

VALUE	CL%	DOCUMENT ID		TECN	COMMENT
<2 $\times 10^{-7}$	90	[1] AUBERT	08BK	BABR	$e^+e^- \to \Upsilon(4S)$
• • • We do not use the following data for averages, fits, limits, etc. • • •					
<1.5 $\times 10^{-6}$	90	[1] AUBERT,B	04X	BABR	Repl. by AUBERT 08BK
<3.21 $\times 10^{-4}$	90	[2] ABE	00C	SLD	$e^+e^- \to Z$
<1.2 $\times 10^{-5}$	90	[1] BERGFELD	98	CLE2	
<3.9 $\times 10^{-5}$	90	ASNER	96	CLE2	$e^+e^- \to \Upsilon(4S)$

[1] Assumes equal production of B^+ and B^0 at the $\Upsilon(4S)$.

[2] ABE 00C assumes $B(Z \to b\overline{b})=(21.7 \pm 0.1)\%$ and the B fractions $f_{B^0}=f_{B^+}=(39.7^{+1.8}_{-2.2})\%$ and $f_{B_s}=(10.5^{+1.8}_{-2.2})\%$.

$\Gamma(a_0(980)^\pm\pi^\mp\times B(a_0(980)^\pm\to\eta\pi^\pm))/\Gamma_{total}$ Γ_{379}/Γ

VALUE (units 10^{-6})	CL%	DOCUMENT ID		TECN	COMMENT
<3.1	90	[1] AUBERT	07Y	BABR	$e^+e^- \to \Upsilon(4S)$
• • • We do not use the following data for averages, fits, limits, etc. • • •					
<5.1	90	[1] AUBERT,BE	04	BABR	Repl. by AUBERT 07Y

[1] Assumes equal production of B^+ and B^0 at the $\Upsilon(4S)$.

$\Gamma(a_0(1450)^\pm\pi^\mp\times B(a_0(1450)^\pm\to\eta\pi^\pm))/\Gamma_{total}$ Γ_{380}/Γ

VALUE (units 10^{-6})	CL%	DOCUMENT ID		TECN	COMMENT
<2.3	90	[1] AUBERT	07Y	BABR	$e^+e^- \to \Upsilon(4S)$

[1] Assumes equal production of B^+ and B^0 at the $\Upsilon(4S)$.

$\Gamma(\pi^+\pi^-\pi^0)/\Gamma_{total}$ Γ_{381}/Γ

VALUE	CL%	DOCUMENT ID		TECN	COMMENT
<7.2 $\times 10^{-4}$	90	[1] ALBRECHT	90B	ARG	$e^+e^- \to \Upsilon(4S)$

[1] ALBRECHT 90B limit assumes equal production of $B^0\overline{B}^0$ and B^+B^- at $\Upsilon(4S)$.

$\Gamma(\rho^0\pi^0)/\Gamma_{total}$ Γ_{382}/Γ

VALUE (units 10^{-6})	CL%	DOCUMENT ID		TECN	COMMENT
2.0 ±0.5 OUR AVERAGE					
3.0 ±0.5 ±0.7		[1,2] KUSAKA	08	BELL	$e^+e^- \to \Upsilon(4S)$
1.4 ±0.6 ±0.3		[1] AUBERT	04Z	BABR	$e^+e^- \to \Upsilon(4S)$
$1.6\ ^{+2.0}_{-1.4}$ ±0.8		[1] JESSOP	00	CLEO	$e^+e^- \to \Upsilon(4S)$
• • • We do not use the following data for averages, fits, limits, etc. • • •					
$3.12^{+0.88+0.60}_{-0.82-0.76}$		[1] DRAGIC	06	BELL	Repl. by KUSAKA 08
5.1 ±1.6 ±0.9		DRAGIC	04	BELL	Repl. by DRAGIC 06
< 5.3	90	[1] GORDON	02	BELL	Repl. by DRAGIC 04
< 24	90	ASNER	96	CLEO	Repl. by JESSOP 00
<400	90	[1] ALBRECHT	90B	ARG	$e^+e^- \to \Upsilon(4S)$

[1] Assumes equal production of B^+ and B^0 at the $\Upsilon(4S)$.

[2] This is the first measurement that excludes contributions from $\rho(1450)$ and $\rho(1570)$ resonances.

$\Gamma(\rho^\mp\pi^\pm)/\Gamma_{total}$ Γ_{383}/Γ

VALUE (units 10^{-6})	CL%	DOCUMENT ID		TECN	COMMENT
23.0±2.3 OUR AVERAGE					
22.6±1.1±4.4		[1,2] KUSAKA	08	BELL	$e^+e^- \to \Upsilon(4S)$
22.6±1.8±2.2		[1] AUBERT	03T	BABR	$e^+e^- \to \Upsilon(4S)$
$27.6^{+8.4}_{-7.4}$ ±4.2		[1] JESSOP	00	CLE2	$e^+e^- \to \Upsilon(4S)$
• • • We do not use the following data for averages, fits, limits, etc. • • •					
$20.8^{+6.0+2.8}_{-6.3-3.1}$		[1] GORDON	02	BELL	Repl. by KUSAKA 08
< 88	90	ASNER	96	CLE2	Repl. by JESSOP 00
< 520	90	[1] ALBRECHT	90B	ARG	$e^+e^- \to \Upsilon(4S)$
<5200	90	[3] BEBEK	87	CLEO	$e^+e^- \to \Upsilon(4S)$

[1] Assumes equal production of B^+ and B^0 at the $\Upsilon(4S)$.

[2] This is the first measurement that excludes contributions from $\rho(1450)$ and $\rho(1570)$ resonances.

[3] BEBEK 87 reports $< 6.1\times10^{-3}$ assuming the $\Upsilon(4S)$ decays 43% to $B^0\overline{B}^0$. We rescale to 50%.

$\Gamma(\pi^+\pi^-\pi^+\pi^-)/\Gamma_{total}$ Γ_{384}/Γ

VALUE	CL%	DOCUMENT ID		TECN	COMMENT
<19.3 $\times 10^{-6}$	90	[1] CHIANG	08	BELL	$e^+e^- \to \Upsilon(4S)$
• • • We do not use the following data for averages, fits, limits, etc. • • •					
<23.1 $\times 10^{-6}$	90	[1] AUBERT	08BB	BABR	$e^+e^- \to \Upsilon(4S)$
< 2.3 $\times 10^{-4}$	90	[2] ADAM	96D	DLPH	$e^+e^- \to Z$
< 2.8 $\times 10^{-4}$	90	[3] ABREU	95N	DLPH	Sup. by ADAM 96D
< 6.7 $\times 10^{-4}$	90	[1] ALBRECHT	90B	ARG	$e^+e^- \to \Upsilon(4S)$

[1] Assumes equal production of B^+ and B^0 at the $\Upsilon(4S)$.

[2] ADAM 96D assumes $f_{B^0} = f_{B^-} = 0.39$ and $f_{B_s} = 0.12$.

[3] Assumes a B^0, B^- production fraction of 0.39 and a B_s production fraction of 0.12.

Meson Particle Listings

B^0

$\Gamma(\rho^0\pi^+\pi^-)/\Gamma_{total}$ Γ_{385}/Γ

VALUE (units 10^{-6})	CL%	DOCUMENT ID		TECN	COMMENT
< 8.8	90	[1] AUBERT	08BB	BABR	$e^+e^- \to \Upsilon(4S)$
• • • We do not use the following data for averages, fits, limits, etc. • • •					
<12.0	90	[1] CHIANG	08	BELL	$e^+e^- \to \Upsilon(4S)$

[1] Assumes equal production of B^+ and B^0 at the $\Upsilon(4S)$.

$\Gamma(\rho^0\rho^0)/\Gamma_{total}$ Γ_{386}/Γ

VALUE (units 10^{-6})	CL%	DOCUMENT ID		TECN	COMMENT
0.73±0.28 OUR AVERAGE					
0.92±0.32±0.14		[1] AUBERT	08BB	BABR	$e^+e^- \to \Upsilon(4S)$
0.4 ±0.4 $^{+0.2}_{-0.3}$		[1] CHIANG	08	BELL	$e^+e^- \to \Upsilon(4S)$
• • • We do not use the following data for averages, fits, limits, etc. • • •					
1.07±0.33±0.19		[1] AUBERT	07G	BABR	Repl. by AUBERT 08BB
< 1.1	90	[1] AUBERT	05I	BABR	Repl. by AUBERT 07G
< 2.1	90	[1] AUBERT	03V	BABR	Repl. by AUBERT 05I
< 18	90	[2] GODANG	02	CLE2	$e^+e^- \to \Upsilon(4S)$
<136	90	[3] ABE	00C	SLD	$e^+e^- \to Z$
<280	90	[1] ALBRECHT	90B	ARG	$e^+e^- \to \Upsilon(4S)$
<290	90	[4] BORTOLETTO	89	CLEO	$e^+e^- \to \Upsilon(4S)$
<430	90	[4] BEBEK	87	CLEO	$e^+e^- \to \Upsilon(4S)$

[1] Assumes equal production of B^+ and B^0 at the $\Upsilon(4S)$.
[2] Assumes a helicity 00 configuration. For a helicity 11 configuration, the limit decreases to 1.4×10^{-5}.
[3] ABE 00C assumes $B(Z \to b\overline{b})=(21.7 \pm 0.1)\%$ and the B fractions $f_{B^0}=f_{B^+}=(39.7^{+1.8}_{-2.2})\%$ and $f_{B_s}=(10.5^{+1.8}_{-2.2})\%$.
[4] Paper assumes the $\Upsilon(4S)$ decays 43% to $B^0\overline{B}^0$. We rescale to 50%.

$\Gamma(f_0(980)\pi^+\pi^-)/\Gamma_{total}$ Γ_{387}/Γ

VALUE (units 10^{-6})	CL%	DOCUMENT ID		TECN	COMMENT
<3.8	90	[1] CHIANG	08	BELL	$e^+e^- \to \Upsilon(4S)$

[1] Assumes equal production of B^+ and B^0 at the $\Upsilon(4S)$.

$\Gamma(\rho^0 f_0(980)\times B(f_0(980)\to\pi^+\pi^-))/\Gamma_{total}$ Γ_{388}/Γ

VALUE (units 10^{-6})	CL%	DOCUMENT ID		TECN	COMMENT
<0.3	90	[1] CHIANG	08	BELL	$e^+e^- \to \Upsilon(4S)$
• • • We do not use the following data for averages, fits, limits, etc. • • •					
<0.40	90	[1] AUBERT	08BB	BABR	$e^+e^- \to \Upsilon(4S)$
<0.53	90	[1] AUBERT	07G	BABR	Repl. by AUBERT 08BB

[1] Assumes equal production of B^+ and B^0 at the $\Upsilon(4S)$.

$\Gamma(f_0(980) f_0(980)\times B^2(f_0(980)\to\pi^+\pi^-))/\Gamma_{total}$ Γ_{389}/Γ

VALUE (units 10^{-6})	CL%	DOCUMENT ID		TECN	COMMENT
<0.1	90	[1] CHIANG	08	BELL	$e^+e^- \to \Upsilon(4S)$
• • • We do not use the following data for averages, fits, limits, etc. • • •					
<0.19	90	[1] AUBERT	08BB	BABR	$e^+e^- \to \Upsilon(4S)$
<0.16	90	[1] AUBERT	07G	BABR	Repl. by AUBERT 08BB

[1] Assumes equal production of B^+ and B^0 at the $\Upsilon(4S)$.

$\Gamma(f_0(980) f_0(980)\times B(f_0\to\pi^+\pi^-)\times B(f_0\to K^+K^-))/\Gamma_{total}$ Γ_{390}/Γ

VALUE (units 10^{-6})	CL%	DOCUMENT ID		TECN	COMMENT
<0.23	90	[1] AUBERT	08BK	BABR	$e^+e^- \to \Upsilon(4S)$

[1] Assumes equal production of B^+ and B^0 at the $\Upsilon(4S)$.

$\Gamma(a_1(1260)^\mp\pi^\pm)/\Gamma_{total}$ Γ_{391}/Γ

VALUE (units 10^{-6})	CL%	DOCUMENT ID		TECN	COMMENT
26 ±5 OUR AVERAGE		Error includes scale factor of 1.9.			
22.2±2.0±2.8		[1,2] DALSENO	12	BELL	$e^+e^- \to \Upsilon(4S)$
33.2±3.8±3.0		[2,3] AUBERT	06V	BABR	$e^+e^- \to \Upsilon(4S)$
• • • We do not use the following data for averages, fits, limits, etc. • • •					
< 630	90	[2] ALBRECHT	90B	ARG	$e^+e^- \to \Upsilon(4S)$
< 490	90	[4] BORTOLETTO	89	CLEO	$e^+e^- \to \Upsilon(4S)$
<1000	90	[4] BEBEK	87	CLEO	$e^+e^- \to \Upsilon(4S)$

[1] DALSENO 12 reports $B(B^0 \to a_1^\pm\pi^\mp)\, B(a_1^\pm \to \pi^\pm\pi^+\pi^-) = (11.1 \pm 1.0 \pm 1.4) \times 10^{-6}$ which we rescaled assuming $a_1(1260)$ decays only to 3π and $B(a_1^\pm \to \pi^\pm\pi^+\pi^-) = 0.5$.
[2] Assumes equal production of B^+ and B^0 at the $\Upsilon(4S)$.
[3] Assumes $a_1(1260)$ decays only to 3π and $B(a_1^\pm \to \pi^\pm\pi^\mp\pi^\pm) = 0.5$.
[4] Paper assumes the $\Upsilon(4S)$ decays 43% to $B^0\overline{B}^0$. We rescale to 50%.

$\Gamma(a_2(1320)^\mp\pi^\pm)/\Gamma_{total}$ Γ_{392}/Γ

VALUE	CL%	DOCUMENT ID		TECN	COMMENT
$<6.3 \times 10^{-6}$	90	[1] DALSENO	12	BELL	$e^+e^- \to \Upsilon(4S)$
• • • We do not use the following data for averages, fits, limits, etc. • • •					
$<3.0 \times 10^{-4}$	90	[2] BORTOLETTO	89	CLEO	$e^+e^- \to \Upsilon(4S)$
$<1.4 \times 10^{-3}$	90	[2] BEBEK	87	CLEO	$e^+e^- \to \Upsilon(4S)$

[1] DALSENO 12 reports $B(B^0 \to a_2^\pm\pi^\mp)\, B(a_2^\pm \to \pi^\pm\pi^+\pi^-) < 2.2 \times 10^{-6}$ which we rescaled using $B(a_2^\pm \to \pi^\pm\pi^+\pi^-) = 1/2\, B(a_2^\pm \to 3\pi) = 0.35 \pm 0.013$.
[2] Paper assumes the $\Upsilon(4S)$ decays 43% to $B^0\overline{B}^0$. We rescale to 50%.

$\Gamma(\pi^+\pi^-\pi^0\pi^0)/\Gamma_{total}$ Γ_{393}/Γ

VALUE	CL%	DOCUMENT ID		TECN	COMMENT
$<3.1 \times 10^{-3}$	90	[1] ALBRECHT	90B	ARG	$e^+e^- \to \Upsilon(4S)$

[1] ALBRECHT 90B limit assumes equal production of $B^0\overline{B}^0$ and B^+B^- at $\Upsilon(4S)$.

$\Gamma(\rho^+\rho^-)/\Gamma_{total}$ Γ_{394}/Γ

VALUE (units 10^{-6})	CL%	DOCUMENT ID		TECN	COMMENT
24.2±3.1 OUR AVERAGE					
25.5 $\pm 2.1^{+3.6}_{-3.9}$		[1] AUBERT	07BF	BABR	$e^+e^- \to \Upsilon(4S)$
22.8 $\pm 3.8^{+2.3}_{-2.6}$		[1] SOMOV	06	BELL	$e^+e^- \to \Upsilon(4S)$
• • • We do not use the following data for averages, fits, limits, etc. • • •					
25 $^{+7}_{-6}$ $^{+5}_{-6}$		[1] AUBERT	04G	BABR	Repl. by AUBERT,B 04R
30 ±4 ±5		[1,2] AUBERT,B	04R	BABR	Repl. by AUBERT 07BF
<2200	90	[1] ALBRECHT	90B	ARG	$e^+e^- \to \Upsilon(4S)$

[1] Assumes equal production of B^+ and B^0 at the $\Upsilon(4S)$.
[2] The quoted result is obtained after combining with AUBERT 04G result by AUBERT 04R alone gives $(33 \pm 4 \pm 5) \times 10^{-6}$.

$\Gamma(a_1(1260)^0\pi^0)/\Gamma_{total}$ Γ_{395}/Γ

VALUE	CL%	DOCUMENT ID		TECN	COMMENT
$<1.1 \times 10^{-3}$	90	[1] ALBRECHT	90B	ARG	$e^+e^- \to \Upsilon(4S)$

[1] ALBRECHT 90B limit assumes equal production of $B^0\overline{B}^0$ and B^+B^- at $\Upsilon(4S)$.

$\Gamma(\omega\pi^0)/\Gamma_{total}$ Γ_{396}/Γ

VALUE (units 10^{-6})	CL%	DOCUMENT ID		TECN	COMMENT
< 0.5	90	[1] AUBERT	08AH	BABR	$e^+e^- \to \Upsilon(4S)$
• • • We do not use the following data for averages, fits, limits, etc. • • •					
< 2.0	90	[1] JEN	06	BELL	$e^+e^- \to \Upsilon(4S)$
< 1.2	90	[1] AUBERT,B	04D	BABR	Repl. by AUBERT 08AH
< 1.9	90	[1] WANG	04A	BELL	$e^+e^- \to \Upsilon(4S)$
< 3	90	[1] AUBERT	01G	BABR	$e^+e^- \to \Upsilon(4S)$
< 5.5	90	[1] JESSOP	00	CLE2	$e^+e^- \to \Upsilon(4S)$
< 14	90	[1] BERGFELD	98	CLE2	Repl. by JESSOP 00
<460	90	[2] ALBRECHT	90B	ARG	$e^+e^- \to \Upsilon(4S)$

[1] Assumes equal production of B^+ and B^0 at the $\Upsilon(4S)$.
[2] ALBRECHT 90B limit assumes equal production of $B^0\overline{B}^0$ and B^+B^- at $\Upsilon(4S)$.

$\Gamma(\pi^+\pi^+\pi^-\pi^-\pi^0)/\Gamma_{total}$ Γ_{397}/Γ

VALUE	CL%	DOCUMENT ID		TECN	COMMENT
$<9.0 \times 10^{-3}$	90	[1] ALBRECHT	90B	ARG	$e^+e^- \to \Upsilon(4S)$

[1] ALBRECHT 90B limit assumes equal production of $B^0\overline{B}^0$ and B^+B^- at $\Upsilon(4S)$.

$\Gamma(a_1(1260)^+\rho^-)/\Gamma_{total}$ Γ_{398}/Γ

VALUE (units 10^{-6})	CL%	DOCUMENT ID		TECN	COMMENT
< 61	90	[1,2] AUBERT,B	06O	BABR	$e^+e^- \to \Upsilon(4S)$
• • • We do not use the following data for averages, fits, limits, etc. • • •					
<3400	90	[1] ALBRECHT	90B	ARG	$e^+e^- \to \Upsilon(4S)$

[1] Assumes equal production of B^+ and B^0 at the $\Upsilon(4S)$.
[2] Assumes $a_1(1260)$ decays only to 3π and $B(a_1^\pm \to \pi^\pm\pi^\mp\pi^\pm) = 0.5$.

$\Gamma(a_1(1260)^0\rho^0)/\Gamma_{total}$ Γ_{399}/Γ

VALUE	CL%	DOCUMENT ID		TECN	COMMENT
$<2.4 \times 10^{-3}$	90	[1] ALBRECHT	90B	ARG	$e^+e^- \to \Upsilon(4S)$

[1] ALBRECHT 90B limit assumes equal production of $B^0\overline{B}^0$ and B^+B^- at $\Upsilon(4S)$.

$\Gamma(b_1^\mp\pi^\pm\times B(b_1^\mp\to\omega\pi^\mp))/\Gamma_{total}$ Γ_{400}/Γ

VALUE (units 10^{-6})	CL%	DOCUMENT ID		TECN	COMMENT
10.9±1.2±0.9		[1] AUBERT	07BI	BABR	$e^+e^- \to \Upsilon(4S)$

[1] Assumes equal production of B^+ and B^0 at the $\Upsilon(4S)$.

$\Gamma(b_1^0\pi^0\times B(b_1^0\to\omega\pi^0))/\Gamma_{total}$ Γ_{401}/Γ

VALUE (units 10^{-6})	CL%	DOCUMENT ID		TECN	COMMENT
<1.9	90	[1] AUBERT	08AG	BABR	$e^+e^- \to \Upsilon(4S)$

[1] Assumes equal production of B^+ and B^0 at the $\Upsilon(4S)$.

$\Gamma(b_1^-\rho^+\times B(b_1^-\to\omega\pi^-))/\Gamma_{total}$ Γ_{402}/Γ

VALUE	CL%	DOCUMENT ID		TECN	COMMENT
$<1.4 \times 10^{-6}$	90	[1] AUBERT	09AF	BABR	$e^+e^- \to \Upsilon(4S)$

[1] Assumes equal production of B^+ and B^0 at the $\Upsilon(4S)$.

$\Gamma(b_1^0\rho^0\times B(b_1^0\to\omega\pi^0))/\Gamma_{total}$ Γ_{403}/Γ

VALUE	CL%	DOCUMENT ID		TECN	COMMENT
$<3.4 \times 10^{-6}$	90	[1] AUBERT	09AF	BABR	$e^+e^- \to \Upsilon(4S)$

[1] Assumes equal production of B^+ and B^0 at the $\Upsilon(4S)$.

$\Gamma(\pi^+\pi^+\pi^+\pi^-\pi^-\pi^-)/\Gamma_{total}$ Γ_{404}/Γ

VALUE	CL%	DOCUMENT ID		TECN	COMMENT
$<3.0\times10^{-3}$	90	[1] ALBRECHT	90B	ARG	$e^+e^-\to\Upsilon(4S)$

[1] ALBRECHT 90B limit assumes equal production of $B^0\overline{B}^0$ and B^+B^- at $\Upsilon(4S)$.

$\Gamma(a_1(1260)^+a_1(1260)^-\times B^2(a_1^+\to2\pi^+\pi^-))/\Gamma_{total}$ Γ_{405}/Γ

VALUE (units 10^{-6})	CL%	DOCUMENT ID		TECN	COMMENT
$11.8\pm2.6\pm1.6$		[1] AUBERT	09AL	BABR	$e^+e^-\to\Upsilon(4S)$
• • • We do not use the following data for averages, fits, limits, etc. • • •					
<6000	90	[1] ALBRECHT	90B	ARG	$e^+e^-\to\Upsilon(4S)$
<2800	90	[2] BORTOLETTO	89	CLEO	$e^+e^-\to\Upsilon(4S)$

[1] Assumes equal production of $B^0\overline{B}^0$ and B^+B^- at $\Upsilon(4S)$.
[2] BORTOLETTO 89 reports $<3.2\times10^{-3}$ assuming the $\Upsilon(4S)$ decays 43% to $B^0\overline{B}^0$. We rescale to 50%.

$\Gamma(\pi^+\pi^+\pi^+\pi^-\pi^-\pi^-\pi^0)/\Gamma_{total}$ Γ_{406}/Γ

VALUE	CL%	DOCUMENT ID		TECN	COMMENT
$<1.1\times10^{-2}$	90	[1] ALBRECHT	90B	ARG	$e^+e^-\to\Upsilon(4S)$

[1] ALBRECHT 90B limit assumes equal production of $B^0\overline{B}^0$ and B^+B^- at $\Upsilon(4S)$.

$\Gamma(p\overline{p})/\Gamma_{total}$ Γ_{407}/Γ

VALUE (units 10^{-8})	CL%	DOCUMENT ID		TECN	COMMENT
$1.47^{+0.62}_{-0.51}\pm0.35\pm0.14$		[1] AAIJ	13BQ	LHCB	pp at 7 TeV
• • • We do not use the following data for averages, fits, limits, etc. • • •					
$<$ 11	90	[2] TSAI	07	BELL	$e^+e^-\to\Upsilon(4S)$
$<$ 41	90	[2] CHANG	05	BELL	$e^+e^-\to\Upsilon(4S)$
$<$ 27	90	[2] AUBERT	04U	BABR	$e^+e^-\to\Upsilon(4S)$
$<$ 140	90	[2] BORNHEIM	03	CLE2	$e^+e^-\to\Upsilon(4S)$
$<$ 120	90	[2] ABE	02O	BELL	$e^+e^-\to\Upsilon(4S)$
$<$ 700	90	[2] COAN	99	CLE2	$e^+e^-\to\Upsilon(4S)$
$<$ 1800	90	[3] BUSKULIC	96V	ALEP	$e^+e^-\to Z$
<35000	90	[4] ABREU	95N	DLPH	Sup. by ADAM 96D
$<$ 3400	90	[5] BORTOLETTO	89	CLEO	$e^+e^-\to\Upsilon(4S)$
<12000	90	[6] ALBRECHT	88F	ARG	$e^+e^-\to\Upsilon(4S)$
<17000	90	[5] BEBEK	87	CLEO	$e^+e^-\to\Upsilon(4S)$

[1] Uses normalization mode $B(B^0\to K^+\pi^-)=(19.55\pm0.54)\times10^{-6}$.
[2] Assumes equal production of B^+ and B^0 at the $\Upsilon(4S)$.
[3] BUSKULIC 96V assumes PDG 96 production fractions for B^0, B^+, B_s, b baryons.
[4] Assumes a B^0, B^- production fraction of 0.39 and a B_s production fraction of 0.12.
[5] Paper assumes the $\Upsilon(4S)$ decays 43% to $B^0\overline{B}^0$. We rescale to 50%.
[6] ALBRECHT 88F reports $<1.3\times10^{-4}$ assuming the $\Upsilon(4S)$ decays 45% to $B^0\overline{B}^0$. We rescale to 50%.

$\Gamma(p\overline{p}\pi^+\pi^-)/\Gamma_{total}$ Γ_{408}/Γ

VALUE (units 10^{-4})	CL%	DOCUMENT ID		TECN	COMMENT
<2.5	90	[1] BEBEK	89	CLEO	$e^+e^-\to\Upsilon(4S)$
• • • We do not use the following data for averages, fits, limits, etc. • • •					
<9.5	90	[2] ABREU	95N	DLPH	Sup. by ADAM 96D
$5.4\pm1.8\pm2.0$		[3] ALBRECHT	88F	ARG	$e^+e^-\to\Upsilon(4S)$

[1] BEBEK 89 reports $<2.9\times10^{-4}$ assuming the $\Upsilon(4S)$ decays 43% to $B^0\overline{B}^0$. We rescale to 50%.
[2] Assumes a B^0, B^- production fraction of 0.39 and a B_s production fraction of 0.12.
[3] ALBRECHT 88F reports $6.0\pm2.0\pm2.2$ assuming the $\Upsilon(4S)$ decays 45% to $B^0\overline{B}^0$. We rescale to 50%.

$\Gamma(p\overline{p}K^0)/\Gamma_{total}$ Γ_{409}/Γ

VALUE (units 10^{-6})	CL%	DOCUMENT ID		TECN	COMMENT
2.66 ± 0.32 OUR AVERAGE					
$2.51^{+0.35}_{-0.29}\pm0.21$		[1,2] CHEN	08C	BELL	$e^+e^-\to\Upsilon(4S)$
$3.0\pm0.5\pm0.3$		[2] AUBERT	07AV	BABR	$e^+e^-\to\Upsilon(4S)$
• • • We do not use the following data for averages, fits, limits, etc. • • •					
$2.40^{+0.64}_{-0.44}\pm0.28$		[2,3,4] WANG	05A	BELL	Repl. by CHEN 08C
$1.88^{+0.77}_{-0.60}\pm0.23$		[2,3,5] WANG	04	BELL	Repl. by WANG 05A
<7.2	90	[2,3] ABE	02K	BELL	Repl. by WANG 04

[1] Explicitly vetoes resonant production of $p\overline{p}$ from charmonium states.
[2] Assumes equal production of B^+ and B^0 at the $\Upsilon(4S)$.
[3] Explicitly vetoes resonant production of $p\overline{p}$ from charmonium states and pK^0 production from Λ_c.
[4] Provides also results with $M_{p\overline{p}}<2.85$ GeV/c^2 and angular asymmetry of $p\overline{p}$ system.
[5] The branching fraction for $M_{p\overline{p}}<2.85$ is also reported.

$\Gamma(\Theta(1540)^+\overline{p},\ \Theta^+\to pK_S^0)/\Gamma_{total}$ Γ_{410}/Γ

VALUE (units 10^{-6})	CL%	DOCUMENT ID		TECN	COMMENT
<0.05	90	[1] AUBERT	07AV	BABR	$e^+e^-\to\Upsilon(4S)$
• • • We do not use the following data for averages, fits, limits, etc. • • •					
<0.23	90	[1] WANG	05A	BELL	$e^+e^-\to\Upsilon(4S)$

[1] Assumes equal production of B^+ and B^0 at the $\Upsilon(4S)$.

$\Gamma(f_J(2220)K^0,\ f_J\to p\overline{p})/\Gamma_{total}$ Γ_{411}/Γ

VALUE (units 10^{-6})	CL%	DOCUMENT ID		TECN	COMMENT
<0.45	90	[1] AUBERT	07AV	BABR	$e^+e^-\to\Upsilon(4S)$

[1] Assumes equal production of B^+ and B^0 at the $\Upsilon(4S)$.

$\Gamma(p\overline{p}K^*(892)^0)/\Gamma_{total}$ Γ_{412}/Γ

VALUE (units 10^{-6})	CL%	DOCUMENT ID		TECN	COMMENT
$1.24^{+0.28}_{-0.25}$ OUR AVERAGE					
$1.18^{+0.29}_{-0.25}\pm0.11$		[1,2] CHEN	08C	BELL	$e^+e^-\to\Upsilon(4S)$
$1.47\pm0.45\pm0.40$		[2] AUBERT	07AV	BABR	$e^+e^-\to\Upsilon(4S)$
• • • We do not use the following data for averages, fits, limits, etc. • • •					
<7.6	90	[2] WANG	04	BELL	$e^+e^-\to\Upsilon(4S)$

[1] Explicitly vetoes resonant production of $p\overline{p}$ from charmonium states.
[2] Assumes equal production of B^+ and B^0 at the $\Upsilon(4S)$.

$\Gamma(f_J(2220)K_0^*,\ f_J\to p\overline{p})/\Gamma_{total}$ Γ_{413}/Γ

VALUE (units 10^{-6})	CL%	DOCUMENT ID		TECN	COMMENT
<0.15	90	[1] AUBERT	07AV	BABR	$e^+e^-\to\Upsilon(4S)$

[1] Assumes equal production of B^+ and B^0 at the $\Upsilon(4S)$.

$\Gamma(p\overline{\Lambda}\pi^-)/\Gamma_{total}$ Γ_{414}/Γ

VALUE (units 10^{-6})	CL%	DOCUMENT ID		TECN	COMMENT
3.14 ± 0.29 OUR AVERAGE					
$3.07\pm0.31\pm0.23$		[1] AUBERT	09AC	BABR	$e^+e^-\to\Upsilon(4S)$
$3.23^{+0.33}_{-0.29}\pm0.29$		[1] WANG	07C	BELL	$e^+e^-\to\Upsilon(4S)$
• • • We do not use the following data for averages, fits, limits, etc. • • •					
$2.62^{+0.44}_{-0.40}\pm0.31$		[1,2] WANG	05A	BELL	Repl. by WANG 07C
$3.97^{+1.00}_{-0.80}\pm0.56$		[1] WANG	03	BELL	Repl. by WANG 05A
$<$ 13	90	[1] COAN	99	CLE2	$e^+e^-\to\Upsilon(4S)$
<180	90	[3] ALBRECHT	88F	ARG	$e^+e^-\to\Upsilon(4S)$

[1] Assumes equal production of B^+ and B^0 at the $\Upsilon(4S)$.
[2] Provides also results with $M_{p\overline{\Lambda}}<2.85$ GeV/c^2 and angular asymmetry of $p\overline{\Lambda}$ system.
[3] ALBRECHT 88F reports $<2.0\times10^{-4}$ assuming the $\Upsilon(4S)$ decays 45% to $B^0\overline{B}^0$. We rescale to 50%.

$\Gamma(p\overline{\Sigma}(1385)^-)/\Gamma_{total}$ Γ_{415}/Γ

VALUE (units 10^{-6})	CL%	DOCUMENT ID		TECN	COMMENT
<0.26	90	[1] WANG	07C	BELL	$e^+e^-\to\Upsilon(4S)$

[1] Assumes equal production of B^+ and B^0 at the $\Upsilon(4S)$.

$\Gamma(\Delta^0\overline{\Lambda})/\Gamma_{total}$ Γ_{416}/Γ

VALUE (units 10^{-6})	CL%	DOCUMENT ID		TECN	COMMENT
<0.93	90	[1] WANG	07C	BELL	$e^+e^-\to\Upsilon(4S)$

[1] Assumes equal production of B^+ and B^0 at the $\Upsilon(4S)$.

$\Gamma(p\overline{\Lambda}K^-)/\Gamma_{total}$ Γ_{417}/Γ

VALUE (units 10^{-6})	CL%	DOCUMENT ID		TECN	COMMENT
<0.82	90	[1] WANG	03	BELL	$e^+e^-\to\Upsilon(4S)$

[1] Assumes equal production of B^+ and B^0 at the $\Upsilon(4S)$.

$\Gamma(p\overline{\Sigma}^0\pi^-)/\Gamma_{total}$ Γ_{418}/Γ

VALUE	CL%	DOCUMENT ID		TECN	COMMENT
$<3.8\times10^{-6}$	90	[1] WANG	03	BELL	$e^+e^-\to\Upsilon(4S)$

[1] Assumes equal production of B^+ and B^0 at the $\Upsilon(4S)$.

$\Gamma(\overline{\Lambda}\Lambda)/\Gamma_{total}$ Γ_{419}/Γ

VALUE (units 10^{-6})	CL%	DOCUMENT ID		TECN	COMMENT
<0.32	90	[1] TSAI	07	BELL	$e^+e^-\to\Upsilon(4S)$
• • • We do not use the following data for averages, fits, limits, etc. • • •					
<0.69	90	[1] CHANG	05	BELL	Repl. by TSAI 07
<1.2	90	[1] BORNHEIM	03	CLE2	$e^+e^-\to\Upsilon(4S)$
<1.0	90	[1] ABE	02O	BELL	Repl. by CHANG 05
<3.9	90	[1] COAN	99	CLE2	$e^+e^-\to\Upsilon(4S)$

[1] Assumes equal production of B^+ and B^0 at the $\Upsilon(4S)$.

$\Gamma(\overline{\Lambda}\Lambda K^0)/\Gamma_{total}$ Γ_{420}/Γ

VALUE (units 10^{-6})	DOCUMENT ID		TECN	COMMENT
$4.76^{+0.84}_{-0.68}\pm0.61$	[1,2] CHANG	09	BELL	$e^+e^-\to\Upsilon(4S)$

[1] Excluding charmonium events in $2.85<m_{\Lambda\overline{\Lambda}}<3.128$ GeV/c^2 and $3.315<m_{\Lambda\overline{\Lambda}}<3.735$ GeV/c^2. Measurements in various $m_{\Lambda\overline{\Lambda}}$ bins are also reported.
[2] Assumes equal production of B^+ and B^0 at the $\Upsilon(4S)$.

Meson Particle Listings

B^0

$\Gamma(\overline{\Lambda}\Lambda K^{*0})/\Gamma_{total}$ Γ_{421}/Γ

VALUE (units 10^{-6})		DOCUMENT ID		TECN	COMMENT
$2.46^{+0.87}_{-0.72}\pm0.34$	[1,2]	CHANG	09	BELL	$e^+e^-\to\Upsilon(4S)$

[1] Excluding charmonium events in $2.85 < m_{\Lambda\overline{\Lambda}} < 3.128$ GeV/c^2 and $3.315 < m_{\Lambda\overline{\Lambda}} < 3.735$ GeV/c^2. Measurements in various $m_{\Lambda\overline{\Lambda}}$ bins are also reported.
[2] Assumes equal production of B^+ and B^0 at the $\Upsilon(4S)$.

$\Gamma(\overline{\Lambda}\Lambda D^0)/\Gamma_{total}$ Γ_{422}/Γ

VALUE (units 10^{-5})		DOCUMENT ID		TECN	COMMENT
$1.05^{+0.57}_{-0.44}\pm0.14$	[1]	CHANG	09	BELL	$e^+e^-\to\Upsilon(4S)$

[1] Assumes equal production of B^+ and B^0 at the $\Upsilon(4S)$.

$\Gamma(\Delta^0\overline{\Delta}^0)/\Gamma_{total}$ Γ_{423}/Γ

VALUE	CL%	DOCUMENT ID		TECN	COMMENT
<0.0015	90	[1] BORTOLETTO89		CLEO	$e^+e^-\to\Upsilon(4S)$

[1] BORTOLETTO 89 reports < 0.0018 assuming $\Upsilon(4S)$ decays 43% to $B^0\overline{B}^0$. We rescale to 50%.

$\Gamma(\Delta^{++}\overline{\Delta}^{--})/\Gamma_{total}$ Γ_{424}/Γ

VALUE	CL%	DOCUMENT ID		TECN	COMMENT
$<1.1\times10^{-4}$	90	[1] BORTOLETTO89		CLEO	$e^+e^-\to\Upsilon(4S)$

[1] BORTOLETTO 89 reports $< 1.3\times10^{-4}$ assuming $\Upsilon(4S)$ decays 43% to $B^0\overline{B}^0$. We rescale to 50%.

$\Gamma(\overline{D}^0 p\overline{p})/\Gamma_{total}$ Γ_{425}/Γ

VALUE (units 10^{-4})		DOCUMENT ID		TECN	COMMENT
1.04±0.07 OUR AVERAGE					
$1.02\pm0.04\pm0.06$	[1,2]	DEL-AMO-SA...12		BABR	$e^+e^-\to\Upsilon(4S)$
$1.18\pm0.15\pm0.16$	[2]	ABE	02W	BELL	$e^+e^-\to\Upsilon(4S)$
• • • We do not use the following data for averages, fits, limits, etc. • • •					
$1.13\pm0.06\pm0.08$	[2]	AUBERT,B	06S	BABR	Repl. by DEL-AMO-SANCHEZ 12

[1] Uses the values of D and D^* branching fractions from PDG 08.
[2] Assumes equal production of B^+ and B^0 at the $\Upsilon(4S)$.

$\Gamma(D_s^-\overline{\Lambda}p)/\Gamma_{total}$ Γ_{426}/Γ

VALUE (units 10^{-5})		DOCUMENT ID		TECN	COMMENT
2.8±0.8±0.3	[1,2]	MEDVEDEVA	07	BELL	$e^+e^-\to\Upsilon(4S)$

[1] Assumes equal production of B^+ and B^0 at the $\Upsilon(4S)$.
[2] MEDVEDEVA 07 reports $(2.9\pm0.7\pm0.5\pm0.4)\times10^{-5}$ from a measurement of $[\Gamma(B^0\to D_s^-\overline{\Lambda}p)/\Gamma_{total}]\times[B(D_s^+\to\phi\pi^+)]$ assuming $B(D_s^+\to\phi\pi^+)=(4.4\pm0.6)\times10^{-2}$, which we rescale to our best value $B(D_s^+\to\phi\pi^+)=(4.5\pm0.4)\times10^{-2}$. Our first error is their experiment's error and our second error is the systematic error from using our best value.

$\Gamma(\overline{D}^*(2007)^0 p\overline{p})/\Gamma_{total}$ Γ_{427}/Γ

VALUE (units 10^{-4})		DOCUMENT ID		TECN	COMMENT
0.99±0.11 OUR AVERAGE					
$0.97\pm0.07\pm0.09$	[1,2]	DEL-AMO-SA...12		BABR	$e^+e^-\to\Upsilon(4S)$
$1.20^{+0.33}_{-0.29}\pm0.21$	[2]	ABE	02W	BELL	$e^+e^-\to\Upsilon(4S)$
• • • We do not use the following data for averages, fits, limits, etc. • • •					
$1.01\pm0.10\pm0.09$	[2]	AUBERT,B	06S	BABR	Repl. by DEL-AMO-SANCHEZ 12

[1] Uses the values of D and D^* branching fractions from PDG 08.
[2] Assumes equal production of B^+ and B^0 at the $\Upsilon(4S)$.

$\Gamma(D^*(2010)^-p\overline{n})/\Gamma_{total}$ Γ_{428}/Γ

VALUE (units 10^{-4})		DOCUMENT ID		TECN	COMMENT
$14.5^{+3.4}_{-3.0}\pm2.7$	[1]	ANDERSON	01	CLE2	$e^+e^-\to\Upsilon(4S)$

[1] Assumes equal production of B^+ and B^0 at the $\Upsilon(4S)$.

$\Gamma(D^-p\overline{p}\pi^+)/\Gamma_{total}$ Γ_{429}/Γ

VALUE (units 10^{-4})		DOCUMENT ID		TECN	COMMENT
3.32±0.10±0.29	[1,2]	DEL-AMO-SA...12		BABR	$e^+e^-\to\Upsilon(4S)$
• • • We do not use the following data for averages, fits, limits, etc. • • •					
$3.38\pm0.14\pm0.29$	[2]	AUBERT,B	06S	BABR	Repl. by DEL-AMO-SANCHEZ 12

[1] Uses the values of D and D^* branching fractions from PDG 08.
[2] Assumes equal production of B^+ and B^0 at the $\Upsilon(4S)$.

$\Gamma(D^*(2010)^-p\overline{p}\pi^+)/\Gamma_{total}$ Γ_{430}/Γ

VALUE (units 10^{-4})		DOCUMENT ID		TECN	COMMENT
4.7 ±0.5 OUR AVERAGE Error includes scale factor of 1.2.					
$4.55\pm0.16\pm0.39$	[1,2]	DEL-AMO-SA...12		BABR	$e^+e^-\to\Upsilon(4S)$
$6.5\ ^{+1.3}_{-1.2}\ \pm1.0$	[2]	ANDERSON	01	CLE2	$e^+e^-\to\Upsilon(4S)$
• • • We do not use the following data for averages, fits, limits, etc. • • •					
$4.81\pm0.22\pm0.44$	[2]	AUBERT,B	06S	BABR	Repl. by DEL-AMO-SANCHEZ 12

[1] Uses the values of D and D^* branching fractions from PDG 08.
[2] Assumes equal production of B^+ and B^0 at the $\Upsilon(4S)$.

$\Gamma(\overline{D}^0 p\overline{p}\pi^+\pi^-)/\Gamma_{total}$ Γ_{431}/Γ

VALUE (units 10^{-4})		DOCUMENT ID		TECN	COMMENT
2.99±0.21±0.45	[1,2]	DEL-AMO-SA...12		BABR	$e^+e^-\to\Upsilon(4S)$

[1] Uses the values of D and D^* branching fractions from PDG 08.
[2] Assumes equal production of B^+ and B^0 at the $\Upsilon(4S)$.

$\Gamma(\overline{D}^{*0} p\overline{p}\pi^+\pi^-)/\Gamma_{total}$ Γ_{432}/Γ

VALUE (units 10^{-4})		DOCUMENT ID		TECN	COMMENT
1.91±0.36±0.29	[1,2]	DEL-AMO-SA...12		BABR	$e^+e^-\to\Upsilon(4S)$

[1] Uses the values of D and D^* branching fractions from PDG 08.
[2] Assumes equal production of B^+ and B^0 at the $\Upsilon(4S)$.

$\Gamma(\Theta_c\overline{p}\pi^+,\ \Theta_c\to D^-p)/\Gamma_{total}$ Γ_{433}/Γ

VALUE (units 10^{-6})	CL%	DOCUMENT ID		TECN	COMMENT
<9	90	[1] AUBERT,B	06S	BABR	$e^+e^-\to\Upsilon(4S)$

[1] Assumes equal production of B^+ and B^0 at the $\Upsilon(4S)$.

$\Gamma(\Theta_c\overline{p}\pi^+,\ \Theta_c\to D^{*-}p)/\Gamma_{total}$ Γ_{434}/Γ

VALUE (units 10^{-6})	CL%	DOCUMENT ID		TECN	COMMENT
<14	90	[1] AUBERT,B	06S	BABR	$e^+e^-\to\Upsilon(4S)$

[1] Assumes equal production of B^+ and B^0 at the $\Upsilon(4S)$.

$\Gamma(\Sigma_c^{--}\Delta^{++})/\Gamma_{total}$ Γ_{435}/Γ

VALUE	CL%	DOCUMENT ID		TECN	COMMENT
$<1.0\times10^{-3}$	90	[1] PROCARIO	94	CLE2	$e^+e^-\to\Upsilon(4S)$

[1] PROCARIO 94 reports < 0.0012 from a measurement of $[\Gamma(B^0\to\overline{\Sigma}_c^{--}\Delta^{++})/\Gamma_{total}]\times[B(\Lambda_c^+\to pK^-\pi^+)]$ assuming $B(\Lambda_c^+\to pK^-\pi^+)=0.043$, which we rescale to our best value $B(\Lambda_c^+\to pK^-\pi^+)=5.0\times10^{-2}$.

$\Gamma(\overline{\Lambda}_c^- p\pi^+\pi^-)/\Gamma_{total}$ Γ_{436}/Γ

VALUE (units 10^{-3})		DOCUMENT ID		TECN	COMMENT
1.3 ±0.4 OUR AVERAGE					
$1.7\ ^{+0.3}_{-0.2}\ \pm0.4$	[1]	DYTMAN	02	CLE2	$e^+e^-\to\Upsilon(4S)$
$1.10\pm0.20\pm0.29$	[2]	GABYSHEV	02	BELL	$e^+e^-\to\Upsilon(4S)$
• • • We do not use the following data for averages, fits, limits, etc. • • •					
$1.33^{+0.46}_{-0.42}\pm0.37$	[3]	FU	97	CLE2	Repl. by DYTMAN 02

[1] DYTMAN 02 reports $(1.67^{+0.27}_{-0.25})\times10^{-3}$ from a measurement of $[\Gamma(B^0\to\overline{\Lambda}_c^- p\pi^+\pi^-)/\Gamma_{total}]\times[B(\Lambda_c^+\to pK^-\pi^+)]$ assuming $B(\Lambda_c^+\to pK^-\pi^+)=0.05$, which we rescale to our best value $B(\Lambda_c^+\to pK^-\pi^+)=(5.0\pm1.3)\times10^{-2}$. Our first error is their experiment's error and our second error is the systematic error from using our best value.
[2] GABYSHEV 02 reports $(1.1\pm0.2)\times10^{-3}$ from a measurement of $[\Gamma(B^0\to\overline{\Lambda}_c^- p\pi^+\pi^-)/\Gamma_{total}]\times[B(\Lambda_c^+\to pK^-\pi^+)]$ assuming $B(\Lambda_c^+\to pK^-\pi^+)=0.05$, which we rescale to our best value $B(\Lambda_c^+\to pK^-\pi^+)=(5.0\pm1.3)\times10^{-2}$. Our first error is their experiment's error and our second error is the systematic error from using our best value.
[3] FU 97 uses PDG 96 values of Λ_c branching fraction.

$\Gamma(\overline{\Lambda}_c^- p)/\Gamma_{total}$ Γ_{437}/Γ

VALUE (units 10^{-5})	CL%	DOCUMENT ID		TECN	COMMENT
2.0 ±0.4 OUR AVERAGE					
$1.9\ \pm0.2\ \pm0.5$		[1,2] AUBERT	08BN	BABR	$e^+e^-\to\Upsilon(4S)$
$2.19^{+0.56}_{-0.49}\pm0.65$		[1,3] GABYSHEV	03	BELL	$e^+e^-\to\Upsilon(4S)$
• • • We do not use the following data for averages, fits, limits, etc. • • •					
$2.10^{+0.67+0.77}_{-0.55-0.46}$		[1,4] AUBERT	07AV	BABR	Repl. by AUBERT 08BN
< 9	90	[1,5] DYTMAN	02	CLE2	$e^+e^-\to\Upsilon(4S)$
< 3.1	90	[1,4] GABYSHEV	02	BELL	$e^+e^-\to\Upsilon(4S)$
<21	90	[6] FU	97	CLE2	$e^+e^-\to\Upsilon(4S)$

[1] Assumes equal production of B^+ and B^0 at the $\Upsilon(4S)$.
[2] AUBERT 08BN reports $(1.89\pm0.21\pm0.49)\times10^{-5}$ from a measurement of $[\Gamma(B^0\to\overline{\Lambda}_c^- p)/\Gamma_{total}]\times[B(\Lambda_c^+\to pK^-\pi^+)]$ assuming $B(\Lambda_c^+\to pK^-\pi^+)=(5.0\pm1.3)\times10^{-2}$.
[3] The second error for GABYSHEV 03 includes the systematic and the error of $\Lambda_c\to\overline{p}K^+\pi^-$ decay branching fraction.
[4] Uses the value for $\Lambda_c\to pK^-\pi^+$ branching ratio (5.0 ± 1.3)%.
[5] DYTMAN 02 measurement uses $B(\Lambda_c^-\to\overline{p}K^+\pi^-)=5.0\pm1.3$%. The second error includes the systematic and the uncertainty of the branching ratio.
[6] FU 97 uses PDG 96 values of Λ_c branching ratio.

$\Gamma(\overline{\Lambda}_c^- p\pi^0)/\Gamma_{total}$ Γ_{438}/Γ

VALUE (units 10^{-4})	CL%	DOCUMENT ID		TECN	COMMENT
1.9±0.2±0.5		[1,2] AUBERT	10H	BABR	$e^+e^-\to\Upsilon(4S)$
• • • We do not use the following data for averages, fits, limits, etc. • • •					
<5.9	90	[3] FU	97	CLE2	$e^+e^-\to\Upsilon(4S)$

[1] AUBERT 10H reports $(1.94 \pm 0.17 \pm 0.52) \times 10^{-4}$ from a measurement of $[\Gamma(B^0 \to \overline{\Lambda}_c^- p\pi^0)/\Gamma_{\rm total}] \times [B(\Lambda_c^+ \to pK^-\pi^+)]$ assuming $B(\Lambda_c^+ \to pK^-\pi^+) = (5.0 \pm 1.3) \times 10^{-2}$.

[2] Assumes equal production of B^+ and B^0 at the $\Upsilon(4S)$.

[3] FU 97 uses PDG 96 values of Λ_c branching ratio.

$\Gamma(\Sigma_c(2455)^- p)/\Gamma_{\rm total}$ Γ_{439}/Γ

VALUE (units 10^{-6})		DOCUMENT ID		TECN	COMMENT
<30	[1,2]	AUBERT	10H	BABR	$e^+e^- \to \Upsilon(4S)$

[1] AUBERT 10H reports $[\Gamma(B^0 \to \Sigma_c(2455)^- p)/\Gamma_{\rm total}] \times [B(\Lambda_c^+ \to pK^-\pi^+)] < 1.5 \times 10^{-6}$ which we divide by our best value $B(\Lambda_c^+ \to pK^-\pi^+) = 5.0 \times 10^{-2}$.

[2] Assumes equal production of B^+ and B^0 at the $\Upsilon(4S)$.

$\Gamma(\overline{\Lambda}_c^- p\pi^+\pi^-\pi^0)/\Gamma_{\rm total}$ Γ_{440}/Γ

VALUE	CL%	DOCUMENT ID		TECN	COMMENT
$<5.07 \times 10^{-3}$	90	[1] FU	97	CLE2	$e^+e^- \to \Upsilon(4S)$

[1] FU 97 uses PDG 96 values of Λ_c branching ratio.

$\Gamma(\overline{\Lambda}_c^- p\pi^+\pi^-\pi^+\pi^-)/\Gamma_{\rm total}$ Γ_{441}/Γ

VALUE	CL%	DOCUMENT ID		TECN	COMMENT
$<2.74 \times 10^{-3}$	90	[1] FU	97	CLE2	$e^+e^- \to \Upsilon(4S)$

[1] FU 97 uses PDG 96 values of Λ_c branching ratio.

$\Gamma(\overline{\Lambda}_c^- p\pi^+\pi^-)/\Gamma_{\rm total}$ Γ_{442}/Γ

VALUE (units 10^{-4})		DOCUMENT ID		TECN	COMMENT
11.7±2.3 OUR AVERAGE					
12.3±0.5±3.3	[1,2]	LEES	13H	BABR	$e^+e^- \to \Upsilon(4S)$
11.2±0.5±3.2	[1,3]	PARK	07	BELL	$e^+e^- \to \Upsilon(4S)$

[1] Assumes equal production of B^+ and B^0 at the $\Upsilon(4S)$.

[2] Uses $\Lambda_c^+ \to pK^-\pi^+$ mode. The second error includes the uncertainty of the branching fraction of the Λ_c decay, $B(\Lambda_c^+ \to pK^-\pi^+) = (5.0 \pm 1.3)\%$.

[3] PARK 07 reports $(11.2 \pm 0.5 \pm 3.2) \times 10^{-4}$ from a measurement of $[\Gamma(B^0 \to \overline{\Lambda}_c^- p\pi^+\pi^-)/\Gamma_{\rm total}] \times [B(\Lambda_c^+ \to pK^-\pi^+)]$ assuming $B(\Lambda_c^+ \to pK^-\pi^+) = (5.0 \pm 1.3) \times 10^{-2}$.

$\Gamma(\overline{\Lambda}_c^- p\pi^+\pi^-(\text{nonresonant}))/\Gamma_{\rm total}$ Γ_{443}/Γ

VALUE (units 10^{-4})		DOCUMENT ID		TECN	COMMENT
7.1±1.4 OUR AVERAGE					
7.9±0.4±2.0	[1,2]	LEES	13H	BABR	$e^+e^- \to \Upsilon(4S)$
6.4±0.4±1.9	[1,3]	PARK	07	BELL	$e^+e^- \to \Upsilon(4S)$

[1] Assumes equal production of B^+ and B^0 at the $\Upsilon(4S)$.

[2] Uses $\Lambda_c^+ \to pK^-\pi^+$ mode. The second error includes the uncertainty of the branching fraction of the Λ_c decay, $B(\Lambda_c^+ \to pK^-\pi^+) = (5.0 \pm 1.3)\%$.

[3] PARK 07 reports $(6.4 \pm 0.4 \pm 1.9) \times 10^{-4}$ from a measurement of $[\Gamma(B^0 \to \overline{\Lambda}_c^- p\pi^+\pi^-(\text{nonresonant}))/\Gamma_{\rm total}] \times [B(\Lambda_c^+ \to pK^-\pi^+)]$ assuming $B(\Lambda_c^+ \to pK^-\pi^+) = (5.0 \pm 1.3) \times 10^{-2}$.

$\Gamma(\overline{\Sigma}_c(2520)^{--} p\pi^+)/\Gamma_{\rm total}$ Γ_{444}/Γ

VALUE (units 10^{-4})		DOCUMENT ID		TECN	COMMENT
1.17±0.25 OUR AVERAGE					
1.15±0.10±0.30	[1,2]	LEES	13H	BABR	$e^+e^- \to \Upsilon(4S)$
1.2 ±0.1 ±0.4	[1,3]	PARK	07	BELL	$e^+e^- \to \Upsilon(4S)$
• • • We do not use the following data for averages, fits, limits, etc. • • •					
1.6 ±0.6 ±0.4	[4]	GABYSHEV	02	BELL	Repl. by PARK 07

[1] Assumes equal production of B^+ and B^0 at the $\Upsilon(4S)$.

[2] Uses $\Lambda_c^+ \to pK^-\pi^+$ mode. The second error includes the uncertainty of the branching fraction of the Λ_c decay, $B(\Lambda_c^+ \to pK^-\pi^+) = (5.0 \pm 1.3)\%$.

[3] PARK 07 reports $(1.2 \pm 0.1 \pm 0.4) \times 10^{-4}$ from a measurement of $[\Gamma(B^0 \to \overline{\Sigma}_c(2520)^{--} p\pi^+)/\Gamma_{\rm total}] \times [B(\Lambda_c^+ \to pK^-\pi^+)]$ assuming $B(\Lambda_c^+ \to pK^-\pi^+) = (5.0 \pm 1.3) \times 10^{-2}$.

[4] GABYSHEV 02 reports $(1.63^{+0.64}_{-0.58}) \times 10^{-4}$ from a measurement of $[\Gamma(B^0 \to \overline{\Sigma}_c(2520)^{--} p\pi^+)/\Gamma_{\rm total}] \times [B(\Lambda_c^+ \to pK^-\pi^+)]$ assuming $B(\Lambda_c^+ \to pK^-\pi^+) = 0.05$, which we rescale to our best value $B(\Lambda_c^+ \to pK^-\pi^+) = (5.0 \pm 1.3) \times 10^{-2}$. Our first error is their experiment's error and our second error is the systematic error from using our best value.

$\Gamma(\overline{\Sigma}_c(2520)^0 p\pi^-)/\Gamma_{\rm total}$ Γ_{445}/Γ

VALUE	CL%	DOCUMENT ID		TECN	COMMENT
$<0.31 \times 10^{-4}$	90	[1,2] LEES	13H	BABR	$e^+e^- \to \Upsilon(4S)$
• • • We do not use the following data for averages, fits, limits, etc. • • •					
$<0.38 \times 10^{-4}$	90	[1] PARK	07	BELL	$e^+e^- \to \Upsilon(4S)$
$<1.21 \times 10^{-4}$	90	[1,2] GABYSHEV	02	BELL	Repl. by PARK 07

[1] Assumes equal production of B^+ and B^0 at the $\Upsilon(4S)$.

[2] Uses the value for $\Lambda_c \to pK^-\pi^+$ branching ratio (5.0 ± 1.3)%.

$\Gamma(\overline{\Sigma}_c(2455)^0 N^0,\ N^0 \to p\pi^-)/\Gamma_{\rm total}$ Γ_{447}/Γ

N^0 is the $N(1440)$ P_{11} or $N(1535)$ S_{11} or an admixture of the two baryonic states.

VALUE (units 10^{-4})		DOCUMENT ID		TECN	COMMENT
0.80±0.15±0.25	[1,2]	KIM	08	BELL	$e^+e^- \to \Upsilon(4S)$

[1] Assumes equal production of B^+ and B^0 at the $\Upsilon(4S)$.

[2] KIM 08 reports $(0.80 \pm 0.15 \pm 0.25) \times 10^{-4}$ from a measurement of $[\Gamma(B^0 \to \overline{\Sigma}_c(2455)^0 N^0,\ N^0 \to p\pi^-)/\Gamma_{\rm total}] \times [B(\Lambda_c^+ \to pK^-\pi^+)]$ assuming $B(\Lambda_c^+ \to pK^-\pi^+) = (5.0 \pm 1.3) \times 10^{-2}$.

$\Gamma(\overline{\Sigma}_c(2455)^0 p\pi^-)/\Gamma_{\rm total}$ Γ_{446}/Γ

VALUE (units 10^{-4})	CL%	DOCUMENT ID		TECN	COMMENT
1.04±0.22 OUR AVERAGE					
0.91±0.07±0.24		[1,2] LEES	13H	BABR	$e^+e^- \to \Upsilon(4S)$
1.4 ±0.2 ±0.4		[1,3] PARK	07	BELL	$e^+e^- \to \Upsilon(4S)$
2.2 ±0.7 ±0.6		[4] DYTMAN	02	CLE2	$e^+e^- \to \Upsilon(4S)$
• • • We do not use the following data for averages, fits, limits, etc. • • •					
$0.5\ ^{+0.5}_{-0.4}$ ±0.1	90	[5] GABYSHEV	02	BELL	Repl. by PARK 07

[1] Assumes equal production of B^+ and B^0 at the $\Upsilon(4S)$.

[2] Uses $\Lambda_c^+ \to pK^-\pi^+$ mode. The second error includes the uncertainty of the branching fraction of the Λ_c decay, $B(\Lambda_c^+ \to pK^-\pi^+) = (5.0 \pm 1.3)\%$.

[3] PARK 07 reports $(1.4 \pm 0.2 \pm 0.4) \times 10^{-4}$ from a measurement of $[\Gamma(B^0 \to \overline{\Sigma}_c(2455)^0 p\pi^-)/\Gamma_{\rm total}] \times [B(\Lambda_c^+ \to pK^-\pi^+)]$ assuming $B(\Lambda_c^+ \to pK^-\pi^+) = (5.0 \pm 1.3) \times 10^{-2}$.

[4] DYTMAN 02 reports $(2.2 \pm 0.7) \times 10^{-4}$ from a measurement of $[\Gamma(B^0 \to \overline{\Sigma}_c(2455)^0 p\pi^-)/\Gamma_{\rm total}] \times [B(\Lambda_c^+ \to pK^-\pi^+)]$ assuming $B(\Lambda_c^+ \to pK^-\pi^+) = 0.05$, which we rescale to our best value $B(\Lambda_c^+ \to pK^-\pi^+) = (5.0 \pm 1.3) \times 10^{-2}$. Our first error is their experiment's error and our second error is the systematic error from using our best value.

[5] GABYSHEV 02 reports $(0.48^{+0.46}_{-0.41}) \times 10^{-4}$ from a measurement of $[\Gamma(B^0 \to \overline{\Sigma}_c(2455)^0 p\pi^-)/\Gamma_{\rm total}] \times [B(\Lambda_c^+ \to pK^-\pi^+)]$ assuming $B(\Lambda_c^+ \to pK^-\pi^+) = 0.05$, which we rescale to our best value $B(\Lambda_c^+ \to pK^-\pi^+) = (5.0 \pm 1.3) \times 10^{-2}$. Our first error is their experiment's error and our second error is the systematic error from using our best value.

$\Gamma(\overline{\Sigma}_c(2455)^{--} p\pi^+)/\Gamma_{\rm total}$ Γ_{448}/Γ

VALUE (units 10^{-4})		DOCUMENT ID		TECN	COMMENT
2.2 ±0.4 OUR AVERAGE					
2.13±0.10±0.56	[1,2]	LEES	13H	BABR	$e^+e^- \to \Upsilon(4S)$
2.1 ±0.2 ±0.6	[1,3]	PARK	07	BELL	$e^+e^- \to \Upsilon(4S)$
3.7 ±1.1 ±1.0	[4]	DYTMAN	02	CLE2	$e^+e^- \to \Upsilon(4S)$
• • • We do not use the following data for averages, fits, limits, etc. • • •					
$2.4\ ^{+0.8}_{-0.7}$ ±0.6	[5]	GABYSHEV	02	BELL	Repl. by PARK 07

[1] Assumes equal production of B^+ and B^0 at the $\Upsilon(4S)$.

[2] Uses $\Lambda_c^+ \to pK^-\pi^+$ mode. The second error includes the uncertainty of the branching fraction of the Λ_c decay, $B(\Lambda_c^+ \to pK^-\pi^+) = (5.0 \pm 1.3)\%$.

[3] PARK 07 reports $(2.1 \pm 0.2 \pm 0.6) \times 10^{-4}$ from a measurement of $[\Gamma(B^0 \to \overline{\Sigma}_c(2455)^{--} p\pi^+)/\Gamma_{\rm total}] \times [B(\Lambda_c^+ \to pK^-\pi^+)]$ assuming $B(\Lambda_c^+ \to pK^-\pi^+) = (5.0 \pm 1.3) \times 10^{-2}$.

[4] DYTMAN 02 reports $(3.7 \pm 1.1) \times 10^{-4}$ from a measurement of $[\Gamma(B^0 \to \overline{\Sigma}_c(2455)^{--} p\pi^+)/\Gamma_{\rm total}] \times [B(\Lambda_c^+ \to pK^-\pi^+)]$ assuming $B(\Lambda_c^+ \to pK^-\pi^+) = 0.05$, which we rescale to our best value $B(\Lambda_c^+ \to pK^-\pi^+) = (5.0 \pm 1.3) \times 10^{-2}$. Our first error is their experiment's error and our second error is the systematic error from using our best value.

[5] GABYSHEV 02 reports $(2.38^{+0.75}_{-0.69}) \times 10^{-4}$ from a measurement of $[\Gamma(B^0 \to \overline{\Sigma}_c(2455)^{--} p\pi^+)/\Gamma_{\rm total}] \times [B(\Lambda_c^+ \to pK^-\pi^+)]$ assuming $B(\Lambda_c^+ \to pK^-\pi^+) = 0.05$, which we rescale to our best value $B(\Lambda_c^+ \to pK^-\pi^+) = (5.0 \pm 1.3) \times 10^{-2}$. Our first error is their experiment's error and our second error is the systematic error from using our best value.

$\Gamma(\Lambda_c^- pK^+\pi^-)/\Gamma_{\rm total}$ Γ_{449}/Γ

VALUE (units 10^{-5})		DOCUMENT ID		TECN	COMMENT
4.3±0.8±1.2	[1,2]	AUBERT	09AG	BABR	$e^+e^- \to \Upsilon(4S)$

[1] AUBERT 09AG reports $(4.33 \pm 0.82 \pm 0.33 \pm 1.13) \times 10^{-5}$ from a measurement of $[\Gamma(B^0 \to \Lambda_c^- pK^+\pi^-)/\Gamma_{\rm total}] \times [B(\Lambda_c^+ \to pK^-\pi^+)]$ assuming $B(\Lambda_c^+ \to pK^-\pi^+) = (5.0 \pm 1.3) \times 10^{-2}$.

[2] Assumes equal production of B^+ and B^0 at the $\Upsilon(4S)$.

$\Gamma(\overline{\Sigma}_c(2455)^{--} pK^+,\ \overline{\Sigma}_c^{--} \to \overline{\Lambda}_c^- \pi^-)/\Gamma_{\rm total}$ Γ_{450}/Γ

VALUE (units 10^{-5})		DOCUMENT ID		TECN	COMMENT
1.11±0.30±0.30	[1,2]	AUBERT	09AG	BABR	$e^+e^- \to \Upsilon(4S)$

[1] AUBERT 09AG reports $(1.11 \pm 0.30 \pm 0.09 \pm 0.29) \times 10^{-5}$ from a measurement of $[\Gamma(B^0 \to \overline{\Sigma}_c(2455)^{--} pK^+,\ \overline{\Sigma}_c^{--} \to \overline{\Lambda}_c^- \pi^-)/\Gamma_{\rm total}] \times [B(\Lambda_c^+ \to pK^-\pi^+)]$ assuming $B(\Lambda_c^+ \to pK^-\pi^+) = (5.0 \pm 1.3) \times 10^{-2}$.

[2] Assumes equal production of B^+ and B^0 at the $\Upsilon(4S)$.

Meson Particle Listings

B^0

$\Gamma(\Lambda_c^- p K^*(892)^0)/\Gamma_{total}$ Γ_{451}/Γ

VALUE (units 10^{-5})	CL%	DOCUMENT ID		TECN	COMMENT
<2.42	90	[1] AUBERT	09AG	BABR	$e^+e^- \to \Upsilon(4S)$

[1] Assumes equal production of B^+ and B^0 at the $\Upsilon(4S)$.

$\Gamma(\overline{\Lambda}_c^- \Lambda K^+)/\Gamma_{total}$ Γ_{452}/Γ

VALUE (units 10^{-5})	DOCUMENT ID		TECN	COMMENT
3.8±0.8±1.0	[1,2] LEES	11F	BABR	$e^+e^- \to \Upsilon(4S)$

[1] Assumes equal production of B^0 and B^+ from Upsilon(4S) decays.
[2] LEES 11F reports $(3.8 \pm 0.8 \pm 0.2 \pm 1.0) \times 10^{-5}$ from a measurement of $[\Gamma(B^0 \to \overline{\Lambda}_c^- \Lambda K^+)/\Gamma_{total}] / [B(\Lambda_c^+ \to p K^- \pi^+)] / [B(\Lambda \to p\pi^-)]$ assuming $B(\Lambda_c^+ \to p K^- \pi^+) = (5.0 \pm 1.3) \times 10^{-2}$, $B(\Lambda \to p\pi^-) = (63.9 \pm 0.5) \times 10^{-2}$. The reported uncertainties are statistical, systematic, and $\overline{\Lambda}_c^-$ branching fraction uncertainty.

$\Gamma(\overline{\Lambda}_c^- \Lambda_c^+)/\Gamma_{total}$ Γ_{453}/Γ

VALUE (units 10^{-5})	CL%	DOCUMENT ID		TECN	COMMENT
<6.2	90	[1] UCHIDA	08	BELL	$e^+e^- \to \Upsilon(4S)$

[1] Assumes equal production of B^+ and B^0 at the $\Upsilon(4S)$.

$\Gamma(\overline{\Lambda}_c(2593)^- / \overline{\Lambda}_c(2625)^- p)/\Gamma_{total}$ Γ_{454}/Γ

VALUE	CL%	DOCUMENT ID		TECN	COMMENT
<1.1 × 10⁻⁴	90	[1,2] DYTMAN	02	CLE2	$e^+e^- \to \Upsilon(4S)$

[1] Assumes equal production of B^+ and B^0 at the $\Upsilon(4S)$.
[2] DYTMAN 02 measurement uses $B(\Lambda_c^- \to \overline{p} K^+ \pi^-) = 5.0 \pm 1.3\%$. The second error includes the systematic and the uncertainty of the branching ratio.

$\Gamma(\Xi_c^- \Lambda_c^+, \Xi_c^- \to \Xi^+ \pi^- \pi^-)/\Gamma_{total}$ Γ_{455}/Γ

VALUE (units 10^{-5})	DOCUMENT ID		TECN	COMMENT
2.2±2.3 OUR AVERAGE Error includes scale factor of 1.9.				
1.5 ± 1.1 ± 0.4	[1,2] AUBERT	08H	BABR	$e^+e^- \to \Upsilon(4S)$
$9.3^{+3.7}_{-2.8} \pm 3.1$	[2,3] CHISTOV	06A	BELL	$e^+e^- \to \Upsilon(4S)$

[1] AUBERT 08H reports $(1.5 \pm 1.07 \pm 0.44) \times 10^{-5}$ from a measurement of $[\Gamma(B^0 \to \Xi_c^- \Lambda_c^+, \Xi_c^- \to \Xi^+ \pi^- \pi^-)/\Gamma_{total}] \times [B(\Lambda_c^+ \to p K^- \pi^+)]$ assuming $B(\Lambda_c^+ \to p K^- \pi^+) = (5.0 \pm 1.3) \times 10^{-2}$.
[2] Assumes equal production of B^+ and B^0 at the $\Upsilon(4S)$.
[3] CHISTOV 06A reports $(9.3^{+3.7}_{-2.8} \pm 3.1) \times 10^{-5}$ from a measurement of $[\Gamma(B^0 \to \Xi_c^- \Lambda_c^+, \Xi_c^- \to \Xi^+ \pi^- \pi^-)/\Gamma_{total}] \times [B(\Lambda_c^+ \to p K^- \pi^+)]$ assuming $B(\Lambda_c^+ \to p K^- \pi^+) = (5.0 \pm 1.3) \times 10^{-2}$.

$\Gamma(\Lambda_c^+ \Lambda_c^- K^0)/\Gamma_{total}$ Γ_{456}/Γ

VALUE (units 10^{-4})	DOCUMENT ID		TECN	COMMENT
5.4±3.2 OUR AVERAGE				
3.8 ± 3.1 ± 2.1	[1,2] AUBERT	08H	BABR	$e^+e^- \to \Upsilon(4S)$
$8\ ^{+3}_{-2} \pm 4$	[2,3] GABYSHEV	06	BELL	$e^+e^- \to \Upsilon(4S)$

[1] AUBERT 08H reports $(0.38 \pm 0.31 \pm 0.21) \times 10^{-3}$ from a measurement of $[\Gamma(B^0 \to \Lambda_c^+ \Lambda_c^- K^0)/\Gamma_{total}] \times [B(\Lambda_c^+ \to p K^- \pi^+)]$ assuming $B(\Lambda_c^+ \to p K^- \pi^+) = (5.0 \pm 1.3) \times 10^{-2}$.
[2] Assumes equal production of B^+ and B^0 at the $\Upsilon(4S)$.
[3] GABYSHEV 06 reports $(7.9^{+2.9}_{-2.3} \pm 4.3) \times 10^{-4}$ from a measurement of $[\Gamma(B^0 \to \Lambda_c^+ \Lambda_c^- K^0)/\Gamma_{total}] \times [B(\Lambda_c^+ \to p K^- \pi^+)]$ assuming $B(\Lambda_c^+ \to p K^- \pi^+) = (5.0 \pm 1.3) \times 10^{-2}$.

$\Gamma(\gamma\gamma)/\Gamma_{total}$ Γ_{457}/Γ

Test for ΔB=1 weak neutral current. Allowed by higher-order electroweak interactions.

VALUE	CL%	DOCUMENT ID		TECN	COMMENT
<3.2 × 10⁻⁷	90	[1] DEL-AMO-SA...11A		BABR	$e^+e^- \to \Upsilon(4S)$
• • • We do not use the following data for averages, fits, limits, etc. • • •					
$<6.2 \times 10^{-7}$	90	[1] VILLA	06	BELL	$e^+e^- \to \Upsilon(4S)$
$<1.7 \times 10^{-6}$	90	[1] AUBERT	01I	BABR	$e^+e^- \to \Upsilon(4S)$
$<3.9 \times 10^{-5}$	90	[2] ACCIARRI	95I	L3	$e^+e^- \to Z$

[1] Assumes equal production of B^+ and B^0 at the $\Upsilon(4S)$.
[2] ACCIARRI 95I assumes $f_{B^0} = 39.5 \pm 4.0$ and $f_{B_s} = 12.0 \pm 3.0\%$.

$\Gamma(e^+e^-)/\Gamma_{total}$ Γ_{458}/Γ

Test for ΔB=1 weak neutral current. Allowed by higher-order electroweak interactions.

VALUE	CL%	DOCUMENT ID		TECN	COMMENT
< 8.3 × 10⁻⁸	90	AALTONEN	09P	CDF	$p\overline{p}$ at 1.96 TeV
• • • We do not use the following data for averages, fits, limits, etc. • • •					
$<11.3 \times 10^{-8}$	90	[1] AUBERT	08P	BABR	$e^+e^- \to \Upsilon(4S)$
$< 6.1 \times 10^{-8}$	90	[1] AUBERT	05W	BABR	Repl. by AUBERT 08P
$< 1.9 \times 10^{-7}$	90	[1] CHANG	03	BELL	$e^+e^- \to \Upsilon(4S)$
$< 8.3 \times 10^{-7}$	90	[1] BERGFELD	00B	CLE2	$e^+e^- \to \Upsilon(4S)$
$< 1.4 \times 10^{-5}$	90	[2] ACCIARRI	97B	L3	$e^+e^- \to Z$
$< 5.9 \times 10^{-6}$	90	AMMAR	94	CLE2	Repl. by BERGFELD 00B
$< 2.6 \times 10^{-5}$	90	[3] AVERY	89B	CLEO	$e^+e^- \to \Upsilon(4S)$
$< 7.6 \times 10^{-5}$	90	[4] ALBRECHT	87D	ARG	$e^+e^- \to \Upsilon(4S)$
$< 6.4 \times 10^{-5}$	90	[5] AVERY	87	CLEO	$e^+e^- \to \Upsilon(4S)$
$< 3 \times 10^{-4}$	90	GILES	84	CLEO	Repl. by AVERY 87

[1] Assumes equal production of B^+ and B^0 at the $\Upsilon(4S)$.
[2] ACCIARRI 97B assume PDG 96 production fractions for B^+, B^0, B_s, and Λ_b.
[3] AVERY 89B reports $< 3 \times 10^{-5}$ assuming the $\Upsilon(4S)$ decays 43% to $B^0\overline{B}^0$. We rescale to 50%.
[4] ALBRECHT 87D reports $< 8.5 \times 10^{-5}$ assuming the $\Upsilon(4S)$ decays 45% to $B^0\overline{B}^0$. We rescale to 50%.
[5] AVERY 87 reports $< 8 \times 10^{-5}$ assuming the $\Upsilon(4S)$ decays 40% to $B^0\overline{B}^0$. We rescale to 50%.

$\Gamma(e^+e^-\gamma)/\Gamma_{total}$ Γ_{459}/Γ

Test for ΔB=1 weak neutral current. Allowed by higher-order electroweak interactions.

VALUE	CL%	DOCUMENT ID		TECN	COMMENT
<1.2 × 10⁻⁷	90	AUBERT	08C	BABR	$e^+e^- \to \Upsilon(4S)$

$\Gamma(\mu^+\mu^-)/\Gamma_{total}$ Γ_{460}/Γ

Test for ΔB=1 weak neutral current. Allowed by higher-order electroweak interactions.

VALUE	CL%	DOCUMENT ID		TECN	COMMENT
<6.3 × 10⁻¹⁰	90	[1] AAIJ	13BA	LHCB	pp at 7, 8 TeV
• • • We do not use the following data for averages, fits, limits, etc. • • •					
$<8.0 \times 10^{-10}$	90	[2] AAIJ	13B	LHCB	Repl. by AAIJ 13BA
$<3.8 \times 10^{-9}$	90	[3] AALTONEN	13F	CDF	$p\overline{p}$ at 1.96 TeV
$<9.2 \times 10^{-10}$	90	[4] CHATRCHYAN	13AW	CMS	pp at 7, 8 TeV
$<2.6 \times 10^{-9}$	90	[2] AAIJ	12A	LHCB	Repl. by AAIJ 12W
$<0.81 \times 10^{-9}$	90	[5] AAIJ	12W	LHCB	Repl. by AAIJ 13B
$<1.4 \times 10^{-9}$	90	[5] CHATRCHYAN	12A	CMS	pp at 7 TeV
$<1.2 \times 10^{-8}$	90	[6] AAIJ	11B	LHCB	Repl. by AAIJ 12A
$<5.0 \times 10^{-9}$	90	[5] AALTONEN	11AG	CDF	$p\overline{p}$ at 1.96 TeV
$<3.7 \times 10^{-9}$	90	[5] CHATRCHYAN	11T	CMS	Repl. by CHATRCHYAN 12A
$<1.5 \times 10^{-8}$	90	[7] AALTONEN	08I	CDF	Repl. by AALTONEN 11AG
$<5.2 \times 10^{-8}$	90	[8] AUBERT	08P	BABR	$e^+e^- \to \Upsilon(4S)$
$<3.9 \times 10^{-8}$	90	[9] ABULENCIA	05	CDF	Repl. by AALTONEN 08I
$<8.3 \times 10^{-8}$	90	[8] AUBERT	05W	BABR	$e^+e^- \to \Upsilon(4S)$
$<1.5 \times 10^{-7}$	90	[10] ACOSTA	04D	CDF	$p\overline{p}$ at 1.96 TeV
$<1.6 \times 10^{-7}$	90	[8] CHANG	03	BELL	$e^+e^- \to \Upsilon(4S)$
$<6.1 \times 10^{-7}$	90	[8] BERGFELD	00B	CLE2	$e^+e^- \to \Upsilon(4S)$
$<4.0 \times 10^{-5}$	90	ABBOTT	98B	D0	$p\overline{p}$ 1.8 TeV
$<6.8 \times 10^{-7}$	90	[11] ABE	98	CDF	$p\overline{p}$ at 1.8 TeV
$<1.0 \times 10^{-5}$	90	[12] ACCIARRI	97B	L3	$e^+e^- \to Z$
$<1.6 \times 10^{-6}$	90	[13] ABE	96L	CDF	Repl. by ABE 98
$<5.9 \times 10^{-6}$	90	AMMAR	94	CLE2	$e^+e^- \to \Upsilon(4S)$
$<8.3 \times 10^{-6}$	90	[14] ALBAJAR	91C	UA1	$E_{cm}^{p\overline{p}}$= 630 GeV
$<1.2 \times 10^{-5}$	90	[15] ALBAJAR	91C	UA1	$E_{cm}^{p\overline{p}}$= 630 GeV
$<4.3 \times 10^{-5}$	90	[16] AVERY	89B	CLEO	$e^+e^- \to \Upsilon(4S)$
$<4.5 \times 10^{-5}$	90	[17] ALBRECHT	87D	ARG	$e^+e^- \to \Upsilon(4S)$
$<7.7 \times 10^{-5}$	90	[18] AVERY	87	CLEO	$e^+e^- \to \Upsilon(4S)$
$<2 \times 10^{-4}$	90	GILES	84	CLEO	Repl. by AVERY 87

[1] Reports also a limit of $< 7.4 \times 10^{-10}$ at 95% CL. Uses normalization modes $B^+ \to J/\psi K^+ \to \mu^+\mu^- K^+$ and $B^0 \to K^+\pi^-$.
[2] Uses $B(B^+ \to J/\psi K^+ \to \mu^+\mu^- K^+) = (6.01 \pm 0.21) \times 10^{-5}$ and $B(B^0 \to K^+\pi^-) = (1.94 \pm 0.06) \times 10^{-5}$ for normalization.
[3] Uses normalization mode $B(B^+ \to J/\psi K^+) = (10.22 \pm 0.35) \times 10^{-4}$.
[4] Uses $B(B^+ \to J/\psi K^+ \to \mu^+\mu^- K^+) = (6.0 \pm 0.2) \times 10^{-5}$ for normalization.
[5] Uses $B(B^+ \to J/\psi K^+ \to \mu^+\mu^- K^+) = (6.01 \pm 0.21) \times 10^{-5}$.
[6] Uses B production ratio $f(\overline{b} \to B^+)/f(\overline{b} \to B_s^0) = 3.71 \pm 0.47$ and three normalization modes.
[7] Uses $B(B^+ \to J/\psi K^+)\, B(J/\psi \to \mu^+\mu^-) = (5.94 \pm 0.21) \times 10^{-5}$.
[8] Assumes equal production of B^+ and B^0 at the $\Upsilon(4S)$.
[9] Uses $B(B^+ \to J/\psi K^+)\, B(J/\psi \to \mu^+\mu^-) = (5.88 \pm 0.26) \times 10^{-5}$.
[10] Assumes production cross-section $\sigma(B_s)/\sigma(B^+) = 0.100/0.391$ and the CDF measured value of $\sigma(B^+) = 3.6 \pm 0.6\ \mu$b.
[11] ABE 98 assumes production of $\sigma(B^0) = \sigma(B^+)$ and $\sigma(B_s)/\sigma(B^0) = 1/3$. They normalize to their measured $\sigma(B^0, p_T(B) > 6, |y| < 1.0) = 2.39 \pm 0.32 \pm 0.44\ \mu$b.
[12] ACCIARRI 97B assume PDG 96 production fractions for B^+, B^0, B_s, and Λ_b.
[13] ABE 96L assumes equal B^0 and B^+ production. They normalize to their measured $\sigma(B^+, p_T(B) > 6\ \text{GeV}/c, |y| < 1) = 2.39 \pm 0.54\ \mu$b.
[14] B^0 and B_s^0 are not separated.
[15] Obtained from unseparated B^0 and B_s^0 measurement by assuming a B^0:B_s^0 ratio 2:1.
[16] AVERY 89B reports $< 5 \times 10^{-3}$ assuming the $\Upsilon(4S)$ decays 43% to $B^0\overline{B}^0$. We rescale to 50%.
[17] ALBRECHT 87D reports $< 5 \times 10^{-5}$ assuming the $\Upsilon(4S)$ decays 45% to $B^0\overline{B}^0$. We rescale to 50%.
[18] AVERY 87 reports $< 9 \times 10^{-5}$ assuming the $\Upsilon(4S)$ decays 40% to $B^0\overline{B}^0$. We rescale to 50%.

$\Gamma(\mu^+\mu^-\gamma)/\Gamma_{total}$ Γ_{461}/Γ

Test for ΔB=1 weak neutral current. Allowed by higher-order electroweak interactions.

VALUE	CL%	DOCUMENT ID		TECN	COMMENT
<1.6 × 10⁻⁷	90	AUBERT	08C	BABR	$e^+e^- \to \Upsilon(4S)$

$\Gamma(\tau^+\tau^-)/\Gamma_{total}$ Γ_{464}/Γ

Test for ΔB=1 weak neutral current. Allowed by higher-order electroweak interactions.

VALUE	CL%	DOCUMENT ID		TECN	COMMENT
<4.1 × 10⁻³	90	[1] AUBERT	06S	BABR	$e^+e^- \to \Upsilon(4S)$

[1] Assumes equal production of B^+ and B^0 at the $\Upsilon(4S)$.

$\Gamma(\mu^+\mu^-\mu^+\mu^-)/\Gamma_{total}$ Γ_{462}/Γ

VALUE	CL%	DOCUMENT ID		TECN	COMMENT
$<5.3\times10^{-9}$	90	[1] AAIJ	13AW	LHCB	pp at 7 TeV

[1] Also reports a limit of $<6.6\times10^{-9}$ at 95% CL.

$\Gamma(SP,\ S\to\mu^+\mu^-,\ P\to\mu^+\mu^-)/\Gamma_{total}$ Γ_{463}/Γ

Here S and P are the hypothetical scalar and pseudoscalar particles with masses of 2.5 GeV/c^2 and 214.3 MeV/c^2, respectively.

VALUE	CL%	DOCUMENT ID		TECN	COMMENT
$<5.1\times10^{-9}$	90	[1] AAIJ	13AW	LHCB	pp at 7 TeV

[1] Also reports a limit of $<6.3\times10^{-9}$ at 95% CL.

$\Gamma(\pi^0\ell^+\ell^-)/\Gamma_{total}$ Γ_{465}/Γ

VALUE	CL%	DOCUMENT ID		TECN	COMMENT
$<5.3\times10^{-8}$	90	[1] LEES	13M	BABR	$e^+e^-\to\Upsilon(4S)$
• • • We do not use the following data for averages, fits, limits, etc. • • •					
$<1.5\times10^{-7}$	90	[1] WEI	08A	BELL	$e^+e^-\to\Upsilon(4S)$
$<1.2\times10^{-7}$	90	[1] AUBERT	07AG	BABR	Repl. by LEES 13M

[1] Assumes equal production of B^+ and B^0 at the $\Upsilon(4S)$.

$\Gamma(\pi^0\nu\overline{\nu})/\Gamma_{total}$ Γ_{471}/Γ

Test for $\Delta B=1$ weak neutral current. Allowed by higher-order electroweak interaction.

VALUE	CL%	DOCUMENT ID		TECN	COMMENT
$<6.9\times10^{-5}$	90	[1] LUTZ	13	BELL	$e^+e^-\to\Upsilon(4S)$
• • • We do not use the following data for averages, fits, limits, etc. • • •					
$<2.2\times10^{-4}$	90	[1] CHEN	07D	BELL	Repl. by LUTZ 13

[1] Assumes equal production of B^+ and B^0 at the $\Upsilon(4S)$.

$\Gamma(\pi^0e^+e^-)/\Gamma_{total}$ Γ_{466}/Γ

VALUE	CL%	DOCUMENT ID		TECN	COMMENT
$<8.4\times10^{-8}$	90	[1] LEES	13M	BABR	$e^+e^-\to\Upsilon(4S)$
• • • We do not use the following data for averages, fits, limits, etc. • • •					
$<2.3\times10^{-7}$	90	[1] WEI	08A	BELL	$e^+e^-\to\Upsilon(4S)$
$<1.4\times10^{-7}$	90	[1] AUBERT	07AG	BABR	Repl. by LEES 13M

[1] Assumes equal production of B^+ and B^0 at the $\Upsilon(4S)$.

$\Gamma(\pi^0\mu^+\mu^-)/\Gamma_{total}$ Γ_{467}/Γ

VALUE	CL%	DOCUMENT ID		TECN	COMMENT
$<6.9\times10^{-8}$	90	[1] LEES	13M	BABR	$e^+e^-\to\Upsilon(4S)$
• • • We do not use the following data for averages, fits, limits, etc. • • •					
$<1.8\times10^{-7}$	90	[1] WEI	08A	BELL	$e^+e^-\to\Upsilon(4S)$
$<5.1\times10^{-7}$	90	[1] AUBERT	07AG	BABR	$e^+e^-\to\Upsilon(4S)$

[1] Assumes equal production of B^+ and B^0 at the $\Upsilon(4S)$.

$\Gamma(\eta\ell^+\ell^-)/\Gamma_{total}$ Γ_{468}/Γ

VALUE	CL%	DOCUMENT ID		TECN	COMMENT
$<6.4\times10^{-8}$	90	[1] LEES	13M	BABR	$e^+e^-\to\Upsilon(4S)$

[1] Assumes equal production of B^+ and B^0 at the $\Upsilon(4S)$.

$\Gamma(\eta e^+e^-)/\Gamma_{total}$ Γ_{469}/Γ

VALUE	CL%	DOCUMENT ID		TECN	COMMENT
$<10.8\times10^{-8}$	90	[1] LEES	13M	BABR	$e^+e^-\to\Upsilon(4S)$

[1] Assumes equal production of B^+ and B^0 at the $\Upsilon(4S)$.

$\Gamma(\eta\mu^+\mu^-)/\Gamma_{total}$ Γ_{470}/Γ

VALUE	CL%	DOCUMENT ID		TECN	COMMENT
$<11.2\times10^{-8}$	90	[1] LEES	13M	BABR	$e^+e^-\to\Upsilon(4S)$

[1] Assumes equal production of B^+ and B^0 at the $\Upsilon(4S)$.

$\Gamma(K^0\ell^+\ell^-)/\Gamma_{total}$ Γ_{472}/Γ

VALUE (units 10^{-7})	CL%	DOCUMENT ID		TECN	COMMENT
$3.1^{+0.8}_{-0.7}$ OUR AVERAGE					
$2.1^{+1.5}_{-1.3}\pm0.2$		[1] AUBERT	09T	BABR	$e^+e^-\to\Upsilon(4S)$
$3.4^{+0.9}_{-0.8}\pm0.2$		[1] WEI	09A	BELL	$e^+e^-\to\Upsilon(4S)$
• • • We do not use the following data for averages, fits, limits, etc. • • •					
$2.9^{+1.6}_{-1.3}\pm0.3$		[1] AUBERT,B	06J	BABR	Repl. by AUBERT 09T
<6.8	90	[1] ISHIKAWA	03	BELL	$e^+e^-\to\Upsilon(4S)$

[1] Assumes equal production of B^0 and B^+ at $\Upsilon(4S)$.

$\Gamma(K^0e^+e^-)/\Gamma_{total}$ Γ_{473}/Γ

Test for $\Delta B=1$ weak neutral current. Allowed by higher-order electroweak interactions.

VALUE (units 10^{-7})	CL%	DOCUMENT ID		TECN	COMMENT
$1.6^{+1.0}_{-0.8}$ OUR AVERAGE					
$0.8^{+1.5}_{-1.2}\pm0.1$		[1] AUBERT	09T	BABR	$e^+e^-\to\Upsilon(4S)$
$2.0^{+1.4}_{-1.0}\pm0.1$		[1] WEI	09A	BELL	$e^+e^-\to\Upsilon(4S)$
• • • We do not use the following data for averages, fits, limits, etc. • • •					
$1.3^{+1.6}_{-1.1}\pm0.2$		[1] AUBERT,B	06J	BABR	Repl. by AUBERT 09T
$-$ $2.1^{+2.3}_{-1.6}\pm0.8$		[1] AUBERT	03U	BABR	$e^+e^-\to\Upsilon(4S)$
$<$ 5.4	90	[2] ISHIKAWA	03	BELL	$e^+e^-\to\Upsilon(4S)$
$<$ 27	90	[1] ABE	02	BELL	Repl. by ISHIKAWA 03
$<$ 38	90	[1] AUBERT	02L	BABR	$e^+e^-\to\Upsilon(4S)$
$<$ 84.5	90	[3] ANDERSON	01B	CLE2	$e^+e^-\to\Upsilon(4S)$
$<$ 3000	90	ALBRECHT	91E	ARG	$e^+e^-\to\Upsilon(4S)$
$<$ 5200	90	[4] AVERY	87	CLEO	$e^+e^-\to\Upsilon(4S)$

[1] Assumes equal production of B^+ and B^0 at the $\Upsilon(4S)$.
[2] Assumes equal production of B^0 and B^+ at $\Upsilon(4S)$.
[3] The result is for di-lepton masses above 0.5 GeV.
[4] AVERY 87 reports $<6.5\times10^{-4}$ assuming the $\Upsilon(4S)$ decays 40% to $B^0\overline{B}^0$. We rescale to 50%.

$\Gamma(K^0\nu\overline{\nu})/\Gamma_{total}$ Γ_{475}/Γ

Test for $\Delta B=1$ weak neutral current. Allowed by higher-order electroweak interaction.

VALUE	CL%	DOCUMENT ID		TECN	COMMENT
$<4.9\times10^{-5}$	90	[1,2] LEES	13I	BABR	$e^+e^-\to\Upsilon(4S)$
• • • We do not use the following data for averages, fits, limits, etc. • • •					
$<19.4\times10^{-5}$	90	[1] LUTZ	13	BELL	$e^+e^-\to\Upsilon(4S)$
$<5.6\times10^{-5}$	90	[1] DEL-AMO-SA...10Q		BABR	Repl. by LEES 13I
$<1.6\times10^{-4}$	90	[1] CHEN	07D	BELL	$e^+e^-\to\Upsilon(4S)$

[1] Assumes equal production of B^+ and B^0 at the $\Upsilon(4S)$.
[2] Also reported a limit $<8.1\times10^{-5}$ at 90% CL obtained using a fully reconstructed hadronic B-tag evnets.

$\Gamma(\rho^0\nu\overline{\nu})/\Gamma_{total}$ Γ_{476}/Γ

Test for $\Delta B=1$ weak neutral current. Allowed by higher-order electroweak interaction.

VALUE	CL%	DOCUMENT ID		TECN	COMMENT
$<2.08\times10^{-4}$	90	[1] LUTZ	13	BELL	$e^+e^-\to\Upsilon(4S)$
• • • We do not use the following data for averages, fits, limits, etc. • • •					
$<4.4\ \times10^{-4}$	90	[1] CHEN	07D	BELL	Repl. by LUTZ 13

[1] Assumes equal production of B^+ and B^0 at the $\Upsilon(4S)$.

$\Gamma(K^0\mu^+\mu^-)/\Gamma_{total}$ Γ_{474}/Γ

Test for $\Delta B=1$ weak neutral current. Allowed by higher-order electroweak interactions.

VALUE (units 10^{-7})	CL%	DOCUMENT ID		TECN	COMMENT
3.4 ±0.5 OUR FIT					
$3.5^{+0.6}_{-0.5}$ OUR AVERAGE					
$3.1^{+0.7}_{-0.6}$		AAIJ	12AH	LHCB	pp at 7 TeV
$4.9^{+2.9}_{-2.5}\pm0.3$		[1] AUBERT	09T	BABR	$e^+e^-\to\Upsilon(4S)$
$4.4^{+1.3}_{-1.1}\pm0.3$		[1] WEI	09A	BELL	$e^+e^-\to\Upsilon(4S)$
• • • We do not use the following data for averages, fits, limits, etc. • • •					
$5.9^{+3.3}_{-2.6}\pm0.7$		[1] AUBERT,B	06J	BABR	Repl. by AUBERT 09T
$1.63^{+0.82}_{-0.63}\pm0.14$		[1] AUBERT	03U	BABR	Repl. by AUBERT,B 06J
$5.6^{+2.9}_{-2.3}\pm0.5$		[2] ISHIKAWA	03	BELL	Repl. by WEI 09A
<33	90	[1] ABE	02	BELL	Repl. by ISHIKAWA 03
<36	90	AUBERT	02L	BABR	$e^+e^-\to\Upsilon(4S)$
<66.4	90	[3] ANDERSON	01B	CLE2	$e^+e^-\to\Upsilon(4S)$
<5200	90	ALBRECHT	91E	ARG	$e^+e^-\to\Upsilon(4S)$
<3600	90	[4] AVERY	87	CLEO	$e^+e^-\to\Upsilon(4S)$

[1] Assumes equal production of B^+ and B^0 at the $\Upsilon(4S)$.
[2] Assumes equal production of B^0 and B^+ at $\Upsilon(4S)$. The second error is a total of systematic uncertainties including model dependence.
[3] The result is for di-lepton masses above 0.5 GeV.
[4] AVERY 87 reports $<4.5\times10^{-4}$ assuming the $\Upsilon(4S)$ decays 40% to $B^0\overline{B}^0$. We rescale to 50%.

$\Gamma(K^0\mu^+\mu^-)/\Gamma(J/\psi(1S)K^0)$ $\Gamma_{474}/\Gamma_{169}$

VALUE (units 10^{-3})	DOCUMENT ID		TECN	COMMENT
0.39±0.06 OUR FIT				
0.37±0.12±0.02	AALTONEN	11AI	CDF	$p\overline{p}$ at 1.96 TeV

$\Gamma(K^*(892)^0\ell^+\ell^-)/\Gamma_{total}$ Γ_{477}/Γ

Test for $\Delta B=1$ weak neutral current. Allowed by higher-order electroweak interactions.

VALUE (units 10^{-7})	DOCUMENT ID		TECN	COMMENT
$9.9^{+1.2}_{-1.1}$ OUR AVERAGE				
$10.3^{+2.2}_{-2.1}\pm0.7$	[1] AUBERT	09T	BABR	$e^+e^-\to\Upsilon(4S)$
$9.7^{+1.3}_{-1.1}\pm0.7$	[1] WEI	09A	BELL	$e^+e^-\to\Upsilon(4S)$
• • • We do not use the following data for averages, fits, limits, etc. • • •				
$8.1^{+2.1}_{-1.9}\pm0.9$	[1] AUBERT,B	06J	BABR	Repl. by AUBERT 09T
$11.7^{+3.0}_{-2.7}\pm0.9$	[1] ISHIKAWA	03	BELL	Repl. by WEI 09A

[1] Assumes equal production of B^0 and B^+ at $\Upsilon(4S)$.

Meson Particle Listings

B^0

$\Gamma(K^*(892)^0 e^+ e^-)/\Gamma_{total}$ Γ_{478}/Γ

Test for ΔB=1 weak neutral current. Allowed by higher-order electroweak interactions.

VALUE (units 10^{-7})	CL%	DOCUMENT ID		TECN	COMMENT
$10.3^{+1.9}_{-1.7}$ OUR AVERAGE					
$8.6^{+2.6}_{-2.4}\pm0.5$		[1] AUBERT	09T	BABR	$e^+e^- \to \Upsilon(4S)$
$11.8^{+2.7}_{-2.2}\pm0.9$		[1] WEI	09A	BELL	$e^+e^- \to \Upsilon(4S)$
• • • We do not use the following data for averages, fits, limits, etc. • • •					
$10.4^{+3.3}_{-2.9}\pm1.1$		[1] AUBERT,B	06J	BABR	Repl. by AUBERT 09T
$11.1^{+5.6}_{-4.7}\pm1.1$		[1] AUBERT	03U	BABR	$e^+e^- \to \Upsilon(4S)$
< 24	90	[2] ISHIKAWA	03	BELL	$e^+e^- \to \Upsilon(4S)$
< 64	90	[1] ABE	02	BELL	Repl. by ISHIKAWA 03
< 67	90	[1] AUBERT	02L	BABR	$e^+e^- \to \Upsilon(4S)$
<2900	90	ALBRECHT	91E	ARG	$e^+e^- \to \Upsilon(4S)$

[1] Assumes equal production of B^+ and B^0 at the $\Upsilon(4S)$.
[2] Assumes equal production of B^0 and B^+ at $\Upsilon(4S)$.

$\Gamma(K^*(892)^0 \mu^+ \mu^-)/\Gamma_{total}$ Γ_{479}/Γ

Test for ΔB=1 weak neutral current. Allowed by higher-order electroweak interactions.

VALUE (units 10^{-7})	CL%	DOCUMENT ID		TECN	COMMENT
10.5 ± 1.0 OUR FIT					
$11.1^{+1.8}_{-1.4}$ OUR AVERAGE					
$13.5^{+4.0}_{-3.7}\pm1.0$		[1] AUBERT	09T	BABR	$e^+e^- \to \Upsilon(4S)$
$10.6^{+1.9}_{-1.4}\pm0.7$		[1] WEI	09A	BELL	$e^+e^- \to \Upsilon(4S)$
• • • We do not use the following data for averages, fits, limits, etc. • • •					
$8.7^{+3.8}_{-3.3}\pm1.2$		[1] AUBERT,B	06J	BABR	Repl. by AUBERT 09T
$8.6^{+7.9}_{-5.8}\pm1.1$		[1] AUBERT	03U	BABR	Repl. by AUBERT,B 06J
$13.3^{+4.2}_{-3.7}\pm1.1$		[2] ISHIKAWA	03	BELL	Repl. by WEI 09A
< 42	90	[1] ABE	02	BELL	$e^+e^- \to \Upsilon(4S)$
< 33	90	AUBERT	02L	BABR	$e^+e^- \to \Upsilon(4S)$
< 40	90	[3] AFFOLDER	99B	CDF	$p\overline{p}$ at 1.8 TeV
< 250	90	[4] ABE	96L	CDF	Repl. by AFFOLDER 99B
< 230	90	[5] ALBAJAR	91C	UA1	$E^{p\overline{p}}_{cm}$= 630 GeV
<3400	90	ALBRECHT	91E	ARG	$e^+e^- \to \Upsilon(4S)$

[1] Assumes equal production of B^+ and B^0 at the $\Upsilon(4S)$.
[2] Assumes equal production of B^0 and B^+ at $\Upsilon(4S)$. The second error is a total of systematic uncertainties including model dependence.
[3] AFFOLDER 99B measured relative to $B^0 \to J/\psi(1S)\,K^*(892)^0$.
[4] ABE 96L measured relative to $B^0 \to J/\psi(1S)\,K^*(892)^0$ using PDG 94 branching ratios.
[5] ALBAJAR 91C assumes 36% of $\overline{b}$ quarks give B^0 mesons.

$\Gamma(K^*(892)^0 \mu^+ \mu^-)/\Gamma(J/\psi(1S)\,K^*(892)^0)$ $\Gamma_{479}/\Gamma_{171}$

VALUE (units 10^{-3})	DOCUMENT ID		TECN	COMMENT
0.79 ± 0.07 OUR FIT				
$0.77\pm0.08\pm0.03$	AALTONEN	11AI	CDF	$p\overline{p}$ at 1.96 TeV
• • • We do not use the following data for averages, fits, limits, etc. • • •				
$0.80\pm0.10\pm0.06$	AALTONEN	11L	CDF	Repl. by AALTONEN 11AI
$0.61\pm0.23\pm0.07$	AALTONEN	09B	CDF	Repl. by AALTONEN 11L

$\Gamma(K^*(892)^0 \nu\overline{\nu})/\Gamma_{total}$ Γ_{480}/Γ

Test for ΔB=1 weak neutral current. Allowed by higher-order electroweak interactions.

VALUE	CL%	DOCUMENT ID		TECN	COMMENT
$< 5.5 \times 10^{-5}$	90	[1] LUTZ	13	BELL	$e^+e^- \to \Upsilon(4S)$
• • • We do not use the following data for averages, fits, limits, etc. • • •					
$<1.2 \times 10^{-4}$	90	[1,2] LEES	13I	BABR	$e^+e^- \to \Upsilon(4S)$
$<1.2 \times 10^{-4}$	90	AUBERT	08BC	BABR	Repl. by LEES 13I
$<3.4 \times 10^{-4}$	90	[1] CHEN	07D	BELL	$e^+e^- \to \Upsilon(4S)$
$<1.0 \times 10^{-3}$	90	[3] ADAM	96D	DLPH	$e^+e^- \to Z$

[1] Assumes equal production of B^+ and B^0 at the $\Upsilon(4S)$.
[2] Also reported a limit $< 9.3 \times 10^{-5}$ at 90% CL obtained using a fully reconstructed hadronic B-tag evnets.
[3] ADAM 96D assumes $f_{B^0} = f_{B^-} = 0.39$ and $f_{B_s} = 0.12$.

$\Gamma(\phi\nu\overline{\nu})/\Gamma_{total}$ Γ_{481}/Γ

Test for $\Delta B = 1$ weak neutral current. Allowed by higher-order electroweak interaction.

VALUE	CL%	DOCUMENT ID		TECN	COMMENT
$< 1.27 \times 10^{-4}$	90	[1] LUTZ	13	BELL	$e^+e^- \to \Upsilon(4S)$
• • • We do not use the following data for averages, fits, limits, etc. • • •					
$<5.8 \times 10^{-5}$	90	[1] CHEN	07D	BELL	Repl. by LUTZ 13

[1] Assumes equal production of B^+ and B^0 at the $\Upsilon(4S)$.

$\Gamma(e^\pm \mu^\mp)/\Gamma_{total}$ Γ_{482}/Γ

Test of lepton family number conservation. Allowed by higher-order electroweak interactions.

VALUE	CL%	DOCUMENT ID		TECN	COMMENT
$< 2.8 \times 10^{-9}$	90	[1] AAIJ	13BM	LHCB	pp at 7 TeV
• • • We do not use the following data for averages, fits, limits, etc. • • •					
$< 6.4 \times 10^{-8}$	90	AALTONEN	09P	CDF	$p\overline{p}$ at 1.96 TeV
$< 9.2 \times 10^{-8}$	90	[2] AUBERT	08P	BABR	$e^+e^- \to \Upsilon(4S)$
$< 1.8 \times 10^{-7}$	90	[2] AUBERT	05W	BABR	$e^+e^- \to \Upsilon(4S)$
$< 1.7 \times 10^{-7}$	90	[2] CHANG	03	BELL	$e^+e^- \to \Upsilon(4S)$
$<15 \times 10^{-7}$	90	[2] BERGFELD	00B	CLE2	$e^+e^- \to \Upsilon(4S)$
$< 3.5 \times 10^{-6}$	90	ABE	98V	CDF	$p\overline{p}$ at 1.8 TeV
$< 1.6 \times 10^{-5}$	90	[3] ACCIARRI	97B	L3	$e^+e^- \to Z$
$< 5.9 \times 10^{-6}$	90	AMMAR	94	CLE2	$e^+e^- \to \Upsilon(4S)$
$< 3.4 \times 10^{-5}$	90	[4] AVERY	89B	CLEO	$e^+e^- \to \Upsilon(4S)$
$< 4.5 \times 10^{-5}$	90	[5] ALBRECHT	87D	ARG	$e^+e^- \to \Upsilon(4S)$
$< 7.7 \times 10^{-5}$	90	[6] AVERY	87	CLEO	$e^+e^- \to \Upsilon(4S)$
$< 3 \times 10^{-4}$	90	GILES	84	CLEO	Repl. by AVERY 87

[1] Uses normalization mode $B(B^0 \to K^+\pi^-) = (19.4 \pm 0.6) \times 10^{-6}$.
[2] Assumes equal production of B^+ and B^0 at the $\Upsilon(4S)$.
[3] ACCIARRI 97B assume PDG 96 production fractions for B^+, B^0, B_s, and Λ_b.
[4] Paper assumes the $\Upsilon(4S)$ decays 43% to $B^0\overline{B}^0$. We rescale to 50%.
[5] ALBRECHT 87D reports $< 5 \times 10^{-5}$ assuming the $\Upsilon(4S)$ decays 45% to $B^0\overline{B}^0$. We rescale to 50%.
[6] AVERY 87 reports $< 9 \times 10^{-5}$ assuming the $\Upsilon(4S)$ decays 40% to $B^0\overline{B}^0$. We rescale to 50%.

$\Gamma(\pi^0 e^\pm \mu^\mp)/\Gamma_{total}$ Γ_{483}/Γ

VALUE	CL%	DOCUMENT ID		TECN	COMMENT
$< 1.4 \times 10^{-7}$	90	[1] AUBERT	07AG	BABR	$e^+e^- \to \Upsilon(4S)$

[1] Assumes equal production of B^+ and B^0 at the $\Upsilon(4S)$.

$\Gamma(K^0 e^\pm \mu^\mp)/\Gamma_{total}$ Γ_{484}/Γ

Test of lepton family number conservation.

VALUE (units 10^{-7})	CL%	DOCUMENT ID		TECN	COMMENT
< 2.7	90	[1] AUBERT,B	06J	BABR	$e^+e^- \to \Upsilon(4S)$
• • • We do not use the following data for averages, fits, limits, etc. • • •					
<40	90	[1] AUBERT	02L	BABR	Repl. by AUBERT,B 06J

[1] Assumes equal production of B^+ and B^0 at the $\Upsilon(4S)$.

$\Gamma(K^*(892)^0 e^+ \mu^-)/\Gamma_{total}$ Γ_{485}/Γ

VALUE (units 10^{-7})	CL%	DOCUMENT ID		TECN	COMMENT
< 5.3	90	[1] AUBERT,B	06J	BABR	$e^+e^- \to \Upsilon(4S)$

[1] Assumes equal production of B^0 and B^+ at $\Upsilon(4S)$.

$\Gamma(K^*(892)^0 e^- \mu^+)/\Gamma_{total}$ Γ_{486}/Γ

VALUE (units 10^{-7})	CL%	DOCUMENT ID		TECN	COMMENT
< 3.4	90	[1] AUBERT,B	06J	BABR	$e^+e^- \to \Upsilon(4S)$

[1] Assumes equal production of B^0 and B^+ at $\Upsilon(4S)$.

$\Gamma(K^*(892)^0 e^\pm \mu^\mp)/\Gamma_{total}$ Γ_{487}/Γ

Test of lepton family number conservation.

VALUE (units 10^{-7})	CL%	DOCUMENT ID		TECN	COMMENT
< 5.8	90	[1] AUBERT,B	06J	BABR	$e^+e^- \to \Upsilon(4S)$
• • • We do not use the following data for averages, fits, limits, etc. • • •					
<34	90	[1] AUBERT	02L	BABR	Repl. by AUBERT,B 06J

[1] Assumes equal production of B^+ and B^0 at the $\Upsilon(4S)$.

$\Gamma(e^\pm \tau^\mp)/\Gamma_{total}$ Γ_{488}/Γ

Test of lepton family number conservation. Allowed by higher-order electroweak interactions.

VALUE	CL%	DOCUMENT ID		TECN	COMMENT
$< 2.8 \times 10^{-5}$	90	[1] AUBERT	08AD	BABR	$e^+e^- \to \Upsilon(4S)$
• • • We do not use the following data for averages, fits, limits, etc. • • •					
$<1.1 \times 10^{-4}$	90	BORNHEIM	04	CLE2	$e^+e^- \to \Upsilon(4S)$
$<5.3 \times 10^{-4}$	90	AMMAR	94	CLE2	Repl. by BORNHEIM 04

[1] Assumes equal production of B^+ and B^0 at the $\Upsilon(4S)$.

$\Gamma(\mu^\pm \tau^\mp)/\Gamma_{total}$ Γ_{489}/Γ

Test of lepton family number conservation. Allowed by higher-order electroweak interactions.

VALUE	CL%	DOCUMENT ID		TECN	COMMENT
$< 2.2 \times 10^{-5}$	90	[1] AUBERT	08AD	BABR	$e^+e^- \to \Upsilon(4S)$
• • • We do not use the following data for averages, fits, limits, etc. • • •					
$<3.8 \times 10^{-5}$	90	BORNHEIM	04	CLE2	$e^+e^- \to \Upsilon(4S)$
$<8.3 \times 10^{-4}$	90	AMMAR	94	CLE2	Repl. by BORNHEIM 04

[1] Assumes equal production of B^+ and B^0 at the $\Upsilon(4S)$.

Γ(invisible)/Γ_{total} Γ_{490}/Γ

VALUE (units 10^{-5})	CL%	DOCUMENT ID		TECN	COMMENT
< 2.4	90	[1] LEES	12T	BABR	$e^+e^- \to \Upsilon(4S)$
• • • We do not use the following data for averages, fits, limits, etc. • • •					
<13	90	[2] HSU	12	BELL	$e^+e^- \to \Upsilon(4S)$
<22	90	[1] AUBERT,B	04J	BABR	$e^+e^- \to \Upsilon(4S)$

[1] Uses the fully reconstructed $B^0 \to D^{(*)-}\ell^+\nu_\ell$ events as a tag.
[2] Identified by fully reconstructing a hadronic decay of the accompanying B meson and requiring no other particles in the event.

$\Gamma(\nu\overline{\nu}\gamma)/\Gamma_{total}$ Γ_{491}/Γ

VALUE (units 10^{-5})	CL%	DOCUMENT ID		TECN	COMMENT
<1.7	90	[1] LEES	12T	BABR	$e^+e^- \to \Upsilon(4S)$
• • • We do not use the following data for averages, fits, limits, etc. • • •					
<4.7	90	[1] AUBERT,B	04J	BABR	Repl. by LEES 12T

[1] Uses the fully reconstructed $B^0 \to D^{(*)-}\ell^+\nu_\ell$ events as a tag.

$\Gamma(\Lambda_c^+\mu^-)/\Gamma_{total}$ Γ_{492}/Γ

VALUE	CL%	DOCUMENT ID		TECN	COMMENT
$<1.8\times10^{-6}$	90	[1,2] DEL-AMO-SA...11K		BABR	$e^+e^- \to \Upsilon(4S)$

[1] DEL-AMO-SANCHEZ 11K reports $< 180\times10^{-8}$ from a measurement of $[\Gamma(B^0 \to \Lambda_c^+\mu^-)/\Gamma_{total}] \times [B(\Lambda_c^+ \to pK^-\pi^+)]$ assuming $B(\Lambda_c^+ \to pK^-\pi^+) = (5.0 \pm 1.3)\times10^{-2}$.
[2] Uses $B(\Upsilon(4S) \to B^0\overline{B}^0) = (51.6\pm0.6)\%$ and $B(\Upsilon(4S) \to B^+B^-) = (48.4\pm0.6)\%$.

$\Gamma(\Lambda_c^+ e^-)/\Gamma_{total}$ Γ_{493}/Γ

VALUE	CL%	DOCUMENT ID		TECN	COMMENT
$<5\times10^{-6}$	90	[1,2] DEL-AMO-SA...11K		BABR	$e^+e^- \to \Upsilon(4S)$

[1] DEL-AMO-SANCHEZ 11K reports $< 520\times10^{-8}$ from a measurement of $[\Gamma(B^0 \to \Lambda_c^+ e^-)/\Gamma_{total}] \times [B(\Lambda_c^+ \to pK^-\pi^+)]$ assuming $B(\Lambda_c^+ \to pK^-\pi^+) = (5.0 \pm 1.3)\times10^{-2}$.
[2] Uses $B(\Upsilon(4S) \to B^0\overline{B}^0) = (51.6\pm0.6)\%$ and $B(\Upsilon(4S) \to B^+B^-) = (48.4\pm0.6)\%$.

POLARIZATION IN B DECAYS

Revised December 2013 by A. V. Gritsan (Johns Hopkins University) and J. G. Smith (University of Colorado at Boulder).

We review the notation used in polarization measurements in particle production and decay, with a particular emphasis on the B decays and the CP-violating observables in polarization measurements. We look at several examples of vector-vector and vector-tensor B meson decays, while more details about the theory and experimental results in B decays can be found in a separate mini-review [1] in this *Review*.

Figure 1 illustrates angular observables in an example of the sequential process $ab \to X \to P_1P_2 \to (p_{11}p_{12})(p_{21}p_{22})$ [2]. The angular distributions are of particular interest because they are sensitive to spin correlations and reveal properties of particles and their interactions, such as quantum numbers and couplings. In the case of a spin-zero particle X, such as B meson or a Higgs boson, there are no spin correlations in the production mechanism and the decay chain is to be analyzed. The angular distribution of decay products can be expressed as a function of three helicity angles which describe the alignment of the particles in the decay chain. The analyzer of the B-daughter polarization is normally chosen for two-body decays, as the direction of the daughters in the center-of-mass of the parent (*e.g.*, $\rho \to 2\pi$) [3], and for three-body decays as the normal to the decay plane (*e.g.*, $\omega \to 3\pi$) [4]. An equivalent set of transversity angles is sometimes used in polarization analyses [5]. The differential decay width depends on complex amplitudes $A_{\lambda_1\lambda_2}$, corresponding to the X-daughter helicity states λ_i.

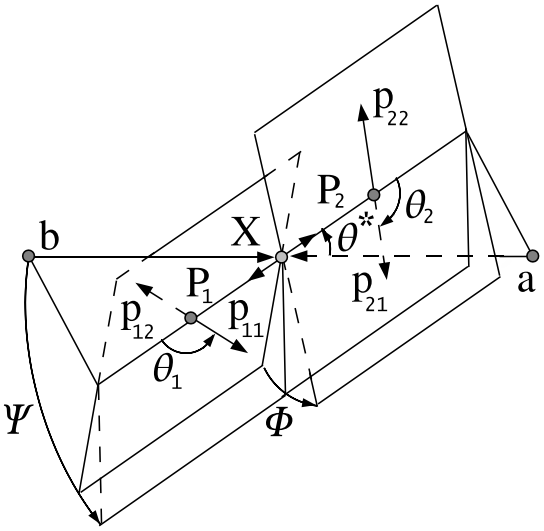

Figure 1: Definition of the production and helicity angles in the sequential process $ab \to X \to P_1P_2 \to (p_{11}p_{12})(p_{21}p_{22})$. The three helicity angles include θ_1 and θ_2, defined in the rest frame of the two daughters P_1 and P_2, and Φ, defined in the X frame as the angle between the two decay planes. The two production angles θ^* and Ψ are defined in the X frame, where Ψ is the angle between the production plane and the average of the two decay planes.

In the case of a spin-zero B-meson decay, its daughter helicities are constrained to $\lambda_1 = \lambda_2 = \lambda$. Therefore we simplify amplitude notation as A_λ. Moreover, most B-decay polarization analyses are limited to the case when the spin of one of the B-meson daughters is 1. In that case, there are only three independent amplitudes corresponding to $\lambda = 0$ or ±1 [6], where the last two can be expressed in terms of parity-even and parity-odd amplitudes $A_{\parallel,\perp} = (A_{+1} \pm A_{-1})/\sqrt{2}$. The overall decay amplitude involves three complex terms proportional to the above amplitudes and the Wigner d functions of helicity angles. The exact angular dependence would depend on the quantum numbers of the B-meson daughters and of their decay products, and can be found in the literature [6,7]. The differential decay rate would involve six real quantities α_i, including interference terms,

$$\frac{d\Gamma}{\Gamma\, d\cos\theta_1\, d\cos\theta_2\, d\Phi} = \sum_i \alpha_i \;\; f_i(\cos\theta_1,\, \cos\theta_2,\, \Phi)\,, \qquad (1)$$

where each $f_i(\cos\theta_1, \cos\theta_2, \Phi)$ has unique angular dependence specific to particle quantum numbers, and the α_i parameters are defined as:

$$\alpha_1 = \frac{|A_0|^2}{\Sigma|A_\lambda|^2} = f_L\,, \qquad (2)$$

$$\alpha_2 = \frac{|A_\parallel|^2 + |A_\perp|^2}{\Sigma|A_\lambda|^2} = (1 - f_L)\,, \qquad (3)$$

$$\alpha_3 = \frac{|A_\parallel|^2 - |A_\perp|^2}{\Sigma|A_\lambda|^2} = (1 - f_L - 2\,f_\perp)\,, \qquad (4)$$

$$\alpha_4 = \frac{\Im m(A_\perp A_\parallel^*)}{\Sigma|A_\lambda|^2} = \sqrt{f_\perp(1-f_L-f_\perp)}\,\sin(\phi_\perp-\phi_\parallel)\,, \quad (5)$$

$$\alpha_5 = \frac{\Re e(A_\parallel A_0^*)}{\Sigma|A_\lambda|^2} = \sqrt{f_L\,(1-f_L-f_\perp)}\,\cos(\phi_\parallel)\,, \quad (6)$$

$$\alpha_6 = \frac{\Im m(A_\perp A_0^*)}{\Sigma|A_\lambda|^2} = \sqrt{f_\perp\,f_L}\,\sin(\phi_\perp)\,, \quad (7)$$

where the amplitudes have been expressed with the help of polarization parameters f_L, $f_\perp$, $\phi_\parallel$, and $\phi_\perp$ defined in Table 1. Note that the terms proportional to $\Re e(A_\perp A_\parallel^*)$, $\Im m(A_\parallel A_0^*)$, and $\Re e(A_\perp A_0^*)$ are absent in Eqs. (2-7). However, these terms may appear for some three-body decays of a B-meson daughter, see Ref. 7.

Table 1: Rate, polarization, and *CP*-asymmetry parameters defined for the B-meson decays to mesons with non-zero spin. Numerical examples are shown for the 2013 HFAG average of the $B^0 \to \varphi K^*(892)^0$ decay obtained from BABAR [8] and Belle [9] measurements. The first six parameters are defined under the assumption of no *CP* violation in decay, while they are averaged between the $\overline{B}$ and B parameters in general. The last six parameters involve differences between the $\overline{B}$ and B meson decay parameters. The phase convention δ_0 is chosen with respect to a single A_{00} amplitude from a reference B decay mode, which is $B^0 \to \varphi K_0^*(1430)^0$ for numerical results.

parameter	definition	average
$\mathcal{B}$	$\Gamma/\Gamma_{\rm total}$	$(9.8 \pm 0.6) \times 10^{-6}$
f_L	$\lvert A_0\rvert^2/\Sigma\lvert A_\lambda\rvert^2$	0.497 ± 0.025
$f_\perp$	$\lvert A_\perp\rvert^2/\Sigma\lvert A_\lambda\rvert^2$	0.228 ± 0.021
$\phi_\parallel - \pi$	$\arg(A_\parallel/A_0) - \pi$	-0.86 ± 0.09
$\phi_\perp - \pi$	$\arg(A_\perp/A_0) - \pi$	-0.78 ± 0.09
$\delta_0 - \pi$	$\arg(A_{00}/A_0) - \pi$	-0.26 ± 0.10
A_{CP}	$(\bar\Gamma - \Gamma)/(\bar\Gamma + \Gamma)$	0.00 ± 0.04
A_{CP}^0	$(\bar f_L - f_L)/(\bar f_L + f_L)$	-0.01 ± 0.05
$A_{CP}^\perp$	$(\bar f_\perp - f_\perp)/(\bar f_\perp + f_\perp)$	-0.11 ± 0.09
$\Delta\phi_\parallel$	$(\bar\phi_\parallel - \phi_\parallel)/2$	$+0.06 \pm 0.08$
$\Delta\phi_\perp$	$(\bar\phi_\perp - \phi_\perp - \pi)/2$	$+0.10 \pm 0.09$
$\Delta\delta_0$	$(\bar\delta_0 - \delta_0)/2$	$+0.13 \pm 0.08$

Overall, six real parameters describe three complex amplitudes A_0, $A_\parallel$, and $A_\perp$. These could be chosen to be the four polarization parameters f_L, $f_\perp$, $\phi_\parallel$, and $\phi_\perp$, one overall size normalization, such as decay rate Γ, or branching fraction $\mathcal{B}$, and one overall phase δ_0. The phase convention is arbitrary for an isolated B decay mode. However, for several B decays, the relative phase could produce meaningful and observable effects through interference with other B decays with the same final states, such as for $B \to VK_J^*$ with $J = 0, 1, 2, 3, 4, ...$ The phase could be referenced to the single $B \to VK_0^*$ amplitude A_{00} in such a case, as shown in Table 1. Here V stands for any spin-one vector meson.

Moreover, *CP* violation can be tested in the angular distribution of the decay as the difference between the B and $\overline{B}$. Each of the six real parameters describing the three complex amplitudes would have a counterpart *CP*-asymmetry term, corresponding to three direct-*CP* asymmetries in three amplitudes, and three *CP*-violating phase differences, equivalent to the phase measurements from the mixing-induced *CP* asymmetries in the time evolution of B-decays [1]. In Table 1 and Ref. 10, these are chosen to be the direct-*CP* asymmetries in the overall decay rate $\mathcal{A}_{CP}$, in the f_L fraction $\mathcal{A}_{CP}^0$, and in the $f_\perp$ fraction $\mathcal{A}_{CP}^\perp$, and three weak phase differences:

$$\Delta\phi_\parallel = \frac{1}{2}\arg(\bar A_\parallel A_0/A_\parallel \bar A_0)\,, \quad (8)$$

$$\Delta\phi_\perp = \frac{1}{2}\arg(\bar A_\perp A_0/A_\perp \bar A_0) - \frac{\pi}{2}\,, \quad (9)$$

$$\Delta\delta_0 = \frac{1}{2}\arg(\bar A_{00} A_0/A_{00} \bar A_0)\,. \quad (10)$$

The $\frac{\pi}{2}$ term in Eq. (9) reflects the fact that $A_\perp$ and $\bar A_\perp$ differ in phase by π if *CP* is conserved. The two parameters $\Delta\phi_\parallel$ and $\Delta\phi_\perp$ are equivalent to triple-product asymmetries constructed from the vectors describing the decay angular distribution [11]. The *CP*-violating phase difference in the reference decay mode [10] is, in the Wolfenstein CKM quark-mixing phase convention,

$$\Delta\phi_{00} = \frac{1}{2}\arg(A_{00}/\bar A_{00})\,. \quad (11)$$

This can be measured only together with the mixing-induced phase difference for some of the neutral B-meson decays similar to other mixing-induced *CP* asymmetry measurements [1].

It may not always be possible to have a phase-reference decay mode which would define δ_0 and $\Delta\delta_0$ parameters. In that case, it may be possible to define the phase difference directly similarly to Eq. (11):

$$\Delta\phi_0 = \frac{1}{2}\arg(A_0/\bar A_0)\,. \quad (12)$$

One can measure the angles of the CKM unitarity triangle, assuming Standard Model contributions to the $\Delta\phi_0$ and B-mixing phases. Examples include measurements of $\beta = \phi_1$ with $B \to J/\psi K^*$ and $\alpha = \phi_2$ with $B \to \rho\rho$.

Most of the B decays that arise from tree-level $b \to c$ transitions have the amplitude hierarchy $|A_0| > |A_+| > |A_-|$ which is expected from analyses based on quark-helicity conservation [12]. The larger the mass of the vector-meson daughters, the weaker the inequality. The B meson decays to heavy vector particles with charm, such as $B \to J/\psi K^*$, $\psi(2S)K^*$, $\chi_{c1}K^*$, $D^*\rho$, D^*K^*, D^*D^*, and $D^*D_s^*$, show a substantial fraction of the amplitudes corresponding to transverse polarization of the vector mesons ($A_{\pm 1}$), in agreement with the factorization prediction. The detailed amplitude analysis of the $B \to J/\psi K^*$ decays has been performed by the BABAR [13], Belle [14], CDF [15], CLEO [16], and D0 [17] collaborations. Most analyses are performed under the assumption of the absence of

direct *CP* violation. The parameter values are given in the particle listing of this *Review*. The difference between the strong phases $\phi_\parallel$ and $\phi_\perp$ deviates significantly from zero. The recent measurements [13,14] of *CP*-violating terms similar to those in $B \to \varphi K^*$ [10] shown in Table 1 are consistent with zero.

In addition, the mixing-induced *CP*-violating asymmetry is measured in the $B^0 \to J/\psi K^{*0}$ decay [1,13,14] where angular analysis allows one to separate *CP*-eigenstate amplitudes. This allows one to resolve the sign ambiguity of the $\cos 2\beta$ ($\cos 2\phi_1$) term that appears in the time-dependent angular distribution due to interference of parity-even and parity-odd terms. This analysis relies on the knowledge of discrete ambiguities in the strong phases $\phi_\parallel$ and $\phi_\perp$, as discussed below. The BABAR experiment used a method based on the dependence on the $K\pi$ invariant mass of the interference between the *S*- and *P*-waves to resolve the discrete ambiguity in the determination of the strong phases $(\phi_\parallel, \phi_\perp)$ in $B \to J/\psi K^*$ decays [13]. The result is in agreement with the amplitude hierarchy expectation [12]. The CDF [18], D0 [19], and LHCb [20] experiments have studied the $B_s^0 \to J/\psi\varphi$ decay and provided the lifetime, polarization, and phase measurements.

The amplitude hierarchy $|A_0| \gg |A_+| \gg |A_-|$ was expected in B decays to light vector particles in both penguin transitions [21,22] and tree-level transitions [12]. There is confirmation by the BABAR and Belle experiments of predominantly longitudinal polarization in the tree-level $b \to u$ transition, such as $B^0 \to \rho^+\rho^-$ [23], $B^+ \to \rho^0\rho^+$ [24], and $B^+ \to \omega\rho^+$ [25]; this is consistent with the analysis of the quark helicity conservation [12]. Because the longitudinal amplitude dominates the decay, a detailed amplitude analysis is not possible with current B samples, and limits on the transverse amplitude fraction are obtained. The fraction of transverse polarization is large in decays to heavier mesons such as $B^0 \to a_1(1260)^+ a_1(1260)^-$ [26]. Only limits have been set for $B^0 \to \omega\rho^0, \omega\omega$ [25]; there is some evidence for $B^0 \to \rho^0\rho^0$ [27] decays. The small values for these branching fractions indicates that $b \to d$ penguin pollution is small in the charmless, strangeless vector-vector B decays.

The interest in the polarization and *CP*-asymmetry measurements in penguin transition, such as $b \to s$ decays $B \to \varphi K^*$, ρK^*, ωK^*, or $B_s^0 \to \varphi\varphi$, and $b \to d$ decay $B \to K^*\bar{K}^*$, is motivated by their potential sensitivity to physics beyond the Standard Model. The decay amplitudes for $B \to \varphi K^*$ have been measured by the BABAR and Belle experiments [10,9,28,29]. The fractions of longitudinal polarization are $f_L = 0.50 \pm 0.05$ for the $B^+ \to \varphi K^{*+}$ decay and $f_L = 0.497 \pm 0.025$ for the $B^0 \to \varphi K^{*0}$ decay. These indicate significant departure from the naive expectation of predominant longitudinal polarization, suggesting other contributions to the decay amplitude, previously neglected, either within the Standard Model, such as penguin annihilation [30] or QCD rescattering [31], or from physics beyond the Standard Model [32]. The complete set of twelve amplitude parameters measured in the $B^0 \to \varphi K^{*0}$ decay is given in Table 1. Several other parameters could be constructed from the above twelve parameters, as suggested in Ref. 33.

The discrete ambiguity in the phase $(\phi_\parallel, \phi_\perp, \Delta\phi_\parallel, \Delta\phi_\perp)$ measurements has been resolved by BABAR in favor of $|A_+| \gg |A_-|$ through interference between the *S*- and *P*-waves of $K\pi$. The search for vector-tensor and vector-axialvector $B \to \varphi K_J^{(*)}$ decays with $J = 1, 2, 3, 4$ revealed a large fraction of longitudinal polarization in the decay $B \to \varphi K_2^*(1430)$ with $f_L = 0.90^{+0.06}_{-0.07}$ [10,34], but large contribution of transverse amplitude in $B \to \varphi K_1(1270)$ with $f_L = 0.46^{+0.13}_{-0.15}$ [35].

Like $B \to \varphi K^*$, the decays $B \to \rho K^*$ and $B \to \omega K^*$ may be sensitive to New Physics. Measurements of the longitudinal polarization fraction in $B^+ \to \rho^0 K^{*0}$, $B^+ \to \rho^+ K^{*0}$ [36] and in both vector-vector and vector-tensor final states of $B \to \omega K_J^*$ [25] reveal a large fraction of transverse polarization, indicating an anomaly similar to $B \to \varphi K^*$ except for a different pattern in vector-tensor final states. A large transverse polarization is also observed in the $B_s^0 \to \varphi\varphi$ decay by CDF [37] and LHCb [38], $B_s^0 \to K^{*0}\bar{K}^{*0}$ decays by LHCb [39], and $B_s^0 \to \varphi K^{*0}$ decays by LHCb [40]. At the same time, first measurement of the polarization in the $b \to d$ penguin decays $B \to K^*\bar{K}^*$ indicates a large fraction of longitudinal polarization [41]. The polarization pattern in penguin-dominated B-meson decays is not fully understood [30,31,32].

The three-body semileptonic B-meson decays, such as $B \to V\ell_1\ell_2$, share many features with the two-body $B \to VV$ decays. Their differential decay width can be parameterized with the two helicity angles defined in the V and $(\ell_1\ell_2)$ frames and with the azimuthal angle, as defined in Fig. 1. However, since the $(\ell_1\ell_2)$ pair does not come from an on-shell particle, the angular distribution is unique to each point in the dilepton mass $m_{\ell\ell}$ spectrum. The polarization measurements as a function of $m_{\ell\ell}$ provide complementary information on physics beyond the Standard Model, as discussed for $B \to K^*\ell^+\ell^-$ decay in Ref. 42. The current data in this mode has been analyzed by the BABAR, Belle, and CDF, LHCb, and CMS experiments [43].

The examples of the angular distributions and observables in $B \to K^*\ell^+\ell^-$ are discussed in Ref. 42. Typically two angular observables have been measured in this decay in certain ranges of the dilepton mass $m_{\ell\ell}$ [43]. One parameter is the fraction of longitudinal polarization F_L, which is determined by the K^* angular distribution and is similar to f_L defined for exclusive two-body decays. The other parameter is the forward-backward asymmetry of the lepton pair A_{FB}, which is the asymmetry of the decay rate with positive and negative values of $\cos\theta_1$.

In summary, there has been considerable recent interest in the polarization measurements of B-meson decays because they reveal both weak- and strong-interaction dynamics [30–32,44]. New measurements will further elucidate the pattern of spin alignment measurements in rare B decays, and further test the Standard Model and strong interaction dynamics, including the non-factorizable contributions to the B-decay amplitudes.

References

1. Y. Kwon, G. Punzi, and J. G. Smith, "Production and Decay of b-Flavored Hadrons," mini-review in this *Review*.
2. For a recent example and further references see Y. Y. Gao *et al.*, Phys. Rev. **D81**, 075022 (2010).
3. M. Jacob and G. C. Wick, Ann. Phys. **7**, 404 (1959).
4. S. M. Berman and M. Jacob, Phys. Rev. **139**, 1023 (1965).
5. I. Dunietz *et al.*, Phys. Rev. **D43**, 2193 (1991).
6. G. Kramer and W. F. Palmer, Phys. Rev. **D45**, 193 (1992).
7. A. Datta *et al.*, Phys. Rev. **D77**, 114025 (2008).
8. BABAR Collab., B. Aubert *et al.*, Phys. Rev. **D78**, 092008 (2008).
9. Belle Collab., M. Prim *et al.*, Phys. Rev. **D88**, 072004 (2013).
10. BABAR Collab., B. Aubert *et al.*, Phys. Rev. Lett. **93**, 231804 (2004); Phys. Rev. Lett. **98**, 051801 (2007); Phys. Rev. **D78**, 092008 (2008).
11. G. Valencia, Phys. Rev. **D39**, 3339 (1998); A. Datta and D. London, Int. J. Mod. Phys. **A19**, 2505 (2004).
12. A. Ali *et al.*, Z. Physik **C1**, 269 (1979); M. Suzuki, Phys. Rev. **D64**, 117503 (2001).
13. BABAR Collab., B. Aubert *et al.*, Phys. Rev. **D71**, 032005 (2005); Phys. Rev. **D76**, 031102 (2007).
14. Belle Collab., R. Itoh *et al.*, Phys. Rev. Lett. **95**, 091601 (2005) Phys. Rev. **D88**, 072004 (2013).
15. CDF Collab., T. Affolder *et al.*, Phys. Rev. Lett. **85**, 4668 (2000); CDF Collab., D. Acosta *et al.*, Phys. Rev. Lett. **94**, 101803 (2005).
16. CLEO Collab., C. P. Jessop, Phys. Rev. Lett. **79**, 4533 (1997).
17. D0 Collab., V. M. Abazov *et al.*, Phys. Rev. Lett. **102**, 032001 (2009).
18. CDF Collab., T. Aaltonen *et al.*, Phys. Rev. Lett. **100**, 121803 (2008); Phys. Rev. **D85**, 072002 (2012).
19. D0 Collab., V. M. Abazov *et al.*, Phys. Rev. Lett. **98**, 121801 (2007); Phys. Rev. **D85**, 032006 (2012)..
20. LHCb Collab., R. Aaij *et al.*, Phys. Rev. Lett. **108**, 101803 (2012).
21. H. Y. Cheng and K. C. Yang, Phys. Lett. **B511**, 40 (2001); C. H. Chen, Y. Y. Keum, and H. n. Li, Phys. Rev. **D66**, 054013 (2002).
22. A. L. Kagan, Phys. Lett. **B601**, 151 (2004); Y. Grossman, Int. J. Mod. Phys. **A19**, 907 (2004).
23. Belle Collab., A. Somov *et al.*, Phys. Rev. Lett. **96**, 171801 (2006); BABAR Collab., B. Aubert *et al.*, Phys. Rev. **D76**, 052007 (2007).
24. Belle Collab., J. Zhang *et al.*, Phys. Rev. Lett. **91**, 221801 (2003); BABAR Collab., B. Aubert *et al.*, Phys. Rev. Lett. **102**, 141802 (2009).
25. BABAR Collab., B. Aubert *et al.*, Phys. Rev. **D74**, 051102 (2006); Phys. Rev. **D79**, 052005 (2009).
26. BABAR Collab., B. Aubert *et al.*, Phys. Rev. **D80**, 092007 (2009).
27. BABAR Collab., B. Aubert *et al.*, Phys. Rev. **D78**, 071104 (2008).
28. Belle Collab., K. F. Chen *et al.*, Phys. Rev. Lett. **94**, 221804 (2005).
29. BABAR Collab., B. Aubert *et al.*, Phys. Rev. Lett. **99**, 201802 (2007).
30. A. L. Kagan, Phys. Lett. **B601**, 151 (2004); H. n. Li and S. Mishima, Phys. Rev. **D71**, 054025 (2005); C.-H. Chen *et al.*, Phys. Rev. **D72**, 054011 (2005); M. Beneke *et al.*, Phys. Rev. Lett. **96**, 141801 (2006); C.-H. Chen and C.-Q. Geng, Phys. Rev. **D75**, 054010 (2007); A. Datta *et al.*, Phys. Rev. **D76**, 034015 (2007); M. Beneke, J. Rohrer, and D. Yang, Nucl. Phys. **B774**, 64 (2007); H.-Y. Cheng and K.-C. Yang, Phys. Rev. **D78**, 094001 (2008).
31. C. W. Bauer *et al.*, Phys. Rev. **D70**, 054015 (2004); P. Colangelo *et al.*, Phys. Lett. **B597**, 291 (2004); M. Ladisa *et al.*, Phys. Rev. **D70**, 114025 (2004); H. Y. Cheng *et al.*, Phys. Rev. **D71**, 014030 (2005); H. Y. Cheng and K. C. Yang, Phys. Rev. **D83**, 034001 (2011).
32. Y. Grossman, Int. J. Mod. Phys. A **19**, 907 (2004); E. Alvarez *et al.*, Phys. Rev. **D70**, 115014 (2004); P. K. Das and K. C. Yang, Phys. Rev. **D71**, 094002 (2005); C. H. Chen and C. Q. Geng, Phys. Rev. **D71**, 115004 (2005); Y. D. Yang *et al.*, Phys. Rev. **D72**, 015009 (2005); K. C. Yang, Phys. Rev. **72**, 034009 (2005); S. Baek,Phys. Rev. **D72**, 094008 (2005); C. S. Huang *et al.*, Phys. Rev. **D73**, 034026 (2006); C. H. Chen and H. Hatanaka, Phys. Rev. **D73**, 075003 (2006); A. Faessler *et al.*, Phys. Rev. **D75**, 074029 (2007).
33. D. London, N. Sinha, and R. Sinha, Phys. Rev. **D69**, 114013 (2004).
34. BABAR Collab., B. Aubert *et al.*, Phys. Rev. **D76**, 051103 (2007).
35. BABAR Collab., B. Aubert *et al.*, Phys. Rev. Lett. **101**, 161801 (2008).
36. Belle Collab., J. Zhang *et al.*, Phys. Rev. Lett. **95**, 141801 (2005); BABAR Collab., B. Aubert *et al.*, Phys. Rev. Lett. **97**, 201801 (2006); Phys. Rev. **D83**, 051101 (2011); Phys. Rev. **D85**, 072005 (2012).
37. CDF Collab., T. Aaltonen *et al.*, Phys. Rev. Lett. **107**, 261802 (2011).
38. LHCb Collab., R. Aaij *et al.*, Phys. Lett. B **713**, 369 (2012).
39. LHCb Collab., R. Aaij *et al.*, Phys. Lett. B **709**, 50 (2012).
40. LHCb Collab., R. Aaij *et al.*, JHEP **1311**, 092 (2013).
41. BABAR Collab., B. Aubert *et al.*, Phys. Rev. Lett. **100**, 081801 (2008), Phys. Rev. **D79**, 051102 (2009).
42. G. Burdman, Phys. Rev. **D52**, 6400 (1995); F. Kruger and J. Matias, Phys. Rev. **D71**, 094009 (2005); E. Lunghi and J. Matias, JHEP **0704**, 058 (2007); J. Matias *et al.*, JHEP **1204**, 104 (2012).
43. Belle Collab., J.-T. Wei *et al.*, Phys. Rev. Lett. **103**, 171801 (2009); BABAR Collab., B. Aubert *et al.*, Phys. Rev. **D79**, 031102 (2009); CDF Collab., T. Aaltonen *et al.*, Phys. Rev. Lett. **108**, 081807 (2012); LHCb Collab., R. Aaij *et al.*, JHEP **1308**, 131 (2013); CMS Collab., S. Chatrchyan *et al.*, Phys. Lett. **B727**, 77 (2013).
44. C. H. Chen and H. n. Li, Phys. Rev. **D71**, 114008 (2005).

See key on page 547

POLARIZATION IN B^0 DECAY

In decays involving two vector mesons, one can distinguish among the states in which meson polarizations are both longitudinal (L) or both are transverse and parallel ($\|$) or perpendicular ($\perp$) to each other with the parameters Γ_L/Γ, $\Gamma_\perp/\Gamma$, and the relative phases $\phi_\|$ and $\phi_\perp$. See the definitions in the note on "Polarization in B Decays" review in the B^0 Particle Listings.

Γ_L/Γ in $B^0 \to J/\psi(1S)K^*(892)^0$

VALUE	EVTS	DOCUMENT ID		TECN	COMMENT
0.571±0.007 OUR AVERAGE					
0.572±0.006±0.014		[1] AAIJ	13AT	LHCB	pp at 7 TeV
0.587±0.011±0.013		[2] ABAZOV	09E	D0	$p\overline{p}$ at 1.96 TeV
0.556±0.009±0.010		[3] AUBERT	07AD	BABR	$e^+e^- \to \Upsilon(4S)$
0.562±0.026±0.018		ACOSTA	05	CDF	$p\overline{p}$ at 1.96 TeV
0.574±0.012±0.009		ITOH	05	BELL	$e^+e^- \to \Upsilon(4S)$
0.59 ±0.06 ±0.01		[4] AFFOLDER	00N	CDF	$p\overline{p}$ at 1.8 TeV
0.52 ±0.07 ±0.04		[5] JESSOP	97	CLE2	$e^+e^- \to \Upsilon(4S)$
0.65 ±0.10 ±0.04	65	ABE	95Z	CDF	$p\overline{p}$ at 1.8 TeV
0.97 ±0.16 ±0.15	13	[6] ALBRECHT	94G	ARG	$e^+e^- \to \Upsilon(4S)$
• • • We do not use the following data for averages, fits, limits, etc. • • •					
0.566±0.012±0.005		[3] AUBERT	05P	BABR	Repl. by AUBERT 07AD
0.62 ±0.02 ±0.03		[7] ABE	02N	BELL	Repl. by ITOH 05
0.597±0.028±0.024		[8] AUBERT	01H	BABR	Repl. by AUBERT 07AD
0.80 ±0.08 ±0.05	42	[6] ALAM	94	CLE2	Sup. by JESSOP 97

[1] AAIJ 13AT obtains $\Gamma_\|/\Gamma = 0.227 \pm 0.004 \pm 0.011$. The relation $1 = (\Gamma_L + \Gamma_\perp + \Gamma_\|)/\Gamma$ is used to obtain Γ_L/Γ.

[2] Measured the angular and lifetime parameters for the time-dependent angular untagged decays $B^0_d \to J/\psi K^{*0}$ and $B^0_s \to J/\psi\phi$.

[3] Obtained by combining the B^0 and B^+ modes.

[4] AFFOLDER 00N measurements are based on 190 B^0 candidates obtained from a data sample of 89 pb^{-1}. The P-wave fraction is found to be $0.13^{+0.12}_{-0.09} \pm 0.06$.

[5] JESSOP 97 is the average over a mixture of B^0 and B^+ decays. The P-wave fraction is found to be $0.16 \pm 0.08 \pm 0.04$.

[6] Averaged over an admixture of B^0 and B^+ decays.

[7] Averaged over an admixture of B^0 and B^+ decays and the P wave fraction is $(19 \pm 2 \pm 3)\%$.

[8] Averaged over an admixture of B^0 and B^- decays and the P wave fraction is $(16.0 \pm 3.2 \pm 1.4) \times 10^{-2}$.

$\Gamma_\perp/\Gamma$ in $B^0 \to J/\psi K^{*0}$

VALUE	DOCUMENT ID		TECN	COMMENT
0.211±0.008 OUR AVERAGE	Error includes scale factor of 1.3.			See the ideogram below.
0.201±0.004±0.008	AAIJ	13AT	LHCB	pp at 7 TeV
0.230±0.013±0.025	[1] ABAZOV	09E	D0	$p\overline{p}$ at 1.96 TeV
0.233±0.010±0.005	[2] AUBERT	07AD	BABR	$e^+e^- \to \Upsilon(4S)$
0.215±0.032±0.006	ACOSTA	05	CDF	$p\overline{p}$ at 1.96 TeV
0.195±0.012±0.008	ITOH	05	BELL	$e^+e^- \to \Upsilon(4S)$

[1] Measured the angular and lifetime parameters for the time-dependent angular untagged decays $B^0_d \to J/\psi K^{*0}$ and $B^0_s \to J/\psi\phi$.

[2] Obtained by combining the B^0 and B^+ modes.

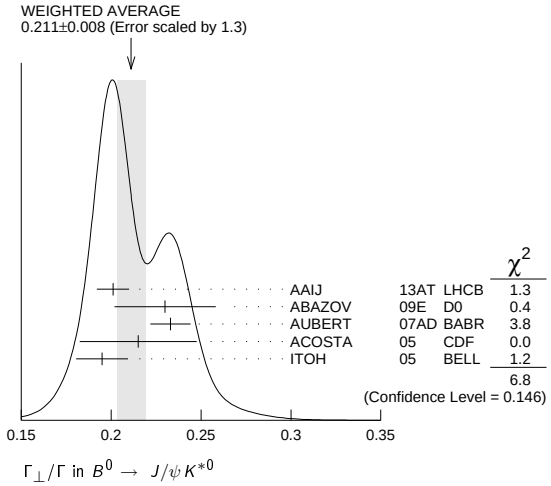

$\phi_\|$ in $B^0 \to J/\psi K^{*0}$

VALUE (rad)	DOCUMENT ID		TECN	COMMENT
−2.92±0.04 OUR AVERAGE	Error includes scale factor of 1.3.			See the ideogram below.
−2.94±0.02±0.03	AAIJ	13AT	LHCB	pp at 7 TeV
−2.69±0.08±0.11	[1] ABAZOV	09E	D0	$p\overline{p}$ at 1.96 TeV
−2.93±0.08±0.04	[2] AUBERT	07AD	BABR	$e^+e^- \to \Upsilon(4S)$

[1] Obtained $\phi_\|$ as $\delta_2 - \delta_1$, assuming they are uncorrelated.

[2] Obtained by combining the B^0 and B^+ modes.

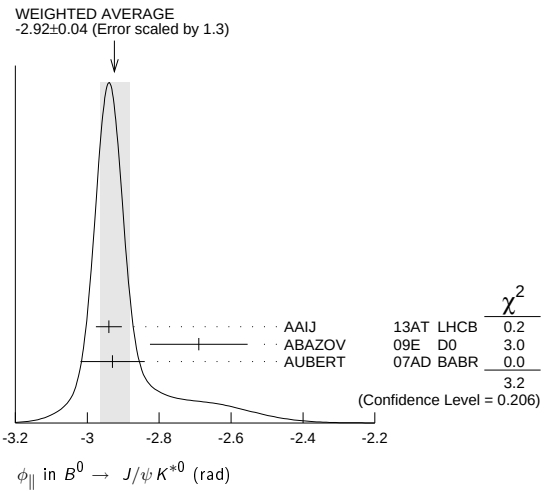

$\phi_\perp$ in $B^0 \to J/\psi K^{*0}$

VALUE (rad)	DOCUMENT ID		TECN	COMMENT
2.96±0.05 OUR AVERAGE	Error includes scale factor of 2.2.			See the ideogram below.
2.94±0.02±0.02	AAIJ	13AT	LHCB	pp at 7 TeV
3.21±0.06±0.06	ABAZOV	09E	D0	$p\overline{p}$ at 1.96 TeV
2.91±0.05±0.03	[1] AUBERT	07AD	BABR	$e^+e^- \to \Upsilon(4S)$

[1] Obtained by combining the B^0 and B^+ modes.

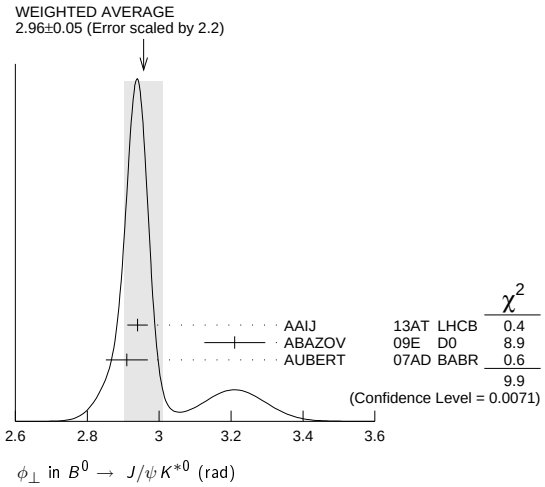

Γ_L/Γ in $B^0 \to \psi(2S)K^*(892)^0$

VALUE	DOCUMENT ID		TECN	COMMENT
$0.463^{+0.028}_{-0.040}$ OUR AVERAGE				
$0.455^{+0.031}_{-0.029}{}^{+0.014}_{-0.049}$	CHILIKIN	13	BELL	$e^+e^- \to \Upsilon(4S)$
0.48 ±0.05 ±0.02	[1] AUBERT	07AD	BABR	$e^+e^- \to \Upsilon(4S)$
0.45 ±0.11 ±0.04	[2] RICHICHI	01	CLE2	$e^+e^- \to \Upsilon(4S)$
• • • We do not use the following data for averages, fits, limits, etc. • • •				
$0.448^{+0.040}_{-0.027}{}^{+0.040}_{-0.053}$	MIZUK	09	BELL	$e^+e^- \to \Upsilon(4S)$

[1] Obtained by combining the B^0 and B^+ modes.

[2] Averages between charged and neutral B mesons.

$\Gamma_\perp/\Gamma$ in $B^0 \to \psi(2S)K^{*0}$

VALUE	DOCUMENT ID		TECN	COMMENT
0.30±0.06±0.02	[1] AUBERT	07AD	BABR	$e^+e^- \to \Upsilon(4S)$

[1] Obtained by combining the B^0 and B^+ modes.

$\phi_\|$ in $B^0 \to \psi(2S)K^{*0}$

VALUE (rad)	DOCUMENT ID		TECN	COMMENT
−2.8±0.4±0.1	[1] AUBERT	07AD	BABR	$e^+e^- \to \Upsilon(4S)$

[1] Obtained by combining the B^0 and B^+ modes.

Meson Particle Listings

B^0

$\phi_\perp$ in $B^0 \to \psi(2S) K^{*0}$

VALUE (rad)	DOCUMENT ID		TECN	COMMENT
2.8±0.3±0.1	[1] AUBERT	07AD	BABR	$e^+e^- \to \Upsilon(4S)$

[1] Obtained by combining the B^0 and B^+ modes.

Γ_L/Γ in $B^0 \to \chi_{c1} K^*(892)^0$

VALUE	DOCUMENT ID		TECN	COMMENT
0.83 $^{+0.06}_{-0.08}$ OUR AVERAGE	Error includes scale factor of 1.3.			
$0.947 ^{+0.038}_{-0.048} ^{+0.046}_{-0.099}$	MIZUK	08	BELL	$e^+e^- \to \Upsilon(4S)$
0.77 ±0.07 ±0.04	[1] AUBERT	07AD	BABR	$e^+e^- \to \Upsilon(4S)$

[1] Obtained by combining the B^0 and B^+ modes.

$\Gamma_\perp/\Gamma$ in $B^0 \to \chi_{c1} K^*(892)^0$

VALUE	DOCUMENT ID		TECN	COMMENT
0.03±0.04±0.02	[1] AUBERT	07AD	BABR	$e^+e^- \to \Upsilon(4S)$

[1] Obtained by combining the B^0 and B^+ modes.

$\phi_\parallel$ in $B^0 \to \chi_{c1} K^*(892)^0$

VALUE (rad)	DOCUMENT ID		TECN	COMMENT
0.0±0.3±0.1	[1] AUBERT	07AD	BABR	$e^+e^- \to \Upsilon(4S)$

[1] Obtained by combining the B^0 and B^+ modes.

Γ_L/Γ in $B^0 \to D_s^{*+} D^{*-}$

VALUE	DOCUMENT ID		TECN	COMMENT
0.52 ±0.05 OUR AVERAGE				
0.519±0.050±0.028	[1] AUBERT	03I	BABR	$e^+e^- \to \Upsilon(4S)$
0.506±0.139±0.036	AHMED	00B	CLE2	$e^+e^- \to \Upsilon(4S)$

[1] Measurement performed using partial reconstruction of D^{*-} decay.

Γ_L/Γ in $B^0 \to D^{*-} \rho^+$

VALUE	EVTS	DOCUMENT ID		TECN	COMMENT
0.885±0.016±0.012		CSORNA	03	CLE2	$e^+e^- \to \Upsilon(4S)$
• • • We do not use the following data for averages, fits, limits, etc. • • •					
0.93 ±0.05 ±0.05	76	ALAM	94	CLE2	$e^+e^- \to \Upsilon(4S)$

Γ_L/Γ in $B^0 \to D_s^{*+} \rho^-$

VALUE	DOCUMENT ID		TECN	COMMENT
0.84 $^{+0.26}_{-0.28}$ ±0.13	[1] AUBERT	08AJ	BABR	$e^+e^- \to \Upsilon(4S)$

[1] Assumes equal production of B^+ and B^0 at the $\Upsilon(4S)$.

Γ_L/Γ in $B^0 \to D_s^{*+} K^{*-}$

VALUE	DOCUMENT ID		TECN	COMMENT
0.92 $^{+0.37}_{-0.31}$ ±0.07	[1] AUBERT	08AJ	BABR	$e^+e^- \to \Upsilon(4S)$

[1] Assumes equal production of B^+ and B^0 at the $\Upsilon(4S)$.

Γ_L/Γ in $B^0 \to D^{*+} D^{*-}$

VALUE	DOCUMENT ID		TECN	COMMENT
0.624±0.029±0.011	KRONENBITT..12		BELL	$e^+e^- \to \Upsilon(4S)$
• • • We do not use the following data for averages, fits, limits, etc. • • •				
0.57 ±0.08 ±0.02	MIYAKE	05	BELL	Repl. by KRONENBITTER 12

$\Gamma_\perp/\Gamma$ in $B^0 \to D^{*+} D^{*-}$

VALUE	DOCUMENT ID		TECN	COMMENT
0.147±0.019 OUR AVERAGE				
0.138±0.024±0.006	KRONENBITT..12		BELL	$e^+e^- \to \Upsilon(4S)$
0.158±0.028±0.006	AUBERT	09C	BABR	$e^+e^- \to \Upsilon(4S)$
• • • We do not use the following data for averages, fits, limits, etc. • • •				
0.125±0.043±0.023	VERVINK	09	BELL	Repl. by KRONENBITTER 12
0.143±0.034±0.008	AUBERT	07BO	BABR	Repl. by AUBERT 09C
0.125±0.044±0.007	AUBERT,BE	05A	BABR	Repl. by AUBERT 07BO
0.19 ±0.08 ±0.01	MIYAKE	05	BELL	Repl. by VERVINK 09
0.063±0.055±0.009	AUBERT	03Q	BABR	Repl. by AUBERT,BE 05A

Γ_L/Γ in $B^0 \to \overline{D}^{*0} \omega$

VALUE	DOCUMENT ID		TECN	COMMENT
0.665±0.047±0.015	LEES	11M	BABR	$e^+e^- \to \Upsilon(4S)$

Γ_L/Γ in $B^0 \to D^{*-} \omega \pi^+$

VALUE	DOCUMENT ID		TECN	COMMENT
0.654±0.042±0.016	[1] AUBERT	06L	BABR	$e^+e^- \to \Upsilon(4S)$

[1] Invariant mass of the $[\omega\pi]$ system is restricted in the region 1.1 and 1.9 GeV.

Γ_L/Γ in $B^0 \to \omega K^{*0}$

VALUE	DOCUMENT ID		TECN	COMMENT
0.69±0.13 OUR AVERAGE				
0.72±0.14±0.02	AUBERT	09H	BABR	$e^+e^- \to \Upsilon(4S)$
$0.56 \pm 0.29 ^{+0.18}_{-0.08}$	GOLDENZWE..08		BELL	$e^+e^- \to \Upsilon(4S)$

Γ_L/Γ in $B^0 \to \omega K_2^*(1430)^0$

VALUE	DOCUMENT ID		TECN	COMMENT
0.45±0.12±0.02	AUBERT	09H	BABR	$e^+e^- \to \Upsilon(4S)$

Γ_L/Γ in $B^0 \to K^{*0} \overline{K}^{*0}$

VALUE	DOCUMENT ID		TECN	COMMENT
0.80 $^{+0.10}_{-0.12}$ ±0.06	AUBERT	08I	BABR	$e^+e^- \to \Upsilon(4S)$

Γ_L/Γ in $B^0 \to \phi K^*(892)^0$

VALUE	DOCUMENT ID		TECN	COMMENT
0.497±0.025 OUR AVERAGE				
0.499±0.030±0.018	PRIM	13	BELL	$e^+e^- \to \Upsilon(4S)$
0.494±0.034±0.013	AUBERT	08BG	BABR	$e^+e^- \to \Upsilon(4S)$
• • • We do not use the following data for averages, fits, limits, etc. • • •				
0.506±0.040±0.015	AUBERT	07D	BABR	Repl. by AUBERT 08BG
0.45 ±0.05 ±0.02	CHEN	05A	BELL	Repl. by PRIM 13
0.52 ±0.05 ±0.02	[1] AUBERT,B	04W	BABR	Repl. by AUBERT 07D
0.65 ±0.07 ±0.02	AUBERT	03V	BABR	Repl. by AUBERT,B 04W
0.41 ±0.10 ±0.04	CHEN	03B	BELL	Repl. by CHEN 05A

[1] AUBERT,B 04W also measures the fraction of parity-odd transverse contribution $f_\perp = 0.22 \pm 0.05 \pm 0.02$ and the phases of the parity-even and parity-odd transverse amplitudes relative to the longitudinal amplitude.

$\Gamma_\perp/\Gamma$ in $B^0 \to \phi K^*(892)^0$

VALUE	DOCUMENT ID		TECN	COMMENT
0.228±0.021 OUR AVERAGE				
0.238±0.026±0.008	PRIM	13	BELL	$e^+e^- \to \Upsilon(4S)$
0.212±0.032±0.013	AUBERT	08BG	BABR	$e^+e^- \to \Upsilon(4S)$
• • • We do not use the following data for averages, fits, limits, etc. • • •				
0.227±0.038±0.013	AUBERT	07D	BABR	Repl. by AUBERT 08BG
0.31 $^{+0.06}_{-0.05}$ ±0.02	[1] CHEN	05A	BELL	Repl. by PRIM 13
0.22 ±0.05 ±0.02	AUBERT,B	04W	BABR	Repl. by AUBERT 07D

[1] This quantity was recalculated by the BELLE authors from numbers in the original paper.

$\phi_\parallel$ in $B^0 \to \phi K^*(892)^0$

VALUE (rad)	DOCUMENT ID		TECN	COMMENT
2.28±0.08 OUR AVERAGE				
2.23±0.10±0.02	PRIM	13	BELL	$e^+e^- \to \Upsilon(4S)$
2.40±0.13±0.08	AUBERT	08BG	BABR	$e^+e^- \to \Upsilon(4S)$
• • • We do not use the following data for averages, fits, limits, etc. • • •				
2.31±0.14±0.08	AUBERT	07D	BABR	Repl. by AUBERT 08BG
2.40 $^{+0.28}_{-0.24}$ ±0.07	[1] CHEN	05A	BELL	Repl. by PRIM 13
2.34 $^{+0.23}_{-0.20}$ ±0.05	AUBERT,B	04W	BABR	Repl. by AUBERT 07D

[1] This quantity was recalculated by the BELLE authors from numbers in the original paper.

$\phi_\perp$ in $B^0 \to \phi K^*(892)^0$

VALUE (rad)	DOCUMENT ID		TECN	COMMENT
2.36±0.09 OUR AVERAGE				
2.37±0.10±0.04	PRIM	13	BELL	$e^+e^- \to \Upsilon(4S)$
2.35±0.13±0.09	AUBERT	08BG	BABR	$e^+e^- \to \Upsilon(4S)$
• • • We do not use the following data for averages, fits, limits, etc. • • •				
2.24±0.15±0.09	AUBERT	07D	BABR	Repl. by AUBERT 08BG
2.51±0.25±0.06	[1] CHEN	05A	BELL	Repl. by PRIM 13
2.47±0.25±0.05	AUBERT,B	04W	BABR	Repl. by AUBERT 07D

[1] This quantity was recalculated by the BELLE authors from numbers in the original paper.

$\delta_0(B^0 \to \phi K^*(892)^0)$

VALUE (rad)	DOCUMENT ID		TECN	COMMENT
2.88±0.10 OUR AVERAGE				
2.91±0.10±0.08	PRIM	13	BELL	$e^+e^- \to \Upsilon(4S)$
2.82±0.15±0.09	AUBERT	08BG	BABR	$e^+e^- \to \Upsilon(4S)$
• • • We do not use the following data for averages, fits, limits, etc. • • •				
2.78±0.17±0.09	AUBERT	07D	BABR	Repl. by AUBERT 08BG

A_{CP}^0 in $B^0 \to \phi K^*(892)^0$

VALUE	DOCUMENT ID		TECN	COMMENT
−0.01 ±0.05 OUR AVERAGE				
−0.030±0.061±0.007	PRIM	13	BELL	$e^+e^- \to \Upsilon(4S)$
0.01 ±0.07 ±0.02	AUBERT	08BG	BABR	$e^+e^- \to \Upsilon(4S)$
• • • We do not use the following data for averages, fits, limits, etc. • • •				
−0.03 ±0.08 ±0.02	AUBERT	07D	BABR	Repl. by AUBERT 08BG
0.13 ±0.12 ±0.04	[1] CHEN	05A	BELL	Repl. by PRIM 13
−0.06 ±0.10 ±0.01	AUBERT,B	04W	BABR	Repl. by AUBERT 07D

[1] This quantity was recalculated by the BELLE authors from numbers in the original paper.

See key on page 547

$A_{CP}^{\perp}$ in $B^0 \to \phi K^*(892)^0$

VALUE	DOCUMENT ID		TECN	COMMENT
-0.11 ± 0.09 OUR AVERAGE				
$-0.14 \pm 0.11 \pm 0.01$	PRIM	13	BELL	$e^+e^- \to \Upsilon(4S)$
$-0.04 \pm 0.15 \pm 0.06$	AUBERT	08BG	BABR	$e^+e^- \to \Upsilon(4S)$
• • • We do not use the following data for averages, fits, limits, etc. • • •				
$-0.03 \pm 0.16 \pm 0.05$	AUBERT	07D	BABR	Repl. by AUBERT 08BG
$-0.20 \pm 0.18 \pm 0.04$	[1] CHEN	05A	BELL	Repl. by PRIM 13
$-0.10 \pm 0.24 \pm 0.05$	AUBERT,B	04W	BABR	Repl. by AUBERT 07D

[1] This quantity was recalculated by the BELLE authors from numbers in the original paper.

$\Delta\phi_{\parallel}$ in $B^0 \to \phi K^*(892)^0$

VALUE (rad)	DOCUMENT ID		TECN	COMMENT
0.06 ± 0.11 OUR AVERAGE Error includes scale factor of 1.4.				
$-0.02 \pm 0.10 \pm 0.01$	PRIM	13	BELL	$e^+e^- \to \Upsilon(4S)$
$0.22 \pm 0.12 \pm 0.08$	AUBERT	08BG	BABR	$e^+e^- \to \Upsilon(4S)$
• • • We do not use the following data for averages, fits, limits, etc. • • •				
$0.24 \pm 0.14 \pm 0.08$	AUBERT	07D	BABR	Repl. by AUBERT 08BG
$-0.32 \pm 0.27 \pm 0.07$	[1] CHEN	05A	BELL	Repl. by PRIM 13
$0.27^{+0.20}_{-0.23} \pm 0.05$	AUBERT,B	04W	BABR	Repl. by AUBERT 07D

[1] This quantity was recalculated by the BELLE authors from numbers in the original paper.

$\Delta\phi_{\perp}$ in $B^0 \to \phi K^*(892)^0$

VALUE (rad)	DOCUMENT ID		TECN	COMMENT
0.10 ± 0.08 OUR AVERAGE				
$0.05 \pm 0.10 \pm 0.02$	PRIM	13	BELL	$e^+e^- \to \Upsilon(4S)$
$0.21 \pm 0.13 \pm 0.08$	AUBERT	08BG	BABR	$e^+e^- \to \Upsilon(4S)$
• • • We do not use the following data for averages, fits, limits, etc. • • •				
$0.19 \pm 0.15 \pm 0.08$	AUBERT	07D	BABR	Repl. by AUBERT 08BG
$-0.30 \pm 0.25 \pm 0.06$	[1] CHEN	05A	BELL	Repl. by PRIM 13
$0.36 \pm 0.25 \pm 0.05$	AUBERT,B	04W	BABR	Repl. by AUBERT 07D

[1] This quantity was recalculated by the BELLE authors from numbers in the original paper.

$\Delta\delta_0(B^0 \to \phi K^*(892)^0)$

VALUE (rad)	DOCUMENT ID		TECN	COMMENT
0.13 ± 0.09 OUR AVERAGE				
$0.08 \pm 0.10 \pm 0.01$	PRIM	13	BELL	$e^+e^- \to \Upsilon(4S)$
$0.27 \pm 0.14 \pm 0.08$	AUBERT	08BG	BABR	$e^+e^- \to \Upsilon(4S)$
• • • We do not use the following data for averages, fits, limits, etc. • • •				
$0.21 \pm 0.17 \pm 0.08$	AUBERT	07D	BABR	Repl. by AUBERT 08BG

$\Delta\phi_{00}(B^0 \to \phi K_0^*(1430)^0)$

VALUE (rad)	DOCUMENT ID		TECN	COMMENT
$0.28 \pm 0.42 \pm 0.04$	AUBERT	08BG	BABR	$e^+e^- \to \Upsilon(4S)$

Γ_L/Γ in $B^0 \to \phi K_2^*(1430)^0$

VALUE	DOCUMENT ID		TECN	COMMENT
$0.913^{+0.028}_{-0.050}$ OUR AVERAGE				
$0.918^{+0.029}_{-0.060} \pm 0.012$	PRIM	13	BELL	$e^+e^- \to \Upsilon(4S)$
$0.901^{+0.046}_{-0.058} \pm 0.037$	AUBERT	08BG	BABR	$e^+e^- \to \Upsilon(4S)$
• • • We do not use the following data for averages, fits, limits, etc. • • •				
$0.853^{+0.061}_{-0.069} \pm 0.036$	AUBERT	07D	BABR	Repl. by AUBERT 08BG

$\Gamma_{\perp}/\Gamma$ in $B^0 \to \phi K_2^*(1430)^0$

VALUE	DOCUMENT ID		TECN	COMMENT
$0.027^{+0.031}_{-0.025}$ OUR AVERAGE Error includes scale factor of 1.1.				
$0.056^{+0.050}_{-0.035} \pm 0.009$	PRIM	13	BELL	$e^+e^- \to \Upsilon(4S)$
$0.002^{+0.018}_{-0.002} \pm 0.031$	AUBERT	08BG	BABR	$e^+e^- \to \Upsilon(4S)$
• • • We do not use the following data for averages, fits, limits, etc. • • •				
$0.045^{+0.049}_{-0.040} \pm 0.013$	AUBERT	07D	BABR	Repl. by AUBERT 08BG

$\phi_{\parallel}$ in $B^0 \to \phi K_2^*(1430)^0$

VALUE (rad)	DOCUMENT ID		TECN	COMMENT
4.0 ±0.4 OUR AVERAGE				
$3.76 \pm 2.88 \pm 1.32$	PRIM	13	BELL	$e^+e^- \to \Upsilon(4S)$
$3.96 \pm 0.38 \pm 0.06$	AUBERT	08BG	BABR	$e^+e^- \to \Upsilon(4S)$
• • • We do not use the following data for averages, fits, limits, etc. • • •				
$2.90 \pm 0.39 \pm 0.06$	AUBERT	07D	BABR	Repl. by AUBERT 08BG

$\phi_{\perp}$ in $B^0 \to \phi K_2^*(1430)^0$

VALUE (rad)	DOCUMENT ID		TECN	COMMENT
$4.45^{+0.43}_{-0.38} \pm 0.13$	PRIM	13	BELL	$e^+e^- \to \Upsilon(4S)$
• • • We do not use the following data for averages, fits, limits, etc. • • •				
$5.72^{+0.55}_{-0.87} \pm 0.11$	AUBERT	07D	BABR	Repl. by AUBERT 08BG

$\delta_0(B^0 \to \phi K_2^*(1430)^0)$

VALUE (rad)	DOCUMENT ID		TECN	COMMENT
3.46±0.14 OUR AVERAGE				
$3.53 \pm 0.11 \pm 0.19$	PRIM	13	BELL	$e^+e^- \to \Upsilon(4S)$
$3.41 \pm 0.13 \pm 0.13$	AUBERT	08BG	BABR	$e^+e^- \to \Upsilon(4S)$
• • • We do not use the following data for averages, fits, limits, etc. • • •				
$3.54^{+0.12}_{-0.14} \pm 0.06$	AUBERT	07D	BABR	Repl. by AUBERT 08BG

A_{CP}^0 in $B^0 \to \phi K_2^*(1430)^0$

VALUE	DOCUMENT ID		TECN	COMMENT
-0.03 ± 0.04 OUR AVERAGE				
$-0.016^{+0.066}_{-0.051} \pm 0.008$	PRIM	13	BELL	$e^+e^- \to \Upsilon(4S)$
$-0.05 \pm 0.06 \pm 0.01$	AUBERT	08BG	BABR	$e^+e^- \to \Upsilon(4S)$

$A_{CP}^{\perp}$ in $B^0 \to \phi K_2^*(1430)^0$

VALUE	DOCUMENT ID		TECN	COMMENT
$-0.01^{+0.85}_{-0.67} \pm 0.09$	PRIM	13	BELL	$e^+e^- \to \Upsilon(4S)$

$\Delta\phi_{\parallel}(B^0 \to \phi K_2^*(1430)^0)$

VALUE (rad)	DOCUMENT ID		TECN	COMMENT
-0.9 ± 0.4 OUR AVERAGE				
$-0.02 \pm 1.08 \pm 1.01$	PRIM	13	BELL	$e^+e^- \to \Upsilon(4S)$
$-1.00 \pm 0.38 \pm 0.09$	AUBERT	08BG	BABR	$e^+e^- \to \Upsilon(4S)$

$\Delta\phi_{\perp}(B^0 \to \phi K_2^*(1430)^0)$

VALUE	DOCUMENT ID		TECN	COMMENT
$-0.19 \pm 0.42 \pm 0.11$	PRIM	13	BELL	$e^+e^- \to \Upsilon(4S)$

$\Delta\delta_0$ in $B^0 \to \phi K_2^*(1430)^0$

VALUE (rad)	DOCUMENT ID		TECN	COMMENT
0.08±0.09 OUR AVERAGE				
$0.06 \pm 0.11 \pm 0.02$	PRIM	13	BELL	$e^+e^- \to \Upsilon(4S)$
$0.11 \pm 0.13 \pm 0.06$	AUBERT	08BG	BABR	$e^+e^- \to \Upsilon(4S)$

Γ_L/Γ in $B^0 \to K^*(892)^0\rho^0$

VALUE	DOCUMENT ID		TECN	COMMENT
$0.40 \pm 0.08 \pm 0.11$	LEES	12K	BABR	$e^+e^- \to \Upsilon(4S)$
• • • We do not use the following data for averages, fits, limits, etc. • • •				
$0.57 \pm 0.09 \pm 0.08$	AUBERT,B	06G	BABR	Repl. by LEES 12K

Γ_L/Γ in $B^0 \to K^{*+}\rho^-$

VALUE	DOCUMENT ID		TECN	COMMENT
$0.38 \pm 0.13 \pm 0.03$	LEES	12K	BABR	$e^+e^- \to \Upsilon(4S)$

Γ_L/Γ in $B^0 \to \rho^+\rho^-$

VALUE	DOCUMENT ID		TECN	COMMENT
$0.977^{+0.028}_{-0.024}$ OUR AVERAGE				
$0.992 \pm 0.024^{+0.026}_{-0.013}$	AUBERT	07BF	BABR	$e^+e^- \to \Upsilon(4S)$
$0.941^{+0.034}_{-0.040} \pm 0.030$	SOMOV	06	BELL	$e^+e^- \to \Upsilon(4S)$
• • • We do not use the following data for averages, fits, limits, etc. • • •				
$0.978 \pm 0.014^{+0.021}_{-0.029}$	AUBERT,B	05C	BABR	Repl. by AUBERT 07BF
$0.98 \ ^{+0.02}_{-0.08} \pm 0.03$	AUBERT	04G	BABR	Repl. by AUBERT,B 04R
$0.99 \pm 0.03 \ ^{+0.04}_{-0.03}$	AUBERT,B	04R	BABR	Repl. by AUBERT,B 05C

Γ_L/Γ in $B^0 \to \rho^0\rho^0$

VALUE	DOCUMENT ID		TECN	COMMENT
$0.75^{+0.11}_{-0.14} \pm 0.05$	AUBERT	08BB	BABR	$e^+e^- \to \Upsilon(4S)$
• • • We do not use the following data for averages, fits, limits, etc. • • •				
$0.87 \pm 0.13 \pm 0.04$	AUBERT	07G	BABR	Repl. by AUBERT 08BB

Γ_L/Γ in $B^0 \to a_1(1260)^+ a_1(1260)^-$

VALUE	DOCUMENT ID		TECN	COMMENT
$0.31 \pm 0.22 \pm 0.10$	AUBERT	09AL	BABR	$e^+e^- \to \Upsilon(4S)$

Γ_L/Γ in $B^0 \to p\bar{p}K^*(892)^0$

VALUE	DOCUMENT ID		TECN	COMMENT
$1.01 \pm 0.13 \pm 0.03$	CHEN	08C	BELL	$e^+e^- \to \Upsilon(4S)$

Γ_L/Γ in $B^0 \to \Lambda\bar{\Lambda}K^*(892)^0$

VALUE	DOCUMENT ID		TECN	COMMENT
$0.60 \pm 0.22 \pm 0.08$	CHANG	09	BELL	$e^+e^- \to \Upsilon(4S)$

B^0–$\overline{B}^0$ MIXING

Updated April 2014 by O. Schneider (Ecole Polytechnique Fédérale de Lausanne).

There are two neutral B^0–$\overline{B}^0$ meson systems, B^0_d–$\overline{B}^0_d$ and B^0_s–$\overline{B}^0_s$ (generically denoted B^0_q–$\overline{B}^0_q$, $q = s, d$), which exhibit particle-antiparticle mixing [1]. This mixing phenomenon is described in Ref. 2. In the following, we adopt the notation introduced in Ref. 2, and assume CPT conservation throughout. In each system, the light (L) and heavy (H) mass eigenstates,

$$|B_{\rm L,H}\rangle = p|B^0_q\rangle \pm q|\overline{B}^0_q\rangle\,, \tag{1}$$

have a mass difference $\Delta m_q = m_{\rm H} - m_{\rm L} > 0$, and a total decay width difference $\Delta\Gamma_q = \Gamma_{\rm L} - \Gamma_{\rm H}$. In the absence of CP violation in the mixing, $|q/p| = 1$, these differences are given by $\Delta m_q = 2|M_{12}|$ and $|\Delta\Gamma_q| = 2|\Gamma_{12}|$, where M_{12} and Γ_{12} are the off-diagonal elements of the mass and decay matrices [2]. The evolution of a pure $|B^0_q\rangle$ or $|\overline{B}^0_q\rangle$ state at $t = 0$ is given by

$$|B^0_q(t)\rangle = g_+(t)\,|B^0_q\rangle + \frac{q}{p}\,g_-(t)\,|\overline{B}^0_q\rangle\,, \tag{2}$$

$$|\overline{B}^0_q(t)\rangle = g_+(t)\,|\overline{B}^0_q\rangle + \frac{p}{q}g_-(t)\,|B^0_q\rangle\,, \tag{3}$$

which means that the flavor states remain unchanged (+) or oscillate into each other (−) with time-dependent probabilities proportional to

$$|g_\pm(t)|^2 = \frac{e^{-\Gamma_q t}}{2}\left[\cosh\left(\frac{\Delta\Gamma_q}{2}\,t\right) \pm \cos(\Delta m_q\,t)\right]\,, \tag{4}$$

where $\Gamma_q = (\Gamma_{\rm H} + \Gamma_{\rm L})/2$. In the absence of CP violation, the time-integrated mixing probability $\int |g_-(t)|^2\,dt/(\int |g_-(t)|^2\,dt + \int |g_+(t)|^2\,dt)$ is given by

$$\chi_q = \frac{x_q^2 + y_q^2}{2(x_q^2+1)}\,, \quad \text{where} \quad x_q = \frac{\Delta m_q}{\Gamma_q}\,, \quad y_q = \frac{\Delta\Gamma_q}{2\Gamma_q}\,. \tag{5}$$

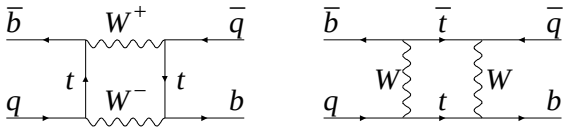

Figure 1: Dominant box diagrams for the $B^0_q \to \overline{B}^0_q$ transitions ($q = d$ or s). Similar diagrams exist where one or both t quarks are replaced with c or u quarks.

Standard Model predictions and phenomenology

In the Standard Model, the transitions $B^0_q \to \overline{B}^0_q$ and $\overline{B}^0_q \to B^0_q$ are due to the weak interaction. They are described, at the lowest order, by box diagrams involving two W bosons and two up-type quarks (see Fig. 1), as is the case for K^0–$\overline{K}^0$ mixing. However, the long range interactions arising from intermediate virtual states are negligible for the neutral B meson systems, because the large B mass is off the region of hadronic resonances. The calculation of the dispersive and absorptive parts of the box diagrams yields the following predictions for the off-diagonal element of the mass and decay matrices [3],

$$M_{12} = -\frac{G_F^2 m_W^2 \eta_B m_{B_q} B_{B_q} f_{B_q}^2}{12\pi^2}\,S_0(m_t^2/m_W^2)\,(V_{tq}^* V_{tb})^2\,, \tag{6}$$

$$\Gamma_{12} = \frac{G_F^2 m_b^2 \eta'_B m_{B_q} B_{B_q} f_{B_q}^2}{8\pi} \times \left[(V_{tq}^* V_{tb})^2 + V_{tq}^* V_{tb} V_{cq}^* V_{cb}\;\mathcal{O}\left(\frac{m_c^2}{m_b^2}\right) + (V_{cq}^* V_{cb})^2\;\mathcal{O}\left(\frac{m_c^4}{m_b^4}\right)\right]\,, \tag{7}$$

where G_F is the Fermi constant, m_W the W boson mass, and m_i the mass of quark i; m_{B_q}, f_{B_q} and B_{B_q} are the B^0_q mass, weak decay constant and bag parameter, respectively. The known function $S_0(x_t)$ can be approximated very well by $0.784\,x_t^{0.76}$ [4], and V_{ij} are the elements of the CKM matrix [5]. The QCD corrections η_B and η'_B are of order unity. The only non-negligible contributions to M_{12} are from box diagrams involving two top quarks. The phases of M_{12} and Γ_{12} satisfy

$$\phi_M - \phi_\Gamma = \pi + \mathcal{O}\left(\frac{m_c^2}{m_b^2}\right)\,, \tag{8}$$

implying that the mass eigenstates have mass and width differences of opposite signs. This means that, like in the K^0–$\overline{K}^0$ system, the heavy state is expected to have a smaller decay width than that of the light state: $\Gamma_{\rm H} < \Gamma_{\rm L}$. Hence, $\Delta\Gamma = \Gamma_{\rm L} - \Gamma_{\rm H}$ is expected to be positive in the Standard Model.

Furthermore, the quantity

$$\left|\frac{\Gamma_{12}}{M_{12}}\right| \simeq \frac{3\pi}{2}\frac{m_b^2}{m_W^2}\frac{1}{S_0(m_t^2/m_W^2)} \sim \mathcal{O}\left(\frac{m_b^2}{m_t^2}\right) \tag{9}$$

is small, and a power expansion of $|q/p|^2$ yields

$$\left|\frac{q}{p}\right|^2 = 1 + \left|\frac{\Gamma_{12}}{M_{12}}\right|\sin(\phi_M - \phi_\Gamma) + \mathcal{O}\left(\left|\frac{\Gamma_{12}}{M_{12}}\right|^2\right)\,. \tag{10}$$

Therefore, considering both Eqs. (8) and (9), the CP-violating parameter

$$1 - \left|\frac{q}{p}\right|^2 \simeq \mathrm{Im}\left(\frac{\Gamma_{12}}{M_{12}}\right) \tag{11}$$

is expected to be very small: $\sim \mathcal{O}(10^{-3})$ for the B^0_d–$\overline{B}^0_d$ system and $\lesssim \mathcal{O}(10^{-4})$ for the B^0_s–$\overline{B}^0_s$ system [6].

In the approximation of negligible CP violation in mixing, the ratio $\Delta\Gamma_q/\Delta m_q$ is equal to the small quantity $|\Gamma_{12}/M_{12}|$ of Eq. (9); it is hence independent of CKM matrix elements, *i.e.*, the same for the B^0_d–$\overline{B}^0_d$ and B^0_s–$\overline{B}^0_s$ systems. Calculations [7] yield $\sim 5\times10^{-3}$ with a $\sim 20\%$ uncertainty. Given the published experimental knowledge [8] on the mixing parameter x_q

$$\begin{cases} x_d = 0.774 \pm 0.006 & (B^0_d\text{–}\overline{B}^0_d \text{ system}) \\ x_s = 26.85 \pm 0.13 & (B^0_s\text{–}\overline{B}^0_s \text{ system}) \end{cases}\,, \tag{12}$$

the Standard Model thus predicts that $\Delta\Gamma_d/\Gamma_d$ is very small (below 1%), but $\Delta\Gamma_s/\Gamma_s$ considerably larger ($\sim 10\%$). These width differences are caused by the existence of final states to which both the B^0_q and $\overline{B}^0_q$ mesons can decay. Such decays

involve $b \to c\bar{c}q$ quark-level transitions, which are Cabibbo-suppressed if $q = d$ and Cabibbo-allowed if $q = s$.

A complete set of Standard Model predictions for all mixing parameters in both the B^0_d–$\overline{B}{}^0_d$ and B^0_s–$\overline{B}{}^0_s$ systems can be found in Ref. 7.

Experimental issues and methods for oscillation analyses

Time-integrated measurements of B^0–$\overline{B}{}^0$ mixing were published for the first time in 1987 by UA1 [9] and ARGUS [10], and since then by many other experiments. These measurements are typically based on counting same-sign and opposite-sign lepton pairs from the semileptonic decay of the produced $b\overline{b}$ pairs. Such analyses cannot easily separate the contributions from the different b-hadron species, therefore, the clean environment of $\Upsilon(4S)$ machines (where only B^0_d and charged B_u mesons are produced) is in principle best suited to measure χ_d.

However, better sensitivity is obtained from time-dependent analyses aiming at the direct measurement of the oscillation frequencies Δm_d and Δm_s, from the proper time distributions of B^0_d or B^0_s candidates identified through their decay in (mostly) flavor-specific modes, and suitably tagged as mixed or unmixed. This is particularly true for the B^0_s–$\overline{B}{}^0_s$ system, where the large value of x_s implies maximal mixing, *i.e.*, $\chi_s \simeq 1/2$. In such analyses, the B^0_d or B^0_s mesons are either fully reconstructed, partially reconstructed from a charm meson, selected from a lepton with the characteristics of a $b \to \ell^-$ decay, or selected from a reconstructed displaced vertex. At high-energy colliders (LEP, SLC, Tevatron, LHC), the proper time $t = \dfrac{m_B}{p}L$ is measured from the distance L between the production vertex and the B decay vertex, and from an estimate of the B momentum p. At asymmetric B factories (KEKB, PEP-II), producing $e^+e^- \to \Upsilon(4S) \to B^0_d\overline{B}{}^0_d$ events with a boost $\beta\gamma$ ($= 0.425$, 0.55), the proper time difference between the two B candidates is estimated as $\Delta t \simeq \dfrac{\Delta z}{\beta\gamma c}$, where Δz is the spatial separation between the two B decay vertices along the boost direction. In all cases, the good resolution needed on the vertex positions is obtained with silicon detectors.

The average statistical significance $\mathcal{S}$ of a B^0_d or B^0_s oscillation signal can be approximated as [11]

$$\mathcal{S} \approx \sqrt{N/2}\, f_{\rm sig}\, (1-2\eta)\, e^{-(\Delta m\, \sigma_t)^2/2}\,, \qquad (13)$$

where N is the number of selected and tagged candidates, $f_{\rm sig}$ is the fraction of signal in that sample, η is the total mistag probability, and σ_t is the resolution on proper time (or proper time difference). The quantity $\mathcal{S}$ decreases very quickly as Δm increases; this dependence is controlled by σ_t, which is therefore a critical parameter for Δm_s analyses. At high-energy colliders, the proper time resolution $\sigma_t \sim \dfrac{m_B}{\langle p\rangle}\sigma_L \oplus t\dfrac{\sigma_p}{p}$ includes a constant contribution due to the decay length resolution σ_L (typically 0.04–0.3 ps), and a term due to the relative momentum resolution σ_p/p (typically 10–20% for partially reconstructed decays), which increases with proper time. At B factories, the boost of the B mesons is estimated from the known beam energies, and the term due to the spatial resolution dominates (typically 1–1.5 ps because of the much smaller B boost).

In order to tag a B candidate as mixed or unmixed, it is necessary to determine its flavor both in the initial state and in the final state. The initial and final state mistag probabilities, η_i and η_f, degrade $\mathcal{S}$ by a total factor $(1-2\eta) = (1-2\eta_i)(1-2\eta_f)$. In lepton-based analyses, the final state is tagged by the charge of the lepton from $b \to \ell^-$ decays; the largest contribution to η_f is then due to $\overline{b} \to \overline{c} \to \ell^-$ decays. Alternatively, the charge of a reconstructed charm meson (D^{*-} from B^0_d or D^-_s from B^0_s), or that of a kaon hypothesized to come from a $b \to c \to s$ decay [12], can be used. For fully-inclusive analyses based on topological vertexing, final-state tagging techniques include jet-charge [13] and charge-dipole [14,15] methods. At high-energy colliders, the methods to tag the initial state (*i.e.*, the state at production), can be divided into two groups: the ones that tag the initial charge of the $\overline{b}$ quark contained in the B candidate itself (same-side tag), and the ones that tag the initial charge of the other b quark produced in the event (opposite-side tag). On the same side, the sign of a charged pion or kaon from the primary vertex is correlated with the production state of the B^0_d or B^0_s if that particle is a decay product of a B^{**} state or the first in the fragmentation chain [16,17]. Jet- and vertex-charge techniques work on both sides and on the opposite side, respectively. Finally, the charge of a lepton from $b \to \ell^-$ or of a kaon from $b \to c \to s$ can be used as opposite side tags, keeping in mind that their performance is degraded due to integrated mixing. At SLC, the beam polarization produced a sizeable forward-backward asymmetry in the $Z \to b\overline{b}$ decays, and provided another very interesting and effective initial state tag based on the polar angle of the B candidate [14]. Initial state tags have also been combined to reach $\eta_i \sim 26\%$ at LEP [17,18], or even 22% at SLD [14] with full efficiency. In the case $\eta_f = 0$, this corresponds to an effective tagging efficiency $Q = \epsilon D^2 = \epsilon(1-2\eta)^2$, where ϵ is the tagging efficiency, in the range $23-31\%$. The equivalent figure achieved by CDF during Tevatron Run I was $\sim 3.5\%$ [19], reflecting the fact that tagging is more difficult at hadron colliders. The CDF and DØ analyses of Tevatron Run II data reached $\epsilon D^2 = (1.8 \pm 0.1)\%$ [20] and $(2.5 \pm 0.2)\%$ [21] for opposite-side tagging, while same-side kaon tagging (for B^0_s analyses) contributed an additional $3.7-4.8\%$ at CDF [20], and pushed the combined performance to $(4.7 \pm 0.5)\%$ at DØ [22]. LHCb, operating in the forward region at the LHC where the environment is different in terms of track multiplicity and b-hadron production kinematics, has reported $\epsilon D^2 = (2.10 \pm 0.25)\%$ [23] for opposite-side tagging and $(1.5 \pm 0.4)\%$ [24] for same-side kaon tagging, with a combined figure of $(3.8 \pm 0.7)\%$ [24].

At B factories, the flavor of a B^0_d meson at production cannot be determined, since the two neutral B mesons produced in a $\Upsilon(4S)$ decay evolve in a coherent P-wave state where they keep opposite flavors at any time. However, as soon as one of them decays, the other follows a time-evolution given by

Eqs. (2) or (3), where t is replaced with Δt (which will take negative values half of the time). Hence, the "initial state" tag of a B can be taken as the final-state tag of the other B. Effective tagging efficiencies Q of 30% are achieved by BaBar and Belle [25], using different techniques including $b \to \ell^-$ and $b \to c \to s$ tags. It is worth noting that, in this case, mixing of the other B (*i.e.*, the coherent mixing occurring before the first B decay) does not contribute to the mistag probability.

Before the experimental observation of a decay-width difference, oscillation analyses typically neglected $\Delta\Gamma$ in Eq. (4), and described the physics with the functions $\Gamma e^{-\Gamma t}(1 \pm \cos(\Delta m t))/2$ (high-energy colliders) or $\Gamma e^{-\Gamma|\Delta t|}(1 \pm \cos(\Delta m \Delta t))/4$ (asymmetric $\Upsilon(4S)$ machines). As can be seen from Eq. (4), a non-zero value of $\Delta\Gamma$ would effectively reduce the oscillation amplitude with a small time-dependent factor that would be very difficult to distinguish from time resolution effects. Measurements of Δm are usually extracted from the data using a maximum likelihood fit.

Δm_d and $\Delta\Gamma_d$ measurements

Many B^0_d–$\overline{B}{}^0_d$ oscillations analyses have been published [26] by the ALEPH [27], DELPHI [15,28], L3 [29], OPAL [30,31] BaBar [32], Belle [33], CDF [16], DØ [21], and LHCb [34–36] collaborations. Although a variety of different techniques have been used, the individual Δm_d results obtained at LEP and Tevatron have remarkably similar precision. Their average is compatible with the recent and more precise measurements from the asymmetric B factories and the LHC. The systematic uncertainties are not negligible; they are often dominated by sample composition, mistag probability, or b-hadron lifetime contributions. Before being combined, the measurements are adjusted on the basis of a common set of input values, including the b-hadron lifetimes and fractions published in this *Review*. Some measurements are statistically correlated. Systematic correlations arise both from common physics sources (fragmentation fractions, lifetimes, branching ratios of b hadrons), and from purely experimental or algorithmic effects (efficiency, resolution, tagging, background description). Combining all published measurements [15,16,21,27–36] and accounting for all identified correlations yields $\Delta m_d = 0.510 \pm 0.003(\text{stat}) \pm 0.002(\text{syst})$ ps^{-1} [8], a result dominated by the BaBar, Belle and LHCb.

On the other hand, ARGUS and CLEO have published time-integrated measurements [37–39], which average to $\chi_d = 0.182 \pm 0.015$. Following Ref. 39, the width difference $\Delta\Gamma_d$ could in principle be extracted from the measured value of Γ_d and the above averages for Δm_d and χ_d (see Eq. (5)), provided that $\Delta\Gamma_d$ has a negligible impact on the Δm_d measurements. However, direct time-dependent studies published by DELPHI [15], BaBar [40], Belle [41], DØ [42] and LHCb [43] provide stronger constraints, which can be combined to yield [8]

$$\Delta\Gamma_d/\Gamma_d = 0.001 \pm 0.010\,. \tag{14}$$

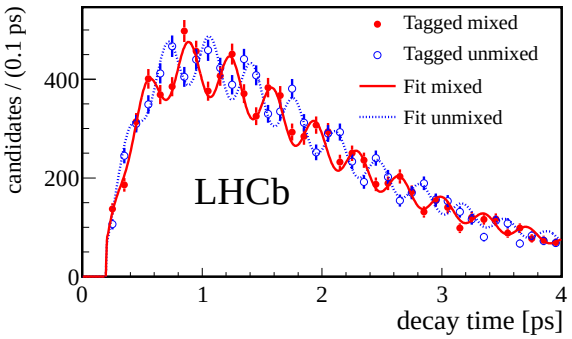

Figure 2: Proper time distribution of $B^0_s \to D^-_s\pi^+$ candidates tagged as mixed (red) or unmixed (blue) in the LHCb experiment, displaying B^0_s–$\overline{B}{}^0_s$ oscillations (from Ref. [46]) .

Assuming $\Delta\Gamma_d = 0$ and no CP violation in mixing, and using the measured B^0_d lifetime of 1.519 ± 0.005 ps, the Δm_d and χ_d results are combined to yield the world average

$$\Delta m_d = 0.510 \pm 0.003 \text{ ps}^{-1} \tag{15}$$

or, equivalently,

$$\chi_d = 0.1874 \pm 0.0018\,. \tag{16}$$

This Δm_d value provides an estimate of $2|M_{12}|$, and can be used with Eq. (6) to extract $|V_{td}|$ within the Standard Model [44]. The main experimental uncertainties on the result come from m_t and Δm_d, but are completely negligible with respect to the uncertainty due to the hadronic matrix element $f_{B_d}\sqrt{B_{B_d}} = 216 \pm 15$ MeV [45] obtained from unquenched lattice QCD calculations.

Δm_s and $\Delta\Gamma_s$ measurements

After many years of intense search at LEP and SLC, B^0_s–$\overline{B}{}^0_s$ oscillations were first observed in 2006 by CDF using 1 fb^{-1} of Tevatron Run II data [20]. More recently LHCb observed B^0_s–$\overline{B}{}^0_s$ oscillations independently with $B^0_s \to D^-_s\pi^+$ [34,46], $B^0_s \to D^-_s\mu^+\nu$X [36] and even $B^0_s \to J/\psi K^+K^-$ [47] decays, using 1 fb^{-1} of data collected at the LHC until the end of 2011. Taking systematic correlations into account, the average of all published measurements of Δm_s [20,34,36,46,47] is

$$\Delta m_s = 17.761 \pm 0.021(\text{stat}) \pm 0.007(\text{syst}) \text{ ps}^{-1}\,, \tag{17}$$

dominated by LHCb (see Fig. 2) and still statistically limited.

The information on $|V_{ts}|$ obtained in the framework of the Standard Model is hampered by the hadronic uncertainty, as in the B^0_d case. However, several uncertainties cancel in the frequency ratio

$$\frac{\Delta m_s}{\Delta m_d} = \frac{m_{B_s}}{m_{B_d}}\,\xi^2\left|\frac{V_{ts}}{V_{td}}\right|^2\,, \tag{18}$$

where $\xi = (f_{B_s}\sqrt{B_{B_s}})/(f_{B_d}\sqrt{B_{B_d}}) = 1.268 \pm 0.063$ is an SU(3) flavor-symmetry breaking factor obtained from unquenched

lattice QCD calculations [45]. Using the measurements of Eqs. (15) and (17), one can extract

$$\left|\frac{V_{td}}{V_{ts}}\right| = 0.2166 \pm 0.0007(\text{exp}) \pm 0.0108(\text{lattice})\,, \qquad (19)$$

in good agreement with (but much more precise than) the value obtained from the ratio of the $b \to d\gamma$ and $b \to s\gamma$ transition rates observed at the B factories [44].

The CKM matrix can be constrained using experimental results on observables such as Δm_d, Δm_s, $|V_{ub}/V_{cb}|$, ϵ_K, and $\sin(2\beta)$ together with theoretical inputs and unitarity conditions [44,48,49]. The constraint from our knowledge on the ratio $\Delta m_s/\Delta m_d$ is more effective in limiting the position of the apex of the CKM unitarity triangle than the one obtained from the Δm_d measurements alone, due to the reduced hadronic uncertainty in Eq. (18). We also note that the measured value of Δm_s is consistent with the Standard Model prediction obtained from CKM fits where no experimental information on Δm_s is used, *e.g.*, 17.4 ± 1.1 ps^{-1} [48] or $16.5\,^{+1.8}_{-1.4}$ ps^{-1} [49].

Information on $\Delta\Gamma_s$ can be obtained from the study of the proper time distribution of untagged B_s^0 samples [50]. In the case of an inclusive B_s^0 selection [51], or a flavor-specific (semileptonic or hadronic) B_s^0 decay selection [18,52,53], both the short- and long-lived components are present, and the proper time distribution is a superposition of two exponentials with decay constants $\Gamma_{\rm L,H} = \Gamma_s \pm \Delta\Gamma_s/2$. In principle, this provides sensitivity to both Γ_s and $(\Delta\Gamma_s/\Gamma_s)^2$. Ignoring $\Delta\Gamma_s$ and fitting for a single exponential leads to an estimate of Γ_s with a relative bias proportional to $(\Delta\Gamma_s/\Gamma_s)^2$. An alternative approach, which is directly sensitive to first order in $\Delta\Gamma_s/\Gamma_s$, is to determine the effective lifetime of untagged B_s^0 candidates decaying to pure CP eigenstates; measurements exist for $B_s^0 \to K^+K^-$ [54], $B_s^0 \to D_s^+D_s^-$ [53], $B_s^0 \to J/\psi f_0(980)$ [55], $B_s^0 \to J/\psi\pi^+\pi^-$ [47] and $B_s^0 \to J/\psi K_{\rm S}^0$ [56]. The extraction of $1/\Gamma_s$ and $\Delta\Gamma_s$ from such measurements, discussed in detail in Ref. [57], requires additional information in the form of theoretical assumptions or external inputs on weak phases and hadronic parameters. In what follows, the effective lifetimes from the above decays to pure CP eigenstates will be assumed to be dominated by a single weak phase.

The best sensitivity to $1/\Gamma_s$ and $\Delta\Gamma_s$ is achieved by the time-dependent measurements of the $B_s^0 \to J/\psi\phi$ (or more generally $B_s^0 \to J/\psi K^+K^-$) decay rates performed at CDF [58], DØ [59], ATLAS [60], and LHCb [47], where the CP-even and CP-odd amplitudes are separated statistically through a full angular analysis. The LHCb collaboration analyzes the $B_s^0 \to J/\psi K^+K^-$ decay considering that the K^+K^- system can be in a P-wave or S-wave state, and measures the dependence of the strong phase difference between the P-wave and S-wave amplitudes as a function of the K^+K^- invariant mass [47,61]; this allows the unambiguous determination of the sign of $\Delta\Gamma_s$, which is found to be positive. All these studies use both untagged and tagged B_s^0 candidates and are optimized for the measurement of the CP-violating phase ϕ_s, defined as the weak phase difference between the B_s^0–$\overline{B}_s^0$ mixing amplitude and the $b \to c\bar{c}s$ decay amplitude. As reported further below, the central value of the current experimental average of ϕ_s is zero. Assuming no CP violation (*i.e.*, $\phi_s = 0$) a combination [8] of the published $B_s^0 \to J/\psi\phi$, $J/\psi K^+K^-$ analyses [47,58–60] and of the effective lifetime measurements with flavor-specific [18,52,53] and pure CP [47,53–56] final states yields

$$\Delta\Gamma_s = +0.091 \pm 0.008 \text{ ps}^{-1} \quad \text{and} \quad 1/\Gamma_s = 1.512 \pm 0.007 \text{ ps}\,, \qquad (20)$$

or, equivalently,

$$1/\Gamma_{\rm L} = 1.414 \pm 0.010 \text{ ps} \quad \text{and} \quad 1/\Gamma_{\rm H} = 1.624 \pm 0.014 \text{ ps}\,, \qquad (21)$$

in good agreement with the Standard Model prediction $\Delta\Gamma_s = 0.087 \pm 0.021$ ps^{-1} [7].

Independent estimates of $\Delta\Gamma_s/\Gamma_s$ obtained from measurements of the $B_s^0 \to D_s^{(*)+}D_s^{(*)-}$ branching fractions are not included in the average, since they are based on the questionable [7] assumption that these decays account for all CP-even final states.

Average b-hadron mixing probability and b-hadron production fractions at high energy

Mixing measurements can significantly improve our knowledge on the fractions f_u, f_d, f_s, and $f_{\rm baryon}$, defined as the fractions of B_u, B_d^0, B_s^0, and b-baryons in an unbiased sample of weakly decaying b hadrons produced in high-energy collisions. Indeed, time-integrated mixing analyses using lepton pairs from $b\bar{b}$ events at high energy measure the quantity

$$\overline{\chi} = f'_d\,\chi_d + f'_s\,\chi_s\,, \qquad (22)$$

where f'_d and f'_s are the fractions of B_d^0 and B_s^0 hadrons in a sample of semileptonic b-hadron decays. Assuming that all b hadrons have the same semileptonic decay width implies $f'_q = f_q/(\Gamma_q\tau_b)$ $(q = s, d)$, where τ_b is the average b-hadron lifetime. Hence $\overline{\chi}$ measurements performed at LEP [62] and Tevatron [63–65], together with the χ_d average of Eq. (16) and the very good approximation $\chi_s = 1/2$ (in fact $\chi_s = 0.499311 \pm 0.000007$ from Eqs. (5), (17) and (20)), provide constraints on the fractions f_d and f_s. In what follows, we use the preliminary $\overline{\chi}$ result from CDF [64] instead of the published one [63]. Averages based on published data only can be found in the full listings of this *Review*.

The LEP experiments have measured $\mathcal{B}(\bar{b} \to B_s^0) \times \mathcal{B}(B_s^0 \to D_s^-\ell^+\nu_\ell X)$ [66], $\mathcal{B}(b \to \Lambda_b^0) \times \mathcal{B}(\Lambda_b^0 \to \Lambda_c^+\ell^-\overline{\nu}_\ell X)$ [67], and $\mathcal{B}(b \to \Xi_b^-) \times \mathcal{B}(\Xi_b^- \to \Xi^-\ell^-\overline{\nu}_\ell X)$ [68] from partially reconstructed final states including a lepton, $f_{\rm baryon}$ from protons identified in b events [69], and the production rate of charged b hadrons [70]. The b-hadron fraction ratios measured at CDF are based on double semileptonic $K^*\mu\mu$ and $\phi\mu\mu$ final states [71] and lepton-charm final states [72]; in addition CDF and DØ have both measured strange b-baryon production [73]. On the

other hand, fraction ratios have been studied by LHCb using fully reconstructed hadronic B_s^0 and B_d^0 decays [74], as well as semileptonic decays [75]. Both CDF and LHCb observe that the ratio $f_{\Lambda_b^0}/(f_u + f_d)$ decreases with the transverse momentum of the lepton+charm system, indicating that the b-hadron fractions are not the same in different environments. We therefore provide sets of fractions separately for LEP and Tevatron (and no complete set for LHCb, where strange b-baryon production has not been measured yet). A combination of all the available information under the constraints $f_u = f_d$, $f_u + f_d + f_s + f_{\rm baryon} = 1$, and Eq. (22), yields the averages shown in Table 1.

Table 1: $\overline{\chi}$ and b-hadron fractions (see text).

	in Z decays [8]	at Tevatron [8]	at LHCb [74]
$\overline{\chi}$	0.1259 ± 0.0042	0.127 ± 0.008	
$f_u = f_d$	0.404 ± 0.009	0.330 ± 0.030	
f_s	0.103 ± 0.009	0.103 ± 0.012	
$f_{\rm baryon}$	0.089 ± 0.015	0.237 ± 0.067	
f_s/f_d	0.254 ± 0.025	0.311 ± 0.037	0.256 ± 0.020

CP-violation studies

Evidence for CP violation in B_q^0–$\overline{B}_q^0$ mixing has been searched for, both with flavor-specific and inclusive B_q^0 decays, in samples where the initial flavor state is tagged, usually with a lepton from the other b-hadron in the event. In the case of semileptonic (or other flavor-specific) decays, where the final-state tag is also available, the following asymmetry [2]

$$\mathcal{A}_{\rm SL}^q = \frac{N(\overline{B}_q^0(t) \to \ell^+\nu_\ell X) - N(B_q^0(t) \to \ell^-\overline{\nu}_\ell X)}{N(\overline{B}_q^0(t) \to \ell^+\nu_\ell X) + N(B_q^0(t) \to \ell^-\overline{\nu}_\ell X)} \simeq 1 - |q/p|_q^2 \tag{23}$$

has been measured either in time-integrated analyses at CLEO [39,76], CDF [77], DØ [42,78,79] and LHCb [80], or in time-dependent analyses at LEP [31,81], BaBar [40,82] and Belle [83]. In the inclusive case, also investigated at LEP [81,84], no final-state tag is used, and the asymmetry [85]

$$\frac{N(B_q^0(t) \to \text{all}) - N(\overline{B}_q^0(t) \to \text{all})}{N(B_q^0(t) \to \text{all}) + N(\overline{B}_q^0(t) \to \text{all})} \simeq \mathcal{A}_{\rm SL}^q \left[\frac{x_q}{2}\sin(\Delta m_q\, t) - \sin^2\left(\frac{\Delta m_q\, t}{2}\right)\right] \tag{24}$$

must be measured as a function of the proper time to extract information on CP violation.

The DØ collaboration measures a like-sign dimuon charge asymmetry in semileptonic b decays that deviates by $2.8\,\sigma$ from the tiny Standard Model prediction and concludes, from a more refined analysis in bins of muon impact parameters, that the overall discrepancy is at the level of $3.6\,\sigma$ [42]. In all other cases, asymmetries compatible with zero (and the Standard Model [7]) have been found, with a precision limited by the available statistics. Several of the analyses at high energy don't disentangle the B_d^0 and B_s^0 contributions, and either quote a mean asymmetry or a measurement of $\mathcal{A}_{\rm SL}^d$ assuming $\mathcal{A}_{\rm SL}^s = 0$: we no longer include these in the average. An exception is the latest dimuon DØ analysis [42], which separates the two contributions by exploiting their dependence on the muon impact parameter cut. The resulting measurements of $\mathcal{A}_{\rm SL}^d$ and $\mathcal{A}_{\rm SL}^s$ are then both compatible with the Standard Model. They are also correlated. We therefore perform a two-dimensional average of the measurements of Refs. [39,40,42,76,78–80,82,83] and obtain [8]

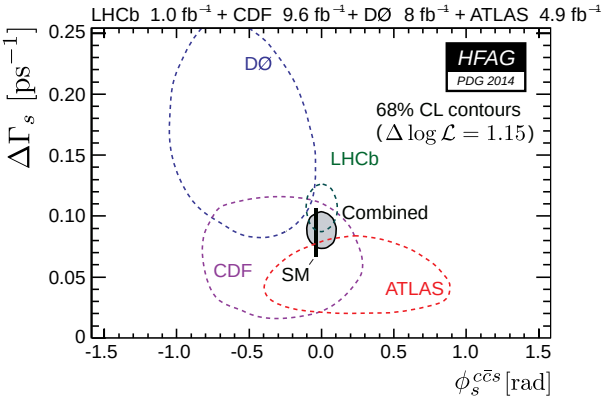

Figure 3: 68% CL contours in the $(\phi_s, \Delta\Gamma_s)$ plane, showing the measurements from CDF [58], DØ [59], ATLAS [60] and LHCb [47], with their combination [8]. The thin rectangle represents the Standard Model predictions of ϕ_s [49] and $\Delta\Gamma_s$ [7].

$$\mathcal{A}_{\rm SL}^d = -0.0009 \pm 0.0021\,, \quad \text{or} \quad |q/p|_d = 1.0005 \pm 0.0011\,, \tag{25}$$

$$\mathcal{A}_{\rm SL}^s = -0.0077 \pm 0.0042\,, \quad \text{or} \quad |q/p|_s = 1.0039 \pm 0.0021\,, \tag{26}$$

with a correlation coefficient of -0.19 between $\mathcal{A}_{\rm SL}^d$ and $\mathcal{A}_{\rm SL}^s$. These results show no evidence of CP violation and don't constrain yet the Standard Model.

CP violation induced by B_s^0–$\overline{B}_s^0$ mixing in $b \to c\bar{c}s$ decays has been a field of very active study in the past few years. In addition to the previously mentioned $B_s^0 \to J/\psi\phi$ and $B_s^0 \to J/\psi K^+K^-$ studies, the decay mode $B_s^0 \to J/\psi\pi^+\pi^-$ (including $B_s^0 \to J/\psi f_0(980)$) has also been analyzed by LHCb to measure ϕ_s [47], without the need for an angular analysis since the $J/\psi\pi^+\pi^-$ final state has been shown to be (very close to) a pure CP-odd state [86]. A two-dimensional fit [8] of all published analyses [47,58–60] in the $(\phi_s, \Delta\Gamma_s)$ plane, shown on Fig. 3, yields

$$\phi_s = 0.00 \pm 0.07\,. \tag{27}$$

This is consistent with the Standard Model prediction for ϕ_s, which is equal to $-2\beta_s = -2\arg(-(V_{ts}V_{tb}^*)/(V_{cs}V_{cb}^*)) = -0.0363\,^{+0.0016}_{-0.0015}$ [49], assuming negligible Penguin pollution.

Summary

B^0–$\overline{B}^0$ mixing has been and still is a field of intense study. While relatively little experimental progress was achieved in the B_d^0 sector during the past years, impressive new B_s^0

results became available from CDF, DØ and LHCb. The mass difference in the B_s^0–$\overline{B}_s^0$ system is now known to a relative precision of 0.12%, which is significantly better than that in the B_d^0–$\overline{B}_d^0$ system (0.68%). The non-zero decay width difference in the B_s^0–$\overline{B}_s^0$ system is now established, with a relative difference of $\Delta\Gamma_s/\Gamma_s = (13.8 \pm 1.2)\%$. Its sign has been determined: the heavy state of the B_s^0–$\overline{B}_s^0$ system lives longer than the light state. In contrast, the relative decay width difference in the B_d^0–$\overline{B}_d^0$ system, $\Delta\Gamma_d/\Gamma_d = (0.1 \pm 1.0)\%$, is still consistent with zero. CP violation in mixing has not been observed yet, with precisions on the semileptonic asymmetries below 0.5%. An impressive progress has been achieved in the measurement of the mixing-induced phase ϕ_s in B_s^0 decays proceeding through the $b \to c\bar{c}s$ transition, with a Gaussian uncertainty reaching the 0.07 radian level. Despite these significant improvements, all observations remain consistent with the Standard Model expectations.

However, the measurements where New Physics might show up are still statistically limited. More results are expected in the future, especially from LHCb in the B_s^0 sector, with promising prospects for the investigation of the CP-violating phase $\arg(-M_{12}/\Gamma_{12})$ and an expected uncertainty on ϕ_s of ~ 0.03 radian by the time of the next edition of this *Review*.

Mixing studies have clearly reached the stage of precision measurements, where much effort is needed, both on the experimental and theoretical sides, in particular to further reduce the hadronic uncertainties of lattice QCD calculations. In the long term, a stringent check of the consistency of the B_d^0 and B_s^0 mixing amplitudes (magnitudes and phases) with all other measured flavor-physics observables will be possible within the Standard Model, leading to very tight limits on (or otherwise a long-awaited surprize about) New Physics.

References

1. T.D. Lee and C.S. Wu, Ann. Rev. Nucl. Sci. **16**, 511 (1966); I.I. Bigi and A.I. Sanda, "CP violation," Cambridge Univ. Press, 2000; G.C. Branco, L. Lavoura, and J.P. Silva, "CP violation," Clarendon Press Oxford, 1999.
2. See the review on CP violation in meson decays by D. Kirkby and Y. Nir in this publication.
3. A.J. Buras, W. Slominski, and H. Steger, Nucl. Phys. **B245**, 369 (1984).
4. T. Inami and C.S. Lim, Prog. Theor. Phys. **65**, 297 (1981); for the power-like approximation, see A.J. Buras and R. Fleischer, page 91 in "Heavy Flavours II," eds. A.J. Buras and M. Lindner, Singapore World Scientific, 1998.
5. M. Kobayashi and K. Maskawa, Prog. Theor. Phys. **49**, 652 (1973).
6. I.I. Bigi *et al.*, in "CP violation," ed. C. Jarlskog, Singapore World Scientific, 1989.
7. A. Lenz and U. Nierste, `arXiv:1102.4274 [hep-ph]`; A. Lenz and U. Nierste, JHEP **0607**, 072 (2007).
8. Y. Amhis *et al.* (HFAG), "Averages of b-hadron, c-hadron, and τ-lepton properties as of early 2012," `arXiv:1207.1158v2 [hep-ex]`, August 2013;
the combined results on b-hadron fractions, lifetimes and mixing parameters published in this *Review* have been obtained by the B oscillations working group of the Heavy Flavor Averaging Group (HFAG), using the methods and procedures described in Chapter 3 of the above paper, after updating the list of inputs; for more information, see `http://www.slac.stanford.edu/xorg/hfag/osc/`.
9. C. Albajar *et al.* (UA1 Collab.), Phys. Lett. **B186**, 247 (1987).
10. H. Albrecht *et al.* (ARGUS Collab.), Phys. Lett. **B192**, 245 (1987).
11. H.-G. Moser and A. Roussarie, Nucl. Instrum. Methods **384**, 491 (1997).
12. SLD Collab., SLAC-PUB-7228, SLAC-PUB-7229, and SLAC-PUB-7230, *28th Int. Conf. on High Energy Physics,* Warsaw, 1996; J. Wittlin, PhD thesis, SLAC-R-582, 2001.
13. ALEPH Collab., contrib. 596 to *Int. Europhysics Conf. on High Energy Physics,* Jerusalem, 1997.
14. K. Abe *et al.* (SLD Collab.), Phys. Rev. **D67**, 012006 (2003).
15. J. Abdallah *et al.* (DELPHI Collab.), Eur. Phys. J. **C28**, 155 (2003).
16. F. Abe *et al.* (CDF Collab.), Phys. Rev. Lett. **80**, 2057 (1998) and Phys. Rev. **D59**, 032001 (1999); Phys. Rev. **D60**, 051101 (1999); Phys. Rev. **D60**, 072003 (1999); T. Affolder *et al.* (CDF Collab.), Phys. Rev. **D60**, 112004 (1999).
17. R. Barate *et al.* (ALEPH Collab.), Eur. Phys. J. **C4**, 367 (1998); Eur. Phys. J. **C7**, 553 (1999).
18. P. Abreu *et al.* (DELPHI Collab.), Eur. Phys. J. **C16**, 555 (2000).
19. See tagging summary on page 160 of K. Anikeev *et al.*, "B physics at the Tevatron: Run II and beyond," FERMILAB-PUB-01/97, `hep-ph/0201071`, and references therein.
20. A. Abulencia *et al.* (CDF Collab.), Phys. Rev. Lett. **97**, 242003 (2006).
21. V.M. Abazov *et al.* (DØ Collab.), Phys. Rev. **D74**, 112002 (2006).
22. V.M. Abazov *et al.* (DØ Collab.), Phys. Rev. Lett. **101**, 241801 (2008).
23. R. Aaij *et al.* (LHCb Collab.), Eur. Phys. J. **C72**, 2022 (2012).
24. LHCb Collab., LHCb note CERN-LHCb-CONF-2012-033, November 2012.
25. B. Aubert *et al.* (BaBar Collab.), Phys. Rev. Lett. **94**, 161803 (2005); K.-F. Chen *et al.* (Belle Collab.), Phys. Rev. **D72**, 012004 (2005).
26. Throughout this paper, we omit references of results that have been superseded by new published measurements.
27. D. Buskulic *et al.* (ALEPH Collab.), Z. Phys. **C75**, 397 (1997).
28. P. Abreu *et al.* (DELPHI Collab.), Z. Phys. **C76**, 579 (1997).
29. M. Acciarri *et al.* (L3 Collab.), Eur. Phys. J. **C5**, 195 (1998).
30. G. Alexander *et al.* (OPAL Collab.), Z. Phys. **C72**, 377 (1996); K. Ackerstaff *et al.* (OPAL Collab.), Z. Phys. **C76**, 417 (1997); G. Abbiendi *et al.* (OPAL Collab.), Phys. Lett. **B493**, 266 (2000).
31. K. Ackerstaff *et al.* (OPAL Collab.), Z. Phys. **C76**, 401 (1997).

32. B. Aubert *et al.* (BaBar Collab.), Phys. Rev. Lett. **88**, 221802 (2002) and Phys. Rev. **D66**, 032003 (2002); Phys. Rev. Lett. **88**, 221803 (2002); Phys. Rev. **D67**, 072002 (2003); Phys. Rev. **D73**, 012004 (2006).
33. N.C. Hastings *et al.* (Belle Collab.), Phys. Rev. **D67**, 052004 (2003); Y. Zheng *et al.* (Belle Collab.), Phys. Rev. **D67**, 092004 (2003); K. Abe *et al.* (Belle Collab.), Phys. Rev. **D71**, 072003 (2005).
34. R. Aaij *et al.* (LHCb Collab.), Phys. Lett. **B709**, 177 (2012).
35. R. Aaij *et al.* (LHCb Collab.), Phys. Lett. **B719**, 318 (2013).
36. R. Aaij *et al.* (LHCb Collab.), Eur. Phys. J. **C73**, 2655 (2013).
37. H. Albrecht *et al.* (ARGUS Collab.), Z. Phys. **C55**, 357 (1992); Phys. Lett. **B324**, 249 (1994).
38. J. Bartelt *et al.* (CLEO Collab.), Phys. Rev. Lett. **71**, 1680 (1993).
39. B.H. Behrens *et al.* (CLEO Collab.), Phys. Lett. **B490**, 36 (2000).
40. B. Aubert *et al.* (BaBar Collab.), Phys. Rev. Lett. **92**, 181801 (2004) and Phys. Rev. **D70**, 012007 (2004).
41. T. Higuchi *et al.* (Belle Collab.), Phys. Rev. **D85**, 071105 (2012).
42. V.M. Abazov *et al.* (DØ Collab.), Phys. Rev. **D89**, 012002 (2014).
43. R. Aaij *et al.* (LHCb Collab.), `arXiv:1402.2554 [hep-ex]`, to appear in JHEP.
44. See the review on the CKM quark-mixing matrix by A. Ceccucci, Z. Ligeti, and Y. Sakai in this publication.
45. S. Aoki *et al.* (FLAG working group), `arXiv:1310.8555 [hep-lat]`; see also `http://itpwiki.unibe.ch/flag/`.
46. R. Aaij *et al.* (LHCb Collab.), New J. Phys. **15**, 053021 (2013).
47. R. Aaij *et al.* (LHCb Collab.), Phys. Rev. **D87**, 112010 (2013).
48. M. Bona *et al.* (UTfit Collab.), `arXiv:hep-ph/0606167v2`; updated results at `http://www.utfit.org/`.
49. J. Charles *et al.* (CKMfitter Group), Phys. Rev. **D84**, 033005 (2011); updated results at `http://ckmfitter.in2p3.fr/`.
50. K. Hartkorn and H.-G. Moser, Eur. Phys. J. **C8**, 381 (1999).
51. M. Acciarri *et al.* (L3 Collab.), Phys. Lett. **B438**, 417 (1998).
52. D. Buskulic *et al.* (ALEPH Collab.), Phys. Lett. **B377**, 205 (1996); K. Ackerstaff *et al.* (OPAL Collab.), Phys. Lett. **B426**, 161 (1998); F. Abe *et al.* (CDF Collab.), Phys. Rev. **D59**, 032004 (1999); V.M. Abazov *et al.* (DØ Collab.), Phys. Rev. Lett. **97**, 241801 (2006); T. Aaltonen *et al.* (CDF Collab.), Phys. Rev. Lett. **107**, 272001 (2011).
53. R. Aaij *et al.* (LHCb Collab.), Phys. Rev. Lett. **112**, 111802 (2014).
54. R. Aaij *et al.* (LHCb Collab.), Phys. Lett. **B707**, 349 (2012); Phys. Lett. **B716**, 393 (2012).
55. T. Aaltonen *et al.* (CDF Collab.), Phys. Rev. **D84**, 052012 (2011).
56. R. Aaij *et al.* (LHCb Collab.), Nucl. Phys. **B873**, 275 (2013).
57. R. Fleischer and R. Knegjens, Eur. Phys. J. **C71**, 1789 (2011).
58. T. Aaltonen *et al.* (CDF Collab.), Phys. Rev. Lett. **109**, 171802 (2012).
59. V.M. Abazov *et al.* (DØ Collab.), Phys. Rev. **D85**, 032006 (2012).
60. G. Aad *et al.* (ATLAS Collab.), JHEP **1212**, 072 (2012).
61. R. Aaij *et al.* (LHCb Collab.), Phys. Rev. Lett. **108**, 241801 (2012).
62. ALEPH, DELPHI, L3, OPAL, and SLD Collabs.; Physics Reports **427**, 257 (2006); we use the $\overline{\chi}$ average given in Eq. (5.39).
63. D. Acosta *et al.* (CDF Collab.), Phys. Rev. **D69**, 012002 (2004).
64. CDF Collab., CDF note 10335, January 2011.
65. V.M. Abazov *et al.* (DØ Collab.), Phys. Rev. **D74**, 092001 (2006).
66. P. Abreu *et al.* (DELPHI Collab.), Phys. Lett. **B289**, 199 (1992); P.D. Acton *et al.* (OPAL Collab.), Phys. Lett. **B295**, 357 (1992); D. Buskulic *et al.* (ALEPH Collab.), Phys. Lett. **B361**, 221 (1995).
67. P. Abreu *et al.* (DELPHI Collab.), Z. Phys. **C68**, 375 (1995); R. Barate *et al.* (ALEPH Collab.), Eur. Phys. J. **C2**, 197 (1998).
68. D. Buskulic *et al.* (ALEPH Collab.), Phys. Lett. **B384**, 449 (1996); J. Abdallah *et al.* (DELPHI Collab.), Eur. Phys. J. **C44**, 299 (2005).
69. R. Barate *et al.* (ALEPH Collab.), Eur. Phys. J. **C5**, 205 (1998).
70. J. Abdallah *et al.* (DELPHI Collab.), Phys. Lett. **B576**, 29 (2003).
71. F. Abe *et al.* (CDF Collab.), Phys. Rev. **D60**, 092005 (1999).
72. T. Aaltonen *et al.* (CDF Collab.), Phys. Rev. **D77**, 072003 (2008); T. Affolder *et al.* (CDF Collab.), Phys. Rev. Lett. **84**, 1663 (2000); the measurement of $f_{\rm baryon}/f_d$ in the latter paper has been updated based on T. Aaltonen *et al.* (CDF Collab.), Phys. Rev. **D79**, 032001 (2009).
73. V.M. Abazov *et al.* (DØ Collab.), Phys. Rev. Lett. **99**, 052001 (2007); V.M. Abazov *et al.* (DØ Collab.), Phys. Rev. Lett. **101**, 232002 (2008); T. Aaltonen *et al.* (CDF Collab.), Phys. Rev. **D80**, 072003 (2009).
74. R. Aaij *et al.* (LHCb Collab.), JHEP **1304**, 001 (2013).
75. R. Aaij *et al.* (LHCb Collab.), Phys. Rev. **D85**, 032008 (2012).
76. D.E. Jaffe *et al.* (CLEO Collab.), Phys. Rev. Lett. **86**, 5000 (2001).
77. F. Abe *et al.* (CDF Collab.), Phys. Rev. **D55**, 2546 (1997).
78. V.M. Abazov *et al.* (DØ Collab.), Phys. Rev. **D86**, 072009 (2012).
79. V.M. Abazov *et al.* (DØ Collab.), Phys. Rev. Lett. **110**, 011801 (2013).
80. R. Aaij *et al.* (LHCb Collab.), Phys. Lett. **B728**, 607 (2014).
81. R. Barate *et al.* (ALEPH Collab.), Eur. Phys. J. **C20**, 431 (2001).
82. B. Aubert *et al.* (BaBar Collab.), Phys. Rev. Lett. **96**, 251802 (2006); J.P. Lees *et al.* (BaBar Collab.), Phys. Rev. Lett. **111**, 101802 (2013).

83. E. Nakano *et al.* (Belle Collab.), Phys. Rev. **D73**, 112002 (2006).

84. G. Abbiendi *et al.* (OPAL Collab.), Eur. Phys. J. **C12**, 609 (2000).

85. M. Beneke, G. Buchalla, and I. Dunietz, Phys. Lett. **B393**, 132 (1997); I. Dunietz, Eur. Phys. J. **C7**, 197 (1999).

86. R. Aaij *et al.* (LHCb Collab.), Phys. Rev. **D86**, 052006 (2012).

B^0-$\overline{B}^0$ MIXING PARAMETERS

For a discussion of B^0-$\overline{B}^0$ mixing see the note on "B^0-$\overline{B}^0$ Mixing" in the B^0 Particle Listings above.

χ_d is a measure of the time-integrated B^0-$\overline{B}^0$ mixing probability that a produced $B^0(\overline{B}^0)$ decays as a $\overline{B}^0(B^0)$. Mixing violates $\Delta B \neq 2$ rule.

$$\chi_d = \frac{x_d^2}{2(1+x_d^2)}$$

$$x_d = \frac{\Delta m_{B^0}}{\Gamma_{B^0}} = (m_{B^0_H} - m_{B^0_L})\,\tau_{B^0}\ ,$$

where H, L stand for heavy and light states of two B^0 CP eigenstates and $\tau_{B^0} = \frac{1}{0.5(\Gamma_{B^0_H}+\Gamma_{B^0_L})}$.

χ_d

This B^0-$\overline{B}^0$ mixing parameter is the probability (integrated over time) that a produced B^0 (or $\overline{B}^0$) decays as a $\overline{B}^0$ (or B^0), e.g. for inclusive lepton decays

$\chi_d = \Gamma(B^0 \to \ell^- X \text{ (via } \overline{B}^0)) / \Gamma(B^0 \to \ell^\pm X)$

$= \Gamma(\overline{B}^0 \to \ell^+ X \text{ (via } B^0)) / \Gamma(\overline{B}^0 \to \ell^\pm X)$

Where experiments have measured the parameter $r = \chi/(1-\chi)$, we have converted to χ. Mixing violates the $\Delta B \neq 2$ rule.

Note that the measurement of χ at energies higher than the $\Upsilon(4S)$ have not separated χ_d from χ_s where the subscripts indicate $B^0(\overline{b}d)$ or $B^0_s(\overline{b}s)$. They are listed in the $B^\pm/B^0/B^0_s$/b-baryon ADMIXTURE section.

The experiments at $\Upsilon(4S)$ make an assumption about the $B^0\overline{B}^0$ fraction and about the ratio of the $B^\pm$ and B^0 semileptonic branching ratios (usually that it equals one).

"OUR EVALUATION" is an average using rescaled values of the data listed below. The average and rescaling were performed by the Heavy Flavor Averaging Group (HFAG) and are described at http://www.slac.stanford.edu/xorg/hfag/. The averaging/rescaling procedure takes into account correlations between the measurements, includes χ_d calculated from Δm_{B^0} and τ_{B^0}.

VALUE	CL%	DOCUMENT ID		TECN	COMMENT
0.1874±0.0018 OUR EVALUATION					
0.182 ±0.015 OUR AVERAGE					
0.198 ±0.013 ±0.014		[1] BEHRENS	00B	CLE2	$e^+e^- \to \Upsilon(4S)$
0.16 ±0.04 ±0.04		[2] ALBRECHT	94	ARG	$e^+e^- \to \Upsilon(4S)$
0.149 ±0.023 ±0.022		[3] BARTELT	93	CLE2	$e^+e^- \to \Upsilon(4S)$
0.171 ±0.048		[4] ALBRECHT	92L	ARG	$e^+e^- \to \Upsilon(4S)$
• • • We do not use the following data for averages, fits, limits, etc. • • •					
0.20 ±0.13 ±0.12		[5] ALBRECHT	96D	ARG	$e^+e^- \to \Upsilon(4S)$
0.19 ±0.07 ±0.09		[6] ALBRECHT	96D	ARG	$e^+e^- \to \Upsilon(4S)$
0.24 ±0.12		[7] ELSEN	90	JADE	e^+e^- 35–44 GeV
0.158 $^{+0.052}_{-0.059}$		ARTUSO	89	CLEO	$e^+e^- \to \Upsilon(4S)$
0.17 ±0.05		[8] ALBRECHT	87I	ARG	$e^+e^- \to \Upsilon(4S)$
<0.19	90	[9] BEAN	87B	CLEO	$e^+e^- \to \Upsilon(4S)$
<0.27	90	[10] AVERY	84	CLEO	$e^+e^- \to \Upsilon(4S)$

[1] BEHRENS 00B uses high-momentum lepton tags and partially reconstructed $\overline{B}^0 \to D^{*+}\pi^-$, ρ^- decays to determine the flavor of the B meson.

[2] ALBRECHT 94 reports r=0.194 ± 0.062 ± 0.054. We convert to χ for comparison. Uses tagged events (lepton + pion from D^*).

[3] BARTELT 93 analysis performed using tagged events (lepton+pion from D^*). Using dilepton events they obtain $0.157 \pm 0.016^{+0.033}_{-0.028}$.

[4] ALBRECHT 92L is a combined measurement employing several lepton-based techniques. It uses all previous ARGUS data in addition to new data and therefore supersedes ALBRECHT 87I. A value of $r = 20.6 \pm 7.0\%$ is directly measured. The value can be used to measure $x = \Delta M/\Gamma = 0.72 \pm 0.15$ for the B_d meson. Assumes $f_{+-}/f_0 = 1.0 \pm 0.05$ and uses $\tau_{B^\pm}/\tau_{B^0} = (0.95 \pm 0.14)$ (f_{+-}/f_0).

[5] Uses $D^{*+}K^\pm$ correlations.

[6] Uses $(D^{*+}\ell^-)\,K^\pm$ correlations.

[7] These experiments see a combination of B_s and B_d mesons.

[8] ALBRECHT 87I is inclusive measurement with like-sign dileptons, with tagged B decays plus leptons, and one fully reconstructed event. Measures r=0.21 ± 0.08. We convert to χ for comparison. Superseded by ALBRECHT 92L.

[9] BEAN 87B measured $r <$ 0.24; we converted to χ.

[10] Same-sign dilepton events. Limit assumes semileptonic BR for B^+ and B^0 equal. If $B^0/B^\pm$ ratio <0.58, no limit exists. The limit was corrected in BEAN 87B from $r <$ 0.30 to $r <$ 0.37. We converted this limit to χ.

$\Delta m_{B^0} = m_{B^0_H} - m_{B^0_L}$

Δm_{B^0} is a measure of 2π times the B^0-$\overline{B}^0$ oscillation frequency in time-dependent mixing experiments.

The second "OUR EVALUATION" is an average using rescaled values of the data listed below. The average and rescaling were performed by the Heavy Flavor Averaging Group (HFAG) and are described at http://www.slac.stanford.edu/xorg/hfag/. The averaging/rescaling procedure takes into account correlations between the measurements.

The first "OUR EVALUATION", also provided by the HFAG, includes Δm_d calculated from χ_d measured at $\Upsilon(4S)$.

VALUE ($10^{12}\ \hbar\ s^{-1}$)	DOCUMENT ID		TECN	COMMENT
0.510 ±0.003 OUR EVALUATION First				
0.510 ±0.003 OUR EVALUATION Second				
0.503 ±0.011 ±0.013	AAIJ	13CF	LHCB	pp at 7 TeV
0.5156 ±0.0051 ±0.0033	[1] AAIJ	13F	LHCB	pp at 7 TeV
0.499 ±0.032 ±0.003	[2] AAIJ	12I	LHCB	pp at 7 TeV
0.506 ±0.020 ±0.016	[3] ABAZOV	06W	D0	$p\overline{p}$ at 1.96 TeV
0.511 ±0.007 $^{+0.007}_{-0.006}$	[4] AUBERT	06G	BABR	$e^+e^- \to \Upsilon(4S)$
0.511 ±0.005 ±0.006	[5] ABE	05B	BELL	$e^+e^- \to \Upsilon(4S)$
0.531 ±0.025 ±0.007	[6] ABDALLAH	03B	DLPH	$e^+e^- \to Z$
0.503 ±0.008 ±0.010	[7] HASTINGS	03	BELL	$e^+e^- \to \Upsilon(4S)$
0.509 ±0.017 ±0.020	[8] ZHENG	03	BELL	$e^+e^- \to \Upsilon(4S)$
0.516 ±0.016 ±0.010	[9] AUBERT	02I	BABR	$e^+e^- \to \Upsilon(4S)$
0.493 ±0.012 ±0.009	[10] AUBERT	02J	BABR	$e^+e^- \to \Upsilon(4S)$
0.497 ±0.024 ±0.025	[11] ABBIENDI,G	00B	OPAL	$e^+e^- \to Z$
0.503 ±0.064 ±0.071	[12] ABE	99K	CDF	$p\overline{p}$ at 1.8 TeV
0.500 ±0.052 ±0.043	[13] ABE	99Q	CDF	$p\overline{p}$ at 1.8 TeV
0.516 ±0.099 $^{+0.029}_{-0.035}$	[14] AFFOLDER	99C	CDF	$p\overline{p}$ at 1.8 TeV
0.471 $^{+0.078}_{-0.068}$ $^{+0.033}_{-0.034}$	[15] ABE	98C	CDF	$p\overline{p}$ at 1.8 TeV
0.458 ±0.046 ±0.032	[16] ACCIARRI	98D	L3	$e^+e^- \to Z$
0.437 ±0.043 ±0.044	[17] ACCIARRI	98D	L3	$e^+e^- \to Z$
0.472 ±0.049 ±0.053	[18] ACCIARRI	98D	L3	$e^+e^- \to Z$
0.523 ±0.072 ±0.043	[19] ABREU	97N	DLPH	$e^+e^- \to Z$
0.493 ±0.042 ±0.027	[17] ABREU	97N	DLPH	$e^+e^- \to Z$
0.499 ±0.053 ±0.015	[20] ABREU	97N	DLPH	$e^+e^- \to Z$
0.480 ±0.040 ±0.051	[16] ABREU	97N	DLPH	$e^+e^- \to Z$
0.444 ±0.029 $^{+0.020}_{-0.017}$	[17] ACKERSTAFF	97U	OPAL	$e^+e^- \to Z$
0.430 ±0.043 $^{+0.028}_{-0.030}$	[16] ACKERSTAFF	97V	OPAL	$e^+e^- \to Z$
0.482 ±0.044 ±0.024	[21] BUSKULIC	97D	ALEP	$e^+e^- \to Z$
0.404 ±0.045 ±0.027	[17] BUSKULIC	97D	ALEP	$e^+e^- \to Z$
0.452 ±0.039 ±0.044	[16] BUSKULIC	97D	ALEP	$e^+e^- \to Z$
0.539 ±0.060 ±0.024	[22] ALEXANDER	96V	OPAL	$e^+e^- \to Z$
0.567 ±0.089 $^{+0.029}_{-0.023}$	[23] ALEXANDER	96V	OPAL	$e^+e^- \to Z$
• • • We do not use the following data for averages, fits, limits, etc. • • •				
0.492 ±0.018 ±0.013	[24] AUBERT	03C	BABR	Repl. by AUBERT 06G
0.516 ±0.016 ±0.010	[25] AUBERT	02N	BABR	$e^+e^- \to \Upsilon(4S)$
0.494 ±0.012 ±0.015	[26] HARA	02	BELL	Repl. by ABE 05B
0.528 ±0.017 ±0.011	[27] TOMURA	02	BELL	Repl. by ABE 05B
0.463 ±0.008 ±0.016	[10] ABE	01D	BELL	Repl. by HASTINGS 03
0.444 ±0.028 ±0.028	[28] ACCIARRI	98D	L3	$e^+e^- \to Z$
0.497 ±0.035	[29] ABREU	97N	DLPH	$e^+e^- \to Z$
0.467 ±0.022 $^{+0.017}_{-0.015}$	[30] ACKERSTAFF	97V	OPAL	$e^+e^- \to Z$
0.446 ±0.032	[31] BUSKULIC	97D	ALEP	$e^+e^- \to Z$
0.531 $^{+0.050}_{-0.046}$ ±0.078	[32] ABREU	96Q	DLPH	Sup. by ABREU 97N
0.496 $^{+0.055}_{-0.051}$ ±0.043	[16] ACCIARRI	96E	L3	Repl. by ACCIARRI 98D
0.548 ±0.050 $^{+0.023}_{-0.019}$	[33] ALEXANDER	96V	OPAL	$e^+e^- \to Z$
0.496 ±0.046	[34] AKERS	95J	OPAL	Repl. by ACKERSTAFF 97V
0.462 $^{+0.040}_{-0.053}$ $^{+0.052}_{-0.035}$	[16] AKERS	95J	OPAL	Repl. by ACKERSTAFF 97V
0.50 ±0.12 ±0.06	[19] ABREU	94M	DLPH	Sup. by ABREU 97N
0.508 ±0.075 ±0.025	[22] AKERS	94C	OPAL	Repl. by ALEXANDER 96V
0.57 ±0.11 ±0.02	[23] AKERS	94H	OPAL	Repl. by ALEXANDER 96V
0.50 $^{+0.07}_{-0.06}$ $^{+0.11}_{-0.10}$	[16] BUSKULIC	94B	ALEP	Sup. by BUSKULIC 97D
0.52 $^{+0.10}_{-0.11}$ $^{+0.04}_{-0.03}$	[23] BUSKULIC	93K	ALEP	Sup. by BUSKULIC 97D

[1] Measured using $B^0 \to D^-\pi^+$ and $B^0 \to J/\psi K^*(892)^0$ decays.

[2] Measured using $B^0 \to D^-\pi^+$.

[3] Uses opposite-side flavor-tagging with $B \to D^{(*)}\mu\nu_\mu X$ events.

[4] Measured using a simultaneous fit of the B^0 lifetime and $\overline{B}^0B^0$ oscillation frequency Δm_d in the partially reconstructed $B^0 \to D^{*-}\ell\nu$ decays.

[5] Measurement performed using a combined fit of CP-violation, mixing and lifetimes.

[6] Events with a high transverse momentum lepton were removed and an inclusively reconstructed vertex was required.

[7] HASTINGS 03 measurement based on the time evolution of dilepton events. It also reports $f_+/f_0 = 1.01 \pm 0.03 \pm 0.09$ and CPT violation parameters in B^0-$\overline{B}^0$ mixing.

[8] ZHENG 03 data analyzed using partially reconstructed $\overline{B}^0 \to D^{*-}\pi^+$ decay and a flavor tag based on the charge of the lepton from the accompanying B decay.
[9] Uses a tagged sample of fully-reconstructed neutral B decays at $\Upsilon(4S)$.
[10] Measured based on the time evolution of dilepton events in $\Upsilon(4S)$ decays.
[11] Data analyzed using partially reconstructed $\overline{B}^0 \to D^{*+}\ell^-\overline{\nu}$ decay and a combination of flavor tags from the rest of the event.
[12] Uses di-muon events.
[13] Uses jet-charge and lepton-flavor tagging.
[14] Uses $\ell^- D^{*+} -\ell$ events.
[15] Uses π-B in the same side.
[16] Uses ℓ-ℓ.
[17] Uses ℓ-$Q_{\rm hem}$.
[18] Uses ℓ-ℓ with impact parameters.
[19] Uses $D^{*\pm}$-$Q_{\rm hem}$.
[20] Uses $\pi_s^{\pm}$ ℓ-$Q_{\rm hem}$.
[21] Uses $D^{*\pm}$-$\ell/Q_{\rm hem}$.
[22] Uses $D^{*\pm}$ ℓ-$Q_{\rm hem}$.
[23] Uses $D^{*\pm}$-ℓ.
[24] AUBERT 03C uses a sample of approximately 14,000 exclusively reconstructed $B^0 \to D^*(2010)^-\ell\nu$ and simultaneously measures the lifetime and oscillation frequency.
[25] AUBERT 02N result based on the same analysis and data sample reported in AUBERT 02I.
[26] Uses a tagged sample of B^0 decays reconstructed in the mode $B^0 \to D^*\ell\nu$.
[27] Uses a tagged sample of fully-reconstructed hadronic B^0 decays at $\Upsilon(4S)$.
[28] ACCIARRI 98D combines results from ℓ-ℓ, ℓ-$Q_{\rm hem}$, and ℓ-ℓ with impact parameters.
[29] ABREU 97N combines results from $D^{*\pm}$-$Q_{\rm hem}$, ℓ-$Q_{\rm hem}$, $\pi_s^{\pm}$ ℓ-$Q_{\rm hem}$, and ℓ-ℓ.
[30] ACKERSTAFF 97V combines results from ℓ-ℓ, ℓ-$Q_{\rm hem}$, D^*-ℓ, and $D^{*\pm}$-$Q_{\rm hem}$.
[31] BUSKULIC 97D combines results from $D^{*\pm}$-$\ell/Q_{\rm hem}$, ℓ-$Q_{\rm hem}$, and ℓ-ℓ.
[32] ABREU 96Q analysis performed using lepton, kaon, and jet-charge tags.
[33] ALEXANDER 96V combines results from $D^{*\pm}$-ℓ and $D^{*\pm}$ ℓ-$Q_{\rm hem}$.
[34] AKERS 95J combines results from charge measurement, $D^{*\pm}$ ℓ-$Q_{\rm hem}$ and ℓ-ℓ.

$x_d = \Delta m_{B^0}/\Gamma_{B^0}$

The second "OUR EVALUATION" is an average using rescaled values of the data listed below. The average and rescaling were performed by the Heavy Flavor Averaging Group (HFAG) and are described at http://www.slac.stanford.edu/xorg/hfag/. The averaging/rescaling procedure takes into account correlations between the measurements.

The first "OUR EVALUATION", also provided by the HFAG, includes χ_d measured at $\Upsilon(4S)$.

VALUE	DOCUMENT ID
0.774±0.006 OUR EVALUATION	First
0.774±0.006 OUR EVALUATION	Second

Re(λ_{CP} / $|\lambda_{CP}|$) Re(z)

The λ_{CP} characterizes B^0 and $\overline{B}^0$ decays to states of charmonium plus K^0_L. Parameter z is used to describe CPT violation in mixing, see the review on "CP Violation" in the reviews section.

VALUE	DOCUMENT ID		TECN	COMMENT
0.014±0.035±0.034	[1] AUBERT,B	04C	BABR	$e^+e^- \to \Upsilon(4S)$

[1] Corresponds to 90% confidence range [−0.072, 0.101].

ΔΓ Re(z)

VALUE	DOCUMENT ID		TECN	COMMENT
−0.0071±0.0039±0.0020	AUBERT	06T	BABR	$e^+e^- \to \Upsilon(4S)$

Re(z)

VALUE (units 10^{-2})	DOCUMENT ID		TECN	COMMENT
1.9± 3.7±3.3	[1] HIGUCHI	12	BELL	$e^+e^- \to \Upsilon(4S)$
• • • We do not use the following data for averages, fits, limits, etc. • • •				
0 ±12 ±1	[2] HASTINGS	03	BELL	Repl. by HIGUCHI 12

[1] Measured using $B^0 \to J/\psi K^0_S$, $J/\psi K^0_L$, $D^-\pi^+$, $D^{*-}\pi^+$, $D^{*-}\rho^+$, and $D^{*-}\ell^+\nu$ decays.
[2] Measured using inclusive dilepton events from B^0 decay.

Im(z)

VALUE (units 10^{-2})	DOCUMENT ID		TECN	COMMENT
−0.8 ±0.4 OUR AVERAGE				
−0.57±0.33±0.33	[1] HIGUCHI	12	BELL	$e^+e^- \to \Upsilon(4S)$
−1.39±0.73±0.32	[2] AUBERT	06T	BABR	$e^+e^- \to \Upsilon(4S)$
• • • We do not use the following data for averages, fits, limits, etc. • • •				
3.8 ±2.9 ±2.5	[3] AUBERT,B	04C	BABR	Repl. by AUBERT 06T
−3 ±1 ±3	[4] HASTINGS	03	BELL	Repl. by HIGUCHI 12

[1] Measured using $B^0 \to J/\psi K^0_S$, $J/\psi K^0_L$, $D^-\pi^+$, $D^{*-}\pi^+$, $D^{*-}\rho^+$, and $D^{*-}\ell^+\nu$ decays.
[2] Assuming $\Delta\Gamma = 0$, the result becomes Im(z) = −0.0037 ± 0.0046.
[3] Corresponds to 90% confidence range [−0.028, 0.104].
[4] Measured using inclusive dilepton events from B^0 decay.

CP VIOLATION PARAMETERS

Re(ϵ_{B^0})/(1+$|\epsilon_{B^0}|^2$)

CP impurity in B^0_d system. It is obtained from either $a_{\ell\ell}$, the charge asymmetry in like-sign dilepton events or a_{cp}, the time-dependent asymmetry of inclusive B^0 and $\overline{B}^0$ decays.

The second "OUR EVALUATION" is an average using rescaled values of the data listed below. The average and rescaling were performed by the Heavy Flavor Averaging Group (HFAG) and are described at http://www.slac.stanford.edu/xorg/hfag/. The averaging/rescaling procedure takes into account correlations between the measurements. It assumes there is no CP violation in B_S mixing.

The first "OUR EVALUATION", also provided by the HFAG, uses the measurements from B-factories only.

VALUE (units 10^{-3})	DOCUMENT ID		TECN	COMMENT
0.1 ± 0.8 OUR EVALUATION	first eval			
− 0.2 ± 0.5 OUR EVALUATION	second eval			
0.9 ± 0.5 OUR AVERAGE				
1.55± 1.05	[1] ABAZOV	14	D0	$p\overline{p}$ at 1.96 TeV
0.15± 0.42$^{+0.94}_{-0.81}$	[2] LEES	13N	BABR	$e^+e^- \to \Upsilon(4S)$
1.7 ± 1.1 ±0.4	[3] ABAZOV	12AC	D0	$p\overline{p}$ at 1.96 TeV
0.4 ± 1.3 ±0.9	[4] AUBERT	06T	BABR	$e^+e^- \to \Upsilon(4S)$
− 0.3 ± 2.0 ±2.1	[5] NAKANO	06	BELL	$e^+e^- \to \Upsilon(4S)$
1.2 ± 2.9 ±3.6	[6] AUBERT	02K	BABR	$e^+e^- \to \Upsilon(4S)$
− 3.2 ± 6.5	[7] BARATE	01D	ALEP	$e^+e^- \to Z$
3.5 ±10.3 ±1.5	[8] JAFFE	01	CLE2	$e^+e^- \to \Upsilon(4S)$
1.2 ±13.8 ±3.2	[9] ABBIENDI	99J	OPAL	$e^+e^- \to Z$
2 ± 7 ±3	[10] ACKERSTAFF	97U	OPAL	$e^+e^- \to Z$
• • • We do not use the following data for averages, fits, limits, etc. • • •				
− 0.3 ± 1.3	[11] ABAZOV	11U	D0	Repl. by ABAZOV 14
− 2.3 ± 1.1 ±0.8	[12] ABAZOV	06S	D0	Repl. by ABAZOV 11U
−14.7 ± 6.7 ±5.7	[13] AUBERT,B	04C	BABR	Repl. by AUBERT 06T
4 ±18 ±3	[14] BEHRENS	00B	CLE2	Repl. by JAFFE 01
< 45	[15] BARTELT	93	CLE2	$e^+e^- \to \Upsilon(4S)$

[1] ABAZOV 14 uses the dimuon charge asymmetry with different impact parameters from which it reports $A^d_{SL} = (-0.62 \pm 0.42) \times 10^{-2}$.
[2] Uses $B^0 \to D^{*-}X\ell^+\nu_\ell$ and a kaon-tagged sample which yields measurement of A^d_{SL} = (0.06±0.17$^{+0.38}_{-0.32}$)%, corresponding to $\Delta_{CP} = 1-|q/p| = (0.29\pm0.84^{+1.88}_{-1.61})\times10^{-3}$.
[3] ABAZOV 12AC uses $B^0 \to D^-\mu^+X$ and $B^0 \to D^*(2010)^-\mu^+X$ decays without initial state flavor tagging which yields measurement of $A^d_{SL} = (6.8 \pm 4.5 \pm 1.4) \times 10^{-3}$.
[4] AUBERT 06T reports $|q/p|-1=(-0.8\pm2.7\pm1.9)\times10^{-3}$. We convert to $(1-|q/p|^2)/4$.
[5] Uses the charge asymmetry in like-sign dilepton events and reports $|q/p| = 1.0005 \pm 0.0040 \pm 0.0043$.
[6] AUBERT 02K uses the charge asymmetry in like-sign dilepton events.
[7] BARATE 01D measured by investigating time-dependent asymmetries in semileptonic and fully inclusive B^0_d decays.
[8] JAFFE 01 finds $a_{\ell\ell} = 0.013 \pm 0.050 \pm 0.005$ and combines with the previous BEHRENS 00B independent measurement.
[9] Data analyzed using the time-dependent asymmetry of inclusive B^0 decay. The production flavor of B^0 mesons is determined using both the jet charge and the charge of secondary vertex in the opposite hemisphere.
[10] ACKERSTAFF 97U assumes CPT and is based on measuring the charge asymmetry in a sample of B^0 decays defined by lepton and $Q_{\rm hem}$ tags. If CPT is not invoked, Re(ϵ_B) = −0.006 ± 0.010 ± 0.006 is found. The indirect CPT violation parameter is determined to Im(δB) = −0.020 ± 0.016 ± 0.006.
[11] ABAZOV 11U uses the dimuon charge asymmetry with different impact parameters from which it reports $A^d_{SL} = (-1.2 \pm 5.2) \times 10^{-3}$.
[12] Uses the dimuon charge asymmetry.
[13] AUBERT 04C reports $|q/p| = 1.029\pm0.013\pm0.011$ and we converted it to (1- $|q/p|^2$)/4.
[14] BEHRENS 00B uses high-momentum lepton tags and partially reconstructed $\overline{B}^0 \to D^{*+}\pi^-$, ρ^- decays to determine the flavor of the B meson.
[15] BARTELT 93 finds $a_{\ell\ell} = 0.031 \pm 0.096 \pm 0.032$ which corresponds to $|a_{\ell\ell}| < 0.18$, which yields the above $|{\rm Re}(\epsilon_{B^0})/(1+|\epsilon_{B^0}|^2|$.

$A_{T/CP}$

$A_{T/CP}$ is defined as

$$\frac{P(\overline{B}^0 \to B^0) - P(B^0 \to \overline{B}^0)}{P(\overline{B}^0 \to B^0) + P(B^0 \to \overline{B}^0)},$$

the CPT invariant asymmetry between the oscillation probabilities P($\overline{B}^0 \to B^0$) and P($B^0 \to \overline{B}^0$).

VALUE	DOCUMENT ID		TECN	COMMENT
0.005±0.012±0.014	[1] AUBERT	02K	BABR	$e^+e^- \to \Upsilon(4S)$

[1] AUBERT 02K uses the charge asymmetry in like-sign dilepton events.

$A_{CP}(B^0 \to D^*(2010)^+ D^-)$

A_{CP} is defined as

$$\frac{B(\overline{B}^0 \to \overline{f}) - B(B^0 \to f)}{B(\overline{B}^0 \to \overline{f}) + B(B^0 \to f)},$$

the CP-violation charge asymmetry of exclusive B^0 and $\overline{B}^0$ decay.

VALUE	DOCUMENT ID		TECN	COMMENT
0.037±0.034 OUR AVERAGE				
0.06 ±0.05 ±0.02	ROHRKEN	12	BELL	$e^+e^- \to \Upsilon(4S)$
0.008±0.048±0.013	AUBERT	09C	BABR	$e^+e^- \to \Upsilon(4S)$
0.07 ±0.08 ±0.04	[1] AUSHEV	04	BELL	$e^+e^- \to \Upsilon(4S)$
• • • We do not use the following data for averages, fits, limits, etc. • • •				
−0.12 ±0.06 ±0.02	AUBERT	07AI	BABR	Repl. by AUBERT 09C
−0.03 ±0.10 ±0.02	AUBERT,B	06A	BABR	Repl. by AUBERT 07AI
−0.03 ±0.11 ±0.05	AUBERT	03J	BABR	Repl. by AUBERT,B 06B

[1] Combines results from fully and partially reconstructed $B^0 \to D^{*\pm} D^{\mp}$ decays.

$A_{CP}(B^0 \to [K^+K^-]_D K^*(892)^0)$

VALUE	DOCUMENT ID		TECN	COMMENT
−0.45±0.23±0.02	AAIJ	13L	LHCB	pp at 7 TeV

$A_{CP}(B^0 \to [K^+\pi^-]_D K^*(892)^0)$

VALUE	DOCUMENT ID		TECN	COMMENT
−0.08±0.08±0.01	AAIJ	13L	LHCB	pp at 7 TeV

$A_{CP}(B^0 \to K^+\pi^-)$

VALUE	DOCUMENT ID		TECN	COMMENT
−0.082±0.006 OUR AVERAGE				
−0.080±0.007±0.003	AAIJ	13AX	LHCB	pp at 7 TeV
−0.069±0.014±0.007	DUH	13	BELL	$e^+e^- \to \Upsilon(4S)$
$-0.107\pm0.016^{+0.006}_{-0.004}$	LEES	13D	BABR	$e^+e^- \to \Upsilon(4S)$
−0.086±0.023±0.009	AALTONEN	11N	CDF	$p\overline{p}$ at 1.96 TeV
−0.04 ±0.16	[1] CHEN	00	CLE2	$e^+e^- \to \Upsilon(4S)$
• • • We do not use the following data for averages, fits, limits, etc. • • •				
−0.088±0.011±0.008	AAIJ	12V	LHCB	Repl. by AAIJ 13AX
−0.094±0.018±0.008	LIN	08	BELL	Repl. by DUH 13
$-0.107\pm0.018^{+0.007}_{-0.004}$	AUBERT	07AF	BABR	Repl. by LEES 13D
−0.013±0.078±0.012	ABULENCIA,A	06D	CDF	Repl. by AALTONEN 11N
−0.088±0.035±0.013	[2] CHAO	05A	BELL	Repl. by CHAO 04B
−0.133±0.030±0.009	[3] AUBERT,B	04K	BABR	Repl. by AUBERT 07AF
−0.101±0.025±0.005	[4] CHAO	04B	BELL	Repl. by LIN 08
−0.07 ±0.08 ±0.02	[5] AUBERT	02D	BABR	Repl. by AUBERT 02Q
−0.102±0.050±0.016	[6] AUBERT	02Q	BABR	Repl. by AUBERT,B 04K
$-0.06 \pm 0.09\ ^{+0.01}_{-0.02}$	[7] CASEY	02	BELL	Repl. by CHAO 04B
$0.044^{+0.186+0.018}_{-0.167-0.021}$	[8] ABE	01K	BELL	Repl. by CASEY 02
−0.19 ±0.10 ±0.03	[9] AUBERT	01E	BABR	Repl. by AUBERT 02Q

[1] Corresponds to 90% confidence range $-0.30 < A_{CP} < 0.22$.
[2] Corresponds to a 90% CL interval of $-0.15 < A_{CP} < -0.03$.
[3] Based on a total signal yield of $N(K^-\pi^+) + N(K^+\pi^-) = 1606 \pm 51$ events.
[4] CHAO 04B reports significance of 3.9 standard deviation for deviation of A_{CP} from zero.
[5] Corresponds to 90% confidence range $-0.21 < A_{CP} < 0.07$.
[6] Corresponds to 90% confidence range $-0.188 < A_{CP} < -0.016$.
[7] Corresponds to 90% confidence range $-0.21 < A_{CP} < +0.09$.
[8] Corresponds to 90% confidence range $-0.25 < A_{CP} < 0.37$.
[9] Corresponds to 90% confidence range $-0.35 < A_{CP} < -0.03$.

$A_{CP}(B^0 \to \eta' K^*(892)^0)$

VALUE	DOCUMENT ID		TECN	COMMENT
0.02±0.23±0.02	DEL-AMO-SA...10A		BABR	$e^+e^- \to \Upsilon(4S)$
• • • We do not use the following data for averages, fits, limits, etc. • • •				
0.08±0.25±0.02	[1] AUBERT	07E	BABR	Repl. by DEL-AMO-SANCHEZ 10A

[1] Reports A_{CP} with the opposite sign convention.

$A_{CP}(B^0 \to \eta' K_0^*(1430)^0)$

VALUE	DOCUMENT ID		TECN	COMMENT
−0.19±0.17±0.02	DEL-AMO-SA...10A		BABR	$e^+e^- \to \Upsilon(4S)$

$A_{CP}(B^0 \to \eta' K_2^*(1430)^0)$

VALUE	DOCUMENT ID		TECN	COMMENT
0.14±0.18±0.02	DEL-AMO-SA...10A		BABR	$e^+e^- \to \Upsilon(4S)$

$A_{CP}(B^0 \to \eta K^*(892)^0)$

VALUE	DOCUMENT ID		TECN	COMMENT
0.19±0.05 OUR AVERAGE				
0.17±0.08±0.01	WANG	07B	BELL	$e^+e^- \to \Upsilon(4S)$
0.21±0.06±0.02	AUBERT,B	06H	BABR	$e^+e^- \to \Upsilon(4S)$
• • • We do not use the following data for averages, fits, limits, etc. • • •				
0.02±0.11±0.02	AUBERT,B	04D	BABR	Repl. by AUBERT,B 06H

$A_{CP}(B^0 \to \eta K_0^*(1430)^0)$

VALUE	DOCUMENT ID		TECN	COMMENT
0.06±0.13±0.02	AUBERT,B	06H	BABR	$e^+e^- \to \Upsilon(4S)$

$A_{CP}(B^0 \to \eta K_2^*(1430)^0)$

VALUE	DOCUMENT ID		TECN	COMMENT
−0.07±0.19±0.02	AUBERT,B	06H	BABR	$e^+e^- \to \Upsilon(4S)$

$A_{CP}(B^0 \to b_1 K^+)$

VALUE	DOCUMENT ID		TECN	COMMENT
−0.07±0.12±0.02	AUBERT	07BI	BABR	$e^+e^- \to \Upsilon(4S)$

$A_{CP}(B^0 \to \omega K^{*0})$

VALUE	DOCUMENT ID		TECN	COMMENT
0.45±0.25±0.02	AUBERT	09H	BABR	$e^+e^- \to \Upsilon(4S)$

$A_{CP}(B^0 \to \omega (K\pi)_0^{*0})$

VALUE	DOCUMENT ID		TECN	COMMENT
−0.07±0.09±0.02	AUBERT	09H	BABR	$e^+e^- \to \Upsilon(4S)$

$A_{CP}(B^0 \to \omega K_2^*(1430)^0)$

VALUE	DOCUMENT ID		TECN	COMMENT
−0.37±0.17±0.02	AUBERT	09H	BABR	$e^+e^- \to \Upsilon(4S)$

$A_{CP}(B^0 \to K^+\pi^-\pi^0)$

VALUE (units 10^{-2})	DOCUMENT ID		TECN	COMMENT
0 ± 6 OUR AVERAGE				
$-3.0^{+4.5}_{-5.1} \pm 5.5$	[1] AUBERT	08AQ	BABR	$e^+e^- \to \Upsilon(4S)$
7 ±11 ±1	[2] CHANG	04	BELL	$e^+e^- \to \Upsilon(4S)$

[1] Uses Dalitz plot analysis of $B^0 \to K^+\pi^-\pi^0$ decays.
[2] Corresponds to 90% confidence range $-0.12 < A^{CP} < 0.26$.

$A_{CP}(B^0 \to \rho^- K^+)$

VALUE	DOCUMENT ID		TECN	COMMENT
0.20±0.11 OUR AVERAGE				
0.20±0.09±0.08	[1] LEES	11	BABR	$e^+e^- \to \Upsilon(4S)$
$0.22^{+0.22+0.06}_{-0.23-0.02}$	[2] CHANG	04	BELL	$e^+e^- \to \Upsilon(4S)$
• • • We do not use the following data for averages, fits, limits, etc. • • •				
$0.11^{+0.14}_{-0.15} \pm 0.07$	[1] AUBERT	08AQ	BABR	Repl. by LEES 11
−0.28±0.17±0.08	[3] AUBERT	03T	BABR	Repl. by AUBERT 08AQ

[1] Uses Dalitz plot analysis of $B^0 \to K^+\pi^-\pi^0$ decays.
[2] Corresponds to 90% confidence range $-0.18 < A_{CP} < 0.64$.
[3] The result reported corresponds to $-A_{CP}$.

$A_{CP}(B^0 \to \rho(1450)^- K^+)$

VALUE	DOCUMENT ID		TECN	COMMENT
−0.10±0.32±0.09	[1] LEES	11	BABR	$e^+e^- \to \Upsilon(4S)$

[1] Uses Dalitz plot analysis of $B^0 \to K^+\pi^-\pi^0$ decays.

$A_{CP}(B^0 \to \rho(1700)^- K^+)$

VALUE	DOCUMENT ID		TECN	COMMENT
−0.36±0.57±0.23	[1] LEES	11	BABR	$e^+e^- \to \Upsilon(4S)$

[1] Uses Dalitz plot analysis of $B^0 \to K^+\pi^-\pi^0$ decays.

$A_{CP}(B^0 \to K^+\pi^-\pi^0 \text{ nonresonant})$

VALUE	DOCUMENT ID		TECN	COMMENT
0.10±0.16±0.08	[1] LEES	11	BABR	$e^+e^- \to \Upsilon(4S)$
• • • We do not use the following data for averages, fits, limits, etc. • • •				
$0.23^{+0.19+0.11}_{-0.27-0.10}$	[1] AUBERT	08AQ	BABR	Repl. by LEES 11

[1] Uses Dalitz plot analysis of $B^0 \to K^+\pi^-\pi^0$ decays. The quoted value is only for the flat part of the non-resonant component.

$A_{CP}(B^0 \to K^0\pi^+\pi^-)$

VALUE	DOCUMENT ID		TECN	COMMENT
−0.01±0.05±0.01	[1] AUBERT	09AU	BABR	$e^+e^- \to \Upsilon(4S)$

[1] Uses Dalitz plot analysis of $B^0 \to K^0\pi^+\pi^-$ decays and the first of two equivalent solutions is used.

$A_{CP}(B^0 \to K^*(892)^+\pi^-)$

VALUE	DOCUMENT ID		TECN	COMMENT
−0.22±0.06 OUR AVERAGE				
−0.29±0.11±0.02	[1] LEES	11	BABR	$e^+e^- \to \Upsilon(4S)$
−0.21±0.10±0.02	[2,3] AUBERT	09AU	BABR	$e^+e^- \to \Upsilon(4S)$
−0.21±0.11±0.07	[4] DALSENO	09	BELL	$e^+e^- \to \Upsilon(4S)$
$0.26^{+0.33+0.10}_{-0.34-0.08}$	[5] EISENSTEIN	03	CLE2	$e^+e^- \to \Upsilon(4S)$
• • • We do not use the following data for averages, fits, limits, etc. • • •				
$-0.19^{+0.20}_{-0.15} \pm 0.04$	[1] AUBERT	08AQ	BABR	Repl. by LEES 11
−0.11±0.14±0.05	[2] AUBERT	06I	BABR	Repl. by AUBERT 09AU
$0.23 \pm 0.18^{+0.09}_{-0.06}$	AUBERT,B	04O	BABR	Repl. by AUBERT 06I

[1] Uses Dalitz plot analysis of $B^0 \to K^+\pi^-\pi^0$ decays.
[2] Uses Dalitz plot analysis of $B^0 \to K^0\pi^+\pi^-$ decays.
[3] The first of two equivalent solutions is used.
[4] Uses Dalitz plot analysis of $B^0 \to K^0\pi^+\pi^-$ decays and the first of two consistent solutions that may be preferred.
[5] Corresponds to 90% confidence range $-0.31 < A_{CP} < 0.78$.

$A_{CP}(B^0 \to (K\pi)_0^{*+}\pi^-)$

VALUE	DOCUMENT ID		TECN	COMMENT
0.09±0.07 OUR AVERAGE				
0.07±0.14±0.01	[1] LEES	11	BABR	$e^+e^- \to \Upsilon(4S)$
0.09±0.07±0.03	[2] AUBERT	09AU	BABR	$e^+e^- \to \Upsilon(4S)$
• • • We do not use the following data for averages, fits, limits, etc. • • •				
$0.17^{+0.11}_{-0.16}\pm0.22$	[1] AUBERT	08AQ	BABR	Repl. by LEES 11

[1] Uses Dalitz plot analysis of $B^0 \to K^+\pi^-\pi^0$ decays.
[2] Uses Dalitz plot analysis of $B^0 \to K^0\pi^+\pi^-$ decays and the first of two equivalent solutions is used.

$A_{CP}(B^0 \to (K\pi)_0^{*0}\pi^0)$

VALUE	DOCUMENT ID		TECN	COMMENT
−0.15±0.10±0.04	[1] LEES	11	BABR	$e^+e^- \to \Upsilon(4S)$
• • • We do not use the following data for averages, fits, limits, etc. • • •				
$-0.22\pm0.12^{+0.30}_{-0.29}$	[1] AUBERT	08AQ	BABR	Repl. by LEES 11

[1] Uses Dalitz plot analysis of $B^0 \to K^+\pi^-\pi^0$ decays.

$A_{CP}(B^0 \to K^{*0}\pi^0)$

VALUE	DOCUMENT ID		TECN	COMMENT
−0.15±0.12±0.04	[1] LEES	11	BABR	$e^+e^- \to \Upsilon(4S)$
• • • We do not use the following data for averages, fits, limits, etc. • • •				
$-0.09^{+0.21}_{-0.24}\pm0.09$	[1] AUBERT	08AQ	BABR	Repl. by LEES 11

[1] Uses Dalitz plot analysis of $B^0 \to K^+\pi^-\pi^0$ decays.

$A_{CP}(B^0 \to K^*(892)^0\pi^+\pi^-)$

VALUE	DOCUMENT ID	TECN	COMMENT
0.07±0.04±0.03	AUBERT	07AS	BABR	$e^+e^- \to \Upsilon(4S)$

$A_{CP}(B^0 \to K^*(892)^0\rho^0)$

VALUE	DOCUMENT ID		TECN	COMMENT
−0.06±0.09±0.02	LEES	12K	BABR	$e^+e^- \to \Upsilon(4S)$
• • • We do not use the following data for averages, fits, limits, etc. • • •				
0.09±0.19±0.02	AUBERT,B	06G	BABR	Repl. by LEES 12K

$A_{CP}(B^0 \to K^{*0}f_0(980))$

VALUE	DOCUMENT ID		TECN	COMMENT
0.07±0.10±0.02	LEES	12K	BABR	$e^+e^- \to \Upsilon(4S)$
• • • We do not use the following data for averages, fits, limits, etc. • • •				
−0.17±0.28±0.02	AUBERT,B	06G	BABR	Repl. by LEES 12K

$A_{CP}(B^0 \to K^{*+}\rho^-)$

VALUE	DOCUMENT ID		TECN	COMMENT
0.21±0.15±0.02	LEES	12K	BABR	$e^+e^- \to \Upsilon(4S)$

$A_{CP}(B^0 \to K^*(892)^0K^+K^-)$

VALUE	DOCUMENT ID		TECN	COMMENT
0.01±0.05±0.02	AUBERT	07AS	BABR	$e^+e^- \to \Upsilon(4S)$

$A_{CP}(B^0 \to a_1^-K^+)$

VALUE	DOCUMENT ID		TECN	COMMENT
−0.16±0.12±0.01	AUBERT	08F	BABR	$e^+e^- \to \Upsilon(4S)$

$A_{CP}(B^0 \to K^0K^0)$

VALUE	DOCUMENT ID		TECN	COMMENT
$\mathbf{-0.58^{+0.73}_{-0.66}\pm0.04}$	LIN	07	BELL	$e^+e^- \to \Upsilon(4S)$

$A_{CP}(B^0 \to K^*(892)^0\phi)$

VALUE	DOCUMENT ID		TECN	COMMENT
(0 ±4) × 10^{-2} OUR AVERAGE				
− 0.007±0.048±0.021	PRIM	13	BELL	$e^+e^- \to \Upsilon(4S)$
0.01 ±0.06 ±0.03	AUBERT	08BG	BABR	$e^+e^- \to \Upsilon(4S)$
• • • We do not use the following data for averages, fits, limits, etc. • • •				
− 0.03 ±0.07 ±0.03	AUBERT	07D	BABR	Repl. by AUBERT 08BG
0.02 ±0.09 ±0.02	[1] CHEN	05A	BELL	Repl. by PRIM 13
− 0.01 ±0.09 ±0.02	AUBERT,B	04W	BABR	Repl. by AUBERT 07D
0.04 ±0.12 ±0.02	AUBERT	03V	BABR	Repl. by AUBERT 04W
0.07 ±0.15 $^{+0.05}_{-0.03}$	[2] CHEN	03B	BELL	Repl. by CHEN 05A
0.00 ±0.27 ±0.03	[3] AUBERT	02E	BABR	Repl. by AUBERT 03V

[1] Corresponds to 90% confidence range $-0.14 < A_{CP} < 0.17$.
[2] Corresponds to 90% confidence range $-0.18 < A_{CP} < 0.33$.
[3] Corresponds to 90% confidence range $-0.44 < A_{CP} < 0.44$.

$A_{CP}(B^0 \to K^*(892)^0K^-\pi^+)$

VALUE	DOCUMENT ID		TECN	COMMENT
0.22±0.33±0.20	AUBERT	07AS	BABR	$e^+e^- \to \Upsilon(4S)$

$A_{CP}(B^0 \to \phi(K\pi)_0^{*0})$

VALUE	DOCUMENT ID		TECN	COMMENT
0.12 ±0.08 OUR AVERAGE				
0.093±0.094±0.017	PRIM	13	BELL	$e^+e^- \to \Upsilon(4S)$
0.20 ±0.14 ±0.06	AUBERT	08BG	BABR	$e^+e^- \to \Upsilon(4S)$
• • • We do not use the following data for averages, fits, limits, etc. • • •				
0.17 ±0.15 ±0.03	AUBERT	07D	BABR	Repl. by AUBERT 08BG

$A_{CP}(B^0 \to \phi K_2^*(1430)^0)$

VALUE	DOCUMENT ID		TECN	COMMENT
−0.11 ±0.10 OUR AVERAGE				
$-0.155^{+0.152}_{-0.133}\pm0.033$	PRIM	13	BELL	$e^+e^- \to \Upsilon(4S)$
−0.08 ±0.12 ±0.05	AUBERT	08BG	BABR	$e^+e^- \to \Upsilon(4S)$
• • • We do not use the following data for averages, fits, limits, etc. • • •				
−0.12 ±0.14 ±0.04	AUBERT	07D	BABR	Repl. by AUBERT 08BG

$A_{CP}(B^0 \to K^*(892)^0\gamma)$

VALUE	DOCUMENT ID		TECN	COMMENT
−0.002±0.015 OUR AVERAGE				
0.008±0.017±0.009	AAIJ	13	LHCB	pp at 7 TeV
−0.016±0.022±0.007	AUBERT	09AO	BABR	$e^+e^- \to \Upsilon(4S)$

$A_{CP}(B^0 \to K_2^*(1430)^0\gamma)$

VALUE	DOCUMENT ID		TECN	COMMENT
−0.08±0.15±0.01	AUBERT,B	04U	BABR	$e^+e^- \to \Upsilon(4S)$

$A_{CP}(B^0 \to \rho^+\pi^-)$

VALUE	DOCUMENT ID		TECN	COMMENT
0.13±0.06 OUR AVERAGE Error includes scale factor of 1.1.				
$0.09^{+0.05}_{-0.06}\pm0.04$	[1] LEES	13J	BABR	$e^+e^- \to \Upsilon(4S)$
0.21±0.08±0.04	[1] KUSAKA	07	BELL	$e^+e^- \to \Upsilon(4S)$
• • • We do not use the following data for averages, fits, limits, etc. • • •				
0.03±0.07±0.04	AUBERT	07AA	BABR	Repl. by LEES 13J
$-0.02\pm0.16^{+0.05}_{-0.02}$	WANG	05	BELL	Repl. by KUSAKA 07
−0.18±0.08±0.03	AUBERT	03T	BABR	Repl. by AUBERT 07AA

[1] Uses time-dependent Dalitz plot analysis of $B^0 \to \pi^+\pi^-\pi^0$ decays.

$A_{CP}(B^0 \to \rho^-\pi^+)$

VALUE	DOCUMENT ID		TECN	COMMENT
−0.08±0.08 OUR AVERAGE				
$-0.12\pm0.08^{+0.04}_{-0.05}$	[1] LEES	13J	BABR	$e^+e^- \to \Upsilon(4S)$
0.08±0.16±0.11	[1] KUSAKA	07	BELL	$e^+e^- \to \Upsilon(4S)$
• • • We do not use the following data for averages, fits, limits, etc. • • •				
$-0.37\pm0.16^{+0.09}_{-0.10}$	AUBERT	07AA	BABR	Repl. by LEES 13J
$-0.53\pm0.29^{+0.09}_{-0.04}$	WANG	05	BELL	Repl. by KUSAKA 07

[1] Uses time-dependent Dalitz plot analysis of $B^0 \to \pi^+\pi^-\pi^0$ decays.

$A_{CP}(B^0 \to a_1(1260)^\pm\pi^\mp)$

VALUE	DOCUMENT ID		TECN	COMMENT
−0.07±0.06 OUR AVERAGE				
−0.06±0.05±0.07	DALSENO	12	BELL	$e^+e^- \to \Upsilon(4S)$
−0.07±0.07±0.02	AUBERT	07O	BABR	$e^+e^- \to \Upsilon(4S)$

$A_{CP}(B^0 \to b_1^-\pi^+)$

VALUE	DOCUMENT ID		TECN	COMMENT
−0.05±0.10±0.02	AUBERT	07BI	BABR	$e^+e^- \to \Upsilon(4S)$

$A_{CP}(B^0 \to p\overline{p}K^*(892)^0)$

VALUE	DOCUMENT ID		TECN	COMMENT
0.05±0.12 OUR AVERAGE				
−0.08±0.20±0.02	CHEN	08C	BELL	$e^+e^- \to \Upsilon(4S)$
0.11±0.13±0.06	AUBERT	07AV	BABR	$e^+e^- \to \Upsilon(4S)$

$A_{CP}(B^0 \to p\overline{\Lambda}\pi^-)$

VALUE	DOCUMENT ID		TECN	COMMENT
0.04±0.07 OUR AVERAGE				
0.10±0.10±0.02	AUBERT	09AC	BABR	$e^+e^- \to \Upsilon(4S)$
−0.02±0.10±0.03	WANG	07C	BELL	$e^+e^- \to \Upsilon(4S)$

$A_{CP}(B^0 \to K^{*0}\ell^+\ell^-)$

VALUE	DOCUMENT ID		TECN	COMMENT
−0.05±0.10 OUR AVERAGE				
0.02±0.20±0.02	AUBERT	09T	BABR	$e^+e^- \to \Upsilon(4S)$
−0.08±0.12±0.02	WEI	09A	BELL	$e^+e^- \to \Upsilon(4S)$

$A_{CP}(B^0 \to K^{*0} e^+ e^-)$

VALUE	DOCUMENT ID		TECN	COMMENT
$-0.21 \pm 0.19 \pm 0.02$	WEI	09A	BELL	$e^+ e^- \to \Upsilon(4S)$

$A_{CP}(B^0 \to K^{*0} \mu^+ \mu^-)$

VALUE	DOCUMENT ID		TECN	COMMENT
-0.07 ± 0.04 OUR AVERAGE				
$-0.072 \pm 0.040 \pm 0.005$	AAIJ	13E	LHCB	pp at 7 TeV
$0.00 \pm 0.15 \pm 0.03$	WEI	09A	BELL	$e^+ e^- \to \Upsilon(4S)$

$C_{D^*(2010)^- D^+}$ $(B^0 \to D^*(2010)^- D^+)$

VALUE	DOCUMENT ID		TECN	COMMENT
-0.01 ± 0.11 OUR AVERAGE				
$-0.13 \pm 0.16 \pm 0.05$	[1] ROHRKEN	12	BELL	$e^+ e^- \to \Upsilon(4S)$
$0.00 \pm 0.17 \pm 0.03$	AUBERT	09C	BABR	$e^+ e^- \to \Upsilon(4S)$
$0.23 \pm 0.25 \pm 0.06$	[2] AUSHEV	04	BELL	$e^+ e^- \to \Upsilon(4S)$
• • • We do not use the following data for averages, fits, limits, etc. • • •				
$0.23 \pm 0.15 \pm 0.04$	AUBERT	07AI	BABR	Repl. by AUBERT 09C
$0.17 \pm 0.24 \pm 0.04$	AUBERT,B	05Z	BABR	Repl. by AUBERT 07AI
$-0.22 \pm 0.37 \pm 0.10$	AUBERT	03J	BABR	Repl. by AUBERT,B 05Z

[1] ROHRKEN 12 reports the measurements of C = $-0.01 \pm 0.11 \pm 0.04$ and $\Delta C = 0.12 \pm 0.11 \pm 0.03$ such that $C_{D^*(2010)^- D^+} = C - \Delta C$.

[2] Combines results from fully and partially reconstructed $B^0 \to D^{*\pm} D^{\mp}$ decays.

$S_{D^*(2010)^- D^+}$ $(B^0 \to D^*(2010)^- D^+)$

VALUE	DOCUMENT ID		TECN	COMMENT
-0.72 ± 0.15 OUR AVERAGE				
$-0.65 \pm 0.22 \pm 0.07$	[1] ROHRKEN	12	BELL	$e^+ e^- \to \Upsilon(4S)$
$-0.73 \pm 0.23 \pm 0.050$	AUBERT	09C	BABR	$e^+ e^- \to \Upsilon(4S)$
$-0.96 \pm 0.43 \pm 0.12$	[2] AUSHEV	04	BELL	$e^+ e^- \to \Upsilon(4S)$
• • • We do not use the following data for averages, fits, limits, etc. • • •				
$-0.44 \pm 0.22 \pm 0.06$	AUBERT	07AI	BABR	Repl. by AUBERT 09C
$-0.29 \pm 0.33 \pm 0.07$	AUBERT,B	05Z	BABR	Repl. by AUBERT 07AI
$-0.24 \pm 0.69 \pm 0.12$	AUBERT	03J	BABR	Repl. by AUBERT,B 05Z

[1] ROHRKEN 12 reports the measurements of S = $-0.78 \pm 0.15 \pm 0.05$ and $\Delta S = -0.13 \pm 0.15 \pm 0.04$ such that $S_{D^*(2010)^+ D^-} = S - \Delta S$.

[2] Combines results from fully and partially reconstructed $B^0 \to D^{*\pm} D^{\mp}$ decays.

$C_{D^*(2010)^+ D^-}$ $(B^0 \to D^*(2010)^+ D^-)$

VALUE	DOCUMENT ID		TECN	COMMENT
0.00 ± 0.13 OUR AVERAGE	Error includes scale factor of 1.3. See the ideogram below.			
$0.11 \pm 0.14 \pm 0.06$	[1] ROHRKEN	12	BELL	$e^+ e^- \to \Upsilon(4S)$
$0.08 \pm 0.17 \pm 0.04$	AUBERT	09C	BABR	$e^+ e^- \to \Upsilon(4S)$
$-0.37 \pm 0.22 \pm 0.06$	[2] AUSHEV	04	BELL	$e^+ e^- \to \Upsilon(4S)$
• • • We do not use the following data for averages, fits, limits, etc. • • •				
$0.18 \pm 0.15 \pm 0.04$	AUBERT	07AI	BABR	Repl. by AUBERT 09C
$0.09 \pm 0.25 \pm 0.06$	AUBERT,B	05Z	BABR	Repl. by AUBERT 07AI
$-0.47 \pm 0.40 \pm 0.12$	AUBERT	03J	BABR	Repl. by AUBERT,B 05Z

[1] ROHRKEN 12 reports the measurements of C = $-0.01 \pm 0.11 \pm 0.04$ and $\Delta C = 0.12 \pm 0.11 \pm 0.03$ such that $C_{D^*(2010)^+ D^-} = C + \Delta C$.

[2] Combines results from fully and partially reconstructed $B^0 \to D^{*\pm} D^{\mp}$ decays.

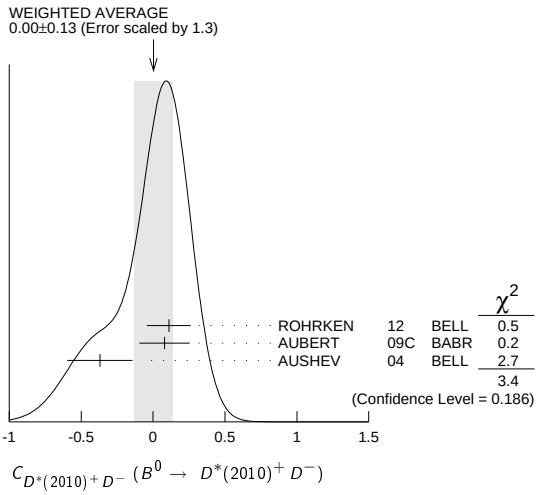

$C_{D^*(2010)^+ D^-}$ $(B^0 \to D^*(2010)^+ D^-)$

$S_{D^*(2010)^+ D^-}$ $(B^0 \to D^*(2010)^+ D^-)$

VALUE	DOCUMENT ID		TECN	COMMENT
-0.73 ± 0.14 OUR AVERAGE				
$-0.90 \pm 0.21 \pm 0.07$	[1] ROHRKEN	12	BELL	$e^+ e^- \to \Upsilon(4S)$
$-0.62 \pm 0.21 \pm 0.03$	AUBERT	09C	BABR	$e^+ e^- \to \Upsilon(4S)$
$-0.55 \pm 0.39 \pm 0.12$	[2] AUSHEV	04	BELL	$e^+ e^- \to \Upsilon(4S)$
• • • We do not use the following data for averages, fits, limits, etc. • • •				
$-0.79 \pm 0.21 \pm 0.06$	AUBERT	07AI	BABR	Repl. by AUBERT 09C
$-0.54 \pm 0.35 \pm 0.07$	AUBERT,B	05Z	BABR	Repl. by AUBERT 07AI
$-0.82 \pm 0.75 \pm 0.14$	AUBERT	03J	BABR	Repl. by AUBERT,B 05Z

[1] ROHRKEN 12 reports the measurements of S = $-0.78 \pm 0.15 \pm 0.05$ and $\Delta S = -0.13 \pm 0.15 \pm 0.04$ such that $S_{D^*(2010)^+ D^-} = S + \Delta S$.

[2] Combines results from fully and partially reconstructed $B^0 \to D^{*\pm} D^{\mp}$ decays.

$C_{D^{*+} D^{*-}}$ $(B^0 \to D^{*+} D^{*-})$

VALUE	DOCUMENT ID		TECN	COMMENT
0.01 ± 0.09 OUR AVERAGE	Error includes scale factor of 1.6. See the ideogram below.			
$-0.15 \pm 0.08 \pm 0.04$	[1,2] KRONENBITT..12		BELL	$e^+ e^- \to \Upsilon(4S)$
$+0.15 \pm 0.09 \pm 0.04$	[3] LEES	12AF	BABR	$e^+ e^- \to \Upsilon(4S)$
$0.05 \pm 0.09 \pm 0.02$	AUBERT	09C	BABR	$e^+ e^- \to \Upsilon(4S)$
• • • We do not use the following data for averages, fits, limits, etc. • • •				
$-0.15 \pm 0.13 \pm 0.04$	[2] VERVINK	09	BELL	Repl. by KRONENBITTER 12
$-0.02 \pm 0.11 \pm 0.02$	[1] AUBERT	07BO	BABR	Repl. by AUBERT 09C
$0.26 \pm 0.26 \pm 0.06$	[2] MIYAKE	05	BELL	Repl. by VERVINK 09
$0.28 \pm 0.23 \pm 0.02$	[4] AUBERT	03Q	BABR	Repl. by AUBERT 07BO

[1] Assumes both *CP*-even and *CP*-odd states having the *CP* asymmetry.

[2] Belle Collab. quotes $A_{D^{*+} D^{*-}}$ which is equal to $-C_{D^{*+} D^{*-}}$.

[3] Measured partially reconstructed candidates when one D^0 meson is not excplicitely reconstructed. Analysis does not separate *CP*-even and *CP*-odd component.

[4] AUBERT 03Q reports $|\lambda| = 0.75 \pm 0.19 \pm 0.02$ and $\mathrm{Im}(\lambda) = 0.05 \pm 0.29 \pm 0.10$. We convert them to *S* and *C* parameters taking into account correlations.

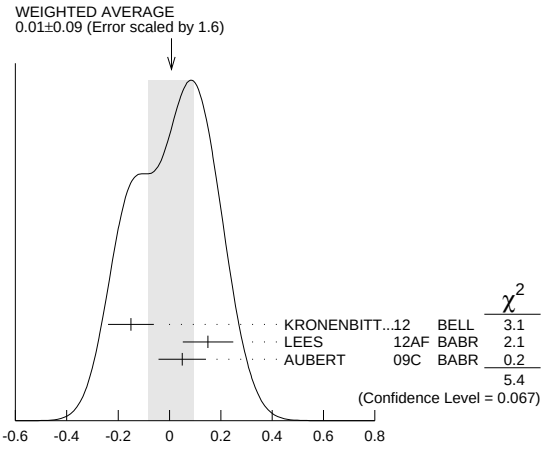

$C_{D^{*+} D^{*-}}$ $(B^0 \to D^{*+} D^{*-})$

$S_{D^{*+} D^{*-}}$ $(B^0 \to D^{*+} D^{*-})$

VALUE	DOCUMENT ID		TECN	COMMENT
-0.59 ± 0.14 OUR AVERAGE	Error includes scale factor of 1.8. See the ideogram below.			
$-0.79 \pm 0.13 \pm 0.03$	[1] KRONENBITT..12		BELL	$e^+ e^- \to \Upsilon(4S)$
$-0.34 \pm 0.12 \pm 0.05$	[2] LEES	12AF	BABR	$e^+ e^- \to \Upsilon(4S)$
$-0.70 \pm 0.16 \pm 0.03$	[1] AUBERT	09C	BABR	$e^+ e^- \to \Upsilon(4S)$
• • • We do not use the following data for averages, fits, limits, etc. • • •				
$-0.96 \pm 0.25^{+0.13}_{-0.16}$	VERVINK	09	BELL	Repl. by KRONENBITTER 12
$-0.66 \pm 0.19 \pm 0.04$	[1] AUBERT	07BO	BABR	Repl. by AUBERT 09C
$-0.75 \pm 0.56 \pm 0.12$	MIYAKE	05	BELL	Repl. by VERVINK 09
$0.06 \pm 0.37 \pm 0.13$	[3] AUBERT	03Q	BABR	Repl. by AUBERT 07BO

[1] Assumes both *CP*-even and *CP*-odd states having the *CP* asymmetry.

[2] Measured partially reconstructed candidates when one D^0 meson is not excplicitely reconstructed. Analysis does not separate *CP*-even and *CP*-odd component.

[3] AUBERT 03Q reports $|\lambda| = 0.75 \pm 0.19 \pm 0.02$ and $\mathrm{Im}(\lambda) = 0.05 \pm 0.29 \pm 0.10$. We convert them to *S* and *C* parameters taking into account correlations.

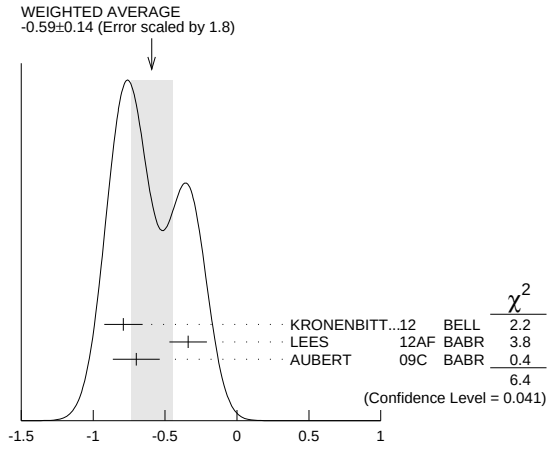

$S_{D^{*+}D^{*-}}$ ($B^0 \to D^{*+}D^{*-}$)

C_+ ($B^0 \to D^{*+}D^{*-}$)

See the note in the $C_{\pi\pi}$ datablock, but for *CP* even final state.

VALUE	DOCUMENT ID		TECN	COMMENT
0.00±0.10 OUR AVERAGE	Error includes scale factor of 1.6. See the ideogram below.			
−0.18±0.10±0.05	[1] KRONENBITT.12		BELL	$e^+e^- \to \Upsilon(4S)$
+0.15±0.09±0.04	[2] LEES	12AF	BABR	$e^+e^- \to \Upsilon(4S)$
0.00±0.12±0.02	AUBERT	09C	BABR	$e^+e^- \to \Upsilon(4S)$
• • • We do not use the following data for averages, fits, limits, etc. • • •				
−0.05±0.14±0.02	AUBERT	07BO	BABR	Repl. by AUBERT 09C
0.06±0.17±0.03	[3] AUBERT,BE	05A	BABR	Repl. by AUBERT 07BO

[1] Belle Collab. quotes $A_{D^{*+}D^{*-}}$ which is equal to $-C_{D^{*+}D^{*-}}$.

[2] Measured partially reconstructed candidates when one D^0 meson is not excplicitely reconstructed. Extracted under assumption of equal C_+ and C_-.

[3] AUBERT,BE 05A reports a *CP*-odd fraction $R_\perp = 0.125 \pm 0.044 \pm 0.007$.

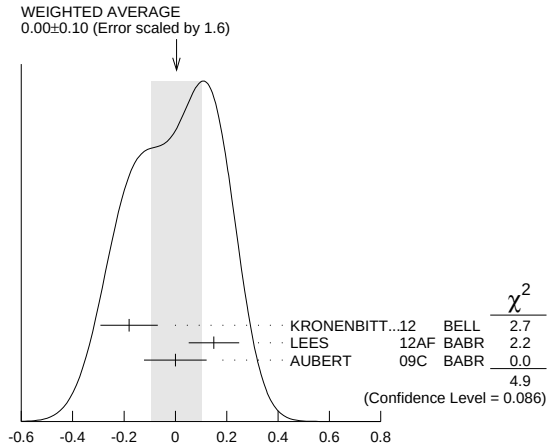

C_+ ($B^0 \to D^{*+}D^{*-}$)

S_+ ($B^0 \to D^{*+}D^{*-}$)

See the note in the $S_{\pi\pi}$ datablock, but for *CP* even final state.

VALUE	DOCUMENT ID		TECN	COMMENT
−0.73±0.09 OUR AVERAGE				
−0.81±0.13±0.03	KRONENBITT.12		BELL	$e^+e^- \to \Upsilon(4S)$
−0.49±0.18±0.08	[1] LEES	12AF	BABR	$e^+e^- \to \Upsilon(4S)$
−0.76±0.16±0.04	AUBERT	09C	BABR	$e^+e^- \to \Upsilon(4S)$
• • • We do not use the following data for averages, fits, limits, etc. • • •				
−0.72±0.19±0.05	AUBERT	07BO	BABR	Repl. by AUBERT 09C
−0.75±0.25±0.03	[2] AUBERT,BE	05A	BABR	Repl. by AUBERT 07BO

[1] Measured partially reconstructed candidates when one D^0 meson is not excplicitely reconstructed. Analysis does not separate *CP*-even and *CP*-odd component. Value is obtained from $S = -0.34 \pm 0.12 \pm 0.05$ using $S = S_+ (1 - 2R_\perp)$ with $R_\perp = 0.158 \pm 0.029$.

[2] AUBERT,BE 05A reports a *CP*-odd fraction $R_\perp = 0.125 \pm 0.044 \pm 0.007$.

C_- ($B^0 \to D^{*+}D^{*-}$)

See the note in the $C_{\pi\pi}$ datablock, but for *CP* odd final state.

VALUE	DOCUMENT ID		TECN	COMMENT
0.19±0.31 OUR AVERAGE				
0.05±0.39±0.08	[1] KRONENBITT.12		BELL	$e^+e^- \to \Upsilon(4S)$
0.41±0.49±0.08	AUBERT	09C	BABR	$e^+e^- \to \Upsilon(4S)$
• • • We do not use the following data for averages, fits, limits, etc. • • •				
0.23±0.67±0.10	AUBERT	07BO	BABR	Repl. by AUBERT 09C
−0.20±0.96±0.11	[2] AUBERT,BE	05A	BABR	Repl. by AUBERT 07BO

[1] Belle Collab. quotes $A_{D^{*+}D^{*-}}$ which is equal to $-C_{D^{*+}D^{*-}}$.

[2] AUBERT,BE 05A reports a *CP*-odd fraction $R_\perp = 0.125 \pm 0.044 \pm 0.007$.

S_- ($B^0 \to D^{*+}D^{*-}$)

See the note in the $S_{\pi\pi}$ datablock, but for *CP* odd final state.

VALUE	DOCUMENT ID		TECN	COMMENT
0.1 ±1.6 OUR AVERAGE	Error includes scale factor of 3.5.			
1.52±0.62±0.12	KRONENBITT.12		BELL	$e^+e^- \to \Upsilon(4S)$
−1.80±0.70±0.16	AUBERT	09C	BABR	$e^+e^- \to \Upsilon(4S)$
• • • We do not use the following data for averages, fits, limits, etc. • • •				
−1.83±1.04±0.23	AUBERT	07BO	BABR	Repl. by AUBERT 09C
−1.75±1.78±0.22	[1] AUBERT,BE	05A	BABR	Repl. by AUBERT 07BO

[1] AUBERT,BE 05A reports a *CP*-odd fraction $R_\perp = 0.125 \pm 0.044 \pm 0.007$.

C ($B^0 \to D^*(2010)^+ D^*(2010)^- K^0_S$)

VALUE	DOCUMENT ID		TECN	COMMENT
0.01±0.28±0.09	[1] DALSENO	07	BELL	$e^+e^- \to \Upsilon(4S)$

[1] Reports value of A which is equal to $-C$.

S ($B^0 \to D^*(2010)^+ D^*(2010)^- K^0_S$)

VALUE	DOCUMENT ID		TECN	COMMENT
$0.06^{+0.45}_{-0.44}$±0.06	[1] DALSENO	07	BELL	$e^+e^- \to \Upsilon(4S)$

[1] This value includes an unknown *CP* dilution factor D due to possible contributions from intermediate resonances and different partial waves.

$C_{D^+D^-}$ ($B^0 \to D^+D^-$)

VALUE	DOCUMENT ID		TECN	COMMENT
−0.46±0.21 OUR AVERAGE	Error includes scale factor of 1.8. See the ideogram below.			
−0.43±0.16±0.05	ROHRKEN	12	BELL	$e^+e^- \to \Upsilon(4S)$
−0.07±0.23±0.03	AUBERT	09C	BABR	$e^+e^- \to \Upsilon(4S)$
−0.91±0.23±0.06	[1] FRATINA	07	BELL	$e^+e^- \to \Upsilon(4S)$
• • • We do not use the following data for averages, fits, limits, etc. • • •				
0.11±0.22±0.07	AUBERT	07AI	BABR	Repl. by AUBERT 09C
0.11±0.35±0.06	AUBERT,B	05Z	BABR	Repl. by AUBERT 07AI

[1] The paper reports A, which is equal to $-C$.

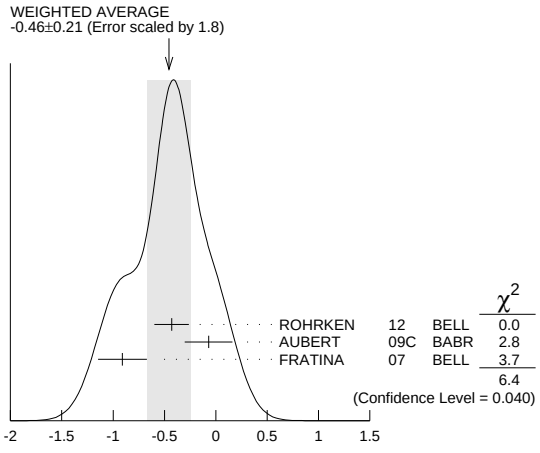

$C_{D^+D^-}$ ($B^0 \to D^+D^-$)

$S_{D^+D^-}$ ($B^0 \to D^+D^-$)

VALUE	DOCUMENT ID		TECN	COMMENT
$-0.99^{+0.17}_{-0.14}$ OUR AVERAGE				
$-1.06^{+0.21}_{-0.14}$±0.08	ROHRKEN	12	BELL	$e^+e^- \to \Upsilon(4S)$
−0.63±0.36±0.05	AUBERT	09C	BABR	$e^+e^- \to \Upsilon(4S)$
−1.13±0.37±0.09	FRATINA	07	BELL	$e^+e^- \to \Upsilon(4S)$
• • • We do not use the following data for averages, fits, limits, etc. • • •				
−0.54±0.34±0.06	AUBERT	07AI	BABR	Repl. by AUBERT 09C
−0.29±0.63±0.06	AUBERT,B	05Z	BABR	Repl. by AUBERT 07AI

$C_{J/\psi(1S)\pi^0}$ ($B^0 \to J/\psi(1S)\pi^0$)

VALUE	DOCUMENT ID		TECN	COMMENT
-0.13 ± 0.13 OUR AVERAGE				
$-0.20\pm0.19\pm0.03$	AUBERT	08AU	BABR	$e^+e^- \to \Upsilon(4S)$
$-0.08\pm0.16\pm0.05$	[1] LEE	08A	BELL	$e^+e^- \to \Upsilon(4S)$
• • • We do not use the following data for averages, fits, limits, etc. • • •				
$-0.21\pm0.26\pm0.06$	AUBERT,B	06B	BABR	Repl. by AUBERT 08AU
$0.01\pm0.29\pm0.03$	[1] KATAOKA	04	BELL	Repl. by LEE 08A
$0.38\pm0.41\pm0.09$	AUBERT	03N	BABR	Repl. by AUBERT,B 06B

[1] BELLE Collab. quotes $A_{J/\psi\pi^0}$ which is equal to $-C_{J/\psi\pi^0}$.

$S_{J/\psi(1S)\pi^0}$ ($B^0 \to J/\psi(1S)\pi^0$)

VALUE	DOCUMENT ID		TECN	COMMENT
-0.94 ± 0.29 OUR AVERAGE	Error includes scale factor of 1.9.			
$-1.23\pm0.21\pm0.04$	AUBERT	08AU	BABR	$e^+e^- \to \Upsilon(4S)$
$-0.65\pm0.21\pm0.05$	LEE	08A	BELL	$e^+e^- \to \Upsilon(4S)$
• • • We do not use the following data for averages, fits, limits, etc. • • •				
$-0.68\pm0.30\pm0.04$	AUBERT,B	06B	BABR	Repl. by AUBERT 08AU
$-0.72\pm0.42\pm0.09$	KATAOKA	04	BELL	Repl. by LEE 08A
$0.05\pm0.49\pm0.16$	AUBERT	03N	BABR	Repl. by AUBERT,B 06B

$C_{D^{(*)}_{CP}h^0}$ ($B^0 \to D^{(*)}_{CP}h^0$)

VALUE	DOCUMENT ID		TECN	COMMENT
$-0.23\pm0.16\pm0.04$	AUBERT	07AJ	BABR	$e^+e^- \to \Upsilon(4S)$

$S_{D^{(*)}_{CP}h^0}$ ($B^0 \to D^{(*)}_{CP}h^0$)

VALUE	DOCUMENT ID		TECN	COMMENT
$-0.56\pm0.23\pm0.05$	AUBERT	07AJ	BABR	$e^+e^- \to \Upsilon(4S)$

$C_{K^0\pi^0}$ ($B^0 \to K^0\pi^0$)

VALUE	DOCUMENT ID		TECN	COMMENT
0.00 ± 0.13 OUR AVERAGE	Error includes scale factor of 1.4.			
$-0.14\pm0.13\pm0.06$	[1] FUJIKAWA	10A	BELL	$e^+e^- \to \Upsilon(4S)$
$0.13\pm0.13\pm0.03$	AUBERT	09I	BABR	$e^+e^- \to \Upsilon(4S)$
• • • We do not use the following data for averages, fits, limits, etc. • • •				
$0.24\pm0.15\pm0.03$	AUBERT	08E	BABR	Repl. by AUBERT 09I
$0.05\pm0.14\pm0.05$	[1] CHAO	07	BELL	Repl. by FUJIKAWA 10A
$0.06\pm0.18\pm0.03$	AUBERT	05Y	BABR	Repl. by AUBERT 08E
$-0.16\pm0.29\pm0.05$	[1,2] CHAO	05A	BELL	Repl. by CHEN 05B
$0.11\pm0.20\pm0.09$	[1] CHEN	05B	BELL	Repl. by CHAO 07
$-0.03\pm0.36\pm0.11$	[1] AUBERT	04M	BABR	Repl. by AUBERT,B 04M
$0.40^{+0.27}_{-0.28}\pm0.09$	[3] AUBERT,B	04M	BABR	Repl. by AUBERT 05Y

[1] Reports A which is equal to $-C$.
[2] Corresponds to a 90% CL interval of $-0.33 < A_{CP} < 0.64$.
[3] Based on a total signal yield of 122 ± 16 events.

$S_{K^0\pi^0}$ ($B^0 \to K^0\pi^0$)

VALUE	DOCUMENT ID		TECN	COMMENT
0.58 ± 0.17 OUR AVERAGE				
$0.67\pm0.31\pm0.08$	FUJIKAWA	10A	BELL	$e^+e^- \to \Upsilon(4S)$
$0.55\pm0.20\pm0.03$	AUBERT	09I	BABR	$e^+e^- \to \Upsilon(4S)$
• • • We do not use the following data for averages, fits, limits, etc. • • •				
$0.40\pm0.23\pm0.03$	AUBERT	08E	BABR	Repl. by AUBERT 09I
$0.33\pm0.35\pm0.08$	CHAO	07	BELL	Repl. by FUJIKAWA 10A
$0.35^{+0.30}_{-0.33}\pm0.04$	AUBERT	05Y	BABR	Repl. by AUBERT 08E
$0.32\pm0.61\pm0.13$	CHEN	05B	BELL	Repl. by CHAO 07
$0.48^{+0.38}_{-0.47}\pm0.06$	[1] AUBERT,B	04M	BABR	Repl. by AUBERT 05Y

[1] Based on a total signal yield of 122 ± 16 events.

$C_{\eta'(958)K^0_S}$ ($B^0 \to \eta'(958)K^0_S$)

See updated measurements in $C_{\eta' K^0}$

VALUE	DOCUMENT ID		TECN	COMMENT
-0.04 ± 0.20 OUR AVERAGE	Error includes scale factor of 2.5.			
$-0.21\pm0.10\pm0.02$	AUBERT	05M	BABR	$e^+e^- \to \Upsilon(4S)$
$0.19\pm0.11\pm0.05$	[1] CHEN	05B	BELL	$e^+e^- \to \Upsilon(4S)$
• • • We do not use the following data for averages, fits, limits, etc. • • •				
$-0.26\pm0.22\pm0.03$	[1] ABE	03C	BELL	Repl. by ABE 03H
$0.01\pm0.16\pm0.04$	[1] ABE	03H	BELL	Repl. by CHEN 05B
$0.10\pm0.22\pm0.04$	AUBERT	03W	BABR	Repl. by AUBERT 05M
$-0.13\pm0.32^{+0.06}_{-0.09}$	[1] CHEN	02B	BELL	Repl. by ABE 03C

[1] BELLE Collab. quotes $A_{\eta'(958)K^0_S}$ which is equal to $-C_{\eta'(958)K^0_S}$.

$S_{\eta'(958)K^0_S}$ ($B^0 \to \eta'(958)K^0_S$)

See updated measurements in $S_{\eta' K^0}$

VALUE	DOCUMENT ID		TECN	COMMENT
0.43 ± 0.17 OUR AVERAGE	Error includes scale factor of 1.5.			
$0.30\pm0.14\pm0.02$	AUBERT	05M	BABR	$e^+e^- \to \Upsilon(4S)$
$0.65\pm0.18\pm0.04$	CHEN	05B	BELL	$e^+e^- \to \Upsilon(4S)$
• • • We do not use the following data for averages, fits, limits, etc. • • •				
$0.71\pm0.37^{+0.05}_{-0.06}$	ABE	03C	BELL	Repl. by ABE 03H
$0.43\pm0.27\pm0.05$	ABE	03H	BELL	Repl. by CHEN 05B
$0.02\pm0.34\pm0.03$	AUBERT	03W	BABR	Repl. by AUBERT 05M
$0.28\pm0.55^{+0.07}_{-0.08}$	CHEN	02B	BELL	Repl. by ABE 03C

$C_{\eta' K^0}$ ($B^0 \to \eta' K^0$)

VALUE	DOCUMENT ID		TECN	COMMENT
-0.05 ± 0.05 OUR AVERAGE				
$-0.08\pm0.06\pm0.02$	AUBERT	09I	BABR	$e^+e^- \to \Upsilon(4S)$
$0.01\pm0.07\pm0.05$	[1,2] CHEN	07	BELL	$e^+e^- \to \Upsilon(4S)$
• • • We do not use the following data for averages, fits, limits, etc. • • •				
$-0.16\pm0.07\pm0.03$	[1] AUBERT	07A	BABR	Repl. by AUBERT 09I

[1] The mixing-induced CP violation is reported with a significance of more than 5 standard deviations in this $b \to s$ penguin dominated mode.
[2] The paper reports A, which is equal to $-C$.

$S_{\eta' K^0}$ ($B^0 \to \eta' K^0$)

VALUE	DOCUMENT ID		TECN	COMMENT
0.60±0.07 OUR AVERAGE				
$0.57\pm0.08\pm0.02$	AUBERT	09I	BABR	$e^+e^- \to \Upsilon(4S)$
$0.64\pm0.10\pm0.04$	[1] CHEN	07	BELL	$e^+e^- \to \Upsilon(4S)$
• • • We do not use the following data for averages, fits, limits, etc. • • •				
$0.58\pm0.10\pm0.03$	[1] AUBERT	07A	BABR	Repl. by AUBERT 09I

[1] The mixing-induced CP violation is reported with a significance of more than 5 standard deviations in this $b \to s$ penguin dominated mode.

$C_{\omega K^0_S}$ ($B^0 \to \omega K^0_S$)

VALUE	DOCUMENT ID		TECN	COMMENT
-0.30 ± 0.28 OUR AVERAGE	Error includes scale factor of 1.6.			
$-0.52^{+0.22}_{-0.20}\pm0.03$	AUBERT	09I	BABR	$e^+e^- \to \Upsilon(4S)$
$0.09\pm0.29\pm0.06$	[1] CHAO	07	BELL	$e^+e^- \to \Upsilon(4S)$
• • • We do not use the following data for averages, fits, limits, etc. • • •				
$-0.55^{+0.28}_{-0.26}\pm0.03$	AUBERT,B	06E	BABR	Repl. by AUBERT 09I
$-0.27\pm0.48\pm0.15$	[1] CHEN	05B	BELL	Repl. by CHAO 07

[1] Belle Collab. quotes $A_{\omega K^0_S}$ which is equal to $-C_{\omega K^0_S}$.

$S_{\omega K^0_S}$ ($B^0 \to \omega K^0_S$)

VALUE	DOCUMENT ID		TECN	COMMENT
0.43±0.24 OUR AVERAGE				
$0.55^{+0.26}_{-0.29}\pm0.02$	AUBERT	09I	BABR	$e^+e^- \to \Upsilon(4S)$
$0.11\pm0.46\pm0.07$	CHAO	07	BELL	$e^+e^- \to \Upsilon(4S)$
• • • We do not use the following data for averages, fits, limits, etc. • • •				
$0.51^{+0.35}_{-0.39}\pm0.02$	AUBERT,B	06E	BABR	Repl. by AUBERT 09I
$0.76\pm0.65^{+0.13}_{-0.16}$	CHEN	05B	BELL	Repl. by CHAO 07

C ($B^0 \to K^0_S\pi^0\pi^0$)

VALUE	DOCUMENT ID		TECN	COMMENT
0.23±0.52±0.13	AUBERT	07AQ	BABR	$e^+e^- \to \Upsilon(4S)$

S ($B^0 \to K^0_S\pi^0\pi^0$)

VALUE	DOCUMENT ID		TECN	COMMENT
0.72±0.71±0.08	AUBERT	07AQ	BABR	$e^+e^- \to \Upsilon(4S)$

$C_{\rho^0 K^0_S}$ ($B^0 \to \rho^0 K^0_S$)

VALUE	DOCUMENT ID		TECN	COMMENT
-0.04 ± 0.20 OUR AVERAGE				
$-0.05\pm0.26\pm0.10$	[1] AUBERT	09AU	BABR	$e^+e^- \to \Upsilon(4S)$
$-0.03^{+0.24}_{-0.23}\pm0.15$	[2,3] DALSENO	09	BELL	$e^+e^- \to \Upsilon(4S)$
• • • We do not use the following data for averages, fits, limits, etc. • • •				
$0.64\pm0.41\pm0.20$	AUBERT	07F	BABR	Repl. by AUBERT 09AU

[1] Uses Dalitz plot analysis of $B^0 \to K^0\pi^+\pi^-$ decays and the first of two equivalent solutions is used.
[2] Quotes $A_{\rho^0(KS)^0}$ which is equal to $-C_{\rho^0 K^0_S}$.
[3] Uses Dalitz plot analysis of $B^0 \to K^0\pi^+\pi^-$ decays and the first of two consistent solutions that may be preferred.

Meson Particle Listings

B^0

$S_{\rho^0 K^0_S}$ ($B^0 \to \rho^0 K^0_S$)

VALUE	DOCUMENT ID		TECN	COMMENT
$0.50^{+0.17}_{-0.21}$ OUR AVERAGE				
$0.35^{+0.26}_{-0.31} \pm 0.07$	[1] AUBERT	09AU	BABR	$e^+e^- \to \Upsilon(4S)$
$0.64^{+0.19}_{-0.25} \pm 0.13$	[2] DALSENO	09	BELL	$e^+e^- \to \Upsilon(4S)$
• • • We do not use the following data for averages, fits, limits, etc. • • •				
$0.20 \pm 0.52 \pm 0.24$	AUBERT	07F	BABR	Repl. by AUBERT 09AU

[1] Uses Dalitz plot analysis of $B^0 \to K^0\pi^+\pi^-$ decays and the first of two equivalent solutions is used.
[2] Uses Dalitz plot analysis of $B^0 \to K^0\pi^+\pi^-$ decays and the first of two consistent solutions that may be preferred.

$C_{f_0(980) K^0_S}$ ($B^0 \to f_0(980) K^0_S$)

VALUE	DOCUMENT ID		TECN	COMMENT
0.29 ± 0.20 OUR AVERAGE				
$0.28 \pm 0.24 \pm 0.09$	[1] LEES	12O	BABR	$e^+e^- \to \Upsilon(4S)$
$0.30 \pm 0.29 \pm 0.14$	[2,3] NAKAHAMA	10	BELL	$e^+e^- \to \Upsilon(4S)$
• • • We do not use the following data for averages, fits, limits, etc. • • •				
$0.08 \pm 0.19 \pm 0.05$	[4] AUBERT	09AU	BABR	Repl. by LEES 12O
$0.06 \pm 0.17 \pm 0.11$	[2,5] DALSENO	09	BELL	Repl. by NAKAHAMA 10
$-0.41 \pm 0.23 \pm 0.07$	[2] AUBERT	07AX	BABR	Repl. by AUBERT 09AU
$0.15 \pm 0.15 \pm 0.07$	[2] CHAO	07	BELL	Repl. by DALSENO 09
$0.39 \pm 0.27 \pm 0.09$	[2] CHEN	05B	BELL	Repl. by CHAO 07

[1] Uses Dalitz plot analysis of the $B^0 \to K^0_S K^+ K^-$ decay.
[2] Quotes $A_{f_0(980) K^0_S}$ which is equal to $-C_{f_0(980) K^0_S}$.
[3] Uses Dalitz plot analysis of $B^0 \to K^0_S K^+ K^-$ decays and the first of four consistent solutions that may be preferred.
[4] Uses Dalitz plot analysis of $B^0 \to K^0\pi^+\pi^-$ decays and the first of two equivalent solutions is used.
[5] Uses Dalitz plot analysis of $B^0 \to K^0\pi^+\pi^-$ decays and the first of two consistent solutions that may be preferred.

$S_{f_0(980) K^0_S}$ ($B^0 \to f_0(980) K^0_S$)

VALUE	DOCUMENT ID		TECN	COMMENT
-0.50 ± 0.16 OUR AVERAGE				
$-0.55 \pm 0.18 \pm 0.12$	[1] LEES	12O	BABR	$e^+e^- \to \Upsilon(4S)$
$-0.43^{+0.22}_{-0.20} \pm 0.14$	[2] DALSENO	09	BELL	$e^+e^- \to \Upsilon(4S)$
• • • We do not use the following data for averages, fits, limits, etc. • • •				
$-0.96^{+0.21}_{-0.04} \pm 0.04$	[3] AUBERT	09AU	BABR	Repl. by LEES 12O
$-0.25 \pm 0.26 \pm 0.10$	[4] AUBERT	07AX	BABR	Repl. by AUBERT 09AU
$0.18 \pm 0.23 \pm 0.11$	CHAO	07	BELL	Repl. by DALSENO 09
$0.47 \pm 0.41 \pm 0.08$	CHEN	05B	BELL	Repl. by CHAO 07

[1] Uses Dalitz plot analysis of the $B^0 \to K^0_S K^+ K^-$ decay.
[2] Uses Dalitz plot analysis of $B^0 \to K^0\pi^+\pi^-$ decays and the first of two consistent solutions that may be preferred.
[3] Uses Dalitz plot analysis of $B^0 \to K^0\pi^+\pi^-$ decays and the first of two equivalent solutions is used.
[4] Reports β_{eff}. We quote S obtained from epaps: E-PRLTAO-99-076741.

$S_{f_2(1270) K^0_S}$ ($B^0 \to f_2(1270) K^0_S$)

VALUE	DOCUMENT ID		TECN	COMMENT
$-0.48 \pm 0.52 \pm 0.12$	[1] AUBERT	09AU	BABR	$e^+e^- \to \Upsilon(4S)$

[1] Uses Dalitz plot analysis of $B^0 \to K^0\pi^+\pi^-$ decays and the first of two equivalent solutions is used.

$C_{f_2(1270) K^0_S}$ ($B^0 \to f_2(1270) K^0_S$)

VALUE	DOCUMENT ID		TECN	COMMENT
$0.28^{+0.35}_{-0.40} \pm 0.11$	[1] AUBERT	09AU	BABR	$e^+e^- \to \Upsilon(4S)$

[1] Uses Dalitz plot analysis of $B^0 \to K^0\pi^+\pi^-$ decays and the first of two equivalent solutions is used.

$S_{f_x(1300) K^0_S}$ ($B^0 \to f_x(1300) K^0_S$)

VALUE	DOCUMENT ID		TECN	COMMENT
$-0.20 \pm 0.52 \pm 0.10$	[1] AUBERT	09AU	BABR	$e^+e^- \to \Upsilon(4S)$

[1] Uses Dalitz plot analysis of $B^0 \to K^0\pi^+\pi^-$ decays and the first of two equivalent solutions is used.

$C_{f_x(1300) K^0_S}$ ($B^0 \to f_x(1300) K^0_S$)

VALUE	DOCUMENT ID		TECN	COMMENT
$0.13^{+0.33}_{-0.35} \pm 0.10$	[1] AUBERT	09AU	BABR	$e^+e^- \to \Upsilon(4S)$

[1] Uses Dalitz plot analysis of $B^0 \to K^0\pi^+\pi^-$ decays and the first of two equivalent solutions is used.

$S_{K^0\pi^+\pi^-}$ ($B^0 \to K^0\pi^+\pi^-$ nonresonant)

VALUE	DOCUMENT ID		TECN	COMMENT
$-0.01 \pm 0.31 \pm 0.10$	[1] AUBERT	09AU	BABR	$e^+e^- \to \Upsilon(4S)$

[1] Uses Dalitz plot analysis of $B^0 \to K^0\pi^+\pi^-$ decays and the first of two equivalent solutions is used.

$C_{K^0\pi^+\pi^-}$ ($B^0 \to K^0\pi^+\pi^-$ nonresonant)

VALUE	DOCUMENT ID		TECN	COMMENT
$0.01 \pm 0.25 \pm 0.08$	[1] AUBERT	09AU	BABR	$e^+e^- \to \Upsilon(4S)$

[1] Uses Dalitz plot analysis of $B^0 \to K^0\pi^+\pi^-$ decays and the first of two equivalent solutions is used.

$C_{K^0_S K^0_S}$ ($B^0 \to K^0_S K^0_S$)

VALUE	DOCUMENT ID		TECN	COMMENT
0.0 ± 0.4 OUR AVERAGE Error includes scale factor of 1.4.				
$0.38 \pm 0.38 \pm 0.05$	[1] NAKAHAMA	08	BELL	$e^+e^- \to \Upsilon(4S)$
$-0.40 \pm 0.41 \pm 0.06$	AUBERT,BE	06C	BABR	$e^+e^- \to \Upsilon(4S)$

[1] Reports $A_{K^0_S K^0_S}$ which equals to $-C_{K^0_S K^0_S}$.

$S_{K^0_S K^0_S}$ ($B^0 \to K^0_S K^0_S$)

VALUE	DOCUMENT ID		TECN	COMMENT
-0.8 ± 0.5 OUR AVERAGE				
$-0.38^{+0.69}_{-0.77} \pm 0.09$	NAKAHAMA	08	BELL	$e^+e^- \to \Upsilon(4S)$
$-1.28^{+0.80}_{-0.73} \pm 0.11$	AUBERT,BE	06C	BABR	$e^+e^- \to \Upsilon(4S)$

$C_{K^+K^-K^0_S}$ ($B^0 \to K^+K^-K^0_S$ nonresonant)

VALUE	DOCUMENT ID		TECN	COMMENT
0.06 ± 0.08 OUR AVERAGE				
$0.02 \pm 0.09 \pm 0.03$	[1,2] LEES	12O	BABR	$e^+e^- \to \Upsilon(4S)$
$0.14 \pm 0.11 \pm 0.09$	[3,4] NAKAHAMA	10	BELL	$e^+e^- \to \Upsilon(4S)$
• • • We do not use the following data for averages, fits, limits, etc. • • •				
$0.054 \pm 0.102 \pm 0.060$	[3,5] AUBERT	07AX	BABR	Repl. by LEES 12O
$0.09 \pm 0.10 \pm 0.05$	[3,5] CHAO	07	BELL	Repl. by NAKAHAMA 10
$0.10 \pm 0.14 \pm 0.04$	[5] AUBERT	05T	BABR	Repl. by AUBERT 07AX
$0.09 \pm 0.12 \pm 0.07$	[3] CHEN	05B	BELL	Repl. by CHAO 07
$-0.10 \pm 0.19 \pm 0.10$	[5] AUBERT,B	04V	BABR	Repl. by AUBERT 05T
$0.40 \pm 0.33^{+0.28}_{-0.10}$	[3] ABE	03C	BELL	Repl. by ABE 03H
$0.17 \pm 0.16 \pm 0.04$	[3,5] ABE	03H	BELL	Repl. by CHEN 05B

[1] Uses Dalitz plot analysis of the $B^0 \to K^0_S K^+ K^-$ decay.
[2] This measurement is performed on all the isobar components, excluding ϕK^0_S and $f_0(980) K^0_S$.
[3] Quotes $A_{K^+K^-K^0_S}$ which is equal to $-C_{K^+K^-K^0_S}$.
[4] Uses Dalitz plot analysis of $B^0 \to K^0_S K^+ K^-$ decays and the first of four consistent solutions that may be preferred.
[5] Excludes the events from $B^0 \to \phi K^0_S$ decay. The results are derived from a combined sample of $K^+K^-K^0_S$ and $K^+K^-K^0_L$ decays.

$S_{K^+K^-K^0_S}$ ($B^0 \to K^+K^-K^0_S$ nonresonant)

VALUE	DOCUMENT ID		TECN	COMMENT
-0.66 ± 0.11 OUR AVERAGE				
$-0.65 \pm 0.12 \pm 0.03$	[1,2] LEES	12O	BABR	$e^+e^- \to \Upsilon(4S)$
$-0.68 \pm 0.15^{+0.21}_{-0.13}$	[3] CHAO	07	BELL	$e^+e^- \to \Upsilon(4S)$
• • • We do not use the following data for averages, fits, limits, etc. • • •				
$-0.764 \pm 0.111^{+0.071}_{-0.040}$	[3,4] AUBERT	07AX	BABR	Repl. by LEES 12O
$-0.42 \pm 0.17 \pm 0.03$	[3,5] AUBERT	05T	BABR	Repl. by AUBERT 07AX
$-0.49 \pm 0.18 \pm 0.04$	CHEN	05B	BELL	Repl. by CHAO 07
$-0.56 \pm 0.25 \pm 0.04$	[3,6] AUBERT,B	04V	BABR	Repl. by AUBERT 05T
$-0.49 \pm 0.43 \pm 0.11$	ABE	03C	BELL	Repl. by ABE 03H
$-0.51 \pm 0.26 \pm 0.05$	[3,7] ABE	03H	BELL	Repl. by CHEN 05B

[1] Uses Dalitz plot analysis of the $B^0 \to K^0_S K^+ K^-$ decay.
[2] This measurement is performed on all the isobar components, excluding ϕK^0_S and $f_0(980) K^0_S$. Note that the nonresonant component is not a CP eigenstate.
[3] Excludes events from $B^0 \to \phi K^0_S$ decay. The results are derived from a combined sample of $K^+K^-K^0_S$ and $K^+K^-K^0_L$ decays.
[4] Reports β_{eff}. We quote S obtained from epaps: E-PRLTAO-99-076741.
[5] The measured CP-even final states fraction is $0.89 \pm 0.08 \pm 0.06$.
[6] The measured CP-even final states fraction is $0.98 \pm 0.15 \pm 0.04$.
[7] The measured CP-even final states fraction is $1.03 \pm 0.15 \pm 0.05$.

$C_{K^+K^-K^0_S}$ ($B^0 \to K^+K^-K^0_S$ inclusive)

VALUE	DOCUMENT ID		TECN	COMMENT
$0.015 \pm 0.077 \pm 0.053$	[1,2] AUBERT	07AX	BABR	$e^+e^- \to \Upsilon(4S)$

[1] Measured using full Dalitz plot fit including ϕ component.
[2] The results are derived from a combined sample of $K^+K^-K^0_S$ and $K^+K^-K^0_L$ decays.

$S_{K^+K^-K^0_S}$ ($B^0 \to K^+K^-K^0_S$ inclusive)

VALUE	DOCUMENT ID		TECN	COMMENT
$-0.647 \pm 0.116 \pm 0.040$	[1] AUBERT	07AX	BABR	$e^+e^- \to \Upsilon(4S)$

[1] Measured using full Dalitz plot fit including ϕ component.

$C_{\phi K^0_S}$ ($B^0 \to \phi K^0_S$)

VALUE	DOCUMENT ID		TECN	COMMENT
0.01±0.14 OUR AVERAGE				
0.05±0.18±0.05	[1] LEES	12O	BABR	$e^+e^- \to \Upsilon(4S)$
−0.04±0.20±0.10	[2,3] NAKAHAMA	10	BELL	$e^+e^- \to \Upsilon(4S)$
• • • We do not use the following data for averages, fits, limits, etc. • • •				
0.08±0.18±0.04	[2,4] AUBERT	07AX	BABR	Repl. by LEES 12O
−0.07±0.15±0.05	[2,4] CHEN	07	BELL	Repl. by NAKAHAMA 10
0.00±0.23±0.05	[4] AUBERT	05T	BABR	Repl. by AUBERT 07AX
−0.08±0.22±0.09	[2,4] CHEN	05B	BELL	Repl. by CHEN 07
0.01±0.33±0.10	[4] AUBERT,B	04G	BABR	Repl. by AUBERT 05T
0.56±0.41±0.16	[2] ABE	03C	BELL	Repl. by ABE 03H
0.15±0.29±0.07	[2] ABE	03H	BELL	Repl. by CHEN 05B

[1] Uses Dalitz plot analysis of the $B^0 \to K^0_S K^+ K^-$ decay.

[2] Quotes $A_{\phi K^0_S}$ which is equal to $-C_{\phi K^0_S}$.

[3] Uses Dalitz plot analysis of $B^0 \to K^0_S K^+ K^-$ decays and the first of four consistent solutions that may be preferred.

[4] Result combines B-meson final states ϕK^0_S and ϕK^0_L by assuming $S_{\phi K^0_S} = -S_{\phi K^0_L}$

$S_{\phi K^0_S}$ ($B^0 \to \phi K^0_S$)

VALUE	DOCUMENT ID		TECN	COMMENT
0.59±0.14 OUR AVERAGE				
0.66±0.17±0.07	[1] LEES	12O	BABR	$e^+e^- \to \Upsilon(4S)$
0.50±0.21±0.06	[2] CHEN	07	BELL	$e^+e^- \to \Upsilon(4S)$
• • • We do not use the following data for averages, fits, limits, etc. • • •				
0.21±0.26±0.11	[2,3] AUBERT	07AX	BABR	Repl. by LEES 12O
$0.50 \pm 0.25^{+0.07}_{-0.04}$	[2] AUBERT	05T	BABR	Repl. by AUBERT 07AX
0.08±0.33±0.09	[2] CHEN	05B	BELL	Repl. by CHEN 07
$0.47 \pm 0.34^{+0.08}_{-0.06}$	[2] AUBERT,B	04G	BABR	Repl. by AUBERT 05T
−0.73±0.64±0.22	ABE	03C	BELL	Repl. by ABE 03H
$-0.96 \pm 0.50^{+0.09}_{-0.11}$	ABE	03H	BELL	Repl. by CHEN 05B

[1] Uses Dalitz plot analysis of the $B^0 \to K^0_S K^+ K^-$ decay.

[2] Result combines B-meson final states ϕK^0_S and ϕK^0_L by assuming $S_{\phi K^0_S} = -S_{\phi K^0_L}$

[3] Reports β_{eff}. We quote S obtained from epaps: E-PRLTAO-99-076741.

$C_{K_S K_S K_S}(B^0 \to K_S K_S K_S)$

VALUE	DOCUMENT ID		TECN	COMMENT
−0.23±0.14 OUR AVERAGE				
−0.17±0.18±0.04	LEES	12I	BABR	$e^+e^- \to \Upsilon(4S)$
−0.31±0.20±0.07	[1] CHEN	07	BELL	$e^+e^- \to \Upsilon(4S)$
• • • We do not use the following data for averages, fits, limits, etc. • • •				
0.02±0.21±0.05	AUBERT	07AT	BABR	Repl. by LEES 12I
$-0.34 \pm 0.28^{+0.05}_{-0.25}$	AUBERT,B	05	BABR	Repl. by AUBERT 07AT
−0.54±0.34±0.09	[1] SUMISAWA	05	BELL	Repl. by CHEN 07

[1] Belle Collab. quotes $A_{K_S K_S K_S}$ which is equal to $-C_{K_S K_S K_S}$.

$S_{K_S K_S K_S}(B^0 \to K_S K_S K_S)$

VALUE	DOCUMENT ID		TECN	COMMENT
−0.5 ±0.6 OUR AVERAGE	Error includes scale factor of 3.0.			
$-0.94 \pm 0.24^{+0.06}_{-0.21}$	LEES	12I	BABR	$e^+e^- \to \Upsilon(4S)$
0.30±0.32±0.08	CHEN	07	BELL	$e^+e^- \to \Upsilon(4S)$
• • • We do not use the following data for averages, fits, limits, etc. • • •				
−0.71±0.24±0.04	AUBERT	07AT	BABR	Repl. by LEES 12I
$-0.71 \pm 0.38^{+0.04}_{-0.32}$	AUBERT,B	05	BABR	Repl. by AUBERT 07AT
1.26±0.68±0.20	SUMISAWA	05	BELL	Repl. by CHEN 07.

$C_{K^0_S\pi^0\gamma}(B^0 \to K^0_S\pi^0\gamma)$

VALUE	DOCUMENT ID		TECN	COMMENT
0.36±0.33±0.04	[1] AUBERT	08BA	BABR	$e^+e^- \to \Upsilon(4S)$
• • • We do not use the following data for averages, fits, limits, etc. • • •				
0.20±0.20±0.06	[2,3] USHIRODA	06	BELL	$e^+e^- \to \Upsilon(4S)$
−1.0 ±0.5 ±0.2	[1] AUBERT,B	05P	BABR	Repl. by AUBERT 08BA
−0.03±0.34±0.11	[3] USHIRODA	05	BELL	Repl. by USHIRODA 06

[1] Requires $1.1 < M_{K^0_S\pi^0} < 1.8$ GeV/c^2.

[2] Requires $M_{K^0_S\pi^0} < 1.8$ GeV/c^2.

[3] Reports $A_{K^0_S\pi^0\gamma}$, which is $-C_{K^0_S\pi^0\gamma}$.

$S_{K^0_S\pi^0\gamma}(B^0 \to K^0_S\pi^0\gamma)$

VALUE	DOCUMENT ID		TECN	COMMENT
−0.78±0.59±0.09	[1] AUBERT	08BA	BABR	$e^+e^- \to \Upsilon(4S)$
• • • We do not use the following data for averages, fits, limits, etc. • • •				
−0.10±0.31±0.07	[2] USHIRODA	06	BELL	$e^+e^- \to \Upsilon(4S)$
0.9 ±1.0 ±0.2	[1] AUBERT,B	05P	BABR	Repl. by AUBERT 08BA
$-0.58^{+0.46}_{-0.38} \pm 0.11$	USHIRODA	05	BELL	Repl. by USHIRODA 06

[1] Requires $1.1 < M_{K^0_S\pi^0} < 1.8$ GeV/c^2.

[2] Requires $M_{K^0_S\pi^0} < 1.8$ GeV/c^2.

$C_{K^*(892)^0\gamma}$ ($B^0 \to K^*(892)^0\gamma$)

VALUE	DOCUMENT ID		TECN	COMMENT
−0.04±0.16 OUR AVERAGE	Error includes scale factor of 1.2.			
−0.14±0.16±0.03	[1] AUBERT	08BA	BABR	$e^+e^- \to \Upsilon(4S)$
0.20±0.24±0.05	[1,2] USHIRODA	06	BELL	$e^+e^- \to \Upsilon(4S)$
• • • We do not use the following data for averages, fits, limits, etc. • • •				
−0.40±0.23±0.03	AUBERT,B	05P	BABR	Repl. by AUBERT 08BA
−0.57±0.32±0.09	[3] AUBERT,B	04Z	BABR	Repl. by AUBERT,B 05P

[1] Requires $0.8 < M_{K^0_S\pi^0} < 1.0$ GeV/c^2.

[2] Reports value of A which is equal to $-C$.

[3] Based on a total signal of 105 ± 14 events with $K^*(892)^0 \to K^0_S\pi^0$ only.

$S_{K^*(892)^0\gamma}$ ($B^0 \to K^*(892)^0\gamma$)

VALUE	DOCUMENT ID		TECN	COMMENT
−0.15±0.22 OUR AVERAGE				
−0.03±0.29±0.03	[1] AUBERT	08BA	BABR	$e^+e^- \to \Upsilon(4S)$
$-0.32^{+0.36}_{-0.33} \pm 0.05$	[1] USHIRODA	06	BELL	$e^+e^- \to \Upsilon(4S)$
• • • We do not use the following data for averages, fits, limits, etc. • • •				
−0.21±0.40±0.05	AUBERT,B	05P	BABR	Repl. by AUBERT 08BA
$-0.79^{+0.63}_{-0.50} \pm 0.10$	[2] USHIRODA	05	BELL	Repl. by USHIRODA 06
0.25±0.63±0.14	[3] AUBERT,B	04Z	BABR	Repl. by AUBERT,B 05P

[1] Requires $0.8 < M_{K^0_S\pi^0} < 1.0$ GeV/c^2.

[2] Assumes $C(B^0 \to K^*(892)^0\gamma) = 0$.

[3] Based on a total signal of 105 ± 14 events with $K^*(892)^0 \to K^0_S\pi^0$ only.

$C_{\eta K^0\gamma}$ ($B^0 \to \eta K^0\gamma$)

VALUE	DOCUMENT ID		TECN	COMMENT
$\mathbf{-0.32^{+0.40}_{-0.39} \pm 0.07}$	[1] AUBERT	09	BABR	$e^+e^- \to \Upsilon(4S)$

[1] $m_{\eta K} < 3.25$ GeV/c^2.

$S_{\eta K^0\gamma}$ ($B^0 \to \eta K^0\gamma$)

VALUE	DOCUMENT ID		TECN	COMMENT
$\mathbf{-0.18^{+0.49}_{-0.46} \pm 0.12}$	[1] AUBERT	09	BABR	$e^+e^- \to \Upsilon(4S)$

[1] $m_{\eta K} < 3.25$ GeV/c^2.

$C_{K^0\phi\gamma}$ ($B^0 \to K^0\phi\gamma$)

VALUE	DOCUMENT ID		TECN	COMMENT
$\mathbf{-0.35 \pm 0.58^{+0.10}_{-0.23}}$	[1] SAHOO	11A	BELL	$e^+e^- \to \Upsilon(4S)$

[1] Reports value of A, which is equal to $-C$.

$S_{K^0\phi\gamma}$ ($B^0 \to K^0\phi\gamma$)

VALUE	DOCUMENT ID		TECN	COMMENT
$\mathbf{0.74^{+0.72}_{-1.05} {}^{+0.10}_{-0.24}}$	SAHOO	11A	BELL	$e^+e^- \to \Upsilon(4S)$

$C(B^0 \to K^0_S\rho^0\gamma)$

VALUE	DOCUMENT ID		TECN	COMMENT
−0.05±0.18±0.06	[1,2] LI	08F	BELL	$e^+e^- \to \Upsilon(4S)$

[1] Requires $M_{K^0_S\pi^+\pi^-} < 1.8$ GeV/c^2 and $0.6 < M_{\pi^+\pi^-} < 0.9$ GeV/c^2 .

[2] Reports value of $A_{\rm eff}$ which is equal to $-C$, and includes the non-resonant $\pi^+\pi^-$ contribution in the ρ^0 region.

$S(B^0 \to K^0_S\rho^0\gamma)$

VALUE	DOCUMENT ID		TECN	COMMENT
$\mathbf{0.11 \pm 0.33^{+0.05}_{-0.09}}$	[1] LI	08F	BELL	$e^+e^- \to \Upsilon(4S)$

[1] Requires $M_{K^0_S\pi^+\pi^-} < 1.8$ GeV/c^2.

$C(B^0 \to \rho^0\gamma)$

VALUE	DOCUMENT ID		TECN	COMMENT
0.44±0.49±0.14	[1] USHIRODA	08	BELL	$e^+e^- \to \Upsilon(4S)$

[1] Reports value of A which is equal to $-C$.

S ($B^0 \to \rho^0\gamma$)

VALUE	DOCUMENT ID		TECN	COMMENT
$-0.83\pm0.65\pm0.18$	USHIRODA	08	BELL	$e^+e^- \to \Upsilon(4S)$

$C_{\pi\pi}$ ($B^0 \to \pi^+\pi^-$)

$C_{\pi\pi}$ is defined as $(1-|\lambda|^2)/(1+|\lambda|^2)$, where the quantity $\lambda = q/p\,\overline{A}_f/A_f$ is a phase convention independent observable quantity for the final state f. For details, see the review on "CP Violation" in the Reviews section.

VALUE	DOCUMENT ID		TECN	COMMENT
-0.31 ± 0.05 OUR AVERAGE				
$-0.38\pm0.15\pm0.02$	AAIJ	13BO	LHCB	pp at 7 TeV
$-0.33\pm0.06\pm0.03$	[1] DALSENO	13	BELL	$e^+e^- \to \Upsilon(4S)$
$-0.25\pm0.08\pm0.02$	LEES	13D	BABR	$e^+e^- \to \Upsilon(4S)$
• • • We do not use the following data for averages, fits, limits, etc. • • •				
$-0.21\pm0.09\pm0.02$	AUBERT	07AF	BABR	Repl. by LEES 13D
$-0.55\pm0.08\pm0.05$	[1] ISHINO	07	BELL	Repl. by DALSENO 13
$-0.56\pm0.12\pm0.06$	[1] ABE	05D	BELL	Repl. by ISHINO 07
$-0.09\pm0.15\pm0.04$	AUBERT,BE	05	BABR	Repl. by AUBERT 07AF
$-0.58\pm0.15\pm0.07$	[1] ABE	04E	BELL	Repl. by ABE 05D
$-0.77\pm0.27\pm0.08$	[1] ABE	03G	BELL	Repl. by ABE 04E.
$-0.94^{+0.31}_{-0.25}\pm0.09$	[1] ABE	02M	BELL	Repl. by ABE 03G
$-0.25^{+0.45}_{-0.47}\pm0.14$	[2] AUBERT	02D	BABR	Repl. by AUBERT 02Q
$-0.30\pm0.25\pm0.04$	[3] AUBERT	02Q	BABR	Repl. by AUBERT,BE 05

[1] Paper reports $A_{\pi\pi}$ which equals to $-C_{\pi\pi}$.
[2] Corresponds to 90% confidence range $-1.0 < C_{\pi\pi} < 0.47$.
[3] Corresponds to 90% confidence range $-0.72 < C_{\pi\pi} < 0.12$.

$S_{\pi\pi}$ ($B^0 \to \pi^+\pi^-$)

$S_{\pi\pi} = 2\mathrm{Im}\lambda/(1+|\lambda|^2)$, see the note in the $C_{\pi\pi}$ datablock above.

VALUE	DOCUMENT ID		TECN	COMMENT
-0.67 ± 0.06 OUR AVERAGE				
$-0.71\pm0.13\pm0.02$	AAIJ	13BO	LHCB	pp at 7 TeV
$-0.64\pm0.08\pm0.03$	[1] DALSENO	13	BELL	$e^+e^- \to \Upsilon(4S)$
$-0.68\pm0.10\pm0.03$	LEES	13D	BABR	$e^+e^- \to \Upsilon(4S)$
• • • We do not use the following data for averages, fits, limits, etc. • • •				
$-0.60\pm0.11\pm0.03$	AUBERT	07AF	BABR	Repl. by LEES 13D
$-0.61\pm0.10\pm0.04$	ISHINO	07	BELL	Repl. by DALSENO 13
$-0.67\pm0.16\pm0.06$	[2] ABE	05D	BELL	Repl. by ISHINO 07
$-0.30\pm0.17\pm0.03$	AUBERT,BE	05	BABR	Repl. by AUBERT 07AF
$-1.00\pm0.21\pm0.07$	[3] ABE	04E	BELL	Repl. by ABE 05D
$-1.23\pm0.41^{+0.08}_{-0.07}$	ABE	03G	BELL	Repl. by ABE 04E.
$-1.21^{+0.38+0.16}_{-0.27-0.13}$	ABE	02M	BELL	Repl. by ABE 03G
$0.03^{+0.52}_{-0.56}\pm0.11$	[4] AUBERT	02D	BABR	Repl. by AUBERT 02Q
$0.02\pm0.34\pm0.05$	[5] AUBERT	02Q	BABR	Repl. by AUBERT,BE 05

[1] An isospin analysis using other BELLE measurements, disfavors the region of $23.8^\circ < \phi_2 < 66.8^\circ$ at 68% CL.
[2] Rule out the CP-conserving case, $C_{\pi\pi} = S_{\pi\pi} = 0$, at the 5.4 sigma level.
[3] Rule out the CP-conserving case, $C_{\pi\pi} = S_{\pi\pi} = 0$, at the 5.2 sigma level.
[4] Corresponds to 90% confidence range $-0.89 < S_{\pi\pi} < 0.85$.
[5] Corresponds to 90% confidence range $-0.54 < S_{\pi\pi} < 0.58$.

$C_{\pi^0\pi^0}$($B^0 \to \pi^0\pi^0$)

VALUE	DOCUMENT ID		TECN	COMMENT
-0.43 ± 0.24 OUR AVERAGE				
$-0.43\pm0.26\pm0.05$	LEES	13D	BABR	$e^+e^- \to \Upsilon(4S)$
$-0.44^{+0.52}_{-0.53}\pm0.17$	[1] CHAO	05	BELL	$e^+e^- \to \Upsilon(4S)$
• • • We do not use the following data for averages, fits, limits, etc. • • •				
$-0.49\pm0.35\pm0.05$	AUBERT	07BC	BABR	Repl. by LEES 13D
$-0.12\pm0.56\pm0.06$	[2] AUBERT	05L	BABR	Repl. by AUBERT 07BC

[1] BELLE Collab. quotes $A_{\pi^0\pi^0}$ which is equal to $-C_{\pi^0\pi^0}$.
[2] Corresponds to a 90% CL interval of $-0.88 < A_{CP} < 0.64$.

$C_{\rho\pi}$ ($B^0 \to \rho^+\pi^-$)

VALUE	DOCUMENT ID		TECN	COMMENT
$-0.03\ \pm0.07$ OUR AVERAGE	Error includes scale factor of 1.2.			
$0.016\pm0.059\pm0.036$	[1] LEES	13J	BABR	$e^+e^- \to \Upsilon(4S)$
$-0.13\ \pm0.09\ \pm0.05$	[1] KUSAKA	07	BELL	$e^+e^- \to \Upsilon(4S)$
• • • We do not use the following data for averages, fits, limits, etc. • • •				
$0.15\ \pm0.09\ \pm0.05$	AUBERT	07AA	BABR	Repl. by LEES 13J
$0.25\ \pm0.17\ ^{+0.02}_{-0.06}$	WANG	05	BELL	Repl. by KUSAKA 07
$0.36\ \pm0.18\ \pm0.04$	AUBERT	03T	BABR	Repl. by AUBERT 07AA

[1] Uses time-dependent Dalitz plot analysis of $B^0 \to \pi^+\pi^-\pi^0$ decays.

$S_{\rho\pi}$ ($B^0 \to \rho^+\pi^-$)

VALUE	DOCUMENT ID		TECN	COMMENT
$0.05\ \pm0.07$ OUR AVERAGE				
$0.053\pm0.081\pm0.034$	[1] LEES	13J	BABR	$e^+e^- \to \Upsilon(4S)$
$0.06\ \pm0.13\ \pm0.05$	[1] KUSAKA	07	BELL	$e^+e^- \to \Upsilon(4S)$
• • • We do not use the following data for averages, fits, limits, etc. • • •				
$-0.03\ \pm0.11\ \pm0.04$	AUBERT	07AA	BABR	Repl. by LEES 13J
$-0.28\ \pm0.23\ ^{+0.10}_{-0.08}$	WANG	05	BELL	Repl. by KUSAKA 07
$0.19\ \pm0.24\ \pm0.03$	AUBERT	03T	BABR	Repl. by AUBERT 07AA

[1] Uses time-dependent Dalitz plot analysis of $B^0 \to \pi^+\pi^-\pi^0$ decays.

$\Delta C_{\rho\pi}$ ($B^0 \to \rho^+\pi^-$)

$\Delta C_{\rho\pi}$ describes the asymmetry between the rates $\Gamma(B^0 \to \rho^+\pi^-) + \Gamma(\overline{B}^0 \to \rho^-\pi^+)$ and $\Gamma(B^0 \to \rho^-\pi^+) + \Gamma(\overline{B}^0 \to \rho^+\pi^-)$.

VALUE	DOCUMENT ID		TECN	COMMENT
$0.27\ \pm0.06$ OUR AVERAGE				
$0.234\pm0.061\pm0.048$	[1] LEES	13J	BABR	$e^+e^- \to \Upsilon(4S)$
$0.36\ \pm0.10\ \pm0.05$	[1] KUSAKA	07	BELL	$e^+e^- \to \Upsilon(4S)$
• • • We do not use the following data for averages, fits, limits, etc. • • •				
$0.39\ \pm0.09\ \pm0.09$	AUBERT	07AA	BABR	Repl. by LEES 13J
$0.38\ \pm0.18\ ^{+0.02}_{-0.04}$	WANG	05	BELL	Repl. by KUSAKA 07
$0.28\ ^{+0.18}_{-0.19}\ \pm0.04$	AUBERT	03T	BABR	Repl. by AUBERT 07AA

[1] Uses time-dependent Dalitz plot analysis of $B^0 \to \pi^+\pi^-\pi^0$ decays.

$\Delta S_{\rho\pi}$ ($B^0 \to \rho^+\pi^-$)

$\Delta S_{\rho\pi}$ is related to the strong phase difference between the amplitudes contributing to $B^0 \to \rho^+\pi^-$.

VALUE	DOCUMENT ID		TECN	COMMENT
$0.01\ \pm0.08$ OUR AVERAGE				
$0.054\pm0.082\pm0.039$	[1] LEES	13J	BABR	$e^+e^- \to \Upsilon(4S)$
$-0.08\ \pm0.13\ \pm0.05$	[1] KUSAKA	07	BELL	$e^+e^- \to \Upsilon(4S)$
• • • We do not use the following data for averages, fits, limits, etc. • • •				
$-0.01\ \pm0.14\ \pm0.06$	AUBERT	07AA	BABR	Repl. by LEES 13J
$-0.30\ \pm0.24\ \pm0.09$	WANG	05	BELL	Repl. by KUSAKA 07
$0.15\ \pm0.25\ \pm0.03$	AUBERT	03T	BABR	Repl. by AUBERT 07AA

[1] Uses time-dependent Dalitz plot analysis of $B^0 \to \pi^+\pi^-\pi^0$ decays.

$C_{\rho^0\pi^0}$ ($B^0 \to \rho^0\pi^0$)

VALUE	DOCUMENT ID		TECN	COMMENT
0.27 ± 0.24 OUR AVERAGE				
$0.19\pm0.23\pm0.15$	[1] LEES	13J	BABR	$e^+e^- \to \Upsilon(4S)$
$0.49\pm0.36\pm0.28$	[1,2] KUSAKA	07	BELL	$e^+e^- \to \Upsilon(4S)$
• • • We do not use the following data for averages, fits, limits, etc. • • •				
$-0.10\pm0.40\pm0.53$	AUBERT	07AA	BABR	Repl. by LEES 13J
$0.53^{+0.67+0.10}_{-0.84-0.15}$	[2] DRAGIC	06	BELL	Repl. by KUSAKA 07

[1] Uses time-dependent Dalitz plot analysis of $B^0 \to \pi^+\pi^-\pi^0$ decays.
[2] Quotes $A_{\rho^0\pi^0}$ which is equal to $-C_{\rho^0\pi^0}$.

$S_{\rho^0\pi^0}$ ($B^0 \to \rho^0\pi^0$)

VALUE	DOCUMENT ID		TECN	COMMENT
-0.23 ± 0.34 OUR AVERAGE				
$-0.37\pm0.34\pm0.20$	[1] LEES	13J	BABR	$e^+e^- \to \Upsilon(4S)$
$0.17\pm0.57\pm0.35$	[1] KUSAKA	07	BELL	$e^+e^- \to \Upsilon(4S)$
• • • We do not use the following data for averages, fits, limits, etc. • • •				
$0.04\pm0.44\pm0.18$	AUBERT	07AA	BABR	Repl. by LEES 13J

[1] Uses time-dependent Dalitz plot analysis of $B^0 \to \pi^+\pi^-\pi^0$ decays.

$C_{a_1\pi}$ ($B^0 \to a_1(1260)^+\pi^-$)

VALUE	DOCUMENT ID		TECN	COMMENT
-0.05 ± 0.11 OUR AVERAGE				
$-0.01\pm0.11\pm0.09$	DALSENO	12	BELL	$e^+e^- \to \Upsilon(4S)$
$-0.10\pm0.15\pm0.09$	AUBERT	07O	BABR	$e^+e^- \to \Upsilon(4S)$

$S_{a_1\pi}$ ($B^0 \to a_1(1260)^+\pi^-$)

VALUE	DOCUMENT ID		TECN	COMMENT
$-0.2\ \pm0.4$ OUR AVERAGE	Error includes scale factor of 3.2.			
$-0.51\pm0.14\pm0.08$	DALSENO	12	BELL	$e^+e^- \to \Upsilon(4S)$
$0.37\pm0.21\pm0.07$	AUBERT	07O	BABR	$e^+e^- \to \Upsilon(4S)$

$\Delta C_{a_1\pi}$ ($B^0 \to a_1(1260)^+\pi^-$)

$\Delta C_{a_1\pi}$ describes the asymmetry between the rates $\Gamma(B^0 \to a_1^+\pi^-) + \Gamma(\overline{B}^0 \to a_1^-\pi^+)$ and $\Gamma(B^0 \to a_1^-\pi^+) + \Gamma(\overline{B}^0 \to a_1^+\pi^-)$.

VALUE	DOCUMENT ID		TECN	COMMENT
0.43 ± 0.14 OUR AVERAGE	Error includes scale factor of 1.3.			
$0.54\pm0.11\pm0.07$	DALSENO	12	BELL	$e^+e^- \to \Upsilon(4S)$
$0.26\pm0.15\pm0.07$	AUBERT	07O	BABR	$e^+e^- \to \Upsilon(4S)$

$\Delta S_{a_1\pi}$ ($B^0 \to a_1(1260)^+\pi^-$)

$\Delta S_{a_1\pi}$ is related to the strong phase difference between the amplitudes contributing to $B^0 \to a_1\pi$ decays.

VALUE	DOCUMENT ID		TECN	COMMENT
-0.11 ± 0.12 OUR AVERAGE				
$-0.09\pm0.14\pm0.06$	DALSENO	12	BELL	$e^+e^- \to \Upsilon(4S)$
$-0.14\pm0.21\pm0.06$	AUBERT	07O	BABR	$e^+e^- \to \Upsilon(4S)$

C ($B^0 \to b_1^- K^+$)

VALUE	DOCUMENT ID		TECN	COMMENT
$-0.22\pm0.23\pm0.05$	AUBERT	07BI	BABR	$e^+e^- \to \Upsilon(4S)$

ΔC ($B^0 \to b_1^-\pi^+$)

VALUE	DOCUMENT ID		TECN	COMMENT
$-1.04\pm0.23\pm0.08$	AUBERT	07BI	BABR	$e^+e^- \to \Upsilon(4S)$

$C_{\rho^0\rho^0}$ ($B^0 \to \rho^0\rho^0$)

VALUE	DOCUMENT ID		TECN	COMMENT
$0.2\pm0.8\pm0.3$	AUBERT	08BB	BABR	$e^+e^- \to \Upsilon(4S)$

$S_{\rho^0\rho^0}$ ($B^0 \to \rho^0\rho^0$)

VALUE	DOCUMENT ID		TECN	COMMENT
$0.3\pm0.7\pm0.2$	AUBERT	08BB	BABR	$e^+e^- \to \Upsilon(4S)$

$C_{\rho\rho}$ ($B^0 \to \rho^+\rho^-$)

VALUE	DOCUMENT ID		TECN	COMMENT
-0.05 ± 0.13 OUR AVERAGE				
$0.01\pm0.15\pm0.06$	AUBERT	07BF	BABR	$e^+e^- \to \Upsilon(4S)$
$-0.16\pm0.21\pm0.08$	[1] SOMOV	07	BELL	$e^+e^- \to \Upsilon(4S)$
• • • We do not use the following data for averages, fits, limits, etc. • • •				
$-0.00\pm0.30\pm0.09$	[1] SOMOV	06	BELL	Repl. by SOMOV 07
$-0.03\pm0.18\pm0.09$	AUBERT,B	05C	BABR	Repl. by AUBERT 07BF
$-0.17\pm0.27\pm0.14$	AUBERT,B	04R	BABR	Repl. by AUBERT,B 05C

[1] BELLE Collab. quotes A_{CP} which is equal to $-C$.

$S_{\rho\rho}$ ($B^0 \to \rho^+\rho^-$)

VALUE	DOCUMENT ID		TECN	COMMENT
-0.06 ± 0.17 OUR AVERAGE				
$-0.17\pm0.20^{+0.05}_{-0.06}$	AUBERT	07BF	BABR	$e^+e^- \to \Upsilon(4S)$
$0.19\pm0.30\pm0.08$	SOMOV	07	BELL	$e^+e^- \to \Upsilon(4S)$
• • • We do not use the following data for averages, fits, limits, etc. • • •				
$0.08\pm0.41\pm0.09$	SOMOV	06	BELL	Repl. by SOMOV 07
$-0.33\pm0.24^{+0.08}_{-0.14}$	AUBERT,B	05C	BABR	Repl. by AUBERT 07BF
$-0.42\pm0.42\pm0.14$	AUBERT,B	04R	BABR	Repl. by AUBERT,B 05C

$|\lambda|$ ($B^0 \to J/\psi K^*(892)^0$)

VALUE	CL%	DOCUMENT ID		TECN	COMMENT
<0.25	95	[1] AUBERT,B	04H	BABR	$e^+e^- \to \Upsilon(4S)$

[1] Uses the measured cosine coefficients C and $\overline{C}$ and assumes $|q/p| = 1$.

cos 2β ($B^0 \to J/\psi K^*(892)^0$)

$\beta(\phi_1)$ is one of the angles of CMK unitarity triangle, see the review on "*CP* Violation in the Reviews section.

VALUE	DOCUMENT ID		TECN	COMMENT
$1.7\ ^{+0.7}_{-0.9}$ OUR AVERAGE Error includes scale factor of 1.6.				
$2.72^{+0.50}_{-0.79}\pm0.27$	[1] AUBERT	05P	BABR	$e^+e^- \to \Upsilon(4S)$
$0.87\pm0.74\pm0.12$	[2] ITOH	05	BELL	$e^+e^- \to \Upsilon(4S)$

[1] The measurement is obtained when sin 2β is fixed to 0.726 and the sign of cos 2β is positive with 86% confidence level.
[2] The measurement is obtained with sin 2β fixed to 0.731.

cos 2β ($B^0 \to [K^0_S\pi^+\pi^-]_{D^{(*)}}\, h^0$)

VALUE	DOCUMENT ID		TECN	COMMENT
$1.0\ ^{+0.6}_{-0.7}$ OUR AVERAGE Error includes scale factor of 1.8.				
$0.42\pm0.49\pm0.16$	[1] AUBERT	07BH	BABR	$e^+e^- \to \Upsilon(4S)$
$1.87^{+0.40+0.22}_{-0.53-0.32}$	[2] KROKOVNY	06	BELL	$e^+e^- \to \Upsilon(4S)$

[1] AUBERT 07BH evaluates the likelihoods for the positive and negative solutions assuming $\sin(2\beta_{eff}) = 0.678$. It quotes $L_+/(L_+ + L_-) = 0.86$ corresponding to a likelihood ratio of $L_+/L_- = 6.14$ in favor of the positive solution.
[2] KROKOVNY 06 evaluates the likelihoods for the positive and negative solutions assuming $\sin(2\beta_{eff}) = 0.689$. It quotes $L_+/(L_+ + L_-) = 0.983$ corresponding to a likelihood ratio of $L_+/L_- = 57.8$ in favor of the positive solution.

$(S_+ + S_-)/2$ ($B^0 \to D^{*-}\pi^+$)

$S_\pm = -\frac{2Im(\lambda_\pm)}{1+|\lambda_\pm|^2}$ where λ_+ and λ_- are defined in the $C_{\pi\pi}$ datablock above for $B^0 \to D^{*-}\pi^+$ and $\overline{B}^0 \to D^{*+}\pi^-$.

VALUE	DOCUMENT ID		TECN	COMMENT
-0.039 ± 0.011 OUR AVERAGE				
$-0.046\pm0.013\pm0.015$	[1] BAHINIPATI	11	BELL	$e^+e^- \to \Upsilon(4S)$
$-0.040\pm0.023\pm0.010$	[2] AUBERT	06Y	BABR	$e^+e^- \to \Upsilon(4S)$
$-0.034\pm0.014\pm0.009$	[1] AUBERT	05Z	BABR	$e^+e^- \to \Upsilon(4S)$
• • • We do not use the following data for averages, fits, limits, etc. • • •				
$-0.039\pm0.020\pm0.013$	[3] RONGA	06	BELL	Repl. by BAHINIPATI 11
$-0.030\pm0.028\pm0.018$	[1] GERSHON	05	BELL	Repl. by RONGA 06
$-0.068\pm0.038\pm0.020$	[2] AUBERT	04V	BABR	Repl. by AUBERT 06Y
$-0.063\pm0.024\pm0.014$	[1] AUBERT	04W	BABR	Repl. by AUBERT 05Z
$0.060\pm0.040\pm0.019$	[2] SARANGI	04	BELL	Repl. by RONGA 06

[1] Uses partially reconstructed $B^0 \to D^{*\pm}\pi^\mp$ decays.
[2] Uses fully reconstructed $B^0 \to D^{*\pm}\pi^\mp$ decays.
[3] Combines the results from fully reconstructed and partially reconstructed $D^*\pi$ events by taking weighted averages. Assumes that systematic errors from physics parameters and fit biases in the two measurements are 100% correlated.

$(S_- - S_+)/2$ ($B^0 \to D^{*-}\pi^+$)

VALUE	DOCUMENT ID		TECN	COMMENT
-0.009 ± 0.015 OUR AVERAGE				
$-0.015\pm0.013\pm0.015$	[1] BAHINIPATI	11	BELL	$e^+e^- \to \Upsilon(4S)$
$0.049\pm0.042\pm0.015$	[2] AUBERT	06Y	BABR	$e^+e^- \to \Upsilon(4S)$
$-0.019\pm0.022\pm0.013$	[1] AUBERT	05Z	BABR	$e^+e^- \to \Upsilon(4S)$
• • • We do not use the following data for averages, fits, limits, etc. • • •				
$-0.011\pm0.020\pm0.013$	[3] RONGA	06	BELL	Repl. by BAHINIPATI 11
$-0.005\pm0.028\pm0.018$	[1] GERSHON	05	BELL	Repl. by RONGA 06
$0.031\pm0.070\pm0.033$	[2] AUBERT	04V	BABR	Repl. by AUBERT 06Y
$-0.004\pm0.037\pm0.014$	[1] AUBERT	04W	BABR	Repl. by AUBERT 05Z
$0.049\pm0.040\pm0.019$	[2] SARANGI	04	BELL	Repl. by RONGA 06

[1] Uses partially reconstructed $B^0 \to D^{*\pm}\pi^\mp$ decays.
[2] Uses fully reconstructed $B^0 \to D^{*\pm}\pi^\mp$ decays.
[3] Combines the results from fully reconstructed and partially reconstructed $D^*\pi$ events by taking weighted averages. Assumes that systematic errors from physics parameters and fit biases in the two measurements are 100% correlated.

$(S_+ + S_-)/2$ ($B^0 \to D^-\pi^+$)

VALUE	DOCUMENT ID		TECN	COMMENT
-0.046 ± 0.023 OUR AVERAGE				
$-0.010\pm0.023\pm0.07$	[1] AUBERT	06Y	BABR	$e^+e^- \to \Upsilon(4S)$
$-0.050\pm0.021\pm0.012$	[2] RONGA	06	BELL	$e^+e^- \to \Upsilon(4S)$
• • • We do not use the following data for averages, fits, limits, etc. • • •				
$-0.022\pm0.038\pm0.020$	[1] AUBERT	04V	BABR	Repl. by AUBERT 06Y
$-0.062\pm0.037\pm0.018$	[1] SARANGI	04	BELL	Repl. by RONGA 06

[1] Uses fully reconstructed $B^0 \to D^\pm\pi^\mp$ decays.
[2] Combines the results from fully reconstructed and partially reconstructed $D\pi$ events by taking weighted averages. Assumes that systematic errors from physics parameters and fit biases in the two measurements are 100% correlated.

$(S_- - S_+)/2$ ($B^0 \to D^-\pi^+$)

VALUE	DOCUMENT ID		TECN	COMMENT
-0.022 ± 0.021 OUR AVERAGE				
$-0.033\pm0.042\pm0.012$	[1] AUBERT	06Y	BABR	$e^+e^- \to \Upsilon(4S)$
$-0.019\pm0.021\pm0.012$	[2] RONGA	06	BELL	$e^+e^- \to \Upsilon(4S)$
• • • We do not use the following data for averages, fits, limits, etc. • • •				
$0.025\pm0.068\pm0.033$	[1] AUBERT	04V	BABR	Repl. by AUBERT 06Y
$-0.025\pm0.037\pm0.018$	[1] SARANGI	04	BELL	Repl. by RONGA 06

[1] Uses fully reconstructed $B^0 \to D^\pm\pi^\mp$ decays.
[2] Combines the results from fully reconstructed and partially reconstructed $D\pi$ events by taking weighted averages. Assumes that systematic errors from physics parameters and fit biases in the two measurements are 100% correlated.

$(S_+ + S_-)/2$ ($B^0 \to D^-\rho^+$)

VALUE	DOCUMENT ID		TECN	COMMENT
$-0.024\pm0.031\pm0.009$	[1] AUBERT	06Y	BABR	$e^+e^- \to \Upsilon(4S)$

[1] Uses fully reconstructed $B^0 \to D^-\rho^+$ decays.

$(S_- - S_+)/2$ ($B^0 \to D^-\rho^+$)

VALUE	DOCUMENT ID		TECN	COMMENT
$-0.098\pm0.055\pm0.018$	[1] AUBERT	06Y	BABR	$e^+e^- \to \Upsilon(4S)$

[1] Uses fully reconstructed $B^0 \to D^-\rho^+$ decays.

$C_{\eta_c K^0_S}$ ($B^0 \to \eta_c K^0_S$)

VALUE	DOCUMENT ID		TECN	COMMENT
$0.080\pm0.124\pm0.029$	AUBERT	09K	BABR	$e^+e^- \to \Upsilon(4S)$

$S_{\eta_c K^0_S}$ ($B^0 \to \eta_c K^0_S$)

VALUE	DOCUMENT ID		TECN	COMMENT
$0.925\pm0.160\pm0.057$	AUBERT	09K	BABR	$e^+e^- \to \Upsilon(4S)$

Meson Particle Listings

B^0

$C_{c\overline{c}K(*)0}$ ($B^0 \to c\overline{c}K^{(*)0}$)

"OUR EVALUATION" is an average using rescaled values of the data listed below. The average and rescaling were performed by the Heavy Flavor Averaging Group (HFAG) and are described at http://www.slac.stanford.edu/xorg/hfag/. The averaging/rescaling procedure takes into account correlations between the measurements.

VALUE (units 10^{-2})	DOCUMENT ID		TECN	COMMENT
0.5 ± 1.7 OUR EVALUATION				
0.5 ± 1.6 OUR AVERAGE				
− 0.6 ± 1.6 ± 1.2	[1] ADACHI	12A	BELL	$e^+e^- \to \Upsilon(4S)$
−29 $^{+53}_{-44}$ ± 6	[2] AUBERT	09AU	BABR	$e^+e^- \to \Upsilon(4S)$
2.4 ± 2.0 ± 1.6	[3] AUBERT	09K	BABR	$e^+e^- \to \Upsilon(4S)$
• • • We do not use the following data for averages, fits, limits, etc. • • •				
− 4 ± 7 ± 5	[4] SAHOO	08	BELL	Repl. by ADACHI 12A
4.9 ± 2.3 ± 1.8	[3] AUBERT	07AY	BABR	Repl. by AUBERT 09K
− 1.8 ± 2.1 ± 1.4	[5] CHEN	07	BELL	Repl. by ADACHI 12A
− 0.7 ± 4.1 ± 3.3	[6] ABE	05B	BELL	Repl. by CHEN 07
5.1 ± 3.2 ± 1.4	[7] AUBERT	05F	BABR	Repl. by AUBERT 07AY
5.1 ± 5.1 ± 2.6	[8] ABE	02Z	BELL	Repl. by ABE 05B
5.3 ± 5.4 ± 3.2	[9] AUBERT	02P	BABR	Repl. by AUBERT 05F

[1] Measurement based on $B^0 \to J/\psi K^0_S$, $B^0 \to \psi(2S) K^0_S$, $B^0 \to J/\psi K^0_L$, and $B^0 \to \chi_{c1}(1P) K^0_S$ decays.
[2] Uses Dalitz plot analysis of $B^0 \to K^0\pi^+\pi^-$ decays and the first of two equivalent solutions is used.
[3] Measurement based on $B^0 \to c\overline{c}K^{(*)0}$ decays.
[4] Reports value of A of $B^0 \to \psi(2S) K^0$ which is equal to $-C$.
[5] Reports value of A of $B^0 \to J/\psi K^0$ which is equal to $-C$.
[6] Measurement based on 152×10^6 $B\overline{B}$ pairs.
[7] Measurement based on 227×10^6 $B\overline{B}$ pairs.
[8] Measured with both $\eta_f = \pm 1$ samples.
[9] Measured with the high purity of $\eta_f = -1$ samples.

sin(2β)

For a discussion of CP violation, see the review on "CP Violation" in the Reviews section. sin(2β) is a measure of the CP-violating amplitude in the $B^0_d \to J/\psi(1S) K^0_S$.

"OUR EVALUATION" is an average using rescaled values of the data listed below. The average and rescaling were performed by the Heavy Flavor Averaging Group (HFAG) and are described at http://www.slac.stanford.edu/xorg/hfag/. The averaging/rescaling procedure takes into account correlations between the measurements.

VALUE	DOCUMENT ID		TECN	COMMENT
0.682 ± 0.019 OUR EVALUATION				
0.675 ± 0.020 OUR AVERAGE				
0.667 ± 0.023 ± 0.012	[1] ADACHI	12A	BELL	$e^+e^- \to \Upsilon(4S)$
0.57 ± 0.58 ± 0.06	[2] SATO	12	BELL	$e^+e^- \to \Upsilon(5S)$
−0.69 ± 0.52 ± 0.08	[3] AUBERT	09AU	BABR	$e^+e^- \to \Upsilon(4S)$
0.687 ± 0.028 ± 0.012	[4] AUBERT	09K	BABR	$e^+e^- \to \Upsilon(4S)$
1.56 ± 0.42 ± 0.21	[5] AUBERT	04R	BABR	$e^+e^- \to \Upsilon(4S)$
0.79 $^{+0.41}_{-0.44}$	[6] AFFOLDER	00C	CDF	$p\overline{p}$ at 1.8 TeV
0.84 $^{+0.82}_{-1.04}$ ± 0.16	[7] BARATE	00Q	ALEP	$e^+e^- \to Z$
3.2 $^{+1.8}_{-2.0}$ ± 0.5	[8] ACKERSTAFF	98Z	OPAL	$e^+e^- \to Z$
• • • We do not use the following data for averages, fits, limits, etc. • • •				
0.72 ± 0.09 ± 0.03	[9] SAHOO	08	BELL	Repl. by ADACHI 12A
0.714 ± 0.032 ± 0.018	[4] AUBERT	07AY	BABR	Repl. by AUBERT 09K
0.642 ± 0.031 ± 0.017	CHEN	07	BELL	Repl. by ADACHI 12A
0.728 ± 0.056 ± 0.023	[10] ABE	05B	BELL	Repl. by CHEN 07
0.722 ± 0.040 ± 0.023	[11] AUBERT	05F	BABR	Repl. by AUBERT 07AY
0.99 ± 0.14 ± 0.06	[12] ABE	02U	BELL	$e^+e^- \to \Upsilon(4S)$
0.719 ± 0.074 ± 0.035	[13] ABE	02Z	BELL	Repl. by ABE 05B
0.59 ± 0.14 ± 0.05	[14] AUBERT	02N	BABR	$e^+e^- \to \Upsilon(4S)$
0.741 ± 0.067 ± 0.034	[15] AUBERT	02P	BABR	Repl. by AUBERT 05F
0.58 $^{+0.32}_{-0.34}$ $^{+0.09}_{-0.10}$	ABASHIAN	01	BELL	Repl. by ABE 01G
0.99 ± 0.14 ± 0.06	[16] ABE	01G	BELL	Repl. by ABE 02Z
0.34 ± 0.20 ± 0.05	AUBERT	01	BABR	Repl. by AUBERT 01B
0.59 ± 0.14 ± 0.05	[16] AUBERT	01B	BABR	Repl. by AUBERT 02P
1.8 ± 1.1 ± 0.3	[17] ABE	98U	CDF	Repl. by AFFOLDER 00C

[1] Measurement based on $B^0 \to J/\psi K^0_S$, $B^0 \to \psi(2S) K^0_S$, $B^0 \to J/\psi K^0_L$, and $B^0 \to \chi_{c1}(1P) K^0_S$ decays.
[2] SATO 12 uses 121 fb^{-1} data collected on $\Upsilon(5S)$ resonance. Uses the "$B-\pi$ tagging" where $B\pi^+$ and $B\pi^-$ tagged $J/\psi K^0_S$ events are compared.
[3] Uses Dalitz plot analysis of $B^0 \to K^0\pi^+\pi^-$ decays and the first of two equivalent solutions.
[4] Measurement based on $B^0 \to c\overline{c}K^{(*)0}$ decays.
[5] Measurement in which the J/ψ decays to hadrons or to muons that do not satisfy the standard identification criteria.
[6] AFFOLDER 00C uses about 400 $B^0 \to J/\psi(1S) K^0_S$ events. The production flavor of B^0 was determined using three tagging algorithms: a same-side tag, a jet-charge tag, and a soft-lepton tag.
[7] BARATE 00Q uses 23 candidates for $B^0 \to J/\psi(1S) K^0_S$ decays. A combination of jet-charge, vertex-charge, and same-side tagging techniques were used to determine the B^0 production flavor.
[8] ACKERSTAFF 98Z uses 24 candidates for $B^0_d \to J/\psi(1S) K^0_S$ decay. A combination of jet-charge and vertex-charge techniques were used to tag the B^0_d production flavor.
[9] Based on $B^0 \to \psi(2S) K^0_S$ decays.
[10] Measurement based on 152×10^6 $B\overline{B}$ pairs.
[11] Measurement based on 227×10^6 $B\overline{B}$ pairs.
[12] ABE 02U result is based on the same analysis and data sample reported in ABE 01G.
[13] ABE 02Z result is based on 85×10^6 $B\overline{B}$ pairs.
[14] AUBERT 02N result based on the same analysis and data sample reported in AUBERT 01B.
[15] AUBERT 02P result is based on 88×10^6 $B\overline{B}$ pairs.
[16] First observation of CP violation in B^0 meson system.
[17] ABE 98U uses 198 ± 17 $B^0_d \to J/\psi(1S) K^0$ events. The production flavor of B^0 was determined using the same side tagging technique.

$C_{J/\psi(nS)K^0}$ ($B^0 \to J/\psi(nS) K^0$)

"OUR EVALUATION" is an average using rescaled values of the data listed below. The average and rescaling were performed by the Heavy Flavor Averaging Group (HFAG) and are described at http://www.slac.stanford.edu/xorg/hfag/. The averaging/rescaling procedure takes into account correlations between the measurements.

VALUE (units 10^{-2})	DOCUMENT ID		TECN	COMMENT
0.5 ± 2.0 OUR EVALUATION				
0.3 ± 1.8 OUR AVERAGE				
3 ± 9 ± 1	[1] AAIJ	13K	LHCB	pp at 7 TeV
1.5 ± 2.1 $^{+2.3}_{-4.5}$	[2,3] ADACHI	12A	BELL	$e^+e^- \to \Upsilon(4S)$
−10.4 ± 5.5 $^{+2.7}_{-4.7}$	[3,4] ADACHI	12A	BELL	$e^+e^- \to \Upsilon(4S)$
− 1.9 ± 2.6 $^{+4.1}_{-1.7}$	[3,5] ADACHI	12A	BELL	$e^+e^- \to \Upsilon(4S)$
8.9 ± 7.6 ± 2.0	[4] AUBERT	09K	BABR	$e^+e^- \to \Upsilon(4S)$
1.6 ± 2.3 ± 1.8	AUBERT	09K	BABR	$e^+e^- \to \Upsilon(4S)$
• • • We do not use the following data for averages, fits, limits, etc. • • •				
− 4 ± 7 ± 5	[3,4] SAHOO	08	BELL	Repl. by ADACHI 12A
− 1.8 ± 2.1 ± 1.4	[3] CHEN	07	BELL	Repl. by ADACHI 12A

[1] AAIJ 13K uses 8200 flavor-tagged $B_d \to J/\psi K^0_S$ events from 1 fb^{-1} of integrated luminosity. Provides the correlation coefficient $\rho = 0.42$ between the statistical uncertainties of $S_{J/\psi(nS)K^0}$ ($B^0 \to J/\psi(nS) K^0$) and $C_{J/\psi(nS)K^0}$ ($B^0 \to J/\psi(nS) K^0$) measurements.
[2] Uses $B^0 \to J/\psi K^0_S$ decays.
[3] The paper reports A, which is equal to $-C$.
[4] Uses $B^0 \to \psi(2S) K^0_S$ decays.
[5] Uses $B^0 \to J/\psi K^0_L$ decays.

$S_{J/\psi(nS)K^0}$ ($B^0 \to J/\psi(nS) K^0$)

"OUR EVALUATION" is an average using rescaled values of the data listed below. The average and rescaling were performed by the Heavy Flavor Averaging Group (HFAG) and are described at http://www.slac.stanford.edu/xorg/hfag/. The averaging/rescaling procedure takes into account correlations between the measurements.

VALUE	DOCUMENT ID		TECN	COMMENT
0.676 ± 0.021 OUR EVALUATION				
0.680 ± 0.021 OUR AVERAGE Error includes scale factor of 1.1.				
0.73 ± 0.07 ± 0.04	[1] AAIJ	13K	LHCB	pp at 7 TeV
0.670 ± 0.029 ± 0.013	[2] ADACHI	12A	BELL	$e^+e^- \to \Upsilon(4S)$
0.738 ± 0.079 ± 0.036	[3] ADACHI	12A	BELL	$e^+e^- \to \Upsilon(4S)$
0.642 ± 0.047 ± 0.021	[4] ADACHI	12A	BELL	$e^+e^- \to \Upsilon(4S)$
0.57 ± 0.58 ± 0.06	[5] SATO	12	BELL	$e^+e^- \to \Upsilon(5S)$
0.897 ± 0.100 ± 0.036	[3] AUBERT	09K	BABR	$e^+e^- \to \Upsilon(4S)$
0.666 ± 0.031 ± 0.013	AUBERT	09K	BABR	$e^+e^- \to \Upsilon(4S)$
0.79 $^{+0.41}_{-0.44}$	[6] AFFOLDER	00C	CDF	$p\overline{p}$ at 1.8 TeV
0.84 $^{+0.82}_{-1.04}$ ± 0.16	[7] BARATE	00Q	ALEP	$e^+e^- \to Z$
3.2 $^{+1.8}_{-2.0}$ ± 0.5	[8] ACKERSTAFF	98Z	OPAL	$e^+e^- \to Z$
• • • We do not use the following data for averages, fits, limits, etc. • • •				
0.650 ± 0.029 ± 0.018	[9] SAHOO	08	BELL	Repl. by ADACHI 12A
0.72 ± 0.09 ± 0.03	[3] SAHOO	08	BELL	Repl. by ADACHI 12A
0.642 ± 0.031 ± 0.017	CHEN	07	BELL	Repl. by ADACHI 12A

[1] AAIJ 13K uses 8200 flavor-tagged $B_d \to J/\psi K^0_S$ events from 1 fb^{-1} of integrated luminosity. Provides the correlation coefficient $\rho = 0.42$ between the statistical uncertainties of $S_{J/\psi(nS)K^0}$ ($B^0 \to J/\psi(nS) K^0$) and $C_{J/\psi(nS)K^0}$ ($B^0 \to J/\psi(nS) K^0$) measurements.
[2] Uses $B^0 \to J/\psi K^0_S$ decays.
[3] Based on $B^0 \to \psi(2S) K^0_S$ decays.
[4] Uses $B^0 \to J/\psi K^0_L$ decays.
[5] SATO 12 uses 121 fb^{-1} data collected at $\Upsilon(5S)$ resonance. Uses the "$B-\pi$ tagging" where $B\pi^+$ and $B\pi^-$ tagged $J/\psi K^0_S$ events are compared.
[6] AFFOLDER 00C uses about 400 $B^0 \to J/\psi(1S) K^0_S$ events. The production flavor of B^0 was determined using three tagging algorithms: a same-side tag, a jet-charge tag, and a soft-lepton tag.
[7] BARATE 00Q uses 23 candidates for $B^0 \to J/\psi(1S) K^0_S$ decays. A combination of jet-charge, vertex-charge, and same-side tagging techniques were used to determine the B^0 production flavor.
[8] ACKERSTAFF 98Z uses 24 candidates for $B^0_d \to J/\psi(1S) K^0_S$ decay. A combination of jet-charge and vertex-charge techniques were used to tag the B^0_d production flavor.
[9] Combined result of CHEN 07 and SAHOO 08.

$C_{J/\psi K^{*0}}$ ($B^0 \to J/\psi K^{*0}$)

VALUE	DOCUMENT ID		TECN	COMMENT
$0.025 \pm 0.083 \pm 0.054$	[1] AUBERT	09K	BABR	$e^+e^- \to \Upsilon(4S)$

[1] Based on $B^0 \to J/\psi K^{*0}$, $K^{*0} \to K^0_S\pi^0$.

$S_{J/\psi K^{*0}}$ ($B^0 \to J/\psi K^{*0}$)

VALUE	DOCUMENT ID		TECN	COMMENT
$0.601 \pm 0.239 \pm 0.087$	[1,2] AUBERT	09K	BABR	$e^+e^- \to \Upsilon(4S)$

[1] Based on $B^0 \to J/\psi K^{*0}$, $K^{*0} \to K^0_S\pi^0$.

[2] This $S_{J/\psi K^{*0}}$ value has been corrected for the dilution of the $\sin(\Delta M\,\Delta t)$ coefficient of the CP asymmetry by a factor of $1-R_\perp$, which arises from the mixture of CP-even and CP-odd B decay amplitudes.

$C_{\chi_{c0}K^0_S}$ ($B^0 \to \chi_{c0}K^0_S$)

VALUE	DOCUMENT ID		TECN	COMMENT
$-0.29^{+0.53}_{-0.44} \pm 0.06$	[1] AUBERT	09AU	BABR	$e^+e^- \to \Upsilon(4S)$

[1] Uses Dalitz plot analysis of $B^0 \to K^0\pi^+\pi^-$ decays and the first of two equivalent solutions is used.

$S_{\chi_{c0}K^0_S}$ ($B^0 \to \chi_{c0}K^0_S$)

VALUE	DOCUMENT ID		TECN	COMMENT
$-0.69 \pm 0.52 \pm 0.08$	[1] AUBERT	09AU	BABR	$e^+e^- \to \Upsilon(4S)$

[1] Uses Dalitz plot analysis of $B^0 \to K^0\pi^+\pi^-$ decays and the first of two equivalent solutions is used.

$C_{\chi_{c1}K^0_S}$ ($B^0 \to \chi_{c1}K^0_S$)

VALUE	DOCUMENT ID		TECN	COMMENT
0.06 ± 0.07 OUR AVERAGE				
$0.017 \pm 0.083^{+0.026}_{-0.046}$	ADACHI	12A	BELL	$e^+e^- \to \Upsilon(4S)$
$0.129 \pm 0.109 \pm 0.025$	AUBERT	09K	BABR	$e^+e^- \to \Upsilon(4S)$

$S_{\chi_{c1}K^0_S}$ ($B^0 \to \chi_{c1}K^0_S$)

VALUE	DOCUMENT ID		TECN	COMMENT
0.63 ± 0.10 OUR AVERAGE				
$0.640 \pm 0.117 \pm 0.040$	ADACHI	12A	BELL	$e^+e^- \to \Upsilon(4S)$
$0.614 \pm 0.160 \pm 0.040$	AUBERT	09K	BABR	$e^+e^- \to \Upsilon(4S)$

$\sin(2\beta_{\rm eff})$ ($B^0 \to \phi K^0$)

VALUE	DOCUMENT ID		TECN	COMMENT
$0.22 \pm 0.27 \pm 0.12$	AUBERT	07AX	BABR	$e^+e^- \to \Upsilon(4S)$
• • • We do not use the following data for averages, fits, limits, etc. • • •				
$0.50 \pm 0.25^{+0.07}_{-0.04}$	[1] AUBERT	05T	BABR	Repl. by AUBERT 07AX

[1] Obtained by constraining $C = 0$.

$\sin(2\beta_{\rm eff})$ ($B^0 \to \phi K^*_0(1430)^0$)

VALUE	DOCUMENT ID		TECN	COMMENT
$0.97^{+0.03}_{-0.52}$	[1] AUBERT	08BG	BABR	$e^+e^- \to \Upsilon(4S)$

[1] Measured using the CP-violation phase difference $\Delta\phi_{00}$ between the B and $\overline{B}$ decay amplitude.

$\sin(2\beta_{\rm eff})$ ($B^0 \to K^+K^-K^0_S$)

VALUE	DOCUMENT ID		TECN	COMMENT
$0.77 \pm 0.11^{+0.07}_{-0.04}$	AUBERT	07AX	BABR	$e^+e^- \to \Upsilon(4S)$
• • • We do not use the following data for averages, fits, limits, etc. • • •				
$0.55 \pm 0.22 \pm 0.12$	[1] AUBERT	05T	BABR	Repl. by AUBERT 07AX

[1] Obtained by constraining $C = 0$.

$\sin(2\beta_{\rm eff})$ ($B^0 \to [K^0_S\pi^+\pi^-]_{D(*)}\,h^0$)

VALUE	DOCUMENT ID		TECN	COMMENT
0.45 ± 0.28 OUR AVERAGE				
$0.29 \pm 0.34 \pm 0.06$	AUBERT	07BH	BABR	$e^+e^- \to \Upsilon(4S)$
$0.78 \pm 0.44 \pm 0.22$	KROKOVNY	06	BELL	$e^+e^- \to \Upsilon(4S)$

$|\lambda|$ ($B^0 \to [K^0_S\pi^+\pi^-]_{D(*)}\,h^0$)

VALUE	DOCUMENT ID		TECN	COMMENT
$1.01 \pm 0.08 \pm 0.02$	AUBERT	07BH	BABR	$e^+e^- \to \Upsilon(4S)$

$|\sin(2\beta+\gamma)|$

β (ϕ_1) and γ (ϕ_3) are angles of CKM unitarity triangle, see the review on "CP Violation" in the Reviews section.

VALUE	CL%	DOCUMENT ID		TECN	COMMENT
>0.40	90	[1] AUBERT	06Y	BABR	$e^+e^- \to \Upsilon(4S)$
• • • We do not use the following data for averages, fits, limits, etc. • • •					
>0.13	95	[2] RONGA	06	BELL	$e^+e^- \to \Upsilon(4S)$
>0.07	95	[2] RONGA	06	BELL	$e^+e^- \to \Upsilon(4S)$
>0.35	90	[3] AUBERT	05Z	BABR	$e^+e^- \to \Upsilon(4S)$
>0.69	68	[4] AUBERT	04V	BABR	$e^+e^- \to \Upsilon(4S)$
>0.58	95	[5] AUBERT	04W	BABR	Repl. by AUBERT 05Z

[1] Uses fully reconstructed $B^0 \to D^{(*)\pm}\pi^\mp$ and $D^\pm\rho^\mp$ decays and some theoretical assumptions.

[2] Combines the results from fully reconstructed and partially reconstructed $D^{(*)}\pi$ events by taking weighted averages. Assumes that systematic errors from physics parameters and fit biases in the two measurements are 100% correlated.

[3] Uses partially reconstructed $B^0 \to D^{*\pm}\pi^\mp$ decays and some theoretical assumptions.

[4] Uses fully reconstructed $B^0 \to D^{(*)\pm}\pi^\mp$ decays and some theoretical assumptions, such as the SU(3) symmetry relation.

[5] Combining this measurement with the results from AUBERT 04V for fully reconstructed $B^0 \to D^{(*)\pm}\pi^\mp$ and some theoretical assumptions, such as the SU(3) symmetry relation.

$2\beta+\gamma$

VALUE (°)	DOCUMENT ID		TECN	COMMENT
$83 \pm 53 \pm 20$	[1] AUBERT	08AC	BABR	$e^+e^- \to \Upsilon(4S)$

[1] Used a time-dependent Dalitz-plot analysis of $B^0 \to D^\mp K^0\pi^\pm$ assuming the ratio of the $b \to u$ and $b \to c$ decay amplitudes to be 0.3.

$\gamma(B^0 \to D^0K^{*0})$

VALUE (°)	DOCUMENT ID		TECN	COMMENT
162 ± 56	[1] AUBERT	09R	BABR	$e^+e^- \to \Upsilon(4S)$

[1] Uses Dalitz plot analysis of $D^0 \to K^0_S\pi^+\pi^-$ decays coming from $B^0 \to D^0K^{*0}$ modes. The corresponding 95% CL interval is $77^\circ < \gamma < 247^\circ$. A 180 degree ambiguity is implied.

α

For angle $\alpha(\phi_2)$ of the CKM unitarity triangle, see the review on "CP violation" in the reviews section.

VALUE (°)	DOCUMENT ID		TECN	COMMENT
90 ± 5 OUR AVERAGE				
$79 \pm 7 \pm 11$	[1] AUBERT	10D	BABR	$e^+e^- \to \Upsilon(4S)$
$92.4^{+6.0}_{-6.5}$	[2] AUBERT	09G	BABR	$e^+e^- \to \Upsilon(4S)$
88 ± 17	[3] SOMOV	06	BELL	$e^+e^- \to \Upsilon(4S)$
• • • We do not use the following data for averages, fits, limits, etc. • • •				
78.6 ± 7.3	[4] AUBERT	07O	BABR	$e^+e^- \to \Upsilon(4S)$
100 ± 13	[5] AUBERT,B	05C	BABR	Repl. by AUBERT 09G
$102\ ^{+16}_{-12} \pm 14$	[6] AUBERT,B	04R	BABR	Repl. by AUBERT,B 05C

[1] Obtained using the time dependent analysis of $B^0 \to a_1(1260)^\pm\pi^\mp$ and branching fraction measurements of $B \to a_1(1260)K$ and $B \to K_1\pi$.

[2] Based on the favored $B \to \rho\rho$ isospin method.

[3] Obtained using isospin relation and selecting a solution closest to the CKM best fit average; the 90% CL allowed interval is $59^\circ < \phi_2\ (\equiv\alpha) < 115^\circ$.

[4] The angle $\alpha_{\rm eff}$ is obtained using the measured CP parameters of $B^0 \to a_1(1260)^\pm\pi^\mp$ and choosing one of the four solutions that is compatible with the result of SM-based fits.

[5] Obtained using isospin relation and selecting a solution closest to the CKM best fit average; 90% CL allowed interval is $79^\circ < \alpha < 123^\circ$.

[6] Obtained from the measured CP parameters of the longitudinal polarization by selecting the solution closest to the CKM best fit central value of $\alpha = 95^\circ$ – 98°.

T and CPT VIOLATION PARAMETERS

Measured values of the T-, CP-, and CPT-asymmetry parameters, defined as the differences in $S^\pm_{\alpha,\beta}$ and $C^\pm_{\alpha,\beta}$ between symmetry-transformed transitions. The indices $\alpha = \ell^+$, ℓ^- and $\beta = K^0_S$, K^0_L stand for reconstructed the flavor final state and the CP final states from $\Upsilon(4S)$ decay. The sign $\pm$ indicates whether the decay to the flavor final state α occurs before or after the decay to the CP final state.

ΔS^+_T ($S^-_{\ell^-,K^0_S} - S^+_{\ell^+,K^0_S}$)

VALUE	DOCUMENT ID		TECN	COMMENT
$-1.37 \pm 0.14 \pm 0.06$	LEES	12W	BABR	$e^+e^- \to \Upsilon(4S)$

ΔS^-_T ($S^+_{\ell^-,K^0_S} - S^-_{\ell^+,K^0_S}$)

VALUE	DOCUMENT ID		TECN	COMMENT
$1.17 \pm 0.18 \pm 0.11$	LEES	12W	BABR	$e^+e^- \to \Upsilon(4S)$

ΔC^+_T ($C^-_{\ell^-,K^0_S} - C^+_{\ell^+,K^0_S}$)

VALUE	DOCUMENT ID		TECN	COMMENT
$0.10 \pm 0.14 \pm 0.08$	LEES	12W	BABR	$e^+e^- \to \Upsilon(4S)$

ΔC^-_T ($C^+_{\ell^-,K^0_S} - C^-_{\ell^+,K^0_S}$)

VALUE	DOCUMENT ID		TECN	COMMENT
$0.04 \pm 0.14 \pm 0.08$	LEES	12W	BABR	$e^+e^- \to \Upsilon(4S)$

ΔS^+_{CP} ($S^+_{\ell^-,K^0_S} - S^+_{\ell^+,K^0_S}$)

VALUE	DOCUMENT ID		TECN	COMMENT
$-1.30 \pm 0.11 \pm 0.07$	LEES	12W	BABR	$e^+e^- \to \Upsilon(4S)$

ΔS^-_{CP} ($S^-_{\ell^-,K^0_S} - S^-_{\ell^+,K^0_S}$)

VALUE	DOCUMENT ID		TECN	COMMENT
$1.33 \pm 0.12 \pm 0.06$	LEES	12W	BABR	$e^+e^- \to \Upsilon(4S)$

ΔC^+_{CP} ($C^+_{\ell^-,K^0_S}$ − $C^+_{\ell^+,K^0_S}$)

VALUE	DOCUMENT ID		TECN	COMMENT
0.07±0.09±0.03	LEES	12W	BABR	$e^+e^- \to \Upsilon(4S)$

ΔC^-_{CP} ($C^-_{\ell^-,K^0_S}$ − $C^-_{\ell^+,K^0_S}$)

VALUE	DOCUMENT ID		TECN	COMMENT
0.08±0.10±0.04	LEES	12W	BABR	$e^+e^- \to \Upsilon(4S)$

ΔS^+_{CPT} ($S^-_{\ell^+,K^0_S}$ − $S^+_{\ell^+,K^0_S}$)

VALUE	DOCUMENT ID		TECN	COMMENT
0.16±0.21±0.09	LEES	12W	BABR	$e^+e^- \to \Upsilon(4S)$

ΔS^-_{CPT} ($S^+_{\ell^+,K^0_S}$ − $S^-_{\ell^+,K^0_S}$)

VALUE	DOCUMENT ID		TECN	COMMENT
−0.03±0.13±0.06	LEES	12W	BABR	$e^+e^- \to \Upsilon(4S)$

ΔC^+_{CPT} ($C^-_{\ell^+,K^0_S}$ − $C^+_{\ell^+,K^0_S}$)

VALUE	DOCUMENT ID		TECN	COMMENT
0.14±0.15±0.07	LEES	12W	BABR	$e^+e^- \to \Upsilon(4S)$

ΔC^-_{CPT} ($C^+_{\ell^+,K^0_S}$ − $C^-_{\ell^+,K^0_S}$)

VALUE	DOCUMENT ID		TECN	COMMENT
0.03±0.12±0.08	LEES	12W	BABR	$e^+e^- \to \Upsilon(4S)$

$B^0 \to D^{*-}\ell^+\nu_\ell$ FORM FACTORS

R_1 (form factor ratio $\sim V/A_1$)

VALUE	DOCUMENT ID		TECN	COMMENT
1.41 ±0.04 OUR AVERAGE				
1.401±0.034±0.018	[1] DUNGEL	10	BELL	$e^+e^- \to \Upsilon(4S)$
1.56 ±0.07 ±0.15	AUBERT	09A	BABR	$e^+e^- \to \Upsilon(4S)$
1.18 ±0.30 ±0.12	DUBOSCQ	96	CLE2	$e^+e^- \to \Upsilon(4S)$
• • • We do not use the following data for averages, fits, limits, etc. • • •				
1.429±0.061±0.044	AUBERT	08R	BABR	Repl. by AUBERT 09A
1.396±0.060±0.044	AUBERT,B	06Z	BABR	Repl. by AUBERT 08R

[1] Uses fully reconstructed $D^{*-}\ell^+\nu$ events ($\ell = e$ or μ).

R_2 (form factor ratio $\sim A_2/A_1$)

VALUE	DOCUMENT ID		TECN	COMMENT
0.85 ±0.05 OUR AVERAGE	Error includes scale factor of 1.9.			
0.864±0.024±0.008	[1] DUNGEL	10	BELL	$e^+e^- \to \Upsilon(4S)$
0.66 ±0.05 ±0.09	AUBERT	09A	BABR	$e^+e^- \to \Upsilon(4S)$
0.71 ±0.22 ±0.07	DUBOSCQ	96	CLE2	$e^+e^- \to \Upsilon(4S)$
• • • We do not use the following data for averages, fits, limits, etc. • • •				
0.827±0.038±0.022	AUBERT	08R	BABR	Repl. by AUBERT 09A
0.885±0.040±0.026	AUBERT,B	06Z	BABR	Repl. by AUBERT 08R

[1] Uses fully reconstructed $D^{*-}\ell^+\nu$ events ($\ell = e$ or μ).

$\rho^2_{A_1}$ (form factor slope)

VALUE	DOCUMENT ID		TECN	COMMENT
1.204±0.031 OUR AVERAGE				
1.214±0.034±0.009	[1] DUNGEL	10	BELL	$e^+e^- \to \Upsilon(4S)$
1.22 ±0.02 ±0.07	AUBERT	09A	BABR	$e^+e^- \to \Upsilon(4S)$
0.91 ±0.15 ±0.06	DUBOSCQ	96	CLE2	$e^+e^- \to \Upsilon(4S)$
• • • We do not use the following data for averages, fits, limits, etc. • • •				
1.191±0.048±0.028	AUBERT	08R	BABR	Repl. by AUBERT 09A
1.145±0.059±0.046	AUBERT,B	06Z	BABR	Repl. by AUBERT 08R

[1] Uses fully reconstructed $D^{*-}\ell^+\nu$ events ($\ell = e$ or μ).

PARTIAL BRANCHING FRACTIONS IN $B^0 \to K^{(*)0}\ell^+\ell^-$

B($B^0 \to K^{*0}e^+e^-$) ($0.0009 < q^2 < 1.0$ GeV$^2/c^4$)

VALUE (units 10^{-7})	DOCUMENT ID		TECN	COMMENT
$\mathbf{3.1^{+0.9+0.2}_{-0.8-0.3}\pm0.2}$	[1] AAIJ	13U	LHCB	pp at 7 TeV

[1] The last uncertainty is due to uncertainties of B($B^0 \to J/\psi K^{*0}$) and B($J/\psi \to e^+e^-$) branching fraction measurements.

B($B^0 \to K^{*0}\ell^+\ell^-$) ($0.1 < q^2 < 2.0$ GeV$^2/c^4$)

VALUE (units 10^{-7})	DOCUMENT ID		TECN	COMMENT
$\mathbf{0.66^{+0.08}_{-0.10}}$ **OUR AVERAGE**				
$0.60\pm0.06^{+0.06}_{-0.08}$	AAIJ	13Y	LHCB	pp at 7 TeV, $K^{*0}\mu^+\mu^-$
1.80±0.36±0.11	AALTONEN	11AI	CDF	$p\overline{p}$ at 1.96 TeV
• • • We do not use the following data for averages, fits, limits, etc. • • •				
$0.48^{+0.14}_{-0.12}\pm0.04$	[1] CHATRCHYAN	13BL	CMS	pp at 7 TeV
1.16±0.23±0.11	AAIJ	12U	LHCB	Repl. by AAIJ 13Y

[1] CHATRCHYAN 13BL uses, for this bin, $1.0 < q^2 < 2.0$ GeV$^2/c^4$.

B($B^0 \to K^{*0}\ell^+\ell^-$) ($2.0 < q^2 < 4.3$ GeV$^2/c^4$)

VALUE (units 10^{-7})	DOCUMENT ID		TECN	COMMENT
0.33±0.04 OUR AVERAGE				
0.30±0.03±0.04	AAIJ	13Y	LHCB	pp at 7 TeV, $K^{*0}\mu^+\mu^-$
0.38±0.07±0.03	CHATRCHYAN	13BL	CMS	pp at 7 TeV
0.84±0.28±0.06	AALTONEN	11AI	CDF	$p\overline{p}$ at 1.96 TeV
• • • We do not use the following data for averages, fits, limits, etc. • • •				
0.78±0.21±0.05	AAIJ	12U	LHCB	Repl. by AAIJ 13Y

B($B^0 \to K^{*0}\ell^+\ell^-$) ($4.3 < q^2 < 8.68$ GeV$^2/c^4$)

VALUE (units 10^{-7})	DOCUMENT ID		TECN	COMMENT
0.46±0.06 OUR AVERAGE	Error includes scale factor of 1.2.			
$0.49\pm0.04^{+0.05}_{-0.06}$	AAIJ	13Y	LHCB	pp at 7 TeV, $K^{*0}\mu^+\mu^-$
0.37±0.07±0.04	CHATRCHYAN	13BL	CMS	pp at 7 TeV
1.73±0.43±0.15	AALTONEN	11AI	CDF	$p\overline{p}$ at 1.96 TeV
• • • We do not use the following data for averages, fits, limits, etc. • • •				
3.02±0.35±0.22	AAIJ	12U	LHCB	Repl. by AAIJ 13Y

B($B^0 \to K^{*0}\ell^+\ell^-$) ($10.09 < q^2 < 12.86$ GeV$^2/c^4$)

VALUE (units 10^{-7})	DOCUMENT ID		TECN	COMMENT
0.48±0.06 OUR AVERAGE				
$0.43\pm0.04^{+0.05}_{-0.06}$	AAIJ	13Y	LHCB	pp at 7 TeV, $K^{*0}\mu^+\mu^-$
0.54±0.09±0.09	CHATRCHYAN	13BL	CMS	pp at 7 TeV
1.77±0.36±0.12	AALTONEN	11AI	CDF	$p\overline{p}$ at 1.96 TeV
• • • We do not use the following data for averages, fits, limits, etc. • • •				
1.52±0.25±0.19	AAIJ	12U	LHCB	Repl. by AAIJ 13Y

B($B^0 \to K^{*0}\ell^+\ell^-$) ($14.18 < q^2 < 16.0$ GeV$^2/c^4$)

VALUE (units 10^{-7})	DOCUMENT ID		TECN	COMMENT
0.56±0.14 OUR AVERAGE	Error includes scale factor of 2.1.			See the ideogram below.
$0.56\pm0.06^{+0.06}_{-0.08}$	AAIJ	13Y	LHCB	pp at 7 TeV, $K^{*0}\mu^+\mu^-$
$0.46^{+0.09}_{-0.08}\pm0.05$	CHATRCHYAN	13BL	CMS	pp at 7 TeV
1.34±0.26±0.08	AALTONEN	11AI	CDF	$p\overline{p}$ at 1.96 TeV
• • • We do not use the following data for averages, fits, limits, etc. • • •				
1.15±0.20±0.09	AAIJ	12U	LHCB	Repl. by AAIJ 13Y

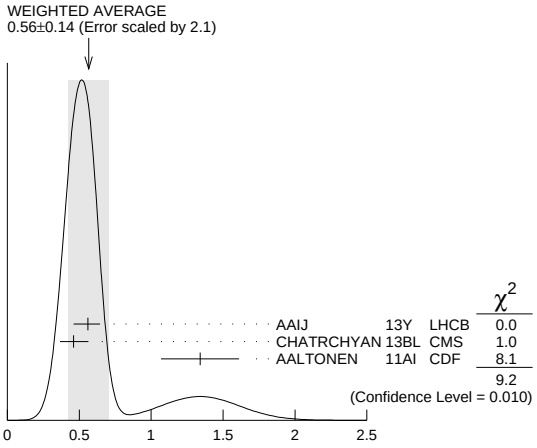

B($B^0 \to K^{*0}\ell^+\ell^-$) ($14.18 < q^2 < 16.0$ GeV$^2/c^4$) (units 10^{-7})

B($B^0 \to K^{*0}\ell^+\ell^-$) ($16.0 < q^2 < 19.0$ GeV$^2/c^4$)

VALUE (units 10^{-7})	DOCUMENT ID		TECN	COMMENT
0.47±0.06 OUR AVERAGE	Error includes scale factor of 1.1.			
$0.41\pm0.04^{+0.05}_{-0.06}$	AAIJ	13Y	LHCB	pp at 7 TeV, $K^{*0}\mu^+\mu^-$
0.52±0.06±0.05	CHATRCHYAN	13BL	CMS	pp at 7 TeV
0.97±0.26±0.07	AALTONEN	11AI	CDF	$p\overline{p}$ at 1.96 TeV
• • • We do not use the following data for averages, fits, limits, etc. • • •				
1.50±0.24±0.15	AAIJ	12U	LHCB	Repl. by AAIJ 13Y

B($B^0 \to K^{*0}\ell^+\ell^-$) ($1.0 < q^2 < 6.0$ GeV$^2/c^4$)

VALUE (units 10^{-7})	DOCUMENT ID		TECN	COMMENT
0.38±0.05 OUR AVERAGE	Error includes scale factor of 1.2.			
$0.34\pm0.03^{+0.04}_{-0.05}$	AAIJ	13Y	LHCB	pp at 7 TeV, $K^{*0}\mu^+\mu^-$
0.44±0.06±0.04	CHATRCHYAN	13BL	CMS	pp at 7 TeV
1.42±0.41±0.12	AALTONEN	11AI	CDF	$p\overline{p}$ at 1.96 TeV
• • • We do not use the following data for averages, fits, limits, etc. • • •				
2.10±0.30±0.15	AAIJ	12U	LHCB	Repl. by AAIJ 13Y

B($B^0 \to K^{*0}\ell^+\ell^-$) ($0.0 < q^2 < 4.3$ GeV$^2/c^4$)

VALUE (units 10^{-7})	DOCUMENT ID		TECN	COMMENT
2.60±0.45±0.17	AALTONEN	11AI	CDF	$p\overline{p}$ at 1.96 TeV

B(B^0 → $K^0\ell^+\ell^-$) (q^2 < 2.0 GeV$^2/c^4$)

VALUE (units 10^{-7})	DOCUMENT ID		TECN	COMMENT
$0.24^{+0.22}_{-0.20}$ OUR AVERAGE				
$0.21^{+0.27}_{-0.23}$	AAIJ	12AH	LHCB	pp at 7 TeV
$0.31 \pm 0.37 \pm 0.02$	AALTONEN	11AI	CDF	$p\overline{p}$ at 1.96 TeV

B(B^0 → $K^0\ell^+\ell^-$) (2.0 < q^2 < 4.3 GeV$^2/c^4$)

VALUE (units 10^{-7})	DOCUMENT ID		TECN	COMMENT
$0.24^{+0.35}_{-0.30}$ OUR AVERAGE Error includes scale factor of 1.6.				
$0.07^{+0.25}_{-0.21}$	AAIJ	12AH	LHCB	pp at 7 TeV
$0.93 \pm 0.49 \pm 0.07$	AALTONEN	11AI	CDF	$p\overline{p}$ at 1.96 TeV

B(B^0 → $K^0\ell^+\ell^-$) (4.3 < q^2 < 8.68 GeV$^2/c^4$)

VALUE (units 10^{-7})	DOCUMENT ID		TECN	COMMENT
1.08 ± 0.27 OUR AVERAGE				
1.23 ± 0.31	AAIJ	12AH	LHCB	pp at 7 TeV
$0.66 \pm 0.51 \pm 0.05$	AALTONEN	11AI	CDF	$p\overline{p}$ at 1.96 TeV

B(B^0 → $K^0\ell^+\ell^-$) (10.09 < q^2 < 12.86 GeV$^2/c^4$)

VALUE (units 10^{-7})	DOCUMENT ID		TECN	COMMENT
0.27 ± 0.27 OUR AVERAGE Error includes scale factor of 1.8.				
$0.50^{+0.22}_{-0.19}$	AAIJ	12AH	LHCB	pp at 7 TeV
$-0.03 \pm 0.22 \pm 0.01$	AALTONEN	11AI	CDF	$p\overline{p}$ at 1.96 TeV

B(B^0 → $K^0\ell^+\ell^-$) (14.18 < q^2 < 16.0 GeV$^2/c^4$)

VALUE (units 10^{-7})	DOCUMENT ID		TECN	COMMENT
$0.29^{+0.21}_{-0.15}$ OUR AVERAGE Error includes scale factor of 1.8.				
$0.20^{+0.13}_{-0.09}$	AAIJ	12AH	LHCB	pp at 7 TeV
$0.73 \pm 0.26 \pm 0.06$	AALTONEN	11AI	CDF	$p\overline{p}$ at 1.96 TeV

B(B^0 → $K^0\ell^+\ell^-$) (q^2 > 16.0 GeV$^2/c^4$)

VALUE (units 10^{-7})	DOCUMENT ID		TECN	COMMENT
$0.31^{+0.16}_{-0.12}$ OUR AVERAGE				
$0.35^{+0.21}_{-0.14}$	AAIJ	12AH	LHCB	pp at 7 TeV
$0.21 \pm 0.18 \pm 0.16$	AALTONEN	11AI	CDF	$p\overline{p}$ at 1.96 TeV

B(B^0 → $K^0\ell^+\ell^-$) (1.0 < q^2 < 6.0 GeV$^2/c^4$)

VALUE (units 10^{-7})	DOCUMENT ID		TECN	COMMENT
$0.75^{+0.40}_{-0.30}$ OUR AVERAGE				
$0.65^{+0.45}_{-0.35}$	AAIJ	12AH	LHCB	pp at 7 TeV
$0.98 \pm 0.61 \pm 0.08$	AALTONEN	11AI	CDF	$p\overline{p}$ at 1.96 TeV

B(B^0 → $K^0\ell^+\ell^-$) (0.0 < q^2 < 4.3 GeV$^2/c^4$)

VALUE (units 10^{-7})	DOCUMENT ID	TECN	COMMENT
$1.27 \pm 0.62 \pm 0.10$	AALTONEN 11AI	CDF	$p\overline{p}$ at 1.96 TeV

B^0 REFERENCES

AAIJ	14E	JHEP 1404 114	R. Aaij *et al.*	(LHCb Collab.)
ABAZOV	14	PR D89 012002	V.M. Abazov *et al.*	(D0 Collab.)
LEES	14	PR D89 051101	J.P. Lees *et al.*	(BABAR Collab.)
AAD	13U	PR D87 032002	G. Aad *et al.*	(ATLAS Collab.)
AAIJ	13	NP B867 1	R. Aaij *et al.*	(LHCb Collab.)
AAIJ	13A	NP B867 547	R. Aaij *et al.*	(LHCb Collab.)
AAIJ	13AA	NP B871 403	R. Aaij *et al.*	(LHCb Collab.)
AAIJ	13AC	NP B874 663	R. Aaij *et al.*	(LHCb Collab.)
AAIJ	13AO	PR D87 092001	R. Aaij *et al.*	(LHCb Collab.)
AAIJ	13AP	PR D87 092007	R. Aaij *et al.*	(LHCb Collab.)
AAIJ	13AQ	PR D87 112009	R. Aaij *et al.*	(LHCb Collab.)
AAIJ	13AT	PR D88 052002	R. Aaij *et al.*	(LHCb Collab.)
AAIJ	13AW	PRL 110 211801	R. Aaij *et al.*	(LHCb Collab.)
AAIJ	13AX	PRL 110 221601	R. Aaij *et al.*	(LHCb Collab.)
AAIJ	13B	PRL 110 021801	R. Aaij *et al.*	(LHCb Collab.)
AAIJ	13BA	PRL 111 101805	R. Aaij *et al.*	(LHCb Collab.)
AAIJ	13BM	PRL 111 141801	R. Aaij *et al.*	(LHCb Collab.)
AAIJ	13BO	JHEP 1310 183	R. Aaij *et al.*	(LHCb Collab.)
AAIJ	13BP	JHEP 1310 143	R. Aaij *et al.*	(LHCb Collab.)
AAIJ	13BQ	JHEP 1310 005	R. Aaij *et al.*	(LHCb Collab.)
AAIJ	13BT	PR D88 072005	R. Aaij *et al.*	(LHCb Collab.)
AAIJ	13CF	EPJ C73 2655	R. Aaij *et al.*	(LHCb Collab.)
AAIJ	13E	PRL 110 031801	R. Aaij *et al.*	(LHCb Collab.)
AAIJ	13F	PL B719 318	R. Aaij *et al.*	(LHCb Collab.)
AAIJ	13K	PL B721 24	R. Aaij *et al.*	(LHCb Collab.)
AAIJ	13L	JHEP 1303 067	R. Aaij *et al.*	(LHCb Collab.)
AAIJ	13M	PR D87 052001	R. Aaij *et al.*	(LHCb Collab.)
AAIJ	13P	JHEP 1304 001	R. Aaij *et al.*	(LHCb Collab.)
AAIJ	13U	JHEP 1305 159	R. Aaij *et al.*	(LHCb Collab.)
AAIJ	13Y	JHEP 1308 131	R. Aaij *et al.*	(LHCb Collab.)
AAIJ	13Z	JHEP 1309 006	R. Aaij *et al.*	(LHCb Collab.)
AALTONEN	13F	PR D87 072003	T. Aaltonen *et al.*	(CDF Collab.)
CHATRCHYAN	13AW	PRL 111 101804	S. Chatrchyan *et al.*	(CMS Collab.)
CHATRCHYAN	13BL	PL B727 77	S. Chatrchyan *et al.*	(CMS Collab.)
CHILIKIN	13	PR D88 074026	K. Chilikin *et al.*	(BELLE Collab.)
DALSENO	13	PR D88 092003	J. Dalseno *et al.*	(BELLE Collab.)
DUH	13	PR D87 031103	Y. T. Duh *et al.*	(BELLE Collab.)
GAUR	13	PR D87 091101	V. Gaur *et al.*	(BELLE Collab.)
LEES	13D	PR D87 052009	J.P. Lees *et al.*	(BABAR Collab.)
LEES	13H	PR D87 092004	J.P. Lees *et al.*	(BABAR Collab.)
LEES	13I	PR D87 112005	J.P. Lees *et al.*	(BABAR Collab.)
LEES	13J	PR D88 012003	J.P. Lees *et al.*	(BABAR Collab.)
LEES	13M	PR D88 032012	J.P. Lees *et al.*	(BABAR Collab.)
LEES	13N	PRL 111 101802	J.P. Lees *et al.*	(BABAR Collab.)
Also		PRL 111 159901(errat.)	J.P. Lees *et al.*	(BABAR Collab.)
LUTZ	13	PR D87 111103	O. Lutz *et al.*	(BELLE Collab.)
PRIM	13	PR D88 072004	M. Prim *et al.*	(BELLE Collab.)
SIBIDANOV	13	PR D88 032005	A. Sibidanov *et al.*	(BELLE Collab.)
AAIJ	12A	PL B708 55	R. Aaij *et al.*	(LHCb Collab.)
AAIJ	12AH	JHEP 1207 133	R. Aaij *et al.*	(LHCb Collab.)
AAIJ	12AM	PRL 109 131801	R. Aaij *et al.*	(LHCb Collab.)
AAIJ	12AR	JHEP 1210 037	R. Aaij *et al.*	(LHCb Collab.)
AAIJ	12AX	PR D86 112005	R. Aaij *et al.*	(LHCb Collab.)
AAIJ	12E	PL B708 241	R. Aaij *et al.*	(LHCb Collab.)
AAIJ	12I	PL B709 177	R. Aaij *et al.*	(LHCb Collab.)
AAIJ	12L	EPJ C72 2118	R. Aaij *et al.*	(LHCb Collab.)
AAIJ	12T	PRL 108 161801	R. Aaij *et al.*	(LHCb Collab.)
AAIJ	12U	PRL 108 181806	R. Aaij *et al.*	(LHCb Collab.)
AAIJ	12V	PRL 108 201601	R. Aaij *et al.*	(LHCb Collab.)
AAIJ	12W	PRL 108 231801	R. Aaij *et al.*	(LHCb Collab.)
AALTONEN	12L	PRL 108 211803	T. Aaltonen *et al.*	(CDF Collab.)
ABAZOV	12AC	PR D86 072009	V.M. Abazov *et al.*	(D0 Collab.)
ABAZOV	12U	PR D85 112003	V.M. Abazov *et al.*	(D0 Collab.)
ADACHI	12A	PRL 108 171802	I. Adachi *et al.*	(BELLE Collab.)
CHANG	12	PR D85 091102	M.-C. Chang *et al.*	(BELLE Collab.)
CHATRCHYAN	12A	JHEP 1204 033	S. Chatrchyan *et al.*	(CMS Collab.)
DALSENO	12	PR D86 092012	J. Dalseno *et al.*	(BELLE Collab.)
DEL-AMO-SA...	12	PR D85 092017	P. del Amo Sanchez *et al.*	(BABAR Collab.)
HIGUCHI	12	PR D85 071105	T. Higuchi *et al.*	(BELLE Collab.)
HOI	12	PRL 108 031801	C.-T. Hoi *et al.*	(BELLE Collab.)
HSU	12	PR D86 032002	C.-L. Hsu *et al.*	(BELLE Collab.)
KIM	12A	PR D86 031101	J.H. Kim *et al.*	(BELLE Collab.)
KRONENBITT...	12	PR D86 071103	B. Kronenbitter *et al.*	(BELLE Collab.)
LEES	12AA	PR D86 092004	J.P. Lees *et al.*	(BABAR Collab.)
LEES	12AF	PR D86 112006	J.P. Lees *et al.*	(BABAR Collab.)
LEES	12B	PR D85 052003	J.P. Lees *et al.*	(BABAR Collab.)
LEES	12D	PRL 109 101802	J.P. Lees *et al.*	(BABAR Collab.)
Also		PR D88 072012	J.P. Lees *et al.*	(BABAR Collab.)
LEES	12I	PR D85 054023	J.P. Lees *et al.*	(BABAR Collab.)
LEES	12K	PR D85 072005	J.P. Lees *et al.*	(BABAR Collab.)
LEES	12O	PR D85 112010	J.P. Lees *et al.*	(BABAR Collab.)
LEES	12T	PR D86 051105	J.P. Lees *et al.*	(BABAR Collab.)
LEES	12W	PRL 109 211801	J.P. Lees *et al.*	(BABAR Collab.)
NEGISHI	12	PR D86 011101	K. Negishi *et al.*	(BELLE Collab.)
ROHRKEN	12	PR D85 091106	M. Rohrken *et al.*	(BELLE Collab.)
SATO	12	PRL 108 171801	Y. Sato *et al.*	(BELLE Collab.)
AAIJ	11B	PL B699 330	R. Aaij *et al.*	(LHCb Collab.)
AAIJ	11E	PR D84 092001	R. Aaij *et al.*	(LHCb Collab.)
Also		PR D85 039904 (errat)	R. Aaij *et al.*	(LHCb Collab.)
AAIJ	11F	PRL 107 211801	R. Aaij *et al.*	(LHCb Collab.)
AALTONEN	11	PRL 106 121804	T. Aaltonen *et al.*	(CDF Collab.)
AALTONEN	11AG	PRL 107 191801	T. Aaltonen *et al.*	(CDF Collab.)
Also		PRL 107 239903 (errat)	T. Aaltonen *et al.*	(CDF Collab.)
AALTONEN	11AI	PRL 107 201802	T. Aaltonen *et al.*	(CDF Collab.)
AALTONEN	11L	PRL 106 161801	T. Aaltonen *et al.*	(CDF Collab.)
AALTONEN	11N	PRL 106 181802	T. Aaltonen *et al.*	(CDF Collab.)
ABAZOV	11U	PR D84 052007	V.M. Abazov *et al.*	(D0 Collab.)
AUSHEV	11	PR D83 051102	T. Aushev *et al.*	(BELLE Collab.)
BAHINIPATI	11	PR D84 021101	S. Bahinipati *et al.*	(BELLE Collab.)
BHARDWAJ	11	PRL 107 091803	V. Bhardwaj *et al.*	(BELLE Collab.)
CHATRCHYAN	11T	PRL 107 191802	S. Chatrchyan *et al.*	(CMS Collab.)
CHOI	11	PR D84 052004	S.-K. Choi *et al.*	(BELLE Collab.)
DEL-AMO-SA...	11A	PR D83 032006	P. del Amo Sanchez *et al.*	(BABAR Collab.)
DEL-AMO-SA...	11B	PR D83 032004	P. del Amo Sanchez *et al.*	(BABAR Collab.)
DEL-AMO-SA...	11C	PR D83 032007	P. del Amo Sanchez *et al.*	(BABAR Collab.)
DEL-AMO-SA...	11F	PR D83 052011	P. del Amo Sanchez *et al.*	(BABAR Collab.)
DEL-AMO-SA...	11K	PR D83 091101	P. del Amo Sanchez *et al.*	(BABAR Collab.)
HA	11	PR D83 071101	H. Ha *et al.*	(BELLE Collab.)
LEES	11	PR D83 112010	J.P. Lees *et al.*	(BABAR Collab.)
LEES	11A	PR D84 012001	J.P. Lees *et al.*	(BABAR Collab.)
LEES	11F	PR D84 071102	J.P. Lees *et al.*	(BABAR Collab.)
LEES	11M	PR D84 112007	J.P. Lees *et al.*	(BABAR Collab.)
Also		PR D87 039901 (errat)	J.P. Lees *et al.*	(BABAR Collab.)
SAHOO	11A	PR D84 071101	H. Sahoo *et al.*	(BELLE Collab.)
AUBERT	10	PRL 104 011802	B. Aubert *et al.*	(BABAR Collab.)
AUBERT	10D	PR D81 052009	B. Aubert *et al.*	(BABAR Collab.)
AUBERT	10H	PR D82 031102	B. AUBERT *et al.*	(BABAR Collab.)
AUSHEV	10	PR D81 031103	T. Aushev *et al.*	(BELLE Collab.)
CHIANG	10	PR D81 071101	C.-C. Chiang *et al.*	(BELLE Collab.)
DAS	10	PR D82 051103	A. Das *et al.*	(BELLE Collab.)
DEL-AMO-SA...	10A	PR D82 011502	P. del Amo Sanchez *et al.*	(BABAR Collab.)
DEL-AMO-SA...	10B	PR D82 011101	P. del Amo Sanchez *et al.*	(BABAR Collab.)
DEL-AMO-SA...	10E	PR D82 031101	P. del Amo Sanchez *et al.*	(BABAR Collab.)
DEL-AMO-SA...	10Q	PR D82 112002	P. del Amo Sanchez *et al.*	(BABAR Collab.)
DUNGEL	10	PR D82 112007	W. Dungel *et al.*	(BELLE Collab.)
FUJIKAWA	10A	PR D81 011101	M. Fujikawa *et al.*	(BELLE Collab.)
HYUN	10	PRL 105 091801	H.J. Hyun *et al.*	(BELLE Collab.)
JOSHI	10	PR D81 031101	N.J. Joshi *et al.*	(BELLE Collab.)
NAKAHAMA	10	PR D82 073011	Y. Nakahama *et al.*	(BELLE Collab.)
WEDD	10	PR D81 111104	R. Wedd *et al.*	(BELLE Collab.)
AALTONEN	09B	PR D79 011104	T. Aaltonen *et al.*	(CDF Collab.)
AALTONEN	09C	PRL 103 031801	T. Aaltonen *et al.*	(CDF Collab.)
AALTONEN	09E	PR D79 032001	T. Aaltonen *et al.*	(CDF Collab.)
AALTONEN	09P	PRL 102 201801	T. Aaltonen *et al.*	(CDF Collab.)
ABAZOV	09E	PRL 102 032001	V.M. Abazov *et al.*	(D0 Collab.)
AUBERT	09	PR D79 011102	B. Aubert *et al.*	(BABAR Collab.)
AUBERT	09A	PR D79 012002	B. Aubert *et al.*	(BABAR Collab.)
AUBERT	09AA	PR D79 112001	B. Aubert *et al.*	(BABAR Collab.)
AUBERT	09AC	PR D79 112009	B. Aubert *et al.*	(BABAR Collab.)
AUBERT	09AD	PR D80 011101	B. Aubert *et al.*	(BABAR Collab.)
AUBERT	09AE	PR D80 031102	B. Aubert *et al.*	(BABAR Collab.)
AUBERT	09AF	PR D80 051101	B. Aubert *et al.*	(BABAR Collab.)
AUBERT	09AG	PR D80 051105	B. Aubert *et al.*	(BABAR Collab.)
AUBERT	09AL	PR D80 092007	B. Aubert *et al.*	(BABAR Collab.)
AUBERT	09AO	PRL 103 211802	B. Aubert *et al.*	(BABAR Collab.)
AUBERT	09AU	PR D80 112001	B. Aubert *et al.*	(BABAR Collab.)
AUBERT	09AV	PR D80 112002	B. Aubert *et al.*	(BABAR Collab.)
AUBERT	09B	PRL 102 132001	B. Aubert *et al.*	(BABAR Collab.)
AUBERT	09C	PR D79 032002	B. Aubert *et al.*	(BABAR Collab.)
AUBERT	09G	PRL 102 141802	B. Aubert *et al.*	(BABAR Collab.)
AUBERT	09H	PR D79 052005	B. Aubert *et al.*	(BABAR Collab.)
AUBERT	09I	PR D79 052003	B. Aubert *et al.*	(BABAR Collab.)
AUBERT	09K	PR D79 072009	B. Aubert *et al.*	(BABAR Collab.)
AUBERT	09R	PR D79 072003	B. Aubert *et al.*	(BABAR Collab.)
AUBERT	09S	PR D79 092002	B. Aubert *et al.*	(BABAR Collab.)
AUBERT	09T	PRL 102 091803	B. Aubert *et al.*	(BABAR Collab.)
Also		EPAPS Document No. E-PRLTAO-102-060910		(BABAR Collab.)
AUBERT	09Y	PRL 103 051803	B. Aubert *et al.*	(BABAR Collab.)
CHANG	09	PR D79 052006	Y.-W. Chang *et al.*	(BELLE Collab.)
DALSENO	09	PR D79 072004	J. Dalseno *et al.*	(BELLE Collab.)
KYEONG	09	PR D80 051103	S.-H. Kyeong *et al.*	(BELLE Collab.)

Meson Particle Listings

B^0

MIZUK 09 PR D80 031104 R. Mizuk *et al.* (BELLE Collab.)
VERVINK 09 PR D80 111104 K. Vervink *et al.* (BELLE Collab.)
WEI 09A PRL 103 171801 J.-T. Wei *et al.* (BELLE Collab.)
Also EPAPS Supplement EPAPS_appendix.pdf (BELLE Collab.)
AALTONEN 08I PRL 100 101802 T. Aaltonen *et al.* (CDF Collab.)
ADACHI 08 PR D77 091101 I. Adachi *et al.* (BELLE Collab.)
AUBERT 08AB PR D78 012006 B. Aubert *et al.* (BABAR Collab.)
AUBERT 08AC PR D77 071102 B. Aubert *et al.* (BABAR Collab.)
AUBERT 08AD PR D77 091104 B. Aubert *et al.* (BABAR Collab.)
AUBERT 08AF PR D78 011103 B. Aubert *et al.* (BABAR Collab.)
AUBERT 08AG PR D78 011104 B. Aubert *et al.* (BABAR Collab.)
AUBERT 08AH PR D78 011107 B. Aubert *et al.* (BABAR Collab.)
AUBERT 08AJ PR D78 032005 B. Aubert *et al.* (BABAR Collab.)
AUBERT 08AP PR D78 051103 B. Aubert *et al.* (BABAR Collab.)
AUBERT 08AQ PR D78 052005 B. Aubert *et al.* (BABAR Collab.)
AUBERT 08AU PRL 101 021801 B. Aubert *et al.* (BABAR Collab.)
AUBERT 08AV PRL 101 081801 B. Aubert *et al.* (BABAR Collab.)
AUBERT 08B PR D77 011102 B. Aubert *et al.* (BABAR Collab.)
AUBERT 08BA PR D78 071102 B. Aubert *et al.* (BABAR Collab.)
AUBERT 08BB PR D78 071104 B. Aubert *et al.* (BABAR Collab.)
AUBERT 08BC PR D78 072007 B. Aubert *et al.* (BABAR Collab.)
AUBERT 08BD PR D78 091101 B. Aubert *et al.* (BABAR Collab.)
AUBERT 08BG PR D78 092008 B. Aubert *et al.* (BABAR Collab.)
AUBERT 08BH PR D78 112001 B. Aubert *et al.* (BABAR Collab.)
AUBERT 08BK PRL 101 201801 B. Aubert *et al.* (BABAR Collab.)
AUBERT 08BL PRL 101 261802 B. Aubert *et al.* (BABAR Collab.)
AUBERT 08BN PR D78 112003 B. Aubert *et al.* (BABAR Collab.)
AUBERT 08C PR D77 011104 B. Aubert *et al.* (BABAR Collab.)
AUBERT 08E PR D77 012003 B. Aubert *et al.* (BABAR Collab.)
AUBERT 08F PRL 100 051803 B. Aubert *et al.* (BABAR Collab.)
AUBERT 08G PRL 100 171803 B. Aubert *et al.* (BABAR Collab.)
AUBERT 08H PR D77 031101 B. Aubert *et al.* (BABAR Collab.)
AUBERT 08I PRL 100 081801 B. Aubert *et al.* (BABAR Collab.)
AUBERT 08N PRL 100 021801 B. Aubert *et al.* (BABAR Collab.)
Also PR D79 092002 B. Aubert *et al.* (BABAR Collab.)
AUBERT 08P PR D77 032007 B. Aubert *et al.* (BABAR Collab.)
AUBERT 08Q PRL 100 151802 B. Aubert *et al.* (BABAR Collab.)
AUBERT 08R PR D77 032002 B. Aubert *et al.* (BABAR Collab.)
AUBERT 08W PRL 101 082001 B. Aubert *et al.* (BABAR Collab.)
AUBERT 08Y PR D77 111101 B. Aubert *et al.* (BABAR Collab.)
CHEN 08C PRL 100 251801 J.-H. Chen *et al.* (BELLE Collab.)
CHIANG 08 PR D78 111102 C.C. Chiang *et al.* (BELLE Collab.)
CHOI 08 PRL 100 142001 S.-K. Choi *et al.* (BELLE Collab.)
GOLDENZWE...08 PRL 101 231801 P. Goldenzweig *et al.* (BELLE Collab.)
KIM 08 PL B669 287 H.O. Kim *et al.* (BELLE Collab.)
KUMAR 08 PR D78 091104 R. Kumar *et al.* (BELLE Collab.)
KUSAKA 08 PR D77 072001 A. Kusaka *et al.* (BELLE Collab.)
LEE 08A PR D77 071101 S.E. Lee *et al.* (BELLE Collab.)
LI 08F PRL 101 251601 J. Li *et al.* (BELLE Collab.)
LIN 08 NAT 452 332 S.-W. Lin *et al.* (BELLE Collab.)
LIU 08I PR D78 011106 Y. Liu *et al.* (BELLE Collab.)
LIVENTSEV 08 PR D77 091503 D. Liventsev *et al.* (BELLE Collab.)
MIZUK 08 PR D78 072004 R. Mizuk *et al.* (BELLE Collab.)
NAKAHAMA 08 PRL 100 121601 Y. Nakahama *et al.* (BELLE Collab.)
PDG 08 PL B667 1 C. Amsler *et al.* (PDG Collab.)
SAHOO 08 PR D77 091103 H. Sahoo *et al.* (BELLE Collab.)
TANIGUCHI 08 PRL 101 111801 N. Taniguchi *et al.* (BELLE Collab.)
UCHIDA 08 PR D77 051101 Y. Uchida *et al.* (BELLE Collab.)
USHIRODA 08 PRL 100 021602 Y. Ushiroda *et al.* (BELLE Collab.)
WEI 08A PR D78 011101 J.-T. Wei *et al.* (BELLE Collab.)
ABAZOV 07S PRL 99 142001 V.M. Abazov *et al.* (D0 Collab.)
ABULENCIA 07A PRL 98 122001 A. Abulencia *et al.* (FNAL CDF Collab.)
ADAM 07 PRL 99 041802 N.E. Adam *et al.* (CLEO Collab.)
Also PR D76 012007 D.M. Asner *et al.* (CLEO Collab.)
AUBERT 07A PRL 98 031801 B. Aubert *et al.* (BABAR Collab.)
AUBERT 07AA PR D76 012004 B. Aubert *et al.* (BABAR Collab.)
AUBERT 07AC PR D76 031101 B. Aubert *et al.* (BABAR Collab.)
AUBERT 07AD PR D76 031102 B. Aubert *et al.* (BABAR Collab.)
AUBERT 07AE PR D76 031103 B. Aubert *et al.* (BABAR Collab.)
AUBERT 07AF PRL 99 021603 B. Aubert *et al.* (BABAR Collab.)
AUBERT 07AG PRL 99 051801 B. Aubert *et al.* (BABAR Collab.)
AUBERT 07AI PRL 99 071801 B. Aubert *et al.* (BABAR Collab.)
AUBERT 07AJ PRL 99 081801 B. Aubert *et al.* (BABAR Collab.)
AUBERT 07AN PR D76 051101 B. Aubert *et al.* (BABAR Collab.)
AUBERT 07AO PR D76 051103 B. Aubert *et al.* (BABAR Collab.)
AUBERT 07AQ PR D76 071101 B. Aubert *et al.* (BABAR Collab.)
AUBERT 07AS PR D76 071104 B. Aubert *et al.* (BABAR Collab.)
AUBERT 07AT PR D76 091101 B. Aubert *et al.* (BABAR Collab.)
AUBERT 07AV PR D76 092004 B. Aubert *et al.* (BABAR Collab.)
AUBERT 07AX PRL 99 161802 B. Aubert *et al.* (BABAR Collab.)
AUBERT 07AY PRL 99 171803 B. Aubert *et al.* (BABAR Collab.)
AUBERT 07B PR D75 012008 B. Aubert *et al.* (BABAR Collab.)
AUBERT 07BC PR D76 091102 B. Aubert *et al.* (BABAR Collab.)
AUBERT 07BF PR D76 052007 B. Aubert *et al.* (BABAR Collab.)
AUBERT 07BH PRL 99 231802 B. Aubert *et al.* (BABAR Collab.)
AUBERT 07BI PRL 99 241803 B. Aubert *et al.* (BABAR Collab.)
AUBERT 07BO PR D76 111102 B. Aubert *et al.* (BABAR Collab.)
AUBERT 07D PRL 98 051801 B. Aubert *et al.* (BABAR Collab.)
AUBERT 07E PRL 98 051802 B. Aubert *et al.* (BABAR Collab.)
AUBERT 07F PRL 98 051803 B. Aubert *et al.* (BABAR Collab.)
AUBERT 07G PRL 98 111801 B. Aubert *et al.* (BABAR Collab.)
AUBERT 07H PR D75 031101 B. Aubert *et al.* (BABAR Collab.)
AUBERT 07J PRL 98 091801 B. Aubert *et al.* (BABAR Collab.)
AUBERT 07K PRL 98 081801 B. Aubert *et al.* (BABAR Collab.)
AUBERT 07L PRL 98 151802 B. Aubert *et al.* (BABAR Collab.)
AUBERT 07N PR D75 072002 B. Aubert *et al.* (BABAR Collab.)
AUBERT 07O PRL 98 181803 B. Aubert *et al.* (BABAR Collab.)
AUBERT 07Q PR D75 051102 B. Aubert *et al.* (BABAR Collab.)
AUBERT 07R PRL 98 211804 B. Aubert *et al.* (BABAR Collab.)
Also PRL 100 189903E B. Aubert *et al.* (BABAR Collab.)
Also PRL 100 199905E B. Aubert *et al.* (BABAR Collab.)
AUBERT 07Y PR D75 111102 B. Aubert *et al.* (BABAR Collab.)
CHANG 07A PRL 98 131803 M.-C. Chang *et al.* (BELLE Collab.)
CHANG 07B PR D75 071104 P. Chang *et al.* (BELLE Collab.)
CHAO 07 PR D76 091103 Y. Chao *et al.* (BELLE Collab.)
CHEN 07 PRL 98 031802 K.-F. Chen *et al.* (BELLE Collab.)
CHEN 07D PRL 99 221802 K.-F. Chen *et al.* (BELLE Collab.)
DALSENO 07 PR D76 072004 J. Dalseno *et al.* (BELLE Collab.)
FRATINA 07 PRL 98 221802 S. Fratina *et al.* (BELLE Collab.)
GARMASH 07 PR D75 012006 A. Garmash *et al.* (BELLE Collab.)
HOKUUE 07 PL B648 139 T. Hokuue *et al.* (BELLE Collab.)
ISHINO 07 PRL 98 211801 H. Ishino *et al.* (BELLE Collab.)
KUSAKA 07 PRL 98 221602 A. Kusaka *et al.* (BELLE Collab.)
Also PR D77 072001 A. Kusaka *et al.* (BELLE Collab.)
KUZMIN 07 PR D76 012006 A. Kuzmin *et al.* (BELLE Collab.)
LIN 07 PRL 98 181804 S.-W. Lin *et al.* (BELLE Collab.)
LIN 07A PRL 99 121601 S.-W. Lin *et al.* (BELLE Collab.)
MATYJA 07 PRL 99 191807 A. Matyja *et al.* (BELLE Collab.)
MEDVEDEVA 07 PR D76 051102 T. Medvedeva *et al.* (BELLE Collab.)
PARK 07 PR D75 011101 K.S. Park *et al.* (BELLE Collab.)
SCHUEMANN 07 PR D75 092002 J. Schuemann *et al.* (BELLE Collab.)
SOMOV 07 PR D76 011104 A. Somov *et al.* (BELLE Collab.)
TSAI 07 PR D75 111101 Y.-T. Tsai *et al.* (BELLE Collab.)
URQUIJO 07 PR D75 032001 P. Urquijo *et al.* (BELLE Collab.)
WANG 07B PR D75 092005 C.H. Wang *et al.* (BELLE Collab.)
WANG 07C PR D76 052004 M.-Z. Wang *et al.* (BELLE Collab.)
XIE 07 PR D75 017101 Q.L. Xie *et al.* (BELLE Collab.)
ZUPANC 07 PR D75 091102 A. Zupanc *et al.* (BELLE Collab.)
ABAZOV 06S PR D74 092001 V.M. Abazov *et al.* (D0 Collab.)
ABAZOV 06W PR D74 112002 V.M. Abazov *et al.* (D0 Collab.)
ABULENCIA,A 06D PRL 97 211802 A. Abulencia *et al.* (CDF Collab.)
ACOSTA 06 PRL 96 202001 D. Acosta *et al.* (CDF Collab.)
AUBERT 06 PR D73 011101 B. Aubert *et al.* (BABAR Collab.)
AUBERT 06A PRL 96 011803 B. Aubert *et al.* (BABAR Collab.)
AUBERT 06E PRL 96 052002 B. Aubert *et al.* (BABAR Collab.)
AUBERT 06G PR D73 012004 B. Aubert *et al.* (BABAR Collab.)
AUBERT 06I PR D73 031101 B. Aubert *et al.* (BABAR Collab.)
AUBERT 06L PR D74 012001 B. Aubert *et al.* (BABAR Collab.)
AUBERT 06N PR D74 031103 B. Aubert *et al.* (BABAR Collab.)
AUBERT 06S PRL 96 241802 B. Aubert *et al.* (BABAR Collab.)
AUBERT 06T PRL 96 251802 B. Aubert *et al.* (BABAR Collab.)
AUBERT 06V PRL 97 051802 B. Aubert *et al.* (BABAR Collab.)
AUBERT 06W PR D73 071102 B. Aubert *et al.* (BABAR Collab.)
AUBERT 06X PR D73 071103 B. Aubert *et al.* (BABAR Collab.)
AUBERT 06Y PR D73 111101 B. Aubert *et al.* (BABAR Collab.)
AUBERT,B 06A PR D73 112004 B. Aubert *et al.* (BABAR Collab.)
AUBERT,B 06B PR D74 011101 B. Aubert *et al.* (BABAR Collab.)
AUBERT,B 06C PR D74 011102 B. Aubert *et al.* (BABAR Collab.)
AUBERT,B 06E PR D74 011106 B. Aubert *et al.* (BABAR Collab.)
AUBERT,B 06G PRL 97 201801 B. Aubert *et al.* (BABAR Collab.)
AUBERT,B 06H PRL 97 201802 B. Aubert *et al.* (BABAR Collab.)
AUBERT,B 06J PR D73 092001 B. Aubert *et al.* (BABAR Collab.)
AUBERT,B 06K PRL 97 211801 B. Aubert *et al.* (BABAR Collab.)
AUBERT,B 06L PR D74 031101 B. Aubert *et al.* (BABAR Collab.)
AUBERT,B 06M PR D74 031102 B. Aubert *et al.* (BABAR Collab.)
AUBERT,B 06O PR D74 031104 B. Aubert *et al.* (BABAR Collab.)
AUBERT,B 06P PR D74 031105 B. Aubert *et al.* (BABAR Collab.)
AUBERT,B 06Q PR D74 091101 B. Aubert *et al.* (BABAR Collab.)
AUBERT,B 06R PR D74 032005 B. Aubert *et al.* (BABAR Collab.)
AUBERT,B 06S PR D74 051101 B. Aubert *et al.* (BABAR Collab.)
AUBERT,B 06T PR D74 051102 B. Aubert *et al.* (BABAR Collab.)
AUBERT,B 06V PR D74 051106 B. Aubert *et al.* (BABAR Collab.)
AUBERT,B 06Y PR D74 091105 B. Aubert *et al.* (BABAR Collab.)
AUBERT,B 06Z PR D74 092004 B. Aubert *et al.* (BABAR Collab.)
AUBERT,BE 06C PRL 97 171805 B. Aubert *et al.* (BABAR Collab.)
AUBERT,BE 06H PRL 97 261803 B. Aubert *et al.* (BABAR Collab.)
AUBERT,BE 06J PR D74 111102 B. Aubert *et al.* (BABAR Collab.)
AUBERT,BE 06N PR D74 072008 B. Aubert *et al.* (BABAR Collab.)
BLYTH 06 PR D74 092002 S. Blyth *et al.* (BELLE Collab.)
CHISTOV 06A PR D74 111105 R. Chistov *et al.* (BELLE Collab.)
DRAGIC 06 PR D73 111105 J. Dragic *et al.* (BELLE Collab.)
GABYSHEV 06 PRL 97 202003 N. Gabyshev *et al.* (BELLE Collab.)
GOKHROO 06 PRL 97 162002 G. Gokhroo *et al.* (BELLE Collab.)
JEN 06 PR D74 111101 C.-M. Jen *et al.* (BELLE Collab.)
KROKOVNY 06 PRL 97 081801 P. Krokovny *et al.* (BELLE Collab.)
MOHAPATRA 06 PRL 96 221601 D. Mohapatra *et al.* (BELLE Collab.)
NAKANO 06 PR D73 112002 E. Nakano *et al.* (BELLE Collab.)
RONGA 06 PR D73 092003 F.J. Ronga *et al.* (BELLE Collab.)
SCHUEMANN 06 PRL 97 061802 J. Schuemann *et al.* (BELLE Collab.)
SOMOV 06 PRL 96 171801 A. Somov *et al.* (BELLE Collab.)
SONI 06 PL B634 155 N. Soni *et al.* (BELLE Collab.)
USHIRODA 06 PR D74 111104 Y. Ushiroda *et al.* (BELLE Collab.)
VILLA 06 PR D73 051107 S. Villa *et al.* (BELLE Collab.)
ABAZOV 05B PRL 94 042001 V.M. Abazov *et al.* (D0 Collab.)
ABAZOV 05C PRL 94 102001 V.M. Abazov *et al.* (D0 Collab.)
ABAZOV 05D PRL 94 182001 V.M. Abazov *et al.* (D0 Collab.)
ABAZOV 05W PRL 95 171801 V.M. Abazov *et al.* (D0 Collab.)
ABE 05A PRL 94 221805 K. Abe *et al.* (BELLE Collab.)
ABE 05B PR D71 072003 K. Abe *et al.* (BELLE Collab.)
Also PR D71 079903 (errat.) K. Abe *et al.* (BELLE Collab.)
ABE 05D PRL 95 101801 K. Abe *et al.* (BELLE Collab.)
ABE 05G PRL 95 231802 K. Abe *et al.* (BELLE Collab.)
ABULENCIA 05 PRL 95 221805 A. Abulencia *et al.* (CDF Collab.)
Also PRL 95 249905 (errat) A. Abulencia *et al.* (CDF Collab.)
ACOSTA 05 PRL 94 101803 D. Acosta *et al.* (CDF Collab.)
AUBERT 05 PRL 94 011801 B. Aubert *et al.* (BABAR Collab.)
AUBERT 05B PR D71 031501 B. Aubert *et al.* (BABAR Collab.)
AUBERT 05E PR D71 051502 B. Aubert *et al.* (BABAR Collab.)
AUBERT 05F PRL 94 161803 B. Aubert *et al.* (BABAR Collab.)
AUBERT 05I PRL 94 131801 B. Aubert *et al.* (BABAR Collab.)
AUBERT 05J PRL 94 141801 B. Aubert *et al.* (BABAR Collab.)
AUBERT 05K PRL 94 171801 B. Aubert *et al.* (BABAR Collab.)
AUBERT 05L PRL 94 181802 B. Aubert *et al.* (BABAR Collab.)
AUBERT 05M PRL 94 191802 B. Aubert *et al.* (BABAR Collab.)
AUBERT 05O PR D71 031103 B. Aubert *et al.* (BABAR Collab.)
AUBERT 05P PR D71 032005 B. Aubert *et al.* (BABAR Collab.)
AUBERT 05T PR D71 091102 B. Aubert *et al.* (BABAR Collab.)
AUBERT 05U PR D71 091103 B. Aubert *et al.* (BABAR Collab.)
AUBERT 05V PR D71 091104 B. Aubert *et al.* (BABAR Collab.)
AUBERT 05W PRL 94 221803 B. Aubert *et al.* (BABAR Collab.)
AUBERT 05Y PR D71 111102 B. Aubert *et al.* (BABAR Collab.)
AUBERT 05Z PR D71 112003 B. Aubert *et al.* (BABAR Collab.)
AUBERT,B 05 PRL 95 011801 B. Aubert *et al.* (BABAR Collab.)
AUBERT,B 05C PRL 95 041805 B. Aubert *et al.* (BABAR Collab.)
AUBERT,B 05K PRL 95 131803 B. Aubert *et al.* (BABAR Collab.)
AUBERT,B 05O PR D72 051102 B. Aubert *et al.* (BABAR Collab.)
AUBERT,B 05P PR D72 051103 B. Aubert *et al.* (BABAR Collab.)
AUBERT,B 05Q PR D72 051106 B. Aubert *et al.* (BABAR Collab.)
AUBERT,B 05Z PRL 95 131802 B. Aubert *et al.* (BABAR Collab.)
AUBERT,BE 05 PRL 95 151803 B. Aubert *et al.* (BABAR Collab.)
AUBERT,BE 05A PRL 95 151804 B. Aubert *et al.* (BABAR Collab.)
AUBERT,BE 05B PRL 95 171802 B. Aubert *et al.* (BABAR Collab.)
AUBERT,BE 05C PR D72 091103 B. Aubert *et al.* (BABAR Collab.)
AUBERT,BE 05E PRL 95 221801 B. Aubert *et al.* (BABAR Collab.)
AUBERT,BE 05F PR D72 111101 B. Aubert *et al.* (BABAR Collab.)
CHANG 05 PR D71 072007 M.-C. Chang *et al.* (BELLE Collab.)
CHANG 05A PR D71 091106 P. Chang *et al.* (BELLE Collab.)
CHAO 05 PRL 94 181803 Y. Chao *et al.* (BELLE Collab.)
CHAO 05A PR D71 031502 Y. Chao *et al.* (BELLE Collab.)
CHEN 05A PRL 94 221804 K.-F. Chen *et al.* (BELLE Collab.)
CHEN 05B PR D72 012004 K.-F. Chen *et al.* (BELLE Collab.)
DRUTSKOY 05 PRL 94 061802 A. Drutskoy *et al.* (BELLE Collab.)
GERSHON 05 PL B624 11 T. Gershon *et al.* (BELLE Collab.)
ITOH 05 PRL 95 091601 R. Itoh *et al.* (BELLE Collab.)
LIVENTSEV 05 PR D72 051109 D. Liventsev *et al.* (BELLE Collab.)
MAJUMDER 05 PRL 95 041803 G. Majumder *et al.* (BELLE Collab.)
MIYAKE 05 PL B618 34 H. Miyake *et al.* (BELLE Collab.)
MOHAPATRA 05 PR D72 011101 D. Mohapatra *et al.* (BELLE Collab.)
NISHIDA 05 PL B610 23 S. Nishida *et al.* (BELLE Collab.)
OKABE 05 PL B614 27 T. Okabe *et al.* (BELLE Collab.)
PARK 05 PRL 94 021801 H.K. Park *et al.* (FNAL HyperCP Collab.)
SCHUMANN 05 PR D72 011103 J. Schumann *et al.* (BELLE Collab.)
SUMISAWA 05 PRL 95 061801 K. Sumisawa *et al.* (BELLE Collab.)

USHIRODA 05 PRL 94 231601 Y. Ushiroda *et al.* (BELLE Collab.)
WANG 05 PRL 94 121801 C.C. Wang *et al.* (BELLE Collab.)
WANG 05A PL B617 141 M.-Z. Wang *et al.* (BELLE Collab.)
XIE 05 PR D72 051105 Q.L. Xie *et al.* (BELLE Collab.)
YANG 05 PRL 94 111802 H. Yang *et al.* (BELLE Collab.)
ZHANG 05B PR D71 091107 L.M. Zhang *et al.* (BELLE Collab.)
ABDALLAH 04D EPJ C33 213 J. Abdallah *et al.* (DELPHI Collab.)
ABDALLAH 04E EPJ C33 307 J. Abdallah *et al.* (DELPHI Collab.)
ABE 04E PRL 93 021601 K. Abe *et al.* (BELLE Collab.)
ACOSTA 04D PRL 93 032001 D. Acosta *et al.* (CDF Collab.)
AUBERT 04A PR D69 011102 B. Aubert *et al.* (BABAR Collab.)
AUBERT 04B PR D69 032004 B. Aubert *et al.* (BABAR Collab.)
AUBERT 04C PRL 92 111801 B. Aubert *et al.* (BaBar Collab.)
AUBERT 04G PR D69 031102 B. Aubert *et al.* (BABAR Collab.)
AUBERT 04H PRL 92 061801 B. Aubert *et al.* (BABAR Collab.)
AUBERT 04M PRL 92 201802 B. Aubert *et al.* (BABAR Collab.)
AUBERT 04R PR D69 052001 B. Aubert *et al.* (BABAR Collab.)
AUBERT 04U PR D69 091503 B. Aubert *et al.* (BABAR Collab.)
AUBERT 04V PRL 92 251801 B. Aubert *et al.* (BABAR Collab.)
AUBERT 04W PRL 92 251802 B. Aubert *et al.* (BABAR Collab.)
AUBERT 04Y PRL 93 041801 B. Aubert *et al.* (BaBar Collab.)
AUBERT 04Z PRL 93 051802 B. Aubert *et al.* (BABAR Collab.)
AUBERT,B 04B PR D70 011101 B. Aubert *et al.* (BABAR Collab.)
AUBERT,B 04C PR D70 012007 B. Aubert *et al.* (BABAR Collab.)
Also PRL 92 181801 B. Aubert *et al.* (BABAR Collab.)
AUBERT,B 04D PR D70 032006 B. Aubert *et al.* (BABAR Collab.)
AUBERT,B 04G PRL 93 071801 B. Aubert *et al.* (BABAR Collab.)
AUBERT,B 04H PRL 93 081801 B. Aubert *et al.* (BABAR Collab.)
AUBERT,B 04J PRL 93 091802 B. Aubert *et al.* (BABAR Collab.)
AUBERT,B 04K PRL 93 131801 B. Aubert *et al.* (BABAR Collab.)
AUBERT,B 04M PRL 93 131805 B. Aubert (BABAR Collab.)
AUBERT,B 04O PR D70 091103 B. Aubert *et al.* (BABAR Collab.)
AUBERT,B 04R PRL 93 231801 B. Aubert *et al.* (BABAR Collab.)
AUBERT,B 04S PRL 93 181801 B. Aubert *et al.* (BABAR Collab.)
AUBERT,B 04T PR D70 091104 B. Aubert *et al.* (BABAR Collab.)
AUBERT,B 04U PR D70 091105 B. Aubert *et al.* (BABAR Collab.)
AUBERT,B 04V PRL 93 181805 B. Aubert *et al.* (BABAR Collab.)
AUBERT,B 04W PRL 93 231804 B. Aubert *et al.* (BABAR Collab)
AUBERT,B 04X PRL 93 181806 B. Aubert *et al.* (BABAR Collab.)
AUBERT,B 04Z PRL 93 201801 B. Aubert *et al.* (BABAR Collab.)
AUBERT,BE 04 PR D70 111102 B. Aubert *et al.* (BABAR Collab.)
AUBERT,BE 04A PR D70 112006 B. Aubert *et al.* (BABAR Collab.)
AUBERT,BE 04B PR D70 091106 B. Aubert *et al.* (BABAR Collab.)
AUSHEV 04 PRL 93 201802 T. Aushev *et al.* (BELLE Collab.)
BORNHEIM 04 PRL 93 241802 A. Bornheim *et al.* (CLEO Collab.)
CHANG 04 PL B599 148 P. Chang *et al.* (BELLE Collab.)
CHAO 04 PR D69 111102 Y. Chao *et al.* (BELLE Collab.)
CHAO 04B PRL 93 191802 Y. Chao *et al.* (BELLE Collab.)
DRAGIC 04 PRL 93 131802 J. Dragic (BELLE Collab.)
DRUTSKOY 04 PRL 92 051801 A. Drutskoy *et al.* (BELLE Collab.)
GARMASH 04 PR D69 012001 A. Garmash *et al.* (BELLE Collab.)
KATAOKA 04 PRL 93 261801 S.U. Kataoka *et al.* (BELLE Collab.)
MAJUMDER 04 PR D70 111103 G. Majumder *et al.* (BELLE Collab.)
NAKAO 04 PR D69 112001 M. Nakao *et al.* (BELLE Collab.)
SARANGI 04 PRL 93 031802 T.R. Sarangi *et al.* (BELLE Collab.)
WANG 04 PRL 92 131801 M.Z. Wang *et al.* (BELLE Collab.)
WANG 04A PR D70 012001 C.H. Wang *et al.* (BELLE Collab.)
ABDALLAH 03B EPJ C28 155 J. Abdallah *et al.* (DELPHI Collab.)
ABE 03B PR D67 032003 K. Abe *et al.* (BELLE Collab.)
ABE 03C PR D67 031102 K. Abe *et al.* (BELLE Collab.)
ABE 03G PR D68 012001 K. Abe *et al.* (BELLE Collab.)
ABE 03H PRL 91 261602 K. Abe *et al.* (BELLE Collab.)
ADAM 03 PR D67 032001 N.E. Adam *et al.* (CLEO Collab.)
ATHAR 03 PR D68 072003 S.B. Athar *et al.* (CLEO Collab.)
AUBERT 03B PRL 90 091801 B. Aubert *et al.* (BaBar Collab.)
AUBERT 03C PR D67 072002 B. Aubert *et al.* (BaBar Collab.)
AUBERT 03D PRL 90 181803 B. Aubert *et al.* (BaBar Collab.)
AUBERT 03E PRL 90 181801 B. Aubert *et al.* (BaBar Collab.)
AUBERT 03H PR D67 091101 B. Aubert *et al.* (BaBar Collab.)
AUBERT 03I PR D67 092003 B. Aubert *et al.* (BaBar Collab.)
AUBERT 03J PRL 90 221801 B. Aubert *et al.* (BaBar Collab.)
AUBERT 03K PRL 90 231801 B. Aubert *et al.* (BaBar Collab.)
AUBERT 03L PRL 91 021801 B. Aubert *et al.* (BaBar Collab.)
AUBERT 03N PRL 91 061802 B. Aubert *et al.* (BaBar Collab.)
AUBERT 03O PRL 91 071801 B. Aubert *et al.* (BaBar Collab.)
AUBERT 03Q PRL 91 131801 B. Aubert *et al.* (BaBar Collab.)
AUBERT 03S PRL 91 241801 B. Aubert *et al.* (BaBar Collab.)
AUBERT 03T PRL 91 201802 B. Aubert *et al.* (BaBar Collab.)
AUBERT 03U PRL 91 221802 B. Aubert *et al.* (BaBar Collab.)
AUBERT 03V PRL 91 171802 B. Aubert *et al.* (BaBar Collab.)
AUBERT 03W PRL 91 161801 B. Aubert *et al.* (BaBar Collab.)
AUBERT 03X PR D68 092001 B. Aubert *et al.* (BaBar Collab.)
BORNHEIM 03 PR D68 052002 A. Bornheim *et al.* (CLEO Collab.)
CHANG 03 PR D68 111101 M.-C. Chang *et al.* (BELLE Collab.)
CHEN 03B PRL 91 201801 K.-F. Chen *et al.* (BELLE Collab.)
CSORNA 03 PR D67 112002 S.E. Csorna *et al.* (CLEO Collab.)
EISENSTEIN 03 PR D68 017101 B.I. Eisenstein *et al.* (CLEO Collab.)
FANG 03 PRL 90 071801 F. Fang *et al.* (BELLE Collab.)
GABYSHEV 03 PRL 90 121802 N. Gabyshev *et al.* (BELLE Collab.)
HASTINGS 03 PR D67 052004 N.C. Hastings *et al.* (BELLE Collab.)
ISHIKAWA 03 PRL 91 261601 A. Ishikawa *et al.* (BELLE Collab.)
KROKOVNY 03 PRL 90 141802 P. Krokovny *et al.* (BELLE Collab.)
KROKOVNY 03B PRL 91 262002 P. Krokovny *et al.* (BELLE Collab.)
LEE 03 PRL 91 261801 S.H. Lee *et al.* (BELLE Collab.)
SATPATHY 03 PL B553 159 A. Satpathy *et al.* (BELLE Collab.)
WANG 03 PRL 90 201802 M.-Z. Wang *et al.* (BELLE Collab.)
ZHENG 03 PR D67 092004 Y. Zheng *et al.* (BELLE Collab.)
ABE 02 PRL 88 021801 K. Abe *et al.* (BELLE Collab.)
ABE 02E PL B526 258 K. Abe *et al.* (BELLE Collab.)
ABE 02F PL B526 247 K. Abe *et al.* (BELLE Collab.)
ABE 02H PRL 88 171801 K. Abe *et al.* (BELLE Collab.)
ABE 02J PRL 88 052002 K. Abe *et al.* (BELLE Collab.)
ABE 02K PRL 88 181803 K. Abe *et al.* (BELLE Collab.)
ABE 02M PRL 89 071801 K. Abe *et al.* (BELLE Collab.)
ABE 02N PL B538 11 K. Abe *et al.* (BELLE Collab.)
ABE 02O PR D65 091103 K. Abe *et al.* (BELLE Collab.)
ABE 02Q PRL 89 122001 K. Abe *et al.* (BELLE Collab.)
ABE 02U PR D66 032007 K. Abe *et al.* (BELLE Collab.)
ABE 02W PRL 89 151802 K. Abe *et al.* (BELLE Collab.)
ABE 02Z PR D66 071102 K. Abe *et al.* (BELLE Collab.)
ACOSTA 02C PR D65 092009 D. Acosta *et al.* (CDF Collab.)
ACOSTA 02G PR D66 112002 D. Acosta *et al.* (CDF Collab.)
AFFOLDER 02B PRL 88 071801 T. Affolder *et al.* (CDF Collab.)
AHMED 02B PR D66 031101 S. Ahmed *et al.* (CLEO Collab.)
ASNER 02 PR D65 031103 D.M. Asner *et al.* (CLEO Collab.)
AUBERT 02 PR D65 032001 B. Aubert *et al.* (BaBar Collab.)
AUBERT 02C PRL 88 101805 B. Aubert *et al.* (BaBar Collab.)
AUBERT 02D PR D65 051502 B. Aubert *et al.* (BaBar Collab.)
AUBERT 02E PR D65 051101 B. Aubert *et al.* (BaBar Collab.)
AUBERT 02H PRL 89 011802 B. Aubert *et al.* (BaBar Collab.)
Also PRL 89 169903 (errat) B. Aubert *et al.* (BaBar Collab.)
AUBERT 02I PRL 88 221802 B. Aubert *et al.* (BaBar Collab.)
AUBERT 02J PRL 88 221803 B. Aubert *et al.* (BaBar Collab.)
AUBERT 02K PR D66 071103 B. Aubert *et al.* (BaBar Collab.)
AUBERT 02L PRL 89 061801 B. Aubert *et al.* (BaBar Collab.)
AUBERT 02M PR D66 032003 B. Aubert *et al.* (BaBar Collab.)
AUBERT 02N PRL 89 201802 B. Aubert *et al.* (BaBar Collab.)
AUBERT 02P PRL 89 281802 B. Aubert *et al.* (BaBar Collab.)
AUBERT 02Q PRL 89 081803 R. Briere *et al.* (CLEO Collab.)
BRIERE 02 PR D66 092002 B.C.K. Casey *et al.* (BELLE Collab.)
CASEY 02 PL B546 196 K.-F. Chen *et al.* (BELLE Collab.)
CHEN 02B PR 88 062001 T.E. Coan *et al.* (CLEO Collab.)
COAN 02 PRL 88 069902 (errat) T.E. Coan *et al.* (CLEO Collab.)
Also PL B542 171 A. Drutskoy *et al.* (BELLE Collab.)
DRUTSKOY 02 PR D66 091101 S.A. Dytman *et al.* (CLEO Collab.)
DYTMAN 02 PRL 89 251801 E. Eckhart *et al.* (CLEO Collab.)
ECKHART 02 PR D65 012002 K.W. Edwards *et al.* (CLEO Collab.)
EDWARDS 02 PR D66 091102 N. Gabyshev *et al.* (BELLE Collab.)
GABYSHEV 02 PRL 88 021802 R. Godang *et al.* (CLEO Collab.)
GODANG 02 PL B542 183 A. Gordon *et al.* (BELLE Collab.)
GORDON 02 PRL 89 251803 K. Hara *et al.* (BELLE Collab.)
HARA 02 PRL 89 231804 P. Korkovny *et al.* (BELLE Collab.)
KROKOVNY 02 PRL 88 101803 R. Mahapatra *et al.* (CLEO Collab.)
MAHAPATRA 02 PRL 89 231801 S. Nishida *et al.* (BELLE Collab.)
NISHIDA 02 PL B542 207 T. Tomura *et al.* (BELLE Collab.)
TOMURA 02 PRL 86 2509 A. Abashian *et al.* (BELLE Collab.)
ABASHIAN 01 PRL 86 3228 K. Abe *et al.* (BELLE Collab.)
ABE 01D PRL 87 091802 K. Abe *et al.* (BELLE Collab.)
ABE 01G PRL 87 101801 K. Abe *et al.* (BELLE Collab.)
ABE 01H PRL 87 111801 K. Abe *et al.* (BELLE Collab.)
ABE 01I PR D64 071101 K. Abe *et al.* (BELLE Collab.)
ABE 01K PRL 87 161601 K. Abe *et al.* (BELLE Collab.)
ABE 01L PL B517 309 K. Abe *et al.* (BELLE Collab.)
ABE 01M PL B510 55 P. Abreu *et al.* (DELPHI Collab.)
ABREU 01H PR D64 092001 J.P. Alexander *et al.* (CLEO Collab.)
ALEXANDER 01B PRL 87 271801 R. Ammar *et al.* (CLEO Collab.)
AMMAR 01B PRL 86 2732 S. Anderson *et al.* (CLEO Collab.)
ANDERSON 01 PRL 87 181803 S. Anderson *et al.* (CLEO Collab.)
ANDERSON 01B PRL 86 2515 B. Aubert *et al.* (BaBar Collab.)
AUBERT 01 PRL 87 091801 B. Aubert *et al.* (BaBar Collab.)
AUBERT 01B PRL 87 151801 B. Aubert *et al.* (BaBar Collab.)
AUBERT 01D PRL 87 151802 B. Aubert *et al.* (BaBar Collab.)
AUBERT 01E PRL 87 201803 B. Aubert *et al.* (BaBar Collab.)
AUBERT 01F PRL 87 221802 B. Aubert *et al.* (BaBar Collab.)
AUBERT 01G PRL 87 241801 B. Aubert *et al.* (BaBar Collab.)
AUBERT 01H PRL 87 241803 B. Aubert *et al.* (BaBar Collab.)
AUBERT 01I PR D64 031101 R. Barate *et al.* (ALEPH Collab.)
BARATE 01D EPJ C20 431 R.A. Briere *et al.* (CLEO Collab.)
BRIERE 01 PRL 86 3718 K.W. Edwards *et al.* (CLEO Collab.)
EDWARDS 01 PRL 86 30 D. Jaffe *et al.* (CLEO Collab.)
JAFFE 01 PRL 86 5000 S.J. Richichi *et al.* (CLEO Collab.)
RICHICHI 01 PR D63 031103 G. Abbiendi *et al.* (OPAL Collab.)
ABBIENDI 00Q PL B482 15 G. Abbiendi *et al.* (OPAL Collab.)
ABBIENDI,G 00B PL B493 266 K. Abe *et al.* (SLD Collab.)
ABE 00C PR D62 071101 T. Affolder *et al.* (CDF Collab.)
AFFOLDER 00C PR D61 072005 T. Affolder *et al.* (CDF Collab.)
AFFOLDER 00N PRL 85 4668 S. Ahmed *et al.* (CLEO Collab.)
AHMED 00B PR D62 112003 A. Anastassov *et al.* (CLEO Collab.)
ANASTASSOV 00 PRL 84 1393 M. Artuso *et al.* (CLEO Collab.)
ARTUSO 00 PRL 84 4292 P. Avery *et al.* (CLEO Collab.)
AVERY 00 PR D62 051101 R. Barate *et al.* (ALEPH Collab.)
BARATE 00Q PL B492 259 R. Barate *et al.* (ALEPH Collab.)
BARATE 00R PL B492 275 M. Artuso *et al.* (CLEO Collab.)
BEHRENS 00 PR D61 052001 B.H. Behrens *et al.* (CLEO Collab.)
BEHRENS 00B PL B490 36 T. Bergfeld *et al.* (CLEO Collab.)
BERGFELD 00B PR D62 091102 S. Chen *et al.* (CLEO Collab.)
CHEN 00 PRL 85 525 T.E. Coan *et al.* (CLEO Collab.)
COAN 00 PRL 84 5283 D. Cronin-Hennessy *et al.* (CLEO Collab.)
CRONIN-HEN... 00 PRL 85 515 S.E. Csorna *et al.* (CLEO Collab.)
CSORNA 00 PR D61 111101 C.P. Jessop *et al.* (CLEO Collab.)
JESSOP 00 PRL 85 2881 E. Lipeles *et al.* (CLEO Collab.)
LIPELES 00 PR D62 032005 S.J. Richichi *et al.* (CLEO Collab.)
RICHICHI 00 PRL 85 520 G. Abbiendi *et al.* (OPAL Collab.)
ABBIENDI 99J EPJ C12 609 F. Abe *et al.* (CDF Collab.)
ABE 99K PR D60 051101 F. Abe *et al.* (CDF Collab.)
ABE 99Q PR D60 072003 T. Affolder *et al.* (CDF Collab.)
AFFOLDER 99B PRL 83 3378 T. Affolder *et al.* (CDF Collab.)
AFFOLDER 99C PR D60 112004 M. Artuso *et al.* (CLEO Collab.)
ARTUSO 99 PRL 82 3020 J. Bartelt *et al.* (CLEO Collab.)
BARTELT 99 PRL 82 3746 T.E. Coan *et al.* (CLEO Collab.)
COAN 99 PR D59 111101 B. Abbott *et al.* (D0 Collab.)
ABBOTT 98B PL B423 419 F. Abe *et al.* (CDF Collab.)
ABE 98 PR D57 R3811 F. Abe *et al.* (CDF Collab.)
ABE 98B PR D57 5382 F. Abe *et al.* (CDF Collab.)
ABE 98C PRL 80 2057 F. Abe *et al.* (CDF Collab.)
Also PR D59 032001 F. Abe *et al.* (CDF Collab.)
ABE 98O PR D58 072001 F. Abe *et al.* (CDF Collab.)
ABE 98Q PR D58 092002 F. Abe *et al.* (CDF Collab.)
ABE 98U PRL 81 5513 F. Abe *et al.* (CDF Collab.)
ABE 98V PRL 81 5742 F. Abe *et al.* (CDF Collab.)
ACCIARRI 98D EPJ C5 195 M. Acciarri *et al.* (L3 Collab.)
ACCIARRI 98S PL B438 417 M. Acciarri *et al.* (L3 Collab.)
ACKERSTAFF 98Z EPJ C5 379 K. Ackerstaff *et al.* (OPAL Collab.)
BARATE 98Q EPJ C4 387 R. Barate *et al.* (ALEPH Collab.)
BEHRENS 98 PRL 80 3710 B.H. Behrens *et al.* (CLEO Collab.)
BERGFELD 98 PRL 81 272 T. Bergfeld *et al.* (CLEO Collab.)
BRANDENB... 98 PRL 80 2762 G. Brandenbrug *et al.* (CLEO Collab.)
GODANG 98 PRL 80 3456 R. Godang *et al.* (CLEO Collab.)
NEMATI 98 PR D57 5363 B. Nemati *et al.* (CLEO Collab.)
ABE 97J PRL 79 590 K. Abe *et al.* (SLD Collab.)
ABREU 97F ZPHY C74 19 P. Abreu *et al.* (DELPHI Collab.)
Also ZPHY C75 579 (erratum) P. Abreu *et al.* (DELPHI Collab.)
ABREU 97N ZPHY C76 579 P. Abreu *et al.* (DELPHI Collab.)
ACCIARRI 97B PL B391 474 M. Acciarri *et al.* (L3 Collab.)
ACCIARRI 97C PL B391 481 M. Acciarri *et al.* (L3 Collab.)
ACKERSTAFF 97G PL B395 128 K. Ackerstaff *et al.* (OPAL Collab.)
ACKERSTAFF 97U ZPHY C76 401 K. Ackerstaff *et al.* (OPAL Collab.)
ACKERSTAFF 97V ZPHY C76 417 K. Ackerstaff *et al.* (OPAL Collab.)
ARTUSO 97 PL B399 321 M. Artuso *et al.* (CLEO Collab.)
ASNER 97 PRL 79 799 D. Asner *et al.* (CLEO Collab.)
ATHANAS 97 PRL 79 2208 M. Athanas *et al.* (CLEO Collab.)
BUSKULIC 97 PL B395 373 D. Buskulic *et al.* (ALEPH Collab.)
BUSKULIC 97D ZPHY C75 397 D. Buskulic *et al.* (ALEPH Collab.)
FU 97 PRL 79 3125 X. Fu *et al.* (CLEO Collab.)
JESSOP 97 PRL 79 4533 C.P. Jessop *et al.* (CLEO Collab.)
ABE 96B PR D53 3496 F. Abe *et al.* (CDF Collab.)
ABE 96C PRL 76 4462 F. Abe *et al.* (CDF Collab.)
ABE 96H PRL 76 2015 F. Abe *et al.* (CDF Collab.)
ABE 96L PRL 76 4675 F. Abe *et al.* (CDF Collab.)
ABE 96Q PR D54 6596 F. Abe *et al.* (CDF Collab.)
ABREU 96P ZPHY C71 539 P. Abreu *et al.* (DELPHI Collab.)
ABREU 96Q ZPHY C72 17 P. Abreu *et al.* (DELPHI Collab.)
ACCIARRI 96E PL B383 487 M. Acciarri *et al.* (L3 Collab.)
ADAM 96D ZPHY C72 207 W. Adam *et al.* (DELPHI Collab.)

ALBRECHT	96D	PL B374 256	H. Albrecht *et al.*	(ARGUS Collab.)
ALEXANDER	96T	PRL 77 5000	J.P. Alexander *et al.*	(CLEO Collab.)
ALEXANDER	96V	ZPHY C72 377	G. Alexander *et al.*	(OPAL Collab.)
ASNER	96	PR D53 1039	D.M. Asner *et al.*	(CLEO Collab.)
BARISH	96B	PRL 76 1570	B.C. Barish *et al.*	(CLEO Collab.)
BISHAI	96	PL B369 186	M. Bishai *et al.*	(CLEO Collab.)
BUSKULIC	96J	ZPHY C71 31	D. Buskulic *et al.*	(ALEPH Collab.)
BUSKULIC	96V	PL B384 471	D. Buskulic *et al.*	(ALEPH Collab.)
DUBOSCQ	96	PRL 76 3898	J.E. Duboscq *et al.*	(CLEO Collab.)
GIBAUT	96	PR D53 4734	D. Gibaut *et al.*	(CLEO Collab.)
PDG	96	PR D54 1	R. M. Barnett *et al.*	(PDG Collab.)
ABE	95Z	PRL 75 3068	F. Abe *et al.*	(CDF Collab.)
ABREU	95N	PL B357 255	P. Abreu *et al.*	(DELPHI Collab.)
ABREU	95Q	ZPHY C68 13	P. Abreu *et al.*	(DELPHI Collab.)
ACCIARRI	95H	PL B363 127	M. Acciarri *et al.*	(L3 Collab.)
ACCIARRI	95I	PL B363 137	M. Acciarri *et al.*	(L3 Collab.)
ADAM	95	ZPHY C68 363	W. Adam *et al.*	(DELPHI Collab.)
AKERS	95J	ZPHY C66 555	R. Akers *et al.*	(OPAL Collab.)
AKERS	95T	ZPHY C67 379	R. Akers *et al.*	(OPAL Collab.)
ALEXANDER	95	PL B341 435	J. Alexander *et al.*	(CLEO Collab.)
Also		PL B347 469 (erratum)	J. Alexander *et al.*	(CLEO Collab.)
BARISH	95	PR D51 1014	B.C. Barish *et al.*	(CLEO Collab.)
BUSKULIC	95N	PL B359 236	D. Buskulic *et al.*	(ALEPH Collab.)
ABE	94D	PRL 72 3456	F. Abe *et al.*	(CDF Collab.)
ABREU	94M	PL B338 409	P. Abreu *et al.*	(DELPHI Collab.)
AKERS	94C	PL B327 411	R. Akers *et al.*	(OPAL Collab.)
AKERS	94H	PL B336 585	R. Akers *et al.*	(OPAL Collab.)
AKERS	94J	PL B337 196	R. Akers *et al.*	(OPAL Collab.)
AKERS	94L	PL B337 393	R. Akers *et al.*	(OPAL Collab.)
ALAM	94	PR D50 43	M.S. Alam *et al.*	(CLEO Collab.)
ALBRECHT	94	PL B324 249	H. Albrecht *et al.*	(ARGUS Collab.)
ALBRECHT	94G	PL B340 217	H. Albrecht *et al.*	(ARGUS Collab.)
AMMAR	94	PR D49 5701	R. Ammar *et al.*	(CLEO Collab.)
ATHANAS	94	PRL 73 3503	M. Athanas *et al.*	(CLEO Collab.)
Also		PRL 74 3090 (erratum)	M. Athanas *et al.*	(CLEO Collab.)
BUSKULIC	94B	PL B322 441	D. Buskulic *et al.*	(ALEPH Collab.)
PDG	94	PR D50 1173	L. Montanet *et al.*	(CERN, LBL, BOST+)
PROCARIO	94	PRL 73 1472	M. Procario *et al.*	(CLEO Collab.)
STONE	94	HEPSY 93-11	S. Stone	
Published in B Decays, 2nd Edition, World Scientific, Singapore				
ABREU	93D	ZPHY C57 181	P. Abreu *et al.*	(DELPHI Collab.)
ABREU	93G	PL B312 253	P. Abreu *et al.*	(DELPHI Collab.)
ACTON	93C	PL B307 247	P.D. Acton *et al.*	(OPAL Collab.)
ALBRECHT	93	ZPHY C57 533	H. Albrecht *et al.*	(ARGUS Collab.)
ALBRECHT	93E	ZPHY C60 11	H. Albrecht *et al.*	(ARGUS Collab.)
ALEXANDER	93B	PL B319 365	J. Alexander *et al.*	(CLEO Collab.)
AMMAR	93	PRL 71 674	R. Ammar *et al.*	(CLEO Collab.)
BARTELT	93	PRL 71 1680	J.E. Bartelt *et al.*	(CLEO Collab.)
BATTLE	93	PRL 71 3922	M. Battle *et al.*	(CLEO Collab.)
BEAN	93B	PRL 70 2681	A. Bean *et al.*	(CLEO Collab.)
BUSKULIC	93D	PL B307 194	D. Buskulic *et al.*	(ALEPH Collab.)
Also		PL B325 537 (erratum)	D. Buskulic *et al.*	(ALEPH Collab.)
BUSKULIC	93K	PL B313 498	D. Buskulic *et al.*	(ALEPH Collab.)
SANGHERA	93	PR D47 791	S. Sanghera *et al.*	(CLEO Collab.)
ALBRECHT	92C	PL B275 195	H. Albrecht *et al.*	(ARGUS Collab.)
ALBRECHT	92G	ZPHY C54 1	H. Albrecht *et al.*	(ARGUS Collab.)
ALBRECHT	92L	ZPHY C55 357	H. Albrecht *et al.*	(ARGUS Collab.)
BORTOLETTO	92	PR D45 21	D. Bortoletto *et al.*	(CLEO Collab.)
HENDERSON	92	PR D45 2212	S. Henderson *et al.*	(CLEO Collab.)
KRAMER	92	PL B279 181	G. Kramer, W.F. Palmer	(HAMB, OSU)
ALBAJAR	91C	PL B262 163	C. Albajar *et al.*	(UA1 Collab.)
ALBAJAR	91E	PL B273 540	C. Albajar *et al.*	(UA1 Collab.)
ALBRECHT	91B	PL B254 288	H. Albrecht *et al.*	(ARGUS Collab.)
ALBRECHT	91C	PL B255 297	H. Albrecht *et al.*	(ARGUS Collab.)
ALBRECHT	91E	PL B262 148	H. Albrecht *et al.*	(ARGUS Collab.)
BERKELMAN	91	ARNPS 41 1	K. Berkelman, S. Stone	(CORN, SYRA)
"Decays of B Mesons"				
FULTON	91	PR D43 651	R. Fulton *et al.*	(CLEO Collab.)
ALBRECHT	90B	PL B241 278	H. Albrecht *et al.*	(ARGUS Collab.)
ALBRECHT	90J	ZPHY C48 543	H. Albrecht *et al.*	(ARGUS Collab.)
ANTREASYAN	90B	ZPHY C48 553	D. Antreasyan *et al.*	(Crystal Ball Collab.)
BORTOLETTO	90	PRL 64 2117	D. Bortoletto *et al.*	(CLEO Collab.)
ELSEN	90	ZPHY C46 349	E. Elsen *et al.*	(JADE Collab.)
ROSNER	90	PR D42 3732	J.L. Rosner	
WAGNER	90	PRL 64 1095	S.R. Wagner *et al.*	(Mark II Collab.)
ALBRECHT	89C	PL B219 121	H. Albrecht *et al.*	(ARGUS Collab.)
ALBRECHT	89G	PL B229 304	H. Albrecht *et al.*	(ARGUS Collab.)
ALBRECHT	89J	PL B229 175	H. Albrecht *et al.*	(ARGUS Collab.)
ALBRECHT	89L	PL B232 554	H. Albrecht *et al.*	(ARGUS Collab.)
ARTUSO	89	PRL 62 2233	M. Artuso *et al.*	(CLEO Collab.)
AVERILL	89	PR D39 123	D.A. Averill *et al.*	(HRS Collab.)
AVERY	89B	PL B223 470	P. Avery *et al.*	(CLEO Collab.)
BEBEK	89	PRL 62 8	C. Bebek *et al.*	(CLEO Collab.)
BORTOLETTO	89	PRL 62 2436	D. Bortoletto *et al.*	(CLEO Collab.)
BORTOLETTO	89B	PRL 63 1667	D. Bortoletto *et al.*	(CLEO Collab.)
ALBRECHT	88F	PL B209 119	H. Albrecht *et al.*	(ARGUS Collab.)
ALBRECHT	88K	PL B215 424	H. Albrecht *et al.*	(ARGUS Collab.)
ALBRECHT	87C	PL B185 218	H. Albrecht *et al.*	(ARGUS Collab.)
ALBRECHT	87D	PL B199 451	H. Albrecht *et al.*	(ARGUS Collab.)
ALBRECHT	87I	PL B192 245	H. Albrecht *et al.*	(ARGUS Collab.)
ALBRECHT	87J	PL B197 452	H. Albrecht *et al.*	(ARGUS Collab.)
AVERY	87	PL B183 429	P. Avery *et al.*	(CLEO Collab.)
BEAN	87B	PRL 58 183	A. Bean *et al.*	(CLEO Collab.)
BEBEK	87	PR D36 1289	C. Bebek *et al.*	(CLEO Collab.)
ALAM	86	PR D34 3279	M.S. Alam *et al.*	(CLEO Collab.)
ALBRECHT	86F	PL B182 95	H. Albrecht *et al.*	(ARGUS Collab.)
PDG	86	PL 170B 1	M. Aguilar-Benitez *et al.*	(CERN, CIT+)
CHEN	85	PR D31 2386	A. Chen *et al.*	(CLEO Collab.)
HAAS	85	PRL 55 1248	J. Haas *et al.*	(CLEO Collab.)
AVERY	84	PRL 53 1309	P. Avery *et al.*	(CLEO Collab.)
GILES	84	PR D30 2279	R. Giles *et al.*	(CLEO Collab.)
BEHRENDS	83	PRL 50 881	S. Behrends *et al.*	(CLEO Collab.)

$B^\pm/B^0$ ADMIXTURE

B DECAY MODES

The branching fraction measurements are for an admixture of B mesons at the $\Upsilon(4S)$. The values quoted assume that $B(\Upsilon(4S) \to B\overline{B}) = 100\%$.

For inclusive branching fractions, *e.g.*, $B \to D^\pm$ *anything*, the treatment of multiple D's in the final state must be defined. One possibility would be to count the number of events with one-or-more D's and divide by the total number of B's. Another possibility would be to count the total number of D's and divide by the total number of B's, which is the definition of average multiplicity. The two definitions are identical if only one D is allowed in the final state. Even though the "one-or-more" definition seems sensible, for practical reasons inclusive branching fractions are almost always measured using the multiplicity definition. For heavy final state particles, authors call their results inclusive branching fractions while for light particles some authors call their results multiplicities. In the B sections, we list all results as inclusive branching fractions, adopting a multiplicity definition. This means that inclusive branching fractions can exceed 100% and that inclusive partial widths can exceed total widths, just as inclusive cross sections can exceed total cross section.

$\overline{B}$ modes are charge conjugates of the modes below. Reactions indicate the weak decay vertex and do not include mixing.

	Mode		Fraction (Γ_i/Γ)	Scale factor/ Confidence level
	Semileptonic and leptonic modes			
Γ_1	$e^+\nu_e$ anything	[a]	(10.86 ± 0.16) %	
Γ_2	$\overline{p}e^+\nu_e$ anything		< 5.9	$\times 10^{-4}$ CL=90%
Γ_3	$\mu^+\nu_\mu$ anything	[a]	(10.86 ± 0.16) %	
Γ_4	$\ell^+\nu_\ell$ anything	[a,b]	(10.86 ± 0.16) %	
Γ_5	$D^-\ell^+\nu_\ell$ anything	[b]	(2.8 ± 0.9) %	
Γ_6	$\overline{D}^0\ell^+\nu_\ell$ anything	[b]	(7.3 ± 1.5) %	
Γ_7	$\overline{D}\ell^+\nu_\ell$		(2.42 ± 0.12) %	
Γ_8	$\overline{D}\tau^+\nu_\tau$		(1.07 ± 0.18) %	
Γ_9	$D^{*-}\ell^+\nu_\ell$ anything	[c]	(6.7 ± 1.3) $\times 10^{-3}$	
Γ_{10}	$D^{*0}\ell^+\nu_\ell$ anything			
Γ_{11}	$D^*\ell^+\nu_\ell$	[d]	(4.95 ± 0.11) %	
Γ_{12}	$D^*\tau^+\nu_\tau$		(1.64 ± 0.15) %	
Γ_{13}	$\overline{D}^{**}\ell^+\nu_\ell$	[b,e]	(2.7 ± 0.7) %	
Γ_{14}	$\overline{D}_1(2420)\ell^+\nu_\ell$ anything		(3.8 ± 1.3) $\times 10^{-3}$	S=2.4
Γ_{15}	$D\pi\ell^+\nu_\ell$ anything + $D^*\pi\ell^+\nu_\ell$ anything		(2.6 ± 0.5) %	S=1.5
Γ_{16}	$D\pi\ell^+\nu_\ell$ anything		(1.5 ± 0.6) %	
Γ_{17}	$D^*\pi\ell^+\nu_\ell$ anything		(1.9 ± 0.4) %	
Γ_{18}	$\overline{D}_2^*(2460)\ell^+\nu_\ell$ anything		(4.4 ± 1.6) $\times 10^{-3}$	
Γ_{19}	$D^{*-}\pi^+\ell^+\nu_\ell$ anything		(1.00 ± 0.34) %	
Γ_{20}	$D_s^-\ell^+\nu_\ell$ anything	[b]	< 7	$\times 10^{-3}$ CL=90%
Γ_{21}	$D_s^-\ell^+\nu_\ell K^+$ anything	[b]	< 5	$\times 10^{-3}$ CL=90%
Γ_{22}	$D_s^-\ell^+\nu_\ell K^0$ anything	[b]	< 7	$\times 10^{-3}$ CL=90%
Γ_{23}	$X_c\ell^+\nu_\ell$		(10.65 ± 0.16) %	
Γ_{24}	$X_u\ell^+\nu_\ell$		(2.14 ± 0.31) $\times 10^{-3}$	
Γ_{25}	$K^+\ell^+\nu_\ell$ anything	[b]	(6.3 ± 0.6) %	
Γ_{26}	$K^-\ell^+\nu_\ell$ anything	[b]	(10 ± 4) $\times 10^{-3}$	
Γ_{27}	$K^0/\overline{K}^0\ell^+\nu_\ell$ anything	[b]	(4.6 ± 0.5) %	
	***D*, *D**, or D_s modes**			
Γ_{28}	$D^\pm$ anything		(23.7 ± 1.3) %	
Γ_{29}	$D^0/\overline{D}^0$ anything		(62.7 ± 2.9) %	S=1.3
Γ_{30}	$D^*(2010)^\pm$ anything		(22.5 ± 1.5) %	
Γ_{31}	$D^*(2007)^0$ anything		(26.0 ± 2.7) %	
Γ_{32}	$D_s^\pm$ anything	[f]	(8.3 ± 0.8) %	
Γ_{33}	$D_s^{*\pm}$ anything		(6.3 ± 1.0) %	
Γ_{34}	$D_s^{*\pm}\overline{D}^{(*)}$		(3.4 ± 0.6) %	
Γ_{35}	$\overline{D}D_{s0}(2317)$			
Γ_{36}	$\overline{D}D_{sJ}(2457)$			
Γ_{37}	$D^{(*)}\overline{D}^{(*)}K^0 + D^{(*)}\overline{D}^{(*)}K^\pm$	[f,g]	(7.1 $^{+\ 2.7}_{-\ 1.7}$) %	
Γ_{38}	$b \to c\overline{c}s$		(22 ± 4) %	
Γ_{39}	$D_s^{(*)}\overline{D}^{(*)}$	[f,g]	(3.9 ± 0.4) %	
Γ_{40}	$D^*D^*(2010)^\pm$	[f]	< 5.9	$\times 10^{-3}$ CL=90%
Γ_{41}	$DD^*(2010)^\pm + D^*D^\pm$	[f]	< 5.5	$\times 10^{-3}$ CL=90%
Γ_{42}	$DD^\pm$	[f]	< 3.1	$\times 10^{-3}$ CL=90%
Γ_{43}	$D_s^{(*)\pm}\overline{D}^{(*)}X(n\pi^\pm)$	[f,g]	(9 $^{+\ 5}_{-\ 4}$) %	

Γ_{44}	$D^*(2010)\gamma$		<	1.1	$\times 10^{-3}$	CL=90%
Γ_{45}	$D_s^+\pi^-$, $D_s^{*+}\pi^-$, $D_s^+\rho^-$, $D_s^{*+}\rho^-$, $D_s^+\pi^0$, $D_s^{*+}\pi^0$, $D_s^+\eta$, $D_s^{*+}\eta$, $D_s^+\rho^0$, $D_s^{*+}\rho^0$, $D_s^+\omega$, $D_s^{*+}\omega$	[f]	<	4	$\times 10^{-4}$	CL=90%
Γ_{46}	$D_{s1}(2536)^+$ anything		<	9.5	$\times 10^{-3}$	CL=90%

Charmonium modes

Γ_{47}	$J/\psi(1S)$ anything		(	1.094 ± 0.032)	%	S=1.1
Γ_{48}	$J/\psi(1S)$ (direct) anything		(	7.8 ± 0.4)	$\times 10^{-3}$	S=1.1
Γ_{49}	$\psi(2S)$ anything		(	3.07 ± 0.21)	$\times 10^{-3}$	
Γ_{50}	$\chi_{c1}(1P)$ anything		(	3.86 ± 0.27)	$\times 10^{-3}$	
Γ_{51}	$\chi_{c1}(1P)$ (direct) anything		(	3.24 ± 0.25)	$\times 10^{-3}$	
Γ_{52}	$\chi_{c2}(1P)$ anything		(	1.4 ± 0.4)	$\times 10^{-3}$	S=1.9
Γ_{53}	$\chi_{c2}(1P)$ (direct) anything		(	1.65 ± 0.31)	$\times 10^{-3}$	
Γ_{54}	$\eta_c(1S)$ anything		<	9	$\times 10^{-3}$	CL=90%
Γ_{55}	$KX(3872)\times$ B($X \to D^0\overline{D}^0\pi^0$)		(	1.2 ± 0.4)	$\times 10^{-4}$	
Γ_{56}	$KX(3872)\times$ B($X \to D^{*0}D^0$)		(	8.0 ± 2.2)	$\times 10^{-5}$	
Γ_{57}	$KX(3940)\times$ B($X \to D^{*0}D^0$)		<	6.7	$\times 10^{-5}$	CL=90%
Γ_{58}	$K\chi_{c0}(2P)$, $\chi_{c0} \to \omega J/\psi$	[h]	(	7.1 ± 3.4)	$\times 10^{-5}$	

K* or *K* **modes**

Γ_{59}	$K^{\pm}$ anything	[f]	(	78.9 ± 2.5)	%	
Γ_{60}	K^+ anything		(	66 ± 5)	%	
Γ_{61}	K^- anything		(	13 ± 4)	%	
Γ_{62}	$K^0/\overline{K}^0$ anything	[f]	(	64 ± 4)	%	
Γ_{63}	$K^*(892)^{\pm}$ anything		(	18 ± 6)	%	
Γ_{64}	$K^*(892)^0/\overline{K}^*(892)^0$ anything	[f]	(	14.6 ± 2.6)	%	
Γ_{65}	$K^*(892)\gamma$		(	4.2 ± 0.6)	$\times 10^{-5}$	
Γ_{66}	$\eta K\gamma$		(	8.5 $^{+1.8}_{-1.6}$)	$\times 10^{-6}$	
Γ_{67}	$K_1(1400)\gamma$		<	1.27	$\times 10^{-4}$	CL=90%
Γ_{68}	$K_2^*(1430)\gamma$		(	1.7 $^{+0.6}_{-0.5}$)	$\times 10^{-5}$	
Γ_{69}	$K_2(1770)\gamma$		<	1.2	$\times 10^{-3}$	CL=90%
Γ_{70}	$K_3^*(1780)\gamma$		<	3.7	$\times 10^{-5}$	CL=90%
Γ_{71}	$K_4^*(2045)\gamma$		<	1.0	$\times 10^{-3}$	CL=90%
Γ_{72}	$K\eta'(958)$		(	8.3 ± 1.1)	$\times 10^{-5}$	
Γ_{73}	$K^*(892)\eta'(958)$		(	4.1 ± 1.1)	$\times 10^{-6}$	
Γ_{74}	$K\eta$		<	5.2	$\times 10^{-6}$	CL=90%
Γ_{75}	$K^*(892)\eta$		(	1.8 ± 0.5)	$\times 10^{-5}$	
Γ_{76}	$K\phi\phi$		(	2.3 ± 0.9)	$\times 10^{-6}$	
Γ_{77}	$\overline{b} \to \overline{s}\gamma$		(	3.40 ± 0.21)	$\times 10^{-4}$	
Γ_{78}	$\overline{b} \to \overline{d}\gamma$		(	9.2 ± 3.0)	$\times 10^{-6}$	
Γ_{79}	$\overline{b} \to \overline{s}$gluon		<	6.8	%	CL=90%
Γ_{80}	η anything		(	2.6 $^{+0.5}_{-0.8}$)	$\times 10^{-4}$	
Γ_{81}	η' anything		(	4.2 ± 0.9)	$\times 10^{-4}$	
Γ_{82}	K^+ gluon (charmless)		<	1.87	$\times 10^{-4}$	CL=90%
Γ_{83}	K^0 gluon (charmless)		(	1.9 ± 0.7)	$\times 10^{-4}$	

Light unflavored meson modes

Γ_{84}	$\rho\gamma$		(	1.39 ± 0.25)	$\times 10^{-6}$	S=1.2
Γ_{85}	$\rho/\omega\gamma$		(	1.30 ± 0.23)	$\times 10^{-6}$	S=1.2
Γ_{86}	$\pi^{\pm}$ anything	[f,i]	(	358 ± 7)	%	
Γ_{87}	π^0 anything		(	235 ±11)	%	
Γ_{88}	η anything		(	17.6 ± 1.6)	%	
Γ_{89}	ρ^0 anything		(	21 ± 5)	%	
Γ_{90}	ω anything		<	81	%	CL=90%
Γ_{91}	ϕ anything		(	3.43 ± 0.12)	%	
Γ_{92}	$\phi K^*(892)$		<	2.2	$\times 10^{-5}$	CL=90%
Γ_{93}	$\overline{b} \to \overline{d}$ gluon					
Γ_{94}	π^+ gluon (charmless)		(	3.7 ± 0.8)	$\times 10^{-4}$	

Baryon modes

Γ_{95}	Λ_c^+ / $\overline{\Lambda}_c^-$ anything		(	4.5 ± 1.2)	%	
Γ_{96}	Λ_c^+ anything		<	1.7	%	CL=90%
Γ_{97}	$\overline{\Lambda}_c^-$ anything		<	9	%	CL=90%
Γ_{98}	$\overline{\Lambda}_c^-\ell^+$ anything		<	1.1	$\times 10^{-3}$	CL=90%
Γ_{99}	$\overline{\Lambda}_c^- e^+$ anything		<	2.3	$\times 10^{-3}$	CL=90%
Γ_{100}	$\overline{\Lambda}_c^-\mu^+$ anything		<	1.8	$\times 10^{-3}$	CL=90%
Γ_{101}	$\overline{\Lambda}_c^- p$ anything		(	2.6 ± 0.8)	%	
Γ_{102}	$\overline{\Lambda}_c^- p e^+\nu_e$		<	1.0	$\times 10^{-3}$	CL=90%
Γ_{103}	$\overline{\Sigma}_c^{--}$ anything		(	4.2 ± 2.4)	$\times 10^{-3}$	
Γ_{104}	$\overline{\Sigma}_c^-$ anything		<	9.6	$\times 10^{-3}$	CL=90%
Γ_{105}	$\overline{\Sigma}_c^0$ anything		(	4.6 ± 2.4)	$\times 10^{-3}$	
Γ_{106}	$\overline{\Sigma}_c^0 N(N = p$ or $n)$		<	1.5	$\times 10^{-3}$	CL=90%
Γ_{107}	Ξ_c^0 anything $\times$ B($\Xi_c^0 \to \Xi^-\pi^+$)		(	1.93 ± 0.30)	$\times 10^{-4}$	S=1.1
Γ_{108}	Ξ_c^+ anything $\times$ B($\Xi_c^+ \to \Xi^-\pi^+\pi^+$)		(	4.5 $^{+1.3}_{-1.2}$)	$\times 10^{-4}$	
Γ_{109}	$p/\overline{p}$ anything	[f]	(	8.0 ± 0.4)	%	
Γ_{110}	$p/\overline{p}$ (direct) anything	[f]	(	5.5 ± 0.5)	%	
Γ_{111}	$\Lambda/\overline{\Lambda}$ anything	[f]	(	4.0 ± 0.5)	%	
Γ_{112}	Λ anything					
Γ_{113}	$\overline{\Lambda}$ anything					
Γ_{114}	$\Xi^-/\overline{\Xi}^+$ anything	[f]	(	2.7 ± 0.6)	$\times 10^{-3}$	
Γ_{115}	baryons anything		(	6.8 ± 0.6)	%	
Γ_{116}	$p\overline{p}$ anything		(	2.47 ± 0.23)	%	
Γ_{117}	$\Lambda\overline{p}/\overline{\Lambda}p$ anything	[f]	(	2.5 ± 0.4)	%	
Γ_{118}	$\Lambda\overline{\Lambda}$ anything		<	5	$\times 10^{-3}$	CL=90%

Lepton Family number (*LF*) violating modes or $\Delta B = 1$ weak neutral current (*B1*) modes

Γ_{119}	$s e^+ e^-$	*B1*		(	4.7 ± 1.3)	$\times 10^{-6}$	
Γ_{120}	$s\mu^+\mu^-$	*B1*		(	4.3 ± 1.2)	$\times 10^{-6}$	
Γ_{121}	$s\ell^+\ell^-$	*B1*	[b]	(	4.5 ± 1.0)	$\times 10^{-6}$	
Γ_{122}	$\pi\ell^+\ell^-$	*B1*		<	5.9	$\times 10^{-8}$	CL=90%
Γ_{123}	$\pi e^+ e^-$			<	1.10	$\times 10^{-7}$	CL=90%
Γ_{124}	$\pi\mu^+\mu^-$			<	5.0	$\times 10^{-8}$	CL=90%
Γ_{125}	$K e^+ e^-$	*B1*		(	4.4 ± 0.6)	$\times 10^{-7}$	
Γ_{126}	$K^*(892) e^+ e^-$	*B1*		(	1.19 ± 0.20)	$\times 10^{-6}$	S=1.2
Γ_{127}	$K\mu^+\mu^-$	*B1*		(	4.4 ± 0.4)	$\times 10^{-7}$	
Γ_{128}	$K^*(892)\mu^+\mu^-$	*B1*		(	1.06 ± 0.09)	$\times 10^{-6}$	
Γ_{129}	$K\ell^+\ell^-$	*B1*		(	4.8 ± 0.4)	$\times 10^{-7}$	
Γ_{130}	$K^*(892)\ell^+\ell^-$	*B1*		(	1.05 ± 0.10)	$\times 10^{-6}$	
Γ_{131}	$K\nu\overline{\nu}$	*B1*		<	1.7	$\times 10^{-5}$	CL=90%
Γ_{132}	$K^*\nu\overline{\nu}$	*B1*		<	7.6	$\times 10^{-5}$	CL=90%
Γ_{133}	$s e^{\pm}\mu^{\mp}$	*LF*	[f]	<	2.2	$\times 10^{-5}$	CL=90%
Γ_{134}	$\pi e^{\pm}\mu^{\mp}$	*LF*		<	9.2	$\times 10^{-8}$	CL=90%
Γ_{135}	$\rho e^{\pm}\mu^{\mp}$	*LF*		<	3.2	$\times 10^{-6}$	CL=90%
Γ_{136}	$K e^{\pm}\mu^{\mp}$	*LF*		<	3.8	$\times 10^{-8}$	CL=90%
Γ_{137}	$K^*(892) e^{\pm}\mu^{\mp}$	*LF*		<	5.1	$\times 10^{-7}$	CL=90%

[a] These values are model dependent.

[b] An ℓ indicates an e or a μ mode, not a sum over these modes.

[c] Here "anything" means at least one particle observed.

[d] This is a B($B^0 \to D^{*-}\ell^+\nu_\ell$) value.

[e] D^{**} stands for the sum of the $D(1\,^1P_1)$, $D(1\,^3P_0)$, $D(1\,^3P_1)$, $D(1\,^3P_2)$, $D(2\,^1S_0)$, and $D(2\,^1S_1)$ resonances.

[f] The value is for the sum of the charge states or particle/antiparticle states indicated.

[g] $D^{(*)}\overline{D}^{(*)}$ stands for the sum of $D^*\overline{D}^*$, $D^*\overline{D}$, $D\overline{D}^*$, and $D\overline{D}$.

[h] $X(3915)$ denotes a near-threshold enhancement in the $\omega J/\psi$ mass spectrum.

[i] Inclusive branching fractions have a multiplicity definition and can be greater than 100%.

$B^{\pm}/B^0$ ADMIXTURE BRANCHING RATIOS

$\Gamma(e^+\nu_e \text{anything})/\Gamma_{\text{total}}$ Γ_1/Γ

These branching fraction values are model dependent.

"OUR EVALUATION" is an average using rescaled values of the data listed below. The average and rescaling were performed by the Heavy Flavor Averaging Group (HFAG) and are described at http://www.slac.stanford.edu/xorg/hfag/. The averaging/rescaling procedure takes into account correlations between the measurements.

VALUE	DOCUMENT ID		TECN	COMMENT
The data in this block is included in the average printed for a previous datablock.				
0.1086±0.0016 OUR EVALUATION				
0.1044±0.0025 OUR AVERAGE Error includes scale factor of 1.5. See the ideogram below.				
0.1028±0.0018±0.0024	[1] URQUIJO	07	BELL	$e^+e^- \to \Upsilon(4S)$
0.0996±0.0019±0.0032	[2] AUBERT,B	06Y	BABR	$e^+e^- \to \Upsilon(4S)$
0.1091±0.0009±0.0024	[3] MAHMOOD	04	CLEO	$e^+e^- \to \Upsilon(4S)$
0.097 ±0.005 ±0.004	[4] ALBRECHT	93H	ARG	$e^+e^- \to \Upsilon(4S)$

• • • We do not use the following data for averages, fits, limits, etc. • • •

0.1085±0.0021±0.0036	[5] OKABE	05	BELL	Repl. by URQUIJO 07	
0.1083±0.0016±0.0006	[6] AUBERT	04X	BABR	Repl. by AUBERT,B 06Y	
0.1036±0.0006±0.0023	[7] AUBERT,B	04A	BABR	$e^+e^- \to \Upsilon(4S)$	
0.1087±0.0018±0.0030	[8] AUBERT	03	BABR	Repl. by AUBERT 04X	
0.109 ±0.0012±0.0049	[9] ABE	02Y	BELL	Repl. by OKABE 05	
0.1049±0.0017±0.0043	[10] BARISH	96B	CLE2	Repl. by MAHMOOD 04	
0.100 ±0.004 ±0.003	[11] YANAGISAWA	91	CSB2	$e^+e^- \to \Upsilon(4S)$	
0.103 ±0.006 ±0.002	[12] ALBRECHT	90H	ARG	$e^+e^- \to \Upsilon(4S)$	
0.117 ±0.004 ±0.010	[13] WACHS	89	CBAL	Direct e at $\Upsilon(4S)$	
0.120 ±0.007 ±0.005	CHEN	84	CLEO	Direct e at $\Upsilon(4S)$	
0.132 ±0.008 ±0.014	[14] KLOPFEN...	83B	CUSB	Direct e at $\Upsilon(4S)$	

[1] URQUIJO 07 report a measurement of (10.07 ± 0.18 ± 0.21)% for the partial branching fraction of $B \to e\nu_e X_c$ decay with electron energy above 0.6 GeV. We converted the result to $B \to e\nu_e X$ branching fraction.

[2] The measurements are obtained for charged and neutral B mesons partial rates of semileptonic decay to electrons with momentum above 0.6 GeV/c in the B rest frame. The best precision on the ratio is achieved for a momentum threshold of 1.0 GeV: $B(B^+ \to e^+\nu_e X) / B(B^0 \to e^+\nu_e X) = 1.074 \pm 0.041 \pm 0.026$.

[3] Uses charge and angular correlations in $\Upsilon(4S)$ events with a high-momentum lepton and an additional electron.

[4] ALBRECHT 93H analysis performed using tagged semileptonic decays of the B. This technique is almost model independent for the lepton branching ratio.

[5] The measurements are obtained for charged and neutral B mesons partial rates of semileptonic decay to electrons with momentum above 0.6 GeV/c in the B rest frame, and their ratio of $B(B^+ \to e^+\nu_e X)/B(B^0 \to e^+\nu_e X) = 1.08 \pm 0.05 \pm 0.02$.

[6] The semileptonic branching ratio, $|V_{cb}|$ and other heavy-quark parameters are determined from a simultaneous fit to moments of the hadronic-mass and lepton-energy distribution.

[7] Uses the high-momentum lepton tag method and requires the electron energy above 0.6 GeV.

[8] Uses the high-momentum lepton tag method. They also report $|V_{cb}| = 0.0423 \pm 0.0007(\text{exp}) \pm 0.0020(\text{theo.})$.

[9] Uses the high-momentum lepton tag method. ABE 02Y also reports $|V_{cb}| = 0.0408 \pm 0.0010(\text{exp}) \pm 0.0025(\text{theo.})$. The second error is due to uncertainties of theoretical inputs.

[10] BARISH 96B analysis performed using tagged semileptonic decays of the B. This technique is almost model independent for the lepton branching ratio.

[11] YANAGISAWA 91 also measures an average semileptonic branching ratio at the $\Upsilon(5S)$ of 9.6–10.5% depending on assumptions about the relative production of different B meson species.

[12] ALBRECHT 90H uses the model of ALTARELLI 82 to correct over all lepton momenta. 0.099 ± 0.006 is obtained using ISGUR 89B.

[13] Using data above $p(e) = 2.4$ GeV, WACHS 89 determine $\sigma(B \to e\nu\text{up})/\sigma(B \to e\nu\text{charm}) < 0.065$ at 90% CL.

[14] Ratio $\sigma(b \to e\nu\text{up})/\sigma(b \to e\nu\text{charm}) < 0.055$ at CL = 90%.

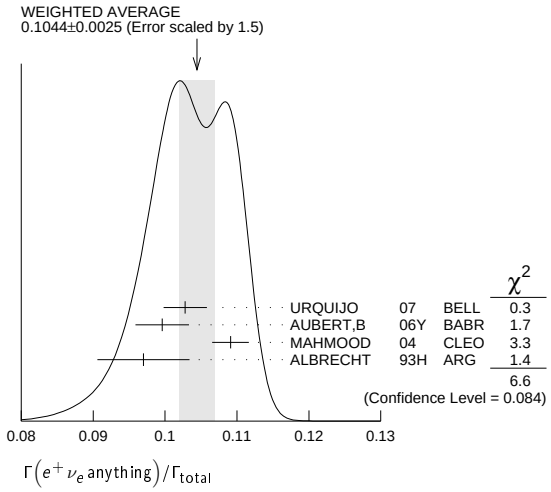

$\Gamma(\overline{p}e^+\nu_e \text{ anything})/\Gamma_{\text{total}}$ — Γ_2/Γ

VALUE	CL%	DOCUMENT ID		TECN	COMMENT
<5.9 ×10⁻⁴	90	[1] ADAM	03B	CLE2	$e^+e^- \to \Upsilon(4S)$

• • • We do not use the following data for averages, fits, limits, etc. • • •

<0.0016	90	ALBRECHT	90H	ARG	$e^+e^- \to \Upsilon(4S)$

[1] Based on $V-A$ model.

$\Gamma(\mu^+\nu_\mu \text{anything})/\Gamma_{\text{total}}$ — Γ_3/Γ

These branching fraction values are model dependent.

"OUR EVALUATION" is an average using rescaled values of the data listed below. The average and rescaling were performed by the Heavy Flavor Averaging Group (HFAG) and are described at http://www.slac.stanford.edu/xorg/hfag/. The averaging/rescaling procedure takes into account correlations between the measurements.

VALUE	DOCUMENT ID	TECN	COMMENT
The data in this block is included in the average printed for a previous datablock.			

0.1086±0.0016 OUR EVALUATION

• • • We do not use the following data for averages, fits, limits, etc. • • •

0.100 ±0.006 ±0.002	[1] ALBRECHT	90H	ARG	$e^+e^- \to \Upsilon(4S)$	
0.108 ±0.006 ±0.01	CHEN	84	CLEO	Direct μ at $\Upsilon(4S)$	
0.112 ±0.009 ±0.01	LEVMAN	84	CUSB	Direct μ at $\Upsilon(4S)$	

[1] ALBRECHT 90H uses the model of ALTARELLI 82 to correct over all lepton momenta. 0.097 ± 0.006 is obtained using ISGUR 89B.

$\Gamma(\ell^+\nu_\ell \text{anything})/\Gamma_{\text{total}}$ — Γ_4/Γ

These branching fraction values are model dependent.

"OUR EVALUATION" is an average using rescaled values of the data listed below. The average and rescaling were performed by the Heavy Flavor Averaging Group (HFAG) and are described at http://www.slac.stanford.edu/xorg/hfag/. The averaging/rescaling procedure takes into account correlations between the measurements.

VALUE	DOCUMENT ID	TECN	COMMENT
0.1086±0.0016 OUR EVALUATION			
0.1044±0.0025 OUR AVERAGE Includes data from the 2 datablocks that follow this one. Error includes scale factor of 1.5. See the ideogram below.			

• • • We do not use the following data for averages, fits, limits, etc. • • •

0.108 ±0.002 ±0.0056	[1] HENDERSON	92	CLEO	$e^+e^- \to \Upsilon(4S)$	

[1] HENDERSON 92 measurement employs e and μ. The systematic error contains 0.004 in quadrature from model dependence. The authors average a variation of the Isgur, Scora, Grinstein, and Wise model with that of the Altarelli-Cabibbo-Corbò-Maiani-Martinelli model for semileptonic decays to correct the acceptance.

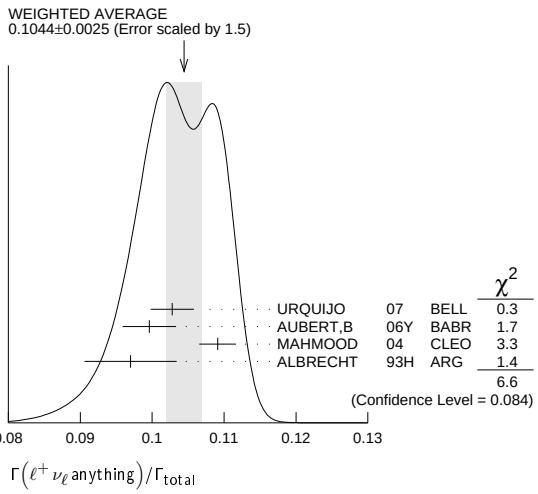

$\Gamma(D^-\ell^+\nu_\ell \text{anything})/\Gamma(\ell^+\nu_\ell \text{anything})$ — Γ_5/Γ_4

$\ell = e$ or μ.

VALUE	DOCUMENT ID		TECN	COMMENT
0.26±0.07±0.04	[1] FULTON	91	CLEO	$e^+e^- \to \Upsilon(4S)$

[1] FULTON 91 uses $B(D^+ \to K^-\pi^+\pi^+) = (9.1 \pm 1.3 \pm 0.4)\%$ as measured by MARK III.

$\Gamma(\overline{D}^0\ell^+\nu_\ell \text{anything})/\Gamma(\ell^+\nu_\ell \text{anything})$ — Γ_6/Γ_4

$\ell = e$ or μ.

VALUE	DOCUMENT ID		TECN	COMMENT
0.67±0.09±0.10	[1] FULTON	91	CLEO	$e^+e^- \to \Upsilon(4S)$

[1] FULTON 91 uses $B(D^0 \to K^-\pi^+) = (4.2 \pm 0.4 \pm 0.4)\%$ as measured by MARK III.

$\Gamma(\overline{D}\ell^+\nu_\ell)/\Gamma(\ell^+\nu_\ell \text{anything})$ — Γ_7/Γ_4

VALUE	DOCUMENT ID		TECN	COMMENT
0.223±0.006±0.009	[1] AUBERT	10	BABR	$e^+e^- \to \Upsilon(4S)$

[1] Uses a fully reconstructed B meson as a tag on the recoil side.

$\Gamma(\overline{D}\tau^+\nu_\tau)/\Gamma(\overline{D}\ell^+\nu_\ell)$ — Γ_8/Γ_7

VALUE (units 10^{-2})	DOCUMENT ID		TECN	COMMENT
44.0 ± 5.8±4.2	[1,2] LEES	12D	BABR	$e^+e^- \to \Upsilon(4S)$

• • • We do not use the following data for averages, fits, limits, etc. • • •

4.16±11.7±5.2	[1] AUBERT	08N	BABR	Repl. by LEES 12D

[1] Uses a fully reconstructed B meson as a tag on the recoil side.

[2] Uses $\tau^+ \to e^+\nu_e\overline{\nu}_\tau$ and $\tau^+ \to \mu^+\nu_\mu\overline{\nu}_\tau$ and e^+ or μ^+ as ℓ^+. Obtained from simultaneous fit to B+ and B0 assuming isospin symmetry.

$\Gamma(D^{*-}\ell^+\nu_\ell \text{anything})/\Gamma_{\text{total}}$ — Γ_9/Γ

VALUE (units 10^{-2})	DOCUMENT ID		TECN	COMMENT
0.67±0.08±0.10	ABDALLAH	04D	DLPH	$e^+e^- \to Z^0$

• • • We do not use the following data for averages, fits, limits, etc. • • •

0.6 ±0.3 ±0.1	[1] BARISH	95	CLE2	$e^+e^- \to \Upsilon(4S)$	

[1] BARISH 95 use $B(D^0 \to K^-\pi^+) = (3.91 \pm 0.08 \pm 0.17)\%$ and $B(D^{*+} \to D^0\pi^+) = (68.1 \pm 1.0 \pm 1.3)\%$.

$\Gamma(D^{*0}\ell^+\nu_\ell\text{anything})/\Gamma_{\text{total}}$ Γ_{10}/Γ

VALUE (units 10^{-2})	DOCUMENT ID		TECN	COMMENT
• • • We do not use the following data for averages, fits, limits, etc. • • •				
$0.6\pm0.6\pm0.1$	[1] BARISH	95	CLE2	$e^+e^- \to \Upsilon(4S)$

[1] BARISH 95 use $B(D^0 \to K^-\pi^+) = (3.91 \pm 0.08 \pm 0.17)\%$, $B(D^{*+} \to D^0\pi^+) = (68.1 \pm 1.0 \pm 1.3)\%$, $B(D^{*0} \to D^0\pi^0) = (63.6 \pm 2.3 \pm 3.3)\%$.

$\Gamma(D^*\tau^+\nu_\tau)/\Gamma(D^*\ell^+\nu_\ell)$ Γ_{12}/Γ_{11}

VALUE (units 10^{-2})	DOCUMENT ID		TECN	COMMENT
$33.2\pm2.4\pm1.8$	[1] LEES	12D	BABR	$e^+e^- \to \Upsilon(4S)$
• • • We do not use the following data for averages, fits, limits, etc. • • •				
$29.7\pm5.6\pm1.8$	[2] AUBERT	08N	BABR	Repl. by LEES 12D

[1] Uses $\tau^+ \to e^+\nu_e\overline{\nu}_\tau$ and $\tau^+ \to \mu^+\nu_\mu\overline{\nu}_\tau$ and e^+ or μ^+ as ℓ^+. Obtained from simultaneous fit to B+ and B0 assuming isospin symmetry. Uses a fully reconstructed B meson as a tag on the recoil side.

[2] Uses a fully reconstructed B meson as a tag on the recoil side. The results are normalized to the B^+ decay rate.

$\Gamma(\overline{D}^{**}\ell^+\nu_\ell)/\Gamma_{\text{total}}$ Γ_{13}/Γ

D^{**} stands for the sum of the $D(1\,^1P_1)$, $D(1\,^3P_0)$, $D(1\,^3P_1)$, $D(1\,^3P_2)$, $D(2\,^1S_0)$, and $D(2\,^1S_1)$ resonances. $\ell = e$ or μ, not sum over e and μ modes.

VALUE	CL%	EVTS	DOCUMENT ID		TECN	COMMENT
$0.027\pm0.005\pm0.005$		63	[1] ALBRECHT	93	ARG	$e^+e^- \to \Upsilon(4S)$
• • • We do not use the following data for averages, fits, limits, etc. • • •						
<0.028	95		[2] BARISH	95	CLE2	$e^+e^- \to \Upsilon(4S)$

[1] ALBRECHT 93 assumes the GISW model to correct for unseen modes. Using the BHKT model, the result becomes $0.023 \pm 0.006 \pm 0.004$. Assumes $B(D^{*+} \to D^0\pi^+) = 68.1\%$, $B(D^0 \to K^-\pi^+) = 3.65\%$, $B(D^0 \to K^-\pi^+\pi^-\pi^+) = 7.5\%$. We have taken their average e and μ value.

[2] BARISH 95 use $B(D^0 \to K^-\pi^+) = (3.91 \pm 0.08 \pm 0.17)\%$, assume all nonresonant channels are zero, and use GISW model for relative abundances of D^{**} states.

$\Gamma(\overline{D}_1(2420)\ell^+\nu_\ell\text{anything})/\Gamma_{\text{total}}$ Γ_{14}/Γ

VALUE	DOCUMENT ID		TECN	COMMENT
0.0038 ± 0.0013 OUR AVERAGE	Error includes scale factor of 2.4.			
0.0033 ± 0.0006	[1] ABAZOV	05O	D0	$p\overline{p}$ at 1.96 TeV
0.0074 ± 0.0016	[2] BUSKULIC	97B	ALEP	$e^+e^- \to Z$
• • • We do not use the following data for averages, fits, limits, etc. • • •				
seen	[3] BUSKULIC	95B	ALEP	Repl. by BUSKULIC 97B

[1] Assumes $B(D_1 \to D^*\pi) = 1$, $B(D_1 \to D^*\pi^\pm) = 2/3$, and $B(b \to B) = 0.397$.

[2] BUSKULIC 97B assumes $B(D_1(2420) \to D^*\pi) = 1$, $B(D_1(2420) \to D^*\pi^\pm) = 2/3$, and $B(b \to B) = 0.378 \pm 0.022$.

[3] BUSKULIC 95B reports $f_B \times B(B \to \overline{D}_1(2420)^0\ell^+\nu_\ell\text{anything}) \times B(\overline{D}_1(2420)^0 \to \overline{D}^*(2010)^-\pi^+) = (2.04 \pm 0.58 \pm 0.34)10^{-3}$, where f_B is the production fraction for a single B charge state.

$[\Gamma(D\pi\ell^+\nu_\ell\text{anything}) + \Gamma(D^*\pi\ell^+\nu_\ell\text{anything})]/\Gamma_{\text{total}}$ Γ_{15}/Γ

VALUE	DOCUMENT ID		TECN	COMMENT
$0.026\ \pm0.005$ OUR AVERAGE	Error includes scale factor of 1.5.			
$0.0340\pm0.0052\pm0.0032$	[1] ABREU	00R	DLPH	$e^+e^- \to Z$
$0.0226\pm0.0029\pm0.0033$	[2] BUSKULIC	97B	ALEP	$e^+e^- \to Z$

[1] Assumes no contribution from B_s and b baryons. Further assumes contributions from single pion ($D\pi$ and $D^*\pi$) states only, allowing isospin conservation to relate the relative π^0 and π^+ rates.

[2] BUSKULIC 97B assumes $B(b \to B) = 0.378 \pm 0.022$ and uses isospin invariance by assuming that all observed $D^0\pi^+$, $D^{*0}\pi^+$, $D^+\pi^-$, and $D^{*+}\pi^-$ are from D^{**} states. A correction has been applied to account for the production of B_s^0 and Λ_b^0.

$\Gamma(D\pi\ell^+\nu_\ell\text{anything})/\Gamma_{\text{total}}$ Γ_{16}/Γ

VALUE	DOCUMENT ID	TECN	COMMENT
0.0154 ± 0.0061	ABREU 00R	DLPH	$e^+e^- \to Z$

$\Gamma(D^*\pi\ell^+\nu_\ell\text{anything})/\Gamma_{\text{total}}$ Γ_{17}/Γ

VALUE	DOCUMENT ID	TECN	COMMENT
0.0186 ± 0.0038	ABREU 00R	DLPH	$e^+e^- \to Z$

$\Gamma(\overline{D}_2^*(2460)\ell^+\nu_\ell\text{anything})/\Gamma_{\text{total}}$ Γ_{18}/Γ

VALUE	CL%	DOCUMENT ID		TECN	COMMENT
0.0044 ± 0.0016		[1] ABAZOV	05O	D0	$p\overline{p}$ at 1.96 TeV
• • • We do not use the following data for averages, fits, limits, etc. • • •					
<0.0065	95	[2] BUSKULIC	97B	ALEP	$e^+e^- \to Z$
not seen		[3] BUSKULIC	95B	ALEP	$e^+e^- \to Z$

[1] Assumes $B(D_2^* \to D^*\pi^\pm) = 0.30 \pm 0.06$ and $B(b \to B) = 0.397$.

[2] A revised number based on BUSKULIC 97B which assumes $B(D_2^*(2460) \to D^*\pi^\pm) = 0.20$ and $B(b \to B) = 0.378 \pm 0.022$.

[3] BUSKULIC 95B reports $f_B \times B(B \to \overline{D}_2^*(2460)^0\ell^+\nu_\ell\text{anything}) \times B(\overline{D}_2^*(2460)^0 \to \overline{D}^*(2010)^-\pi^+) \leq 0.81 \times 10^{-3}$ at CL=95%, where f_B is the production fraction for a single B charge state.

$\frac{\Gamma(B \to \overline{D}_2^*(2460)\ell^+\nu_\ell\text{anything}) \times B(D_2^*(2460) \to D^{*-}\pi^+)}{\Gamma(B \to D_1(2420)\ell^+\nu_\ell\text{anything}) \times B(D_1(2420) \to D^{*-}\pi^+)}$

VALUE	DOCUMENT ID		TECN	COMMENT
$0.39\pm0.09\pm0.12$	ABAZOV	05O	D0	$p\overline{p}$ at 1.96 TeV

$\Gamma(D^{*-}\pi^+\ell^+\nu_\ell\text{anything})/\Gamma_{\text{total}}$ Γ_{19}/Γ

Includes resonant and nonresonant contributions.

VALUE (units 10^{-3})	DOCUMENT ID		TECN	COMMENT
$10.0\pm2.7\pm2.1$	[1] BUSKULIC	95B	ALEP	$e^+e^- \to Z$

[1] BUSKULIC 95B reports $f_B \times B(B \to \overline{D}^*(2010)^-\pi^+\ell^+\nu_\ell\text{anything}) = (3.7 \pm 1.0 \pm 0.7)10^{-3}$. Above value assumes $f_B = 0.37 \pm 0.03$.

$\Gamma(D_s^-\ell^+\nu_\ell\text{anything})/\Gamma_{\text{total}}$ Γ_{20}/Γ

VALUE	CL%	DOCUMENT ID		TECN	COMMENT
$<7\times10^{-3}$	90	[1] ALBRECHT	93E	ARG	$e^+e^- \to \Upsilon(4S)$

[1] ALBRECHT 93E reports < 0.012 from a measurement of $[\Gamma(B \to D_s^-\ell^+\nu_\ell\text{anything})/\Gamma_{\text{total}}] \times [B(D_s^+ \to \phi\pi^+)]$ assuming $B(D_s^+ \to \phi\pi^+) = 0.027$, which we rescale to our best value $B(D_s^+ \to \phi\pi^+) = 4.5 \times 10^{-2}$.

$\Gamma(D_s^-\ell^+\nu_\ell K^+\text{anything})/\Gamma_{\text{total}}$ Γ_{21}/Γ

VALUE	CL%	DOCUMENT ID		TECN	COMMENT
$<5\times10^{-3}$	90	[1] ALBRECHT	93E	ARG	$e^+e^- \to \Upsilon(4S)$

[1] ALBRECHT 93E reports < 0.008 from a measurement of $[\Gamma(B \to D_s^-\ell^+\nu_\ell K^+\text{anything})/\Gamma_{\text{total}}] \times [B(D_s^+ \to \phi\pi^+)]$ assuming $B(D_s^+ \to \phi\pi^+) = 0.027$, which we rescale to our best value $B(D_s^+ \to \phi\pi^+) = 4.5 \times 10^{-2}$.

$\Gamma(D_s^-\ell^+\nu_\ell K^0\text{anything})/\Gamma_{\text{total}}$ Γ_{22}/Γ

VALUE	CL%	DOCUMENT ID		TECN	COMMENT
$<7\times10^{-3}$	90	[1] ALBRECHT	93E	ARG	$e^+e^- \to \Upsilon(4S)$

[1] ALBRECHT 93E reports < 0.012 from a measurement of $[\Gamma(B \to D_s^-\ell^+\nu_\ell K^0\text{anything})/\Gamma_{\text{total}}] \times [B(D_s^+ \to \phi\pi^+)]$ assuming $B(D_s^+ \to \phi\pi^+) = 0.027$, which we rescale to our best value $B(D_s^+ \to \phi\pi^+) = 4.5 \times 10^{-2}$.

$\Gamma(X_c\ell^+\nu_\ell)/\Gamma_{\text{total}}$ Γ_{23}/Γ

"OUR EVALUATION" is an average using rescaled values of the data listed below. The average and rescaling were performed by the Heavy Flavor Averaging Group (HFAG) and are described at http://www.slac.stanford.edu/xorg/hfag/. The averaging/rescaling procedure takes into account correlations between the measurements.

VALUE	DOCUMENT ID		TECN	COMMENT
0.1065 ± 0.0016 OUR EVALUATION				
0.1058 ± 0.0015 OUR AVERAGE				
$0.1064\pm0.0017\pm0.0006$	[1] AUBERT	10A	BABR	$e^+e^- \to \Upsilon(4S)$
$0.1044\pm0.0019\pm0.0022$	[2] URQUIJO	07	BELL	$e^+e^- \to \Upsilon(4S)$
• • • We do not use the following data for averages, fits, limits, etc. • • •				
$0.1061\pm0.0016\pm0.0006$	[3] AUBERT	04X	BABR	Repl. by AUBERT 10A

[1] Obtained from a combined fit to the moments of observed spectra in inclusive $B \to X_c\ell^+\nu_\ell$ decay.

[2] Measured the independent B^+ and B^0 partial branching fractions with electron energy above 0.4 GeV.

[3] The semileptonic branching ratio, $|V_{cb}|$ and other heavy-quark parameters are determined from a simultaneous fit to moments of the hadronic-mass and lepton-energy distribution.

$\Gamma(X_u\ell^+\nu_\ell)/\Gamma_{\text{total}}$ Γ_{24}/Γ

"OUR EVALUATION" is an average using rescaled values of the data listed below. The average and rescaling were performed by the Heavy Flavor Averaging Group (HFAG) and are described at http://www.slac.stanford.edu/xorg/hfag/. The averaging/rescaling procedure takes into account correlations between the measurements.

VALUE (units 10^{-3})	DOCUMENT ID		TECN	COMMENT
$2.14\ \pm0.31$ OUR EVALUATION				
$2.01\ \pm0.15\ \pm0.25$	[1] LEES	12R	BABR	$e^+e^- \to \Upsilon(4S)$
$2.27\ \pm0.26\ ^{+0.37}_{-0.33}$	[2] AUBERT	06H	BABR	$e^+e^- \to \Upsilon(4S)$
$2.53\ \pm0.24\ \pm0.24$	[3] AUBERT,B	05X	BABR	$e^+e^- \to \Upsilon(4S)$
$2.80\ \pm0.52\ \pm0.41$	[4] LIMOSANI	05	BELL	$e^+e^- \to \Upsilon(4S)$
$1.77\ \pm0.29\ \pm0.38$	[5] BORNHEIM	02	CLE2	$e^+e^- \to \Upsilon(4S)$
• • • We do not use the following data for averages, fits, limits, etc. • • •				
$1.963\pm0.173\pm0.159$	[6] URQUIJO	10	BELL	$e^+e^- \to \Upsilon(4S)$
$1.18\ \pm0.09\ \pm0.07$	[7] AUBERT	08AS	BABR	Repl. by LEES 12R
$2.24\ \pm0.27\ \pm0.47$	[8,9] AUBERT	04I	BABR	Repl. by AUBERT,B 05X

[1] Measures several partial branching fractions in different phase space regions. The most precise result on the full branching fraction is obtained in the region for lepton momentum in B rest frame $p_\ell^* > 1$ GeV/c, where the measured partial branching fraction is $\Delta B = (1.80 \pm 0.13 \pm 0.15) \times 10^{-3}$. The acceptance in that region is reported in a private communication by the Authors to be 0.894. The corresponding $|V_{ub}|$ from the BLNP method is $(4.28 \pm 0.15 \pm 0.18 \pm 0.19) \times 10^{-3}$, where the last uncertainty comes from theoretical prediction.

[2] Obtained from the partial rate $\Delta B = (0.572 \pm 0.041 \pm 0.065) \times 10^{-3}$ for the electron momentum interval of 2.0–2.6 GeV/c based on BLNP method.

[3] Determined from the partial rate $\Delta B = (4.41 \pm 0.42 \pm 0.42) \times 10^{-4}$ measured for electron energy > 2 GeV and hadronic mass squared < 3.5 GeV^2, and calculated acceptance 0.174 in that region. The V_{ub} is measured as $(4.41 \pm 0.30^{+0.65}_{-0.47} \pm 0.28) \times 10^{-3}$.

[4] Uses electrons in the momentum interval 1.9–2.6 GeV/c in the center-of-mass frame. The V_{ub} is found to be $(5.08 \pm 0.47^{+0.49}_{-0.48}) \times 10^{-3}$.

[5] BORNHEIM 02 uses the observed yield of leptons from semileptonic B decays in the end-point momentum interval 2.2–2.6 GeV/c with recent CLEO-2 data on $B \to X_s\gamma$. The V_{ub} is found to be $(4.08 \pm 0.34 \pm 0.53) \times 10^{-3}$.

[6] Uses a multivariate analysis method and requires lepton momentum in the B rest frame, $p_l^{*B} > 1.0$ GeV/c.

[7] Measures several partial branching fractions in different phase space regions. The most precise result is obtained in the region for hadronic mass $M_X < 1.55$ GeV/c^2, and is $\Delta B = (1.18 \pm 0.09 \pm 0.07) \times 10^{-3}$. The corresponding $|V_{ub}|$ from the BLNP method is $(4.27 \pm 0.16 \pm 0.13 \pm 0.30) \times 10^{-3}$, where the last uncertainty comes from the theoretical prediction of the partial rate in the given phase-space region.

[8] Used BaBar measurement of Semileptonic branching fraction $B(B \to X \ell \nu_\ell) = (10.87 \pm 0.18 \pm 0.30)\%$ to convert the ratio of rates to branching fraction.

[9] The third error includes the systematics and theoretical errors summed in quadrature.

$\Gamma(X_u \ell^+ \nu_\ell)/\Gamma(\ell^+ \nu_\ell \text{anything})$ Γ_{24}/Γ_4

ℓ denotes e or μ, not the sum. These experiments measure this ratio in very limited momentum intervals.

VALUE (units 10^{-2})	CL%	EVTS	DOCUMENT ID		TECN	COMMENT
2.06±0.25±0.42			[1] AUBERT	04I	BABR	$e^+e^- \to \Upsilon(4S)$
• • • We do not use the following data for averages, fits, limits, etc. • • •						
			[2] ALBRECHT	94C	ARG	$e^+e^- \to \Upsilon(4S)$
		107	[3] BARTELT	93B	CLE2	$e^+e^- \to \Upsilon(4S)$
		77	[4] ALBRECHT	91C	ARG	$e^+e^- \to \Upsilon(4S)$
		41	[5] ALBRECHT	90	ARG	$e^+e^- \to \Upsilon(4S)$
		76	[6] FULTON	90	CLEO	$e^+e^- \to \Upsilon(4S)$
<4.0	90		[7] BEHRENDS	87	CLEO	$e^+e^- \to \Upsilon(4S)$
<4.0	90		CHEN	84	CLEO	Direct e at $\Upsilon(4S)$
<5.5	90		KLOPFEN...	83B	CUSB	Direct e at $\Upsilon(4S)$

[1] The third error includes the systematics and theoretical errors summed in quadrature.

[2] ALBRECHT 94C find $\Gamma(b \to c)/\Gamma(b \to \text{all}) = 0.99 \pm 0.02 \pm 0.04$.

[3] BARTELT 93B (CLEO II) measures an excess of $107 \pm 15 \pm 11$ leptons in the lepton momentum interval 2.3–2.6 GeV/c which is attributed to $b \to u\ell\nu_\ell$. This corresponds to a model-dependent partial branching ratio ΔB_{ub} between $(1.15 \pm 0.16 \pm 0.15) \times 10^{-4}$, as evaluated using the KS model (KOERNER 88), and $(1.54 \pm 0.22 \pm 0.20) \times 10^{-4}$ using the ACCMM model (ARTUSO 93). The corresponding values of $|V_{ub}|/|V_{cb}|$ are 0.056 ± 0.006 and 0.076 ± 0.008, respectively.

[4] ALBRECHT 91C result supersedes ALBRECHT 90. Two events are fully reconstructed providing evidence for the $b \to u$ transition. Using the model of ALTARELLI 82, they obtain $|V_{ub}/V_{cb}| = 0.11 \pm 0.012$ from 77 leptons in the 2.3–2.6 GeV momentum range.

[5] ALBRECHT 90 observes 41 ± 10 excess e and μ (lepton) events in the momentum interval $p = 2.3$–2.6 GeV signaling the presence of the $b \to u$ transition. The events correspond to a model-dependent measurement of $|V_{ub}/V_{cb}| = 0.10 \pm 0.01$.

[6] FULTON 90 observe 76 ± 20 excess e and μ (lepton) events in the momentum interval $p = 2.4$–2.6 GeV signaling the presence of the $b \to u$ transition. The average branching ratio, $(1.8 \pm 0.4 \pm 0.3) \times 10^{-4}$, corresponds to a model-dependent measurement of approximately $|V_{ub}/V_{cb}| = 0.1$ using $B(b \to c\ell\nu) = 10.2 \pm 0.2 \pm 0.7\%$.

[7] The quoted possible limits range from 0.018 to 0.04 for the ratio, depending on which model or momentum range is chosen. We select the most conservative limit they have calculated. This corresponds to a limit on $|V_{ub}|/|V_{cb}| < 0.20$. While the endpoint technique employed is more robust than their previous results in CHEN 84, these results do not provide a numerical improvement in the limit.

$\Gamma(K^+ \ell^+ \nu_\ell \text{anything})/\Gamma(\ell^+ \nu_\ell \text{anything})$ Γ_{25}/Γ_4

ℓ denotes e or μ, not the sum.

VALUE	DOCUMENT ID		TECN	COMMENT
0.58 ±0.05 OUR AVERAGE				
0.594±0.021±0.056	ALBRECHT	94C	ARG	$e^+e^- \to \Upsilon(4S)$
0.54 ±0.07 ±0.06	[1] ALAM	87B	CLEO	$e^+e^- \to \Upsilon(4S)$

[1] ALAM 87B measurement relies on lepton-kaon correlations.

$\Gamma(K^- \ell^+ \nu_\ell \text{anything})/\Gamma(\ell^+ \nu_\ell \text{anything})$ Γ_{26}/Γ_4

ℓ denotes e or μ, not the sum.

VALUE	DOCUMENT ID		TECN	COMMENT
0.092±0.035 OUR AVERAGE				
0.086±0.011±0.044	ALBRECHT	94C	ARG	$e^+e^- \to \Upsilon(4S)$
0.10 ±0.05 ±0.02	[1] ALAM	87B	CLEO	$e^+e^- \to \Upsilon(4S)$

[1] ALAM 87B measurement relies on lepton-kaon correlations.

$\Gamma(K^0/\overline{K}^0 \ell^+ \nu_\ell \text{anything})/\Gamma(\ell^+ \nu_\ell \text{anything})$ Γ_{27}/Γ_4

ℓ denotes e or μ, not the sum. Sum over K^0 and $\overline{K}^0$ states.

VALUE	DOCUMENT ID		TECN	COMMENT
0.42 ±0.05 OUR AVERAGE				
0.452±0.038±0.056	[1] ALBRECHT	94C	ARG	$e^+e^- \to \Upsilon(4S)$
0.39 ±0.06 ±0.04	[2] ALAM	87B	CLEO	$e^+e^- \to \Upsilon(4S)$

[1] ALBRECHT 94C assume a $K^0/\overline{K}^0$ multiplicity twice that of K^0_S.

[2] ALAM 87B measurement relies on lepton-kaon correlations.

$\langle n_c \rangle$

VALUE	DOCUMENT ID		TECN	COMMENT
1.10±0.05	[1] GIBBONS	97B	CLE2	$e^+e^- \to \Upsilon(4S)$
• • • We do not use the following data for averages, fits, limits, etc. • • •				
0.98±0.16±0.12	[2] ALAM	87B	CLEO	$e^+e^- \to \Upsilon(4S)$

[1] GIBBONS 97B from charm counting using $B(D_s^+ \to \phi\pi) = 0.036 \pm 0.009$ and $B(\Lambda_c^+ \to pK^-\pi^+) = 0.044 \pm 0.006$.

[2] From the difference between K^- and K^+ widths. ALAM 87B measurement relies on lepton-kaon correlations. It does not consider the possibility of $B\overline{B}$ mixing. We have thus removed it from the average.

$\Gamma(D^{\pm} \text{anything})/\Gamma_{\text{total}}$ Γ_{28}/Γ

VALUE	EVTS	DOCUMENT ID		TECN	COMMENT
0.237±0.013 OUR AVERAGE					
0.237±0.013±0.005		[1] GIBBONS	97B	CLE2	$e^+e^- \to \Upsilon(4S)$
0.25 ±0.04 ±0.01		[2] BORTOLETTO92		CLEO	$e^+e^- \to \Upsilon(4S)$
0.229±0.053±0.005		[3] ALBRECHT	91H	ARG	$e^+e^- \to \Upsilon(4S)$
• • • We do not use the following data for averages, fits, limits, etc. • • •					
0.208±0.049±0.004	20k	[4] BORTOLETTO87		CLEO	Sup. by BORTOLETTO 92

[1] GIBBONS 97B reports $[\Gamma(B \to D^{\pm}\text{anything})/\Gamma_{\text{total}}] \times [B(D^+ \to K^-2\pi^+)] = 0.0216 \pm 0.0008 \pm 0.00082$ which we divide by our best value $B(D^+ \to K^-2\pi^+) = (9.13 \pm 0.19) \times 10^{-2}$. Our first error is their experiment's error and our second error is the systematic error from using our best value.

[2] BORTOLETTO 92 reports $[\Gamma(B \to D^{\pm}\text{anything})/\Gamma_{\text{total}}] \times [B(D^+ \to K^-2\pi^+)] = 0.0226 \pm 0.0030 \pm 0.0018$ which we divide by our best value $B(D^+ \to K^-2\pi^+) = (9.13 \pm 0.19) \times 10^{-2}$. Our first error is their experiment's error and our second error is the systematic error from using our best value.

[3] ALBRECHT 91H reports $[\Gamma(B \to D^{\pm}\text{anything})/\Gamma_{\text{total}}] \times [B(D^+ \to K^-2\pi^+)] = 0.0209 \pm 0.0027 \pm 0.0040$ which we divide by our best value $B(D^+ \to K^-2\pi^+) = (9.13 \pm 0.19) \times 10^{-2}$. Our first error is their experiment's error and our second error is the systematic error from using our best value.

[4] BORTOLETTO 87 reports $[\Gamma(B \to D^{\pm}\text{anything})/\Gamma_{\text{total}}] \times [B(D^+ \to K^-2\pi^+)] = 0.019 \pm 0.004 \pm 0.002$ which we divide by our best value $B(D^+ \to K^-2\pi^+) = (9.13 \pm 0.19) \times 10^{-2}$. Our first error is their experiment's error and our second error is the systematic error from using our best value.

$\Gamma(D^0/\overline{D}^0 \text{anything})/\Gamma_{\text{total}}$ Γ_{29}/Γ

VALUE	EVTS	DOCUMENT ID		TECN	COMMENT
0.627±0.029 OUR AVERAGE		Error includes scale factor of 1.3. See the ideogram below.			
$0.647 \pm 0.025^{+0.007}_{-0.008}$		[1] GIBBONS	97B	CLE2	$e^+e^- \to \Upsilon(4S)$
0.60 ±0.05 ±0.01		[2] BORTOLETTO92		CLEO	$e^+e^- \to \Upsilon(4S)$
0.50 ±0.08 ±0.01		[3] ALBRECHT	91H	ARG	$e^+e^- \to \Upsilon(4S)$
• • • We do not use the following data for averages, fits, limits, etc. • • •					
0.54 ±0.07 ±0.01	21k	[4] BORTOLETTO87		CLEO	$e^+e^- \to \Upsilon(4S)$
0.62 ±0.19 ±0.01		[5] GREEN	83	CLEO	Repl. by BORTOLETTO 87

[1] GIBBONS 97B reports $[\Gamma(B \to D^0/\overline{D}^0\text{anything})/\Gamma_{\text{total}}] \times [B(D^0 \to K^-\pi^+)] = 0.0251 \pm 0.0006 \pm 0.00075$ which we divide by our best value $B(D^0 \to K^-\pi^+) = (3.88 \pm 0.05) \times 10^{-2}$. Our first error is their experiment's error and our second error is the systematic error from using our best value.

[2] BORTOLETTO 92 reports $[\Gamma(B \to D^0/\overline{D}^0\text{anything})/\Gamma_{\text{total}}] \times [B(D^0 \to K^-\pi^+)] = 0.0233 \pm 0.0012 \pm 0.0014$ which we divide by our best value $B(D^0 \to K^-\pi^+) = (3.88 \pm 0.05) \times 10^{-2}$. Our first error is their experiment's error and our second error is the systematic error from using our best value.

[3] ALBRECHT 91H reports $[\Gamma(B \to D^0/\overline{D}^0\text{anything})/\Gamma_{\text{total}}] \times [B(D^0 \to K^-\pi^+)] = 0.0194 \pm 0.0015 \pm 0.0025$ which we divide by our best value $B(D^0 \to K^-\pi^+) = (3.88 \pm 0.05) \times 10^{-2}$. Our first error is their experiment's error and our second error is the systematic error from using our best value.

[4] BORTOLETTO 87 reports $[\Gamma(B \to D^0/\overline{D}^0\text{anything})/\Gamma_{\text{total}}] \times [B(D^0 \to K^-\pi^+)] = 0.0210 \pm 0.0015 \pm 0.0021$ which we divide by our best value $B(D^0 \to K^-\pi^+) = (3.88 \pm 0.05) \times 10^{-2}$. Our first error is their experiment's error and our second error is the systematic error from using our best value.

[5] GREEN 83 reports $[\Gamma(B \to D^0/\overline{D}^0\text{anything})/\Gamma_{\text{total}}] \times [B(D^0 \to K^-\pi^+)] = 0.024 \pm 0.006 \pm 0.004$ which we divide by our best value $B(D^0 \to K^-\pi^+) = (3.88 \pm 0.05) \times 10^{-2}$. Our first error is their experiment's error and our second error is the systematic error from using our best value.

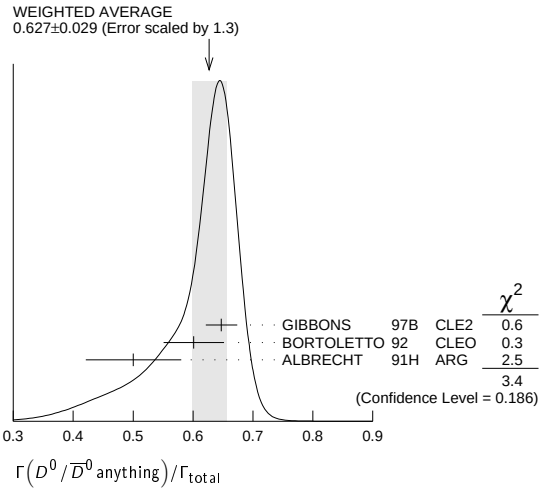

$\Gamma(D^*(2010)^{\pm}\text{anything})/\Gamma_{\text{total}}$ — Γ_{30}/Γ

VALUE	EVTS	DOCUMENT ID		TECN	COMMENT
0.225±0.015 OUR AVERAGE					
0.247±0.019±0.01		[1] GIBBONS	97B	CLE2	$e^+e^- \to \Upsilon(4S)$
0.205±0.019±0.007		[2] ALBRECHT	96D	ARG	$e^+e^- \to \Upsilon(4S)$
0.230±0.028±0.009		[3] BORTOLETTO	92	CLEO	$e^+e^- \to \Upsilon(4S)$
• • • We do not use the following data for averages, fits, limits, etc. • • •					
0.283±0.053±0.002		[4] ALBRECHT	91H	ARG	Sup. by ALBRECHT 96D
0.22 ±0.04 $^{+0.07}_{-0.04}$	5200	[5] BORTOLETTO	87	CLEO	$e^+e^- \to \Upsilon(4S)$
0.27 ±0.06 $^{+0.08}_{-0.06}$	510	[6] CSORNA	85	CLEO	Repl. by BORTOLETTO 87

[1] GIBBONS 97B reports $B(B \to D^*(2010)^+\text{anything}) = 0.239 \pm 0.015 \pm 0.014 \pm 0.009$ using CLEO measured D and D^* branching fractions. We rescale to our PDG 96 values of D and D^* branching ratios. Our first error is their experiment's error and our second error is the systematic error from using our best value.

[2] ALBRECHT 96D reports $B(B \to D^*(2010)^+\text{anything})$ 0.196 ± 0.019 using CLEO measured $B(D^*(2010)^+ \to D^0\pi^+) = 0.681 \pm 0.01 \pm 0.013$, $B(D^0 \to K^-\pi^+) = 0.0401 \pm 0.0014$, $B(D^0 \to K^-\pi^+\pi^+\pi^-) = 0.081 \pm 0.005$., We rescale to our PDG 96 values of D and D^* branching ratios. Our first error is their experiment's error and our second error is the systematic error from using our best value.

[3] BORTOLETTO 92 reports $B(B \to D^*(2010)^+\text{anything}) = 0.25 \pm 0.03 \pm 0.04$ using MARK II $B(D^*(2010)^+ \to D^0\pi^+) = 0.57 \pm 0.06$ and $B(D^0 \to K^-\pi^+) = 0.042 \pm 0.008$. We rescale to our PDG 96 values of D and D^* branching ratios. Our first error is their experiment's error and our second error is the systematic error from using our best value.

[4] ALBRECHT 91H reports 0.348 ± 0.060 ± 0.035 from a measurement of $[\Gamma(B \to D^*(2010)^{\pm}\text{anything})/\Gamma_{\text{total}}] \times [B(D^*(2010)^+ \to D^0\pi^+)]$ assuming $B(D^*(2010)^+ \to D^0\pi^+) = 0.55 \pm 0.04$, which we rescale to our best value $B(D^*(2010)^+ \to D^0\pi^+) = (67.7 \pm 0.5) \times 10^{-2}$. Our first error is their experiment's error and our second error is the systematic error from using our best value. Uses the PDG 90 $B(D^0 \to K^-\pi^+) = 0.0371 \pm 0.0025$.

[5] BORTOLETTO 87 uses old MARK III (BALTRUSAITIS 86E) branching ratios $B(D^0 \to K^-\pi^+) = 0.056 \pm 0.004 \pm 0.003$ and also assumes $B(D^*(2010)^+ \to D^0\pi^+) = 0.60^{+0.08}_{-0.15}$. The product branching ratio for $B(B \to D^*(2010)^+)\, B(D^*(2010)^+ \to D^0\pi^+)$ is 0.13 ± 0.02 ± 0.012. Superseded by BORTOLETTO 92.

[6] $V-A$ momentum spectrum used to extrapolate below $p = 1$ GeV. We correct the value assuming $B(D^0 \to K^-\pi^+) = 0.042 \pm 0.006$ and $B(D^{*+} \to D^0\pi^+) = 0.6^{+0.08}_{-0.15}$. The product branching fraction is $B(B \to D^{*+}X)\cdot B(D^{*+} \to \pi^+D^0)\cdot B(D^0 \to K^-\pi^+) = (68 \pm 15 \pm 9) \times 10^{-4}$.

$\Gamma(D^*(2007)^0\text{anything})/\Gamma_{\text{total}}$ — Γ_{31}/Γ

VALUE	DOCUMENT ID		TECN	COMMENT
0.260±0.023±0.015	[1] GIBBONS	97B	CLE2	$e^+e^- \to \Upsilon(4S)$

[1] GIBBONS 97B reports $B(B \to D^*(2007)^0\text{anything})$ 0.247 ± 0.012 ± 0.018 ± 0.018 using CLEO measured D and D^* branching fractions. We rescale to our PDG 96 values of D and D^* branching ratios. Our first error is their experiment's error and our second error is the systematic error from using our best value.

$\Gamma(D_s^{\pm}\text{anything})/\Gamma_{\text{total}}$ — Γ_{32}/Γ

VALUE	EVTS	DOCUMENT ID		TECN	COMMENT
0.083±0.008 OUR AVERAGE					
0.089±0.010±0.008		[1] ARTUSO	05B	CLE2	$e^+e^- \to \Upsilon(5S)$
0.087±0.005±0.008		[2] AUBERT	02G	BABR	$e^+e^- \to \Upsilon(4S)$
0.065±0.011±0.006		[3] ALBRECHT	92G	ARG	$e^+e^- \to \Upsilon(4S)$
0.068±0.010±0.006	257	[4] BORTOLETTO	90	CLEO	$e^+e^- \to \Upsilon(4S)$
0.085±0.022±0.008		[5] HAAS	86	CLEO	$e^+e^- \to \Upsilon(4S)$
• • • We do not use the following data for averages, fits, limits, etc. • • •					
0.094±0.007±0.008		[6] GIBAUT	96	CLE2	Repl. by ARTUSO 05B
0.094±0.024±0.008		[7] ALBRECHT	87H	ARG	$e^+e^- \to \Upsilon(4S)$

[1] ARTUSO 05B reports 0.0905 ± 0.0025 ± 0.0140 from a measurement of $[\Gamma(B \to D_s^{\pm}\text{anything})/\Gamma_{\text{total}}] \times [B(D_s^+ \to \phi\pi^+)]$ assuming $B(D_s^+ \to \phi\pi^+) = (4.4 \pm 0.5) \times 10^{-2}$, which we rescale to our best value $B(D_s^+ \to \phi\pi^+) = (4.5 \pm 0.4) \times 10^{-2}$. Our first error is their experiment's error and our second error is the systematic error from using our best value.

[2] AUBERT 02G reports $[\Gamma(B \to D_s^{\pm}\text{anything})/\Gamma_{\text{total}}] \times [B(D_s^+ \to \phi\pi^+)] = 0.00393 \pm 0.00007 \pm 0.00021$ which we divide by our best value $B(D_s^+ \to \phi\pi^+) = (4.5 \pm 0.4) \times 10^{-2}$. Our first error is their experiment's error and our second error is the systematic error from using our best value.

[3] ALBRECHT 92G reports $[\Gamma(B \to D_s^{\pm}\text{anything})/\Gamma_{\text{total}}] \times [B(D_s^+ \to \phi\pi^+)] = 0.00292 \pm 0.00039 \pm 0.00031$ which we divide by our best value $B(D_s^+ \to \phi\pi^+) = (4.5 \pm 0.4) \times 10^{-2}$. Our first error is their experiment's error and our second error is the systematic error from using our best value.

[4] BORTOLETTO 90 reports $[\Gamma(B \to D_s^{\pm}\text{anything})/\Gamma_{\text{total}}] \times [B(D_s^+ \to \phi\pi^+)] = 0.00306 \pm 0.00047$ which we divide by our best value $B(D_s^+ \to \phi\pi^+) = (4.5 \pm 0.4) \times 10^{-2}$. Our first error is their experiment's error and our second error is the systematic error from using our best value.

[5] HAAS 86 reports $[\Gamma(B \to D_s^{\pm}\text{anything})/\Gamma_{\text{total}}] \times [B(D_s^+ \to \phi\pi^+)] = 0.0038 \pm 0.0010$ which we divide by our best value $B(D_s^+ \to \phi\pi^+) = (4.5 \pm 0.4) \times 10^{-2}$. Our first error is their experiment's error and our second error is the systematic error from using our best value. 64 ± 22% decays are 2-body.

[6] GIBAUT 96 reports 0.1211 ± 0.0039 ± 0.0088 from a measurement of $[\Gamma(B \to D_s^{\pm}\text{anything})/\Gamma_{\text{total}}] \times [B(D_s^+ \to \phi\pi^+)]$ assuming $B(D_s^+ \to \phi\pi^+) = 0.035$, which we rescale to our best value $B(D_s^+ \to \phi\pi^+) = (4.5 \pm 0.4) \times 10^{-2}$. Our first error is their experiment's error and our second error is the systematic error from using our best value.

[7] ALBRECHT 87H reports $[\Gamma(B \to D_s^{\pm}\text{anything})/\Gamma_{\text{total}}] \times [B(D_s^+ \to \phi\pi^+)] = 0.0042 \pm 0.0009 \pm 0.0006$ which we divide by our best value $B(D_s^+ \to \phi\pi^+) = (4.5 \pm 0.4) \times 10^{-2}$. Our first error is their experiment's error and our second error is the systematic error from using our best value. 46 ± 16% of $B \to D_s X$ decays are 2-body. Superseded by ALBRECHT 92G.

$\Gamma(D_s^{*\pm}\text{anything})/\Gamma_{\text{total}}$ — Γ_{33}/Γ

VALUE	DOCUMENT ID		TECN	COMMENT
0.063±0.009±0.006	[1] AUBERT	02G	BABR	$e^+e^- \to \Upsilon(4S)$

[1] AUBERT 02G reports $[\Gamma(B \to D_s^{*\pm}\text{anything})/\Gamma_{\text{total}}] \times [B(D_s^+ \to \phi\pi^+)] = 0.00284 \pm 0.00029 \pm 0.00025$ which we divide by our best value $B(D_s^+ \to \phi\pi^+) = (4.5 \pm 0.4) \times 10^{-2}$. Our first error is their experiment's error and our second error is the systematic error from using our best value.

$\Gamma(D_s^{*\pm}\overline{D}^{(*)})/\Gamma(D_s^{*\pm}\text{anything})$ — Γ_{34}/Γ_{33}

Sum over modes

VALUE	DOCUMENT ID		TECN	COMMENT
0.533±0.037±0.037	AUBERT	02G	BABR	$e^+e^- \to \Upsilon(4S)$

$\Gamma(\overline{D}D_{s0}(2317))/\Gamma_{\text{total}}$ — Γ_{35}/Γ

VALUE	DOCUMENT ID		TECN	COMMENT
seen	[1] KROKOVNY	03B	BELL	$e^+e^- \to \Upsilon(4S)$

[1] The product branching ratio for $B(B \to \overline{D}D_{s0}(2317)^+)\times B(D_{s0}(2317)^+ \to D_s\pi^0)$ is measured to be $(8.5^{+2.1}_{-1.9} \pm 2.6) \times 10^{-4}$.

$\Gamma(\overline{D}D_{sJ}(2457))/\Gamma_{\text{total}}$ — Γ_{36}/Γ

VALUE	DOCUMENT ID		TECN	COMMENT
seen	[1] KROKOVNY	03B	BELL	$e^+e^- \to \Upsilon(4S)$

[1] The product branching ratio for $B(B \to \overline{D}D_{sJ}(2457)^+)\times B(D_{sJ}(2457)^+ \to D_s^{*+}\pi^0, D_s^+\gamma)$ are measured to be $(17.8^{+4.5}_{-3.9} \pm 5.3) \times 10^{-4}$ and $(6.7^{+1.3}_{-1.2} \pm 2.0) \times 10^{-4}$, respectively.

$[\Gamma(D^{(*)}\overline{D}^{(*)}K^0) + \Gamma(D^{(*)}\overline{D}^{(*)}K^{\pm})]/\Gamma_{\text{total}}$ — Γ_{37}/Γ

VALUE	DOCUMENT ID		TECN	COMMENT
0.071 $^{+0.025}_{-0.015}$ $^{+0.010}_{-0.009}$	[1] BARATE	98Q	ALEP	$e^+e^- \to Z$

[1] The systematic error includes the uncertainties due to the charm branching ratios.

$\Gamma(b \to c\overline{c}s)/\Gamma_{\text{total}}$ — Γ_{38}/Γ

VALUE	DOCUMENT ID		TECN	COMMENT
0.219±0.037	[1] COAN	98	CLE2	$e^+e^- \to \Upsilon(4S)$

[1] COAN 98 uses D-ℓ correlation.

$\Gamma(D_s^{(*)}\overline{D}^{(*)})/\Gamma(D_s^{\pm}\text{anything})$ — Γ_{39}/Γ_{32}

Sum over modes.

VALUE	DOCUMENT ID		TECN	COMMENT
0.469±0.017 OUR AVERAGE				
0.464±0.013±0.015	AUBERT	02G	BABR	$e^+e^- \to \Upsilon(4S)$
0.56 $^{+0.21}_{-0.15}$ $^{+0.09}_{-0.08}$	[1] BARATE	98Q	ALEP	$e^+e^- \to Z$
0.457±0.019±0.037	GIBAUT	96	CLE2	$e^+e^- \to \Upsilon(4S)$
0.58 ±0.07 ±0.09	ALBRECHT	92G	ARG	$e^+e^- \to \Upsilon(4S)$
0.56 ±0.10	BORTOLETTO	90	CLEO	$e^+e^- \to \Upsilon(4S)$

[1] BARATE 98Q measures $B(B \to D_s^{(*)}\overline{D}^{(*)}) = 0.056^{+0.021}_{-0.015}{}^{+0.009}_{-0.008}{}^{+0.019}_{-0.011}$, where the third error results from the uncertainty on the different D branching ratios and is dominated by the uncertainty on $B(D_s^+ \to \phi\pi^+)$. We divide $B(B \to D_s^{(*)}\overline{D}^{(*)})$ by our best value of $B(B \to D_s\text{ anything}) = 0.1 \pm 0.025$.

Meson Particle Listings

$B^{\pm}/B^{0}$ ADMIXTURE

$\Gamma(D^{*}D^{*}(2010)^{\pm})/\Gamma_{total}$ Γ_{40}/Γ

VALUE	CL%	DOCUMENT ID		TECN	COMMENT
$<5.9\times10^{-3}$	90	BARATE	98Q	ALEP	$e^+e^-\to Z$

$[\Gamma(DD^{*}(2010)^{\pm})+\Gamma(D^{*}D^{\pm})]/\Gamma_{total}$ Γ_{41}/Γ

VALUE	CL%	DOCUMENT ID		TECN	COMMENT
$<5.5\times10^{-3}$	90	BARATE	98Q	ALEP	$e^+e^-\to Z$

$\Gamma(DD^{\pm})/\Gamma_{total}$ Γ_{42}/Γ

VALUE	CL%	DOCUMENT ID		TECN	COMMENT
$<3.1\times10^{-3}$	90	BARATE	98Q	ALEP	$e^+e^-\to Z$

$\Gamma(D_s^{(*)\pm}\overline{D}^{(*)}X(n\pi^{\pm}))/\Gamma_{total}$ Γ_{43}/Γ

VALUE	DOCUMENT ID		TECN	COMMENT
$0.094^{+0.040+0.034}_{-0.031-0.024}$	[1] BARATE	98Q	ALEP	$e^+e^-\to Z$

[1] The systematic error includes the uncertainties due to the charm branching ratios.

$\Gamma(D^{*}(2010)\gamma)/\Gamma_{total}$ Γ_{44}/Γ

VALUE	CL%	DOCUMENT ID		TECN	COMMENT
$<1.1\times10^{-3}$	90	[1] LESIAK	92	CBAL	$e^+e^-\to\Upsilon(4S)$

[1] LESIAK 92 set a limit on the inclusive process $B(b\to s\gamma)<2.8\times10^{-3}$ at 90% CL for the range of masses of 892–2045 MeV, independent of assumptions about s-quark hadronization.

$\Gamma(D_s^{+}\pi^{-}, D_s^{*+}\pi^{-}, D_s^{+}\rho^{-}, D_s^{*+}\rho^{-}, D_s^{+}\pi^{0}, D_s^{*+}\pi^{0}, D_s^{+}\eta, D_s^{*+}\eta, D_s^{+}\rho^{0}, D_s^{*+}\rho^{0}, D_s^{+}\omega, D_s^{*+}\omega)/\Gamma_{total}$ Γ_{45}/Γ

Sum over modes.

VALUE	CL%	DOCUMENT ID		TECN	COMMENT
$<4\times10^{-4}$	90	[1] ALEXANDER	93B	CLE2	$e^+e^-\to\Upsilon(4S)$

[1] ALEXANDER 93B reports $<4.8\times10^{-4}$ from a measurement of $[\Gamma(B\to D_s^{+}\pi^{-}, D_s^{*+}\pi^{-}, D_s^{+}\rho^{-}, D_s^{*+}\rho^{-}, D_s^{+}\pi^{0}, D_s^{*+}\pi^{0}, D_s^{+}\eta, D_s^{*+}\eta, D_s^{+}\rho^{0}, D_s^{*+}\rho^{0}, D_s^{+}\omega, D_s^{*+}\omega)/\Gamma_{total}]\times[B(D_s^{+}\to\phi\pi^{+})]$ assuming $B(D_s^{+}\to\phi\pi^{+})=0.037$, which we rescale to our best value $B(D_s^{+}\to\phi\pi^{+})=4.5\times10^{-2}$. This branching ratio limit provides a model-dependent upper limit $|V_{ub}|/|V_{cb}|<0.16$ at CL=90%.

$\Gamma(D_{s1}(2536)^{+}\text{anything})/\Gamma_{total}$ Γ_{46}/Γ

$D_{s1}(2536)^{+}$ is the narrow P-wave D_s^{+} meson with $J^{P}=1^{+}$.

VALUE	CL%	DOCUMENT ID		TECN	COMMENT
<0.0095	90	[1] BISHAI	98	CLE2	$e^+e^-\to\Upsilon(4S)$

[1] Assuming factorization, the decay constant $f_{D_{s1}^{+}}$ is at least a factor of 2.5 times smaller than $f_{D_s^{+}}$.

$\Gamma(J/\psi(1S)\text{anything})/\Gamma_{total}$ Γ_{47}/Γ

VALUE (units 10^{-2})	EVTS	DOCUMENT ID		TECN	COMMENT
1.094 ± 0.032 OUR AVERAGE		Error includes scale factor of 1.1.			
$1.057\pm0.012\pm0.040$		[1] AUBERT	03F	BABR	$e^+e^-\to\Upsilon(4S)$
$1.121\pm0.013\pm0.042$		ANDERSON	02	CLE2	$e^+e^-\to\Upsilon(4S)$
$1.29\ \pm0.45\ \pm0.01$	27	[2] MASCHMANN	90	CBAL	$e^+e^-\to\Upsilon(4S)$
$1.24\ \pm0.27\ \pm0.01$	120	[3] ALBRECHT	87D	ARG	$e^+e^-\to\Upsilon(4S)$
$1.35\ \pm0.24\ \pm0.01$	52	[4] ALAM	86	CLEO	$e^+e^-\to\Upsilon(4S)$
• • • We do not use the following data for averages, fits, limits, etc. • • •					
$1.12\ \pm0.06\ \pm0.01$	1489	[5] BALEST	95B	CLE2	$e^+e^-\to\Upsilon(4S)$
$1.4\ ^{+0.6}_{-0.5}$	7	[6] ALBRECHT	85H	ARG	$e^+e^-\to\Upsilon(4S)$
$1.1\ \pm0.21\ \pm0.23$	46	[7] HAAS	85	CLEO	Repl. by ALAM 86

[1] AUBERT 03F also reports the momentum distribution and helicity of $J/\psi\to\ell^{+}\ell^{-}$ in the $\Upsilon(4S)$ center-of-mass frame.

[2] MASCHMANN 90 reports $(1.12\pm0.33\pm0.25)\times10^{-2}$ from a measurement of $[\Gamma(B\to J/\psi(1S)\text{anything})/\Gamma_{total}]\times[B(J/\psi(1S)\to e^+e^-)]$ assuming $B(J/\psi(1S)\to e^+e^-)=0.069\pm0.009$, which we rescale to our best value $B(J/\psi(1S)\to e^+e^-)=(5.971\pm0.032)\times10^{-2}$. Our first error is their experiment's error and our second error is the systematic error from using our best value.

[3] ALBRECHT 87D reports $(1.07\pm0.16\pm0.22)\times10^{-2}$ from a measurement of $[\Gamma(B\to J/\psi(1S)\text{anything})/\Gamma_{total}]\times[B(J/\psi(1S)\to e^+e^-)]$ assuming $B(J/\psi(1S)\to e^+e^-)=0.069\pm0.009$, which we rescale to our best value $B(J/\psi(1S)\to e^+e^-)=(5.971\pm0.032)\times10^{-2}$. Our first error is their experiment's error and our second error is the systematic error from using our best value. ALBRECHT 87D find the branching ratio for J/ψ not from $\psi(2S)$ to be 0.0081 ± 0.0023.

[4] ALAM 86 reports $(1.09\pm0.16\pm0.21)\times10^{-2}$ from a measurement of $[\Gamma(B\to J/\psi(1S)\text{anything})/\Gamma_{total}]\times[B(J/\psi(1S)\to\mu^+\mu^-)]$ assuming $B(J/\psi(1S)\to\mu^+\mu^-)=0.074\pm0.012$, which we rescale to our best value $B(J/\psi(1S)\to\mu^+\mu^-)=(5.961\pm0.033)\times10^{-2}$. Our first error is their experiment's error and our second error is the systematic error from using our best value.

[5] BALEST 95B reports $(1.12\pm0.04\pm0.06)\times10^{-2}$ from a measurement of $[\Gamma(B\to J/\psi(1S)\text{anything})/\Gamma_{total}]\times[B(J/\psi(1S)\to e^+e^-)]$ assuming $B(J/\psi(1S)\to e^+e^-)=0.0599\pm0.0025$, which we rescale to our best value $B(J/\psi(1S)\to e^+e^-)=(5.971\pm0.032)\times10^{-2}$. Our first error is their experiment's error and our second error is the systematic error from using our best value. They measure $J/\psi(1S)\to e^+e^-$ and $\mu^+\mu^-$ and use PDG 1994 values for the branching fractions. The rescaling is the same for either mode so we use e^+e^-.

[6] Statistical and systematic errors were added in quadrature. ALBRECHT 85H also report a CL = 90% limit of 0.007 for $B\to J/\psi(1S)+X$ where $m_X<1$ GeV.

[7] Dimuon and dielectron events used.

$\Gamma(J/\psi(1S)(\text{direct})\text{anything})/\Gamma_{total}$ Γ_{48}/Γ

VALUE	DOCUMENT ID		TECN	COMMENT
0.0078 ± 0.0004 OUR AVERAGE	Error includes scale factor of 1.1.			
$0.00740\pm0.00023\pm0.00043$	[1] AUBERT	03F	BABR	$e^+e^-\to\Upsilon(4S)$
$0.00813\pm0.00017\pm0.00037$	[2] ANDERSON	02	CLE2	$e^+e^-\to\Upsilon(4S)$
• • • We do not use the following data for averages, fits, limits, etc. • • •				
$0.0080\ \pm0.0008$	[3] BALEST	95B	CLE2	$e^+e^-\to\Upsilon(4S)$

[1] AUBERT 03F also reports the helicity of $J/\psi\to\ell^{+}\ell^{-}$ produced directly in B decay.

[2] Also reports the measurement of $J/\psi\to\ell^{+}\ell^{-}$ polarization produced directly from B decay.

[3] BALEST 95B assume PDG 1994 values for sub mode branching ratios. $J/\psi(1S)$ mesons are reconstructed in $J/\psi(1S)\to e^+e^-$ and $J/\psi(1S)\to\mu^+\mu^-$. The $B\to J/\psi(1S)X$ branching ratio contains $J/\psi(1S)$ mesons directly from B decays and also from feeddown through $\psi(2S)\to J/\psi(1S)$, $\chi_{c1}(1P)\to J/\psi(1S)$, or $\chi_{c2}(1P)\to J/\psi(1S)$. Using the measured inclusive rates, BALEST 95B corrects for the feeddown and finds the $B\to J/\psi(1S)$ (direct) X branching ratio.

$\Gamma(\psi(2S)\text{anything})/\Gamma_{total}$ Γ_{49}/Γ

VALUE	EVTS	DOCUMENT ID		TECN	COMMENT
0.00307 ± 0.00021 OUR AVERAGE					
$0.00297\pm0.00020\pm0.00020$		AUBERT	03F	BABR	$e^+e^-\to\Upsilon(4S)$
$0.00316\pm0.00014\pm0.00028$		[1] ANDERSON	02	CLE2	$e^+e^-\to\Upsilon(4S)$
$0.0046\ \pm0.0017\ \pm0.0011$	8	ALBRECHT	87D	ARG	$e^+e^-\to\Upsilon(4S)$
• • • We do not use the following data for averages, fits, limits, etc. • • •					
$0.0034\ \pm0.0004\ \pm0.0003$	240	[2] BALEST	95B	CLE2	$e^+e^-\to\Upsilon(4S)$

[1] Also reports the measurement of $\psi(2S)\to\ell^{+}\ell^{-}$ polarization produced directly from B decay.

[2] BALEST 95B assume PDG 1994 values for sub mode branching ratios. They find $B(B\to\psi(2S)X, \psi(2S)\to\ell^{+}\ell^{-})=0.30\pm0.05\pm0.04$ and $B(B\to\psi(2S)X, \psi(2S)\to J/\psi(1S)\pi^{+}\pi^{-})=0.37\pm0.05\pm0.05$. Weighted average is quoted for $B(B\to\psi(2S)X)$.

$\Gamma(\chi_{c1}(1P)\text{anything})/\Gamma_{total}$ Γ_{50}/Γ

VALUE	EVTS	DOCUMENT ID		TECN	COMMENT
0.00386 ± 0.00027 OUR AVERAGE					
$0.00367\pm0.00035\pm0.00044$		AUBERT	03F	BABR	$e^+e^-\to\Upsilon(4S)$
$0.00363\pm0.00022\pm0.00034$		[1] ABE	02L	BELL	$e^+e^-\to\Upsilon(4S)$
$0.00435\pm0.00029\pm0.00040$		ANDERSON	02	CLE2	$e^+e^-\to\Upsilon(4S)$
• • • We do not use the following data for averages, fits, limits, etc. • • •					
$0.0033\ \pm0.0004\ \pm0.0001$		[2] CHEN	01	CLE2	$e^+e^-\to\Upsilon(4S)$
$0.0040\ \pm0.0006\ \pm0.0004$	112	[3] BALEST	95B	CLE2	Repl. by CHEN 01
$0.0105\ \pm0.0035\ \pm0.0025$		[4] ALBRECHT	92E	ARG	$e^+e^-\to\Upsilon(4S)$

[1] ABE 02L uses PDG 01 values for $B(J/\psi(1S)\to\ell^{+}\ell^{-})$ and $B(\chi_{c1,c2}\to J/\psi(1S)\gamma)$.

[2] CHEN 01 reports $0.00414\pm0.00031\pm0.00040$ from a measurement of $[\Gamma(B\to\chi_{c1}(1P)\text{anything})/\Gamma_{total}]\times[B(\chi_{c1}(1P)\to\gamma J/\psi(1S))]$ assuming $B(\chi_{c1}(1P)\to\gamma J/\psi(1S))=0.273\pm0.016$, which we rescale to our best value $B(\chi_{c1}(1P)\to\gamma J/\psi(1S))=(33.9\pm1.2)\times10^{-2}$. Our first error is their experiment's error and our second error is the systematic error from using our best value. Assumes equal production of B^{+} and B^{0} at the $\Upsilon(4S)$.

[3] BALEST 95B assume $B(\chi_{c1}(1P)\to J/\psi(1S)\gamma)=(27.3\pm1.6)\times10^{-2}$, the PDG 1994 value. Fit to ψ-photon invariant mass distribution allows for a $\chi_{c1}(1P)$ and a $\chi_{c2}(1P)$ component.

[4] ALBRECHT 92E assumes no $\chi_{c2}(1P)$ production.

$\Gamma(\chi_{c1}(1P)(\text{direct})\text{anything})/\Gamma_{total}$ Γ_{51}/Γ

VALUE	DOCUMENT ID		TECN	COMMENT
0.00324 ± 0.00025 OUR AVERAGE				
$0.00341\pm0.00035\pm0.00042$	AUBERT	03F	BABR	$e^+e^-\to\Upsilon(4S)$
$0.00332\pm0.00022\pm0.00034$	[1] ABE	02L	BELL	$e^+e^-\to\Upsilon(4S)$
$0.0031\ \pm0.0004\ \pm0.0001$	[2] CHEN	01	CLE2	$e^+e^-\to\Upsilon(4S)$
• • • We do not use the following data for averages, fits, limits, etc. • • •				
$0.0037\ \pm0.0007$	[3] BALEST	95B	CLE2	Repl. by CHEN 01

[1] ABE 02L uses PDG 01 values for $B(J/\psi(1S)\to\ell^{+}\ell^{-})$ and $B(\chi_{c1,c2}\to J/\psi(1S)\gamma)$.

[2] CHEN 01 reports $0.00383\pm0.00031\pm0.00040$ from a measurement of $[\Gamma(B\to\chi_{c1}(1P)(\text{direct})\text{anything})/\Gamma_{total}]\times[B(\chi_{c1}(1P)\to\gamma J/\psi(1S))]$ assuming $B(\chi_{c1}(1P)\to\gamma J/\psi(1S))=0.273\pm0.016$, which we rescale to our best value $B(\chi_{c1}(1P)\to\gamma J/\psi(1S))=(33.9\pm1.2)\times10^{-2}$. Our first error is their experiment's error and our second error is the systematic error from using our best value. Assumes equal production of B^{+} and B^{0} at the $\Upsilon(4S)$.

[3] BALEST 95B assume PDG 1994 values. $J/\psi(1S)$ mesons are reconstructed in the e^+e^- and $\mu^+\mu^-$ modes. The $B\to\chi_{c1}(1P)X$ branching ratio contains $\chi_{c1}(1P)$ mesons directly from B decays and also from feeddown through $\psi(2S)\to\chi_{c1}(1P)\gamma$. Using the measured inclusive rates, BALEST 95B corrects for the feeddown and finds the $B\to\chi_{c1}(1P)$ (direct) X branching ratio.

$\Gamma(\chi_{c2}(1P)\text{anything})/\Gamma_{total}$ Γ_{52}/Γ

VALUE (units 10^{-4})	CL%	EVTS	DOCUMENT ID		TECN	COMMENT
14 ±4 OUR AVERAGE			Error includes scale factor of 1.9. See the ideogram below.			
$21.0\pm4.5\pm3.1$			AUBERT	03F	BABR	$e^+e^-\to\Upsilon(4S)$
$18.0^{+2.3}_{-2.8}\pm2.6$			[1] ABE	02L	BELL	$e^+e^-\to\Upsilon(4S)$
$6.9\pm3.5\pm0.3$			[2] CHEN	01	CLE2	$e^+e^-\to\Upsilon(4S)$
• • • We do not use the following data for averages, fits, limits, etc. • • •						
<38	90	35	[3] BALEST	95B	CLE2	Repl. by CHEN 01

[1] ABE 02L uses PDG 01 values for $B(J/\psi(1S) \to \ell^+\ell^-)$ and $B(\chi_{c1,c2} \to J/\psi(1S)\gamma)$.

[2] CHEN 01 reports $(9.8 \pm 4.8 \pm 1.5) \times 10^{-4}$ from a measurement of $[\Gamma(B \to \chi_{c2}(1P)\text{anything})/\Gamma_{\text{total}}] \times [B(\chi_{c2}(1P) \to \gamma J/\psi(1S))]$ assuming $B(\chi_{c2}(1P) \to \gamma J/\psi(1S)) = 0.135 \pm 0.011$, which we rescale to our best value $B(\chi_{c2}(1P) \to \gamma J/\psi(1S)) = (19.2 \pm 0.7) \times 10^{-2}$. Our first error is their experiment's error and our second error is the systematic error from using our best value. Assumes equal production of B^+ and B^0 at the $\Upsilon(4S)$.

[3] BALEST 95B assume $B(\chi_{c2}(1P) \to J/\psi(1S)\gamma) = (13.5 \pm 1.1) \times 10^{-2}$, the PDG 1994 value. $J/\psi(1S)$ mesons are reconstructed in the e^+e^- and $\mu^+\mu^-$ modes, and PDG 1994 branching fractions are used. If interpreted as signal, the 35 ± 13 events correspond to $B(B \to \chi_{c2}(1P)X) = (0.25 \pm 0.10 \pm 0.03) \times 10^{-2}$.

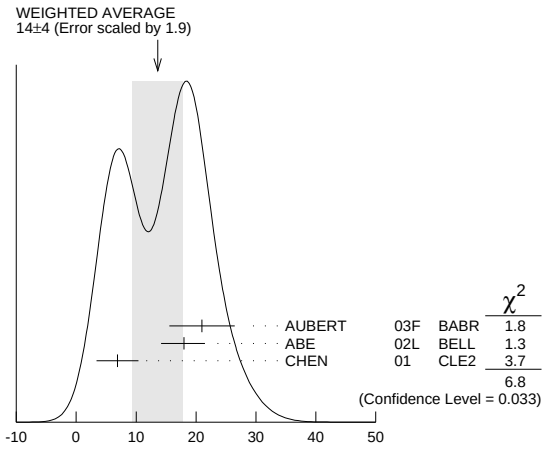

$\Gamma(\chi_{c2}(1P)\text{anything})/\Gamma_{\text{total}}$ Γ_{52}/Γ

$\Gamma(\chi_{c2}(1P)\text{(direct) anything})/\Gamma_{\text{total}}$ Γ_{53}/Γ

VALUE	DOCUMENT ID		TECN	COMMENT
0.00165±0.00031 OUR AVERAGE				
$0.00190 \pm 0.00045 \pm 0.00029$	AUBERT	03F	BABR	$e^+e^- \to \Upsilon(4S)$
$0.00153^{+0.00023}_{-0.00028} \pm 0.00027$	[1] ABE	02L	BELL	$e^+e^- \to \Upsilon(4S)$

[1] ABE 02L uses PDG 01 values for $B(J/\psi(1S) \to \ell^+\ell^-)$ and $B(\chi_{c1,c2} \to J/\psi(1S)\gamma)$.

$\Gamma(\eta_c(1S)\text{anything})/\Gamma_{\text{total}}$ Γ_{54}/Γ

VALUE	CL%	DOCUMENT ID		TECN	COMMENT
<0.009	90	[1] BALEST	95B	CLE2	$e^+e^- \to \Upsilon(4S)$

[1] BALEST 95B assume PDG 1994 values for sub mode branching ratios. $J/\psi(1S)$ mesons are reconstructed in $J/\psi(1S) \to e^+e^-$ and $J/\psi(1S) \to \mu^+\mu^-$. Search region $2960 < m_{\eta_c(1S)} < 3010$ MeV/c^2.

$\Gamma(KX(3872) \times B(X \to D^0\overline{D}{}^0\pi^0))/\Gamma_{\text{total}}$ Γ_{55}/Γ

VALUE (units 10^{-4})	DOCUMENT ID		TECN	COMMENT
$\mathbf{1.22 \pm 0.31^{+0.23}_{-0.30}}$	[1] GOKHROO	06	BELL	$e^+e^- \to \Upsilon(4S)$

[1] Measure the near-threshold enhancements in the $(D^0\overline{D}{}^0\pi^0)$ system at a mass $3875.2 \pm 0.7^{+0.3}_{-1.6} \pm 0.8$ MeV/c^2.

$\Gamma(KX(3872) \times B(X \to D^{*0}D^0))/\Gamma_{\text{total}}$ Γ_{56}/Γ

VALUE (units 10^{-4})	DOCUMENT ID		TECN	COMMENT
0.80±0.20±0.10	AUSHEV	10	BELL	$e^+e^- \to \Upsilon(4S)$

$\Gamma(KX(3940) \times B(X \to D^{*0}D^0))/\Gamma_{\text{total}}$ Γ_{57}/Γ

VALUE (units 10^{-4})	CL%	DOCUMENT ID		TECN	COMMENT
<0.67	90	AUSHEV	10	BELL	$e^+e^- \to \Upsilon(4S)$

$\Gamma(K\chi_{c0}(2P), \chi_{c0} \to \omega J/\psi)/\Gamma_{\text{total}}$ Γ_{58}/Γ

VALUE (units 10^{-5})	DOCUMENT ID		TECN	COMMENT
7.1±1.3±3.1	[1] CHOI	05	BELL	$e^+e^- \to \Upsilon(4S)$

[1] CHOI 05 reports the observation of a near-threshold enhancement in the $\omega J/\psi$ mass spectrum in exclusive $B \to K\omega J/\psi$. The new state, denoted as $X(3915)$, is measured to have a mass of $3943 \pm 11 \pm 13$ GeV/c^2 and a width $\Gamma = 87 \pm 22 \pm 26$ MeV.

$\Gamma(K^{\pm}\text{anything})/\Gamma_{\text{total}}$ Γ_{59}/Γ

VALUE	DOCUMENT ID		TECN	COMMENT
0.789±0.025 OUR AVERAGE				
$0.82 \pm 0.01 \pm 0.05$	ALBRECHT	94C	ARG	$e^+e^- \to \Upsilon(4S)$
$0.775 \pm 0.015 \pm 0.025$	[1] ALBRECHT	93I	ARG	$e^+e^- \to \Upsilon(4S)$
$0.85 \pm 0.07 \pm 0.09$	ALAM	87B	CLEO	$e^+e^- \to \Upsilon(4S)$
• • • We do not use the following data for averages, fits, limits, etc. • • •				
seen	[2] BRODY	82	CLEO	$e^+e^- \to \Upsilon(4S)$
seen	[3] GIANNINI	82	CUSB	$e^+e^- \to \Upsilon(4S)$

[1] ALBRECHT 93I value is not independent of the sum of $B \to K^+$ anything and $B \to K^-$ anything ALBRECHT 94C values.

[2] Assuming $\Upsilon(4S) \to B\overline{B}$, a total of $3.38 \pm 0.34 \pm 0.68$ kaons per $\Upsilon(4S)$ decay is found (the second error is systematic). In the context of the standard B-decay model, this leads to a value for (b-quark $\to$ c-quark)/(b-quark $\to$ all) of $1.09 \pm 0.33 \pm 0.13$.

[3] GIANNINI 82 at CESR-CUSB observed 1.58 ± 0.35 K^0 per hadronic event much higher than 0.82 ± 0.10 below threshold. Consistent with predominant $b \to c$X decay.

$\Gamma(K^+\text{anything})/\Gamma_{\text{total}}$ Γ_{60}/Γ

VALUE	DOCUMENT ID		TECN	COMMENT
0.66 ±0.05	[1] ALBRECHT	94C	ARG	$e^+e^- \to \Upsilon(4S)$
• • • We do not use the following data for averages, fits, limits, etc. • • •				
$0.620 \pm 0.013 \pm 0.038$	[2] ALBRECHT	94C	ARG	$e^+e^- \to \Upsilon(4S)$
$0.66 \pm 0.05 \pm 0.07$	[2] ALAM	87B	CLEO	$e^+e^- \to \Upsilon(4S)$

[1] Measurement relies on lepton-kaon correlations. It is for the weak decay vertex and does not include mixing of the neutral B meson. Mixing effects were corrected for by assuming a mixing parameter r of $(18.1 \pm 4.3)\%$.

[2] Measurement relies on lepton-kaon correlations. It includes production through mixing of the neutral B meson.

$\Gamma(K^-\text{anything})/\Gamma_{\text{total}}$ Γ_{61}/Γ

VALUE	DOCUMENT ID		TECN	COMMENT
0.13 ±0.04	[1] ALBRECHT	94C	ARG	$e^+e^- \to \Upsilon(4S)$
• • • We do not use the following data for averages, fits, limits, etc. • • •				
$0.165 \pm 0.011 \pm 0.036$	[2] ALBRECHT	94C	ARG	$e^+e^- \to \Upsilon(4S)$
$0.19 \pm 0.05 \pm 0.02$	[2] ALAM	87B	CLEO	$e^+e^- \to \Upsilon(4S)$

[1] Measurement relies on lepton-kaon correlations. It is for the weak decay vertex and does not include mixing of the neutral B meson. Mixing effects were corrected for by assuming a mixing parameter r of $(18.1 \pm 4.3)\%$.

[2] Measurement relies on lepton-kaon correlations. It includes production through mixing of the neutral B meson.

$\Gamma(K^0/\overline{K}{}^0\text{anything})/\Gamma_{\text{total}}$ Γ_{62}/Γ

VALUE	DOCUMENT ID		TECN	COMMENT
0.64 ±0.04 OUR AVERAGE				
$0.642 \pm 0.010 \pm 0.042$	[1] ALBRECHT	94C	ARG	$e^+e^- \to \Upsilon(4S)$
$0.63 \pm 0.06 \pm 0.06$	ALAM	87B	CLEO	$e^+e^- \to \Upsilon(4S)$

[1] ALBRECHT 94C assume a $K^0/\overline{K}{}^0$ multiplicity twice that of K^0_S.

$\Gamma(K^*(892)^{\pm}\text{anything})/\Gamma_{\text{total}}$ Γ_{63}/Γ

VALUE	DOCUMENT ID		TECN	COMMENT
0.182±0.054±0.024	ALBRECHT	94J	ARG	$e^+e^- \to \Upsilon(4S)$

$\Gamma(K^*(892)^0/\overline{K}{}^*(892)^0\text{anything})/\Gamma_{\text{total}}$ Γ_{64}/Γ

VALUE	DOCUMENT ID		TECN	COMMENT
0.146±0.016±0.020	ALBRECHT	94J	ARG	$e^+e^- \to \Upsilon(4S)$

$\Gamma(K^*(892)\gamma)/\Gamma_{\text{total}}$ Γ_{65}/Γ

VALUE (units 10^{-5})	CL%	DOCUMENT ID		TECN	COMMENT
4.24±0.54±0.32		[1] COAN	00	CLE2	$e^+e^- \to \Upsilon(4S)$
• • • We do not use the following data for averages, fits, limits, etc. • • •					
<150	90	[2] LESIAK	92	CBAL	$e^+e^- \to \Upsilon(4S)$
< 24	90	ALBRECHT	88H	ARG	$e^+e^- \to \Upsilon(4S)$

[1] An average of $B(B^+ \to K^*(892)^+\gamma)$ and $B(B^0 \to K^*(892)^0\gamma)$ measurements reported in COAN 00 by assuming full correlated systematic errors.

[2] LESIAK 92 set a limit on the inclusive process $B(b \to s\gamma) < 2.8 \times 10^{-3}$ at 90% CL for the range of masses of 892–2045 MeV, independent of assumptions about s-quark hadronization.

$\Gamma(\eta K\gamma)/\Gamma_{\text{total}}$ Γ_{66}/Γ

VALUE (units 10^{-6})	DOCUMENT ID		TECN	COMMENT
$\mathbf{8.5 \pm 1.3^{+1.2}_{-0.9}}$	[1] NISHIDA	05	BELL	$e^+e^- \to \Upsilon(4S)$

[1] $m_{\eta K} < 2.4$ GeV/c^2

$\Gamma(K_1(1400)\gamma)/\Gamma_{\text{total}}$ Γ_{67}/Γ

VALUE	CL%	DOCUMENT ID		TECN	COMMENT
<12.7 × 10⁻⁵	90	[1] COAN	00	CLE2	$e^+e^- \to \Upsilon(4S)$
• • • We do not use the following data for averages, fits, limits, etc. • • •					
$< 1.6 \times 10^{-3}$	90	[2] LESIAK	92	CBAL	$e^+e^- \to \Upsilon(4S)$
$< 4.1 \times 10^{-4}$	90	ALBRECHT	88H	ARG	$e^+e^- \to \Upsilon(4S)$

[1] Assumes equal production of B^+ and B^0 at the $\Upsilon(4S)$.

[2] LESIAK 92 set a limit on the inclusive process $B(b \to s\gamma) < 2.8 \times 10^{-3}$ at 90% CL for the range of masses of 892–2045 MeV, independent of assumptions about s-quark hadronization.

$\Gamma(K_2^*(1430)\gamma)/\Gamma_{\text{total}}$ Γ_{68}/Γ

VALUE (units 10^{-5})	CL%	DOCUMENT ID		TECN	COMMENT
$\mathbf{1.66^{+0.59}_{-0.53} \pm 0.13}$		[1] COAN	00	CLE2	$e^+e^- \to \Upsilon(4S)$
• • • We do not use the following data for averages, fits, limits, etc. • • •					
<83	90	ALBRECHT	88H	ARG	$e^+e^- \to \Upsilon(4S)$

[1] COAN 00 obtains a fitted signal yield of $15.9^{+5.7}_{-5.2}$ events. A search for contamination by $K^*(1410)$ yielded a rate consistent with 0; the central value assumes no contamination.

$\Gamma(K_2(1770)\gamma)/\Gamma_{total}$ Γ_{69}/Γ

VALUE	CL%	DOCUMENT ID		TECN	COMMENT
$<1.2\times10^{-3}$	90	[1] LESIAK	92	CBAL	$e^+e^-\to\Upsilon(4S)$

[1] LESIAK 92 set a limit on the inclusive process $B(b\to s\gamma)<2.8\times10^{-3}$ at 90% CL for the range of masses of 892–2045 MeV, independent of assumptions about s-quark hadronization.

$\Gamma(K_3^*(1780)\gamma)/\Gamma_{total}$ Γ_{70}/Γ

VALUE	CL%	DOCUMENT ID		TECN	COMMENT
$<3.7\times10^{-5}$	90	[1] NISHIDA	05	BELL	$e^+e^-\to\Upsilon(4S)$
• • • We do not use the following data for averages, fits, limits, etc. • • •					
$<3.0\times10^{-3}$	90	ALBRECHT	88H	ARG	$e^+e^-\to\Upsilon(4S)$

[1] Uses $B(K_3^*(1780)\to\eta K)=0.11^{+0.05}_{-0.04}$.

$\Gamma(K_4^*(2045)\gamma)/\Gamma_{total}$ Γ_{71}/Γ

VALUE	CL%	DOCUMENT ID		TECN	COMMENT
$<1.0\times10^{-3}$	90	[1] LESIAK	92	CBAL	$e^+e^-\to\Upsilon(4S)$

[1] LESIAK 92 set a limit on the inclusive process $B(b\to s\gamma)<2.8\times10^{-3}$ at 90% CL for the range of masses of 892–2045 MeV, independent of assumptions about s-quark hadronization.

$\Gamma(K\eta'(958))/\Gamma_{total}$ Γ_{72}/Γ

VALUE	DOCUMENT ID		TECN	COMMENT
$(8.3^{+0.9}_{-0.8}\pm0.7)\times10^{-5}$	[1] RICHICHI	00	CLE2	$e^+e^-\to\Upsilon(4S)$

[1] Assumes equal production of B^+ and B^0 at the $\Upsilon(4S)$.

$\Gamma(K^*(892)\eta'(958))/\Gamma_{total}$ Γ_{73}/Γ

VALUE (units 10^{-6})	CL%	DOCUMENT ID		TECN	COMMENT
$4.1^{+1.0}_{-0.9}\pm0.5$		[1] AUBERT	07E	BABR	$e^+e^-\to\Upsilon(4S)$
• • • We do not use the following data for averages, fits, limits, etc. • • •					
<22	90	[1] RICHICHI	00	CLE2	$e^+e^-\to\Upsilon(4S)$

[1] Assumes equal production of B^+ and B^0 at the $\Upsilon(4S)$.

$\Gamma(K\eta)/\Gamma_{total}$ Γ_{74}/Γ

VALUE	CL%	DOCUMENT ID		TECN	COMMENT
$<5.2\times10^{-6}$	90	[1] RICHICHI	00	CLE2	$e^+e^-\to\Upsilon(4S)$

[1] Assumes equal production of B^+ and B^0 at the $\Upsilon(4S)$.

$\Gamma(K^*(892)\eta)/\Gamma_{total}$ Γ_{75}/Γ

VALUE	DOCUMENT ID		TECN	COMMENT
$(1.80^{+0.49}_{-0.43}\pm0.18)\times10^{-5}$	[1] RICHICHI	00	CLE2	$e^+e^-\to\Upsilon(4S)$

[1] Assumes equal production of B^+ and B^0 at the $\Upsilon(4S)$.

$\Gamma(K\phi\phi)/\Gamma_{total}$ Γ_{76}/Γ

VALUE (units 10^{-6})	DOCUMENT ID		TECN	COMMENT
$2.3^{+0.9}_{-0.8}\pm0.3$	[1] HUANG	03	BELL	$e^+e^-\to\Upsilon(4S)$

[1] Assumes equal production of charged and neutral B meson pairs and isospin symmetry.

$\Gamma(\bar{b}\to\bar{s}\gamma)/\Gamma_{total}$ Γ_{77}/Γ

VALUE (units 10^{-4})	DOCUMENT ID		TECN	COMMENT
3.40±0.21 OUR AVERAGE				
$3.52\pm0.20\pm0.51$	[1,2] LEES	12U	BABR	$e^+e^-\to\Upsilon(4S)$
$3.32\pm0.16\pm0.31$	[1,3] LEES	12V	BABR	$e^+e^-\to\Upsilon(4S)$
$3.47\pm0.15\pm0.40$	[1,4] LIMOSANI	09	BELL	$e^+e^-\to\Upsilon(4S)$
$3.90\pm0.91\pm0.64$	[1,5] AUBERT	08O	BABR	$e^+e^-\to\Upsilon(4S)$
$3.36\pm0.53^{+0.65}_{-0.68}$	[6] ABE	01F	BELL	$e^+e^-\to\Upsilon(4S)$
$3.29\pm0.44\pm0.29$	[1,7] CHEN	01C	CLE2	$e^+e^-\to\Upsilon(4S)$
• • • We do not use the following data for averages, fits, limits, etc. • • •				
$2.30\pm0.08\pm0.30$	[8] DEL-AMO-SA...10M		BABR	$e^+e^-\to\Upsilon(4S)$
$4.3\ \pm0.3\ \pm0.7$	[9] AUBERT	09U	BABR	Repl. by DEL-AMO-SANCHEZ 10M
$3.92\pm0.31\pm0.47$	[1,10] AUBERT,BE	06B	BABR	Repl. by LEES 12V
$3.49\pm0.20^{+0.59}_{-0.46}$	[1,11] AUBERT,B	05R	BABR	Repl. by LEES 12U
$3.50\pm0.32\pm0.31$	[1,12] KOPPENBURG	04	BELL	Repl. by LIMOSANI 09
$2.32\pm0.57\pm0.35$	ALAM	95	CLE2	Repl. by CHEN 01C

[1] We correct it to $E_\gamma>1.6$ GeV using the method of BUCHMULLER 06 (average of three theoretical models).

[2] Reports $(3.29\pm0.19\pm0.48)\times10^{-4}$ for $E_\gamma>1.9$ GeV.

[3] Reports $(3.21\pm0.15\pm0.29\pm0.08)\times10^{-4}$ for $1.8<E_\gamma<2.8$ GeV, where the last systematic uncertainty is for model dependency. Results with other cutoffs are also reported.

[4] The measurement reported is $(3.45\pm0.15\pm0.40)\times10^{-4}$ for $E_\gamma>1.7$ GeV.

[5] Uses a fully reconstructed B meson as a tag on the recoil side. The measurement reported is $(3.66\pm0.85\pm0.60)\times10^{-4}$ for $E_\gamma>1.9$ GeV.

[6] ABE 01F reports their systematic errors $(\pm0.42^{+0.50}_{-0.54})\times10^{-4}$, where the second error is due to the theoretical uncertainty. We combine them in quadrature.

[7] The measurement reported is $(3.21\pm0.43^{+0.32}_{-0.29})\times10^{-4}$ for $E_\gamma>2.0$ GeV.

[8] Measured using sums of seven exclusive final states $B\to X_{d(s)}\gamma$ where $X_{d(s)}$ is a nonstrange (strange) charmless hadronic system in mass range 0.5–2.0 GeV/c^2.

[9] Measured using sums of seven exclusive final states $B\to X_{d(s)}\gamma$ where $X_{d(s)}$ is a nonstrange (strange) charmless hadronic system in mass range 0.6–1.8 GeV/c^2.

[10] The measurement reported is $(3.67\pm0.29\pm0.45)\times10^{-4}$ for $E_\gamma>1.9$ GeV.

[11] The measurement reported is $(3.27\pm0.18^{+0.55}_{-0.42})\times10^{-4}$ for $E_\gamma>1.9$ GeV.

[12] The measurement reported is $(3.55\pm0.32\pm0.32)\times10^{-4}$ for $E_\gamma>1.8$ GeV.

$\Gamma(\bar{b}\to\bar{d}\gamma)/\Gamma_{total}$ Γ_{78}/Γ

VALUE (units 10^{-6})	DOCUMENT ID		TECN	COMMENT
$9.2\pm2.0\pm2.3$	[1] DEL-AMO-SA...10M		BABR	$e^+e^-\to\Upsilon(4S)$
• • • We do not use the following data for averages, fits, limits, etc. • • •				
$14\ \pm5\ \pm4$	[2] AUBERT	09U	BABR	Repl. by DEL-AMO-SANCHEZ 10M

[1] Measured using sums of seven exclusive final states $B\to X_{d(s)}\gamma$ where $X_{d(s)}$ is a nonstrange (strange) charmless hadronic system in mass range 0.5–2.0 GeV/c^2.

[2] Measured using sums of seven exclusive final states $B\to X_{d(s)}\gamma$ where $X_{d(s)}$ is a nonstrange (strange) charmless hadronic system in mass range 0.6–1.8 GeV/c^2.

$\Gamma(\bar{b}\to\bar{d}\gamma)/\Gamma(\bar{b}\to\bar{s}\gamma)$ Γ_{78}/Γ_{77}

VALUE	DOCUMENT ID		TECN	COMMENT
$0.040\pm0.009\pm0.010$	[1] DEL-AMO-SA...10M		BABR	$e^+e^-\to\Upsilon(4S)$
• • • We do not use the following data for averages, fits, limits, etc. • • •				
$0.033\pm0.013\pm0.009$	[2] AUBERT	09U	BABR	Repl. by DEL-AMO-SANCHEZ 10M

[1] Measured using sums of seven exclusive final states $B\to X_{d(s)}\gamma$ where $X_{d(s)}$ is a nonstrange (strange) charmless hadronic system in mass range 0.5–2.0 GeV/c^2.

[2] Measured using sums of seven exclusive final states $B\to X_{d(s)}\gamma$ where $X_{d(s)}$ is a nonstrange (strange) charmless hadronic system in mass range 0.6–1.8 GeV/c^2.

$\Gamma(\bar{b}\to\bar{s}\text{gluon})/\Gamma_{total}$ Γ_{79}/Γ

VALUE	CL%	EVTS	DOCUMENT ID		TECN	COMMENT
<0.068	90		[1] COAN	98	CLE2	$e^+e^-\to\Upsilon(4S)$
• • • We do not use the following data for averages, fits, limits, etc. • • •						
<0.08		2	[2] ALBRECHT	95D	ARG	$e^+e^-\to\Upsilon(4S)$

[1] COAN 98 uses D-ℓ correlation.

[2] ALBRECHT 95D use full reconstruction of one B decay as tag. Two candidate events for charmless B decay can be interpreted as either $b\to s$gluon or $b\to u$ transition. If interpreted as $b\to s$gluon they find a branching ratio of ~0.026 or the upper limit quoted above. Result is highly model dependent.

$\Gamma(\eta\text{ anything})/\Gamma_{total}$ Γ_{80}/Γ

VALUE (units 10^{-4})	CL%	DOCUMENT ID		TECN	COMMENT
$2.61\pm0.30^{+0.44}_{-0.74}$		[1] NISHIMURA	10	BELL	$e^+e^-\to\Upsilon(4S)$
• • • We do not use the following data for averages, fits, limits, etc. • • •					
$1.69\pm0.29^{+0.36}_{-0.62}$		[2] NISHIMURA	10	BELL	$e^+e^-\to\Upsilon(4S)$
<4.4	90	[3] BROWDER	98	CLE2	$e^+e^-\to\Upsilon(4S)$

[1] Uses $B\to\eta X_s$ with $0.4<m_{X_s}<2.6$ GeV/c^2.

[2] Uses $B\to\eta X_s$ with $1.8<m_{X_s}<2.6$ GeV/c^2.

[3] BROWDER 98 search for high momentum $B\to\eta X_s$ between 2.1 and 2.7 GeV/c.

$\Gamma(\eta'\text{ anything})/\Gamma_{total}$ Γ_{81}/Γ

VALUE (units 10^{-4})	DOCUMENT ID		TECN	COMMENT
4.2±0.9 OUR AVERAGE				
$3.9\pm0.8\pm0.9$	[1] AUBERT,B	04F	BABR	$e^+e^-\to\Upsilon(4S)$
$4.6\pm1.1\pm0.6$	[2] BONVICINI	03	CLE2	$e^+e^-\to\Upsilon(4S)$
• • • We do not use the following data for averages, fits, limits, etc. • • •				
$6.2\pm1.6^{+1.3}_{-2.0}$	[3] BROWDER	98	CLE2	$e^+e^-\to\Upsilon(4S)$

[1] AUBERT,B 04F reports branching ratio $B\to\eta' X_s$ for high momentum η' between 2.0 and 2.7 GeV/c in the $\Upsilon(4S)$ center-of-mass frame. X_s represents a recoil system consisting of a kaon and zero to four pions.

[2] BONVICINI 03 observed a signal of 61.2 ± 13.9 events in $B\to\eta' X_{nc}$ production for high momentum η' between 2.0 and 2.7 GeV/c in the $\Upsilon(4S)$ center-of-mass frame. The X_{nc} denotes "charmless" hadronic states recoiling against η'. The second error combines systematic and background subtraction uncertainties in quadrature.

[3] BROWDER 98 observed a signal of 39.0 ± 11.6 events in high momentum $B\to\eta' X_s$ production between 2.0 and 2.7 GeV/c. The branching fraction is based on the interpretation of $b\to sg$, where the last error includes additional uncertainties due to the color-suppressed $b\to$ backgrounds.

$\Gamma(K^+\text{gluon (charmless)})/\Gamma_{total}$ Γ_{82}/Γ

VALUE (units 10^{-4})	CL%	DOCUMENT ID		TECN	COMMENT
<1.87	90	[1] DEL-AMO-SA...11		BABR	$e^+e^-\to\Upsilon(4S)$

[1] $B\to K^+X$ with $m_X<1.69$ GeV/c^2.

$\Gamma(K^0\text{gluon (charmless)})/\Gamma_{total}$ Γ_{83}/Γ

VALUE (units 10^{-4})	DOCUMENT ID		TECN	COMMENT
$1.95^{+0.51}_{-0.45}\pm0.50$	[1] DEL-AMO-SA...11		BABR	$e^+e^-\to\Upsilon(4S)$

[1] $B\to K^0X$ with $m_X<1.69$ GeV/c^2.

$\Gamma(\rho\gamma)/\Gamma_{\text{total}}$ Γ_{84}/Γ

VALUE (units 10^{-6})	CL%	DOCUMENT ID		TECN	COMMENT
1.39±0.25 OUR AVERAGE		Error includes scale factor of 1.2.			
$1.73^{+0.34}_{-0.32}\pm0.17$		[1,2] AUBERT	08BH	BABR	$e^+e^- \to \Upsilon(4S)$
$1.21^{+0.24}_{-0.22}\pm0.12$		[1,2] TANIGUCHI	08	BELL	$e^+e^- \to \Upsilon(4S)$
• • • We do not use the following data for averages, fits, limits, etc. • • •					
$1.36^{+0.29}_{-0.27}\pm0.10$		[1,3] AUBERT	07L	BABR	Repl. by AUBERT 08BH
< 1.9	90	[1,3] AUBERT	04C	BABR	Repl. by AUBERT 07L
<14	90	[1,4] COAN	00	CLE2	$e^+e^- \to \Upsilon(4S)$

[1] Assumes equal production of B^+ and B^0 at the $\Upsilon(4S)$.
[2] Assumes $\Gamma(B \to \rho\gamma) = \Gamma(B^+ \to \rho^+\gamma) = 2\,\Gamma(B^0 \to \rho^0\gamma)$ and uses lifetime ratio of $\tau_{B^+}/\tau_{B^0} = 1.071 \pm 0.009$.
[3] Assumes $\Gamma(B \to \rho\gamma) = \Gamma(B^+ \to \rho^+\gamma) = 2\,\Gamma(B^0 \to \rho^0\gamma)$ and uses lifetime ratio of $\tau_{B^+}/\tau_{B^0} = 1.083 \pm 0.017$.
[4] COAN 00 reports $B(B \to \rho\gamma)/B(B \to K^*(892)\gamma) < 0.32$ at 90%CL and scaled by the central value of $B(B \to K^*(892)\gamma)=(4.24 \pm 0.54 \pm 0.32) \times 10^{-5}$.

$\Gamma(\rho\gamma)/\Gamma(K^*(892)\gamma)$ Γ_{84}/Γ_{65}

VALUE (units 10^{-2})	DOCUMENT ID		TECN	COMMENT
$\mathbf{3.02^{+0.60+0.26}_{-0.55-0.28}}$	TANIGUCHI	08	BELL	$e^+e^- \to \Upsilon(4S)$

$\Gamma(\rho/\omega\gamma)/\Gamma_{\text{total}}$ Γ_{85}/Γ

VALUE (units 10^{-6})	CL%	DOCUMENT ID		TECN	COMMENT
1.30±0.23 OUR AVERAGE		Error includes scale factor of 1.2.			
$1.63^{+0.30}_{-0.28}\pm0.16$		[1,2,3] AUBERT	08BH	BABR	$e^+e^- \to \Upsilon(4S)$
$1.14\pm0.20^{+0.10}_{-0.12}$		[1,3] TANIGUCHI	08	BELL	$e^+e^- \to \Upsilon(4S)$
• • • We do not use the following data for averages, fits, limits, etc. • • •					
$1.25^{+0.25}_{-0.24}\pm0.09$		[4] AUBERT	07L	BABR	Repl. by AUBERT 08BH
$1.32^{+0.34+0.10}_{-0.31-0.09}$		[4] MOHAPATRA	06	BELL	Repl. by TANIGUCHI 08
0.6 ±0.3 ±0.1		[4] AUBERT	05	BABR	Repl. by AUBERT 07L
<1.4	90	[4] MOHAPATRA	05	BELL	$e^+e^- \to \Upsilon(4S)$

[1] Assumes $\Gamma(B \to \rho\gamma) = \Gamma(B^+ \to \rho^+\gamma) = 2\,\Gamma(B^0 \to \rho^0\gamma)$ and uses lifetime ratio of $\tau_{B^+}/\tau_{B^0} = 1.071 \pm 0.009$.
[2] Also reports $|V_{td}/V_{ts}| = 0.233^{+0.025+0.022}_{-0.024-0.021}$.
[3] Assumes equal production of B^+ and B^0 at the $\Upsilon(4S)$.
[4] Assumes $\Gamma(B \to \rho\gamma) = \Gamma(B^+ \to \rho^+\gamma) = 2\,\Gamma(B^0 \to \rho^0\gamma)$ and uses lifetime ratio of $\tau_{B^+}/\tau_{B^0} = 1.083 \pm 0.017$.

$\Gamma(\rho/\omega\gamma)/\Gamma(K^*(892)\gamma)$ Γ_{85}/Γ_{65}

VALUE (units 10^{-2})	CL%	DOCUMENT ID		TECN	COMMENT
$\mathbf{2.84\pm0.50^{+0.27}_{-0.29}}$		[1] TANIGUCHI	08	BELL	$e^+e^- \to \Upsilon(4S)$
• • • We do not use the following data for averages, fits, limits, etc. • • •					
<3.5	90	MOHAPATRA	05	BELL	Repl. by TANIGUCHI 08

[1] Also reports $|V_{td}/V_{ts}| = 0.195^{+0.020}_{-0.019} \pm 0.015$.

$\Gamma(\pi^{\pm}\text{ anything})/\Gamma_{\text{total}}$ Γ_{86}/Γ

VALUE	DOCUMENT ID		TECN	COMMENT
3.585±0.025±0.070	[1] ALBRECHT	93I	ARG	$e^+e^- \to \Upsilon(4S)$

[1] ALBRECHT 93 excludes $\pi^{\pm}$ from K^0_S and Λ decays. If included, they find 4.105 ± 0.025 ± 0.080.

$\Gamma(\pi^0\text{ anything})/\Gamma_{\text{total}}$ Γ_{87}/Γ

VALUE	DOCUMENT ID		TECN	COMMENT
2.35±0.02±0.11	[1] ABE	01J	BELL	$e^+e \to \Upsilon(4S)$

[1] From fully inclusive π^0 yield with no corrections from decays of K^0_S or other particles.

$\Gamma(\eta\text{ anything})/\Gamma_{\text{total}}$ Γ_{88}/Γ

VALUE	DOCUMENT ID		TECN	COMMENT
0.176±0.011±0.012	KUBOTA	96	CLE2	$e^+e^- \to \Upsilon(4S)$

$\Gamma(\rho^0\text{ anything})/\Gamma_{\text{total}}$ Γ_{89}/Γ

VALUE	DOCUMENT ID		TECN	COMMENT
0.208±0.042±0.032	ALBRECHT	94J	ARG	$e^+e^- \to \Upsilon(4S)$

$\Gamma(\omega\text{ anything})/\Gamma_{\text{total}}$ Γ_{90}/Γ

VALUE	CL%	DOCUMENT ID		TECN	COMMENT
<0.81	90	ALBRECHT	94J	ARG	$e^+e^- \to \Upsilon(4S)$

$\Gamma(\phi\text{ anything})/\Gamma_{\text{total}}$ Γ_{91}/Γ

VALUE	DOCUMENT ID		TECN	COMMENT
0.0343±0.0012 OUR AVERAGE				
0.0353±0.0005±0.0030	HUANG	07	CLEO	$e^+e^- \to \Upsilon(4S)$
0.0341±0.0006±0.0012	AUBERT	04S	BABR	$e^+e^- \to \Upsilon(4S)$
0.0390±0.0030±0.0035	ALBRECHT	94J	ARG	$e^+e^- \to \Upsilon(4S)$
0.023 ±0.006 ±0.005	BORTOLETTO	86	CLEO	$e^+e^- \to \Upsilon(4S)$

$\Gamma(\phi K^*(892))/\Gamma_{\text{total}}$ Γ_{92}/Γ

VALUE	CL%	DOCUMENT ID		TECN
<2.2 × 10^{-5}	90	[1] BERGFELD	98	CLE2

[1] Assumes equal production of B^+ and B^0 at the $\Upsilon(4S)$.

$\Gamma(\pi^+\text{ gluon (charmless)})/\Gamma_{\text{total}}$ Γ_{94}/Γ

VALUE (units 10^{-4})	DOCUMENT ID		TECN	COMMENT
$\mathbf{3.72^{+0.50}_{-0.47}\pm0.59}$	[1] DEL-AMO-SA...11		BABR	$e^+e^- \to \Upsilon(4S)$

[1] $B \to \pi^+ X$ with $m_X < 1.71$ GeV/c^2.

$\Gamma(\Lambda_c^+ / \overline{\Lambda}_c^-\text{ anything})/\Gamma_{\text{total}}$ Γ_{95}/Γ

VALUE	CL%	DOCUMENT ID		TECN	COMMENT
0.045±0.003±0.012		[1] AUBERT	07C	BABR	$e^+e^- \to \Upsilon(4S)$
• • • We do not use the following data for averages, fits, limits, etc. • • •					
0.064±0.008±0.008		[2] CRAWFORD	92	CLEO	$e^+e^- \to \Upsilon(4S)$
0.14 ±0.09		[3] ALBRECHT	88E	ARG	$e^+e^- \to \Upsilon(4S)$
<0.112	90	[4] ALAM	87	CLEO	$e^+e^- \to \Upsilon(4S)$

[1] AUBERT 07C reports 0.045 ± 0.003 ± 0.012 from a measurement of $[\Gamma(B \to \Lambda_c^+ / \overline{\Lambda}_c^-\text{ anything})/\Gamma_{\text{total}}] \times [B(\Lambda_c^+ \to p K^-\pi^+)]$ assuming $B(\Lambda_c^+ \to p K^-\pi^+) = (5.0 \pm 1.3) \times 10^{-2}$.
[2] CRAWFORD 92 result derived from lepton baryon correlations. Assumes all charmed baryons in B^0 and $B^{\pm}$ decay are Λ_c.
[3] ALBRECHT 88E measured $B(B \to \Lambda_c^+ X)\cdot B(\Lambda_c^+ \to p K^-\pi^+) = (0.30 \pm 0.12 \pm 0.06)\%$ and used $B(\Lambda_c^+ \to p K^-\pi^+) = (2.2 \pm 1.0)\%$ from ABRAMS 80 to obtain above number.
[4] Assuming all baryons result from charmed baryons, ALAM 86 conclude the branching fraction is 7.4 ± 2.9%. The limit given above is model independent.

$\Gamma(\Lambda_c^+\text{ anything})/\Gamma(\overline{\Lambda}_c^-\text{ anything})$ Γ_{96}/Γ_{97}

VALUE	DOCUMENT ID		TECN	COMMENT
0.19±0.13±0.04	[1] AMMAR	97	CLE2	$e^+e^- \to \Upsilon(4S)$

[1] AMMAR 97 uses a high-momentum lepton tag ($P_\ell > 1.4$ GeV/c^2).

$\Gamma(\overline{\Lambda}_c^-\mu^+\text{ anything})/\Gamma(\overline{\Lambda}_c^-\text{ anything})$ Γ_{100}/Γ_{97}

VALUE (units 10^{-2})	DOCUMENT ID		TECN	COMMENT
−2.0±2.0±1.9	LEES	12	BABR	$e^+e^- \to \Upsilon(4S)$

$\Gamma(\overline{\Lambda}_c^-\ell^+\text{ anything})/\Gamma(\Lambda_c^+ / \overline{\Lambda}_c^-\text{ anything})$ Γ_{98}/Γ_{95}

VALUE	CL%	DOCUMENT ID		TECN	COMMENT
<2.5 × 10^{-2}	90	[1] LEES	12	BABR	$e^+e^- \to \Upsilon(4S)$

[1] LEES 12 quotes also the measurement $\Gamma(B \to \overline{\Lambda}_c^-\ell^+\text{ anything})/\Gamma(B \to \Lambda_c^+ / \overline{\Lambda}_c^-\text{ anything}) = (1.2 \pm 0.7 \pm 0.4) \times 10^{-2}$.

$\Gamma(\overline{\Lambda}_c^- e^+\text{ anything})/\Gamma(\Lambda_c^+ / \overline{\Lambda}_c^-\text{ anything})$ Γ_{99}/Γ_{95}

VALUE	CL%	DOCUMENT ID		TECN	COMMENT
<0.05	90	[1] BONVICINI	98	CLE2	$e^+e^- \to \Upsilon(4S)$

[1] BONVICINI 98 uses the electron with momentum above 0.6 GeV/c.

$\Gamma(\overline{\Lambda}_c^- e^+\text{ anything})/\Gamma(\overline{\Lambda}_c^-\text{ anything})$ Γ_{99}/Γ_{97}

VALUE (units 10^{-2})	DOCUMENT ID		TECN	COMMENT
2.5±1.1±0.6	[1] LEES	12	BABR	$e^+e^- \to \Upsilon(4S)$

[1] Uses the full reconstruction of the recoiling B in a hadronic decay as a tag.

$\Gamma(\overline{\Lambda}_c^-\ell^+\text{ anything})/\Gamma(\overline{\Lambda}_c^-\text{ anything})$ Γ_{98}/Γ_{97}

VALUE	CL%	DOCUMENT ID		TECN	COMMENT
<3.5 × 10^{-2}	90	[1] LEES	12	BABR	$e^+e^- \to \Upsilon(4S)$

[1] LEES 12 quotes also the measurement $\Gamma(B \to \overline{\Lambda}_c^-\ell^+\text{ anything})/\Gamma(B \to \overline{\Lambda}_c^-\text{ anything}) = (1.7 \pm 1.0 \pm 0.6) \times 10^{-2}$.

$\Gamma(\overline{\Lambda}_c^- p\text{ anything})/\Gamma(\Lambda_c^+ / \overline{\Lambda}_c^-\text{ anything})$ Γ_{101}/Γ_{95}

VALUE	DOCUMENT ID		TECN	COMMENT
0.57±0.05±0.05	BONVICINI	98	CLE2	$e^+e^- \to \Upsilon(4S)$

$\Gamma(\overline{\Lambda}_c^- p e^+\nu_e)/\Gamma(\overline{\Lambda}_c^- p\text{ anything})$ $\Gamma_{102}/\Gamma_{101}$

VALUE	CL%	DOCUMENT ID		TECN	COMMENT
<0.04	90	[1] BONVICINI	98	CLE2	$e^+e^- \to \Upsilon(4S)$

[1] BONVICINI 98 uses the electron with momentum above 0.6 GeV/c.

$\Gamma(\overline{\Sigma}_c^{--}\text{anything})/\Gamma_{\text{total}}$ Γ_{103}/Γ

VALUE	EVTS	DOCUMENT ID		TECN	COMMENT
0.0042±0.0021±0.0011	77	[1] PROCARIO	94	CLE2	$e^+e^- \to \Upsilon(4S)$

[1] PROCARIO 94 reports $[\Gamma(B \to \overline{\Sigma}_c^{--}\text{anything})/\Gamma_{\text{total}}] \times [B(\Lambda_c^+ \to p K^-\pi^+)] = 0.00021 \pm 0.00008 \pm 0.00007$ which we divide by our best value $B(\Lambda_c^+ \to p K^-\pi^+) = (5.0 \pm 1.3) \times 10^{-2}$. Our first error is their experiment's error and our second error is the systematic error from using our best value.

$\Gamma(\Sigma_c^- \text{anything})/\Gamma_{\text{total}}$ Γ_{104}/Γ

VALUE	CL%	DOCUMENT ID		TECN	COMMENT
<0.010	90	[1] PROCARIO	94	CLE2	$e^+e^- \to \Upsilon(4S)$

[1] PROCARIO 94 reports $[\Gamma(B \to \overline{\Sigma}_c^- \text{anything})/\Gamma_{\text{total}}] \times [B(\Lambda_c^+ \to pK^-\pi^+)] < 0.00048$ which we divide by our best value $B(\Lambda_c^+ \to pK^-\pi^+) = 5.0 \times 10^{-2}$.

$\Gamma(\Sigma_c^0 \text{anything})/\Gamma_{\text{total}}$ Γ_{105}/Γ

VALUE	EVTS	DOCUMENT ID		TECN	COMMENT
0.0046±0.0021±0.0012	76	[1] PROCARIO	94	CLE2	$e^+e^- \to \Upsilon(4S)$

[1] PROCARIO 94 reports $[\Gamma(B \to \overline{\Sigma}_c^0 \text{anything})/\Gamma_{\text{total}}] \times [B(\Lambda_c^+ \to pK^-\pi^+)] = 0.00023 \pm 0.00008 \pm 0.00007$ which we divide by our best value $B(\Lambda_c^+ \to pK^-\pi^+) = (5.0 \pm 1.3) \times 10^{-2}$. Our first error is their experiment's error and our second error is the systematic error from using our best value.

$\Gamma(\Sigma_c^0 N (N = p \text{ or } n))/\Gamma_{\text{total}}$ Γ_{106}/Γ

VALUE	CL%	DOCUMENT ID		TECN	COMMENT
$<1.5 \times 10^{-3}$	90	[1] PROCARIO	94	CLE2	$e^+e^- \to \Upsilon(4S)$

[1] PROCARIO 94 reports < 0.0017 from a measurement of $[\Gamma(B \to \overline{\Sigma}_c^0 N(N = p \text{ or } n))/\Gamma_{\text{total}}] \times [B(\Lambda_c^+ \to pK^-\pi^+)]$ assuming $B(\Lambda_c^+ \to pK^-\pi^+) = 0.043$, which we rescale to our best value $B(\Lambda_c^+ \to pK^-\pi^+) = 5.0 \times 10^{-2}$.

$\Gamma(\Xi_c^0 \text{anything} \times B(\Xi_c^0 \to \Xi^-\pi^+))/\Gamma_{\text{total}}$ Γ_{107}/Γ

VALUE (units 10^{-3})	DOCUMENT ID		TECN	COMMENT
0.193±0.030 OUR AVERAGE	Error includes scale factor of 1.1.			
0.211±0.019±0.025	[1] AUBERT,B	05M	BABR	$e^+e^- \to \Upsilon(4S)$
0.144±0.048±0.021	[2] BARISH	97	CLE2	$e^+e^- \to \Upsilon(4S)$

[1] The yield is obtained by requiring the momentum $P < 2.15$ GeV/c.
[2] BARISH 97 find 79 ± 27 Ξ_c^0 events.

$\Gamma(\Xi_c^+ \text{anything} \times B(\Xi_c^+ \to \Xi^-\pi^+\pi^+))/\Gamma_{\text{total}}$ Γ_{108}/Γ

VALUE (units 10^{-3})	DOCUMENT ID		TECN	COMMENT
$0.453 \pm 0.096 {}^{+0.085}_{-0.065}$	[1] BARISH	97	CLE2	$e^+e^- \to \Upsilon(4S)$

[1] BARISH 97 find 125 ± 28 Ξ_c^+ events.

$\Gamma(p/\overline{p} \text{anything})/\Gamma_{\text{total}}$ Γ_{109}/Γ

Includes p and $\overline{p}$ from Λ and $\overline{\Lambda}$ decay.

VALUE	EVTS	DOCUMENT ID		TECN	COMMENT
0.080±0.004 OUR AVERAGE					
0.080±0.005±0.005		ALBRECHT	93I	ARG	$e^+e^- \to \Upsilon(4S)$
0.080±0.005±0.003		CRAWFORD	92	CLEO	$e^+e^- \to \Upsilon(4S)$
$0.082 \pm 0.005 {}^{+0.013}_{-0.010}$	2163	[1] ALBRECHT	89K	ARG	$e^+e^- \to \Upsilon(4S)$
• • • We do not use the following data for averages, fits, limits, etc. • • •					
>0.021		[2] ALAM	83B	CLEO	$e^+e^- \to \Upsilon(4S)$

[1] ALBRECHT 89K include direct and nondirect protons.
[2] ALAM 83B reported their result as $> 0.036 \pm 0.006 \pm 0.009$. Data are consistent with equal yields of p and $\overline{p}$. Using assumed yields below cut, $B(B \to p + X) = 0.03$ not including protons from Λ decays.

$\Gamma(p/\overline{p} \text{ (direct) anything})/\Gamma_{\text{total}}$ Γ_{110}/Γ

VALUE	EVTS	DOCUMENT ID		TECN	COMMENT
0.055±0.005 OUR AVERAGE					
0.055±0.005±0.0035		ALBRECHT	93I	ARG	$e^+e^- \to \Upsilon(4S)$
0.056±0.006±0.005		CRAWFORD	92	CLEO	$e^+e^- \to \Upsilon(4S)$
0.055±0.016	1220	[1] ALBRECHT	89K	ARG	$e^+e^- \to \Upsilon(4S)$

[1] ALBRECHT 89K subtract contribution of Λ decay from the inclusive proton yield.

$\Gamma(\Lambda/\overline{\Lambda} \text{anything})/\Gamma_{\text{total}}$ Γ_{111}/Γ

VALUE	EVTS	DOCUMENT ID		TECN	COMMENT
0.040±0.005 OUR AVERAGE					
0.038±0.004±0.006	2998	CRAWFORD	92	CLEO	$e^+e^- \to \Upsilon(4S)$
0.042±0.005±0.006	943	ALBRECHT	89K	ARG	$e^+e^- \to \Upsilon(4S)$
• • • We do not use the following data for averages, fits, limits, etc. • • •					
0.022±0.003±0.0022		[1] ACKERSTAFF	97N	OPAL	$e^+e^- \to Z$
>0.011		[2] ALAM	83B	CLEO	$e^+e^- \to \Upsilon(4S)$

[1] ACKERSTAFF 97N assumes $B(b \to B) = 0.868 \pm 0.041$, *i.e.*, an admixture of B^0, $B^{\pm}$, and B_s.
[2] ALAM 83B reported their result as $> 0.022 \pm 0.007 \pm 0.004$. Values are for $(B(\Lambda X)+B(\overline{\Lambda} X))/2$. Data are consistent with equal yields of p and $\overline{p}$. Using assumed yields below cut, $B(B \to \Lambda X) = 0.03$.

$\Gamma(\Lambda \text{anything})/\Gamma(\overline{\Lambda} \text{anything})$ $\Gamma_{112}/\Gamma_{113}$

VALUE	DOCUMENT ID		TECN	COMMENT
0.43±0.09±0.07	[1] AMMAR	97	CLE2	$e^+e^- \to \Upsilon(4S)$

[1] AMMAR 97 uses a high-momentum lepton tag ($P_\ell > 1.4$ GeV/c^2).

$\Gamma(\Xi^-/\overline{\Xi}^+ \text{anything})/\Gamma_{\text{total}}$ Γ_{114}/Γ

VALUE	EVTS	DOCUMENT ID		TECN	COMMENT
0.0027±0.0006 OUR AVERAGE					
0.0027±0.0005±0.0004	147	CRAWFORD	92	CLEO	$e^+e^- \to \Upsilon(4S)$
0.0028±0.0014	54	ALBRECHT	89K	ARG	$e^+e^- \to \Upsilon(4S)$

$\Gamma(\text{baryons anything})/\Gamma_{\text{total}}$ Γ_{115}/Γ

VALUE	DOCUMENT ID		TECN	COMMENT
0.068±0.005±0.003	[1] ALBRECHT	92O	ARG	$e^+e^- \to \Upsilon(4S)$
• • • We do not use the following data for averages, fits, limits, etc. • • •				
0.076±0.014	[2] ALBRECHT	89K	ARG	$e^+e^- \to \Upsilon(4S)$

[1] ALBRECHT 92O result is from simultaneous analysis of p and Λ yields, $p\overline{p}$ and $\Lambda\overline{p}$ correlations, and various lepton-baryon and lepton-baryon-antibaryon correlations. Supersedes ALBRECHT 89K.
[2] ALBRECHT 89K obtain this result by adding their their measurements $(5.5 \pm 1.6)\%$ for direct protons and $(4.2 \pm 0.5 \pm 0.6)\%$ for inclusive Λ production. They then assume $(5.5 \pm 1.6)\%$ for neutron production and add it in also. Since each B decay has two baryons, they divide by 2 to obtain $(7.6 \pm 1.4)\%$.

$\Gamma(p\overline{p} \text{ anything})/\Gamma_{\text{total}}$ Γ_{116}/Γ

Includes p and $\overline{p}$ from Λ and $\overline{\Lambda}$ decay.

VALUE	EVTS	DOCUMENT ID		TECN	COMMENT
0.0247±0.0023 OUR AVERAGE					
0.024 ±0.001 ±0.004		CRAWFORD	92	CLEO	$e^+e^- \to \Upsilon(4S)$
0.025 ±0.002 ±0.002	918	ALBRECHT	89K	ARG	$e^+e^- \to \Upsilon(4S)$

$\Gamma(p\overline{p} \text{ anything})/\Gamma(p/\overline{p} \text{ anything})$ $\Gamma_{116}/\Gamma_{109}$

Includes p and $\overline{p}$ from Λ and $\overline{\Lambda}$ decay.

VALUE	DOCUMENT ID		TECN	COMMENT
• • • We do not use the following data for averages, fits, limits, etc. • • •				
0.30±0.02±0.05	[1] CRAWFORD	92	CLEO	$e^+e^- \to \Upsilon(4S)$

[1] CRAWFORD 92 value is not independent of their $\Gamma(p\overline{p} \text{anything})/\Gamma_{\text{total}}$ value.

$\Gamma(\Lambda\overline{p}/\overline{\Lambda}p \text{ anything})/\Gamma_{\text{total}}$ Γ_{117}/Γ

Includes p and $\overline{p}$ from Λ and $\overline{\Lambda}$ decay.

VALUE	EVTS	DOCUMENT ID		TECN	COMMENT
0.025±0.004 OUR AVERAGE					
0.029±0.005±0.005		CRAWFORD	92	CLEO	$e^+e^- \to \Upsilon(4S)$
0.023±0.004±0.003	165	ALBRECHT	89K	ARG	$e^+e^- \to \Upsilon(4S)$

$\Gamma(\Lambda\overline{p}/\overline{\Lambda}p \text{ anything})/\Gamma(\Lambda/\overline{\Lambda} \text{ anything})$ $\Gamma_{117}/\Gamma_{111}$

Includes p and $\overline{p}$ from Λ and $\overline{\Lambda}$ decay.

VALUE	DOCUMENT ID		TECN	COMMENT
• • • We do not use the following data for averages, fits, limits, etc. • • •				
0.76±0.11±0.08	[1] CRAWFORD	92	CLEO	$e^+e^- \to \Upsilon(4S)$

[1] CRAWFORD 92 value is not independent of their $[\Gamma(\Lambda\overline{p} \text{anything})+\Gamma(\overline{\Lambda}p \text{anything})]/\Gamma_{\text{total}}$ value.

$\Gamma(\Lambda\overline{\Lambda} \text{ anything})/\Gamma_{\text{total}}$ Γ_{118}/Γ

VALUE	CL%	EVTS	DOCUMENT ID		TECN	COMMENT
<0.005	90		CRAWFORD	92	CLEO	$e^+e^- \to \Upsilon(4S)$
• • • We do not use the following data for averages, fits, limits, etc. • • •						
<0.0088	90	12	ALBRECHT	89K	ARG	$e^+e^- \to \Upsilon(4S)$

$\Gamma(\Lambda\overline{\Lambda} \text{ anything})/\Gamma(\Lambda/\overline{\Lambda} \text{ anything})$ $\Gamma_{118}/\Gamma_{111}$

VALUE	CL%	DOCUMENT ID		TECN	COMMENT
• • • We do not use the following data for averages, fits, limits, etc. • • •					
<0.13	90	[1] CRAWFORD	92	CLEO	$e^+e^- \to \Upsilon(4S)$

[1] CRAWFORD 92 value is not independent of their $\Gamma(\Lambda\overline{\Lambda} \text{anything})/\Gamma_{\text{total}}$ value.

$\Gamma(se^+e^-)/\Gamma_{\text{total}}$ Γ_{119}/Γ

Test for $\Delta B = 1$ weak neutral current. Allowed by higher-order electroweak interactions.

VALUE (units 10^{-6})	CL%	DOCUMENT ID		TECN	COMMENT
4.7 ±1.3 OUR AVERAGE					
$4.04 \pm 1.30 {}^{+0.87}_{-0.83}$		[1] IWASAKI	05	BELL	$e^+e^- \to \Upsilon(4S)$
6.0 ±1.7 ±1.3		[2] AUBERT,B	04I	BABR	$e^+e^- \to \Upsilon(4S)$
• • • We do not use the following data for averages, fits, limits, etc. • • •					
$5.0 \pm 2.3 {}^{+1.3}_{-1.1}$		[2] KANEKO	03	BELL	Repl. by IWASAKI 05
< 57	90	GLENN	98	CLEO	$e^+e^- \to \Upsilon(4S)$
<50000	90	BEBEK	81	CLEO	$e^+e^- \to \Upsilon(4S)$

[1] Requires $M_{\ell^+\ell^-} > 0.2$ GeV/c^2.
[2] Requires $M_{e^+e^-} > 0.2$ GeV/c^2.

$\Gamma(s\mu^+\mu^-)/\Gamma_{\text{total}}$ Γ_{120}/Γ

Test for $\Delta B = 1$ weak neutral current. Allowed by higher-order electroweak interactions.

VALUE (units 10^{-6})	CL%	DOCUMENT ID		TECN	COMMENT
4.3 ±1.2 OUR AVERAGE					
$4.13 \pm 1.05 {}^{+0.85}_{-0.81}$		[1] IWASAKI	05	BELL	$e^+e^- \to \Upsilon(4S)$
5.0 ±2.8 ±1.2		AUBERT,B	04I	BABR	$e^+e^- \to \Upsilon(4S)$
• • • We do not use the following data for averages, fits, limits, etc. • • •					
7.9 ±2.1 $+2.1$ -1.5		KANEKO	03	BELL	Repl. by IWASAKI 05
< 58	90	GLENN	98	CLEO	$e^+e^- \to \Upsilon(4S)$
<17000	90	CHADWICK	81	CLEO	$e^+e^- \to \Upsilon(4S)$

[1] Requires $M_{\ell^+\ell^-} > 0.2$ GeV/c^2.

$[\Gamma(se^+e^-)+\Gamma(s\mu^+\mu^-)]/\Gamma_{total}$ $(\Gamma_{119}+\Gamma_{120})/\Gamma$

Test for $\Delta B = 1$ weak neutral current. Allowed by higher-order electroweak interactions.

VALUE	CL%	DOCUMENT ID		TECN	COMMENT
<4.2 ×10⁻⁵	90	GLENN	98	CLEO	$e^+e^- \to \Upsilon(4S)$
• • • We do not use the following data for averages, fits, limits, etc. • • •					
<0.0024	90	[1] BEAN	87	CLEO	Repl. by GLENN 98
<0.0062	90	[2] AVERY	84	CLEO	Repl. by BEAN 87

[1] BEAN 87 reports $[(\mu^+\mu^-)+(e^+e^-)]/2$ and we converted it.
[2] Determine ratio of B^+ to B^0 semileptonic decays to be in the range 0.25–2.9.

$\Gamma(s\ell^+\ell^-)/\Gamma_{total}$ Γ_{121}/Γ

Test for $\Delta B = 1$ weak neutral current.

VALUE (units 10^{-6})	DOCUMENT ID		TECN	COMMENT
4.5 ±1.0 OUR AVERAGE				
$4.11\pm0.83^{+0.85}_{-0.81}$	[1] IWASAKI	05	BELL	$e^+e^- \to \Upsilon(4S)$
5.6 ±1.5 ±1.3	[2] AUBERT,B	04I	BABR	$e^+e^- \to \Upsilon(4S)$
• • • We do not use the following data for averages, fits, limits, etc. • • •				
$6.1 \pm1.4 ^{+1.4}_{-1.1}$	[2] KANEKO	03	BELL	Repl. by IWASAKI 05

[1] Requires $M_{\ell^+\ell^-} > 0.2$ GeV/c^2.
[2] Requires $M_{e^+e^-} > 0.2$ GeV/c^2.

$\Gamma(\pi\ell^+\ell^-)/\Gamma_{total}$ Γ_{122}/Γ

VALUE	CL%	DOCUMENT ID		TECN	COMMENT
<5.9 × 10⁻⁸	90	[1] LEES	13M	BABR	$e^+e^- \to \Upsilon(4S)$
• • • We do not use the following data for averages, fits, limits, etc. • • •					
$<6.2\times10^{-8}$	90	[1] WEI	08A	BELL	$e^+e^- \to \Upsilon(4S)$
$<9.1\times10^{-8}$	90	[1] AUBERT	07AG	BABR	$e^+e^- \to \Upsilon(4S)$

[1] Assumes equal production of B^+ and B^0 at the $\Upsilon(4S)$.

$\Gamma(\pi e^+e^-)/\Gamma_{total}$ Γ_{123}/Γ

VALUE	CL%	DOCUMENT ID		TECN	COMMENT
<11.0 × 10⁻⁸	90	[1] LEES	13M	BABR	$e^+e^- \to \Upsilon(4S)$

[1] Assumes equal production of B^+ and B^0 at the $\Upsilon(4S)$.

$\Gamma(\pi\mu^+\mu^-)/\Gamma_{total}$ Γ_{124}/Γ

VALUE	CL%	DOCUMENT ID		TECN	COMMENT
<5.0 × 10⁻⁸	90	[1] LEES	13M	BABR	$e^+e^- \to \Upsilon(4S)$

[1] Assumes equal production of B^+ and B^0 at the $\Upsilon(4S)$.

$\Gamma(Ke^+e^-)/\Gamma_{total}$ Γ_{125}/Γ

Test for $\Delta B = 1$ weak neutral current. Allowed by higher-order electroweak interactions.

VALUE (units 10^{-7})	CL%	DOCUMENT ID		TECN	COMMENT
4.4±0.6 OUR AVERAGE					
$3.9^{+0.9}_{-0.8}\pm0.2$		[1] AUBERT	09T	BABR	$e^+e^- \to \Upsilon(4S)$
$4.8^{+0.8}_{-0.7}\pm0.3$		[1] WEI	09A	BELL	$e^+e^- \to \Upsilon(4S)$
• • • We do not use the following data for averages, fits, limits, etc. • • •					
$3.3^{+0.9}_{-0.8}\pm0.2$		[1] AUBERT,B	06J	BABR	Repl. by AUBERT 09T
$7.4^{+1.8}_{-1.6}\pm0.5$		[1] AUBERT	03U	BABR	Repl. by AUBERT,B 06J
$4.8^{+1.5}_{-1.3}\pm0.3$		[1,2] ISHIKAWA	03	BELL	Repl. by WEI 09A
<13	90	ABE	02	BELL	Repl. by ISHIKAWA 03

[1] Assumes equal production of B^+ and B^0 at the $\Upsilon(4S)$.
[2] The second error is a total of systematic uncertainties including model dependence.

$\Gamma(K^*(892)e^+e^-)/\Gamma_{total}$ Γ_{126}/Γ

Test for $\Delta B = 1$ weak neutral current. Allowed by higher-order electroweak interactions.

VALUE (units 10^{-7})	CL%	DOCUMENT ID		TECN	COMMENT
11.9±2.0 OUR AVERAGE	Error includes scale factor of 1.2.				
$9.9^{+2.3}_{-2.1}\pm0.6$		[1] AUBERT	09T	BABR	$e^+e^- \to \Upsilon(4S)$
$13.9^{+2.3}_{-2.0}\pm1.2$		[1] WEI	09A	BELL	$e^+e^- \to \Upsilon(4S)$
• • • We do not use the following data for averages, fits, limits, etc. • • •					
$9.7^{+3.0}_{-2.7}\pm1.4$		[1] AUBERT,B	06J	BABR	Repl. by AUBERT 09T
$9.8^{+5.0}_{-4.2}\pm1.1$		[1] AUBERT	03U	BABR	Repl. by AUBERT,B 06J
$14.9^{+5.2}_{-4.6}{}^{+1.2}_{-1.3}$		[2] ISHIKAWA	03	BELL	Repl. by WEI 09A
<56	90	ABE	02	BELL	Repl. by ISHIKAWA 03

[1] Assumes equal production of B^+ and B^0 at the $\Upsilon(4S)$.
[2] Assumes equal production of B^0 and B^+ at $\Upsilon(4S)$. The second error is a total of systematic uncertainties including model dependence.

$\Gamma(K\mu^+\mu^-)/\Gamma_{total}$ Γ_{127}/Γ

Test for $\Delta B = 1$ weak neutral current. Allowed by higher-order electroweak interactions.

VALUE (units 10^{-7})	DOCUMENT ID		TECN	COMMENT
4.4±0.4 OUR AVERAGE				
4.2±0.4±0.2	AALTONEN	11AI	CDF	$p\overline{p}$ at 1.96 TeV
$4.1^{+1.3}_{-1.2}\pm0.2$	[1] AUBERT	09T	BABR	$e^+e^- \to \Upsilon(4S)$
5.0±0.6±0.3	[1] WEI	09A	BELL	$e^+e^- \to \Upsilon(4S)$
• • • We do not use the following data for averages, fits, limits, etc. • • •				
$3.5^{+1.3}_{-1.1}\pm0.3$	[1] AUBERT,B	06J	BABR	Repl. by AUBERT 09T
$4.5^{+2.3}_{-1.9}\pm0.4$	[1] AUBERT	03U	BABR	Repl. by AUBERT,B 06J
$4.8^{+1.2}_{-1.1}\pm0.4$	[1,2] ISHIKAWA	03	BELL	Repl. by WEI 09A
$9.9^{+4.0}_{-3.2}{}^{+1.3}_{-1.0}$	ABE	02	BELL	Repl. by ISHIKAWA 03

[1] Assumes equal production of B^+ and B^0 at the $\Upsilon(4S)$.
[2] The second error is a total of systematic uncertainties including model dependence.

$\Gamma(K\mu^+\mu^-)/\Gamma(Ke^+e^-)$ $\Gamma_{127}/\Gamma_{125}$

VALUE	DOCUMENT ID		TECN	COMMENT
1.01±0.15 OUR AVERAGE				
$1.00^{+0.31}_{-0.25}\pm0.07$	[1] LEES	12S	BABR	$e^+e^- \to \Upsilon(4S)$
$0.96^{+0.44}_{-0.34}\pm0.05$	AUBERT	09T	BABR	$e^+e^- \to \Upsilon(4S)$
1.03±0.19±0.06	WEI	09A	BELL	$e^+e^- \to \Upsilon(4S)$
• • • We do not use the following data for averages, fits, limits, etc. • • •				
1.06±0.48±0.08	AUBERT,B	06J	BABR	Repl. by AUBERT 09T

[1] Measured in the union of $0.10 < q^2 < 8.12$ GeV$^2/c^4$ and $q^2 > 10.11$ GeV$^2/c^4$. LEES 12S reports also individual measurements $\Gamma(B \to K\mu^+\mu^-)/\Gamma(B \to Ke^+e^-) = 0.74^{+0.40}_{-0.31} \pm 0.06$ for $0.10 < q^2 < 8.12$ GeV$^2/c^4$ and $\Gamma(B \to K\mu^+\mu^-)/\Gamma(B \to Ke^+e^-) = 1.43^{+0.65}_{-0.44} \pm 0.12$ for $q^2 > 10.11$ GeV$^2/c^4$.

$\Gamma(K^*(892)\mu^+\mu^-)/\Gamma_{total}$ Γ_{128}/Γ

Test for $\Delta B = 1$ weak neutral current. Allowed by higher-order electroweak interactions.

VALUE (units 10^{-7})	CL%	DOCUMENT ID		TECN	COMMENT
10.6±0.9 OUR AVERAGE					
10.1±1.0±0.5		AALTONEN	11AI	CDF	$p\overline{p}$ at 1.96 TeV
$13.5^{+3.5}_{-3.3}\pm1.0$		[1] AUBERT	09T	BABR	$e^+e^- \to \Upsilon(4S)$
$11.0^{+1.6}_{-1.4}\pm0.8$		[1] WEI	09A	BELL	$e^+e^- \to \Upsilon(4S)$
• • • We do not use the following data for averages, fits, limits, etc. • • •					
$8.8^{+3.5}_{-3.0}\pm1.2$		[1] AUBERT,B	06J	BABR	Repl. by AUBERT 09T
$12.7^{+7.6}_{-6.1}\pm1.6$		[1] AUBERT	03U	BABR	Repl. by AUBERT,B 06J
$11.7^{+3.6}_{-3.1}\pm1.0$		[2] ISHIKAWA	03	BELL	Repl. by WEI 09A
<31	90	ABE	02	BELL	Repl. by ISHIKAWA 03

[1] Assumes equal production of B^+ and B^0 at the $\Upsilon(4S)$.
[2] Assumes equal production of B^0 and B^+ at $\Upsilon(4S)$. The second error is a total of systematic uncertainties including model dependence.

$\Gamma(K^*(892)\mu^+\mu^-)/\Gamma(K^*(892)e^+e^-)$ $\Gamma_{128}/\Gamma_{126}$

VALUE	DOCUMENT ID		TECN	COMMENT
0.98±0.15 OUR AVERAGE				
$1.13^{+0.34}_{-0.26}\pm0.10$	[1] LEES	12S	BABR	$e^+e^- \to \Upsilon(4S)$
$1.37^{+0.53}_{-0.40}\pm0.09$	AUBERT	09T	BABR	$e^+e^- \to \Upsilon(4S)$
0.83±0.17±0.08	WEI	09A	BELL	$e^+e^- \to \Upsilon(4S)$
• • • We do not use the following data for averages, fits, limits, etc. • • •				
0.91±0.45±0.06	AUBERT,B	06J	BABR	Repl. by AUBERT 09T

[1] Measured in the union of $0.10 < q^2 < 8.12$ GeV$^2/c^4$ and $q^2 > 10.11$ GeV$^2/c^4$. LEES 12S reports also individual measurements $\Gamma(B \to K^*(892)\mu^+\mu^-)/\Gamma(B \to K^*(892)e^+e^-) = 1.06^{+0.48}_{-0.33} \pm 0.08$ for $0.10 < q^2 < 8.12$ GeV$^2/c^4$ and $\Gamma(B \to K^*(892)\mu^+\mu^-)/\Gamma(B \to K^*(892)e^+e^-) = 1.18^{+0.55}_{-0.37} \pm 0.11$ for $q^2 > 10.11$ GeV$^2/c^4$.

$\Gamma(K\ell^+\ell^-)/\Gamma_{total}$ Γ_{129}/Γ

Test for $\Delta B = 1$ weak neutral current. Allowed by higher-order electroweak interactions.

VALUE (units 10^{-7})	CL%	DOCUMENT ID		TECN	COMMENT
4.8±0.4 OUR AVERAGE					
4.7±0.6±0.2		LEES	12S	BABR	$e^+e^- \to \Upsilon(4S)$
$4.8^{+0.5}_{-0.4}\pm0.3$		WEI	09A	BELL	$e^+e^- \to \Upsilon(4S)$

• • • We do not use the following data for averages, fits, limits, etc. • • •

$3.9\pm0.7\pm0.2$		[1] AUBERT	09T	BABR	Repl. by LEES 12S	
$3.4\pm0.7\pm0.2$		[1] AUBERT,B	06J	BABR	Repl. by AUBERT 09T	
$6.5^{+1.4}_{-1.3}\pm0.4$		[2] AUBERT	03U	BABR	Repl. by AUBERT,B 06J	
$4.8^{+1.0}_{-0.9}\pm0.3$		[3] ISHIKAWA	03	BELL	Repl. by WEI 09A	
$7.5^{+2.5}_{-2.1}\pm0.6$		[4] ABE	02	BELL	Repl. by ISHIKAWA 03	
<5.1	90	[1] AUBERT	02L	BABR	$e^+e^-\to\Upsilon(4S)$	
<17	90	[5] ANDERSON	01B	CLE2	$e^+e^-\to\Upsilon(4S)$	

[1] Assumes equal production of B^+ and B^0 at the $\Upsilon(4S)$.
[2] Assumes all four $B\to K\ell^+\ell^-$ modes having equal partial widths in the fit.
[3] Assumes equal production rate for charge and neutral B meson pairs, isospin invariance, lepton universality for $B\to K\ell^+\ell^-$, and $B(B\to K^*(892)\mu^+\mu^-)=1.33$. The second error is total systematic uncertainties including model dependence.
[4] Assumes lepton universality.
[5] The result is for di-lepton masses above 0.5 GeV.

$\Gamma(K^*(892)\ell^+\ell^-)/\Gamma_{total}$ Γ_{130}/Γ

Test for $\Delta B=1$ weak neutral current. Allowed by higher-order electroweak interactions.

VALUE (units 10^{-7})	CL%	DOCUMENT ID		TECN	COMMENT
10.5 ± 1.0 OUR AVERAGE					
$10.2^{+1.4}_{-1.3}\pm0.5$		LEES	12S	BABR	$e^+e^-\to\Upsilon(4S)$
$10.7^{+1.1}_{-1.0}\pm0.9$		WEI	09A	BELL	$e^+e^-\to\Upsilon(4S)$

• • • We do not use the following data for averages, fits, limits, etc. • • •

$11.1^{+1.9}_{-1.8}\pm0.7$		[1] AUBERT	09T	BABR	Repl. by LEES 12S	
$7.8^{+1.9}_{-1.7}\pm1.1$		[1] AUBERT,B	06J	BABR	Repl. by AUBERT 09T	
$8.8^{+3.3}_{-2.9}\pm1.0$		[2] AUBERT	03U	BABR	Repl. by AUBERT,B 06J	
$11.5^{+2.6}_{-2.4}\pm0.8$		[3] ISHIKAWA	03	BELL	Repl. by WEI 09A	
<31	90	[1,4] AUBERT	02L	BABR	Repl. by AUBERT 03U	
<33	90	[5] ANDERSON	01B	CLE2	$e^+e^-\to\Upsilon(4S)$	

[1] Assumes equal production of B^+ and B^0 at the $\Upsilon(4S)$.
[2] Assumes the partial width ratio of electron and muon modes to be $\Gamma(B\to K^*(892)e^+e^-)/\Gamma(B\to K^*(892)\mu^+\mu^-)=1.33$.
[3] Assumes equal production rate for charge and neutral B meson pairs, isospin invariance, lepton universality for $B\to K\ell^+\ell^-$, and $B(B\to K^*(892)\mu^+\mu^-)=1.33$. The second error is total systematic uncertainties including model dependence.
[4] For averaging $K^*(892)\mu^+\mu^-$ and $K^*(892)e^+e^-$ modes, AUBERT 02L assumed $B(B\to K^*(892)e^+e^-)/B(B\to K^*(892)\mu^+\mu^-)=1.2$.
[5] The result is for di-lepton masses above 0.5 GeV.

$\Gamma(K\nu\overline{\nu})/\Gamma_{total}$ Γ_{131}/Γ

Test for $\Delta B=1$ weak neutral current.

VALUE	CL%	DOCUMENT ID		TECN	COMMENT
$<1.7\times10^{-5}$	90	[1,2] LEES	13I	BABR	$e^+e^-\to\Upsilon(4S)$

• • • We do not use the following data for averages, fits, limits, etc. • • •

$<1.4\times10^{-5}$	90	[1] DEL-AMO-SA...10Q		BABR	Repl. by LEES 13I

[1] Assumes equal production of B^+ and B^0 at the $\Upsilon(4S)$.
[2] Also reported a limit $<3.2\times10^{-5}$ at 90% CL obtained using a fully reconstructed hadronic B-tag evnets.

$\Gamma(K^*\nu\overline{\nu})/\Gamma_{total}$ Γ_{132}/Γ

Test for $\Delta B=1$ weak neutral current.

VALUE	CL%	DOCUMENT ID		TECN	COMMENT
$<7.6\times10^{-5}$	90	[1,2] LEES	13I	BABR	$e^+e^-\to\Upsilon(4S)$

• • • We do not use the following data for averages, fits, limits, etc. • • •

$<8\ \times10^{-5}$	90	AUBERT	08BC	BABR	Repl. by LEES 13I

[1] Assumes equal production of B^+ and B^0 at the $\Upsilon(4S)$.
[2] Also reported a limit $<7.9\times10^{-5}$ at 90% CL obtained using a fully reconstructed hadronic B-tag evnets.

$\Gamma(se^{\pm}\mu^{\mp})/\Gamma_{total}$ Γ_{133}/Γ

Test for lepton family number conservation. Allowed by higher-order electroweak interactions.

VALUE	CL%	DOCUMENT ID		TECN	COMMENT
$<2.2\times10^{-5}$	90	GLENN	98	CLEO	$e^+e^-\to\Upsilon(4S)$

$\Gamma(\pi e^{\pm}\mu^{\mp})/\Gamma_{total}$ Γ_{134}/Γ

Test of lepton family number conservation.

VALUE	CL%	DOCUMENT ID		TECN	COMMENT
$<9.2\times10^{-8}$	90	[1] AUBERT	07AG	BABR	$e^+e^-\to\Upsilon(4S)$

• • • We do not use the following data for averages, fits, limits, etc. • • •

$<1.6\times10^{-6}$	90	[1] EDWARDS	02B	CLE2	$e^+e^-\to\Upsilon(4S)$

[1] Assumes equal production of B^+ and B^0 at the $\Upsilon(4S)$.

$\Gamma(\rho e^{\pm}\mu^{\mp})/\Gamma_{total}$ Γ_{135}/Γ

Test of lepton family number conservation.

VALUE	CL%	DOCUMENT ID		TECN	COMMENT
$<3.2\times10^{-6}$	90	[1] EDWARDS	02B	CLE2	$e^+e^-\to\Upsilon(4S)$

[1] Assumes equal production of B^+ and B^0 at the $\Upsilon(4S)$.

$\Gamma(Ke^{\pm}\mu^{\mp})/\Gamma_{total}$ Γ_{136}/Γ

Test of lepton family number conservation.

VALUE (units 10^{-7})	CL%	DOCUMENT ID		TECN	COMMENT
<0.38	90	[1] AUBERT,B	06J	BABR	$e^+e^-\to\Upsilon(4S)$

• • • We do not use the following data for averages, fits, limits, etc. • • •

<16	90	[1] EDWARDS	02B	CLE2	$e^+e^-\to\Upsilon(4S)$	

[1] Assumes equal production of B^+ and B^0 at the $\Upsilon(4S)$.

$\Gamma(K^*(892)e^{\pm}\mu^{\mp})/\Gamma_{total}$ Γ_{137}/Γ

Test of lepton family number conservation.

VALUE (units 10^{-7})	CL%	DOCUMENT ID		TECN	COMMENT
<5.1	90	[1] AUBERT,B	06J	BABR	$e^+e^-\to\Upsilon(4S)$

• • • We do not use the following data for averages, fits, limits, etc. • • •

<62	90	[1] EDWARDS	02B	CLE2	$e^+e^-\to\Upsilon(4S)$	

[1] Assumes equal production of B^+ and B^0 at the $\Upsilon(4S)$.

CP VIOLATION

A_{CP} is defined as

$$\frac{B(\overline{B}\to\overline{f})-B(B\to f)}{B(\overline{B}\to\overline{f})+B(B\to f)},$$

the *CP*-violation charge asymmetry of inclusive $B^{\pm}$ and B^0 decay.

$A_{CP}(B\to K^*(892)\gamma)$

VALUE	DOCUMENT ID		TECN	COMMENT
-0.003 ± 0.017 OUR AVERAGE				
$-0.003\pm0.017\pm0.007$	[1] AUBERT	09AO	BABR	$e^+e^-\to\Upsilon(4S)$
$-0.015\pm0.044\pm0.012$	[2] NAKAO	04	BELL	$e^+e^-\to\Upsilon(4S)$
$+0.08\ \pm0.13\ \pm0.03$	[2] COAN	00	CLE2	$e^+e^-\to\Upsilon(4S)$

• • • We do not use the following data for averages, fits, limits, etc. • • •

$-0.013\pm0.036\pm0.010$	[3] AUBERT,BE	04A	BABR	Repl. by AUBERT 09AO	
$-0.044\pm0.076\pm0.012$	[4] AUBERT	02C	BABR	Repl. by AUBERT,BE 04A	

[1] Corresponds to a 90% CL interval $-0.033<A_{CP}<0.028$.
[2] Assumes equal production of B^+ and B^0 at the $\Upsilon(4S)$.
[3] Corresponds to a 90% CL allowed region, $-0.074<A_{CP}<0.049$.
[4] A 90% CL range is $-0.170<A_{CP}<0.082$.

$A_{CP}(b\to s\gamma)$

VALUE	DOCUMENT ID		TECN	COMMENT
-0.008 ± 0.029 OUR AVERAGE				
$-0.011\pm0.030\pm0.014$	[1] AUBERT	08BJ	BABR	$e^+e^-\to\Upsilon(4S)$
$0.002\pm0.050\pm0.030$	[2] NISHIDA	04	BELL	$e^+e^-\to\Upsilon(4S)$

• • • We do not use the following data for averages, fits, limits, etc. • • •

$0.025\pm0.050\pm0.015$	[3] AUBERT,B	04E	BABR	Repl. by AUBERT 08BJ	

[1] Uses a sum of exclusively reconstructed $B\to X_s$ decay modes, with X_s mass between 0.6 and 2.8 GeV/c^2.
[2] This measurement is performed inclusively for recoil mass X_s less than 2.1 GeV, which corresponds to $-0.093<A_{CP}<0.096$ at 90% CL.
[3] Corresponds to $-0.06<A_{CP}<0.11$ at 90% CL.

$A_{CP}(b\to(s+d)\gamma)$

VALUE	DOCUMENT ID		TECN	COMMENT
$-0.01\ \pm0.05$ OUR AVERAGE				
$0.057\pm0.060\pm0.018$	LEES	12V	BABR	$e^+e^-\to\Upsilon(4S)$
$-0.10\ \pm0.18\ \pm0.05$	[1] AUBERT	08O	BABR	$e^+e^-\to\Upsilon(4S)$
$-0.110\pm0.115\pm0.017$	AUBERT,BE	06B	BABR	$e^+e^-\to\Upsilon(4S)$
$-0.079\pm0.108\pm0.022$	[2] COAN	01	CLE2	$e^+e^-\to\Upsilon(4S)$

[1] Uses a fully reconstructed B meson as a tag on the recoil side. Requires $E_\gamma>2.2$ GeV.
[2] Corresponds to $-0.27<A_{CP}<0.10$ at 90% CL.

$A_{CP}(B\to X_s\ell^+\ell^-)$

VALUE	DOCUMENT ID		TECN	COMMENT
$-0.22\pm0.26\pm0.02$	[1] AUBERT,B	04I	BABR	$e^+e^-\to\Upsilon(4S)$

[1] The final state flavor is determined by the kaon and pion charges where modes with $X_s=K^0_S$, $K^0_S\pi^0$ or $K^0_S\pi^+\pi^-$ are not used.

$A_{CP}(B\to K^*e^+e^-)$

VALUE	DOCUMENT ID		TECN	COMMENT
$-0.18\pm0.15\pm0.01$	WEI	09A	BELL	$e^+e^-\to\Upsilon(4S)$

$A_{CP}(B\to K^*\mu^+\mu^-)$

VALUE	DOCUMENT ID		TECN	COMMENT
$-0.03\pm0.13\pm0.02$	WEI	09A	BELL	$e^+e^-\to\Upsilon(4S)$

$A_{CP}(B \to K^*\ell^+\ell^-)$

VALUE	DOCUMENT ID		TECN	COMMENT
-0.04 ± 0.07 OUR AVERAGE				
$0.03\pm0.13\pm0.01$	[1] LEES	12S	BABR	$e^+e^- \to \Upsilon(4S)$
$+0.01^{+0.16}_{-0.15}\pm0.01$	AUBERT	09T	BABR	$e^+e^- \to \Upsilon(4S)$
$-0.10\pm0.10\pm0.01$	WEI	09A	BELL	$e^+e^- \to \Upsilon(4S)$

[1] Measured in the union of $0.10 < q^2 < 8.12$ GeV$^2/c^4$ and $q^2 > 10.11$ GeV$^2/c^4$. LEES 12S reports also individual measurements $A_{CP}(B \to K^*\ell^+\ell^-) = -0.13^{+0.18}_{-0.19}\pm 0.01$ for $0.10 < q^2 < 8.12$ GeV$^2/c^4$ and $A_{CP}(B \to K^*\ell^+\ell^-) = 0.16^{+0.18}_{-0.19}\pm 0.01$ for $q^2 > 10.11$ GeV$^2/c^4$.

$A_{CP}(B \to \eta$anything$)$

VALUE	DOCUMENT ID		TECN	COMMENT
$-0.13\pm0.04^{+0.02}_{-0.03}$	[1] NISHIMURA	10	BELL	$e^+e^- \to \Upsilon(4S)$

[1] Uses $B \to \eta X_s$ with $0.4 < m_{X_s} < 2.6$ GeV/c^2.

POLARIZATION IN B DECAY

In decays involving two vector mesons, one can distinguish among the states in which meson polarizations are both longitudinal (L) or both are transverse and parallel ($\|$) or perpendicular ($\perp$) to each other with the parameters Γ_L/Γ, $\Gamma_\perp/\Gamma$, and the relative phases $\phi_\|$ and $\phi_\perp$. See the definitions in the note on "Polarization in B Decays" review in the B^0 Particle Listings.

$F_L(B \to K^*\ell^+\ell^-)$ ($q^2 > 0.1$ GeV$^2/c^4$)

VALUE	DOCUMENT ID		TECN	COMMENT
$0.63^{+0.18}_{-0.19}\pm0.05$	[1] AUBERT,B	06J	BABR	$e^+e^- \to \Upsilon(4S)$

[1] Results with different q^2 cuts are also reported.

$F_L(B \to K^*\ell^+\ell^-)$ ($m_{\ell\ell} < 2.5$ GeV/c^2)

VALUE	DOCUMENT ID		TECN	COMMENT
$0.35\pm0.16\pm0.04$	AUBERT	09N	BABR	$e^+e^- \to \Upsilon(4S)$

$F_L(B \to K^*\ell^+\ell^-)$ ($m_{\ell\ell} > 3.2$ GeV/c^2)

VALUE	DOCUMENT ID		TECN	COMMENT
$0.71^{+0.20}_{-0.22}\pm0.04$	AUBERT	09N	BABR	$e^+e^- \to \Upsilon(4S)$

$F_L(B \to K^*\ell^+\ell^-)$ ($0.1 < q^2 < 2.0$ GeV$^2/c^4$)

VALUE	DOCUMENT ID		TECN	COMMENT
$0.34^{+0.08}_{-0.07}$ OUR AVERAGE				
$0.37^{+0.10}_{-0.09}{}^{+0.04}_{-0.03}$	AAIJ	13Y	LHCB	pp at 7 TeV, $K^{*0}\mu^+\mu^-$
$0.30\pm0.16\pm0.02$	AALTONEN	12I	CDF	$p\overline{p}$ at 1.96 TeV
$0.29^{+0.21}_{-0.18}\pm0.02$	WEI	09A	BELL	$e^+e^- \to \Upsilon(4S)$
• • • We do not use the following data for averages, fits, limits, etc. • • •				
$0.60^{+0.00}_{-0.28}\pm0.19$	[1] CHATRCHYAN	13BL	CMS	pp at 7 TeV
$0.00^{+0.13}_{-0.00}\pm0.02$	AAIJ	12U	LHCB	Repl. by AAIJ 13Y
$0.53^{+0.32}_{-0.34}\pm0.07$	AALTONEN	11L	CDF	Repl. by AALTONEN 12I

[1] CHATRCHYAN 13BL uses, for this bin, $1.0 < q^2 < 2.0$ GeV$^2/c^4$.

$F_L(B \to K^*\ell^+\ell^-)$ ($2.0 < q^2 < 4.3$ GeV$^2/c^4$)

VALUE	DOCUMENT ID		TECN	COMMENT
0.69 ± 0.08 OUR AVERAGE				
$0.74^{+0.10}_{-0.09}{}^{+0.02}_{-0.03}$	AAIJ	13Y	LHCB	pp at 7 TeV, $K^{*0}\mu^+\mu^-$
$0.65\pm0.17\pm0.03$	CHATRCHYAN	13BL	CMS	pp at 7 TeV
$0.37^{+0.25}_{-0.24}\pm0.10$	AALTONEN	12I	CDF	$p\overline{p}$ at 1.96 TeV
$0.71\pm0.24\pm0.05$	WEI	09A	BELL	$e^+e^- \to \Upsilon(4S)$
• • • We do not use the following data for averages, fits, limits, etc. • • •				
$0.77\pm0.15\pm0.03$	AAIJ	12U	LHCB	Repl. by AAIJ 13Y
$0.40^{+0.32}_{-0.33}\pm0.08$	AALTONEN	11L	CDF	Repl. by AALTONEN 12I

$F_L(B \to K^*\ell^+\ell^-)$ ($4.3 < q^2 < 8.6$ GeV$^2/c^4$)

VALUE	DOCUMENT ID		TECN	COMMENT
0.64 ± 0.06 OUR AVERAGE				
$0.57\pm0.07\pm0.03$	AAIJ	13Y	LHCB	pp at 7 TeV, $K^{*0}\mu^+\mu^-$
$0.81^{+0.13}_{-0.12}\pm0.05$	CHATRCHYAN	13BL	CMS	pp at 7 TeV
$0.68^{+0.15}_{-0.17}\pm0.09$	AALTONEN	12I	CDF	$p\overline{p}$ at 1.96 TeV
$0.64^{+0.23}_{-0.24}\pm0.07$	WEI	09A	BELL	$e^+e^- \to \Upsilon(4S)$
• • • We do not use the following data for averages, fits, limits, etc. • • •				
$0.60^{+0.06}_{-0.07}\pm0.01$	AAIJ	12U	LHCB	Repl. by AAIJ 13Y
$0.82^{+0.19}_{-0.23}\pm0.07$	AALTONEN	11L	CDF	Repl. by AALTONEN 12I

$F_L(B \to K^*\ell^+\ell^-)$ ($10.09 < q^2 < 12.86$ GeV$^2/c^4$)

VALUE	DOCUMENT ID		TECN	COMMENT
0.43 ± 0.06 OUR AVERAGE				
$0.48^{+0.08}_{-0.09}\pm0.03$	AAIJ	13Y	LHCB	pp at 7 TeV, $K^{*0}\mu^+\mu^-$
$0.45^{+0.10}_{-0.11}\pm0.04$	CHATRCHYAN	13BL	CMS	pp at 7 TeV
$0.47\pm0.14\pm0.03$	AALTONEN	12I	CDF	$p\overline{p}$ at 1.96 TeV
$0.17^{+0.17}_{-0.15}\pm0.03$	WEI	09A	BELL	$e^+e^- \to \Upsilon(4S)$
• • • We do not use the following data for averages, fits, limits, etc. • • •				
$0.41\pm0.11\pm0.03$	AAIJ	12U	LHCB	Repl. by AAIJ 13Y
$0.31^{+0.19}_{-0.18}\pm0.02$	AALTONEN	11L	CDF	Repl. by AALTONEN 12I

$F_L(B \to K^*\ell^+\ell^-)$ ($14.18 < q^2 < 16.0$ GeV$^2/c^4$)

VALUE	DOCUMENT ID		TECN	COMMENT
0.35 ± 0.08 OUR AVERAGE Error includes scale factor of 1.4. See the ideogram below.				
$0.33^{+0.08}_{-0.07}{}^{+0.02}_{-0.03}$	AAIJ	13Y	LHCB	pp at 7 TeV, $K^{*0}\mu^+\mu^-$
$0.53\pm0.12\pm0.03$	CHATRCHYAN	13BL	CMS	pp at 7 TeV
$0.29^{+0.14}_{-0.13}\pm0.05$	AALTONEN	12I	CDF	$p\overline{p}$ at 1.96 TeV
$-0.15^{+0.27}_{-0.23}\pm0.07$	WEI	09A	BELL	$e^+e^- \to \Upsilon(4S)$
• • • We do not use the following data for averages, fits, limits, etc. • • •				
$0.37\pm0.09\pm0.05$	AAIJ	12U	LHCB	Repl. by AAIJ 13Y
$0.55^{+0.17}_{-0.18}\pm0.02$	AALTONEN	11L	CDF	Repl. by AALTONEN 12I

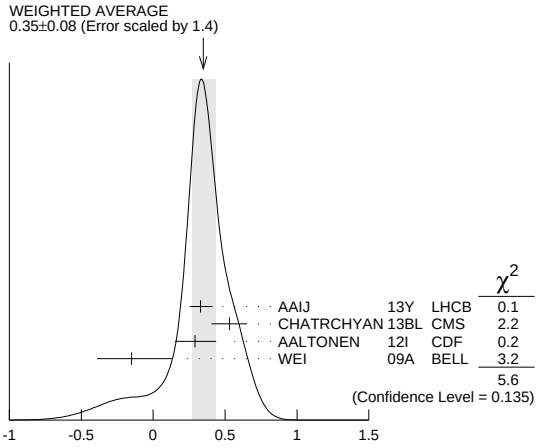

$F_L(B \to K^*\ell^+\ell^-)$ ($14.18 < q^2 < 16.0$ GeV$^2/c^4$)

$F_L(B \to K^*\ell^+\ell^-)$ ($16.0 < q^2 < 19.0$ GeV$^2/c^4$)

VALUE	DOCUMENT ID		TECN	COMMENT
0.37 ± 0.06 OUR AVERAGE Error includes scale factor of 1.2.				
$0.38^{+0.09}_{-0.07}\pm0.03$	AAIJ	13Y	LHCB	pp at 7 TeV, $K^{*0}\mu^+\mu^-$
$0.44\pm0.07\pm0.03$	CHATRCHYAN	13BL	CMS	pp at 7 TeV
$0.20^{+0.19}_{-0.17}\pm0.05$	AALTONEN	12I	CDF	$p\overline{p}$ at 1.96 TeV
$0.12^{+0.15}_{-0.13}\pm0.02$	WEI	09A	BELL	$e^+e^- \to \Upsilon(4S)$
• • • We do not use the following data for averages, fits, limits, etc. • • •				
$0.26^{+0.10}_{-0.08}\pm0.03$	AAIJ	12U	LHCB	Repl. by AAIJ 13Y
$0.09^{+0.18}_{-0.14}\pm0.03$	AALTONEN	11L	CDF	Repl. by AALTONEN 12I

$F_L(B \to K^*\ell^+\ell^-)$ ($1.0 < q^2 < 6.0$ GeV$^2/c^4$)

VALUE	DOCUMENT ID		TECN	COMMENT
0.66 ± 0.06 OUR AVERAGE				
$0.65^{+0.08}_{-0.07}\pm0.03$	AAIJ	13Y	LHCB	pp at 7 TeV, $K^{*0}\mu^+\mu^-$
$0.68\pm0.10\pm0.02$	CHATRCHYAN	13BL	CMS	pp at 7 TeV
$0.69^{+0.19}_{-0.21}\pm0.08$	AALTONEN	12I	CDF	$p\overline{p}$ at 1.96 TeV
$0.67\pm0.23\pm0.05$	WEI	09A	BELL	$e^+e^- \to \Upsilon(4S)$
• • • We do not use the following data for averages, fits, limits, etc. • • •				
$0.55\pm0.10\pm0.03$	AAIJ	12U	LHCB	Repl. by AAIJ 13Y
$0.50^{+0.27}_{-0.30}\pm0.03$	AALTONEN	11L	CDF	Repl. by AALTONEN 12I

$F_L(B \to K^*\ell^+\ell^-)$ ($0.0 < q^2 < 4.3$ GeV$^2/c^4$)

VALUE	DOCUMENT ID		TECN	COMMENT
$0.33^{+0.14}_{-0.13}\pm0.03$	AALTONEN	12I	CDF	$p\overline{p}$ at 1.96 TeV
• • • We do not use the following data for averages, fits, limits, etc. • • •				
$0.47^{+0.23}_{-0.24}\pm0.03$	AALTONEN	11L	CDF	Repl. by AALTONEN 12I

Meson Particle Listings

$B^{\pm}/B^{0}$ ADMIXTURE

PARTIAL BRANCHING FRACTIONS IN $B \to K^{(*)}\ell^+\ell^-$

B($B \to K^*\ell^+\ell^-$) ($q^2 < 2.0$ GeV$^2/c^4$)

VALUE (units 10^{-7})	DOCUMENT ID		TECN	COMMENT
1.68±0.23 OUR AVERAGE				
$1.89^{+0.52}_{-0.46}\pm0.06$	[1] LEES	12S	BABR	$e^+e^- \to \Upsilon(4S)$
$1.73\pm0.33\pm0.10$	AALTONEN	11AI	CDF	$p\overline{p}$ at 1.96 TeV
$1.46^{+0.40}_{-0.35}\pm0.11$	WEI	09A	BELL	$e^+e^- \to \Upsilon(4S)$
• • • We do not use the following data for averages, fits, limits, etc. • • •				
$0.98\pm0.40\pm0.09$	AALTONEN	11L	CDF	Repl. by AALTONEN 11AI

[1] The value reported here from LEES 12S refers to $0.1 < q^2 < 2.0$ GeV$^2/c^2$.

B($B \to K^*\ell^+\ell^-$) ($2.0 < q^2 < 4.3$ GeV$^2/c^4$)

VALUE (units 10^{-7})	DOCUMENT ID		TECN	COMMENT
0.87±0.17 OUR AVERAGE				
$0.95^{+0.35}_{-0.30}\pm0.04$	LEES	12S	BABR	$e^+e^- \to \Upsilon(4S)$
$0.82\pm0.26\pm0.06$	AALTONEN	11AI	CDF	$p\overline{p}$ at 1.96 TeV
$0.86^{+0.31}_{-0.27}\pm0.07$	WEI	09A	BELL	$e^+e^- \to \Upsilon(4S)$
• • • We do not use the following data for averages, fits, limits, etc. • • •				
$1.00\pm0.38\pm0.09$	AALTONEN	11L	CDF	Repl. by AALTONEN 11AI

B($B \to K^*\ell^+\ell^-$) ($4.3 < q^2 < 8.68$ GeV$^2/c^4$)

VALUE (units 10^{-7})	DOCUMENT ID		TECN	COMMENT
1.67±0.29 OUR AVERAGE				
$1.82^{+0.56}_{-0.52}\pm0.09$	[1] LEES	12S	BABR	$e^+e^- \to \Upsilon(4S)$
$1.72\pm0.41\pm0.14$	AALTONEN	11AI	CDF	$p\overline{p}$ at 1.96 TeV
$1.37^{+0.47}_{-0.42}\pm0.39$	WEI	09A	BELL	$e^+e^- \to \Upsilon(4S)$
• • • We do not use the following data for averages, fits, limits, etc. • • •				
$1.69\pm0.57\pm0.15$	AALTONEN	11L	CDF	Repl. by AALTONEN 11AI

[1] The value reported here from LEES 12S refers to $4.3 < q^2 < 8.12$ GeV$^2/c^2$.

B($B \to K^*\ell^+\ell^-$) ($10.09 < q^2 < 12.86$ GeV$^2/c^4$)

VALUE (units 10^{-7})	DOCUMENT ID		TECN	COMMENT
1.93±0.25 OUR AVERAGE				
$1.86^{+0.52}_{-0.48}\pm0.10$	[1] LEES	12S	BABR	$e^+e^- \to \Upsilon(4S)$
$1.77\pm0.34\pm0.11$	AALTONEN	11AI	CDF	$p\overline{p}$ at 1.96 TeV
$2.24^{+0.44}_{-0.40}\pm0.19$	WEI	09A	BELL	$e^+e^- \to \Upsilon(4S)$
• • • We do not use the following data for averages, fits, limits, etc. • • •				
$1.97\pm0.47\pm0.17$	AALTONEN	11L	CDF	Repl. by AALTONEN 11AI

[1] The value reported here from LEES 12S refers to $10.11 < q^2 < 12.89$ GeV$^2/c^2$.

B($B \to K^*\ell^+\ell^-$) ($14.18 < q^2 < 16.0$ GeV$^2/c^4$)

VALUE (units 10^{-7})	DOCUMENT ID		TECN	COMMENT
1.21±0.17 OUR AVERAGE				
$1.46^{+0.41}_{-0.36}\pm0.06$	[1] LEES	12S	BABR	$e^+e^- \to \Upsilon(4S)$
$1.21\pm0.24\pm0.07$	AALTONEN	11AI	CDF	$p\overline{p}$ at 1.96 TeV
$1.05^{+0.29}_{-0.26}\pm0.08$	WEI	09A	BELL	$e^+e^- \to \Upsilon(4S)$
• • • We do not use the following data for averages, fits, limits, etc. • • •				
$1.51\pm0.36\pm0.13$	AALTONEN	11L	CDF	Repl. by AALTONEN 11AI

[1] The value reported here from LEES 12S refers to $14.21 < q^2 < 16.0$ GeV$^2/c^2$.

B($B \to K^*\ell^+\ell^-$) ($16.0 < q^2$ GeV$^2/c^4$)

VALUE (units 10^{-7})	DOCUMENT ID		TECN	COMMENT
1.3 ±0.4 OUR AVERAGE	Error includes scale factor of 2.3. See the ideogram below.			
$1.02^{+0.47}_{-0.42}\pm0.06$	LEES	12S	BABR	$e^+e^- \to \Upsilon(4S)$
$0.88\pm0.22\pm0.05$	AALTONEN	11AI	CDF	$p\overline{p}$ at 1.96 TeV
$2.04^{+0.27}_{-0.24}\pm0.16$	WEI	09A	BELL	$e^+e^- \to \Upsilon(4S)$
• • • We do not use the following data for averages, fits, limits, etc. • • •				
$1.35\pm0.37\pm0.12$	AALTONEN	11L	CDF	Repl. by AALTONEN 11AI

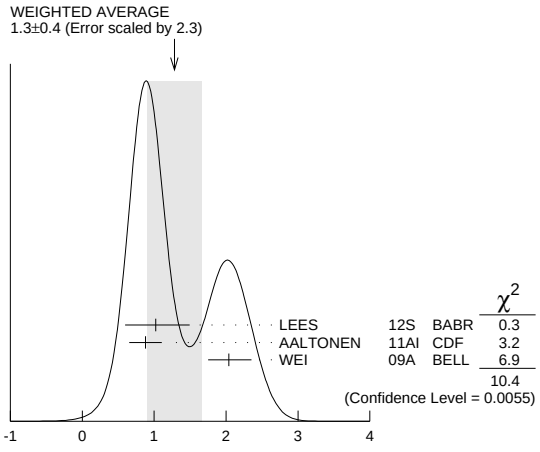

B($B \to K^*\ell^+\ell^-$) ($16.0 < q^2$ GeV$^2/c^4$) (units 10^{-7})

B($B \to K^*\ell^+\ell^-$) ($1.0 < q^2 < 6.0$ GeV$^2/c^4$)

VALUE (units 10^{-7})	DOCUMENT ID		TECN	COMMENT
1.64±0.26 OUR AVERAGE				
$2.05^{+0.53}_{-0.48}\pm0.07$	LEES	12S	BABR	$e^+e^- \to \Upsilon(4S)$
$1.48\pm0.39\pm0.12$	AALTONEN	11AI	CDF	$p\overline{p}$ at 1.96 TeV
$1.49^{+0.45}_{-0.40}\pm0.12$	WEI	09A	BELL	$e^+e^- \to \Upsilon(4S)$
• • • We do not use the following data for averages, fits, limits, etc. • • •				
$1.60\pm0.54\pm0.14$	AALTONEN	11L	CDF	Repl. by AALTONEN 11AI

B($B \to K^*\ell^+\ell^-$) ($0.0 < q^2 < 4.3$ GeV$^2/c^4$)

VALUE (units 10^{-7})	DOCUMENT ID		TECN	COMMENT
2.53±0.43±0.15	AALTONEN	11AI	CDF	$p\overline{p}$ at 1.96 TeV
• • • We do not use the following data for averages, fits, limits, etc. • • •				
$1.98\pm0.55\pm0.18$	AALTONEN	11L	CDF	Repl. by AALTONEN 11AI

B($B \to K\ell^+\ell^-$) ($q^2 < 2.0$ GeV$^2/c^4$)

VALUE (units 10^{-7})	DOCUMENT ID		TECN	COMMENT
0.51±0.16 OUR AVERAGE	Error includes scale factor of 1.9. See the ideogram below.			
$0.71^{+0.20}_{-0.18}\pm0.02$	[1] LEES	12S	BABR	$e^+e^- \to \Upsilon(4S)$
$0.33\pm0.10\pm0.02$	AALTONEN	11AI	CDF	$p\overline{p}$ at 1.96 TeV
$0.81^{+0.18}_{-0.16}\pm0.05$	WEI	09A	BELL	$e^+e^- \to \Upsilon(4S)$
• • • We do not use the following data for averages, fits, limits, etc. • • •				
$0.38\pm0.16\pm0.03$	AALTONEN	11L	CDF	Repl. by AALTONEN 11AI

[1] The value reported here from LEES 12S refers to $0.1 < q^2 < 2.0$ GeV$^2/c^2$.

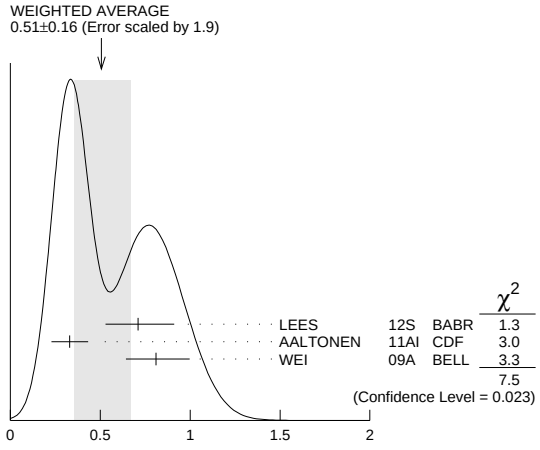

B($B \to K\ell^+\ell^-$) ($q^2 < 2.0$ GeV$^2/c^4$) (units 10^{-7})

B($B \to K\ell^+\ell^-$) ($2.0 < q^2 < 4.3$ GeV$^2/c^4$)

VALUE (units 10^{-7})	DOCUMENT ID		TECN	COMMENT
$\mathbf{0.57^{+0.10}_{-0.09}}$ **OUR AVERAGE**	Error includes scale factor of 1.2.			
$0.49^{+0.15}_{-0.13}\pm0.01$	LEES	12S	BABR	$e^+e^- \to \Upsilon(4S)$
$0.77\pm0.14\pm0.05$	AALTONEN	11AI	CDF	$p\overline{p}$ at 1.96 TeV
$0.46^{+0.14}_{-0.12}\pm0.03$	WEI	09A	BELL	$e^+e^- \to \Upsilon(4S)$
• • • We do not use the following data for averages, fits, limits, etc. • • •				
$0.58\pm0.19\pm0.04$	AALTONEN	11L	CDF	Repl. by AALTONEN 11AI

B($B \to K\ell^+\ell^-$) ($4.3 < q^2 < 8.68$ GeV$^2/c^4$)

VALUE (units 10^{-7})	DOCUMENT ID		TECN	COMMENT
1.00 ± 0.11 OUR AVERAGE				
$0.94^{+0.20}_{-0.19}\pm0.02$	[1] LEES	12S	BABR	$e^+e^- \to \Upsilon(4S)$
$1.05\pm0.17\pm0.07$	AALTONEN	11AI	CDF	$p\overline{p}$ at 1.96 TeV
$1.00^{+0.19}_{-0.18}\pm0.06$	WEI	09A	BELL	$e^+e^- \to \Upsilon(4S)$
• • • We do not use the following data for averages, fits, limits, etc. • • •				
$0.93\pm0.25\pm0.06$	AALTONEN	11L	CDF	Repl. by AALTONEN 11AI

[1] The value reported here from LEES 12S refers to $4.3 < q^2 < 8.12$ GeV$^2/c^2$.

B($B \to K\ell^+\ell^-$) ($10.09 < q^2 < 12.86$ GeV$^2/c^4$)

VALUE (units 10^{-7})	DOCUMENT ID		TECN	COMMENT
0.57 ± 0.11 OUR AVERAGE	Error includes scale factor of 1.4. See the ideogram below.			
$0.90^{+0.20}_{-0.19}\pm0.04$	[1] LEES	12S	BABR	$e^+e^- \to \Upsilon(4S)$
$0.48\pm0.10\pm0.03$	AALTONEN	11AI	CDF	$p\overline{p}$ at 1.96 TeV
$0.55^{+0.16}_{-0.14}\pm0.03$	WEI	09A	BELL	$e^+e^- \to \Upsilon(4S)$
• • • We do not use the following data for averages, fits, limits, etc. • • •				
$0.72\pm0.17\pm0.05$	AALTONEN	11L	CDF	Repl. by AALTONEN 11AI

[1] The value reported here from LEES 12S refers to $10.11 < q^2 < 12.89$ GeV$^2/c^2$.

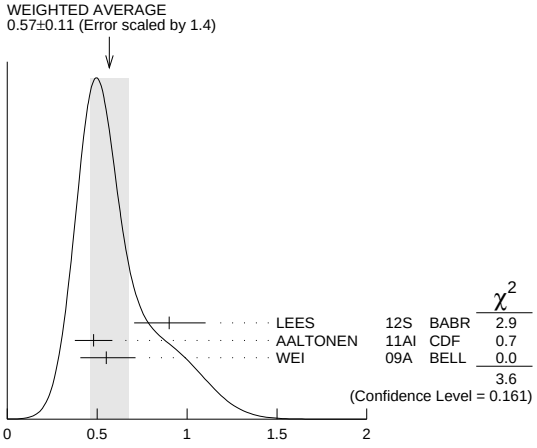

B($B \to K\ell^+\ell^-$) ($14.18 < q^2 < 16.0$ GeV$^2/c^4$)

VALUE (units 10^{-7})	DOCUMENT ID		TECN	COMMENT
0.49 ± 0.07 OUR AVERAGE				
$0.49^{+0.15}_{-0.14}\pm0.02$	[1] LEES	12S	BABR	$e^+e^- \to \Upsilon(4S)$
$0.52\pm0.09\pm0.03$	AALTONEN	11AI	CDF	$p\overline{p}$ at 1.96 TeV
$0.38^{+0.19}_{-0.12}\pm0.02$	WEI	09A	BELL	$e^+e^- \to \Upsilon(4S)$
• • • We do not use the following data for averages, fits, limits, etc. • • •				
$0.38\pm0.12\pm0.03$	AALTONEN	11L	CDF	Repl. by AALTONEN 11AI

[1] The value reported here from LEES 12S refers to $14.21 < q^2 < 16.0$ GeV$^2/c^2$.

B($B \to K\ell^+\ell^-$) ($16.0 < q^2$ GeV$^2/c^4$)

VALUE (units 10^{-7})	DOCUMENT ID		TECN	COMMENT
0.52 ± 0.16 OUR AVERAGE	Error includes scale factor of 2.1. See the ideogram below.			
$0.67^{+0.23}_{-0.21}\pm0.05$	LEES	12S	BABR	$e^+e^- \to \Upsilon(4S)$
$0.38\pm0.09\pm0.02$	AALTONEN	11AI	CDF	$p\overline{p}$ at 1.96 TeV
$0.98^{+0.20}_{-0.18}\pm0.06$	WEI	09A	BELL	$e^+e^- \to \Upsilon(4S)$
• • • We do not use the following data for averages, fits, limits, etc. • • •				
$0.35\pm0.13\pm0.02$	AALTONEN	11L	CDF	Repl. by AALTONEN 11AI

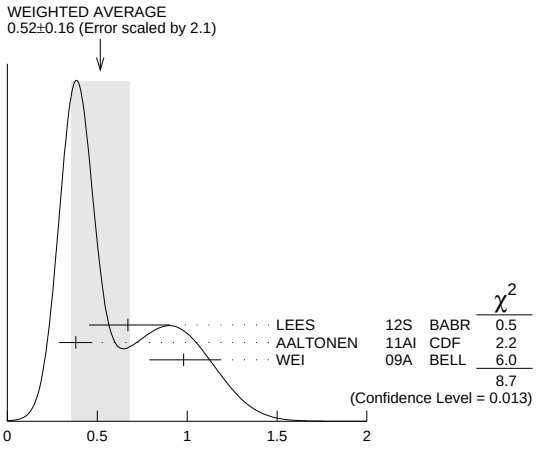

B($B \to K\ell^+\ell^-$) ($1.0 < q^2 < 6.0$ GeV$^2/c^4$)

VALUE (units 10^{-7})	DOCUMENT ID		TECN	COMMENT
1.33 ± 0.13 OUR AVERAGE				
$1.36^{+0.27}_{-0.24}\pm0.03$	LEES	12S	BABR	$e^+e^- \to \Upsilon(4S)$
$1.29\pm0.18\pm0.08$	AALTONEN	11AI	CDF	$p\overline{p}$ at 1.96 TeV
$1.36^{+0.23}_{-0.21}\pm0.08$	WEI	09A	BELL	$e^+e^- \to \Upsilon(4S)$
• • • We do not use the following data for averages, fits, limits, etc. • • •				
$1.01\pm0.26\pm0.07$	AALTONEN	11L	CDF	Repl. by AALTONEN 11AI

B($B \to K\ell^+\ell^-$) ($0.0 < q^2 < 4.3$ GeV$^2/c^4$)

VALUE (units 10^{-7})	DOCUMENT ID		TECN	COMMENT
$1.07\pm0.17\pm0.07$	AALTONEN	11AI	CDF	$p\overline{p}$ at 1.96 TeV
• • • We do not use the following data for averages, fits, limits, etc. • • •				
$0.96\pm0.25\pm0.06$	AALTONEN	11L	CDF	Repl. by AALTONEN 11AI

LEPTON FORWARD-BACKWARD ASYMMETRY IN $B \to K^{(*)}\ell^+\ell^-$ DECAY

The forward-backward angular asymmetry of the lepton pair in $B \to K^{(*)}\ell^+\ell^-$ decay is defined as

$$A_{FB}(s) = \frac{N(cos\theta>0)-N(cos\theta<0)}{N(cos\theta>0)+N(cos\theta<0)},$$

where $s=q^2/m_B^2$, and θ is the angle of the lepton with respect to the flight direction of the B meson, measured in the dilepton rest frame. In addition, the fraction of longitudinal polarization F_L of the K^* and F_S, the relative contribution from scalar and pseudoscalar penguin amplitudes in $B \to K\ell^+\ell^-$, can be measured from the angular distribution of its decay products.

A_{FB}($B \to K^*\ell^+\ell^-$) ($q^2 > 0.1$ GeV$^2/c^4$)

VALUE	CL%	DOCUMENT ID		TECN	COMMENT
$0.50\pm0.15\pm0.02$		[1] ISHIKAWA	06	BELL	$e^+e^- \to \Upsilon(4S)$
• • • We do not use the following data for averages, fits, limits, etc. • • •					
>0.55	95	[2] AUBERT,B	06J	BABR	$e^+e^- \to \Upsilon(4S)$

[1] Using an unbinned max. likelihood fits to the M_{bc} distribution in five q^2 bins for $\cos\theta > 0$ and $\cos\theta < 0$.
[2] Results with different q^2 cuts are also reported.

A_{FB}($B \to K^*\ell^+\ell^-$) ($0.1 < q^2 < 2.0$ GeV$^2/c^4$)

VALUE	DOCUMENT ID		TECN	COMMENT
-0.01 ± 0.14 OUR AVERAGE	Error includes scale factor of 1.4. See the ideogram below.			
$-0.02\pm0.12\pm0.01$	AAIJ	13Y	LHCB	pp at 7 TeV, $K^{*0}\mu^+\mu^-$
$-0.35^{+0.26}_{-0.23}\pm0.10$	AALTONEN	12I	CDF	$p\overline{p}$ at 1.96 TeV
$0.47^{+0.26}_{-0.32}\pm0.03$	WEI	09A	BELL	$e^+e^- \to \Upsilon(4S)$
• • • We do not use the following data for averages, fits, limits, etc. • • •				
$-0.29^{+0.37}_{-0.00}\pm0.18$	[1] CHATRCHYAN	13BL	CMS	pp at 7 TeV
$-0.15\pm0.20\pm0.06$	AAIJ	12U	LHCB	Repl. by AAIJ 13Y
$0.13^{+1.65}_{-0.75}\pm0.25$	AALTONEN	11L	CDF	Repl. by AALTONEN 12I

[1] CHATRCHYAN 13BL uses, for this bin, $1.0 < q^2 < 2.0$ GeV$^2/c^4$.

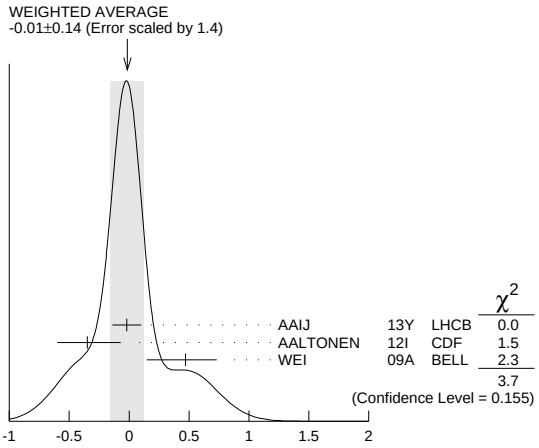

$A_{FB}(B \to K^* \ell^+ \ell^-)$ $(0.1 < q^2 < 2.0$ GeV$^2/c^4)$

$A_{FB}(B \to K^* \ell^+ \ell^-)$ ($m_{\ell\ell} < 2.5$ GeV/c^4)

VALUE	DOCUMENT ID		TECN	COMMENT
$0.24^{+0.18}_{-0.23} \pm 0.05$	AUBERT	09N	BABR	$e^+e^- \to \Upsilon(4S)$

$A_{FB}(B \to K^* \ell^+ \ell^-)$ ($m_{\ell\ell} > 3.2$ GeV/c^4)

VALUE	DOCUMENT ID		TECN	COMMENT
$0.76^{+0.52}_{-0.32} \pm 0.07$	AUBERT	09N	BABR	$e^+e^- \to \Upsilon(4S)$

$A_{FB}(B \to K^* \ell^+ \ell^-)$ ($2.0 < q^2 < 4.3$ GeV$^2/c^4$)

VALUE	DOCUMENT ID		TECN	COMMENT
-0.15 ± 0.07 OUR AVERAGE				
$-0.20 \pm 0.08 \pm 0.01$	AAIJ	13Y	LHCB	pp at 7 TeV, $K^{*0}\mu^+\mu^-$
$-0.07 \pm 0.20 \pm 0.02$	CHATRCHYAN	13BL	CMS	pp at 7 TeV
$0.29^{+0.32}_{-0.35} \pm 0.15$	AALTONEN	12I	CDF	$p\overline{p}$ at 1.96 TeV
$0.11^{+0.31}_{-0.36} \pm 0.07$	WEI	09A	BELL	$e^+e^- \to \Upsilon(4S)$
• • • We do not use the following data for averages, fits, limits, etc. • • •				
$0.05^{+0.16}_{-0.20} \pm 0.04$	AAIJ	12U	LHCB	Repl. by AAIJ 13Y
$0.19^{+0.40}_{-0.41} \pm 0.14$	AALTONEN	11L	CDF	Repl. by AALTONEN 12I

$A_{FB}(B \to K^* \ell^+ \ell^-)$ ($0.0 < q^2 < 4.3$ GeV$^2/c^4$)

VALUE	DOCUMENT ID		TECN	COMMENT
$\mathbf{-0.08^{+0.21}_{-0.20} \pm 0.05}$	AALTONEN	12I	CDF	$p\overline{p}$ at 1.96 TeV
• • • We do not use the following data for averages, fits, limits, etc. • • •				
$0.21^{+0.31}_{-0.33} \pm 0.05$	AALTONEN	11L	CDF	Repl. by AALTONEN 12I

$A_{FB}(B \to K^* \ell^+ \ell^-)$ ($1.0 < q^2 < 6.0$ GeV$^2/c^4$)

VALUE	DOCUMENT ID		TECN	COMMENT
-0.12 ± 0.07 OUR AVERAGE	Error includes scale factor of 1.3. See the ideogram below.			
$-0.17 \pm 0.06 \pm 0.01$	AAIJ	13Y	LHCB	pp at 7 TeV, $K^{*0}\mu^+\mu^-$
$-0.07 \pm 0.12 \pm 0.01$	CHATRCHYAN	13BL	CMS	pp at 7 TeV
$0.29^{+0.20}_{-0.23} \pm 0.07$	AALTONEN	12I	CDF	$p\overline{p}$ at 1.96 TeV
$0.26^{+0.27}_{-0.30} \pm 0.07$	WEI	09A	BELL	$e^+e^- \to \Upsilon(4S)$
• • • We do not use the following data for averages, fits, limits, etc. • • •				
$-0.06^{+0.13}_{-0.14} \pm 0.07$	AAIJ	12U	LHCB	Repl. by AAIJ 13Y
$0.43^{+0.36}_{-0.37} \pm 0.06$	AALTONEN	11L	CDF	Repl. by AALTONEN 12I

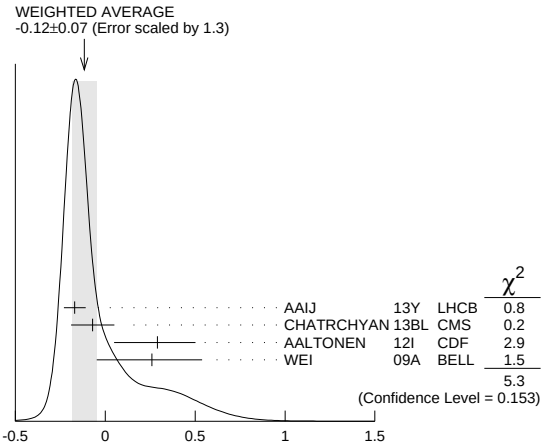

$A_{FB}(B \to K^* \ell^+ \ell^-)$ $(1.0 < q^2 < 6.0$ GeV$^2/c^4)$

$A_{FB}(B \to K^* \ell^+ \ell^-)$ ($4.3 < q^2 < 8.6$ GeV$^2/c^4$)

VALUE	DOCUMENT ID		TECN	COMMENT
$0.13^{+0.06}_{-0.05}$ OUR AVERAGE	Error includes scale factor of 1.1.			
$0.16^{+0.06}_{-0.05} \pm 0.01$	AAIJ	13Y	LHCB	pp at 7 TeV, $K^{*0}\mu^+\mu^-$
$-0.01 \pm 0.11 \pm 0.03$	CHATRCHYAN	13BL	CMS	pp at 7 TeV
$0.01 \pm 0.20 \pm 0.09$	AALTONEN	12I	CDF	$p\overline{p}$ at 1.96 TeV
$0.45^{+0.15}_{-0.21} \pm 0.15$	WEI	09A	BELL	$e^+e^- \to \Upsilon(4S)$
• • • We do not use the following data for averages, fits, limits, etc. • • •				
$0.27^{+0.06}_{-0.08} \pm 0.02$	AAIJ	12U	LHCB	Repl. by AAIJ 13Y
$-0.06^{+0.30}_{-0.28} \pm 0.05$	AALTONEN	11L	CDF	Repl. by AALTONEN 12I

$A_{FB}(B \to K^* \ell^+ \ell^-)$ ($10.09 < q^2 < 12.86$ GeV$^2/c^4$)

VALUE	DOCUMENT ID		TECN	COMMENT
0.34 ± 0.05 OUR AVERAGE				
$0.28^{+0.07}_{-0.06} \pm 0.02$	AAIJ	13Y	LHCB	pp at 7 TeV, $K^{*0}\mu^+\mu^-$
$0.40 \pm 0.08 \pm 0.05$	CHATRCHYAN	13BL	CMS	pp at 7 TeV
$0.38^{+0.16}_{-0.19} \pm 0.09$	AALTONEN	12I	CDF	$p\overline{p}$ at 1.96 TeV
$0.43^{+0.18}_{-0.20} \pm 0.03$	WEI	09A	BELL	$e^+e^- \to \Upsilon(4S)$
• • • We do not use the following data for averages, fits, limits, etc. • • •				
$0.27^{+0.11}_{-0.13} \pm 0.02$	AAIJ	12U	LHCB	Repl. by AAIJ 13Y
$0.66^{+0.23}_{-0.20} \pm 0.07$	AALTONEN	11L	CDF	Repl. by AALTONEN 12I

$A_{FB}(B \to K^* \ell^+ \ell^-)$ ($14.18 < q^2 < 16.0$ GeV$^2/c^4$)

VALUE	DOCUMENT ID		TECN	COMMENT
$0.47^{+0.07}_{-0.06}$ OUR AVERAGE	Error includes scale factor of 1.2.			
$0.51^{+0.07}_{-0.05} \pm 0.02$	AAIJ	13Y	LHCB	pp at 7 TeV, $K^{*0}\mu^+\mu^-$
$0.29 \pm 0.09 \pm 0.05$	CHATRCHYAN	13BL	CMS	pp at 7 TeV
$0.44^{+0.18}_{-0.21} \pm 0.10$	AALTONEN	12I	CDF	$p\overline{p}$ at 1.96 TeV
$0.70^{+0.16}_{-0.22} \pm 0.10$	WEI	09A	BELL	$e^+e^- \to \Upsilon(4S)$
• • • We do not use the following data for averages, fits, limits, etc. • • •				
$0.47^{+0.06}_{-0.08} \pm 0.03$	AAIJ	12U	LHCB	Repl. by AAIJ 13Y
$0.42 \pm 0.16 \pm 0.09$	AALTONEN	11L	CDF	Repl. by AALTONEN 12I

$A_{FB}(B \to K^* \ell^+ \ell^-)$ ($16.0 < q^2 < 19.0$ GeV$^2/c^4$)

VALUE	DOCUMENT ID		TECN	COMMENT
0.40 ± 0.06 OUR AVERAGE	Error includes scale factor of 1.3. See the ideogram below.			
$0.30 \pm 0.08^{+0.01}_{-0.02}$	AAIJ	13Y	LHCB	pp at 7 TeV, $K^{*0}\mu^+\mu^-$
$0.41 \pm 0.05 \pm 0.03$	CHATRCHYAN	13BL	CMS	pp at 7 TeV
$0.65^{+0.17}_{-0.18} \pm 0.16$	AALTONEN	12I	CDF	$p\overline{p}$ at 1.96 TeV
$0.66^{+0.11}_{-0.16} \pm 0.04$	WEI	09A	BELL	$e^+e^- \to \Upsilon(4S)$
• • • We do not use the following data for averages, fits, limits, etc. • • •				
$0.16^{+0.11}_{-0.13} \pm 0.06$	AAIJ	12U	LHCB	Repl. by AAIJ 13Y
$0.70^{+0.16}_{-0.25} \pm 0.10$	AALTONEN	11L	CDF	Repl. by AALTONEN 12I

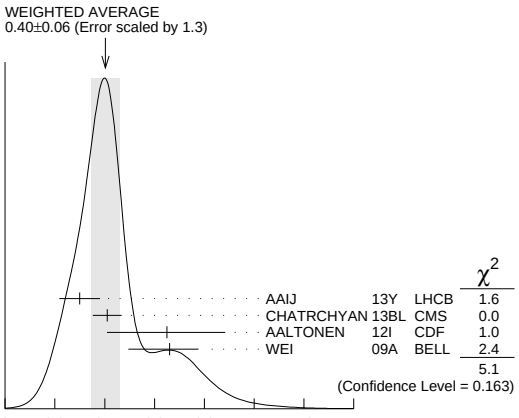

$A_{FB}(B \to K\ell^+\ell^-)$ ($q^2 > 0.1$ GeV$^2/c^4$)

VALUE	DOCUMENT ID		TECN	COMMENT
0.11±0.12 OUR AVERAGE				
$0.15^{+0.21}_{-0.23}\pm0.08$	[1] AUBERT,B	06J	BABR	$e^+e^- \to \Upsilon(4S)$
$0.10\pm0.14\pm0.01$	[2] ISHIKAWA	06	BELL	$e^+e^- \to \Upsilon(4S)$

[1] Results with different q^2 cuts are also reported.
[2] Using an unbinned max. likelihood fits to the M_{bc} distribution in five q^2 bins for $\cos\theta > 0$ and $\cos\theta < 0$.

$A_{FB}(B \to K\ell^+\ell^-)$ ($q^2 < 2.0$ GeV$^2/c^4$)

VALUE	DOCUMENT ID		TECN	COMMENT
$0.00^{+0.06}_{-0.05}$ OUR AVERAGE				
$0.00^{+0.06}_{-0.05}{}^{+0.03}_{-0.01}$	AAIJ	13H	LHCB	pp at 7 TeV
$0.13^{+0.42}_{-0.43}\pm0.07$	AALTONEN	12I	CDF	$p\overline{p}$ at 1.96 TeV
$0.06^{+0.32}_{-0.35}\pm0.02$	WEI	09A	BELL	$e^+e^- \to \Upsilon(4S)$
• • • We do not use the following data for averages, fits, limits, etc. • • •				
$-0.15^{+0.46}_{-0.39}\pm0.08$	AALTONEN	11L	CDF	Repl. by AALTONEN 12I

$A_{FB}(B \to K\ell^+\ell^-)$ ($2.0 < q^2 < 4.3$ GeV$^2/c^4$)

VALUE	DOCUMENT ID		TECN	COMMENT
$0.09^{+0.10}_{-0.07}$ OUR AVERAGE Error includes scale factor of 1.4.				
$0.07^{+0.08}_{-0.05}{}^{+0.02}_{-0.01}$	AAIJ	13H	LHCB	pp at 7 TeV
$0.32^{+0.15}_{-0.16}\pm0.05$	AALTONEN	12I	CDF	$p\overline{p}$ at 1.96 TeV
$-0.43^{+0.38}_{-0.40}\pm0.09$	WEI	09A	BELL	$e^+e^- \to \Upsilon(4S)$
• • • We do not use the following data for averages, fits, limits, etc. • • •				
$0.72^{+0.40}_{-0.35}\pm0.07$	AALTONEN	11L	CDF	Repl. by AALTONEN 12I

$A_{FB}(B \to K\ell^+\ell^-)$ ($0.0 < q^2 < 4.3$ GeV$^2/c^4$)

VALUE	DOCUMENT ID	TECN	COMMENT
0.31±0.16±0.04	AALTONEN	12I	CDF $p\overline{p}$ at 1.96 TeV
• • • We do not use the following data for averages, fits, limits, etc. • • •			
$0.36^{+0.24}_{-0.26}\pm0.06$	AALTONEN	11L	CDF Repl. by AALTONEN 12I

$A_{FB}(B \to K\ell^+\ell^-)$ ($1.0 < q^2 < 6.0$ GeV$^2/c^4$)

VALUE	DOCUMENT ID		TECN	COMMENT
$0.034^{+0.040}_{-0.029}$ OUR AVERAGE				
$0.02\ ^{+0.05}_{-0.03}\ ^{+0.02}_{-0.01}$	AAIJ	13H	LHCB	pp at 7 TeV
$0.13\ \pm0.09\ \pm0.02$	AALTONEN	12I	CDF	$p\overline{p}$ at 1.96 TeV
$-0.04\ ^{+0.13}_{-0.16}\ \pm0.05$	WEI	09A	BELL	$e^+e^- \to \Upsilon(4S)$
• • • We do not use the following data for averages, fits, limits, etc. • • •				
$0.08\ ^{+0.27}_{-0.22}\ \pm0.07$	AALTONEN	11L	CDF	Repl. by AALTONEN 12I

$A_{FB}(B \to K\ell^+\ell^-)$ ($4.3 < q^2 < 8.6$ GeV$^2/c^4$)

VALUE	DOCUMENT ID		TECN	COMMENT
$-0.04^{+0.04}_{-0.05}$ OUR AVERAGE				
$-0.02^{+0.03}_{-0.05}\pm0.03$	AAIJ	13H	LHCB	pp at 7 TeV
$0.01^{+0.13}_{-0.10}\pm0.01$	AALTONEN	12I	CDF	$p\overline{p}$ at 1.96 TeV
$-0.20^{+0.12}_{-0.14}\pm0.03$	WEI	09A	BELL	$e^+e^- \to \Upsilon(4S)$
• • • We do not use the following data for averages, fits, limits, etc. • • •				
$-0.20^{+0.17}_{-0.28}\pm0.03$	AALTONEN	11L	CDF	Repl. by AALTONEN 12I

$A_{FB}(B \to K\ell^+\ell^-)$ ($10.09 < q^2 < 12.86$ GeV$^2/c^4$)

VALUE	DOCUMENT ID		TECN	COMMENT
−0.05±0.06 OUR AVERAGE				
$-0.03\pm0.07\pm0.01$	AAIJ	13H	LHCB	pp at 7 TeV
$-0.03^{+0.11}_{-0.10}\pm0.04$	AALTONEN	12I	CDF	$p\overline{p}$ at 1.96 TeV
$-0.21^{+0.17}_{-0.15}\pm0.06$	WEI	09A	BELL	$e^+e^- \to \Upsilon(4S)$
• • • We do not use the following data for averages, fits, limits, etc. • • •				
$-0.10^{+0.17}_{-0.15}\pm0.07$	AALTONEN	11L	CDF	Repl. by AALTONEN 12I

$A_{FB}(B \to K\ell^+\ell^-)$ ($14.18 < q^2 < 16.0$ GeV$^2/c^4$)

VALUE	DOCUMENT ID		TECN	COMMENT
$-0.02^{+0.07}_{-0.05}$ OUR AVERAGE				
$-0.01^{+0.12}_{-0.06}\pm0.01$	AAIJ	13H	LHCB	pp at 7 TeV
$-0.05^{+0.09}_{-0.11}\pm0.03$	AALTONEN	12I	CDF	$p\overline{p}$ at 1.96 TeV
$0.04^{+0.32}_{-0.26}\pm0.05$	WEI	09A	BELL	$e^+e^- \to \Upsilon(4S)$
• • • We do not use the following data for averages, fits, limits, etc. • • •				
$0.03^{+0.49}_{-0.16}\pm0.04$	AALTONEN	11L	CDF	Repl. by AALTONEN 12I

$A_{FB}(B \to K\ell^+\ell^-)$ ($16.0 < q^2 < 18.0$ GeV$^2/c^4$)

VALUE	DOCUMENT ID		TECN	COMMENT
$-0.09^{+0.07}_{-0.09}{}^{+0.02}_{-0.01}$	AAIJ	13H	LHCB	pp at 7 TeV

$A_{FB}(B \to K\ell^+\ell^-)$ ($18.0 < q^2 < 22.0$ GeV$^2/c^4$)

VALUE	DOCUMENT ID		TECN	COMMENT
0.02±0.11±0.01	AAIJ	13H	LHCB	pp at 7 TeV

$A_{FB}(B \to K\ell^+\ell^-)$ ($q^2 > 16.0$ GeV$^2/c^4$)

VALUE	DOCUMENT ID		TECN	COMMENT
$0.04^{+0.09}_{-0.07}$ OUR AVERAGE				
$0.09^{+0.17}_{-0.13}\pm0.03$	AALTONEN	12I	CDF	$p\overline{p}$ at 1.96 TeV
$0.02^{+0.11}_{-0.08}\pm0.02$	WEI	09A	BELL	$e^+e^- \to \Upsilon(4S)$
• • • We do not use the following data for averages, fits, limits, etc. • • •				
$0.07^{+0.30}_{-0.23}\pm0.02$	AALTONEN	11L	CDF	Repl. by AALTONEN 12I

$F_S(B \to K\ell^+\ell^-)$ ($q^2 > 0.1$ GeV$^2/c^4$)

VALUE	DOCUMENT ID		TECN	COMMENT
$0.81^{+0.58}_{-0.61}\pm0.46$	[1] AUBERT,B	06J	BABR	$e^+e^- \to \Upsilon(4S)$

[1] Results with different q^2 cuts are also reported.

ISOSPIN ASYMMETRY

Δ_{0-} is defined as

$$\frac{\Gamma(B^0 \to f_d) - \Gamma(B^+ \to f_u)}{\Gamma(B^0 \to f) + \Gamma(B^+ \to f)},$$

the isospin asymmetry of inclusive neutral and charged B decay.

$\Delta_{0-}(B(B \to X_s\gamma))$

VALUE	DOCUMENT ID		TECN	COMMENT
−0.01 ±0.06 OUR AVERAGE				
$-0.06\ \pm0.15\ \pm0.07$	[1,2] AUBERT	08O	BABR	$e^+e^- \to \Upsilon(4S)$
$-0.006\pm0.058\pm0.026$	AUBERT,B	05R	BABR	$e^+e^- \to \Upsilon(4S)$

[1] The result is for $E_\gamma > 2.2$ GeV.
[2] Uses a fully reconstructed B meson as a tag on the recoil side.

$\Delta_{0+}(B \to K^*(892)\gamma)$

Δ_{0+} describes the isospin asymmetry between $\Gamma(B^0 \to K^*(892)^0\gamma)$ and $\Gamma(B^+ \to K^*(892)^+\gamma)$.

VALUE	DOCUMENT ID		TECN	COMMENT
0.052±0.026 OUR AVERAGE				
$0.066\pm0.021\pm0.022$	[1] AUBERT	09AO	BABR	$e^+e^- \to \Upsilon(4S)$
$0.012\pm0.044\pm0.026$	NAKAO	04	BELL	$e^+e^- \to \Upsilon(4S)$
• • • We do not use the following data for averages, fits, limits, etc. • • •				
$0.050\pm0.045\pm0.037$	[2] AUBERT,BE	04A	BABR	Repl. by AUBERT 09AO

[1] Uses the production ratio of charged and neutral B from $\Upsilon(4S)$ decays and the lifetime ratio $\tau_{B^+}/\tau_{B^0} = 1.071 \pm 0.009$. The 90% CL interval is $0.017 < \Delta_{0+} < 0.116$
[2] Uses the production ratio of charged and neutral B from $\Upsilon(4S)$ decays $R^{+/0} = 1.006 \pm 0.048$ and the lifetime ratio of $\tau_{B^+}/\tau_{B^0} = 1.083 \pm 0.017$. The 90% CL interval is $-0.046 < \Delta_{0+} < 0.146$.

$\Delta_{\rho\gamma} = \Gamma(B^+ \to \rho^+\gamma) / (2 \cdot \Gamma(B^0 \to \rho^0\gamma)) - 1$

VALUE	DOCUMENT ID		TECN	COMMENT
−0.46±0.17 OUR AVERAGE				
$-0.43^{+0.25}_{-0.22}\pm0.10$	AUBERT	08BH	BABR	$e^+e^- \to \Upsilon(4S)$
$-0.48^{+0.21}_{-0.19}{}^{+0.08}_{-0.09}$	TANIGUCHI	08	BELL	$e^+e^- \to \Upsilon(4S)$

Δ_{0-}(B($B \to K\ell^+\ell^-$))

VALUE	DOCUMENT ID		TECN	COMMENT
-0.37 ± 0.13 OUR AVERAGE				
$-0.35^{+0.23}_{-0.27}$	[1] AAIJ	12AH	LHCB	pp at 7 TeV
$-0.58^{+0.29}_{-0.37}\pm0.02$	[2] LEES	12S	BABR	$e^+e^- \to \Upsilon(4S)$
$-0.31^{+0.17}_{-0.14}\pm0.08$	[3] WEI	09A	BELL	$e^+e^- \to \Upsilon(4S)$
• • • We do not use the following data for averages, fits, limits, etc. • • •				
$-1.43^{+0.56}_{-0.85}\pm0.05$	[4,5] AUBERT	09T	BABR	Repl. by LEES 12S

[1] For $1 < q^2 < 6$ GeV$^2/c^4$.
[2] For $0.10 < q^2 < 8.12$ GeV$^2/c^4$. Measurements in other q^2 bins are also reported.
[3] For $q^2 < 8.68$ GeV$^2/c^4$.
[4] For $0.1 < m^2_{\ell^+\ell^-} < 7.02$ GeV$^2/c^4$.
[5] Assumes equal production of B^+ and B^0 at the $\Upsilon(4S)$.

Δ_{0-}(B($B \to K^*\ell^+\ell^-$))

VALUE	DOCUMENT ID		TECN	COMMENT
-0.22 ± 0.10 OUR AVERAGE				
-0.15 ± 0.16	[1] AAIJ	12AH	LHCB	pp at 7 TeV
$-0.25^{+0.20}_{-0.17}\pm0.03$	[2] LEES	12S	BABR	$e^+e^- \to \Upsilon(4S)$
$-0.29\pm0.16\pm0.09$	[3] WEI	09A	BELL	$e^+e^- \to \Upsilon(4S)$
• • • We do not use the following data for averages, fits, limits, etc. • • •				
$-0.56^{+0.17}_{-0.15}\pm0.03$	[4,5] AUBERT	09T	BABR	Repl. by LEES 12S

[1] For $1 < q^2 < 6$ GeV$^2/c^4$.
[2] For $0.10 < q^2 < 8.12$ GeV$^2/c^4$. Measurements in other q^2 bins are also reported.
[3] For $q^2 < 8.68$ GeV$^2/c^4$.
[4] For $0.1 < m^2_{\ell^+\ell^-} < 7.02$ GeV$^2/c^4$.
[5] Assumes equal production of B^+ and B^0 at the $\Upsilon(4S)$.

Δ_{0-}(B($B \to K^{(*)}\ell^+\ell^-$))

VALUE	DOCUMENT ID		TECN	COMMENT
-0.45 ± 0.17 OUR AVERAGE Error includes scale factor of 1.7.				
$-0.64^{+0.15}_{-0.14}\pm0.03$	[1,2] AUBERT	09T	BABR	$e^+e^- \to \Upsilon(4S)$
$-0.30^{+0.12}_{-0.11}\pm0.08$	[3] WEI	09A	BELL	$e^+e^- \to \Upsilon(4S)$

[1] For $0.1 < m^2_{\ell^+\ell^-} < 7.02$ GeV$^2/c^4$.
[2] Assumes equal production of B^+ and B^0 at the $\Upsilon(4S)$.
[3] For $q^2 < 8.68$ GeV$^2/c^2$.

$B \to X_c\ell\nu$ HADRONIC MASS MOMENTS

$\langle M_X^2 - \overline{M}_D^2 \rangle$ (First Moments)

VALUE (GeV^2)	DOCUMENT ID		TECN	COMMENT
0.36 ±0.08 OUR AVERAGE Error includes scale factor of 1.8.				
$0.467\pm0.038\pm0.068$	[1] ACOSTA	05F	CDF	$p\overline{p}$ at 1.96 TeV
$0.293\pm0.012\pm0.058$	[2] CSORNA	04	CLE2	$e^+e^- \to \Upsilon(4S)$
• • • We do not use the following data for averages, fits, limits, etc. • • •				
$0.251\pm0.023\pm0.062$	[3] CRONIN-HEN..	01B	CLE2	$e^+e^- \to \Upsilon(4S)$

[1] Moments are measured with a minimum lepton momentum of 0.7 GeV/c in the B rest frame;
[2] Uses minimum lepton energy of 1.5 GeV and also reports moments with $E_\ell > 1.0$ GeV.
[3] The leptons are required to have $P_\ell > 1.5$ GeV/c.

$\langle M_X^2 \rangle$ (First Moments)

VALUE (GeV^2)	DOCUMENT ID		TECN	COMMENT
4.156±0.029 OUR AVERAGE				
$4.144\pm0.028\pm0.022$	[1] SCHWANDA	07	BELL	$e^+e^- \to \Upsilon(4S)$
$4.18\ \pm0.04\ \pm0.03$	[1] AUBERT,B	04	BABR	$e^+e^- \to \Upsilon(4S)$

[1] The leptons are required to have $E_\ell > 1.5$ GeV/c.

$\langle (M_X^2 - \overline{M}_X^2)^2 \rangle$ (Second Moments)

VALUE (GeV^4)	DOCUMENT ID		TECN	COMMENT
0.55 ±0.08 OUR AVERAGE				
$0.515\pm0.061\pm0.064$	[1] SCHWANDA	07	BELL	$e^+e^- \to \Upsilon(4S)$
$0.629\pm0.031\pm0.143$	[2] CSORNA	04	CLE2	$e^+e^- \to \Upsilon(4S)$
• • • We do not use the following data for averages, fits, limits, etc. • • •				
$1.05\ \pm0.26\ \pm0.13$	[3] ACOSTA	05F	CDF	$p\overline{p}$ at 1.96 TeV
$0.576\pm0.048\pm0.168$	[1] CRONIN-HEN..	01B	CLE2	$e^+e^- \to \Upsilon(4S)$

[1] The leptons are required to have $E_\ell > 1.5$ GeV/c.
[2] Uses minimum lepton energy of 1.5 GeV and also reports moments with $E_\ell > 1.0$ GeV.
[3] Moments are measured with a minimum lepton momentum of 0.7 GeV/c in the B rest frame;

$\langle (M_X^2 - \overline{M}_D^2)^2 \rangle$ (Second Moments)

VALUE (GeV^4)	DOCUMENT ID		TECN	COMMENT
0.639±0.056±0.178	[1] CRONIN-HEN..	01B	CLE2	$e^+e^- \to \Upsilon(4S)$

[1] The leptons are required to have $E_\ell > 1.5$ GeV/c.

$B \to X_c\ell\nu$ LEPTON MOMENTUM MOMENTS

R_0 ($\Gamma_{E_l>1.7GeV}$ / $\Gamma_{E_l>1.5GeV}$)

VALUE	DOCUMENT ID		TECN	COMMENT
0.6187±0.0014±0.0016	[1] MAHMOOD	03	CLE2	$e^+e^- \to \Upsilon(4S)$

[1] The leptons are required to have $E_l > 1.5$ GeV in the B rest frame.

R_1 ($\langle E_l \rangle_{E_l>1.5GeV}$)

VALUE	DOCUMENT ID		TECN	COMMENT
1.7797±0.0018 OUR AVERAGE Error includes scale factor of 1.8. See the ideogram below.				
$1.7743\pm0.0019\pm0.0014$	[1] AUBERT,B	04A	BABR	$e^+e^- \to \Upsilon(4S)$
$1.7792\pm0.0021\pm0.0027$	[2] MAHMOOD	04	CLEO	$e^+e^- \to \Upsilon(4S)$
$1.7810\pm0.0007\pm0.0009$	[3] MAHMOOD	03	CLE2	$e^+e^- \to \Upsilon(4S)$

[1] The leptons are required to have $E_l > 1.5$ GeV in the B rest frame. The result with $E_l > 0.6$ GeV is also given.
[2] Uses $E_e > 1.5$ GeV and also reports moments with other minimum minimum E_e conditions, as low as $E_e > 0.6$ GeV.
[3] The leptons are required to have $E_l > 1.5$ GeV in the B rest frame.

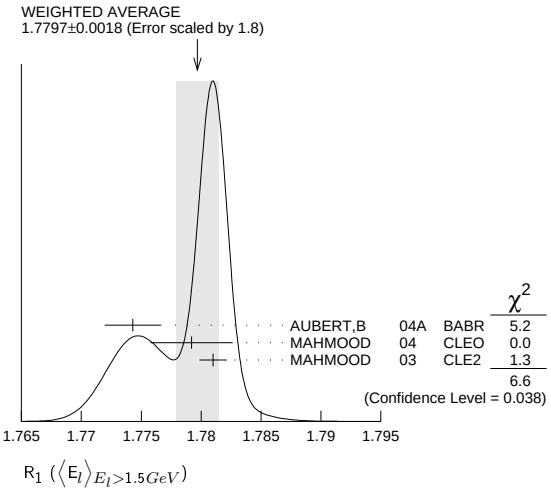

R_2 ($\langle E_l^2 - \overline{E}_l^2 \rangle_{E_l>1.5GeV}$)

VALUE (10^{-3} GeV^2)	DOCUMENT ID		TECN	COMMENT
30.8±0.8 OUR AVERAGE				
$30.3\pm0.9\pm0.5$	[1] AUBERT,B	04A	BABR	$e^+e^- \to \Upsilon(4S)$
$31.6\pm0.8\pm1.0$	[2] MAHMOOD	04	CLEO	$e^+e^- \to \Upsilon(4S)$

[1] The leptons are required to have $E_l > 1.5$ GeV in the B rest frame. The result with $E_l > 0.6$ GeV is also given.
[2] Uses $E_e > 1.5$ GeV and also reports moments with other minimum minimum E_e conditions, as low as $E_e > 0.6$ GeV.

R_3 ($\langle E_l^3 - \overline{E}_l^3 \rangle_{E_l>1.5GeV}$)

VALUE (10^{-3} GeV^3)	DOCUMENT ID		TECN	COMMENT
2.12±0.47±0.20	[1] AUBERT,B	04A	BABR	$e^+e^- \to \Upsilon(4S)$

[1] The leptons are required to have $E_l > 1.5$ GeV in the B rest frame. The result with $E_l > 0.6$ GeV is also given.

$B \to X_s\gamma$ PHOTON ENERGY MOMENTS

$\langle E_\gamma \rangle$

VALUE (GeV)	DOCUMENT ID		TECN	COMMENT
2.314±0.011 OUR AVERAGE				
$2.346\pm0.018^{+0.027}_{-0.022}$	[1,2] LEES	12U	BABR	$e^+e^- \to \Upsilon(4S)$
$2.304\pm0.014\pm0.017$	[2,3] LEES	12V	BABR	$e^+e^- \to \Upsilon(4S)$
$2.311\pm0.009\pm0.015$	[3] LIMOSANI	09	BELL	$e^+e^- \to \Upsilon(4S)$
$2.289\pm0.058\pm0.027$	[3,4] AUBERT	08O	BABR	$e^+e^- \to \Upsilon(4S)$
$2.309\pm0.023\pm0.023$	[2,3] SCHWANDA	08	BELL	$e^+e^- \to \Upsilon(4S)$
• • • We do not use the following data for averages, fits, limits, etc. • • •				
$2.288\pm0.025\pm0.023$	[3] AUBERT,BE	06B	BABR	Repl. by LEES 12V

[1] LEES 12U uses $E_\gamma > 1.897$ GeV to calculate the moments; the moments are used to calculate the HQET parameters $m_b = 4.579^{+0.032}_{-0.029}$ GeV/c^2 and $\mu_\pi^2 = 0.257^{+0.034}_{-0.039}$ GeV^2 in the shape function model. The same HQET parameters are also determined in the kinetic model.
[2] Results for different E_γ threshold values are also measured.
[3] The result is for $E_\gamma > 1.9$ GeV.
[4] Uses a fully reconstructed B meson as a tag on the recoil side.

$\langle E_\gamma^2 \rangle - \langle E_\gamma \rangle^2$

VALUE (10^{-2} GeV^2)	DOCUMENT ID		TECN	COMMENT
3.03±0.25 OUR AVERAGE				
$2.11 \pm 0.57^{+0.55}_{-0.69}$	[1,2] LEES	12U	BABR	$e^+e^- \to \Upsilon(4S)$
$3.62 \pm 0.33 \pm 0.33$	[2,3] LEES	12V	BABR	$e^+e^- \to \Upsilon(4S)$
$3.02 \pm 0.19 \pm 0.30$	[3] LIMOSANI	09	BELL	$e^+e^- \to \Upsilon(4S)$
$3.34 \pm 1.24 \pm 0.62$	[3,4] AUBERT	08O	BABR	$e^+e^- \to \Upsilon(4S)$
$2.17 \pm 0.60 \pm 0.55$	[2,3] SCHWANDA	08	BELL	$e^+e^- \to \Upsilon(4S)$
• • • We do not use the following data for averages, fits, limits, etc. • • •				
$3.28 \pm 0.40 \pm 0.43$	[3] AUBERT,BE	06B	BABR	Repl. by LEES 12V

[1] LEES 12U uses $E_\gamma > 1.897$ GeV to calculate the moments; the moments are used to calculate the HQET parameters $m_b = 4.579^{+0.032}_{-0.029}$ GeV/c^2 and $\mu_\pi^2 = 0.257^{+0.034}_{-0.039}$ GeV^2 in the shape function model. The same HQET parameters are also determined in the kinetic model.

[2] Results for different E_γ threshold values are also measured.

[3] The result is for $E_\gamma > 1.9$ GeV.

[4] Uses a fully reconstructed B meson as a tag on the recoil side.

$B^{\pm}/B^0$ ADMIXTURE REFERENCES

AAIJ	13H	JHEP 1302 105	R. Aaij *et al.*	(LHCb Collab.)
AAIJ	13Y	JHEP 1308 131	R. Aaij *et al.*	(LHCb Collab.)
CHATRCHYAN	13BL	PL B727 77	S. Chatrchyan *et al.*	(CMS Collab.)
LEES	13I	PR D87 112005	J.P. Lees *et al.*	(BABAR Collab.)
LEES	13M	PR D88 032012	J.P. Lees *et al.*	(BABAR Collab.)
AAIJ	12AH	JHEP 1207 133	R. Aaij *et al.*	(LHCb Collab.)
AAIJ	12U	PRL 108 181806	R. Aaij *et al.*	(LHCb Collab.)
AALTONEN	12I	PRL 108 081807	T. Aaltonen *et al.*	(CDF Collab.)
LEES	12	PR D85 011102	J.P. Lees *et al.*	(BABAR Collab.)
LEES	12D	PRL 109 101802	J.P. Lees *et al.*	(BABAR Collab.)
Also		PR D88 072012	J.P. Lees *et al.*	(BABAR Collab.)
LEES	12R	PR D86 032004	J.P. Lees *et al.*	(BABAR Collab.)
LEES	12S	PR D86 032012	J.P. Lees *et al.*	(BABAR Collab.)
LEES	12U	PR D86 052012	J.P. Lees *et al.*	(BABAR Collab.)
LEES	12V	PRL 109 191801	J.P. Lees	(BABAR Collab.)
Also		PR D86 112008	J.P. Lees *et al.*	(BABAR Collab.)
AALTONEN	11AI	PRL 107 201802	T. Aaltonen *et al.*	(CDF Collab.)
AALTONEN	11L	PRL 106 161801	T. Aaltonen *et al.*	(CDF Collab.)
DEL-AMO-SA...	11	PR D83 031103	P. del Amo Sanchez *et al.*	(BABAR Collab.)
AUBERT	10	PRL 104 011802	B. Aubert *et al.*	(BABAR Collab.)
AUBERT	10A	PR D81 032003	B. Aubert *et al.*	(BABAR Collab.)
AUSHEV	10	PR D81 031103	T. Aushev *et al.*	(BELLE Collab.)
DEL-AMO-SA...	10M	PR D82 051101	P. del Amo Sanchez *et al.*	(BABAR Collab.)
DEL-AMO-SA...	10Q	PR D82 112002	P. del Amo Sanchez *et al.*	(BABAR Collab.)
NISHIMURA	10	PRL 105 191803	K. Nishimura *et al.*	(BELLE Collab.)
URQUIJO	10	PRL 104 021801	P. Urquijo *et al.*	(BELLE Collab.)
AUBERT	09AO	PRL 103 211802	B. Aubert *et al.*	(BABAR Collab.)
AUBERT	09N	PR D79 031102	B. Aubert *et al.*	(BABAR Collab.)
AUBERT	09T	PRL 102 091803	B. Aubert *et al.*	(BABAR Collab.)
Also		EPAPS Document No. E-PRLTAO-102-060910		(BABAR Collab.)
AUBERT	09U	PRL 102 161803	B. Aubert *et al.*	(BABAR Collab.)
LIMOSANI	09	PRL 103 241801	A. Limosani *et al.*	(BELLE Collab.)
WEI	09A	PRL 103 171801	J.-T. Wei *et al.*	(BELLE Collab.)
Also		EPAPS Supplement EPAPS_appendix.pdf		(BELLE Collab.)
AUBERT	08AS	PRL 100 171802	B. Aubert *et al.*	(BABAR Collab.)
AUBERT	08BC	PR D78 072007	B. Aubert *et al.*	(BABAR Collab.)
AUBERT	08BH	PR D78 112001	B. Aubert *et al.*	(BABAR Collab.)
AUBERT	08BJ	PRL 101 171804	B. Aubert *et al.*	(BABAR Collab.)
AUBERT	08N	PRL 100 021801	B. Aubert *et al.*	(BABAR Collab.)
Also		PR D79 092002	B. Aubert *et al.*	(BABAR Collab.)
AUBERT	08O	PR D77 051103	B. Aubert *et al.*	(BABAR Collab.)
SCHWANDA	08	PR D78 032016	C. Schwanda *et al.*	(BELLE Collab.)
TANIGUCHI	08	PRL 101 111801	N. Taniguchi *et al.*	(BELLE Collab.)
WEI	08A	PR D78 011101	J.-T. Wei *et al.*	(BELLE Collab.)
AUBERT	07AG	PRL 99 051801	B. Aubert *et al.*	(BABAR Collab.)
AUBERT	07C	PR D75 012003	B. Aubert *et al.*	(BABAR Collab.)
AUBERT	07E	PRL 98 051802	B. Aubert *et al.*	(BABAR Collab.)
AUBERT	07L	PRL 98 151802	B. Aubert *et al.*	(BABAR Collab.)
HUANG	07	PR D75 012002	G.S. Huang *et al.*	(CLEO Collab.)
SCHWANDA	07	PR D75 032005	C. Schwanda *et al.*	(BELLE Collab.)
URQUIJO	07	PR D75 032001	P. Urquijo *et al.*	(BELLE Collab.)
AUBERT	06H	PR D73 012006	B. Aubert *et al.*	(BABAR Collab.)
AUBERT,B	06J	PR D73 092001	B. Aubert *et al.*	(BABAR Collab.)
AUBERT,B	06Y	PR D74 091105	B. Aubert *et al.*	(BABAR Collab.)
AUBERT,BE	06B	PRL 97 171803	B. Aubert *et al.*	(BABAR Collab.)
BUCHMULLER	06	PR D73 073008	O.L. Buchmuller, H.U. Flacher	(RHBL)
GOKHROO	06	PRL 97 162002	G. Gokhroo *et al.*	(BELLE Collab.)
ISHIKAWA	06	PRL 96 251801	A. Ishikawa *et al.*	(BELLE Collab.)
MOHAPATRA	06	PRL 96 221601	D. Mohapatra *et al.*	(BELLE Collab.)
ABAZOV	05O	PRL 95 171803	V.M. Abazov *et al.*	(D0 Collab.)
ACOSTA	05F	PR D71 051103	D. Acosta *et al.*	(CDF Collab.)
ARTUSO	05B	PRL 95 261801	M. Artuso *et al.*	(CLEO Collab.)
AUBERT	05	PRL 94 011801	B. Aubert *et al.*	(BABAR Collab.)
AUBERT,B	05M	PRL 95 142003	B. Aubert *et al.*	(BABAR Collab.)
AUBERT,B	05R	PR D72 052004	B. Aubert *et al.*	(BABAR Collab.)
AUBERT,B	05X	PRL 95 111801	B. Aubert *et al.*	(BABAR Collab.)
Also		PRL 97 019903 (errat.)	B. Aubert *et al.*	(BABAR Collab.)
CHOI	05	PRL 94 182002	S.-K. Choi *et al.*	(BELLE Collab.)
IWASAKI	05	PR D72 092005	M. Iwasaki *et al.*	(BELLE Collab.)
LIMOSANI	05	PL B621 28	A. Limosani *et al.*	(BELLE Collab.)
MOHAPATRA	05	PR D72 011101	D. Mohapatra *et al.*	(BELLE Collab.)
NISHIDA	05	PL B610 23	S. Nishida *et al.*	(BELLE Collab.)
OKABE	05	PL B614 27	T. Okabe *et al.*	(BELLE Collab.)
ABDALLAH	04D	EPJ C33 213	J. Abdallah *et al.*	(DELPHI Collab.)
AUBERT	04C	PRL 92 111801	B. Aubert *et al.*	(BaBar Collab.)
AUBERT	04I	PRL 92 071802	B. Aubert *et al.*	(BABAR Collab.)
AUBERT	04S	PR D69 052005	B. Aubert *et al.*	(BABAR Collab.)
AUBERT	04X	PRL 93 011803	B. Aubert *et al.*	(BABAR Collab.)
AUBERT,B	04	PR D69 111103	B. Aubert *et al.*	(BABAR Collab.)
AUBERT,B	04A	PR D69 111104	B. Aubert *et al.*	(BABAR Collab.)
AUBERT,B	04E	PRL 93 021804	B. Aubert *et al.*	(BABAR Collab.)
AUBERT,B	04F	PRL 93 061801	B. Aubert *et al.*	(BABAR Collab.)
AUBERT,B	04I	PRL 93 081802	B. Aubert *et al.*	(BABAR Collab.)
AUBERT,BE	04A	PR D70 112006	B. Aubert *et al.*	(BABAR Collab.)
CSORNA	04	PR D70 032002	S.E. Csorna *et al.*	(CLEO Collab.)
KOPPENBURG	04	PRL 93 061803	P. Koppenburg *et al.*	(BELLE Collab.)
MAHMOOD	04	PR D70 032003	A.H. Mahmood *et al.*	(CLEO Collab.)
NAKAO	04	PR D69 112001	M. Nakao *et al.*	(BELLE Collab.)
NISHIDA	04	PRL 93 031803	S. Nishida *et al.*	(BELLE Collab.)
ADAM	03B	PR D68 012004	N.E. Adam *et al.*	(CLEO Collab.)
AUBERT	03	PR D67 031101	B. Aubert *et al.*	(BaBar Collab.)
AUBERT	03F	PR D67 032002	B. Aubert *et al.*	(BaBar Collab.)
AUBERT	03U	PRL 91 221802	B. Aubert *et al.*	(BaBar Collab.)
BONVICINI	03	PR D68 011101	G. Bonvicini *et al.*	(CLEO Collab.)
HUANG	03	PRL 91 241802	H.-C. Huang *et al.*	(BELLE Collab.)
ISHIKAWA	03	PRL 91 261601	A. Ishikawa *et al.*	(BELLE Collab.)
KANEKO	03	PRL 90 021801	J. Kaneko *et al.*	(BELLE Collab.)
KROKOVNY	03B	PRL 91 262002	P. Krokovny *et al.*	(BELLE Collab.)
MAHMOOD	03	PR D67 072001	A.H. Mahmood *et al.*	(CLEO Collab.)
ABE	02	PRL 88 021801	K. Abe *et al.*	(BELLE Collab.)
ABE	02L	PRL 89 011803	K. Abe *et al.*	(BELLE Collab.)
ABE	02Y	PL B547 181	K. Abe *et al.*	(BELLE Collab.)
ANDERSON	02	PRL 89 282001	S. Anderson *et al.*	(CLEO Collab.)
AUBERT	02C	PRL 88 101805	B. Aubert *et al.*	(BaBar Collab.)
AUBERT	02G	PR D65 091104	B. Aubert *et al.*	(BaBar Collab.)
AUBERT	02L	PRL 88 241801	B. Aubert *et al.*	(BaBar Collab.)
BORNHEIM	02	PRL 88 231803	A. Bornheim *et al.*	(CLEO Collab.)
EDWARDS	02B	PR D65 111102	K.W. Edwards *et al.*	(CLEO Collab.)
ABE	01F	PL B511 151	K. Abe *et al.*	(BELLE Collab.)
ABE	01J	PR D64 072001	K. Abe *et al.*	(BELLE Collab.)
ANDERSON	01B	PRL 87 181803	S. Anderson *et al.*	(CLEO Collab.)
CHEN	01	PR D63 031102	S. Chen *et al.*	(CLEO Collab.)
CHEN	01C	PRL 87 251807	S. Chen *et al.*	(CLEO Collab.)
COAN	01	PRL 86 5661	T.E. Coan *et al.*	(CLEO Collab.)
CRONIN-HEN...	01B	PRL 87 251808	D. Cronin-Hennessy *et al.*	(CLEO Collab.)
PDG	01	Unofficial 2001 WWW edition		
ABREU	00R	PL B475 407	P. Abreu *et al.*	(DELPHI Collab.)
COAN	00	PRL 84 5283	T.E. Coan *et al.*	(CLEO Collab.)
RICHICHI	00	PRL 85 520	S.J. Richichi *et al.*	(CLEO Collab.)
BARATE	98Q	EPJ C4 387	R. Barate *et al.*	(ALEPH Collab.)
BERGFELD	98	PRL 81 272	T. Bergfeld *et al.*	(CLEO Collab.)
BISHAI	98	PR D57 3847	M. Bishai *et al.*	(CLEO Collab.)
BONVICINI	98	PR D57 6604	G. Bonvicini *et al.*	(CLEO Collab.)
BROWDER	98	PRL 81 1786	T.E. Browder *et al.*	(CLEO Collab.)
COAN	98	PRL 80 1150	T.E. Coan *et al.*	(CLEO Collab.)
GLENN	98	PRL 80 2289	S. Glenn *et al.*	(CLEO Collab.)
ACKERSTAFF	97N	ZPHY C74 423	K. Ackerstaff *et al.*	(OPAL Collab.)
AMMAR	97	PR D55 13	R. Ammar *et al.*	(CLEO Collab.)
BARISH	97	PRL 79 3599	B. Barish *et al.*	(CLEO Collab.)
BUSKULIC	97B	ZPHY C73 601	D. Buskulic *et al.*	(ALEPH Collab.)
GIBBONS	97B	PR D56 3783	L. Gibbons *et al.*	(CLEO Collab.)
ALBRECHT	96D	PL B374 256	H. Albrecht *et al.*	(ARGUS Collab.)
BARISH	96B	PRL 76 1570	B.C. Barish *et al.*	(CLEO Collab.)
GIBAUT	96	PR D53 4734	D. Gibaut *et al.*	(CLEO Collab.)
KUBOTA	96	PR D53 6033	Y. Kubota *et al.*	(CLEO Collab.)
PDG	96	PR D54 1	R. M. Barnett *et al.*	(PDG Collab.)
ALAM	95	PRL 74 2885	M.S. Alam *et al.*	(CLEO Collab.)
ALBRECHT	95D	PL B353 554	H. Albrecht *et al.*	(ARGUS Collab.)
BALEST	95B	PR D52 2661	R. Balest *et al.*	(CLEO Collab.)
BARISH	95	PR D51 1014	B.C. Barish *et al.*	(CLEO Collab.)
BUSKULIC	95B	PL B345 103	D. Buskulic *et al.*	(ALEPH Collab.)
ALBRECHT	94C	ZPHY C62 371	H. Albrecht *et al.*	(ARGUS Collab.)
ALBRECHT	94J	ZPHY C61 1	H. Albrecht *et al.*	(ARGUS Collab.)
PROCARIO	94	PRL 73 1472	M. Procario *et al.*	(CLEO Collab.)
ALBRECHT	93	ZPHY C57 533	H. Albrecht *et al.*	(ARGUS Collab.)
ALBRECHT	93E	ZPHY C60 11	H. Albrecht *et al.*	(ARGUS Collab.)
ALBRECHT	93H	PL B318 397	H. Albrecht *et al.*	(ARGUS Collab.)
ALBRECHT	93I	ZPHY C58 191	H. Albrecht *et al.*	(ARGUS Collab.)
ALEXANDER	93B	PL B319 365	J. Alexander *et al.*	(CLEO Collab.)
ARTUSO	93	PL B311 307	M. Artuso	(SYRA)
BARTELT	93B	PRL 71 4111	J.E. Bartelt *et al.*	(CLEO Collab.)
ALBRECHT	92E	PL B277 209	H. Albrecht *et al.*	(ARGUS Collab.)
ALBRECHT	92G	ZPHY C54 1	H. Albrecht *et al.*	(ARGUS Collab.)
ALBRECHT	92O	ZPHY C56 1	H. Albrecht *et al.*	(ARGUS Collab.)
BORTOLETTO	92	PR D45 21	D. Bortoletto *et al.*	(CLEO Collab.)
CRAWFORD	92	PR D45 752	G. Crawford *et al.*	(CLEO Collab.)
HENDERSON	92	PR D45 2212	S. Henderson *et al.*	(CLEO Collab.)
LESIAK	92	ZPHY C55 33	T. Lesiak *et al.*	(Crystal Ball Collab.)
ALBRECHT	91C	PL B255 297	H. Albrecht *et al.*	(ARGUS Collab.)
ALBRECHT	91H	ZPHY C52 353	H. Albrecht *et al.*	(ARGUS Collab.)
FULTON	91	PR D43 651	R. Fulton *et al.*	(CLEO Collab.)
YANAGISAWA	91	PRL 66 2436	C. Yanagisawa *et al.*	(CUSB II Collab.)
ALBRECHT	90	PL B234 409	H. Albrecht *et al.*	(ARGUS Collab.)
ALBRECHT	90H	PL B249 359	H. Albrecht *et al.*	(ARGUS Collab.)
BORTOLETTO	90	PRL 64 2117	D. Bortoletto *et al.*	(CLEO Collab.)
Also		PR D45 21	D. Bortoletto *et al.*	(CLEO Collab.)
FULTON	90	PRL 64 16	R. Fulton *et al.*	(CLEO Collab.)
MASCHMANN	90	ZPHY C46 555	W.S. Maschmann *et al.*	(Crystal Ball Collab.)
PDG	90	PL B239 1	J.J. Hernandez *et al.*	(IFIC, BOST, CIT+)
ALBRECHT	89K	ZPHY C42 519	H. Albrecht *et al.*	(ARGUS Collab.)
ISGUR	89B	PR D39 799	N. Isgur *et al.*	(TNTO, CIT)
WACHS	89	ZPHY C42 33	K. Wachs *et al.*	(Crystal Ball Collab.)
ALBRECHT	88E	PL B210 263	H. Albrecht *et al.*	(ARGUS Collab.)
ALBRECHT	88H	PL B210 258	H. Albrecht *et al.*	(ARGUS Collab.)
KOERNER	88	ZPHY C38 511	J.G. Korner, G.A. Schuler	(MANZ, DESY)
ALAM	87	PRL 59 22	M.S. Alam *et al.*	(CLEO Collab.)
ALAM	87B	PR 58 1814	M.S. Alam *et al.*	(CLEO Collab.)
ALBRECHT	87D	PL B199 451	H. Albrecht *et al.*	(ARGUS Collab.)
ALBRECHT	87H	PL B187 425	H. Albrecht *et al.*	(ARGUS Collab.)
BEAN	87	PR D35 3533	A. Bean *et al.*	(CLEO Collab.)
BEHRENDS	87	PRL 59 407	S. Behrends *et al.*	(CLEO Collab.)
BORTOLETTO	87	PR D35 19	D. Bortoletto *et al.*	(CLEO Collab.)
ALAM	86	PR D34 3279	M.S. Alam *et al.*	(CLEO Collab.)
BALTRUSAIT...	86E	PRL 56 2140	R.M. Baltrusaitis *et al.*	(Mark III Collab.)
BORTOLETTO	86	PRL 56 800	D. Bortoletto *et al.*	(CLEO Collab.)
HAAS	86	PRL 56 2781	J. Haas *et al.*	(CLEO Collab.)
ALBRECHT	85H	PL 162B 395	H. Albrecht *et al.*	(ARGUS Collab.)
CSORNA	85	PRL 54 1894	S.E. Csorna *et al.*	(CLEO Collab.)
HAAS	85	PRL 55 1248	J. Haas *et al.*	(CLEO Collab.)
AVERY	84	PRL 53 1309	P. Avery *et al.*	(CLEO Collab.)
CHEN	84	PRL 52 1084	A. Chen *et al.*	(CLEO Collab.)
LEVMAN	84	PL 141B 271	G.M. Levman *et al.*	(CUSB Collab.)
ALAM	83B	PRL 51 1143	M.S. Alam *et al.*	(CLEO Collab.)
GREEN	83	PRL 51 347	J. Green *et al.*	(CLEO Collab.)
KLOPFEN...	83B	PL 130B 444	C. Klopfenstein *et al.*	(CUSB Collab.)
ALTARELLI	82	NP B208 365	G. Altarelli *et al.*	(ROMA, INFN, FRAS)
BRODY	82	PRL 48 1070	A.D. Brody *et al.*	(CLEO Collab.)
GIANNINI	82	NP B206 1	G. Giannini *et al.*	(CUSB Collab.)
BEBEK	81	PRL 46 84	C. Bebek *et al.*	(CLEO Collab.)
CHADWICK	81	PRL 46 88	K. Chadwick *et al.*	(CLEO Collab.)
ABRAMS	80	PRL 44 10	G.S. Abrams *et al.*	(SLAC, LBL)

$B^{\pm}/B^0/B^0_s/b$-baryon ADMIXTURE

$B^{\pm}/B^0/B^0_s/b$-baryon ADMIXTURE MEAN LIFE

Each measurement of the B mean life is an average over an admixture of various bottom mesons and baryons which decay weakly. Different techniques emphasize different admixtures of produced particles, which could result in a different B mean life.

"OUR EVALUATION" is an average using rescaled values of the data listed below. The average and rescaling were performed by the Heavy Flavor Averaging Group (HFAG) and are described at http://www.slac.stanford.edu/xorg/hfag/. The averaging/rescaling procedure takes into account correlations between the measurements and asymmetric lifetime errors, but ignores the small differences due to different techniques.

VALUE (10^{-12} s)	EVTS	DOCUMENT ID		TECN	COMMENT
1.568±0.009 OUR EVALUATION					
1.570±0.005±0.008		[1] ABDALLAH	04E	DLPH	$e^+e^- \to Z$
1.533±0.015 $^{+0.035}_{-0.031}$		[2] ABE	98B	CDF	$p\overline{p}$ at 1.8 TeV
1.549±0.009±0.015		[3] ACCIARRI	98	L3	$e^+e^- \to Z$
1.611±0.010±0.027		[4] ACKERSTAFF	97F	OPAL	$e^+e^- \to Z$
1.582±0.011±0.027		[4] ABREU	96E	DLPH	$e^+e^- \to Z$
1.533±0.013±0.022	19.8k	[5] BUSKULIC	96F	ALEP	$e^+e^- \to Z$
1.564±0.030±0.036		[6] ABE,K	95B	SLD	$e^+e^- \to Z$
1.542±0.021±0.045		[7] ABREU	94L	DLPH	$e^+e^- \to Z$
1.523±0.034±0.038	5372	[8] ACTON	93L	OPAL	$e^+e^- \to Z$
1.511±0.022±0.078		[9] BUSKULIC	93O	ALEP	$e^+e^- \to Z$
• • • We do not use the following data for averages, fits, limits, etc. • • •					
1.575±0.010±0.026		[10] ABREU	96E	DLPH	$e^+e^- \to Z$
1.50 $^{+0.24}_{-0.21}$ ±0.03		[11] ABREU	94P	DLPH	$e^+e^- \to Z$
1.46 ±0.06 ±0.06	5344	[12] ABE	93J	CDF	Repl. by ABE 98B
1.23 $^{+0.14}_{-0.13}$ ±0.15	188	[13] ABREU	93D	DLPH	Sup. by ABREU 94L
1.49 ±0.11 ±0.12	253	[14] ABREU	93G	DLPH	Sup. by ABREU 94L
1.51 $^{+0.16}_{-0.14}$ ±0.11	130	[15] ACTON	93C	OPAL	$e^+e^- \to Z$
1.535±0.035±0.028	7357	[8] ADRIANI	93K	L3	Repl. by ACCIARRI 98
1.28 ±0.10		[16] ABREU	92	DLPH	Sup. by ABREU 94L
1.37 ±0.07 ±0.06	1354	[17] ACTON	92	OPAL	Sup. by ACTON 93L
1.49 ±0.03 ±0.06		[18] BUSKULIC	92F	ALEP	Sup. by BUSKULIC 96F
1.35 $^{+0.19}_{-0.17}$ ±0.05		[19] BUSKULIC	92G	ALEP	$e^+e^- \to Z$
1.32 ±0.08 ±0.09	1386	[20] ADEVA	91H	L3	Sup. by ADRIANI 93K
1.32 $^{+0.31}_{-0.25}$ ±0.15	37	[21] ALEXANDER	91G	OPAL	$e^+e^- \to Z$
1.29 ±0.06 ±0.10	2973	[22] DECAMP	91C	ALEP	Sup. by BUSKULIC 92F
1.36 $^{+0.25}_{-0.23}$		[23] HAGEMANN	90	JADE	E^{ee}_{cm} = 35 GeV
1.13 ±0.15		[24] LYONS	90	RVUE	
1.35 ±0.10 ±0.24		BRAUNSCH...	89B	TASS	E^{ee}_{cm} = 35 GeV
0.98 ±0.12 ±0.13		ONG	89	MRK2	E^{ee}_{cm} = 29 GeV
1.17 $^{+0.27}_{-0.22}$ $^{+0.17}_{-0.16}$		KLEM	88	DLCO	E^{ee}_{cm} = 29 GeV
1.29 ±0.20 ±0.21		[25] ASH	87	MAC	E^{ee}_{cm} = 29 GeV
1.02 $^{+0.42}_{-0.39}$	301	[26] BROM	87	HRS	E^{ee}_{cm} = 29 GeV

[1] Measurement performed using an inclusive reconstruction and B flavor identification technique.
[2] Measured using inclusive $J/\psi(1S) \to \mu^+\mu^-$ vertex.
[3] ACCIARRI 98 uses inclusively reconstructed secondary vertex and lepton impact parameter.
[4] ACKERSTAFF 97F uses inclusively reconstructed secondary vertices.
[5] BUSKULIC 96F analyzed using 3D impact parameter.
[6] ABE,K 95B uses an inclusive topological technique.
[7] ABREU 94L uses charged particle impact parameters. Their result from inclusively reconstructed secondary vertices is superseded by ABREU 96E.
[8] ACTON 93L and ADRIANI 93K analyzed using lepton (e and μ) impact parameter at Z.
[9] BUSKULIC 93O analyzed using dipole method.
[10] Combines ABREU 96E secondary vertex result with ABREU 94L impact parameter result.
[11] From proper time distribution of $b \to J/\psi(1S)$ anything.
[12] ABE 93J analyzed using $J/\psi(1S) \to \mu\mu$ vertices.
[13] ABREU 93D data analyzed using $D/D^*\ell$anything event vertices.
[14] ABREU 93G data analyzed using charged and neutral vertices.
[15] ACTON 93C analysed using $D/D^*\ell$anything event vertices.
[16] ABREU 92 is combined result of muon and hadron impact parameter analyses. Hadron tracks gave $(12.7 \pm 0.4 \pm 1.2) \times 10^{-13}$ s for an admixture of B species weighted by production fraction and mean charge multiplicity, while muon tracks gave $(13.0 \pm 1.0 \pm 0.8) \times 10^{-13}$ s for an admixture weighted by production fraction and semileptonic branching fraction.
[17] ACTON 92 is combined result of muon and electron impact parameter analyses.
[18] BUSKULIC 92F uses the lepton impact parameter distribution for data from the 1991 run.
[19] BUSKULIC 92G use $J/\psi(1S)$ tags to measure the average b lifetime. This is comparable to other methods only if the $J/\psi(1S)$ branching fractions of the different b-flavored hadrons are in the same ratio.
[20] Using $Z \to e^+$X or μ^+X, ADEVA 91H determined the average lifetime for an admixture of B hadrons from the impact parameter distribution of the lepton.
[21] Using $Z \to J/\psi(1S)$X, $J/\psi(1S) \to \ell^+\ell^-$, ALEXANDER 91G determined the average lifetime for an admixture of B hadrons from the decay point of the $J/\psi(1S)$.
[22] Using $Z \to e$X or μX, DECAMP 91C determines the average lifetime for an admixture of B hadrons from the signed impact parameter distribution of the lepton.
[23] HAGEMANN 90 uses electrons and muons in an impact parameter analysis.
[24] LYONS 90 combine the results of the B lifetime measurements of ONG 89, BRAUNSCHWEIG 89B, KLEM 88, and ASH 87, and JADE data by private communication. They use statistical techniques which include variation of the error with the mean life, and possible correlations between the systematic errors. This result is not independent of the measured results used in our average.
[25] We have combined an overall scale error of 15% in quadrature with the systematic error of ±0.7 to obtain ±2.1 systematic error.
[26] Statistical and systematic errors were combined by BROM 87.

CHARGED b-HADRON ADMIXTURE MEAN LIFE

VALUE (10^{-12} s)	DOCUMENT ID		TECN	COMMENT
1.72±0.08±0.06	[1] ADAM	95	DLPH	$e^+e^- \to Z$

[1] ADAM 95 data analyzed using vertex-charge technique to tag b-hadron charge.

NEUTRAL b-HADRON ADMIXTURE MEAN LIFE

VALUE (10^{-12} s)	DOCUMENT ID		TECN	COMMENT
1.58±0.11±0.09	[1] ADAM	95	DLPH	$e^+e^- \to Z$

[1] ADAM 95 data analyzed using vertex-charge technique to tag b-hadron charge.

MEAN LIFE RATIO $\tau_{\text{charged } b\text{-hadron}}/\tau_{\text{neutral } b\text{-hadron}}$

VALUE	DOCUMENT ID		TECN	COMMENT
1.09 $^{+0.11}_{-0.10}$ ±0.08	[1] ADAM	95	DLPH	$e^+e^- \to Z$

[1] ADAM 95 data analyzed using vertex-charge technique to tag b-hadron charge.

$|\Delta\tau_b|/\tau_{b,\overline{b}}$

$\tau_{b,\overline{b}}$ and $|\Delta\tau_b|$ are the mean life average and difference between b and $\overline{b}$ hadrons.

VALUE	DOCUMENT ID		TECN	COMMENT
−0.001±0.012±0.008	[1] ABBIENDI	99J	OPAL	$e^+e^- \to Z$

[1] Data analyzed using both the jet charge and the charge of secondary vertex in the opposite hemisphere.

$\overline{b}$ PRODUCTION FRACTIONS AND DECAY MODES

The branching fraction measurements are for an admixture of B mesons and baryons at energies above the $\Upsilon(4S)$. Only the highest energy results (LHC, LEP, Tevatron, S$p\overline{p}$S) are used in the branching fraction averages. In the following, we assume that the production fractions are the same at the LHC, LEP, and at the Tevatron.

For inclusive branching fractions, *e.g.*, $B \to D^{\pm}$anything, the values usually are multiplicities, not branching fractions. They can be greater than one.

The modes below are listed for a $\overline{b}$ initial state. b modes are their charge conjugates. Reactions indicate the weak decay vertex and do not include mixing.

Mode	Fraction (Γ_i/Γ)	Scale factor/ Confidence level

PRODUCTION FRACTIONS

The production fractions for weakly decaying b-hadrons at high energy have been calculated from the best values of mean lives, mixing parameters, and branching fractions in this edition by the Heavy Flavor Averaging Group (HFAG) as described in the note "B^0-$\overline{B}^0$ Mixing" in the B^0 Particle Listings. The production fractions in b-hadronic Z decay or $p\overline{p}$ collisions at the Tevatron are also listed at the end of the section. Values assume

$$B(\overline{b} \to B^+) = B(\overline{b} \to B^0)$$
$$B(\overline{b} \to B^+) + B(\overline{b} \to B^0) + B(\overline{b} \to B^0_s) + B(b \to b\text{-baryon}) = 100\ \%.$$

The correlation coefficients between production fractions are also reported:

$cor(B^0_s, b\text{-baryon}) = -0.291$
$cor(B^0_s, B^{\pm}{=}B^0) = -0.083$
$cor(b\text{-baryon}, B^{\pm}{=}B^0) = -0.929.$

The notation for production fractions varies in the literature (f_d, d_{B^0}, $f(b \to \overline{B}^0)$, $Br(b \to \overline{B}^0)$). We use our own branching fraction notation here, $B(\overline{b} \to B^0)$.

Note these production fractions are b-hadronization fractions, not the conventional branching fractions of b-quark to a B-hadron, which may have

considerable dependence on the initial and final state kinematic and production environment.

Γ_1	B^+		(40.2 ± 0.7) %
Γ_2	B^0		(40.2 ± 0.7) %
Γ_3	B_s^0		(10.5 ± 0.6) %
Γ_4	b-baryon		(9.2 ± 1.5) %

DECAY MODES

Semileptonic and leptonic modes

Γ_5	ν anything		(23.1 ± 1.5) %	
Γ_6	$\ell^+\nu_\ell$ anything	[a]	(10.69 ± 0.22) %	
Γ_7	$e^+\nu_e$ anything		(10.86 ± 0.35) %	
Γ_8	$\mu^+\nu_\mu$ anything		($10.95^{+0.29}_{-0.25}$) %	
Γ_9	$D^-\ell^+\nu_\ell$ anything	[a]	(2.27 ± 0.35) %	S=1.7
Γ_{10}	$D^-\pi^+\ell^+\nu_\ell$ anything		(4.9 ± 1.9) × 10^{-3}	
Γ_{11}	$D^-\pi^-\ell^+\nu_\ell$ anything		(2.6 ± 1.6) × 10^{-3}	
Γ_{12}	$\overline{D}^0\ell^+\nu_\ell$ anything	[a]	(6.84 ± 0.35) %	
Γ_{13}	$\overline{D}^0\pi^-\ell^+\nu_\ell$ anything		(1.07 ± 0.27) %	
Γ_{14}	$\overline{D}^0\pi^+\ell^+\nu_\ell$ anything		(2.3 ± 1.6) × 10^{-3}	
Γ_{15}	$D^{*-}\ell^+\nu_\ell$ anything	[a]	(2.75 ± 0.19) %	
Γ_{16}	$D^{*-}\pi^-\ell^+\nu_\ell$ anything		(6 ± 7) × 10^{-4}	
Γ_{17}	$D^{*-}\pi^+\ell^+\nu_\ell$ anything		(4.8 ± 1.0) × 10^{-3}	
Γ_{18}	$\overline{D}_j^0\ell^+\nu_\ell$ anything × B($\overline{D}_j^0 \to D^{*+}\pi^-$)	[a,b]	(2.6 ± 0.9) × 10^{-3}	
Γ_{19}	$D_j^-\ell^+\nu_\ell$ anything × B($D_j^- \to D^0\pi^-$)	[a,b]	(7.0 ± 2.3) × 10^{-3}	
Γ_{20}	$\overline{D}_2^*(2460)^0\ell^+\nu_\ell$ anything × B($\overline{D}_2^*(2460)^0 \to D^{*-}\pi^+$)		< 1.4 × 10^{-3}	CL=90%
Γ_{21}	$D_2^*(2460)^-\ell^+\nu_\ell$ anything × B($D_2^*(2460)^- \to D^0\pi^-$)		($4.2^{+1.5}_{-1.8}$) × 10^{-3}	
Γ_{22}	$\overline{D}_2^*(2460)^0\ell^+\nu_\ell$ anything × B($\overline{D}_2^*(2460)^0 \to D^-\pi^+$)		(1.6 ± 0.8) × 10^{-3}	
Γ_{23}	charmless $\ell\overline{\nu}_\ell$	[a]	(1.7 ± 0.5) × 10^{-3}	
Γ_{24}	$\tau^+\nu_\tau$ anything		(2.41 ± 0.23) %	
Γ_{25}	$D^{*-}\tau\nu_\tau$ anything		(9 ± 4) × 10^{-3}	
Γ_{26}	$\overline{c} \to \ell^-\overline{\nu}_\ell$ anything	[a]	(8.02 ± 0.19) %	
Γ_{27}	$c \to \ell^+\nu$ anything		($1.6^{+0.4}_{-0.5}$) %	

Charmed meson and baryon modes

Γ_{28}	$\overline{D}^0$ anything		(59.8 ± 2.9) %	
Γ_{29}	$D^0 D_s^\pm$ anything	[c]	($9.1^{+4.0}_{-2.8}$) %	
Γ_{30}	$D^\mp D_s^\pm$ anything	[c]	($4.0^{+2.3}_{-1.8}$) %	
Γ_{31}	$\overline{D}^0 D^0$ anything	[c]	($5.1^{+2.0}_{-1.8}$) %	
Γ_{32}	$D^0 D^\pm$ anything	[c]	($2.7^{+1.8}_{-1.6}$) %	
Γ_{33}	$D^\pm D^\mp$ anything	[c]	< 9 × 10^{-3}	CL=90%
Γ_{34}	D^0 anything			
Γ_{35}	D^+ anything			
Γ_{36}	D^- anything		(23.3 ± 1.7) %	
Γ_{37}	$D^*(2010)^+$ anything		(17.3 ± 2.0) %	
Γ_{38}	$D_1(2420)^0$ anything		(5.0 ± 1.5) %	
Γ_{39}	$D^*(2010)^\mp D_s^\pm$ anything	[c]	($3.3^{+1.6}_{-1.3}$) %	
Γ_{40}	$D^0 D^*(2010)^\pm$ anything	[c]	($3.0^{+1.1}_{-0.9}$) %	
Γ_{41}	$D^*(2010)^\pm D^\mp$ anything	[c]	($2.5^{+1.2}_{-1.0}$) %	
Γ_{42}	$D^*(2010)^\pm D^*(2010)^\mp$ anything	[c]	(1.2 ± 0.4) %	
Γ_{43}	$\overline{D}\,D$ anything		(10^{+11}_{-10}) %	
Γ_{44}	$D_2^*(2460)^0$ anything		(4.7 ± 2.7) %	
Γ_{45}	D_s^- anything		(14.7 ± 2.1) %	
Γ_{46}	D_s^+ anything		(10.1 ± 3.1) %	
Γ_{47}	Λ_c^+ anything		(9.7 ± 2.9) %	
Γ_{48}	$\overline{c}/c$ anything	[d]	(116.2 ± 3.2) %	

Charmonium modes

Γ_{49}	$J/\psi(1S)$ anything		(1.16 ± 0.10) %	
Γ_{50}	$\psi(2S)$ anything		(2.83 ± 0.29) × 10^{-3}	
Γ_{51}	$\chi_{c1}(1P)$ anything		(1.4 ± 0.4) %	

K or K^* modes

Γ_{52}	$\overline{s}\gamma$		(3.1 ± 1.1) × 10^{-4}		
Γ_{53}	$\overline{s}\overline{\nu}\nu$	B1	< 6.4 × 10^{-4}		CL=90%
Γ_{54}	$K^\pm$ anything		(74 ± 6) %		
Γ_{55}	K_S^0 anything		(29.0 ± 2.9) %		

Pion modes

Γ_{56}	$\pi^\pm$ anything		(397 ±21) %	
Γ_{57}	π^0 anything	[d]	(278 ±60) %	
Γ_{58}	ϕ anything		(2.82 ± 0.23) %	

Baryon modes

Γ_{59}	$p/\overline{p}$ anything		(13.1 ± 1.1) %	
Γ_{60}	$\Lambda/\overline{\Lambda}$ anything		(5.9 ± 0.6) %	
Γ_{61}	b-baryon anything		(10.2 ± 2.8) %	

Other modes

Γ_{62}	charged anything	[d]	(497 ± 7) %	
Γ_{63}	hadron$^+$ hadron$^-$		($1.7^{+1.0}_{-0.7}$) × 10^{-5}	
Γ_{64}	charmless		(7 ±21) × 10^{-3}	

$\Delta B = 1$ weak neutral current ($B1$) modes

Γ_{65}	e^+e^- anything	B1			
Γ_{66}	$\mu^+\mu^-$ anything	B1	< 3.2 × 10^{-4}		CL=90%
Γ_{67}	$\nu\overline{\nu}$ anything	B1			

[a] An ℓ indicates an e or a μ mode, not a sum over these modes.

[b] D_j represents an unresolved mixture of pseudoscalar and tensor D^{**} (P-wave) states.

[c] The value is for the sum of the charge states or particle/antiparticle states indicated.

[d] Inclusive branching fractions have a multiplicity definition and can be greater than 100%.

$B^{\pm}/B^0/B_s^0/b$-baryon ADMIXTURE BRANCHING RATIOS

$\Gamma(B^+)/\Gamma_{total}$ Γ_1/Γ

"OUR EVALUATION" is an average using rescaled values of the data listed below and from the best values of mean lives, mixing parameters, and branching fractions in this edition by the Heavy Flavor Averaging Group (HFAG) as described at http://www.slac.stanford.edu/xorg/hfag/.

VALUE	DOCUMENT ID		TECN	COMMENT
0.402 ±0.007 OUR EVALUATION				
0.4099±0.0082±0.0111	[1] ABDALLAH	03K	DLPH	$e^+e^- \to Z$

[1] The analysis is based on a neural network, to estimate the charge of the weakly-decaying b hadron by distinguishing its decay products from particles produced at the primary vertex.

$\Gamma(B^+)/\Gamma(B^0)$ Γ_1/Γ_2

VALUE	DOCUMENT ID		TECN	COMMENT
$1.054\pm0.018^{+0.062}_{-0.074}$	AALTONEN	08N	CDF	$p\overline{p}$ at 1.96 TeV

$\Gamma(B_s^0)/[\Gamma(B^+)+\Gamma(B^0)]$ $\Gamma_3/(\Gamma_1+\Gamma_2)$

VALUE	DOCUMENT ID		TECN	COMMENT
0.131 ±0.008 OUR EVALUATION				
0.134 ±0.008 OUR AVERAGE				
0.134 ±0.004 $^{+0.011}_{-0.010}$	[1] AAIJ	12J	LHCB	pp at 7 TeV
0.1265 ± 0.0085 ± 0.0131	[2] AAIJ	11F	LHCB	pp at 7 TeV
0.128 $^{+0.011}_{-0.010}$ ±0.011	[3] AALTONEN	08N	CDF	$p\overline{p}$ at 1.96 TeV
0.213 ±0.068	[4] AFFOLDER	00E	CDF	$p\overline{p}$ at 1.8 TeV
0.21 ±0.036 $^{+0.038}_{-0.030}$	[5] ABE	99P	CDF	$\overline{p}p$ at 1.8 TeV

[1] Measured using b-hadron semileptonic decays and assuming isospin symmetry.

[2] AAIJ 11F measured $f_s/f_d = 0.253 \pm 0.017 \pm 0.017 \pm 0.020$, where the errors are statistical, systematic, and theoretical. We divide their value by 2. Our second error combines systematic and theoretical uncertainties.

[3] AALTONEN 08N reports $[\Gamma(\overline{b} \to B_s^0)/\left[\Gamma(\overline{b} \to B^+) + \Gamma(\overline{b} \to B^0)\right]] \times [\mathrm{B}(D_s^+ \to \phi\pi^+)] = (5.76 \pm 0.18^{+0.45}_{-0.42}) \times 10^{-3}$ which we divide by our best value $\mathrm{B}(D_s^+ \to \phi\pi^+) = (4.5 \pm 0.4) \times 10^{-2}$. Our first error is their experiment's error and our second error is the systematic error from using our best value.

[4] AFFOLDER 00E uses several electron-charm final states in $b \to ce^-\mathrm{X}$.

[5] ABE 99P uses the numbers of $K^*(892)^0$, $K^*(892)^+$, and $\phi(1020)$ events produced in association with the double semileptonic decays $b \to c\mu^-\mathrm{X}$ with $c \to s\mu^+\mathrm{X}$.

Meson Particle Listings

$B^{\pm}/B^0/B_s^0/b$-baryon ADMIXTURE

$\Gamma(B_s^0)/\Gamma(B^0)$ Γ_3/Γ_2

VALUE	DOCUMENT ID		TECN	COMMENT
0.261±0.015 OUR EVALUATION				
0.238±0.004±0.015±0.021	[1] AAIJ	13P	LHCB	pp at 7 TeV

[1] AAIJ 13P studies also separately the $p_T(B)$ and $\eta(B)$ dependency of $\Gamma(\overline{b}\to B_s^0)/\Gamma(\overline{b}\to B^0)$, finding $f_s/f_d(p_T)= (0.256\pm0.020)+(-2.0\pm0.6)\,10^{-3}$ /GeV/c $(p_T-\langle p_T\rangle)$ and $f_s/f_d(\eta)= (0.256\pm0.020)+(0.005\pm0.006)\,(\eta-\langle\eta\rangle)$, where $\langle p_T\rangle = 10.4$ GeV/c and $\langle\eta\rangle = 3.28$.

$\Gamma(b\text{-baryon})/\left[\Gamma(B^+)+\Gamma(B^0)\right]$ $\Gamma_4/(\Gamma_1+\Gamma_2)$

VALUE	DOCUMENT ID		TECN	COMMENT
0.114±0.021 OUR EVALUATION				
0.30 ±0.06 OUR AVERAGE				
$0.305\pm0.010\pm0.081$	[1] AAIJ	12J	LHCB	pp at 7 TeV
$0.31\ \pm0.11\ ^{+0.12}_{-0.08}$	[2] AALTONEN	09E	CDF	$p\overline{p}$ at 1.8 TeV
$0.28\ ^{+0.11}_{-0.09}\ \pm0.07$	[3] AALTONEN	08N	CDF	$p\overline{p}$ at 1.96 TeV
• • • We do not use the following data for averages, fits, limits, etc. • • •				
0.118 ± 0.042	[4] AFFOLDER	00E	CDF	$p\overline{p}$ at 1.8 TeV

[1] Measured the ratio to be $(0.404\pm0.017\pm0.027\pm0.105)\times[1-(0.031\pm0.004\pm0.003)\times P_T]$ using b-hadron semileptonic decays where the P_T is the momentum of charmed hadron-muon pair in GeV/c. We quote their weighted average value where the second error combines systematic and the error on $B(\Lambda_c^+\to pK^-\pi^+)$.

[2] Errata to the measurement reported in AFFOLDER 00E using the p_T spectra from fully reconstructed B^0 and Λ_b decays.

[3] AALTONEN 08N reports $[\Gamma(\overline{b}\to b\text{-baryon})/\left[\Gamma(\overline{b}\to B^+)+\Gamma(\overline{b}\to B^0)\right]]\times[B(\Lambda_c^+\to pK^-\pi^+)] = (14.1\pm0.6^{+5.3}_{-4.4})\times10^{-3}$ which we divide by our best value $B(\Lambda_c^+\to pK^-\pi^+) = (5.0\pm1.3)\times10^{-2}$. Our first error is their experiment's error and our second error is the systematic error from using our best value.

[4] AFFOLDER 00E uses several electron-charm final states in $b\to ce^-X$.

$\Gamma(\nu\text{anything})/\Gamma_{\text{total}}$ Γ_5/Γ

VALUE	DOCUMENT ID		TECN	COMMENT
0.2308±0.0077±0.0124	[1,2] ACCIARRI	96C	L3	$e^+e^-\to Z$

[1] ACCIARRI 96C assumes relative b semileptonic decay rates $e{:}\mu{:}\tau$ of 1:1:0.25. Based on missing-energy spectrum.

[2] Assumes Standard Model value for R_B.

$\Gamma(\ell^+\nu_\ell\text{anything})/\Gamma_{\text{total}}$ Γ_6/Γ

"OUR EVALUATION" is an average of the data listed below, excluding all asymmetry measurements, performed by the LEP Electroweak Working Group as described in the "Note on the Z boson" in the Z Particle Listings.

VALUE	DOCUMENT ID		TECN	COMMENT
0.1069±0.0022 OUR EVALUATION				
0.1064±0.0016 OUR AVERAGE				
$0.1070\pm0.0010\pm0.0035$	[1] HEISTER	02G	ALEP	$e^+e^-\to Z$
$0.1070\pm0.0008^{+0.0037}_{-0.0049}$	[2] ABREU	01L	DLPH	$e^+e^-\to Z$
$0.1083\pm0.0010^{+0.0028}_{-0.0024}$	[3] ABBIENDI	00E	OPAL	$e^+e^-\to Z$
$0.1016\pm0.0013\pm0.0030$	[4] ACCIARRI	00	L3	$e^+e^-\to Z$
$0.1085\pm0.0012\pm0.0047$	[5,6] ACCIARRI	96C	L3	$e^+e^-\to Z$
• • • We do not use the following data for averages, fits, limits, etc. • • •				
$0.1106\pm0.0039\pm0.0022$	[7] ABREU	95D	DLPH	$e^+e^-\to Z$
$0.114\ \pm0.003\ \pm0.004$	[8] BUSKULIC	94G	ALEP	$e^+e^-\to Z$
$0.100\ \pm0.007\ \pm0.007$	[9] ABREU	93C	DLPH	$e^+e^-\to Z$
$0.105\ \pm0.006\ \pm0.005$	[10] AKERS	93B	OPAL	Repl. by ABBIENDI 00E

[1] Uses the combination of lepton transverse momentum spectrum and the correlation between the charge of the lepton and opposite jet charge. The first error is statistic and the second error is the total systematic error including the modeling.

[2] The experimental systematic and model uncertainties are combined in quadrature.

[3] ABBIENDI 00E result is determined by comparing the distribution of several kinematic variables of leptonic events in a lifetime tagged $Z\to b\overline{b}$ sample using artificial neural network techniques. The first error is statistic; the second error is the total systematic error.

[4] ACCIARRI 00 result obtained from a combined fit of $R_b=\Gamma(Z\to b\overline{b})/\Gamma(Z\to\text{hadrons})$ and $B(b\to\ell\nu X)$, using double-tagging method.

[5] ACCIARRI 96C result obtained by a fit to the single lepton spectrum.

[6] Assumes Standard Model value for R_B.

[7] ABREU 95D give systematic errors ±0.0019 (model) and 0.0012 (R_C). We combine these in quadrature.

[8] BUSKULIC 94G uses e and μ events. This value is from a global fit to the lepton p and p_T (relative to jet) spectra which also determines the b and c production fractions, the fragmentation functions, and the forward-backward asymmetries. This branching ratio depends primarily on the ratio of dileptons to single leptons at high p_T, but the lower p_T portion of the lepton spectrum is included in the global fit to reduce the model dependence. The model dependence is ±0.0026 and is included in the systematic error.

[9] ABREU 93C event count includes ee events. Combining ee, $\mu\mu$, and $e\mu$ events, they obtain 0.100 ± 0.007 ± 0.007.

[10] AKERS 93B analysis performed using single and dilepton events.

$\Gamma(e^+\nu_e\text{anything})/\Gamma_{\text{total}}$ Γ_7/Γ

VALUE	EVTS	DOCUMENT ID		TECN	COMMENT
0.1086±0.0035 OUR AVERAGE					
$0.1078\pm0.0008^{+0.0050}_{-0.0046}$		[1] ABBIENDI	00E	OPAL	$e^+e^-\to Z$
$0.1089\pm0.0020\pm0.0051$		[2,3] ACCIARRI	96C	L3	$e^+e^-\to Z$
$0.107\ \pm0.015\ \pm0.007$	260	[4] ABREU	93C	DLPH	$e^+e^-\to Z$
$0.138\ \pm0.032\ \pm0.008$		[5] ADEVA	91C	L3	$e^+e^-\to Z$
• • • We do not use the following data for averages, fits, limits, etc. • • •					
$0.086\ \pm0.027\ \pm0.008$		[6] ABE	93E	VNS	$E_{\text{cm}}^{ee}=58$ GeV
$0.109\ ^{+0.014}_{-0.013}\ \pm0.0055$	2719	[7] AKERS	93B	OPAL	Repl. by ABBIENDI 00E
$0.111\ \pm0.028\ \pm0.026$		BEHREND	90D	CELL	$E_{\text{cm}}^{ee}=43$ GeV
$0.150\ \pm0.011\ \pm0.022$		BEHREND	90D	CELL	$E_{\text{cm}}^{ee}=35$ GeV
$0.112\ \pm0.009\ \pm0.011$		ONG	88	MRK2	$E_{\text{cm}}^{ee}=29$ GeV
$0.149\ ^{+0.022}_{-0.019}$		PAL	86	DLCO	$E_{\text{cm}}^{ee}=29$ GeV
$0.110\ \pm0.018\ \pm0.010$		AIHARA	85	TPC	$E_{\text{cm}}^{ee}=29$ GeV
$0.111\ \pm0.034\ \pm0.040$		ALTHOFF	84J	TASS	$E_{\text{cm}}^{ee}=34.6$ GeV
$0.146\ \pm0.028$		KOOP	84	DLCO	Repl. by PAL 86
$0.116\ \pm0.021\ \pm0.017$		NELSON	83	MRK2	$E_{\text{cm}}^{ee}=29$ GeV

[1] ABBIENDI 00E result is determined by comparing the distribution of several kinematic variables of leptonic events in a lifetime tagged $Z\to b\overline{b}$ sample using artificial neural network techniques. The first error is statistic; the second error is the total systematic error.

[2] ACCIARRI 96C result obtained by a fit to the single lepton spectrum.

[3] Assumes Standard Model value for R_B.

[4] ABREU 93C event count includes ee events. Combining ee, $\mu\mu$, and $e\mu$ events, they obtain 0.100 ± 0.007 ± 0.007.

[5] ADEVA 91C measure the average $B(b\to eX)$ branching ratio using single and double tagged b enhanced Z events. Combining e and μ results, they obtain $0.113\pm0.010\pm0.006$. Constraining the initial number of b quarks by the Standard Model prediction (378 ± 3 MeV) for the decay of the Z into $b\overline{b}$, the electron result gives $0.112\pm0.004\pm0.008$. They obtain $0.119\pm0.003\pm0.006$ when e and μ results are combined. Used to measure the $b\overline{b}$ width itself, this electron result gives 370 ± 12 ± 24 MeV and combined with the muon result gives 385 ± 7 ± 22 MeV.

[6] ABE 93E experiment also measures forward-backward asymmetries and fragmentation functions for b and c.

[7] AKERS 93B analysis performed using single and dilepton events.

$\Gamma(\mu^+\nu_\mu\text{anything})/\Gamma_{\text{total}}$ Γ_8/Γ

VALUE	EVTS	DOCUMENT ID		TECN	COMMENT
0.1095 $^{+0.0029}_{-0.0025}$ OUR AVERAGE					
$0.1096\pm0.0008^{+0.0034}_{-0.0027}$		[1] ABBIENDI	00E	OPAL	$e^+e^-\to Z$
$0.1082\pm0.0015\pm0.0059$		[2,3] ACCIARRI	96C	L3	$e^+e^-\to Z$
$0.110\ \pm0.012\ \pm0.007$	656	[4] ABREU	93C	DLPH	$e^+e^-\to Z$
$0.113\ \pm0.012\ \pm0.006$		[5] ADEVA	91C	L3	$e^+e^-\to Z$
• • • We do not use the following data for averages, fits, limits, etc. • • •					
$0.122\ \pm0.006\ \pm0.007$		[3] UENO	96	AMY	e^+e^- at 57.9 GeV
$0.101\ ^{+0.010}_{-0.009}\ \pm0.0055$	4248	[6] AKERS	93B	OPAL	Repl. by ABBIENDI 00E
$0.104\ \pm0.023\ \pm0.016$		BEHREND	90D	CELL	$E_{\text{cm}}^{ee}=43$ GeV
$0.148\ \pm0.010\ \pm0.016$		BEHREND	90D	CELL	$E_{\text{cm}}^{ee}=35$ GeV
$0.118\ \pm0.012\ \pm0.010$		ONG	88	MRK2	$E_{\text{cm}}^{ee}=29$ GeV
$0.117\ \pm0.016\ \pm0.015$		BARTEL	87	JADE	$E_{\text{cm}}^{ee}=34.6$ GeV
$0.114\ \pm0.018\ \pm0.025$		BARTEL	85J	JADE	Repl. by BARTEL 87
$0.117\ \pm0.028\ \pm0.010$		ALTHOFF	84G	TASS	$E_{\text{cm}}^{ee}=34.5$ GeV
$0.105\ \pm0.015\ \pm0.013$		ADEVA	83B	MRKJ	$E_{\text{cm}}^{ee}=33$–38.5 GeV
$0.155\ ^{+0.054}_{-0.029}$		FERNANDEZ	83D	MAC	$E_{\text{cm}}^{ee}=29$ GeV

[1] ABBIENDI 00E result is determined by comparing the distribution of several kinematic variables of leptonic events in a lifetime tagged $Z\to b\overline{b}$ sample using artificial neural network techniques. The first error is statistic; the second error is the total systematic error.

[2] ACCIARRI 96C result obtained by a fit to the single lepton spectrum.

[3] Assumes Standard Model value for R_B.

[4] ABREU 93C event count includes $\mu\mu$ events. Combining ee, $\mu\mu$, and $e\mu$ events, they obtain 0.100 ± 0.007 ± 0.007.

[5] ADEVA 91C measure the average $B(b\to eX)$ branching ratio using single and double tagged b enhanced Z events. Combining e and μ results, they obtain $0.113\pm0.010\pm0.006$. Constraining the initial number of b quarks by the Standard Model prediction $(378\pm3$ MeV) for the decay of the Z into $b\overline{b}$, the muon result gives $0.123\pm0.003\pm0.006$. They obtain $0.119\pm0.003\pm0.006$ when e and μ results are combined. Used to measure the $b\overline{b}$ width itself, this muon result gives 394 ± 9 ± 22 MeV and combined with the electron result gives 385 ± 7 ± 22 MeV.

[6] AKERS 93B analysis performed using single and dilepton events.

$\Gamma(D^-\ell^+\nu_\ell\text{anything})/\Gamma_{\text{total}}$ Γ_9/Γ

VALUE	DOCUMENT ID		TECN	COMMENT
0.0227±0.0035 OUR AVERAGE	Error includes scale factor of 1.7.			
$0.0272\pm0.0028\pm0.0018$	[1] ABREU	00R	DLPH	$e^+e^-\to Z$
$0.0199\pm0.0026\pm0.0004$	[2] AKERS	95Q	OPAL	$e^+e^-\to Z$

[1] ABREU 00R reports their experiment's uncertainties $\pm0.0019\pm0.0016\pm0.0018$, where the first error is statistical, the second is systematic, and the third is the uncertainty due to the D branching fraction. We combine first two in quadrature.

[2] AKERS 95Q reports $[\Gamma(\overline{b}\to D^-\ell^+\nu_\ell\text{anything})/\Gamma_{\text{total}}]\times[B(D^+\to K^-2\pi^+)] = (1.82\pm0.20\pm0.12)\times10^{-3}$ which we divide by our best value $B(D^+\to K^-2\pi^+) = (9.13\pm0.19)\times10^{-2}$. Our first error is their experiment's error and our second error is the systematic error from using our best value.

$\Gamma(D^-\pi^+\ell^+\nu_\ell\text{anything})/\Gamma_{total}$ Γ_{10}/Γ

VALUE	DOCUMENT ID		TECN	COMMENT
0.0049±0.0018±0.0007	ABREU	00R	DLPH	$e^+e^-\to Z$

$\Gamma(D^-\pi^-\ell^+\nu_\ell\text{anything})/\Gamma_{total}$ Γ_{11}/Γ

VALUE	DOCUMENT ID		TECN	COMMENT
0.0026±0.0015±0.0004	ABREU	00R	DLPH	$e^+e^-\to Z$

$\Gamma(\overline{D}^0\ell^+\nu_\ell\text{anything})/\Gamma_{total}$ Γ_{12}/Γ

VALUE	DOCUMENT ID		TECN	COMMENT
0.0684±0.0035 OUR AVERAGE				
0.0704±0.0040±0.0017	[1] ABREU	00R	DLPH	$e^+e^-\to Z$
0.065 ±0.006 ±0.001	[2] AKERS	95Q	OPAL	$e^+e^-\to Z$

[1] ABREU 00R reports their experiment's uncertainties ±0.0034 ± 0.0036 ± 0.0017, where the first error is statistical, the second is systematic, and the third is the uncertainty due to the D branching fraction. We combine first two in quadrature.

[2] AKERS 95Q reports $[\Gamma(\overline{b}\to\ \overline{D}^0\ell^+\nu_\ell\text{anything})/\Gamma_{total}]\times[\mathrm{B}(D^0\to\ K^-\pi^+)] = (2.52\pm0.14\pm0.17)\times10^{-3}$ which we divide by our best value $\mathrm{B}(D^0\to\ K^-\pi^+) = (3.88\pm0.05)\times10^{-2}$. Our first error is their experiment's error and our second error is the systematic error from using our best value.

$\Gamma(\overline{D}^0\pi^-\ell^+\nu_\ell\text{anything})/\Gamma_{total}$ Γ_{13}/Γ

VALUE	DOCUMENT ID		TECN	COMMENT
0.0107±0.0025±0.0011	ABREU	00R	DLPH	$e^+e^-\to Z$

$\Gamma(\overline{D}^0\pi^+\ell^+\nu_\ell\text{anything})/\Gamma_{total}$ Γ_{14}/Γ

VALUE	DOCUMENT ID		TECN	COMMENT
0.0023±0.0015±0.0004	ABREU	00R	DLPH	$e^+e^-\to Z$

$\Gamma(D^{*-}\ell^+\nu_\ell\text{anything})/\Gamma_{total}$ Γ_{15}/Γ

VALUE	DOCUMENT ID		TECN	COMMENT
0.0275±0.0019 OUR AVERAGE				
0.0275±0.0021±0.0009	[1] ABREU	00R	DLPH	$e^+e^-\to Z$
0.0276±0.0027±0.0011	[2] AKERS	95Q	OPAL	$e^+e^-\to Z$

[1] ABREU 00R reports their experiment's uncertainties ±0.0017 ± 0.0013 ± 0.0009, where the first error is statistical, the second is systematic, and the third is the uncertainty due to the D branching fraction. We combine first two in quadrature.

[2] AKERS 95Q reports $[\mathrm{B}(\overline{b}\to\ D^*\ell^+\nu_\ell\mathrm{X})\times\mathrm{B}(D^{*+}\to\ D^0\pi^+)\times\mathrm{B}(D^0\to\ K^-\pi^+)] = ((7.53\pm0.47\pm0.56)\times10^{-4})$ and uses $\mathrm{B}(D^{*+}\to\ D^0\pi^+) = 0.681\pm0.013$ and $\mathrm{B}(D^0\to\ K^-\pi^+) = 0.0401\pm0.0014$ to obtain the above result. The first error is the experiments error and the second error is the systematic error from the D^{*+} and D^0 branching ratios.

$\Gamma(D^{*-}\pi^-\ell^+\nu_\ell\text{anything})/\Gamma_{total}$ Γ_{16}/Γ

VALUE	DOCUMENT ID		TECN	COMMENT
0.0006±0.0007±0.0002	ABREU	00R	DLPH	$e^+e^-\to Z$

$\Gamma(D^{*-}\pi^+\ell^+\nu_\ell\text{anything})/\Gamma_{total}$ Γ_{17}/Γ

VALUE	DOCUMENT ID		TECN	COMMENT
0.0048±0.0009±0.0005	ABREU	00R	DLPH	$e^+e^-\to Z$

$\Gamma(\overline{D}_j^0\ell^+\nu_\ell\text{anything}\times\mathrm{B}(\overline{D}_j^0\to D^{*+}\pi^-))/\Gamma_{total}$ Γ_{18}/Γ

D_j represents an unresolved mixture of pseudoscalar and tensor D^{**} (P-wave) states.

VALUE (units 10^{-3})	DOCUMENT ID		TECN	COMMENT
2.64±0.79±0.39	ABBIENDI	03M	OPAL	$e^+e^-\to Z$
• • • We do not use the following data for averages, fits, limits, etc. • • •				
6.1 ±1.3 ±1.3	AKERS	95Q	OPAL	Repl. by ABBIENDI 03M

$\Gamma(D_j^-\ell^+\nu_\ell\text{anything}\times\mathrm{B}(D_j^-\to D^0\pi^-))/\Gamma_{total}$ Γ_{19}/Γ

D_j represents an unresolved mixture of pseudoscalar and tensor D^{**} (P-wave) states.

VALUE (units 10^{-3})	DOCUMENT ID		TECN	COMMENT
$\mathbf{7.0\pm1.9^{+1.2}_{-1.3}}$	AKERS	95Q	OPAL	$e^+e^-\to Z$

$\Gamma(\overline{D}_2^*(2460)^0\ell^+\nu_\ell\text{anything}\times\mathrm{B}(\overline{D}_2^*(2460)^0\to D^{*-}\pi^+))/\Gamma_{total}$ Γ_{20}/Γ

VALUE (units 10^{-3})	CL%	DOCUMENT ID		TECN	COMMENT
<1.4	90	ABBIENDI	03M	OPAL	$e^+e^-\to Z$

$\Gamma(D_2^*(2460)^-\ell^+\nu_\ell\text{anything}\times\mathrm{B}(D_2^*(2460)^-\to D^0\pi^-))/\Gamma_{total}$ Γ_{21}/Γ

VALUE (units 10^{-3})	DOCUMENT ID		TECN	COMMENT
$\mathbf{4.2\pm1.3^{+0.7}_{-1.2}}$	AKERS	95Q	OPAL	$e^+e^-\to Z$

$\Gamma(\overline{D}_2^*(2460)^0\ell^+\nu_\ell\text{anything}\times\mathrm{B}(\overline{D}_2^*(2460)^0\to D^-\pi^+))/\Gamma_{total}$ Γ_{22}/Γ

VALUE (units 10^{-3})	DOCUMENT ID		TECN	COMMENT
1.6±0.7±0.3	AKERS	95Q	OPAL	$e^+e^-\to Z$

$\Gamma(\text{charmless }\ell\overline{\nu}_\ell)/\Gamma_{total}$ Γ_{23}/Γ

"OUR EVALUATION" is an average of the data listed below performed by the LEP Heavy Flavour Steering Group. The averaging procedure takes into account correlations between the measurements.

VALUE	DOCUMENT ID		TECN	COMMENT
0.00171±0.00052 OUR EVALUATION				
0.0017 ±0.0004 OUR AVERAGE				
$0.00163\pm0.00053^{+0.00055}_{-0.00062}$	[1] ABBIENDI	01R	OPAL	$e^+e^-\to Z$
0.00157±0.00035±0.00055	[2] ABREU	00D	DLPH	$e^+e^-\to Z$
0.00173±0.00055±0.00055	[3] BARATE	99G	ALEP	$e^+e^-\to Z$
0.0033 ±0.0010 ±0.0017	[4] ACCIARRI	98K	L3	$e^+e^-\to Z$

[1] Obtained from the best fit of the MC simulated events to the data based on the $b\to X_u\ell\nu$ neutral network output distributions.

[2] ABREU 00D result obtained from a fit to the numbers of decays in $b\to\ u$ enriched and depleted samples and their lepton spectra, and assuming $|V_{cb}|= 0.0384\pm0.0033$ and $\tau_b= 1.564\pm0.014$ ps.

[3] Uses lifetime tagged $b\overline{b}$ sample.

[4] ACCIARRI 98K assumes $R_b= 0.2174\pm0.0009$ at Z decay.

$\Gamma(\tau^+\nu_\tau\text{anything})/\Gamma_{total}$ Γ_{24}/Γ

VALUE (units 10^{-2})	EVTS	DOCUMENT ID		TECN	COMMENT
2.41±0.23 OUR AVERAGE					
2.78±0.18±0.51		[1] ABBIENDI	01Q	OPAL	$e^+e^-\to Z$
2.43±0.20±0.25		[2] BARATE	01E	ALEP	$e^+e^-\to Z$
2.19±0.24±0.39		[3] ABREU	00C	DLPH	$e^+e^-\to Z$
1.7 ±0.5 ±1.1		[4,5] ACCIARRI	96C	L3	$e^+e^-\to Z$
2.4 ±0.7 ±0.8	1032	[6] ACCIARRI	94C	L3	$e^+e^-\to Z$
• • • We do not use the following data for averages, fits, limits, etc. • • •					
2.75±0.30±0.37	405	[7] BUSKULIC	95	ALEP	Repl. by BARATE 01E
4.08±0.76±0.62		BUSKULIC	93B	ALEP	Repl. by BUSKULIC 95

[1] ABBIENDI 01Q uses a missing energy technique.

[2] The energy-flow and b-tagging algorithms were used.

[3] Uses the missing energy in $Z\to\ b\overline{b}$ decays without identifying leptons.

[4] ACCIARRI 96C result obtained from missing energy spectrum.

[5] Assumes Standard Model value for R_B.

[6] This is a direct result using tagged $b\overline{b}$ events at the Z, but species are not separated.

[7] BUSKULIC 95 uses missing-energy technique.

$\Gamma(D^{*-}\tau\nu_\tau\text{anything})/\Gamma_{total}$ Γ_{25}/Γ

VALUE	DOCUMENT ID		TECN	COMMENT
$\mathbf{(0.88\pm0.31\pm0.28)\times10^{-2}}$	[1] BARATE	01E	ALEP	$e^+e^-\to Z$

[1] The energy-flow and b-tagging algorithms were used.

$\Gamma(\overline{b}\to\ \overline{c}\to\ \ell^-\overline{\nu}_\ell\text{anything})/\Gamma_{total}$ Γ_{26}/Γ

"OUR EVALUATION" is an average of the data listed below, excluding all asymmetry measurements, performed by the LEP Electroweak Working Group as described in the "Note on the Z boson" in the Z Particle Listings.

VALUE	DOCUMENT ID		TECN	COMMENT
0.0802±0.0019 OUR EVALUATION				
0.0817±0.0020 OUR AVERAGE				
$0.0818\pm0.0015^{+0.0024}_{-0.0026}$	[1] HEISTER	02G	ALEP	$e^+e^-\to Z$
$0.0798\pm0.0022^{+0.0025}_{-0.0029}$	[2] ABREU	01L	DLPH	$e^+e^-\to Z$
$0.0840\pm0.0016^{+0.0039}_{-0.0036}$	[3] ABBIENDI	00E	OPAL	$e^+e^-\to Z$
• • • We do not use the following data for averages, fits, limits, etc. • • •				
0.0770±0.0097±0.0046	[4] ABREU	95D	DLPH	$e^+e^-\to Z$
0.082 ±0.003 ±0.012	[5] BUSKULIC	94G	ALEP	$e^+e^-\to Z$
0.077 ±0.004 ±0.007	[6] AKERS	93B	OPAL	Repl. by ABBIENDI 00E

[1] Uses the combination of lepton transverse momentum spectrum and the correlation between the charge of the lepton and opposite jet charge. The first error is statistic and the second error is the total systematic error including the modeling.

[2] The experimental systematic and model uncertainties are combined in quadrature.

[3] ABBIENDI 00E result is determined by comparing the distribution of several kinematic variables of leptonic events in a lifetime tagged $Z\to\ b\overline{b}$ sample using artificial neural network techniques. The first error is statistic; the second error is the total systematic error.

[4] ABREU 95D give systematic errors ±0.0033 (model) and 0.0032 (R_C). We combine these in quadrature. This result is from the same global fit as their $\Gamma(\overline{b}\to\ \ell^+\nu_\ell\mathrm{X})$ data.

[5] BUSKULIC 94G uses e and μ events. This value is from the same global fit as their $\Gamma(\overline{b}\to\ \ell^+\nu_\ell\text{anything})/\Gamma_{total}$ data.

[6] AKERS 93B analysis performed using single and dilepton events.

$\Gamma(c\to\ \ell^+\nu\text{anything})/\Gamma_{total}$ Γ_{27}/Γ

VALUE	DOCUMENT ID		TECN	COMMENT
$\mathbf{0.0161\pm0.0020^{+0.0034}_{-0.0047}}$	[1] ABREU	01L	DLPH	$e^+e^-\to Z$

[1] The experimental systematic and model uncertainties are combined in quadrature.

Meson Particle Listings

$B^{\pm}/B^0/B_s^0/b$-baryon ADMIXTURE

$\Gamma(\overline{D}^0 \text{ anything})/\Gamma_{\text{total}}$ Γ_{28}/Γ

VALUE	DOCUMENT ID		TECN	COMMENT
0.598±0.028±0.007	[1] BUSKULIC	96Y	ALEP	$e^+e^- \to Z$

[1] BUSKULIC 96Y reports 0.605 ± 0.024 ± 0.016 from a measurement of $[\Gamma(\overline{b} \to \overline{D}^0 \text{ anything})/\Gamma_{\text{total}}] \times [\text{B}(D^0 \to K^-\pi^+)]$ assuming $\text{B}(D^0 \to K^-\pi^+) = 0.0383$, which we rescale to our best value $\text{B}(D^0 \to K^-\pi^+) = (3.88 \pm 0.05) \times 10^{-2}$. Our first error is their experiment's error and our second error is the systematic error from using our best value.

$\Gamma(D^0 D_s^{\pm} \text{ anything})/\Gamma_{\text{total}}$ Γ_{29}/Γ

VALUE	DOCUMENT ID		TECN	COMMENT
$\mathbf{0.091^{+0.020}_{-0.018}{}^{+0.034}_{-0.022}}$	[1] BARATE	98Q	ALEP	$e^+e^- \to Z$

[1] The systematic error includes the uncertainties due to the charm branching ratios.

$\Gamma(D^{\mp} D_s^{\pm} \text{ anything})/\Gamma_{\text{total}}$ Γ_{30}/Γ

VALUE	DOCUMENT ID		TECN	COMMENT
$\mathbf{0.040^{+0.017}_{-0.014}{}^{+0.016}_{-0.011}}$	[1] BARATE	98Q	ALEP	$e^+e^- \to Z$

[1] The systematic error includes the uncertainties due to the charm branching ratios.

$[\Gamma(D^0 D_s^{\pm} \text{ anything}) + \Gamma(D^{\mp} D_s^{\pm} \text{ anything})]/\Gamma_{\text{total}}$ $(\Gamma_{29}+\Gamma_{30})/\Gamma$

VALUE	DOCUMENT ID		TECN	COMMENT
$\mathbf{0.131^{+0.026}_{-0.022}{}^{+0.048}_{-0.031}}$	[1] BARATE	98Q	ALEP	$e^+e^- \to Z$

[1] The systematic error includes the uncertainties due to the charm branching ratios.

$\Gamma(\overline{D}^0 D^0 \text{ anything})/\Gamma_{\text{total}}$ Γ_{31}/Γ

VALUE	DOCUMENT ID		TECN	COMMENT
$\mathbf{0.051^{+0.016}_{-0.014}{}^{+0.012}_{-0.011}}$	[1] BARATE	98Q	ALEP	$e^+e^- \to Z$

[1] The systematic error includes the uncertainties due to the charm branching ratios.

$\Gamma(D^0 D^{\pm} \text{ anything})/\Gamma_{\text{total}}$ Γ_{32}/Γ

VALUE	DOCUMENT ID		TECN	COMMENT
$\mathbf{0.027^{+0.015}_{-0.013}{}^{+0.010}_{-0.009}}$	[1] BARATE	98Q	ALEP	$e^+e^- \to Z$

[1] The systematic error includes the uncertainties due to the charm branching ratios.

$[\Gamma(\overline{D}^0 D^0 \text{ anything}) + \Gamma(D^0 D^{\pm} \text{ anything})]/\Gamma_{\text{total}}$ $(\Gamma_{31}+\Gamma_{32})/\Gamma$

VALUE	DOCUMENT ID		TECN	COMMENT
$\mathbf{0.078^{+0.020}_{-0.018}{}^{+0.018}_{-0.016}}$	[1] BARATE	98Q	ALEP	$e^+e^- \to Z$

[1] The systematic error includes the uncertainties due to the charm branching ratios.

$\Gamma(D^{\pm} D^{\mp} \text{ anything})/\Gamma_{\text{total}}$ Γ_{33}/Γ

VALUE	CL%	DOCUMENT ID		TECN	COMMENT
<0.009	90	BARATE	98Q	ALEP	$e^+e^- \to Z$

$[\Gamma(D^0 \text{ anything}) + \Gamma(D^+ \text{ anything})]/\Gamma_{\text{total}}$ $(\Gamma_{34}+\Gamma_{35})/\Gamma$

VALUE	DOCUMENT ID		TECN	COMMENT
0.093±0.017±0.014	[1] ABDALLAH	03E	DLPH	$e^+e^- \to Z$

[1] The second error is the total of systematic uncertainties including the branching fractions used in the measurement.

$\Gamma(D^- \text{ anything})/\Gamma_{\text{total}}$ Γ_{36}/Γ

VALUE	DOCUMENT ID		TECN	COMMENT
0.233±0.016±0.005	[1] BUSKULIC	96Y	ALEP	$e^+e^- \to Z$

[1] BUSKULIC 96Y reports 0.234 ± 0.013 ± 0.010 from a measurement of $[\Gamma(\overline{b} \to D^- \text{ anything})/\Gamma_{\text{total}}] \times [\text{B}(D^+ \to K^-2\pi^+)]$ assuming $\text{B}(D^+ \to K^-2\pi^+) = 0.091$, which we rescale to our best value $\text{B}(D^+ \to K^-2\pi^+) = (9.13 \pm 0.19) \times 10^{-2}$. Our first error is their experiment's error and our second error is the systematic error from using our best value.

$\Gamma(D^*(2010)^+ \text{ anything})/\Gamma_{\text{total}}$ Γ_{37}/Γ

VALUE	DOCUMENT ID		TECN	COMMENT
0.173±0.016±0.012	[1] ACKERSTAFF	98E	OPAL	$e^+e^- \to Z$

[1] Uses lepton tags to select $Z \to b\overline{b}$ events.

$\Gamma(D_1(2420)^0 \text{ anything})/\Gamma_{\text{total}}$ Γ_{38}/Γ

VALUE	DOCUMENT ID		TECN	COMMENT
0.050±0.014±0.006	[1] ACKERSTAFF	97W	OPAL	$e^+e^- \to Z$

[1] ACKERSTAFF 97W assumes $\text{B}(D_2^*(2460)^0 \to D^{*+}\pi^-) = 0.21 \pm 0.04$ and $\Gamma_{b\overline{b}}/\Gamma_{\text{hadrons}} = 0.216$ at Z decay.

$\Gamma(D^*(2010)^{\mp} D_s^{\pm} \text{ anything})/\Gamma_{\text{total}}$ Γ_{39}/Γ

VALUE	DOCUMENT ID		TECN	COMMENT
$\mathbf{0.033^{+0.010}_{-0.009}{}^{+0.012}_{-0.009}}$	[1] BARATE	98Q	ALEP	$e^+e^- \to Z$

[1] The systematic error includes the uncertainties due to the charm branching ratios.

$\Gamma(D^0 D^*(2010)^{\pm} \text{ anything})/\Gamma_{\text{total}}$ Γ_{40}/Γ

VALUE	DOCUMENT ID		TECN	COMMENT
$\mathbf{0.030^{+0.009}_{-0.008}{}^{+0.007}_{-0.005}}$	[1] BARATE	98Q	ALEP	$e^+e^- \to Z$

[1] The systematic error includes the uncertainties due to the charm branching ratios.

$\Gamma(D^*(2010)^{\pm} D^{\mp} \text{ anything})/\Gamma_{\text{total}}$ Γ_{41}/Γ

VALUE	DOCUMENT ID		TECN	COMMENT
$\mathbf{0.025^{+0.010}_{-0.009}{}^{+0.006}_{-0.005}}$	[1] BARATE	98Q	ALEP	$e^+e^- \to Z$

[1] The systematic error includes the uncertainties due to the charm branching ratios.

$\Gamma(D^*(2010)^{\pm} D^*(2010)^{\mp} \text{ anything})/\Gamma_{\text{total}}$ Γ_{42}/Γ

VALUE	DOCUMENT ID		TECN	COMMENT
$\mathbf{0.012^{+0.004}_{-0.003}\pm0.002}$	[1] BARATE	98Q	ALEP	$e^+e^- \to Z$

[1] The systematic error includes the uncertainties due to the charm branching ratios.

$\Gamma(\overline{D}\,D \text{ anything})/\Gamma_{\text{total}}$ Γ_{43}/Γ

VALUE	DOCUMENT ID		TECN	COMMENT
$\mathbf{0.10\pm0.032^{+0.107}_{-0.095}}$	[1] ABBIENDI	04I	OPAL	$e^+e^- \to Z$

[1] Measurement performed using an inclusive identification of B mesons and the D candidates.

$\Gamma(D_2^*(2460)^0 \text{ anything})/\Gamma_{\text{total}}$ Γ_{44}/Γ

VALUE	DOCUMENT ID		TECN	COMMENT
0.047±0.024±0.013	[1] ACKERSTAFF	97W	OPAL	$e^+e^- \to Z$

[1] ACKERSTAFF 97W assumes $\text{B}(D_2^*(2460)^0 \to D^{*+}\pi^-) = 0.21 \pm 0.04$ and $\Gamma_{b\overline{b}}/\Gamma_{\text{hadrons}} = 0.216$ at Z decay.

$\Gamma(D_s^- \text{ anything})/\Gamma_{\text{total}}$ Γ_{45}/Γ

VALUE	DOCUMENT ID		TECN	COMMENT
0.147±0.017±0.013	[1] BUSKULIC	96Y	ALEP	$e^+e^- \to Z$

[1] BUSKULIC 96Y reports 0.183 ± 0.019 ± 0.009 from a measurement of $[\Gamma(\overline{b} \to D_s^- \text{ anything})/\Gamma_{\text{total}}] \times [\text{B}(D_s^+ \to \phi\pi^+)]$ assuming $\text{B}(D_s^+ \to \phi\pi^+) = 0.036$, which we rescale to our best value $\text{B}(D_s^+ \to \phi\pi^+) = (4.5 \pm 0.4) \times 10^{-2}$. Our first error is their experiment's error and our second error is the systematic error from using our best value.

$\Gamma(D_s^+ \text{ anything})/\Gamma_{\text{total}}$ Γ_{46}/Γ

VALUE	DOCUMENT ID		TECN	COMMENT
0.101±0.010±0.029	[1] ABDALLAH	03E	DLPH	$e^+e^- \to Z$

[1] The second error is the total of systematic uncertainties including the branching fractions used in the measurement.

$\Gamma(b \to \Lambda_c^+ \text{ anything})/\Gamma_{\text{total}}$ Γ_{47}/Γ

VALUE	DOCUMENT ID		TECN	COMMENT
0.097±0.013±0.025	[1] BUSKULIC	96Y	ALEP	$e^+e^- \to Z$

[1] BUSKULIC 96Y reports 0.110 ± 0.014 ± 0.006 from a measurement of $[\Gamma(b \to \Lambda_c^+ \text{ anything})/\Gamma_{\text{total}}] \times [\text{B}(\Lambda_c^+ \to pK^-\pi^+)]$ assuming $\text{B}(\Lambda_c^+ \to pK^-\pi^+) = 0.044$, which we rescale to our best value $\text{B}(\Lambda_c^+ \to pK^-\pi^+) = (5.0 \pm 1.3) \times 10^{-2}$. Our first error is their experiment's error and our second error is the systematic error from using our best value.

$\Gamma(\overline{c}/c \text{ anything})/\Gamma_{\text{total}}$ Γ_{48}/Γ

VALUE	DOCUMENT ID		TECN	COMMENT
1.162±0.032 OUR AVERAGE				
$1.12\ ^{+0.11}_{-0.10}$	[1] ABBIENDI	04I	OPAL	$e^+e^- \to Z$
1.166±0.031±0.080	[2] ABREU	00	DLPH	$e^+e^- \to Z$
1.147±0.041	[3] ABREU	98D	DLPH	$e^+e^- \to Z$
1.230±0.036±0.065	[4] BUSKULIC	96Y	ALEP	$e^+e^- \to Z$

[1] Measurement performed using an inclusive identification of B mesons and the D candidates.
[2] Evaluated via summation of exclusive and inclusive channels.
[3] ABREU 98D results are extracted from a fit to the b-tagging probability distribution based on the impact parameter.
[4] BUSKULIC 96Y assumes PDG 96 production fractions for B^0, B^+, B_s, b baryons, and PDG 96 branching ratios for charm decays. This is sum of their inclusive $\overline{D}^0$, D^-, $\overline{D}_s$, and Λ_c branching ratios, corrected to include inclusive Ξ_c and charmonium.

$\Gamma(J/\psi(1S) \text{ anything})/\Gamma_{\text{total}}$ Γ_{49}/Γ

VALUE (units 10^{-2})	CL%	EVTS	DOCUMENT ID		TECN	COMMENT
1.16±0.10 OUR AVERAGE						
1.12±0.12±0.10			[1] ABREU	94P	DLPH	$e^+e^- \to Z$
1.16±0.16±0.14		121	[2] ADRIANI	93J	L3	$e^+e^- \to Z$
1.21±0.13±0.08			BUSKULIC	92G	ALEP	$e^+e^- \to Z$
• • • We do not use the following data for averages, fits, limits, etc. • • •						
1.3 ±0.2 ±0.2			[3] ADRIANI	92	L3	$e^+e^- \to Z$
<4.9	90		MATTEUZZI	83	MRK2	E_{cm}^{ee}= 29 GeV

[1] ABREU 94P is an inclusive measurement from b decays at the Z. Uses $J/\psi(1S) \to e^+e^-$ and $\mu^+\mu^-$ channels. Assumes $\Gamma(Z \to b\overline{b})/\Gamma_{\text{hadron}}$=0.22.
[2] ADRIANI 93J is an inclusive measurement from b decays at the Z. Uses $J/\psi(1S) \to \mu^+\mu^-$ and $J/\psi(1S) \to e^+e^-$ channels.
[3] ADRIANI 92 measurement is an inclusive result for $\text{B}(Z \to J/\psi(1S)\text{X}) = (4.1 \pm 0.7 \pm 0.3) \times 10^{-3}$ which is used to extract the b-hadron contribution to $J/\psi(1S)$ production.

$\Gamma(\psi(2S)\text{anything})/\Gamma_{\text{total}}$ Γ_{50}/Γ

VALUE	DOCUMENT ID	TECN	COMMENT
• • • We do not use the following data for averages, fits, limits, etc. • • •			
$0.0048\pm0.0022\pm0.0010$	[1] ABREU 94P	DLPH	$e^+e^-\to Z$

[1] ABREU 94P is an inclusive measurement from b decays at the Z. Uses $\psi(2S)\to J/\psi(1S)\pi^+\pi^-$, $J/\psi(1S)\to\mu^+\mu^-$ channels. Assumes $\Gamma(Z\to b\overline{b})/\Gamma_{\text{hadron}}=0.22$.

$\Gamma(\psi(2S)\text{anything})/\Gamma(J/\psi(1S)\text{anything})$ Γ_{50}/Γ_{49}

VALUE	DOCUMENT ID	TECN	COMMENT
0.243±0.014 OUR AVERAGE			
$0.239\pm0.015\pm0.005$	[1,2] AAIJ 12BD	LHCB	pp at 7 TeV
$0.260\pm0.015\pm0.029$	[3,4] CHATRCHYAN 12AK	CMS	pp at 7 TeV

[1] AAIJ 12BD reports $0.235\pm0.005\pm0.015$ from a measurement of $[\Gamma(\overline{b}\to\psi(2S)\text{anything})/\Gamma(\overline{b}\to J/\psi(1S)\text{anything})]\times[B(J/\psi(1S)\to\mu^+\mu^-)]$ / $[B(\psi(2S)\to e^+e^-)]$ assuming $B(J/\psi(1S)\to\mu^+\mu^-)=(5.93\pm0.06)\times10^{-2}$, $B(\psi(2S)\to e^+e^-)=(7.72\pm0.17)\times10^{-3}$, which we rescale to our best values $B(J/\psi(1S)\to\mu^+\mu^-)=(5.961\pm0.033)\times10^{-2}$, $B(\psi(2S)\to e^+e^-)=(7.89\pm0.17)\times10^{-3}$. Our first error is their experiment's error and our second error is the systematic error from using our best values.

[2] Assumes lepton universality imposing $B(\psi(2s)\to\mu^+\mu^-)=B(\psi(2s)\to e^+e^-)$.

[3] CHATRCHYAN 12AK really reports $\Gamma_{50}/\Gamma=(3.08\pm0.12\pm0.13\pm0.42)\times10^{-3}$ assuming PDG 10 value of $\Gamma_{49}/\Gamma=(1.16\pm0.10)\times10^{-2}$ which we present as a ratio of $\Gamma_{50}/\Gamma_{49}=(26.5\pm1.0\pm1.1\pm2.8)\times10^{-2}$.

[4] CHATRCHYAN 12AK reports $(26.5\pm1.0\pm1.1\pm2.8)\times10^{-2}$ from a measurement of $[\Gamma(\overline{b}\to\psi(2S)\text{anything})/\Gamma(\overline{b}\to J/\psi(1S)\text{anything})]\times[B(\psi(2S)\to\mu^+\mu^-)]$ / $[B(J/\psi(1S)\to\mu^+\mu^-)]$ assuming $B(\psi(2S)\to\mu^+\mu^-)=(7.7\pm0.8)\times10^{-3}$, $B(J/\psi(1S)\to\mu^+\mu^-)=(5.93\pm0.06)\times10^{-2}$, which we rescale to our best values $B(\psi(2S)\to\mu^+\mu^-)=(7.9\pm0.9)\times10^{-3}$, $B(J/\psi(1S)\to\mu^+\mu^-)=(5.961\pm0.033)\times10^{-2}$. Our first error is their experiment's error and our second error is the systematic error from using our best values.

$\Gamma(\chi_{c1}(1P)\text{anything})/\Gamma_{\text{total}}$ Γ_{51}/Γ

VALUE	EVTS	DOCUMENT ID	TECN	COMMENT
0.014 ±0.004 OUR AVERAGE				
$0.0113^{+0.0058}_{-0.0050}\pm0.0004$		[1] ABREU 94P	DLPH	$e^+e^-\to Z$
$0.019\pm0.007\pm0.001$	19	[2] ADRIANI 93J	L3	$e^+e^-\to Z$

[1] ABREU 94P reports $0.014\pm0.006^{+0.004}_{-0.002}$ from a measurement of $[\Gamma(\overline{b}\to\chi_{c1}(1P)\text{anything})/\Gamma_{\text{total}}]\times[B(\chi_{c1}(1P)\to\gamma J/\psi(1S))]$ assuming $B(\chi_{c1}(1P)\to\gamma J/\psi(1S))=0.273\pm0.016$, which we rescale to our best value $B(\chi_{c1}(1P)\to\gamma J/\psi(1S))=(33.9\pm1.2)\times10^{-2}$. Our first error is their experiment's error and our second error is the systematic error from using our best value. Assumes no $\chi_{c2}(1P)$ and $\Gamma(Z\to b\overline{b})/\Gamma_{\text{hadron}}=0.22$.

[2] ADRIANI 93J reports $0.024\pm0.009\pm0.002$ from a measurement of $[\Gamma(\overline{b}\to\chi_{c1}(1P)\text{anything})/\Gamma_{\text{total}}]\times[B(\chi_{c1}(1P)\to\gamma J/\psi(1S))]$ assuming $B(\chi_{c1}(1P)\to\gamma J/\psi(1S))=0.273\pm0.016$, which we rescale to our best value $B(\chi_{c1}(1P)\to\gamma J/\psi(1S))=(33.9\pm1.2)\times10^{-2}$. Our first error is their experiment's error and our second error is the systematic error from using our best value.

$\Gamma(\chi_{c1}(1P)\text{anything})/\Gamma(J/\psi(1S)\text{anything})$ Γ_{51}/Γ_{49}

VALUE	EVTS	DOCUMENT ID	TECN	COMMENT
• • • We do not use the following data for averages, fits, limits, etc. • • •				
1.92 ± 0.82	121	[1] ADRIANI 93J	L3	$e^+e^-\to Z$

[1] ADRIANI 93J is a ratio of inclusive measurements from b decays at the Z using only the $J/\psi(1S)\to\mu^+\mu^-$ channel since some systematics cancel.

$\Gamma(\overline{s}\gamma)/\Gamma_{\text{total}}$ Γ_{52}/Γ

VALUE (units 10^{-4})	CL%	DOCUMENT ID	TECN	COMMENT
3.11±0.80±0.72		[1] BARATE 98I	ALEP	$e^+e^-\to Z$
• • • We do not use the following data for averages, fits, limits, etc. • • •				
<5.4	90	[2] ADAM 96D	DLPH	$e^+e^-\to Z$
<12	90	[3] ADRIANI 93L	L3	$e^+e^-\to Z$

[1] BARATE 98I uses lifetime tagged $Z\to b\overline{b}$ sample.

[2] ADAM 96D assumes $f_{B^0}=f_{B^-}=0.39$ and $f_{B_s}=0.12$.

[3] ADRIANI 93L result is for $\overline{b}\to\overline{s}\gamma$ is performed inclusively.

$\Gamma(\overline{s}\overline{\nu}\nu)/\Gamma_{\text{total}}$ Γ_{53}/Γ

VALUE	CL%	DOCUMENT ID	TECN	COMMENT
<6.4 × 10⁻⁴	90	[1] BARATE 01E	ALEP	$e^+e^-\to Z$

[1] The energy-flow and b-tagging algorithms were used.

$\Gamma(K^{\pm}\text{anything})/\Gamma_{\text{total}}$ Γ_{54}/Γ

VALUE	DOCUMENT ID	TECN	COMMENT
0.74±0.06 OUR AVERAGE			
$0.72\pm0.02\pm0.06$	BARATE 98V	ALEP	$e^+e^-\to Z$
$0.88\pm0.05\pm0.18$	ABREU 95C	DLPH	$e^+e^-\to Z$

$\Gamma(K^0_S\text{anything})/\Gamma_{\text{total}}$ Γ_{55}/Γ

VALUE	DOCUMENT ID	TECN	COMMENT
0.290±0.011±0.027	ABREU 95C	DLPH	$e^+e^-\to Z$

$\Gamma(\pi^{\pm}\text{anything})/\Gamma_{\text{total}}$ Γ_{56}/Γ

VALUE	DOCUMENT ID	TECN	COMMENT
3.97±0.02±0.21	BARATE 98V	ALEP	$e^+e^-\to Z$

$\Gamma(\pi^0\text{anything})/\Gamma_{\text{total}}$ Γ_{57}/Γ

VALUE	DOCUMENT ID	TECN	COMMENT
2.78±0.15±0.60	[1] ADAM 96	DLPH	$e^+e^-\to Z$

[1] ADAM 96 measurement obtained from a fit to the rapidity distribution of $\pi^{0\prime s}$ in $Z\to b\,b$ events.

$\Gamma(\phi\text{anything})/\Gamma_{\text{total}}$ Γ_{58}/Γ

VALUE	DOCUMENT ID	TECN	COMMENT
0.0282±0.0013±0.0019	ABBIENDI 00Z	OPAL	$e^+e^-\to Z$

$\Gamma(p/\overline{p}\text{anything})/\Gamma_{\text{total}}$ Γ_{59}/Γ

VALUE	DOCUMENT ID	TECN	COMMENT
0.131±0.011 OUR AVERAGE			
$0.131\pm0.004\pm0.011$	BARATE 98V	ALEP	$e^+e^-\to Z$
$0.141\pm0.018\pm0.056$	ABREU 95C	DLPH	$e^+e^-\to Z$

$\Gamma(\Lambda/\overline{\Lambda}\text{anything})/\Gamma_{\text{total}}$ Γ_{60}/Γ

VALUE	DOCUMENT ID	TECN	COMMENT
0.059 ±0.006 OUR AVERAGE			
$0.0587\pm0.0046\pm0.0048$	ACKERSTAFF 97N	OPAL	$e^+e^-\to Z$
$0.059\pm0.007\pm0.009$	ABREU 95C	DLPH	$e^+e^-\to Z$

$\Gamma(b\text{-baryon anything})/\Gamma_{\text{total}}$ Γ_{61}/Γ

VALUE	DOCUMENT ID	TECN	COMMENT
0.102±0.007±0.027	[1] BARATE 98V	ALEP	$e^+e^-\to Z$

[1] BARATE 98V assumes $B(B_s\to pX)=8\pm4\%$ and $B(b\text{-baryon}\to pX)=58\pm6\%$.

$\Gamma(\text{charged anything})/\Gamma_{\text{total}}$ Γ_{62}/Γ

VALUE	DOCUMENT ID	TECN	COMMENT
4.97±0.03±0.06	[1] ABREU 98H	DLPH	$e^+e^-\to Z$
• • • We do not use the following data for averages, fits, limits, etc. • • •			
$5.84\pm0.04\pm0.38$	ABREU 95C	DLPH	Repl. by ABREU 98H

[1] ABREU 98H measurement excludes the contribution from K^0 and Λ decay.

$\Gamma(\text{hadron}^+\,\text{hadron}^-)/\Gamma_{\text{total}}$ Γ_{63}/Γ

VALUE (units 10^{-5})	DOCUMENT ID	TECN	COMMENT
1.7$^{+1.0}_{-0.7}$±0.2	[1,2] BUSKULIC 96V	ALEP	$e^+e^-\to Z$

[1] BUSKULIC 96V assumes PDG 96 production fractions for B^0, B^+, B_s, b baryons.

[2] Average branching fraction of weakly decaying B hadrons into two long-lived charged hadrons, weighted by their production cross section and lifetimes.

$\Gamma(\text{charmless})/\Gamma_{\text{total}}$ Γ_{64}/Γ

VALUE	DOCUMENT ID	TECN	COMMENT
0.007±0.021	[1] ABREU 98D	DLPH	$e^+e^-\to Z$

[1] ABREU 98D results are extracted from a fit to the b-tagging probability distribution based on the impact parameter. The expected hidden charm contribution of 0.026 ± 0.004 has been subtracted.

$\Gamma(\mu^+\mu^-\text{anything})/\Gamma_{\text{total}}$ Γ_{66}/Γ

Test for $\Delta B=1$ weak neutral current.

VALUE	CL%	DOCUMENT ID	TECN	COMMENT
<3.2 × 10⁻⁴	90	ABBOTT 98B	D0	$p\overline{p}$ 1.8 TeV
• • • We do not use the following data for averages, fits, limits, etc. • • •				
$<5.0\times10^{-5}$	90	[1] ALBAJAR 91C	UA1	$E^{p\overline{p}}_{\text{cm}}=630$ GeV
<0.02	95	ALTHOFF 84G	TASS	$E^{ee}_{\text{cm}}=34.5$ GeV
<0.007	95	ADEVA 83	MRKJ	$E^{ee}_{\text{cm}}=30$–38 GeV
<0.007	95	BARTEL 83B	JADE	$E^{ee}_{\text{cm}}=33$–37 GeV

[1] Both ABBOTT 98B and GLENN 98 claim that the efficiency quoted in ALBAJAR 91C was overestimated by a large factor.

$[\Gamma(e^+e^-\text{anything})+\Gamma(\mu^+\mu^-\text{anything})]/\Gamma_{\text{total}}$ $(\Gamma_{65}+\Gamma_{66})/\Gamma$

Test for $\Delta B=1$ weak neutral current.

VALUE	CL%	DOCUMENT ID	TECN	COMMENT
• • • We do not use the following data for averages, fits, limits, etc. • • •				
<0.008	90	MATTEUZZI 83	MRK2	$E^{ee}_{\text{cm}}=29$ GeV

$\Gamma(\nu\overline{\nu}\text{anything})/\Gamma_{\text{total}}$ Γ_{67}/Γ

VALUE	DOCUMENT ID	TECN	COMMENT
• • • We do not use the following data for averages, fits, limits, etc. • • •			
$<3.9\times10^{-4}$	[1] GROSSMAN 96	RVUE	$e^+e^-\to Z$

[1] GROSSMAN 96 limit is derived from the ALEPH BUSKULIC 95 limit $B(B^+ \to \tau^+\nu_\tau) < 1.8 \times 10^{-3}$ at CL=90% using conservative simplifying assumptions.

χ_b AT HIGH ENERGY

For a discussion of B-$\overline{B}$ mixing, see the note on "B^0-$\overline{B}^0$ Mixing" in the B^0 Particle Listings.

χ_b is the average B-$\overline{B}$ mixing parameter at high-energy $\chi_b = f'_d\chi_d + f'_s\chi_s$ where f'_d and f'_s are the fractions of B^0 and B_s^0 hadrons in an unbiased sample of semileptonic b-hadron decays.

"OUR EVALUATION" is an average using rescaled values of the data listed below. The average and rescaling were performed by the Heavy Flavor Averaging Group (HFAG) and are described at http://www.slac.stanford.edu/xorg/hfag/. The averaging/rescaling procedure takes into account correlations between the measurements.

VALUE	EVTS	DOCUMENT ID		TECN	COMMENT
0.1284±0.0069 OUR EVALUATION					
0.129 ±0.004 OUR AVERAGE					
0.132 ±0.001 ±0.024		[1] ABAZOV	06S	D0	$p\overline{p}$ at 1.96 TeV
0.152 ±0.007 ±0.011		[2] ACOSTA	04A	CDF	$p\overline{p}$ at 1.8 TeV
0.1312±0.0049±0.0042		[3] ABBIENDI	03P	OPAL	$e^+e^- \to Z$
0.127 ±0.013 ±0.006		[4] ABREU	01L	DLPH	$e^+e^- \to Z$
0.1192±0.0068±0.0051		[5] ACCIARRI	99D	L3	$e^+e^- \to Z$
0.121 ±0.016 ±0.006		[6] ABREU	94J	DLPH	$e^+e^- \to Z$
0.114 ±0.014 ±0.008		[7] BUSKULIC	94G	ALEP	$e^+e^- \to Z$
0.129 ±0.022		[8] BUSKULIC	92B	ALEP	$e^+e^- \to Z$
0.176 ±0.031 ±0.032	1112	[9] ABE	91G	CDF	$p\overline{p}$ 1.8 TeV
0.148 ±0.029 ±0.017		[10] ALBAJAR	91D	UA1	$p\overline{p}$ 630 GeV
• • • We do not use the following data for averages, fits, limits, etc. • • •					
0.131 ±0.020 ±0.016		[11] ABE	97I	CDF	Repl. by ACOSTA 04A
0.1107±0.0062±0.0055		[12] ALEXANDER	96	OPAL	Rep. by ABBIENDI 03P
0.136 ±0.037 ±0.040		[13] UENO	96	AMY	e^+e^- at 57.9 GeV
0.144 ±0.014 $^{+0.017}_{-0.011}$		[14] ABREU	94F	DLPH	Sup. by ABREU 94J
0.131 ±0.014		[15] ABREU	94J	DLPH	$e^+e^- \to Z$
0.123 ±0.012 ±0.008		ACCIARRI	94D	L3	Repl. by ACCIARRI 99D
0.157 ±0.020 ±0.032		[16] ALBAJAR	94	UA1	$\sqrt{s}$ = 630 GeV
0.121 $^{+0.044}_{-0.040}$ ±0.017	1665	[17] ABREU	93C	DLPH	Sup. by ABREU 94J
0.143 $^{+0.022}_{-0.021}$ ±0.007		[18] AKERS	93B	OPAL	Sup. by ALEXANDER 96
0.145 $^{+0.041}_{-0.035}$ ±0.018		[19] ACTON	92C	OPAL	$e^+e^- \to Z$
0.121 ±0.017 ±0.006		[20] ADEVA	92C	L3	Sup. by ACCIARRI 94D
0.132 ±0.22 $^{+0.015}_{-0.012}$	823	[21] DECAMP	91	ALEP	$e^+e^- \to Z$
0.178 $^{+0.049}_{-0.040}$ ±0.020		[22] ADEVA	90P	L3	$e^+e^- \to Z$
0.17 $^{+0.15}_{-0.08}$		[23,24] WEIR	90	MRK2	e^+e^- 29 GeV
0.21 $^{+0.29}_{-0.15}$		[23] BAND	88	MAC	E_{cm}^{ee}= 29 GeV
>0.02 at 90% CL		[23] BAND	88	MAC	E_{cm}^{ee}= 29 GeV
0.121 ±0.047		[23,25] ALBAJAR	87C	UA1	Repl. by ALBAJAR 91D
<0.12 at 90% CL		[23,26] SCHAAD	85	MRK2	E_{cm}^{ee}= 29 GeV

[1] Uses the dimuon charge asymmetry. Averaged over the mix of b-flavored hadrons.
[2] Measurement performed using events containing a dimuon or an e/μ pair.
[3] The average B mixing parameter is determined simultaneously with b and c forward-backward asymmetries in the fit.
[4] The experimental systematic and model uncertainties are combined in quadrature.
[5] ACCIARRI 99D uses maximum-likelihood fits to extract χ_b as well as the A_{FB}^b in $Z \to b\overline{b}$ events containing prompt leptons.
[6] This ABREU 94J result is from 5182 $\ell\ell$ and 279 $\Lambda\ell$ events. The systematic error includes 0.004 for model dependence.
[7] BUSKULIC 94G data analyzed using ee, $e\mu$, and $\mu\mu$ events.
[8] BUSKULIC 92B uses a jet charge technique combined with electrons and muons.
[9] ABE 91G measurement of χ is done with $e\mu$ and ee events.
[10] ALBAJAR 91D measurement of χ is done with dimuons.
[11] Uses di-muon events.
[12] ALEXANDER 96 uses a maximum likelihood fit to simultaneously extract χ as well as the forward-backward asymmetries in $e^+e^- \to Z \to b\overline{b}$ and $c\overline{c}$.
[13] UENO 96 extracted χ from the energy dependence of the forward-backward asymmetry.
[14] ABREU 94F uses the average electric charge sum of the jets recoiling against a b-quark jet tagged by a high p_T muon. The result is for $\overline{\chi} = f_d\chi_d + 0.9 f_s\chi_s$.
[15] This ABREU 94J result combines $\ell\ell$, $\Lambda\ell$, and jet-charge ℓ (ABREU 94F) analyses. It is for $\overline{\chi} = f_d\chi_d + 0.96 f_s\chi_s$.
[16] ALBAJAR 94 uses dimuon events. Not independent of ALBAJAR 91D.
[17] ABREU 93C data analyzed using ee, $e\mu$, and $\mu\mu$ events.
[18] AKERS 93B analysis performed using dilepton events.
[19] ACTON 92C uses electrons and muons. Superseded by AKERS 93B.
[20] ADEVA 92C uses electrons and muons.
[21] DECAMP 91 done with opposite and like-sign dileptons. Superseded by BUSKULIC 92B.
[22] ADEVA 90P measurement uses ee, $\mu\mu$, and $e\mu$ events from 118k events at the Z. Superseded by ADEVA 92C.
[23] These experiments are not in the average because the combination of B_s and B_d mesons which they see could differ from those at higher energy.
[24] The WEIR 90 measurement supersedes the limit obtained in SCHAAD 85. The 90% CL are 0.06 and 0.38.
[25] ALBAJAR 87C measured $\chi = (\overline{B}^0 \to B^0 \to \mu^+ X)$ divided by the average production weighted semileptonic branching fraction for B hadrons at 546 and 630 GeV.
[26] Limit is average probability for hadron containing B quark to produce a positive lepton.

CP VIOLATION PARAMETERS in semileptonic b-hadron decays.

Re(ϵ_b) / (1 + $|\epsilon_b|^2$)

CP impurity in semileptonic b-hadron decays.

VALUE (units 10^{-3})	DOCUMENT ID		TECN	COMMENT
1.24±0.38±0.18	[1] ABAZOV	14	D0	$p\overline{p}$ at 1.96 TeV
• • • We do not use the following data for averages, fits, limits, etc. • • •				
−1.97±0.43±0.23	[2] ABAZOV	11U	D0	Repl. by ABAZOV 14
−2.39±0.63±0.37	[3] ABAZOV	10H	D0	Repl. by ABAZOV 11U

[1] ABAZOV 14 reports a measurement of like-sign dimuon charge asymmetry of $A_{SL}^b = (-4.96 \pm 1.53 \pm 0.72) \times 10^{-3}$ in semileptonic b-hadron decays.
[2] ABAZOV 11U reports a measurement of like-sign dimuon charge asymmetry of $A_{SL}^b = (-7.87 \pm 1.72 \pm 0.93) \times 10^{-3}$ in semileptonic b-hadron decays.
[3] ABAZOV 10H reports a measurement of like-sign dimuon charge asymmetry of $A_{SL}^b = (-9.57 \pm 2.51 \pm 1.46) \times 10^{-3}$ in semileptonic b-hadron decays. Using the measured production ratio of B_d^0 and B_s^0, and the asymmetry of B_d^0 $A_{SL}^d = (-4.7 \pm 4.6) \times 10^{-3}$ measured from B-factories, they obtain the asymmetry for B_s^0 as $A_{SL}^s = (-14.6 \pm 7.5) \times 10^{-3}$.

B-HADRON PRODUCTION FRACTIONS IN HADRONIC Z DECAY

The production fractions of b-hadrons in hadronic Z decays have been calculated using the best values of mean lives, mixing parameters and branching fractions in this edition by the Heavy Flavor Averaging Group (HFAG) (see http://www.slac.stanford.edu/xorg/hfag/).

The values reported below assume:

$f(\overline{b} \to B^+) = f(\overline{b} \to B^0)$

$f(\overline{b} \to B^+) + f(\overline{b} \to B^0) + f(\overline{b} \to B_s^0) + f(b \to b\text{-baryon}) = 1$

The values are:

$f(\overline{b} \to B^+) = f(\overline{b} \to B^0) = 0.404 \pm 0.009$

$f(\overline{b} \to B_s^0) = 0.103 \pm 0.009$

$f(b \to b\text{-baryon}) = 0.089 \pm 0.015$

and their correlation coefficients are:

$cor(B_s^0, b\text{-baryon}) = +0.052$

$cor(B_s^0, B^+ = B^0) = -0.534$

$cor(b\text{-baryon}, B^+ = B^0) = -0.872$

as obtained using a time-integrated mixing parameter $\overline{\chi} = 0.1259 \pm 0.0042$ given by a fit to heavy quark quantities with asymmetries removed (see the note "The Z boson").

B-HADRON PRODUCTION FRACTIONS IN $p\overline{p}$ COLLISIONS AT Tevatron

The production fractions for b-hadrons in $p\overline{p}$ collisions at the Tevatron have been calculated from the best values of mean lifetimes, mixing parameters, and branching fractions in this edition by the Heavy Flavor Averaging Group (HFAG) (see http://www.slac.stanford.edu/xorg/hfag/).

The values reported below assume:

$f(\overline{b} \to B^+) = f(\overline{b} \to B^0)$

$f(\overline{b} \to B^+) + f(\overline{b} \to B^0) + f(\overline{b} \to B_s^0) + f(b \to b\text{-baryon}) = 1$

The values are:

$f(\overline{b} \to B^+) = f(\overline{b} \to B^0) = 0.339 \pm 0.031$

$f(\overline{b} \to B_s^0) = 0.111 \pm 0.014$

$f(b \to b\text{-baryon}) = 0.212 \pm 0.069$

and their correlation coefficients are:

$cor(B_s^0, b\text{-baryon}) = -0.581$

$cor(B_s^0, B^+ = B^0) = +0.425$

$cor(b\text{-baryon}, B^+ = B^0) = -0.984$

as obtained with the Tevatron average of time-integrated mixing parameter $\overline{\chi} = 0.147 \pm 0.011$.

$B^{\pm}/B^0/B_s^0/b$-baryon ADMIXTURE REFERENCES

ABAZOV	14	PR D89 012002	V.M. Abazov *et al.*	(D0 Collab.)
AAIJ	13P	JHEP 1304 001	R. Aaij *et al.*	(LHCb Collab.)
AAIJ	12BD	EPJ C72 2100	R. Aaij *et al.*	(LHCb Collab.)
AAIJ	12J	PR D85 032008	R. Aaji *et al.*	(LHCb Collab.)
CHATRCHYAN	12AK	JHEP 1202 011	S. Chatrchyan *et al.*	(CMS Collab.)
AAIJ	11F	PRL 107 211801	R. Aaij *et al.*	(LHCb Collab.)
ABAZOV	11U	PR D84 052007	V.M. Abazov *et al.*	(D0 Collab.)
ABAZOV	10H	PR D82 032001	V.M. Abazov *et al.*	(D0 Collab.)
Also		PRL 105 081801	V.M. Abazov *et al.*	(D0 Collab.)
PDG	10	JP G37 075021	K. Nakamura *et al.*	(PDG Collab.)
AALTONEN	09E	PR D79 032001	T. Aaltonen *et al.*	(CDF Collab.)
AALTONEN	08N	PR D77 072003	T. Aaltonen *et al.*	(CDF Collab.)
ABAZOV	06S	PR D74 092001	V.M. Abazov *et al.*	(D0 Collab.)
ABBIENDI	04I	EPJ C35 149	G. Abbiendi *et al.*	(OPAL Collab.)
ABDALLAH	04E	EPJ C33 307	J. Abdallah *et al.*	(DELPHI Collab.)
ACOSTA	04A	PR D69 012002	D. Acosta *et al.*	(CDF Collab.)
ABBIENDI	03M	EPJ C30 467	G. Abbiendi *et al.*	(OPAL Collab.)

ABBIENDI	03P	PL B577 18	G. Abbiendi *et al.*	(OPAL Collab.)
ABDALLAH	03E	PL B561 26	J. Abdallah *et al.*	(DELPHI Collab.)
ABDALLAH	03K	PL B576 29	J. Abdallah *et al.*	(DELPHI Collab.)
HEISTER	02G	EPJ C22 613	A. Heister *et al.*	(ALEPH Collab.)
ABBIENDI	01Q	PL B520 1	G. Abbiendi *et al.*	(OPAL Collab.)
ABBIENDI	01R	EPJ C21 399	G. Abbiendi *et al.*	(OPAL Collab.)
ABREU	01L	EPJ C20 455	P. Abreu *et al.*	(DELPHI Collab.)
BARATE	01E	EPJ C19 213	R. Barate *et al.*	(ALEPH Collab.)
ABBIENDI	00E	EPJ C13 225	G. Abbiendi *et al.*	(OPAL Collab.)
ABBIENDI	00Z	PL B492 13	G. Abbiendi *et al.*	(OPAL Collab.)
ABREU	00	EPJ C12 225	P. Abreu *et al.*	(DELPHI Collab.)
ABREU	00C	PL B496 43	P. Abreu *et al.*	(DELPHI Collab.)
ABREU	00D	PL B478 14	P. Abreu *et al.*	(DELPHI Collab.)
ABREU	00R	PL B475 407	P. Abreu *et al.*	(DELPHI Collab.)
ACCIARRI	00	EPJ C13 47	M. Acciarri *et al.*	(L3 Collab.)
AFFOLDER	00E	PRL 84 1663	T. Affolder *et al.*	(CDF Collab.)
ABBIENDI	99J	EPJ C12 609	G. Abbiendi *et al.*	(OPAL Collab.)
ABE	99P	PR D60 092005	F. Abe *et al.*	(CDF Collab.)
ACCIARRI	99D	PL B448 152	M. Acciarri *et al.*	(L3 Collab.)
BARATE	99G	EPJ C6 555	R. Barate *et al.*	(ALEPH Collab.)
ABBOTT	98B	PL B423 419	B. Abbott *et al.*	(D0 Collab.)
ABE	98B	PR D57 5382	F. Abe *et al.*	(CDF Collab.)
ABREU	98D	PL B426 193	P. Abreu *et al.*	(DELPHI Collab.)
ABREU	98H	PL B425 399	P. Abreu *et al.*	(DELPHI Collab.)
ACCIARRI	98	PL B416 220	M. Acciarri *et al.*	(L3 Collab.)
ACCIARRI	98K	PL B436 174	M. Acciarri *et al.*	(L3 Collab.)
ACKERSTAFF	98E	EPJ C1 439	K. Ackerstaff *et al.*	(OPAL Collab.)
BARATE	98I	PL B429 169	R. Barate *et al.*	(ALEPH Collab.)
BARATE	98Q	EPJ C4 387	R. Barate *et al.*	(ALEPH Collab.)
BARATE	98V	EPJ C5 205	R. Barate *et al.*	(ALEPH Collab.)
GLENN	98	PRL 80 2289	S. Glenn *et al.*	(CLEO Collab.)
ABE	97I	PR D55 2546	F. Abe *et al.*	(CDF Collab.)
ACKERSTAFF	97F	ZPHY C73 397	K. Ackerstaff *et al.*	(OPAL Collab.)
ACKERSTAFF	97N	ZPHY C74 423	K. Ackerstaff *et al.*	(OPAL Collab.)
ACKERSTAFF	97W	ZPHY C76 425	K. Ackerstaff *et al.*	(OPAL Collab.)
ABREU	96E	PL B377 195	P. Abreu *et al.*	(DELPHI Collab.)
ACCIARRI	96C	ZPHY C71 379	M. Acciarri *et al.*	(L3 Collab.)
ADAM	96	ZPHY C69 561	W. Adam *et al.*	(DELPHI Collab.)
ADAM	96D	ZPHY C72 207	W. Adam *et al.*	(DELPHI Collab.)
ALEXANDER	96	ZPHY C70 357	G. Alexander *et al.*	(OPAL Collab.)
BUSKULIC	96F	PL B369 151	D. Buskulic *et al.*	(ALEPH Collab.)
BUSKULIC	96V	PL B384 471	D. Buskulic *et al.*	(ALEPH Collab.)
BUSKULIC	96Y	PL B388 648	D. Buskulic *et al.*	(ALEPH Collab.)
GROSSMAN	96	NP B465 369	Y. Grossman, Z. Ligeti, E. Nardi	(REHO, CIT)
Also		NP B480 753 (erratum)	Y. Grossman, Z. Ligeti, E. Nardi	
PDG	96	PR D54 1	R. M. Barnett *et al.*	(PDG Collab.)
UENO	96	PL B381 365	K. Ueno *et al.*	(AMY Collab.)
ABE,K	95B	PRL 75 3624	K. Abe *et al.*	(SLD Collab.)
ABREU	95C	PL B347 447	P. Abreu *et al.*	(DELPHI Collab.)
ABREU	95D	ZPHY C66 323	P. Abreu *et al.*	(DELPHI Collab.)
ADAM	95	ZPHY C68 363	W. Adam *et al.*	(DELPHI Collab.)
AKERS	95Q	ZPHY C67 57	R. Akers *et al.*	(OPAL Collab.)
BUSKULIC	95	PL B343 444	D. Buskulic *et al.*	(ALEPH Collab.)
ABREU	94F	PL B322 459	P. Abreu *et al.*	(DELPHI Collab.)
ABREU	94J	PL B332 488	P. Abreu *et al.*	(DELPHI Collab.)
ABREU	94L	ZPHY C63 3	P. Abreu *et al.*	(DELPHI Collab.)
ABREU	94P	PL B341 109	P. Abreu *et al.*	(DELPHI Collab.)
ACCIARRI	94C	PL B332 201	M. Acciarri *et al.*	(L3 Collab.)
ACCIARRI	94D	PL B335 542	M. Acciarri *et al.*	(L3 Collab.)
ALBAJAR	94	ZPHY C61 41	C. Albajar *et al.*	(UA1 Collab.)
BUSKULIC	94G	ZPHY C62 179	D. Buskulic *et al.*	(ALEPH Collab.)
ABE	93E	PL B313 288	K. Abe *et al.*	(VENUS Collab.)
ABE	93J	PRL 71 3421	F. Abe *et al.*	(CDF Collab.)
ABREU	93C	PL B301 145	P. Abreu *et al.*	(DELPHI Collab.)
ABREU	93D	ZPHY C57 181	P. Abreu *et al.*	(DELPHI Collab.)
ABREU	93G	PL B312 253	P. Abreu *et al.*	(DELPHI Collab.)
ACTON	93C	PL B307 247	P.D. Acton *et al.*	(OPAL Collab.)
ACTON	93L	ZPHY C60 217	P.D. Acton *et al.*	(OPAL Collab.)
ADRIANI	93J	PL B317 467	O. Adriani *et al.*	(L3 Collab.)
ADRIANI	93K	PL B317 474	O. Adriani *et al.*	(L3 Collab.)
ADRIANI	93L	PL B317 637	O. Adriani *et al.*	(L3 Collab.)
AKERS	93B	ZPHY C60 199	R. Akers *et al.*	(OPAL Collab.)
BUSKULIC	93B	PL B298 479	D. Buskulic *et al.*	(ALEPH Collab.)
BUSKULIC	93O	PL B314 459	D. Buskulic *et al.*	(ALEPH Collab.)
ABREU	92	ZPHY C53 567	P. Abreu *et al.*	(DELPHI Collab.)
ACTON	92	PL B274 513	D.P. Acton *et al.*	(OPAL Collab.)
ACTON	92C	PL B276 379	D.P. Acton *et al.*	(OPAL Collab.)
ADEVA	92C	PL B288 395	B. Adeva *et al.*	(L3 Collab.)
ADRIANI	92	PL B288 412	O. Adriani *et al.*	(L3 Collab.)
BUSKULIC	92B	PL B284 177	D. Buskulic *et al.*	(ALEPH Collab.)
BUSKULIC	92F	PL B295 174	D. Buskulic *et al.*	(ALEPH Collab.)
BUSKULIC	92G	PL B295 396	D. Buskulic *et al.*	(ALEPH Collab.)
ABE	91G	PRL 67 3351	F. Abe *et al.*	(CDF Collab.)
ADEVA	91C	PL B261 177	B. Adeva *et al.*	(L3 Collab.)
ADEVA	91H	PL B270 111	B. Adeva *et al.*	(L3 Collab.)
ALBAJAR	91C	PL B262 163	C. Albajar *et al.*	(UA1 Collab.)
ALBAJAR	91D	PL B262 171	C. Albajar *et al.*	(UA1 Collab.)
ALEXANDER	91G	PL B266 485	G. Alexander *et al.*	(OPAL Collab.)
DECAMP	91	PL B258 236	D. Decamp *et al.*	(ALEPH Collab.)
DECAMP	91C	PL B257 492	D. Decamp *et al.*	(ALEPH Collab.)
ADEVA	90P	PL B252 703	B. Adeva *et al.*	(L3 Collab.)
BEHREND	90D	ZPHY C47 333	H.J. Behrend *et al.*	(CELLO Collab.)
HAGEMANN	90	ZPHY C48 401	J. Hagemann *et al.*	(JADE Collab.)
LYONS	90	PR D41 982	L. Lyons, A.J. Martin, D.H. Saxon	(OXF, BRIS+)
WEIR	90	PL B240 289	A.J. Weir *et al.*	(Mark II Collab.)
BRAUNSCH...	89B	ZPHY C44 1	R. Braunschweig *et al.*	(TASSO Collab.)
ONG	89	PRL 62 1236	R.A. Ong *et al.*	(Mark II Collab.)
BAND	88	PL B200 221	H.R. Band *et al.*	(MAC Collab.)
KLEM	88	PR D37 41	D.E. Klem *et al.*	(DELCO Collab.)
ONG	88	PRL 60 2587	R.A. Ong *et al.*	(Mark II Collab.)
ALBAJAR	87C	PL B186 247	C. Albajar *et al.*	(UA1 Collab.)
ASH	87	PRL 58 640	W.W. Ash *et al.*	(MAC Collab.)
BARTEL	87	ZPHY C33 339	W. Bartel *et al.*	(JADE Collab.)
BROM	87	PL B195 301	J.M. Brom *et al.*	(HRS Collab.)
PAL	86	PR D33 2708	T. Pal *et al.*	(DELCO Collab.)
AIHARA	85	ZPHY C27 39	H. Aihara *et al.*	(TPC Collab.)
BARTEL	85J	PL 163B 277	W. Bartel *et al.*	(JADE Collab.)
SCHAAD	85	PL 160B 188	T. Schaad *et al.*	(Mark II Collab.)
ALTHOFF	84G	ZPHY C22 219	M. Althoff *et al.*	(TASSO Collab.)
ALTHOFF	84J	PL 146B 443	M. Althoff *et al.*	(TASSO Collab.)
KOOP	84	PRL 52 970	D.E. Koop *et al.*	(DELCO Collab.)
ADEVA	83	PRL 50 799	B. Adeva *et al.*	(Mark-J Collab.)
ADEVA	83B	PRL 51 443	B. Adeva *et al.*	(Mark-J Collab.)
BARTEL	83B	PL 132B 241	W. Bartel *et al.*	(JADE Collab.)
FERNANDEZ	83D	PRL 50 2054	E. Fernandez *et al.*	(MAC Collab.)
MATTEUZZI	83	PL 129B 141	C. Matteuzzi *et al.*	(Mark II Collab.)
NELSON	83	PRL 50 1542	M.E. Nelson *et al.*	(Mark II Collab.)

V_{cb} and V_{ub} CKM Matrix Elements

OMITTED FROM SUMMARY TABLE

SEMILEPTONIC B MESON DECAYS AND THE DETERMINATION OF V_{cb} AND V_{ub}

Updated February 2014 by R. Kowalewski (Univ. of Victoria, Canada) and T. Mannel (Univ. of Siegen, Germany)

INTRODUCTION

Semileptonic B meson decay amplitudes allow determinations of $|V_{ub}|$ and $|V_{cb}|$ which are assumed to be largely free from any impact of non-standard model physics, since they are dominated by the standard-model W boson exchange. A charged Higgs boson, present in many models of new physics, will couple to the mass of the lepton and hence it will have practically no impact in decays into e and μ. However, decays to tau leptons, which are also discussed in this review, provide sensitivity to these models.

Precision determinations of $|V_{ub}|$ and $|V_{cb}|$ are central to testing the CKM sector of the Standard Model, and complement the measurements of CP asymmetries in B decays. The length of the side of the unitarity triangle opposite the well-measured angle β is proportional to the ratio $|V_{ub}|/|V_{cb}|$, making its determination a high priority of the heavy-flavor physics program.

The semileptonic transitions $b \to c\ell\overline{\nu}_\ell$ and $b \to u\ell\overline{\nu}_\ell$ (where ℓ refers to an electron or muon) each provide two avenues for determining these CKM matrix elements, namely through inclusive and exclusive final states. Recent measurements and calculations are reflected in the values quoted in this article, which is an update of the previous review [1]. The leptonic decay $B^- \to \tau\overline{\nu}$ can also be used to extract $|V_{ub}|$; we do not use this information at present since none of the current experimental measurements has reached the significance level of an observation.

The theory underlying the determination of $|V_{qb}|$ is mature, in particular for $|V_{cb}|$. Most of the theoretical approaches use the fact that the mass m_b of the b quark is large compared to the scale $\Lambda_{\rm QCD}$ that determines low-energy hadronic physics. The basis for precise calculations is a systematic expansion in powers of Λ/m_b, where $\Lambda \sim 500 - 700$ MeV is a hadronic scale of the order of $\Lambda_{\rm QCD}$, based on effective-field-theory methods described in a separate RPP mini-review.

The large data samples available at the B factories enable analyses where one B meson from an $\Upsilon(4S)$ decay is fully reconstructed, allowing a recoiling semileptonic B decay to be studied with high purity. Improved knowledge of $\overline{B} \to X_c\ell\overline{\nu}_\ell$ decays allows partial rates for $\overline{B} \to X_u\ell\overline{\nu}_\ell$ transitions to be measured in regions previously considered inaccessible, increasing the acceptance for $\overline{B} \to X_u\ell\overline{\nu}_\ell$ transitions and reducing theoretical uncertainties.

Experimental measurements of the exclusive $\overline{B} \to \pi\ell\overline{\nu}_\ell$ decay are quite precise, and recent improvements in the theoretical calculation of the form factor normalization have enabled

a determination of $|V_{ub}|$ from this decay with an uncertainty below 10%.

The decays $\overline{B} \to D^{(*)}\tau\overline{\nu}_\ell$ provide sensitivity to possible non-universalities in the couplings to the third generation leptons that are present at tree level in models involving new charged mediators. The constraints on these models are weak at present, and the enhanced decay rates seen in recent measurements of these decay modes, if they turn out to be robust, are an indication of new physics.

Throughout this review the numerical results quoted are based on the methods of the Heavy Flavor Averaging Group [2].

DETERMINATION OF $|V_{cb}|$

Summary: The determination of $|V_{cb}|$ from $\overline{B} \to D^*\ell\overline{\nu}_\ell$ decays has a relative precision of about 2%, with the main uncertainty coming from knowledge of the form factor near the maximum momentum transfer to the leptons. The $\overline{B} \to D\ell\overline{\nu}_\ell$ decay provides a determination with an uncertainty of 5%.

Inclusive decays provide a determination of $|V_{cb}|$ with a relative uncertainty of about 2%. The limitations arise mainly from our ignorance of higher-order perturbative and non-perturbative corrections.

The values obtained from inclusive and exclusive determinations are marginally consistent with each other:

$$|V_{cb}| = (42.2 \pm 0.7) \times 10^{-3} \text{ (inclusive)} \quad (1)$$

$$|V_{cb}| = (39.5 \pm 0.8) \times 10^{-3} \text{ (exclusive);} \quad (2)$$

as a result, their combination should be treated with caution. An average of these determinations has $p(\chi^2) = 0.01$, so we scale the error by $\sqrt{\chi^2/1} = 2.6$ to find

$$|V_{cb}| = (41.1 \pm 1.3) \times 10^{-3} \ . \quad (3)$$

$|V_{cb}|$ from exclusive decays

Exclusive determinations of $|V_{cb}|$ are based on a study of semileptonic B decays into the ground state charmed mesons D and D^*. The main uncertainties in this approach stem from our ignorance of the form factors describing the $B \to D$ and $B \to D^*$ transitions. However, in the limit of infinite bottom and charm quark masses only a single form factor appears, the Isgur-Wise function [3], which depends on the product of the four-velocities v and v' of the initial and final-state hadrons.

The extraction of $|V_{cb}|$ is based on the distribution of the variable $w \equiv v \cdot v'$, which corresponds to the energy of the final state $D^{(*)}$ meson in the rest frame of the decay. Heavy Quark Symmetry (HQS) [3,4] predicts the normalization of the rate at $w = 1$, the point of maximum momentum transfer to the leptons, and $|V_{cb}|$ is obtained from an extrapolation of the measured spectrum to $w = 1$. This extrapolation relies on a parametrization of the form factor, as explained below.

A precise determination requires corrections to the HQS prediction for the normalization as well as some information on the slope of the form factors near the point $w = 1$. The framework for this is "Heavy Quark Effective Theory", which is discussed in a separate mini-review. The corrections to the HQS prediction are due to finite quark masses and are essentially of the order $\Lambda_{\rm QCD}/m_c$. Form factors that are normalized due to HQS are protected against linear corrections of this order and hence the corrections are here of order $\Lambda^2_{\rm QCD}/m_c^2$ due to Luke's Theorem [5], which is an application of the Ademollo-Gatto theorem [6] to heavy quarks. For the form factors that vanish in the infinite mass limit the corrections are in general linear in $\Lambda_{\rm QCD}/m_c$, and thus we have, using the definitions as in Eq. (2.84) of Ref. 7

$$\begin{aligned} h_i(1) &= 1 + \mathcal{O}(\Lambda^2_{\rm QCD}/m_c^2) && \text{for } i = +, V, A_1, A_3 \ , \\ h_i(1) &= \mathcal{O}(\Lambda_{\rm QCD}/m_c) && \text{for } i = -, A_2 \ . \end{aligned} \quad (4)$$

In addition to these corrections, there are perturbatively calculable radiative corrections from hard gluons and photons, which will be discussed in the relevant sections.

$\overline{B} \to D^*\ell\overline{\nu}_\ell$

The decay rate for $\overline{B} \to D^*\ell\overline{\nu}_\ell$ is given by

$$\frac{d\Gamma}{dw}(\overline{B} \to D^*\ell\overline{\nu}_\ell) = \frac{G_F^2 m_B^5}{48\pi^3}|V_{cb}|^2(w^2-1)^{1/2}P(w)(\eta_{\rm ew}\mathcal{F}(w))^2, \quad (5)$$

where $P(w)$ is a phase space factor,

$$P(w) = r^3(1-r)^2(w+1)^2\left(1 + \frac{4w}{w+1}\frac{1-2rw+r^2}{(1-r)^2}\right).$$

with $r = m_{D^*}/m_B$. The form factor $\mathcal{F}(w)$ is dominated by the axial vector form factor h_{A_1} as $w \to 1$. Furthermore, $\eta_{\rm ew} = 1.007$ accounts for the electroweak corrections to the four-fermion operator mediating the semileptonic decay [8]. In the infinite-mass limit, the HQS normalization gives $\mathcal{F}(1) = 1$.

The form factor $\mathcal{F}(w)$ must be parametrized to perform an extrapolation to the zero-recoil point. A frequently used one-parameter form motivated by analyticity and unitarity is [9,10]

$$\begin{aligned} h_{\rm A1}(w) = \eta_{\rm A}&\left[1 + \delta_{1/m^2} + \cdots\right] \\ &\left[1 - 8\rho^2_{\rm A1}z + (53\rho^2_{\rm A1} - 15)z^2 - (231\rho^2_{\rm A1} - 91)z^3\right] \end{aligned} \quad (6)$$

with $z = (\sqrt{w+1} - \sqrt{2})/(\sqrt{w+1} + \sqrt{2})$ originating from a conformal transformation. The parameter $\rho^2_{\rm A1}$ is the slope of the form factor at $w = 1$. The factor $\eta_{\rm A}$ is the QCD short-distance radiative correction [11] to the form factor

$$\eta_{\rm A} = 0.960 \pm 0.007, \quad (7)$$

and δ_{1/m^2} comes from non-perturbative $1/m^2$ corrections.

Precise lattice determinations of the $B \to D^{(*)}$ form factors naturally build in heavy-quark symmetries, so all uncertainties scale with the deviation of the form factor from unity. Unquenched calculations, i.e. calculations with realistic sea quarks, obtain quite precise predictions of the form factors; the relevant calculations for the form factor $\mathcal{F}(\omega)$ in Refs. [12,13] quote a total uncertainty at the 2% level. The main contributions to this uncertainty are from the chiral extrapolation from

the light quark masses used in the numerical lattice computation to realistic up and down quark masses, and from discretization errors. These sources of uncertainty will be reduced with larger lattice sizes and smaller lattice spacings.

Including effects from finite quark masses to calculate the deviation of $\mathcal{F}(1)$ from unity, the current lattice prediction is

$$\mathcal{F}(1) = 0.902 \pm 0.017, \quad (8)$$

where the factor $\eta_{\rm ew}$ has been divided out from the value quoted in Ref. 14 and the errors have been added in quadrature. The leading uncertainties are due to heavy-quark discretization and chiral extrapolation errors.

Non-lattice estimates based on sum rules for the form factor tend to yield lower values for $\mathcal{F}(1)$ [15,16,17]. Omitting the contributions from excited states, the sum rules indicate that $\mathcal{F}(1) < 0.93$. Including an estimate for the contribution of the excited states yields $\mathcal{F}(1) = 0.86 \pm 0.01 \pm 0.02$ [17,18] where the second uncertainty originates from the estimate for the excited states.

Many experiments [19–27] have measured the differential rate as a function of w. These measurements are input to a four-dimensional fit [28] for $\mathcal{F}(1)|V_{cb}|$, $\rho^2_{A_1}$ and the form factor ratios $R_1 \propto A_2/A_1$ and $R_2 \propto V/A_1$. The leading sources of uncertainty on $\mathcal{F}(1)\,|V_{cb}|$ are due to detection efficiencies and $D^{(*)}$ decay branching fractions, while for $\rho^2_{A_1}$ the uncertainties in R_1 and R_2 still dominate. Recent BABAR measurements, one using $\overline{B}^0 \to D^{*0}\ell\overline{\nu}_\ell$ decays [25] and the other using a global fit to $\overline{B} \to D\ell\overline{\nu}_\ell X$ decays [26] are completely insensitive to uncertainties related to the reconstruction of the charged pion from $D^* \to D\pi$ decays; both measurements agree with the average given below.

The fit gives [29] $\eta_{\rm ew}\mathcal{F}(1)\,|V_{cb}| = (35.85 \pm 0.45) \times 10^{-3}$ with a p-value of 0.15. Along with the lattice value given above for $\mathcal{F}(1)$ this yields

$$|V_{cb}| = (39.48 \pm 0.50_{\rm exp} \pm 0.74_{\rm theo}) \times 10^{-3}\ (\overline{B} \to D^*\ell\overline{\nu}_\ell,\ \text{LQCD}). \quad (9)$$

The value of $\mathcal{F}(1)$ obtained from QCD sum rules results in a larger value for $|V_{cb}|$:

$$|V_{cb}| = (41.4 \pm 0.5_{\rm exp} \pm 1.0_{\rm theo}) \times 10^{-3}\ (\overline{B} \to D^*\ell\overline{\nu}_\ell,\ \text{SR}). \quad (10)$$

$\overline{B} \to D\ell\overline{\nu}_\ell$

The differential rate for $\overline{B} \to D\ell\overline{\nu}_\ell$ is given by

$$\frac{d\Gamma}{dw}(\overline{B} \to D\ell\overline{\nu}_\ell) = \frac{G_F^2}{48\pi^3}|V_{cb}|^2(m_B + m_D)^2 m_D^3 (w^2-1)^{3/2}(\eta_{\rm ew}\mathcal{G}(w))^2. \quad (11)$$

The form factor is

$$\mathcal{G}(w) = h_+(w) - \frac{m_B - m_D}{m_B + m_D} h_-(w), \quad (12)$$

where h_+ is normalized to unity in the infinite-mass limit due to HQS and h_- vanishes in the heavy-mass limit. Thus

$$\mathcal{G}(1) = 1 + \mathcal{O}\left(\frac{m_B - m_D}{m_B + m_D}\frac{\Lambda_{\rm QCD}}{m_c}\right) \quad (13)$$

and the corrections to the HQET predictions are parametrically larger than was the case for $\overline{B} \to D^*\ell\overline{\nu}_\ell$.

In order to get a more precise prediction for the form factor $\mathcal{G}(1)$ the heavy-quark expansion can be supplemented by additional assumptions. It has been argued in Ref. 30 that in a limit in which the kinetic energy μ_π^2 is equal to the chromomagnetic moment μ_G^2 (these quantities are discussed below in more detail) one may obtain the value

$$\mathcal{G}(1) = 1.04 \pm 0.01_{\rm power} \pm 0.01_{\rm pert}. \quad (14)$$

Lattice calculations including effects beyond the heavy mass limit have become available, and hence the fact that deviations from the HQET predictions are parametrically larger than in the case $\overline{B} \to D^*\ell\overline{\nu}_\ell$ is irrelevant. These unquenched calculations quote a value (preliminary, from 2005) [31]

$$\mathcal{G}(1) = 1.074 \pm 0.018 \pm 0.016. \quad (15)$$

Recent, yet unpublished results indicate that the updated lattice value for $\mathcal{G}(1)$ will become slightly smaller, making it better compatible with Eq. (14).

Recent measurements of $\overline{B} \to D\ell\overline{\nu}_\ell$ [26,32] are consistent with earlier measurements [19,33,34] but are significantly more precise. The average of these inputs [29] gives $\eta_{\rm ew}\mathcal{G}(1)|V_{cb}| = (42.5 \pm 1.6) \times 10^{-3}$. Using the value from Eq. (15) for $\mathcal{G}(1)$, accounting for the electroweak correction and conservatively adding the theory uncertainties linearly gives

$$|V_{cb}| = (39.3 \pm 1.4 \pm 1.3) \times 10^{-3}\quad (\overline{B} \to D\ell\overline{\nu}_\ell,\ \text{LQCD}), \quad (16)$$

where the first uncertainty is from experiment and the second from theory.

Using the non-lattice estimate from Eq. (14) one finds $|V_{cb}| = (40.6 \pm 1.5 \pm 0.8) \times 10^{-3}$.

Measuring the differential rate at $w = 1$ is more difficult in $\overline{B} \to D\ell\overline{\nu}_\ell$ decays than in $\overline{B} \to D^*\ell\overline{\nu}_\ell$ decays, since the rate is smaller and the background from mis-reconstructed $\overline{B} \to D^*\ell\overline{\nu}_\ell$ decays is significant; this is reflected in the larger experimental uncertainty. The B factories study decays recoiling against fully reconstructed B mesons or perform a global fit to $\bar{B} \to D(X)\ell\nu$ decays. Theoretical input on the shape of the w spectrum in $\overline{B} \to D\ell\overline{\nu}_\ell$ is valuable, as precise measurements of the total rate are easier; recent measurements [26,32] of $\mathcal{B}(\overline{B} \to D\ell\overline{\nu}_\ell)$ have uncertainties of $\sim 5\%$.

The determinations from $\overline{B} \to D^*\ell\overline{\nu}_\ell$ and $\overline{B} \to D\ell\overline{\nu}_\ell$ decays are consistent, and their uncertainties are largely uncorrelated. Averaging the two lattice-based results quoted above gives

$$|V_{cb}| = (39.5 \pm 0.8) \times 10^{-3}\quad (\text{exclusive}). \quad (17)$$

$|V_{cb}|$ from inclusive decays

At present the most precise determination of $|V_{cb}|$ comes from inclusive decays. The method is based on a measurement of the total semileptonic decay rate, together with the leptonic energy and the hadronic invariant mass spectra of inclusive

semileptonic decays. The total decay rate can be calculated quite reliably in terms of non-perturbative parameters that can be extracted from the information contained in the spectra.

Inclusive semileptonic rate

The theoretical foundation for the calculation of the total semileptonic rate is the Operator Product Expansion (OPE) which yields the Heavy Quark Expansion (HQE) [35,36]. Details of this can be found in the separate mini-review on Effective Theories. The validity of the OPE is proven in the deep Euclidean region for the momenta (which is satisfied, *e.g.*, in deep inelastic scattering), but its application to heavy-quark decays requires a continuation to time-like momenta $p_B^2 = M_B^2$, where possible contributions that are exponentially damped in the Euclidean region could become oscillatory. The validity of the OPE for inclusive decays is equivalent to the assumption of parton-hadron duality, and any violation of this assumption would imply the presence of terms which do not appear in the $1/m_b$ expansion [37]. However, fits of the HQE predictions to the data show no evidence for such terms and hence for duality violations. Thus duality or, equivalently, the validity of the OPE, is assumed in the analysis.

The OPE result for the total rate can be written schematically (the details of the expression can be found, *e.g.*, in Ref. 38) as

$$\begin{aligned}\Gamma =& |V_{cb}|^2 \hat{\Gamma}_0 m_b^5(\mu)(1+A_{\rm ew})\times \\ & \left[z_0^{(0)}(r) + \frac{\alpha_s(\mu)}{\pi} z_0^{(1)}(r) + \left(\frac{\alpha_s(\mu)}{\pi}\right)^2 z_0^{(2)}(r) + \cdots \right. \\ & + \frac{\mu_\pi^2}{m_b^2}\left(z_2^{(0)}(r) + \frac{\alpha_s(\mu)}{\pi} z_2^{(1)}(r) + \cdots \right) \\ & + \frac{\mu_G^2}{m_b^2}\left(y_2^{(0)}(r) + \frac{\alpha_s(\mu)}{\pi} y_2^{(1)}(r) + \cdots \right) \\ & + \frac{\rho_{\rm D}^3}{m_b^3}\left(z_3^{(0)}(r) + \frac{\alpha_s(\mu)}{\pi} z_3^{(1)}(r) + \cdots \right) \\ & \left. + \frac{\rho_{\rm LS}^3}{m_b^3}\left(y_3^{(0)}(r) + \frac{\alpha_s(\mu)}{\pi} y_3^{(1)}(r) + \cdots \right) + ... \right] \end{aligned} \quad (18)$$

where $\eta_{\rm ew} = 1 + A_{\rm ew}$ denotes the electroweak corrections, r is the ratio m_c/m_b and the y_i and z_i are functions which appear in the perturbative expansion of the different orders of the heavy mass expansion. A similar expansion can be set up for moments of the distributions of charged-lepton energy, hadronic invariant mass and hadronic energy.

This expression is known up to order $1/m_b^5$, where the terms of order $1/m_b^n$ with $n > 2$ have been computed only at tree level [39–42]. The leading term is the parton model, which is known completely to order α_s and α_s^2 [43–45], and the terms of order $\alpha_s^{n+1}\beta_0^n$ (where β_0 is the first coefficient of the QCD β function, $\beta_0 = (33-2n_f)/3$) have been included by the usual BLM procedure [38,46,47]. Furthermore, the corrections of order $\alpha_s\mu_\pi^2/m_b^2$ have been computed [48,49].

Starting at order $1/m_b^3$ contributions with an infrared sensitivity to the charm mass m_c appear [41,50,51]. At order $1/m_b^3$ this "intrinsic charm" contribution is a $\log(m_c)$ in the coefficient of the Darwin term ρ_D^3. At higher orders, terms such as $1/m_b^3 \times 1/m_c^2$ and $\alpha_s(m_c)1/m_b^3 \times 1/m_c$ appear, which are comparable in size to the contributions of order $1/m_b^4$

The HQE parameters are given in terms of forward matrix elements; the parameters entering the expansion for orders up to $1/m_b^3$ are

$$\begin{aligned} \overline{\Lambda} &= M_B - m_b\,, \\ \mu_\pi^2 &= -\langle B|\overline{b}(iD_\perp)^2 b|B\rangle\,, \\ \mu_G^2 &= \langle B|\overline{b}(iD_\perp^\mu)(iD_\perp^\nu)\sigma_{\mu\nu} b|B\rangle\,, \\ \rho_{\rm D}^3 &= \langle B|\overline{b}(iD_{\perp\mu})(ivD)(iD_\perp^\nu) b|B\rangle\,, \\ \rho_{\rm LS}^3 &= \langle B|\overline{b}(iD_\perp^\mu)(ivD)(iD_\perp^\nu)\sigma_{\mu\nu} b|B\rangle. \end{aligned} \quad (19)$$

These parameters still depend on the heavy quark mass. Sometimes the infinite mass limits of these parameters $\overline{\Lambda} \to \overline{\Lambda}_{\rm HQET}$, $\mu_\pi^2 \to -\lambda_1$, $\mu_G^2 \to 3\lambda_2$, $\rho_D^3 \to \rho_1$ and $\rho_{LS}^3 \to 3\rho_2$, are used instead. The hadronic parameters of the orders $1/m_b^4$ and $1/m_b^5$ have been defined and estimated in Ref. 42 while the five hadronic parameters s_i of the order $1/m_b^4$ can be found in Ref. 40; these have not yet been included in the fits.

The rates and the spectra depend strongly on m_b (or equivalently on $\overline{\Lambda}$), This makes the discussion of renormalization issues mandatory, since the size of the QCD corrections is strongly correlated with the definitions used for the quark masses. Using the pole mass definition for the heavy quark masses, it is well known that the corresponding perturbative series of decay rates does not converge very well, making a precision determination of $|V_{cb}|$ in such a scheme impossible.

The solution to this problem is to choose an appropriate "short-distance" mass definition. Frequently used mass definitions are the kinetic scheme [15], or the 1S scheme [52]. Both of these schemes have been applied to semileptonic $b \to c$ transitions, yielding comparable results and uncertainties.

The 1S scheme eliminates the b quark pole mass by relating it to the perturbative expression for the mass of the 1S state of the Υ system. The physical mass of the $\Upsilon(1S)$ contains non-perturbative contributions, which have been estimated in Ref. 53. These non-perturbative contributions are small; nevertheless, the best determination of the b quark mass in the 1S scheme is obtained from sum rules for $e^+e^- \to b\bar{b}$ [54].

Alternatively one may use a short-distance mass definition such as the $\overline{\rm MS}$ mass $m_b^{\overline{\rm MS}}(m_b)$. However, it has been argued that the scale m_b is unnaturally high for B decays, while for smaller scales $\mu \sim 1\,{\rm GeV}$ $m_b^{\overline{\rm MS}}(\mu)$ is under poor control. For this reason the so-called "kinetic mass" $m_b^{\rm kin}(\mu)$, has been proposed. It is the mass entering the non-relativistic expression for the kinetic energy of a heavy quark, and is defined using heavy-quark sum rules [15].

Determination of HQE Parameters and $|V_{cb}|$

Several experiments have measured moments in $\overline{B} \to X_c\ell\overline{\nu}_\ell$ decays [55–63] as a function of the minimum lepton momentum. The measurements of the moments of the electron energy spectrum ($0^{\rm th}$-$3^{\rm rd}$) and of the squared hadronic mass spectrum ($0^{\rm th}$-$2^{\rm nd}$) have statistical uncertainties that are roughly equal to

their systematic uncertainties. The sets of moments measured by each experiment have strong correlations; the full statistical and systematic correlation matrices are required to allow these to be used in a global fit. Measurements of photon energy moments ($0^{\rm th}$-$2^{\rm nd}$) in $B \to X_s\gamma$ decays [64–68] as a function of the minimum accepted photon energy are still primarily statistics limited.

Global fits to the full set of moments [63,65,69–72] have been performed in the 1S and kinetic schemes. The semileptonic moments alone determine a linear combination of m_b and m_c very accurately but leave the orthogonal combination poorly determined [73]; additional input is required to allow a precise determination of m_b. This additional information can come from the radiative $B \to X_s\gamma$ moments, which provide complementary information on m_b and μ_π^2, or from precise determinations of the charm quark mass [74,75]. The values obtained in the kinetic scheme fits [71] with these two constraints are consistent. Based on the charm quark mass constraint [76], $m_c^{\overline{\rm MS}}(3\,{\rm GeV}) = 0.986 \pm 0.013\,{\rm GeV}$, a recent analysis [77] obtains

$$|V_{cb}| = (42.42 \pm 0.86) \times 10^{-3} \quad (20)$$
$$m_b^{\rm kin} = 4.541 \pm 0.023\,{\rm GeV} \quad (21)$$
$$\mu_\pi^2({\rm kin}) = 0.414 \pm 0.078\,{\rm GeV}^2, \quad (22)$$

where the error on $|V_{cb}|$ includes experimental and theoretical uncertainties.

Theoretical uncertainties are estimated and included in performing the fits. Similar values for the parameters are obtained with a variety of assumptions about the theoretical uncertainties and their correlations. The χ^2/dof is substantially below unity in all fits, suggesting that the theoretical uncertainties may be overestimated. While one could obtain a satisfactory fit with smaller uncertainties, this would make the use of the extracted values for the HQE parameters in other processes unsafe. In any case, the low χ^2 shows no evidence for duality violations at a significant level. The mass in the $\overline{\rm MS}$ scheme corresponding to Eq. (21) is $m_b^{\overline{\rm MS}} = 4.17 \pm 0.04\,{\rm GeV}$, which can be compared with a recent value obtained using relativistic sum rules [76], $m_b^{\overline{\rm MS}} = 4.163 \pm 0.016\,{\rm GeV}$, and provides a non-trivial cross-check.

A fit in the 1S scheme [72] to the measured moments gives

$$|V_{cb}| = (41.96 \pm 0.45 \pm 0.07) \times 10^{-3} \quad (23)$$
$$m_b^{\rm 1S} = 4.691 \pm 0.037\,{\rm GeV} \quad (24)$$
$$\lambda_1({\rm 1S}) = -0.362 \pm 0.067\,{\rm GeV}^2, \quad (25)$$

where the last error on $|V_{cb}|$ is due to the uncertainties in the B meson lifetimes. This fit uses semileptonic and radiative moments and constrains the chromomagnetic operator using the mass difference between the pseudoscalar and vector mesons (for both B abd D); however, the fit does not include the constraint on m_c nor the full NNLO corrections.

The fits in the two renormalization schemes give consistent results for $|V_{cb}|$ and, after translation to a common renormalization scheme, for m_b and μ_π^2. We take the arithmetic average of the $|V_{cb}|$ values and of the quoted uncertainties to find

$$|V_{cb}| = (42.2 \pm 0.7) \times 10^{-3}\ ({\rm inclusive}). \quad (26)$$

The precision of the global fit results can be further improved by calculating higher order perturbative corrections to the coefficients of the HQE parameters, in particular the still missing $\alpha_s\mu_G^2$ corrections, which are presently only known for $B \to X_s\gamma$ [78]. The inclusion of still higher order moments may improve the sensitivity of the fits to higher order terms in the HQE.

Determination of $|V_{ub}|$

Summary: The determination of $|V_{ub}|$ is the focus of significant experimental and theoretical work. The determinations based on inclusive semileptonic decays using different calculational ansätze are consistent. The largest parametric uncertainty comes from the error on m_b. The best determinations of $|V_{ub}|$ from $\overline{B} \to \pi\ell\overline{\nu}_\ell$ decays come from combined fits to theory and experimental data as a function of q^2; the precision is limited by the form factor normalization.

The values obtained from inclusive and exclusive determinations are

$$|V_{ub}| = (4.41 \pm 0.15\ ^{+\ 0.15}_{-\ 0.17}) \times 10^{-3} \quad ({\rm inclusive}), \quad (27)$$
$$|V_{ub}| = (3.28 \pm 0.29) \times 10^{-3} \quad ({\rm exclusive}). \quad (28)$$

The two determinations are independent, and the dominant uncertainties are on multiplicative factors. Given the marginal agreement between the inclusive and exclusive values their combination should be treated with caution. To combine these values, the inclusive and exclusive values are weighted by their relative errors and the uncertainties are treated as normally distributed. The resulting average has $p(\chi^2) = 0.01$, so we scale the error by $\sqrt{\chi^2/1} = 2.7$ to find

$$|V_{ub}| = (4.13 \pm 0.49) \times 10^{-3}. \quad (29)$$

Given the poor consistency between the two determinations, this average should be treated with caution.

$|V_{ub}|$ from inclusive decays

The theoretical description of inclusive $\overline{B} \to X_u\ell\overline{\nu}_\ell$ decays is based on the Heavy Quark Expansion, as for $\overline{B} \to X_c\ell\overline{\nu}_\ell$ decays, and leads to a predicted total decay rate with uncertainties below 5% [79,80]. Unfortunately, the total decay rate is hard to measure due to the large background from CKM-favored $\overline{B} \to X_c\ell\overline{\nu}_\ell$ transitions. Technically, the calculation of the partial decay rate in regions of phase space where $\overline{B} \to X_c\ell\overline{\nu}_\ell$ decays are suppressed requires the introduction of a non-perturbative distribution function, the "shape function" (SF) [81,82], whose form is unknown. The shape function becomes important when the light-cone momentum component $P_+ \equiv E_X - |P_X|$ is not large compared to Λ_{QCD}. This additional difficulty can be

addressed in two complementary ways. The leading shape function can either be measured in the radiative decay $\overline{B} \to X_s\gamma$, or be modeled with constraints on the 0^{th}-2^{nd} moments, and the results applied to the calculation of the $\overline{B} \to X_u\ell\overline{\nu}_\ell$ partial decay rate [83–85]; in such an approach the largest challenges are for the theory. Alternatively, measurements of $\overline{B} \to X_u\ell\overline{\nu}_\ell$ partial decay rates can be extended further into the $\overline{B} \to X_c\ell\overline{\nu}_\ell$-allowed region, enabling a simplified theoretical (pure HQE) treatment [86] but requiring precise experimental knowledge of the $\overline{B} \to X_c\ell\overline{\nu}_\ell$ background.

At leading order a single shape function appears, which is universal for all heavy-to-light transitions [81,82], and thus it can be measured in $\overline{B} \to X_s\gamma$ decays. However, at sub-leading order in $1/m_b$ several shape functions appear [87] rendering a simple comparison of semileptonic and radiative B decays impossible.

The form of the SFs cannot be calculated from first principles. Prescriptions that relate directly the partial rates for $\overline{B} \to X_s\gamma$ and $\overline{B} \to X_u\ell\overline{\nu}_\ell$ decays are available [88–91]; however, this approach is limited to the leading order in $1/m_b$.

Existing approaches have tended to use parameterizations of the leading SF that respect constraints on the zeroth, first and second moments, which are given in terms of the HQE parameters $\overline{\Lambda} = M_B - m_b$ and μ_π^2, respectively. The relations between SF moments and the HQE parameters are known to second order in α_s [92]. As a result, measurements of HQE parameters from global fits to $\overline{B} \to X_c\ell\overline{\nu}_\ell$ and $\overline{B} \to X_s\gamma$ moments can be used to constrain the SF moments, as well as provide accurate values of m_b and other parameters for use in determining $|V_{ub}|$.

A recent development is to use appropriate basis functions to approximate the shape function, thereby also including the known short-distance contributions as well as the renormalization properties of the SF [93], in order to allow a global fit of all inclusive B meson decay data.

The calculations that are used for the fits performed by HFAG are documented in Refs. [83] (BLNP), [94] (GGOU), [95] (DGE) and [86] (BLL).

The triple diffential rate in the variables

$$P_l = M_B - 2E_l, \quad P_- = E_X + |\vec{P}_X|, \quad P_+ = E_X - |\vec{P}_X| \quad (30)$$

is

$$\frac{d^3\Gamma}{dP_+\,dP_-\,dP_l} = \frac{G_F^2|V_{ub}|^2}{16\pi^2}(M_B - P_+) \quad (31)$$
$$\Big\{(P_- - P_l)(M_B - P_- + P_l - P_+)\mathcal{F}_1$$
$$+(M_B - P_-)(P_- - P_+)\mathcal{F}_2 + (P_- - P_l)(P_l - P_+)\mathcal{F}_3\Big\}.$$

The "structure functions" $\mathcal{F}_i$ can be calculated using factorization theorems that have been proven to subleading order in the $1/m_b$ expansion.

The BLNP [83] calculation uses these factorization theorems to write the $\mathcal{F}_i$ in terms of perturbatively calculable hard coefficients H and jet functions J, which are convolved with the (soft) light-cone distribution functions S, the shape functions of the B meson. The partial calculation of the $\mathcal{O}(\alpha_S^2)$ contributions in Ref. 96 has recently been completed [97]. However, the full calculation is not yet included in the fit.

The leading order term in the $1/m_b$ expansion of the $\mathcal{F}_i$ contains a single non-perturbative function and is calculated to subleading order in α_s, while at subleading order in the $1/m_b$ expansion there are several independent non-perturbative functions which have been calculated only at tree level in the α_s expansion.

To extract the non-perturbative input one can study the photon energy spectrum in $B \to X_s\gamma$ [85]. This spectrum is known to a similar accuracy as the P_+ spectrum in $B \to X_u\ell\overline{\nu}_\ell$. Going to subleading order in the $1/m_b$ expansion requires the modeling of subleading SFs, a large variety of which were studied in Ref. 83.

A distinct approach (GGOU) [94] uses a hard, Wilsonian cut-off that matches the definition of the kinetic mass. The non-perturbative input is similar to what is used in BLNP, but the shape functions are defined differently. In particular, they are defined at finite m_b and depend on the light-cone component k_+ of the b quark momentum and on the momentum transfer q^2 to the leptons. These functions include sub-leading effects to all orders; as a result they are non-universal, with one shape function corresponding to each structure function in Eq. (31). Their k_+ moments can be computed in the OPE and related to observables and to the shape functions defined in Ref. 83.

Going to subleading order in α_s requires the definition of a renormalization scheme for the HQE parameters and for the SF. It has been noted that the relation between the moments of the SF and the forward matrix elements of local operators is plagued by ultraviolet problems which require additional renormalization. A possible scheme for improving this behavior has been suggested in Refs. [83,85], which introduce a particular definition of the quark mass (the so-called shape function scheme) based on the first moment of the measured spectrum. Likewise, the HQE parameters can be defined from measured moments of spectra, corresponding to moments of the SF.

One can also attempt to calculate the SF by using additional assumptions. One possible approach (DGE) is the so-called "dressed gluon exponentiation" [95], where the perturbative result is continued into the infrared regime using the renormalon structure obtained in the large β_0 limit, where β_0 has been defined following Eq. (18).

While attempts to quantify the SF are important, the impact of uncertainties in the SF is significantly reduced in some recent measurements that cover a larger portion of the $\overline{B} \to X_u\ell\overline{\nu}_\ell$ phase space. Several measurements using a combination of cuts on the leptonic momentum transfer q^2 and the hadronic invariant mass m_X as suggested in Ref. 98 have been made. Measurements of the electron spectrum in $\overline{B} \to X_u\ell\overline{\nu}_\ell$ decays have been made down to momenta of 1.9 GeV, where SF

uncertainties are not dominant; however, determining $\overline{B} \to X_u \ell \overline{\nu}_\ell$ partial rates in charm-dominated regions can bring in a strong dependence on the modeling of the $\overline{B} \to X_u \ell \overline{\nu}_\ell$ spectrum, which is problematic. The measurements quoted below have used a variety of functional forms to parameterize the leading SF; in no case does this lead to more than a 2% uncertainty on $|V_{ub}|$.

Weak Annihilation [99,100,94] (WA) can in principle contribute significantly in the high-q^2 region accepted by measurements of $\overline{B} \to X_u \ell \overline{\nu}_\ell$ decays. Estimates based on semileptonic D_s decays [100,51,86] lead to a $\sim 2\%$ uncertainty on the total $\overline{B} \to X_u \ell \overline{\nu}_\ell$ rate from the $\Upsilon(4S)$. The q^2 spectrum of the WA contribution is not well known, but from the OPE it is expected to contribute predominantly at high q^2. More recent investigations [51,101,102] indicate that WA is a small effect, but may become a significant source of uncertainty for $|V_{ub}|$ measurements that only accept a small fraction of the full $\overline{B} \to X_u \ell \overline{\nu}_\ell$ phase space. Model-dependent limits on WA were determined in Ref. 103, where the CLEO data were fitted to combinations of WA models and a spectator $\overline{B} \to X_u \ell \overline{\nu}_\ell$ component and background. More direct experimental constraints [104] on WA have been made by comparing the $\overline{B} \to X_u \ell \overline{\nu}_\ell$ decay rates of charged and neutral B mesons, although these constraints are not sensitive to the isoscalar contribution to WA.

Measurements

We summarize the measurements used in the determination of $|V_{ub}|$ below. Given the improved precision and more rigorous theoretical interpretation of the recent measurements, earlier determinations [105–108] will not be further considered in this review.

Inclusive electron momentum measurements [109–111] reconstruct a single charged electron to determine a partial decay rate for $\overline{B} \to X_u \ell \overline{\nu}_\ell$ near the kinematic endpoint. This results in a high $\mathcal{O}(50\%)$ selection efficiency and only modest sensitivity to the modeling of detector response. The decay rate can be cleanly extracted for $E_e > 2.3\,\text{GeV}$, but this is deep in the SF region, where theoretical uncertainties are large. Measurements down to 2.0 or 1.9 GeV have a low ($< 1/10$) signal-to-background (S/B) ratio. The inclusive electron momentum spectrum from $B\overline{B}$ events, after subtraction of the $e^+e^- \to q\overline{q}$ continuum background, is fitted to a model $\overline{B} \to X_u \ell \overline{\nu}_\ell$ spectrum and several components ($D\ell\overline{\nu}_\ell$, $D^*\ell\overline{\nu}_\ell$, ...) of the $\overline{B} \to X_c \ell \overline{\nu}_\ell$ background; the dominant uncertainties are related to this subtraction and modelling. The resulting $|V_{ub}|$ values for various E_e cuts are given in Table 1.

An untagged "neutrino reconstruction" measurement [112] from BABAR uses a combination [113] of a high-energy electron with a measurement of the missing momentum vector. This allows a much higher S/B~ 0.7 at the same E_e cut and a $\mathcal{O}(5\%)$ selection efficiency, but at the cost of a smaller accepted phase space for $\overline{B} \to X_u \ell \overline{\nu}_\ell$ decays and uncertainties associated with the determination of the missing momentum. The corresponding values for $|V_{ub}|$ are given in Table 1.

The large samples accumulated at the B factories allow studies in which one B meson is fully reconstructed and the recoiling B decays semileptonically [114–118]. The experiments can fully reconstruct a "tag" B candidate in about 0.5% (0.3%) of B^+B^- ($B^0\overline{B}^0$) events. An electron or muon with center-of-mass momentum above 1.0 GeV is required amongst the charged tracks not assigned to the tag B and the remaining particles are assigned to the X_u system. The full set of kinematic properties (E_ℓ, m_X, q^2, *etc.*) are available for studying the semileptonically decaying B, making possible selections that accept up to 90% of the full $\overline{B} \to X_u \ell \overline{\nu}_\ell$ rate. Despite requirements (e.g. on the square of the missing mass) aimed at rejecting events with additional missing particles, undetected or mis-measured particles from $\overline{B} \to X_c \ell \overline{\nu}_\ell$ decay (e.g., K_L^0 and additional neutrinos) remain an important source of uncertainty. Measurements with the largest kinematic acceptance (i.e. $E_\ell > 1\,\text{GeV}$) lead to the smallest theoretical and overall uncertainties on $|V_{ub}|$.

BABAR [114] and BELLE [115,116] have measured partial rates with cuts on m_X, m_X and q^2, P_+ and E_ℓ based on large samples of $B\overline{B}$ events; the corresponding $|V_{ub}|$ values are given in Table 1. In each case the experimental systematics have significant contributions from the modeling of $\overline{B} \to X_u \ell \overline{\nu}_\ell$ and $\overline{B} \to X_c \ell \overline{\nu}_\ell$ decays and from the detector response to charged particles, photons and neutral hadrons.

Determination of $|V_{ub}|$

The determination of $|V_{ub}|$ from the measured partial rates requires input from theory. The BLNP, GGOU and DGE calculations described previously are used to determine $|V_{ub}|$ from all measured partial $\overline{B} \to X_u \ell \overline{\nu}_\ell$ rates; the values [28] are given in Table 1. The HFAG averages quoted here are based on the following m_b values: $m_b^{SF} = 4.588 \pm 0.025$ GeV for BLNP, $m_b^{\rm kin} = 4.560 \pm 0.023$ GeV for GGOU, and $m_b^{\overline{MS}} = 4.194 \pm 0.043$ GeV for DGE. The $m_b^{\rm kin}$ value is determined in a global fit to moments in the kinetic scheme; this value is translated into m_b^{SF} and $m_b^{\overline{MS}}$ at fixed order in α_s. These input values are based on an earlier determination of $m_b^{\rm kin}$ than is quoted in equation Eq. (21); using the latest value would increase the $|V_{ub}|$ averages by 1-2%.

As an illustration of the relative sizes of the uncertainties entering $|V_{ub}|$ we give the error breakdown for the GGOU average: statistical—2.0%; experimental—1.7%; $\overline{B} \to X_c \ell \overline{\nu}_\ell$ modeling—1.3%; $\overline{B} \to X_u \ell \overline{\nu}_\ell$ modeling—1.9%; HQE parameters —1.9%; higher-order corrections—1.4%; q^2 modeling—1.3%; Weak Annihilation—$^{+0}_{-1.9}$%; SF form—0.2%. The uncertainty on m_b dominates the uncertainty on $|V_{ub}|$ from HQE parameters, but no longer dominates the overall uncertainty.

The correlations amongst the multiple BABAR recoil-based measurements [114] are fully accounted for in the average. The statistical correlations amongst the other measurements used in the average are tiny (due to small overlaps among signal events and large differences in S/B ratios) and have been ignored. Correlated systematic and theoretical errors are taken into account, both within an experiment and between experiments.

Table 1: $|V_{ub}|$ (in units of 10^{-5}) from inclusive $\overline{B} \to X_u \ell \overline{\nu}_\ell$ measurements. The first uncertainty on $|V_{ub}|$ is experimental, while the second includes both theoretical and HQE parameter uncertainties. The values are listed in order of increasing f_u (0.19 to 0.90); those below the horizontal bar are based on recoil methods.

Ref.	cut	BLNP	GGOU	DGE
[109]	$E_e > 2.1$	$419 \pm 49 \,^{+\,26}_{-\,34}$	$393 \pm 46 \,^{+\,22}_{-\,29}$	$382 \pm 45 \,^{+\,23}_{-\,26}$
[112]	E_e-q^2	$466 \pm 31 \,^{+\,31}_{-\,36}$	not available	$432 \pm 29 \,^{+\,24}_{-\,29}$
[111]	$E_e > 2.0$	$448 \pm 25 \,^{+\,27}_{-\,28}$	$429 \pm 24 \,^{+\,18}_{-\,24}$	$428 \pm 24 \,^{+\,22}_{-\,24}$
[110]	$E_e > 1.9$	$488 \pm 45 \,^{+\,24}_{-\,27}$	$475 \pm 44 \,^{+\,17}_{-\,22}$	$479 \pm 44 \,^{+\,21}_{-\,24}$
[114]	m_X-q^2	$425 \pm 23 \,^{+\,23}_{-\,25}$	$417 \pm 22 \,^{+\,22}_{-\,25}$	$419 \pm 22 \,^{+\,18}_{-\,19}$
[114]	P_+	$402 \pm 25 \,^{+\,24}_{-\,23}$	$375 \pm 23 \,^{+\,30}_{-\,32}$	$410 \pm 25 \,^{+\,37}_{-\,28}$
[114]	m_X	$397 \pm 22 \,^{+\,20}_{-\,20}$	$394 \pm 22 \,^{+\,16}_{-\,17}$	$416 \pm 23 \,^{+\,26}_{-\,22}$
[114]	$E_e > 1$	$428 \pm 24 \,^{+\,18}_{-\,20}$	$435 \pm 24 \,^{+\,09}_{-\,10}$	$440 \pm 24 \,^{+\,12}_{-\,13}$
[116]	$E_e > 1$	$447 \pm 27 \,^{+\,19}_{-\,21}$	$454 \pm 27 \,^{+\,10}_{-\,11}$	$460 \pm 27 \,^{+\,11}_{-\,13}$
		$440 \pm 15 \,^{+\,19}_{-\,21}$	$439 \pm 15 \,^{+\,12}_{-\,14}$	$445 \pm 15 \,^{+\,15}_{-\,16}$

The theoretical calculations produce very similar results for $|V_{ub}|$; the standard deviation of the theory predictions for the endpoint rate is 4.6%, for the m_X-q^2 rate is 2.2%, and for the $E_e > 1\,\mathrm{GeV}$ rate is 0.8%. The $|V_{ub}|$ values do not show a marked trend versus the kinematic acceptance, f_u, for $\overline{B} \to X_u \ell \overline{\nu}_\ell$ decays. The p-values of the averages are in the range 34-44%, indicating that the ratios of calculated partial widths in the different phase space regions are in good agreement with ratios of measured partial branching fractions.

All calculations yield compatible $|V_{ub}|$ values and similar error estimates. We take the arithmetic mean of the values and errors to find

$$|V_{ub}| = (4.41 \pm 0.15_{\rm exp}\,{}^{+0.15}_{-0.17\,\rm theo}) \times 10^{-3} \quad \text{(inclusive)}. \qquad (32)$$

Hadronization uncertainties also impact the $|V_{ub}|$ determination. The theoretical expressions are valid at the parton level and do not incorporate any resonant structure (*e.g.* $\overline{B} \to \pi \ell \overline{\nu}_\ell$); this must be added to the simulated $\overline{B} \to X_u \ell \overline{\nu}_\ell$ event samples, since the detailed final state multiplicity and structure impacts the estimates of experimental acceptance and efficiency. The experiments have adopted procedures to input resonant structure while preserving the appropriate behavior in the kinematic variables (q^2, E_ℓ, m_X) averaged over the sample, but these prescriptions are not unique. The resulting uncertainties have been estimated to be $\sim$ 1-2% on $|V_{ub}|$.

A separate class of analyses follows the strategy discussed in Refs. [88–91], where integrals of differential distributions in $\overline{B} \to X_u \ell \overline{\nu}_\ell$ decays are compared with corresponding integrals in $\overline{B} \to X_s \gamma$ decays to extract $|V_{ub}|$, thereby eliminating the need to model the leading shape function. A study [117] using the measured BABAR electron spectrum in $\overline{B} \to X_u \ell \overline{\nu}_\ell$ decays provides $|V_{ub}|$ determinations using all available "SF-free" calculations; the resulting $|V_{ub}|$ values have total uncertainties of $\sim 12\%$ and are compatible with the average quoted above.

The BLL [98] calculation can be used for measurements [115,118,119] with cuts on m_X and q^2. Using the same HQE parameter input as above yields a $|V_{ub}|$ value of $(4.62 \pm 0.20 \pm 0.29) \times 10^{-3}$, which is about 7% higher than the values obtained from the calculations used in Table 1 for these same measurements.

Status and outlook

At present, as indicated by the average given above, the uncertainty on $|V_{ub}|$ from inclusive decays is at the 5% level. The uncertainty on m_b was discussed in detail above. The uncertainties quoted in the calculations due to matching scales, higher order corrections, etc., are at the few percent level on $|V_{ub}|$. While these uncertainties are inherently difficult to quantify, the calculations take different approaches and yet yield similar estimates. The recent calculation of the full NNLO contributions in Ref. 97 indicates, that the NNLO terms are indeed dominated by the contributions of the order $\alpha_s^2\beta_0$, which are included in both the GGOU and DGE fits. To this end, the sizeable shift of V_{ub} in the BLNP approach induced by including the partial $\mathcal{O}(\alpha_s^2)$ corrections computed in [96] seems to be an artifact.

Experimental uncertainties have been assessed independently by BaBar and Belle. An important common source of uncertainty comes from the modelling of hadronization in inclusive $\overline{B} \to X_u \ell \overline{\nu}_\ell$ decays. Better measurements of these exclusive decays, as in Ref. 120, are helpful in this regard, as would improved knowledge of the main $\overline{B} \to X_c \ell \overline{\nu}_\ell$ decays.

$|V_{ub}|$ from exclusive decays

Exclusive charmless semileptonic decays offer a complementary means of determining $|V_{ub}|$. For the experiments, the specification of the final state provides better background rejection, but the lower branching fraction reflects itself in lower yields compared with inclusive decays. For theory, the calculation of the form factors for $\overline{B} \to X_u \ell \overline{\nu}_\ell$ decays is challenging, but brings in a different set of uncertainties from those encountered in inclusive decays. In this review we focus on $\overline{B} \to \pi \ell \overline{\nu}_\ell$, as it is the most promising mode for both experiment and theory, and recent improvements have been made in both areas. Measurements of other exclusive states can be found in Refs. [121–127].

$\overline{B} \to \pi \ell \overline{\nu}_\ell$ form factor calculations

The relevant form factors for the decay $\overline{B} \to \pi \ell \overline{\nu}_\ell$ are usually defined as

$$\langle \pi(p_\pi) | V^\mu | B(p_B) \rangle = \qquad (33)$$
$$f_+(q^2) \left[p_B^\mu + p_\pi^\mu - \frac{m_B^2 - m_\pi^2}{q^2} q^\mu \right] + f_0(q^2) \frac{m_B^2 - m_\pi^2}{q^2} q^\mu$$

in terms of which the rate becomes (in the limit $m_\ell \to 0$)

$$\frac{d\Gamma}{dq^2} = \frac{G_F^2 |V_{ub}|^2}{24\pi^3} |p_\pi|^3 |f_+(q^2)|^2, \qquad (34)$$

where p_π is the pion momentum in the B meson rest frame.

Currently available non-perturbative methods for the calculation of the form factors include lattice QCD (LQCD) and light-cone sum rules (LCSR). The two methods are complementary in phase space, since the lattice calculation is restricted to the kinematical range of high momentum transfer q^2 to the leptons, while light-cone sum rules provide information near $q^2 = 0$. Interpolations between these two regions can be constrained by unitarity and analyticity.

Unquenched simulations, i.e. where quark loop effects are fully incorporated, have become quite common, and the commonly used results based on these simulations for the $\overline{B} \to \pi\ell\overline{\nu}_\ell$ form factors have been obtained by the Fermilab/MILC collaboration [128] and the HPQCD collaboration [129]. The two calculations differ in the way the b quark is simulated, with HPQCD using nonrelativistic QCD and Fermilab/MILC the so-called Fermilab heavy-quark method; they agree within the quoted errors.

The extrapolation to small values of q^2 can be performed by using analyticity and unitarity bounds. Making use of the heavy-quark limit, stringent constraints on the shape of the form factor can be derived [130], and the conformal mapping of the kinematical variables onto the complex unit disc yields a rapidly converging series in the variable

$$z = \frac{\sqrt{t_+ - t_-} - \sqrt{t_+ - q^2}}{\sqrt{t_+ - t_-} + \sqrt{t_+ - q^2}}$$

where $t_\pm = (M_B \pm m_\pi)^2$. The use of lattice data in combination with a data point at small q^2 from SCET or sum rules provides a stringent constraint on the shape of the form factor [131]. The form factor parametrization given in Ref. 131 has been applied to the extraction of $|V_{ub}|$ from $B \to \pi\ell\bar{\nu}_\ell$ using lattice data in Ref. 128.

Much work remains to be done, since the current combined statistical plus systematic errors in the lattice results are still at the $\sim 10\%$ level on $|V_{ub}|$ and need to be reduced. Reduction of errors to the $\sim$ 5-6% level for $|V_{ub}|$ will be feasible within the next few years, with the inclusion of numerical data at lighter pion masses and finer lattice spacings, as well as possibly two-loop or nonperturbative matching between lattice and continuum heavy-to-light current operators.

Another established non-perturbative approach to obtain the form factors is through Light-Cone QCD Sum Rules (LCSR), where the heavy mass limit has been discussed from the point of view of SCET in Ref. 132. The sum-rule approach provides an approximation for the product $f_B f_+(q^2)$, valid in the region $0 < q^2 <\sim 12$ GeV^2. The determination of $f_+(q^2)$ itself requires knowledge of the decay constant f_B, which usually is obtained by replacing f_B by its two-point QCD (SVZ) sum rule [133] in terms of perturbative and condensate contributions. The advantage of this procedure is the approximate cancellation of various theoretical uncertainties in the ratio $(f_B f_+)/(f_B)$. The LCSR for $f_B f_+$ is based on the light-cone OPE of the relevant vacuum-to-pion correlation function, calculated in full QCD at finite b-quark mass. The resulting expressions actually comprise a triple expansion: in the twist t of the operators near the light-cone, in α_s, and in the deviation of the pion distribution amplitudes from their asymptotic form, which is fixed from conformal symmetry.

There are multiple sources of uncertainties in the LCSR calculation, which are discussed in Refs. [134,135]. Currently, a total uncertainty slightly larger than 10% on $|V_{ub}|$ is extracted from a LCSR calculation of

$$\Delta\zeta(0, q^2_{max}) = \frac{G_F^2}{24\pi^3} \int_0^{q^2_{max}} dq^2\, p_\pi^3 |f_+(q^2)|^2$$
$$= \frac{1}{|V_{ub}|^2 \tau_{B_0}} \int_0^{q^2_{max}} dq^2 \frac{d\mathcal{B}(B \to \pi\ell\nu)}{dq^2} \qquad (35)$$

which gives [136]

$$\Delta\zeta(0, 12\,\mathrm{GeV}^2) = 4.59^{+1.00}_{-0.85}\,\mathrm{ps}^{-1}. \qquad (36)$$

The recent calculation of two loop contributions to the LCQCD sum rules [137] only yields a small effect.

It is interesting to note that the results from LQCD extrapolate smoothly onto the LCSR results when employing the parametrizations based on conformal mappings [131,138]. This increases confidence in the theoretical predictions for the rate of $\overline{B} \to \pi\ell\overline{\nu}_\ell$.

$\overline{B} \to \pi\ell\overline{\nu}_\ell$ measurements

The $\overline{B} \to \pi\ell\overline{\nu}_\ell$ measurements fall into two broad classes: untagged, in which case the reconstruction of the missing momentum of the event serves as an estimator for the unseen neutrino, and tagged, in which the second B meson in the event is fully reconstructed in either a hadronic or semileptonic decay mode. The tagged measurements have high and uniform acceptance, S/B as high as 10, but low statistics. The untagged measurements have somewhat higher background levels (S/B $<$ 1) and make slightly more restrictive kinematic cuts, but have adequate statistics to measure the q^2 dependence of the form factor.

CLEO has analyzed $\overline{B} \to \pi\ell\overline{\nu}_\ell$ and $\overline{B} \to \rho\ell\overline{\nu}_\ell$ using an untagged analysis [125]. Similar analyses have been done at BABAR [126,127] and BELLE [139]. The leading systematic uncertainties in the untagged $\overline{B} \to \pi\ell\overline{\nu}_\ell$ analyses are associated with modeling the missing momentum reconstruction, with backgrounds from $\overline{B} \to X_u\ell\overline{\nu}_\ell$ decays and $e^+e^- \to q\overline{q}$ continuum events, and with varying the form factor for the $\overline{B} \to \rho\ell\overline{\nu}_\ell$ decay. The values obtained for the full and partial branching fractions [28] are listed in Table 2 above the horizontal line. These BABAR and BELLE measurements provide the differential $\overline{B} \to \pi\ell\overline{\nu}_\ell$ rate versus q^2, shown in Fig. 1, which is used in the determination of $|V_{ub}|$ discussed below.

Table 2: Total and partial branching fractions for $\overline{B}^0 \to \pi^+\ell^-\overline{\nu}_\ell$. B-tagged analyses are indicated (SL *for semileptonic*, had *for hadronic*). The uncertainties are from statistics and systematics. Measurements of $\mathcal{B}(B^- \to \pi^0\ell^-\overline{\nu}_\ell)$ have been multiplied by a factor $2\tau_{B^0}/\tau_{B^+}$ to obtain the values below.

	$\mathcal{B}\times10^4$	$\mathcal{B}(q^2>16)\times10^4$
CLEO π^+,π^0 [125]	$1.38\pm0.15\pm0.11$	$0.41\pm0.08\pm0.04$
BABAR π^+,π^0 [126]	$1.41\pm0.05\pm0.08$	$0.32\pm0.02\pm0.03$
BABAR π^+ [127]	$1.44\pm0.04\pm0.06$	$0.37\pm0.02\pm0.02$
BELLE π^+,π^0 [139]	$1.48\pm0.04\pm0.07$	$0.40\pm0.02\pm0.02$
BELLE SL π^+ [140]	$1.41\pm0.19\pm0.15$	$0.37\pm0.10\pm0.04$
BELLE SL π^0 [140]	$1.41\pm0.26\pm0.15$	$0.37\pm0.15\pm0.04$
BELLE had π^+ [120]	$1.49\pm0.09\pm0.07$	$0.45\pm0.05\pm0.02$
BELLE had π^0 [120]	$1.48\pm0.15\pm0.08$	$0.36\pm0.07\pm0.02$
BABAR SL π^+ [141]	$1.39\pm0.21\pm0.08$	$0.46\pm0.13\pm0.03$
BABAR SL π^0 [141]	$1.78\pm0.28\pm0.15$	$0.44\pm0.17\pm0.06$
BABAR had π^+ [142]	$1.07\pm0.27\pm0.19$	$0.65\pm0.20\pm0.13$
BABAR had π^0 [142]	$1.52\pm0.41\pm0.30$	$0.48\pm0.22\pm0.12$
Average	$1.45\pm0.02\pm0.04$	$0.38\pm0.01\pm0.01$

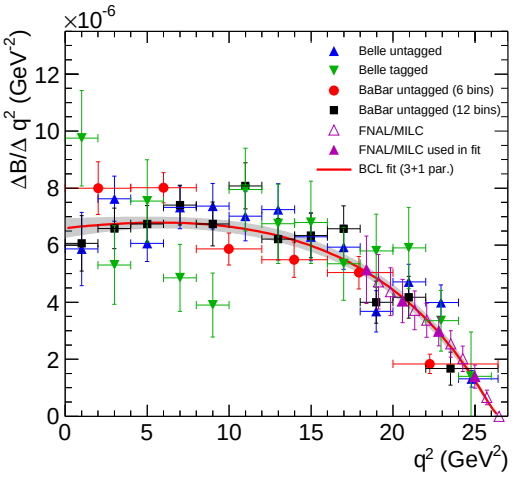

Figure 1: The untagged measurements of the differential $\overline{B} \to \pi\ell\overline{\nu}_\ell$ branching fraction versus q^2 that are used together with lattice calculations in the determination of $|V_{ub}|$.

Analyses [140,141] based on reconstructing a B in the $\overline{D}^{(*)}\ell^+\nu_\ell$ decay mode and looking for a $\overline{B} \to \pi\ell\overline{\nu}_\ell$ or $\overline{B} \to \rho\ell\overline{\nu}_\ell$ decay amongst the remaining particles in the event make use of the fact that the B and $\overline{B}$ are back-to-back in the $\Upsilon(4S)$ frame to construct a discriminant variable that provides a signal-to-noise ratio above unity for all q^2 bins. A related technique was discussed in Ref. 143. BABAR [141] and [120] have also used their samples of B mesons reconstructed in hadronic decay modes to measure exclusive charmless semileptonic decays giving very clean but low-yield samples. The resulting full and partial branching fractions are given in Table 2. The averages take account of correlations and common systematic uncertainties, and have $p(\chi^2) > 0.5$ in each case.

$|V_{ub}|$ can be obtained from the average $\overline{B} \to \pi\ell\overline{\nu}_\ell$ branching fraction and the measured q^2 spectrum. Using the average [28] of partial branching fractions in the $q^2 < 12\,\mathrm{GeV}^2$ region, $(0.81\pm0.02\pm0.02)\times10^{-4}$, along with an LCSR calculation of the theoretical rate [136] gives

$$|V_{ub}| = (3.41\pm0.06_{\rm exp}{}^{+0.37}_{-0.32\ \rm theo})\times10^{-3} \quad (\mathrm{LCSR}, q^2<12\,\mathrm{GeV}^2). \tag{37}$$

Fits to the measured q^2 spectrum using a theoretically motivated parameterization (e.g. "BCL" from Ref. 138) remove most of the model dependence from theoretical uncertainties in the shape of the spectrum. Recent determinations [28,128] of $|V_{ub}|$ from $\overline{B} \to \pi\ell\overline{\nu}_\ell$ decays have used simultaneous fits (see also Ref. 144) to the experimental partial rate and lattice points versus q^2. A fit [28] to the untagged measurements incorporates the full statistical and systematic uncertainties in the measured spectrum and uses four lattice points in the region $q^2 > 16\,\mathrm{GeV}^2$, taking into account their correlations. The fit, shown in Fig. 1, has $p(\chi^2) = 2.2\%$. If the tagged measurements, which are less consistent in the $q^2 < 8\,\mathrm{GeV}^2$ region, are included, the fit gives $p(\chi^2) < 0.01\%$. We quote the result from the untagged measurements and add the difference (0.09×10^{-3}) between the $|V_{ub}|$ values from the two fits as an additional uncertainty to find

$$|V_{ub}| = (3.28\pm0.29)\times10^{-3} \quad \text{(exclusive)}. \tag{38}$$

The largest contributions to the uncertainty come from lattice systematic and statistical errors, which will be further improved in the future.

$\overline{B} \to D^{(*)}\tau\overline{\nu}_\ell$

Summary: Semileptonic decays to third-generation leptons provide sensitivity to non-standard model amplitudes, such as from a charged Higgs boson [145]. The ratios of branching fractions of semileptonic decays involving tau leptons to those involving e/μ, $\mathcal{R}_{D^{(*)}} \equiv \mathcal{B}(\overline{B} \to \mathcal{D}^{(*)}\tau\overline{\nu}_\ell)/\mathcal{B}(\overline{B} \to \mathcal{D}^{(*)}\ell\overline{\nu}_\ell)$, are predicted with good precision in the standard model: [146]

$$\mathcal{R}_D^{\rm SM} = 0.297\pm0.017$$
$$\mathcal{R}_{D^*}^{\rm SM} = 0.252\pm0.003. \tag{39}$$

Measurements [146–150] of these ratios yield higher values; using B-tagged measurements only we find

$$\mathcal{R}_D^{\rm meas} = 0.462\pm0.067$$
$$\mathcal{R}_{D^*}^{\rm meas} = 0.341\pm0.029 \tag{40}$$

These values exceed standard model predictions by 2.4σ and 3.0σ, respectively. A variety of new physics models have been proposed [145,151–154] to explain this excess. The potential impact of any new physics in this decay mode on the $|V_{ub}|$ and $|V_{cb}|$ results given above is expected to be negligible.

Sensitivity of $\overline{B} \to D^{(*)}\tau\overline{\nu}_\ell$ to additional amplitudes

In addition to the helicity amplitudes present for decays to $e\overline{\nu}_e$ and $\mu\overline{\nu}_\mu$, decays proceeding through $\tau\overline{\nu}_\tau$ include a scalar amplitude H_s. The differential decay rate is given by [155]

$$\frac{d\Gamma}{dq^2} = \frac{G_F^2\,|V_{cb}|^2\,|\mathbf{p}^*_{D^{(*)}}|q^2}{96\pi^3 m_B^2}\left(1-\frac{m_\tau^2}{q^2}\right)^2 \left[(|H_+|^2+|H_-|^2+|H_0|^2)\left(1+\frac{m_\tau^2}{2q^2}\right)+\frac{3m_\tau^2}{2q^2}|H_s|^2\right], \quad (41)$$

where $|\mathbf{p}^*_{D^{(*)}}|$ is the 3-momentum of the $D^{(*)}$ in the $\bar{B}$ rest frame and the helicity amplitudes depend on q^2. All four helicity amplitudes contribute to $\overline{B} \to D^*\tau\overline{\nu}_\ell$, while only H_0 and H_s contribute to $\overline{B} \to D\tau\overline{\nu}_\ell$; as a result, new physics contributions tend to produce larger effects in the latter mode. The use of the ratios of decay rates, $\mathcal{R}_{D^{(*)}}$, allows a partial cancellation of uncertainties in standard model form factors, and reduces the impact of many experimental uncertainties.

The (semi)-leptonic B decays into a τ lepton provide a stringent test of the two-Higgs doublet model of type II (2HDMII), i.e. where the two Higgs doublets couple separately to up- and down-type quarks. This is also of relevance for Supersymmetry, since this corresponds to the Higgs sector of any commonly used supersymmetric model. These models involve additional charged scalar particles, which contribute at tree level to the (semi)-leptonic B decays into a τ. The distinct feature of the 2HDMII is that the contributions of the charged scalars scale as $m_\tau^2/m_{H^+}^2$, since the couplings to the charged Higgs particles are proportional to the mass of the lepton. As a consequence, one may expect visible effects in decays into a τ, but only small effects for decays into e and μ.

As discussed in the next section, the observations cannot be fitted to the expectations from the 2HDMII. To this end one has to extend the analysis to other models, where the scaling of the new contributions with the lepton mass is different.

Measurement of $\mathcal{R}_{D^{(*)}}$

The $\overline{B} \to D^{(*)}\tau\overline{\nu}_\ell$ decays have been studied at the $\Upsilon(4S)$ resonance, where the experimental signature consists of a D or D^* meson, an electron or muon from the decay $\tau \to \ell\nu_\tau\overline{\nu}_\ell$, a fully-reconstructed hadronic decay of the second B meson in the event and multiple missing neutrinos. The signal decays are separated from $\overline{B} \to D^{(*)}\ell\overline{\nu}_\ell$ decays using the measured missing mass squared; decays with only a single missing neutrino peak sharply at zero in this variable, while the signal is spread out to positive values. Background from $\overline{B} \to D^{**}\ell\overline{\nu}_\ell$ decays with one or more unreconstructed particles is harder to separate from signal.

Measurements from BELLE [147–149] and BABAR [150,146] have consistently resulted in values for $\mathcal{R}_D$ and $\mathcal{R}_{D^*}$ that exceed standard model predictions. The largest uncertainty is statistical; leading sources of systematic uncertainty include the modelling of semileptonic decays to charm final states with masses above m_{D^*} and the modelling of the selection efficiency for signal events. The first two BELLE measurements were untagged and are subject to larger systematic uncertainties. We choose to average the tagged measurements [149,146], and take the systematic uncertainties of the BELLE measurements to have a 50% correlation with each other and a 25% correlation with the BABAR measurements to find the values quoted in Eq. (40). If we include the untagged measurements (assuming 50%/25% correlation in systematic errors with other BELLE/BABAR measurements) we find $\mathcal{R}_D^{\rm meas} = 0.427 \pm 0.060$ and $\mathcal{R}_{D^*}^{\rm meas} = 0.345 \pm 0.028$. Some improvement should be possible with existing B-factory data sets.

Table 3 lists the inputs used in calculating the averages quoted here. Where the ratios $\mathcal{R}_{D^{(*)}}$ were not directly measured, the branching fractions used to obtain these results were $\mathcal{B}(\overline{B}^0 \to D^{*+}\ell\overline{\nu}_\ell) = 0.0495 \pm 0.0011$ and $\mathcal{B}(\overline{B}^0 \to D^{+}\ell\overline{\nu}_\ell) = 0.0213 \pm 0.0010$, with the corresponding B^- branching fractions obtained by multiplying by the lifetime ratio $\tau_{B^+}/\tau_{B^0} = 1.079 \pm 0.007$.

Table 3: Measurements of $\mathcal{R}_D$ and $\mathcal{R}_{D^*}$ times 10^2.

	$\mathcal{R}_D$	$\mathcal{R}_{D^*}$
BABAR [146] all B, tag	$44.0 \pm 5.8 \pm 4.2$	$33.2 \pm 2.4 \pm 1.8$
BELLE [149] B^+, tag	$70 \pm 19 \pm 10$	$47 \pm 11 \pm 7$
BELLE [149] B^0, tag	$48 \pm 21 \pm 6$	$48 \pm 13 \pm 5$
BELLE [147] B^+, no tag	$34 \pm 10 \pm 5$	$40 \pm 5 \pm 5$
BELLE [148] B^0, no tag		$41 \pm 8 \pm 7$

The tension between the SM prediction and the measurements at the level of 2.4σ and 3.0σ lead to various speculations on possible new physics contributions. It is striking that an interpretation in terms of the 2HDMII seems to be ruled out by the data. Fig. 2 shows that the interpretation of the deviation of $\mathcal{R}_D$ in terms of the 2HDMII requires vastly different values of the relevant parameter $\tan\beta/m_{H^+}$ than for $\mathcal{R}_{D^*}$, excluding this possibility.

A more general approach has been formulated in [153] on the basis of an effective field theory consideration. Assuming lepton-flavour universality (LFU) violating operators of dimension six and eight the observed values can be fitted to the coefficients of these operators. Although a detailed analysis along these lines requires to have more data on related decays (such as $B \to \pi\tau\nu$), there are indications that the tension in $\mathcal{R}_{D^{(*)}}$ cannot be explained by a minimally flavor-violating scenario with only left-handed interactions; a better fit is obtained once right-handed and scalar currents are involved.

Conclusion

The study of semileptonic B meson decays continues to be an active area for both theory and experiment. Substantial progress has been made in the application of HQE calculations to inclusive decays, where fits to moments of $\overline{B} \to X_c\ell\overline{\nu}_\ell$ decays provide precise values for $|V_{cb}|$ and, in conjunction with $B \to X_s\gamma$ decays or input on m_c, provide precise and consistent

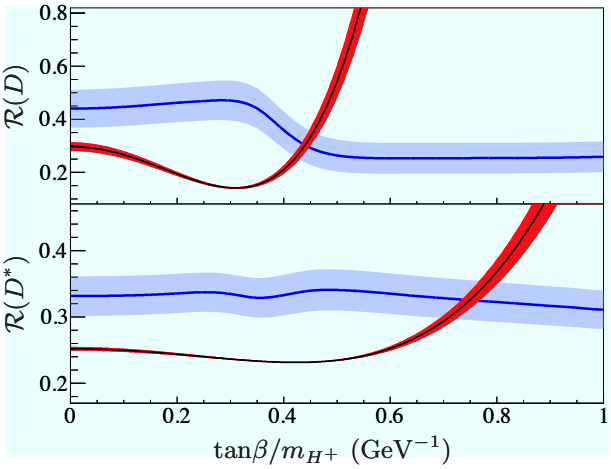

Figure 2: The $\mathcal{R}_{D^{(*)}}$ measured in Ref. 146 along with expectations in the 2HDMII as a function of $\tan\beta/m_{H^+}$.

values for m_b. The values from the inclusive and exclusive $|V_{cb}|$ determinations are marginally consistent.

Continued improvements in measurements of inclusive $\overline{B} \to X_u \ell \overline{\nu}_\ell$ decays, along with additional theoretical studies of higher order contributions and improved knowledge of m_b, have strengthened our determination of $|V_{ub}|$. Further progress in this area is possible, but will require better theoretical control over higher order terms, and improved experimental knowledge of the $\overline{B} \to X_c \ell \overline{\nu}_\ell$ background.

Progress in both $b \to u$ and $b \to c$ exclusive channels depends crucially on progress in lattice QCD calculations. Here the prospects are good, since unquenched calculations are now available for the semileptonic form factors discussed here, as well as for other hadronic weak matrix elements needed to obtain the elements and phase of the CKM matrix [156,157]. Projections for future uncertainties from lattice calculations can be found in Ref. 158.

The measurements of the $\overline{B} \to \pi \ell \overline{\nu}_\ell$ branching fraction have uncertainties below 4%, and the measured q^2 dependence is reasonably precise. Reducing the theoretical uncertainties to a comparable level will require significant effort, but is essential.

The tension between the values for $|V_{ub}|$ obtained from inclusive and exclusive decays has persisted for many years, despite significant improvements in both theory and experiment for both methods. How to reconcile these results remains an intriguing puzzle.

Both $|V_{cb}|$ and $|V_{ub}|$ are indispensable inputs into unitarity triangle fits. In particular, knowing $|V_{ub}|$ with good precision allows a test of CKM unitarity in the most direct way, by comparing the length of the $|V_{ub}|$ side of the unitarity triangle with the measurement of $\sin(2\beta)$. This comparison of a "tree" process ($b \to u$) with a "loop-induced" process ($B^0 - \overline{B}^0$ mixing) provides sensitivity to possible contributions from new physics.

The observation of semileptonic decays into τ leptons has opened a new window to the physics of the third generation. The data indicate a tension between the data and the standard model prediction, which could be a hint to new physics. However, the most prominent and simplest candidate, the 2HDMII, cannot explain the current data. More general ansätze can fit the data, but do not lead to a deeper insight unless measurements of related processes (such as $B \to \pi\tau\bar{\nu}$) are available.

The authors would like to acknowledge helpful input from F. Bernlochner, P. Gambino and C. Schwanda.

References

1. See R. Kowalewski and T. Mannel in Phys. Rev. **D86**, 010001 (2012).
2. Y. Amhis *et al.*, arXiv:1207.1158.
3. N. Isgur and M.B. Wise, Phys. Lett. **B232**, 113 (1989); *ibid.* **B237**, 527 (1990).
4. M.A. Shifman and M.B. Voloshin, Sov. J. Nucl. Phys. **47**, 511 (1988) [Yad. Fiz. **47**, 801 (1988)].
5. M.E. Luke, Phys. Lett. **B252**, 447 (1990).
6. M. Ademollo and R. Gatto, Phys. Rev. Lett. **13**, 264 (1964).
7. A.V. Manohar and M.B. Wise, Camb. Monogr. Part. Phys. Nucl. Phys. Cosmol. **10**,1(2000); H. Georgi, Phys. Lett. **B240**, 447 (1990); A.F. Falk *et al.*, Nucl. Phys. **B343**, 1 (1990); E. Eichten and B. Hill, Phys. Lett. **B234**, 511 (1990).
8. A. Sirlin, Nucl. Phys. **B196**, 83 (1982).
9. C.G. Boyd, B. Grinstein, and R.F. Lebed, Phys. Rev. **D56**, 6895 (1997); *ibid.*, Phys. Rev. Lett. **74**, 4603 (1995); C.G. Boyd and M.J. Savage, Phys. Rev. **D56**, 303 (1997).
10. I. Caprini *et al.*, Nucl. Phys. **B530**, 153 (1998).
11. A. Czarnecki and K. Melnikov, Nucl. Phys. **B505**, 65 (1997).
12. S. Hashimoto *et al.*, Phys. Rev. **D66**, 014503 (2002).
13. S. Hashimoto *et al.*, Phys. Rev. **D61**, 014502 (2000).
14. Jon A. Bailey *et al.*, Fermilab Lattice and MILC collaborations, *Proceedings of Science LATTICE2010* (2010) 311. This is an update of C. Bernard *et al.*, Phys. Rev. **D79**, 014506 (2009).
15. I.I.Y. Bigi *et al.*, Phys. Rev. **D52**, 196 (1995).
16. A. Kapustin *et al.*, Phys. Lett. B **375**, 327 (1996).
17. P. Gambino, T. Mannel, and N. Uraltsev, Phys. Rev. **D81**, 113002 (2010).
18. P. Gambino, T. Mannel and N. Uraltsev, JHEP **1210**, 169 (2012).
19. D. Buskulic *et al.*, (ALEPH Collab.), Phys. Lett. **B395**, 373 (1997).
20. G. Abbiendi *et al.*, (OPAL Collab.), Phys. Lett. **B482**, 15 (2000).
21. P. Abreu *et al.*, (DELPHI Collab.), Phys. Lett. **B510**, 55 (2001).
22. J. Abdallah *et al.*, (DELPHI Collab.), Eur. Phys. J. **C33**, 213 (2004).
23. N.E. Adam *et al.*, (CLEO Collab.), Phys. Rev. **D67**, 032001 (2003).

24. B. Aubert *et al.*, (BABAR Collab.), Phys. Rev. **D77**, 032002 (2008).
25. B. Aubert *et al.*, (BABAR Collab.), Phys. Rev. Lett. **100**, 231803 (2008).
26. B. Aubert *et al.*, (BABAR Collab.), Phys. Rev. **D79**, 012002 (2009).
27. W. Dungel *et al.*, (BELLE Collab.), Phys. Rev. **D82**, 112007 (2010).
28. See `slac.stanford.edu/xorg/hfag/semi/` update to Ref. [2] for PDG 2013.
29. J. Beringer *et al.*(Particle Data Group), Phys. Rev. **D86**, 010001 (2012) and 2013 partial update for the 2014 edition.
30. N. Uraltsev, Phys. Lett. **B585**, 253 (2004).
31. M. Okamoto *et al.*, Nucl. Phys. (Proc. Supp.) **B140**, 461 (2005). A. Kronfeld, talk presented at the workshop CKM05, San Diego, CA - Workshop on the Unitarity Triangle, 15-18 March 2005.
32. B. Aubert *et al.*, (BABAR Collab.), Phys. Rev. Lett. **104**, 011802 (2010).
33. J. E. Bartelt *et al.*, (CLEO Collab.), Phys. Rev. Lett. **82**, 3746 (1999).
34. K. Abe *et al.*, (BELLE Collab.), Phys. Lett. **B526**, 247 (2002).
35. A.V. Manohar and M.B. Wise, Phys. Rev. **D49**, 1310 (1994).
36. I.I.Y. Bigi *et al.*, Phys. Rev. Lett. **71**, 496 (1993), Phys. Lett. **B323**, 408 (1994).
37. M.A. Shifman, I.I.Y. Bigi, and N. Uraltsev, Int. J. Mod. Phys. **A16**, 5201 (2001).
38. D. Benson *et al.*, Nucl. Phys. **B665**, 367 (2003).
39. M. Gremm and A. Kapustin, Phys. Rev. **D55**, 6924 (1997).
40. B. M. Dassinger, T. Mannel, and S. Turczyk, JHEP **0703**, 087 (2007).
41. I. I. Bigi, N. Uraltsev, and R. Zwicky, Eur. Phys. J. **C50**, 539 (2007).
42. T. Mannel, S. Turczyk, and N. Uraltsev, JHEP **1011**, 109 (2010).
43. A. Pak and A. Czarnecki, Phys. Rev. D **78**, 114015 (2008).
44. S. Biswas and K. Melnikov, JHEP **1002**, 089 (2010).
45. P. Gambino, JHEP **1109**, 055 (2011).
46. P. Gambino and N. Uraltsev, Eur. Phys. J. **C34**, 181 (2004).
47. V. Aquila *et al.*, Nucl. Phys. B **719**, 77 (2005).
48. T. Becher, H. Boos, and E. Lunghi, JHEP **0712**, 062 (2007).
49. A. Alberti *et al.*, Nucl. Phys. B **870**, 16 (2013).
50. C. Breidenbach *et al.*, Phys. Rev. D **78**, 014022 (2008).
51. I. Bigi *et al.*, JHEP **1004** , 073 (2010).
52. A.H. Hoang *et al.*, Phys. Rev. **D59**, 074017 (1999).
53. H. Leutwyler, Phys. Lett. **B98**, 447 (1981); M.B. Voloshin, Sov. J. Nucl. Phys. **36**, 143 (1982).
54. A.H. Hoang, Phys. Rev. D **61**, 034005 (2000).
55. S.E. Csorna *et al.*, (CLEO Collab.), Phys. Rev. **D70**, 032002 (2004).
56. A.H. Mahmood *et al.*, (CLEO Collab.), Phys. Rev. **D70**, 032003 (2004).
57. B. Aubert *et al.*, (BABAR Collab.), Phys. Rev. **D69**, 111103 (2004).
58. B. Aubert *et al.*, (BABAR Collab.), Phys. Rev. **D69**, 111104 (2004).
59. C. Schwanda *et al.*, (BELLE Collab.), Phys. Rev. **D75**, 032005 (2007).
60. P. Urquijo *et al.*, (BELLE Collab.), Phys. Rev. **D75**, 032001 (2007).
61. J. Abdallah *et al.*, (DELPHI Collab.), Eur. Phys. J. **C45**, 35 (2006).
62. D. Acosta *et al.*, (CDF Collab.), Phys. Rev. **D71**, 051103 (2005).
63. B. Aubert *et al.*, (BABAR Collab.), Phys. Rev. **D81**, 032003 (2010).
64. A. Limosani *et al.* [BELLE Collab.], Phys. Rev. Lett. **103**, 241801 (2009).
65. C. Schwanda *et al.*, (BELLE Collab.), Phys. Rev. **D78**, 032016 (2008).
66. B. Aubert *et al.*, (BABAR Collab.), Phys. Rev. **D72**, 052004 (2005).
67. B. Aubert *et al.*, (BABAR Collab.), Phys. Rev. Lett. **97**, 171803 (2006).
68. S. Chen *et al.*, (CLEO Collab.), Phys. Rev. Lett. **87**, 251807 (2001).
69. M. Battaglia *et al.*, Phys. Lett. **B556**, 41 (2003).
70. B. Aubert *et al.*, (BABAR Collab.), Phys. Rev. Lett. **93**, 011803 (2004).
71. O. Buchmüller and H. Flächer, `hep-ph/0507253`; updated in Ref. 28.
72. C. W. Bauer *et al.*, Phys. Rev. **D70**, 094017 (2004); updated in Ref. 28.
73. See section 5.4.2 of M. Antonelli *et al.*, Phys. Reports **494**, 197 (2010).
74. B.Dehnadi, *et al.*, `arXiv:1102.2264`.
75. I. Allison *et al.*, (HPQCD Collab.), Phys. Rev. **D78**, 054513 (2008).
76. Chetyrkin *et al.*, Phys. Rev. **D80**, 074010 (2009).
77. P. Gambino and C. Schwanda, Phys. Rev. **D89**, 014022 (2014).
78. T. Ewerth, P. Gambino, and S. Nandi, Nucl. Phys. B **830**, 278 (2010).
79. A. H. Hoang *et al.*, Phys. Rev. **D59**, 074017 (1999).
80. N. Uraltsev, Int. J. Mod. Phys. **A14**, 4641 (1999).
81. M. Neubert, Phys. Rev. **D49**, 4623 (1994); *ibid.* **D49**, 3392 (1994).
82. I. Bigi *et al.*, Int. J. Mod. Phys. **A9**, 2467 (1994).
83. B.O. Lange, M. Neubert, and G. Paz, Phys. Rev. **D72**, 073006 (2005).
84. C. W. Bauer *et al.*, Phys. Lett. **B543**, 261 (2002).
85. T. Mannel and S. Recksiegel, Phys. Rev. **D60**, 114040 (1999).
86. C. W. Bauer, Z. Ligeti, and M. E. Luke, Phys. Rev. **D64**, 113004 (2001).
87. C. W. Bauer *et al.*, Phys. Rev. **D68**, 094001 (2003).
88. M. Neubert, Phys. Lett. **B513**, 88 (2001); Phys. Lett. **B543**, 269 (2002).
89. A.K. Leibovich *et al.*, Phys. Rev. **D61**, 053006 (2000); **62**, 014010 (2000); Phys. Lett. **B486**, 86 (2000); **513**, 83 (2001).

90. A.H. Hoang *et al.*, Phys. Rev. **D71**, 093007 (2005).
91. B. Lange *et al.*, JHEP **0510**, 084 (2005); B. Lange, JHEP **0601**, 104 (2006).
92. M. Neubert, Phys. Lett. **B612**, 13 (2005).
93. Z. Ligeti, I. W. Stewart, and F. J. Tackmann, Phys. Rev. D **78**, 114014 (2008).
94. P. Gambino *et al.*, JHEP **0710**, 058 (2007).
95. J.R. Andersen and E. Gardi, JHEP **0601**, 097 (2006).
96. C. Greub, M. Neubert, and B.D. Pecjak, Eur. Phys. J. C**65**, 501(2010).
97. M. Brucherseifer, F. Caola, and K. Melnikov, Phys. Lett. B **721**, 107 (2013).
98. C. W. Bauer *et al.*, Phys. Rev. **D64**, 113004 (2001); Phys. Lett. **B479**, 395 (2000).
99. I. I. Y. Bigi and N. G. Uraltsev, Nucl. Phys. **B423**, 33 (1994).
100. M.B. Voloshin, Phys. Lett. **B515**, 74 (2001).
101. Z. Ligeti, M. Luke, and A. V. Manohar, Phys. Rev. **D82**, 033003 (2010).
102. P. Gambino and J. F. Kamenik, Nucl. Phys. **B840**,424 (2010).
103. J.L. Rosner *et al.*, (CLEO Collab.), Phys. Rev. Lett. **96**, 121801 (2006).
104. B. Aubert *et al.*, (BABAR Collab.), arXiv:0708.1753.
105. R. Barate *et al.*, (ALEPH Collab.), Eur. Phys. J. **C6**, 555 (1999).
106. M. Acciarri *et al.*, (L3 Collab.), Phys. Lett. **B436**, 174 (1998).
107. G. Abbiendi *et al.*, (OPAL Collab.), Eur. Phys. J. **C21**, 399 (2001).
108. P. Abreu *et al.*, (DELPHI Collab.), Phys. Lett. **B478**, 14 (2000).
109. A. Bornheim *et al.*, (CLEO Collab.), Phys. Rev. Lett. **88**, 231803 (2002).
110. A. Limosani *et al.*, (BELLE Collab.), Phys. Lett. **B621**, 28 (2005).
111. B. Aubert *et al.*, (BABAR Collab.), Phys. Rev. **D73**, 012006 (2006).
112. B. Aubert *et al.*, (BABAR Collab.), Phys. Rev. Lett. **95**, 111801 (2005), Erratum-*ibid.* **97**, 019903(E) (2006).
113. R. Kowalewski and S. Menke, Phys. Lett. **B541**, 29 (2002).
114. J. P. Lees *et al.*, (BABAR Collab.), arXiv:1112.0702.
115. I. Bizjak *et al.*, (BELLE Collab.), Phys. Rev. Lett. **95**, 241801 (2005).
116. P. Urquijo *et al.*, (BELLE Collab.), Phys. Rev. Lett. **104**, 021801 (2010).
117. V. Golubev, Y. Skovpen, and V. Luth, Phys. Rev. **D76**, 114003 (2007).
118. B. Aubert *et al.*, (BABAR Collab.), Phys. Rev. Lett. **96**, 221801 (2006).
119. H. Kakuno *et al.*, (BELLE Collab.), Phys. Rev. Lett. **92**, 101801 (2004).
120. A. Sibidanov *et al.*, (BELLE Collab.), Phys. Rev. **D88**, 032005 (2013).
121. B. Aubert *et al.*, (BABAR Collab.), Phys. Rev. Lett. **90**, 181801 (2003).
122. T. Hokuue *et al.*, (BELLE Collab.), Phys. Lett. **B648**, 139 (2007).
123. B. Aubert *et al.*, (BABAR Collab.), Phys. Rev. **D79**, 052011 (2008).
124. C. Schwanda *et al.*, (BELLE Collab.), Phys. Rev. Lett. **93**, 131803 (2004).
125. N. E. Adam *et al.*, (CLEO Collab.), Phys. Rev. Lett. **99**, 041802 (2007); Phys. Rev. **D76**, 012007 (2007); supercedes Phys. Rev. **D68**, 072003 (2003).
126. P. del Amo Sanchez *et al.*, (BABAR Collab.), Phys. Rev. **D83**, 032007 (2011); supercedes B. Aubert *et al.*, (BABAR Collab.), Phys. Rev. **D72**, 051102 (2005).
127. P. del Amo Sanchez *et al.*, (BABAR Collab.), Phys. Rev. **D83**, 052011 (2011); updated in J. P. Lees *et al.*, (BABAR Collab.), Phys. Rev. **D86**, 092004 (2012).
128. J. Bailey *et al.*, (Fermilab/MILC), Phys. Rev. **D79**, 054507 (2009).
129. E. Dalgic *et al.*, (HPQCD), Phys. Rev. **D73**, 074502 (2006), Erratum-*ibid.* **D75** 119906 (2007).
130. T. Becher and R. J. Hill, Phys. Lett. **B633**, 61 (2006).
131. M. C. Arnesen *et al.*, Phys. Rev. Lett. **95**, 071802 (2005).
132. T. Hurth *et al.*, hep-ph/0509167.
133. M.A. Shifman, A.I. Vainshtein, and V.I. Zakharov, Nucl. Phys. **B147**, 385 (1979); *ibid.* **B147**, 448 (1979).
134. P. Ball and R. Zwicky, Phys. Rev. **D71**, 014015 (2005).
135. G. Duplancic *et al.*, JHEP **0804**, 014 (2008).
136. A. Khodjamirian *et al.*, Phys. Rev. **D83**, 094031 (2011).
137. A. Bharucha, JHEP **1205**, 092 (2012).
138. C. Bourrely, I. Caprini, and L. Lellouch, Phys. Rev. **D79**, 013008 (2009).
139. H. Ha *et al.*, (BELLE Collab.), Phys. Rev. **D83**, 071101 (2011).
140. K. Abe *et al.*, (BELLE Collab.), Phys. Lett. **B648**, 139 (2007).
141. B. Aubert *et al.*, (BABAR Collab.), Phys. Rev. Lett. **101**, 081801 (2008).
142. B. Aubert *et al.*, (BABAR Collab.), Phys. Rev. Lett. **97**, 211801 (2006).
143. W. Brower and H. Paar, Nucl. Instrum. Methods **A421**, 411 (1999).
144. P. Ball, arXiv:0705.2290;
J.M. Flynn and J. Nieves, Phys. Lett. **B649**, 269 (2007);
T. Becher and R.J. Hill, Phys. Lett. **B633**, 61 (2006);
M. Arnesen *et al.*, Phys. Rev. Lett. **95**, 071802 (2005).
145. M. Tanaka, Z. Phys. **C67**, 321 (1995);
H. Itoh, S. Komine, and Y. Okada, Prog. Theor. Phys. **114**, 179 (2005);
U. Nierste, S. Trine, and S. Westhoff, Phys. Rev. **D78**, 015006 (2008);
M. Tanaka and R. Watanabe, Phys. Rev. **D82**, 034027 (2010);
S. Fajfer, J. F. Kamenik, and I. Nišandžić, Phys. Rev. **D85**, 094025 (2012).
146. J. Lees *et al.*, (Babar Collab.), Phys. Rev. Lett. **109**, 101802 (2012).
147. A. Bozek *et al.*, (Belle Collab.), Phys. Rev. **D82**, 072005 (2010).
148. A. Matyja *et al.*, (Belle Collab.), Phys. Rev. Lett. **99**, 191807 (2007).
149. I. Adachi *et al.*, (Belle Collab.), arXiv:0910.430.
150. B. Aubert *et al.*, (Babar Collab.), Phys. Rev. Lett. **100**, 021801 (2008).

151. A. Datta, M. Duraisamy, and D. Ghosh, Phys. Rev. **D86**, 034027 (2012).

152. D. Becirevic, N. Kosnik, and A. Tayduganov, Phys. Lett. **B716**, 208 (2012).

153. S. Fajfer *et al.*, Phys. Rev. Lett. **109**, 161801 (2012).

154. A. Crivellin, C. Greub, and A. Kokulu, Phys. Rev. **D86**, 054014 (2012).

155. J. G. Körner and G. A. Schuler, Z. Phys. **C46**, 93 (1990).

156. J. Laiho, E. Lunghi, and R. S. Van de Water, Phys. Rev. D **81**, 034503 (2010).

157. G. Colangelo, *et al.*, Eur. Phys. J. C **71**, 1695 (2011).

158. USQCD Collab. (2011), www.usqcd.org/documents/HiIntensityFlavor.pdf.

V_{cb} MEASUREMENTS

For the discussion of V_{cb} measurements, which is not repeated here, see the review on "Determination of $|V_{cb}|$ and $|V_{ub}|$."

The CKM matrix element $|V_{cb}|$ can be determined by studying the rate of the semileptonic decay $B \to D^{(*)} \ell\nu$ as a function of the recoil kinematics of $D^{(*)}$ mesons. Taking advantage of theoretical constraints on the normalization and a linear ω dependence of the form factors ($F(\omega)$, $G(\omega)$) provided by Heavy Quark Effective Theory (HQET), the $|V_{cb}|\times F(\omega)$ and ρ^2 (a^2) can be simultaneously extracted from data, where ω is the scalar product of the two-meson four velocities, $F(1)$ is the form factor at zero recoil (ω=1) and ρ^2 is the slope, sometimes denoted as a^2. Using the theoretical input of $F(1)$, a value of $|V_{cb}|$ can be obtained.

"OUR EVALUATION" is an average using rescaled values of the data listed below. The average and rescaling were performed by the Heavy Flavor Averaging Group (HFAG) and are described at http://www.slac.stanford.edu/xorg/hfag/. The averaging/rescaling procedure takes into account correlations between the measurements.

$|V_{cb}| \times F(1)$ (from $B^0 \to D^{*-}\ell^+\nu$)

VALUE		DOCUMENT ID		TECN	COMMENT
0.03581 ± 0.00045 OUR EVALUATION		with ρ^2=1.207 ± 0.026 and a correlation 0.324. The fitted χ^2 is 30.0 for 23 degrees of freedom.			
0.0360 ± 0.0009 OUR AVERAGE		Error includes scale factor of 1.5. See the ideogram below.			
0.0346	±0.0002 ±0.0010	[1] DUNGEL	10	BELL	$e^+e^- \to \Upsilon(4S)$
0.0359	±0.0002 ±0.0012	[2] AUBERT	09A	BABR	$e^+e^- \to \Upsilon(4S)$
0.0359	±0.0006 ±0.0014	[3] AUBERT	08AT	BABR	$e^+e^- \to \Upsilon(4S)$
0.0392	±0.0018 ±0.0023	[4] ABDALLAH	04D	DLPH	$e^+e^- \to Z^0$
0.0431	±0.0013 ±0.0018	[5] ADAM	03	CLE2	$e^+e^- \to \Upsilon(4S)$
0.0355	±0.0014 $^{+0.0023}_{-0.0024}$	[6] ABREU	01H	DLPH	$e^+e^- \to Z$
0.0371	±0.0010 ±0.0020	[7] ABBIENDI	00Q	OPAL	$e^+e^- \to Z$
0.0319	±0.0018 ±0.0019	[8] BUSKULIC	97	ALEP	$e^+e^- \to Z$
• • • We do not use the following data for averages, fits, limits, etc. • • •					
0.0344	±0.0003 ±0.0011	[9] AUBERT	08R	BABR	Repl. by AUBERT 09A
0.0355	±0.0003 ±0.0016	[10] AUBERT	05E	BABR	Repl. by AUBERT 08R
0.0377	±0.0011 ±0.0019	[11] ABDALLAH	04D	DLPH	$e^+e^- \to Z^0$
0.0354	±0.0019 ±0.0018	[12] ABE	02F	BELL	Repl. by DUNGEL 10
0.0431	±0.0013 ±0.0018	[13] BRIERE	02	CLE2	$e^+e^- \to \Upsilon(4S)$
0.0328	±0.0019 ±0.0022	ACKERSTAFF	97G	OPAL	Repl. by ABBIENDI 00Q
0.0350	±0.0019 ±0.0023	[14] ABREU	96P	DLPH	Repl. by ABREU 01H
0.0351	±0.0019 ±0.0020	[15] BARISH	95	CLE2	Repl. by ADAM 03
0.0314	±0.0023 ±0.0025	BUSKULIC	95N	ALEP	Repl. by BUSKULIC 97

[1] Uses fully reconstructed $D^{*-}\ell^+\nu$ events ($\ell = e$ or μ).

[2] Obtained from a global fit to $B \to D^{(*)}\ell\nu_\ell$ events, with reconstructed $D^0\ell$ and $D^+\ell$ final states and $\rho^2 = 1.22 \pm 0.02 \pm 0.07$.

[3] Measured using the dependence of $B^- \to D^{*0}e^-\overline{\nu}_e$ decay differential rate and the form factor description by CAPRINI 98 with $\rho^2 = 1.16 \pm 0.06 \pm 0.08$.

[4] Measurement using fully reconstructed D^* sample with a $\rho^2 = 1.32 \pm 0.15 \pm 0.33$.

[5] Average of the $B^0 \to D^*(2010)^-\ell^+\nu$ and $B^+ \to \overline{D}^*(2007))\ell^+\nu$ modes with $\rho^2 = 1.61 \pm 0.09 \pm 0.21$ and $f_{+-} = 0.521 \pm 0.012$.

[6] ABREU 01H measured using about 5000 partial reconstructed D^* sample with a ρ^2=1.34 ± 0.14 $^{+0.24}_{-0.22}$.

[7] ABBIENDI 00Q: measured using both inclusively and exclusively reconstructed $D^{*\pm}$ samples with a ρ^2=1.21 ± 0.12 ± 0.20. The statistical and systematic correlations between $|V_{cb}|\times F(1)$ and ρ^2 are 0.90 and 0.54 respectively.

[8] BUSKULIC 97: measured using exclusively reconstructed $D^{*\pm}$ with a a^2=0.31 ± 0.17 ± 0.08. The statistical correlation is 0.92.

[9] Measured using fully reconstructed D^* sample and a simultaneous fit to the Caprini-Lellouch-Neubert form factor parameters: $\rho^2 = 1.191 \pm 0.048 \pm 0.028$, $R_1(1) = 1.429 \pm 0.061 \pm 0.044$, and $R_2(1) = 0.827 \pm 0.038 \pm 0.022$.

[10] Measurement using fully reconstructed D^* sample with a $\rho^2 = 1.29 \pm 0.03 \pm 0.27$.

[11] Combines with previous partial reconstructed D^* measurement with a $\rho^2 = 1.39 \pm 0.10 \pm 0.33$.

[12] Measured using exclusive $B^0 \to D^*(892)^-e^+\nu$ decays with ρ^2= 1.35 ± 0.17 ± 0.19 and a correlation of 0.91.

[13] BRIERE 02 result is based on the same analysis and data sample reported in ADAM 03.

[14] ABREU 96P: measured using both inclusively and exclusively reconstructed $D^{*\pm}$ samples.

[15] BARISH 95: measured using both exclusive reconstructed $B^0 \to D^{*-}\ell^+\nu$ and $B^+ \to D^{*0}\ell^+\nu$ samples. They report their experiment's uncertainties ±0.0019 ± 0.0018 ± 0.0008, where the first error is statistical, the second is systematic, and the third is the uncertainty in the lifetimes. We combine the last two in quadrature.

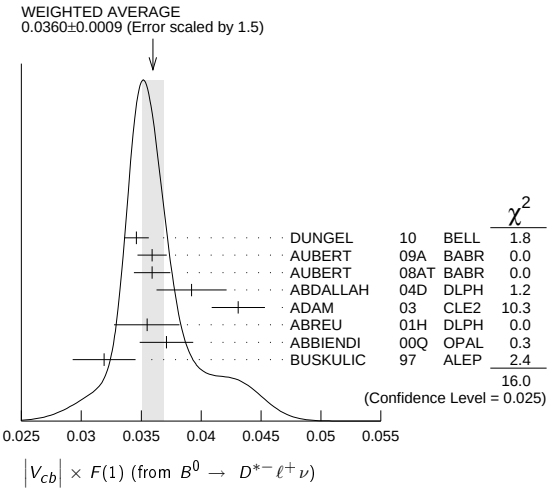

$|V_{cb}| \times G(1)$ (from $B \to D^-\ell^+\nu$)

VALUE		DOCUMENT ID		TECN	COMMENT
0.04265 ± 0.00153 OUR EVALUATION		with ρ^2=1.190 ± 0.054 and a correlation 0.83. The fitted χ^2 is 0.5 for 8 degrees of freedom.			
0.0421 ± 0.0016 OUR AVERAGE					
0.0423	±0.0019 ±0.0014	[16] AUBERT	10	BABR	$e^+e^- \to \Upsilon(4S)$
0.0431	±0.0008 ±0.0023	[17] AUBERT	09A	BABR	$e^+e^- \to \Upsilon(4S)$
0.0411	±0.0044 ±0.0052	[18] ABE	02E	BELL	$e^+e^- \to \Upsilon(4S)$
0.0416	±0.0047 ±0.0037	[19] BARTELT	99	CLE2	$e^+e^- \to \Upsilon(4S)$
0.0278	±0.0068 ±0.0065	[20] BUSKULIC	97	ALEP	$e^+e^- \to Z$
• • • We do not use the following data for averages, fits, limits, etc. • • •					
0.0337	±0.0044 $^{+0.0072}_{-0.0049}$	[21] ATHANAS	97	CLE2	Repl. by BARTELT 99

[16] Obtained from a fit to the combined $B \to \overline{D}\ell^+\nu_\ell$ sample in which a hadronic decay of the second B meson is fully reconstructed and $\rho^2 = 1.20 \pm 0.09 \pm 0.04$.

[17] Obtained from a global fit to $B \to D^{(*)}\ell\nu_\ell$ events, with reconstructed $D^0\ell$ and $D^+\ell$ final states and $\rho^2 = 1.20 \pm 0.04 \pm 0.07$.

[18] Using the missing energy and momentum to extract kinematic information about the undetected neutrino in the $B^0 \to D^-\ell^+\nu$ decay.

[19] BARTELT 99: measured using both exclusive reconstructed $B^0 \to D^-\ell^+\nu$ and $B^+ \to D^0\ell^+\nu$ samples.

[20] BUSKULIC 97: measured using exclusively reconstructed $D^\pm$ with a a^2=−0.05 ± 0.53 ± 0.38. The statistical correlation is 0.99.

[21] ATHANAS 97: measured using both exclusive reconstructed $B^0 \to D^-\ell^+\nu$ and $B^+ \to D^0\ell^+\nu$ samples with a ρ^2=0.59 ± 0.22 ± 0.12 $^{+0.59}_{-0}$. They report their experiment's uncertainties ±0.0044 ± 0.0048 $^{+0.0053}_{-0.0012}$, where the first error is statistical, the second is systematic, and the third is the uncertainty due to the form factor model variations. We combine the last two in quadrature.

V_{ub} MEASUREMENTS

For the discussion of V_{ub} measurements, which is not repeated here, see the review on "Determination of $|V_{cb}|$ and $|V_{ub}|$."

The CKM matrix element $|V_{ub}|$ can be determined by studying the rate of the charmless semileptonic decay $b \to u\ell\nu$. The relevant branching ratio measurements based on exclusive and inclusive decays can be found in the B Listings, and are not repeated here.

V_{cb} and V_{ub} CKM Matrix Elements REFERENCES

AUBERT	10	PRL 104 011802	B. Aubert *et al.*	(BABAR Collab.)
DUNGEL	10	PR D82 112007	W. Dungel *et al.*	(BELLE Collab.)
AUBERT	09A	PR D79 012002	B. Aubert *et al.*	(BABAR Collab.)
AUBERT	08AT	PRL 100 231803	B. Aubert *et al.*	(BABAR Collab.)
AUBERT	08R	PR D77 032002	B. Aubert *et al.*	(BABAR Collab.)
AUBERT	05E	PR D71 051502	B. Aubert *et al.*	(BABAR Collab.)
ABDALLAH	04D	EPJ C33 213	J. Abdallah *et al.*	(DELPHI Collab.)
ADAM	03	PR D67 032001	N.E. Adam *et al.*	(CLEO Collab.)
ABE	02E	PL B526 258	K. Abe *et al.*	(BELLE Collab.)
ABE	02F	PL B526 247	K. Abe *et al.*	(BELLE Collab.)
BRIERE	02	PRL 89 081803	R. Briere *et al.*	(CLEO Collab.)

ABREU	01H	PL B510 55	P. Abreu *et al.*	(DELPHI Collab.)
ABBIENDI	00Q	PL B482 15	G. Abbiendi *et al.*	(OPAL Collab.)
BARTELT	99	PRL 82 3746	J. Bartelt *et al.*	(CLEO Collab.)
CAPRINI	98	NP B530 153	I. Caprini, L. Lellouch, M. Neubert	(BCIP, CERN)
ACKERSTAFF	97G	PL B395 128	K. Ackerstaff *et al.*	(OPAL Collab.)
ATHANAS	97	PRL 79 2208	M. Athanas *et al.*	(CLEO Collab.)
BUSKULIC	97	PL B395 373	D. Buskulic *et al.*	(ALEPH Collab.)
ABREU	96P	ZPHY C71 539	P. Abreu *et al.*	(DELPHI Collab.)
BARISH	95	PR D51 1014	B.C. Barish *et al.*	(CLEO Collab.)
BUSKULIC	95N	PL B359 236	D. Buskulic *et al.*	(ALEPH Collab.)

B^*

$I(J^P) = \frac{1}{2}(1^-)$

I, *J*, *P* need confirmation. Quantum numbers shown are quark-model predictions.

B^* MASS

From mass difference below and the average of our B masses $(m_{B^\pm} + m_{B^0})/2$.

VALUE (MeV)	DOCUMENT ID
5325.2±0.4 OUR FIT	

$m_{B^*} - m_B$

VALUE (MeV)	EVTS	DOCUMENT ID		TECN	COMMENT
45.78±0.35 OUR FIT					
45.78±0.35 OUR AVERAGE					
46.2 ±0.3 ±0.8		[1] ACKERSTAFF	97M	OPAL	$e^+e^- \to Z$
45.3 ±0.35±0.87	4227	[1] BUSKULIC	96D	ALEP	E_{cm}^{ee}= 88–94 GeV
45.5 ±0.3 ±0.8		[1] ABREU	95R	DLPH	E_{cm}^{ee}= 88–94 GeV
46.3 ±1.9	1378	[1] ACCIARRI	95B	L3	E_{cm}^{ee}= 88–94 GeV
46.4 ±0.3 ±0.8		[2] AKERIB	91	CLE2	$e^+e^- \to \gamma X$
45.6 ±0.8		[2] WU	91	CSB2	$e^+e^- \to \gamma X, \gamma \ell X$
45.4 ±1.0		[3] LEE-FRANZINI	90	CSB2	$e^+e^- \to \Upsilon(5S)$
• • • We do not use the following data for averages, fits, limits, etc. • • •					
52 ±2 ±4	1400	[4] HAN	85	CUSB	$e^+e^- \to \gamma e X$

[1] *u*, *d*, *s* flavor averaged.
[2] These papers report E_γ in the B^* center of mass. The $m_{B^*} - m_B$ is 0.2 MeV higher. E_{cm} = 10.61–10.7 GeV. Admixture of B^0 and B^+ mesons, but not B_s.
[3] LEE-FRANZINI 90 value is for an admixture of B^0 and B^+. They measure 46.7 ± 0.4 ± 0.2 MeV for an admixture of B^0, B^+, and B_s, and use the shape of the photon line to separate the above value.
[4] HAN 85 is for E_{cm} = 10.6–11.2 GeV, giving an admixture of B^0, B^+, and B_s.

$m_{B^{*+}} - m_{B^+}$

VALUE (MeV)	DOCUMENT ID		TECN	COMMENT
45.01±0.30±0.23	[5] AAIJ	13O	LHCB	pp at 7 TeV

[5] Obtained the mass difference between $B^{*+}K^-$ and B^+K^- from $B_{s2}^*(5840)^0$ decay.

$|(m_{B^{*+}} - m_{B^+}) - (m_{B^{*0}} - m_{B^0})|$

VALUE (MeV)	CL%	DOCUMENT ID		TECN	COMMENT
<6	95	ABREU	95R	DLPH	E_{cm}^{ee}= 88–94 GeV

B^* DECAY MODES

	Mode	Fraction (Γ_i/Γ)
Γ_1	$B\gamma$	dominant

B^* REFERENCES

AAIJ	13O	PRL 110 151803	R. Aaij *et al.*	(LHCb Collab.)
ACKERSTAFF	97M	ZPHY C74 413	K. Ackerstaff *et al.*	(OPAL Collab.)
BUSKULIC	96D	ZPHY C69 393	D. Buskulic *et al.*	(ALEPH Collab.)
ABREU	95R	ZPHY C68 353	P. Abreu *et al.*	(DELPHI Collab.)
ACCIARRI	95B	PL B345 589	M. Acciarri *et al.*	(L3 Collab.)
AKERIB	91	PRL 67 1692	D.S. Akerib *et al.*	(CLEO Collab.)
WU	91	PL B273 177	Q.W. Wu *et al.*	(CUSB II Collab.)
LEE-FRANZINI	90	PRL 65 2947	J. Lee-Franzini *et al.*	(CUSB II Collab.)
HAN	85	PRL 55 36	K. Han *et al.*	(COLU, LSU, MPIM, STON)

$B_J^*(5732)$ or B^{**}

$I(J^P) = ?(?^?)$
I, *J*, *P* need confirmation.

OMITTED FROM SUMMARY TABLE
Signal can be interpreted as stemming from several narrow and broad resonances. Needs confirmation.

$B_J^*(5732)$ MASS

VALUE (MeV)	EVTS	DOCUMENT ID		TECN	COMMENT
5698± 8 OUR AVERAGE Error includes scale factor of 1.2.					
5710±20		[1] AFFOLDER	01F	CDF	$p\overline{p}$ at 1.8 TeV
5695^{+17}_{-19}		[2] BARATE	98L	ALEP	$e^+e^- \to Z$
5704± 4±10	1944	[3] BUSKULIC	96D	ALEP	E_{cm}^{ee}= 88–94 GeV
5732± 5±20	2157	ABREU	95B	DLPH	E_{cm}^{ee}= 88–94 GeV
5681±11	1738	AKERS	95E	OPAL	E_{cm}^{ee}= 88–94 GeV
• • • We do not use the following data for averages, fits, limits, etc. • • •					
5713± 2		[4] ACCIARRI	99N	L3	$e^+e^- \to Z$

[1] AFFOLDER 01F uses the reconstructed B meson through semileptonic decay channels. The fraction of light B mesons that are produced at L=1 B^{**} states is measured to be 0.28 ± 0.06 ± 0.03.
[2] BARATE 98L uses fully reconstructed B mesons to search for B^{**} production in the $B\pi^\pm$ system. In the framework of heavy quark symmetry (HQS), they also measured the mass of B_2^* to be $5739^{+8}_{-11}{}^{+6}_{-4}$ MeV/c^2 and the relative production rate of $B(b \to B_2^* \to B^{(*)}\pi)/B(b \to B_{u,d})$ = $(31 \pm 9^{+6}_{-5})$%.
[3] Using $m_{B\pi} - m_B$ = 424 ± 4 ± 10 MeV.
[4] ACCIARRI 99N uses inclusive reconstructed B mesons to search for B^{**} production in the $B^{(*)}\pi^\pm$ system. In the framework of HQET, they measured the mass of B_1^* and B_2^* to be 5670±10±13 MeV and 5768±5±6 with the $B(b \to B^{**}) = (32 \pm 3 \pm 6) \times 10^{-2}$. They also reported the evidence for the existence of an excited B-meson state or mixture of states in the region 5.9–6.0 GeV.

$B_J^*(5732)$ WIDTH

VALUE (MeV)	EVTS	DOCUMENT ID		TECN	COMMENT
128±18 OUR AVERAGE					
145±28	2157	ABREU	95B	DLPH	E_{cm}^{ee}= 88–94 GeV
116±24	1738	AKERS	95E	OPAL	E_{cm}^{ee}= 88–94 GeV

$B_J^*(5732)$ DECAY MODES

	Mode	Fraction (Γ_i/Γ)
Γ_1	$B^*\pi + B\pi$	dominant
Γ_2	$B^*\pi$(X)	[a] (85±29) %

[a] X refers to decay modes with or without additional accompanying decay particles.

$B_J^*(5732)$ BRANCHING RATIOS

X refers to decay modes with or without additional accompanying decay particles.

$\Gamma(B^*\pi(X))/\Gamma_{total}$ **Γ_2/Γ**

VALUE	DOCUMENT ID		TECN	COMMENT
$\mathbf{0.85^{+0.26}_{-0.27}\pm0.12}$	ABBIENDI	02E	OPAL	$e^+e^- \to Z$

$B_J^*(5732)$ REFERENCES

ABBIENDI	02E	EPJ C23 437	G. Abbiendi *et al.*	(OPAL Collab.)
AFFOLDER	01F	PR D64 072002	T. Affolder *et al.*	(CDF Collab.)
ACCIARRI	99N	PL B465 323	M. Acciarri *et al.*	(L3 Collab.)
BARATE	98L	PL B425 215	R. Barate *et al.*	(ALEPH Collab.)
BUSKULIC	96D	ZPHY C69 393	D. Buskulic *et al.*	(ALEPH Collab.)
ABREU	95B	PL B345 598	P. Abreu *et al.*	(DELPHI Collab.)
AKERS	95E	ZPHY C66 19	R. Akers *et al.*	(OPAL Collab.)

$B_1(5721)^0$

$I(J^P) = \frac{1}{2}(1^+)$ Status: ***

I, J, P need confirmation.

Quantum numbers shown are quark-model predictions.

$B_1(5721)^0$ MASS

OUR FIT uses m_{B^+} and $m_{B_1^0} - m_{B^+}$ to determine $m_{B_1(5721)^0}$.

VALUE (MeV)	DOCUMENT ID
5723.5±2.0 OUR FIT Error includes scale factor of 1.1.	

$m_{B_1^0} - m_{B^+}$

VALUE (MeV)	DOCUMENT ID		TECN	COMMENT
444.3±2.0 OUR FIT Error includes scale factor of 1.1.				
444.2±2.3 OUR AVERAGE Error includes scale factor of 1.3.				
$446.2^{+1.9}_{-2.1}{}^{+1.0}_{-1.2}$	[1] AALTONEN	09D	CDF	$p\overline{p}$ at 1.96 TeV
441.5±2.4±1.3	ABAZOV	07T	D0	$p\overline{p}$ at 1.96 TeV

[1] Observed in $B_1^0 \to B^{*+}\pi^-$.

$B_1(5721)^0$ DECAY MODES

	Mode	Fraction (Γ_i/Γ)
Γ_1	$B^{*+}\pi^-$	dominant

$B_1(5721)^0$ BRANCHING RATIOS

$\Gamma(B^{*+}\pi^-)/\Gamma_{total}$ **Γ_1/Γ**

VALUE	DOCUMENT ID		TECN	COMMENT
dominant	AALTONEN	09D	CDF	$p\overline{p}$ at 1.96 TeV
dominant	[2] ABAZOV	07T	D0	$p\overline{p}$ at 1.96 TeV

[2] Observed in $B_1^0 \to B^{*+}\pi^-$ with $B^{*+} \to B^+\gamma$ and $B^+ \to J/\psi\pi^+$.

$B_1(5721)^0$ REFERENCES

AALTONEN	09D	PRL 102 102003	T. Aaltonen *et al.*	(CDF Collab.)
ABAZOV	07T	PRL 99 172001	V.M. Abazov *et al.*	(D0 Collab.)

$B_2^*(5747)^0$

$I(J^P) = \frac{1}{2}(2^+)$ Status: ***

I, J, P need confirmation.

Quantum numbers shown are quark-model predictions.

$B_2^*(5747)^0$ MASS

OUR FIT uses m_{B^+}, $m_{B_1^0} - m_{B^+}$, and $m_{B_2^{*0}} - m_{B_1^0}$ to determine $m_{B_2^*(5747)^0}$. The −0.659 correlation between statistical uncertainties of $m_{B_1^0} - m_{B^+}$ and $m_{B_2^{*0}} - m_{B_1^0}$ measurements reported by ABAZOV 07T is taken into account.

VALUE (MeV)	DOCUMENT ID
5743±5 OUR FIT Error includes scale factor of 2.9.	

$B_2^*(5747)^0$ WIDTH

VALUE (MeV)	DOCUMENT ID		TECN	COMMENT
$\mathbf{22.7^{+3.8}_{-3.2}{}^{+3.2}_{-10.2}}$	AALTONEN	09D	CDF	$p\overline{p}$ at 1.96 TeV

$m_{B_2^{*0}} - m_{B_1^0}$

VALUE (MeV)	DOCUMENT ID		TECN	COMMENT
19 ±6 OUR FIT Error includes scale factor of 3.0.				
19 ±6 OUR AVERAGE Error includes scale factor of 2.8.				
$14.9^{+2.2}_{-2.5}{}^{+1.2}_{-1.4}$	[1] AALTONEN	09D	CDF	$p\overline{p}$ at 1.96 TeV
26.2±3.1±0.9	[1] ABAZOV	07T	D0	$p\overline{p}$ at 1.96 TeV

[1] Observed in $B_2^{*0} \to B^{*+}\pi^-$ and $B_2^{*0} \to B^+\pi^-$.

$B_2^*(5747)^0$ DECAY MODES

	Mode	Fraction (Γ_i/Γ)
Γ_1	$B^+\pi^-$	dominant
Γ_2	$B^{*+}\pi^-$	dominant

$B_2^*(5747)^0$ BRANCHING RATIOS

$\Gamma(B^+\pi^-)/\Gamma_{total}$ **Γ_1/Γ**

VALUE	DOCUMENT ID		TECN	COMMENT
dominant	AALTONEN	09D	CDF	$p\overline{p}$ at 1.96 TeV
dominant	ABAZOV	07T	D0	$p\overline{p}$ at 1.96 TeV

$\Gamma(B^{*+}\pi^-)/\Gamma_{total}$ **Γ_2/Γ**

VALUE	DOCUMENT ID		TECN	COMMENT
dominant	AALTONEN	09D	CDF	$p\overline{p}$ at 1.96 TeV
dominant	ABAZOV	07T	D0	$p\overline{p}$ at 1.96 TeV

$\Gamma(B^{*+}\pi^-)/\Gamma(B^+\pi^-)$ **Γ_2/Γ_1**

VALUE	DOCUMENT ID		TECN	COMMENT
1.10±0.42±0.31	[2] ABAZOV	07T	D0	$p\overline{p}$ at 1.96 TeV

[2] Converted from measured ratio of $R = B(B_2^{*0} \to B^{*+}\pi^-) / B(B_2^{*0} \to B^{(*)+}\pi^-) = 0.475 \pm 0.095 \pm 0.069$.

$B_2^*(5747)^0$ REFERENCES

AALTONEN	09D	PRL 102 102003	T. Aaltonen *et al.*	(CDF Collab.)
ABAZOV	07T	PRL 99 172001	V.M. Abazov *et al.*	(D0 Collab.)

BOTTOM, STRANGE MESONS ($B = \pm 1, S = \mp 1$)

$B_s^0 = s\overline{b}$, $\overline{B}_s^0 = \overline{s}b$, similarly for B_s^*'s

B_s^0

$I(J^P) = 0(0^-)$

I, *J*, *P* need confirmation. Quantum numbers shown are quark-model predictions.

B_s^0 MASS

VALUE (MeV)	EVTS	DOCUMENT ID		TECN	COMMENT
5366.77± 0.24 OUR FIT					
5366.7 ± 0.4 OUR AVERAGE		Error includes scale factor of 1.3. See the ideogram below.			
5366.90± 0.28±0.23		[1] AAIJ	12E	LHCB	pp at 7 TeV
5364.4 ± 1.3 ±0.7		LOUVOT	09	BELL	$e^+e^- \to \Upsilon(5S)$
5366.01± 0.73±0.33		[2] ACOSTA	06	CDF	$p\overline{p}$ at 1.96 TeV
5369.9 ± 2.3 ±1.3	32	[3] ABE	96B	CDF	$p\overline{p}$ at 1.8 TeV
5374 ±16 ±2	3	ABREU	94D	DLPH	$e^+e^- \to Z$
5359 ±19 ±7	1	[3] AKERS	94J	OPAL	$e^+e^- \to Z$
5368.6 ± 5.6 ±1.5	2	BUSKULIC	93G	ALEP	$e^+e^- \to Z$
• • • We do not use the following data for averages, fits, limits, etc. • • •					
5370 ± 1 ±3		DRUTSKOY	07A	BELL	Repl. by LOUVOT 09
5370 ±40	6	[4] AKERS	94J	OPAL	$e^+e^- \to Z$
5383.3 ± 4.5 ±5.0	14	ABE	93F	CDF	Repl. by ABE 96B

[1] Uses $B_s^0 \to J/\psi\phi$ fully reconstructed decays.
[2] Uses exclusively reconstructed final states containing a $J/\psi \to \mu^+\mu^-$ decays.
[3] From the decay $B_s \to J/\psi(1S)\phi$.
[4] From the decay $B_s \to D_s^-\pi^+$.

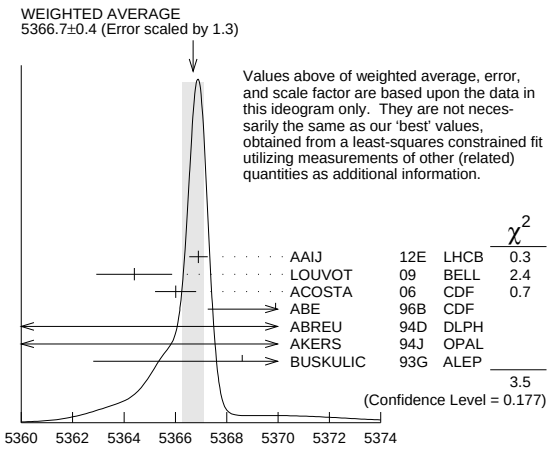

$m_{B_s^0} - m_B$

m_B is the average of our B masses $(m_{B^\pm} + m_{B^0})/2$.

VALUE (MeV)	CL%	DOCUMENT ID		TECN	COMMENT
87.35±0.23 OUR FIT					
87.34±0.29 OUR AVERAGE					
87.42±0.30±0.09		[1] AAIJ	12E	LHCB	pp at 7 TeV
86.64±0.80±0.08		[2] ACOSTA	06	CDF	$p\overline{p}$ at 1.96 TeV
• • • We use the following data for averages but not for fits. • • •					
89.7 ±2.7 ±1.2		ABE	96B	CDF	$p\overline{p}$ at 1.8 TeV
• • • We do not use the following data for averages, fits, limits, etc. • • •					
80 to 130	68	LEE-FRANZINI 90		CSB2	$e^+e^- \to \Upsilon(5S)$

[1] The reported result is $m_{B_s^0} - m_{B^+} = 87.52 \pm 0.30 \pm 0.12$ MeV. We convert it to the mass difference with respect to the average of $(m_{B^\pm} + m_{B^0})/2$.
[2] The reported result is $m_{B_s^0} - m_{B^0} = 86.38 \pm 0.90 \pm 0.06$ MeV. We convert it to the mass difference with respect to the average of $(m_{B^\pm} + m_{B^0})/2$.

$m_{B_{sH}^0} - m_{B_{sL}^0}$

See the B_s^0-$\overline{B}_s^0$ MIXING section near the end of these B_s^0 Listings.

B_s^0 MEAN LIFE

"OUR EVALUATION" is an average using rescaled values of the data listed below. The average and rescaling were performed by the Heavy Flavor Averaging Group (HFAG) and are described at http://www.slac.stanford.edu/xorg/hfag/. The averaging/rescaling procedure takes into account correlations between the measurements and asymmetric lifetime errors.

The
First "OUR EVALUATION" is an average of 1 / [0.5 ($\Gamma_{B^0_{sL}} + \Gamma_{B^0_{sH}}$)].
The Second "OUR EVALUATION" is the average of $B_s \to D_s X$ data listed below.

VALUE (10^{-12} s)	EVTS	DOCUMENT ID		TECN	COMMENT
1.512±0.007 OUR EVALUATION		First			
1.469±0.031 OUR EVALUATION		Second			
1.518±0.041±0.027		[1] AALTONEN	11AP	CDF	$p\overline{p}$ at 1.96 TeV
1.398±0.044$^{+0.028}_{-0.025}$		[2] ABAZOV	06V	D0	$p\overline{p}$ at 1.96 TeV
1.42 $^{+0.14}_{-0.13}$ ±0.03		[3] ABREU	00Y	DLPH	$e^+e^- \to Z$
1.53 $^{+0.16}_{-0.15}$ ±0.07		[4] ABREU,P	00G	DLPH	$e^+e^- \to Z$
1.36 ±0.09 $^{+0.06}_{-0.05}$		[5] ABE	99D	CDF	$p\overline{p}$ at 1.8 TeV
1.72 $^{+0.20}_{-0.19}$ $^{+0.18}_{-0.17}$		[6] ACKERSTAFF	98F	OPAL	$e^+e^- \to Z$
1.50 $^{+0.16}_{-0.15}$ ±0.04		[5] ACKERSTAFF	98G	OPAL	$e^+e^- \to Z$
1.47 ±0.14 ±0.08		[4] BARATE	98C	ALEP	$e^+e^- \to Z$
1.54 $^{+0.14}_{-0.13}$ ±0.04		[5] BUSKULIC	96M	ALEP	$e^+e^- \to Z$
• • • We do not use the following data for averages, fits, limits, etc. • • •					
1.51 ±0.11		[7] BARATE	98C	ALEP	$e^+e^- \to Z$
1.56 $^{+0.29}_{-0.26}$ $^{+0.08}_{-0.07}$		[5] ABREU	96F	DLPH	Repl. by ABREU 00Y
1.65 $^{+0.34}_{-0.31}$ ±0.12		[4] ABREU	96F	DLPH	Repl. by ABREU 00Y
1.76 ±0.20 $^{+0.15}_{-0.10}$		[8] ABREU	96F	DLPH	Repl. by ABREU 00Y
1.60 ±0.26 $^{+0.13}_{-0.15}$		[9] ABREU	96F	DLPH	Repl. by ABREU,P 00G
1.67 ±0.14		[10] ABREU	96F	DLPH	$e^+e^- \to Z$
1.61 $^{+0.30}_{-0.29}$ $^{+0.18}_{-0.16}$	90	[4] BUSKULIC	96E	ALEP	Repl. by BARATE 98C
1.42 $^{+0.27}_{-0.23}$ ±0.11	76	[5] ABE	95R	CDF	Repl. by ABE 99D
1.74 $^{+1.08}_{-0.69}$ ±0.07	8	[11] ABE	95R	CDF	Sup. by ABE 96N
1.54 $^{+0.25}_{-0.21}$ ±0.06	79	[5] AKERS	95G	OPAL	Repl. by ACKERSTAFF 98G
1.59 $^{+0.17}_{-0.15}$ ±0.03	134	[5] BUSKULIC	95O	ALEP	Sup. by BUSKULIC 96M
0.96 ±0.37	41	[12] ABREU	94E	DLPH	Sup. by ABREU 96F
1.92 $^{+0.45}_{-0.35}$ ±0.04	31	[5] BUSKULIC	94C	ALEP	Sup. by BUSKULIC 95O
1.13 $^{+0.35}_{-0.26}$ ±0.09	22	[5] ACTON	93H	OPAL	Sup. by AKERS 95G

[1] AALTONEN 11AP combines the fully reconstrcuted $B_s^0 \to D_s^-\pi^+$ decays and partially reconstructed $B_s^0 \to D_s X$ decays.
[2] Measured using $D_s\mu^+$ vertices.
[3] Uses $D_s^-\ell^+$, and $\phi\ell^+$ vertices.
[4] Measured using D_s hadron vertices.
[5] Measured using $D_s^-\ell^+$ vertices.
[6] ACKERSTAFF 98F use fully reconstructed $D_s^- \to \phi\pi^-$ and $D_s^- \to K^{*0}K^-$ in the inclusive B_s^0 decay.
[7] Combined results from $D_s^-\ell^+$ and D_s hadron.
[8] Measured using $\phi\ell$ vertices.
[9] Measured using inclusive D_s vertices.
[10] Combined result for the four ABREU 96F methods.
[11] Exclusive reconstruction of $B_s \to \psi\phi$.
[12] ABREU 94E uses the flight-distance distribution of D_s vertices, ϕ-lepton vertices, and $D_s\mu$ vertices.

B_s^0 MEAN LIFE (Flavor specific)

VALUE (10^{-12} s)	DOCUMENT ID		TECN	COMMENT
1.465±0.031 OUR EVALUATION				
1.459±0.031 OUR AVERAGE				
1.52 ±0.15 ±0.01	[1] AAIJ	14F	LHCB	pp at 7, 8 TeV
1.518±0.041±0.027	[2] AALTONEN	11AP	CDF	$p\overline{p}$ at 1.96 TeV
1.398±0.044$^{+0.028}_{-0.025}$	[3] ABAZOV	06V	D0	$p\overline{p}$ at 1.96 TeV
1.42 $^{+0.14}_{-0.13}$ ±0.03	[4] ABREU	00Y	DLPH	$e^+e^- \to Z$
1.36 ±0.09 $^{+0.06}_{-0.05}$	[5] ABE	99D	CDF	$p\overline{p}$ at 1.8 TeV
1.50 $^{+0.16}_{-0.15}$ ±0.04	[5] ACKERSTAFF	98G	OPAL	$e^+e^- \to Z$
1.54 $^{+0.14}_{-0.13}$ ±0.04	[5] BUSKULIC	96M	ALEP	$e^+e^- \to Z$

[1] Measured using $B_s^0 \to D^+ D_s^-$.

[2] AALTONEN 11AP combines the fully reconstrcuted $B_s^0 \to D_s^- \pi^+$ decays and partially reconstructed $B_s^0 \to D_s X$ decays.

[3] Measured using $D_s^- \mu^+$ vertices.

[4] Uses $D_s^- \ell^+$, and $\phi \ell^+$ vertices.

[5] Measured using $D_s^- \ell^+$ vertices.

B_s^0 MEAN LIFE ($B_S \to J/\psi\phi$)

VALUE (10^{-12} s)	DOCUMENT ID		TECN	COMMENT
1.479±0.012 OUR EVALUATION				
1.486±0.018 OUR AVERAGE Error includes scale factor of 1.6.				
1.480±0.011±0.005	[1] AAIJ	14E	LHCB	pp at 7 TeV
1.529±0.025±0.012	[2] AALTONEN	12D	CDF	$p\overline{p}$ at 1.96 TeV
$1.444^{+0.098}_{-0.090}$±0.020	[1] ABAZOV	05B	D0	$p\overline{p}$ at 1.96 TeV
$1.40\ ^{+0.15}_{-0.13}$ ±0.02	[2] ACOSTA	05	CDF	$p\overline{p}$ at 1.96 TeV
$1.34\ ^{+0.23}_{-0.19}$ ±0.05	[2] ABE	98B	CDF	$p\overline{p}$ at 1.8 TeV
• • • We do not use the following data for averages, fits, limits, etc. • • •				
$1.39\ ^{+0.13}_{-0.16}\ ^{+0.01}_{-0.02}$	[2] ABAZOV	05W	D0	$p\overline{p}$ at 1.96 TeV
$1.34\ ^{+0.23}_{-0.19}$ ±0.05	[3] ABE	96N	CDF	Repl. by ABE 98B

[1] Measured using fully reconstructed $B_s \to J/\psi\phi$ decays.

[2] Measured using the time-dependent angular analysis of $B_s^0 \to J/\psi\phi$ decays.

[3] ABE 96N uses 58 ± 12 exclusive $B_s \to J/\psi\phi$ events.

$\tau_{B_s^0}/\tau_{B^0}$ MEAN LIFE RATIO

$\tau_{B_s^0}/\tau_{B^0}$ (direct measurements)

VALUE	DOCUMENT ID		TECN	COMMENT
0.995±0.006 OUR EVALUATION				
0.973±0.010 OUR AVERAGE				
0.971±0.009±0.004	[1] AAIJ	14E	LHCB	pp at 7 TeV
1.052±0.061±0.015	[2] ABAZOV	09E	D0	$p\overline{p}$ at 1.96 TeV
• • • We do not use the following data for averages, fits, limits, etc. • • •				
$0.980^{+0.076}_{-0.071}$±0.003	[3] ABAZOV	05B	D0	Repl. by ABAZOV 05W
0.91 ±0.09 ±0.003	[4] ABAZOV	05W	D0	Repl. by ABAZOV 09E

[1] Measured using $B_s^0 \to J/\psi\phi$ and $B^0 \to J/\psi K^{*0}$ decays.

[2] Measured the angular and lifetime parameters for the time-dependent angular untagged decays $B_d^0 \to J/\psi K^{*0}$ and $B_s^0 \to J/\psi\phi$.

[3] Measured mean life ratio using fully reconstructed decays.

[4] Measured using the time-dependent angular analysis of $B_s^0 \to J/\psi\phi$ decays.

B_{sH}^0 MEAN LIFE

B_{sH}^0 is the heavy mass state of two B_s^0 CP eigenstates.

"OUR EVALUATION" has been obtained by the Heavy Flavor Averaging Group (HFAG) using the constraint of the flavor-specific lifetime average in a way similar to $\Delta\Gamma_{B_s^0}/\Gamma_{B_s^0}$.

VALUE (10^{-12} s)	DOCUMENT ID		TECN	COMMENT
1.661±0.032 OUR EVALUATION				
1.70 ±0.04 OUR AVERAGE				
1.75 ±0.12 ±0.07	[1] AAIJ	13AB	LHCB	pp at 7 TeV
1.700±0.040±0.026	[2] AAIJ	12AN	LHCB	pp at 7 TeV
$1.70\ ^{+0.12}_{-0.11}$ ±0.03	[2] AALTONEN	11AB	CDF	$p\overline{p}$ at 1.96 TeV
• • • We do not use the following data for averages, fits, limits, etc. • • •				
	[3] AALTONEN	12D	CDF	$p\overline{p}$ at 1.96 TeV
$1.613^{+0.123}_{-0.113}$	[4,5] AALTONEN	08J	CDF	Repl. by AALTONEN 12D
$1.58\ ^{+0.39}_{-0.42}\ ^{+0.01}_{-0.02}$	[5] ABAZOV	05W	D0	Repl. by ABAZOV 08AM
$2.07\ ^{+0.58}_{-0.46}$ ±0.03	[5] ACOSTA	05	CDF	Repl. by AALTONEN 08J

[1] Measured using a pure CP-odd final state $J/\psi K_S^0$ with the assumption that contributions from penguin diagrams are small.

[2] Measured using a pure CP-odd final state $J/\psi f_0(980)$.

[3] Uses the time-dependent angular analysis of $B_s^0 \to J/\psi\phi$ decays assuming CP-violating angle $\beta_s(B^0 \to J/\psi\phi) = 0.02$.

[4] Obtained from $\Delta\Gamma_s$ and Γ_s fit with a correlation of 0.6.

[5] Measured using the time-dependent angular analysis of $B_s^0 \to J/\psi\phi$ decays.

B_{sL}^0 MEAN LIFE

B_{sL}^0 is the light mass state of two B_s^0 CP eigenstates.

"OUR EVALUATION" has been obtained by the Heavy Flavor Averaging Group (HFAG) using the constraint of the flavor-specific lifetime average in a way similar to $\Delta\Gamma_{B_s^0}/\Gamma_{B_s^0}$.

VALUE (10^{-12} s)	DOCUMENT ID		TECN	COMMENT
1.405±0.025 OUR EVALUATION				
1.405±0.025 OUR AVERAGE				
1.379±0.026±0.017	[1] AAIJ	14F	LHCB	pp at 7, 8 TeV
1.440±0.096±0.009	[2] AAIJ	12	LHCB	pp at 7 TeV
1.455±0.046±0.006	[2] AAIJ	12R	LHCB	pp at 7 TeV
• • • We do not use the following data for averages, fits, limits, etc. • • •				
	[3] AALTONEN	12D	CDF	$p\overline{p}$ at 1.96 TeV
$1.437^{+0.054}_{-0.047}$	[4,5] AALTONEN	08J	CDF	Repl. by AALTONEN 12D
$1.24\ ^{+0.14}_{-0.11}\ ^{+0.01}_{-0.02}$	[5] ABAZOV	05W	D0	Repl. by ABAZOV 08AM
$1.05\ ^{+0.16}_{-0.13}$ ±0.02	[5] ACOSTA	05	CDF	Repl. by AALTONEN 08J
1.27 ±0.33 ±0.08	[6] BARATE	00K	ALEP	$e^+e^- \to Z$

[1] Measured using $B_s^0 \to D_s^- D_s^+$. The effective lifetime is translated into a decay width of $\Gamma_L = 0.725 \pm 0.014 \pm 0.009$ ps^{-1}.

[2] Measured using decays $B_s^0 \to K^+K^-$.

[3] Uses the time-dependent angular analysis of $B_s^0 \to J/\psi\phi$ decays and assuming CP-violating angle $\beta_s(B^0 \to J/\psi\phi) = 0.02$.

[4] Obtained from $\Delta\Gamma_s$ and Γ_s fit with a correlation of 0.6.

[5] Measured using the time-dependent angular analysis of $B_s^0 \to J/\psi\phi$ decays.

[6] Uses $\phi\phi$ correlations from $B_s^0 \to D_s^{(*)+} D_s^{(*)-}$.

$\Delta\Gamma_{B_s^0}/\Gamma_{B_s^0}$

$\Gamma_{B_s^0}$ and $\Delta\Gamma_{B_s^0}$ are the decay rate average and difference between two B_s^0 CP eigenstates (light − heavy).

"OUR EVALUATION" is an average of all available B_s flavor-specific lifetime measurements with the $\Delta\Gamma_{B_s^0}/\Gamma_s$ analyses performed by the Heavy Flavor Averaging Group (HFAG) as described in our "Review on B-$\overline{B}$ Mixing" in the B^0 Section of these Listings.

VALUE	CL%	DOCUMENT ID		TECN	COMMENT
0.138±0.012 OUR EVALUATION					
		[1] AAIJ	12D	LHCB	pp at 7 TeV
		[2] ABAZOV	12D	D0	$p\overline{p}$ at 1.96 TeV
• • • We do not use the following data for averages, fits, limits, etc. • • •					
0.090±0.009±0.023		[3] ESEN	13	BELL	$e^+e^- \to \Upsilon(5S)$
		[4] AALTONEN	12D	CDF	$p\overline{p}$ at 1.96 TeV
$0.147^{+0.036}_{-0.030}\ ^{+0.042}_{-0.041}$		[3] ESEN	10	BELL	$e^+e^- \to \Upsilon(5S)$
$0.116^{+0.09}_{-0.10}$ ±0.010		[5] AALTONEN	08J	CDF	Repl. by AALTONEN 12D
$0.24\ ^{+0.28}_{-0.38}\ ^{+0.03}_{-0.04}$		[5,6] ABAZOV	05W	D0	Repl. by ABAZOV 08AM
$0.65\ ^{+0.25}_{-0.33}$ ±0.01		[5] ACOSTA	05	CDF	Repl. by AALTONEN 08J
<0.46	95	[7] ABREU	00Y	DLPH	$e^+e^- \to Z$
<0.69	95	[8] ABREU,P	00G	DLPH	$e^+e^- \to Z$
<0.83	95	[9] ABE	99D	CDF	$p\overline{p}$ at 1.8 TeV
<0.67	95	[10] ACCIARRI	98S	L3	$e^+e^- \to Z$

[1] Measured using the time-dependent angular analysis of $B_s^0 \to J/\psi\phi$ decays.

[2] Measured using fully reconstructed $B_s \to J/\psi\phi$ decays.

[3] Assumes CP violation is negligible.

[4] Uses the time-dependent angular analysis of $B_s^0 \to J/\psi\phi$ decays and assuming CP-violating angle $\beta_s(B^0 \to J/\psi\phi) = 0.02$.

[5] Measured using the time-dependent angular analysis of $B_s^0 \to J/\psi\phi$ decays.

[6] Uses $|A_0|^2 - |A_\parallel|^2 = 0.355 \pm 0.066$ from ACOSTA 05.

[7] Uses $D_s^- \ell^+$, and $\phi\ell^+$ vertices.

[8] Measured using D_s hadron vertices.

[9] ABE 99D assumes $\tau_{B_s^0} = 1.55 \pm 0.05$ ps.

[10] ACCIARRI 98S assumes $\tau_{B_s^0} = 1.49 \pm 0.06$ ps and PDG 98 values of b production fraction.

Meson Particle Listings

B_s^0

$\Delta\Gamma_{B_s^0}$

"OUR EVALUATION" has been obtained by the Heavy Flavor Averaging Group (HFAG) using the constraint of the flavor-specific lifetime average in a way similar to $\Delta\Gamma_{B_s^0}/\Gamma_{B_s^0}$.

VALUE (10^{12} s^{-1})	DOCUMENT ID		TECN	COMMENT
0.091±0.008 OUR EVALUATION				
0.091±0.016 OUR AVERAGE	Error includes scale factor of 1.5. See the ideogram below.			
0.106±0.011±0.007	[1] AAIJ	13AR	LHCB	pp at 7 TeV
0.053±0.021±0.010	[2] AAD	12CV	ATLS	pp at 7 TeV
0.068±0.026±0.007	[2] AALTONEN	12AJ	CDF	$p\overline{p}$ at 1.96 TeV
$0.163^{+0.065}_{-0.064}$	[3,4] ABAZOV	12D	D0	$p\overline{p}$ at 1.96 TeV
• • • We do not use the following data for averages, fits, limits, etc. • • •				
0.123±0.029±0.011	[2] AAIJ	12D	LHCB	Repl. by AAIJ 13AR
0.075±0.035±0.006	[5] AALTONEN	12D	CDF	Repl. by AALTONEN 12AJ
$0.085^{+0.072}_{-0.078}\pm0.001$	[6] ABAZOV	09E	D0	Repl. by ABAZOV 08AM
$0.076^{+0.059}_{-0.063}\pm0.006$	[7] AALTONEN	08J	CDF	Repl. by AALTONEN 12D
$0.19\ \pm0.07\ ^{+0.02}_{-0.01}$	[4,8] ABAZOV	08AM	D0	Repl. by ABAZOV 12D
$0.12\ ^{+0.08}_{-0.10}\ \pm0.02$	[7,9] ABAZOV	07	D0	Repl. by ABAZOV 07N
0.13 ±0.09	[10] ABAZOV	07N	D0	Repl. by ABAZOV 09E
$0.47\ ^{+0.19}_{-0.24}\ \pm0.01$	[7] ACOSTA	05	CDF	Repl. by AALTONEN 08J

[1] AAIJ 13AR result comes from a combined fit to $B_s^0 \to J/\psi K^+K^-$ and $B_s^0 \to J/\psi\pi^+\pi^-$ data sets. Also reports $\Delta\Gamma_s = 0.100 \pm 0.016 \pm 0.003$ ps^{-1} from a fit to $B_s^0 \to J/\psi K^+K^-$ decays.
[2] Measured using the time-dependent angular analysis of $B_s^0 \to J/\psi\phi$ decays.
[3] The error includes both statistical and systematic uncertainties.
[4] Measured using fully reconstructed $B_s \to J/\psi\phi$ decays.
[5] Uses the time-dependent angular analysis of $B_s^0 \to J/\psi\phi$ decays and assuming CP-violating angle $\beta_s(B^0 \to J/\psi\phi) = 0.02$.
[6] Measured the angular and lifetime parameters for the time-dependent angular untagged decays $B_d^0 \to J/\psi K^{*0}$ and $B_s^0 \to J/\psi\phi$.
[7] Measured using the time-dependent angular analysis of $B_s^0 \to J/\psi\phi$ decays and assuming CP-violating phase $\phi_s = 0$.
[8] Obtaines 90% CL interval $-0.06 < \Delta\Gamma_s < 0.30$.
[9] ABAZOV 07 reports $0.17 \pm 0.09 \pm 0.02$ with CP-violating phase ϕ_s as a free parameter.
[10] Combines D^0 measurements of time-dependent angular distributions in $B_s^0 \to J/\psi\phi$ and charge asymmetry in semileptonic decays. There is a 4-fold ambiguity in the solution.

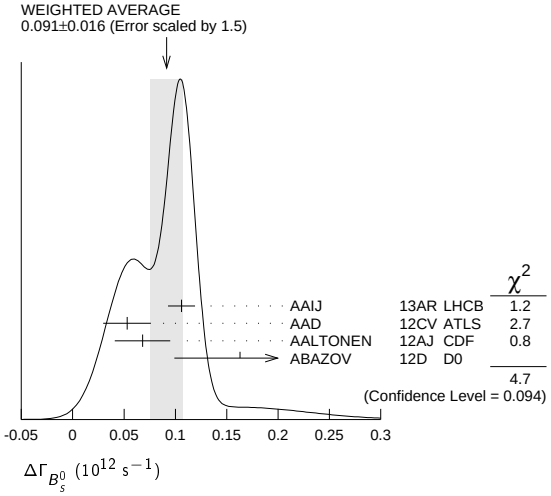

$\Delta\Gamma_s^{CP}$ / Γ_s

Γ_s and $\Delta\Gamma_s^{CP}$ are the decay rate average and difference between even, $\Gamma_s^{CP-even}$, and odd, Γ_s^{CP-odd}, CP eigenstates.

VALUE	CL%	DOCUMENT ID		TECN	COMMENT
• • • We do not use the following data for averages, fits, limits, etc. • • •					
0.072±0.021±0.022		[1] ABAZOV	09I	D0	$p\overline{p}$ at 1.96 TeV
>0.012	95	[1] AALTONEN	08F	CDF	$p\overline{p}$ at 1.96 TeV
$0.079^{+0.038+0.031}_{-0.035-0.030}$		[1] ABAZOV	07Y	D0	Repl. by ABAZOV 09I
$0.25\ ^{+0.21}_{-0.14}$		[2] BARATE	00K	ALEP	$e^+e^- \to Z$

[1] Assumes 2 B($B_s^0 \to D_s^{(*)}D_s^{(*)}$) $\simeq \Delta\Gamma_s^{CP}/\Gamma_s$.
[2] Uses $\phi\phi$ correlations from $B_s^0 \to D_s^{(*)+}D_s^{(*)-}$.

$1/\Gamma_{B_s^0}$

"OUR EVALUATION" has been obtained by the Heavy Flavor Averaging Group (HFAG) using the constraint of the flavor-specific lifetime average in a way similar to $\Delta\Gamma_{B_s^0}/\Gamma_{B_s^0}$.

VALUE (10^{-12} s)	DOCUMENT ID		TECN	COMMENT
1.512±0.007 OUR EVALUATION				
1.500±0.015 OUR AVERAGE	Error includes scale factor of 1.5. See the ideogram below.			
1.513±0.009±0.014	[1] AAIJ	13AR	LHCB	pp at 7 TeV
1.477±0.015±0.009	[2] AAD	12CV	ATLS	pp at 7 TeV
1.528±0.019±0.009	[3] AALTONEN	12AJ	CDF	$p\overline{p}$ at 1.96 TeV
$1.443^{+0.038}_{-0.035}$	[3,4] ABAZOV	12D	D0	$p\overline{p}$ at 1.96 TeV
• • • We do not use the following data for averages, fits, limits, etc. • • •				
1.522±0.021±0.019	[5] AAIJ	12D	LHCB	Repl. by AAIJ 13AR
1.529±0.025±0.012	[3] AALTONEN	12D	CDF	Repl. by AALTONEN 12AJ
1.487±0.060±0.028	[3] ABAZOV	09E	D0	Repl. by ABAZOV 08AM
1.52 ±0.04 ±0.02	[3] AALTONEN	08J	CDF	Repl. by AALTONEN 12D
1.52 ±0.05 ±0.01	[3] ABAZOV	08AM	D0	Repl. by ABAZOV 12D

[1] AAIJ 13AR reports $\Gamma_s = 0.661 \pm 0.004 \pm 0.006$ ps^{-1} obtained from combined fit to $B_s^0 \to J/\psi K^+K^-$ and $B_s^0 \to J/\psi\pi^+\pi^-$ data sets. Also reports a separate measurement of $\Gamma_s = 0.663 \pm 0.005 \pm 0.006$ ps^{-1} from $B_s^0 \to J/\psi K^+K^-$ decays.
[2] AAD 12CV reports $\Gamma_{B_s^0} = 0.677 \pm 0.007 \pm 0.004$ ps^{-1} measured using a time-dependent angular analysis of $B_s^0 \to J/\psi\phi$ decays.
[3] Measured using the time-dependent angular analysis of $B_s^0 \to J/\psi\phi$ decays.
[4] The error includes both statistical and systematic uncertainties.
[5] AAIJ 12D reports average deacy width of B_s^0, $\Gamma_{B_s^0} = 0.657 \pm 0.009 \pm 0.008$ ps^{-1} that we converted to $1/\Gamma_{B_s^0}$.

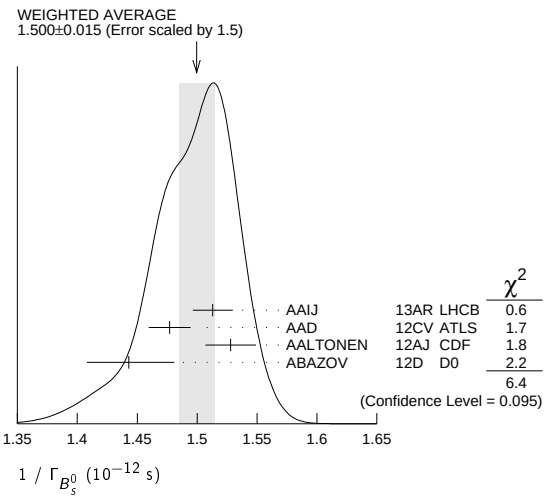

B_s^0 DECAY MODES

These branching fractions all scale with B($\overline{b} \to B_s^0$).

The branching fraction B($B_s^0 \to D_s^-\ell^+\nu_\ell$anything) is not a pure measurement since the measured product branching fraction B($\overline{b} \to B_s^0$) × B($B_s^0 \to D_s^-\ell^+\nu_\ell$anything) was used to determine B($\overline{b} \to B_s^0$), as described in the note on "B^0-$\overline{B}^0$ Mixing"

For inclusive branching fractions, *e.g.*, $B \to D^\pm$anything, the values usually are multiplicities, not branching fractions. They can be greater than one.

	Mode	Fraction (Γ_i/Γ)	Scale factor/ Confidence level
Γ_1	D_s^- anything	(93 ±25) %	
Γ_2	$\ell\nu_\ell X$	(10.5 ± 0.8) %	
Γ_3	$D_s^-\ell^+\nu_\ell$anything	[a] (7.9 ± 2.4) %	
Γ_4	$D_{s1}(2536)^-\mu^+\nu_\mu$, $D_{s1}^- \to D^{*-}K_S^0$	(2.5 ± 0.7) × 10^{-3}	
Γ_5	$D_{s1}(2536)^- X\,\mu^+\nu$, $D_{s1}^- \to \overline{D}^0K^+$	(4.3 ± 1.7) × 10^{-3}	

Γ_6	$D_{s2}(2573)^- X\,\mu^+\nu$, $D_{s2}^- \to \overline{D}^0 K^+$		$(\ 2.6 \pm 1.2\ )\times10^{-3}$		
Γ_7	$D_s^-\pi^+$		$(\ 3.04\pm 0.23)\times10^{-3}$		
Γ_8	$D_s^-\rho^+$		$(\ 7.0 \pm 1.5\ )\times10^{-3}$		
Γ_9	$D_s^-\pi^+\pi^+\pi^-$		$(\ 6.3 \pm 1.1\ )\times10^{-3}$		
Γ_{10}	$D_{s1}(2536)^-\pi^+$, $D_{s1}^- \to D_s^-\pi^+\pi^-$		$(\ 2.5 \pm 0.8\ )\times10^{-5}$		
Γ_{11}	$D_s^\mp K^\pm$		$(\ 2.03\pm 0.28)\times10^{-4}$		S=1.3
Γ_{12}	$D_s^- K^+\pi^+\pi^-$		$(\ 3.3 \pm 0.7\ )\times10^{-4}$		
Γ_{13}	$D_s^+ D_s^-$		$(\ 4.4 \pm 0.5\ )\times10^{-3}$		
Γ_{14}	$D_s^- D^+$		$(\ 3.6 \pm 0.8\ )\times10^{-4}$		
Γ_{15}	$D^+ D^-$		$(\ 2.2 \pm 0.6\ )\times10^{-4}$		
Γ_{16}	$D^0\overline{D}^0$		$(\ 1.9 \pm 0.5\ )\times10^{-4}$		
Γ_{17}	$D_s^{*-}\pi^+$		$(\ 2.0 \pm 0.5\ )\times10^{-3}$		
Γ_{18}	$D_s^{*-}\rho^+$		$(\ 9.7 \pm 2.2\ )\times10^{-3}$		
Γ_{19}	$D_s^{*+} D_s^- + D_s^{*-} D_s^+$		$(\ 1.28\pm 0.23)$ %		S=1.2
Γ_{20}	$D_s^{*+} D_s^{*-}$		$(\ 1.85\pm 0.30)$ %		
Γ_{21}	$D_s^{(*)+} D_s^{(*)-}$		$(\ 4.5 \pm 1.4\ )$ %		
Γ_{22}	$\overline{D}^0 K^-\pi^+$		$(\ 9.9 \pm 1.5\ )\times10^{-4}$		
Γ_{23}	$\overline{D}^0\overline{K}^*(892)^0$		$(\ 3.5 \pm 0.6\ )\times10^{-4}$		
Γ_{24}	$\overline{D}^0 K^+ K^-$		$(\ 4.2 \pm 1.9\ )\times10^{-5}$		
Γ_{25}	$\overline{D}^0\phi$		$(\ 2.4 \pm 0.7\ )\times10^{-5}$		
Γ_{26}	$D^{*\mp}\pi^\pm$		$< 6.1 \times10^{-6}$		CL=90%
Γ_{27}	$J/\psi(1S)\phi$		$(\ 1.07\pm 0.09)\times10^{-3}$		
Γ_{28}	$J/\psi(1S)\pi^0$		$< 1.2 \times10^{-3}$		CL=90%
Γ_{29}	$J/\psi(1S)\eta$		$(\ 4.0 \pm 0.7\ )\times10^{-4}$		S=1.3
Γ_{30}	$J/\psi(1S) K_S^0$		$(\ 1.87\pm 0.17)\times10^{-5}$		
Γ_{31}	$J/\psi(1S) K^*(892)^0$		$(\ 4.4 \pm 0.9\ )\times10^{-5}$		
Γ_{32}	$J/\psi(1S)\eta'$		$(\ 3.4 \pm 0.5\ )\times10^{-4}$		
Γ_{33}	$J/\psi(1S)\pi^+\pi^-$		$(\ 2.12\pm 0.19)\times10^{-4}$		
Γ_{34}	$J/\psi(1S) f_0(980)$, $f_0 \to \pi^+\pi^-$		$(\ 1.39\pm 0.14)\times10^{-4}$		
Γ_{35}	$J/\psi(1S) f_0(1370)$, $f_0 \to \pi^+\pi^-$		$(\ 3.9\ ^{+\ 0.8}_{-\ 1.8}\ )\times10^{-5}$		
Γ_{36}	$J/\psi(1S) f_2(1270)$, $f_2 \to \pi^+\pi^-$		$(\ 1.1 \pm 0.4\ )\times10^{-6}$		
Γ_{37}	$J/\psi(1S)\pi^+\pi^-$ (nonresonant)		$(\ 1.8\ ^{+\ 1.1}_{-\ 0.4}\ )\times10^{-5}$		
Γ_{38}	$J/\psi(1S) K^+ K^-$		$(\ 7.9 \pm 0.7\ )\times10^{-4}$		
Γ_{39}	$J/\psi(1S) f_2'(1525)$		$(\ 2.6 \pm 0.6\ )\times10^{-4}$		
Γ_{40}	$J/\psi(1S)\, p\overline{p}$		$< 4.8 \times10^{-6}$		CL=90%
Γ_{41}	$\psi(2S)\eta$		$(\ 3.3 \pm 0.9\ )\times10^{-4}$		
Γ_{42}	$\psi(2S)\pi^+\pi^-$		$(\ 7.2 \pm 1.2\ )\times10^{-5}$		
Γ_{43}	$\psi(2S)\phi$		$(\ 5.4 \pm 0.6\ )\times10^{-4}$		
Γ_{44}	$\chi_{c1}\phi$		$(\ 2.02\pm 0.30)\times10^{-4}$		
Γ_{45}	$\pi^+\pi^-$		$(\ 7.6 \pm 1.9\ )\times10^{-7}$		S=1.4
Γ_{46}	$\pi^0\pi^0$		$< 2.1 \times10^{-4}$		CL=90%
Γ_{47}	$\eta\pi^0$		$< 1.0 \times10^{-3}$		CL=90%
Γ_{48}	$\eta\eta$		$< 1.5 \times10^{-3}$		CL=90%
Γ_{49}	$\rho^0\rho^0$		$< 3.20 \times10^{-4}$		CL=90%
Γ_{50}	$\phi\rho^0$		$< 6.17 \times10^{-4}$		CL=90%
Γ_{51}	$\phi\phi$		$(\ 1.91\pm 0.31)\times10^{-5}$		
Γ_{52}	$\pi^+ K^-$		$(\ 5.5 \pm 0.6\ )\times10^{-6}$		
Γ_{53}	$K^+ K^-$		$(\ 2.49\pm 0.17)\times10^{-5}$		
Γ_{54}	$K^0\overline{K}^0$		$< 6.6 \times10^{-5}$		CL=90%
Γ_{55}	$K^0\pi^+\pi^-$		$(\ 1.9 \pm 0.5\ )\times10^{-5}$		
Γ_{56}	$K^0 K^\pm\pi^\mp$		$(\ 9.7 \pm 1.7\ )\times10^{-5}$		
Γ_{57}	$K^0 K^+ K^-$		$< 4 \times10^{-6}$		CL=90%
Γ_{58}	$\overline{K}^*(892)^0\rho^0$		$< 7.67 \times10^{-4}$		CL=90%
Γ_{59}	$\overline{K}^*(892)^0 K^*(892)^0$		$(\ 2.8 \pm 0.7\ )\times10^{-5}$		
Γ_{60}	$\phi K^*(892)^0$		$(\ 1.13\pm 0.30)\times10^{-6}$		
Γ_{61}	$p\overline{p}$		$(\ 2.8\ ^{+\ 2.2}_{-\ 1.7}\ )\times10^{-8}$		
Γ_{62}	$\Lambda_c^-\Lambda\pi^+$		$(\ 3.6 \pm 1.6\ )\times10^{-4}$		
Γ_{63}	$\gamma\gamma$	*B1*	$< 8.7 \times10^{-6}$		CL=90%
Γ_{64}	$\phi\gamma$		$(\ 3.6 \pm 0.4\ )\times10^{-5}$		

Lepton Family number (LF) violating modes or $\Delta B = 1$ weak neutral current ($B1$) modes

Γ_{65}	$\mu^+\mu^-$	*B1*	$(\ 3.1 \pm 0.7\ )\times10^{-9}$		
Γ_{66}	$e^+ e^-$	*B1*	$< 2.8 \times10^{-7}$		CL=90%
Γ_{67}	$e^\pm\mu^\mp$	*LF*	[b] $< 1.1 \times10^{-8}$		CL=90%
Γ_{68}	$\mu^+\mu^-\mu^+\mu^-$		$< 1.2 \times10^{-8}$		CL=90%
Γ_{69}	SP, $S \to \mu^+\mu^-$, $P \to \mu^+\mu^-$		[c] $< 1.2 \times10^{-8}$		CL=90%
Γ_{70}	$\phi(1020)\mu^+\mu^-$	*B1*	$(\ 7.6 \pm 1.5\ )\times10^{-7}$		
Γ_{71}	$\phi\nu\overline{\nu}$	*B1*	$< 5.4 \times10^{-3}$		CL=90%

[a] Not a pure measurement. See note at head of B_s^0 Decay Modes.

[b] The value is for the sum of the charge states or particle/antiparticle states indicated.

[c] Here S and P are the hypothetical scalar and pseudoscalar particles with masses of 2.5 GeV/c^2 and 214.3 MeV/c^2, respectively.

CONSTRAINED FIT INFORMATION

An overall fit to 10 branching ratios uses 18 measurements and one constraint to determine 7 parameters. The overall fit has a $\chi^2 = 5.6$ for 12 degrees of freedom.

The following *off-diagonal* array elements are the correlation coefficients $\langle \delta x_i \delta x_j \rangle / (\delta x_i \cdot \delta x_j)$, in percent, from the fit to the branching fractions, $x_i \equiv \Gamma_i/\Gamma_{\rm total}$. The fit constrains the x_i whose labels appear in this array to sum to one.

	x_7	x_9	x_{11}	x_{27}	x_{34}
x_9	28				
x_{11}	55	16			
x_{27}	0	0	0		
x_{34}	0	0	0	78	
x_{35}	0	0	0	16	12

B_s^0 BRANCHING RATIOS

$\Gamma(D_s^-\ \text{anything})/\Gamma_{\rm total}$ Γ_1/Γ

VALUE	EVTS	DOCUMENT ID		TECN	COMMENT
0.93±0.25 OUR AVERAGE					
0.91±0.18±0.41		[1] DRUTSKOY	07	BELL	$e^+e^- \to \Upsilon(4S)$
0.81±0.24±0.22	90	[2] BUSKULIC	96E	ALEP	$e^+e^- \to Z$
1.56±0.58±0.44	147	[3] ACTON	92N	OPAL	$e^+e^- \to Z$

[1] The extraction of this result takes into account the correlation between the measurements of $B(\Upsilon(5S) \to D_s X)$ and $B(\Upsilon(5S) \to D^0 X)$.

[2] BUSKULIC 96E separate $c\overline{c}$ and $b\overline{b}$ sources of D_s^+ mesons using a lifetime tag, subtract generic $\overline{b} \to W^+ \to D_s^+$ events, and obtain $B(\overline{b} \to B_s^0) \times B(B_s^0 \to D_s^-\ \text{anything}) = 0.088 \pm 0.020 \pm 0.020$ assuming $B(D_s \to \phi\pi) = (3.5 \pm 0.4)\times10^{-2}$ and PDG 1994 values for the relative partial widths to other D_s channels. We evaluate using our current values $B(\overline{b} \to B_s^0) = 0.107 \pm 0.014$ and $B(D_s \to \phi\pi) = 0.036 \pm 0.009$. Our first error is their experiment's and our second error is that due to $B(\overline{b} \to B_s^0)$ and $B(D_s \to \phi\pi)$.

[3] ACTON 92N assume that excess of 147 ± 48 D_s^0 events over that expected from B^0, B^+, and $c\overline{c}$ is all from B_s^0 decay. The product branching fraction is measured to be $B(\overline{b} \to B_s^0) B(B_s^0 \to D_s^-\ \text{anything}) \times B(D_s^- \to \phi\pi^-) = (5.9 \pm 1.9 \pm 1.1)\times10^{-3}$. We evaluate using our current values $B(\overline{b} \to B_s^0) = 0.107 \pm 0.014$ and $B(D_s \to \phi\pi) = 0.036 \pm 0.009$. Our first error is their experiment's and our second error is that due to $B(\overline{b} \to B_s^0)$ and $B(D_s \to \phi\pi)$.

$\Gamma(\ell\nu_\ell X)/\Gamma_{\rm total}$ Γ_2/Γ

VALUE (units 10^{-2})	DOCUMENT ID		TECN	COMMENT
10.5±0.8 OUR AVERAGE				
10.6±0.5±0.7	[1] OSWALD	13	BELL	$e^+e^- \to \Upsilon(5S)$
$9.5\ ^{+2.5}_{-2.0}\ ^{+1.1}_{-1.9}$	[2] LEES	12A	BABR	e^+e^-

[1] The measurement corresponds to the average of the electron and muon branching fractions. OSWALD 13 also reports separate branching fractions for muons and electrons.

[2] The measurement corresponds to a branching fraction where the lepton originates from bottom decay and is the average between the electron and muon branching fractions. LEES 12A uses the correlation of the production of ϕ mesons in association with a lepton in e^+e^- data taken at center-of-mass energies between 10.54 and 11.2 GeV.

$\Gamma(D_s^-\ell^+\nu_\ell\ \text{anything})/\Gamma_{\rm total}$ Γ_3/Γ

The values and averages in this section serve only to show what values result if one assumes our $B(\overline{b} \to B_s^0)$. They cannot be thought of as measurements since the underlying product branching fractions were also used to determine $B(\overline{b} \to B_s^0)$ as described in the note on "Production and Decay of b-Flavored Hadrons."

VALUE	EVTS	DOCUMENT ID		TECN	COMMENT
0.079±0.024 OUR AVERAGE					
0.076±0.012±0.021	134	[1] BUSKULIC	95O	ALEP	$e^+e^- \to Z$
0.107±0.043±0.029		[2] ABREU	92M	DLPH	$e^+e^- \to Z$
0.103±0.036±0.028	18	[3] ACTON	92N	OPAL	$e^+e^- \to Z$
• • • We do not use the following data for averages, fits, limits, etc. • • •					
0.13 ±0.04 ±0.04	27	[4] BUSKULIC	92E	ALEP	$e^+e^- \to Z$

Meson Particle Listings

B_s^0

[1] BUSKULIC 95O use $D_s\ell$ correlations. The measured product branching ratio is $B(\overline{b}\to B_s)\times B(B_s\to D_s^-\ell^+\nu_\ell \text{anything}) = (0.82\pm0.09^{+0.13}_{-0.14})\%$ assuming $B(D_s\to\phi\pi) = (3.5\pm0.4)\times10^{-2}$ and PDG 1994 values for the relative partial widths to the six other D_s channels used in this analysis. Combined with results from $\Upsilon(4S)$ experiments this can be used to extract $B(\overline{b}\to B_s) = (11.0\pm1.2^{+2.5}_{-2.6})\%$. We evaluate using our current values $B(\overline{b}\to B_s^0) = 0.107\pm0.014$ and $B(D_s\to\phi\pi) = 0.036\pm0.009$. Our first error is their experiment's and our second error is that due to $B(\overline{b}\to B_s^0)$ and $B(D_s\to\phi\pi)$.

[2] ABREU 92M measured muons only and obtained product branching ratio $B(Z\to b\text{or }\overline{b})\times B(\overline{b}\to B_s)\times B(B_s\to D_s\mu^+\nu_\mu \text{anything})\times B(D_s\to\phi\pi) = (18\pm8)\times10^{-5}$. We evaluate using our current values $B(\overline{b}\to B_s^0) = 0.107\pm0.014$ and $B(D_s\to\phi\pi) = 0.036\pm0.009$. Our first error is their experiment's and our second error is that due to $B(\overline{b}\to B_s^0)$ and $B(D_s\to\phi\pi)$. We use $B(Z\to b\text{or }\overline{b}) = 2B(Z\to b\overline{b}) = 2\times(0.2212\pm0.0019)$.

[3] ACTON 92N is measured using $D_s\to\phi\pi^+$ and $K^*(892)^0K^+$ events. The product branching fraction measured is measured to be $B(\overline{b}\to B_s^0)B(B_s^0\to D_s^-\ell^+\nu_\ell \text{anything})\times B(D_s^-\to\phi\pi^-) = (3.9\pm1.1\pm0.8)\times10^{-4}$. We evaluate using our current values $B(\overline{b}\to B_s^0) = 0.107\pm0.014$ and $B(D_s\to\phi\pi) = 0.036\pm0.009$. Our first error is their experiment's and our second error is that due to $B(\overline{b}\to B_s^0)$ and $B(D_s\to\phi\pi)$.

[4] BUSKULIC 92E is measured using $D_s\to\phi\pi^+$ and $K^*(892)^0K^+$ events. They use $2.7\pm0.7\%$ for the $\phi\pi^+$ branching fraction. The average product branching fraction is measured to be $B(\overline{b}\to B_s^0)B(B_s^0\to D_s^-\ell^+\nu_\ell \text{anything}) = 0.020\pm0.0055^{+0.005}_{-0.006}$. We evaluate using our current values $B(\overline{b}\to B_s^0) = 0.107\pm0.014$ and $B(D_s\to\phi\pi) = 0.036\pm0.009$. Our first error is their experiment's and our second error is that due to $B(\overline{b}\to B_s^0)$ and $B(D_s\to\phi\pi)$. Superseded by BUSKULIC 95O.

$\Gamma(D_{s1}(2536)^-\mu^+\nu_\mu,\ D_{s1}^-\to D^{*-}K_S^0)/\Gamma_{\text{total}}$ Γ_4/Γ

VALUE (units 10^{-3})	DOCUMENT ID		TECN	COMMENT
2.5±0.7±0.1	[1] ABAZOV	09G	D0	$p\overline{p}$ at 1.96 TeV

[1] ABAZOV 09G reports $[\Gamma(B_s^0\to D_{s1}(2536)^-\mu^+\nu_\mu,\ D_{s1}^-\to D^{*-}K_S^0)/\Gamma_{\text{total}}]\times[B(\overline{b}\to B_s^0)] = (2.66\pm0.52\pm0.45)\times10^{-4}$ which we divide by our best value $B(\overline{b}\to B_s^0) = (10.5\pm0.6)\times10^{-2}$. Our first error is their experiment's error and our second error is the systematic error from using our best value.

$\Gamma(D_{s1}(2536)^-X\mu^+\nu,\ D_{s1}^-\to\overline{D}^0K^+)/\Gamma(D_s^-\ell^+\nu_\ell \text{anything})$ Γ_5/Γ_3

VALUE (units 10^{-2})	DOCUMENT ID		TECN	COMMENT
5.4±1.2±0.5	AAIJ	11A	LHCB	pp at 7 TeV

$\Gamma(D_{s2}(2573)^-X\mu^+\nu,\ D_{s2}^-\to\overline{D}^0K^+)/\Gamma(D_s^-\ell^+\nu_\ell \text{anything})$ Γ_6/Γ_3

VALUE (units 10^{-2})	DOCUMENT ID		TECN	COMMENT
3.3±1.0±0.4	AAIJ	11A	LHCB	pp at 7 TeV

$\Gamma(D_{s1}(2536)^-X\mu^+\nu,\ D_{s1}^-\to\overline{D}^0K^+)/\Gamma(D_{s2}(2573)^-X\mu^+\nu,\ D_{s2}^-\to\overline{D}^0K^+)$ Γ_5/Γ_6

VALUE	DOCUMENT ID		TECN	COMMENT
• • • We do not use the following data for averages, fits, limits, etc. • • •				
$0.61\pm0.14\pm0.05$	[1] AAIJ	11A	LHCB	pp at 7 TeV

[1] Not independent of other AAIJ 11A measurements.

$\Gamma(D_s^-\pi^+)/\Gamma_{\text{total}}$ Γ_7/Γ

VALUE (units 10^{-3})	EVTS	DOCUMENT ID		TECN	COMMENT
3.04±0.23 OUR FIT					
3.02±0.24 OUR AVERAGE					
$2.95\pm0.05^{+0.25}_{-0.28}$		[1] AAIJ	12AG	LHCB	pp at 7 TeV
3.6 ±0.5 ±0.5		[2] LOUVOT	09	BELL	$e^+e^-\to\Upsilon(5S)$
3.0 ±0.7 ±0.1		[3] ABULENCIA	07C	CDF	$p\overline{p}$ at 1.96 TeV
• • • We do not use the following data for averages, fits, limits, etc. • • •					
6.8 ±2.2 ±1.6		DRUTSKOY	07A	BELL	Repl. by LOUVOT 09
3.5 ±1.1 ±0.2		[4] ABULENCIA	06J	CDF	Repl. by ABULENCIA 07C
<130	6	[5] AKERS	94J	OPAL	$e^+e^-\to Z$
seen	1	BUSKULIC	93G	ALEP	$e^+e^-\to Z$

[1] AAIJ 12AG reports $(2.95\pm0.05\pm0.17^{+0.18}_{-0.22})\times10^{-3}$ where the last uncertainty comes from the semileptonic f_s/f_d measurement. We combined the systematics in quadrature.

[2] LOUVOT 09 reports $(3.67^{+0.35+0.65}_{-0.33-0.645})\times10^{-3}$ from a measurement of $[\Gamma(B_s^0\to D_s^-\pi^+)/\Gamma_{\text{total}}]\times[B(\Upsilon(10860)\to B_s^{(*)}\overline{B}_s^{(*)})]$ assuming $B(\Upsilon(10860)\to B_s^{(*)}\overline{B}_s^{(*)}) = (19.5\pm2.6)\times10^{-2}$, which we rescale to our best value $B(\Upsilon(10860)\to B_s^{(*)}\overline{B}_s^{(*)}) = (20.1\pm3.1)\times10^{-2}$. Our first error is their experiment's error and our second error is the systematic error from using our best value.

[3] ABULENCIA 07C reports $[\Gamma(B_s^0\to D_s^-\pi^+)/\Gamma_{\text{total}}]\ /\ [B(B^0\to D^-\pi^+)] = 1.13\pm0.08\pm0.23$ which we multiply by our best value $B(B^0\to D^-\pi^+) = (2.68\pm0.13)\times10^{-3}$. Our first error is their experiment's error and our second error is the systematic error from using our best value.

[4] ABULENCIA 06J reports $[\Gamma(B_s^0\to D_s^-\pi^+)/\Gamma_{\text{total}}]\ /\ [B(B^0\to D^-\pi^+)] = 1.32\pm0.18\pm0.38$ which we multiply by our best value $B(B^0\to D^-\pi^+) = (2.68\pm0.13)\times10^{-3}$. Our first error is their experiment's error and our second error is the systematic error from using our best value.

[5] AKERS 94J sees ≤ 6 events and measures the limit on the product branching fraction $f(\overline{b}\to B_s^0)\cdot B(B_s^0\to D_s^-\pi^+) < 1.3\%$ at CL = 90%. We divide by our current value $B(\overline{b}\to B_s^0) = 0.105$.

$\Gamma(D_s^-\rho^+)/\Gamma_{\text{total}}$ Γ_8/Γ

VALUE (units 10^{-3})	DOCUMENT ID		TECN	COMMENT
7.0±1.4±0.5	[1] LOUVOT	10	BELL	$e^+e^-\to\Upsilon(5S)$

[1] LOUVOT 10 reports $[\Gamma(B_s^0\to D_s^-\rho^+)/\Gamma_{\text{total}}]\ /\ [B(B_s^0\to D_s^-\pi^+)] = 2.3\pm0.4\pm0.2$ which we multiply by our best value $B(B_s^0\to D_s^-\pi^+) = (3.04\pm0.23)\times10^{-3}$. Our first error is their experiment's error and our second error is the systematic error from using our best value.

$\Gamma(D_s^-\pi^+\pi^+\pi^-)/\Gamma_{\text{total}}$ Γ_9/Γ

VALUE (units 10^{-3})	DOCUMENT ID		TECN	COMMENT
6.3±1.1 OUR FIT				
6.7±1.5±0.7	[1] ABULENCIA	07C	CDF	$p\overline{p}$ at 1.96 TeV

[1] ABULENCIA 07C reports $[\Gamma(B_s^0\to D_s^-\pi^+\pi^+\pi^-)/\Gamma_{\text{total}}]\ /\ [B(B^0\to D^-\pi^+\pi^+\pi^-)] = 1.05\pm0.10\pm0.22$ which we multiply by our best value $B(B^0\to D^-\pi^+\pi^+\pi^-) = (6.4\pm0.7)\times10^{-3}$. Our first error is their experiment's error and our second error is the systematic error from using our best value.

$\Gamma(D_s^-\pi^+\pi^+\pi^-)/\Gamma(D_s^-\pi^+)$ Γ_9/Γ_7

VALUE	DOCUMENT ID		TECN	COMMENT
2.08±0.34 OUR FIT				
2.01±0.37±0.20	AAIJ	11E	LHCB	pp at 7 TeV

$\Gamma(D_{s1}(2536)^-\pi^+,\ D_{s1}^-\to D_s^-\pi^+\pi^-)/\Gamma(D_s^-\pi^+\pi^+\pi^-)$ Γ_{10}/Γ_9

VALUE (units 10^{-3})	DOCUMENT ID		TECN	COMMENT
4.0±1.0±0.4	AAIJ	12AX	LHCB	pp at 7 TeV

$\Gamma(D_s^{\mp}K^{\pm})/\Gamma_{\text{total}}$ Γ_{11}/Γ

VALUE (units 10^{-4})	DOCUMENT ID		TECN	COMMENT
2.03±0.28 OUR FIT Error includes scale factor of 1.3.				
2.3 $^{+1.2}_{-1.0}$ $^{+0.4}_{-0.3}$	[1] LOUVOT	09	BELL	$e^+e^-\to\Upsilon(5S)$

[1] LOUVOT 09 reports $(2.4^{+1.2}_{-1.0}\pm0.42)\times10^{-4}$ from a measurement of $[\Gamma(B_s^0\to D_s^{\mp}K^{\pm})/\Gamma_{\text{total}}]\times[B(\Upsilon(10860)\to B_s^{(*)}\overline{B}_s^{(*)})]$ assuming $B(\Upsilon(10860)\to B_s^{(*)}\overline{B}_s^{(*)}) = (19.5\pm2.6)\times10^{-2}$, which we rescale to our best value $B(\Upsilon(10860)\to B_s^{(*)}\overline{B}_s^{(*)}) = (20.1\pm3.1)\times10^{-2}$. Our first error is their experiment's error and our second error is the systematic error from using our best value.

$\Gamma(D_s^{\mp}K^{\pm})/\Gamma(D_s^-\pi^+)$ Γ_{11}/Γ_7

VALUE	DOCUMENT ID		TECN	COMMENT
0.067 ±0.008 OUR FIT Error includes scale factor of 1.6.				
0.066 ±0.008 OUR AVERAGE Error includes scale factor of 1.6.				
$0.0646\pm0.0043\pm0.0025$	AAIJ	12AG	LHCB	pp at 7 TeV
0.097 ±0.018 ±0.009	AALTONEN	09AQ	CDF	$p\overline{p}$ at 1.96 TeV

$\Gamma(D_s^-K^+\pi^+\pi^-)/\Gamma(D_s^-\pi^+\pi^+\pi^-)$ Γ_{12}/Γ_9

VALUE (units 10^{-2})	DOCUMENT ID		TECN	COMMENT
5.2±0.5±0.3	AAIJ	12AX	LHCB	pp at 7 TeV

$\Gamma(D_s^+D_s^-)/\Gamma_{\text{total}}$ Γ_{13}/Γ

VALUE (units 10^{-3})	CL%	DOCUMENT ID		TECN	COMMENT
4.4±0.5 OUR AVERAGE					
$4.0\pm0.2\pm0.5$		[1] AAIJ	13AP	LHCB	pp at 7 TeV
$5.8^{+1.1}_{-0.9}\pm1.3$		[2] ESEN	13	BELL	$e^+e^-\to\Upsilon(5S)$
$5.1\pm0.7\pm0.6$		[3] AALTONEN	12C	CDF	$p\overline{p}$ at 1.96 TeV
• • • We do not use the following data for averages, fits, limits, etc. • • •					
$10.3^{+3.9+2.6}_{-3.2-2.5}$		[4] ESEN	10	BELL	Repl. by ESEN 13
$10.4^{+3.5}_{-3.2}\pm1.1$		[5] AALTONEN	08F	CDF	Repl. by AALTONEN 12C
<67	90	DRUTSKOY	07A	BELL	Repl. by ESEN 10

[1] Uses $B(B^0\to D^-D_s^+) = (7.2\pm0.8)\times10^{-3}$.

[2] Use $\Upsilon(5S)\to B_s^*\overline{B}_s^*$ decays assuming $B(\Upsilon(5S)\to B_s^*\overline{B}_s^*) = (17.1\pm3.0)\%$ and $\Gamma(\Upsilon(5S)\to B_s^*\overline{B}_s^*)\ /\ \Gamma(\Upsilon(5S)\to B_s^{(*)}\overline{B}_s^{(*)}) = (87.0\pm1.7)\%$.

[3] AALTONEN 12C reports $(f_s/f_d)\ (B(B_s^0\to D_s^+D_s^-)\ /\ B(B^0\to D^-D_s^+)) = 0.183\pm0.021\pm0.017$. We multiply this result by our best value of $B(B^0\to D^-D_s^+) = (7.2\pm0.8)\times10^{-3}$ and divide by our best value of f_s/f_d, where $1/2\ f_s/f_d = 0.131\pm0.008$. Our first quoted uncertainty is the combined experiment's uncertainty and our second is the systematic uncertainty from using out best values.

[4] Uses $\Upsilon(10860)\to B_s^*\overline{B}_s^*$ assuming $B(\Upsilon(10860)\to B_s^{(*)}\overline{B}_s^{(*)}) = (19.3\pm2.9)\%$ and $\Gamma(\Upsilon(10860)\to B_s^*\overline{B}_s^*)\ /\ \Gamma(\Upsilon(10860)\to B_s^{(*)}\overline{B}_s^{(*)}) = (90.1^{+3.8}_{-4.0})\%$.

[5] AALTONEN 08F reports $[\Gamma(B_s^0\to D_s^+D_s^-)/\Gamma_{\text{total}}]\ /\ [B(B^0\to D^-D_s^+)] = 1.44^{+0.48}_{-0.44}$ which we multiply by our best value $B(B^0\to D^-D_s^+) = (7.2\pm0.8)\times10^{-3}$. Our first error is their experiment's error and our second error is the systematic error from using our best value.

$\Gamma(D_s^-D^+)/\Gamma_{\text{total}}$ Γ_{14}/Γ

VALUE (units 10^{-4})	DOCUMENT ID		TECN	COMMENT
3.6±0.6±0.5	[1] AAIJ	13AP	LHCB	pp at 7 TeV

[1] Uses $B(B^0\to D^-D_s^+) = (7.2\pm0.8)\times10^{-3}$.

$\Gamma(D^+ D^-)/\Gamma_{total}$ Γ_{15}/Γ

VALUE (units 10^{-4})	DOCUMENT ID		TECN	COMMENT
2.2±0.4±0.4	[1] AAIJ	13AP	LHCB	pp at 7 TeV

[1] Uses B($B^0 \to D^- D^+$) = (2.11 ± 0.31) × 10^{-4} and B($B^+ \to \overline{D}^0 D_s^+$) = (10.1 ± 1.7) × 10^{-3}.

$\Gamma(D^0 \overline{D}^0)/\Gamma_{total}$ Γ_{16}/Γ

VALUE (units 10^{-4})	DOCUMENT ID		TECN	COMMENT
1.9±0.3±0.4	[1] AAIJ	13AP	LHCB	pp at 7 TeV

[1] Uses B($B^0 \to D^- D^+$) = (2.11 ± 0.31) × 10^{-4} and B($B^+ \to \overline{D}^0 D_s^+$) = (10.1 ± 1.7) × 10^{-3}.

$\Gamma(D_s^{*-} \pi^+)/\Gamma_{total}$ Γ_{17}/Γ

VALUE (units 10^{-3})	DOCUMENT ID		TECN	COMMENT
$2.0^{+0.5+0.1}_{-0.4-0.2}$	[1] LOUVOT	10	BELL	$e^+e^- \to \Upsilon(5S)$

[1] LOUVOT 10 reports [$\Gamma(B_s^0 \to D_s^{*-}\pi^+)/\Gamma_{total}$] / [B($B_s^0 \to D_s^-\pi^+$)] = $0.65^{+0.15}_{-0.13}$ ± 0.07 which we multiply by our best value B($B_s^0 \to D_s^-\pi^+$) = (3.04 ± 0.23) × 10^{-3}. Our first error is their experiment's error and our second error is the systematic error from using our best value.

$\Gamma(D_s^{*-} \rho^+)/\Gamma_{total}$ Γ_{18}/Γ

VALUE (units 10^{-3})	DOCUMENT ID		TECN	COMMENT
$9.7 \pm 2.0^{+0.7}_{-0.8}$	[1] LOUVOT	10	BELL	$e^+e^- \to \Upsilon(5S)$

[1] LOUVOT 10 reports [$\Gamma(B_s^0 \to D_s^{*-}\rho^+)/\Gamma_{total}$] / [B($B_s^0 \to D_s^-\pi^+$)] = 3.2±0.6±0.3 which we multiply by our best value B($B_s^0 \to D_s^-\pi^+$) = (3.04 ± 0.23) × 10^{-3}. Our first error is their experiment's error and our second error is the systematic error from using our best value.

$\Gamma(D_s^{*-} \rho^+)/\Gamma(D_s^- \rho^+)$ Γ_{18}/Γ_8

VALUE	DOCUMENT ID		TECN	COMMENT
• • • We do not use the following data for averages, fits, limits, etc. • • •				
1.4±0.3±0.1	LOUVOT	10	BELL	$e^+e^- \to \Upsilon(5S)$

$[\Gamma(D_s^{*+} D_s^-) + \Gamma(D_s^{*-} D_s^+)]/\Gamma_{total}$ Γ_{19}/Γ

VALUE (units 10^{-3})	CL%	DOCUMENT ID		TECN	COMMENT
12.8±2.3 OUR AVERAGE		Error includes scale factor of 1.2.			
$17.6^{+2.3}_{-2.2}$±4.0		[1] ESEN	13	BELL	$e^+e^- \to \Upsilon(5S)$
11.7±1.6±1.4		[2] AALTONEN	12C	CDF	$p\overline{p}$ at 1.96 TeV
• • • We do not use the following data for averages, fits, limits, etc. • • •					
$27.5^{+8.3}_{-7.1}$±6.9		[3] ESEN	10	BELL	Repl. by ESEN 13
<121	90	DRUTSKOY	07A	BELL	Repl. by ESEN 10

[1] Use $\Upsilon(5S) \to B_s^* \overline{B}_s^*$ decays assuming B($\Upsilon(5S) \to B_s^* \overline{B}_s^*$) = (17.1 ± 3.0)% and $\Gamma(\Upsilon(5S) \to B_s^* \overline{B}_s^*)$ / $\Gamma(\Upsilon(5S) \to B_s^{(*)} \overline{B}_s^{(*)})$ = (87.0 ± 1.7)%.

[2] AALTONEN 12C reports (f_s/f_d) (B($B_s^0 \to D_s^{*+} D_s^-$ + $D_s^{*-} D_s^+$) / B($B^0 \to D^- D_s^+$)) = 0.424 ± 0.046 ± 0.035. We multiply this result by our best value of B($B^0 \to D^- D_s^+$) = (7.2 ± 0.8) × 10^{-3} and divide by our best value of f_s/f_d, where 1/2 f_s/f_d = 0.131 ± 0.008. Our first quoted uncertainty is the combined experiment's uncertainty and our second is the systematic uncertainty from using out best values.

[3] Uses $\Upsilon(10860) \to B_s^* \overline{B}_s^*$ assuming B($\Upsilon(10860) \to B_s^{(*)} \overline{B}_s^{(*)}$) = (19.3 ± 2.9)% and $\Gamma(\Upsilon(10860) \to B_s^* \overline{B}_s^*)$ / $\Gamma(\Upsilon(10860) \to B_s^{(*)} \overline{B}_s^{(*)})$ = $(90.1^{+3.8}_{-4.0})$%.

$\Gamma(D_s^{*+} D_s^{*-})/\Gamma_{total}$ Γ_{20}/Γ

VALUE (units 10^{-3})	CL%	DOCUMENT ID		TECN	COMMENT
18.5± 3.0 OUR AVERAGE					
$19.8^{+3.3+5.2}_{-3.1-5.0}$		[1] ESEN	13	BELL	$e^+e^- \to \Upsilon(5S)$
18.1± 2.7±2.2		[2] AALTONEN	12C	CDF	$p\overline{p}$ at 1.96 TeV
• • • We do not use the following data for averages, fits, limits, etc. • • •					
$30.8^{+12.2+8.5}_{-10.4-8.6}$		[3] ESEN	10	BELL	Repl. by ESEN 13
<257	90	DRUTSKOY	07A	BELL	Repl. by ESEN 10

[1] Use $\Upsilon(5S) \to B_s^* \overline{B}_s^*$ decays assuming B($\Upsilon(5S) \to B_s^* \overline{B}_s^*$) = (17.1 ± 3.0)% and $\Gamma(\Upsilon(5S) \to B_s^* \overline{B}_s^*)$ / $\Gamma(\Upsilon(5S) \to B_s^{(*)} \overline{B}_s^{(*)})$ = (87.0 ± 1.7)%.

[2] AALTONEN 12C reports (f_s/f_d) (B($B_s^0 \to D_s^{*+} D_s^{*-}$) / B($B^0 \to D^- D_s^+$)) = 0.654 ± 0.072 ± 0.065. We multiply this result by our best value of B($B^0 \to D^- D_s^+$) = (7.2 ± 0.8) × 10^{-3} and divide by our best value of f_s/f_d, where 1/2 f_s/f_d = 0.131 ± 0.008. Our first quoted uncertainty is the combined experiment's uncertainty and our second is the systematic uncertainty from using out best values.

[3] Uses $\Upsilon(10860) \to B_s^* \overline{B}_s^*$ assuming B($\Upsilon(10860) \to B_s^{(*)} \overline{B}_s^{(*)}$) = (19.3 ± 2.9)% and $\Gamma(\Upsilon(10860) \to B_s^* \overline{B}_s^*)$ / $\Gamma(\Upsilon(10860) \to B_s^{(*)} \overline{B}_s^{(*)})$ = $(90.1^{+3.8}_{-4.0})$%.

$\Gamma(D_s^{(*)+} D_s^{(*)-})/\Gamma_{total}$ Γ_{21}/Γ

"OUR EVALUATION" is an average using rescaled values of the data listed below. The average and rescaling were performed by the Heavy Flavor Averaging Group (HFAG) and are described at http://www.slac.stanford.edu/xorg/hfag/. The averaging/rescaling procedure takes into account correlations between the measurements.

VALUE (%)	CL%	DOCUMENT ID		TECN	COMMENT
4.5 ±1.4 OUR EVALUATION					
3.7 ±0.5 OUR AVERAGE					
$4.32^{+0.42+1.04}_{-0.39-1.03}$		[1] ESEN	13	BELL	$e^+e^- \to \Upsilon(5S)$
3.5 ±0.4 ±0.4		[2] AALTONEN	12C	CDF	$p\overline{p}$ at 1.96 TeV
3.5 ±1.0 ±1.1		[3] ABAZOV	09I	D0	$p\overline{p}$ at 1.96 TeV
14 ±6 ±3		[4,5] BARATE	00K	ALEP	$e^+e^- \to Z$
• • • We do not use the following data for averages, fits, limits, etc. • • •					
$6.85^{+1.53+1.79}_{-1.30-1.80}$		[6,7] ESEN	10	BELL	Repl. by ESEN 13
$3.9^{+1.9+1.6}_{-1.7-1.5}$		[3] ABAZOV	07Y	D0	Repl. by ABAZOV 09I
<0.218	90	BARATE	98Q	ALEP	$e^+e^- \to Z$

[1] Use $\Upsilon(5S) \to B_s^* \overline{B}_s^*$ decays assuming B($\Upsilon(5S) \to B_s^* \overline{B}_s^*$) = (17.1 ± 3.0)% and $\Gamma(\Upsilon(5S) \to B_s^* \overline{B}_s^*)$ / $\Gamma(\Upsilon(5S) \to B_s^{(*)} \overline{B}_s^{(*)})$ = (87.0 ± 1.7)%.

[2] AALTONEN 12C reports (f_s/f_d) (B($B_s^0 \to D_s^{(*)+} D_s^{(*)-}$) / B($B^0 \to D^- D_s^+$)) = 1.261 ± 0.095 ± 0.112. We multiply this result by our best value of B($B^0 \to D^- D_s^+$) = (7.2 ± 0.8) × 10^{-3} and divide by our best value of f_s/f_d, where 1/2 f_s/f_d = 0.131 ± 0.008. Our first quoted uncertainty is the combined experiment's uncertainty and our second is the systematic uncertainty from using out best values.

[3] Uses the final states where $D_s^+ \to \phi\pi^+$ and $D_s^- \to \phi\mu^-\overline{\nu}_\mu$.

[4] Reports B(B_s^0(short) $\to D_s^{(*)} D_s^{(*)}$) = (0.23 ± 0.10 ± 0.05) · [0.17/B($D_s \to \phi\chi$)]^2 assuming B($B_s^0 \to B_s^0$(short)) = 50%. We use our best value of B($D_s \to \phi\chi$) = 15.7 ± 1.0% to obtain the quoted result.

[5] Uses $\phi\phi$ correlations from B_s^0(short) $\to D_s^{(*)+} D_s^{(*)-}$.

[6] Sum of exclusive $B_s \to D_s^+ D_s^-$, $B_s \to D_s^{*\pm} D_s^{\mp}$ and $B_s \to D_s^{*+} D_s^{*-}$.

[7] Uses $\Upsilon(10860) \to B_s^* \overline{B}_s^*$ assuming B($\Upsilon(10860) \to B_s^{(*)} \overline{B}_s^{(*)}$) = (19.3 ± 2.9)% and $\Gamma(\Upsilon(10860) \to B_s^* \overline{B}_s^*)$ / $\Gamma(\Upsilon(10860) \to B_s^{(*)} \overline{B}_s^{(*)})$ = $(90.1^{+3.8}_{-4.0})$%.

$\Gamma(\overline{D}^0 K^- \pi^+)/\Gamma_{total}$ Γ_{22}/Γ

VALUE (units 10^{-4})	DOCUMENT ID		TECN	COMMENT
9.9±1.1±1.1	[1] AAIJ	13AQ	LHCB	pp at 7 TeV

[1] AAIJ 13AQ reports [$\Gamma(B_s^0 \to \overline{D}^0 K^-\pi^+)/\Gamma_{total}$] / [B($B^0 \to \overline{D}^0\pi^+\pi^-$)] = 1.18 ± 0.05 ± 0.12 which we multiply by our best value B($B^0 \to \overline{D}^0\pi^+\pi^-$) = (8.4 ± 0.9) × 10^{-4}. Our first error is their experiment's error and our second error is the systematic error from using our best value.

$\Gamma(\overline{D}^0 \overline{K}^*(892)^0)/\Gamma_{total}$ Γ_{23}/Γ

VALUE (units 10^{-4})	DOCUMENT ID		TECN	COMMENT
3.5±0.6 OUR AVERAGE				
3.3±0.4±0.5	[1] AAIJ	13BX	LHCB	pp at 7 TeV
4.7±1.2±0.7	[2] AAIJ	11D	LHCB	pp at 7 TeV

[1] AAIJ 13BX reports [$\Gamma(B_s^0 \to \overline{D}^0 \overline{K}^*(892)^0)/\Gamma_{total}$] / [B($B^0 \to \overline{D}^0 K^*(892)^0$)] = 7.8 ± 0.7 ± 0.3 ± 0.6 which we multiply by our best value B($B^0 \to \overline{D}^0 K^*(892)^0$) = (4.2 ± 0.6) × 10^{-5}. Our first error is their experiment's error and our second error is the systematic error from using our best value.

[2] AAIJ 11D reports [$\Gamma(B_s^0 \to \overline{D}^0 \overline{K}^*(892)^0)/\Gamma_{total}$] / [B($B^0 \to \overline{D}^0\rho^0$)] = 1.48 ± 0.34 ± 0.19 which we multiply by our best value B($B^0 \to \overline{D}^0\rho^0$) = (3.2 ± 0.5) × 10^{-4}. Our first error is their experiment's error and our second error is the systematic error from using our best value.

$\Gamma(\overline{D}^0 K^+ K^-)/\Gamma_{total}$ Γ_{24}/Γ

VALUE (units 10^{-5})	DOCUMENT ID		TECN	COMMENT
4.2±1.6±1.1	[1,2] AAIJ	12AM	LHCB	pp at 7 TeV

[1] AAIJ 12AM reports [$\Gamma(B_s^0 \to \overline{D}^0 K^+ K^-)/\Gamma_{total}$] / [B($B^0 \to \overline{D}^0 K^+ K^-$)] = 0.90 ± 0.27 ± 0.20 which we multiply by our best value B($B^0 \to \overline{D}^0 K^+ K^-$) = (4.7 ± 1.2) × 10^{-5}. Our first error is their experiment's error and our second error is the systematic error from using our best value.

[2] Uses B($b \to B_s^0$)/B($b \to B^0$) = $0.267^{+0.023}_{-0.020}$ measured by the same authors.

$\Gamma(\overline{D}^0 \phi)/\Gamma(\overline{D}^0 \overline{K}^*(892)^0)$ Γ_{25}/Γ_{23}

VALUE	DOCUMENT ID		TECN	COMMENT
0.069±0.013±0.007	AAIJ	13BX	LHCB	pp at 7 TeV

$\Gamma(D^{*\mp}\pi^{\pm})/\Gamma_{total}$ Γ_{26}/Γ

VALUE	CL%	DOCUMENT ID		TECN	COMMENT
$<6.1 \times 10^{-6}$	90	[1] AAIJ	13AL	LHCB	pp at 7 TeV

[1] Uses f_s/f_d = 0.256 ± 0.020 and B($B^0 \to D^{*-}\pi^+$) = (2.76 ± 0.13) × 10^{-3}.

Meson Particle Listings

B_s^0

$\Gamma(J/\psi(1S)\phi)/\Gamma_{total}$ Γ_{27}/Γ

VALUE (units 10^{-3})	EVTS	DOCUMENT ID		TECN	COMMENT
1.07 ±0.09 OUR FIT					
1.10 ±0.09 OUR AVERAGE					
1.050±0.013±0.104		[1] AAIJ	13AN	LHCB	pp at 7 TeV
1.25 ±0.07 ±0.23		[2] THORNE	13	BELL	$e^+e^- \to \Upsilon(5S)$
1.4 ±0.4 ±0.1		[3] ABE	96Q	CDF	$p\overline{p}$
• • • We do not use the following data for averages, fits, limits, etc. • • •					
<6	1	[4] AKERS	94J	OPAL	$e^+e^- \to Z$
seen	14	[5] ABE	93F	CDF	$p\overline{p}$ at 1.8 TeV
seen	1	[6] ACTON	92N	OPAL	Sup. by AKERS 94J

[1] Uses $f_s/f_d = 0.256 \pm 0.020$ and $B(B^+ \to J/\psi K^+) = (10.18 \pm 0.42) \times 10^{-4}$.

[2] Uses $f_s = (17.2 \pm 3.0)\%$ as the fraction of $\Upsilon(5S)$ decaying to $B_s^{(*)}\overline{B}_s^{(*)}$.

[3] ABE 96Q reports $[\Gamma(B_s^0 \to J/\psi(1S)\phi)/\Gamma_{total}] \times [\Gamma(\overline{b} \to B_s^0)/\left[\Gamma(\overline{b} \to B^+) + \Gamma(\overline{b} \to B^0)\right]] = (0.185 \pm 0.055 \pm 0.020) \times 10^{-3}$ which we divide by our best value $\Gamma(\overline{b} \to B_s^0)/\left[\Gamma(\overline{b} \to B^+) + \Gamma(\overline{b} \to B^0)\right] = 0.131 \pm 0.008$. Our first error is their experiment's error and our second error is the systematic error from using our best value.

[4] AKERS 94J sees one event and measures the limit on the product branching fraction $f(\overline{b} \to B_s^0) \cdot B(B_s^0 \to J/\psi(1S)\phi) < 7 \times 10^{-4}$ at CL = 90%. We divide by $B(\overline{b} \to B_s^0) = 0.112$.

[5] ABE 93F measured using $J/\psi(1S) \to \mu^+\mu^-$ and $\phi \to K^+K^-$.

[6] In ACTON 92N a limit on the product branching fraction is measured to be $f(\overline{b} \to B_s^0) \cdot B(B_s^0 \to J/\psi(1S)\phi) \leq 0.22 \times 10^{-2}$.

$\Gamma(J/\psi(1S)\pi^0)/\Gamma_{total}$ Γ_{28}/Γ

VALUE	CL%	DOCUMENT ID		TECN
$<1.2 \times 10^{-3}$	90	[1] ACCIARRI	97C	L3

[1] ACCIARRI 97C assumes B^0 production fraction (39.5 ± 4.0%) and B_S (12.0 ± 3.0%).

$\Gamma(J/\psi(1S)\eta)/\Gamma_{total}$ Γ_{29}/Γ

VALUE (units 10^{-4})	CL%	DOCUMENT ID		TECN	COMMENT
4.0 ±0.7 OUR AVERAGE		Error includes scale factor of 1.3.			
$3.6 \ ^{+0.5}_{-0.6} \pm 0.3$		[1] AAIJ	13A	LHCB	pp at 7 TeV
$5.10 \pm 0.50 \ ^{+1.17}_{-0.83}$		[2] LI	12	BELL	$e^+e^- \to \Upsilon(4S)$
• • • We do not use the following data for averages, fits, limits, etc. • • •					
<38	90	[3] ACCIARRI	97C	L3	

[1] AAIJ 13A reports $[\Gamma(B_s^0 \to J/\psi(1S)\eta)/\Gamma_{total}] / [B(B^0 \to J/\psi(1S)\rho^0)] = 14.0 \pm 1.2 \ ^{+1.1}_{-1.5} \ ^{+1.1}_{-1.0}$ which we multiply by our best value $B(B^0 \to J/\psi(1S)\rho^0) = (2.58 \pm 0.21) \times 10^{-5}$. Our first error is their experiment's error and our second error is the systematic error from using our best value.

[2] Observed for the first time with significances over 10 σ. The second error are total systematic uncertainties including the error on $N(B_s^{(*)}\overline{B}_s^{(*)})$.

[3] ACCIARRI 97C assumes B^0 production fraction (39.5 ± 4.0%) and B_S (12.0 ± 3.0%).

$\Gamma(J/\psi(1S)K_S^0)/\Gamma_{total}$ Γ_{30}/Γ

VALUE (units 10^{-5})	DOCUMENT ID		TECN	COMMENT
1.87±0.17 OUR AVERAGE				
1.88±0.15±0.13	[1] AAIJ	13AB	LHCB	pp at 7 TeV
1.8 ±0.4 ±0.1	[2] AALTONEN	11A	CDF	$p\overline{p}$ at 1.96 TeV
• • • We do not use the following data for averages, fits, limits, etc. • • •				
1.88±0.24±0.13	[3] AAIJ	12O	LHCB	Repl. by AAIJ 13AB

[1] AAIJ 13AB reports $(1.97 \pm 0.14 \pm 0.07 \pm 0.15 \pm 0.08) \times 10^{-5}$ from a measurement of $[\Gamma(B_s^0 \to J/\psi(1S)K_S^0)/\Gamma_{total}] / [B(B^0 \to J/\psi(1S)K^0)] \times [\Gamma(\overline{b} \to B_s^0)/\Gamma(\overline{b} \to B^0)]$ assuming $B(B^0 \to J/\psi(1S)K^0) = (8.98 \pm 0.35) \times 10^{-4}$, $\Gamma(\overline{b} \to B_s^0)/\Gamma(\overline{b} \to B^0) = 0.256 \pm 0.020$, which we rescale to our best values $B(B^0 \to J/\psi(1S)K^0) = (8.73 \pm 0.32) \times 10^{-4}$, $\Gamma(\overline{b} \to B_s^0)/\Gamma(\overline{b} \to B^0) = 0.261 \pm 0.015$. Our first error is their experiment's error and our second error is the systematic error from using our best values.

[2] AALTONEN 11A reports $[\Gamma(B_s^0 \to J/\psi(1S)K_S^0)/\Gamma_{total}] \times [B(\overline{b} \to B_s^0)] / [B(\overline{b} \to B^0)] / [B(B^0 \to J/\psi(1S)K_S^0)] = (1.09 \pm 0.19 \pm 0.11) \times 10^{-2}$ which we multiply or divide by our best values $B(\overline{b} \to B_s^0) = (10.5 \pm 0.6) \times 10^{-2}$, $B(\overline{b} \to B^0) = (40.2 \pm 0.7) \times 10^{-2}$, $B(B^0 \to J/\psi(1S)K_S^0) = 1/2 \times B(B^0 \to J/\psi(1S)K^0) = 1/2 \times (8.73 \pm 0.32) \times 10^{-4}$. Our firs t error is their experiment's error and our second error is the systematic error from using our best values.

[3] AAIJ 12O reports $(1.83 \pm 0.21 \pm 0.10 \pm 0.14 \pm 0.07) \times 10^{-5}$ from a measurement of $[\Gamma(B_s^0 \to J/\psi(1S)K_S^0)/\Gamma_{total}] / [B(B^0 \to J/\psi(1S)K^0)] \times [\Gamma(\overline{b} \to B_s^0)/\Gamma(\overline{b} \to B^0)]$ assuming $B(B^0 \to J/\psi(1S)K^0) = (8.71 \pm 0.32) \times 10^{-4}$, $\Gamma(\overline{b} \to B_s^0)/\Gamma(\overline{b} \to B^0) = 0.267 \ ^{+0.021}_{-0.02}$, which we rescale to our best values $B(B^0 \to J/\psi(1S)K^0) = (8.73 \pm 0.32) \times 10^{-4}$, $\Gamma(\overline{b} \to B_s^0)/\Gamma(\overline{b} \to B^0) = 0.261 \pm 0.015$. Our first error is their experiment's error and our second error is the systematic error from using our best values.

$\Gamma(J/\psi(1S)K^*(892)^0)/\Gamma_{total}$ Γ_{31}/Γ

VALUE (units 10^{-5})	DOCUMENT ID		TECN	COMMENT
$4.4 \ ^{+0.5}_{-0.4} \pm 0.8$	[1] AAIJ	12AP	LHCB	pp at 7 TeV
• • • We do not use the following data for averages, fits, limits, etc. • • •				
8 ±4 ±1	[2] AALTONEN	11A	CDF	$p\overline{p}$ at 1.96 TeV

[1] AAIJ 12AP reports $B(B_s^0 \to J/\psi(1S)K^*(892)^0)/B(B^0 \to J/\psi(1S)K^*(892)^0) = (3.43 \ ^{+0.34}_{-0.36} \pm 0.50) \times 10^{-2}$ and $B(B^0 \to J/\psi(1S)K^*(892)^0) = (1.29 \pm 0.05 \pm 0.13) \times 10^{-3}$ after correcting for the contribution from $K\pi$ S-wave beneath the K^* peak.

[2] AALTONEN 11A reports $[\Gamma(B_s^0 \to J/\psi(1S)K^*(892)^0)/\Gamma_{total}] \times [B(\overline{b} \to B_s^0)] / [B(\overline{b} \to B^0)] / [B(B^0 \to J/\psi(1S)K^*(892)^0)] = 0.0168 \pm 0.0024 \pm 0.0068$ which we multiply or divide by our best values $B(\overline{b} \to B_s^0) = (10.5 \pm 0.6) \times 10^{-2}$, $B(\overline{b} \to B^0) = (40.2 \pm 0.7) \times 10^{-2}$, $B(B^0 \to J/\psi(1S)K^*(892)^0) = (1.32 \pm 0.06) \times 10^{-3}$. Our first error is their experiment's error and our second error is the systematic error from using our best values.

$\Gamma(J/\psi(1S)\eta')/\Gamma_{total}$ Γ_{32}/Γ

VALUE (units 10^{-4})	DOCUMENT ID		TECN	COMMENT
3.4 ±0.5 OUR AVERAGE				
$3.3 \ ^{+0.4}_{-0.5} \pm 0.3$	[1] AAIJ	13A	LHCB	pp at 7 TeV
$3.71 \pm 0.61 \ ^{+0.85}_{-0.60}$	[2] LI	12	BELL	$e^+e^- \to \Upsilon(4S)$

[1] AAIJ 13A reports $[\Gamma(B_s^0 \to J/\psi(1S)\eta')/\Gamma_{total}] / [B(B^0 \to J/\psi(1S)\rho^0)] = 12.7 \pm 1.1 \ ^{+0.5}_{-1.3} \ ^{+1.0}_{-0.9}$ which we multiply by our best value $B(B^0 \to J/\psi(1S)\rho^0) = (2.58 \pm 0.21) \times 10^{-5}$. Our first error is their experiment's error and our second error is the systematic error from using our best value.

[2] Observed for the first time with significances over 10 σ. The second error are total systematic uncertainties including the error on $N(B_s^{(*)}\overline{B}_s^{(*)})$.

$\Gamma(J/\psi(1S)\eta')/\Gamma(J/\psi(1S)\eta)$ Γ_{32}/Γ_{29}

VALUE	DOCUMENT ID		TECN	COMMENT
$0.85 \ ^{+0.09}_{-0.08}$ OUR AVERAGE				
$0.90 \pm 0.09 \ ^{+0.06}_{-0.02}$	[1] AAIJ	13A	LHCB	pp at 7 TeV
0.73±0.14±0.02	[1] LI	12	BELL	$e^+e^- \to \Upsilon(4S)$

[1] Strongly correlated with measurements of $\Gamma(J/\psi(1S)\eta)/\Gamma$ and $\Gamma(J/\psi(1S)\eta')/\Gamma$ reported in the same reference.

$\Gamma(J/\psi(1S)\pi^+\pi^-)/\Gamma(J/\psi(1S)\phi)$ Γ_{33}/Γ_{27}

VALUE (units 10^{-2})	DOCUMENT ID		TECN	COMMENT
19.8±0.5±0.5	[1] AAIJ	12AO	LHCB	pp at 7 TeV

[1] AAIJ 12AO reports $(19.79 \pm 0.47 \pm 0.52) \times 10^{-2}$ from a measurement of $[\Gamma(B_s^0 \to J/\psi(1S)\pi^+\pi^-)/\Gamma(B_s^0 \to J/\psi(1S)\phi)] / [B(\phi(1020) \to K^+K^-)]$ assuming $B(\phi(1020) \to K^+K^-) = (48.9 \pm 0.5) \times 10^{-2}$.

$\Gamma(J/\psi(1S)f_0(980),\ f_0 \to \pi^+\pi^-)/\Gamma_{total}$ Γ_{34}/Γ

VALUE (units 10^{-4})	DOCUMENT ID		TECN	COMMENT
1.39±0.14 OUR FIT				
$1.16 \ ^{+0.31}_{-0.19} \ ^{+0.30}_{-0.25}$	[1] LI	11	BELL	$e^+e^- \to \Upsilon(5S)$

[1] The second error includes both the detector systematic and the uncertainty in the number of produced $Y(5S) \to B_s^{(*)}\overline{B}_s^{(*)}$ pairs.

$\Gamma(J/\psi(1S)f_0(980),\ f_0 \to \pi^+\pi^-)/\Gamma(J/\psi(1S)\phi)$ Γ_{34}/Γ_{27}

VALUE	DOCUMENT ID		TECN	COMMENT
0.129±0.008 OUR FIT				
$0.130 \pm 0.010 \pm 0.008$ OUR AVERAGE				
$0.139 \pm 0.006 \ ^{+0.025}_{-0.012}$	[1,2] AAIJ	12AO	LHCB	pp at 7 TeV
0.135±0.036±0.001	[3] ABAZOV	12C	D0	$p\overline{p}$ at 1.96 TeV
$0.123 \ ^{+0.026}_{-0.022} \pm 0.001$	[4] AAIJ	11	LHCB	pp at 7 TeV
0.126±0.012±0.001	[5] AALTONEN	11AB	CDF	$p\overline{p}$ at 1.96 TeV

[1] AAIJ 12AO reports $(13.9 \pm 0.6 \ ^{+2.5}_{-1.2}) \times 10^{-2}$ from a measurement of $[\Gamma(B_s^0 \to J/\psi(1S)f_0(980),\ f_0 \to \pi^+\pi^-)/\Gamma(B_s^0 \to J/\psi(1S)\phi)] / [B(\phi(1020) \to K^+K^-)]$ assuming $B(\phi(1020) \to K^+K^-) = (48.9 \pm 0.5) \times 10^{-2}$.

[2] Measured in Dalitz plot like analysis of $B_s \to J/\psi\pi^+\pi^-$ decays.

[3] ABAZOV 12C reports $[\Gamma(B_s^0 \to J/\psi(1S)f_0(980),\ f_0 \to \pi^+\pi^-)/\Gamma(B_s^0 \to J/\psi(1S)\phi)] / [B(\phi(1020) \to K^+K^-)] = 0.275 \pm 0.041 \pm 0.061$ which we multiply by our best value $B(\phi(1020) \to K^+K^-) = (48.9 \pm 0.5) \times 10^{-2}$. Our first error is their experiment's error and our second error is the systematic error from using our best value.

[4] AAIJ 11 reports $[\Gamma(B_s^0 \to J/\psi(1S)f_0(980),\ f_0 \to \pi^+\pi^-)/\Gamma(B_s^0 \to J/\psi(1S)\phi)] / [B(\phi(1020) \to K^+K^-)] = 0.252 \ ^{+0.046}_{-0.032} \ ^{+0.027}_{-0.033}$ which we multiply by our best value $B(\phi(1020) \to K^+K^-) = (48.9 \pm 0.5) \times 10^{-2}$. Our first error is their experiment's error and our second error is the systematic error from using our best value.

[5] AALTONEN 11AB reports $[\Gamma(B_s^0 \to J/\psi(1S)f_0(980),\ f_0 \to \pi^+\pi^-)/\Gamma(B_s^0 \to J/\psi(1S)\phi)] / [B(\phi(1020) \to K^+K^-)] = 0.257 \pm 0.020 \pm 0.014$ which we multiply by our best value $B(\phi(1020) \to K^+K^-) = (48.9 \pm 0.5) \times 10^{-2}$. Our first error is their experiment's error and our second error is the systematic error from using our best value.

$\Gamma(J/\psi(1S)f_0(1370),\ f_0\to\pi^+\pi^-)/\Gamma_{total}$ Γ_{35}/Γ

VALUE (units 10^{-4})	DOCUMENT ID		TECN	COMMENT
$0.39^{+0.08}_{-0.18}$ OUR FIT				
$0.34^{+0.11}_{-0.14}{}^{+0.085}_{-0.054}$	[1] LI	11	BELL	$e^+e^-\to\Upsilon(5S)$

[1] The second error includes both the detector systematic and the uncertainty in the number of produced $Y(5S)\to B_s^{(*)}\overline{B}_s^{(*)}$ pairs.

$\Gamma(J/\psi(1S)f_0(1370),\ f_0\to\pi^+\pi^-)/\Gamma(J/\psi(1S)\phi)$ Γ_{35}/Γ_{27}

VALUE (units 10^{-2})	DOCUMENT ID		TECN	COMMENT
$3.7^{+0.8}_{-1.7}$ OUR FIT				
$4.2\pm0.5^{+0.1}_{-3.7}$	[1,2] AAIJ	12AO	LHCB	pp at 7 TeV

[1] AAIJ 12AO reports $(4.19\pm0.53^{+0.12}_{-3.7})\times10^{-2}$ from a measurement of $[\Gamma(B_s^0\to J/\psi(1S)f_0(1370),\ f_0\to\pi^+\pi^-)/\Gamma(B_s^0\to J/\psi(1S)\phi)]$ / $[B(\phi(1020)\to K^+K^-)]$ assuming $B(\phi(1020)\to K^+K^-)=(48.9\pm0.5)\times10^{-2}$.

[2] Measured in Dalitz plot like analysis of $B_s\to J/\psi\pi^+\pi^-$ decays.

$\Gamma(J/\psi(1S)f_2(1270),\ f_2\to\pi^+\pi^-)/\Gamma(J/\psi(1S)\phi)$ Γ_{36}/Γ_{27}

VALUE (units 10^{-4})	DOCUMENT ID		TECN	COMMENT
$9.8\pm3.3^{+0.6}_{-1.5}$	[1,2] AAIJ	12AO	LHCB	pp at 7 TeV

[1] AAIJ 12AO reports $(0.098\pm0.033^{+0.006}_{-0.015})\times10^{-2}$ from a measurement of $[\Gamma(B_s^0\to J/\psi(1S)f_2(1270),\ f_2\to\pi^+\pi^-)/\Gamma(B_s^0\to J/\psi(1S)\phi)]$ / $[B(\phi(1020)\to K^+K^-)]$ assuming $B(\phi(1020)\to K^+K^-)=(48.9\pm0.5)\times10^{-2}$.

[2] Measured in Dalitz plot like analysis of $B_s\to J/\psi\pi^+\pi^-$ decays for the f_2 helicity state $\lambda=0$.

$\Gamma(J/\psi(1S)\pi^+\pi^-\text{(nonresonant)})/\Gamma(J/\psi(1S)\phi)$ Γ_{37}/Γ_{27}

VALUE (units 10^{-2})	DOCUMENT ID		TECN	COMMENT
$1.66\pm0.31^{+0.96}_{-0.08}$	[1,2] AAIJ	12AO	LHCB	pp at 7 TeV

[1] AAIJ 12AO reports $(1.66\pm0.31^{+0.96}_{-0.08})\times10^{-2}$ from a measurement of $[\Gamma(B_s^0\to J/\psi(1S)\pi^+\pi^-\text{(nonresonant)})/\Gamma(B_s^0\to J/\psi(1S)\phi)]$ / $[B(\phi(1020)\to K^+K^-)]$ assuming $B(\phi(1020)\to K^+K^-)=(48.9\pm0.5)\times10^{-2}$.

[2] Measured in Dalitz plot like analysis of $B_s\to J/\psi\pi^+\pi^-$ decays.

$\Gamma(J/\psi(1S)K^+K^-)/\Gamma_{total}$ Γ_{38}/Γ

VALUE (units 10^{-4})	DOCUMENT ID		TECN	COMMENT
7.9 ±0.7 OUR AVERAGE				
$7.70\pm0.08\pm0.72$	[1] AAIJ	13AN	LHCB	pp at 7 TeV
10.1 ±0.9 ±2.1	[2] THORNE	13	BELL	$e^+e^-\to\Upsilon(5S)$

[1] Uses $f_s/f_d=0.256\pm0.020$ and $B(B^+\to J/\psi K^+)=(10.18\pm0.42)\times10^{-4}$.

[2] Uses $f_s=(17.2\pm3.0)\%$ as the fraction of $\Upsilon(5S)$ decaying to $B_s^{(*)}\overline{B}_s^{(*)}$.

$\Gamma(J/\psi(1S)f_2'(1525))/\Gamma(J/\psi(1S)\phi)$ Γ_{39}/Γ_{27}

VALUE (units 10^{-2})	DOCUMENT ID		TECN	COMMENT
21 ±4 OUR AVERAGE				
$21.5\pm4.9\pm2.6$	[1] THORNE	13	BELL	$e^+e^-\to\Upsilon(5S)$
21 ±7 ±1	[2,3] ABAZOV	12AF	D0	$p\overline{p}$ at 1.96 TeV
• • • We do not use the following data for averages, fits, limits, etc. • • •				
$26.4\pm3.5\pm0.7$	[4] AAIJ	12S	LHCB	Repl. by AAIJ 13AN

[1] Uses $B(f_2'(1525)\to K^+K^-)=(44.4\pm1.1)\%$.

[2] ABAZOV 12AF reports $[\Gamma(B_s^0\to J/\psi(1S)f_2'(1525))/\Gamma(B_s^0\to J/\psi(1S)\phi)]\times B(f_2'(1525)\to K^+K^-)$ / $B(\phi(1020)\to K^+K^-)=0.19\pm0.05\pm0.04$ which we divide and multiply by our best values $B(f_2'(1525)\to K^+K^-)=\frac{1}{2}(88.7\pm2.2)\times10^{-2}$, $B(\phi(1020)\to K^+K^-)=(48.9\pm0.5)\times10^{-2}$. Our first error is their experiment's error and our second error is the systematic error from using our best values.

[3] ABAZOV 12AF fits the invariant masses of the K^+K^- pair in the range $1.35<M(K^+K^-)<2$ GeV.

[4] AAIJ 12S reports $[(26.4\pm2.7\pm2.4)\times10^{-2}$ from a measurement of $\Gamma(B_s^0\to J/\psi(1S)f_2'(1525))/\Gamma(B_s^0\to J/\psi(1S)\phi)]\times B(f_2'(1525)\to K^+K^-)$ / $B(\phi(1020)\to K^+K^-)$ assuming $B(f_2'(1525)\to K^+K^-)=(44.4\pm1.1)\times10^{-2}$, $B(\phi(1020)\to K^+K^-)=(48.9\pm0.5)\times10^{-2}$, which we rescale to our best values $B(f_2'(1525)\to K^+K^-)=\frac{1}{2}(88.7\pm2.2)\times10^{-2}$, $B(\phi(1020)\to K^+K^-)=(48.9\pm0.5)\times10^{-2}$. Our first error is their experiment's error and our second error is the systematic error from using our best values.

$\Gamma(J/\psi(1S)f_2'(1525))/\Gamma_{total}$ Γ_{39}/Γ

VALUE (units 10^{-4})	DOCUMENT ID		TECN	COMMENT
$2.61\pm0.20^{+0.56}_{-0.50}$	[1] AAIJ	13AN	LHCB	pp at 7 TeV

[1] Uses $f_s/f_d=0.256\pm0.020$ and $B(B^+\to J/\psi K^+)=(10.18\pm0.42)\times10^{-4}$.

$\Gamma(\psi(2S)\eta)/\Gamma(J/\psi(1S)\eta)$ Γ_{41}/Γ_{29}

VALUE	DOCUMENT ID		TECN	COMMENT
$0.83\pm0.14\pm0.12$	[1] AAIJ	13AA	LHCB	pp at 7 TeV

[1] Assuming lepton universality for dimuon decay modes of J/ψ and $\psi(2S)$ mesons, the ratio $B(J/\psi\to\mu^+\mu^-)/B(\psi(2S)\to\mu^+\mu^-)=B(J/\psi\to e^+e^-)/B(\psi(2S)\to e^+e^-)=7.69\pm0.19$ was used.

$\Gamma(J/\psi(1S)p\overline{p})/\Gamma_{total}$ Γ_{40}/Γ

VALUE	CL%	DOCUMENT ID		TECN	COMMENT
$<4.8\times10^{-6}$	90	[1] AAIJ	13Z	LHCB	pp at 7 TeV

[1] Uses $B(B_s^0\to J/\psi(1S)\pi^+\pi^-)=(1.98\pm0.20)\times10^{-4}$.

$\Gamma(\psi(2S)\phi)/\Gamma_{total}$ Γ_{43}/Γ

VALUE (units 10^{-4})	EVTS	DOCUMENT ID		TECN	COMMENT
• • • We do not use the following data for averages, fits, limits, etc. • • •					
seen	1	BUSKULIC	93G	ALEP	$e^+e^-\to Z$

$\Gamma(\psi(2S)\phi)/\Gamma(J/\psi(1S)\phi)$ Γ_{43}/Γ_{27}

VALUE	DOCUMENT ID		TECN	COMMENT
0.501±0.034 OUR AVERAGE				
$0.497\pm0.034\pm0.011$	[1,2] AAIJ	12L	LHCB	pp at 7 TeV
0.53 ±0.10 ±0.09	ABAZOV	09Y	D0	$p\overline{p}$ at 1.96 TeV
0.52 ±0.13 ±0.07	ABULENCIA	06N	CDF	$p\overline{p}$ at 1.96 TeV

[1] AAIJ 12L reports $0.489\pm0.026\pm0.021\pm0.012$ from a measurement of $[\Gamma(B_s^0\to\psi(2S)\phi)/\Gamma(B_s^0\to J/\psi(1S)\phi)]\times[B(J/\psi(1S)\to e^+e^-)]$ / $[B(\psi(2S)\to e^+e^-)]$ assuming $B(J/\psi(1S)\to e^+e^-)=(5.94\pm0.06)\times10^{-2}$, $B(\psi(2S)\to e^+e^-)=(7.72\pm0.17)\times10^{-3}$, which we rescale to our best values $B(J/\psi(1S)\to e^+e^-)=(5.971\pm0.032)\times10^{-2}$, $B(\psi(2S)\to e^+e^-)=(7.89\pm0.17)\times10^{-3}$. Our first error is their experiment's error and our second error is the systematic error from using our best values.

[2] Assumes $B(J/\psi\to\mu^+\mu^-)$ / $B(\psi(2S)\to\mu^+\mu^-)=B(J/\psi\to e^+e^-)$ / $B(\psi(2S)\to e^+e^-)=7.69\pm0.19$.

$\Gamma(\chi_{c1}\phi)/\Gamma(J/\psi(1S)\phi)$ Γ_{44}/Γ_{27}

VALUE (units 10^{-2})	DOCUMENT ID		TECN	COMMENT
18.9±1.8±1.5	[1] AAIJ	13AC	LHCB	pp at 7 TeV

[1] Uses $B(\chi_{c1}\to J/\psi\gamma)=(34.4\pm1.5)\%$.

$\Gamma(\psi(2S)\pi^+\pi^-)/\Gamma(J/\psi(1S)\pi^+\pi^-)$ Γ_{42}/Γ_{33}

VALUE	DOCUMENT ID		TECN	COMMENT
0.34±0.04±0.03	[1] AAIJ	13AA	LHCB	pp at 7 TeV

[1] Assuming lepton universality for dimuon decay modes of J/ψ and $\psi(2S)$ mesons, the ratio $B(J/\psi\to\mu^+\mu^-)/B(\psi(2S)\to\mu^+\mu^-)=B(J/\psi\to e^+e^-)/B(\psi(2S)\to e^+e^-)=7.69\pm0.19$ was used.

$\Gamma(\pi^+\pi^-)/\Gamma_{total}$ Γ_{45}/Γ

VALUE (10^{-6})	CL%	DOCUMENT ID		TECN	COMMENT
0.76±0.19 OUR AVERAGE		Error includes scale factor of 1.4.			
$0.98^{+0.23}_{-0.19}\pm0.07$		[1] AAIJ	12AR	LHCB	pp at 7 TeV
$0.60\pm0.17\pm0.04$		[2] AALTONEN	12L	CDF	$p\overline{p}$ at 1.96 TeV
• • • We do not use the following data for averages, fits, limits, etc. • • •					
< 12	90	[3] PENG	10	BELL	$e^+e^-\to\Upsilon(5S)$
< 1.2	90	[4] AALTONEN	09C	CDF	Repl. by AALTONEN 12L
< 1.7	90	[5] ABULENCIA,A	06D	CDF	Repl. by AALTONEN 09C
<232	90	[6] ABE	00C	SLD	$e^+e^-\to Z$
<170	90	[7] BUSKULIC	96V	ALEP	$e^+e^-\to Z$

[1] AAIJ 12AR reports $[\Gamma(B_s^0\to\pi^+\pi^-)/\Gamma_{total}]$ / $[B(B^0\to\pi^+\pi^-)]\times[\Gamma(\overline{b}\to B_s^0)/\Gamma(\overline{b}\to B^0)]=0.050^{+0.011}_{-0.009}\pm0.004$ which we multiply or divide by our best values $B(B^0\to\pi^+\pi^-)=(5.12\pm0.19)\times10^{-6}$, $\Gamma(\overline{b}\to B_s^0)/\Gamma(\overline{b}\to B^0)=0.261\pm0.015$. Our first error is their experiment's error and our second error is the systematic error from using our best values.

[2] AALTONEN 12L reports $[\Gamma(B_s^0\to\pi^+\pi^-)/\Gamma_{total}]$ / $[B(B^0\to K^+\pi^-)]\times[\Gamma(\overline{b}\to B_s^0)/\Gamma(\overline{b}\to B^0)]=0.008\pm0.002\pm0.001$ which we multiply or divide by our best values $B(B^0\to K^+\pi^-)=(1.96\pm0.05)\times10^{-5}$, $\Gamma(\overline{b}\to B_s^0)/\Gamma(\overline{b}\to B^0)=0.261\pm0.015$. Our first error is their experiment's error and our second error is the systematic error from using our best values.

[3] Uses $\Upsilon(10860)\to B_s^*\overline{B}_s^*$ and assumes $B(\Upsilon(10860)\to B_s^{(*)}\overline{B}_s^{(*)})=(19.3\pm2.9)\%$ and $\Gamma(\Upsilon(10860)\to B_s^*\overline{B}_s^*)$ / $\Gamma(\Upsilon(10860)\to B_s^{(*)}\overline{B}_s^{(*)})=(90.1^{+3.8}_{-4.0})\%$.

[4] Obtains this result from $(f_s/f_d)\cdot B(B_s\to\pi^+\pi^-)/B(B^0\to K^+\pi^-)=0.007\pm0.004\pm0.005$, assuming $f_s/f_d=0.276\pm0.034$ and $B(B^0\to K^+\pi^-)=(19.4\pm0.6)\times10^{-6}$.

[5] ABULENCIA,A 06D obtains this from $B(B_s\to\pi^+\pi^-)$ / $B(B_s\to K^+K^-)<0.05$ at 90% CL, assuming $B(B_s\to K^+K^-)=(33\pm6\pm7)\times10^{-6}$.

[6] ABE 00C assumes $B(Z\to b\overline{b})=(21.7\pm0.1)\%$ and the B fractions $f_{B^0}=f_{B^+}=(39.7^{+1.8}_{-2.2})\%$ and $f_{B_s}=(10.5^{+1.8}_{-2.2})\%$.

[7] BUSKULIC 96V assumes PDG 96 production fractions for B^0, B^+, B_s, b baryons.

Meson Particle Listings

B_s^0

$\Gamma(\pi^0\pi^0)/\Gamma_{total}$ Γ_{46}/Γ

VALUE	CL%	DOCUMENT ID		TECN	COMMENT
$<2.1\times10^{-4}$	90	[1] ACCIARRI	95H	L3	$e^+e^-\to Z$

[1] ACCIARRI 95H assumes $f_{B^0}=39.5\pm4.0$ and $f_{B_s}=12.0\pm3.0$%.

$\Gamma(\eta\pi^0)/\Gamma_{total}$ Γ_{47}/Γ

VALUE	CL%	DOCUMENT ID		TECN	COMMENT
$<1.0\times10^{-3}$	90	[1] ACCIARRI	95H	L3	$e^+e^-\to Z$

[1] ACCIARRI 95H assumes $f_{B^0}=39.5\pm4.0$ and $f_{B_s}=12.0\pm3.0$%.

$\Gamma(\eta\eta)/\Gamma_{total}$ Γ_{48}/Γ

VALUE	CL%	DOCUMENT ID		TECN	COMMENT
$<1.5\times10^{-3}$	90	[1] ACCIARRI	95H	L3	$e^+e^-\to Z$

[1] ACCIARRI 95H assumes $f_{B^0}=39.5\pm4.0$ and $f_{B_s}=12.0\pm3.0$%.

$\Gamma(\rho^0\rho^0)/\Gamma_{total}$ Γ_{49}/Γ

VALUE	CL%	DOCUMENT ID		TECN	COMMENT
$<3.20\times10^{-4}$	90	[1] ABE	00C	SLD	$e^+e^-\to Z$

[1] ABE 00C assumes $B(Z\to b\overline{b})=(21.7\pm0.1)$% and the B fractions $f_{B^0}=f_{B^+}=(39.7^{+1.8}_{-2.2})$% and $f_{B_s}=(10.5^{+1.8}_{-2.2})$%.

$\Gamma(\phi\rho^0)/\Gamma_{total}$ Γ_{50}/Γ

VALUE	CL%	DOCUMENT ID		TECN	COMMENT
$<6.17\times10^{-4}$	90	[1] ABE	00C	SLD	$e^+e^-\to Z$

[1] ABE 00C assumes $B(Z\to b\overline{b})=(21.7\pm0.1)$% and the B fractions $f_{B^0}=f_{B^+}=(39.7^{+1.8}_{-2.2})$% and $f_{B_s}=(10.5^{+1.8}_{-2.2})$%.

$\Gamma(\phi\phi)/\Gamma_{total}$ Γ_{51}/Γ

VALUE (units 10^{-6})	CL%	DOCUMENT ID		TECN	COMMENT
$19.1\pm2.6\pm1.6$		[1] AALTONEN	11AN	CDF	$p\overline{p}$ at 1.96 TeV
• • • We do not use the following data for averages, fits, limits, etc. • • •					
$14\ ^{+6}_{-5}\ \pm6$		[2] ACOSTA	05J	CDF	Repl. by AALTONEN 11AN
<1183	90	[3] ABE	00C	SLD	$e^+e^-\to Z$

[1] AALTONEN 11AN reports $[\Gamma(B_s^0\to\phi\phi)/\Gamma_{total}]$ / $[B(B_s^0\to J/\psi(1S)\phi)]=(1.78\pm0.14\pm0.20)\times10^{-2}$ which we multiply by our best value $B(B_s^0\to J/\psi(1S)\phi)=(1.07\pm0.09)\times10^{-3}$. Our first error is their experiment's error and our second error is the systematic error from using our best value.

[2] Uses $B(B^0\to J/\psi\phi)=(1.38\pm0.49)\times10^{-3}$ and production cross-section ratio of $\sigma(B_s)/\sigma(B^0)=0.26\pm0.04$.

[3] ABE 00C assumes $B(Z\to b\overline{b})=(21.7\pm0.1)$% and the B fractions $f_{B^0}=f_{B^+}=(39.7^{+1.8}_{-2.2})$% and $f_{B_s}=(10.5^{+1.8}_{-2.2})$%.

$\Gamma(\pi^+K^-)/\Gamma_{total}$ Γ_{52}/Γ

VALUE (units 10^{-6})	CL%	DOCUMENT ID		TECN	COMMENT
5.5 ± 0.6 OUR AVERAGE					
$5.6\pm0.6\pm0.3$		[1] AAIJ	12AR	LHCB	pp at 7 TeV
$5.3\pm0.9\pm0.3$		[2] AALTONEN	09C	CDF	$p\overline{p}$ at 1.96 TeV
• • • We do not use the following data for averages, fits, limits, etc. • • •					
< 26	90	[3] PENG	10	BELL	$e^+e^-\to\Upsilon(5S)$
< 5.6	90	[4] ABULENCIA,A	06D	CDF	Repl. by AALTONEN 09C
<261	90	[5] ABE	00C	SLD	$e^+e^-\to Z$
<210	90	[6] BUSKULIC	96V	ALEP	$e^+e^-\to Z$
<260	90	[7] AKERS	94L	OPAL	$e^+e^-\to Z$

[1] AAIJ 12AR reports $[\Gamma(B_s^0\to\pi^+K^-)/\Gamma_{total}]$ / $[B(B^0\to K^+\pi^-)]\times[\Gamma(\overline{b}\to B_s^0)/\Gamma(\overline{b}\to B^0)]=0.074\pm0.006\pm0.006$ which we multiply or divide by our best values $B(B^0\to K^+\pi^-)=(1.96\pm0.05)\times10^{-5}$, $\Gamma(\overline{b}\to B_s^0)/\Gamma(\overline{b}\to B^0)=0.261\pm0.015$. Our first error is their experiment's error and our second error is the systematic error from using our best values.

[2] AALTONEN 09C reports $[\Gamma(B_s^0\to\pi^+K^-)/\Gamma_{total}]$ / $[B(B^0\to K^+\pi^-)]\times[B(\overline{b}\to B_s^0)]$ / $[B(\overline{b}\to B^0)]=0.071\pm0.010\pm0.007$ which we multiply or divide by our best values $B(B^0\to K^+\pi^-)=(1.96\pm0.05)\times10^{-5}$, $B(\overline{b}\to B_s^0)=(10.5\pm0.6)\times10^{-2}$, $B(\overline{b}\to B^0)=(40.2\pm0.7)\times10^{-2}$. Our first error is their experiment's error and our second error is the systematic error from using our best values.

[3] Uses $\Upsilon(10860)\to B_s^*\overline{B}_s^*$ and assumes $B(\Upsilon(10860)\to B_s^{(*)}\overline{B}_s^{(*)})=(19.3\pm2.9)$% and $\Gamma(\Upsilon(10860)\to B_s^*\overline{B}_s^*)$ / $\Gamma(\Upsilon(10860)\to B_s^{(*)}\overline{B}_s^{(*)})=(90.1^{+3.8}_{-4.0})$%.

[4] ABULENCIA,A 06D obtains this from (f_s/f_d) $(B(B_s\to K^+K^-)$ / $B(B^0\to K^+\pi^-))<0.08$ at 90% CL, assuming $f_s/f_d=0.260\pm0.039$ and $B(B^0\to K^+\pi^-)=(18.9\pm0.7)\times10^{-6}$.

[5] ABE 00C assumes $B(Z\to b\overline{b})=(21.7\pm0.1)$% and the B fractions $f_{B^0}=f_{B^+}=(39.7^{+1.8}_{-2.2})$% and $f_{B_s}=(10.5^{+1.8}_{-2.2})$%.

[6] BUSKULIC 96V assumes PDG 96 production fractions for B^0, B^+, B_s, b baryons.

[7] Assumes $B(Z\to b\overline{b})=0.217$ and B_d^0 (B_s^0) fraction 39.5% (12%).

$\Gamma(K^+K^-)/\Gamma_{total}$ Γ_{53}/Γ

VALUE (units 10^{-6})	CL%	DOCUMENT ID		TECN	COMMENT
24.9 ± 1.7 OUR AVERAGE					
$23.7\pm1.6\pm1.5$		[1] AAIJ	12AR	LHCB	pp at 7 TeV
$25.9\pm2.2\pm1.7$		[2] AALTONEN	11N	CDF	$p\overline{p}$ at 1.96 TeV
$38\ ^{+10}_{-9}\ \pm7$		[3] PENG	10	BELL	$e^+e^-\to\Upsilon(5S)$
• • • We do not use the following data for averages, fits, limits, etc. • • •					
<310	90	DRUTSKOY	07A	BELL	$e^+e^-\to\Upsilon(5S)$
$33\ \pm6\ \pm7$		[4] ABULENCIA,A	06D	CDF	Repl. by AALTONEN 11N
<283	90	[5] ABE	00C	SLD	$e^+e^-\to Z$
< 59	90	[6] BUSKULIC	96V	ALEP	$e^+e^-\to Z$
<140	90	[7] AKERS	94L	OPAL	$e^+e^-\to Z$

[1] AAIJ 12AR reports $[\Gamma(B_s^0\to K^+K^-)/\Gamma_{total}]$ / $[B(B^0\to K^+\pi^-)]\times[\Gamma(\overline{b}\to B_s^0)/\Gamma(\overline{b}\to B^0)]=0.316\pm0.009\pm0.019$ which we multiply or divide by our best values $B(B^0\to K^+\pi^-)=(1.96\pm0.05)\times10^{-5}$, $\Gamma(\overline{b}\to B_s^0)/\Gamma(\overline{b}\to B^0)=0.261\pm0.015$. Our first error is their experiment's error and our second error is the systematic error from using our best values.

[2] AALTONEN 11N reports (f_s/f_d) $(B(B_s^0\to K^+K^-)$ / $B(B^0\to K^+\pi^-))=0.347\pm0.020\pm0.021$. We multiply this result by our best value of $B(B^0\to K^+\pi^-)=(1.96\pm0.05)\times10^{-5}$ and divide by our best value of f_s/f_d, where $1/2\ f_s/f_d=0.131\pm0.008$. Our first quoted uncertainty is the combined experiment's uncertainty and our second is the systematic uncertainty from using out best values.

[3] Uses $\Upsilon(10860)\to B_s^*\overline{B}_s^*$ and assumes $B(\Upsilon(10860)\to B_s^{(*)}\overline{B}_s^{(*)})=(19.3\pm2.9)$% and $\Gamma(\Upsilon(10860)\to B_s^*\overline{B}_s^*)$ / $\Gamma(\Upsilon(10860)\to B_s^{(*)}\overline{B}_s^{(*)})=(90.1^{+3.8}_{-4.0})$%.

[4] ABULENCIA,A 06D obtains this from (f_s/f_d) $(B(B_s\to K^+K^-)$ / $B(B^0\to K^+\pi^-))=0.46\pm0.08\pm0.07$, assuming $f_s/f_d=0.260\pm0.039$ and $B(B^0\to K^+\pi^-)=(18.9\pm0.7)\times10^{-6}$.

[5] ABE 00C assumes $B(Z\to b\overline{b})=(21.7\pm0.1)$% and the B fractions $f_{B^0}=f_{B^+}=(39.7^{+1.8}_{-2.2})$% and $f_{B_s}=(10.5^{+1.8}_{-2.2})$%.

[6] BUSKULIC 96V assumes PDG 96 production fractions for B^0, B^+, B_s, b baryons.

[7] Assumes $B(Z\to b\overline{b})=0.217$ and B_d^0 (B_s^0) fraction 39.5% (12%).

$\Gamma(K^0\overline{K}^0)/\Gamma_{total}$ Γ_{54}/Γ

VALUE (units 10^{-5})	CL%	DOCUMENT ID		TECN	COMMENT
<6.6	90	[1] PENG	10	BELL	$e^+e^-\to\Upsilon(5S)$

[1] Uses $\Upsilon(10860)\to B_s^*\overline{B}_s^*$ and assumes $B(\Upsilon(10860)\to B_s^{(*)}\overline{B}_s^{(*)})=(19.3\pm2.9)$% and $\Gamma(\Upsilon(10860)\to B_s^*\overline{B}_s^*)$ / $\Gamma(\Upsilon(10860)\to B_s^{(*)}\overline{B}_s^{(*)})=(90.1^{+3.8}_{-4.0})$%.

$\Gamma(K^0\pi^+\pi^-)/\Gamma_{total}$ Γ_{55}/Γ

VALUE (units 10^{-6})	DOCUMENT ID		TECN	COMMENT
$19\pm5\pm2$	[1] AAIJ	13BP	LHCB	pp at 7 TeV

[1] AAIJ 13BP reports $[\Gamma(B_s^0\to K^0\pi^+\pi^-)/\Gamma_{total}]$ / $[B(B^0\to K^0\pi^+\pi^-)]=0.29\pm0.06\pm0.04$ which we multiply by our best value $B(B^0\to K^0\pi^+\pi^-)=(6.5\pm0.8)\times10^{-5}$. Our first error is their experiment's error and our second error is the systematic error from using our best value.

$\Gamma(K^0K^\pm\pi^\mp)/\Gamma_{total}$ Γ_{56}/Γ

VALUE (units 10^{-5})	DOCUMENT ID		TECN	COMMENT
$9.7\pm1.2\pm1.2$	[1] AAIJ	13BP	LHCB	pp at 7 TeV

[1] AAIJ 13BP reports $[\Gamma(B_s^0\to K^0K^\pm\pi^\mp)/\Gamma_{total}]$ / $[B(B^0\to K^0\pi^+\pi^-)]=1.48\pm0.12\pm0.14$ which we multiply by our best value $B(B^0\to K^0\pi^+\pi^-)=(6.5\pm0.8)\times10^{-5}$. Our first error is their experiment's error and our second error is the systematic error from using our best value.

$\Gamma(K^0K^+K^-)/\Gamma_{total}$ Γ_{57}/Γ

VALUE	CL%	DOCUMENT ID		TECN	COMMENT
$<4\times10^{-6}$	90	[1] AAIJ	13BP	LHCB	pp at 7 TeV

[1] AAIJ 13BP reports $[\Gamma(B_s^0\to K^0K^+K^-)/\Gamma_{total}]$ / $[B(B^0\to K^0\pi^+\pi^-)]<0.068$ which we multiply by our best value $B(B^0\to K^0\pi^+\pi^-)=6.5\times10^{-5}$.

$\Gamma(\overline{K}^*(892)^0\rho^0)/\Gamma_{total}$ Γ_{58}/Γ

VALUE	CL%	DOCUMENT ID		TECN	COMMENT
$<7.67\times10^{-4}$	90	[1] ABE	00C	SLD	$e^+e^-\to Z$

[1] ABE 00C assumes $B(Z\to b\overline{b})=(21.7\pm0.1)$% and the B fractions $f_{B^0}=f_{B^+}=(39.7^{+1.8}_{-2.2})$% and $f_{B_s}=(10.5^{+1.8}_{-2.2})$%.

$\Gamma(\overline{K}^*(892)^0K^*(892)^0)/\Gamma_{total}$ Γ_{59}/Γ

VALUE (units 10^{-5})	CL%	DOCUMENT ID		TECN	COMMENT
$2.81\pm0.46\pm0.56$		[1] AAIJ	12F	LHCB	pp at 7 TeV
• • • We do not use the following data for averages, fits, limits, etc. • • •					
<168.1	90	[2] ABE	00C	SLD	$e^+e^-\to Z$

[1] Uses $B^0\to J/\psi K^{*0}$ for normalization and assumes $B(B^0\to J/\psi K^{*0})$ $B(J/\psi\to\mu^+\mu^-)$ $B(K^{*0}\to K^+\pi^-)=(1.33\pm0.06)\times10^{-3}$ and $f_s/f_d=0.253\pm0.031$. The second quoted error is total uncertainty including the error of 0.34 on f_s/f_d.

[2] ABE 00C assumes $B(Z\to b\overline{b})=(21.7\pm0.1)$% and the B fractions $f_{B^0}=f_{B^+}=(39.7^{+1.8}_{-2.2})$% and $f_{B_s}=(10.5^{+1.8}_{-2.2})$%.

$\Gamma(\phi K^*(892)^0)/\Gamma_{total}$ Γ_{60}/Γ

VALUE (units 10^{-6})	CL%	DOCUMENT ID		TECN	COMMENT
1.13±0.29±0.06		[1] AAIJ	13BW	LHCB	pp at 7 TeV
• • • We do not use the following data for averages, fits, limits, etc. • • •					
<1013	90	[2] ABE	00C	SLD	$e^+e^- \to Z$

[1] AAIJ 13BW reports $[\Gamma(B_s^0 \to \phi K^*(892)^0)/\Gamma_{total}] / [B(B^0 \to K^*(892)^0\phi)] = 0.113 \pm 0.024 \pm 0.016$ which we multiply by our best value $B(B^0 \to K^*(892)^0\phi) = (1.00 \pm 0.05) \times 10^{-5}$. Our first error is their experiment's error and our second error is the systematic error from using our best value.

[2] ABE 00C assumes $B(Z \to b\overline{b})$=(21.7 ± 0.1)% and the B fractions $f_{B^0}=f_{B^+}=(39.7^{+1.8}_{-2.2})$% and $f_{B_s}=(10.5^{+1.8}_{-2.2})$%.

$\Gamma(p\overline{p})/\Gamma_{total}$ Γ_{61}/Γ

Test for ΔB=1 weak neutral current. Allowed by higher-order electroweak interactions.

VALUE (units 10^{-8})	CL%	DOCUMENT ID		TECN	COMMENT
$\mathbf{2.84^{+2.03+0.85}_{-1.68-0.18}}$		[1] AAIJ	13BQ	LHCB	pp at 7 TeV
• • • We do not use the following data for averages, fits, limits, etc. • • •					
<5900	90	[2] BUSKULIC	96V	ALEP	$e^+e^- \to Z$

[1] Uses normalization mode $B(B^0 \to K^+\pi^-) = (19.55 \pm 0.54) \times 10^{-6}$ and B production ratio $f(\overline{b} \to B_s^0)/f(\overline{b} \to B_d^0) = 0.256 \pm 0.020$.

[2] BUSKULIC 96V assumes PDG 96 production fractions for B^0, B^+, B_s, b baryons.

$\Gamma(\Lambda_c^- \Lambda\pi^+)/\Gamma_{total}$ Γ_{62}/Γ

VALUE (units 10^{-4})	DOCUMENT ID		TECN	COMMENT
3.6±1.1±1.2	[1] SOLOVIEVA	13	BELL	$e^+e^- \to \Upsilon(4S)$

[1] The second error is the total systematic uncertainty including the Λ_c absolute branching fractions and the normalizion number of B_s events.

$\Gamma(\gamma\gamma)/\Gamma_{total}$ Γ_{63}/Γ

Test for ΔB=1 weak neutral current.

VALUE (units 10^{-6})	CL%	DOCUMENT ID		TECN	COMMENT
< 8.7	90	[1] WICHT	08A	BELL	$e^+e^- \to \Upsilon(5S)$
• • • We do not use the following data for averages, fits, limits, etc. • • •					
< 53	90	DRUTSKOY	07A	BELL	Repl. by WICHT 08A
<148	90	[2] ACCIARRI	95I	L3	$e^+e^- \to Z$

[1] Assumes $\Upsilon(5S) \to B_s^*\overline{B}_s^*$ = $(19.5^{+3.0}_{-2.3})$%.

[2] ACCIARRI 95I assumes $f_{B^0} = 39.5 \pm 4.0$ and $f_{B_s} = 12.0 \pm 3.0$%.

$\Gamma(\phi\gamma)/\Gamma_{total}$ Γ_{64}/Γ

VALUE (units 10^{-6})	CL%	DOCUMENT ID		TECN	COMMENT
36 ± 4 OUR AVERAGE					
35.1± 3.5± 1.2		[1] AAIJ	13	LHCB	pp at 7 TeV
$57\ ^{+18}_{-15}\ ^{+12}_{-11}$		[2] WICHT	08A	BELL	$e^+e^- \to \Upsilon(5S)$
• • • We do not use the following data for averages, fits, limits, etc. • • •					
39 ± 5		[3] AAIJ	12AE	LHCB	Repl. by AAIJ 13
<390	90	DRUTSKOY	07A	BELL	$e^+e^- \to \Upsilon(5S)$
<120	90	ACOSTA	02G	CDF	$p\overline{p}$ at 1.8 TeV
<700	90	[4] ADAM	96D	DLPH	$e^+e^- \to Z$

[1] AAIJ 13 reports $[\Gamma(B_s^0 \to \phi\gamma)/\Gamma_{total}] / [B(B^0 \to K^*(892)^0\gamma)] = 0.81 \pm 0.04 \pm 0.07$ which we multiply by our best value $B(B^0 \to K^*(892)^0\gamma) = (4.33 \pm 0.15) \times 10^{-5}$. Our first error is their experiment's error and our second error is the systematic error from using our best value.

[2] Assumes $\Upsilon(5S) \to B_s^*\overline{B}_s^*$ = $(19.5^{+3.0}_{-2.3})$%.

[3] Measures $B(B^0 \to K^{*0}\gamma)/B(B_s \to \phi\gamma) = 1.12 \pm 0.08(\text{stat})^{+0.06}_{-0.04}(\text{sys})^{+0.09}_{-0.08}(f_s/f_d)$ and uses current world-average value of $B(B^0 \to K^{*0}\gamma) = (4.33 \pm 0.15) \times 10^{-5}$.

[4] ADAM 96D assumes $f_{B^0} = f_{B^-} = 0.39$ and $f_{B_s} = 0.12$.

$\Gamma(\mu^+\mu^-)/\Gamma_{total}$ Γ_{65}/Γ

Test for $\Delta B = 1$ weak neutral current.

VALUE (units 10^{-9})	CL%	DOCUMENT ID		TECN	COMMENT
3.1±0.7 OUR AVERAGE					
$2.9^{+1.1+0.3}_{-1.0-0.1}$		[1] AAIJ	13BA	LHCB	pp at 7, 8 TeV
$13\ ^{+9}_{-7}$		[2] AALTONEN	13F	CDF	$p\overline{p}$ at 1.96 TeV
$3.0^{+1.0}_{-0.9}$		[3] CHATRCHYAN	13AW	CMS	pp at 7, 8 TeV
• • • We do not use the following data for averages, fits, limits, etc. • • •					
$3.2^{+1.4+0.5}_{-1.2-0.3}$		[4] AAIJ	13B	LHCB	Repl. by AAIJ 13BA
< 12	90	[5] ABAZOV	13C	D0	$p\overline{p}$ at 1.96 TeV
< 19	90	[6] AAD	12AE	ATLS	pp at 7 TeV
< 12	90	[7] AAIJ	12A	LHCB	Repl. by AAIJ 12W
< 3.8	90	[8] AAIJ	12W	LHCB	Repl. by AAIJ 13B
< 6.4	90	[9] CHATRCHYAN	12A	CMS	pp at 7 TeV
< 43	90	[10] AAIJ	11B	LHCB	Repl. by AAIJ 12A
< 35	90	[11] AALTONEN	11AG	CDF	$p\overline{p}$ at 1.96 TeV
< 16	90	[12] CHATRCHYAN	11T	CMS	Repl. by CHATRCHYAN 12A
< 42	90	[13] ABAZOV	10S	D0	$p\overline{p}$ at 1.96 TeV
< 47	90	[13] AALTONEN	08I	CDF	Repl. by AALTONEN 11AG
< 94	90	[14] ABAZOV	07Q	D0	Repl. by ABAZOV 10S
< 410	90	[15] ABAZOV	05E	D0	$p\overline{p}$ at 1.96 TeV
< 150	90	[16] ABULENCIA	05	CDF	$p\overline{p}$ at 1.96 TeV
< 580	90	[17] ACOSTA	04D	CDF	$p\overline{p}$ at 1.96 TeV
< 2000	90	[18] ABE	98	CDF	$p\overline{p}$ at 1.8 TeV
<38000	90	[19] ACCIARRI	97B	L3	$e^+e^- \to Z$
< 8400	90	[20] ABE	96L	CDF	Repl. by ABE 98

[1] Uses B production ratio $f(\overline{b} \to B_s^0)/f(\overline{b} \to B_d^0) = 0.259 \pm 0.015$ and normalization modes $B^+ \to J/\psi K^+ \to \mu^+\mu^- K^+$ and $B^0 \to K^+\pi^-$.

[2] Uses normalization mode $B(B^+ \to J/\psi K^+) = (10.22 \pm 0.35) \times 10^{-4}$ and B production ratio $f(\overline{b} \to B_s^0)/f(\overline{b} \to B_d^0) = 0.28 \pm 0.04$.

[3] Uses B production ratio $f(\overline{b} \to B_s^0)/f(\overline{b} \to B_d^0) = 0.256 \pm 0.020$ and $B(B^+ \to J/\psi K^+ \to \mu^+\mu^- K^+) = (6.0 \pm 0.2) \times 10^{-5}$ for normalization.

[4] Uses B production ratio $f(\overline{b} \to B_s^0)/f(\overline{b} \to B_d^0) = 0.256 \pm 0.020$ and two normalization modes: $B(B^+ \to J/\psi K^+ \to \mu^+\mu^- K^+) = (6.01 \pm 0.21) \times 10^{-5}$ and $B(B^0 \to K^+\pi^-) = (1.94 \pm 0.06) \times 10^{-5}$.

[5] Uses normalization mode $B(B^+ \to J/\psi K^+ \to \mu^+\mu^- K^+) = (6.01 \pm 0.21) \times 10^{-5}$ and B production ratio $f(\overline{b} \to B_s^0)/f(\overline{b} \to B_d^0) = 0.263 \pm 0.017$.

[6] Uses B production ratio $f(\overline{b} \to B^+)/f(\overline{b} \to B_s^0) = 3.75 \pm 0.29$ and $B(B^+ \to J/\psi K^+ \to \mu^+\mu^- K^+) = (6.0 \pm 0.2) \times 10^{-5}$.

[7] Uses B production ratio $f(\overline{b} \to B_s^0)/f(\overline{b} \to B_d^0) = 0.267^{+0.021}_{-0.020}$ and three normalization modes $B(B^+ \to J/\psi K^+ \to \mu^+\mu^- K^+) = (6.01 \pm 0.21) \times 10^{-5}$, $B(B^0 \to K^+\pi^-) = (1.94 \pm 0.06) \times 10^{-5}$, and $B(B_s^0 \to J/\psi\phi \to \mu^+\mu^- K^+ K^-) = (3.4 \pm 0.9) \times 10^{-5}$.

[8] Uses B production ratio $f(\overline{b} \to B_s^0)/f(\overline{b} \to B_d^0) = 0.267^{+0.021}_{-0.020}$ and three normalization modes of $B^+ \to J/\psi K^+$, $B^0 \to K^+\pi^-$, and $B_s^0 \to J/\psi\phi$.

[9] Uses $f_s/f_u = 0.267 \pm 0.021$ and $B(B^+ \to J/\psi K^+ \to \mu^+\mu^- K^+) = (6.0 \pm 0.2) \times 10^{-5}$.

[10] Uses B production ratio $f(\overline{b} \to B^+)/f(\overline{b} \to B_s^0) = 3.71 \pm 0.47$ and three normalization modes.

[11] Uses B production ratio $f(\overline{b} \to B^+)/f(\overline{b} \to B_s^0) = 3.55 \pm 0.47$ and $B(B^+ \to J/\psi K^+ \to \mu^+\mu^- K^+) = (6.01 \pm 0.21) \times 10^{-5}$.

[12] Uses B production ratio $f(\overline{b} \to B^+)/f(\overline{b} \to B_s^0) = 3.55 \pm 0.42$ and $B(B^+ \to J/\psi K^+ \to \mu^+\mu^- K^+) = (6.0 \pm 0.2) \times 10^{-5}$.

[13] Uses B production ratio $f(\overline{b} \to B^+)/f(\overline{b} \to B_s^0) = 3.86 \pm 0.59$, and the number of $B^+ \to J/\psi K^+$ decays.

[14] Uses B production ratio $f(\overline{b} \to B^+)/f(\overline{b} \to B_s^0) = 3.86 \pm 0.54$ and the number of $B^+ \to J/\psi K^+$ decays.

[15] Assumes production cross-section $\sigma(B_s)/\sigma(B^+) = 0.270 \pm 0.034$.

[16] Assumes production cross section $\sigma(B^+)/\sigma(B_s) = 3.71 \pm 0.41$ and $B(B^+ \to J/\psi K^+ \to \mu^+\mu^- K^+) = (5.88 \pm 0.26) \times 10^{-5}$.

[17] Assumes production cross-section $\sigma(B_s)/\sigma(B^+) = 0.100/0.391$ and the CDF measured value of $\sigma(B^+) = 3.6 \pm 0.6$ μb.

[18] ABE 98 assumes production of $\sigma(B^0) = \sigma(B^+)$ and $\sigma(B_s)/\sigma(B^0) = 1/3$. They normalize to their measured $\sigma(B^0, p_T(B) > 6, |y| < 1.0) = 2.39 \pm 0.32 \pm 0.44$ μb.

[19] ACCIARRI 97B assume PDG 96 production fractions for B^+, B^0, B_s, and Λ_b.

[20] ABE 96L assumes B^+/B_s production ratio 3/1. They normalize to their measured $\sigma(B^+, p_T(B) > 6$ GeV/c, $|y| < 1) = 2.39 \pm 0.54$ μb.

$\Gamma(e^+e^-)/\Gamma_{total}$ Γ_{66}/Γ

Test for $\Delta B = 1$ weak neutral current.

VALUE	CL%	DOCUMENT ID		TECN	COMMENT
$<2.8 \times 10^{-7}$	90	AALTONEN	09P	CDF	$p\overline{p}$ at 1.96 TeV
• • • We do not use the following data for averages, fits, limits, etc. • • •					
$<5.4 \times 10^{-5}$	90	[1] ACCIARRI	97B	L3	$e^+e^- \to Z$

[1] ACCIARRI 97B assume PDG 96 production fractions for B^+, B^0, B_s, and Λ_b.

$\Gamma(e^\pm\mu^\mp)/\Gamma_{total}$ Γ_{67}/Γ

Test of lepton family number conservation.

VALUE	CL%	DOCUMENT ID		TECN	COMMENT
$<1.1 \times 10^{-8}$	90	[1] AAIJ	13BM	LHCB	pp at 7 TeV
• • • We do not use the following data for averages, fits, limits, etc. • • •					
$<2.0 \times 10^{-7}$	90	AALTONEN	09P	CDF	$p\overline{p}$ at 1.96 TeV
$<6.1 \times 10^{-6}$	90	ABE	98V	CDF	Repl. by AALTONEN 09P
$<4.1 \times 10^{-5}$	90	[2] ACCIARRI	97B	L3	$e^+e^- \to Z$

[1] Uses normalization mode $B(B^0 \to K^+\pi^-) = (19.4 \pm 0.6) \times 10^{-6}$ and B production ratio $f(\overline{b} \to B_s^0)/f(\overline{b} \to B_d^0) = 0.256 \pm 0.020$.

[2] ACCIARRI 97B assume PDG 96 production fractions for B^+, B^0, B_s, and Λ_b.

$\Gamma(\mu^+\mu^-\mu^+\mu^-)/\Gamma_{total}$ Γ_{68}/Γ

VALUE	CL%	DOCUMENT ID		TECN	COMMENT
$<1.2 \times 10^{-8}$	90	[1] AAIJ	13AW	LHCB	pp at 7 TeV

[1] Also reports a limit of $< 1.6 \times 10^{-8}$ at 95% CL.

$\Gamma(SP, S \to \mu^+\mu^-, P \to \mu^+\mu^-)/\Gamma_{total}$ Γ_{69}/Γ

Here S and P are the hypothetical scalar and pseudoscalar particles with masses of 2.5 GeV/c^2 and 214.3 MeV/c^2, respectively.

VALUE	CL%	DOCUMENT ID		TECN	COMMENT
$<1.2 \times 10^{-8}$	90	[1] AAIJ	13AW	LHCB	pp at 7 TeV

[1] Also reports a limit of $< 1.6 \times 10^{-8}$ at 95% CL.

Meson Particle Listings

B_s^0

$\Gamma(\phi(1020)\mu^+\mu^-)/\Gamma_{\text{total}}$ Γ_{70}/Γ

Test for $\Delta B = 1$ weak neutral current.

VALUE	CL%	DOCUMENT ID		TECN	COMMENT
• • • We do not use the following data for averages, fits, limits, etc. • • •					
$<3.2\times10^{-6}$	90	[1] ABAZOV	06G	D0	$p\overline{p}$ at 1.96 TeV
$<4.7\times10^{-5}$	90	ACOSTA	02D	CDF	$p\overline{p}$ at 1.8 TeV

[1] Uses $B(B_s^0 \to J/\psi\phi) = 9.3\times10^{-4}$.

$\Gamma(\phi(1020)\mu^+\mu^-)/\Gamma(J/\psi(1S)\phi)$ Γ_{70}/Γ_{27}

VALUE (units 10^{-3})	CL%	DOCUMENT ID		TECN	COMMENT
0.71 ±0.13 OUR AVERAGE		Error includes scale factor of 2.2.			
$0.674^{+0.061}_{-0.056}\pm0.016$		AAIJ	13X	LHCB	pp at 7 TeV
1.13 ±0.19 ±0.07		AALTONEN	11AI	CDF	$p\overline{p}$ at 1.96 TeV
• • • We do not use the following data for averages, fits, limits, etc. • • •					
1.11 ±0.25 ±0.09		AALTONEN	11L	CDF	Repl. by AALTONEN 11AI
< 2.3	90	AALTONEN	09B	CDF	Repl. by AALTONEN 11L

$\Gamma(\phi\nu\overline{\nu})/\Gamma_{\text{total}}$ Γ_{71}/Γ

Test for $\Delta B = 1$ weak neutral current.

VALUE	CL%	DOCUMENT ID		TECN	COMMENT
$<5.4\times10^{-3}$	90	[1] ADAM	96D	DLPH	$e^+e^- \to Z$

[1] ADAM 96D assumes $f_{B^0} = f_{B^-} = 0.39$ and $f_{B_s} = 0.12$.

POLARIZATION IN B_s^0 DECAY

In decays involving two vector mesons, one can distinguish among the states in which meson polarizations are both longitudinal (L), or both are transverse and parallel ($\|$), or perpendicular ($\perp$) to each other with the parameters Γ_L/Γ, $\Gamma_\perp/\Gamma$, and the relative phases $\phi_\|$ and $\phi_\perp$. See the definitions in the note on "Polarization in B Decays" review in the B^0 Particle Listings.

Γ_L/Γ in $B_s^0 \to D_s^{*}\rho^+$

VALUE	DOCUMENT ID		TECN	COMMENT
$1.05^{+0.08+0.03}_{-0.10-0.04}$	LOUVOT	10	BELL	$e^+e^- \to \Upsilon(5S)$

Γ_L/Γ in $B_s^0 \to J/\psi(1S)\phi$

VALUE	EVTS	DOCUMENT ID		TECN	COMMENT
0.542±0.011 OUR AVERAGE					
0.539±0.014±0.016		[1] AAD	12CV	ATLS	pp at 7 TeV
0.524±0.013±0.015		[1] AALTONEN	12D	CDF	$p\overline{p}$ at 1.96 TeV
$0.558^{+0.017}_{-0.019}$		[1,2] ABAZOV	12D	D0	$p\overline{p}$ at 1.96 TeV
0.61 ±0.14 ±0.02		[3] AFFOLDER	00N	CDF	$p\overline{p}$ at 1.8 TeV
0.56 ±0.21 $^{+0.02}_{-0.04}$	19	ABE	95Z	CDF	$p\overline{p}$ at 1.8 TeV
• • • We do not use the following data for averages, fits, limits, etc. • • •					
0.555±0.027±0.006		[4] ABAZOV	09E	D0	Repl. by ABAZOV 12D
0.531±0.020±0.007		[1] AALTONEN	08J	CDF	Repl. by AALTONEN 12D
0.62 ±0.06 ±0.01		ACOSTA	05	CDF	Repl. by AALTONEN 08J

[1] Measured using the time-dependent angular analysis of $B_s^0 \to J/\psi\phi$ decays.
[2] The error includes both statistical and systematic uncertainties.
[3] AFFOLDER 00N measurements are based on 40 B_s^0 candidates obtained from a data sample of 89 pb^{-1}. The P-wave fraction is found to be $0.23 \pm 0.19 \pm 0.04$.
[4] Measured the angular and lifetime parameters for the time-dependent angular untagged decays $B_d^0 \to J/\psi K^{*0}$ and $B_s^0 \to J/\psi\phi$.

Γ_L/Γ in $B_s^0 \to D_s^{*+}D_s^{*-}$

VALUE	DOCUMENT ID		TECN	COMMENT
$0.06^{+0.18}_{-0.17}\pm0.03$	ESEN	13	BELL	$e^+e^- \to \Upsilon(5S)$

$\Gamma_\|/\Gamma$ in $B_s^0 \to J/\psi(1S)\phi$

VALUE	DOCUMENT ID		TECN	COMMENT
0.227±0.010 OUR AVERAGE				
0.224±0.010±0.009	[1] AAD	12CV	ATLS	pp at 7 TeV
0.231±0.014±0.015	[1] AALTONEN	12D	CDF	$p\overline{p}$ at 1.96 TeV
$0.231^{+0.024}_{-0.030}$	[1,2] ABAZOV	12D	D0	$p\overline{p}$ at 1.96 TeV
• • • We do not use the following data for averages, fits, limits, etc. • • •				
0.244±0.032±0.014	[3] ABAZOV	09E	D0	Repl. by ABAZOV 12D
0.230±0.029±0.011	[1] AALTONEN	08J	CDF	Repl. by AALTONEN 12D
0.260±0.084±0.013	ACOSTA	05	CDF	Repl. by AALTONEN 08J

[1] Measured using the time-dependent angular analysis of $B_s^0 \to J/\psi\phi$ decays.
[2] The error includes both statistical and systematic uncertainties.
[3] Measured the angular and lifetime parameters for the time-dependent angular untagged decays $B_d^0 \to J/\psi K^{*0}$ and $B_s^0 \to J/\psi\phi$.

$\phi_\|$ in $B_s^0 \to J/\psi(1S)\phi$

VALUE (rad)	DOCUMENT ID		TECN	COMMENT
3.15±0.22	[1] ABAZOV	12D	D0	$p\overline{p}$ at 1.96 TeV
• • • We do not use the following data for averages, fits, limits, etc. • • •				
$2.72^{+1.12}_{-0.27}\pm0.26$	ABAZOV	09E	D0	Repl. by ABAZOV 12D

[1] The error includes both statistical and systematic uncertainties.

Γ_L/Γ for $B_s^0 \to J/\psi(1S)K^*(892)^0$

Longitudinal polarization fraction, equals to f_L using notation of "Polarization in B decays" review.

VALUE	DOCUMENT ID		TECN	COMMENT
0.50±0.08±0.02	[1] AAIJ	12AP	LHCB	pp at 7 TeV

[1] The non-resonant $K\pi$ background contributions are subtracted. Also reports an S-wave amplitude $|A_S|^2 = 0.07^{+0.15}_{-0.07}$.

$\Gamma_\|/\Gamma$ for $B_s^0 \to J/\psi(1S)K^*(892)^0$

Parallel polarization fraction, equals to $1 - f_L - f_\perp$ using notation of "Polarization in B decays" review.

VALUE	DOCUMENT ID		TECN	COMMENT
$0.19^{+0.10}_{-0.08}\pm0.02$	[1] AAIJ	12AP	LHCB	pp at 7 TeV

[1] The non-resonant $K\pi$ background contributions are subtracted. Also reports an S-wave amplitude $|A_S|^2 = 0.07^{+0.15}_{-0.07}$.

Γ_L/Γ in $B_s^0 \to \phi\phi$

VALUE	DOCUMENT ID		TECN	COMMENT
0.361±0.022 OUR AVERAGE				
0.365±0.022±0.012	AAIJ	12P	LHCB	pp at 7 TeV
0.348±0.041±0.021	AALTONEN	11AN	CDF	$p\overline{p}$ at 1.96 TeV

$\Gamma_\perp/\Gamma$ in $B_s^0 \to \phi\phi$

VALUE	DOCUMENT ID		TECN	COMMENT
0.306±0.030 OUR AVERAGE	Error includes scale factor of 1.3.			
0.291±0.024±0.010	AAIJ	12P	LHCB	pp at 7 TeV
0.365±0.044±0.027	AALTONEN	11AN	CDF	$p\overline{p}$ at 1.96 TeV

$\phi_\|$ in $B_s^0 \to \phi\phi$

VALUE (rad)	DOCUMENT ID		TECN	COMMENT
2.59±0.15 OUR AVERAGE				
2.57±0.15±0.06	[1] AAIJ	12P	LHCB	pp at 7 TeV
$2.71^{+0.31}_{-0.36}\pm0.22$	[2] AALTONEN	11AN	CDF	$p\overline{p}$ at 1.96 TeV

[1] AAIJ 12P quotes $\cos\phi_\| = -0.844 \pm 0.068 \pm 0.029$ which we convert to $\phi_\|$, taking the smaller solution.
[2] AALTONEN 11AN quotes $\cos\phi_\| = -0.91^{+0.15}_{-0.13} \pm 0.09$ which we convert to $\phi_\|$ taking the smaller solution.

Γ_L/Γ in $B_s^0 \to K^{*0}\overline{K}^{*0}$

VALUE	DOCUMENT ID		TECN	COMMENT
0.31±0.12±0.04	AAIJ	12F	LHCB	pp at 7 TeV

$\Gamma_\perp/\Gamma$ in $B_s^0 \to K^{*0}\overline{K}^{*0}$

VALUE	DOCUMENT ID		TECN	COMMENT
0.38±0.11±0.04	AAIJ	12F	LHCB	pp at 7 TeV

Γ_L/Γ in $B_s^0 \to \phi\overline{K}^{*0}$

VALUE	DOCUMENT ID		TECN	COMMENT
0.51±0.15±0.07	AAIJ	13BW	LHCB	pp at 7 TeV

$\Gamma_\|/\Gamma$ in $B_s^0 \to \phi\overline{K}^{*0}$

VALUE	DOCUMENT ID		TECN	COMMENT
0.21±0.11±0.02	AAIJ	13BW	LHCB	pp at 7 TeV

$\phi_\|$ in $B_s^0 \to \phi\overline{K}^{*0}$

VALUE (rad)	DOCUMENT ID		TECN	COMMENT
1.75±0.53±0.29	[1] AAIJ	13BW	LHCB	pp at 7 TeV

[1] Measures $\cos(\phi_\|) = -0.18 \pm 0.52 \pm 0.29$, which we convert to $\phi_\|$ by taking the smaller solution.

$F_L(B_s^0 \to \phi\mu^+\mu^-)$ $(0.10 < q^2 < 2.00\ \text{GeV}^2/c^4)$

VALUE	DOCUMENT ID		TECN	COMMENT
$0.37^{+0.19}_{-0.17}\pm0.07$	AAIJ	13X	LHCB	pp at 7 TeV

$F_L(B_s^0 \to \phi\mu^+\mu^-)$ $(2.00 < q^2 < 4.30\ \text{GeV}^2/c^4)$

VALUE	DOCUMENT ID		TECN	COMMENT
$0.53^{+0.25}_{-0.23}\pm0.10$	AAIJ	13X	LHCB	pp at 7 TeV

$F_L(B_s^0 \to \phi\mu^+\mu^-)$ $(4.30 < q^2 < 8.68\ \text{GeV}^2/c^4)$

VALUE	DOCUMENT ID		TECN	COMMENT
$0.81^{+0.11}_{-0.13}\pm0.05$	AAIJ	13X	LHCB	pp at 7 TeV

$F_L(B_s^0 \to \phi\mu^+\mu^-)$ ($10.09 < q^2 < 12.90$ GeV$^2/c^4$)

VALUE	DOCUMENT ID		TECN	COMMENT
$0.33^{+0.14}_{-0.12} \pm 0.06$	AAIJ	13X	LHCB	pp at 7 TeV

$F_L(B_s^0 \to \phi\mu^+\mu^-)$ ($14.18 < q^2 < 16.00$ GeV$^2/c^4$)

VALUE	DOCUMENT ID		TECN	COMMENT
$0.34^{+0.18}_{-0.17} \pm 0.07$	AAIJ	13X	LHCB	pp at 7 TeV

$F_L(B_s^0 \to \phi\mu^+\mu^-)$ ($16.00 < q^2 < 19.00$ GeV$^2/c^4$)

VALUE	DOCUMENT ID		TECN	COMMENT
$0.16^{+0.17}_{-0.10} \pm 0.07$	AAIJ	13X	LHCB	pp at 7 TeV

$F_L(B_s^0 \to \phi\mu^+\mu^-)$ ($1.00 < q^2 < 6.00$ GeV$^2/c^4$)

VALUE	DOCUMENT ID		TECN	COMMENT
$0.56^{+0.17}_{-0.16} \pm 0.09$	AAIJ	13X	LHCB	pp at 7 TeV

B_s^0-$\overline{B}_s^0$ MIXING

For a discussion of B_s^0-$\overline{B}_s^0$ mixing see the note on "B^0-$\overline{B}^0$ Mixing" in the B^0 Particle Listings above.

χ_s is a measure of the time-integrated B_s^0-$\overline{B}_s^0$ mixing probability that produced $B_s^0(\overline{B}_s^0)$ decays as a $\overline{B}_s^0(B_s^0)$. Mixing violates $\Delta B \neq 2$ rule.

$$\chi_s = \frac{x_s^2}{2(1+x_s^2)}$$

$$x_s = \frac{\Delta m_{B_s^0}}{\Gamma_{B_s^0}} = (m_{B_{sH}^0} - m_{B_{sL}^0})\,\tau_{B_s^0},$$

where H, L stand for heavy and light states of two B_s^0 CP eigenstates and $\tau_{B_s^0} = \frac{1}{0.5(\Gamma_{B_{sH}^0} + \Gamma_{B_{sL}^0})}$.

$\Delta m_{B_s^0} = m_{B_{sH}^0} - m_{B_{sL}^0}$

$\Delta m_{B_s^0}$ is a measure of 2π times the B_s^0-$\overline{B}_s^0$ oscillation frequency in time-dependent mixing experiments.

"OUR EVALUATION" is provided by the Heavy Flavor Averaging Group (HFAG) by taking into account correlations between measurements.

VALUE ($10^{12}\ \hbar\,s^{-1}$)	CL%	DOCUMENT ID		TECN	COMMENT
17.761±0.022 OUR EVALUATION					
17.769±0.023 OUR AVERAGE					
17.768±0.023±0.006		[1] AAIJ	13BI	LHCB	pp at 7 TeV
17.93 ±0.22 ±0.15		[2] AAIJ	13CF	LHCB	pp at 7 TeV
17.77 ±0.10 ±0.07		[3] ABULENCIA,A	06G	CDF	$p\overline{p}$ at 1.96 TeV
• • • We do not use the following data for averages, fits, limits, etc. • • •					
17.63 ±0.11 ±0.02		[4] AAIJ	12I	LHCB	Repl. by AAIJ 13BI
17–21	90	[5] ABAZOV	06B	D0	$p\overline{p}$ at 1.96 TeV
17.31 $^{+0.33}_{-0.18}$ ±0.07		[6] ABULENCIA	06Q	CDF	Repl. by ABULENCIA,A 06G
> 8.0	95	[7] ABDALLAH	04J	DLPH	$e^+e^- \to Z^0$
> 4.9	95	[8] ABDALLAH	04J	DLPH	$e^+e^- \to Z^0$
> 8.5	95	[9] ABDALLAH	04J	DLPH	$e^+e^- \to Z^0$
> 5.0	95	[10] ABDALLAH	03B	DLPH	$e^+e^- \to Z$
>10.3	95	[11] ABE	03	SLD	$e^+e^- \to Z$
>10.9	95	[12] HEISTER	03E	ALEP	$e^+e^- \to Z$
> 5.3	95	[13] ABE	02V	SLD	$e^+e^- \to Z$
> 1.0	95	[14] ABBIENDI	01D	OPAL	$e^+e^- \to Z$
> 7.4	95	[15] ABREU	00Y	DLPH	Repl. by ABDALLAH 04J
> 4.0	95	[16] ABREU,P	00G	DLPH	$e^+e^- \to Z$
> 5.2	95	[17] ABBIENDI	99S	OPAL	$e^+e^- \to Z$
<96	95	[18] ABE	99D	CDF	$p\overline{p}$ at 1.8 TeV
> 5.8	95	[19] ABE	99J	CDF	$p\overline{p}$ at 1.8 TeV
> 9.6	95	[20] BARATE	99J	ALEP	$e^+e^- \to Z$
> 7.9	95	[21] BARATE	98C	ALEP	Repl. by BARATE 99J
> 3.1	95	[22] ACKERSTAFF	97U	OPAL	Repl. by ABBIENDI 99S
> 2.2	95	[23] ACKERSTAFF	97V	OPAL	Repl. by ABBIENDI 99S
> 6.5	95	[24] ADAM	97	DLPH	Repl. by ABREU 00Y
> 6.6	95	[25] BUSKULIC	96M	ALEP	Repl. by BARATE 98C
> 2.2	95	[23] AKERS	95J	OPAL	Sup. by ACKERSTAFF 97V
> 5.7	95	[26] BUSKULIC	95J	ALEP	$e^+e^- \to Z$
> 1.8	95	[23] BUSKULIC	94B	ALEP	$e^+e^- \to Z$

[1] Measured using $B_s^0 \to D_s^-\pi^+$ decays.
[2] Measured using $B_s^0 \to D_s^-\mu^+\nu_\mu X$ decays.
[3] Significance of oscillation signal is 5.4 σ. Also reports $|V_{td}\ /\ V_{ts}| = 0.2060 \pm 0.0007^{+0.0081}_{-0.0060}$.
[4] Measured using $B_s^0 \to D_s^-\pi^+$ and $D_s^-\pi^+\pi^-\pi^+$ decays.
[5] A likelihood scan over the oscillation frequency, Δm_s, gives a most probable value of 19 ps^{-1} and a range of $17 < \Delta m_s < 21$ (ps^{-1}) at 90% C.L. assuming Gaussian uncertainties. Also excludes $\Delta m_s < 14.8$ ps^{-1} at 95% C.L.
[6] Significance of oscillation signal is 0.2%. Also reported the value $|V_{td}\ /\ V_{ts}| = 0.208^{+0.001+0.008}_{-0.002-0.006}$.
[7] Uses leptons emitted with large momentum transverse to a jet and improved techniques for vertexing and flavor-tagging.
[8] Updates of D_s-lepton analysis.
[9] Combined results from all Delphi analyses.
[10] Events with a high transverse momentum lepton were removed and an inclusively reconstructed vertex was required.
[11] ABE 03 uses the novel "charge dipole" technique to reconstruct separate secondary and tertiary vertices originating from the $B \to D$ decay chain. The analysis excludes $\Delta m_s < 4.9$ ps^{-1} and $7.9 < \Delta m_s < 10.3$ ps^{-1}.
[12] Three analyses based on complementary event selections: (1) fully-reconstructed hadronic decays; (2) semileptonic decays with D_s exclusively reconstructed; (3) inclusive semileptonic decays.
[13] ABE 02V uses exclusively reconstructed D_s^- mesons and excludes $\Delta m_s < 1.4$ ps^{-1} and $2.4 < \Delta m_s < 5.3$ ps^{-1} at 95%CL.
[14] Uses fully or partially reconstructed $D_s\ell$ vertices and a mixing tag as a flavor tagging.
[15] Replaced by ABDALLAH 04A. Uses $D_s^-\ell^+$, and $\phi\ell^+$ vertices, and a multi-variable discriminant as a flavor tagging.
[16] Uses inclusive D_s vertices and fully reconstructed B_s decays and a multi-variable discriminant as a flavor tagging.
[17] Uses ℓ-$Q_{\rm hem}$ and ℓ-ℓ.
[18] ABE 99D assumes $\tau_{B_s^0} = 1.55 \pm 0.05$ ps and $\Delta\Gamma/\Delta m = (5.6 \pm 2.6) \times 10^{-3}$.
[19] ABE 99J uses ϕ ℓ-ℓ correlation.
[20] BARATE 99J uses combination of an inclusive lepton and D_s^--based analyses.
[21] BARATE 98C combines results from $D_s h$-$\ell/Q_{\rm hem}$, $D_s h$-K in the same side, $D_s\ell$-$\ell/Q_{\rm hem}$ and $D_s\ell$-K in the same side.
[22] Uses ℓ-$Q_{\rm hem}$.
[23] Uses ℓ-ℓ.
[24] ADAM 97 combines results from $D_s\ell$-$Q_{\rm hem}$, ℓ-$Q_{\rm hem}$, and ℓ-ℓ.
[25] BUSKULIC 96M uses D_s lepton correlations and lepton, kaon, and jet charge tags.
[26] BUSKULIC 95J uses ℓ-$Q_{\rm hem}$. They find $\Delta m_s > 5.6$ [> 6.1] for f_s=10% [12%]. We interpolate to our central value f_s=10.5%.

$x_s = \Delta m_{B_s^0}/\Gamma_{B_s^0}$

This is derived by the Heavy Flavor Averaging Group (HFAG) from the results on $\Delta m_{B_s^0}$ and "OUR EVALUATION" of the B_s^0 mean lifetime.

VALUE	DOCUMENT ID
26.85±0.13 OUR EVALUATION	

χ_s

This is a B_s^0-$\overline{B}_s^0$ integrated mixing parameter derived from x_s above and OUR EVALUATION of $\Delta\Gamma_{B_s^0}/\Gamma_{B_s^0}$.

VALUE	DOCUMENT ID
0.499311±0.000007 OUR EVALUATION	

CP VIOLATION PARAMETERS in B_s^0

$\mathrm{Re}(\epsilon_{B_s^0})\ /\ (1 + |\epsilon_{B_s^0}|^2)$

CP impurity in B_s^0 system.

"OUR EVALUATION" is an average using rescaled values of the data listed below. The average and rescaling were performed by the Heavy Flavor Averaging Group (HFAG) and are described at http://www.slac.stanford.edu/xorg/hfag/. The averaging/scaling procedure takes into account correlation between the measurements. The value has been obtained from a 2D fit of the B_d and B_s asymmetries, which includes the B_s measurements listed below and the B factory average for the B_d.

VALUE (units 10^{-3})	DOCUMENT ID		TECN	COMMENT
−1.9 ±1.0 OUR EVALUATION				
−1.3 ±0.9 OUR AVERAGE				
−0.15±1.25±0.90	[1] AAIJ	14D	LHCB	pp at 7 TeV
−2.15±1.85	[2] ABAZOV	14	D0	$p\overline{p}$ at 1.96 TeV
−2.8 ±1.9 ±0.4	[3] ABAZOV	13	D0	$p\overline{p}$ at 1.96 TeV
−0.4 ±2.3 ±0.4	[4] ABAZOV	10E	D0	$p\overline{p}$ at 1.96 TeV
• • • We do not use the following data for averages, fits, limits, etc. • • •				
−4.5 ±2.7	[5] ABAZOV	11U	D0	Repl. by ABAZOV 14
−3.6 ±1.9	[6] ABAZOV	10H	D0	Repl. by ABAZOV 11U
6.1 ±4.8 ±0.9	[7] ABAZOV	07A	D0	Repl. by ABAZOV 10E

Meson Particle Listings

B_s^0

[1] AAIJ 14D reports a measurement of time-integrated flavor-specific asymmetry in $B_s^0 \to \mu^+ D_s^- X$ decays $a_{sl}^s = (-0.06 \pm 0.50 \pm 0.36)\%$ which is approximately equal to $4 \times \mathrm{Re}(\epsilon_{B_s^0}) / (1 + |\epsilon_{B_s^0}|^2)$.

[2] ABAZOV 14 uses the dimuon charge asymmetry with different impact parameters from which it reports $A_{SL}^s = (-0.86 \pm 0.74) \times 10^{-2}$.

[3] ABAZOV 13 reports a measurement of time-integrated flavor-specific asymmetry in mixed semileptonic $B_s^0 \to \mu^+ D_s^- X$ decays $A_s^{SL} = (-1.12 \pm 0.74 \pm 0.17)\%$ which is approximately equal to $4 \times \mathrm{Re}(\epsilon_{B_s^0}) / (1 + |\epsilon_{B_s^0}|^2)$.

[4] ABAZOV 10E reports a measurement of flavor-specific asymmetry in $B_{(s)}^0 \to \mu^+ D_{(s)}^{*-} X$ decays with a decay-time analysis including initial-state flavor tagging, $A_{SL}^s = (-1.7 \pm 9.1^{+1.4}_{-1.5}) \times 10^{-3}$ which is approximately equal to $4 \times \mathrm{Re}(\epsilon_{B_s^0}) / (1 + |\epsilon_{B_s^0}|^2)$.

[5] ABAZOV 11U uses the dimuon charge asymmetry with different impact parameters from which it reports $A_{SL}^s = (-18.1 \pm 10.6) \times 10^{-3}$.

[6] ABAZOV 10H reports a measurement of like-sign dimuon charge asymmetry of $A_{SL}^b = (-9.57 \pm 2.51 \pm 1.46) \times 10^{-3}$ in semileptonic b-hadron decays. Using the measured production ratio of B_d^0 and B_s^0, and the asymmetry of B_d^0 $A_{SL}^d = (-4.7 \pm 4.6) \times 10^{-3}$ measured from B-factories, they obtain the asymmetry for B_s^0.

[7] The first direct measurement of the time integrated flavor untagged charge asymmetry in semileptonic B_s^0 decays is reported as $2xA_{SL}^s(\text{untagged}) = A_{SL}^s = (2.45 \pm 1.93 \pm 0.35) \times 10^{-2}$.

$C_{KK}(B_s^0 \to K^+K^-)$

VALUE	DOCUMENT ID		TECN	COMMENT
0.14±0.11±0.03	AAIJ	13BO	LHCB	pp at 7 TeV

$S_{KK}(B_s^0 \to K^+K^-)$

VALUE	DOCUMENT ID		TECN	COMMENT
0.30±0.12±0.04	AAIJ	13BO	LHCB	pp at 7 TeV

CP Violation phase β_s

$-2\beta_s$ is the weak phase difference between B_s^0 mixing amplitude and the $B_s^0 \to J/\psi\phi$ decay amplitude. The Standard Model value of β_s is $\arg(-\frac{V_{ts}V_{tb}^*}{V_{cs}V_{cb}^*})$.

"OUR EVALUATION" is an average using rescaled values of the data listed below. The average and rescaling were performed by the Heavy Flavor Averaging Group (HFAG) and are described at http://www.slac.stanford.edu/xorg/hfag/. The averaging/scaling procedure takes into account correlation between the measurements.

VALUE (units 10^{-2})			DOCUMENT ID		TECN	COMMENT
0.0 ± 3.5	**OUR EVALUATION**					
0.1 ± 3.4	**OUR AVERAGE**					
− 0.5 ± 3.5	±0.5		[1] AAIJ	13AR	LHCB	pp at 7 TeV
−11.0 ±20.5	±5.0		[2] AAD	12CV	ATLS	pp at 7 TeV
			[3] AALTONEN	12AJ	CDF	$p\overline{p}$ at 1.96 TeV
28	$^{+18}_{-19}$		[4,5,6] ABAZOV	12D	D0	$p\overline{p}$ at 1.96 TeV
• • • We do not use the following data for averages, fits, limits, etc. • • •						
			[7] AAIJ	13AY	LHCB	pp at 7 TeV
22	±22	±1	[8] AAIJ	12B	LHCB	Repl. by AAIJ 12Q
− 8	± 9	±3	[9] AAIJ	12D	LHCB	Repl. by AAIJ 13AR
0.95	$^{+\ 8.70}_{-\ 8.65}$	$^{+0.15}_{-0.20}$	[10] AAIJ	12Q	LHCB	Repl. by AAIJ 13AR
			[11] AALTONEN	12D	CDF	Repl. by AALTONEN 12AJ
			[12] AALTONEN	08G	CDF	Repl. by AALTONEN 12D
28	$^{+12}_{-15}$	$^{+4}_{-1}$	[5,13] ABAZOV	08AM	D0	Repl. by ABAZOV 12D
39.5	±28.0	$^{+0.5}_{-7.0}$	[6,14] ABAZOV	07	D0	Repl. by ABAZOV 07N
35	$^{+20}_{-24}$		[6,15] ABAZOV	07N	D0	Repl. by ABAZOV 08AM

[1] AAIJ 13AR reports $\phi_S = -2\beta_S = 0.01 \pm 0.07 \pm 0.01$ radians obtained from combined fit to $B_s^0 \to J/\psi K^+K^-$ and $B_s^0 \to J/\psi\pi^+\pi^-$ data sets. Also reports separate results of $\phi_S = 0.07 \pm 0.09 \pm 0.01$ radians from $B_s^0 \to J/\psi K^+K^-$ decays and $\phi_S = -0.14^{+0.17}_{-0.16} \pm 0.01$ radians from $B_s^0 \to J/\psi\pi^+\pi^-$ decays.

[2] AAD 12CV reports $\phi_s = -2\beta_S = 0.22 \pm 0.41 \pm 0.10$ rad. that was measured using a time-dependent angular analysis of $B_s^0 \to J/\psi\phi$ decays.

[3] AALTONEN 12AJ reports $-\pi/2 < \beta_S < -1.51$ or $-0.06 < \beta_S < 0.30$, or $1.26 < \beta_S < \pi/2$ at 68% CL. Measured using the time-dependent angular analysis of $B_s^0 \to J/\psi\phi$ decays.

[4] The error includes both statistical and systematic uncertainties.

[5] Measured using fully reconstructed $B_s \to J/\psi\phi$ decays.

[6] Reports ϕ_S which equals to $-2\beta_S$.

[7] Uses $B_s^0 \to \phi\phi$ mode, and reports the 68% CL interval of $\phi_S = -2\beta_S$ as $[-2.46, -0.76]$.

[8] Reports $\phi_S = -2\beta_S = -0.44 \pm 0.44 \pm 0.02$ that was measured using a time-dependent fit to $B_s^0 \to J/\psi f_0(980)$ decays.

[9] Reports $\phi_S = -2\beta_S = 0.15 \pm 0.18 \pm 0.06$ that was measured using a time-dependent angular analysis of $B_s^0 \to J/\psi\phi$ decays.

[10] Reports $\phi_S = -2\beta_S = -0.019^{+0.173+0.004}_{-0.174-0.003}$ radians which was measured using a time-dependent fit to $B_s^0 \to J/\psi\pi^+\pi^-$ decays, with the $\pi^+\pi^-$ mass within 775–1550 MeV. Searches for, but finds no evidence, for direct CP violation in $B_s^0 \to J/\psi\pi\pi$ decays.

[11] Reports $0.02 < \phi_S < 0.52$ or $1.08 < \phi_S < 1.55$ at 68% C.L. confidence regions in the two-dimensional space of ϕ_S and $\Delta\Gamma_{B_s^0}$ from $B_s^0 \to J/\psi\phi$ decays.

[12] Reports $0.32 < 2\beta_S < 2.82$ at 68% C.L. and confidence regions in the two-dimensional space of $2\beta_S$ and $\Delta\Gamma$ from the first measurement of $B_s^0 \to J/\psi\phi$ decays using flavor tagging. The probability of a deviation from SM prediction as large as the level of observed data is 15%.

[13] Reports $\phi_S = -2\beta_S$ and obtains 90% CL interval $-0.03 < \beta_S < 0.60$.

[14] The first direct measurement of the CP-violating mixing phase is reported from the time-dependent analysis of flavor untagged $B_s^0 \to J/\psi\phi$ decays.

[15] Combines D0 collaboration measurements of time-dependent angular distributions in $B_s^0 \to J/\psi\phi$ and charge asymmetry in semileptonic decays. There is a 4-fold ambiguity in the solution.

$A_{CP}(B_s \to \pi^+K^-)$

A_{CP} is defined as

$$\frac{B(\overline{B}_s^0 \to f) - B(B_s^0 \to \overline{f})}{B(\overline{B}_s^0 \to f) + B(B_s^0 \to \overline{f})},$$

the CP-violation asymmetry of exclusive B_s^0 and $\overline{B}_s^0$ decay.

VALUE	DOCUMENT ID		TECN	COMMENT
0.28±0.04 OUR AVERAGE				
0.27±0.04±0.01	AAIJ	13AX	LHCB	pp at 7 TeV
0.39±0.15±0.08	AALTONEN	11N	CDF	$p\overline{p}$ at 1.96 TeV
• • • We do not use the following data for averages, fits, limits, etc. • • •				
0.27±0.08±0.02	AAIJ	12V	LHCB	Repl. by AAIJ 13AX

$A_{CP}(B_s^0 \to [K^+K^-]_D \overline{K}^*(892)^0)$

VALUE	DOCUMENT ID		TECN	COMMENT
0.04±0.16±0.01	AAIJ	13L	LHCB	pp at 7 TeV

PARTIAL BRANCHING FRACTIONS IN $B_s \to \phi\ell^+\ell^-$

$B(B_s \to \phi\ell^+\ell^-)$ ($0.1 < q^2 < 2.0$ GeV$^2/c^4$)

VALUE (units 10^{-7})	DOCUMENT ID		TECN	COMMENT
0.49 ±0.11 OUR AVERAGE				
$0.472^{+0.109}_{-0.098}$±0.051	AAIJ	13X	LHCB	pp at 7 TeV, $B_s^0 \to \phi\mu^+\mu^-$
2.78 ±0.95 ±0.89	AALTONEN	11AI	CDF	$p\overline{p}$ at 1.96 TeV

$B(B_s \to \phi\ell^+\ell^-)$ ($2.0 < q^2 < 4.3$ GeV$^2/c^4$)

VALUE (units 10^{-7})	DOCUMENT ID		TECN	COMMENT
0.24 $^{+0.08}_{-0.07}$ OUR AVERAGE				
$0.230^{+0.079}_{-0.069}$±0.025	AAIJ	13X	LHCB	pp at 7 TeV, $B_s^0 \to \phi\mu^+\mu^-$
0.58 ±0.55 ±0.19	AALTONEN	11AI	CDF	$p\overline{p}$ at 1.96 TeV

$B(B_s \to \phi\ell^+\ell^-)$ ($4.3 < q^2 < 8.68$ GeV$^2/c^4$)

VALUE (units 10^{-7})	DOCUMENT ID		TECN	COMMENT
0.32 ±0.06 OUR AVERAGE				
$0.315^{+0.058}_{-0.053}$±0.033	AAIJ	13X	LHCB	pp at 7 TeV, $B_s^0 \to \phi\mu^+\mu^-$
1.34 ±0.83 ±0.43	AALTONEN	11AI	CDF	$p\overline{p}$ at 1.96 TeV

$B(B_s \to \phi\ell^+\ell^-)$ ($10.09 < q^2 < 12.86$ GeV$^2/c^4$)

VALUE (units 10^{-7})	DOCUMENT ID		TECN	COMMENT
0.44 ±0.09 OUR AVERAGE				
$0.426^{+0.081}_{-0.075}$±0.050	AAIJ	13X	LHCB	pp at 7 TeV, $B_s^0 \to \phi\mu^+\mu^-$
2.98 ±0.95 ±0.95	AALTONEN	11AI	CDF	$p\overline{p}$ at 1.96 TeV

$B(B_s \to \phi\ell^+\ell^-)$ ($14.18 < q^2 < 16.0$ GeV$^2/c^4$)

VALUE (units 10^{-7})	DOCUMENT ID		TECN	COMMENT
0.44 ±0.11 OUR AVERAGE				
$0.417^{+0.104}_{-0.093}$±0.048	AAIJ	13X	LHCB	pp at 7 TeV, $B_s^0 \to \phi\mu^+\mu^-$
1.86 ±0.66 ±0.59	AALTONEN	11AI	CDF	$p\overline{p}$ at 1.96 TeV

$B(B_s \to \phi\ell^+\ell^-)$ ($16.0 < q^2 < 19.0$ GeV$^2/c^4$)

VALUE (units 10^{-7})	DOCUMENT ID		TECN	COMMENT
0.36 ±0.08 OUR AVERAGE				
$0.352^{+0.076}_{-0.070}$±0.040	AAIJ	13X	LHCB	pp at 7 TeV, $B_s^0 \to \phi\mu^+\mu^-$
2.32 ±0.76 ±0.74	AALTONEN	11AI	CDF	$p\overline{p}$ at 1.96 TeV

$B(B_s \to \phi\ell^+\ell^-)$ ($1.0 < q^2 < 6.0$ GeV$^2/c^4$)

VALUE (units 10^{-7})	DOCUMENT ID		TECN	COMMENT
0.23 ±0.05 OUR AVERAGE				
$0.227^{+0.050}_{-0.046}$±0.025	AAIJ	13X	LHCB	pp at 7 TeV, $B_s^0 \to \phi\mu^+\mu^-$
1.14 ±0.79 ±0.36	AALTONEN	11AI	CDF	$p\overline{p}$ at 1.96 TeV

B($B_s \to \phi\ell^+\ell^-$) ($0.0 < q^2 < 4.3$ GeV$^2/c^4$)

VALUE (units 10^{-7})	DOCUMENT ID		TECN	COMMENT
3.30±1.09±1.05	AALTONEN	11AI	CDF	$p\overline{p}$ at 1.96 TeV

B_s^0 REFERENCES

AAIJ	14D	PL B728 607	R. Aaij *et al.*	(LHCb Collab.)
AAIJ	14E	JHEP 1404 114	R. Aaij *et al.*	(LHCb Collab.)
AAIJ	14F	PRL 112 111802	R. Aaij *et al.*	(LHCb Collab.)
ABAZOV	14	PR D89 012002	V.M. Abazov *et al.*	(D0 Collab.)
AAIJ	13	NP B867 1	R. Aaij *et al.*	(LHCb Collab.)
AAIJ	13A	NP B867 547	R. Aaij *et al.*	(LHCb Collab.)
AAIJ	13AA	NP B871 403	R. Aaij *et al.*	(LHCb Collab.)
AAIJ	13AB	NP B873 275	R. Aaij *et al.*	(LHCb Collab.)
AAIJ	13AC	NP B874 663	R. Aaij *et al.*	(LHCb Collab.)
AAIJ	13AL	PR D87 071101	R. Aaij *et al.*	(LHCb Collab.)
AAIJ	13AN	PR D87 072004	R. Aaij *et al.*	(LHCb Collab.)
AAIJ	13AP	PR D87 092007	R. Aaij *et al.*	(LHCb Collab.)
AAIJ	13AQ	PR D87 112009	R. Aaij *et al.*	(LHCb Collab.)
AAIJ	13AR	PR D87 112010	R. Aaij *et al.*	(LHCb Collab.)
AAIJ	13AW	PRL 110 211801	R. Aaij *et al.*	(LHCb Collab.)
AAIJ	13AX	PRL 110 221601	R. Aaij *et al.*	(LHCb Collab.)
AAIJ	13AY	PRL 110 241802	R. Aaij *et al.*	(LHCb Collab.)
AAIJ	13B	PRL 110 021801	R. Aaij *et al.*	(LHCb Collab.)
AAIJ	13BA	PRL 111 101805	R. Aaij *et al.*	(LHCb Collab.)
AAIJ	13BI	NJP 15 053021	R. Aaij *et al.*	(LHCb Collab.)
AAIJ	13BM	PRL 111 141801	R. Aaij *et al.*	(LHCb Collab.)
AAIJ	13BO	JHEP 1310 183	R. Aaij *et al.*	(LHCb Collab.)
AAIJ	13BP	JHEP 1310 143	R. Aaij *et al.*	(LHCb Collab.)
AAIJ	13BQ	JHEP 1310 005	R. Aaij *et al.*	(LHCb Collab.)
AAIJ	13BW	JHEP 1311 092	R. Aaij *et al.*	(LHCb Collab.)
AAIJ	13BX	PL B727 403	R. Aaij *et al.*	(LHCb Collab.)
AAIJ	13CF	EPJ C73 2655	R. Aaij *et al.*	(LHCb Collab.)
AAIJ	13L	JHEP 1303 067	R. Aaij *et al.*	(LHCb Collab.)
AAIJ	13X	JHEP 1307 084	R. Aaij *et al.*	(LHCb Collab.)
AAIJ	13Z	JHEP 1309 006	R. Aaij *et al.*	(LHCb Collab.)
AALTONEN	13F	PR D87 072003	T. Aaltonen *et al.*	(CDF Collab.)
ABAZOV	13	PRL 110 011801	V.M. Abazov *et al.*	(D0 Collab.)
ABAZOV	13C	PR D87 072006	V.M. Abazov *et al.*	(D0 Collab.)
CHATRCHYAN	13AW	PRL 111 101804	S. Chatrchyan *et al.*	(CMS Collab.)
ESEN	13	PR D87 031101	S. Esen *et al.*	(BELLE Collab.)
OSWALD	13	PR D87 072008	C. Oswald *et al.*	(BELLE Collab.)
SOLOVIEVA	13	PL B726 206	E. Solovieva *et al.*	(BELLE Collab.)
THORNE	13	PR D88 114006	F. Thorne *et al.*	(BELLE Collab.)
AAD	12AE	PL B713 387	G. Aad *et al.*	(ATLAS Collab.)
AAD	12CV	JHEP 1212 072	G. Aad *et al.*	(ATLAS Collab.)
AAIJ	12	PL B707 349	R. Aaij *et al.*	(LHCb Collab.)
AAIJ	12A	PL B708 55	R. Aaij *et al.*	(LHCb Collab.)
AAIJ	12AE	PR D85 112013	R. Aaij *et al.*	(LHCb Collab.)
AAIJ	12AG	JHEP 1206 115	R. Aaij *et al.*	(LHCb Collab.)
AAIJ	12AM	PRL 109 131801	R. Aaij *et al.*	(LHCb Collab.)
AAIJ	12AN	PRL 109 152002	R. Aaij *et al.*	(LHCb Collab.)
AAIJ	12AO	PR D86 052006	R. Aaij *et al.*	(LHCb Collab.)
AAIJ	12AP	PR D86 071102	R. Aaij *et al.*	(LHCb Collab.)
AAIJ	12AR	JHEP 1210 037	R. Aaij *et al.*	(LHCb Collab.)
AAIJ	12AX	PR D86 112005	R. Aaij *et al.*	(LHCb Collab.)
AAIJ	12B	PL B707 497	R. Aaij *et al.*	(LHCb Collab.)
AAIJ	12D	PRL 108 101803	R. Aaij *et al.*	(LHCb Collab.)
AAIJ	12E	PL B708 241	R. Aaij *et al.*	(LHCb Collab.)
AAIJ	12F	PL B709 50	R. Aaij *et al.*	(LHCb Collab.)
AAIJ	12I	PL B709 177	R. Aaij *et al.*	(LHCb Collab.)
AAIJ	12L	EPJ C72 2118	R. Aaij *et al.*	(LHCb Collab.)
AAIJ	12O	PL B713 172	R. Aaij *et al.*	(LHCb Collab.)
AAIJ	12P	PL B713 369	R. Aaij *et al.*	(LHCb Collab.)
AAIJ	12Q	PL B713 378	R. Aaij *et al.*	(LHCb Collab.)
AAIJ	12R	PL B716 393	R. Aaij *et al.*	(LHCb Collab.)
AAIJ	12S	PRL 108 151801	R. Aaij *et al.*	(LHCb Collab.)
AAIJ	12V	PRL 108 201601	R. Aaij *et al.*	(LHCb Collab.)
AAIJ	12W	PRL 108 231801	R. Aaij *et al.*	(LHCb Collab.)
AALTONEN	12AJ	PRL 109 171802	T. Aaltonen *et al.*	(CDF Collab.)
AALTONEN	12C	PRL 108 201801	T. Aaltonen *et al.*	(CDF Collab.)
AALTONEN	12D	PR D85 072002	T. Aaltonen *et al.*	(CDF Collab.)
AALTONEN	12L	PRL 108 211803	T. Aaltonen *et al.*	(CDF Collab.)
ABAZOV	12AF	PR D86 092011	V.M. Abazov *et al.*	(D0 Collab.)
ABAZOV	12C	PR D85 011103	V.M. Abazov *et al.*	(D0 Collab.)
ABAZOV	12D	PR D85 032006	V.M. Abazov *et al.*	(D0 Collab.)
CHATRCHYAN	12A	JHEP 1204 033	S. Chatrchyan *et al.*	(CMS Collab.)
LEES	12A	PR D85 011101	J.P. Lees *et al.*	(BABAR Collab.)
LI	12	PRL 108 181808	J. Li *et al.*	(BELLE Collab.)
AAIJ	11	PL B698 115	R. Aaij *et al.*	(LHCb Collab.)
AAIJ	11A	PL B698 14	R. Aaij *et al.*	(LHCb Collab.)
AAIJ	11B	PL B699 330	R. Aaij *et al.*	(LHCb Collab.)
AAIJ	11D	PL B706 32	R. Aaij, et al	(LHCb Collab.)
AAIJ	11E	PR D84 092001	R. Aaij *et al.*	(LHCb Collab.)
Also		PR D85 039904 (errat)	R. Aaij *et al.*	(LHCb Collab.)
AALTONEN	11A	PR D83 052012	T. Aaltonen *et al.*	(CDF Collab.)
AALTONEN	11AB	PR D84 052012	T. Aaltonen *et al.*	(CDF Collab.)
AALTONEN	11AG	PRL 107 191801	T. Aaltonen *et al.*	(CDF Collab.)
Also		PRL 107 239903 (errat)	T. Aaltonen *et al.*	(CDF Collab.)
AALTONEN	11AI	PRL 107 201802	T. Aaltonen *et al.*	(CDF Collab.)
AALTONEN	11AN	PRL 107 261802	T. Aaltonen *et al.*	(CDF Collab.)
AALTONEN	11AP	PRL 107 272001	T. Aaltonen *et al.*	(CDF Collab.)
AALTONEN	11L	PRL 106 161801	T. Aaltonen *et al.*	(CDF Collab.)
AALTONEN	11N	PRL 106 181802	T. Aaltonen *et al.*	(CDF Collab.)
ABAZOV	11U	PR D84 052007	V.M. Abazov *et al.*	(D0 Collab.)
CHATRCHYAN	11T	PRL 107 191802	S. Chatrchyan *et al.*	(CMS Collab.)
LI	11	PRL 106 121802	J. Li *et al.*	(BELLE Collab.)
ABAZOV	10E	PR D82 012003	V.M. Abazov *et al.*	(D0 Collab.)
ABAZOV	10H	PR D82 032001	V.M. Abazov *et al.*	(D0 Collab.)
ABAZOV	10S	PL B693 539	V.M. Abazov *et al.*	(D0 Collab.)
ESEN	10	PRL 105 201802	S. Esen *et al.*	(BELLE Collab.)
LOUVOT	10	PRL 104 231801	R. LOUVOT *et al.*	(BELLE Collab.)
PENG	10	PR D82 072007	C.-C. Peng *et al.*	(BELLE Collab.)
AALTONEN	09AQ	PRL 103 191802	T. Aaltonen *et al.*	(CDF Collab.)
AALTONEN	09B	PR D79 011104	T. Aaltonen *et al.*	(CDF Collab.)
AALTONEN	09C	PRL 103 031801	T. Aaltonen *et al.*	(CDF Collab.)
AALTONEN	09P	PRL 102 201801	T. Aaltonen *et al.*	(CDF Collab.)
ABAZOV	09E	PRL 102 032001	V.M. Abazov *et al.*	(D0 Collab.)
ABAZOV	09G	PRL 102 051801	V.M. Abazov *et al.*	(D0 Collab.)
ABAZOV	09I	PRL 102 091801	V.M. Abazov *et al.*	(D0 Collab.)
ABAZOV	09Y	PR D79 111102	V.M. Abazov *et al.*	(D0 Collab.)
LOUVOT	09	PRL 102 021801	R. Louvot *et al.*	(BELLE Collab.)
AALTONEN	08F	PRL 100 021803	T. Aaltonen *et al.*	(CDF Collab.)
AALTONEN	08G	PRL 100 161802	T. Aaltonen *et al.*	(CDF Collab.)
AALTONEN	08I	PRL 100 101802	T. Aaltonen *et al.*	(CDF Collab.)
AALTONEN	08J	PRL 100 121803	T. Aaltonen *et al.*	(CDF Collab.)
ABAZOV	08AM	PRL 101 241801	V.M. Abazov *et al.*	(D0 Collab.)
WICHT	08A	PRL 100 121801	J. Wicht *et al.*	(BELLE Collab.)
ABAZOV	07	PRL 98 121801	V.M. Abazov *et al.*	(D0 Collab.)
ABAZOV	07A	PRL 98 151801	V.M. Abazov *et al.*	(D0 Collab.)
ABAZOV	07N	PR D76 057101	V.M. Abazov *et al.*	(D0 Collab.)
ABAZOV	07Q	PR D76 092001	V.M. Abazov *et al.*	(D0 Collab.)
ABAZOV	07Y	PRL 99 241801	V.M. Abazov *et al.*	(D0 Collab.)
ABULENCIA	07C	PRL 98 061802	A. Abulencia *et al.*	(CDF Collab.)
DRUTSKOY	07	PRL 98 052001	A. Drutskoy *et al.*	(BELLE Collab.)
DRUTSKOY	07A	PR D76 012002	A. Drutskoy *et al.*	(BELLE Collab.)
ABAZOV	06B	PRL 97 021802	V.M. Abazov *et al.*	(D0 Collab.)
ABAZOV	06G	PR D74 031107	V.M. Abazov *et al.*	(D0 Collab.)
ABAZOV	06V	PRL 97 241801	V.M. Abazov *et al.*	(D0 Collab.)
ABULENCIA	06J	PRL 96 191801	A. Abulencia *et al.*	(CDF Collab.)
ABULENCIA	06N	PRL 96 231801	A. Abulencia *et al.*	(CDF Collab.)
ABULENCIA	06Q	PRL 97 062003	A. Abulencia *et al.*	(CDF Collab.)
ABULENCIA,A	06D	PRL 97 211802	A. Abulencia *et al.*	(CDF Collab.)
ABULENCIA,A	06G	PRL 97 242003	A. Abulencia *et al.*	(CDF Collab.)
ACOSTA	06	PRL 96 202001	D. Acosta *et al.*	(CDF Collab.)
ABAZOV	05B	PRL 94 042001	V.M. Abazov *et al.*	(D0 Collab.)
ABAZOV	05E	PRL 94 071802	V.M. Abazov *et al.*	(D0 Collab.)
ABAZOV	05W	PRL 95 171801	V.M. Abazov *et al.*	(D0 Collab.)
ABULENCIA	05	PRL 95 221805	A. Abulencia *et al.*	(CDF Collab.)
Also		PRL 95 249905 (errat)	A. Abulencia *et al.*	(CDF Collab.)
ACOSTA	05	PRL 94 101803	D. Acosta *et al.*	(CDF Collab.)
ACOSTA	05J	PRL 95 031801	D. Acosta *et al.*	(CDF Collab.)
ABDALLAH	04A	PL B585 63	J. Abdallah *et al.*	(DELPHI Collab.)
ABDALLAH	04J	EPJ C35 35	J. Abdallah *et al.*	(DELPHI Collab.)
ACOSTA	04D	PRL 93 032001	D. Acosta *et al.*	(CDF Collab.)
ABDALLAH	03B	EPJ C28 155	J. Abdallah *et al.*	(DELPHI Collab.)
ABE	03	PR D67 012006	K. Abe *et al.*	(SLD Collab.)
HEISTER	03E	EPJ C29 143	A. Heister *et al.*	(ALEPH Collab.)
ABE	02V	PR D66 032009	K. Abe *et al.*	(SLD Collab.)
ACOSTA	02D	PR D65 111101	D. Acosta *et al.*	(CDF Collab.)
ACOSTA	02G	PR D66 112002	D. Acosta *et al.*	(CDF Collab.)
ABBIENDI	01D	EPJ C19 241	G. Abbiendi *et al.*	(OPAL Collab.)
ABE	00C	PR D62 071101	K. Abe *et al.*	(SLD Collab.)
ABREU	00Y	EPJ C16 555	P. Abreu *et al.*	(DELPHI Collab.)
ABREU,P	00G	EPJ C18 229	P. Abreu *et al.*	(DELPHI Collab.)
AFFOLDER	00N	PRL 85 4668	T. Affolder *et al.*	(CDF Collab.)
BARATE	00K	PL B486 286	R. Barate *et al.*	(ALEPH Collab.)
ABBIENDI	99S	EPJ C11 587	G. Abbiendi *et al.*	(OPAL Collab.)
ABE	99D	PR D59 032004	F. Abe *et al.*	(CDF Collab.)
ABE	99J	PRL 82 3576	F. Abe *et al.*	(CDF Collab.)
BARATE	99J	EPJ C7 553	R. Barate *et al.*	(ALEPH Collab.)
Also		EPJ C12 181 (errat)	R. Barate *et al.*	(ALEPH Collab.)
ABE	98	PR D57 R3811	F. Abe *et al.*	(CDF Collab.)
ABE	98B	PR D57 5382	F. Abe *et al.*	(CDF Collab.)
ABE	98V	PRL 81 5742	F. Abe *et al.*	(CDF Collab.)
ACCIARRI	98S	PL B438 417	M. Acciarri *et al.*	(L3 Collab.)
ACKERSTAFF	98F	EPJ C2 407	K. Ackerstaff *et al.*	(OPAL Collab.)
ACKERSTAFF	98G	PL B426 161	K. Ackerstaff *et al.*	(OPAL Collab.)
BARATE	98C	EPJ C4 367	R. Barate *et al.*	(ALEPH Collab.)
BARATE	98Q	EPJ C4 387	R. Barate *et al.*	(ALEPH Collab.)
PDG	98	EPJ C3 1	C. Caso *et al.*	(PDG Collab.)
ACCIARRI	97B	PL B391 474	M. Acciarri *et al.*	(L3 Collab.)
ACCIARRI	97C	PL B391 481	M. Acciarri *et al.*	(L3 Collab.)
ACKERSTAFF	97U	ZPHY C76 401	K. Ackerstaff *et al.*	(OPAL Collab.)
ACKERSTAFF	97V	ZPHY C76 417	K. Ackerstaff *et al.*	(OPAL Collab.)
ADAM	97	PL B414 382	W. Adam *et al.*	(DELPHI Collab.)
ABE	96B	PR D53 3496	F. Abe *et al.*	(CDF Collab.)
ABE	96L	PRL 76 4675	F. Abe *et al.*	(CDF Collab.)
ABE	96N	PRL 77 1945	F. Abe *et al.*	(CDF Collab.)
ABE	96Q	PR D54 6596	F. Abe *et al.*	(CDF Collab.)
ABREU	96F	ZPHY C71 11	P. Abreu *et al.*	(DELPHI Collab.)
ADAM	96D	ZPHY C72 207	W. Adam *et al.*	(DELPHI Collab.)
BUSKULIC	96E	ZPHY C69 585	D. Buskulic *et al.*	(ALEPH Collab.)
BUSKULIC	96M	PL B377 205	D. Buskulic *et al.*	(ALEPH Collab.)
BUSKULIC	96V	PL B384 471	D. Buskulic *et al.*	(ALEPH Collab.)
PDG	96	PR D54 1	R. M. Barnett *et al.*	(PDG Collab.)
ABE	95R	PRL 74 4988	F. Abe *et al.*	(CDF Collab.)
ABE	95Z	PRL 75 3068	F. Abe *et al.*	(CDF Collab.)
ACCIARRI	95H	PL B363 127	M. Acciarri *et al.*	(L3 Collab.)
ACCIARRI	95I	PL B363 137	M. Acciarri *et al.*	(L3 Collab.)
AKERS	95G	PL B350 273	R. Akers *et al.*	(OPAL Collab.)
AKERS	95J	ZPHY C66 555	R. Akers *et al.*	(OPAL Collab.)
BUSKULIC	95J	PL B356 409	D. Buskulic *et al.*	(ALEPH Collab.)
BUSKULIC	95O	PL B361 221	D. Buskulic *et al.*	(ALEPH Collab.)
ABREU	94D	PL B324 500	P. Abreu *et al.*	(DELPHI Collab.)
ABREU	94E	ZPHY C61 407	P. Abreu *et al.*	(DELPHI Collab.)
Also		PL B289 199	P. Abreu *et al.*	(DELPHI Collab.)
AKERS	94J	PL B337 196	R. Akers *et al.*	(OPAL Collab.)
AKERS	94L	PL B337 393	R. Akers *et al.*	(OPAL Collab.)
BUSKULIC	94B	PL B322 441	D. Buskulic *et al.*	(ALEPH Collab.)
BUSKULIC	94C	PL B322 275	D. Buskulic *et al.*	(ALEPH Collab.)
ABE	93F	PRL 71 1685	F. Abe *et al.*	(CDF Collab.)
ACTON	93H	PL B312 501	P.D. Acton *et al.*	(OPAL Collab.)
BUSKULIC	93G	PL B311 425	D. Buskulic *et al.*	(ALEPH Collab.)
ABREU	92M	PL B289 199	P. Abreu *et al.*	(DELPHI Collab.)
ACTON	92N	PL B295 357	P.D. Acton *et al.*	(OPAL Collab.)
BUSKULIC	92E	PL B294 145	D. Buskulic *et al.*	(ALEPH Collab.)
LEE-FRANZINI	90	PRL 65 2947	J. Lee-Franzini *et al.*	(CUSB II Collab.)

B_s^*

$I(J^P) = 0(1^-)$

I, *J*, *P* need confirmation. Quantum numbers shown are quark-model predictions.

B_s^* MASS

From mass difference below and the B_s^0 mass.

VALUE (MeV)	DOCUMENT ID		TECN	COMMENT
$5415.4^{+2.4}_{-2.1}$ OUR FIT	Error includes scale factor of 3.0.			
5415.8±1.5 OUR AVERAGE	Error includes scale factor of 2.6.			
5416.4±0.4±0.5	LOUVOT	09	BELL	$e^+e^- \to \Upsilon(5S)$
5411.7±1.6±0.6	[1] AQUINES	06	CLEO	$e^+e^- \to \Upsilon(5S)$
• • • We do not use the following data for averages, fits, limits, etc. • • •				
5418 ±1 ±3	DRUTSKOY	07A	BELL	Repl. by LOUVOT 09
5414 ±1 ±3	[2] BONVICINI	06	CLEO	$e^+e^- \to \Upsilon(5S)$

Meson Particle Listings

B_s^*, $B_{s1}(5830)^0$, $B_{s2}^*(5840)^0$, $B_{sJ}^*(5850)$

[1] Utilized the beam constrained invariant mass peak positions for B^* and B_s^* to extract the measurement.
[2] Uses 14 candidates consistent with B_s decays into final states with a J/ψ and a $D_s^{(*)-}$.

$m_{B_s^*} - m_{B_s}$

VALUE (MeV)	DOCUMENT ID		TECN	COMMENT
$48.7^{+2.3}_{-2.1}$ OUR FIT Error includes scale factor of 2.8.				
46.1±1.5 OUR AVERAGE				
45.7±1.7±0.7	[3] AQUINES	06	CLEO	$e^+e^- \to \Upsilon(5S)$
47.0±2.6	[4] LEE-FRANZINI	90	CSB2	$e^+e^- \to \Upsilon(5S)$
• • • We do not use the following data for averages, fits, limits, etc. • • •				
48 ±1 ±3	[5] BONVICINI	06	CLEO	Repl. by AQUINES 06

[3] Utilized the beam constrained invariant mass peak positions for B^* and B_s^* to extract the measurement.
[4] LEE-FRANZINI 90 measure 46.7 ± 0.4 ± 0.2 MeV for an admixture of B^0, B^+, and B_s. They use the shape of the photon line to separate the above value for B_s.
[5] Uses 14 candidates consistent with B_s decays into final states with a J/ψ and a $D_s^{(*)-}$.

$|(m_{B_s^*} - m_{B_s}) - (m_{B^*} - m_B)|$

VALUE (MeV)	CL%	DOCUMENT ID		TECN	COMMENT
<6	95	ABREU	95R	DLPH	$E_{\rm cm}^{ee}$= 88–94 GeV

B_s^* DECAY MODES

	Mode	Fraction (Γ_i/Γ)
Γ_1	$B_s\gamma$	dominant

B_s^* REFERENCES

LOUVOT	09	PRL 102 021801	R. Louvot *et al.*	(BELLE Collab.)
DRUTSKOY	07A	PR D76 012002	A. Drutskoy *et al.*	(BELLE Collab.)
AQUINES	06	PRL 96 152001	O. Aquines *et al.*	(CLEO Collab.)
BONVICINI	06	PRL 96 022002	G. Bonvicini *et al.*	(CLEO Collab.)
ABREU	95R	ZPHY C68 353	P. Abreu *et al.*	(DELPHI Collab.)
LEE-FRANZINI	90	PRL 65 2947	J. Lee-Franzini *et al.*	(CUSB II Collab.)

$B_{s1}(5830)^0$

$I(J^P) = 0(1^+)$ Status: ***
I, J, P need confirmation.

Quantum numbers shown are quark-model predictions.

$B_{s1}(5830)^0$ MASS

VALUE (MeV)	DOCUMENT ID		TECN	COMMENT
5828.7 ±0.4 OUR AVERAGE	Error includes scale factor of 1.2.			
5828.40±0.04±0.41	[1] AAIJ	13O	LHCB	pp at 7 TeV
5829.4 ±0.7	[2] AALTONEN	08K	CDF	$p\overline{p}$ at 1.96 TeV

[1] Uses $B_{s1}(5830)^0 \to B^{*+}K^-$ decay.
[2] Uses two-body decays into K^- and B^+ mesons reconstructed as $B^+ \to J/\psi K^+$, $J/\psi \to \mu^+\mu^-$ or $B^+ \to \overline{D}^0\pi^+$, $\overline{D}^0 \to K^+\pi^-$.

$m_{B_{s1}^0} - m_{B^{*+}}$

VALUE (MeV)	DOCUMENT ID		TECN	COMMENT
504.41±0.21±0.14	[3] AALTONEN	08K	CDF	$p\overline{p}$ at 1.96 TeV

[3] Uses two-body decays into K^- and B^+ mesons reconstructed as $B^+ \to J/\psi K^+$, $J/\psi \to \mu^+\mu^-$ or $B^+ \to \overline{D}^0\pi^+$, $\overline{D}^0 \to K^+\pi^-$.

$B_{s1}(5830)^0$ DECAY MODES

	Mode	Fraction (Γ_i/Γ)
Γ_1	$B^{*+}K^-$	dominant

$B_{s1}(5830)^0$ BRANCHING RATIOS

$\Gamma(B^{*+}K^-)/\Gamma_{\rm total}$ **Γ_1/Γ**

VALUE	DOCUMENT ID		TECN	COMMENT
dominant	AALTONEN	08K	CDF	$p\overline{p}$ at 1.96 TeV

$B_{s1}(5830)^0$ REFERENCES

AAIJ	13O	PRL 110 151803	R. Aaij *et al.*	(LHCb Collab.)
AALTONEN	08K	PRL 100 082001	T. Aaltonen *et al.*	(CDF Collab.)

$B_{s2}^*(5840)^0$

$I(J^P) = 0(2^+)$ Status: ***
I, J, P need confirmation.

Quantum numbers shown are quark-model predictions.

$B_{s2}^*(5840)^0$ MASS

VALUE (MeV)	DOCUMENT ID		TECN	COMMENT
5839.96±0.20 OUR AVERAGE				
5839.99±0.05±0.20	AAIJ	13O	LHCB	pp at 7 TeV
5839.7 ±0.7	[1] AALTONEN	08K	CDF	$p\overline{p}$ at 1.96 TeV
5839.6 ±1.1 ±0.7	[2] ABAZOV	08E	D0	$p\overline{p}$ at 1.96 TeV

[1] Uses two-body decays into K^- and B^+ mesons reconstructed as $B^+ \to J/\psi K^+$, $J/\psi \to \mu^+\mu^-$ or $B^+ \to \overline{D}^0\pi^+$, $\overline{D}^0 \to K^+\pi^-$.
[2] Observed in $B_{s2}^{*0} \to B^+K^-$. Measured production rate of B_{s2}^{*0} relative to B^+ to be (1.15 ± 0.23 ± 0.13)%.

$m_{B_{s2}^{*0}} - m_{B_{s1}^0}$

VALUE (MeV)	DOCUMENT ID		TECN	COMMENT
10.5±0.6	[3] AALTONEN	08K	CDF	$p\overline{p}$ at 1.96 TeV

[3] Uses two-body decays into K^- and B^+ mesons reconstructed as $B^+ \to J/\psi K^+$, $J/\psi \to \mu^+\mu^-$ or $B^+ \to \overline{D}^0\pi^+$, $\overline{D}^0 \to K^+\pi^-$.

$B_{s2}^*(5840)^0$ WIDTH

VALUE (MeV)	DOCUMENT ID		TECN	COMMENT
1.56±0.13±0.47	[4] AAIJ	13O	LHCB	pp at 7 TeV

[4] Uses $B_{s2}^*(5840)^0 \to B^{*+}K^-$ decays.

$B_{s2}^*(5840)^0$ DECAY MODES

	Mode	Fraction (Γ_i/Γ)
Γ_1	B^+K^-	dominant
Γ_2	$B^{*+}K^-$	

$B_{s2}^*(5840)^0$ BRANCHING RATIOS

$\Gamma(B^+K^-)/\Gamma_{\rm total}$ **Γ_1/Γ**

VALUE	DOCUMENT ID		TECN	COMMENT
dominant	AALTONEN	08K	CDF	$p\overline{p}$ at 1.96 TeV
dominant	[5] ABAZOV	08E	D0	$p\overline{p}$ at 1.96 TeV

[5] Measured production rate of B_{s2}^{*0} relative to B^+ to be (1.15 ± 0.23 ± 0.13)%.

$\Gamma(B^{*+}K^-)/\Gamma(B^+K^-)$ **Γ_2/Γ_1**

VALUE	DOCUMENT ID		TECN	COMMENT
0.093±0.013±0.012	AAIJ	13O	LHCB	pp at 7 TeV

$B_{s2}^*(5840)^0$ REFERENCES

AAIJ	13O	PRL 110 151803	R. Aaij *et al.*	(LHCb Collab.)
AALTONEN	08K	PRL 100 082001	T. Aaltonen *et al.*	(CDF Collab.)
ABAZOV	08E	PRL 100 082002	V.M. Abazov *et al.*	(D0 Collab.)

$B_{sJ}^*(5850)$

$I(J^P) = ?(?^?)$
I, J, P need confirmation.

OMITTED FROM SUMMARY TABLE

Signal can be interpreted as coming from $\overline{b}s$ states. Needs confirmation.

$B_{sJ}^*(5850)$ MASS

VALUE (MeV)	EVTS	DOCUMENT ID		TECN	COMMENT
5853±15	141	AKERS	95E	OPAL	$E_{\rm cm}^{ee}$= 88–94 GeV

$B_{sJ}^*(5850)$ WIDTH

VALUE (MeV)	EVTS	DOCUMENT ID		TECN	COMMENT
47±22	141	AKERS	95E	OPAL	$E_{\rm cm}^{ee}$= 88–94 GeV

$B_{sJ}^*(5850)$ REFERENCES

AKERS	95E	ZPHY C66 19	R. Akers *et al.*	(OPAL Collab.)

BOTTOM, CHARMED MESONS ($B = C = \pm 1$)

$B_c^+ = c\overline{b}$, $B_c^- = \overline{c}b$, similarly for B_c^*'s

$B_c^{\pm}$

$I(J^P) = 0(0^-)$
I, J, P need confirmation.

Quantum numbers shown are quark-model predictions.

$B_c^{\pm}$ MASS

VALUE (GeV)		DOCUMENT ID		TECN	COMMENT
6.2756 ±0.0011 OUR AVERAGE					
6.27628 ±0.00144	±0.00036	[1] AAIJ	13AS	LHCB	pp at 7, 8 TeV
6.2737 ±0.0013	±0.0016	[2] AAIJ	12AV	LHCB	pp at 7 TeV
6.2756 ±0.0029	±0.0025	[3] AALTONEN	08M	CDF	$p\overline{p}$ at 1.96 TeV
6.300 ±0.014	±0.005	[3] ABAZOV	08T	D0	$p\overline{p}$ at 1.96 TeV
6.4 ±0.39	±0.13	[4] ABE	98M	CDF	$p\overline{p}$ at 1.8 TeV
• • • We do not use the following data for averages, fits, limits, etc. • • •					
6.2857 ±0.0053	±0.0012	[3] ABULENCIA	06C	CDF	Repl. by AALTONEN 08M
6.32 ±0.06		[5] ACKERSTAFF	98O	OPAL	$e^+e^- \to Z$

[1] AAIJ 13AS uses the $B_c^+ \to J/\psi D_s^+$.

[2] AAIJ 12AV uses the $B_c^+ \to J/\psi\pi^+$ mode and also measures the mass difference $M(B_c^+) - M(B^+) = 994.6 \pm 1.3 \pm 0.6$ MeV/c^2.

[3] Measured using a fully reconstructed decay mode of $B_c \to J/\psi\pi$.

[4] ABE 98M observed $20.4^{+6.2}_{-5.5}$ events in the $B_c^+ \to J/\psi(1s)\ell\nu_\ell$ with a significance of > 4.8 standard deviations. The mass value is estimated from $m(J/\psi(1S)\ell)$.

[5] ACKERSTAFF 98O observed 2 candidate events in the $B_c^+ \to J/\psi(1S)\pi^+$ channel with an estimated background of 0.63 ± 0.20 events.

$B_c^{\pm}$ MEAN LIFE

"OUR EVALUATION" is an average using rescaled values of the data listed below. The average and rescaling were performed by the Heavy Flavor Averaging Group (HFAG) and are described at http://www.slac.stanford.edu/xorg/hfag/. The averaging/rescaling procedure takes into account correlations between the measurements.

VALUE (10^{-12} s)	DOCUMENT ID		TECN	COMMENT
0.452±0.033 OUR EVALUATION				
0.500±0.013 OUR AVERAGE				
0.509±0.008±0.012	[6] AAIJ	14G	LHCB	pp at 8 TeV
0.452±0.048±0.027	[7] AALTONEN	13	CDF	$p\overline{p}$ at 1.96 TeV
$0.448^{+0.038}_{-0.036}$±0.032	[8] ABAZOV	09H	D0	$p\overline{p}$ at 1.96 TeV
$0.463^{+0.073}_{-0.065}$±0.036	[8] ABULENCIA	06O	CDF	$p\overline{p}$ at 1.96 TeV
$0.46\ ^{+0.18}_{-0.16}$ ±0.03	[8] ABE	98M	CDF	$p\overline{p}$ 1.8 TeV

[6] Measured using $B_c^+ \to J/\psi\mu^+\nu_\mu X$ decays.

[7] Uses fully reconstructed $B_c^+ \to J/\psi\pi^+$ decays.

[8] The lifetime is measured from the $J/\psi e$ decay vertices.

B_c^+ DECAY MODES × B($\overline{b} \to B_c$)

B_c^- modes are charge conjugates of the modes below.

	Mode	Fraction (Γ_i/Γ)		Confidence level
	The following quantities are not pure branching ratios; rather the fraction $\Gamma_i/\Gamma \times B(\overline{b} \to B_c)$.			
Γ_1	$J/\psi(1S)\ell^+\nu_\ell$ anything	$(5.2\ ^{+2.4}_{-2.1}) \times 10^{-5}$		
Γ_2	$J/\psi(1S)\pi^+$	seen		
Γ_3	$J/\psi(1S)K^+$	seen		
Γ_4	$J/\psi(1S)\pi^+\pi^+\pi^-$	seen		
Γ_5	$J/\psi(1S)a_1(1260)$	< 1.2	$\times 10^{-3}$	90%
Γ_6	$J/\psi(1S)K^+K^-\pi^+$	seen		
Γ_7	$\psi(2S)\pi^+$	seen		
Γ_8	$J/\psi(1S)D_s^+$	seen		
Γ_9	$J/\psi(1S)D_s^{*+}$	seen		
Γ_{10}	$D^*(2010)^+\overline{D}^0$	< 6.2	$\times 10^{-3}$	90%
Γ_{11}	D^+K^{*0}	< 0.20	$\times 10^{-6}$	90%
Γ_{12}	$D^+\overline{K}^{*0}$	< 0.16	$\times 10^{-6}$	90%
Γ_{13}	$D_s^+K^{*0}$	< 0.28	$\times 10^{-6}$	90%
Γ_{14}	$D_s^+\overline{K}^{*0}$	< 0.4	$\times 10^{-6}$	90%
Γ_{15}	$D_s^+\phi$	< 0.32	$\times 10^{-6}$	90%
Γ_{16}	K^+K^0	< 4.6	$\times 10^{-7}$	90%
Γ_{17}	$B_s^0\pi^+$ / B($\overline{b} \to B_s$)	$(2.37^{+0.37}_{-0.35}) \times 10^{-3}$		

B_c^+ BRANCHING RATIOS

$\Gamma(J/\psi(1S)\ell^+\nu_\ell \text{anything})/\Gamma_{\text{total}} \times B(\overline{b} \to B_c)$ — $\Gamma_1/\Gamma \times B$

VALUE	CL%	DOCUMENT ID		TECN	COMMENT
$(5.2^{+2.4}_{-2.1}) \times 10^{-5}$		[9] ABE	98M	CDF	$p\overline{p}$ 1.8 TeV
• • • We do not use the following data for averages, fits, limits, etc. • • •					
$< 1.6 \times 10^{-4}$	90	[10] ACKERSTAFF	98O	OPAL	$e^+e^- \to Z$
$< 1.9 \times 10^{-4}$	90	[11] ABREU	97E	DLPH	$e^+e^- \to Z$
$< 1.2 \times 10^{-4}$	90	[12] BARATE	97H	ALEP	$e^+e^- \to Z$

[9] ABE 98M result is derived from the measurement of $[\sigma(B_c)\times B(B_c \to J/\psi(1S)\ell\nu_\ell)] / [\sigma(B^+)\times B(B^+ \to J/\psi(1S)K^+)] = 0.132^{+0.041}_{-0.037}(\text{stat}) \pm 0.031(\text{sys})^{+0.032}_{-0.020}(\text{lifetime})$ by using PDG 98 values of $B(b \to B^+)$ and $B(B^+ \to J/\psi(1S)K^+)$.

[10] ACKERSTAFF 98O reports $B(Z \to B_c X)/B(Z \to q\overline{q})\times B(B_c \to J/\psi(1S)\ell\nu_\ell) < 6.95 \times 10^{-5}$ at 90%CL. We rescale to our PDG 98 values of $B(Z \to b\overline{b})$.

[11] ABREU 97E value listed is for an assumed $\tau_{B_c} = 0.4$ ps and improves to 1.6×10^{-4} for $\tau_{B_c} = 1.4$ ps.

[12] BARATE 97H reports $B(Z \to B_c X)/B(Z \to q\overline{q})\cdot B(B_c \to J/\psi(1S)\ell\nu_\ell) < 5.2\times 10^{-5}$ at 90%CL. We rescale to our PDG 96 values of $B(Z \to b\overline{b})$. A $B_c^+ \to J/\psi(1S)\mu^+\nu_\mu$ candidate event is found, compared to all the known background sources 2×10^{-3}, which gives $m_{B_c} = 5.96^{+0.25}_{-0.19}$ GeV and $\tau_{B_c} = 1.77 \pm 0.17$ ps.

$\Gamma(J/\psi(1S)\pi^+)/\Gamma_{\text{total}} \times B(\overline{b} \to B_c)$ — $\Gamma_2/\Gamma \times B$

VALUE	CL%	DOCUMENT ID		TECN	COMMENT
seen		AALTONEN	13	CDF	$p\overline{p}$ at 1.96 TeV
seen		[13] AAIJ	12AV	LHCB	pp at 7 TeV
seen		AALTONEN	08M	CDF	$p\overline{p}$ at 1.96 TeV
seen		ABAZOV	08T	D0	$p\overline{p}$ at 1.96 TeV
• • • We do not use the following data for averages, fits, limits, etc. • • •					
$<2.4 \times 10^{-4}$	90	[14] ACKERSTAFF	98O	OPAL	$e^+e^- \to Z$
$<3.4 \times 10^{-4}$	90	[15] ABREU	97E	DLPH	$e^+e^- \to Z$
$<8.2 \times 10^{-5}$	90	[16] BARATE	97H	ALEP	$e^+e^- \to Z$
$<2.0 \times 10^{-5}$	95	[17] ABE	96R	CDF	$p\overline{p}$ 1.8 TeV

[13] AAIJ 12AV reports a measurement of $B(B_c^+ \to J/\psi\pi^+)/B(B^+ \to J/\psi K^+)\ f_c/f_u = (0.68 \pm 0.10 \pm 0.03 \pm 0.05)\%$ at $p_T(B) > 4$ GeV and $2.5 < \eta(B) < 4.5$.

[14] ACKERSTAFF 98O reports $B(Z \to B_c X)/B(Z \to q\overline{q})\times B(B_c \to J/\psi(1S)\pi^+) < 1.06 \times 10^{-4}$ at 90%CL. We rescale to our PDG 98 values of $B(Z \to b\overline{b})$.

[15] ABREU 97E value listed is for an assumed $\tau_{B_c} = 0.4$ ps and improves to 2.7×10^{-4} for $\tau_{B_c} = 1.4$ ps.

[16] BARATE 97H reports $B(Z \to B_c X)/B(Z \to q\overline{q})\cdot B(B_c \to J/\psi(1S)\pi) < 3.6 \times 10^{-5}$ at 90%CL. We rescale to our PDG 96 values of $B(Z \to b\overline{b})$.

[17] ABE 96R reports $B(b \to B_c X)/B(b \to B^+X)\cdot B(B_c^+ \to J/\psi(1S)\pi^+)/B(B^+ \to J/\psi(1S)K^+) < 0.053$ at 95%CL for $\tau_{B_c} = 0.8$ ps. It changes from 0.15 to 0.04 for 0.17 ps$< \tau_{B_c} <$ 1.6 ps. We rescale to our PDG 96 values of $B(b \to B^+) = 0.378 \pm 0.022$ and $B(B^+ \to J/\psi(1S)K^+) = 0.00101 \pm 0.00014$.

$\Gamma(J/\psi(1S)K^+)/\Gamma(J/\psi(1S)\pi^+)$ — Γ_3/Γ_2

VALUE	EVTS	DOCUMENT ID		TECN	COMMENT
0.069±0.019±0.005	50	AAIJ	13BY	LHCB	pp at 7 TeV

$\Gamma(J/\psi(1S)\pi^+\pi^+\pi^-)/\Gamma_{\text{total}} \times B(\overline{b} \to B_c)$ — $\Gamma_4/\Gamma \times B$

VALUE	CL%	DOCUMENT ID		TECN	COMMENT
seen		AAIJ	12Y	LHCB	pp at 7 TeV
• • • We do not use the following data for averages, fits, limits, etc. • • •					
$<5.7 \times 10^{-4}$	90	[18] ABREU	97E	DLPH	$e^+e^- \to Z$

[18] ABREU 97E value listed is independent of 0.4 ps$< \tau_{B_c} <$ 1.4 ps.

$\Gamma(J/\psi(1S)\pi^+\pi^+\pi^-)/\Gamma(J/\psi(1S)\pi^+)$ — Γ_4/Γ_2

VALUE	DOCUMENT ID		TECN	COMMENT
2.41±0.30±0.33	AAIJ	12Y	LHCB	pp at 7 TeV

$\Gamma(J/\psi(1S)a_1(1260))/\Gamma_{\text{total}} \times B(\overline{b} \to B_c)$ — $\Gamma_5/\Gamma \times B$

VALUE	CL%	DOCUMENT ID		TECN	COMMENT
$<1.2 \times 10^{-3}$	90	[19] ACKERSTAFF	98O	OPAL	$e^+e^- \to Z$

[19] ACKERSTAFF 98O reports $B(Z \to B_c X)/B(Z \to q\overline{q})\times B(B_c \to J/\psi(1S)a_1(1260)) < 5.29 \times 10^{-4}$ at 90%CL. We rescale to our PDG 98 values of $B(Z \to b\overline{b})$.

$\Gamma(J/\psi(1S)K^+K^-\pi^+)/\Gamma_{\rm total}\times B(\overline{b}\to B_c)$ $\Gamma_6/\Gamma\times B$

VALUE	DOCUMENT ID		TECN	COMMENT
seen	[20] AAIJ	13CA	LHCB	pp at 7, 8 TeV

[20] A signal yield of 78 ± 14 decays is reported with a significance of 6.2 standard deviations using an integrated luminosity of 3 fb^{-1} data.

$\Gamma(J/\psi(1S)K^+K^-\pi^+)/\Gamma(J/\psi(1S)\pi^+)$ Γ_6/Γ_2

VALUE	DOCUMENT ID		TECN	COMMENT
0.53±0.10±0.05	[21] AAIJ	13CA	LHCB	pp at 7, 8 TeV

[21] A signal yield of 78 ± 14 decays is reported with a significance of 6.2 standard deviations using an integrated luminosity of 3 fb^{-1} data.

$\Gamma(\psi(2S)\pi^+)/\Gamma(J/\psi(1S)\pi^+)$ Γ_7/Γ_2

VALUE	DOCUMENT ID		TECN	COMMENT
0.250±0.068±0.015	[22] AAIJ	13AM	LHCB	pp at 7 TeV

[22] The last uncertainty is due to the measurement of $B(\psi(2S)\to\mu^+\mu^-)/B(J/\psi\to\mu^+\mu^-)$.

$\Gamma(J/\psi(1S)D_s^+)/\Gamma(J/\psi(1S)\pi^+)$ Γ_8/Γ_2

VALUE	DOCUMENT ID		TECN	COMMENT
2.90±0.57±0.24	AAIJ	13AS	LHCB	pp at 7, 8 TeV

$\Gamma(J/\psi(1S)D_s^{*+})/\Gamma(J/\psi(1S)D_s^+)$ Γ_9/Γ_8

VALUE	DOCUMENT ID		TECN	COMMENT
2.37±0.56±0.10	AAIJ	13AS	LHCB	pp at 7, 8 TeV

$\Gamma(D^*(2010)^+\overline{D}^0)/\Gamma_{\rm total}\times B(\overline{b}\to B_c)$ $\Gamma_{10}/\Gamma\times B$

VALUE	CL%	DOCUMENT ID		TECN	COMMENT
$<6.2\times10^{-3}$	90	[23] BARATE	98Q	ALEP	$e^+e^-\to Z$

[23] BARATE 98Q reports $B(Z\to B_c X)\times B(B_c\to D^*(2010)^+\overline{D}^0)<1.9\times10^{-3}$ at 90%CL. We rescale to our PDG 98 values of $B(Z\to b\overline{b})$.

$\Gamma(D^+K^{*0})/\Gamma_{\rm total}\times B(\overline{b}\to B_c)$ $\Gamma_{11}/\Gamma\times B$

VALUE (units 10^{-6})	CL%	DOCUMENT ID		TECN	COMMENT
<0.20	90	[24] AAIJ	13R	LHCB	pp at 7 TeV

[24] AAIJ 13R reports $[\Gamma(B_c^+\to D^+K^{*0})/\Gamma_{\rm total}\times B(\overline{b}\to B_c)]\ /\ [B(\overline{b}\to B^+)]<0.5\times10^{-6}$ which we multiply by our best value $B(\overline{b}\to B^+)=40.2\times10^{-2}$.

$\Gamma(D^+\overline{K}^{*0})/\Gamma_{\rm total}\times B(\overline{b}\to B_c)$ $\Gamma_{12}/\Gamma\times B$

VALUE (units 10^{-6})	CL%	DOCUMENT ID		TECN	COMMENT
<0.16	90	[25] AAIJ	13R	LHCB	pp at 7 TeV

[25] AAIJ 13R reports $[\Gamma(B_c^+\to D^+\overline{K}^{*0})/\Gamma_{\rm total}\times B(\overline{b}\to B_c)]\ /\ [B(\overline{b}\to B^+)]<0.4\times10^{-6}$ which we multiply by our best value $B(\overline{b}\to B^+)=40.2\times10^{-2}$.

$\Gamma(D_s^+K^{*0})/\Gamma_{\rm total}\times B(\overline{b}\to B_c)$ $\Gamma_{13}/\Gamma\times B$

VALUE (units 10^{-6})	CL%	DOCUMENT ID		TECN	COMMENT
<0.28	90	[26] AAIJ	13R	LHCB	pp at 7 TeV

[26] AAIJ 13R reports $[\Gamma(B_c^+\to D_s^+K^{*0})/\Gamma_{\rm total}\times B(\overline{b}\to B_c)]\ /\ [B(\overline{b}\to B^+)]<0.7\times10^{-6}$ which we multiply by our best value $B(\overline{b}\to B^+)=40.2\times10^{-2}$.

$\Gamma(D_s^+\overline{K}^{*0})/\Gamma_{\rm total}\times B(\overline{b}\to B_c)$ $\Gamma_{14}/\Gamma\times B$

VALUE (units 10^{-6})	CL%	DOCUMENT ID		TECN	COMMENT
<0.4	90	[27] AAIJ	13R	LHCB	pp at 7 TeV

[27] AAIJ 13R reports $[\Gamma(B_c^+\to D_s^+\overline{K}^{*0})/\Gamma_{\rm total}\times B(\overline{b}\to B_c)]\ /\ [B(\overline{b}\to B^+)]<1.1\times10^{-6}$ which we multiply by our best value $B(\overline{b}\to B^+)=40.2\times10^{-2}$.

$\Gamma(D_s^+\phi)/\Gamma_{\rm total}\times B(\overline{b}\to B_c)$ $\Gamma_{15}/\Gamma\times B$

VALUE (units 10^{-6})	CL%	DOCUMENT ID		TECN	COMMENT
<0.32	90	[28] AAIJ	13R	LHCB	pp at 7 TeV

[28] AAIJ 13R reports $[\Gamma(B_c^+\to D_s^+\phi)/\Gamma_{\rm total}\times B(\overline{b}\to B_c)]\ /\ [B(\overline{b}\to B^+)]<0.8\times10^{-6}$ which we multiply by our best value $B(\overline{b}\to B^+)=40.2\times10^{-2}$.

$\Gamma(K^+K^0)/\Gamma_{\rm total}\times B(\overline{b}\to B_c)$ $\Gamma_{16}/\Gamma\times B$

VALUE	CL%	DOCUMENT ID		TECN	COMMENT
$<4.6\times10^{-7}$	90	[29] AAIJ	13BS	LHCB	pp at 7 TeV

[29] Derived from $\Gamma(K^+K^0)/\Gamma\times B(\overline{b}\to B_c)\ /\ (B(B^+\to K^0\pi^+)\,B(\overline{b}\to B^+))<5.8\%$ at 90% CL using normalization mode $B(B^+\to K^0\pi^+)=(23.97\pm0.53\pm0.71)\times10^{-6}$ and assuming a B production ratio $f(\overline{b}\to B_u^+)=0.33$.

$\Gamma(B_s^0\pi^+/B(\overline{b}\to B_s))/\Gamma_{\rm total}\times B(\overline{b}\to B_c)$ $\Gamma_{17}/\Gamma\times B$

VALUE (units 10^{-3})	DOCUMENT ID		TECN	COMMENT
$2.37\pm0.31\pm0.11^{+0.17}_{-0.13}$	[30] AAIJ	13BU	LHCB	pp at 7, 8 TeV

[30] The last uncertainty is due to the uncertainty of the B_c^+ lifetime measurement.

POLARIZATION IN B_c^+ DECAY

In decays involving two vector mesons, one can distinguish among the states in which meson polarizations are both longitudinal (L) or both are transverse and parallel ($\|$) or perpendicular ($\perp$) to each other with the parameters Γ_L/Γ, $\Gamma_\perp/\Gamma$, and the relative phases $\phi_\|$ and $\phi_\perp$. See the definitions in the note on "Polarization in B Decays" review in the B^0 Particle Listings.

Γ_L/Γ in $B_c^+\to J/\psi D_s^{*+}$

VALUE	DOCUMENT ID		TECN	COMMENT
0.48±0.20	[31] AAIJ	13AS	LHCB	pp at 7, 8 TeV

[31] AAIJ 13AS measures $1-\Gamma_L/\Gamma=0.52\pm0.20$.

$B_c^\pm$ REFERENCES

AAIJ	14G	EPJ C74 2839	R. Aaij *et al.*	(LHCb Collab.)
AAIJ	13AM	PR D87 071103	R. Aaij *et al.*	(LHCb Collab.)
AAIJ	13AS	PR D87 112012	R. Aaij *et al.*	(LHCb Collab.)
Also		PR D89 019901 (errat.)	R. Aaij *et al.*	(LHCb Collab.)
AAIJ	13BS	PL B726 646	R. Aaij *et al.*	(LHCb Collab.)
AAIJ	13BU	PRL 111 181801	R. Aaij *et al.*	(LHCb Collab.)
AAIJ	13BY	JHEP 1309 075	R. Aaij *et al.*	(LHCb Collab.)
AAIJ	13CA	JHEP 1311 094	R. Aaij *et al.*	(LHCb Collab.)
AAIJ	13R	JHEP 1302 043	R. Aaij *et al.*	(LHCb Collab.)
AALTONEN	13	PR D87 011101	T. Aaltonen *et al.*	(CDF Collab.)
AAIJ	12AV	PRL 109 232001	R. Aaij *et al.*	(LHCb Collab.)
AAIJ	12Y	PRL 108 251802	R. Aaij *et al.*	(LHCb Collab.)
ABAZOV	09H	PRL 102 092001	V.M. Abazov *et al.*	(D0 Collab.)
AALTONEN	08M	PRL 100 182002	T. Aaltonen *et al.*	(CDF Collab.)
ABAZOV	08T	PRL 101 012001	V.M. Abazov *et al.*	(D0 Collab.)
ABULENCIA	06C	PRL 96 082002	A. Abulencia *et al.*	(CDF Collab.)
ABULENCIA	06O	PRL 97 012002	A. Abulencia *et al.*	(CDF Collab.)
ABE	98M	PRL 81 2432	F. Abe *et al.*	(CDF Collab.)
Also		PR D58 112004	F. Abe *et al.*	(CDF Collab.)
ACKERSTAFF	98O	PL B420 157	K. Ackerstaff *et al.*	(OPAL Collab.)
BARATE	98Q	EPJ C4 387	R. Barate *et al.*	(ALEPH Collab.)
PDG	98	EPJ C3 1	C. Caso *et al.*	(PDG Collab.)
ABREU	97E	PL B398 207	P. Abreu *et al.*	(DELPHI Collab.)
BARATE	97H	PL B402 213	R. Barate *et al.*	(ALEPH Collab.)
ABE	96R	PRL 77 5176	F. Abe *et al.*	(CDF Collab.)
PDG	96	PR D54 1	R. M. Barnett *et al.*	(PDG Collab.)

DEVELOPMENTS IN HEAVY QUARKONIUM SPECTROSCOPY

Updated March 2014 by S. Eidelman (Budker Inst. and Novosibirsk State Univ.), C. Hanhart (Forschungszentrum Jülich), B.K. Heltsley (Cornell Univ.), J.J. Hernandez-Rey (Univ. Valencia–CSIC), S. Navas (Univ. Granada), and C. Patrignani (Univ. Genova, INFN).

A golden age for heavy quarkonium physics dawned at the turn of this century, initiated by the confluence of exciting advances in quantum chromodynamics (QCD) and an explosion of related experimental activity. The subsequent broad spectrum of breakthroughs, surprises, and continuing puzzles had not been anticipated. In that period, the BESII program concluded only to give birth to BESIII; the B-factories and CLEO-c flourished; quarkonium production and polarization measurements at HERA and the Tevatron matured; and heavy-ion collisions at RHIC opened a window on the deconfinement regime. Recently also ATLAS, CMS and LHCb started to contribute to the field. For an extensive presentation of the status of heavy quarkonium physics, the reader is referred to several reviews [1–7], the last of which covers developments through the middle of 2010, and which supplies some tabular information and phrasing reproduced here (with kind permission, copyright 2011, Springer). This note focuses solely on experimental developments in heavy quarkonium spectroscopy, and in particular on those too recent to have been included in Ref. 7.

In this mini-review we display the newly discovered states, where "newly" is interpreted to include the period since 2003. In earlier versions of this write-up the particles were sorted according to an assumed *conventional* or *unconventional* nature with respect to the quark model. However, since this classification is not always unambiguous, we here follow Ref. [8] and sort

Table 1: New states below the open flavor thresholds in the $c\bar{c}$, $b\bar{c}$, and $b\bar{b}$ regions, ordered by mass. Masses m and widths Γ represent the weighted averages from the listed sources. Quoted uncertainties reflect quadrature summation from individual experiments. Ellipses (...) in the Process column indicate inclusively selected event topologies; *i.e.*, additional particles not required by the Experiments to be present. A question mark (?) indicates an unmeasured value. For each Experiment a citation is given, as well as the statistical significance ($\#\sigma$), or "(np)" for "not provided". The Year column gives the date of the first measurement cited. The Status column indicates that the state has been observed by at most one (NC!-needs confirmation) or at least two independent experiments with significance of $>5\sigma$ (OK). The state labelled $\chi_{c2}(2P)$ has previously been called $Z(3930)$. In the publication $X(3823)$ is called $\psi_2(1D)$, however, only the C–parity is measured; $J^P = 2^+$ are assigned from quark model. Adapted from [7] with kind permission, copyright (2011), Springer, and [8] with kind permission from the authors.

State	m (MeV)	Γ (MeV)	J^{PC}	Process (mode)	Experiment ($\#\sigma$)	Year	Status
$h_c(1P)$	3525.41 ± 0.16	<1	1^{+-}	$\psi(2S) \to \pi^0\,(\gamma\eta_c(1S))$	CLEO [9–11] (13.2)	2004	OK
				$\psi(2S) \to \pi^0\,(\gamma...)$	CLEO [9–11] (10), BES [12] (19)		
				$p\bar{p} \to (\gamma\eta_c) \to (\gamma\gamma\gamma)$	E835 [13] (3.1)		
				$\psi(2S) \to \pi^0\,(...)$	BESIII [12] (9.5)		
$\eta_c(2S)$	3638.9 ± 1.3	10±4	0^{-+}	$B \to K\,(K^0_S K^-\pi^+)$	Belle [14,15] (6.0)	2002	OK
				$e^+e^- \to e^+e^-\,(K^0_S K^-\pi^+)$	BABAR [16,17] (7.8),		
					CLEO [18] (6.5), Belle [19] (6)		
				$e^+e^- \to J/\psi\,(...)$	BABAR [20] (np), Belle [21] (8.1)		
$X(3823)$	3823.1 ± 1.9	< 24	$?^{?-}$	$B \to K(\gamma\,\chi_{c1})$	Belle [22](3.8)	2013	NC!
B_c^+	6277 ± 6	-	0^-	$\bar{p}p \to (\pi^+ J/\psi)...$	CDF [23,24] (8.0), D0 [25] (5.2)	2007	OK
$\eta_b(1S)$	9395.8 ± 3.0	$12.4^{+12.7}_{-5.7}$	0^{-+}	$\Upsilon(3S) \to \gamma\,(...)$	BABAR [26] (10), CLEO [27] (4.0)	2008	OK
				$\Upsilon(2S) \to \gamma\,(...)$	BABAR [28] (3.0)		
				$h_b(1P,2P) \to \gamma\,(...)$	Belle [29](14)	2012	NC!
				$\Upsilon(10860) \to \pi^+\pi^-\gamma\,(...)$	Belle [30] (14)		
$h_b(1P)$	9898.6 ± 1.4	?	1^{+-}	$\Upsilon(10860) \to \pi^+\pi^-\,(...)$	Belle [31,30] (5.5)	2011	NC!
				$\Upsilon(3S) \to \pi^0\,(...)$	BABAR [32] (3.0)		
$\eta_b(2S)$	9999 ± 4	< 24	0^{-+}	$h_b(2P) \to \gamma\,(...)$	Belle [29](4.2)	2012	NC!
$\Upsilon(1^3D_2)$	10163.7 ± 1.4	?	2^{--}	$\Upsilon(3S) \to \gamma\gamma\,(\gamma\gamma\Upsilon(1S))$	CLEO [33] (10.2)	2004	OK
				$\Upsilon(3S) \to \gamma\gamma\,(\pi^+\pi^-\Upsilon(1S))$	BABAR [34] (5.8)		
				$\Upsilon(10860) \to \pi^+\pi^-\,(...)$	Belle [31] (2.4)		
$h_b(2P)$	$10259.8^{+1.5}_{-1.2}$	?	1^{+-}	$\Upsilon(10860) \to \pi^+\pi^-\,(...)$	Belle [31,30] (11.2)	2011	NC!
$\chi_{bJ}(3P)$	10530 ± 10	?	?	$pp \to (\gamma\mu^+\mu^-)...$	ATLAS [35] (>6), D0 [36] (3.6)	2011	OK

the states into three groups, namely states below (*cf.* Table 1), near (*cf.* Table 2) and above (*cf.* Table 3) the lowest open flavor thresholds.

Table 1 lists properties of newly observed heavy quarkonium states located below the lowest open flavor thresholds. Those are expected to be (at least prominently) conventional quarkonia. The h_c is the $^1P_1$ state of charmonium, singlet partner of the long-known χ_{cJ} triplet ^3P_J. The $\eta_c(2S)$ is the first excited state of the pseudoscalar ground state $\eta_c(1S)$, lying just below the mass of its vector counterpart, $\psi(2S)$. The ground state of bottomonium is the $\eta_b(1S)$, recently confirmed with a second observation of more than 5σ significance at Belle. In addition, in the same experiment strong evidence was collected for $\eta_b(2S)$ [29], but it still needs experimental confirmation at the 5σ level. The $\Upsilon(1D)$ is the lowest-lying D-wave triplet of the $b\bar{b}$ system. Both the $h_b(1P)$, the bottomonium counterpart of $h_c(1P)$, and the next excited state, $h_b(2P)$, were recently observed by Belle [31], as described further below, in dipion transitions from either the $\Upsilon(10860)$ or $Y_b(10888)$. In addition, Belle recently reported a measurement of $\psi_2(1D)$ which would be a $J^{PC} = 2^{+-}$ state [22]. While the negative C-parity is indeed established by the measurement, the assignment of $J = 2$ was done by matching to the closest quark model state. In the table this state is therefore simply called $X(3823)$, according to

Table 2: As in Table 1, but for new states near the first open flavor thresholds in the $c\bar{c}$ and $b\bar{b}$ regions, ordered by mass. For $X(3872)$, the values given are based only upon decays to $\pi^+\pi^- J/\psi$. Updated from [7] with kind permission, copyright (2011), Springer, and [8] with kind permission from the authors.

State	m (MeV)	Γ (MeV)	J^{PC}	Process (mode)	Experiment ($\#\sigma$)	Year	Status
$X(3872)$	3871.68±0.17	< 1.2	1^{++}	$B \to K\,(\pi^+\pi^- J/\psi)$	Belle [37,38] (12.8), BABAR [39] (8.6)	2003	OK
				$p\bar{p} \to (\pi^+\pi^- J/\psi) + ...$	CDF [40–42] (np), D0 [43] (5.2)		
				$B \to K\,(\omega J/\psi)$	Belle [44] (4.3), BABAR [45] (4.0)		
				$B \to K\,(D^{*0}\overline{D}^0)$	Belle [46,47] (6.4), BABAR [48] (4.9)		
				$B \to K\,(\gamma J/\psi)$	Belle [49] (4.0), BABAR [50,51] (3.6), LHCb [52] (>10)		
				$B \to K\,(\gamma\psi(2S))$	BABAR [51] (3.5), Belle [49] (0.4), LHCb [52] (4.4)		
				$pp \to (\pi^+\pi^- J/\psi) + ...$	LHCb [53,54] (np)		
$Z_c(3900)^+$	3883.9 ± 4.5	25 ± 12	1^{+-}	$Y(4260) \to \pi^-(D\bar{D}^*)^+$	BESIII [55](np)	2013	NC!
	3891.2 ± 3.3	40 ± 8	$?^{?-}$	$Y(4260) \to \pi^-(\pi^+ J/\psi)$	BESIII [56](8), Belle [57](5.2) T. Xiao *et al.* [CLEO data] [58](>5)	2013	OK
$Z_c(4020)^+$	4022.9 ± 2.8	7.9 ± 3.7	$?^{?-}$	$Y(4260, 4360) \to \pi^-(\pi^+ h_c)$	BESIII [59](8.9)	2013	NC!
	4026.3 ± 4.5	24.8 ± 9.5	$?^{?-}$	$Y(4260) \to \pi^-(D^*\bar{D}^*)^+$	BESIII [60](10)	2013	NC!
$Z_b(10610)^+$	10607.2 ± 2.0	18.4 ± 2.4	1^{+-}	$\Upsilon(10860) \to \pi(\pi\Upsilon(1S, 2S, 3S))$	Belle [61,62,63](>10)	2011	OK
				$\Upsilon(10860) \to \pi^-(\pi^+ h_b(1P, 2P))$	Belle [62](16)	2011	OK
				$\Upsilon(10860) \to \pi^-(B\bar{B}^*)^+$	Belle [64](8)	2012	NC!
$Z_b(10650)^+$	10652.2 ± 1.5	11.5 ± 2.2	1^{+-}	$\Upsilon(10860) \to \pi^-(\pi^+\Upsilon(1S, 2S, 3S))$	Belle [61,62](>10)	2011	OK
				$\Upsilon(10860) \to \pi^-(\pi^+ h_b(1P, 2P))$	Belle [62](16)	2011	OK
				$\Upsilon(10860) \to \pi^-(B^*\bar{B}^*)^+$	Belle [64](6.8)	2012	NC!

the PDG name convention. After the mass of the $\eta_b(1S)$ was shifted upwards by about 11 MeV based on a new Belle measurement [29], all states mentioned in this paragraph fit into their respective spectroscopies roughly where expected. Their exact masses, production mechanisms, and decay modes provide guidance to their descriptions within QCD.

There is a large number of newly discovered states both near and above the lowest open flavor thresholds. They are displayed in Table 2 and Table 3, respectively*; notice that just a few of them have been confirmed experimentally. With the possible exception of the tensor state located at 3930 MeV, neither can unambiguously be assigned a place in the hierarchy of charmonia or bottomonia nor has a universally accepted unconventional origin. The $X(3872)$ is widely studied, yet its interpretation demands additional experimental attention: after the quantum numbers were fixed at LHCb [54] the next experimental challenge will be a measurement of its line shape. The state originally dubbed $Z(3930)$ is now regarded by many as the first observed $2P$ state of χ_{cJ}, the $\chi_{c2}(2P)$. The scalar state at 3915 MeV is now called $\chi_{c0}(3915)$. It might be the first radial excitation of $\chi_{c0}(1P)$, but this interpretation is not generally accepted [100]. The $Y(4260)$ and $Y(4360)$ are vector states decaying to $\pi^+\pi^- J/\psi$ and $\pi^+\pi^-\psi(2S)$, respectively, yet, unlike most conventional vector charmonia, do not correspond to enhancements in the e^+e^- hadronic cross section.

Based on a full amplitude analysis of the $B^0 \to K^+\pi^-\psi(2S)$ decays, Belle determined the spin-parity of the $Z(4430)^{\pm}$** to be $J^P = 1^+$ [92]. Very recently this state as well as its quantum numbers were confirmed at LHCb [94] with much higher statistics. Improved values for mass and width from LHCb are consistent with earlier measurements; our new average is in Table 3; the experiment even reports a resonant behavior of the $Z(4430)^{\pm}$ amplitude. This state as well as $Z(4050)^{\pm}$ and $Z(4250)^{\pm}$ seen in $\pi^{\pm}\chi_{c1}$ are, however, not confirmed (nor excluded) by BaBar (see [93] for the $Z(4430)$ and [74] for the $Z(4050)^{\pm}$ and $Z(4250)^{\pm}$). Belle observes signals of significances 5.0σ, 5.0σ, and 6.4σ for $Z_1(4050)^+$, $Z_2(4250)^+$, and $Z(4430)^+$, respectively, whereas BABAR reports 1.1σ, 2.0σ, and 2.4σ effects, setting upper limits on product branching fractions that are not inconsistent with Belle's and LHCb's measured rates. For $Z_1(4050)^+$ and $Z_2(4250)^+$ the situation remains unresolved.

In addition to the three Z_c^+ discussed in the previous paragraph, in 2013 two more states named $Z_c(3900)^+$ and $Z_c(4020)^+$ were unearthed in the charmonium region. Note that in this write-up as well as the RPP listings we combined $Z_c(3900)^+$ (seen in $J/\psi\pi\pi$) and $Z_c(3885)^+$ (seen in $D\bar{D}^*$) as well as $Z_c(4020)^+$ (seen in $h_c\pi\pi$) and $Z_c(4025)^+$ (seen in $D^*\bar{D}^*$)

* For consistency with the literature, we preserve the use of X, Y and Z, contrary to the practice of the PDG, which exclusively uses X for unidentified states.

** There are currently various candidates for isotriplet states in the spectrum. For some of them both charged states are already established and sometimes there is also evidence for the neutral partner. We still chose to put the charge as superscript since it is an explicit marker of the exotic nature of the states.

Table 3: As in Table 1, but for new states above the first open flavor thresholds in the $c\bar{c}$ and $b\bar{b}$ regions, ordered by mass. $X(3945)$ and $Y(3940)$ have been subsumed under $X(3915)$ due to compatible properties. The quantum numbers of the state were measured at BaBar [65]. The state known as $Z(3930)$ appears as the $\chi_{c2}(2P)$ in Table 1. In some cases experiment still allows two J^{PC} values, in which case both appear. See also the reviews in [1–7]. Updated from [7] with kind permission, copyright (2011), Springer, and [8] with kind permission from the authors.

State	m (MeV)	Γ (MeV)	J^{PC}	Process (mode)	Experiment ($\#\sigma$)	Year	Status
$\chi_{c0}(3915)$	3917.4 ± 2.7	$28^{+10}_{-\ 9}$	0^{++}	$B \to K\,(\omega J/\psi)$	Belle [66] (8.1), BABAR [67,65] (19)	2004	OK
$\chi_{c2}(2P)$	3927.2 ± 2.6	24 ± 6	2^{++}	$e^+e^- \to e^+e^-(D\bar{D})$	Belle [68] (5.3), BABAR [69,45] (5.8)	2005	OK
				$e^+e^- \to e^+e^-\,(\omega J/\psi)$	Belle [70] (7.7), BABAR [45] (np)		
$X(3940)$	3942^{+9}_{-8}	37^{+27}_{-17}	$?^{?+}$	$e^+e^- \to J/\psi\,(D\overline{D}^*)$	Belle [71] (6.0)	2007	NC!
				$e^+e^- \to J/\psi\,(...)$	Belle [21] (5.0)		
$Y(4008)$	$4008^{+121}_{-\ 49}$	226 ± 97	1^{--}	$e^+e^- \to \gamma(\pi^+\pi^- J/\psi)$	Belle [72] (7.4)	2007	NC!
$Z_1(4050)^+$	4051^{+24}_{-43}	82^{+51}_{-55}	?	$B \to K\,(\pi^+\chi_{c1}(1P))$	Belle [73] (5.0), BABAR [74] (1.1)	2008	NC!
$Y(4140)$	4145.8 ± 2.6	18 ± 8	$?^{?+}$	$B^+ \to K^+(\phi J/\psi)$	CDF [75,76](5.0), Belle [77](1.9), LHCb [78](1.4), CMS [79](>5) D0 [80](3.1)	2009	NC!
$X(4160)$	4156^{+29}_{-25}	139^{+113}_{-65}	$?^{?+}$	$e^+e^- \to J/\psi\,(D\overline{D}^*)$	Belle [71] (5.5)	2007	NC!
$Z_2(4250)^+$	$4248^{+185}_{-\ 45}$	$177^{+321}_{-\ 72}$	?	$B \to K\,(\pi^+\chi_{c1}(1P))$	Belle [73] (5.0), BABAR [74] (2.0)	2008	NC!
$Y(4260)$	4263^{+8}_{-9}	95 ± 14	1^{--}	$e^+e^- \to \gamma\,(\pi^+\pi^- J/\psi)$	BABAR [81,82] (8.0) CLEO [83] (5.4), Belle [72] (15)	2005	OK
				$e^+e^- \to (\pi^+\pi^- J/\psi)$	CLEO [84] (11)		
				$e^+e^- \to (\pi^0\pi^0 J/\psi)$	CLEO [84] (5.1)		
				$e^+e^- \to (f_0(980)J/\psi)$	BaBar [85](np), Belle [57](np)	2012	OK
				$e^+e^- \to (\pi^- Z_c(3900)^+)$	BESIII [56](8), Belle [57](5.2)	2013	OK
				$e^+e^- \to (\gamma\,X(3872))$	BESIII [86](5.3)	2013	NC!
$Y(4274)$	4293 ± 20	35 ± 16	$?^{?+}$	$B^+ \to K^+(\phi J/\psi)$	CDF [76](3.1), LHCb [78](1.0), CMS [79](>3), D0 [80](np)	2011	NC!
$X(4350)$	$4350.6^{+4.6}_{-5.1}$	$13.3^{+18.4}_{-10.0}$	$0/2^{++}$	$e^+e^- \to e^+e^-\,(\phi J/\psi)$	Belle [87] (3.2)	2009	NC!
$Y(4360)$	4361 ± 13	74 ± 18	1^{--}	$e^+e^- \to \gamma\,(\pi^+\pi^-\psi(2S))$	BABAR [88] (np), Belle [89] (8.0)	2007	OK
$Z(4430)^+$	4458 ± 15	166^{+37}_{-32}	1^{+-}	$\bar{B}^0 \to K^-(\pi^+ J/\psi)$	Belle [90,91,92](6.4), BaBar [93](2.4)	2007	OK
				$B^0 \to \psi(2S)\pi^- K^+$	LHCb [94](13.9)		
$X(4630)$	$4634^{+\ 9}_{-11}$	92^{+41}_{-32}	1^{--}	$e^+e^- \to \gamma\,(\Lambda_c^+\Lambda_c^-)$	Belle [95] (8.2)	2007	NC!
$Y(4660)$	4664 ± 12	48 ± 15	1^{--}	$e^+e^- \to \gamma\,(\pi^+\pi^-\psi(2S))$	Belle [89] (5.8)	2007	NC!
$\Upsilon(10860)$	10876 ± 11	55 ± 28	1^{--}	$e^+e^- \to (B_{(s)}^{(*)}\bar{B}_{(s)}^{(*)}(\pi))$	PDG [96]	1985	OK
				$e^+e^- \to (\pi\pi\Upsilon(1S,2S,3S))$	Belle [97,62,63](>10)	2007	OK
				$e^+e^- \to (f_0(980)\Upsilon(1S))$	Belle [62,63](>5)	2011	OK
				$e^+e^- \to (\pi Z_b(10610,10650))$	Belle [62,63](>10)	2011	OK
				$e^+e^- \to (\eta\Upsilon(1S,2S))$	Belle [98](10)	2012	OK
				$e^+e^- \to (\pi^+\pi^-\Upsilon(1D))$	Belle [98](9)	2012	OK
$Y_b(10888)$	10888.4 ± 3.0	$30.7^{+8.9}_{-7.7}$	1^{--}	$e^+e^- \to (\pi^+\pi^-\Upsilon(nS))$	Belle [99](2.3)	2008	NC!

into only two states due to their close proximity in mass. In various respects $Z_c(3900)^+$ and $Z_c(4020)^+$ seem to be the charmed partners of $Z_b(10610)^+$ and $Z_b(10650)^+$ as will be outlined below.

Although $\eta_c(2S)$ measurements began to converge towards a mass and a width some time ago, refinements are still in progress. In particular, Belle [15] has revisited its analysis of $B \to K\eta_c(2S)$, $\eta_c(2S) \to KK\pi$ decays with more data and methods that account for interference between the above decay chain, an equivalent one with the $\eta_c(1S)$ instead, and one with no intermediate resonance. The net effect of this interference is far from trivial; it shifts the apparent mass by $\sim$+10 MeV and blows up the apparent width by a factor of six. The updated $\eta_c(2S)$ mass and width are in better accordance with other measurements than the previous treatment [14], which did not include interference. Complementing this measurement in B-decay, BABAR [16] updated their previous [17] $\eta_c(2S)$ mass and width measurements in two-photon production, where interference effects, judging from studies of $\eta_c(1S)$, appear to be small. In combination, precision on the $\eta_c(2S)$ mass has improved dramatically.

The $Y(4140)$ observed in 2008 by CDF [75,76] was confirmed at CMS and D0 [79,80], however, a second structure related to $Y(4274)$ could not be established unambiguously. The two states were neither seen in B decays at Belle [77] and LHCb [78] nor in $\gamma\gamma$ collisions at Belle [87]. Thus the situation for $Y(4140)$ and $Y(4274)$ is still controversial.

New results on η_b, h_b, and Z_b^+ mostly come from Belle, all from analyses of 121.4 fb^{-1} of e^+e^- collision data collected near the peak of the $\Upsilon(10860)$ resonance. They all appear in the same types of decay chains: $\Upsilon(10860) \to \pi^- Z_b^+$, $Z_b^+ \to \pi^+(b\bar{b})$, and, when the $b\bar{b}$ forms an $h_b(1P)$, frequently decaying as $h_b(1P) \to \gamma\eta_b$.

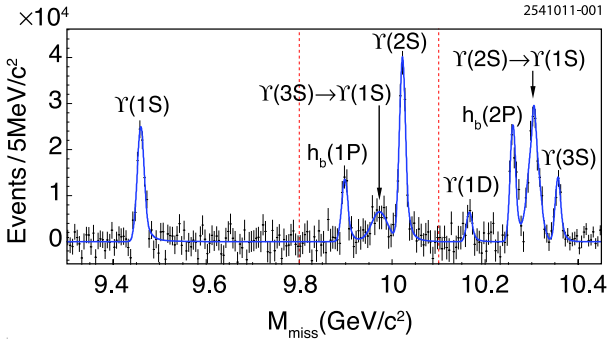

Figure 1: From Belle [31], the mass recoiling against $\pi^+\pi^-$ pairs, $M_{\rm miss}$, in e^+e^- collision data taken near the peak of the $\Upsilon(10860)$ (*points with error bars*). The smooth combinatoric and $K_S^0 \to \pi^+\pi^-$ background contributions have already been subtracted. The fit to the various labeled signal contributions overlaid (*curve*). Adapted from [31] with kind permission, copyright (2011) The American Physical Society.

The Belle h_b discovery analysis [31] selects hadronic events and searches for peaks in the mass recoiling against $\pi^+\pi^-$ pairs, the spectrum for which, after subtraction of smooth combinatoric and $K_S^0 \to \pi^+\pi^-$ backgrounds, appears in Fig. 1. Prominent and unmistakable $h_b(1P)$ and $h_b(2P)$ peaks are present. This search was directly inspired by a CLEO result [101], which found the surprisingly copious transitions $\psi(4160) \to \pi^+\pi^- h_c(1P)$ and an indication that $Y(4260) \to \pi^+\pi^- h_c(1P)$ occurs at a comparable rate as the signature mode, $Y(4260) \to \pi^+\pi^- J/\psi$. The presence of $\Upsilon(nS)$ peaks in Fig. 1 at rates two orders of magnitude larger than expected for transitions requiring a heavy-quark spin-flip, along with separate studies with exclusive decays $\Upsilon(nS) \to \mu^+\mu^-$, allow precise calibration of the $\pi^+\pi^-$ recoil mass spectrum and very accurate measurements of $h_b(1P)$ and $h_b(2P)$ masses. Both corresponding hyperfine splittings are consistent with zero within an uncertainty of about 1.5 MeV (lowered to ± 1.1 MeV for $h_b(1P)$ in Ref. [30]) .

Belle soon noticed that, for events in the peaks of Fig. 1, there seemed to be two intermediate charged states nearby. For example, Fig. 2 shows a Dalitz plot for events restricted to the $\Upsilon(2S)$ region of $\pi^+\pi^-$ recoil mass. The two bands observed in the maximum of the two $M[\pi^\pm\Upsilon(2S)]^2$ values also appear for $\Upsilon(1S)$, $\Upsilon(3S)$, $h_b(1P)$, and $h_b(2P)$ samples but not in the respective $[b\bar{b}]$ sidebands. Belle fits all subsamples to resonant plus non-resonant amplitudes, allowing for interference (notably, between $\pi^- Z_b^+$ and $\pi^+ Z_b^-$), and finds consistent pairs of Z_b^+ masses for all bottomonium transitions, and comparable strengths of the two states. A recent angular analysis assigned $J^P = 1^+$ for both Z_b^+ states [102], which must also have negative G-parity. Transitions through Z_b^+ to the $h_b(nP)$ saturate the observed $\pi^+\pi^- h_b(nP)$ cross sections. The two masses of Z_b^+ states are just a few MeV above the $B^*\bar{B}$ and $B^*\bar{B}^*$ thresholds, respectively. Still, they predominantly decay into these channels [64], regardless the small phase space, with branching fractions that exceed 80% and 70%, respectively, at 90% CL. This feature provides strong evidence for their molecular nature—note that the Z_b^+ states cannot be simple mesons because they are charged and have $b\bar{b}$ content.

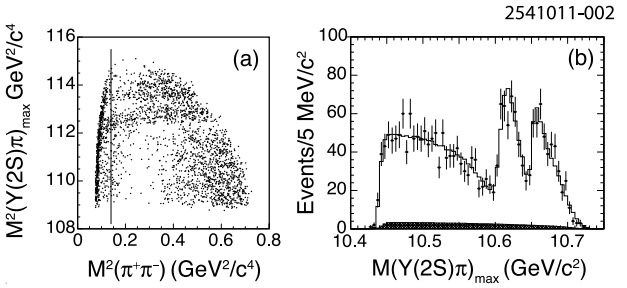

Figure 2: From Belle [62] e^+e^- collision data taken near the peak of the $\Upsilon(10860)$ for events with a $\pi^+\pi^-$-missing mass consistent with a $\Upsilon(nS)2$, (a) the maximum of the two possible single $\pi^\pm$-missing-mass-squared combinations vs. the $\pi^+\pi^-$-mass-squared; and (b) projection of the maximum of the two possible single $\pi^\pm$-missing-mass combinations (*points with error bars*) overlaid with a fit (*curve*). Events to the left of the vertical line in (a) are excluded from further analysis. The two horizontal stripes in (a) and two peaks in (b) correspond to the two Z_b^+ states. Adapted from [62] with kind permission, copyright (2011) The American Physical Society.

The third Belle result to follow from these data is the confirmation of the $\eta_b(1S)$ and measurement of the $h_b(1P) \to \gamma\eta_b(1S)$ branching fraction, expected to be several tens of percent. To accomplish this, events with the $\pi^+\pi^-$ recoil mass in the $h_b(1P)$ mass window and a radiative photon candidate are selected, and the $\pi^+\pi^-\gamma$ recoil mass queried for correlation with non-zero $h_b(1P)$ population in the $\pi^+\pi^-$ missing mass spectrum, as shown in Fig. 3. A clear peak is observed, corresponding to the $\eta_b(1S)$. A fit is performed to extract the $\eta_b(1S)$ mass, and determine its width and the branching fraction for $h_b(1P) \to \gamma\eta_b(1S)$ (the latter of which is $(49.8 \pm 6.8^{+10.9}_{-5.2})\%$) for the first time. The mass determination has comparable uncertainty and a larger central value (by 10 MeV, or 2.4σ) than the average of previous measurements, thereby reducing the new world average hyperfine splitting by nearly 5 MeV. An independent experimental confirmation of the shifted mass is very important to pursue.

The $\chi_{bJ}(nP)$ states have recently been observed at the LHC by ATLAS [35] and confirmed by D0 [36] for $n = 1, 2, 3$,

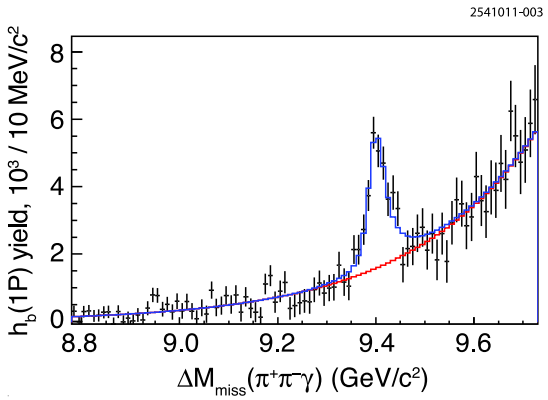

Figure 3: From Belle [30] e^+e^- collision data taken near the peak of the $\Upsilon(10860)$, the $h_b(1P)$ event yield vs. the mass recoiling against the $\pi^+\pi^-\gamma$ (corrected for misreconstructed $\pi^+\pi^-$), where the $h_b(1P)$ yield is obtained by fitting the mass recoiling against the $\pi^+\pi^-$ (*points with error bars*). The fit results (*solid histograms*) for signal plus background and background alone are superimposed. Adapted from [30] with kind permission, copyright (2011) The American Physical Society.

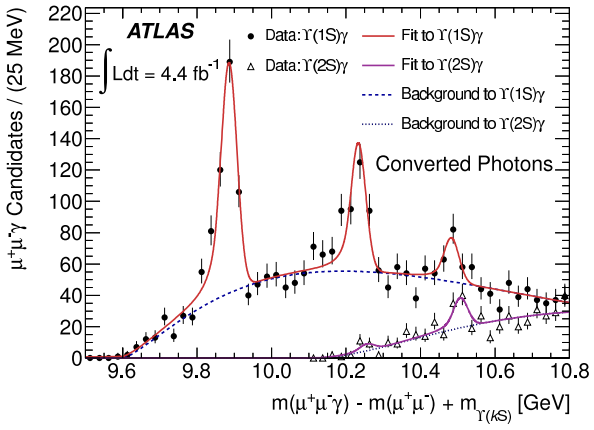

Figure 4: From ATLAS [35] pp collision data (*points with error bars*) taken at $\sqrt{s}$ = 7 TeV, the effective mass of $\chi_{bJ}(1P, 2P, 3P) \to \gamma\Upsilon(1S, 2S)$ candidates in which $\Upsilon(1S, 2S) \to \mu^+\mu^-$ and the photon is reconstructed as an e^+e^- conversion in the tracking system. Fits (*smooth curves*) show significant signals for each triplet (merged-J) on top of a smooth background. From [35] with kind permission, copyright (2012) The American Physical Society.

although in each case the three J states are not distinguished from one another. Events are sought which have both a photon and an $\Upsilon(1S, 2S) \to \mu^+\mu^-$ candidate which together form a mass in the χ_b region. Observation of all three J-merged peaks is seen with significance in excess of 6σ for both unconverted and converted photons. The mass plot for converted photons, which provide better mass resolution, is shown in Fig. 4. This marks the first observation of the $\chi_{bJ}(3P)$ triplet, quite near the expected mass.

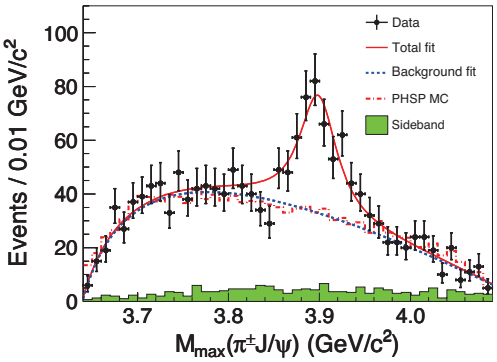

Figure 5: $J/\psi\pi$ invariant mass distributions from BES-III [56] e^+e^- collision data taken near the peak of the $Y(4260)$. Adapted from [56] with kind permission, copyright (2013) The American Physical Society.

In 2013 at BESIII [56] and shortly after at Belle [57] a charged state called $Z_c(3900)^+$ was found near the $D\bar{D}^*$ threshold—the corresponding spectrum from BESIII is shown in Fig. 5. In addition to confirming these findings, Ref. [58] also provided evidence for a neutral partner. A nearby signal was also seen in the $D\bar{D}^*$ channel [55] whose quantum numbers were fixed to 1^{+-}. The masses extracted from these experiments agree only within 2σ. However, since the extraction did not allow for an interference with the background and used Breit-Wigner line shapes, which is not justified near thresholds, there might be some additional systematic uncertainty in the mass values. Therefore in the RPP listings as well as Table 2 both structures appear under the name $Z_c(3900)^+$. Analogously, $Z_c(4020)^+$ (seen in in $h_c\pi\pi$ [59]) and $Z_c^+(4025)$ (seen in $D^*\bar{D}^*$ [60]) are listed as one state, $Z_c(4020)^+$. The Z_c^+ states show some remarkable similarities to the Z_b^+ states, e.g. they decay dominantly to the $D^{(*)}\bar{D}^*$ channels. However, current analyses suggest that the mass of especially the $Z_c(3900)^+$ might be somewhat above the $D\bar{D}^*$ threshold. If confirmed, this feature would clearly challenge a possible $D\bar{D}^*$–molecular interpretation.

References

1. N. Brambilla *et al.*, CERN-2005-005, (CERN, Geneva, 2005), arXiv:hep-ph/0412158.
2. E. Eichten *et al.*, Rev. Mod. Phys. **80**, 1161 (2008) arXiv:hep-ph/0701208.
3. S. Eidelman, H. Mahlke-Kruger, and C. Patrignani, in C. Amsler *et al.* (Particle Data Group), Phys. Lett. **B667**, 1029 (2008).
4. S. Godfrey and S.L. Olsen, Ann. Rev. Nucl. Part. Sci. **58** 51 (2008), arXiv:0801.3867 [hep-ph].

5. T. Barnes and S.L. Olsen, Int. J. Mod. Phys. **A24**, 305 (2009).
6. G.V. Pakhlova, P.N. Pakhlov, and S.I. Eidelman, Phys. Usp. **53**, 219 (2010), [Usp. Fiz. Nauk **180**, 225 (2010)].
7. N. Brambilla *et al.*, Eur. Phys. J. **C71**, 1534 (2011) arXiv:1010.5827 [hep-ph].
8. N. Brambilla, S. Eidelman, P. Foka, S.V. Gardner, A.S. Kronfeld et al., "QCD and strongly coupled gauge theories: challenges and perspectives" Preprint TUM-EFT 46/14.
9. P. Rubin *et al.* (CLEO Collab.), Phys. Rev. **D72**, 092004 (2005) arXiv:hep-ex/0508037.
10. J.L. Rosner *et al.* (CLEO Collab.), Phys. Rev. Lett. **95**, 102003 (2005) arXiv:hep-ex/0505073.
11. S. Dobbs *et al.* (CLEO Collab.), Phys. Rev. Lett. **101**, 182003 (2008) arXiv:0805.4599 [hep-ex].
12. M. Ablikim *et al.* (BESIII Collab.), Phys. Rev. Lett. **104**, 132003 (2010) arXiv:1002.0501 [hep-ex].
13. M. Andreotti *et al.* (E835 Collab.), Phys. Rev. **D72**, 032001 (2005).
14. S.K. Choi *et al.* (Belle Collab.), Phys. Rev. Lett. **89**, 102001 (2002) [Erratum-ibid. **89**, 129901 (2002)], arXiv:hep-ex/0206002.
15. A. Vinokurova *et al.* (Belle Collab.), Phys. Lett. **B706**, 139 (2011) arXiv:1105.0978 [hep-ex].
16. P. del Amo Sanchez *et al.* (BABAR Collab.), Phys. Rev. **D84**, 021004 (2011) arXiv:1103.3971 [hep-ex]].
17. B. Aubert *et al.* (BABAR Collab.), Phys. Rev. Lett. **92**, 142002 (2004) arXiv:hep-ex/0311038.
18. D.M. Asner *et al.* (CLEO Collab.), Phys. Rev. Lett. **92**, 142001 (2004) arXiv:hep-ex/0312058.
19. H. Nakazawa (Belle Collab.), Nucl. Phys. (Proc. Supp.) **184**, 220 (2008).
20. B. Aubert *et al.* (BABAR Collab.), Phys. Rev. **D72**, 031101 (2005) arXiv:hep-ex/0506062.
21. K. Abe *et al.* (Belle Collab.), Phys. Rev. Lett. **98**, 082001 (2007) arXiv:hep-ex/0507019.
22. V. Bhardwaj et al. (Belle Collaboration), Phys. Rev. Lett. **111**, 032001 (2013), arXiv:1304.3975.
23. F. Abe *et al.* [CDF Collab.], Phys. Rev. Lett. **81**, 2432 (1998) arXiv:hep-ex/9805034.
24. T. Aaltonen *et al.* (CDF Collab.), Phys. Rev. Lett. **100**, 182002 (2008) arXiv:0712.1506 [hep-ex].
25. V.M. Abazov *et al.* (D0 Collab.), Phys. Rev. Lett. **101**, 012001 (2008) arXiv:0802.4258 [hep-ex].
26. B. Aubert *et al.* (BABAR Collab.), Phys. Rev. Lett. **101**, 071801 (2008) [Erratum-ibid. **102**, 029901 (2009)], arXiv:0807.1086 [hep-ex].
27. G. Bonvicini *et al.* (CLEO Collab.), Phys. Rev. **D81**, 031104 (2010) arXiv:0909.5474 [hep-ex].
28. B. Aubert *et al.* (BABAR Collab.), Phys. Rev. Lett. **103**, 161801 (2009) arXiv:0903.1124 [hep-ex].
29. R. Mizuk et al. (Belle Collaboration), Phys. Rev. Lett. **109**, 232002 (2012), arXiv:1205.6351.
30. I. Adachi *et al.* (Belle Collab.), arXiv:1110.3934 [hep-ex].
31. I. Adachi *et al.* (Belle Collab.), Phys. Rev. Lett. **108**, 032001 (2012) arXiv:1103.3419 [hep-ex].
32. J.P. Lees *et al.* (BABAR Collab.), Phys. Rev. **D84**, 091101 (2011) arXiv:1102.4565 [hep-ex].
33. G. Bonvicini *et al.* (CLEO Collab.), Phys. Rev. **D70**, 032001 (2004) arXiv:hep-ex/0404021.
34. P. del Amo Sanchez *et al.* (BABAR Collab.), Phys. Rev. **D82**, 111102 (2010) arXiv:1004.0175 [hep-ex].
35. G. Aad *et al.* (ATLAS Collab.), Phys. Rev. Lett. **108**, 152001 (2012) arXiv:1112.5154 [hep-ex].
36. V. M. Abazov (D0 Collaboration), Phys.Rev. D **86**, 031103 (2012), arXiv:1203.6034.
37. S.K. Choi *et al.* (Belle Collab.), Phys. Rev. Lett. **91**, 262001 (2003) arXiv:hep-ex/0309032.
38. S.-K. Choi *et al.* (Belle Collab.), Phys. Rev. **D84**, 052004R (2011) arXiv:1107.0163 [hep-ex].
39. B. Aubert *et al.* (BABAR Collab.), Phys. Rev. **D77**, 111101 (2008) arXiv:0803.2838 [hep-ex].
40. D.E. Acosta *et al.* (CDF II Collab.), Phys. Rev. Lett. **93**, 072001 (2004) arXiv:hep-ex/0312021.
41. A. Abulencia *et al.* (CDF Collab.), Phys. Rev. Lett. **98**, 132002 (2007) arXiv:hep-ex/0612053.
42. T. Aaltonen *et al.* (CDF Collab.), Phys. Rev. Lett. **103**, 152001 (2009) arXiv:0906.5218 [hep-ex].
43. V.M. Abazov *et al.* (D0 Collab.), Phys. Rev. Lett. **93**, 162002 (2004) arXiv:hep-ex/0405004.
44. K. Abe *et al.* (Belle Collab.), arXiv:hep-ex/0505037.
45. P. del Amo Sanchez *et al.* (BABAR Collab.), Phys. Rev. **D82**, 011101R (2010) arXiv:1005.5190 [hep-ex].
46. G. Gokhroo *et al.* (Belle Collab.), Phys. Rev. Lett. **97**, 162002 (2006) arXiv:hep-ex/0606055.
47. T. Aushev *et al.*, Phys. Rev. **D81**, 031103R (2010), arXiv:0810.0358 [hep-ex].
48. B. Aubert *et al.* (BABAR Collab.), Phys. Rev. **D77**, 011102 (2008) arXiv:0708.1565 [hep-ex].
49. V. Bhardwaj *et al.* (Belle Collab.), Phys. Rev. Lett. **107**, 091803 (2011) arXiv:1105.0177 [hep-ex].
50. B. Aubert *et al.* (BABAR Collab.), Phys. Rev. **D74**, 071101 (2006) arXiv:hep-ex/0607050.
51. B. Aubert *et al.* (BABAR Collab.), Phys. Rev. Lett. **102**, 132001 (2009) arXiv:0809.0042 [hep-ex].
52. R. Aaij *et al.* (LHCb Collab.), arXiv:1404.0275 [hep-ex].
53. R. Aaij *et al.* (LHCb Collab.), Eur. Phys. J. **C72**, 1972 (2012) arXiv:1112.5310 [hep-ex].
54. R. Aaij *et al.* [LHCb Collaboration], Phys. Rev. Lett. **110**, 222001 (2013) arXiv:1302.6269 [hep-ex].
55. M. Ablikim *et al.* [BESIII Collaboration], Phys. Rev. Lett. **112**, 022001 (2014) arXiv:1310.1163.
56. M. Ablikim *et al.* [BESIII Collaboration], Phys. Rev. Lett. **110**, 252001 (2013) arXiv:1303.5949.
57. Z. Q. Liu *et al.* [Belle Collaboration], Phys. Rev. Lett. **110**, 252002 (2013) arXiv:1304.0121.
58. T. Xiao, S. Dobbs, A. Tomaradze and K. K. Seth, Phys. Lett. **B727**, 366 (2013) arXiv:304.3036.
59. M. Ablikim *et al.* [BESIII Collaboration], Phys. Rev. Lett. **111**, 242001 (2013) arXiv:1309.1896.
60. M. Ablikim et al. (BESIII Collaboration) (2013),arXiv:1308.2760.
61. I. Adachi *et al.* (Belle Collab.), arxiv:arXiv:1105.4583 [hep-ex].
62. A. Bondar *et al.* (Belle Collab.), Phys. Rev. Lett. **108**, 122001 (2012) arXiv:1110.2251 [hep-ex].

See key on page 547

63. P. Krokovny et al. (Belle Collaboration), Phys.Rev. D **88**, 052016 (2013), arXiv:1308.2646.
64. I. Adachi et al. (Belle Collaboration) (2012), arXiv:1209.6450.
65. J. P. Lees *et al.* [BaBar Collaboration], Phys. Rev. D 86, 072002 (2012) arXiv:1207.2651 [hep-ex].
66. K. Abe *et al.* (Belle Collab.), Phys. Rev. Lett. **94**, 182002 (2005) arXiv:hep-ex/0408126.
67. B. Aubert *et al.* (BABAR Collab.), Phys. Rev. Lett. **101**, 082001 (2008) arXiv:0711.2047 [hep-ex].
68. S. Uehara *et al.* (Belle Collab.), Phys. Rev. Lett. **96**, 082003 (2006) arXiv:hep-ex/0512035.
69. B. Aubert *et al.* (BABAR Collab.), Phys. Rev. **D81**, 092003 (2010) arXiv:1002.0281 [hep-ex].
70. S. Uehara *et al.* (Belle Collab.), Phys. Rev. Lett. **104**, 092001 (2010) arXiv:0912.4451 [hep-ex].
71. P. Pakhlov *et al.* (Belle Collab.), Phys. Rev. Lett. **100**, 202001 (2008) arXiv:0708.3812 [hep-ex].
72. C.Z. Yuan *et al.* (Belle Collab.), Phys. Rev. Lett. **99**, 182004 (2007) arXiv:0707.2541 [hep-ex].
73. R. Mizuk *et al.* (Belle Collab.), Phys. Rev. **D78**, 072004 (2008) arXiv:0806.4098 [hep-ex].
74. J.P. Lees *et al.* (BABAR Collab.), Phys. Rev. **D85**, 052003 (2011) arXiv:1111.5919 [hep-ex].
75. T. Aaltonen *et al.* (CDF Collab.), Phys. Rev. Lett. **102**, 242002 (2009) arXiv:0903.2229 [hep-ex].
76. T. Aaltonen *et al.* (CDF Collab.), arXiv:1101.6058 [hep-ex].
77. J. Brodzicka, Conf.Proc. C0908171, 299 (2009).
78. R. Aaij et al. (LHCb Collaboration), Phys. Rev. D **85**,091103 (2012), arXiv:1202.5087.
79. S. Chatrchyan et al. (CMS Collaboration) (2013), arXiv:1309.6920rm.
80. V. Abazov et al. (D0 Collaboration), Phys.Rev. D **89**, 012004 (2014), arXiv:1309.6580.
81. B. Aubert *et al.* (BABAR Collab.), Phys. Rev. Lett. **95**, 142001 (2005) arXiv:hep-ex/0506081.
82. B. Aubert *et al.* (BABAR Collab.), arXiv:0808.1543v2 [hep-ex].
83. Q. He *et al.* (CLEO Collab.), Phys. Rev. **D74**, 091104 (2006) arXiv:hep-ex/0611021.
84. T.E. Coan *et al.* (CLEO Collab.), Phys. Rev. Lett. **96**, 162003 (2006) arXiv:hep-ex/0602034.
85. J. Lees et al. (BABAR Collaboration), Phys.Rev. D **86**, 051102 (2012), arXiv:1204.2158.
86. M. Ablikim et al. (BESIII Collaboration), Phys.Rev.Lett. **112**, 092001 (2014), arXiv:1310.4101.
87. C.P. Shen *et al.* (Belle Collab.), Phys. Rev. Lett. **104**, 112004 (2010) arXiv:0912.2383 [hep-ex].
88. B. Aubert *et al.* (BABAR Collab.), Phys. Rev. Lett. **98**, 212001 (2007) arXiv:hep-ex/0610057.
89. X.L. Wang *et al.* (Belle Collab.), Phys. Rev. Lett. **99**, 142002 (2007) arXiv:0707.3699 [hep-ex].
90. S.K. Choi *et al.* (Belle Collab.), Phys. Rev. Lett. **100**, 142001 (2008) arXiv:0708.1790 [hep-ex].
91. R. Mizuk *et al.* (Belle Collab.), Phys. Rev. **D80**, 031104 (2009) arXiv:0905.2869 [hep-ex].
92. K. Chilikin et al. (Belle Collaboration), Phys.Rev. D **88**,074026 (2013), arXiv:1306.4894.
93. B. Aubert et al. (BABAR Collaboration), Phys. Rev. D **79**, 112001 (2009), arXiv:0811.0564.
94. R. Aaij *et al.* [LHCb Collaboration], arXiv:1404.1903 [hep-ex].
95. G. Pakhlova *et al.* (Belle Collab.), Phys. Rev. Lett. **101**, 172001 (2008) arXiv:0807.4458 [hep-ex].
96. J. Beringer et al. (Particle Data Group), Phys. Rev. D **86**, 010001 (2012).
97. K.F. Chen *et al.* (Belle Collab.), Phys. Rev. Lett. **100**, 112001 (2008) arXiv:0710.2577 [hep-ex].
98. P. Krokovny, talk given at Les Rencontres de Physique de la Vallee d'Aoste, La Thuile, Aosta Valley, Italy, 2012.
99. K.-F. Chen et al. (Belle Collaboration), Phys. Rev. D 82, 091106 (2010), arXiv:0810.3829.
100. F. -K. Guo and U. -G. Meissner, Phys. Rev. D 86, 091501 (2012), arXiv:1208.1134.
101. T.K. Pedlar *et al.* (CLEO Collab.), Phys. Rev. Lett. **107**, 041803 (2011) arXiv:1104.2025 [hep-ex].
102. A. Garmash *et al.* [Belle Collab.], arXiv:1403.0992.

$c\overline{c}$ MESONS

THE CHARMONIUM SYSTEM

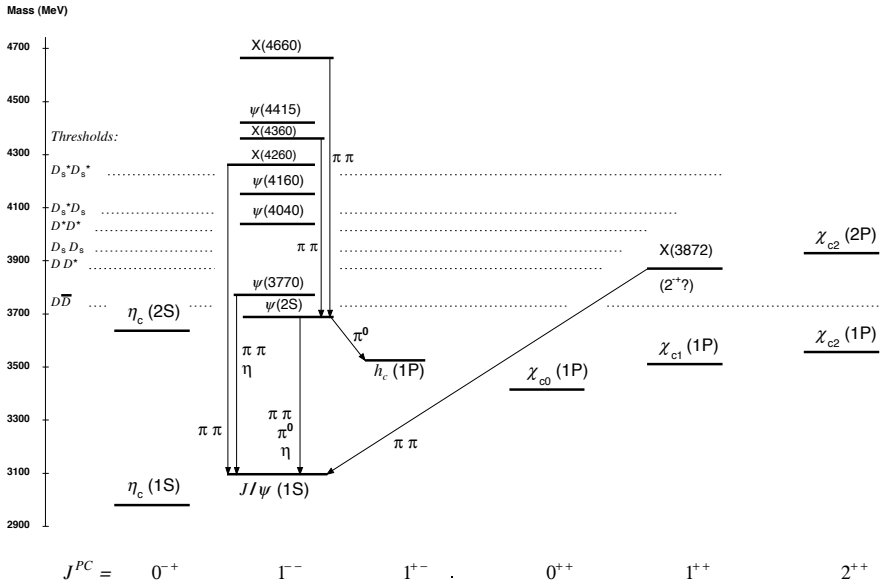

The level scheme of the $c\overline{c}$ states showing experimentally established states with solid lines. Singlet states are called η_c and h_c, triplet states ψ and χ_{cJ}, and unassigned charmonium-like states X. In parentheses it is sufficient to give the radial quantum number and the orbital angular momentum to specify the states with all their quantum numbers. Only observed hadronic transitions are shown; the single photon transitions $\psi(nS) \to \gamma\eta_c(mP)$, $\psi(nS) \to \gamma\chi_{cJ}(mP)$, and $\chi_{cJ}(1P) \to \gamma J/\psi$ are omitted for clarity.

$\eta_c(1S)$

$I^G(J^{PC}) = 0^+(0^{-+})$

$\eta_c(1S)$ MASS

VALUE (MeV)	EVTS	DOCUMENT ID		TECN	COMMENT
2983.6 ± 0.7 OUR AVERAGE		Error includes scale factor of 1.3. See the ideogram below.			
2984.3 ± 0.6 ± 0.6		[1,2] ABLIKIM	12F	BES3	$\psi(2S) \to \gamma\eta_c$
2984.49 ± 1.16 ± 0.52	832	[3] ABLIKIM	12N	BES3	$\psi(2S) \to \pi^0\gamma$ hadrons
2982.7 ± 1.8 ± 2.2	486	ZHANG	12A	BELL	$e^+e^- \to e^+e^-\eta'\pi^+\pi^-$
2984.5 ± 0.8 ± 3.1	11k	DEL-AMO-SA...	11M	BABR	$\gamma\gamma \to K^+K^-\pi^+\pi^-\pi^0$
2985.4 ± 1.5 $^{+0.5}_{-2.0}$	920	[2] VINOKUROVA	11	BELL	$B^\pm \to K^\pm(K^0_S K^\pm\pi^\mp)$
2982.2 ± 0.4 ± 1.6	14k	[4] LEES	10	BABR	10.6 $e^+e^- \to e^+e^- K^0_S K^\pm\pi^\mp$
2985.8 ± 1.5 ± 3.1	0.9k	AUBERT	08AB	BABR	$B \to \eta_C(1S)K^{(*)} \to K\overline{K}\pi K^{(*)}$
2986.1 ± 1.0 ± 2.5	7.5k	UEHARA	08	BELL	$\gamma\gamma \to \eta_c \to$ hadrons
2970 ± 5 ± 6	501	[5] ABE	07	BELL	$e^+e^- \to J/\psi(c\overline{c})$
2971 ± 3 $^{+2}_{-1}$	195	WU	06	BELL	$B^+ \to p\overline{p}K^+$
2974 ± 7 $^{+2}_{-1}$	20	WU	06	BELL	$B^+ \to \Lambda\overline{\Lambda}K^+$
2981.8 ± 1.3 ± 1.5	592	ASNER	04	CLEO	$\gamma\gamma \to \eta_c \to K^0_S K^\pm\pi^\mp$
2984.1 ± 2.1 ± 1.0	190	[6] AMBROGIANI	03	E835	$\overline{p}p \to \eta_c \to \gamma\gamma$
• • • We do not use the following data for averages, fits, limits, etc. • • •					
2982.5 ± 0.4 ± 1.4	12k	[7] DEL-AMO-SA...	11M	BABR	$\gamma\gamma \to K^0_S K^\pm\pi^\mp$
2982.2 ± 0.6		[8] MITCHELL	09	CLEO	$e^+e^- \to \gamma X$
2982 ± 5	270	[9] AUBERT	06E	BABR	$B^\pm \to K^\pm X_{c\overline{c}}$
2982.5 ± 1.1 ± 0.9	2.5k	[10] AUBERT	04D	BABR	$\gamma\gamma \to \eta_c(1S) \to K\overline{K}\pi$
2977.5 ± 1.0 ± 1.2		[8,11] BAI	03	BES	$J/\psi \to \gamma\eta_c$
2979.6 ± 2.3 ± 1.6	180	[12] FANG	03	BELL	$B \to \eta_c K$
2976.3 ± 2.3 ± 1.2		[8,13] BAI	00F	BES	$J/\psi,\ \psi(2S) \to \gamma\eta_c$
2976.6 ± 2.9 ± 1.3	140	[8,14] BAI	00F	BES	$J/\psi \to \gamma\eta_c$
2980.4 ± 2.3 ± 0.6		[15] BRANDENB...	00B	CLE2	$\gamma\gamma \to \eta_c \to K^\pm K^0_S\pi^\mp$
2975.8 ± 3.9 ± 1.2		[14] BAI	99B	BES	Sup. by BAI 00F
2999 ± 8	25	ABREU	98O	DLPH	$e^+e^- \to e^+e^-$ +hadrons
2988.3 $^{+3.3}_{-3.1}$		ARMSTRONG	95F	E760	$\overline{p}p \to \gamma\gamma$
2974.4 ± 1.9		[8,16] BISELLO	91	DM2	$J/\psi \to \eta_c\gamma$
2969 ± 4 ± 4	80	[8] BAI	90B	MRK3	$J/\psi \to \gamma K^+K^-K^+K^-$
2956 ±12 ±12		[8] BAI	90B	MRK3	$J/\psi \to \gamma K^+K^-K^0_S K^0_L$
2982.6 $^{+2.7}_{-2.3}$	12	BAGLIN	87B	SPEC	$\overline{p}p \to \gamma\gamma$
2980.2 ± 1.6		[8,16] BALTRUSAIT...	86	MRK3	$J/\psi \to \eta_c\gamma$
2984 ± 2.3 ± 4.0		[8] GAISER	86	CBAL	$J/\psi \to \gamma X,\ \psi(2S) \to \gamma X$
2976 ± 8		[8,17] BALTRUSAIT...	84	MRK3	$J/\psi \to 2\phi\gamma$
2982 ± 8	18	[18] HIMEL	80B	MRK2	e^+e^-
2980 ± 9		[18] PARTRIDGE	80B	CBAL	e^+e^-

[1] From a simultaneous fit to six decay modes of the η_C.
[2] Accounts for interference with non-resonant continuum.
[3] With floating width.
[4] Taking into account interference with the non-resonant $J^P = 0^-$ amplitude.
[5] From a fit of the J/ψ recoil mass spectrum. Supersedes ABE,K 02 and ABE 04G.
[6] Using mass of $\psi(2S) = 3686.00$ MeV.
[7] Not independent from the measurements reported by LEES 10.
[8] MITCHELL 09 observes a significant asymmetry in the lineshapes of $\psi(2S) \to \gamma\eta_C$ and $J/\psi \to \gamma\eta_C$ transitions. If ignored, this asymmetry could lead to significant bias whenever the mass and width are measured in $\psi(2S)$ or J/ψ radiative decays.
[9] From the fit of the kaon momentum spectrum. Systematic errors not evaluated.
[10] Superseded by LEES 10.
[11] From a simultaneous fit of five decay modes of the η_C.
[12] Superseded by VINOKUROVA 11.
[13] Weighted average of the $\psi(2S)$ and $J/\psi(1S)$ samples. Using an η_C width of 13.2 MeV.
[14] Average of several decay modes. Using an η_C width of 13.2 MeV.
[15] Superseded by ASNER 04.
[16] Average of several decay modes.
[17] $\eta_C \to \phi\phi$.
[18] Mass adjusted by us to correspond to $J/\psi(1S)$ mass = 3097 MeV.

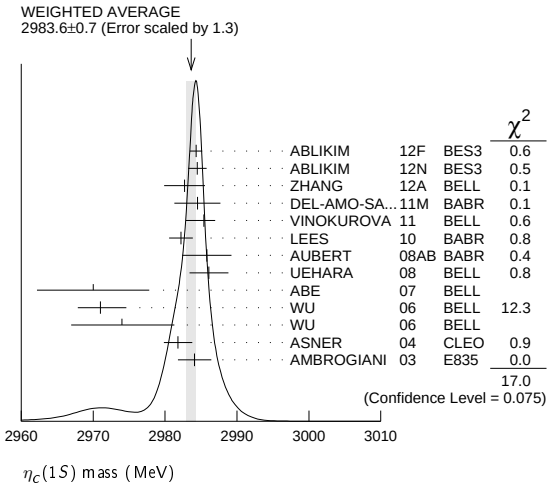

$\eta_c(1S)$ WIDTH

VALUE (MeV)	EVTS	DOCUMENT ID		TECN	COMMENT
32.2± 0.9 OUR FIT					
32.3± 1.0 OUR AVERAGE		Error includes scale factor of 1.2.			
32.0± 1.2±1.0		[1,2] ABLIKIM	12F	BES3	$\psi(2S) \to \gamma\eta_c$
36.4± 3.2±1.7	832	[3] ABLIKIM	12N	BES3	$\psi(2S) \to \pi^0\gamma$ hadrons
$37.8^{+5.8}_{-5.3}\pm3.1$	486	ZHANG	12A	BELL	$e^+e^- \to e^+e^-\eta'\pi^+\pi^-$
36.2± 2.8±3.0	11k	DEL-AMO-SA...	11M	BABR	$\gamma\gamma \to K^+K^-\pi^+\pi^-\pi^0$
$35.1\pm 3.1^{+1.0}_{-1.6}$	920	[2] VINOKUROVA	11	BELL	$B^\pm \to K^\pm(K^0_S K^\pm\pi^\mp)$
31.7± 1.2±0.8	14k	[4] LEES	10	BABR	$10.6\ e^+e^- \to e^+e^- K^0_S K^\pm\pi^\mp$
$36.3^{+3.7}_{-3.6}\pm4.4$	0.9k	AUBERT	08AB	BABR	$B \to \eta_c(1S)K^{(*)} \to K\overline{K}\pi K^{(*)}$
28.1± 3.2±2.2	7.5k	UEHARA	08	BELL	$\gamma\gamma \to \eta_c \to$ hadrons
$48\ ^{+8}_{-7}\ \pm5$	195	WU	06	BELL	$B^+ \to p\overline{p}K^+$
40 ±19 ±5	20	WU	06	BELL	$B^+ \to \Lambda\overline{\Lambda}K^+$
24.8± 3.4±3.5	592	ASNER	04	CLEO	$\gamma\gamma \to \eta_c \to K^0_S K^\pm\pi^\mp$
$20.4^{+7.7}_{-6.7}\pm2.0$	190	AMBROGIANI	03	E835	$\overline{p}p \to \eta_c \to \gamma\gamma$
$23.9^{+12.6}_{-7.1}$		ARMSTRONG	95F	E760	$\overline{p}p \to \gamma\gamma$
• • • We do not use the following data for averages, fits, limits, etc. • • •					
32.1± 1.1±1.3	12k	[5] DEL-AMO-SA...	11M	BABR	$\gamma\gamma \to K^0_S K^\pm\pi^\mp$
34.3± 2.3±0.9	2.5k	[6] AUBERT	04D	BABR	$\gamma\gamma \to \eta_c(1S) \to K\overline{K}\pi$
17.0± 3.7±7.4		[7] BAI	03	BES	$J/\psi \to \gamma\eta_c$
29 ± 8 ±6	180	[8] FANG	03	BELL	$B \to \eta_c K$
11.0± 8.1±4.1		[9] BAI	00F	BES	$J/\psi \to \gamma\eta_c$ and $\psi(2S) \to \gamma\eta_c$
27.0± 5.8±1.4		[10] BRANDENB...	00B	CLE2	$\gamma\gamma \to \eta_c \to K^\pm K^0_S\pi^\mp$
$7.0^{+7.5}_{-7.0}$	12	BAGLIN	87B	SPEC	$\overline{p}p \to \gamma\gamma$
$10.1^{+33.0}_{-8.2}$	23	[11] BALTRUSAIT...	86	MRK3	$J/\psi \to \gamma p\overline{p}$
11.5± 4.5		GAISER	86	CBAL	$J/\psi \to \gamma$X, $\psi(2S) \to \gamma$X
< 40 90% CL	18	HIMEL	80B	MRK2	e^+e^-
< 20 90% CL		PARTRIDGE	80B	CBAL	e^+e^-

[1] From a simultaneous fit to six decay modes of the η_c.
[2] Accounts for interference with non-resonant continuum.
[3] With floating mass.
[4] Taking into account interference with the non-resonant $J^P = 0^-$ amplitude.
[5] Not independent from the measurements reported by LEES 10.
[6] Superseded by LEES 10.
[7] From a simultaneous fit of five decay modes of the η_c.
[8] Superseded by VINOKUROVA 11.
[9] From a fit to the 4-prong invariant mass in $\psi(2S) \to \gamma\eta_c$ and $J/\psi(1S) \to \gamma\eta_c$ decays.
[10] Superseded by ASNER 04.
[11] Positive and negative errors correspond to 90% confidence level.

$\eta_c(1S)$ DECAY MODES

	Mode	Fraction (Γ_i/Γ)		Confidence level
	Decays involving hadronic resonances			
Γ_1	$\eta'(958)\pi\pi$	(4.1 ±1.7) %		
Γ_2	$\rho\rho$	(1.8 ±0.5) %		
Γ_3	$K^*(892)^0K^-\pi^+$ + c.c.	(2.0 ±0.7) %		
Γ_4	$K^*(892)\overline{K}^*(892)$	(7.0 ±1.3)	$\times10^{-3}$	
Γ_5	$K^{*0}\overline{K}^{*0}\pi^+\pi^-$	(1.1 ±0.5) %		
Γ_6	ϕK^+K^-	(2.9 ±1.4)	$\times10^{-3}$	
Γ_7	$\phi\phi$	(1.76±0.20)	$\times10^{-3}$	
Γ_8	$\phi2(\pi^+\pi^-)$	< 4	$\times10^{-3}$	90%
Γ_9	$a_0(980)\pi$	< 2	%	90%
Γ_{10}	$a_2(1320)\pi$	< 2	%	90%
Γ_{11}	$K^*(892)\overline{K}$ + c.c.	< 1.28	%	90%
Γ_{12}	$f_2(1270)\eta$	< 1.1	%	90%
Γ_{13}	$\omega\omega$	< 3.1	$\times10^{-3}$	90%
Γ_{14}	$\omega\phi$	< 1.7	$\times10^{-3}$	90%
Γ_{15}	$f_2(1270)f_2(1270)$	(9.8 ±2.5)	$\times10^{-3}$	
Γ_{16}	$f_2(1270)f'_2(1525)$	(9.7 ±3.2)	$\times10^{-3}$	
	Decays into stable hadrons			
Γ_{17}	$K\overline{K}\pi$	(7.3 ±0.5) %		
Γ_{18}	$\eta\pi^+\pi^-$	(1.7 ±0.5) %		
Γ_{19}	$\eta2(\pi^+\pi^-)$	(4.4 ±1.3) %		
Γ_{20}	$K^+K^-\pi^+\pi^-$	(6.9 ±1.1)	$\times10^{-3}$	
Γ_{21}	$K^+K^-\pi^+\pi^-\pi^0$	(3.5 ±0.6) %		
Γ_{22}	$K^0K^-\pi^+\pi^-\pi^+$ + c.c.	(5.6 ±1.5) %		
Γ_{23}	$K^+K^-2(\pi^+\pi^-)$	(7.5 ±2.4)	$\times10^{-3}$	
Γ_{24}	$2(K^+K^-)$	(1.47±0.31)	$\times10^{-3}$	
Γ_{25}	$\pi^+\pi^-\pi^0\pi^0$	(4.7 ±1.0) %		
Γ_{26}	$2(\pi^+\pi^-)$	(9.7 ±1.2)	$\times10^{-3}$	
Γ_{27}	$2(\pi^+\pi^-\pi^0)$	(17.4 ±3.3) %		
Γ_{28}	$3(\pi^+\pi^-)$	(1.8 ±0.4) %		
Γ_{29}	$p\overline{p}$	(1.52±0.16)	$\times10^{-3}$	
Γ_{30}	$p\overline{p}\pi^0$	(3.6 ±1.3)	$\times10^{-3}$	
Γ_{31}	$\Lambda\overline{\Lambda}$	(1.09±0.24)	$\times10^{-3}$	
Γ_{32}	$\Sigma^+\overline{\Sigma}^-$	(2.1 ±0.6)	$\times10^{-3}$	
Γ_{33}	$\Xi^-\overline{\Xi}^+$	(8.9 ±2.7)	$\times10^{-4}$	
Γ_{34}	$K\overline{K}\eta$	(10 ±5)	$\times10^{-3}$	
Γ_{35}	$\pi^+\pi^-p\overline{p}$	(5.3 ±1.8)	$\times10^{-3}$	
	Radiative decays			
Γ_{36}	$\gamma\gamma$	(1.57±0.12)	$\times10^{-4}$	
	Charge conjugation (C), Parity (P), Lepton family number (LF) violating modes			
Γ_{37}	$\pi^+\pi^-$	P,CP < 1.1	$\times10^{-4}$	90%
Γ_{38}	$\pi^0\pi^0$	P,CP < 3.5	$\times10^{-5}$	90%
Γ_{39}	K^+K^-	P,CP < 6	$\times10^{-4}$	90%
Γ_{40}	$K^0_SK^0_S$	P,CP < 3.1	$\times10^{-4}$	90%

CONSTRAINED FIT INFORMATION

An overall fit to the total width, 8 combinations of partial widths obtained from integrated cross section, and 17 branching ratios uses 80 measurements and one constraint to determine 12 parameters. The overall fit has a $\chi^2 = 113.0$ for 69 degrees of freedom.

The following *off-diagonal* array elements are the correlation coefficients $\langle\delta p_i\delta p_j\rangle/(\delta p_i\cdot\delta p_j)$, in percent, from the fit to parameters p_i, including the branching fractions, $x_i \equiv \Gamma_i/\Gamma_{\rm total}$. The fit constrains the x_i whose labels appear in this array to sum to one.

x_7	18									
x_{15}	3	6								
x_{17}	22	42	7							
x_{20}	11	21	4	25						
x_{24}	9	16	3	25	10					
x_{26}	14	25	5	31	16	12				
x_{29}	14	26	5	36	16	13	20			
x_{31}	3	6	1	9	4	3	5	25		
x_{36}	−29	−54	−10	−66	−34	−27	−41	−45	−11	
Γ	−2	−3	−1	−4	−2	−2	−2	7	2	−29
	x_4	x_7	x_{15}	x_{17}	x_{20}	x_{24}	x_{26}	x_{29}	x_{31}	x_{36}

Meson Particle Listings

$\eta_c(1S)$

	Mode	Rate (MeV)
Γ_4	$K^*(892)\overline{K}^*(892)$	0.23 ±0.04
Γ_7	$\phi\phi$	0.057 ±0.007
Γ_{15}	$f_2(1270)f_2(1270)$	0.32 ±0.08
Γ_{17}	$K\overline{K}\pi$	2.36 ±0.17
Γ_{20}	$K^+K^-\pi^+\pi^-$	0.223 ±0.035
Γ_{24}	$2(K^+K^-)$	0.047 ±0.010
Γ_{26}	$2(\pi^+\pi^-)$	0.31 ±0.04
Γ_{29}	$p\overline{p}$	0.049 ±0.005
Γ_{31}	$\Lambda\overline{\Lambda}$	0.035 ±0.008
Γ_{36}	$\gamma\gamma$	0.0050±0.0004

$\eta_c(1S)$ PARTIAL WIDTHS

$\Gamma(\gamma\gamma)$ Γ_{36}

VALUE (keV)	EVTS	DOCUMENT ID		TECN	COMMENT
5.0± 0.4 OUR FIT					
• • • We do not use the following data for averages, fits, limits, etc. • • •					
5.8± 1.1	486	[1] ZHANG	12A	BELL	$e^+e^- \to e^+e^-\eta'\pi^+\pi^-$
5.2± 1.2	273 ± 43	[2,3] AUBERT	06E	BABR	$B^\pm \to K^\pm X_{c\overline{c}}$
5.5± 1.2± 1.8	157 ± 33	[4] KUO	05	BELL	$\gamma\gamma \to p\overline{p}$
7.4± 0.4± 2.3		[5] ASNER	04	CLEO	$\gamma\gamma \to \eta_c \to K^0_S K^\pm\pi^\mp$
13.9± 2.0± 3.0	41	[6] ABDALLAH	03J	DLPH	$\gamma\gamma \to \eta_c$
$3.8^{+\ 1.1+\ 1.9}_{-\ 1.0-\ 1.0}$	190	[7] AMBROGIANI	03	E835	$\overline{p}p \to \eta_c \to \gamma\gamma$
7.6± 0.8± 2.3		[5,8] BRANDENB...	00B	CLE2	$\gamma\gamma \to \eta_c \to K^\pm K^0_S\pi^\mp$
6.9± 1.7± 2.1	76	[9] ACCIARRI	99T	L3	$e^+e^- \to e^+e^-\eta_c$
27 ±16 ±10	5	[5] SHIRAI	98	AMY	58 e^+e^-
$6.7^{+\ 2.4}_{-\ 1.7}$± 2.3		[4] ARMSTRONG	95F	E760	$\overline{p}p \to \gamma\gamma$
11.3± 4.2		[10] ALBRECHT	94H	ARG	$e^+e^- \to e^+e^-\eta_c$
8.0± 2.3± 2.4	17	[11] ADRIANI	93N	L3	$e^+e^- \to e^+e^-\eta_c$
$5.9^{+\ 2.1}_{-\ 1.8}$± 1.9		[7] CHEN	90B	CLEO	$e^+e^- \to e^+e^-\eta_c$
$6.4^{+\ 5.0}_{-\ 3.4}$		[12] AIHARA	88D	TPC	$e^+e^- \to e^+e^-X$
$4.3^{+\ 3.4}_{-\ 3.7}$± 2.4		[4] BAGLIN	87B	SPEC	$\overline{p}p \to \gamma\gamma$
28 ±15		[5,13] BERGER	86	PLUT	$\gamma\gamma \to K\overline{K}\pi$

[1] Assuming there is no interference with the non-resonant background.
[2] Calculated by us using $\Gamma(\eta_c \to K\overline{K}\pi) \times \Gamma(\eta_c \to \gamma\gamma) / \Gamma = 0.44 \pm 0.05$ keV from PDG 06 and $B(\eta_c \to K\overline{K}\pi) = (8.5 \pm 1.8)\%$ from AUBERT 06E.
[3] Systematic errors not evaluated.
[4] Normalized to $B(\eta_c \to p\overline{p}) = (1.3 \pm 0.4) \times 10^{-3}$.
[5] Normalized to $B(\eta_c \to K^\pm K^0_S\pi^\mp)$.
[6] Average of $K^0_S K^\pm\pi^\mp$, $\pi^+\pi^-K^+K^-$, and $2(K^+K^-)$ decay modes.
[7] Normalized to the sum of $B(\eta_c \to K^\pm K^0_S\pi^\mp)$, $B(\eta_c \to K^+K^-\pi^+\pi^-)$, and $B(\eta_c \to 2\pi^+2\pi^-)$.
[8] Superseded by ASNER 04.
[9] Normalized to the sum of 9 branching ratios.
[10] Normalized to the sum of $B(\eta_c \to K^\pm K^0_S\pi^\mp)$, $B(\eta_c \to \phi\phi)$, $B(\eta_c \to K^+K^-\pi^+\pi^-)$, and $B(\eta_c \to 2\pi^+2\pi^-)$.
[11] Superseded by ACCIARRI 99T.
[12] Normalized to the sum of $B(\eta_c \to K^\pm K^0_S\pi^\mp)$, $B(\eta_c \to 2K^+2K^-)$, $B(\eta_c \to K^+K^-\pi^+\pi^-)$, and $B(\eta_c \to 2\pi^+2\pi^-)$.
[13] Re-evaluated by AIHARA 88D.

$\eta_c(1S)$ Γ(i)$\Gamma(\gamma\gamma)/\Gamma$(total)

$\Gamma(\eta'(958)\pi\pi) \times \Gamma(\gamma\gamma)/\Gamma_{total}$ $\Gamma_1\Gamma_{36}/\Gamma$

VALUE (keV)	EVTS	DOCUMENT ID		TECN	COMMENT
$\mathbf{75.8^{+\ 6.3}_{-\ 6.2}\pm 8.4}$	486	[1] ZHANG	12A	BELL	$e^+e^- \to e^+e^-\eta'\pi^+\pi^-$

[1] Assuming there is no interference with the non-resonant background.

$\Gamma(\rho\rho) \times \Gamma(\gamma\gamma)/\Gamma_{total}$ $\Gamma_2\Gamma_{36}/\Gamma$

VALUE (eV)	CL%	EVTS	DOCUMENT ID		TECN	COMMENT
• • • We do not use the following data for averages, fits, limits, etc. • • •						
<39	90	< 1556	UEHARA	08	BELL	$\gamma\gamma \to 2(\pi^+\pi^-)$

$\Gamma(K^*(892)\overline{K}^*(892)) \times \Gamma(\gamma\gamma)/\Gamma_{total}$ $\Gamma_4\Gamma_{36}/\Gamma$

VALUE (eV)	EVTS	DOCUMENT ID		TECN	COMMENT
35 ±6 OUR FIT					
32.4±4.2±5.8	882 ± 115	UEHARA	08	BELL	$\gamma\gamma \to \pi^+\pi^-K^+K^-$

$\Gamma(\phi\phi) \times \Gamma(\gamma\gamma)/\Gamma_{total}$ $\Gamma_7\Gamma_{36}/\Gamma$

VALUE (eV)	EVTS	DOCUMENT ID		TECN	COMMENT
8.9 ±0.8 OUR FIT					
7.75±0.66±0.62	386 ± 31	[1] LIU	12B	BELL	$\gamma\gamma \to 2(K^+K^-)$
• • • We do not use the following data for averages, fits, limits, etc. • • •					
6.8 ±1.2 ±1.3	132 ± 23	UEHARA	08	BELL	$\gamma\gamma \to 2(K^+K^-)$

[1] Supersedes UEHARA 08. Using $B(\phi \to K^+K^-) = (48.9 \pm 0.5)\%$.

$\Gamma(\omega\omega) \times \Gamma(\gamma\gamma)/\Gamma_{total}$ $\Gamma_{13}\Gamma_{36}/\Gamma$

VALUE (eV)	EVTS	DOCUMENT ID		TECN	COMMENT
8.67±2.86±0.96	85 ± 29	[1] LIU	12B	BELL	$\gamma\gamma \to 2(\pi^+\pi^-\pi^0)$

[1] Using $B(\omega \to \pi^+\pi^-\pi^0) = (89.2 \pm 0.7)\%$.

$\Gamma(\omega\phi) \times \Gamma(\gamma\gamma)/\Gamma_{total}$ $\Gamma_{14}\Gamma_{36}/\Gamma$

VALUE (eV)	CL%	DOCUMENT ID		TECN	COMMENT
• • • We do not use the following data for averages, fits, limits, etc. • • •					
<0.49	90	[1] LIU	12B	BELL	$\gamma\gamma \to K^+K^-\pi^+\pi^-\pi^0$

[1] Using $B(\phi \to K^+K^-) = (48.9 \pm 0.5)\%$ and $B(\omega \to \pi^+\pi^-\pi^0) = (89.2 \pm 0.7)\%$.

$\Gamma(f_2(1270)f_2(1270)) \times \Gamma(\gamma\gamma)/\Gamma_{total}$ $\Gamma_{15}\Gamma_{36}/\Gamma$

VALUE (eV)	EVTS	DOCUMENT ID		TECN	COMMENT
49±13 OUR FIT					
69±17±12	3182±766	UEHARA	08	BELL	$\gamma\gamma \to 2(\pi^+\pi^-)$

$\Gamma(f_2(1270)f'_2(1525)) \times \Gamma(\gamma\gamma)/\Gamma_{total}$ $\Gamma_{16}\Gamma_{36}/\Gamma$

VALUE (eV)	EVTS	DOCUMENT ID		TECN	COMMENT
49±9±13	1128±206	UEHARA	08	BELL	$\gamma\gamma \to \pi^+\pi^-K^+K^-$

$\Gamma(K\overline{K}\pi) \times \Gamma(\gamma\gamma)/\Gamma_{total}$ $\Gamma_{17}\Gamma_{36}/\Gamma$

VALUE (keV)	CL%	EVTS	DOCUMENT ID		TECN	COMMENT
0.369±0.021 OUR FIT						
0.407±0.027 OUR AVERAGE Error includes scale factor of 1.2.						
0.374±0.009±0.031		14k	[1] LEES	10	BABR	10.6 $e^+e^- \to e^+e^-K^0_S K^\pm\pi^\mp$
0.407±0.022±0.028			[2,3] ASNER	04	CLEO	$\gamma\gamma \to \eta_c \to K^0_S K^\pm\pi^\mp$
0.60 ±0.12 ±0.09		41	[3,4] ABDALLAH	03J	DLPH	$\gamma\gamma \to K^0_S K^\pm\pi^\mp$
1.47 ±0.87 ±0.27			[3] SHIRAI	98	AMY	$\gamma\gamma \to \eta_c \to K^\pm K^0_S\pi^\mp$
0.84 ±0.21			[3] ALBRECHT	94H	ARG	$\gamma\gamma \to K^\pm K^0_S\pi^\mp$
$0.60\ ^{+0.23}_{-0.20}$			[3] CHEN	90B	CLEO	$\gamma\gamma \to \eta_c K^\pm K^0_S\pi^\mp$
1.06 ±0.41 ±0.27		11	[3] BRAUNSCH...	89	TASS	$\gamma\gamma \to K\overline{K}\pi$
$1.5\ ^{+0.60}_{-0.45}$ ±0.3		7	[3] BERGER	86	PLUT	$\gamma\gamma \to K\overline{K}\pi$
• • • We do not use the following data for averages, fits, limits, etc. • • •						
0.386±0.008±0.021		12k	[5] DEL-AMO-SA...	11M	BABR	$\gamma\gamma \to K^0_S K^\pm\pi^\mp$
0.418±0.044±0.022			[3,6] BRANDENB...	00B	CLE2	$\gamma\gamma \to \eta_c \to K^\pm K^0_S\pi^\mp$
<0.63	95		[3] BEHREND	89	CELL	$\gamma\gamma \to K^0_S K^\pm\pi^\mp$
<4.4	95		ALTHOFF	85B	TASS	$\gamma\gamma \to K\overline{K}\pi$

[1] From the corrected and unfolded mass spectrum.
[2] Calculated by us from the value reported in ASNER 04 that assumes $B(\eta_c \to K\overline{K}\pi) = 5.5 \pm 1.7\%$
[3] We have multiplied $K^\pm K^0_S\pi^\mp$ measurement by 3 to obtain $K\overline{K}\pi$.
[4] Calculated by us from the value reported in ABDALLAH 03J, which uses $B(\eta_c \to K^0_S K^\pm\pi^\mp) = (1.5 \pm 0.4)\%$.
[5] Not independent from the measurements reported by LEES 10.
[6] Superseded by ASNER 04.

$\Gamma(K^+K^-\pi^+\pi^-) \times \Gamma(\gamma\gamma)/\Gamma_{total}$ $\Gamma_{20}\Gamma_{36}/\Gamma$

VALUE (eV)	EVTS	DOCUMENT ID		TECN	COMMENT
35 ± 5 OUR FIT					
27 ± 6 OUR AVERAGE					
25.7± 3.2± 4.9	2019±248	UEHARA	08	BELL	$\gamma\gamma \to \pi^+\pi^-K^+K^-$
280 ±100 ±60	42	[1] ABDALLAH	03J	DLPH	$\gamma\gamma \to \pi^+\pi^-K^+K^-$
170 ± 80 ±20	13.9 ± 6.6	ALBRECHT	94H	ARG	$\gamma\gamma \to \pi^+\pi^-K^+K^-$

[1] Calculated by us from the value reported in ABDALLAH 03J, which uses $B(\eta_c \to \pi^+\pi^-K^+K^-) = (2.0 \pm 0.7)\%$.

$\Gamma(K^+K^-\pi^+\pi^-\pi^0) \times \Gamma(\gamma\gamma)/\Gamma_{total}$ $\Gamma_{21}\Gamma_{36}/\Gamma$

VALUE (keV)	EVTS	DOCUMENT ID		TECN	COMMENT
• • • We do not use the following data for averages, fits, limits, etc. • • •					
0.190±0.006±0.028	11k	[1] DEL-AMO-SA...	11M	BABR	$\gamma\gamma \to K^+K^-\pi^+\pi^-\pi^0$

[1] Not independent from other measurements reported in DEL-AMO-SANCHEZ 11M.

$\Gamma(2(K^+K^-)) \times \Gamma(\gamma\gamma)/\Gamma_{total}$ $\Gamma_{24}\Gamma_{36}/\Gamma$

VALUE (eV)	EVTS	DOCUMENT ID		TECN	COMMENT
7.4± 1.5 OUR FIT					
5.8± 1.9 OUR AVERAGE					
5.6± 1.1± 1.6	216 ± 42	UEHARA	08	BELL	$\gamma\gamma \to 2(K^+K^-)$
350 ±90 ±60	46	[1] ABDALLAH	03J	DLPH	$\gamma\gamma \to 2(K^+K^-)$
231 ±90 ±23	9.1 ± 3.3	[2] ALBRECHT	94H	ARG	$\gamma\gamma \to 2(K^+K^-)$

[1] Calculated by us from the value reported in ABDALLAH 03J, which uses $B(\eta_c \to 2(K^+K^-)) = (2.1 \pm 1.2)\%$.
[2] Includes all topological modes except $\eta_c \to \phi\phi$.

$\Gamma(2(\pi^+\pi^-)) \times \Gamma(\gamma\gamma)/\Gamma_{total}$ $\Gamma_{26}\Gamma_{36}/\Gamma$

VALUE (eV)	EVTS	DOCUMENT ID		TECN	COMMENT
49 ± 6 OUR FIT					
42 ± 6 OUR AVERAGE					
40.7± 3.7± 5.3	5381 ±492	UEHARA	08	BELL	$\gamma\gamma \to 2(\pi^+\pi^-)$
180 ±70 ±20	21.4 ± 8.6	ALBRECHT	94H	ARG	$\gamma\gamma \to 2(\pi^+\pi^-)$

$\Gamma(p\overline{p}) \times \Gamma(\gamma\gamma)/\Gamma_{total}$ $\Gamma_{29}\Gamma_{36}/\Gamma$

VALUE (eV)	EVTS	DOCUMENT ID		TECN	COMMENT
7.6 ±0.8 OUR FIT					
$7.20 \pm 1.53^{+0.67}_{-0.75}$	157 ± 33	[1] KUO	05	BELL	$\gamma\gamma \to p\overline{p}$
• • • We do not use the following data for averages, fits, limits, etc. • • •					
$4.6\ ^{+1.3}_{-1.1}\ \pm 0.4$	190	[1] AMBROGIANI	03	E835	$\overline{p}p \to \gamma\gamma$
$8.1\ ^{+2.9}_{-2.0}$		[1] ARMSTRONG	95F	E760	$\overline{p}p \to \gamma\gamma$

[1] Not independent from the $\Gamma_{\gamma\gamma}$ reported by the same experiment.

$\Gamma(K^0_S K^0_S) \times \Gamma(\gamma\gamma)/\Gamma_{total}$ $\Gamma_{40}\Gamma_{36}/\Gamma$

VALUE (eV)	CL%	DOCUMENT ID		TECN	COMMENT
<1.6	90	[1] UEHARA	13	BELL	$\gamma\gamma \to K^0_S K^0_S$
• • • We do not use the following data for averages, fits, limits, etc. • • •					
<0.29	90	[2] UEHARA	13	BELL	$\gamma\gamma \to K^0_S K^0_S$

[1] Taking into account interference with the non-resonant continuum.
[2] Neglecting interference with the non-resonant continuum.

$\eta_c(1S)$ BRANCHING RATIOS

HADRONIC DECAYS

$\Gamma(\eta'(958)\pi\pi)/\Gamma_{total}$ Γ_1/Γ

VALUE	EVTS	DOCUMENT ID		TECN	COMMENT
0.041±0.017	14	[1] BALTRUSAIT...86		MRK3	$J/\psi \to \eta_c\gamma$

[1] The quoted branching ratios use $B(J/\psi(1S) \to \gamma\eta_c(1S)) = 0.0127 \pm 0.0036$.

$\Gamma(\rho\rho)/\Gamma_{total}$ Γ_2/Γ

VALUE (units 10^{-3})	CL%	EVTS	DOCUMENT ID		TECN	COMMENT
18 ± 5 OUR AVERAGE						
12.6± 3.8±5.1		72	[1] ABLIKIM	05L	BES2	$J/\psi \to \pi^+\pi^-\pi^+\pi^-\gamma$
26.0± 2.4±8.8		113	[1] BISELLO	91	DM2	$J/\psi \to \gamma\rho^0\rho^0$
23.6±10.6±8.2		32	[1] BISELLO	91	DM2	$J/\psi \to \gamma\rho^+\rho^-$
• • • We do not use the following data for averages, fits, limits, etc. • • •						
<14	90		[1] BALTRUSAIT...86		MRK3	$J/\psi \to \eta_c\gamma$

[1] The quoted branching ratios use $B(J/\psi(1S) \to \gamma\eta_c(1S)) = 0.0127 \pm 0.0036$. Where relevant, the error in this branching ratio is treated as a common systematic in computing averages.

$\Gamma(K^*(892)^0 K^-\pi^+ + \text{c.c.})/\Gamma_{total}$ Γ_3/Γ

VALUE	EVTS	DOCUMENT ID		TECN	COMMENT
0.02±0.007	63	[1,2] BALTRUSAIT...86		MRK3	$J/\psi \to \eta_c\gamma$

[1] BALTRUSAITIS 86 has an error according to Partridge.
[2] The quoted branching ratios use $B(J/\psi(1S) \to \gamma\eta_c(1S)) = 0.0127 \pm 0.0036$.

$\Gamma(K^*(892)\overline{K}^*(892))/\Gamma_{total}$ Γ_4/Γ

VALUE (units 10^{-4})	EVTS	DOCUMENT ID		TECN	COMMENT
70±13 OUR FIT					
91±26 OUR AVERAGE					
108±25±44	60	[1] ABLIKIM	05L	BES2	$J/\psi \to K^+K^-\pi^+\pi^-\gamma$
82±28±27	14	[1] BISELLO	91	DM2	$e^+e^- \to \gamma K^+K^-\pi^+\pi^-$
90±50	9	[1] BALTRUSAIT...86		MRK3	$J/\psi \to \eta_c\gamma$

[1] The quoted branching ratios use $B(J/\psi(1S) \to \gamma\eta_c(1S)) = 0.0127 \pm 0.0036$. Where relevant, the error in this branching ratio is treated as a common systematic in computing averages.

$\Gamma(K^{*0}\overline{K}^{*0}\pi^+\pi^-)/\Gamma_{total}$ Γ_5/Γ

VALUE (units 10^{-4})	EVTS	DOCUMENT ID		TECN	COMMENT
113±47±25	45	[1] ABLIKIM	06A	BES2	$J/\psi \to K^{*0}\overline{K}^{*0}\pi^+\pi^-\gamma$

[1] ABLIKIM 06A reports $[\Gamma(\eta_c(1S) \to K^{*0}\overline{K}^{*0}\pi^+\pi^-)/\Gamma_{total}] \times [B(J/\psi(1S) \to \gamma\eta_c(1S))] = (1.91\pm0.64\pm0.48)\times10^{-4}$ which we divide by our best value $B(J/\psi(1S) \to \gamma\eta_c(1S)) = (1.7\pm0.4)\times10^{-2}$. Our first error is their experiment's error and our second error is the systematic error from using our best value.

$\Gamma(\phi K^+K^-)/\Gamma_{total}$ Γ_6/Γ

VALUE (units 10^{-3})	EVTS	DOCUMENT ID		TECN	COMMENT
$\mathbf{2.9^{+0.9}_{-0.8}\pm1.1}$	$14.1^{+4.4}_{-3.7}$	[1] HUANG	03	BELL	$B^+ \to (\phi K^+K^-)\ K^+$

[1] Using $B(B^+ \to \eta_c K^+) = (1.25 \pm 0.12^{+0.10}_{-0.12}) \times 10^{-3}$ from FANG 03 and $B(\eta_c \to K\overline{K}\pi) = (5.5 \pm 1.7) \times 10^{-2}$.

$\Gamma(\phi\phi)/\Gamma_{total}$ Γ_7/Γ

VALUE (units 10^{-4})	EVTS	DOCUMENT ID		TECN	COMMENT
17.6± 2.0 OUR FIT					
30 ± 5 OUR AVERAGE					
25.3± 5.1± 9.1	72	[1] ABLIKIM	05L	BES2	$J/\psi \to K^+K^-K^+K^-\gamma$
26 ± 9	357 ± 64	[1] BAI	04	BES	$J/\psi \to \gamma K^+K^-K^+K^-$
31 ± 7 ±10	19	[1] BISELLO	91	DM2	$J/\psi \to \gamma K^+K^-K^+K^-$
$30\ ^{+18}_{-12}\ \pm10$	5	[1] BISELLO	91	DM2	$J/\psi \to \gamma K^+K^-K^0_S K^0_L$
74 ±18 ±24	80	[1] BAI	90B	MRK3	$J/\psi \to \gamma K^+K^-K^+K^-$
67 ±21 ±24		[1] BAI	90B	MRK3	$J/\psi \to \gamma K^+K^-K^0_S K^0_L$
• • • We do not use the following data for averages, fits, limits, etc. • • •					
$18\ ^{+\ 8}_{-\ 6}\ \pm\ 7$	$7.0^{+3.0}_{-2.3}$	[2] HUANG	03	BELL	$B^+ \to (\phi\phi)\ K^+$

[1] The quoted branching ratios use $B(J/\psi(1S) \to \gamma\eta_c(1S)) = 0.0127 \pm 0.0036$. Where relevant, the error in this branching ratio is treated as a common systematic in computing averages.
[2] Using $B(B^+ \to \eta_c K^+) = (1.25 \pm 0.12^{+0.10}_{-0.12}) \times 10^{-3}$ from FANG 03 and $B(\eta_c \to K\overline{K}\pi) = (5.5 \pm 1.7) \times 10^{-2}$.

$\Gamma(\phi\phi)/\Gamma(K\overline{K}\pi)$ Γ_7/Γ_{17}

VALUE	EVTS	DOCUMENT ID		TECN	COMMENT
0.0240±0.0026 OUR FIT					
$\mathbf{0.044\ ^{+0.012}_{-0.010}}$ **OUR AVERAGE**					
0.055 ±0.014 ±0.005		AUBERT,B	04B	BABR	$B^\pm \to K^\pm\eta_c$
$0.032\ ^{+0.014}_{-0.010}\ \pm0.009$	7	[1] HUANG	03	BELL	$B^\pm \to K^\pm\phi\phi$

[1] Using $B(B^+ \to \eta_c K^+) = (1.25 \pm 0.12^{+0.10}_{-0.12}) \times 10^{-3}$ from FANG 03 and $B(\eta_c \to K\overline{K}\pi) = (5.5 \pm 1.7) \times 10^{-2}$.

$\Gamma(\phi 2(\pi^+\pi^-))/\Gamma_{total}$ Γ_8/Γ

VALUE (units 10^{-4})	CL%	DOCUMENT ID		TECN	COMMENT
<40	90	[1] ABLIKIM	06A	BES2	$J/\psi \to \phi 2(\pi^+\pi^-)\gamma$

[1] ABLIKIM 06A reports $[\Gamma(\eta_c(1S) \to \phi 2(\pi^+\pi^-))/\Gamma_{total}] \times [B(J/\psi(1S) \to \gamma\eta_c(1S))] < 0.603 \times 10^{-4}$ which we divide by our best value $B(J/\psi(1S) \to \gamma\eta_c(1S)) = 1.7 \times 10^{-2}$.

$\Gamma(a_0(980)\pi)/\Gamma_{total}$ Γ_9/Γ

VALUE	CL%	DOCUMENT ID		TECN	COMMENT
<0.02	90	[1,2] BALTRUSAIT...86		MRK3	$J/\psi \to \eta_c\gamma$

[1] The quoted branching ratios use $B(J/\psi(1S) \to \gamma\eta_c(1S)) = 0.0127 \pm 0.0036$.
[2] We are assuming $B(a_0(980) \to \eta\pi) > 0.5$.

$\Gamma(a_2(1320)\pi)/\Gamma_{total}$ Γ_{10}/Γ

VALUE	CL%	DOCUMENT ID		TECN	COMMENT
<0.02	90	[1] BALTRUSAIT...86		MRK3	$J/\psi \to \eta_c\gamma$

[1] The quoted branching ratios use $B(J/\psi(1S) \to \gamma\eta_c(1S)) = 0.0127 \pm 0.0036$.

$\Gamma(K^*(892)\overline{K} + \text{c.c.})/\Gamma_{total}$ Γ_{11}/Γ

VALUE	CL%	DOCUMENT ID		TECN	COMMENT
<0.0128	90	BISELLO	91	DM2	$J/\psi \to \gamma K^0_S K^\pm\pi^\mp$
<0.0132	90	[1] BISELLO	91	DM2	$J/\psi \to \gamma K^+K^-\pi^0$

[1] The quoted branching ratios use $B(J/\psi(1S) \to \gamma\eta_c(1S)) = 0.0127 \pm 0.0036$.

$\Gamma(f_2(1270)\eta)/\Gamma_{total}$ Γ_{12}/Γ

VALUE	CL%	DOCUMENT ID		TECN	COMMENT
<0.011	90	[1] BALTRUSAIT...86		MRK3	$J/\psi \to \eta_c\gamma$

[1] The quoted branching ratios use $B(J/\psi(1S) \to \gamma\eta_c(1S)) = 0.0127 \pm 0.0036$.

$\Gamma(\omega\omega)/\Gamma_{total}$ Γ_{13}/Γ

VALUE	CL%	DOCUMENT ID		TECN	COMMENT
<0.0031	90	[1] BALTRUSAIT...86		MRK3	$J/\psi \to \eta_c\gamma$
• • • We do not use the following data for averages, fits, limits, etc. • • •					
<0.0063	90	[1] ABLIKIM	05L	BES2	$J/\psi \to \pi^+\pi^-\pi^0\pi^+\pi^-\pi^0\gamma$
<0.0063		[1] BISELLO	91	DM2	$J/\psi \to \gamma\omega\omega$

[1] The quoted branching ratios use $B(J/\psi(1S) \to \gamma\eta_c(1S)) = 0.0127 \pm 0.0036$. Where relevant, the error in this branching ratio is treated as a common systematic in computing averages.

$\Gamma(\omega\phi)/\Gamma_{total}$ Γ_{14}/Γ

VALUE	CL%	DOCUMENT ID		TECN	COMMENT
<0.0017	90	[1] ABLIKIM	05L	BES2	$J/\psi \to \pi^+\pi^-\pi^0 K^+K^-\gamma$

[1] The quoted branching ratios use $B(J/\psi(1S) \to \gamma\eta_c(1S)) = 0.0127 \pm 0.0036$.

Meson Particle Listings

$\eta_c(1S)$

$\Gamma(f_2(1270)f_2(1270))/\Gamma_{total}$ Γ_{15}/Γ

VALUE (units 10^{-2})	EVTS	DOCUMENT ID		TECN	COMMENT
0.98±0.25 OUR FIT					
$0.77^{+0.25}_{-0.30}\pm0.17$	91.2 ± 19.8	[1] ABLIKIM	04M	BES	$J/\psi \to \gamma 2\pi^+ 2\pi^-$

[1] ABLIKIM 04M reports $[\Gamma(\eta_c(1S) \to f_2(1270)f_2(1270))/\Gamma_{total}] \times [B(J/\psi(1S) \to \gamma\eta_c(1S))] = (1.3 \pm 0.3^{+0.3}_{-0.4}) \times 10^{-4}$ which we divide by our best value $B(J/\psi(1S) \to \gamma\eta_c(1S)) = (1.7 \pm 0.4) \times 10^{-2}$. Our first error is their experiment's error and our second error is the systematic error from using our best value.

$\Gamma(K\overline{K}\pi)/\Gamma_{total}$ Γ_{17}/Γ

VALUE (units 10^{-2})	EVTS	DOCUMENT ID		TECN	COMMENT
7.3 ±0.5 OUR FIT					
6.5 ±0.6 OUR AVERAGE					
6.3 ±1.3 ±0.6	55	[1,2] ABLIKIM	12N	BES3	$\psi(2S) \to \pi^0\gamma K^+ K^-\pi^0$
7.9 ±1.4 ±0.7	107	[3,4] ABLIKIM	12N	BES3	$\psi(2S) \to \pi^0\gamma K^0_S K^\mp\pi^\pm$
8.5 ±1.8		[5] AUBERT	06E	BABR	$B^\pm \to K^\pm X_{c\overline{c}}$
5.1 ±2.1	0.6k	[6] BAI	04	BES	$J/\psi \to \gamma K^\pm\pi^\mp K^0_S$
6.90±1.42±1.32	33	[6] BISELLO	91	DM2	$J/\psi \to \gamma K^+ K^-\pi^0$
5.43±0.94±0.94	68	[6] BISELLO	91	DM2	$J/\psi \to \gamma K^\pm\pi^\mp K^0_S$
4.8 ±1.7	95	[6,7] BALTRUSAIT...86		MRK3	$J/\psi \to \eta_c\gamma$
$16.1\ ^{+9.2}_{-7.3}$		[8,9] HIMEL	80B	MRK2	$\psi(2S) \to \eta_c\gamma$
• • • We do not use the following data for averages, fits, limits, etc. • • •					
< 10.7 90% CL		[6,10] PARTRIDGE	80B	CBAL	$J/\psi \to \eta_c\gamma$

[1] ABLIKIM 12N quotes $B(\psi(2S) \to \pi^0 h_c) \cdot B(h_c \to \gamma\eta_c) \cdot B(\eta_c \to K^+K^-\pi^0) = (4.54 \pm 0.76 \pm 0.48) \times 10^{-6}$ which we multiply by 6 to account for isospin symmetry.

[2] ABLIKIM 12N reports $[\Gamma(\eta_c(1S) \to K\overline{K}\pi)/\Gamma_{total}] \times [\Gamma(h_c(1P) \to \eta_c(1S)\gamma)/\Gamma_{total} \times \Gamma(\psi(2S) \to \pi^0 h_c(1P))/\Gamma_{total}] = (27.24 \pm 4.56 \pm 2.88) \times 10^{-6}$ which we divide by our best value $\Gamma(h_c(1P) \to \eta_c(1S)\gamma)/\Gamma_{total} \times \Gamma(\psi(2S) \to \pi^0 h_c(1P))/\Gamma_{total} = (4.3 \pm 0.4) \times 10^{-4}$. Our first error is their experiment's error and our second error is the systematic error from using our best value.

[3] ABLIKIM 12N quotes $B(\psi(2S) \to \pi^0 h_c) \cdot B(h_c \to \gamma\eta_c) \cdot B(\eta_c \to K^0_S K^\pm\pi^\mp) = (11.35 \pm 1.25 \pm 1.50) \times 10^{-6}$ which we multiply by 3 to account for isospin symmetry.

[4] ABLIKIM 12N reports $[\Gamma(\eta_c(1S) \to K\overline{K}\pi)/\Gamma_{total}] \times [\Gamma(h_c(1P) \to \eta_c(1S)\gamma)/\Gamma_{total} \times \Gamma(\psi(2S) \to \pi^0 h_c(1P))/\Gamma_{total}] = (34.05 \pm 3.75 \pm 4.50) \times 10^{-6}$ which we divide by our best value $\Gamma(h_c(1P) \to \eta_c(1S)\gamma)/\Gamma_{total} \times \Gamma(\psi(2S) \to \pi^0 h_c(1P))/\Gamma_{total} = (4.3 \pm 0.4) \times 10^{-4}$. Our first error is their experiment's error and our second error is the systematic error from using our best value.

[5] Determined from the ratio of $B(B^\pm \to K^\pm\eta_c)\, B(\eta_c \to K\overline{K}\pi) = (7.4 \pm 0.5 \pm 0.7) \times 10^{-5}$ reported in AUBERT,B 04B and $B(B^\pm \to K^\pm\eta_c) = (8.7 \pm 1.5) \times 10^{-3}$ reported in AUBERT 06E.

[6] The quoted branching ratios use $B(J/\psi(1S) \to \gamma\eta_c(1S)) = 0.0127 \pm 0.0036$. Where relevant, the error in this branching ratio is treated as a common systematic in computing averages.

[7] Average from $K^+K^-\pi^0$ and $K^\pm K^0_S\pi^\mp$ decay channels.

[8] $K^\pm K^0_S\pi^\mp$ corrected to $K\overline{K}\pi$ by factor 3. KS, MR.

[9] Estimated using $B(\psi(2S) \to \gamma\eta_c(1S)) = 0.0028 \pm 0.0006$.

[10] $K^+K^-\pi^0$ corrected to $K\overline{K}\pi$ by factor 6. KS, MR

$\Gamma(\phi K^+K^-)/\Gamma(K\overline{K}\pi)$ Γ_6/Γ_{17}

VALUE	EVTS	DOCUMENT ID		TECN	COMMENT
$0.052^{+0.016}_{-0.014}\pm0.014$	7	[1] HUANG	03	BELL	$B^\pm \to K^\pm\phi\phi$

[1] Using $B(B^+ \to \eta_c K^+) = (1.25 \pm 0.12^{+0.10}_{-0.12}) \times 10^{-3}$ from FANG 03 and $B(\eta_c \to K\overline{K}\pi) = (5.5 \pm 1.7) \times 10^{-2}$.

$\Gamma(\eta\pi^+\pi^-)/\Gamma_{total}$ Γ_{18}/Γ

VALUE (units 10^{-2})	EVTS	DOCUMENT ID		TECN	COMMENT
1.7±0.4±0.1	33	[1] ABLIKIM	12N	BES3	$\psi(2S) \to \pi^0\gamma\eta\pi^+\pi^-$
• • • We do not use the following data for averages, fits, limits, etc. • • •					
5.4±2.0	75	[2] BALTRUSAIT...86		MRK3	$J/\psi \to \eta_c\gamma$
3.7±1.3±2.0	18	[2] PARTRIDGE	80B	CBAL	$J/\psi \to \eta\pi^+\pi^-\gamma$

[1] ABLIKIM 12N reports $[\Gamma(\eta_c(1S) \to \eta\pi^+\pi^-)/\Gamma_{total}] \times [\Gamma(h_c(1P) \to \eta_c(1S)\gamma)/\Gamma_{total} \times \Gamma(\psi(2S) \to \pi^0 h_c(1P))/\Gamma_{total}] = (7.22 \pm 1.47 \pm 1.11) \times 10^{-6}$ which we divide by our best value $\Gamma(h_c(1P) \to \eta_c(1S)\gamma)/\Gamma_{total} \times \Gamma(\psi(2S) \to \pi^0 h_c(1P))/\Gamma_{total} = (4.3 \pm 0.4) \times 10^{-4}$. Our first error is their experiment's error and our second error is the systematic error from using our best value.

[2] The quoted branching ratios use $B(J/\psi(1S) \to \gamma\eta_c(1S)) = 0.0127 \pm 0.0036$. Where relevant, the error in this branching ratio is treated as a common systematic in computing averages.

$\Gamma(\eta 2(\pi^+\pi^-))/\Gamma_{total}$ Γ_{19}/Γ

VALUE (units 10^{-2})	EVTS	DOCUMENT ID		TECN	COMMENT
4.4±1.2±0.4	39	[1] ABLIKIM	12N	BES3	$\psi(2S) \to \pi^0\gamma\eta 2(\pi^+\pi^-)$

[1] ABLIKIM 12N reports $[\Gamma(\eta_c(1S) \to \eta 2(\pi^+\pi^-))/\Gamma_{total}] \times [\Gamma(h_c(1P) \to \eta_c(1S)\gamma)/\Gamma_{total} \times \Gamma(\psi(2S) \to \pi^0 h_c(1P))/\Gamma_{total}] = (19.17 \pm 3.77 \pm 3.72) \times 10^{-6}$ which we divide by our best value $\Gamma(h_c(1P) \to \eta_c(1S)\gamma)/\Gamma_{total} \times \Gamma(\psi(2S) \to \pi^0 h_c(1P))/\Gamma_{total} = (4.3 \pm 0.4) \times 10^{-4}$. Our first error is their experiment's error and our second error is the systematic error from using our best value.

$\Gamma(K^+K^-\pi^+\pi^-)/\Gamma_{total}$ Γ_{20}/Γ

VALUE (units 10^{-3})	EVTS	DOCUMENT ID		TECN	COMMENT
6.9± 1.1 OUR FIT					
11.2± 1.9 OUR AVERAGE					
9.7± 2.2±0.9	38	[1] ABLIKIM	12N	BES3	$\psi(2S) \to \pi^0\gamma K^+K^-\pi^+\pi^-$
12 ± 4	0.4k	[2] BAI	04	BES	$J/\psi \to \gamma K^+K^-\pi^+\pi^-$
21 ± 7	110	[2] BALTRUSAIT...86		MRK3	$J/\psi \to \eta_c\gamma$
$14\ ^{+22}_{-9}$		[3] HIMEL	80B	MRK2	$\psi(2S) \to \eta_c\gamma$

[1] ABLIKIM 12N reports $[\Gamma(\eta_c(1S) \to K^+K^-\pi^+\pi^-)/\Gamma_{total}] \times [\Gamma(h_c(1P) \to \eta_c(1S)\gamma)/\Gamma_{total} \times \Gamma(\psi(2S) \to \pi^0 h_c(1P))/\Gamma_{total}] = (4.16 \pm 0.76 \pm 0.59) \times 10^{-6}$ which we divide by our best value $\Gamma(h_c(1P) \to \eta_c(1S)\gamma)/\Gamma_{total} \times \Gamma(\psi(2S) \to \pi^0 h_c(1P))/\Gamma_{total} = (4.3 \pm 0.4) \times 10^{-4}$. Our first error is their experiment's error and our second error is the systematic error from using our best value.

[2] The quoted branching ratios use $B(J/\psi(1S) \to \gamma\eta_c(1S)) = 0.0127 \pm 0.0036$. Where relevant, the error in this branching ratio is treated as a common systematic in computing averages.

[3] Estimated using $B(\psi(2S) \to \gamma\eta_c(1S)) = 0.0028 \pm 0.0006$.

$\Gamma(K^+K^-\pi^+\pi^-\pi^0)/\Gamma(K\overline{K}\pi)$ Γ_{21}/Γ_{17}

VALUE	EVTS	DOCUMENT ID		TECN	COMMENT
0.477±0.017±0.070	11k	[1] DEL-AMO-SA...11M		BABR	$\gamma\gamma \to K^+K^-\pi^+\pi^-\pi^0$

[1] We have multiplied the value of $\Gamma(K^+K^-\pi^+\pi^-\pi^0)/\Gamma(K^0_S K^\pm\pi^\mp)$ reported in DEL-AMO-SANCHEZ 11M by a factor 1/3 to obtain $\Gamma(K^+K^-\pi^+\pi^-\pi^0)/\Gamma(K\overline{K}\pi)$. Not independent from other measurements reported in DEL-AMO-SANCHEZ 11M.

$\Gamma(K^0K^-\pi^+\pi^-\pi^+ + \text{c.c.})/\Gamma_{total}$ Γ_{22}/Γ

VALUE (units 10^{-2})	EVTS	DOCUMENT ID		TECN	COMMENT
5.6±1.4±0.5	43	[1,2] ABLIKIM	12N	BES3	$\psi(2S) \to \pi^0\gamma K^0_S K^\mp\pi^\mp 2\pi^\pm$

[1] ABLIKIM 12N quotes $B(\psi(2S) \to \pi^0 h_c) \cdot B(h_c \to \gamma\eta_c) \cdot B(\eta_c \to K^0_S K^-\pi^- 2\pi^+) = (12.01 \pm 2.22 \pm 2.04) \times 10^{-6}$ which we multiply by 2 to take c.c. into account.

[2] ABLIKIM 12N reports $[\Gamma(\eta_c(1S) \to K^0K^-\pi^+\pi^-\pi^+ + \text{c.c.})/\Gamma_{total}] \times [\Gamma(h_c(1P) \to \eta_c(1S)\gamma)/\Gamma_{total} \times \Gamma(\psi(2S) \to \pi^0 h_c(1P))/\Gamma_{total}] = (24.02 \pm 4.44 \pm 4.08) \times 10^{-6}$ which we divide by our best value $\Gamma(h_c(1P) \to \eta_c(1S)\gamma)/\Gamma_{total} \times \Gamma(\psi(2S) \to \pi^0 h_c(1P))/\Gamma_{total} = (4.3 \pm 0.4) \times 10^{-4}$. Our first error is their experiment's error and our second error is the systematic error from using our best value.

$\Gamma(K^+K^-2(\pi^+\pi^-))/\Gamma_{total}$ Γ_{23}/Γ

VALUE (units 10^{-3})	EVTS	DOCUMENT ID		TECN	COMMENT
7.5±2.4 OUR AVERAGE					
8 ±4 ±1	10	[1] ABLIKIM	12N	BES3	$\psi(2S) \to \pi^0\gamma K^+K^-2(\pi^+\pi^-)$
7.2±2.4±1.6	100	[2] ABLIKIM	06A	BES2	$J/\psi \to K^+K^-2(\pi^+\pi^-)\gamma$

[1] ABLIKIM 12N reports $[\Gamma(\eta_c(1S) \to K^+K^-2(\pi^+\pi^-))/\Gamma_{total}] \times [\Gamma(h_c(1P) \to \eta_c(1S)\gamma)/\Gamma_{total} \times \Gamma(\psi(2S) \to \pi^0 h_c(1P))/\Gamma_{total}] = (3.60 \pm 1.71 \pm 0.64) \times 10^{-6}$ which we divide by our best value $\Gamma(h_c(1P) \to \eta_c(1S)\gamma)/\Gamma_{total} \times \Gamma(\psi(2S) \to \pi^0 h_c(1P))/\Gamma_{total} = (4.3 \pm 0.4) \times 10^{-4}$. Our first error is their experiment's error and our second error is the systematic error from using our best value.

[2] ABLIKIM 06A reports $[\Gamma(\eta_c(1S) \to K^+K^-2(\pi^+\pi^-))/\Gamma_{total}] \times [B(J/\psi(1S) \to \gamma\eta_c(1S))] = (1.21 \pm 0.32 \pm 0.24) \times 10^{-4}$ which we divide by our best value $B(J/\psi(1S) \to \gamma\eta_c(1S)) = (1.7 \pm 0.4) \times 10^{-2}$. Our first error is their experiment's error and our second error is the systematic error from using our best value.

$\Gamma(2(K^+K^-))/\Gamma_{total}$ Γ_{24}/Γ

VALUE (units 10^{-3})	EVTS	DOCUMENT ID		TECN	COMMENT
1.47± 0.31 OUR FIT					
2.2 ± 0.9 ±0.2	7	[1] ABLIKIM	12N	BES3	$\psi(2S) \to \pi^0\gamma 2(K^+K^-)$
• • • We do not use the following data for averages, fits, limits, etc. • • •					
$1.4\ ^{+\ 0.5}_{-\ 0.4}$ ±0.6	$14.5^{+4.6}_{-3.0}$	[2] HUANG	03	BELL	$B^+ \to 2(K^+K^-)\,K^+$
21 ±10 ±6		[3] ALBRECHT	94H	ARG	$\gamma\gamma \to K^+K^-K^+K^-$

[1] ABLIKIM 12N reports $[\Gamma(\eta_c(1S) \to 2(K^+K^-))/\Gamma_{total}] \times [\Gamma(h_c(1P) \to \eta_c(1S)\gamma)/\Gamma_{total} \times \Gamma(\psi(2S) \to \pi^0 h_c(1P))/\Gamma_{total}] = (0.94 \pm 0.37 \pm 0.14) \times 10^{-6}$ which we divide by our best value $\Gamma(h_c(1P) \to \eta_c(1S)\gamma)/\Gamma_{total} \times \Gamma(\psi(2S) \to \pi^0 h_c(1P))/\Gamma_{total} = (4.3 \pm 0.4) \times 10^{-4}$. Our first error is their experiment's error and our second error is the systematic error from using our best value.

[2] Using $B(B^+ \to \eta_c K^+) = (1.25 \pm 0.12^{+0.10}_{-0.12}) \times 10^{-3}$ from FANG 03 and $B(\eta_c \to K\overline{K}\pi) = (5.5 \pm 1.7) \times 10^{-2}$.

[3] Normalized to the sum of $B(\eta_c \to K^\pm K^0_S\pi^\mp)$, $B(\eta_c \to \phi\phi)$, $B(\eta_c \to K^+K^-\pi^+\pi^-)$, and $B(\eta_c \to 2\pi^+2\pi^-)$.

$\Gamma(2(K^+K^-))/\Gamma(K\overline{K}\pi)$ Γ_{24}/Γ_{17}

VALUE	EVTS	DOCUMENT ID		TECN	COMMENT
0.020±0.004 OUR FIT					
0.024±0.007 OUR AVERAGE					
0.023±0.007±0.006		AUBERT,B	04B	BABR	$B^\pm \to K^\pm\eta_c$
$0.026^{+0.009}_{-0.007}\pm0.007$	15	[1] HUANG	03	BELL	$B^\pm \to K^\pm(2K^+2K^-)$

[1] Using $B(B^+ \to \eta_c K^+) = (1.25 \pm 0.12^{+0.10}_{-0.12}) \times 10^{-3}$ from FANG 03 and $B(\eta_c \to K\overline{K}\pi) = (5.5 \pm 1.7) \times 10^{-2}$.

$\Gamma(\pi^+\pi^-\pi^0\pi^0)/\Gamma_{total}$ Γ_{25}/Γ

VALUE (units 10^{-2})	EVTS	DOCUMENT ID		TECN	COMMENT
4.7±0.9±0.4	118	[1] ABLIKIM	12N	BES3	$\psi(2S) \to \pi^0\gamma\pi^+\pi^-2\pi^0$

[1] ABLIKIM 12N reports $[\Gamma(\eta_c(1S) \to \pi^+\pi^-\pi^0\pi^0)/\Gamma_{total}] \times [\Gamma(h_c(1P) \to \eta_c(1S)\gamma)/\Gamma_{total} \times \Gamma(\psi(2S) \to \pi^0 h_c(1P))/\Gamma_{total}] = (20.31 \pm 2.20 \pm 3.33) \times 10^{-6}$ which we divide by our best value $\Gamma(h_c(1P) \to \eta_c(1S)\gamma)/\Gamma_{total} \times \Gamma(\psi(2S) \to \pi^0 h_c(1P))/\Gamma_{total} = (4.3 \pm 0.4) \times 10^{-4}$. Our first error is their experiment's error and our second error is the systematic error from using our best value.

$\Gamma(2(\pi^+\pi^-))/\Gamma_{total}$ Γ_{26}/Γ

VALUE (units 10^{-2})	EVTS	DOCUMENT ID		TECN	COMMENT
0.97±0.12 OUR FIT					
1.35±0.21 OUR AVERAGE					
1.74±0.32±0.15	100	[1] ABLIKIM	12N	BES3	$\psi(2S) \to \pi^0\gamma 2(\pi^+\pi^-)$
1.0 ±0.5	542 ± 75	[2] BAI	04	BES	$J/\psi \to \gamma\, 2(\pi^+\pi^-)$
1.05±0.17±0.34	137	[2] BISELLO	91	DM2	$J/\psi \to \gamma 2\pi^+ 2\pi^-$
1.3 ±0.6	25	[2] BALTRUSAIT...86		MRK3	$J/\psi \to \eta_c\gamma$
$2.0\ ^{+1.5}_{-1.0}$		[3] HIMEL	80B	MRK2	$\psi(2S) \to \eta_c\gamma$

[1] ABLIKIM 12N reports $[\Gamma(\eta_c(1S) \to 2(\pi^+\pi^-))/\Gamma_{total}] \times [\Gamma(h_c(1P) \to \eta_c(1S)\gamma)/\Gamma_{total} \times \Gamma(\psi(2S) \to \pi^0 h_c(1P))/\Gamma_{total}] = (7.51 \pm 0.85 \pm 1.11) \times 10^{-6}$ which we divide by our best value $\Gamma(h_c(1P) \to \eta_c(1S)\gamma)/\Gamma_{total} \times \Gamma(\psi(2S) \to \pi^0 h_c(1P))/\Gamma_{total} = (4.3 \pm 0.4) \times 10^{-4}$. Our first error is their experiment's error and our second error is the systematic error from using our best value.

[2] The quoted branching ratios use $B(J/\psi(1S) \to \gamma\eta_c(1S)) = 0.0127 \pm 0.0036$. Where relevant, the error in this branching ratio is treated as a common systematic in computing averages.

[3] Estimated using $B(\psi(2S) \to \gamma\eta_c(1S)) = 0.0028 \pm 0.0006$.

$\Gamma(2(\pi^+\pi^-\pi^0))/\Gamma_{total}$ Γ_{27}/Γ

VALUE (units 10^{-2})	EVTS	DOCUMENT ID		TECN	COMMENT
17.4±2.9±1.5	175	[1] ABLIKIM	12N	BES3	$\psi(2S) \to \pi^0\gamma 2(\pi^+\pi^-2\pi^0)$

[1] ABLIKIM 12N reports $[\Gamma(\eta_c(1S) \to 2(\pi^+\pi^-\pi^0))/\Gamma_{total}] \times [\Gamma(h_c(1P) \to \eta_c(1S)\gamma)/\Gamma_{total} \times \Gamma(\psi(2S) \to \pi^0 h_c(1P))/\Gamma_{total}] = (75.13 \pm 7.42 \pm 9.99) \times 10^{-6}$ which we divide by our best value $\Gamma(h_c(1P) \to \eta_c(1S)\gamma)/\Gamma_{total} \times \Gamma(\psi(2S) \to \pi^0 h_c(1P))/\Gamma_{total} = (4.3 \pm 0.4) \times 10^{-4}$. Our first error is their experiment's error and our second error is the systematic error from using our best value.

$\Gamma(3(\pi^+\pi^-))/\Gamma_{total}$ Γ_{28}/Γ

VALUE (units 10^{-3})	EVTS	DOCUMENT ID		TECN	COMMENT
18 ±4 OUR AVERAGE					
20 ±5 ±2	51	[1] ABLIKIM	12N	BES3	$\psi(2S) \to \pi^0\gamma 3(\pi^+\pi^-)$
15.3±3.4±3.3	479	[2] ABLIKIM	06A	BES2	$J/\psi \to 3(\pi^+\pi^-)\gamma$

[1] ABLIKIM 12N reports $[\Gamma(\eta_c(1S) \to 3(\pi^+\pi^-))/\Gamma_{total}] \times [\Gamma(h_c(1P) \to \eta_c(1S)\gamma)/\Gamma_{total} \times \Gamma(\psi(2S) \to \pi^0 h_c(1P))/\Gamma_{total}] = (8.82 \pm 1.57 \pm 1.59) \times 10^{-6}$ which we divide by our best value $\Gamma(h_c(1P) \to \eta_c(1S)\gamma)/\Gamma_{total} \times \Gamma(\psi(2S) \to \pi^0 h_c(1P))/\Gamma_{total} = (4.3 \pm 0.4) \times 10^{-4}$. Our first error is their experiment's error and our second error is the systematic error from using our best value.

[2] ABLIKIM 06A reports $[\Gamma(\eta_c(1S) \to 3(\pi^+\pi^-))/\Gamma_{total}] \times [B(J/\psi(1S) \to \gamma\eta_c(1S))] = (2.59 \pm 0.32 \pm 0.47) \times 10^{-4}$ which we divide by our best value $B(J/\psi(1S) \to \gamma\eta_c(1S)) = (1.7 \pm 0.4) \times 10^{-2}$. Our first error is their experiment's error and our second error is the systematic error from using our best value.

$\Gamma(p\overline{p})/\Gamma_{total}$ Γ_{29}/Γ

VALUE (units 10^{-4})	EVTS	DOCUMENT ID		TECN	COMMENT
15.2± 1.6 OUR FIT					
13.2± 2.7 OUR AVERAGE					
15 ± 5 ±1	15	[1] ABLIKIM	12N	BES3	$\psi(2S) \to \pi^0\gamma p\overline{p}$
15 ± 6	213 ± 33	[2] BAI	04	BES	$J/\psi \to \gamma p\overline{p}$
10 ± 3 ±4	18	[2] BISELLO	91	DM2	$J/\psi \to \gamma p\overline{p}$
11 ± 6	23	[2] BALTRUSAIT...86		MRK3	$J/\psi \to \eta_c\gamma$
$29\ ^{+29}_{-15}$		[3] HIMEL	80B	MRK2	$\psi(2S) \to \eta_c\gamma$
• • • We do not use the following data for averages, fits, limits, etc. • • •					
$14.8^{+\ 2.0+1.7}_{-\ 2.4-1.8}$	195	[4] WU	06	BELL	$B^+ \to p\overline{p}K^+$

[1] ABLIKIM 12N reports $[\Gamma(\eta_c(1S) \to p\overline{p})/\Gamma_{total}] \times [\Gamma(h_c(1P) \to \eta_c(1S)\gamma)/\Gamma_{total} \times \Gamma(\psi(2S) \to \pi^0 h_c(1P))/\Gamma_{total}] = (0.65 \pm 0.19 \pm 0.10) \times 10^{-6}$ which we divide by our best value $\Gamma(h_c(1P) \to \eta_c(1S)\gamma)/\Gamma_{total} \times \Gamma(\psi(2S) \to \pi^0 h_c(1P))/\Gamma_{total} = (4.3 \pm 0.4) \times 10^{-4}$. Our first error is their experiment's error and our second error is the systematic error from using our best value.

[2] The quoted branching ratios use $B(J/\psi(1S) \to \gamma\eta_c(1S)) = 0.0127 \pm 0.0036$. Where relevant, the error in this branching ratio is treated as a common systematic in computing averages.

[3] Estimated using $B(\psi(2S) \to \gamma\eta_c(1S)) = 0.0028 \pm 0.0006$.

[4] WU 06 reports $[\Gamma(\eta_c(1S) \to p\overline{p})/\Gamma_{total}] \times [B(B^+ \to \eta_c K^+)] = (1.42 \pm 0.11\ ^{+0.16}_{-0.20}) \times 10^{-6}$ which we divide by our best value $B(B^+ \to \eta_c K^+) = (9.6 \pm 1.1) \times 10^{-4}$. Our first error is their experiment's error and our second error is the systematic error from using our best value.

$\Gamma(p\overline{p})/\Gamma(K\overline{K}\pi)$ Γ_{29}/Γ_{17}

VALUE	EVTS	DOCUMENT ID		TECN	COMMENT
0.0207±0.0021 OUR FIT					
$\mathbf{0.021\ \pm 0.002\ ^{+0.004}_{-0.006}}$	195	[1] WU	06	BELL	$B^\pm \to K^\pm p\overline{p}$

[1] Using $B(B^+ \to \eta_c K^+) = (1.25 \pm 0.12\ ^{+0.10}_{-0.12}) \times 10^{-3}$ from FANG 03 and $B(\eta_c \to K\overline{K}\pi) = (5.5 \pm 1.7) \times 10^{-2}$.

$\Gamma(p\overline{p})/\Gamma_{total} \times \Gamma(\phi\phi)/\Gamma_{total}$ $\Gamma_{29}/\Gamma \times \Gamma_7/\Gamma$

VALUE (units 10^{-5})	DOCUMENT ID		TECN	COMMENT
0.27±0.05 OUR FIT				
$\mathbf{4.0\ ^{+3.5}_{-3.2}}$	BAGLIN	89	SPEC	$\overline{p}p \to K^+K^-K^+K^-$

$\Gamma(p\overline{p}\pi^0)/\Gamma_{total}$ Γ_{30}/Γ

VALUE (units 10^{-2})	EVTS	DOCUMENT ID		TECN	COMMENT
0.36±0.13±0.03	14	[1] ABLIKIM	12N	BES3	$\psi(2S) \to \pi^0\gamma p\overline{p}\pi^0$

[1] ABLIKIM 12N reports $[\Gamma(\eta_c(1S) \to p\overline{p}\pi^0)/\Gamma_{total}] \times [\Gamma(h_c(1P) \to \eta_c(1S)\gamma)/\Gamma_{total} \times \Gamma(\psi(2S) \to \pi^0 h_c(1P))/\Gamma_{total}] = (1.53 \pm 0.49 \pm 0.23) \times 10^{-6}$ which we divide by our best value $\Gamma(h_c(1P) \to \eta_c(1S)\gamma)/\Gamma_{total} \times \Gamma(\psi(2S) \to \pi^0 h_c(1P))/\Gamma_{total} = (4.3 \pm 0.4) \times 10^{-4}$. Our first error is their experiment's error and our second error is the systematic error from using our best value.

$\Gamma(\Lambda\overline{\Lambda})/\Gamma_{total}$ Γ_{31}/Γ

VALUE (units 10^{-4})	CL%	EVTS	DOCUMENT ID		TECN	COMMENT
10.9±2.4 OUR FIT						
11.7±2.3±2.6			[1] ABLIKIM	12B	BES3	
• • • We do not use the following data for averages, fits, limits, etc. • • •						
$9.9^{+\ 2.7}_{-\ 2.6}$±1.2		20	[2] WU	06	BELL	$B^+ \to \Lambda\overline{\Lambda}K^+$
<20	90		[3] BISELLO	91	DM2	$e^+e^- \to \gamma\Lambda\overline{\Lambda}$

[1] ABLIKIM 12B reports $[\Gamma(\eta_c(1S) \to \Lambda\overline{\Lambda})/\Gamma_{total}] \times [B(J/\psi(1S) \to \gamma\eta_c(1S))] = (0.198 \pm 0.021 \pm 0.032) \times 10^{-4}$ which we divide by our best value $B(J/\psi(1S) \to \gamma\eta_c(1S)) = (1.7 \pm 0.4) \times 10^{-2}$. Our first error is their experiment's error and our second error is the systematic error from using our best value.

[2] WU 06 reports $[\Gamma(\eta_c(1S) \to \Lambda\overline{\Lambda})/\Gamma_{total}] \times [B(B^+ \to \eta_c K^+)] = (0.95\ ^{+0.25+0.08}_{-0.22-0.11}) \times 10^{-6}$ which we divide by our best value $B(B^+ \to \eta_c K^+) = (9.6 \pm 1.1) \times 10^{-4}$. Our first error is their experiment's error and our second error is the systematic error from using our best value.

[3] The quoted branching ratios use $B(J/\psi(1S) \to \gamma\eta_c(1S)) = 0.0127 \pm 0.0036$.

$\Gamma(\Lambda\overline{\Lambda})/\Gamma(p\overline{p})$ Γ_{31}/Γ_{29}

VALUE	DOCUMENT ID		TECN	COMMENT
0.72±0.16 OUR FIT				
$\mathbf{0.67\ ^{+0.19}_{-0.16}\pm 0.12}$	[1] WU	06	BELL	$B^+ \to p\overline{p}K^+, \Lambda\overline{\Lambda}K^+$

[1] Not independent from other $\eta_c \to \Lambda\overline{\Lambda}$, $p\overline{p}$ branching ratios reported by WU 06.

$\Gamma(\Sigma^+\overline{\Sigma}^-)/\Gamma_{total}$ Γ_{32}/Γ

VALUE (units 10^{-3})	EVTS	DOCUMENT ID		TECN	COMMENT
2.1±0.3±0.5	112	[1] ABLIKIM	13C	BES3	$J/\psi \to \gamma p\overline{p}\pi^0\pi^0$

[1] ABLIKIM 13C reports $[\Gamma(\eta_c(1S) \to \Sigma^+\overline{\Sigma}^-)/\Gamma_{total}] \times [B(J/\psi(1S) \to \gamma\eta_c(1S))] = (3.60 \pm 0.48 \pm 0.31) \times 10^{-5}$ which we divide by our best value $B(J/\psi(1S) \to \gamma\eta_c(1S)) = (1.7 \pm 0.4) \times 10^{-2}$. Our first error is their experiment's error and our second error is the systematic error from using our best value.

$\Gamma(\Xi^-\overline{\Xi}^+)/\Gamma_{total}$ Γ_{33}/Γ

VALUE (units 10^{-3})	EVTS	DOCUMENT ID		TECN	COMMENT
0.89±0.18±0.19	78	[1] ABLIKIM	13C	BES3	$J/\psi \to \gamma\Lambda\overline{\Lambda}\pi^+\pi^-$

[1] ABLIKIM 13C reports $[\Gamma(\eta_c(1S) \to \Xi^-\overline{\Xi}^+)/\Gamma_{total}] \times [B(J/\psi(1S) \to \gamma\eta_c(1S))] = (1.51 \pm 0.27 \pm 0.14) \times 10^{-5}$ which we divide by our best value $B(J/\psi(1S) \to \gamma\eta_c(1S)) = (1.7 \pm 0.4) \times 10^{-2}$. Our first error is their experiment's error and our second error is the systematic error from using our best value.

$\Gamma(K\overline{K}\eta)/\Gamma_{total}$ Γ_{34}/Γ

VALUE (units 10^{-2})	CL%	EVTS	DOCUMENT ID		TECN	COMMENT
1.0±0.5±0.1		7	[1,2] ABLIKIM	12N	BES3	$\psi(2S) \to \pi^0\gamma K^+K^-$
• • • We do not use the following data for averages, fits, limits, etc. • • •						
<3.1	90		[3] BALTRUSAIT...86		MRK3	$J/\psi \to \eta_c\gamma$

[1] ABLIKIM 12N quotes $B(\psi(2S) \to \pi^0 h_c) \cdot B(h_c \to \gamma\eta_c) \cdot B(\eta_c \to K^+K^-\eta) = (12.01 \pm 2.22 \pm 2.04) \times 10^{-6}$ which we multiply by 2 to account for isospin symmetry.

[2] ABLIKIM 12N reports $[\Gamma(\eta_c(1S) \to K\overline{K}\eta)/\Gamma_{total}] \times [\Gamma(h_c(1P) \to \eta_c(1S)\gamma)/\Gamma_{total} \times \Gamma(\psi(2S) \to \pi^0 h_c(1P))/\Gamma_{total}] = (4.22 \pm 2.02 \pm 0.64) \times 10^{-6}$ which we divide by our best value $\Gamma(h_c(1P) \to \eta_c(1S)\gamma)/\Gamma_{total} \times \Gamma(\psi(2S) \to \pi^0 h_c(1P))/\Gamma_{total} = (4.3 \pm 0.4) \times 10^{-4}$. Our first error is their experiment's error and our second error is the systematic error from using our best value.

[3] The quoted branching ratios use $B(J/\psi(1S) \to \gamma\eta_c(1S)) = 0.0127 \pm 0.0036$.

Meson Particle Listings

$\eta_c(1S)$

$\Gamma(\pi^+\pi^- p\overline{p})/\Gamma_{\rm total}$ Γ_{35}/Γ

VALUE (units 10^{-3})	CL%	EVTS	DOCUMENT ID		TECN	COMMENT
5.3±1.7±0.5		19	[1] ABLIKIM	12N	BES3	$\psi(2S) \to \pi^0\gamma p\overline{p}\pi^+\pi^-$
• • • We do not use the following data for averages, fits, limits, etc. • • •						
<12	90		HIMEL	80B	MRK2	$\psi(2S) \to \eta_c\gamma$

[1] ABLIKIM 12N reports $[\Gamma(\eta_c(1S) \to \pi^+\pi^- p\overline{p})/\Gamma_{\rm total}] \times [\Gamma(h_c(1P) \to \eta_c(1S)\gamma)/\Gamma_{\rm total} \times \Gamma(\psi(2S) \to \pi^0 h_c(1P))/\Gamma_{\rm total}] = (2.30 \pm 0.65 \pm 0.36) \times 10^{-6}$ which we divide by our best value $\Gamma(h_c(1P) \to \eta_c(1S)\gamma)/\Gamma_{\rm total} \times \Gamma(\psi(2S) \to \pi^0 h_c(1P))/\Gamma_{\rm total} = (4.3 \pm 0.4) \times 10^{-4}$. Our first error is their experiment's error and our second error is the systematic error from using our best value.

RADIATIVE DECAYS

$\Gamma(\gamma\gamma)/\Gamma_{\rm total}$ Γ_{36}/Γ

VALUE (units 10^{-4})	CL%	EVTS	DOCUMENT ID		TECN	COMMENT
1.57±0.12 OUR FIT						
1.9 $^{+0.7}_{-0.6}$ OUR AVERAGE						
2.7 ±0.8 ±0.6			[1] ABLIKIM	13I	BES3	
1.4 $^{+0.7}_{-0.5}$ ±0.3		1.2 $^{+2.8}_{-1.1}$	[2] ADAMS	08	CLEO	$\psi(2S) \to \pi^+\pi^- J/\psi$
• • • We do not use the following data for averages, fits, limits, etc. • • •						
2.3 $^{+1.0}_{-0.8}$ ±0.3		13	[3] WICHT	08	BELL	$B^\pm \to K^\pm\gamma\gamma$
2.80 $^{+0.67}_{-0.58}$ ±1.0			[4] ARMSTRONG	95F	E760	$\overline{p}p \to \gamma\gamma$
< 9	90		[5] BISELLO	91	DM2	$J/\psi \to \gamma\gamma\gamma$
6 $^{+4}_{-3}$ ±4			[4] BAGLIN	87B	SPEC	$\overline{p}p \to \gamma\gamma$
< 18	90		[6] BLOOM	83	CBAL	$J/\psi \to \eta_c\gamma$

[1] ABLIKIM 13I reports $[\Gamma(\eta_c(1S) \to \gamma\gamma)/\Gamma_{\rm total}] \times [B(J/\psi(1S) \to \gamma\eta_c(1S))] = (4.5 \pm 1.2 \pm 0.6) \times 10^{-6}$ which we divide by our best value $B(J/\psi(1S) \to \gamma\eta_c(1S)) = (1.7 \pm 0.4) \times 10^{-2}$. Our first error is their experiment's error and our second error is the systematic error from using our best value.

[2] ADAMS 08 reports $[\Gamma(\eta_c(1S) \to \gamma\gamma)/\Gamma_{\rm total}] \times [B(J/\psi(1S) \to \gamma\eta_c(1S))] = (2.4 \pm 0.8 \pm 0.3) \times 10^{-6}$ which we divide by our best value $B(J/\psi(1S) \to \gamma\eta_c(1S)) = (1.7 \pm 0.4) \times 10^{-2}$. Our first error is their experiment's error and our second error is the systematic error from using our best value.

[3] WICHT 08 reports $[\Gamma(\eta_c(1S) \to \gamma\gamma)/\Gamma_{\rm total}] \times [B(B^+ \to \eta_c K^+)] = (2.2 \pm 0.9 \pm 0.4) \times 10^{-7}$ which we divide by our best value $B(B^+ \to \eta_c K^+) = (9.6 \pm 1.1) \times 10^{-4}$. Our first error is their experiment's error and our second error is the systematic error from using our best value.

[4] Not independent from the values of the total and two-photon width quoted by the same experiment.

[5] The quoted branching ratios use $B(J/\psi(1S) \to \gamma\eta_c(1S)) = 0.0127 \pm 0.0036$.

[6] Using $B(J/\psi(1S) \to \gamma\eta_c(1S)) = 0.0127 \pm 0.0036$.

$\Gamma(\gamma\gamma)/\Gamma(K\overline{K}\pi)$ Γ_{36}/Γ_{17}

VALUE (units 10^{-3})	EVTS	DOCUMENT ID		TECN	COMMENT
2.13±0.29 OUR FIT					
3.2 $^{+1.3}_{-1.0}$ $^{+0.8}_{-0.6}$	13	[1] WICHT	08	BELL	$B^\pm \to K^\pm\gamma\gamma$

[1] Using $B(B^+ \to \eta_c K^+) = (1.25 \pm 0.12^{+0.10}_{-0.12}) \times 10^{-3}$ from FANG 03 and $B(\eta_c \to K\overline{K}\pi) = (5.5 \pm 1.7) \times 10^{-2}$.

$\Gamma(p\overline{p})/\Gamma_{\rm total} \times \Gamma(\gamma\gamma)/\Gamma_{\rm total}$ $\Gamma_{29}/\Gamma \times \Gamma_{36}/\Gamma$

VALUE (units 10^{-6})	EVTS	DOCUMENT ID		TECN	COMMENT
0.237±0.024 OUR FIT					
0.26 ±0.05 OUR AVERAGE Error includes scale factor of 1.4.					
0.224 $^{+0.038}_{-0.037}$ ±0.020	190	AMBROGIANI	03	E835	$\overline{p}p \to \eta_c \to \gamma\gamma$
0.336 $^{+0.080}_{-0.070}$		ARMSTRONG	95F	E760	$\overline{p}p \to \gamma\gamma$
0.68 $^{+0.42}_{-0.31}$	12	BAGLIN	87B	SPEC	$\overline{p}p \to \gamma\gamma$

Charge conjugation (C), Parity (P), Lepton family number (LF) violating modes

$\Gamma(\pi^+\pi^-)/\Gamma_{\rm total}$ Γ_{37}/Γ

VALUE (units 10^{-5})	CL%	DOCUMENT ID		TECN	COMMENT
<11	90	[1] ABLIKIM	11G	BES3	$J/\psi \to \gamma\pi^+\pi^-$
• • • We do not use the following data for averages, fits, limits, etc. • • •					
<70	90	[2] ABLIKIM	06B	BES2	$J/\psi \to \pi^+\pi^-\gamma$

[1] ABLIKIM 11G reports $[\Gamma(\eta_c(1S) \to \pi^+\pi^-)/\Gamma_{\rm total}] \times [B(J/\psi(1S) \to \gamma\eta_c(1S))] < 1.82\times10^{-6}$ which we divide by our best value $B(J/\psi(1S) \to \gamma\eta_c(1S)) = 1.7\times10^{-2}$.

[2] ABLIKIM 06B reports $[\Gamma(\eta_c(1S) \to \pi^+\pi^-)/\Gamma_{\rm total}] \times [B(J/\psi(1S) \to \gamma\eta_c(1S))] < 1.1\times10^{-5}$ which we divide by our best value $B(J/\psi(1S) \to \gamma\eta_c(1S)) = 1.7\times10^{-2}$.

$\Gamma(\pi^0\pi^0)/\Gamma_{\rm total}$ Γ_{38}/Γ

VALUE (units 10^{-5})	CL%	DOCUMENT ID		TECN	COMMENT
< 3.5	90	[1] ABLIKIM	11G	BES3	$J/\psi \to \gamma\pi^0\pi^0$
• • • We do not use the following data for averages, fits, limits, etc. • • •					
<40	90	[2] ABLIKIM	06B	BES2	$J/\psi \to \pi^0\pi^0\gamma$

[1] ABLIKIM 11G reports $[\Gamma(\eta_c(1S) \to \pi^0\pi^0)/\Gamma_{\rm total}] \times [B(J/\psi(1S) \to \gamma\eta_c(1S))] < 6.0\times10^{-7}$ which we divide by our best value $B(J/\psi(1S) \to \gamma\eta_c(1S)) = 1.7\times10^{-2}$.

[2] ABLIKIM 06B reports $[\Gamma(\eta_c(1S) \to \pi^0\pi^0)/\Gamma_{\rm total}] \times [B(J/\psi(1S) \to \gamma\eta_c(1S))] < 0.71\times10^{-5}$ which we divide by our best value $B(J/\psi(1S) \to \gamma\eta_c(1S)) = 1.7\times10^{-2}$.

$\Gamma(K^+K^-)/\Gamma_{\rm total}$ Γ_{39}/Γ

VALUE (units 10^{-5})	CL%	DOCUMENT ID		TECN	COMMENT
<60	90	[1] ABLIKIM	06B	BES2	$J/\psi \to K^+K^-\gamma$

[1] ABLIKIM 06B reports $[\Gamma(\eta_c(1S) \to K^+K^-)/\Gamma_{\rm total}] \times [B(J/\psi(1S) \to \gamma\eta_c(1S))] < 0.96\times10^{-5}$ which we divide by our best value $B(J/\psi(1S) \to \gamma\eta_c(1S)) = 1.7\times10^{-2}$.

$\Gamma(K^0_S K^0_S)/\Gamma_{\rm total}$ Γ_{40}/Γ

VALUE (units 10^{-5})	CL%	DOCUMENT ID		TECN	COMMENT
<31	90	[1] ABLIKIM	06B	BES2	$J/\psi \to K^0_S K^0_S\gamma$
• • • We do not use the following data for averages, fits, limits, etc. • • •					
<32	90	[2] UEHARA	13	BELL	$\gamma\gamma \to K^0_S K^0_S$
< 5.6	90	[3] UEHARA	13	BELL	$\gamma\gamma \to K^0_S K^0_S$

[1] ABLIKIM 06B reports $[\Gamma(\eta_c(1S) \to K^0_S K^0_S)/\Gamma_{\rm total}] \times [B(J/\psi(1S) \to \gamma\eta_c(1S))] < 0.53\times10^{-5}$ which we divide by our best value $B(J/\psi(1S) \to \gamma\eta_c(1S)) = 1.7\times10^{-2}$.

[2] Taking into account interference with the non-resonant continuum.

[3] Neglecting interference with the non-resonant continuum.

$\eta_c(1S)$ REFERENCES

ABLIKIM	13C	PR D87 012003	M. Ablikim *et al.*	(BES III Collab.)
ABLIKIM	13I	PR D87 032003	M. Ablikim *et al.*	(BES III Collab.)
UEHARA	13	PTEP 2013 123C01	S. Uehara *et al.*	(BELLE Collab.)
ABLIKIM	12B	PR D86 032008	M. Ablikim *et al.*	(BES III Collab.)
ABLIKIM	12F	PRL 108 222002	M. Ablikim *et al.*	(BES III Collab.)
ABLIKIM	12N	PR D86 092009	M. Ablikim *et al.*	(BES III Collab.)
LIU	12B	PRL 108 232001	Z.Q. Liu *et al.*	(BELLE Collab.)
ZHANG	12A	PR D86 052002	C.C. Zhang *et al.*	(BELLE Collab.)
ABLIKIM	11G	PR D84 032006	M. Ablikim *et al.*	(BES III Collab.)
DEL-AMO-SA...	11M	PR D84 012004	P. del Amo Sanchez *et al.*	(BABAR Collab.)
VINOKUROVA	11	PL B706 139	A. Vinokurova *et al.*	(BELLE Collab.)
LEES	10	PR D81 052010	J.P. Lees *et al.*	(BABAR Collab.)
MITCHELL	09	PRL 102 011801	R.E. Mitchell *et al.*	(CLEO Collab.)
ADAMS	08	PRL 101 101801	G.S. Adams *et al.*	(CLEO Collab.)
AUBERT	08AB	PR D78 012006	B. Aubert *et al.*	(BABAR Collab.)
UEHARA	08	EPJ C53 1	S. Uehara *et al.*	(BELLE Collab.)
WICHT	08	PL B662 323	J. Wicht *et al.*	(BELLE Collab.)
ABE	07	PRL 98 082001	K. Abe *et al.*	(BELLE Collab.)
ABLIKIM	06A	PL B633 19	M. Ablikim *et al.*	(BES Collab.)
ABLIKIM	06B	EPJ C45 337	M. Ablikim *et al.*	(BES Collab.)
AUBERT	06E	PRL 96 052002	B. Aubert *et al.*	(BABAR Collab.)
PDG	06	JP G33 1	W.-M. Yao *et al.*	(PDG Collab.)
WU	06	PRL 97 162003	C.-H. Wu *et al.*	(BELLE Collab.)
ABLIKIM	05L	PR D72 072005	M. Ablikim *et al.*	(BES Collab.)
KUO	05	PL B621 41	C.C. Kuo *et al.*	(BELLE Collab.)
ABE	04G	PR D70 071102	K. Abe *et al.*	(BELLE Collab.)
ABLIKIM	04M	PR D70 112008	M. Ablikim *et al.*	(BES Collab.)
ASNER	04	PRL 92 142001	D.M. Asner *et al.*	(CLEO Collab.)
AUBERT	04D	PRL 92 142002	B. Aubert *et al.*	(BABAR Collab.)
AUBERT,B	04B	PR D70 011101	B. Aubert *et al.*	(BABAR Collab.)
BAI	04	PL B578 16	J.Z. Bai *et al.*	(BES Collab.)
ABDALLAH	03J	EPJ C31 481	J. Abdallah *et al.*	(DELPHI Collab.)
AMBROGIANI	03	PL B566 45	M. Ambrogiani *et al.*	(FNAL E835 Collab.)
BAI	03	PL B555 174	J.Z. Bai *et al.*	(BES Collab.)
FANG	03	PRL 90 071801	F. Fang *et al.*	(BELLE Collab.)
HUANG	03	PRL 91 241802	H.-C. Huang *et al.*	(BELLE Collab.)
ABE,K	02	PRL 89 142001	K. Abe *et al.*	(BELLE Collab.)
BAI	00F	PR D62 072001	J.Z. Bai *et al.*	(BES Collab.)
BRANDENB...	00B	PRL 85 3095	G. Brandenburg *et al.*	(CLEO Collab.)
ACCIARRI	99T	PL B461 155	M. Acciarri *et al.*	(L3 Collab.)
BAI	99B	PR D60 072001	J.Z. Bai *et al.*	(BES Collab.)
ABREU	98O	PL B441 479	P. Abreu *et al.*	(DELPHI Collab.)
SHIRAI	98	PL B424 405	M. Shirai *et al.*	(AMY Collab.)
ARMSTRONG	95F	PR D52 4839	T.A. Armstrong *et al.*	(FNAL, FERR, GENO+)
ALBRECHT	94H	PL B338 390	H. Albrecht *et al.*	(ARGUS Collab.)
ADRIANI	93N	PL B318 575	O. Adriani *et al.*	(L3 Collab.)
BISELLO	91	NP B350 1	D. Bisello *et al.*	(DM2 Collab.)
BAI	90B	PRL 65 1309	Z. Bai *et al.*	(Mark III Collab.)
CHEN	90B	PL B243 169	W.Y. Chen *et al.*	(CLEO Collab.)
BAGLIN	89	PL B231 557	C. Baglin, S. Baird, G. Bassompierre	(R704 Collab.)
BEHREND	89	ZPHY C42 367	H.J. Behrend *et al.*	(CELLO Collab.)
BRAUNSCH...	89	ZPHY C41 533	W. Braunschweig *et al.*	(TASSO Collab.)
AIHARA	88D	PRL 60 2355	H. Aihara *et al.*	(TPC Collab.)
BAGLIN	87B	PL B187 191	C. Baglin *et al.*	(R704 Collab.)
BALTRUSAIT...	86	PR D33 629	R.M. Baltrusaitis *et al.*	(Mark III Collab.)
BERGER	86	PL 167B 120	C. Berger *et al.*	(PLUTO Collab.)
GAISER	86	PR D34 711	J. Gaiser *et al.*	(Crystal Ball Collab.)
ALTHOFF	85B	ZPHY C29 189	M. Althoff *et al.*	(TASSO Collab.)
BALTRUSAIT...	84	PRL 52 2126	R.M. Baltrusaitis *et al.*	(CIT, UCSC+) JP
BLOOM	83	ARNS 33 143	E.D. Bloom, C. Peck	(SLAC, CIT)
HIMEL	80B	PRL 45 1146	T.M. Himel *et al.*	(SLAC, LBL, UCB)
PARTRIDGE	80B	PRL 45 1150	R. Partridge *et al.*	(CIT, HARV, PRIN+)

$J/\psi(1S)$

$I^G(J^{PC}) = 0^-(1^{--})$

$J/\psi(1S)$ MASS

VALUE (MeV)	EVTS	DOCUMENT ID		TECN	COMMENT
3096.916±0.011 OUR AVERAGE					
3096.917±0.010±0.007		AULCHENKO	03	KEDR	$e^+e^- \to$ hadrons
3096.89 ±0.09	502	[1] ARTAMONOV	00	OLYA	$e^+e^- \to$ hadrons
3096.91 ±0.03 ±0.01		[2] ARMSTRONG	93B	E760	$\overline{p}p \to e^+e^-$
3096.95 ±0.1 ±0.3	193	BAGLIN	87	SPEC	$\overline{p}p \to e^+e^-$X
• • • We do not use the following data for averages, fits, limits, etc. • • •					
3097.5 ±0.3		GRIBUSHIN	96	FMPS	515 π^-Be $\to 2\mu X$
3098.4 ±2.0	38k	LEMOIGNE	82	GOLI	185 π^-Be $\to \gamma\mu^+\mu^-$A
3096.93 ±0.09	502	[3] ZHOLENTZ	80	REDE	e^+e^-
3097.0 ±1		[4] BRANDELIK	79C	DASP	e^+e^-

[1] Reanalysis of ZHOLENTZ 80 using new electron mass (COHEN 87) and radiative corrections (KURAEV 85).
[2] Mass central value and systematic error recalculated by us according to Eq. (16) in ARMSTRONG 93B, using the value for the $\psi(2S)$ mass from AULCHENKO 03.
[3] Superseded by ARTAMONOV 00.
[4] From a simultaneous fit to e^+e^-, $\mu^+\mu^-$ and hadronic channels assuming $\Gamma(e^+e^-) = \Gamma(\mu^+\mu^-)$.

$J/\psi(1S)$ WIDTH

VALUE (keV)	EVTS	DOCUMENT ID		TECN	COMMENT
92.9± 2.8 OUR AVERAGE Error includes scale factor of 1.1.					
96.1± 3.2	13k	[1] ADAMS	06A	CLEO	$e^+e^- \to \mu^+\mu^-\gamma$
84.4± 8.9		BAI	95B	BES	e^+e^-
91 ±11 ±6		[2] ARMSTRONG	93B	E760	$\overline{p}p \to e^+e^-$
$85.5^{+\ 6.1}_{-\ 5.8}$		[3] HSUEH	92	RVUE	See Υ mini-review
• • • We do not use the following data for averages, fits, limits, etc. • • •					
94.1± 2.7		[4] ANASHIN	10	KEDR	3.097 $e^+e^- \to e^+e^-$, $\mu^+\mu^-$
93.7± 3.5	7.8k	[1] AUBERT	04	BABR	$e^+e^- \to \mu^+\mu^-\gamma$

[1] Calculated by us from the reported values of $\Gamma(e^+e^-)\times B(\mu^+\mu^-)$ using $B(e^+e^-) = (5.94 \pm 0.06)\%$ and $B(\mu^+\mu^-) = (5.93 \pm 0.06)\%$.
[2] The initial-state radiation correction reevaluated by ANDREOTTI 07 in its Ref. [4].
[3] Using data from COFFMAN 92, BALDINI-CELIO 75, BOYARSKI 75, ESPOSITO 75B, BRANDELIK 79C.
[4] Assuming $\Gamma(e^+e^-) = \Gamma(\mu^+\mu^-)$ and using $\Gamma(e^+e^-)/\Gamma_{total} = (5.94 \pm 0.06)\%$.

$J/\psi(1S)$ DECAY MODES

	Mode		Fraction (Γ_i/Γ)	Scale factor/ Confidence level
Γ_1	hadrons		(87.7 ±0.5) %	
Γ_2	virtual$\gamma \to$ hadrons		(13.50 ±0.30) %	
Γ_3	ggg		(64.1 ±1.0) %	
Γ_4	γgg		(8.8 ±1.1) %	
Γ_5	e^+e^-		(5.971±0.032) %	
Γ_6	$e^+e^-\gamma$	[a]	(8.8 ±1.4) $\times 10^{-3}$	
Γ_7	$\mu^+\mu^-$		(5.961±0.033) %	
	Decays involving hadronic resonances			
Γ_8	$\rho\pi$		(1.69 ±0.15) %	S=2.4
Γ_9	$\rho^0\pi^0$		(5.6 ±0.7) $\times 10^{-3}$	
Γ_{10}	$a_2(1320)\rho$		(1.09 ±0.22) %	
Γ_{11}	$\omega\pi^+\pi^+\pi^-\pi^-$		(8.5 ±3.4) $\times 10^{-3}$	
Γ_{12}	$\omega\pi^+\pi^-\pi^0$		(4.0 ±0.7) $\times 10^{-3}$	
Γ_{13}	$\omega\pi^+\pi^-$		(8.6 ±0.7) $\times 10^{-3}$	S=1.1
Γ_{14}	$\omega f_2(1270)$		(4.3 ±0.6) $\times 10^{-3}$	
Γ_{15}	$K^*(892)^0\overline{K}^*(892)^0$		(2.3 ±0.7) $\times 10^{-4}$	
Γ_{16}	$K^*(892)^\pm K^*(892)^\mp$		(1.00 $^{+0.22}_{-0.40}$) $\times 10^{-3}$	
Γ_{17}	$K^*(892)^\pm K^*(800)^\mp$		(1.1 $^{+1.0}_{-0.6}$) $\times 10^{-3}$	
Γ_{18}	$\eta K^*(892)^0\overline{K}^*(892)^0$		(1.15 ±0.26) $\times 10^{-3}$	
Γ_{19}	$K^*(892)^0\overline{K}_2^*(1430)^0$ + c.c.		(6.0 ±0.6) $\times 10^{-3}$	
Γ_{20}	$K^*(892)^0\overline{K}_2(1770)^0$ + c.c. $\to$ $K^*(892)^0K^-\pi^+$ + c.c.		(6.9 ±0.9) $\times 10^{-4}$	
Γ_{21}	$\omega K^*(892)\overline{K}$ + c.c.		(6.1 ±0.9) $\times 10^{-3}$	
Γ_{22}	$K^+K^*(892)^-$ + c.c.		(5.12 ±0.30) $\times 10^{-3}$	
Γ_{23}	$K^+K^*(892)^-$ + c.c. $\to$ $K^+K^-\pi^0$		(1.97 ±0.20) $\times 10^{-3}$	
Γ_{24}	$K^+K^*(892)^-$ + c.c. $\to$ $K^0K^\pm\pi^\mp$ + c.c.		(3.0 ±0.4) $\times 10^{-3}$	
Γ_{25}	$K^0\overline{K}^*(892)^0$ + c.c.		(4.39 ±0.31) $\times 10^{-3}$	
Γ_{26}	$K^0\overline{K}^*(892)^0$ + c.c. $\to$ $K^0K^\pm\pi^\mp$ + c.c.		(3.2 ±0.4) $\times 10^{-3}$	
Γ_{27}	$K_1(1400)^\pm K^\mp$		(3.8 ±1.4) $\times 10^{-3}$	
Γ_{28}	$\overline{K}^*(892)^0K^+\pi^-$ + c.c.		seen	
Γ_{29}	$\omega\pi^0\pi^0$		(3.4 ±0.8) $\times 10^{-3}$	
Γ_{30}	$b_1(1235)^\pm\pi^\mp$	[b]	(3.0 ±0.5) $\times 10^{-3}$	
Γ_{31}	$\omega K^\pm K_S^0\pi^\mp$	[b]	(3.4 ±0.5) $\times 10^{-3}$	
Γ_{32}	$b_1(1235)^0\pi^0$		(2.3 ±0.6) $\times 10^{-3}$	
Γ_{33}	$\eta K^\pm K_S^0\pi^\mp$	[b]	(2.2 ±0.4) $\times 10^{-3}$	
Γ_{34}	$\phi K^*(892)\overline{K}$ + c.c.		(2.18 ±0.23) $\times 10^{-3}$	
Γ_{35}	$\omega K\overline{K}$		(1.70 ±0.32) $\times 10^{-3}$	
Γ_{36}	$\omega f_0(1710) \to \omega K\overline{K}$		(4.8 ±1.1) $\times 10^{-4}$	
Γ_{37}	$\phi 2(\pi^+\pi^-)$		(1.66 ±0.23) $\times 10^{-3}$	
Γ_{38}	$\Delta(1232)^{++}\overline{p}\pi^-$		(1.6 ±0.5) $\times 10^{-3}$	
Γ_{39}	$\omega\eta$		(1.74 ±0.20) $\times 10^{-3}$	S=1.6
Γ_{40}	$\phi K\overline{K}$		(1.83 ±0.24) $\times 10^{-3}$	S=1.5
Γ_{41}	$\phi f_0(1710) \to \phi K\overline{K}$		(3.6 ±0.6) $\times 10^{-4}$	
Γ_{42}	$\phi f_2(1270)$		(7.2 ±1.3) $\times 10^{-4}$	
Γ_{43}	$\Delta(1232)^{++}\overline{\Delta}(1232)^{--}$		(1.10 ±0.29) $\times 10^{-3}$	
Γ_{44}	$\Sigma(1385)^-\overline{\Sigma}(1385)^+$ (or c.c.)	[b]	(1.10 ±0.12) $\times 10^{-3}$	
Γ_{45}	$\phi f_2'(1525)$		(8 ±4) $\times 10^{-4}$	S=2.7
Γ_{46}	$\phi\pi^+\pi^-$		(9.4 ±0.9) $\times 10^{-4}$	S=1.2
Γ_{47}	$\phi\pi^0\pi^0$		(5.6 ±1.6) $\times 10^{-4}$	
Γ_{48}	$\phi K^\pm K_S^0\pi^\mp$	[b]	(7.2 ±0.8) $\times 10^{-4}$	
Γ_{49}	$\omega f_1(1420)$		(6.8 ±2.4) $\times 10^{-4}$	
Γ_{50}	$\phi\eta$		(7.5 ±0.8) $\times 10^{-4}$	S=1.5
Γ_{51}	$\Xi^0\overline{\Xi}^0$		(1.20 ±0.24) $\times 10^{-3}$	
Γ_{52}	$\Xi(1530)^-\overline{\Xi}^+$		(5.9 ±1.5) $\times 10^{-4}$	
Γ_{53}	$pK^-\overline{\Sigma}(1385)^0$		(5.1 ±3.2) $\times 10^{-4}$	
Γ_{54}	$\omega\pi^0$		(4.5 ±0.5) $\times 10^{-4}$	S=1.4
Γ_{55}	$\phi\eta'(958)$		(4.0 ±0.7) $\times 10^{-4}$	S=2.1
Γ_{56}	$\phi f_0(980)$		(3.2 ±0.9) $\times 10^{-4}$	S=1.9
Γ_{57}	$\phi f_0(980) \to \phi\pi^+\pi^-$		(1.8 ±0.4) $\times 10^{-4}$	
Γ_{58}	$\phi f_0(980) \to \phi\pi^0\pi^0$		(1.7 ±0.7) $\times 10^{-4}$	
Γ_{59}	$\eta\phi f_0(980) \to \eta\phi\pi^+\pi^-$		(3.2 ±1.0) $\times 10^{-4}$	
Γ_{60}	$\phi a_0(980)^0 \to \phi\eta\pi^0$		(5 ±4) $\times 10^{-6}$	
Γ_{61}	$\Xi(1530)^0\overline{\Xi}^0$		(3.2 ±1.4) $\times 10^{-4}$	
Γ_{62}	$\Sigma(1385)^-\overline{\Sigma}^+$ (or c.c.)	[b]	(3.1 ±0.5) $\times 10^{-4}$	
Γ_{63}	$\phi f_1(1285)$		(2.6 ±0.5) $\times 10^{-4}$	S=1.1
Γ_{64}	$\eta\pi^+\pi^-$		(4.0 ±1.7) $\times 10^{-4}$	
Γ_{65}	$\rho\eta$		(1.93 ±0.23) $\times 10^{-4}$	
Γ_{66}	$\omega\eta'(958)$		(1.82 ±0.21) $\times 10^{-4}$	
Γ_{67}	$\omega f_0(980)$		(1.4 ±0.5) $\times 10^{-4}$	
Γ_{68}	$\rho\eta'(958)$		(1.05 ±0.18) $\times 10^{-4}$	
Γ_{69}	$a_2(1320)^\pm\pi^\mp$	[b]	< 4.3 $\times 10^{-3}$	CL=90%
Γ_{70}	$K\overline{K}_2^*(1430)$ + c.c.		< 4.0 $\times 10^{-3}$	CL=90%
Γ_{71}	$K_1(1270)^\pm K^\mp$		< 3.0 $\times 10^{-3}$	CL=90%
Γ_{72}	$K_2^*(1430)^0\overline{K}_2^*(1430)^0$		< 2.9 $\times 10^{-3}$	CL=90%
Γ_{73}	$\phi\pi^0$		< 6.4 $\times 10^{-6}$	CL=90%
Γ_{74}	$\phi\eta(1405) \to \phi\eta\pi\pi$		< 2.5 $\times 10^{-4}$	CL=90%
Γ_{75}	$\omega f_2'(1525)$		< 2.2 $\times 10^{-4}$	CL=90%
Γ_{76}	$\omega X(1835) \to \omega p\overline{p}$		< 3.9 $\times 10^{-6}$	CL=95%
Γ_{77}	$\eta\phi(2170) \to \eta K^*(892)^0\overline{K}^*(892)^0$		< 2.52 $\times 10^{-4}$	CL=90%
Γ_{78}	$\Sigma(1385)^0\overline{\Lambda}$ + c.c.		< 8.2 $\times 10^{-6}$	CL=90%
Γ_{79}	$\Delta(1232)^+\overline{p}$		< 1 $\times 10^{-4}$	CL=90%
Γ_{80}	$\Lambda(1520)\overline{\Lambda}$ + c.c. $\to \gamma\Lambda\overline{\Lambda}$		< 4.1 $\times 10^{-6}$	CL=90%
Γ_{81}	$\Theta(1540)\overline{\Theta}(1540) \to K_S^0pK^-\overline{n}$ + c.c.		< 1.1 $\times 10^{-5}$	CL=90%
Γ_{82}	$\Theta(1540)K^-\overline{n} \to K_S^0pK^-\overline{n}$		< 2.1 $\times 10^{-5}$	CL=90%
Γ_{83}	$\Theta(1540)K_S^0\overline{p} \to K_S^0\overline{p}K^+n$		< 1.6 $\times 10^{-5}$	CL=90%
Γ_{84}	$\overline{\Theta}(1540)K^+n \to K_S^0\overline{p}K^+n$		< 5.6 $\times 10^{-5}$	CL=90%
Γ_{85}	$\overline{\Theta}(1540)K_S^0p \to K_S^0pK^-\overline{n}$		< 1.1 $\times 10^{-5}$	CL=90%
Γ_{86}	$\Sigma^0\overline{\Lambda}$		< 9 $\times 10^{-5}$	CL=90%
	Decays into stable hadrons			
Γ_{87}	$2(\pi^+\pi^-)\pi^0$		(4.1 ±0.5) %	S=2.4
Γ_{88}	$3(\pi^+\pi^-)\pi^0$		(2.9 ±0.6) %	
Γ_{89}	$\pi^+\pi^-\pi^0$		(2.11 ±0.07) %	S=1.5
Γ_{90}	$\pi^+\pi^-\pi^0K^+K^-$		(1.79 ±0.29) %	S=2.2
Γ_{91}	$4(\pi^+\pi^-)\pi^0$		(9.0 ±3.0) $\times 10^{-3}$	
Γ_{92}	$\pi^+\pi^-K^+K^-$		(6.6 ±0.5) $\times 10^{-3}$	
Γ_{93}	$\pi^+\pi^-K^+K^-\eta$		(1.84 ±0.28) $\times 10^{-3}$	
Γ_{94}	$\pi^0\pi^0K^+K^-$		(2.45 ±0.31) $\times 10^{-3}$	
Γ_{95}	$K\overline{K}\pi$		(6.1 ±1.0) $\times 10^{-3}$	
Γ_{96}	$2(\pi^+\pi^-)$		(3.57 ±0.30) $\times 10^{-3}$	
Γ_{97}	$3(\pi^+\pi^-)$		(4.3 ±0.4) $\times 10^{-3}$	

Meson Particle Listings

$J/\psi(1S)$

Γ_{98}	$2(\pi^+\pi^-\pi^0)$		(1.62	$\pm$0.21)	%	
Γ_{99}	$2(\pi^+\pi^-)\eta$		(2.29	$\pm$0.24)	$\times 10^{-3}$	
Γ_{100}	$3(\pi^+\pi^-)\eta$		(7.2	$\pm$1.5)	$\times 10^{-4}$	
Γ_{101}	$p\overline{p}$		(2.120	$\pm$0.029)	$\times 10^{-3}$	
Γ_{102}	$p\overline{p}\pi^0$		(1.19	$\pm$0.08)	$\times 10^{-3}$	S=1.1
Γ_{103}	$p\overline{p}\pi^+\pi^-$		(6.0	$\pm$0.5)	$\times 10^{-3}$	S=1.3
Γ_{104}	$p\overline{p}\pi^+\pi^-\pi^0$	[c]	(2.3	$\pm$0.9)	$\times 10^{-3}$	S=1.9
Γ_{105}	$p\overline{p}\eta$		(2.00	$\pm$0.12)	$\times 10^{-3}$	
Γ_{106}	$p\overline{p}\rho$		< 3.1		$\times 10^{-4}$	CL=90%
Γ_{107}	$p\overline{p}\omega$		(9.8	$\pm$1.0)	$\times 10^{-4}$	S=1.3
Γ_{108}	$p\overline{p}\eta'(958)$		(2.1	$\pm$0.4)	$\times 10^{-4}$	
Γ_{109}	$p\overline{p}\phi$		(4.5	$\pm$1.5)	$\times 10^{-5}$	
Γ_{110}	$n\overline{n}$		(2.09	$\pm$0.16)	$\times 10^{-3}$	
Γ_{111}	$n\overline{n}\pi^+\pi^-$		(4	$\pm$4)	$\times 10^{-3}$	
Γ_{112}	$\Sigma^+\overline{\Sigma}^-$		(1.50	$\pm$0.24)	$\times 10^{-3}$	
Γ_{113}	$\Sigma^0\overline{\Sigma}^0$		(1.29	$\pm$0.09)	$\times 10^{-3}$	
Γ_{114}	$2(\pi^+\pi^-)K^+K^-$		(4.7	$\pm$0.7)	$\times 10^{-3}$	S=1.3
Γ_{115}	$p\overline{n}\pi^-$		(2.12	$\pm$0.09)	$\times 10^{-3}$	
Γ_{116}	$nN(1440)$		seen			
Γ_{117}	$nN(1520)$		seen			
Γ_{118}	$nN(1535)$		seen			
Γ_{119}	$\Xi^-\overline{\Xi}^+$		(8.6	$\pm$1.1)	$\times 10^{-4}$	S=1.2
Γ_{120}	$\Lambda\overline{\Lambda}$		(1.61	$\pm$0.15)	$\times 10^{-3}$	S=1.9
Γ_{121}	$\Lambda\overline{\Sigma}^-\pi^+$ (or c.c.)	[b]	(8.3	$\pm$0.7)	$\times 10^{-4}$	S=1.2
Γ_{122}	$pK^-\overline{\Lambda}$		(8.9	$\pm$1.6)	$\times 10^{-4}$	
Γ_{123}	$2(K^+K^-)$		(7.6	$\pm$0.9)	$\times 10^{-4}$	
Γ_{124}	$pK^-\overline{\Sigma}^0$		(2.9	$\pm$0.8)	$\times 10^{-4}$	
Γ_{125}	K^+K^-		(2.70	$\pm$0.17)	$\times 10^{-4}$	
Γ_{126}	$K^0_S K^0_L$		(2.1	$\pm$0.4)	$\times 10^{-4}$	S=3.2
Γ_{127}	$\Lambda\overline{\Lambda}\pi^+\pi^-$		(4.3	$\pm$1.0)	$\times 10^{-3}$	
Γ_{128}	$\Lambda\overline{\Lambda}\eta$		(1.62	$\pm$0.17)	$\times 10^{-4}$	
Γ_{129}	$\Lambda\overline{\Lambda}\pi^0$		(3.8	$\pm$0.4)	$\times 10^{-5}$	
Γ_{130}	$\overline{\Lambda}nK^0_S$ + c.c.		(6.5	$\pm$1.1)	$\times 10^{-4}$	
Γ_{131}	$\pi^+\pi^-$		(1.47	$\pm$0.14)	$\times 10^{-4}$	
Γ_{132}	$\Lambda\overline{\Sigma}$ + c.c.		(2.83	$\pm$0.23)	$\times 10^{-5}$	
Γ_{133}	$K^0_S K^0_S$		< 1		$\times 10^{-6}$	CL=95%

Radiative decays

Γ_{134}	3γ		(1.16	$\pm$0.22)	$\times 10^{-5}$	
Γ_{135}	4γ		< 9		$\times 10^{-6}$	CL=90%
Γ_{136}	5γ		< 1.5		$\times 10^{-5}$	CL=90%
Γ_{137}	$\gamma\eta_c(1S)$		(1.7	$\pm$0.4)	%	S=1.6
Γ_{138}	$\gamma\eta_c(1S) \rightarrow 3\gamma$		(3.8	$^{+1.3}_{-1.0}$)	$\times 10^{-6}$	S=1.1
Γ_{139}	$\gamma\pi^+\pi^-2\pi^0$		(8.3	$\pm$3.1)	$\times 10^{-3}$	
Γ_{140}	$\gamma\eta\pi\pi$		(6.1	$\pm$1.0)	$\times 10^{-3}$	
Γ_{141}	$\gamma\eta_2(1870) \rightarrow \gamma\eta\pi^+\pi^-$		(6.2	$\pm$2.4)	$\times 10^{-4}$	
Γ_{142}	$\gamma\eta(1405/1475) \rightarrow \gamma K\overline{K}\pi$	[d]	(2.8	$\pm$0.6)	$\times 10^{-3}$	S=1.6
Γ_{143}	$\gamma\eta(1405/1475) \rightarrow \gamma\gamma\rho^0$		(7.8	$\pm$2.0)	$\times 10^{-5}$	S=1.8
Γ_{144}	$\gamma\eta(1405/1475) \rightarrow \gamma\eta\pi^+\pi^-$		(3.0	$\pm$0.5)	$\times 10^{-4}$	
Γ_{145}	$\gamma\eta(1405/1475) \rightarrow \gamma\gamma\phi$		< 8.2		$\times 10^{-5}$	CL=95%
Γ_{146}	$\gamma\rho\rho$		(4.5	$\pm$0.8)	$\times 10^{-3}$	
Γ_{147}	$\gamma\rho\omega$		< 5.4		$\times 10^{-4}$	CL=90%
Γ_{148}	$\gamma\rho\phi$		< 8.8		$\times 10^{-5}$	CL=90%
Γ_{149}	$\gamma\eta'(958)$		(5.15	$\pm$0.16)	$\times 10^{-3}$	S=1.2
Γ_{150}	$\gamma 2\pi^+2\pi^-$		(2.8	$\pm$0.5)	$\times 10^{-3}$	S=1.9
Γ_{151}	$\gamma f_2(1270) f_2(1270)$		(9.5	$\pm$1.7)	$\times 10^{-4}$	
Γ_{152}	$\gamma f_2(1270) f_2(1270)$(non resonant)		(8.2	$\pm$1.9)	$\times 10^{-4}$	
Γ_{153}	$\gamma K^+K^-\pi^+\pi^-$		(2.1	$\pm$0.6)	$\times 10^{-3}$	
Γ_{154}	$\gamma f_4(2050)$		(2.7	$\pm$0.7)	$\times 10^{-3}$	
Γ_{155}	$\gamma\omega\omega$		(1.61	$\pm$0.33)	$\times 10^{-3}$	
Γ_{156}	$\gamma\eta(1405/1475) \rightarrow \gamma\rho^0\rho^0$		(1.7	$\pm$0.4)	$\times 10^{-3}$	S=1.3
Γ_{157}	$\gamma f_2(1270)$		(1.43	$\pm$0.11)	$\times 10^{-3}$	
Γ_{158}	$\gamma f_0(1710) \rightarrow \gamma K\overline{K}$		(8.5	$^{+1.2}_{-0.9}$)	$\times 10^{-4}$	S=1.2
Γ_{159}	$\gamma f_0(1710) \rightarrow \gamma\pi\pi$		(4.0	$\pm$1.0)	$\times 10^{-4}$	
Γ_{160}	$\gamma f_0(1710) \rightarrow \gamma\omega\omega$		(3.1	$\pm$1.0)	$\times 10^{-4}$	
Γ_{161}	$\gamma\eta$		(1.104	$\pm$0.034)	$\times 10^{-3}$	
Γ_{162}	$\gamma f_1(1420) \rightarrow \gamma K\overline{K}\pi$		(7.9	$\pm$1.3)	$\times 10^{-4}$	
Γ_{163}	$\gamma f_1(1285)$		(6.1	$\pm$0.8)	$\times 10^{-4}$	
Γ_{164}	$\gamma f_1(1510) \rightarrow \gamma\eta\pi^+\pi^-$		(4.5	$\pm$1.2)	$\times 10^{-4}$	
Γ_{165}	$\gamma f'_2(1525)$		(4.5	$^{+0.7}_{-0.4}$)	$\times 10^{-4}$	
Γ_{166}	$\gamma f_2(1640) \rightarrow \gamma\omega\omega$		(2.8	$\pm$1.8)	$\times 10^{-4}$	
Γ_{167}	$\gamma f_2(1910) \rightarrow \gamma\omega\omega$		(2.0	$\pm$1.4)	$\times 10^{-4}$	
Γ_{168}	$\gamma f_0(1800) \rightarrow \gamma\omega\phi$		(2.5	$\pm$0.6)	$\times 10^{-4}$	
Γ_{169}	$\gamma f_2(1950) \rightarrow \gamma K^*(892)\overline{K}^*(892)$		(7.0	$\pm$2.2)	$\times 10^{-4}$	
Γ_{170}	$\gamma K^*(892)\overline{K}^*(892)$		(4.0	$\pm$1.3)	$\times 10^{-3}$	
Γ_{171}	$\gamma\phi\phi$		(4.0	$\pm$1.2)	$\times 10^{-4}$	S=2.1
Γ_{172}	$\gamma p\overline{p}$		(3.8	$\pm$1.0)	$\times 10^{-4}$	
Γ_{173}	$\gamma\eta(2225)$		(3.3	$\pm$0.5)	$\times 10^{-4}$	
Γ_{174}	$\gamma\eta(1760) \rightarrow \gamma\rho^0\rho^0$		(1.3	$\pm$0.9)	$\times 10^{-4}$	
Γ_{175}	$\gamma\eta(1760) \rightarrow \gamma\omega\omega$		(1.98	$\pm$0.33)	$\times 10^{-3}$	
Γ_{176}	$\gamma X(1835) \rightarrow \gamma\pi^+\pi^-\eta'$		(2.6	$\pm$0.4)	$\times 10^{-4}$	
Γ_{177}	$\gamma X(1835) \rightarrow \gamma p\overline{p}$		(7.7	$^{+1.5}_{-0.9}$)	$\times 10^{-5}$	
Γ_{178}	$\gamma X(1840) \rightarrow \gamma 3(\pi^+\pi^-)$		(2.4	$^{+0.7}_{-0.8}$)	$\times 10^{-5}$	
Γ_{179}	$\gamma(K\overline{K}\pi)$ [$J^{PC} = 0^{-+}$]		(7	$\pm$4)	$\times 10^{-4}$	S=2.1
Γ_{180}	$\gamma\pi^0$		(3.49	$^{+0.33}_{-0.30}$)	$\times 10^{-5}$	
Γ_{181}	$\gamma p\overline{p}\pi^+\pi^-$		< 7.9		$\times 10^{-4}$	CL=90%
Γ_{182}	$\gamma\Lambda\overline{\Lambda}$		< 1.3		$\times 10^{-4}$	CL=90%
Γ_{183}	$\gamma f_0(2200)$					
Γ_{184}	$\gamma f_J(2220)$		> 2.50		$\times 10^{-3}$	CL=99.9%
Γ_{185}	$\gamma f_J(2220) \rightarrow \gamma\pi\pi$		(8	$\pm$4)	$\times 10^{-5}$	
Γ_{186}	$\gamma f_J(2220) \rightarrow \gamma K\overline{K}$		< 3.6		$\times 10^{-5}$	
Γ_{187}	$\gamma f_J(2220) \rightarrow \gamma p\overline{p}$		(1.5	$\pm$0.8)	$\times 10^{-5}$	
Γ_{188}	$\gamma f_0(1500)$		(1.01	$\pm$0.32)	$\times 10^{-4}$	
Γ_{189}	$\gamma A \rightarrow \gamma$ invisible	[e]	< 6.3		$\times 10^{-6}$	CL=90%
Γ_{190}	$\gamma A^0 \rightarrow \gamma\mu^+\mu^-$	[f]	< 2.1		$\times 10^{-5}$	CL=90%

Weak decays

Γ_{191}	$D^- e^+\nu_e$ + c.c.	< 1.2	$\times 10^{-5}$	CL=90%
Γ_{192}	$\overline{D}^0 e^+ e^-$ + c.c.	< 1.1	$\times 10^{-5}$	CL=90%
Γ_{193}	$D^-_s e^+\nu_e$ + c.c.	< 3.6	$\times 10^{-5}$	CL=90%
Γ_{194}	$D^-\pi^+$ + c.c.	< 7.5	$\times 10^{-5}$	CL=90%
Γ_{195}	$\overline{D}^0\overline{K}^0$ + c.c.	< 1.7	$\times 10^{-4}$	CL=90%
Γ_{196}	$D^-_s\pi^+$ + c.c.	< 1.3	$\times 10^{-4}$	CL=90%

Charge conjugation (C), Parity (P), Lepton Family number (LF) violating modes

Γ_{197}	$\gamma\gamma$	C	< 5	$\times 10^{-6}$	CL=90%
Γ_{198}	$e^\pm\mu^\mp$	LF	< 1.6	$\times 10^{-7}$	CL=90%
Γ_{199}	$e^\pm\tau^\mp$	LF	< 8.3	$\times 10^{-6}$	CL=90%
Γ_{200}	$\mu^\pm\tau^\mp$	LF	< 2.0	$\times 10^{-6}$	CL=90%

Other decays

Γ_{201}	invisible	< 7	$\times 10^{-4}$	CL=90%

[a] For $E_\gamma > 100$ MeV.

[b] The value is for the sum of the charge states or particle/antiparticle states indicated.

[c] Includes $p\overline{p}\pi^+\pi^-\gamma$ and excludes $p\overline{p}\eta$, $p\overline{p}\omega$, $p\overline{p}\eta'$.

[d] See the "Note on the $\eta(1405)$" in the $\eta(1405)$ Particle Listings.

[e] For a narrow state A with mass less than 960 MeV.

[f] For a narrow scalar or pseudoscalar A^0 with mass 0.21–3.0 GeV.

$J/\psi(1S)$ PARTIAL WIDTHS

Γ(hadrons) Γ_1

VALUE (keV)	DOCUMENT ID		TECN	COMMENT
• • • We do not use the following data for averages, fits, limits, etc. • • •				
74.1 $\pm$ 8.1	BAI	95B	BES	e^+e^-
59 $\pm$24	BALDINI-...	75	FRAG	e^+e^-
59 $\pm$14	BOYARSKI	75	MRK1	e^+e^-
50 $\pm$25	ESPOSITO	75B	FRAM	e^+e^-

$\Gamma(e^+e^-)$ Γ_5

VALUE (keV)	EVTS	DOCUMENT ID		TECN	COMMENT
5.55 $\pm$ 0.14 $\pm$ 0.02 OUR EVALUATION					
• • • We do not use the following data for averages, fits, limits, etc. • • •					
5.71 $\pm$ 0.16	13k	[1] ADAMS	06A	CLEO	$e^+e^- \rightarrow \mu^+\mu^-\gamma$
5.57 $\pm$ 0.19	7.8k	[1] AUBERT	04	BABR	$e^+e^- \rightarrow \mu^+\mu^-\gamma$
5.14 $\pm$ 0.39		BAI	95B	BES	e^+e^-
$5.36^{+0.29}_{-0.28}$		[2] HSUEH	92	RVUE	See Υ mini-review
4.72 $\pm$ 0.35		ALEXANDER	89	RVUE	See Υ mini-review
4.4 $\pm$0.6		[2] BRANDELIK	79C	DASP	e^+e^-
4.6 $\pm$0.8		[3] BALDINI-...	75	FRAG	e^+e^-
4.8 $\pm$0.6		BOYARSKI	75	MRK1	e^+e^-
4.6 $\pm$1.0		ESPOSITO	75B	FRAM	e^+e^-

[1] Calculated by us from the reported values of $\Gamma(e^+e^-)\times B(\mu^+\mu^-)$ using $B(\mu^+\mu^-) = (5.93 \pm 0.06)\%$.
[2] From a simultaneous fit to e^+e^-, $\mu^+\mu^-$, and hadronic channels assuming $\Gamma(e^+e^-) = \Gamma(\mu^+\mu^-)$.
[3] Assuming equal partial widths for e^+e^- and $\mu^+\mu^-$.

$\Gamma(\mu^+\mu^-)$ Γ_7

VALUE (keV)	DOCUMENT ID		TECN	COMMENT
• • • We do not use the following data for averages, fits, limits, etc. • • •				
5.13±0.52	BAI	95B	BES	e^+e^-
4.8 ±0.6	BOYARSKI	75	MRK1	e^+e^-
5 ±1	ESPOSITO	75B	FRAM	e^+e^-

$\Gamma(\gamma\gamma)$ Γ_{197}

VALUE (eV)	CL%	DOCUMENT ID		TECN	COMMENT
<5.4	90	BRANDELIK	79C	DASP	e^+e^-

$J/\psi(1S)$ $\Gamma(i)\Gamma(e^+e^-)/\Gamma(\text{total})$

This combination of a partial width with the partial width into e^+e^- and with the total width is obtained from the integrated cross section into channel$_i$ in the e^+e^- annihilation.

$\Gamma(\text{hadrons}) \times \Gamma(e^+e^-)/\Gamma_{\text{total}}$ $\Gamma_1\Gamma_5/\Gamma$

VALUE (keV)	DOCUMENT ID		TECN	COMMENT
• • • We do not use the following data for averages, fits, limits, etc. • • •				
4 ±0.8	[1] BALDINI-...	75	FRAG	e^+e^-
3.9±0.8	[1] ESPOSITO	75B	FRAM	e^+e^-

[1] Data redundant with branching ratios or partial widths above.

$\Gamma(e^+e^-) \times \Gamma(e^+e^-)/\Gamma_{\text{total}}$ $\Gamma_5\Gamma_5/\Gamma$

VALUE (eV)	DOCUMENT ID		TECN	COMMENT
332.3± 6.4±4.8	ANASHIN	10	KEDR	3.097 $e^+e^- \to e^+e^-$
• • • We do not use the following data for averages, fits, limits, etc. • • •				
350 ± 20	BRANDELIK	79C	DASP	e^+e^-
320 ± 70	[1] BALDINI-...	75	FRAG	e^+e^-
340 ± 90	[1] ESPOSITO	75B	FRAM	e^+e^-
360 ±100	[1] FORD	75	SPEC	e^+e^-

[1] Data redundant with branching ratios or partial widths above.

$\Gamma(\mu^+\mu^-) \times \Gamma(e^+e^-)/\Gamma_{\text{total}}$ $\Gamma_7\Gamma_5/\Gamma$

VALUE (eV)	EVTS	DOCUMENT ID		TECN	COMMENT
334 ± 5 OUR AVERAGE					
331.8± 5.2±6.3		ANASHIN	10	KEDR	3.097 $e^+e^- \to \mu^+\mu^-$
338.4± 5.8±7.1	13k	ADAMS	06A	CLEO	$e^+e^- \to \mu^+\mu^-\gamma$
330.1± 7.7±7.3	7.8k	AUBERT	04	BABR	$e^+e^- \to \mu^+\mu^-\gamma$
• • • We do not use the following data for averages, fits, limits, etc. • • •					
510 ±90		DASP	75	DASP	e^+e^-
380 ±50		[1] ESPOSITO	75B	FRAM	e^+e^-

[1] Data redundant with branching ratios or partial widths above.

$\Gamma(\omega\pi^+\pi^-\pi^0) \times \Gamma(e^+e^-)/\Gamma_{\text{total}}$ $\Gamma_{12}\Gamma_5/\Gamma$

VALUE (10^{-2} keV)	EVTS	DOCUMENT ID		TECN	COMMENT
2.2±0.3±0.2	170	AUBERT	06D	BABR	10.6 $e^+e^- \to \omega\pi^+\pi^-\pi^0\gamma$

$\Gamma(\omega\pi^+\pi^-) \times \Gamma(e^+e^-)/\Gamma_{\text{total}}$ $\Gamma_{13}\Gamma_5/\Gamma$

VALUE (eV)	EVTS	DOCUMENT ID		TECN	COMMENT
53.6±5.0±0.4	788	[1] AUBERT	07AU	BABR	10.6 $e^+e^- \to \omega\pi^+\pi^-\gamma$

[1] AUBERT 07AU reports $[\Gamma(J/\psi(1S) \to \omega\pi^+\pi^-) \times \Gamma(J/\psi(1S) \to e^+e^-)/\Gamma_{\text{total}}] \times [B(\omega(782) \to \pi^+\pi^-\pi^0)] = 47.8 \pm 3.1 \pm 3.2$ eV which we divide by our best value $B(\omega(782) \to \pi^+\pi^-\pi^0) = (89.2 \pm 0.7) \times 10^{-2}$. Our first error is their experiment's error and our second error is the systematic error from using our best value.

$\Gamma(K^*(892)^0\overline{K}_2^*(1430)^0 + \text{c.c.}) \times \Gamma(e^+e^-)/\Gamma_{\text{total}}$ $\Gamma_{19}\Gamma_5/\Gamma$

VALUE (eV)	EVTS	DOCUMENT ID		TECN	COMMENT
33±4±1	317 ± 23	[1,2] AUBERT	07AK	BABR	10.6 $e^+e^- \to \pi^+\pi^-K^+K^-\gamma$

[1] Dividing by 2/3 to take into account that $B(K^{*0} \to K^+\pi^-) = 2/3$.
[2] AUBERT 07AK reports $[\Gamma(J/\psi(1S) \to K^*(892)^0\overline{K}_2^*(1430)^0 + \text{c.c.}) \times \Gamma(J/\psi(1S) \to e^+e^-)/\Gamma_{\text{total}}] \times [B(K_2^*(1430) \to K\pi)] = 16.4 \pm 1.1 \pm 1.4$ eV which we divide by our best value $B(K_2^*(1430) \to K\pi) = (49.9 \pm 1.2) \times 10^{-2}$. Our first error is their experiment's error and our second error is the systematic error from using our best value.

$\Gamma(K^*(892)^0\overline{K}_2(1770)^0 + \text{c.c.} \to K^*(892)^0K^-\pi^+ + \text{c.c.}) \times \Gamma(e^+e^-)/\Gamma_{\text{total}}$ $\Gamma_{20}\Gamma_5/\Gamma$

VALUE (eV)	EVTS	DOCUMENT ID		TECN	COMMENT
3.8±0.4±0.3	110 ± 14	[1] AUBERT	07AK	BABR	10.6 $e^+e^- \to \pi^+\pi^-K^+K^-\gamma$

[1] Dividing by 2/3 to take into account that $B(K^{*0} \to K^+\pi^-) = 2/3$.

$\Gamma(K^+K^*(892)^- + \text{c.c.}) \times \Gamma(e^+e^-)/\Gamma_{\text{total}}$ $\Gamma_{22}\Gamma_5/\Gamma$

VALUE (eV)	DOCUMENT ID		TECN	COMMENT
29.0±1.7±1.3	AUBERT	08S	BABR	10.6 $e^+e^- \to K^+K^*(892)^-\gamma$

$\Gamma(K^+K^*(892)^- + \text{c.c.} \to K^+K^-\pi^0) \times \Gamma(e^+e^-)/\Gamma_{\text{total}}$ $\Gamma_{23}\Gamma_5/\Gamma$

VALUE (eV)	EVTS	DOCUMENT ID		TECN	COMMENT
10.96±0.85±0.70	155	AUBERT	08S	BABR	10.6 $e^+e^- \to K^+K^-\pi^0\gamma$

$\Gamma(K^+K^*(892)^- + \text{c.c.} \to K^0K^\pm\pi^\mp + \text{c.c.}) \times \Gamma(e^+e^-)/\Gamma_{\text{total}}$ $\Gamma_{24}\Gamma_5/\Gamma$

VALUE (eV)	EVTS	DOCUMENT ID		TECN	COMMENT
16.76±1.70±1.00	89	AUBERT	08S	BABR	10.6 $e^+e^- \to K_S^0K^\pm\pi^\mp\gamma$

$\Gamma(K^0\overline{K}^*(892)^0 + \text{c.c.}) \times \Gamma(e^+e^-)/\Gamma_{\text{total}}$ $\Gamma_{25}\Gamma_5/\Gamma$

VALUE (eV)	DOCUMENT ID		TECN	COMMENT
26.6±2.5±1.5	AUBERT	08S	BABR	10.6 $e^+e^- \to K^0\overline{K}^*(892)^0\gamma$

$\Gamma(K^0\overline{K}^*(892)^0 + \text{c.c.} \to K^0K^\pm\pi^\mp + \text{c.c.}) \times \Gamma(e^+e^-)/\Gamma_{\text{total}}$ $\Gamma_{26}\Gamma_5/\Gamma$

VALUE (eV)	EVTS	DOCUMENT ID		TECN	COMMENT
17.70±1.70±1.00	94	AUBERT	08S	BABR	10.6 $e^+e^- \to K_S^0K^\pm\pi^\mp\gamma$

$\Gamma(\omega K\overline{K}) \times \Gamma(e^+e^-)/\Gamma_{\text{total}}$ $\Gamma_{35}\Gamma_5/\Gamma$

VALUE (eV)	EVTS	DOCUMENT ID		TECN	COMMENT
3.70±1.98±0.03	24	[1] AUBERT	07AU	BABR	10.6 $e^+e^- \to \omega K^+K^-\gamma$

[1] AUBERT 07AU reports $[\Gamma(J/\psi(1S) \to \omega K\overline{K}) \times \Gamma(J/\psi(1S) \to e^+e^-)/\Gamma_{\text{total}}] \times [B(\omega(782) \to \pi^+\pi^-\pi^0)] = 3.3 \pm 1.3 \pm 1.2$ eV which we divide by our best value $B(\omega(782) \to \pi^+\pi^-\pi^0) = (89.2 \pm 0.7) \times 10^{-2}$. Our first error is their experiment's error and our second error is the systematic error from using our best value.

$\Gamma(\phi 2(\pi^+\pi^-)) \times \Gamma(e^+e^-)/\Gamma_{\text{total}}$ $\Gamma_{37}\Gamma_5/\Gamma$

VALUE (10^{-2} keV)	EVTS	DOCUMENT ID		TECN	COMMENT
0.96±0.19±0.01	35	[1] AUBERT	06D	BABR	10.6 $e^+e^- \to \phi 2(\pi^+\pi^-)\gamma$

[1] AUBERT 06D reports $[\Gamma(J/\psi(1S) \to \phi 2(\pi^+\pi^-)) \times \Gamma(J/\psi(1S) \to e^+e^-)/\Gamma_{\text{total}}] \times [B(\phi(1020) \to K^+K^-)] = (0.47 \pm 0.09 \pm 0.03) \times 10^{-2}$ keV which we divide by our best value $B(\phi(1020) \to K^+K^-) = (48.9 \pm 0.5) \times 10^{-2}$. Our first error is their experiment's error and our second error is the systematic error from using our best value.

$\Gamma(\phi\pi^+\pi^-) \times \Gamma(e^+e^-)/\Gamma_{\text{total}}$ $\Gamma_{46}\Gamma_5/\Gamma$

VALUE (eV)	EVTS	DOCUMENT ID		TECN	COMMENT
4.8 ±0.4 OUR AVERAGE					
4.52±0.48±0.04	254 ± 23	[1] SHEN	09	BELL	10.6 $e^+e^- \to K^+K^-\pi^+\pi^-\gamma$
5.33±0.71±0.05	103	[2] AUBERT,BE	06D	BABR	10.6 $e^+e^- \to K^+K^-\pi^+\pi^-\gamma$

[1] SHEN 09 reports $4.50 \pm 0.41 \pm 0.26$ eV from a measurement of $[\Gamma(J/\psi(1S) \to \phi\pi^+\pi^-) \times \Gamma(J/\psi(1S) \to e^+e^-)/\Gamma_{\text{total}}] \times [B(\phi(1020) \to K^+K^-)]$ assuming $B(\phi(1020) \to K^+K^-) = (49.2 \pm 0.6) \times 10^{-2}$, which we rescale to our best value $B(\phi(1020) \to K^+K^-) = (48.9 \pm 0.5) \times 10^{-2}$. Our first error is their experiment's error and our second error is the systematic error from using our best value.
[2] AUBERT,BE 06D reports $[\Gamma(J/\psi(1S) \to \phi\pi^+\pi^-) \times \Gamma(J/\psi(1S) \to e^+e^-)/\Gamma_{\text{total}}] \times [B(\phi(1020) \to K^+K^-)] = 2.61 \pm 0.30 \pm 0.18$ eV which we divide by our best value $B(\phi(1020) \to K^+K^-) = (48.9 \pm 0.5) \times 10^{-2}$. Our first error is their experiment's error and our second error is the systematic error from using our best value.

$\Gamma(\phi\pi^0\pi^0) \times \Gamma(e^+e^-)/\Gamma_{\text{total}}$ $\Gamma_{47}\Gamma_5/\Gamma$

VALUE (eV)	EVTS	DOCUMENT ID		TECN	COMMENT
3.15±0.88±0.03	23	[1] AUBERT,BE	06D	BABR	10.6 $e^+e^- \to K^+K^-\pi^0\pi^0\gamma$

[1] AUBERT,BE 06D reports $[\Gamma(J/\psi(1S) \to \phi\pi^0\pi^0) \times \Gamma(J/\psi(1S) \to e^+e^-)/\Gamma_{\text{total}}] \times [B(\phi(1020) \to K^+K^-)] = 1.54 \pm 0.40 \pm 0.16$ eV which we divide by our best value $B(\phi(1020) \to K^+K^-) = (48.9 \pm 0.5) \times 10^{-2}$. Our first error is their experiment's error and our second error is the systematic error from using our best value.

$\Gamma(\phi\eta) \times \Gamma(e^+e^-)/\Gamma_{\text{total}}$ $\Gamma_{50}\Gamma_5/\Gamma$

VALUE (eV)	EVTS	DOCUMENT ID		TECN	COMMENT
6.1±2.7±0.4	6	[1] AUBERT	07AU	BABR	10.6 $e^+e^- \to \phi\eta\gamma$

[1] AUBERT 07AU quotes $\Gamma_{ee}^{J/\psi} \cdot B(J/\psi \to \phi\eta) \cdot B(\phi \to K^+K^-) \cdot B(\eta \to 3\pi) = 0.84 \pm 0.37 \pm 0.05$ eV.

$\Gamma(\phi f_0(980) \to \phi\pi^+\pi^-) \times \Gamma(e^+e^-)/\Gamma_{\text{total}}$ $\Gamma_{57}\Gamma_5/\Gamma$

VALUE (eV)	EVTS	DOCUMENT ID		TECN	COMMENT
1.21±0.23 OUR AVERAGE		Error includes scale factor of 1.2.			
1.48±0.27±0.09	60±11	[1] SHEN	09	BELL	10.6 $e^+e^- \to K^+K^-\pi^+\pi^-\gamma$
1.02±0.24±0.01	20 ± 5	[2] AUBERT	07AK	BABR	10.6 $e^+e^- \to \pi^+\pi^-K^+K^-\gamma$

[1] Multiplied by 2/3 to take into account the $\phi\pi^+\pi^-$ mode only. Using $B(\phi \to K^+K^-) = (49.2 \pm 0.6)\%$.
[2] AUBERT 07AK reports $[\Gamma(J/\psi(1S) \to \phi f_0(980) \to \phi\pi^+\pi^-) \times \Gamma(J/\psi(1S) \to e^+e^-)/\Gamma_{\text{total}}] \times [B(\phi(1020) \to K^+K^-)] = 0.50 \pm 0.11 \pm 0.04$ eV which we divide by our best value $B(\phi(1020) \to K^+K^-) = (48.9 \pm 0.5) \times 10^{-2}$. Our first error is their experiment's error and our second error is the systematic error from using our best value.

$\Gamma(\phi f_0(980) \to \phi\pi^0\pi^0) \times \Gamma(e^+e^-)/\Gamma_{\text{total}}$ $\Gamma_{58}\Gamma_5/\Gamma$

VALUE (eV)	EVTS	DOCUMENT ID		TECN	COMMENT
0.96±0.40±0.01	7.0 ± 2.8	[1] AUBERT	07AK	BABR	10.6 $e^+e^- \to \pi^0\pi^0K^+K^-\gamma$

[1] AUBERT 07AK reports $[\Gamma(J/\psi(1S) \to \phi f_0(980) \to \phi\pi^0\pi^0) \times \Gamma(J/\psi(1S) \to e^+e^-)/\Gamma_{\text{total}}] \times [B(\phi(1020) \to K^+K^-)] = 0.47 \pm 0.19 \pm 0.05$ eV which we divide by our best value $B(\phi(1020) \to K^+K^-) = (48.9 \pm 0.5) \times 10^{-2}$. Our first error is their experiment's error and our second error is the systematic error from using our best value.

Meson Particle Listings

$J/\psi(1S)$

$\Gamma(\eta\pi^+\pi^-) \times \Gamma(e^+e^-)/\Gamma_{total}$ $\Gamma_{64}\Gamma_5/\Gamma$

VALUE (eV)	EVTS	DOCUMENT ID		TECN	COMMENT
2.23±0.97±0.03	9	[1] AUBERT	07AU	BABR	10.6 $e^+e^- \to \eta\pi^+\pi^-\gamma$

[1] AUBERT 07AU reports $[\Gamma(J/\psi(1S) \to \eta\pi^+\pi^-) \times \Gamma(J/\psi(1S) \to e^+e^-)/\Gamma_{total}] \times [B(\eta \to \pi^+\pi^-\pi^0)] = 0.51 \pm 0.22 \pm 0.03$ eV which we divide by our best value $B(\eta \to \pi^+\pi^-\pi^0) = (22.92 \pm 0.28) \times 10^{-2}$. Our first error is their experiment's error and our second error is the systematic error from using our best value.

$\Gamma(K^*(892)^0\overline{K}^*(892)^0) \times \Gamma(e^+e^-)/\Gamma_{total}$ $\Gamma_{15}\Gamma_5/\Gamma$

VALUE (eV)	EVTS	DOCUMENT ID		TECN	COMMENT
1.28±0.40±0.11	25 ± 8	[1] AUBERT	07AK	BABR	10.6 $e^+e^- \to \pi^+\pi^- K^+K^-\gamma$

[1] Dividing by $(2/3)^2$ to take twice into account that $B(K^{*0} \to K^+\pi^-) = 2/3$.

$\Gamma(\phi f_2(1270)) \times \Gamma(e^+e^-)/\Gamma_{total}$ $\Gamma_{42}\Gamma_5/\Gamma$

VALUE (eV)	EVTS	DOCUMENT ID		TECN	COMMENT
4.0±0.7±0.1	44 ± 7	[1,2] AUBERT	07AK	BABR	10.6 $e^+e^- \to \pi^+\pi^- K^+K^-\gamma$

[1] Using $B(\phi \to (K+K)^-) = (49.3 \pm 0.6)\%$.

[2] AUBERT 07AK reports $[\Gamma(J/\psi(1S) \to \phi f_2(1270)) \times \Gamma(J/\psi(1S) \to e^+e^-)/\Gamma_{total}] \times [B(f_2(1270) \to \pi\pi)] = 3.41 \pm 0.55 \pm 0.28$ eV which we divide by our best value $B(f_2(1270) \to \pi\pi) = (84.8^{+2.4}_{-1.2}) \times 10^{-2}$. Our first error is their experiment's error and our second error is the systematic error from using our best value.

$\Gamma(2(\pi^+\pi^-)\pi^0) \times \Gamma(e^+e^-)/\Gamma_{total}$ $\Gamma_{87}\Gamma_5/\Gamma$

VALUE (eV)	EVTS	DOCUMENT ID		TECN	COMMENT
303±5±18	4990	AUBERT	07AU	BABR	10.6 $e^+e^- \to 2(\pi^+\pi^-)\pi^0\gamma$

$\Gamma(\pi^+\pi^-\pi^0) \times \Gamma(e^+e^-)/\Gamma_{total}$ $\Gamma_{89}\Gamma_5/\Gamma$

VALUE (keV)	DOCUMENT ID		TECN	COMMENT
0.122±0.005±0.008	AUBERT,B	04N	BABR	10.6 $e^+e^- \to \pi^+\pi^-\pi^0\gamma$

$\Gamma(\pi^+\pi^-\pi^0 K^+K^-) \times \Gamma(e^+e^-)/\Gamma_{total}$ $\Gamma_{90}\Gamma_5/\Gamma$

VALUE (eV)	EVTS	DOCUMENT ID		TECN	COMMENT
107.0±4.3±6.4	768	AUBERT	07AU	BABR	10.6 $e^+e^- \to K^+K^-\pi^+\pi^-\pi^0\gamma$

$\Gamma(\pi^+\pi^- K^+K^-) \times \Gamma(e^+e^-)/\Gamma_{total}$ $\Gamma_{92}\Gamma_5/\Gamma$

VALUE (eV)	EVTS	DOCUMENT ID		TECN	COMMENT
36.3±1.3±2.1	1586 ± 58	AUBERT	07AK	BABR	10.6 $e^+e^- \to \pi^+\pi^- K^+K^-\gamma$
• • • We do not use the following data for averages, fits, limits, etc. • • •					
33.6±2.7±2.7	233	[1] AUBERT	05D	BABR	10.6 $e^+e^- \to K^+K^-\pi^+\pi^-\gamma$

[1] Superseded by AUBERT 07AK.

$\Gamma(\pi^+\pi^- K^+K^-\eta) \times \Gamma(e^+e^-)/\Gamma_{total}$ $\Gamma_{93}\Gamma_5/\Gamma$

VALUE (eV)	EVTS	DOCUMENT ID		TECN	COMMENT
25.9±3.9±0.1	73	[1] AUBERT	07AU	BABR	10.6 $e^+e^- \to K^+K^-\pi^+\pi^-\eta\gamma$

[1] AUBERT 07AU reports $[\Gamma(J/\psi(1S) \to \pi^+\pi^- K^+K^-\eta) \times \Gamma(J/\psi(1S) \to e^+e^-)/\Gamma_{total}] \times [B(\eta \to 2\gamma)] = 10.2 \pm 1.3 \pm 0.8$ eV which we divide by our best value $B(\eta \to 2\gamma) = (39.41 \pm 0.20) \times 10^{-2}$. Our first error is their experiment's error and our second error is the systematic error from using our best value.

$\Gamma(\pi^0\pi^0 K^+K^-) \times \Gamma(e^+e^-)/\Gamma_{total}$ $\Gamma_{94}\Gamma_5/\Gamma$

VALUE (eV)	EVTS	DOCUMENT ID		TECN	COMMENT
13.6±1.1±1.3	203 ± 16	AUBERT	07AK	BABR	10.6 $e^+e^- \to \pi^0\pi^0 K^+K^-\gamma$

$\Gamma(2(\pi^+\pi^-)) \times \Gamma(e^+e^-)/\Gamma_{total}$ $\Gamma_{96}\Gamma_5/\Gamma$

VALUE (eV)	EVTS	DOCUMENT ID		TECN	COMMENT
20.4±0.9±0.4		LEES	12E	BABR	10.6 $e^+e^- \to 2\pi^+2\pi^-\gamma$
• • • We do not use the following data for averages, fits, limits, etc. • • •					
19.5±1.4±1.3	270	[1] AUBERT	05D	BABR	10.6 $e^+e^- \to 2(\pi^+\pi^-)\gamma$

[1] Superseded by LEES 12E.

$\Gamma(3(\pi^+\pi^-)) \times \Gamma(e^+e^-)/\Gamma_{total}$ $\Gamma_{97}\Gamma_5/\Gamma$

VALUE (10^{-2} keV)	EVTS	DOCUMENT ID		TECN	COMMENT
2.37±0.16±0.14	496	AUBERT	06D	BABR	10.6 $e^+e^- \to 3(\pi^+\pi^-)\gamma$

$\Gamma(2(\pi^+\pi^-\pi^0)) \times \Gamma(e^+e^-)/\Gamma_{total}$ $\Gamma_{98}\Gamma_5/\Gamma$

VALUE (10^{-2} keV)	EVTS	DOCUMENT ID		TECN	COMMENT
8.9±0.5±1.0	761	AUBERT	06D	BABR	10.6 $e^+e^- \to 2(\pi^+\pi^-\pi^0)\gamma$

$\Gamma(2(\pi^+\pi^-)\eta) \times \Gamma(e^+e^-)/\Gamma_{total}$ $\Gamma_{99}\Gamma_5/\Gamma$

VALUE (eV)	EVTS	DOCUMENT ID		TECN	COMMENT
13.1±2.4±0.1	85	[1] AUBERT	07AU	BABR	10.6 $e^+e^- \to 2(\pi^+\pi^-)\eta\gamma$

[1] AUBERT 07AU reports $[\Gamma(J/\psi(1S) \to 2(\pi^+\pi^-)\eta) \times \Gamma(J/\psi(1S) \to e^+e^-)/\Gamma_{total}] \times [B(\eta \to 2\gamma)] = 5.16 \pm 0.85 \pm 0.39$ eV which we divide by our best value $B(\eta \to 2\gamma) = (39.41 \pm 0.20) \times 10^{-2}$. Our first error is their experiment's error and our second error is the systematic error from using our best value.

$\Gamma(p\overline{p}) \times \Gamma(e^+e^-)/\Gamma_{total}$ $\Gamma_{101}\Gamma_5/\Gamma$

VALUE (eV)	EVTS	DOCUMENT ID		TECN	COMMENT
11.9±0.5 OUR AVERAGE		Error includes scale factor of 1.4. See the ideogram below.			
11.3±0.4±0.3	821	LEES	13O	BABR	$e^+e^- \to p\overline{p}\gamma$
12.9±0.4±0.4	918	LEES	13Y	BABR	$e^+e^- \to p\overline{p}\gamma$
12.0±0.6±0.5	438	AUBERT	06B		$e^+e^- \to p\overline{p}\gamma$
9.7±1.7		[1] ARMSTRONG	93B	E760	$\overline{p}p \to e^+e^-$

[1] Using $\Gamma_{total} = 85.5^{+6.1}_{-5.8}$ MeV.

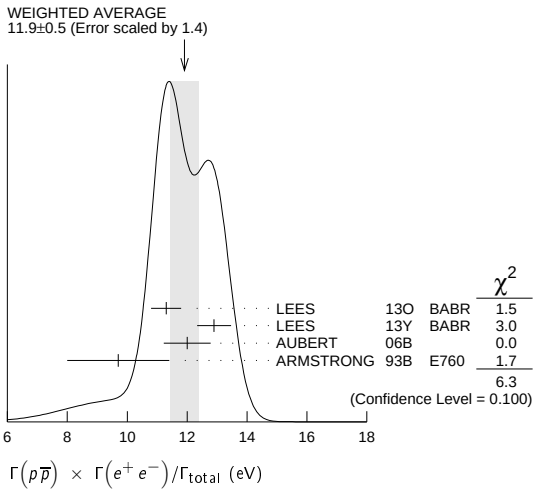

$\Gamma(\Sigma^0\overline{\Sigma}^0) \times \Gamma(e^+e^-)/\Gamma_{total}$ $\Gamma_{113}\Gamma_5/\Gamma$

VALUE (eV)	DOCUMENT ID		TECN	COMMENT
6.4±1.2±0.6	AUBERT	07BD	BABR	10.6 $e^+e^- \to \Sigma^0\overline{\Sigma}^0\gamma$

$\Gamma(2(\pi^+\pi^-)K^+K^-) \times \Gamma(e^+e^-)/\Gamma_{total}$ $\Gamma_{114}\Gamma_5/\Gamma$

VALUE (10^{-2} keV)	EVTS	DOCUMENT ID		TECN	COMMENT
2.75±0.23±0.17	205	AUBERT	06D	BABR	10.6 $e^+e^- \to K^+K^-2(\pi^+\pi^-)\gamma$

$\Gamma(\Lambda\overline{\Lambda}) \times \Gamma(e^+e^-)/\Gamma_{total}$ $\Gamma_{120}\Gamma_5/\Gamma$

VALUE (eV)	DOCUMENT ID		TECN	COMMENT
10.7±0.9±0.7	AUBERT	07BD	BABR	10.6 $e^+e^- \to \Lambda\overline{\Lambda}\gamma$

$\Gamma(2(K^+K^-)) \times \Gamma(e^+e^-)/\Gamma_{total}$ $\Gamma_{123}\Gamma_5/\Gamma$

VALUE (eV)	EVTS	DOCUMENT ID		TECN	COMMENT
4.11±0.39±0.30	156 ± 15	AUBERT	07AK	BABR	10.6 $e^+e^- \to 2(K^+K^-)\gamma$
• • • We do not use the following data for averages, fits, limits, etc. • • •					
4.0 ±0.7 ±0.6	38	[1] AUBERT	05D	BABR	10.6 $e^+e^- \to 2(K^+K^-)\gamma$

[1] Superseded by AUBERT 07AK.

$\Gamma(K^+K^-) \times \Gamma(e^+e^-)/\Gamma_{total}$ $\Gamma_{125}\Gamma_5/\Gamma$

VALUE (eV)	EVTS	DOCUMENT ID		TECN	COMMENT
1.42±0.23±0.08	51	LEES	13Q	BABR	$e^+e^- \to K^+K^-\gamma$

$J/\psi(1S)$ BRANCHING RATIOS

For the first four branching ratios, see also the partial widths, and (partial widths) $\times \Gamma(e^+e^-)/\Gamma_{total}$ above.

$\Gamma(\text{hadrons})/\Gamma_{total}$ Γ_1/Γ

VALUE	DOCUMENT ID		TECN	COMMENT
0.877±0.005 OUR AVERAGE				
0.878±0.005	BAI	95B	BES	e^+e^-
0.86 ±0.02	BOYARSKI	75	MRK1	e^+e^-

$\Gamma(\text{virtual}\gamma \to \text{hadrons})/\Gamma_{total}$ Γ_2/Γ

VALUE	DOCUMENT ID		TECN	COMMENT
0.135±0.003	[1,2] SETH	04	RVUE	e^+e^-
• • • We do not use the following data for averages, fits, limits, etc. • • •				
0.17 ±0.02	[1] BOYARSKI	75	MRK1	e^+e^-

[1] Included in $\Gamma(\text{hadrons})/\Gamma_{total}$.

[2] Using $B(J/\psi \to \ell^+\ell^-) = (5.90 \pm 0.09)\%$ from RPP-2002 and $R = 2.28 \pm 0.04$ determined by a fit to data from BAI 00 and BAI 02C.

$\Gamma(ggg)/\Gamma_{total}$ Γ_3/Γ

VALUE (units 10^{-2})	EVTS	DOCUMENT ID		TECN	COMMENT
64.1±1.0	6 M	[1] BESSON	08	CLEO	$\psi(2S) \to \pi^+\pi^-$ + hadrons

[1] Calculated using the value $\Gamma(\gamma gg)/\Gamma(ggg) = 0.137 \pm 0.001 \pm 0.016 \pm 0.004$ from BESSON 08 and the PDG 08 values of $B(\ell^+\ell^-)$, B(virtual $\gamma \to$ hadrons), and $B(\gamma\eta_c)$. The statistical error is negligible and the systematic error is partially correlated with that of $\Gamma(\gamma gg)/\Gamma_{total}$ measurement of BESSON 08.

$\Gamma(\gamma gg)/\Gamma_{total}$ Γ_4/Γ

VALUE (units 10^{-2})	EVTS	DOCUMENT ID		TECN	COMMENT
8.79±1.05	200 k	[1] BESSON	08	CLEO	$\psi(2S) \to \pi^+\pi^-\gamma$ + hadrons

[1] Calculated using the value $\Gamma(\gamma gg)/\Gamma(ggg) = 0.137 \pm 0.001 \pm 0.016 \pm 0.004$ from BESSON 08 and the value of $\Gamma(ggg)/\Gamma_{total}$. The statistical error is negligible and the systematic error is partially correlated with that of $\Gamma(ggg)/\Gamma_{total}$ measurement of BESSON 08.

$\Gamma(\gamma gg)/\Gamma(ggg)$ Γ_4/Γ_3

VALUE (units 10^{-2})	EVTS	DOCUMENT ID		TECN	COMMENT
13.7±0.1±0.7	6 M	BESSON	08	CLEO	$\psi(2S) \to \pi^+\pi^- J/\psi$

$\Gamma(e^+e^-)/\Gamma_{total}$ Γ_5/Γ

VALUE (units 10^{-2})	EVTS	DOCUMENT ID		TECN	COMMENT
5.971±0.032 OUR AVERAGE					
5.983±0.007±0.037	720k	ABLIKIM	13R	BES3	$\psi(2S) \to J/\psi\pi^+\pi^-$
5.945±0.067±0.042	15k	LI	05C	CLEO	$\psi(2S) \to J/\psi\pi^+\pi^-$
5.90 ±0.05 ±0.10		BAI	98D	BES	$\psi(2S) \to J/\psi\pi^+\pi^-$
6.09 ±0.33		BAI	95B	BES	e^+e^-
5.92 ±0.15 ±0.20		COFFMAN	92	MRK3	$\psi(2S) \to J/\psi\pi^+\pi^-$
6.9 ±0.9		BOYARSKI	75	MRK1	e^+e^-

$\Gamma(e^+e^-\gamma)/\Gamma_{total}$ Γ_6/Γ

VALUE (units 10^{-3})	DOCUMENT ID		TECN	COMMENT
8.8±1.3±0.4	[1] ARMSTRONG	96	E760	$\overline{p}p \to e^+e^-\gamma$

[1] For $E_\gamma > 100$ MeV.

$\Gamma(\mu^+\mu^-)/\Gamma_{total}$ Γ_7/Γ

VALUE (units 10^{-2})	EVTS	DOCUMENT ID		TECN	COMMENT
5.961±0.033 OUR AVERAGE					
5.973±0.007±0.038	770k	ABLIKIM	13R	BES3	$\psi(2S) \to J/\psi\pi^+\pi^-$
5.960±0.065±0.050	17k	LI	05C	CLEO	$\psi(2S) \to J/\psi\pi^+\pi^-$
5.84 ±0.06 ±0.10		BAI	98D	BES	$\psi(2S) \to J/\psi\pi^+\pi^-$
6.08 ±0.33		BAI	95B	BES	e^+e^-
5.90 ±0.15 ±0.19		COFFMAN	92	MRK3	$\psi(2S) \to J/\psi\pi^+\pi^-$
6.9 ±0.9		BOYARSKI	75	MRK1	e^+e^-

$\Gamma(e^+e^-)/\Gamma(\mu^+\mu^-)$ Γ_5/Γ_7

VALUE	DOCUMENT ID		TECN	COMMENT
1.0016±0.0031 OUR AVERAGE				
1.0022±0.0044±0.0048	[1] AULCHENKO	14	KEDR	3.097 $e^+e^- \to e^+e^-,\mu^+\mu^-$
1.0017±0.0017±0.0033	[2] ABLIKIM	13R	BES3	$\psi(2S) \to J/\psi\pi^+\pi^-$
1.002 ±0.021 ±0.013	[3] ANASHIN	10	KEDR	3.097 $e^+e^- \to e^+e^-,\mu^+\mu^-$
0.997 ±0.012 ±0.006	LI	05C	CLEO	$\psi(2S) \to J/\psi\pi^+\pi^-$
• • • We do not use the following data for averages, fits, limits, etc. • • •				
1.011 ±0.013 ±0.016	BAI	98D	BES	$\psi(2S) \to J/\psi\pi^+\pi^-$
1.00 ±0.07	BAI	95B	BES	e^+e^-
1.00 ±0.05	BOYARSKI	75	MRK1	e^+e^-
0.91 ±0.15	ESPOSITO	75B	FRAM	e^+e^-
0.93 ±0.10	FORD	75	SPEC	e^+e^-

[1] From 235.3k $J/\psi \to e^+e^-$ and 156.6k $J/\psi \to \mu^+\mu^-$ observed events.

[2] Not independent of the corresponding measurements of $\Gamma(e+ e-)/\Gamma_{total}$ and $\Gamma(mu+ mu-)/\Gamma_{total}$.

[3] Not independent of the corresponding measurements of $\Gamma(e^+e^-) \times \Gamma(e^+e^-)/\Gamma_{total}$ and $\Gamma(\mu^+\mu^-) \times \Gamma(e^+e^-)/\Gamma_{total}$.

HADRONIC DECAYS

$\Gamma(\rho\pi)/\Gamma_{total}$ Γ_8/Γ

VALUE (units 10^{-2})	EVTS	DOCUMENT ID		TECN	COMMENT
1.69 ±0.15 OUR AVERAGE		Error includes scale factor of 2.4. See the ideogram below.			
2.18 ±0.19		[1,2] AUBERT,B	04N	BABR	10.6 $e^+e^- \to \pi^+\pi^-\pi^0\gamma$
2.184±0.005±0.201	220k	[2,3] BAI	04H	BES	$e^+e^- \to J/\psi \to \pi^+\pi^-\pi^0$
2.091±0.021±0.116		[2,4] BAI	04H	BES	$\psi(2S) \to \pi^+\pi^- J/\psi$
1.21 ±0.20		BAI	96D	BES	$e^+e^- \to \rho\pi$
1.42 ±0.01 ±0.19		COFFMAN	88	MRK3	e^+e^-
1.3 ±0.3	150	FRANKLIN	83	MRK2	e^+e^-
1.6 ±0.4	183	ALEXANDER	78	PLUT	e^+e^-
1.33 ±0.21		BRANDELIK	78B	DASP	e^+e^-
1.0 ±0.2	543	BARTEL	76	CNTR	e^+e^-
1.3 ±0.3	153	JEAN-MARIE	76	MRK1	e^+e^-

[1] From the ratio of $\Gamma(e^+e^-)\ B(\pi^+\pi^-\pi^0)$ and $\Gamma(e^+e^-)\ B(\mu^+\mu^-)$ (AUBERT 04).

[2] Not independent of their $B(\pi^+\pi^-\pi^0)$.

[3] From $J/\psi \to \pi^+\pi^-\pi^0$ events directly.

[4] Obtained comparing the rates for $\pi^+\pi^-\pi^0$ and $\mu^+\mu^-$, using J/ψ events produced via $\psi(2S) \to \pi^+\pi^- J/\psi$ and with $B(J/\psi \to \mu^+\mu^-) = 5.88 \pm 0.10\%$.

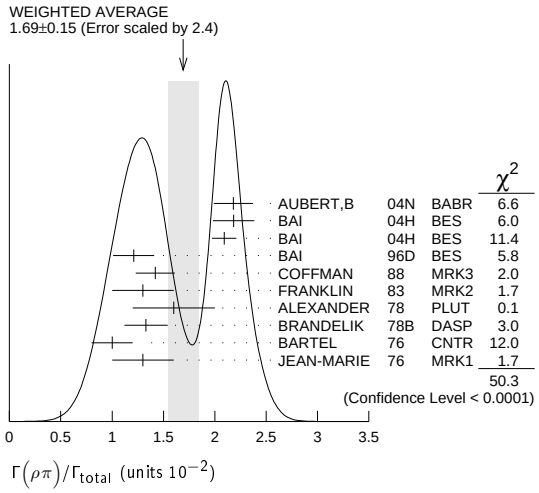

$\Gamma(\rho^0\pi^0)/\Gamma(\rho\pi)$ Γ_9/Γ_8

VALUE	DOCUMENT ID		TECN	COMMENT
0.328±0.005±0.027	COFFMAN	88	MRK3	e^+e^-
• • • We do not use the following data for averages, fits, limits, etc. • • •				
0.35 ±0.08	ALEXANDER	78	PLUT	e^+e^-
0.32 ±0.08	BRANDELIK	78B	DASP	e^+e^-
0.39 ±0.11	BARTEL	76	CNTR	e^+e^-
0.37 ±0.09	JEAN-MARIE	76	MRK1	e^+e^-

$\Gamma(a_2(1320)\rho)/\Gamma_{total}$ Γ_{10}/Γ

VALUE (units 10^{-3})	EVTS	DOCUMENT ID		TECN	COMMENT
10.9±2.2 OUR AVERAGE					
11.7±0.7±2.5	7584	AUGUSTIN	89	DM2	$J/\psi \to \rho^0\rho^\pm\pi^\mp$
8.4±4.5	36	VANNUCCI	77	MRK1	$e^+e^- \to 2(\pi^+\pi^-)\pi^0$

$\Gamma(\omega\pi^+\pi^+\pi^-\pi^-)/\Gamma_{total}$ Γ_{11}/Γ

VALUE (units 10^{-4})	EVTS	DOCUMENT ID	TECN	COMMENT
85±34	140	VANNUCCI 77	MRK1	$e^+e^- \to 3(\pi^+\pi^-)\pi^0$

$\Gamma(\omega\pi^+\pi^-\pi^0)/\Gamma_{total}$ Γ_{12}/Γ

VALUE (units 10^{-2})	EVTS	DOCUMENT ID		TECN	COMMENT
0.40±0.06±0.04	170	[1] AUBERT	06D	BABR	10.6 $e^+e^- \to \omega\pi^+\pi^-\pi^0\gamma$

[1] Using $\Gamma(J/\psi \to e^+e^-) = 5.52 \pm 0.14 \pm 0.04$ keV.

$\Gamma(\omega\pi^+\pi^-)/\Gamma_{total}$ Γ_{13}/Γ

VALUE (units 10^{-3})	EVTS	DOCUMENT ID		TECN	COMMENT
8.6±0.7 OUR AVERAGE		Error includes scale factor of 1.1.			
9.7±0.6±0.6	788	[1] AUBERT	07AU	BABR	10.6 $e^+e^- \to \omega\pi^+\pi^-\gamma$
7.0±1.6	18058	AUGUSTIN	89	DM2	$J/\psi \to 2(\pi^+\pi^-)\pi^0$
7.8±1.6	215	BURMESTER	77D	PLUT	e^+e^-
6.8±1.9	348	VANNUCCI	77	MRK1	$e^+e^- \to 2(\pi^+\pi^-)\pi^0$

[1] AUBERT 07AU quotes $\Gamma^{J/\psi}_{ee} \cdot B(J/\psi \to \omega\pi^+\pi^-) \cdot B(\omega \to 3\pi) = 47.8 \pm 3.1 \pm 3.2$ eV.

$\Gamma(\omega f_2(1270))/\Gamma_{total}$ Γ_{14}/Γ

VALUE (units 10^{-3})	EVTS	DOCUMENT ID		TECN	COMMENT
4.3±0.6 OUR AVERAGE					
4.3±0.2±0.6	5860	AUGUSTIN	89	DM2	e^+e^-
4.0±1.6	70	BURMESTER	77D	PLUT	e^+e^-
• • • We do not use the following data for averages, fits, limits, etc. • • •					
1.9±0.8	81	VANNUCCI	77	MRK1	$e^+e^- \to 2(\pi^+\pi^-)\pi^0$

$\Gamma(K^*(892)^0\overline{K}^*(892)^0)/\Gamma_{total}$ Γ_{15}/Γ

VALUE (units 10^{-4})	CL%	EVTS	DOCUMENT ID		TECN	COMMENT
2.3±0.7±0.1		25 ± 8	[1] AUBERT	07AK	BABR	10.6 $e^+e^- \to \pi^+\pi^- K^+K^-\gamma$
• • • We do not use the following data for averages, fits, limits, etc. • • •						
<5		90	VANNUCCI	77	MRK1	$e^+e^- \to \pi^+\pi^- K^+K^-$

[1] AUBERT 07AK reports $[\Gamma(J/\psi(1S) \to K^*(892)^0\overline{K}^*(892)^0)/\Gamma_{total}] \times [\Gamma(J/\psi(1S) \to e^+e^-)] = (1.28 \pm 0.40 \pm 0.11) \times 10^{-3}$ keV which we divide by our best value $\Gamma(J/\psi(1S) \to e^+e^-) = 5.55 \pm 0.14 \pm 0.02$ keV. Our first error is their experiment's error and our second error is the systematic error from using our best value.

Meson Particle Listings

$J/\psi(1S)$

$\Gamma(K^*(892)^\pm K^*(892)^\mp)/\Gamma_{total}$ Γ_{16}/Γ

VALUE (units 10^{-3})	EVTS	DOCUMENT ID		TECN	COMMENT
$1.00\pm0.19^{+0.11}_{-0.32}$	323	ABLIKIM	10E	BES2	$J/\psi \to K^\pm K^0_S \pi^\mp \pi^0$

$\Gamma(K^*(892)^\pm K^*(800)^\mp)/\Gamma_{total}$ Γ_{17}/Γ

VALUE (units 10^{-3})	EVTS	DOCUMENT ID		TECN	COMMENT
$1.09\pm0.18^{+0.94}_{-0.54}$	655	ABLIKIM	10E	BES2	$J/\psi \to K^\pm K^0_S \pi^\mp \pi^0$

$\Gamma(\eta K^*(892)^0 \overline{K}^*(892)^0)/\Gamma_{total}$ Γ_{18}/Γ

VALUE (units 10^{-3})	EVTS	DOCUMENT ID		TECN	COMMENT
$1.15\pm0.13\pm0.22$	209	ABLIKIM	10C	BES2	$J/\psi \to \eta K^+ \pi^- K^- \pi^+$

$\Gamma(K^*(892)^0 \overline{K}^*_2(1430)^0 + \text{c.c.})/\Gamma_{total}$ Γ_{19}/Γ

VALUE (units 10^{-3})	EVTS	DOCUMENT ID		TECN	COMMENT
6.0 ± 0.6 OUR AVERAGE					
$5.9\pm0.6\pm0.2$	317 ± 23	[1,2] AUBERT	07AK	BABR	$10.6\ e^+e^- \to \pi^+\pi^- K^+ K^- \gamma$
6.7 ± 2.6	40	VANNUCCI	77	MRK1	$e^+e^- \to \pi^+\pi^- K^+ K^-$

[1] Using $B(K^*_2(1430)^0 \to K\pi) = (49.9\pm1.2)\%$.

[2] AUBERT 07AK reports $[\Gamma(J/\psi(1S) \to K^*(892)^0 \overline{K}^*_2(1430)^0 + \text{c.c.})/\Gamma_{total}] \times [\Gamma(J/\psi(1S) \to e^+e^-)] = (32.9\pm2.3\pm2.7)\times10^{-3}$ keV which we divide by our best value $\Gamma(J/\psi(1S) \to e^+e^-) = 5.55\pm0.14\pm0.02$ keV. Our first error is their experiment's error and our second error is the systematic error from using our best value.

$\Gamma(\omega K^*(892)\overline{K} + \text{c.c.})/\Gamma_{total}$ Γ_{21}/Γ

VALUE (units 10^{-4})	EVTS	DOCUMENT ID		TECN	COMMENT
$61\ \pm9$ OUR AVERAGE					
$62.0\pm6.8\pm10.6$	899 ± 98	ABLIKIM	08E	BES2	$J/\psi \to \omega K^0_S K^\pm \pi^\mp$
$65.3\pm10.2\pm13.5$	176 ± 28	ABLIKIM	08E	BES2	$J/\psi \to \omega K^+ K^- \pi^0$
$53\ \pm14\ \pm14$	530 ± 140	BECKER	87	MRK3	$e^+e^- \to$ hadrons

$\Gamma(K^+ K^*(892)^- + \text{c.c.})/\Gamma_{total}$ Γ_{22}/Γ

VALUE (units 10^{-3})	EVTS	DOCUMENT ID		TECN	COMMENT
5.12 ± 0.30 OUR AVERAGE					
$5.2\ \pm0.4\ \pm0.1$		[1] AUBERT	08S	BABR	$10.6\ e^+e^- \to K^+ K^*(892)^- \gamma$
$4.57\pm0.17\pm0.70$	2285	JOUSSET	90	DM2	$J/\psi \to$ hadrons
$5.26\pm0.13\pm0.53$		COFFMAN	88	MRK3	$J/\psi \to K^\pm K^0_S \pi^\mp, K^+ K^- \pi^0$
• • • We do not use the following data for averages, fits, limits, etc. • • •					
$2.6\ \pm0.6$	24	FRANKLIN	83	MRK2	$J/\psi \to K^+ K^- \pi^0$
$3.2\ \pm0.6$	48	VANNUCCI	77	MRK1	$J/\psi \to K^\pm K^0_S \pi^\mp$
$4.1\ \pm1.2$	39	BRAUNSCH...	76	DASP	$J/\psi \to K^\pm X$

[1] AUBERT 08S reports $[\Gamma(J/\psi(1S) \to K^+ K^*(892)^- + \text{c.c.})/\Gamma_{total}] \times [\Gamma(J/\psi(1S) \to e^+e^-)] = (29.0\pm1.7\pm1.3)\times10^{-3}$ keV which we divide by our best value $\Gamma(J/\psi(1S) \to e^+e^-) = 5.55\pm0.14\pm0.02$ keV. Our first error is their experiment's error and our second error is the systematic error from using our best value.

$\Gamma(K^+ K^*(892)^- + \text{c.c.} \to K^+ K^- \pi^0)/\Gamma_{total}$ Γ_{23}/Γ

VALUE (units 10^{-3})	EVTS	DOCUMENT ID		TECN	COMMENT
$1.97\pm0.20\pm0.05$	155	[1] AUBERT	08S	BABR	$10.6\ e^+e^- \to K^+ K^- \pi^0 \gamma$

[1] AUBERT 08S reports $[\Gamma(J/\psi(1S) \to K^+ K^*(892)^- + \text{c.c.} \to K^+ K^- \pi^0)/\Gamma_{total}] \times [\Gamma(J/\psi(1S) \to e^+e^-)] = (10.96\pm0.85\pm0.70)\times10^{-3}$ keV which we divide by our best value $\Gamma(J/\psi(1S) \to e^+e^-) = 5.55\pm0.14\pm0.02$ keV. Our first error is their experiment's error and our second error is the systematic error from using our best value.

$\Gamma(K^+ K^*(892)^- + \text{c.c.} \to K^0 K^\pm \pi^\mp + \text{c.c.})/\Gamma_{total}$ Γ_{24}/Γ

VALUE (units 10^{-3})	EVTS	DOCUMENT ID		TECN	COMMENT
$3.0\pm0.4\pm0.1$	89	[1] AUBERT	08S	BABR	$10.6\ e^+e^- \to K^0_S K^\pm \pi^\mp \gamma$

[1] AUBERT 08S reports $[\Gamma(J/\psi(1S) \to K^+ K^*(892)^- + \text{c.c.} \to K^0 K^\pm \pi^\mp + \text{c.c.})/\Gamma_{total}] \times [\Gamma(J/\psi(1S) \to e^+e^-)] = (16.76\pm1.70\pm1.00)\times10^{-3}$ keV which we divide by our best value $\Gamma(J/\psi(1S) \to e^+e^-) = 5.55\pm0.14\pm0.02$ keV. Our first error is their experiment's error and our second error is the systematic error from using our best value.

$\Gamma(K^0 \overline{K}^*(892)^0 + \text{c.c.})/\Gamma_{total}$ Γ_{25}/Γ

VALUE (units 10^{-3})	EVTS	DOCUMENT ID		TECN	COMMENT
4.39 ± 0.31 OUR AVERAGE					
$4.8\ \pm0.5\ \pm0.1$		[1] AUBERT	08S	BABR	$10.6\ e^+e^- \to K^0 \overline{K}^*(892)^0 \gamma$
$3.96\pm0.15\pm0.60$	1192	JOUSSET	90	DM2	$J/\psi \to$ hadrons
$4.33\pm0.12\pm0.45$		COFFMAN	88	MRK3	$J/\psi \to K^\pm K^0_S \pi^\mp$
• • • We do not use the following data for averages, fits, limits, etc. • • •					
$2.7\ \pm0.6$	45	VANNUCCI	77	MRK1	$J/\psi \to K^\pm K^0_S \pi^\mp$

[1] AUBERT 08S reports $[\Gamma(J/\psi(1S) \to K^0 \overline{K}^*(892)^0 + \text{c.c.})/\Gamma_{total}] \times [\Gamma(J/\psi(1S) \to e^+e^-)] = (26.6\pm2.5\pm1.5)\times10^{-3}$ keV which we divide by our best value $\Gamma(J/\psi(1S) \to e^+e^-) = 5.55\pm0.14\pm0.02$ keV. Our first error is their experiment's error and our second error is the systematic error from using our best value.

$\Gamma(K^0 \overline{K}^*(892)^0 + \text{c.c.})/\Gamma(K^+ K^*(892)^- + \text{c.c.})$ Γ_{25}/Γ_{22}

VALUE	DOCUMENT ID		TECN	COMMENT
$0.82\pm0.05\pm0.09$	COFFMAN	88	MRK3	$J/\psi \to K\overline{K}^*(892) + \text{c.c.}$

$\Gamma(K^0 \overline{K}^*(892)^0 + \text{c.c.} \to K^0 K^\pm \pi^\mp + \text{c.c.})/\Gamma_{total}$ Γ_{26}/Γ

VALUE (units 10^{-3})	EVTS	DOCUMENT ID		TECN	COMMENT
$3.2\pm0.4\pm0.1$	94	[1] AUBERT	08S	BABR	$10.6\ e^+e^- \to K^0_S K^\pm \pi^\mp \gamma$

[1] AUBERT 08S reports $[\Gamma(J/\psi(1S) \to K^0 \overline{K}^*(892)^0 + \text{c.c.} \to K^0 K^\pm \pi^\mp + \text{c.c.})/\Gamma_{total}] \times [\Gamma(J/\psi(1S) \to e^+e^-)] = (17.70\pm1.70\pm1.00)\times10^{-3}$ keV which we divide by our best value $\Gamma(J/\psi(1S) \to e^+e^-) = 5.55\pm0.14\pm0.02$ keV. Our first error is their experiment's error and our second error is the systematic error from using our best value.

$\Gamma(K_1(1400)^\pm K^\mp)/\Gamma_{total}$ Γ_{27}/Γ

VALUE (units 10^{-3})	DOCUMENT ID		TECN	COMMENT
$3.8\pm0.8\pm1.2$	[1] BAI	99C	BES	e^+e^-

[1] Assuming $B(K_1(1400) \to K^*\pi) = 0.94\pm0.06$

$\Gamma(\overline{K}^*(892)^0 K^+\pi^- + \text{c.c.})/\Gamma_{total}$ Γ_{28}/Γ

VALUE	DOCUMENT ID		TECN	COMMENT
seen	[1] ABLIKIM	06C	BES2	$J/\psi \to \overline{K}^*(892)^0 K^+\pi^-$

[1] A $K^*_0(800)$ is observed by ABLIKIM 06C in the $K^+\pi^-$ mass spectrum of the $\overline{K}^*(892)^0 K^+\pi^-$ final state against the $\overline{K}^*(892)$. A corresponding branching fraction of the $J/\psi(1S)$ is not presented.

$\Gamma(\omega\pi^0\pi^0)/\Gamma_{total}$ Γ_{29}/Γ

VALUE (units 10^{-3})	EVTS	DOCUMENT ID		TECN	COMMENT
$3.4\pm0.3\pm0.7$	509	AUGUSTIN	89	DM2	$J/\psi \to \pi^+\pi^- 3\pi^0$

$\Gamma(b_1(1235)^\pm\pi^\mp)/\Gamma_{total}$ Γ_{30}/Γ

VALUE (units 10^{-4})	EVTS	DOCUMENT ID		TECN	COMMENT
30 ± 5 OUR AVERAGE					
31 ± 6	4600	AUGUSTIN	89	DM2	$J/\psi \to 2(\pi^+\pi^-)\pi^0$
29 ± 7	87	BURMESTER	77D	PLUT	e^+e^-

$\Gamma(\omega K^\pm K^0_S \pi^\mp)/\Gamma_{total}$ Γ_{31}/Γ

VALUE (units 10^{-4})	EVTS	DOCUMENT ID		TECN	COMMENT
$34\ \pm5$ OUR AVERAGE					
$37.7\pm0.8\pm5.8$	1972 ± 41	ABLIKIM	08E	BES2	$e^+e^- \to J/\psi$
$29.5\pm1.4\pm7.0$	879 ± 41	BECKER	87	MRK3	$e^+e^- \to$ hadrons

$\Gamma(b_1(1235)^0\pi^0)/\Gamma_{total}$ Γ_{32}/Γ

VALUE (units 10^{-4})	EVTS	DOCUMENT ID		TECN	COMMENT
$23\pm3\pm5$	229	AUGUSTIN	89	DM2	e^+e^-

$\Gamma(\eta K^\pm K^0_S \pi^\mp)/\Gamma_{total}$ Γ_{33}/Γ

VALUE (units 10^{-4})	EVTS	DOCUMENT ID		TECN	COMMENT
$21.8\pm2.2\pm3.4$	232 ± 23	ABLIKIM	08E	BES2	$e^+e^- \to J/\psi$

$\Gamma(\phi K^*(892)\overline{K} + \text{c.c.})/\Gamma_{total}$ Γ_{34}/Γ

VALUE (units 10^{-4})	EVTS	DOCUMENT ID		TECN	COMMENT
21.8 ± 2.3 OUR AVERAGE					
$20.8\pm2.7\pm3.9$	195 ± 25	ABLIKIM	08E	BES2	$J/\psi \to \phi K^0_S K^\pm \pi^\mp$
$29.6\pm3.7\pm4.7$	238 ± 30	ABLIKIM	08E	BES2	$J/\psi \to \phi K^+ K^- \pi^0$
$20.7\pm2.4\pm3.0$		FALVARD	88	DM2	$J/\psi \to$ hadrons
$20\ \pm3\ \pm3$	155 ± 20	BECKER	87	MRK3	$e^+e^- \to$ hadrons

$\Gamma(\omega K\overline{K})/\Gamma_{total}$ Γ_{35}/Γ

VALUE (units 10^{-4})	EVTS	DOCUMENT ID		TECN	COMMENT
$17.0\pm\ 3.2$ OUR AVERAGE					
$13.6\pm\ 5.0\pm1.0$	24	[1] AUBERT	07AU	BABR	$10.6\ e^+e^- \to \omega K^+ K^- \gamma$
$19.8\pm\ 2.1\pm3.9$		[2] FALVARD	88	DM2	$J/\psi \to$ hadrons
$16\ \pm10$	22	FELDMAN	77	MRK1	e^+e^-

[1] AUBERT 07AU quotes $\Gamma^{J/\psi}_{ee} \cdot B(J/\psi \to \omega K^+ K^-) \cdot B(\eta \to 3\pi) = 3.3\pm1.3\pm0.2$ eV.

[2] Addition of $\omega K^+ K^-$ and $\omega K^0 \overline{K}^0$ branching ratios.

$\Gamma(\omega f_0(1710) \to \omega K\overline{K})/\Gamma_{total}$ Γ_{36}/Γ

VALUE (units 10^{-4})	DOCUMENT ID		TECN	COMMENT
$4.8\pm1.1\pm0.3$	[1,2] FALVARD	88	DM2	$J/\psi \to$ hadrons

[1] Includes unknown branching fraction $f_0(1710) \to K\overline{K}$.

[2] Addition of $f_0(1710) \to K^+ K^-$ and $f_0(1710) \to K^0 \overline{K}^0$ branching ratios.

$\Gamma(\phi 2(\pi^+\pi^-))/\Gamma_{total}$ Γ_{37}/Γ

VALUE (units 10^{-4})	EVTS	DOCUMENT ID		TECN	COMMENT
16.6 ± 2.3 OUR AVERAGE					
$17.3\pm3.3\pm1.2$	35	[1] AUBERT	06D	BABR	$10.6\ e^+e^- \to \phi 2(\pi^+\pi^-)\gamma$
$16.0\pm1.0\pm3.0$		FALVARD	88	DM2	$J/\psi \to$ hadrons

[1] Using $\Gamma(J/\psi \to e^+e^-) = 5.52\pm0.14\pm0.04$ keV.

$\Gamma(\Delta(1232)^{++}\overline{p}\pi^-)/\Gamma_{total}$ Γ_{38}/Γ

VALUE (units 10^{-3})	EVTS	DOCUMENT ID		TECN	COMMENT
1.58±0.23±0.40	332	EATON	84	MRK2	e^+e^-

$\Gamma(\omega\eta)/\Gamma_{total}$ Γ_{39}/Γ

VALUE (units 10^{-3})	EVTS	DOCUMENT ID		TECN	COMMENT
1.74 ±0.20 OUR AVERAGE		Error includes scale factor of 1.6.			See the ideogram below.
2.352±0.273	5k	[1] ABLIKIM	06F	BES2	$J/\psi \to \omega\eta$
1.44 ±0.40 ±0.14	13	[2] AUBERT	06D	BABR	10.6 $e^+e^- \to \omega\eta\gamma$
1.43 ±0.10 ±0.21	378	JOUSSET	90	DM2	$J/\psi \to$ hadrons
1.71 ±0.08 ±0.20		COFFMAN	88	MRK3	$e^+e^- \to 3\pi\eta$

[1] Using B($\eta \to 2\gamma$) = (39.43 ± 0.26)%, B($\eta \to \pi^+\pi^-\pi^0$) = 22.6 ± 0.4%, B($\eta \to \pi^+\pi^-\gamma$) = 4.68 ± 0.11%, and B($\omega \to \pi^+\pi^-\pi^0$) = (89.1 ± 0.7)%.
[2] Using $\Gamma(J/\psi \to e^+e^-)$ = 5.52 ± 0.14 ± 0.04 keV.

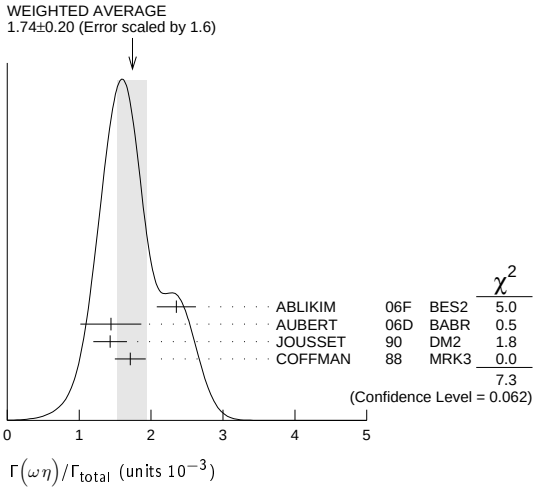

$\Gamma(\phi K\overline{K})/\Gamma_{total}$ Γ_{40}/Γ

VALUE (units 10^{-4})	EVTS	DOCUMENT ID		TECN	COMMENT
18.3± 2.4 OUR AVERAGE		Error includes scale factor of 1.5.			See the ideogram below.
21.4± 0.4±2.2		ABLIKIM	05	BES2	$J/\psi \to \phi\pi^+\pi^-$
48 $^{+20}_{-16}$ ±6	9.0 $^{+3.7}_{-3.0}$	[1,2] HUANG	03	BELL	$B^+ \to (\phi K^+K^-)\,K^+$
14.6± 0.8±2.1		[3] FALVARD	88	DM2	$J/\psi \to$ hadrons
18 ± 8	14	FELDMAN	77	MRK1	e^+e^-

[1] We have multiplied K^+K^- measurement by 2 to obtain $K\overline{K}$.
[2] Using B($B^+ \to J/\psi K^+$) = (1.01 ± 0.05) × 10^{-3}.
[3] Addition of ϕK^+K^- and $\phi K^0\overline{K}^0$ branching ratios.

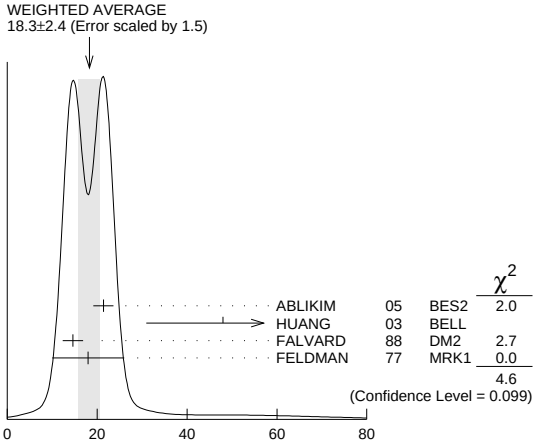

$\Gamma(\phi f_0(1710) \to \phi K\overline{K})/\Gamma_{total}$ Γ_{41}/Γ

VALUE (units 10^{-4})	DOCUMENT ID		TECN	COMMENT
3.6±0.2±0.6	[1,2] FALVARD	88	DM2	$J/\psi \to$ hadrons

[1] Including interference with $f_2'(1525)$.
[2] Includes unknown branching fraction $f_0(1710) \to K\overline{K}$.

$\Gamma(\phi f_2(1270))/\Gamma_{total}$ Γ_{42}/Γ

VALUE (units 10^{-3})	CL%	EVTS	DOCUMENT ID		TECN	COMMENT
0.72±0.13±0.02		44 ± 7	[1,2] AUBERT	07AK	BABR	10.6 $e^+e^- \to \pi^+\pi^- K^+K^-\gamma$
• • • We do not use the following data for averages, fits, limits, etc. • • •						
< 0.45	90		FALVARD	88	DM2	$J/\psi \to$ hadrons
< 0.37	90		VANNUCCI	77	MRK1	$e^+e^- \to \pi^+\pi^- K^+K^-$

[1] Using B($f_2(1270) \to \pi\pi$) = (84.8 $^{+2.4}_{-1.2}$)%
[2] AUBERT 07AK reports [$\Gamma(J/\psi(1S) \to \phi f_2(1270))/\Gamma_{total}$] × [$\Gamma(J/\psi(1S) \to e^+e^-)$] = (4.02 ± 0.65 ± 0.33) × 10^{-3} keV which we divide by our best value $\Gamma(J/\psi(1S) \to e^+e^-)$ = 5.55 ± 0.14 ± 0.02 keV. Our first error is their experiment's error and our second error is the systematic error from using our best value.

$\Gamma(\Delta(1232)^{++}\overline{\Delta}(1232)^{--})/\Gamma_{total}$ Γ_{43}/Γ

VALUE (units 10^{-3})	EVTS	DOCUMENT ID		TECN	COMMENT
1.10±0.09±0.28	233	EATON	84	MRK2	e^+e^-

$\Gamma(\Sigma(1385)^-\overline{\Sigma}(1385)^+ (\text{or c.c.}))/\Gamma_{total}$ Γ_{44}/Γ

VALUE (units 10^{-3})	EVTS	DOCUMENT ID		TECN	COMMENT
1.10±0.12 OUR AVERAGE					
1.23±0.07±0.30	0.8k	ABLIKIM	12P	BES2	$J/\psi \to \Sigma(1385)^-\overline{\Sigma}(1385)^+$
1.50±0.08±0.38	1k	ABLIKIM	12P	BES2	$J/\psi \to \Sigma(1385)^+\overline{\Sigma}(1385)^-$
1.00±0.04±0.21	0.6k	HENRARD	87	DM2	$e^+e^- \to \Sigma^{*-}$
1.19±0.04±0.25	0.7k	HENRARD	87	DM2	$e^+e^- \to \Sigma^{*+}$
0.86±0.18±0.22	56	EATON	84	MRK2	$e^+e^- \to \Sigma^{*-}$
1.03±0.24±0.25	68	EATON	84	MRK2	$e^+e^- \to \Sigma^{*+}$

$\Gamma(\phi f_2'(1525))/\Gamma_{total}$ Γ_{45}/Γ

VALUE (units 10^{-4})	EVTS	DOCUMENT ID		TECN	COMMENT
8 ±4 OUR AVERAGE		Error includes scale factor of 2.7.			
12.3±0.6±2.0		[1,2] FALVARD	88	DM2	$J/\psi \to$ hadrons
4.8±1.8	46	[1] GIDAL	81	MRK2	$J/\psi \to K^+K^-K^+K^-$

[1] Re-evaluated using B($f_2'(1525) \to K\overline{K}$) = 0.713.
[2] Including interference with $f_0(1710)$.

$\Gamma(\phi\pi^+\pi^-)/\Gamma_{total}$ Γ_{46}/Γ

VALUE (units 10^{-3})	EVTS	DOCUMENT ID		TECN	COMMENT
0.94±0.09 OUR AVERAGE		Error includes scale factor of 1.2.			
0.96±0.13	103	[1] AUBERT,BE	06D	BABR	10.6 $e^+e^- \to K^+K^-\pi^+\pi^-\gamma$
1.09±0.02±0.13		ABLIKIM	05	BES2	$J/\psi \to \phi\pi^+\pi^-$
0.78±0.03±0.12		FALVARD	88	DM2	$J/\psi \to$ hadrons
2.1 ±0.9	23	FELDMAN	77	MRK1	e^+e^-

[1] Derived by us. AUBERT,BE 06D measures $\Gamma(J/\psi \to e^+e^-) \times$ B($J/\psi \to \phi\pi^+\pi^-$) × B($\phi \to K^+K^-$) = (2.61 ± 0.30 ± 0.18) eV

$\Gamma(\phi\pi^0\pi^0)/\Gamma_{total}$ Γ_{47}/Γ

VALUE (units 10^{-3})	EVTS	DOCUMENT ID		TECN	COMMENT
0.56±0.16	23	[1] AUBERT,BE	06D	BABR	10.6 $e^+e^- \to K^+K^-\pi^0\pi^0\gamma$

[1] Derived by us. AUBERT,BE 06D measures $\Gamma(J/\psi \to e^+e^-) \times$ B($J/\psi \to \phi\pi^0\pi^0$) × B($\phi \to K^+K^-$) = (1.54 ± 0.40 ± 0.16) eV

$\Gamma(\phi K^\pm K_S^0\pi^\mp)/\Gamma_{total}$ Γ_{48}/Γ

VALUE (units 10^{-4})	EVTS	DOCUMENT ID		TECN	COMMENT
7.2±0.8 OUR AVERAGE					
7.4±0.6±1.4	227 ± 19	ABLIKIM	08E	BES2	$e^+e^- \to J/\psi$
7.4±0.9±1.1		FALVARD	88	DM2	$J/\psi \to$ hadrons
7 ±0.6±1.0	163 ± 15	BECKER	87	MRK3	$e^+e^- \to$ hadrons

$\Gamma(\omega f_1(1420))/\Gamma_{total}$ Γ_{49}/Γ

VALUE (units 10^{-4})	EVTS	DOCUMENT ID	TECN	COMMENT
6.8 $^{+1.9}_{-1.6}$ ±1.7	111 $^{+31}_{-26}$	BECKER	87	MRK3	$e^+e^- \to$ hadrons

$\Gamma(\phi\eta)/\Gamma_{total}$ Γ_{50}/Γ

VALUE (units 10^{-3})	EVTS	DOCUMENT ID		TECN	COMMENT
0.75 ±0.08 OUR AVERAGE		Error includes scale factor of 1.5.			See the ideogram below.
1.4 ±0.6 ±0.1	6	[1] AUBERT	07AU	BABR	10.6 $e^+e^- \to \phi\eta\gamma$
0.898±0.024±0.089		ABLIKIM	05B	BES2	$e^+e^- \to J/\psi \to$ hadr
0.64 ±0.04 ±0.11	346	JOUSSET	90	DM2	$J/\psi \to$ hadrons
0.661±0.045±0.078		COFFMAN	88	MRK3	$e^+e^- \to K^+K^-\eta$

[1] AUBERT 07AU quotes $\Gamma_{ee}^{J/\psi}$ · B($J/\psi \to \phi\eta$) · B($\phi \to K^+K^-$) · B($\eta \to \gamma\gamma$)= 0.84 ± 0.37 ± 0.05 eV.

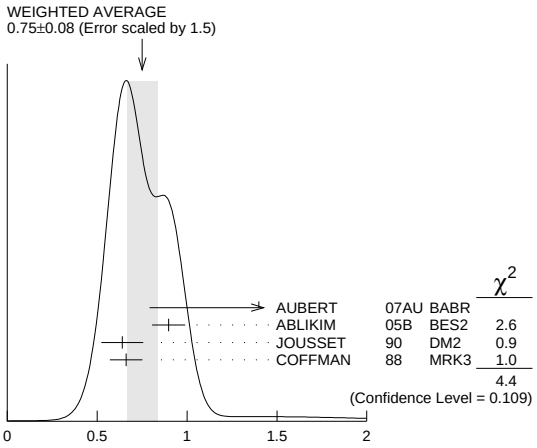

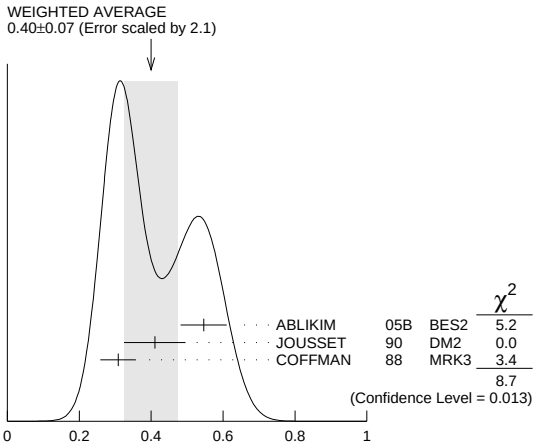

$\Gamma(\Xi^0\overline{\Xi}^0)/\Gamma_{total}$ Γ_{51}/Γ

VALUE (units 10^{-3})	EVTS	DOCUMENT ID		TECN	COMMENT
1.20±0.12±0.21	206	ABLIKIM	08O	BES2	$e^+e^- \to J/\psi$

$\Gamma(\Xi(1530)^-\overline{\Xi}^+)/\Gamma_{total}$ Γ_{52}/Γ

VALUE (units 10^{-3})	EVTS	DOCUMENT ID		TECN	COMMENT
0.59±0.09±0.12	75 ± 11	HENRARD	87	DM2	e^+e^-

$\Gamma(pK^-\overline{\Sigma}(1385)^0)/\Gamma_{total}$ Γ_{53}/Γ

VALUE (units 10^{-3})	EVTS	DOCUMENT ID		TECN	COMMENT
0.51±0.26±0.18	89	EATON	84	MRK2	e^+e^-

$\Gamma(\omega\pi^0)/\Gamma_{total}$ Γ_{54}/Γ

VALUE (units 10^{-3})	EVTS	DOCUMENT ID		TECN	COMMENT
0.45 ±0.05 OUR AVERAGE		Error includes scale factor of 1.4. See the ideogram below.			
0.538±0.012±0.065	2090	[1] ABLIKIM	06F	BES2	$J/\psi \to \omega\pi^0$
0.360±0.028±0.054	222	JOUSSET	90	DM2	$J/\psi \to$ hadrons
0.482±0.019±0.064		COFFMAN	88	MRK3	$e^+e^- \to \pi^0\pi^+\pi^-\pi^0$

[1] Using B($\omega \to \pi^+\pi^-\pi^0$) = (89.1 ± 0.7)%.

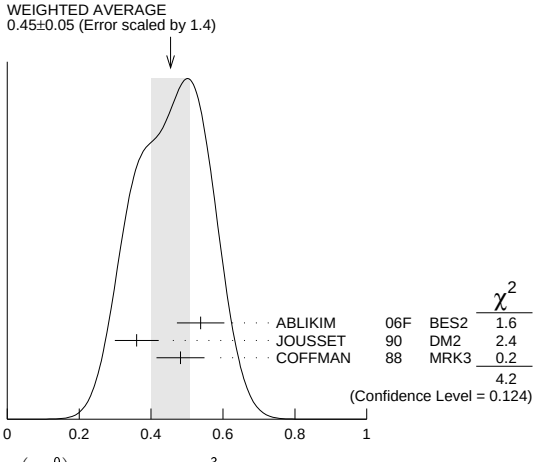

$\Gamma(\phi\eta'(958))/\Gamma_{total}$ Γ_{55}/Γ

VALUE (units 10^{-3})	CL%	EVTS	DOCUMENT ID		TECN	COMMENT
0.40 ±0.07 OUR AVERAGE			Error includes scale factor of 2.1. See the ideogram below.			
0.546±0.031±0.056			ABLIKIM	05B	BES2	$e^+e^- \to J/\psi \to$ hadr
0.41 ±0.03 ±0.08		167	JOUSSET	90	DM2	$J/\psi \to$ hadrons
0.308±0.034±0.036			COFFMAN	88	MRK3	$e^+e^- \to K^+K^-\eta'$
• • • We do not use the following data for averages, fits, limits, etc. • • •						
< 1.3	90		VANNUCCI	77	MRK1	e^+e^-

$\Gamma(\phi f_0(980))/\Gamma_{total}$ Γ_{56}/Γ

VALUE (units 10^{-4})	EVTS	DOCUMENT ID		TECN	COMMENT
3.2±0.9 OUR AVERAGE		Error includes scale factor of 1.9.			
4.6±0.4±0.8		[1] FALVARD	88	DM2	$J/\psi \to$ hadrons
2.6±0.6	50	[1] GIDAL	81	MRK2	$J/\psi \to K^+K^-K^+K^-$

[1] Assuming B($f_0(980) \to \pi\pi$) = 0.78.

$\Gamma(\phi f_0(980) \to \phi\pi^+\pi^-)/\Gamma_{total}$ Γ_{57}/Γ

VALUE (units 10^{-3})	EVTS	DOCUMENT ID		TECN	COMMENT
0.182±0.042±0.005	19.5 ± 4.5	[1,2] AUBERT	07AK	BABR	10.6 $e^+e^- \to \pi^+\pi^-K^+K^-\gamma$

[1] Using B($\phi \to K^+K^-$) = (49.3 ± 0.6)%.

[2] AUBERT 07AK reports $[\Gamma(J/\psi(1S) \to \phi f_0(980) \to \phi\pi^+\pi^-)/\Gamma_{total}] \times [\Gamma(J/\psi(1S) \to e^+e^-)] = (1.01 \pm 0.22 \pm 0.08) \times 10^{-3}$ keV which we divide by our best value $\Gamma(J/\psi(1S) \to e^+e^-) = 5.55 \pm 0.14 \pm 0.02$ keV. Our first error is their experiment's error and our second error is the systematic error from using our best value.

$\Gamma(\phi f_0(980) \to \phi\pi^0\pi^0)/\Gamma_{total}$ Γ_{58}/Γ

VALUE (units 10^{-3})	EVTS	DOCUMENT ID		TECN	COMMENT
0.171±0.073±0.004	7.0 ± 2.8	[1,2] AUBERT	07AK	BABR	10.6 $e^+e^- \to \pi^0\pi^0K^+K^-\gamma$

[1] Using B($\phi \to K^+K^-$) = (49.3 ± 0.6)%.

[2] AUBERT 07AK reports $[\Gamma(J/\psi(1S) \to \phi f_0(980) \to \phi\pi^0\pi^0)/\Gamma_{total}] \times [\Gamma(J/\psi(1S) \to e^+e^-)] = (0.95 \pm 0.39 \pm 0.10) \times 10^{-3}$ keV which we divide by our best value $\Gamma(J/\psi(1S) \to e^+e^-) = 5.55 \pm 0.14 \pm 0.02$ keV. Our first error is their experiment's error and our second error is the systematic error from using our best value.

$\Gamma(\eta\phi f_0(980) \to \eta\phi\pi^+\pi^-)/\Gamma_{total}$ Γ_{59}/Γ

VALUE (units 10^{-4})	EVTS	DOCUMENT ID		TECN	COMMENT
3.23±0.75±0.73	52	ABLIKIM	08F	BES	$J/\psi \to \eta\phi f_0(980)$

$\Gamma(\phi a_0(980)^0 \to \phi\eta\pi^0)/\Gamma_{total}$ Γ_{60}/Γ

VALUE (units 10^{-6})	DOCUMENT ID		TECN	COMMENT
5.0±2.7±2.5	[1] ABLIKIM	11D	BES3	$J/\psi \to \phi\eta\pi^0$

[1] Assuming $a_0(980) - f_0(980)$ mixing and isospin breaking via γ^* and K^*K loops.

$\Gamma(\Xi(1530)^0\overline{\Xi}^0)/\Gamma_{total}$ Γ_{61}/Γ

VALUE (units 10^{-3})	EVTS	DOCUMENT ID		TECN	COMMENT
0.32±0.12±0.07	24 ± 9	HENRARD	87	DM2	e^+e^-

$\Gamma(\Sigma(1385)^-\overline{\Sigma}^+ \text{(or c.c.)})/\Gamma_{total}$ Γ_{62}/Γ

VALUE (units 10^{-3})	EVTS	DOCUMENT ID		TECN	COMMENT
0.31±0.05 OUR AVERAGE					
0.30±0.03±0.07	74 ± 8	HENRARD	87	DM2	$e^+e^- \to \Sigma^{*-}$
0.34±0.04±0.07	77 ± 9	HENRARD	87	DM2	$e^+e^- \to \Sigma^{*+}$
0.29±0.11±0.10	26	EATON	84	MRK2	$e^+e^- \to \Sigma^{*-}$
0.31±0.11±0.11	28	EATON	84	MRK2	$e^+e^- \to \Sigma^{*+}$

$\Gamma(\phi f_1(1285))/\Gamma_{total}$ Γ_{63}/Γ

VALUE (units 10^{-4})	EVTS	DOCUMENT ID		TECN	COMMENT
2.6±0.5 OUR AVERAGE		Error includes scale factor of 1.1.			
3.2±0.6±0.4		JOUSSET	90	DM2	$J/\psi \to \phi 2(\pi^+\pi^-)$
2.1±0.5±0.4	25	[1] JOUSSET	90	DM2	$J/\psi \to \phi\eta\pi^+\pi^-$
• • • We do not use the following data for averages, fits, limits, etc. • • •					
0.6±0.2±0.1	16 ± 6	BECKER	87	MRK3	$J/\psi \to \phi K\overline{K}\pi$

[1] We attribute to the $f_1(1285)$ the signal observed in the $\pi^+\pi^-\eta$ invariant mass distribution at 1297 MeV.

$\Gamma(\eta\pi^+\pi^-)/\Gamma_{total}$ Γ_{64}/Γ

VALUE (units 10^{-3})	EVTS	DOCUMENT ID		TECN	COMMENT
0.40±0.17±0.03	9	[1] AUBERT	07AU	BABR	10.6 $e^+e^-\to\eta\pi^+\pi^-\gamma$

[1] AUBERT 07AU quotes $\Gamma_{ee}^{J/\psi}\cdot B(J/\psi\to\eta\pi^+\pi^-)\cdot B(\eta\to 3\pi)=0.51\pm0.22\pm0.03$ eV.

$\Gamma(\rho\eta)/\Gamma_{total}$ Γ_{65}/Γ

VALUE (units 10^{-3})	EVTS	DOCUMENT ID		TECN	COMMENT
0.193±0.023 OUR AVERAGE					
0.194±0.017±0.029	299	JOUSSET	90	DM2	$J/\psi\to$ hadrons
0.193±0.013±0.029		COFFMAN	88	MRK3	$e^+e^-\to\pi^+\pi^-\eta$

$\Gamma(\omega\eta'(958))/\Gamma_{total}$ Γ_{66}/Γ

VALUE (units 10^{-3})	EVTS	DOCUMENT ID		TECN	COMMENT
0.182±0.021 OUR AVERAGE					
0.226±0.043	218	[1] ABLIKIM	06F	BES2	$J/\psi\to\omega\eta'$
$0.18\ ^{+0.10}_{-0.08}\pm0.03$	6	JOUSSET	90	DM2	$J/\psi\to$ hadrons
0.166±0.017±0.019		COFFMAN	88	MRK3	$e^+e^-\to 3\pi\eta'$

[1] Using $B(\eta'\to\pi^+\pi^-\eta)=(44.3\pm1.5)\%$, $B(\eta'\to\pi^+\pi^-\gamma)=29.5\pm1.0\%$, $B(\eta\to 2\gamma)=39.43\pm0.26\%$, and $B(\omega\to\pi^+\pi^-\pi^0)=(89.1\pm0.7)\%$.

$\Gamma(\omega f_0(980))/\Gamma_{total}$ Γ_{67}/Γ

VALUE (units 10^{-4})	DOCUMENT ID		TECN	COMMENT
1.41±0.27±0.47	[1] AUGUSTIN	89	DM2	$J/\psi\to 2(\pi^+\pi^-)\pi^0$

[1] Assuming $B(f_0(980)\to\pi\pi)=0.78$.

$\Gamma(\rho\eta'(958))/\Gamma_{total}$ Γ_{68}/Γ

VALUE (units 10^{-3})	EVTS	DOCUMENT ID		TECN	COMMENT
0.105±0.018 OUR AVERAGE					
0.083±0.030±0.012	19	JOUSSET	90	DM2	$J/\psi\to$ hadrons
0.114±0.014±0.016		COFFMAN	88	MRK3	$J/\psi\to\pi^+\pi^-\eta'$

$\Gamma(a_2(1320)^\pm\pi^\mp)/\Gamma_{total}$ Γ_{69}/Γ

VALUE (units 10^{-4})	CL%	DOCUMENT ID		TECN	COMMENT
<43	90	BRAUNSCH...	76	DASP	e^+e^-

$\Gamma(K\overline{K}_2^*(1430)+\text{c.c.})/\Gamma_{total}$ Γ_{70}/Γ

VALUE (units 10^{-4})	CL%	DOCUMENT ID		TECN	COMMENT
<40	90	VANNUCCI	77	MRK1	$e^+e^-\to K^0\overline{K}_2^{*0}$
• • • We do not use the following data for averages, fits, limits, etc. • • •					
<66	90	BRAUNSCH...	76	DASP	$e^+e^-\to K^\pm\overline{K}_2^{*\mp}$

$\Gamma(K_1(1270)^\pm K^\mp)/\Gamma_{total}$ Γ_{71}/Γ

VALUE (units 10^{-3})	CL%	DOCUMENT ID		TECN	COMMENT
<3.0	90	[1] BAI	99C	BES	e^+e^-

[1] Assuming $B(K_1(1270)\to K\rho)=0.42\pm0.06$

$\Gamma(K_2^*(1430)^0\overline{K}_2^*(1430)^0)/\Gamma_{total}$ Γ_{72}/Γ

VALUE (units 10^{-4})	CL%	DOCUMENT ID		TECN	COMMENT
<29	90	VANNUCCI	77	MRK1	$e^+e^-\to\pi^+\pi^-K^+K^-$

$\Gamma(\phi\pi^0)/\Gamma_{total}$ Γ_{73}/Γ

VALUE (units 10^{-6})	CL%	DOCUMENT ID		TECN	COMMENT
<6.4	90	ABLIKIM	05B	BES2	$e^+e^-\to J/\psi\to\phi\gamma\gamma$
• • • We do not use the following data for averages, fits, limits, etc. • • •					
<6.8	90	COFFMAN	88	MRK3	$e^+e^-\to K^+K^-\pi^0$

$\Gamma(\phi\eta(1405)\to\phi\eta\pi\pi)/\Gamma_{total}$ Γ_{74}/Γ

VALUE (units 10^{-4})	CL%	DOCUMENT ID		TECN	COMMENT
<2.5	90	[1] FALVARD	88	DM2	$J/\psi\to$ hadrons

[1] Includes unknown branching fraction $\eta(1405)\to\eta\pi\pi$.

$\Gamma(\omega f_2'(1525))/\Gamma_{total}$ Γ_{75}/Γ

VALUE (units 10^{-4})	CL%	DOCUMENT ID		TECN	COMMENT
<2.2	90	[1] VANNUCCI	77	MRK1	$e^+e^-\to\pi^+\pi^-\pi^0K^+K^-$
• • • We do not use the following data for averages, fits, limits, etc. • • •					
<2.8	90	[1] FALVARD	88	DM2	$J/\psi\to$ hadrons

[1] Re-evaluated assuming $B(f_2'(1525)\to K\overline{K})=0.713$.

$\Gamma(\omega X(1835)\to\omega p\overline{p})/\Gamma_{total}$ Γ_{76}/Γ

VALUE (units 10^{-6})	CL%	DOCUMENT ID		TECN	COMMENT
<3.9	95	ABLIKIM	13P	BES3	$J/\psi\to\gamma\pi^0p\overline{p}$

$\Gamma(\eta\phi(2170)\to\eta K^*(892)^0\overline{K}^*(892)^0)/\Gamma_{total}$ Γ_{77}/Γ

VALUE (units 10^{-4})	CL%	DOCUMENT ID		TECN	COMMENT
<2.52	90	ABLIKIM	10C	BES2	$J/\psi\to\eta K^+\pi^-K^-\pi^+$

$\Gamma(\Sigma(1385)^0\overline{\Lambda}+\text{c.c.})/\Gamma_{total}$ Γ_{78}/Γ

VALUE (units 10^{-5})	CL%	DOCUMENT ID		TECN	COMMENT
< 0.82	90	ABLIKIM	13F	BES3	$J/\psi\to p\overline{p}\pi^+\pi^-\gamma\gamma$
• • • We do not use the following data for averages, fits, limits, etc. • • •					
<20	90	HENRARD	87	DM2	e^+e^-

$\Gamma(\Delta(1232)^+\overline{p})/\Gamma_{total}$ Γ_{79}/Γ

VALUE (units 10^{-3})	CL%	DOCUMENT ID		TECN	COMMENT
<0.1	90	HENRARD	87	DM2	e^+e^-

$\Gamma(\Lambda(1520)\overline{\Lambda}+\text{c.c.}\to\gamma\Lambda\overline{\Lambda})/\Gamma_{total}$ Γ_{80}/Γ

VALUE (units 10^{-6})	CL%	DOCUMENT ID		TECN	COMMENT
<4.1	90	ABLIKIM	12B	BES3	$J/\psi\to\Lambda\overline{\Lambda}\gamma$

$\Gamma(\Theta(1540)\overline{\Theta}(1540)\to K_S^0pK^-\overline{n}+\text{c.c.})/\Gamma_{total}$ Γ_{81}/Γ

VALUE (units 10^{-5})	CL%	DOCUMENT ID		TECN	COMMENT
<1.1	90	BAI	04G	BES2	e^+e^-

$\Gamma(\Theta(1540)K^-\overline{n}\to K_S^0pK^-\overline{n})/\Gamma_{total}$ Γ_{82}/Γ

VALUE (units 10^{-5})	CL%	DOCUMENT ID		TECN	COMMENT
<2.1	90	BAI	04G	BES2	e^+e^-

$\Gamma(\Theta(1540)K_S^0\overline{p}\to K_S^0\overline{p}K^+n)/\Gamma_{total}$ Γ_{83}/Γ

VALUE (units 10^{-5})	CL%	DOCUMENT ID		TECN	COMMENT
<1.6	90	BAI	04G	BES2	e^+e^-

$\Gamma(\overline{\Theta}(1540)K^+n\to K_S^0\overline{p}K^+n)/\Gamma_{total}$ Γ_{84}/Γ

VALUE (units 10^{-5})	CL%	DOCUMENT ID		TECN	COMMENT
<5.6	90	BAI	04G	BES2	e^+e^-

$\Gamma(\overline{\Theta}(1540)K_S^0p\to K_S^0pK^-\overline{n})/\Gamma_{total}$ Γ_{85}/Γ

VALUE (units 10^{-5})	CL%	DOCUMENT ID		TECN	COMMENT
<1.1	90	BAI	04G	BES2	e^+e^-

$\Gamma(\Sigma^0\overline{\Lambda})/\Gamma_{total}$ Γ_{86}/Γ

VALUE (units 10^{-4})	CL%	DOCUMENT ID		TECN	COMMENT
<0.9	90	HENRARD	87	DM2	e^+e^-

STABLE HADRONS

$\Gamma(2(\pi^+\pi^-)\pi^0)/\Gamma_{total}$ Γ_{87}/Γ

VALUE (units 10^{-2})	EVTS	DOCUMENT ID		TECN	COMMENT
4.1 ±0.5 OUR AVERAGE		Error includes scale factor of 2.4. See the ideogram below.			
5.46±0.34±0.14	4990	[1] AUBERT	07AU	BABR	10.6 $e^+e^-\to 2(\pi^+\pi^-)\pi^0\gamma$
3.25±0.49	46055	AUGUSTIN	89	DM2	$J/\psi\to 2(\pi^+\pi^-)\pi^0$
3.17±0.42	147	FRANKLIN	83	MRK2	$e^+e^-\to$ hadrons
3.64±0.52	1500	BURMESTER	77D	PLUT	e^+e^-
4 ±1	675	JEAN-MARIE	76	MRK1	e^+e^-

[1] AUBERT 07AU reports $[\Gamma(J/\psi(1S)\to 2(\pi^+\pi^-)\pi^0)/\Gamma_{total}]\times[\Gamma(J/\psi(1S)\to e^+e^-)]=0.303\pm0.005\pm0.018$ keV which we divide by our best value $\Gamma(J/\psi(1S)\to e^+e^-)=5.55\pm0.14\pm0.02$ keV. Our first error is their experiment's error and our second error is the systematic error from using our best value.

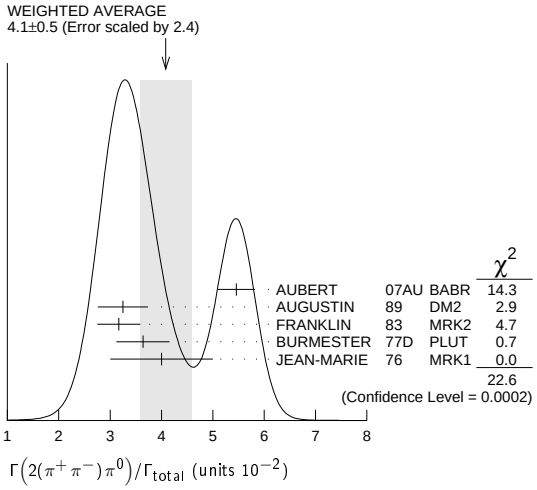

$\Gamma(\omega\pi^+\pi^-)/\Gamma(2(\pi^+\pi^-)\pi^0)$ Γ_{13}/Γ_{87}

VALUE	DOCUMENT ID		TECN	COMMENT
• • • We do not use the following data for averages, fits, limits, etc. • • •				
0.3	[1] JEAN-MARIE	76	MRK1	e^+e^-

[1] Final state $(\pi^+\pi^-)\pi^0$ under the assumption that $\pi\pi$ is isospin 0.

Meson Particle Listings

$J/\psi(1S)$

$\Gamma(3(\pi^+\pi^-)\pi^0)/\Gamma_{total}$ Γ_{88}/Γ

VALUE	EVTS	DOCUMENT ID		TECN	COMMENT
0.029±0.006 OUR AVERAGE					
0.028±0.009	11	FRANKLIN	83	MRK2	$e^+e^- \to$ hadrons
0.029±0.007	181	JEAN-MARIE	76	MRK1	e^+e^-

$\Gamma(\pi^+\pi^-\pi^0)/\Gamma_{total}$ Γ_{89}/Γ

VALUE (units 10^{-3})	EVTS	DOCUMENT ID		TECN	COMMENT
21.1 ±0.7 OUR AVERAGE		Error includes scale factor of 1.5. See the ideogram below.			
$21.37\pm0.04^{+0.64}_{-0.62}$	1.8M	[1,2] ABLIKIM	12H	BES3	$e^+e^- \to J/\psi$
22.9 ±2.0 ±0.4	256	[3] AUBERT	07AU	BABR	10.6 $e^+e^- \to J/\psi\pi^+\pi^-\gamma$
21.8 ±1.9		[4,5] AUBERT,B	04N	BABR	10.6 $e^+e^- \to \pi^+\pi^-\pi^0\gamma$
21.84±0.05±2.01	220k	[1,5] BAI	04H	BES	e^+e^-
20.91±0.21±1.16		[5,6] BAI	04H	BES	e^+e^-
15 ±2	168	FRANKLIN	83	MRK2	e^+e^-

[1] From $J/\psi \to \pi^+\pi^-\pi^0$ events directly.
[2] The quoted systematic error includes a contribution of 1.23% (added in quadrature) from the uncertainty on the number of J/ψ events.
[3] AUBERT 07AU reports $[\Gamma(J/\psi(1S) \to \pi^+\pi^-\pi^0)/\Gamma_{total}] \times [\Gamma(\psi(2S) \to J/\psi(1S)\pi^+\pi^-) \times \Gamma(\psi(2S) \to e^+e^-)/\Gamma_{total}] = (18.6\pm1.2\pm1.1)\times10^{-3}$ keV which we divide by our best value $\Gamma(\psi(2S) \to J/\psi(1S)\pi^+\pi^-) \times \Gamma(\psi(2S) \to e^+e^-)/\Gamma_{total} = 0.813 \pm 0.013$ keV. Our first error is their experiment's error and our second error is the systematic error from using our best value.
[4] From the ratio of $\Gamma(e^+e^-)\,B(\pi^+\pi^-\pi^0)$ and $\Gamma(e^+e^-)\,B(\mu^+\mu^-)$ (AUBERT 04).
[5] Mostly $\rho\pi$, see also $\rho\pi$ subsection.
[6] Obtained comparing the rates for $\pi^+\pi^-\pi^0$ and $\mu^+\mu^-$, using J/ψ events produced via $\psi(2S) \to \pi^+\pi^- J/\psi$ and with $B(J/\psi \to \mu^+\mu^-) = 5.88 \pm 0.10\%$.

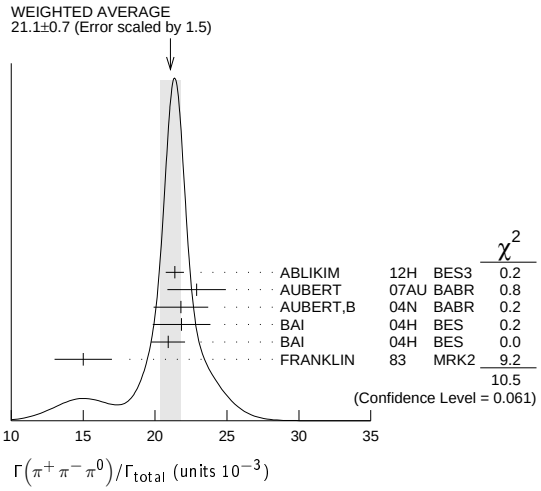

$\Gamma(\pi^+\pi^-K^+K^-)/\Gamma_{total}$ Γ_{90}/Γ

VALUE (units 10^{-2})	EVTS	DOCUMENT ID		TECN	COMMENT
1.79±0.29 OUR AVERAGE		Error includes scale factor of 2.2.			
1.93±0.14±0.05	768	[1] AUBERT	07AU	BABR	10.6 $e^+e^- \to K^+K^-\pi^+\pi^-\pi^0\gamma$
1.2 ±0.3	309	VANNUCCI	77	MRK1	e^+e^-

[1] AUBERT 07AU reports $[\Gamma(J/\psi(1S) \to \pi^+\pi^-\pi^0K^+K^-)/\Gamma_{total}] \times [\Gamma(J/\psi(1S) \to e^+e^-)] = 0.1070\pm0.0043\pm0.0064$ keV which we divide by our best value $\Gamma(J/\psi(1S) \to e^+e^-) = 5.55 \pm 0.14 \pm 0.02$ keV. Our first error is their experiment's error and our second error is the systematic error from using our best value.

$\Gamma(4(\pi^+\pi^-)\pi^0)/\Gamma_{total}$ Γ_{91}/Γ

VALUE (units 10^{-4})	EVTS	DOCUMENT ID		TECN	COMMENT
90±30	13	JEAN-MARIE	76	MRK1	e^+e^-

$\Gamma(\pi^+\pi^-K^+K^-)/\Gamma_{total}$ Γ_{92}/Γ

VALUE (units 10^{-3})	EVTS	DOCUMENT ID		TECN	COMMENT
6.6±0.5 OUR AVERAGE					
6.5±0.4±0.2	1.6k	[1] AUBERT	07AK	BABR	10.6 $e^+e^- \to \pi^+\pi^-K^+K^-\gamma$
7.2±2.3	205	VANNUCCI	77	MRK1	e^+e^-
• • • We do not use the following data for averages, fits, limits, etc. • • •					
6.1±0.7±0.2	233	[2] AUBERT	05D	BABR	10.6 $e^+e^- \to K^+K^-\pi^+\pi^-\gamma$

[1] AUBERT 07AK reports $[\Gamma(J/\psi(1S) \to \pi^+\pi^-K^+K^-)/\Gamma_{total}] \times [\Gamma(J/\psi(1S) \to e^+e^-)] = (36.3\pm1.3\pm2.1)\times10^{-3}$ keV which we divide by our best value $\Gamma(J/\psi(1S) \to e^+e^-) = 5.55 \pm 0.14 \pm 0.02$ keV. Our first error is their experiment's error and our second error is the systematic error from using our best value.
[2] Superseded by AUBERT 07AK. AUBERT 05D reports $[\Gamma(J/\psi(1S) \to \pi^+\pi^-K^+K^-)/\Gamma_{total}] \times [\Gamma(J/\psi(1S) \to e^+e^-)] = (33.6 \pm 2.7 \pm 2.7)\times10^{-3}$ keV which we divide by our best value $\Gamma(J/\psi(1S) \to e^+e^-) = 5.55 \pm 0.14 \pm 0.02$ keV. Our first error is their experiment's error and our second error is the systematic error from using our best value.

$\Gamma(\pi^+\pi^-K^+K^-\eta)/\Gamma_{total}$ Γ_{93}/Γ

VALUE (units 10^{-3})	EVTS	DOCUMENT ID		TECN	COMMENT
1.84±0.28±0.05	73	[1] AUBERT	07AU	BABR	10.6 $e^+e^- \to K^+K^-\pi^+\pi^-\eta\gamma$

[1] AUBERT 07AU reports $[\Gamma(J/\psi(1S) \to \pi^+\pi^-K^+K^-\eta)/\Gamma_{total}] \times [\Gamma(J/\psi(1S) \to e^+e^-)] = (10.2\pm1.3\pm0.8)\times10^{-3}$ keV which we divide by our best value $\Gamma(J/\psi(1S) \to e^+e^-) = 5.55 \pm 0.14 \pm 0.02$ keV. Our first error is their experiment's error and our second error is the systematic error from using our best value.

$\Gamma(\pi^0\pi^0K^+K^-)/\Gamma_{total}$ Γ_{94}/Γ

VALUE (units 10^{-3})	EVTS	DOCUMENT ID		TECN	COMMENT
2.45±0.31±0.06	203 ± 16	[1] AUBERT	07AK	BABR	10.6 $e^+e^- \to \pi^0\pi^0K^+K^-\gamma$

[1] AUBERT 07AK reports $[\Gamma(J/\psi(1S) \to \pi^0\pi^0K^+K^-)/\Gamma_{total}] \times [\Gamma(J/\psi(1S) \to e^+e^-)] = (13.6\pm1.1\pm1.3)\times10^{-3}$ keV which we divide by our best value $\Gamma(J/\psi(1S) \to e^+e^-) = 5.55 \pm 0.14 \pm 0.02$ keV. Our first error is their experiment's error and our second error is the systematic error from using our best value.

$\Gamma(K\overline{K}\pi)/\Gamma_{total}$ Γ_{95}/Γ

VALUE (units 10^{-4})	EVTS	DOCUMENT ID		TECN	COMMENT
61 ±10 OUR AVERAGE					
55.2±12.0	25	FRANKLIN	83	MRK2	$e^+e^- \to K^+K^-\pi^0$
78.0±21.0	126	VANNUCCI	77	MRK1	$e^+e^- \to K^0_S K^\pm\pi^\mp$

$\Gamma(2(\pi^+\pi^-))/\Gamma_{total}$ Γ_{96}/Γ

VALUE (units 10^{-3})	EVTS	DOCUMENT ID		TECN	COMMENT
3.57±0.30 OUR AVERAGE					
3.53±0.12±0.29	1107	[1] ABLIKIM	05H	BES2	$e^+e^- \to \psi(2S) \to J/\psi\pi^+\pi^-$, $J/\psi \to 2(\pi^+\pi^-)$
4.0 ±1.0	76	JEAN-MARIE	76	MRK1	e^+e^-
• • • We do not use the following data for averages, fits, limits, etc. • • •					
3.51±0.34±0.09	270	[2] AUBERT	05D	BABR	10.6 $e^+e^- \to 2(\pi^+\pi^-)\gamma$

[1] Computed using $B(J/\psi \to \mu^+\mu^-) = 0.0588 \pm 0.0010$.
[2] AUBERT 05D reports $[\Gamma(J/\psi(1S) \to 2(\pi^+\pi^-))/\Gamma_{total}] \times [\Gamma(J/\psi(1S) \to e^+e^-)] = (19.5 \pm 1.4 \pm 1.3) \times 10^{-3}$ keV which we divide by our best value $\Gamma(J/\psi(1S) \to e^+e^-) = 5.55 \pm 0.14 \pm 0.02$ keV. Our first error is their experiment's error and our second error is the systematic error from using our best value. Superseded by LEES 12E.

$\Gamma(3(\pi^+\pi^-))/\Gamma_{total}$ Γ_{97}/Γ

VALUE (units 10^{-4})	EVTS	DOCUMENT ID		TECN	COMMENT
43 ± 4 OUR AVERAGE					
43.0± 2.9±2.8	496	[1] AUBERT	06D	BABR	10.6 $e^+e^- \to 3(\pi^+\pi^-)\gamma$
40 ±20	32	JEAN-MARIE	76	MRK1	e^+e^-

[1] Using $\Gamma(J/\psi \to e^+e^-) = 5.52 \pm 0.14 \pm 0.04$ keV.

$\Gamma(2(\pi^+\pi^-\pi^0))/\Gamma_{total}$ Γ_{98}/Γ

VALUE (units 10^{-2})	EVTS	DOCUMENT ID		TECN	COMMENT
1.62±0.09±0.19	761	[1] AUBERT	06D	BABR	10.6 $e^+e^- \to 2(\pi^+\pi^-\pi^0)\gamma$

[1] Using $\Gamma(J/\psi \to e^+e^-) = 5.52 \pm 0.14 \pm 0.04$ keV.

$\Gamma(2(\pi^+\pi^-)\eta)/\Gamma_{total}$ Γ_{99}/Γ

VALUE (units 10^{-3})	EVTS	DOCUMENT ID		TECN	COMMENT
2.29±0.24 OUR AVERAGE					
2.35±0.39±0.20	85	[1] AUBERT	07AU	BABR	10.6 $e^+e^- \to 2(\pi^+\pi^-)\eta\gamma$
2.26±0.08±0.27	4839	ABLIKIM	05C	BES2	$e^+e^- \to 2(\pi^+\pi^-)\eta$

[1] AUBERT 07AU quotes $\Gamma_{ee}^{J/\psi} \cdot B(J/\psi \to 2(\pi^+\pi^-)\eta) \cdot B(\eta \to \gamma\gamma) = 5.16 \pm 0.85 \pm 0.39$ eV.

$\Gamma(3(\pi^+\pi^-)\eta)/\Gamma_{total}$ Γ_{100}/Γ

VALUE (units 10^{-4})	EVTS	DOCUMENT ID		TECN	COMMENT
7.24±0.96±1.11	616	ABLIKIM	05C	BES2	$e^+e^- \to 3(\pi^+\pi^-)\eta$

$\Gamma(p\overline{p})/\Gamma_{total}$ Γ_{101}/Γ

VALUE (units 10^{-3})	EVTS	DOCUMENT ID		TECN	COMMENT
2.120±0.029 OUR AVERAGE					
2.112±0.004±0.031	314k	ABLIKIM	12C	BES3	e^+e^-
2.15 ±0.16 ±0.06	317	[1] WU	06	BELL	$B^+ \to p\overline{p}K^+$
2.26 ±0.01 ±0.14	63316	BAI	04E	BES2	$e^+e^- \to J/\psi$
1.97 ±0.22	99	BALDINI	98	FENI	e^+e^-
1.91 ±0.04 ±0.30		PALLIN	87	DM2	e^+e^-
2.16 ±0.07 ±0.15	1420	EATON	84	MRK2	e^+e^-
2.5 ±0.4	133	BRANDELIK	79C	DASP	e^+e^-
2.0 ±0.5		BESCH	78	BONA	e^+e^-
2.2 ±0.2	331	[2] PERUZZI	78	MRK1	e^+e^-
• • • We do not use the following data for averages, fits, limits, etc. • • •					
2.0 ±0.3	48	ANTONELLI	93	SPEC	e^+e^-

[1] WU 06 reports $[\Gamma(J/\psi(1S) \to p\overline{p})/\Gamma_{total}] \times [B(B^+ \to J/\psi(1S)K^+)] = (2.21 \pm 0.13 \pm 0.10) \times 10^{-6}$ which we divide by our best value $B(B^+ \to J/\psi(1S)K^+) = (1.027 \pm 0.031) \times 10^{-3}$. Our first error is their experiment's error and our second error is the systematic error from using our best value.
[2] Assuming angular distribution $(1+\cos^2\theta)$.

$\Gamma(p\overline{p}\pi^0)/\Gamma_{total}$ Γ_{102}/Γ

VALUE (units 10^{-3})	EVTS	DOCUMENT ID		TECN	COMMENT
1.19±0.08 OUR AVERAGE		Error includes scale factor of 1.1.			
1.33±0.02±0.11	11k	ABLIKIM	09B	BES2	e^+e^-
1.13±0.09±0.09	685	EATON	84	MRK2	e^+e^-
1.4 ±0.4		BRANDELIK	79C	DASP	e^+e^-
1.00±0.15	109	PERUZZI	78	MRK1	e^+e^-

$\Gamma(p\overline{p}\pi^+\pi^-)/\Gamma_{total}$ Γ_{103}/Γ

VALUE (units 10^{-3})	EVTS	DOCUMENT ID		TECN	COMMENT
6.0 ±0.5 OUR AVERAGE		Error includes scale factor of 1.3. See the ideogram below.			
6.46±0.17±0.43	1435	EATON	84	MRK2	e^+e^-
3.8 ±1.6	48	BESCH	81	BONA	e^+e^-
5.5 ±0.6	533	PERUZZI	78	MRK1	e^+e^-

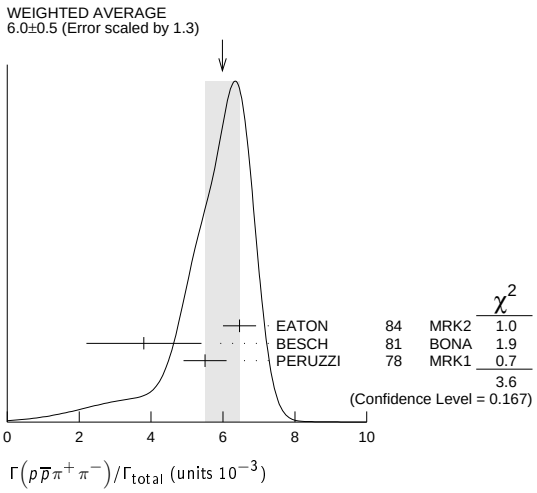

$\Gamma(p\overline{p}\pi^+\pi^-\pi^0)/\Gamma_{total}$ Γ_{104}/Γ

Including $p\overline{p}\pi^+\pi^-\gamma$ and excluding ω, η, η'

VALUE (units 10^{-3})	EVTS	DOCUMENT ID		TECN	COMMENT
2.3 ±0.9 OUR AVERAGE		Error includes scale factor of 1.9.			
3.36±0.65±0.28	364	EATON	84	MRK2	e^+e^-
1.6 ±0.6	39	PERUZZI	78	MRK1	e^+e^-

$\Gamma(p\overline{p}\eta)/\Gamma_{total}$ Γ_{105}/Γ

VALUE (units 10^{-3})	EVTS	DOCUMENT ID		TECN	COMMENT
2.00±0.12 OUR AVERAGE					
1.91±0.02±0.17	13k	[1] ABLIKIM	09	BES2	e^+e^-
2.03±0.13±0.15	826	EATON	84	MRK2	e^+e^-
2.5 ±1.2		BRANDELIK	79C	DASP	e^+e^-
2.3 ±0.4	197	PERUZZI	78	MRK1	e^+e^-

[1] From the combination of $p\overline{p}\eta \to p\overline{p}\gamma\gamma$ and $p\overline{p}\eta \to p\overline{p}\pi^+\pi^-\pi^0$ channels.

$\Gamma(p\overline{p}\rho)/\Gamma_{total}$ Γ_{106}/Γ

VALUE (units 10^{-3})	CL%	DOCUMENT ID		TECN	COMMENT
<0.31	90	EATON	84	MRK2	$e^+e^- \to$ hadronsγ

$\Gamma(p\overline{p}\omega)/\Gamma_{total}$ Γ_{107}/Γ

VALUE (units 10^{-3})	EVTS	DOCUMENT ID		TECN	COMMENT
0.98±0.10 OUR AVERAGE		Error includes scale factor of 1.3. See the ideogram below.			
0.90±0.02±0.09	2670	ABLIKIM	13P	BES3	e^+e^-
0.98±0.03±0.14	2449	ABLIKIM	08	BES2	e^+e^-
1.10±0.17±0.18	486	EATON	84	MRK2	e^+e^-
1.6 ±0.3	77	PERUZZI	78	MRK1	e^+e^-

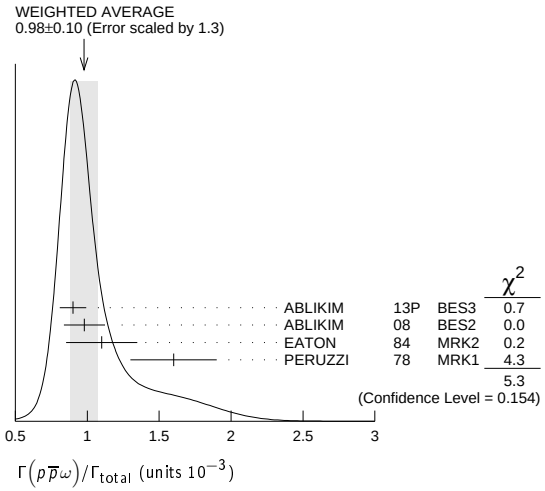

$\Gamma(p\overline{p}\eta'(958))/\Gamma_{total}$ Γ_{108}/Γ

VALUE (units 10^{-3})	EVTS	DOCUMENT ID		TECN	COMMENT
0.21 ±0.04 OUR AVERAGE					
0.200±0.023±0.028	265 ± 31	[1] ABLIKIM	09	BES2	e^+e^-
0.68 ±0.23 ±0.17	19	EATON	84	MRK2	e^+e^-
1.8 ±0.6	19	PERUZZI	78	MRK1	e^+e^-

[1] From the combination of $p\overline{p}\eta' \to p\overline{p}\pi^+\pi^-\eta$ and $p\overline{p}\eta' \to p\overline{p}\gamma\rho^0$ channels.

$\Gamma(p\overline{p}\phi)/\Gamma_{total}$ Γ_{109}/Γ

VALUE (units 10^{-4})	DOCUMENT ID		TECN	COMMENT
0.45±0.13±0.07	FALVARD	88	DM2	$J/\psi \to$ hadrons

$\Gamma(n\overline{n})/\Gamma_{total}$ Γ_{110}/Γ

VALUE (units 10^{-3})	EVTS	DOCUMENT ID		TECN	COMMENT
2.09±0.16 OUR AVERAGE					
2.07±0.01±0.17	36k	ABLIKIM	12C	BES3	e^+e^-
2.31±0.49	79	BALDINI	98	FENI	e^+e^-
1.8 ±0.9		BESCH	78	BONA	e^+e^-
• • • We do not use the following data for averages, fits, limits, etc. • • •					
1.90±0.55	40	ANTONELLI	93	SPEC	e^+e^-

$\Gamma(n\overline{n}\pi^+\pi^-)/\Gamma_{total}$ Γ_{111}/Γ

VALUE (units 10^{-3})	EVTS	DOCUMENT ID		TECN	COMMENT
3.8±3.6	5	BESCH	81	BONA	e^+e^-

$\Gamma(\Sigma^+\overline{\Sigma}^-)/\Gamma_{total}$ Γ_{112}/Γ

VALUE (units 10^{-3})	EVTS	DOCUMENT ID		TECN	COMMENT
1.50±0.10±0.22	399	ABLIKIM	08O	BES2	$e^+e^- \to J/\psi$

$\Gamma(\Sigma^0\overline{\Sigma}^0)/\Gamma_{total}$ Γ_{113}/Γ

VALUE (units 10^{-3})	EVTS	DOCUMENT ID		TECN	COMMENT
1.29±0.09 OUR AVERAGE					
1.15±0.24±0.03		[1] AUBERT	07BD	BABR	10.6 $e^+e^- \to \Sigma^0\overline{\Sigma}^0\gamma$
1.33±0.04±0.11	1779	ABLIKIM	06	BES2	$J/\psi \to \Sigma^0\overline{\Sigma}^0$
1.06±0.04±0.23	884 ± 30	PALLIN	87	DM2	$e^+e^- \to \Sigma^0\overline{\Sigma}^0$
1.58±0.16±0.25	90	EATON	84	MRK2	$e^+e^- \to \Sigma^0\overline{\Sigma}^0$
1.3 ±0.4	52	PERUZZI	78	MRK1	$e^+e^- \to \Sigma^0\overline{\Sigma}^0$
• • • We do not use the following data for averages, fits, limits, etc. • • •					
2.4 ±2.6	3	BESCH	81	BONA	$e^+e^- \to \Sigma^+\overline{\Sigma}^-$

[1] AUBERT 07BD reports $[\Gamma(J/\psi(1S) \to \Sigma^0\overline{\Sigma}^0)/\Gamma_{total}] \times [\Gamma(J/\psi(1S) \to e^+e^-)] = (6.4 \pm 1.2 \pm 0.6) \times 10^{-3}$ keV which we divide by our best value $\Gamma(J/\psi(1S) \to e^+e^-) = 5.55 \pm 0.14 \pm 0.02$ keV. Our first error is their experiment's error and our second error is the systematic error from using our best value.

$\Gamma(2(\pi^+\pi^-)K^+K^-)/\Gamma_{total}$ Γ_{114}/Γ

VALUE (units 10^{-4})	EVTS	DOCUMENT ID		TECN	COMMENT
47 ± 7 OUR AVERAGE		Error includes scale factor of 1.3.			
49.8± 4.2±3.4	205	[1] AUBERT	06D	BABR	10.6 $e^+e^- \to \omega K^+K^-2(\pi^+\pi^-)\gamma$
31 ±13	30	VANNUCCI	77	MRK1	e^+e^-

[1] Using $\Gamma(J/\psi \to e^+e^-) = 5.52 \pm 0.14 \pm 0.04$ keV.

Meson Particle Listings

$J/\psi(1S)$

$\Gamma(p\overline{n}\pi^-)/\Gamma_{total}$ Γ_{115}/Γ

VALUE (units 10^{-3})	EVTS	DOCUMENT ID		TECN	COMMENT
2.12±0.09 OUR AVERAGE					
2.36±0.02±0.21	59k	ABLIKIM	06K	BES2	$J/\psi \to p\pi^-\overline{n}$
2.47±0.02±0.24	55k	ABLIKIM	06K	BES2	$J/\psi \to \overline{p}\pi^+ n$
2.02±0.07±0.16	1288	EATON	84	MRK2	$e^+e^- \to p\pi^-$
1.93±0.07±0.16	1191	EATON	84	MRK2	$e^+e^- \to \overline{p}\pi^+$
1.7 ±0.7	32	BESCH	81	BONA	$e^+e^- \to p\pi^-$
1.6 ±1.2	5	BESCH	81	BONA	$e^+e^- \to \overline{p}\pi^+$
2.16±0.29	194	PERUZZI	78	MRK1	$e^+e^- \to p\pi^-$
2.04±0.27	204	PERUZZI	78	MRK1	$e^+e^- \to \overline{p}\pi^+$

$\Gamma(\Xi^-\overline{\Xi}^+)/\Gamma_{total}$ Γ_{119}/Γ

VALUE (units 10^{-3})	EVTS	DOCUMENT ID		TECN	COMMENT
0.86±0.11 OUR AVERAGE Error includes scale factor of 1.2.					
0.90±0.03±0.18	961 ± 35	ABLIKIM	12P	BES2	$J/\psi \to \Xi^-\overline{\Xi}^+$
0.70±0.06±0.12	132 ± 11	HENRARD	87	DM2	$e^+e^- \to \Xi^-\overline{\Xi}^+$
1.14±0.08±0.20	194	EATON	84	MRK2	$e^+e^- \to \Xi^-\overline{\Xi}^+$
1.4 ±0.5	51	PERUZZI	78	MRK1	$e^+e^- \to \Xi^-\overline{\Xi}^+$

$\Gamma(\Lambda\overline{\Lambda})/\Gamma_{total}$ Γ_{120}/Γ

VALUE (units 10^{-3})	EVTS	DOCUMENT ID		TECN	COMMENT
1.61±0.15 OUR AVERAGE Error includes scale factor of 1.9. See the ideogram below.					
1.93±0.21±0.05		[1] AUBERT	07BD	BABR	10.6 $e^+e^- \to \Lambda\overline{\Lambda}\gamma$
2.03±0.03±0.15	8887	ABLIKIM	06	BES2	$J/\psi \to \Lambda\overline{\Lambda}$
$1.9\ ^{+0.5}_{-0.4}$ ±0.1	46	[2] WU	06	BELL	$B^+ \to \Lambda\overline{\Lambda}K^+$
1.08±0.06±0.24	631	BAI	98G	BES	e^+e^-
1.38±0.05±0.20	1847	PALLIN	87	DM2	e^+e^-
1.58±0.08±0.19	365	EATON	84	MRK2	e^+e^-
2.6 ±1.6	5	BESCH	81	BONA	e^+e^-
1.1 ±0.2	196	PERUZZI	78	MRK1	e^+e^-

[1] AUBERT 07BD reports $[\Gamma(J/\psi(1S) \to \Lambda\overline{\Lambda})/\Gamma_{total}] \times [\Gamma(J/\psi(1S) \to e^+e^-)] = (10.7 \pm 0.9 \pm 0.7) \times 10^{-3}$ keV which we divide by our best value $\Gamma(J/\psi(1S) \to e^+e^-) = 5.55 \pm 0.14 \pm 0.02$ keV. Our first error is their experiment's error and our second error is the systematic error from using our best value.

[2] WU 06 reports $[\Gamma(J/\psi(1S) \to \Lambda\overline{\Lambda})/\Gamma_{total}] \times [B(B^+ \to J/\psi(1S)K^+)] = (2.00\ ^{+0.34}_{-0.29} \pm 0.34) \times 10^{-6}$ which we divide by our best value $B(B^+ \to J/\psi(1S)K^+) = (1.027 \pm 0.031) \times 10^{-3}$. Our first error is their experiment's error and our second error is the systematic error from using our best value.

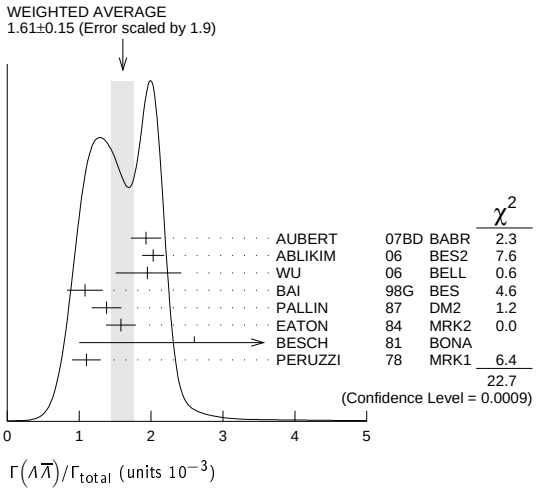

$\Gamma(\Lambda\overline{\Lambda})/\Gamma(p\overline{p})$ $\Gamma_{120}/\Gamma_{101}$

VALUE	DOCUMENT ID		TECN	COMMENT
$\mathbf{0.90\ ^{+0.15}_{-0.14} \pm 0.10}$	[1] WU	06	BELL	$B^+ \to p\overline{p}K^+, \Lambda\overline{\Lambda}K^+$

[1] Not independent of other $J/\psi \to \Lambda\overline{\Lambda}$, $p\overline{p}$ branching ratios reported by WU 06.

$\Gamma(\Lambda\overline{\Sigma}^-\pi^+ \text{(or c.c.)})/\Gamma_{total}$ Γ_{121}/Γ

VALUE (units 10^{-3})	EVTS	DOCUMENT ID		TECN	COMMENT
0.83 ±0.07 OUR AVERAGE Error includes scale factor of 1.2.					
0.770±0.051±0.083	335	[1] ABLIKIM	07H	BES2	$e^+e^- \to \overline{\Lambda}\Sigma^+\pi^-$
0.747±0.056±0.076	254	[1] ABLIKIM	07H	BES2	$e^+e^- \to \Lambda\overline{\Sigma}^-\pi^+$
0.90 ±0.06 ±0.16	225 ± 15	HENRARD	87	DM2	$e^+e^- \to \overline{\Lambda}\Sigma^+\pi^-$
1.11 ±0.06 ±0.20	342 ± 18	HENRARD	87	DM2	$e^+e^- \to \Lambda\overline{\Sigma}^-\pi^+$
1.53 ±0.17 ±0.38	135	EATON	84	MRK2	$e^+e^- \to \overline{\Lambda}\Sigma^+\pi^-$
1.38 ±0.21 ±0.35	118	EATON	84	MRK2	$e^+e^- \to \Lambda\overline{\Sigma}^-\pi^+$

[1] Using $B(\Lambda \to \pi^-p) = 63.9\%$ and $B(\Sigma^+ \to \pi^0p) = 51.6\%$.

$\Gamma(pK^-\overline{\Lambda})/\Gamma_{total}$ Γ_{122}/Γ

VALUE (units 10^{-3})	EVTS	DOCUMENT ID		TECN	COMMENT
0.89±0.07±0.14	307	EATON	84	MRK2	e^+e^-

$\Gamma(2(K^+K^-))/\Gamma_{total}$ Γ_{123}/Γ

VALUE (units 10^{-3})	EVTS	DOCUMENT ID		TECN	COMMENT
0.76±0.09 OUR AVERAGE					
0.74±0.09±0.02	156 ± 15	[1] AUBERT	07AK	BABR	10.6 $e^+e^- \to 2(K^+K^-)\gamma$
$1.4\ ^{+0.5}_{-0.4}$ ±0.2	$11.0 \pm ^{4.3}_{3.5}$	[2] HUANG	03	BELL	$B^+ \to 2(K^+K^-)\ K^+$
0.7 ±0.3		VANNUCCI	77	MRK1	e^+e^-
• • • We do not use the following data for averages, fits, limits, etc. • • •					
0.72±0.17±0.02	38	[3] AUBERT	05D	BABR	10.6 $e^+e^- \to 2(K^+K^-)\gamma$

[1] AUBERT 07AK reports $[\Gamma(J/\psi(1S) \to 2(K^+K^-))/\Gamma_{total}] \times [\Gamma(J/\psi(1S) \to e^+e^-)] = (4.11 \pm 0.39 \pm 0.30) \times 10^{-3}$ keV which we divide by our best value $\Gamma(J/\psi(1S) \to e^+e^-) = 5.55 \pm 0.14 \pm 0.02$ keV. Our first error is their experiment's error and our second error is the systematic error from using our best value.

[2] Using $B(B^+ \to J/\psi K^+) = (1.01 \pm 0.05) \times 10^{-3}$.

[3] Superseded by AUBERT 07AK. AUBERT 05D reports $[\Gamma(J/\psi(1S) \to 2(K^+K^-))/\Gamma_{total}] \times [\Gamma(J/\psi(1S) \to e^+e^-)] = (4.0 \pm 0.7 \pm 0.6) \times 10^{-3}$ keV which we divide by our best value $\Gamma(J/\psi(1S) \to e^+e^-) = 5.55 \pm 0.14 \pm 0.02$ keV. Our first error is their experiment's error and our second error is the systematic error from using our best value.

$\Gamma(pK^-\overline{\Sigma}^0)/\Gamma_{total}$ Γ_{124}/Γ

VALUE (units 10^{-3})	EVTS	DOCUMENT ID		TECN	COMMENT
0.29±0.06±0.05	90	EATON	84	MRK2	e^+e^-

$\Gamma(K^+K^-)/\Gamma_{total}$ Γ_{125}/Γ

VALUE (units 10^{-4})	EVTS	DOCUMENT ID		TECN	COMMENT
2.70±0.17 OUR AVERAGE					
2.86±0.09±0.19	1k	[1] METREVELI	12		$\psi(2S) \to \pi^+\pi^-K^+K^-$
2.39±0.24±0.22	107	BALTRUSAIT...85D		MRK3	e^+e^-
2.2 ±0.9	6	BRANDELIK	79C	DASP	e^+e^-

[1] Obtained by analyzing CLEO-c data but not authored by the CLEO Collaboration.

$\Gamma(K^0_SK^0_L)/\Gamma_{total}$ Γ_{126}/Γ

VALUE (units 10^{-4})	EVTS	DOCUMENT ID		TECN	COMMENT
2.1 ±0.4 OUR AVERAGE Error includes scale factor of 3.2.					
2.62±0.15±0.14	0.3k	[1] METREVELI	12		$\psi(2S) \to \pi^+\pi^-K^0_SK^0_L$
1.82±0.04±0.13	2.1k	[2] BAI	04A	BES2	$J/\psi \to K^0_SK^0_L \to \pi^+\pi^-X$
• • • We do not use the following data for averages, fits, limits, etc. • • •					
1.18±0.12±0.18		JOUSSET	90	DM2	$J/\psi \to$ hadrons
1.01±0.16±0.09	74	BALTRUSAIT...85D		MRK3	e^+e^-

[1] Obtained by analyzing CLEO-c data but not authored by the CLEO Collaboration.

[2] Using $B(K^0_S \to \pi^+\pi^-) = 0.6868 \pm 0.0027$.

$\Gamma(\Lambda\overline{\Lambda}\pi^+\pi^-)/\Gamma_{total}$ Γ_{127}/Γ

VALUE (units 10^{-3})	EVTS	DOCUMENT ID		TECN	COMMENT
4.30±0.13±0.99	2.4k	ABLIKIM	12P	BES2	J/ψ

$\Gamma(\Lambda\overline{\Lambda}\eta)/\Gamma_{total}$ Γ_{128}/Γ

VALUE (units 10^{-5})	EVTS	DOCUMENT ID		TECN	COMMENT
16.2±1.7 OUR AVERAGE					
15.7±0.80±1.54	454	[1] ABLIKIM	13F	BES3	$J/\psi \to p\overline{p}\pi^+\pi^-\gamma\gamma$
26.2±6.0 ±4.4	44	[2] ABLIKIM	07H	BES2	$e^+e^- \to \psi(2S)$

[1] Using $B(\Lambda \to \pi^-p) = 63.9\%$ and $B(\eta \to \gamma\gamma) = 39.31\%$.

[2] Using $B(\Lambda \to \pi^-p) = 63.9\%$ and $B(\eta \to \gamma\gamma) = 39.4\%$.

$\Gamma(\Lambda\overline{\Lambda}\pi^0)/\Gamma_{total}$ Γ_{129}/Γ

VALUE (units 10^{-5})	CL%	EVTS	DOCUMENT ID		TECN	COMMENT
3.78±0.27±0.30		323	[1] ABLIKIM	13F	BES3	$J/\psi \to p\overline{p}\pi^+\pi^-\gamma\gamma$
• • • We do not use the following data for averages, fits, limits, etc. • • •						
< 6.4	90		[2] ABLIKIM	07H	BES2	$e^+e^- \to \psi(2S)$
23 ±7 ±8		11	BAI	98G	BES	e^+e^-
22 ±5 ±5		19	HENRARD	87	DM2	e^+e^-

[1] Using $B(\Lambda \to \pi^-p) = 63.9\%$ and $B(\pi^0 \to \gamma\gamma) = 98.8\%$.

[2] Using $B(\Lambda \to \pi^-p) = 63.9\%$.

$\Gamma(\overline{\Lambda}nK^0_S + \text{c.c.})/\Gamma_{total}$ Γ_{130}/Γ

VALUE (units 10^{-4})	EVTS	DOCUMENT ID		TECN	COMMENT
6.46±0.20±1.07	1058	[1] ABLIKIM	08C	BES2	$e^+e^- \to J/\psi$

[1] Using $B(\overline{\Lambda} \to \overline{p}\pi^+) = 63.9\%$ and $B(K^0_S \to \pi^+\pi^-) = 69.2\%$.

$\Gamma(\pi^+\pi^-)/\Gamma_{total}$ Γ_{131}/Γ

VALUE (units 10^{-4})	EVTS	DOCUMENT ID		TECN	COMMENT
1.47±0.14 OUR AVERAGE					
1.47±0.13±0.13	140	[1] METREVELI	12		$\psi(2S) \to 2(\pi^+\pi^-)$
1.58±0.20±0.15	84	BALTRUSAIT...85D		MRK3	e^+e^-
1.0 ±0.5	5	BRANDELIK	78B	DASP	e^+e^-
1.6 ±1.6	1	VANNUCCI	77	MRK1	e^+e^-

[1] Obtained by analyzing CLEO-c data but not authored by the CLEO Collaboration.

$\Gamma(\Lambda\overline{\Sigma}+\text{c.c.})/\Gamma_{\text{total}}$ Γ_{132}/Γ

VALUE (units 10^{-5})	CL%	EVTS	DOCUMENT ID		TECN	COMMENT
2.83±0.23 OUR AVERAGE						
2.74±0.24±0.22		234 ± 21	[1] ABLIKIM	12B	BES3	$J/\psi \to \Lambda\overline{\Sigma}^0$
2.92±0.22±0.24		308 ± 24	[2] ABLIKIM	12B	BES3	$J/\psi \to \overline{\Lambda}\Sigma^0$
• • • We do not use the following data for averages, fits, limits, etc. • • •						
<15	90		PERUZZI	78	MRK1	$e^+e^- \to \Lambda X$

[1] ABLIKIM 12B quotes $B(J/\psi \to \Lambda\overline{\Sigma}^0)$ which we multiply by 2.
[2] ABLIKIM 12B quotes $B(J/\psi \to \overline{\Lambda}\Sigma^0)$ which we multiply by 2.

$\Gamma(K^0_S K^0_S)/\Gamma_{\text{total}}$ Γ_{133}/Γ

VALUE (units 10^{-4})	CL%	DOCUMENT ID		TECN	COMMENT
<0.01	95	[1] BAI	04D	BES	e^+e^-
• • • We do not use the following data for averages, fits, limits, etc. • • •					
<0.052	90	[1] BALTRUSAIT...	85C	MRK3	e^+e^-

[1] Forbidden by *CP*.

RADIATIVE DECAYS

$\Gamma(3\gamma)/\Gamma_{\text{total}}$ Γ_{134}/Γ

VALUE (units 10^{-6})	CL%	EVTS	DOCUMENT ID		TECN	COMMENT
11.6±2.2 OUR AVERAGE						
11.3±1.8±2.0		113 ± 18	ABLIKIM	13I	BES3	$\psi(2S) \to \pi^+\pi^- J/\psi$
12 ±3 ±2		$24.2^{+7.2}_{-6.0}$	ADAMS	08	CLEO	$\psi(2S) \to \pi^+\pi^- J/\psi$
• • • We do not use the following data for averages, fits, limits, etc. • • •						
<55	90		PARTRIDGE	80	CBAL	e^+e^-

$\Gamma(4\gamma)/\Gamma_{\text{total}}$ Γ_{135}/Γ

VALUE (units 10^{-6})	CL%	DOCUMENT ID		TECN	COMMENT
<9	90	ADAMS	08	CLEO	$\psi(2S) \to \pi^+\pi^- J/\psi$

$\Gamma(5\gamma)/\Gamma_{\text{total}}$ Γ_{136}/Γ

VALUE (units 10^{-6})	CL%	DOCUMENT ID		TECN	COMMENT
<15	90	ADAMS	08	CLEO	$\psi(2S) \to \pi^+\pi^- J/\psi$

$\Gamma(\gamma\eta_c(1S))/\Gamma_{\text{total}}$ Γ_{137}/Γ

VALUE (units 10^{-2})	EVTS	DOCUMENT ID		TECN	COMMENT
1.7 ±0.4 OUR AVERAGE Error includes scale factor of 1.6.					
2.01±0.32±0.02		[1] MITCHELL	09	CLEO	$e^+e^- \to \gamma X$
1.27±0.36		GAISER	86	CBAL	$J/\psi \to \gamma X$
• • • We do not use the following data for averages, fits, limits, etc. • • •					
0.79±0.20	273 ± 43	[2] AUBERT	06E	BABR	$B^\pm \to K^\pm X_{c\overline{c}}$
seen	16	BALTRUSAIT...84		MRK3	$J/\psi \to 2\phi\gamma$

[1] MITCHELL 09 reports $(1.98 \pm 0.09 \pm 0.30) \times 10^{-2}$ from a measurement of $[\Gamma(J/\psi(1S) \to \gamma\eta_c(1S))/\Gamma_{\text{total}}] \times [B(\psi(2S) \to J/\psi(1S)\pi^+\pi^-)]$ assuming $B(\psi(2S) \to J/\psi(1S)\pi^+\pi^-) = (35.04 \pm 0.07 \pm 0.77) \times 10^{-2}$, which we rescale to our best value $B(\psi(2S) \to J/\psi(1S)\pi^+\pi^-) = (34.45 \pm 0.30) \times 10^{-2}$. Our first error is their experiment's error and our second error is the systematic error from using our best value.
[2] Calculated by the authors using an average of $B(J/\psi \to \gamma\eta_c) \times B(\eta_c \to K\overline{K}\pi)$ from BALTRUSAITIS 86, BISELLO 91, BAI 04 and $B(\eta_c \to K\overline{K}\pi) = (8.5 \pm 1.8)\%$ from AUBERT 06E.

$\Gamma(\gamma\eta_c(1S) \to 3\gamma)/\Gamma_{\text{total}}$ Γ_{138}/Γ

VALUE (units 10^{-6})	EVTS	DOCUMENT ID		TECN	COMMENT
$\mathbf{3.8^{+1.3}_{-1.0}}$ **OUR AVERAGE** Error includes scale factor of 1.1.					
4.5±1.2±0.6	33 ± 9	ABLIKIM	13I	BES3	$\psi(2S) \to \pi^+\pi^- J/\psi$
$1.2^{+2.7}_{-1.1}$±0.3	$1.2^{+2.8}_{-1.1}$	ADAMS	08	CLEO	$\psi(2S) \to \pi^+\pi^- J/\psi$

$\Gamma(\gamma\pi^+\pi^-2\pi^0)/\Gamma_{\text{total}}$ Γ_{139}/Γ

VALUE (units 10^{-3})	DOCUMENT ID		TECN	COMMENT
8.3±0.2±3.1	[1] BALTRUSAIT...	86B	MRK3	$J/\psi \to 4\pi\gamma$

[1] 4π mass less than 2.0 GeV.

$\Gamma(\gamma\eta\pi\pi)/\Gamma_{\text{total}}$ Γ_{140}/Γ

VALUE (units 10^{-3})	DOCUMENT ID		TECN	COMMENT
6.1 ±1.0 OUR AVERAGE				
5.85±0.3±1.05	[1] EDWARDS	83B	CBAL	$J/\psi \to \eta\pi^+\pi^-$
7.8 ±1.2±2.4	[1] EDWARDS	83B	CBAL	$J/\psi \to \eta 2\pi^0$

[1] Broad enhancement at 1700 MeV.

$\Gamma(\gamma\eta_2(1870) \to \gamma\eta\pi^+\pi^-)/\Gamma_{\text{total}}$ Γ_{141}/Γ

VALUE (units 10^{-4})	DOCUMENT ID		TECN	COMMENT
6.2±2.2±0.9	BAI	99	BES	$J/\psi \to \gamma\eta\pi^+\pi^-$

$\Gamma(\gamma\eta(1405/1475) \to \gamma K\overline{K}\pi)/\Gamma_{\text{total}}$ Γ_{142}/Γ

VALUE (units 10^{-3})	DOCUMENT ID		TECN	COMMENT
2.8 ±0.6 OUR AVERAGE Error includes scale factor of 1.6. See the ideogram below.				
1.66±0.1 ±0.58	[1,2] BAI	00D	BES	$J/\psi \to \gamma K^\pm K^0_S \pi^\mp$
3.8 ±0.3 ±0.6	[3] AUGUSTIN	90	DM2	$J/\psi \to \gamma K\overline{K}\pi$
4.0 ±0.7 ±1.0	[3] EDWARDS	82E	CBAL	$J/\psi \to K^+K^-\pi^0\gamma$
4.3 ±1.7	[3,4] SCHARRE	80	MRK2	e^+e^-
• • • We do not use the following data for averages, fits, limits, etc. • • •				
1.78±0.21±0.33	[3,5,6] AUGUSTIN	92	DM2	$J/\psi \to \gamma K\overline{K}\pi$
0.83±0.13±0.18	[3,7,8] AUGUSTIN	92	DM2	$J/\psi \to \gamma K\overline{K}\pi$
$0.66^{+0.17}_{-0.16}{}^{+0.24}_{-0.15}$	[3,6,9] BAI	90C	MRK3	$J/\psi \to \gamma K^0_S K^\pm\pi^\mp$
$1.03^{+0.21}_{-0.18}{}^{+0.26}_{-0.19}$	[3,8,10] BAI	90C	MRK3	$J/\psi \to \gamma K^0_S K^\pm\pi^\mp$

[1] Interference with the $J/\psi(1S)$ radiative transition to the broad $K\overline{K}\pi$ pseudoscalar state around 1800 is $(0.15 \pm 0.01 \pm 0.05) \times 10^{-3}$.
[2] Interference with $J/\psi \to \gamma f_1(1420)$ is $(-0.03 \pm 0.01 \pm 0.01) \times 10^{-3}$.
[3] Includes unknown branching fraction $\eta(1405) \to K\overline{K}\pi$.
[4] Corrected for spin-zero hypothesis for $\eta(1405)$.
[5] From fit to the $a_0(980)\pi$ 0^{-+} partial wave.
[6] $a_0(980)\pi$ mode.
[7] From fit to the $K^*(892)K$ 0^{-+} partial wave.
[8] K^*K mode.
[9] From $a_0(980)\pi$ final state.
[10] From $K^*(890)K$ final state.

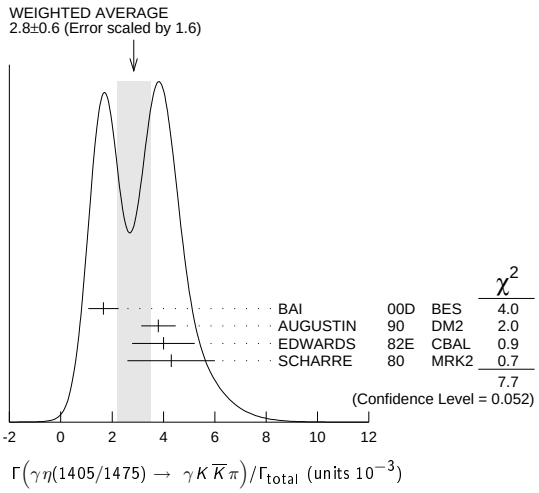

$\Gamma(\gamma\eta(1405/1475) \to \gamma\gamma\rho^0)/\Gamma_{\text{total}}$ Γ_{143}/Γ

VALUE (units 10^{-4})	DOCUMENT ID		TECN	COMMENT
0.78±0.20 OUR AVERAGE Error includes scale factor of 1.8.				
1.07±0.17±0.11	[1] BAI	04J	BES2	$J/\psi \to \gamma\gamma\pi^+\pi^-$
0.64±0.12±0.07	[1] COFFMAN	90	MRK3	$J/\psi \to \gamma\gamma\pi^+\pi^-$

[1] Includes unknown branching fraction $\eta(1405) \to \gamma\rho^0$.

$\Gamma(\gamma\eta(1405/1475) \to \gamma\eta\pi^+\pi^-)/\Gamma_{\text{total}}$ Γ_{144}/Γ

VALUE (units 10^{-4})	EVTS	DOCUMENT ID		TECN	COMMENT
3.0 ±0.5 OUR AVERAGE					
2.6 ±0.7 ±0.4		BAI	99	BES	$J/\psi \to \gamma\eta\pi^+\pi^-$
3.38±0.33±0.64		[1] BOLTON	92B	MRK3	$J/\psi \to \gamma\eta\pi^+\pi^-$
• • • We do not use the following data for averages, fits, limits, etc. • • •					
7.0 ±0.6 ±1.1	261	[2] AUGUSTIN	90	DM2	$J/\psi \to \gamma\eta\pi^+\pi^-$

[1] Via $a_0(980)\pi$.
[2] Includes unknown branching fraction to $\eta\pi^+\pi^-$.

$\Gamma(\gamma\eta(1405/1475) \to \gamma\gamma\phi)/\Gamma_{\text{total}}$ Γ_{145}/Γ

VALUE (units 10^{-4})	CL%	DOCUMENT ID		TECN	COMMENT
<0.82	95	BAI	04J	BES2	$J/\psi \to \gamma\gamma K^+K^-$

$\Gamma(\gamma\rho\rho)/\Gamma_{\text{total}}$ Γ_{146}/Γ

VALUE (units 10^{-3})	CL%	DOCUMENT ID		TECN	COMMENT
4.5 ±0.8 OUR AVERAGE					
4.7 ±0.3 ±0.9		[1] BALTRUSAIT...	86B	MRK3	$J/\psi \to 4\pi\gamma$
3.75±1.05±1.20		[2] BURKE	82	MRK2	$J/\psi \to 4\pi\gamma$
• • • We do not use the following data for averages, fits, limits, etc. • • •					
<0.09	90	[3] BISELLO	89B		$J/\psi \to 4\pi\gamma$

[1] 4π mass less than 2.0 GeV.
[2] 4π mass less than 2.0 GeV. We have multiplied $2\rho^0$ measurement by 3 to obtain 2ρ.
[3] 4π mass in the range 2.0–25 GeV.

Meson Particle Listings

$J/\psi(1S)$

$\Gamma(\gamma\rho\omega)/\Gamma_{\text{total}}$ Γ_{147}/Γ

VALUE (units 10^{-4})	CL%	DOCUMENT ID		TECN	COMMENT
<5.4	90	ABLIKIM	08A	BES2	$e^+e^- \to J/\psi$

$\Gamma(\gamma\rho\phi)/\Gamma_{\text{total}}$ Γ_{148}/Γ

VALUE (units 10^{-5})	CL%	DOCUMENT ID		TECN	COMMENT
<8.8	90	ABLIKIM	08A	BES2	$e^+e^- \to J/\psi$

$\Gamma(\gamma\eta'(958))/\Gamma_{\text{total}}$ Γ_{149}/Γ

VALUE (units 10^{-3})	EVTS	DOCUMENT ID		TECN	COMMENT
5.15±0.16 OUR AVERAGE		Error includes scale factor of 1.2.			
4.82±0.23±0.08		[1] ABLIKIM	11	BES3	$J/\psi \to \eta'\gamma$
5.24±0.12±0.11		PEDLAR	09	CLE3	$J/\psi \to \eta'\gamma$
5.55±0.44	35k	ABLIKIM	06E	BES2	$J/\psi \to \eta'\gamma$
• • • We do not use the following data for averages, fits, limits, etc. • • •					
4.50±0.14±0.53		BOLTON	92B	MRK3	$J/\psi \to \gamma\pi^+\pi^-\eta,\ \eta \to \gamma\gamma$
4.30±0.31±0.71		BOLTON	92B	MRK3	$J/\psi \to \gamma\pi^+\pi^-\eta,\ \eta \to \pi^+\pi^-\pi^0$
4.04±0.16±0.85	622	AUGUSTIN	90	DM2	$J/\psi \to \gamma\eta\pi^+\pi^-$
4.39±0.09±0.66	2420	AUGUSTIN	90	DM2	$J/\psi \to \gamma\gamma\pi^+\pi^-$
4.1 ±0.3 ±0.6		BLOOM	83	CBAL	$e^+e^- \to 3\gamma$ + hadrons
2.9 ±1.1	6	BRANDELIK	79C	DASP	$e^+e^- \to 3\gamma$
2.4 ±0.7	57	BARTEL	76	CNTR	$e^+e^- \to 2\gamma\rho$

[1] ABLIKIM 11 reports $(4.84 \pm 0.03 \pm 0.24) \times 10^{-3}$ from a measurement of $[\Gamma(J/\psi(1S) \to \gamma\eta'(958))/\Gamma_{\text{total}}]$ / $[B(\eta'(958) \to \pi^+\pi^-\eta)]$ / $[B(\eta \to 2\gamma)]$ assuming $B(\eta'(958) \to \pi^+\pi^-\eta) = (43.2 \pm 0.7) \times 10^{-2}$, $B(\eta \to 2\gamma) = (39.31 \pm 0.20) \times 10^{-2}$, which we rescale to our best values $B(\eta'(958) \to \pi^+\pi^-\eta) = (42.9 \pm 0.7) \times 10^{-2}$, $B(\eta \to 2\gamma) = (39.41 \pm 0.20) \times 10^{-2}$. Our first error is their experiment's error and our second error is the systematic error from using our best values.

$\Gamma(\gamma 2\pi^+ 2\pi^-)/\Gamma_{\text{total}}$ Γ_{150}/Γ

VALUE (units 10^{-3})	DOCUMENT ID			TECN	COMMENT
2.8 ±0.5 OUR AVERAGE	Error includes scale factor of 1.9. See the ideogram below.				
4.32±0.14±0.73	[1] BISELLO		89B	DM2	$J/\psi \to 4\pi\gamma$
2.08±0.13±0.35	[2] BISELLO		89B	DM2	$J/\psi \to 4\pi\gamma$
3.05±0.08±0.45	[2] BALTRUSAIT...		86B	MRK3	$J/\psi \to 4\pi\gamma$
4.85±0.45±1.20	[3] BURKE		82	MRK2	e^+e^-

[1] 4π mass less than 3.0 GeV.
[2] 4π mass less than 2.0 GeV.
[3] 4π mass less than 2.5 GeV.

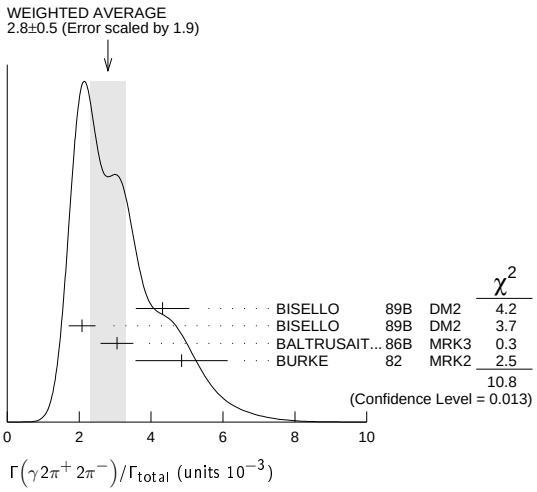

$\Gamma(\gamma f_2(1270) f_2(1270))/\Gamma_{\text{total}}$ Γ_{151}/Γ

VALUE (units 10^{-4})	EVTS	DOCUMENT ID		TECN	COMMENT
9.5±0.7±1.6	646 ± 45	ABLIKIM	04M	BES	$J/\psi \to \gamma 2\pi^+ 2\pi^-$

$\Gamma(\gamma f_2(1270) f_2(1270)\,(\text{non resonant}))/\Gamma_{\text{total}}$ Γ_{152}/Γ

VALUE (units 10^{-4})	DOCUMENT ID			TECN	COMMENT
8.2±0.8±1.7	[1] ABLIKIM		04M	BES	$J/\psi \to \gamma 2\pi^+ 2\pi^-$

[1] Subtracting contribution from intermediate $\eta_c(1S)$ decays.

$\Gamma(\gamma K^+ K^- \pi^+ \pi^-)/\Gamma_{\text{total}}$ Γ_{153}/Γ

VALUE (units 10^{-3})	EVTS	DOCUMENT ID		TECN	COMMENT
2.1±0.1±0.6	1516	BAI	00B	BES	$J/\psi \to \gamma K^+ K^0 \pi^+ \pi^-$

$\Gamma(\gamma f_4(2050))/\Gamma_{\text{total}}$ Γ_{154}/Γ

VALUE (units 10^{-3})	DOCUMENT ID			TECN	COMMENT
2.7±0.5±0.5	[1] BALTRUSAIT...87			MRK3	$J/\psi \to \gamma\pi^+\pi^-$

[1] Assuming branching fraction $f_4(2050) \to \pi\pi$/ total = 0.167.

$\Gamma(\gamma\omega\omega)/\Gamma_{\text{total}}$ Γ_{155}/Γ

VALUE (units 10^{-3})	EVTS	DOCUMENT ID		TECN	COMMENT
1.61±0.33 OUR AVERAGE					
6.0 ±4.8 ±1.8		ABLIKIM	08A	BES2	$J/\psi \to \gamma\omega\pi^+\pi^-$
1.41±0.2 ±0.42	120 ± 17	BISELLO	87	SPEC	e^+e^-, hadronsγ
1.76±0.09±0.45		BALTRUSAIT...85C		MRK3	$e^+e^- \to$ hadronsγ

$\Gamma(\gamma\eta(1405/1475) \to \gamma\rho^0\rho^0)/\Gamma_{\text{total}}$ Γ_{156}/Γ

VALUE (units 10^{-3})	DOCUMENT ID			TECN	COMMENT
1.7 ±0.4 OUR AVERAGE	Error includes scale factor of 1.3.				
2.1 ±0.4	BUGG		95	MRK3	$J/\psi \to \gamma\pi^+\pi^-\pi^+\pi^-$
1.36±0.38	[1,2] BISELLO		89B	DM2	$J/\psi \to 4\pi\gamma$

[1] Estimated by us from various fits.
[2] Includes unknown branching fraction to $\rho^0\rho^0$.

$\Gamma(\gamma f_2(1270))/\Gamma_{\text{total}}$ Γ_{157}/Γ

VALUE (units 10^{-3})	EVTS	DOCUMENT ID		TECN	COMMENT
1.43±0.11 OUR AVERAGE					
$1.62 \pm 0.26^{+0.02}_{-0.05}$		[1] ABLIKIM	06V	BES2	$e^+e^- \to J/\psi \to \gamma\pi^+\pi^-$
$1.42 \pm 0.21^{+0.02}_{-0.04}$		[2] ABLIKIM	06V	BES2	$e^+e^- \to J/\psi \to \gamma\pi^0\pi^0$
1.33±0.05±0.20		[3] AUGUSTIN	87	DM2	$J/\psi \to \gamma\pi^+\pi^-$
1.36±0.09±0.23		[3] BALTRUSAIT...87		MRK3	$J/\psi \to \gamma\pi^+\pi^-$
1.48±0.25±0.30	178	EDWARDS	82B	CBAL	$e^+e^- \to 2\pi^0\gamma$
2.0 ±0.7	35	ALEXANDER	78	PLUT	e^+e^-
1.2 ±0.6	30	[4] BRANDELIK	78B	DASP	$e^+e^- \to \pi^+\pi^-\gamma$

[1] ABLIKIM 06V reports $[\Gamma(J/\psi(1S) \to \gamma f_2(1270))/\Gamma_{\text{total}}] \times [B(f_2(1270) \to \pi\pi)] = (1.371 \pm 0.010 \pm 0.222) \times 10^{-3}$ which we divide by our best value $B(f_2(1270) \to \pi\pi) = (84.8^{+2.4}_{-1.2}) \times 10^{-2}$. Our first error is their experiment's error and our second error is the systematic error from using our best value.
[2] ABLIKIM 06V reports $[\Gamma(J/\psi(1S) \to \gamma f_2(1270))/\Gamma_{\text{total}}] \times [B(f_2(1270) \to \pi\pi)] = (1.200 \pm 0.027 \pm 0.174) \times 10^{-3}$ which we divide by our best value $B(f_2(1270) \to \pi\pi) = (84.8^{+2.4}_{-1.2}) \times 10^{-2}$. Our first error is their experiment's error and our second error is the systematic error from using our best value.
[3] Estimated using $B(f_2(1270) \to \pi\pi)$=0.843 ± 0.012. The errors do not contain the uncertainty in the $f_2(1270)$ decay.
[4] Restated by us to take account of spread of E1, M2, E3 transitions.

$\Gamma(\gamma f_0(1710) \to \gamma K\overline{K})/\Gamma_{\text{total}}$ Γ_{158}/Γ

VALUE (units 10^{-4})	CL%	DOCUMENT ID		TECN	COMMENT
$8.5\ ^{+\ 1.2}_{-\ 0.9}$ OUR AVERAGE	Error includes scale factor of 1.2.				
$9.62 \pm 029\ ^{+3.51}_{-1.86}$		[1] BAI	03G	BES	$J/\psi \to \gamma K\overline{K}$
$5.0 \pm 0.8^{+1.8}_{-0.4}$		[2,3] BAI	96C	BES	$J/\psi \to \gamma K^+ K^-$
9.2 ± 1.4±1.4		[3] AUGUSTIN	88	DM2	$J/\psi \to \gamma K^+ K^-$
10.4 ± 1.2±1.6		[3] AUGUSTIN	88	DM2	$J/\psi \to \gamma K^0_S K^0_S$
9.6 ± 1.2±1.8		[3] BALTRUSAIT...87		MRK3	$J/\psi \to \gamma K^+ K^-$
• • • We do not use the following data for averages, fits, limits, etc. • • •					
$1.6 \pm 0.2^{+0.6}_{-0.2}$		[3,4] BAI	96C	BES	$J/\psi \to \gamma K^+ K^-$
< 0.8	90	[5] BISELLO	89B		$J/\psi \to 4\pi\gamma$
1.6 ± 0.4±0.3		[6] BALTRUSAIT...87		MRK3	$J/\psi \to \gamma\pi^+\pi^-$
3.8 ± 1.6		[7] EDWARDS	82D	CBAL	$e^+e^- \to \eta\eta\gamma$

[1] Includes unknown branching ratio to K^+K^- or $K^0_S K^0_S$.
[2] Assuming $J^P = 2^+$ for $f_0(1710)$.
[3] Includes unknown branching fraction to K^+K^- or $K^0_S K^0_S$. We have multiplied K^+K^- measurement by 2, and $K^0_S K^0_S$ by 4 to obtain $K\overline{K}$ result.
[4] Assuming $J^P = 0^+$ for $f_0(1710)$.
[5] Includes unknown branching fraction to $\rho^0\rho^0$.
[6] Includes unknown branching fraction to $\pi^+\pi^-$.
[7] Includes unknown branching fraction to $\eta\eta$.

$\Gamma(\gamma f_0(1710) \to \gamma\pi\pi)/\Gamma_{\text{total}}$ Γ_{159}/Γ

VALUE (units 10^{-4})	DOCUMENT ID			TECN	COMMENT
4.0 ±1.0 OUR AVERAGE					
3.96±0.06±1.12	[1] ABLIKIM		06V	BES2	$e^+e^- \to J/\psi \to \gamma\pi^+\pi^-$
3.99±0.15±2.64	[1] ABLIKIM		06V	BES2	$e^+e^- \to J/\psi \to \gamma\pi^0\pi^0$
• • • We do not use the following data for averages, fits, limits, etc. • • •					
2.5 ±1.6 ±0.8	BAI		98H	BES	$J/\psi \to \gamma\pi^0\pi^0$

[1] Including unknown branching fraction to $\pi\pi$.

$\Gamma(\gamma f_0(1710) \to \gamma\omega\omega)/\Gamma_{\text{total}}$ Γ_{160}/Γ

VALUE (units 10^{-3})	EVTS	DOCUMENT ID		TECN	COMMENT
0.31±0.06±0.08	180	ABLIKIM	06H	BES	$J/\psi \to \gamma\omega\omega$

$\Gamma(\gamma\eta)/\Gamma_{total}$ Γ_{161}/Γ

VALUE (units 10^{-3})	EVTS	DOCUMENT ID		TECN	COMMENT
1.104±0.034 OUR AVERAGE					
1.101±0.029±0.022		PEDLAR	09	CLE3	$J/\psi \to \eta\gamma$
1.123±0.089	11k	ABLIKIM	06E	BES2	$J/\psi \to \eta\gamma$
• • • We do not use the following data for averages, fits, limits, etc. • • •					
0.88 ±0.08 ±0.11		BLOOM	83	CBAL	e^+e^-
0.82 ±0.10		BRANDELIK	79C	DASP	e^+e^-
1.3 ±0.4	21	BARTEL	77	CNTR	e^+e^-

$\Gamma(\gamma f_1(1420) \to \gamma K\overline{K}\pi)/\Gamma_{total}$ Γ_{162}/Γ

VALUE (units 10^{-3})	DOCUMENT ID		TECN	COMMENT
0.79±0.13 OUR AVERAGE				
0.68±0.04±0.24	BAI	00D	BES	$J/\psi \to \gamma K^\pm K_S^0 \pi^\mp$
0.76±0.15±0.21	[1,2] AUGUSTIN	92	DM2	$J/\psi \to \gamma K\overline{K}\pi$
$0.87\pm0.14^{+0.14}_{-0.11}$	[1] BAI	90C	MRK3	$J/\psi \to \gamma K_S^0 K^\pm\pi^\mp$

[1] Included unknown branching fraction $f_1(1420) \to K\overline{K}\pi$.
[2] From fit to the $K^*(892)\,K$ 1^{++} partial wave.

$\Gamma(\gamma f_1(1285))/\Gamma_{total}$ Γ_{163}/Γ

VALUE (units 10^{-3})	DOCUMENT ID		TECN	COMMENT
0.61 ±0.08 OUR AVERAGE				
0.69 ±0.16 ±0.20	[1] BAI	04J	BES2	$J/\psi \to \gamma\gamma\rho^0$
0.61 ±0.04 ±0.21	[2] BAI	00D	BES	$J/\psi \to \gamma K^\pm K_S^0 \pi^\mp$
0.45 ±0.09 ±0.17	[3] BAI	99	BES	$J/\psi \to \gamma\eta\pi^+\pi^-$
0.625±0.063±0.103	[4] BOLTON	92	MRK3	$J/\psi \to \gamma f_1(1285)$
0.70 ±0.08 ±0.16	[5] BOLTON	92B	MRK3	$J/\psi \to \gamma\eta\pi^+\pi^-$

[1] Assuming $B(f_1(1285) \to \rho^0\gamma) = 0.055 \pm 0.013$.
[2] Assuming $\Gamma(f_1(1285) \to K\overline{K}\pi)/\Gamma_{total} = 0.090 \pm 0.004$.
[3] Assuming $\Gamma(f_1(1285) \to \eta\pi\pi)/\Gamma_{total} = 0.5 \pm 0.18$.
[4] Obtained summing the sequential decay channels
$B(J/\psi \to \gamma f_1(1285), f_1(1285) \to \pi\pi\pi\pi) = (1.44 \pm 0.39 \pm 0.27) \times 10^{-4}$;
$B(J/\psi \to \gamma f_1(1285), f_1(1285) \to a_0(980)\pi, a_0(980) \to \eta\pi) = (3.90 \pm 0.42 \pm 0.87) \times 10^{-4}$;
$B(J/\psi \to \gamma f_1(1285), f_1(1285) \to a_0(980)\pi, a_0(980) \to K\overline{K}) = (0.66 \pm 0.26 \pm 0.29) \times 10^{-4}$;
$B(J/\psi \to \gamma f_1(1285), f_1(1285) \to \gamma\rho^0) = (0.25 \pm 0.07 \pm 0.03) \times 10^{-4}$.
[5] Using $B(f_1(1285) \to a_0(980)\pi) = 0.37$, and including unknown branching ratio for $a_0(980) \to \eta\pi$.

$\Gamma(\gamma f_1(1510) \to \gamma\eta\pi^+\pi^-)/\Gamma_{total}$ Γ_{164}/Γ

VALUE (units 10^{-4})	DOCUMENT ID		TECN	COMMENT
4.5±1.0±0.7	BAI	99	BES	$J/\psi \to \gamma\eta\pi^+\pi^-$

$\Gamma(\gamma f_2'(1525))/\Gamma_{total}$ Γ_{165}/Γ

VALUE (units 10^{-4})	CL%	EVTS	DOCUMENT ID		TECN	COMMENT
4.5 $^{+0.7}_{-0.4}$ OUR AVERAGE						
$3.85\pm0.17^{+1.91}_{-0.73}$			[1] BAI	03G	BES	$J/\psi \to \gamma K\overline{K}$
$3.6 \pm0.4\ ^{+1.4}_{-0.4}$			[1] BAI	96C	BES	$J/\psi \to \gamma K^+K^-$
5.6 ±1.4 ±0.9			[1] AUGUSTIN	88	DM2	$J/\psi \to \gamma K^+K^-$
4.5 ±0.4 ±0.9			[1] AUGUSTIN	88	DM2	$J/\psi \to \gamma K_S^0 K_S^0$
6.8 ±1.6 ±1.4			[1] BALTRUSAIT...87		MRK3	$J/\psi \to \gamma K^+K^-$
• • • We do not use the following data for averages, fits, limits, etc. • • •						
<3.4	90	4	[2] BRANDELIK	79C	DASP	$e^+e^- \to \pi^+\pi^-\gamma$
<2.3	90	3	ALEXANDER	78	PLUT	$e^+e^- \to K^+K^-\gamma$

[1] Using $B(f_2'(1525) \to K\overline{K}) = 0.888$.
[2] Assuming isotropic production and decay of the $f_2'(1525)$ and isospin.

$\Gamma(\gamma f_2(1640) \to \gamma\omega\omega)/\Gamma_{total}$ Γ_{166}/Γ

VALUE (units 10^{-3})	EVTS	DOCUMENT ID		TECN	COMMENT
0.28±0.05±0.17	141	ABLIKIM	06H	BES	$J/\psi \to \gamma\omega\omega$

$\Gamma(\gamma f_2(1910) \to \gamma\omega\omega)/\Gamma_{total}$ Γ_{167}/Γ

VALUE (units 10^{-3})	EVTS	DOCUMENT ID		TECN	COMMENT
0.20±0.04±0.13	151	ABLIKIM	06H	BES	$J/\psi \to \gamma\omega\omega$

$\Gamma(\gamma f_0(1800) \to \gamma\omega\phi)/\Gamma_{total}$ Γ_{168}/Γ

VALUE (units 10^{-4})	EVTS	DOCUMENT ID		TECN	COMMENT
2.5 ±0.6 OUR AVERAGE					
$2.00\pm0.08^{+1.38}_{-1.64}$	1.3k	ABLIKIM	13J	BES3	$J/\psi \to \gamma\omega\phi$
2.61±0.27±0.65	95	ABLIKIM	06J	BES2	$J/\psi \to \gamma\omega\phi$

$\Gamma(\gamma f_2(1950) \to \gamma K^*(892)\overline{K}^*(892))/\Gamma_{total}$ Γ_{169}/Γ

VALUE (units 10^{-3})	DOCUMENT ID		TECN	COMMENT
0.7±0.1±0.2	BAI	00B	BES	$J/\psi \to \gamma K^+K^0\pi^+\pi^-$

$\Gamma(\gamma K^*(892)\overline{K}^*(892))/\Gamma_{total}$ Γ_{170}/Γ

VALUE (units 10^{-3})	EVTS	DOCUMENT ID		TECN	COMMENT
4.0±0.3±1.3	320	[1] BAI	00B	BES	$J/\psi \to \gamma K^+K^0\pi^+\pi^-$

[1] Summed over all charges.

$\Gamma(\gamma\phi\phi)/\Gamma_{total}$ Γ_{171}/Γ

VALUE (units 10^{-4})	EVTS	DOCUMENT ID		TECN	COMMENT
4.0±1.2 OUR AVERAGE Error includes scale factor of 2.1. See the ideogram below.					
7.5±0.6±1.2	168	BAI	90B	MRK3	$J/\psi \to \gamma 4K$
3.4±0.8±0.6	33 ± 7	[1] BISELLO	90	DM2	$J/\psi \to \gamma K^+K^-K_S^0K_L^0$
3.1±0.7±0.4		[1] BISELLO	86B	DM2	$J/\psi \to \gamma K^+K^-K^+K^-$

[1] $\phi\phi$ mass less than 2.9 GeV, η_c excluded.

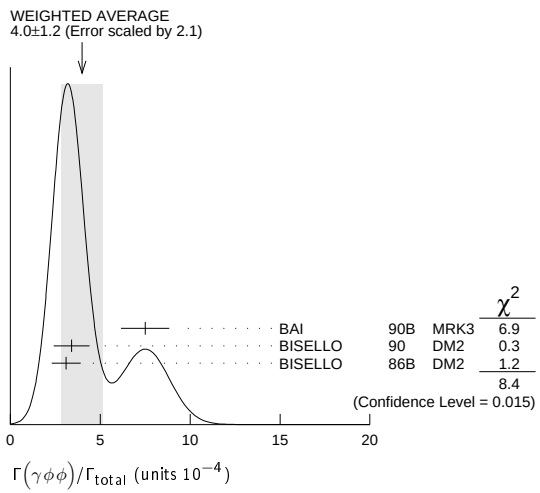

$\Gamma(\gamma p\overline{p})/\Gamma_{total}$ Γ_{172}/Γ

VALUE (units 10^{-3})	CL%	EVTS	DOCUMENT ID		TECN	COMMENT
0.38±0.07±0.07		49	EATON	84	MRK2	e^+e^-
• • • We do not use the following data for averages, fits, limits, etc. • • •						
<0.11	90		PERUZZI	78	MRK1	e^+e^-

$\Gamma(\gamma\eta(2225))/\Gamma_{total}$ Γ_{173}/Γ

VALUE (units 10^{-3})	EVTS	DOCUMENT ID		TECN	COMMENT
0.33±0.05 OUR AVERAGE					
0.44±0.04±0.08	196 ± 19	[1] ABLIKIM	08I	BES	$J/\psi \to \gamma K^+K^-K_S^0K_L^0$
0.33±0.08±0.05		[1] BAI	90B	MRK3	$J/\psi \to \gamma K^+K^-K^+K^-$
0.27±0.06±0.06		[1] BAI	90B	MRK3	$J/\psi \to \gamma K^+K^-K_S^0K_L^0$
$0.24^{+0.15}_{-0.10}$		[2,3] BISELLO	89B	DM2	$J/\psi \to 4\pi\gamma$

[1] Includes unknown branching fraction to $\phi\phi$.
[2] Estimated by us from various fits.
[3] Includes unknown branching fraction to $\rho^0\rho^0$.

$\Gamma(\gamma\eta(1760) \to \gamma\rho^0\rho^0)/\Gamma_{total}$ Γ_{174}/Γ

VALUE (units 10^{-3})	DOCUMENT ID		TECN	COMMENT
0.13±0.09	[1,2] BISELLO	89B	DM2	$J/\psi \to 4\pi\gamma$

[1] Estimated by us from various fits.
[2] Includes unknown branching fraction to $\rho^0\rho^0$.

$\Gamma(\gamma\eta(1760) \to \gamma\omega\omega)/\Gamma_{total}$ Γ_{175}/Γ

VALUE (units 10^{-3})	EVTS	DOCUMENT ID		TECN	COMMENT
1.98±0.08±0.32	1045	ABLIKIM	06H	BES	$J/\psi \to \gamma\omega\omega$

$\Gamma(\gamma X(1835) \to \gamma\pi^+\pi^-\eta')/\Gamma_{total}$ Γ_{176}/Γ

VALUE (units 10^{-4})	EVTS	DOCUMENT ID		TECN	COMMENT
2.6 ±0.4 OUR AVERAGE					
$2.87\pm0.09^{+0.49}_{-0.52}$	4265	[1] ABLIKIM	11C	BES3	$J/\psi \to \gamma\pi^+\pi^-\eta'$
2.2 ±0.4 ±0.4	264	ABLIKIM	05R	BES2	$J/\psi \to \gamma\pi^+\pi^-\eta'$

[1] From a fit of the $\pi^+\pi^-\eta'$ mass distribution to a combination of $\gamma f_1(1510)$, $\gamma X(1835)$, and two unconfirmed states $\gamma X(2120)$, and $\gamma X(2370)$, for $M(p\overline{p}) < 2.8$ GeV, and accounting for backgrounds from non-η' events and $J/\psi \to \pi^0\pi^+\pi^-\eta'$.

$\Gamma(\gamma X(1835) \to \gamma p\overline{p})/\Gamma_{total}$ Γ_{177}/Γ

VALUE (units 10^{-4})	EVTS	DOCUMENT ID		TECN	COMMENT
$0.77^{+0.15}_{-0.09}$ OUR AVERAGE					
$0.90^{+0.04}_{-0.11}\pm0.27_{-0.55}$		[1] ABLIKIM	12D	BES3	$J/\psi \to \gamma p\overline{p}$
$1.14^{+0.43}_{-0.30}\pm0.42_{-0.26}$	231	[2] ALEXANDER	10	CLEO	$J/\psi \to \gamma p\overline{p}$
$0.70\pm0.04^{+0.19}_{-0.08}$		BAI	03F	BES2	$J/\psi \to \gamma p\overline{p}$

[1] From the fit including final state interaction effects in isospin 0 S-wave according to SIBIRTSEV 05A.
[2] From a fit of the $p\overline{p}$ mass distribution to a combination of $\gamma X(1835)$, γR with $M(R) = 2100$ MeV and $\Gamma(R) = 160$ MeV, and $\gamma p\overline{p}$ phase space, for $M(p\overline{p}) < 2.85$ GeV.

$\Gamma(\gamma X(1840) \to \gamma 3(\pi^+\pi^-))/\Gamma_{total}$ Γ_{178}/Γ

VALUE (units 10^{-5})	EVTS	DOCUMENT ID		TECN	COMMENT
$2.44 \pm 0.36^{+0.60}_{-0.74}$	0.6k	ABLIKIM	13U	BES3	$J/\psi \to \gamma 3(\pi^+\pi^-)$

$\Gamma(\gamma(K\overline{K}\pi)\,[J^{PC} = 0^{-+}])/\Gamma_{total}$ Γ_{179}/Γ

VALUE (units 10^{-3})	DOCUMENT ID		TECN	COMMENT
0.7 ±0.4 OUR AVERAGE	Error includes scale factor of 2.1.			
$0.58 \pm 0.03 \pm 0.20$	[1] BAI	00D	BES	$J/\psi \to \gamma K^\pm K^0_S \pi^\mp$
$2.1 \pm 0.1 \pm 0.7$	[2] BAI	00D	BES	$J/\psi \to \gamma K^\pm K^0_S \pi^\mp$

[1] For a broad structure around 1800 MeV.
[2] For a broad structure around 2040 MeV.

$\Gamma(\gamma\pi^0)/\Gamma_{total}$ Γ_{180}/Γ

VALUE (units 10^{-5})	EVTS	DOCUMENT ID		TECN	COMMENT
$3.49^{+0.33}_{-0.30}$ OUR AVERAGE					
$3.63 \pm 0.36 \pm 0.13$		PEDLAR	09	CLE3	$J/\psi \to \pi^0\gamma$
$3.13^{+0.65}_{-0.47}$	586	ABLIKIM	06E	BES2	$J/\psi \to \pi^0\gamma$
• • • We do not use the following data for averages, fits, limits, etc. • • •					
$3.6 \pm 1.1 \pm 0.7$		BLOOM	83	CBAL	e^+e^-
7.3 ± 4.7	10	BRANDELIK	79C	DASP	e^+e^-

$\Gamma(\gamma p\overline{p}\pi^+\pi^-)/\Gamma_{total}$ Γ_{181}/Γ

VALUE (units 10^{-3})	CL%	DOCUMENT ID		TECN	COMMENT
<0.79	90	EATON	84	MRK2	e^+e^-

$\Gamma(\gamma\Lambda\overline{\Lambda})/\Gamma_{total}$ Γ_{182}/Γ

VALUE (units 10^{-3})	CL%	DOCUMENT ID		TECN	COMMENT
<0.13	90	HENRARD	87	DM2	e^+e^-
• • • We do not use the following data for averages, fits, limits, etc. • • •					
<0.16	90	BAI	98G	BES	e^+e^-

$\Gamma(\gamma f_0(2200))/\Gamma_{total}$ Γ_{183}/Γ

VALUE (units 10^{-4})	DOCUMENT ID		TECN	COMMENT
• • • We do not use the following data for averages, fits, limits, etc. • • •				
1.5	[1] AUGUSTIN	88	DM2	$J/\psi \to \gamma K^0_S K^0_S$

[1] Includes unknown branching fraction to $K^0_S K^0_S$.

$\Gamma(\gamma f_J(2220))/\Gamma_{total}$ Γ_{184}/Γ

VALUE (units 10^{-5})	CL%	EVTS	DOCUMENT ID		TECN	COMMENT
>250	99.9		[1] HASAN	96	SPEC	$\overline{p}p \to \pi^+\pi^-$
• • • We do not use the following data for averages, fits, limits, etc. • • •						
>300			[2] BAI	96B	BES	$e^+e^- \to \gamma\overline{p}p,\ K\overline{K}$
< 2.3	95		[3] AUGUSTIN	88	DM2	$J/\psi \to \gamma K^+K^-$
< 1.6	95		[3] AUGUSTIN	88	DM2	$J/\psi \to \gamma K^0_S K^0_S$
$12.4^{+6.4}_{-5.2} \pm 2.8$		23	[3] BALTRUSAIT...	86D	MRK3	$J/\psi \to \gamma K^0_S K^0_S$
$8.4^{+3.4}_{-2.8} \pm 1.6$		93	[3] BALTRUSAIT...	86D	MRK3	$J/\psi \to \gamma K^+K^-$

[1] Using BAI 96B.
[2] Using BARNES 93.
[3] Includes unknown branching fraction to K^+K^- or $K^0_S K^0_S$.

$\Gamma(\gamma f_J(2220) \to \gamma\pi\pi)/\Gamma_{total}$ Γ_{185}/Γ

VALUE (units 10^{-4})	DOCUMENT ID		TECN	COMMENT
$0.84 \pm 0.26 \pm 0.30$	BAI	96B	BES	$e^+e^- \to J/\psi \to \gamma\pi^+\pi^-$
• • • We do not use the following data for averages, fits, limits, etc. • • •				
$1.4 \pm 0.8 \pm 0.4$	BAI	98H	BES	$J/\psi \to \gamma\pi^0\pi^0$

$\Gamma(\gamma f_J(2220) \to \gamma K\overline{K})/\Gamma_{total}$ Γ_{186}/Γ

VALUE (units 10^{-5})	DOCUMENT ID		TECN	COMMENT
< 3.6	[1] DEL-AMO-SA...	10O	BABR	$e^+e^- \to J/\psi \to \gamma K^+K^-$
• • • We do not use the following data for averages, fits, limits, etc. • • •				
< 2.9	[1] DEL-AMO-SA...	10O	BABR	$e^+e^- \to J/\psi \to \gamma K^0_S K^0_S$
$6.6 \pm 2.9 \pm 2.4$	BAI	96B	BES	$e^+e^- \to J/\psi \to \gamma K^+K^-$
$10.8 \pm 4.0 \pm 3.2$	BAI	96B	BES	$e^+e^- \to J/\psi \to \gamma K^0_S K^0_S$

[1] For spin 2 and helicity 0; other combinations lead to more stringent upper limits.

$\Gamma(\gamma f_J(2220) \to \gamma p\overline{p})/\Gamma_{total}$ Γ_{187}/Γ

VALUE (units 10^{-5})	DOCUMENT ID		TECN	COMMENT
$1.5 \pm 0.6 \pm 0.5$	BAI	96B	BES	$e^+e^- \to J/\psi \to \gamma p\overline{p}$

$\Gamma(\gamma f_0(1500))/\Gamma_{total}$ Γ_{188}/Γ

VALUE (units 10^{-4})	DOCUMENT ID		TECN	COMMENT
1.01 ± 0.32 OUR AVERAGE				
$1.00 \pm 0.03 \pm 0.45$	[1] ABLIKIM	06V	BES2	$e^+e^- \to J/\psi \to \gamma\pi^+\pi^-$
$1.02 \pm 0.09 \pm 0.45$	[1] ABLIKIM	06V	BES2	$e^+e^- \to J/\psi \to \gamma\pi^0\pi^0$
• • • We do not use the following data for averages, fits, limits, etc. • • •				
>5.7 ±0.8	[2,3] BUGG	95	MRK3	$J/\psi \to \gamma\pi^+\pi^-\pi^+\pi^-$

[1] Including unknown branching fraction to $\pi\pi$.
[2] Including unknown branching ratio for $f_0(1500) \to \pi^+\pi^-\pi^+\pi^-$.
[3] Assuming that $f_0(1500)$ decays only to two S-wave dipions.

$\Gamma(\gamma A \to \gamma$invisible$)/\Gamma_{total}$ Γ_{189}/Γ
(narrow state A with m_A < 960 MeV)

VALUE (units 10^{-6})	CL%	DOCUMENT ID		TECN	COMMENT
<6.3	90	[1] INSLER	10	CLEO	$e^+e^- \to \pi^+\pi^- J/\psi$

[1] The limit varies with mass m_A of a narrow state A and is 4.3×10^{-6} for $m_A = 0$ MeV, reaches its largest value of 6.3×10^{-6} at $m_A = 500$ MeV, and is 3.6×10^{-6} at $m_A = 960$ MeV.

$\Gamma(\gamma A^0 \to \gamma\mu^+\mu^-)/\Gamma_{total}$ Γ_{190}/Γ
(narrow state A^0 with 0.2 GeV $< m_{A^0} <$ 3 GeV)

VALUE (units 10^{-5})	CL%	DOCUMENT ID		TECN	COMMENT
<2.1	90	[1] ABLIKIM	12	BES3	$J/\psi \to \gamma\mu^+\mu^-$

[1] For a narrow scalar or pseudoscalar, A^0, with a mass in the range 0.21–3.00 GeV. The measured 90% CL limit as a function of m_{A^0} ranges from 4×10^{-7} to 2.1×10^{-5}.

WEAK DECAYS

$\Gamma(D^- e^+\nu_e + \text{c.c.})/\Gamma_{total}$ Γ_{191}/Γ

VALUE (units 10^{-5})	CL%	DOCUMENT ID		TECN	COMMENT
<1.2	90	ABLIKIM	06M	BES2	$e^+e^- \to J/\psi$

$\Gamma(\overline{D}^0 e^+ e^- + \text{c.c.})/\Gamma_{total}$ Γ_{192}/Γ

VALUE (units 10^{-5})	CL%	DOCUMENT ID		TECN	COMMENT
<1.1	90	ABLIKIM	06M	BES2	$e^+e^- \to J/\psi$

$\Gamma(D_s^- e^+\nu_e + \text{c.c.})/\Gamma_{total}$ Γ_{193}/Γ

VALUE (units 10^{-5})	CL%	DOCUMENT ID		TECN	COMMENT
<3.6	90	[1] ABLIKIM	06M	BES2	$e^+e^- \to J/\psi$

[1] Using $B(D_s^- \to \phi\pi^-) = 4.4 \pm 0.5$ %.

$\Gamma(D^-\pi^+ + \text{c.c.})/\Gamma_{total}$ Γ_{194}/Γ

VALUE	CL%	DOCUMENT ID		TECN	COMMENT
$<7.5 \times 10^{-5}$	90	ABLIKIM	08J	BES2	$e^+e^- \to J/\psi$

$\Gamma(\overline{D}^0\overline{K}^0 + \text{c.c.})/\Gamma_{total}$ Γ_{195}/Γ

VALUE	CL%	DOCUMENT ID		TECN	COMMENT
$<1.7 \times 10^{-4}$	90	ABLIKIM	08J	BES2	$e^+e^- \to J/\psi$

$\Gamma(D_s^-\pi^+ + \text{c.c.})/\Gamma_{total}$ Γ_{196}/Γ

VALUE	CL%	DOCUMENT ID		TECN	COMMENT
$<1.3 \times 10^{-4}$	90	ABLIKIM	08J	BES2	$e^+e^- \to J/\psi$

$\Gamma(\gamma\gamma)/\Gamma_{total}$ Γ_{197}/Γ

VALUE (units 10^{-5})	CL%	DOCUMENT ID		TECN	COMMENT
< 0.5	90	ADAMS	08	CLEO	$\psi(2S) \to \pi^+\pi^- J/\psi$
• • • We do not use the following data for averages, fits, limits, etc. • • •					
<16	90	[1] WICHT	08	BELL	$B^\pm \to K^\pm\gamma\gamma$
< 2.2	90	ABLIKIM	07J	BES2	$\psi(2S) \to J/\psi\pi^+\pi^-$
<50	90	BARTEL	77	CNTR	e^+e^-

[1] WICHT 08 reports $[\Gamma(J/\psi(1S) \to \gamma\gamma)/\Gamma_{total}] \times [B(B^+ \to J/\psi(1S)K^+)] < 0.16 \times 10^{-6}$ which we divide by our best value $B(B^+ \to J/\psi(1S)K^+) = 1.027 \times 10^{-3}$.

LEPTON FAMILY NUMBER (LF) VIOLATING MODES

$\Gamma(e^\pm\mu^\mp)/\Gamma_{total}$ Γ_{198}/Γ

VALUE (units 10^{-7})	CL%	DOCUMENT ID		TECN	COMMENT
< 1.6	90	ABLIKIM	13L	BES3	$e^+e^- \to J/\psi$
• • • We do not use the following data for averages, fits, limits, etc. • • •					
<11	90	BAI	03D	BES	$e^+e^- \to J/\psi$

$\Gamma(e^\pm\tau^\mp)/\Gamma_{total}$ Γ_{199}/Γ

VALUE (units 10^{-6})	CL%	DOCUMENT ID		TECN	COMMENT
<8.3	90	ABLIKIM	04	BES	$e^+e^- \to J/\psi$

$\Gamma(\mu^\pm\tau^\mp)/\Gamma_{\rm total}$ Γ_{200}/Γ

VALUE (units 10^{-6})	CL%	DOCUMENT ID		TECN	COMMENT
<2.0	90	ABLIKIM	04	BES	$e^+e^- \to J/\psi$

OTHER DECAYS

Γ(invisible)/$\Gamma(e^+e^-)$ Γ_{201}/Γ_5

VALUE	CL%	DOCUMENT ID		TECN	COMMENT
$<6.6\times10^{-2}$	90	LEES	13I	BABR	$B \to K^{(*)}J/\psi$

Γ(invisible)/$\Gamma(\mu^+\mu^-)$ Γ_{201}/Γ_7

VALUE	CL%	DOCUMENT ID		TECN	COMMENT
$<1.2\times10^{-2}$	90	ABLIKIM	08G	BES2	$\psi(2S) \to \pi^+\pi^- J/\psi$

$J/\psi(1S)$ REFERENCES

AULCHENKO 14 PL B731 227 V.M. Aulchenko *et al.* (KEDR Collab.)
ABLIKIM 13F PR D87 052007 M. Ablikim *et al.* (BES III Collab.)
ABLIKIM 13I PR D87 032003 M. Ablikim *et al.* (BES III Collab.)
ABLIKIM 13J PR D87 032008 M. Ablikim *et al.* (BES III Collab.)
ABLIKIM 13L PR D87 112007 Ablikim M. *et al.* (BES III Collab.)
ABLIKIM 13P PR D87 112004 M. Ablikim *et al.* (BES III Collab.)
ABLIKIM 13R PR D88 032007 M. Ablikim *et al.* (BES III Collab.)
ABLIKIM 13U PR D88 091502 M. Ablikim *et al.* (BES III Collab.)
LEES 13I PR D87 112005 J.P. Lees *et al.* (BABAR Collab.)
LEES 13O PR D87 092005 J.P. Lees *et al.* (BABAR Collab.)
LEES 13Q PR D88 032013 J.P. Lees *et al.* (BABAR Collab.)
LEES 13Y PR D88 072009 J.P. Lees *et al.* (BABAR Collab.)
ABLIKIM 12 PR D85 092012 M. Ablikim *et al.* (BES III Collab.)
ABLIKIM 12B PR D86 032008 M. Ablikim *et al.* (BES III Collab.)
ABLIKIM 12C PR D86 032014 M. Ablikim *et al.* (BES III Collab.)
ABLIKIM 12D PRL 108 112003 M. Ablikim *et al.* (BES III Collab.)
ABLIKIM 12H PL B710 594 M. Ablikim *et al.* (BES III Collab.)
ABLIKIM 12P CP C36 1031 M. Ablikim *et al.* (BES II Collab.)
LEES 12E PR D85 112009 J.P. Lees *et al.* (BABAR Collab.)
METREVELI 12 PR D85 092007 Z. Metreveli *et al.* (NWES, FLOR, WAYN+)
ABLIKIM 11 PR D83 012003 M. Ablikim *et al.* (BES III Collab.)
ABLIKIM 11C PRL 106 072002 M. Ablikim *et al.* (BES III Collab.)
ABLIKIM 11D PR D83 032003 M. Ablikim *et al.* (BES III Collab.)
ABLIKIM 10C PL B685 27 M. Ablikim *et al.* (BES II Collab.)
ABLIKIM 10E PL B693 88 M. Ablikim *et al.* (BES II Collab.)
ALEXANDER 10 PR D82 092002 J.P. Alexander *et al.* (CLEO Collab.)
ANASHIN 10 PL B685 134 V.V. Anashin *et al.* (KEDR Collab.)
DEL-AMO-SA... 10O PRL 105 172001 P. del Amo Sanchez *et al.* (BABAR Collab.)
INSLER 10 PR D81 091101 J. Insler *et al.* (CLEO Collab.)
ABLIKIM 09 PL B676 25 M. Ablikim *et al.* (BES Collab.)
ABLIKIM 09B PR D80 052004 M. Ablikim *et al.* (BES II Collab.)
MITCHELL 09 PRL 102 011801 R.E. Mitchell *et al.* (CLEO Collab.)
PEDLAR 09 PR D79 111101 T.K. Pedlar *et al.* (CLEO Collab.)
SHEN 09 PR D80 031101 C.P. Shen *et al.* (BELLE Collab.)
ABLIKIM 08 EPJ C53 15 M. Ablikim *et al.* (BES Collab.)
ABLIKIM 08A PR D77 012001 M. Ablikim *et al.* (BES Collab.)
ABLIKIM 08C PL B659 789 M. Ablikim *et al.* (BES Collab.)
ABLIKIM 08E PR D77 032005 M. Ablikim *et al.* (BES Collab.)
ABLIKIM 08F PRL 100 102003 M. Ablikim *et al.* (BES Collab.)
ABLIKIM 08G PRL 100 192001 M. Ablikim *et al.* (BES Collab.)
ABLIKIM 08I PL B662 330 M. Ablikim *et al.* (BES Collab.)
ABLIKIM 08J PL B663 297 M. Ablikim *et al.* (BES Collab.)
ABLIKIM 08O PR D78 092005 M. Ablikim *et al.* (BES Collab.)
ADAMS 08 PRL 101 101801 G.S. Adams *et al.* (CLEO Collab.)
AUBERT 08S PR D77 092002 B. Aubert *et al.* (BABAR Collab.)
BESSON 08 PR D78 032012 D. Besson *et al.* (CLEO Collab.)
PDG 08 PL B667 1 C. Amsler *et al.* (PDG Collab.)
WICHT 08 PL B662 323 J. Wicht *et al.* (BELLE Collab.)
ABLIKIM 07H PR D76 092003 M. Ablikim *et al.* (BES Collab.)
ABLIKIM 07J PR D76 117101 M. Ablikim *et al.* (BES Collab.)
ANDREOTTI 07 PL B654 74 M. Andreotti *et al.* (Fermilab E835 Collab.)
AUBERT 07AK PR D76 012008 B. Aubert *et al.* (BABAR Collab.)
AUBERT 07AU PR D76 092005 B. Aubert *et al.* (BABAR Collab.)
Also PR D77 119902E (errat.) B. Aubert *et al.* (BABAR Collab.)
AUBERT 07BD PR D76 092006 B. Aubert *et al.* (BABAR Collab.)
ABLIKIM 06 PL B632 181 M. Ablikim *et al.* (BES Collab.)
ABLIKIM 06C PL B633 681 M. Ablikim *et al.* (BES Collab.)
ABLIKIM 06E PR D73 052008 M. Ablikim *et al.* (BES Collab.)
ABLIKIM 06F PR D73 052007 M. Ablikim *et al.* (BES Collab.)
ABLIKIM 06H PR D73 112007 M. Ablikim *et al.* (BES Collab.)
ABLIKIM 06J PRL 96 162002 M. Ablikim *et al.* (BES Collab.)
ABLIKIM 06K PRL 97 062001 M. Ablikim *et al.* (BES II Collab.)
ABLIKIM 06M PL B639 418 M. Ablikim *et al.* (BES Collab.)
ABLIKIM 06V PL B642 441 M. Ablikim *et al.* (BES Collab.)
ADAMS 06A PR D73 051103 G.S. Adams *et al.* (CLEO Collab.)
AUBERT 06B PR D73 012005 B. Aubert *et al.* (BABAR Collab.)
AUBERT 06D PR D73 052003 B. Aubert *et al.* (BABAR Collab.)
AUBERT 06E PRL 96 052002 B. Aubert *et al.* (BABAR Collab.)
AUBERT,BE 06D PR D74 091103 B. Aubert *et al.* (BABAR Collab.)
WU 06 PRL 97 162003 C.-H. Wu *et al.* (BELLE Collab.)
ABLIKIM 05 PL B607 243 M. Ablikim *et al.* (BES Collab.)
ABLIKIM 05B PR D71 032003 M. Ablikim *et al.* (BES Collab.)
ABLIKIM 05C PL B610 192 M. Ablikim *et al.* (BES Collab.)
ABLIKIM 05H PR D72 012002 M. Ablikim *et al.* (BES Collab.)
ABLIKIM 05R PRL 95 262001 M. Ablikim *et al.* (BES Collab.)
AUBERT 05D PR D71 052001 B. Aubert *et al.* (BABAR Collab.)
LI 05C PR D71 111103 Z. Li *et al.* (CLEO Collab.)
SIBIRTSEV 05A PR D71 054010 A. Sibirtsev, J. Haidenbauer
ABLIKIM 04 PL B598 172 M. Ablikim *et al.* (BES Collab.)
ABLIKIM 04M PR D70 112008 M. Ablikim *et al.* (BES Collab.)
AUBERT 04 PR D69 011103 B. Aubert *et al.* (BaBar Collab.)
AUBERT,B 04N PR D70 072004 B. Aubert *et al.* (BABAR Collab.)
BAI 04 PL B578 16 J.Z. Bai *et al.* (BES Collab.)
BAI 04A PR D69 012003 J.Z. Bai *et al.* (BES Collab.)
BAI 04D PL B589 7 J.Z. Bai *et al.* (BES Collab.)
BAI 04E PL B591 42 J.Z. Bai *et al.* (BES Collab.)
BAI 04G PR D70 012004 J.Z. Bai *et al.* (BES Collab.)
BAI 04H PR D70 012005 J.Z. Bai *et al.* (BES Collab.)
BAI 04J PL B594 47 J.Z. Bai *et al.* (BES Collab.)
SETH 04 PR D69 097503 K.K. Seth
AULCHENKO 03 PL B573 63 V.M. Aulchenko *et al.* (KEDR Collab.)
BAI 03D PL B561 49 J.Z. Bai *et al.* (BES Collab.)
BAI 03F PRL 91 022001 J.Z. Bai *et al.* (BES II Collab.)
BAI 03G PR D68 052003 J.Z. Bai *et al.* (BES Collab.)
HUANG 03 PRL 91 241802 H.-C. Huang *et al.* (BELLE Collab.)
BAI 02C PRL 88 101802 J.Z. Bai *et al.* (BES Collab.)
ARTAMONOV 00 PL B474 427 A.S. Artamonov *et al.*
BAI 00 PRL 84 594 J.Z. Bai *et al.* (BES Collab.)
BAI 00B PL B472 200 J.Z. Bai *et al.* (BES Collab.)
BAI 00D PL B476 25 J.Z. Bai *et al.* (BES Collab.)
BAI 99 PL B446 356 J.Z. Bai *et al.* (BES Collab.)
BAI 99C PRL 83 1918 J.Z. Bai *et al.* (BES Collab.)
BAI 98D PR D58 092006 J.Z. Bai *et al.* (BES Collab.)
BAI 98G PL B424 213 J.Z. Bai *et al.* (BES Collab.)
BAI 98H PRL 81 1179 J.Z. Bai *et al.* (BES Collab.)
BALDINI 98 PL B444 111 R. Baldini *et al.* (FENICE Collab.)
ARMSTRONG 96 PR D54 7067 T.A. Armstrong *et al.* (E760 Collab.)
BAI 96B PRL 76 3502 J.Z. Bai *et al.* (BES Collab.)
BAI 96C PRL 77 3959 J.Z. Bai *et al.* (BES Collab.)
BAI 96D PR D54 1221 J.Z. Bai *et al.* (BES Collab.)
GRIBUSHIN 96 PR D53 4723 A. Gribushin *et al.* (E672 Collab., E706 Collab.)
HASAN 96 PL B388 376 A. Hasan, D.V. Bugg (BRUN, LOQM)
BAI 95B PL B355 374 J.Z. Bai *et al.* (BES Collab.)
BUGG 95 PL B353 378 D.V. Bugg *et al.* (LOQM, PNPI, WASH)
ANTONELLI 93 PL B301 317 A. Antonelli *et al.* (FENICE Collab.)
ARMSTRONG 93B PR D47 772 T.A. Armstrong *et al.* (FNAL E760 Collab.)
BARNES 93 PL B309 469 P.D. Barnes *et al.* (PS185 Collab.)
AUGUSTIN 92 PR D46 1951 J.E. Augustin, G. Cosme (DM2 Collab.)
BOLTON 92 PL B278 495 T. Bolton *et al.* (Mark III Collab.)
BOLTON 92B PRL 69 1328 T. Bolton *et al.* (Mark III Collab.)
COFFMAN 92 PRL 68 282 D.M. Coffman *et al.* (Mark III Collab.)
HSUEH 92 PR D45 R2181 S. Hsueh, S. Palestini (FNAL, TORI)
BISELLO 91 NP B350 1 D. Bisello *et al.* (DM2 Collab.)
AUGUSTIN 90 PR D42 10 J.E. Augustin *et al.* (DM2 Collab.)
BAI 90B PRL 65 1309 Z. Bai *et al.* (Mark III Collab.)
BAI 90C PRL 65 2507 Z. Bai *et al.* (Mark III Collab.)
BISELLO 90 PL B241 617 D. Bisello *et al.* (DM2 Collab.)
COFFMAN 90 PR D41 1410 D.M. Coffman *et al.* (Mark III Collab.)
JOUSSET 90 PR D41 1389 J. Jousset *et al.* (DM2 Collab.)
ALEXANDER 89 NP B320 45 J.P. Alexander *et al.* (LBL, MICH, SLAC)
AUGUSTIN 89 NP B320 1 J.E. Augustin, G. Cosme (DM2 Collab.)
BISELLO 89B PR D39 701 G. Busetto *et al.* (DM2 Collab.)
AUGUSTIN 88 PRL 60 2238 J.E. Augustin *et al.* (DM2 Collab.)
COFFMAN 88 PR D38 2695 D.M. Coffman *et al.* (Mark III Collab.)
FALVARD 88 PR D38 2706 A. Falvard *et al.* (CLER, FRAS, LALO+)
AUGUSTIN 87 ZPHY C36 369 J.E. Augustin *et al.* (LALO, CLER, FRAS+)
BAGLIN 87 NP B286 592 C. Baglin *et al.* (LAPP, CERN, GENO, LYON+)
BALTRUSAIT... 87 PR D35 2077 R.M. Baltrusaitis *et al.* (Mark III Collab.)
BECKER 87 PRL 59 186 J.J. Becker *et al.* (Mark III Collab.)
BISELLO 87 PL B192 239 D. Bisello *et al.* (PADO, CLER, FRAS+)
COHEN 87 RMP 59 1121 E.R. Cohen, B.N. Taylor (RISC, NBS)
HENRARD 87 NP B292 670 P. Henrard *et al.* (CLER, FRAS, LALO+)
PALLIN 87 NP B292 653 D. Pallin *et al.* (CLER, FRAS, LALO, PADO)
BALTRUSAIT... 86 PR D33 629 R.M. Baltrusaitis *et al.* (Mark III Collab.)
BALTRUSAIT... 86B PR D33 1222 R.M. Baltrusaitis *et al.* (Mark III Collab.)
BALTRUSAIT... 86D PRL 56 107 R.M. Baltrusaitis (CIT, UCSC, ILL, SLAC+)
BISELLO 86B PL B179 294 D. Bisello *et al.* (DM2 Collab.)
GAISER 86 PR D34 711 J. Gaiser *et al.* (Crystal Ball Collab.)
BALTRUSAIT... 85C PRL 55 1723 R.M. Baltrusaitis *et al.* (CIT, UCSC+)
BALTRUSAIT... 85D PR D32 566 R.M. Baltrusaitis *et al.* (CIT, UCSC+)
KURAEV 85 SJNP 41 466 E.A. Kuraev, V.S. Fadin (NOVO)
Translated from YAF 41 733.
BALTRUSAIT... 84 PRL 52 2126 R.M. Baltrusaitis *et al.* (CIT, UCSC+)
EATON 84 PR D29 804 M.W. Eaton *et al.* (LBL, SLAC)
BLOOM 83 ARNS 33 143 E.D. Bloom, C. Peck (SLAC, CIT)
EDWARDS 83B PRL 51 859 C. Edwards *et al.* (CIT, HARV, PRIN+)
FRANKLIN 83 PRL 51 963 M.E.B. Franklin *et al.* (LBL, SLAC)
BURKE 82 PRL 49 632 D.L. Burke *et al.* (LBL, SLAC)
EDWARDS 82B PR D25 3065 C. Edwards *et al.* (CIT, HARV, PRIN+)
EDWARDS 82D PRL 48 458 C. Edwards *et al.* (CIT, HARV, PRIN+)
Also ARNS 33 143 E.D. Bloom, C. Peck (SLAC, CIT)
EDWARDS 82E PRL 49 259 C. Edwards *et al.* (CIT, HARV, PRIN+)
LEMOIGNE 82 PL 113B 509 Y. Lemoigne *et al.* (SACL, LOIC, SHMP+)
BESCH 81 ZPHY C8 1 H.J. Besch *et al.* (BONN, DESY, MANZ)
GIDAL 81 PL 107B 153 G. Gidal *et al.* (SLAC, LBL)
PARTRIDGE 80 PRL 44 712 R. Partridge *et al.* (CIT, HARV, PRIN+)
SCHARRE 80 PL 97B 329 D.L. Scharre *et al.* (SLAC, LBL)
ZHOLENTZ 80 PL 96B 214 A.A. Zholents *et al.* (NOVO)
Also SJNP 34 814 A.A. Zholents *et al.* (NOVO)
Translated from YAF 34 1471.
BRANDELIK 79C ZPHY C1 233 R. Brandelik *et al.* (DASP Collab.)
ALEXANDER 78 PL 72B 493 G. Alexander *et al.* (DESY, HAMB, SIEG+)
BESCH 78 PL 78B 347 H.J. Besch *et al.* (BONN, DESY, MANZ)
BRANDELIK 78B PL 74B 292 R. Brandelik *et al.* (DASP Collab.)
PERUZZI 78 PR D17 2901 I. Peruzzi *et al.* (SLAC, LBL)
BARTEL 77 PL 66B 489 W. Bartel *et al.* (DESY, HEIDP)
BURMESTER 77D PL 72B 135 J. Burmester *et al.* (DESY, HAMB, SIEG+)
FELDMAN 77 PRPL 33C 285 G.J. Feldman, M.L. Perl (LBL, SLAC)
VANNUCCI 77 PR D15 1814 F. Vannucci *et al.* (SLAC, LBL)
BARTEL 76 PL 64B 483 W. Bartel *et al.* (DESY, HEIDP)
BRAUNSCH... 76 PL 63B 487 W. Braunschweig *et al.* (DASP Collab.)
JEAN-MARIE 76 PRL 36 291 B. Jean-Marie *et al.* (SLAC, LBL) IG
BALDINI-... 75 PL 58B 471 R. Baldini-Celio *et al.* (FRAS, ROMA)
BOYARSKI 75 PRL 34 1357 A.M. Boyarski *et al.* (SLAC, LBL) JPC
DASP 75 PL 56B 491 W. Braunschweig *et al.* (DASP Collab.)
ESPOSITO 75B LNC 14 73 B. Esposito *et al.* (FRAS, NAPL, PADO+)
FORD 75 PRL 34 604 R.L. Ford *et al.* (SLAC, PENN)

BRANCHING RATIOS OF $\psi(2S)$ AND $\chi_{c0,1,2}$

Updated May 2012 by J.J. Hernández-Rey (IFIC, Valencia), S. Navas (University of Granada), and C. Patrignani (INFN, Genova)

Since 2002, the treatment of the branching ratios of the $\psi(2S)$ and $\chi_{c0,1,2}$ has undergone an important restructuring.

When measuring a branching ratio experimentally, it is not always possible to normalize the number of events observed in the corresponding decay mode to the total number of particles produced. Therefore, the experimenters sometimes report the number of observed decays with respect to another decay mode of the same or another particle in the relevant decay chain. This is actually equivalent to measuring combinations of branching fractions of several decay modes.

To extract the branching ratio of a given decay mode, the collaborations use some previously reported measurements of the required branching ratios. However, the values are frequently taken from the *Review of Particle Physics* (RPP), which in turn uses the branching ratio reported by the experiment in the following edition, giving rise either to correlations or to plain vicious circles Ref. 1,Ref. 2 as discussed in more detail in earlier editions of this mini-review.

The way to avoid these dependencies and correlations is to extract the branching ratios through a fit that uses the truly measured combinations of branching fractions and partial widths. This fit, in fact, should involve decays from the four concerned particles, $\psi(2S)$, χ_{c0}, χ_{c1}, and χ_{c2}, and occasionally some combinations of branching ratios of more than one of them. This is what is done since the 2002 edition [3].

The PDG policy is to quote the results of the collaborations in a manner as close as possible to what appears in their original publications. However, in order to avoid the problems mentioned above, we had in some cases to work out the values originally measured, using the number of events and detection efficiencies given by the collaborations, or rescaling back the published results. The information was sometimes spread over several articles, and some articles referred to papers still unpublished, which in turn contained the relevant numbers in footnotes.

Even though the experimental collaborations are entitled to extract whatever branching ratios they consider appropriate by using other published results, we would like to encourage them to also quote explicitly in their articles the actual quantities measured, so that they can be used directly in averages and fits of different experimental determinations.

To inform the reader how we computed some of the values used in this edition of RPP, we use footnotes to indicate the branching ratios actually given by the experiments and the quantities they use to derive them from the true combination of branching ratios actually measured.

None of the branching ratios of the $\chi_{c0,1,2}$ are measured independently of the $\psi(2S)$ radiative decays. We tried to identify those branching ratios which can be correlated in a non-trivial way, and although we cannot preclude the existence of other cases, we are confident that the most relevant correlations have already been removed. Nevertheless, correlations in the errors of different quantities measured by the same experiment have not been taken into account.

FIT INFORMATION

This is an overall fit to 4 total widths, 1 partial width, 25 combinations of partial widths, 7 branching ratios, and 77 combinations of branching ratios. Of the latter 57 involve decays of more than one particle.

The overall fit uses 223 measurements to determine 49 parameters and has a χ^2 of 312.2 for 174 degrees of freedom.

The relatively high χ^2 of the fit, 1.8 per d.o.f., can be traced back to a few specific discrepancies in the data. No rescaling of errors has been applied.

In the listing we provide the correlation coefficients $< \delta x_i \delta x_j > / (\delta x_i \cdot \delta x_j)$, in percent, from the fit to the corresponding parameter x_i.

References

1. Y.F. Gu and X.H. Li, Phys. Lett. **B449**, 361 (1999).
2. C. Patrignani, Phys. Rev. **D64**, 034017 (2001).
3. Particle Data Group, K.Hagiwara *et al.*, Phys. Rev. **D68**, 010001 (2002).

$\chi_{c0}(1P)$ $I^G(J^{PC}) = 0^+(0^{++})$

$\chi_{c0}(1P)$ MASS

VALUE (MeV)	EVTS	DOCUMENT ID		TECN	COMMENT
3414.75 ± 0.31 OUR AVERAGE					
3414.2 ± 0.5 ± 2.3	5.4k	UEHARA	08	BELL	$\gamma\gamma \to \chi_{c0} \to$ hadrons
3406 ± 7 ± 6	230	[1] ABE	07	BELL	$e^+e^- \to J/\psi(c\overline{c})$
3414.21 ± 0.39 ± 0.27		ABLIKIM	05G	BES2	$\psi(2S) \to \gamma\chi_{c0}$
3414.7 $^{+0.7}_{-0.6}$ ± 0.2		[2] ANDREOTTI	03	E835	$\overline{p}p \to \chi_{c0} \to \pi^0\pi^0$
3415.5 ± 0.4 ± 0.4	392	[3] BAGNASCO	02	E835	$\overline{p}p \to \chi_{c0} \to J/\psi\gamma$
3417.4 $^{+1.8}_{-1.9}$ ± 0.2		[2] AMBROGIANI	99B	E835	$\overline{p}p \to e^+e^-\gamma$
3414.1 ± 0.6 ± 0.8		BAI	99B	BES	$\psi(2S) \to \gamma$X
3417.8 ± 0.4 ± 4		[2] GAISER	86	CBAL	$\psi(2S) \to \gamma$X
3416 ± 3 ± 4		[4] TANENBAUM	78	MRK1	e^+e^-
• • • We do not use the following data for averages, fits, limits, etc. • • •					
3414.6 ± 1.1	266	UEHARA	13	BELL	$\gamma\gamma \to K^0_S K^0_S$
3416.5 ± 3.0		EISENSTEIN	01	CLE2	$e^+e^- \to e^+e^-\chi_{c0}$
3422 ±10		[4] BARTEL	78B	CNTR	$e^+e^- \to J/\psi 2\gamma$
3415 ± 9		[4] BIDDICK	77	CNTR	$e^+e^- \to \gamma$X

[1] From a fit of the J/ψ recoil mass spectrum. Supersedes ABE,K 02 and ABE 04G.
[2] Using mass of $\psi(2S) = 3686.0$ MeV.
[3] Recalculated by ANDREOTTI 05A, using the value of $\psi(2S)$ mass from AULCHENKO 03.
[4] Mass value shifted by us by amount appropriate for $\psi(2S)$ mass = 3686 MeV and $J/\psi(1S)$ mass = 3097 MeV.

$\chi_{c0}(1P)$ WIDTH

VALUE (MeV)	EVTS	DOCUMENT ID		TECN	COMMENT
10.5±0.6 OUR FIT					
10.5±0.8 OUR AVERAGE Error includes scale factor of 1.1.					
10.6±1.9±2.6	5.4k	UEHARA	08	BELL	$\gamma\gamma \to \chi_{c0} \to$ hadrons
$12.6^{+1.5}_{-1.6}{}^{+0.9}_{-1.1}$		ABLIKIM	05G	BES2	$\psi(2S) \to \gamma\chi_{c0}$
$8.6^{+1.7}_{-1.3}$±0.1		ANDREOTTI	03	E835	$\overline{p}p \to \chi_{c0} \to \pi^0\pi^0$
9.7±1.0	392	[1] BAGNASCO	02	E835	$\overline{p}p \to \chi_{c0} \to J/\psi\gamma$
$16.6^{+5.2}_{-3.7}$±0.1		AMBROGIANI	99B	E835	$\overline{p}p \to e^+e^-\gamma$
14.3±2.0±3.0		BAI	98I	BES	$\psi(2S) \to \gamma\pi^+\pi^-$
13.5±3.3±4.2		GAISER	86	CBAL	$\psi(2S) \to \gamma$X, $\gamma\pi^0\pi^0$
• • • We do not use the following data for averages, fits, limits, etc. • • •					
13.2±2.1	266	UEHARA	13	BELL	$\gamma\gamma \to K^0_S K^0_S$

[1] Recalculated by ANDREOTTI 05A.

$\chi_{c0}(1P)$ DECAY MODES

	Mode	Fraction (Γ_i/Γ)	Scale factor/ Confidence level
	Hadronic decays		
Γ_1	$2(\pi^+\pi^-)$	(2.24±0.18) %	
Γ_2	$\rho^0\pi^+\pi^-$	(8.7 ±2.8) × 10^{-3}	
Γ_3	$\rho^0\rho^0$		
Γ_4	$f_0(980)f_0(980)$	(6.5 ±2.1) × 10^{-4}	
Γ_5	$\pi^+\pi^-\pi^0\pi^0$	(3.3 ±0.4) %	
Γ_6	$\rho^+\pi^-\pi^0$ + c.c.	(2.8 ±0.4) %	
Γ_7	$4\pi^0$	(3.2 ±0.4) × 10^{-3}	
Γ_8	$\pi^+\pi^-K^+K^-$	(1.75±0.14) %	
Γ_9	$K_0^*(1430)^0\overline{K}_0^*(1430)^0 \to \pi^+\pi^-K^+K^-$	(9.6 $^{+3.5}_{-2.8}$) × 10^{-4}	
Γ_{10}	$K_0^*(1430)^0\overline{K}_2^*(1430)^0$ + c.c. $\to \pi^+\pi^-K^+K^-$	(7.8 $^{+1.9}_{-2.4}$) × 10^{-4}	
Γ_{11}	$K_1(1270)^+K^-$ + c.c. $\to \pi^+\pi^-K^+K^-$	(6.1 ±1.9) × 10^{-3}	

Γ_{12}	$K_1(1400)^+ K^-$ + c.c. → $\pi^+\pi^- K^+ K^-$	< 2.6	$\times 10^{-3}$	CL=90%
Γ_{13}	$f_0(980)\, f_0(980)$	$(1.6\ ^{+1.0}_{-0.9}) \times 10^{-4}$		
Γ_{14}	$f_0(980)\, f_0(2200)$	$(7.8\ ^{+2.0}_{-2.5}) \times 10^{-4}$		
Γ_{15}	$f_0(1370)\, f_0(1370)$	< 2.7	$\times 10^{-4}$	CL=90%
Γ_{16}	$f_0(1370)\, f_0(1500)$	< 1.7	$\times 10^{-4}$	CL=90%
Γ_{17}	$f_0(1370)\, f_0(1710)$	$(6.6\ ^{+3.5}_{-2.3}) \times 10^{-4}$		
Γ_{18}	$f_0(1500)\, f_0(1370)$	< 1.3	$\times 10^{-4}$	CL=90%
Γ_{19}	$f_0(1500)\, f_0(1500)$	< 5	$\times 10^{-5}$	CL=90%
Γ_{20}	$f_0(1500)\, f_0(1710)$	< 7	$\times 10^{-5}$	CL=90%
Γ_{21}	$K^+ K^- \pi^+ \pi^- \pi^0$	(1.11 ± 0.26) %		
Γ_{22}	$K^+ K^- \pi^0 \pi^0$	$(5.4\ \pm 0.9\ ) \times 10^{-3}$		
Γ_{23}	$K^+ \pi^- \overline{K}^0 \pi^0$ + c.c.	(2.44 ± 0.33) %		
Γ_{24}	$\rho^+ K^- K^0$ + c.c.	(1.18 ± 0.21) %		
Γ_{25}	$K^*(892)^- K^+ \pi^0$ → $K^+ \pi^- \overline{K}^0 \pi^0$ + c.c.	$(4.5\ \pm 1.1\ ) \times 10^{-3}$		
Γ_{26}	$K^0_S K^0_S \pi^+ \pi^-$	$(5.6\ \pm 1.0\ ) \times 10^{-3}$		
Γ_{27}	$K^+ K^- \eta \pi^0$	$(3.0\ \pm 0.7\ ) \times 10^{-3}$		
Γ_{28}	$3(\pi^+\pi^-)$	(1.20 ± 0.18) %		
Γ_{29}	$K^+ \overline{K}^*(892)^0 \pi^-$ + c.c.	$(7.2\ \pm 1.6\ ) \times 10^{-3}$		
Γ_{30}	$K^*(892)^0 \overline{K}^*(892)^0$	$(1.7\ \pm 0.6\ ) \times 10^{-3}$		
Γ_{31}	$\pi\pi$	$(8.33 \pm 0.35) \times 10^{-3}$		
Γ_{32}	$\pi^0 \eta$	< 1.8	$\times 10^{-4}$	
Γ_{33}	$\pi^0 \eta'$	< 1.1	$\times 10^{-3}$	
Γ_{34}	$\eta\eta$	$(2.95 \pm 0.19) \times 10^{-3}$		
Γ_{35}	$\eta\eta'$	< 2.3	$\times 10^{-4}$	CL=90%
Γ_{36}	$\eta'\eta'$	$(1.96 \pm 0.21) \times 10^{-3}$		
Γ_{37}	$\omega\omega$	$(9.5\ \pm 1.1\ ) \times 10^{-4}$		
Γ_{38}	$\omega\phi$	$(1.16 \pm 0.21) \times 10^{-4}$		
Γ_{39}	$K^+ K^-$	$(5.91 \pm 0.32) \times 10^{-3}$		
Γ_{40}	$K^0_S K^0_S$	$(3.10 \pm 0.18) \times 10^{-3}$		
Γ_{41}	$\pi^+\pi^-\eta$	< 1.9	$\times 10^{-4}$	CL=90%
Γ_{42}	$\pi^+\pi^-\eta'$	< 3.5	$\times 10^{-4}$	CL=90%
Γ_{43}	$\overline{K}^0 K^+ \pi^-$ + c.c.	< 9	$\times 10^{-5}$	CL=90%
Γ_{44}	$K^+ K^- \pi^0$	< 6	$\times 10^{-5}$	CL=90%
Γ_{45}	$K^+ K^- \eta$	< 2.2	$\times 10^{-4}$	CL=90%
Γ_{46}	$K^+ K^- K^0_S K^0_S$	$(1.4\ \pm 0.5\ ) \times 10^{-3}$		
Γ_{47}	$K^+ K^- K^+ K^-$	$(2.75 \pm 0.28) \times 10^{-3}$		
Γ_{48}	$K^+ K^- \phi$	$(9.5\ \pm 2.4\ ) \times 10^{-4}$		
Γ_{49}	$\phi\phi$	$(7.7\ \pm 0.7\ ) \times 10^{-4}$		
Γ_{50}	$p\overline{p}$	$(2.25 \pm 0.09) \times 10^{-4}$		
Γ_{51}	$p\overline{p}\pi^0$	$(6.8\ \pm 0.7\ ) \times 10^{-4}$		S=1.3
Γ_{52}	$p\overline{p}\eta$	$(3.5\ \pm 0.4\ ) \times 10^{-4}$		
Γ_{53}	$p\overline{p}\omega$	$(5.1\ \pm 0.6\ ) \times 10^{-4}$		
Γ_{54}	$p\overline{p}\phi$	$(5.9\ \pm 1.4\ ) \times 10^{-5}$		
Γ_{55}	$p\overline{p}\pi^+\pi^-$	$(2.1\ \pm 0.7\ ) \times 10^{-3}$		S=1.4
Γ_{56}	$p\overline{p}\pi^0\pi^0$	$(1.02 \pm 0.27) \times 10^{-3}$		
Γ_{57}	$p\overline{p}K^+K^-$ (non-resonant)	$(1.19 \pm 0.26) \times 10^{-4}$		
Γ_{58}	$p\overline{p}K^0_S K^0_S$	< 8.8	$\times 10^{-4}$	CL=90%
Γ_{59}	$p\overline{n}\pi^-$	$(1.24 \pm 0.11) \times 10^{-3}$		
Γ_{60}	$\overline{p}n\pi^+$	$(1.34 \pm 0.12) \times 10^{-3}$		
Γ_{61}	$p\overline{n}\pi^-\pi^0$	$(2.29 \pm 0.21) \times 10^{-3}$		
Γ_{62}	$\overline{p}n\pi^+\pi^0$	$(2.16 \pm 0.18) \times 10^{-3}$		
Γ_{63}	$\Lambda\overline{\Lambda}$	$(3.21 \pm 0.25) \times 10^{-4}$		
Γ_{64}	$\Lambda\overline{\Lambda}\pi^+\pi^-$	$(1.15 \pm 0.13) \times 10^{-3}$		
Γ_{65}	$\Lambda\overline{\Lambda}\pi^+\pi^-$ (non-resonant)	< 5	$\times 10^{-4}$	CL=90%
Γ_{66}	$\Sigma(1385)^+\overline{\Lambda}\pi^-$ + c.c.	< 5	$\times 10^{-4}$	CL=90%
Γ_{67}	$\Sigma(1385)^-\overline{\Lambda}\pi^+$ + c.c.	< 5	$\times 10^{-4}$	CL=90%
Γ_{68}	$K^+\overline{p}\Lambda$ + c.c.	$(1.22 \pm 0.12) \times 10^{-3}$		S=1.3
Γ_{69}	$K^+\overline{p}\Lambda(1520)$ + c.c.	$(2.9\ \pm 0.7\ ) \times 10^{-4}$		
Γ_{70}	$\Lambda(1520)\overline{\Lambda}(1520)$	$(3.1\ \pm 1.2\ ) \times 10^{-4}$		
Γ_{71}	$\Sigma^0\overline{\Sigma}^0$	$(4.4\ \pm 0.4\ ) \times 10^{-4}$		
Γ_{72}	$\Sigma^+\overline{\Sigma}^-$	$(3.9\ \pm 0.7\ ) \times 10^{-4}$		S=1.7
Γ_{73}	$\Sigma(1385)^+\overline{\Sigma}(1385)^-$	$(1.6\ \pm 0.6\ ) \times 10^{-4}$		
Γ_{74}	$\Sigma(1385)^-\overline{\Sigma}(1385)^+$	$(2.3\ \pm 0.6\ ) \times 10^{-4}$		
Γ_{75}	$\Xi^0\overline{\Xi}^0$	$(3.1\ \pm 0.8\ ) \times 10^{-4}$		
Γ_{76}	$\Xi^-\overline{\Xi}^+$	$(4.7\ \pm 0.7\ ) \times 10^{-4}$		

Radiative decays

Γ_{77}	$\gamma J/\psi(1S)$	(1.27 ± 0.06) %		
Γ_{78}	$\gamma\rho^0$	< 9	$\times 10^{-6}$	CL=90%
Γ_{79}	$\gamma\omega$	< 8	$\times 10^{-6}$	CL=90%
Γ_{80}	$\gamma\phi$	< 6	$\times 10^{-6}$	CL=90%
Γ_{81}	$\gamma\gamma$	$(2.23 \pm 0.13) \times 10^{-4}$		

CONSTRAINED FIT INFORMATION

A multiparticle fit to $\chi_{c1}(1P)$, $\chi_{c0}(1P)$, $\chi_{c2}(1P)$, and $\psi(2S)$ with 4 total widths, a partial width, 25 combinations of partial widths obtained from integrated cross section, and 84 branching ratios uses 238 measurements to determine 49 parameters. The overall fit has a $\chi^2 = 339.7$ for 189 degrees of freedom.

The following *off-diagonal* array elements are the correlation coefficients $\langle \delta p_i \delta p_j \rangle / (\delta p_i \cdot \delta p_j)$, in percent, from the fit to parameters p_i, including the branching fractions, $x_i \equiv \Gamma_i / \Gamma_{\rm total}$.

x_2	25									
x_8	14	4								
x_{29}	7	2	29							
x_{31}	15	4	16	5						
x_{34}	8	2	9	3	21					
x_{39}	13	3	14	5	28	17				
x_{40}	12	3	13	4	27	16	22			
x_{47}	9	2	8	3	14	8	12	11		
x_{49}	10	3	10	4	14	9	12	12	7	
x_{50}	7	2	9	3	13	6	15	15	8	8
x_{63}	8	2	9	3	20	12	17	16	8	9
x_{77}	4	1	5	1	14	9	10	10	5	5
x_{81}	−16	−4	−9	−6	5	4	2	4	−2	−4
Γ	−22	−6	−17	−8	−16	−9	−15	−14	−10	−13
	x_1	x_2	x_8	x_{29}	x_{31}	x_{34}	x_{39}	x_{40}	x_{47}	x_{49}

x_{63}	11			
x_{77}	−21	8		
x_{81}	2	4	9	
Γ	−7	−9	−8	−48
	x_{50}	x_{63}	x_{77}	x_{81}

$\chi_{c0}(1P)$ PARTIAL WIDTHS

$\chi_{c0}(1P)$ Γ(i)Γ($\gamma J/\psi(1S)$)/Γ(total)

$\Gamma(p\overline{p}) \times \Gamma(\gamma J/\psi(1S))/\Gamma_{\rm total}$ — **$\Gamma_{50}\Gamma_{77}/\Gamma$**

VALUE (eV)	EVTS	DOCUMENT ID		TECN	COMMENT
30.0± 2.3 OUR FIT					
• • • We do not use the following data for averages, fits, limits, etc. • • •					
26.6± 2.6±1.4	392	[1,2] BAGNASCO	02	E835	$\overline{p}p \to \chi_{c0} \to J/\psi\gamma$
$48.7^{+11.3}_{-8.9} \pm 2.4$		[1,2] AMBROGIANI	99B	E835	$\overline{p}p \to \gamma J/\psi$

[1] Calculated by us using $B(J/\psi(1S) \to e^+e^-) = 0.0593 \pm 0.0010$.

[2] Values in $(\Gamma(p\overline{p}) \times \Gamma(\gamma J/\psi(1S))/\Gamma_{\rm total})$ and $(\Gamma(p\overline{p})/\Gamma_{\rm total} \times \Gamma(\gamma J/\psi(1S))/\Gamma_{\rm total})$ are not independent. The latter is used in the fit since it is less correlated to the total width.

$\chi_{c0}(1P)$ Γ(i)Γ($\gamma\gamma$)/Γ(total)

$\Gamma(2(\pi^+\pi^-)) \times \Gamma(\gamma\gamma)/\Gamma_{\rm total}$ — **$\Gamma_1\Gamma_{81}/\Gamma$**

VALUE (eV)	EVTS	DOCUMENT ID		TECN	COMMENT
52 ± 4 OUR FIT					
49 ±10 OUR AVERAGE	Error includes scale factor of 1.8.				
44.7± 3.6±4.9	3.6k	UEHARA	08	BELL	$\gamma\gamma \to \chi_{c0} \to 2(\pi^+\pi^-)$
75 ±13 ±8		EISENSTEIN	01	CLE2	$e^+e^- \to e^+e^-\chi_{c0}$

$\Gamma(\rho^0\rho^0) \times \Gamma(\gamma\gamma)/\Gamma_{\rm total}$ — **$\Gamma_3\Gamma_{81}/\Gamma$**

VALUE (eV)	CL%	EVTS	DOCUMENT ID		TECN	COMMENT
• • • We do not use the following data for averages, fits, limits, etc. • • •						
<12	90	<252	UEHARA	08	BELL	$\gamma\gamma \to \chi_{c0} \to 2(\pi^+\pi^-)$

$\Gamma(\pi^+\pi^- K^+ K^-) \times \Gamma(\gamma\gamma)/\Gamma_{\rm total}$ — **$\Gamma_8\Gamma_{81}/\Gamma$**

VALUE (eV)	EVTS	DOCUMENT ID		TECN	COMMENT
41 ±4 OUR FIT					
38.8±3.7±4.7	1.7k	UEHARA	08	BELL	$\gamma\gamma \to \chi_{c0} \to K^+K^-\pi^+\pi^-$

$\Gamma(K^+K^-\pi^+\pi^-\pi^0) \times \Gamma(\gamma\gamma)/\Gamma_{\rm total}$ — **$\Gamma_{21}\Gamma_{81}/\Gamma$**

VALUE (eV)	EVTS	DOCUMENT ID		TECN	COMMENT
26±4±4	1094	DEL-AMO-SA...11M		BABR	$\gamma\gamma \to K^+K^-\pi^+\pi^-\pi^0$

$\Gamma(K^+\overline{K}^*(892)^0\pi^- + \text{c.c.}) \times \Gamma(\gamma\gamma)/\Gamma_{\rm total}$ — **$\Gamma_{29}\Gamma_{81}/\Gamma$**

VALUE (eV)	EVTS	DOCUMENT ID		TECN	COMMENT
17 ±4 OUR FIT					
16.7±6.1±3.0	495 ± 182	UEHARA	08	BELL	$\gamma\gamma \to \chi_{c0} \to K^+K^-\pi^+\pi^-$

Meson Particle Listings

$\chi_{c0}(1P)$

$\Gamma(K^*(892)^0\overline{K}^*(892)^0) \times \Gamma(\gamma\gamma)/\Gamma_{total}$ $\Gamma_{30}\Gamma_{81}/\Gamma$

VALUE (eV)	CL%	EVTS	DOCUMENT ID		TECN	COMMENT
• • • We do not use the following data for averages, fits, limits, etc. • • •						
<6	90	<148	UEHARA	08	BELL	$\gamma\gamma \to \chi_{c0} \to K^+K^-\pi^+\pi^-$

$\Gamma(\pi\pi) \times \Gamma(\gamma\gamma)/\Gamma_{total}$ $\Gamma_{31}\Gamma_{81}/\Gamma$

VALUE (eV)	EVTS	DOCUMENT ID		TECN	COMMENT
19.5± 1.4 OUR FIT					
23 ± 5 OUR AVERAGE					
$29.7^{+17.4}_{-12.0}\pm4.8$	103^{+60}_{-42}	[1] UEHARA	09	BELL	10.6 $e^+e^- \to e^+e^-\pi^0\pi^0$
22.7± 3.2±3.5	129 ± 18	[2] NAKAZAWA	05	BELL	10.6 $e^+e^- \to e^+e^-\pi^+\pi^-$

[1] We multiplied the measurement by 3 to convert from $\pi^0\pi^0$ to $\pi\pi$. Interference with the continuum included.
[2] We have multiplied $\pi^+\pi^-$ measurement by 3/2 to obtain $\pi\pi$.

$\Gamma(\eta\eta) \times \Gamma(\gamma\gamma)/\Gamma_{total}$ $\Gamma_{34}\Gamma_{81}/\Gamma$

VALUE (eV)	EVTS	DOCUMENT ID		TECN	COMMENT
9.4±2.3±1.2	22	[1] UEHARA	10A	BELL	10.6 $e^+e^- \to e^+e^-\eta\eta$

[1] Interference with the continuum not included.

$\Gamma(\omega\omega) \times \Gamma(\gamma\gamma)/\Gamma_{total}$ $\Gamma_{37}\Gamma_{81}/\Gamma$

VALUE (eV)	CL%	DOCUMENT ID		TECN	COMMENT
• • • We do not use the following data for averages, fits, limits, etc. • • •					
<3.9	90	[1] LIU	12B	BELL	$\gamma\gamma \to 2(\pi^+\pi^-\pi^0)$

[1] Using B($\omega \to \pi^+\pi^-\pi^0$) = (89.2 ± 0.7)%.

$\Gamma(\omega\phi) \times \Gamma(\gamma\gamma)/\Gamma_{total}$ $\Gamma_{38}\Gamma_{81}/\Gamma$

VALUE (eV)	CL%	DOCUMENT ID		TECN	COMMENT
• • • We do not use the following data for averages, fits, limits, etc. • • •					
<0.34	90	[1] LIU	12B	BELL	$\gamma\gamma \to K^+K^-\pi^+\pi^-\pi^0$

[1] Using B($\phi \to K^+K^-$) = (48.9 ± 0.5)% and B($\omega \to \pi^+\pi^-\pi^0$) = (89.2 ± 0.7)%.

$\Gamma(K^+K^-) \times \Gamma(\gamma\gamma)/\Gamma_{total}$ $\Gamma_{39}\Gamma_{81}/\Gamma$

VALUE (eV)	EVTS	DOCUMENT ID		TECN	COMMENT
13.9±1.1 OUR FIT					
14.3±1.6±2.3	153 ± 17	NAKAZAWA	05	BELL	10.6 $e^+e^- \to e^+e^-K^+K^-$

$\Gamma(K^0_SK^0_S) \times \Gamma(\gamma\gamma)/\Gamma_{total}$ $\Gamma_{40}\Gamma_{81}/\Gamma$

VALUE (eV)	EVTS	DOCUMENT ID		TECN	COMMENT
7.3 ±0.6 OUR FIT					
8.7 ±1.7 ±0.9	266	[1] UEHARA	13	BELL	$\gamma\gamma \to K^0_SK^0_S$
• • • We do not use the following data for averages, fits, limits, etc. • • •					
7.00±0.65±0.71	134 ± 12	CHEN	07B	BELL	$e^+e^- \to e^+e^-\chi_{c0}$

[1] Supersedes CHEN 07B.

$\Gamma(K^+K^-K^+K^-) \times \Gamma(\gamma\gamma)/\Gamma_{total}$ $\Gamma_{47}\Gamma_{81}/\Gamma$

VALUE (eV)	EVTS	DOCUMENT ID	TECN	COMMENT
6.4±0.7 OUR FIT				
7.9±1.3±1.1	215 ± 36	UEHARA 08	BELL	$\gamma\gamma \to \chi_{c0} \to 2(K^+K^-)$

$\Gamma(\phi\phi) \times \Gamma(\gamma\gamma)/\Gamma_{total}$ $\Gamma_{49}\Gamma_{81}/\Gamma$

VALUE (eV)	EVTS	DOCUMENT ID		TECN	COMMENT
1.82±0.19 OUR FIT					
1.72±0.33±0.14	56 ± 11	[1] LIU	12B	BELL	$\gamma\gamma \to 2(K^+K^-)$
• • • We do not use the following data for averages, fits, limits, etc. • • •					
2.3 ±0.9 ±0.4	23.6 ± 9.6	UEHARA	08	BELL	$\gamma\gamma \to \chi_{c0} \to 2(K^+K^-)$

[1] Supersedes UEHARA 08. Using B($\phi \to K^+K^-$) = (48.9 ± 0.5)%.

$\chi_{c0}(1P)$ BRANCHING RATIOS

HADRONIC DECAYS

$\Gamma(2(\pi^+\pi^-))/\Gamma_{total}$ Γ_1/Γ

VALUE	DOCUMENT ID
0.0224±0.0018 OUR FIT	

$\Gamma(\rho^0\pi^+\pi^-)/\Gamma(2(\pi^+\pi^-))$ Γ_2/Γ_1

VALUE	DOCUMENT ID		TECN	COMMENT
0.39±0.12 OUR FIT				
0.39±0.12	TANENBAUM	78	MRK1	$\psi(2S) \to \gamma\chi_{c0}$

$\Gamma(\rho^0\pi^+\pi^-)/\Gamma_{total}$ Γ_2/Γ

VALUE	DOCUMENT ID
0.0087±0.0028 OUR FIT	

$\Gamma(f_0(980)f_0(980))/\Gamma_{total}$ Γ_4/Γ

VALUE (units 10^{-4})	EVTS	DOCUMENT ID		TECN	COMMENT
6.5±2.1±0.2	36 ± 9	[1] ABLIKIM	04G	BES	$\psi(2S) \to \gamma 2\pi^+ 2\pi^-$

[1] ABLIKIM 04G reports $[\Gamma(\chi_{c0}(1P) \to f_0(980)f_0(980))/\Gamma_{total}] \times [B(\psi(2S) \to \gamma\chi_{c0}(1P))] = (6.5 \pm 1.6 \pm 1.3) \times 10^{-5}$ which we divide by our best value $B(\psi(2S) \to \gamma\chi_{c0}(1P)) = (9.99 \pm 0.27) \times 10^{-2}$. Our first error is their experiment's error and our second error is the systematic error from using our best value.

$\Gamma(\pi^+\pi^-\pi^0\pi^0)/\Gamma_{total}$ Γ_5/Γ

VALUE (%)	EVTS	DOCUMENT ID		TECN	COMMENT
3.3±0.4±0.1	1751.4	[1] HE	08B	CLEO	$e^+e^- \to \gamma h^+h^-h^0h^0$

[1] HE 08B reports 3.54 ± 0.10 ± 0.43 ± 0.18 % from a measurement of $[\Gamma(\chi_{c0}(1P) \to \pi^+\pi^-\pi^0\pi^0)/\Gamma_{total}] \times [B(\psi(2S) \to \gamma\chi_{c0}(1P))]$ assuming $B(\psi(2S) \to \gamma\chi_{c0}(1P)) = (9.22 \pm 0.11 \pm 0.46) \times 10^{-2}$, which we rescale to our best value $B(\psi(2S) \to \gamma\chi_{c0}(1P)) = (9.99 \pm 0.27) \times 10^{-2}$. Our first error is their experiment's error and our second error is the systematic error from using our best value.

$\Gamma(\rho^+\pi^-\pi^0 + \text{c.c.})/\Gamma_{total}$ Γ_6/Γ

VALUE (%)	EVTS	DOCUMENT ID		TECN	COMMENT
2.8±0.4±0.1	1358.5	[1,2] HE	08B	CLEO	$e^+e^- \to \gamma h^+h^-h^0h^0$

[1] HE 08B reports 3.04 ± 0.18 ± 0.42 ± 0.16 % from a measurement of $[\Gamma(\chi_{c0}(1P) \to \rho^+\pi^-\pi^0 + \text{c.c.})/\Gamma_{total}] \times [B(\psi(2S) \to \gamma\chi_{c0}(1P))]$ assuming $B(\psi(2S) \to \gamma\chi_{c0}(1P)) = (9.22 \pm 0.11 \pm 0.46) \times 10^{-2}$, which we rescale to our best value $B(\psi(2S) \to \gamma\chi_{c0}(1P)) = (9.99 \pm 0.27) \times 10^{-2}$. Our first error is their experiment's error and our second error is the systematic error from using our best value.
[2] Calculated by us. We have added the values from HE 08B for $\rho^+\pi^-\pi^0$ and $\rho^-\pi^+\pi^0$ decays assuming uncorrelated statistical and fully correlated systematic uncertainties.

$\Gamma(4\pi^0)/\Gamma_{total}$ Γ_7/Γ

VALUE (units 10^{-3})	EVTS	DOCUMENT ID		TECN	COMMENT
3.2±0.4±0.1	3296	[1] ABLIKIM	11A	BES3	$e^+e^- \to \psi(2S) \to \gamma\chi_{c0}$

[1] ABLIKIM 11A reports $(3.34 \pm 0.06 \pm 0.44) \times 10^{-3}$ from a measurement of $[\Gamma(\chi_{c0}(1P) \to 4\pi^0)/\Gamma_{total}] \times [B(\psi(2S) \to \gamma\chi_{c0}(1P))]$ assuming $B(\psi(2S) \to \gamma\chi_{c0}(1P)) = (9.62 \pm 0.31) \times 10^{-2}$, which we rescale to our best value $B(\psi(2S) \to \gamma\chi_{c0}(1P)) = (9.99 \pm 0.27) \times 10^{-2}$. Our first error is their experiment's error and our second error is the systematic error from using our best value.

$\Gamma(\pi^+\pi^-K^+K^-)/\Gamma_{total}$ Γ_8/Γ

VALUE (units 10^{-3})	DOCUMENT ID
17.5±1.4 OUR FIT	

$\Gamma(K^+\overline{K}^*(892)^0\pi^- + \text{c.c.})/\Gamma(\pi^+\pi^-K^+K^-)$ Γ_{29}/Γ_8

VALUE	DOCUMENT ID		TECN	COMMENT
0.41±0.09 OUR FIT				
0.41±0.10	TANENBAUM	78	MRK1	$\psi(2S) \to \gamma\chi_{c0}$

$\Gamma(K^*_0(1430)^0\overline{K}^*_0(1430)^0 \to \pi^+\pi^-K^+K^-)/\Gamma_{total}$ Γ_9/Γ

VALUE (units 10^{-4})	EVTS	DOCUMENT ID		TECN	COMMENT
$\mathbf{9.6^{+3.5}_{-2.8}\pm0.3}$	83	[1] ABLIKIM	05Q	BES2	$\psi(2S) \to \gamma\pi^+\pi^-K^+K^-$

[1] ABLIKIM 05Q reports $(10.44 \pm 2.37^{+3.05}_{-1.90}) \times 10^{-4}$ from a measurement of $[\Gamma(\chi_{c0}(1P) \to K^*_0(1430)^0\overline{K}^*_0(1430)^0 \to \pi^+\pi^-K^+K^-)/\Gamma_{total}] \times [B(\psi(2S) \to \gamma\chi_{c0}(1P))]$ assuming $B(\psi(2S) \to \gamma\chi_{c0}(1P)) = (9.22 \pm 0.11 \pm 0.46) \times 10^{-2}$, which we rescale to our best value $B(\psi(2S) \to \gamma\chi_{c0}(1P)) = (9.99 \pm 0.27) \times 10^{-2}$. Our first error is their experiment's error and our second error is the systematic error from using our best value.

$\Gamma(K^*_0(1430)^0\overline{K}^*_2(1430)^0 + \text{c.c.} \to \pi^+\pi^-K^+K^-)/\Gamma_{total}$ Γ_{10}/Γ

VALUE (units 10^{-4})	EVTS	DOCUMENT ID		TECN	COMMENT
$\mathbf{7.8^{+1.9}_{-2.4}\pm0.2}$	62	[1] ABLIKIM	05Q	BES2	$\psi(2S) \to \gamma\pi^+\pi^-K^+K^-$

[1] ABLIKIM 05Q reports $(8.49 \pm 1.66^{+1.32}_{-1.99}) \times 10^{-4}$ from a measurement of $[\Gamma(\chi_{c0}(1P) \to K^*_0(1430)^0\overline{K}^*_2(1430)^0 + \text{c.c.} \to \pi^+\pi^-K^+K^-)/\Gamma_{total}] \times [B(\psi(2S) \to \gamma\chi_{c0}(1P))]$ assuming $B(\psi(2S) \to \gamma\chi_{c0}(1P)) = (9.22 \pm 0.11 \pm 0.46) \times 10^{-2}$, which we rescale to our best value $B(\psi(2S) \to \gamma\chi_{c0}(1P)) = (9.99 \pm 0.27) \times 10^{-2}$. Our first error is their experiment's error and our second error is the systematic error from using our best value.

$\Gamma(K_1(1270)^+K^- + \text{c.c.} \to \pi^+\pi^-K^+K^-)/\Gamma_{total}$ Γ_{11}/Γ

VALUE (units 10^{-3})	EVTS	DOCUMENT ID		TECN	COMMENT
$\mathbf{6.1^{+1.9}_{-1.8}\pm0.2}$	68	[1] ABLIKIM	05Q	BES2	$\psi(2S) \to \gamma\pi^+\pi^-K^+K^-$

[1] ABLIKIM 05Q reports $(6.66 \pm 1.31^{+1.60}_{-1.51}) \times 10^{-3}$ from a measurement of $[\Gamma(\chi_{c0}(1P) \to K_1(1270)^+K^- + \text{c.c.} \to \pi^+\pi^-K^+K^-)/\Gamma_{total}] \times [B(\psi(2S) \to \gamma\chi_{c0}(1P))]$ assuming $B(\psi(2S) \to \gamma\chi_{c0}(1P)) = (9.22 \pm 0.11 \pm 0.46) \times 10^{-2}$, which we rescale to our best value $B(\psi(2S) \to \gamma\chi_{c0}(1P)) = (9.99 \pm 0.27) \times 10^{-2}$. Our first error is their experiment's error and our second error is the systematic error from using our best value. The measurement assumes $B(K_1(1270) \to K\rho(770)) = 42 \pm 6\%$.

$\Gamma(K_1(1400)^+K^- + \text{c.c.} \to \pi^+\pi^-K^+K^-)/\Gamma_{total}$ Γ_{12}/Γ

VALUE (units 10^{-3})	CL%	DOCUMENT ID		TECN	COMMENT
<2.6	90	[1] ABLIKIM	05Q	BES2	$\psi(2S) \to \gamma\pi^+\pi^-K^+K^-$

[1] ABLIKIM 05Q reports $< 2.85 \times 10^{-3}$ from a measurement of $[\Gamma(\chi_{c0}(1P) \to K_1(1400)^+K^- + \text{c.c.} \to \pi^+\pi^-K^+K^-)/\Gamma_{total}] \times [B(\psi(2S) \to \gamma\chi_{c0}(1P))]$ assuming $B(\psi(2S) \to \gamma\chi_{c0}(1P)) = (9.22 \pm 0.11 \pm 0.46) \times 10^{-2}$, which we rescale to our best value $B(\psi(2S) \to \gamma\chi_{c0}(1P)) = 9.99 \times 10^{-2}$. The measurement assumes $B(K_1(1400) \to K^*(892)\pi) = 94 \pm 6\%$.

$\Gamma(f_0(980)\,f_0(980))/\Gamma_{total}$ Γ_{13}/Γ

VALUE (units 10^{-5})	EVTS	DOCUMENT ID		TECN	COMMENT
$15.9^{+10.2}_{-8.8}\pm0.4$	28	[1] ABLIKIM	05Q	BES2	$\psi(2S)\to\gamma\pi^+\pi^-K^+K^-$

[1] ABLIKIM 05Q reports $[\Gamma(\chi_{c0}(1P)\to f_0(980)\,f_0(980))/\Gamma_{total}]\times[B(\psi(2S)\to\gamma\chi_{c0}(1P))] = (1.59\pm0.50^{+0.89}_{-0.72})\times10^{-5}$ which we divide by our best value $B(\psi(2S)\to\gamma\chi_{c0}(1P)) = (9.99\pm0.27)\times10^{-2}$. Our first error is their experiment's error and our second error is the systematic error from using our best value. One of the $f_0(980)$ mesons is identified via decay to $\pi^+\pi^-$ while the other via K^+K^- decay.

$\Gamma(f_0(980)\,f_0(2200))/\Gamma_{total}$ Γ_{14}/Γ

VALUE (units 10^{-4})	EVTS	DOCUMENT ID		TECN	COMMENT
$7.8^{+2.0}_{-2.5}\pm0.2$	77	[1] ABLIKIM	05Q	BES2	$\psi(2S)\to\gamma\pi^+\pi^-K^+K^-$

[1] ABLIKIM 05Q reports $(8.42\pm1.42^{+1.65}_{-2.29})\times10^{-4}$ from a measurement of $[\Gamma(\chi_{c0}(1P)\to f_0(980)\,f_0(2200))/\Gamma_{total}]\times[B(\psi(2S)\to\gamma\chi_{c0}(1P))]$ assuming $B(\psi(2S)\to\gamma\chi_{c0}(1P)) = (9.22\pm0.11\pm0.46)\times10^{-2}$, which we rescale to our best value $B(\psi(2S)\to\gamma\chi_{c0}(1P)) = (9.99\pm0.27)\times10^{-2}$. Our first error is their experiment's error and our second error is the systematic error from using our best value. The f_0 mesons are identified via $f_0(980)\to\pi^+\pi^-$ and $f_0(2200)\to K^+K^-$ decays.

$\Gamma(f_0(1370)\,f_0(1370))/\Gamma_{total}$ Γ_{15}/Γ

VALUE (units 10^{-4})	CL%	DOCUMENT ID		TECN	COMMENT
<2.7	90	[1] ABLIKIM	05Q	BES2	$\psi(2S)\to\gamma\pi^+\pi^-K^+K^-$

[1] ABLIKIM 05Q reports $<2.9\times10^{-4}$ from a measurement of $[\Gamma(\chi_{c0}(1P)\to f_0(1370)\,f_0(1370))/\Gamma_{total}]\times[B(\psi(2S)\to\gamma\chi_{c0}(1P))]$ assuming $B(\psi(2S)\to\gamma\chi_{c0}(1P)) = (9.22\pm0.11\pm0.46)\times10^{-2}$, which we rescale to our best value $B(\psi(2S)\to\gamma\chi_{c0}(1P)) = 9.99\times10^{-2}$. One of the $f_0(1370)$ mesons is identified via decay to $\pi^+\pi^-$ while the other via K^+K^- decay. Both branching fractions for these f_0 decays are implicitly included in the quoted result.

$\Gamma(f_0(1370)\,f_0(1500))/\Gamma_{total}$ Γ_{16}/Γ

VALUE (units 10^{-4})	CL%	DOCUMENT ID		TECN	COMMENT
<1.7	90	[1] ABLIKIM	05Q	BES2	$\psi(2S)\to\gamma\pi^+\pi^-K^+K^-$

[1] ABLIKIM 05Q reports $<1.8\times10^{-4}$ from a measurement of $[\Gamma(\chi_{c0}(1P)\to f_0(1370)\,f_0(1500))/\Gamma_{total}]\times[B(\psi(2S)\to\gamma\chi_{c0}(1P))]$ assuming $B(\psi(2S)\to\gamma\chi_{c0}(1P)) = (9.22\pm0.11\pm0.46)\times10^{-2}$, which we rescale to our best value $B(\psi(2S)\to\gamma\chi_{c0}(1P)) = 9.99\times10^{-2}$. The f_0 mesons are identified via $f_0(1370)\to\pi^+\pi^-$ and $f_0(1500)\to K^+K^-$ decays. Both branching fractions for these f_0 decays are implicitly included in the quoted result.

$\Gamma(f_0(1370)\,f_0(1710))/\Gamma_{total}$ Γ_{17}/Γ

VALUE (units 10^{-4})	EVTS	DOCUMENT ID		TECN	COMMENT
$6.6^{+3.5}_{-2.3}\pm0.2$	61	[1] ABLIKIM	05Q	BES2	$\psi(2S)\to\gamma\pi^+\pi^-K^+K^-$

[1] ABLIKIM 05Q reports $(7.12\pm1.85^{+3.28}_{-1.68})\times10^{-4}$ from a measurement of $[\Gamma(\chi_{c0}(1P)\to f_0(1370)\,f_0(1710))/\Gamma_{total}]\times[B(\psi(2S)\to\gamma\chi_{c0}(1P))]$ assuming $B(\psi(2S)\to\gamma\chi_{c0}(1P)) = (9.22\pm0.11\pm0.46)\times10^{-2}$, which we rescale to our best value $B(\psi(2S)\to\gamma\chi_{c0}(1P)) = (9.99\pm0.27)\times10^{-2}$. Our first error is their experiment's error and our second error is the systematic error from using our best value. The f_0 mesons are identified via $f_0(1370)\to\pi^+\pi^-$ and $f_0(1710)\to K^+K^-$ decays. Both branching fractions for these f_0 decays are implicitly included in the quoted result.

$\Gamma(f_0(1500)\,f_0(1370))/\Gamma_{total}$ Γ_{18}/Γ

VALUE (units 10^{-4})	CL%	DOCUMENT ID		TECN	COMMENT
<1.3	90	[1] ABLIKIM	05Q	BES2	$\psi(2S)\to\gamma\pi^+\pi^-K^+K^-$

[1] ABLIKIM 05Q reports $<1.4\times10^{-4}$ from a measurement of $[\Gamma(\chi_{c0}(1P)\to f_0(1500)\,f_0(1370))/\Gamma_{total}]\times[B(\psi(2S)\to\gamma\chi_{c0}(1P))]$ assuming $B(\psi(2S)\to\gamma\chi_{c0}(1P)) = (9.22\pm0.11\pm0.46)\times10^{-2}$, which we rescale to our best value $B(\psi(2S)\to\gamma\chi_{c0}(1P)) = 9.99\times10^{-2}$. The f_0 mesons are identified via $f_0(1500)\to\pi^+\pi^-$ and $f_0(1370)\to K^+K^-$ decays. Both branching fractions for these f_0 decays are implicitly included in the quoted result.

$\Gamma(f_0(1500)\,f_0(1500))/\Gamma_{total}$ Γ_{19}/Γ

VALUE (units 10^{-4})	CL%	DOCUMENT ID		TECN	COMMENT
<0.5	90	[1] ABLIKIM	05Q	BES2	$\psi(2S)\to\gamma\pi^+\pi^-K^+K^-$

[1] ABLIKIM 05Q reports $<0.55\times10^{-4}$ from a measurement of $[\Gamma(\chi_{c0}(1P)\to f_0(1500)\,f_0(1500))/\Gamma_{total}]\times[B(\psi(2S)\to\gamma\chi_{c0}(1P))]$ assuming $B(\psi(2S)\to\gamma\chi_{c0}(1P)) = (9.22\pm0.11\pm0.46)\times10^{-2}$, which we rescale to our best value $B(\psi(2S)\to\gamma\chi_{c0}(1P)) = 9.99\times10^{-2}$. One of the $f_0(1500)$ is identified via decay to $\pi^+\pi^-$ while the other via K^+K^- decay. Both branching fractions for these f_0 decays are implicitly included in the quoted result.

$\Gamma(f_0(1500)\,f_0(1710))/\Gamma_{total}$ Γ_{20}/Γ

VALUE (units 10^{-4})	CL%	DOCUMENT ID		TECN	COMMENT
<0.7	90	[1] ABLIKIM	05Q	BES2	$\psi(2S)\to\gamma\pi^+\pi^-K^+K^-$

[1] ABLIKIM 05Q reports $<0.73\times10^{-4}$ from a measurement of $[\Gamma(\chi_{c0}(1P)\to f_0(1500)\,f_0(1710))/\Gamma_{total}]\times[B(\psi(2S)\to\gamma\chi_{c0}(1P))]$ assuming $B(\psi(2S)\to\gamma\chi_{c0}(1P)) = (9.22\pm0.11\pm0.46)\times10^{-2}$, which we rescale to our best value $B(\psi(2S)\to\gamma\chi_{c0}(1P)) = 9.99\times10^{-2}$. The f_0 mesons are identified via $f_0(1500)\to\pi^+\pi^-$ and $f_0(1710)\to K^+K^-$ decays. Both branching fractions for these f_0 decays are implicitly included in the quoted result.

$\Gamma(K^+K^-\pi^0\pi^0)/\Gamma_{total}$ Γ_{22}/Γ

VALUE (%)	EVTS	DOCUMENT ID		TECN	COMMENT
$0.54\pm0.09\pm0.01$	213.5	[1] HE	08B	CLEO	$e^+e^-\to\gamma h^+h^-h^0h^0$

[1] HE 08B reports $0.59\pm0.05\pm0.08\pm0.03$ % from a measurement of $[\Gamma(\chi_{c0}(1P)\to K^+K^-\pi^0\pi^0)/\Gamma_{total}]\times[B(\psi(2S)\to\gamma\chi_{c0}(1P))]$ assuming $B(\psi(2S)\to\gamma\chi_{c0}(1P)) = (9.22\pm0.11\pm0.46)\times10^{-2}$, which we rescale to our best value $B(\psi(2S)\to\gamma\chi_{c0}(1P)) = (9.99\pm0.27)\times10^{-2}$. Our first error is their experiment's error and our second error is the systematic error from using our best value.

$\Gamma(K^+\pi^-\overline{K}^0\pi^0+\text{c.c.})/\Gamma_{total}$ Γ_{23}/Γ

VALUE (%)	EVTS	DOCUMENT ID		TECN	COMMENT
$2.44\pm0.32\pm0.07$	401.7	[1] HE	08B	CLEO	$e^+e^-\to\gamma h^+h^-h^0h^0$

[1] HE 08B reports $2.64\pm0.15\pm0.31\pm0.14$ % from a measurement of $[\Gamma(\chi_{c0}(1P)\to K^+\pi^-\overline{K}^0\pi^0+\text{c.c.})/\Gamma_{total}]\times[B(\psi(2S)\to\gamma\chi_{c0}(1P))]$ assuming $B(\psi(2S)\to\gamma\chi_{c0}(1P)) = (9.22\pm0.11\pm0.46)\times10^{-2}$, which we rescale to our best value $B(\psi(2S)\to\gamma\chi_{c0}(1P)) = (9.99\pm0.27)\times10^{-2}$. Our first error is their experiment's error and our second error is the systematic error from using our best value.

$\Gamma(\rho^+K^-K^0+\text{c.c.})/\Gamma_{total}$ Γ_{24}/Γ

VALUE (%)	EVTS	DOCUMENT ID		TECN	COMMENT
$1.18\pm0.20\pm0.03$	179.7	[1] HE	08B	CLEO	$e^+e^-\to\gamma h^+h^-h^0h^0$

[1] HE 08B reports $1.28\pm0.16\pm0.15\pm0.07$ % from a measurement of $[\Gamma(\chi_{c0}(1P)\to\rho^+K^-K^0+\text{c.c.})/\Gamma_{total}]\times[B(\psi(2S)\to\gamma\chi_{c0}(1P))]$ assuming $B(\psi(2S)\to\gamma\chi_{c0}(1P)) = (9.22\pm0.11\pm0.46)\times10^{-2}$, which we rescale to our best value $B(\psi(2S)\to\gamma\chi_{c0}(1P)) = (9.99\pm0.27)\times10^{-2}$. Our first error is their experiment's error and our second error is the systematic error from using our best value.

$\Gamma(K^*(892)^-K^+\pi^0\to K^+\pi^-\overline{K}^0\pi^0+\text{c.c.})/\Gamma_{total}$ Γ_{25}/Γ

VALUE (%)	EVTS	DOCUMENT ID		TECN	COMMENT
$0.45\pm0.11\pm0.01$	64.1	[1] HE	08B	CLEO	$e^+e^-\to\gamma h^+h^-h^0h^0$

[1] HE 08B reports $0.49\pm0.10\pm0.07\pm0.03$ % from a measurement of $[\Gamma(\chi_{c0}(1P)\to K^*(892)^-K^+\pi^0\to K^+\pi^-\overline{K}^0\pi^0+\text{c.c.})/\Gamma_{total}]\times[B(\psi(2S)\to\gamma\chi_{c0}(1P))]$ assuming $B(\psi(2S)\to\gamma\chi_{c0}(1P)) = (9.22\pm0.11\pm0.46)\times10^{-2}$, which we rescale to our best value $B(\psi(2S)\to\gamma\chi_{c0}(1P)) = (9.99\pm0.27)\times10^{-2}$. Our first error is their experiment's error and our second error is the systematic error from using our best value.

$\Gamma(K^0_SK^0_S\pi^+\pi^-)/\Gamma_{total}$ Γ_{26}/Γ

VALUE (units 10^{-3})	EVTS	DOCUMENT ID		TECN	COMMENT
$5.6\pm1.0\pm0.2$	152 ± 14	[1] ABLIKIM	05O	BES2	$\psi(2S)\to\gamma\chi_{c0}$

[1] ABLIKIM 05O reports $[\Gamma(\chi_{c0}(1P)\to K^0_SK^0_S\pi^+\pi^-)/\Gamma_{total}]\times[B(\psi(2S)\to\gamma\chi_{c0}(1P))] = (0.558\pm0.051\pm0.089)\times10^{-3}$ which we divide by our best value $B(\psi(2S)\to\gamma\chi_{c0}(1P)) = (9.99\pm0.27)\times10^{-2}$. Our first error is their experiment's error and our second error is the systematic error from using our best value.

$\Gamma(K^+K^-\eta\pi^0)/\Gamma_{total}$ Γ_{27}/Γ

VALUE (%)	EVTS	DOCUMENT ID		TECN	COMMENT
$0.30\pm0.07\pm0.01$	56.4	[1] HE	08B	CLEO	$e^+e^-\to\gamma h^+h^-h^0h^0$

[1] HE 08B reports $0.32\pm0.05\pm0.05\pm0.02$ % from a measurement of $[\Gamma(\chi_{c0}(1P)\to K^+K^-\eta\pi^0)/\Gamma_{total}]\times[B(\psi(2S)\to\gamma\chi_{c0}(1P))]$ assuming $B(\psi(2S)\to\gamma\chi_{c0}(1P)) = (9.22\pm0.11\pm0.46)\times10^{-2}$, which we rescale to our best value $B(\psi(2S)\to\gamma\chi_{c0}(1P)) = (9.99\pm0.27)\times10^{-2}$. Our first error is their experiment's error and our second error is the systematic error from using our best value.

$\Gamma(3(\pi^+\pi^-))/\Gamma_{total}$ Γ_{28}/Γ

VALUE (units 10^{-3})	DOCUMENT ID		TECN	COMMENT
12.0±1.8 OUR EVALUATION	Treating systematic error as correlated.			
12.0±1.7 OUR AVERAGE				
$11.7\pm1.0\pm1.9$	[1] BAI	99B	BES	$\psi(2S)\to\gamma\chi_{c0}$
$12.5\pm2.9\pm0.5$	[1] TANENBAUM	78	MRK1	$\psi(2S)\to\gamma\chi_{c0}$

[1] Rescaled by us using $B(\psi(2S)\to\gamma\chi_{c0}) = (9.4\pm0.4)\%$ and $B(\psi(2S)\to J/\psi(1S)\pi^+\pi^-) = (32.6\pm0.5)\%$.

$\Gamma(K^+\overline{K}^*(892)^0\pi^-+\text{c.c.})/\Gamma_{total}$ Γ_{29}/Γ

VALUE	DOCUMENT ID
0.0072±0.0016 OUR FIT	

$\Gamma(K^*(892)^0\overline{K}^*(892)^0)/\Gamma_{total}$ Γ_{30}/Γ

VALUE (units 10^{-3})	EVTS	DOCUMENT ID		TECN	COMMENT
$1.68^{+0.59}_{-0.53}\pm0.05$	64	[1] ABLIKIM	05Q	BES2	$\psi(2S)\to\gamma\pi^+\pi^-K^+K^-$
• • • We do not use the following data for averages, fits, limits, etc. • • •					
$1.53\pm0.39\pm0.04$	30 ± 6	[2,3] ABLIKIM	04H	BES	Repl. by ABLIKIM 05Q

[1] ABLIKIM 05Q reports $[\Gamma(\chi_{c0}(1P)\to K^*(892)^0\overline{K}^*(892)^0)/\Gamma_{total}]\times[B(\psi(2S)\to\gamma\chi_{c0}(1P))] = (0.168\pm0.035^{+0.047}_{-0.040})\times10^{-3}$ which we divide by our best value $B(\psi(2S)\to\gamma\chi_{c0}(1P)) = (9.99\pm0.27)\times10^{-2}$. Our first error is their experiment's error and our second error is the systematic error from using our best value.

[2] Assumes $B(K^*(892)^0\to K^-\pi^+) = 2/3$.

[3] ABLIKIM 04H reports $[\Gamma(\chi_{c0}(1P)\to K^*(892)^0\overline{K}^*(892)^0)/\Gamma_{total}]\times[B(\psi(2S)\to\gamma\chi_{c0}(1P))] = (1.53\pm0.29\pm0.26)\times10^{-4}$ which we divide by our best value $B(\psi(2S)\to\gamma\chi_{c0}(1P)) = (9.99\pm0.27)\times10^{-2}$. Our first error is their experiment's error and our second error is the systematic error from using our best value.

Meson Particle Listings

$\chi_{c0}(1P)$

$\Gamma(\pi\pi)/\Gamma_{\text{total}}$ Γ_{31}/Γ

VALUE (units 10^{-3})	DOCUMENT ID
8.33±0.35 OUR FIT	

$\Gamma(\eta\eta)/\Gamma_{\text{total}}$ Γ_{34}/Γ

VALUE (units 10^{-3})	DOCUMENT ID
2.95±0.19 OUR FIT	

$\Gamma(\eta\eta)/\Gamma(\pi\pi)$ Γ_{34}/Γ_{31}

VALUE	DOCUMENT ID	TECN	COMMENT
0.354±0.025 OUR FIT			
• • • We do not use the following data for averages, fits, limits, etc. • • •			
$0.26 \pm 0.09\ ^{+0.03}_{-0.02}$	[1] ANDREOTTI 05C	E835	$\overline{p}p \to$ 2 mesons
$0.24 \pm 0.10 \pm 0.08$	[1] BAI 03C	BES	$\psi(2S) \to 5\gamma$

[1] We have multiplied $\pi^0\pi^0$ measurement by 3 to obtain $\pi\pi$.

$\Gamma(\eta\eta')/\Gamma_{\text{total}}$ Γ_{35}/Γ

VALUE (units 10^{-3})	CL%	EVTS	DOCUMENT ID	TECN	COMMENT
<0.23	90	35 ± 13	[1] ASNER 09	CLEO	$\psi(2S) \to \gamma\eta'\eta$
• • • We do not use the following data for averages, fits, limits, etc. • • •					
<0.5	90		[2] ADAMS 07	CLEO	$\psi(2S) \to \gamma\chi_{c0}$

[1] ASNER 09 reports $< 0.25 \times 10^{-3}$ from a measurement of $[\Gamma(\chi_{c0}(1P) \to \eta\eta')/\Gamma_{\text{total}}] \times [B(\psi(2S) \to \gamma\chi_{c0}(1P))]$ assuming $B(\psi(2S) \to \gamma\chi_{c0}(1P)) = (9.22 \pm 0.11 \pm 0.46) \times 10^{-2}$, which we rescale to our best value $B(\psi(2S) \to \gamma\chi_{c0}(1P)) = 9.99 \times 10^{-2}$.

[2] Superseded by ASNER 09. ADAMS 07 reports $< 0.5 \times 10^{-3}$ from a measurement of $[\Gamma(\chi_{c0}(1P) \to \eta\eta')/\Gamma_{\text{total}}] \times [B(\psi(2S) \to \gamma\chi_{c0}(1P))]$ assuming $B(\psi(2S) \to \gamma\chi_{c0}(1P)) = (9.22 \pm 0.11 \pm 0.46) \times 10^{-2}$, which we rescale to our best value $B(\psi(2S) \to \gamma\chi_{c0}(1P)) = 9.99 \times 10^{-2}$.

$\Gamma(\eta'\eta')/\Gamma_{\text{total}}$ Γ_{36}/Γ

VALUE (units 10^{-3})	EVTS	DOCUMENT ID	TECN	COMMENT
1.96±0.20±0.05	0.4k	[1] ASNER 09	CLEO	$\psi(2S) \to \gamma\eta'\eta'$
• • • We do not use the following data for averages, fits, limits, etc. • • •				
$1.57 \pm 0.40 \pm 0.04$	23	[2] ADAMS 07	CLEO	$\psi(2S) \to \gamma\chi_{c0}$

[1] ASNER 09 reports $(2.12 \pm 0.13 \pm 0.21) \times 10^{-3}$ from a measurement of $[\Gamma(\chi_{c0}(1P) \to \eta'\eta')/\Gamma_{\text{total}}] \times [B(\psi(2S) \to \gamma\chi_{c0}(1P))]$ assuming $B(\psi(2S) \to \gamma\chi_{c0}(1P)) = (9.22 \pm 0.11 \pm 0.46) \times 10^{-2}$, which we rescale to our best value $B(\psi(2S) \to \gamma\chi_{c0}(1P)) = (9.99 \pm 0.27) \times 10^{-2}$. Our first error is their experiment's error and our second error is the systematic error from using our best value.

[2] Superseded by ASNER 09. ADAMS 07 reports $(1.7 \pm 0.4 \pm 0.2) \times 10^{-3}$ from a measurement of $[\Gamma(\chi_{c0}(1P) \to \eta'\eta')/\Gamma_{\text{total}}] \times [B(\psi(2S) \to \gamma\chi_{c0}(1P))]$ assuming $B(\psi(2S) \to \gamma\chi_{c0}(1P)) = 0.0922 \pm 0.0011 \pm 0.0046$, which we rescale to our best value $B(\psi(2S) \to \gamma\chi_{c0}(1P)) = (9.99 \pm 0.27) \times 10^{-2}$. Our first error is their experiment's error and our second error is the systematic error from using our best value.

$\Gamma(\omega\omega)/\Gamma_{\text{total}}$ Γ_{37}/Γ

VALUE (units 10^{-3})	EVTS	DOCUMENT ID	TECN	COMMENT
0.95±0.11 OUR AVERAGE				
$0.91 \pm 0.11 \pm 0.02$	991	[1] ABLIKIM 11K	BES3	$\psi(2S) \to \gamma$ hadrons
$2.1 \pm 0.6 \pm 0.1$	38.1 ± 9.6	[2] ABLIKIM 05N	BES2	$\psi(2S) \to \gamma\chi_{c0} \to \gamma 6\pi$

[1] ABLIKIM 11K reports $(0.95 \pm 0.03 \pm 0.11) \times 10^{-3}$ from a measurement of $[\Gamma(\chi_{c0}(1P) \to \omega\omega)/\Gamma_{\text{total}}] \times [B(\psi(2S) \to \gamma\chi_{c0}(1P))]$ assuming $B(\psi(2S) \to \gamma\chi_{c0}(1P)) = (9.62 \pm 0.31) \times 10^{-2}$, which we rescale to our best value $B(\psi(2S) \to \gamma\chi_{c0}(1P)) = (9.99 \pm 0.27) \times 10^{-2}$. Our first error is their experiment's error and our second error is the systematic error from using our best value.

[2] ABLIKIM 05N reports $[\Gamma(\chi_{c0}(1P) \to \omega\omega)/\Gamma_{\text{total}}] \times [B(\psi(2S) \to \gamma\chi_{c0}(1P))] = (0.212 \pm 0.053 \pm 0.037) \times 10^{-3}$ which we divide by our best value $B(\psi(2S) \to \gamma\chi_{c0}(1P)) = (9.99 \pm 0.27) \times 10^{-2}$. Our first error is their experiment's error and our second error is the systematic error from using our best value.

$\Gamma(\omega\phi)/\Gamma_{\text{total}}$ Γ_{38}/Γ

VALUE (units 10^{-4})	EVTS	DOCUMENT ID	TECN	COMMENT
1.16±0.21±0.03	76	[1] ABLIKIM 11K	BES3	$\psi(2S) \to \gamma$ hadrons

[1] ABLIKIM 11K reports $(1.2 \pm 0.1 \pm 0.2) \times 10^{-4}$ from a measurement of $[\Gamma(\chi_{c0}(1P) \to \omega\phi)/\Gamma_{\text{total}}] \times [B(\psi(2S) \to \gamma\chi_{c0}(1P))]$ assuming $B(\psi(2S) \to \gamma\chi_{c0}(1P)) = (9.62 \pm 0.31) \times 10^{-2}$, which we rescale to our best value $B(\psi(2S) \to \gamma\chi_{c0}(1P)) = (9.99 \pm 0.27) \times 10^{-2}$. Our first error is their experiment's error and our second error is the systematic error from using our best value.

$\Gamma(K^+K^-)/\Gamma_{\text{total}}$ Γ_{39}/Γ

VALUE (units 10^{-3})	DOCUMENT ID
5.91±0.32 OUR FIT	

$\Gamma(K^0_S K^0_S)/\Gamma_{\text{total}}$ Γ_{40}/Γ

VALUE (units 10^{-3})	DOCUMENT ID
3.10±0.18 OUR FIT	

$\Gamma(K^0_S K^0_S)/\Gamma(\pi\pi)$ Γ_{40}/Γ_{31}

VALUE	DOCUMENT ID	TECN	COMMENT
0.372±0.023 OUR FIT			
• • • We do not use the following data for averages, fits, limits, etc. • • •			
$0.31 \pm 0.05 \pm 0.05$	[1,2] CHEN 07B	BELL	$e^+e^- \to e^+e^-\chi_{c0}$

[1] Using $\Gamma(\pi\pi) \times \Gamma(\gamma\gamma)/\Gamma_{\text{total}}$ from the $\pi^+\pi^-$ measurement of NAKAZAWA 05 rescaled by 3/2 to convert to $\pi\pi$.

[2] Not independent from other measurements.

$\Gamma(K^0_S K^0_S)/\Gamma(K^+K^-)$ Γ_{40}/Γ_{39}

VALUE	DOCUMENT ID	TECN	COMMENT
0.52±0.04 OUR FIT			
• • • We do not use the following data for averages, fits, limits, etc. • • •			
$0.49 \pm 0.07 \pm 0.08$	[1,2] CHEN 07B	BELL	$e^+e^- \to e^+e^-\chi_{c0}$

[1] Using $\Gamma(K^+K^-) \times \Gamma(\gamma\gamma)/\Gamma_{\text{total}}$ from NAKAZAWA 05.

[2] Not independent from other measurements.

$\Gamma(\pi^+\pi^-\eta)/\Gamma_{\text{total}}$ Γ_{41}/Γ

VALUE (units 10^{-3})	CL%	DOCUMENT ID	TECN	COMMENT
<0.19	90	[1] ATHAR 07	CLEO	$\psi(2S) \to \gamma h^+h^-h^0$
• • • We do not use the following data for averages, fits, limits, etc. • • •				
<1.0	90	[2] ABLIKIM 06R	BES2	$\psi(2S) \to \gamma\chi_{c0}$

[1] ATHAR 07 reports $< 0.21 \times 10^{-3}$ from a measurement of $[\Gamma(\chi_{c0}(1P) \to \pi^+\pi^-\eta)/\Gamma_{\text{total}}] \times [B(\psi(2S) \to \gamma\chi_{c0}(1P))]$ assuming $B(\psi(2S) \to \gamma\chi_{c0}(1P)) = (9.22 \pm 0.11 \pm 0.46) \times 10^{-2}$, which we rescale to our best value $B(\psi(2S) \to \gamma\chi_{c0}(1P)) = 9.99 \times 10^{-2}$.

[2] ABLIKIM 06R reports $< 1.1 \times 10^{-3}$ from a measurement of $[\Gamma(\chi_{c0}(1P) \to \pi^+\pi^-\eta)/\Gamma_{\text{total}}] \times [B(\psi(2S) \to \gamma\chi_{c0}(1P))]$ assuming $B(\psi(2S) \to \gamma\chi_{c0}(1P)) = (9.2 \pm 0.4) \times 10^{-2}$, which we rescale to our best value $B(\psi(2S) \to \gamma\chi_{c0}(1P)) = 9.99 \times 10^{-2}$.

$\Gamma(\pi^+\pi^-\eta')/\Gamma_{\text{total}}$ Γ_{42}/Γ

VALUE (units 10^{-3})	CL%	DOCUMENT ID	TECN	COMMENT
<0.35	90	[1] ATHAR 07	CLEO	$\psi(2S) \to \gamma h^+h^-h^0$

[1] ATHAR 07 reports $< 0.38 \times 10^{-3}$ from a measurement of $[\Gamma(\chi_{c0}(1P) \to \pi^+\pi^-\eta')/\Gamma_{\text{total}}] \times [B(\psi(2S) \to \gamma\chi_{c0}(1P))]$ assuming $B(\psi(2S) \to \gamma\chi_{c0}(1P)) = (9.22 \pm 0.11 \pm 0.46) \times 10^{-2}$, which we rescale to our best value $B(\psi(2S) \to \gamma\chi_{c0}(1P)) = 9.99 \times 10^{-2}$.

$\Gamma(\overline{K}^0K^+\pi^- + \text{c.c.})/\Gamma_{\text{total}}$ Γ_{43}/Γ

VALUE (units 10^{-3})	CL%	DOCUMENT ID	TECN	COMMENT
<0.09	90	[1] ATHAR 07	CLEO	$\psi(2S) \to \gamma h^+h^-h^0$
• • • We do not use the following data for averages, fits, limits, etc. • • •				
<0.6	90	[2,3] ABLIKIM 06R	BES2	$\psi(2S) \to \gamma\chi_{c0}$
<0.7	90	[3,4] BAI 99B	BES	$\psi(2S) \to \gamma\chi_{c0}$

[1] ATHAR 07 reports $< 0.10 \times 10^{-3}$ from a measurement of $[\Gamma(\chi_{c0}(1P) \to \overline{K}^0K^+\pi^- + \text{c.c.})/\Gamma_{\text{total}}] \times [B(\psi(2S) \to \gamma\chi_{c0}(1P))]$ assuming $B(\psi(2S) \to \gamma\chi_{c0}(1P)) = (9.22 \pm 0.11 \pm 0.46) \times 10^{-2}$, which we rescale to our best value $B(\psi(2S) \to \gamma\chi_{c0}(1P)) = 9.99 \times 10^{-2}$.

[2] ABLIKIM 06R reports $< 0.70 \times 10^{-3}$ from a measurement of $[\Gamma(\chi_{c0}(1P) \to \overline{K}^0K^+\pi^- + \text{c.c.})/\Gamma_{\text{total}}] \times [B(\psi(2S) \to \gamma\chi_{c0}(1P))]$ assuming $B(\psi(2S) \to \gamma\chi_{c0}(1P)) = (9.2 \pm 0.4) \times 10^{-2}$, which we rescale to our best value $B(\psi(2S) \to \gamma\chi_{c0}(1P)) = 9.99 \times 10^{-2}$.

[3] We have multiplied the $K^0_S K^+\pi^-$ measurement by a factor of 2 to convert to $K^0K^+\pi^-$.

[4] Rescaled by us using $B(\psi(2S) \to \gamma\chi_{c0}) = (9.4 \pm 0.4)\%$ and $B(\psi(2S) \to J/\psi(1S)\pi^+\pi^-) = (32.6 \pm 0.5)\%$.

$\Gamma(K^+K^-\pi^0)/\Gamma_{\text{total}}$ Γ_{44}/Γ

VALUE (units 10^{-3})	CL%	DOCUMENT ID	TECN	COMMENT
<0.06	90	[1] ATHAR 07	CLEO	$\psi(2S) \to \gamma h^+h^-h^0$

[1] ATHAR 07 reports $< 0.06 \times 10^{-3}$ from a measurement of $[\Gamma(\chi_{c0}(1P) \to K^+K^-\pi^0)/\Gamma_{\text{total}}] \times [B(\psi(2S) \to \gamma\chi_{c0}(1P))]$ assuming $B(\psi(2S) \to \gamma\chi_{c0}(1P)) = (9.22 \pm 0.11 \pm 0.46) \times 10^{-2}$, which we rescale to our best value $B(\psi(2S) \to \gamma\chi_{c0}(1P)) = 9.99 \times 10^{-2}$.

$\Gamma(K^+K^-\eta)/\Gamma_{\text{total}}$ Γ_{45}/Γ

VALUE (units 10^{-3})	CL%	DOCUMENT ID	TECN	COMMENT
<0.22	90	[1] ATHAR 07	CLEO	$\psi(2S) \to \gamma h^+h^-h^0$

[1] ATHAR 07 reports $< 0.24 \times 10^{-3}$ from a measurement of $[\Gamma(\chi_{c0}(1P) \to K^+K^-\eta)/\Gamma_{\text{total}}] \times [B(\psi(2S) \to \gamma\chi_{c0}(1P))]$ assuming $B(\psi(2S) \to \gamma\chi_{c0}(1P)) = (9.22 \pm 0.11 \pm 0.46) \times 10^{-2}$, which we rescale to our best value $B(\psi(2S) \to \gamma\chi_{c0}(1P)) = 9.99 \times 10^{-2}$.

$\Gamma(K^+K^-K^0_S K^0_S)/\Gamma_{\text{total}}$ Γ_{46}/Γ

VALUE (units 10^{-3})	EVTS	DOCUMENT ID	TECN	COMMENT
1.38±0.46±0.04	16.8 ± 4.8	[1] ABLIKIM 05O	BES2	$\psi(2S) \to \gamma\chi_{c0}$

[1] ABLIKIM 05O reports $[\Gamma(\chi_{c0}(1P) \to K^+K^-K^0_S K^0_S)/\Gamma_{\text{total}}] \times [B(\psi(2S) \to \gamma\chi_{c0}(1P))] = (0.138 \pm 0.039 \pm 0.025) \times 10^{-3}$ which we divide by our best value $B(\psi(2S) \to \gamma\chi_{c0}(1P)) = (9.99 \pm 0.27) \times 10^{-2}$. Our first error is their experiment's error and our second error is the systematic error from using our best value.

$\Gamma(K^+K^-K^+K^-)/\Gamma_{total}$ Γ_{47}/Γ

VALUE (units 10^{-3})	DOCUMENT ID
2.75±0.28 OUR FIT	

$\Gamma(K^+K^-\phi)/\Gamma_{total}$ Γ_{48}/Γ

VALUE (units 10^{-3})	EVTS	DOCUMENT ID		TECN	COMMENT
0.95±0.24±0.03	38	[1] ABLIKIM	06T	BES2	$\psi(2S) \to \gamma 2K^+2K^-$

[1] ABLIKIM 06T reports $(1.03\pm0.22\pm0.15)\times10^{-3}$ from a measurement of $[\Gamma(\chi_{c0}(1P) \to K^+K^-\phi)/\Gamma_{total}] \times [B(\psi(2S) \to \gamma\chi_{c0}(1P))]$ assuming $B(\psi(2S) \to \gamma\chi_{c0}(1P)) = (9.2 \pm 0.4) \times 10^{-2}$, which we rescale to our best value $B(\psi(2S) \to \gamma\chi_{c0}(1P)) = (9.99 \pm 0.27) \times 10^{-2}$. Our first error is their experiment's error and our second error is the systematic error from using our best value.

$\Gamma(\phi\phi)/\Gamma_{total}$ Γ_{49}/Γ

VALUE (units 10^{-3})	DOCUMENT ID
0.77±0.07 OUR FIT	

$\Gamma(p\overline{p})/\Gamma_{total}$ Γ_{50}/Γ

VALUE (units 10^{-4})	DOCUMENT ID
2.25±0.09 OUR FIT	

$\Gamma(p\overline{p}\pi^0)/\Gamma_{total}$ Γ_{51}/Γ

VALUE (units 10^{-3})	DOCUMENT ID		TECN	COMMENT
0.68±0.07 OUR AVERAGE Error includes scale factor of 1.3.				
0.72±0.06±0.02	[1] ONYISI	10	CLE3	$\psi(2S) \to \gamma p\overline{p}X$
0.54±0.11±0.01	[2] ATHAR	07	CLEO	$\psi(2S) \to \gamma h^+h^-h^0$

[1] ONYISI 10 reports $(7.76 \pm 0.37 \pm 0.51 \pm 0.39) \times 10^{-4}$ from a measurement of $[\Gamma(\chi_{c0}(1P) \to p\overline{p}\pi^0)/\Gamma_{total}] \times [B(\psi(2S) \to \gamma\chi_{c0}(1P))]$ assuming $B(\psi(2S) \to \gamma\chi_{c0}(1P)) = (9.22\pm0.11\pm0.46)\times10^{-2}$, which we rescale to our best value $B(\psi(2S) \to \gamma\chi_{c0}(1P)) = (9.99 \pm 0.27) \times 10^{-2}$. Our first error is their experiment's error and our second error is the systematic error from using our best value.

[2] ATHAR 07 reports $(0.59 \pm 0.10 \pm 0.08) \times 10^{-3}$ from a measurement of $[\Gamma(\chi_{c0}(1P) \to p\overline{p}\pi^0)/\Gamma_{total}] \times [B(\psi(2S) \to \gamma\chi_{c0}(1P))]$ assuming $B(\psi(2S) \to \gamma\chi_{c0}(1P)) = (9.22\pm0.11\pm0.46)\times10^{-2}$, which we rescale to our best value $B(\psi(2S) \to \gamma\chi_{c0}(1P)) = (9.99\pm0.27)\times10^{-2}$. Our first error is their experiment's error and our second error is the systematic error from using our best value.

$\Gamma(p\overline{p}\eta)/\Gamma_{total}$ Γ_{52}/Γ

VALUE (units 10^{-3})	DOCUMENT ID		TECN	COMMENT
0.35±0.04 OUR AVERAGE				
0.34±0.04±0.01	[1] ONYISI	10	CLE3	$\psi(2S) \to \gamma p\overline{p}X$
0.36±0.11±0.01	[2] ATHAR	07	CLEO	$\psi(2S) \to \gamma h^+h^-h^0$

[1] ONYISI 10 reports $(3.73 \pm 0.38 \pm 0.28 \pm 0.19) \times 10^{-4}$ from a measurement of $[\Gamma(\chi_{c0}(1P) \to p\overline{p}\eta)/\Gamma_{total}] \times [B(\psi(2S) \to \gamma\chi_{c0}(1P))]$ assuming $B(\psi(2S) \to \gamma\chi_{c0}(1P)) = (9.22\pm0.11\pm0.46)\times10^{-2}$, which we rescale to our best value $B(\psi(2S) \to \gamma\chi_{c0}(1P)) = (9.99 \pm 0.27) \times 10^{-2}$. Our first error is their experiment's error and our second error is the systematic error from using our best value.

[2] ATHAR 07 reports $(0.39 \pm 0.11 \pm 0.04) \times 10^{-3}$ from a measurement of $[\Gamma(\chi_{c0}(1P) \to p\overline{p}\eta)/\Gamma_{total}] \times [B(\psi(2S) \to \gamma\chi_{c0}(1P))]$ assuming $B(\psi(2S) \to \gamma\chi_{c0}(1P)) = (9.22 \pm 0.11 \pm 0.46) \times 10^{-2}$, which we rescale to our best value $B(\psi(2S) \to \gamma\chi_{c0}(1P)) = (9.99 \pm 0.27) \times 10^{-2}$. Our first error is their experiment's error and our second error is the systematic error from using our best value.

$\Gamma(p\overline{p}\omega)/\Gamma_{total}$ Γ_{53}/Γ

VALUE (units 10^{-3})	DOCUMENT ID		TECN	COMMENT
0.51±0.05±0.01	[1] ONYISI	10	CLE3	$\psi(2S) \to \gamma p\overline{p}X$

[1] ONYISI 10 reports $(5.57 \pm 0.48 \pm 0.42 \pm 0.14) \times 10^{-4}$ from a measurement of $[\Gamma(\chi_{c0}(1P) \to p\overline{p}\omega)/\Gamma_{total}] \times [B(\psi(2S) \to \gamma\chi_{c0}(1P))]$ assuming $B(\psi(2S) \to \gamma\chi_{c0}(1P)) = (9.22\pm0.11\pm0.46)\times10^{-2}$, which we rescale to our best value $B(\psi(2S) \to \gamma\chi_{c0}(1P)) = (9.99 \pm 0.27) \times 10^{-2}$. Our first error is their experiment's error and our second error is the systematic error from using our best value.

$\Gamma(p\overline{p}\phi)/\Gamma_{total}$ Γ_{54}/Γ

VALUE (units 10^{-5})	EVTS	DOCUMENT ID		TECN	COMMENT
5.9±1.4±0.2	42 ± 8	[1] ABLIKIM	11F	BES3	$\psi(2S) \to \gamma p\overline{p}K^+K^-$

[1] ABLIKIM 11F reports $(6.12\pm1.18\pm0.86)\times10^{-5}$ from a measurement of $[\Gamma(\chi_{c0}(1P) \to p\overline{p}\phi)/\Gamma_{total}] \times [B(\psi(2S) \to \gamma\chi_{c0}(1P))]$ assuming $B(\psi(2S) \to \gamma\chi_{c0}(1P)) = (9.62\pm0.31) \times 10^{-2}$, which we rescale to our best value $B(\psi(2S) \to \gamma\chi_{c0}(1P)) = (9.99 \pm 0.27) \times 10^{-2}$. Our first error is their experiment's error and our second error is the systematic error from using our best value.

$\Gamma(p\overline{p}\pi^+\pi^-)/\Gamma_{total}$ Γ_{55}/Γ

VALUE (units 10^{-3})	DOCUMENT ID		TECN	COMMENT
2.1 ±0.7 OUR EVALUATION Error includes scale factor of 1.4. Treating systematic error as correlated.				
2.1 ±1.0 OUR AVERAGE Error includes scale factor of 2.0.				
1.57±0.21±0.53	[1] BAI	99B	BES	$\psi(2S) \to \gamma\chi_{c0}$
4.20±1.15±0.18	[1] TANENBAUM	78	MRK1	$\psi(2S) \to \gamma\chi_{c0}$

[1] Rescaled by us using $B(\psi(2S) \to \gamma\chi_{c0}) = (9.4 \pm 0.4)\%$ and $B(\psi(2S) \to J/\psi(1S)\pi^+\pi^-) = (32.6 \pm 0.5)\%$.

$\Gamma(p\overline{p}\pi^0\pi^0)/\Gamma_{total}$ Γ_{56}/Γ

VALUE (%)	EVTS	DOCUMENT ID		TECN	COMMENT
0.102±0.027±0.003	39.5	[1] HE	08B	CLEO	$e^+e^- \to \gamma h^+h^-h^0h^0$

[1] HE 08B reports 0.11 ± 0.02 ± 0.02 ± 0.01 % from a measurement of $[\Gamma(\chi_{c0}(1P) \to p\overline{p}\pi^0\pi^0)/\Gamma_{total}] \times [B(\psi(2S) \to \gamma\chi_{c0}(1P))]$ assuming $B(\psi(2S) \to \gamma\chi_{c0}(1P)) = (9.22 \pm 0.11 \pm 0.46) \times 10^{-2}$, which we rescale to our best value $B(\psi(2S) \to \gamma\chi_{c0}(1P)) = (9.99 \pm 0.27) \times 10^{-2}$. Our first error is their experiment's error and our second error is the systematic error from using our best value.

$\Gamma(p\overline{p}K^+K^-(\text{non-resonant}))/\Gamma_{total}$ Γ_{57}/Γ

VALUE (units 10^{-4})	EVTS	DOCUMENT ID		TECN	COMMENT
1.19±0.26±0.03	48 ± 8	[1] ABLIKIM	11F	BES3	$\psi(2S) \to \gamma p\overline{p}K^+K^-$

[1] ABLIKIM 11F reports $(1.24\pm0.20\pm0.18)\times10^{-4}$ from a measurement of $[\Gamma(\chi_{c0}(1P) \to p\overline{p}K^+K^-(\text{non-resonant}))/\Gamma_{total}] \times [B(\psi(2S) \to \gamma\chi_{c0}(1P))]$ assuming $B(\psi(2S) \to \gamma\chi_{c0}(1P)) = (9.62 \pm 0.31) \times 10^{-2}$, which we rescale to our best value $B(\psi(2S) \to \gamma\chi_{c0}(1P)) = (9.99 \pm 0.27) \times 10^{-2}$. Our first error is their experiment's error and our second error is the systematic error from using our best value.

$\Gamma(p\overline{p}K^0_SK^0_S)/\Gamma_{total}$ Γ_{58}/Γ

VALUE (units 10^{-4})	CL%	DOCUMENT ID		TECN	COMMENT
<8.8	90	[1] ABLIKIM	06D	BES2	$\psi(2S) \to \chi_{c0}\gamma$

[1] Using $B(\psi(2S) \to \chi_{c0}\gamma) = (9.2 \pm 0.5)\%$

$\Gamma(p\overline{n}\pi^-)/\Gamma_{total}$ Γ_{59}/Γ

VALUE (units 10^{-4})	EVTS	DOCUMENT ID		TECN	COMMENT
12.4±1.1 OUR AVERAGE					
12.6±1.1±0.3	5150	[1] ABLIKIM	12J	BES3	$\psi(2S) \to \gamma p\overline{n}\pi^-$
11.0±3.0±0.3		[2] ABLIKIM	06I	BES2	$\psi(2S) \to \gamma p\pi^-X$

[1] ABLIKIM 12J reports $[\Gamma(\chi_{c0}(1P) \to p\overline{n}\pi^-)/\Gamma_{total}] \times [B(\psi(2S) \to \gamma\chi_{c0}(1P))] = (1.26 \pm 0.02 \pm 0.11) \times 10^{-4}$ which we divide by our best value $B(\psi(2S) \to \gamma\chi_{c0}(1P)) = (9.99 \pm 0.27) \times 10^{-2}$. Our first error is their experiment's error and our second error is the systematic error from using our best value.

[2] ABLIKIM 06I reports $[\Gamma(\chi_{c0}(1P) \to p\overline{n}\pi^-)/\Gamma_{total}] \times [B(\psi(2S) \to \gamma\chi_{c0}(1P))] = (1.10 \pm 0.24 \pm 0.18) \times 10^{-4}$ which we divide by our best value $B(\psi(2S) \to \gamma\chi_{c0}(1P)) = (9.99 \pm 0.27) \times 10^{-2}$. Our first error is their experiment's error and our second error is the systematic error from using our best value.

$\Gamma(\overline{p}n\pi^+)/\Gamma_{total}$ Γ_{60}/Γ

VALUE (units 10^{-4})	EVTS	DOCUMENT ID		TECN	COMMENT
13.4±1.1±0.4	5808	[1] ABLIKIM	12J	BES3	$\psi(2S) \to \gamma\overline{p}n\pi^+$

[1] ABLIKIM 12J reports $[\Gamma(\chi_{c0}(1P) \to \overline{p}n\pi^+)/\Gamma_{total}] \times [B(\psi(2S) \to \gamma\chi_{c0}(1P))] = (1.34 \pm 0.03 \pm 0.11) \times 10^{-4}$ which we divide by our best value $B(\psi(2S) \to \gamma\chi_{c0}(1P)) = (9.99 \pm 0.27) \times 10^{-2}$. Our first error is their experiment's error and our second error is the systematic error from using our best value.

$\Gamma(p\overline{n}\pi^-\pi^0)/\Gamma_{total}$ Γ_{61}/Γ

VALUE (units 10^{-4})	EVTS	DOCUMENT ID		TECN	COMMENT
22.9±2.0±0.6	2480	[1] ABLIKIM	12J	BES3	$\psi(2S) \to \gamma p\overline{n}\pi^-\pi^0$

[1] ABLIKIM 12J reports $[\Gamma(\chi_{c0}(1P) \to p\overline{n}\pi^-\pi^0)/\Gamma_{total}] \times [B(\psi(2S) \to \gamma\chi_{c0}(1P))] = (2.29 \pm 0.08 \pm 0.18) \times 10^{-4}$ which we divide by our best value $B(\psi(2S) \to \gamma\chi_{c0}(1P)) = (9.99 \pm 0.27) \times 10^{-2}$. Our first error is their experiment's error and our second error is the systematic error from using our best value.

$\Gamma(\overline{p}n\pi^+\pi^0)/\Gamma_{total}$ Γ_{62}/Γ

VALUE (units 10^{-4})	EVTS	DOCUMENT ID		TECN	COMMENT
21.6±1.7±0.6	2757	[1] ABLIKIM	12J	BES3	$\psi(2S) \to \gamma\overline{p}n\pi^+\pi^0$

[1] ABLIKIM 12J reports $[\Gamma(\chi_{c0}(1P) \to \overline{p}n\pi^+\pi^0)/\Gamma_{total}] \times [B(\psi(2S) \to \gamma\chi_{c0}(1P))] = (2.16 \pm 0.07 \pm 0.16) \times 10^{-4}$ which we divide by our best value $B(\psi(2S) \to \gamma\chi_{c0}(1P)) = (9.99 \pm 0.27) \times 10^{-2}$. Our first error is their experiment's error and our second error is the systematic error from using our best value.

$\Gamma(\Lambda\overline{\Lambda})/\Gamma_{total}$ Γ_{63}/Γ

VALUE (units 10^{-4})	DOCUMENT ID
3.21±0.25 OUR FIT	

$\Gamma(\Lambda\overline{\Lambda}\pi^+\pi^-)/\Gamma_{total}$ Γ_{64}/Γ

VALUE (units 10^{-5})	CL%	EVTS	DOCUMENT ID		TECN	COMMENT
115±12±3		426	[1] ABLIKIM	12I	BES3	$\psi(2S) \to \gamma\Lambda\overline{\Lambda}\pi^+\pi^-$
• • • We do not use the following data for averages, fits, limits, etc. • • •						
<400	90		[2] ABLIKIM	06D	BES2	$\psi(2S) \to \chi_{c0}\gamma$

[1] ABLIKIM 12I reports $(119.0\pm6.4\pm11.4)\times10^{-5}$ from a measurement of $[\Gamma(\chi_{c0}(1P) \to \Lambda\overline{\Lambda}\pi^+\pi^-)/\Gamma_{total}] \times [B(\psi(2S) \to \gamma\chi_{c0}(1P))]$ assuming $B(\psi(2S) \to \gamma\chi_{c0}(1P)) = (9.68 \pm 0.31) \times 10^{-2}$, which we rescale to our best value $B(\psi(2S) \to \gamma\chi_{c0}(1P)) = (9.99 \pm 0.27) \times 10^{-2}$. Our first error is their experiment's error and our second error is the systematic error from using our best value.

[2] Using $B(\psi(2S) \to \chi_{c0}\gamma) = (9.2 \pm 0.5)\%$

Meson Particle Listings

$\chi_{c0}(1P)$

$\Gamma(\Lambda\overline{\Lambda}\pi^+\pi^-(\text{non-resonant}))/\Gamma_{\text{total}}$ Γ_{65}/Γ

VALUE (units 10^{-5})	CL%	DOCUMENT ID		TECN	COMMENT
<50	90	[1] ABLIKIM	12I	BES3	$\psi(2S) \to \gamma\Lambda\overline{\Lambda}\pi^+\pi^-$

[1] ABLIKIM 12I reports $< 54 \times 10^{-5}$ from a measurement of $[\Gamma(\chi_{c0}(1P) \to \Lambda\overline{\Lambda}\pi^+\pi^-(\text{non-resonant}))/\Gamma_{\text{total}}] \times [B(\psi(2S) \to \gamma\chi_{c0}(1P))]$ assuming $B(\psi(2S) \to \gamma\chi_{c0}(1P)) = (9.68 \pm 0.31) \times 10^{-2}$, which we rescale to our best value $B(\psi(2S) \to \gamma\chi_{c0}(1P)) = 9.99 \times 10^{-2}$.

$\Gamma(\Sigma(1385)^+\overline{\Lambda}\pi^- + \text{c.c.})/\Gamma_{\text{total}}$ Γ_{66}/Γ

VALUE (units 10^{-5})	CL%	DOCUMENT ID		TECN	COMMENT
<50	90	[1] ABLIKIM	12I	BES3	$\psi(2S) \to \gamma\Sigma(1385)^+\overline{\Lambda}\pi^-$

[1] ABLIKIM 12I reports $< 55 \times 10^{-5}$ from a measurement of $[\Gamma(\chi_{c0}(1P) \to \Sigma(1385)^+\overline{\Lambda}\pi^- + \text{c.c.})/\Gamma_{\text{total}}] \times [B(\psi(2S) \to \gamma\chi_{c0}(1P))]$ assuming $B(\psi(2S) \to \gamma\chi_{c0}(1P)) = (9.68 \pm 0.31) \times 10^{-2}$, which we rescale to our best value $B(\psi(2S) \to \gamma\chi_{c0}(1P)) = 9.99 \times 10^{-2}$.

$\Gamma(\Sigma(1385)^-\overline{\Lambda}\pi^+ + \text{c.c.})/\Gamma_{\text{total}}$ Γ_{67}/Γ

VALUE (units 10^{-5})	CL%	DOCUMENT ID		TECN	COMMENT
<50	90	[1] ABLIKIM	12I	BES3	$\psi(2S) \to \gamma\Sigma(1385)^-\overline{\Lambda}\pi^+$

[1] ABLIKIM 12I reports $< 50 \times 10^{-5}$ from a measurement of $[\Gamma(\chi_{c0}(1P) \to \Sigma(1385)^-\overline{\Lambda}\pi^+ + \text{c.c.})/\Gamma_{\text{total}}] \times [B(\psi(2S) \to \gamma\chi_{c0}(1P))]$ assuming $B(\psi(2S) \to \gamma\chi_{c0}(1P)) = (9.68 \pm 0.31) \times 10^{-2}$, which we rescale to our best value $B(\psi(2S) \to \gamma\chi_{c0}(1P)) = 9.99 \times 10^{-2}$.

$\Gamma(K^+\overline{p}\Lambda + \text{c.c.})/\Gamma_{\text{total}}$ Γ_{68}/Γ

VALUE (units 10^{-3})	EVTS	DOCUMENT ID		TECN	COMMENT
1.22±0.12 OUR AVERAGE		Error includes scale factor of 1.3.			
$1.28 \pm 0.09 \pm 0.03$	9k	[1,2] ABLIKIM	13D	BES3	$\psi(2S) \to \gamma\Lambda\overline{p}K^+$
$0.99 \pm 0.19 \pm 0.03$		[3] ATHAR	07	CLEO	$\psi(2S) \to \gamma h^+ h^- h^0$

[1] ABLIKIM 13D reports $(1.32 \pm 0.03 \pm 0.10) \times 10^{-3}$ from a measurement of $[\Gamma(\chi_{c0}(1P) \to K^+\overline{p}\Lambda + \text{c.c.})/\Gamma_{\text{total}}] \times [B(\psi(2S) \to \gamma\chi_{c0}(1P))]$ assuming $B(\psi(2S) \to \gamma\chi_{c0}(1P)) = (9.68 \pm 0.31) \times 10^{-2}$, which we rescale to our best value $B(\psi(2S) \to \gamma\chi_{c0}(1P)) = (9.99 \pm 0.27) \times 10^{-2}$. Our first error is their experiment's error and our second error is the systematic error from using our best value.

[2] Using $B(\Lambda \to p\pi^-) = 63.9\%$.

[3] ATHAR 07 reports $(1.07 \pm 0.17 \pm 0.12) \times 10^{-3}$ from a measurement of $[\Gamma(\chi_{c0}(1P) \to K^+\overline{p}\Lambda + \text{c.c.})/\Gamma_{\text{total}}] \times [B(\psi(2S) \to \gamma\chi_{c0}(1P))]$ assuming $B(\psi(2S) \to \gamma\chi_{c0}(1P)) = (9.22 \pm 0.11 \pm 0.46) \times 10^{-2}$, which we rescale to our best value $B(\psi(2S) \to \gamma\chi_{c0}(1P)) = (9.99 \pm 0.27) \times 10^{-2}$. Our first error is their experiment's error and our second error is the systematic error from using our best value.

$\Gamma(K^+\overline{p}\Lambda(1520) + \text{c.c.})/\Gamma_{\text{total}}$ Γ_{69}/Γ

VALUE (units 10^{-4})	EVTS	DOCUMENT ID		TECN	COMMENT
2.9±0.7±0.1	62 ± 12	[1] ABLIKIM	11F	BES3	$\psi(2S) \to \gamma p\overline{p}K^+K^-$

[1] ABLIKIM 11F reports $(3.00 \pm 0.58 \pm 0.50) \times 10^{-4}$ from a measurement of $[\Gamma(\chi_{c0}(1P) \to K^+\overline{p}\Lambda(1520) + \text{c.c.})/\Gamma_{\text{total}}] \times [B(\psi(2S) \to \gamma\chi_{c0}(1P))]$ assuming $B(\psi(2S) \to \gamma\chi_{c0}(1P)) = (9.62 \pm 0.31) \times 10^{-2}$, which we rescale to our best value $B(\psi(2S) \to \gamma\chi_{c0}(1P)) = (9.99 \pm 0.27) \times 10^{-2}$. Our first error is their experiment's error and our second error is the systematic error from using our best value.

$\Gamma(\Lambda(1520)\overline{\Lambda}(1520))/\Gamma_{\text{total}}$ Γ_{70}/Γ

VALUE (units 10^{-4})	EVTS	DOCUMENT ID		TECN	COMMENT
3.1±1.2±0.1	28 ± 10	[1] ABLIKIM	11F	BES3	$\psi(2S) \to \gamma p\overline{p}K^+K^-$

[1] ABLIKIM 11F reports $(3.18 \pm 1.11 \pm 0.53) \times 10^{-4}$ from a measurement of $[\Gamma(\chi_{c0}(1P) \to \Lambda(1520)\overline{\Lambda}(1520))/\Gamma_{\text{total}}] \times [B(\psi(2S) \to \gamma\chi_{c0}(1P))]$ assuming $B(\psi(2S) \to \gamma\chi_{c0}(1P)) = (9.62 \pm 0.31) \times 10^{-2}$, which we rescale to our best value $B(\psi(2S) \to \gamma\chi_{c0}(1P)) = (9.99 \pm 0.27) \times 10^{-2}$. Our first error is their experiment's error and our second error is the systematic error from using our best value.

$\Gamma(\Sigma^0\overline{\Sigma}^0)/\Gamma_{\text{total}}$ Γ_{71}/Γ

VALUE (units 10^{-4})	EVTS	DOCUMENT ID		TECN	COMMENT
4.4±0.4 OUR AVERAGE					
$4.6 \pm 0.5 \pm 0.1$	243	[1] ABLIKIM	13H	BES3	$\psi(2S) \to \gamma\Sigma^0\overline{\Sigma}^0$
$4.1 \pm 0.6 \pm 0.1$	78 ± 10	[2] NAIK	08	CLEO	$\psi(2S) \to \gamma\Sigma^0\overline{\Sigma}^0$

[1] ABLIKIM 13H reports $(4.78 \pm 0.34 \pm 0.39) \times 10^{-4}$ from a measurement of $[\Gamma(\chi_{c0}(1P) \to \Sigma^0\overline{\Sigma}^0)/\Gamma_{\text{total}}] \times [B(\psi(2S) \to \gamma\chi_{c0}(1P))]$ assuming $B(\psi(2S) \to \gamma\chi_{c0}(1P)) = (9.62 \pm 0.31) \times 10^{-2}$, which we rescale to our best value $B(\psi(2S) \to \gamma\chi_{c0}(1P)) = (9.99 \pm 0.27) \times 10^{-2}$. Our first error is their experiment's error and our second error is the systematic error from using our best value.

[2] NAIK 08 reports $(4.41 \pm 0.56 \pm 0.47) \times 10^{-4}$ from a measurement of $[\Gamma(\chi_{c0}(1P) \to \Sigma^0\overline{\Sigma}^0)/\Gamma_{\text{total}}] \times [B(\psi(2S) \to \gamma\chi_{c0}(1P))]$ assuming $B(\psi(2S) \to \gamma\chi_{c0}(1P)) = (9.22 \pm 0.11 \pm 0.46) \times 10^{-2}$, which we rescale to our best value $B(\psi(2S) \to \gamma\chi_{c0}(1P)) = (9.99 \pm 0.27) \times 10^{-2}$. Our first error is their experiment's error and our second error is the systematic error from using our best value.

$\Gamma(\Sigma^+\overline{\Sigma}^-)/\Gamma_{\text{total}}$ Γ_{72}/Γ

VALUE (units 10^{-4})	EVTS	DOCUMENT ID		TECN	COMMENT
3.9±0.7 OUR AVERAGE		Error includes scale factor of 1.7.			
$4.4 \pm 0.5 \pm 0.1$	148	[1] ABLIKIM	13H	BES3	$\psi(2S) \to \gamma\Sigma^+\overline{\Sigma}^-$
$3.0 \pm 0.6 \pm 0.1$	39 ± 7	[2] NAIK	08	CLEO	$\psi(2S) \to \gamma\Sigma^+\overline{\Sigma}^-$

[1] ABLIKIM 13H reports $(4.54 \pm 0.42 \pm 0.30) \times 10^{-4}$ from a measurement of $[\Gamma(\chi_{c0}(1P) \to \Sigma^+\overline{\Sigma}^-)/\Gamma_{\text{total}}] \times [B(\psi(2S) \to \gamma\chi_{c0}(1P))]$ assuming $B(\psi(2S) \to \gamma\chi_{c0}(1P)) = (9.62 \pm 0.31) \times 10^{-2}$, which we rescale to our best value $B(\psi(2S) \to \gamma\chi_{c0}(1P)) = (9.99 \pm 0.27) \times 10^{-2}$. Our first error is their experiment's error and our second error is the systematic error from using our best value.

[2] NAIK 08 reports $(3.25 \pm 0.57 \pm 0.43) \times 10^{-4}$ from a measurement of $[\Gamma(\chi_{c0}(1P) \to \Sigma^+\overline{\Sigma}^-)/\Gamma_{\text{total}}] \times [B(\psi(2S) \to \gamma\chi_{c0}(1P))]$ assuming $B(\psi(2S) \to \gamma\chi_{c0}(1P)) = (9.22 \pm 0.11 \pm 0.46) \times 10^{-2}$, which we rescale to our best value $B(\psi(2S) \to \gamma\chi_{c0}(1P)) = (9.99 \pm 0.27) \times 10^{-2}$. Our first error is their experiment's error and our second error is the systematic error from using our best value.

$\Gamma(\Sigma(1385)^+\overline{\Sigma}(1385)^-)/\Gamma_{\text{total}}$ Γ_{73}/Γ

VALUE (units 10^{-5})	EVTS	DOCUMENT ID		TECN	COMMENT
15.9±5.7±0.4	27	[1] ABLIKIM	12I	BES3	$\psi(2S) \to \gamma\Lambda\overline{\Lambda}\pi^+\pi^-$

[1] ABLIKIM 12I reports $(16.4 \pm 5.7 \pm 1.6) \times 10^{-5}$ from a measurement of $[\Gamma(\chi_{c0}(1P) \to \Sigma(1385)^+\overline{\Sigma}(1385)^-)/\Gamma_{\text{total}}] \times [B(\psi(2S) \to \gamma\chi_{c0}(1P))]$ assuming $B(\psi(2S) \to \gamma\chi_{c0}(1P)) = (9.68 \pm 0.31) \times 10^{-2}$, which we rescale to our best value $B(\psi(2S) \to \gamma\chi_{c0}(1P)) = (9.99 \pm 0.27) \times 10^{-2}$. Our first error is their experiment's error and our second error is the systematic error from using our best value.

$\Gamma(\Sigma(1385)^-\overline{\Sigma}(1385)^+)/\Gamma_{\text{total}}$ Γ_{74}/Γ

VALUE (units 10^{-5})	EVTS	DOCUMENT ID		TECN	COMMENT
23±6±1	33	[1] ABLIKIM	12I	BES3	$\psi(2S) \to \gamma\Lambda\overline{\Lambda}\pi^+\pi^-$

[1] ABLIKIM 12I reports $(23.5 \pm 6.2 \pm 2.3) \times 10^{-5}$ from a measurement of $[\Gamma(\chi_{c0}(1P) \to \Sigma(1385)^-\overline{\Sigma}(1385)^+)/\Gamma_{\text{total}}] \times [B(\psi(2S) \to \gamma\chi_{c0}(1P))]$ assuming $B(\psi(2S) \to \gamma\chi_{c0}(1P)) = (9.68 \pm 0.31) \times 10^{-2}$, which we rescale to our best value $B(\psi(2S) \to \gamma\chi_{c0}(1P)) = (9.99 \pm 0.27) \times 10^{-2}$. Our first error is their experiment's error and our second error is the systematic error from using our best value.

$\Gamma(\Xi^0\overline{\Xi}^0)/\Gamma_{\text{total}}$ Γ_{75}/Γ

VALUE (units 10^{-4})	EVTS	DOCUMENT ID		TECN	COMMENT
3.1±0.8±0.1	23.3 ± 4.9	[1] NAIK	08	CLEO	$\psi(2S) \to \gamma\Xi^0\overline{\Xi}^0$

[1] NAIK 08 reports $(3.34 \pm 0.70 \pm 0.48) \times 10^{-4}$ from a measurement of $[\Gamma(\chi_{c0}(1P) \to \Xi^0\overline{\Xi}^0)/\Gamma_{\text{total}}] \times [B(\psi(2S) \to \gamma\chi_{c0}(1P))]$ assuming $B(\psi(2S) \to \gamma\chi_{c0}(1P)) = (9.22 \pm 0.11 \pm 0.46) \times 10^{-2}$, which we rescale to our best value $B(\psi(2S) \to \gamma\chi_{c0}(1P)) = (9.99 \pm 0.27) \times 10^{-2}$. Our first error is their experiment's error and our second error is the systematic error from using our best value.

$\Gamma(\Xi^-\overline{\Xi}^+)/\Gamma_{\text{total}}$ Γ_{76}/Γ

VALUE (units 10^{-4})	CL%	EVTS	DOCUMENT ID		TECN	COMMENT
4.7±0.7±0.1		95 ± 11	[1] NAIK	08	CLEO	$\psi(2S) \to \gamma\Xi^+\overline{\Xi}^-$
• • • We do not use the following data for averages, fits, limits, etc. • • •						
<10.3	90		[2] ABLIKIM	06D	BES2	$\psi(2S) \to \chi_{c0}\gamma$

[1] NAIK 08 reports $(5.14 \pm 0.60 \pm 0.47) \times 10^{-4}$ from a measurement of $[\Gamma(\chi_{c0}(1P) \to \Xi^-\overline{\Xi}^+)/\Gamma_{\text{total}}] \times [B(\psi(2S) \to \gamma\chi_{c0}(1P))]$ assuming $B(\psi(2S) \to \gamma\chi_{c0}(1P)) = (9.22 \pm 0.11 \pm 0.46) \times 10^{-2}$, which we rescale to our best value $B(\psi(2S) \to \gamma\chi_{c0}(1P)) = (9.99 \pm 0.27) \times 10^{-2}$. Our first error is their experiment's error and our second error is the systematic error from using our best value.

[2] Using $B(\psi(2S) \to \chi_{c0}\gamma) = (9.2 \pm 0.5)\%$

$\Gamma(p\overline{p})/\Gamma_{\text{total}} \times \Gamma(\pi\pi)/\Gamma_{\text{total}}$ $\Gamma_{50}/\Gamma \times \Gamma_{31}/\Gamma$

VALUE (units 10^{-7})	DOCUMENT ID		TECN	COMMENT
18.8±1.2 OUR FIT				
15.3±2.4±0.8	[1] ANDREOTTI	03	E835	$\overline{p}p \to \chi_{c0} \to \pi^0\pi^0$

[1] We have multiplied $B(p\overline{p})\cdot B(\pi^0\pi^0)$ measurement by 3 to obtain $B(p\overline{p})\cdot B(\pi\pi)$.

$\Gamma(p\overline{p})/\Gamma_{\text{total}} \times \Gamma(\pi^0\eta)/\Gamma_{\text{total}}$ $\Gamma_{50}/\Gamma \times \Gamma_{32}/\Gamma$

VALUE (units 10^{-7})	DOCUMENT ID		TECN	COMMENT
<0.4	ANDREOTTI	05C	E835	$\overline{p}p \to \pi^0\eta$

$\Gamma(p\overline{p})/\Gamma_{\text{total}} \times \Gamma(\pi^0\eta')/\Gamma_{\text{total}}$ $\Gamma_{50}/\Gamma \times \Gamma_{33}/\Gamma$

VALUE (units 10^{-7})	DOCUMENT ID		TECN	COMMENT
<2.5	ANDREOTTI	05C	E835	$\overline{p}p \to \pi^0\eta$

$\Gamma(p\overline{p})/\Gamma_{\text{total}} \times \Gamma(\eta\eta)/\Gamma_{\text{total}}$ $\Gamma_{50}/\Gamma \times \Gamma_{34}/\Gamma$

VALUE (units 10^{-7})	DOCUMENT ID		TECN	COMMENT
6.6±0.5 OUR FIT				
$4.0 \pm 1.2^{+0.5}_{-0.3}$	ANDREOTTI	05C	E835	$\overline{p}p \to \eta\eta$

$\Gamma(p\overline{p})/\Gamma_{\text{total}} \times \Gamma(\eta\eta')/\Gamma_{\text{total}}$ $\Gamma_{50}/\Gamma \times \Gamma_{35}/\Gamma$

VALUE (units 10^{-6})	DOCUMENT ID		TECN	COMMENT
• • • We do not use the following data for averages, fits, limits, etc. • • •				
$2.1^{+2.3}_{-1.5}$	ANDREOTTI	05C	E835	$\overline{p}p \to \pi^0\eta$

RADIATIVE DECAYS

$\Gamma(\gamma J/\psi(1S))/\Gamma_{total}$ Γ_{77}/Γ

VALUE (units 10^{-4})	DOCUMENT ID	TECN	COMMENT
127± 6 OUR FIT			
• • • We do not use the following data for averages, fits, limits, etc. • • •			
200±20±20	[1] ADAM 05A	CLEO	$e^+e^- \to \psi(2S) \to \gamma\chi_{c0}$

[1] Uses $B(\psi(2S) \to \gamma\chi_{c0} \to \gamma\gamma J/\psi)$ from ADAM 05A and $B(\psi(2S) \to \gamma\chi_{c0})$ from ATHAR 04.

$\Gamma(\gamma\rho^0)/\Gamma_{total}$ Γ_{78}/Γ

VALUE (units 10^{-6})	CL%	EVTS	DOCUMENT ID	TECN	COMMENT
< 9	90	1.2 ± 4.5	[1] BENNETT 08A	CLEO	$\psi(2S) \to \gamma\gamma\rho^0$
• • • We do not use the following data for averages, fits, limits, etc. • • •					
<10	90	6 ± 12	[2] ABLIKIM 11E	BES3	$\psi(2S) \to \gamma\gamma\rho^0$

[1] BENNETT 08A reports $< 9.6 \times 10^{-6}$ from a measurement of $[\Gamma(\chi_{c0}(1P) \to \gamma\rho^0)/\Gamma_{total}] \times [B(\psi(2S) \to \gamma\chi_{c0}(1P))]$ assuming $B(\psi(2S) \to \gamma\chi_{c0}(1P)) = (9.2 \pm 0.4) \times 10^{-2}$, which we rescale to our best value $B(\psi(2S) \to \gamma\chi_{c0}(1P)) = 9.99 \times 10^{-2}$.

[2] ABLIKIM 11E reports $< 10.5 \times 10^{-6}$ from a measurement of $[\Gamma(\chi_{c0}(1P) \to \gamma\rho^0)/\Gamma_{total}] \times [B(\psi(2S) \to \gamma\chi_{c0}(1P))]$ assuming $B(\psi(2S) \to \gamma\chi_{c0}(1P)) = (9.62 \pm 0.31) \times 10^{-2}$, which we rescale to our best value $B(\psi(2S) \to \gamma\chi_{c0}(1P)) = 9.99 \times 10^{-2}$.

$\Gamma(\gamma\omega)/\Gamma_{total}$ Γ_{79}/Γ

VALUE (units 10^{-6})	CL%	EVTS	DOCUMENT ID	TECN	COMMENT
< 8	90	0.0 ± 2.8	[1] BENNETT 08A	CLEO	$\psi(2S) \to \gamma\gamma\omega$
• • • We do not use the following data for averages, fits, limits, etc. • • •					
<12	90	5 ± 11	[2] ABLIKIM 11E	BES3	$\psi(2S) \to \gamma\gamma\omega$

[1] BENNETT 08A reports $< 8.8 \times 10^{-6}$ from a measurement of $[\Gamma(\chi_{c0}(1P) \to \gamma\omega)/\Gamma_{total}] \times [B(\psi(2S) \to \gamma\chi_{c0}(1P))]$ assuming $B(\psi(2S) \to \gamma\chi_{c0}(1P)) = (9.2 \pm 0.4) \times 10^{-2}$, which we rescale to our best value $B(\psi(2S) \to \gamma\chi_{c0}(1P)) = 9.99 \times 10^{-2}$.

[2] ABLIKIM 11E reports $< 12.9 \times 10^{-6}$ from a measurement of $[\Gamma(\chi_{c0}(1P) \to \gamma\omega)/\Gamma_{total}] \times [B(\psi(2S) \to \gamma\chi_{c0}(1P))]$ assuming $B(\psi(2S) \to \gamma\chi_{c0}(1P)) = (9.62 \pm 0.31) \times 10^{-2}$, which we rescale to our best value $B(\psi(2S) \to \gamma\chi_{c0}(1P)) = 9.99 \times 10^{-2}$.

$\Gamma(\gamma\phi)/\Gamma_{total}$ Γ_{80}/Γ

VALUE (units 10^{-6})	CL%	EVTS	DOCUMENT ID	TECN	COMMENT
< 6	90	0.1 ± 1.6	[1] BENNETT 08A	CLEO	$\psi(2S) \to \gamma\gamma\phi$
• • • We do not use the following data for averages, fits, limits, etc. • • •					
<16	90	15 ± 7	[2] ABLIKIM 11E	BES3	$\psi(2S) \to \gamma\gamma\phi$

[1] BENNETT 08A reports $< 6.4 \times 10^{-6}$ from a measurement of $[\Gamma(\chi_{c0}(1P) \to \gamma\phi)/\Gamma_{total}] \times [B(\psi(2S) \to \gamma\chi_{c0}(1P))]$ assuming $B(\psi(2S) \to \gamma\chi_{c0}(1P)) = (9.2 \pm 0.4) \times 10^{-2}$, which we rescale to our best value $B(\psi(2S) \to \gamma\chi_{c0}(1P)) = 9.99 \times 10^{-2}$.

[2] ABLIKIM 11E reports $< 16.2 \times 10^{-6}$ from a measurement of $[\Gamma(\chi_{c0}(1P) \to \gamma\phi)/\Gamma_{total}] \times [B(\psi(2S) \to \gamma\chi_{c0}(1P))]$ assuming $B(\psi(2S) \to \gamma\chi_{c0}(1P)) = (9.62 \pm 0.31) \times 10^{-2}$, which we rescale to our best value $B(\psi(2S) \to \gamma\chi_{c0}(1P)) = 9.99 \times 10^{-2}$.

$\Gamma(\gamma\gamma)/\Gamma_{total}$ Γ_{81}/Γ

VALUE (units 10^{-4})	CL%	DOCUMENT ID	TECN	COMMENT
2.23±0.13 OUR FIT				
• • • We do not use the following data for averages, fits, limits, etc. • • •				
<7	90	[1] WICHT 08	BELL	$B^\pm \to K^\pm\gamma\gamma$

[1] WICHT 08 reports $[\Gamma(\chi_{c0}(1P) \to \gamma\gamma)/\Gamma_{total}] \times [B(B^+ \to \chi_{c0}(1P)K^+)] < 0.11 \times 10^{-6}$ which we divide by our best value $B(B^+ \to \chi_{c0}(1P)K^+) = 1.50 \times 10^{-4}$.

$\Gamma(\gamma\gamma)/\Gamma(\gamma J/\psi(1S))$ Γ_{81}/Γ_{77}

VALUE (units 10^{-2})	DOCUMENT ID	TECN	COMMENT
1.76±0.13 OUR FIT			
2.0 ±0.4 OUR AVERAGE			
2.2 ±0.4 $^{+0.1}_{-0.2}$	[1] ANDREOTTI 04 E835		$p\overline{p} \to \chi_{c0} \to \gamma\gamma$
1.45±0.74	[2] AMBROGIANI 00B E835		$\overline{p}p \to \chi_{c2} \to \gamma\gamma, \gamma J/\psi$

[1] The values of $B(p\overline{p})B(\gamma\gamma)$ and $B(\gamma\gamma)B(\gamma J/\psi)$ measured by ANDREOTTI 04 are not independent. The latter is used in the fit because of smaller systematics.

[2] Calculated by us using $B(J/\psi(1S) \to e^+e^-) = 0.0593 \pm 0.0010$.

$\Gamma(p\overline{p})/\Gamma_{total} \times \Gamma(\gamma J/\psi(1S))/\Gamma_{total}$ $\Gamma_{50}/\Gamma \times \Gamma_{77}/\Gamma$

VALUE (units 10^{-7})	EVTS	DOCUMENT ID	TECN	COMMENT
28.5±1.6 OUR FIT				
28.2±2.1 OUR AVERAGE				
28.0±1.9±1.3	392	[1,2,3] BAGNASCO 02 E835		$\overline{p}p \to \chi_{c0} \to J/\psi\gamma$
$29.3^{+5.7}_{-4.7}$±1.5	89	[1,2] AMBROGIANI 99B		$\overline{p}p \to \chi_{c0} \to J/\psi\gamma$

[1] Values in $(\Gamma(p\overline{p}) \times \Gamma(\gamma J/\psi(1S))/\Gamma_{total})$ and $(\Gamma(p\overline{p})/\Gamma_{total} \times \Gamma(\gamma J/\psi(1S))/\Gamma_{total})$ are not independent. The latter is used in the fit since it is less correlated to the total width.

[2] Calculated by us using $B(J/\psi(1S) \to e^+e^-) = 0.0593 \pm 0.0010$.

[3] Recalculated by ANDREOTTI 05A.

$\Gamma(p\overline{p})/\Gamma_{total} \times \Gamma(\gamma\gamma)/\Gamma_{total}$ $\Gamma_{50}/\Gamma \times \Gamma_{81}/\Gamma$

VALUE (units 10^{-8})	DOCUMENT ID	TECN	COMMENT
5.0 ±0.4 OUR FIT			
• • • We do not use the following data for averages, fits, limits, etc. • • •			
$6.52 \pm 1.18^{+0.48}_{-0.72}$	[1] ANDREOTTI 04 E835		$p\overline{p} \to \chi_{c0} \to \gamma\gamma$

[1] The values of $B(p\overline{p})B(\gamma\gamma)$ and $B(\gamma\gamma)B(\gamma J/\psi)$ measured by ANDREOTTI 04 are not independent. The latter is used in the fit because of smaller systematics.

$\chi_{c0}(1P)$ CROSS-PARTICLE BRANCHING RATIOS

$\Gamma(\chi_{c0}(1P) \to p\overline{p})/\Gamma_{total} \times \Gamma(\psi(2S) \to \gamma\chi_{c0}(1P))/\Gamma_{total}$ $\Gamma_{50}/\Gamma \times \Gamma_{128}^{\psi(2S)}/\Gamma^{\psi(2S)}$

VALUE (units 10^{-6})	EVTS	DOCUMENT ID	TECN	COMMENT
22.5±0.9 OUR FIT				
23.7±1.0 OUR AVERAGE				
23.7±0.8±0.9	1222	ABLIKIM 13V	BES3	$\psi(2S) \to \gamma p\overline{p}$
23.7±1.4±1.4	383 ± 22	[1] NAIK 08	CLEO	$\psi(2S) \to \gamma p\overline{p}$
$23.6^{+3.7}_{-3.4}$±3.4	89.5^{+14}_{-13}	BAI 04F	BES	$\psi(2S) \to \gamma\chi_{c0}(1P) \to \gamma\overline{p}p$

[1] Calculated by us. NAIK 08 reports $B(\chi_{c0} \to p\overline{p}) = (25.7 \pm 1.5 \pm 1.5 \pm 1.3) \times 10^{-5}$ using $B(\psi(2S) \to \gamma\chi_{c0}) = (9.22 \pm 0.11 \pm 0.46)\%$.

$\Gamma(\chi_{c0}(1P) \to p\overline{p})/\Gamma_{total} \times \Gamma(\psi(2S) \to \gamma\chi_{c0}(1P))/\Gamma(\psi(2S) \to J/\psi(1S)\pi^+\pi^-)$ $\Gamma_{50}/\Gamma \times \Gamma_{128}^{\psi(2S)}/\Gamma_{11}^{\psi(2S)}$

VALUE (units 10^{-5})	DOCUMENT ID	TECN	COMMENT
6.54±0.27 OUR FIT			
4.6 ±1.9	[1] BAI 98I	BES	$\psi(2S) \to \gamma\chi_{c0} \to \gamma\overline{p}p$

[1] Calculated by us. The value for $B(\chi_{c0} \to p\overline{p})$ reported in BAI 98I is derived using $B(\psi(2S) \to \gamma\chi_{c0}) = (9.3 \pm 0.8)\%$ and $B(\psi(2S) \to J/\psi(1S)\pi^+\pi^-) = (32.4 \pm 2.6)\%$ [BAI 98D].

$\Gamma(\chi_{c0}(1P) \to \Lambda\overline{\Lambda})/\Gamma_{total} \times \Gamma(\psi(2S) \to \gamma\chi_{c0}(1P))/\Gamma_{total}$ $\Gamma_{63}/\Gamma \times \Gamma_{128}^{\psi(2S)}/\Gamma^{\psi(2S)}$

VALUE (units 10^{-6})	EVTS	DOCUMENT ID	TECN	COMMENT
32.0±2.3 OUR FIT				
31.7±2.3 OUR AVERAGE				
32.0±1.9±2.2	369	[1] ABLIKIM 13H	BES3	$\psi(2S) \to \gamma\Lambda\overline{\Lambda}$
31.2±3.3±2.0	131 ± 12	[2] NAIK 08	CLEO	$\psi(2S) \to \gamma\Lambda\overline{\Lambda}$

[1] Calculated by us. ABLIKIM 13H reports $B(\chi_{c0} \to \Lambda\overline{\Lambda}) = (33.3 \pm 2.0 \pm 2.6) \times 10^{-5}$ from a measurement of $B(\chi_{c0} \to \Lambda\overline{\Lambda}) \times B(\psi(2S) \to \gamma\chi_{c0})$ assuming $B(\psi(2S) \to \gamma\chi_{c0}) = (9.62 \pm 0.31)\%$.

[2] Calculated by us. NAIK 08 reports $B(\chi_{c0} \to \Lambda\overline{\Lambda}) = (33.8 \pm 3.6 \pm 2.2 \pm 1.7) \times 10^{-5}$ using $B(\psi(2S) \to \gamma\chi_{c0}) = (9.22 \pm 0.11 \pm 0.46)\%$.

$\Gamma(\chi_{c0}(1P) \to \Lambda\overline{\Lambda})/\Gamma_{total} \times \Gamma(\psi(2S) \to \gamma\chi_{c0}(1P))/\Gamma(\psi(2S) \to J/\psi(1S)\pi^+\pi^-)$ $\Gamma_{63}/\Gamma \times \Gamma_{128}^{\psi(2S)}/\Gamma_{11}^{\psi(2S)}$

VALUE (units 10^{-5})	EVTS	DOCUMENT ID	TECN	COMMENT
9.3±0.7 OUR FIT				
13.0$^{+3.6}_{-3.5}$±2.5	$15.2^{+4.2}_{-4.0}$	[1] BAI 03E	BES	$\psi(2S) \to \gamma\Lambda\overline{\Lambda}$

[1] BAI 03E reports $[B(\chi_{c0} \to \Lambda\overline{\Lambda})\, B(\psi(2S) \to \gamma\chi_{c0}) / B(\psi(2S) \to J/\psi\pi^+\pi^-)] \times [B^2(\Lambda \to \pi^- p) / B(J/\psi \to p\overline{p})] = (2.45^{+0.68}_{-0.65} \pm 0.46)\%$. We calculate from this measurement the presented value using $B(\Lambda \to \pi^- p) = (63.9 \pm 0.5)\%$ and $B(J/\psi \to p\overline{p}) = (2.17 \pm 0.07) \times 10^{-3}$.

$\Gamma(\chi_{c0}(1P) \to \gamma J/\psi(1S))/\Gamma_{total} \times \Gamma(\psi(2S) \to \gamma\chi_{c0}(1P))/\Gamma_{total}$ $\Gamma_{77}/\Gamma \times \Gamma_{128}^{\psi(2S)}/\Gamma^{\psi(2S)}$

VALUE (units 10^{-2})	EVTS	DOCUMENT ID	TECN	COMMENT
0.126±0.006 OUR FIT				
0.131±0.035 OUR AVERAGE Error includes scale factor of 3.9.				
0.151±0.003±0.010	4.3k	ABLIKIM 12O	BES3	$\psi(2S) \to \gamma\chi_{c0}$
0.069±0.018		[1] OREGLIA 82	CBAL	$\psi(2S) \to \gamma\chi_{c0}$
0.4 ±0.3		[2] BRANDELIK 79B	DASP	$\psi(2S) \to \gamma\chi_{c0}$
0.16 ±0.11		[2] BARTEL 78B	CNTR	$\psi(2S) \to \gamma\chi_{c0}$
3.3 ±1.7		[3] BIDDICK 77	CNTR	$e^+e^- \to \gamma X$
• • • We do not use the following data for averages, fits, limits, etc. • • •				
0.125±0.007±0.013	560	[4] MENDEZ 08	CLEO	$\psi(2S) \to \gamma\chi_{c0}$
0.18 ±0.01 ±0.02	172	[5] ADAM 05A	CLEO	Repl. by MENDEZ 08

[1] Recalculated by us using $B(J/\psi(1S) \to \ell^+\ell^-) = 0.1181 \pm 0.0020$.

[2] Recalculated by us using $B(J/\psi(1S) \to \mu^+\mu^-) = 0.0588 \pm 0.0010$.

[3] Assumes isotropic gamma distribution.

[4] Not independent from other measurements of MENDEZ 08.

[5] Not independent from other values reported by ADAM 05A.

Meson Particle Listings

$\chi_{c0}(1P)$

$\Gamma(\chi_{c0}(1P) \to \gamma J/\psi(1S))/\Gamma_{\text{total}} \times \Gamma(\psi(2S) \to \gamma\chi_{c0}(1P))/\Gamma(\psi(2S) \to J/\psi(1S)\text{anything})$ $\Gamma_{77}/\Gamma \times \Gamma_{128}^{\psi(2S)}/\Gamma_{9}^{\psi(2S)}$

$\Gamma_{77}/\Gamma \times \Gamma_{128}^{\psi(2S)}/\Gamma_{9}^{\psi(2S)} = \Gamma_{77}/\Gamma \times \Gamma_{128}^{\psi(2S)}/(\Gamma_{11}^{\psi(2S)} + \Gamma_{12}^{\psi(2S)} + \Gamma_{13}^{\psi(2S)} + 0.339\Gamma_{129}^{\psi(2S)} + 0.192\Gamma_{130}^{\psi(2S)})$

VALUE (units 10^{-2})	EVTS	DOCUMENT ID		TECN	COMMENT
0.208±0.011 OUR FIT					
• • • We do not use the following data for averages, fits, limits, etc. • • •					
0.201±0.011±0.021	560	[1] MENDEZ	08	CLEO	$\psi(2S) \to \gamma\chi_{c0}$
0.31 ±0.02 ±0.03	172	ADAM	05A	CLEO	Repl. by MENDEZ 08

[1] Not independent from other measurements of MENDEZ 08.

$\Gamma(\chi_{c0}(1P) \to \gamma J/\psi(1S))/\Gamma_{\text{total}} \times \Gamma(\psi(2S) \to \gamma\chi_{c0}(1P))/\Gamma(\psi(2S) \to J/\psi(1S)\pi^+\pi^-)$ $\Gamma_{77}/\Gamma \times \Gamma_{128}^{\psi(2S)}/\Gamma_{11}^{\psi(2S)}$

VALUE (units 10^{-2})	EVTS	DOCUMENT ID		TECN	COMMENT
0.367±0.019 OUR FIT					
0.358±0.020±0.037	560	MENDEZ	08	CLEO	$\psi(2S) \to \gamma\chi_{c0}$
• • • We do not use the following data for averages, fits, limits, etc. • • •					
0.55 ±0.04 ±0.06	172	[1] ADAM	05A	CLEO	Repl. by MENDEZ 08

[1] Not independent from other values reported by ADAM 05A.

$\Gamma(\chi_{c0}(1P) \to \gamma\gamma)/\Gamma_{\text{total}} \times \Gamma(\psi(2S) \to \gamma\chi_{c0}(1P))/\Gamma_{\text{total}}$ $\Gamma_{81}/\Gamma \times \Gamma_{128}^{\psi(2S)}/\Gamma^{\psi(2S)}$

VALUE (units 10^{-5})	EVTS	DOCUMENT ID		TECN	COMMENT
2.23±0.14 OUR FIT					
2.18±0.18 OUR AVERAGE					
2.17±0.17±0.12	0.8k	ABLIKIM	12A	BES3	$\psi(2S) \to \gamma\chi_{c0} \to 3\gamma$
2.17±0.32±0.10	0.2k	ECKLUND	08A	CLEO	$\psi(2S) \to \gamma\chi_{c0} \to 3\gamma$
3.7 ±1.8 ±1.0		LEE	85	CBAL	$\psi(2S) \to \gamma\chi_{c0}$

$\Gamma(\chi_{c0}(1P) \to \pi\pi)/\Gamma_{\text{total}} \times \Gamma(\psi(2S) \to \gamma\chi_{c0}(1P))/\Gamma_{\text{total}}$ $\Gamma_{31}/\Gamma \times \Gamma_{128}^{\psi(2S)}/\Gamma^{\psi(2S)}$

VALUE (units 10^{-4})	EVTS	DOCUMENT ID		TECN	COMMENT
8.32±0.29 OUR FIT					
8.80±0.34 OUR AVERAGE					
9.11±0.08±0.65	17k	[1] ABLIKIM	10A	BES3	$e^+e^- \to \psi(2S) \to \gamma\chi_{c0}$
8.81±0.11±0.43	8.9k	[2] ASNER	09	CLEO	$\psi(2S) \to \gamma\pi^+\pi^-$
8.13±0.19±0.89	2.8k	[3] ASNER	09	CLEO	$\psi(2S) \to \gamma\pi^0\pi^0$

[1] Calculated by us. ABLIKIM 10A reports $B(\chi_{c0} \to \pi^0\pi^0) = (3.23 \pm 0.03 \pm 0.23 \pm 0.14) \times 10^{-3}$ using $B(\psi(2S) \to \gamma\chi_{c0}) = (9.4 \pm 0.4)\%$. We have multiplied the $\pi^0\pi^0$ measurement by 3 to obtain $\pi\pi$.

[2] Calculated by us. ASNER 09 reports $B(\chi_{c0} \to \pi^+\pi^-) = (6.37 \pm 0.08 \pm 0.31 \pm 0.32) \times 10^{-3}$ using $B(\psi(2S) \to \gamma\chi_{c0}) = (9.22 \pm 0.11 \pm 0.46)\%$. We have multiplied the $\pi^+\pi^-$ measurement by 3/2 to obtain $\pi\pi$.

[3] Calculated by us. ASNER 09 reports $B(\chi_{c0} \to \pi^0\pi^0) = (2.94 \pm 0.07 \pm 0.32 \pm 0.15) \times 10^{-3}$ using $B(\psi(2S) \to \gamma\chi_{c0}) = (9.22 \pm 0.11 \pm 0.46)\%$. We have multiplied the $\pi^0\pi^0$ measurement by 3 to obtain $\pi\pi$.

$\Gamma(\chi_{c0}(1P) \to \pi\pi)/\Gamma_{\text{total}} \times \Gamma(\psi(2S) \to \gamma\chi_{c0}(1P))/\Gamma(\psi(2S) \to J/\psi(1S)\pi^+\pi^-)$ $\Gamma_{31}/\Gamma \times \Gamma_{128}^{\psi(2S)}/\Gamma_{11}^{\psi(2S)}$

VALUE (units 10^{-4})	EVTS	DOCUMENT ID		TECN	COMMENT
24.2±0.8 OUR FIT					
20.7±1.7 OUR AVERAGE					
23.9±2.7±4.1	97 ± 11	[1] BAI	03C	BES	$\psi(2S) \to \gamma\chi_{c0} \to \gamma\pi^0\pi^0$
20.2±1.1±1.5	720 ± 32	[2] BAI	98I	BES	$\psi(2S) \to \gamma\chi_{c0} \to \gamma\pi^+\pi^-$

[1] We have multiplied $\pi^0\pi^0$ measurement by 3 to obtain $\pi\pi$.

[2] Calculated by us. The value for $B(\chi_{c0} \to \pi^+\pi^-)$ reported in BAI 98I is derived using $B(\psi' \to \gamma\chi_{c0}) = (9.3 \pm 0.8)\%$ and $B(\psi' \to J/\psi\pi^+\pi^-) = (32.4 \pm 2.6)\%$ [BAI 98D]. We have multiplied $\pi^+\pi^-$ measurement by 3/2 to obtain $\pi\pi$.

$\Gamma(\chi_{c0}(1P) \to \eta\eta)/\Gamma_{\text{total}} \times \Gamma(\psi(2S) \to \gamma\chi_{c0}(1P))/\Gamma_{\text{total}}$ $\Gamma_{34}/\Gamma \times \Gamma_{128}^{\psi(2S)}/\Gamma^{\psi(2S)}$

VALUE (units 10^{-4})	EVTS	DOCUMENT ID		TECN	COMMENT
2.95±0.18 OUR FIT					
3.12±0.19 OUR AVERAGE					
3.23±0.09±0.23	2132	[1] ABLIKIM	10A	BES3	$e^+e^- \to \psi(2S) \to \gamma\chi_{c0}$
2.93±0.12±0.29	0.9k	[2] ASNER	09	CLEO	$\psi(2S) \to \gamma\eta\eta$
• • • We do not use the following data for averages, fits, limits, etc. • • •					
2.86±0.46±0.37	48	[3] ADAMS	07	CLEO	$\psi(2S) \to \gamma\chi_{c0}$

[1] Calculated by us. ABLIKIM 10A reports $B(\chi_{c0} \to \eta\eta) = (3.44 \pm 0.10 \pm 0.24 \pm 0.13) \times 10^{-3}$ using $B(\psi(2S) \to \gamma\chi_{c0}) = (9.4 \pm 0.4)\%$.

[2] Calculated by us. ASNER 09 reports $B(\chi_{c0} \to \eta\eta) = (3.18 \pm 0.13 \pm 0.31 \pm 0.16) \times 10^{-3}$ using $B(\psi(2S) \to \gamma\chi_{c0}) = (9.22 \pm 0.11 \pm 0.46)\%$.

[3] Superseded by ASNER 09. Calculated by us. The value of $B(\chi_{c0}(1P) \to \eta\eta)$ reported by ADAMS 07 was derived using $B(\psi(2S) \to \gamma\chi_{c0}(1P)) = (9.22 \pm 0.11 \pm 0.46)\%$ (ATHAR 04).

$\Gamma(\chi_{c0}(1P) \to \eta\eta)/\Gamma_{\text{total}} \times \Gamma(\psi(2S) \to \gamma\chi_{c0}(1P))/\Gamma(\psi(2S) \to J/\psi(1S)\pi^+\pi^-)$ $\Gamma_{34}/\Gamma \times \Gamma_{128}^{\psi(2S)}/\Gamma_{11}^{\psi(2S)}$

VALUE (units 10^{-3})	DOCUMENT ID		TECN	COMMENT
0.86 ±0.05 OUR FIT				
0.578±0.241±0.158	BAI	03C	BES	$\psi(2S) \to \gamma\eta\eta$

$\Gamma(\chi_{c0}(1P) \to K^+K^-)/\Gamma_{\text{total}} \times \Gamma(\psi(2S) \to \gamma\chi_{c0}(1P))/\Gamma_{\text{total}}$ $\Gamma_{39}/\Gamma \times \Gamma_{128}^{\psi(2S)}/\Gamma^{\psi(2S)}$

VALUE (units 10^{-4})	EVTS	DOCUMENT ID		TECN	COMMENT
5.90±0.28 OUR FIT					
5.97±0.07±0.32	8.1k	[1] ASNER	09	CLEO	$\psi(2S) \to \gamma K^+K^-$

[1] Calculated by us. ASNER 09 reports $B(\chi_{c0} \to K^+K^-) = (6.47 \pm 0.08 \pm 0.35 \pm 0.32) \times 10^{-3}$ using $B(\psi(2S) \to \gamma\chi_{c0}) = (9.22 \pm 0.11 \pm 0.46)\%$.

$\Gamma(\chi_{c0}(1P) \to K^+K^-)/\Gamma_{\text{total}} \times \Gamma(\psi(2S) \to \gamma\chi_{c0}(1P))/\Gamma(\psi(2S) \to J/\psi(1S)\pi^+\pi^-)$ $\Gamma_{39}/\Gamma \times \Gamma_{128}^{\psi(2S)}/\Gamma_{11}^{\psi(2S)}$

VALUE (units 10^{-3})	EVTS	DOCUMENT ID		TECN	COMMENT
1.71±0.08 OUR FIT					
1.63±0.10±0.15	774 ± 38	[1] BAI	98I	BES	$\psi(2S) \to \gamma K^+K^-$

[1] Calculated by us. The value for $B(\chi_{c0} \to K^+K^-)$ reported by BAI 98I is derived using $B(\psi(2S) \to \gamma\chi_{c0}) = (9.3 \pm 0.8)\%$ and $B(\psi(2S) \to J/\psi\pi^+\pi^-) = (32.4 \pm 2.6)\%$ [BAI 98D].

$\Gamma(\chi_{c0}(1P) \to K^0_S K^0_S)/\Gamma_{\text{total}} \times \Gamma(\psi(2S) \to \gamma\chi_{c0}(1P))/\Gamma_{\text{total}}$ $\Gamma_{40}/\Gamma \times \Gamma_{128}^{\psi(2S)}/\Gamma^{\psi(2S)}$

VALUE (units 10^{-4})	EVTS	DOCUMENT ID		TECN	COMMENT
3.09±0.16 OUR FIT					
3.18±0.17 OUR AVERAGE					
3.22±0.07±0.17	2.1k	[1] ASNER	09	CLEO	$\psi(2S) \to \gamma K^0_S K^0_S$
3.02±0.19±0.33	322	ABLIKIM	05O	BES2	$\psi(2S) \to \gamma K^0_S K^0_S$

[1] Calculated by us. ASNER 09 reports $B(\chi_{c0} \to K^0_S K^0_S) = (3.49 \pm 0.08 \pm 0.18 \pm 0.17) \times 10^{-3}$ using $B(\psi(2S) \to \gamma\chi_{c0}) = (9.22 \pm 0.11 \pm 0.46)\%$.

$\Gamma(\chi_{c0}(1P) \to K^0_S K^0_S)/\Gamma_{\text{total}} \times \Gamma(\psi(2S) \to \gamma\chi_{c0}(1P))/\Gamma(\psi(2S) \to J/\psi(1S)\pi^+\pi^-)$ $\Gamma_{40}/\Gamma \times \Gamma_{128}^{\psi(2S)}/\Gamma_{11}^{\psi(2S)}$

VALUE (units 10^{-4})	DOCUMENT ID		TECN	COMMENT
9.0±0.5 OUR FIT				
5.6±0.8±1.3	[1] BAI	99B	BES	$\psi(2S) \to \gamma K^0_S K^0_S$

[1] Calculated by us. The value of $B(\chi_{c0} \to K^0_S K^0_S)$ reported by BAI 99B was derived using $B(\psi(2S) \to \gamma\chi_{c0}(1P)) = (9.3 \pm 0.8)\%$ and $B(\psi(2S) \to J/\psi\pi^+\pi^-) = (32.4 \pm 2.6)\%$ [BAI 98D].

$\Gamma(\chi_{c0}(1P) \to 2(\pi^+\pi^-))/\Gamma_{\text{total}} \times \Gamma(\psi(2S) \to \gamma\chi_{c0}(1P))/\Gamma(\psi(2S) \to J/\psi(1S)\pi^+\pi^-)$ $\Gamma_{1}/\Gamma \times \Gamma_{128}^{\psi(2S)}/\Gamma_{11}^{\psi(2S)}$

VALUE (units 10^{-3})	DOCUMENT ID		TECN	COMMENT
6.5±0.5 OUR FIT				
6.9±2.4 OUR AVERAGE Error includes scale factor of 3.8.				
4.4±0.1±0.9	[1] BAI	99B	BES	$\psi(2S) \to \gamma\chi_{c0}$
9.3±0.9	[2] TANENBAUM	78	MRK1	$\psi(2S) \to \gamma\chi_{c0}$

[1] Calculated by us. The value for $B(\chi_{c0} \to 2\pi^+2\pi^-)$ reported in BAI 99B is derived using $B(\psi(2S) \to \gamma\chi_{c0}) = (9.3 \pm 0.8)\%$ and $B(\psi(2S) \to J/\psi(1S)\pi^+\pi^-) = (32.4 \pm 2.6)\%$ [BAI 98D].

[2] The value $B(\psi(1S) \to \gamma\chi_{c0}) \times B(\chi_{c0} \to 2\pi^+2\pi^-)$ reported in TANENBAUM 78 is derived using $B(\psi(2S) \to J/\psi(1S)\pi^+\pi^-) \times B(J/\psi(1S) \to \ell^+\ell^-) = (4.6 \pm 0.7)\%$. Calculated by us using $B(J/\psi(1S) \to \ell^+\ell^-) = 0.1181 \pm 0.0020$.

$\Gamma(\chi_{c0}(1P) \to \pi^+\pi^-K^+K^-)/\Gamma_{\text{total}} \times \Gamma(\psi(2S) \to \gamma\chi_{c0}(1P))/\Gamma_{\text{total}}$ $\Gamma_{8}/\Gamma \times \Gamma_{128}^{\psi(2S)}/\Gamma^{\psi(2S)}$

VALUE (units 10^{-3})	DOCUMENT ID		TECN	COMMENT
1.75±0.14 OUR FIT				
1.64±0.05±0.2	ABLIKIM	05Q	BES2	$\psi(2S) \to \gamma\chi_{c0}$

$\Gamma(\chi_{c0}(1P) \to \pi^+\pi^-K^+K^-)/\Gamma_{\text{total}} \times \Gamma(\psi(2S) \to \gamma\chi_{c0}(1P))/\Gamma(\psi(2S) \to J/\psi(1S)\pi^+\pi^-)$ $\Gamma_{8}/\Gamma \times \Gamma_{128}^{\psi(2S)}/\Gamma_{11}^{\psi(2S)}$

VALUE (units 10^{-3})	DOCUMENT ID		TECN	COMMENT
5.1 ±0.4 OUR FIT				
5.8 ±1.6 OUR AVERAGE Error includes scale factor of 2.3.				
4.22±0.20±0.97	BAI	99B	BES	$\psi(2S) \to \gamma\chi_{c0}$
7.4 ±1.0	[1] TANENBAUM	78	MRK1	$\psi(2S) \to \gamma\chi_{c0}$

[1] The reported value is derived using $B(\psi(2S) \to \pi^+\pi^- J/\psi) \times B(J/\psi \to \ell^+\ell^-) = (4.6 \pm 0.7)\%$. Calculated by us using $B(J/\psi \to \ell^+\ell^-) = 0.1181 \pm 0.0020$.

$\Gamma(\chi_{c0}(1P) \to K^+K^-K^+K^-)/\Gamma_{\text{total}} \times \Gamma(\psi(2S) \to \gamma\chi_{c0}(1P))/\Gamma_{\text{total}}$ $\Gamma_{47}/\Gamma \times \Gamma_{128}^{\psi(2S)}/\Gamma^{\psi(2S)}$

VALUE (units 10^{-4})	EVTS	DOCUMENT ID		TECN	COMMENT
2.74±0.28 OUR FIT					
3.20±0.11±0.41	278	[1] ABLIKIM	06T	BES2	$\psi(2S) \to \gamma 2K^+2K^-$

[1] Calculated by us. The value of $B(\chi_{c0} \to 2K^+2K^-)$ reported by ABLIKIM 06T was derived using $B(\psi(2S) \to \gamma\chi_{c0}(1P)) = (9.2 \pm 0.4)\%$.

$\Gamma(\chi_{c0}(1P) \to K^+K^-K^+K^-)/\Gamma_{total} \times \Gamma(\psi(2S) \to \gamma\chi_{c0}(1P))/\Gamma(\psi(2S) \to J/\psi(1S)\pi^+\pi^-)$ $\Gamma_{47}/\Gamma \times \Gamma_{128}^{\psi(2S)}/\Gamma_{11}^{\psi(2S)}$

VALUE (units 10^{-4})	DOCUMENT ID		TECN	COMMENT
8.0±0.8 OUR FIT				
6.1±0.8±0.9	[1] BAI	99B	BES	$\psi(2S) \to \gamma 2K^+2K^-$

[1] Calculated by us. The value of $B(\chi_{c0} \to 2K^+2K^-)$ reported by BAI 99B was derived using $B(\psi(2S) \to \gamma\chi_{c0}(1P)) = (9.3 \pm 0.8)\%$ and $B(\psi(2S) \to J/\psi\pi^+\pi^-) = (32.4 \pm 2.6)\%$ [BAI 98D].

$\Gamma(\chi_{c0}(1P) \to \phi\phi)/\Gamma_{total} \times \Gamma(\psi(2S) \to \gamma\chi_{c0}(1P))/\Gamma_{total}$ $\Gamma_{49}/\Gamma \times \Gamma_{128}^{\psi(2S)}/\Gamma^{\psi(2S)}$

VALUE (units 10^{-4})	EVTS	DOCUMENT ID		TECN	COMMENT
0.77±0.07 OUR FIT					
0.78±0.08 OUR AVERAGE					
0.77±0.03±0.08	612	[1] ABLIKIM	11K	BES3	$\psi(2S) \to \gamma$ hadrons
0.86±0.19±0.12	26	[2] ABLIKIM	06T	BES2	$\psi(2S) \to \gamma 2K^+2K^-$

[1] Calculated by us. The value of $B(\chi_{c0} \to \phi\phi)$ reported by ABLIKIM 11K was derived using $B(\psi(2S) \to \gamma\chi_{c0}(1P)) = (9.62 \pm 0.31)\%$.

[2] Calculated by us. The value of $B(\chi_{c0} \to \phi\phi)$ reported by ABLIKIM 06T was derived using $B(\psi(2S) \to \gamma\chi_{c0}(1P)) = (9.2 \pm 0.4)\%$.

$\Gamma(\chi_{c0}(1P) \to \phi\phi)/\Gamma_{total} \times \Gamma(\psi(2S) \to \gamma\chi_{c0}(1P))/\Gamma(\psi(2S) \to J/\psi(1S)\pi^+\pi^-)$ $\Gamma_{49}/\Gamma \times \Gamma_{128}^{\psi(2S)}/\Gamma_{11}^{\psi(2S)}$

VALUE (units 10^{-4})	DOCUMENT ID		TECN	COMMENT
2.24±0.21 OUR FIT				
2.6 ±1.0 ±1.1	[1] BAI	99B	BES	$\psi(2S) \to \gamma 2K^+2K^-$

[1] Calculated by us. The value of $B(\chi_{c0} \to \phi\phi)$ reported by BAI 99B was derived using $B(\psi(2S) \to \gamma\chi_{c0}(1P)) = (9.3 \pm 0.8)\%$ and $B(\psi(2S) \to J/\psi\pi^+\pi^-) = (32.4 \pm 2.6)\%$ [BAI 98D].

$\chi_{c0}(1P)$ REFERENCES

ABLIKIM	13D	PR D87 012007	M. Ablikim *et al.*	(BES III Collab.)
ABLIKIM	13H	PR D87 032007	M. Ablikim *et al.*	(BES III Collab.)
ABLIKIM	13V	PR D88 112001	M. Ablikim *et al.*	(BES III Collab.)
UEHARA	13	PTEP 2013 123C01	S. Uehara *et al.*	(BELLE Collab.)
ABLIKIM	12A	PR D85 112008	M. Ablikim *et al.*	(BES III Collab.)
ABLIKIM	12I	PR D86 052004	M. Ablikim *et al.*	(BES III Collab.)
ABLIKIM	12J	PR D86 052011	M. Ablikim *et al.*	(BES III Collab.)
ABLIKIM	12O	PRL 109 172002	M. Ablikim *et al.*	(BES III Collab.)
LIU	12B	PRL 108 232001	Z.Q. Liu *et al.*	(BELLE Collab.)
ABLIKIM	11A	PR D83 012006	M. Ablikim *et al.*	(BES III Collab.)
ABLIKIM	11E	PR D83 112005	M. Ablikim *et al.*	(BES III Collab.)
ABLIKIM	11F	PR D83 112009	M. Ablikim *et al.*	(BES III Collab.)
ABLIKIM	11K	PRL 107 092001	M. Ablikim *et al.*	(BES III Collab.)
DEL-AMO-SA...	11M	PR D84 012004	P. del Amo Sanchez *et al.*	(BABAR Collab.)
ABLIKIM	10A	PR D81 052005	M. Ablikim *et al.*	(BES III Collab.)
ONYISI	10	PR D82 011103	P.U.E. Onyisi *et al.*	(CLEO Collab.)
UEHARA	10A	PR D82 114031	S. Uehara *et al.*	(BELLE Collab.)
ASNER	09	PR D79 072007	D.M. Asner *et al.*	(CLEO Collab.)
UEHARA	09	PR D79 052009	S. Uehara *et al.*	(BELLE Collab.)
BENNETT	08A	PRL 101 151801	J.V. Bennett *et al.*	(CLEO Collab.)
ECKLUND	08A	PR D78 091501	K.M. Ecklund *et al.*	(CLEO Collab.)
HE	08B	PR D78 092004	Q. He *et al.*	(CLEO Collab.)
MENDEZ	08	PR D78 011102	H. Mendez *et al.*	(CLEO Collab.)
NAIK	08	PR D78 031101	P. Naik *et al.*	(CLEO Collab.)
UEHARA	08	EPJ C53 1	S. Uehara *et al.*	(BELLE Collab.)
WICHT	08	PL B662 323	J. Wicht *et al.*	(BELLE Collab.)
ABE	07	PRL 98 082001	K. Abe *et al.*	(BELLE Collab.)
ADAMS	07	PR D75 071101	G.S. Adams *et al.*	(CLEO Collab.)
ATHAR	07	PR D75 032002	S.B. Athar *et al.*	(CLEO Collab.)
CHEN	07B	PL B651 15	W.T. Chen *et al.*	(BELLE Collab.)
ABLIKIM	06D	PR D73 052006	M. Ablikim *et al.*	(BES Collab.)
ABLIKIM	06I	PR D74 012004	M. Ablikim *et al.*	(BES Collab.)
ABLIKIM	06R	PR D74 072001	M. Ablikim *et al.*	(BES Collab.)
ABLIKIM	06T	PL B642 197	M. Ablikim *et al.*	(BES Collab.)
ABLIKIM	05G	PR D71 092002	M. Ablikim *et al.*	(BES Collab.)
ABLIKIM	05N	PL B630 7	M. Ablikim *et al.*	(BES Collab.)
ABLIKIM	05O	PL B630 21	M. Ablikim *et al.*	(BES Collab.)
ABLIKIM	05Q	PR D72 092002	M. Ablikim *et al.*	(BES Collab.)
ADAM	05A	PRL 94 232002	N.E. Adam *et al.*	(CLEO Collab.)
ANDREOTTI	05A	NP B717 34	M. Andreotti *et al.*	(FNAL E835 Collab.)
ANDREOTTI	05C	PR D72 112002	M. Andreotti *et al.*	(FNAL E835 Collab.)
NAKAZAWA	05	PL B615 39	H. Nakazawa *et al.*	(BELLE Collab.)
ABE	04G	PR D70 071102	K. Abe *et al.*	(BELLE Collab.)
ABLIKIM	04G	PR D70 092002	M. Ablikim *et al.*	(BES Collab.)
ABLIKIM	04H	PR D70 092003	M. Ablikim *et al.*	(BES Collab.)
ANDREOTTI	04	PL B584 16	M. Andreotti *et al.*	(E835 Collab.)
ATHAR	04	PR D70 112002	S.B. Athar *et al.*	(CLEO Collab.)
BAI	04F	PR D69 092001	J.Z. Bai *et al.*	(BES Collab.)
ANDREOTTI	03	PRL 91 091801	M. Andreotti *et al.*	(FNAL E835 Collab.)
AULCHENKO	03	PL B573 63	V.M. Aulchenko *et al.*	(KEDR Collab.)
BAI	03C	PR D67 032004	J.Z. Bai *et al.*	(BES Collab.)
BAI	03E	PR D67 112001	J.Z. Bai *et al.*	(BES Collab.)
ABE,K	02	PRL 89 142001	K. Abe *et al.*	(BELLE Collab.)
BAGNASCO	02	PL B533 237	S. Bagnasco *et al.*	(FNAL E835 Collab.)
EISENSTEIN	01	PRL 87 061801	B.I. Eisenstein *et al.*	(CLEO Collab.)
AMBROGIANI	00B	PR D62 052002	M. Ambrogiani *et al.*	(FNAL E835 Collab.)
AMBROGIANI	99B	PRL 83 2902	M. Ambrogiani *et al.*	(FNAL E835 Collab.)
BAI	99B	PR D60 072001	J.Z. Bai *et al.*	(BES Collab.)
BAI	98D	PR D58 092006	J.Z. Bai *et al.*	(BES Collab.)
BAI	98I	PRL 81 3091	J.Z. Bai *et al.*	(BES Collab.)
GAISER	86	PR D34 711	J. Gaiser *et al.*	(Crystal Ball Collab.)
LEE	85	SLAC 282	R.A. Lee	(SLAC)
OREGLIA	82	PR D25 2259	M.J. Oreglia *et al.*	(SLAC, CIT, HARV+)
BRANDELIK	79B	NP B160 426	R. Brandelik *et al.*	(DASP Collab.)
BARTEL	78B	PL 79B 492	W. Bartel *et al.*	(DESY, HEIDP)
TANENBAUM	78	PR D17 1731	W.M. Tanenbaum *et al.*	(SLAC, LBL)
Also		Private Comm.	G. Trilling	(LBL, UCB)
BIDDICK	77	PRL 38 1324	C.J. Biddick *et al.*	(UCSD, UMD, PAVI+)

$\chi_{c1}(1P)$ $I^G(J^{PC}) = 0^+(1^{++})$

See the Review on "$\psi(2S)$ and χ_c branching ratios" before the $\chi_{c0}(1P)$ Listings.

$\chi_{c1}(1P)$ MASS

VALUE (MeV)	EVTS	DOCUMENT ID		TECN	COMMENT
3510.66 ± 0.07 OUR AVERAGE		Error includes scale factor of 1.5. See the ideogram below.			
3510.30 ± 0.14 ±0.16		ABLIKIM	05G	BES2	$\psi(2S) \to \gamma\chi_{c1}$
3510.719± 0.051±0.019		ANDREOTTI	05A	E835	$p\overline{p} \to e^+e^-\gamma$
3509.4 ± 0.9		BAI	99B	BES	$\psi(2S) \to \gamma$X
3510.60 ± 0.087±0.019	513	[1] ARMSTRONG	92	E760	$\overline{p}p \to e^+e^-\gamma$
3511.3 ± 0.4 ±0.4	30	BAGLIN	86B	SPEC	$\overline{p}p \to e^+e^-$X
3512.3 ± 0.3 ±4.0		[2] GAISER	86	CBAL	$\psi(2S) \to \gamma$X
3507.4 ± 1.7	91	[3] LEMOIGNE	82	GOLI	185 π^-Be $\to \gamma\mu^+\mu^-$A
3510.4 ± 0.6		OREGLIA	82	CBAL	$e^+e^- \to J/\psi 2\gamma$
3510.1 ± 1.1	254	[4] HIMEL	80	MRK2	$e^+e^- \to J/\psi 2\gamma$
3509 ±11	21	BRANDELIK	79B	DASP	$e^+e^- \to J/\psi 2\gamma$
3507 ± 3		[4] BARTEL	78B	CNTR	$e^+e^- \to J/\psi 2\gamma$
3505.0 ± 4 ±4		[4,5] TANENBAUM	78	MRK1	e^+e^-
3513 ± 7	367	[4] BIDDICK	77	CNTR	$\psi(2S) \to \gamma$X
• • • We do not use the following data for averages, fits, limits, etc. • • •					
3500 ±10	40	TANENBAUM	75	MRK1	Hadrons γ

[1] Recalculated by ANDREOTTI 05A, using the value of $\psi(2S)$ mass from AULCHENKO 03.

[2] Using mass of $\psi(2S) = 3686.0$ MeV.

[3] $J/\psi(1S)$ mass constrained to 3097 MeV.

[4] Mass value shifted by us by amount appropriate for $\psi(2S)$ mass = 3686 MeV and $J/\psi(1S)$ mass = 3097 MeV.

[5] From a simultaneous fit to radiative and hadronic decay channels.

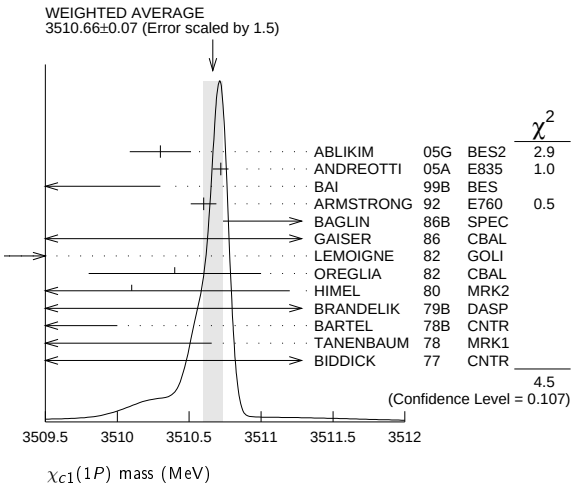

$\chi_{c1}(1P)$ WIDTH

VALUE (MeV)	CL%	EVTS	DOCUMENT ID		TECN	COMMENT
0.84 ±0.04 OUR FIT						
0.88 ±0.05 OUR AVERAGE						
1.39 $^{+0.40}_{-0.38}$ $^{+0.26}_{-0.77}$			ABLIKIM	05G	BES2	$\psi(2S) \to \gamma\chi_{c1}$
0.876±0.045±0.026			ANDREOTTI	05A	E835	$p\overline{p} \to e^+e^-\gamma$
0.87 ±0.11 ±0.08		513	[1] ARMSTRONG	92	E760	$\overline{p}p \to e^+e^-\gamma$
• • • We do not use the following data for averages, fits, limits, etc. • • •						
<1.3	95		BAGLIN	86B	SPEC	$\overline{p}p \to e^+e^-$X
<3.8	90		GAISER	86	CBAL	$\psi(2S) \to \gamma$X

[1] Recalculated by ANDREOTTI 05A.

Meson Particle Listings

$\chi_{c1}(1P)$

$\chi_{c1}(1P)$ DECAY MODES

	Mode	Fraction (Γ_i/Γ)	Scale factor/ Confidence level
	Hadronic decays		
Γ_1	$3(\pi^+\pi^-)$	$(5.8 \pm 1.4) \times 10^{-3}$	S=1.2
Γ_2	$2(\pi^+\pi^-)$	$(7.6 \pm 2.6) \times 10^{-3}$	
Γ_3	$\pi^+\pi^-\pi^0\pi^0$	(1.22 ± 0.16) %	
Γ_4	$\rho^+\pi^-\pi^0$ + c.c.	(1.48 ± 0.25) %	
Γ_5	$\rho^0\pi^+\pi^-$	$(3.9 \pm 3.5) \times 10^{-3}$	
Γ_6	$4\pi^0$	$(5.5 \pm 0.8) \times 10^{-4}$	
Γ_7	$\pi^+\pi^-K^+K^-$	$(4.5 \pm 1.0) \times 10^{-3}$	
Γ_8	$K^+K^-\pi^0\pi^0$	$(1.14 \pm 0.28) \times 10^{-3}$	
Γ_9	$K^+\pi^-\overline{K}^0\pi^0$ + c.c.	$(8.7 \pm 1.4) \times 10^{-3}$	
Γ_{10}	$\rho^-K^+\overline{K}^0$ + c.c.	$(5.1 \pm 1.2) \times 10^{-3}$	
Γ_{11}	$K^*(892)^0\overline{K}^0\pi^0 \to K^+\pi^-\overline{K}^0\pi^0$ + c.c.	$(2.4 \pm 0.7) \times 10^{-3}$	
Γ_{12}	$K^+K^-\eta\pi^0$	$(1.14 \pm 0.35) \times 10^{-3}$	
Γ_{13}	$\pi^+\pi^-K^0_SK^0_S$	$(7.0 \pm 3.0) \times 10^{-4}$	
Γ_{14}	$K^+K^-\eta$	$(3.2 \pm 1.0) \times 10^{-4}$	
Γ_{15}	$\overline{K}^0K^+\pi^-$ + c.c.	$(7.1 \pm 0.6) \times 10^{-3}$	
Γ_{16}	$K^*(892)^0\overline{K}^0$ + c.c.	$(1.0 \pm 0.4) \times 10^{-3}$	
Γ_{17}	$K^*(892)^+K^-$ + c.c.	$(1.5 \pm 0.7) \times 10^{-3}$	
Γ_{18}	$K^*_J(1430)^0\overline{K}^0$ + c.c. $\to K^0_SK^+\pi^-$ + c.c.	$< 8 \times 10^{-4}$	CL=90%
Γ_{19}	$K^*_J(1430)^+K^-$ + c.c. $\to K^0_SK^+\pi^-$ + c.c.	$< 2.2 \times 10^{-3}$	CL=90%
Γ_{20}	$K^+K^-\pi^0$	$(1.85 \pm 0.25) \times 10^{-3}$	
Γ_{21}	$\eta\pi^+\pi^-$	$(4.9 \pm 0.5) \times 10^{-3}$	
Γ_{22}	$a_0(980)^+\pi^-$ + c.c. $\to \eta\pi^+\pi^-$	$(1.8 \pm 0.6) \times 10^{-3}$	
Γ_{23}	$f_2(1270)\eta$	$(2.7 \pm 0.8) \times 10^{-3}$	
Γ_{24}	$\pi^+\pi^-\eta'$	$(2.3 \pm 0.5) \times 10^{-3}$	
Γ_{25}	$\pi^0f_0(980) \to \pi^0\pi^+\pi^-$	$< 6 \times 10^{-6}$	CL=90%
Γ_{26}	$K^+\overline{K}^*(892)^0\pi^-$ + c.c.	$(3.2 \pm 2.1) \times 10^{-3}$	
Γ_{27}	$K^*(892)^0\overline{K}^*(892)^0$	$(1.5 \pm 0.4) \times 10^{-3}$	
Γ_{28}	$K^+K^-K^0_SK^0_S$	$< 4 \times 10^{-4}$	CL=90%
Γ_{29}	$K^+K^-K^+K^-$	$(5.5 \pm 1.1) \times 10^{-4}$	
Γ_{30}	$K^+K^-\phi$	$(4.2 \pm 1.6) \times 10^{-4}$	
Γ_{31}	$\omega\omega$	$(5.8 \pm 0.7) \times 10^{-4}$	
Γ_{32}	$\omega\phi$	$(2.1 \pm 0.6) \times 10^{-5}$	
Γ_{33}	$\phi\phi$	$(4.2 \pm 0.5) \times 10^{-4}$	
Γ_{34}	$p\overline{p}$	$(7.72 \pm 0.35) \times 10^{-5}$	
Γ_{35}	$p\overline{p}\pi^0$	$(1.59 \pm 0.19) \times 10^{-4}$	
Γ_{36}	$p\overline{p}\eta$	$(1.48 \pm 0.25) \times 10^{-4}$	
Γ_{37}	$p\overline{p}\omega$	$(2.16 \pm 0.31) \times 10^{-4}$	
Γ_{38}	$p\overline{p}\phi$	$< 1.8 \times 10^{-5}$	CL=90%
Γ_{39}	$p\overline{p}\pi^+\pi^-$	$(5.0 \pm 1.9) \times 10^{-4}$	
Γ_{40}	$p\overline{p}\pi^0\pi^0$		
Γ_{41}	$p\overline{p}K^+K^-$ (non-resonant)	$(1.30 \pm 0.23) \times 10^{-4}$	
Γ_{42}	$p\overline{p}K^0_SK^0_S$	$< 4.5 \times 10^{-4}$	CL=90%
Γ_{43}	$p\overline{n}\pi^-$	$(3.9 \pm 0.5) \times 10^{-4}$	
Γ_{44}	$\overline{p}n\pi^+$	$(4.0 \pm 0.5) \times 10^{-4}$	
Γ_{45}	$p\overline{n}\pi^-\pi^0$	$(1.05 \pm 0.12) \times 10^{-3}$	
Γ_{46}	$\overline{p}n\pi^+\pi^0$	$(1.03 \pm 0.12) \times 10^{-3}$	
Γ_{47}	$\Lambda\overline{\Lambda}$	$(1.16 \pm 0.12) \times 10^{-4}$	
Γ_{48}	$\Lambda\overline{\Lambda}\pi^+\pi^-$	$(3.0 \pm 0.5) \times 10^{-4}$	
Γ_{49}	$\Lambda\overline{\Lambda}\pi^+\pi^-$ (non-resonant)	$(2.5 \pm 0.6) \times 10^{-4}$	
Γ_{50}	$\Sigma(1385)^+\overline{\Lambda}\pi^-$ + c.c.	$< 1.3 \times 10^{-4}$	CL=90%
Γ_{51}	$\Sigma(1385)^-\overline{\Lambda}\pi^+$ + c.c.	$< 1.3 \times 10^{-4}$	CL=90%
Γ_{52}	$K^+\overline{p}\Lambda$	$(4.2 \pm 0.4) \times 10^{-4}$	S=1.1
Γ_{53}	$K^+\overline{p}\Lambda(1520)$ + c.c.	$(1.7 \pm 0.5) \times 10^{-4}$	
Γ_{54}	$\Lambda(1520)\overline{\Lambda}(1520)$	$< 1.0 \times 10^{-4}$	CL=90%
Γ_{55}	$\Sigma^0\overline{\Sigma}^0$	$< 4 \times 10^{-5}$	CL=90%
Γ_{56}	$\Sigma^+\overline{\Sigma}^-$	$< 6 \times 10^{-5}$	CL=90%
Γ_{57}	$\Sigma(1385)^+\overline{\Sigma}(1385)^-$	$< 1.0 \times 10^{-4}$	CL=90%
Γ_{58}	$\Sigma(1385)^-\overline{\Sigma}(1385)^+$	$< 5 \times 10^{-5}$	CL=90%
Γ_{59}	$\Xi^0\overline{\Xi}^0$	$< 6 \times 10^{-5}$	CL=90%
Γ_{60}	$\Xi^-\overline{\Xi}^+$	$(8.2 \pm 2.2) \times 10^{-5}$	
Γ_{61}	$\pi^+\pi^- + K^+K^-$	$< 2.1 \times 10^{-3}$	
Γ_{62}	$K^0_SK^0_S$	$< 6 \times 10^{-5}$	CL=90%
	Radiative decays		
Γ_{63}	$\gamma J/\psi(1S)$	(33.9 ± 1.2) %	
Γ_{64}	$\gamma\rho^0$	$(2.20 \pm 0.18) \times 10^{-4}$	
Γ_{65}	$\gamma\omega$	$(6.9 \pm 0.8) \times 10^{-5}$	
Γ_{66}	$\gamma\phi$	$(2.5 \pm 0.5) \times 10^{-5}$	
Γ_{67}	$\gamma\gamma$		

CONSTRAINED FIT INFORMATION

A multiparticle fit to $\chi_{c1}(1P)$, $\chi_{c0}(1P)$, $\chi_{c2}(1P)$, and $\psi(2S)$ with 4 total widths, a partial width, 25 combinations of partial widths obtained from integrated cross section, and 84 branching ratios uses 238 measurements to determine 49 parameters. The overall fit has a $\chi^2 = 339.7$ for 189 degrees of freedom.

The following *off-diagonal* array elements are the correlation coefficients $\langle \delta p_i \delta p_j \rangle / (\delta p_i \cdot \delta p_j)$, in percent, from the fit to parameters p_i, including the branching fractions, $x_i \equiv \Gamma_i/\Gamma_{\rm total}$.

x_{29}	6				
x_{34}	8	3			
x_{47}	13	5	7		
x_{63}	31	13	6	26	
Γ	−19	−8	−62	−16	−51
	x_{15}	x_{29}	x_{34}	x_{47}	x_{63}

$\chi_{c1}(1P)$ PARTIAL WIDTHS

$\chi_{c1}(1P)\ \Gamma(i)\Gamma(\gamma J/\psi(1S))/\Gamma(\text{total})$

$\Gamma(p\overline{p}) \times \Gamma(\gamma J/\psi(1S))/\Gamma_{\rm total}$ $\Gamma_{34}\Gamma_{63}/\Gamma$

VALUE (eV)	DOCUMENT ID		TECN	COMMENT
21.9±0.8 OUR FIT				
21.4±0.9 OUR AVERAGE				
21.5±0.5±0.8	[1] ANDREOTTI	05A	E835	$p\overline{p} \to e^+e^-\gamma$
21.4±1.5±2.2	[1,2] ARMSTRONG	92	E760	$\overline{p}p \to e^+e^-\gamma$
$19.9^{+4.4}_{-4.0}$	[1] BAGLIN	86B	SPEC	$\overline{p}p \to e^+e^-$X

[1] Calculated by us using $B(J/\psi(1S) \to e^+e^-) = 0.0593 \pm 0.0010$.
[2] Recalculated by ANDREOTTI 05A.

$\chi_{c1}(1P)$ BRANCHING RATIOS

HADRONIC DECAYS

$\Gamma(3(\pi^+\pi^-))/\Gamma_{\rm total}$ Γ_1/Γ

VALUE (units 10^{-3})	DOCUMENT ID		TECN	COMMENT
5.8±1.4 OUR EVALUATION Error includes scale factor of 1.2. Treating systematic error as correlated.				
5.8±1.1 OUR AVERAGE				
5.4±0.7±0.9	[1] BAI	99B	BES	$\psi(2S) \to \gamma\chi_{c1}$
16.0±5.9±0.8	[1] TANENBAUM	78	MRK1	$\psi(2S) \to \gamma\chi_{c1}$

[1] Rescaled by us using $B(\psi(2S) \to \gamma\chi_{c1}) = (8.8 \pm 0.4)\%$ and $B(\psi(2S) \to J/\psi(1S)\pi^+\pi^-) = (32.6 \pm 0.5)\%$.

$\Gamma(2(\pi^+\pi^-))/\Gamma_{\rm total}$ Γ_2/Γ

VALUE (units 10^{-3})	DOCUMENT ID		TECN	COMMENT
7.6±2.6 OUR EVALUATION Treating systematic error as correlated.				
8 ±4 OUR AVERAGE Error includes scale factor of 1.5.				
4.6±2.1±2.6	[1] BAI	99B	BES	$\psi(2S) \to \gamma\chi_{c1}$
12.5±4.2±0.6	[1] TANENBAUM	78	MRK1	$\psi(2S) \to \gamma\chi_{c1}$

[1] Rescaled by us using $B(\psi(2S) \to \gamma\chi_{c1}) = (8.8 \pm 0.4)\%$ and $B(\psi(2S) \to J/\psi(1S)\pi^+\pi^-) = (32.6 \pm 0.5)\%$.

$\Gamma(\pi^+\pi^-\pi^0\pi^0)/\Gamma_{\rm total}$ Γ_3/Γ

VALUE (%)	EVTS	DOCUMENT ID		TECN	COMMENT
1.22±0.15±0.04	604.7	[1] HE	08B	CLEO	$e^+e^- \to \gamma h^+h^-h^0h^0$

[1] HE 08B reports $1.28 \pm 0.06 \pm 0.15 \pm 0.08$ % from a measurement of $[\Gamma(\chi_{c1}(1P) \to \pi^+\pi^-\pi^0\pi^0)/\Gamma_{\rm total}] \times [B(\psi(2S) \to \gamma\chi_{c1}(1P))]$ assuming $B(\psi(2S) \to \gamma\chi_{c1}(1P)) = (9.07 \pm 0.11 \pm 0.54) \times 10^{-2}$, which we rescale to our best value $B(\psi(2S) \to \gamma\chi_{c1}(1P)) = (9.55 \pm 0.31) \times 10^{-2}$. Our first error is their experiment's error and our second error is the systematic error from using our best value.

$\Gamma(\rho^+\pi^-\pi^0 + \text{c.c.})/\Gamma_{\rm total}$ Γ_4/Γ

VALUE (%)	EVTS	DOCUMENT ID		TECN	COMMENT
1.48±0.24±0.05	712.3	[1,2] HE	08B	CLEO	$e^+e^- \to \gamma h^+h^-h^0h^0$

[1] HE 08B reports $1.56 \pm 0.13 \pm 0.22 \pm 0.10$ % from a measurement of $[\Gamma(\chi_{c1}(1P) \to \rho^+\pi^-\pi^0 + \text{c.c.})/\Gamma_{\rm total}] \times [B(\psi(2S) \to \gamma\chi_{c1}(1P))]$ assuming $B(\psi(2S) \to \gamma\chi_{c1}(1P)) = (9.07 \pm 0.11 \pm 0.54) \times 10^{-2}$, which we rescale to our best value $B(\psi(2S) \to \gamma\chi_{c1}(1P)) = (9.55 \pm 0.31) \times 10^{-2}$. Our first error is their experiment's error and our second error is the systematic error from using our best value.
[2] Calculated by us. We have added the values from HE 08B for $\rho^+\pi^-\pi^0$ and $\rho^-\pi^+\pi^0$ decays assuming uncorrelated statistical and fully correlated systematic uncertainties.

$\Gamma(\rho^0\pi^+\pi^-)/\Gamma_{total}$ Γ_5/Γ

VALUE (units 10^{-4})	DOCUMENT ID		TECN	COMMENT
39±35	[1] TANENBAUM	78	MRK1	$\psi(2S) \to \gamma\chi_{c1}$

[1] Estimated using $B(\psi(2S) \to \gamma\chi_{c1}(1P)) = 0.087$. The errors do not contain the uncertainty in the $\psi(2S)$ decay.

$\Gamma(4\pi^0)/\Gamma_{total}$ Γ_6/Γ

VALUE (units 10^{-3})	EVTS	DOCUMENT ID		TECN	COMMENT
0.55±0.08±0.02	608	[1] ABLIKIM	11A	BES3	$e^+e^- \to \psi(2S) \to \gamma\chi_{c1}$

[1] ABLIKIM 11A reports $(0.57\pm0.03\pm0.08)\times10^{-3}$ from a measurement of $[\Gamma(\chi_{c1}(1P) \to 4\pi^0)/\Gamma_{total}] \times [B(\psi(2S) \to \gamma\chi_{c1}(1P))]$ assuming $B(\psi(2S) \to \gamma\chi_{c1}(1P)) = (9.2 \pm 0.4) \times 10^{-2}$, which we rescale to our best value $B(\psi(2S) \to \gamma\chi_{c1}(1P)) = (9.55 \pm 0.31) \times 10^{-2}$. Our first error is their experiment's error and our second error is the systematic error from using our best value.

$\Gamma(\pi^+\pi^-K^+K^-)/\Gamma_{total}$ Γ_7/Γ

VALUE (units 10^{-3})	DOCUMENT ID		TECN	COMMENT
4.5±1.0 OUR EVALUATION	Treating systematic error as correlated.			
4.5±0.9 OUR AVERAGE				
4.2±0.4±0.9	[1] BAI	99B	BES	$\psi(2S) \to \gamma\chi_{c1}$
7.3±3.0±0.4	[1] TANENBAUM	78	MRK1	$\psi(2S) \to \gamma\chi_{c1}$

[1] Rescaled by us using $B(\psi(2S) \to \gamma\chi_{c1}) = (8.8 \pm 0.4)\%$ and $B(\psi(2S) \to J/\psi(1S)\pi^+\pi^-) = (32.6 \pm 0.5)\%$.

$\Gamma(K^+K^-\pi^0\pi^0)/\Gamma_{total}$ Γ_8/Γ

VALUE (%)	EVTS	DOCUMENT ID		TECN	COMMENT
0.114±0.028±0.004	45.1	[1] HE	08B	CLEO	$e^+e^- \to \gamma h^+h^-h^0h^0$

[1] HE 08B reports $0.12 \pm 0.02 \pm 0.02 \pm 0.01$ % from a measurement of $[\Gamma(\chi_{c1}(1P) \to K^+K^-\pi^0\pi^0)/\Gamma_{total}] \times [B(\psi(2S) \to \gamma\chi_{c1}(1P))]$ assuming $B(\psi(2S) \to \gamma\chi_{c1}(1P)) = (9.07 \pm 0.11 \pm 0.54) \times 10^{-2}$, which we rescale to our best value $B(\psi(2S) \to \gamma\chi_{c1}(1P)) = (9.55 \pm 0.31) \times 10^{-2}$. Our first error is their experiment's error and our second error is the systematic error from using our best value.

$\Gamma(K^+\pi^-\overline{K}^0\pi^0 + c.c.)/\Gamma_{total}$ Γ_9/Γ

VALUE (%)	EVTS	DOCUMENT ID		TECN	COMMENT
0.87±0.14±0.03	141.3	[1] HE	08B	CLEO	$e^+e^- \to \gamma h^+h^-h^0h^0$

[1] HE 08B reports $0.92 \pm 0.09 \pm 0.11 \pm 0.06$ % from a measurement of $[\Gamma(\chi_{c1}(1P) \to K^+\pi^-\overline{K}^0\pi^0 + c.c.)/\Gamma_{total}] \times [B(\psi(2S) \to \gamma\chi_{c1}(1P))]$ assuming $B(\psi(2S) \to \gamma\chi_{c1}(1P)) = (9.07\pm0.11\pm0.54)\times10^{-2}$, which we rescale to our best value $B(\psi(2S) \to \gamma\chi_{c1}(1P)) = (9.55 \pm 0.31) \times 10^{-2}$. Our first error is their experiment's error and our second error is the systematic error from using our best value.

$\Gamma(\rho^-K^+\overline{K}^0 + c.c.)/\Gamma_{total}$ Γ_{10}/Γ

VALUE (%)	EVTS	DOCUMENT ID		TECN	COMMENT
0.51±0.12±0.02	141.3	[1] HE	08B	CLEO	$e^+e^- \to \gamma h^+h^-h^0h^0$

[1] HE 08B reports $0.54 \pm 0.11 \pm 0.07 \pm 0.03$ % from a measurement of $[\Gamma(\chi_{c1}(1P) \to \rho^-K^+\overline{K}^0 + c.c.)/\Gamma_{total}] \times [B(\psi(2S) \to \gamma\chi_{c1}(1P))]$ assuming $B(\psi(2S) \to \gamma\chi_{c1}(1P)) = (9.07\pm0.11\pm0.54)\times10^{-2}$, which we rescale to our best value $B(\psi(2S) \to \gamma\chi_{c1}(1P)) = (9.55 \pm 0.31) \times 10^{-2}$. Our first error is their experiment's error and our second error is the systematic error from using our best value.

$\Gamma(K^*(892)^0\overline{K}^0\pi^0 \to K^+\pi^-\overline{K}^0\pi^0 + c.c.)/\Gamma_{total}$ Γ_{11}/Γ

VALUE (%)	EVTS	DOCUMENT ID		TECN	COMMENT
0.24±0.06±0.01	141.3	[1] HE	08B	CLEO	$e^+e^- \to \gamma h^+h^-h^0h^0$

[1] HE 08B reports $0.25 \pm 0.06 \pm 0.03 \pm 0.02$ % from a measurement of $[\Gamma(\chi_{c1}(1P) \to K^*(892)^0\overline{K}^0\pi^0 \to K^+\pi^-\overline{K}^0\pi^0 + c.c.)/\Gamma_{total}] \times [B(\psi(2S) \to \gamma\chi_{c1}(1P))]$ assuming $B(\psi(2S) \to \gamma\chi_{c1}(1P)) = (9.07 \pm 0.11 \pm 0.54) \times 10^{-2}$, which we rescale to our best value $B(\psi(2S) \to \gamma\chi_{c1}(1P)) = (9.55 \pm 0.31) \times 10^{-2}$. Our first error is their experiment's error and our second error is the systematic error from using our best value.

$\Gamma(K^+K^-\eta\pi^0)/\Gamma_{total}$ Γ_{12}/Γ

VALUE (%)	EVTS	DOCUMENT ID		TECN	COMMENT
0.114±0.035±0.004	141.3	[1] HE	08B	CLEO	$e^+e^- \to \gamma h^+h^-h^0h^0$

[1] HE 08B reports $0.12 \pm 0.03 \pm 0.02 \pm 0.01$ % from a measurement of $[\Gamma(\chi_{c1}(1P) \to K^+K^-\eta\pi^0)/\Gamma_{total}] \times [B(\psi(2S) \to \gamma\chi_{c1}(1P))]$ assuming $B(\psi(2S) \to \gamma\chi_{c1}(1P)) = (9.07 \pm 0.11 \pm 0.54) \times 10^{-2}$, which we rescale to our best value $B(\psi(2S) \to \gamma\chi_{c1}(1P)) = (9.55 \pm 0.31) \times 10^{-2}$. Our first error is their experiment's error and our second error is the systematic error from using our best value.

$\Gamma(\pi^+\pi^-K^0_SK^0_S)/\Gamma_{total}$ Γ_{13}/Γ

VALUE (units 10^{-4})	EVTS	DOCUMENT ID		TECN	COMMENT
7.0±3.0±0.2	19.8±7.7	[1] ABLIKIM	05O	BES2	$\psi(2S) \to \chi_{c1}\gamma$

[1] ABLIKIM 05O reports $[\Gamma(\chi_{c1}(1P) \to \pi^+\pi^-K^0_SK^0_S)/\Gamma_{total}] \times [B(\psi(2S) \to \gamma\chi_{c1}(1P))] = (0.67\pm0.26\pm0.11)\times10^{-4}$ which we divide by our best value $B(\psi(2S) \to \gamma\chi_{c1}(1P)) = (9.55 \pm 0.31) \times 10^{-2}$. Our first error is their experiment's error and our second error is the systematic error from using our best value.

$\Gamma(K^+K^-\eta)/\Gamma_{total}$ Γ_{14}/Γ

VALUE (units 10^{-3})	DOCUMENT ID		TECN	COMMENT
0.32±0.10±0.01	[1] ATHAR	07	CLEO	$\psi(2S) \to \gamma h^+h^-h^0$

[1] ATHAR 07 reports $(0.34 \pm 0.10 \pm 0.04) \times 10^{-3}$ from a measurement of $[\Gamma(\chi_{c1}(1P) \to K^+K^-\eta)/\Gamma_{total}] \times [B(\psi(2S) \to \gamma\chi_{c1}(1P))]$ assuming $B(\psi(2S) \to \gamma\chi_{c1}(1P)) = 0.0907 \pm 0.0011 \pm 0.0054$, which we rescale to our best value $B(\psi(2S) \to \gamma\chi_{c1}(1P)) = (9.55 \pm 0.31) \times 10^{-2}$. Our first error is their experiment's error and our second error is the systematic error from using our best value.

$\Gamma(\overline{K}^0K^+\pi^- + c.c.)/\Gamma_{total}$ Γ_{15}/Γ

VALUE (units 10^{-3})	DOCUMENT ID
7.1±0.6 OUR FIT	

$\Gamma(K^*(892)^0\overline{K}^0 + c.c.)/\Gamma_{total}$ Γ_{16}/Γ

VALUE (units 10^{-3})	EVTS	DOCUMENT ID		TECN	COMMENT
1.00±0.37±0.03	22	[1] ABLIKIM	06R	BES2	$\psi(2S) \to \gamma\chi_{c1}$

[1] ABLIKIM 06R reports $(1.1 \pm 0.4 \pm 0.1) \times 10^{-3}$ from a measurement of $[\Gamma(\chi_{c1}(1P) \to K^*(892)^0\overline{K}^0 + c.c.)/\Gamma_{total}] \times [B(\psi(2S) \to \gamma\chi_{c1}(1P))]$ assuming $B(\psi(2S) \to \gamma\chi_{c1}(1P)) = (8.7 \pm 0.4) \times 10^{-2}$, which we rescale to our best value $B(\psi(2S) \to \gamma\chi_{c1}(1P)) = (9.55 \pm 0.31) \times 10^{-2}$. Our first error is their experiment's error and our second error is the systematic error from using our best value.

$\Gamma(K^*(892)^+K^- + c.c.)/\Gamma_{total}$ Γ_{17}/Γ

VALUE (units 10^{-3})	EVTS	DOCUMENT ID		TECN	COMMENT
1.46±0.66±0.05	27	[1] ABLIKIM	06R	BES2	$\psi(2S) \to \gamma\chi_{c1}$

[1] ABLIKIM 06R reports $(1.6 \pm 0.7 \pm 0.2) \times 10^{-3}$ from a measurement of $[\Gamma(\chi_{c1}(1P) \to K^*(892)^+K^- + c.c.)/\Gamma_{total}] \times [B(\psi(2S) \to \gamma\chi_{c1}(1P))]$ assuming $B(\psi(2S) \to \gamma\chi_{c1}(1P)) = (8.7 \pm 0.4) \times 10^{-2}$, which we rescale to our best value $B(\psi(2S) \to \gamma\chi_{c1}(1P)) = (9.55 \pm 0.31) \times 10^{-2}$. Our first error is their experiment's error and our second error is the systematic error from using our best value.

$\Gamma(K^*_J(1430)^0\overline{K}^0 + c.c. \to K^0_SK^+\pi^- + c.c.)/\Gamma_{total}$ Γ_{18}/Γ

VALUE (units 10^{-3})	CL%	DOCUMENT ID		TECN	COMMENT
<0.8	90	[1] ABLIKIM	06R	BES2	$\psi(2S) \to \gamma\chi_{c1}$

[1] ABLIKIM 06R reports $< 0.9 \times 10^{-3}$ from a measurement of $[\Gamma(\chi_{c1}(1P) \to K^*_J(1430)^0\overline{K}^0 + c.c. \to K^0_SK^+\pi^- + c.c.)/\Gamma_{total}] \times [B(\psi(2S) \to \gamma\chi_{c1}(1P))]$ assuming $B(\psi(2S) \to \gamma\chi_{c1}(1P)) = (8.7 \pm 0.4) \times 10^{-2}$, which we rescale to our best value $B(\psi(2S) \to \gamma\chi_{c1}(1P)) = 9.55 \times 10^{-2}$.

$\Gamma(K^*_J(1430)^+K^- + c.c. \to K^0_SK^+\pi^- + c.c.)/\Gamma_{total}$ Γ_{19}/Γ

VALUE (units 10^{-3})	CL%	DOCUMENT ID		TECN	COMMENT
<2.2	90	[1] ABLIKIM	06R	BES2	$\psi(2S) \to \gamma\chi_{c1}$

[1] ABLIKIM 06R reports $< 2.4 \times 10^{-3}$ from a measurement of $[\Gamma(\chi_{c1}(1P) \to K^*_J(1430)^+K^- + c.c. \to K^0_SK^+\pi^- + c.c.)/\Gamma_{total}] \times [B(\psi(2S) \to \gamma\chi_{c1}(1P))]$ assuming $B(\psi(2S) \to \gamma\chi_{c1}(1P)) = (8.7 \pm 0.4) \times 10^{-2}$, which we rescale to our best value $B(\psi(2S) \to \gamma\chi_{c1}(1P)) = 9.55 \times 10^{-2}$.

$\Gamma(K^+K^-\pi^0)/\Gamma_{total}$ Γ_{20}/Γ

VALUE (units 10^{-3})	DOCUMENT ID		TECN	COMMENT
1.85±0.24±0.06	[1] ATHAR	07	CLEO	$\psi(2S) \to \gamma h^+h^-h^0$

[1] ATHAR 07 reports $(1.95 \pm 0.16 \pm 0.23) \times 10^{-3}$ from a measurement of $[\Gamma(\chi_{c1}(1P) \to K^+K^-\pi^0)/\Gamma_{total}] \times [B(\psi(2S) \to \gamma\chi_{c1}(1P))]$ assuming $B(\psi(2S) \to \gamma\chi_{c1}(1P)) = 0.0907 \pm 0.0011 \pm 0.0054$, which we rescale to our best value $B(\psi(2S) \to \gamma\chi_{c1}(1P)) = (9.55 \pm 0.31) \times 10^{-2}$. Our first error is their experiment's error and our second error is the systematic error from using our best value.

$\Gamma(\eta\pi^+\pi^-)/\Gamma_{total}$ Γ_{21}/Γ

VALUE (units 10^{-3})	EVTS	DOCUMENT ID		TECN	COMMENT
4.9±0.5 OUR AVERAGE					
4.7±0.5±0.2		[1] ATHAR	07	CLEO	$\psi(2S) \to \gamma h^+h^-h^0$
5.4±0.9±0.2	222	[2] ABLIKIM	06R	BES2	$\psi(2S) \to \gamma\chi_{c1}$

[1] ATHAR 07 reports $(5.0 \pm 0.3 \pm 0.5) \times 10^{-3}$ from a measurement of $[\Gamma(\chi_{c1}(1P) \to \eta\pi^+\pi^-)/\Gamma_{total}] \times [B(\psi(2S) \to \gamma\chi_{c1}(1P))]$ assuming $B(\psi(2S) \to \gamma\chi_{c1}(1P)) = 0.0907 \pm 0.0011 \pm 0.0054$, which we rescale to our best value $B(\psi(2S) \to \gamma\chi_{c1}(1P)) = (9.55 \pm 0.31) \times 10^{-2}$. Our first error is their experiment's error and our second error is the systematic error from using our best value.

[2] ABLIKIM 06R reports $(5.9 \pm 0.7 \pm 0.8) \times 10^{-3}$ from a measurement of $[\Gamma(\chi_{c1}(1P) \to \eta\pi^+\pi^-)/\Gamma_{total}] \times [B(\psi(2S) \to \gamma\chi_{c1}(1P))]$ assuming $B(\psi(2S) \to \gamma\chi_{c1}(1P)) = (8.7 \pm 0.4) \times 10^{-2}$, which we rescale to our best value $B(\psi(2S) \to \gamma\chi_{c1}(1P)) = (9.55 \pm 0.31) \times 10^{-2}$. Our first error is their experiment's error and our second error is the systematic error from using our best value.

$\Gamma(a_0(980)^+\pi^- + c.c. \to \eta\pi^+\pi^-)/\Gamma_{total}$ Γ_{22}/Γ

VALUE (units 10^{-3})	EVTS	DOCUMENT ID		TECN	COMMENT
1.8±0.6±0.1	58	[1] ABLIKIM	06R	BES2	$\psi(2S) \to \gamma\chi_{c1}$

[1] ABLIKIM 06R reports $(2.0 \pm 0.5 \pm 0.5) \times 10^{-3}$ from a measurement of $[\Gamma(\chi_{c1}(1P) \to a_0(980)^+\pi^- + c.c. \to \eta\pi^+\pi^-)/\Gamma_{total}] \times [B(\psi(2S) \to \gamma\chi_{c1}(1P))]$ assuming $B(\psi(2S) \to \gamma\chi_{c1}(1P)) = (8.7 \pm 0.4) \times 10^{-2}$, which we rescale to our best value $B(\psi(2S) \to \gamma\chi_{c1}(1P)) = (9.55 \pm 0.31) \times 10^{-2}$. Our first error is their experiment's error and our second error is the systematic error from using our best value.

$\chi_{c1}(1P)$

$\Gamma(f_2(1270)\eta)/\Gamma_{\text{total}}$ Γ_{23}/Γ

VALUE (units 10^{-3})	EVTS	DOCUMENT ID		TECN	COMMENT
2.7±0.8±0.1	53	[1] ABLIKIM	06R	BES2	$\psi(2S) \to \gamma\chi_{c1}$

[1] ABLIKIM 06R reports $(3.0 \pm 0.7 \pm 0.5) \times 10^{-3}$ from a measurement of $[\Gamma(\chi_{c1}(1P) \to f_2(1270)\eta)/\Gamma_{\text{total}}] \times [B(\psi(2S) \to \gamma\chi_{c1}(1P))]$ assuming $B(\psi(2S) \to \gamma\chi_{c1}(1P)) = (8.7 \pm 0.4) \times 10^{-2}$, which we rescale to our best value $B(\psi(2S) \to \gamma\chi_{c1}(1P)) = (9.55 \pm 0.31) \times 10^{-2}$. Our first error is their experiment's error and our second error is the systematic error from using our best value.

$\Gamma(\pi^+\pi^-\eta')/\Gamma_{\text{total}}$ Γ_{24}/Γ

VALUE (units 10^{-3})	DOCUMENT ID		TECN	COMMENT
2.3±0.5±0.1	[1] ATHAR	07	CLEO	$\psi(2S) \to \gamma h^+ h^- h^0$

[1] ATHAR 07 reports $(2.4 \pm 0.4 \pm 0.3) \times 10^{-3}$ from a measurement of $[\Gamma(\chi_{c1}(1P) \to \pi^+\pi^-\eta')/\Gamma_{\text{total}}] \times [B(\psi(2S) \to \gamma\chi_{c1}(1P))]$ assuming $B(\psi(2S) \to \gamma\chi_{c1}(1P)) = 0.0907 \pm 0.0011 \pm 0.0054$, which we rescale to our best value $B(\psi(2S) \to \gamma\chi_{c1}(1P)) = (9.55 \pm 0.31) \times 10^{-2}$. Our first error is their experiment's error and our second error is the systematic error from using our best value.

$\Gamma(\pi^0 f_0(980) \to \pi^0\pi^+\pi^-)/\Gamma_{\text{total}}$ Γ_{25}/Γ

VALUE	CL%	DOCUMENT ID		TECN	COMMENT
$<6 \times 10^{-6}$	90	[1] ABLIKIM	11D	BES3	$\psi(2S) \to \gamma\pi^0\pi^+\pi^-$

[1] ABLIKIM 11D reports $[\Gamma(\chi_{c1}(1P) \to \pi^0 f_0(980) \to \pi^0\pi^+\pi^-)/\Gamma_{\text{total}}] \times [B(\psi(2S) \to \gamma\chi_{c1}(1P))] < 6.0 \times 10^{-7}$ which we divide by our best value $B(\psi(2S) \to \gamma\chi_{c1}(1P)) = 9.55 \times 10^{-2}$.

$\Gamma(K^+\overline{K}^*(892)^0\pi^- + \text{c.c.})/\Gamma_{\text{total}}$ Γ_{26}/Γ

VALUE (units 10^{-4})	DOCUMENT ID		TECN	COMMENT
32±21	[1] TANENBAUM	78	MRK1	$\psi(2S) \to \gamma\chi_{c1}$

[1] Estimated using $B(\psi(2S) \to \gamma\chi_{c1}(1P)) = 0.087$. The errors do not contain the uncertainty in the $\psi(2S)$ decay.

$\Gamma(K^*(892)^0\overline{K}^*(892)^0)/\Gamma_{\text{total}}$ Γ_{27}/Γ

VALUE (units 10^{-3})	EVTS	DOCUMENT ID		TECN	COMMENT
1.47±0.36±0.05	28.4±5.5	[1,2] ABLIKIM	04H	BES	$\psi(2S) \to \gamma K^+ K^- \pi^+ \pi^-$

[1] ABLIKIM 04H reports $[\Gamma(\chi_{c1}(1P) \to K^*(892)^0\overline{K}^*(892)^0)/\Gamma_{\text{total}}] \times [B(\psi(2S) \to \gamma\chi_{c1}(1P))] = (1.40 \pm 0.27 \pm 0.22) \times 10^{-4}$ which we divide by our best value $B(\psi(2S) \to \gamma\chi_{c1}(1P)) = (9.55 \pm 0.31) \times 10^{-2}$. Our first error is their experiment's error and our second error is the systematic error from using our best value.

[2] Assumes $B(K^*(892)^0 \to K^-\pi^+) = 2/3$.

$\Gamma(K^+K^-K^0_S K^0_S)/\Gamma_{\text{total}}$ Γ_{28}/Γ

VALUE (units 10^{-4})	CL%	EVTS	DOCUMENT ID		TECN	COMMENT
<4	90	3.2 ± 2.4	[1] ABLIKIM	05O	BES2	$\psi(2S) \to \chi_{c1}\gamma$

[1] ABLIKIM 05O reports $[\Gamma(\chi_{c1}(1P) \to K^+K^-K^0_S K^0_S)/\Gamma_{\text{total}}] \times [B(\psi(2S) \to \gamma\chi_{c1}(1P))] < 4.2 \times 10^{-5}$ which we divide by our best value $B(\psi(2S) \to \gamma\chi_{c1}(1P)) = 9.55 \times 10^{-2}$.

$\Gamma(K^+K^-K^+K^-)/\Gamma_{\text{total}}$ Γ_{29}/Γ

VALUE (units 10^{-3})	DOCUMENT ID
0.55±0.11 OUR FIT	

$\Gamma(K^+K^-\phi)/\Gamma_{\text{total}}$ Γ_{30}/Γ

VALUE (units 10^{-3})	EVTS	DOCUMENT ID		TECN	COMMENT
0.42±0.15±0.01	17	[1] ABLIKIM	06T	BES2	$\psi(2S) \to \gamma 2K^+ 2K^-$

[1] ABLIKIM 06T reports $(0.46 \pm 0.16 \pm 0.06) \times 10^{-3}$ from a measurement of $[\Gamma(\chi_{c1}(1P) \to K^+K^-\phi)/\Gamma_{\text{total}}] \times [B(\psi(2S) \to \gamma\chi_{c1}(1P))]$ assuming $B(\psi(2S) \to \gamma\chi_{c1}(1P)) = (8.7 \pm 0.4) \times 10^{-2}$, which we rescale to our best value $B(\psi(2S) \to \gamma\chi_{c1}(1P)) = (9.55 \pm 0.31) \times 10^{-2}$. Our first error is their experiment's error and our second error is the systematic error from using our best value.

$\Gamma(\omega\omega)/\Gamma_{\text{total}}$ Γ_{31}/Γ

VALUE (units 10^{-4})	EVTS	DOCUMENT ID		TECN	COMMENT
5.8±0.7±0.2	597	[1] ABLIKIM	11K	BES3	$\psi(2S) \to \gamma$ hadrons

[1] ABLIKIM 11K reports $(6.0 \pm 0.3 \pm 0.7) \times 10^{-4}$ from a measurement of $[\Gamma(\chi_{c1}(1P) \to \omega\omega)/\Gamma_{\text{total}}] \times [B(\psi(2S) \to \gamma\chi_{c1}(1P))]$ assuming $B(\psi(2S) \to \gamma\chi_{c1}(1P)) = (9.2 \pm 0.4) \times 10^{-2}$, which we rescale to our best value $B(\psi(2S) \to \gamma\chi_{c1}(1P)) = (9.55 \pm 0.31) \times 10^{-2}$. Our first error is their experiment's error and our second error is the systematic error from using our best value.

$\Gamma(\omega\phi)/\Gamma_{\text{total}}$ Γ_{32}/Γ

VALUE (units 10^{-4})	EVTS	DOCUMENT ID		TECN	COMMENT
0.21±0.06±0.01	15	[1] ABLIKIM	11K	BES3	$\psi(2S) \to \gamma$ hadrons

[1] ABLIKIM 11K reports $(0.22 \pm 0.06 \pm 0.02) \times 10^{-4}$ from a measurement of $[\Gamma(\chi_{c1}(1P) \to \omega\phi)/\Gamma_{\text{total}}] \times [B(\psi(2S) \to \gamma\chi_{c1}(1P))]$ assuming $B(\psi(2S) \to \gamma\chi_{c1}(1P)) = (9.2 \pm 0.4) \times 10^{-2}$, which we rescale to our best value $B(\psi(2S) \to \gamma\chi_{c1}(1P)) = (9.55 \pm 0.31) \times 10^{-2}$. Our first error is their experiment's error and our second error is the systematic error from using our best value.

$\Gamma(\phi\phi)/\Gamma_{\text{total}}$ Γ_{33}/Γ

VALUE (units 10^{-4})	EVTS	DOCUMENT ID		TECN	COMMENT
4.2±0.5±0.1	366	[1] ABLIKIM	11K	BES3	$\psi(2S) \to \gamma$ hadrons

[1] ABLIKIM 11K reports $(4.4 \pm 0.3 \pm 0.5) \times 10^{-4}$ from a measurement of $[\Gamma(\chi_{c1}(1P) \to \phi\phi)/\Gamma_{\text{total}}] \times [B(\psi(2S) \to \gamma\chi_{c1}(1P))]$ assuming $B(\psi(2S) \to \gamma\chi_{c1}(1P)) = (9.2 \pm 0.4) \times 10^{-2}$, which we rescale to our best value $B(\psi(2S) \to \gamma\chi_{c1}(1P)) = (9.55 \pm 0.31) \times 10^{-2}$. Our first error is their experiment's error and our second error is the systematic error from using our best value.

$\Gamma(p\overline{p})/\Gamma_{\text{total}}$ Γ_{34}/Γ

VALUE (units 10^{-4})	DOCUMENT ID
0.772±0.035 OUR FIT	

$\Gamma(p\overline{p}\pi^0)/\Gamma_{\text{total}}$ Γ_{35}/Γ

VALUE (units 10^{-3})	DOCUMENT ID		TECN	COMMENT
0.159±0.019 OUR AVERAGE				
0.166±0.020±0.005	[1] ONYISI	10	CLE3	$\psi(2S) \to \gamma p\overline{p}X$
0.114±0.048±0.004	[2] ATHAR	07	CLEO	$\psi(2S) \to \gamma h^+ h^- h^0$

[1] ONYISI 10 reports $(1.75 \pm 0.16 \pm 0.13 \pm 0.11) \times 10^{-4}$ from a measurement of $[\Gamma(\chi_{c1}(1P) \to p\overline{p}\pi^0)/\Gamma_{\text{total}}] \times [B(\psi(2S) \to \gamma\chi_{c1}(1P))]$ assuming $B(\psi(2S) \to \gamma\chi_{c1}(1P)) = (9.07 \pm 0.11 \pm 0.54) \times 10^{-2}$, which we rescale to our best value $B(\psi(2S) \to \gamma\chi_{c1}(1P)) = (9.55 \pm 0.31) \times 10^{-2}$. Our first error is their experiment's error and our second error is the systematic error from using our best value.

[2] ATHAR 07 reports $(1.2 \pm 0.5 \pm 0.1) \times 10^{-4}$ from a measurement of $[\Gamma(\chi_{c1}(1P) \to p\overline{p}\pi^0)/\Gamma_{\text{total}}] \times [B(\psi(2S) \to \gamma\chi_{c1}(1P))]$ assuming $B(\psi(2S) \to \gamma\chi_{c1}(1P)) = (9.07 \pm 0.11 \pm 0.54) \times 10^{-2}$, which we rescale to our best value $B(\psi(2S) \to \gamma\chi_{c1}(1P)) = (9.55 \pm 0.31) \times 10^{-2}$. Our first error is their experiment's error and our second error is the systematic error from using our best value.

$\Gamma(p\overline{p}\eta)/\Gamma_{\text{total}}$ Γ_{36}/Γ

VALUE (units 10^{-3})	CL%	DOCUMENT ID		TECN	COMMENT
0.148±0.025±0.005		[1] ONYISI	10	CLE3	$\psi(2S) \to \gamma p\overline{p}X$
• • • We do not use the following data for averages, fits, limits, etc. • • •					
<0.15	90	[2] ATHAR	07	CLEO	$\psi(2S) \to \gamma h^+ h^- h^0$

[1] ONYISI 10 reports $(1.56 \pm 0.22 \pm 0.14 \pm 0.10) \times 10^{-4}$ from a measurement of $[\Gamma(\chi_{c1}(1P) \to p\overline{p}\eta)/\Gamma_{\text{total}}] \times [B(\psi(2S) \to \gamma\chi_{c1}(1P))]$ assuming $B(\psi(2S) \to \gamma\chi_{c1}(1P)) = (9.07 \pm 0.11 \pm 0.54) \times 10^{-2}$, which we rescale to our best value $B(\psi(2S) \to \gamma\chi_{c1}(1P)) = (9.55 \pm 0.31) \times 10^{-2}$. Our first error is their experiment's error and our second error is the systematic error from using our best value.

[2] ATHAR 07 reports $< 0.16 \times 10^{-3}$ from a measurement of $[\Gamma(\chi_{c1}(1P) \to p\overline{p}\eta)/\Gamma_{\text{total}}] \times [B(\psi(2S) \to \gamma\chi_{c1}(1P))]$ assuming $B(\psi(2S) \to \gamma\chi_{c1}(1P)) = (9.07 \pm 0.11 \pm 0.54) \times 10^{-2}$, which we rescale to our best value $B(\psi(2S) \to \gamma\chi_{c1}(1P)) = 9.55 \times 10^{-2}$.

$\Gamma(p\overline{p}\omega)/\Gamma_{\text{total}}$ Γ_{37}/Γ

VALUE (units 10^{-3})	DOCUMENT ID		TECN	COMMENT
0.216±0.031±0.007	[1] ONYISI	10	CLE3	$\psi(2S) \to \gamma p\overline{p}X$

[1] ONYISI 10 reports $(2.28 \pm 0.28 \pm 0.16 \pm 0.14) \times 10^{-4}$ from a measurement of $[\Gamma(\chi_{c1}(1P) \to p\overline{p}\omega)/\Gamma_{\text{total}}] \times [B(\psi(2S) \to \gamma\chi_{c1}(1P))]$ assuming $B(\psi(2S) \to \gamma\chi_{c1}(1P)) = (9.07 \pm 0.11 \pm 0.54) \times 10^{-2}$, which we rescale to our best value $B(\psi(2S) \to \gamma\chi_{c1}(1P)) = (9.55 \pm 0.31) \times 10^{-2}$. Our first error is their experiment's error and our second error is the systematic error from using our best value.

$\Gamma(p\overline{p}\phi)/\Gamma_{\text{total}}$ Γ_{38}/Γ

VALUE (units 10^{-5})	CL%	DOCUMENT ID		TECN	COMMENT
<1.8	90	[1] ABLIKIM	11F	BES3	$\psi(2S) \to \gamma p\overline{p}K^+K^-$

[1] ABLIKIM 11F reports $< 1.82 \times 10^{-5}$ from a measurement of $[\Gamma(\chi_{c1}(1P) \to p\overline{p}\phi)/\Gamma_{\text{total}}] \times [B(\psi(2S) \to \gamma\chi_{c1}(1P))]$ assuming $B(\psi(2S) \to \gamma\chi_{c1}(1P)) = (9.2 \pm 0.4) \times 10^{-2}$, which we rescale to our best value $B(\psi(2S) \to \gamma\chi_{c1}(1P)) = 9.55 \times 10^{-2}$.

$\Gamma(p\overline{p}\pi^+\pi^-)/\Gamma_{\text{total}}$ Γ_{39}/Γ

VALUE (units 10^{-3})	DOCUMENT ID		TECN	COMMENT
0.50±0.19 OUR EVALUATION	Treating systematic error as correlated.			
0.50±0.19 OUR AVERAGE				
0.46±0.12±0.15	[1] BAI	99B	BES	$\psi(2S) \to \gamma\chi_{c1}$
1.08±0.77±0.05	[1] TANENBAUM	78	MRK1	$\psi(2S) \to \gamma\chi_{c1}$

[1] Rescaled by us using $B(\psi(2S) \to \gamma\chi_{c1}) = (8.8 \pm 0.4)\%$ and $B(\psi(2S) \to J/\psi(1S)\pi^+\pi^-) = (32.6 \pm 0.5)\%$.

$\Gamma(p\overline{p}\pi^0\pi^0)/\Gamma_{\text{total}}$ Γ_{40}/Γ

VALUE (%)	CL%	DOCUMENT ID		TECN	COMMENT
<0.05	90	[1] HE	08B	CLEO	$e^+e^- \to \gamma h^+ h^- h^0 h^0$

[1] HE 08B reports < 0.05 % from a measurement of $[\Gamma(\chi_{c1}(1P) \to p\overline{p}\pi^0\pi^0)/\Gamma_{\text{total}}] \times [B(\psi(2S) \to \gamma\chi_{c1}(1P))]$ assuming $B(\psi(2S) \to \gamma\chi_{c1}(1P)) = (9.07 \pm 0.11 \pm 0.54) \times 10^{-2}$, which we rescale to our best value $B(\psi(2S) \to \gamma\chi_{c1}(1P)) = 9.55 \times 10^{-2}$.

$\Gamma(p\overline{p}K^+K^-(\text{non-resonant}))/\Gamma_{\text{total}}$ Γ_{41}/Γ

VALUE (units 10^{-4})	EVTS	DOCUMENT ID		TECN	COMMENT
1.30±0.23±0.04	82 ± 9	[1] ABLIKIM	11F	BES3	$\psi(2S) \to \gamma p\overline{p}K^+K^-$

[1] ABLIKIM 11F reports $(1.35 \pm 0.15 \pm 0.19) \times 10^{-4}$ from a measurement of $[\Gamma(\chi_{c1}(1P) \to p\overline{p}K^+K^-(\text{non-resonant}))/\Gamma_{\text{total}}] \times [B(\psi(2S) \to \gamma\chi_{c1}(1P))]$ assuming $B(\psi(2S) \to \gamma\chi_{c1}(1P)) = (9.2 \pm 0.4) \times 10^{-2}$, which we rescale to our best value $B(\psi(2S) \to \gamma\chi_{c1}(1P)) = (9.55 \pm 0.31) \times 10^{-2}$. Our first error is their experiment's error and our second error is the systematic error from using our best value.

$\Gamma(p\overline{p}K^0_S K^0_S)/\Gamma_{total}$ Γ_{42}/Γ

VALUE (units 10^{-4})	CL%	DOCUMENT ID		TECN	COMMENT
<4.5	90	[1] ABLIKIM	06D	BES2	$\psi(2S) \to \gamma\chi_{c1}$

[1] Using B($\psi(2S) \to \chi_{c1}\gamma$) (9.1 ± 0.6)%.

$\Gamma(p\overline{n}\pi^-)/\Gamma_{total}$ Γ_{43}/Γ

VALUE (units 10^{-4})	EVTS	DOCUMENT ID		TECN	COMMENT
3.9±0.5±0.1	1412	[1] ABLIKIM	12J	BES3	$\psi(2S) \to \gamma p\overline{n}\pi^-$

[1] ABLIKIM 12J reports $[\Gamma(\chi_{c1}(1P) \to p\overline{n}\pi^-)/\Gamma_{total}] \times [B(\psi(2S) \to \gamma\chi_{c1}(1P))] = (0.37 \pm 0.02 \pm 0.04) \times 10^{-4}$ which we divide by our best value $B(\psi(2S) \to \gamma\chi_{c1}(1P)) = (9.55 \pm 0.31) \times 10^{-2}$. Our first error is their experiment's error and our second error is the systematic error from using our best value.

$\Gamma(\overline{p}n\pi^+)/\Gamma_{total}$ Γ_{44}/Γ

VALUE (units 10^{-4})	EVTS	DOCUMENT ID		TECN	COMMENT
4.0±0.5±0.1	1625	[1] ABLIKIM	12J	BES3	$\psi(2S) \to \gamma\overline{p}n\pi^+$

[1] ABLIKIM 12J reports $[\Gamma(\chi_{c1}(1P) \to \overline{p}n\pi^+)/\Gamma_{total}] \times [B(\psi(2S) \to \gamma\chi_{c1}(1P))] = (0.38 \pm 0.02 \pm 0.04) \times 10^{-4}$ which we divide by our best value $B(\psi(2S) \to \gamma\chi_{c1}(1P)) = (9.55 \pm 0.31) \times 10^{-2}$. Our first error is their experiment's error and our second error is the systematic error from using our best value.

$\Gamma(p\overline{n}\pi^-\pi^0)/\Gamma_{total}$ Γ_{45}/Γ

VALUE (units 10^{-4})	EVTS	DOCUMENT ID		TECN	COMMENT
10.5±1.2±0.3	1082	[1] ABLIKIM	12J	BES3	$\psi(2S) \to \gamma p\overline{n}\pi^-\pi^0$

[1] ABLIKIM 12J reports $[\Gamma(\chi_{c1}(1P) \to p\overline{n}\pi^-\pi^0)/\Gamma_{total}] \times [B(\psi(2S) \to \gamma\chi_{c1}(1P))] = (1.00 \pm 0.05 \pm 0.10) \times 10^{-4}$ which we divide by our best value $B(\psi(2S) \to \gamma\chi_{c1}(1P)) = (9.55 \pm 0.31) \times 10^{-2}$. Our first error is their experiment's error and our second error is the systematic error from using our best value.

$\Gamma(\overline{p}n\pi^+\pi^0)/\Gamma_{total}$ Γ_{46}/Γ

VALUE (units 10^{-4})	EVTS	DOCUMENT ID		TECN	COMMENT
10.3±1.2±0.3	1261	[1] ABLIKIM	12J	BES3	$\psi(2S) \to \gamma\overline{p}n\pi^+\pi^0$

[1] ABLIKIM 12J reports $[\Gamma(\chi_{c1}(1P) \to \overline{p}n\pi^+\pi^0)/\Gamma_{total}] \times [B(\psi(2S) \to \gamma\chi_{c1}(1P))] = (0.98 \pm 0.05 \pm 0.10) \times 10^{-4}$ which we divide by our best value $B(\psi(2S) \to \gamma\chi_{c1}(1P)) = (9.55 \pm 0.31) \times 10^{-2}$. Our first error is their experiment's error and our second error is the systematic error from using our best value.

$\Gamma(\Lambda\overline{\Lambda})/\Gamma_{total}$ Γ_{47}/Γ

VALUE (units 10^{-4})	DOCUMENT ID
1.16±0.12 OUR FIT	

$\Gamma(\Lambda\overline{\Lambda}\pi^+\pi^-)/\Gamma_{total}$ Γ_{48}/Γ

VALUE (units 10^{-5})	CL%	EVTS	DOCUMENT ID		TECN	COMMENT
30±5±1		105	[1] ABLIKIM	12I	BES3	$\psi(2S) \to \gamma\Lambda\overline{\Lambda}\pi^+\pi^-$
• • • We do not use the following data for averages, fits, limits, etc. • • •						
<150	90		[2] ABLIKIM	06D	BES2	$\psi(2S) \to \gamma\chi_{c1}$

[1] ABLIKIM 12I reports $(31.1 \pm 3.4 \pm 3.9) \times 10^{-5}$ from a measurement of $[\Gamma(\chi_{c1}(1P) \to \Lambda\overline{\Lambda}\pi^+\pi^-)/\Gamma_{total}] \times [B(\psi(2S) \to \gamma\chi_{c1}(1P))]$ assuming $B(\psi(2S) \to \gamma\chi_{c1}(1P)) = (9.2 \pm 0.4) \times 10^{-2}$, which we rescale to our best value $B(\psi(2S) \to \gamma\chi_{c1}(1P)) = (9.55 \pm 0.31) \times 10^{-2}$. Our first error is their experiment's error and our second error is the systematic error from using our best value.

[2] Using B($\psi(2S) \to \chi_{c1}\gamma$) (9.1 ± 0.6)%.

$\Gamma(\Lambda\overline{\Lambda}\pi^+\pi^-(\text{non-resonant}))/\Gamma_{total}$ Γ_{49}/Γ

VALUE (units 10^{-5})	EVTS	DOCUMENT ID		TECN	COMMENT
25±6±1	13	[1] ABLIKIM	12I	BES3	$\psi(2S) \to \gamma\Lambda\overline{\Lambda}\pi^+\pi^-$

[1] ABLIKIM 12I reports $(26.2 \pm 5.5 \pm 3.3) \times 10^{-5}$ from a measurement of $[\Gamma(\chi_{c1}(1P) \to \Lambda\overline{\Lambda}\pi^+\pi^-(\text{non-resonant}))/\Gamma_{total}] \times [B(\psi(2S) \to \gamma\chi_{c1}(1P))]$ assuming $B(\psi(2S) \to \gamma\chi_{c1}(1P)) = (9.2 \pm 0.4) \times 10^{-2}$, which we rescale to our best value $B(\psi(2S) \to \gamma\chi_{c1}(1P)) = (9.55 \pm 0.31) \times 10^{-2}$. Our first error is their experiment's error and our second error is the systematic error from using our best value.

$\Gamma(\Sigma(1385)^+\overline{\Lambda}\pi^- + \text{c.c.})/\Gamma_{total}$ Γ_{50}/Γ

VALUE (units 10^{-5})	CL%	DOCUMENT ID		TECN	COMMENT
<13	90	[1] ABLIKIM	12I	BES3	$\psi(2S) \to \gamma\Sigma(1385)^+\overline{\Lambda}\pi^-$

[1] ABLIKIM 12I reports $< 14 \times 10^{-5}$ from a measurement of $[\Gamma(\chi_{c1}(1P) \to \Sigma(1385)^+\overline{\Lambda}\pi^- + \text{c.c.})/\Gamma_{total}] \times [B(\psi(2S) \to \gamma\chi_{c1}(1P))]$ assuming $B(\psi(2S) \to \gamma\chi_{c1}(1P)) = (9.2 \pm 0.4) \times 10^{-2}$, which we rescale to our best value $B(\psi(2S) \to \gamma\chi_{c1}(1P)) = 9.55 \times 10^{-2}$.

$\Gamma(\Sigma(1385)^-\overline{\Lambda}\pi^+ + \text{c.c.})/\Gamma_{total}$ Γ_{51}/Γ

VALUE (units 10^{-5})	CL%	DOCUMENT ID		TECN	COMMENT
<13	90	[1] ABLIKIM	12I	BES3	$\psi(2S) \to \gamma\Sigma(1385)^-\overline{\Lambda}\pi^+$

[1] ABLIKIM 12I reports $< 14 \times 10^{-5}$ from a measurement of $[\Gamma(\chi_{c1}(1P) \to \Sigma(1385)^-\overline{\Lambda}\pi^+ + \text{c.c.})/\Gamma_{total}] \times [B(\psi(2S) \to \gamma\chi_{c1}(1P))]$ assuming $B(\psi(2S) \to \gamma\chi_{c1}(1P)) = (9.2 \pm 0.4) \times 10^{-2}$, which we rescale to our best value $B(\psi(2S) \to \gamma\chi_{c1}(1P)) = 9.55 \times 10^{-2}$.

$\Gamma(K^+\overline{p}\Lambda)/\Gamma_{total}$ Γ_{52}/Γ

VALUE (units 10^{-4})	EVTS	DOCUMENT ID		TECN	COMMENT
4.2±0.4 OUR AVERAGE Error includes scale factor of 1.1.					
4.3±0.4±0.1	3k	[1,2] ABLIKIM	13D	BES3	$\psi(2S) \to \gamma\Lambda\overline{p}K^+$
3.1±0.9±0.1		[3] ATHAR	07	CLEO	$\psi(2S) \to \gamma h^+h^-h^0$

[1] ABLIKIM 13D reports $(4.5 \pm 0.2 \pm 0.4) \times 10^{-4}$ from a measurement of $[\Gamma(\chi_{c1}(1P) \to K^+\overline{p}\Lambda)/\Gamma_{total}] \times [B(\psi(2S) \to \gamma\chi_{c1}(1P))]$ assuming $B(\psi(2S) \to \gamma\chi_{c1}(1P)) = (9.2 \pm 0.4) \times 10^{-2}$, which we rescale to our best value $B(\psi(2S) \to \gamma\chi_{c1}(1P)) = (9.55 \pm 0.31) \times 10^{-2}$. Our first error is their experiment's error and our second error is the systematic error from using our best value.

[2] Using B($\Lambda \to p\pi^-$) = 63.9%.

[3] ATHAR 07 reports $(3.3 \pm 0.9 \pm 0.4) \times 10^{-4}$ from a measurement of $[\Gamma(\chi_{c1}(1P) \to K^+\overline{p}\Lambda)/\Gamma_{total}] \times [B(\psi(2S) \to \gamma\chi_{c1}(1P))]$ assuming $B(\psi(2S) \to \gamma\chi_{c1}(1P)) = (9.07 \pm 0.11 \pm 0.54) \times 10^{-2}$, which we rescale to our best value $B(\psi(2S) \to \gamma\chi_{c1}(1P)) = (9.55 \pm 0.31) \times 10^{-2}$. Our first error is their experiment's error and our second error is the systematic error from using our best value.

$\Gamma(K^+\overline{p}\Lambda(1520) + \text{c.c.})/\Gamma_{total}$ Γ_{53}/Γ

VALUE (units 10^{-4})	EVTS	DOCUMENT ID		TECN	COMMENT
1.7±0.4±0.1	48 ± 10	[1] ABLIKIM	11F	BES3	$\psi(2S) \to \gamma p\overline{p}K^+K^-$

[1] ABLIKIM 11F reports $(1.81 \pm 0.38 \pm 0.28) \times 10^{-4}$ from a measurement of $[\Gamma(\chi_{c1}(1P) \to K^+\overline{p}\Lambda(1520) + \text{c.c.})/\Gamma_{total}] \times [B(\psi(2S) \to \gamma\chi_{c1}(1P))]$ assuming $B(\psi(2S) \to \gamma\chi_{c1}(1P)) = (9.2 \pm 0.4) \times 10^{-2}$, which we rescale to our best value $B(\psi(2S) \to \gamma\chi_{c1}(1P)) = (9.55 \pm 0.31) \times 10^{-2}$. Our first error is their experiment's error and our second error is the systematic error from using our best value.

$\Gamma(\Lambda(1520)\overline{\Lambda}(1520))/\Gamma_{total}$ Γ_{54}/Γ

VALUE (units 10^{-4})	CL%	DOCUMENT ID		TECN	COMMENT
<1.0	90	[1] ABLIKIM	11F	BES3	$\psi(2S) \to \gamma p\overline{p}K^+K^-$

[1] ABLIKIM 11F reports $< 1.00 \times 10^{-4}$ from a measurement of $[\Gamma(\chi_{c1}(1P) \to \Lambda(1520)\overline{\Lambda}(1520))/\Gamma_{total}] \times [B(\psi(2S) \to \gamma\chi_{c1}(1P))]$ assuming $B(\psi(2S) \to \gamma\chi_{c1}(1P)) = (9.2 \pm 0.4) \times 10^{-2}$, which we rescale to our best value $B(\psi(2S) \to \gamma\chi_{c1}(1P)) = 9.55 \times 10^{-2}$.

$\Gamma(\Sigma^0\overline{\Sigma}^0)/\Gamma_{total}$ Γ_{55}/Γ

VALUE (units 10^{-4})	CL%	EVTS	DOCUMENT ID		TECN	COMMENT
<0.4	90	3.8 ± 2.5	[1] NAIK	08	CLEO	$\psi(2S) \to \gamma\Sigma^0\overline{\Sigma}^0$
• • • We do not use the following data for averages, fits, limits, etc. • • •						
<0.6	90		[2] ABLIKIM	13H	BES3	$\psi(2S) \to \gamma\Sigma^0\overline{\Sigma}^0$

[1] NAIK 08 reports $< 0.44 \times 10^{-4}$ from a measurement of $[\Gamma(\chi_{c1}(1P) \to \Sigma^0\overline{\Sigma}^0)/\Gamma_{total}] \times [B(\psi(2S) \to \gamma\chi_{c1}(1P))]$ assuming $B(\psi(2S) \to \gamma\chi_{c1}(1P)) = (9.07 \pm 0.11 \pm 0.54) \times 10^{-2}$, which we rescale to our best value $B(\psi(2S) \to \gamma\chi_{c1}(1P)) = 9.55 \times 10^{-2}$.

[2] ABLIKIM 13H reports $< 0.62 \times 10^{-4}$ from a measurement of $[\Gamma(\chi_{c1}(1P) \to \Sigma^0\overline{\Sigma}^0)/\Gamma_{total}] \times [B(\psi(2S) \to \gamma\chi_{c1}(1P))]$ assuming $B(\psi(2S) \to \gamma\chi_{c1}(1P)) = (9.2 \pm 0.4) \times 10^{-2}$, which we rescale to our best value $B(\psi(2S) \to \gamma\chi_{c1}(1P)) = 9.55 \times 10^{-2}$.

$\Gamma(\Sigma^+\overline{\Sigma}^-)/\Gamma_{total}$ Γ_{56}/Γ

VALUE (units 10^{-4})	CL%	EVTS	DOCUMENT ID		TECN	COMMENT
<0.6	90	4.3 ± 2.3	[1] NAIK	08	CLEO	$\psi(2S) \to \gamma\Sigma^+\overline{\Sigma}^-$
• • • We do not use the following data for averages, fits, limits, etc. • • •						
<0.8	90		[2] ABLIKIM	13H	BES3	$\psi(2S) \to \gamma\Sigma^+\overline{\Sigma}^-$

[1] NAIK 08 reports $< 0.65 \times 10^{-4}$ from a measurement of $[\Gamma(\chi_{c1}(1P) \to \Sigma^+\overline{\Sigma}^-)/\Gamma_{total}] \times [B(\psi(2S) \to \gamma\chi_{c1}(1P))]$ assuming $B(\psi(2S) \to \gamma\chi_{c1}(1P)) = (9.07 \pm 0.11 \pm 0.54) \times 10^{-2}$, which we rescale to our best value $B(\psi(2S) \to \gamma\chi_{c1}(1P)) = 9.55 \times 10^{-2}$.

[2] ABLIKIM 13H reports $< 0.87 \times 10^{-4}$ from a measurement of $[\Gamma(\chi_{c1}(1P) \to \Sigma^+\overline{\Sigma}^-)/\Gamma_{total}] \times [B(\psi(2S) \to \gamma\chi_{c1}(1P))]$ assuming $B(\psi(2S) \to \gamma\chi_{c1}(1P)) = (9.2 \pm 0.4) \times 10^{-2}$, which we rescale to our best value $B(\psi(2S) \to \gamma\chi_{c1}(1P)) = 9.55 \times 10^{-2}$.

$\Gamma(\Sigma(1385)^+\overline{\Sigma}(1385)^-)/\Gamma_{total}$ Γ_{57}/Γ

VALUE (units 10^{-5})	CL%	DOCUMENT ID		TECN	COMMENT
<10	90	[1] ABLIKIM	12I	BES3	$\psi(2S) \to \gamma\Lambda\overline{\Lambda}\pi^+\pi^-$

[1] ABLIKIM 12I reports $< 10 \times 10^{-5}$ from a measurement of $[\Gamma(\chi_{c1}(1P) \to \Sigma(1385)^+\overline{\Sigma}(1385)^-)/\Gamma_{total}] \times [B(\psi(2S) \to \gamma\chi_{c1}(1P))]$ assuming $B(\psi(2S) \to \gamma\chi_{c1}(1P)) = (9.2 \pm 0.4) \times 10^{-2}$, which we rescale to our best value $B(\psi(2S) \to \gamma\chi_{c1}(1P)) = 9.55 \times 10^{-2}$.

$\Gamma(\Sigma(1385)^-\overline{\Sigma}(1385)^+)/\Gamma_{total}$ Γ_{58}/Γ

VALUE (units 10^{-5})	CL%	DOCUMENT ID		TECN	COMMENT
<5	90	[1] ABLIKIM	12I	BES3	$\psi(2S) \to \gamma\Lambda\overline{\Lambda}\pi^+\pi^-$

[1] ABLIKIM 12I reports $< 5.7 \times 10^{-5}$ from a measurement of $[\Gamma(\chi_{c1}(1P) \to \Sigma(1385)^-\overline{\Sigma}(1385)^+)/\Gamma_{total}] \times [B(\psi(2S) \to \gamma\chi_{c1}(1P))]$ assuming $B(\psi(2S) \to \gamma\chi_{c1}(1P)) = (9.2 \pm 0.4) \times 10^{-2}$, which we rescale to our best value $B(\psi(2S) \to \gamma\chi_{c1}(1P)) = 9.55 \times 10^{-2}$.

Meson Particle Listings

$\chi_{c1}(1P)$

$\Gamma(\Xi^0\overline{\Xi}^0)/\Gamma_{\rm total}$ Γ_{59}/Γ

VALUE (units 10^{-4})	CL%	EVTS	DOCUMENT ID		TECN	COMMENT
<0.6	90	1.7 ± 2.4	[1] NAIK	08	CLEO	$\psi(2S) \to \gamma\Xi^0\overline{\Xi}^0$

[1] NAIK 08 reports $< 0.60\times10^{-4}$ from a measurement of $[\Gamma(\chi_{c1}(1P) \to \Xi^0\overline{\Xi}^0)/\Gamma_{\rm total}] \times [B(\psi(2S) \to \gamma\chi_{c1}(1P))]$ assuming $B(\psi(2S) \to \gamma\chi_{c1}(1P)) = (9.07 \pm 0.11 \pm 0.54)\times 10^{-2}$, which we rescale to our best value $B(\psi(2S) \to \gamma\chi_{c1}(1P)) = 9.55 \times 10^{-2}$.

$\Gamma(\Xi^-\overline{\Xi}^+)/\Gamma_{\rm total}$ Γ_{60}/Γ

VALUE (units 10^{-4})	CL%	EVTS	DOCUMENT ID		TECN	COMMENT
0.82±0.22±0.03		16.4 ± 4.3	[1] NAIK	08	CLEO	$\psi(2S) \to \gamma\Xi^+\overline{\Xi}^-$
• • • We do not use the following data for averages, fits, limits, etc. • • •						
< 3.4	90		[2] ABLIKIM	06D	BES2	$\psi(2S) \to \gamma\chi_{c1}$

[1] NAIK 08 reports $(0.86 \pm 0.22 \pm 0.08) \times 10^{-4}$ from a measurement of $[\Gamma(\chi_{c1}(1P) \to \Xi^-\overline{\Xi}^+)/\Gamma_{\rm total}] \times [B(\psi(2S) \to \gamma\chi_{c1}(1P))]$ assuming $B(\psi(2S) \to \gamma\chi_{c1}(1P)) = (9.07 \pm 0.11 \pm 0.54)\times10^{-2}$, which we rescale to our best value $B(\psi(2S) \to \gamma\chi_{c1}(1P)) = (9.55 \pm 0.31) \times 10^{-2}$. Our first error is their experiment's error and our second error is the systematic error from using our best value.

[2] Using $B(\psi(2S) \to \chi_{c1}\gamma)$ $(9.1 \pm 0.6)\%$.

$[\Gamma(\pi^+\pi^-) + \Gamma(K^+K^-)]/\Gamma_{\rm total}$ Γ_{61}/Γ

VALUE (units 10^{-4})	CL%	DOCUMENT ID		TECN	COMMENT
<21		[1] FELDMAN	77	MRK1	$\psi(2S) \to \gamma\chi_{c1}$
• • • We do not use the following data for averages, fits, limits, etc. • • •					
<38	90	[1] BRANDELIK	79B	DASP	$\psi(2S) \to \gamma\chi_{c1}$

[1] Estimated using $B(\psi(2S) \to \gamma\chi_{c1}(1P)) = 0.087$. The errors do not contain the uncertainty in the $\psi(2S)$ decay.

$\Gamma(K^0_S K^0_S)/\Gamma_{\rm total}$ Γ_{62}/Γ

VALUE (units 10^{-4})	CL%	DOCUMENT ID		TECN	COMMENT
<0.6	90	[1] ABLIKIM	05O	BES2	$\psi(2S) \to \chi_{c1}\gamma$

[1] ABLIKIM 05O reports $[\Gamma(\chi_{c1}(1P) \to K^0_S K^0_S)/\Gamma_{\rm total}] \times [B(\psi(2S) \to \gamma\chi_{c1}(1P))] < 0.6\times10^{-5}$ which we divide by our best value $B(\psi(2S) \to \gamma\chi_{c1}(1P)) = 9.55\times10^{-2}$.

RADIATIVE DECAYS

$\Gamma(\gamma J/\psi(1S))/\Gamma_{\rm total}$ Γ_{63}/Γ

VALUE	DOCUMENT ID		TECN	COMMENT
0.339±0.012 OUR FIT				
• • • We do not use the following data for averages, fits, limits, etc. • • •				
$0.379 \pm 0.008 \pm 0.021$	[1] ADAM	05A	CLEO	$e^+e^- \to \psi(2S) \to \gamma\chi_{c1}$

[1] Uses $B(\psi(2S) \to \gamma\chi_{c1} \to \gamma\gamma J/\psi)$ from ADAM 05A and $B(\psi(2S) \to \gamma\chi_{c1})$ from ATHAR 04.

$\Gamma(\gamma\rho^0)/\Gamma_{\rm total}$ Γ_{64}/Γ

VALUE (units 10^{-6})	EVTS	DOCUMENT ID		TECN	COMMENT
220±18 OUR AVERAGE					
$220 \pm 23 \pm 7$	432 ± 25	[1] ABLIKIM	11E	BES3	$\psi(2S) \to \gamma\gamma\rho^0$
$221 \pm 24 \pm 7$	186 ± 15	[2] BENNETT	08A	CLEO	$\psi(2S) \to \gamma\gamma\rho^0$

[1] ABLIKIM 11E reports $(228 \pm 13 \pm 22) \times 10^{-6}$ from a measurement of $[\Gamma(\chi_{c1}(1P) \to \gamma\rho^0)/\Gamma_{\rm total}] \times [B(\psi(2S) \to \gamma\chi_{c1}(1P))]$ assuming $B(\psi(2S) \to \gamma\chi_{c1}(1P)) = (9.2 \pm 0.4) \times 10^{-2}$, which we rescale to our best value $B(\psi(2S) \to \gamma\chi_{c1}(1P)) = (9.55 \pm 0.31) \times 10^{-2}$. Our first error is their experiment's error and our second error is the systematic error from using our best value.

[2] BENNETT 08A reports $(243 \pm 19 \pm 22) \times 10^{-6}$ from a measurement of $[\Gamma(\chi_{c1}(1P) \to \gamma\rho^0)/\Gamma_{\rm total}] \times [B(\psi(2S) \to \gamma\chi_{c1}(1P))]$ assuming $B(\psi(2S) \to \gamma\chi_{c1}(1P)) = (8.7 \pm 0.4) \times 10^{-2}$, which we rescale to our best value $B(\psi(2S) \to \gamma\chi_{c1}(1P)) = (9.55 \pm 0.31) \times 10^{-2}$. Our first error is their experiment's error and our second error is the systematic error from using our best value.

$\Gamma(\gamma\omega)/\Gamma_{\rm total}$ Γ_{65}/Γ

VALUE (units 10^{-6})	EVTS	DOCUMENT ID		TECN	COMMENT
69± 8 OUR AVERAGE					
$67 \pm 9 \pm 2$	136 ± 14	[1] ABLIKIM	11E	BES3	$\psi(2S) \to \gamma\gamma\omega$
$76 \pm 17 \pm 2$	39 ± 7	[2] BENNETT	08A	CLEO	$\psi(2S) \to \gamma\gamma\omega$

[1] ABLIKIM 11E reports $(69.7 \pm 7.2 \pm 6.6) \times 10^{-6}$ from a measurement of $[\Gamma(\chi_{c1}(1P) \to \gamma\omega)/\Gamma_{\rm total}] \times [B(\psi(2S) \to \gamma\chi_{c1}(1P))]$ assuming $B(\psi(2S) \to \gamma\chi_{c1}(1P)) = (9.2 \pm 0.4) \times 10^{-2}$, which we rescale to our best value $B(\psi(2S) \to \gamma\chi_{c1}(1P)) = (9.55 \pm 0.31) \times 10^{-2}$. Our first error is their experiment's error and our second error is the systematic error from using our best value.

[2] BENNETT 08A reports $(83 \pm 15 \pm 12) \times 10^{-6}$ from a measurement of $[\Gamma(\chi_{c1}(1P) \to \gamma\omega)/\Gamma_{\rm total}] \times [B(\psi(2S) \to \gamma\chi_{c1}(1P))]$ assuming $B(\psi(2S) \to \gamma\chi_{c1}(1P)) = (8.7 \pm 0.4) \times 10^{-2}$, which we rescale to our best value $B(\psi(2S) \to \gamma\chi_{c1}(1P)) = (9.55 \pm 0.31) \times 10^{-2}$. Our first error is their experiment's error and our second error is the systematic error from using our best value.

$\Gamma(\gamma\phi)/\Gamma_{\rm total}$ Γ_{66}/Γ

VALUE (units 10^{-6})	CL%	EVTS	DOCUMENT ID		TECN	COMMENT
25±5±1		43 ± 9	[1] ABLIKIM	11E	BES3	$\psi(2S) \to \gamma\gamma\phi$
• • • We do not use the following data for averages, fits, limits, etc. • • •						
<24	90	5.2 ± 3.1	[2] BENNETT	08A	CLEO	$\psi(2S) \to \gamma\gamma\phi$

[1] ABLIKIM 11E reports $(25.8 \pm 5.2 \pm 2.3) \times 10^{-6}$ from a measurement of $[\Gamma(\chi_{c1}(1P) \to \gamma\phi)/\Gamma_{\rm total}] \times [B(\psi(2S) \to \gamma\chi_{c1}(1P))]$ assuming $B(\psi(2S) \to \gamma\chi_{c1}(1P)) = (9.2 \pm 0.4) \times 10^{-2}$, which we rescale to our best value $B(\psi(2S) \to \gamma\chi_{c1}(1P)) = (9.55 \pm 0.31) \times 10^{-2}$. Our first error is their experiment's error and our second error is the systematic error from using our best value.

[2] BENNETT 08A reports $< 26\times10^{-6}$ from a measurement of $[\Gamma(\chi_{c1}(1P) \to \gamma\phi)/\Gamma_{\rm total}] \times [B(\psi(2S) \to \gamma\chi_{c1}(1P))]$ assuming $B(\psi(2S) \to \gamma\chi_{c1}(1P)) = (8.7 \pm 0.4) \times 10^{-2}$, which we rescale to our best value $B(\psi(2S) \to \gamma\chi_{c1}(1P)) = 9.55 \times 10^{-2}$.

$\Gamma(\gamma\gamma)/\Gamma_{\rm total}$ Γ_{67}/Γ

VALUE (units 10^{-5})	CL%	DOCUMENT ID		TECN	COMMENT
• • • We do not use the following data for averages, fits, limits, etc. • • •					
< 3.5	90	ECKLUND	08A	CLEO	$\psi(2S) \to \gamma\chi_{c1} \to 3\gamma$
<150	90	[1] YAMADA	77	DASP	$e^+e^- \to 3\gamma$

[1] Estimated using $B(\psi(2S) \to \gamma\chi_{c1}(1P)) = 0.087$. The errors do not contain the uncertainty in the $\psi(2S)$ decay.

$\chi_{c1}(1P)$ CROSS-PARTICLE BRANCHING RATIOS

$\Gamma(\chi_{c1}(1P) \to p\overline{p})/\Gamma_{\rm total} \times \Gamma(\psi(2S) \to \gamma\chi_{c1}(1P))/\Gamma(\psi(2S) \to J/\psi(1S)\pi^+\pi^-)$ $\Gamma_{34}/\Gamma \times \Gamma^{\psi(2S)}_{129}/\Gamma^{\psi(2S)}_{11}$

VALUE (units 10^{-5})	DOCUMENT ID		TECN	COMMENT
2.14±0.11 OUR FIT				
1.1 ±1.0	[1] BAI	98I	BES	$\psi(2S) \to \gamma\chi_{c1} \to \gamma\overline{p}p$

[1] Calculated by us. The value for $B(\chi_{c1} \to p\overline{p})$ reported in BAI 98I is derived using $B(\psi(2S) \to \gamma\chi_{c1}) = (8.7 \pm 0.8)\%$ and $B(\psi(2S) \to J/\psi(1S)\pi^+\pi^-) = (32.4 \pm 2.6)\%$ [BAI 98D].

$\Gamma(\chi_{c1}(1P) \to \Lambda\overline{\Lambda})/\Gamma_{\rm total} \times \Gamma(\psi(2S) \to \gamma\chi_{c1}(1P))/\Gamma_{\rm total}$ $\Gamma_{47}/\Gamma \times \Gamma^{\psi(2S)}_{129}/\Gamma^{\psi(2S)}$

VALUE (units 10^{-6})	EVTS	DOCUMENT ID		TECN	COMMENT
11.1±1.1 OUR FIT					
10.9±1.1 OUR AVERAGE					
$11.2 \pm 1.0 \pm 0.9$	136	[1] ABLIKIM	13H	BES3	$\psi(2S) \to \gamma\Lambda\overline{\Lambda}$
$10.5 \pm 1.6 \pm 0.6$	46 ± 7	[2] NAIK	08	CLEO	$\psi(2S) \to \gamma\Lambda\overline{\Lambda}$

[1] Calculated by us. ABLIKIM 13H reports $B(\chi_{c1} \to \Lambda\overline{\Lambda}) = (12.2 \pm 1.1 \pm 1.1) \times 10^{-5}$ from a measurement of $B(\chi_{c1} \to \Lambda\overline{\Lambda}) \times B(\psi(2S) \to \gamma\chi_{c1})$ assuming $B(\psi(2S) \to \gamma\chi_{c1}) = (9.2 \pm 0.4)\%$.

[2] Calculated by us. NAIK 08 reports $B(\chi_{c1} \to \Lambda\overline{\Lambda}) = (11.6 \pm 1.8 \pm 0.7 \pm 0.7) \times 10^{-5}$ using $B(\psi(2S) \to \gamma\chi_{c1}) = (9.07 \pm 0.11 \pm 0.54)\%$.

$\Gamma(\chi_{c1}(1P) \to \Lambda\overline{\Lambda})/\Gamma_{\rm total} \times \Gamma(\psi(2S) \to \gamma\chi_{c1}(1P))/\Gamma(\psi(2S) \to J/\psi(1S)\pi^+\pi^-)$ $\Gamma_{47}/\Gamma \times \Gamma^{\psi(2S)}_{129}/\Gamma^{\psi(2S)}_{11}$

VALUE (units 10^{-5})	EVTS	DOCUMENT ID		TECN	COMMENT
3.22±0.31 OUR FIT					
7.1 $^{+2.8}_{-2.4}$ ±1.3	$9.0^{+3.5}_{-3.1}$	[1] BAI	03E	BES	$\psi(2S) \to \gamma\Lambda\overline{\Lambda}$

[1] BAI 03E reports [$B(\chi_{c1} \to \Lambda\overline{\Lambda})$ $B(\psi(2S) \to \gamma\chi_{c1})$ / $B(\psi(2S) \to J/\psi\pi^+\pi^-)$] × [$B^2(\Lambda \to \pi^- p)$ / $B(J/\psi \to p\overline{p})$] = $(1.33^{+0.52}_{-0.46} \pm 0.25)\%$. We calculate from this measurement the presented value using $B(\Lambda \to \pi^- p) = (63.9 \pm 0.5)\%$ and $B(J/\psi \to p\overline{p}) = (2.17 \pm 0.07) \times 10^{-3}$.

$\Gamma(\chi_{c1}(1P) \to \gamma J/\psi(1S))/\Gamma_{\rm total} \times \Gamma(\psi(2S) \to \gamma\chi_{c1}(1P))/\Gamma_{\rm total}$ $\Gamma_{63}/\Gamma \times \Gamma^{\psi(2S)}_{129}/\Gamma^{\psi(2S)}$

VALUE (units 10^{-2})	EVTS	DOCUMENT ID		TECN	COMMENT
3.24 ±0.07 OUR FIT					
2.93 ±0.15 OUR AVERAGE		Error includes scale factor of 1.4. See the ideogram below.			
$3.377 \pm 0.009 \pm 0.183$	142k	ABLIKIM	12O	BES3	$\psi(2S) \to \gamma\chi_{c1}$
2.81 ±0.05 ±0.23	13k	BAI	04I	BES2	$\psi(2S) \to J/\psi\gamma\gamma$
2.56 ±0.12 ±0.20		GAISER	86	CBAL	$\psi(2S) \to \gamma$X
2.78 ±0.30		[1] OREGLIA	82	CBAL	$\psi(2S) \to \gamma\chi_{c1}$
2.2 ±0.5		[2] BRANDELIK	79B	DASP	$\psi(2S) \to \gamma\chi_{c1}$
2.9 ±0.5		[2] BARTEL	78B	CNTR	$\psi(2S) \to \gamma\chi_{c1}$
5.0 ±1.5		[3] BIDDICK	77	CNTR	$e^+e^- \to \gamma$X
2.8 ±0.9		[1] WHITAKER	76	MRK1	e^+e^-
• • • We do not use the following data for averages, fits, limits, etc. • • •					
3.56 ±0.03 ±0.12	24.9k	[4] MENDEZ	08	CLEO	$\psi(2S) \to \gamma\chi_{c1}$
3.44 ±0.06 ±0.13	3.7k	[5] ADAM	05A	CLEO	Repl. by MENDEZ 08

[1] Recalculated by us using $B(J/\psi(1S) \to \ell^+\ell^-) = 0.1181 \pm 0.0020$.
[2] Recalculated by us using $B(J/\psi(1S) \to \mu^+\mu^-) = 0.0588 \pm 0.0010$.
[3] Assumes isotropic gamma distribution.
[4] Not independent from other measurements of MENDEZ 08.
[5] Not independent from other values reported by ADAM 05A.

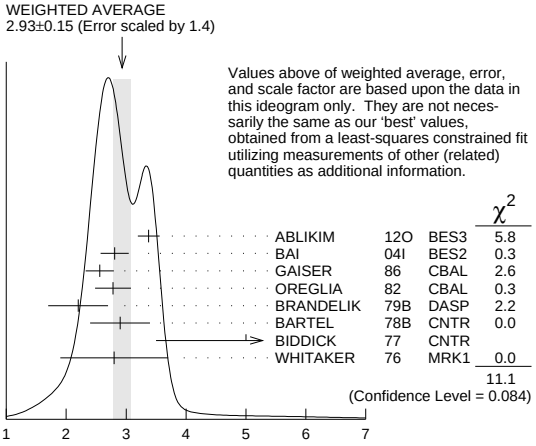

$\Gamma\left(\chi_{c1}(1P) \to \gamma J/\psi(1S)\right)/\Gamma_{\text{total}} \times \Gamma\left(\psi(2S) \to \gamma\chi_{c1}(1P)\right)/\Gamma_{\text{total}}$ (units 10^{-2})

$\Gamma(\chi_{c1}(1P) \to \gamma J/\psi(1S))/\Gamma_{\text{total}} \times \Gamma(\psi(2S) \to \gamma\chi_{c1}(1P))/\Gamma(\psi(2S) \to J/\psi(1S)\text{anything})$ $\Gamma_{63}/\Gamma \times \Gamma_{129}^{\psi(2S)}/\Gamma_{9}^{\psi(2S)}$

$\Gamma_{63}/\Gamma \times \Gamma_{129}^{\psi(2S)}/\Gamma_{9}^{\psi(2S)} = \Gamma_{63}/\Gamma \times \Gamma_{129}^{\psi(2S)}/(\Gamma_{11}^{\psi(2S)} + \Gamma_{12}^{\psi(2S)} + \Gamma_{13}^{\psi(2S)} + 0.339\Gamma_{129}^{\psi(2S)} + 0.192\Gamma_{130}^{\psi(2S)})$

VALUE (units 10^{-2})	EVTS	DOCUMENT ID		TECN	COMMENT
5.32±0.11 OUR FIT					
• • • We do not use the following data for averages, fits, limits, etc. • • •					
5.70±0.04±0.15	24.9k	[1] MENDEZ	08	CLEO	$\psi(2S) \to \gamma\chi_{c1}$
5.77±0.10±0.12	3.7k	ADAM	05A	CLEO	Repl. by MENDEZ 08

[1] Not independent from other measurements of MENDEZ 08.

$\Gamma(\chi_{c1}(1P) \to \gamma J/\psi(1S))/\Gamma_{\text{total}} \times \Gamma(\psi(2S) \to \gamma\chi_{c1}(1P))/\Gamma(\psi(2S) \to J/\psi(1S)\pi^+\pi^-)$ $\Gamma_{63}/\Gamma \times \Gamma_{129}^{\psi(2S)}/\Gamma_{11}^{\psi(2S)}$

VALUE (units 10^{-2})	EVTS	DOCUMENT ID		TECN	COMMENT
9.41±0.21 OUR FIT					
10.15±0.28 OUR AVERAGE					
10.17±0.07±0.27	24.9k	MENDEZ	08	CLEO	$\psi(2S) \to \gamma\chi_{c1}$
12.6 ±0.3 ±3.8	3k	[1] ABLIKIM	04B	BES	$\psi(2S) \to J/\psi X$
8.5 ±2.1		[2] HIMEL	80	MRK2	$\psi(2S) \to \gamma\chi_{c1}$
• • • We do not use the following data for averages, fits, limits, etc. • • •					
10.24±0.17±0.23	3.7k	[3] ADAM	05A	CLEO	Repl. by MENDEZ 08

[1] From a fit to the J/ψ recoil mass spectra.
[2] The value for $B(\psi(2S) \to \gamma\chi_{c1}) \times B(\chi_{c1} \to \gamma J/\psi(1S))$ quoted in HIMEL 80 is derived using $B(\psi(2S) \to J/\psi(1S)\pi^+\pi^-) = (33 \pm 3)\%$ and $B(J/\psi(1S) \to \ell^+\ell^-) = 0.138 \pm 0.018$. Calculated by us using $B(J/\psi(1S) \to \ell^+\ell^-) = 0.1181 \pm 0.0020$.
[3] Not independent from other values reported by ADAM 05A.

$\Gamma(\chi_{c1}(1P) \to \overline{K}^0 K^+\pi^- + \text{c.c.})/\Gamma_{\text{total}} \times \Gamma(\psi(2S) \to \gamma\chi_{c1}(1P))/\Gamma_{\text{total}}$ $\Gamma_{15}/\Gamma \times \Gamma_{129}^{\psi(2S)}/\Gamma^{\psi(2S)}$

VALUE (units 10^{-4})	DOCUMENT ID			TECN	COMMENT
6.8±0.5 OUR FIT					
7.2±0.6 OUR AVERAGE					
7.3±0.5±0.5	[1] ATHAR	07	CLEO		$\psi(2S) \to \gamma K_S^0 K^+\pi^-$
7.0±0.5±0.9	[2] ABLIKIM	06R	BES2		$\psi(2S) \to \gamma\chi_{c1}$

[1] Calculated by us. The value of $B(\chi_{c1} \to K^0 K^+\pi^- + \text{c.c.})$ reported by ATHAR 07 was derived using $B(\psi(2S) \to \gamma\chi_{c1}(1P)) = (9.07 \pm 0.11 \pm 0.54)\%$.
[2] Calculated by us. ABLIKIM 06R reports $B(\chi_{c1} \to K_S^0 K^+\pi^-) = (4.0 \pm 0.3 \pm 0.5) \times 10^{-3}$. We use $B(\psi(2S) \to \gamma\chi_{c1}) = (8.7 \pm 0.4) \times 10^{-2}$.

$\Gamma(\chi_{c1}(1P) \to \overline{K}^0 K^+\pi^- + \text{c.c.})/\Gamma_{\text{total}} \times \Gamma(\psi(2S) \to \gamma\chi_{c1}(1P))/\Gamma(\psi(2S) \to J/\psi(1S)\pi^+\pi^-)$ $\Gamma_{15}/\Gamma \times \Gamma_{129}^{\psi(2S)}/\Gamma_{11}^{\psi(2S)}$

VALUE (units 10^{-4})	DOCUMENT ID			TECN	COMMENT
19.7±1.6 OUR FIT					
13.2±2.4±3.2	[1] BAI	99B	BES		$\psi(2S) \to \gamma K_S^0 K^+\pi^-$

[1] Calculated by us. The value of $B(\chi_{c1} \to K_S^0 K^+\pi^-)$ reported by BAI 99B was derived using $B(\psi(2S) \to \gamma\chi_{c1}(1P)) = (8.7 \pm 0.8)\%$ and $B(\psi(2S) \to J/\psi\pi^+\pi^-) = (32.4 \pm 2.6)\%$ [BAI 98D].

$\Gamma(\chi_{c1}(1P) \to K^+K^-K^+K^-)/\Gamma_{\text{total}} \times \Gamma(\psi(2S) \to \gamma\chi_{c1}(1P))/\Gamma_{\text{total}}$ $\Gamma_{29}/\Gamma \times \Gamma_{129}^{\psi(2S)}/\Gamma^{\psi(2S)}$

VALUE (units 10^{-4})	EVTS	DOCUMENT ID		TECN	COMMENT
0.52±0.11 OUR FIT					
0.61±0.11±0.08	54	[1] ABLIKIM	06T	BES2	$\psi(2S) \to \gamma K^+K^+K^-K^-$

[1] Calculated by us. The value of $B(\chi_{c1} \to 2K^+2K^-)$ reported by ABLIKIM 06T was derived using $B(\psi(2S) \to \gamma\chi_{c1}(1P)) = (8.7 \pm 0.8)\%$.

$\Gamma(\chi_{c1}(1P) \to K^+K^-K^+K^-)/\Gamma_{\text{total}} \times \Gamma(\psi(2S) \to \gamma\chi_{c1}(1P))/\Gamma(\psi(2S) \to J/\psi(1S)\pi^+\pi^-)$ $\Gamma_{29}/\Gamma \times \Gamma_{129}^{\psi(2S)}/\Gamma_{11}^{\psi(2S)}$

VALUE (units 10^{-4})	DOCUMENT ID			TECN	COMMENT
1.52±0.31 OUR FIT					
1.13±0.40±0.29	[1] BAI	99B	BES		$\psi(2S) \to \gamma K^+K^+K^-K^-$

[1] Calculated by us. The value of $B(\chi_{c1} \to 2K^+2K^-)$ reported by BAI 99B was derived using $B(\psi(2S) \to \gamma\chi_{c1}(1P)) = (8.7 \pm 0.8)\%$ and $B(\psi(2S) \to J/\psi\pi^+\pi^-) = (32.4 \pm 2.6)\%$ [BAI 98D].

$\Gamma(\chi_{c1}(1P) \to p\overline{p})/\Gamma_{\text{total}} \times \Gamma(\psi(2S) \to \gamma\chi_{c1}(1P))/\Gamma_{\text{total}}$ $\Gamma_{34}/\Gamma \times \Gamma_{129}^{\psi(2S)}/\Gamma^{\psi(2S)}$

VALUE (units 10^{-6})	EVTS	DOCUMENT ID		TECN	COMMENT
7.4±0.4 OUR FIT					
7.8±0.6 OUR AVERAGE Error includes scale factor of 1.4. See the ideogram below.					
7.9±0.4±0.3	453	ABLIKIM	13V	BES3	$\psi(2S) \to \gamma p\overline{p}$
8.2±0.7±0.4	141 ± 13	[1] NAIK	08	CLEO	$\psi(2S) \to \gamma p\overline{p}$
$4.8^{+1.4}_{-1.3}\pm0.6$	$18.2^{+5.5}_{-4.9}$	BAI	04F	BES	$\psi(2S) \to \gamma\chi_{c1}(1P) \to \gamma\overline{p}p$

[1] Calculated by us. NAIK 08 reports $B(\chi_{c1} \to p\overline{p}) = (9.0 \pm 0.8 \pm 0.4 \pm 0.5) \times 10^{-5}$ using $B(\psi(2S) \to \gamma\chi_{c1}) = (9.07 \pm 0.11 \pm 0.54)\%$.

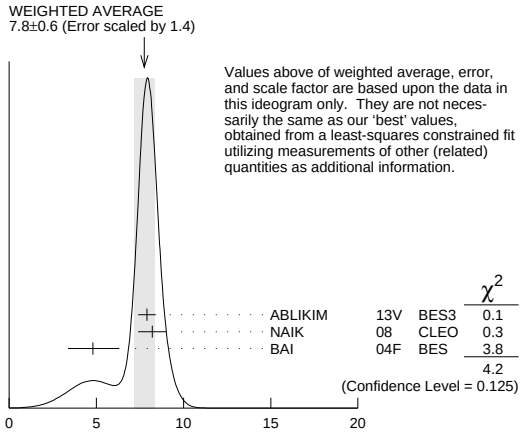

$\Gamma\left(\chi_{c1}(1P) \to p\overline{p}\right)/\Gamma_{\text{total}} \times \Gamma\left(\psi(2S) \to \gamma\chi_{c1}(1P)\right)/\Gamma_{\text{total}}$ (units 10^{-6})

MULTIPOLE AMPLITUDES IN $\chi_{c1}(1P) \to \gamma J/\psi(1S)$

$a_2 = M2/\sqrt{E1^2 + M2^2}$ Magnetic quadrupole fractional transition amplitude

VALUE (units 10^{-2})	EVTS	DOCUMENT ID		TECN	COMMENT
$-5.4\ ^{+1.2}_{-1.5}$ **OUR AVERAGE**		Error includes scale factor of 2.4. See the ideogram below.			
−6.26±0.63±0.24	39k	ARTUSO	09	CLEO	$\psi(2S) \to \gamma\gamma\ell^+\ell^-$
0.2 ±3.2 ±0.4	2090	AMBROGIANI	02	E835	$p\overline{p} \to \chi_{c1} \to J/\psi\gamma$
$-0.2\ ^{+0.8}_{-2.0}$	921	OREGLIA	82	CBAL	$\psi(2S) \to \chi_{c1}\gamma \to J/\psi\gamma\gamma$

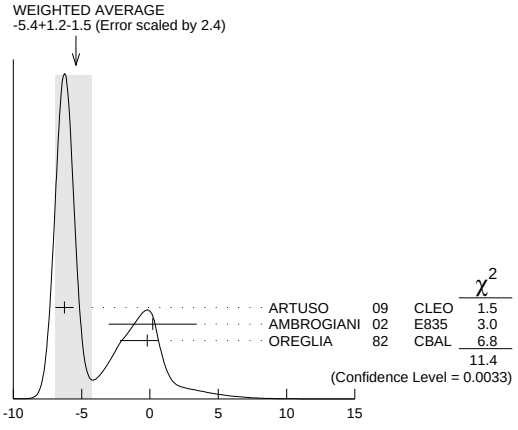

$a_2 = M2/\sqrt{E1^2 + M2^2}$ (units 10^{-2})

Meson Particle Listings

$\chi_{c1}(1P)$, $h_c(1P)$

MULTIPOLE AMPLITUDES IN $\psi(2S) \to \gamma\chi_{c1}(1S)$ RADIATIVE DECAY

$b_2 = M2/\sqrt{E1^2 + M2^2}$ Magnetic quadrupole fractional transition amplitude

VALUE (units 10^{-2})	EVTS	DOCUMENT ID		TECN	COMMENT
2.9 ±0.8 OUR AVERAGE					
$2.76 \pm 0.73 \pm 0.23$	39k	ARTUSO	09	CLEO	$\psi(2S) \to \gamma\gamma\ell^+\ell^-$
$7.7\ ^{+5.0}_{-4.5}$	921	OREGLIA	82	CBAL	$\psi(2S) \to \gamma\gamma\ell^+\ell^-$

MULTIPOLE AMPLITUDE RATIOS IN RADIATIVE DECAYS $\psi(2S) \to \gamma\chi_{c1}(1S)$ and $\chi_{c1} \to \gamma J/\psi(1S)$

a_2/b_2 Magnetic quadrupole transition amplitude ratio

VALUE	EVTS	DOCUMENT ID		TECN	COMMENT
$\mathbf{-2.27^{+0.57}_{-0.99}}$	39k	[1] ARTUSO	09	CLEO	$\psi(2S) \to \gamma\gamma\ell^+\ell^-$

[1] Statistical and systematic errors combined. Not independent of $a_2(\chi_{c1})$ and $b_2(\chi_{c1})$ values from ARTUSO 09.

$\chi_{c1}(1P)$ REFERENCES

ABLIKIM	13D	PR D87 012007	M. Ablikim *et al.*	(BES III Collab.)
ABLIKIM	13H	PR D87 032007	M. Ablikim *et al.*	(BES III Collab.)
ABLIKIM	13V	PR D88 112001	M. Ablikim *et al.*	(BES III Collab.)
ABLIKIM	12I	PR D86 052004	M. Ablikim *et al.*	(BES III Collab.)
ABLIKIM	12J	PR D86 052011	M. Ablikim *et al.*	(BES III Collab.)
ABLIKIM	12O	PRL 109 172002	M. Ablikim *et al.*	(BES III Collab.)
ABLIKIM	11A	PR D83 012006	M. Ablikim *et al.*	(BES III Collab.)
ABLIKIM	11D	PR D83 032003	M. Ablikim *et al.*	(BES III Collab.)
ABLIKIM	11E	PR D83 112005	M. Ablikim *et al.*	(BES III Collab.)
ABLIKIM	11F	PR D83 112009	M. Ablikim *et al.*	(BES III Collab.)
ABLIKIM	11K	PRL 107 092001	M. Ablikim *et al.*	(BES III Collab.)
ONYISI	10	PR D82 011103	P.U.E. Onyisi *et al.*	(CLEO Collab.)
ARTUSO	09	PR D80 112003	M. Artuso *et al.*	(CLEO Collab.)
BENNETT	08A	PRL 101 151801	J.V. Bennett *et al.*	(CLEO Collab.)
ECKLUND	08A	PR D78 091501	K.M. Ecklund *et al.*	(CLEO Collab.)
HE	08B	PR D78 092004	Q. He *et al.*	(CLEO Collab.)
MENDEZ	08	PR D78 011102	H. Mendez *et al.*	(CLEO Collab.)
NAIK	08	PR D78 031101	P. Naik *et al.*	(CLEO Collab.)
ATHAR	07	PR D75 032002	S.B. Athar *et al.*	(CLEO Collab.)
ABLIKIM	06D	PR D73 052006	M. Ablikim *et al.*	(BES Collab.)
ABLIKIM	06R	PR D74 072001	M. Ablikim *et al.*	(BES Collab.)
ABLIKIM	06T	PL B642 197	M. Ablikim *et al.*	(BES Collab.)
ABLIKIM	05G	PR D71 092002	M. Ablikim *et al.*	(BES Collab.)
ABLIKIM	05O	PL B630 21	M. Ablikim *et al.*	(BES Collab.)
ADAM	05A	PRL 94 232002	N.E. Adam *et al.*	(CLEO Collab.)
ANDREOTTI	05A	NP B717 34	M. Andreotti *et al.*	(FNAL E835 Collab.)
ABLIKIM	04B	PR D70 012003	M. Ablikim *et al.*	(BES Collab.)
ABLIKIM	04H	PR D70 092003	M. Ablikim *et al.*	(BES Collab.)
ATHAR	04	PR D70 112002	S.B. Athar *et al.*	(CLEO Collab.)
BAI	04F	PR D69 092001	J.Z. Bai *et al.*	(BES Collab.)
BAI	04I	PR D70 012006	J.Z. Bai *et al.*	(BES Collab.)
AULCHENKO	03	PL B573 63	V.M. Aulchenko *et al.*	(KEDR Collab.)
BAI	03E	PR D67 112001	J.Z. Bai *et al.*	(BES Collab.)
AMBROGIANI	02	PR D65 052002	M. Ambrogiani *et al.*	(FNAL E835 Collab.)
BAI	99B	PR D60 072001	J.Z. Bai *et al.*	(BES Collab.)
BAI	98D	PR D58 092006	J.Z. Bai *et al.*	(BES Collab.)
BAI	98I	PRL 81 3091	J.Z. Bai *et al.*	(BES Collab.)
ARMSTRONG	92	NP B373 35	T.A. Armstrong *et al.*	(FNAL, FERR, GENO+)
Also		PRL 68 1468	T.A. Armstrong *et al.*	(FNAL, FERR, GENO+)
BAGLIN	86B	PL B172 455	C. Baglin	(LAPP, CERN, GENO, LYON, OSLO+)
GAISER	86	PR D34 711	J. Gaiser *et al.*	(Crystal Ball Collab.)
LEMOIGNE	82	PL 113B 509	Y. Lemoigne *et al.*	(SACL, LOIC, SHMP+)
OREGLIA	82	PR D25 2259	M.J. Oreglia *et al.*	(SLAC, CIT, HARV+)
Also		Private Comm.	M.J. Oreglia	(EFI)
HIMEL	80	PRL 44 920	T. Himel *et al.*	(LBL, SLAC)
Also		Private Comm.	G. Trilling	(LBL, UCB)
BRANDELIK	79B	NP B160 426	R. Brandelik *et al.*	(DASP Collab.)
BARTEL	78B	PL 79B 492	W. Bartel *et al.*	(DESY, HEIDP)
TANENBAUM	78	PR D17 1731	W.M. Tanenbaum *et al.*	(SLAC, LBL)
Also		Private Comm.	G. Trilling	(LBL, UCB)
BIDDICK	77	PRL 38 1324	C.J. Biddick *et al.*	(UCSD, UMD, PAVI+)
FELDMAN	77	PRPL 33C 285	G.J. Feldman, M.L. Perl	(LBL, SLAC)
YAMADA	77	Hamburg Conf. 69	S. Yamada	(DASP Collab.)
WHITAKER	76	PRL 37 1596	J.S. Whitaker *et al.*	(SLAC, LBL)
TANENBAUM	75	PRL 35 1323	W.M. Tanenbaum *et al.*	(LBL, SLAC)

$h_c(1P)$

$I^G(J^{PC}) = ?^?(1^{+-})$

Quantum numbers are quark model prediction, $C = -$ established by $\eta_c\gamma$ decay.

$h_c(1P)$ MASS

VALUE (MeV)	EVTS	DOCUMENT ID		TECN	COMMENT
3525.38±0.11 OUR AVERAGE					
$3525.31 \pm 0.11 \pm 0.14$	832	[1] ABLIKIM	12N	BES3	$\psi(2S) \to \pi^0\gamma$ hadrons
$3525.40 \pm 0.13 \pm 0.18$	3679	ABLIKIM	10B	BES3	$\psi(2S) \to \pi^0\gamma\eta_c$
$3525.20 \pm 0.18 \pm 0.12$	1282	[2] DOBBS	08A	CLEO	$\psi(2S) \to \pi^0\eta_c\gamma$
$3525.8 \pm 0.2 \pm 0.2$	13	ANDREOTTI	05B	E835	$\overline{p}p \to \eta_c\gamma$
• • • We do not use the following data for averages, fits, limits, etc. • • •					
3525.6 ± 0.5	92^{+23}_{-22}	ADAMS	09	CLEO	$\psi(2S) \to 2(\pi^+\pi^-\pi^0)$
$3524.4 \pm 0.6 \pm 0.4$	168 ± 40	[3] ROSNER	05	CLEO	$\psi(2S) \to \pi^0\eta_c\gamma$
3527 ± 8	42	ANTONIAZZI	94	E705	300 $\pi^\pm$, pLi $\to J/\psi\pi^0$X
$3526.28 \pm 0.18 \pm 0.19$	59	[4] ARMSTRONG	92D	E760	$\overline{p}p \to J/\psi\pi^0$
$3525.4 \pm 0.8 \pm 0.4$	5	BAGLIN	86	SPEC	$\overline{p}p \to J/\psi$X

[1] With floating width.
[2] Combination of exclusive and inclusive analyses for the reaction $\psi(2S) \to \pi^0 h_c \to \pi^0\eta_c\gamma$. This result is the average of DOBBS 08A and ROSNER 05.
[3] Superseded by DOBBS 08A.
[4] Mass central value and systematic error recalculated by us according to Eq. (16) in ARMSTRONG 93B, using the value for the $\psi(2S)$ mass from AULCHENKO 03.

$h_c(1P)$ WIDTH

VALUE (MeV)	CL%	EVTS	DOCUMENT ID		TECN	COMMENT
0.70±0.28±0.22		832	[5] ABLIKIM	12N	BES3	$\psi(2S) \to \pi^0\gamma$ hadrons
• • • We do not use the following data for averages, fits, limits, etc. • • •						
< 1.44	90	3679	[6] ABLIKIM	10B	BES3	$\psi(2S) \to \pi^0\gamma\eta_c$
< 1		13	ANDREOTTI	05B	E835	$\overline{p}p \to \eta_c\gamma$
< 1.1	90	59	ARMSTRONG	92D	E760	$\overline{p}p \to J/\psi\pi^0$

[5] With floating mass.
[6] The central value is $\Gamma = 0.73 \pm 0.45 \pm 0.28$ MeV.

$h_c(1P)$ DECAY MODES

	Mode	Fraction (Γ_i/Γ)	Confidence level
Γ_1	$J/\psi(1S)\pi^0$		
Γ_2	$J/\psi(1S)\pi\pi$	not seen	
Γ_3	$p\overline{p}$	$< 1.5 \times 10^{-4}$	90%
Γ_4	$\eta_c(1S)\gamma$	(51 ±6) %	
Γ_5	$\pi^+\pi^-\pi^0$	$< 2.2 \times 10^{-3}$	
Γ_6	$2\pi^+2\pi^-\pi^0$	$(\ 2.2^{+0.8}_{-0.7})$ %	
Γ_7	$3\pi^+3\pi^-\pi^0$	< 2.9 %	

$h_c(1P)$ PARTIAL WIDTHS

$h_c(1P)$ Γ(i)$\Gamma(\overline{p}p)/\Gamma$(total)

$\Gamma(\eta_c(1S)\gamma) \times \Gamma(p\overline{p})/\Gamma_{\text{total}}$ **$\Gamma_4\Gamma_3/\Gamma$**

VALUE (eV)	EVTS	DOCUMENT ID		TECN	COMMENT
• • • We do not use the following data for averages, fits, limits, etc. • • •					
12.0 ± 4.5	13	[7] ANDREOTTI	05B	E835	$\overline{p}p \to \eta_c\gamma$

[7] Assuming $\Gamma = 1$ MeV.

$h_c(1P)$ BRANCHING RATIOS

$\Gamma(J/\psi(1S)\pi\pi)/\Gamma(J/\psi(1S)\pi^0)$ **Γ_2/Γ_1**

VALUE	CL%	DOCUMENT ID		TECN	COMMENT
<0.18	90	ARMSTRONG	92D	E760	$\overline{p}p \to J/\psi\pi^0$

$\Gamma(\eta_c(1S)\gamma)/\Gamma_{\text{total}}$ **Γ_4/Γ**

VALUE (units 10^{-2})	EVTS	DOCUMENT ID		TECN	COMMENT
51 ± 6 OUR AVERAGE					
$54.3 \pm 6.7 \pm 5.2$	3679	ABLIKIM	10B	BES3	$\psi(2S) \to \pi^0\gamma\eta_c$
48 ± 6 ±7		[8] DOBBS	08A	CLEO	$\psi(2S) \to \pi^0\eta_c\gamma$
• • • We do not use the following data for averages, fits, limits, etc. • • •					
48 ± 6 ±7	1282	[9] DOBBS	08A	CLEO	$\psi(2S) \to \pi^0\eta_c\gamma$
46 ±12 ±7	168	[10] ROSNER	05	CLEO	$\psi(2S) \to \pi^0\eta_c\gamma$

[8] Average of DOBBS 08A and ROSNER 05. DOBBS 08A reports $[\Gamma(h_c(1P) \to \eta_c(1S)\gamma)/\Gamma_{\text{total}}] \times [B(\psi(2S) \to \pi^0 h_c(1P))] = (4.16 \pm 0.30 \pm 0.37) \times 10^{-4}$ which we divide by our best value $B(\psi(2S) \to \pi^0 h_c(1P)) = (8.6 \pm 1.3) \times 10^{-4}$. Our first error is their experiment's error and our second error is the systematic error from using our best value.
[9] DOBBS 08A reports $[\Gamma(h_c(1P) \to \eta_c(1S)\gamma)/\Gamma_{\text{total}}] \times [B(\psi(2S) \to \pi^0 h_c(1P))] = (4.19 \pm 0.32 \pm 0.45) \times 10^{-4}$ which we divide by our best value $B(\psi(2S) \to \pi^0 h_c(1P)) = (8.6 \pm 1.3) \times 10^{-4}$. Our first error is their experiment's error and our second error is the systematic error from using our best value.
[10] ROSNER 05 reports $[\Gamma(h_c(1P) \to \eta_c(1S)\gamma)/\Gamma_{\text{total}}] \times [B(\psi(2S) \to \pi^0 h_c(1P))] = (4.0 \pm 0.8 \pm 0.7) \times 10^{-4}$ which we divide by our best value $B(\psi(2S) \to \pi^0 h_c(1P)) = (8.6 \pm 1.3) \times 10^{-4}$. Our first error is their experiment's error and our second error is the systematic error from using our best value.

$\Gamma(\pi^+\pi^-\pi^0)/\Gamma_{\text{total}}$ **Γ_5/Γ**

VALUE (units 10^{-3})	DOCUMENT ID		TECN	COMMENT
<2.2	[11] ADAMS	09	CLEO	$\psi(2S) \to \pi^0\gamma\eta_c$

[11] ADAMS 09 reports $[\Gamma(h_c(1P) \to \pi^+\pi^-\pi^0)/\Gamma_{\text{total}}] \times [B(\psi(2S) \to \pi^0 h_c(1P))] < 0.19 \times 10^{-5}$ which we divide by our best value $B(\psi(2S) \to \pi^0 h_c(1P)) = 8.6 \times 10^{-4}$.

$\Gamma(2\pi^+2\pi^-\pi^0)/\Gamma_{\text{total}}$ **Γ_6/Γ**

VALUE (units 10^{-2})	EVTS	DOCUMENT ID		TECN	COMMENT
$\mathbf{2.2^{+0.8}_{-0.6} \pm 0.3}$	92	[12] ADAMS	09	CLEO	$\psi(2S) \to \pi^0\gamma\eta_c$

[12] ADAMS 09 reports $[\Gamma(h_c(1P) \to 2\pi^+2\pi^-\pi^0)/\Gamma_{\text{total}}] \times [B(\psi(2S) \to \pi^0 h_c(1P))] = (1.88^{+0.48}_{-0.45} \pm 0.47) \times 10^{-5}$ which we divide by our best value $B(\psi(2S) \to \pi^0 h_c(1P)) = (8.6 \pm 1.3) \times 10^{-4}$. Our first error is their experiment's error and our second error is the systematic error from using our best value.

$\Gamma(3\pi^+3\pi^-\pi^0)/\Gamma_{\rm total}$ Γ_7/Γ

VALUE (units 10^{-2})	DOCUMENT ID		TECN	COMMENT
<2.9	[13] ADAMS	09	CLEO	$\psi(2S) \to \pi^0\gamma\eta_c$

[13] ADAMS 09 reports $[\Gamma(h_c(1P) \to 3\pi^+3\pi^-\pi^0)/\Gamma_{\rm total}] \times [B(\psi(2S) \to \pi^0 h_c(1P))] < 2.5\times10^{-5}$ which we divide by our best value $B(\psi(2S) \to \pi^0 h_c(1P)) = 8.6\times10^{-4}$.

$\Gamma(h_c(1P) \to \eta_c(1S)\gamma)/\Gamma_{\rm total} \times \Gamma(\psi(2S) \to \pi^0 h_c(1P))/\Gamma_{\rm total}$ $\Gamma_4/\Gamma \times \Gamma_{15}^{\psi(2S)}/\Gamma^{\psi(2S)}$

VALUE (units 10^{-4})	EVTS	DOCUMENT ID		TECN	COMMENT
4.3 ±0.4 OUR AVERAGE					
4.58±0.40±0.50	3679	[14] ABLIKIM	10B	BES3	$\psi(2S) \to \pi^0\gamma X$
4.16±0.30±0.37	1430	[15] DOBBS	08A	CLEO	$\psi(2S) \to \pi^0\gamma\eta_c$

[14] Not independent of other branching fractions in ABLIKIM 10B.
[15] Not independent of other branching fractions in DOBBS 08A.

$\Gamma(h_c(1P) \to p\overline{p})/\Gamma_{\rm total} \times \Gamma(\psi(2S) \to \pi^0 h_c(1P))/\Gamma_{\rm total}$ $\Gamma_3/\Gamma \times \Gamma_{15}^{\psi(2S)}/\Gamma^{\psi(2S)}$

VALUE	CL%	DOCUMENT ID		TECN	COMMENT
$<1.3\times10^{-7}$	90	ABLIKIM	13V	BES3	$\psi(2S) \to \gamma p\overline{p}$

$h_c(1P)$ REFERENCES

ABLIKIM	13V	PR D88 112001	M. Ablikim *et al.*	(BES III Collab.)
ABLIKIM	12N	PR D86 092009	M. Ablikim *et al.*	(BES III Collab.)
ABLIKIM	10B	PRL 104 132002	M. Ablikim *et al.*	(BES III Collab.)
ADAMS	09	PR D80 051106	G.S. Adams *et al.*	(CLEO Collab.)
DOBBS	08A	PRL 101 182003	S. Dobbs *et al.*	(CLEO Collab.)
ANDREOTTI	05B	PR D72 032001	M. Andreotti *et al.*	(FNAL E835 Collab.)
ROSNER	05	PRL 95 102003	J.L. Rosner *et al.*	(CLEO Collab.)
AULCHENKO	03	PL B573 63	V.M. Aulchenko *et al.*	(KEDR Collab.)
ANTONIAZZI	94	PR D50 4258	L. Antoniazzi *et al.*	(E705 Collab.)
ARMSTRONG	93B	PR D47 772	T.A. Armstrong *et al.*	(FNAL E760 Collab.)
ARMSTRONG	92D	PRL 69 2337	T.A. Armstrong *et al.*	(FNAL, FERR, GENO+)
BAGLIN	86	PL B171 135	C. Baglin *et al.*	(LAPP, CERN, TORI, STRB+)

$\chi_{c2}(1P)$

$I^G(J^{PC}) = 0^+(2^{++})$

See the Review on "$\psi(2S)$ and χ_c branching ratios" before the $\chi_{c0}(1P)$ Listings.

$\chi_{c2}(1P)$ MASS

VALUE (MeV)			EVTS	DOCUMENT ID		TECN	COMMENT
3556.20 ± 0.09 OUR AVERAGE							
3555.3	± 0.6	±2.2	2.5k	UEHARA	08	BELL	$\gamma\gamma \to$ hadrons
3555.70	± 0.59	±0.39		ABLIKIM	05G	BES2	$\psi(2S) \to \gamma\chi_{c2}$
3556.173	± 0.123	±0.020		ANDREOTTI	05A	E835	$p\overline{p} \to e^+e^-\gamma$
3559.9	± 2.9			EISENSTEIN	01	CLE2	$e^+e^- \to e^+e^-\chi_{c2}$
3556.4	± 0.7			BAI	99B	BES	$\psi(2S) \to \gamma$X
3556.22	± 0.131	±0.020	585	[1] ARMSTRONG	92	E760	$\overline{p}p \to e^+e^-\gamma$
3556.9	± 0.4	±0.5	50	BAGLIN	86B	SPEC	$\overline{p}p \to e^+e^-$X
3557.8	± 0.2	±4		[2] GAISER	86	CBAL	$\psi(2S) \to \gamma$X
3553.4	± 2.2		66	[3] LEMOIGNE	82	GOLI	185 π^-Be $\to \gamma\mu^+\mu^-$A
3555.9	± 0.7			[4] OREGLIA	82	CBAL	$e^+e^- \to J/\psi 2\gamma$
3557	± 1.5		69	[5] HIMEL	80	MRK2	$e^+e^- \to J/\psi 2\gamma$
3551	±11		15	BRANDELIK	79B	DASP	$e^+e^- \to J/\psi 2\gamma$
3553	± 4			[5] BARTEL	78B	CNTR	$e^+e^- \to J/\psi 2\gamma$
3553	± 4	±4		[5,6] TANENBAUM	78	MRK1	e^+e^-
3563	± 7		360	[5] BIDDICK	77	CNTR	$e^+e^- \to \gamma$X
• • • We do not use the following data for averages, fits, limits, etc. • • •							
3555.4	± 1.3		53	UEHARA	13	BELL	$\gamma\gamma \to K^0_S K^0_S$
3543	±10		4	WHITAKER	76	MRK1	$e^+e^- \to J/\psi 2\gamma$

[1] Recalculated by ANDREOTTI 05A, using the value of $\psi(2S)$ mass from AULCHENKO 03.
[2] Using mass of $\psi(2S) = 3686.0$ MeV.
[3] $J/\psi(1S)$ mass constrained to 3097 MeV.
[4] Assuming $\psi(2S)$ mass = 3686 MeV and $J/\psi(1S)$ mass = 3097 MeV.
[5] Mass value shifted by us by amount appropriate for $\psi(2S)$ mass = 3686 MeV and $J/\psi(1S)$ mass = 3097 MeV.
[6] From a simultaneous fit to radiative and hadronic decay channels.

$\chi_{c2}(1P)$ WIDTH

VALUE (MeV)	EVTS	DOCUMENT ID		TECN	COMMENT
1.93 ±0.11 OUR FIT					
1.95 ±0.13 OUR AVERAGE					
1.915±0.188±0.013		ANDREOTTI	05A	E835	$p\overline{p} \to e^+e^-\gamma$
1.96 ±0.17 ±0.07	585	[1] ARMSTRONG	92	E760	$\overline{p}p \to e^+e^-\gamma$
$2.6\ ^{+1.4}_{-1.0}$	50	BAGLIN	86B	SPEC	$\overline{p}p \to e^+e^-$X
$2.8\ ^{+2.1}_{-2.0}$		[2] GAISER	86	CBAL	$\psi(2S) \to \gamma$X

[1] Recalculated by ANDREOTTI 05A.
[2] Errors correspond to 90% confidence level; authors give only width range.

$\chi_{c2}(1P)$ DECAY MODES

	Mode	Fraction (Γ_i/Γ)	Confidence level
	Hadronic decays		
Γ_1	$2(\pi^+\pi^-)$	(1.07±0.10) %	
Γ_2	$\rho\rho$		
Γ_3	$\pi^+\pi^-\pi^0\pi^0$	(1.92±0.25) %	
Γ_4	$\rho^+\pi^-\pi^0$ + c.c.	(2.3 ±0.4) %	
Γ_5	$4\pi^0$	(1.16±0.16) $\times10^{-3}$	
Γ_6	$K^+K^-\pi^0\pi^0$	(2.2 ±0.4) $\times10^{-3}$	
Γ_7	$K^+\pi^-\overline{K}^0\pi^0$ + c.c.	(1.44±0.21) %	
Γ_8	$\rho^-K^+\overline{K}^0$ + c.c.	(4.3 ±1.3) $\times10^{-3}$	
Γ_9	$K^*(892)^0K^-\pi^+ \to K^-\pi^+K^0\pi^0$ + c.c.	(3.1 ±0.8) $\times10^{-3}$	
Γ_{10}	$K^*(892)^0\overline{K}^0\pi^0 \to K^+\pi^-\overline{K}^0\pi^0$ + c.c.	(4.0 ±0.9) $\times10^{-3}$	
Γ_{11}	$K^*(892)^-K^+\pi^0 \to K^+\pi^-\overline{K}^0\pi^0$ + c.c.	(3.9 ±0.9) $\times10^{-3}$	
Γ_{12}	$K^*(892)^+\overline{K}^0\pi^- \to K^+\pi^-\overline{K}^0\pi^0$ + c.c.	(3.1 ±0.8) $\times10^{-3}$	
Γ_{13}	$K^+K^-\eta\pi^0$	(1.3 ±0.5) $\times10^{-3}$	
Γ_{14}	$K^+K^-\pi^+\pi^-$	(8.8 ±1.0) $\times10^{-3}$	
Γ_{15}	$K^+K^-\pi^+\pi^-\pi^0$	(1.23±0.34) %	
Γ_{16}	$K^+\overline{K}^*(892)^0\pi^-$ + c.c.	(2.2 ±1.1) $\times10^{-3}$	
Γ_{17}	$K^*(892)^0\overline{K}^*(892)^0$	(2.4 ±0.5) $\times10^{-3}$	
Γ_{18}	$3(\pi^+\pi^-)$	(8.6 ±1.8) $\times10^{-3}$	
Γ_{19}	$\phi\phi$	(1.12±0.10) $\times10^{-3}$	
Γ_{20}	$\omega\omega$	(8.8 ±1.1) $\times10^{-4}$	
Γ_{21}	$\omega\phi$		
Γ_{22}	$\pi\pi$	(2.33±0.12) $\times10^{-3}$	
Γ_{23}	$\rho^0\pi^+\pi^-$	(3.8 ±1.6) $\times10^{-3}$	
Γ_{24}	$\pi^+\pi^-\eta$	(5.0 ±1.3) $\times10^{-4}$	
Γ_{25}	$\pi^+\pi^-\eta'$	(5.2 ±1.9) $\times10^{-4}$	
Γ_{26}	$\eta\eta$	(5.7 ±0.5) $\times10^{-4}$	
Γ_{27}	K^+K^-	(1.05±0.07) $\times10^{-3}$	
Γ_{28}	$K^0_S K^0_S$	(5.5 ±0.4) $\times10^{-4}$	
Γ_{29}	$\overline{K}^0K^+\pi^-$ + c.c.	(1.34±0.19) $\times10^{-3}$	
Γ_{30}	$K^+K^-\pi^0$	(3.2 ±0.8) $\times10^{-4}$	
Γ_{31}	$K^+K^-\eta$	< 3.4 $\times10^{-4}$	90%
Γ_{32}	$\eta\eta'$	< 6 $\times10^{-5}$	90%
Γ_{33}	$\eta'\eta'$	< 1.0 $\times10^{-4}$	90%
Γ_{34}	$\pi^+\pi^-K^0_S K^0_S$	(2.3 ±0.6) $\times10^{-3}$	
Γ_{35}	$K^+K^-K^0_S K^0_S$	< 4 $\times10^{-4}$	90%
Γ_{36}	$K^+K^-K^+K^-$	(1.73±0.21) $\times10^{-3}$	
Γ_{37}	$K^+K^-\phi$	(1.48±0.31) $\times10^{-3}$	
Γ_{38}	$p\overline{p}$	(7.5 ±0.4) $\times10^{-5}$	
Γ_{39}	$p\overline{p}\pi^0$	(4.9 ±0.4) $\times10^{-4}$	
Γ_{40}	$p\overline{p}\eta$	(1.82±0.26) $\times10^{-4}$	
Γ_{41}	$p\overline{p}\omega$	(3.8 ±0.5) $\times10^{-4}$	
Γ_{42}	$p\overline{p}\phi$	(2.9 ±0.9) $\times10^{-5}$	
Γ_{43}	$p\overline{p}\pi^+\pi^-$	(1.32±0.34) $\times10^{-3}$	
Γ_{44}	$p\overline{p}\pi^0\pi^0$	(8.2 ±2.5) $\times10^{-4}$	
Γ_{45}	$p\overline{p}K^+K^-$(non-resonant)	(2.00±0.34) $\times10^{-4}$	
Γ_{46}	$p\overline{p}K^0_S K^0_S$	< 7.9 $\times10^{-4}$	90%
Γ_{47}	$p\overline{n}\pi^-$	(8.9 ±1.0) $\times10^{-4}$	
Γ_{48}	$\overline{p}n\pi^+$	(9.3 ±0.9) $\times10^{-4}$	
Γ_{49}	$p\overline{n}\pi^-\pi^0$	(2.27±0.19) $\times10^{-3}$	
Γ_{50}	$\overline{p}n\pi^+\pi^0$	(2.21±0.20) $\times10^{-3}$	
Γ_{51}	$\Lambda\overline{\Lambda}$	(1.92±0.16) $\times10^{-4}$	
Γ_{52}	$\Lambda\overline{\Lambda}\pi^+\pi^-$	(1.31±0.17) $\times10^{-3}$	
Γ_{53}	$\Lambda\overline{\Lambda}\pi^+\pi^-$(non-resonant)	(6.9 ±1.6) $\times10^{-4}$	
Γ_{54}	$\Sigma(1385)^+\overline{\Lambda}\pi^-$ + c.c.	< 4 $\times10^{-4}$	90%
Γ_{55}	$\Sigma(1385)^-\overline{\Lambda}\pi^+$ + c.c.	< 6 $\times10^{-4}$	90%
Γ_{56}	$K^+\overline{p}\Lambda$ + c.c.	(8.1 ±0.6) $\times10^{-4}$	
Γ_{57}	$K^+\overline{p}\Lambda(1520)$ + c.c.	(2.9 ±0.7) $\times10^{-4}$	
Γ_{58}	$\Lambda(1520)\overline{\Lambda}(1520)$	(4.8 ±1.5) $\times10^{-4}$	
Γ_{59}	$\Sigma^0\overline{\Sigma}^0$	< 6 $\times10^{-5}$	90%
Γ_{60}	$\Sigma^+\overline{\Sigma}^-$	< 7 $\times10^{-5}$	90%
Γ_{61}	$\Sigma(1385)^+\overline{\Sigma}(1385)^-$	< 1.6 $\times10^{-4}$	90%
Γ_{62}	$\Sigma(1385)^-\overline{\Sigma}(1385)^+$	< 8 $\times10^{-5}$	90%
Γ_{63}	$\Xi^0\overline{\Xi}^0$	< 1.1 $\times10^{-4}$	90%
Γ_{64}	$\Xi^-\overline{\Xi}^+$	(1.48±0.33) $\times10^{-4}$	
Γ_{65}	$J/\psi(1S)\pi^+\pi^-\pi^0$	< 1.5 %	90%
Γ_{66}	$\eta_c(1S)\pi^+\pi^-$	< 2.2 %	90%

Meson Particle Listings

$\chi_{c2}(1P)$

Radiative decays

Γ_{67}	$\gamma J/\psi(1S)$	(19.2 ±0.7) %		
Γ_{68}	$\gamma\rho^0$	< 2.0	$\times 10^{-5}$	90%
Γ_{69}	$\gamma\omega$	< 6	$\times 10^{-6}$	90%
Γ_{70}	$\gamma\phi$	< 8	$\times 10^{-6}$	90%
Γ_{71}	$\gamma\gamma$	(2.74±0.14)	$\times 10^{-4}$	

CONSTRAINED FIT INFORMATION

A multiparticle fit to $\chi_{c1}(1P)$, $\chi_{c0}(1P)$, $\chi_{c2}(1P)$, and $\psi(2S)$ with 4 total widths, a partial width, 25 combinations of partial widths obtained from integrated cross section, and 84 branching ratios uses 238 measurements to determine 49 parameters. The overall fit has a $\chi^2 = 339.7$ for 189 degrees of freedom.

The following *off-diagonal* array elements are the correlation coefficients $\left\langle \delta p_i \delta p_j \right\rangle / (\delta p_i \cdot \delta p_j)$, in percent, from the fit to parameters p_i, including the branching fractions, $x_i \equiv \Gamma_i/\Gamma_{\rm total}$.

x_{14}	13									
x_{16}	3	21								
x_{17}	8	7	1							
x_{19}	14	12	3	7						
x_{22}	19	16	3	10	24					
x_{23}	19	3	1	2	3	4				
x_{26}	11	9	2	6	14	27	2			
x_{27}	14	12	3	7	17	33	3	19		
x_{28}	13	11	2	6	15	28	3	17	20	
x_{29}	7	6	1	4	8	16	1	9	11	10
x_{36}	9	8	2	5	10	18	2	10	13	11
x_{38}	16	13	3	8	16	24	4	14	17	15
x_{51}	11	9	2	6	14	28	2	16	20	17
x_{67}	24	21	4	12	29	55	5	32	40	34
x_{71}	−8	−6	−1	−3	1	19	−2	13	13	10
Γ	−28	−23	−5	−14	−28	−43	−6	−25	−32	−28
	x_1	x_{14}	x_{16}	x_{17}	x_{19}	x_{22}	x_{23}	x_{26}	x_{27}	x_{28}

x_{36}	6					
x_{38}	8	10				
x_{51}	9	11	14			
x_{67}	19	22	19	33		
x_{71}	6	4	26	13	30	
Γ	−15	−19	−54	−25	−61	−52
	x_{29}	x_{36}	x_{38}	x_{51}	x_{67}	x_{71}

$\chi_{c2}(1P)$ PARTIAL WIDTHS

$\chi_{c2}(1P)$ Γ(i)$\Gamma(\gamma J/\psi(1S))/\Gamma$(total)

$\Gamma(p\overline{p}) \times \Gamma(\gamma J/\psi(1S))/\Gamma_{\rm total}$ — $\Gamma_{38}\Gamma_{67}/\Gamma$

VALUE (eV)	DOCUMENT ID		TECN	COMMENT
27.9±1.3 OUR FIT				
27.5±1.5 OUR AVERAGE				
27.0±1.5±1.1	[1] ANDREOTTI	05A	E835	$p\overline{p} \to e^+e^-\gamma$
27.7±1.5±2.0	[1,2] ARMSTRONG	92	E760	$\overline{p}p \to e^+e^-\gamma$
36 ±8	[1] BAGLIN	86B	SPEC	$\overline{p}p \to e^+e^-$X

[1] Calculated by us using B($J/\psi(1S) \to e^+e^-$) = 0.0593 ± 0.0010.
[2] Recalculated by ANDREOTTI 05A.

$\Gamma(\gamma\gamma) \times \Gamma(\gamma J/\psi(1S))/\Gamma_{\rm total}$ — $\Gamma_{71}\Gamma_{67}/\Gamma$

VALUE (eV)	EVTS	DOCUMENT ID		TECN	COMMENT
102± 5 OUR FIT					
117± 10 OUR AVERAGE					
111± 12± 9	147 ± 15	[1] DOBBS	06	CLE3	10.4 $e^+e^- \to e^+e^-\chi_{c2}$
114± 11± 9	136 ± 13.3	[1,2] ABE	02T	BELL	$e^+e^- \to e^+e^-\chi_{c2}$
139± 55± 21		[1,3] ACCIARRI	99E	L3	$e^+e^- \to e^+e^-\chi_{c2}$
242± 65± 51		[1,4] ACKER...,K...	98	OPAL	$e^+e^- \to e^+e^-\chi_{c2}$
150± 42± 36		[1,5] DOMINICK	94	CLE2	$e^+e^- \to e^+e^-\chi_{c2}$
470±240±120		[1,6] BAUER	93	TPC	$e^+e^- \to e^+e^-\chi_{c2}$

[1] Calculated by us using B($J/\psi \to \ell^+\ell^-$) = 0.1187 ± 0.0008.
[2] All systematic errors added in quadrature.
[3] The value for $\Gamma(\chi_{c2} \to \gamma\gamma)$ reported in ACCIARRI 99E is derived using B($\chi_{c2} \to \gamma J/\psi(1S)$)×B($J/\psi(1S) \to \ell^+\ell^-$) = 0.0162 ± 0.0014.
[4] The value for $\Gamma(\chi_{c2} \to \gamma\gamma)$ reported in ACKERSTAFF,K 98 is derived using B($\chi_{c2} \to \gamma J/\psi(1S)$) = 0.135 ± 0.011 and B($J/\psi(1S) \to \ell^+\ell^-$) = 0.1203 ± 0.0038.
[5] The value for $\Gamma(\chi_{c2} \to \gamma\gamma)$ reported in DOMINICK 94 is derived using B($\chi_{c2} \to \gamma J/\psi(1S)$)= 0.135 ± 0.011, B($J/\psi(1S) \to e^+e^-$) = 0.0627 ± 0.0020, and B($J/\psi(1S) \to \mu^+\mu^-$) = 0.0597 ± 0.0025.
[6] The value for $\Gamma(\chi_{c2} \to \gamma\gamma)$ reported in BAUER 93 is derived using B($\chi_{c2} \to \gamma J/\psi(1S)$)= 0.135 ± 0.011, B($J/\psi(1S) \to e^+e^-$) = 0.0627 ± 0.0020, and B($J/\psi(1S) \to \mu^+\mu^-$) = 0.0597 ± 0.0025.

$\chi_{c2}(1P)$ Γ(i)$\Gamma(\gamma\gamma)/\Gamma$(total)

$\Gamma(2(\pi^+\pi^-)) \times \Gamma(\gamma\gamma)/\Gamma_{\rm total}$ — $\Gamma_1\Gamma_{71}/\Gamma$

VALUE (eV)	EVTS	DOCUMENT ID		TECN	COMMENT
5.7 ±0.5 OUR FIT					
5.2 ±0.7 OUR AVERAGE					
5.01±0.44±0.55	1597±138	UEHARA	08	BELL	$\gamma\gamma \to \chi_{c2} \to 2(\pi^+\pi^-)$
6.4 ±1.8 ±0.8		EISENSTEIN	01	CLE2	$e^+e^- \to e^+e^-\chi_{c2}$

$\Gamma(\rho\rho) \times \Gamma(\gamma\gamma)/\Gamma_{\rm total}$ — $\Gamma_2\Gamma_{71}/\Gamma$

VALUE (eV)	CL%	EVTS	DOCUMENT ID		TECN	COMMENT
• • • We do not use the following data for averages, fits, limits, etc. • • •						
<7.8	90	<598	UEHARA	08	BELL	$\gamma\gamma \to \chi_{c2} \to 2(\pi^+\pi^-)$

$\Gamma(K^+K^-\pi^+\pi^-) \times \Gamma(\gamma\gamma)/\Gamma_{\rm total}$ — $\Gamma_{14}\Gamma_{71}/\Gamma$

VALUE (eV)	EVTS	DOCUMENT ID		TECN	COMMENT
4.7 ±0.5 OUR FIT					
4.42±0.42±0.53	780 ± 74	UEHARA	08	BELL	$\gamma\gamma \to \chi_{c2} \to K^+K^-\pi^+\pi^-$

$\Gamma(K^+K^-\pi^+\pi^-\pi^0) \times \Gamma(\gamma\gamma)/\Gamma_{\rm total}$ — $\Gamma_{15}\Gamma_{71}/\Gamma$

VALUE (eV)	EVTS	DOCUMENT ID		TECN	COMMENT
6.5±0.9±1.5	1250	DEL-AMO-SA...11M		BABR	$\gamma\gamma \to K^+K^-\pi^+\pi^-\pi^0$

$\Gamma(K^*(892)^0\overline{K}^*(892)^0) \times \Gamma(\gamma\gamma)/\Gamma_{\rm total}$ — $\Gamma_{17}\Gamma_{71}/\Gamma$

VALUE (eV)	EVTS	DOCUMENT ID		TECN	COMMENT
1.26±0.24 OUR FIT					
0.8 ±0.17±0.27	151 ± 30	UEHARA	08	BELL	$\gamma\gamma \to \chi_{c2} \to K^+K^-\pi^+\pi^-$

$\Gamma(\phi\phi) \times \Gamma(\gamma\gamma)/\Gamma_{\rm total}$ — $\Gamma_{19}\Gamma_{71}/\Gamma$

VALUE (eV)	EVTS	DOCUMENT ID		TECN	COMMENT
0.59±0.05 OUR FIT					
0.62±0.07±0.05	89 ± 11	[1] LIU	12B	BELL	$\gamma\gamma \to 2(K^+K^-)$
• • • We do not use the following data for averages, fits, limits, etc. • • •					
0.58±0.18±0.16	26.5 ± 8.1	UEHARA	08	BELL	$\gamma\gamma \to \chi_{c2} \to 2(K^+K^-)$

[1] Supersedes UEHARA 08. Using B($\phi \to K^+K^-$) = (48.9 ± 0.5)%.

$\Gamma(\omega\omega) \times \Gamma(\gamma\gamma)/\Gamma_{\rm total}$ — $\Gamma_{20}\Gamma_{71}/\Gamma$

VALUE (eV)	CL%	DOCUMENT ID		TECN	COMMENT
• • • We do not use the following data for averages, fits, limits, etc. • • •					
<0.64	90	[1] LIU	12B	BELL	$\gamma\gamma \to 2(\pi^+\pi^-\pi^0)$

[1] Using B($\omega \to \pi^+\pi^-\pi^0$) = (89.2 ± 0.7)%.

$\Gamma(\omega\phi) \times \Gamma(\gamma\gamma)/\Gamma_{\rm total}$ — $\Gamma_{21}\Gamma_{71}/\Gamma$

VALUE (eV)	CL%	DOCUMENT ID		TECN	COMMENT
• • • We do not use the following data for averages, fits, limits, etc. • • •					
<0.04	90	[1] LIU	12B	BELL	$\gamma\gamma \to K^+K^-\pi^+\pi^-\pi^0$

[1] Using B($\phi \to K^+K^-$) = (48.9 ± 0.5)% and B($\omega \to \pi^+\pi^-\pi^0$) = (89.2 ± 0.7)%.

$\Gamma(\pi\pi) \times \Gamma(\gamma\gamma)/\Gamma_{\rm total}$ — $\Gamma_{22}\Gamma_{71}/\Gamma$

VALUE (eV)	EVTS	DOCUMENT ID		TECN	COMMENT
1.23±0.08 OUR FIT					
1.18±0.25 OUR AVERAGE					
1.44±0.54±0.47	34 ± 13	[1] UEHARA	09	BELL	10.6 $e^+e^- \to e^+e^-\pi^0\pi^0$
1.14±0.21±0.17	54 ± 10	[2] NAKAZAWA	05	BELL	10.6 $e^+e^- \to e^+e^-\pi^+\pi^-$

[1] We multiplied the measurement by 3 to convert from $\pi^0\pi^0$ to $\pi\pi$. Interference with the continuum included.
[2] We have multiplied $\pi^+\pi^-$ measurement by 3/2 to obtain $\pi\pi$.

$\Gamma(\rho^0\pi^+\pi^-) \times \Gamma(\gamma\gamma)/\Gamma_{\rm total}$ — $\Gamma_{23}\Gamma_{71}/\Gamma$

VALUE (eV)	EVTS	DOCUMENT ID		TECN	COMMENT
2.0±0.9 OUR FIT					
3.2±1.9±0.5	986 ± 578	UEHARA	08	BELL	$\gamma\gamma \to \chi_{c2} \to 2(\pi^+\pi^-)$

$\Gamma(\eta\eta) \times \Gamma(\gamma\gamma)/\Gamma_{\rm total}$ — $\Gamma_{26}\Gamma_{71}/\Gamma$

VALUE (eV)	EVTS	DOCUMENT ID		TECN	COMMENT
0.53±0.22±0.09	8	[1] UEHARA	10A	BELL	10.6 $e^+e^- \to e^+e^-\eta\eta$

[1] Interference with the continuum not included.

$\Gamma(K^+K^-) \times \Gamma(\gamma\gamma)/\Gamma_{\rm total}$ — $\Gamma_{27}\Gamma_{71}/\Gamma$

VALUE (eV)	EVTS	DOCUMENT ID		TECN	COMMENT
0.56±0.04 OUR FIT					
0.44±0.11±0.07	33 ± 8	NAKAZAWA	05	BELL	10.6 $e^+e^- \to e^+e^-K^+K^-$

$\Gamma(K_S^0 K_S^0) \times \Gamma(\gamma\gamma)/\Gamma_{\text{total}}$ $\Gamma_{28}\Gamma_{71}/\Gamma$

VALUE (eV)	EVTS	DOCUMENT ID		TECN	COMMENT
0.291±0.025 OUR FIT					
0.27 $^{+0.07}_{-0.06}$ ±0.03	53	[1] UEHARA	13	BELL	$\gamma\gamma \to K_S^0 K_S^0$
• • • We do not use the following data for averages, fits, limits, etc. • • •					
0.31 ±0.05 ±0.03	38 ± 7	CHEN	07B	BELL	$e^+e^- \to e^+e^-\chi_{c2}$

[1] Supersedes CHEN 07B.

$\Gamma(\overline{K}^0 K^+\pi^- + \text{c.c.}) \times \Gamma(\gamma\gamma)/\Gamma_{\text{total}}$ $\Gamma_{29}\Gamma_{71}/\Gamma$

VALUE (eV)	EVTS	DOCUMENT ID		TECN	COMMENT
0.71±0.11 OUR FIT					
1.20±0.33±0.13	126	[1] DEL-AMO-SA...11M		BABR	$\gamma\gamma \to K_S^0 K^\pm\pi^\mp$

[1] We have multiplied $\overline{K}K\pi$ by 2/3 to obtain $\overline{K}^0 K^+\pi^-$ + c.c.

$\Gamma(K^+K^-K^+K^-) \times \Gamma(\gamma\gamma)/\Gamma_{\text{total}}$ $\Gamma_{36}\Gamma_{71}/\Gamma$

VALUE (eV)	EVTS	DOCUMENT ID		TECN	COMMENT
0.91±0.12 OUR FIT					
1.10±0.21±0.15	126 ± 24	UEHARA	08	BELL	$\gamma\gamma \to \chi_{c2} \to 2(K^+K^-)$

$\Gamma(\eta_c(1S)\pi^+\pi^-) \times \Gamma(\gamma\gamma)/\Gamma_{\text{total}}$ $\Gamma_{66}\Gamma_{71}/\Gamma$

VALUE (eV)	CL%	DOCUMENT ID		TECN	COMMENT
<15.7	90	LEES	12AE	BABR	$e^+e^- \to e^+e^-\pi^+\pi^-\eta_c$

$\chi_{c2}(1P)$ BRANCHING RATIOS

HADRONIC DECAYS

$\Gamma(2(\pi^+\pi^-))/\Gamma_{\text{total}}$ Γ_1/Γ

VALUE	DOCUMENT ID
0.0107±0.0010 OUR FIT	

$\Gamma(\rho^0\pi^+\pi^-)/\Gamma(2(\pi^+\pi^-))$ Γ_{23}/Γ_1

VALUE	DOCUMENT ID		TECN	COMMENT
0.36±0.15 OUR FIT				
0.31±0.17	TANENBAUM	78	MRK1	$\psi(2S) \to \gamma\chi_{c2}$

$\Gamma(\pi^+\pi^-\pi^0\pi^0)/\Gamma_{\text{total}}$ Γ_3/Γ

VALUE (%)	EVTS	DOCUMENT ID		TECN	COMMENT
1.92±0.24±0.07	903.5	[1] HE	08B	CLEO	$e^+e^- \to \gamma h^+h^-h^0h^0$

[1] HE 08B reports 1.87 ± 0.07 ± 0.22 ± 0.13 % from a measurement of $[\Gamma(\chi_{c2}(1P) \to \pi^+\pi^-\pi^0\pi^0)/\Gamma_{\text{total}}] \times [\text{B}(\psi(2S) \to \gamma\chi_{c2}(1P))]$ assuming $\text{B}(\psi(2S) \to \gamma\chi_{c2}(1P)) = (9.33 \pm 0.14 \pm 0.61) \times 10^{-2}$, which we rescale to our best value $\text{B}(\psi(2S) \to \gamma\chi_{c2}(1P)) = (9.11 \pm 0.31) \times 10^{-2}$. Our first error is their experiment's error and our second error is the systematic error from using our best value.

$\Gamma(\rho^+\pi^-\pi^0 + \text{c.c.})/\Gamma_{\text{total}}$ Γ_4/Γ

VALUE (%)	EVTS	DOCUMENT ID		TECN	COMMENT
2.28±0.35±0.08	1031.9	[1,2] HE	08B	CLEO	$e^+e^- \to \gamma h^+h^-h^0h^0$

[1] HE 08B reports 2.23 ± 0.11 ± 0.32 ± 0.16 % from a measurement of $[\Gamma(\chi_{c2}(1P) \to \rho^+\pi^-\pi^0 + \text{c.c.})/\Gamma_{\text{total}}] \times [\text{B}(\psi(2S) \to \gamma\chi_{c2}(1P))]$ assuming $\text{B}(\psi(2S) \to \gamma\chi_{c2}(1P)) = (9.33 \pm 0.14 \pm 0.61) \times 10^{-2}$, which we rescale to our best value $\text{B}(\psi(2S) \to \gamma\chi_{c2}(1P)) = (9.11 \pm 0.31) \times 10^{-2}$. Our first error is their experiment's error and our second error is the systematic error from using our best value.

[2] Calculated by us. We have added the values from HE 08B for $\rho^+\pi^-\pi^0$ and $\rho^-\pi^+\pi^0$ decays assuming uncorrelated statistical and fully correlated systematic uncertainties.

$\Gamma(4\pi^0)/\Gamma_{\text{total}}$ Γ_5/Γ

VALUE (units 10^{-3})	EVTS	DOCUMENT ID		TECN	COMMENT
1.16±0.15±0.04	1164	[1] ABLIKIM	11A	BES3	$e^+e^- \to \psi(2S) \to \gamma\chi_{c2}$

[1] ABLIKIM 11A reports $(1.21 \pm 0.05 \pm 0.16) \times 10^{-3}$ from a measurement of $[\Gamma(\chi_{c2}(1P) \to 4\pi^0)/\Gamma_{\text{total}}] \times [\text{B}(\psi(2S) \to \gamma\chi_{c2}(1P))]$ assuming $\text{B}(\psi(2S) \to \gamma\chi_{c2}(1P)) = (8.74 \pm 0.35) \times 10^{-2}$, which we rescale to our best value $\text{B}(\psi(2S) \to \gamma\chi_{c2}(1P)) = (9.11 \pm 0.31) \times 10^{-2}$. Our first error is their experiment's error and our second error is the systematic error from using our best value.

$\Gamma(K^+K^-\pi^0\pi^0)/\Gamma_{\text{total}}$ Γ_6/Γ

VALUE (%)	EVTS	DOCUMENT ID		TECN	COMMENT
0.22±0.04±0.01	76.9	[1] HE	08B	CLEO	$e^+e^- \to \gamma h^+h^-h^0h^0$

[1] HE 08B reports 0.21 ± 0.03 ± 0.03 ± 0.01 % from a measurement of $[\Gamma(\chi_{c2}(1P) \to K^+K^-\pi^0\pi^0)/\Gamma_{\text{total}}] \times [\text{B}(\psi(2S) \to \gamma\chi_{c2}(1P))]$ assuming $\text{B}(\psi(2S) \to \gamma\chi_{c2}(1P)) = (9.33 \pm 0.14 \pm 0.61) \times 10^{-2}$, which we rescale to our best value $\text{B}(\psi(2S) \to \gamma\chi_{c2}(1P)) = (9.11 \pm 0.31) \times 10^{-2}$. Our first error is their experiment's error and our second error is the systematic error from using our best value.

$\Gamma(K^+\pi^-\overline{K}^0\pi^0 + \text{c.c.})/\Gamma_{\text{total}}$ Γ_7/Γ

VALUE (%)	EVTS	DOCUMENT ID		TECN	COMMENT
1.44±0.20±0.05	211.6	[1] HE	08B	CLEO	$e^+e^- \to \gamma h^+h^-h^0h^0$

[1] HE 08B reports 1.41 ± 0.11 ± 0.16 ± 0.10 % from a measurement of $[\Gamma(\chi_{c2}(1P) \to K^+\pi^-\overline{K}^0\pi^0 + \text{c.c.})/\Gamma_{\text{total}}] \times [\text{B}(\psi(2S) \to \gamma\chi_{c2}(1P))]$ assuming $\text{B}(\psi(2S) \to \gamma\chi_{c2}(1P)) = (9.33 \pm 0.14 \pm 0.61) \times 10^{-2}$, which we rescale to our best value $\text{B}(\psi(2S) \to \gamma\chi_{c2}(1P)) = (9.11 \pm 0.31) \times 10^{-2}$. Our first error is their experiment's error and our second error is the systematic error from using our best value.

$\Gamma(\rho^-K^+\overline{K}^0 + \text{c.c.})/\Gamma_{\text{total}}$ Γ_8/Γ

VALUE (%)	EVTS	DOCUMENT ID		TECN	COMMENT
0.43±0.13±0.01	62.9	[1] HE	08B	CLEO	$e^+e^- \to \gamma h^+h^-h^0h^0$

[1] HE 08B reports 0.42 ± 0.11 ± 0.06 ± 0.03 % from a measurement of $[\Gamma(\chi_{c2}(1P) \to \rho^-K^+\overline{K}^0 + \text{c.c.})/\Gamma_{\text{total}}] \times [\text{B}(\psi(2S) \to \gamma\chi_{c2}(1P))]$ assuming $\text{B}(\psi(2S) \to \gamma\chi_{c2}(1P)) = (9.33 \pm 0.14 \pm 0.61) \times 10^{-2}$, which we rescale to our best value $\text{B}(\psi(2S) \to \gamma\chi_{c2}(1P)) = (9.11 \pm 0.31) \times 10^{-2}$. Our first error is their experiment's error and our second error is the systematic error from using our best value.

$\Gamma(K^*(892)^0K^-\pi^+ \to K^-\pi^+K^0\pi^0 + \text{c.c.})/\Gamma_{\text{total}}$ Γ_9/Γ

VALUE (%)	EVTS	DOCUMENT ID		TECN	COMMENT
0.31±0.08±0.01	38.7	[1] HE	08B	CLEO	$e^+e^- \to \gamma h^+h^-h^0h^0$

[1] HE 08B reports 0.30 ± 0.07 ± 0.04 ± 0.02 % from a measurement of $[\Gamma(\chi_{c2}(1P) \to K^*(892)^0K^-\pi^+ \to K^-\pi^+K^0\pi^0 + \text{c.c.})/\Gamma_{\text{total}}] \times [\text{B}(\psi(2S) \to \gamma\chi_{c2}(1P))]$ assuming $\text{B}(\psi(2S) \to \gamma\chi_{c2}(1P)) = (9.33 \pm 0.14 \pm 0.61) \times 10^{-2}$, which we rescale to our best value $\text{B}(\psi(2S) \to \gamma\chi_{c2}(1P)) = (9.11 \pm 0.31) \times 10^{-2}$. Our first error is their experiment's error and our second error is the systematic error from using our best value.

$\Gamma(K^*(892)^0\overline{K}^0\pi^0 \to K^+\pi^-\overline{K}^0\pi^0 + \text{c.c.})/\Gamma_{\text{total}}$ Γ_{10}/Γ

VALUE (%)	EVTS	DOCUMENT ID		TECN	COMMENT
0.40±0.09±0.01	63.0	[1] HE	08B	CLEO	$e^+e^- \to \gamma h^+h^-h^0h^0$

[1] HE 08B reports 0.39 ± 0.07 ± 0.05 ± 0.03 % from a measurement of $[\Gamma(\chi_{c2}(1P) \to K^*(892)^0\overline{K}^0\pi^0 \to K^+\pi^-\overline{K}^0\pi^0 + \text{c.c.})/\Gamma_{\text{total}}] \times [\text{B}(\psi(2S) \to \gamma\chi_{c2}(1P))]$ assuming $\text{B}(\psi(2S) \to \gamma\chi_{c2}(1P)) = (9.33 \pm 0.14 \pm 0.61) \times 10^{-2}$, which we rescale to our best value $\text{B}(\psi(2S) \to \gamma\chi_{c2}(1P)) = (9.11 \pm 0.31) \times 10^{-2}$. Our first error is their experiment's error and our second error is the systematic error from using our best value.

$\Gamma(K^*(892)^-K^+\pi^0 \to K^+\pi^-\overline{K}^0\pi^0 + \text{c.c.})/\Gamma_{\text{total}}$ Γ_{11}/Γ

VALUE (%)	EVTS	DOCUMENT ID		TECN	COMMENT
0.39±0.08±0.01	51.1	[1] HE	08B	CLEO	$e^+e^- \to \gamma h^+h^-h^0h^0$

[1] HE 08B reports 0.38 ± 0.07 ± 0.04 ± 0.03 % from a measurement of $[\Gamma(\chi_{c2}(1P) \to K^*(892)^-K^+\pi^0 \to K^+\pi^-\overline{K}^0\pi^0 + \text{c.c.})/\Gamma_{\text{total}}] \times [\text{B}(\psi(2S) \to \gamma\chi_{c2}(1P))]$ assuming $\text{B}(\psi(2S) \to \gamma\chi_{c2}(1P)) = (9.33 \pm 0.14 \pm 0.61) \times 10^{-2}$, which we rescale to our best value $\text{B}(\psi(2S) \to \gamma\chi_{c2}(1P)) = (9.11 \pm 0.31) \times 10^{-2}$. Our first error is their experiment's error and our second error is the systematic error from using our best value.

$\Gamma(K^*(892)^+\overline{K}^0\pi^- \to K^+\pi^-\overline{K}^0\pi^0 + \text{c.c.})/\Gamma_{\text{total}}$ Γ_{12}/Γ

VALUE (%)	EVTS	DOCUMENT ID		TECN	COMMENT
0.31±0.08±0.01	39.3	[1] HE	08B	CLEO	$e^+e^- \to \gamma h^+h^-h^0h^0$

[1] HE 08B reports 0.30 ± 0.07 ± 0.04 ± 0.02 % from a measurement of $[\Gamma(\chi_{c2}(1P) \to K^*(892)^+\overline{K}^0\pi^- \to K^+\pi^-\overline{K}^0\pi^0 + \text{c.c.})/\Gamma_{\text{total}}] \times [\text{B}(\psi(2S) \to \gamma\chi_{c2}(1P))]$ assuming $\text{B}(\psi(2S) \to \gamma\chi_{c2}(1P)) = (9.33 \pm 0.14 \pm 0.61) \times 10^{-2}$, which we rescale to our best value $\text{B}(\psi(2S) \to \gamma\chi_{c2}(1P)) = (9.11 \pm 0.31) \times 10^{-2}$. Our first error is their experiment's error and our second error is the systematic error from using our best value.

$\Gamma(K^+K^-\eta\pi^0)/\Gamma_{\text{total}}$ Γ_{13}/Γ

VALUE (%)	EVTS	DOCUMENT ID		TECN	COMMENT
0.133±0.046±0.005	22.9	[1] HE	08B	CLEO	$e^+e^- \to \gamma h^+h^-h^0h^0$

[1] HE 08B reports 0.13 ± 0.04 ± 0.02 ± 0.01 % from a measurement of $[\Gamma(\chi_{c2}(1P) \to K^+K^-\eta\pi^0)/\Gamma_{\text{total}}] \times [\text{B}(\psi(2S) \to \gamma\chi_{c2}(1P))]$ assuming $\text{B}(\psi(2S) \to \gamma\chi_{c2}(1P)) = (9.33 \pm 0.14 \pm 0.61) \times 10^{-2}$, which we rescale to our best value $\text{B}(\psi(2S) \to \gamma\chi_{c2}(1P)) = (9.11 \pm 0.31) \times 10^{-2}$. Our first error is their experiment's error and our second error is the systematic error from using our best value.

$\Gamma(K^+K^-\pi^+\pi^-)/\Gamma_{\text{total}}$ Γ_{14}/Γ

VALUE (units 10^{-3})	DOCUMENT ID
8.8±1.0 OUR FIT	

$\Gamma(K^+\overline{K}^*(892)^0\pi^- + \text{c.c.})/\Gamma(K^+K^-\pi^+\pi^-)$ Γ_{16}/Γ_{14}

VALUE	DOCUMENT ID		TECN	COMMENT
0.25±0.13 OUR FIT				
0.25±0.13	TANENBAUM	78	MRK1	$\psi(2S) \to \gamma\chi_{c2}$

$\Gamma(K^+\overline{K}^*(892)^0\pi^- + \text{c.c.})/\Gamma_{\text{total}}$ Γ_{16}/Γ

VALUE (units 10^{-4})	DOCUMENT ID
22±11 OUR FIT	

$\Gamma(K^*(892)^0\overline{K}^*(892)^0)/\Gamma_{\text{total}}$ Γ_{17}/Γ

VALUE (units 10^{-3})	DOCUMENT ID
2.4±0.5 OUR FIT	

$\Gamma(3(\pi^+\pi^-))/\Gamma_{\text{total}}$ Γ_{18}/Γ

VALUE (units 10^{-3})	DOCUMENT ID		TECN	COMMENT
8.6±1.8 OUR EVALUATION	Treating systematic error as correlated.			
8.6±1.8 OUR AVERAGE				
8.6±0.9±1.6	[1] BAI	99B	BES	$\psi(2S) \to \gamma\chi_{c2}$
8.7±5.9±0.4	[1] TANENBAUM	78	MRK1	$\psi(2S) \to \gamma\chi_{c2}$

[1] Rescaled by us using $\text{B}(\psi(2S) \to \gamma\chi_{c2}) = (8.3 \pm 0.4)\%$ and $\text{B}(\psi(2S) \to J/\psi(1S)\pi^+\pi^-) = (32.6 \pm 0.5)\%$. Multiplied by a factor of 2 to convert from $K_S^0 K^+\pi^-$ to $K^0 K^+\pi^-$ decay.

Meson Particle Listings

$\chi_{c2}(1P)$

$\Gamma(\phi\phi)/\Gamma_{\text{total}}$ Γ_{19}/Γ

VALUE (units 10^{-3})	DOCUMENT ID
1.12±0.10 OUR FIT	

$\Gamma(\omega\omega)/\Gamma_{\text{total}}$ Γ_{20}/Γ

VALUE (units 10^{-3})	EVTS	DOCUMENT ID		TECN	COMMENT
0.88±0.11 OUR AVERAGE					
0.85±0.10±0.03	762	[1] ABLIKIM	11K	BES3	$\psi(2S) \to \gamma$ hadrons
1.8 ±0.6 ±0.1	27.7±7.4	[2] ABLIKIM	05N	BES2	$\psi(2S) \to \gamma\chi_{c2} \to \gamma 6\pi$

[1] ABLIKIM 11K reports $(8.9 \pm 0.3 \pm 1.1) \times 10^{-4}$ from a measurement of $[\Gamma(\chi_{c2}(1P) \to \omega\omega)/\Gamma_{\text{total}}] \times [\text{B}(\psi(2S) \to \gamma\chi_{c2}(1P))]$ assuming $\text{B}(\psi(2S) \to \gamma\chi_{c2}(1P)) = (8.74 \pm 0.35) \times 10^{-2}$, which we rescale to our best value $\text{B}(\psi(2S) \to \gamma\chi_{c2}(1P)) = (9.11 \pm 0.31) \times 10^{-2}$. Our first error is their experiment's error and our second error is the systematic error from using our best value.

[2] ABLIKIM 05N reports $[\Gamma(\chi_{c2}(1P) \to \omega\omega)/\Gamma_{\text{total}}] \times [\text{B}(\psi(2S) \to \gamma\chi_{c2}(1P))] = (0.165 \pm 0.044 \pm 0.032) \times 10^{-3}$ which we divide by our best value $\text{B}(\psi(2S) \to \gamma\chi_{c2}(1P)) = (9.11 \pm 0.31) \times 10^{-2}$. Our first error is their experiment's error and our second error is the systematic error from using our best value.

$\Gamma(\omega\phi)/\Gamma_{\text{total}}$ Γ_{21}/Γ

VALUE (units 10^{-5})	CL%	DOCUMENT ID		TECN	COMMENT
<1.9	90	[1] ABLIKIM	11K	BES3	$\psi(2S) \to \gamma$ hadrons

[1] ABLIKIM 11K reports $< 2 \times 10^{-5}$ from a measurement of $[\Gamma(\chi_{c2}(1P) \to \omega\phi)/\Gamma_{\text{total}}] \times [\text{B}(\psi(2S) \to \gamma\chi_{c2}(1P))]$ assuming $\text{B}(\psi(2S) \to \gamma\chi_{c2}(1P)) = (8.74 \pm 0.35) \times 10^{-2}$, which we rescale to our best value $\text{B}(\psi(2S) \to \gamma\chi_{c2}(1P)) = 9.11 \times 10^{-2}$.

$\Gamma(\pi\pi)/\Gamma_{\text{total}}$ Γ_{22}/Γ

VALUE (units 10^{-3})	DOCUMENT ID
2.33±0.12 OUR FIT	

$\Gamma(\rho^0\pi^+\pi^-)/\Gamma_{\text{total}}$ Γ_{23}/Γ

VALUE (units 10^{-4})	DOCUMENT ID
38±16 OUR FIT	

$\Gamma(\pi^+\pi^-\eta)/\Gamma_{\text{total}}$ Γ_{24}/Γ

VALUE (units 10^{-3})	CL%	DOCUMENT ID		TECN	COMMENT
0.50±0.13±0.02		[1] ATHAR	07	CLEO	$\psi(2S) \to \gamma h^+ h^- h^0$
• • • We do not use the following data for averages, fits, limits, etc. • • •					
<1.5	90	[2] ABLIKIM	06R	BES2	$\psi(2S) \to \gamma\chi_{c2}$

[1] ATHAR 07 reports $(0.49 \pm 0.12 \pm 0.06) \times 10^{-3}$ from a measurement of $[\Gamma(\chi_{c2}(1P) \to \pi^+\pi^-\eta)/\Gamma_{\text{total}}] \times [\text{B}(\psi(2S) \to \gamma\chi_{c2}(1P))]$ assuming $\text{B}(\psi(2S) \to \gamma\chi_{c2}(1P)) = (9.33 \pm 0.14 \pm 0.61) \times 10^{-2}$, which we rescale to our best value $\text{B}(\psi(2S) \to \gamma\chi_{c2}(1P)) = (9.11 \pm 0.31) \times 10^{-2}$. Our first error is their experiment's error and our second error is the systematic error from using our best value.

[2] ABLIKIM 06R reports $< 1.7 \times 10^{-3}$ from a measurement of $[\Gamma(\chi_{c2}(1P) \to \pi^+\pi^-\eta)/\Gamma_{\text{total}}] \times [\text{B}(\psi(2S) \to \gamma\chi_{c2}(1P))]$ assuming $\text{B}(\psi(2S) \to \gamma\chi_{c2}(1P)) = (8.1 \pm 0.4) \times 10^{-2}$, which we rescale to our best value $\text{B}(\psi(2S) \to \gamma\chi_{c2}(1P)) = 9.11 \times 10^{-2}$.

$\Gamma(\pi^+\pi^-\eta')/\Gamma_{\text{total}}$ Γ_{25}/Γ

VALUE (units 10^{-3})	DOCUMENT ID		TECN	COMMENT
0.52±0.19±0.02	[1] ATHAR	07	CLEO	$\psi(2S) \to \gamma h^+ h^- h^0$

[1] ATHAR 07 reports $(0.51 \pm 0.18 \pm 0.06) \times 10^{-3}$ from a measurement of $[\Gamma(\chi_{c2}(1P) \to \pi^+\pi^-\eta')/\Gamma_{\text{total}}] \times [\text{B}(\psi(2S) \to \gamma\chi_{c2}(1P))]$ assuming $\text{B}(\psi(2S) \to \gamma\chi_{c2}(1P)) = (9.33 \pm 0.14 \pm 0.61) \times 10^{-2}$, which we rescale to our best value $\text{B}(\psi(2S) \to \gamma\chi_{c2}(1P)) = (9.11 \pm 0.31) \times 10^{-2}$. Our first error is their experiment's error and our second error is the systematic error from using our best value.

$\Gamma(\eta\eta)/\Gamma_{\text{total}}$ Γ_{26}/Γ

VALUE (units 10^{-4})	DOCUMENT ID
5.7±0.5 OUR FIT	

$\Gamma(K^+K^-)/\Gamma_{\text{total}}$ Γ_{27}/Γ

VALUE (units 10^{-3})	DOCUMENT ID
1.05±0.07 OUR FIT	

$\Gamma(K^0_S K^0_S)/\Gamma_{\text{total}}$ Γ_{28}/Γ

VALUE (units 10^{-3})	DOCUMENT ID
0.55±0.04 OUR FIT	

$\Gamma(K^0_S K^0_S)/\Gamma(\pi\pi)$ Γ_{28}/Γ_{22}

VALUE	DOCUMENT ID		TECN	COMMENT
0.235±0.019 OUR FIT				
• • • We do not use the following data for averages, fits, limits, etc. • • •				
0.27 ±0.07 ±0.04	[1,2] CHEN	07B	BELL	$e^+e^- \to e^+e^-\chi_{c2}$

[1] Using $\Gamma(\pi\pi) \times \Gamma(\gamma\gamma)/\Gamma_{\text{total}}$ from the $\pi^+\pi^-$ measurement of NAKAZAWA 05 rescaled by 3/2 to convert to $\pi\pi$.

[2] Not independent from other measurements.

$\Gamma(K^0_S K^0_S)/\Gamma(K^+K^-)$ Γ_{28}/Γ_{27}

VALUE	DOCUMENT ID		TECN	COMMENT
0.52±0.05 OUR FIT				
• • • We do not use the following data for averages, fits, limits, etc. • • •				
0.70±0.21±0.12	[1,2] CHEN	07B	BELL	$e^+e^- \to e^+e^-\chi_{c2}$

[1] Using $\Gamma(K^+K^-) \times \Gamma(\gamma\gamma)/\Gamma_{\text{total}}$ from NAKAZAWA 05.

[2] Not independent from other measurements.

$\Gamma(K^+K^-\pi^0)/\Gamma_{\text{total}}$ Γ_{30}/Γ

VALUE (units 10^{-3})	DOCUMENT ID		TECN	COMMENT
0.32±0.08±0.01	[1] ATHAR	07	CLEO	$\psi(2S) \to \gamma h^+ h^- h^0$

[1] ATHAR 07 reports $(0.31 \pm 0.07 \pm 0.04) \times 10^{-3}$ from a measurement of $[\Gamma(\chi_{c2}(1P) \to K^+K^-\pi^0)/\Gamma_{\text{total}}] \times [\text{B}(\psi(2S) \to \gamma\chi_{c2}(1P))]$ assuming $\text{B}(\psi(2S) \to \gamma\chi_{c2}(1P)) = (9.33 \pm 0.14 \pm 0.61) \times 10^{-2}$, which we rescale to our best value $\text{B}(\psi(2S) \to \gamma\chi_{c2}(1P)) = (9.11 \pm 0.31) \times 10^{-2}$. Our first error is their experiment's error and our second error is the systematic error from using our best value.

$\Gamma(K^+K^-\eta)/\Gamma_{\text{total}}$ Γ_{31}/Γ

VALUE (units 10^{-3})	CL%	DOCUMENT ID		TECN	COMMENT
<0.34	90	[1] ATHAR	07	CLEO	$\psi(2S) \to \gamma h^+ h^- h^0$

[1] ATHAR 07 reports $< 0.33 \times 10^{-3}$ from a measurement of $[\Gamma(\chi_{c2}(1P) \to K^+K^-\eta)/\Gamma_{\text{total}}] \times [\text{B}(\psi(2S) \to \gamma\chi_{c2}(1P))]$ assuming $\text{B}(\psi(2S) \to \gamma\chi_{c2}(1P)) = (9.33 \pm 0.14 \pm 0.61) \times 10^{-2}$, which we rescale to our best value $\text{B}(\psi(2S) \to \gamma\chi_{c2}(1P)) = 9.11 \times 10^{-2}$.

$\Gamma(\eta\eta')/\Gamma_{\text{total}}$ Γ_{32}/Γ

VALUE (units 10^{-4})	CL%	EVTS	DOCUMENT ID		TECN	COMMENT
<0.6	90	3.3±8.0	[1] ASNER	09	CLEO	$\psi(2S) \to \gamma\eta\eta'$
• • • We do not use the following data for averages, fits, limits, etc. • • •						
<2.4	90		[2] ADAMS	07	CLEO	$\psi(2S) \to \gamma\chi_{c2}$

[1] ASNER 09 reports $< 0.6 \times 10^{-4}$ from a measurement of $[\Gamma(\chi_{c2}(1P) \to \eta\eta')/\Gamma_{\text{total}}] \times [\text{B}(\psi(2S) \to \gamma\chi_{c2}(1P))]$ assuming $\text{B}(\psi(2S) \to \gamma\chi_{c2}(1P)) = (9.33 \pm 0.14 \pm 0.61) \times 10^{-2}$, which we rescale to our best value $\text{B}(\psi(2S) \to \gamma\chi_{c2}(1P)) = 9.11 \times 10^{-2}$.

[2] Superseded by ASNER 09. ADAMS 07 reports $< 2.3 \times 10^{-4}$ from a measurement of $[\Gamma(\chi_{c2}(1P) \to \eta\eta')/\Gamma_{\text{total}}] \times [\text{B}(\psi(2S) \to \gamma\chi_{c2}(1P))]$ assuming $\text{B}(\psi(2S) \to \gamma\chi_{c2}(1P)) = 0.0933 \pm 0.0014 \pm 0.0061$, which we rescale to our best value $\text{B}(\psi(2S) \to \gamma\chi_{c2}(1P)) = 9.11 \times 10^{-2}$.

$\Gamma(\eta'\eta')/\Gamma_{\text{total}}$ Γ_{33}/Γ

VALUE (units 10^{-4})	CL%	EVTS	DOCUMENT ID		TECN	COMMENT
<1.0	90	12 ± 7	[1] ASNER	09	CLEO	$\psi(2S) \to \gamma\eta'\eta'$
• • • We do not use the following data for averages, fits, limits, etc. • • •						
<3.2	90		[2] ADAMS	07	CLEO	$\psi(2S) \to \gamma\chi_{c2}$

[1] ASNER 09 reports $< 1.0 \times 10^{-4}$ from a measurement of $[\Gamma(\chi_{c2}(1P) \to \eta'\eta')/\Gamma_{\text{total}}] \times [\text{B}(\psi(2S) \to \gamma\chi_{c2}(1P))]$ assuming $\text{B}(\psi(2S) \to \gamma\chi_{c2}(1P)) = (9.33 \pm 0.14 \pm 0.61) \times 10^{-2}$, which we rescale to our best value $\text{B}(\psi(2S) \to \gamma\chi_{c2}(1P)) = 9.11 \times 10^{-2}$.

[2] Superseded by ASNER 09. ADAMS 07 reports $< 3.1 \times 10^{-4}$ from a measurement of $[\Gamma(\chi_{c2}(1P) \to \eta'\eta')/\Gamma_{\text{total}}] \times [\text{B}(\psi(2S) \to \gamma\chi_{c2}(1P))]$ assuming $\text{B}(\psi(2S) \to \gamma\chi_{c2}(1P)) = 0.0933 \pm 0.0014 \pm 0.0061$, which we rescale to our best value $\text{B}(\psi(2S) \to \gamma\chi_{c2}(1P)) = 9.11 \times 10^{-2}$.

$\Gamma(\pi^+\pi^- K^0_S K^0_S)/\Gamma_{\text{total}}$ Γ_{34}/Γ

VALUE (units 10^{-3})	EVTS	DOCUMENT ID		TECN	COMMENT
2.3±0.6±0.1	57 ± 11	[1] ABLIKIM	05O	BES2	$\psi(2S) \to \gamma\chi_{c2}$

[1] ABLIKIM 05O reports $[\Gamma(\chi_{c2}(1P) \to \pi^+\pi^- K^0_S K^0_S)/\Gamma_{\text{total}}] \times [\text{B}(\psi(2S) \to \gamma\chi_{c2}(1P))] = (0.207 \pm 0.039 \pm 0.033) \times 10^{-3}$ which we divide by our best value $\text{B}(\psi(2S) \to \gamma\chi_{c2}(1P)) = (9.11 \pm 0.31) \times 10^{-2}$. Our first error is their experiment's error and our second error is the systematic error from using our best value.

$\Gamma(K^+K^- K^0_S K^0_S)/\Gamma_{\text{total}}$ Γ_{35}/Γ

VALUE (units 10^{-4})	CL%	EVTS	DOCUMENT ID		TECN	COMMENT
<4	90	2.3 ± 2.2	[1] ABLIKIM	05O	BES2	$e^+e^- \to \chi_{c2}\gamma$

[1] ABLIKIM 05O reports $[\Gamma(\chi_{c2}(1P) \to K^+K^- K^0_S K^0_S)/\Gamma_{\text{total}}] \times [\text{B}(\psi(2S) \to \gamma\chi_{c2}(1P))] < 3.5 \times 10^{-5}$ which we divide by our best value $\text{B}(\psi(2S) \to \gamma\chi_{c2}(1P)) = 9.11 \times 10^{-2}$.

$\Gamma(K^+K^-K^+K^-)/\Gamma_{\text{total}}$ Γ_{36}/Γ

VALUE (units 10^{-3})	DOCUMENT ID
1.73±0.21 OUR FIT	

$\Gamma(K^+K^-\phi)/\Gamma_{\text{total}}$ Γ_{37}/Γ

VALUE (units 10^{-3})	EVTS	DOCUMENT ID		TECN	COMMENT
1.48±0.31±0.05	52	[1] ABLIKIM	06T	BES2	$\psi(2S) \to \gamma 2K^+ 2K^-$

[1] ABLIKIM 06T reports $(1.67 \pm 0.26 \pm 0.24) \times 10^{-3}$ from a measurement of $[\Gamma(\chi_{c2}(1P) \to K^+K^-\phi)/\Gamma_{\text{total}}] \times [\text{B}(\psi(2S) \to \gamma\chi_{c2}(1P))]$ assuming $\text{B}(\psi(2S) \to \gamma\chi_{c2}(1P)) = (8.1 \pm 0.4) \times 10^{-2}$, which we rescale to our best value $\text{B}(\psi(2S) \to \gamma\chi_{c2}(1P)) = (9.11 \pm 0.31) \times 10^{-2}$. Our first error is their experiment's error and our second error is the systematic error from using our best value.

$\Gamma(p\overline{p})/\Gamma_{total}$ Γ_{38}/Γ

VALUE (units 10^{-4})	DOCUMENT ID
0.75±0.04 OUR FIT	

$\Gamma(p\overline{p}\pi^0)/\Gamma_{total}$ Γ_{39}/Γ

VALUE (units 10^{-3})	DOCUMENT ID		TECN	COMMENT
0.49±0.04 OUR AVERAGE				
0.49±0.04±0.02	[1] ONYISI	10	CLE3	$\psi(2S) \to \gamma p\overline{p}X$
0.45±0.09±0.02	[2] ATHAR	07	CLEO	$\psi(2S) \to \gamma h^+ h^- h^0$

[1] ONYISI 10 reports $(4.83 \pm 0.25 \pm 0.35 \pm 0.31) \times 10^{-4}$ from a measurement of $[\Gamma(\chi_{c2}(1P) \to p\overline{p}\pi^0)/\Gamma_{total}] \times [B(\psi(2S) \to \gamma\chi_{c2}(1P))]$ assuming $B(\psi(2S) \to \gamma\chi_{c2}(1P)) = (9.33\pm0.14\pm0.61)\times10^{-2}$, which we rescale to our best value $B(\psi(2S) \to \gamma\chi_{c2}(1P)) = (9.11 \pm 0.31) \times 10^{-2}$. Our first error is their experiment's error and our second error is the systematic error from using our best value.

[2] ATHAR 07 reports $(0.44 \pm 0.08 \pm 0.05) \times 10^{-3}$ from a measurement of $[\Gamma(\chi_{c2}(1P) \to p\overline{p}\pi^0)/\Gamma_{total}] \times [B(\psi(2S) \to \gamma\chi_{c2}(1P))]$ assuming $B(\psi(2S) \to \gamma\chi_{c2}(1P)) = (9.33\pm0.14\pm0.61)\times10^{-2}$, which we rescale to our best value $B(\psi(2S) \to \gamma\chi_{c2}(1P)) = (9.11 \pm 0.31) \times 10^{-2}$. Our first error is their experiment's error and our second error is the systematic error from using our best value.

$\Gamma(p\overline{p}\eta)/\Gamma_{total}$ Γ_{40}/Γ

VALUE (units 10^{-3})	DOCUMENT ID		TECN	COMMENT
0.182±0.026 OUR AVERAGE				
0.180±0.027±0.006	[1] ONYISI	10	CLE3	$\psi(2S) \to \gamma p\overline{p}X$
0.19 ±0.07 ±0.01	[2] ATHAR	07	CLEO	$\psi(2S) \to \gamma h^+ h^- h^0$

[1] ONYISI 10 reports $(1.76 \pm 0.23 \pm 0.14 \pm 0.11) \times 10^{-4}$ from a measurement of $[\Gamma(\chi_{c2}(1P) \to p\overline{p}\eta)/\Gamma_{total}] \times [B(\psi(2S) \to \gamma\chi_{c2}(1P))]$ assuming $B(\psi(2S) \to \gamma\chi_{c2}(1P)) = (9.33\pm0.14\pm0.61)\times10^{-2}$, which we rescale to our best value $B(\psi(2S) \to \gamma\chi_{c2}(1P)) = (9.11 \pm 0.31) \times 10^{-2}$. Our first error is their experiment's error and our second error is the systematic error from using our best value.

[2] ATHAR 07 reports $(0.19 \pm 0.07 \pm 0.02) \times 10^{-3}$ from a measurement of $[\Gamma(\chi_{c2}(1P) \to p\overline{p}\eta)/\Gamma_{total}] \times [B(\psi(2S) \to \gamma\chi_{c2}(1P))]$ assuming $B(\psi(2S) \to \gamma\chi_{c2}(1P)) = (9.33 \pm 0.14 \pm 0.61) \times 10^{-2}$, which we rescale to our best value $B(\psi(2S) \to \gamma\chi_{c2}(1P)) = (9.11 \pm 0.31) \times 10^{-2}$. Our first error is their experiment's error and our second error is the systematic error from using our best value.

$\Gamma(p\overline{p}\omega)/\Gamma_{total}$ Γ_{41}/Γ

VALUE (units 10^{-3})	DOCUMENT ID		TECN	COMMENT
0.38±0.04±0.01	[1] ONYISI	10	CLE3	$\psi(2S) \to \gamma p\overline{p}X$

[1] ONYISI 10 reports $(3.68 \pm 0.35 \pm 0.26 \pm 0.24) \times 10^{-4}$ from a measurement of $[\Gamma(\chi_{c2}(1P) \to p\overline{p}\omega)/\Gamma_{total}] \times [B(\psi(2S) \to \gamma\chi_{c2}(1P))]$ assuming $B(\psi(2S) \to \gamma\chi_{c2}(1P)) = (9.33\pm0.14\pm0.61)\times10^{-2}$, which we rescale to our best value $B(\psi(2S) \to \gamma\chi_{c2}(1P)) = (9.11 \pm 0.31) \times 10^{-2}$. Our first error is their experiment's error and our second error is the systematic error from using our best value.

$\Gamma(p\overline{p}\phi)/\Gamma_{total}$ Γ_{42}/Γ

VALUE (units 10^{-5})	EVTS	DOCUMENT ID		TECN	COMMENT
2.9±0.9±0.1	24 ± 7	[1] ABLIKIM	11F	BES3	$\psi(2S) \to \gamma p\overline{p}K^+K^-$

[1] ABLIKIM 11F reports $(3.04\pm0.85\pm0.43)\times10^{-5}$ from a measurement of $[\Gamma(\chi_{c2}(1P) \to p\overline{p}\phi)/\Gamma_{total}] \times [B(\psi(2S) \to \gamma\chi_{c2}(1P))]$ assuming $B(\psi(2S) \to \gamma\chi_{c2}(1P)) = (8.74 \pm 0.35) \times 10^{-2}$, which we rescale to our best value $B(\psi(2S) \to \gamma\chi_{c2}(1P)) = (9.11 \pm 0.31) \times 10^{-2}$. Our first error is their experiment's error and our second error is the systematic error from using our best value.

$\Gamma(p\overline{p}\pi^+\pi^-)/\Gamma_{total}$ Γ_{43}/Γ

VALUE (units 10^{-3})	DOCUMENT ID		TECN	COMMENT
1.32±0.34 OUR EVALUATION Treating systematic error as correlated.				
1.3 ±0.4 OUR AVERAGE Error includes scale factor of 1.3.				
1.17±0.19±0.30	[1] BAI	99B	BES	$\psi(2S) \to \gamma\chi_{c2}$
2.64±1.03±0.14	[1] TANENBAUM	78	MRK1	$\psi(2S) \to \gamma\chi_{c2}$

[1] Rescaled by us using $B(\psi(2S) \to \gamma\chi_{c2}) = (8.3 \pm 0.4)\%$ and $B(\psi(2S) \to J/\psi(1S)\pi^+\pi^-) = (32.6 \pm 0.5)\%$. Multiplied by a factor of 2 to convert from $K^0_S K^+\pi^-$ to $K^0 K^+\pi^-$ decay.

$\Gamma(p\overline{p}\pi^0\pi^0)/\Gamma_{total}$ Γ_{44}/Γ

VALUE (%)	EVTS	DOCUMENT ID		TECN	COMMENT
0.082±0.024±0.003	29.2	[1] HE	08B	CLEO	$e^+e^- \to \gamma h^+ h^- h^0 h^0$

[1] HE 08B reports $0.08 \pm 0.02 \pm 0.01 \pm 0.01$ % from a measurement of $[\Gamma(\chi_{c2}(1P) \to p\overline{p}\pi^0\pi^0)/\Gamma_{total}] \times [B(\psi(2S) \to \gamma\chi_{c2}(1P))]$ assuming $B(\psi(2S) \to \gamma\chi_{c2}(1P)) = (9.33\pm0.14\pm0.61)\times10^{-2}$, which we rescale to our best value $B(\psi(2S) \to \gamma\chi_{c2}(1P)) = (9.11 \pm 0.31) \times 10^{-2}$. Our first error is their experiment's error and our second error is the systematic error from using our best value.

$\Gamma(p\overline{p}K^+K^-(\text{non-resonant}))/\Gamma_{total}$ Γ_{45}/Γ

VALUE (units 10^{-4})	EVTS	DOCUMENT ID		TECN	COMMENT
2.00±0.33±0.07	131 ± 12	[1] ABLIKIM	11F	BES3	$\psi(2S) \to \gamma p\overline{p}K^+K^-$

[1] ABLIKIM 11F reports $(2.08\pm0.19\pm0.30)\times10^{-4}$ from a measurement of $[\Gamma(\chi_{c2}(1P) \to p\overline{p}K^+K^-(\text{non-resonant}))/\Gamma_{total}] \times [B(\psi(2S) \to \gamma\chi_{c2}(1P))]$ assuming $B(\psi(2S) \to \gamma\chi_{c2}(1P)) = (8.74 \pm 0.35) \times 10^{-2}$, which we rescale to our best value $B(\psi(2S) \to \gamma\chi_{c2}(1P)) = (9.11 \pm 0.31) \times 10^{-2}$. Our first error is their experiment's error and our second error is the systematic error from using our best value.

$\Gamma(p\overline{p}K^0_S K^0_S)/\Gamma_{total}$ Γ_{46}/Γ

VALUE (units 10^{-4})	CL%	DOCUMENT ID		TECN	COMMENT
<7.9	90	[1] ABLIKIM	06D	BES2	$\psi(2S) \to \chi_{c2}\gamma$

[1] Using $B(\psi(2S) \to \chi_{c2}\gamma) = (9.3 \pm 0.6)\%$.

$\Gamma(p\overline{n}\pi^-)/\Gamma_{total}$ Γ_{47}/Γ

VALUE (units 10^{-4})	EVTS	DOCUMENT ID		TECN	COMMENT
8.9±1.0 OUR AVERAGE					
8.8±1.0±0.3	3309	[1] ABLIKIM	12J	BES3	$\psi(2S) \to \gamma p\overline{n}\pi^-$
10.6±3.6±0.4		[2] ABLIKIM	06I	BES2	$\psi(2S) \to \gamma p\pi^- X$

[1] ABLIKIM 12J reports $[\Gamma(\chi_{c2}(1P) \to p\overline{n}\pi^-)/\Gamma_{total}] \times [B(\psi(2S) \to \gamma\chi_{c2}(1P))] = (0.80 \pm 0.02 \pm 0.09) \times 10^{-4}$ which we divide by our best value $B(\psi(2S) \to \gamma\chi_{c2}(1P)) = (9.11 \pm 0.31) \times 10^{-2}$. Our first error is their experiment's error and our second error is the systematic error from using our best value.

[2] ABLIKIM 06I reports $[\Gamma(\chi_{c2}(1P) \to p\overline{n}\pi^-)/\Gamma_{total}] \times [B(\psi(2S) \to \gamma\chi_{c2}(1P))] = (0.97 \pm 0.20 \pm 0.26) \times 10^{-4}$ which we divide by our best value $B(\psi(2S) \to \gamma\chi_{c2}(1P)) = (9.11 \pm 0.31) \times 10^{-2}$. Our first error is their experiment's error and our second error is the systematic error from using our best value.

$\Gamma(\overline{p}n\pi^+)/\Gamma_{total}$ Γ_{48}/Γ

VALUE (units 10^{-4})	EVTS	DOCUMENT ID		TECN	COMMENT
9.3±0.8±0.3	3732	[1] ABLIKIM	12J	BES3	$\psi(2S) \to \gamma\overline{p}n\pi^+$

[1] ABLIKIM 12J reports $[\Gamma(\chi_{c2}(1P) \to \overline{p}n\pi^+)/\Gamma_{total}] \times [B(\psi(2S) \to \gamma\chi_{c2}(1P))] = (0.85 \pm 0.02 \pm 0.07) \times 10^{-4}$ which we divide by our best value $B(\psi(2S) \to \gamma\chi_{c2}(1P)) = (9.11 \pm 0.31) \times 10^{-2}$. Our first error is their experiment's error and our second error is the systematic error from using our best value.

$\Gamma(p\overline{n}\pi^-\pi^0)/\Gamma_{total}$ Γ_{49}/Γ

VALUE (units 10^{-4})	EVTS	DOCUMENT ID		TECN	COMMENT
22.7±1.8±0.8	2128	[1] ABLIKIM	12J	BES3	$\psi(2S) \to \gamma p\overline{n}\pi^-\pi^0$

[1] ABLIKIM 12J reports $[\Gamma(\chi_{c2}(1P) \to p\overline{n}\pi^-\pi^0)/\Gamma_{total}] \times [B(\psi(2S) \to \gamma\chi_{c2}(1P))] = (2.07 \pm 0.06 \pm 0.15) \times 10^{-4}$ which we divide by our best value $B(\psi(2S) \to \gamma\chi_{c2}(1P)) = (9.11 \pm 0.31) \times 10^{-2}$. Our first error is their experiment's error and our second error is the systematic error from using our best value.

$\Gamma(\overline{p}n\pi^+\pi^0)/\Gamma_{total}$ Γ_{50}/Γ

VALUE (units 10^{-4})	EVTS	DOCUMENT ID		TECN	COMMENT
22.1±1.9±0.8	2352	[1] ABLIKIM	12J	BES3	$\psi(2S) \to \gamma\overline{p}n\pi^+\pi^0$

[1] ABLIKIM 12J reports $[\Gamma(\chi_{c2}(1P) \to \overline{p}n\pi^+\pi^0)/\Gamma_{total}] \times [B(\psi(2S) \to \gamma\chi_{c2}(1P))] = (2.01 \pm 0.06 \pm 0.16) \times 10^{-4}$ which we divide by our best value $B(\psi(2S) \to \gamma\chi_{c2}(1P)) = (9.11 \pm 0.31) \times 10^{-2}$. Our first error is their experiment's error and our second error is the systematic error from using our best value.

$\Gamma(\Lambda\overline{\Lambda})/\Gamma_{total}$ Γ_{51}/Γ

VALUE (units 10^{-4})	DOCUMENT ID
1.92±0.16 OUR FIT	

$\Gamma(\Lambda\overline{\Lambda}\pi^+\pi^-)/\Gamma_{total}$ Γ_{52}/Γ

VALUE (units 10^{-5})	CL%	EVTS	DOCUMENT ID		TECN	COMMENT
131±16±5		371	[1] ABLIKIM	12I	BES3	$\psi(2S) \to \gamma\Lambda\overline{\Lambda}\pi^+\pi^-$
• • • We do not use the following data for averages, fits, limits, etc. • • •						
<350	90		[2] ABLIKIM	06D	BES2	$\psi(2S) \to \chi_{c2}\gamma$

[1] ABLIKIM 12I reports $(137.0\pm7.6\pm15.7)\times10^{-5}$ from a measurement of $[\Gamma(\chi_{c2}(1P) \to \Lambda\overline{\Lambda}\pi^+\pi^-)/\Gamma_{total}] \times [B(\psi(2S) \to \gamma\chi_{c2}(1P))]$ assuming $B(\psi(2S) \to \gamma\chi_{c2}(1P)) = (8.72 \pm 0.34) \times 10^{-2}$, which we rescale to our best value $B(\psi(2S) \to \gamma\chi_{c2}(1P)) = (9.11 \pm 0.31) \times 10^{-2}$. Our first error is their experiment's error and our second error is the systematic error from using our best value.

[2] Using $B(\psi(2S) \to \chi_{c2}\gamma) = (9.3 \pm 0.6)\%$.

$\Gamma(\Lambda\overline{\Lambda}\pi^+\pi^-(\text{non-resonant}))/\Gamma_{total}$ Γ_{53}/Γ

VALUE (units 10^{-5})	EVTS	DOCUMENT ID		TECN	COMMENT
69±16±2	36	[1] ABLIKIM	12I	BES3	$\psi(2S) \to \gamma\Lambda\overline{\Lambda}\pi^+\pi^-$

[1] ABLIKIM 12I reports $(71.8\pm14.5\pm8.2)\times10^{-5}$ from a measurement of $[\Gamma(\chi_{c2}(1P) \to \Lambda\overline{\Lambda}\pi^+\pi^-(\text{non-resonant}))/\Gamma_{total}] \times [B(\psi(2S) \to \gamma\chi_{c2}(1P))]$ assuming $B(\psi(2S) \to \gamma\chi_{c2}(1P)) = (8.72 \pm 0.34) \times 10^{-2}$, which we rescale to our best value $B(\psi(2S) \to \gamma\chi_{c2}(1P)) = (9.11 \pm 0.31) \times 10^{-2}$. Our first error is their experiment's error and our second error is the systematic error from using our best value.

$\Gamma(\Sigma(1385)^+\overline{\Lambda}\pi^- + \text{c.c.})/\Gamma_{total}$ Γ_{54}/Γ

VALUE (units 10^{-5})	CL%	DOCUMENT ID		TECN	COMMENT
<40	90	[1] ABLIKIM	12I	BES3	$\psi(2S) \to \gamma\Sigma(1385)^+\overline{\Lambda}\pi^-$

[1] ABLIKIM 12I reports $< 42 \times 10^{-5}$ from a measurement of $[\Gamma(\chi_{c2}(1P) \to \Sigma(1385)^+\overline{\Lambda}\pi^- + \text{c.c.})/\Gamma_{total}] \times [B(\psi(2S) \to \gamma\chi_{c2}(1P))]$ assuming $B(\psi(2S) \to \gamma\chi_{c2}(1P)) = (8.72 \pm 0.34) \times 10^{-2}$, which we rescale to our best value $B(\psi(2S) \to \gamma\chi_{c2}(1P)) = 9.11 \times 10^{-2}$.

Meson Particle Listings

$\chi_{c2}(1P)$

$\Gamma(\Sigma(1385)^-\overline{\Lambda}\pi^+ + \text{c.c.})/\Gamma_{\text{total}}$ Γ_{55}/Γ

VALUE (units 10^{-5})	CL%	DOCUMENT ID		TECN	COMMENT
<60	90	[1] ABLIKIM	12I	BES3	$\psi(2S) \to \gamma\Sigma(1385)^-\overline{\Lambda}\pi^+$

[1] ABLIKIM 12I reports $< 61 \times 10^{-5}$ from a measurement of $[\Gamma(\chi_{c2}(1P) \to \Sigma(1385)^-\overline{\Lambda}\pi^+ + \text{c.c.})/\Gamma_{\text{total}}] \times [B(\psi(2S) \to \gamma\chi_{c2}(1P))]$ assuming $B(\psi(2S) \to \gamma\chi_{c2}(1P)) = (8.72 \pm 0.34) \times 10^{-2}$, which we rescale to our best value $B(\psi(2S) \to \gamma\chi_{c2}(1P)) = 9.11 \times 10^{-2}$.

$\Gamma(K^+\overline{p}\Lambda + \text{c.c.})/\Gamma_{\text{total}}$ Γ_{56}/Γ

VALUE (units 10^{-4})	EVTS	DOCUMENT ID		TECN	COMMENT
8.1±0.6 OUR AVERAGE					
8.0±0.6±0.3	5k	[1,2] ABLIKIM	13D	BES3	$\psi(2S) \to \gamma\Lambda\overline{p}K^+$
8.7±1.7±0.3		[3] ATHAR	07	CLEO	$\psi(2S) \to \gamma h^+ h^- h^0$

[1] ABLIKIM 13D reports $(8.4 \pm 0.3 \pm 0.6) \times 10^{-4}$ from a measurement of $[\Gamma(\chi_{c2}(1P) \to K^+\overline{p}\Lambda + \text{c.c.})/\Gamma_{\text{total}}] \times [B(\psi(2S) \to \gamma\chi_{c2}(1P))]$ assuming $B(\psi(2S) \to \gamma\chi_{c2}(1P)) = (8.72 \pm 0.34) \times 10^{-2}$, which we rescale to our best value $B(\psi(2S) \to \gamma\chi_{c2}(1P)) = (9.11 \pm 0.31) \times 10^{-2}$. Our first error is their experiment's error and our second error is the systematic error from using our best value.

[2] Using $B(\Lambda \to p\pi^-) = 63.9\%$.

[3] ATHAR 07 reports $(8.5 \pm 1.4 \pm 1.0) \times 10^{-4}$ from a measurement of $[\Gamma(\chi_{c2}(1P) \to K^+\overline{p}\Lambda + \text{c.c.})/\Gamma_{\text{total}}] \times [B(\psi(2S) \to \gamma\chi_{c2}(1P))]$ assuming $B(\psi(2S) \to \gamma\chi_{c2}(1P)) = (9.33 \pm 0.14 \pm 0.61) \times 10^{-2}$, which we rescale to our best value $B(\psi(2S) \to \gamma\chi_{c2}(1P)) = (9.11 \pm 0.31) \times 10^{-2}$. Our first error is their experiment's error and our second error is the systematic error from using our best value.

$\Gamma(K^+\overline{p}\Lambda(1520) + \text{c.c.})/\Gamma_{\text{total}}$ Γ_{57}/Γ

VALUE (units 10^{-4})	EVTS	DOCUMENT ID		TECN	COMMENT
2.9±0.7±0.1	79 ± 13	[1] ABLIKIM	11F	BES3	$\psi(2S) \to \gamma p\overline{p}K^+K^-$

[1] ABLIKIM 11F reports $(3.06 \pm 0.50 \pm 0.54) \times 10^{-4}$ from a measurement of $[\Gamma(\chi_{c2}(1P) \to K^+\overline{p}\Lambda(1520) + \text{c.c.})/\Gamma_{\text{total}}] \times [B(\psi(2S) \to \gamma\chi_{c2}(1P))]$ assuming $B(\psi(2S) \to \gamma\chi_{c2}(1P)) = (8.74 \pm 0.35) \times 10^{-2}$, which we rescale to our best value $B(\psi(2S) \to \gamma\chi_{c2}(1P)) = (9.11 \pm 0.31) \times 10^{-2}$. Our first error is their experiment's error and our second error is the systematic error from using our best value.

$\Gamma(\Lambda(1520)\overline{\Lambda}(1520))/\Gamma_{\text{total}}$ Γ_{58}/Γ

VALUE (units 10^{-4})	EVTS	DOCUMENT ID		TECN	COMMENT
4.8±1.5±0.2	29 ± 7	[1] ABLIKIM	11F	BES3	$\psi(2S) \to \gamma p\overline{p}K^+K^-$

[1] ABLIKIM 11F reports $(5.05 \pm 1.29 \pm 0.93) \times 10^{-4}$ from a measurement of $[\Gamma(\chi_{c2}(1P) \to \Lambda(1520)\overline{\Lambda}(1520))/\Gamma_{\text{total}}] \times [B(\psi(2S) \to \gamma\chi_{c2}(1P))]$ assuming $B(\psi(2S) \to \gamma\chi_{c2}(1P)) = (8.74 \pm 0.35) \times 10^{-2}$, which we rescale to our best value $B(\psi(2S) \to \gamma\chi_{c2}(1P)) = (9.11 \pm 0.31) \times 10^{-2}$. Our first error is their experiment's error and our second error is the systematic error from using our best value.

$\Gamma(\Sigma^0\overline{\Sigma}^0)/\Gamma_{\text{total}}$ Γ_{59}/Γ

VALUE (units 10^{-4})	CL%	EVTS	DOCUMENT ID		TECN	COMMENT
<0.6	90		[1] ABLIKIM	13H	BES3	$\psi(2S) \to \gamma\Sigma^0\overline{\Sigma}^0$
• • • We do not use the following data for averages, fits, limits, etc. • • •						
<0.8	90	7.5 ± 3.4	[2] NAIK	08	CLEO	$\psi(2S) \to \gamma\Sigma^0\overline{\Sigma}^0$

[1] ABLIKIM 13H reports $< 0.65 \times 10^{-4}$ from a measurement of $[\Gamma(\chi_{c2}(1P) \to \Sigma^0\overline{\Sigma}^0)/\Gamma_{\text{total}}] \times [B(\psi(2S) \to \gamma\chi_{c2}(1P))]$ assuming $B(\psi(2S) \to \gamma\chi_{c2}(1P)) = (8.74 \pm 0.35) \times 10^{-2}$, which we rescale to our best value $B(\psi(2S) \to \gamma\chi_{c2}(1P)) = 9.11 \times 10^{-2}$.

[2] NAIK 08 reports $< 0.75 \times 10^{-4}$ from a measurement of $[\Gamma(\chi_{c2}(1P) \to \Sigma^0\overline{\Sigma}^0)/\Gamma_{\text{total}}] \times [B(\psi(2S) \to \gamma\chi_{c2}(1P))]$ assuming $B(\psi(2S) \to \gamma\chi_{c2}(1P)) = (9.33 \pm 0.14 \pm 0.61) \times 10^{-2}$, which we rescale to our best value $B(\psi(2S) \to \gamma\chi_{c2}(1P)) = 9.11 \times 10^{-2}$.

$\Gamma(\Sigma^+\overline{\Sigma}^-)/\Gamma_{\text{total}}$ Γ_{60}/Γ

VALUE (units 10^{-4})	CL%	EVTS	DOCUMENT ID		TECN	COMMENT
<0.7	90	4.0 ± 3.5	[1] NAIK	08	CLEO	$\psi(2S) \to \gamma\Sigma^+\overline{\Sigma}^-$
• • • We do not use the following data for averages, fits, limits, etc. • • •						
<0.8	90		[2] ABLIKIM	13H	BES3	$\psi(2S) \to \gamma\Sigma^+\overline{\Sigma}^-$

[1] NAIK 08 reports $< 0.67 \times 10^{-4}$ from a measurement of $[\Gamma(\chi_{c2}(1P) \to \Sigma^+\overline{\Sigma}^-)/\Gamma_{\text{total}}] \times [B(\psi(2S) \to \gamma\chi_{c2}(1P))]$ assuming $B(\psi(2S) \to \gamma\chi_{c2}(1P)) = (9.33 \pm 0.14 \pm 0.61) \times 10^{-2}$, which we rescale to our best value $B(\psi(2S) \to \gamma\chi_{c2}(1P)) = 9.11 \times 10^{-2}$.

[2] ABLIKIM 13H reports $< 0.88 \times 10^{-4}$ from a measurement of $[\Gamma(\chi_{c2}(1P) \to \Sigma^+\overline{\Sigma}^-)/\Gamma_{\text{total}}] \times [B(\psi(2S) \to \gamma\chi_{c2}(1P))]$ assuming $B(\psi(2S) \to \gamma\chi_{c2}(1P)) = (8.74 \pm 0.35) \times 10^{-2}$, which we rescale to our best value $B(\psi(2S) \to \gamma\chi_{c2}(1P)) = 9.11 \times 10^{-2}$.

$\Gamma(\Sigma(1385)^+\overline{\Sigma}(1385)^-)/\Gamma_{\text{total}}$ Γ_{61}/Γ

VALUE (units 10^{-5})	CL%	DOCUMENT ID		TECN	COMMENT
<16	90	[1] ABLIKIM	12I	BES3	$\psi(2S) \to \gamma\Sigma(1385)^+\overline{\Sigma}(1385)^-$

[1] ABLIKIM 12I reports $< 17 \times 10^{-5}$ from a measurement of $[\Gamma(\chi_{c2}(1P) \to \Sigma(1385)^+\overline{\Sigma}(1385)^-)/\Gamma_{\text{total}}] \times [B(\psi(2S) \to \gamma\chi_{c2}(1P))]$ assuming $B(\psi(2S) \to \gamma\chi_{c2}(1P)) = (8.72 \pm 0.34) \times 10^{-2}$, which we rescale to our best value $B(\psi(2S) \to \gamma\chi_{c2}(1P)) = 9.11 \times 10^{-2}$.

$\Gamma(\Sigma(1385)^-\overline{\Sigma}(1385)^+)/\Gamma_{\text{total}}$ Γ_{62}/Γ

VALUE (units 10^{-5})	CL%	DOCUMENT ID		TECN	COMMENT
<8	90	[1] ABLIKIM	12I	BES3	$\psi(2S) \to \gamma\Sigma(1385)^-\overline{\Sigma}(1385)^+$

[1] ABLIKIM 12I reports $< 8.5 \times 10^{-5}$ from a measurement of $[\Gamma(\chi_{c2}(1P) \to \Sigma(1385)^-\overline{\Sigma}(1385)^+)/\Gamma_{\text{total}}] \times [B(\psi(2S) \to \gamma\chi_{c2}(1P))]$ assuming $B(\psi(2S) \to \gamma\chi_{c2}(1P)) = (8.72 \pm 0.34) \times 10^{-2}$, which we rescale to our best value $B(\psi(2S) \to \gamma\chi_{c2}(1P)) = 9.11 \times 10^{-2}$.

$\Gamma(\Xi^0\overline{\Xi}^0)/\Gamma_{\text{total}}$ Γ_{63}/Γ

VALUE (units 10^{-4})	CL%	EVTS	DOCUMENT ID		TECN	COMMENT
<1.1	90	2.9 ± 1.7	[1] NAIK	08	CLEO	$\psi(2S) \to \gamma\Xi^0\overline{\Xi}^0$

[1] NAIK 08 reports $< 1.06 \times 10^{-4}$ from a measurement of $[\Gamma(\chi_{c2}(1P) \to \Xi^0\overline{\Xi}^0)/\Gamma_{\text{total}}] \times [B(\psi(2S) \to \gamma\chi_{c2}(1P))]$ assuming $B(\psi(2S) \to \gamma\chi_{c2}(1P)) = (9.33 \pm 0.14 \pm 0.61) \times 10^{-2}$, which we rescale to our best value $B(\psi(2S) \to \gamma\chi_{c2}(1P)) = 9.11 \times 10^{-2}$.

$\Gamma(\Xi^-\overline{\Xi}^+)/\Gamma_{\text{total}}$ Γ_{64}/Γ

VALUE (units 10^{-4})	CL%	EVTS	DOCUMENT ID		TECN	COMMENT
1.48±0.33±0.05		29 ± 5	[1] NAIK	08	CLEO	$\psi(2S) \to \gamma\Xi^+\overline{\Xi}^-$
• • • We do not use the following data for averages, fits, limits, etc. • • •						
< 3.7	90		[2] ABLIKIM	06D	BES2	$\psi(2S) \to \chi_{c2}\gamma$

[1] NAIK 08 reports $(1.45 \pm 0.30 \pm 0.15) \times 10^{-4}$ from a measurement of $[\Gamma(\chi_{c2}(1P) \to \Xi^-\overline{\Xi}^+)/\Gamma_{\text{total}}] \times [B(\psi(2S) \to \gamma\chi_{c2}(1P))]$ assuming $B(\psi(2S) \to \gamma\chi_{c2}(1P)) = (9.33 \pm 0.14 \pm 0.61) \times 10^{-2}$, which we rescale to our best value $B(\psi(2S) \to \gamma\chi_{c2}(1P)) = (9.11 \pm 0.31) \times 10^{-2}$. Our first error is their experiment's error and our second error is the systematic error from using our best value.

[2] Using $B(\psi(2S) \to \chi_{c2}\gamma) = (9.3 \pm 0.6)\%$.

$\Gamma(J/\psi(1S)\pi^+\pi^-\pi^0)/\Gamma_{\text{total}}$ Γ_{65}/Γ

VALUE	CL%	DOCUMENT ID		TECN	COMMENT
<0.015	90	BARATE	81	SPEC	190 GeV π^- Be $\to 2\pi 2\mu$

$\Gamma(\eta_c(1S)\pi^+\pi^-)/\Gamma(\overline{K}^0K^+\pi^- + \text{c.c.})$ Γ_{66}/Γ_{29}

VALUE	CL%	DOCUMENT ID		TECN	COMMENT
<16.4	90	[1] LEES	12AE	BABR	$e^+e^- \to e^+e^-\pi^+\pi^-\eta_c$

[1] We divided the reported limit by 2 to take into account the $K^0_L K^+\pi^-$ mode.

RADIATIVE DECAYS

$\Gamma(\gamma J/\psi(1S))/\Gamma_{\text{total}}$ Γ_{67}/Γ

VALUE	DOCUMENT ID		TECN	COMMENT
0.192±0.007 OUR FIT				
• • • We do not use the following data for averages, fits, limits, etc. • • •				
0.199±0.005±0.012	[1] ADAM	05A	CLEO	$e^+e^- \to \psi(2S) \to \gamma\chi_{c2}$

[1] Uses $B(\psi(2S) \to \gamma\chi_{c2} \to \gamma\gamma J/\psi)$ from ADAM 05A and $B(\psi(2S) \to \gamma\chi_{c2})$ from ATHAR 04.

$\Gamma(\gamma\rho^0)/\Gamma_{\text{total}}$ Γ_{68}/Γ

VALUE (units 10^{-6})	CL%	EVTS	DOCUMENT ID		TECN	COMMENT
<20	90	13 ± 11	[1] ABLIKIM	11E	BES3	$\psi(2S) \to \gamma\gamma\rho^0$
• • • We do not use the following data for averages, fits, limits, etc. • • •						
<40	90	17.2 ± 6.8	[2] BENNETT	08A	CLEO	$\psi(2S) \to \gamma\gamma\rho^0$

[1] ABLIKIM 11E reports $< 20.8 \times 10^{-6}$ from a measurement of $[\Gamma(\chi_{c2}(1P) \to \gamma\rho^0)/\Gamma_{\text{total}}] \times [B(\psi(2S) \to \gamma\chi_{c2}(1P))]$ assuming $B(\psi(2S) \to \gamma\chi_{c2}(1P)) = (8.74 \pm 0.35) \times 10^{-2}$, which we rescale to our best value $B(\psi(2S) \to \gamma\chi_{c2}(1P)) = 9.11 \times 10^{-2}$.

[2] BENNETT 08A reports $< 50 \times 10^{-6}$ from a measurement of $[\Gamma(\chi_{c2}(1P) \to \gamma\rho^0)/\Gamma_{\text{total}}] \times [B(\psi(2S) \to \gamma\chi_{c2}(1P))]$ assuming $B(\psi(2S) \to \gamma\chi_{c2}(1P)) = (8.1 \pm 0.4) \times 10^{-2}$, which we rescale to our best value $B(\psi(2S) \to \gamma\chi_{c2}(1P)) = 9.11 \times 10^{-2}$.

$\Gamma(\gamma\omega)/\Gamma_{\text{total}}$ Γ_{69}/Γ

VALUE (units 10^{-6})	CL%	EVTS	DOCUMENT ID		TECN	COMMENT
<6	90	1 ± 6	[1] ABLIKIM	11E	BES3	$\psi(2S) \to \gamma\gamma\omega$
• • • We do not use the following data for averages, fits, limits, etc. • • •						
<6	90	0.0 ± 1.8	[2] BENNETT	08A	CLEO	$\psi(2S) \to \gamma\gamma\omega$

[1] ABLIKIM 11E reports $< 6.1 \times 10^{-6}$ from a measurement of $[\Gamma(\chi_{c2}(1P) \to \gamma\omega)/\Gamma_{\text{total}}] \times [B(\psi(2S) \to \gamma\chi_{c2}(1P))]$ assuming $B(\psi(2S) \to \gamma\chi_{c2}(1P)) = (8.74 \pm 0.35) \times 10^{-2}$, which we rescale to our best value $B(\psi(2S) \to \gamma\chi_{c2}(1P)) = 9.11 \times 10^{-2}$.

[2] BENNETT 08A reports $< 7.0 \times 10^{-6}$ from a measurement of $[\Gamma(\chi_{c2}(1P) \to \gamma\omega)/\Gamma_{\text{total}}] \times [B(\psi(2S) \to \gamma\chi_{c2}(1P))]$ assuming $B(\psi(2S) \to \gamma\chi_{c2}(1P)) = (8.1 \pm 0.4) \times 10^{-2}$, which we rescale to our best value $B(\psi(2S) \to \gamma\chi_{c2}(1P)) = 9.11 \times 10^{-2}$.

$\Gamma(\gamma\phi)/\Gamma_{\text{total}}$ Γ_{70}/Γ

VALUE (units 10^{-6})	CL%	EVTS	DOCUMENT ID		TECN	COMMENT
< 8	90	5 ± 5	[1] ABLIKIM	11E	BES3	$\psi(2S) \to \gamma\gamma\phi$
• • • We do not use the following data for averages, fits, limits, etc. • • •						
<12	90	1.3 ± 2.5	[2] BENNETT	08A	CLEO	$\psi(2S) \to \gamma\gamma\phi$

[1] ABLIKIM 11E reports $< 8.1 \times 10^{-6}$ from a measurement of $[\Gamma(\chi_{c2}(1P) \to \gamma\phi)/\Gamma_{\text{total}}] \times [B(\psi(2S) \to \gamma\chi_{c2}(1P))]$ assuming $B(\psi(2S) \to \gamma\chi_{c2}(1P)) = (8.74 \pm 0.35) \times 10^{-2}$, which we rescale to our best value $B(\psi(2S) \to \gamma\chi_{c2}(1P)) = 9.11 \times 10^{-2}$.

[2] BENNETT 08A reports $< 13 \times 10^{-6}$ from a measurement of $[\Gamma(\chi_{c2}(1P) \to \gamma\phi)/\Gamma_{\text{total}}] \times [B(\psi(2S) \to \gamma\chi_{c2}(1P))]$ assuming $B(\psi(2S) \to \gamma\chi_{c2}(1P)) = (8.1 \pm 0.4) \times 10^{-2}$, which we rescale to our best value $B(\psi(2S) \to \gamma\chi_{c2}(1P)) = 9.11 \times 10^{-2}$.

$\Gamma(\gamma\gamma)/\Gamma_{\text{total}}$ Γ_{71}/Γ

VALUE (units 10^{-4})	DOCUMENT ID
2.74±0.14 OUR FIT	

$\Gamma(\gamma\gamma)/\Gamma(\gamma J/\psi(1S))$ Γ_{71}/Γ_{67}

VALUE (units 10^{-3})	DOCUMENT ID	TECN	COMMENT
1.43±0.08 OUR FIT			
0.99±0.18	[1] AMBROGIANI 00B	E835	$\overline{p}p \to \chi_{c2} \to \gamma\gamma, \gamma J/\psi$

[1] Calculated by us using $B(J/\psi(1S) \to e^+e^-) = 0.0593 \pm 0.0010$.

$\Gamma(\gamma\gamma)/\Gamma_{\text{total}} \times \Gamma(p\overline{p})/\Gamma_{\text{total}}$ $\Gamma_{71}/\Gamma \times \Gamma_{38}/\Gamma$

VALUE (units 10^{-8})	DOCUMENT ID	TECN	COMMENT
2.06±0.16 OUR FIT			
1.7 ±0.4 OUR AVERAGE			
1.60±0.42	ARMSTRONG 93	E760	$\overline{p}p \to \gamma\gamma X$
9.9 ±4.5	BAGLIN 87B	SPEC	$\overline{p}p \to \gamma\gamma X$

$\chi_{c2}(1P)$ CROSS-PARTICLE BRANCHING RATIOS

$\Gamma(\chi_{c2}(1P) \to K^+K^-\pi^+\pi^-)/\Gamma_{\text{total}} \times \Gamma(\psi(2S) \to \gamma\chi_{c2}(1P))/\Gamma(\psi(2S) \to J/\psi(1S)\pi^+\pi^-)$ $\Gamma_{14}/\Gamma \times \Gamma_{130}^{\psi(2S)}/\Gamma_{11}^{\psi(2S)}$

VALUE (units 10^{-3})	DOCUMENT ID	TECN	COMMENT
2.34±0.26 OUR FIT			
2.5 ±0.9 OUR AVERAGE Error includes scale factor of 2.3.			
1.90±0.14±0.44	BAI 99B	BES	$\psi(2S) \to \gamma\chi_{c2}$
3.8 ±0.67	[1] TANENBAUM 78	MRK1	$\psi(2S) \to \gamma\chi_{c2}$

[1] The reported value is derived using $B(\psi(2S) \to \pi^+\pi^- J/\psi) \times B(J/\psi \to \ell^+\ell^-) = (4.6 \pm 0.7)\%$. Calculated by us using $B(J/\psi \to \ell^+\ell^-) = 0.1181 \pm 0.0020$.

$\Gamma(\chi_{c2}(1P) \to K^*(892)^0\overline{K}^*(892)^0)/\Gamma_{\text{total}} \times \Gamma(\psi(2S) \to \gamma\chi_{c2}(1P))/\Gamma_{\text{total}}$ $\Gamma_{17}/\Gamma \times \Gamma_{130}^{\psi(2S)}/\Gamma^{\psi(2S)}$

VALUE (units 10^{-4})	DOCUMENT ID	TECN	COMMENT
2.2 ±0.4 OUR FIT			
3.11±0.36±0.48	ABLIKIM 04H	BES2	$\psi(2S) \to \gamma\chi_{c2}$

$\Gamma(\chi_{c2}(1P) \to p\overline{p})/\Gamma_{\text{total}} \times \Gamma(\psi(2S) \to \gamma\chi_{c2}(1P))/\Gamma(\psi(2S) \to J/\psi(1S)\pi^+\pi^-)$ $\Gamma_{38}/\Gamma \times \Gamma_{130}^{\psi(2S)}/\Gamma_{11}^{\psi(2S)}$

VALUE (units 10^{-5})	DOCUMENT ID	TECN	COMMENT
1.99±0.10 OUR FIT			
1.4 ±1.1	[1] BAI 98I	BES	$\psi(2S) \to \gamma\chi_{c2} \to \gamma p\overline{p}$

[1] Calculated by us. The value for $B(\chi_{c2} \to p\overline{p})$ reported in BAI 98I is derived using $B(\psi(2S) \to \gamma\chi_{c2}) = (7.8 \pm 0.8)\%$ and $B(\psi(2S) \to J/\psi(1S)\pi^+\pi^-) = (32.4 \pm 2.6)\%$ [BAI 98D].

$\Gamma(\chi_{c2}(1P) \to p\overline{p})/\Gamma_{\text{total}} \times \Gamma(\psi(2S) \to \gamma\chi_{c2}(1P))/\Gamma_{\text{total}}$ $\Gamma_{38}/\Gamma \times \Gamma_{130}^{\psi(2S)}/\Gamma^{\psi(2S)}$

VALUE (units 10^{-6})	EVTS	DOCUMENT ID	TECN	COMMENT
6.85±0.33 OUR FIT				
7.1 ±0.5 OUR AVERAGE Error includes scale factor of 1.2.				
7.3 ±0.4 ±0.3	405	ABLIKIM 13V	BES3	$\psi(2S) \to \gamma p\overline{p}$
7.2 ±0.7 ±0.4	121 ± 12	[1] NAIK 08	CLEO	$\psi(2S) \to \gamma p\overline{p}$
$4.4\ ^{+1.6}_{-1.4}$ ±0.6	$14.3^{+5.2}_{-4.7}$	BAI 04F	BES	$\psi(2S) \to \gamma\chi_{c2}(1P) \to \gamma\overline{p}p$

[1] Calculated by us. NAIK 08 reports $B(\chi_{c2} \to p\overline{p}) = (7.7 \pm 0.8 \pm 0.4 \pm 0.5) \times 10^{-5}$ using $B(\psi(2S) \to \gamma\chi_{c2}) = (9.33 \pm 0.14 \pm 0.61)\%$.

$\Gamma(\chi_{c2}(1P) \to \Lambda\overline{\Lambda})/\Gamma_{\text{total}} \times \Gamma(\psi(2S) \to \gamma\chi_{c2}(1P))/\Gamma_{\text{total}}$ $\Gamma_{51}/\Gamma \times \Gamma_{130}^{\psi(2S)}/\Gamma^{\psi(2S)}$

VALUE (units 10^{-6})	EVTS	DOCUMENT ID	TECN	COMMENT
17.5±1.3 OUR FIT				
17.4±1.4 OUR AVERAGE				
18.2±1.4±0.9	207	[1] ABLIKIM 13H	BES3	$\psi(2S) \to \gamma\Lambda\overline{\Lambda}$
15.9±2.1±1.0	71 ± 9	[2] NAIK 08	CLEO	$\psi(2S) \to \gamma\Lambda\overline{\Lambda}$

[1] Calculated by us. ABLIKIM 13H reports $B(\chi_{c2} \to \Lambda\overline{\Lambda}) = (20.8 \pm 1.6 \pm 2.3) \times 10^{-5}$ from a measurement of $B(\chi_{c2} \to \Lambda\overline{\Lambda}) \times B(\psi(2S) \to \gamma\chi_{c2})$ assuming $B(\psi(2S) \to \gamma\chi_{c2}) = (8.74 \pm 0.35)\%$.

[2] Calculated by us. NAIK 08 reports $B(\chi_{c2} \to \Lambda\overline{\Lambda}) = (17.0 \pm 2.2 \pm 1.1 \pm 1.1) \times 10^{-5}$ using $B(\psi(2S) \to \gamma\chi_{c2}) = (9.33 \pm 0.14 \pm 0.61)\%$.

$\Gamma(\chi_{c2}(1P) \to \Lambda\overline{\Lambda})/\Gamma_{\text{total}} \times \Gamma(\psi(2S) \to \gamma\chi_{c2}(1P))/\Gamma(\psi(2S) \to J/\psi(1S)\pi^+\pi^-)$ $\Gamma_{51}/\Gamma \times \Gamma_{130}^{\psi(2S)}/\Gamma_{11}^{\psi(2S)}$

VALUE (units 10^{-5})	EVTS	DOCUMENT ID	TECN	COMMENT
5.1±0.4 OUR FIT				
$\mathbf{7.1^{+3.1}_{-2.9}\pm1.3}$	$8.3^{+3.7}_{-3.4}$	[1] BAI 03E	BES	$\psi(2S) \to \gamma\Lambda\overline{\Lambda}$

[1] BAI 03E reports $[\ B(\chi_{c2} \to \Lambda\overline{\Lambda})\ B(\psi(2S) \to \gamma\chi_{c2})\ /\ B(\psi(2S) \to J/\psi\pi^+\pi^-)\ ] \times [B^2(\Lambda \to \pi^- p)\ /\ B(J/\psi \to p\overline{p})\ ] = (1.33^{+0.59}_{-0.55} \pm 0.25)\%$. We calculate from this measurement the presented value using $B(\Lambda \to \pi^- p) = (63.9 \pm 0.5)\%$ and $B(J/\psi \to p\overline{p}) = (2.17 \pm 0.07) \times 10^{-3}$.

$\Gamma(\chi_{c2}(1P) \to \pi\pi)/\Gamma_{\text{total}} \times \Gamma(\psi(2S) \to \gamma\chi_{c2}(1P))/\Gamma_{\text{total}}$ $\Gamma_{22}/\Gamma \times \Gamma_{130}^{\psi(2S)}/\Gamma^{\psi(2S)}$

VALUE (units 10^{-4})	EVTS	DOCUMENT ID	TECN	COMMENT
2.12±0.08 OUR FIT				
2.17±0.09 OUR AVERAGE				
2.19±0.05±0.15	4.5k	[1] ABLIKIM 10A	BES3	$e^+e^- \to \psi(2S) \to \gamma\chi_{c2}$
2.23±0.06±0.10	2.5k	[2] ASNER 09	CLEO	$\psi(2S) \to \gamma\pi^+\pi^-$
1.90±0.08±0.20	0.8k	[3] ASNER 09	CLEO	$\psi(2S) \to \gamma\pi^0\pi^0$

[1] Calculated by us. ABLIKIM 10A reports $B(\chi_{c2} \to \pi^0\pi^0) = (0.88 \pm 0.02 \pm 0.06 \pm 0.04) \times 10^{-3}$ using $B(\psi(2S) \to \gamma\chi_{c2}) = (8.3 \pm 0.4)\%$. We have multiplied the $\pi^0\pi^0$ measurement by 3 to obtain $\pi\pi$.

[2] Calculated by us. ASNER 09 reports $B(\chi_{c2} \to \pi^+\pi^-) = (1.59 \pm 0.04 \pm 0.07 \pm 0.10) \times 10^{-3}$ using $B(\psi(2S) \to \gamma\chi_{c2}) = (9.33 \pm 0.14 \pm 0.61)\%$. We have multiplied the $\pi^+\pi^-$ measurement by 3/2 to obtain $\pi\pi$.

[3] Calculated by us. ASNER 09 reports $B(\chi_{c2} \to \pi^0\pi^0) = (0.68 \pm 0.03 \pm 0.07 \pm 0.04) \times 10^{-3}$ using $B(\psi(2S) \to \gamma\chi_{c2}) = (9.33 \pm 0.14 \pm 0.61)\%$. We have multiplied the $\pi^0\pi^0$ measurement by 3 to obtain $\pi\pi$.

$\Gamma(\chi_{c2}(1P) \to \pi\pi)/\Gamma_{\text{total}} \times \Gamma(\psi(2S) \to \gamma\chi_{c2}(1P))/\Gamma(\psi(2S) \to J/\psi(1S)\pi^+\pi^-)$ $\Gamma_{22}/\Gamma \times \Gamma_{130}^{\psi(2S)}/\Gamma_{11}^{\psi(2S)}$

VALUE (units 10^{-3})	EVTS	DOCUMENT ID	TECN	COMMENT
0.616±0.023 OUR FIT				
0.54 ±0.06 OUR AVERAGE				
0.66 ±0.18 ±0.37	21 ± 6	[1] BAI 03C	BES	$\psi(2S) \to \gamma\pi^0\pi^0$
0.54 ±0.05 ±0.04	185 ± 16	[2] BAI 98I	BES	$\psi(2S) \to \gamma\pi^+\pi^-$

[1] We have multiplied $\pi^0\pi^0$ measurement by 3 to obtain $\pi\pi$.

[2] Calculated by us. The value for $B(\chi_{c2} \to \pi^+\pi^-)$ reported by BAI 98I is derived using $B(\psi(2S) \to \gamma\chi_{c2}) = (7.8 \pm 0.8)\%$ and $B(\psi(2S) \to J/\psi\pi^+\pi^-) = (32.4 \pm 2.6)\%$ [BAI 98D]. We have multiplied $\pi^+\pi^-$ measurement by 3/2 to obtain $\pi\pi$.

$\Gamma(\chi_{c2}(1P) \to \eta\eta)/\Gamma_{\text{total}} \times \Gamma(\psi(2S) \to \gamma\chi_{c2}(1P))/\Gamma_{\text{total}}$ $\Gamma_{26}/\Gamma \times \Gamma_{130}^{\psi(2S)}/\Gamma^{\psi(2S)}$

VALUE (units 10^{-4})	CL%	EVTS	DOCUMENT ID	TECN	COMMENT
0.52±0.04 OUR FIT					
0.52±0.04 OUR AVERAGE					
0.54±0.03±0.04		386	[1] ABLIKIM 10A	BES3	$e^+e^- \to \psi(2S) \to \gamma\chi_{c2}$
0.47±0.05±0.05		156 ± 14	ASNER 09	CLEO	$\psi(2S) \to \gamma\eta\eta$
• • • We do not use the following data for averages, fits, limits, etc. • • •					
< 0.44	90		[2] ADAMS 07	CLEO	$\psi(2S) \to \gamma\chi_{c2}$
< 3	90		BAI 03C	BES	$\psi(2S) \to \gamma\eta\eta \to 5\gamma$
0.62±0.31±0.19			LEE 85	CBAL	$\psi(2S) \to$ photons

[1] Calculated by us. ABLIKIM 10A reports $B(\chi_{c2} \to \eta\eta) = (0.65 \pm 0.04 \pm 0.05 \pm 0.03) \times 10^{-3}$ using $B(\psi(2S) \to \gamma\chi_{c2}) = (8.3 \pm 0.4)\%$.

[2] Superseded by ASNER 09.

$\Gamma(\chi_{c2}(1P) \to K^+K^-)/\Gamma_{\text{total}} \times \Gamma(\psi(2S) \to \gamma\chi_{c2}(1P))/\Gamma_{\text{total}}$ $\Gamma_{27}/\Gamma \times \Gamma_{130}^{\psi(2S)}/\Gamma^{\psi(2S)}$

VALUE (units 10^{-5})	EVTS	DOCUMENT ID	TECN	COMMENT
9.6±0.6 OUR FIT				
10.5±0.3±0.6	1.6k	[1] ASNER 09	CLEO	$\psi(2S) \to \gamma K^+K^-$

[1] Calculated by us. ASNER 09 reports $B(\chi_{c2} \to K^+K^-) = (1.13 \pm 0.03 \pm 0.06 \pm 0.07) \times 10^{-3}$ using $B(\psi(2S) \to \gamma\chi_{c2}) = (9.33 \pm 0.14 \pm 0.61)\%$.

$\Gamma(\chi_{c2}(1P) \to K^+K^-)/\Gamma_{\text{total}} \times \Gamma(\psi(2S) \to \gamma\chi_{c2}(1P))/\Gamma(\psi(2S) \to J/\psi(1S)\pi^+\pi^-)$ $\Gamma_{27}/\Gamma \times \Gamma_{130}^{\psi(2S)}/\Gamma_{11}^{\psi(2S)}$

VALUE (units 10^{-3})	EVTS	DOCUMENT ID	TECN	COMMENT
0.278±0.017 OUR FIT				
0.190±0.034±0.019	115 ± 13	[1] BAI 98I	BES	$\psi(2S) \to \gamma K^+K^-$

[1] Calculated by us. The value for $B(\chi_{c2} \to K^+K^-)$ reported by BAI 98I is derived using $B(\psi(2S) \to \gamma\chi_{c2}) = (7.8 \pm 0.8)\%$ and $B(\psi(2S) \to J/\psi\pi^+\pi^-) = (32.4 \pm 2.6)\%$ [BAI 98D].

$\Gamma(\chi_{c2}(1P) \to K^0_S K^0_S)/\Gamma_{\text{total}} \times \Gamma(\psi(2S) \to \gamma\chi_{c2}(1P))/\Gamma_{\text{total}}$ $\Gamma_{28}/\Gamma \times \Gamma_{130}^{\psi(2S)}/\Gamma^{\psi(2S)}$

VALUE (units 10^{-5})	EVTS	DOCUMENT ID	TECN	COMMENT
5.0 ±0.4 OUR FIT				
5.0 ±0.4 OUR AVERAGE				
4.9 ±0.3 ±0.3	373 ± 20	[1] ASNER 09	CLEO	$\psi(2S) \to \gamma K^0_S K^0_S$
5.72±0.76±0.63	65	ABLIKIM 05O	BES2	$\psi(2S) \to \gamma K^0_S K^0_S$

[1] Calculated by us. ASNER 09 reports $B(\chi_{c2} \to K^0_S K^0_S) = (0.53 \pm 0.03 \pm 0.03 \pm 0.03) \times 10^{-3}$ using $B(\psi(2S) \to \gamma\chi_{c2}) = (9.33 \pm 0.14 \pm 0.61)\%$.

Meson Particle Listings

$\chi_{c2}(1P)$

$\Gamma(\chi_{c2}(1P) \to K^0_S K^0_S)/\Gamma_{\rm total} \times \Gamma(\psi(2S) \to \gamma\chi_{c2}(1P))/\Gamma(\psi(2S) \to J/\psi(1S)\pi^+\pi^-)$ $\Gamma_{28}/\Gamma \times \Gamma^{\psi(2S)}_{130}/\Gamma^{\psi(2S)}_{11}$

VALUE (units 10^{-5})		DOCUMENT ID		TECN	COMMENT
14.5±1.1 OUR FIT					
14.7±4.1±3.3		[1] BAI	99B	BES	$\psi(2S) \to \gamma K^0_S K^0_S$

[1] Calculated by us. The value of $B(\chi_{c2} \to K^0_S K^0_S)$ reported by BAI 99B was derived using $B(\psi(2S) \to \gamma\chi_{c2}(1P)) = (7.8 \pm 0.8)\%$ and $B(\psi(2S) \to J/\psi\pi^+\pi^-) = (32.4 \pm 2.6)\%$ [BAI 98D].

$\Gamma(\chi_{c2}(1P) \to \overline{K}^0 K^+\pi^- + \text{c.c.})/\Gamma_{\rm total} \times \Gamma(\psi(2S) \to \gamma\chi_{c2}(1P))/\Gamma_{\rm total}$ $\Gamma_{29}/\Gamma \times \Gamma^{\psi(2S)}_{130}/\Gamma^{\psi(2S)}$

VALUE (units 10^{-4})	EVTS	DOCUMENT ID		TECN	COMMENT
1.22±0.17 OUR FIT					
1.15±0.18 OUR AVERAGE					
1.21±0.19±0.09	37	[1] ATHAR	07	CLEO	$\psi(2S) \to \gamma K^0_S K^\pm\pi^\mp$
0.97±0.32±0.13	28	[2] ABLIKIM	06R	BES2	$\psi(2S) \to \gamma K^0_S K^\pm\pi^\mp$

[1] Calculated by us. ATHAR 07 reports $B(\chi_{c2} \to \overline{K}^0 K^+\pi^- + \text{c.c.}) = (1.3 \pm 0.2 \pm 0.1 \pm 0.1) \times 10^{-3}$ using $B(\psi(2S) \to \gamma\chi_{c2}) = (9.33 \pm 0.14 \pm 0.61)\%$.

[2] Calculated by us. ABLIKIM 06R reports $B(\chi_{c2} \to K^0_S K^\pm\pi^\mp) = (0.6 \pm 0.2 \pm 0.1) \times 10^{-3}$ using $B(\psi(2S) \to \gamma\chi_{c2}) = (8.1 \pm 0.6)\%$. We have multiplied by 2 to obtain $\overline{K}^0 K^+\pi^-$ + c.c. from $K^0_S K^\pm\pi^\mp$.

$\Gamma(\chi_{c2}(1P) \to 2(\pi^+\pi^-))/\Gamma_{\rm total} \times \Gamma(\psi(2S) \to \gamma\chi_{c2}(1P))/\Gamma(\psi(2S) \to J/\psi(1S)\pi^+\pi^-)$ $\Gamma_1/\Gamma \times \Gamma^{\psi(2S)}_{130}/\Gamma^{\psi(2S)}_{11}$

VALUE (units 10^{-3})		DOCUMENT ID		TECN	COMMENT
2.83±0.27 OUR FIT					
3.1 ±1.0 OUR AVERAGE	Error includes scale factor of 2.5.				
2.3 ±0.1 ±0.5		[1] BAI	99B	BES	$\psi(2S) \to \gamma\chi_{c2}$
4.3 ±0.6		[2] TANENBAUM	78	MRK1	$\psi(2S) \to \gamma\chi_{c2}$

[1] Calculated by us. The value for $B(\chi_{c2} \to 2\pi^+ 2\pi^-)$ reported in BAI 99B is derived using $B(\psi(2S) \to \gamma\chi_{c2}) = (7.8 \pm 0.8)\%$ and $B(\psi(2S) \to J/\psi(1S)\pi^+\pi^-) = (32.4 \pm 2.6)\%$ [BAI 98D].

[2] The value for $B(\psi(2S) \to \gamma\chi_{c2}) \times B(\chi_{c2} \to 2\pi^+\pi^-)$ reported in TANENBAUM 78 is derived using $B(\psi(2S) \to J/\psi(1S)\pi^+\pi^-) \times B(J/\psi(1S) \ell^+\ell^-) = (4.6 \pm 0.7)\%$. Calculated by us using $B(J/\psi(1S) \to \ell^+\ell^-) = 0.1181 \pm 0.0020$.

$\Gamma(\chi_{c2}(1P) \to K^+K^-K^+K^-)/\Gamma_{\rm total} \times \Gamma(\psi(2S) \to \gamma\chi_{c2}(1P))/\Gamma_{\rm total}$ $\Gamma_{36}/\Gamma \times \Gamma^{\psi(2S)}_{130}/\Gamma^{\psi(2S)}$

VALUE (units 10^{-4})	EVTS	DOCUMENT ID		TECN	COMMENT
1.57±0.19 OUR FIT					
1.76±0.16±0.24	160	[1] ABLIKIM	06T	BES2	$\psi(2S) \to \gamma 2K^+2K^-$

[1] Calculated by us. The value of $B(\chi_{c2} \to 2K^+2K^-)$ reported by ABLIKIM 06T was derived using $B(\psi(2S) \to \gamma\chi_{c2}(1P)) = (8.1 \pm 0.4)\%$.

$\Gamma(\chi_{c2}(1P) \to K^+K^-K^+K^-)/\Gamma_{\rm total} \times \Gamma(\psi(2S) \to \gamma\chi_{c2}(1P))/\Gamma(\psi(2S) \to J/\psi(1S)\pi^+\pi^-)$ $\Gamma_{36}/\Gamma \times \Gamma^{\psi(2S)}_{130}/\Gamma^{\psi(2S)}_{11}$

VALUE (units 10^{-4})		DOCUMENT ID		TECN	COMMENT
4.6±0.5 OUR FIT					
3.6±0.6±0.6		[1] BAI	99B	BES	$\psi(2S) \to \gamma 2K^+2K^-$

[1] Calculated by us. The value of $B(\chi_{c2} \to 2K^+2K^-)$ reported by BAI 99B was derived using $B(\psi(2S) \to \gamma\chi_{c2}(1P)) = (7.8 \pm 0.8)\%$ and $B(\psi(2S) \to J/\psi\pi^+\pi^-) = (32.4 \pm 2.6)\%$ [BAI 98D].

$\Gamma(\chi_{c2}(1P) \to \phi\phi)/\Gamma_{\rm total} \times \Gamma(\psi(2S) \to \gamma\chi_{c2}(1P))/\Gamma_{\rm total}$ $\Gamma_{19}/\Gamma \times \Gamma^{\psi(2S)}_{130}/\Gamma^{\psi(2S)}$

VALUE (units 10^{-4})	EVTS	DOCUMENT ID		TECN	COMMENT
1.02±0.08 OUR FIT					
0.98±0.13 OUR AVERAGE	Error includes scale factor of 1.3.				
0.94±0.03±0.10	849	[1] ABLIKIM	11K	BES3	$\psi(2S) \to \gamma$ hadrons
1.38±0.24±0.23	41	[2] ABLIKIM	06T	BES2	$\psi(2S) \to \gamma 2K^+2K^-$

[1] Calculated by us. The value of $B(\chi_{c2} \to \phi\phi)$ reported by ABLIKIM 11K was derived using $B(\psi(2S) \to \gamma\chi_{c2}(1P)) = (8.74 \pm 0.35)\%$.

[2] Calculated by us. The value of $B(\chi_{c2} \to \phi\phi)$ reported by ABLIKIM 06T was derived using $B(\psi(2S) \to \gamma\chi_{c2}(1P)) = (8.1 \pm 0.4)\%$.

$\Gamma(\chi_{c2}(1P) \to \phi\phi)/\Gamma_{\rm total} \times \Gamma(\psi(2S) \to \gamma\chi_{c2}(1P))/\Gamma(\psi(2S) \to J/\psi(1S)\pi^+\pi^-)$ $\Gamma_{19}/\Gamma \times \Gamma^{\psi(2S)}_{130}/\Gamma^{\psi(2S)}_{11}$

VALUE (units 10^{-4})		DOCUMENT ID		TECN	COMMENT
2.95±0.24 OUR FIT					
4.8 ±1.3 ±1.3		[1] BAI	99B	BES	$\psi(2S) \to \gamma 2K^+2K^-$

[1] Calculated by us. The value of $B(\chi_{c2} \to \phi\phi)$ reported by BAI 99B was derived using $B(\psi(2S) \to \gamma\chi_{c2}(1P)) = (7.8 \pm 0.8)\%$ and $B(\psi(2S) \to J/\psi\pi^+\pi^-) = (32.4 \pm 2.6)\%$ [BAI 98D].

$\Gamma(\chi_{c2}(1P) \to \gamma J/\psi(1S))/\Gamma_{\rm total} \times \Gamma(\psi(2S) \to \gamma\chi_{c2}(1P))/\Gamma_{\rm total}$ $\Gamma_{67}/\Gamma \times \Gamma^{\psi(2S)}_{130}/\Gamma^{\psi(2S)}$

VALUE (units 10^{-2})	EVTS	DOCUMENT ID		TECN	COMMENT
1.75 ±0.04 OUR FIT					
1.52 ±0.15 OUR AVERAGE	Error includes scale factor of 2.6. See the ideogram below.				
1.874±0.007±0.102	76k	ABLIKIM	12O	BES3	$\psi(2S) \to \gamma\chi_{c2}$
1.62 ±0.04 ±0.12	5.8k	BAI	04I	BES2	$\psi(2S) \to J/\psi\gamma\gamma$
0.99 ±0.10 ±0.08		GAISER	86	CBAL	$\psi(2S) \to \gamma$X
1.47 ±0.17		[1] OREGLIA	82	CBAL	$\psi(2S) \to \gamma\chi_{c2}$
1.8 ±0.5		[2] BRANDELIK	79B	DASP	$\psi(2S) \to \gamma\chi_{c2}$
1.2 ±0.2		[2] BARTEL	78B	CNTR	$\psi(2S) \to \gamma\chi_{c2}$
2.2 ±1.2		[3] BIDDICK	77	CNTR	$e^+e^- \to \gamma$X
1.2 ±0.7		[1] WHITAKER	76	MRK1	e^+e^-
• • • We do not use the following data for averages, fits, limits, etc. • • •					
1.95 ±0.02 ±0.07	12.4k	[4] MENDEZ	08	CLEO	$\psi(2S) \to \gamma\chi_{c2}$
1.85 ±0.04 ±0.07	1.9k	[5] ADAM	05A	CLEO	Repl. by MENDEZ 08

[1] Recalculated by us using $B(J/\psi(1S) \to \ell^+\ell^-) = 0.1181 \pm 0.0020$.

[2] Recalculated by us using $B(J/\psi(1S) \to \mu^+\mu^-) = 0.0588 \pm 0.0010$.

[3] Assumes isotropic gamma distribution.

[4] Not independent from other measurements of MENDEZ 08.

[5] Not independent from other values reported by ADAM 05A.

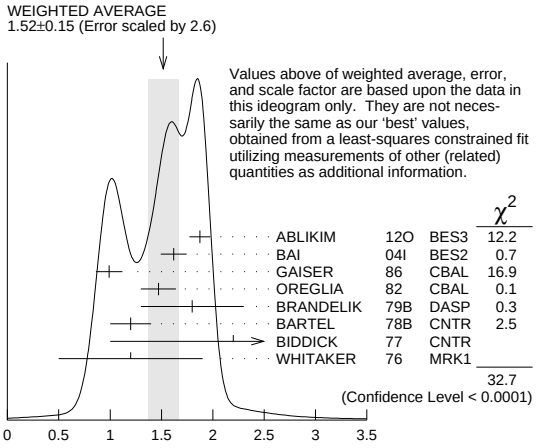

$\Gamma(\chi_{c2}(1P) \to \gamma J/\psi(1S))/\Gamma_{\rm total} \times \Gamma(\psi(2S) \to \gamma\chi_{c2}(1P))/\Gamma_{\rm total}$ (units 10^{-2})

$\Gamma(\chi_{c2}(1P) \to \gamma J/\psi(1S))/\Gamma_{\rm total} \times \Gamma(\psi(2S) \to \gamma\chi_{c2}(1P))/\Gamma(\psi(2S) \to J/\psi(1S)\text{anything})$ $\Gamma_{67}/\Gamma \times \Gamma^{\psi(2S)}_{130}/\Gamma^{\psi(2S)}_{9}$

$\Gamma_{67}/\Gamma \times \Gamma^{\psi(2S)}_{130}/\Gamma^{\psi(2S)}_{9} = \Gamma_{67}/\Gamma \times \Gamma^{\psi(2S)}_{130}/(\Gamma^{\psi(2S)}_{11} + \Gamma^{\psi(2S)}_{12} + \Gamma^{\psi(2S)}_{13} + 0.339\Gamma^{\psi(2S)}_{129} + 0.192\Gamma^{\psi(2S)}_{130})$

VALUE (units 10^{-2})	EVTS	DOCUMENT ID		TECN	COMMENT
2.87±0.07 OUR FIT					
• • • We do not use the following data for averages, fits, limits, etc. • • •					
3.12±0.03±0.09	12.4k	[1] MENDEZ	08	CLEO	$\psi(2S) \to \gamma\chi_{c2}$
3.11±0.07±0.07	1.9k	ADAM	05A	CLEO	Repl. by MENDEZ 08

[1] Not independent from other measurements of MENDEZ 08.

$\Gamma(\chi_{c2}(1P) \to \gamma J/\psi(1S))/\Gamma_{\rm total} \times \Gamma(\psi(2S) \to \gamma\chi_{c2}(1P))/\Gamma(\psi(2S) \to J/\psi(1S)\pi^+\pi^-)$ $\Gamma_{67}/\Gamma \times \Gamma^{\psi(2S)}_{130}/\Gamma^{\psi(2S)}_{11}$

VALUE (units 10^{-2})	EVTS	DOCUMENT ID		TECN	COMMENT
5.08±0.12 OUR FIT					
5.53±0.17 OUR AVERAGE					
5.56±0.05±0.16	12.4k	MENDEZ	08	CLEO	$\psi(2S) \to \gamma\chi_{c2}$
6.0 ±2.8	1.3k	[1] ABLIKIM	04B	BES	$\psi(2S) \to J/\psi$X
3.9 ±1.2		[2] HIMEL	80	MRK2	$\psi(2S) \to \gamma\chi_{c2}$
• • • We do not use the following data for averages, fits, limits, etc. • • •					
5.52±0.13±0.13	1.9k	[3] ADAM	05A	CLEO	Repl. by MENDEZ 08

[1] From a fit to the J/ψ recoil mass spectra.

[2] The value for $B(\psi(2S) \to \gamma\chi_{c2}) \times B(\chi_{c2} \to \gamma J/\psi(1S))$ reported in HIMEL 80 is derived using $B(\psi(2S) \to J/\psi(1S)\pi^+\pi^-) = (33 \pm 3)\%$ and $B(J/\psi(1S) \to \ell^+\ell^-) = 0.138 \pm 0.018$. Calculated by us using $B(J/\psi(1S) \to \ell^+\ell^-) = (0.1181 \pm 0.0020)$.

[3] Not independent from other values reported by ADAM 05A.

$\Gamma(\chi_{c2}(1P)\to\gamma\gamma)/\Gamma_{\rm total}\times\Gamma(\psi(2S)\to\gamma\chi_{c2}(1P))/\Gamma_{\rm total}$ $\Gamma_{71}/\Gamma\times\Gamma_{130}^{\psi(2S)}/\Gamma^{\psi(2S)}$

VALUE (units 10^{-5})	EVTS	DOCUMENT ID		TECN	COMMENT
2.50±0.13 OUR FIT					
2.78±0.18 OUR AVERAGE					
2.81±0.17±0.15	1.1k	[1] ABLIKIM	12A	BES3	$\psi(2S)\to\gamma\chi_{c2}\to 3\gamma$
2.68±0.28±0.15	0.3k	ECKLUND	08A	CLEO	$\psi(2S)\to\gamma\chi_{c2}\to 3\gamma$
7.0 ±2.1 ±2.0		LEE	85	CBAL	$\psi(2S)\to\gamma\chi_{c2}$

[1] ABLIKIM 12A measures the ratio of two-photon partial widths for the helicity $\lambda=0$ and helicity $\lambda=2$ components to be $f_{0/2}=\Gamma_{\gamma\gamma}^{\lambda=0}/\Gamma_{\gamma\gamma}^{\lambda=2}=0.00\pm0.02\pm0.02$.

$\Gamma(\chi_{c2}(1P)\to\gamma\gamma)/\Gamma(\chi_{c0}(1P)\to\gamma\gamma)$ $\Gamma_{71}/\Gamma_{81}^{\chi_{c0}(1P)}$

VALUE	EVTS	DOCUMENT ID		TECN	COMMENT
0.273±0.035 OUR AVERAGE					
0.271±0.029±0.030	1.9k	[1] ABLIKIM	12A	BES3	$\psi(2S)\to\gamma\chi_{cJ}\to 3\gamma$
0.278±0.050±0.036	0.5k	[1] ECKLUND	08A	CLEO	$\psi(2S)\to\gamma\chi_{cJ}\to 3\gamma$

[1] Not independent from the values of $\Gamma(\chi_{c0},\chi_{c2})$ and $B(\psi(2S)\to\chi_{c0},\chi_{c2})$.

MULTIPOLE AMPLITUDES IN $\chi_{c2}(1P)\to\gamma J/\psi(1S)$ RADIATIVE DECAY

$a_2 = M2/\sqrt{E1^2+M2^2+E3^2}$ Magnetic quadrupole fractional transition amplitude

VALUE (units 10^{-2})	EVTS	DOCUMENT ID		TECN	COMMENT
−10.0± 1.5 OUR AVERAGE					
− 9.3± 1.6±0.3	19.8k	[1] ARTUSO	09	CLEO	$\psi(2S)\to\gamma\gamma\ell^+\ell^-$
$-\ 9.3^{+\ 3.9}_{-\ 4.1}\pm0.6$	5.9k	[2] AMBROGIANI	02	E835	$p\overline{p}\to\chi_{c2}\to J/\psi\gamma$
−14 ± 6	1.9k	[2] ARMSTRONG	93E	E760	$p\overline{p}\to\chi_{c2}\to J/\psi\gamma$
$-33.3^{+11.6}_{-29.2}$	441	[2] OREGLIA	82	CBAL	$\psi(2S)\to\chi_{c1}\gamma\to J/\psi\gamma\gamma$
• • • We do not use the following data for averages, fits, limits, etc. • • •					
− 7.9± 1.9±0.3	19.8k	[3] ARTUSO	09	CLEO	$\psi(2S)\to\gamma\gamma\ell^+\ell^-$

[1] From a fit with floating $M2$ amplitudes a_2 and b_2, and fixed $E3$ amplitudes $a_3=b_3=0$.
[2] Assuming $a_3=0$.
[3] From a fit with floating $M2$ and $E3$ amplitudes a_2, b_2, and a_3, and b_3.

$a_3 = E3/\sqrt{E1^2+M2^2+E3^2}$ Electric octupole fractional transition amplitude

VALUE (units 10^{-2})	EVTS	DOCUMENT ID		TECN	COMMENT
1.6±1.3 OUR AVERAGE					
1.7±1.4±0.3	19.8k	[1] ARTUSO	09	CLEO	$\psi(2S)\to\gamma\gamma\ell^+\ell^-$
$2.0^{+5.5}_{-4.4}\pm0.9$	5908	AMBROGIANI	02	E835	$p\overline{p}\to\chi_{c2}\to J/\psi\gamma$
$0\ ^{+6}_{-5}$	1904	ARMSTRONG	93E	E760	$p\overline{p}\to\chi_{c2}\to J/\psi\gamma$

[1] From a fit with floating $M2$ and $E3$ amplitudes a_2, b_2, and a_3, and b_3.

MULTIPOLE AMPLITUDES IN $\psi(2S)\to\gamma\chi_{c2}(1P)$ RADIATIVE DECAY

$b_2 = M2/\sqrt{E1^2+M2^2+E3^2}$ Magnetic quadrupole fractional transition amplitude

VALUE (units 10^{-2})	EVTS	DOCUMENT ID		TECN	COMMENT
2.2±1.8 OUR AVERAGE		Error includes scale factor of 1.7. See the ideogram below.			
4.6±1.0±1.3	13.8k	[1] ABLIKIM	11I	BES3	$\psi(2S)\to\gamma\pi^+\pi^-,\gamma K^+K^-$
0.2±1.5±0.4	19.8k	[2] ARTUSO	09	CLEO	$\psi(2S)\to\gamma\gamma\ell^+\ell^-$
$-\ 5.1^{+5.4}_{-3.6}$	721	[1] ABLIKIM	04I	BES2	$\psi(2S)\to\gamma\pi^+\pi^-,\gamma K^+K^-$
$13.2^{+9.8}_{-7.5}$	441	[3] OREGLIA	82	CBAL	$\psi(2S)\to\gamma\gamma\ell^+\ell^-$
• • • We do not use the following data for averages, fits, limits, etc. • • •					
1.0±1.3±0.3	19.8k	[3] ARTUSO	09	CLEO	$\psi(2S)\to\gamma\gamma\ell^+\ell^-$

[1] From a fit with floating $M2$ and $E3$ amplitudes b_2 and b_3.
[2] From a fit with floating $M2$ and $E3$ amplitudes a_2, b_2, and a_3, and b_3.
[3] From a fit with floating $M2$ amplitudes a_2 and b_2, and fixed $E3$ amplitudes $a_3=b_3=0$.

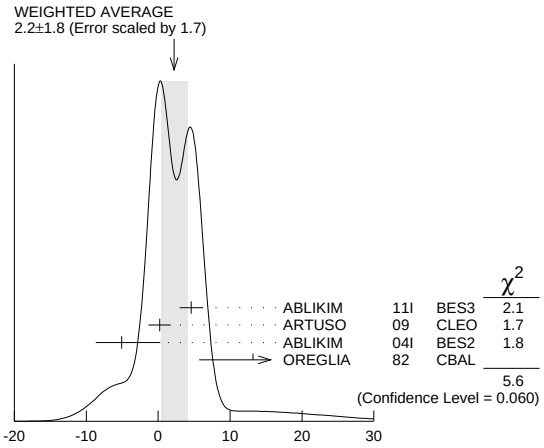

$b_2 = M2/\sqrt{E1^2+M2^2+E3^2}$ Magnetic quadrupole fractional transition amplitude (units 10^{-2})

$b_3 = E3/\sqrt{E1^2+M2^2+E3^2}$ Electric octupole fractional transition amplitude

VALUE (units 10^{-2})	EVTS	DOCUMENT ID		TECN	COMMENT
−0.3±1.0 OUR AVERAGE					
1.5±0.8±1.8	13.8k	[1] ABLIKIM	11I	BES3	$\psi(2S)\to\gamma\pi^+\pi^-,\gamma K^+K^-$
−0.8±1.2±0.2	19.8k	ARTUSO	09	CLEO	$\psi(2S)\to\gamma\gamma\ell^+\ell^-$
$-2.7^{+4.3}_{-2.9}$	721	[1] ABLIKIM	04I	BES2	$\psi(2S)\to\gamma\pi^+\pi^-,\gamma K^+K^-$

[1] From a fit with floating $M2$ and $E3$ amplitudes b_2 and b_3.

MULTIPOLE AMPLITUDE RATIOS IN RADIATIVE DECAYS $\psi(2S)\to\gamma\chi_{c2}(1P)$ and $\chi_{c2}\to\gamma J/\psi(1S)$

b_2/a_2 Magnetic quadrupole transition amplitude ratio

VALUE (units 10^{-2})	EVTS	DOCUMENT ID		TECN	COMMENT
$\mathbf{-11^{+14}_{-15}}$	19.8k	[1] ARTUSO	09	CLEO	$\psi(2S)\to\gamma\gamma\ell^+\ell^-$

[1] Statistical and systematic errors combined. From a fit with floating $M2$ amplitudes a_2 and b_2, and fixed $E3$ amplitudes $a_3=b_3=0$. Not independent of values for $a_2(\chi_{c2}(1P))$ and $b_2(\chi_{c2}(1P))$ from ARTUSO 09.

$\chi_{c2}(1P)$ REFERENCES

ABLIKIM	13D	PR D87 012007	M. Ablikim *et al.*	(BES III Collab.)
ABLIKIM	13H	PR D87 032007	M. Ablikim *et al.*	(BES III Collab.)
ABLIKIM	13V	PR D88 112001	M. Ablikim *et al.*	(BES III Collab.)
UEHARA	13	PTEP 2013 123C01	S. Uehara *et al.*	(BELLE Collab.)
ABLIKIM	12A	PR D85 112008	M. Ablikim *et al.*	(BES III Collab.)
ABLIKIM	12I	PR D86 052004	M. Ablikim *et al.*	(BES III Collab.)
ABLIKIM	12J	PR D86 052011	M. Ablikim *et al.*	(BES III Collab.)
ABLIKIM	12O	PRL 109 172002	M. Ablikim *et al.*	(BES III Collab.)
LEES	12AE	PR D86 092005	J.P. Lees *et al.*	(BABAR Collab.)
LIU	12B	PRL 108 232001	Z.Q. Liu *et al.*	(BELLE Collab.)
ABLIKIM	11A	PR D83 012006	M. Ablikim *et al.*	(BES III Collab.)
ABLIKIM	11E	PR D83 112005	M. Ablikim *et al.*	(BES III Collab.)
ABLIKIM	11F	PR D83 112009	M. Ablikim *et al.*	(BES III Collab.)
ABLIKIM	11I	PR D84 092006	M. Ablikim *et al.*	(BES III Collab.)
ABLIKIM	11K	PRL 107 092001	M. Ablikim *et al.*	(BES III Collab.)
DEL-AMO-SA...	11M	PR D84 012004	P. del Amo Sanchez *et al.*	(BABAR Collab.)
ABLIKIM	10A	PR D81 052005	M. Ablikim *et al.*	(BES III Collab.)
ONYISI	10	PR D82 011103	P.U.E. Onyisi *et al.*	(CLEO Collab.)
UEHARA	10A	PR D82 114031	S. Uehara *et al.*	(BELLE Collab.)
ARTUSO	09	PR D80 112003	M. Artuso *et al.*	(CLEO Collab.)
ASNER	09	PR D79 072007	D.M. Asner *et al.*	(CLEO Collab.)
UEHARA	09	PR D79 052009	S. Uehara *et al.*	(BELLE Collab.)
BENNETT	08A	PRL 101 151801	J.V. Bennett *et al.*	(CLEO Collab.)
ECKLUND	08A	PR D78 091501	K.M. Ecklund *et al.*	(CLEO Collab.)
HE	08B	PR D78 092004	Q. He *et al.*	(CLEO Collab.)
MENDEZ	08	PR D78 011102	H. Mendez *et al.*	(CLEO Collab.)
NAIK	08	PR D78 031101	P. Naik *et al.*	(CLEO Collab.)
UEHARA	08	EPJ C53 1	S. Uehara *et al.*	(BELLE Collab.)
ADAMS	07	PR D75 071101	G.S. Adams *et al.*	(CLEO Collab.)
ATHAR	07	PR D75 032002	S.B. Athar *et al.*	(CLEO Collab.)
CHEN	07B	PL B651 15	W.T. Chen *et al.*	(BELLE Collab.)
ABLIKIM	06D	PR D73 052006	M. Ablikim *et al.*	(BES Collab.)
ABLIKIM	06I	PR D74 012004	M. Ablikim *et al.*	(BES Collab.)
ABLIKIM	06R	PR D74 072001	M. Ablikim *et al.*	(BES Collab.)
ABLIKIM	06T	PL B642 197	M. Ablikim *et al.*	(BES Collab.)
DOBBS	06	PR D73 071101	S. Dobbs *et al.*	(CLEO Collab.)
ABLIKIM	05G	PR D71 092002	M. Ablikim *et al.*	(BES Collab.)
ABLIKIM	05N	PL B630 7	M. Ablikim *et al.*	(BES Collab.)
ABLIKIM	05O	PL B630 21	M. Ablikim *et al.*	(BES Collab.)
ADAM	05A	PRL 94 232002	N.E. Adam *et al.*	(CLEO Collab.)
ANDREOTTI	05A	NP B717 34	M. Andreotti *et al.*	(FNAL E835 Collab.)
NAKAZAWA	05	PL B615 39	H. Nakazawa *et al.*	(BELLE Collab.)
ABLIKIM	04B	PR D70 012003	M. Ablikim *et al.*	(BES Collab.)
ABLIKIM	04H	PR D70 092003	M. Ablikim *et al.*	(BES Collab.)
ABLIKIM	04I	PR D70 092004	M. Ablikim *et al.*	(BES Collab.)
ATHAR	04	PR D70 112002	S.B. Athar *et al.*	(CLEO Collab.)
BAI	04F	PR D69 092001	J.Z. Bai *et al.*	(BES Collab.)
BAI	04I	PR D70 012006	J.Z. Bai *et al.*	(BES Collab.)
AULCHENKO	03	PL B573 63	V.M. Aulchenko *et al.*	(KEDR Collab.)
BAI	03C	PR D67 032004	J.Z. Bai *et al.*	(BES Collab.)
BAI	03E	PR D67 112001	J.Z. Bai *et al.*	(BES Collab.)

Meson Particle Listings

$\chi_{c2}(1P)$, $\eta_c(2S)$

ABE	02T	PL B540 33	K. Abe *et al.*	(BELLE Collab.)
AMBROGIANI	02	PR D65 052002	M. Ambrogiani *et al.*	(FNAL E835 Collab.)
EISENSTEIN	01	PRL 87 061801	B.I. Eisenstein *et al.*	(CLEO Collab.)
AMBROGIANI	00B	PR D62 052002	M. Ambrogiani *et al.*	(FNAL E835 Collab.)
ACCIARRI	99E	PL B453 73	M. Acciarri *et al.*	(L3 Collab.)
BAI	99B	PR D60 072001	J.Z. Bai *et al.*	(BES Collab.)
ACKER...K...	98	PL B439 197	K. Ackerstaff *et al.*	(OPAL Collab.)
BAI	98D	PR D58 092006	J.Z. Bai *et al.*	(BES Collab.)
BAI	98I	PRL 81 3091	J.Z. Bai *et al.*	(BES Collab.)
DOMINICK	94	PR D50 4265	J. Dominick *et al.*	(CLEO Collab.)
ARMSTRONG	93	PRL 70 2988	T.A. Armstrong *et al.*	(FNAL E760 Collab.)
ARMSTRONG	93E	PR D48 3037	T.A. Armstrong *et al.*	(FNAL-E760 Collab.)
BAUER	93	PL B302 345	D.A. Bauer *et al.*	(TPC Collab.)
ARMSTRONG	92	NP B373 35	T.A. Armstrong *et al.*	(FNAL, FERR, GENO+)
Also		PRL 68 1468	T.A. Armstrong *et al.*	(FNAL, FERR, GENO+)
BAGLIN	87B	PL B187 191	C. Baglin *et al.*	(R704 Collab.)
BAGLIN	86B	PL B172 455	C. Baglin	(LAPP, CERN, GENO, LYON, OSLO+)
GAISER	86	PR D34 711	J. Gaiser *et al.*	(Crystal Ball Collab.)
LEE	85	SLAC 282	R.A. Lee	(SLAC)
LEMOIGNE	82	PL 113B 509	Y. Lemoigne *et al.*	(SACL, LOIC, SHMP+)
OREGLIA	82	PR D25 2259	M.J. Oreglia *et al.*	(SLAC, CIT, HARV+)
Also		Private Comm.	M.J. Oreglia	(EFI)
BARATE	81	PR D24 2994	R. Barate *et al.*	(SACL, LOIC, SHMP, CERN+)
HIMEL	80	PRL 44 920	T. Himel *et al.*	(LBL, SLAC)
Also		Private Comm.	G. Trilling	(LBL, UCB)
BRANDELIK	79B	NP B160 426	R. Brandelik *et al.*	(DASP Collab.)
BARTEL	78B	PL 79B 492	W. Bartel *et al.*	(DESY, HEIDP)
TANENBAUM	78	PR D17 1731	W.M. Tanenbaum *et al.*	(SLAC, LBL)
Also		Private Comm.	G. Trilling	(LBL, UCB)
BIDDICK	77	PRL 38 1324	C.J. Biddick *et al.*	(UCSD, UMD, PAVI+)
WHITAKER	76	PRL 37 1596	J.S. Whitaker *et al.*	(SLAC, LBL)

$\eta_c(2S)$

$I^G(J^{PC}) = 0^+(0^{-+})$

Quantum numbers are quark model predictions.

$\eta_c(2S)$ MASS

VALUE (MeV)	EVTS	DOCUMENT ID		TECN	COMMENT
3639.4±1.3 OUR AVERAGE		Error includes scale factor of 1.2.			
3646.9±1.6±3.6	57 ± 17	ABLIKIM	13K	BES3	$\psi(2S) \to \gamma K^0_S K^\pm \pi^\mp \pi^+ \pi^-$
3637.6±2.9±1.6	127 ± 18	[1] ABLIKIM	12G	BES3	$\psi(2S) \to \gamma K^0 K \pi$, $K K \pi^0$
3638.5±1.5±0.8	624	[2] DEL-AMO-SA...11M		BABR	$\gamma\gamma \to K^0_S K^\pm \pi^\mp$
3640.5±3.2±2.5	1201	[2] DEL-AMO-SA...11M		BABR	$\gamma\gamma \to K^+ K^- \pi^+ \pi^- \pi^0$
$3636.1^{+3.9}_{-4.2}{}^{+0.7}_{-2.0}$	128	[3] VINOKUROVA	11	BELL	$B^\pm \to K^\pm (K^0_S K^\pm \pi^\mp)$
3626 ±5 ±6	311	[4] ABE	07	BELL	$e^+e^- \to J/\psi(c\overline{c})$
$3645.0 \pm 5.5^{+4.9}_{-7.8}$	121 ± 27	AUBERT	05C	BABR	$e^+e^- \to J/\psi c\overline{c}$
3642.9±3.1±1.5	61	ASNER	04	CLEO	$\gamma\gamma \to \eta_c \to K^0_S K^\pm \pi^\mp$
• • • We do not use the following data for averages, fits, limits, etc. • • •					
3639 ±7	98 ± 52	[5] AUBERT	06E	BABR	$B^\pm \to K^\pm X_{c\overline{c}}$
3630.8±3.4±1.0	112 ± 24	[6] AUBERT	04D	BABR	$\gamma\gamma \to \eta_c(2S) \to K\overline{K}\pi$
3654 ±6 ±8	39 ± 11	[7] CHOI	02	BELL	$B \to K K_S K^- \pi^+$
3594 ±5		[8] EDWARDS	82C	CBAL	$e^+e^- \to \gamma X$

[1] From a simultaneous fit to $K^0_S K^\pm \pi^\mp$ and $K^+ K^- \pi^0$ decay modes.
[2] Ignoring possible interference with continuum.
[3] Accounts for interference with non-resonant continuum.
[4] From a fit of the J/ψ recoil mass spectrum. Supersedes ABE,K 02 and ABE 04G.
[5] From the fit of the kaon momentum spectrum. Systematic errors not evaluated.
[6] Superseded by DEL-AMO-SANCHEZ 11M.
[7] Superseded by VINOKUROVA 11.
[8] Assuming mass of $\psi(2S) = 3686$ MeV.

$\eta_c(2S)$ WIDTH

VALUE (MeV)	CL%	EVTS	DOCUMENT ID		TECN	COMMENT
$\mathbf{11.3^{+\ 3.2}_{-\ 2.9}}$ **OUR AVERAGE**						
$9.9 \pm 4.8 \pm 2.9$		57 ± 17	ABLIKIM	13K	BES3	$\psi(2S) \to \gamma K^0_S K^\pm \pi^\mp \pi^+ \pi^-$
16.9± 6.4±4.8		127 ± 18	[9] ABLIKIM	12G	BES3	$\psi(2S) \to \gamma K^0 K \pi$, $K K \pi^0$
13.4± 4.6±3.2		624	[10] DEL-AMO-SA...11M		BABR	$\gamma\gamma \to K^0_S K^\pm \pi^\mp$
$6.6^{+\ 8.4}_{-\ 5.1}{}^{+2.6}_{-0.9}$		128	[11] VINOKUROVA	11	BELL	$B^\pm \to K^\pm (K^0_S K^\pm \pi^\mp)$
6.3±12.4±4.0		61	ASNER	04	CLEO	$\gamma\gamma \to \eta_c \to K^0_S K^\pm \pi^\mp$
• • • We do not use the following data for averages, fits, limits, etc. • • •						
< 23	90	98 ± 52	[12] AUBERT	06E	BABR	$B^\pm \to K^\pm X_{c\overline{c}}$
22 ±14		121 ± 27	AUBERT	05C	BABR	$e^+e^- \to J/\psi c\overline{c}$
17.0± 8.3±2.5		112 ± 24	[13] AUBERT	04D	BABR	$\gamma\gamma \to \eta_c(2S) \to K\overline{K}\pi$
<55	90	39 ± 11	[14] CHOI	02	BELL	$B \to K K_S K^- \pi^+$
<8.0	95		[15] EDWARDS	82C	CBAL	$e^+e^- \to \gamma X$

[9] From a simultaneous fit to $K^0_S K^\pm \pi^\mp$ and $K^+ K^- \pi^0$ decay modes.
[10] Ignoring possible interference with continuum.
[11] Accounts for interference with non-resonant continuum.
[12] From the fit of the kaon momentum spectrum. Systematic errors not evaluated.
[13] Superseded by DEL-AMO-SANCHEZ 11M.
[14] For a mass value of 3654 ± 6 MeV. Superseded by VINOKUROVA 11.
[15] For a mass value of 3594 ± 5 MeV

$\eta_c(2S)$ DECAY MODES

	Mode	Fraction (Γ_i/Γ)	Confidence level
Γ_1	hadrons	not seen	
Γ_2	$K\overline{K}\pi$	(1.9±1.2) %	
Γ_3	$2\pi^+ 2\pi^-$	not seen	
Γ_4	$\rho^0\rho^0$	not seen	
Γ_5	$3\pi^+ 3\pi^-$	not seen	
Γ_6	$K^+ K^- \pi^+ \pi^-$	not seen	
Γ_7	$K^{*0}\overline{K}{}^{*0}$	not seen	
Γ_8	$K^+ K^- \pi^+ \pi^- \pi^0$	(1.4±1.0) %	
Γ_9	$K^+ K^- 2\pi^+ 2\pi^-$	not seen	
Γ_{10}	$K^0_S K^- 2\pi^+ \pi^-$ + c.c.	seen	
Γ_{11}	$2K^+ 2K^-$	not seen	
Γ_{12}	$\phi\phi$	not seen	
Γ_{13}	$p\overline{p}$	$< 2.0 \times 10^{-3}$	90%
Γ_{14}	$\gamma\gamma$	$(1.9 \pm 1.3) \times 10^{-4}$	
Γ_{15}	$\pi^+\pi^-\eta$	not seen	
Γ_{16}	$\pi^+\pi^-\eta'$	not seen	
Γ_{17}	$K^+ K^- \eta$	not seen	
Γ_{18}	$\pi^+\pi^-\eta_c(1S)$	< 25 %	90%

$\eta_c(2S)$ PARTIAL WIDTHS

$\Gamma(\gamma\gamma)$ Γ_{14}

VALUE (keV)	DOCUMENT ID		TECN	COMMENT
• • • We do not use the following data for averages, fits, limits, etc. • • •				
1.3±0.6	[16] ASNER	04	CLEO	$\gamma\gamma \to \eta_c \to K^0_S K^\pm \pi^\mp$

[16] They measure $\Gamma(\eta_c(2S)\gamma\gamma)\ B(\eta_c(2S) \to K\overline{K}\pi) = (0.18 \pm 0.05 \pm 0.02)\ \Gamma(\eta_c(1S)\gamma\gamma)\ B(\eta_c(1S) \to K\overline{K}\pi)$. The value for $\Gamma(\eta_c(2S) \to \gamma\gamma)$ is derived assuming that the branching fractions for $\eta_c(2S)$ and $\eta_c(1S)$ decays to $K_S K\pi$ are equal and using $\Gamma(\eta_c(1S) \to \gamma\gamma) = 7.4 \pm 0.4 \pm 2.3$ keV.

$\eta_c(2S)\ \Gamma(i)\Gamma(\gamma\gamma)/\Gamma(\text{total})$

$\Gamma(2\pi^+ 2\pi^-) \times \Gamma(\gamma\gamma)/\Gamma_{\text{total}}$ $\Gamma_3\Gamma_{14}/\Gamma$

VALUE (eV)	CL%	DOCUMENT ID		TECN	COMMENT
<6.5	90	UEHARA	08	BELL	$\gamma\gamma \to \eta_c(2S) \to 2(\pi^+\pi^-)$

$\Gamma(K\overline{K}\pi) \times \Gamma(\gamma\gamma)/\Gamma_{\text{total}}$ $\Gamma_2\Gamma_{14}/\Gamma$

VALUE (eV)	EVTS	DOCUMENT ID		TECN	COMMENT
41±4±6	624	[17] DEL-AMO-SA...11M		BABR	$\gamma\gamma \to K^0_S K^\pm \pi^\mp$

[17] Not independent from other measurements reported in DEL-AMO-SANCHEZ 11M.

$\Gamma(K^+ K^- \pi^+ \pi^-) \times \Gamma(\gamma\gamma)/\Gamma_{\text{total}}$ $\Gamma_6\Gamma_{14}/\Gamma$

VALUE (eV)	CL%	DOCUMENT ID		TECN	COMMENT
<5.0	90	UEHARA	08	BELL	$\gamma\gamma \to \eta_c(2S) \to K^+ K^- \pi^+ \pi^-$

$\Gamma(K^+ K^- \pi^+ \pi^- \pi^0) \times \Gamma(\gamma\gamma)/\Gamma_{\text{total}}$ $\Gamma_8\Gamma_{14}/\Gamma$

VALUE (eV)	EVTS	DOCUMENT ID		TECN	COMMENT
30±6±5	1201	[18] DEL-AMO-SA...11M		BABR	$\gamma\gamma \to K^+ K^- \pi^+ \pi^- \pi^0$

[18] Not independent from other measurements reported in DEL-AMO-SANCHEZ 11M.

$\Gamma(2K^+ 2K^-) \times \Gamma(\gamma\gamma)/\Gamma_{\text{total}}$ $\Gamma_{11}\Gamma_{14}/\Gamma$

VALUE (eV)	CL%	DOCUMENT ID		TECN	COMMENT
<2.9	90	UEHARA	08	BELL	$\gamma\gamma \to \eta_c(2S) \to 2(K^+ K^-)$

$\Gamma(\pi^+\pi^-\eta_c(1S)) \times \Gamma(\gamma\gamma)/\Gamma_{\text{total}}$ $\Gamma_{18}\Gamma_{14}/\Gamma$

VALUE (eV)	CL%	DOCUMENT ID		TECN	COMMENT
<133	90	LEES	12AE	BABR	$e^+e^- \to e^+e^-\pi^+\pi^-\eta_c$

$\eta_c(2S)\ \Gamma(i)\Gamma(\gamma\gamma)/\Gamma^2(\text{total})$

$\Gamma(p\overline{p})/\Gamma_{\text{total}} \times \Gamma(\gamma\gamma)/\Gamma_{\text{total}}$ $\Gamma_{13}/\Gamma \times \Gamma_{14}/\Gamma$

VALUE ($\text{units } 10^{-8}$)	CL%	DOCUMENT ID		TECN	COMMENT
< 5.6	90	[19,20,21] AMBROGIANI	01	E835	$\overline{p}p \to \gamma\gamma$
• • • We do not use the following data for averages, fits, limits, etc. • • •					
< 8.0	90	[19,20,22] AMBROGIANI	01	E835	$\overline{p}p \to \gamma\gamma$
<12.0	90	[20,22] AMBROGIANI	01	E835	$\overline{p}p \to \gamma\gamma$

[19] Including the measurements of of ARMSTRONG 95F in the AMBROGIANI 01 analysis.
[20] For a total width Γ=5 MeV.
[21] For the resonance mass region 3589–3599 MeV/c^2.
[22] For the resonance mass region 3575–3660 MeV/c^2.

$\eta_c(2S)$ BRANCHING RATIOS

$\Gamma(\text{hadrons})/\Gamma_{\text{total}}$ Γ_1/Γ

VALUE	DOCUMENT ID		TECN	COMMENT
not seen	ABREU	98O	DLPH	$e^+e^- \to e^+e^-$ + hadrons

• • • We do not use the following data for averages, fits, limits, etc. • • •

seen	[23] EDWARDS	82C	CBAL	$e^+e^- \to \gamma X$	

[23] For a mass value of 3594 ± 5 MeV

$\Gamma(K\overline{K}\pi)/\Gamma_{\text{total}}$ Γ_2/Γ

VALUE (units 10^{-2})	EVTS	DOCUMENT ID		TECN	COMMENT
1.9±0.4±1.1	59 ± 12	[24] AUBERT	08AB	BABR	$B \to \eta_c(2S)K \to K\overline{K}\pi K$

• • • We do not use the following data for averages, fits, limits, etc. • • •

seen	127 ± 18	ABLIKIM	13K	BES3	$\psi(2S) \to \gamma K\overline{K}\pi$	
seen	39 ± 11	[25] CHOI	02	BELL	$B \to K K_S K^-\pi^+$	

[24] Derived from a measurement of $[B(B^+ \to \eta_c(2S)K^+) \times B(\eta_c(2S) \to K\overline{K}\pi)] / [B(B^+ \to \eta_c K^+) \times B(\eta_c \to K\overline{K}\pi)] = (9.6^{+2.0}_{-1.9} \pm 2.5)\%$ and using $B(B^+ \to \eta_c(2S)K^+) = (3.4 \pm 1.8) \times 10^{-4}$, and $[B(B^+ \to \eta_c K^+) \times B(\eta_c \to K\overline{K}\pi)] = (6.88 \pm 0.77^{+0.55}_{-0.66}) \times 10^{-5}$.

[25] For a mass value of 3654 ± 6 MeV

$\Gamma(2\pi^+2\pi^-)/\Gamma_{\text{total}}$ Γ_3/Γ

VALUE	DOCUMENT ID		TECN	COMMENT
not seen	UEHARA	08	BELL	$\gamma\gamma \to \eta_c(2S)$

$\Gamma(\rho^0\rho^0)/\Gamma_{\text{total}}$ Γ_4/Γ

VALUE	DOCUMENT ID		TECN	COMMENT
not seen	ABLIKIM	11H	BES3	$\psi(2S) \to \gamma 2\pi^+ 2\pi^-$

$\Gamma(K^+K^-\pi^+\pi^-)/\Gamma_{\text{total}}$ Γ_6/Γ

VALUE	DOCUMENT ID		TECN	COMMENT
not seen	UEHARA	08	BELL	$\gamma\gamma \to \eta_c(2S)$

$\Gamma(K^+K^-\pi^+\pi^-\pi^0)/\Gamma(K\overline{K}\pi)$ Γ_8/Γ_2

VALUE	EVTS	DOCUMENT ID		TECN	COMMENT
0.73±0.17±0.17	1201	[26] DEL-AMO-SA...11M		BABR	$\gamma\gamma \to K^+K^-\pi^+\pi^-\pi^0$

[26] We have multiplied the value of $\Gamma(K^+K^-\pi^+\pi^-\pi^0)/\Gamma(K^0_S K^\pm\pi^\mp)$ reported in DEL-AMO-SANCHEZ 11M by a factor 1/3 to obtain $\Gamma(K^+K^-\pi^+\pi^-\pi^0)/\Gamma(K\overline{K}\pi)$. Not independent from other measurements reported in DEL-AMO-SANCHEZ 11M.

$\Gamma(K^{*0}\overline{K}^{*0})/\Gamma_{\text{total}}$ Γ_7/Γ

VALUE	DOCUMENT ID		TECN	COMMENT
not seen	ABLIKIM	11H	BES3	$\psi(2S) \to \gamma K^+K^-\pi^+\pi^-$

$\Gamma(K^0_S K^-2\pi^+\pi^- + \text{c.c.})/\Gamma_{\text{total}}$ Γ_{10}/Γ

VALUE	EVTS	DOCUMENT ID		TECN	COMMENT
seen	57±17	ABLIKIM	13K	BES3	$\psi(2S) \to \gamma K^0_S K^\pm\pi^\mp\pi^+\pi^-$

$\Gamma(2K^+2K^-)/\Gamma_{\text{total}}$ Γ_{11}/Γ

VALUE	DOCUMENT ID		TECN	COMMENT
not seen	UEHARA	08	BELL	$\gamma\gamma \to \eta_c(2S)$

$\Gamma(\phi\phi)/\Gamma_{\text{total}}$ Γ_{12}/Γ

VALUE	DOCUMENT ID		TECN	COMMENT
not seen	ABLIKIM	11H	BES3	$\psi(2S) \to \gamma K^+K^-K^+K^-$

$\Gamma(\gamma\gamma)/\Gamma_{\text{total}}$ Γ_{14}/Γ

VALUE	CL%	DOCUMENT ID		TECN	COMMENT

• • • We do not use the following data for averages, fits, limits, etc. • • •

$<5 \times 10^{-4}$	90	[27] WICHT	08	BELL	$B^\pm \to K^\pm\gamma\gamma$	
not seen		AMBROGIANI	01	E835	$\overline{p}p \to \gamma\gamma$	
<0.01	90	LEE	85	CBAL	$\psi' \to$ photons	

[27] WICHT 08 reports $[\Gamma(\eta_c(2S) \to \gamma\gamma)/\Gamma_{\text{total}}] \times [B(B^+ \to \eta_c(2S)K^+)] < 0.18 \times 10^{-6}$ which we divide by our best value $B(B^+ \to \eta_c(2S)K^+) = 3.4 \times 10^{-4}$.

$\Gamma(\pi^+\pi^-\eta_c(1S))/\Gamma(K\overline{K}\pi)$ Γ_{18}/Γ_2

VALUE	CL%	DOCUMENT ID		TECN	COMMENT
<3.33	90	[28] LEES	12AE	BABR	$e^+e^- \to e^+e^-\pi^+\pi^-\eta_c$

[28] We divided the reported limit by 3 to take into account isospin relations.

$\eta_c(2S)$ CROSS-PARTICLE BRANCHING RATIOS

$\Gamma(\eta_c(2S) \to 2\pi^+2\pi^-)/\Gamma_{\text{total}} \times \Gamma(\psi(2S) \to \gamma\eta_c(2S))/\Gamma_{\text{total}}$ $\Gamma_3/\Gamma \times \Gamma^{\psi(2S)}_{132}/\Gamma^{\psi(2S)}$

VALUE	CL%	DOCUMENT ID		TECN	COMMENT
<14.6 × 10⁻⁶	90	[29] CRONIN-HEN...10		CLEO	$\psi(2S) \to \gamma 2\pi^+ 2\pi^-$

[29] Assuming $\Gamma(\eta_c(2S)) = 14$ MeV. CRONIN-HENNESSY 10 gives the analytic dependence of limits on width.

$\Gamma(\eta_c(2S) \to \rho^0\rho^0)/\Gamma_{\text{total}} \times \Gamma(\psi(2S) \to \gamma\eta_c(2S))/\Gamma_{\text{total}}$ $\Gamma_4/\Gamma \times \Gamma^{\psi(2S)}_{132}/\Gamma^{\psi(2S)}$

VALUE	CL%	DOCUMENT ID		TECN	COMMENT
<12.7 × 10⁻⁷	90	ABLIKIM	11H	BES3	$\psi(2S) \to \gamma 2\pi^+ 2\pi^-$

$\Gamma(\eta_c(2S) \to 3\pi^+3\pi^-)/\Gamma_{\text{total}} \times \Gamma(\psi(2S) \to \gamma\eta_c(2S))/\Gamma_{\text{total}}$ $\Gamma_5/\Gamma \times \Gamma^{\psi(2S)}_{132}/\Gamma^{\psi(2S)}$

VALUE	CL%	DOCUMENT ID		TECN	COMMENT
<13.2 × 10⁻⁶	90	[30] CRONIN-HEN...10		CLEO	$\psi(2S) \to \gamma 3\pi^+ 3\pi^-$

[30] Assuming $\Gamma(\eta_c(2S)) = 14$ MeV. CRONIN-HENNESSY 10 gives the analytic dependence of limits on width.

$\Gamma(\eta_c(2S) \to K^+K^-\pi^+\pi^-)/\Gamma_{\text{total}} \times \Gamma(\psi(2S) \to \gamma\eta_c(2S))/\Gamma_{\text{total}}$ $\Gamma_6/\Gamma \times \Gamma^{\psi(2S)}_{132}/\Gamma^{\psi(2S)}$

VALUE	CL%	DOCUMENT ID		TECN	COMMENT
<9.6 × 10⁻⁶	90	[31] CRONIN-HEN...10		CLEO	$\psi(2S) \to \gamma K^+K^-\pi^+\pi^-$

[31] Assuming $\Gamma(\eta_c(2S)) = 14$ MeV. CRONIN-HENNESSY 10 gives the analytic dependence of limits on width.

$\Gamma(\eta_c(2S) \to K^{*0}\overline{K}^{*0})/\Gamma_{\text{total}} \times \Gamma(\psi(2S) \to \gamma\eta_c(2S))/\Gamma_{\text{total}}$ $\Gamma_7/\Gamma \times \Gamma^{\psi(2S)}_{132}/\Gamma^{\psi(2S)}$

VALUE	CL%	DOCUMENT ID		TECN	COMMENT
<19.6 × 10⁻⁷	90	ABLIKIM	11H	BES3	$\psi(2S) \to \gamma K^+K^-\pi^+\pi^-$

$\Gamma(\eta_c(2S) \to K^+K^-\pi^+\pi^-\pi^0)/\Gamma_{\text{total}} \times \Gamma(\psi(2S) \to \gamma\eta_c(2S))/\Gamma_{\text{total}}$ $\Gamma_8/\Gamma \times \Gamma^{\psi(2S)}_{132}/\Gamma^{\psi(2S)}$

VALUE	CL%	DOCUMENT ID		TECN	COMMENT
<43.0 × 10⁻⁶	90	[32] CRONIN-HEN...10		CLEO	$\psi(2S) \to \gamma K^+K^-\pi^+\pi^-\pi^0$

[32] Assuming $\Gamma(\eta_c(2S)) = 14$ MeV. CRONIN-HENNESSY 10 gives the analytic dependence of limits on width.

$\Gamma(\eta_c(2S) \to K^+K^-2\pi^+2\pi^-)/\Gamma_{\text{total}} \times \Gamma(\psi(2S) \to \gamma\eta_c(2S))/\Gamma_{\text{total}}$ $\Gamma_9/\Gamma \times \Gamma^{\psi(2S)}_{132}/\Gamma^{\psi(2S)}$

VALUE	CL%	DOCUMENT ID		TECN	COMMENT
<9.7 × 10⁻⁶	90	[33] CRONIN-HEN...10		CLEO	$\psi(2S) \to \gamma K^+K^-2\pi^+2\pi^-$

[33] Assuming $\Gamma(\eta_c(2S)) = 14$ MeV. CRONIN-HENNESSY 10 gives the analytic dependence of limits on width.

$\Gamma(\eta_c(2S) \to K^0_S K^-2\pi^+\pi^- + \text{c.c.})/\Gamma_{\text{total}} \times \Gamma(\psi(2S) \to \gamma\eta_c(2S))/\Gamma_{\text{total}}$ $\Gamma_{10}/\Gamma \times \Gamma^{\psi(2S)}_{132}/\Gamma^{\psi(2S)}$

VALUE (units 10^{-6})	CL%	EVTS	DOCUMENT ID		TECN	COMMENT
7.03±2.10±0.7	60		ABLIKIM	13K	BES3	$\psi(2S) \to \gamma K^0_S K^-2\pi^+\pi^-$ +c.c.

• • • We do not use the following data for averages, fits, limits, etc. • • •

< 15.2	90	[34] CRONIN-HEN...10		CLEO	$\psi(2S) \to \gamma K^0_S K^-2\pi^+\pi^-$ +c.c.	

[34] Assuming $\Gamma(\eta_c(2S)) = 14$ MeV. CRONIN-HENNESSY 10 gives the analytic dependence of limits on width.

$\Gamma(\eta_c(2S) \to \phi\phi)/\Gamma_{\text{total}} \times \Gamma(\psi(2S) \to \gamma\eta_c(2S))/\Gamma_{\text{total}}$ $\Gamma_{12}/\Gamma \times \Gamma^{\psi(2S)}_{132}/\Gamma^{\psi(2S)}$

VALUE	CL%	DOCUMENT ID		TECN	COMMENT
<7.8 × 10⁻⁷	90	ABLIKIM	11H	BES3	$\psi(2S) \to \gamma K^+K^-K^+K^-$

$\Gamma(\eta_c(2S) \to \pi^+\pi^-\eta)/\Gamma_{\text{total}} \times \Gamma(\psi(2S) \to \gamma\eta_c(2S))/\Gamma_{\text{total}}$ $\Gamma_{15}/\Gamma \times \Gamma^{\psi(2S)}_{132}/\Gamma^{\psi(2S)}$

VALUE	CL%	DOCUMENT ID		TECN	COMMENT
<4.3 × 10⁻⁶	90	[35] CRONIN-HEN...10		CLEO	$\psi(2S) \to \gamma\pi^+\pi^-\eta$

[35] Assuming $\Gamma(\eta_c(2S)) = 14$ MeV. CRONIN-HENNESSY 10 gives the analytic dependence of limits on width.

$\Gamma(\eta_c(2S) \to \pi^+\pi^-\eta')/\Gamma_{\text{total}} \times \Gamma(\psi(2S) \to \gamma\eta_c(2S))/\Gamma_{\text{total}}$ $\Gamma_{16}/\Gamma \times \Gamma^{\psi(2S)}_{132}/\Gamma^{\psi(2S)}$

VALUE	CL%	DOCUMENT ID		TECN	COMMENT
<14.2 × 10⁻⁶	90	[36] CRONIN-HEN...10		CLEO	$\psi(2S) \to \gamma\pi^+\pi^-\eta'$

[36] Assuming $\Gamma(\eta_c(2S)) = 14$ MeV. CRONIN-HENNESSY 10 gives the analytic dependence of limits on width.

$\Gamma(\eta_c(2S) \to K^+K^-\eta)/\Gamma_{\text{total}} \times \Gamma(\psi(2S) \to \gamma\eta_c(2S))/\Gamma_{\text{total}}$ $\Gamma_{17}/\Gamma \times \Gamma^{\psi(2S)}_{132}/\Gamma^{\psi(2S)}$

VALUE	CL%	DOCUMENT ID		TECN	COMMENT
<5.9 × 10⁻⁶	90	[37] CRONIN-HEN...10		CLEO	$\psi(2S) \to \gamma K^+K^-\eta$

[37] Assuming $\Gamma(\eta_c(2S)) = 14$ MeV. CRONIN-HENNESSY 10 gives the analytic dependence of limits on width.

Meson Particle Listings

$\eta_c(2S)$, $\psi(2S)$

$\Gamma(\eta_c(2S) \to \pi^+\pi^-\eta_c(1S))/\Gamma_{total} \times \Gamma(\psi(2S) \to \gamma\eta_c(2S))/\Gamma_{total}$

$\Gamma_{18}/\Gamma \times \Gamma_{132}^{\psi(2S)}/\Gamma^{\psi(2S)}$

VALUE	CL%	DOCUMENT ID	TECN	COMMENT
$<1.7 \times 10^{-4}$	90	[38] CRONIN-HEN..10	CLEO	$\psi(2S) \to \gamma\pi^+\pi^-\eta_c(1S)$

[38] Assuming $\Gamma(\eta_c(2S)) = 14$ MeV. CRONIN-HENNESSY 10 gives the analytic dependence of limits on width.

$\Gamma(\eta_c(2S) \to p\overline{p})/\Gamma_{total} \times \Gamma(\psi(2S) \to \gamma\eta_c(2S))/\Gamma_{total}$

$\Gamma_{13}/\Gamma \times \Gamma_{132}^{\psi(2S)}/\Gamma^{\psi(2S)}$

VALUE	CL%	DOCUMENT ID	TECN	COMMENT
$<1.4 \times 10^{-6}$	90	ABLIKIM 13V	BES3	$\psi(2S) \to \gamma p\overline{p}$

$\eta_c(2S)$ REFERENCES

ABLIKIM	13K	PR D87 052005	M. Ablikim *et al.*	(BES III Collab.)
ABLIKIM	13V	PR D88 112001	M. Ablikim *et al.*	(BES III Collab.)
ABLIKIM	12G	PRL 109 042003	M. Ablikim *et al.*	(BES III Collab.)
LEES	12AE	PR D86 092005	J.P. Lees *et al.*	(BABAR Collab.)
ABLIKIM	11H	PR D84 091102	M. Ablikim *et al.*	(BES III Collab.)
DEL-AMO-SA...	11M	PR D84 012004	P. del Amo Sanchez *et al.*	(BABAR Collab.)
VINOKUROVA	11	PL B706 139	A. Vinokurova *et al.*	(BELLE Collab.)
CRONIN-HEN...	10	PR D81 052002	D. Cronin-Hennessey *et al.*	(CLEO Collab.)
AUBERT	08AB	PR D78 012006	B. Aubert *et al.*	(BABAR Collab.)
UEHARA	08	EPJ C53 1	S. Uehara *et al.*	(BELLE Collab.)
WICHT	08	PL B662 323	J. Wicht *et al.*	(BELLE Collab.)
ABE	07	PRL 98 082001	K. Abe *et al.*	(BELLE Collab.)
AUBERT	06E	PRL 96 052002	B. Aubert *et al.*	(BABAR Collab.)
AUBERT	05C	PR D72 031101	B. Aubert *et al.*	(BABAR Collab.)
ABE	04G	PR D70 071102	K. Abe *et al.*	(BELLE Collab.)
ASNER	04	PRL 92 142001	D.M. Asner *et al.*	(CLEO Collab.)
AUBERT	04D	PRL 92 142002	B. Aubert *et al.*	(BABAR Collab.)
ABE,K	02	PRL 89 142001	K. Abe *et al.*	(BELLE Collab.)
CHOI	02	PRL 89 102001	S.-K. Choi *et al.*	(BELLE Collab.)
AMBROGIANI	01	PR D64 052003	M. Ambrogiani *et al.*	(FNAL E835 Collab.)
ABREU	98O	PL B441 479	P. Abreu *et al.*	(DELPHI Collab.)
ARMSTRONG	95F	PR D52 4839	T.A. Armstrong *et al.*	(FNAL, FERR, GENO+)
LEE	85	SLAC 282	R.A. Lee	(SLAC)
EDWARDS	82C	PRL 48 70	C. Edwards *et al.*	(CIT, HARV, PRIN+)

$\psi(2S)$

$I^G(J^{PC}) = 0^-(1^{--})$

See the Review on "$\psi(2S)$ and χ_c branching ratios" before the $\chi_{c0}(1P)$ Listings.

$\psi(2S)$ MASS

OUR FIT includes measurements of $m_{\psi(2S)}$, $m_{\psi(3770)}$, and $m_{\psi(3770)} - m_{\psi(2S)}$.

VALUE (MeV)	EVTS	DOCUMENT ID	TECN	COMMENT
$3686.109^{+0.012}_{-0.014}$ OUR FIT				
$3686.108^{+0.011}_{-0.014}$ OUR AVERAGE				
$3686.12 \pm 0.06 \pm 0.10$	4k	AAIJ 12H	LHCB	$pp \to J/\psi\pi^+\pi^- X$
$3686.114 \pm 0.007^{+0.011}_{-0.016}$		[1] ANASHIN 12	KEDR	$e^+e^- \to$ hadrons
$3686.111 \pm 0.025 \pm 0.009$		AULCHENKO 03	KEDR	$e^+e^- \to$ hadrons
3685.95 ± 0.10	413	[2] ARTAMONOV 00	OLYA	$e^+e^- \to$ hadrons
$3685.98 \pm 0.09 \pm 0.04$		[3] ARMSTRONG 93B	E760	$\overline{p}p \to e^+e^-$
• • • We do not use the following data for averages, fits, limits, etc. • • •				
3686.00 ± 0.10	413	[4] ZHOLENTZ 80	OLYA	e^+e^-

[1] From the scans in 2004 and 2006. ANASHIN 12 reports the value $3686.114 \pm 0.007 \pm 0.011^{+0.002}_{-0.012}$ MeV, where the third uncertainty is due to assumptions on the interference between the resonance and hadronic continuum. We combined the two systematic uncertainties.

[2] Reanalysis of ZHOLENTZ 80 using new electron mass (COHEN 87) and radiative corrections (KURAEV 85).

[3] Mass central value and systematic error recalculated by us according to Eq. (16) in ARMSTRONG 93B, using the value for the $J/\psi(1S)$ mass from AULCHENKO 03.

[4] Superseded by ARTAMONOV 00.

$m_{\psi(2S)} - m_{J/\psi(1S)}$

VALUE (MeV)	DOCUMENT ID	TECN	COMMENT
589.188 ± 0.028 OUR AVERAGE			
$589.194 \pm 0.027 \pm 0.011$	[1] AULCHENKO 03	KEDR	$e^+e^- \to$ hadrons
589.7 ± 1.2	LEMOIGNE 82	GOLI	185 π^- Be $\to \gamma\mu^+\mu^-$ A
589.07 ± 0.13	[1] ZHOLENTZ 80	OLYA	e^+e^-
588.7 ± 0.8	LUTH 75	MRK1	
• • • We do not use the following data for averages, fits, limits, etc. • • •			
588 ± 1	[2] BAI 98E	BES	e^+e^-

[1] Redundant with data in mass above.

[2] Systematic errors not evaluated.

$\psi(2S)$ WIDTH

VALUE (keV)	EVTS	DOCUMENT ID	TECN	COMMENT
299 ± 8 OUR FIT				
286 ± 16 OUR AVERAGE				
$358 \pm 88 \pm 4$		ABLIKIM 08B	BES2	$e^+e^- \to$ hadrons
$290 \pm 25 \pm 4$	2.7k	ANDREOTTI 07	E835	$p\overline{p} \to e^+e^-$, $J/\psi X$
$331 \pm 58 \pm 2$		ABLIKIM 06L	BES2	$e^+e^- \to$ hadrons
264 ± 27		[1] BAI 02B	BES2	e^+e^-
$287 \pm 37 \pm 16$		[2] ARMSTRONG 93B	E760	$\overline{p}p \to e^+e^-$

[1] From a simultaneous fit to the hadronic and $\mu^+\mu^-$ cross section, assuming $\Gamma = \Gamma_h + \Gamma_e + \Gamma_\mu + \Gamma_\tau$ and lepton universality. Does not include vacuum polarization correction.

[2] The initial-state radiation correction reevaluated by ANDREOTTI 07 in its Ref. [4].

$\psi(2S)$ DECAY MODES

	Mode	Fraction (Γ_i/Γ)	Scale factor/ Confidence level
Γ_1	hadrons	(97.85 ± 0.13) %	
Γ_2	virtual$\gamma \to$ hadrons	(1.73 ± 0.14) %	S=1.5
Γ_3	ggg	(10.6 ± 1.6) %	
Γ_4	γgg	(1.03 ± 0.29) %	
Γ_5	light hadrons	(15.4 ± 1.5) %	
Γ_6	e^+e^-	$(7.89 \pm 0.17) \times 10^{-3}$	
Γ_7	$\mu^+\mu^-$	$(7.9 \pm 0.9) \times 10^{-3}$	
Γ_8	$\tau^+\tau^-$	$(3.1 \pm 0.4) \times 10^{-3}$	
	Decays into $J/\psi(1S)$ and anything		
Γ_9	$J/\psi(1S)$anything	(60.9 ± 0.6) %	
Γ_{10}	$J/\psi(1S)$neutrals	(25.10 ± 0.33) %	
Γ_{11}	$J/\psi(1S)\pi^+\pi^-$	(34.45 ± 0.30) %	
Γ_{12}	$J/\psi(1S)\pi^0\pi^0$	(18.13 ± 0.31) %	
Γ_{13}	$J/\psi(1S)\eta$	(3.36 ± 0.05) %	
Γ_{14}	$J/\psi(1S)\pi^0$	$(1.268 \pm 0.032) \times 10^{-3}$	
	Hadronic decays		
Γ_{15}	$\pi^0 h_c(1P)$	$(8.6 \pm 1.3) \times 10^{-4}$	
Γ_{16}	$3(\pi^+\pi^-)\pi^0$	$(3.5 \pm 1.6) \times 10^{-3}$	
Γ_{17}	$2(\pi^+\pi^-)\pi^0$	$(2.9 \pm 1.0) \times 10^{-3}$	S=4.7
Γ_{18}	$\rho a_2(1320)$	$(2.6 \pm 0.9) \times 10^{-4}$	
Γ_{19}	$p\overline{p}$	$(2.80 \pm 0.11) \times 10^{-4}$	
Γ_{20}	$\Delta^{++}\overline{\Delta}^{--}$	$(1.28 \pm 0.35) \times 10^{-4}$	
Γ_{21}	$\Lambda\overline{\Lambda}\pi^0$	$< 2.9 \times 10^{-6}$	CL=90%
Γ_{22}	$\Lambda\overline{\Lambda}\eta$	$(2.5 \pm 0.4) \times 10^{-5}$	
Γ_{23}	$\Lambda\overline{p}K^+$	$(1.00 \pm 0.14) \times 10^{-4}$	
Γ_{24}	$\Lambda\overline{p}K^+\pi^+\pi^-$	$(1.8 \pm 0.4) \times 10^{-4}$	
Γ_{25}	$\Lambda\overline{\Lambda}\pi^+\pi^-$	$(2.8 \pm 0.6) \times 10^{-4}$	
Γ_{26}	$\Lambda\overline{\Lambda}$	$(2.8 \pm 0.5) \times 10^{-4}$	S=2.6
Γ_{27}	$\Lambda\overline{\Sigma}^+\pi^-$ + c.c.	$(1.40 \pm 0.13) \times 10^{-4}$	
Γ_{28}	$\Lambda\overline{\Sigma}^-\pi^+$ + c.c.	$(1.54 \pm 0.14) \times 10^{-4}$	
Γ_{29}	$\Sigma^0\overline{p}K^+$ + c.c.	$(1.67 \pm 0.18) \times 10^{-5}$	
Γ_{30}	$\Sigma^+\overline{\Sigma}^-$	$(2.6 \pm 0.8) \times 10^{-4}$	
Γ_{31}	$\Sigma^0\overline{\Sigma}^0$	$(2.2 \pm 0.4) \times 10^{-4}$	S=1.5
Γ_{32}	$\Sigma(1385)^+\overline{\Sigma}(1385)^-$	$(1.1 \pm 0.4) \times 10^{-4}$	
Γ_{33}	$\Xi^-\overline{\Xi}^+$	$(1.8 \pm 0.6) \times 10^{-4}$	S=2.8
Γ_{34}	$\Xi^0\overline{\Xi}^0$	$(2.8 \pm 0.9) \times 10^{-4}$	
Γ_{35}	$\Xi(1530)^0\overline{\Xi}(1530)^0$	$(5.2 \pm 3.2 \pm 1.2) \times 10^{-5}$	
Γ_{36}	$\Omega^-\overline{\Omega}^+$	$< 7.3 \times 10^{-5}$	CL=90%
Γ_{37}	$\pi^0 p\overline{p}$	$(1.53 \pm 0.07) \times 10^{-4}$	
Γ_{38}	$N(940)\overline{p}$+ c.c. $\to \pi^0 p\overline{p}$	$(6.4 \pm 1.8 \pm 1.3) \times 10^{-5}$	
Γ_{39}	$N(1440)\overline{p}$+ c.c. $\to \pi^0 p\overline{p}$	$(7.3 \pm 1.7 \pm 1.5) \times 10^{-5}$	S=2.5
Γ_{40}	$N(1520)\overline{p}$+ c.c. $\to \pi^0 p\overline{p}$	$(6.4 \pm 2.3 \pm 1.8) \times 10^{-6}$	
Γ_{41}	$N(1535)\overline{p}$+ c.c. $\to \pi^0 p\overline{p}$	$(2.5 \pm 1.0) \times 10^{-5}$	
Γ_{42}	$N(1650)\overline{p}$+ c.c. $\to \pi^0 p\overline{p}$	$(3.8 \pm 1.4 \pm 1.7) \times 10^{-5}$	
Γ_{43}	$N(1720)\overline{p}$+ c.c. $\to \pi^0 p\overline{p}$	$(1.79 \pm 0.26 \pm 0.70) \times 10^{-5}$	
Γ_{44}	$N(2300)\overline{p}$+ c.c. $\to \pi^0 p\overline{p}$	$(2.6 \pm 1.2 \pm 0.7) \times 10^{-5}$	
Γ_{45}	$N(2570)\overline{p}$+ c.c. $\to \pi^0 p\overline{p}$	$(2.13 \pm 0.40 \pm 0.31) \times 10^{-5}$	
Γ_{46}	$\pi^0 f_0(2100) \to \pi^0 p\overline{p}$	$(1.1 \pm 0.4) \times 10^{-5}$	
Γ_{47}	$\eta p\overline{p}$	$(6.0 \pm 0.4) \times 10^{-5}$	
Γ_{48}	$\eta f_0(2100) \to \eta p\overline{p}$	$(1.2 \pm 0.4) \times 10^{-5}$	
Γ_{49}	$N(1535)\overline{p} \to \eta p\overline{p}$	$(4.4 \pm 0.7) \times 10^{-5}$	

Γ_{50}	$\omega p\overline{p}$	(6.9	± 2.1)	$\times 10^{-5}$	
Γ_{51}	$\phi p\overline{p}$	< 2.4		$\times 10^{-5}$	CL=90%
Γ_{52}	$\pi^+\pi^- p\overline{p}$	(6.0	± 0.4)	$\times 10^{-4}$	
Γ_{53}	$p\overline{n}\pi^-$ or c.c.	(2.48	± 0.17)	$\times 10^{-4}$	
Γ_{54}	$p\overline{n}\pi^-\pi^0$	(3.2	± 0.7)	$\times 10^{-4}$	
Γ_{55}	$2(\pi^+\pi^-\pi^0)$	(4.7	± 1.5)	$\times 10^{-3}$	
Γ_{56}	$\eta\pi^+\pi^-$	< 1.6		$\times 10^{-4}$	CL=90%
Γ_{57}	$\eta\pi^+\pi^-\pi^0$	(9.5	± 1.7)	$\times 10^{-4}$	
Γ_{58}	$2(\pi^+\pi^-)\eta$	(1.2	± 0.6)	$\times 10^{-3}$	
Γ_{59}	$\eta'\pi^+\pi^-\pi^0$	(4.5	± 2.1)	$\times 10^{-4}$	
Γ_{60}	$\omega\pi^+\pi^-$	(7.3	± 1.2)	$\times 10^{-4}$	S=2.1
Γ_{61}	$b_1^\pm\pi^\mp$	(4.0	± 0.6)	$\times 10^{-4}$	S=1.1
Γ_{62}	$b_1^0\pi^0$	(2.4	± 0.6)	$\times 10^{-4}$	
Γ_{63}	$\omega f_2(1270)$	(2.2	± 0.4)	$\times 10^{-4}$	
Γ_{64}	$\pi^+\pi^- K^+K^-$	(7.5	± 0.9)	$\times 10^{-4}$	S=1.9
Γ_{65}	$\rho^0 K^+K^-$	(2.2	± 0.4)	$\times 10^{-4}$	
Γ_{66}	$K^*(892)^0\overline{K}_2^*(1430)^0$	(1.9	± 0.5)	$\times 10^{-4}$	
Γ_{67}	$K^+K^-\pi^+\pi^-\eta$	(1.3	± 0.7)	$\times 10^{-3}$	
Γ_{68}	$K^+K^-2(\pi^+\pi^-)\pi^0$	(1.00	± 0.31)	$\times 10^{-3}$	
Γ_{69}	$K^+K^-2(\pi^+\pi^-)$	(1.9	± 0.9)	$\times 10^{-3}$	
Γ_{70}	$K_1(1270)^\pm K^\mp$	(1.00	± 0.28)	$\times 10^{-3}$	
Γ_{71}	$K_S^0 K_S^0\pi^+\pi^-$	(2.2	± 0.4)	$\times 10^{-4}$	
Γ_{72}	$\rho^0 p\overline{p}$	(5.0	± 2.2)	$\times 10^{-5}$	
Γ_{73}	$K^+\overline{K}^*(892)^0\pi^-$ + c.c.	(6.7	± 2.5)	$\times 10^{-4}$	
Γ_{74}	$2(\pi^+\pi^-)$	(2.4	± 0.6)	$\times 10^{-4}$	S=2.2
Γ_{75}	$\rho^0\pi^+\pi^-$	(2.2	± 0.6)	$\times 10^{-4}$	S=1.4
Γ_{76}	$K^+K^-\pi^+\pi^-\pi^0$	(1.26	± 0.09)	$\times 10^{-3}$	
Γ_{77}	$\omega f_0(1710) \to \omega K^+K^-$	(5.9	± 2.2)	$\times 10^{-5}$	
Γ_{78}	$K^*(892)^0 K^-\pi^+\pi^0$ + c.c.	(8.6	± 2.2)	$\times 10^{-4}$	
Γ_{79}	$K^*(892)^+ K^-\pi^+\pi^-$ + c.c.	(9.6	± 2.8)	$\times 10^{-4}$	
Γ_{80}	$K^*(892)^+ K^-\rho^0$ + c.c.	(7.3	± 2.6)	$\times 10^{-4}$	
Γ_{81}	$K^*(892)^0 K^-\rho^+$ + c.c.	(6.1	± 1.8)	$\times 10^{-4}$	
Γ_{82}	ηK^+K^-, no $\eta\phi$	(3.1	± 0.4)	$\times 10^{-5}$	
Γ_{83}	ωK^+K^-	(1.85	± 0.25)	$\times 10^{-4}$	S=1.1
Γ_{84}	$\omega K^*(892)^+ K^-$ + c.c.	(2.07	± 0.26)	$\times 10^{-4}$	
Γ_{85}	$\omega K_2^*(1430)^+ K^-$ + c.c.	(6.1	± 1.2)	$\times 10^{-5}$	
Γ_{86}	$\omega\overline{K}^*(892)^0 K^0$	(1.68	± 0.30)	$\times 10^{-4}$	
Γ_{87}	$\omega\overline{K}_2^*(1430)^0 K^0$	(5.8	± 2.2)	$\times 10^{-5}$	
Γ_{88}	$\omega X(1440) \to \omega K_S^0 K^-\pi^+$ + c.c.	(1.6	± 0.4)	$\times 10^{-5}$	
Γ_{89}	$\omega X(1440) \to \omega K^+K^-\pi^0$	(1.09	± 0.26)	$\times 10^{-5}$	
Γ_{90}	$\omega f_1(1285) \to \omega K_S^0 K^-\pi^+$ + c.c.	(3.0	± 1.0)	$\times 10^{-6}$	
Γ_{91}	$\omega f_1(1285) \to \omega K^+K^-\pi^0$	(1.2	± 0.7)	$\times 10^{-6}$	
Γ_{92}	$3(\pi^+\pi^-)$	(3.5	± 2.0)	$\times 10^{-4}$	S=2.8
Γ_{93}	$p\overline{p}\pi^+\pi^-\pi^0$	(7.3	± 0.7)	$\times 10^{-4}$	
Γ_{94}	K^+K^-	(7.1	± 0.5)	$\times 10^{-5}$	S=1.5
Γ_{95}	$K_S^0 K_L^0$	(5.34	± 0.33)	$\times 10^{-5}$	
Γ_{96}	$\pi^+\pi^-\pi^0$	(2.01	± 0.17)	$\times 10^{-4}$	S=1.7
Γ_{97}	$\rho(2150)\pi \to \pi^+\pi^-\pi^0$	(1.9	$^{+1.2}_{-0.4}$)	$\times 10^{-4}$	
Γ_{98}	$\rho(770)\pi \to \pi^+\pi^-\pi^0$	(3.2	± 1.2)	$\times 10^{-5}$	S=1.8
Γ_{99}	$\pi^+\pi^-$	(7.8	± 2.6)	$\times 10^{-6}$	
Γ_{100}	$K_1(1400)^\pm K^\mp$	< 3.1		$\times 10^{-4}$	CL=90%
Γ_{101}	$K_2^*(1430)^\pm K^\mp$	(7.1	$^{+1.3}_{-0.9}$)	$\times 10^{-5}$	
Γ_{102}	$K^+K^-\pi^0$	(4.07	± 0.31)	$\times 10^{-5}$	
Γ_{103}	$K^+K^*(892)^-$ + c.c.	(2.9	± 0.4)	$\times 10^{-5}$	S=1.2
Γ_{104}	$K^*(892)^0\overline{K}^0$ + c.c.	(1.09	± 0.20)	$\times 10^{-4}$	
Γ_{105}	$\phi\pi^+\pi^-$	(1.17	± 0.29)	$\times 10^{-4}$	S=1.7
Γ_{106}	$\phi f_0(980) \to \pi^+\pi^-$	(6.8	± 2.4)	$\times 10^{-5}$	S=1.1
Γ_{107}	$2(K^+K^-)$	(6.0	± 1.4)	$\times 10^{-5}$	
Γ_{108}	ϕK^+K^-	(7.0	± 1.6)	$\times 10^{-5}$	
Γ_{109}	$2(K^+K^-)\pi^0$	(1.10	± 0.28)	$\times 10^{-4}$	
Γ_{110}	$\phi\eta$	(3.10	± 0.31)	$\times 10^{-5}$	
Γ_{111}	$\phi\eta'$	(3.1	± 1.6)	$\times 10^{-5}$	
Γ_{112}	$\omega\eta'$	(3.2	$^{+2.5}_{-2.1}$)	$\times 10^{-5}$	
Γ_{113}	$\omega\pi^0$	(2.1	± 0.6)	$\times 10^{-5}$	
Γ_{114}	$\rho\eta'$	(1.9	$^{+1.7}_{-1.2}$)	$\times 10^{-5}$	
Γ_{115}	$\rho\eta$	(2.2	± 0.6)	$\times 10^{-5}$	S=1.1
Γ_{116}	$\omega\eta$	< 1.1		$\times 10^{-5}$	CL=90%
Γ_{117}	$\phi\pi^0$	< 4		$\times 10^{-7}$	CL=90%
Γ_{118}	$\eta_c\pi^+\pi^-\pi^0$	< 1.0		$\times 10^{-3}$	CL=90%
Γ_{119}	$p\overline{p}K^+K^-$	(2.7	± 0.7)	$\times 10^{-5}$	
Γ_{120}	$\overline{\Lambda}n K_S^0$ + c.c.	(8.1	± 1.8)	$\times 10^{-5}$	
Γ_{121}	$\phi f_2'(1525)$	(4.4	± 1.6)	$\times 10^{-5}$	
Γ_{122}	$\Theta(1540)\overline{\Theta}(1540) \to K_S^0 p K^-\overline{n}$ + c.c.	< 8.8		$\times 10^{-6}$	CL=90%
Γ_{123}	$\Theta(1540) K^-\overline{n} \to K_S^0 p K^-\overline{n}$	< 1.0		$\times 10^{-5}$	CL=90%
Γ_{124}	$\Theta(1540) K_S^0\overline{p} \to K_S^0\overline{p}K^+ n$	< 7.0		$\times 10^{-6}$	CL=90%
Γ_{125}	$\overline{\Theta}(1540) K^+ n \to K_S^0\overline{p}K^+ n$	< 2.6		$\times 10^{-5}$	CL=90%
Γ_{126}	$\overline{\Theta}(1540) K_S^0 p \to K_S^0 p K^-\overline{n}$	< 6.0		$\times 10^{-6}$	CL=90%
Γ_{127}	$K_S^0 K_S^0$	< 4.6		$\times 10^{-6}$	

Radiative decays

Γ_{128}	$\gamma\chi_{c0}(1P)$	(9.99	± 0.27)	%	
Γ_{129}	$\gamma\chi_{c1}(1P)$	(9.55	± 0.31)	%	
Γ_{130}	$\gamma\chi_{c2}(1P)$	(9.11	± 0.31)	%	
Γ_{131}	$\gamma\eta_c(1S)$	(3.4	± 0.5)	$\times 10^{-3}$	S=1.3
Γ_{132}	$\gamma\eta_c(2S)$	(7	± 5)	$\times 10^{-4}$	
Γ_{133}	$\gamma\pi^0$	(1.6	± 0.4)	$\times 10^{-6}$	
Γ_{134}	$\gamma\eta'(958)$	(1.23	± 0.06)	$\times 10^{-4}$	
Γ_{135}	$\gamma f_2(1270)$	(2.1	± 0.4)	$\times 10^{-4}$	
Γ_{136}	$\gamma f_0(1710)$				
Γ_{137}	$\gamma f_0(1710) \to \gamma\pi\pi$	(3.0	± 1.3)	$\times 10^{-5}$	
Γ_{138}	$\gamma f_0(1710) \to \gamma K\overline{K}$	(6.0	± 1.6)	$\times 10^{-5}$	
Γ_{139}	$\gamma\gamma$	< 1.4		$\times 10^{-4}$	CL=90%
Γ_{140}	$\gamma\eta$	(1.4	± 0.5)	$\times 10^{-6}$	
Γ_{141}	$\gamma\eta\pi^+\pi^-$	(8.7	± 2.1)	$\times 10^{-4}$	
Γ_{142}	$\gamma\eta(1405)$				
Γ_{143}	$\gamma\eta(1405) \to \gamma K\overline{K}\pi$	< 9		$\times 10^{-5}$	CL=90%
Γ_{144}	$\gamma\eta(1405) \to \eta\pi^+\pi^-$	(3.6	± 2.5)	$\times 10^{-5}$	
Γ_{145}	$\gamma\eta(1475)$				
Γ_{146}	$\gamma\eta(1475) \to K\overline{K}\pi$	< 1.4		$\times 10^{-4}$	CL=90%
Γ_{147}	$\gamma\eta(1475) \to \eta\pi^+\pi^-$	< 8.8		$\times 10^{-5}$	CL=90%
Γ_{148}	$\gamma 2(\pi^+\pi^-)$	(4.0	± 0.6)	$\times 10^{-4}$	
Γ_{149}	$\gamma K^{*0} K^+\pi^-$ + c.c.	(3.7	± 0.9)	$\times 10^{-4}$	
Γ_{150}	$\gamma K^{*0}\overline{K}^{*0}$	(2.4	± 0.7)	$\times 10^{-4}$	
Γ_{151}	$\gamma K_S^0 K^+\pi^-$ + c.c.	(2.6	± 0.5)	$\times 10^{-4}$	
Γ_{152}	$\gamma K^+K^-\pi^+\pi^-$	(1.9	± 0.5)	$\times 10^{-4}$	
Γ_{153}	$\gamma p\overline{p}$	(3.9	± 0.5)	$\times 10^{-5}$	S=2.0
Γ_{154}	$\gamma f_2(1950) \to \gamma p\overline{p}$	(1.20	± 0.22)	$\times 10^{-5}$	
Γ_{155}	$\gamma f_2(2150) \to \gamma p\overline{p}$	(7.2	± 1.8)	$\times 10^{-6}$	
Γ_{156}	$\gamma X(1835) \to \gamma p\overline{p}$	(4.6	$^{+1.8}_{-4.0}$)	$\times 10^{-6}$	
Γ_{157}	$\gamma X \to \gamma p\overline{p}$	[a] < 2		$\times 10^{-6}$	CL=90%
Γ_{158}	$\gamma\pi^+\pi^- p\overline{p}$	(2.8	± 1.4)	$\times 10^{-5}$	
Γ_{159}	$\gamma 2(\pi^+\pi^-) K^+K^-$	< 2.2		$\times 10^{-4}$	CL=90%
Γ_{160}	$\gamma 3(\pi^+\pi^-)$	< 1.7		$\times 10^{-4}$	CL=90%
Γ_{161}	$\gamma K^+K^-K^+K^-$	< 4		$\times 10^{-5}$	CL=90%
Γ_{162}	$\gamma\gamma J/\psi$	(3.1	$^{+1.0}_{-1.2}$)	$\times 10^{-4}$	

Other decays

Γ_{163}	invisible	< 1.6		%	CL=90%

[a] For a narrow resonance in the range $2.2 < M(X) < 2.8$ GeV.

CONSTRAINED FIT INFORMATION

A multiparticle fit to $\chi_{c1}(1P)$, $\chi_{c0}(1P)$, $\chi_{c2}(1P)$, and $\psi(2S)$ with 4 total widths, a partial width, 25 combinations of partial widths obtained from integrated cross section, and 84 branching ratios uses 238 measurements to determine 49 parameters. The overall fit has a $\chi^2 = 339.7$ for 189 degrees of freedom.

The following *off-diagonal* array elements are the correlation coefficients $\langle \delta p_i \delta p_j \rangle / (\delta p_i \cdot \delta p_j)$, in percent, from the fit to parameters p_i, including the branching fractions, $x_i \equiv \Gamma_i/\Gamma_{\rm total}$.

x_7	3									
x_8	1	0								
x_{11}	30	8	2							
x_{12}	29	5	1	49						
x_{13}	13	3	1	37	16					
x_{19}	0	1	0	6	4	3				
x_{128}	1	0	0	3	1	1	0			
x_{129}	2	0	0	4	1	1	0	0		
x_{130}	1	0	0	4	2	1	0	0	0	
Γ	−79	−3	−1	−40	−35	−17	−11	−1	−2	−2
	x_6	x_7	x_8	x_{11}	x_{12}	x_{13}	x_{19}	x_{128}	x_{129}	x_{130}

$\psi(2S)$ PARTIAL WIDTHS

Γ(hadrons) Γ_1

VALUE (keV)	DOCUMENT ID		TECN	COMMENT
• • • We do not use the following data for averages, fits, limits, etc. • • •				
258±26	BAI	02B	BES2	e^+e^-
224±56	LUTH	75	MRK1	e^+e^-

$\Gamma(e^+e^-)$ Γ_6

VALUE (keV)	DOCUMENT ID		TECN	COMMENT
2.36 ±0.04 OUR FIT				
2.33 ±0.07 OUR AVERAGE				
2.338±0.037±0.096	ABLIKIM	08B	BES2	$e^+e^-\to$ hadrons
2.330±0.036±0.110	ABLIKIM	06L	BES2	$e^+e^-\to$ hadrons
2.44 ±0.21	[1] BAI	02B	BES2	e^+e^-
2.14 ±0.21	ALEXANDER	89	RVUE	See Υ mini-review
• • • We do not use the following data for averages, fits, limits, etc. • • •				
2.0 ±0.3	BRANDELIK	79C	DASP	e^+e^-
2.1 ±0.3	[2] LUTH	75	MRK1	e^+e^-

[1] From a simultaneous fit to e^+e^-, $\mu^+\mu^-$, and hadronic channel, assuming $\Gamma_e=\Gamma_\mu=\Gamma_\tau/0.38847$.
[2] From a simultaneous fit to e^+e^-, $\mu^+\mu^-$, and hadronic channels assuming $\Gamma(e^+e^-)=\Gamma(\mu^+\mu^-)$.

$\Gamma(\gamma\gamma)$ Γ_{139}

VALUE (eV)	CL%	DOCUMENT ID		TECN	COMMENT
<43	90	BRANDELIK	79C	DASP	e^+e^-

$\psi(2S)$ Γ(i)$\Gamma(e^+e^-)/\Gamma$(total)

This combination of a partial width with the partial width into e^+e^- and with the total width is obtained from the integrated cross section into channel(i) in the e^+e^- annihilation. We list only data that have not been used to determine the partial width Γ(i) or the branching ratio Γ(i)/total.

Γ(hadrons) × $\Gamma(e^+e^-)/\Gamma_{\rm total}$ $\Gamma_1\Gamma_6/\Gamma$

VALUE (keV)	DOCUMENT ID		TECN	COMMENT
2.233±0.015±0.042	[1] ANASHIN	12	KEDR	$e^+e^-\to$ hadrons
• • • We do not use the following data for averages, fits, limits, etc. • • •				
2.2 ±0.4	ABRAMS	75	MRK1	e^+e^-

[1] ANASHIN 12 reports the value 2.233 ± 0.015 ± 0.037 ± 0.020 keV, where the third uncertainty is due to assumptions on the interference between the resonance and hadronic continuum. We combined the two systematic uncertainties.

$\Gamma(\tau^+\tau^-)$ × $\Gamma(e^+e^-)/\Gamma_{\rm total}$ $\Gamma_8\Gamma_6/\Gamma$

VALUE (eV)	EVTS	DOCUMENT ID		TECN	COMMENT
• • • We do not use the following data for averages, fits, limits, etc. • • •					
9.0±2.6	79	[1] ANASHIN	07	KEDR	$e^+e^-\to\psi(2S)\to\tau^+\tau^-$

[1] Using $\psi(2S)$ total width of 337 ± 13 keV. Systematic errors not evaluated.

$\Gamma(J/\psi(1S)\pi^+\pi^-)$ × $\Gamma(e^+e^-)/\Gamma_{\rm total}$ $\Gamma_{11}\Gamma_6/\Gamma$

VALUE (keV)	EVTS	DOCUMENT ID		TECN	COMMENT
0.813±0.013 OUR FIT					
0.837±0.025 OUR AVERAGE		Error includes scale factor of 1.3. See the ideogram below.			
0.837±0.028±0.005		[1] LEES	12E	BABR	10.6 $e^+e^-\to 2\pi^+2\pi^-\gamma$
0.852±0.010±0.026	19.5k	ADAM	06	CLEO	3.773 $e^+e^-\to\gamma\psi(2S)$
0.68 ±0.09		[2] BAI	98E	BES	e^+e^-
• • • We do not use the following data for averages, fits, limits, etc. • • •					
0.88 ±0.08 ±0.03	256	[3] AUBERT	07AU	BABR	10.6 $e^+e^-\to J/\psi\pi^+\pi^-\gamma$
0.755±0.048±0.004	544	[4] AUBERT	05D	BABR	10.6 $e^+e^-\to\pi^+\pi^-\mu^+\mu^-\gamma$

[1] LEES 12E reports $[\Gamma(\psi(2S)\to J/\psi(1S)\pi^+\pi^-)\times\Gamma(\psi(2S)\to e^+e^-)/\Gamma_{\rm total}]\times[B(J/\psi(1S)\to\mu^+\mu^-)]=(49.9\pm1.3\pm1.0)\times10^{-3}$ keV which we divide by our best value $B(J/\psi(1S)\to\mu^+\mu^-)=(5.961\pm0.033)\times10^{-2}$. Our first error is their experiment's error and our second error is the systematic error from using our best value.
[2] The value of $\Gamma(e^+e^-)$ quoted in BAI 98E is derived using $B(\psi(2S)\to J/\psi(1S)\pi^+\pi^-)=(32.4\pm2.6)\times10^{-2}$ and $B(J/\psi(1S)\to\ell^+\ell^-)=0.1203\pm0.0038$. Recalculated by us using $B(J/\psi(1S)\to\ell^+\ell^-)=0.1181\pm0.0020$.
[3] AUBERT 07AU reports $[\Gamma(\psi(2S)\to J/\psi(1S)\pi^+\pi^-)\times\Gamma(\psi(2S)\to e^+e^-)/\Gamma_{\rm total}]\times[B(J/\psi(1S)\to\pi^+\pi^-\pi^0)]=0.0186\pm0.0012\pm0.0011$ keV which we divide by our best value $B(J/\psi(1S)\to\pi^+\pi^-\pi^0)=(2.11\pm0.07)\times10^{-2}$. Our first error is their experiment's error and our second error is the systematic error from using our best value.
[4] AUBERT 05D reports $[\Gamma(\psi(2S)\to J/\psi(1S)\pi^+\pi^-)\times\Gamma(\psi(2S)\to e^+e^-)/\Gamma_{\rm total}]\times[B(J/\psi(1S)\to\mu^+\mu^-)]=0.0450\pm0.0018\pm0.0022$ keV which we divide by our best value $B(J/\psi(1S)\to\mu^+\mu^-)=(5.961\pm0.033)\times10^{-2}$. Our first error is their experiment's error and our second error is the systematic error from using our best value. Superseded by LEES 12E.

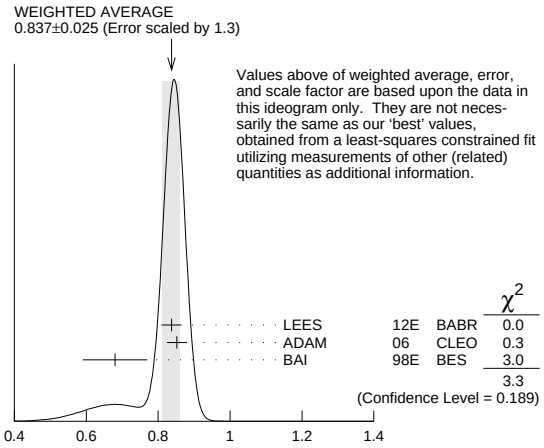

$\Gamma(J/\psi(1S)\pi^0\pi^0)\times\Gamma(e^+e^-)/\Gamma_{\rm total}$ $\Gamma_{12}\Gamma_6/\Gamma$

VALUE (keV)	EVTS	DOCUMENT ID		TECN	COMMENT
0.428±0.009 OUR FIT					
0.411±0.008±0.018	3.6k±96	ADAM	06	CLEO	3.773 $e^+e^-\to\gamma\psi(2S)$

$\Gamma(J/\psi(1S)\eta)\times\Gamma(e^+e^-)/\Gamma_{\rm total}$ $\Gamma_{13}\Gamma_6/\Gamma$

VALUE (eV)	EVTS	DOCUMENT ID		TECN	COMMENT
79.2± 1.7 OUR FIT					
87 ± 9 OUR AVERAGE					
83 ±25 ±5	14	[1] AUBERT	07AU	BABR	10.6 $e^+e^-\to J/\psi\pi^+\pi^-\pi^0\gamma$
88 ± 6 ±7	291 ± 24	ADAM	06	CLEO	3.773 $e^+e^-\to\gamma\psi(2S)$

[1] AUBERT 07AU quotes $\Gamma^{\psi(2S)}_{ee}\cdot B(\psi(2S)\to J/\psi\eta)\cdot B(J/\psi\to\mu^+\mu^-)\cdot B(\eta\to\pi^+\pi^-\pi^0)=1.11\pm0.33\pm0.07$ eV.

$\Gamma(J/\psi(1S)\pi^0)\times\Gamma(e^+e^-)/\Gamma_{\rm total}$ $\Gamma_{14}\Gamma_6/\Gamma$

VALUE (eV)	CL%	EVTS	DOCUMENT ID		TECN	COMMENT
<8	90	<37	ADAM	06	CLEO	3.773 $e^+e^-\to\gamma\psi(2S)$

$\Gamma(p\overline{p})\times\Gamma(e^+e^-)/\Gamma_{\rm total}$ $\Gamma_{19}\Gamma_6/\Gamma$

VALUE (eV)	EVTS	DOCUMENT ID		TECN	COMMENT
0.661±0.026 OUR FIT					
0.64 ±0.04 OUR AVERAGE					
0.67 ±0.12 ±0.02	43	LEES	13O	BABR	$e^+e^-\to p\overline{p}\gamma$
0.74 ±0.07 ±0.04	142	LEES	13Y	BABR	$e^+e^-\to p\overline{p}\gamma$
0.579±0.038±0.036	2.7k	ANDREOTTI	07	E835	$p\overline{p}\to e^+e^-,\ J/\psi X$
0.70 ±0.17 ±0.03	22	AUBERT	06B		$e^+e^-\to p\overline{p}\gamma$

$\Gamma(\Lambda\overline{\Lambda})\times\Gamma(e^+e^-)/\Gamma_{\rm total}$ $\Gamma_{26}\Gamma_6/\Gamma$

VALUE (eV)	DOCUMENT ID		TECN	COMMENT
1.5±0.4±0.1	AUBERT	07BD	BABR	10.6 $e^+e^-\to\Lambda\overline{\Lambda}\gamma$

$\Gamma(2(\pi^+\pi^-\pi^0))\times\Gamma(e^+e^-)/\Gamma_{\rm total}$ $\Gamma_{55}\Gamma_6/\Gamma$

VALUE (eV)	EVTS	DOCUMENT ID		TECN	COMMENT
11.2±3.3±1.3	43	AUBERT	06D	BABR	10.6 $e^+e^-\to 2(\pi^+\pi^-\pi^0)\gamma$

$\Gamma(K^+K^-2(\pi^+\pi^-))\times\Gamma(e^+e^-)/\Gamma_{\rm total}$ $\Gamma_{69}\Gamma_6/\Gamma$

VALUE (eV)	EVTS	DOCUMENT ID		TECN	COMMENT
4.4±2.1±0.3	26	AUBERT	06D	BABR	10.6 $e^+e^-\to K^+K^-2(\pi^+\pi^-)\gamma$

$\Gamma(\pi^+\pi^-K^+K^-)\times\Gamma(e^+e^-)/\Gamma_{\rm total}$ $\Gamma_{64}\Gamma_6/\Gamma$

VALUE (eV)	EVTS	DOCUMENT ID		TECN	COMMENT
2.56±0.42±0.16	85	AUBERT	07AK	BABR	10.6 $e^+e^-\to\pi^+\pi^-K^+K^-\gamma$

$\Gamma(\phi f_0(980)\to\pi^+\pi^-)\times\Gamma(e^+e^-)/\Gamma_{\rm total}$ $\Gamma_{106}\Gamma_6/\Gamma$

VALUE (eV)	EVTS	DOCUMENT ID		TECN	COMMENT
0.347±0.169±0.003	6 ± 3	[1] AUBERT	07AK	BABR	10.6 $e^+e^-\to\pi^+\pi^-K^+K^-\gamma$

[1] AUBERT 07AK reports $[\Gamma(\psi(2S)\to\phi f_0(980)\to\pi^+\pi^-)\times\Gamma(\psi(2S)\to e^+e^-)/\Gamma_{\rm total}]\times[B(\phi(1020)\to K^+K^-)]=0.17\pm0.08\pm0.02$ eV which we divide by our best value $B(\phi(1020)\to K^+K^-)=(48.9\pm0.5)\times10^{-2}$. Our first error is their experiment's error and our second error is the systematic error from using our best value.

$\Gamma(\phi\pi^+\pi^-)\times\Gamma(e^+e^-)/\Gamma_{\rm total}$ $\Gamma_{105}\Gamma_6/\Gamma$

VALUE (eV)	EVTS	DOCUMENT ID		TECN	COMMENT
0.57±0.23±0.01	10	[1] AUBERT,BE	06D	BABR	10.6 $e^+e^-\to K^+K^-\pi^+\pi^-\gamma$

[1] AUBERT,BE 06D reports $[\Gamma(\psi(2S)\to\phi\pi^+\pi^-)\times\Gamma(\psi(2S)\to e^+e^-)/\Gamma_{\rm total}]\times[B(\phi(1020)\to K^+K^-)]=0.28\pm0.11\pm0.02$ eV which we divide by our best value $B(\phi(1020)\to K^+K^-)=(48.9\pm0.5)\times10^{-2}$. Our first error is their experiment's error and our second error is the systematic error from using our best value.

$\Gamma(2(\pi^+\pi^-)\pi^0) \times \Gamma(e^+e^-)/\Gamma_{total}$ $\Gamma_{17}\Gamma_6/\Gamma$

VALUE (eV)	EVTS	DOCUMENT ID		TECN	COMMENT
29.7±2.2±1.8	410	AUBERT	07AU	BABR	10.6 $e^+e^- \to 2(\pi^+\pi^-)\pi^0\gamma$

$\Gamma(\omega\pi^+\pi^-) \times \Gamma(e^+e^-)/\Gamma_{total}$ $\Gamma_{60}\Gamma_6/\Gamma$

VALUE (eV)	EVTS	DOCUMENT ID		TECN	COMMENT
3.01±0.84±0.02	37	[1] AUBERT	07AU	BABR	10.6 $e^+e^- \to \omega\pi^+\pi^-\gamma$

[1] AUBERT 07AU reports $[\Gamma(\psi(2S) \to \omega\pi^+\pi^-) \times \Gamma(\psi(2S) \to e^+e^-)/\Gamma_{total}] \times [B(\omega(782) \to \pi^+\pi^-\pi^0)] = 2.69 \pm 0.73 \pm 0.16$ eV which we divide by our best value $B(\omega(782) \to \pi^+\pi^-\pi^0) = (89.2 \pm 0.7) \times 10^{-2}$. Our first error is their experiment's error and our second error is the systematic error from using our best value.

$\Gamma(2(\pi^+\pi^-)\eta) \times \Gamma(e^+e^-)/\Gamma_{total}$ $\Gamma_{58}\Gamma_6/\Gamma$

VALUE (eV)	EVTS	DOCUMENT ID		TECN	COMMENT
2.87±1.41±0.01	16	[1] AUBERT	07AU	BABR	10.6 $e^+e^- \to 2(\pi^+\pi^-)\eta\gamma$

[1] AUBERT 07AU reports $[\Gamma(\psi(2S) \to 2(\pi^+\pi^-)\eta) \times \Gamma(\psi(2S) \to e^+e^-)/\Gamma_{total}] \times [B(\eta \to 2\gamma)] = 1.13 \pm 0.55 \pm 0.08$ eV which we divide by our best value $B(\eta \to 2\gamma) = (39.41 \pm 0.20) \times 10^{-2}$. Our first error is their experiment's error and our second error is the systematic error from using our best value.

$\Gamma(K^+K^-\pi^+\pi^-\pi^0) \times \Gamma(e^+e^-)/\Gamma_{total}$ $\Gamma_{76}\Gamma_6/\Gamma$

VALUE (eV)	EVTS	DOCUMENT ID		TECN	COMMENT
4.4±1.3±0.3	32	AUBERT	07AU	BABR	10.6 $e^+e^- \to K^+K^-\pi^+\pi^-\pi^0\gamma$

$\Gamma(K^+K^-\pi^+\pi^-\eta) \times \Gamma(e^+e^-)/\Gamma_{total}$ $\Gamma_{67}\Gamma_6/\Gamma$

VALUE (eV)	EVTS	DOCUMENT ID		TECN	COMMENT
3.04±1.79±0.02	7	[1] AUBERT	07AU	BABR	10.6 $e^+e^- \to K^+K^-\pi^+\pi^-\eta\gamma$

[1] AUBERT 07AU reports $[\Gamma(\psi(2S) \to K^+K^-\pi^+\pi^-\eta) \times \Gamma(\psi(2S) \to e^+e^-)/\Gamma_{total}] \times [B(\eta \to 2\gamma)] = 1.2 \pm 0.7 \pm 0.1$ eV which we divide by our best value $B(\eta \to 2\gamma) = (39.41 \pm 0.20) \times 10^{-2}$. Our first error is their experiment's error and our second error is the systematic error from using our best value.

$\Gamma(K^+K^-) \times \Gamma(e^+e^-)/\Gamma_{total}$ $\Gamma_{94}\Gamma_6/\Gamma$

VALUE (eV)	EVTS	DOCUMENT ID		TECN	COMMENT
0.35±0.14±0.03	11	LEES	13Q	BABR	$e^+e^- \to K^+K^-\gamma$

$\psi(2S)$ BRANCHING RATIOS

$\Gamma(\text{hadrons})/\Gamma_{total}$ Γ_1/Γ

VALUE	DOCUMENT ID		TECN	COMMENT
0.9785±0.0013 OUR AVERAGE				
0.9779±0.0015	[1] BAI	02B	BES2	e^+e^-
0.981 ±0.003	[1] LUTH	75	MRK1	e^+e^-

[1] Includes cascade decay into $J/\psi(1S)$.

$\Gamma(\text{virtual}\,\gamma \to \text{hadrons})/\Gamma_{total}$ Γ_2/Γ

VALUE	DOCUMENT ID		TECN	COMMENT
0.0173±0.0014 OUR AVERAGE Error includes scale factor of 1.5.				
0.0166±0.0010	[1,2] SETH	04	RVUE	e^+e^-
0.0199±0.0019	[1] BAI	02B	BES2	e^+e^-
• • • We do not use the following data for averages, fits, limits, etc. • • •				
0.029 ±0.004	[1] LUTH	75	MRK1	e^+e^-

[1] Included in $\Gamma(\text{hadrons})/\Gamma_{total}$.
[2] Using $B(\psi(2S) \to \ell^+\ell^-) = (0.73 \pm 0.04)\%$ from RPP-2002 and $R = 2.28 \pm 0.04$ determined by a fit to data from BAI 00 and BAI 02C.

$\Gamma(ggg)/\Gamma_{total}$ Γ_3/Γ

VALUE (units 10^{-2})	EVTS	DOCUMENT ID		TECN	COMMENT
10.58±1.62	2.9 M	[1] LIBBY	09	CLEO	$\psi(2S) \to$ hadrons

[1] Calculated using $\Gamma(\gamma gg)/\Gamma(ggg) = 0.097 \pm 0.026 \pm 0.016$ from LIBBY 09, $B(\psi(2S) \to X J/\psi)$ relative and absolute branching fractions from MENDEZ 08, $B(\psi(2S) \to \gamma\eta_c)$ from MITCHELL 09, and $B(\psi(2S) \to$ virtual $\gamma \to$ hadrons), $B(\psi(2S) \to \gamma\chi_{cJ})$, and $B(\psi(2S) \to \ell^+\ell^-)$ from PDG 08. The statistical error is negligible and the systematic error is largely uncorrelated with that of $\Gamma(\gamma gg)/\Gamma_{total}$ LIBBY 09 measurement.

$\Gamma(\gamma gg)/\Gamma_{total}$ Γ_4/Γ

VALUE (units 10^{-2})	EVTS	DOCUMENT ID		TECN	COMMENT
1.025±0.288	200 k	[1] LIBBY	09	CLEO	$\psi(2S) \to \gamma +$ hadrons

[1] Calculated using $\Gamma(\gamma gg)/\Gamma(ggg) = 0.097 \pm 0.026 \pm 0.016$ from LIBBY 09. The statistical error is negligible and the systematic error is largely uncorrelated with that of $\Gamma(ggg)/\Gamma_{total}$ LIBBY 09 measurement.

$\Gamma(\gamma gg)/\Gamma(ggg)$ Γ_4/Γ_3

VALUE (units 10^{-2})	EVTS	DOCUMENT ID		TECN	COMMENT
9.7±2.6±1.6	2.9 M	LIBBY	09	CLEO	$\psi(2S) \to (\gamma +)$ hadrons

$\Gamma(\text{light hadrons})/\Gamma_{total}$ Γ_5/Γ

VALUE	DOCUMENT ID		TECN	COMMENT
0.154±0.015	[1] MENDEZ	08	CLEO	$e^+e^- \to \psi(2S)$
• • • We do not use the following data for averages, fits, limits, etc. • • •				
0.169±0.026	[2] ADAM	05A	CLEO	$e^+e^- \to \psi(2S)$

[1] Uses $B(\psi(2S) \to J/\psi X)$ from MENDEZ 08 and other branching fractions from PDG 07.
[2] Uses $B(J/\psi X)$ from ADAM 05A, $B(\chi_{cJ}\gamma)$, $B(\eta_c\gamma)$ from ATHAR 04 and $B(\ell^+\ell^-)$ from PDG 04. Superseded by MENDEZ 08.

$\Gamma(e^+e^-)/\Gamma_{total}$ Γ_6/Γ

VALUE (units 10^{-4})	DOCUMENT ID		TECN	COMMENT
78.9± 1.7 OUR FIT				
• • • We do not use the following data for averages, fits, limits, etc. • • •				
88 ±13	[1] FELDMAN	77	RVUE	e^+e^-

[1] From an overall fit assuming equal partial widths for e^+e^- and $\mu^+\mu^-$. For a measurement of the ratio see the entry $\Gamma(\mu^+\mu^-)/\Gamma(e^+e^-)$ below. Includes LUTH 75, HILGER 75, BURMESTER 77.

$\Gamma(\mu^+\mu^-)/\Gamma_{total}$ Γ_7/Γ

VALUE (units 10^{-4})	DOCUMENT ID
79±9 OUR FIT	

$\Gamma(\mu^+\mu^-)/\Gamma(e^+e^-)$ Γ_7/Γ_6

VALUE	DOCUMENT ID		TECN	COMMENT
1.00±0.11 OUR FIT				
• • • We do not use the following data for averages, fits, limits, etc. • • •				
0.89±0.16	BOYARSKI	75C	MRK1	e^+e^-

$\Gamma(\tau^+\tau^-)/\Gamma_{total}$ Γ_8/Γ

VALUE (units 10^{-4})	DOCUMENT ID		TECN	COMMENT
31 ±4 OUR FIT				
30.8±2.1±3.8	[1] ABLIKIM	06W	BES	$e^+e^- \to \psi(2S)$

[1] Computed using PDG 02 value of $B(\psi(2S) \to$ hadrons$) = 0.9810 \pm 0.0030$ to estimate the total number of $\psi(2S)$ events.

DECAYS INTO $J/\psi(1S)$ AND ANYTHING

$\Gamma(J/\psi(1S)\text{anything})/\Gamma_{total}$ Γ_9/Γ

VALUE	EVTS	DOCUMENT ID		TECN	COMMENT
0.609 ±0.006 OUR FIT					
0.55 ±0.07 OUR AVERAGE					
0.51 ±0.12		BRANDELIK	79C	DASP	$e^+e^- \to \mu^+\mu^-X$
0.57 ±0.08		ABRAMS	75B	MRK1	$e^+e^- \to \mu^+\mu^-X$
• • • We do not use the following data for averages, fits, limits, etc. • • •					
0.6254±0.0016±0.0155	1.1M	[1] MENDEZ	08	CLEO	$\psi(2S) \to \ell^+\ell^-X$
0.5950±0.0015±0.0190	151k	ADAM	05A	CLEO	Repl. by MENDEZ 08

[1] Not independent from other measurements of MENDEZ 08.

$\Gamma(e^+e^-)/\Gamma(J/\psi(1S)\text{anything})$
$\Gamma_6/\Gamma_9 = \Gamma_6/(\Gamma_{11}+\Gamma_{12}+\Gamma_{13}+0.339\Gamma_{129}+0.192\Gamma_{130})$

VALUE (units 10^{-2})	EVTS	DOCUMENT ID		TECN	COMMENT
1.295±0.026 OUR FIT					
1.28 ±0.04 OUR AVERAGE Error includes scale factor of 1.6. See the ideogram below.					
1.22 ±0.02 ±0.05	5097 ± 73	[1] ANDREOTTI	05	E835	$p\overline{p} \to \psi(2S) \to e^+e^-$
1.28 ±0.03 ±0.02		[1] AMBROGIANI	00A	E835	$p\overline{p} \to \psi(2S)$
1.44 ±0.08 ±0.02		[1] ARMSTRONG	97	E760	$\overline{p}p \to \psi(2S)$

[1] Using $B(J/\psi(1S) \to e^+e^-) = 0.0593 \pm 0.0010$.

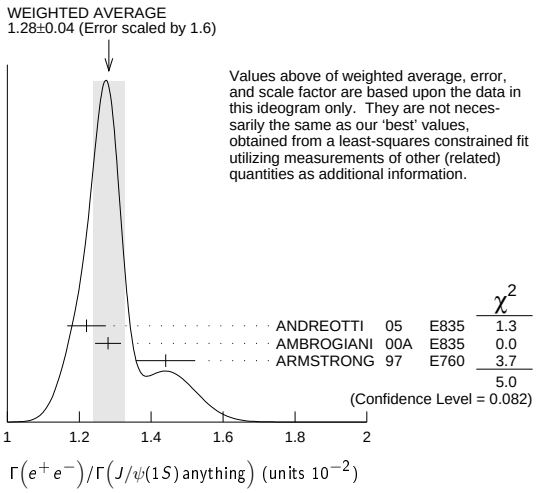

$\Gamma(\mu^+\mu^-)/\Gamma(J/\psi(1S)\text{anything})$
$\Gamma_7/\Gamma_9 = \Gamma_7/(\Gamma_{11}+\Gamma_{12}+\Gamma_{13}+0.339\Gamma_{129}+0.192\Gamma_{130})$

VALUE	DOCUMENT ID		TECN	COMMENT
0.0130±0.0014 OUR FIT				
0.014 ±0.003	HILGER	75	SPEC	e^+e^-

$\Gamma(J/\psi(1S)\text{neutrals})/\Gamma_{total}$ Γ_{10}/Γ

VALUE	DOCUMENT ID
0.2510±0.0033 OUR FIT	

$\Gamma(J/\psi(1S)\pi^+\pi^-)/\Gamma_{total}$ Γ_{11}/Γ

VALUE	EVTS	DOCUMENT ID		TECN	COMMENT
0.3445±0.0030 OUR FIT					
0.348 ±0.005 OUR AVERAGE Error includes scale factor of 1.3. See the ideogram below.					
0.3498±0.0002±0.0045	20M	ABLIKIM	13R	BES3	$\psi(2S)\to J/\psi\pi^+\pi^-$
0.3504±0.0007±0.0077	565k	MENDEZ	08	CLEO	$\psi(2S)\to \ell^+\ell^-\pi^+\pi^-$
0.323 ±0.014		BAI	02B	BES2	e^+e^-
0.32 ±0.04		ABRAMS	75B	MRK1	$e^+e^-\to J/\psi\pi^+\pi^-$
• • • We do not use the following data for averages, fits, limits, etc. • • •					
0.3354±0.0014±0.0110	60k	[1] ADAM	05A	CLEO	Repl. by MENDEZ 08

[1] Not independent from other values reported by ADAM 05A.

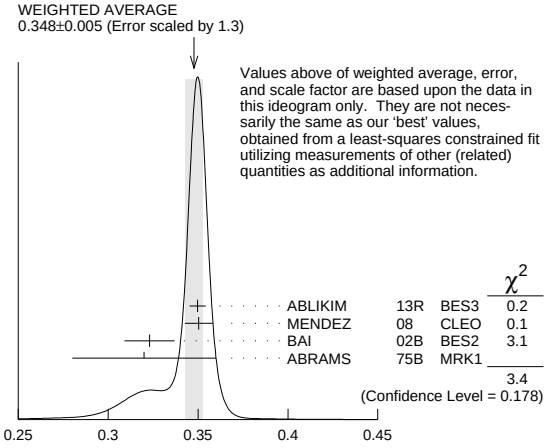

$\Gamma\left(J/\psi(1S)\pi^+\pi^-\right)/\Gamma_{total}$

$\Gamma(e^+e^-)/\Gamma(J/\psi(1S)\pi^+\pi^-)$ Γ_6/Γ_{11}

VALUE	DOCUMENT ID		TECN	COMMENT
0.0229±0.0005 OUR FIT				
0.0252±0.0028±0.0011	[1] AUBERT	02B	BABR	e^+e^-

[1] Using B($J/\psi(1S)\to e^+e^-$) = 0.0593 ± 0.0010.

$\Gamma(\mu^+\mu^-)/\Gamma(J/\psi(1S)\pi^+\pi^-)$ Γ_7/Γ_{11}

VALUE	DOCUMENT ID		TECN	COMMENT
0.0229±0.0025 OUR FIT				
0.0224±0.0029 OUR AVERAGE				
0.0216±0.0026±0.0014	[1] AUBERT	02B	BABR	e^+e^-
0.0327±0.0077±0.0072	[1] GRIBUSHIN	96	FMPS	515 π^- Be $\to 2\mu X$

[1] Using B($J/\psi(1S)\to\mu^+\mu^-$) = 0.0588 ± 0.0010.

$\Gamma(\tau^+\tau^-)/\Gamma(J/\psi(1S)\pi^+\pi^-)$ Γ_8/Γ_{11}

VALUE (units 10^{-3})	DOCUMENT ID		TECN	COMMENT
8.9 ±1.1 OUR FIT				
8.73±1.39±1.57	BAI	02	BES	e^+e^-

$\Gamma(J/\psi(1S)\pi^+\pi^-)/\Gamma(J/\psi(1S)\text{anything})$ Γ_{11}/Γ_9

VALUE	EVTS	DOCUMENT ID		TECN	COMMENT
0.5654±0.0026 OUR FIT					
0.554 ±0.008 OUR AVERAGE Error includes scale factor of 1.3. See the ideogram below.					
0.5604±0.0009±0.0062	565k	MENDEZ	08	CLEO	$\psi(2S)\to \ell^+\ell^-\pi^+\pi^-$
0.525 ±0.009 ±0.022	4k	ANDREOTTI	05	E835	$\psi(2S)\to J/\psi X$
0.536 ±0.007 ±0.016	20k	[1,2] ABLIKIM	04B	BES	$\psi(2S)\to J/\psi X$
0.496 ±0.037		ARMSTRONG	97	E760	$\overline{p}p\to\psi(2S)$
• • • We do not use the following data for averages, fits, limits, etc. • • •					
0.5637±0.0027±0.0046	60k	ADAM	05A	CLEO	Repl. by MENDEZ 08

[1] From a fit to the J/ψ recoil mass spectra.
[2] ABLIKIM 04B quotes B($\psi(2S)\to J/\psi X$) / B($\psi(2S)\to J/\psi\pi^+\pi^-$).

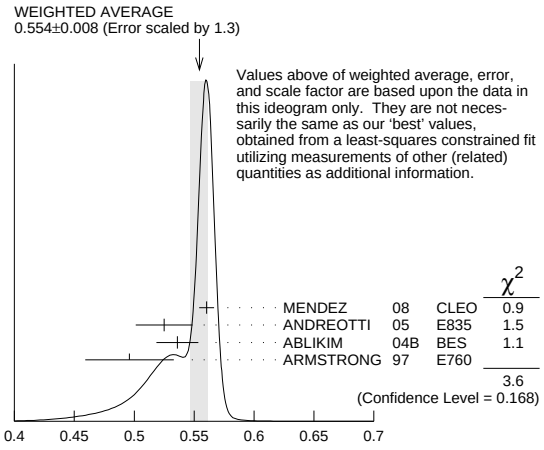

$\Gamma\left(J/\psi(1S)\pi^+\pi^-\right)/\Gamma\left(J/\psi(1S)\text{anything}\right)$ Γ_{11}/Γ_9

$\Gamma(J/\psi(1S)\text{neutrals})/\Gamma(J/\psi(1S)\pi^+\pi^-)$ $\Gamma_{10}/\Gamma_{11}=(0.9761\Gamma_{12}+0.719\Gamma_{13}+0.339\Gamma_{129}+0.192\Gamma_{130})/\Gamma_{11}$

VALUE	DOCUMENT ID		TECN	COMMENT
0.729±0.008 OUR FIT				
0.73 ±0.09	TANENBAUM	76	MRK1	e^+e^-

$\Gamma(J/\psi(1S)\pi^0\pi^0)/\Gamma_{total}$ Γ_{12}/Γ

VALUE	EVTS	DOCUMENT ID		TECN	COMMENT
0.1813±0.0031 OUR FIT					
• • • We do not use the following data for averages, fits, limits, etc. • • •					
0.1769±0.0008±0.0053	61k	[1] MENDEZ	08	CLEO	$\psi(2S)\to \ell^+\ell^-2\pi^0$
0.1652±0.0014±0.0058	13.4k	[2] ADAM	05A	CLEO	Repl. by MENDEZ 08

[1] Not independent from other measurements of MENDEZ 08.
[2] Not independent from other values reported by ADAM 05A.

$\Gamma(J/\psi(1S)\pi^0\pi^0)/\Gamma(J/\psi(1S)\text{anything})$ Γ_{12}/Γ_9

VALUE	EVTS	DOCUMENT ID		TECN	COMMENT
0.2976±0.0031 OUR FIT					
0.320 ±0.012 OUR AVERAGE					
0.300 ±0.008 ±0.022	1655 ± 44	ANDREOTTI	05	E835	$\psi(2S)\to J/\psi X$
0.328 ±0.013 ±0.008		AMBROGIANI	00A	E835	$p\overline{p}\to\psi(2S)$
0.323 ±0.033		ARMSTRONG	97	E760	$\overline{p}p\to\psi(2S)$
• • • We do not use the following data for averages, fits, limits, etc. • • •					
0.2829±0.0012±0.0056	61k	MENDEZ	08	CLEO	$\psi(2S)\to \ell^+\ell^-2\pi^0$
0.2776±0.0025±0.0043	13.4k	ADAM	05A	CLEO	Repl. by MENDEZ 08

$\Gamma(J/\psi(1S)\pi^0\pi^0)/\Gamma(J/\psi(1S)\pi^+\pi^-)$ Γ_{12}/Γ_{11}

VALUE	EVTS	DOCUMENT ID		TECN	COMMENT
0.526 ±0.008 OUR FIT					
0.513 ±0.022 OUR AVERAGE Error includes scale factor of 2.2.					
0.5047±0.0022±0.0102	61k	MENDEZ	08	CLEO	$\psi(2S)\to \ell^+\ell^-2\pi^0$
0.570 ±0.009 ±0.026	14k	[1] ABLIKIM	04B	BES	$\psi(2S)\to J/\psi X$
• • • We do not use the following data for averages, fits, limits, etc. • • •					
0.4924±0.0047±0.0086	73k	[2,3] ADAM	05A	CLEO	Repl. by MENDEZ 08
0.571 ±0.018 ±0.044		[4] ANDREOTTI	05	E835	$\psi(2S)\to J/\psi X$
0.53 ±0.06		TANENBAUM	76	MRK1	e^+e^-
0.64 ±0.15		[5] HILGER	75	SPEC	e^+e^-

[1] From a fit to the J/ψ recoil mass spectra.
[2] Not independent from other values reported by ADAM 05A.
[3] Using 13,217 $J/\psi\pi^0\pi^0$ and 60,010 $J/\psi\pi^+\pi^-$ events.
[4] Not independent from other values reported by ANDREOTTI 05.
[5] Ignoring the $J/\psi(1S)\eta$ and $J/\psi(1S)\gamma\gamma$ decays.

$\Gamma(J/\psi(1S)\eta)/\Gamma_{total}$ Γ_{13}/Γ

VALUE (units 10^{-3})	EVTS	DOCUMENT ID		TECN	COMMENT
33.6 ± 0.5 OUR FIT					
32.9 ± 1.7 OUR AVERAGE Error includes scale factor of 2.1. See the ideogram below.					
33.75± 0.17±0.86	68.2k	ABLIKIM	12M	BES3	$e^+e^-\to \ell^+\ell^-2\gamma$
29.8 ± 0.9 ±2.3	5.7k	BAI	04I	BES2	$\psi(2S)\to J/\psi\gamma\gamma$
25.5 ± 2.9	386	[1] OREGLIA	80	CBAL	$e^+e^-\to J/\psi 2\gamma$
45 ±12	17	[2] BRANDELIK	79B	DASP	$e^+e^-\to J/\psi 2\gamma$
42 ± 6	164	[2] BARTEL	78B	CNTR	e^+e^-
• • • We do not use the following data for averages, fits, limits, etc. • • •					
34.3 ± 0.4 ±0.9	18.4k	[3] MENDEZ	08	CLEO	$\psi(2S)\to \ell^+\ell^-\eta$
32.5 ± 0.6 ±1.1	2.8k	[4] ADAM	05A	CLEO	Repl. by MENDEZ 08
43 ± 8	44	TANENBAUM	76	MRK1	e^+e^-

[1] Recalculated by us using $B(J/\psi(1S) \to \ell^+\ell^-) = 0.1181 \pm 0.0020$.
[2] Recalculated by us using $B(J/\psi(1S) \to \mu^+\mu^-) = 0.0588 \pm 0.0010$.
[3] Not independent from other measurements of MENDEZ 08.
[4] Not independent from other values reported by ADAM 05A.

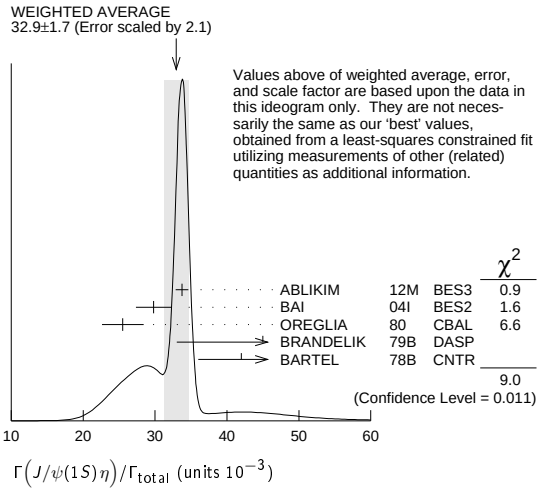

$\Gamma(J/\psi(1S)\eta)/\Gamma(J/\psi(1S)\text{anything})$ Γ_{13}/Γ_9

VALUE	EVTS	DOCUMENT ID		TECN	COMMENT
0.0551±0.0008 OUR FIT					
0.058 ±0.007 OUR AVERAGE Error includes scale factor of 1.4. See the ideogram below.					
0.050 ±0.006 ±0.003	298 ± 20	ANDREOTTI	05	E835	$\psi(2S) \to J/\psi X$
0.072 ±0.009		AMBROGIANI	00A	E835	$p\overline{p} \to \psi(2S)$
0.061 ±0.015		ARMSTRONG	97	E760	$\overline{p}p \to \psi(2S)$
• • • We do not use the following data for averages, fits, limits, etc. • • •					
0.0549±0.0006±0.0009	18.4k	[1] MENDEZ	08	CLEO	$\psi(2S) \to \ell^+\ell^-\eta$
0.0546±0.0010±0.0007	2.8k	ADAM	05A	CLEO	Repl. by MENDEZ 08

[1] Not independent from other measurements of MENDEZ 08.

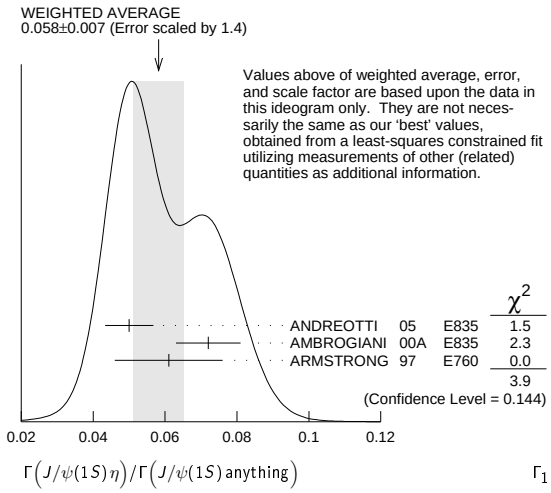

Γ_{13}/Γ_9

$\Gamma(J/\psi(1S)\eta)/\Gamma(J/\psi(1S)\pi^+\pi^-)$ Γ_{13}/Γ_{11}

VALUE	EVTS	DOCUMENT ID		TECN	COMMENT
0.0975±0.0014 OUR FIT					
0.0979±0.0018 OUR AVERAGE					
0.0979±0.0010±0.0015	18.4k	MENDEZ	08	CLEO	$\psi(2S) \to \ell^+\ell^-\eta$
0.098 ±0.005 ±0.010	2k	[1] ABLIKIM	04B	BES	$\psi(2S) \to J/\psi X$
0.091 ±0.021		[2] HIMEL	80	MRK2	$e^+e^- \to \psi(2S)X$
• • • We do not use the following data for averages, fits, limits, etc. • • •					
0.0968±0.0019±0.0013	2.8k	[3] ADAM	05A	CLEO	Repl. by MENDEZ 08
0.095 ±0.007 ±0.007		[4] ANDREOTTI	05	E835	$\psi(2S) \to J/\psi X$

[1] From a fit to the J/ψ recoil mass spectra.
[2] The value for $B(\psi(2S) \to J/\psi(1s)\eta)$ reported in HIMEL 80 is derived using $B(\psi(2S)) \to J/\psi(1S)\pi^+\pi^-) = (33 \pm 3))\%$ and $B(J/\psi(1S) \to \ell^+\ell^-) = 0.138 \pm 0.018$. Calculated by us using $B(J/\psi(1S) \to \ell^+\ell^-) = (0.1181 \pm 0.0020)$.
[3] Not independent from other values reported by ADAM 05A.
[4] Not independent from other values reported by ANDREOTTI 05.

$\Gamma(J/\psi(1S)\pi^0)/\Gamma_{\text{total}}$ Γ_{14}/Γ

VALUE (units 10^{-4})	EVTS	DOCUMENT ID		TECN	COMMENT
12.68±0.32 OUR AVERAGE					
12.6 ±0.2 ±0.3	4.1k	ABLIKIM	12M	BES3	$e^+e^- \to \ell^+\ell^-2\gamma$
13.3 ±0.8 ±0.3	530	MENDEZ	08	CLEO	$\psi(2S) \to \ell^+\ell^-2\gamma$
14.3 ±1.4 ±1.2	280	BAI	04I	BES2	$\psi(2S) \to J/\psi\gamma\gamma$
14 ±6	7	HIMEL	80	MRK2	e^+e^-
9 ±2 ±1	23	[1] OREGLIA	80	CBAL	$\psi(2S) \to J/\psi 2\gamma$
• • • We do not use the following data for averages, fits, limits, etc. • • •					
13 ±1 ±1	88	ADAM	05A	CLEO	Repl. by MENDEZ 08

[1] Recalculated by us using $B(J/\psi(1S) \to \ell^+\ell^-) = 0.1181 \pm 0.0020$.

$\Gamma(J/\psi(1S)\pi^0)/\Gamma(J/\psi(1S)\text{anything})$ $\Gamma_{14}/\Gamma_9 = \Gamma_{14}/(\Gamma_{11}+\Gamma_{12}+\Gamma_{13}+0.339\Gamma_{129}+0.192\Gamma_{130})$

VALUE (units 10^{-2})	EVTS	DOCUMENT ID		TECN	COMMENT
• • • We do not use the following data for averages, fits, limits, etc. • • •					
0.213±0.012±0.003	527	[1] MENDEZ	08	CLEO	$e^+e^- \to J/\psi\gamma\gamma$
0.22 ±0.02 ±0.01		[2] ADAM	05A	CLEO	$e^+e^- \to \psi(2S) \to J/\psi\gamma\gamma$

[1] Not independent from other values reported by MENDEZ 08. Supersedes ADAM 05A.
[2] Not independent from other values reported by ADAM 05A.

$\Gamma(J/\psi(1S)\pi^0)/\Gamma(J/\psi(1S)\pi^+\pi^-)$ Γ_{14}/Γ_{11}

VALUE (units 10^{-2})	EVTS	DOCUMENT ID		TECN	COMMENT
• • • We do not use the following data for averages, fits, limits, etc. • • •					
0.380±0.022±0.005	527	[1] MENDEZ	08	CLEO	$e^+e^- \to J/\psi\gamma\gamma$
0.39 ±0.04 ±0.01		[2] ADAM	05A	CLEO	$e^+e^- \to \psi(2S) \to J/\psi\gamma\gamma$

[1] Not independent from other values reported by MENDEZ 08. Supersedes ADAM 05A.
[2] Not independent from other values reported by ADAM 05A.

HADRONIC DECAYS

$\Gamma(\pi^0 h_c(1P))/\Gamma_{\text{total}}$ Γ_{15}/Γ

VALUE (units 10^{-4})	EVTS	DOCUMENT ID		TECN	COMMENT
8.6±1.3 OUR AVERAGE					
9.0±1.5±1.3	3k	[1] GE	11	CLEO	$\psi(2S) \to \pi^0$ anything
8.4±1.3±1.0	11k	ABLIKIM	10B	BES3	$\psi(2S) \to \pi^0 h_c$
• • • We do not use the following data for averages, fits, limits, etc. • • •					
seen	92^{+23}_{-22}	ADAMS	09	CLEO	$\psi(2S) \to 2\pi^+2\pi^-2\pi^0$
seen	1282	DOBBS	08A	CLEO	$\psi(2S) \to \pi^0\eta_c\gamma$
seen	168 ± 40	ROSNER	05	CLEO	$\psi(2S) \to \pi^0\eta_c\gamma$

[1] Assuming a width $\Gamma(h_c(1P)) = 0.86$ MeV $\equiv \Gamma_0$, a measured dependence of the central value of $B = (7.6 +1.4 \times \Gamma(h_c(1P)/\Gamma_0) \times 10^{-4}$, and with a systematic error that accounts for the width variation range 0.43–1.29 MeV.

$\Gamma(3(\pi^+\pi^-)\pi^0)/\Gamma_{\text{total}}$ Γ_{16}/Γ

VALUE (units 10^{-4})	EVTS	DOCUMENT ID		TECN	COMMENT
35±16	6	FRANKLIN	83	MRK2	$e^+e^- \to$ hadrons

$\Gamma(2(\pi^+\pi^-)\pi^0)/\Gamma_{\text{total}}$ Γ_{17}/Γ

VALUE (units 10^{-4})	EVTS	DOCUMENT ID		TECN	COMMENT
29 ±10 OUR AVERAGE		Error includes scale factor of 4.7. See the ideogram below.			
24.9± 0.7±3.6	2173	ABLIKIM	07D	BES2	$e^+e^- \to \psi(2S)$
126 ±12 ±2	410	[1] AUBERT	07AU	BABR	10.6 $e^+e^- \to 2(\pi^+\pi^-)\pi^0\gamma$
26.1± 0.7±3.0	1703	BRIERE	05	CLEO	$e^+e^- \to \psi(2S) \to 2(\pi^+\pi^-)\pi^0$
30 ± 8	42	FRANKLIN	83	MRK2	e^+e^-

[1] AUBERT 07AU reports $[\Gamma(\psi(2S) \to 2(\pi^+\pi^-)\pi^0)/\Gamma_{\text{total}}] \times [\Gamma(\psi(2S) \to e^+e^-)] = (297 \pm 22 \pm 18) \times 10^{-4}$ keV which we divide by our best value $\Gamma(\psi(2S) \to e^+e^-) = 2.36 \pm 0.04$ keV. Our first error is their experiment's error and our second error is the systematic error from using our best value.

Meson Particle Listings

$\psi(2S)$

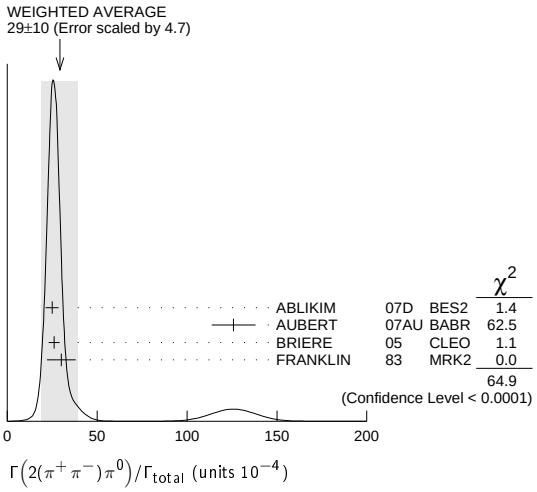

$\Gamma(\rho a_2(1320))/\Gamma_{total}$ Γ_{18}/Γ

VALUE (units 10^{-4})	CL%	EVTS	DOCUMENT ID		TECN	COMMENT
2.55±0.73±0.47		112 ± 31	BAI	04C	BES2	$\psi(2S) \to 2(\pi^+\pi^-)\pi^0$
• • • We do not use the following data for averages, fits, limits, etc. • • •						
<2.3	90		BAI	98J	BES	e^+e^-

$\Gamma(p\overline{p})/\Gamma_{total}$ Γ_{19}/Γ

VALUE (units 10^{-4})	EVTS	DOCUMENT ID		TECN	COMMENT
2.80±0.11 OUR FIT					
2.95±0.23 OUR AVERAGE	Error includes scale factor of 1.5. See the ideogram below.				
3.36±0.09±0.25	1618	ABLIKIM	07C	BES	$e^+e^- \to \psi(2S) \to p\overline{p}$
2.87±0.12±0.15	557	PEDLAR	05	CLEO	$e^+e^- \to \psi(2S) \to p\overline{p}$
1.4 ±0.8	4	BRANDELIK	79C	DASP	$e^+e^- \to \psi(2S) \to p\overline{p}$
2.3 ±0.7		FELDMAN	77	MRK1	$e^+e^- \to \psi(2S) \to p\overline{p}$

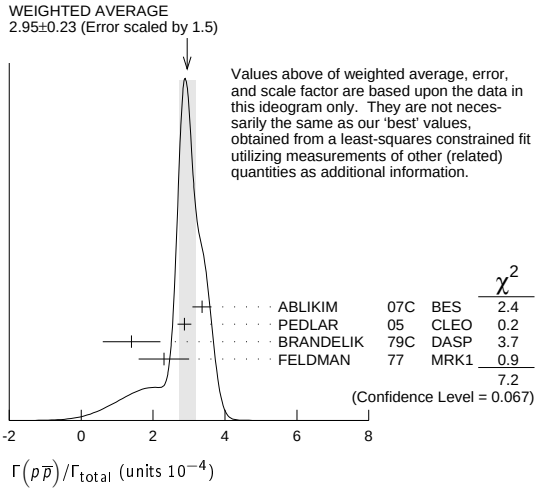

$\Gamma(p\overline{p})/\Gamma(J/\psi(1S)\pi^+\pi^-)$ Γ_{19}/Γ_{11}

VALUE (units 10^{-4})	DOCUMENT ID		TECN	COMMENT
8.13±0.32 OUR FIT				
6.98±0.49±0.97	BAI	01	BES	$e^+e^- \to \psi(2S) \to p\overline{p}$

$\Gamma(\Delta^{++}\overline{\Delta}^{--})/\Gamma_{total}$ Γ_{20}/Γ

VALUE (units 10^{-5})	EVTS	DOCUMENT ID		TECN	COMMENT
12.8±1.0±3.4	157	[1] BAI	01	BES	$e^+e^- \to \psi(2S) \to$ hadrons

[1] Estimated using B($\psi(2S) \to J/\psi\pi^+\pi^-$)= 0.310 ± 0.028.

$\Gamma(\Lambda\overline{\Lambda}\pi^0)/\Gamma_{total}$ Γ_{21}/Γ

VALUE (units 10^{-5})	CL%	DOCUMENT ID		TECN	COMMENT
< 0.29	90	[1] ABLIKIM	13F	BES3	$\psi(2S) \to p\overline{p}\pi^+\pi^-\gamma\gamma$
• • • We do not use the following data for averages, fits, limits, etc. • • •					
<12	90	[2] ABLIKIM	07H	BES2	$e^+e^- \to \psi(2S)$

[1] Using B($\Lambda \to \pi^- p$) = 63.9% and B($\pi^0 \to \gamma\gamma$) = 98.8%.
[2] Using B($\Lambda \to \pi^- p$) = 63.9% and B($\eta \to \gamma\gamma$) = 39.4%.

$\Gamma(\Lambda\overline{\Lambda}\eta)/\Gamma_{total}$ Γ_{22}/Γ

VALUE (units 10^{-5})	CL%	EVTS	DOCUMENT ID		TECN	COMMENT
2.48±0.34±0.19		60	[1] ABLIKIM	13F	BES3	$\psi(2S) \to p\overline{p}\pi^+\pi^-\gamma\gamma$
• • • We do not use the following data for averages, fits, limits, etc. • • •						
<4.9	90		[2] ABLIKIM	07H	BES2	$e^+e^- \to \psi(2S)$

[1] Using B($\Lambda \to \pi^- p$) = 63.9% and B($\eta \to \gamma\gamma$) = 39.31%.
[2] Using B($\Lambda \to \pi^- p$) = 63.9%.

$\Gamma(\Lambda\overline{p}K^+)/\Gamma_{total}$ Γ_{23}/Γ

VALUE (units 10^{-4})	EVTS	DOCUMENT ID		TECN	COMMENT
1.0±0.1±0.1	74.0	BRIERE	05	CLEO	$e^+e^- \to \psi(2S) \to p\overline{p}K^+\pi^-$

$\Gamma(\Lambda\overline{p}K^+\pi^+\pi^-)/\Gamma_{total}$ Γ_{24}/Γ

VALUE (units 10^{-4})	EVTS	DOCUMENT ID		TECN	COMMENT
1.8±0.3±0.3	45.8	BRIERE	05	CLEO	$e^+e^- \to \psi(2S) \to p\overline{p}K^+\pi^+\pi^-\pi^-$

$\Gamma(\Lambda\overline{\Lambda}\pi^+\pi^-)/\Gamma_{total}$ Γ_{25}/Γ

VALUE (units 10^{-4})	EVTS	DOCUMENT ID		TECN	COMMENT
2.8±0.4±0.5	73.4	BRIERE	05	CLEO	$e^+e^- \to \psi(2S) \to p\overline{p}2(\pi^+\pi^-)$

$\Gamma(\Lambda\overline{\Lambda})/\Gamma_{total}$ Γ_{26}/Γ

VALUE (units 10^{-4})	CL%	EVTS	DOCUMENT ID		TECN	COMMENT
2.8 ±0.5 OUR AVERAGE		Error includes scale factor of 2.6. See the ideogram below.				
3.39±0.20±0.32		337	ABLIKIM	07C	BES	$e^+e^- \to \psi(2S) \to$ hadrons
6.4 ±1.7 ±0.1			[1] AUBERT	07BD	BABR	10.6 $e^+e^- \to \Lambda\overline{\Lambda}\gamma$
3.28±0.23±0.25		208	PEDLAR	05	CLEO	$e^+e^- \to \psi(2S) \to$ hadrons
1.81±0.20±0.27		80	[2] BAI	01	BES	$e^+e^- \to \psi(2S) \to$ hadrons
• • • We do not use the following data for averages, fits, limits, etc. • • •						
< 4	90		FELDMAN	77	MRK1	$e^+e^- \to \psi(2S) \to$ hadrons

[1] AUBERT 07BD reports $[\Gamma(\psi(2S) \to \Lambda\overline{\Lambda})/\Gamma_{total}] \times [\Gamma(\psi(2S) \to e^+e^-)] = (15 \pm 4 \pm 1) \times 10^{-4}$ keV which we divide by our best value $\Gamma(\psi(2S) \to e^+e^-) = 2.36 \pm 0.04$ keV. Our first error is their experiment's error and our second error is the systematic error from using our best value.
[2] Estimated using B($\psi(2S) \to J/\psi\pi^+\pi^-$)= 0.310 ± 0.028.

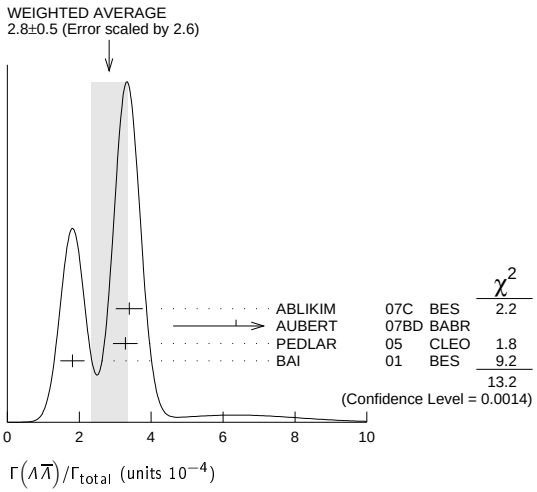

$\Gamma(\Lambda\overline{\Sigma}^+\pi^- + c.c.)/\Gamma_{total}$ Γ_{27}/Γ

VALUE (units 10^{-4})	EVTS	DOCUMENT ID		TECN	COMMENT
1.40±0.03±0.13	2.8k	ABLIKIM	13W	BES3	$\psi(2S) \to$ hadrons

$\Gamma(\Lambda\overline{\Sigma}^-\pi^+ + c.c.)/\Gamma_{total}$ Γ_{28}/Γ

VALUE (units 10^{-4})	EVTS	DOCUMENT ID		TECN	COMMENT
1.54±0.04±0.13	2.8k	ABLIKIM	13W	BES3	$\psi(2S) \to$ hadrons

$\Gamma(\Sigma^0\overline{p}K^+ + c.c.)/\Gamma_{total}$ Γ_{29}/Γ

VALUE (units 10^{-5})	EVTS	DOCUMENT ID		TECN	COMMENT
1.67±0.13±0.12	276	[1] ABLIKIM	13D	BES3	$\psi(2S) \to \gamma\Lambda\overline{p}K^+$

[1] Using B($\Lambda \to p\pi^-$) = 63.9%, and B($\Sigma^0 \to \Lambda\gamma$) = 100%.

$\Gamma(\Sigma^+\overline{\Sigma}^-)/\Gamma_{total}$ Γ_{30}/Γ

VALUE (units 10^{-5})	EVTS	DOCUMENT ID		TECN	COMMENT
25.7±4.4±6.8	35	PEDLAR	05	CLEO	$e^+e^- \to \psi(2S) \to$ hadrons

$\Gamma(\Sigma^0\overline{\Sigma}^0)/\Gamma_{total}$ Γ_{31}/Γ

VALUE (units 10^{-5})	EVTS	DOCUMENT ID		TECN	COMMENT
22 ±4 OUR AVERAGE		Error includes scale factor of 1.5. See the ideogram below.			
23.5±3.6±3.2	59	ABLIKIM	07C	BES	$e^+e^- \to \psi(2S) \to$ hadrons
26.3±3.5±2.1	58	PEDLAR	05	CLEO	$e^+e^- \to \psi(2S) \to$ hadrons
12 ±4 ±4	8	[1] BAI	01	BES	$e^+e^- \to \psi(2S) \to$ hadrons

[1] Estimated using $B(\psi(2S) \to J/\psi\pi^+\pi^-) = 0.310 \pm 0.028$.

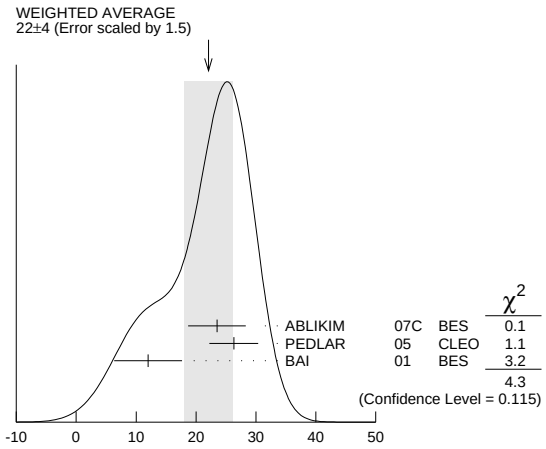

$\Gamma(\Sigma(1385)^+\overline{\Sigma}(1385)^-)/\Gamma_{total}$ Γ_{32}/Γ

VALUE (units 10^{-5})	EVTS	DOCUMENT ID		TECN	COMMENT
11±3±3	14	[1] BAI	01	BES	$e^+e^- \to \psi(2S) \to$ hadrons

[1] Estimated using $B(\psi(2S) \to J/\psi\pi^+\pi^-) = 0.310 \pm 0.028$.

$\Gamma(\Xi^-\overline{\Xi}^+)/\Gamma_{total}$ Γ_{33}/Γ

VALUE (units 10^{-5})	CL%	EVTS	DOCUMENT ID		TECN	COMMENT
18 ±6 OUR AVERAGE			Error includes scale factor of 2.8. See the ideogram below.			
30.3±4.0±3.2		67	ABLIKIM	07C	BES	$e^+e^- \to \psi(2S) \to$ hadrons
23.8±3.0±2.1		63	PEDLAR	05	CLEO	$e^+e^- \to \psi(2S) \to$ hadrons
9.4±2.7±1.5		12	[1] BAI	01	BES	$e^+e^- \to \psi(2S) \to$ hadrons
• • • We do not use the following data for averages, fits, limits, etc. • • •						
<20	90		FELDMAN	77	MRK1	$e^+e^- \to \psi(2S) \to$ hadrons

[1] Estimated using $B(\psi(2S) \to J/\psi\pi^+\pi^-) = 0.310 \pm 0.028$.

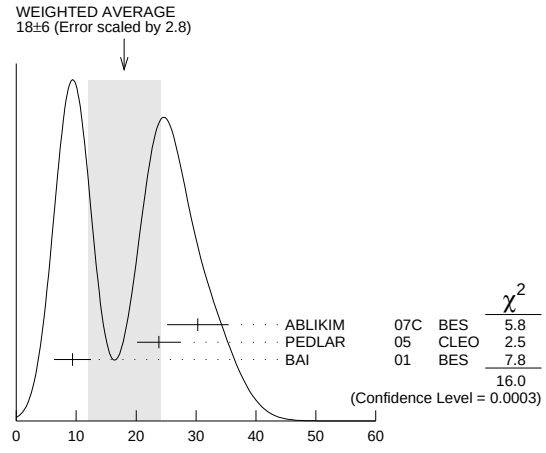

$\Gamma(\Xi^0\overline{\Xi}^0)/\Gamma_{total}$ Γ_{34}/Γ

VALUE (units 10^{-5})	EVTS	DOCUMENT ID		TECN	COMMENT
27.5±6.4±6.1	19	PEDLAR	05	CLEO	$e^+e^- \to \psi(2S) \to$ hadrons

$\Gamma(\Xi(1530)^0\overline{\Xi}(1530)^0)/\Gamma_{total}$ Γ_{35}/Γ

VALUE (units 10^{-5})	CL%	EVTS	DOCUMENT ID		TECN	COMMENT
5.2±0.3$^{+3.2}_{-1.2}$		527	[1] ABLIKIM	13S	BES3	$\psi(2S) \to \eta p\overline{p}$
• • • We do not use the following data for averages, fits, limits, etc. • • •						
<32	90		PEDLAR	05	CLEO	$e^+e^- \to \psi(2S) \to$ hadrons
< 8.1	90		[2] BAI	01	BES	$e^+e^- \to \psi(2S) \to$ hadrons

[1] With $N(1535)$ decaying to $p\eta$.
[2] Estimated using $B(\psi(2S) \to J/\psi\pi^+\pi^-) = 0.310 \pm 0.028$.

$\Gamma(\Omega^-\overline{\Omega}^+)/\Gamma_{total}$ Γ_{36}/Γ

VALUE (units 10^{-5})	CL%	DOCUMENT ID		TECN	COMMENT
< 7.3	90	[1] BAI	01	BES	$e^+e^- \to \psi(2S) \to$ hadrons
• • • We do not use the following data for averages, fits, limits, etc. • • •					
<15	90	ABLIKIM	12Q	BES2	$e^+e^- \to \psi(2S) \to$ hadrons
<16	90	PEDLAR	05	CLEO	$e^+e^- \to \psi(2S) \to$ hadrons

[1] Estimated using $B(\psi(2S) \to J/\psi\pi^+\pi^-) = 0.310 \pm 0.028$.

$\Gamma(\pi^0 p\overline{p})/\Gamma_{total}$ Γ_{37}/Γ

VALUE (units 10^{-4})	EVTS	DOCUMENT ID		TECN	COMMENT
1.53±0.07 OUR AVERAGE					
1.65±0.03±0.15	4.5k	ABLIKIM	13A	BES3	$\psi(2S) \to p\overline{p}\pi^0$
1.54±0.06±0.06	948	ALEXANDER	10	CLEO	$\psi(2S) \to \pi^0 p\overline{p}$
1.32±0.10±0.15	256 ± 18	[1] ABLIKIM	05E	BES2	$e^+e^- \to \psi(2S) \to p\overline{p}\gamma\gamma$
1.4 ±0.5	9	FRANKLIN	83	MRK2	e^+e^-

[1] Computed using $B(\pi^0 \to \gamma\gamma) = (98.80 \pm 0.03)\%$.

$\Gamma(N(940)\overline{p}+\text{c.c.} \to \pi^0 p\overline{p})/\Gamma_{total}$ Γ_{38}/Γ

VALUE (units 10^{-5})	EVTS	DOCUMENT ID		TECN	COMMENT
6.42±0.20$^{+1.78}_{-1.28}$	1.9k	[1] ABLIKIM	13A	BES3	$\psi(2S) \to p\overline{p}\pi^0$

[1] From a fit of $\pi^0 p\overline{p}$ data to eight distinct intermediate $N\overline{p}$ resonant states.

$\Gamma(N(1440)\overline{p}+\text{c.c.} \to \pi^0 p\overline{p})/\Gamma_{total}$ Γ_{39}/Γ

VALUE (units 10^{-5})	EVTS	DOCUMENT ID		TECN	COMMENT
7.3 $^{+1.7}_{-1.5}$ OUR AVERAGE		Error includes scale factor of 2.5.			
3.58±0.25$^{+1.59}_{-0.84}$	1.1k	[1] ABLIKIM	13A	BES3	$\psi(2S) \to p\overline{p}\pi^0$
8.1 ±0.7 ±0.3	474	[2] ALEXANDER	10	CLEO	$\psi(2S) \to \pi^0 p\overline{p}$

[1] From a fit of $\pi^0 p\overline{p}$ data to eight distinct intermediate $N\overline{p}$ resonant states.
[2] From a fit of the $p\overline{p}$ and $p\pi^0$ mass distributions to a combination of $N(1440)\overline{p}$, $\pi^0 f_0(2100)$, and two other broad, unestablished resonances.

$\Gamma(N(1520)\overline{p}+\text{c.c.} \to \pi^0 p\overline{p})/\Gamma_{total}$ Γ_{40}/Γ

VALUE (units 10^{-5})	EVTS	DOCUMENT ID		TECN	COMMENT
0.64±0.05$^{+0.22}_{-0.17}$	0.2k	[1] ABLIKIM	13A	BES3	$\psi(2S) \to p\overline{p}\pi^0$

[1] From a fit of $\pi^0 p\overline{p}$ data to eight distinct intermediate $N\overline{p}$ resonant states.

$\Gamma(N(1535)\overline{p}+\text{c.c.} \to \pi^0 p\overline{p})/\Gamma_{total}$ Γ_{41}/Γ

VALUE (units 10^{-5})	EVTS	DOCUMENT ID		TECN	COMMENT
2.47±0.28$^{+0.99}_{-0.97}$	0.7k	[1] ABLIKIM	13A	BES3	$\psi(2S) \to p\overline{p}\pi^0$

[1] From a fit of $\pi^0 p\overline{p}$ data to eight distinct intermediate $N\overline{p}$ resonant states.

$\Gamma(N(1650)\overline{p}+\text{c.c.} \to \pi^0 p\overline{p})/\Gamma_{total}$ Γ_{42}/Γ

VALUE (units 10^{-5})	EVTS	DOCUMENT ID		TECN	COMMENT
3.76±0.28$^{+1.37}_{-1.66}$	1.1k	[1] ABLIKIM	13A	BES3	$\psi(2S) \to p\overline{p}\pi^0$

[1] From a fit of $\pi^0 p\overline{p}$ data to eight distinct intermediate $N\overline{p}$ resonant states.

$\Gamma(N(1720)\overline{p}+\text{c.c.} \to \pi^0 p\overline{p})/\Gamma_{total}$ Γ_{43}/Γ

VALUE (units 10^{-5})	EVTS	DOCUMENT ID		TECN	COMMENT
1.79±0.10$^{+0.24}_{-0.71}$	0.5k	[1] ABLIKIM	13A	BES3	$\psi(2S) \to p\overline{p}\pi^0$

[1] From a fit of $\pi^0 p\overline{p}$ data to eight distinct intermediate $N\overline{p}$ resonant states.

$\Gamma(N(2300)\overline{p}+\text{c.c.} \to \pi^0 p\overline{p})/\Gamma_{total}$ Γ_{44}/Γ

VALUE (units 10^{-5})	EVTS	DOCUMENT ID		TECN	COMMENT
2.62±0.28$^{+1.12}_{-0.64}$	0.9k	[1] ABLIKIM	13A	BES3	$\psi(2S) \to p\overline{p}\pi^0$

[1] From a fit of $\pi^0 p\overline{p}$ data to eight distinct intermediate $N\overline{p}$ resonant states.

$\Gamma(N(2570)\overline{p}+\text{c.c.} \to \pi^0 p\overline{p})/\Gamma_{total}$ Γ_{45}/Γ

VALUE (units 10^{-5})	EVTS	DOCUMENT ID		TECN	COMMENT
2.13±0.08$^{+0.40}_{-0.30}$	0.8k	[1] ABLIKIM	13A	BES3	$\psi(2S) \to p\overline{p}\pi^0$

[1] From a fit of $\pi^0 p\overline{p}$ data to eight distinct intermediate $N\overline{p}$ resonant states.

$\Gamma(\pi^0 f_0(2100) \to \pi^0 p\overline{p})/\Gamma_{total}$ Γ_{46}/Γ

VALUE (units 10^{-5})	EVTS	DOCUMENT ID		TECN	COMMENT
1.1±0.4±0.1	76	[1] ALEXANDER	10	CLEO	$\psi(2S) \to \pi^0 p\overline{p}$

[1] From a fit of the $p\overline{p}$ and $p\pi^0$ mass distributions to a combination of $N_1^*(1440)\overline{p}$, $\pi^0 f_0(2100)$, and two other broad, unestablished resonances.

$\Gamma(\eta p\overline{p})/\Gamma_{total}$ Γ_{47}/Γ

VALUE (units 10^{-5})	EVTS	DOCUMENT ID		TECN	COMMENT
6.0±0.4 OUR AVERAGE					
6.4±0.2±0.6	679	[1] ABLIKIM	13S	BES3	$\psi(2S) \to \eta p\overline{p}$
5.6±0.6±0.3	154	[1] ALEXANDER	10	CLEO	$\psi(2S) \to \eta p\overline{p}$
5.8±1.1±0.7	44.8 ± 8.5	[2] ABLIKIM	05E	BES2	$e^+e^- \to \psi(2S) \to p\overline{p}\gamma\gamma$
8 ±3 ±3	9.8	BRIERE	05	CLEO	$e^+e^- \to \psi(2S) \to p\overline{p}\pi^+\pi^-\pi^0$

[1] With $N(1535)$ decaying to $p\eta$.
[2] Computed using $B(\eta \to \gamma\gamma) = (39.43 \pm 0.26)\%$.

$\Gamma(\eta f_0(2100) \to \eta p\overline{p})/\Gamma_{total}$ Γ_{48}/Γ

VALUE (units 10^{-5})	EVTS	DOCUMENT ID		TECN	COMMENT
1.2±0.4±0.1	31	[1] ALEXANDER	10	CLEO	$\psi(2S) \to \eta p\overline{p}$

[1] From a fit of the $p\overline{p}$ and $p\eta$ distributions to a combination of $N^*(1535)\overline{p}$ and $\eta f_0(2100)$.

$\Gamma(N(1535)\overline{p} \to \eta p\overline{p})/\Gamma_{total}$ Γ_{49}/Γ

VALUE (units 10^{-5})	EVTS	DOCUMENT ID		TECN	COMMENT
4.4±0.6±0.3	123	[1] ALEXANDER	10	CLEO	$\psi(2S) \to \eta p\overline{p}$

[1] From a fit of the $p\overline{p}$ and $p\eta$ distributions to a combination of $N^*(1535)\overline{p}$ and $\eta f_0(2100)$.

$\Gamma(\omega p\overline{p})/\Gamma_{total}$ Γ_{50}/Γ

VALUE (units 10^{-4})	EVTS	DOCUMENT ID		TECN	COMMENT
0.69±0.21 OUR AVERAGE					
0.6 ±0.2 ±0.2	21.2	BRIERE	05	CLEO	$e^+e^- \to \psi(2S) \to p\overline{p}\pi^+\pi^-\pi^0$
0.8 ±0.3 ±0.1	14.9 ± 0.1	[1] BAI	03B	BES	$\psi(2S) \to p\overline{p}\pi^+\pi^-\pi^0$

[1] Normalized to $B(\psi(2S) \to J/\psi\pi^+\pi^-) = 0.305 \pm 0.016$.

$\Gamma(\phi p\overline{p})/\Gamma_{total}$ Γ_{51}/Γ

VALUE (units 10^{-4})	CL%	DOCUMENT ID		TECN	COMMENT
<0.24	90	BRIERE	05	CLEO	$e^+e^- \to \psi(2S) \to p\overline{p}K^+K^-$
• • • We do not use the following data for averages, fits, limits, etc. • • •					
<0.26	90	[1] BAI	03B	BES	$\psi(2S) \to K^+K^-p\overline{p}$

[1] Normalized to $B(\psi(2S) \to J/\psi\pi^+\pi^-) = 0.305 \pm 0.016$.

$\Gamma(\pi^+\pi^- p\overline{p})/\Gamma_{total}$ Γ_{52}/Γ

VALUE (units 10^{-4})	EVTS	DOCUMENT ID		TECN	COMMENT
6.0±0.4 OUR AVERAGE					
5.9±0.2±0.4	904.5	BRIERE	05	CLEO	$e^+e^- \to \psi(2S) \to p\overline{p}\pi^+\pi^-$
8 ±2		[1] TANENBAUM	78	MRK1	e^+e^-

[1] Assuming entirely strong decay.

$\Gamma(p\overline{n}\pi^-$ or c.c.$)/\Gamma_{total}$ Γ_{53}/Γ

VALUE (units 10^{-4})	EVTS	DOCUMENT ID		TECN	COMMENT
2.48±0.17 OUR AVERAGE					
2.45±0.11±0.21	851	ABLIKIM	06I	BES2	$e^+e^- \to p\pi^- X$
2.52±0.12±0.22	849	ABLIKIM	06I	BES2	$e^+e^- \to \overline{p}\pi^+ X$

$\Gamma(p\overline{n}\pi^-\pi^0)/\Gamma_{total}$ Γ_{54}/Γ

VALUE (units 10^{-4})	EVTS	DOCUMENT ID		TECN	COMMENT
3.18±0.50±0.50	135 ± 21	ABLIKIM	06I	BES2	$e^+e^- \to p\pi^-\pi^0 X$

$\Gamma(\eta\pi^+\pi^-)/\Gamma_{total}$ Γ_{56}/Γ

VALUE (units 10^{-4})	CL%	DOCUMENT ID		TECN	COMMENT
<1.6	90	BRIERE	05	CLEO	$e^+e^- \to \psi(2S) \to 2(\pi^+\pi^-)\pi^0$

$\Gamma(\eta\pi^+\pi^-\pi^0)/\Gamma_{total}$ Γ_{57}/Γ

VALUE (units 10^{-4})	EVTS	DOCUMENT ID		TECN	COMMENT
9.5±0.7±1.5		[1] BRIERE	05	CLEO	$e^+e^- \to \psi(2S) \to$ hadr
• • • We do not use the following data for averages, fits, limits, etc. • • •					
10.3±0.8±1.4	201.7	[2] BRIERE	05	CLEO	$e^+e^- \to \psi(2S) \to \eta 3\pi(\eta \to \gamma\gamma)$
8.1±1.4±1.6	50.0	[2] BRIERE	05	CLEO	$e^+e^- \to \psi(2S) \to \eta 3\pi(\eta \to 3\pi)$

[1] Average of $\eta \to \gamma\gamma$ and $\eta \to 3\pi$.
[2] Not independent from other values reported by BRIERE 05.

$\Gamma(2(\pi^+\pi^-)\eta)/\Gamma_{total}$ Γ_{58}/Γ

VALUE (units 10^{-3})	EVTS	DOCUMENT ID		TECN	COMMENT
1.2±0.6±0.1	16	[1] AUBERT	07AU	BABR	10.6 $e^+e^- \to 2(\pi^+\pi^-)\eta\gamma$

[1] AUBERT 07AU quotes $\Gamma_{ee}^{\psi(2S)} \cdot B(\psi(2S) \to 2(\pi^+\pi)\eta) \cdot B(\eta \to \gamma\gamma) = 1.2 \pm 0.7 \pm 0.1$ eV.

$\Gamma(\eta'\pi^+\pi^-\pi^0)/\Gamma_{total}$ Γ_{59}/Γ

VALUE (units 10^{-4})	EVTS	DOCUMENT ID		TECN	COMMENT
4.5±1.6±1.3	12.8	BRIERE	05	CLEO	$e^+e^- \to \psi(2S) \to$ hadr

$\Gamma(\omega\pi^+\pi^-)/\Gamma_{total}$ Γ_{60}/Γ

VALUE (units 10^{-4})	EVTS	DOCUMENT ID		TECN	COMMENT
7.3±1.2 OUR AVERAGE	Error includes scale factor of 2.1. See the ideogram below.				
8.4±0.5±1.2	386	ABLIKIM	07D	BES2	$e^+e^- \to \psi(2S)$
12.2±2.2±0.7	37	[1] AUBERT	07AU	BABR	10.6 $e^+e^- \to \omega\pi^+\pi^-\gamma$
8.2±0.5±0.7	391	BRIERE	05	CLEO	$e^+e^- \to \psi(2S) \to 2(\pi^+\pi^-)\pi^0$
4.8±0.6±0.7	100 ± 22	[2] BAI	03B	BES	$\psi(2S) \to 2(\pi^+\pi^-)\pi^0$

[1] AUBERT 07AU quotes $\Gamma_{ee}^{\psi(2S)} \cdot B(\psi(2S) \to \omega\pi^+\pi^-) \cdot B(\omega \to 3\pi) = 2.69 \pm 0.73 \pm 0.16$ eV.
[2] Normalized to $B(\psi(2S) \to J/\psi\pi^+\pi^-) = 0.305 \pm 0.016$.

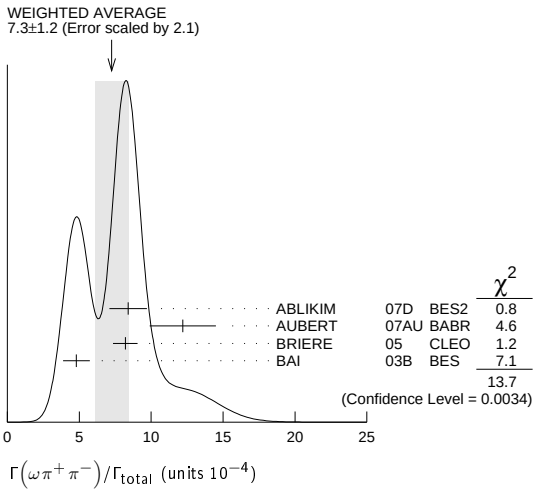

$\Gamma(b_1^\pm\pi^\mp)/\Gamma_{total}$ Γ_{61}/Γ

VALUE (units 10^{-4})	EVTS	DOCUMENT ID		TECN	COMMENT
4.0 ±0.6 OUR AVERAGE	Error includes scale factor of 1.1.				
5.1 ±0.6 ±0.8	202	ABLIKIM	07D	BES2	$e^+e^- \to \psi(2S)$
$4.18^{+0.43}_{-0.42} \pm 0.92$	170	ADAM	05	CLEO	$e^+e^- \to \psi(2S)$
3.2 ±0.6 ±0.5	61 ± 11	[1,2] BAI	03B	BES	$\psi(2S) \to 2(\pi^+\pi^-)\pi^0$
• • • We do not use the following data for averages, fits, limits, etc. • • •					
5.2 ±0.8 ±1.0		[1] BAI	99C	BES	Repl. by BAI 03B

[1] Assuming $B(b_1 \to \omega\pi)=1$.
[2] Normalized to $B(\psi(2S) \to J/\psi\pi^+\pi^-) = 0.305 \pm 0.016$.

$\Gamma(b_1^0\pi^0)/\Gamma_{total}$ Γ_{62}/Γ

VALUE (units 10^{-4})	EVTS	DOCUMENT ID		TECN	COMMENT
$2.35^{+0.47}_{-0.42}$±0.40	45	ADAM	05	CLEO	$e^+e^- \to \psi(2S)$

$\Gamma(\omega f_2(1270))/\Gamma_{total}$ Γ_{63}/Γ

VALUE (units 10^{-4})	CL%	EVTS	DOCUMENT ID		TECN	COMMENT
2.2 ±0.4 OUR AVERAGE						
2.3 ±0.5 ±0.4		57	ABLIKIM	07D	BES2	$e^+e^- \to \psi(2S)$
2.05±0.41±0.38		62±12	BAI	04C	BES2	$\psi(2S) \to 2(\pi^+\pi^-)\pi^0$
• • • We do not use the following data for averages, fits, limits, etc. • • •						
<1.5	90		[1] BAI	03B	BES	$\psi(2S) \to 2(\pi^+\pi^-)\pi^0$
<1.7	90		BAI	98J	BES	Repl. by BAI 03B

[1] Normalized to $B(\psi(2S) \to J/\psi\pi^+\pi^-) = 0.305 \pm 0.016$.

$\Gamma(\pi^+\pi^- K^+K^-)/\Gamma_{total}$ Γ_{64}/Γ

VALUE (units 10^{-4})	EVTS	DOCUMENT ID		TECN	COMMENT
7.5±0.9 OUR AVERAGE	Error includes scale factor of 1.9.				
10.9±1.9±0.2	85	[1] AUBERT	07AK	BABR	10.6 $e^+e^- \to \pi^+\pi^- K^+K^-\gamma$
7.1±0.3±0.4	817.2	BRIERE	05	CLEO	$e^+e^- \to \psi(2S) \to K^+K^-\pi^+\pi^-$
16 ±4		[2] TANENBAUM	78	MRK1	e^+e^-

[1] AUBERT 07AK reports $[\Gamma(\psi(2S) \to \pi^+\pi^- K^+ K^-)/\Gamma_{\rm total}] \times [\Gamma(\psi(2S) \to e^+e^-)] = (2.56 \pm 0.42 \pm 0.16) \times 10^{-3}$ keV which we divide by our best value $\Gamma(\psi(2S) \to e^+e^-) = 2.36 \pm 0.04$ keV. Our first error is their experiment's error and our second error is the systematic error from using our best value.

[2] Assuming entirely strong decay.

$\Gamma(\rho^0 K^+ K^-)/\Gamma_{\rm total}$ Γ_{65}/Γ

VALUE (units 10^{-4})	EVTS	DOCUMENT ID		TECN	COMMENT
2.2±0.2±0.4	223.8	BRIERE	05	CLEO	$e^+e^- \to \psi(2S) \to K^+K^-\pi^+\pi^-$

$\Gamma(K^*(892)^0 \overline{K}{}^*_2(1430)^0)/\Gamma_{\rm total}$ Γ_{66}/Γ

VALUE (units 10^{-4})	CL%	EVTS	DOCUMENT ID		TECN	COMMENT
1.86±0.32±0.43		93 ± 16	BAI	04C		$\psi(2S) \to K^+K^-\pi^+\pi^-$
• • • We do not use the following data for averages, fits, limits, etc. • • •						
<1.2	90		BAI	98J	BES	e^+e^-

$\Gamma(K^+K^-\pi^+\pi^-\eta)/\Gamma_{\rm total}$ Γ_{67}/Γ

VALUE (units 10^{-3})	EVTS	DOCUMENT ID		TECN	COMMENT
1.3±0.7±0.1	7	[1] AUBERT	07AU	BABR	10.6 $e^+e^- \to K^+K^-\pi^+\pi^-\eta\gamma$

[1] AUBERT 07AU quotes $\Gamma_{ee}^{\psi(2S)} \cdot B(\psi(2S) \to 2(\pi^+\pi)\eta) \cdot B(\eta \to \gamma\gamma) = 1.2 \pm 0.7 \pm 0.1$ eV.

$\Gamma(K^+K^-2(\pi^+\pi^-)\pi^0)/\Gamma_{\rm total}$ Γ_{68}/Γ

VALUE (units 10^{-4})	EVTS	DOCUMENT ID		TECN	COMMENT
10.0±2.5±1.8	65	ABLIKIM	07D	BES2	$e^+e^- \to \psi(2S)$

$\Gamma(K_1(1270)^\pm K^\mp)/\Gamma_{\rm total}$ Γ_{70}/Γ

VALUE (units 10^{-4})	DOCUMENT ID		TECN	COMMENT
10.0±1.8±2.1	[1] BAI	99C	BES	e^+e^-

[1] Assuming $B(K_1(1270) \to K\rho) = 0.42 \pm 0.06$

$\Gamma(K^0_S K^0_S \pi^+\pi^-)/\Gamma_{\rm total}$ Γ_{71}/Γ

VALUE (units 10^{-4})	EVTS	DOCUMENT ID		TECN	COMMENT
2.20±0.25±0.37	83 ± 9	ABLIKIM	05O	BES2	$e^+e^- \to \psi(2S)$

$\Gamma(\rho^0 p\overline{p})/\Gamma_{\rm total}$ Γ_{72}/Γ

VALUE (units 10^{-4})	EVTS	DOCUMENT ID		TECN	COMMENT
0.5±0.1±0.2	61.1	BRIERE	05	CLEO	$e^+e^- \to \psi(2S) \to p\overline{p}\pi^+\pi^-$

$\Gamma(K^+\overline{K}{}^*(892)^0\pi^- + \text{c.c.})/\Gamma_{\rm total}$ Γ_{73}/Γ

VALUE (units 10^{-4})	DOCUMENT ID		TECN	COMMENT
6.7±2.5	TANENBAUM	78	MRK1	e^+e^-

$\Gamma(2(\pi^+\pi^-))/\Gamma_{\rm total}$ Γ_{74}/Γ

VALUE (units 10^{-4})	EVTS	DOCUMENT ID		TECN	COMMENT
2.4±0.6 OUR AVERAGE Error includes scale factor of 2.2.					
2.2±0.2±0.2	308	BRIERE	05	CLEO	$e^+e^- \to \psi(2S) \to 2(\pi^+\pi^-)$
4.5±1.0		TANENBAUM	78	MRK1	e^+e^-

$\Gamma(\rho^0\pi^+\pi^-)/\Gamma_{\rm total}$ Γ_{75}/Γ

VALUE (units 10^{-4})	EVTS	DOCUMENT ID		TECN	COMMENT
2.2±0.6 OUR AVERAGE Error includes scale factor of 1.4.					
2.0±0.2±0.4	285.5	BRIERE	05	CLEO	$e^+e^- \to \psi(2S) \to 2(\pi^+\pi^-)$
4.2±1.5		TANENBAUM	78	MRK1	e^+e^-

$\Gamma(K^+K^-\pi^+\pi^-\pi^0)/\Gamma_{\rm total}$ Γ_{76}/Γ

VALUE (units 10^{-4})	EVTS	DOCUMENT ID		TECN	COMMENT
12.6±0.9 OUR AVERAGE					
18.6±5.7±0.3	32	[1] AUBERT	07AU	BABR	10.6 $e^+e^- \to K^+K^-\pi^+\pi^-\pi^0\gamma$
11.7±1.0±1.5	597	ABLIKIM	06G	BES2	$\psi(2S) \to K^+K^-\pi^+\pi^-\pi^0$
12.7±0.5±1.0	711.6	BRIERE	05	CLEO	$e^+e^- \to \psi(2S) \to K^+K^-\pi^+\pi^-\pi^0$

[1] AUBERT 07AU reports $[\Gamma(\psi(2S) \to K^+K^-\pi^+\pi^-\pi^0)/\Gamma_{\rm total}] \times [\Gamma(\psi(2S) \to e^+e^-)] = (44 \pm 13 \pm 3) \times 10^{-4}$ keV which we divide by our best value $\Gamma(\psi(2S) \to e^+e^-) = 2.36 \pm 0.04$ keV. Our first error is their experiment's error and our second error is the systematic error from using our best value.

$\Gamma(\omega f_0(1710) \to \omega K^+K^-)/\Gamma_{\rm total}$ Γ_{77}/Γ

VALUE (units 10^{-5})	EVTS	DOCUMENT ID		TECN	COMMENT
5.9±2.0±0.9	19	ABLIKIM	06G	BES2	$\psi(2S) \to K^+K^-\pi^+\pi^-\pi^0$

$\Gamma(K^*(892)^0 K^-\pi^+\pi^0 + \text{c.c.})/\Gamma_{\rm total}$ Γ_{78}/Γ

VALUE (units 10^{-4})	EVTS	DOCUMENT ID		TECN	COMMENT
8.6±1.3±1.8	238	ABLIKIM	06G	BES2	$\psi(2S) \to K^+K^-\pi^+\pi^-\pi^0$

$\Gamma(K^*(892)^+ K^-\pi^+\pi^- + \text{c.c.})/\Gamma_{\rm total}$ Γ_{79}/Γ

VALUE (units 10^{-4})	EVTS	DOCUMENT ID		TECN	COMMENT
9.6±2.2±1.7	133	ABLIKIM	06G	BES2	$\psi(2S) \to K^+K^-\pi^+\pi^-\pi^0$

$\Gamma(K^*(892)^+ K^-\rho^0 + \text{c.c.})/\Gamma_{\rm total}$ Γ_{80}/Γ

VALUE (units 10^{-4})	EVTS	DOCUMENT ID		TECN	COMMENT
7.3±2.2±1.4	78	ABLIKIM	06G	BES2	$\psi(2S) \to K^+K^-\pi^+\pi^-\pi^0$

$\Gamma(K^*(892)^0 K^-\rho^+ + \text{c.c.})/\Gamma_{\rm total}$ Γ_{81}/Γ

VALUE (units 10^{-4})	EVTS	DOCUMENT ID		TECN	COMMENT
6.1±1.3±1.2	125	ABLIKIM	06G	BES2	$\psi(2S) \to K^+K^-\pi^+\pi^-\pi^0$

$\Gamma(\eta K^+K^-, \text{no } \eta\phi)/\Gamma_{\rm total}$ Γ_{82}/Γ

VALUE (units 10^{-5})	CL%	EVTS	DOCUMENT ID		TECN	COMMENT
3.08±0.29±0.25		0.3k	[1] ABLIKIM	12L	BES3	$\psi(2S) \to K^+K^-\gamma\gamma$
• • • We do not use the following data for averages, fits, limits, etc. • • •						
<13	90		BRIERE	05	CLEO	$e^+e^- \to \psi(2S) \to K^+K^-\pi^+\pi^-\pi^0$

[1] Excluding $\eta\phi$.

$\Gamma(\omega K^+K^-)/\Gamma_{\rm total}$ Γ_{83}/Γ

VALUE (units 10^{-4})	EVTS	DOCUMENT ID		TECN	COMMENT
1.85±0.25 OUR AVERAGE Error includes scale factor of 1.1.					
2.38±0.37±0.29	78	ABLIKIM	06G	BES2	$\psi(2S) \to K^+K^-\pi^+\pi^-\pi^0$
1.9 ±0.3 ±0.3	76.8	BRIERE	05	CLEO	$e^+e^- \to \psi(2S) \to K^+K^-\pi^+\pi^-\pi^0$
1.5 ±0.3 ±0.2	23.0 ± 5.2	[1] BAI	03B	BES	$\psi(2S) \to K^+K^-\pi^+\pi^-\pi^0$

[1] Normalized to $B(\psi(2S) \to J/\psi\pi^+\pi^-) = 0.305 \pm 0.016$.

$\Gamma(\omega K^*(892)^+ K^- + \text{c.c.})/\Gamma_{\rm total}$ Γ_{84}/Γ

VALUE (units 10^{-5})	EVTS	DOCUMENT ID		TECN	COMMENT
20.7±2.6 OUR AVERAGE					
18.9±2.9±2.2	396	ABLIKIM	13M	BES3	$\psi(2S) \to \omega K^0_S K^-\pi^+$
22.6±3.0±2.4	535	ABLIKIM	13M	BES3	$\psi(2S) \to \omega K^+K^-\pi^0$

$\Gamma(\omega K^*_2(1430)^+ K^- + \text{c.c.})/\Gamma_{\rm total}$ Γ_{85}/Γ

VALUE (units 10^{-5})	EVTS	DOCUMENT ID		TECN	COMMENT
6.1 ±1.2 OUR AVERAGE					
6.39±1.50±0.78	128	ABLIKIM	13M	BES3	$\psi(2S) \to \omega K^0_S K^-\pi^+$
5.86±1.61±0.83	143	ABLIKIM	13M	BES3	$\psi(2S) \to \omega K^+K^-\pi^0$

$\Gamma(\omega \overline{K}{}^*(892)^0 K^0)/\Gamma_{\rm total}$ Γ_{86}/Γ

VALUE (units 10^{-5})	EVTS	DOCUMENT ID		TECN	COMMENT
16.8±2.5±1.6	356	ABLIKIM	13M	BES3	$\psi(2S) \to \omega K^0_S K^-\pi^+$

$\Gamma(\omega \overline{K}{}^*_2(1430)^0 K^0)/\Gamma_{\rm total}$ Γ_{87}/Γ

VALUE (units 10^{-5})	EVTS	DOCUMENT ID		TECN	COMMENT
5.82±2.08±0.72	116	ABLIKIM	13M	BES3	$\psi(2S) \to \omega K^0_S K^-\pi^+$

$\Gamma(\omega X(1440) \to \omega K^0_S K^-\pi^+ + \text{c.c.})/\Gamma_{\rm total}$ Γ_{88}/Γ

VALUE (units 10^{-5})	EVTS	DOCUMENT ID		TECN	COMMENT
1.60±0.27±0.24	109	[1] ABLIKIM	13M	BES3	$\psi(2S) \to \omega K^0_S K^-\pi^+$

[1] $X(1440)$ compatible with $\eta(1405)$ and $\eta(1475)$. A $f_1(1420)$ is also possible.

$\Gamma(\omega X(1440) \to \omega K^+K^-\pi^0)/\Gamma_{\rm total}$ Γ_{89}/Γ

VALUE (units 10^{-5})	EVTS	DOCUMENT ID		TECN	COMMENT
1.09±0.20±0.16	82	[1] ABLIKIM	13M	BES3	$\psi(2S) \to \omega K^+K^-\pi^0$

[1] $X(1440)$ compatible with $\eta(1405)$ and $\eta(1475)$. A $f_1(1420)$ is also possible.

$\Gamma(\omega f_1(1285) \to \omega K^0_S K^-\pi^+ + \text{c.c.})/\Gamma_{\rm total}$ Γ_{90}/Γ

VALUE (units 10^{-5})	EVTS	DOCUMENT ID		TECN	COMMENT
0.302±0.098±0.027	22	[1] ABLIKIM	13M	BES3	$\psi(2S) \to \omega K^0_S K^-\pi^+$

[1] Statistical signficance 4.5 σ. This measurement is equivalent to a limit of $< 0.478 \times 10^{-5}$ at 90% C.L.

$\Gamma(\omega f_1(1285) \to \omega K^+K^-\pi^0)/\Gamma_{\rm total}$ Γ_{91}/Γ

VALUE (units 10^{-5})	EVTS	DOCUMENT ID		TECN	COMMENT
0.125±0.070±0.013	10	[1] ABLIKIM	13M	BES3	$\psi(2S) \to \omega K^+K^-\pi^0$

[1] Statistical signficance 3.2 σ. This measurement is equivalent to a limit of $< 0.221 \times 10^{-5}$ at 90% C.L.

Meson Particle Listings

$\psi(2S)$

$\Gamma(3(\pi^+\pi^-))/\Gamma_{total}$ Γ_{92}/Γ

VALUE (units 10^{-4})	EVTS	DOCUMENT ID		TECN	COMMENT
3.5 ±2.0 OUR AVERAGE	Error includes scale factor of 2.8.				
5.45±0.42±0.87	671	ABLIKIM	05H	BES2	$e^+e^- \to \psi(2S) \to 3(\pi^+\pi^-)$
1.5 ±1.0		[1] TANENBAUM	78	MRK1	e^+e^-

[1] Assuming entirely strong decay.

$\Gamma(p\overline{p}\pi^+\pi^-\pi^0)/\Gamma_{total}$ Γ_{93}/Γ

VALUE (units 10^{-4})	EVTS	DOCUMENT ID		TECN	COMMENT
7.3±0.4±0.6	434.9	BRIERE	05	CLEO	$e^+e^- \to \psi(2S) \to p\overline{p}\pi^+\pi^-\pi^0$

$\Gamma(K^+K^-)/\Gamma_{total}$ Γ_{94}/Γ

VALUE (units 10^{-5})	CL%	EVTS	DOCUMENT ID		TECN	COMMENT
7.1 ±0.5 OUR AVERAGE		Error includes scale factor of 1.5.				
7.48±0.23±0.39		1.3k	[1] METREVELI	12		$\psi(2S) \to K^+K^-$
6.3 ±0.6 ±0.3			DOBBS	06A	CLEO	e^+e^-
10 ±7			BRANDELIK	79C	DASP	e^+e^-
• • • We do not use the following data for averages, fits, limits, etc. • • •						
< 5	90		FELDMAN	77	MRK1	e^+e^-

[1] Obtained by analyzing CLEO-c data but not authored by the CLEO Collaboration.

$\Gamma(K^0_S K^0_L)/\Gamma_{total}$ Γ_{95}/Γ

VALUE (units 10^{-5})	EVTS	DOCUMENT ID		TECN	COMMENT
5.34±0.33 OUR AVERAGE					
5.28±0.25±0.34	478 ± 23	[1] METREVELI	12		$\psi(2S) \to K^0_S K^0_L$
5.8 ±0.8 ±0.4		DOBBS	06A	CLEO	e^+e^-
5.24±0.47±0.48	156 ± 14	[2] BAI	04B	BES2	$\psi(2S) \to K^0_S K^0_L \to \pi^+\pi^- X$

[1] Obtained by analyzing CLEO-c data but not authored by the CLEO Collaboration.
[2] Using $B(K^0_S \to \pi^+\pi^-) = 0.6860 \pm 0.0027$.

$\Gamma(\pi^+\pi^-\pi^0)/\Gamma_{total}$ Γ_{96}/Γ

VALUE (units 10^{-4})	EVTS	DOCUMENT ID		TECN	COMMENT
2.01±0.17 OUR AVERAGE	Error includes scale factor of 1.7. See the ideogram below.				
$2.14\pm0.03^{+0.12}_{-0.11}$	7k	[1] ABLIKIM	12H	BES3	$e^+e^- \to \psi(2S)$
1.81±0.18±0.19	260 ± 19	[2] ABLIKIM	05J	BES2	$e^+e^- \to \psi(2S)$
$1.88^{+0.16}_{-0.15}\pm0.28$	194	ADAM	05	CLEO	$e^+e^- \to \psi(2S)$
0.85±0.46	4	FRANKLIN	83	MRK2	$e^+e^- \to$ hadrons

[1] From $\psi(2S) \to \pi^+\pi^-\pi^0$ events directly. The quoted systematic error includes a contribution of 4% (added in quadrature) from the uncertainty on the number of $\psi(2S)$ events.
[2] From a PW analysis of $\psi(2S) \to \pi^+\pi^-\pi^0$.

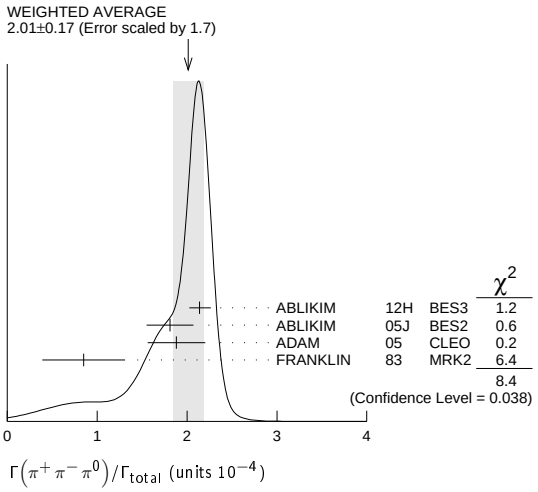

$\Gamma(\rho(2150)\pi \to \pi^+\pi^-\pi^0)/\Gamma_{total}$ Γ_{97}/Γ

VALUE (units 10^{-4})	DOCUMENT ID		TECN	COMMENT
$\mathbf{1.94\pm0.25^{+1.15}_{-0.34}}$	[1] ABLIKIM	05J	BES2	$\psi(2S) \to \rho(2150)\pi \to \pi^+\pi^-\pi^0$

[1] From a PW analysis of $\psi(2S) \to \pi^+\pi^-\pi^0$.

$\Gamma(\rho(770)\pi \to \pi^+\pi^-\pi^0)/\Gamma_{total}$ Γ_{98}/Γ

VALUE (units 10^{-4})	CL%	EVTS	DOCUMENT ID		TECN	COMMENT
0.32±0.12 OUR AVERAGE		Error includes scale factor of 1.8.				
0.51±0.07±0.11			[1] ABLIKIM	05J	BES2	$\psi(2S) \to \rho(770)\pi \to \pi^+\pi^-\pi^0$
$0.24^{+0.08}_{-0.07}\pm0.02$		22	ADAM	05	CLEO	$e^+e^- \to \psi(2S)$
• • • We do not use the following data for averages, fits, limits, etc. • • •						
<0.83	90	1	FRANKLIN	83	MRK2	e^+e^-
<10	90		BARTEL	76	CNTR	e^+e^-
<10	90		[2] ABRAMS	75	MRK1	e^+e^-

[1] From a PW analysis of $\psi(2S) \to \pi^+\pi^-\pi^0$.
[2] Final state $\rho^0\pi^0$.

$\Gamma(\pi^+\pi^-)/\Gamma_{total}$ Γ_{99}/Γ

VALUE (units 10^{-5})	CL%	EVTS	DOCUMENT ID		TECN	COMMENT
0.78±0.26 OUR AVERAGE						
0.76±0.25±0.06		30	[1] METREVELI	12		$\psi(2S) \to \pi^+\pi^-$
8 ±5			BRANDELIK	79C	DASP	e^+e^-
• • • We do not use the following data for averages, fits, limits, etc. • • •						
<2.1	90		DOBBS	06A	CLEO	$e^+e^- \to \psi(2S)$
<5	90		FELDMAN	77	MRK1	e^+e^-

[1] Obtained by analyzing CLEO-c data but not authored by the CLEO Collaboration. Using $\psi(3770) \to \pi^+\pi^-$ for continuum subtraction.

$\Gamma(K_1(1400)^\pm K^\mp)/\Gamma_{total}$ Γ_{100}/Γ

VALUE (units 10^{-4})	CL%	DOCUMENT ID		TECN	COMMENT
<3.1	90	[1] BAI	99C	BES	e^+e^-

[1] Assuming $B(K_1(1400) \to K^*\pi) = 0.94 \pm 0.06$

$\Gamma(K_2^*(1430)^\pm K^\mp)/\Gamma_{total}$ Γ_{101}/Γ

VALUE (units 10^{-5})	EVTS	DOCUMENT ID		TECN	COMMENT
$\mathbf{7.12\pm0.62^{+1.13}_{-0.61}}$	251 ± 22	ABLIKIM	12L	BES3	$e^+e^- \to \psi(2S)$

$\Gamma(K^+K^-\pi^0)/\Gamma_{total}$ Γ_{102}/Γ

VALUE (units 10^{-5})	CL%	EVTS	DOCUMENT ID		TECN	COMMENT
4.07±0.16±0.26		0.9k	ABLIKIM	12L	BES3	$e^+e^- \to \psi(2S)$
• • • We do not use the following data for averages, fits, limits, etc. • • •						
<8.9	90	1	FRANKLIN	83	MRK2	$e^+e^- \to$ hadrons

$\Gamma(K^+K^*(892)^- + \text{c.c.})/\Gamma_{total}$ Γ_{103}/Γ

VALUE (units 10^{-5})	CL%	EVTS	DOCUMENT ID		TECN	COMMENT
2.9 ±0.4 OUR AVERAGE		Error includes scale factor of 1.2.				
$3.18\pm0.30^{+0.26}_{-0.31}$		0.2k	ABLIKIM	12L	BES3	$e^+e^- \to \psi(2S)$
$2.9\ ^{+1.3}_{-1.7}\ \pm0.4$		9.6 ± 4.2	ABLIKIM	05I	BES2	$e^+e^- \to \psi(2S)$
$1.3\ ^{+1.0}_{-0.7}\ \pm0.3$		7	ADAM	05	CLEO	$e^+e^- \to \psi(2S)$
• • • We do not use the following data for averages, fits, limits, etc. • • •						
<5.4	90		FRANKLIN	83	MRK2	$e^+e^- \to$ hadrons

$\Gamma(K^*(892)^0\overline{K}^0 + \text{c.c.})/\Gamma_{total}$ Γ_{104}/Γ

VALUE (units 10^{-5})	EVTS	DOCUMENT ID		TECN	COMMENT
10.9±2.0 OUR AVERAGE					
$13.3^{+2.4}_{-2.8}\pm1.7$	65.6 ± 9.0	ABLIKIM	05I	BES2	$e^+e^- \to \psi(2S)$
$9.2^{+2.7}_{-2.2}\pm0.9$	25	ADAM	05	CLEO	$e^+e^- \to \psi(2S)$

$\Gamma(K^+K^*(892)^- + \text{c.c.})/\Gamma(K^*(892)^0\overline{K}^0 + \text{c.c.})$ $\Gamma_{103}/\Gamma_{104}$

VALUE	DOCUMENT ID		TECN	COMMENT
0.16±0.06 OUR AVERAGE				
$0.22^{+0.10}_{-0.14}$	ABLIKIM	05I	BES2	$e^+e^- \to \psi(2S)$
$0.14^{+0.08}_{-0.06}$	ADAM	05	CLEO	$e^+e^- \to \psi(2S)$

$\Gamma(\phi\pi^+\pi^-)/\Gamma_{total}$ Γ_{105}/Γ

VALUE (units 10^{-4})	EVTS	DOCUMENT ID		TECN	COMMENT
1.17±0.29 OUR AVERAGE	Error includes scale factor of 1.7.				
2.42±0.95±0.04	10 ± 4	[1,2] AUBERT	07AK	BABR	$10.6\ e^+e^- \to \pi^+\pi^- K^+K^-\gamma$
0.9 ±0.2 ±0.1	47.6	BRIERE	05	CLEO	$e^+e^- \to \psi(2S) \to K^+K^-\pi^+\pi^-$
1.5 ±0.2 ±0.2	51.5±8.3	[3] BAI	03B	BES	$\psi(2S) \to K^+K^-\pi^+\pi^-$

[1] AUBERT 07AK reports $[\Gamma(\psi(2S) \to \phi\pi^+\pi^-)/\Gamma_{total}] \times [\Gamma(\psi(2S) \to e^+e^-)] = (0.57 \pm 0.22 \pm 0.04) \times 10^{-3}$ keV which we divide by our best value $\Gamma(\psi(2S) \to e^+e^-) = 2.36 \pm 0.04$ keV. Our first error is their experiment's error and our second error is the systematic error from using our best value.
[2] Using $B(\phi \to K^+K^-) = (49.3 \pm 0.6)\%$.
[3] Normalized to $B(\psi(2S) \to J/\psi\pi^+\pi^-) = 0.305 \pm 0.016$.

$\Gamma(\phi f_0(980) \to \pi^+\pi^-)/\Gamma_{total}$ Γ_{106}/Γ

VALUE (units 10^{-4})	EVTS	DOCUMENT ID		TECN	COMMENT
0.68±0.24 OUR AVERAGE	Error includes scale factor of 1.1.				
1.44±0.70±0.02	6 ± 3	[1,2] AUBERT	07AK	BABR	$10.6\ e^+e^- \to \pi^+\pi^- K^+K^-\gamma$
0.6 ±0.2 ±0.1	18.4±6.4	[3] BAI	03B	BES	$\psi(2S) \to K^+K^-\pi^+\pi^-$

[1] AUBERT 07AK reports $[\Gamma(\psi(2S) \to \phi f_0(980) \to \pi^+\pi^-)/\Gamma_{total}] \times [\Gamma(\psi(2S) \to e^+e^-)] = (0.34 \pm 0.16 \pm 0.04) \times 10^{-3}$ keV which we divide by our best value $\Gamma(\psi(2S) \to e^+e^-) = 2.36 \pm 0.04$ keV. Our first error is their experiment's error and our second error is the systematic error from using our best value.
[2] Using $B(\phi \to K^+K^-) = (49.3 \pm 0.6)\%$.
[3] Normalized to $B(\psi(2S) \to J/\psi\pi^+\pi^-) = 0.305 \pm 0.016$.

$\Gamma(2(K^+K^-))/\Gamma_{total}$ Γ_{107}/Γ

VALUE (units 10^{-4})	EVTS	DOCUMENT ID		TECN	COMMENT
0.6±0.1±0.1	59.2	BRIERE	05	CLEO	$e^+e^- \to \psi(2S) \to 2(K^+K^-)$

$\Gamma(\phi K^+K^-)/\Gamma_{total}$ Γ_{108}/Γ

VALUE (units 10^{-4})	EVTS	DOCUMENT ID		TECN	COMMENT
0.70±0.16 OUR AVERAGE					
0.8 ±0.2 ±0.1	36.8	BRIERE	05	CLEO	$e^+e^- \to \psi(2S) \to 2(K^+K^-)$
0.6 ±0.2 ±0.1	16.1 ± 5.0	[1] BAI	03B	BES	$\psi(2S) \to 2(K^+K^-)$

[1] Normalized to $B(\psi(2S) \to J/\psi\pi^+\pi^-) = 0.305 \pm 0.016$.

$\Gamma(2(K^+K^-)\pi^0)/\Gamma_{total}$ Γ_{109}/Γ

VALUE (units 10^{-4})	EVTS	DOCUMENT ID		TECN	COMMENT
1.1±0.2±0.2	44.7	BRIERE	05	CLEO	$e^+e^- \to \psi(2S) \to 2(K^+K^-)\pi^0$

$\Gamma(\phi\eta)/\Gamma_{total}$ Γ_{110}/Γ

VALUE (units 10^{-5})	EVTS	DOCUMENT ID		TECN	COMMENT
3.10±0.31 OUR AVERAGE					
3.14±0.23±0.23	0.2k	ABLIKIM	12L	BES3	$e^+e^- \to \psi(2S)$
2.0 $^{+1.5}_{-1.1}$ ±0.4	6	ADAM	05	CLEO	$e^+e^- \to \psi(2S)$
3.3 ±1.1 ±0.5	17	ABLIKIM	04K	BES	$e^+e^- \to \psi(2S)$

$\Gamma(\phi\eta')/\Gamma_{total}$ Γ_{111}/Γ

VALUE (units 10^{-5})	EVTS	DOCUMENT ID		TECN	COMMENT
3.1±1.4±0.7	8	[1] ABLIKIM	04K	BES	$e^+e^- \to \psi(2S)$

[1] Calculated combining $\eta' \to \gamma\rho$ and $\eta\pi^+\pi^-$ channels.

$\Gamma(\omega\eta')/\Gamma_{total}$ Γ_{112}/Γ

VALUE (units 10^{-5})	EVTS	DOCUMENT ID		TECN	COMMENT
3.2$^{+2.4}_{-2.0}$±0.7	4	[1] ABLIKIM	04K	BES	$e^+e^- \to \psi(2S)$

[1] Calculated combining $\eta' \to \gamma\rho$ and $\eta\pi^+\pi^-$ channels.

$\Gamma(\omega\pi^0)/\Gamma_{total}$ Γ_{113}/Γ

VALUE (units 10^{-5})	EVTS	DOCUMENT ID		TECN	COMMENT
2.1 ±0.6 OUR AVERAGE					
2.5 $^{+1.2}_{-1.0}$ ±0.2	14	ADAM	05	CLEO	$e^+e^- \to \psi(2S)$
1.87$^{+0.68}_{-0.62}$±0.28	14	ABLIKIM	04L	BES	$e^+e^- \to \psi(2S)$

$\Gamma(\rho\eta')/\Gamma_{total}$ Γ_{114}/Γ

VALUE (units 10^{-5})	EVTS	DOCUMENT ID		TECN	COMMENT
1.87$^{+1.64}_{-1.11}$±0.33	2	ABLIKIM	04L	BES	$e^+e^- \to \psi(2S)$

$\Gamma(\rho\eta)/\Gamma_{total}$ Γ_{115}/Γ

VALUE (units 10^{-5})	EVTS	DOCUMENT ID		TECN	COMMENT
2.2 ±0.6 OUR AVERAGE Error includes scale factor of 1.1.					
3.0 $^{+1.1}_{-0.9}$ ±0.2	18	ADAM	05	CLEO	$e^+e^- \to \psi(2S)$
1.78$^{+0.67}_{-0.62}$±0.17	13	ABLIKIM	04L	BES	$e^+e^- \to \psi(2S)$

$\Gamma(\omega\eta)/\Gamma_{total}$ Γ_{116}/Γ

VALUE (units 10^{-5})	CL%	DOCUMENT ID		TECN	COMMENT
<1.1	90	ADAM	05	CLEO	$e^+e^- \to \psi(2S)$
• • • We do not use the following data for averages, fits, limits, etc. • • •					
<3.1	90	ABLIKIM	04K	BES	$e^+e^- \to \psi(2S)$

$\Gamma(\phi\pi^0)/\Gamma_{total}$ Γ_{117}/Γ

VALUE (units 10^{-5})	CL%	DOCUMENT ID		TECN	COMMENT
<0.04	90	ABLIKIM	12L	BES3	$e^+e^- \to \psi(2S)$
• • • We do not use the following data for averages, fits, limits, etc. • • •					
<0.7	90	ADAM	05	CLEO	$e^+e^- \to \psi(2S)$
<0.4	90	ABLIKIM	04K	BES	$e^+e^- \to \psi(2S)$

$\Gamma(\eta_c\pi^+\pi^-\pi^0)/\Gamma_{total}$ Γ_{118}/Γ

VALUE (units 10^{-3})	CL%	DOCUMENT ID		TECN	COMMENT
<1.0	90	PEDLAR	07	CLEO	$e^+e^- \to \psi(2S)$

$\Gamma(p\bar{p}K^+K^-)/\Gamma_{total}$ Γ_{119}/Γ

VALUE (units 10^{-5})	EVTS	DOCUMENT ID		TECN	COMMENT
2.7±0.6±0.4	30.1	BRIERE	05	CLEO	$e^+e^- \to \psi(2S) \to p\bar{p}K^+K^-$

$\Gamma(\overline{\Lambda}nK^0_S + \text{c.c.})/\Gamma_{total}$ Γ_{120}/Γ

VALUE (units 10^{-4})	EVTS	DOCUMENT ID		TECN	COMMENT
0.81±0.11±0.14	50	[1] ABLIKIM	08C	BES2	$e^+e^- \to J/\psi$

[1] Using $B(\overline{\Lambda} \to \bar{p}\pi^+) = 63.9\%$ and $B(K^0_S \to \pi^+\pi^-) = 69.2\%$.

$\Gamma(\phi f'_2(1525))/\Gamma_{total}$ Γ_{121}/Γ

VALUE (units 10^{-4})	CL%	EVTS	DOCUMENT ID		TECN	COMMENT
0.44±0.12±0.11		20 ± 6	BAI	04C		$\psi(2S) \to 2(K^+K^-)$
• • • We do not use the following data for averages, fits, limits, etc. • • •						
<0.45	90		BAI	98J	BES	$e^+e^- \to 2(K^+K^-)$

$\Gamma(\Theta(1540)\overline{\Theta}(1540) \to K^0_S pK^-\overline{n} + \text{c.c.})/\Gamma_{total}$ Γ_{122}/Γ

VALUE (units 10^{-5})	CL%	DOCUMENT ID		TECN	COMMENT
<0.88	90	BAI	04G	BES2	e^+e^-

$\Gamma(\Theta(1540)K^-\overline{n} \to K^0_S pK^-\overline{n})/\Gamma_{total}$ Γ_{123}/Γ

VALUE (units 10^{-5})	CL%	DOCUMENT ID		TECN	COMMENT
<1.0	90	BAI	04G	BES2	e^+e^-

$\Gamma(\Theta(1540)K^0_S\overline{p} \to K^0_S\overline{p}K^+n)/\Gamma_{total}$ Γ_{124}/Γ

VALUE (units 10^{-5})	CL%	DOCUMENT ID		TECN	COMMENT
<0.70	90	BAI	04G	BES2	e^+e^-

$\Gamma(\overline{\Theta}(1540)K^+n \to K^0_S\overline{p}K^+n)/\Gamma_{total}$ Γ_{125}/Γ

VALUE (units 10^{-5})	CL%	DOCUMENT ID		TECN	COMMENT
<2.6	90	BAI	04G	BES2	e^+e^-

$\Gamma(\overline{\Theta}(1540)K^0_S p \to K^0_S pK^-\overline{n})/\Gamma_{total}$ Γ_{126}/Γ

VALUE (units 10^{-5})	CL%	DOCUMENT ID		TECN	COMMENT
<0.60	90	BAI	04G	BES2	e^+e^-

$\Gamma(K^0_S K^0_S)/\Gamma_{total}$ Γ_{127}/Γ

VALUE (units 10^{-4})	DOCUMENT ID		TECN	COMMENT
<0.046	[1] BAI	04D	BES	e^+e^-

[1] Forbidden by *CP*.

RADIATIVE DECAYS

$\Gamma(\gamma\chi_{c0}(1P))/\Gamma_{total}$ Γ_{128}/Γ

VALUE (units 10^{-2})	EVTS	DOCUMENT ID		TECN	COMMENT
9.99±0.27 OUR FIT					
9.2 ±0.4 OUR AVERAGE					
9.22±0.11±0.46	72600	ATHAR	04	CLEO	$e^+e^- \to \gamma X$
9.9 ±0.5 ±0.8		[1] GAISER	86	CBAL	$e^+e^- \to \gamma X$
7.2 ±2.3		[1] BIDDICK	77	CNTR	$e^+e^- \to \gamma X$
7.5 ±2.6		[1] WHITAKER	76	MRK1	e^+e^-

[1] Angular distribution $(1+\cos^2\theta)$ assumed.

$\Gamma(\gamma\chi_{c1}(1P))/\Gamma_{total}$ Γ_{129}/Γ

VALUE (units 10^{-2})	EVTS	DOCUMENT ID		TECN	COMMENT
9.55±0.31 OUR FIT					
8.9 ±0.5 OUR AVERAGE					
9.07±0.11±0.54	76700	ATHAR	04	CLEO	$e^+e^- \to \gamma X$
9.0 ±0.5 ±0.7		[1] GAISER	86	CBAL	$e^+e^- \to \gamma X$
7.1 ±1.9		[2] BIDDICK	77	CNTR	$e^+e^- \to \gamma X$

[1] Angular distribution $(1-0.189\cos^2\theta)$ assumed.
[2] Valid for isotropic distribution of the photon.

$\Gamma(\gamma\chi_{c2}(1P))/\Gamma_{total}$ Γ_{130}/Γ

VALUE (units 10^{-2})	EVTS	DOCUMENT ID		TECN	COMMENT
9.11±0.31 OUR FIT					
8.8 ±0.5 OUR AVERAGE Error includes scale factor of 1.1.					
9.33±0.14±0.61	79300	ATHAR	04	CLEO	$e^+e^- \to \gamma X$
8.0 ±0.5 ±0.7		[1] GAISER	86	CBAL	$e^+e^- \to \gamma X$
7.0 ±2.0		[2] BIDDICK	77	CNTR	$e^+e^- \to \gamma X$

[1] Angular distribution $(1-0.052\cos^2\theta)$ assumed.
[2] Valid for isotropic distribution of the photon.

$[\Gamma(\gamma\chi_{c0}(1P)) + \Gamma(\gamma\chi_{c1}(1P)) + \Gamma(\gamma\chi_{c2}(1P))]/\Gamma_{total}$ $(\Gamma_{128}+\Gamma_{129}+\Gamma_{130})/\Gamma$

VALUE	DOCUMENT ID		TECN	COMMENT
• • • We do not use the following data for averages, fits, limits, etc. • • •				
27.6±0.3±2.0	[1] ATHAR	04	CLEO	$e^+e^- \to \gamma X$

[1] Not independent from ATHAR 04 measurements of $B(\gamma\chi_{cJ})$.

$\Gamma(\gamma\chi_{c0}(1P))/\Gamma(\gamma\chi_{c1}(1P))$ $\Gamma_{128}/\Gamma_{129}$

VALUE	DOCUMENT ID		TECN	COMMENT
• • • We do not use the following data for averages, fits, limits, etc. • • •				
1.02±0.01±0.07	[1] ATHAR	04	CLEO	$e^+e^- \to \gamma X$

[1] Not independent from ATHAR 04 measurements of $B(\gamma\chi_{cJ})$.

$\Gamma(\gamma\chi_{c2}(1P))/\Gamma(\gamma\chi_{c1}(1P))$ $\Gamma_{130}/\Gamma_{129}$

VALUE	DOCUMENT ID		TECN	COMMENT
• • • We do not use the following data for averages, fits, limits, etc. • • •				
1.03±0.02±0.03	[1] ATHAR	04	CLEO	$e^+e^- \to \gamma X$

[1] Not independent from ATHAR 04 measurements of $B(\gamma\chi_{cJ})$.

$\Gamma(\gamma\chi_{c0}(1P))/\Gamma(\gamma\chi_{c2}(1P))$ $\Gamma_{128}/\Gamma_{130}$

VALUE	DOCUMENT ID		TECN	COMMENT
• • • We do not use the following data for averages, fits, limits, etc. • • •				
0.99±0.02±0.08	[1] ATHAR	04	CLEO	$e^+e^- \to \gamma X$

[1] Not independent from ATHAR 04 measurements of $B(\gamma\chi_{cJ})$.

$\Gamma(\gamma\eta_c(1S))/\Gamma_{\text{total}}$ Γ_{131}/Γ

VALUE (units 10^{-2})	EVTS	DOCUMENT ID		TECN	COMMENT
0.34 ±0.05 OUR AVERAGE		Error includes scale factor of 1.3. See the ideogram below.			
0.432±0.016±0.060		MITCHELL	09	CLEO	$e^+e^- \to \gamma X$
0.32 ±0.04 ±0.06	2560	[1] ATHAR	04	CLEO	$e^+e^- \to \gamma X$
0.28 ±0.06		[2] GAISER	86	CBAL	$e^+e^- \to \gamma X$

[1] ATHAR 04 used $\Gamma_{\eta_c(1S)} = 24.8 \pm 4.9$ MeV to obtain this result.

[2] GAISER 86 used $\Gamma_{\eta_c(1S)} = 11.5 \pm 4.5$ MeV to obtain this result.

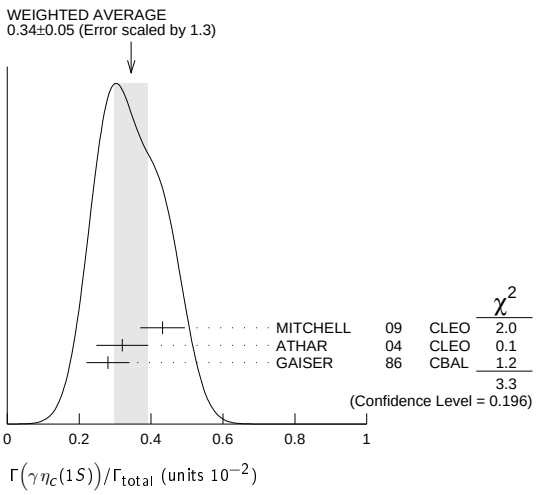

$\Gamma(\gamma\eta_c(2S))/\Gamma_{\text{total}}$ Γ_{132}/Γ

VALUE (units 10^{-4})	CL%	DOCUMENT ID		TECN	COMMENT
7±2±4		[1] ABLIKIM	12G	BES3	$\psi(2S) \to \gamma K^0 K\pi$, $KK\pi^0$
• • • We do not use the following data for averages, fits, limits, etc. • • •					
< 8	90	[2] CRONIN-HEN..10		CLEO	$\psi(2S) \to \gamma K\overline{K}\pi$
<20	90	ATHAR	04	CLEO	$e^+e^- \to \gamma X$
20–130	95	EDWARDS	82C	CBAL	$e^+e^- \to \gamma X$

[1] ABLIKIM 12G reports $[\Gamma(\psi(2S) \to \gamma\eta_c(2S))/\Gamma_{\text{total}}] \times [B(\eta_c(2S) \to K\overline{K}\pi)] = (1.30 \pm 0.20 \pm 0.30) \times 10^{-5}$ which we divide by our best value $B(\eta_c(2S) \to K\overline{K}\pi) = (1.9 \pm 1.2) \times 10^{-2}$. Our first error is their experiment's error and our second error is the systematic error from using our best value.

[2] CRONIN-HENNESSY 10 reports $[\Gamma(\psi(2S) \to \gamma\eta_c(2S))/\Gamma_{\text{total}}] \times [B(\eta_c(2S) \to K\overline{K}\pi)] < 14.5 \times 10^{-6}$ which we divide by our best value $B(\eta_c(2S) \to K\overline{K}\pi) = 1.9 \times 10^{-2}$. This measurement assumes $\Gamma(\eta_c(2S)) = 14$ MeV. CRONIN-HENNESSY 10 gives the analytic dependence of limits on width.

$\Gamma(\gamma\pi^0)/\Gamma_{\text{total}}$ Γ_{133}/Γ

VALUE (units 10^{-6})	CL%	EVTS	DOCUMENT ID		TECN	COMMENT
1.58±0.40±0.13		37	ABLIKIM	10F	BES3	$\psi(2S) \to \gamma\pi^0$
• • • We do not use the following data for averages, fits, limits, etc. • • •						
< 5	90		PEDLAR	09	CLE3	$\psi(2S) \to \gamma X$
<5400	95		[1] LIBERMAN	75	SPEC	e^+e^-
$< 1 \times 10^4$	90		WIIK	75	DASP	e^+e^-

[1] Restated by us using $B(\psi(2S) \to \mu^+\mu^-) = 0.0077$.

$\Gamma(\gamma\eta'(958))/\Gamma_{\text{total}}$ Γ_{134}/Γ

VALUE (units 10^{-4})	CL%	EVTS	DOCUMENT ID		TECN	COMMENT
1.23±0.06 OUR AVERAGE						
1.26±0.03±0.08		2226	[1] ABLIKIM	10F	BES3	$\psi(2S) \to 3\gamma\pi^+\pi^-$, $2\gamma\pi^+\pi^-$
1.19±0.08±0.03			PEDLAR	09	CLE3	$\psi(2S) \to \gamma X$
1.24±0.27±0.15		23	ABLIKIM	06R	BES2	$e^+e^- \to \psi(2S)$
1.54±0.31±0.20		~ 43	BAI	98F	BES	$\psi(2S) \to \pi^+\pi^-2\gamma$, $\pi^+\pi^-3\gamma$
• • • We do not use the following data for averages, fits, limits, etc. • • •						
< 60	90		[2] BRAUNSCH...	77	DASP	e^+e^-
< 11	90		[3] BARTEL	76	CNTR	e^+e^-

[1] Combining the results from $\eta' \to \pi^+\pi^-\eta$ and $\eta' \to \pi^+\pi^-\gamma$ decay modes.

[2] Restated by us using total decay width 228 keV.

[3] The value is normalized to the branching ratio for $\Gamma(J/\psi(1S)\eta)/\Gamma_{\text{total}}$.

$\Gamma(\gamma f_2(1270))/\Gamma_{\text{total}}$ Γ_{135}/Γ

VALUE (units 10^{-4})	EVTS	DOCUMENT ID		TECN	COMMENT
2.12±0.19±0.32		[1,2] BAI	03C	BES	$\psi(2S) \to \gamma\pi\pi$
• • • We do not use the following data for averages, fits, limits, etc. • • •					
2.08±0.19±0.33	200.6 ± 18.8	[1] BAI	03C	BES	$\psi(2S) \to \gamma\pi^+\pi^-$
2.90±1.08±1.07	29.9 ± 11.1	[1] BAI	03C	BES	$\psi(2S) \to \gamma\pi^0\pi^0$

[1] Normalized to $B(\psi(2S) \to J/\psi\pi^+\pi^-) = 0.305 \pm 0.016$.

[2] Combining the results from $\pi^+\pi^-$ and $\pi^0\pi^0$ decay modes.

$\Gamma(\gamma f_0(1710) \to \gamma\pi\pi)/\Gamma_{\text{total}}$ Γ_{137}/Γ

VALUE (units 10^{-4})	EVTS	DOCUMENT ID		TECN	COMMENT
0.301±0.041±0.124	35.6 ± 4.8	[1] BAI	03C	BES	$\psi(2S) \to \gamma\pi^+\pi^-$

[1] Normalized to $B(\psi(2S) \to J/\psi\pi^+\pi^-) = 0.305 \pm 0.016$.

$\Gamma(\gamma f_0(1710) \to \gamma K\overline{K})/\Gamma_{\text{total}}$ Γ_{138}/Γ

VALUE (units 10^{-4})	CL%	EVTS	DOCUMENT ID		TECN	COMMENT
0.604±0.090±0.132		39.6 ± 5.9	[1,2] BAI	03C	BES	$\psi(2S) \to \gamma K^+K^-$
• • • We do not use the following data for averages, fits, limits, etc. • • •						
< 1.56	90	6.8 ± 3.1	[1,2] BAI	03C	BES	$\psi(2S) \to \gamma K^0_S K^0_S$

[1] Includes unknown branching fractions to K^+K^- or $K^0_S K^0_S$. We have multiplied the K^+K^- result by a factor of 2 and the $K^0_S K^0_S$ result by a factor of 4 to obtain the $K\overline{K}$ result.

[2] Normalized to $B(\psi(2S) \to J/\psi\pi^+\pi^-) = 0.305 \pm 0.016$.

$\Gamma(\gamma\eta)/\Gamma_{\text{total}}$ Γ_{140}/Γ

VALUE (units 10^{-6})	CL%	EVTS	DOCUMENT ID		TECN	COMMENT
1.38±0.48±0.09		13	[1] ABLIKIM	10F	BES3	$\psi(2S) \to \gamma\pi^+\pi^-\pi^0$, $\gamma 3\pi^0$
• • • We do not use the following data for averages, fits, limits, etc. • • •						
< 2	90		PEDLAR	09	CLE3	$\psi(2S) \to \gamma X$
< 90	90		BAI	98F	BES	$\psi(2S) \to \pi^+\pi^-3\gamma$
<200	90		YAMADA	77	DASP	$e^+e^- \to 3\gamma$

[1] Combining the results from $\eta \to \pi^+\pi^-\pi^0$ and $\eta \to 3\pi^0$ decay modes.

$\Gamma(\gamma\eta\pi^+\pi^-)/\Gamma_{\text{total}}$ Γ_{141}/Γ

VALUE (units 10^{-4})	EVTS	DOCUMENT ID		TECN	COMMENT
8.71±1.25±1.64	418	ABLIKIM	06R	BES2	$\psi(2S) \to \gamma\eta\pi^+\pi^-$

$\Gamma(\gamma\eta(1405) \to \gamma K\overline{K}\pi)/\Gamma_{\text{total}}$ Γ_{143}/Γ

VALUE (units 10^{-4})	CL%	DOCUMENT ID		TECN	COMMENT
<0.9	90	ABLIKIM	06R	BES2	$\psi(2S) \to \gamma K^0_S K^+\pi^- +$ c.c.
• • • We do not use the following data for averages, fits, limits, etc. • • •					
<1.3	90	ABLIKIM	06R	BES2	$\psi(2S) \to \gamma K^+K^-\pi^0$
<1.2	90	[1] SCHARRE	80	MRK1	e^+e^-

[1] Includes unknown branching fraction $\eta(1405) \to K\overline{K}\pi$.

$\Gamma(\gamma\eta(1405) \to \eta\pi^+\pi^-)/\Gamma_{\text{total}}$ Γ_{144}/Γ

VALUE (units 10^{-4})	EVTS	DOCUMENT ID		TECN	COMMENT
0.36±0.25±0.05	10	ABLIKIM	06R	BES2	$\psi(2S) \to \gamma\eta\pi^+\pi^-$

$\Gamma(\gamma\eta(1475) \to K\overline{K}\pi)/\Gamma_{\text{total}}$ Γ_{146}/Γ

VALUE (units 10^{-4})	CL%	DOCUMENT ID		TECN	COMMENT
<1.4	90	ABLIKIM	06R	BES2	$\psi(2S) \to \gamma K^+K^-\pi^0$
• • • We do not use the following data for averages, fits, limits, etc. • • •					
<1.5	90	ABLIKIM	06R	BES2	$\psi(2S) \to \gamma K^0_S K^+\pi^- +$ c.c.

$\Gamma(\gamma\eta(1475) \to \eta\pi^+\pi^-)/\Gamma_{\text{total}}$ Γ_{147}/Γ

VALUE (units 10^{-4})	CL%	DOCUMENT ID		TECN	COMMENT
<0.88	90	ABLIKIM	06R	BES2	$\psi(2S) \to \gamma\eta\pi^+\pi^-$

$\Gamma(\gamma 2(\pi^+\pi^-))/\Gamma_{\text{total}}$ Γ_{148}/Γ

VALUE (units 10^{-5})	EVTS	DOCUMENT ID		TECN	COMMENT
39.6±2.8±5.0	583	ABLIKIM	07D	BES2	$e^+e^- \to \psi(2S)$

$\Gamma(\gamma K^{*0} K^+ \pi^- + \text{c.c.})/\Gamma_{\text{total}}$ Γ_{149}/Γ

VALUE (units 10^{-5})	EVTS	DOCUMENT ID		TECN	COMMENT
37.0±6.1±7.2	237	ABLIKIM	07D	BES2	$e^+e^- \to \psi(2S)$

$\Gamma(\gamma K^{*0} \overline{K}^{*0})/\Gamma_{\text{total}}$ Γ_{150}/Γ

VALUE (units 10^{-5})	EVTS	DOCUMENT ID		TECN	COMMENT
24.0±4.5±5.0	41	ABLIKIM	07D	BES2	$e^+e^- \to \psi(2S)$

$\Gamma(\gamma K^0_S K^+ \pi^- + \text{c.c.})/\Gamma_{\text{total}}$ Γ_{151}/Γ

VALUE (units 10^{-5})	EVTS	DOCUMENT ID		TECN	COMMENT
25.6±3.6±3.6	115	ABLIKIM	07D	BES2	$e^+e^- \to \psi(2S)$

$\Gamma(\gamma K^+ K^- \pi^+ \pi^-)/\Gamma_{\text{total}}$ Γ_{152}/Γ

VALUE (units 10^{-5})	EVTS	DOCUMENT ID		TECN	COMMENT
19.1±2.7±4.3	132	ABLIKIM	07D	BES2	$e^+e^- \to \psi(2S)$

$\Gamma(\gamma p\overline{p})/\Gamma_{\text{total}}$ Γ_{153}/Γ

VALUE (units 10^{-5})	EVTS	DOCUMENT ID		TECN	COMMENT
3.9 ±0.5 OUR AVERAGE Error includes scale factor of 2.0.					
4.18±0.26±0.18	348	[1] ALEXANDER	10	CLEO	$\psi(2S) \to \gamma p\overline{p}$
2.9 ±0.4 ±0.4	142	ABLIKIM	07D	BES2	$e^+e^- \to \psi(2S)$

[1] From a fit of the $p\overline{p}$ mass distribution to a combination of $\gamma f_2(1950)$, $\gamma f_2(2150)$, and $\gamma p\overline{p}$ phase space, for $M(p\overline{p} < 2.85$ GeV, and accounting for backgrounds from $\psi(2S) \to \pi^0 p\overline{p}$ and continuum.

$\Gamma(\gamma f_2(1950) \to \gamma p\overline{p})/\Gamma_{\text{total}}$ Γ_{154}/Γ

VALUE (units 10^{-5})	EVTS	DOCUMENT ID		TECN	COMMENT
1.2±0.2±0.1	111	[1] ALEXANDER	10	CLEO	$\psi(2S) \to \gamma p\overline{p}$

[1] From a fit of the $p\overline{p}$ mass distribution to a combination of $\gamma f_2(1950)$, $\gamma f_2(2150)$, and $\gamma p\overline{p}$ phase space, for $M(p\overline{p} < 2.85$ GeV, and accounting for backgrounds from $\psi(2S) \to \pi^0 p\overline{p}$ and continuum.

$\Gamma(\gamma f_2(2150) \to \gamma p\overline{p})/\Gamma_{\text{total}}$ Γ_{155}/Γ

VALUE (units 10^{-5})	EVTS	DOCUMENT ID		TECN	COMMENT
0.72±0.18±0.03	73	[1] ALEXANDER	10	CLEO	$\psi(2S) \to \gamma p\overline{p}$

[1] From a fit of the $p\overline{p}$ mass distribution to a combination of $\gamma f_2(1950)$, $\gamma f_2(2150)$, and $\gamma p\overline{p}$ phase space, for $M(p\overline{p} < 2.85$ GeV, and accounting for backgrounds from $\psi(2S) \to \pi^0 p\overline{p}$ and continuum.

$\Gamma(\gamma X(1835) \to \gamma p\overline{p})/\Gamma_{\text{total}}$ Γ_{156}/Γ

VALUE (units 10^{-6})	CL%	DOCUMENT ID		TECN	COMMENT
$4.57 \pm 0.36^{+1.77}_{-4.26}$		ABLIKIM	12D	BES3	$J/\psi \to \gamma p\overline{p}$
• • • We do not use the following data for averages, fits, limits, etc. • • •					
<1.6	90	ALEXANDER	10	CLEO	$\psi(2S) \to \gamma p\overline{p}$
<5.4	90	ABLIKIM	07D	BES	$\psi(2S) \to \gamma p\overline{p}$

$\Gamma(\gamma X \to \gamma p\overline{p})/\Gamma_{\text{total}}$ Γ_{157}/Γ

For a narrow resonance in the range $2.2 < M(X) < 2.8$ GeV.

VALUE (units 10^{-6})	CL%	DOCUMENT ID		TECN	COMMENT
<2	90	ALEXANDER	10	CLEO	$\psi(2S) \to \gamma p\overline{p}$

$\Gamma(\gamma \pi^+ \pi^- p\overline{p})/\Gamma_{\text{total}}$ Γ_{158}/Γ

VALUE (units 10^{-5})	EVTS	DOCUMENT ID		TECN	COMMENT
2.8±1.2±0.7	17	ABLIKIM	07D	BES2	$e^+e^- \to \psi(2S)$

$\Gamma(\gamma 2(\pi^+ \pi^-) K^+ K^-)/\Gamma_{\text{total}}$ Γ_{159}/Γ

VALUE (units 10^{-5})	CL%	DOCUMENT ID		TECN	COMMENT
<22	90	ABLIKIM	07D	BES2	$e^+e^- \to \psi(2S)$

$\Gamma(\gamma 3(\pi^+ \pi^-))/\Gamma_{\text{total}}$ Γ_{160}/Γ

VALUE (units 10^{-5})	CL%	DOCUMENT ID		TECN	COMMENT
<17	90	ABLIKIM	07D	BES2	$e^+e^- \to \psi(2S)$

$\Gamma(\gamma K^+ K^- K^+ K^-)/\Gamma_{\text{total}}$ Γ_{161}/Γ

VALUE (units 10^{-5})	CL%	DOCUMENT ID		TECN	COMMENT
<4	90	ABLIKIM	07D	BES2	$e^+e^- \to \psi(2S)$

$\Gamma(\gamma\gamma J/\psi)/\Gamma_{\text{total}}$ Γ_{162}/Γ

VALUE (units 10^{-4})	EVTS	DOCUMENT ID		TECN	COMMENT
$3.1 \pm 0.6^{+0.8}_{-1.0}$	1.1k	ABLIKIM	12O	BES3	$e^+e^- \to \psi(2S)$

OTHER DECAYS

$\Gamma(\text{invisible})/\Gamma(e^+e^-)$ Γ_{163}/Γ_6

VALUE	CL%	DOCUMENT ID		TECN	COMMENT
<2.0	90	LEES	13I	BABR	$B \to K^{(*)}\psi(2S)$

$\psi(2S)$ CROSS-PARTICLE BRANCHING RATIOS

For measurements involving $B(\psi(2S) \to \gamma\chi_{cJ}(1P)) \times B(\chi_{cJ}(1P) \to X)$ see the corresponding entries in the $\chi_{cJ}(1P)$ sections.

MULTIPOLE AMPLITUDE RATIOS IN RADIATIVE DECAYS $\psi(2S) \to \gamma\chi_{cJ}(1P)$ and $\chi_{cJ} \to \gamma J/\psi(1S)$

$a_2(\chi_{c1})/a_2(\chi_{c2})$ Magnetic quadrupole transition amplitude ratio

VALUE (units 10^{-2})	EVTS	DOCUMENT ID		TECN	COMMENT
67^{+19}_{-13}	59k	[1] ARTUSO	09	CLEO	$\psi(2S) \to \gamma\gamma\ell^+\ell^-$

[1] Statistical and systematic errors combined. Using values from fits with floating $M2$ amplitudes $a_2(\chi_{c1})$, $a_2(\chi_{c2})$, $b_2(\chi_{c1})$, $b_2(\chi_{c2})$ and fixed $E3$ amplitudes of $a_3(\chi_{c2}) = b_3(\chi_{c2}) = 0$. Not independent of values for $a_2(\chi_{c1}(1P))$ and $a_2(\chi_{c2}(1P))$ from ARTUSO 09.

$b_2(\chi_{c2})/b_2(\chi_{c1})$ Magnetic quadrupole transition amplitude ratio

VALUE (units 10^{-2})	EVTS	DOCUMENT ID		TECN	COMMENT
37^{+53}_{-47}	59k	[1] ARTUSO	09	CLEO	$\psi(2S) \to \gamma\gamma\ell^+\ell^-$

[1] Statistical and systematic errors combined. Using values from fits with floating $M2$ amplitudes $a_2(\chi_{c1})$, $a_2(\chi_{c2})$, $b_2(\chi_{c1})$, $b_2(\chi_{c2})$ and fixed $E3$ amplitudes of $a_3(\chi_{c2}) = b_3(\chi_{c2}) = 0$. Not independent of values for $b_2(\chi_{c1}(1P))$ and $b_2(\chi_{c2}(1P))$ from ARTUSO 09.

$\psi(2S)$ REFERENCES

ABLIKIM	13A	PRL 110 022001	M. Ablikim *et al.*	(BES III Collab.)
ABLIKIM	13D	PR D87 012007	M. Ablikim *et al.*	(BES III Collab.)
ABLIKIM	13F	PR D87 052007	M. Ablikim *et al.*	(BES III Collab.)
ABLIKIM	13M	PR D87 092006	M. Ablikim *et al.*	(BES III Collab.)
ABLIKIM	13R	PR D88 032007	M. Ablikim *et al.*	(BES III Collab.)
ABLIKIM	13S	PR D88 032010	M. Ablikim *et al.*	(BES III Collab.)
ABLIKIM	13W	PR D88 112007	M. Ablikim *et al.*	(BES III Collab.)
LEES	13I	PR D87 112005	J.P. Lees *et al.*	(BABAR Collab.)
LEES	13O	PR D87 092005	J.P. Lees *et al.*	(BABAR Collab.)
LEES	13Q	PR D88 032013	J.P. Lees *et al.*	(BABAR Collab.)
LEES	13Y	PR D88 072009	J.P. Lees *et al.*	(BABAR Collab.)
AAIJ	12H	EPJ C72 1972	R. Aaij *et al.*	(LHCb Collab.)
ABLIKIM	12D	PRL 108 112003	M. Ablikim *et al.*	(BES III Collab.)
ABLIKIM	12G	PRL 109 042003	M. Ablikim *et al.*	(BES III Collab.)
ABLIKIM	12H	PL B710 594	M. Ablikim *et al.*	(BES III Collab.)
ABLIKIM	12L	PR D86 072011	M. Ablikim *et al.*	(BES III Collab.)
ABLIKIM	12M	PR D86 092008	M. Ablikim *et al.*	(BES III Collab.)
ABLIKIM	12O	PRL 109 172002	M. Ablikim *et al.*	(BES III Collab.)
ABLIKIM	12Q	CP C36 1040	M. Ablikim *et al.*	(BES II Collab.)
ANASHIN	12	PL B711 280	V.V. Anashin *et al.*	(KEDR Collab.)
LEES	12E	PR D85 112009	J.P. Lees *et al.*	(BABAR Collab.)
METREVELI	12	PR D85 092007	Z. Metreveli *et al.*	(NWES, FLOR, WAYN+)
GE	11	PR D84 032008	J.Y. Ge *et al.*	(CLEO Collab.)
ABLIKIM	10B	PRL 104 132002	M. Ablikim *et al.*	(BES III Collab.)
ABLIKIM	10F	PRL 105 261801	M. Ablikim *et al.*	(BES III Collab.)
ALEXANDER	10	PR D82 092002	J.P. Alexander *et al.*	(CLEO Collab.)
CRONIN-HEN...	10	PR D81 052002	D. Cronin-Hennessey *et al.*	(CLEO Collab.)
ADAMS	09	PR D80 051106	G.S. Adams *et al.*	(CLEO Collab.)
ARTUSO	09	PR D80 112003	M. Artuso *et al.*	(CLEO Collab.)
LIBBY	09	PR D80 072002	J. Libby *et al.*	(CLEO Collab.)
MITCHELL	09	PRL 102 011801	R.E. Mitchell *et al.*	(CLEO Collab.)
PEDLAR	09	PR D79 111101	T.K. Pedlar *et al.*	(CLEO Collab.)
ABLIKIM	08B	PL B659 74	M. Ablikim *et al.*	(BES Collab.)
ABLIKIM	08C	PL B659 789	M. Ablikim *et al.*	(BES Collab.)
DOBBS	08A	PRL 101 182003	S. Dobbs *et al.*	(CLEO Collab.)
MENDEZ	08	PR D78 011102	H. Mendez *et al.*	(CLEO Collab.)
PDG	08	PL B667 1	C. Amsler *et al.*	(PDG Collab.)
ABLIKIM	07C	PL B648 149	M. Ablikim *et al.*	(BES Collab.)
ABLIKIM	07D	PRL 99 011802	M. Ablikim *et al.*	(BES II Collab.)
ABLIKIM	07H	PR D76 092003	M. Ablikim *et al.*	(BES Collab.)
ANASHIN	07	JETPL 85 347 Translated from ZETFP 85 429.	V.V. Anashin *et al.*	(KEDR Collab.)
ANDREOTTI	07	PL B654 74	M. Andreotti *et al.*	(Femilab E835 Collab.)
AUBERT	07AK	PR D76 012008	B. Aubert *et al.*	(BABAR Collab.)
AUBERT	07AU	PR D76 092005	B. Aubert *et al.*	(BABAR Collab.)
Also		PR D77 119902E (errat.)	B. Aubert *et al.*	(BABAR Collab.)
AUBERT	07BD	PR D76 092006	B. Aubert *et al.*	(BABAR Collab.)
PDG	07	Unofficial 2007 WWW edition		(PDG Collab.)
PEDLAR	07	PR D75 011102	T.K. Pedlar *et al.*	(CLEO Collab.)
ABLIKIM	06G	PR D73 052004	M. Ablikim *et al.*	(BES Collab.)
ABLIKIM	06I	PR D74 012004	M. Ablikim *et al.*	(BES Collab.)
ABLIKIM	06L	PRL 97 121801	M. Ablikim *et al.*	(BES Collab.)
ABLIKIM	06R	PR D74 072001	M. Ablikim *et al.*	(BES Collab.)
ABLIKIM	06W	PR D74 112003	M. Ablikim *et al.*	(BES Collab.)
ADAM	06	PRL 96 082004	N.E. Adam *et al.*	(CLEO Collab.)
AUBERT	06B	PR D73 012005	B. Aubert *et al.*	(BABAR Collab.)
AUBERT	06D	PR D73 052003	B. Aubert *et al.*	(BABAR Collab.)
AUBERT,BE	06D	PR D74 091103	B. Aubert *et al.*	(BABAR Collab.)
DOBBS	06A	PR D74 011105	S. Dobbs *et al.*	(CLEO Collab.)
ABLIKIM	05E	PR D71 072006	M. Ablikim *et al.*	(BES Collab.)
ABLIKIM	05H	PR D72 012002	M. Ablikim *et al.*	(BES Collab.)
ABLIKIM	05I	PL B614 37	M. Ablikim *et al.*	(BES Collab.)
ABLIKIM	05J	PL B619 247	M. Ablikim *et al.*	(BES Collab.)
ABLIKIM	05O	PL B630 21	M. Ablikim *et al.*	(BES Collab.)
ADAM	05	PRL 94 012005	N.E. Adam *et al.*	(CLEO Collab.)
ADAM	05A	PRL 94 232002	N.E. Adam *et al.*	(CLEO Collab.)
ANDREOTTI	05	PR D71 032006	M. Andreotti *et al.*	(FNAL E835 Collab.)
AUBERT	05D	PR D71 052001	B. Aubert *et al.*	(BABAR Collab.)
BRIERE	05	PRL 95 062001	R.A. Briere *et al.*	(CLEO Collab.)
PEDLAR	05	PR D72 051108	T.K. Pedlar *et al.*	(CLEO Collab.)
ROSNER	05	PRL 95 102003	J.L. Rosner *et al.*	(CLEO Collab.)
ABLIKIM	04B	PR D70 012003	M. Ablikim *et al.*	(BES Collab.)
ABLIKIM	04K	PR D70 112003	M. Ablikim *et al.*	(BES Collab.)
ABLIKIM	04L	PR D70 112007	M. Ablikim *et al.*	(BES Collab.)
ATHAR	04	PR D70 112002	S.B. Athar *et al.*	(CLEO Collab.)
BAI	04B	PRL 92 052001	J.Z. Bai *et al.*	(BES Collab.)
BAI	04C	PR D69 072001	J.Z. Bai *et al.*	(BES Collab.)
BAI	04D	PL B589 7	J.Z. Bai *et al.*	(BES Collab.)
BAI	04G	PR D70 012004	J.Z. Bai *et al.*	(BES Collab.)
BAI	04I	PR D70 012006	J.Z. Bai *et al.*	(BES Collab.)
PDG	04	PL B592 1	S. Eidelman *et al.*	(PDG Collab.)
SETH	04	PR D69 097503	K.K. Seth	

Meson Particle Listings

$\psi(2S)$, $\psi(3770)$

AULCHENKO	03	PL B573 63	V.M. Aulchenko *et al.*	(KEDR Collab.)
BAI	03B	PR D67 052002	J.Z. Bai *et al.*	(BES Collab.)
BAI	03C	PR D67 032004	J.Z. Bai *et al.*	(BES Collab.)
AUBERT	02B	PR D65 031101	B. Aubert *et al.*	(BaBar Collab.)
BAI	02	PR D65 052004	J.Z. Bai *et al.*	(BES Collab.)
BAI	02B	PL B550 24	J.Z. Bai *et al.*	(BES Collab.)
BAI	02C	PRL 88 101802	J.Z. Bai *et al.*	(BES Collab.)
PDG	02	PR D66 010001	K. Hagiwara *et al.*	
BAI	01	PR D63 032002	J.Z. Bai *et al.*	(BES Collab.)
AMBROGIANI	00A	PR D62 032004	M. Ambrogiani *et al.*	(FNAL E835 Collab.)
ARTAMONOV	00	PL B474 427	A.S. Artamonov *et al.*	
BAI	00	PRL 84 594	J.Z. Bai *et al.*	(BES Collab.)
BAI	99C	PRL 83 1918	J.Z. Bai *et al.*	(BES Collab.)
BAI	98E	PR D57 3854	J.Z. Bai *et al.*	(BES Collab.)
BAI	98F	PR D58 097101	J.Z. Bai *et al.*	(BES Collab.)
BAI	98J	PRL 81 5080	J.Z. Bai *et al.*	(BES Collab.)
ARMSTRONG	97	PR D55 1153	T.A. Armstrong *et al.*	(E760 Collab.)
GRIBUSHIN	96	PR D53 4723	A. Gribushin *et al.*	(E672 Collab., E706 Collab.)
ARMSTRONG	93B	PR D47 772	T.A. Armstrong *et al.*	(FNAL E760 Collab.)
ALEXANDER	89	NP B320 45	J.P. Alexander *et al.*	(LBL, MICH, SLAC)
COHEN	87	RMP 59 1121	E.R. Cohen, B.N. Taylor	(RISC, NBS)
GAISER	86	PR D34 711	J. Gaiser *et al.*	(Crystal Ball Collab.)
KURAEV	85	SJNP 41 466	E.A. Kuraev, V.S. Fadin	(NOVO)
		Translated from YAF 41 733.		
FRANKLIN	83	PRL 51 963	M.E.B. Franklin *et al.*	(LBL, SLAC)
EDWARDS	82C	PRL 48 70	C. Edwards *et al.*	(CIT, HARV, PRIN+)
LEMOIGNE	82	PL 113B 509	Y. Lemoigne *et al.*	(SACL, LOIC, SHMP+)
HIMEL	80	PRL 44 920	T. Himel *et al.*	(LBL, SLAC)
OREGLIA	80	PRL 45 959	M.J. Oreglia *et al.*	(SLAC, CIT, HARV+)
SCHARRE	80	PL 97B 329	D.L. Scharre *et al.*	(SLAC, LBL)
ZHOLENTZ	80	PL 96B 214	A.A. Zholents *et al.*	(NOVO)
Also		SJNP 34 814	A.A. Zholents *et al.*	(NOVO)
		Translated from YAF 34 1471.		
BRANDELIK	79B	NP B160 426	R. Brandelik *et al.*	(DASP Collab.)
BRANDELIK	79C	ZPHY C1 233	R. Brandelik *et al.*	(DASP Collab.)
BARTEL	78B	PL 79B 492	W. Bartel *et al.*	(DESY, HEIDP)
TANENBAUM	78	PR D17 1731	W.M. Tanenbaum *et al.*	(SLAC, LBL)
BIDDICK	77	PRL 38 1324	C.J. Biddick *et al.*	(UCSD, UMD, PAVI+)
BRAUNSCH...	77	PL 67B 249	W. Braunschweig *et al.*	(DASP Collab.)
BURMESTER	77	PL 66B 395	J. Burmester *et al.*	(DESY, HAMB, SIEG+)
FELDMAN	77	PRPL 33C 285	G.J. Feldman, M.L. Perl	(LBL, SLAC)
YAMADA	77	Hamburg Conf. 69	S. Yamada	(DASP Collab.)
BARTEL	76	PL 64B 483	W. Bartel *et al.*	(DESY, HEIDP)
TANENBAUM	76	PRL 36 402	W.M. Tanenbaum *et al.*	(SLAC, LBL) IG
WHITAKER	76	PRL 37 1596	J.S. Whitaker *et al.*	(SLAC, LBL)
ABRAMS	75	Stanford Symp. 25	G.S. Abrams	(LBL)
ABRAMS	75B	PRL 34 1181	G.S. Abrams *et al.*	(LBL, SLAC)
BOYARSKI	75C	Palermo Conf. 54	A.M. Boyarski *et al.*	(SLAC, LBL)
HILGER	75	PRL 35 625	E. Hilger *et al.*	(STAN, PENN)
LIBERMAN	75	Stanford Symp. 55	A.D. Liberman	(STAN)
LUTH	75	PRL 35 1124	V. Luth *et al.*	(SLAC, LBL) JPC
WIIK	75	Stanford Symp. 69	B.H. Wiik	(DESY)

$\psi(3770)$

$I^G(J^{PC}) = 0^-(1^{--})$

$\psi(3770)$ MASS (MeV)

OUR FIT includes measurements of $m_{\psi(2S)}$, $m_{\psi(3770)}$, and $m_{\psi(3770)} - m_{\psi(2S)}$.

VALUE (MeV)	EVTS	DOCUMENT ID		TECN	COMMENT
3773.15±0.33 OUR FIT					
3778.1 ±1.2 OUR AVERAGE					
$3779.2\ ^{+1.8}_{-1.7}\ ^{+0.6}_{-0.8}$		[1] ANASHIN	12A	KEDR	$e^+e^- \to D\overline{D}$
3775.5 ±2.4 ±0.5	57	AUBERT	08B	BABR	$B \to D\overline{D}K$
3776 ±5 ±4	68	BRODZICKA	08	BELL	$B^+ \to D^0\overline{D}^0K^+$
3778.8 ±1.9 ±0.9		AUBERT	07BE	BABR	$e^+e^- \to D\overline{D}\gamma$
• • • We do not use the following data for averages, fits, limits, etc. • • •					
3772.0 ±1.9		[2,3] ABLIKIM	08D	BES2	$e^+e^- \to$ hadrons
3778.4 ±3.0 ±1.3	34	CHISTOV	04	BELL	Sup. by BRODZICKA 08

[1] Taking into account interference between the resonant and non-resonant $D\overline{D}$ production.
[2] Reanalysis of data presented in BAI 02C. From a global fit over the center-of-mass energy region 3.7–5.0 GeV covering the $\psi(3770)$, $\psi(4040)$, $\psi(4160)$, and $\psi(4415)$ resonances. Phase angle fixed in the fit to $\delta = 0^\circ$.
[3] Interference between the resonant and non-resonant $D\overline{D}$ production not taken into account.

$m_{\psi(3770)} - m_{\psi(2S)}$

OUR FIT includes measurements of $m_{\psi(2S)}$, $m_{\psi(3770)}$, and $m_{\psi(3770)} - m_{\psi(2S)}$.

VALUE (MeV)	DOCUMENT ID		TECN	COMMENT
87.04±0.33 OUR FIT				
86.6 ±0.7 OUR AVERAGE	Error includes scale factor of 2.0. See the ideogram below.			
86.9 ±0.4	[4] ABLIKIM	07E	BES2	$e^+e^- \to$ hadrons
86.7 ±0.7	ABLIKIM	06L	BES2	$e^+e^- \to$ hadrons
80 ±2	SCHINDLER	80	MRK2	e^+e^-
86 ±2	[5] BACINO	78	DLCO	e^+e^-
88 ±3	RAPIDIS	77	LGW	e^+e^-

[4] BES-II $\psi(2S)$ mass subtracted (see ABLIKIM 06L).
[5] SPEAR $\psi(2S)$ mass subtracted (see SCHINDLER 80).

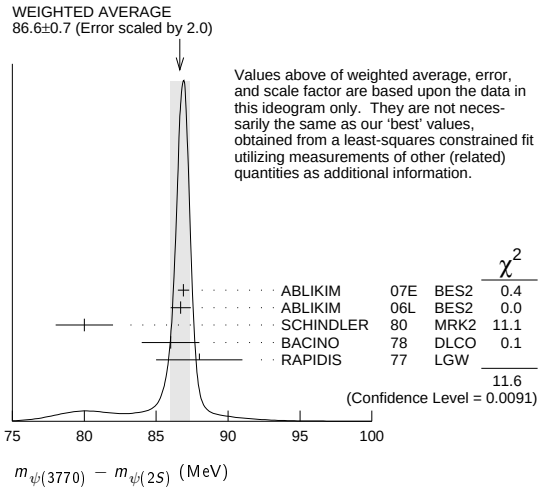

$\psi(3770)$ WIDTH

VALUE (MeV)	EVTS	DOCUMENT ID		TECN	COMMENT
27.2± 1.0 OUR FIT					
27.5± 0.9 OUR AVERAGE					
$24.9\ ^{+\ 4.6+0.5}_{-\ 4.0-1.1}$		[6] ANASHIN	12A	KEDR	$e^+e^- \to D\overline{D}$
30.4± 8.5		[7,8] ABLIKIM	08D	BES2	$e^+e^- \to$ hadrons
27 ±10 ±5	68	BRODZICKA	08	BELL	$B^+ \to D^0\overline{D}^0K^+$
28.5± 1.2±0.2		[8] ABLIKIM	07E	BES2	$e^+e^- \to$ hadrons
23.5± 3.7±0.9		AUBERT	07BE	BABR	$e^+e^- \to D\overline{D}\gamma$
26.9± 2.4±0.3		[8] ABLIKIM	06L	BES2	$e^+e^- \to$ hadrons
24 ± 5		[8] SCHINDLER	80	MRK2	e^+e^-
24 ± 5		[8] BACINO	78	DLCO	e^+e^-
28 ± 5		[8] RAPIDIS	77	LGW	e^+e^-

[6] Taking into account interference between the resonant and non-resonant $D\overline{D}$ production.
[7] Reanalysis of data presented in BAI 02C. From a global fit over the center-of-mass energy region 3.7–5.0 GeV covering the $\psi(3770)$, $\psi(4040)$, $\psi(4160)$, and $\psi(4415)$ resonances. Phase angle fixed in the fit to $\delta = 0^\circ$.
[8] Interference between the resonant and non-resonant $D\overline{D}$ production not taken into account.

$\psi(3770)$ DECAY MODES

In addition to the dominant decay mode to $D\overline{D}$, $\psi(3770)$ was found to decay into the final states containing the J/ψ (BAI 05, ADAM 06). ADAMS 06 and HUANG 06A searched for various decay modes with light hadrons and found a statistically significant signal for the decay to $\phi\eta$ only (ADAMS 06).

	Mode	Fraction (Γ_i/Γ)	Scale factor/ Confidence level
Γ_1	$D\overline{D}$	$(93\ ^{+8}_{-9})$ %	S=2.0
Γ_2	$D^0\overline{D}^0$	(52 ±5) %	S=2.0
Γ_3	D^+D^-	(41 ±4) %	S=2.0
Γ_4	$J/\psi\pi^+\pi^-$	$(1.93\pm0.28)\times10^{-3}$	
Γ_5	$J/\psi\pi^0\pi^0$	$(8.0\pm3.0)\times10^{-4}$	
Γ_6	$J/\psi\eta$	$(9\pm4)\times10^{-4}$	
Γ_7	$J/\psi\pi^0$	$<2.8\times10^{-4}$	CL=90%
Γ_8	e^+e^-	$(9.6\pm0.7)\times10^{-6}$	S=1.3
	Decays to light hadrons		
Γ_9	$b_1(1235)\pi$	$<1.4\times10^{-5}$	CL=90%
Γ_{10}	$\phi\eta'$	$<7\times10^{-4}$	CL=90%
Γ_{11}	$\omega\eta'$	$<4\times10^{-4}$	CL=90%
Γ_{12}	$\rho^0\eta'$	$<6\times10^{-4}$	CL=90%
Γ_{13}	$\phi\eta$	$(3.1\pm0.7)\times10^{-4}$	
Γ_{14}	$\omega\eta$	$<1.4\times10^{-5}$	CL=90%
Γ_{15}	$\rho^0\eta$	$<5\times10^{-4}$	CL=90%
Γ_{16}	$\phi\pi^0$	$<3\times10^{-5}$	CL=90%
Γ_{17}	$\omega\pi^0$	$<6\times10^{-4}$	CL=90%
Γ_{18}	$\pi^+\pi^-\pi^0$	$<5\times10^{-6}$	CL=90%
Γ_{19}	$\rho\pi$	$<5\times10^{-6}$	CL=90%
Γ_{20}	$K^*(892)^+K^-$ + c.c.	$<1.4\times10^{-5}$	CL=90%
Γ_{21}	$K^*(892)^0\overline{K}^0$ + c.c.	$<1.2\times10^{-3}$	CL=90%
Γ_{22}	$K^0_SK^0_L$	$<1.2\times10^{-5}$	CL=90%
Γ_{23}	$2(\pi^+\pi^-)$	$<1.12\times10^{-3}$	CL=90%
Γ_{24}	$2(\pi^+\pi^-)\pi^0$	$<1.06\times10^{-3}$	CL=90%
Γ_{25}	$2(\pi^+\pi^-\pi^0)$	<5.85 %	CL=90%

Γ_{26}	$\omega\pi^+\pi^-$	<	6.0	$\times10^{-4}$	CL=90%
Γ_{27}	$3(\pi^+\pi^-)$	<	9.1	$\times10^{-3}$	
Γ_{28}	$3(\pi^+\pi^-)\pi^0$	<	1.37	%	
Γ_{29}	$3(\pi^+\pi^-)2\pi^0$	<	11.74	%	CL=90%
Γ_{30}	$\eta\pi^+\pi^-$	<	1.24	$\times10^{-3}$	CL=90%
Γ_{31}	$\pi^+\pi^-2\pi^0$	<	8.9	$\times10^{-3}$	CL=90%
Γ_{32}	$\rho^0\pi^+\pi^-$	<	6.9	$\times10^{-3}$	CL=90%
Γ_{33}	$\eta3\pi$	<	1.34	$\times10^{-3}$	CL=90%
Γ_{34}	$\eta2(\pi^+\pi^-)$	<	2.43	%	
Γ_{35}	$\eta\rho^0\pi^+\pi^-$	<	1.45	%	CL=90%
Γ_{36}	$\eta'3\pi$	<	2.44	$\times10^{-3}$	CL=90%
Γ_{37}	$K^+K^-\pi^+\pi^-$	<	9.0	$\times10^{-4}$	CL=90%
Γ_{38}	$\phi\pi^+\pi^-$	<	4.1	$\times10^{-4}$	CL=90%
Γ_{39}	$K^+K^-2\pi^0$	<	4.2	$\times10^{-3}$	CL=90%
Γ_{40}	$4(\pi^+\pi^-)$	<	1.67	%	CL=90%
Γ_{41}	$4(\pi^+\pi^-)\pi^0$	<	3.06	%	CL=90%
Γ_{42}	$\phi f_0(980)$	<	4.5	$\times10^{-4}$	CL=90%
Γ_{43}	$K^+K^-\pi^+\pi^-\pi^0$	<	2.36	$\times10^{-3}$	CL=90%
Γ_{44}	$K^+K^-\rho^0\pi^0$	<	8	$\times10^{-4}$	CL=90%
Γ_{45}	$K^+K^-\rho^+\pi^-$	<	1.46	%	CL=90%
Γ_{46}	ωK^+K^-	<	3.4	$\times10^{-4}$	CL=90%
Γ_{47}	$\phi\pi^+\pi^-\pi^0$	<	3.8	$\times10^{-3}$	CL=90%
Γ_{48}	$K^{*0}K^-\pi^+\pi^0$ + c.c.	<	1.62	%	CL=90%
Γ_{49}	$K^{*+}K^-\pi^+\pi^-$ + c.c.	<	3.23	%	CL=90%
Γ_{50}	$K^+K^-\pi^+\pi^-2\pi^0$	<	2.67	%	CL=90%
Γ_{51}	$K^+K^-2(\pi^+\pi^-)$	<	1.03	%	CL=90%
Γ_{52}	$K^+K^-2(\pi^+\pi^-)\pi^0$	<	3.60	%	CL=90%
Γ_{53}	ηK^+K^-	<	4.1	$\times10^{-4}$	CL=90%
Γ_{54}	$\eta K^+K^-\pi^+\pi^-$	<	1.24	%	CL=90%
Γ_{55}	$\rho^0K^+K^-$	<	5.0	$\times10^{-3}$	CL=90%
Γ_{56}	$2(K^+K^-)$	<	6.0	$\times10^{-4}$	CL=90%
Γ_{57}	ϕK^+K^-	<	7.5	$\times10^{-4}$	CL=90%
Γ_{58}	$2(K^+K^-)\pi^0$	<	2.9	$\times10^{-4}$	CL=90%
Γ_{59}	$2(K^+K^-)\pi^+\pi^-$	<	3.2	$\times10^{-3}$	CL=90%
Γ_{60}	$K^0_S K^-\pi^+$	<	3.2	$\times10^{-3}$	CL=90%
Γ_{61}	$K^0_S K^-\pi^+\pi^0$	<	1.33	%	CL=90%
Γ_{62}	$K^0_S K^-\rho^+$	<	6.6	$\times10^{-3}$	CL=90%
Γ_{63}	$K^0_S K^-2\pi^+\pi^-$	<	8.7	$\times10^{-3}$	CL=90%
Γ_{64}	$K^0_S K^-\pi^+\rho^0$	<	1.6	%	CL=90%
Γ_{65}	$K^0_S K^-\pi^+\eta$	<	1.3	%	CL=90%
Γ_{66}	$K^0_S K^-2\pi^+\pi^-\pi^0$	<	4.18	%	CL=90%
Γ_{67}	$K^0_S K^-2\pi^+\pi^-\eta$	<	4.8	%	CL=90%
Γ_{68}	$K^0_S K^-\pi^+2(\pi^+\pi^-)$	<	1.22	%	CL=90%
Γ_{69}	$K^0_S K^-\pi^+2\pi^0$	<	2.65	%	CL=90%
Γ_{70}	$K^0_S K^-K^+K^-\pi^+$	<	4.9	$\times10^{-3}$	CL=90%
Γ_{71}	$K^0_S K^-K^+K^-\pi^+\pi^0$	<	3.0	%	CL=90%
Γ_{72}	$K^0_S K^-K^+K^-\pi^+\eta$	<	2.2	%	CL=90%
Γ_{73}	$K^{*0}K^-\pi^+$ + c.c.	<	9.7	$\times10^{-3}$	CL=90%
Γ_{74}	$p\overline{p}\pi^0$	<	1.2	$\times10^{-3}$	
Γ_{75}	$p\overline{p}\pi^+\pi^-$	<	5.8	$\times10^{-4}$	CL=90%
Γ_{76}	$\Lambda\overline{\Lambda}$	<	1.2	$\times10^{-4}$	CL=90%
Γ_{77}	$p\overline{p}\pi^+\pi^-\pi^0$	<	1.85	$\times10^{-3}$	CL=90%
Γ_{78}	$\omega p\overline{p}$	<	2.9	$\times10^{-4}$	CL=90%
Γ_{79}	$\Lambda\overline{\Lambda}\pi^0$	<	7	$\times10^{-5}$	CL=90%
Γ_{80}	$p\overline{p}2(\pi^+\pi^-)$	<	2.6	$\times10^{-3}$	CL=90%
Γ_{81}	$\eta p\overline{p}$	<	5.4	$\times10^{-4}$	CL=90%
Γ_{82}	$\eta p\overline{p}\pi^+\pi^-$	<	3.3	$\times10^{-3}$	CL=90%
Γ_{83}	$\rho^0 p\overline{p}$	<	1.7	$\times10^{-3}$	CL=90%
Γ_{84}	$p\overline{p}K^+K^-$	<	3.2	$\times10^{-4}$	CL=90%
Γ_{85}	$\eta p\overline{p}K^+K^-$	<	6.9	$\times10^{-3}$	CL=90%
Γ_{86}	$\pi^0 p\overline{p}K^+K^-$	<	1.2	$\times10^{-3}$	CL=90%
Γ_{87}	$\phi p\overline{p}$	<	1.3	$\times10^{-4}$	CL=90%
Γ_{88}	$\Lambda\overline{\Lambda}\pi^+\pi^-$	<	2.5	$\times10^{-4}$	CL=90%
Γ_{89}	$\Lambda\overline{p}K^+$	<	2.8	$\times10^{-4}$	CL=90%
Γ_{90}	$\Lambda\overline{p}K^+\pi^+\pi^-$	<	6.3	$\times10^{-4}$	CL=90%
Γ_{91}	$\Lambda\overline{\Lambda}\eta$	<	1.9	$\times10^{-4}$	CL=90%
Γ_{92}	$\Sigma^+\overline{\Sigma}^-$	<	1.0	$\times10^{-4}$	CL=90%
Γ_{93}	$\Sigma^0\overline{\Sigma}^0$	<	4	$\times10^{-5}$	CL=90%
Γ_{94}	$\Xi^+\overline{\Xi}^-$	<	1.5	$\times10^{-4}$	CL=90%
Γ_{95}	$\Xi^0\overline{\Xi}^0$	<	1.4	$\times10^{-4}$	CL=90%

Radiative decays

Γ_{96}	$\gamma\chi_{c2}$	<	9	$\times10^{-4}$	CL=90%
Γ_{97}	$\gamma\chi_{c1}$	(	2.9 ±0.6)	$\times10^{-3}$	
Γ_{98}	$\gamma\chi_{c0}$	(	7.3 ±0.9)	$\times10^{-3}$	
Γ_{99}	$\gamma\eta'$	<	1.8	$\times10^{-4}$	CL=90%
Γ_{100}	$\gamma\eta$	<	1.5	$\times10^{-4}$	CL=90%
Γ_{101}	$\gamma\pi^0$	<	2	$\times10^{-4}$	CL=90%

CONSTRAINED FIT INFORMATION

An overall fit to the total width, a partial width, and 3 branching ratios uses 23 measurements and one constraint to determine 5 parameters. The overall fit has a $\chi^2 = 20.0$ for 19 degrees of freedom.

The following *off-diagonal* array elements are the correlation coefficients $\langle\delta p_i\delta p_j\rangle/(\delta p_i\cdot\delta p_j)$, in percent, from the fit to parameters p_i, including the branching fractions, $x_i \equiv \Gamma_i/\Gamma_{\rm total}$. The fit constrains the x_i whose labels appear in this array to sum to one.

x_3	98		
x_8	0	0	
Γ	0	0	−44
	x_2	x_3	x_8

	Mode	Rate (MeV)	Scale factor
Γ_2	$D^0\overline{D}^0$	14.1 ±1.4	1.7
Γ_3	D^+D^-	11.2 ±1.1	1.7
Γ_8	e^+e^-	(2.62±0.18) $\times10^{-4}$	1.4

$\psi(3770)$ PARTIAL WIDTHS

$\Gamma(e^+e^-)$ Γ_8

VALUE (keV)	EVTS	DOCUMENT ID		TECN	COMMENT
0.262±0.018 OUR FIT	Error includes scale factor of 1.4.				
0.256±0.016 OUR AVERAGE	Error includes scale factor of 1.2.				
$0.154^{+0.079}_{-0.058}\pm0.021$		[9,10] ANASHIN	12A	KEDR	$e^+e^-\to D\overline{D}$
0.22 ±0.05		[11,12] ABLIKIM	08D	BES2	$e^+e^-\to$ hadrons
0.277±0.011±0.013		[12] ABLIKIM	07E	BES2	$e^+e^-\to$ hadrons
$0.203\pm0.003^{+0.041}_{-0.027}$	1.4M	[12,13] BESSON	06	CLEO	$e^+e^-\to$ hadrons
0.276±0.050		[12] SCHINDLER	80	MRK2	e^+e^-
0.18 ±0.06		[12] BACINO	78	DLCO	e^+e^-
• • • We do not use the following data for averages, fits, limits, etc. • • •					
$0.414^{+0.072}_{-0.080}\pm0.093$		[10,14] ANASHIN	12A	KEDR	$e^+e^-\to D\overline{D}$
0.37 ±0.09		[15] RAPIDIS	77	LGW	e^+e^-

[9] Solution I of the two solutions.
[10] Taking into account interference between the resonant and non-resonant $D\overline{D}$ production.
[11] Reanalysis of data presented in BAI 02C. From a global fit over the center-of-mass energy region 3.7–5.0 GeV covering the $\psi(3770)$, $\psi(4040)$, $\psi(4160)$, and $\psi(4415)$ resonances. Phase angle fixed in the fit to $\delta = 0^\circ$.
[12] Interference between the resonant and non-resonant $D\overline{D}$ production not taken into account.
[13] BESSON 06 (as corrected in BESSON 10) measure $\sigma(e^+e^-\to\psi(3770)\to$ hadrons) $= 6.36 \pm 0.08^{+0.41}_{-0.30}$ nb at $\sqrt{s} = 3773 \pm 1$ MeV, and obtain Γ_{ee} from the Born-level cross section calculated using $\psi(3770)$ mass and width from our 2004 edition, PDG 04.
[14] Solution II of the two solutions.
[15] See also $\Gamma(e^+e^-)/\Gamma_{\rm total}$ below.

$\psi(3770)$ BRANCHING RATIOS

$\Gamma(D\overline{D})/\Gamma_{\rm total}$ $\Gamma_1/\Gamma = (\Gamma_2+\Gamma_3)/\Gamma$

VALUE	EVTS	DOCUMENT ID		TECN	COMMENT
0.93 $^{+0.08}_{-0.09}$ OUR FIT	Error includes scale factor of 2.0.				
0.93 $^{+0.08}_{-0.09}$ OUR AVERAGE	Error includes scale factor of 2.1.				
0.849±0.056±0.018		[16] ABLIKIM	08B	BES2	$e^+e^-\to$ non-$D\overline{D}$
$1.033\pm0.014^{+0.048}_{-0.066}$	1.427M	[17] BESSON	06	CLEO	$e^+e^-\to$ hadrons
• • • We do not use the following data for averages, fits, limits, etc. • • •					
0.866±0.050±0.036		[18,19] ABLIKIM	07K	BES2	$e^+e^-\to$ non-$D\overline{D}$
0.836±0.073±0.042		[19] ABLIKIM	06L	BES2	$e^+e^-\to D\overline{D}$
0.855±0.017±0.058		[19,20] ABLIKIM	06N	BES2	$e^+e^-\to D\overline{D}$

$\Gamma(D^0\overline{D}^0)/\Gamma_{\rm total}$ Γ_2/Γ

VALUE	DOCUMENT ID		TECN	COMMENT
0.52 ±0.05 OUR FIT	Error includes scale factor of 2.0.			
• • • We do not use the following data for averages, fits, limits, etc. • • •				
0.467±0.047±0.023	ABLIKIM	06L	BES2	$e^+e^-\to D^0\overline{D}^0$
0.499±0.013±0.038	[20] ABLIKIM	06N	BES2	$e^+e^-\to D^0\overline{D}^0$

Meson Particle Listings

$\psi(3770)$

$\Gamma(D^+D^-)/\Gamma_{total}$ Γ_3/Γ

VALUE	DOCUMENT ID		TECN	COMMENT
0.41 ±0.04 OUR FIT Error includes scale factor of 2.0.				
• • • We do not use the following data for averages, fits, limits, etc. • • •				
0.369±0.037±0.028	ABLIKIM	06L	BES2	$e^+e^- \to D^+D^-$
0.357±0.011±0.034 [20]	ABLIKIM	06N	BES2	$e^+e^- \to D^+D^-$

$\Gamma(D^0\overline{D}^0)/\Gamma(D^+D^-)$ Γ_2/Γ_3

VALUE	EVTS	DOCUMENT ID		TECN	COMMENT
1.260±0.021 OUR FIT					
1.260±0.021 OUR AVERAGE					
1.39 ±0.31 ±0.12		PAKHLOVA	08	BELL	10.6 $e^+e^- \to D\overline{D}\gamma$
1.78 ±0.33 ±0.24		AUBERT	07BE	BABR	$e^+e^- \to D\overline{D}\gamma$
1.258±0.016±0.014		DOBBS	07	CLEO	$e^+e^- \to D\overline{D}$
1.27 ±0.12 ±0.08		ABLIKIM	06L	BES2	$e^+e^- \to D\overline{D}$
2.43 ±1.50 ±0.43	34	[21] CHISTOV	04	BELL	$B^+ \to \psi(3770)K^+$

$\Gamma(J/\psi\pi^+\pi^-)/\Gamma_{total}$ Γ_4/Γ

VALUE (units 10^{-3})	EVTS	DOCUMENT ID		TECN	COMMENT
1.93±0.28 OUR AVERAGE					
1.89±0.20±0.20	231 ± 33	ADAM	06	CLEO	$e^+e^- \to \psi(3770)$
3.4 ±1.4 ±0.9	17.8 ± 4.8	BAI	05	BES2	$e^+e^- \to \psi(3770)$

$\Gamma(J/\psi\pi^0\pi^0)/\Gamma_{total}$ Γ_5/Γ

VALUE (units 10^{-2})	EVTS	DOCUMENT ID		TECN	COMMENT
0.080±0.025±0.016	39 ± 14	ADAM	06	CLEO	$e^+e^- \to \psi(3770)$

$\Gamma(J/\psi\eta)/\Gamma_{total}$ Γ_6/Γ

VALUE (units 10^{-5})	EVTS	DOCUMENT ID		TECN	COMMENT
87±33±22	22 ± 10	ADAM	06	CLEO	$e^+e^- \to \psi(3770)$

$\Gamma(J/\psi\pi^0)/\Gamma_{total}$ Γ_7/Γ

VALUE (units 10^{-5})	CL%	EVTS	DOCUMENT ID		TECN	COMMENT
<28	90	<10	ADAM	06	CLEO	$e^+e^- \to \psi(3770)$

$\Gamma(e^+e^-)/\Gamma_{total}$ Γ_8/Γ

VALUE (units 10^{-5})	DOCUMENT ID		TECN	COMMENT
0.96±0.07 OUR FIT Error includes scale factor of 1.3.				
1.3 ±0.2	RAPIDIS	77	LGW	e^+e^-

[16] Neglecting interference.
[17] Obtained by comparing a measurement of the total cross section (corrected in BESSON 10) with that of $D\overline{D}$ reported by CLEO in DOBBS 07.
[18] Using $\sigma^{obs} = 7.07 \pm 0.58$ nb and neglecting interference.
[19] Not independent of ABLIKIM 08B.
[20] From a measurement of $\sigma(e^+e^- \to D\overline{D})$ at $\sqrt{s} = 3773$ MeV, using the $\psi(3770)$ resonance parameters measured by ABLIKIM 06L.
[21] See ADLER 88C for older measurements of this quantity.

DECAYS TO LIGHT HADRONS

$\Gamma(b_1(1235)\pi)/\Gamma_{total}$ Γ_9/Γ

VALUE (units 10^{-5})	CL%	DOCUMENT ID		TECN	COMMENT
<1.4	90	[22] ADAMS	06	CLEO	$e^+e^- \to \psi(3770)$

$\Gamma(\phi\eta')/\Gamma_{total}$ Γ_{10}/Γ

VALUE (units 10^{-4})	CL%	DOCUMENT ID		TECN	COMMENT
<7	90	[22] ADAMS	06	CLEO	$e^+e^- \to \psi(3770)$

$\Gamma(\omega\eta')/\Gamma_{total}$ Γ_{11}/Γ

VALUE (units 10^{-4})	CL%	DOCUMENT ID		TECN	COMMENT
<4	90	[22] ADAMS	06	CLEO	$e^+e^- \to \psi(3770)$

$\Gamma(\rho^0\eta')/\Gamma_{total}$ Γ_{12}/Γ

VALUE (units 10^{-4})	CL%	DOCUMENT ID		TECN	COMMENT
<6	90	[22] ADAMS	06	CLEO	$e^+e^- \to \psi(3770)$

$\Gamma(\phi\eta)/\Gamma_{total}$ Γ_{13}/Γ

VALUE (units 10^{-4})	DOCUMENT ID		TECN	COMMENT
3.1±0.6±0.3	[22] ADAMS	06	CLEO	3.773 $e^+e^- \to \phi\eta$
• • • We do not use the following data for averages, fits, limits, etc. • • •				
<19	[23] ABLIKIM	07B	BES2	$e^+e^- \to \psi(3770)$

$\Gamma(\omega\eta)/\Gamma_{total}$ Γ_{14}/Γ

VALUE (units 10^{-5})	CL%	DOCUMENT ID		TECN	COMMENT
<1.4	90	[22] ADAMS	06	CLEO	$e^+e^- \to \psi(3770)$

$\Gamma(\rho^0\eta)/\Gamma_{total}$ Γ_{15}/Γ

VALUE (units 10^{-4})	CL%	DOCUMENT ID		TECN	COMMENT
<5	90	[22] ADAMS	06	CLEO	$e^+e^- \to \psi(3770)$

$\Gamma(\phi\pi^0)/\Gamma_{total}$ Γ_{16}/Γ

VALUE (units 10^{-5})	CL%	DOCUMENT ID		TECN	COMMENT
< 3	90	[22] ADAMS	06	CLEO	$e^+e^- \to \psi(3770)$
• • • We do not use the following data for averages, fits, limits, etc. • • •					
<50		[23] ABLIKIM	07B	BES2	$e^+e^- \to \psi(3770)$

$\Gamma(\omega\pi^0)/\Gamma_{total}$ Γ_{17}/Γ

VALUE (units 10^{-4})	CL%	DOCUMENT ID		TECN	COMMENT
<6	90	[22] ADAMS	06	CLEO	$e^+e^- \to \psi(3770)$

$\Gamma(\pi^+\pi^-\pi^0)/\Gamma_{total}$ Γ_{18}/Γ

VALUE (units 10^{-6})	CL%	DOCUMENT ID		TECN	COMMENT
<5	90	[22,24] ADAMS	06	CLEO	$e^+e^- \to \psi(3770)$

$\Gamma(\rho\pi)/\Gamma_{total}$ Γ_{19}/Γ

VALUE (units 10^{-6})	CL%	DOCUMENT ID		TECN	COMMENT
<5	90	[22,24] ADAMS	06	CLEO	$e^+e^- \to \psi(3770)$

$\Gamma(K^*(892)^+K^- + \text{c.c.})/\Gamma_{total}$ Γ_{20}/Γ

VALUE (units 10^{-5})	CL%	DOCUMENT ID		TECN	COMMENT
<1.4	90	[22] ADAMS	06	CLEO	$e^+e^- \to \psi(3770)$

$\Gamma(K^*(892)^0\overline{K}^0 + \text{c.c.})/\Gamma_{total}$ Γ_{21}/Γ

VALUE (units 10^{-3})	CL%	DOCUMENT ID		TECN	COMMENT
<1.2	90	[22] ADAMS	06	CLEO	$e^+e^- \to \psi(3770)$

$\Gamma(K^0_S K^0_L)/\Gamma_{total}$ Γ_{22}/Γ

VALUE (units 10^{-5})	CL%	DOCUMENT ID		TECN	COMMENT
< 1.2	90	[25] CRONIN-HEN..06		CLEO	$e^+e^- \to \psi(3770)$
• • • We do not use the following data for averages, fits, limits, etc. • • •					
<21	90	[26] ABLIKIM	04F	BES	$e^+e^- \to \psi(3770)$

$\Gamma(2(\pi^+\pi^-))/\Gamma_{total}$ Γ_{23}/Γ

VALUE (units 10^{-4})	CL%	DOCUMENT ID		TECN	COMMENT
<11.2	90	[27] HUANG	06A	CLEO	$e^+e^- \to \psi(3770)$
• • • We do not use the following data for averages, fits, limits, etc. • • •					
<48		[23] ABLIKIM	07B	BES2	$e^+e^- \to \psi(3770)$

$\Gamma(2(\pi^+\pi^-)\pi^0)/\Gamma_{total}$ Γ_{24}/Γ

VALUE (units 10^{-4})	CL%	DOCUMENT ID		TECN	COMMENT
<10.6	90	[27] HUANG	06A	CLEO	$e^+e^- \to \psi(3770)$
• • • We do not use the following data for averages, fits, limits, etc. • • •					
<62		[23] ABLIKIM	07B	BES2	$e^+e^- \to \psi(3770)$

$\Gamma(2(\pi^+\pi^-\pi^0))/\Gamma_{total}$ Γ_{25}/Γ

VALUE (units 10^{-3})	CL%	EVTS	DOCUMENT ID		TECN	COMMENT
<58.5	90	305	ABLIKIM	08N	BES2	$e^+e^- \to \psi(3770)$

$\Gamma(\omega\pi^+\pi^-)/\Gamma_{total}$ Γ_{26}/Γ

VALUE (units 10^{-4})	CL%	DOCUMENT ID		TECN	COMMENT
< 6.0	90	[27] HUANG	06A	CLEO	$e^+e^- \to \psi(3770)$
• • • We do not use the following data for averages, fits, limits, etc. • • •					
<55	90	[23] ABLIKIM	07I	BES2	3.77 e^+e^-

$\Gamma(3(\pi^+\pi^-))/\Gamma_{total}$ Γ_{27}/Γ

VALUE (units 10^{-4})	DOCUMENT ID		TECN	COMMENT
<91	[23] ABLIKIM	07B	BES2	$e^+e^- \to \psi(3770)$

$\Gamma(3(\pi^+\pi^-)\pi^0)/\Gamma_{total}$ Γ_{28}/Γ

VALUE (units 10^{-4})	DOCUMENT ID		TECN	COMMENT
<137	[23] ABLIKIM	07B	BES2	$e^+e^- \to \psi(3770)$

$\Gamma(3(\pi^+\pi^-)2\pi^0)/\Gamma_{total}$ Γ_{29}/Γ

VALUE (units 10^{-3})	CL%	EVTS	DOCUMENT ID		TECN	COMMENT
<117.4	90	59	ABLIKIM	08N	BES2	$e^+e^- \to \psi(3770)$

$\Gamma(\eta\pi^+\pi^-)/\Gamma_{total}$ Γ_{30}/Γ

VALUE (units 10^{-3})	CL%	DOCUMENT ID		TECN	COMMENT
<1.24	90	[27] HUANG	06A	CLEO	$e^+e^- \to \psi(3770)$
• • • We do not use the following data for averages, fits, limits, etc. • • •					
<2.3	90	[23] ABLIKIM	10D	BES2	$e^+e^- \to \psi(3770)$

$\Gamma(\pi^+\pi^-2\pi^0)/\Gamma_{total}$ Γ_{31}/Γ

VALUE (units 10^{-3})	CL%	EVTS	DOCUMENT ID		TECN	COMMENT
<8.9	90	218	ABLIKIM	08N	BES2	$e^+e^- \to \psi(3770)$

See key on page 547

$\Gamma(\rho^0\pi^+\pi^-)/\Gamma_{total}$ Γ_{32}/Γ

VALUE (units 10^{-3})	CL%	DOCUMENT ID		TECN	COMMENT
<6.9	90	[23] ABLIKIM	07F	BES2	$e^+e^- \to \psi(3770)$

$\Gamma(\eta 3\pi)/\Gamma_{total}$ Γ_{33}/Γ

VALUE (units 10^{-4})	CL%	DOCUMENT ID		TECN	COMMENT
<13.4	90	[27] HUANG	06A	CLEO	$e^+e^- \to \psi(3770)$

$\Gamma(\eta 2(\pi^+\pi^-))/\Gamma_{total}$ Γ_{34}/Γ

VALUE (units 10^{-4})	DOCUMENT ID		TECN	COMMENT
<243	[23] ABLIKIM	07B	BES2	$e^+e^- \to \psi(3770)$

$\Gamma(\eta\rho^0\pi^+\pi^-)/\Gamma_{total}$ Γ_{35}/Γ

VALUE (units 10^{-2})	CL%	DOCUMENT ID		TECN	COMMENT
<1.45	90	[23] ABLIKIM	10D	BES2	$e^+e^- \to \psi(3770)$

$\Gamma(\eta' 3\pi)/\Gamma_{total}$ Γ_{36}/Γ

VALUE (units 10^{-4})	CL%	DOCUMENT ID		TECN	COMMENT
<24.4	90	[27] HUANG	06A	CLEO	$e^+e^- \to \psi(3770)$

$\Gamma(K^+K^-\pi^+\pi^-)/\Gamma_{total}$ Γ_{37}/Γ

VALUE (units 10^{-4})	CL%	DOCUMENT ID		TECN	COMMENT
< 9.0	90	[27] HUANG	06A	CLEO	$e^+e^- \to \psi(3770)$
• • • We do not use the following data for averages, fits, limits, etc. • • •					
<48		[23] ABLIKIM	07B	BES2	$e^+e^- \to \psi(3770)$

$\Gamma(\phi\pi^+\pi^-)/\Gamma_{total}$ Γ_{38}/Γ

VALUE (units 10^{-4})	CL%	DOCUMENT ID		TECN	COMMENT
< 4.1	90	[27] HUANG	06A	CLEO	$e^+e^- \to \psi(3770)$
• • • We do not use the following data for averages, fits, limits, etc. • • •					
<16		[23] ABLIKIM	07B	BES2	$e^+e^- \to \psi(3770)$

$\Gamma(K^+K^-2\pi^0)/\Gamma_{total}$ Γ_{39}/Γ

VALUE (units 10^{-3})	CL%	EVTS	DOCUMENT ID		TECN	COMMENT
<4.2	90	14	ABLIKIM	08N	BES2	$e^+e^- \to \psi(3770)$

$\Gamma(4(\pi^+\pi^-))/\Gamma_{total}$ Γ_{40}/Γ

VALUE (units 10^{-3})	CL%	DOCUMENT ID		TECN	COMMENT
<16.7	90	[23] ABLIKIM	07F	BES2	$e^+e^- \to \psi(3770)$

$\Gamma(4(\pi^+\pi^-)\pi^0)/\Gamma_{total}$ Γ_{41}/Γ

VALUE (units 10^{-3})	CL%	DOCUMENT ID		TECN	COMMENT
<30.6	90	[23] ABLIKIM	07F	BES2	$e^+e^- \to \psi(3770)$

$\Gamma(\phi f_0(980))/\Gamma_{total}$ Γ_{42}/Γ

VALUE (units 10^{-4})	CL%	DOCUMENT ID		TECN	COMMENT
<4.5	90	[27] HUANG	06A	CLEO	$e^+e^- \to \psi(3770)$

$\Gamma(K^+K^-\pi^+\pi^-\pi^0)/\Gamma_{total}$ Γ_{43}/Γ

VALUE (units 10^{-4})	CL%	DOCUMENT ID		TECN	COMMENT
< 23.6	90	[27] HUANG	06A	CLEO	$e^+e^- \to \psi(3770)$
• • • We do not use the following data for averages, fits, limits, etc. • • •					
<111		[23] ABLIKIM	07B	BES2	$e^+e^- \to \psi(3770)$

$\Gamma(K^+K^-\rho^0\pi^0)/\Gamma_{total}$ Γ_{44}/Γ

VALUE (units 10^{-4})	CL%	DOCUMENT ID		TECN	COMMENT
<8	90	[23] ABLIKIM	07I	BES2	3.77 e^+e^-

$\Gamma(K^+K^-\rho^+\pi^-)/\Gamma_{total}$ Γ_{45}/Γ

VALUE (units 10^{-4})	CL%	DOCUMENT ID		TECN	COMMENT
<146	90	[23] ABLIKIM	07I	BES2	3.77 e^+e^-

$\Gamma(\omega K^+K^-)/\Gamma_{total}$ Γ_{46}/Γ

VALUE (units 10^{-4})	CL%	DOCUMENT ID		TECN	COMMENT
< 3.4	90	[27] HUANG	06A	CLEO	$e^+e^- \to \psi(3770)$
• • • We do not use the following data for averages, fits, limits, etc. • • •					
<66	90	[23] ABLIKIM	07I	BES2	3.77 e^+e^-

$\Gamma(\phi\pi^+\pi^-\pi^0)/\Gamma_{total}$ Γ_{47}/Γ

VALUE (units 10^{-4})	CL%	DOCUMENT ID		TECN	COMMENT
<38	90	[23] ABLIKIM	07I	BES2	3.77 e^+e^-

$\Gamma(K^{*0}K^-\pi^+\pi^0 + \text{c.c.})/\Gamma_{total}$ Γ_{48}/Γ

VALUE (units 10^{-4})	CL%	DOCUMENT ID		TECN	COMMENT
<162	90	[23] ABLIKIM	07I	BES2	3.77 e^+e^-

$\Gamma(K^{*+}K^-\pi^+\pi^- + \text{c.c.})/\Gamma_{total}$ Γ_{49}/Γ

VALUE (units 10^{-4})	CL%	DOCUMENT ID		TECN	COMMENT
<323	90	[23] ABLIKIM	07I	BES2	3.77 e^+e^-

$\Gamma(K^+K^-\pi^+\pi^-2\pi^0)/\Gamma_{total}$ Γ_{50}/Γ

VALUE (units 10^{-3})	CL%	EVTS	DOCUMENT ID		TECN	COMMENT
<26.7	90	24	ABLIKIM	08N	BES2	$e^+e^- \to \psi(3770)$

$\Gamma(K^+K^-2(\pi^+\pi^-))/\Gamma_{total}$ Γ_{51}/Γ

VALUE (units 10^{-3})	CL%	DOCUMENT ID		TECN	COMMENT
<10.3	90	[23] ABLIKIM	07F	BES2	$e^+e^- \to \psi(3770)$

$\Gamma(K^+K^-2(\pi^+\pi^-)\pi^0)/\Gamma_{total}$ Γ_{52}/Γ

VALUE (units 10^{-3})	CL%	DOCUMENT ID		TECN	COMMENT
<36.0	90	[23] ABLIKIM	07F	BES2	$e^+e^- \to \psi(3770)$

$\Gamma(\eta K^+K^-)/\Gamma_{total}$ Γ_{53}/Γ

VALUE (units 10^{-4})	CL%	DOCUMENT ID		TECN	COMMENT
< 4.1	90	[27] HUANG	06A	CLEO	$e^+e^- \to \psi(3770)$
• • • We do not use the following data for averages, fits, limits, etc. • • •					
<31	90	[23] ABLIKIM	10D	BES2	$e^+e^- \to \psi(3770)$

$\Gamma(\eta K^+K^-\pi^+\pi^-)/\Gamma_{total}$ Γ_{54}/Γ

VALUE (units 10^{-2})	CL%	DOCUMENT ID		TECN	COMMENT
<1.24	90	[23] ABLIKIM	10D	BES2	$e^+e^- \to \psi(3770)$

$\Gamma(\rho^0K^+K^-)/\Gamma_{total}$ Γ_{55}/Γ

VALUE (units 10^{-3})	CL%	DOCUMENT ID		TECN	COMMENT
<5.0	90	[23] ABLIKIM	07F	BES2	$e^+e^- \to \psi(3770)$

$\Gamma(2(K^+K^-))/\Gamma_{total}$ Γ_{56}/Γ

VALUE (units 10^{-4})	CL%	DOCUMENT ID		TECN	COMMENT
< 6.0	90	[27] HUANG	06A	CLEO	$e^+e^- \to \psi(3770)$
• • • We do not use the following data for averages, fits, limits, etc. • • •					
<17		[23] ABLIKIM	07B	BES2	$e^+e^- \to \psi(3770)$

$\Gamma(\phi K^+K^-)/\Gamma_{total}$ Γ_{57}/Γ

VALUE (units 10^{-4})	CL%	DOCUMENT ID		TECN	COMMENT
< 7.5	90	[27] HUANG	06A	CLEO	$e^+e^- \to \psi(3770)$
• • • We do not use the following data for averages, fits, limits, etc. • • •					
<24		[23] ABLIKIM	07B	BES2	$e^+e^- \to \psi(3770)$

$\Gamma(2(K^+K^-)\pi^0)/\Gamma_{total}$ Γ_{58}/Γ

VALUE (units 10^{-4})	CL%	DOCUMENT ID		TECN	COMMENT
< 2.9	90	[27] HUANG	06A	CLEO	$e^+e^- \to \psi(3770)$
• • • We do not use the following data for averages, fits, limits, etc. • • •					
<46		[23] ABLIKIM	07B	BES2	$e^+e^- \to \psi(3770)$

$\Gamma(2(K^+K^-)\pi^+\pi^-)/\Gamma_{total}$ Γ_{59}/Γ

VALUE (units 10^{-3})	CL%	DOCUMENT ID		TECN	COMMENT
<3.2	90	[23] ABLIKIM	07F	BES2	$e^+e^- \to \psi(3770)$

$\Gamma(K^0_S K^-\pi^+)/\Gamma_{total}$ Γ_{60}/Γ

VALUE (units 10^{-3})	CL%	EVTS	DOCUMENT ID		TECN	COMMENT
<3.2	90	18	ABLIKIM	08M	BES2	$e^+e^- \to \psi(3770)$

$\Gamma(K^0_S K^-\pi^+\pi^0)/\Gamma_{total}$ Γ_{61}/Γ

VALUE (units 10^{-3})	CL%	EVTS	DOCUMENT ID		TECN	COMMENT
<13.3	90	40	ABLIKIM	08M	BES2	$e^+e^- \to \psi(3770)$

$\Gamma(K^0_S K^-\rho^+)/\Gamma_{total}$ Γ_{62}/Γ

VALUE (units 10^{-3})	CL%	DOCUMENT ID		TECN	COMMENT
<6.6	90	ABLIKIM	09C	BES2	$e^+e^- \to \psi(3770)$

$\Gamma(K^0_S K^-2\pi^+\pi^-)/\Gamma_{total}$ Γ_{63}/Γ

VALUE (units 10^{-3})	CL%	EVTS	DOCUMENT ID		TECN	COMMENT
<8.7	90	39	ABLIKIM	08M	BES2	$e^+e^- \to \psi(3770)$

$\Gamma(K^0_S K^-\pi^+\rho^0)/\Gamma_{total}$ Γ_{64}/Γ

VALUE (units 10^{-2})	CL%	DOCUMENT ID		TECN	COMMENT
<1.6	90	ABLIKIM	09C	BES2	$e^+e^- \to \psi(3770)$

$\Gamma(K^0_S K^-\pi^+\eta)/\Gamma_{total}$ Γ_{65}/Γ

VALUE (units 10^{-2})	CL%	DOCUMENT ID		TECN	COMMENT
<1.3	90	ABLIKIM	09C	BES2	$e^+e^- \to \psi(3770)$

$\Gamma(K^0_S K^-2\pi^+\pi^-\pi^0)/\Gamma_{total}$ Γ_{66}/Γ

VALUE (units 10^{-3})	CL%	EVTS	DOCUMENT ID		TECN	COMMENT
<41.8	90	23	ABLIKIM	08M	BES2	$e^+e^- \to \psi(3770)$

$\Gamma(K_S^0 K^- 2\pi^+\pi^-\eta)/\Gamma_{total}$ Γ_{67}/Γ

VALUE (units 10^{-2})	CL%	DOCUMENT ID		TECN	COMMENT
<4.8	90	ABLIKIM	09C	BES2	$e^+e^- \to \psi(3770)$

$\Gamma(K_S^0 K^- \pi^+ 2(\pi^+\pi^-))/\Gamma_{total}$ Γ_{68}/Γ

VALUE (units 10^{-3})	CL%	EVTS	DOCUMENT ID		TECN	COMMENT
<12.2	90	4	ABLIKIM	08M	BES2	$e^+e^- \to \psi(3770)$

$\Gamma(K_S^0 K^- \pi^+ 2\pi^0)/\Gamma_{total}$ Γ_{69}/Γ

VALUE (units 10^{-3})	CL%	EVTS	DOCUMENT ID		TECN	COMMENT
<26.5	90	17	ABLIKIM	08M	BES2	$e^+e^- \to \psi(3770)$

$\Gamma(K_S^0 K^- K^+ K^- \pi^+)/\Gamma_{total}$ Γ_{70}/Γ

VALUE (units 10^{-3})	CL%	DOCUMENT ID		TECN	COMMENT
<4.9	90	ABLIKIM	09C	BES2	$e^+e^- \to \psi(3770)$

$\Gamma(K_S^0 K^- K^+ K^- \pi^+\pi^0)/\Gamma_{total}$ Γ_{71}/Γ

VALUE (units 10^{-2})	CL%	DOCUMENT ID		TECN	COMMENT
<3.0	90	ABLIKIM	09C	BES2	$e^+e^- \to \psi(3770)$

$\Gamma(K_S^0 K^- K^+ K^- \pi^+\eta)/\Gamma_{total}$ Γ_{72}/Γ

VALUE (units 10^{-2})	CL%	DOCUMENT ID		TECN	COMMENT
<2.2	90	ABLIKIM	09C	BES2	$e^+e^- \to \psi(3770)$

$\Gamma(K^{*0} K^- \pi^+ + \text{c.c.})/\Gamma_{total}$ Γ_{73}/Γ

VALUE (units 10^{-3})	CL%	DOCUMENT ID		TECN	COMMENT
<9.7	90	[23] ABLIKIM	07F	BES2	$e^+e^- \to \psi(3770)$

$\Gamma(p\overline{p}\pi^0)/\Gamma_{total}$ Γ_{74}/Γ

VALUE (units 10^{-4})	DOCUMENT ID		TECN	COMMENT
<12	[23] ABLIKIM	07B	BES2	$e^+e^- \to \psi(3770)$

$\Gamma(p\overline{p}\pi^+\pi^-)/\Gamma_{total}$ Γ_{75}/Γ

VALUE (units 10^{-4})	CL%	DOCUMENT ID		TECN	COMMENT
< 5.8	90	[27] HUANG	06A	CLEO	$e^+e^- \to \psi(3770)$
• • • We do not use the following data for averages, fits, limits, etc. • • •					
<16		[23] ABLIKIM	07B	BES2	$e^+e^- \to \psi(3770)$

$\Gamma(\Lambda\overline{\Lambda})/\Gamma_{total}$ Γ_{76}/Γ

VALUE (units 10^{-4})	CL%	DOCUMENT ID		TECN	COMMENT
<1.2	90	[27] HUANG	06A	CLEO	$e^+e^- \to \psi(3770)$
• • • We do not use the following data for averages, fits, limits, etc. • • •					
<4	90	[23] ABLIKIM	07F	BES2	$e^+e^- \to \psi(3770)$

$\Gamma(p\overline{p}\pi^+\pi^-\pi^0)/\Gamma_{total}$ Γ_{77}/Γ

VALUE (units 10^{-4})	CL%	DOCUMENT ID		TECN	COMMENT
<18.5	90	[27] HUANG	06A	CLEO	$e^+e^- \to \psi(3770)$
• • • We do not use the following data for averages, fits, limits, etc. • • •					
<73		[23] ABLIKIM	07B	BES2	$e^+e^- \to \psi(3770)$

$\Gamma(\omega p\overline{p})/\Gamma_{total}$ Γ_{78}/Γ

VALUE (units 10^{-4})	CL%	DOCUMENT ID		TECN	COMMENT
< 2.9	90	[27] HUANG	06A	CLEO	$e^+e^- \to \psi(3770)$
• • • We do not use the following data for averages, fits, limits, etc. • • •					
<30	90	[28] ABLIKIM	07I	BES2	3.77 e^+e^-

$\Gamma(\Lambda\overline{\Lambda}\pi^0)/\Gamma_{total}$ Γ_{79}/Γ

VALUE (units 10^{-4})	CL%	DOCUMENT ID		TECN	COMMENT
< 0.7	90	[29] ABLIKIM	13Q	BES3	$e^+e^- \to \psi(3770)$
• • • We do not use the following data for averages, fits, limits, etc. • • •					
<12	90	[23] ABLIKIM	07I	BES2	3.77 e^+e^-

$\Gamma(p\overline{p}2(\pi^+\pi^-))/\Gamma_{total}$ Γ_{80}/Γ

VALUE (units 10^{-3})	CL%	DOCUMENT ID		TECN	COMMENT
<2.6	90	[23] ABLIKIM	07F	BES2	$e^+e^- \to \psi(3770)$

$\Gamma(\eta p\overline{p})/\Gamma_{total}$ Γ_{81}/Γ

VALUE (units 10^{-4})	CL%	DOCUMENT ID		TECN	COMMENT
< 5.4	90	[27] HUANG	06A	CLEO	$e^+e^- \to \psi(3770)$
• • • We do not use the following data for averages, fits, limits, etc. • • •					
<11	90	[23] ABLIKIM	10D	BES2	$e^+e^- \to \psi(3770)$

$\Gamma(\eta p\overline{p}\pi^+\pi^-)/\Gamma_{total}$ Γ_{82}/Γ

VALUE (units 10^{-3})	CL%	DOCUMENT ID		TECN	COMMENT
<3.3	90	[23] ABLIKIM	10D	BES2	$e^+e^- \to \psi(3770)$

$\Gamma(\rho^0 p\overline{p})/\Gamma_{total}$ Γ_{83}/Γ

VALUE (units 10^{-3})	CL%	DOCUMENT ID		TECN	COMMENT
<1.7	90	[23] ABLIKIM	07F	BES2	$e^+e^- \to \psi(3770)$

$\Gamma(p\overline{p}K^+K^-)/\Gamma_{total}$ Γ_{84}/Γ

VALUE (units 10^{-4})	CL%	DOCUMENT ID		TECN	COMMENT
< 3.2	90	[27] HUANG	06A	CLEO	$e^+e^- \to \psi(3770)$
• • • We do not use the following data for averages, fits, limits, etc. • • •					
<11		[23] ABLIKIM	07B	BES2	$e^+e^- \to \psi(3770)$

$\Gamma(\eta p\overline{p}K^+K^-)/\Gamma_{total}$ Γ_{85}/Γ

VALUE (units 10^{-3})	CL%	DOCUMENT ID		TECN	COMMENT
<6.9	90	[23] ABLIKIM	10D	BES2	$e^+e^- \to \psi(3770)$

$\Gamma(\pi^0 p\overline{p}K^+K^-)/\Gamma_{total}$ Γ_{86}/Γ

VALUE (units 10^{-3})	CL%	DOCUMENT ID		TECN	COMMENT
<1.2	90	[23] ABLIKIM	10D	BES2	$e^+e^- \to \psi(3770)$

$\Gamma(\phi p\overline{p})/\Gamma_{total}$ Γ_{87}/Γ

VALUE (units 10^{-4})	CL%	DOCUMENT ID		TECN	COMMENT
<1.3	90	[27] HUANG	06A	CLEO	$e^+e^- \to \psi(3770)$
• • • We do not use the following data for averages, fits, limits, etc. • • •					
<9		[23] ABLIKIM	07B	BES2	$e^+e^- \to \psi(3770)$

$\Gamma(\Lambda\overline{\Lambda}\pi^+\pi^-)/\Gamma_{total}$ Γ_{88}/Γ

VALUE (units 10^{-4})	CL%	DOCUMENT ID		TECN	COMMENT
< 2.5	90	[27] HUANG	06A	CLEO	$e^+e^- \to \psi(3770)$
• • • We do not use the following data for averages, fits, limits, etc. • • •					
< 4.7	90	[29] ABLIKIM	13Q	BES3	$e^+e^- \to \psi(3770)$
<39	90	[23] ABLIKIM	07F	BES2	$e^+e^- \to \psi(3770)$

$\Gamma(\Lambda\overline{p}K^+)/\Gamma_{total}$ Γ_{89}/Γ

VALUE (units 10^{-4})	CL%	DOCUMENT ID		TECN	COMMENT
<2.8	90	[27] HUANG	06A	CLEO	$e^+e^- \to \psi(3770)$

$\Gamma(\Lambda\overline{p}K^+\pi^+\pi^-)/\Gamma_{total}$ Γ_{90}/Γ

VALUE (units 10^{-4})	CL%	DOCUMENT ID		TECN	COMMENT
<6.3	90	[27] HUANG	06A	CLEO	$e^+e^- \to \psi(3770)$

$\Gamma(\Lambda\overline{\Lambda}\eta)/\Gamma_{total}$ Γ_{91}/Γ

VALUE (units 10^{-4})	CL%	DOCUMENT ID		TECN	COMMENT
<1.9	90	[29] ABLIKIM	13Q	BES3	$e^+e^- \to \psi(3770)$

$\Gamma(\Sigma^+\overline{\Sigma}^-)/\Gamma_{total}$ Γ_{92}/Γ

VALUE (units 10^{-4})	CL%	DOCUMENT ID		TECN	COMMENT
<1.0	90	[29] ABLIKIM	13Q	BES3	$e^+e^- \to \psi(3770)$

$\Gamma(\Sigma^0\overline{\Sigma}^0)/\Gamma_{total}$ Γ_{93}/Γ

VALUE (units 10^{-4})	CL%	DOCUMENT ID		TECN	COMMENT
<0.4	90	[29] ABLIKIM	13Q	BES3	$e^+e^- \to \psi(3770)$

$\Gamma(\Xi^+\overline{\Xi}^-)/\Gamma_{total}$ Γ_{94}/Γ

VALUE (units 10^{-4})	CL%	DOCUMENT ID		TECN	COMMENT
<1.5	90	[29] ABLIKIM	13Q	BES3	$e^+e^- \to \psi(3770)$

$\Gamma(\Xi^0\overline{\Xi}^0)/\Gamma_{total}$ Γ_{95}/Γ

VALUE (units 10^{-4})	CL%	DOCUMENT ID		TECN	COMMENT
<1.4	90	[29] ABLIKIM	13Q	BES3	$e^+e^- \to \psi(3770)$

[22] Comparing cross sections at $\sqrt{s} = 3.773$ GeV and $\sqrt{s} = 3.671$ GeV, neglecting interference, and using $\sigma(\psi(3770) \to D\overline{D}) = 6.39 \pm 0.20$ nb.

[23] Assuming that interference effects between resonance and continuum can be neglected and using $\sigma^{obs}(e^+e^- \to \psi(3770)) = 7.15 \pm 0.38$ nb.

[24] Data suggest possible destructive interference with continuum.

[25] Using $\sigma(e^+e^- \to \psi(3770) \to \text{hadrons}) = (6.38 \pm 0.08^{+0.41}_{-0.30})$ nb from BESSON 06 and $B(K_S^0 \to \pi^+\pi^-) = 0.6895 \pm 0.0014$.

[26] Using $B(K_S^0 \to \pi^+\pi^-) = 0.6860 \pm 0.0027$.

[27] Using $\sigma_{tot}(e^+e^- \to \psi(3770)) = 7.9 \pm 0.6$ nb at the resonance.

[28] Using $\sigma^{obs} = 7.15 \pm 0.27 \pm 0.27$ nb and neglecting interference.

[29] Assuming that interference effects between resonance and continuum can be neglected.

RADIATIVE DECAYS

$\Gamma(\gamma\chi_{c2})/\Gamma_{total}$ Γ_{96}/Γ

VALUE (units 10^{-3})	CL%	DOCUMENT ID		TECN	COMMENT
<0.9	90	[30] COAN	06A	CLEO	$e^+e^- \to \psi(3770) \to \gamma\gamma J/\psi$
• • • We do not use the following data for averages, fits, limits, etc. • • •					
<2.0	90	[31] BRIERE	06	CLEO	$e^+e^- \to \psi(3770) \to \gamma +$ hadrons

$\Gamma(\gamma\chi_{c1})/\Gamma_{total}$ Γ_{97}/Γ

VALUE (units 10^{-3})	EVTS	DOCUMENT ID		TECN	COMMENT
2.9±0.5±0.4		[32] BRIERE	06	CLEO	$e^+e^- \to \psi(3770) \to \gamma +$ hadrons, $\gamma\gamma J/\psi$
• • • We do not use the following data for averages, fits, limits, etc. • • •					
3.9±1.4±0.6	54 ± 17	[33] BRIERE	06	CLEO	$e^+e^- \to \psi(3770) \to \gamma +$ hadrons
2.8±0.5±0.4	53 ± 10	[30] COAN	06A	CLEO	$e^+e^- \to \psi(3770) \to \gamma\gamma J/\psi$

$\Gamma(\gamma\chi_{c1})/\Gamma(J/\psi\pi^+\pi^-)$ Γ_{97}/Γ_4

VALUE	EVTS	DOCUMENT ID		TECN	COMMENT
1.49±0.31±0.26	53 ± 10	[34] COAN	06A	CLEO	$e^+e^- \to \psi(3770) \to \gamma\gamma J/\psi$

$\Gamma(\gamma\chi_{c0})/\Gamma_{total}$ Γ_{98}/Γ

VALUE (units 10^{-3})	CL%	EVTS	DOCUMENT ID		TECN	COMMENT
7.3±0.7±0.6		274 ± 27	[35] BRIERE	06	CLEO	$e^+e^- \to \psi(3770) \to \gamma +$ hadrons
• • • We do not use the following data for averages, fits, limits, etc. • • •						
< 44	90		[30] COAN	06A	CLEO	$e^+e^- \to \psi(3770) \to \gamma\gamma J/\psi$

$\Gamma(\gamma\chi_{c0})/\Gamma(\gamma\chi_{c2})$ Γ_{98}/Γ_{96}

VALUE	CL%	DOCUMENT ID		TECN	COMMENT
• • • We do not use the following data for averages, fits, limits, etc. • • •					
>8	90	[36] BRIERE	06	CLEO	$e^+e^- \to \psi(3770)$

$\Gamma(\gamma\chi_{c0})/\Gamma(\gamma\chi_{c1})$ Γ_{98}/Γ_{97}

VALUE	DOCUMENT ID		TECN	COMMENT
• • • We do not use the following data for averages, fits, limits, etc. • • •				
2.5 ± 0.6	[36] BRIERE	06	CLEO	$e^+e^- \to \psi(3770)$

$\Gamma(\gamma\eta')/\Gamma_{total}$ Γ_{99}/Γ

VALUE (units 10^{-4})	CL%	DOCUMENT ID		TECN	COMMENT
<1.8	90	[37] PEDLAR	09	CLE3	$\psi(2S) \to \gamma X$

$\Gamma(\gamma\eta)/\Gamma_{total}$ Γ_{100}/Γ

VALUE (units 10^{-4})	CL%	DOCUMENT ID		TECN	COMMENT
<1.5	90	[37] PEDLAR	09	CLE3	$\psi(2S) \to \gamma X$

$\Gamma(\gamma\pi^0)/\Gamma_{total}$ Γ_{101}/Γ

VALUE (units 10^{-4})	CL%	DOCUMENT ID		TECN	COMMENT
<2	90	PEDLAR	09	CLE3	$\psi(2S) \to \gamma X$

[30] Using $\Gamma_{ee}(\psi(2S)) = (2.54 \pm 0.03 \pm 0.11)$ keV from ADAM 06 and taking $\sigma(e^+e^- \to D\overline{D})$ from HE 05 for $\sigma(e^+e^- \to \psi(3770))$.

[31] Uses $B(\psi(2S) \to \gamma\chi_{c2}) = 9.22 \pm 0.11 \pm 0.46\,\%$ from ATHAR 04, $\psi(2S)$ mass and width from PDG 04, and $\Gamma_{ee}(\psi(2S)) = 2.54 \pm 0.03 \pm 0.11$ keV from ADAM 06.

[32] Averages the two measurements from COAN 06A and BRIERE 06.

[33] Uses $B(\psi(2S) \to \gamma\chi_{c1}) = 9.07 \pm 0.11 \pm 0.54\,\%$ from ATHAR 04, $\psi(2S)$ mass and width from PDG 04, and $\Gamma_{ee}(\psi(2S)) = 2.54 \pm 0.03 \pm 0.11$ keV from ADAM 06.

[34] Using $B(\psi(3770) \to J/\psi\pi^+\pi^-) = (1.89 \pm 0.20 \pm 0.20) \times 10^{-3}$ from ADAM 06.

[35] Uses $B(\psi(2S) \to \gamma\chi_{c0}) = 9.33 \pm 0.14 \pm 0.61\,\%$ from ATHAR 04, $\psi(2S)$ mass and width from PDG 04, and $\Gamma_{ee}(\psi(2S)) = 2.54 \pm 0.03 \pm 0.11$ keV from ADAM 06.

[36] Not independent of other results in BRIERE 06.

[37] Assuming maximal destructive interference between $\psi(3770)$ and continuum sources.

$\psi(3770)$ REFERENCES

ABLIKIM	13Q	PR D87 112011	Ablikim M. *et al.*	(BES III Collab.)
ANASHIN	12A	PL B711 292	V.V. Anashin *et al.*	(KEDR Collab.)
ABLIKIM	10D	EPJ C66 11	M. Ablikim *et al.*	(BES II Collab.)
BESSON	10	PRL 104 159901E	D. Besson *et al.*	(CLEO Collab.)
ABLIKIM	09C	EPJ C64 243	M. Ablikim *et al.*	(BES Collab.)
PEDLAR	09	PR D79 111101	T.K. Pedlar *et al.*	(CLEO Collab.)
ABLIKIM	08B	PL B659 74	M. Ablikim *et al.*	(BES Collab.)
ABLIKIM	08D	PL B660 315	M. Ablikim *et al.*	(BES Collab.)
ABLIKIM	08M	PL B670 179	M. Ablikim *et al.*	(BES Collab.)
ABLIKIM	08N	PL B670 184	M. Ablikim *et al.*	(BES Collab.)
AUBERT	08B	PR D77 011102	B. Aubert *et al.*	(BABAR Collab.)
BRODZICKA	08	PRL 100 092001	J. Brodzicka *et al.*	(BELLE Collab.)
PAKHLOVA	08	PR D77 011103	G. Pakhlova *et al.*	(BELLE Collab.)
ABLIKIM	07B	PL B650 111	M. Ablikim *et al.*	(BES Collab.)
ABLIKIM	07E	PL B652 238	M. Ablikim *et al.*	(BES Collab.)
ABLIKIM	07F	PL B656 30	M. Ablikim *et al.*	(BES Collab.)
ABLIKIM	07I	EPJ C52 805	M. Ablikim *et al.*	(BES Collab.)
ABLIKIM	07K	PR D76 122002	M. Ablikim *et al.*	(BES Collab.)
AUBERT	07BE	PR D76 111105	B. Aubert *et al.*	(BABAR Collab.)
DOBBS	07	PR D76 112001	S. Dobbs *et al.*	(CLEO Collab.)
ABLIKIM	06L	PRL 97 121801	M. Ablikim *et al.*	(BES Collab.)
ABLIKIM	06N	PL B641 145	M. Ablikim *et al.*	(BES Collab.)
ADAM	06	PRL 96 082004	N.E. Adam *et al.*	(CLEO Collab.)
ADAMS	06	PR D73 012002	G.S. Adams *et al.*	(CLEO Collab.)
BESSON	06	PRL 96 092002	D. Besson *et al.*	(CLEO Collab.)
Also		PRL 104 159901E	D. Besson *et al.*	(CLEO Collab.)
BRIERE	06	PR D74 031106	R.A. Briere *et al.*	(CLEO Collab.)
COAN	06A	PRL 96 182002	T.E. Coan *et al.*	(CLEO Collab.)
CRONIN-HEN...	06	PR D74 012005	D. Cronin-Hennessy *et al.*	(CLEO Collab.)
HUANG	06A	PRL 96 032003	G.S. Huang *et al.*	(CLEO Collab.)
BAI	05	PL B605 63	J.Z. Bai *et al.*	(BES Collab.)
HE	05	PRL 95 121801	Q. He *et al.*	(CLEO Collab.)
Also		PRL 96 199903 (errat.)	Q. He *et al.*	(CLEO Collab.)
ABLIKIM	04F	PR D70 077101	M. Ablikim *et al.*	(BES Collab.)
ATHAR	04	PR D70 112002	S.B. Athar *et al.*	(CLEO Collab.)
CHISTOV	04	PRL 93 051803	R. Chistov *et al.*	(BELLE Collab.)
PDG	04	PL B592 1	S. Eidelman *et al.*	(PDG Collab.)
BAI	02C	PRL 88 101802	J.Z. Bai *et al.*	(BES Collab.)
ADLER	88C	PRL 60 89	J. Adler *et al.*	(Mark III Collab.)
SCHINDLER	80	PR D21 2716	R.H. Schindler *et al.*	(Mark II Collab.)
BACINO	78	PRL 40 671	W.J. Bacino *et al.*	(SLAC, UCLA, UCI)
RAPIDIS	77	PRL 39 526	P.A. Rapidis *et al.*	(LGW Collab.)

$X(3823)$

$I^G(J^{PC}) = ?^?(?^{?-})$

OMITTED FROM SUMMARY TABLE

Seen by BHARDWAJ 13 in $B \to \chi_{c1}\gamma K$ decays as a narrow peak in the invariant mass distribution of the $\chi_{c1}\gamma$ system. Properties consistent with the $\psi_2(1^3D_2)$ $c\overline{c}$ state.

$X(3823)$ MASS

VALUE (MeV)	EVTS	DOCUMENT ID		TECN	COMMENT
3823.1±1.8±0.7	33 ± 10	[1] BHARDWAJ	13	BELL	$B \to \chi_{c1}\gamma K$

[1] From a simultaneous fit to $B^\pm \to (\chi_{c1}\gamma)K^\pm$ and $B^0 \to (\chi_{c1}\gamma)K^0_S$ with significance 4.0σ including systematics. Corrected for the measured $\psi(2S)$ mass using $B \to \psi(2S)K \to (\gamma\chi_{c1})K$ decays.

$X(3823)$ WIDTH

VALUE (MeV)	CL%	DOCUMENT ID		TECN	COMMENT
<24	90	[1] BHARDWAJ	13	BELL	$B \to \chi_{c1}\gamma K$

[1] From a simultaneous fit to $B^\pm \to (\chi_{c1}\gamma)K^\pm$ and $B^0 \to (\chi_{c1}\gamma)K^0_S$ with significance 4.0σ including systematics.

$X(3823)$ DECAY MODES

	Mode	Fraction (Γ_i/Γ)
Γ_1	$\chi_{c1}\gamma$	seen
Γ_2	$\chi_{c2}\gamma$	not seen

$X(3823)$ BRANCHING RATIOS

$\Gamma(\chi_{c1}\gamma)/\Gamma_{total}$ Γ_1/Γ

VALUE	EVTS	DOCUMENT ID		TECN	COMMENT
seen	33 ± 10	[1] BHARDWAJ	13	BELL	$B^+ \to \chi_{c1}\gamma K^+$

[1] Reported $B(B^\pm \to X(3823)K^\pm) \times B(X(3823) \to \gamma\chi_{c1}) = (9.7 \pm 2.8 \pm 1.1) \times 10^{-6}$ with statistical significance 3.8σ.

$\Gamma(\chi_{c2}\gamma)/\Gamma_{total}$ Γ_2/Γ

VALUE	DOCUMENT ID		TECN	COMMENT
not seen	[1] BHARDWAJ	13	BELL	$B^+ \to \chi_{c2}\gamma K^+$

[1] Reported $B(B^\pm \to X(3823)K^\pm) \times B(X(3823) \to \gamma\chi_{c2}) < 3.6 \times 10^{-6}$ at 90% CL.

$\Gamma(\chi_{c2}\gamma)/\Gamma(\chi_{c1}\gamma)$ Γ_2/Γ_1

VALUE	CL%	DOCUMENT ID		TECN	COMMENT
<0.41	90	BHARDWAJ	13	BELL	$B^+ \to \chi_{c1/c2}\gamma K^+$

$X(3823)$ REFERENCES

BHARDWAJ	13	PRL 111 032001	V. Bhardwaj *et al.*	(BELLE Collab.)

X(3872)

$I^G(J^{PC}) = 0^+(1^{++})$

First observed by CHOI 03 in $B \to K\pi^+\pi^- J/\psi(1S)$ decays as a narrow peak in the invariant mass distribution of the $\pi^+\pi^- J/\psi(1S)$ final state. Isovector hypothesis excluded by AUBERT 05B and CHOI 11.

AAIJ 13Q perform a full five-dimensional amplitude analysis of the angular correlations between the decay products in $B^+ \to X(3872)K^+$ decays, where $X(3872) \to J/\psi\pi^+\pi^-$ and $J/\psi \to \mu^+\mu^-$, which unambiguously gives the $J^{PC} = 1^{++}$ assignment.

See our note on "Developments in Heavy Quarkonium Spectroscopy".

X(3872) MASS FROM $J/\psi X$ MODE

VALUE (MeV)	EVTS	DOCUMENT ID		TECN	COMMENT
3871.69± 0.17 OUR AVERAGE					
3871.9 ± 0.7 ±0.2	20 ± 5	ABLIKIM	14	BES3	$e^+e^- \to J/\psi\pi^+\pi^-\gamma$
3871.95± 0.48±0.12	0.6k	AAIJ	12H	LHCB	$pp \to J/\psi\pi^+\pi^- X$
3871.85± 0.27±0.19	∼ 170	[1] CHOI	11	BELL	$B \to K\pi^+\pi^- J/\psi$
3873 $^{+1.8}_{-1.6}$ ±1.3	27 ± 8	[2] DEL-AMO-SA.	10B	BABR	$B \to \omega J/\psi K$
3871.61± 0.16±0.19	6k	[2,3] AALTONEN	09AU	CDF2	$p\overline{p} \to J/\psi\pi^+\pi^- X$
3871.4 ± 0.6 ±0.1	93.4	AUBERT	08Y	BABR	$B^+ \to K^+ J/\psi\pi^+\pi^-$
3868.7 ± 1.5 ±0.4	9.4	AUBERT	08Y	BABR	$B^0 \to K^0_S J/\psi\pi^+\pi^-$
3871.8 ± 3.1 ±3.0	522	[2,4] ABAZOV	04F	D0	$p\overline{p} \to J/\psi\pi^+\pi^- X$
• • • We do not use the following data for averages, fits, limits, etc. • • •					
3868.6 ± 1.2 ±0.2	8	[5] AUBERT	06	BABR	$B^0 \to K^0_S J/\psi\pi^+\pi^-$
3871.3 ± 0.6 ±0.1	61	[5] AUBERT	06	BABR	$B^- \to K^- J/\psi\pi^+\pi^-$
3873.4 ± 1.4	25	[6] AUBERT	05R	BABR	$B^+ \to K^+ J/\psi\pi^+\pi^-$
3871.3 ± 0.7 ±0.4	730	[2,7] ACOSTA	04	CDF2	$p\overline{p} \to J/\psi\pi^+\pi^- X$
3872.0 ± 0.6 ±0.5	36	[8] CHOI	03	BELL	$B \to K\pi^+\pi^- J/\psi$
3836 ±13	58	[2,9] ANTONIAZZI	94	E705	300 $\pi^\pm$Li → $J/\psi\pi^+\pi^- X$

[1] The mass difference for the $X(3872)$ produced in B^+ and B^0 decays is $(-0.71 \pm 0.96 \pm 0.19)$ MeV.
[2] Width consistent with detector resolution.
[3] A possible equal mixture of two states with a mass difference greater than 3.6 MeV/c^2 is excluded at 95% CL.
[4] Calculated from the corresponding $m_{X(3872)} - m_{J/\psi}$ using $m_{J/\psi}$=3096.916 MeV.
[5] Calculated from the corresponding $m_{X(3872)} - m_{\psi(2S)}$ using $m_{\psi(2S)}$ = 3686.093 MeV. Superseded by AUBERT 08Y.
[6] Calculated from the corresponding $m_{X(3872)} - m_{\psi(2S)}$ using $m_{\psi(2S)}$ = 3685.96MeV. Superseded by AUBERT 06.
[7] Superseded by AALTONEN 09AU.
[8] Superseded by CHOI 11.
[9] A lower mass value can be due to an incorrect momentum scale for soft pions.

X(3872) MASS FROM $\overline{D}^{*0}D^0$ MODE

VALUE (MeV)	EVTS	DOCUMENT ID		TECN	COMMENT
• • • We do not use the following data for averages, fits, limits, etc. • • •					
3872.9 $^{+0.6}_{-0.4}$ $^{+0.4}_{-0.5}$	50 [10,11]	AUSHEV	10	BELL	$B \to \overline{D}^{*0} D^0 K$
3875.1 $^{+0.7}_{-0.5}$ ±0.5	33 ± 6 [11]	AUBERT	08B	BABR	$B \to \overline{D}^{*0} D^0 K$
3875.2±0.7 $^{+0.9}_{-1.8}$	24 ± 6 [11,12]	GOKHROO	06	BELL	$B \to D^0\overline{D}^0\pi^0 K$

[10] Calculated from the measured $m_{X(3872)} - m_{D^{*0}} - m_{\overline{D}^0} = 1.1^{+0.6}_{-0.4}{}^{+0.1}_{-0.3}$ MeV.
[11] Experiments report $D^{*0}\overline{D}^0$ invariant mass above $D^{*0}\overline{D}^0$ threshold because D^{*0} decay products are kinematically constrained to the D^{*0} mass, even though the D^{*0} may decay off-shell.
[12] Superseded by AUSHEV 10.

$m_{X(3872)} - m_{J/\psi}$

VALUE (MeV)	EVTS	DOCUMENT ID		TECN	COMMENT
774.9±3.1±3.0	522	ABAZOV	04F	D0	$p\overline{p} \to J/\psi\pi^+\pi^- X$

$m_{X(3872)} - m_{\psi(2S)}$

VALUE (MeV)	EVTS	DOCUMENT ID		TECN	COMMENT
• • • We do not use the following data for averages, fits, limits, etc. • • •					
187.4±1.4	25	[13] AUBERT	05R	BABR	$B^+ \to K^+ J/\psi\pi^+\pi^-$

[13] Superseded by AUBERT 06.

X(3872) WIDTH

VALUE (MeV)	CL%	EVTS	DOCUMENT ID		TECN	COMMENT
<1.2	90		CHOI	11	BELL	$B \to K\pi^+\pi^- J/\psi$
• • • We do not use the following data for averages, fits, limits, etc. • • •						
<2.4	90		ABLIKIM	14	BES3	$e^+e^- \to J/\psi\pi^+\pi^-\gamma$
<3.3	90		AUBERT	08Y	BABR	$B^+ \to K^+ J/\psi\pi^+\pi^-$
<4.1	90	69	AUBERT	06	BABR	$B \to K\pi^+\pi^- J/\psi$
<2.3	90	36	[14] CHOI	03	BELL	$B \to K\pi^+\pi^- J/\psi$

[14] Superseded by CHOI 11.

X(3872) WIDTH FROM $\overline{D}^{*0}D^0$ MODE

VALUE (MeV)	EVTS	DOCUMENT ID		TECN	COMMENT
• • • We do not use the following data for averages, fits, limits, etc. • • •					
3.9 $^{+2.8}_{-1.4}$ $^{+0.2}_{-1.1}$	50	[15] AUSHEV	10	BELL	$B \to \overline{D}^{*0} D^0 K$
3.0 $^{+1.9}_{-1.4}$ ±0.9	33 ± 6	AUBERT	08B	BABR	$B \to \overline{D}^{*0} D^0 K$

[15] With a measured value of $B(B \to X(3872)K) \times B(X(3872) \to D^{*0}\overline{D}^0) = (0.80 \pm 0.20 \pm 0.10) \times 10^{-4}$, assumed to be equal for both charged and neutral modes.

X(3872) DECAY MODES

	Mode	Fraction (Γ_i/Γ)
Γ_1	e^+e^-	
Γ_2	$\pi^+\pi^- J/\psi(1S)$	> 2.6 %
Γ_3	$\rho^0 J/\psi(1S)$	
Γ_4	$\omega J/\psi(1S)$	> 1.9 %
Γ_5	$D^0\overline{D}^0\pi^0$	>32 %
Γ_6	$\overline{D}^{*0}D^0$	>24 %
Γ_7	$\gamma\gamma$	
Γ_8	$D^0\overline{D}^0$	
Γ_9	D^+D^-	
Γ_{10}	$\gamma\chi_{c1}$	
Γ_{11}	$\gamma\chi_{c2}$	
Γ_{12}	$\eta J/\psi$	
Γ_{13}	$\gamma J/\psi$	> 6 × 10^{-3}
Γ_{14}	$\gamma\psi(2S)$	[a] > 3.0 %
Γ_{15}	$\pi^+\pi^-\eta_c(1S)$	not seen
Γ_{16}	$p\overline{p}$	not seen

[a] BHARDWAJ 11 does not observe this decay and presents a stronger 90% CL limit than this value. See measurements listings for details.

X(3872) PARTIAL WIDTHS

$\Gamma(e^+e^-)$ Γ_1

VALUE (keV)	CL%	DOCUMENT ID		TECN	COMMENT
• • • We do not use the following data for averages, fits, limits, etc. • • •					
<0.28	90	[16] YUAN	04	RVUE	$e^+e^- \to \pi^+\pi^- J/\psi$

[16] Using BAI 98E data on $e^+e^- \to \pi^+\pi^-\ell^+\ell^-$. Assuming that $\Gamma(\pi^+\pi^- J/\psi)$ of $X(3872)$ is the same as that of $\psi(2S)$ (85.4 keV).

X(3872) Γ(i)Γ(e^+e^-)/Γ(total)

$\Gamma(\pi^+\pi^- J/\psi(1S)) \times \Gamma(e^+e^-)/\Gamma_{total}$ $\Gamma_2\Gamma_1/\Gamma$

VALUE (eV)	CL%	DOCUMENT ID		TECN	COMMENT
< 6.2	90	[17,18] AUBERT	05D	BABR	10.6 $e^+e^- \to K^+K^-\pi^+\pi^-\gamma$
• • • We do not use the following data for averages, fits, limits, etc. • • •					
< 8.3	90	[18] DOBBS	05	CLE3	$e^+e^- \to \pi^+\pi^- J/\psi$
<10	90	[19] YUAN	04	RVUE	$e^+e^- \to \pi^+\pi^- J/\psi$

[17] Using $B(X(3872) \to J/\psi\pi^+\pi^-) \cdot B(J/\psi \to \mu^+\mu^-) \cdot \Gamma(X(3872) \to e^+e^-) < 0.37$ eV from AUBERT 05D and $B(J/\psi \to \mu^+\mu^-) = 0.0588 \pm 0.0010$ from the PDG 04.
[18] Assuming $X(3872)$ has $J^{PC} = 1^{--}$.
[19] Using BAI 98E data on $e^+e^- \to \pi^+\pi^-\ell^+\ell^-$. From theoretical calculation of the production cross section and using $B(J/\psi \to \mu^+\mu^-) = (5.88 \pm 0.10)\%$.

X(3872) Γ(i)Γ(γγ)/Γ(total)

$\Gamma(\pi^+\pi^- J/\psi(1S)) \times \Gamma(\gamma\gamma)/\Gamma_{total}$ $\Gamma_2\Gamma_7/\Gamma$

VALUE (eV)	CL%	DOCUMENT ID		TECN	COMMENT
• • • We do not use the following data for averages, fits, limits, etc. • • •					
<12.9	90	[20] DOBBS	05	CLE3	$e^+e^- \to \pi^+\pi^- J/\psi\gamma$

[20] Assuming $X(3872)$ has positive C parity and spin 0.

$\Gamma(\omega J/\psi(1S)) \times \Gamma(\gamma\gamma)/\Gamma_{total}$ $\Gamma_4\Gamma_7/\Gamma$

VALUE (eV)	CL%	DOCUMENT ID		TECN	COMMENT
• • • We do not use the following data for averages, fits, limits, etc. • • •					
<1.7	90	[21] LEES	12AD	BABR	$e^+e^- \to e^+e^-\omega J/\psi$

[21] Assuming $X(3872)$ has spin 2.

$\Gamma(\pi^+\pi^-\eta_c(1S)) \times \Gamma(\gamma\gamma)/\Gamma_{total}$ $\Gamma_{15}\Gamma_7/\Gamma$

VALUE (eV)	CL%	DOCUMENT ID		TECN	COMMENT
<11.1	90	LEES	12AE	BABR	$e^+e^- \to e^+e^-\pi^+\pi^-\eta_C$

$X(3872)$ BRANCHING RATIOS

$\Gamma(\pi^+\pi^- J/\psi(1S))/\Gamma_{total}$ Γ_2/Γ

VALUE	EVTS	DOCUMENT ID		TECN	COMMENT
>0.026	93 ± 17	[22] AUBERT	08Y	BABR	$B \to X(3872)K$
• • • We do not use the following data for averages, fits, limits, etc. • • •					
>0.04	30	[23] AUBERT	05R	BABR	$B^+ \to K^+ J/\psi\pi^+\pi^-$
>0.04	36 ± 7	[24] CHOI	03	BABR	$B^+ \to K^+ J/\psi\pi^+\pi^-$

[22] AUBERT 08Y reports $[\Gamma(X(3872) \to \pi^+\pi^- J/\psi(1S))/\Gamma_{total}] \times [B(B^+ \to X(3872)K^+)] = (8.4 \pm 1.5 \pm 0.7)\times10^{-6}$ which we divide by our best value $B(B^+ \to X(3872)K^+) < 3.2\times10^{-4}$.

[23] Superseded by AUBERT 08Y. AUBERT 05R reports $[\Gamma(X(3872) \to \pi^+\pi^- J/\psi(1S))/\Gamma_{total}] \times [B(B^+ \to X(3872)K^+)] = (1.28 \pm 0.41)\times10^{-5}$ which we divide by our best value $B(B^+ \to X(3872)K^+) < 3.2\times10^{-4}$.

[24] CHOI 03 reports $[\Gamma(X(3872) \to \pi^+\pi^- J/\psi(1S))/\Gamma_{total}] \times [B(B^+ \to X(3872)K^+)] / [B(B^+ \to \psi(2S)K^+)] / [B(\psi(2S) \to J/\psi(1S)\pi^+\pi^-)] = 0.063 \pm 0.012 \pm 0.007$ which we multiply or divide by our best values $B(B^+ \to X(3872)K^+) < 3.2\times10^{-4}$, $B(B^+ \to \psi(2S)K^+) = (6.27 \pm 0.24)\times10^{-4}$, $B(\psi(2S) \to J/\psi(1S)\pi^+\pi^-) = (34.45 \pm 0.30)\times10^{-2}$.

$\Gamma(\omega J/\psi(1S))/\Gamma_{total}$ Γ_4/Γ

VALUE	EVTS	DOCUMENT ID		TECN	COMMENT
>0.019	21 ± 7	[25] DEL-AMO-SA..10B		BABR	$B^+ \to \omega J/\psi K^+$

[25] DEL-AMO-SANCHEZ 10B reports $[\Gamma(X(3872) \to \omega J/\psi(1S))/\Gamma_{total}] \times [B(B^+ \to X(3872)K^+)] = (6 \pm 2 \pm 1)\times10^{-6}$ which we divide by our best value $B(B^+ \to X(3872)K^+) < 3.2\times10^{-4}$. DEL-AMO-SANCHEZ 10B also reports $B(B^0 \to X(3872)K^0) \times B(X(3872) \to J/\psi\omega) = (6 \pm 3 \pm 1)\times10^{-6}$.

$\Gamma(\omega J/\psi(1S))/\Gamma(\pi^+\pi^- J/\psi(1S))$ Γ_4/Γ_2

VALUE	DOCUMENT ID		TECN	COMMENT
0.8±0.3	[26] DEL-AMO-SA..10B		BABR	$B \to \omega J/\psi K$

[26] Statistical and systematic errors added in quadrature. Uses the values of $B(B \to X(3872)K) \times B(X(3872) \to J/\psi\pi^+\pi^-)$ reported in AUBERT 08Y, taking into account the common systematics.

$\Gamma(D^0\overline{D}{}^0\pi^0)/\Gamma_{total}$ Γ_5/Γ

VALUE	EVTS	DOCUMENT ID		TECN	COMMENT
>0.32	17 ± 5	[27] GOKHROO	06	BELL	$B^+ \to D^0\overline{D}{}^0\pi^0K^+$

[27] GOKHROO 06 reports $[\Gamma(X(3872) \to D^0\overline{D}{}^0\pi^0)/\Gamma_{total}] \times [B(B^+ \to X(3872)K^+)] = (1.02\pm0.31^{+0.21}_{-0.29})\times10^{-4}$ which we divide by our best value $B(B^+ \to X(3872)K^+) < 3.2\times10^{-4}$.

$\Gamma(\overline{D}{}^{*0}D^0)/\Gamma_{total}$ Γ_6/Γ

VALUE	EVTS	DOCUMENT ID		TECN	COMMENT
>0.24	41^{+9}_{-8}	[28] AUSHEV	10	BELL	$B^+ \to \overline{D}{}^{*0}\overline{D}{}^0K^+$
• • • We do not use the following data for averages, fits, limits, etc. • • •					
>0.5	27 ± 6	[29] AUBERT	08B	BABR	$B^+ \to \overline{D}{}^{*0}D^0K^+$

[28] AUSHEV 10 reports $[\Gamma(X(3872) \to \overline{D}{}^{*0}D^0)/\Gamma_{total}] \times [B(B^+ \to X(3872)K^+)] = (0.77 \pm 0.16 \pm 0.10)\times10^{-4}$ which we divide by our best value $B(B^+ \to X(3872)K^+) < 3.2\times10^{-4}$.

[29] AUBERT 08B reports $[\Gamma(X(3872) \to \overline{D}{}^{*0}D^0)/\Gamma_{total}] \times [B(B^+ \to X(3872)K^+)] = (1.67 \pm 0.36 \pm 0.47)\times10^{-4}$ which we divide by our best value $B(B^+ \to X(3872)K^+) < 3.2\times10^{-4}$.

$\Gamma(D^0\overline{D}{}^0\pi^0)/\Gamma(\pi^+\pi^- J/\psi(1S))$ Γ_5/Γ_2

VALUE	DOCUMENT ID		TECN	COMMENT
seen	[30] GOKHROO	06	BELL	$B \to D^0\overline{D}{}^0\pi^0K$
• • • We do not use the following data for averages, fits, limits, etc. • • •				
seen	AUSHEV	10	BELL	$B \to D^0\overline{D}{}^0\pi^0K$

[30] May not necessarily be the same state as that observed in the $J/\psi\pi^+\pi^-$ mode. Supersedes CHISTOV 04.

$\Gamma(D^0\overline{D}{}^0)/\Gamma(\pi^+\pi^- J/\psi(1S))$ Γ_8/Γ_2

VALUE	DOCUMENT ID		TECN	COMMENT
• • • We do not use the following data for averages, fits, limits, etc. • • •				
not seen	CHISTOV	04	BELL	$B \to KD^0\overline{D}{}^0$

$\Gamma(D^+D^-)/\Gamma(\pi^+\pi^- J/\psi(1S))$ Γ_9/Γ_2

VALUE	DOCUMENT ID		TECN	COMMENT
• • • We do not use the following data for averages, fits, limits, etc. • • •				
not seen	CHISTOV	04	BELL	$B \to KD^+D^-$

$\Gamma(\gamma\chi_{c1})/\Gamma(\pi^+\pi^- J/\psi(1S))$ Γ_{10}/Γ_2

VALUE	CL%	DOCUMENT ID		TECN	COMMENT
not seen		[31] BHARDWAJ	13	BELL	$B^+ \to \chi_{c1}\gamma K^+$
<0.89	90	CHOI	03	BELL	$B \to K\pi^+\pi^- J/\psi$

[31] Reported $B(B^\pm \to X(3872)K^\pm) \times B(X(3872) \to \gamma\chi_{c1}) < 1.9\times10^{-6}$ at 90% CL.

$\Gamma(\gamma\chi_{c2})/\Gamma(\pi^+\pi^- J/\psi(1S))$ Γ_{11}/Γ_2

VALUE	DOCUMENT ID		TECN	COMMENT
not seen	[32] BHARDWAJ	13	BELL	$B^\pm \to \chi_{c2}\gamma K^+$

[32] Reported $B(B^\pm \to X(3872)K^\pm) \times B(X(3872) \to \gamma\chi_{c2}) < 6.7\times10^{-6}$ at 90% CL.

$\Gamma(\eta J/\psi)/\Gamma(\pi^+\pi^- J/\psi(1S))$ Γ_{12}/Γ_2

VALUE	CL%	DOCUMENT ID		TECN	COMMENT
• • • We do not use the following data for averages, fits, limits, etc. • • •					
<0.6	90	AUBERT	04Y	BABR	$B \to K\eta J/\psi$

$\Gamma(\gamma J/\psi)/\Gamma_{total}$ Γ_{13}/Γ

VALUE	EVTS	DOCUMENT ID		TECN	COMMENT
>6 $\times10^{-3}$		[33] BHARDWAJ	11	BELL	$B^\pm \to \gamma J/\psi K^\pm$
• • • We do not use the following data for averages, fits, limits, etc. • • •					
>9 $\times10^{-3}$	20	[34] AUBERT	09B	BABR	$B^+ \to \gamma J/\psi K^+$
>0.010	19	[35] AUBERT,BE	06M	BABR	$B^+ \to \gamma J/\psi K^+$

[33] BHARDWAJ 11 reports $[\Gamma(X(3872) \to \gamma J/\psi)/\Gamma_{total}] \times [B(B^+ \to X(3872)K^+)] = (1.78^{+0.48}_{-0.44} \pm 0.12)\times10^{-6}$ which we divide by our best value $B(B^+ \to X(3872)K^+) < 3.2\times10^{-4}$.

[34] AUBERT 09B reports $[\Gamma(X(3872) \to \gamma J/\psi)/\Gamma_{total}] \times [B(B^+ \to X(3872)K^+)] = (2.8 \pm 0.8 \pm 0.1)\times10^{-6}$ which we divide by our best value $B(B^+ \to X(3872)K^+) < 3.2\times10^{-4}$.

[35] Superseded by AUBERT 09B. AUBERT,BE 06M reports $[\Gamma(X(3872) \to \gamma J/\psi)/\Gamma_{total}] \times [B(B^+ \to X(3872)K^+)] = (3.3 \pm 1.0 \pm 0.3)\times10^{-6}$ which we divide by our best value $B(B^+ \to X(3872)K^+) < 3.2\times10^{-4}$.

$\Gamma(\gamma\psi(2S))/\Gamma_{total}$ Γ_{14}/Γ

VALUE	EVTS	DOCUMENT ID		TECN	COMMENT
not seen		[36] BHARDWAJ	11	BELL	$B^+ \to \gamma\psi(2S)K^+$
>0.030	25 ± 7	[37] AUBERT	09B	BABR	$B^+ \to \gamma\psi(2S)K^+$

[36] BHARDWAJ 11 reports $B(B^+ \to K^+X(3872)) \times B(X \to \gamma\psi(2S)) < 3.45\times10^{-6}$ at 90% CL.

[37] AUBERT 09B reports $[\Gamma(X(3872) \to \gamma\psi(2S))/\Gamma_{total}] \times [B(B^+ \to X(3872)K^+)] = (9.5 \pm 2.7 \pm 0.6)\times10^{-6}$ which we divide by our best value $B(B^+ \to X(3872)K^+) < 3.2\times10^{-4}$.

$\Gamma(\gamma\psi(2S))/\Gamma(\gamma J/\psi)$ Γ_{14}/Γ_{13}

VALUE	CL%	DOCUMENT ID		TECN	COMMENT
<2.1	90	BHARDWAJ	11	BELL	$B^+ \to K^+\psi(2S)\gamma$
3.4±1.4		AUBERT	09B	BABR	$B^+ \to \gamma c\overline{c}K'$

$\Gamma(p\overline{p})/\Gamma(\pi^+\pi^- J/\psi(1S))$ Γ_{16}/Γ_2

VALUE	CL%	DOCUMENT ID		TECN	COMMENT
<2.0 $\times10^{-3}$	95	[38] AAIJ	13S	LHCB	$B^+ \to p\overline{p}K^+$

[38] AAIJ 13S reports $[\Gamma(X(3872) \to p\overline{p})/\Gamma(X(3872) \to \pi^+\pi^- J/\psi(1S))] \times [B(B^+ \to X(3872)K^+,\ X \to J/\psi\pi^+\pi^-)] < 1.7\times10^{-8}$ which we divide by our best value $B(B^+ \to X(3872)K^+,\ X \to J/\psi\pi^+\pi^-) = 8.6\times10^{-6}$.

$X(3872)$ REFERENCES

ABLIKIM	14	PRL 112 092001	M. Ablikim *et al.*	(BES III Collab.)
AAIJ	13Q	PRL 110 222001	R. Aaij *et al.*	(LHCb Collab.) JP
AAIJ	13S	EPJ C73 2462	R. Aaij *et al.*	(LHCb Collab.)
BHARDWAJ	13	PRL 111 032001	V. Bhardwaj *et al.*	(BELLE Collab.)
AAIJ	12H	EPJ C72 1972	R. Aaij *et al.*	(LHCb Collab.)
LEES	12AD	PR D86 072002	J.P. Lees *et al.*	(BABAR Collab.)
LEES	12AE	PR D86 092005	J.P. Lees *et al.*	(BABAR Collab.)
BHARDWAJ	11	PRL 107 091803	V. Bhardwaj *et al.*	(BELLE Collab.)
CHOI	11	PR D84 052004	S.-K. Choi *et al.*	(BELLE Collab.)
AUSHEV	10	PR D81 031103	T. Aushev *et al.*	(BELLE Collab.)
DEL-AMO-SA...	10B	PR D82 011101	P. del Amo Sanchez *et al.*	(BABAR Collab.)
AALTONEN	09AU	PRL 103 152001	T. Aaltonen *et al.*	(CDF Collab.)
AUBERT	09B	PRL 102 132001	B. Aubert *et al.*	(BABAR Collab.)
AUBERT	08B	PR D77 011102	B. Aubert *et al.*	(BABAR Collab.)
AUBERT	08Y	PR D77 111101	B. Aubert *et al.*	(BABAR Collab.)
AUBERT	06	PR D73 011101	B. Aubert *et al.*	(BABAR Collab.)
AUBERT,BE	06M	PR D74 071101	B. Aubert *et al.*	(BABAR Collab.)
GOKHROO	06	PRL 97 162002	G. Gokhroo *et al.*	(BELLE Collab.)
AUBERT	05B	PR D71 031501	B. Aubert *et al.*	(BABAR Collab.)
AUBERT	05D	PR D71 052001	B. Aubert *et al.*	(BABAR Collab.)
AUBERT	05R	PR D71 071103	B. Aubert *et al.*	(BABAR Collab.)
DOBBS	05	PRL 94 032004	S. Dobbs *et al.*	(CLEO Collab.)
ABAZOV	04F	PRL 93 162002	V.M. Abazov *et al.*	(D0 Collab.)
ACOSTA	04	PRL 93 072001	D. Acosta *et al.*	(CDF Collab.)
AUBERT	04Y	PRL 93 041801	B. Aubert *et al.*	(BaBar Collab.)
CHISTOV	04	PRL 93 051803	R. Chistov *et al.*	(BELLE Collab.)
PDG	04	PL B592 1	S. Eidelman *et al.*	(PDG Collab.)
YUAN	04	PL B579 74	C.Z. Yuan *et al.*	
CHOI	03	PRL 91 262001	S.-K. Choi *et al.*	(BELLE Collab.)
BAI	98E	PR D57 3854	J.Z. Bai *et al.*	(BES Collab.)
ANTONIAZZI	94	PR D50 4258	L. Antoniazzi *et al.*	(E705 Collab.)

Meson Particle Listings

$X(3900)^{\pm}$, $X(3900)^0$, $\chi_{c0}(2P)$

$X(3900)^{\pm}$

$I(J^P) = ?(1^+)$

Seen as a peak in the invariant mass distribution of the $J/\psi\pi^{\pm}$ system by BES3 (ABLIKIM 13T) in $e^+e^- \to \pi^+\pi^- J/\psi$ at c.m. energy of 4.42 GeV and by radiative return from e^+e^- collisions at $\sqrt{s}$ from 9.46 to 10.86 GeV at BELLE (LIU 13B). Angular analysis of ABLIKIM 14A favors the $J^P = 1^+$ assignment. Needs confirmation.

$X(3900)^{\pm}$ MASS

VALUE (MeV)	EVTS	DOCUMENT ID		TECN	COMMENT
3888.7±3.4 OUR AVERAGE		Error includes scale factor of 1.3. See the ideogram below.			
3883.9±1.5±4.2	1.2k	[1,2] ABLIKIM	14A	BES3	$e^+e^- \to \pi^{\pm}(D\overline{D}^*)^{\mp}$
3899.0±3.6±4.9	307 ± 48	[1] ABLIKIM	13T	BES3	$e^+e^- \to \pi^+\pi^- J/\psi$
3894.5±6.6±4.5	159 ± 49	[1] LIU	13B	BELL	$e^+e^- \to \gamma\pi^+\pi^- J/\psi$
3886 ±4 ±2	81 ± 16	[3] XIAO	13A		4.17 $e^+e^- \to \pi^+\pi^- J/\psi$

[1] Neglecting interference between the $X(3900)$ and non-resonant continuum.
[2] With estimated statistical signifance of more than 18 σ.
[3] For $M^2(\pi^+\pi^-) < 0.65$ GeV^2. Signal has 5.7σ significance including systematic uncertainties. Obtained by analyzing CLEO-c data but not authored by the CLEO Collaboration.

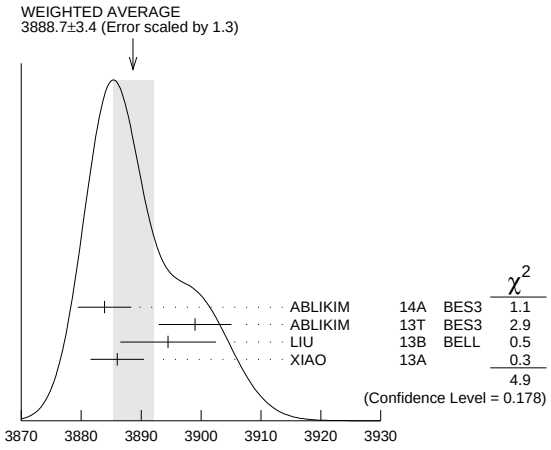

$X(3900)^{\pm}$ WIDTH

VALUE (MeV)	EVTS	DOCUMENT ID		TECN	COMMENT
35 ± 7 OUR AVERAGE					
24.8± 3.3±11.0	1.2k	[1,2] ABLIKIM	14A	BES3	$e^+e^- \to \pi^{\pm}(D\overline{D}^*)^{\mp}$
46 ±10 ±20	307 ± 48	[1] ABLIKIM	13T	BES3	$e^+e^- \to \pi^+\pi^- J/\psi$
63 ±24 ±26	159 ± 49	[1] LIU	13B	BELL	$e^+e^- \to \gamma\pi^+\pi^- J/\psi$
37 ± 4 ± 8	81 ± 16	[3] XIAO	13A		4.17 $e^+e^- \to \pi^+\pi^- J/\psi$

[1] Neglecting interference between the $X(3900)$ and non-resonant continuum.
[2] With estimated statistical signifance of more than 18 σ.
[3] For $M^2(\pi^+\pi^-) < 0.65$ GeV^2. Signal has 5.7σ significance including systematic uncertainties. Obtained by analyzing CLEO-c data but not authored by the CLEO Collaboration.

$X(3900)^{\pm}$ DECAY MODES

	Mode	Fraction (Γ_i/Γ)
Γ_1	$J/\psi\pi^{\pm}$	seen
Γ_2	$h_c\pi^{\pm}$	not seen
Γ_3	$(D\overline{D}^*)^{\pm}$	seen

$X(3900)^{\pm}$ BRANCHING RATIOS

$\Gamma(J/\psi\pi^{\pm})/\Gamma_{total}$ — **Γ_1/Γ**

VALUE	EVTS	DOCUMENT ID	TECN	COMMENT
seen	307 ± 48	ABLIKIM 13T	BES3	$e^+e^- \to \pi^+\pi^- J/\psi$

$\Gamma(h_c\pi^{\pm})/\Gamma_{total}$ — **Γ_2/Γ**

VALUE	DOCUMENT ID	TECN	COMMENT
not seen	ABLIKIM 13X	BES3	$e^+e^- \to h_c\pi^{\pm}$

$\Gamma((D\overline{D}^*)^{\pm})/\Gamma(J/\psi\pi^{\pm})$ — **Γ_3/Γ_1**

VALUE	EVTS	DOCUMENT ID		TECN	COMMENT
6.2±1.1±2.7	1.2k	[1] ABLIKIM	14A	BES3	$e^+e^- \to \pi^{\pm}(D\overline{D}^*)^{\mp}$

[1] Assuming the same origin of the $(D\overline{D}^*)^{\pm}$ and $\pi^{\pm}J/\psi$ decay modes.

$X(3900)^{\pm}$ REFERENCES

ABLIKIM	14A	PRL 112 022001	M. Ablikim *et al.*	(BES III Collab.) JP
ABLIKIM	13T	PRL 110 252001	M. Ablikim *et al.*	(BES III Collab.)
ABLIKIM	13X	PRL 111 242001	M. Ablikim *et al.*	(BES III Collab.)
LIU	13B	PRL 110 252002	Z.Q. Liu *et al.*	(BELLE Collab.)
XIAO	13A	PL B727 366	T. Xiao *et al.*	(NWES)

$X(3900)^0$

$I(J^P) = ?(?^?)$

OMITTED FROM SUMMARY TABLE

Seen by XIAO 13A in $e^+e^- \to \pi^0 X^0$, $X^0 \to \pi^0 J/\psi$ at $\sqrt{s}$ = 4170 MeV. Likely the isospin partner of the $X(3900)^{\pm}$.

$X(3900)^0$ MASS

VALUE (MeV)	EVTS	DOCUMENT ID		TECN	COMMENT
3904±9±5	25 ± 7	[1] XIAO	13A		4.17 $e^+e^- \to \pi^+\pi^- J/\psi$

[1] For $M^2(\pi^0\pi^0) < 0.65$ GeV^2 and fixed width of 37 MeV. The signal has 3.5σ significance including systematic uncertainties. Obtained by analyzing CLEO-c data but not authored by the CLEO Collaboration.

$X(3900)^0$ DECAY MODES

	Mode	Fraction (Γ_i/Γ)
Γ_1	$J/\psi\pi^0$	seen

$X(3900)^0$ BRANCHING RATIOS

$\Gamma(J/\psi\pi^0)/\Gamma_{total}$ — **Γ_1/Γ**

VALUE	EVTS	DOCUMENT ID		COMMENT
seen	25 ± 7	[1] XIAO	13A	4.17 $e^+e^- \to \pi^+\pi^- J/\psi$

[1] Obtained by analyzing CLEO-c data but not authored by the CLEO Collaboration.

$X(3900)^0$ REFERENCES

XIAO	13A	PL B727 366	T. Xiao *et al.*	(NWES)

$\chi_{c0}(2P)$ was $X(3915)$

$I^G(J^{PC}) = 0^+(0^{++})$

$\chi_{c0}(2P)$ MASS

VALUE (MeV)	EVTS	DOCUMENT ID		TECN	COMMENT
3918.4± 1.9 OUR AVERAGE					
3919.4± 2.2± 1.6	59 ± 10	LEES	12AD	BABR	$e^+e^- \to e^+e^-\omega J/\psi$
$3919.1^{+3.8}_{-3.4}$± 2.0		DEL-AMO-SA..10B		BABR	$B \to \omega J/\psi K$
3915 ± 3 ± 2	49 ± 15	UEHARA	10	BELL	10.6 $e^+e^- \to e^+e^-\omega J/\psi$
3943 ±11 ±13	58 ± 11	[1] CHOI	05	BELL	$B \to \omega J/\psi K$
• • • We do not use the following data for averages, fits, limits, etc. • • •					
$3914.6^{+3.8}_{-3.4}$± 2.0		[1] AUBERT	08W	BABR	Superseded by DEL-AMO-SANCHEZ 10B

[1] $\omega J/\psi$ threshold enhancement fitted as an S-wave Breit-Wigner resonance.

$\chi_{c0}(2P)$ WIDTH

VALUE (MeV)	EVTS	DOCUMENT ID		TECN	COMMENT
20± 5 OUR AVERAGE		Error includes scale factor of 1.1.			
13± 6± 3	59 ± 10	LEES	12AD	BABR	$e^+e^- \to e^+e^-\omega J/\psi$
31^{+10}_{-8}± 5		DEL-AMO-SA..10B		BABR	$B \to \omega J/\psi K$
17±10± 3	49 ± 15	UEHARA	10	BELL	10.6 $e^+e^- \to e^+e^-\omega J/\psi$
87±22±26	58 ± 11	[2] CHOI	05	BELL	$B \to \omega J/\psi K$
• • • We do not use the following data for averages, fits, limits, etc. • • •					
34^{+12}_{-8}± 5		[2] AUBERT	08W	BABR	Superseded by DEL-AMO-SANCHEZ 10B

[2] $\omega J/\psi$ threshold enhancement fitted as an S-wave Breit-Wigner resonance.

$\chi_{c0}(2P)$ DECAY MODES

	Mode	Fraction (Γ_i/Γ)
Γ_1	$\omega J/\psi$	seen
Γ_2	$\overline{D}^{*0}D^0$	
Γ_3	$\pi^+\pi^-\eta_c(1S)$	not seen
Γ_4	$K\overline{K}$	not seen
Γ_5	$\gamma\gamma$	seen

$\chi_{c0}(2P)$ Γ(i)$\Gamma(\gamma\gamma)/\Gamma$(total)

$\Gamma(\omega J/\psi) \times \Gamma(\gamma\gamma)/\Gamma_{total}$ $\Gamma_1\Gamma_5/\Gamma$

VALUE (eV)	EVTS	DOCUMENT ID		TECN	COMMENT
54± 9 OUR AVERAGE					
52±10±3	59 ± 10	[3] LEES	12AD	BABR	$e^+e^- \to e^+e^-\omega J/\psi$
61±17±8	49 ± 15	[3] UEHARA	10	BELL	10.6 $e^+e^- \to e^+e^-\omega J/\psi$
• • • We do not use the following data for averages, fits, limits, etc. • • •					
18± 5±2	49 ± 15	[4] UEHARA	10	BELL	10.6 $e^+e^- \to e^+e^-\omega J/\psi$

[3] For $J^P = 0^+$.
[4] For $J^P = 2^+$, helicity-2.

$\Gamma(\pi^+\pi^-\eta_c(1S)) \times \Gamma(\gamma\gamma)/\Gamma_{total}$ $\Gamma_3\Gamma_5/\Gamma$

VALUE (eV)	CL%	DOCUMENT ID		TECN	COMMENT
<16	90	LEES	12AE	BABR	$e^+e^- \to e^+e^-\pi^+\pi^-\eta_c$

$\Gamma(K\overline{K}) \times \Gamma(\gamma\gamma)/\Gamma_{total}$ $\Gamma_4\Gamma_5/\Gamma$

VALUE (eV)	CL%	DOCUMENT ID		TECN	COMMENT
<1.96	90	UEHARA	13	BELL	$\gamma\gamma \to K^0_S K^0_S$

$\chi_{c0}(2P)$ BRANCHING RATIOS

$\Gamma(\gamma\gamma)/\Gamma_{total}$ Γ_5/Γ

VALUE	EVTS	DOCUMENT ID		TECN	COMMENT
seen	59 ± 10	LEES	12AD	BABR	$e^+e^- \to e^+e^-\omega J/\psi$
seen		UEHARA	10	BELL	10.6 $e^+e^- \to e^+e^-\omega J/\psi$

$\Gamma(\omega J/\psi)/\Gamma(\overline{D}^{*0}D^0)$ Γ_1/Γ_2

VALUE	CL%	DOCUMENT ID		TECN	COMMENT
>0.71	90	[5] AUSHEV	10	BELL	$B \to \overline{D}^{*0}D^0K$

[5] By combining the upper limit $B(B \to X(3915)K) \times B(X(3915) \to D^{*0}\overline{D}^0) < 0.67 \times 10^{-4}$ from AUSHEV 10 with the average of CHOI 05 and AUBERT 08W measurements $B(B \to X(3915)K) \times B(X(3915) \to \omega J/\psi) = (0.51 \pm 0.11) \times 10^{-4}$.

$\Gamma(\omega J/\psi)/\Gamma_{total}$ Γ_1/Γ

VALUE	DOCUMENT ID		TECN	COMMENT
seen	[6] DEL-AMO-SA...	10B	BABR	$B \to \omega J/\psi K$
seen	[7] CHOI	05	BELL	$B \to \omega J/\psi K$

[6] DEL-AMO-SANCHEZ 10B reports $B(B^\pm \to X(3915)K^\pm) \times B(X(3915) \to J/\psi\omega) = (3.0^{+0.7+0.5}_{-0.6-0.3}) \times 10^{-5}$ and $B(B^0 \to X(3915)K^0) \times B(X(3915) \to J/\psi\omega) = (2.1 \pm 0.9 \pm 0.3) \times 10^{-5}$.
[7] CHOI 05 reports $B(B \to X(3915)K) \times B(X(3915) \to J/\psi\omega) = (7.1 \pm 1.3 \pm 3.1) \times 10^{-5}$.

$\chi_{c0}(2P)$ REFERENCES

UEHARA	13	PTEP 2013 123C01	S. Uehara *et al.*	(BELLE Collab.)
LEES	12AD	PR D86 072002	J.P. Lees *et al.*	(BABAR Collab.)
LEES	12AE	PR D86 092005	J.P. Lees *et al.*	(BABAR Collab.)
AUSHEV	10	PR D81 031103	T. Aushev *et al.*	(BELLE Collab.)
DEL-AMO-SA...	10B	PR D82 011101	P. del Amo Sanchez *et al.*	(BABAR Collab.)
UEHARA	10	PRL 104 092001	S. Uehara *et al.*	(BELLE Collab.)
AUBERT	08W	PRL 101 082001	B. Aubert *et al.*	(BABAR Collab.)
CHOI	05	PRL 94 182002	S.-K. Choi *et al.*	(BELLE Collab.)

$\chi_{c2}(2P)$

$I^G(J^{PC}) = 0^+(2^{++})$

$\chi_{c2}(2P)$ MASS

VALUE (MeV)	EVTS	DOCUMENT ID		TECN	COMMENT
3927.2±2.6 OUR AVERAGE					
3926.7±2.7±1.1	76 ± 17	AUBERT	10G	BABR	10.6 $e^+e^- \to e^+e^-D\overline{D}$
3929 ±5 ±2	64	UEHARA	06	BELL	10.6 $e^+e^- \to e^+e^-D\overline{D}$

$\chi_{c2}(2P)$ WIDTH

VALUE (MeV)	EVTS	DOCUMENT ID		TECN	COMMENT
24 ± 6 OUR AVERAGE					
21.3± 6.8±3.6	76 ± 17	AUBERT	10G	BABR	10.6 $e^+e^- \to e^+e^-D\overline{D}$
29 ±10 ±2	64	UEHARA	06	BELL	10.6 $e^+e^- \to e^+e^-D\overline{D}$

$\chi_{c2}(2P)$ DECAY MODES

	Mode	Fraction (Γ_i/Γ)
Γ_1	$\gamma\gamma$	seen
Γ_2	$K\overline{K}\pi$	
Γ_3	$K^+K^-\pi^+\pi^-\pi^0$	
Γ_4	$D\overline{D}$	seen
Γ_5	D^+D^-	seen
Γ_6	$D^0\overline{D}^0$	seen
Γ_7	$\pi^+\pi^-\eta_c(1S)$	not seen
Γ_8	$K\overline{K}$	not seen

$\chi_{c2}(2P)$ PARTIAL WIDTHS

$\chi_{c2}(2P)$ Γ(i)$\Gamma(\gamma\gamma)/\Gamma$(total)

$\Gamma(K\overline{K}\pi) \times \Gamma(\gamma\gamma)/\Gamma_{total}$ $\Gamma_2\Gamma_1/\Gamma$

VALUE (eV)	CL%	DOCUMENT ID		TECN	COMMENT
<2.1	90	DEL-AMO-SA...	11M	BABR	$\gamma\gamma \to K^0_S K^\pm\pi^\mp$

$\Gamma(K^+K^-\pi^+\pi^-\pi^0) \times \Gamma(\gamma\gamma)/\Gamma_{total}$ $\Gamma_3\Gamma_1/\Gamma$

VALUE (eV)	CL%	DOCUMENT ID		TECN	COMMENT
<3.4	90	DEL-AMO-SA...	11M	BABR	$\gamma\gamma \to K^+K^-\pi^+\pi^-\pi^0$

$\Gamma(D\overline{D}) \times \Gamma(\gamma\gamma)/\Gamma_{total}$ $\Gamma_4\Gamma_1/\Gamma$

VALUE (keV)	EVTS	DOCUMENT ID		TECN	COMMENT
0.21±0.04 OUR AVERAGE					
0.24±0.05±0.04	76 ± 17	AUBERT	10G	BABR	10.6 $e^+e^- \to e^+e^-D\overline{D}$
0.18±0.05±0.03	64	[1] UEHARA	06	BELL	10.6 $e^+e^- \to e^+e^-D\overline{D}$

[1] Assuming $B(D^+D^-) = 0.89\ B(D^0\overline{D}^0)$.

$\Gamma(\pi^+\pi^-\eta_c(1S)) \times \Gamma(\gamma\gamma)/\Gamma_{total}$ $\Gamma_7\Gamma_1/\Gamma$

VALUE (eV)	CL%	DOCUMENT ID		TECN	COMMENT
<18	90	LEES	12AE	BABR	$e^+e^- \to e^+e^-\pi^+\pi^-\eta_c$

$\Gamma(K\overline{K}) \times \Gamma(\gamma\gamma)/\Gamma_{total}$ $\Gamma_8\Gamma_1/\Gamma$

VALUE (eV)	CL%	DOCUMENT ID		TECN	COMMENT
<0.256	90	UEHARA	13	BELL	$\gamma\gamma \to K^0_S K^0_S$

$\chi_{c2}(2P)$ BRANCHING RATIOS

$\Gamma(D^+D^-)/\Gamma(D^0\overline{D}^0)$ Γ_5/Γ_6

VALUE	EVTS	DOCUMENT ID		TECN	COMMENT
0.74±0.43±0.16	64	UEHARA	06	BELL	10.6 $e^+e^- \to e^+e^-D\overline{D}$

$\chi_{c2}(2P)$ REFERENCES

UEHARA	13	PTEP 2013 123C01	S. Uehara *et al.*	(BELLE Collab.)
LEES	12AE	PR D86 092005	J.P. Lees *et al.*	(BABAR Collab.)
DEL-AMO-SA...	11M	PR D84 012004	P. del Amo Sanchez *et al.*	(BABAR Collab.)
AUBERT	10G	PR D81 092003	B. Aubert *et al.*	(BABAR Collab.)
UEHARA	06	PRL 96 082003	S. Uehara *et al.*	(BELLE Collab.)

$X(3940)$

$I^G(J^{PC}) = ?^?(?^{??})$

OMITTED FROM SUMMARY TABLE
Reported by ABE 07, observed in $e^+e^- \to J/\psi X$.

$X(3940)$ MASS

VALUE (MeV)	EVTS	DOCUMENT ID		TECN	COMMENT
$3942^{+\ 7}_{-\ 6}\pm6$	52	PAKHLOV	08	BELL	$e^+e^- \to J/\psi X$
• • • We do not use the following data for averages, fits, limits, etc. • • •					
3943± 6±6	25	[1] ABE	07	BELL	$e^+e^- \to J/\psi X$
3936±14	266	[2] ABE	07	BELL	$e^+e^- \to J/\psi(c\overline{c})$

[1] From a fit to $D^{*+}D^-$ and $D^{*0}\overline{D}^0$ events.
[2] From the inclusive fit. Not independent of the exclusive measurement by ABE 07.

$X(3940)$ WIDTH

VALUE (MeV)	CL%	EVTS	DOCUMENT ID		TECN	COMMENT
$37^{+26}_{-15}\pm8$		52	PAKHLOV	08	BELL	$e^+e^- \to J/\psi X$
• • • We do not use the following data for averages, fits, limits, etc. • • •						
<52	90	25	ABE	07	BELL	$e^+e^- \to J/\psi X$

$X(3940)$ DECAY MODES

	Mode	Fraction (Γ_i/Γ)
Γ_1	$D\overline{D}^*$ + c.c.	seen
Γ_2	$D\overline{D}$	not seen
Γ_3	$J/\psi\omega$	not seen

$X(3940)$ BRANCHING RATIOS

$\Gamma(D\overline{D}^*$ + c.c.$)/\Gamma_{total}$ Γ_1/Γ

VALUE	CL%	EVTS	DOCUMENT ID		TECN	COMMENT
• • • We do not use the following data for averages, fits, limits, etc. • • •						
>0.45	90	25	[3,4] ABE	07	BELL	$e^+e^- \to J/\psi X$

[3] For $X(3940)$ decaying to final states with more than two tracks.
[4] PAKHLOV 08 finds that the inclusive peak near 3940 MeV/c^2 may consist of several states.

Meson Particle Listings

$X(3940)$, $X(4020)^{\pm}$, $\psi(4040)$

$\Gamma(D\overline{D})/\Gamma_{total}$ Γ_2/Γ

VALUE	CL%	DOCUMENT ID		TECN	COMMENT
• • • We do not use the following data for averages, fits, limits, etc. • • •					
<0.41	90	[5,6] ABE	07	BELL	$e^+e^- \to J/\psi X$

[5] For $X(3940)$ decaying to final states with more than two tracks.
[6] PAKHLOV 08 finds that the inclusive peak near 3940 MeV/c^2 may consist of several states.

$\Gamma(J/\psi\omega)/\Gamma_{total}$ Γ_3/Γ

VALUE	CL%	DOCUMENT ID		TECN	COMMENT
• • • We do not use the following data for averages, fits, limits, etc. • • •					
<0.26	90	[7,8] ABE	07	BELL	$e^+e^- \to J/\psi X$

[7] For $X(3940)$ decaying to final states with more than two tracks.
[8] PAKHLOV 08 finds that the inclusive peak near 3940 MeV/c^2 may consist of several states.

$X(3940)$ REFERENCES

PAKHLOV 08 PRL 100 202001 P. Pakhlov *et al.* (BELLE Collab.)
ABE 07 PRL 98 082001 K. Abe *et al.* (BELLE Collab.)

$X(4020)^{\pm}$ $I(J^P) = ?(?^?)$

OMITTED FROM SUMMARY TABLE

Seen by ABLIKIM 13X in $e^+e^- \to \pi^+\pi^- h_c$ at c.m. energy from 3.90 to 4.42 GeV as a peak in the invariant mass distribution of the $h_c\pi^{\pm}$ system. Needs confirmation.

$X(4020)^{\pm}$ MASS

VALUE (MeV)	EVTS	DOCUMENT ID		TECN	COMMENT
4023.9±2.4 OUR AVERAGE					
4026.3±2.6±3.7	0.4k	[1] ABLIKIM	14B	BES3	$e^+e^- \to (D^*\overline{D}^*)^{\pm}\pi^{\mp}$
4022.9±0.8±2.7	253	ABLIKIM	13X	BES3	$e^+e^- \to \pi^+\pi^- h_c$

[1] Neglecting interference between the $X(4020)$ and non-resonant continuum. Assuming the same origin of the $(D^*\overline{D}^*)^+$ and $h_c\pi^+$ decay modes.

$X(4020)^{\pm}$ WIDTH

VALUE (MeV)	EVTS	DOCUMENT ID		TECN	COMMENT
10 ±6 OUR AVERAGE Error includes scale factor of 1.7.					
24.8±5.6±7.7	0.4k	[1] ABLIKIM	14B	BES3	$e^+e^- \to (D^*\overline{D}^*)^{\pm}\pi^{\mp}$
7.9±2.7±2.6	253	ABLIKIM	13X	BES3	$e^+e^- \to \pi^+\pi^- h_c$

[1] Neglecting interference between the $X(4020)$ and non-resonant continuum. Assuming the same origin of the $(D^*\overline{D}^*)^+$ and $h_c\pi^+$ decay modes.

$X(4020)^{\pm}$ DECAY MODES

	Mode	Fraction (Γ_i/Γ)
Γ_1	$h_c\pi^{\pm}$	seen
Γ_2	$D^*\overline{D}^*$	seen

$X(4020)^{\pm}$ BRANCHING RATIOS

$\Gamma(h_c\pi^{\pm})/\Gamma_{total}$ Γ_1/Γ

VALUE	EVTS	DOCUMENT ID		TECN	COMMENT
seen	253	ABLIKIM	13X	BES3	$e^+e^- \to \pi^+\pi^- h_c$

$\Gamma(D^*\overline{D}^*)/\Gamma_{total}$ Γ_2/Γ

VALUE	EVTS	DOCUMENT ID		TECN	COMMENT
seen	0.4k	[1] ABLIKIM	14B	BES3	$e^+e^- \to (D^*\overline{D}^*)^{\pm}\pi^{\mp}$

[1] Neglecting interference between the $X(4020)$ and non-resonant continuum.

$X(4020)^{\pm}$ REFERENCES

ABLIKIM 14B PRL 112 132001 M. Ablikim *et al.* (BES III Collab.)
ABLIKIM 13X PRL 111 242001 M. Ablikim *et al.* (BES III Collab.)

$\psi(4040)$ $I^G(J^{PC}) = 0^-(1^{--})$

$\psi(4040)$ MASS

VALUE (MeV)	DOCUMENT ID		TECN	COMMENT
4039 ± 1 OUR ESTIMATE				
4039.6± 4.3	[1] ABLIKIM	08D	BES2	$e^+e^- \to$ hadrons
• • • We do not use the following data for averages, fits, limits, etc. • • •				
4034 ± 6	[2] MO	10	RVUE	$e^+e^- \to$ hadrons
4037 ± 2	[3] SETH	05A	RVUE	$e^+e^- \to$ hadrons
4040 ± 1	[4] SETH	05A	RVUE	$e^+e^- \to$ hadrons
4040 ±10	BRANDELIK	78C	DASP	e^+e^-

[1] Reanalysis of data presented in BAI 02C. From a global fit over the center-of-mass energy region 3.7–5.0 GeV covering the $\psi(3770)$, $\psi(4040)$, $\psi(4160)$, and $\psi(4415)$ resonances. Phase angle fixed in the fit to $\delta = (130 \pm 46)^{\circ}$.
[2] Reanalysis of data presented in BAI 00 and BAI 02C. From a global fit over the center-of-mass energy 3.8–4.8 GeV covering the $\psi(4040)$, $\psi(4160)$ and $\psi(4415)$ resonances and including interference effects.
[3] From a fit to Crystal Ball (OSTERHELD 86) data.
[4] From a fit to BES (BAI 02C) data.

$\psi(4040)$ WIDTH

VALUE (MeV)	DOCUMENT ID		TECN	COMMENT
80 ±10 OUR ESTIMATE				
84.5±12.3	[5] ABLIKIM	08D	BES2	$e^+e^- \to$ hadrons
• • • We do not use the following data for averages, fits, limits, etc. • • •				
87 ±11	[6] MO	10	RVUE	$e^+e^- \to$ hadrons
85 ±10	[7] SETH	05A	RVUE	$e^+e^- \to$ hadrons
89 ± 6	[8] SETH	05A	RVUE	$e^+e^- \to$ hadrons
52 ±10	BRANDELIK	78C	DASP	e^+e^-

[5] Reanalysis of data presented in BAI 02C. From a global fit over the center-of-mass energy region 3.7–5.0 GeV covering the $\psi(3770)$, $\psi(4040)$, $\psi(4160)$, and $\psi(4415)$ resonances. Phase angle fixed in the fit to $\delta = (130 \pm 46)^{\circ}$.
[6] Reanalysis of data presented in BAI 00 and BAI 02C. From a global fit over the center-of-mass energy 3.8–4.8 GeV covering the $\psi(4040)$, $\psi(4160)$ and $\psi(4415)$ resonances and including interference effects.
[7] From a fit to Crystal Ball (OSTERHELD 86) data.
[8] From a fit to BES (BAI 02C) data.

$\psi(4040)$ DECAY MODES

Due to the complexity of the $c\overline{c}$ threshold region, in this listing, "seen" ("not seen") means that a cross section for the mode in question has been measured at effective $\sqrt{s}$ near this particle's central mass value, more (less) than 2σ above zero, without regard to any peaking behavior in $\sqrt{s}$ or absence thereof. See mode listing(s) for details and references.

	Mode	Fraction (Γ_i/Γ)		Confidence level
Γ_1	e^+e^-	$(1.07\pm0.16)\times10^{-5}$		
Γ_2	$D\overline{D}$	seen		
Γ_3	$D^0\overline{D}^0$	seen		
Γ_4	D^+D^-	seen		
Γ_5	$D^*\overline{D}$ + c.c.	seen		
Γ_6	$D^*(2007)^0\overline{D}^0$ + c.c.	seen		
Γ_7	$D^*(2010)^+D^-$ + c.c.	seen		
Γ_8	$D^*\overline{D}^*$	seen		
Γ_9	$D^*(2007)^0\overline{D}^*(2007)^0$	seen		
Γ_{10}	$D^*(2010)^+D^*(2010)^-$	seen		
Γ_{11}	$D\overline{D}\pi$ (excl. $D^*\overline{D}$)			
Γ_{12}	$D^0D^-\pi^+$ + c.c. (excl. $D^*(2007)^0\overline{D}^0$ + c.c., $D^*(2010)^+D^-$ + c.c.)	not seen		
Γ_{13}	$D\overline{D}^*\pi$ (excl. $D^*\overline{D}^*$)	not seen		
Γ_{14}	$D^0\overline{D}^{*-}\pi^+$ + c.c. (excl. $D^*(2010)^+D^*(2010)^-$)	seen		
Γ_{15}	$D_s^+D_s^-$	seen		
Γ_{16}	$J/\psi(1S)$ hadrons			
Γ_{17}	$J/\psi\pi^+\pi^-$	< 4	$\times10^{-3}$	90%
Γ_{18}	$J/\psi\pi^0\pi^0$	< 2	$\times10^{-3}$	90%
Γ_{19}	$J/\psi\eta$	$(5.2\ \pm0.7\ )\times10^{-3}$		
Γ_{20}	$J/\psi\pi^0$	< 2.8	$\times10^{-4}$	90%
Γ_{21}	$J/\psi\pi^+\pi^-\pi^0$	< 2	$\times10^{-3}$	90%
Γ_{22}	$\chi_{c1}\gamma$	< 1.1	%	90%
Γ_{23}	$\chi_{c2}\gamma$	< 1.7	%	90%
Γ_{24}	$\chi_{c1}\pi^+\pi^-\pi^0$	< 1.1	%	90%
Γ_{25}	$\chi_{c2}\pi^+\pi^-\pi^0$	< 3.2	%	90%

Γ_{26}	$h_c(1P)\pi^+\pi^-$	< 3	$\times 10^{-3}$	90%
Γ_{27}	$\phi\pi^+\pi^-$	< 3	$\times 10^{-3}$	90%
Γ_{28}	$\Lambda\overline{\Lambda}\pi^+\pi^-$	< 2.9	$\times 10^{-4}$	90%
Γ_{29}	$\Lambda\overline{\Lambda}\pi^0$	< 9	$\times 10^{-5}$	90%
Γ_{30}	$\Lambda\overline{\Lambda}\eta$	< 3.0	$\times 10^{-4}$	90%
Γ_{31}	$\Sigma^+\overline{\Sigma}{}^-$	< 1.3	$\times 10^{-4}$	90%
Γ_{32}	$\Sigma^0\overline{\Sigma}{}^0$	< 7	$\times 10^{-5}$	90%
Γ_{33}	$\Xi^+\overline{\Xi}{}^-$	< 1.6	$\times 10^{-4}$	90%
Γ_{34}	$\Xi^0\overline{\Xi}{}^0$	< 1.8	$\times 10^{-4}$	90%
Γ_{35}	$\mu^+\mu^-$			

$\psi(4040)$ PARTIAL WIDTHS

$\Gamma(e^+e^-)$ Γ_1

VALUE (keV)	DOCUMENT ID		TECN	COMMENT
0.86±0.07 OUR ESTIMATE				
0.83±0.20	[9] ABLIKIM	08D	BES2	$e^+e^- \to$ hadrons
• • • We do not use the following data for averages, fits, limits, etc. • • •				
0.6 to 1.4	[10] MO	10	RVUE	$e^+e^- \to$ hadrons
0.88±0.11	[11] SETH	05A	RVUE	$e^+e^- \to$ hadrons
0.91±0.13	[12] SETH	05A	RVUE	$e^+e^- \to$ hadrons
0.75±0.15	BRANDELIK	78C	DASP	e^+e^-

[9] Reanalysis of data presented in BAI 02C. From a global fit over the center-of-mass energy region 3.7–5.0 GeV covering the $\psi(3770)$, $\psi(4040)$, $\psi(4160)$, and $\psi(4415)$ resonances. Phase angle fixed in the fit to $\delta = (130 \pm 46)^\circ$.

[10] Reanalysis of data presented in BAI 00 and BAI 02C. From a global fit over the center-of-mass energy 3.8–4.8 GeV covering the $\psi(4040)$, $\psi(4160)$ and $\psi(4415)$ resonances and including interference effects. Four sets of solutions are obtained with the same fit quality, mass and total width, but with different e^+e^- partial widths. We quote only the range of values.

[11] From a fit to Crystal Ball (OSTERHELD 86) data.

[12] From a fit to BES (BAI 02C) data.

$\psi(4040)$ $\Gamma(i)\Gamma(e^+e^-)/\Gamma^2(\text{total})$

$\Gamma(J/\psi\eta)/\Gamma_{\text{total}} \times \Gamma(e^+e^-)/\Gamma_{\text{total}}$ $\Gamma_{19}/\Gamma \times \Gamma_1/\Gamma$

VALUE (units 10^{-8})	DOCUMENT ID		TECN	COMMENT
• • • We do not use the following data for averages, fits, limits, etc. • • •				
5.1±1.4±1.5	[13] WANG	13B	BELL	$e^+e^- \to J/\psi\eta\gamma$
12.8±2.1±1.9	[14] WANG	13B	BELL	$e^+e^- \to J/\psi\eta\gamma$

[13] Solution I of two equivalent solutions in a fit using two interfering resonances. Mass and width fixed at 4039 MeV and 80 MeV, respectively.

[14] Solution II of two equivalent solutions in a fit using two interfering resonances. Mass and width fixed at 4039 MeV and 80 MeV, respectively.

$\psi(4040)$ BRANCHING RATIOS

$\Gamma(e^+e^-)/\Gamma_{\text{total}}$ Γ_1/Γ

VALUE (units 10^{-5})	DOCUMENT ID		TECN	COMMENT
• • • We do not use the following data for averages, fits, limits, etc. • • •				
~ 1.0	FELDMAN	77	MRK1	e^+e^-

$\Gamma(D^0\overline{D}{}^0)/\Gamma_{\text{total}}$ Γ_3/Γ

VALUE	DOCUMENT ID		TECN	COMMENT
seen	AUBERT	09M	BABR	$e^+e^- \to D^0\overline{D}{}^0\gamma$
seen	CRONIN-HEN..	09	CLEO	$e^+e^- \to D^0\overline{D}{}^0$
seen	PAKHLOVA	08	BELL	$e^+e^- \to D^0\overline{D}{}^0\gamma$

$\Gamma(D^+D^-)/\Gamma_{\text{total}}$ Γ_4/Γ

VALUE	DOCUMENT ID		TECN	COMMENT
seen	AUBERT	09M	BABR	$e^+e^- \to D^+D^-\gamma$
seen	CRONIN-HEN..	09	CLEO	$e^+e^- \to D^+D^-$
seen	PAKHLOVA	08	BELL	$e^+e^- \to D^+D^-\gamma$

$\Gamma(D\overline{D})/\Gamma(D^*\overline{D}+\text{c.c.})$ Γ_2/Γ_5

VALUE	DOCUMENT ID		TECN	COMMENT
0.24±0.05±0.12	AUBERT	09M	BABR	$e^+e^- \to \gamma D^{(*)}\overline{D}$

$\Gamma(D^0\overline{D}{}^0)/\Gamma(D^*(2007)^0\overline{D}{}^0+\text{c.c.})$ Γ_3/Γ_6

VALUE	DOCUMENT ID		TECN	COMMENT
0.05±0.03	[15] GOLDHABER	77	MRK1	e^+e^-

[15] Phase-space factor (p^3) explicitly removed.

$\Gamma(D^*(2007)^0\overline{D}{}^0+\text{c.c.})/\Gamma_{\text{total}}$ Γ_6/Γ

VALUE	DOCUMENT ID		TECN	COMMENT
seen	AUBERT	09M	BABR	$e^+e^- \to D^{*0}\overline{D}{}^0\gamma$
seen	CRONIN-HEN..	09	CLEO	$e^+e^- \to D^{*0}\overline{D}{}^0$

$\Gamma(D^*(2010)^+D^-+\text{c.c.})/\Gamma_{\text{total}}$ Γ_7/Γ

VALUE	DOCUMENT ID		TECN	COMMENT
seen	AUBERT	09M	BABR	$e^+e^- \to D^{*+}D^-\gamma$
seen	CRONIN-HEN..	09	CLEO	$e^+e^- \to D^{*+}D^-$
seen	PAKHLOVA	07	BELL	$e^+e^- \to D^{*+}D^-\gamma$

$\Gamma(D^*(2010)^+D^-+\text{c.c.})/\Gamma(D^*(2007)^0\overline{D}{}^0+\text{c.c.})$ Γ_7/Γ_6

VALUE	DOCUMENT ID		TECN	COMMENT
0.95±0.09±0.10	AUBERT	09M	BABR	$e^+e^- \to \gamma D^*\overline{D}$

$\Gamma(D^*\overline{D}{}^*)/\Gamma(D^*\overline{D}+\text{c.c.})$ Γ_8/Γ_5

VALUE	DOCUMENT ID		TECN	COMMENT
0.18±0.14±0.03	AUBERT	09M	BABR	$e^+e^- \to \gamma D^{(*)}\overline{D}{}^{(*)}$

$\Gamma(D^*(2007)^0\overline{D}{}^*(2007)^0)/\Gamma_{\text{total}}$ Γ_9/Γ

VALUE	DOCUMENT ID		TECN	COMMENT
seen	AUBERT	09M	BABR	$e^+e^- \to D^{*0}\overline{D}{}^{*0}\gamma$
seen	CRONIN-HEN..	09	CLEO	$e^+e^- \to D^{*0}\overline{D}{}^{*0}$

$\Gamma(D^*(2007)^0\overline{D}{}^*(2007)^0)/\Gamma(D^*(2007)^0\overline{D}{}^0+\text{c.c.})$ Γ_9/Γ_6

VALUE	DOCUMENT ID		TECN	COMMENT
32.0±12.0	[16] GOLDHABER	77	MRK1	e^+e^-

[16] Phase-space factor (p^3) explicitly removed.

$\Gamma(D^*(2010)^+D^*(2010)^-)/\Gamma_{\text{total}}$ Γ_{10}/Γ

VALUE	DOCUMENT ID		TECN	COMMENT
seen	AUBERT	09M	BABR	$e^+e^- \to D^{*+}D^{*-}\gamma$
seen	CRONIN-HEN..	09	CLEO	$e^+e^- \to D^{*+}D^{*-}$
seen	PAKHLOVA	07	BELL	$e^+e^- \to D^{*+}D^{*-}\gamma$

$\Gamma(D^0D^-\pi^+ + \text{c.c. (excl. } D^*(2007)^0\overline{D}{}^0 + \text{c.c., } D^*(2010)^+D^- + \text{c.c.}))/\Gamma_{\text{total}}$ Γ_{12}/Γ

VALUE	DOCUMENT ID		TECN	COMMENT
not seen	PAKHLOVA	08A	BELL	$e^+e^- \to D^0D^-\pi^+\gamma$

$\Gamma(D\overline{D}{}^*\pi(\text{excl. } D^*\overline{D}{}^*))/\Gamma_{\text{total}}$ Γ_{13}/Γ

VALUE	DOCUMENT ID		TECN	COMMENT
not seen	CRONIN-HEN..	09	CLEO	$e^+e^- \to D\overline{D}{}^*\pi$

$\Gamma(D^0\overline{D}{}^{*-}\pi^+ + \text{c.c. (excl. } D^*(2010)^+D^*(2010)^-))/\Gamma_{\text{total}}$ Γ_{14}/Γ

VALUE	DOCUMENT ID		TECN	COMMENT
seen	PAKHLOVA	09	BELL	$e^+e^- \to D^0D^{*-}\pi^+\gamma$

$\Gamma(D_s^+D_s^-)/\Gamma_{\text{total}}$ Γ_{15}/Γ

VALUE	DOCUMENT ID		TECN	COMMENT
seen	PAKHLOVA	11	BELL	$e^+e^- \to D_s^+D_s^-\gamma$
seen	DEL-AMO-SA..	10N	BABR	$e^+e^- \to D_s^+D_s^-\gamma$
seen	CRONIN-HEN..	09	CLEO	$e^+e^- \to D_s^+D_s^-$

$\Gamma(J/\psi\pi^+\pi^-)/\Gamma_{\text{total}}$ Γ_{17}/Γ

VALUE (units 10^{-3})	CL%	DOCUMENT ID		TECN	COMMENT
<4	90	COAN	06	CLEO	3.97–4.06 $e^+e^- \to$ hadrons

$\Gamma(J/\psi\pi^0\pi^0)/\Gamma_{\text{total}}$ Γ_{18}/Γ

VALUE (units 10^{-3})	CL%	DOCUMENT ID		TECN	COMMENT
<2	90	COAN	06	CLEO	3.97–4.06 $e^+e^- \to$ hadrons

$\Gamma(J/\psi\eta)/\Gamma_{\text{total}}$ Γ_{19}/Γ

VALUE (units 10^{-3})	CL%	DOCUMENT ID		TECN	COMMENT
5.2±0.5±0.5		[17] ABLIKIM	12K	BES3	$e^+e^- \to \ell^+\ell^-2\gamma$
• • • We do not use the following data for averages, fits, limits, etc. • • •					
<7	90	COAN	06	CLEO	3.97–4.06 $e^+e^- \to$ hadrons

[17] ABLIKIM 12K measure $\sigma(e^+e^- \to J/\psi\eta) = 32.1 \pm 2.8 \pm 1.3$ pb. They assume the $\eta J/\psi$ fully originates from $\psi(4040)$ decays.

$\Gamma(J/\psi\pi^0)/\Gamma_{\text{total}}$ Γ_{20}/Γ

VALUE (units 10^{-3})	CL%	DOCUMENT ID		TECN	COMMENT
<0.28	90	[18] ABLIKIM	12K	BES3	$e^+e^- \to \ell^+\ell^-2\gamma$
• • • We do not use the following data for averages, fits, limits, etc. • • •					
<2	90	COAN	06	CLEO	3.97–4.06 $e^+e^- \to$ hadrons

[18] ABLIKIM 12K measure $\sigma(e^+e^- \to J/\psi\pi^0) < 1.6$ pb. They assume the $\eta J/\psi$ fully originates from $\psi(4040)$ decays.

$\Gamma(J/\psi\pi^+\pi^-\pi^0)/\Gamma_{\text{total}}$ Γ_{21}/Γ

VALUE (units 10^{-3})	CL%	DOCUMENT ID		TECN	COMMENT
<2	90	COAN	06	CLEO	3.97–4.06 $e^+e^- \to$ hadrons

$\Gamma(\chi_{c1}\gamma)/\Gamma_{\text{total}}$ Γ_{22}/Γ

VALUE (units 10^{-3})	CL%	DOCUMENT ID		TECN	COMMENT
<11	90	COAN	06	CLEO	3.97–4.06 $e^+e^- \to$ hadrons

$\Gamma(\chi_{c2}\gamma)/\Gamma_{\text{total}}$ Γ_{23}/Γ

VALUE (units 10^{-3})	CL%	DOCUMENT ID		TECN	COMMENT
<17	90	COAN	06	CLEO	3.97–4.06 $e^+e^- \to$ hadrons

Meson Particle Listings

$\psi(4040)$, $X(4050)^{\pm}$, $X(4140)$

$\Gamma(\chi_{c1}\pi^+\pi^-\pi^0)/\Gamma_{total}$ **Γ_{24}/Γ**

VALUE (units 10^{-3})	CL%	DOCUMENT ID		TECN	COMMENT
<11	90	COAN	06	CLEO	3.97–4.06 e^+e^- → hadrons

$\Gamma(\chi_{c2}\pi^+\pi^-\pi^0)/\Gamma_{total}$ **Γ_{25}/Γ**

VALUE (units 10^{-3})	CL%	DOCUMENT ID		TECN	COMMENT
<32	90	COAN	06	CLEO	3.97–4.06 e^+e^- → hadrons

$\Gamma(h_c(1P)\pi^+\pi^-)/\Gamma_{total}$ **Γ_{26}/Γ**

VALUE (units 10^{-3})	CL%	DOCUMENT ID		TECN	COMMENT
<3	90	[19] PEDLAR	11	CLEO	e^+e^- → $h_c(1P)\pi^+\pi^-$

[19] From several values of $\sqrt{s}$ near the peak of the $\psi(4040)$, PEDLAR 11 measures $\sigma(e^+e^-\to h_c(1P)\pi^+\pi^-) = 1.0\pm8.0\pm5.4\pm0.2$ pb, where the errors are statistical, systematic, and due to uncertainty in $B(\psi(2S)\to\pi^0 h_c(1P))$, respectively.

$\Gamma(\phi\pi^+\pi^-)/\Gamma_{total}$ **Γ_{27}/Γ**

VALUE (units 10^{-3})	CL%	DOCUMENT ID		TECN	COMMENT
<3	90	COAN	06	CLEO	3.97–4.06 e^+e^- → hadrons

$\Gamma(\Lambda\overline{\Lambda}\pi^+\pi^-)/\Gamma_{total}$ **Γ_{28}/Γ**

VALUE (units 10^{-4})	CL%	DOCUMENT ID		TECN	COMMENT
<2.9	90	[20] ABLIKIM	13Q	BES3	e^+e^- → $\psi(4040)$

[20] Assuming that interference effects between resonance and continuum can be neglected.

$\Gamma(\Lambda\overline{\Lambda}\pi^0)/\Gamma_{total}$ **Γ_{29}/Γ**

VALUE (units 10^{-4})	CL%	DOCUMENT ID		TECN	COMMENT
<0.9	90	[21] ABLIKIM	13Q	BES3	e^+e^- → $\psi(4040)$

[21] Assuming that interference effects between resonance and continuum can be neglected.

$\Gamma(\Lambda\overline{\Lambda}\eta)/\Gamma_{total}$ **Γ_{30}/Γ**

VALUE (units 10^{-4})	CL%	DOCUMENT ID		TECN	COMMENT
<3.0	90	[22] ABLIKIM	13Q	BES3	e^+e^- → $\psi(4040)$

[22] Assuming that interference effects between resonance and continuum can be neglected.

$\Gamma(\Sigma^+\overline{\Sigma}^-)/\Gamma_{total}$ **Γ_{31}/Γ**

VALUE (units 10^{-4})	CL%	DOCUMENT ID		TECN	COMMENT
<1.3	90	[23] ABLIKIM	13Q	BES3	e^+e^- → $\psi(4040)$

[23] Assuming that interference effects between resonance and continuum can be neglected.

$\Gamma(\Sigma^0\overline{\Sigma}^0)/\Gamma_{total}$ **Γ_{32}/Γ**

VALUE (units 10^{-4})	CL%	DOCUMENT ID		TECN	COMMENT
<0.7	90	[24] ABLIKIM	13Q	BES3	e^+e^- → $\psi(4040)$

[24] Assuming that interference effects between resonance and continuum can be neglected.

$\Gamma(\Xi^+\overline{\Xi}^-)/\Gamma_{total}$ **Γ_{33}/Γ**

VALUE (units 10^{-4})	CL%	DOCUMENT ID		TECN	COMMENT
<1.6	90	[25] ABLIKIM	13Q	BES3	e^+e^- → $\psi(4040)$

[25] Assuming that interference effects between resonance and continuum can be neglected.

$\Gamma(\Xi^0\overline{\Xi}^0)/\Gamma_{total}$ **Γ_{34}/Γ**

VALUE (units 10^{-4})	CL%	DOCUMENT ID		TECN	COMMENT
<1.8	90	[26] ABLIKIM	13Q	BES3	e^+e^- → $\psi(4040)$

[26] Assuming that interference effects between resonance and continuum can be neglected.

$\psi(4040)$ REFERENCES

ABLIKIM	13Q	PR D87 112011	Ablikim M. *et al.*	(BES III Collab.)
WANG	13B	PR D87 051101	X.L. Wang *et al.*	(BELLE Collab.)
ABLIKIM	12K	PR D86 071101	M. Ablikim *et al.*	(BES III Collab.)
PAKHLOVA	11	PR D83 011101	G. Pakhlova *et al.*	(BELLE Collab.)
PEDLAR	11	PRL 107 041803	T. Pedlar *et al.*	(CLEO Collab.)
DEL-AMO-SA...	10N	PR D82 052004	P. del Amo Sanchez *et al.*	(BABAR Collab.)
MO	10	PR D82 077501	X.H. Mo, C.Z. Yuan, P. Wang	(BHEP)
AUBERT	09M	PR D79 092001	B. Aubert *et al.*	(BABAR Collab.)
CRONIN-HEN...	09	PR D80 072001	D. Cronin-Hennessy *et al.*	(CLEO Collab.)
PAKHLOVA	09	PR D80 091101	G. Pakhlova *et al.*	(BELLE Collab.)
ABLIKIM	08D	PL B660 315	M. Ablikim *et al.*	(BES Collab.)
PAKHLOVA	08	PR D77 011103	G. Pakhlova *et al.*	(BELLE Collab.)
PAKHLOVA	08A	PRL 100 062001	G. Pakhlova *et al.*	(BELLE Collab.)
PAKHLOVA	07	PRL 98 092001	G. Pakhlova *et al.*	(BELLE Collab.)
COAN	06	PRL 96 162003	T.E. Coan *et al.*	(CLEO Collab.)
SETH	05A	PR D72 017501	K.K. Seth	
BAI	02C	PRL 88 101802	J.Z. Bai *et al.*	(BES Collab.)
BAI	00	PRL 84 594	J.Z. Bai *et al.*	(BES Collab.)
OSTERHELD	86	SLAC-PUB-4160	A. Osterheld *et al.*	(SLAC Crystal Ball Collab.)
BRANDELIK	78C	PL 76B 361	R. Brandelik *et al.*	(DASP Collab.)
Also		ZPHY C1 233	R. Brandelik *et al.*	(DASP Collab.)
FELDMAN	77	PRPL 33C 285	G.J. Feldman, M.L. Perl	(LBL, SLAC)
GOLDHABER	77	PL 69B 503	G. Goldhaber *et al.*	(Mark I Collab.)

$X(4050)^{\pm}$

$I(J^P) = ?(?^?)$

OMITTED FROM SUMMARY TABLE

Observed by MIZUK 08 in the $\pi^+\chi_{c1}(1P)$ invariant mass distribution in $\overline{B}^0 \to K^-\pi^+\chi_{c1}(1P)$ decays. Not seen by LEES 12B in this same mode after accounting for $K\pi$ resonant mass and angular structure.

$X(4050)^{\pm}$ MASS

VALUE (MeV)	DOCUMENT ID		TECN	COMMENT
$4051\pm14^{+20}_{-41}$	[1] MIZUK	08	BELL	$\overline{B}^0 \to K^-\pi^+\chi_{c1}(1P)$

[1] From a Dalitz plot analysis with two Breit-Wigner amplitudes.

$X(4050)^{\pm}$ WIDTH

VALUE (MeV)	DOCUMENT ID		TECN	COMMENT
82^{+21+47}_{-17-22}	[2] MIZUK	08	BELL	$\overline{B}^0 \to K^-\pi^+\chi_{c1}(1P)$

[2] From a Dalitz plot analysis with two Breit-Wigner amplitudes.

$X(4050)^{\pm}$ DECAY MODES

	Mode	Fraction (Γ_i/Γ)
Γ_1	$\pi^+\chi_{c1}(1P)$	seen

$X(4050)^{\pm}$ BRANCHING RATIOS

$\Gamma(\pi^+\chi_{c1}(1P))/\Gamma_{total}$ **Γ_1/Γ**

VALUE	DOCUMENT ID		TECN	COMMENT
seen	[3] MIZUK	08	BELL	$\overline{B}^0 \to K^-\pi^+\chi_{c1}(1P)$
• • • We do not use the following data for averages, fits, limits, etc. • • •				
not seen	[4] LEES	12B	BABR	$B \to K\pi\chi_{c1}(1P)$

[3] With a product branching fraction measurement of $B(\overline{B}^0 \to K^-X(4050)^+) \times B(X(4050)^+ \to \pi^+\chi_{c1}(1P)) = (3.0^{+1.5+3.7}_{-0.8-1.6})\times10^{-5}$.

[4] With a product branching fraction limit of $B(\overline{B}^0 \to X(4050)^+K^-)\times B(X(4050)^+ \to \chi_{c1}\pi^+) < 1.8\times10^{-5}$ at 90% CL.

$X(4050)^{\pm}$ REFERENCES

LEES	12B	PR D85 052003	J.P. Lees *et al.*	(BABAR Collab.)
MIZUK	08	PR D78 072004	R. Mizuk *et al.*	(BELLE Collab.)

$X(4140)$

$I^G(J^{PC}) = 0^+(?^{?+})$

OMITTED FROM SUMMARY TABLE

Needs confirmation.

Seen by AALTONEN 09AH and ABAZOV 14A in the $B^+ \to XK^+$, $X \to J/\psi\phi$. Not seen by SHEN 10 in $\gamma\gamma \to J/\psi\phi$ or AAIJ 12AA in $B^+ \to J/\psi\phi K^+$.

$X(4140)$ MASS

VALUE (MeV)	EVTS	DOCUMENT ID		TECN	COMMENT
• • • We do not use the following data for averages, fits, limits, etc. • • •					
$4159.0\pm4.3\pm6.6$	52 ± 19	[1] ABAZOV	14A	D0	$B^+ \to J/\psi\phi K^+$
$4143.0\pm2.9\pm1.2$	14 ± 5	[2] AALTONEN	09AH	CDF	$B^+ \to J/\psi\phi K^+$

[1] Statistical significance of 3.1 σ.

[2] Statistical significance of 3.8 σ.

$X(4140)$ WIDTH

VALUE (MeV)	EVTS	DOCUMENT ID		TECN	COMMENT
• • • We do not use the following data for averages, fits, limits, etc. • • •					
$20\pm13^{+3}_{-8}$	52 ± 19	[3] ABAZOV	14A	D0	$B^+ \to J/\psi\phi K^+$
$11.7^{+8.3}_{-5.0}\pm3.7$	14 ± 5	[4] AALTONEN	09AH	CDF	$B^+ \to J/\psi\phi K^+$

[3] Statistical significance of 3.1 σ.

[4] Statistical significance of 3.8 σ.

$X(4140)$ DECAY MODES

	Mode	Fraction (Γ_i/Γ)
Γ_1	$J/\psi\phi$	not seen
Γ_2	$\gamma\gamma$	not seen

$X(4140)$ Γ(i)$\Gamma(\gamma\gamma)/\Gamma$(total)

$\Gamma(\gamma\gamma) \times \Gamma(J/\psi\phi)/\Gamma_{total}$ $\Gamma_2\Gamma_1/\Gamma$

VALUE (eV)	CL%	DOCUMENT ID		TECN	COMMENT
<41	90	[5] SHEN	10	BELL	10.6 $e^+e^- \to e^+e^- J/\psi\phi$
• • • We do not use the following data for averages, fits, limits, etc. • • •					
< 6	90	[6] SHEN	10	BELL	10.6 $e^+e^- \to e^+e^- J/\psi\phi$

[5] For $J^P = 0^+$.
[6] For $J^P = 2^+$.

$X(4140)$ BRANCHING RATIOS

$\Gamma(J/\psi\phi)/\Gamma_{total}$ Γ_1/Γ

VALUE	EVTS	DOCUMENT ID		TECN	COMMENT
not seen		[7] AAIJ	12AA	LHCB	$pp \to B^+X$ at 7 TeV
• • • We do not use the following data for averages, fits, limits, etc. • • •					
seen	52 ± 19	[8] ABAZOV	14A	D0	$B^+ \to J/\psi\phi K^+$
seen	14 ± 5	[9] AALTONEN	09AH	CDF	$B^+ \to J/\psi\phi K^+$

[7] Reported $B(B^+ \to X(4140)K^+)\cdot B(X(4140) \to J/\psi\phi)/B(B^+ \to J/\psi\phi K^+) < 0.07$ at 90% CL.
[8] ABAZOV 14A reports $B(B^+ \to X(4140)K^+ \to J/\psi\phi K^+)/B(B^+ \to J/\psi\phi K^+) = (19 \pm 7 \pm 4)\%$ with 3.1 σ signficance.
[9] Statistical significance of 3.8 σ.

$\Gamma(\gamma\gamma)/\Gamma_{total}$ Γ_2/Γ

VALUE	DOCUMENT ID		TECN	COMMENT
not seen	SHEN	10	BELL	10.6 $e^+e^- \to e^+e^- J/\psi\phi$

$X(4140)$ REFERENCES

ABAZOV	14A	PR D89 012004	V.M. Abazov *et al.*	(D0 Collab.)
AAIJ	12AA	PR D85 091103	R. Aaij *et al.*	(LHCb Collab.)
SHEN	10	PRL 104 112004	C.P. Shen *et al.*	(BELLE Collab.)
AALTONEN	09AH	PRL 102 242002	T. Aaltonen *et al.*	(CDF Collab.)

$\psi(4160)$

$I^G(J^{PC}) = 0^-(1^{--})$

$\psi(4160)$ MASS

VALUE (MeV)		DOCUMENT ID		TECN	COMMENT
4191 ± 5 OUR AVERAGE					
4191 $^{+9}_{-8}$		AAIJ	13BC	LHCB	$B^+ \to K^+\mu^+\mu^-$
4191.7± 6.5		[1] ABLIKIM	08D	BES2	$e^+e^- \to$ hadrons
• • • We do not use the following data for averages, fits, limits, etc. • • •					
4193 ± 7		[2] MO	10	RVUE	$e^+e^- \to$ hadrons
4151 ± 4		[3] SETH	05A	RVUE	$e^+e^- \to$ hadrons
4155 ± 5		[4] SETH	05A	RVUE	$e^+e^- \to$ hadrons
4159 ±20		BRANDELIK	78C	DASP	e^+e^-

[1] Reanalysis of data presented in BAI 02C. From a global fit over the center-of-mass energy region 3.7–5.0 GeV covering the $\psi(3770)$, $\psi(4040)$, $\psi(4160)$, and $\psi(4415)$ resonances. Phase angle fixed in the fit to $\delta = (293 \pm 57)^\circ$.
[2] Reanalysis of data presented in BAI 00 and BAI 02C. From a global fit over the center-of-mass energy 3.8-4.8 GeV covering the $\psi(4040)$, $\psi(4160)$ and $\psi(4415)$ resonances and including interference effects.
[3] From a fit to Crystal Ball (OSTERHELD 86) data.
[4] From a fit to BES (BAI 02C) data.

$\psi(4160)$ WIDTH

VALUE (MeV)		DOCUMENT ID		TECN	COMMENT
70 ±10 OUR AVERAGE					
65 $^{+22}_{-16}$		AAIJ	13BC	LHCB	$B^+ \to K^+\mu^+\mu^-$
71.8±12.3		[5] ABLIKIM	08D	BES2	$e^+e^- \to$ hadrons
• • • We do not use the following data for averages, fits, limits, etc. • • •					
79 ±14		[6] MO	10	RVUE	$e^+e^- \to$ hadrons
107 ±10		[7] SETH	05A	RVUE	$e^+e^- \to$ hadrons
107 ±16		[8] SETH	05A	RVUE	$e^+e^- \to$ hadrons
78 ±20		BRANDELIK	78C	DASP	e^+e^-

[5] Reanalysis of data presented in BAI 02C. From a global fit over the center-of-mass energy region 3.7–5.0 GeV covering the $\psi(3770)$, $\psi(4040)$, $\psi(4160)$, and $\psi(4415)$ resonances. Phase angle fixed in the fit to $\delta = (293 \pm 57)^\circ$.
[6] Reanalysis of data presented in BAI 00 and BAI 02C. From a global fit over the center-of-mass energy 3.8-4.8 GeV covering the $\psi(4040)$, $\psi(4160)$ and $\psi(4415)$ resonances and including interference effects.
[7] From a fit to Crystal Ball (OSTERHELD 86) data.
[8] From a fit to BES (BAI 02C) data.

$\psi(4160)$ DECAY MODES

Due to the complexity of the $c\overline{c}$ threshold region, in this listing, "seen" ("not seen") means that a cross section for the mode in question has been measured at effective $\sqrt{s}$ near this particle's central mass value, more (less) than 2σ above zero, without regard to any peaking behavior in $\sqrt{s}$ or absence thereof. See mode listing(s) for details and references.

	Mode	Fraction (Γ_i/Γ)		Confidence level
Γ_1	e^+e^-	$(6.9\pm3.3)\times10^{-6}$		
Γ_2	$\mu^+\mu^-$	seen		
Γ_3	$D\overline{D}$	seen		
Γ_4	$D^0\overline{D}^0$	seen		
Γ_5	D^+D^-	seen		
Γ_6	$D^*\overline{D}$ + c.c.	seen		
Γ_7	$D^*(2007)^0\overline{D}^0$ + c.c.	seen		
Γ_8	$D^*(2010)^+D^-$ + c.c.	seen		
Γ_9	$D^*\overline{D}^*$	seen		
Γ_{10}	$D^*(2007)^0\overline{D}^*(2007)^0$	seen		
Γ_{11}	$D^*(2010)^+D^*(2010)^-$	seen		
Γ_{12}	$D^0D^-\pi^+$ + c.c. (excl. $D^*(2007)^0\overline{D}^0$ + c.c., $D^*(2010)^+D^-$ + c.c.)	not seen		
Γ_{13}	$D\overline{D}^*\pi$ + c.c. (excl. $D^*\overline{D}^*$)	seen		
Γ_{14}	$D^0D^{*-}\pi^+$ + c.c. (excl. $D^*(2010)^+D^*(2010)^-$)	not seen		
Γ_{15}	$D_s^+D_s^-$	not seen		
Γ_{16}	$D_s^{*+}D_s^-$ + c.c.	seen		
Γ_{17}	$J/\psi\pi^+\pi^-$	< 3	$\times10^{-3}$	90%
Γ_{18}	$J/\psi\pi^0\pi^0$	< 3	$\times10^{-3}$	90%
Γ_{19}	$J/\psi K^+K^-$	< 2	$\times10^{-3}$	90%
Γ_{20}	$J/\psi\eta$	< 8	$\times10^{-3}$	90%
Γ_{21}	$J/\psi\pi^0$	< 1	$\times10^{-3}$	90%
Γ_{22}	$J/\psi\eta'$	< 5	$\times10^{-3}$	90%
Γ_{23}	$J/\psi\pi^+\pi^-\pi^0$	< 1	$\times10^{-3}$	90%
Γ_{24}	$\psi(2S)\pi^+\pi^-$	< 4	$\times10^{-3}$	90%
Γ_{25}	$\chi_{c1}\gamma$	< 7	$\times10^{-3}$	90%
Γ_{26}	$\chi_{c2}\gamma$	< 1.3	%	90%
Γ_{27}	$\chi_{c1}\pi^+\pi^-\pi^0$	< 2	$\times10^{-3}$	90%
Γ_{28}	$\chi_{c2}\pi^+\pi^-\pi^0$	< 8	$\times10^{-3}$	90%
Γ_{29}	$h_c(1P)\pi^+\pi^-$	< 5	$\times10^{-3}$	90%
Γ_{30}	$h_c(1P)\pi^0\pi^0$	< 2	$\times10^{-3}$	90%
Γ_{31}	$h_c(1P)\eta$	< 2	$\times10^{-3}$	90%
Γ_{32}	$h_c(1P)\pi^0$	< 4	$\times10^{-4}$	90%
Γ_{33}	$\phi\pi^+\pi^-$	< 2	$\times10^{-3}$	90%

$\psi(4160)$ PARTIAL WIDTHS

$\Gamma(e^+e^-)$ Γ_1

VALUE (keV)	DOCUMENT ID		TECN	COMMENT
0.48±0.22	[9] ABLIKIM	08D	BES2	$e^+e^- \to$ hadrons
• • • We do not use the following data for averages, fits, limits, etc. • • •				
0.4 to 1.1	[10] MO	10	RVUE	$e^+e^- \to$ hadrons
0.83±0.08	[11] SETH	05A	RVUE	$e^+e^- \to$ hadrons
0.84±0.13	[12] SETH	05A	RVUE	$e^+e^- \to$ hadrons
0.77±0.23	BRANDELIK	78C	DASP	e^+e^-

[9] Reanalysis of data presented in BAI 02C. From a global fit over the center-of-mass energy region 3.7–5.0 GeV covering the $\psi(3770)$, $\psi(4040)$, $\psi(4160)$, and $\psi(4415)$ resonances. Phase angle fixed in the fit to $\delta = (293 \pm 57)^\circ$.
[10] Reanalysis of data presented in BAI 00 and BAI 02C. From a global fit over the center-of-mass energy 3.8-4.8 GeV covering the $\psi(4040)$, $\psi(4160)$ and $\psi(4415)$ resonances and including interference effects. Four sets of solutions are obtained with the same fit quality, mass and total width, but with different e^+e^- partial widths. We quote only the range of values.
[11] From a fit to Crystal Ball (OSTERHELD 86) data.
[12] From a fit to BES (BAI 02C) data.

$\psi(4160)$ Γ(i)$\Gamma(e^+e^-)/\Gamma^2$(total)

$\Gamma(J/\psi\eta)/\Gamma_{total} \times \Gamma(e^+e^-)/\Gamma_{total}$ $\Gamma_{20}/\Gamma \times \Gamma_1/\Gamma$

VALUE (units 10^{-8})	DOCUMENT ID		TECN	COMMENT
• • • We do not use the following data for averages, fits, limits, etc. • • •				
2.8±0.9±0.9	[13] WANG	13B	BELL	$e^+e^- \to J/\psi\eta\gamma$
12.8±1.7±2.0	[14] WANG	13B	BELL	$e^+e^- \to J/\psi\eta\gamma$

[13] Solution I of two equivalent solutions in a fit using two interfering resonances. Mass and width fixed at 4153 MeV and 103 MeV, respectively.
[14] Solution II of two equivalent solutions in a fit using two interfering resonances. Mass and width fixed at 4153 MeV and 103 MeV, respectively.

$\psi(4160)$ BRANCHING RATIOS

$\Gamma(\mu^+\mu^-)/\Gamma_{total}$ — Γ_2/Γ

VALUE	DOCUMENT ID		TECN	COMMENT
seen	[15] AAIJ	13BC	LHCB	$B^+ \to K^+\mu^+\mu^-$

[15] AAIJ 13BC report $B(B^+ \to K^+\psi(4160))\, B(\psi(4160) \to \mu^+\mu^-) = (3.5^{+0.9}_{-0.8}) \times 10^{-9}$.

$\Gamma(D\overline{D})/\Gamma(D^*\overline{D}^*)$ — Γ_3/Γ_9

VALUE	DOCUMENT ID		TECN	COMMENT
0.02±0.03±0.02	AUBERT	09M	BABR	$e^+e^- \to \gamma D^{(*)}\overline{D}^{(*)}$

$\Gamma(D^0\overline{D}^0)/\Gamma_{total}$ — Γ_4/Γ

VALUE	DOCUMENT ID		TECN	COMMENT
seen	CRONIN-HEN...	09	CLEO	$e^+e^- \to D^0\overline{D}^0$
seen	PAKHLOVA	08	BELL	$e^+e^- \to D^0\overline{D}^0\gamma$
• • • We do not use the following data for averages, fits, limits, etc. • • •				
not seen	AUBERT	09M	BABR	$e^+e^- \to D^0\overline{D}^0\gamma$

$\Gamma(D^+D^-)/\Gamma_{total}$ — Γ_5/Γ

VALUE	DOCUMENT ID		TECN	COMMENT
seen	CRONIN-HEN...	09	CLEO	$e^+e^- \to D^+D^-$
seen	PAKHLOVA	08	BELL	$e^+e^- \to D^+D^-\gamma$
• • • We do not use the following data for averages, fits, limits, etc. • • •				
not seen	AUBERT	09M	BABR	$e^+e^- \to D^+D^-\gamma$

$\Gamma(D^*(2007)^0\overline{D}^0 + \text{c.c.})/\Gamma_{total}$ — Γ_7/Γ

VALUE	DOCUMENT ID		TECN	COMMENT
seen	AUBERT	09M	BABR	$e^+e^- \to D^{*0}\overline{D}^0\gamma$
seen	CRONIN-HEN...	09	CLEO	$e^+e^- \to D^{*0}\overline{D}^0$

$\Gamma(D^*(2010)^+D^- + \text{c.c.})/\Gamma_{total}$ — Γ_8/Γ

VALUE	DOCUMENT ID		TECN	COMMENT
seen	AUBERT	09M	BABR	$e^+e^- \to D^{*+}D^-\gamma$
seen	CRONIN-HEN...	09	CLEO	$e^+e^- \to D^{*+}D^-$
seen	PAKHLOVA	07	BELL	$e^+e^- \to D^{*+}D^-\gamma$

$\Gamma(D^*\overline{D} + \text{c.c.})/\Gamma(D^*\overline{D}^*)$ — Γ_6/Γ_9

VALUE	DOCUMENT ID		TECN	COMMENT
0.34±0.14±0.05	AUBERT	09M	BABR	$e^+e^- \to \gamma D^{(*)}\overline{D}^{(*)}$

$\Gamma(D^*(2007)^0\overline{D}^*(2007)^0)/\Gamma_{total}$ — Γ_{10}/Γ

VALUE	DOCUMENT ID		TECN	COMMENT
seen	AUBERT	09M	BABR	$e^+e^- \to D^{*0}\overline{D}^{*0}\gamma$
seen	CRONIN-HEN...	09	CLEO	$e^+e^- \to D^{*0}\overline{D}^{*0}$

$\Gamma(D^*(2010)^+D^*(2010)^-)/\Gamma_{total}$ — Γ_{11}/Γ

VALUE	DOCUMENT ID		TECN	COMMENT
seen	AUBERT	09M	BABR	$e^+e^- \to D^{*+}D^{*-}\gamma$
seen	CRONIN-HEN...	09	CLEO	$e^+e^- \to D^{*+}D^{*-}$
seen	PAKHLOVA	07	BELL	$e^+e^- \to D^{*+}D^{*-}\gamma$

$\Gamma(D^0D^-\pi^+ + \text{c.c. (excl. } D^*(2007)^0\overline{D}^0 + \text{c.c., } D^*(2010)^+D^- + \text{c.c.}))/\Gamma_{total}$ — Γ_{12}/Γ

VALUE	DOCUMENT ID		TECN	COMMENT
not seen	PAKHLOVA	08A	BELL	$e^+e^- \to D^0D^-\pi^+\gamma$

$\Gamma(D\overline{D}^*\pi + \text{c.c. (excl. } D^*\overline{D}^*))/\Gamma_{total}$ — Γ_{13}/Γ

VALUE	DOCUMENT ID		TECN	COMMENT
seen	CRONIN-HEN...	09	CLEO	$e^+e^- \to D\overline{D}^*\pi$

$\Gamma(D^0D^{*-}\pi^+ + \text{c.c. (excl. } D^*(2010)^+D^*(2010)^-))/\Gamma_{total}$ — Γ_{14}/Γ

VALUE	DOCUMENT ID		TECN	COMMENT
not seen	PAKHLOVA	09	BELL	$e^+e^- \to D^0D^{*-}\pi^+\gamma$

$\Gamma(D_s^+D_s^-)/\Gamma_{total}$ — Γ_{15}/Γ

VALUE	DOCUMENT ID		TECN	COMMENT
not seen	PAKHLOVA	11	BELL	$e^+e^- \to D_s^+D_s^-\gamma$
not seen	DEL-AMO-SA...	10N	BABR	$e^+e^- \to D_s^+D_s^-\gamma$
not seen	CRONIN-HEN...	09	CLEO	$e^+e^- \to D_s^+D_s^-$

$\Gamma(D_s^{*+}D_s^- + \text{c.c.})/\Gamma_{total}$ — Γ_{16}/Γ

VALUE	DOCUMENT ID		TECN	COMMENT
seen	PAKHLOVA	11	BELL	$e^+e^- \to D_s^{*+}D_s^-\gamma$
seen	DEL-AMO-SA...	10N	BABR	$e^+e^- \to D_s^{*+}D_s^-\gamma$
seen	CRONIN-HEN...	09	CLEO	$e^+e^- \to D_s^{*+}D_s^-$

$\Gamma(J/\psi\pi^+\pi^-)/\Gamma_{total}$ — Γ_{17}/Γ

VALUE (units 10^{-3})	CL%	DOCUMENT ID		TECN	COMMENT
<3	90	COAN	06	CLEO	4.12–4.2 $e^+e^- \to$ hadrons

$\Gamma(J/\psi\pi^0\pi^0)/\Gamma_{total}$ — Γ_{18}/Γ

VALUE (units 10^{-3})	CL%	DOCUMENT ID		TECN	COMMENT
<3	90	COAN	06	CLEO	4.12–4.2 $e^+e^- \to$ hadrons

$\Gamma(J/\psi K^+K^-)/\Gamma_{total}$ — Γ_{19}/Γ

VALUE (units 10^{-3})	CL%	DOCUMENT ID		TECN	COMMENT
<2	90	COAN	06	CLEO	4.12–4.2 $e^+e^- \to$ hadrons

$\Gamma(J/\psi\eta)/\Gamma_{total}$ — Γ_{20}/Γ

VALUE (units 10^{-3})	CL%	DOCUMENT ID		TECN	COMMENT
<8	90	COAN	06	CLEO	4.12–4.2 $e^+e^- \to$ hadrons

$\Gamma(J/\psi\pi^0)/\Gamma_{total}$ — Γ_{21}/Γ

VALUE (units 10^{-3})	CL%	DOCUMENT ID		TECN	COMMENT
<1	90	COAN	06	CLEO	4.12–4.2 $e^+e^- \to$ hadrons

$\Gamma(J/\psi\eta')/\Gamma_{total}$ — Γ_{22}/Γ

VALUE (units 10^{-3})	CL%	DOCUMENT ID		TECN	COMMENT
<5	90	COAN	06	CLEO	4.12–4.2 $e^+e^- \to$ hadrons

$\Gamma(J/\psi\pi^+\pi^-\pi^0)/\Gamma_{total}$ — Γ_{23}/Γ

VALUE (units 10^{-3})	CL%	DOCUMENT ID		TECN	COMMENT
<1	90	COAN	06	CLEO	4.12–4.2 $e^+e^- \to$ hadrons

$\Gamma(\psi(2S)\pi^+\pi^-)/\Gamma_{total}$ — Γ_{24}/Γ

VALUE (units 10^{-3})	CL%	DOCUMENT ID		TECN	COMMENT
<4	90	COAN	06	CLEO	4.12–4.2 $e^+e^- \to$ hadrons

$\Gamma(\chi_{c1}\gamma)/\Gamma_{total}$ — Γ_{25}/Γ

VALUE (units 10^{-3})	CL%	DOCUMENT ID		TECN	COMMENT
<7	90	COAN	06	CLEO	4.12–4.2 $e^+e^- \to$ hadrons

$\Gamma(\chi_{c2}\gamma)/\Gamma_{total}$ — Γ_{26}/Γ

VALUE (units 10^{-3})	CL%	DOCUMENT ID		TECN	COMMENT
<13	90	COAN	06	CLEO	4.12–4.2 $e^+e^- \to$ hadrons

$\Gamma(\chi_{c1}\pi^+\pi^-\pi^0)/\Gamma_{total}$ — Γ_{27}/Γ

VALUE (units 10^{-3})	CL%	DOCUMENT ID		TECN	COMMENT
<2	90	COAN	06	CLEO	4.12–4.2 $e^+e^- \to$ hadrons

$\Gamma(\chi_{c2}\pi^+\pi^-\pi^0)/\Gamma_{total}$ — Γ_{28}/Γ

VALUE (units 10^{-3})	CL%	DOCUMENT ID		TECN	COMMENT
<8	90	COAN	06	CLEO	4.12–4.2 $e^+e^- \to$ hadrons

$\Gamma(h_c(1P)\pi^+\pi^-)/\Gamma_{total}$ — Γ_{29}/Γ

VALUE (units 10^{-3})	CL%	DOCUMENT ID		TECN	COMMENT
<5	90	[16] PEDLAR	11	CLEO	$e^+e^- \to h_c(1P)\pi^+\pi^-$

[16] At $\sqrt{s} = 4170$ MeV, PEDLAR 11 measures $\sigma(e^+e^- \to h_c(1P)\pi^+\pi^-) = 15.6 \pm 2.3 \pm 1.9 \pm 3.0$ pb, where the errors are statistical, systematic, and due to uncertainty in $B(\psi(2S) \to \pi^0 h_c(1P))$, respectively.

$\Gamma(h_c(1P)\pi^0\pi^0)/\Gamma_{total}$ — Γ_{30}/Γ

VALUE (units 10^{-3})	CL%	DOCUMENT ID		TECN	COMMENT
<2	90	[17] PEDLAR	11	CLEO	$e^+e^- \to h_c(1P)\pi^0\pi^0$

[17] At $\sqrt{s} = 4170$ MeV, PEDLAR 11 measures $\sigma(e^+e^- \to h_c(1P)\pi^0\pi^0) = 3.0 \pm 3.3 \pm 1.1 \pm 0.6$ pb, where the errors are statistical, systematic, and due to uncertainty in $B(\psi(2S) \to \pi^0 h_c(1P))$, respectively.

$\Gamma(h_c(1P)\eta)/\Gamma_{total}$ — Γ_{31}/Γ

VALUE (units 10^{-3})	CL%	DOCUMENT ID		TECN	COMMENT
<2	90	[18] PEDLAR	11	CLEO	$e^+e^- \to h_c(1P)\eta$

[18] At $\sqrt{s} = 4170$ MeV, PEDLAR 11 measures $\sigma(e^+e^- \to h_c(1P)\eta) = 4.7 \pm 1.7 \pm 1.0 \pm 0.9$ pb, where the errors are statistical, systematic, and due to uncertainty in $B(\psi(2S) \to \pi^0 h_c(1P))$, respectively.

$\Gamma(h_c(1P)\pi^0)/\Gamma_{total}$ — Γ_{32}/Γ

VALUE (units 10^{-3})	CL%	DOCUMENT ID		TECN	COMMENT
<0.4	90	[19] PEDLAR	11	CLEO	$e^+e^- \to h_c(1P)\pi^0$

[19] At $\sqrt{s} = 4170$ MeV, PEDLAR 11 measures $\sigma(e^+e^- \to h_c(1P)\pi^0) = -0.7 \pm 1.8 \pm 0.7 \pm 0.1$ pb, where the errors are statistical, systematic, and due to uncertainty in $B(\psi(2S) \to \pi^0 h_c(1P))$, respectively.

$\Gamma(\phi\pi^+\pi^-)/\Gamma_{total}$ — Γ_{33}/Γ

VALUE (units 10^{-3})	CL%	DOCUMENT ID		TECN	COMMENT
<2	90	COAN	06	CLEO	4.12–4.2 $e^+e^- \to$ hadrons

$\psi(4160)$ REFERENCES

AAIJ	13BC	PRL 111 112003	R. Aaij *et al.*	(LHCb Collab.)
WANG	13B	PR D87 051101	X.L. Wang *et al.*	(BELLE Collab.)
PAKHLOVA	11	PR D83 011101	G. Pakhlova *et al.*	(BELLE Collab.)
PEDLAR	11	PRL 107 041803	T. Pedlar *et al.*	(CLEO Collab.)
DEL-AMO-SA...	10N	PR D82 052004	P. del Amo Sanchez *et al.*	(BABAR Collab.)
MO	10	PR D82 077501	X.H. Mo, C.Z. Yuan, P. Wang	(BHEP)
AUBERT	09M	PR D79 092001	B. Aubert *et al.*	(BABAR Collab.)
CRONIN-HEN...	09	PR D80 072001	D. Cronin-Hennessy *et al.*	(CLEO Collab.)
PAKHLOVA	09	PR D80 091101	G. Pakhlova *et al.*	(BELLE Collab.)
ABLIKIM	08D	PL B660 315	M. Ablikim *et al.*	(BES Collab.)
PAKHLOVA	08	PR D77 011103	G. Pakhlova *et al.*	(BELLE Collab.)
PAKHLOVA	08A	PRL 100 062001	G. Pakhlova *et al.*	(BELLE Collab.)
PAKHLOVA	07	PRL 98 092001	G. Pakhlova *et al.*	(BELLE Collab.)
COAN	06	PRL 96 162003	T.E. Coan *et al.*	(CLEO Collab.)
SETH	05A	PR D72 017501	K.K. Seth	
BAI	02C	PRL 88 101802	J.Z. Bai *et al.*	(BES Collab.)
BAI	00	PRL 84 594	J.Z. Bai *et al.*	(BES Collab.)
OSTERHELD	86	SLAC-PUB-4160	A. Osterheld *et al.*	(SLAC Crystal Ball Collab.)
BRANDELIK	78C	PL 76B 361	R. Brandelik *et al.*	(DASP Collab.)

$X(4160)$

$I^G(J^{PC}) = ?^?(?^{??})$

OMITTED FROM SUMMARY TABLE

Seen by PAKHLOV 08 in $e^+e^- \to J/\psi X$, $X \to D^*\overline{D}^*$

$X(4160)$ MASS

VALUE (MeV)	EVTS	DOCUMENT ID		TECN	COMMENT
$4156^{+25}_{-20} \pm 15$	24	PAKHLOV	08	BELL	$e^+e^- \to J/\psi X$

$X(4160)$ WIDTH

VALUE (MeV)	EVTS	DOCUMENT ID		TECN	COMMENT
$139^{+111}_{-61} \pm 21$	24	PAKHLOV	08	BELL	$e^+e^- \to J/\psi X$

$X(4160)$ DECAY MODES

	Mode	Fraction (Γ_i/Γ)
Γ_1	$D\overline{D}$	not seen
Γ_2	$D^*\overline{D}$ + c.c.	not seen
Γ_3	$D^*\overline{D}^*$	seen

$X(4160)$ BRANCHING RATIOS

$\Gamma(D\overline{D})/\Gamma(D^*\overline{D}^*)$ Γ_1/Γ_3

VALUE	CL%	DOCUMENT ID		TECN	COMMENT
<0.09	90	PAKHLOV	08	BELL	$e^+e^- \to J/\psi X$

$\Gamma(D^*\overline{D}$ + c.c.)$/\Gamma(D^*\overline{D}^*)$ Γ_2/Γ_3

VALUE	CL%	DOCUMENT ID		TECN	COMMENT
<0.22	90	PAKHLOV	08	BELL	$e^+e^- \to J/\psi X$

$X(4160)$ REFERENCES

PAKHLOV	08	PRL 100 202001	P. Pakhlov *et al.*	(BELLE Collab.)

$X(4250)^{\pm}$

$I(J^P) = ?(?^?)$

OMITTED FROM SUMMARY TABLE

Observed by MIZUK 08 in the $\pi^+\chi_{c1}(1P)$ invariant mass distribution in $\overline{B}^0 \to K^-\pi^+\chi_{c1}(1P)$ decays. Not seen by LEES 12B in this same mode after accounting for $K\pi$ resonant mass and angular structure.

$X(4250)^{\pm}$ MASS

VALUE (MeV)	DOCUMENT ID		TECN	COMMENT
$4248^{+44}_{-29}{}^{+180}_{-35}$	[1] MIZUK	08	BELL	$\overline{B}^0 \to K^-\pi^+\chi_{c1}(1P)$

[1] From a Dalitz plot analysis with two Breit-Wigner amplitudes.

$X(4250)^{\pm}$ WIDTH

VALUE (MeV)	DOCUMENT ID		TECN	COMMENT
$177^{+54}_{-39}{}^{+316}_{-61}$	[2] MIZUK	08	BELL	$\overline{B}^0 \to K^-\pi^+\chi_{c1}(1P)$

[2] From a Dalitz plot analysis with two Breit-Wigner amplitudes.

$X(4250)^{\pm}$ DECAY MODES

	Mode	Fraction (Γ_i/Γ)
Γ_1	$\pi^+\chi_{c1}(1P)$	seen

$X(4250)^{\pm}$ BRANCHING RATIOS

$\Gamma(\pi^+\chi_{c1}(1P))/\Gamma_{\text{total}}$ Γ_1/Γ

VALUE	DOCUMENT ID		TECN	COMMENT
seen	[3] MIZUK	08	BELL	$\overline{B}^0 \to K^-\pi^+\chi_{c1}(1P)$
• • • We do not use the following data for averages, fits, limits, etc. • • •				
not seen	[4] LEES	12B	BABR	$B \to K\pi\chi_{c1}(1P)$

[3] With a product branching fraction measurement of $B(\overline{B}^0 \to K^-X(4250)^+) \times B(X(4250)^+ \to \pi^+\chi_{c1}(1P)) = (4.0^{+2.3}_{-0.9}{}^{+19.7}_{-0.5}) \times 10^{-5}$.

[4] With a product branching fraction limit of $B(\overline{B}^0 \to X(4250)^+K^-) \times B(X(4250)^+ \to \chi_{c1}\pi^+) < 4.0 \times 10^{-5}$ at 90% CL.

$X(4250)^{\pm}$ REFERENCES

LEES	12B	PR D85 052003	J.P. Lees *et al.*	(BABAR Collab.)
MIZUK	08	PR D78 072004	R. Mizuk *et al.*	(BELLE Collab.)

$X(4260)$

$I^G(J^{PC}) = ?^?(1^{--})$

Seen in radiative return from e^+e^- collisions at $\sqrt{s} = 9.54$–10.58 GeV by AUBERT,B 05I, HE 06B, and YUAN 07, and in e^+e^- collisions at $\sqrt{s} \approx 4.26$ GeV by COAN 06. Possibly seen by AUBERT 06 in $B^- \to K^-\pi^+\pi^-J/\psi$. See also the mini-review under the $X(3872)$. (See the index for the page number.)

$X(4260)$ MASS

VALUE (MeV)	EVTS	DOCUMENT ID		TECN	COMMENT
4251 ± 9 OUR AVERAGE Error includes scale factor of 1.6. See the ideogram below.					
$4258.6 \pm 8.3 \pm 12.1$		[1] LIU	13B	BELL	$e^+e^- \to \gamma\pi^+\pi^-J/\psi$
$4245 \pm 5 \pm 4$		[2] LEES	12AC	BABR	10.58 $e^+e^- \to \gamma\pi^+\pi^-J/\psi$
$4284\ ^{+17}_{-16} \pm 4\ 13.6$		HE	06B	CLEO	9.4–10.6 $e^+e^- \to \gamma\pi^+\pi^-J/\psi$
• • • We do not use the following data for averages, fits, limits, etc. • • •					
$4247 \pm 12\ ^{+17}_{-32}$		[1,3] YUAN	07	BELL	10.58 $e^+e^- \to \gamma\pi^+\pi^-J/\psi$
$4259 \pm 8\ ^{+2}_{-6}\ 125$		[4] AUBERT,B	05I	BABR	10.58 $e^+e^- \to \gamma\pi^+\pi^-J/\psi$

[1] From a two-resonance fit.
[2] From a single-resonance fit. Supersedes AUBERT,B 05I.
[3] Superseded by LIU 13B.
[4] From a single-resonance fit. Two interfering resonances are not excluded. Superseded by LEES 12AC.

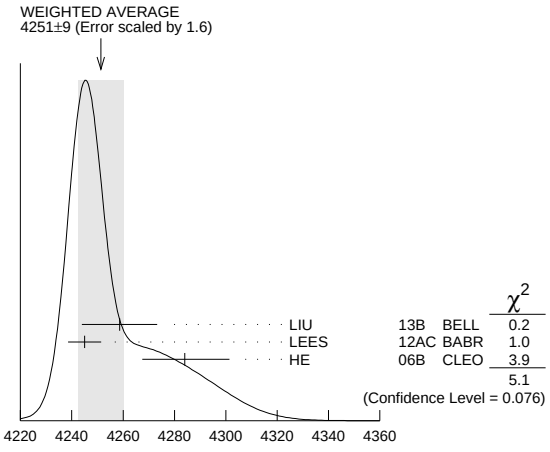

$X(4260)$ WIDTH

VALUE (MeV)	EVTS	DOCUMENT ID		TECN	COMMENT
120 ±12 OUR AVERAGE Error includes scale factor of 1.1.					
$134.1 \pm 16.4 \pm 5.5$		[1] LIU	13B	BELL	$e^+e^- \to \gamma\pi^+\pi^-J/\psi$
$114\ ^{+16}_{-15} \pm 7$		[2] LEES	12AC	BABR	10.58 $e^+e^- \to \gamma\pi^+\pi^-J/\psi$
$73\ ^{+39}_{-25} \pm 5\ 13.6$		HE	06B	CLEO	9.4–10.6 $e^+e^- \to \gamma\pi^+\pi^-J/\psi$
• • • We do not use the following data for averages, fits, limits, etc. • • •					

108	±19	±10		[1,3] YUAN	07	BELL	10.58	$e^+e^- \to \gamma\pi^+\pi^- J/\psi$
88	±23	$^{+\ 6}_{-\ 4}$	125	[4] AUBERT,B	05I	BABR	10.58	$e^+e^- \to \gamma\pi^+\pi^- J/\psi$

[1] From a two-resonance fit.
[2] From a single-resonance fit. Supersedes AUBERT,B 05I.
[3] Superseded by LIU 13B.
[4] From a single-resonance fit. Two interfering resonances are not excluded. Superseded by LEES 12AC.

$X(4260)$ DECAY MODES

	Mode	Fraction (Γ_i/Γ)
Γ_1	e^+e^-	
Γ_2	$J/\psi\pi^+\pi^-$	seen
Γ_3	$J/\psi f_0(980)$, $f_0(980) \to \pi^+\pi^-$	seen
Γ_4	$X(3900)^\pm\pi^\mp$, $X^\pm \to J/\psi\pi^\pm$	seen
Γ_5	$J/\psi\pi^0\pi^0$	seen
Γ_6	$J/\psi K^+K^-$	seen
Γ_7	$X(3872)\gamma$	seen
Γ_8	$J/\psi\eta$	not seen
Γ_9	$J/\psi\pi^0$	not seen
Γ_{10}	$J/\psi\eta'$	not seen
Γ_{11}	$J/\psi\pi^+\pi^-\pi^0$	not seen
Γ_{12}	$J/\psi\eta\eta$	not seen
Γ_{13}	$\psi(2S)\pi^+\pi^-$	not seen
Γ_{14}	$\psi(2S)\eta$	not seen
Γ_{15}	$\chi_{c0}\omega$	not seen
Γ_{16}	$\chi_{c1}\gamma$	not seen
Γ_{17}	$\chi_{c2}\gamma$	not seen
Γ_{18}	$\chi_{c1}\pi^+\pi^-\pi^0$	not seen
Γ_{19}	$\chi_{c2}\pi^+\pi^-\pi^0$	not seen
Γ_{20}	$h_c(1P)\pi^+\pi^-$	not seen
Γ_{21}	$\phi\pi^+\pi^-$	not seen
Γ_{22}	$\phi f_0(980) \to \phi\pi^+\pi^-$	not seen
Γ_{23}	$D\overline{D}$	not seen
Γ_{24}	$D^0\overline{D}^0$	not seen
Γ_{25}	D^+D^-	not seen
Γ_{26}	$D^*\overline{D}$ + c.c.	not seen
Γ_{27}	$D^*(2007)^0\overline{D}^0$ + c.c.	not seen
Γ_{28}	$D^*(2010)^+D^-$ + c.c.	not seen
Γ_{29}	$D^*\overline{D}^*$	not seen
Γ_{30}	$D^*(2007)^0\overline{D}^*(2007)^0$	not seen
Γ_{31}	$D^*(2010)^+D^*(2010)^-$	not seen
Γ_{32}	$D\overline{D}\pi$ + c.c.	
Γ_{33}	$D^0D^-\pi^+$ + c.c. (excl. $D^*(2007)^0\overline{D}^{*0}$ + c.c., $D^*(2010)^+D^-$ + c.c.)	not seen
Γ_{34}	$D\overline{D}^*\pi$ + c.c. (excl. $D^*\overline{D}^*$)	not seen
Γ_{35}	$D^0D^{*-}\pi^+$ + c.c. (excl. $D^*(2010)^+D^*(2010)^-$)	not seen
Γ_{36}	$D^0D^*(2010)^-\pi^+$ + c.c.	not seen
Γ_{37}	$D^*\overline{D}^*\pi$	not seen
Γ_{38}	$D_s^+D_s^-$	not seen
Γ_{39}	$D_s^{*+}D_s^-$ + c.c.	not seen
Γ_{40}	$D_s^{*+}D_s^{*-}$	not seen
Γ_{41}	$p\overline{p}$	not seen
Γ_{42}	$K_S^0K^\pm\pi^\mp$	not seen
Γ_{43}	$K^+K^-\pi^0$	not seen

$X(4260)$ $\Gamma(i)\Gamma(e^+e^-)/\Gamma(\text{total})$

$\Gamma(J/\psi\pi^+\pi^-) \times \Gamma(e^+e^-)/\Gamma_{\text{total}}$ $\quad \Gamma_2\Gamma_1/\Gamma$

VALUE (eV)	EVTS	DOCUMENT ID		TECN	COMMENT
9.2±1.0 OUR AVERAGE					
9.2±0.8±0.7		[1] LEES	12AC	BABR	10.58 $e^+e^- \to \gamma\pi^+\pi^- J/\psi$
$8.9^{+3.9}_{-3.1}$±1.8	8.1	HE	06B	CLEO	9.4–10.6 $e^+e^- \to \gamma\pi^+\pi^- J/\psi$
• • • We do not use the following data for averages, fits, limits, etc. • • •					
6.4±0.8±0.6		[2] LIU	13B	BELL	$e^+e^- \to \gamma\pi^+\pi^- J/\psi$
20.5±1.4±2.0		[3] LIU	13B	BELL	$e^+e^- \to \gamma\pi^+\pi^- J/\psi$
6.0±1.2$^{+4.7}_{-0.5}$		[2,4] YUAN	07	BELL	10.58 $e^+e^- \to \gamma\pi^+\pi^- J/\psi$
20.6±2.3$^{+9.1}_{-1.7}$		[3,4] YUAN	07	BELL	10.58 $e^+e^- \to \gamma\pi^+\pi^- J/\psi$
5.5±1.0$^{+0.8}_{-0.7}$	125	[5] AUBERT,B	05I	BABR	10.58 $e^+e^- \to \gamma\pi^+\pi^- J/\psi$

[1] From a single-resonance fit. Supersedes AUBERT,B 05I.
[2] Solution I of two equivalent solutions in a fit using two interfering resonances.
[3] Solution II of two equivalent solutions in a fit using two interfering resonances.
[4] Superseded by LIU 13B.
[5] From a single-resonance fit. Two interfering resonances are not excluded. Superseded by LEES 12AC.

$\Gamma(J/\psi K^+K^-) \times \Gamma(e^+e^-)/\Gamma_{\text{total}}$ $\quad \Gamma_6\Gamma_1/\Gamma$

VALUE (eV)	CL%	DOCUMENT ID		TECN	COMMENT
• • • We do not use the following data for averages, fits, limits, etc. • • •					
<1.2	90	[1] YUAN	08	BELL	$e^+e^- \to \gamma K^+K^- J/\psi$

[1] From a fit of the broad K^+K^-J/ψ enhancement including a coherent $X(4260)$ amplitude with mass and width from YUAN 07.

$\Gamma(J/\psi\eta) \times \Gamma(e^+e^-)/\Gamma_{\text{total}}$ $\quad \Gamma_8\Gamma_1/\Gamma$

VALUE (eV)	CL%	DOCUMENT ID		TECN	COMMENT
• • • We do not use the following data for averages, fits, limits, etc. • • •					
<14.2	90	WANG	13B	BELL	$e^+e^- \to J/\psi\eta\gamma$

$\Gamma(\psi(2S)\pi^+\pi^-) \times \Gamma(e^+e^-)/\Gamma_{\text{total}}$ $\quad \Gamma_{13}\Gamma_1/\Gamma$

VALUE (eV)	CL%	DOCUMENT ID		TECN	COMMENT
• • • We do not use the following data for averages, fits, limits, etc. • • •					
<4.3	90	[1] LIU	08H	RVUE	10.58 $e^+e^- \to \psi(2S)\pi^+\pi^-\gamma$
$7.4^{+2.1}_{-1.7}$		[2] LIU	08H	RVUE	10.58 $e^+e^- \to \psi(2S)\pi^+\pi^-\gamma$

[1] For constructive interference with the $X(4360)$ in a combined fit of AUBERT 07S and WANG 07D data with three resonances.
[2] For destructive interference with the $X(4360)$ in a combined fit of AUBERT 07S and WANG 07D data with three resonances.

$\Gamma(\phi\pi^+\pi^-) \times \Gamma(e^+e^-)/\Gamma_{\text{total}}$ $\quad \Gamma_{21}\Gamma_1/\Gamma$

VALUE (eV)	CL%	DOCUMENT ID		TECN	COMMENT
<0.4	90	AUBERT,BE	06D	BABR	10.6 $e^+e^- \to K^+K^-\pi^+\pi^-\gamma$

$\Gamma(\phi f_0(980) \to \phi\pi^+\pi^-) \times \Gamma(e^+e^-)/\Gamma_{\text{total}}$ $\quad \Gamma_{22}\Gamma_1/\Gamma$

VALUE (eV)	CL%	DOCUMENT ID		TECN	COMMENT
<0.29	90	[1] AUBERT	07AK	BABR	10.6 $e^+e^- \to \pi^+\pi^-K^+K^-\gamma$

[1] AUBERT 07AK reports $[\Gamma(X(4260) \to \phi f_0(980) \to \phi\pi^+\pi^-) \times \Gamma(X(4260) \to e^+e^-)/\Gamma_{\text{total}}] \times [B(\phi(1020) \to K^+K^-)] < 0.14$ eV which we divide by our best value $B(\phi(1020) \to K^+K^-) = 48.9 \times 10^{-2}$.

$\Gamma(K_S^0K^\pm\pi^\mp) \times \Gamma(e^+e^-)/\Gamma_{\text{total}}$ $\quad \Gamma_{42}\Gamma_1/\Gamma$

VALUE (eV)	CL%	DOCUMENT ID		TECN	COMMENT
• • • We do not use the following data for averages, fits, limits, etc. • • •					
<0.5	90	AUBERT	08S	BABR	10.6 $e^+e^- \to K_S^0K^\pm\pi^\mp\gamma$

$\Gamma(K^+K^-\pi^0) \times \Gamma(e^+e^-)/\Gamma_{\text{total}}$ $\quad \Gamma_{43}\Gamma_1/\Gamma$

VALUE (eV)	CL%	DOCUMENT ID		TECN	COMMENT
• • • We do not use the following data for averages, fits, limits, etc. • • •					
<0.6	90	AUBERT	08S	BABR	10.6 $e^+e^- \to K^+K^-\pi^0\gamma$

$X(4260)$ BRANCHING RATIOS

$\Gamma(J/\psi f_0(980), f_0(980) \to \pi^+\pi^-)/\Gamma(J/\psi\pi^+\pi^-)$ $\quad \Gamma_3/\Gamma_2$

VALUE	DOCUMENT ID		TECN	COMMENT
• • • We do not use the following data for averages, fits, limits, etc. • • •				
0.17±0.13	[1] LEES	12AC	BABR	10.58 $e^+e^- \to \gamma\pi^+\pi^- J/\psi$

[1] Systematic uncertainties not estimated.

$\Gamma(X(3900)^\pm\pi^\mp, X^\pm \to J/\psi\pi^\pm)/\Gamma(J/\psi\pi^+\pi^-)$ $\quad \Gamma_4/\Gamma_2$

VALUE	DOCUMENT ID		TECN	COMMENT
0.215±0.033±0.075	[1] ABLIKIM	13T	BES3	$e^+e^- \to \pi^+\pi^- J/\psi$
• • • We do not use the following data for averages, fits, limits, etc. • • •				
0.29 ±0.08	[2] LIU	13B	BELL	$e^+e^- \to \gamma\pi^+\pi^- J/\psi$

[1] Assuming that the cross section of $e^+e^- \to \pi^+\pi^- J/\psi$ is fully due to the $X(4260)$.
[2] Systematic error not evaluated.

$\Gamma(h_c(1P)\pi^+\pi^-)/\Gamma(J/\psi\pi^+\pi^-)$ $\quad \Gamma_{20}/\Gamma_2$

VALUE	CL%	DOCUMENT ID		TECN	COMMENT
<1.0	90	[1] PEDLAR	11	CLEO	$e^+e^- \to h_c(1P)\pi^+\pi^-$

[1] At $\sqrt{s} = 4260$ MeV, PEDLAR 11 measures $\sigma(e^+e^- \to h_c(1P)\pi^+\pi^-) = 32 \pm 17 \pm 6 \pm 6$ pb, where the errors are statistical, systematic, and due to uncertainty in $B(\psi(2S) \to \pi^0 h_c(1P))$, respectively.

$\Gamma(X(3872)\gamma)/\Gamma_{\text{total}}$ $\quad \Gamma_7/\Gamma$

VALUE	EVTS	DOCUMENT ID		TECN	COMMENT
seen	20 ± 5	ABLIKIM	14	BES3	$e^+e^- \to J/\psi\pi^+\pi^-\gamma$

$\Gamma(D\overline{D})/\Gamma(J/\psi\pi^+\pi^-)$ Γ_{23}/Γ_2

VALUE	CL%	DOCUMENT ID		TECN	COMMENT
<1.0	90	[1] AUBERT	07BE	BABR	$e^+e^- \to D\overline{D}\gamma$
• • • We do not use the following data for averages, fits, limits, etc. • • •					
<4.0	90	CRONIN-HEN..	09	CLEO	e^+e^-

[1] Using 4259 ± 10 MeV for the mass and 88 ± 24 MeV for the width of $X(4260)$.

$\Gamma(D^0\overline{D}^0)/\Gamma_{\text{total}}$ Γ_{24}/Γ

VALUE	DOCUMENT ID		TECN	COMMENT
not seen	CRONIN-HEN..	09	CLEO	$e^+e^- \to D^0\overline{D}^0$
• • • We do not use the following data for averages, fits, limits, etc. • • •				
not seen	AUBERT	09M	BABR	$e^+e^- \to D^0\overline{D}^0\gamma$
not seen	PAKHLOVA	08	BELL	$e^+e^- \to D^0\overline{D}^0\gamma$

$\Gamma(D^+D^-)/\Gamma_{\text{total}}$ Γ_{25}/Γ

VALUE	DOCUMENT ID		TECN	COMMENT
not seen	CRONIN-HEN..	09	CLEO	$e^+e^- \to D^+D^-$
• • • We do not use the following data for averages, fits, limits, etc. • • •				
not seen	AUBERT	09M	BABR	$e^+e^- \to D^+D^-\gamma$
not seen	PAKHLOVA	08	BELL	$e^+e^- \to D^+D^-\gamma$

$\Gamma(D^*\overline{D}+\text{c.c.})/\Gamma(J/\psi\pi^+\pi^-)$ Γ_{26}/Γ_2

VALUE	CL%	DOCUMENT ID		TECN	COMMENT
<34	90	AUBERT	09M	BABR	$e^+e^- \to \gamma D^*\overline{D}$
• • • We do not use the following data for averages, fits, limits, etc. • • •					
<45	90	CRONIN-HEN..	09	CLEO	e^+e^-

$\Gamma(D^*(2007)^0\overline{D}^0+\text{c.c.})/\Gamma_{\text{total}}$ Γ_{27}/Γ

VALUE	DOCUMENT ID		TECN	COMMENT
not seen	CRONIN-HEN..	09	CLEO	$e^+e^- \to D^{*0}\overline{D}^0$
• • • We do not use the following data for averages, fits, limits, etc. • • •				
not seen	AUBERT	09M	BABR	$e^+e^- \to D^{*0}\overline{D}^0\gamma$

$\Gamma(D^*(2010)^+D^-+\text{c.c.})/\Gamma_{\text{total}}$ Γ_{28}/Γ

VALUE	DOCUMENT ID		TECN	COMMENT
not seen	CRONIN-HEN..	09	CLEO	$e^+e^- \to D^{*+}D^-$
not seen	PAKHLOVA	07	BELL	$e^+e^- \to D^{*+}D^-\gamma$
• • • We do not use the following data for averages, fits, limits, etc. • • •				
not seen	AUBERT	09M	BABR	$e^+e^- \to D^{*+}D^-\gamma$

$\Gamma(D^*\overline{D}^*)/\Gamma(J/\psi\pi^+\pi^-)$ Γ_{29}/Γ_2

VALUE	CL%	DOCUMENT ID		TECN	COMMENT
<11	90	CRONIN-HEN..	09	CLEO	e^+e^-
• • • We do not use the following data for averages, fits, limits, etc. • • •					
<40	90	AUBERT	09M	BABR	$e^+e^- \to \gamma D^*\overline{D}^*$

$\Gamma(D^*(2007)^0\overline{D}^*(2007)^0)/\Gamma_{\text{total}}$ Γ_{30}/Γ

VALUE	DOCUMENT ID		TECN	COMMENT
not seen	CRONIN-HEN..	09	CLEO	$e^+e^- \to D^{*0}\overline{D}^{*0}$
• • • We do not use the following data for averages, fits, limits, etc. • • •				
not seen	AUBERT	09M	BABR	$e^+e^- \to D^{*0}\overline{D}^{*0}\gamma$

$\Gamma(D^*(2010)^+D^*(2010)^-)/\Gamma_{\text{total}}$ Γ_{31}/Γ

VALUE	DOCUMENT ID		TECN	COMMENT
not seen	CRONIN-HEN..	09	CLEO	$e^+e^- \to D^{*+}D^{*-}$
not seen	PAKHLOVA	07	BELL	$e^+e^- \to D^{*+}D^{*-}\gamma$
• • • We do not use the following data for averages, fits, limits, etc. • • •				
not seen	AUBERT	09M	BABR	$e^+e^- \to D^{*+}D^{*-}\gamma$

$\Gamma(D^0D^-\pi^++\text{c.c.}\ (\text{excl. } D^*(2007)^0\overline{D}^{*0}+\text{c.c.}, D^*(2010)^+D^-+\text{c.c.}))/\Gamma_{\text{total}}$ Γ_{33}/Γ

VALUE	DOCUMENT ID		TECN	COMMENT
not seen	PAKHLOVA	08A	BELL	10.6 $e^+e^- \to D^0D^-\pi^+\gamma$

$\Gamma(D\overline{D}^*\pi+\text{c.c.}\ (\text{excl. } D^*\overline{D}^*))/\Gamma_{\text{total}}$ Γ_{34}/Γ

VALUE	DOCUMENT ID		TECN	COMMENT
not seen	CRONIN-HEN..	09	CLEO	$e^+e^- \to D^*\overline{D}\pi$

$\Gamma(D\overline{D}^*\pi+\text{c.c.}\ (\text{excl. } D^*\overline{D}^*))/\Gamma(J/\psi\pi^+\pi^-)$ Γ_{34}/Γ_2

VALUE	CL%	DOCUMENT ID		TECN	COMMENT
<15	90	CRONIN-HEN..	09	CLEO	e^+e^-

$\Gamma(D^0D^{*-}\pi^++\text{c.c.}\ (\text{excl. } D^*(2010)^+D^*(2010)^-))/\Gamma_{\text{total}}$ Γ_{35}/Γ

VALUE	DOCUMENT ID		TECN	COMMENT
not seen	PAKHLOVA	09	BELL	$e^+e^- \to D^0D^{*-}\pi^+\gamma$

$\Gamma(D^0D^*(2010)^-\pi^++\text{c.c.})/\Gamma(J/\psi\pi^+\pi^-)$ Γ_{36}/Γ_2

VALUE	CL%	DOCUMENT ID		TECN	COMMENT
<9	90	PAKHLOVA	09	BELL	$e^+e^- \to D^0D^{*-}\pi^+$

$\Gamma(D^0D^*(2010)^-\pi^++\text{c.c.})/\Gamma_{\text{total}} \times \Gamma(e^+e^-)/\Gamma_{\text{total}}$ $\Gamma_{36}/\Gamma \times \Gamma_1/\Gamma$

VALUE	CL%	DOCUMENT ID		TECN	COMMENT
$<0.42 \times 10^{-6}$	90	[1] PAKHLOVA	09	BELL	$e^+e^- \to D^0D^{*-}\pi^+$

[1] Using 4263^{+8}_{-9} MeV for the mass of $X(4260)$.

$\Gamma(D^*\overline{D}^*\pi)/\Gamma_{\text{total}}$ Γ_{37}/Γ

VALUE	DOCUMENT ID		TECN	COMMENT
not seen	CRONIN-HEN..	09	CLEO	$e^+e^- \to D^*\overline{D}^*\pi$

$\Gamma(D^*\overline{D}^*\pi)/\Gamma(J/\psi\pi^+\pi^-)$ Γ_{37}/Γ_2

VALUE	CL%	DOCUMENT ID		TECN	COMMENT
<8.2	90	CRONIN-HEN..	09	CLEO	e^+e^-

$\Gamma(D_s^+D_s^-)/\Gamma_{\text{total}}$ Γ_{38}/Γ

VALUE	DOCUMENT ID		TECN	COMMENT
not seen	DEL-AMO-SA..	10N	BABR	$e^+e^- \to D_s^+D_s^-\gamma$
not seen	CRONIN-HEN..	09	CLEO	$e^+e^- \to D_s^+D_s^-$
• • • We do not use the following data for averages, fits, limits, etc. • • •				
not seen	PAKHLOVA	11	BELL	$e^+e^- \to D_s^+D_s^-\gamma$

$\Gamma(D_s^+D_s^-)/\Gamma(J/\psi\pi^+\pi^-)$ Γ_{38}/Γ_2

VALUE	CL%	DOCUMENT ID		TECN	COMMENT
<0.7	95	DEL-AMO-SA..	10N	BABR	10.6 e^+e^-
• • • We do not use the following data for averages, fits, limits, etc. • • •					
<1.3	90	CRONIN-HEN..	09	CLEO	e^+e^-

$\Gamma(D_s^{*+}D_s^-+\text{c.c.})/\Gamma_{\text{total}}$ Γ_{39}/Γ

VALUE	DOCUMENT ID		TECN	COMMENT
not seen	DEL-AMO-SA..	10N	BABR	$e^+e^- \to D_s^{*+}D_s^-\gamma$
not seen	CRONIN-HEN..	09	CLEO	$e^+e^- \to D_s^{*+}D_s^-$
• • • We do not use the following data for averages, fits, limits, etc. • • •				
not seen	PAKHLOVA	11	BELL	$e^+e^- \to D_s^{*+}D_s^-\gamma$

$\Gamma(D_s^{*+}D_s^-+\text{c.c.})/\Gamma(J/\psi\pi^+\pi^-)$ Γ_{39}/Γ_2

VALUE	CL%	DOCUMENT ID		TECN	COMMENT
< 0.8	90	CRONIN-HEN..	09	CLEO	e^+e^-
• • • We do not use the following data for averages, fits, limits, etc. • • •					
<44	95	DEL-AMO-SA..	10N	BABR	10.6 e^+e^-

$\Gamma(D_s^{*+}D_s^{*-})/\Gamma_{\text{total}}$ Γ_{40}/Γ

VALUE	DOCUMENT ID		TECN	COMMENT
not seen	CRONIN-HEN..	09	CLEO	$e^+e^- \to D_s^{*+}D_s^{*-}$
• • • We do not use the following data for averages, fits, limits, etc. • • •				
not seen	PAKHLOVA	11	BELL	$e^+e^- \to D_s^{*+}D_s^{*-}\gamma$
not seen	DEL-AMO-SA..	10N	BABR	$e^+e^- \to D_s^{*+}D_s^{*-}\gamma$

$\Gamma(D_s^{*+}D_s^{*-})/\Gamma(J/\psi\pi^+\pi^-)$ Γ_{40}/Γ_2

VALUE	CL%	DOCUMENT ID		TECN	COMMENT
< 9.5	90	CRONIN-HEN..	09	CLEO	e^+e^-
• • • We do not use the following data for averages, fits, limits, etc. • • •					
<30	95	DEL-AMO-SA..	10N	BABR	10.6 e^+e^-

$\Gamma(p\overline{p})/\Gamma(J/\psi\pi^+\pi^-)$ Γ_{41}/Γ_2

VALUE	CL%	DOCUMENT ID		COMMENT
<0.13	90	[1] AUBERT	06B	$e^+e^- \to p\overline{p}\gamma$

[1] Using 4259 ± 10 MeV for the mass and 88 ± 24 MeV for the width of $X(4260)$.

$X(4260)$ REFERENCES

ABLIKIM	14	PRL 112 092001	M. Ablikim *et al.*	(BES III Collab.)
ABLIKIM	13T	PR 110 252001	M. Ablikim *et al.*	(BES III Collab.)
LIU	13B	PRL 110 252002	Z.Q. Liu *et al.*	(BELLE Collab.)
WANG	13B	PR D87 051101	X.L. Wang *et al.*	(BELLE Collab.)
LEES	12AC	PR D86 051102	J.P. Lees *et al.*	(BABAR Collab.)
PAKHLOVA	11	PR D83 011101	G. Pakhlova *et al.*	(BELLE Collab.)
PEDLAR	11	PRL 107 041803	T. Pedlar *et al.*	(CLEO Collab.)
DEL-AMO-SA...	10N	PR D82 052004	P. del Amo Sanchez *et al.*	(BABAR Collab.)
AUBERT	09M	PR D79 092001	B. Aubert *et al.*	(BABAR Collab.)
CRONIN-HEN...	09	PR D80 072001	D. Cronin-Hennessy *et al.*	(CLEO Collab.)
PAKHLOVA	09	PR D80 091101	G. Pakhlova *et al.*	(BELLE Collab.)
AUBERT	08S	PR D77 092002	B. Aubert *et al.*	(BABAR Collab.)
LIU	08H	PR D78 014032	Z.Q. Liu, X.S. Qin, C.Z. Yuan	
PAKHLOVA	08	PR D77 011103	G. Pakhlova *et al.*	(BELLE Collab.)
PAKHLOVA	08A	PRL 100 062001	G. Pakhlova *et al.*	(BELLE Collab.)
YUAN	08	PR D77 011105	C.Z. Yuan *et al.*	(BELLE Collab.)
AUBERT	07AK	PR D76 012008	B. Aubert *et al.*	(BABAR Collab.)
AUBERT	07BE	PR D76 111105	B. Aubert *et al.*	(BABAR Collab.)
AUBERT	07S	PRL 98 212001	B. Aubert *et al.*	(BABAR Collab.)
PAKHLOVA	07	PRL 98 092001	G. Pakhlova *et al.*	(BELLE Collab.)
WANG	07D	PRL 99 142002	X.L. Wang *et al.*	(BELLE Collab.)
YUAN	07	PRL 99 182004	C.Z. Yuan *et al.*	(BELLE Collab.)
AUBERT	06	PR D73 011101	B. Aubert *et al.*	(BABAR Collab.)
AUBERT	06B	PR D73 012005	B. Aubert *et al.*	(BABAR Collab.)
AUBERT,BE	06D	PR D74 091103	B. Aubert *et al.*	(BABAR Collab.)
COAN	06	PRL 96 162003	T.E. Coan *et al.*	(CLEO Collab.)
HE	06B	PR D74 091104	Q. He *et al.*	(CLEO Collab.)
AUBERT,B	05I	PRL 95 142001	B. Aubert *et al.*	(BABAR Collab.)

Meson Particle Listings

$X(4350)$, $X(4360)$

$X(4350)$

$I^G(J^{PC}) = 0^+(?^{?+})$

OMITTED FROM SUMMARY TABLE

Seen by SHEN 10 in the $\gamma\gamma \to J/\psi\phi$. Needs confirmation.

$X(4350)$ MASS

VALUE (MeV)	EVTS	DOCUMENT ID		TECN	COMMENT
$4350.6^{+4.6}_{-5.1} \pm 0.7$	$8.8^{+4.2}_{-3.2}$	[1] SHEN	10	BELL	10.6 $e^+e^- \to e^+e^- J/\psi\phi$

[1] Statistical significance of 3.2 σ.

$X(4350)$ WIDTH

VALUE (MeV)	EVTS	DOCUMENT ID		TECN	COMMENT
$13^{+18}_{-9} \pm 4$	$8.8^{+4.2}_{-3.2}$	[2] SHEN	10	BELL	10.6 $e^+e^- \to e^+e^- J/\psi\phi$

[2] Statistical significance of 3.2 σ.

$X(4350)$ DECAY MODES

	Mode	Fraction (Γ_i/Γ)
Γ_1	$J/\psi\phi$	seen
Γ_2	$\gamma\gamma$	seen

$X(4350)$ $\Gamma(i)\Gamma(\gamma\gamma)/\Gamma(\text{total})$

$\Gamma(\gamma\gamma) \times \Gamma(J/\psi\phi)/\Gamma_{\text{total}}$ $\Gamma_2\Gamma_1/\Gamma$

VALUE (eV)	EVTS	DOCUMENT ID		TECN	COMMENT
$6.7^{+3.2}_{-2.4} \pm 1.1$	$8.8^{+4.2}_{-3.2}$	[3] SHEN	10	BELL	10.6 $e^+e^- \to e^+e^- J/\psi\phi$
• • • We do not use the following data for averages, fits, limits, etc. • • •					
$1.5^{+0.7}_{-0.6} \pm 0.3$	$8.8^{+4.2}_{-3.2}$	[4] SHEN	10	BELL	10.6 $e^+e^- \to e^+e^- J/\psi\phi$

[3] For $J^P = 0^+$. Statistical significance of 3.2 σ.
[4] For $J^P = 2^+$. Statistical significance of 3.2 σ.

$X(4350)$ BRANCHING RATIOS

$\Gamma(J/\psi\phi)/\Gamma_{\text{total}}$ Γ_1/Γ

VALUE	DOCUMENT ID		TECN	COMMENT
seen	[5] SHEN	10	BELL	10.6 $e^+e^- \to e^+e^- J/\psi\phi$

[5] Statistical significance of 3.2 σ.

$\Gamma(\gamma\gamma)/\Gamma_{\text{total}}$ Γ_2/Γ

VALUE	DOCUMENT ID		TECN	COMMENT
seen	[6] SHEN	10	BELL	10.6 $e^+e^- \to e^+e^- J/\psi\phi$

[6] Statistical significance of 3.2 σ.

$X(4350)$ REFERENCES

SHEN	10	PRL 104 112004	C.P. Shen *et al.*	(BELLE Collab.)

$X(4360)$

$I^G(J^{PC}) = ?^?(1^{--})$

Seen in radiative return from e^+e^- collisions at $\sqrt{s} = 9.54$–10.58 GeV by AUBERT 07S and WANG 07D. See also the review under the $X(3872)$ particle listings. (See the index for the page number.)

$X(4360)$ MASS

VALUE (MeV)	DOCUMENT ID		TECN	COMMENT
$4361 \pm 9 \pm 9$	[1] WANG	07D	BELL	10.58 $e^+e^- \to \gamma\pi^+\pi^-\psi(2S)$
• • • We do not use the following data for averages, fits, limits, etc. • • •				
$4355^{+9}_{-10} \pm 9$	[2] LIU	08H	RVUE	10.58 $e^+e^- \to \psi(2S)\pi^+\pi^-\gamma$
4324 ± 24	[3] AUBERT	07S	BABR	10.58 $e^+e^- \to \gamma\pi^+\pi^-\psi(2S)$

[1] From a two-resonance fit.
[2] From a combined fit of AUBERT 07S and WANG 07D data with two resonances.
[3] From a single-resonance fit. Systematic errors not estimated.

$X(4360)$ WIDTH

VALUE (MeV)	DOCUMENT ID		TECN	COMMENT
$74 \pm 15 \pm 10$	[4] WANG	07D	BELL	10.58 $e^+e^- \to \gamma\pi^+\pi^-\psi(2S)$
• • • We do not use the following data for averages, fits, limits, etc. • • •				
$103^{+17}_{-15} \pm 11$	[5] LIU	08H	RVUE	10.58 $e^+e^- \to \psi(2S)\pi^+\pi^-\gamma$
172 ± 33	[6] AUBERT	07S	BABR	10.58 $e^+e^- \to \gamma\pi^+\pi^-\psi(2S)$

[4] From a two-resonance fit.
[5] From a combined fit of AUBERT 07S and WANG 07D data with two resonances.
[6] From a single-resonance fit. Systematic errors not estimated.

$X(4360)$ DECAY MODES

	Mode	Fraction (Γ_i/Γ)
Γ_1	e^+e^-	
Γ_2	$\psi(2S)\pi^+\pi^-$	seen
Γ_3	$J/\psi\eta$	
Γ_4	$D^0D^{*-}\pi^+$	

$X(4360)$ $\Gamma(i)\Gamma(e^+e^-)/\Gamma(\text{total})$

$\Gamma(\psi(2S)\pi^+\pi^-) \times \Gamma(e^+e^-)/\Gamma_{\text{total}}$ $\Gamma_2\Gamma_1/\Gamma$

VALUE (eV)	DOCUMENT ID		TECN	COMMENT
• • • We do not use the following data for averages, fits, limits, etc. • • •				
$11.1^{+1.3}_{-1.2}$	[7] LIU	08H	RVUE	10.58 $e^+e^- \to \psi(2S)\pi^+\pi^-\gamma$
12.3 ± 1.2	[8] LIU	08H	RVUE	10.58 $e^+e^- \to \psi(2S)\pi^+\pi^-\gamma$
$10.4 \pm 1.7 \pm 1.5$	[9] WANG	07D	BELL	10.58 $e^+e^- \to \gamma\pi^+\pi^-\psi(2S)$
$11.8 \pm 1.8 \pm 1.4$	[10] WANG	07D	BELL	10.58 $e^+e^- \to \gamma\pi^+\pi^-\psi(2S)$

[7] Solution I in a combined fit of AUBERT 07S and WANG 07D data with two resonances.
[8] Solution II in a combined fit of AUBERT 07S and WANG 07D data with two resonances.
[9] Solution I of two equivalent solutions in a fit using two interfering resonances.
[10] Solution II of two equivalent solutions in a fit using two interfering resonances.

$\Gamma(J/\psi\eta) \times \Gamma(e^+e^-)/\Gamma_{\text{total}}$ $\Gamma_3\Gamma_1/\Gamma$

VALUE (eV)	CL%	DOCUMENT ID		TECN	COMMENT
• • • We do not use the following data for averages, fits, limits, etc. • • •					
<6.8	90	WANG	13B	BELL	$e^+e^- \to J/\psi\eta\gamma$

$X(4360)$ BRANCHING RATIOS

$\Gamma(D^0D^{*-}\pi^+)/\Gamma(\psi(2S)\pi^+\pi^-)$ Γ_4/Γ_2

VALUE	CL%	DOCUMENT ID		TECN	COMMENT
<8	90	PAKHLOVA	09	BELL	$e^+e^- \to X(4360) \to D^0D^{*-}\pi^+$

$\Gamma(D^0D^{*-}\pi^+)/\Gamma_{\text{total}} \times \Gamma(e^+e^-)/\Gamma_{\text{total}}$ $\Gamma_4/\Gamma \times \Gamma_1/\Gamma$

VALUE	CL%	DOCUMENT ID		TECN	COMMENT
$<0.72 \times 10^{-6}$	90	[11] PAKHLOVA	09	BELL	$e^+e^- \to X(4360) \to D^0D^{*-}\pi^+$

[11] Using $4355^{+9}_{-10} \pm 9$ MeV for the mass of $X(4360)$.

$X(4360)$ REFERENCES

WANG	13B	PR D87 051101	X.L. Wang *et al.*	(BELLE Collab.)
PAKHLOVA	09	PR D80 091101	G. Pakhlova *et al.*	(BELLE Collab.)
LIU	08H	PR D78 014032	Z.Q. Liu, X.S. Qin, C.Z. Yuan	
AUBERT	07S	PRL 98 212001	B. Aubert *et al.*	(BABAR Collab.)
WANG	07D	PRL 99 142002	X.L. Wang *et al.*	(BELLE Collab.)

$\psi(4415)$

$I^G(J^{PC}) = 0^-(1^{--})$

$\psi(4415)$ MASS

VALUE (MeV)		DOCUMENT ID		TECN	COMMENT
4421 ± 4 OUR ESTIMATE					
4415.1± 7.9	[1]	ABLIKIM	08D	BES2	$e^+e^- \to$ hadrons
• • • We do not use the following data for averages, fits, limits, etc. • • •					
4412 ±15	[2]	MO	10	RVUE	$e^+e^- \to$ hadrons
4411 ± 7	[3]	PAKHLOVA	08A	BELL	10.6 $e^+e^- \to D^0D^-\pi^+\gamma$
4425 ± 6	[4]	SETH	05A	RVUE	$e^+e^- \to$ hadrons
4429 ± 9	[5]	SETH	05A	RVUE	$e^+e^- \to$ hadrons
4417 ±10		BRANDELIK	78C	DASP	e^+e^-
4414 ± 7		SIEGRIST	76	MRK1	e^+e^-

[1] Reanalysis of data presented in BAI 02C. From a global fit over the center-of-mass energy region 3.7–5.0 GeV covering the $\psi(3770)$, $\psi(4040)$, $\psi(4160)$, and $\psi(4415)$ resonances. Phase angle fixed in the fit to $\delta = (234 \pm 88)^\circ$.

[2] Reanalysis of data presented in BAI 00 and BAI 02C. From a global fit over the center-of-mass energy 3.8-4.8 GeV covering the $\psi(4040)$, $\psi(4160)$ and $\psi(4415)$ resonances and including interference effects.

[3] Systematic uncertainties not estimated.

[4] From a fit to Crystal Ball (OSTERHELD 86) data.

[5] From a fit to BES (BAI 02C) data.

$\psi(4415)$ WIDTH

VALUE (MeV)		DOCUMENT ID		TECN	COMMENT
62 ±20 OUR ESTIMATE					
71.5±19.0	[6]	ABLIKIM	08D	BES2	$e^+e^- \to$ hadrons
• • • We do not use the following data for averages, fits, limits, etc. • • •					
118 ±32	[7]	MO	10	RVUE	$e^+e^- \to$ hadrons
77 ±20	[8]	PAKHLOVA	08A	BELL	10.6 $e^+e^- \to D^0D^-\pi^+\gamma$
119 ±16	[9]	SETH	05A	RVUE	$e^+e^- \to$ hadrons
118 ±35	[10]	SETH	05A	RVUE	$e^+e^- \to$ hadrons
66 ±15		BRANDELIK	78C	DASP	e^+e^-
33 ±10		SIEGRIST	76	MRK1	e^+e^-

[6] Reanalysis of data presented in BAI 02C. From a global fit over the center-of-mass energy region 3.7–5.0 GeV covering the $\psi(3770)$, $\psi(4040)$, $\psi(4160)$, and $\psi(4415)$ resonances. Phase angle fixed in the fit to $\delta = (234 \pm 88)^\circ$.

[7] Reanalysis of data presented in BAI 00 and BAI 02C. From a global fit over the center-of-mass energy 3.8-4.8 GeV covering the $\psi(4040)$, $\psi(4160)$ and $\psi(4415)$ resonances and including interference effects.

[8] Systematic uncertainties not estimated.

[9] From a fit to Crystal Ball (OSTERHELD 86) data.

[10] From a fit to BES (BAI 02C) data.

$\psi(4415)$ DECAY MODES

Due to the complexity of the $c\overline{c}$ threshold region, in this listing, "seen" ("not seen") means that a cross section for the mode in question has been measured at effective $\sqrt{s}$ near this particle's central mass value, more (less) than 2σ above zero, without regard to any peaking behavior in $\sqrt{s}$ or absence thereof. See mode listing(s) for details and references.

	Mode	Fraction (Γ_i/Γ)	Confidence level
Γ_1	$D\overline{D}$	not seen	
Γ_2	$D^0\overline{D}^0$	seen	
Γ_3	D^+D^-	seen	
Γ_4	$D^*\overline{D}$ + c.c.	not seen	
Γ_5	$D^*(2007)^0\overline{D}^0$ + c.c.	seen	
Γ_6	$D^*(2010)^+D^-$ + c.c.	seen	
Γ_7	$D^*\overline{D}^*$	not seen	
Γ_8	$D^*(2007)^0\overline{D}^*(2007)^0$ + c.c.	seen	
Γ_9	$D^*(2010)^+D^*(2010)^-$ + c.c.	seen	
Γ_{10}	$D^0D^-\pi^+$ (excl. $D^*(2007)^0\overline{D}^0$ +c.c., $D^*(2010)^+D^-$ +c.c.	< 2.3 %	90%
Γ_{11}	$D\overline{D}_2^*(2460) \to D^0D^-\pi^+$+c.c.	(10 ±4) %	
Γ_{12}	$D^0\overline{D}^{*-}\pi^+$+c.c.	< 11 %	90%
Γ_{13}	$D_s^+D_s^-$	not seen	
Γ_{14}	$D_s^{*+}D_s^-$+c.c.	seen	
Γ_{15}	$D_s^{*+}D_s^{*-}$	not seen	
Γ_{16}	$J/\psi\eta$	< 6 $\times 10^{-3}$	90%
Γ_{17}	e^+e^-	(9.4±3.2) $\times 10^{-6}$	

$\psi(4415)$ PARTIAL WIDTHS

$\Gamma(e^+e^-)$ Γ_{17}

VALUE (keV)		DOCUMENT ID		TECN	COMMENT
0.58±0.07 OUR ESTIMATE					
0.35±0.12	[11]	ABLIKIM	08D	BES2	$e^+e^- \to$ hadrons
• • • We do not use the following data for averages, fits, limits, etc. • • •					
0.4 to 0.8	[12]	MO	10	RVUE	$e^+e^- \to$ hadrons
0.72±0.11	[13]	SETH	05A	RVUE	$e^+e^- \to$ hadrons
0.64±0.23	[14]	SETH	05A	RVUE	$e^+e^- \to$ hadrons
0.49±0.13		BRANDELIK	78C	DASP	e^+e^-
0.44±0.14		SIEGRIST	76	MRK1	e^+e^-

[11] Reanalysis of data presented in BAI 02C. From a global fit over the center-of-mass energy region 3.7–5.0 GeV covering the $\psi(3770)$, $\psi(4040)$, $\psi(4160)$, and $\psi(4415)$ resonances. Phase angle fixed in the fit to $\delta = (234 \pm 88)^\circ$.

[12] Reanalysis of data presented in BAI 00 and BAI 02C. From a global fit over the center-of-mass energy 3.8-4.8 GeV covering the $\psi(4040)$, $\psi(4160)$ and $\psi(4415)$ resonances and including interference effects. Four sets of solutions are obtained with the same fit quality, mass and total width, but with different e^+e^- partial widths. We quote only the range of values.

[13] From a fit to Crystal Ball (OSTERHELD 86) data.

[14] From a fit to BES (BAI 02C) data.

$\psi(4415)$ $\Gamma(i)\Gamma(e^+e^-)/\Gamma(\text{total})$

$\Gamma(J/\psi\eta) \times \Gamma(e^+e^-)/\Gamma_{\text{total}}$ $\Gamma_{16}\Gamma_{17}/\Gamma$

VALUE (eV)	CL%	DOCUMENT ID		TECN	COMMENT
<3.6	90	WANG	13B	BELL	$e^+e^- \to J/\psi\eta\gamma$

$\psi(4415)$ BRANCHING RATIOS

$\Gamma(D^0\overline{D}^0)/\Gamma_{\text{total}}$ Γ_2/Γ

VALUE	DOCUMENT ID		TECN	COMMENT
seen	PAKHLOVA	08	BELL	$e^+e^- \to D^0\overline{D}^0\gamma$
• • • We do not use the following data for averages, fits, limits, etc. • • •				
not seen	AUBERT	09M	BABR	$e^+e^- \to D^0\overline{D}^0\gamma$

$\Gamma(D^+D^-)/\Gamma_{\text{total}}$ Γ_3/Γ

VALUE	DOCUMENT ID		TECN	COMMENT
seen	PAKHLOVA	08	BELL	$e^+e^- \to D^+D^-\gamma$
• • • We do not use the following data for averages, fits, limits, etc. • • •				
not seen	AUBERT	09M	BABR	$e^+e^- \to D^+D^-\gamma$

$\Gamma(D\overline{D})/\Gamma(D^*\overline{D}^*)$ Γ_1/Γ_7

VALUE	DOCUMENT ID		TECN	COMMENT
0.14±0.12±0.03	AUBERT	09M	BABR	$e^+e^- \to \gamma D^{(*)}\overline{D}^{(*)}$

$\Gamma(D^*(2007)^0\overline{D}^0 + \text{c.c.})/\Gamma_{\text{total}}$ Γ_5/Γ

VALUE	DOCUMENT ID		TECN	COMMENT
seen	AUBERT	09M	BABR	$e^+e^- \to D^{*0}\overline{D}^0\gamma$

$\Gamma(D^*(2010)^+D^- + \text{c.c.})/\Gamma_{\text{total}}$ Γ_6/Γ

VALUE	DOCUMENT ID		TECN	COMMENT
seen	AUBERT	09M	BABR	$e^+e^- \to D^{*+}D^-\gamma$
seen	PAKHLOVA	07	BELL	$e^+e^- \to D^{*+}D^-\gamma$

$\Gamma(D^*\overline{D} + \text{c.c.})/\Gamma(D^*\overline{D}^*)$ Γ_4/Γ_7

VALUE	DOCUMENT ID		TECN	COMMENT
0.17±0.25±0.03	AUBERT	09M	BABR	$e^+e^- \to \gamma D^{(*)}\overline{D}^{(*)}$

$\Gamma(D^*(2007)^0\overline{D}^*(2007)^0 + \text{c.c.})/\Gamma_{\text{total}}$ Γ_8/Γ

VALUE	DOCUMENT ID		TECN	COMMENT
seen	AUBERT	09M	BABR	$e^+e^- \to D^{*0}\overline{D}^{*0}\gamma$

$\Gamma(D^*(2010)^+D^*(2010)^- + \text{c.c.})/\Gamma_{\text{total}}$ Γ_9/Γ

VALUE	DOCUMENT ID		TECN	COMMENT
seen	AUBERT	09M	BABR	$e^+e^- \to D^{*+}D^{*-}\gamma$
seen	PAKHLOVA	07	BELL	$e^+e^- \to D^{*+}D^{*-}\gamma$

$\Gamma(D\overline{D}_2^*(2460) \to D^0D^-\pi^+ + \text{c.c.})/\Gamma_{\text{total}}$ Γ_{11}/Γ

VALUE (units 10^{-2})	DOCUMENT ID		TECN	COMMENT
10.5±2.4±3.8	[15] PAKHLOVA	08A	BELL	10.6 $e^+e^- \to D^0D^-\pi^+\gamma$

[15] Using 4421 ± 4 MeV for the mass and 62 ± 20 MeV for the width of $\psi(4415)$.

$\Gamma(D^0D^-\pi^+$ (excl. $D^*(2007)^0\overline{D}^0$ +c.c., $D^*(2010)^+D^-$ +c.c.)/ $\Gamma(D\overline{D}_2^*(2460) \to D^0D^-\pi^+$ +c.c.) Γ_{10}/Γ_{11}

VALUE	CL%	DOCUMENT ID		TECN	COMMENT
<0.22	90	[16] PAKHLOVA	08A	BELL	10.6 $e^+e^- \to D^0D^-\pi^+\gamma$

[16] Using 4421 ± 4 MeV for the mass and 62 ± 20 MeV for the width of $\psi(4415)$.

Meson Particle Listings

$\psi(4415)$, $X(4430)^{\pm}$, $X(4660)$

$\Gamma(D^0 D^{*-}\pi^+ + \text{c.c.})/\Gamma_{\text{total}} \times \Gamma(e^+e^-)/\Gamma_{\text{total}}$ $\quad \Gamma_{12}/\Gamma \times \Gamma_{17}/\Gamma$

VALUE	CL%	DOCUMENT ID		TECN	COMMENT
$<0.99 \times 10^{-6}$	90	[17] PAKHLOVA	09	BELL	$e^+e^- \to D^0 D^{*-}\pi^+$

[17] Using 4421 ± 4 MeV for the mass of $\psi(4415)$.

$\Gamma(D_s^+ D_s^-)/\Gamma_{\text{total}}$ $\quad \Gamma_{13}/\Gamma$

VALUE	DOCUMENT ID		TECN	COMMENT
not seen	PAKHLOVA	11	BELL	$e^+e^- \to D_s^+ D_s^-\gamma$
not seen	DEL-AMO-SA...10N		BABR	$e^+e^- \to D_s^+ D_s^-\gamma$

$\Gamma(D_s^{*+} D_s^- + \text{c.c.})/\Gamma_{\text{total}}$ $\quad \Gamma_{14}/\Gamma$

VALUE	DOCUMENT ID		TECN	COMMENT
seen	PAKHLOVA	11	BELL	$e^+e^- \to D_s^{*+} D_s^-\gamma$
seen	DEL-AMO-SA...10N		BABR	$e^+e^- \to D_s^{*+} D_s^-\gamma$

$\Gamma(D_s^{*+} D_s^{*-})/\Gamma_{\text{total}}$ $\quad \Gamma_{15}/\Gamma$

VALUE	DOCUMENT ID		TECN	COMMENT
not seen	PAKHLOVA	11	BELL	$e^+e^- \to D_s^{*+} D_s^{*-}\gamma$
not seen	DEL-AMO-SA...10N		BABR	$e^+e^- \to D_s^{*+} D_s^{*-}\gamma$

$\psi(4415)$ REFERENCES

WANG	13B	PR D87 051101	X.L. Wang *et al.*	(BELLE Collab.)
PAKHLOVA	11	PR D83 011101	G. Pakhlova *et al.*	(BELLE Collab.)
DEL-AMO-SA...	10N	PR D82 052004	P. del Amo Sanchez *et al.*	(BABAR Collab.)
MO	10	PR D82 077501	X.H. Mo, C.Z. Yuan, P. Wang	(BHEP)
AUBERT	09M	PR D79 092001	B. Aubert *et al.*	(BABAR Collab.)
PAKHLOVA	09	PR D80 091101	G. Pakhlova *et al.*	(BELLE Collab.)
ABLIKIM	08D	PL B660 315	M. Ablikim *et al.*	(BES Collab.)
PAKHLOVA	08	PR D77 011103	G. Pakhlova *et al.*	(BELLE Collab.)
PAKHLOVA	08A	PRL 100 062001	G. Pakhlova *et al.*	(BELLE Collab.)
PAKHLOVA	07	PRL 98 092001	G. Pakhlova *et al.*	(BELLE Collab.)
SETH	05A	PR D72 017501	K.K. Seth	
BAI	02C	PRL 88 101802	J.Z. Bai *et al.*	(BES Collab.)
BAI	00	PRL 84 594	J.Z. Bai *et al.*	(BES Collab.)
OSTERHELD	86	SLAC-PUB-4160	A. Osterheld *et al.*	(SLAC Crystal Ball Collab.)
BRANDELIK	78C	PL 76B 361	R. Brandelik *et al.*	(DASP Collab.)
SIEGRIST	76	PRL 36 700	J.L. Siegrist *et al.*	(LBL, SLAC)

$X(4430)^{\pm}$

$I(J^P) = ?(1^+)$

OMITTED FROM SUMMARY TABLE

Spin and parity assigment $J^P = 1^+$ is favored over 0^-, 1^-, 2^-, and 2^+ at the levels of 3.4 σ, 3.7 σ, 4.7 σ, and 5.1 σ, respectively, according to the four-dimensional amplitude analysis of CHILIKIN 13. Seen by CHOI 08 in $B \to K\pi^+\psi(2S)$ decays and confirmed by reanalysis of the same data sample in MIZUK 09. Not seen by AUBERT 09AA.

$X(4430)^{\pm}$ MASS

VALUE (MeV)	DOCUMENT ID		TECN	COMMENT
$4485 \pm 22^{+28}_{-11}$	[1] CHILIKIN	13	BELL	$B^0 \to \psi(2S)K^+\pi^-$
• • • We do not use the following data for averages, fits, limits, etc. • • •				
$4443^{+15}_{-12}{}^{+19}_{-13}$	[2] MIZUK	09	BELL	$B \to K\pi^+\psi(2S)$
$4433 \pm 4 \pm 2$	[3] CHOI	08	BELL	$B \to K\pi^+\psi(2S)$

[1] From a four-dimensional amplitude analysis.
[2] From a Dalitz plot analysis. Superseded by CHILIKIN 13.
[3] Superseded by MIZUK 09 and CHILIKIN 13.

$X(4430)^{\pm}$ WIDTH

VALUE (MeV)	DOCUMENT ID		TECN	COMMENT
$200^{+41}_{-46}{}^{+26}_{-35}$	[4] CHILIKIN	13	BELL	$B^0 \to \psi(2S)K^+\pi^-$
• • • We do not use the following data for averages, fits, limits, etc. • • •				
$107^{+86}_{-43}{}^{+74}_{-56}$	[5] MIZUK	09	BELL	$B \to K\pi^+\psi(2S)$
$45^{+18}_{-13}{}^{+30}_{-13}$	[6] CHOI	08	BELL	$B \to K\pi^+\psi(2S)$

[4] From a four-dimensional amplitude analysis.
[5] From a Dalitz plot analysis. Superseded by CHILIKIN 13.
[6] Superseded by MIZUK 09 and CHILIKIN 13.

$X(4430)^{\pm}$ DECAY MODES

	Mode	Fraction (Γ_i/Γ)
Γ_1	$\pi^+\psi(2S)$	seen
Γ_2	$\pi^+ J/\psi$	not seen

$X(4430)^{\pm}$ BRANCHING RATIOS

$\Gamma(\pi^+\psi(2S))/\Gamma_{\text{total}}$ $\quad \Gamma_1/\Gamma$

VALUE	DOCUMENT ID		TECN	COMMENT
seen	[7] CHILIKIN	13	BELL	$B^0 \to \psi(2S)K^+\pi^-$
• • • We do not use the following data for averages, fits, limits, etc. • • •				
not seen	[8] AUBERT	09AA	BABR	$B \to K\pi^+\psi(2S)$
seen	[9] MIZUK	09	BELL	$B \to K\pi^+\psi(2S)$

[7] From a four-dimensional amplitude analysis. Measured a product of branching fractions $B(B^0 \to X(4430)^- K^+) \times B(X(4430)^- \to \psi(2S)\pi^-) = (6.0^{+1.7}_{-2.0}{}^{+2.5}_{-1.4}) \times 10^{-5}$.
[8] AUBERT 09AA quotes $B(B^+ \to \overline{K}^0 X(4430)^+) \times B(X(4430)^+ \to \pi^+\psi(2S)) < 4.7 \times 10^{-5}$ and $B(\overline{B}^0 \to K^- X(4430)^+) \times B(X(4430)^+ \to \pi^+\psi(2S)) < 3.1 \times 10^{-5}$ at 95% CL.
[9] Measured a product of branching fractions $B(\overline{B}^0 \to K^- X(4430)^+) \times B(X(4430)^+ \to \pi^+\psi(2S)) = (3.2^{+1.8}_{-0.9}{}^{+5.3}_{-1.6}) \times 10^{-5}$. Superseded by CHILIKIN 13.

$\Gamma(\pi^+ J/\psi)/\Gamma_{\text{total}}$ $\quad \Gamma_2/\Gamma$

VALUE	DOCUMENT ID		TECN	COMMENT
not seen	[10] AUBERT	09AA	BABR	$B \to K\pi^+ J/\psi$

[10] AUBERT 09AA quotes $B(B^+ \to \overline{K}^0 X(4430)^+) \times B(X(4430)^+ \to \pi^+ J/\psi) < 1.5 \times 10^{-5}$ and $B(\overline{B}^0 \to K^- X(4430)^+) \times B(X(4430)^+ \to \pi^+ J/\psi) < 0.4 \times 10^{-5}$ at 95% CL.

$X(4430)^{\pm}$ REFERENCES

CHILIKIN	13	PR D88 074026	K. Chilikin *et al.*	(BELLE Collab.)
AUBERT	09AA	PR D79 112001	B. Aubert *et al.*	(BABAR Collab.)
MIZUK	09	PR D80 031104	R. Mizuk *et al.*	(BELLE Collab.)
CHOI	08	PRL 100 142001	S.-K. Choi *et al.*	(BELLE Collab.)

$X(4660)$

$I^G(J^{PC}) = ?^?(1^{--})$

Seen in radiative return from e^+e^- collisions at $\sqrt{s}$ = 9.54–10.58 GeV by WANG 07D. Also obtained in a combined fit of WANG 07D and AUBERT 07S. See also the review under the $X(3872)$ particle listings. (See the index for the page number.)

$X(4660)$ MASS

VALUE (MeV)	DOCUMENT ID		TECN	COMMENT
$4664 \pm 11 \pm 5$	WANG	07D	BELL	10.58 $e^+e^- \to \psi(2S)\pi^+\pi^-\gamma$
• • • We do not use the following data for averages, fits, limits, etc. • • •				
$4661^{+\ 9}_{-\ 8} \pm 6$	[1] LIU	08H	RVUE	10.58 $e^+e^- \to \psi(2S)\pi^+\pi^-\gamma$

[1] From a combined fit of AUBERT 07S and WANG 07D data with two resonances.

$X(4660)$ WIDTH

VALUE (MeV)	DOCUMENT ID		TECN	COMMENT
$48 \pm 15 \pm 3$	WANG	07D	BELL	10.58 $e^+e^- \to \psi(2S)\pi^+\pi^-\gamma$
• • • We do not use the following data for averages, fits, limits, etc. • • •				
$42^{+17}_{-12} \pm 6$	[2] LIU	08H	RVUE	10.58 $e^+e^- \to \psi(2S)\pi^+\pi^-\gamma$

[2] From a combined fit of AUBERT 07S and WANG 07D data with two resonances.

$X(4660)$ DECAY MODES

	Mode	Fraction (Γ_i/Γ)
Γ_1	e^+e^-	
Γ_2	$\psi(2S)\pi^+\pi^-$	seen
Γ_3	$J/\psi\eta$	
Γ_4	$D^0 D^{*-}\pi^+$	

$X(4660)$ $\Gamma(i)\Gamma(e^+e^-)/\Gamma(\text{total})$

$\Gamma(\psi(2S)\pi^+\pi^-) \times \Gamma(e^+e^-)/\Gamma_{\text{total}}$ $\quad \Gamma_2\Gamma_1/\Gamma$

VALUE (eV)	DOCUMENT ID		TECN	COMMENT
• • • We do not use the following data for averages, fits, limits, etc. • • •				
$2.2^{+0.7}_{-0.6}$	[3] LIU	08H	RVUE	10.58 $e^+e^- \to \psi(2S)\pi^+\pi^-\gamma$
5.9 ± 1.6	[4] LIU	08H	RVUE	10.58 $e^+e^- \to \psi(2S)\pi^+\pi^-\gamma$
$3.0 \pm 0.9 \pm 0.3$	[5] WANG	07D	BELL	10.58 $e^+e^- \to \psi(2S)\pi^+\pi^-\gamma$
$7.6 \pm 1.8 \pm 0.8$	[6] WANG	07D	BELL	10.58 $e^+e^- \to \psi(2S)\pi^+\pi^-\gamma$

[3] Solution I in a combined fit of AUBERT 07S and WANG 07D data with two resonances.
[4] Solution II in a combined fit of AUBERT 07S and WANG 07D data with two resonances.
[5] Solution I of two equivalent solutions in a fit using two interfering resonances.
[6] Solution II of two equivalent solutions in a fit using two interfering resonances.

See key on page 547

$\Gamma(J/\psi\eta) \times \Gamma(e^+e^-)/\Gamma_{total}$ $\Gamma_3\Gamma_1/\Gamma$

VALUE (eV)	CL%	DOCUMENT ID		TECN	COMMENT
• • • We do not use the following data for averages, fits, limits, etc. • • •					
<0.94	90	WANG	13B	BELL	$e^+e^- \to J/\psi\eta\gamma$

$X(4660)$ BRANCHING RATIOS

$\Gamma(D^0D^{*-}\pi^+)/\Gamma(\psi(2S)\pi^+\pi^-)$ Γ_4/Γ_2

VALUE	CL%	DOCUMENT ID		TECN	COMMENT
<10	90	PAKHLOVA	09	BELL	$e^+e^- \to X(4660) \to D^0D^{*-}\pi^+$

$\Gamma(D^0D^{*-}\pi^+)/\Gamma_{total} \times \Gamma(e^+e^-)/\Gamma_{total}$ $\Gamma_4/\Gamma \times \Gamma_1/\Gamma$

VALUE	CL%	DOCUMENT ID		TECN	COMMENT
$<0.37 \times 10^{-6}$	90	[7] PAKHLOVA	09	BELL	$e^+e^- \to X(4660) \to D^0D^{*-}\pi^+$

[7] Using $4664 \pm 11 \pm 5$ MeV for the mass of $X(4660)$.

$X(4660)$ REFERENCES

WANG	13B	PR D87 051101	X.L. Wang *et al.*	(BELLE Collab.)
PAKHLOVA	09	PR D80 091101	G. Pakhlova *et al.*	(BELLE Collab.)
LIU	08H	PR D78 014032	Z.Q. Liu, X.S. Qin, C.Z. Yuan	
AUBERT	07S	PRL 98 212001	B. Aubert *et al.*	(BABAR Collab.)
WANG	07D	PRL 99 142002	X.L. Wang *et al.*	(BELLE Collab.)

$b\bar{b}$ MESONS

THE BOTTOMONIUM SYSTEM

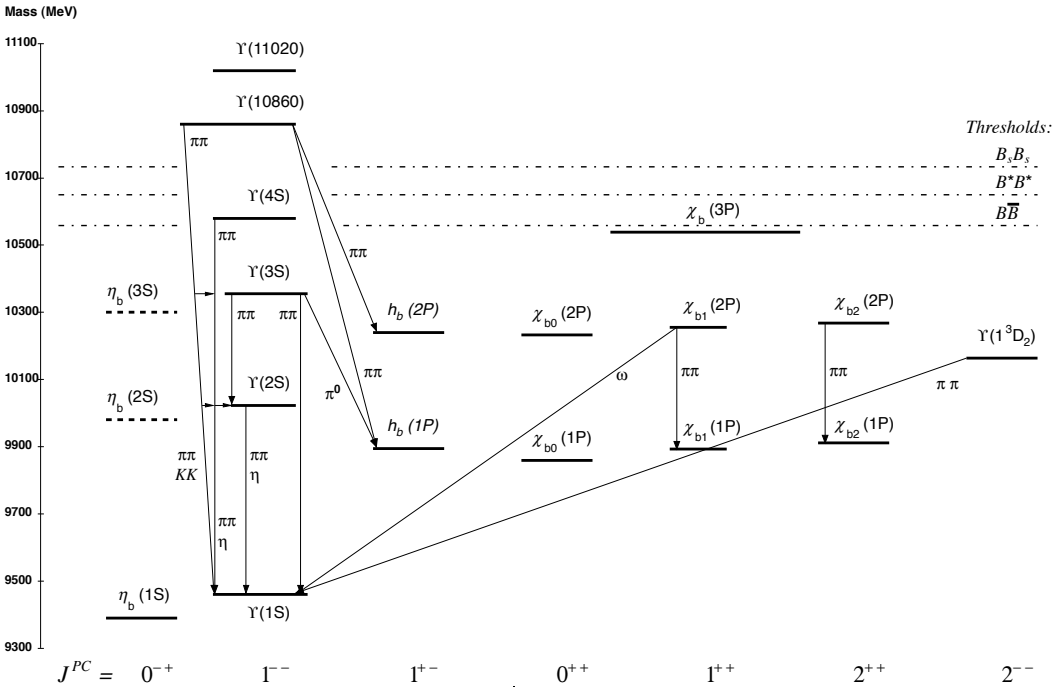

The level scheme of the $b\bar{b}$ states showing experimentally established states with solid lines. Singlet states are called η_b and h_b, triplet states Υ and χ_{bJ}. In parentheses it is sufficient to give the radial quantum number and the orbital angular momentum to specify the states with all their quantum numbers. *E.g.*, $h_b(2P)$ means 2^1P_1 with $n = 2$, $L = 1$, $S = 0$, $J = 1$, $PC = +-$. The figure shows observed hadronic transitions. The single photon transitions $\Upsilon(nS) \to \gamma\eta_b(mS)$, $\Upsilon(nS) \to \gamma\chi_{bJ}(mP)$, and $\chi_{bJ}(nP) \to \gamma\Upsilon(mS)$ are omitted for clarity.

WIDTH DETERMINATIONS OF THE Υ STATES

As is the case for the $J/\psi(1S)$ and $\psi(2S)$, the full widths of the $b\bar{b}$ states $\Upsilon(1S)$, $\Upsilon(2S)$, and $\Upsilon(3S)$ are not directly measurable, since they are much narrower than the energy resolution of the e^+e^- storage rings where these states are produced. The common indirect method to determine Γ starts from

$$\Gamma = \Gamma_{\ell\ell}/B_{\ell\ell} \ , \tag{1}$$

where $\Gamma_{\ell\ell}$ is one leptonic partial width and $B_{\ell\ell}$ is the corresponding branching fraction ($\ell = e$, μ, or τ). One then assumes e-μ-τ universality and uses

$$\Gamma_{\ell\ell} = \Gamma_{ee}$$

$$B_{\ell\ell} = \text{average of } B_{ee},\ B_{\mu\mu}, \text{ and } B_{\tau\tau} \ . \tag{2}$$

The electronic partial width Γ_{ee} is also not directly measurable at e^+e^- storage rings, only in the combination $\Gamma_{ee}\Gamma_{\rm had}/\Gamma$, where $\Gamma_{\rm had}$ is the hadronic partial width and

$$\Gamma_{\rm had} + 3\Gamma_{ee} = \Gamma \ . \tag{3}$$

This combination is obtained experimentally from the energy-integrated hadronic cross section

$$\int_{\text{resonance}} \sigma(e^+e^- \to \Upsilon \to \text{hadrons})dE$$

$$= \frac{6\pi^2}{M^2}\frac{\Gamma_{ee}\Gamma_{\rm had}}{\Gamma}C_r = \frac{6\pi^2}{M^2}\frac{\Gamma^{(0)}_{ee}\Gamma_{\rm had}}{\Gamma}C^{(0)}_r \ , \tag{4}$$

where M is the Υ mass, and C_r and $C^{(0)}_r$ are radiative correction factors. C_r is used for obtaining Γ_{ee} as defined in Eq. (1), and contains corrections from all orders of QED for describing $(b\bar{b}) \to e^+e^-$. The lowest order QED value $\Gamma^{(0)}_{ee}$, relevant for comparison with potential-model calculations, is defined by the lowest order QED graph (Born term) alone, and is about 7% lower than Γ_{ee}.

The Listings give experimental results on B_{ee}, $B_{\mu\mu}$, $B_{\tau\tau}$, and $\Gamma_{ee}\Gamma_{\rm had}/\Gamma$. The entries of the last quantity have been re-evaluated consistently using the correction procedure of KURAEV 85. The partial width Γ_{ee} is obtained from the average values for $\Gamma_{ee}\Gamma_{\rm had}/\Gamma$ and $B_{\ell\ell}$ using

$$\Gamma_{ee} = \frac{\Gamma_{ee}\Gamma_{\rm had}}{\Gamma(1 - 3B_{\ell\ell})} \ . \tag{5}$$

The total width Γ is then obtained from Eq. (1). We do not list Γ_{ee} and Γ values of individual experiments. The Γ_{ee} values in the Meson Summary Table are also those defined in Eq. (1).

$\eta_b(1S)$

$I^G(J^{PC}) = 0^+(0^{-+})$

OMITTED FROM SUMMARY TABLE

Quantum numbers shown are quark-model predictions. Observed in radiative decay of the $\Upsilon(3S)$, therefore $C = +$.

$\eta_b(1S)$ MASS

VALUE (MeV)	EVTS	DOCUMENT ID		TECN	COMMENT
9398.0± 3.2 OUR AVERAGE		Error includes scale factor of 1.8. See the ideogram below.			
9402.4± 1.5± 1.8	34k	[1] MIZUK	12	BELL	$e^+e^- \to \gamma\pi^+\pi^-$ + hadrons
9391.8± 6.6± 2.0	2.3 ± 0.5k	[2] BONVICINI	10	CLEO	$\Upsilon(3S) \to \gamma X$
$9394.2^{+4.8}_{-4.9}$ ± 2.0	13 ± 5k	[2] AUBERT	09AQ	BABR	$\Upsilon(2S) \to \gamma X$
$9388.9^{+3.1}_{-2.3}$ ± 2.7	19 ± 3k	[2] AUBERT	08V	BABR	$\Upsilon(3S) \to \gamma X$
• • • We do not use the following data for averages, fits, limits, etc. • • •					
9393.2± 3.4± 2.3	10^{+5}_{-4}	[2,3] DOBBS	12		$\Upsilon(2S) \to \gamma$ hadrons
9300 ±20 ±20		HEISTER	02D	ALEP	181–209 e^+e^-

[1] With floating width. Not independent of the corresponding mass difference measurement.
[2] Assuming $\Gamma_{\eta_b(1S)} = 10$ MeV. Not independent of the corresponding γ energy or mass difference measurements.
[3] Obtained by analyzing CLEO III data but not authored by the CLEO Collaboration.

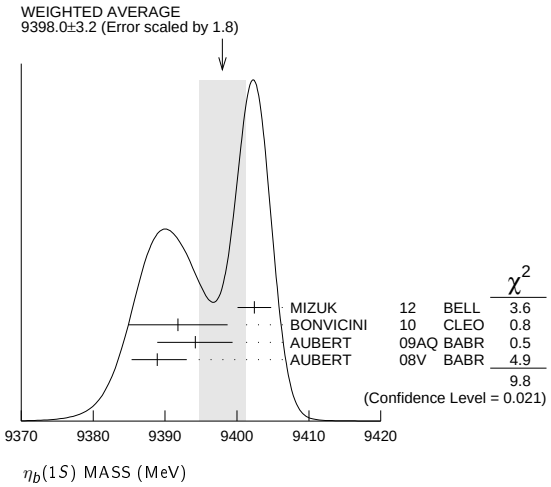

$m_{\Upsilon(1S)} - m_{\eta_b}$

VALUE (MeV)	EVTS	DOCUMENT ID		TECN	COMMENT
62.3±3.2 OUR AVERAGE		Error includes scale factor of 1.8. See the ideogram below.			
57.9±1.5±1.8	34k	[4] MIZUK	12	BELL	$e^+e^- \to \gamma\pi^+\pi^-$ + hadrons
68.5±6.6±2.0	2.3 ± 0.5k	[5] BONVICINI	10	CLEO	$\Upsilon(3S) \to \gamma X$
$66.1^{+4.8}_{-4.9}$ ±2.0	13 ± 5k	[5] AUBERT	09AQ	BABR	$\Upsilon(2S) \to \gamma X$
$71.4^{+2.3}_{-3.1}$ ±2.7	19 ± 3k	[5] AUBERT	08V	BABR	$\Upsilon(3S) \to \gamma X$
• • • We do not use the following data for averages, fits, limits, etc. • • •					
67.1±3.4±2.3	10^{+5}_{-4}	[5,6] DOBBS	12		$\Upsilon(2S) \to \gamma$ hadrons

[4] With floating width. Not independent of the corresponding mass measurement.
[5] Assuming $\Gamma_{\eta_b(1S)} = 10$ MeV. Not independent of the corresponding γ energy or mass measurements.
[6] Obtained by analyzing CLEO III data but not authored by the CLEO Collaboration.

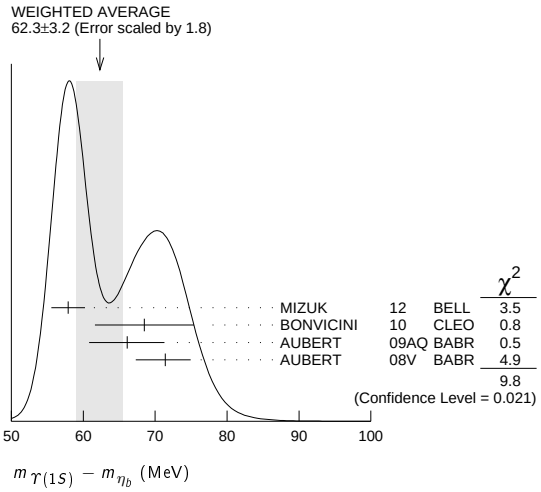

γ ENERGY IN $\Upsilon(3S)$ DECAY

VALUE (MeV)	EVTS	DOCUMENT ID		TECN	COMMENT
$920.6^{+2.8}_{-3.2}$ OUR AVERAGE					
918.6±6.0±1.9	2.3 ± 0.5k	[7] BONVICINI	10	CLEO	$\Upsilon(3S) \to \gamma X$
$921.2^{+2.1}_{-2.8}$ ±2.4	19 ± 3k	[7] AUBERT	08V	BABR	$\Upsilon(3S) \to \gamma X$

[7] Assuming $\Gamma_{\eta_b(1S)} = 10$ MeV. Not independent of the corresponding mass or mass difference measurements.

γ ENERGY IN $\Upsilon(2S)$ DECAY

VALUE (MeV)	EVTS	DOCUMENT ID		TECN	COMMENT
$609.3^{+4.6}_{-4.5}$ ±1.9	13 ± 5k	[8] AUBERT	09AQ	BABR	$\Upsilon(2S) \to \gamma X$

[8] Assuming $\Gamma_{\eta_b(1S)} = 10$ MeV. Not independent of the corresponding mass or mass difference measurements.

$\eta_b(1S)$ WIDTH

VALUE (MeV)	EVTS	DOCUMENT ID		TECN	COMMENT
$10.8^{+4.0}_{-3.7}{}^{+4.5}_{-2.0}$	34k	[9] MIZUK	12	BELL	$e^+e^- \to \gamma\pi^+\pi^-$ + hadrons

[9] With floating mass.

$\eta_b(1S)$ DECAY MODES

	Mode	Fraction (Γ_j/Γ)	Confidence level
Γ_1	hadrons	seen	
Γ_2	$3h^+3h^-$	not seen	
Γ_3	$2h^+2h^-$	not seen	
Γ_4	$4h^+4h^-$		
Γ_5	$\gamma\gamma$	not seen	
Γ_6	$\mu^+\mu^-$	$<9\times10^{-3}$	90%
Γ_7	$\tau^+\tau^-$	<8 %	90%

$\eta_b(1S)$ Γ(i)$\Gamma(\gamma\gamma)/\Gamma$(total)

$\Gamma(3h^+3h^-) \times \Gamma(\gamma\gamma)/\Gamma_{\text{total}}$ **$\Gamma_2\Gamma_5/\Gamma$**

VALUE (eV)	CL%	DOCUMENT ID		TECN	COMMENT
• • • We do not use the following data for averages, fits, limits, etc. • • •					
<470	95	ABDALLAH	06	DLPH	161–209 e^+e^-
<132	95	HEISTER	02D	ALEP	181–209 e^+e^-

$\Gamma(2h^+2h^-) \times \Gamma(\gamma\gamma)/\Gamma_{\text{total}}$ **$\Gamma_3\Gamma_5/\Gamma$**

VALUE (eV)	CL%	DOCUMENT ID		TECN	COMMENT
• • • We do not use the following data for averages, fits, limits, etc. • • •					
<190	95	ABDALLAH	06	DLPH	161–209 e^+e^-
< 48	95	HEISTER	02D	ALEP	181–209 e^+e^-

$\Gamma(4h^+4h^-) \times \Gamma(\gamma\gamma)/\Gamma_{\text{total}}$ **$\Gamma_4\Gamma_5/\Gamma$**

VALUE (eV)	CL%	DOCUMENT ID		TECN	COMMENT
• • • We do not use the following data for averages, fits, limits, etc. • • •					
<660	95	ABDALLAH	06	DLPH	161–209 e^+e^-

Meson Particle Listings

$\eta_b(1S)$, $\Upsilon(1S)$

$\eta_b(1S)$ BRANCHING RATIOS

Γ(hadrons)/Γ_{total} — **Γ_1/Γ**

VALUE	EVTS	DOCUMENT ID		TECN	COMMENT
seen	34k	MIZUK	12	BELL	$e^+e^- \to \gamma\pi^+\pi^-$ + hadrons

$\Gamma(\mu^+\mu^-)/\Gamma_{total}$ — **Γ_6/Γ**

VALUE	CL%	DOCUMENT ID		TECN	COMMENT
$<9\times10^{-3}$	90	[10] AUBERT	09Z	BABR	$e^+e^- \to \Upsilon(2S,3S) \to \gamma\eta_b$

[10] Obtained using $B(\Upsilon(2S) \to \gamma\eta_b) = (4.2^{+1.1}_{-1.0} \pm 0.9)\times10^{-4}$ and $B(\Upsilon(3S) \to \gamma\eta_b) = (4.8 \pm 0.5 \pm 0.6)\times10^{-4}$. This limit is equivalent to $B(\eta_b \to \mu^+\mu^-) = (-0.25 \pm 0.51 \pm 0.33)\%$ measurement.

$\Gamma(\tau^+\tau^-)/\Gamma_{total}$ — **Γ_7/Γ**

VALUE	CL%	DOCUMENT ID	TECN	COMMENT
$<8\times10^{-2}$	90	AUBERT	09P	BABR	$e^+e^- \to \gamma\tau^+\tau^-$

$\eta_b(1S)$ REFERENCES

DOBBS	12	PRL 109 082001	S. Dobbs *et al.*	
MIZUK	12	PRL 109 232002	R. Mizuk *et al.*	(BELLE Collab.)
BONVICINI	10	PR D81 031104	G. Bonvicini *et al.*	(CLEO Collab.)
AUBERT	09AQ	PRL 103 161801	B. Aubert *et al.*	(BABAR Collab.)
AUBERT	09P	PRL 103 181801	B. Aubert *et al.*	(BABAR Collab.)
AUBERT	09Z	PRL 103 081803	B. Aubert *et al.*	(BABAR Collab.)
AUBERT	08V	PRL 101 071801	B. Aubert *et al.*	(BABAR Collab.)
ABDALLAH	06	PL B634 340	J.M. Abdallah *et al.*	(DELPHI Collab.)
HEISTER	02D	PL B530 56	A. Heister *et al.*	(ALEPH Collab.)

$\Upsilon(1S)$

$I^G(J^{PC}) = 0^-(1^{--})$

$\Upsilon(1S)$ MASS

VALUE (MeV)	DOCUMENT ID		TECN	COMMENT
9460.30±0.26 OUR AVERAGE	Error includes scale factor of 3.3.			
9460.51±0.09±0.05	[1] ARTAMONOV	00	MD1	$e^+e^- \to$ hadrons
9459.97±0.11±0.07	MACKAY	84	REDE	$e^+e^- \to$ hadrons
• • • We do not use the following data for averages, fits, limits, etc. • • •				
9460.60±0.09±0.05	[2,3] BARU	92B	REDE	$e^+e^- \to$ hadrons
9460.59±0.12	BARU	86	REDE	$e^+e^- \to$ hadrons
9460.6 ±0.4	[3,4] ARTAMONOV	84	REDE	$e^+e^- \to$ hadrons

[1] Reanalysis of BARU 92B and ARTAMONOV 84 using new electron mass (COHEN 87).
[2] Superseding BARU 86.
[3] Superseded by ARTAMONOV 00.
[4] Value includes data of ARTAMONOV 82.

$\Upsilon(1S)$ WIDTH

VALUE (keV)	DOCUMENT ID
54.02±1.25 OUR EVALUATION	See the Note on "Width Determinations of the Υ States"

$\Upsilon(1S)$ DECAY MODES

	Mode	Fraction (Γ_i/Γ)	Confidence level
Γ_1	$\tau^+\tau^-$	(2.60 ±0.10) %	
Γ_2	e^+e^-	(2.38 ±0.11) %	
Γ_3	$\mu^+\mu^-$	(2.48 ±0.05) %	
	Hadronic decays		
Γ_4	ggg	(81.7 ±0.7) %	
Γ_5	γgg	(2.2 ±0.6) %	
Γ_6	$\eta'(958)$ anything	(2.94 ±0.24) %	
Γ_7	$J/\psi(1S)$ anything	(6.5 ±0.7) $\times10^{-4}$	
Γ_8	χ_{c0} anything	< 5 $\times10^{-3}$	90%
Γ_9	χ_{c1} anything	(2.3 ±0.7) $\times10^{-4}$	
Γ_{10}	χ_{c2} anything	(3.4 ±1.0) $\times10^{-4}$	
Γ_{11}	$\psi(2S)$ anything	(2.7 ±0.9) $\times10^{-4}$	
Γ_{12}	$\rho\pi$	< 3.68 $\times10^{-6}$	90%
Γ_{13}	$\omega\pi^0$	< 3.90 $\times10^{-6}$	90%
Γ_{14}	$\pi^+\pi^-$	< 5 $\times10^{-4}$	90%
Γ_{15}	K^+K^-	< 5 $\times10^{-4}$	90%
Γ_{16}	$p\overline{p}$	< 5 $\times10^{-4}$	90%
Γ_{17}	$\pi^+\pi^-\pi^0$	(2.1 ±0.8) $\times10^{-6}$	
Γ_{18}	ϕK^+K^-	(2.4 ±0.5) $\times10^{-6}$	
Γ_{19}	$\omega\pi^+\pi^-$	(4.5 ±1.0) $\times10^{-6}$	
Γ_{20}	$K^*(892)^0K^-\pi^+$ + c.c.	(4.4 ±0.8) $\times10^{-6}$	
Γ_{21}	$\phi f_2'(1525)$	< 1.63 $\times10^{-6}$	90%
Γ_{22}	$\omega f_2(1270)$	< 1.79 $\times10^{-6}$	90%
Γ_{23}	$\rho(770)a_2(1320)$	< 2.24 $\times10^{-6}$	90%
Γ_{24}	$K^*(892)^0\overline{K}_2^*(1430)^0$ + c.c.	(3.0 ±0.8) $\times10^{-6}$	
Γ_{25}	$K_1(1270)^\pm K^\mp$	< 2.41 $\times10^{-6}$	90%
Γ_{26}	$K_1(1400)^\pm K^\mp$	(1.0 ±0.4) $\times10^{-6}$	
Γ_{27}	$b_1(1235)^\pm\pi^\mp$	< 1.25 $\times10^{-6}$	90%
Γ_{28}	$\pi^+\pi^-\pi^0\pi^0$	(1.28 ±0.30) $\times10^{-5}$	
Γ_{29}	$K_S^0K^+\pi^-$ + c.c.	(1.6 ±0.4) $\times10^{-6}$	
Γ_{30}	$K^*(892)^0\overline{K}^0$ + c.c.	(2.9 ±0.9) $\times10^{-6}$	
Γ_{31}	$K^*(892)^-K^+$ + c.c.	< 1.11 $\times10^{-6}$	90%
Γ_{32}	$D^*(2010)^\pm$ anything	(2.52 ±0.20) %	
Γ_{33}	$\overline{d}$ anything	(2.86 ±0.28) $\times10^{-5}$	
Γ_{34}	Sum of 100 exclusive modes	(1.200±0.017) %	
	Radiative decays		
Γ_{35}	$\gamma\pi^+\pi^-$	(6.3 ±1.8) $\times10^{-5}$	
Γ_{36}	$\gamma\pi^0\pi^0$	(1.7 ±0.7) $\times10^{-5}$	
Γ_{37}	$\gamma\pi^0\eta$	< 2.4 $\times10^{-6}$	90%
Γ_{38}	γK^+K^-	[a] (1.14 ±0.13) $\times10^{-5}$	
Γ_{39}	$\gamma p\overline{p}$	[b] < 6 $\times10^{-6}$	90%
Γ_{40}	$\gamma 2h^+2h^-$	(7.0 ±1.5) $\times10^{-4}$	
Γ_{41}	$\gamma 3h^+3h^-$	(5.4 ±2.0) $\times10^{-4}$	
Γ_{42}	$\gamma 4h^+4h^-$	(7.4 ±3.5) $\times10^{-4}$	
Γ_{43}	$\gamma\pi^+\pi^-K^+K^-$	(2.9 ±0.9) $\times10^{-4}$	
Γ_{44}	$\gamma 2\pi^+2\pi^-$	(2.5 ±0.9) $\times10^{-4}$	
Γ_{45}	$\gamma 3\pi^+3\pi^-$	(2.5 ±1.2) $\times10^{-4}$	
Γ_{46}	$\gamma 2\pi^+2\pi^-K^+K^-$	(2.4 ±1.2) $\times10^{-4}$	
Γ_{47}	$\gamma\pi^+\pi^-p\overline{p}$	(1.5 ±0.6) $\times10^{-4}$	
Γ_{48}	$\gamma 2\pi^+2\pi^-p\overline{p}$	(4 ±6) $\times10^{-5}$	
Γ_{49}	$\gamma 2K^+2K^-$	(2.0 ±2.0) $\times10^{-5}$	
Γ_{50}	$\gamma\eta'(958)$	< 1.9 $\times10^{-6}$	90%
Γ_{51}	$\gamma\eta$	< 1.0 $\times10^{-6}$	90%
Γ_{52}	$\gamma f_0(980)$	< 3 $\times10^{-5}$	90%
Γ_{53}	$\gamma f_2'(1525)$	(3.8 ±0.9) $\times10^{-5}$	
Γ_{54}	$\gamma f_2(1270)$	(1.01 ±0.09) $\times10^{-4}$	
Γ_{55}	$\gamma\eta(1405)$	< 8.2 $\times10^{-5}$	90%
Γ_{56}	$\gamma f_0(1500)$	< 1.5 $\times10^{-5}$	90%
Γ_{57}	$\gamma f_0(1710)$	< 2.6 $\times10^{-4}$	90%
Γ_{58}	$\gamma f_0(1710) \to \gamma K^+K^-$	< 7 $\times10^{-6}$	90%
Γ_{59}	$\gamma f_0(1710) \to \gamma\pi^0\pi^0$	< 1.4 $\times10^{-6}$	90%
Γ_{60}	$\gamma f_0(1710) \to \gamma\eta\eta$	< 1.8 $\times10^{-6}$	90%
Γ_{61}	$\gamma f_4(2050)$	< 5.3 $\times10^{-5}$	90%
Γ_{62}	$\gamma f_0(2200) \to \gamma K^+K^-$	< 2 $\times10^{-4}$	90%
Γ_{63}	$\gamma f_J(2220) \to \gamma K^+K^-$	< 8 $\times10^{-7}$	90%
Γ_{64}	$\gamma f_J(2220) \to \gamma\pi^+\pi^-$	< 6 $\times10^{-7}$	90%
Γ_{65}	$\gamma f_J(2220) \to \gamma p\overline{p}$	< 1.1 $\times10^{-6}$	90%
Γ_{66}	$\gamma\eta(2225) \to \gamma\phi\phi$	< 3 $\times10^{-3}$	90%
Γ_{67}	$\gamma\eta_c(1S)$	< 5.7 $\times10^{-5}$	90%
Γ_{68}	$\gamma\chi_{c0}$	< 6.5 $\times10^{-4}$	90%
Γ_{69}	$\gamma\chi_{c1}$	< 2.3 $\times10^{-5}$	90%
Γ_{70}	$\gamma\chi_{c2}$	< 7.6 $\times10^{-6}$	90%
Γ_{71}	$\gamma X(3872) \to \pi^+\pi^-J/\psi$	< 1.6 $\times10^{-6}$	90%
Γ_{72}	$\gamma X(3872) \to \pi^+\pi^-\pi^0J/\psi$	< 2.8 $\times10^{-6}$	90%
Γ_{73}	$\gamma\chi_{c0}(2P) \to \omega J/\psi$	< 3.0 $\times10^{-6}$	90%
Γ_{74}	$\gamma X(4140) \to \phi J/\psi$	< 2.2 $\times10^{-6}$	90%
Γ_{75}	γX	[c] < 4.5 $\times10^{-6}$	90%
Γ_{76}	$\gamma X\overline{X}(m_X < 3.1$ GeV)	[d] < 1 $\times10^{-3}$	90%
Γ_{77}	$\gamma X\overline{X}(m_X < 4.5$ GeV)	[e] < 2.4 $\times10^{-4}$	90%
Γ_{78}	$\gamma X \to \gamma +\geq 4$ prongs	[f] < 1.78 $\times10^{-4}$	95%
Γ_{79}	$\gamma a_1^0 \to \gamma\mu^+\mu^-$	[g] < 9 $\times10^{-6}$	90%
Γ_{80}	$\gamma a_1^0 \to \gamma\tau^+\tau^-$	[a] < 1.30 $\times10^{-4}$	90%
Γ_{81}	$\gamma a_1^0 \to \gamma gg$	[h] < 1 %	90%
Γ_{82}	$\gamma a_1^0 \to \gamma s\overline{s}$	[h] < 1 $\times10^{-3}$	90%
	Lepton Family number (LF) violating modes		
Γ_{83}	$\mu^\pm\tau^\mp$	LF < 6.0 $\times10^{-6}$	95%
	Other decays		
Γ_{84}	invisible	< 3.0 $\times10^{-4}$	90%

[a] $2m_\tau < M(\tau^+\tau^-) < 9.2$ GeV
[b] 2 GeV $< m_{K^+K^-} <$ 3 GeV
[c] X = scalar with $m < 8.0$ GeV
[d] $X\overline{X}$ = vectors with $m < 3.1$ GeV
[e] X and $\overline{X}$ = zero spin with $m < 4.5$ GeV

[f] 1.5 GeV $< m_X <$ 5.0 GeV

[g] 201 MeV $<$ M($\mu^+\mu^-$) $<$ 3565 MeV

[h] 0.5 GeV $< m_X <$ 9.0 GeV, where m_X is the invariant mass of the hadronic final state.

$\Upsilon(1S)$ Γ(i)$\Gamma(e^+e^-)/\Gamma$(total)

$\Gamma(e^+e^-) \times \Gamma(\mu^+\mu^-)/\Gamma_{total}$ $\Gamma_2\Gamma_3/\Gamma$

VALUE (eV)	DOCUMENT ID		TECN	COMMENT
31.2±1.6±1.7	KOBEL	92	CBAL	$e^+e^- \to \mu^+\mu^-$

Γ(hadrons) $\times \Gamma(e^+e^-)/\Gamma_{total}$ $\Gamma_0\Gamma_2/\Gamma$

VALUE (keV)	DOCUMENT ID		TECN	COMMENT
1.240±0.016 OUR AVERAGE				
1.252±0.004±0.019	[5] ROSNER	06	CLEO	9.5 $e^+e^- \to$ hadrons
1.187±0.023±0.031	[5] BARU	92B	MD1	$e^+e^- \to$ hadrons
1.23 ±0.02 ±0.05	[5] JAKUBOWSKI	88	CBAL	$e^+e^- \to$ hadrons
1.37 ±0.06 ±0.09	[6] GILES	84B	CLEO	$e^+e^- \to$ hadrons
1.23 ±0.08 ±0.04	[6] ALBRECHT	82	DASP	$e^+e^- \to$ hadrons
1.13 ±0.07 ±0.11	[6] NICZYPORUK	82	LENA	$e^+e^- \to$ hadrons
1.09 ±0.25	[6] BOCK	80	CNTR	$e^+e^- \to$ hadrons
1.35 ±0.14	[7] BERGER	79	PLUT	$e^+e^- \to$ hadrons

[5] Radiative corrections evaluated following KURAEV 85.

[6] Radiative corrections reevaluated by BUCHMUELLER 88 following KURAEV 85.

[7] Radiative corrections reevaluated by ALEXANDER 89 using B($\mu\mu$) = 0.026.

$\Upsilon(1S)$ PARTIAL WIDTHS

$\Gamma(e^+e^-)$ Γ_2

VALUE (keV)	DOCUMENT ID
1.340±0.018 OUR EVALUATION	

$\Upsilon(1S)$ BRANCHING RATIOS

$\Gamma(\tau^+\tau^-)/\Gamma_{total}$ Γ_1/Γ

VALUE (units 10^{-2})	EVTS	DOCUMENT ID		TECN	COMMENT
2.60±0.10 OUR AVERAGE					
2.53±0.13±0.05	60k	[8] BESSON	07	CLEO	$e^+e^- \to \Upsilon(1S) \to \tau^+\tau^-$
$2.61\pm0.12^{+0.09}_{-0.13}$	25k	CINABRO	94B	CLE2	$e^+e^- \to \tau^+\tau^-$
2.7 ±0.4 ±0.2		[9] ALBRECHT	85C	ARG	$\Upsilon(2S) \to \pi^+\pi^-\tau^+\tau^-$
3.4 ±0.4 ±0.4		GILES	83	CLEO	$e^+e^- \to \tau^+\tau^-$

[8] BESSON 07 reports [$\Gamma(\Upsilon(1S) \to \tau^+\tau^-)/\Gamma_{total}$] / [B($\Upsilon(1S) \to \mu^+\mu^-$)] = 1.02 ± 0.02 ± 0.05 which we multiply by our best value B($\Upsilon(1S) \to \mu^+\mu^-$) = (2.48 ± 0.05) × 10^{-2}. Our first error is their experiment's error and our second error is the systematic error from using our best value.

[9] Using B($\Upsilon(1S) \to ee$) = B($\Upsilon(1S) \to \mu\mu$) = 0.0256; not used for width evaluations.

$\Gamma(e^+e^-)/\Gamma_{total}$ Γ_2/Γ

VALUE (units 10^{-2})	EVTS	DOCUMENT ID		TECN	COMMENT
2.38±0.11 OUR AVERAGE					
2.29±0.08±0.11		ALEXANDER	98	CLE2	$\Upsilon(2S) \to \pi^+\pi^-e^+e^-$
2.42±0.14±0.14	307	ALBRECHT	87	ARG	$\Upsilon(2S) \to \pi^+\pi^-e^+e^-$
2.8 ±0.3 ±0.2	826	BESSON	84	CLEO	$\Upsilon(2S) \to \pi^+\pi^-e^+e^-$
5.1 ±3.0		BERGER	80C	PLUT	$e^+e^- \to e^+e^-$

$\Gamma(\mu^+\mu^-)/\Gamma_{total}$ Γ_3/Γ

VALUE	EVTS	DOCUMENT ID		TECN	COMMENT
0.0248±0.0005 OUR AVERAGE					
0.0249±0.0002±0.0007	345k	ADAMS	05	CLEO	$e^+e^- \to \mu^+\mu^-$
0.0249±0.0008±0.0013		ALEXANDER	98	CLE2	$\Upsilon(2S) \to \pi^+\pi^-\mu^+\mu^-$
0.0212±0.0020±0.0010		[10] BARU	92	MD1	$e^+e^- \to \mu^+\mu^-$
0.0231±0.0012±0.0010		[10] KOBEL	92	CBAL	$e^+e^- \to \mu^+\mu^-$
0.0252±0.0007±0.0007		CHEN	89B	CLEO	$e^+e^- \to \mu^+\mu^-$
0.0261±0.0009±0.0011		KAARSBERG	89	CSB2	$e^+e^- \to \mu^+\mu^-$
0.0230±0.0025±0.0013	86	ALBRECHT	87	ARG	$\Upsilon(2S) \to \pi^+\pi^-\mu^+\mu^-$
0.029 ±0.003 ±0.002	864	BESSON	84	CLEO	$\Upsilon(2S) \to \pi^+\pi^-\mu^+\mu^-$
0.027 ±0.003 ±0.003		ANDREWS	83	CLEO	$e^+e^- \to \mu^+\mu^-$
0.032 ±0.013 ±0.003		ALBRECHT	82	DASP	$e^+e^- \to \mu^+\mu^-$
0.038 ±0.015 ±0.002		NICZYPORUK	82	LENA	$e^+e^- \to \mu^+\mu^-$
$0.014\ ^{+0.034}_{-0.014}$		BOCK	80	CNTR	$e^+e^- \to \mu^+\mu^-$
0.022 ±0.020		BERGER	79	PLUT	$e^+e^- \to \mu^+\mu^-$

[10] Taking into account interference between the resonance and continuum.

$\Gamma(\tau^+\tau^-)/\Gamma(\mu^+\mu^-)$ Γ_1/Γ_3

VALUE	EVTS	DOCUMENT ID		TECN	COMMENT
1.008±0.023 OUR AVERAGE					
1.005±0.013±0.022	0.7M	[11] DEL-AMO-SA...10C		BABR	$\Upsilon(3S) \to \pi^+\pi^-\Upsilon(1S)$
1.02 ±0.02 ±0.05	60k	BESSON	07	CLEO	$e^+e^- \to \Upsilon(1S)$

[11] Allows any number of extra photons with total energy $<$ 500 MeV.

$\Gamma(ggg)/\Gamma_{total}$ Γ_4/Γ

VALUE (units 10^{-2})	EVTS	DOCUMENT ID		TECN	COMMENT
81.7±0.7	20M	[12] BESSON	06A	CLEO	$\Upsilon(1S) \to$ hadrons

[12] Calculated using the value $\Gamma(\gamma gg)/\Gamma(ggg)$ = (2.70 ± 0.01 ± 0.13 ± 0.24)% from BESSON 06A and PDG 08 values of B($\mu^+\mu^-$) = (2.48 ± 0.05)% and $R_{hadrons}$ = 3.51. The statistical error is negligible and the systematic error is partially correlated with that of $\Gamma(\gamma gg)/\Gamma_{total}$ measurement of BESSON 06A.

$\Gamma(\gamma gg)/\Gamma_{total}$ Γ_5/Γ

VALUE (units 10^{-2})	EVTS	DOCUMENT ID		TECN	COMMENT
2.20±0.60	400k	[13] BESSON	06A	CLEO	$\Upsilon(1S) \to \gamma +$ hadrons

[13] Calculated using BESSON 06A values of $\Gamma(\gamma gg)/\Gamma(ggg)$ = (2.70±0.01±0.13±0.24)% and $\Gamma(ggg)/\Gamma_{total}$. The statistical error is negligible and the systematic error is partially correlated with that of $\Gamma(ggg)/\Gamma_{total}$ measurement of BESSON 06A.

$\Gamma(\gamma gg)/\Gamma(ggg)$ Γ_5/Γ_4

VALUE (units 10^{-2})	EVTS	DOCUMENT ID		TECN	COMMENT
2.70±0.01±0.27	20M	BESSON	06A	CLEO	$\Upsilon(1S) \to (\gamma +)$ hadrons

$\Gamma(\eta'(958)$ anything$)/\Gamma_{total}$ Γ_6/Γ

VALUE	DOCUMENT ID		TECN	COMMENT
0.0294±0.0024 OUR AVERAGE				
0.030 ±0.002 ±0.002	AQUINES	06A	CLE3	$\Upsilon(1S) \to \eta'$ anything
0.028 ±0.004 ±0.002	ARTUSO	03	CLE2	$\Upsilon(1S) \to \eta'$ anything

$\Gamma(J/\psi(1S)$ anything$)/\Gamma_{total}$ Γ_7/Γ

VALUE (units 10^{-3})	CL%	EVTS	DOCUMENT ID		TECN	COMMENT
0.65±0.07 OUR AVERAGE						
0.64±0.04±0.06		730 ± 40	BRIERE	04	CLEO	$e^+e^- \to J/\psi X$
1.1 ±0.4 ±0.2			[14] FULTON	89	CLEO	$e^+e^- \to \mu^+\mu^-$X
• • • We do not use the following data for averages, fits, limits, etc. • • •						
<0.68	90		ALBRECHT	92J	ARG	$e^+e^- \to e^+e^-$X, $\mu^+\mu^-$X
<1.7	90		MASCHMANN	90	CBAL	$e^+e^- \to$ hadrons
<20	90		NICZYPORUK	83	LENA	

[14] Using B($(J/\psi) \to \mu^+\mu^-$) = (6.9 ± 0.9)%.

$\Gamma(\chi_{c0}$ anything$)/\Gamma(J/\psi(1S)$ anything$)$ Γ_8/Γ_7

VALUE	CL%	DOCUMENT ID		TECN	COMMENT
<7.4	90	BRIERE	04	CLEO	$e^+e^- \to J/\psi X$

$\Gamma(\chi_{c1}$ anything$)/\Gamma(J/\psi(1S)$ anything$)$ Γ_9/Γ_7

VALUE	EVTS	DOCUMENT ID		TECN	COMMENT
0.35±0.08±0.06	52 ± 12	BRIERE	04	CLEO	$e^+e^- \to J/\psi X$

$\Gamma(\chi_{c2}$ anything$)/\Gamma(J/\psi(1S)$ anything$)$ Γ_{10}/Γ_7

VALUE	EVTS	DOCUMENT ID		TECN	COMMENT
0.52±0.12±0.09	47 ± 11	BRIERE	04	CLEO	$e^+e^- \to J/\psi X$

$\Gamma(\psi(2S)$ anything$)/\Gamma(J/\psi(1S)$ anything$)$ Γ_{11}/Γ_7

VALUE	EVTS	DOCUMENT ID		TECN	COMMENT
0.41±0.11±0.08	42 ± 11	BRIERE	04	CLEO	$e^+e^- \to J/\psi\pi^+\pi^-X$

$\Gamma(\rho\pi)/\Gamma_{total}$ Γ_{12}/Γ

VALUE (units 10^{-6})	CL%	DOCUMENT ID		TECN	COMMENT
<3.68	90	SHEN	13	BELL	$\Upsilon(1S) \to \pi^+\pi^-\pi^0$
• • • We do not use the following data for averages, fits, limits, etc. • • •					
$<1 \times 10^3$	90	BLINOV	90	MD1	$\Upsilon(1S) \to \rho^0\pi^0$
$<2 \times 10^2$	90	FULTON	90B		$\Upsilon(1S) \to \rho^0\pi^0$
$<2.1 \times 10^3$	90	NICZYPORUK	83	LENA	$\Upsilon(1S) \to \rho^0\pi^0$

$\Gamma(\omega\pi^0)/\Gamma_{total}$ Γ_{13}/Γ

VALUE (units 10^{-6})	CL%	DOCUMENT ID		TECN	COMMENT
<3.90	90	SHEN	13	BELL	$\Upsilon(1S) \to \pi^+\pi^-\pi^0\pi^0$

$\Gamma(\pi^+\pi^-)/\Gamma_{total}$ Γ_{14}/Γ

VALUE (units 10^{-4})	CL%	DOCUMENT ID		TECN	COMMENT
<5	90	BARU	92	MD1	$\Upsilon(1S) \to \pi^+\pi^-$

$\Gamma(K^+K^-)/\Gamma_{total}$ Γ_{15}/Γ

VALUE (units 10^{-4})	CL%	DOCUMENT ID		TECN	COMMENT
<5	90	BARU	92	MD1	$\Upsilon(1S) \to K^+K^-$

$\Gamma(p\overline{p})/\Gamma_{total}$ Γ_{16}/Γ

VALUE (units 10^{-4})	CL%	DOCUMENT ID		TECN	COMMENT
<5	90	[15] BARU	96	MD1	$\Upsilon(1S) \to p\overline{p}$

[15] Supersedes BARU 92 in this node.

Meson Particle Listings

$\Upsilon(1S)$

$\Gamma(\pi^+\pi^-\pi^0)/\Gamma_{total}$ Γ_{17}/Γ

VALUE (units 10^{-6})	CL%	EVTS	DOCUMENT ID		TECN	COMMENT
2.14±0.72±0.34		26 ± 9	SHEN	13	BELL	$\Upsilon(1S) \to \pi^+\pi^-\pi^0$
• • • We do not use the following data for averages, fits, limits, etc. • • •						
<18.4	90		ANASTASSOV	99	CLE2	$e^+e^- \to$ hadrons

$\Gamma(\phi K^+ K^-)/\Gamma_{total}$ Γ_{18}/Γ

VALUE (units 10^{-6})	EVTS	DOCUMENT ID		TECN	COMMENT
2.36±0.37±0.29	56	SHEN	12A	BELL	$\Upsilon(1S) \to 2(K^+K^-)$

$\Gamma(\omega\pi^+\pi^-)/\Gamma_{total}$ Γ_{19}/Γ

VALUE (units 10^{-6})	EVTS	DOCUMENT ID		TECN	COMMENT
4.46±0.67±0.72	64	SHEN	12A	BELL	$\Upsilon(1S) \to 2(\pi^+\pi^-)\pi^0$

$\Gamma(K^*(892)^0 K^-\pi^+ + \text{c.c.})/\Gamma_{total}$ Γ_{20}/Γ

VALUE (units 10^{-6})	EVTS	DOCUMENT ID		TECN	COMMENT
4.42±0.50±0.58	173	SHEN	12A	BELL	$\Upsilon(1S) \to K^+K^-\pi^+\pi^-$

$\Gamma(\phi f_2'(1525))/\Gamma_{total}$ Γ_{21}/Γ

VALUE (units 10^{-6})	CL%	DOCUMENT ID		TECN	COMMENT
<1.63	90	SHEN	12A	BELL	$\Upsilon(1S) \to 2(K^+K^-)$

$\Gamma(\omega f_2(1270))/\Gamma_{total}$ Γ_{22}/Γ

VALUE (units 10^{-6})	CL%	DOCUMENT ID		TECN	COMMENT
<1.79	90	SHEN	12A	BELL	$\Upsilon(1S) \to 2(\pi^+\pi^-)\pi^0$

$\Gamma(\rho(770)a_2(1320))/\Gamma_{total}$ Γ_{23}/Γ

VALUE (units 10^{-6})	CL%	DOCUMENT ID		TECN	COMMENT
<2.24	90	SHEN	12A	BELL	$\Upsilon(1S) \to 2(\pi^+\pi^-)\pi^0$

$\Gamma(K^*(892)^0\overline{K}{}_2^*(1430)^0 + \text{c.c.})/\Gamma_{total}$ Γ_{24}/Γ

VALUE (units 10^{-6})	EVTS	DOCUMENT ID		TECN	COMMENT
3.02±0.68±0.34	42	SHEN	12A	BELL	$\Upsilon(1S) \to K^+K^-\pi^+\pi^-$

$\Gamma(K_1(1270)^\pm K^\mp)/\Gamma_{total}$ Γ_{25}/Γ

VALUE (units 10^{-6})	CL%	DOCUMENT ID		TECN	COMMENT
<2.41	90	SHEN	12A	BELL	$\Upsilon(1S) \to K^+K^-\pi^+\pi^-$

$\Gamma(K_1(1400)^\pm K^\mp)/\Gamma_{total}$ Γ_{26}/Γ

VALUE (units 10^{-6})	EVTS	DOCUMENT ID		TECN	COMMENT
1.02±0.35±0.22	24	SHEN	12A	BELL	$\Upsilon(1S) \to K^+K^-\pi^+\pi^-$

$\Gamma(b_1(1235)^\pm\pi^\mp)/\Gamma_{total}$ Γ_{27}/Γ

VALUE (units 10^{-6})	CL%	DOCUMENT ID		TECN	COMMENT
<1.25	90	SHEN	12A	BELL	$\Upsilon(1S) \to 2(\pi^+\pi^-)\pi^0$

$\Gamma(\pi^+\pi^-\pi^0\pi^0)/\Gamma_{total}$ Γ_{28}/Γ

VALUE (units 10^{-6})	EVTS	DOCUMENT ID		TECN	COMMENT
12.8±2.0±2.3	143 ± 22	SHEN	13	BELL	$\Upsilon(1S) \to \pi^+\pi^-\pi^0\pi^0$

$\Gamma(K_S^0 K^+\pi^- + \text{c.c.})/\Gamma_{total}$ Γ_{29}/Γ

VALUE (units 10^{-6})	CL%	EVTS	DOCUMENT ID		TECN	COMMENT
1.59±0.33±0.18		37 ± 8	SHEN	13	BELL	$\Upsilon(1S) \to K_S^0 K^-\pi^+$
• • • We do not use the following data for averages, fits, limits, etc. • • •						
<3.4	90		[16] DOBBS	12A		$\Upsilon(1S) \to K_S^0 K^-\pi^+$

[16] Obtained by analyzing CLEO III data but not authored by the CLEO Collaboration.

$\Gamma(K^*(892)^0\overline{K}{}^0 + \text{c.c.})/\Gamma_{total}$ Γ_{30}/Γ

VALUE (units 10^{-6})	EVTS	DOCUMENT ID		TECN	COMMENT
2.92±0.85±0.37	16 ± 5	SHEN	13	BELL	$\Upsilon(1S) \to K_S^0 K^-\pi^+$

$\Gamma(K^*(892)^- K^+ + \text{c.c.})/\Gamma_{total}$ Γ_{31}/Γ

VALUE (units 10^{-6})	CL%	DOCUMENT ID		TECN	COMMENT
<1.11	90	SHEN	13	BELL	$\Upsilon(1S) \to K_S^0 K^-\pi^+$

$\Gamma(D^*(2010)^\pm \text{ anything})/\Gamma_{total}$ Γ_{32}/Γ

VALUE (units 10^{-3})	CL%	EVTS	DOCUMENT ID		TECN	COMMENT
25.2±1.3±1.5		≈ 2k	[17] AUBERT	10C	BABR	$\Upsilon(2S) \to \pi^+\pi^-\Upsilon(1S)$
• • • We do not use the following data for averages, fits, limits, etc. • • •						
<19	90		[18] ALBRECHT	92J	ARG	$e^+e^- \to D^0\pi^\pm X$

[17] For $x_p > 0.1$.

[18] For $x_p > 0.2$.

$\Gamma(\overline{d} \text{ anything})/\Gamma_{total}$ Γ_{33}/Γ

VALUE (units 10^{-5})	EVTS	DOCUMENT ID		TECN	COMMENT
2.86±0.19±0.21	455	ASNER	07	CLEO	$e^+e^- \to \overline{d}X$

$\Gamma(\text{Sum of 100 exclusive modes})/\Gamma_{total}$ Γ_{34}/Γ

VALUE (units 10^{-2})	DOCUMENT ID		TECN	COMMENT
1.200±0.017	[19,20] DOBBS	12A		$\Upsilon(1S) \to$ hadrons

[19] DOBBS 12A presents individual exclusive branching fractions or upper limits for 100 modes of four to ten pions, kaons, or protons.

[20] Obtained by analyzing CLEO III data but not authored by the CLEO Collaboration.

$\Gamma(ggg, \gamma gg \to \overline{d} \text{ anything})/\Gamma(ggg, \gamma gg \to \text{anything})$

VALUE (units 10^{-5})	EVTS	DOCUMENT ID		TECN	COMMENT
3.36±0.23±0.25	455	ASNER	07	CLEO	$e^+e^- \to \overline{d}X$

$\Gamma(\gamma\pi^+\pi^-)/\Gamma_{total}$ Γ_{35}/Γ

VALUE (units 10^{-5})	DOCUMENT ID		TECN	COMMENT
6.3±1.2±1.3	[21] ANASTASSOV	99	CLE2	$e^+e^- \to$ hadrons

[21] For $m_{\pi\pi} > 1$ GeV.

$\Gamma(\gamma\pi^0\pi^0)/\Gamma_{total}$ Γ_{36}/Γ

VALUE (units 10^{-5})	DOCUMENT ID		TECN	COMMENT
1.7±0.6±0.3	[22] ANASTASSOV	99	CLE2	$e^+e^- \to$ hadrons

[22] For $m_{\pi\pi} > 1$ GeV.

$\Gamma(\gamma\pi^0\eta)/\Gamma_{total}$ Γ_{37}/Γ

VALUE (units 10^{-6})	CL%	DOCUMENT ID		TECN	COMMENT
<2.4	90	[23] BESSON	07A	CLEO	$e^+e^- \to \Upsilon(1S)$

[23] BESSON 07A obtained this limit for $0.7 < m_{\pi^0\eta} < 3$ GeV.

$\Gamma(\gamma K^+ K^-)/\Gamma_{total}$ Γ_{38}/Γ

($2 < m_{K^+K^-} < 3$ GeV)

VALUE (units 10^{-5})	CL%	DOCUMENT ID		TECN	COMMENT
1.14±0.08±0.10	90	ATHAR	06	CLE3	$\Upsilon(1S) \to \gamma K^+K^-$

$\Gamma(\gamma p\overline{p})/\Gamma_{total}$ Γ_{39}/Γ

($2 < m_{p\overline{p}} < 3$ GeV)

VALUE (units 10^{-5})	CL%	DOCUMENT ID		TECN	COMMENT
<0.6	90	ATHAR	06	CLE3	$\Upsilon(1S) \to \gamma p\overline{p}$

$\Gamma(\gamma 2h^+ 2h^-)/\Gamma_{total}$ Γ_{40}/Γ

VALUE (units 10^{-4})	EVTS	DOCUMENT ID		TECN	COMMENT
7.0±1.1±1.0	80 ± 12	FULTON	90B	CLEO	$e^+e^- \to$ hadrons

$\Gamma(\gamma 3h^+ 3h^-)/\Gamma_{total}$ Γ_{41}/Γ

VALUE (units 10^{-4})	EVTS	DOCUMENT ID		TECN	COMMENT
5.4±1.5±1.3	39 ± 11	FULTON	90B	CLEO	$e^+e^- \to$ hadrons

$\Gamma(\gamma 4h^+ 4h^-)/\Gamma_{total}$ Γ_{42}/Γ

VALUE (units 10^{-4})	EVTS	DOCUMENT ID		TECN	COMMENT
7.4±2.5±2.5	36 ± 12	FULTON	90B	CLEO	$e^+e^- \to$ hadrons

$\Gamma(\gamma\pi^+\pi^- K^+ K^-)/\Gamma_{total}$ Γ_{43}/Γ

VALUE (units 10^{-4})	EVTS	DOCUMENT ID		TECN	COMMENT
2.9±0.7±0.6	29 ± 8	FULTON	90B	CLEO	$e^+e^- \to$ hadrons

$\Gamma(\gamma 2\pi^+ 2\pi^-)/\Gamma_{total}$ Γ_{44}/Γ

VALUE (units 10^{-4})	EVTS	DOCUMENT ID		TECN	COMMENT
2.5±0.7±0.5	26 ± 7	FULTON	90B	CLEO	$e^+e^- \to$ hadrons

$\Gamma(\gamma 3\pi^+ 3\pi^-)/\Gamma_{total}$ Γ_{45}/Γ

VALUE (units 10^{-4})	EVTS	DOCUMENT ID		TECN	COMMENT
2.5±0.9±0.8	17 ± 5	FULTON	90B	CLEO	$e^+e^- \to$ hadrons

$\Gamma(\gamma 2\pi^+ 2\pi^- K^+ K^-)/\Gamma_{total}$ Γ_{46}/Γ

VALUE (units 10^{-4})	EVTS	DOCUMENT ID		TECN	COMMENT
2.4±0.9±0.8	18 ± 7	FULTON	90B	CLEO	$e^+e^- \to$ hadrons

$\Gamma(\gamma\pi^+\pi^- p\overline{p})/\Gamma_{total}$ Γ_{47}/Γ

VALUE (units 10^{-4})	EVTS	DOCUMENT ID		TECN	COMMENT
1.5±0.5±0.3	22 ± 6	FULTON	90B	CLEO	$e^+e^- \to$ hadrons

$\Gamma(\gamma 2\pi^+ 2\pi^- p\overline{p})/\Gamma_{total}$ Γ_{48}/Γ

VALUE (units 10^{-4})	EVTS	DOCUMENT ID		TECN	COMMENT
0.4±0.4±0.4	7 ± 6	FULTON	90B	CLEO	$e^+e^- \to$ hadrons

$\Gamma(\gamma 2K^+ 2K^-)/\Gamma_{total}$ Γ_{49}/Γ

VALUE (units 10^{-4})	EVTS	DOCUMENT ID		TECN	COMMENT
0.2±0.2	2 ± 2	FULTON	90B	CLEO	$e^+e^- \to$ hadrons

$\Gamma(\gamma\eta'(958))/\Gamma_{\text{total}}$ Γ_{50}/Γ

VALUE (units 10^{-6})	CL%	DOCUMENT ID		TECN	COMMENT
< 1.9	90	ATHAR	07A	CLEO	$\Upsilon(1S) \to \gamma\eta' \to \gamma\pi^+\pi^-\eta, \gamma\rho$
• • • We do not use the following data for averages, fits, limits, etc. • • •					
<16	90	RICHICHI	01B	CLE2	$\Upsilon(1S) \to \gamma\eta' \to \gamma\eta\pi^+\pi^-$

$\Gamma(\gamma\eta)/\Gamma_{\text{total}}$ Γ_{51}/Γ

VALUE (units 10^{-6})	CL%	DOCUMENT ID		TECN	COMMENT
< 1.0	90	ATHAR	07A	CLEO	$\Upsilon(1S) \to \gamma\eta \to \gamma\gamma\gamma$, $\gamma\pi^+\pi^-\pi^0$, $\gamma 3\pi^0$
• • • We do not use the following data for averages, fits, limits, etc. • • •					
<21	90	MASEK	02	CLEO	$\Upsilon(1S) \to \gamma\eta$

$\Gamma(\gamma f_0(980))/\Gamma_{\text{total}}$ Γ_{52}/Γ

VALUE (units 10^{-5})	CL%	DOCUMENT ID		TECN	COMMENT
<3	90	[24] ATHAR	06	CLE3	$\Upsilon(1S) \to \gamma\pi^+\pi^-$

[24] Assuming $B(f_0(980) \to \pi\pi) = 1$.

$\Gamma(\gamma f_2'(1525))/\Gamma_{\text{total}}$ Γ_{53}/Γ

VALUE (units 10^{-5})	CL%	EVTS	DOCUMENT ID		TECN	COMMENT
3.8±0.9 OUR AVERAGE						
$4.0\pm1.4\pm0.1$		17 ± 5	[25] BESSON	11	CLEO	$\Upsilon(1S) \to K_S^0 K_S^0$
$3.7^{+0.9}_{-0.7}\pm0.8$			ATHAR	06	CLE3	$\Upsilon(1S) \to \gamma K^+ K^-$
• • • We do not use the following data for averages, fits, limits, etc. • • •						
<14	90		[26] FULTON	90B	CLEO	$\Upsilon(1S) \to \gamma K^+ K^-$
<19.4	90		[26] ALBRECHT	89	ARG	$\Upsilon(1S) \to \gamma K^+ K^-$

[25] BESSON 11 reports $(4.0 \pm 1.3 \pm 0.6) \times 10^{-5}$ from a measurement of $[\Gamma(\Upsilon(1S) \to \gamma f_2'(1525))/\Gamma_{\text{total}}] \times [B(f_2'(1525) \to K\overline{K})]$ assuming $B(f_2'(1525) \to K\overline{K}) = (88.8 \pm 3.1) \times 10^{-2}$, which we rescale to our best value $B(f_2'(1525) \to K\overline{K}) = (88.7 \pm 2.2) \times 10^{-2}$. Our first error is their experiment's error and our second error is the systematic error from using our best value. The result also assumes $B(K_S^0 \to \pi^+\pi^-) = (69.20 \pm 0.05)\%$ and $B(f_2'(1525) \to K\overline{K}) = 4\, B(f_2'(1525) \to K_S^0 K_S^0)$.

[26] Assuming $B(f_2'(1525) \to K\overline{K}) = 0.71$.

$\Gamma(\gamma f_2(1270))/\Gamma_{\text{total}}$ Γ_{54}/Γ

VALUE (units 10^{-5})	CL%	DOCUMENT ID		TECN	COMMENT
10.1±0.9 OUR AVERAGE					
$10.5\pm1.6^{+1.9}_{-1.8}$		[27] BESSON	07A	CLE3	$\Upsilon(1S) \to \gamma\pi^0\pi^0$
$10.2\pm0.8\pm0.7$		ATHAR	06	CLE3	$\Upsilon(1S) \to \gamma\pi^+\pi^-$
$8.1\pm2.3^{+2.9}_{-2.7}$		[28] ANASTASSOV	99	CLE2	$e^+e^- \to$ hadrons
• • • We do not use the following data for averages, fits, limits, etc. • • •					
<21	90	[28] FULTON	90B	CLEO	$\Upsilon(1S) \to \gamma\pi^+\pi^-$
<13	90	[28] ALBRECHT	89	ARG	$\Upsilon(1S) \to \gamma\pi^+\pi^-$
<81	90	SCHMITT	88	CBAL	$\Upsilon(1S) \to \gamma X$

[27] Using $B(f_2(1270) \to \pi^0\pi^0) = B(f_2(1270) \to \pi\pi)/3$ and $B(f_2(1270) \to \pi\pi) = (0.845^{+0.025}_{-0.012})\%$.

[28] Using $B(f_2(1270) \to \pi\pi) = 0.84$.

$\Gamma(\gamma\eta(1405))/\Gamma_{\text{total}}$ Γ_{55}/Γ

VALUE (units 10^{-5})	CL%	DOCUMENT ID		TECN	COMMENT
<8.2	90	[29] FULTON	90B	CLEO	$\Upsilon(1S) \to \gamma K^\pm\pi^\mp K_S^0$

[29] Includes unknown branching ratio of $\eta(1405) \to K^\pm\pi^\mp K_S^0$.

$\Gamma(\gamma f_0(1500))/\Gamma_{\text{total}}$ Γ_{56}/Γ

VALUE (units 10^{-5})	CL%	DOCUMENT ID		TECN	COMMENT
<1.5	90	[30] BESSON	07A	CLEO	$e^+e^- \to \Upsilon(1S) \to \gamma\pi^0\pi^0$
• • • We do not use the following data for averages, fits, limits, etc. • • •					
<6.1	90	[31] BESSON	07A	CLEO	$e^+e^- \to \Upsilon(1S) \to \gamma\eta\eta$

[30] Using $B(f_0(1500) \to \pi^0\pi^0) = B(f_0(1500) \to \pi\pi)/3$ and $B(f_0(1500) \to \pi\pi) = (0.349 \pm 0.023)\%$.

[31] Calculated by us using $B(f_0(1500) \to \eta\eta) = (5.1 \pm 0.9)\%$.

$\Gamma(\gamma f_0(1710))/\Gamma_{\text{total}}$ Γ_{57}/Γ

VALUE (units 10^{-4})	CL%	DOCUMENT ID		TECN	COMMENT
< 2.6	90	[32] ALBRECHT	89	ARG	$\Upsilon(1S) \to \gamma K^+ K^-$
• • • We do not use the following data for averages, fits, limits, etc. • • •					
< 6.3	90	[32] FULTON	90B	CLEO	$\Upsilon(1S) \to \gamma K^+ K^-$
<19	90	[32] FULTON	90B	CLEO	$\Upsilon(1S) \to \gamma K_S^0 K_S^0$
< 8	90	[33] ALBRECHT	89	ARG	$\Upsilon(1S) \to \gamma\pi^+\pi^-$
<24	90	[34] SCHMITT	88	CBAL	$\Upsilon(1S) \to \gamma X$

[32] Assuming $B(f_0(1710) \to K\overline{K}) = 0.38$.

[33] Assuming $B(f_0(1710) \to \pi\pi) = 0.04$.

[34] Assuming $B(f_0(1710) \to \eta\eta) = 0.18$.

$\Gamma(\gamma f_0(1710) \to \gamma K^+ K^-)/\Gamma_{\text{total}}$ Γ_{58}/Γ

VALUE (units 10^{-5})	CL%	DOCUMENT ID		TECN	COMMENT
<0.7	90	ATHAR	06	CLEO	$e^+e^- \to \Upsilon(1S) \to \gamma K^+ K^-$

$\Gamma(\gamma f_0(1710) \to \gamma\pi^0\pi^0)/\Gamma_{\text{total}}$ Γ_{59}/Γ

VALUE (units 10^{-6})	CL%	DOCUMENT ID		TECN	COMMENT
<1.4	90	BESSON	07A	CLEO	$e^+e^- \to \Upsilon(1S) \to \gamma\pi^0\pi^0$

$\Gamma(\gamma f_0(1710) \to \gamma\eta\eta)/\Gamma_{\text{total}}$ Γ_{60}/Γ

VALUE (units 10^{-6})	CL%	DOCUMENT ID		TECN	COMMENT
<1.8	90	BESSON	07A	CLEO	$e^+e^- \to \Upsilon(1S) \to \gamma\eta\eta$

$\Gamma(\gamma f_4(2050))/\Gamma_{\text{total}}$ Γ_{61}/Γ

VALUE (units 10^{-5})	CL%	DOCUMENT ID		TECN	COMMENT
<5.3	90	[35] ATHAR	06	CLE3	$\Upsilon(1S) \to \gamma\pi^+\pi^-$

[35] Assuming $B(f_4(2050) \to \pi\pi) = 0.17$.

$\Gamma(\gamma f_0(2200) \to \gamma K^+ K^-)/\Gamma_{\text{total}}$ Γ_{62}/Γ

VALUE	CL%	DOCUMENT ID		TECN	COMMENT
<0.0002	90	BARU	89	MD1	$\Upsilon(1S) \to \gamma K^+ K^-$

$\Gamma(\gamma f_J(2220) \to \gamma K^+ K^-)/\Gamma_{\text{total}}$ Γ_{63}/Γ

VALUE (units 10^{-7})	CL%	DOCUMENT ID		TECN	COMMENT
< 8	90	ATHAR	06	CLE3	$\Upsilon(1S) \to \gamma K^+ K^-$
• • • We do not use the following data for averages, fits, limits, etc. • • •					
< 160	90	MASEK	02	CLEO	$\Upsilon(1S) \to \gamma K^+ K^-$
< 150	90	FULTON	90B	CLEO	$\Upsilon(1S) \to \gamma K^+ K^-$
< 290	90	ALBRECHT	89	ARG	$\Upsilon(1S) \to \gamma K^+ K^-$
<2000	90	BARU	89	MD1	$\Upsilon(1S) \to \gamma K^+ K^-$

$\Gamma(\gamma f_J(2220) \to \gamma\pi^+\pi^-)/\Gamma_{\text{total}}$ Γ_{64}/Γ

VALUE (units 10^{-7})	CL%	DOCUMENT ID		TECN	COMMENT
< 6	90	ATHAR	06	CLE3	$\Upsilon(1S) \to \gamma\pi^+\pi^-$
• • • We do not use the following data for averages, fits, limits, etc. • • •					
<120	90	MASEK	02	CLEO	$\Upsilon(1S) \to \gamma\pi^+\pi^-$

$\Gamma(\gamma f_J(2220) \to \gamma p\overline{p})/\Gamma_{\text{total}}$ Γ_{65}/Γ

VALUE (units 10^{-7})	CL%	DOCUMENT ID		TECN	COMMENT
< 11	90	ATHAR	06	CLE3	$\Upsilon(1S) \to \gamma p\overline{p}$
• • • We do not use the following data for averages, fits, limits, etc. • • •					
<160	90	MASEK	02	CLEO	$\Upsilon(1S) \to \gamma p\overline{p}$

$\Gamma(\gamma\eta(2225) \to \gamma\phi\phi)/\Gamma_{\text{total}}$ Γ_{66}/Γ

VALUE	CL%	DOCUMENT ID		TECN	COMMENT
<0.003	90	BARU	89	MD1	$\Upsilon(1S) \to \gamma K^+ K^- K^+ K^-$

$\Gamma(\gamma\eta_c(1S))/\Gamma_{\text{total}}$ Γ_{67}/Γ

VALUE (units 10^{-5})	CL%	DOCUMENT ID		TECN	COMMENT
<5.7	90	SHEN	10A	BELL	$\Upsilon(1S) \to \gamma X$

$\Gamma(\gamma\chi_{c0})/\Gamma_{\text{total}}$ Γ_{68}/Γ

VALUE (units 10^{-4})	CL%	DOCUMENT ID		TECN	COMMENT
<6.5	90	SHEN	10A	BELL	$\Upsilon(1S) \to \gamma X$

$\Gamma(\gamma\chi_{c1})/\Gamma_{\text{total}}$ Γ_{69}/Γ

VALUE (units 10^{-5})	CL%	DOCUMENT ID		TECN	COMMENT
<2.3	90	SHEN	10A	BELL	$\Upsilon(1S) \to \gamma X$

$\Gamma(\gamma\chi_{c2})/\Gamma_{\text{total}}$ Γ_{70}/Γ

VALUE (units 10^{-6})	CL%	DOCUMENT ID		TECN	COMMENT
<7.6	90	SHEN	10A	BELL	$\Upsilon(1S) \to \gamma X$

$\Gamma(\gamma X(3872) \to \pi^+\pi^- J/\psi)/\Gamma_{\text{total}}$ Γ_{71}/Γ

VALUE (units 10^{-6})	CL%	DOCUMENT ID		TECN	COMMENT
<1.6	90	SHEN	10A	BELL	$\Upsilon(1S) \to \gamma X$

$\Gamma(\gamma X(3872) \to \pi^+\pi^-\pi^0 J/\psi)/\Gamma_{\text{total}}$ Γ_{72}/Γ

VALUE (units 10^{-6})	CL%	DOCUMENT ID		TECN	COMMENT
<2.8	90	SHEN	10A	BELL	$\Upsilon(1S) \to \gamma X$

$\Gamma(\gamma\chi_{c0}(2P) \to \omega J/\psi)/\Gamma_{\text{total}}$ Γ_{73}/Γ

VALUE (units 10^{-6})	CL%	DOCUMENT ID		TECN	COMMENT
<3.0	90	SHEN	10A	BELL	$\Upsilon(1S) \to \gamma X$

$\Gamma(\gamma X(4140) \to \phi J/\psi)/\Gamma_{\text{total}}$ Γ_{74}/Γ

VALUE (units 10^{-6})	CL%	DOCUMENT ID		TECN	COMMENT
<2.2	90	SHEN	10A	BELL	$\Upsilon(1S) \to \gamma X$

$\Gamma(\gamma X)/\Gamma_{total}$ Γ_{75}/Γ

(X = scalar with $m < 8.0$ GeV)

VALUE (units 10^{-6})	CL%	DOCUMENT ID		TECN	COMMENT
< 4.5	90	[36] DEL-AMO-SA...11J		BABR	$e^+e^- \to \gamma +$ X
• • • We do not use the following data for averages, fits, limits, etc. • • •					
<30	90	[37] BALEST	95	CLEO	$e^+e^- \to \gamma +$ X

[36] For a noninteracting scalar X with mass $m < 8.0$ GeV.
[37] For a noninteracting pseudoscalar X with mass < 7.2 GeV.

$\Gamma(\gamma X\overline{X}(m_X < 3.1\ \text{GeV}))/\Gamma_{total}$ Γ_{76}/Γ

($X\overline{X}$ = vectors with m< 3.1 GeV)

VALUE (units 10^{-3})	CL%	DOCUMENT ID		TECN	COMMENT
<1	90	[38] BALEST	95	CLEO	$e^+e^- \to \gamma +$ $X\overline{X}$

[38] For a noninteracting vector X with mass < 3.1 GeV.

$\Gamma(\gamma X\overline{X}(m_X < 4.5\ \text{GeV}))/\Gamma_{total}$ Γ_{77}/Γ

X and $\overline{X}$ = zero spin with $m < 4.5$ GeV

VALUE (units 10^{-5})	CL%	DOCUMENT ID		TECN	COMMENT
<24	90	[39] DEL-AMO-SA...11J		BABR	$e^+e^- \to \gamma +$ $X\overline{X}$

[39] For a noninteracting scalar X with mass $m < 4.5$ GeV.

$\Gamma(\gamma X \to \gamma + \geq 4\ \text{prongs})/\Gamma_{total}$ Γ_{78}/Γ

(1.5 GeV < m_X < 5.0 GeV)

VALUE (units 10^{-4})	CL%	DOCUMENT ID		TECN	COMMENT
<1.78	95	ROSNER	07A	CLEO	$e^+e^- \to \gamma X$

$\Gamma(\gamma a_1^0 \to \gamma\mu^+\mu^-)/\Gamma_{total}$ Γ_{79}/Γ

(201 < M($\mu^+\mu^-$) < 3565 MeV)

VALUE (units 10^{-6})	CL%	DOCUMENT ID		TECN	COMMENT
<9	90	[40] LOVE	08	CLEO	$e^+e^- \to \gamma a_1^0 \to \gamma\mu^+\mu^-$
• • • We do not use the following data for averages, fits, limits, etc. • • •					
<9.7	90	[41] LEES	13C	BABR	$e^+e^- \to \gamma a_1^0 \to \gamma\mu^+\mu^-$

[40] For a narrow scalar or pseudoscalar a_1^0 with 201 < M($\mu^+\mu^-$) < 3565 MeV, excluding J/ψ. Measured 90% CL limits as a function of M($\mu^+\mu^-$) range from 1–9 $\times 10^{-6}$.
[41] For a narrow scalar or pseudoscalar a_1^0 with mass in the range 212–9200 MeV, excluding J/ψ and $\psi(2S)$. Measured 90% CL limits as a function of $m_{a_1^0}$ range from 0.28–9.7 $\times$ 10^{-6}.

$\Gamma(\gamma a_1^0 \to \gamma\tau^+\tau^-)/\Gamma_{total}$ Γ_{80}/Γ

($2m_\tau$ < M($\tau^+\tau^-$) < 9.2 GeV)

VALUE (units 10^{-6})	CL%	DOCUMENT ID		TECN	COMMENT
<130	90	[42] LEES	13R	BABR	$\Upsilon(2S) \to \gamma\tau^+\tau^-\pi^+\pi^-$
• • • We do not use the following data for averages, fits, limits, etc. • • •					
< 50	90	[43] LOVE	08	CLEO	$e^+e^- \to \gamma a_1^0 \to \gamma\tau^+\tau^-$

[42] For a narrow scalar a_1^0 with $2m_\tau$ < M(a_1^0) < 9.2 GeV, which result in a 90% CL upper limits of 0.9×10^{-5} at M(a_1^0) = $2m_\tau$, $\approx 1.5\times10^{-5}$ at M(a_1^0) = 7.5 GeV, and 13×10^{-5} at M(a_1^0) = 9.2 GeV.
[43] For a narrow scalar or pseudoscalar a_1^0 with $2m_\tau$ < M(a_1^0) < 7.5 GeV, which result in a 90% CL limits ranging from 1×10^{-5} at M(a_1^0)=$2m_\tau$ to 5×10^{-5} at M(a_1^0)=7.5 GeV.

$\Gamma(\gamma a_1^0 \to \gamma gg)/\Gamma_{total}$ Γ_{81}/Γ

(0.5 GeV < m < 9.0 GeV)

VALUE	CL%	DOCUMENT ID		TECN	COMMENT
$<1\times10^{-2}$	90	[44] LEES	13L	BABR	$\Upsilon(1S) \to \gamma X$

[44] For a narrow, CP-odd pseudoscalar a_1^0 searched for in 26 hadronic decay modes with invariant mass 0.5 GeV < m_X < 9.0 GeV. Measured 90% CL limit as a function of m_X range from 10^{-6} to 10^{-2}.

$\Gamma(\gamma a_1^0 \to \gamma s\overline{s})/\Gamma_{total}$ Γ_{82}/Γ

(0.5 GeV < m < 9.0 GeV)

VALUE	CL%	DOCUMENT ID		TECN	COMMENT
$<1\times10^{-3}$	90	[45] LEES	13L	BABR	$\Upsilon(1S) \to \gamma X$

[45] For a narrow, CP-odd pseudoscalar a_1^0 searched for in 14 hadronic decay modes with invariant mass 1.5 GeV < m_X < 9.0 GeV. Measured 90% CL limit as a function of m_X range from 10^{-5} to 10^{-3}.

LEPTON FAMILY NUMBER (LF) VIOLATING MODES

$\Gamma(\mu^\pm\tau^\mp)/\Gamma_{total}$ Γ_{83}/Γ

VALUE (units 10^{-6})	CL%	DOCUMENT ID		TECN	COMMENT
<6.0	95	LOVE	08A	CLEO	$e^+e^- \to \mu^\pm\tau^\mp$

OTHER DECAYS

$\Gamma(\text{invisible})/\Gamma_{total}$ Γ_{84}/Γ

VALUE (units 10^{-4})	CL%	DOCUMENT ID		TECN	COMMENT
< 3.0	90	AUBERT	09AX	BABR	$\Upsilon(3S) \to \pi^+\pi^-\Upsilon(1S)$
• • • We do not use the following data for averages, fits, limits, etc. • • •					
<39	90	RUBIN	07	CLEO	$\Upsilon(2S) \to \pi^+\pi^-\Upsilon(1S)$
<25	90	TAJIMA	07	BELL	$\Upsilon(3S) \to \pi^+\pi^-\Upsilon(1S)$

$\Upsilon(1S)$ REFERENCES

LEES	13C	PR D87 031102	J.P. Lees *et al.*	(BABAR Collab.)
LEES	13L	PR D88 031701	J.P. Lees *et al.*	(BABAR Collab.)
LEES	13R	PR D88 071102	J.P. Lees *et al.*	(BABAR Collab.)
SHEN	13	PR D88 011102	C.P. Shen *et al.*	(BELLE Collab.)
DOBBS	12A	PR D86 052003	S. Dobbs *et al.*	
SHEN	12A	PR D86 031102	C.P. Shen *et al.*	(BELLE Collab.)
BESSON	11	PR D83 037101	D. Besson *et al.*	(CLEO Collab.)
DEL-AMO-SA...	11J	PRL 107 021804	P. del Amo Sanchez *et al.*	(BABAR Collb.)
AUBERT	10C	PR D81 011102	B. Aubert *et al.*	(BABAR Collab.)
DEL-AMO-SA...	10C	PRL 104 191801	P. del Amo Sanchez *et al.*	(BABAR Collab.)
SHEN	10A	PR D82 051504	C.P. Shen *et al.*	(BELLE Collab.)
AUBERT	09AX	PRL 103 251801	B. Aubert *et al.*	(BABAR Collab.)
LOVE	08	PRL 101 151802	W. Love *et al.*	(CLEO Collab.)
LOVE	08A	PRL 101 201601	W. Love *et al.*	(CLEO Collab.)
PDG	08	PL B667 1	C. Amsler *et al.*	(PDG Collab.)
ASNER	07	PR D75 012009	D.M. Asner *et al.*	(CLEO Collab.)
ATHAR	07A	PR D76 072003	S.B. Athar *et al.*	(CLEO Collab.)
BESSON	07	PRL 98 052002	D. Besson *et al.*	(CLEO Collab.)
BESSON	07A	PR D75 072001	D. Besson *et al.*	(CLEO Collab.)
ROSNER	07A	PR D76 117102	J.L. Rosner *et al.*	(CLEO Collab.)
RUBIN	07	PR D75 031104	P. Rubin *et al.*	(CLEO Collab.)
TAJIMA	07	PRL 98 132001	O. Tajima *et al.*	(BELLE Collab.)
AQUINES	06A	PR D74 092006	O. Aquines *et al.*	(CLEO Collab.)
ATHAR	06	PR D73 032001	S.B. Athar *et al.*	(CLEO Collab.)
BESSON	06A	PR D74 012003	D. Besson *et al.*	(CLEO Collab.)
ROSNER	06	PRL 96 092003	J.L. Rosner *et al.*	(CLEO Collab.)
ADAMS	05	PRL 94 012001	G.S. Adams *et al.*	(CLEO Collab.)
BRIERE	04	PR D70 072001	R.A. Briere *et al.*	(CLEO Collab.)
ARTUSO	03	PR D67 052003	M. Artuso *et al.*	(CLEO Collab.)
MASEK	02	PR D65 072002	G. Masek *et al.*	(CLEO Collab.)
RICHICHI	01B	PRL 87 141801	S.J. Richichi *et al.*	(CLEO Collab.)
ARTAMONOV	00	PL B474 427	A.S. Artamonov *et al.*	
ANASTASSOV	99	PRL 82 286	A. Anastassov *et al.*	(CLEO Collab.)
ALEXANDER	98	PR D58 052004	J.P. Alexander *et al.*	(CLEO Collab.)
BARU	96	PRPL 267 71	S.E. Baru *et al.*	(NOVO)
BALEST	95	PR D51 2053	R. Balest *et al.*	(CLEO Collab.)
CINABRO	94B	PL B340 129	D. Cinabro *et al.*	(CLEO Collab.)
ALBRECHT	92J	ZPHY C55 25	H. Albrecht *et al.*	(ARGUS Collab.)
BARU	92	ZPHY C54 229	S.E. Baru *et al.*	(NOVO)
BARU	92B	ZPHY C56 547	S.E. Baru *et al.*	(NOVO)
KOBEL	92	ZPHY C53 193	M. Kobel *et al.*	(Crystal Ball Collab.)
BLINOV	90	PL B245 311	A.E. Blinov *et al.*	(NOVO)
FULTON	90B	PR D41 1401	R. Fulton *et al.*	(CLEO Collab.)
MASCHMANN	90	ZPHY C46 555	W.S. Maschmann *et al.*	(Crystal Ball Collab.)
ALBRECHT	89	ZPHY C42 349	H. Albrecht *et al.*	(ARGUS Collab.)
ALEXANDER	89	NP B320 45	J.P. Alexander *et al.*	(LBL, MICH, SLAC)
BARU	89	ZPHY C42 505	S.E. Baru *et al.*	(NOVO)
CHEN	89B	PR D39 3528	W.Y. Chen *et al.*	(CLEO Collab.)
FULTON	89	PL B224 445	R. Fulton *et al.*	(CLEO Collab.)
KAARSBERG	89	PRL 62 2077	T.M. Kaarsberg *et al.*	(CUSB Collab.)
BUCHMUEL...	88	HE e^+e^- Physics 412	W. Buchmueller, S. Cooper	(HANN, DESY, MIT)
		Editors: A. Ali and P. Soeding, World Scientific, Singapore		
JAKUBOWSKI	88	ZPHY C40 49	Z. Jakubowski *et al.*	(Crystal Ball Collab.) IGJPC
SCHMITT	88	ZPHY C40 199	P. Schmitt *et al.*	(Crystal Ball Collab.)
ALBRECHT	87	ZPHY C35 283	H. Albrecht *et al.*	(ARGUS Collab.)
COHEN	87	RMP 59 1121	E.R. Cohen, B.N. Taylor	(RISC, NBS)
BARU	86	ZPHY C30 551	S.E. Baru *et al.*	(NOVO)
ALBRECHT	85C	PL 154B 452	H. Albrecht *et al.*	(ARGUS Collab.)
KURAEV	85	SJNP 41 466	E.A. Kuraev, V.S. Fadin	(NOVO)
		Translated from YAF 41 733.		
ARTAMONOV	84	PL 137B 272	A.S. Artamonov *et al.*	(NOVO)
BESSON	84	PR D30 1433	D. Besson *et al.*	(CLEO Collab.)
GILES	84B	PR D29 1285	R. Giles *et al.*	(CLEO Collab.)
MACKAY	84	PR D29 2483	W.W. MacKay *et al.*	(CUSB Collab.)
ANDREWS	83	PRL 50 807	D.E. Andrews *et al.*	(CLEO Collab.)
GILES	83	PRL 50 877	R. Giles *et al.*	(HARV, OSU, ROCH, RUTG+)
NICZYPORUK	83	ZPHY C17 197	B. Niczyporuk *et al.*	(LENA Collab.)
ALBRECHT	82	PL 116B 383	H. Albrecht *et al.*	(DESY, DORT, HEIDH+)
ARTAMONOV	82	PL 118B 225	A.S. Artamonov *et al.*	(NOVO)
NICZYPORUK	82	ZPHY C15 299	B. Niczyporuk *et al.*	(LENA Collab.)
BERGER	80C	PL 93B 497	C. Berger *et al.*	(PLUTO Collab.)
BOCK	80	ZPHY C6 125	P. Bock *et al.*	(HEIDP, MPIM, DESY, HAMB)
BERGER	79	ZPHY C1 343	C. Berger *et al.*	(PLUTO Collab.)

$\chi_{b0}(1P)$

$I^G(J^{PC}) = 0^+(0^{++})$
J needs confirmation.

Observed in radiative decay of the $\Upsilon(2S)$, therefore $C = +$. Branching ratio requires E1 transition, M1 is strongly disfavored, therefore $P = +$.

$\chi_{b0}(1P)$ MASS

VALUE (MeV)	DOCUMENT ID
9859.44±0.42±0.31 OUR EVALUATION	From average γ energy below, using $\Upsilon(2S)$ mass = 10023.26 ± 0.31 MeV

γ ENERGY IN $\Upsilon(2S)$ DECAY

VALUE (MeV)	DOCUMENT ID		TECN	COMMENT
162.5 ±0.4 OUR AVERAGE				
162.56±0.19±0.42	ARTUSO	05	CLEO	$\Upsilon(2S) \to \gamma X$
162.0 ±0.8 ±1.2	EDWARDS	99	CLE2	$\Upsilon(2S) \to \gamma\chi(1P)$
162.1 ±0.5 ±1.4	ALBRECHT	85E	ARG	$\Upsilon(2S) \to$ conv.γX
163.8 ±1.6 ±2.7	NERNST	85	CBAL	$\Upsilon(2S) \to \gamma$X
158.0 ±7 ±1	HAAS	84	CLEO	$\Upsilon(2S) \to$ conv.γX
• • • We do not use the following data for averages, fits, limits, etc. • • •				
149.4 ±0.7 ±5.0	KLOPFEN...	83	CUSB	$\Upsilon(2S) \to \gamma$X

$\chi_{b0}(1P)$ DECAY MODES

	Mode	Fraction (Γ_i/Γ)	Confidence level
Γ_1	$\gamma\,\Upsilon(1S)$	(1.76±0.35) %	
Γ_2	$D^0 X$	< 10.4 %	90%
Γ_3	$\pi^+\pi^-K^+K^-\pi^0$	< 1.6 $\times10^{-4}$	90%
Γ_4	$2\pi^+\pi^-K^-K^0_S$	< 5 $\times10^{-5}$	90%
Γ_5	$2\pi^+\pi^-K^-K^0_S2\pi^0$	< 5 $\times10^{-4}$	90%
Γ_6	$2\pi^+2\pi^-2\pi^0$	< 2.1 $\times10^{-4}$	90%
Γ_7	$2\pi^+2\pi^-K^+K^-$	(1.1 ±0.6) $\times10^{-4}$	
Γ_8	$2\pi^+2\pi^-K^+K^-\pi^0$	< 2.7 $\times10^{-4}$	90%
Γ_9	$2\pi^+2\pi^-K^+K^-2\pi^0$	< 5 $\times10^{-4}$	90%
Γ_{10}	$3\pi^+2\pi^-K^-K^0_S\pi^0$	< 1.6 $\times10^{-4}$	90%
Γ_{11}	$3\pi^+3\pi^-$	< 8 $\times10^{-5}$	90%
Γ_{12}	$3\pi^+3\pi^-2\pi^0$	< 6 $\times10^{-4}$	90%
Γ_{13}	$3\pi^+3\pi^-K^+K^-$	(2.4 ±1.2) $\times10^{-4}$	
Γ_{14}	$3\pi^+3\pi^-K^+K^-\pi^0$	< 1.0 $\times10^{-3}$	90%
Γ_{15}	$4\pi^+4\pi^-$	< 8 $\times10^{-5}$	90%
Γ_{16}	$4\pi^+4\pi^-2\pi^0$	< 2.1 $\times10^{-3}$	90%
Γ_{17}	$J/\psi J/\psi$	< 7 $\times10^{-5}$	90%
Γ_{18}	$J/\psi\psi(2S)$	< 1.2 $\times10^{-4}$	90%
Γ_{19}	$\psi(2S)\psi(2S)$	< 3.1 $\times10^{-5}$	90%

$\chi_{b0}(1P)$ BRANCHING RATIOS

$\Gamma(\gamma\,\Upsilon(1S))/\Gamma_{\text{total}}$ Γ_1/Γ

VALUE (%)	CL%	EVTS	DOCUMENT ID		TECN	COMMENT
1.76±0.30±0.18		87	[1,2] KORNICER	11	CLEO	$e^+e^-\to\gamma\gamma\ell^+\ell^-$

• • • We do not use the following data for averages, fits, limits, etc. • • •

< 4.6	90	[3] LEES	11J	BABR	$\Upsilon(2S)\to X\gamma$	
< 6	90	WALK	86	CBAL	$\Upsilon(2S)\to\gamma\gamma\ell^+\ell^-$	
<11	90	PAUSS	83	CUSB	$\Upsilon(2S)\to\gamma\gamma\ell^+\ell^-$	

[1] Assuming B($\Upsilon(1S)\to\ell^+\ell^-$) = (2.48 ± 0.05)%.

[2] KORNICER 11 reports $[\Gamma(\chi_{b0}(1P)\to\gamma\,\Upsilon(1S))/\Gamma_{\text{total}}]\times[\text{B}(\Upsilon(2S)\to\gamma\chi_{b0}(1P))] = (6.59\pm0.96\pm0.60)\times10^{-4}$ which we divide by our best value B($\Upsilon(2S)\to\gamma\chi_{b0}(1P)$) = $(3.8\pm0.4)\times10^{-2}$. Our first error is their experiment's error and our second error is the systematic error from using our best value.

[3] LEES 11J quotes a central value of $\Gamma(\chi_{b0}(1P)\to\gamma\,\Upsilon(1S))/\Gamma_{\text{total}}\times\Gamma(\Upsilon(2S)\to\gamma\chi_{b0}(1P))/\Gamma_{\text{total}} = (8.3\pm5.6^{+3.7}_{-2.6})\times10^{-4}$.

$\Gamma(D^0X)/\Gamma_{\text{total}}$ Γ_2/Γ

VALUE	CL%	DOCUMENT ID		TECN	COMMENT
<10.4 × 10^{-2}	90	[4,5] BRIERE	08	CLEO	$\Upsilon(2S)\to\gamma D^0X$

[4] For $p_{D^0} > 2.5$ GeV/c.

[5] The authors also present their result as $(5.6\pm3.6\pm0.5)\times10^{-2}$.

$\Gamma(\pi^+\pi^-K^+K^-\pi^0)/\Gamma_{\text{total}}$ Γ_3/Γ

VALUE (units 10^{-4})	CL%	DOCUMENT ID		TECN	COMMENT
<1.6	90	[6] ASNER	08A	CLEO	$\Upsilon(2S)\to\gamma\pi^+\pi^-K^+K^-\pi^0$

[6] ASNER 08A reports $[\Gamma(\chi_{b0}(1P)\to\pi^+\pi^-K^+K^-\pi^0)/\Gamma_{\text{total}}]\times[\text{B}(\Upsilon(2S)\to\gamma\chi_{b0}(1P))] < 6\times10^{-6}$ which we divide by our best value B($\Upsilon(2S)\to\gamma\chi_{b0}(1P)$) = 3.8×10^{-2}.

$\Gamma(2\pi^+\pi^-K^-K^0_S)/\Gamma_{\text{total}}$ Γ_4/Γ

VALUE (units 10^{-4})	CL%	DOCUMENT ID		TECN	COMMENT
<0.5	90	[7] ASNER	08A	CLEO	$\Upsilon(2S)\to\gamma2\pi^+\pi^-K^-K^0_S$

[7] ASNER 08A reports $[\Gamma(\chi_{b0}(1P)\to2\pi^+\pi^-K^-K^0_S)/\Gamma_{\text{total}}]\times[\text{B}(\Upsilon(2S)\to\gamma\chi_{b0}(1P))] < 2\times10^{-6}$ which we divide by our best value B($\Upsilon(2S)\to\gamma\chi_{b0}(1P)$) = 3.8×10^{-2}.

$\Gamma(2\pi^+\pi^-K^-K^0_S2\pi^0)/\Gamma_{\text{total}}$ Γ_5/Γ

VALUE (units 10^{-4})	CL%	DOCUMENT ID		TECN	COMMENT
<5	90	[8] ASNER	08A	CLEO	$\Upsilon(2S)\to\gamma2\pi^+\pi^-K^-2\pi^0$

[8] ASNER 08A reports $[\Gamma(\chi_{b0}(1P)\to2\pi^+\pi^-K^-K^0_S2\pi^0)/\Gamma_{\text{total}}]\times[\text{B}(\Upsilon(2S)\to\gamma\chi_{b0}(1P))] < 18\times10^{-6}$ which we divide by our best value B($\Upsilon(2S)\to\gamma\chi_{b0}(1P)$) = 3.8×10^{-2}.

$\Gamma(2\pi^+2\pi^-2\pi^0)/\Gamma_{\text{total}}$ Γ_6/Γ

VALUE (units 10^{-4})	CL%	DOCUMENT ID		TECN	COMMENT
<2.1	90	[9] ASNER	08A	CLEO	$\Upsilon(2S)\to\gamma2\pi^+2\pi^-2\pi^0$

[9] ASNER 08A reports $[\Gamma(\chi_{b0}(1P)\to2\pi^+2\pi^-2\pi^0)/\Gamma_{\text{total}}]\times[\text{B}(\Upsilon(2S)\to\gamma\chi_{b0}(1P))] < 8\times10^{-6}$ which we divide by our best value B($\Upsilon(2S)\to\gamma\chi_{b0}(1P)$) = 3.8×10^{-2}.

$\Gamma(2\pi^+2\pi^-K^+K^-)/\Gamma_{\text{total}}$ Γ_7/Γ

VALUE (units 10^{-4})	EVTS	DOCUMENT ID		TECN	COMMENT
1.1±0.6±0.1	7	[10] ASNER	08A	CLEO	$\Upsilon(2S)\to\gamma2\pi^+2\pi^-K^+K^-$

[10] ASNER 08A reports $[\Gamma(\chi_{b0}(1P)\to2\pi^+2\pi^-K^+K^-)/\Gamma_{\text{total}}]\times[\text{B}(\Upsilon(2S)\to\gamma\chi_{b0}(1P))] = (4\pm2\pm1)\times10^{-6}$ which we divide by our best value B($\Upsilon(2S)\to\gamma\chi_{b0}(1P)$) = $(3.8\pm0.4)\times10^{-2}$. Our first error is their experiment's error and our second error is the systematic error from using our best value.

$\Gamma(2\pi^+2\pi^-K^+K^-\pi^0)/\Gamma_{\text{total}}$ Γ_8/Γ

VALUE (units 10^{-4})	CL%	DOCUMENT ID		TECN	COMMENT
<2.7	90	[11] ASNER	08A	CLEO	$\Upsilon(2S)\to\gamma2\pi^+2\pi^-K^+K^-\pi^0$

[11] ASNER 08A reports $[\Gamma(\chi_{b0}(1P)\to2\pi^+2\pi^-K^+K^-\pi^0)/\Gamma_{\text{total}}]\times[\text{B}(\Upsilon(2S)\to\gamma\chi_{b0}(1P))] < 10\times10^{-6}$ which we divide by our best value B($\Upsilon(2S)\to\gamma\chi_{b0}(1P)$) = 3.8×10^{-2}.

$\Gamma(2\pi^+2\pi^-K^+K^-2\pi^0)/\Gamma_{\text{total}}$ Γ_9/Γ

VALUE (units 10^{-4})	CL%	DOCUMENT ID		TECN	COMMENT
<5	90	[12] ASNER	08A	CLEO	$\Upsilon(2S)\to\gamma2\pi^+2\pi^-K^+K^-2\pi^0$

[12] ASNER 08A reports $[\Gamma(\chi_{b0}(1P)\to2\pi^+2\pi^-K^+K^-2\pi^0)/\Gamma_{\text{total}}]\times[\text{B}(\Upsilon(2S)\to\gamma\chi_{b0}(1P))] < 20\times10^{-6}$ which we divide by our best value B($\Upsilon(2S)\to\gamma\chi_{b0}(1P)$) = 3.8×10^{-2}.

$\Gamma(3\pi^+2\pi^-K^-K^0_S\pi^0)/\Gamma_{\text{total}}$ Γ_{10}/Γ

VALUE (units 10^{-4})	CL%	DOCUMENT ID		TECN	COMMENT
<1.6	90	[13] ASNER	08A	CLEO	$\Upsilon(2S)\to\gamma3\pi^+2\pi^-K^-K^0_S\pi^0$

[13] ASNER 08A reports $[\Gamma(\chi_{b0}(1P)\to3\pi^+2\pi^-K^-K^0_S\pi^0)/\Gamma_{\text{total}}]\times[\text{B}(\Upsilon(2S)\to\gamma\chi_{b0}(1P))] < 6\times10^{-6}$ which we divide by our best value B($\Upsilon(2S)\to\gamma\chi_{b0}(1P)$) = 3.8×10^{-2}.

$\Gamma(3\pi^+3\pi^-)/\Gamma_{\text{total}}$ Γ_{11}/Γ

VALUE (units 10^{-4})	CL%	DOCUMENT ID		TECN	COMMENT
<0.8	90	[14] ASNER	08A	CLEO	$\Upsilon(2S)\to\gamma3\pi^+3\pi^-$

[14] ASNER 08A reports $[\Gamma(\chi_{b0}(1P)\to3\pi^+3\pi^-)/\Gamma_{\text{total}}]\times[\text{B}(\Upsilon(2S)\to\gamma\chi_{b0}(1P))] < 3\times10^{-6}$ which we divide by our best value B($\Upsilon(2S)\to\gamma\chi_{b0}(1P)$) = 3.8×10^{-2}.

$\Gamma(3\pi^+3\pi^-2\pi^0)/\Gamma_{\text{total}}$ Γ_{12}/Γ

VALUE (units 10^{-4})	CL%	DOCUMENT ID		TECN	COMMENT
<6	90	[15] ASNER	08A	CLEO	$\Upsilon(2S)\to\gamma3\pi^+3\pi^-2\pi^0$

[15] ASNER 08A reports $[\Gamma(\chi_{b0}(1P)\to3\pi^+3\pi^-2\pi^0)/\Gamma_{\text{total}}]\times[\text{B}(\Upsilon(2S)\to\gamma\chi_{b0}(1P))] < 22\times10^{-6}$ which we divide by our best value B($\Upsilon(2S)\to\gamma\chi_{b0}(1P)$) = 3.8×10^{-2}.

$\Gamma(3\pi^+3\pi^-K^+K^-)/\Gamma_{\text{total}}$ Γ_{13}/Γ

VALUE (units 10^{-4})	EVTS	DOCUMENT ID		TECN	COMMENT
2.4±1.2±0.2	9	[16] ASNER	08A	CLEO	$\Upsilon(2S)\to\gamma3\pi^+3\pi^-K^+K^-$

[16] ASNER 08A reports $[\Gamma(\chi_{b0}(1P)\to3\pi^+3\pi^-K^+K^-)/\Gamma_{\text{total}}]\times[\text{B}(\Upsilon(2S)\to\gamma\chi_{b0}(1P))] = (9\pm4\pm2)\times10^{-6}$ which we divide by our best value B($\Upsilon(2S)\to\gamma\chi_{b0}(1P)$) = $(3.8\pm0.4)\times10^{-2}$. Our first error is their experiment's error and our second error is the systematic error from using our best value.

$\Gamma(3\pi^+3\pi^-K^+K^-\pi^0)/\Gamma_{\text{total}}$ Γ_{14}/Γ

VALUE (units 10^{-4})	CL%	DOCUMENT ID		TECN	COMMENT
<10	90	[17] ASNER	08A	CLEO	$\Upsilon(2S)\to\gamma3\pi^+3\pi^-K^+K^-\pi^0$

[17] ASNER 08A reports $[\Gamma(\chi_{b0}(1P)\to3\pi^+3\pi^-K^+K^-\pi^0)/\Gamma_{\text{total}}]\times[\text{B}(\Upsilon(2S)\to\gamma\chi_{b0}(1P))] < 37\times10^{-6}$ which we divide by our best value B($\Upsilon(2S)\to\gamma\chi_{b0}(1P)$) = 3.8×10^{-2}.

$\Gamma(4\pi^+4\pi^-)/\Gamma_{\text{total}}$ Γ_{15}/Γ

VALUE (units 10^{-4})	CL%	DOCUMENT ID		TECN	COMMENT
<0.8	90	[18] ASNER	08A	CLEO	$\Upsilon(2S)\to\gamma4\pi^+4\pi^-$

[18] ASNER 08A reports $[\Gamma(\chi_{b0}(1P)\to4\pi^+4\pi^-)/\Gamma_{\text{total}}]\times[\text{B}(\Upsilon(2S)\to\gamma\chi_{b0}(1P))] < 3\times10^{-6}$ which we divide by our best value B($\Upsilon(2S)\to\gamma\chi_{b0}(1P)$) = 3.8×10^{-2}.

$\Gamma(4\pi^+4\pi^-2\pi^0)/\Gamma_{\text{total}}$ Γ_{16}/Γ

VALUE (units 10^{-4})	CL%	DOCUMENT ID		TECN	COMMENT
<21	90	[19] ASNER	08A	CLEO	$\Upsilon(2S)\to\gamma4\pi^+4\pi^-2\pi^0$

[19] ASNER 08A reports $[\Gamma(\chi_{b0}(1P)\to4\pi^+4\pi^-2\pi^0)/\Gamma_{\text{total}}]\times[\text{B}(\Upsilon(2S)\to\gamma\chi_{b0}(1P))] < 77\times10^{-6}$ which we divide by our best value B($\Upsilon(2S)\to\gamma\chi_{b0}(1P)$) = 3.8×10^{-2}.

$\Gamma(J/\psi J/\psi)/\Gamma_{\text{total}}$ Γ_{17}/Γ

VALUE (units 10^{-5})	CL%	DOCUMENT ID		TECN	COMMENT
<7	90	[20] SHEN	12	BELL	$\Upsilon(2S)\to\gamma\psi X$

[20] SHEN 12 reports $< 7.1\times10^{-5}$ from a measurement of $[\Gamma(\chi_{b0}(1P)\to J/\psi J/\psi)/\Gamma_{\text{total}}]\times[\text{B}(\Upsilon(2S)\to\gamma\chi_{b0}(1P))]$ assuming B($\Upsilon(2S)\to\gamma\chi_{b0}(1P)$) = $(3.8\pm0.4)\times10^{-2}$.

Meson Particle Listings

$\chi_{b0}(1P)$, $\chi_{b1}(1P)$

$\Gamma(J/\psi\psi(2S))/\Gamma_{total}$ Γ_{18}/Γ

VALUE (units 10^{-5})	CL%	DOCUMENT ID		TECN	COMMENT
<12	90	[21] SHEN	12	BELL	$\Upsilon(2S) \to \gamma\psi X$

[21] SHEN 12 reports $< 12 \times 10^{-5}$ from a measurement of $[\Gamma(\chi_{b0}(1P) \to J/\psi\psi(2S))/\Gamma_{total}] \times [B(\Upsilon(2S) \to \gamma\chi_{b0}(1P))]$ assuming $B(\Upsilon(2S) \to \gamma\chi_{b0}(1P)) = (3.8 \pm 0.4) \times 10^{-2}$.

$\Gamma(\psi(2S)\psi(2S))/\Gamma_{total}$ Γ_{19}/Γ

VALUE (units 10^{-5})	CL%	DOCUMENT ID		TECN	COMMENT
<3.1	90	[22] SHEN	12	BELL	$\Upsilon(2S) \to \gamma\psi X$

[22] SHEN 12 reports $< 3.1 \times 10^{-5}$ from a measurement of $[\Gamma(\chi_{b0}(1P) \to \psi(2S)\psi(2S))/\Gamma_{total}] \times [B(\Upsilon(2S) \to \gamma\chi_{b0}(1P))]$ assuming $B(\Upsilon(2S) \to \gamma\chi_{b0}(1P)) = (3.8 \pm 0.4) \times 10^{-2}$.

$\chi_{b0}(1P)$ CROSS-PARTICLE BRANCHING RATIOS

$\Gamma(\chi_{b0}(1P) \to \gamma\Upsilon(1S))/\Gamma_{total} \times \Gamma(\Upsilon(2S) \to \gamma\chi_{b0}(1P))/\Gamma_{total}$ $\Gamma_1/\Gamma \times \Gamma_{33}^{\Upsilon(2S)}/\Gamma^{\Upsilon(2S)}$

VALUE	CL%	DOCUMENT ID		TECN	COMMENT
$< 1.7 \times 10^{-3}$	90	[23] LEES	11J	BABR	$\Upsilon(2S) \to X\gamma$

[23] LEES 11J quotes a central value of $\Gamma(\chi_{b0}(1P) \to \gamma\Upsilon(1S))/\Gamma_{total} \times \Gamma(\Upsilon(2S) \to \gamma\chi_{b0}(1P))/\Gamma_{total} = (8.3 \pm 5.6^{+3.7}_{-2.6}) \times 10^{-4}$ and derives a 90% CL upper limit of $\Gamma(\gamma\Upsilon(1S))/\Gamma_{total} < 4.6\%$ using $B(\Upsilon(4S) \to \gamma\chi_{b0}(1P)) = (3.8 \pm 0.4)\%$.

$B(\chi_{b0}(1P) \to \gamma\Upsilon(1S)) \times B(\Upsilon(2S) \to \gamma\chi_{b0}(1P)) \times B(\Upsilon(1S) \to \ell^+\ell^-)$

VALUE (units 10^{-5})	EVTS	DOCUMENT ID	TECN	COMMENT
1.63±0.24±0.15	87	KORNICER 11	CLEO	$e^+e^- \to \gamma\gamma\ell^+\ell^-$

$\chi_{b0}(1P)$ REFERENCES

SHEN	12	PR D85 071102	C.P. Shen *et al.*	(BELLE Collab.)
KORNICER	11	PR D83 054003	M. Kornicer *et al.*	(CLEO Collab.)
LEES	11J	PR D84 072002	J.P. Lees *et al.*	(BABAR Collab.)
ASNER	08A	PR D78 091103	D.M. Asner *et al.*	(CLEO Collab.)
BRIERE	08	PR D78 092007	R.A. Briere *et al.*	(CLEO Collab.)
ARTUSO	05	PRL 94 032001	M. Artuso *et al.*	(CLEO Collab.)
EDWARDS	99	PR D59 032003	K.W. Edwards *et al.*	(CLEO Collab.)
WALK	86	PR D34 2611	W.S. Walk *et al.*	(Crystal Ball Collab.)
ALBRECHT	85E	PL 160B 331	H. Albrecht *et al.*	(ARGUS Collab.)
NERNST	85	PRL 54 2195	R. Nernst *et al.*	(Crystal Ball Collab.)
HAAS	84	PRL 52 799	J. Haas *et al.*	(CLEO Collab.)
KLOPFEN...	83	PRL 51 160	C. Klopfenstein *et al.*	(CUSB Collab.)
PAUSS	83	PL 130B 439	F. Pauss *et al.*	(MPIM, COLU, CORN, LSU+)

$\chi_{b1}(1P)$

$I^G(J^{PC}) = 0^+(1^{++})$
J needs confirmation.

Observed in radiative decay of the $\Upsilon(2S)$, therefore $C = +$. Branching ratio requires E1 transition, M1 is strongly disfavored, therefore $P = +$. $J = 1$ from SKWARNICKI 87.

$\chi_{b1}(1P)$ MASS

VALUE (MeV)	DOCUMENT ID
9892.78±0.26±0.31 OUR EVALUATION	From average γ energy below, using $\Upsilon(2S)$ mass = 10023.26 ± 0.31 MeV

γ ENERGY IN $\Upsilon(2S)$ DECAY

VALUE (MeV)	DOCUMENT ID		TECN	COMMENT
129.63±0.33 OUR AVERAGE	Error includes scale factor of 1.3.			See the ideogram below.
129.58±0.09±0.29	ARTUSO	05	CLEO	$\Upsilon(2S) \to \gamma X$
128.8 ±0.4 ±0.6	EDWARDS	99	CLE2	$\Upsilon(2S) \to \gamma\chi(1P)$
131.7 ±0.9 ±1.3	WALK	86	CBAL	$\Upsilon(2S) \to \gamma\gamma\ell^+\ell^-$
131.7 ±0.3 ±1.1	ALBRECHT	85E	ARG	$\Upsilon(2S) \to$ conv.γX
130.6 ±0.8 ±2.4	NERNST	85	CBAL	$\Upsilon(2S) \to \gamma$X
129 ±0.8 ±1	HAAS	84	CLEO	$\Upsilon(2S) \to$ conv.γX
128.1 ±0.4 ±3.0	KLOPFEN...	83	CUSB	$\Upsilon(2S) \to \gamma$X
130.6 ±3.0	PAUSS	83	CUSB	$\Upsilon(2S) \to \gamma\gamma\ell^+\ell^-$

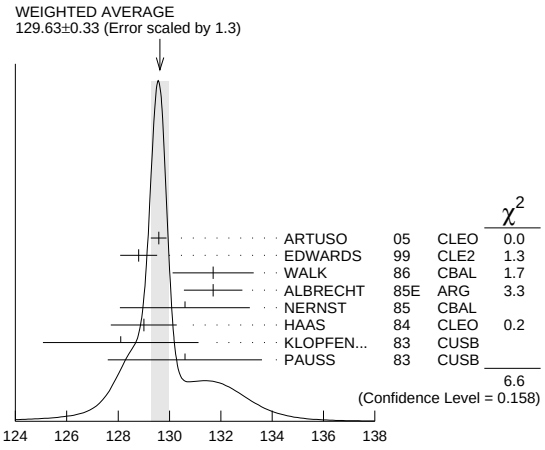

$\chi_{b1}(1P)$ DECAY MODES

	Mode	Fraction (Γ_i/Γ)	Confidence level
Γ_1	$\gamma\Upsilon(1S)$	(33.9±2.2) %	
Γ_2	D^0X	(12.6±2.2) %	
Γ_3	$\pi^+\pi^-K^+K^-\pi^0$	(2.0±0.6) $\times 10^{-4}$	
Γ_4	$2\pi^+\pi^-K^-K^0_S$	(1.3±0.5) $\times 10^{-4}$	
Γ_5	$2\pi^+\pi^-K^-K^0_S2\pi^0$	< 6 $\times 10^{-4}$	90%
Γ_6	$2\pi^+2\pi^-2\pi^0$	(8.0±2.5) $\times 10^{-4}$	
Γ_7	$2\pi^+2\pi^-K^+K^-$	(1.5±0.5) $\times 10^{-4}$	
Γ_8	$2\pi^+2\pi^-K^+K^-\pi^0$	(3.5±1.2) $\times 10^{-4}$	
Γ_9	$2\pi^+2\pi^-K^+K^-2\pi^0$	(8.6±3.2) $\times 10^{-4}$	
Γ_{10}	$3\pi^+2\pi^-K^-K^0_S\pi^0$	(9.3±3.3) $\times 10^{-4}$	
Γ_{11}	$3\pi^+3\pi^-$	(1.9±0.6) $\times 10^{-4}$	
Γ_{12}	$3\pi^+3\pi^-2\pi^0$	(1.7±0.5) $\times 10^{-3}$	
Γ_{13}	$3\pi^+3\pi^-K^+K^-$	(2.6±0.8) $\times 10^{-4}$	
Γ_{14}	$3\pi^+3\pi^-K^+K^-\pi^0$	(7.5±2.6) $\times 10^{-4}$	
Γ_{15}	$4\pi^+4\pi^-$	(2.6±0.9) $\times 10^{-4}$	
Γ_{16}	$4\pi^+4\pi^-2\pi^0$	(1.4±0.6) $\times 10^{-3}$	
Γ_{17}	$J/\psi J/\psi$	< 2.7 $\times 10^{-5}$	90%
Γ_{18}	$J/\psi\psi(2S)$	< 1.7 $\times 10^{-5}$	90%
Γ_{19}	$\psi(2S)\psi(2S)$	< 6 $\times 10^{-5}$	90%

$\chi_{b1}(1P)$ BRANCHING RATIOS

$\Gamma(\gamma\Upsilon(1S))/\Gamma_{total}$ Γ_1/Γ

VALUE	EVTS	DOCUMENT ID		TECN	COMMENT
0.339±0.022 OUR AVERAGE					
0.331±0.018±0.017	3222	[1,2] KORNICER	11	CLEO	$e^+e^- \to \gamma\gamma\ell^+\ell^-$
0.350±0.023±0.018	13k	[3] LEES	11J	BABR	$\Upsilon(2S) \to X\gamma$
0.32 ±0.06 ±0.07		WALK	86	CBAL	$\Upsilon(2S) \to \gamma\gamma\ell^+\ell^-$
0.47 ±0.18		KLOPFEN...	83	CUSB	$\Upsilon(2S) \to \gamma\gamma\ell^+\ell^-$

[1] Assuming $B(\Upsilon(1S) \to \ell^+\ell^-) = (2.48 \pm 0.05)\%$.

[2] KORNICER 11 reports $[\Gamma(\chi_{b1}(1P) \to \gamma\Upsilon(1S))/\Gamma_{total}] \times [B(\Upsilon(2S) \to \gamma\chi_{b1}(1P))] = (22.8 \pm 0.4 \pm 1.2) \times 10^{-3}$ which we divide by our best value $B(\Upsilon(2S) \to \gamma\chi_{b1}(1P)) = (6.9 \pm 0.4) \times 10^{-2}$. Our first error is their experiment's error and our second error is the systematic error from using our best value.

[3] LEES 11J reports $[\Gamma(\chi_{b1}(1P) \to \gamma\Upsilon(1S))/\Gamma_{total}] \times [B(\Upsilon(2S) \to \gamma\chi_{b1}(1P))] = (24.1 \pm 0.6 \pm 1.5) \times 10^{-3}$ which we divide by our best value $B(\Upsilon(2S) \to \gamma\chi_{b1}(1P)) = (6.9 \pm 0.4) \times 10^{-2}$. Our first error is their experiment's error and our second error is the systematic error from using our best value.

$\Gamma(D^0X)/\Gamma_{total}$ Γ_2/Γ

VALUE (units 10^{-2})	EVTS	DOCUMENT ID		TECN	COMMENT
12.6±1.9±1.1	2310	[4] BRIERE	08	CLEO	$\Upsilon(2S) \to \gamma D^0X$

[4] For $p_{D^0} > 2.5$ GeV/c.

$\Gamma(\pi^+\pi^-K^+K^-\pi^0)/\Gamma_{total}$ Γ_3/Γ

VALUE (units 10^{-4})	EVTS	DOCUMENT ID		TECN	COMMENT
2.0±0.6±0.1	18	[5] ASNER	08A	CLEO	$\Upsilon(2S) \to \gamma\pi^+\pi^-K^+K^-\pi^0$

[5] ASNER 08A reports $[\Gamma(\chi_{b1}(1P) \to \pi^+\pi^-K^+K^-\pi^0)/\Gamma_{total}] \times [B(\Upsilon(2S) \to \gamma\chi_{b1}(1P))] = (14 \pm 3 \pm 3) \times 10^{-6}$ which we divide by our best value $B(\Upsilon(2S) \to \gamma\chi_{b1}(1P)) = (6.9 \pm 0.4) \times 10^{-2}$. Our first error is their experiment's error and our second error is the systematic error from using our best value.

$\Gamma(2\pi^+\pi^-K^-K^0_S)/\Gamma_{total}$ Γ_4/Γ

VALUE (units 10^{-4})	EVTS	DOCUMENT ID		TECN	COMMENT
1.3±0.5±0.1	11	[6] ASNER	08A	CLEO	$\Upsilon(2S) \to \gamma 2\pi^+\pi^-K^-K^0_S$

[6] ASNER 08A reports $[\Gamma(\chi_{b1}(1P) \to 2\pi^+\pi^-K^-K^0_S)/\Gamma_{total}] \times [B(\Upsilon(2S) \to \gamma\chi_{b1}(1P))] = (9 \pm 3 \pm 2) \times 10^{-6}$ which we divide by our best value $B(\Upsilon(2S) \to \gamma\chi_{b1}(1P)) = (6.9 \pm 0.4) \times 10^{-2}$. Our first error is their experiment's error and our second error is the systematic error from using our best value.

$\Gamma(2\pi^+\pi^-K^-K^0_S2\pi^0)/\Gamma_{total}$ Γ_5/Γ

VALUE (units 10^{-4})	CL%	DOCUMENT ID		TECN	COMMENT
<6	90	[7] ASNER	08A	CLEO	$\Upsilon(2S) \to \gamma 2\pi^+\pi^-K^-2\pi^0$

[7] ASNER 08A reports $[\Gamma(\chi_{b1}(1P) \to 2\pi^+\pi^-K^-K^0_S2\pi^0)/\Gamma_{total}] \times [B(\Upsilon(2S) \to \gamma\chi_{b1}(1P))] < 42 \times 10^{-6}$ which we divide by our best value $B(\Upsilon(2S) \to \gamma\chi_{b1}(1P)) = 6.9 \times 10^{-2}$.

$\Gamma(2\pi^+2\pi^-2\pi^0)/\Gamma_{total}$ Γ_6/Γ

VALUE (units 10^{-4})	EVTS	DOCUMENT ID		TECN	COMMENT
8.0±2.4±0.4	46	[8] ASNER	08A	CLEO	$\Upsilon(2S) \to \gamma 2\pi^+2\pi^-2\pi^0$

[8] ASNER 08A reports $[\Gamma(\chi_{b1}(1P) \to 2\pi^+2\pi^-2\pi^0)/\Gamma_{total}] \times [B(\Upsilon(2S) \to \gamma\chi_{b1}(1P))] = (55 \pm 9 \pm 14) \times 10^{-6}$ which we divide by our best value $B(\Upsilon(2S) \to \gamma\chi_{b1}(1P)) = (6.9 \pm 0.4) \times 10^{-2}$. Our first error is their experiment's error and our second error is the systematic error from using our best value.

$\Gamma(2\pi^+2\pi^-K^+K^-)/\Gamma_{total}$ Γ_7/Γ

VALUE (units 10^{-4})	EVTS	DOCUMENT ID		TECN	COMMENT
1.5±0.5±0.1	18	[9] ASNER	08A	CLEO	$\Upsilon(2S) \to \gamma 2\pi^+2\pi^-K^+K^-$

[9] ASNER 08A reports $[\Gamma(\chi_{b1}(1P) \to 2\pi^+2\pi^-K^+K^-)/\Gamma_{total}] \times [B(\Upsilon(2S) \to \gamma\chi_{b1}(1P))] = (10 \pm 3 \pm 2) \times 10^{-6}$ which we divide by our best value $B(\Upsilon(2S) \to \gamma\chi_{b1}(1P)) = (6.9 \pm 0.4) \times 10^{-2}$. Our first error is their experiment's error and our second error is the systematic error from using our best value.

$\Gamma(2\pi^+2\pi^-K^+K^-\pi^0)/\Gamma_{total}$ Γ_8/Γ

VALUE (units 10^{-4})	EVTS	DOCUMENT ID		TECN	COMMENT
3.5±1.2±0.2	22	[10] ASNER	08A	CLEO	$\Upsilon(2S) \to \gamma 2\pi^+2\pi^-K^+K^-\pi^0$

[10] ASNER 08A reports $[\Gamma(\chi_{b1}(1P) \to 2\pi^+2\pi^-K^+K^-\pi^0)/\Gamma_{total}] \times [B(\Upsilon(2S) \to \gamma\chi_{b1}(1P))] = (24 \pm 6 \pm 6) \times 10^{-6}$ which we divide by our best value $B(\Upsilon(2S) \to \gamma\chi_{b1}(1P)) = (6.9 \pm 0.4) \times 10^{-2}$. Our first error is their experiment's error and our second error is the systematic error from using our best value.

$\Gamma(2\pi^+2\pi^-K^+K^-2\pi^0)/\Gamma_{total}$ Γ_9/Γ

VALUE (units 10^{-4})	EVTS	DOCUMENT ID		TECN	COMMENT
8.6±3.2±0.4	26	[11] ASNER	08A	CLEO	$\Upsilon(2S) \to \gamma 2\pi^+2\pi^-K^+K^-2\pi^0$

[11] ASNER 08A reports $[\Gamma(\chi_{b1}(1P) \to 2\pi^+2\pi^-K^+K^-2\pi^0)/\Gamma_{total}] \times [B(\Upsilon(2S) \to \gamma\chi_{b1}(1P))] = (59 \pm 14 \pm 17) \times 10^{-6}$ which we divide by our best value $B(\Upsilon(2S) \to \gamma\chi_{b1}(1P)) = (6.9 \pm 0.4) \times 10^{-2}$. Our first error is their experiment's error and our second error is the systematic error from using our best value.

$\Gamma(3\pi^+2\pi^-K^-K^0_S\pi^0)/\Gamma_{total}$ Γ_{10}/Γ

VALUE (units 10^{-4})	EVTS	DOCUMENT ID		TECN	COMMENT
9.3±3.3±0.5	21	[12] ASNER	08A	CLEO	$\Upsilon(2S) \to \gamma 3\pi^+2\pi^-K^-K^0_S\pi^0$

[12] ASNER 08A reports $[\Gamma(\chi_{b1}(1P) \to 3\pi^+2\pi^-K^-K^0_S\pi^0)/\Gamma_{total}] \times [B(\Upsilon(2S) \to \gamma\chi_{b1}(1P))] = (64 \pm 16 \pm 16) \times 10^{-6}$ which we divide by our best value $B(\Upsilon(2S) \to \gamma\chi_{b1}(1P)) = (6.9 \pm 0.4) \times 10^{-2}$. Our first error is their experiment's error and our second error is the systematic error from using our best value.

$\Gamma(3\pi^+3\pi^-)/\Gamma_{total}$ Γ_{11}/Γ

VALUE (units 10^{-4})	EVTS	DOCUMENT ID		TECN	COMMENT
1.9±0.6±0.1	25	[13] ASNER	08A	CLEO	$\Upsilon(2S) \to \gamma 3\pi^+3\pi^-$

[13] ASNER 08A reports $[\Gamma(\chi_{b1}(1P) \to 3\pi^+3\pi^-)/\Gamma_{total}] \times [B(\Upsilon(2S) \to \gamma\chi_{b1}(1P))] = (13 \pm 3 \pm 3) \times 10^{-6}$ which we divide by our best value $B(\Upsilon(2S) \to \gamma\chi_{b1}(1P)) = (6.9 \pm 0.4) \times 10^{-2}$. Our first error is their experiment's error and our second error is the systematic error from using our best value.

$\Gamma(3\pi^+3\pi^-2\pi^0)/\Gamma_{total}$ Γ_{12}/Γ

VALUE (units 10^{-4})	EVTS	DOCUMENT ID		TECN	COMMENT
17±5±1	56	[14] ASNER	08A	CLEO	$\Upsilon(2S) \to \gamma 3\pi^+3\pi^-2\pi^0$

[14] ASNER 08A reports $[\Gamma(\chi_{b1}(1P) \to 3\pi^+3\pi^-2\pi^0)/\Gamma_{total}] \times [B(\Upsilon(2S) \to \gamma\chi_{b1}(1P))] = (119 \pm 18 \pm 32) \times 10^{-6}$ which we divide by our best value $B(\Upsilon(2S) \to \gamma\chi_{b1}(1P)) = (6.9 \pm 0.4) \times 10^{-2}$. Our first error is their experiment's error and our second error is the systematic error from using our best value.

$\Gamma(3\pi^+3\pi^-K^+K^-)/\Gamma_{total}$ Γ_{13}/Γ

VALUE (units 10^{-4})	EVTS	DOCUMENT ID		TECN	COMMENT
2.6±0.8±0.1	21	[15] ASNER	08A	CLEO	$\Upsilon(2S) \to \gamma 3\pi^+3\pi^-K^+K^-$

[15] ASNER 08A reports $[\Gamma(\chi_{b1}(1P) \to 3\pi^+3\pi^-K^+K^-)/\Gamma_{total}] \times [B(\Upsilon(2S) \to \gamma\chi_{b1}(1P))] = (18 \pm 4 \pm 4) \times 10^{-6}$ which we divide by our best value $B(\Upsilon(2S) \to \gamma\chi_{b1}(1P)) = (6.9 \pm 0.4) \times 10^{-2}$. Our first error is their experiment's error and our second error is the systematic error from using our best value.

$\Gamma(3\pi^+3\pi^-K^+K^-\pi^0)/\Gamma_{total}$ Γ_{14}/Γ

VALUE (units 10^{-4})	EVTS	DOCUMENT ID		TECN	COMMENT
7.5±2.6±0.4	28	[16] ASNER	08A	CLEO	$\Upsilon(2S) \to \gamma 3\pi^+3\pi^-K^+K^-\pi^0$

[16] ASNER 08A reports $[\Gamma(\chi_{b1}(1P) \to 3\pi^+3\pi^-K^+K^-\pi^0)/\Gamma_{total}] \times [B(\Upsilon(2S) \to \gamma\chi_{b1}(1P))] = (52 \pm 11 \pm 14) \times 10^{-6}$ which we divide by our best value $B(\Upsilon(2S) \to \gamma\chi_{b1}(1P)) = (6.9 \pm 0.4) \times 10^{-2}$. Our first error is their experiment's error and our second error is the systematic error from using our best value.

$\Gamma(4\pi^+4\pi^-)/\Gamma_{total}$ Γ_{15}/Γ

VALUE (units 10^{-4})	EVTS	DOCUMENT ID		TECN	COMMENT
2.6±0.9±0.1	24	[17] ASNER	08A	CLEO	$\Upsilon(2S) \to \gamma 4\pi^+4\pi^-$

[17] ASNER 08A reports $[\Gamma(\chi_{b1}(1P) \to 4\pi^+4\pi^-)/\Gamma_{total}] \times [B(\Upsilon(2S) \to \gamma\chi_{b1}(1P))] = (18 \pm 4 \pm 5) \times 10^{-6}$ which we divide by our best value $B(\Upsilon(2S) \to \gamma\chi_{b1}(1P)) = (6.9 \pm 0.4) \times 10^{-2}$. Our first error is their experiment's error and our second error is the systematic error from using our best value.

$\Gamma(4\pi^+4\pi^-2\pi^0)/\Gamma_{total}$ Γ_{16}/Γ

VALUE (units 10^{-4})	EVTS	DOCUMENT ID		TECN	COMMENT
14±5±1	26	[18] ASNER	08A	CLEO	$\Upsilon(2S) \to \gamma 4\pi^+4\pi^-2\pi^0$

[18] ASNER 08A reports $[\Gamma(\chi_{b1}(1P) \to 4\pi^+4\pi^-2\pi^0)/\Gamma_{total}] \times [B(\Upsilon(2S) \to \gamma\chi_{b1}(1P))] = (96 \pm 24 \pm 29) \times 10^{-6}$ which we divide by our best value $B(\Upsilon(2S) \to \gamma\chi_{b1}(1P)) = (6.9 \pm 0.4) \times 10^{-2}$. Our first error is their experiment's error and our second error is the systematic error from using our best value.

$\Gamma(J/\psi J/\psi)/\Gamma_{total}$ Γ_{17}/Γ

VALUE (units 10^{-5})	CL%	DOCUMENT ID		TECN	COMMENT
<2.7	90	[19] SHEN	12	BELL	$\Upsilon(2S) \to \gamma\psi X$

[19] SHEN 12 reports $< 2.7 \times 10^{-5}$ from a measurement of $[\Gamma(\chi_{b1}(1P) \to J/\psi J/\psi)/\Gamma_{total}] \times [B(\Upsilon(2S) \to \gamma\chi_{b1}(1P))]$ assuming $B(\Upsilon(2S) \to \gamma\chi_{b1}(1P)) = (6.9 \pm 0.4) \times 10^{-2}$.

$\Gamma(J/\psi\psi(2S))/\Gamma_{total}$ Γ_{18}/Γ

VALUE (units 10^{-5})	CL%	DOCUMENT ID		TECN	COMMENT
<1.7	90	[20] SHEN	12	BELL	$\Upsilon(2S) \to \gamma\psi X$

[20] SHEN 12 reports $< 1.7 \times 10^{-5}$ from a measurement of $[\Gamma(\chi_{b1}(1P) \to J/\psi\psi(2S))/\Gamma_{total}] \times [B(\Upsilon(2S) \to \gamma\chi_{b1}(1P))]$ assuming $B(\Upsilon(2S) \to \gamma\chi_{b1}(1P)) = (6.9 \pm 0.4) \times 10^{-2}$.

$\Gamma(\psi(2S)\psi(2S))/\Gamma_{total}$ Γ_{19}/Γ

VALUE (units 10^{-5})	CL%	DOCUMENT ID		TECN	COMMENT
<6	90	[21] SHEN	12	BELL	$\Upsilon(2S) \to \gamma\psi X$

[21] SHEN 12 reports $< 6.2 \times 10^{-5}$ from a measurement of $[\Gamma(\chi_{b1}(1P) \to \psi(2S)\psi(2S))/\Gamma_{total}] \times [B(\Upsilon(2S) \to \gamma\chi_{b1}(1P))]$ assuming $B(\Upsilon(2S) \to \gamma\chi_{b1}(1P)) = (6.9 \pm 0.4) \times 10^{-2}$.

$\chi_{b1}(1P)$ Cross-Particle Branching Ratios

$\Gamma(\chi_{b1}(1P) \to \gamma\Upsilon(1S))/\Gamma_{total} \times \Gamma(\Upsilon(2S) \to \gamma\chi_{b1}(1P))/\Gamma_{total}$ $\Gamma_1/\Gamma \times \Gamma_{31}^{\Upsilon(2S)}/\Gamma^{\Upsilon(2S)}$

VALUE (units 10^{-3})	EVTS	DOCUMENT ID		TECN	COMMENT
24.1±0.6±1.5	13k	LEES	11J	BABR	$\Upsilon(2S) \to X\gamma$

$B(\chi_{b1}(1P) \to \gamma\Upsilon(1S)) \times B(\Upsilon(2S) \to \gamma\chi_{b1}(1P)) \times B(\Upsilon(1S) \to \ell^+\ell^-)$

VALUE (units 10^{-4})	EVTS	DOCUMENT ID		TECN	COMMENT
5.65±0.11±0.27	3222	KORNICER	11	CLEO	$e^+e^- \to \gamma\gamma\ell^+\ell^-$

$B(\chi_{b1}(1P) \to \gamma\Upsilon(1S)) \times B(\Upsilon(3S) \to \gamma\chi_{b1}(1P)) \times B(\Upsilon(1S) \to \ell^+\ell^-)$

VALUE (units 10^{-5})	EVTS	DOCUMENT ID		TECN	COMMENT
1.33±0.30±0.23	50	KORNICER	11	CLEO	$e^+e^- \to \gamma\gamma\ell^+\ell^-$

$B(\chi_{b2}(1P) \to pX + \bar{p}X)/B(\chi_{b1}(1P) \to pX + \bar{p}X)$

VALUE	DOCUMENT ID		TECN	COMMENT
1.068±0.010±0.040	BRIERE	07	CLEO	$\Upsilon(2S) \to \gamma\chi_{bJ}(1P)$

$B(\chi_{b0}(1P) \to pX + \bar{p}X)/B(\chi_{b1}(1P) \to pX + \bar{p}X)$

VALUE	DOCUMENT ID		TECN	COMMENT
1.11±0.15±0.20	BRIERE	07	CLEO	$\Upsilon(2S) \to \gamma\chi_{bJ}(1P)$

$\chi_{b1}(1P)$ REFERENCES

SHEN	12	PR D85 071102	C.P. Shen *et al.*	(BELLE Collab.)
KORNICER	11	PR D83 054003	M. Kornicer *et al.*	(CLEO Collab.)
LEES	11J	PR D84 072002	J.P. Lees *et al.*	(BABAR Collab.)
ASNER	08A	PR D78 091103	D.M. Asner *et al.*	(CLEO Collab.)
BRIERE	08	PR D78 092007	R.A. Briere *et al.*	(CLEO Collab.)
BRIERE	07	PR D76 012005	R.A. Briere *et al.*	(CLEO Collab.)
ARTUSO	05	PRL 94 032001	M. Artuso *et al.*	(CLEO Collab.)
EDWARDS	99	PR D59 032003	K.W. Edwards *et al.*	(CLEO Collab.)
SKWARNICKI	87	PRL 58 972	T. Skwarnicki *et al.*	(Crystal Ball Collab.) J
WALK	86	PR D34 2611	W.S. Walk *et al.*	(Crystal Ball Collab.)
ALBRECHT	85E	PL 160B 331	H. Albrecht *et al.*	(ARGUS Collab.)
NERNST	85	PRL 54 2195	R. Nernst *et al.*	(Crystal Ball Collab.)
HAAS	84	PRL 52 799	J. Haas *et al.*	(CLEO Collab.)
KLOPFEN...	83	PRL 51 160	C. Klopfenstein *et al.*	(CUSB Collab.)
PAUSS	83	PL 130B 439	F. Pauss *et al.*	(MPIM, COLU, CORN, LSU+)

Meson Particle Listings

$h_b(1P), \chi_{b2}(1P)$

$h_b(1P)$

$I^G(J^{PC}) = ?^?(1^{+-})$

Quantum numbers are quark model predictions, $C = -$ established by $\eta_b\gamma$ decay.

$h_b(1P)$ MASS

VALUE (MeV)	EVTS	DOCUMENT ID		TECN	COMMENT
9899.3±1.0 OUR AVERAGE					
9899.1±0.4±1.0	70k	MIZUK	12	BELL	$e^+e^- \to \pi^+\pi^-$ hadrons
9902 ±4 ±2	10.8k	LEES	11K	BABR	$\Upsilon(3S) \to \eta_b\gamma\pi^0$
• • • We do not use the following data for averages, fits, limits, etc. • • •					
$9898.2^{+1.1}_{-1.0}{}^{+1.0}_{-1.1}$	50.0k	[1] ADACHI	12	BELL	10.86 $e^+e^- \to \pi^+\pi^-$ MM

[1] Superseded by MIZUK 12.

$h_b(1P)$ DECAY MODES

	Mode	Fraction (Γ_i/Γ)
Γ_1	$\eta_b(1S)\gamma$	(49^{+8}_{-7}) %

$h_b(1P)$ BRANCHING RATIOS

$\Gamma(\eta_b(1S)\gamma)/\Gamma_{total}$ **Γ_1/Γ**

VALUE (units 10^{-2})	EVTS	DOCUMENT ID		TECN	COMMENT
$49.2\pm5.7^{+5.6}_{-3.3}$	24k	MIZUK	12	BELL	$e^+e^- \to (\gamma)\pi^+\pi^-$ hadrons
• • • We do not use the following data for averages, fits, limits, etc. • • •					
seen	10.8k	LEES	11K	BABR	$\Upsilon(3S) \to \eta_b\gamma\pi^0$

$h_b(1P)$ REFERENCES

ADACHI	12	PRL 108 032001	I. Adachi *et al.*	(BELLE Collab.)
MIZUK	12	PRL 109 232002	R. Mizuk *et al.*	(BELLE Collab.)
LEES	11K	PR D84 091101	J.P. Lees *et al.*	(BABAR Collab.)

$\chi_{b2}(1P)$

$I^G(J^{PC}) = 0^+(2^{++})$
J needs confirmation.

Observed in radiative decay of the $\Upsilon(2S)$, therefore $C = +$. Branching ratio requires E1 transition, M1 is strongly disfavored, therefore $P = +$. $J = 2$ from SKWARNICKI 87.

$\chi_{b2}(1P)$ MASS

VALUE (MeV)	DOCUMENT ID
9912.21±0.26±0.31 OUR EVALUATION	From average γ energy below, using $\Upsilon(2S)$ mass = 10023.26 ± 0.31 MeV

γ ENERGY IN $\Upsilon(2S)$ DECAY

VALUE (MeV)	DOCUMENT ID		TECN	COMMENT
110.44±0.29 OUR AVERAGE	Error includes scale factor of 1.1.			
110.58±0.08±0.30	ARTUSO	05	CLEO	$\Upsilon(2S) \to \gamma X$
110.8 ±0.3 ±0.6	EDWARDS	99	CLE2	$\Upsilon(2S) \to \gamma\chi(1P)$
107.0 ±1.1 ±1.3	WALK	86	CBAL	$\Upsilon(2S) \to \gamma\gamma\ell^+\ell^-$
110.6 ±0.3 ±0.9	ALBRECHT	85E	ARG	$\Upsilon(2S) \to$ conv.γX
110.4 ±0.8 ±2.2	NERNST	85	CBAL	$\Upsilon(2S) \to \gamma$X
109.5 ±0.7 ±1.0	HAAS	84	CLEO	$\Upsilon(2S) \to$ conv.γX
108.2 ±0.3 ±2.0	KLOPFEN...	83	CUSB	$\Upsilon(2S) \to \gamma$X
108.8 ±4.0	PAUSS	83	CUSB	$\Upsilon(2S) \to \gamma\gamma\ell^+\ell^-$

$\chi_{b2}(1P)$ DECAY MODES

	Mode	Fraction (Γ_i/Γ)	Confidence level
Γ_1	$\gamma\Upsilon(1S)$	(19.1±1.2) %	
Γ_2	D^0X	< 7.9 %	90%
Γ_3	$\pi^+\pi^-K^+K^-\pi^0$	(8 ±5) $\times10^{-5}$	
Γ_4	$2\pi^+\pi^-K^-K^0_S$	< 1.0 $\times10^{-4}$	90%
Γ_5	$2\pi^+\pi^-K^-K^0_S2\pi^0$	(5.3±2.4) $\times10^{-4}$	
Γ_6	$2\pi^+2\pi^-2\pi^0$	(3.5±1.4) $\times10^{-4}$	
Γ_7	$2\pi^+2\pi^-K^+K^-$	(1.1±0.4) $\times10^{-4}$	
Γ_8	$2\pi^+2\pi^-K^+K^-\pi^0$	(2.1±0.9) $\times10^{-4}$	
Γ_9	$2\pi^+2\pi^-K^+K^-2\pi^0$	(3.9±1.8) $\times10^{-4}$	
Γ_{10}	$3\pi^+2\pi^-K^-K^0_S\pi^0$	< 5 $\times10^{-4}$	90%
Γ_{11}	$3\pi^+3\pi^-$	(7.0±3.1) $\times10^{-5}$	
Γ_{12}	$3\pi^+3\pi^-2\pi^0$	(1.0±0.4) $\times10^{-3}$	
Γ_{13}	$3\pi^+3\pi^-K^+K^-$	< 8 $\times10^{-5}$	90%
Γ_{14}	$3\pi^+3\pi^-K^+K^-\pi^0$	(3.6±1.5) $\times10^{-4}$	
Γ_{15}	$4\pi^+4\pi^-$	(8 ±4) $\times10^{-5}$	
Γ_{16}	$4\pi^+4\pi^-2\pi^0$	(1.8±0.7) $\times10^{-3}$	
Γ_{17}	$J/\psi J/\psi$	< 4 $\times10^{-5}$	90%
Γ_{18}	$J/\psi\psi(2S)$	< 5 $\times10^{-5}$	90%
Γ_{19}	$\psi(2S)\psi(2S)$	< 1.6 $\times10^{-5}$	90%

$\chi_{b2}(1P)$ BRANCHING RATIOS

$\Gamma(\gamma\Upsilon(1S))/\Gamma_{total}$ **Γ_1/Γ**

VALUE	EVTS	DOCUMENT ID		TECN	COMMENT
0.191±0.012 OUR AVERAGE					
0.186±0.011±0.009	1770	[1,2] KORNICER	11	CLEO	$e^+e^- \to \gamma\gamma\ell^+\ell^-$
$0.194^{+0.014}_{-0.017}\pm0.009$	8k	[3] LEES	11J	BABR	$\Upsilon(2S) \to X\gamma$
0.27 ±0.06 ±0.06		WALK	86	CBAL	$\Upsilon(2S) \to \gamma\gamma\ell^+\ell^-$
0.20 ±0.05		KLOPFEN...	83	CUSB	$\Upsilon(2S) \to \gamma\gamma\ell^+\ell^-$

[1] Assuming B($\Upsilon(1S) \to \ell^+\ell^-$) = (2.48 ± 0.05)%.
[2] KORNICER 11 reports $[\Gamma(\chi_{b2}(1P) \to \gamma\Upsilon(1S))/\Gamma_{total}] \times [B(\Upsilon(2S) \to \gamma\chi_{b2}(1P))] = (1.33 \pm 0.04 \pm 0.07) \times 10^{-2}$ which we divide by our best value B($\Upsilon(2S) \to \gamma\chi_{b2}(1P)$) = (7.15 ± 0.35) × 10^{-2}. Our first error is their experiment's error and our second error is the systematic error from using our best value.
[3] LEES 11J reports $[\Gamma(\chi_{b2}(1P) \to \gamma\Upsilon(1S))/\Gamma_{total}] \times [B(\Upsilon(2S) \to \gamma\chi_{b2}(1P))] = (13.9 \pm 0.5^{+0.9}_{-1.1}) \times 10^{-3}$ which we divide by our best value B($\Upsilon(2S) \to \gamma\chi_{b2}(1P)$) = (7.15 ± 0.35) × 10^{-2}. Our first error is their experiment's error and our second error is the systematic error from using our best value.

$\Gamma(D^0X)/\Gamma_{total}$ **Γ_2/Γ**

VALUE	CL%	DOCUMENT ID		TECN	COMMENT
<7.9 × 10^{-2}	90	[4,5] BRIERE	08	CLEO	$\Upsilon(2S) \to \gamma D^0X$

[4] For $p_{D^0} > 2.5$ GeV/c.
[5] The authors also present their result as (5.4 ± 1.9 ± 0.5) × 10^{-2}.

$\Gamma(\pi^+\pi^-K^+K^-\pi^0)/\Gamma_{total}$ **Γ_3/Γ**

VALUE (units 10^{-4})	EVTS	DOCUMENT ID		TECN	COMMENT
0.84±0.50±0.04	8	[6] ASNER	08A	CLEO	$\Upsilon(2S) \to \gamma\pi^+\pi^-K^+K^-\pi^0$

[6] ASNER 08A reports $[\Gamma(\chi_{b2}(1P) \to \pi^+\pi^-K^+K^-\pi^0)/\Gamma_{total}] \times [B(\Upsilon(2S) \to \gamma\chi_{b2}(1P))] = (6 \pm 3 \pm 2) \times 10^{-6}$ which we divide by our best value B($\Upsilon(2S) \to \gamma\chi_{b2}(1P)$) = (7.15 ± 0.35) × 10^{-2}. Our first error is their experiment's error and our second error is the systematic error from using our best value.

$\Gamma(2\pi^+\pi^-K^-K^0_S)/\Gamma_{total}$ **Γ_4/Γ**

VALUE (units 10^{-4})	CL%	DOCUMENT ID		TECN	COMMENT
<1.0	90	[7] ASNER	08A	CLEO	$\Upsilon(2S) \to \gamma2\pi^+\pi^-K^-K^0_S$

[7] ASNER 08A reports $[\Gamma(\chi_{b2}(1P) \to 2\pi^+\pi^-K^-K^0_S)/\Gamma_{total}] \times [B(\Upsilon(2S) \to \gamma\chi_{b2}(1P))] < 7 \times 10^{-6}$ which we divide by our best value B($\Upsilon(2S) \to \gamma\chi_{b2}(1P)$) = 7.15 × 10^{-2}.

$\Gamma(2\pi^+\pi^-K^-K^0_S2\pi^0)/\Gamma_{total}$ **Γ_5/Γ**

VALUE (units 10^{-4})	EVTS	DOCUMENT ID		TECN	COMMENT
5.3±2.4±0.3	11	[8] ASNER	08A	CLEO	$\Upsilon(2S) \to \gamma2\pi^+\pi^-K^-2\pi^0$

[8] ASNER 08A reports $[\Gamma(\chi_{b2}(1P) \to 2\pi^+\pi^-K^-K^0_S2\pi^0)/\Gamma_{total}] \times [B(\Upsilon(2S) \to \gamma\chi_{b2}(1P))] = (38 \pm 14 \pm 10) \times 10^{-6}$ which we divide by our best value B($\Upsilon(2S) \to \gamma\chi_{b2}(1P)$) = (7.15 ± 0.35) × 10^{-2}. Our first error is their experiment's error and our second error is the systematic error from using our best value.

$\Gamma(2\pi^+2\pi^-2\pi^0)/\Gamma_{total}$ **Γ_6/Γ**

VALUE (units 10^{-4})	EVTS	DOCUMENT ID		TECN	COMMENT
3.5±1.4±0.2	19	[9] ASNER	08A	CLEO	$\Upsilon(2S) \to \gamma2\pi^+2\pi^-2\pi^0$

[9] ASNER 08A reports $[\Gamma(\chi_{b2}(1P) \to 2\pi^+2\pi^-2\pi^0)/\Gamma_{total}] \times [B(\Upsilon(2S) \to \gamma\chi_{b2}(1P))] = (25 \pm 8 \pm 6) \times 10^{-6}$ which we divide by our best value B($\Upsilon(2S) \to \gamma\chi_{b2}(1P)$) = (7.15 ± 0.35) × 10^{-2}. Our first error is their experiment's error and our second error is the systematic error from using our best value.

$\Gamma(2\pi^+2\pi^-K^+K^-)/\Gamma_{total}$ **Γ_7/Γ**

VALUE (units 10^{-4})	EVTS	DOCUMENT ID		TECN	COMMENT
1.1±0.4±0.1	14	[10] ASNER	08A	CLEO	$\Upsilon(2S) \to \gamma2\pi^+2\pi^-K^+K^-$

[10] ASNER 08A reports $[\Gamma(\chi_{b2}(1P) \to 2\pi^+2\pi^-K^+K^-)/\Gamma_{total}] \times [B(\Upsilon(2S) \to \gamma\chi_{b2}(1P))] = (8 \pm 2 \pm 2) \times 10^{-6}$ which we divide by our best value B($\Upsilon(2S) \to \gamma\chi_{b2}(1P)$) = (7.15 ± 0.35) × 10^{-2}. Our first error is their experiment's error and our second error is the systematic error from using our best value.

$\Gamma(2\pi^+2\pi^-K^+K^-\pi^0)/\Gamma_{total}$ Γ_8/Γ

VALUE (units 10^{-4})	EVTS	DOCUMENT ID		TECN	COMMENT
2.1±0.9±0.1	13	[11] ASNER	08A	CLEO	$\Upsilon(2S) \to \gamma 2\pi^+2\pi^-K^+K^-\pi^0$

[11] ASNER 08A reports $[\Gamma(\chi_{b2}(1P) \to 2\pi^+2\pi^-K^+K^-\pi^0)/\Gamma_{total}] \times [B(\Upsilon(2S) \to \gamma\chi_{b2}(1P))] = (15 \pm 5 \pm 4) \times 10^{-6}$ which we divide by our best value $B(\Upsilon(2S) \to \gamma\chi_{b2}(1P)) = (7.15 \pm 0.35) \times 10^{-2}$. Our first error is their experiment's error and our second error is the systematic error from using our best value.

$\Gamma(2\pi^+2\pi^-K^+K^-2\pi^0)/\Gamma_{total}$ Γ_9/Γ

VALUE (units 10^{-4})	EVTS	DOCUMENT ID		TECN	COMMENT
3.9±1.8±0.2	11	[12] ASNER	08A	CLEO	$\Upsilon(2S) \to \gamma 2\pi^+2\pi^-K^+K^-2\pi^0$

[12] ASNER 08A reports $[\Gamma(\chi_{b2}(1P) \to 2\pi^+2\pi^-K^+K^-2\pi^0)/\Gamma_{total}] \times [B(\Upsilon(2S) \to \gamma\chi_{b2}(1P))] = (28 \pm 11 \pm 7) \times 10^{-6}$ which we divide by our best value $B(\Upsilon(2S) \to \gamma\chi_{b2}(1P)) = (7.15 \pm 0.35) \times 10^{-2}$. Our first error is their experiment's error and our second error is the systematic error from using our best value.

$\Gamma(3\pi^+2\pi^-K^-K^0_S\pi^0)/\Gamma_{total}$ Γ_{10}/Γ

VALUE (units 10^{-4})	CL%	DOCUMENT ID		TECN	COMMENT
<5	90	[13] ASNER	08A	CLEO	$\Upsilon(2S) \to \gamma 3\pi^+2\pi^-K^-K^0_S\pi^0$

[13] ASNER 08A reports $[\Gamma(\chi_{b2}(1P) \to 3\pi^+2\pi^-K^-K^0_S\pi^0)/\Gamma_{total}] \times [B(\Upsilon(2S) \to \gamma\chi_{b2}(1P))] < 36 \times 10^{-6}$ which we divide by our best value $B(\Upsilon(2S) \to \gamma\chi_{b2}(1P)) = 7.15 \times 10^{-2}$.

$\Gamma(3\pi^+3\pi^-)/\Gamma_{total}$ Γ_{11}/Γ

VALUE (units 10^{-4})	EVTS	DOCUMENT ID		TECN	COMMENT
0.70±0.31±0.03	9	[14] ASNER	08A	CLEO	$\Upsilon(2S) \to \gamma 3\pi^+3\pi^-$

[14] ASNER 08A reports $[\Gamma(\chi_{b2}(1P) \to 3\pi^+3\pi^-)/\Gamma_{total}] \times [B(\Upsilon(2S) \to \gamma\chi_{b2}(1P))] = (5 \pm 2 \pm 1) \times 10^{-6}$ which we divide by our best value $B(\Upsilon(2S) \to \gamma\chi_{b2}(1P)) = (7.15 \pm 0.35) \times 10^{-2}$. Our first error is their experiment's error and our second error is the systematic error from using our best value.

$\Gamma(3\pi^+3\pi^-2\pi^0)/\Gamma_{total}$ Γ_{12}/Γ

VALUE (units 10^{-4})	EVTS	DOCUMENT ID		TECN	COMMENT
10.2±3.6±0.5	34	[15] ASNER	08A	CLEO	$\Upsilon(2S) \to \gamma 3\pi^+3\pi^-2\pi^0$

[15] ASNER 08A reports $[\Gamma(\chi_{b2}(1P) \to 3\pi^+3\pi^-2\pi^0)/\Gamma_{total}] \times [B(\Upsilon(2S) \to \gamma\chi_{b2}(1P))] = (73 \pm 16 \pm 20) \times 10^{-6}$ which we divide by our best value $B(\Upsilon(2S) \to \gamma\chi_{b2}(1P)) = (7.15 \pm 0.35) \times 10^{-2}$. Our first error is their experiment's error and our second error is the systematic error from using our best value.

$\Gamma(3\pi^+3\pi^-K^+K^-)/\Gamma_{total}$ Γ_{13}/Γ

VALUE (units 10^{-4})	CL%	DOCUMENT ID		TECN	COMMENT
<0.8	90	[16] ASNER	08A	CLEO	$\Upsilon(2S) \to \gamma 3\pi^+3\pi^-K^+K^-$

[16] ASNER 08A reports $[\Gamma(\chi_{b2}(1P) \to 3\pi^+3\pi^-K^+K^-)/\Gamma_{total}] \times [B(\Upsilon(2S) \to \gamma\chi_{b2}(1P))] < 6 \times 10^{-6}$ which we divide by our best value $B(\Upsilon(2S) \to \gamma\chi_{b2}(1P)) = 7.15 \times 10^{-2}$.

$\Gamma(3\pi^+3\pi^-K^+K^-\pi^0)/\Gamma_{total}$ Γ_{14}/Γ

VALUE (units 10^{-4})	EVTS	DOCUMENT ID		TECN	COMMENT
3.6±1.5±0.2	14	[17] ASNER	08A	CLEO	$\Upsilon(2S) \to \gamma 3\pi^+3\pi^-K^+K^-\pi^0$

[17] ASNER 08A reports $[\Gamma(\chi_{b2}(1P) \to 3\pi^+3\pi^-K^+K^-\pi^0)/\Gamma_{total}] \times [B(\Upsilon(2S) \to \gamma\chi_{b2}(1P))] = (26 \pm 8 \pm 7) \times 10^{-6}$ which we divide by our best value $B(\Upsilon(2S) \to \gamma\chi_{b2}(1P)) = (7.15 \pm 0.35) \times 10^{-2}$. Our first error is their experiment's error and our second error is the systematic error from using our best value.

$\Gamma(4\pi^+4\pi^-)/\Gamma_{total}$ Γ_{15}/Γ

VALUE (units 10^{-4})	EVTS	DOCUMENT ID		TECN	COMMENT
0.84±0.40±0.04	7	[18] ASNER	08A	CLEO	$\Upsilon(2S) \to \gamma 4\pi^+4\pi^-$

[18] ASNER 08A reports $[\Gamma(\chi_{b2}(1P) \to 4\pi^+4\pi^-)/\Gamma_{total}] \times [B(\Upsilon(2S) \to \gamma\chi_{b2}(1P))] = (6 \pm 2 \pm 2) \times 10^{-6}$ which we divide by our best value $B(\Upsilon(2S) \to \gamma\chi_{b2}(1P)) = (7.15 \pm 0.35) \times 10^{-2}$. Our first error is their experiment's error and our second error is the systematic error from using our best value.

$\Gamma(4\pi^+4\pi^-2\pi^0)/\Gamma_{total}$ Γ_{16}/Γ

VALUE (units 10^{-4})	EVTS	DOCUMENT ID		TECN	COMMENT
18±7±1	29	[19] ASNER	08A	CLEO	$\Upsilon(2S) \to \gamma 4\pi^+4\pi^-2\pi^0$

[19] ASNER 08A reports $[\Gamma(\chi_{b2}(1P) \to 4\pi^+4\pi^-2\pi^0)/\Gamma_{total}] \times [B(\Upsilon(2S) \to \gamma\chi_{b2}(1P))] = (132 \pm 31 \pm 40) \times 10^{-6}$ which we divide by our best value $B(\Upsilon(2S) \to \gamma\chi_{b2}(1P)) = (7.15 \pm 0.35) \times 10^{-2}$. Our first error is their experiment's error and our second error is the systematic error from using our best value.

$\Gamma(J/\psi J/\psi)/\Gamma_{total}$ Γ_{17}/Γ

VALUE (units 10^{-5})	CL%	DOCUMENT ID		TECN	COMMENT
<5	90	[20] SHEN	12	BELL	$\Upsilon(2S) \to \gamma\psi X$

[20] SHEN 12 reports $< 4.5 \times 10^{-5}$ from a measurement of $[\Gamma(\chi_{b2}(1P) \to J/\psi J/\psi)/\Gamma_{total}] \times [B(\Upsilon(2S) \to \gamma\chi_{b2}(1P))]$ assuming $B(\Upsilon(2S) \to \gamma\chi_{b2}(1P)) = (7.15 \pm 0.35) \times 10^{-2}$.

$\Gamma(J/\psi\psi(2S))/\Gamma_{total}$ Γ_{18}/Γ

VALUE (units 10^{-5})	CL%	DOCUMENT ID		TECN	COMMENT
<5	90	[21] SHEN	12	BELL	$\Upsilon(2S) \to \gamma\psi X$

[21] SHEN 12 reports $< 4.9 \times 10^{-5}$ from a measurement of $[\Gamma(\chi_{b2}(1P) \to J/\psi\psi(2S))/\Gamma_{total}] \times [B(\Upsilon(2S) \to \gamma\chi_{b2}(1P))]$ assuming $B(\Upsilon(2S) \to \gamma\chi_{b2}(1P)) = (7.15 \pm 0.35) \times 10^{-2}$.

$\Gamma(\psi(2S)\psi(2S))/\Gamma_{total}$ Γ_{19}/Γ

VALUE (units 10^{-5})	CL%	DOCUMENT ID		TECN	COMMENT
<1.6	90	[22] SHEN	12	BELL	$\Upsilon(2S) \to \gamma\psi X$

[22] SHEN 12 reports $< 1.6 \times 10^{-5}$ from a measurement of $[\Gamma(\chi_{b2}(1P) \to \psi(2S)\psi(2S))/\Gamma_{total}] \times [B(\Upsilon(2S) \to \gamma\chi_{b2}(1P))]$ assuming $B(\Upsilon(2S) \to \gamma\chi_{b2}(1P)) = (7.15 \pm 0.35) \times 10^{-2}$.

$\chi_{b2}(1P)$ Cross-Particle Branching Ratios

$\Gamma(\chi_{b2}(1P) \to \gamma\Upsilon(1S))/\Gamma_{total} \times \Gamma(\Upsilon(2S) \to \gamma\chi_{b2}(1P))/\Gamma_{total}$ $\Gamma_1/\Gamma \times \Gamma_{32}^{\Upsilon(2S)}/\Gamma^{\Upsilon(2S)}$

VALUE (units 10^{-3})	EVTS	DOCUMENT ID		TECN	COMMENT
13.9±0.5 $^{+0.9}_{-1.1}$	8k	LEES	11J	BABR	$\Upsilon(2S) \to X\gamma$

$B(\chi_{b2}(1P) \to \gamma\Upsilon(1S)) \times B(\Upsilon(2S) \to \gamma\chi_{b2}(1P)) \times B(\Upsilon(1S) \to \ell^+\ell^-)$

VALUE (units 10^{-4})	EVTS	DOCUMENT ID		TECN	COMMENT
3.29±0.09±0.16	1770	KORNICER	11	CLEO	$e^+e^- \to \gamma\gamma\ell^+\ell^-$

$B(\chi_{b2}(1P) \to \gamma\Upsilon(1S)) \times B(\Upsilon(3S) \to \gamma\chi_{b2}(1P)) \times B(\Upsilon(1S) \to \ell^+\ell^-)$

VALUE (units 10^{-5})	EVTS	DOCUMENT ID		TECN	COMMENT
3.56±0.40±0.41	126	KORNICER	11	CLEO	$e^+e^- \to \gamma\gamma\ell^+\ell^-$

$\chi_{b2}(1P)$ REFERENCES

SHEN	12	PR D85 071102	C.P. Shen *et al.*	(BELLE Collab.)
KORNICER	11	PR D83 054003	M. Kornicer *et al.*	(CLEO Collab.)
LEES	11J	PR D84 072002	J.P. Lees *et al.*	(BABAR Collab.)
ASNER	08A	PR D78 091103	D.M. Asner *et al.*	(CLEO Collab.)
BRIERE	08	PR D78 092007	R.A. Briere *et al.*	(CLEO Collab.)
ARTUSO	05	PRL 94 032001	M. Artuso *et al.*	(CLEO Collab.)
EDWARDS	99	PR D59 032003	K.W. Edwards *et al.*	(CLEO Collab.)
SKWARNICKI	87	PRL 58 972	T. Skwarnicki *et al.*	(Crystal Ball Collab.) J
WALK	86	PR D34 2611	W.S. Walk *et al.*	(Crystal Ball Collab.)
ALBRECHT	85E	PL 160B 331	H. Albrecht *et al.*	(ARGUS Collab.)
NERNST	85	PRL 54 2195	R. Nernst *et al.*	(Crystal Ball Collab.)
HAAS	84	PRL 52 799	J. Haas *et al.*	(CLEO Collab.)
KLOPFEN...	83	PRL 51 160	C. Klopfenstein *et al.*	(CUSB Collab.)
PAUSS	83	PL 130B 439	F. Pauss *et al.*	(MPIM, COLU, CORN, LSU+)

$\eta_b(2S)$

$I^G(J^{PC}) = 0^+(0^{-+})$

OMITTED FROM SUMMARY TABLE

Quantum numbers shown are quark-model predictions.

$\eta_b(2S)$ MASS

VALUE (MeV)	EVTS	DOCUMENT ID		TECN	COMMENT
9999.0±3.5 $^{+2.8}_{-1.9}$	26k	[1] MIZUK	12	BELL	$e^+e^- \to \gamma\pi^+\pi^-$ + hadrons
• • • We do not use the following data for averages, fits, limits, etc. • • •					
9974.6±2.3±2.1	11 ± 4	[2,3] DOBBS	12		$\Upsilon(2S) \to \gamma$ hadrons

[1] Assuming $\Gamma_{\eta_b(2S)} = 4.9$ MeV. Not independent of the corresponding mass difference measurement.
[2] Obtained by analyzing CLEO III data but not authored by the CLEO Collaboration.
[3] Assuming $\Gamma_{\eta_b(2S)} = 5$ MeV. Not independent of the corresponding mass difference measurement.

$m_{\Upsilon(2S)} - m_{\eta_b(2S)}$

VALUE (MeV)	EVTS	DOCUMENT ID		TECN	COMMENT
24.3±3.5 $^{+2.8}_{-1.9}$	26k	[4] MIZUK	12	BELL	$e^+e^- \to \gamma\pi^+\pi^-$ + hadrons
• • • We do not use the following data for averages, fits, limits, etc. • • •					
48.7±2.3±2.1	11 ± 4	[5,6] DOBBS	12		$\Upsilon(2S) \to \gamma$ hadrons

[4] Assuming $\Gamma_{\eta_b(2S)} = 4.9$ MeV. Not independent of the corresponding mass measurement.
[5] Obtained by analyzing CLEO III data but not authored by the CLEO Collaboration.
[6] Assuming $\Gamma_{\eta_b(2S)} = 5$ MeV. Not independent of the corresponding mass measurement.

$\eta_b(2S)$ WIDTH

VALUE (MeV)	CL%	DOCUMENT ID		TECN	COMMENT
<24	90	MIZUK	12	BELL	$e^+e^- \to \gamma\pi^+\pi^-$ hadrons

Meson Particle Listings

$\eta_b(2S)$, $\Upsilon(2S)$

$\eta_b(2S)$ DECAY MODES

	Mode	Fraction (Γ_i/Γ)
Γ_1	hadrons	seen

$\eta_b(2S)$ BRANCHING RATIOS

Γ(hadrons)/Γ_{total} — **Γ_1/Γ**

VALUE	EVTS	DOCUMENT ID		TECN	COMMENT
seen	26k	MIZUK	12	BELL	$e^+e^- \to \gamma\pi^+\pi^-$ hadrons
• • • We do not use the following data for averages, fits, limits, etc. • • •					
seen		[7] DOBBS	12		$\Upsilon(2S) \to \gamma$ hadrons

[7] Obtained by analyzing CLEO III data but not authored by the CLEO Collaboration.

$\eta_b(2S)$ REFERENCES

DOBBS 12 PRL 109 082001 S. Dobbs *et al.*
MIZUK 12 PRL 109 232002 R. Mizuk *et al.* (BELLE Collab.)

$\Upsilon(2S)$

$I^G(J^{PC}) = 0^-(1^{--})$

$\Upsilon(2S)$ MASS

VALUE (MeV)	DOCUMENT ID		TECN	COMMENT
10023.26±0.31 OUR AVERAGE				
10023.5 ±0.5	[1] ARTAMONOV	00	MD1	$e^+e^- \to$ hadrons
10023.1 ±0.4	BARBER	84	REDE	$e^+e^- \to$ hadrons
• • • We do not use the following data for averages, fits, limits, etc. • • •				
10023.6 ±0.5	[2,3] BARU	86B	REDE	$e^+e^- \to$ hadrons

[1] Reanalysis of BARU 86B using new electron mass (COHEN 87).
[2] Reanalysis of ARTAMONOV 84.
[3] Superseded by ARTAMONOV 00.

$m_{\Upsilon(3S)} - m_{\Upsilon(2S)}$

VALUE (MeV)	DOCUMENT ID		TECN	COMMENT
331.50±0.02±0.13	LEES	11C	BABR	$e^+e^- \to \pi^+\pi^- X$

$\Upsilon(2S)$ WIDTH

VALUE (keV)	DOCUMENT ID
31.98±2.63 OUR EVALUATION	See the Note on "Width Determinations of the Υ States"

$\Upsilon(2S)$ DECAY MODES

	Mode	Fraction (Γ_i/Γ)	Scale factor/ Confidence level
Γ_1	$\Upsilon(1S)\pi^+\pi^-$	(17.85± 0.26) %	
Γ_2	$\Upsilon(1S)\pi^0\pi^0$	(8.6 ± 0.4) %	
Γ_3	$\tau^+\tau^-$	(2.00± 0.21) %	
Γ_4	$\mu^+\mu^-$	(1.93± 0.17) %	S=2.2
Γ_5	e^+e^-	(1.91± 0.16) %	
Γ_6	$\Upsilon(1S)\pi^0$	< 4 $\times 10^{-5}$	CL=90%
Γ_7	$\Upsilon(1S)\eta$	(2.9 ± 0.4) $\times 10^{-4}$	S=2.0
Γ_8	$J/\psi(1S)$ anything	< 6 $\times 10^{-3}$	CL=90%
Γ_9	$\overline{d}$ anything	(3.4 ± 0.6) $\times 10^{-5}$	
Γ_{10}	hadrons	(94 ±11) %	
Γ_{11}	ggg	(58.8 ± 1.2) %	
Γ_{12}	γgg	(8.8 ± 1.1) %	
Γ_{13}	ϕK^+K^-	(1.6 ± 0.4) $\times 10^{-6}$	
Γ_{14}	$\omega\pi^+\pi^-$	< 2.58 $\times 10^{-6}$	CL=90%
Γ_{15}	$K^*(892)^0 K^-\pi^+$ + c.c.	(2.3 ± 0.7) $\times 10^{-6}$	
Γ_{16}	$\phi f_2'(1525)$	< 1.33 $\times 10^{-6}$	CL=90%
Γ_{17}	$\omega f_2(1270)$	< 5.7 $\times 10^{-7}$	CL=90%
Γ_{18}	$\rho(770)a_2(1320)$	< 8.8 $\times 10^{-7}$	CL=90%
Γ_{19}	$K^*(892)^0\overline{K}_2^*(1430)^0$ + c.c.	(1.5 ± 0.6) $\times 10^{-6}$	
Γ_{20}	$K_1(1270)^\pm K^\mp$	< 3.22 $\times 10^{-6}$	CL=90%
Γ_{21}	$K_1(1400)^\pm K^\mp$	< 8.3 $\times 10^{-7}$	CL=90%
Γ_{22}	$b_1(1235)^\pm\pi^\mp$	< 4.0 $\times 10^{-7}$	CL=90%
Γ_{23}	$\rho\pi$	< 1.16 $\times 10^{-6}$	CL=90%
Γ_{24}	$\pi^+\pi^-\pi^0$	< 8.0 $\times 10^{-7}$	CL=90%
Γ_{25}	$\omega\pi^0$	< 1.63 $\times 10^{-6}$	CL=90%
Γ_{26}	$\pi^+\pi^-\pi^0\pi^0$	(1.30± 0.28) $\times 10^{-5}$	
Γ_{27}	$K_S^0 K^+\pi^-$ + c.c.	(1.14± 0.33) $\times 10^{-6}$	
Γ_{28}	$K^*(892)^0\overline{K}^0$ + c.c.	< 4.22 $\times 10^{-6}$	CL=90%
Γ_{29}	$K^*(892)^- K^+$ + c.c.	< 1.45 $\times 10^{-6}$	CL=90%
Γ_{30}	Sum of 100 exclusive modes	(2.90± 0.30) $\times 10^{-3}$	

Radiative decays

Γ_{31}	$\gamma\chi_{b1}(1P)$	(6.9 ± 0.4) %		
Γ_{32}	$\gamma\chi_{b2}(1P)$	(7.15± 0.35) %		
Γ_{33}	$\gamma\chi_{b0}(1P)$	(3.8 ± 0.4) %		
Γ_{34}	$\gamma f_0(1710)$	< 5.9	$\times 10^{-4}$	CL=90%
Γ_{35}	$\gamma f_2'(1525)$	< 5.3	$\times 10^{-4}$	CL=90%
Γ_{36}	$\gamma f_2(1270)$	< 2.41	$\times 10^{-4}$	CL=90%
Γ_{37}	$\gamma f_J(2220)$			
Γ_{38}	$\gamma\eta_c(1S)$	< 2.7	$\times 10^{-5}$	CL=90%
Γ_{39}	$\gamma\chi_{c0}$	< 1.0	$\times 10^{-4}$	CL=90%
Γ_{40}	$\gamma\chi_{c1}$	< 3.6	$\times 10^{-6}$	CL=90%
Γ_{41}	$\gamma\chi_{c2}$	< 1.5	$\times 10^{-5}$	CL=90%
Γ_{42}	$\gamma X(3872) \to \pi^+\pi^- J/\psi$	< 8	$\times 10^{-7}$	CL=90%
Γ_{43}	$\gamma X(3872) \to \pi^+\pi^-\pi^0 J/\psi$	< 2.4	$\times 10^{-6}$	CL=90%
Γ_{44}	$\gamma\chi_{c0}(2P) \to \omega J/\psi$	< 2.8	$\times 10^{-6}$	CL=90%
Γ_{45}	$\gamma X(4140) \to \phi J/\psi$	< 1.2	$\times 10^{-6}$	CL=90%
Γ_{46}	$\gamma X(4350) \to \phi J/\psi$	< 1.3	$\times 10^{-6}$	CL=90%
Γ_{47}	$\gamma\eta_b(1S)$	(3.9 ± 1.5)	$\times 10^{-4}$	
Γ_{48}	$\gamma\eta_b(1S) \to \gamma$ Sum of 26 exclusive modes	< 3.7	$\times 10^{-6}$	CL=90%
Γ_{49}	$\gamma X_{b\overline{b}} \to \gamma$ Sum of 26 exclusive modes	< 4.9	$\times 10^{-6}$	CL=90%
Γ_{50}	$\gamma X \to \gamma + \geq 4$ prongs	[a] < 1.95	$\times 10^{-4}$	CL=95%
Γ_{51}	$\gamma A^0 \to \gamma$ hadrons	< 8	$\times 10^{-5}$	CL=90%
Γ_{52}	$\gamma a_1^0 \to \gamma\mu^+\mu^-$	< 8.3	$\times 10^{-6}$	CL=90%

Lepton Family number (LF) violating modes

Γ_{53}	$e^\pm\tau^\mp$	LF	< 3.2	$\times 10^{-6}$	CL=90%
Γ_{54}	$\mu^\pm\tau^\mp$	LF	< 3.3	$\times 10^{-6}$	CL=90%

[a] 1.5 GeV < m_X < 5.0 GeV

CONSTRAINED FIT INFORMATION

An overall fit to 3 branching ratios uses 13 measurements and one constraint to determine 3 parameters. The overall fit has a χ^2 = 11.8 for 11 degrees of freedom.

The following *off-diagonal* array elements are the correlation coefficients $\langle \delta x_i \delta x_j \rangle / (\delta x_i \cdot \delta x_j)$, in percent, from the fit to the branching fractions, $x_i \equiv \Gamma_i/\Gamma_{total}$. The fit constrains the x_i whose labels appear in this array to sum to one.

x_7 | 2

x_1

$\Upsilon(2S)$ Γ(i)$\Gamma(e^+e^-)/\Gamma$(total)

$\Gamma(\mu^+\mu^-) \times \Gamma(e^+e^-)/\Gamma_{total}$ — **$\Gamma_4\Gamma_5/\Gamma$**

VALUE (eV)	DOCUMENT ID		TECN	COMMENT
6.5±1.5±1.0	KOBEL	92	CBAL	$e^+e^- \to \mu^+\mu^-$

$\Gamma(\Upsilon(1S)\pi^+\pi^-) \times \Gamma(e^+e^-)/\Gamma_{total}$ — **$\Gamma_1\Gamma_5/\Gamma$**

VALUE (eV)	EVTS	DOCUMENT ID		TECN	COMMENT
105.4±1.0±4.2	11.8K	[1] AUBERT	08BP	BABR	10.58 $e^+e^- \to \gamma\pi^+\pi^-\ell^+\ell^-$

[1] Using B($\Upsilon(1S) \to e^+e^-$) = (2.38 ± 0.11)% and B($\Upsilon(1S) \to \mu^+\mu^-$) = (2.48 ± 0.05)%.

Γ(hadrons) × $\Gamma(e^+e^-)/\Gamma_{total}$ — **$\Gamma_{10}\Gamma_5/\Gamma$**

VALUE (keV)	DOCUMENT ID		TECN	COMMENT
0.577±0.009 OUR AVERAGE				
0.581±0.004±0.009	[1] ROSNER	06	CLEO	10.0 $e^+e^- \to$ hadrons
0.552±0.031±0.017	[1] BARU	96	MD1	$e^+e^- \to$ hadrons
0.54 ±0.04 ±0.02	[1] JAKUBOWSKI	88	CBAL	$e^+e^- \to$ hadrons
0.58 ±0.03 ±0.04	[2] GILES	84B	CLEO	$e^+e^- \to$ hadrons
0.60 ±0.12 ±0.07	[2] ALBRECHT	82	DASP	$e^+e^- \to$ hadrons
0.54 ±0.07 $^{+0.09}_{-0.05}$	[2] NICZYPORUK	81C	LENA	$e^+e^- \to$ hadrons
0.41 ±0.18	[2] BOCK	80	CNTR	$e^+e^- \to$ hadrons

[1] Radiative corrections evaluated following KURAEV 85.
[2] Radiative corrections reevaluated by BUCHMUELLER 88 following KURAEV 85.

$\Upsilon(2S)$ PARTIAL WIDTHS

$\Gamma(e^+e^-)$ — **Γ_5**

VALUE (keV)	DOCUMENT ID
0.612±0.011 OUR EVALUATION	

$\Upsilon(2S)$ BRANCHING RATIOS

$\Gamma(\Upsilon(1S)\pi^+\pi^-)/\Gamma_{total}$ Γ_1/Γ

Abbreviation MM in the *COMMENT* field below stands for missing mass.

VALUE (units 10^{-2})	EVTS	DOCUMENT ID		TECN	COMMENT
17.85±0.26 OUR FIT					
17.92±0.26 OUR AVERAGE					
16.8 ±1.1 ±1.3	906k	[1] LEES	11C	BABR	$e^+e^- \to \pi^+\pi^- X$
17.80±0.05±0.37	170k	[2] LEES	11L	BABR	$\Upsilon(2S) \to \pi^+\pi^-\mu^+\mu^-$
18.02±0.02±0.61	851k	[3] BHARI	09	CLEO	$e^+e^- \to \pi^+\pi^-$ MM
17.22±0.17±0.75	11.8K	[4] AUBERT	08BP	BABR	$e^+e^- \to \gamma\pi^+\pi^-\ell^+\ell^-$
19.2 ±0.2 ±1.0	52.6k	[5] ALEXANDER	98	CLE2	$\pi^+\pi^-\ell^+\ell^-, \pi^+\pi^-$ MM
18.1 ±0.5 ±1.0	11.6k	ALBRECHT	87	ARG	$e^+e^- \to \pi^+\pi^-$ MM
16.9 ±4.0		GELPHMAN	85	CBAL	$e^+e^- \to e^+e^-\pi^+\pi^-$
19.1 ±1.2 ±0.6		BESSON	84	CLEO	$\pi^+\pi^-$ MM
18.9 ±2.6		FONSECA	84	CUSB	$e^+e^- \to \ell^+\ell^-\pi^+\pi^-$
21 ±7	7	NICZYPORUK	81B	LENA	$e^+e^- \to \ell^+\ell^-\pi^+\pi^-$

[1] LEES 11C reports $[\Gamma(\Upsilon(2S) \to \Upsilon(1S)\pi^+\pi^-)/\Gamma_{total}] \times [B(\Upsilon(3S) \to \Upsilon(2S)\text{anything})] = (1.78 \pm 0.02 \pm 0.11) \times 10^{-2}$ which we divide by our best value $B(\Upsilon(3S) \to \Upsilon(2S)\text{anything}) = (10.6 \pm 0.8) \times 10^{-2}$. Our first error is their experiment's error and our second error is the systematic error from using our best value.

[2] Using $B(\Upsilon(1S) \to \mu^+\mu^-) = (2.48 \pm 0.05)\%$.

[3] A weighted average of the inclusive and exclusive results.

[4] Using $B(\Upsilon(2S) \to e^+e^-) = (1.91 \pm 0.16)\%$, $B(\Upsilon(2S) \to \mu^+\mu^-) = (1.93 \pm 0.17)\%$ and, $\Gamma_{ee}(\Upsilon(2S)) = 0.612 \pm 0.011$ keV.

[5] Using $B(\Upsilon(1S) \to e^+e^-) = (2.52 \pm 0.17)\%$ and $B(\Upsilon(1S) \to \mu^+\mu^-) = (2.48 \pm 0.07)\%$.

$\Gamma(\Upsilon(1S)\pi^0\pi^0)/\Gamma_{total}$ Γ_2/Γ

VALUE (units 10^{-2})	EVTS	DOCUMENT ID		TECN	COMMENT
8.6 ±0.4 OUR AVERAGE					
8.43±0.16±0.42	38k	[1] BHARI	09	CLEO	$e^+e^- \to \pi^0\pi^0\ell^+\ell^-$
9.2 ±0.6 ±0.8	275	[2] ALEXANDER	98	CLE2	$e^+e^- \to \pi^0\pi^0\ell^+\ell^-$
9.5 ±1.9 ±1.9	25	ALBRECHT	87	ARG	$e^+e^- \to \pi^0\pi^0\ell^+\ell^-$
8.0 ±1.5		GELPHMAN	85	CBAL	$e^+e^- \to \pi^0\pi^0\ell^+\ell^-$
10.3 ±2.3		FONSECA	84	CUSB	$e^+e^- \to \pi^0\pi^0\ell^+\ell^-$

[1] Authors assume $B(\Upsilon(1S) \to e^+e^-) + B(\Upsilon(1S) \to \mu^+\mu^-) = 4.96\%$.

[2] Using $B(\Upsilon(1S) \to e^+e^-) = (2.52 \pm 0.17)\%$ and $B(\Upsilon(1S) \to \mu^+\mu^-) = (2.48 \pm 0.07)\%$.

$\Gamma(\Upsilon(1S)\pi^0\pi^0)/\Gamma(\Upsilon(1S)\pi^+\pi^-)$ Γ_2/Γ_1

VALUE	DOCUMENT ID		TECN	COMMENT
• • • We do not use the following data for averages, fits, limits, etc. • • •				
0.462±0.037	[1] BHARI	09	CLEO	$e^+e^- \to \Upsilon(2S)$

[1] Not independent of other values reported by BHARI 09.

$\Gamma(\tau^+\tau^-)/\Gamma_{total}$ Γ_3/Γ

VALUE (units 10^{-2})	EVTS	DOCUMENT ID		TECN	COMMENT
2.00±0.21 OUR AVERAGE					
2.00±0.12±0.18	22k	[1] BESSON	07	CLEO	$e^+e^- \to \Upsilon(2S) \to \tau^+\tau^-$
1.7 ±1.5 ±0.6		HAAS	84B	CLEO	$e^+e^- \to \tau^+\tau^-$

[1] BESSON 07 reports $[\Gamma(\Upsilon(2S) \to \tau^+\tau^-)/\Gamma_{total}] / [B(\Upsilon(2S) \to \mu^+\mu^-)] = 1.04 \pm 0.04 \pm 0.05$ which we multiply by our best value $B(\Upsilon(2S) \to \mu^+\mu^-) = (1.93 \pm 0.17) \times 10^{-2}$. Our first error is their experiment's error and our second error is the systematic error from using our best value.

$\Gamma(\mu^+\mu^-)/\Gamma_{total}$ Γ_4/Γ

VALUE	CL%	EVTS	DOCUMENT ID		TECN	COMMENT
0.0193±0.0017 OUR AVERAGE Error includes scale factor of 2.2. See the ideogram below.						
0.0203±0.0003±0.0008		120k	ADAMS	05	CLEO	$e^+e^- \to \mu^+\mu^-$
0.0122±0.0028±0.0019			[1] KOBEL	92	CBAL	$e^+e^- \to \mu^+\mu^-$
0.0138±0.0025±0.0015			KAARSBERG	89	CSB2	$e^+e^- \to \mu^+\mu^-$
0.009 ±0.006 ±0.006			[2] ALBRECHT	85	ARG	$e^+e^- \to \mu^+\mu^-$
0.018 ±0.008 ±0.005			HAAS	84B	CLEO	$e^+e^- \to \mu^+\mu^-$
• • • We do not use the following data for averages, fits, limits, etc. • • •						
<0.038	90		NICZYPORUK	81C	LENA	$e^+e^- \to \mu^+\mu^-$

[1] Taking into account interference between the resonance and continuum.

[2] Re-evaluated using $B(\Upsilon(1S) \to \mu^+\mu^-) = 0.026$.

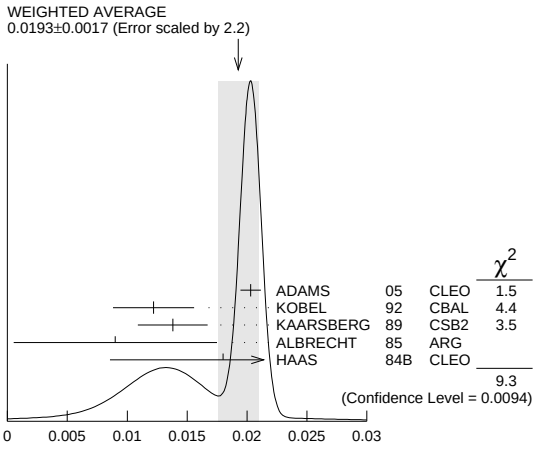

$\Gamma(\tau^+\tau^-)/\Gamma(\mu^+\mu^-)$ Γ_3/Γ_4

VALUE	EVTS	DOCUMENT ID		TECN	COMMENT
1.04±0.04±0.05	22k	BESSON	07	CLEO	$e^+e^- \to \Upsilon(2S)$

$\Gamma(\Upsilon(1S)\pi^0)/\Gamma_{total}$ Γ_6/Γ

VALUE (units 10^{-5})	CL%	DOCUMENT ID		TECN	COMMENT
• • • We do not use the following data for averages, fits, limits, etc. • • •					
< 4	90	[1] TAMPONI	13	BELL	$e^+e^- \to \Upsilon(1S)\pi^0$
< 18	90	[2] HE	08A	CLEO	$e^+e^- \to \ell^+\ell^-\gamma\gamma$
<110	90	ALEXANDER	98	CLE2	$e^+e^- \to \ell^+\ell^-\gamma\gamma$
<800	90	LURZ	87	CBAL	$e^+e^- \to \ell^+\ell^-\gamma\gamma$

[1] TAMPONI 13 reports $[\Gamma(\Upsilon(2S) \to \Upsilon(1S)\pi^0)/\Gamma_{total}] / [B(\Upsilon(2S) \to \Upsilon(1S)\pi^+\pi^-)] < 2.3 \times 10^{-4}$ which we multiply by our best value $B(\Upsilon(2S) \to \Upsilon(1S)\pi^+\pi^-) = 17.85 \times 10^{-2}$.

[2] Authors assume $B(\Upsilon(1S) \to e^+e^-) + B(\Upsilon(1S) \to \mu^+\mu^-) = 4.96\%$.

$\Gamma(\Upsilon(1S)\pi^0)/\Gamma(\Upsilon(1S)\pi^+\pi^-)$ Γ_6/Γ_1

VALUE (units 10^{-4})	CL%	DOCUMENT ID		TECN	COMMENT
<2.3	90	TAMPONI	13	BELL	$e^+e^- \to \Upsilon(1S)\pi^0$

$\Gamma(\Upsilon(1S)\eta)/\Gamma_{total}$ Γ_7/Γ

VALUE (units 10^{-4})	CL%	EVTS	DOCUMENT ID		TECN	COMMENT
2.9 ±0.4 OUR FIT Error includes scale factor of 2.0.						
2.9 ±0.4 OUR AVERAGE Error includes scale factor of 1.9. See the ideogram below.						
2.39±0.31±0.14		112	[1] LEES	11L	BABR	$\Upsilon(2S) \to \ell^+\ell^-\eta$
2.1 $^{+0.7}_{-0.6}$ ±0.3		14	[2] HE	08A	CLEO	$e^+e^- \to \ell^+\ell^-\eta$
• • • We use the following data for averages but not for fits. • • •						
3.55±0.32±0.05		241	[3] TAMPONI	13	BELL	$e^+e^- \to \Upsilon(1S)\eta$
• • • We do not use the following data for averages, fits, limits, etc. • • •						
< 9	90		[1,4] AUBERT	08BP	BABR	$e^+e^- \to \gamma\pi^+\pi^-\pi^0\ell^+\ell^-$
< 28	90		ALEXANDER	98	CLE2	$e^+e^- \to \ell^+\ell^-\eta$
< 50	90		ALBRECHT	87	ARG	$e^+e^- \to \pi^+\pi^-\ell^+\ell^-$ MM
< 70	90		LURZ	87	CBAL	$e^+e^- \to \ell^+\ell^-(\gamma\gamma, 3\pi^0)$
< 100	90		BESSON	84	CLEO	$e^+e^- \to \pi^+\pi^-\ell^+\ell^-$ MM
< 20	90		FONSECA	84	CUSB	$e^+e^- \to \ell^+\ell^-(\gamma\gamma, \pi^+\pi^-\pi^0)$

[1] Using $B(\Upsilon(1S) \to e^+e^-) = (2.38 \pm 0.11)\%$ and $B(\Upsilon(1S) \to \mu^+\mu^-) = (2.48 \pm 0.05)\%$.

[2] Authors assume $B(\Upsilon(1S) \to e^+e^-) + B(\Upsilon(1S) \to \mu^+\mu^-) = 4.96\%$.

[3] TAMPONI 13 reports $[\Gamma(\Upsilon(2S) \to \Upsilon(1S)\eta)/\Gamma_{total}] / [B(\Upsilon(2S) \to \Upsilon(1S)\pi^+\pi^-)] = (1.99 \pm 0.14 \pm 0.11) \times 10^{-3}$ which we multiply by our best value $B(\Upsilon(2S) \to \Upsilon(1S)\pi^+\pi^-) = (17.85 \pm 0.26) \times 10^{-2}$. Our first error is their experiment's error and our second error is the systematic error from using our best value.

[4] Using $\Gamma_{ee}(\Upsilon(2S)) = 0.612 \pm 0.011$ keV.

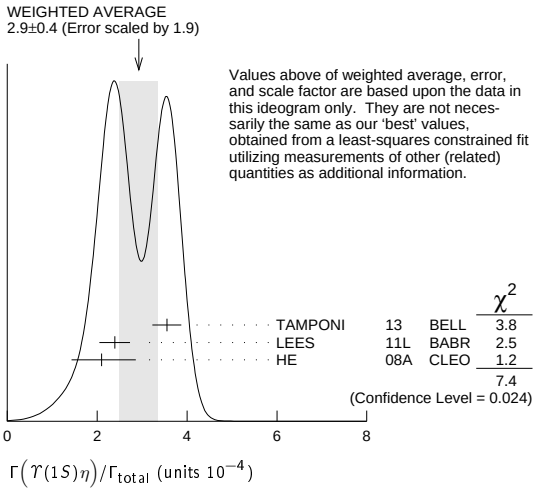

$\Gamma(\Upsilon(1S)\eta)/\Gamma(\Upsilon(1S)\pi^+\pi^-)$ Γ_7/Γ_1

VALUE (units 10^{-3})	CL%	EVTS	DOCUMENT ID		TECN	COMMENT
1.64±0.25 OUR FIT			Error includes scale factor of 2.0.			
1.99±0.14±0.11		241	TAMPONI	13	BELL	$e^+e^- \to \Upsilon(1S)\eta$
• • • We do not use the following data for averages, fits, limits, etc. • • •						
1.35±0.17±0.08			[1] LEES	11L	BABR	$\Upsilon(2S) \to (\pi^+\pi^-)(\gamma\gamma)\mu^+\mu^-$
< 5.2	90		[2] AUBERT	08BP	BABR	$e^+e^- \to \gamma\pi^+\pi^-(\pi^0)\ell^+\ell^-$

[1] Not independent of other values reported by LEES 11L.
[2] Not independent of other values reported by AUBERT 08BP.

$\Gamma(\Upsilon(1S)\pi^0)/\Gamma(\Upsilon(1S)\eta)$ Γ_6/Γ_7

VALUE	CL%	DOCUMENT ID		TECN	COMMENT
• • • We do not use the following data for averages, fits, limits, etc. • • •					
<0.13	90	TAMPONI	13	BELL	$e^+e^- \to \Upsilon(1S)\pi^0$

$\Gamma(J/\psi(1S)\text{ anything})/\Gamma_{\text{total}}$ Γ_8/Γ

VALUE	CL%	DOCUMENT ID		TECN	COMMENT
<0.006	90	MASCHMANN	90	CBAL	$e^+e^- \to$ hadrons

$\Gamma(\overline{d}\text{ anything})/\Gamma_{\text{total}}$ Γ_9/Γ

VALUE (units 10^{-5})	EVTS	DOCUMENT ID		TECN	COMMENT
3.37±0.50±0.25	58	ASNER	07	CLEO	$e^+e^- \to \overline{d}X$

$\Gamma(ggg)/\Gamma_{\text{total}}$ Γ_{11}/Γ

VALUE (units 10^{-2})	EVTS	DOCUMENT ID		TECN	COMMENT
58.8±1.2	6M	[1] BESSON	06A	CLEO	$\Upsilon(2S) \to$ hadrons

[1] Calculated using the value $\Gamma(\gamma gg)/\Gamma(ggg) = (3.18 \pm 0.04 \pm 0.22 \pm 0.41)\%$ from BESSON 06A and PDG 08 values of $B(\pi^+\pi^-\Upsilon(1S)) = (18.1\pm0.4)\%$, $B(\pi^0\pi^0\Upsilon(1S)) = (8.6\pm0.4)\%$, $B(\mu^+\mu^-) = (1.93\pm0.17)\%$, and $R_{\text{hadrons}} = 3.51$. The statistical error is negligible and the systematic error is partially correlated with that of $\Gamma(\gamma gg)/\Gamma_{\text{total}}$ measurement of BESSON 06A.

$\Gamma(\phi K^+K^-)/\Gamma_{\text{total}}$ Γ_{13}/Γ

VALUE (units 10^{-6})	EVTS	DOCUMENT ID		TECN	COMMENT
1.58±0.33±0.18	58	SHEN	12A	BELL	$\Upsilon(1S) \to 2(K^+K^-)$

$\Gamma(\omega\pi^+\pi^-)/\Gamma_{\text{total}}$ Γ_{14}/Γ

VALUE (units 10^{-6})	CL%	DOCUMENT ID		TECN	COMMENT
<2.58	90	SHEN	12A	BELL	$\Upsilon(1S) \to 2(\pi^+\pi^-)\pi^0$

$\Gamma(K^*(892)^0K^-\pi^+ + \text{c.c.})/\Gamma_{\text{total}}$ Γ_{15}/Γ

VALUE (units 10^{-6})	EVTS	DOCUMENT ID		TECN	COMMENT
2.32±0.40±0.54	135	SHEN	12A	BELL	$\Upsilon(1S) \to K^+K^-\pi^+\pi^-$

$\Gamma(\phi f_2'(1525))/\Gamma_{\text{total}}$ Γ_{16}/Γ

VALUE (units 10^{-6})	CL%	DOCUMENT ID		TECN	COMMENT
<1.33	90	SHEN	12A	BELL	$\Upsilon(1S) \to 2(K^+K^-)$

$\Gamma(\omega f_2(1270))/\Gamma_{\text{total}}$ Γ_{17}/Γ

VALUE (units 10^{-6})	CL%	DOCUMENT ID		TECN	COMMENT
<0.57	90	SHEN	12A	BELL	$\Upsilon(1S) \to 2(\pi^+\pi^-)\pi^0$

$\Gamma(\rho(770)a_2(1320))/\Gamma_{\text{total}}$ Γ_{18}/Γ

VALUE (units 10^{-6})	CL%	DOCUMENT ID		TECN	COMMENT
<0.88	90	SHEN	12A	BELL	$\Upsilon(1S) \to 2(\pi^+\pi^-)\pi^0$

$\Gamma(K^*(892)^0\overline{K}_2^*(1430)^0 + \text{c.c.})/\Gamma_{\text{total}}$ Γ_{19}/Γ

VALUE (units 10^{-6})	EVTS	DOCUMENT ID		TECN	COMMENT
1.53±0.52±0.19	32	SHEN	12A	BELL	$\Upsilon(1S) \to K^+K^-\pi^+\pi^-$

$\Gamma(K_1(1270)^\pm K^\mp)/\Gamma_{\text{total}}$ Γ_{20}/Γ

VALUE (units 10^{-6})	CL%	DOCUMENT ID		TECN	COMMENT
<3.22	90	SHEN	12A	BELL	$\Upsilon(1S) \to K^+K^-\pi^+\pi^-$

$\Gamma(K_1(1400)^\pm K^\mp)/\Gamma_{\text{total}}$ Γ_{21}/Γ

VALUE (units 10^{-6})	CL%	DOCUMENT ID		TECN	COMMENT
<0.83	90	SHEN	12A	BELL	$\Upsilon(1S) \to K^+K^-\pi^+\pi^-$

$\Gamma(b_1(1235)^\pm\pi^\mp)/\Gamma_{\text{total}}$ Γ_{22}/Γ

VALUE (units 10^{-6})	CL%	DOCUMENT ID		TECN	COMMENT
<0.40	90	SHEN	12A	BELL	$\Upsilon(1S) \to 2(\pi^+\pi^-)\pi^0$

$\Gamma(\gamma gg)/\Gamma_{\text{total}}$ Γ_{12}/Γ

VALUE (units 10^{-2})	EVTS	DOCUMENT ID		TECN	COMMENT
8.79±1.05	100k	[1] BESSON	06A	CLEO	$\Upsilon(2S) \to \gamma +$ hadrons

[1] Calculated using BESSON 06A values of $\Gamma(\gamma gg)/\Gamma(ggg) = (3.18\pm0.04\pm0.22\pm0.41)\%$ and $\Gamma(ggg)/\Gamma_{\text{total}}$. The statistical error is negligible and the systematic error is partially correlated with that of $\Gamma(ggg)/\Gamma_{\text{total}}$ measurement of BESSON 06A.

$\Gamma(\gamma gg)/\Gamma(ggg)$ Γ_{12}/Γ_{11}

VALUE (units 10^{-2})	EVTS	DOCUMENT ID		TECN	COMMENT
3.18±0.04±0.47	6M	BESSON	06A	CLEO	$\Upsilon(2S) \to (\gamma +)$ hadrons

$\Gamma(\rho\pi)/\Gamma_{\text{total}}$ Γ_{23}/Γ

VALUE (units 10^{-6})	CL%	DOCUMENT ID		TECN	COMMENT
<1.16	90	SHEN	13	BELL	$\Upsilon(2S) \to \pi^+\pi^-\pi^0$

$\Gamma(\pi^+\pi^-\pi^0)/\Gamma_{\text{total}}$ Γ_{24}/Γ

VALUE (units 10^{-6})	CL%	DOCUMENT ID		TECN	COMMENT
<0.80	90	SHEN	13	BELL	$\Upsilon(2S) \to \pi^+\pi^-\pi^0$

$\Gamma(\omega\pi^0)/\Gamma_{\text{total}}$ Γ_{25}/Γ

VALUE (units 10^{-6})	CL%	DOCUMENT ID		TECN	COMMENT
<1.63	90	SHEN	13	BELL	$\Upsilon(2S) \to \pi^+\pi^-\pi^0\pi^0$

$\Gamma(\pi^+\pi^-\pi^0\pi^0)/\Gamma_{\text{total}}$ Γ_{26}/Γ

VALUE (units 10^{-6})	EVTS	DOCUMENT ID		TECN	COMMENT
13.0±1.9±2.1	261 ± 37	SHEN	13	BELL	$\Upsilon(2S) \to \pi^+\pi^-\pi^0\pi^0$

$\Gamma(K_S^0K^+\pi^- + \text{c.c.})/\Gamma_{\text{total}}$ Γ_{27}/Γ

VALUE (units 10^{-6})	CL%	EVTS	DOCUMENT ID		TECN	COMMENT
1.14±0.30±0.13		40 ± 10	SHEN	13	BELL	$\Upsilon(2S) \to K_S^0K^-\pi^+$
• • • We do not use the following data for averages, fits, limits, etc. • • •						
<3.2	90		[1] DOBBS	12A		$\Upsilon(2S) \to K_S^0K^-\pi^+$

[1] Obtained by analyzing CLEO III data but not authored by the CLEO Collaboration.

$\Gamma(K^*(892)^0\overline{K}^0 + \text{c.c.})/\Gamma_{\text{total}}$ Γ_{28}/Γ

VALUE (units 10^{-6})	CL%	DOCUMENT ID		TECN	COMMENT
<4.22	90	SHEN	13	BELL	$\Upsilon(2S) \to K_S^0K^-\pi^+$

$\Gamma(K^*(892)^-K^+ + \text{c.c.})/\Gamma_{\text{total}}$ Γ_{29}/Γ

VALUE (units 10^{-6})	CL%	DOCUMENT ID		TECN	COMMENT
<1.45	90	SHEN	13	BELL	$\Upsilon(2S) \to K_S^0K^-\pi^+$

$\Gamma(\text{Sum of 100 exclusive modes})/\Gamma_{\text{total}}$ Γ_{30}/Γ

VALUE (units 10^{-2})	DOCUMENT ID		COMMENT
0.29±0.03	[1,2] DOBBS	12A	$\Upsilon(2S) \to$ hadrons

[1] DOBBS 12A presents individual exclusive branching fractions or upper limits for 100 modes of four to ten pions, kaons, or protons.
[2] Obtained by analyzing CLEO III data but not authored by the CLEO Collaboration.

$\Gamma(\gamma\chi_{b1}(1P))/\Gamma_{\text{total}}$ Γ_{31}/Γ

VALUE	EVTS	DOCUMENT ID		TECN	COMMENT
0.069 ±0.004 OUR AVERAGE					
0.0693±0.0012±0.0041	407k	ARTUSO	05	CLEO	$e^+e^- \to \gamma X$
0.069 ±0.005 ±0.009		EDWARDS	99	CLE2	$\Upsilon(2S) \to \gamma\chi(1P)$
0.091 ±0.018 ±0.022		ALBRECHT	85E	ARG	$e^+e^- \to \gamma$conv. X
0.065 ±0.007 ±0.012		NERNST	85	CBAL	$e^+e^- \to \gamma X$
0.080 ±0.017 ±0.016		HAAS	84	CLEO	$e^+e^- \to \gamma$conv. X
0.059 ±0.014		KLOPFEN...	83	CUSB	$e^+e^- \to \gamma X$

See key on page 547

$\Gamma(\gamma\chi_{b2}(1P))/\Gamma_{total}$ Γ_{32}/Γ

VALUE	EVTS	DOCUMENT ID		TECN	COMMENT
0.0715±0.0035 OUR AVERAGE					
0.0724±0.0011±0.0040	410k	ARTUSO	05	CLEO	$e^+e^- \to \gamma X$
0.074 ±0.005 ±0.008		EDWARDS	99	CLE2	$\Upsilon(2S) \to \gamma\chi(1P)$
0.098 ±0.021 ±0.024		ALBRECHT	85E	ARG	$e^+e^- \to \gamma$conv. X
0.058 ±0.007 ±0.010		NERNST	85	CBAL	$e^+e^- \to \gamma X$
0.102 ±0.018 ±0.021		HAAS	84	CLEO	$e^+e^- \to \gamma$conv. X
0.061 ±0.014		KLOPFEN...	83	CUSB	$e^+e^- \to \gamma X$

$\Gamma(\gamma\chi_{b0}(1P))/\Gamma_{total}$ Γ_{33}/Γ

VALUE	EVTS	DOCUMENT ID		TECN	COMMENT
0.038 ±0.004 OUR AVERAGE					
0.0375±0.0012±0.0047	198k	ARTUSO	05	CLEO	$e^+e^- \to \gamma X$
0.034 ±0.005 ±0.006		EDWARDS	99	CLE2	$\Upsilon(2S) \to \gamma\chi(1P)$
0.064 ±0.014 ±0.016		ALBRECHT	85E	ARG	$e^+e^- \to \gamma$conv. X
0.036 ±0.008 ±0.009		NERNST	85	CBAL	$e^+e^- \to \gamma X$
0.044 ±0.023 ±0.009		HAAS	84	CLEO	$e^+e^- \to \gamma$conv. X
• • • We do not use the following data for averages, fits, limits, etc. • • •					
0.035 ±0.014		KLOPFEN...	83	CUSB	$e^+e^- \to \gamma X$

$\Gamma(\gamma f_0(1710))/\Gamma_{total}$ Γ_{34}/Γ

VALUE (units 10^{-5})	CL%	DOCUMENT ID		TECN	COMMENT
<59	90	[1] ALBRECHT	89	ARG	$\Upsilon(2S) \to \gamma K^+K^-$
• • • We do not use the following data for averages, fits, limits, etc. • • •					
< 5.9	90	[2] ALBRECHT	89	ARG	$\Upsilon(2S) \to \gamma\pi^+\pi^-$

[1] Re-evaluated assuming $B(f_0(1710) \to K^+K^-) = 0.19$.
[2] Includes unknown branching ratio of $f_0(1710) \to \pi^+\pi^-$.

$\Gamma(\gamma f_2'(1525))/\Gamma_{total}$ Γ_{35}/Γ

VALUE (units 10^{-5})	CL%	DOCUMENT ID		TECN	COMMENT
<53	90	[1] ALBRECHT	89	ARG	$\Upsilon(2S) \to \gamma K^+K^-$

[1] Re-evaluated assuming $B(f_2'(1525) \to K\overline{K}) = 0.71$.

$\Gamma(\gamma f_2(1270))/\Gamma_{total}$ Γ_{36}/Γ

VALUE (units 10^{-5})	CL%	DOCUMENT ID		TECN	COMMENT
<24.1	90	[1] ALBRECHT	89	ARG	$\Upsilon(2S) \to \gamma\pi^+\pi^-$

[1] Using $B(f_2(1270) \to \pi\pi) = 0.84$.

$\Gamma(\gamma f_J(2220))/\Gamma_{total}$ Γ_{37}/Γ

VALUE (units 10^{-5})	CL%	DOCUMENT ID		TECN	COMMENT
• • • We do not use the following data for averages, fits, limits, etc. • • •					
<6.8	90	[1] ALBRECHT	89	ARG	$\Upsilon(2S) \to \gamma K^+K^-$

[1] Includes unknown branching ratio of $f_J(2220) \to K^+K^-$.

$\Gamma(\gamma\eta_c(1S))/\Gamma_{total}$ Γ_{38}/Γ

VALUE	CL%	DOCUMENT ID		TECN	COMMENT
<2.7 × 10⁻⁵	90	WANG	11B	BELL	$\Upsilon(2S) \to \gamma X$

$\Gamma(\gamma\chi_{c0})/\Gamma_{total}$ Γ_{39}/Γ

VALUE	CL%	DOCUMENT ID		TECN	COMMENT
<1.0 × 10⁻⁴	90	WANG	11B	BELL	$\Upsilon(2S) \to \gamma X$

$\Gamma(\gamma\chi_{c1})/\Gamma_{total}$ Γ_{40}/Γ

VALUE	CL%	DOCUMENT ID		TECN	COMMENT
<3.6 × 10⁻⁶	90	WANG	11B	BELL	$\Upsilon(2S) \to \gamma X$

$\Gamma(\gamma\chi_{c2})/\Gamma_{total}$ Γ_{41}/Γ

VALUE	CL%	DOCUMENT ID		TECN	COMMENT
<1.5 × 10⁻⁵	90	WANG	11B	BELL	$\Upsilon(2S) \to \gamma X$

$\Gamma(\gamma X(3872) \to \pi^+\pi^- J/\psi)/\Gamma_{total}$ Γ_{42}/Γ

VALUE	CL%	DOCUMENT ID		TECN	COMMENT
<0.8 × 10⁻⁶	90	WANG	11B	BELL	$\Upsilon(2S) \to \gamma X$

$\Gamma(\gamma X(3872) \to \pi^+\pi^-\pi^0 J/\psi)/\Gamma_{total}$ Γ_{43}/Γ

VALUE	CL%	DOCUMENT ID		TECN	COMMENT
<2.4 × 10⁻⁶	90	WANG	11B	BELL	$\Upsilon(2S) \to \gamma X$

$\Gamma(\gamma\chi_{c0}(2P) \to \omega J/\psi)/\Gamma_{total}$ Γ_{44}/Γ

VALUE	CL%	DOCUMENT ID		TECN	COMMENT
<2.8 × 10⁻⁶	90	WANG	11B	BELL	$\Upsilon(2S) \to \gamma X$

$\Gamma(\gamma X(4140) \to \phi J/\psi)/\Gamma_{total}$ Γ_{45}/Γ

VALUE	CL%	DOCUMENT ID		TECN	COMMENT
<1.2 × 10⁻⁶	90	WANG	11B	BELL	$\Upsilon(2S) \to \gamma X$

$\Gamma(\gamma X(4350) \to \phi J/\psi)/\Gamma_{total}$ Γ_{46}/Γ

VALUE	CL%	DOCUMENT ID		TECN	COMMENT
<1.3 × 10⁻⁶	90	WANG	11B	BELL	$\Upsilon(2S) \to \gamma X$

$\Gamma(\gamma\eta_b(1S))/\Gamma_{total}$ Γ_{47}/Γ

VALUE (units 10^{-4})	CL%	EVTS	DOCUMENT ID		TECN	COMMENT
$3.9\pm1.1^{+1.1}_{-0.9}$		13 ± 5k	[1] AUBERT	09AQ	BABR	$\Upsilon(2S) \to \gamma X$
• • • We do not use the following data for averages, fits, limits, etc. • • •						
<21	90		LEES	11J	BABR	$\Upsilon(2S) \to X\gamma$
< 8.4	90		[1] BONVICINI	10	CLEO	$\Upsilon(2S) \to \gamma X$
< 5.1	90		[2] ARTUSO	05	CLEO	$e^+e^- \to \gamma X$

[1] Assuming $\Gamma_{\eta_b(1S)} = 10$ MeV.
[2] Superseded by BONVICINI 10.

$\Gamma(\gamma\eta_b(1S) \to \gamma$Sum of 26 exclusive modes$)/\Gamma_{total}$ Γ_{48}/Γ

VALUE	CL%	DOCUMENT ID		TECN	COMMENT
<3.7 × 10⁻⁶	90	SANDILYA	13	BELL	$\Upsilon(2S) \to \gamma$ hadrons

$\Gamma(\gamma X_{b\overline{b}} \to \gamma$Sum of 26 exclusive modes$)/\Gamma_{total}$ Γ_{49}/Γ

VALUE (units 10^{-6})	CL%	EVTS	DOCUMENT ID		TECN	COMMENT
< 4.9	90		SANDILYA	13	BELL	$\Upsilon(2S) \to \gamma$ hadrons
• • • We do not use the following data for averages, fits, limits, etc. • • •						
$46.2^{+29.7}_{-14.2}\pm10.6$		10	[1] DOBBS	12		$\Upsilon(2S) \to \gamma$ hadrons

[1] Obtained by analyzing CLEO III data but not authored by the CLEO Collaboration.

$\Gamma(\gamma X \to \gamma+ \geq 4$ prongs$)/\Gamma_{total}$ Γ_{50}/Γ
(1.5 GeV < m_X < 5.0 GeV)

VALUE (units 10^{-4})	CL%	DOCUMENT ID		TECN	COMMENT
<1.95	95	ROSNER	07A	CLEO	$e^+e^- \to \gamma X$

$\Gamma(\gamma A^0 \to \gamma$hadrons$)/\Gamma_{total}$ Γ_{51}/Γ
(0.3 GeV < m_{A^0} < 7 GeV)

VALUE	CL%	DOCUMENT ID		TECN	COMMENT
<8 × 10⁻⁵	90	[1] LEES	11H	BABR	$\Upsilon(2S) \to \gamma$ hadrons

[1] For a narrow scalar or pseudoscalar A^0, excluding known resonances, with mass in the range 0.3–7 GeV. Measured 90% CL limits as a function of m_{A^0} range from 1×10^{-6} to 8×10^{-5}.

$\Gamma(\gamma a_1^0 \to \gamma\mu^+\mu^-)/\Gamma_{total}$ Γ_{52}/Γ

VALUE (units 10^{-6})	CL%	DOCUMENT ID		TECN	COMMENT
<8.3	90	[1] AUBERT	09Z	BABR	$e^+e^- \to \gamma a_1^0 \to \gamma\mu^+\mu^-$

[1] For a narrow scalar or pseudoscalar a_1^0 with mass in the range 212–9300 MeV, excluding J/ψ and $\psi(2S)$. Measured 90% CL limits as a function of $m_{a_1^0}$ range from 0.26–8.3 × 10^{-6}.

LEPTON FAMILY NUMBER (*LF*) VIOLATING MODES

$\Gamma(e^\pm\tau^\mp)/\Gamma_{total}$ Γ_{53}/Γ

VALUE (units 10^{-6})	CL%	DOCUMENT ID		TECN	COMMENT
<3.2	90	LEES	10B	BABR	$e^+e^- \to e^\pm\tau^\mp$

$\Gamma(\mu^\pm\tau^\mp)/\Gamma_{total}$ Γ_{54}/Γ

VALUE (units 10^{-6})	CL%	DOCUMENT ID		TECN	COMMENT
< 3.3	90	LEES	10B	BABR	$e^+e^- \to \mu^\pm\tau^\mp$
• • • We do not use the following data for averages, fits, limits, etc. • • •					
<14.4	95	LOVE	08A	CLEO	$e^+e^- \to \mu^\pm\tau^\mp$

$\Upsilon(2S)$ Cross-Particle Branching Ratios

$B(\Upsilon(2S) \to \pi^+\pi^-) \times B(\Upsilon(3S) \to \Upsilon(2S)X)$

VALUE (units 10^{-2})	EVTS	DOCUMENT ID		TECN	COMMENT
1.78±0.02±0.11	906k	LEES	11C	BABR	$e^+e^- \to \pi^+\pi^- X$

$\Upsilon(2S)$ REFERENCES

SANDILYA	13	PRL 111 112001	S. Sandilya *et al.*	(BELLE Collab.)
SHEN	13	PR D88 011102	C.P. Shen *et al.*	(BELLE Collab.)
TAMPONI	13	PR D87 011104	U. Tamponi *et al.*	(BELLE Collab.)
DOBBS	12	PRL 109 082001	S. Dobbs *et al.*	
DOBBS	12A	PR D86 052003	S. Dobbs *et al.*	
SHEN	12A	PR D86 031102	C.P. Shen *et al.*	(BELLE Collab.)
LEES	11C	PR D84 011104	J.P. Lees *et al.*	(BABAR Collab.)
LEES	11H	PRL 107 221803	J.P. Lees *et al.*	(BABAR Collab.)
LEES	11J	PR D84 072002	J.P. Lees *et al.*	(BABAR Collab.)
LEES	11L	PR D84 092003	J.P. Lees *et al.*	(BABAR Collab.)
WANG	11B	PR D84 071107	X.L. Wang *et al.*	(BELLE Collab.)
BONVICINI	10	PR D81 031104	G. Bonvicini *et al.*	(CLEO Collab.)
LEES	10B	PRL 104 151802	J.P. Lees *et al.*	(BABAR Collab.)
AUBERT	09AQ	PRL 103 161801	B. Aubert *et al.*	(BABAR Collab.)
AUBERT	09Z	PRL 103 081803	B. Aubert *et al.*	(BABAR Collab.)
BHARI	09	PR D79 011103	S.R. Bhari *et al.*	(CLEO Collab.)
AUBERT	08BP	PR D78 112002	B. Aubert *et al.*	(BABAR Collab.)
HE	08A	PRL 101 192001	Q. He *et al.*	(CLEO Collab.)
LOVE	08A	PRL 101 201601	W. Love *et al.*	(CLEO Collab.)
PDG	08	PL B667 1	C. Amsler *et al.*	(PDG Collab.)
ASNER	07	PR D75 012009	D.M. Asner *et al.*	(CLEO Collab.)
BESSON	07	PRL 98 052002	D. Besson *et al.*	(CLEO Collab.)
ROSNER	07A	PR D76 117102	J.L. Rosner *et al.*	(CLEO Collab.)
BESSON	06A	PR D74 012003	D. Besson *et al.*	(CLEO Collab.)
ROSNER	06	PRL 96 092003	J.L. Rosner *et al.*	(CLEO Collab.)

ADAMS	05	PRL 94 012001	G.S. Adams *et al.*	(CLEO Collab.)
ARTUSO	05	PRL 94 032001	M. Artuso *et al.*	(CLEO Collab.)
ARTAMONOV	00	PL B474 427	A.S. Artamonov *et al.*	
EDWARDS	99	PR D59 032003	K.W. Edwards *et al.*	(CLEO Collab.)
ALEXANDER	98	PR D58 052004	J.P. Alexander *et al.*	(CLEO Collab.)
BARU	96	PRPL 267 71	S.E. Baru *et al.*	(NOVO)
KOBEL	92	ZPHY C53 193	M. Kobel *et al.*	(Crystal Ball Collab.)
MASCHMANN	90	ZPHY C46 555	W.S. Maschmann *et al.*	(Crystal Ball Collab.)
ALBRECHT	89	ZPHY C42 349	H. Albrecht *et al.*	(ARGUS Collab.)
KAARSBERG	89	PRL 62 2077	T.M. Kaarsberg *et al.*	(CUSB Collab.)
BUCHMUEL...	88	HE e^+e^- Physics 412 Editors: A. Ali and P. Soeding, World Scientific, Singapore	W. Buchmueller, S. Cooper	(HANN, DESY, MIT)
JAKUBOWSKI	88	ZPHY C40 49	Z. Jakubowski *et al.*	(Crystal Ball Collab.) IGJPC
ALBRECHT	87	ZPHY C35 283	H. Albrecht *et al.*	(ARGUS Collab.)
COHEN	87	RMP 59 1121	E.R. Cohen, B.N. Taylor	(RISC, NBS)
LURZ	87	ZPHY C36 383	B. Lurz *et al.*	(Crystal Ball Collab.)
BARU	86B	ZPHY C32 622 (erratum)	S.E. Baru *et al.*	(NOVO)
ALBRECHT	85	ZPHY C28 45	H. Albrecht *et al.*	(ARGUS Collab.)
ALBRECHT	85E	PL 160B 331	H. Albrecht *et al.*	(ARGUS Collab.)
GELPHMAN	85	PR D32 2893	D. Gelphman *et al.*	(Crystal Ball Collab.)
KURAEV	85	SJNP 41 466 Translated from YAF 41 733.	E.A. Kuraev, V.S. Fadin	(NOVO)
NERNST	85	PRL 54 2195	R. Nernst *et al.*	(Crystal Ball Collab.)
ARTAMONOV	84	PL 137B 272	A.S. Artamonov *et al.*	(NOVO)
BARBER	84	PL 135B 498	D.P. Barber *et al.*	(DESY, ARGUS Collab.+)
BESSON	84	PR D30 1433	D. Besson *et al.*	(CLEO Collab.)
FONSECA	84	NP B242 31	V. Fonseca *et al.*	(CUSB Collab.)
GILES	84B	PR D29 1285	R. Giles *et al.*	(CLEO Collab.)
HAAS	84	PRL 52 799	J. Haas *et al.*	(CLEO Collab.)
HAAS	84B	PR D30 1996	J. Haas *et al.*	(CLEO Collab.)
KLOPFEN...	83	PRL 51 160	C. Klopfenstein *et al.*	(CUSB Collab.)
ALBRECHT	82	PL 116B 383	H. Albrecht *et al.*	(DESY, DORT, HEIDH+)
NICZYPORUK	81B	PL 100B 95	B. Niczyporuk *et al.*	(LENA Collab.)
NICZYPORUK	81C	PL 99B 169	B. Niczyporuk *et al.*	(LENA Collab.)
BOCK	80	ZPHY C6 125	P. Bock *et al.*	(HEIDP, MPIM, DESY, HAMB)

$\Upsilon(1D)$

$I^G(J^{PC}) = 0^-(2^{--})$

First observed by BONVICINI 04 in the decay to $\gamma\gamma\,\Upsilon(1S)$ and confirmed by DEL-AMO-SANCHEZ 10R in the decay to $\pi^+\pi^-\,\Upsilon(1S)$. Data consistent with $J^P = 2^-$. The states with $J = 1$ and 3 also possibly seen, but need confirmation.

$\Upsilon(1D)$ MASS

VALUE (MeV)	EVTS	DOCUMENT ID		TECN	COMMENT
10163.7±1.4 OUR AVERAGE		Error includes scale factor of 1.7.			
10164.5 ± 0.8 ± 0.5		DEL-AMO-SA...10R	BABR		$\Upsilon(3S) \to \gamma\gamma\pi^+\pi^-\ell^+\ell^-$
10161.1 ± 0.6 ± 1.6	38	BONVICINI	04	CLE3	$\Upsilon(3S) \to 4\gamma\ell^+\ell^-$

$\Upsilon(1D)$ DECAY MODES

	Mode	Fraction (Γ_i/Γ)
Γ_1	$\gamma\gamma\,\Upsilon(1S)$	seen
Γ_2	$\gamma\chi_{bJ}(1P)$	seen
Γ_3	$\eta\,\Upsilon(1S)$	not seen
Γ_4	$\pi^+\pi^-\,\Upsilon(1S)$	$(6.6\pm1.6)\times10^{-3}$

$\Upsilon(1D)$ BRANCHING RATIOS

$\Gamma(\eta\,\Upsilon(1S))/\Gamma(\gamma\gamma\,\Upsilon(1S))$ Γ_3/Γ_1

VALUE	CL%	DOCUMENT ID		TECN	COMMENT
<0.25	90	BONVICINI	04	CLE3	$\Upsilon(3S) \to 4\gamma\ell^+\ell^-$

$\Gamma(\pi^+\pi^-\,\Upsilon(1S))/\Gamma_{total}$ Γ_4/Γ

VALUE (units 10^{-2})	DOCUMENT ID		TECN	COMMENT
$0.66^{+0.15}_{-0.14}\pm0.06$	[1] DEL-AMO-SA...10R	BABR		$\Upsilon(3S) \to \gamma\gamma\pi^+\pi^-\ell^+\ell^-$

[1] Using theoretical predictions for $B(\chi_{bJ}(2P) \to \gamma\,\Upsilon(1D))$.

$\Gamma(\pi^+\pi^-\,\Upsilon(1S))/\Gamma(\gamma\gamma\,\Upsilon(1S))$ Γ_4/Γ_1

VALUE	CL%	DOCUMENT ID		TECN	COMMENT
<1.2	90	[2] BONVICINI	04	CLE3	$\Upsilon(3S) \to 4\gamma\ell^+\ell^-$

[2] Assuming $J = 2$.

$\Upsilon(1D)$ REFERENCES

DEL-AMO-SA...	10R	PR D82 111102	P. del Amo Sanchez *et al.*	(BABAR Collab.)
BONVICINI	04	PR D70 032001	G. Bonvicini *et al.*	(CLEO Collab.)

$\chi_{b0}(2P)$

$I^G(J^{PC}) = 0^+(0^{++})$
J needs confirmation.

Observed in radiative decay of the $\Upsilon(3S)$, therefore $C = +$. Branching ratio requires E1 transition, M1 is strongly disfavored, therefore $P = +$.

$\chi_{b0}(2P)$ MASS

VALUE (MeV)	DOCUMENT ID
10232.5±0.4±0.5 OUR EVALUATION	From γ energy below, using $\Upsilon(3S)$ mass = 10355.2 ± 0.5 MeV

γ ENERGY IN $\Upsilon(3S)$ DECAY

VALUE (MeV)	EVTS	DOCUMENT ID		TECN	COMMENT
121.9 ±0.4 OUR EVALUATION		Treating systematic errors as correlated			
122.2 ±0.5 OUR AVERAGE		Error includes scale factor of 1.4. See the ideogram below.			
121.55 ± 0.16 ± 0.46		ARTUSO	05	CLEO	$\Upsilon(3S) \to \gamma X$
123.0 ±0.8	4959	[1] HEINTZ	92	CSB2	$e^+e^- \to \gamma X$
124.6 ±1.4	17	[2] HEINTZ	92	CSB2	$e^+e^- \to \ell^+\ell^-\gamma\gamma$
122.3 ±0.3 ±0.6	9903	MORRISON	91	CLE2	$e^+e^- \to \gamma X$

[1] A systematic uncertainty on the energy scale of 0.9% not included. Supersedes NARAIN 91.
[2] A systematic uncertainty on the energy scale of 0.9% not included. Supersedes HEINTZ 91.

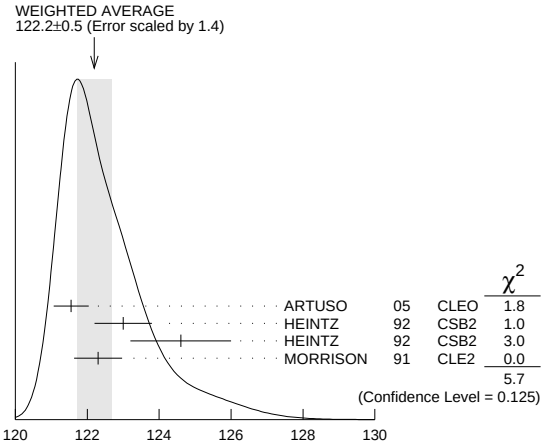

$\chi_{b0}(2P)$ DECAY MODES

	Mode	Fraction (Γ_i/Γ)		Confidence level
Γ_1	$\gamma\,\Upsilon(2S)$	(4.6 ± 2.1) %		
Γ_2	$\gamma\,\Upsilon(1S)$	$(9 \pm 6) \times 10^{-3}$		
Γ_3	D^0X	< 8.2	%	90%
Γ_4	$\pi^+\pi^-K^+K^-\pi^0$	< 3.4	$\times10^{-5}$	90%
Γ_5	$2\pi^+\pi^-K^-K^0_S$	< 5	$\times10^{-5}$	90%
Γ_6	$2\pi^+\pi^-K^-K^0_S2\pi^0$	< 2.2	$\times10^{-4}$	90%
Γ_7	$2\pi^+2\pi^-2\pi^0$	< 2.4	$\times10^{-4}$	90%
Γ_8	$2\pi^+2\pi^-K^+K^-$	< 1.5	$\times10^{-4}$	90%
Γ_9	$2\pi^+2\pi^-K^+K^-\pi^0$	< 2.2	$\times10^{-4}$	90%
Γ_{10}	$2\pi^+2\pi^-K^+K^-2\pi^0$	< 1.1	$\times10^{-3}$	90%
Γ_{11}	$3\pi^+2\pi^-K^-K^0_S\pi^0$	< 7	$\times10^{-4}$	90%
Γ_{12}	$3\pi^+3\pi^-$	< 7	$\times10^{-5}$	90%
Γ_{13}	$3\pi^+3\pi^-2\pi^0$	< 1.2	$\times10^{-3}$	90%
Γ_{14}	$3\pi^+3\pi^-K^+K^-$	< 1.5	$\times10^{-4}$	90%
Γ_{15}	$3\pi^+3\pi^-K^+K^-\pi^0$	< 7	$\times10^{-4}$	90%
Γ_{16}	$4\pi^+4\pi^-$	< 1.7	$\times10^{-4}$	90%
Γ_{17}	$4\pi^+4\pi^-2\pi^0$	< 6	$\times10^{-4}$	90%

$\chi_{b0}(2P)$ BRANCHING RATIOS

$\Gamma(\gamma\,\Upsilon(2S))/\Gamma_{total}$ Γ_1/Γ

VALUE	CL%	DOCUMENT ID		TECN	COMMENT
0.046±0.020±0.007		[3] HEINTZ	92	CSB2	$e^+e^- \to \ell^+\ell^-\gamma\gamma$
• • • We do not use the following data for averages, fits, limits, etc. • • •					
<0.028	90	[4] LEES	11J	BABR	$\Upsilon(3S) \to X\gamma$
<0.089	90	[5] CRAWFORD	92B	CLE2	$e^+e^- \to \ell^+\ell^-\gamma\gamma$

[3] Using B($\Upsilon(2S) \to \mu^+\mu^-$) = (1.44 ± 0.10)%, B($\Upsilon(3S) \to \gamma\chi_{b0}(2P)$) = (6.0 ± 0.4 ± 0.6)% and assuming $e\mu$ universality. Supersedes HEINTZ 91.

[4] LEES 11J quotes a central value of $\Gamma(\chi_{b0}(2P) \to \gamma\Upsilon(2S))/\Gamma_{\text{total}} \times \Gamma(\Upsilon(3S) \to \gamma\chi_{b0}(2P))/\Gamma_{\text{total}} = (-0.3 \pm 0.2^{+0.5}_{-0.4})\%$.

[5] Using B($\Upsilon(2S) \to \mu^+\mu^-$) = (1.37 ± 0.26)%, B($\Upsilon(3S) \to \gamma\gamma\Upsilon(2S)$)×2 B($\Upsilon(2S) \to \mu^+\mu^-$) < 1.19×10^{-4}, and B($\Upsilon(3S) \to \chi_{b0}(2P)\gamma$) = 0.049.

$\Gamma(\gamma\Upsilon(1S))/\Gamma_{\text{total}}$ Γ_2/Γ

VALUE	CL%	DOCUMENT ID		TECN	COMMENT
0.009±0.006±0.001		[6] HEINTZ	92	CSB2	$e^+e^- \to \ell^+\ell^-\gamma\gamma$
• • • We do not use the following data for averages, fits, limits, etc. • • •					
<0.012	90	[7] LEES	11J	BABR	$\Upsilon(3S) \to X\gamma$
<0.025	90	[8] CRAWFORD	92B	CLE2	$e^+e^- \to \ell^+\ell^-\gamma\gamma$

[6] Using B($\Upsilon(1S) \to \mu^+\mu^-$) = (2.57 ± 0.07)%, B($\Upsilon(3S) \to \gamma\chi_{b0}(2P)$) = (6.0 ± 0.4 ± 0.6)% and assuming $e\mu$ universality. Supersedes HEINTZ 91.

[7] LEES 11J quotes a central value of $\Gamma(\chi_{b0}(2P) \to \gamma\Upsilon(1S))/\Gamma_{\text{total}} \times \Gamma(\Upsilon(3S) \to \gamma\chi_{b0}(2P))/\Gamma_{\text{total}} = (3.9 \pm 2.2^{+1.2}_{-0.6}) \times 10^{-4}$.

[8] Using B($\Upsilon(1S) \to \mu^+\mu^-$) = (2.57 ± 0.07)%, B($\Upsilon(3S) \to \gamma\gamma\Upsilon(1S)$)×2 B($\Upsilon(1S) \to \mu^+\mu^-$) < 0.63×10^{-4}, and B($\Upsilon(3S) \to \chi_{b0}(2P)\gamma$) = 0.049.

$\Gamma(D^0X)/\Gamma_{\text{total}}$ Γ_3/Γ

VALUE	CL%	DOCUMENT ID		TECN	COMMENT
<8.2 × 10⁻²	90	[9,10] BRIERE	08	CLEO	$\Upsilon(3S) \to \gamma D^0X$

[9] For $p_{D^0} > 2.5$ GeV/c.

[10] The authors also present their result as $(4.1 \pm 3.0 \pm 0.4) \times 10^{-2}$.

$\Gamma(\pi^+\pi^-K^+K^-\pi^0)/\Gamma_{\text{total}}$ Γ_4/Γ

VALUE (units 10^{-4})	CL%	DOCUMENT ID		TECN	COMMENT
<0.34	90	[11] ASNER	08A	CLEO	$\Upsilon(3S) \to \gamma\pi^+\pi^-K^+K^-\pi^0$

[11] ASNER 08A reports [$\Gamma(\chi_{b0}(2P) \to \pi^+\pi^-K^+K^-\pi^0)/\Gamma_{\text{total}}$] × [B($\Upsilon(3S) \to \gamma\chi_{b0}(2P)$)] < 2×10^{-6} which we divide by our best value B($\Upsilon(3S) \to \gamma\chi_{b0}(2P)$) = 5.9×10^{-2}.

$\Gamma(2\pi^+\pi^-K^-K^0_S)/\Gamma_{\text{total}}$ Γ_5/Γ

VALUE (units 10^{-4})	CL%	DOCUMENT ID		TECN	COMMENT
<0.5	90	[12] ASNER	08A	CLEO	$\Upsilon(3S) \to \gamma 2\pi^+\pi^-K^-K^0_S$

[12] ASNER 08A reports [$\Gamma(\chi_{b0}(2P) \to 2\pi^+\pi^-K^-K^0_S)/\Gamma_{\text{total}}$] × [B($\Upsilon(3S) \to \gamma\chi_{b0}(2P)$)] < 3×10^{-6} which we divide by our best value B($\Upsilon(3S) \to \gamma\chi_{b0}(2P)$) = 5.9×10^{-2}.

$\Gamma(2\pi^+\pi^-K^-K^0_S2\pi^0)/\Gamma_{\text{total}}$ Γ_6/Γ

VALUE (units 10^{-4})	CL%	DOCUMENT ID		TECN	COMMENT
<2.2	90	[13] ASNER	08A	CLEO	$\Upsilon(3S) \to \gamma 2\pi^+\pi^-K^-2\pi^0$

[13] ASNER 08A reports [$\Gamma(\chi_{b0}(2P) \to 2\pi^+\pi^-K^-K^0_S2\pi^0)/\Gamma_{\text{total}}$] × [B($\Upsilon(3S) \to \gamma\chi_{b0}(2P)$)] < 13×10^{-6} which we divide by our best value B($\Upsilon(3S) \to \gamma\chi_{b0}(2P)$) = 5.9×10^{-2}.

$\Gamma(2\pi^+2\pi^-2\pi^0)/\Gamma_{\text{total}}$ Γ_7/Γ

VALUE (units 10^{-4})	CL%	DOCUMENT ID		TECN	COMMENT
<2.4	90	[14] ASNER	08A	CLEO	$\Upsilon(3S) \to \gamma 2\pi^+2\pi^-2\pi^0$

[14] ASNER 08A reports [$\Gamma(\chi_{b0}(2P) \to 2\pi^+2\pi^-2\pi^0)/\Gamma_{\text{total}}$] × [B($\Upsilon(3S) \to \gamma\chi_{b0}(2P)$)] < 14×10^{-6} which we divide by our best value B($\Upsilon(3S) \to \gamma\chi_{b0}(2P)$) = 5.9×10^{-2}.

$\Gamma(2\pi^+2\pi^-K^+K^-)/\Gamma_{\text{total}}$ Γ_8/Γ

VALUE (units 10^{-4})	CL%	DOCUMENT ID		TECN	COMMENT
<1.5	90	[15] ASNER	08A	CLEO	$\Upsilon(3S) \to \gamma 2\pi^+2\pi^-K^+K^-$

[15] ASNER 08A reports [$\Gamma(\chi_{b0}(2P) \to 2\pi^+2\pi^-K^+K^-)/\Gamma_{\text{total}}$] × [B($\Upsilon(3S) \to \gamma\chi_{b0}(2P)$)] < 9×10^{-6} which we divide by our best value B($\Upsilon(3S) \to \gamma\chi_{b0}(2P)$) = 5.9×10^{-2}.

$\Gamma(2\pi^+2\pi^-K^+K^-\pi^0)/\Gamma_{\text{total}}$ Γ_9/Γ

VALUE (units 10^{-4})	CL%	DOCUMENT ID		TECN	COMMENT
<2.2	90	[16] ASNER	08A	CLEO	$\Upsilon(3S) \to \gamma 2\pi^+2\pi^-K^+K^-\pi^0$

[16] ASNER 08A reports [$\Gamma(\chi_{b0}(2P) \to 2\pi^+2\pi^-K^+K^-\pi^0)/\Gamma_{\text{total}}$] × [B($\Upsilon(3S) \to \gamma\chi_{b0}(2P)$)] < 13×10^{-6} which we divide by our best value B($\Upsilon(3S) \to \gamma\chi_{b0}(2P)$) = 5.9×10^{-2}.

$\Gamma(2\pi^+2\pi^-K^+K^-2\pi^0)/\Gamma_{\text{total}}$ Γ_{10}/Γ

VALUE (units 10^{-4})	CL%	DOCUMENT ID		TECN	COMMENT
<11	90	[17] ASNER	08A	CLEO	$\Upsilon(3S) \to \gamma 2\pi^+2\pi^-K^+K^-2\pi^0$

[17] ASNER 08A reports [$\Gamma(\chi_{b0}(2P) \to 2\pi^+2\pi^-K^+K^-2\pi^0)/\Gamma_{\text{total}}$] × [B($\Upsilon(3S) \to \gamma\chi_{b0}(2P)$)] < 63×10^{-6} which we divide by our best value B($\Upsilon(3S) \to \gamma\chi_{b0}(2P)$) = 5.9×10^{-2}.

$\Gamma(3\pi^+2\pi^-K^-K^0_S\pi^0)/\Gamma_{\text{total}}$ Γ_{11}/Γ

VALUE (units 10^{-4})	CL%	DOCUMENT ID		TECN	COMMENT
<7	90	[18] ASNER	08A	CLEO	$\Upsilon(3S) \to \gamma 3\pi^+2\pi^-K^-K^0_S\pi^0$

[18] ASNER 08A reports [$\Gamma(\chi_{b0}(2P) \to 3\pi^+2\pi^-K^-K^0_S\pi^0)/\Gamma_{\text{total}}$] × [B($\Upsilon(3S) \to \gamma\chi_{b0}(2P)$)] < 39×10^{-6} which we divide by our best value B($\Upsilon(3S) \to \gamma\chi_{b0}(2P)$) = 5.9×10^{-2}.

$\Gamma(3\pi^+3\pi^-)/\Gamma_{\text{total}}$ Γ_{12}/Γ

VALUE (units 10^{-4})	CL%	DOCUMENT ID		TECN	COMMENT
<0.7	90	[19] ASNER	08A	CLEO	$\Upsilon(3S) \to \gamma 3\pi^+3\pi^-$

[19] ASNER 08A reports [$\Gamma(\chi_{b0}(2P) \to 3\pi^+3\pi^-)/\Gamma_{\text{total}}$] × [B($\Upsilon(3S) \to \gamma\chi_{b0}(2P)$)] < 4×10^{-6} which we divide by our best value B($\Upsilon(3S) \to \gamma\chi_{b0}(2P)$) = 5.9×10^{-2}.

$\Gamma(3\pi^+3\pi^-2\pi^0)/\Gamma_{\text{total}}$ Γ_{13}/Γ

VALUE (units 10^{-4})	CL%	DOCUMENT ID		TECN	COMMENT
<12	90	[20] ASNER	08A	CLEO	$\Upsilon(3S) \to \gamma 3\pi^+3\pi^-2\pi^0$

[20] ASNER 08A reports [$\Gamma(\chi_{b0}(2P) \to 3\pi^+3\pi^-2\pi^0)/\Gamma_{\text{total}}$] × [B($\Upsilon(3S) \to \gamma\chi_{b0}(2P)$)] < 72×10^{-6} which we divide by our best value B($\Upsilon(3S) \to \gamma\chi_{b0}(2P)$) = 5.9×10^{-2}.

$\Gamma(3\pi^+3\pi^-K^+K^-)/\Gamma_{\text{total}}$ Γ_{14}/Γ

VALUE (units 10^{-4})	CL%	DOCUMENT ID		TECN	COMMENT
<1.5	90	[21] ASNER	08A	CLEO	$\Upsilon(3S) \to \gamma 3\pi^+3\pi^-K^+K^-$

[21] ASNER 08A reports [$\Gamma(\chi_{b0}(2P) \to 3\pi^+3\pi^-K^+K^-)/\Gamma_{\text{total}}$] × [B($\Upsilon(3S) \to \gamma\chi_{b0}(2P)$)] < 9×10^{-6} which we divide by our best value B($\Upsilon(3S) \to \gamma\chi_{b0}(2P)$) = 5.9×10^{-2}.

$\Gamma(3\pi^+3\pi^-K^+K^-\pi^0)/\Gamma_{\text{total}}$ Γ_{15}/Γ

VALUE (units 10^{-4})	CL%	DOCUMENT ID		TECN	COMMENT
<7	90	[22] ASNER	08A	CLEO	$\Upsilon(3S) \to \gamma 3\pi^+3\pi^-K^+K^-\pi^0$

[22] ASNER 08A reports [$\Gamma(\chi_{b0}(2P) \to 3\pi^+3\pi^-K^+K^-\pi^0)/\Gamma_{\text{total}}$] × [B($\Upsilon(3S) \to \gamma\chi_{b0}(2P)$)] < 43×10^{-6} which we divide by our best value B($\Upsilon(3S) \to \gamma\chi_{b0}(2P)$) = 5.9×10^{-2}.

$\Gamma(4\pi^+4\pi^-)/\Gamma_{\text{total}}$ Γ_{16}/Γ

VALUE (units 10^{-4})	CL%	DOCUMENT ID		TECN	COMMENT
<1.7	90	[23] ASNER	08A	CLEO	$\Upsilon(3S) \to \gamma 4\pi^+4\pi^-$

[23] ASNER 08A reports [$\Gamma(\chi_{b0}(2P) \to 4\pi^+4\pi^-)/\Gamma_{\text{total}}$] × [B($\Upsilon(3S) \to \gamma\chi_{b0}(2P)$)] < 10×10^{-6} which we divide by our best value B($\Upsilon(3S) \to \gamma\chi_{b0}(2P)$) = 5.9×10^{-2}.

$\Gamma(4\pi^+4\pi^-2\pi^0)/\Gamma_{\text{total}}$ Γ_{17}/Γ

VALUE (units 10^{-4})	CL%	DOCUMENT ID		TECN	COMMENT
<6	90	[24] ASNER	08A	CLEO	$\Upsilon(3S) \to \gamma 4\pi^+4\pi^-2\pi^0$

[24] ASNER 08A reports [$\Gamma(\chi_{b0}(2P) \to 4\pi^+4\pi^-2\pi^0)/\Gamma_{\text{total}}$] × [B($\Upsilon(3S) \to \gamma\chi_{b0}(2P)$)] < 38×10^{-6} which we divide by our best value B($\Upsilon(3S) \to \gamma\chi_{b0}(2P)$) = 5.9×10^{-2}.

$\Gamma(\chi_{b0}(2P) \to \gamma\Upsilon(1S))/\Gamma_{\text{total}} \times \Gamma(\Upsilon(3S) \to \gamma\chi_{b0}(2P))/\Gamma_{\text{total}}$ $\Gamma_2/\Gamma \times \Gamma^{\Upsilon(3S)}_{21}/\Gamma^{\Upsilon(3S)}$

VALUE (units 10^{-4})	CL%	DOCUMENT ID		TECN	COMMENT
<8.2	90	[25] LEES	11J	BABR	$\Upsilon(3S) \to X\gamma$

[25] LEES 11J quotes a central value of $\Gamma(\chi_{b0}(2P) \to \gamma\Upsilon(1S))/\Gamma_{\text{total}} \times \Gamma(\Upsilon(3S) \to \gamma\chi_{b0}(2P))/\Gamma_{\text{total}} = (3.9 \pm 2.2^{+1.2}_{-0.6}) \times 10^{-4}$ and derives a 90% CL upper limit of B($\chi_{b0}(2P) \to \gamma\Upsilon(1S)$) < 1.2% using B($\Upsilon(3S) \to \gamma\chi_{b0}(2P)$) = (5.9 ± 0.6)%.

$\Gamma(\chi_{b0}(2P) \to \gamma\Upsilon(2S))/\Gamma_{\text{total}} \times \Gamma(\Upsilon(3S) \to \gamma\chi_{b0}(2P))/\Gamma_{\text{total}}$ $\Gamma_1/\Gamma \times \Gamma^{\Upsilon(3S)}_{21}/\Gamma^{\Upsilon(3S)}$

VALUE (units 10^{-3})	CL%	DOCUMENT ID		TECN	COMMENT
<1.6	90	[26] LEES	11J	BABR	$\Upsilon(3S) \to X\gamma$

[26] LEES 11J quotes a central value of $\Gamma(\chi_{b0}(2P) \to \gamma\Upsilon(2S))/\Gamma_{\text{total}} \times \Gamma(\Upsilon(3S) \to \gamma\chi_{b0}(2P))/\Gamma_{\text{total}} = (-0.3 \pm 0.2^{+0.5}_{-0.4})\%$ and derives a 90% CL upper limit of B($\chi_{b0}(2P) \to \gamma\Upsilon(2S)$) < 2.8% using B($\Upsilon(3S) \to \gamma\chi_{b0}(2P)$) = (5.9 ± 0.6)%.

$\chi_{b0}(2P)$ REFERENCES

LEES	11J	PR D84 072002	J.P. Lees *et al.*	(BABAR Collab.)
ASNER	08A	PR D78 091103	D.M. Asner *et al.*	(CLEO Collab.)
BRIERE	08	PR D78 092007	R.A. Briere *et al.*	(CLEO Collab.)
ARTUSO	05	PRL 94 032001	M. Artuso *et al.*	(CLEO Collab.)
CRAWFORD	92B	PL B294 139	G. Crawford, R. Fulton	(CLEO Collab.)
HEINTZ	92	PR D46 1928	U. Heintz *et al.*	(CUSB II Collab.)
HEINTZ	91	PRL 66 1563	U. Heintz *et al.*	(CUSB Collab.)
MORRISON	91	PRL 67 1696	R.J. Morrison *et al.*	(CLEO Collab.)
NARAIN	91	PRL 66 3113	M. Narain *et al.*	(CUSB Collab.)

Meson Particle Listings

$\chi_{b1}(2P)$

$\chi_{b1}(2P)$

$I^G(J^{PC}) = 0^+(1^{++})$
J needs confirmation.

Observed in radiative decay of the $\Upsilon(3S)$, therefore $C = +$. Branching ratio requires E1 transition, M1 is strongly disfavored, therefore $P = +$.

$\chi_{b1}(2P)$ MASS

VALUE (MeV)	DOCUMENT ID
10255.46±0.22±0.50 OUR EVALUATION	From γ energy below, using $\Upsilon(3S)$ mass = 10355.2 ± 0.5 MeV

$m_{\chi_{b1}(2P)} - m_{\chi_{b0}(2P)}$

VALUE (MeV)	DOCUMENT ID		TECN	COMMENT
23.5±0.7±0.7	[1] HEINTZ	92	CSB2	$e^+e^- \to \gamma X, \ell^+\ell^-\gamma\gamma$

[1] From the average photon energy for inclusive and exclusive events. Supersedes NARAIN 91.

γ ENERGY IN $\Upsilon(3S)$ DECAY

VALUE (MeV)	EVTS	DOCUMENT ID		TECN	COMMENT
99.26±0.22 OUR EVALUATION		Treating systematic errors as correlated			
99.53±0.23 OUR AVERAGE		Error includes scale factor of 1.3. See the ideogram below.			
99.15±0.07±0.25		ARTUSO	05	CLEO	$\Upsilon(3S) \to \gamma X$
99 ±1	169	CRAWFORD	92B	CLE2	$e^+e^- \to \ell^+\ell^-\gamma\gamma$
100.1 ±0.4	11147	[2] HEINTZ	92	CSB2	$e^+e^- \to \gamma X$
100.2 ±0.5	223	[3] HEINTZ	92	CSB2	$e^+e^- \to \ell^+\ell^-\gamma\gamma$
99.5 ±0.1 ±0.5	25759	MORRISON	91	CLE2	$e^+e^- \to \gamma X$

[2] A systematic uncertainty on the energy scale of 0.9% not included. Supersedes NARAIN 91.
[3] A systematic uncertainty on the energy scale of 0.9% not included. Supersedes HEINTZ 91.

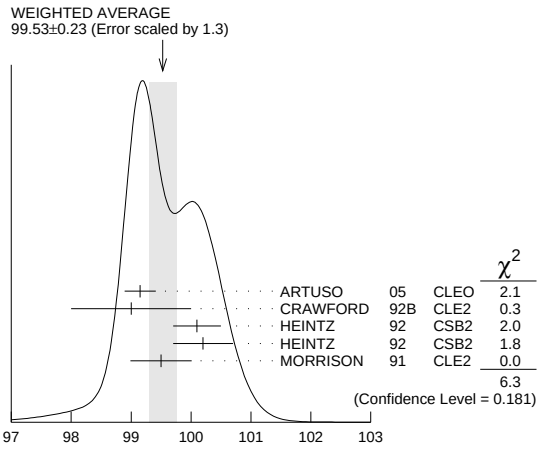

$\chi_{b1}(2P)$ DECAY MODES

	Mode	Fraction (Γ_i/Γ)	Scale factor
Γ_1	$\omega\,\Upsilon(1S)$	$(1.63^{+0.40}_{-0.34})$ %	
Γ_2	$\gamma\,\Upsilon(2S)$	(19.9 ±1.9) %	
Γ_3	$\gamma\,\Upsilon(1S)$	(9.2 ±0.8) %	1.1
Γ_4	$\pi\pi\chi_{b1}(1P)$	(9.1 ±1.3) $\times 10^{-3}$	
Γ_5	D^0X	(8.8 ±1.7) %	
Γ_6	$\pi^+\pi^-K^+K^-\pi^0$	(3.1 ±1.0) $\times 10^{-4}$	
Γ_7	$2\pi^+\pi^-K^-K^0_S$	(1.1 ±0.5) $\times 10^{-4}$	
Γ_8	$2\pi^+\pi^-K^-K^0_S2\pi^0$	(7.7 ±3.2) $\times 10^{-4}$	
Γ_9	$2\pi^+2\pi^-2\pi^0$	(5.9 ±2.0) $\times 10^{-4}$	
Γ_{10}	$2\pi^+2\pi^-K^+K^-$	(10 ±4) $\times 10^{-5}$	
Γ_{11}	$2\pi^+2\pi^-K^+K^-\pi^0$	(5.5 ±1.8) $\times 10^{-4}$	
Γ_{12}	$2\pi^+2\pi^-K^+K^-2\pi^0$	(10 ±4) $\times 10^{-4}$	
Γ_{13}	$3\pi^+2\pi^-K^-K^0_S\pi^0$	(6.7 ±2.6) $\times 10^{-4}$	
Γ_{14}	$3\pi^+3\pi^-$	(1.2 ±0.4) $\times 10^{-4}$	
Γ_{15}	$3\pi^+3\pi^-2\pi^0$	(1.2 ±0.4) $\times 10^{-3}$	
Γ_{16}	$3\pi^+3\pi^-K^+K^-$	(2.0 ±0.8) $\times 10^{-4}$	
Γ_{17}	$3\pi^+3\pi^-K^+K^-\pi^0$	(6.1 ±2.2) $\times 10^{-4}$	
Γ_{18}	$4\pi^+4\pi^-$	(1.7 ±0.6) $\times 10^{-4}$	
Γ_{19}	$4\pi^+4\pi^-2\pi^0$	(1.9 ±0.7) $\times 10^{-3}$	

$\chi_{b1}(2P)$ BRANCHING RATIOS

$\Gamma(\omega\,\Upsilon(1S))/\Gamma_{total}$ Γ_1/Γ

VALUE (units 10^{-2})	EVTS	DOCUMENT ID		TECN	COMMENT
$\mathbf{1.63^{+0.35}_{-0.31}{}^{+0.16}_{-0.15}}$	$32.6^{+6.9}_{-6.1}$	[4] CRONIN-HEN..04		CLE3	$\Upsilon(3S) \to \gamma\omega\,\Upsilon(1S)$

[4] Using B($\Upsilon(3S) \to \gamma\chi_{b1}(2P)$) = (11.3 ± 0.6)% and B($\Upsilon(1S) \to \ell^+\ell^-$) = 2 B($\Upsilon(1S) \to \mu^+\mu^-$) = 2 (2.48 ± 0.06)%.

$\Gamma(\gamma\,\Upsilon(2S))/\Gamma_{total}$ Γ_2/Γ

VALUE	EVTS	DOCUMENT ID		TECN	COMMENT
0.199±0.019 OUR AVERAGE					
0.190±0.018±0.017	4.3k	[5] LEES	11J	BABR	$\Upsilon(3S) \to X\gamma$
0.356±0.042±0.092		[6] CRAWFORD	92B	CLE2	$e^+e^- \to \ell^+\ell^-\gamma\gamma$
0.199±0.020±0.022		[7] HEINTZ	92	CSB2	$e^+e^- \to \ell^+\ell^-\gamma\gamma$

[5] LEES 11J reports $[\Gamma(\chi_{b1}(2P) \to \gamma\,\Upsilon(2S))/\Gamma_{total}] \times [B(\Upsilon(3S) \to \gamma\chi_{b1}(2P))] = (2.4 \pm 0.1 \pm 0.2) \times 10^{-2}$ which we divide by our best value B($\Upsilon(3S) \to \gamma\chi_{b1}(2P)$) = $(12.6 \pm 1.2) \times 10^{-2}$. Our first error is their experiment's error and our second error is the systematic error from using our best value.
[6] Using B($\Upsilon(2S) \to \mu^+\mu^-$) = (1.37 ± 0.26)%, B($\Upsilon(3S) \to \gamma\gamma\,\Upsilon(2S)$)×2 B($\Upsilon(2S) \to \mu^+\mu^-$) = (10.23±1.20±1.26)×$10^{-4}$, and B($\Upsilon(3S) \to \gamma\chi_{b1}(2P)$) = $0.105^{+0.003}_{-0.002}$ ± 0.013.
[7] Using B($\Upsilon(2S) \to \mu^+\mu^-$) = (1.44 ± 0.10)%, B($\Upsilon(3S) \to \gamma\chi_{b1}(2P)$) = (11.5 ± 0.5 ± 0.5)% and assuming $e\mu$ universality. Supersedes HEINTZ 91.

$\Gamma(\gamma\,\Upsilon(1S))/\Gamma_{total}$ Γ_3/Γ

VALUE	EVTS	DOCUMENT ID		TECN	COMMENT
0.092±0.008 OUR AVERAGE		Error includes scale factor of 1.1.			
0.098±0.005±0.009	15k	[8] LEES	11J	BABR	$\Upsilon(3S) \to X\gamma$
0.120±0.021±0.021		[9] CRAWFORD	92B	CLE2	$e^+e^- \to \ell^+\ell^-\gamma\gamma$
0.080±0.009±0.007		[10] HEINTZ	92	CSB2	$e^+e^- \to \ell^+\ell^-\gamma\gamma$

[8] LEES 11J reports $[\Gamma(\chi_{b1}(2P) \to \gamma\,\Upsilon(1S))/\Gamma_{total}] \times [B(\Upsilon(3S) \to \gamma\chi_{b1}(2P))] = (12.4 \pm 0.3 \pm 0.6) \times 10^{-3}$ which we divide by our best value B($\Upsilon(3S) \to \gamma\chi_{b1}(2P)$) = $(12.6 \pm 1.2) \times 10^{-2}$. Our first error is their experiment's error and our second error is the systematic error from using our best value.
[9] Using B($\Upsilon(1S) \to \mu^+\mu^-$) = (2.57 ± 0.07)%, B($\Upsilon(3S) \to \gamma\gamma\,\Upsilon(1S)$)×2 B($\Upsilon(1S) \to \mu^+\mu^-$) = (6.47±1.12±0.82)×$10^{-4}$ and B($\Upsilon(3S) \to \gamma\chi_{b1}(2P)$) = $0.105^{+0.003}_{-0.002}$ ± 0.013.
[10] Using B($\Upsilon(1S) \to \mu^+\mu^-$)=(2.57 ± 0.07)%, B($\Upsilon(3S) \to \gamma\chi_{b1}(2P)$) = (11.5 ± 0.5 ± 0.5)% and assuming $e\mu$ universality. Supersedes HEINTZ 91.

$\Gamma(\pi\pi\chi_{b1}(1P))/\Gamma_{total}$ Γ_4/Γ

VALUE (units 10^{-3})	EVTS	DOCUMENT ID		TECN	COMMENT
9.1±1.3 OUR AVERAGE					
9.2±1.1±0.8	31k	[11] LEES	11C	BABR	$e^+e^- \to \pi^+\pi^-X$
8.6±2.3±2.1		[12] CAWLFIELD	06	CLE3	$\Upsilon(3S) \to 2(\gamma\pi\ell)$

[11] LEES 11C measures B($\Upsilon(3S) \to \chi_{b1}(2P)X$) × B($\chi_{b1}(2P) \to \chi_{b1}(1P)\pi^+\pi^-$) = $(1.16 \pm 0.07 \pm 0.12) \times 10^{-3}$. We derive the value assuming B($\Upsilon(3S) \to \chi_{b1}(2P)X$) = B($\Upsilon(3S) \to \chi_{b1}(2P)\gamma$) = $(12.6 \pm 1.2) \times 10^{-2}$.
[12] CAWLFIELD 06 quote $\Gamma(\chi_b(2P) \to \pi\pi\chi_b(1P)) = 0.83 \pm 0.22 \pm 0.08 \pm 0.19$ keV assuming I-spin conservation, no D-wave contribution, $\Gamma(\chi_{b1}(2P)) = 96 \pm 16$keV, and $\Gamma(\chi_{b2}(2P)) = 138 \pm 19$ keV.

$\Gamma(D^0X)/\Gamma_{total}$ Γ_5/Γ

VALUE (units 10^{-2})	EVTS	DOCUMENT ID		TECN	COMMENT
8.8±1.5±0.8	2243	[13] BRIERE	08	CLEO	$\Upsilon(3S) \to \gamma D^0X$

[13] For $p_{D^0} > 2.5$ GeV/c.

$\Gamma(\pi^+\pi^-K^+K^-\pi^0)/\Gamma_{total}$ Γ_6/Γ

VALUE (units 10^{-4})	EVTS	DOCUMENT ID		TECN	COMMENT
3.1±1.0±0.3	30	[14] ASNER	08A	CLEO	$\Upsilon(3S) \to \gamma\pi^+\pi^-K^+K^-\pi^0$

[14] ASNER 08A reports $[\Gamma(\chi_{b1}(2P) \to \pi^+\pi^-K^+K^-\pi^0)/\Gamma_{total}] \times [B(\Upsilon(3S) \to \gamma\chi_{b1}(2P))] = (39 \pm 8 \pm 9) \times 10^{-6}$ which we divide by our best value B($\Upsilon(3S) \to \gamma\chi_{b1}(2P)$) = $(12.6 \pm 1.2) \times 10^{-2}$. Our first error is their experiment's error and our second error is the systematic error from using our best value.

$\Gamma(2\pi^+\pi^-K^-K^0_S)/\Gamma_{total}$ Γ_7/Γ

VALUE (units 10^{-4})	EVTS	DOCUMENT ID		TECN	COMMENT
1.1±0.5±0.1	10	[15] ASNER	08A	CLEO	$\Upsilon(3S) \to \gamma 2\pi^+\pi^-K^-K^0_S$

[15] ASNER 08A reports $[\Gamma(\chi_{b1}(2P) \to 2\pi^+\pi^-K^-K^0_S)/\Gamma_{total}] \times [B(\Upsilon(3S) \to \gamma\chi_{b1}(2P))] = (14 \pm 5 \pm 3) \times 10^{-6}$ which we divide by our best value B($\Upsilon(3S) \to \gamma\chi_{b1}(2P)$) = $(12.6 \pm 1.2) \times 10^{-2}$. Our first error is their experiment's error and our second error is the systematic error from using our best value.

$\Gamma(2\pi^+\pi^-K^-K^0_S2\pi^0)/\Gamma_{total}$ Γ_8/Γ

VALUE (units 10^{-4})	EVTS	DOCUMENT ID		TECN	COMMENT
7.7±3.1±0.7	15	[16] ASNER	08A	CLEO	$\Upsilon(3S) \to \gamma 2\pi^+\pi^-K^-2\pi^0$

[16] ASNER 08A reports $[\Gamma(\chi_{b1}(2P) \to 2\pi^+\pi^-K^-K^0_S2\pi^0)/\Gamma_{total}] \times [B(\Upsilon(3S) \to \gamma\chi_{b1}(2P))] = (97 \pm 30 \pm 26) \times 10^{-6}$ which we divide by our best value B($\Upsilon(3S) \to \gamma\chi_{b1}(2P)$) = $(12.6 \pm 1.2) \times 10^{-2}$. Our first error is their experiment's error and our second error is the systematic error from using our best value.

$\Gamma(2\pi^+2\pi^-2\pi^0)/\Gamma_{total}$ Γ_9/Γ

VALUE (units 10^{-4})	EVTS	DOCUMENT ID		TECN	COMMENT
5.9±2.0±0.5	36	[17] ASNER	08A	CLEO	$\Upsilon(3S) \to \gamma 2\pi^+2\pi^-2\pi^0$

[17] ASNER 08A reports $[\Gamma(\chi_{b1}(2P) \to 2\pi^+2\pi^-2\pi^0)/\Gamma_{total}] \times [B(\Upsilon(3S) \to \gamma\chi_{b1}(2P))] = (74 \pm 16 \pm 19) \times 10^{-6}$ which we divide by our best value $B(\Upsilon(3S) \to \gamma\chi_{b1}(2P)) = (12.6 \pm 1.2) \times 10^{-2}$. Our first error is their experiment's error and our second error is the systematic error from using our best value.

$\Gamma(2\pi^+2\pi^-K^+K^-)/\Gamma_{total}$ Γ_{10}/Γ

VALUE (units 10^{-4})	EVTS	DOCUMENT ID		TECN	COMMENT
1.0±0.4±0.1	12	[18] ASNER	08A	CLEO	$\Upsilon(3S) \to \gamma 2\pi^+2\pi^-K^+K^-$

[18] ASNER 08A reports $[\Gamma(\chi_{b1}(2P) \to 2\pi^+2\pi^-K^+K^-)/\Gamma_{total}] \times [B(\Upsilon(3S) \to \gamma\chi_{b1}(2P))] = (12 \pm 4 \pm 3) \times 10^{-6}$ which we divide by our best value $B(\Upsilon(3S) \to \gamma\chi_{b1}(2P)) = (12.6 \pm 1.2) \times 10^{-2}$. Our first error is their experiment's error and our second error is the systematic error from using our best value.

$\Gamma(2\pi^+2\pi^-K^+K^-\pi^0)/\Gamma_{total}$ Γ_{11}/Γ

VALUE (units 10^{-4})	EVTS	DOCUMENT ID		TECN	COMMENT
5.5±1.7±0.5	38	[19] ASNER	08A	CLEO	$\Upsilon(3S) \to \gamma 2\pi^+2\pi^-K^+K^-\pi^0$

[19] ASNER 08A reports $[\Gamma(\chi_{b1}(2P) \to 2\pi^+2\pi^-K^+K^-\pi^0)/\Gamma_{total}] \times [B(\Upsilon(3S) \to \gamma\chi_{b1}(2P))] = (69 \pm 13 \pm 17) \times 10^{-6}$ which we divide by our best value $B(\Upsilon(3S) \to \gamma\chi_{b1}(2P)) = (12.6 \pm 1.2) \times 10^{-2}$. Our first error is their experiment's error and our second error is the systematic error from using our best value.

$\Gamma(2\pi^+2\pi^-K^+K^-2\pi^0)/\Gamma_{total}$ Γ_{12}/Γ

VALUE (units 10^{-4})	EVTS	DOCUMENT ID		TECN	COMMENT
9.6±3.5±0.9	27	[20] ASNER	08A	CLEO	$\Upsilon(3S) \to \gamma 2\pi^+2\pi^-K^+K^-2\pi^0$

[20] ASNER 08A reports $[\Gamma(\chi_{b1}(2P) \to 2\pi^+2\pi^-K^+K^-2\pi^0)/\Gamma_{total}] \times [B(\Upsilon(3S) \to \gamma\chi_{b1}(2P))] = (121 \pm 29 \pm 33) \times 10^{-6}$ which we divide by our best value $B(\Upsilon(3S) \to \gamma\chi_{b1}(2P)) = (12.6 \pm 1.2) \times 10^{-2}$. Our first error is their experiment's error and our second error is the systematic error from using our best value.

$\Gamma(3\pi^+2\pi^-K^-K^0_S\pi^0)/\Gamma_{total}$ Γ_{13}/Γ

VALUE (units 10^{-4})	EVTS	DOCUMENT ID		TECN	COMMENT
6.7±2.5±0.6	17	[21] ASNER	08A	CLEO	$\Upsilon(3S) \to \gamma 3\pi^+2\pi^-K^-K^0_S\pi^0$

[21] ASNER 08A reports $[\Gamma(\chi_{b1}(2P) \to 3\pi^+2\pi^-K^-K^0_S\pi^0)/\Gamma_{total}] \times [B(\Upsilon(3S) \to \gamma\chi_{b1}(2P))] = (85 \pm 23 \pm 22) \times 10^{-6}$ which we divide by our best value $B(\Upsilon(3S) \to \gamma\chi_{b1}(2P)) = (12.6 \pm 1.2) \times 10^{-2}$. Our first error is their experiment's error and our second error is the systematic error from using our best value.

$\Gamma(3\pi^+3\pi^-)/\Gamma_{total}$ Γ_{14}/Γ

VALUE (units 10^{-4})	EVTS	DOCUMENT ID		TECN	COMMENT
1.2±0.4±0.1	18	[22] ASNER	08A	CLEO	$\Upsilon(3S) \to \gamma 3\pi^+3\pi^-$

[22] ASNER 08A reports $[\Gamma(\chi_{b1}(2P) \to 3\pi^+3\pi^-)/\Gamma_{total}] \times [B(\Upsilon(3S) \to \gamma\chi_{b1}(2P))] = (15 \pm 4 \pm 3) \times 10^{-6}$ which we divide by our best value $B(\Upsilon(3S) \to \gamma\chi_{b1}(2P)) = (12.6 \pm 1.2) \times 10^{-2}$. Our first error is their experiment's error and our second error is the systematic error from using our best value.

$\Gamma(3\pi^+3\pi^-2\pi^0)/\Gamma_{total}$ Γ_{15}/Γ

VALUE (units 10^{-4})	EVTS	DOCUMENT ID		TECN	COMMENT
12±4±1	44	[23] ASNER	08A	CLEO	$\Upsilon(3S) \to \gamma 3\pi^+3\pi^-2\pi^0$

[23] ASNER 08A reports $[\Gamma(\chi_{b1}(2P) \to 3\pi^+3\pi^-2\pi^0)/\Gamma_{total}] \times [B(\Upsilon(3S) \to \gamma\chi_{b1}(2P))] = (150 \pm 30 \pm 40) \times 10^{-6}$ which we divide by our best value $B(\Upsilon(3S) \to \gamma\chi_{b1}(2P)) = (12.6 \pm 1.2) \times 10^{-2}$. Our first error is their experiment's error and our second error is the systematic error from using our best value.

$\Gamma(3\pi^+3\pi^-K^+K^-)/\Gamma_{total}$ Γ_{16}/Γ

VALUE (units 10^{-4})	EVTS	DOCUMENT ID		TECN	COMMENT
2.0±0.7±0.2	16	[24] ASNER	08A	CLEO	$\Upsilon(3S) \to \gamma 3\pi^+3\pi^-K^+K^-$

[24] ASNER 08A reports $[\Gamma(\chi_{b1}(2P) \to 3\pi^+3\pi^-K^+K^-)/\Gamma_{total}] \times [B(\Upsilon(3S) \to \gamma\chi_{b1}(2P))] = (25 \pm 7 \pm 6) \times 10^{-6}$ which we divide by our best value $B(\Upsilon(3S) \to \gamma\chi_{b1}(2P)) = (12.6 \pm 1.2) \times 10^{-2}$. Our first error is their experiment's error and our second error is the systematic error from using our best value.

$\Gamma(3\pi^+3\pi^-K^+K^-\pi^0)/\Gamma_{total}$ Γ_{17}/Γ

VALUE (units 10^{-4})	EVTS	DOCUMENT ID		TECN	COMMENT
6.1±2.1±0.6	25	[25] ASNER	08A	CLEO	$\Upsilon(3S) \to \gamma 3\pi^+3\pi^-K^+K^-\pi^0$

[25] ASNER 08A reports $[\Gamma(\chi_{b1}(2P) \to 3\pi^+3\pi^-K^+K^-\pi^0)/\Gamma_{total}] \times [B(\Upsilon(3S) \to \gamma\chi_{b1}(2P))] = (77 \pm 17 \pm 21) \times 10^{-6}$ which we divide by our best value $B(\Upsilon(3S) \to \gamma\chi_{b1}(2P)) = (12.6 \pm 1.2) \times 10^{-2}$. Our first error is their experiment's error and our second error is the systematic error from using our best value.

$\Gamma(4\pi^+4\pi^-)/\Gamma_{total}$ Γ_{18}/Γ

VALUE (units 10^{-4})	EVTS	DOCUMENT ID		TECN	COMMENT
1.7±0.6±0.2	16	[26] ASNER	08A	CLEO	$\Upsilon(3S) \to \gamma 4\pi^+4\pi^-$

[26] ASNER 08A reports $[\Gamma(\chi_{b1}(2P) \to 4\pi^+4\pi^-)/\Gamma_{total}] \times [B(\Upsilon(3S) \to \gamma\chi_{b1}(2P))] = (22 \pm 6 \pm 5) \times 10^{-6}$ which we divide by our best value $B(\Upsilon(3S) \to \gamma\chi_{b1}(2P)) = (12.6 \pm 1.2) \times 10^{-2}$. Our first error is their experiment's error and our second error is the systematic error from using our best value.

$\Gamma(4\pi^+4\pi^-2\pi^0)/\Gamma_{total}$ Γ_{19}/Γ

VALUE (units 10^{-4})	EVTS	DOCUMENT ID		TECN	COMMENT
19±7±2	41	[27] ASNER	08A	CLEO	$\Upsilon(3S) \to \gamma 4\pi^+4\pi^-2\pi^0$

[27] ASNER 08A reports $[\Gamma(\chi_{b1}(2P) \to 4\pi^+4\pi^-2\pi^0)/\Gamma_{total}] \times [B(\Upsilon(3S) \to \gamma\chi_{b1}(2P))] = (241 \pm 47 \pm 72) \times 10^{-6}$ which we divide by our best value $B(\Upsilon(3S) \to \gamma\chi_{b1}(2P)) = (12.6 \pm 1.2) \times 10^{-2}$. Our first error is their experiment's error and our second error is the systematic error from using our best value.

$\chi_{b1}(2P)$ Cross-Particle Branching Ratios

$\Gamma(\chi_{b1}(2P) \to \gamma\Upsilon(1S))/\Gamma_{total} \times \Gamma(\Upsilon(3S) \to \gamma\chi_{b1}(2P))/\Gamma_{total}$ $\Gamma_3/\Gamma \times \Gamma^{\Upsilon(3S)}_{20}/\Gamma^{\Upsilon(3S)}$

VALUE (units 10^{-3})	EVTS	DOCUMENT ID		TECN	COMMENT
12.4±0.3±0.6	15k	LEES	11J	BABR	$\Upsilon(3S) \to X\gamma$

$\Gamma(\chi_{b1}(2P) \to \gamma\Upsilon(2S))/\Gamma_{total} \times \Gamma(\Upsilon(3S) \to \gamma\chi_{b1}(2P))/\Gamma_{total}$ $\Gamma_2/\Gamma \times \Gamma^{\Upsilon(3S)}_{20}/\Gamma^{\Upsilon(3S)}$

VALUE (units 10^{-2})	EVTS	DOCUMENT ID		TECN	COMMENT
2.4±0.1±0.2	4.3k	LEES	11J	BABR	$\Upsilon(3S) \to X\gamma$

$B(\chi_{b1}(2P) \to \chi_{b1}(1P)\pi^+\pi^-) \times B(\Upsilon(3S) \to \chi_{b1}(2P)X)$

VALUE (units 10^{-3})	EVTS	DOCUMENT ID		TECN	COMMENT
1.16±0.07±0.12	31k	LEES	11C	BABR	$e^+e^- \to \pi^+\pi^-X$

$B(\chi_{b2}(2P) \to pX + \bar{p}X)/B(\chi_{b1}(2P) \to pX + \bar{p}X)$

VALUE	DOCUMENT ID		TECN	COMMENT
1.109±0.007±0.040	BRIERE	07	CLEO	$\Upsilon(3S) \to \gamma\chi_{bJ}(2P)$

$B(\chi_{b0}(2P) \to pX + \bar{p}X)/B(\chi_{b1}(2P) \to pX + \bar{p}X)$

VALUE	DOCUMENT ID		TECN	COMMENT
1.082±0.025±0.060	BRIERE	07	CLEO	$\Upsilon(3S) \to \gamma\chi_{bJ}(2P)$

$\chi_{b1}(2P)$ REFERENCES

LEES	11C	PR D84 011104	J.P. Lees *et al.*	(BABAR Collab.)
LEES	11J	PR D84 072002	J.P. Lees *et al.*	(BABAR Collab.)
ASNER	08A	PR D78 091103	D.M. Asner *et al.*	(CLEO Collab.)
BRIERE	08	PR D78 092007	R.A. Briere *et al.*	(CLEO Collab.)
BRIERE	07	PR D76 012005	R.A. Briere *et al.*	(CLEO Collab.)
CAWLFIELD	06	PR D73 012003	C. Cawlfield *et al.*	(CLEO Collab.)
ARTUSO	05	PRL 94 032001	M. Artuso *et al.*	(CLEO Collab.)
CRONIN-HEN...	04	PRL 92 222002	D. Cronin-Hennessy *et al.*	(CLEO Collab.)
CRAWFORD	92B	PL B294 139	G. Crawford, R. Fulton	(CLEO Collab.)
HEINTZ	92	PR D46 1928	U. Heintz *et al.*	(CUSB II Collab.)
HEINTZ	91	PRL 66 1563	U. Heintz *et al.*	(CUSB Collab.)
MORRISON	91	PRL 67 1696	R.J. Morrison *et al.*	(CLEO Collab.)
NARAIN	91	PRL 66 3113	M. Narain *et al.*	(CUSB Collab.)

$h_b(2P)$

$I^G(J^{PC}) = ?^?(1^{+-})$

OMITTED FROM SUMMARY TABLE

Quantum numbers are quark model predictions.

$h_b(2P)$ MASS

VALUE (MeV)	EVTS	DOCUMENT ID		TECN	COMMENT
10259.8±0.5±1.1	90k	MIZUK	12	BELL	$e^+e^- \to \pi^+\pi^-$ hadrons
• • • We do not use the following data for averages, fits, limits, etc. • • •					
$10259.8 \pm 0.6^{+1.4}_{-1.0}$	83.9k	[1] ADACHI	12	BELL	10.86 $e^+e^- \to \pi^+\pi^-$ MM

[1] Superseded by MIZUK 12.

$h_b(2P)$ DECAY MODES

	Mode	Fraction (Γ_i/Γ)
Γ_1	hadrons	not seen
Γ_2	$\eta_b(1S)\gamma$	(22± 5) %
Γ_3	$\eta_b(2S)\gamma$	(48±13) %

$h_b(2P)$ BRANCHING RATIOS

$\Gamma(\text{hadrons})/\Gamma_{total}$ Γ_1/Γ

VALUE	EVTS	DOCUMENT ID		TECN	COMMENT
not seen	83.9k	ADACHI	12	BELL	10.86 $e^+e^- \to \pi^+\pi^-$ MM

$\Gamma(\eta_b(1S)\gamma)/\Gamma_{total}$ Γ_2/Γ

VALUE (units 10^{-2})	EVTS	DOCUMENT ID		TECN	COMMENT
$22.3 \pm 3.8^{+3.1}_{-3.3}$	10k	MIZUK	12	BELL	$e^+e^- \to (\gamma)\pi^+\pi^-$ hadrons

Meson Particle Listings

$h_b(2P), \chi_{b2}(2P)$

$\Gamma(\eta_b(2S)\gamma)/\Gamma_{total}$ Γ_3/Γ

VALUE (units 10^{-2})	EVTS	DOCUMENT ID		TECN	COMMENT
$47.5 \pm 10.5^{+6.8}_{-7.7}$	26k	MIZUK	12	BELL	$e^+e^- \to (\gamma)\pi^+\pi^-$ hadrons

$h_b(2P)$ REFERENCES

ADACHI	12	PRL 108 032001	I. Adachi *et al.*	(BELLE Collab.)
MIZUK	12	PRL 109 232002	R. Mizuk *et al.*	(BELLE Collab.)

$\chi_{b2}(2P)$

$I^G(J^{PC}) = 0^+(2^{++})$
J needs confirmation.

Observed in radiative decay of the $\Upsilon(3S)$, therefore $C = +$. Branching ratio requires E1 transition, M1 is strongly disfavored, therefore $P = +$.

$\chi_{b2}(2P)$ MASS

VALUE (MeV)	DOCUMENT ID
$10268.65 \pm 0.22 \pm 0.50$ OUR EVALUATION	From γ energy below, using $\Upsilon(3S)$ mass = 10355.2 ± 0.5 MeV

$m_{\chi_{b2}(2P)} - m_{\chi_{b1}(2P)}$

VALUE (MeV)	DOCUMENT ID		TECN	COMMENT
$13.5 \pm 0.4 \pm 0.5$	[1] HEINTZ	92	CSB2	$e^+e^- \to \gamma X, \ell^+\ell^-\gamma\gamma$

[1] From the average photon energy for inclusive and exclusive events. Supersedes NARAIN 91.

γ ENERGY IN $\Upsilon(3S)$ DECAY

VALUE (MeV)	EVTS	DOCUMENT ID		TECN	COMMENT
86.19 ± 0.22 OUR EVALUATION		Treating systematic errors as correlated			
86.40 ± 0.18 OUR AVERAGE					
$86.04 \pm 0.06 \pm 0.27$		ARTUSO	05	CLEO	$\Upsilon(3S) \to \gamma X$
86 ± 1	101	CRAWFORD	92B	CLE2	$e^+e^- \to \ell^+\ell^-\gamma\gamma$
86.7 ± 0.4	10319	[2] HEINTZ	92	CSB2	$e^+e^- \to \gamma X$
86.9 ± 0.4	157	[3] HEINTZ	92	CSB2	$e^+e^- \to \ell^+\ell^-\gamma\gamma$
$86.4 \pm 0.1 \pm 0.4$	30741	MORRISON	91	CLE2	$e^+e^- \to \gamma X$

[2] A systematic uncertainty on the energy scale of 0.9% not included. Supersedes NARAIN 91.
[3] A systematic uncertainty on the energy scale of 0.9% not included. Supersedes HEINTZ 91.

$\chi_{b2}(2P)$ DECAY MODES

	Mode	Fraction (Γ_i/Γ)	Scale factor/ Confidence level
Γ_1	$\omega\,\Upsilon(1S)$	$(1.10^{+0.34}_{-0.30})$ %	
Γ_2	$\gamma\,\Upsilon(2S)$	(10.6 ±2.6) %	S=2.0
Γ_3	$\gamma\,\Upsilon(1S)$	(7.0 ±0.7) %	
Γ_4	$\pi\pi\chi_{b2}(1P)$	(5.1 ±0.9) $\times 10^{-3}$	
Γ_5	D^0X	< 2.4 %	CL=90%
Γ_6	$\pi^+\pi^-K^+K^-\pi^0$	< 1.1 $\times 10^{-4}$	CL=90%
Γ_7	$2\pi^+\pi^-K^-K^0_S$	< 9 $\times 10^{-5}$	CL=90%
Γ_8	$2\pi^+\pi^-K^-K^0_S2\pi^0$	< 7 $\times 10^{-4}$	CL=90%
Γ_9	$2\pi^+2\pi^-2\pi^0$	(3.9 ±1.6) $\times 10^{-4}$	
Γ_{10}	$2\pi^+2\pi^-K^+K^-$	(9 ±4) $\times 10^{-5}$	
Γ_{11}	$2\pi^+2\pi^-K^+K^-\pi^0$	(2.4 ±1.1) $\times 10^{-4}$	
Γ_{12}	$2\pi^+2\pi^-K^+K^-2\pi^0$	(4.7 ±2.3) $\times 10^{-4}$	
Γ_{13}	$3\pi^+2\pi^-K^-K^0_S\pi^0$	< 4 $\times 10^{-4}$	CL=90%
Γ_{14}	$3\pi^+3\pi^-$	(9 ±4) $\times 10^{-5}$	
Γ_{15}	$3\pi^+3\pi^-2\pi^0$	(1.2 ±0.4) $\times 10^{-3}$	
Γ_{16}	$3\pi^+3\pi^-K^+K^-$	(1.4 ±0.7) $\times 10^{-4}$	
Γ_{17}	$3\pi^+3\pi^-K^+K^-\pi^0$	(4.2 ±1.7) $\times 10^{-4}$	
Γ_{18}	$4\pi^+4\pi^-$	(9 ±5) $\times 10^{-5}$	
Γ_{19}	$4\pi^+4\pi^-2\pi^0$	(1.3 ±0.5) $\times 10^{-3}$	

$\chi_{b2}(2P)$ BRANCHING RATIOS

$\Gamma(\omega\,\Upsilon(1S))/\Gamma_{total}$ Γ_1/Γ

VALUE (units 10^{-2})	EVTS	DOCUMENT ID		TECN	COMMENT
$1.10^{+0.32}_{-0.28}{}^{+0.11}_{-0.10}$	$20.1^{+5.8}_{-5.1}$	[4] CRONIN-HEN..04		CLE3	$\Upsilon(3S) \to \gamma\omega\,\Upsilon(1S)$

[4] Using B($\Upsilon(3S) \to \gamma\chi_{b2}(2P)$) = (11.4 ± 0.8)% and B($\Upsilon(1S) \to \ell^+\ell^-$) = 2 B($\Upsilon(1S) \to \mu^+\mu^-$) = 2 (2.48 ± 0.06)%.

$\Gamma(\gamma\,\Upsilon(2S))/\Gamma_{total}$ Γ_2/Γ

VALUE	EVTS	DOCUMENT ID		TECN	COMMENT
0.106 ± 0.026 OUR AVERAGE		Error includes scale factor of 2.0. See the ideogram below.			
$0.084 \pm 0.011 \pm 0.010$	2.5k	[5] LEES	11J	BABR	$\Upsilon(3S) \to X\gamma$
$0.135 \pm 0.025 \pm 0.035$		[6] CRAWFORD	92B	CLE2	$e^+e^- \to \ell^+\ell^-\gamma\gamma$
$0.173 \pm 0.021 \pm 0.019$		[7] HEINTZ	92	CSB2	$e^+e^- \to \ell^+\ell^-\gamma\gamma$

[5] LEES 11J reports $[\Gamma(\chi_{b2}(2P) \to \gamma\,\Upsilon(2S))/\Gamma_{total}] \times [B(\Upsilon(3S) \to \gamma\chi_{b2}(2P))] = (1.1 \pm 0.1 \pm 0.1) \times 10^{-2}$ which we divide by our best value B($\Upsilon(3S) \to \gamma\chi_{b2}(2P)$) = $(13.1 \pm 1.6) \times 10^{-2}$. Our first error is their experiment's error and our second error is the systematic error from using our best value.
[6] Using B($\Upsilon(2S) \to \mu^+\mu^-$) = (1.37 ± 0.26)%, B($\Upsilon(3S) \to \gamma\gamma\,\Upsilon(2S)$)×2 B($\Upsilon(2S) \to \mu^+\mu^-$) = $(4.98 \pm 0.94 \pm 0.62) \times 10^{-4}$, and B($\Upsilon(3S) \to \gamma\chi_{b2}(2P)$) = 0.135 ± 0.003 ± 0.017.
[7] Using B($\Upsilon(2S) \to \mu^+\mu^-$) = (1.44 ± 0.10)%, B($\Upsilon(3S) \to \gamma\chi_{b2}(2P)$) = (11.1 ± 0.5 ± 0.4)% and assuming $e\mu$ universality. Supersedes HEINTZ 91.

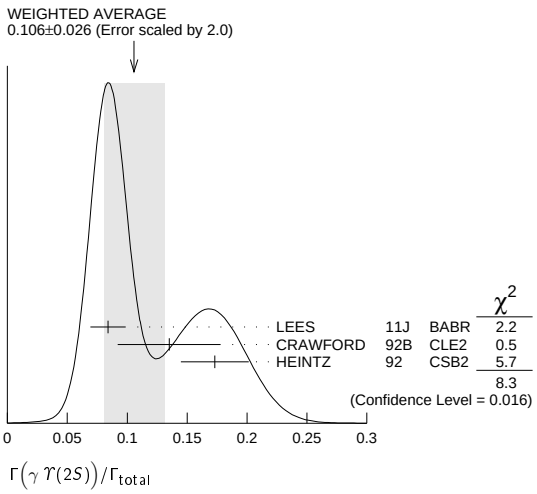

$\Gamma(\gamma\,\Upsilon(1S))/\Gamma_{total}$ Γ_3/Γ

VALUE	EVTS	DOCUMENT ID		TECN	COMMENT
0.070 ± 0.007 OUR AVERAGE					
$0.070 \pm 0.004 \pm 0.008$	11k	[8] LEES	11J	BABR	$\Upsilon(3S) \to X\gamma$
$0.072 \pm 0.014 \pm 0.013$		[9] CRAWFORD	92B	CLE2	$e^+e^- \to \ell^+\ell^-\gamma\gamma$
$0.070 \pm 0.010 \pm 0.006$		[10] HEINTZ	92	CSB2	$e^+e^- \to \ell^+\ell^-\gamma\gamma$

[8] LEES 11J reports $[\Gamma(\chi_{b2}(2P) \to \gamma\,\Upsilon(1S))/\Gamma_{total}] \times [B(\Upsilon(3S) \to \gamma\chi_{b2}(2P))] = (9.2 \pm 0.3 \pm 0.4) \times 10^{-3}$ which we divide by our best value B($\Upsilon(3S) \to \gamma\chi_{b2}(2P)$) = $(13.1 \pm 1.6) \times 10^{-2}$. Our first error is their experiment's error and our second error is the systematic error from using our best value.
[9] Using B($\Upsilon(1S) \to \mu^+\mu^-$) = (2.57 ± 0.07)%, B($\Upsilon(3S) \to \gamma\gamma\,\Upsilon(2S)$)×2 B($\Upsilon(1S) \to \mu^+\mu^-$) = $(5.03 \pm 0.94 \pm 0.63) \times 10^{-4}$, and B($\Upsilon(3S) \to \gamma\chi_{b2}(2P)$) = 0.135 ± 0.003 ± 0.017.
[10] Using B($\Upsilon(1S) \to \mu^+\mu^-$) = (2.57 ± 0.07)%, B($\Upsilon(3S) \to \gamma\chi_{b2}(2P)$) = (11.1 ± 0.5 ± 0.4)% and assuming $e\mu$ universality. Supersedes HEINTZ 91.

$\Gamma(\pi\pi\chi_{b2}(1P))/\Gamma_{total}$ Γ_4/Γ

VALUE (units 10^{-3})	EVTS	DOCUMENT ID		TECN	COMMENT
5.1 ± 0.9 OUR AVERAGE					
$4.9 \pm 0.7 \pm 0.6$	17k	[11] LEES	11C	BABR	$e^+e^- \to \pi^+\pi^-X$
$6.0 \pm 1.6 \pm 1.4$		[12] CAWLFIELD	06	CLE3	$\Upsilon(3S) \to 2(\gamma\pi\ell)$

[11] $(0.64 \pm 0.05 \pm 0.08) \times 10^{-3}$. We derive the value assuming B($\Upsilon(3S) \to \chi_{b2}(2P)X$) = B($\Upsilon(3S) \to \chi_{b2}(2P)\gamma$) = $(13.1 \pm 1.6) \times 10^{-2}$.
[12] CAWLFIELD 06 quote $\Gamma(\chi_b(2P) \to \pi\pi\chi_b(1P)) = 0.83 \pm 0.22 \pm 0.08 \pm 0.19$ keV assuming I-spin conservation, no D-wave contribution, $\Gamma(\chi_{b1}(2P)) = 96 \pm 16$keV, and $\Gamma(\chi_{b2}(2P)) = 138 \pm 19$ keV.

$\Gamma(D^0X)/\Gamma_{total}$ Γ_5/Γ

VALUE	CL%	DOCUMENT ID		TECN	COMMENT
$<2.4 \times 10^{-2}$	90	[13,14] BRIERE	08	CLEO	$\Upsilon(3S) \to \gamma D^0X$

[13] For $p_{D^0} > 2.5$ GeV/c.
[14] The authors also present their result as $(0.2 \pm 1.4 \pm 0.1) \times 10^{-2}$.

$\Gamma(\pi^+\pi^-K^+K^-\pi^0)/\Gamma_{total}$ Γ_6/Γ

VALUE (units 10^{-4})	CL%	DOCUMENT ID		TECN	COMMENT
<1.1	90	[15] ASNER	08A	CLEO	$\Upsilon(3S) \to \gamma\pi^+\pi^-K^+K^-\pi^0$

[15] ASNER 08A reports $[\Gamma(\chi_{b2}(2P) \to \pi^+\pi^-K^+K^-\pi^0)/\Gamma_{total}] \times [B(\Upsilon(3S) \to \gamma\chi_{b2}(2P))] < 14 \times 10^{-6}$ which we divide by our best value B($\Upsilon(3S) \to \gamma\chi_{b2}(2P)$) = 13.1×10^{-2}.

$\Gamma(2\pi^+\pi^-K^-K^0_S)/\Gamma_{total}$ Γ_7/Γ

VALUE (units 10^{-4})	CL%	DOCUMENT ID		TECN	COMMENT
<0.9	90	[16] ASNER	08A	CLEO	$\Upsilon(3S) \to \gamma 2\pi^+\pi^-K^-K^0_S$

[16] ASNER 08A reports $[\Gamma(\chi_{b2}(2P) \to 2\pi^+\pi^-K^-K^0_S)/\Gamma_{total}] \times [B(\Upsilon(3S) \to \gamma\chi_{b2}(2P))] < 12\times10^{-6}$ which we divide by our best value $B(\Upsilon(3S) \to \gamma\chi_{b2}(2P)) = 13.1\times10^{-2}$.

$\Gamma(2\pi^+\pi^-K^-K^0_S2\pi^0)/\Gamma_{total}$ Γ_8/Γ

VALUE (units 10^{-4})	CL%	DOCUMENT ID		TECN	COMMENT
<7	90	[17] ASNER	08A	CLEO	$\Upsilon(3S) \to \gamma 2\pi^+\pi^-K^-K^0_S2\pi^0$

[17] ASNER 08A reports $[\Gamma(\chi_{b2}(2P) \to 2\pi^+\pi^-K^-K^0_S2\pi^0)/\Gamma_{total}] \times [B(\Upsilon(3S) \to \gamma\chi_{b2}(2P))] < 87\times10^{-6}$ which we divide by our best value $B(\Upsilon(3S) \to \gamma\chi_{b2}(2P)) = 13.1\times10^{-2}$.

$\Gamma(2\pi^+2\pi^-2\pi^0)/\Gamma_{total}$ Γ_9/Γ

VALUE (units 10^{-4})	EVTS	DOCUMENT ID		TECN	COMMENT
3.9±1.6±0.5	23	[18] ASNER	08A	CLEO	$\Upsilon(3S) \to \gamma 2\pi^+2\pi^-2\pi^0$

[18] ASNER 08A reports $[\Gamma(\chi_{b2}(2P) \to 2\pi^+2\pi^-2\pi^0)/\Gamma_{total}] \times [B(\Upsilon(3S) \to \gamma\chi_{b2}(2P))] = (51 \pm 16 \pm 13)\times10^{-6}$ which we divide by our best value $B(\Upsilon(3S) \to \gamma\chi_{b2}(2P)) = (13.1 \pm 1.6)\times10^{-2}$. Our first error is their experiment's error and our second error is the systematic error from using our best value.

$\Gamma(2\pi^+2\pi^-K^+K^-)/\Gamma_{total}$ Γ_{10}/Γ

VALUE (units 10^{-4})	EVTS	DOCUMENT ID		TECN	COMMENT
0.9±0.4±0.1	11	[19] ASNER	08A	CLEO	$\Upsilon(3S) \to \gamma 2\pi^+2\pi^-K^+K^-$

[19] ASNER 08A reports $[\Gamma(\chi_{b2}(2P) \to 2\pi^+2\pi^-K^+K^-)/\Gamma_{total}] \times [B(\Upsilon(3S) \to \gamma\chi_{b2}(2P))] = (12 \pm 4 \pm 3)\times10^{-6}$ which we divide by our best value $B(\Upsilon(3S) \to \gamma\chi_{b2}(2P)) = (13.1 \pm 1.6)\times10^{-2}$. Our first error is their experiment's error and our second error is the systematic error from using our best value.

$\Gamma(2\pi^+2\pi^-K^+K^-\pi^0)/\Gamma_{total}$ Γ_{11}/Γ

VALUE (units 10^{-4})	EVTS	DOCUMENT ID		TECN	COMMENT
2.4±1.0±0.3	16	[20] ASNER	08A	CLEO	$\Upsilon(3S) \to \gamma 2\pi^+2\pi^-K^+K^-\pi^0$

[20] ASNER 08A reports $[\Gamma(\chi_{b2}(2P) \to 2\pi^+2\pi^-K^+K^-\pi^0)/\Gamma_{total}] \times [B(\Upsilon(3S) \to \gamma\chi_{b2}(2P))] = (32 \pm 11 \pm 8)\times10^{-6}$ which we divide by our best value $B(\Upsilon(3S) \to \gamma\chi_{b2}(2P)) = (13.1 \pm 1.6)\times10^{-2}$. Our first error is their experiment's error and our second error is the systematic error from using our best value.

$\Gamma(2\pi^+2\pi^-K^+K^-2\pi^0)/\Gamma_{total}$ Γ_{12}/Γ

VALUE (units 10^{-4})	EVTS	DOCUMENT ID		TECN	COMMENT
4.7±2.2±0.6	14	[21] ASNER	08A	CLEO	$\Upsilon(3S) \to \gamma 2\pi^+2\pi^-K^+K^-2\pi^0$

[21] ASNER 08A reports $[\Gamma(\chi_{b2}(2P) \to 2\pi^+2\pi^-K^+K^-2\pi^0)/\Gamma_{total}] \times [B(\Upsilon(3S) \to \gamma\chi_{b2}(2P))] = (62 \pm 23 \pm 17)\times10^{-6}$ which we divide by our best value $B(\Upsilon(3S) \to \gamma\chi_{b2}(2P)) = (13.1 \pm 1.6)\times10^{-2}$. Our first error is their experiment's error and our second error is the systematic error from using our best value.

$\Gamma(3\pi^+2\pi^-K^-K^0_S\pi^0)/\Gamma_{total}$ Γ_{13}/Γ

VALUE (units 10^{-4})	CL%	DOCUMENT ID		TECN	COMMENT
<4	90	[22] ASNER	08A	CLEO	$\Upsilon(3S) \to \gamma 3\pi^+2\pi^-K^-K^0_S\pi^0$

[22] ASNER 08A reports $[\Gamma(\chi_{b2}(2P) \to 3\pi^+2\pi^-K^-K^0_S\pi^0)/\Gamma_{total}] \times [B(\Upsilon(3S) \to \gamma\chi_{b2}(2P))] < 58\times10^{-6}$ which we divide by our best value $B(\Upsilon(3S) \to \gamma\chi_{b2}(2P)) = 13.1\times10^{-2}$.

$\Gamma(3\pi^+3\pi^-)/\Gamma_{total}$ Γ_{14}/Γ

VALUE (units 10^{-4})	EVTS	DOCUMENT ID		TECN	COMMENT
0.9±0.4±0.1	14	[23] ASNER	08A	CLEO	$\Upsilon(3S) \to \gamma 3\pi^+3\pi^-$

[23] ASNER 08A reports $[\Gamma(\chi_{b2}(2P) \to 3\pi^+3\pi^-)/\Gamma_{total}] \times [B(\Upsilon(3S) \to \gamma\chi_{b2}(2P))] = (12 \pm 4 \pm 3)\times10^{-6}$ which we divide by our best value $B(\Upsilon(3S) \to \gamma\chi_{b2}(2P)) = (13.1 \pm 1.6)\times10^{-2}$. Our first error is their experiment's error and our second error is the systematic error from using our best value.

$\Gamma(3\pi^+3\pi^-2\pi^0)/\Gamma_{total}$ Γ_{15}/Γ

VALUE (units 10^{-4})	EVTS	DOCUMENT ID		TECN	COMMENT
12±4±1	45	[24] ASNER	08A	CLEO	$\Upsilon(3S) \to \gamma 3\pi^+3\pi^-2\pi^0$

[24] ASNER 08A reports $[\Gamma(\chi_{b2}(2P) \to 3\pi^+3\pi^-2\pi^0)/\Gamma_{total}] \times [B(\Upsilon(3S) \to \gamma\chi_{b2}(2P))] = (159 \pm 33 \pm 43)\times10^{-6}$ which we divide by our best value $B(\Upsilon(3S) \to \gamma\chi_{b2}(2P)) = (13.1 \pm 1.6)\times10^{-2}$. Our first error is their experiment's error and our second error is the systematic error from using our best value.

$\Gamma(3\pi^+3\pi^-K^+K^-)/\Gamma_{total}$ Γ_{16}/Γ

VALUE (units 10^{-4})	EVTS	DOCUMENT ID		TECN	COMMENT
1.4±0.7±0.2	12	[25] ASNER	08A	CLEO	$\Upsilon(3S) \to \gamma 3\pi^+3\pi^-K^+K^-$

[25] ASNER 08A reports $[\Gamma(\chi_{b2}(2P) \to 3\pi^+3\pi^-K^+K^-)/\Gamma_{total}] \times [B(\Upsilon(3S) \to \gamma\chi_{b2}(2P))] = (19 \pm 7 \pm 5)\times10^{-6}$ which we divide by our best value $B(\Upsilon(3S) \to \gamma\chi_{b2}(2P)) = (13.1 \pm 1.6)\times10^{-2}$. Our first error is their experiment's error and our second error is the systematic error from using our best value.

$\Gamma(3\pi^+3\pi^-K^+K^-\pi^0)/\Gamma_{total}$ Γ_{17}/Γ

VALUE (units 10^{-4})	EVTS	DOCUMENT ID		TECN	COMMENT
4.2±1.7±0.5	16	[26] ASNER	08A	CLEO	$\Upsilon(3S) \to \gamma 3\pi^+3\pi^-K^+K^-\pi^0$

[26] ASNER 08A reports $[\Gamma(\chi_{b2}(2P) \to 3\pi^+3\pi^-K^+K^-\pi^0)/\Gamma_{total}] \times [B(\Upsilon(3S) \to \gamma\chi_{b2}(2P))] = (55 \pm 16 \pm 15)\times10^{-6}$ which we divide by our best value $B(\Upsilon(3S) \to \gamma\chi_{b2}(2P)) = (13.1 \pm 1.6)\times10^{-2}$. Our first error is their experiment's error and our second error is the systematic error from using our best value.

$\Gamma(4\pi^+4\pi^-)/\Gamma_{total}$ Γ_{18}/Γ

VALUE (units 10^{-4})	EVTS	DOCUMENT ID		TECN	COMMENT
0.9±0.4±0.1	9	[27] ASNER	08A	CLEO	$\Upsilon(3S) \to \gamma 4\pi^+4\pi^-$

[27] ASNER 08A reports $[\Gamma(\chi_{b2}(2P) \to 4\pi^+4\pi^-)/\Gamma_{total}] \times [B(\Upsilon(3S) \to \gamma\chi_{b2}(2P))] = (12 \pm 5 \pm 3)\times10^{-6}$ which we divide by our best value $B(\Upsilon(3S) \to \gamma\chi_{b2}(2P)) = (13.1 \pm 1.6)\times10^{-2}$. Our first error is their experiment's error and our second error is the systematic error from using our best value.

$\Gamma(4\pi^+4\pi^-2\pi^0)/\Gamma_{total}$ Γ_{19}/Γ

VALUE (units 10^{-4})	EVTS	DOCUMENT ID		TECN	COMMENT
13±5±2	27	[28] ASNER	08A	CLEO	$\Upsilon(3S) \to \gamma 4\pi^+4\pi^-2\pi^0$

[28] ASNER 08A reports $[\Gamma(\chi_{b2}(2P) \to 4\pi^+4\pi^-2\pi^0)/\Gamma_{total}] \times [B(\Upsilon(3S) \to \gamma\chi_{b2}(2P))] = (165 \pm 46 \pm 50)\times10^{-6}$ which we divide by our best value $B(\Upsilon(3S) \to \gamma\chi_{b2}(2P)) = (13.1 \pm 1.6)\times10^{-2}$. Our first error is their experiment's error and our second error is the systematic error from using our best value.

$\chi_{b2}(2P)$ Cross-Particle Branching Ratios

$\Gamma(\chi_{b2}(2P) \to \gamma\Upsilon(1S))/\Gamma_{total} \times \Gamma(\Upsilon(3S) \to \gamma\chi_{b2}(2P))/\Gamma_{total}$ $\Gamma_3/\Gamma \times \Gamma^{\Upsilon(3S)}_{19}/\Gamma^{\Upsilon(3S)}$

VALUE (units 10^{-3})	EVTS	DOCUMENT ID		TECN	COMMENT
9.2±0.3±0.4	11k	LEES	11J	BABR	$\Upsilon(3S) \to X\gamma$

$\Gamma(\chi_{b2}(2P) \to \gamma\Upsilon(2S))/\Gamma_{total} \times \Gamma(\Upsilon(3S) \to \gamma\chi_{b2}(2P))/\Gamma_{total}$ $\Gamma_2/\Gamma \times \Gamma^{\Upsilon(3S)}_{19}/\Gamma^{\Upsilon(3S)}$

VALUE (units 10^{-2})	EVTS	DOCUMENT ID		TECN	COMMENT
1.1±0.1±0.1	2.5k	LEES	11J	BABR	$\Upsilon(3S) \to X\gamma$

$B(\chi_{b2}(2P) \to \chi_{b2}(1P)\pi^+\pi^-) \times B(\Upsilon(3S) \to \chi_{b2}(2P)X)$

VALUE (units 10^{-3})	EVTS	DOCUMENT ID		TECN	COMMENT
0.64±0.05±0.08	17k	LEES	11C	BABR	$e^+e^- \to \pi^+\pi^-X$

$\chi_{b2}(2P)$ REFERENCES

LEES	11C	PR D84 011104	J.P. Lees *et al.*	(BABAR Collab.)
LEES	11J	PR D84 072002	J.P. Lees *et al.*	(BABAR Collab.)
ASNER	08A	PR D78 091103	D.M. Asner *et al.*	(CLEO Collab.)
BRIERE	08	PR D78 092007	R.A. Briere *et al.*	(CLEO Collab.)
CAWLFIELD	06	PR D73 012003	C. Cawlfield *et al.*	(CLEO Collab.)
ARTUSO	05	PRL 94 032001	M. Artuso *et al.*	(CLEO Collab.)
CRONIN-HEN...	04	PRL 92 222002	D. Cronin-Hennessy *et al.*	(CLEO Collab.)
CRAWFORD	92B	PL B294 139	G. Crawford, R. Fulton	(CLEO Collab.)
HEINTZ	92	PR D46 1928	U. Heintz *et al.*	(CUSB II Collab.)
HEINTZ	91	PRL 66 1563	U. Heintz *et al.*	(CUSB Collab.)
MORRISON	91	PRL 67 1696	R.J. Morrison *et al.*	(CLEO Collab.)
NARAIN	91	PRL 66 3113	M. Narain *et al.*	(CUSB Collab.)

$\Upsilon(3S)$

$I^G(J^{PC}) = 0^-(1^{--})$

$\Upsilon(3S)$ MASS

VALUE (MeV)	DOCUMENT ID		TECN	COMMENT
10355.2±0.5	[1] ARTAMONOV	00	MD1	$e^+e^- \to$ hadrons
• • • We do not use the following data for averages, fits, limits, etc. • • •				
10355.3±0.5	[2,3] BARU	86B	REDE	$e^+e^- \to$ hadrons

[1] Reanalysis of BARU 86B using new electron mass (COHEN 87).
[2] Reanalysis of ARTAMONOV 84.
[3] Superseded by ARTAMONOV 00.

$m_{\Upsilon(3S)} - m_{\Upsilon(2S)}$

VALUE (MeV)	DOCUMENT ID		TECN	COMMENT
331.50±0.02±0.13	LEES	11C	BABR	$e^+e^- \to \pi^+\pi^-X$

$\Upsilon(3S)$ WIDTH

VALUE (keV)	DOCUMENT ID
20.32±1.85 OUR EVALUATION	See the Note on "Width Determinations of the Υ States"

Meson Particle Listings

$\Upsilon(3S)$

$\Upsilon(3S)$ DECAY MODES

	Mode	Fraction (Γ_i/Γ)	Scale factor/ Confidence level
Γ_1	$\Upsilon(2S)$ anything	(10.6 ±0.8) %	
Γ_2	$\Upsilon(2S)\pi^+\pi^-$	(2.82±0.18) %	S=1.6
Γ_3	$\Upsilon(2S)\pi^0\pi^0$	(1.85±0.14) %	
Γ_4	$\Upsilon(2S)\gamma\gamma$	(5.0 ±0.7) %	
Γ_5	$\Upsilon(2S)\pi^0$	< 5.1 $\times 10^{-4}$	CL=90%
Γ_6	$\Upsilon(1S)\pi^+\pi^-$	(4.37±0.08) %	
Γ_7	$\Upsilon(1S)\pi^0\pi^0$	(2.20±0.13) %	
Γ_8	$\Upsilon(1S)\eta$	< 1 $\times 10^{-4}$	CL=90%
Γ_9	$\Upsilon(1S)\pi^0$	< 7 $\times 10^{-5}$	CL=90%
Γ_{10}	$h_b(1P)\pi^0$	< 1.2 $\times 10^{-3}$	CL=90%
Γ_{11}	$h_b(1P)\pi^0 \to \gamma\eta_b(1S)\pi^0$	(4.3 ±1.4) $\times 10^{-4}$	
Γ_{12}	$h_b(1P)\pi^+\pi^-$	< 1.2 $\times 10^{-4}$	CL=90%
Γ_{13}	$\tau^+\tau^-$	(2.29±0.30) %	
Γ_{14}	$\mu^+\mu^-$	(2.18±0.21) %	S=2.1
Γ_{15}	e^+e^-	seen	
Γ_{16}	hadrons		
Γ_{17}	ggg	(35.7 ±2.6) %	
Γ_{18}	γgg	(9.7 ±1.8) $\times 10^{-3}$	
	Radiative decays		
Γ_{19}	$\gamma\chi_{b2}(2P)$	(13.1 ±1.6) %	S=3.4
Γ_{20}	$\gamma\chi_{b1}(2P)$	(12.6 ±1.2) %	S=2.4
Γ_{21}	$\gamma\chi_{b0}(2P)$	(5.9 ±0.6) %	S=1.4
Γ_{22}	$\gamma\chi_{b2}(1P)$	(9.9 ±1.3) $\times 10^{-3}$	S=2.0
Γ_{23}	$\gamma A^0 \to \gamma$ hadrons	< 8 $\times 10^{-5}$	CL=90%
Γ_{24}	$\gamma\chi_{b1}(1P)$	(9 ±5) $\times 10^{-4}$	S=1.9
Γ_{25}	$\gamma\chi_{b0}(1P)$	(2.7 ±0.4) $\times 10^{-3}$	
Γ_{26}	$\gamma\eta_b(2S)$	< 6.2 $\times 10^{-4}$	CL=90%
Γ_{27}	$\gamma\eta_b(1S)$	(5.1 ±0.7) $\times 10^{-4}$	
Γ_{28}	$\gamma X \to \gamma +\geq 4$ prongs	[a] < 2.2 $\times 10^{-4}$	CL=95%
Γ_{29}	$\gamma a_1^0 \to \gamma\mu^+\mu^-$	< 5.5 $\times 10^{-6}$	CL=90%
Γ_{30}	$\gamma a_1^0 \to \gamma\tau^+\tau^-$	[b] < 1.6 $\times 10^{-4}$	CL=90%
	Lepton Family number (LF) violating modes		
Γ_{31}	$e^\pm\tau^\mp$	LF < 4.2 $\times 10^{-6}$	CL=90%
Γ_{32}	$\mu^\pm\tau^\mp$	LF < 3.1 $\times 10^{-6}$	CL=90%

[a] 1.5 GeV $< m_X <$ 5.0 GeV

[b] For $m_{\tau^+\tau^-}$ in the ranges 4.03–9.52 and 9.61–10.10 GeV.

$\Upsilon(3S)$ $\Gamma(i)\Gamma(e^+e^-)/\Gamma(\text{total})$

$\Gamma(\text{hadrons}) \times \Gamma(e^+e^-)/\Gamma_{\text{total}}$ $\Gamma_{16}\Gamma_{15}/\Gamma$

VALUE (keV)	DOCUMENT ID		TECN	COMMENT
0.414±0.007 OUR AVERAGE				
0.413±0.004±0.006	ROSNER	06	CLEO	10.4 $e^+e^- \to$ hadrons
0.45 ±0.03 ±0.03	[4] GILES	84B	CLEO	$e^+e^- \to$ hadrons

[4] Radiative corrections reevaluated by BUCHMUELLER 88 following KURAEV 85.

$\Gamma(\Upsilon(1S)\pi^+\pi^-) \times \Gamma(e^+e^-)/\Gamma_{\text{total}}$ $\Gamma_6\Gamma_{15}/\Gamma$

VALUE (eV)	EVTS	DOCUMENT ID		TECN	COMMENT
18.46±0.27±0.77	6.4K	[5] AUBERT	08BP	BABR	$e^+e^- \to \gamma\pi^+\pi^-\ell^+\ell^-$

[5] Using B($\Upsilon(1S) \to e^+e^-$) = (2.38 ± 0.11)% and B($\Upsilon(1S) \to \mu^+\mu^-$) = (2.48 ± 0.05)%.

$\Upsilon(3S)$ PARTIAL WIDTHS

$\Gamma(e^+e^-)$ Γ_{15}

VALUE (keV)	DOCUMENT ID
0.443±0.008 OUR EVALUATION	

$\Upsilon(3S)$ BRANCHING RATIOS

$\Gamma(\Upsilon(2S)\text{anything})/\Gamma_{\text{total}}$ Γ_1/Γ

VALUE	EVTS	DOCUMENT ID		TECN	COMMENT
0.106 ±0.008 OUR AVERAGE					
0.1023±0.0105	4625	[6,7,8] BUTLER	94B	CLE2	$e^+e^- \to \ell^+\ell^-$X
0.111 ±0.012	4891	[7,8,9] BROCK	91	CLEO	$e^+e^- \to \pi^+\pi^-$X, $\pi^+\pi^-\ell^+\ell^-$

[6] Using B($\Upsilon(2S) \to \Upsilon(1S)\gamma\gamma$) = (0.038 ± 0.007)%, and B($\Upsilon(2S) \to \Upsilon(1S)\pi^0\pi^0$) = (1/2)B($\Upsilon(2S) \to \Upsilon(1S)\pi^+\pi^-$).

[7] Using B($\Upsilon(1S) \to \mu^+\mu^-$) = (2.48 ± 0.06)%. With the assumption of $e\mu$ universality.

[8] Using B($\Upsilon(2S) \to \Upsilon(1S)\pi^+\pi^-$) = (18.5 ± 0.8)%.

[9] Using B($\Upsilon(2S) \to \mu^+\mu^-$) = (1.31 ± 0.21)%, B($\Upsilon(2S) \to \Upsilon(1S)\gamma\gamma$)×2B($\Upsilon(1S) \to \mu^+\mu^-$) = (0.188 ± 0.035)%, and B($\Upsilon(2S) \to \Upsilon(1S)\pi^0\pi^0$)×2B($\Upsilon(1S) \to \mu^+\mu^-$) = (0.436 ± 0.056)%. With the assumption of $e\mu$ universality.

$\Gamma(\Upsilon(2S)\pi^+\pi^-)/\Gamma_{\text{total}}$ Γ_2/Γ

VALUE (units 10^{-2})	EVTS	DOCUMENT ID		TECN	COMMENT
2.82±0.18 OUR AVERAGE Error includes scale factor of 1.6. See the ideogram below.					
3.00±0.02±0.14	543k	LEES	11C	BABR	$e^+e^- \to \pi^+\pi^-X$
2.40±0.10±0.26	800	[10] AUBERT	08BP	BABR	$e^+e^- \to \gamma\pi^+\pi^-e^+e^-$
3.12±0.49	980	[11,12] BUTLER	94B	CLE2	$e^+e^- \to \pi^+\pi^-\ell^+\ell^-$
2.13±0.38	974	[13] BROCK	91	CLEO	$e^+e^- \to \pi^+\pi^-$X, $\pi^+\pi^-\ell^+\ell^-$
• • • We do not use the following data for averages, fits, limits, etc. • • •					
4.82±0.65±0.53	138	[13] WU	93	CUSB	$\Upsilon(3S) \to \pi^+\pi^-\ell^+\ell^-$
3.1 ±2.0	5	MAGERAS	82	CUSB	$\Upsilon(3S) \to \pi^+\pi^-\ell^+\ell^-$

[10] Using B($\Upsilon(1S) \to e^+e^-$) = (2.38 ± 0.11)%, B($\Upsilon(1S) \to \mu^+\mu^-$) = (2.48 ± 0.05)%, and $\Gamma_{ee}(\Upsilon(3S))$ = 0.443 ± 0.008 keV.

[11] From the exclusive mode.

[12] Using B($\Upsilon(2S) \to \Upsilon(1S)\gamma\gamma$) = (0.038 ± 0.007)%, and B($\Upsilon(2S) \to \Upsilon(1S)\pi^0\pi^0$) = (1/2)B($\Upsilon(2S) \to \Upsilon(1S)\pi^+\pi^-$).

[13] Using B($\Upsilon(2S) \to \mu^+\mu^-$) = (1.31 ± 0.21)%, B($\Upsilon(2S) \to \Upsilon(1S)\gamma\gamma$)×2B($\Upsilon(1S) \to \mu^+\mu^-$) = (0.188 ± 0.035)%, and B($\Upsilon(2S) \to \Upsilon(1S)\pi^0\pi^0$)×2B($\Upsilon(1S) \to \mu^+\mu^-$) = (0.436 ± 0.056)%. With the assumption of $e\mu$ universality.

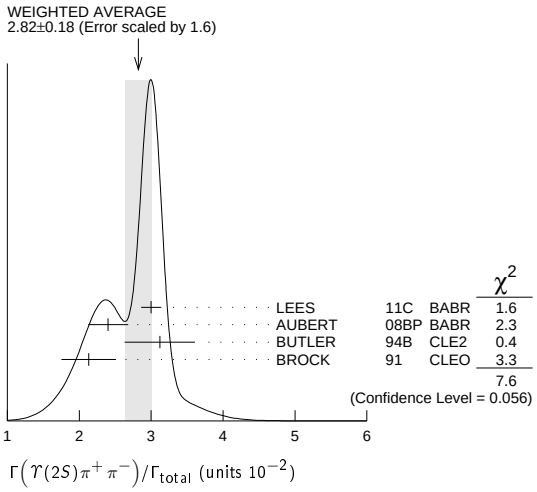

$\Gamma(\Upsilon(2S)\pi^0\pi^0)/\Gamma_{\text{total}}$ Γ_3/Γ

VALUE (units 10^{-2})	EVTS	DOCUMENT ID		TECN	COMMENT
1.85±0.14 OUR AVERAGE					
1.82±0.09±0.12	4391	[14] BHARI	09	CLEO	$e^+e^- \to \pi^0\pi^0\ell^+\ell^-$
2.16±0.39		[15,16] BUTLER	94B	CLE2	$e^+e^- \to \pi^0\pi^0\ell^+\ell^-$
1.7 ±0.5 ±0.2	10	[17] HEINTZ	92	CSB2	$e^+e^- \to \pi^0\pi^0\ell^+\ell^-$

[14] Authors assume B($\Upsilon(1S) \to e^+e^-$) + B($\Upsilon(1S) \to \mu^+\mu^-$) = 4.06%.

[15] B($\Upsilon(2S) \to \mu^+\mu^-$) = (1.31 ± 0.21)% and assuming $e\mu$ universality.

[16] From the exclusive mode.

[17] B($\Upsilon(2S) \to \mu^+\mu^-$) = (1.44 ± 0.10)% and assuming $e\mu$ universality. Supersedes HEINTZ 91.

$\Gamma(\Upsilon(2S)\gamma\gamma)/\Gamma_{\text{total}}$ Γ_4/Γ

VALUE	DOCUMENT ID		TECN	COMMENT
0.0502±0.0069	[18] BUTLER	94B	CLE2	$e^+e^- \to \ell^+\ell^-2\gamma$

[18] From the exclusive mode.

$\Gamma(\Upsilon(2S)\pi^0)/\Gamma_{\text{total}}$ Γ_5/Γ

VALUE (units 10^{-3})	CL%	DOCUMENT ID		TECN	COMMENT
<0.51	90	[19] HE	08A	CLEO	$e^+e^- \to \ell^+\ell^-\gamma\gamma$

[19] Authors assume B($\Upsilon(2S) \to e^+e^-$) + B($\Upsilon(1S) \to \mu^+\mu^-$) = 4.06%.

$\Gamma(\Upsilon(1S)\pi^+\pi^-)/\Gamma_{\text{total}}$ Γ_6/Γ

Abbreviation MM in the *COMMENT* field below stands for missing mass.

VALUE (units 10^{-2})	EVTS	DOCUMENT ID		TECN	COMMENT
4.37±0.08 OUR AVERAGE					
4.32±0.07±0.13	90k	[20] LEES	11L	BABR	$\Upsilon(3S) \to \pi^+\pi^-\ell^+\ell^-$
4.46±0.01±0.13	190k	[21] BHARI	09	CLEO	$e^+e^- \to \pi^+\pi^-$ MM
4.17±0.06±0.19	6.4K	[22] AUBERT	08BP	BABR	10.58 $e^+e^- \to \gamma\pi^+\pi^-\ell^+\ell^-$
4.52±0.35	11830	[23] BUTLER	94B	CLE2	$e^+e^- \to \pi^+\pi^-$X, $\pi^+\pi^-\ell^+\ell^-$
4.46±0.34±0.50	451	[23] WU	93	CUSB	$\Upsilon(3S) \to \pi^+\pi^-\ell^+\ell^-$
4.46±0.30	11221	[23] BROCK	91	CLEO	$e^+e^- \to \pi^+\pi^-$X, $\pi^+\pi^-\ell^+\ell^-$
• • • We do not use the following data for averages, fits, limits, etc. • • •					
4.9 ±1.0	22	GREEN	82	CLEO	$\Upsilon(3S) \to \pi^+\pi^-\ell^+\ell^-$
3.9 ±1.3	26	MAGERAS	82	CUSB	$\Upsilon(3S) \to \pi^+\pi^-\ell^+\ell^-$

[20] Using $B(\Upsilon(1S) \to e^+e^-) = (2.38 \pm 0.11)\%$ and $B(\Upsilon(1S) \to \mu^+\mu^-) = (2.48 \pm 0.05)\%$.

[21] A weighted average of the inclusive and exclusive results.

[22] Using $B(\Upsilon(2S) \to e^+e^-) = (1.91 \pm 0.16)\%$, $B(\Upsilon(2S) \to \mu^+\mu^-) = (1.93 \pm 0.17)\%$, and $\Gamma_{ee}(\Upsilon(3S)) = 0.443 \pm 0.008$ keV.

[23] Using $B(\Upsilon(1S) \to \mu^+\mu^-) = (2.48 \pm 0.06)\%$. With the assumption of $e\mu$ universality.

$\Gamma(\Upsilon(2S)\pi^+\pi^-)/\Gamma(\Upsilon(1S)\pi^+\pi^-)$ Γ_2/Γ_6

VALUE	EVTS	DOCUMENT ID		TECN	COMMENT
• • • We do not use the following data for averages, fits, limits, etc. • • •					
$0.577 \pm 0.026 \pm 0.060$	800	[24] AUBERT	08BP	BABR	$e^+e^- \to \gamma\pi^+\pi^-\ell^+\ell^-$

[24] Using $B(\Upsilon(1S) \to e^+e^-) = (2.38 \pm 0.11)\%$, $B(\Upsilon(1S) \to \mu^+\mu^-) = (2.48 \pm 0.05)\%$, $B(\Upsilon(2S) \to e^+e^-) = (1.91 \pm 0.16)\%$, and $B(\Upsilon(2S) \to \mu^+\mu^-) = (1.93 \pm 0.17)\%$. Not independent of other values reported by AUBERT 08BP.

$\Gamma(\Upsilon(1S)\pi^0\pi^0)/\Gamma_{total}$ Γ_7/Γ

VALUE (units 10^{-2})	EVTS	DOCUMENT ID		TECN	COMMENT
2.20±0.13 OUR AVERAGE					
$2.24 \pm 0.09 \pm 0.11$	6584	[25] BHARI	09	CLEO	$e^+e^- \to \pi^0\pi^0\ell^+\ell^-$
1.99 ± 0.34	56	[26] BUTLER	94B	CLE2	$e^+e^- \to \pi^0\pi^0\ell^+\ell^-$
$2.2 \pm 0.4 \pm 0.3$	33	[27] HEINTZ	92	CSB2	$e^+e^- \to \pi^0\pi^0\ell^+\ell^-$

[25] Authors assume $B(\Upsilon(1S) \to e^+e^-) + B(\Upsilon(1S) \to \mu^+\mu^-) = 4.96\%$.

[26] Using $B(\Upsilon(1S) \to \mu^+\mu^-) = (2.48 \pm 0.06)\%$ and assuming $e\mu$ universality.

[27] Using $B(\Upsilon(1S) \to \mu^+\mu^-) = (2.57 \pm 0.07)\%$ and assuming $e\mu$ universality. Supersedes HEINTZ 91.

$\Gamma(\Upsilon(1S)\pi^0\pi^0)/\Gamma(\Upsilon(1S)\pi^+\pi^-)$ Γ_7/Γ_6

VALUE	DOCUMENT ID		TECN	COMMENT
• • • We do not use the following data for averages, fits, limits, etc. • • •				
0.501 ± 0.043	[28] BHARI	09	CLEO	$e^+e^- \to \Upsilon(3S)$

[28] Not independent of other values reported by BHARI 09.

$\Gamma(\Upsilon(1S)\eta)/\Gamma_{total}$ Γ_8/Γ

VALUE (units 10^{-3})	CL%	DOCUMENT ID		TECN	COMMENT
<0.1	90	[29] LEES	11L	BABR	$\Upsilon(3S) \to (\pi^+\pi^-)(\gamma\gamma)\ell^+\ell^-$
• • • We do not use the following data for averages, fits, limits, etc. • • •					
<0.8	90	[29,30] AUBERT	08BP	BABR	$e^+e^- \to \gamma\pi^+\pi^-\pi^0\ell^+\ell^-$
<0.18	90	[31] HE	08A	CLEO	$e^+e^- \to \ell^+\ell^-\eta$
<2.2	90	BROCK	91	CLEO	$e^+e^- \to \ell^+\ell^-\eta$

[29] Using $B(\Upsilon(1S) \to e^+e^-) = (2.38 \pm 0.11)\%$, $B(\Upsilon(1S) \to \mu^+\mu^-) = (2.48 \pm 0.05)\%$.

[30] Using $\Gamma_{ee}(\Upsilon(3S)) = 0.443 \pm 0.008$ keV.

[31] Authors assume $B(\Upsilon(1S) \to e^+e^-) + B(\Upsilon(1S) \to \mu^+\mu^-) = 4.96\%$.

$\Gamma(\Upsilon(1S)\eta)/\Gamma(\Upsilon(1S)\pi^+\pi^-)$ Γ_8/Γ_6

VALUE (units 10^{-2})	CL%	DOCUMENT ID		TECN	COMMENT
<0.23	90	[32] LEES	11L	BABR	$\Upsilon(3S) \to (\pi^+\pi^-)(\gamma\gamma)\ell^+\ell^-$
• • • We do not use the following data for averages, fits, limits, etc. • • •					
<1.9	90	[33] AUBERT	08BP	BABR	$e^+e^- \to \gamma\pi^+\pi^-(\pi^0)\ell^+\ell^-$

[32] Not independent of other values reported by LEES 11L.

[33] Not independent of other values reported by AUBERT 08BP.

$\Gamma(\Upsilon(1S)\pi^0)/\Gamma_{total}$ Γ_9/Γ

VALUE (units 10^{-3})	CL%	DOCUMENT ID		TECN	COMMENT
<0.07	90	[34] HE	08A	CLEO	$e^+e^- \to \ell^+\ell^-\gamma\gamma$

[34] Authors assume $B(\Upsilon(1S) \to e^+e^-) + B(\Upsilon(1S) \to \mu^+\mu^-) = 4.96\%$.

$\Gamma(h_b(1P)\pi^0)/\Gamma_{total}$ Γ_{10}/Γ

VALUE	CL%	DOCUMENT ID		TECN	COMMENT
$<1.2 \times 10^{-3}$	90	[35] GE	11	CLEO	$\Upsilon(3S) \to \pi^0$ anything

[35] Assuming $M(h_b(1P)) = 9900$ MeV and $\Gamma(h_b(1P)) = 0$ MeV, and allowing $B(h_b(1P) \to \gamma\eta_b(1S))$ to vary from 0–100%.

$\Gamma(h_b(1P)\pi^0 \to \gamma\eta_b(1S)\pi^0)/\Gamma_{total}$ Γ_{11}/Γ

VALUE (units 10^{-4})	DOCUMENT ID		TECN	COMMENT
4.3±1.1±0.9	LEES	11K	BABR	$\Upsilon(3S) \to \eta_b\gamma\pi^0$

$\Gamma(h_b(1P)\pi^+\pi^-)/\Gamma_{total}$ Γ_{12}/Γ

VALUE (units 10^{-4})	CL%	DOCUMENT ID		TECN	COMMENT
< 1.2	90	[36] LEES	11C	BABR	$e^+e^- \to \pi^+\pi^- X$
• • • We do not use the following data for averages, fits, limits, etc. • • •					
<18		[36] BUTLER	94B	CLE2	$e^+e^- \to \pi^+\pi^- X$
<15		[36] BROCK	91	CLEO	$e^+e^- \to \pi^+\pi^- X$

[36] For $M(h_b(1P)) = 9900$ MeV.

$\Gamma(\tau^+\tau^-)/\Gamma_{total}$ Γ_{13}/Γ

VALUE (units 10^{-2})	EVTS	DOCUMENT ID		TECN	COMMENT
2.29±0.21±0.22	15k	[37] BESSON	07	CLEO	$e^+e^- \to \Upsilon(3S) \to \tau^+\tau^-$

[37] BESSON 07 reports $[\Gamma(\Upsilon(3S) \to \tau^+\tau^-)/\Gamma_{total}] / [B(\Upsilon(3S) \to \mu^+\mu^-)] = 1.05 \pm 0.08 \pm 0.05$ which we multiply by our best value $B(\Upsilon(3S) \to \mu^+\mu^-) = (2.18 \pm 0.21) \times 10^{-2}$. Our first error is their experiment's error and our second error is the systematic error from using our best value.

$\Gamma(\tau^+\tau^-)/\Gamma(\mu^+\mu^-)$ Γ_{13}/Γ_{14}

VALUE	EVTS	DOCUMENT ID		TECN	COMMENT
1.05±0.08±0.05	15k	BESSON	07	CLEO	$e^+e^- \to \Upsilon(3S)$

$\Gamma(\mu^+\mu^-)/\Gamma_{total}$ Γ_{14}/Γ

VALUE	EVTS	DOCUMENT ID		TECN	COMMENT
0.0218±0.0021 OUR AVERAGE Error includes scale factor of 2.1. See the ideogram below.					
$0.0239 \pm 0.0007 \pm 0.0010$	81k	ADAMS	05	CLEO	$e^+e^- \to \mu^+\mu^-$
$0.0202 \pm 0.0019 \pm 0.0033$		CHEN	89B	CLEO	$e^+e^- \to \mu^+\mu^-$
$0.0173 \pm 0.0015 \pm 0.0011$		KAARSBERG	89	CSB2	$e^+e^- \to \mu^+\mu^-$
$0.033 \pm 0.013 \pm 0.007$	1096	ANDREWS	83	CLEO	$e^+e^- \to \mu^+\mu^-$

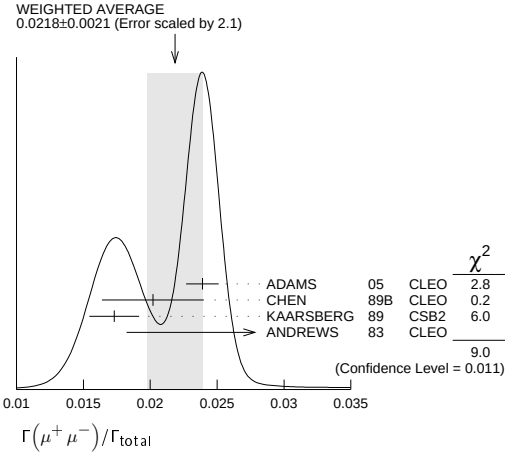

$\Gamma(ggg)/\Gamma_{total}$ Γ_{17}/Γ

VALUE (units 10^{-2})	EVTS	DOCUMENT ID		TECN	COMMENT
35.7±2.6	3M	[38] BESSON	06A	CLEO	$\Upsilon(3S) \to$ hadrons

[38] Calculated using BESSON 06A value of $\Gamma(\gamma gg)/\Gamma(ggg) = (2.72 \pm 0.06 \pm 0.32 \pm 0.37)\%$ and the PDG 08 values of $B(\Upsilon(2S) + \text{anything}) = (10.6 \pm 0.8)\%$, $B(\pi^+\pi^-\Upsilon(1S)) = (4.40 \pm 0.10)\%$, $B(\pi^0\pi^0\Upsilon(1S)) = (2.20 \pm 0.13)\%$, $B(\gamma\chi_{b2}(2P)) = (13.1 \pm 1.6)\%$, $B(\gamma\chi_{b1}(2P)) = (12.6 \pm 1.2)\%$, $B(\gamma\chi_{b0}(2P)) = (5.9 \pm 0.6)\%$, $B(\gamma\chi_{b0}(1P)) = (0.30 \pm 0.11)\%$,$B(\mu^+\mu^-) = (2.18 \pm 0.21)\%$, and $R_{hadrons} = 3.51$. The statistical error is negligible and the systematic error is partially correlated with $\Gamma(\gamma gg)/\Gamma_{total}$ BESSON 06A value.

$\Gamma(\gamma gg)/\Gamma_{total}$ Γ_{18}/Γ

VALUE (units 10^{-2})	EVTS	DOCUMENT ID		TECN	COMMENT
0.97±0.18	60k	[39] BESSON	06A	CLEO	$\Upsilon(3S) \to \gamma +$ hadrons

[39] Calculated using BESSON 06A values of $\Gamma(\gamma gg)/\Gamma(ggg) = (2.72 \pm 0.06 \pm 0.32 \pm 0.37)\%$ and $\Gamma(ggg)/\Gamma_{total}$. The statistical error is negligible and the systematic error is partially correlated with $\Gamma(ggg)/\Gamma_{total}$ BESSON 06A value.

$\Gamma(\gamma gg)/\Gamma(ggg)$ Γ_{18}/Γ_{17}

VALUE (units 10^{-2})	EVTS	DOCUMENT ID		TECN	COMMENT
2.72±0.06±0.49	3M	BESSON	06A	CLEO	$\Upsilon(3S) \to (\gamma +)$ hadrons

$\Gamma(\gamma\chi_{b2}(2P))/\Gamma_{total}$ Γ_{19}/Γ

VALUE	EVTS	DOCUMENT ID		TECN	COMMENT
0.131 ±0.016 OUR AVERAGE Error includes scale factor of 3.4. See the ideogram below.					
$0.1579 \pm 0.0017 \pm 0.0073$	568k	ARTUSO	05	CLEO	$e^+e^- \to \gamma X$
$0.111 \pm 0.005 \pm 0.004$	10319	[40] HEINTZ	92	CSB2	$e^+e^- \to \gamma X$
$0.135 \pm 0.003 \pm 0.017$	30741	MORRISON	91	CLE2	$e^+e^- \to \gamma X$

[40] Supersedes NARAIN 91.

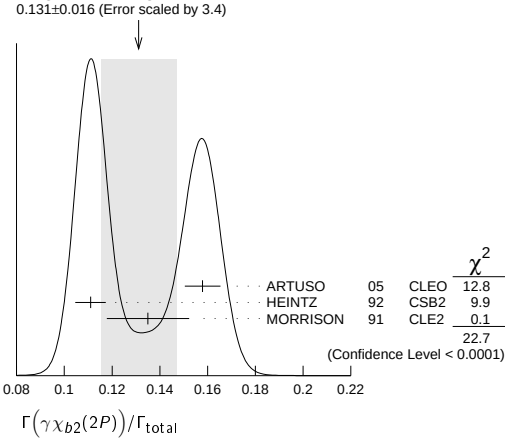

Meson Particle Listings

$\Upsilon(3S)$

$\Gamma(\gamma\chi_{b1}(2P))/\Gamma_{\text{total}}$ Γ_{20}/Γ

VALUE	EVTS	DOCUMENT ID		TECN	COMMENT
0.126 ±0.012 OUR AVERAGE Error includes scale factor of 2.4. See the ideogram below.					
0.1454±0.0018±0.0073	537k	ARTUSO	05	CLEO	$e^+e^- \to \gamma X$
0.115 ±0.005 ±0.005	11147	[41] HEINTZ	92	CSB2	$e^+e^- \to \gamma X$
0.105 $^{+0.003}_{-0.002}$ ±0.013	25759	MORRISON	91	CLE2	$e^+e^- \to \gamma X$

[41] Supersedes NARAIN 91.

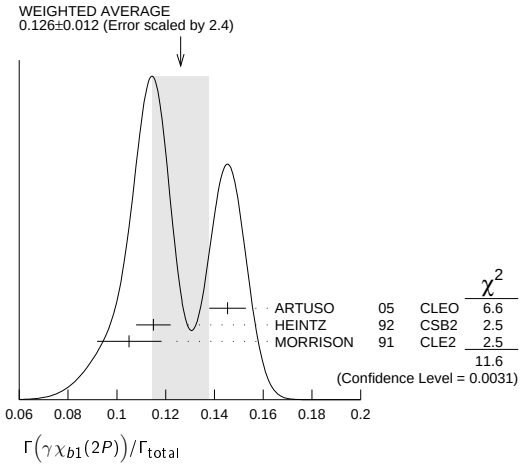

$\Gamma(\gamma\chi_{b0}(2P))/\Gamma_{\text{total}}$ Γ_{21}/Γ

VALUE	EVTS	DOCUMENT ID		TECN	COMMENT
0.059 ±0.006 OUR AVERAGE Error includes scale factor of 1.4. See the ideogram below.					
0.0677±0.0020±0.0065	225k	ARTUSO	05	CLEO	$e^+e^- \to \gamma X$
0.060 ±0.004 ±0.006	4959	[42] HEINTZ	92	CSB2	$e^+e^- \to \gamma X$
0.049 $^{+0.003}_{-0.004}$ ±0.006	9903	MORRISON	91	CLE2	$e^+e^- \to \gamma X$

[42] Supersedes NARAIN 91.

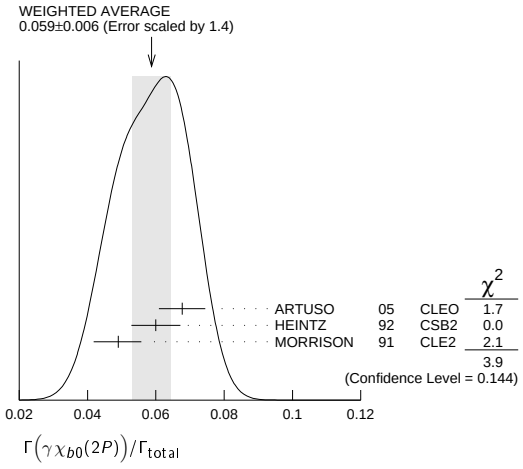

$\Gamma(\gamma\chi_{b2}(1P))/\Gamma_{\text{total}}$ Γ_{22}/Γ

VALUE (units 10^{-3})	CL%	EVTS	DOCUMENT ID		TECN	COMMENT
9.9±1.3 OUR AVERAGE Error includes scale factor of 2.0.						
7.5±1.2±0.5		126	[43,44] KORNICER	11	CLEO	$e^+e^- \to \gamma\gamma\ell^+\ell^-$
10.5±0.3$^{+0.7}_{-0.6}$		9.7k	LEES	11J	BABR	$\Upsilon(3S) \to X\gamma$
• • • We do not use the following data for averages, fits, limits, etc. • • •						
<19	90		[45] ASNER	08A	CLEO	$\Upsilon(3S) \to \gamma+$ hadrons
seen			[46] HEINTZ	92	CSB2	$e^+e^- \to \gamma\gamma\ell^+\ell^-$

[43] Assuming B($\Upsilon(1S) \to \ell^+\ell^-$) = (2.48 ± 0.05)%.

[44] KORNICER 11 reports [$\Gamma(\Upsilon(3S) \to \gamma\chi_{b2}(1P))/\Gamma_{\text{total}}$] × [B($\chi_{b2}(1P) \to \gamma\Upsilon(1S)$)] = (1.435 ± 0.162 ± 0.169) × 10^{-3} which we divide by our best value B($\chi_{b2}(1P) \to \gamma\Upsilon(1S)$) = (19.1 ± 1.2) × 10^{-2}. Our first error is their experiment's error and our second error is the systematic error from using our best value.

[45] ASNER 08A reports [$\Gamma(\Upsilon(3S) \to \gamma\chi_{b2}(1P))/\Gamma_{\text{total}}$] / [B($\Upsilon(2S) \to \gamma\chi_{b2}(1P)$)] < 27.1 × 10^{-2} which we multiply by our best value B($\Upsilon(2S) \to \gamma\chi_{b2}(1P)$) = 7.15 × 10^{-2}.

[46] HEINTZ 92, while unable to distinguish between different J states, measures $\sum_J$B($\Upsilon(3S) \to \gamma\chi_{bJ}$) × B($\chi_{bJ} \to \gamma\Upsilon(1S)$) = (1.7 ± 0.4 ± 0.6) × 10^{-3} for J = 0,1,2 using inclusive $\Upsilon(1S)$ decays and (1.2$^{+0.4}_{-0.3}$ ± 0.09) × 10^{-3} for J = 1,2 using $\Upsilon(1S) \to \ell^+\ell^-$.

$\Gamma(\gamma\chi_{b1}(1P))/\Gamma_{\text{total}}$ Γ_{24}/Γ

VALUE (units 10^{-3})	CL%	EVTS	DOCUMENT ID		TECN	COMMENT
0.9±0.5 OUR AVERAGE Error includes scale factor of 1.9.						
1.6±0.5±0.1		50	[47,48] KORNICER	11	CLEO	$e^+e^- \to \gamma\gamma\ell^+\ell^-$
0.5±0.3$^{+0.2}_{-0.1}$			LEES	11J	BABR	$\Upsilon(3S) \to X\gamma$
• • • We do not use the following data for averages, fits, limits, etc. • • •						
<1.7	90		[49] ASNER	08A	CLEO	$\Upsilon(3S) \to \gamma+$ hadrons
seen			[50] HEINTZ	92	CSB2	$e^+e^- \to \gamma\gamma\ell^+\ell^-$

[47] Assuming B($\Upsilon(1S) \to \ell^+\ell^-$) = (2.48 ± 0.05)%.

[48] KORNICER 11 reports [$\Gamma(\Upsilon(3S) \to \gamma\chi_{b1}(1P))/\Gamma_{\text{total}}$] × [B($\chi_{b1}(1P) \to \gamma\Upsilon(1S)$)] = (5.38 ± 1.20 ± 0.95) × 10^{-4} which we divide by our best value B($\chi_{b1}(1P) \to \gamma\Upsilon(1S)$) = (33.9 ± 2.2) × 10^{-2}. Our first error is their experiment's error and our second error is the systematic error from using our best value.

[49] ASNER 08A reports [$\Gamma(\Upsilon(3S) \to \gamma\chi_{b1}(1P))/\Gamma_{\text{total}}$] / [B($\Upsilon(2S) \to \gamma\chi_{b1}(1P)$)] < 2.5 × 10^{-2} which we multiply by our best value B($\Upsilon(2S) \to \gamma\chi_{b1}(1P)$) = 6.9 × 10^{-2}.

[50] HEINTZ 92, while unable to distinguish between different J states, measures $\sum_J$B($\Upsilon(3S) \to \gamma\chi_{bJ}$) × B($\chi_{bJ} \to \gamma\Upsilon(1S)$) = (1.7 ± 0.4 ± 0.6) × 10^{-3} for J = 0,1,2 using inclusive $\Upsilon(1S)$ decays and (1.2$^{+0.4}_{-0.3}$ ± 0.09) × 10^{-3} for J = 1,2 using $\Upsilon(1S) \to \ell^+\ell^-$.

$\Gamma(\gamma\chi_{b0}(1P))/\Gamma_{\text{total}}$ Γ_{25}/Γ

VALUE (units 10^{-2})	CL%	EVTS	DOCUMENT ID		TECN	COMMENT
0.27±0.04 OUR AVERAGE						
0.27±0.04±0.02		2.3k	LEES	11J	BABR	$\Upsilon(3S) \to X\gamma$
0.30±0.04±0.10		8.7k	ARTUSO	05	CLEO	$e^+e^- \to \gamma X$
• • • We do not use the following data for averages, fits, limits, etc. • • •						
<0.8	90		[51] ASNER	08A	CLEO	$\Upsilon(3S) \to \gamma+$ hadrons

[51] ASNER 08A reports [$\Gamma(\Upsilon(3S) \to \gamma\chi_{b0}(1P))/\Gamma_{\text{total}}$] / [B($\Upsilon(2S) \to \gamma\chi_{b0}(1P)$)] < 21.9 × 10^{-2} which we multiply by our best value B($\Upsilon(2S) \to \gamma\chi_{b0}(1P)$) = 3.8 × 10^{-2}.

$\Gamma(\gamma\eta_b(2S))/\Gamma_{\text{total}}$ Γ_{26}/Γ

VALUE (units 10^{-4})	CL%	DOCUMENT ID		TECN	COMMENT
< 6.2	90	ARTUSO	05	CLEO	$e^+e^- \to \gamma X$
• • • We do not use the following data for averages, fits, limits, etc. • • •					
<19	90	LEES	11J	BABR	$\Upsilon(3S) \to X\gamma$

$\Gamma(\gamma\eta_b(1S))/\Gamma_{\text{total}}$ Γ_{27}/Γ

VALUE (units 10^{-4})	CL%	EVTS	DOCUMENT ID		TECN	COMMENT
5.1±0.7 OUR AVERAGE						
7.1±1.8±1.3		2.3±0.5k	[52] BONVICINI	10	CLEO	$\Upsilon(3S) \to \gamma X$
4.8±0.5±0.6		19 ± 3k	[52] AUBERT	09AQ	BABR	$\Upsilon(3S) \to \gamma X$
• • • We do not use the following data for averages, fits, limits, etc. • • •						
<8.5	90		LEES	11J	BABR	$\Upsilon(3S) \to X\gamma$
4.8±0.5±1.2		19 ± 3k	[52,53] AUBERT	08V	BABR	$\Upsilon(3S) \to \gamma X$
<4.3	90		[54] ARTUSO	05	CLEO	$e^+e^- \to \gamma X$

[52] Assuming $\Gamma_{\eta_b(1S)}$ = 10 MeV.

[53] Systematic error re-evaluated by AUBERT 09AQ.

[54] Superseded by BONVICINI 10.

$\Gamma(\gamma X \to \gamma+ \geq 4 \text{ prongs})/\Gamma_{\text{total}}$ Γ_{28}/Γ

(1.5 GeV < m_X < 5.0 GeV)

VALUE (units 10^{-4})	CL%	DOCUMENT ID		TECN	COMMENT
<2.2	95	ROSNER	07A	CLEO	$e^+e^- \to \gamma X$

$\Gamma(\gamma a_1^0 \to \gamma\mu^+\mu^-)/\Gamma_{\text{total}}$ Γ_{29}/Γ

VALUE (units 10^{-6})	CL%	DOCUMENT ID		TECN	COMMENT
<5.5	90	[55] AUBERT	09Z	BABR	$e^+e^- \to \gamma a_1^0 \to \gamma\mu^+\mu^-$

[55] For a narrow scalar or pseudoscalar a_1^0 with mass in the range 212–9300 MeV, excluding J/ψ and $\psi(2S)$. Measured 90% CL limits as a function of $m_{a_1^0}$ range from 0.27–5.5 × 10^{-6}.

$\Gamma(\gamma a_1^0 \to \gamma\tau^+\tau^-)/\Gamma_{\text{total}}$ Γ_{30}/Γ

VALUE	CL%	DOCUMENT ID		TECN	COMMENT
<1.6 × 10^{-4}	90	[56] AUBERT	09P	BABR	$e^+e^- \to \gamma a_1^0 \to \gamma\tau^+\tau^-$

[56] For a narrow scalar or pseudoscalar a_1^0 with M($\tau^+\tau^-$) in the ranges 4.03–9.52 and 9.61–10.10 GeV. Measured 90% CL limits as a function of M($\tau^+\tau^-$) range from 1.5–16 × 10^{-5}.

$\Gamma(\gamma A^0 \to \gamma\text{hadrons})/\Gamma_{\text{total}}$ Γ_{23}/Γ

(0.3 GeV < m_{A^0} < 7 GeV)

VALUE	CL%	DOCUMENT ID		TECN	COMMENT
<8 × 10^{-5}	90	[57] LEES	11H	BABR	$\Upsilon(3S) \to \gamma$ hadrons

[57] For a narrow scalar or pseudoscalar A^0, excluding known resonances, with mass in the range 0.3–7 GeV. Measured 90% CL limits as a function of m_{A^0} range from 1 × 10^{-6} to 8 × 10^{-5}.

LEPTON FAMILY NUMBER (*LF*) VIOLATING MODES

$\Gamma(e^{\pm}\tau^{\mp})/\Gamma_{total}$ Γ_{31}/Γ

VALUE (units 10^{-6})	CL%	DOCUMENT ID		TECN	COMMENT
<4.2	90	LEES	10B	BABR	$e^+e^- \to e^{\pm}\tau^{\mp}$

$\Gamma(\mu^{\pm}\tau^{\mp})/\Gamma_{total}$ Γ_{32}/Γ

VALUE (units 10^{-6})	CL%	DOCUMENT ID		TECN	COMMENT
< 3.1	90	LEES	10B	BABR	$e^+e^- \to \mu^{\pm}\tau^{\mp}$
• • • We do not use the following data for averages, fits, limits, etc. • • •					
<20.3	95	LOVE	08A	CLEO	$e^+e^- \to \mu^{\pm}\tau^{\mp}$

$\Upsilon(3S)$ REFERENCES

GE	11	PR D84 032008	J.Y. Ge *et al.*	(CLEO Collab.)
KORNICER	11	PR D83 054003	M. Kornicer *et al.*	(CLEO Collab.)
LEES	11C	PR D84 011104	J.P. Lees *et al.*	(BABAR Collab.)
LEES	11H	PRL 107 221803	J.P. Lees *et al.*	(BABAR Collab.)
LEES	11J	PR D84 072002	J.P. Lees *et al.*	(BABAR Collab.)
LEES	11K	PR D84 091101	J.P. Lees *et al.*	(BABAR Collab.)
LEES	11L	PR D84 092003	J.P. Lees *et al.*	(BABAR Collab.)
BONVICINI	10	PR D81 031104	G. Bonvicini *et al.*	(CLEO Collab.)
LEES	10B	PRL 104 151802	J.P. Lees *et al.*	(BABAR Collab.)
AUBERT	09AQ	PRL 103 161801	B. Aubert *et al.*	(BABAR Collab.)
AUBERT	09P	PRL 103 181801	B. Aubert *et al.*	(BABAR Collab.)
AUBERT	09Z	PRL 103 081803	B. Aubert *et al.*	(BABAR Collab.)
BHARI	09	PR D79 011103	S.R. Bhari *et al.*	(CLEO Collab.)
ASNER	08A	PR D78 091103	D.M. Asner *et al.*	(CLEO Collab.)
AUBERT	08BP	PR D78 112002	B. Aubert *et al.*	(BABAR Collab.)
AUBERT	08V	PRL 101 071801	B. Aubert *et al.*	(BABAR Collab.)
HE	08A	PRL 101 192001	Q. He *et al.*	(CLEO Collab.)
LOVE	08A	PRL 101 201601	W. Love *et al.*	(CLEO Collab.)
PDG	08	PL B667 1	C. Amsler *et al.*	(PDG Collab.)
BESSON	07	PRL 98 052002	D. Besson *et al.*	(CLEO Collab.)
ROSNER	07A	PR D76 117102	J.L. Rosner *et al.*	(CLEO Collab.)
BESSON	06A	PR D74 012003	D. Besson *et al.*	(CLEO Collab.)
ROSNER	06	PRL 96 092003	J.L. Rosner *et al.*	(CLEO Collab.)
ADAMS	05	PRL 94 012001	G.S. Adams *et al.*	(CLEO Collab.)
ARTUSO	05	PRL 94 032001	M. Artuso *et al.*	(CLEO Collab.)
ARTAMONOV	00	PL B474 427	A.S. Artamonov *et al.*	
BUTLER	94B	PR D49 40	F. Butler *et al.*	(CLEO Collab.)
WU	93	PL B301 307	Q.W. Wu *et al.*	(CUSB Collab.)
HEINTZ	92	PR D46 1928	U. Heintz *et al.*	(CUSB II Collab.)
BROCK	91	PR D43 1448	I.C. Brock *et al.*	(CLEO Collab.)
HEINTZ	91	PRL 66 1563	U. Heintz *et al.*	(CUSB Collab.)
MORRISON	91	PRL 67 1696	R.J. Morrison *et al.*	(CLEO Collab.)
NARAIN	91	PRL 66 3113	M. Narain *et al.*	(CUSB Collab.)
CHEN	89B	PR D39 3528	W.Y. Chen *et al.*	(CLEO Collab.)
KAARSBERG	89	PRL 62 2077	T.M. Kaarsberg *et al.*	(CUSB Collab.)
BUCHMUEL...	88	HE e^+e^- Physics 412 Editors: A. Ali and P. Soeding, World Scientific, Singapore	W. Buchmueller, S. Cooper	(HANN, DESY, MIT)
COHEN	87	RMP 59 1121	E.R. Cohen, B.N. Taylor	(RISC, NBS)
BARU	86B	ZPHY C32 622 (erratum)	S.E. Baru *et al.*	(NOVO)
KURAEV	85	SJNP 41 466 Translated from YAF 41 733.	E.A. Kuraev, V.S. Fadin	(NOVO)
ARTAMONOV	84	PL 137B 272	A.S. Artamonov *et al.*	(NOVO)
GILES	84B	PR D29 1285	R. Giles *et al.*	(CLEO Collab.)
ANDREWS	83	PRL 50 807	D.E. Andrews *et al.*	(CLEO Collab.)
GREEN	82	PRL 49 617	J. Green *et al.*	(CLEO Collab.)
MAGERAS	82	PL 118B 453	G. Mageras *et al.*	(COLU, CORN, LSU+)

$\chi_b(3P)$

$I^G(J^{PC}) = ?^?(?^{?+})$

A mixture of $J = 0$, 1, and 2 spin components observed in the radiative decay to $\Upsilon(1S)$ and $\Upsilon(2S)$, therefore $C = +$.

$\chi_b(3P)$ MASS

VALUE (MeV)		DOCUMENT ID		TECN	COMMENT
10534± 9 OUR AVERAGE					
10530± 5± 9	[1]	AAD	12A	ATLS	$pp \to \gamma\mu^+\mu^- X$
10551±14±17	[1]	ABAZOV	12Q	D0	$p\overline{p} \to \gamma\mu^+\mu^- X$

[1] The mass barycenter of the merged lineshapes from the $J = 1$ and 2 states.

$\chi_b(3P)$ DECAY MODES

	Mode	Fraction (Γ_i/Γ)
Γ_1	$\Upsilon(1S)\gamma$	seen
Γ_2	$\Upsilon(2S)\gamma$	seen

$\chi_b(3P)$ BRANCHING RATIOS

$\Gamma(\Upsilon(1S)\gamma)/\Gamma_{total}$ Γ_1/Γ

VALUE	DOCUMENT ID		TECN	COMMENT
seen	AAD	12A	ATLS	$pp \to \gamma\mu^+\mu^- X$
• • • We do not use the following data for averages, fits, limits, etc. • • •				
seen	ABAZOV	12Q	D0	$p\overline{p} \to \gamma\mu^+\mu^- X$

$\Gamma(\Upsilon(2S)\gamma)/\Gamma_{total}$ Γ_2/Γ

VALUE	DOCUMENT ID		TECN	COMMENT
seen	AAD	12A	ATLS	$pp \to \gamma\mu^+\mu^- X$

$\chi_b(3P)$ REFERENCES

AAD	12A	PRL 108 152001	G. Aad *et al.*	(ATLAS Collab.)
ABAZOV	12Q	PR D86 031103	V.M. Abazov *et al.*	(D0 Collab.)

$\Upsilon(4S)$ or $\Upsilon(10580)$

$I^G(J^{PC}) = 0^-(1^{--})$

$\Upsilon(4S)$ MASS

VALUE (MeV)		DOCUMENT ID		TECN	COMMENT
10579.4±1.2 OUR AVERAGE					
10579.3±0.4±1.2		AUBERT	05Q	BABR	$e^+e^- \to$ hadrons
10580.0±3.5	[1]	BEBEK	87	CLEO	$e^+e^- \to$ hadrons
• • • We do not use the following data for averages, fits, limits, etc. • • •					
10577.4±1.0	[2]	LOVELOCK	85	CUSB	$e^+e^- \to$ hadrons

[1] Reanalysis of BESSON 85.
[2] No systematic error given.

$\Upsilon(4S)$ WIDTH

VALUE (MeV)	DOCUMENT ID		TECN	COMMENT
20.5±2.5 OUR AVERAGE				
20.7±1.6±2.5	AUBERT	05Q	BABR	$e^+e^- \to$ hadrons
20 ±2 ±4	BESSON	85	CLEO	$e^+e^- \to$ hadrons
• • • We do not use the following data for averages, fits, limits, etc. • • •				
25 ±2.5	LOVELOCK	85	CUSB	$e^+e^- \to$ hadrons

$\Upsilon(4S)$ DECAY MODES

	Mode	Fraction (Γ_i/Γ)		Confidence level
Γ_1	$B\overline{B}$	> 96	%	95%
Γ_2	B^+B^-	(51.4 ±0.6)	%	
Γ_3	D_s^+ anything + c.c.	(17.8 ±2.6)	%	
Γ_4	$B^0\overline{B}{}^0$	(48.6 ±0.6)	%	
Γ_5	$J/\psi K_S^0(J/\psi,\ \eta_c)K_S^0$	< 4	$\times 10^{-7}$	90%
Γ_6	non-$B\overline{B}$	< 4	%	95%
Γ_7	e^+e^-	(1.57±0.08)	$\times 10^{-5}$	
Γ_8	$\rho^+\rho^-$	< 5.7	$\times 10^{-6}$	90%
Γ_9	$K^*(892)^0\overline{K}{}^0$	< 2.0	$\times 10^{-6}$	90%
Γ_{10}	$J/\psi(1S)$ anything	< 1.9	$\times 10^{-4}$	95%
Γ_{11}	D^{*+} anything + c.c.	< 7.4	%	90%
Γ_{12}	ϕ anything	(7.1 ±0.6)	%	
Γ_{13}	$\phi\eta$	< 1.8	$\times 10^{-6}$	90%
Γ_{14}	$\phi\eta'$	< 4.3	$\times 10^{-6}$	90%
Γ_{15}	$\rho\eta$	< 1.3	$\times 10^{-6}$	90%
Γ_{16}	$\rho\eta'$	< 2.5	$\times 10^{-6}$	90%
Γ_{17}	$\Upsilon(1S)$ anything	< 4	$\times 10^{-3}$	90%
Γ_{18}	$\Upsilon(1S)\pi^+\pi^-$	(8.1 ±0.6)	$\times 10^{-5}$	
Γ_{19}	$\Upsilon(1S)\eta$	(1.96±0.28)	$\times 10^{-4}$	
Γ_{20}	$\Upsilon(2S)\pi^+\pi^-$	(8.6 ±1.3)	$\times 10^{-5}$	
Γ_{21}	$h_b(1P)\pi^+\pi^-$	not seen		
Γ_{22}	$\overline{d}$ anything	< 1.3	$\times 10^{-5}$	90%

$\Upsilon(4S)$ PARTIAL WIDTHS

$\Gamma(e^+e^-)$ Γ_7

VALUE (keV)	DOCUMENT ID		TECN	COMMENT
0.272±0.029 OUR AVERAGE	Error includes scale factor of 1.5. See the ideogram below.			
0.321±0.017±0.029	AUBERT	05Q	BABR	$e^+e^- \to$ hadrons
0.28 ±0.05 ±0.01	[3] ALBRECHT	95E	ARG	$e^+e^- \to$ hadrons
0.192±0.007±0.038	BESSON	85	CLEO	$e^+e^- \to$ hadrons
0.283±0.037	LOVELOCK	85	CUSB	$e^+e^- \to$ hadrons

[3] Using LEYAOUANC 77 parametrization of $\Gamma(s)$.

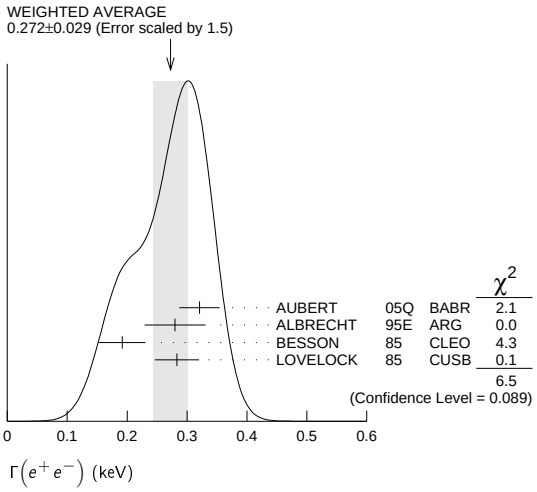

$\Upsilon(4S)$ BRANCHING RATIOS

$B\overline{B}$ DECAYS

The ratio of branching fraction to charged and neutral B mesons is often derived assuming isospin invariance in the decays, and relies on the knowledge of the B^+/B^0 lifetime ratio. "OUR EVALUATION" is obtained based on averages of rescaled data listed below. The average and rescaling were performed by the Heavy Flavor Averaging Group (HFAG) and are described at http://www.slac.stanford.edu/xorg/hfag/. The averaging/rescaling procedure takes into account the common dependence of the measurement on the value of the lifetime ratio.

$\Gamma(B^+B^-)/\Gamma_{total}$ Γ_2/Γ

VALUE	DOCUMENT ID
0.514±0.006 OUR EVALUATION	Assuming B($\Upsilon(4S) \to B\overline{B}$) = 1

$\Gamma(D_s^+ \text{ anything} + \text{c.c.})/\Gamma_{total}$ Γ_3/Γ

VALUE	DOCUMENT ID		TECN	COMMENT
0.178±0.021±0.016	[4] ARTUSO	05B	CLE3	$e^+e^- \to D_X X$

[4] ARTUSO 05B reports $[\Gamma(\Upsilon(4S) \to D_s^+ \text{ anything} + \text{c.c.})/\Gamma_{total}] \times [B(D_s^+ \to \phi\pi^+)] = (8.0 \pm 0.2 \pm 0.9) \times 10^{-3}$ which we divide by our best value $B(D_s^+ \to \phi\pi^+) = (4.5 \pm 0.4) \times 10^{-2}$. Our first error is their experiment's error and our second error is the systematic error from using our best value.

$\Gamma(B^0\overline{B}^0)/\Gamma_{total}$ Γ_4/Γ

VALUE	DOCUMENT ID	TECN	COMMENT
0.486±0.006 OUR EVALUATION	Assuming B($\Upsilon(4S) \to B\overline{B}$) = 1		
• • • We do not use the following data for averages, fits, limits, etc. • • •			
0.487±0.010±0.008	[5] AUBERT,B 05H	BABR	$\Upsilon(4S) \to \overline{B}B \to D^*\ell\nu_\ell$

[5] Direct measurement. This value is averaged with the value extracted from the $\Gamma(B^+B^-)$ / $\Gamma(B^0\overline{B}^0)$ measurements.

$\Gamma(B^+B^-)/\Gamma(B^0\overline{B}^0)$ Γ_2/Γ_4

VALUE	DOCUMENT ID		TECN	COMMENT
1.058±0.024 OUR EVALUATION				
1.006±0.036±0.031	[6] AUBERT	04F	BABR	$\Upsilon(4S) \to B\overline{B} \to J/\psi K$
1.01 ±0.03 ±0.09	[6] HASTINGS	03	BELL	$\Upsilon(4S) \to B\overline{B} \to$ dileptons
1.058±0.084±0.136	[7] ATHAR	02	CLEO	$\Upsilon(4S) \to B\overline{B} \to D^*\ell\nu$
1.10 ±0.06 ±0.05	[8] AUBERT	02	BABR	$\Upsilon(4S) \to B\overline{B} \to (c\overline{c})K^*$
1.04 ±0.07 ±0.04	[9] ALEXANDER	01	CLEO	$\Upsilon(4S) \to B\overline{B} \to J/\psi K^*$

[6] HASTINGS 03 and AUBERT 04F assume $\tau(B^+)$ / $\tau(B^0)$ = 1.083 ± 0.017.
[7] ATHAR 02 assumes $\tau(B^+)$ / $\tau(B^0)$ = 1.074 ± 0.028. Supersedes BARISH 95.
[8] AUBERT 02 assumes $\tau(B^+)$ / $\tau(B^0)$ = 1.062 ± 0.029.
[9] ALEXANDER 01 assumes $\tau(B^+)$ / $\tau(B^0)$ = 1.066 ± 0.024.

$\Gamma(J/\psi K_S^0(J/\psi, \eta_c)K_S^0)/\Gamma_{total}$ Γ_5/Γ

Forbidden by CP invariance.

VALUE (units 10^{-7})	CL%	DOCUMENT ID		TECN	COMMENT
<4	90	[10] TAJIMA	07A	BELL	$\Upsilon(4S) \to B^0\overline{B}^0$

[10] $\Upsilon(4S)$ with $CP = +1$ decays to the final state with $CP = -1$.

non-$B\overline{B}$ DECAYS

$\Gamma(\text{non-}B\overline{B})/\Gamma_{total}$ Γ_6/Γ

VALUE	CL%	DOCUMENT ID		TECN	COMMENT
<0.04	95	BARISH	96B	CLEO	e^+e^-

$\Gamma(e^+e^-)/\Gamma_{total}$ Γ_7/Γ

VALUE (units 10^{-5})	DOCUMENT ID		TECN	COMMENT
1.57±0.08 OUR AVERAGE				
1.55±0.04±0.07	AUBERT	05Q	BABR	$e^+e^- \to$ hadrons
2.77±0.50±0.49	[11] ALBRECHT	95E	ARG	$e^+e^- \to$ hadrons

[11] Using LEYAOUANC 77 parametrization of $\Gamma(s)$.

$\Gamma(\rho^+\rho^-)/\Gamma_{total}$ Γ_8/Γ

VALUE	CL%	DOCUMENT ID		TECN	COMMENT
<5.7 × 10^{-6}	90	AUBERT	08BO	BABR	$e^+e^- \to \pi^+\pi^- 2\pi^0$

$\Gamma(K^*(892)^0\overline{K}^0)/\Gamma_{total}$ Γ_9/Γ

VALUE	CL%	DOCUMENT ID		TECN	COMMENT
<2.0 × 10^{-6}	90	SHEN	13A	BELL	$e^+e^- \to K^*(892)^0\overline{K}^0$

$\Gamma(J/\psi(1S) \text{ anything})/\Gamma_{total}$ Γ_{10}/Γ

VALUE (units 10^{-4})	CL%	DOCUMENT ID		TECN	COMMENT
<1.9	95	[12] ABE	02D	BELL	$e^+e^- \to J/\psi X \to \ell^+\ell^- X$
• • • We do not use the following data for averages, fits, limits, etc. • • •					
<4.7	90	[12] AUBERT	01C	BABR	$e^+e^- \to J/\psi X \to \ell^+\ell^- X$

[12] Uses $B(J/\psi \to e^+e^-) = 0.0593 \pm 0.0010$ and $B(J/\psi \to \mu^+\mu^-) = 0.0588 \pm 0.0010$.

$\Gamma(D^{*+} \text{ anything} + \text{c.c.})/\Gamma_{total}$ Γ_{11}/Γ

VALUE	CL%	DOCUMENT ID		TECN	COMMENT
<0.074	90	[13] ALEXANDER	90C	CLEO	e^+e^-

[13] For $x > 0.473$.

$\Gamma(\phi \text{ anything})/\Gamma_{total}$ Γ_{12}/Γ

VALUE (units 10^{-2})	CL%	DOCUMENT ID		TECN	COMMENT
7.1 ±0.1±0.6		HUANG	07	CLEO	$\Upsilon(4S) \to \phi X$
• • • We do not use the following data for averages, fits, limits, etc. • • •					
<0.23	90	[14] ALEXANDER	90C	CLEO	e^+e^-

[14] For $x > 0.52$.

$\Gamma(\phi\eta)/\Gamma_{total}$ Γ_{13}/Γ

VALUE (units 10^{-6})	CL%	DOCUMENT ID		TECN	COMMENT
<1.8	90	[15] BELOUS	09	BELL	$e^+e^- \to \phi\eta$
• • • We do not use the following data for averages, fits, limits, etc. • • •					
<2.5	90	AUBERT,BE	06F	BABR	$e^+e^- \to \phi\eta$

[15] Using all intermedite branching fraction values from PDG 08.

$\Gamma(\phi\eta')/\Gamma_{total}$ Γ_{14}/Γ

VALUE (units 10^{-6})	CL%	DOCUMENT ID		TECN	COMMENT
<4.3	90	[16] BELOUS	09	BELL	$e^+e^- \to \phi\eta'$

[16] Using all intermedite branching fraction values from PDG 08.

$\Gamma(\rho\eta)/\Gamma_{total}$ Γ_{15}/Γ

VALUE (units 10^{-6})	CL%	DOCUMENT ID		TECN	COMMENT
<1.3	90	[17] BELOUS	09	BELL	$e^+e^- \to \rho\eta$

[17] Using all intermedite branching fraction values from PDG 08.

$\Gamma(\rho\eta')/\Gamma_{total}$ Γ_{16}/Γ

VALUE (units 10^{-6})	CL%	DOCUMENT ID		TECN	COMMENT
<2.5	90	[18] BELOUS	09	BELL	$e^+e^- \to \rho\eta'$

[18] Using all intermedite branching fraction values from PDG 08.

$\Gamma(\Upsilon(1S) \text{ anything})/\Gamma_{total}$ Γ_{17}/Γ

VALUE	CL%	DOCUMENT ID		TECN	COMMENT
<0.004	90	ALEXANDER	90C	CLEO	e^+e^-

$\Gamma(\Upsilon(1S)\pi^+\pi^-)/\Gamma_{total}$ Γ_{18}/Γ

VALUE (units 10^{-5})	CL%	EVTS	DOCUMENT ID		TECN	COMMENT
8.1 ±0.6 OUR AVERAGE						
8.5 ±1.3 ±0.2		113 ± 16	[19] SOKOLOV	09	BELL	$e^+e^- \to \pi^+\pi^-\mu^+\mu^-$
8.00±0.64±0.27		430	[20] AUBERT	08BP	BABR	$\Upsilon(4S) \to \pi^+\pi^-\ell^+\ell^-$
• • • We do not use the following data for averages, fits, limits, etc. • • •						
17.8 ±4.0 ±0.3			[21,22] SOKOLOV	07	BELL	$e^+e^- \to \pi^+\pi^-\mu^+\mu^-$
9.0 ±1.5 ±0.2		167 ± 19	[23] AUBERT	06R	BABR	$e^+e^- \to \pi^+\pi^-\mu^+\mu^-$
<12	90		GLENN	99	CLE2	e^+e^-

[19] SOKOLOV 09 reports $[\Gamma(\Upsilon(4S) \to \Upsilon(1S)\pi^+\pi^-)/\Gamma_{total}] \times [B(\Upsilon(1S) \to \mu^+\mu^-)] = (0.211 \pm 0.030 \pm 0.014) \times 10^{-5}$ which we divide by our best value $B(\Upsilon(1S) \to \mu^+\mu^-) = (2.48 \pm 0.05) \times 10^{-2}$. Our first error is their experiment's error and our second error is the systematic error from using our best value.
[20] Using $B(\Upsilon(1S) \to e^+e^-) = (2.38 \pm 0.11)\%$ and $B(\Upsilon(1S) \to \mu^+\mu^-) = (2.48 \pm 0.05)\%$.
[21] SOKOLOV 07 reports $[\Gamma(\Upsilon(4S) \to \Upsilon(1S)\pi^+\pi^-)/\Gamma_{total}] \times [B(\Upsilon(1S) \to \mu^+\mu^-)] = (4.42 \pm 0.81 \pm 0.56) \times 10^{-6}$ which we divide by our best value $B(\Upsilon(1S) \to \mu^+\mu^-) = (2.48 \pm 0.05) \times 10^{-2}$. Our first error is their experiment's error and our second error is the systematic error from using our best value.
[22] According to the authors, systematic errors were underestimated.
[23] Superseded by AUBERT 08BP. AUBERT 06R reports $[\Gamma(\Upsilon(4S) \to \Upsilon(1S)\pi^+\pi^-)/\Gamma_{total}] \times [B(\Upsilon(1S) \to \mu^+\mu^-)] = (2.23 \pm 0.25 \pm 0.27) \times 10^{-6}$ which we divide by our best value $B(\Upsilon(1S) \to \mu^+\mu^-) = (2.48 \pm 0.05) \times 10^{-2}$. Our first error is their experiment's error and our second error is the systematic error from using our best value.

$\Gamma(\Upsilon(1S)\eta)/\Gamma_{total}$ Γ_{19}/Γ

VALUE (units 10^{-4})	EVTS	DOCUMENT ID		TECN	COMMENT
1.96±0.26±0.09	56	[24] AUBERT	08BP	BABR	$\Upsilon(4S) \to \pi^+\pi^-\pi^0\ell^+\ell^-$

[24] Using B($\Upsilon(1S) \to e^+e^-$) = (2.38 ± 0.11)% and B($\Upsilon(1S) \to \mu^+\mu^-$) = (2.48 ± 0.05)%.

$\Gamma(\Upsilon(1S)\eta)/\Gamma(\Upsilon(1S)\pi^+\pi^-)$ Γ_{19}/Γ_{18}

VALUE	EVTS	DOCUMENT ID		TECN	COMMENT
• • • We do not use the following data for averages, fits, limits, etc. • • •					
2.41±0.40±0.12	56	[25] AUBERT	08BP	BABR	$\Upsilon(4S) \to \pi^+\pi^-(\pi^0)\ell^+\ell^-$

[25] Not independent of other values reported by AUBERT 08BP.

$\Gamma(\Upsilon(2S)\pi^+\pi^-)/\Gamma_{total}$ Γ_{20}/Γ

VALUE (units 10^{-4})	CL%	EVTS	DOCUMENT ID		TECN	COMMENT
0.86±0.11±0.07		220	[26] AUBERT	08BP	BABR	$\Upsilon(4S) \to \pi^+\pi^-\ell^+\ell^-$
• • • We do not use the following data for averages, fits, limits, etc. • • •						
0.88±0.17±0.08		97 ± 15	[27] AUBERT	06R	BABR	$e^+e^- \to \pi^+\pi^-\mu^+\mu^-$
<3.9	90		GLENN	99	CLE2	e^+e^-

[26] Using B($\Upsilon(2S) \to e^+e^-$) = (1.91 ± 0.16)% and B($\Upsilon(2S) \to \mu^+\mu^-$) = (1.93 ± 0.17)%.

[27] Superseded by AUBERT 08BP. AUBERT 06R reports [$\Gamma(\Upsilon(4S) \to \Upsilon(2S)\pi^+\pi^-)/\Gamma_{total}$] × [B($\Upsilon(2S) \to \mu^+\mu^-$)] = (1.69 ± 0.26 ± 0.20) × 10^{-6} which we divide by our best value B($\Upsilon(2S) \to \mu^+\mu^-$) = (1.93 ± 0.17) × 10^{-2}. Our first error is their experiment's error and our second error is the systematic error from using our best value.

$\Gamma(\Upsilon(2S)\pi^+\pi^-)/\Gamma(\Upsilon(1S)\pi^+\pi^-)$ Γ_{20}/Γ_{18}

VALUE	EVTS	DOCUMENT ID		TECN	COMMENT
• • • We do not use the following data for averages, fits, limits, etc. • • •					
1.16±0.16±0.14	220	[28] AUBERT	08BP	BABR	$\Upsilon(4S) \to \pi^+\pi^-\ell^+\ell^-$

[28] Using B($\Upsilon(1S) \to e^+e^-$) = (2.38 ± 0.11)%, B($\Upsilon(1S) \to \mu^+\mu^-$) = (2.48 ± 0.05)%, B($\Upsilon(2S) \to e^+e^-$) = (1.91 ± 0.16)%, and B($\Upsilon(2S) \to \mu^+\mu^-$) = (1.93 ± 0.17)%. Not independent of other values reported by AUBERT 08BP.

$\Gamma(h_b(1P)\pi^+\pi^-)/\Gamma_{total}$ Γ_{21}/Γ

VALUE	EVTS	DOCUMENT ID		TECN	COMMENT
not seen	35 ± 21k	[29] ADACHI	12	BELL	10.58 $e^+e^- \to h_b(1P)\pi^+\pi^-$

[29] From the upper limit on the ratio of $\sigma(e^+e^- \to h_b(1P)\pi^+\pi^-)$ at the $\Upsilon(4S)$ to that at the $\Upsilon(5S)$ of 0.27.

$\Gamma(\bar{d}\ \text{anything})/\Gamma_{total}$ Γ_{22}/Γ

VALUE (units 10^{-5})	CL%	DOCUMENT ID		TECN	COMMENT
<1.3	90	ASNER	07	CLEO	$e^+e^- \to \bar{d}X$

$\Upsilon(4S)$ REFERENCES

SHEN	13A	PR D88 052019	C.P. Shen *et al.*	(BELLE Collab.)
ADACHI	12	PRL 108 032001	I. Adachi *et al.*	(BELLE Collab.)
BELOUS	09	PL B681 400	K. Belous *et al.*	(BELLE Collab.)
SOKOLOV	09	PR D79 051103	A. Sokolov *et al.*	(BELLE Collab.)
AUBERT	08BO	PR D78 071103	B. Aubert *et al.*	(BABAR Collab.)
AUBERT	08BP	PR D78 112002	B. Aubert *et al.*	(BABAR Collab.)
PDG	08	PL B667 1	C. Amsler *et al.*	(PDG Collab.)
ASNER	07	PR D75 012009	D.M. Asner *et al.*	(CLEO Collab.)
HUANG	07	PR D75 012002	G.S. Huang *et al.*	(CLEO Collab.)
SOKOLOV	07	PR D75 071103	A. Sokolov *et al.*	(BELLE Collab.)
TAJIMA	07A	PRL 99 211601	O. Tajima *et al.*	(BELLE Collab.)
AUBERT	06R	PRL 96 232001	B. Aubert *et al.*	(BABAR Collab.)
AUBERT,BE	06F	PR D74 111103	B. Aubert *et al.*	(BABAR Collab.)
ARTUSO	05B	PRL 95 261801	M. Artuso *et al.*	(CLEO Collab.)
AUBERT	05Q	PR D72 032005	B. Aubert *et al.*	(BABAR Collab.)
AUBERT,B	05H	PRL 95 042001	B. Aubert *et al.*	(BABAR Collab.)
AUBERT	04F	PR D69 071101	B.Aubert *et al.*	
HASTINGS	03	PR D67 052004	N.C. Hastings *et al.*	(BELLE Collab.)
ABE	02D	PRL 88 052001	K. Abe *et al.*	(BELLE Collab.)
ATHAR	02	PR D66 052003	S.B. Athar *et al.*	(CLEO Collab.)
AUBERT	02	PR D65 032001	B. Aubert *et al.*	(BaBar Collab.)
ALEXANDER	01	PRL 86 2737	J.P. Alexander *et al.*	(CLEO Collab.)
AUBERT	01C	PRL 87 162002	B. Aubert *et al.*	(BaBar Collab.)
GLENN	99	PR D59 052003	S. Glenn *et al.*	
BARISH	96B	PRL 76 1570	B.C. Barish *et al.*	(CLEO Collab.)
ALBRECHT	95E	ZPHY C65 619	H. Albrecht *et al.*	(ARGUS Collab.)
BARISH	95	PR D51 1014	B.C. Barish *et al.*	(CLEO Collab.)
ALEXANDER	90C	PRL 64 2226	J. Alexander *et al.*	(CLEO Collab.)
BEBEK	87	PR D36 1289	C. Bebek *et al.*	(CLEO Collab.)
BESSON	85	PRL 54 381	D. Besson *et al.*	(CLEO Collab.)
LOVELOCK	85	PRL 54 377	D.M.J. Lovelock *et al.*	(CUSB Collab.)
LEYAOUANC	77	PL B71 397	A. Le Yaouanc *et al.*	(ORSAY)

$X(10610)^{\pm}$ $I^G(J^P) = 1^+(1^+)$

OMITTED FROM SUMMARY TABLE

Observed by BONDAR 12 in $\Upsilon(5S)$ decays to $\Upsilon(nS)\pi^+\pi^-$ (n = 1, 2, 3) and $h_b(mP)\pi^+\pi^-$ (m = 1, 2). $J^P = 1^+$ is favored from angular analyses. Isospin = 1 is favored due to observation by KROKOVNY 13 of a corresponding neutral state produced in $\Upsilon(10860) \to \Upsilon(2S)/\Upsilon(3S)\pi^0\pi^0$ decays at a consistent mass.

$X(10610)^{\pm}$ MASS

VALUE (MeV)	DOCUMENT ID		TECN	COMMENT
10607.2±2.0	[1] BONDAR	12	BELL	$e^+e^- \to$ hadrons
• • • We do not use the following data for averages, fits, limits, etc. • • •				
10611 ±4 ±3	[2] BONDAR	12	BELL	$e^+e^- \to \Upsilon(1S)\pi^+\pi^-$
10609 ±2 ±3	[2] BONDAR	12	BELL	$e^+e^- \to \Upsilon(2S)\pi^+\pi^-$
10608 ±2 ±3	[2] BONDAR	12	BELL	$e^+e^- \to \Upsilon(3S)\pi^+\pi^-$
10605 $\pm 2\ ^{+3}_{-1}$	[2] BONDAR	12	BELL	$e^+e^- \to h_b(1P)\pi^+\pi^-$
10599 $^{+6}_{-3}\ ^{+5}_{-4}$	[2] BONDAR	12	BELL	$e^+e^- \to h_b(2P)\pi^+\pi^-$

[1] Average of the BONDAR 12 measurements in separate channels.
[2] Superseded by the average measurement of BONDAR 12.

$X(10610)^{\pm}$ WIDTH

VALUE (MeV)	DOCUMENT ID		TECN	COMMENT
18.4± 2.4	[3] BONDAR	12	BELL	$e^+e^- \to$ hadrons
• • • We do not use the following data for averages, fits, limits, etc. • • •				
$22.3\pm\ 7.7^{+3.0}_{-4.0}$	[4] BONDAR	12	BELL	$e^+e^- \to \Upsilon(1S)\pi^+\pi^-$
$24.2\pm\ 3.1^{+2.0}_{-3.0}$	[4] BONDAR	12	BELL	$e^+e^- \to \Upsilon(2S)\pi^+\pi^-$
17.6± 3.0±3.0	[4] BONDAR	12	BELL	$e^+e^- \to \Upsilon(3S)\pi^+\pi^-$
$11.4^{+\ 4.5+2.1}_{-\ 3.9-1.2}$	[4] BONDAR	12	BELL	$e^+e^- \to h_b(1P)\pi^+\pi^-$
$13\ ^{+10}_{-\ 8}\ ^{+9}_{-7}$	[4] BONDAR	12	BELL	$e^+e^- \to h_b(2P)\pi^+\pi^-$

[3] Average of the BONDAR 12 measurements in separate channels.
[4] Superseded by the average measurement of BONDAR 12.

$X(10610)^+$ DECAY MODES

$X(10610)^-$ decay modes are charge conjugates of the modes below.

	Mode	Fraction (Γ_j/Γ)
Γ_1	$\Upsilon(1S)\pi^+$	seen
Γ_2	$\Upsilon(2S)\pi^+$	seen
Γ_3	$\Upsilon(3S)\pi^+$	seen
Γ_4	$h_b(1P)\pi^+$	seen
Γ_5	$h_b(2P)\pi^+$	seen

$X(10610)^{\pm}$ BRANCHING RATIOS

$\Gamma(\Upsilon(1S)\pi^+)/\Gamma_{total}$ Γ_1/Γ

VALUE	DOCUMENT ID		TECN	COMMENT
seen	BONDAR	12	BELL	$e^+e^- \to \Upsilon(1S)\pi^+\pi^-$

$\Gamma(\Upsilon(2S)\pi^+)/\Gamma_{total}$ Γ_2/Γ

VALUE	DOCUMENT ID		TECN	COMMENT
seen	BONDAR	12	BELL	$e^+e^- \to \Upsilon(2S)\pi^+\pi^-$

$\Gamma(\Upsilon(3S)\pi^+)/\Gamma_{total}$ Γ_3/Γ

VALUE	DOCUMENT ID		TECN	COMMENT
seen	BONDAR	12	BELL	$e^+e^- \to \Upsilon(3S)\pi^+\pi^-$

$\Gamma(h_b(1P)\pi^+)/\Gamma_{total}$ Γ_4/Γ

VALUE	DOCUMENT ID		TECN	COMMENT
seen	BONDAR	12	BELL	$e^+e^- \to h_b(1P)\pi^+\pi^-$

$\Gamma(h_b(2P)\pi^+)/\Gamma_{total}$ Γ_5/Γ

VALUE	DOCUMENT ID		TECN	COMMENT
seen	BONDAR	12	BELL	$e^+e^- \to h_b(2P)\pi^+\pi^-$

$X(10610)^{\pm}$ REFERENCES

KROKOVNY	13	PR D88 052016	P. Krokovny *et al.*	(BELLE Collab.)
BONDAR	12	PRL 108 122001	A. Bondar *et al.*	(BELLE Collab.)

Meson Particle Listings

$X(10610)^0$, $X(10650)^\pm$, $\Upsilon(10860)$

$X(10610)^0$

$I^G(J^P) = 1^+(1^+)$

OMITTED FROM SUMMARY TABLE

Observed by KROKOVNY 13 in $\Upsilon(10860) \to \Upsilon(nS)\pi^0\pi^0$ (n=2,3). Isospin 1 is favored from the proximity in mass to $X(10610)^\pm$ and their similarity of observed decay modes and cross sections. $J^P = 1^+$ is favored from angular analysis of $X(10610)^\pm$ decays by BONDAR 12.

$X(10610)^0$ MASS

VALUE (MeV)	DOCUMENT ID		TECN	COMMENT
10609±4±4	[1] KROKOVNY	13	BELL	$e^+e^- \to \Upsilon(2S)/\Upsilon(3S)\pi^0\pi^0$

[1] From a simultaneous fit to the KROKOVNY 13 Dalitz analysis of $e^+e^- \to \Upsilon(2S)/\Upsilon(3S)\pi^0\pi^0$ decays with fixed width $\Gamma(X(10610)^0) = 18.4$ MeV.

$X(10610)^0$ DECAY MODES

	Mode	Fraction (Γ_i/Γ)
Γ_1	$\Upsilon(1S)\pi^0$	not seen
Γ_2	$\Upsilon(2S)\pi^0$	seen
Γ_3	$\Upsilon(3S)\pi^0$	seen

$X(10610)^0$ BRANCHING RATIOS

$\Gamma(\Upsilon(1S)\pi^0)/\Gamma_{total}$ **Γ_1/Γ**

VALUE	DOCUMENT ID		TECN	COMMENT
not seen	KROKOVNY	13	BELL	$e^+e^- \to \Upsilon(1S)\pi^0\pi^0$

$\Gamma(\Upsilon(2S)\pi^0)/\Gamma_{total}$ **Γ_2/Γ**

VALUE	DOCUMENT ID		TECN	COMMENT
seen	[2] KROKOVNY	13	BELL	$e^+e^- \to \Upsilon(2S)\pi^0\pi^0$

[2] Combined significance in $e^+e^- \to \Upsilon(2S)/\Upsilon(3S)\pi^0\pi^0$, including systematics, of 6.5σ.

$\Gamma(\Upsilon(3S)\pi^0)/\Gamma_{total}$ **Γ_3/Γ**

VALUE	DOCUMENT ID		TECN	COMMENT
seen	[3] KROKOVNY	13	BELL	$e^+e^- \to \Upsilon(3S)\pi^0\pi^0$

[3] Combined significance in $e^+e^- \to \Upsilon(2S)/\Upsilon(3S)\pi^0\pi^0$, including systematics, of 6.5σ.

$X(10610)^0$ REFERENCES

KROKOVNY	13	PR D88 052016	P. Krokovny *et al.*	(BELLE Collab.)
BONDAR	12	PRL 108 122001	A. Bondar *et al.*	(BELLE Collab.)

$X(10650)^\pm$

$I^G(J^P) = ?^+(1^+)$

OMITTED FROM SUMMARY TABLE

Observed by BONDAR 12 in $\Upsilon(5S)$ decays to $\Upsilon(nS)\pi^+\pi^-$ (n = 1, 2, 3) and $h_b(mP)\pi^+\pi^-$ (m = 1, 2). $J^P = 1^+$ is favored from angular analyses.

$X(10650)^\pm$ MASS

VALUE (MeV)	DOCUMENT ID		TECN	COMMENT
10652.2±1.5	[1] BONDAR	12	BELL	$e^+e^- \to$ hadrons
• • • We do not use the following data for averages, fits, limits, etc. • • •				
10657 ±6 ±3	[2] BONDAR	12	BELL	$e^+e^- \to \Upsilon(1S)\pi^+\pi^-$
10651 ±2 ±3	[2] BONDAR	12	BELL	$e^+e^- \to \Upsilon(2S)\pi^+\pi^-$
10652 ±1 ±2	[2] BONDAR	12	BELL	$e^+e^- \to \Upsilon(3S)\pi^+\pi^-$
10654 ±3 $^{+1}_{-2}$	[2] BONDAR	12	BELL	$e^+e^- \to h_b(1P)\pi^+\pi^-$
10651 $^{+2}_{-3}$ $^{+3}_{-2}$	[2] BONDAR	12	BELL	$e^+e^- \to h_b(2P)\pi^+\pi^-$

[1] Average of the BONDAR 12 measurements in separate channels.
[2] Superseded by the average measurement of BONDAR 12.

$X(10650)^\pm$ WIDTH

VALUE (MeV)	DOCUMENT ID		TECN	COMMENT
11.5±2.2	[3] BONDAR	12	BELL	$e^+e^- \to$ hadrons
• • • We do not use the following data for averages, fits, limits, etc. • • •				
16.3±9.8 $^{+6.0}_{-2.0}$	[4] BONDAR	12	BELL	$e^+e^- \to \Upsilon(1S)\pi^+\pi^-$
13.3±3.3 $^{+4.0}_{-3.0}$	[4] BONDAR	12	BELL	$e^+e^- \to \Upsilon(2S)\pi^+\pi^-$
8.4±2.0± 2.0	[4] BONDAR	12	BELL	$e^+e^- \to \Upsilon(3S)\pi^+\pi^-$
20.9 $^{+5.4}_{-4.7}$ $^{+2.1}_{-5.7}$	[4] BONDAR	12	BELL	$e^+e^- \to h_b(1P)\pi^+\pi^-$
19 ±7 $^{+11}_{-7}$	[4] BONDAR	12	BELL	$e^+e^- \to h_b(2P)\pi^+\pi^-$

[3] Average of the BONDAR 12 measurements in separate channels.
[4] Superseded by the average measurement of BONDAR 12.

$X(10650)^+$ DECAY MODES

$X(10650)^-$ decay modes are charge conjugates of the modes below.

	Mode	Fraction (Γ_i/Γ)
Γ_1	$\Upsilon(1S)\pi^+$	seen
Γ_2	$\Upsilon(2S)\pi^+$	seen
Γ_3	$\Upsilon(3S)\pi^+$	seen
Γ_4	$h_b(1P)\pi^+$	seen
Γ_5	$h_b(2P)\pi^+$	seen

$X(10650)^\pm$ BRANCHING RATIOS

$\Gamma(\Upsilon(1S)\pi^+)/\Gamma_{total}$ **Γ_1/Γ**

VALUE	DOCUMENT ID		TECN	COMMENT
seen	BONDAR	12	BELL	$e^+e^- \to \Upsilon(1S)\pi^+\pi^-$

$\Gamma(\Upsilon(2S)\pi^+)/\Gamma_{total}$ **Γ_2/Γ**

VALUE	DOCUMENT ID		TECN	COMMENT
seen	BONDAR	12	BELL	$e^+e^- \to \Upsilon(2S)\pi^+\pi^-$

$\Gamma(\Upsilon(3S)\pi^+)/\Gamma_{total}$ **Γ_3/Γ**

VALUE	DOCUMENT ID		TECN	COMMENT
seen	BONDAR	12	BELL	$e^+e^- \to \Upsilon(3S)\pi^+\pi^-$

$\Gamma(h_b(1P)\pi^+)/\Gamma_{total}$ **Γ_4/Γ**

VALUE	DOCUMENT ID		TECN	COMMENT
seen	BONDAR	12	BELL	$e^+e^- \to h_b(1P)\pi^+\pi^-$

$\Gamma(h_b(2P)\pi^+)/\Gamma_{total}$ **Γ_5/Γ**

VALUE	DOCUMENT ID		TECN	COMMENT
seen	BONDAR	12	BELL	$e^+e^- \to h_b(2P)\pi^+\pi^-$

$X(10650)^\pm$ REFERENCES

BONDAR	12	PRL 108 122001	A. Bondar *et al.*	(BELLE Collab.)

$\Upsilon(10860)$

$I^G(J^{PC}) = 0^-(1^{--})$

$\Upsilon(10860)$ MASS

VALUE (MeV)	DOCUMENT ID		TECN	COMMENT
10876 ±11 OUR EVALUATION Weighted-average of Belle and BaBar results, but tripling the scaling S-factors applied to the uncertainties to account for model-dependence, handling of radiative corrections, and interference effects.				
• • • We do not use the following data for averages, fits, limits, etc. • • •				
10879 ± 3	[1,2] CHEN	10	BELL	$e^+e^- \to$ hadrons
10888.4 $^{+2.7}_{-2.6}$ ±1.2	[3] CHEN	10	BELL	$e^+e^- \to \Upsilon(1S,2S,3S)\pi^+\pi^-$
10876 ± 2	[1] AUBERT	09E	BABR	$e^+e^- \to$ hadrons
10869 ± 2	[4] AUBERT	09E	BABR	$e^+e^- \to$ hadrons
10868 ± 6 ±5	[5] BESSON	85	CLEO	$e^+e^- \to$ hadrons
10845 ±20	[6] LOVELOCK	85	CUSB	$e^+e^- \to$ hadrons

[1] In a model where a flat non-resonant $b\overline{b}$-continuum is incoherently added to a second flat component interfering with two Breit-Wigner resonances. Systematic uncertainties not estimated.
[2] The parameters of the $\Upsilon(11020)$ are fixed to those in AUBERT 09E.
[3] In a model where a flat nonresonant $\Upsilon(1S,2S,3S)\pi^+\pi^-$ continuum interferes with a single Breit-Wigner resonance.
[4] In a model where a non-resonant $b\overline{b}$-continuum represented by a threshold function at $\sqrt{s}=2m_B$ is incoherently added to a flat component interfering with two Breit-Wigner resonances. Not independent of other AUBERT 09E results. Systematic uncertainties not estimated.
[5] Assuming four Gaussians with radiative tails and a single step in R.
[6] In a coupled-channel model with three resonances and a smooth step in R.

$\Upsilon(10860)$ WIDTH

VALUE (MeV)	DOCUMENT ID		TECN	COMMENT
55 ±28 OUR EVALUATION Weighted-average of Belle and BaBar results, but tripling the scaling S-factors applied to the uncertainties to account for model-dependence, handling of radiative corrections, and interference effects.				
• • • We do not use the following data for averages, fits, limits, etc. • • •				
46 $^{+9}_{-7}$	[7,8] CHEN	10	BELL	$e^+e^- \to$ hadrons
30.7 $^{+8.3}_{-7.0}$ ± 3.1	[9] CHEN	10	BELL	$e^+e^- \to \Upsilon(1S,2S,3S)\pi^+\pi^-$
43 ± 4	[7] AUBERT	09E	BABR	$e^+e^- \to$ hadrons
74 ± 4	[10] AUBERT	09E	BABR	$e^+e^- \to$ hadrons
112 ±17 ±23	[11] BESSON	85	CLEO	$e^+e^- \to$ hadrons
110 ±15	[12] LOVELOCK	85	CUSB	$e^+e^- \to$ hadrons

[7] In a model where a flat non-resonant $b\overline{b}$-continuum is incoherently added to a second flat component interfering with two Breit-Wigner resonances. Systematic uncertainties not estimated.
[8] The parameters of the $\Upsilon(11020)$ are fixed to those in AUBERT 09E.
[9] In a model where a flat nonresonant $\Upsilon(1S,2S,3S)\pi^+\pi^-$ continuum interferes with a single Breit-Wigner resonance.
[10] In a model where a non-resonant $b\overline{b}$-continuum represented by a threshold function at $\sqrt{s}=2m_B$ is incoherently added to a flat component interfering with two Breit-Wigner resonances. Not independent of other AUBERT 09E results. Systematic uncertainties not estimated.
[11] Assuming four Gaussians with radiative tails and a single step in R.
[12] In a coupled-channel model with three resonances and a smooth step in R.

$\Upsilon(10860)$ DECAY MODES

	Mode	Fraction (Γ_i/Γ)	Confidence level
Γ_1	$B\overline{B}X$	$(76.2\ ^{+2.7}_{-4.0})\%$	
Γ_2	$B\overline{B}$	$(5.5\pm1.0)\%$	
Γ_3	$B\overline{B}^*$ + c.c.	$(13.7\pm1.6)\%$	
Γ_4	$B^*\overline{B}^*$	$(38.1\pm3.4)\%$	
Γ_5	$B\overline{B}^{(*)}\pi$	<19.7 %	90%
Γ_6	$B\overline{B}\pi$	$(0.0\pm1.2)\%$	
Γ_7	$B^*\overline{B}\pi + B\overline{B}^*\pi$	$(7.3\pm2.3)\%$	
Γ_8	$B^*\overline{B}^*\pi$	$(1.0\pm1.4)\%$	
Γ_9	$B\overline{B}\pi\pi$	<8.9 %	90%
Γ_{10}	$B_s^{(*)}\overline{B}_s^{(*)}$	$(20.1\pm3.1)\%$	
Γ_{11}	$B_s\overline{B}_s$	$(5\pm5)\times10^{-3}$	
Γ_{12}	$B_s\overline{B}_s^*$ + c.c.	$(1.35\pm0.32)\%$	
Γ_{13}	$B_s^*\overline{B}_s^*$	$(17.6\pm2.7)\%$	
Γ_{14}	no open-bottom	$(3.8\ ^{+5.0}_{-0.5})\%$	
Γ_{15}	e^+e^-	$(5.6\pm3.1)\times10^{-6}$	
Γ_{16}	$K^*(892)^0\overline{K}^0$	$<1.0\times10^{-5}$	90%
Γ_{17}	$\Upsilon(1S)\pi^+\pi^-$	$(5.3\pm0.6)\times10^{-3}$	
Γ_{18}	$\Upsilon(2S)\pi^+\pi^-$	$(7.8\pm1.3)\times10^{-3}$	
Γ_{19}	$\Upsilon(3S)\pi^+\pi^-$	$(4.8\ ^{+1.9}_{-1.7})\times10^{-3}$	
Γ_{20}	$\Upsilon(1S)K^+K^-$	$(6.1\pm1.8)\times10^{-4}$	
Γ_{21}	$h_b(1P)\pi^+\pi^-$	$(3.5\ ^{+1.0}_{-1.3})\times10^{-3}$	
Γ_{22}	$h_b(2P)\pi^+\pi^-$	$(6.0\ ^{+2.1}_{-1.8})\times10^{-3}$	

Inclusive Decays.

These decay modes are submodes of one or more of the decay modes above.

Γ_{23}	ϕ anything	$(13.8\ ^{+2.4}_{-1.7})\%$	
Γ_{24}	D^0 anything + c.c.	$(108\pm8)\%$	
Γ_{25}	D_s anything + c.c.	$(46\pm6)\%$	
Γ_{26}	J/ψ anything	$(2.06\pm0.21)\%$	
Γ_{27}	B^0 anything + c.c.	$(77\pm8)\%$	
Γ_{28}	B^+ anything + c.c.	$(72\pm6)\%$	

$\Upsilon(10860)$ PARTIAL WIDTHS

$\Gamma(e^+e^-)$ Γ_{15}

VALUE (keV)	DOCUMENT ID		TECN	COMMENT
0.31 ±0.07 OUR AVERAGE	Error includes scale factor of 1.3.			
0.22 ±0.05 ±0.07	BESSON	85	CLEO	$e^+e^-\to$ hadrons
0.365±0.070	LOVELOCK	85	CUSB	$e^+e^-\to$ hadrons

$\Upsilon(10860)$ BRANCHING RATIOS

"OUR EVALUATION" is obtained based on averages of rescaled data listed below. The averages and rescaling were performed by the Heavy Flavor Averaging Group (HFAG) and are described at http://www.slac.stanford.edu/xorg/hfag/.

$\Gamma(B\overline{B}X)/\Gamma_{\text{total}}$ Γ_1/Γ

VALUE	EVTS	DOCUMENT ID		TECN	COMMENT
$0.762\ ^{+0.027}_{-0.043}$ OUR EVALUATION					
0.71 ±0.06 OUR AVERAGE					
0.737±0.032±0.051	1063	[13] DRUTSKOY	10	BELL	$\Upsilon(5S)\to B^+X,\ B^0X$
0.589±0.100±0.092		[14] HUANG	07	CLEO	$\Upsilon(5S)\to$ hadrons

$\Gamma(B\overline{B})/\Gamma_{\text{total}}$ Γ_2/Γ

VALUE (units 10^{-2})	CL%	DOCUMENT ID		TECN	COMMENT
$5.5\ ^{+1.0}_{-0.9}\pm0.4$		[15] DRUTSKOY	10	BELL	$\Upsilon(5S)\to B^+X,\ B^0X$
• • • We do not use the following data for averages, fits, limits, etc. • • •					
<13.8	90	[14] HUANG	07	CLEO	$\Upsilon(5S)\to$ hadrons

$\Gamma(B\overline{B})/\Gamma(B\overline{B}X)$ Γ_2/Γ_1

VALUE	CL%	DOCUMENT ID		TECN	COMMENT
<0.22	90	AQUINES	06	CLE3	$\Upsilon(5S)\to$ hadrons

$\Gamma(B\overline{B}^*$ + c.c.)$/\Gamma_{\text{total}}$ Γ_3/Γ

VALUE	DOCUMENT ID		TECN	COMMENT
0.137±0.016 OUR AVERAGE				
0.137±0.013±0.011	[15] DRUTSKOY	10	BELL	$\Upsilon(5S)\to B^+X,\ B^0X$
0.143±0.053±0.027	[14] HUANG	07	CLEO	$\Upsilon(5S)\to$ hadrons

$\Gamma(B\overline{B}^*$ + c.c.)$/\Gamma(B\overline{B}X)$ Γ_3/Γ_1

VALUE	EVTS	DOCUMENT ID		TECN	COMMENT
0.24±0.09±0.03	10	AQUINES	06	CLE3	$\Upsilon(5S)\to$ hadrons

$\Gamma(B^*\overline{B}^*)/\Gamma_{\text{total}}$ Γ_4/Γ

VALUE	DOCUMENT ID		TECN	COMMENT
0.381±0.034 OUR AVERAGE				
$0.375\ ^{+0.021}_{-0.019}\pm0.030$	[15] DRUTSKOY	10	BELL	$\Upsilon(5S)\to B^+X,\ B^0X$
0.436±0.083±0.072	[14] HUANG	07	CLEO	$\Upsilon(5S)\to$ hadrons

$\Gamma(B^*\overline{B}^*)/\Gamma(B\overline{B}X)$ Γ_4/Γ_1

VALUE	EVTS	DOCUMENT ID		TECN	COMMENT
0.74±0.15±0.08	31	AQUINES	06	CLE3	$\Upsilon(5S)\to$ hadrons

$\Gamma(B\overline{B}^{(*)}\pi)/\Gamma_{\text{total}}$ Γ_5/Γ

VALUE	CL%	DOCUMENT ID		TECN	COMMENT
<0.197	90	[14] HUANG	07	CLEO	$\Upsilon(5S)\to$ hadrons

$\Gamma(B\overline{B}^{(*)}\pi)/\Gamma(B\overline{B}X)$ Γ_5/Γ_1

VALUE	CL%	DOCUMENT ID		TECN	COMMENT
<0.32	90	AQUINES	06	CLE3	$\Upsilon(5S)\to$ hadrons

$\Gamma(B\overline{B}\pi)/\Gamma_{\text{total}}$ Γ_6/Γ

VALUE (units 10^{-2})	EVTS	DOCUMENT ID		TECN	COMMENT
0.0±1.2±0.3	0	[15] DRUTSKOY	10	BELL	$\Upsilon(5S)\to B^{+,0}\pi^-X$

$[\Gamma(B^*\overline{B}\pi)+\Gamma(B\overline{B}^*\pi)]/\Gamma_{\text{total}}$ Γ_7/Γ

VALUE (units 10^{-2})	EVTS	DOCUMENT ID		TECN	COMMENT
$7.3\ ^{+2.3}_{-2.1}\pm0.8$	38	[15] DRUTSKOY	10	BELL	$\Upsilon(5S)\to B^{+,0}\pi^-X$

$\Gamma(B^*\overline{B}^*\pi)/\Gamma_{\text{total}}$ Γ_8/Γ

VALUE (units 10^{-2})	EVTS	DOCUMENT ID		TECN	COMMENT
$1.0\ ^{+1.4}_{-1.3}\pm0.4$	5	[15] DRUTSKOY	10	BELL	$\Upsilon(5S)\to B^{+,0}\pi^-X$

$\Gamma(B\overline{B}\pi\pi)/\Gamma_{\text{total}}$ Γ_9/Γ

VALUE	CL%	DOCUMENT ID		TECN	COMMENT
<0.089	90	[14] HUANG	07	CLEO	$\Upsilon(5S)\to$ hadrons

$\Gamma(B\overline{B}\pi\pi)/\Gamma(B\overline{B}X)$ Γ_9/Γ_1

VALUE	CL%	DOCUMENT ID		TECN	COMMENT
<0.14	90	AQUINES	06	CLE3	$\Upsilon(5S)\to$ hadrons

$\Gamma(B_s^{(*)}\overline{B}_s^{(*)})/\Gamma_{\text{total}}$ $\Gamma_{10}/\Gamma=(\Gamma_{11}+\Gamma_{12}+\Gamma_{13})/\Gamma$

VALUE	DOCUMENT ID		TECN	COMMENT
$0.201\ ^{+0.030}_{-0.031}$ OUR EVALUATION				
$0.189\ ^{+0.027}_{-0.021}$ OUR AVERAGE				
0.172±0.030	[16] ESEN	13	BELL	$\Upsilon(5S)\to D^0X,\ D_sX$
$0.21\ ^{+0.06}_{-0.03}$	[17] HUANG	07	CLEO	$\Upsilon(5S)\to D_sX$
• • • We do not use the following data for averages, fits, limits, etc. • • •				
0.180±0.013±0.032	[18] DRUTSKOY	07	BELL	$\Upsilon(5S)\to D^0X,\ D_sX$
0.160±0.026±0.058	[19] ARTUSO	05B	CLEO	$e^+e^-\to D_sX$

$\Gamma(B_s^{(*)}\overline{B}_s^{(*)})/\Gamma(B\overline{B}X)$ Γ_{10}/Γ_1

VALUE	DOCUMENT ID
$0.264\ ^{+0.052}_{-0.045}$ OUR EVALUATION	

$\Gamma(B_s^*\overline{B}_s^*)/\Gamma(B_s^{(*)}\overline{B}_s^{(*)})$ $\Gamma_{13}/\Gamma_{10}=\Gamma_{13}/(\Gamma_{11}+\Gamma_{12}+\Gamma_{13})$

VALUE (units 10^{-2})	EVTS	DOCUMENT ID		TECN	COMMENT
87.8±1.5 OUR AVERAGE					
87.0±1.7		[20,21] ESEN	13	BELL	$B_s^0\to D_s^-\pi^+$
90.5±3.2±0.1	227	[21,22] LI	12	BELL	$B_s^0\to J/\psi\eta^{(\prime)}$
• • • We do not use the following data for averages, fits, limits, etc. • • •					
$90.1\ ^{+3.8}_{-4.0}\pm0.2$		[23] LOUVOT	09	BELL	10.86 $e^+e^-\to B_s^{(*)}\overline{B}_s^{(*)}$
$93\ ^{+7}_{-9}\pm1$		[23] DRUTSKOY	07A	BELL	Superseded by LOUVOT 09

$\Gamma(B_s\overline{B}_s)/\Gamma(B_s^{(*)}\overline{B}_s^{(*)})$ $\Gamma_{11}/\Gamma_{10}=\Gamma_{11}/(\Gamma_{11}+\Gamma_{12}+\Gamma_{13})$

VALUE (units 10^{-2})	DOCUMENT ID		TECN	COMMENT
$2.6^{+2.6}_{-2.5}$	LOUVOT	09	BELL	10.86 $e^+e^-\to B_s^{(*)}\overline{B}_s^{(*)}$

$\Gamma(B_s\overline{B}_s)/\Gamma(B_s^*\overline{B}_s^*)$ Γ_{11}/Γ_{13}

VALUE	CL%	DOCUMENT ID		TECN	COMMENT
<0.16	90	BONVICINI	06	CLE3	e^+e^-

$\Gamma(B_s\overline{B}_s^*+\text{ c.c.})/\Gamma(B_s^{(*)}\overline{B}_s^{(*)})$ $\Gamma_{12}/\Gamma_{10}=\Gamma_{12}/(\Gamma_{11}+\Gamma_{12}+\Gamma_{13})$

VALUE (units 10^{-2})	EVTS	DOCUMENT ID		TECN	COMMENT
6.7±1.2 OUR AVERAGE					
7.3±1.4		[20,21] ESEN	13	BELL	$B_s^0\to D_s^-\pi^+$
4.9±2.5±0.0	227	[21,22] LI	12	BELL	$B_s^0\to J/\psi\eta^{(\prime)}$
• • • We do not use the following data for averages, fits, limits, etc. • • •					
$7.3^{+3.3}_{-3.0}$±0.1		LOUVOT	09	BELL	10.86 $e^+e^-\to B_s^{(*)}\overline{B}_s^{(*)}$

$\Gamma(B_s\overline{B}_s^*+\text{ c.c.})/\Gamma(B_s^*\overline{B}_s^*)$ Γ_{12}/Γ_{13}

VALUE	CL%	DOCUMENT ID		TECN	COMMENT
<0.16	90	BONVICINI	06	CLE3	e^+e^-

$\Gamma(\text{no open-bottom})/\Gamma_{\text{total}}$ Γ_{14}/Γ

VALUE	DOCUMENT ID
$0.038^{+0.051}_{-0.005}$ **OUR EVALUATION**	

$\Gamma(K^*(892)^0\overline{K}^0)/\Gamma_{\text{total}}$ Γ_{16}/Γ

VALUE	CL%	DOCUMENT ID		TECN	COMMENT
$<1.0\times10^{-5}$	90	SHEN	13A	BELL	$e^+e^-\to K^*(892)^0\overline{K}^0$

$\Gamma(\Upsilon(1S)\pi^+\pi^-)/\Gamma_{\text{total}}$ Γ_{17}/Γ

VALUE (units 10^{-3})	EVTS	DOCUMENT ID		TECN	COMMENT
5.3±0.3±0.5	325	[24] CHEN	08	BELL	10.87 $e^+e^-\to\Upsilon(1S)\pi^+\pi^-$

$\Gamma(\Upsilon(2S)\pi^+\pi^-)/\Gamma_{\text{total}}$ Γ_{18}/Γ

VALUE (units 10^{-3})	EVTS	DOCUMENT ID		TECN	COMMENT
7.8±0.6±1.1	186	[24] CHEN	08	BELL	10.87 $e^+e^-\to\Upsilon(2S)\pi^+\pi^-$

$\Gamma(\Upsilon(3S)\pi^+\pi^-)/\Gamma_{\text{total}}$ Γ_{19}/Γ

VALUE (units 10^{-3})	EVTS	DOCUMENT ID		TECN	COMMENT
$4.8^{+1.8}_{-1.5}$±0.7	10	[24] CHEN	08	BELL	10.87 $e^+e^-\to\Upsilon(3S)\pi^+\pi^-$

$\Gamma(\Upsilon(1S)K^+K^-)/\Gamma_{\text{total}}$ Γ_{20}/Γ

VALUE (units 10^{-4})	EVTS	DOCUMENT ID		TECN	COMMENT
$6.1^{+1.6}_{-1.4}$±1.0	20	[24] CHEN	08	BELL	10.87 $e^+e^-\to\Upsilon(1S)K^+K^-$

$\Gamma(h_b(1P)\pi^+\pi^-)/\Gamma(\Upsilon(2S)\pi^+\pi^-)$ Γ_{21}/Γ_{18}

VALUE	DOCUMENT ID		TECN	COMMENT
$0.45\pm0.08^{+0.07}_{-0.12}$	ADACHI	12	BELL	10.86 $e^+e^-\to$ hadrons

$\Gamma(h_b(2P)\pi^+\pi^-)/\Gamma(\Upsilon(2S)\pi^+\pi^-)$ Γ_{22}/Γ_{18}

VALUE	DOCUMENT ID		TECN	COMMENT
$0.77\pm0.08^{+0.22}_{-0.17}$	ADACHI	12	BELL	10.86 $e^+e^-\to$ hadrons

$\Gamma(\phi\text{ anything})/\Gamma_{\text{total}}$ Γ_{23}/Γ

VALUE	DOCUMENT ID		TECN	COMMENT
$0.138\pm0.007^{+0.023}_{-0.015}$	HUANG	07	CLEO	$\Upsilon(5S)\to\phi X$

$\Gamma(D^0\text{ anything + c.c.})/\Gamma_{\text{total}}$ Γ_{24}/Γ

VALUE	DOCUMENT ID		TECN	COMMENT
$1.076\pm0.040\pm0.068$	DRUTSKOY	07	BELL	$\Upsilon(5S)\to D^0X$

$\Gamma(D_s\text{ anything + c.c.})/\Gamma_{\text{total}}$ Γ_{25}/Γ

VALUE	DOCUMENT ID		TECN	COMMENT
0.46 ±0.06 OUR AVERAGE				
0.472±0.024±0.072	[18] DRUTSKOY	07	BELL	$\Upsilon(5S)\to D_sX$
0.44 ±0.09 ±0.04	[25] ARTUSO	05B	CLE3	$e^+e^-\to D_sX$

$\Gamma(J/\psi\text{ anything})/\Gamma_{\text{total}}$ Γ_{26}/Γ

VALUE (units 10^{-2})	DOCUMENT ID		TECN	COMMENT
$2.060\pm0.160\pm0.134$	DRUTSKOY	07	BELL	$\Upsilon(5S)\to J/\psi X$

$\Gamma(B^0\text{ anything + c.c.})/\Gamma_{\text{total}}$ Γ_{27}/Γ

VALUE	EVTS	DOCUMENT ID		TECN	COMMENT
$0.770^{+0.058}_{-0.056}\pm0.061$	352	DRUTSKOY	10	BELL	$\Upsilon(5S)\to B^0X$

$\Gamma(B^+\text{ anything + c.c.})/\Gamma_{\text{total}}$ Γ_{28}/Γ

VALUE	EVTS	DOCUMENT ID		TECN	COMMENT
$0.721^{+0.039}_{-0.038}\pm0.050$	711	DRUTSKOY	10	BELL	$\Upsilon(5S)\to B^+X$

[13] Not independent of DRUTSKOY 10 values for $\Upsilon(5S)\to B^{\pm,0}$ anything.
[14] Using measurements or limits from AQUINES 06.
[15] Assuming isospin conservation.
[16] Supersedes DRUTSKOY 07.
[17] Supersedes ARTUSO 05B. Combining inclusive ϕ, D_s, and B measurements. Using $B(D_s^+\to\phi\pi^+)=4.4\pm0.6\%$ from PDG 06.
[18] Using $B(D_s^+\to\phi\pi^+)=(4.4\pm0.6)\%$ from PDG 06.
[19] Uses a model-dependent estimate $B(B_s\to D_sX)=(92\pm11)\%$.
[20] Supersedes LOUVOT 09.
[21] With $N(B_s^{(*)}\overline{B}_s^{(*)})=(7.11\pm1.30)\times10^6$.
[22] The ratios $N(B_s^*\overline{B}_s^*)$ / $N(B_s^{(*)}\overline{B}_s^{(*)})$ and $N(B_s^*\overline{B}_s^0)$ / $N(B_s^{(*)}\overline{B}_s^{(*)})$ are measured with a correlation coefficient of -0.72.
[23] From a measurement of $\sigma(e^+e^-\to B_s^*\overline{B}_s^*)$ / $\sigma(e^+e^-\to B_s^{(*)}\overline{B}_s^{(*)})$ at $\sqrt{s}=10.86$ GeV.
[24] Assuming that the observed events are solely due to the $\Upsilon(5S)$ resonance.
[25] ARTUSO 05B reports $[\Gamma(\Upsilon(10860)\to D_s\text{ anything + c.c.})/\Gamma_{\text{total}}]\times[B(D_s^+\to\phi\pi^+)]=0.0198\pm0.0019\pm0.0038$ which we divide by our best value $B(D_s^+\to\phi\pi^+)=(4.5\pm0.4)\times10^{-2}$. Our first error is their experiment's error and our second error is the systematic error from using our best value.

$\Upsilon(10860)$ REFERENCES

ESEN	13	PR D87 031101	S. Esen *et al.*	(BELLE Collab.)
SHEN	13A	PR D88 052019	C.P. Shen *et al.*	(BELLE Collab.)
ADACHI	12	PRL 108 032001	I. Adachi *et al.*	(BELLE Collab.)
LI	12	PRL 108 181808	J. Li *et al.*	(BELLE Collab.)
CHEN	10	PR D82 091106	K.-F. Chen *et al.*	(BELLE Collab.)
DRUTSKOY	10	PR D81 112003	A. Drutskoy *et al.*	(BELLE Collab.)
AUBERT	09E	PRL 102 012001	B. Aubert *et al.*	(BABAR Collab.)
LOUVOT	09	PRL 102 021801	R. Louvot *et al.*	(BELLE Collab.)
CHEN	08	PRL 100 112001	K.-F. Chen *et al.*	(BELLE Collab.)
DRUTSKOY	07	PRL 98 052001	A. Drutskoy *et al.*	(BELLE Collab.)
DRUTSKOY	07A	PR D76 012002	A. Drutskoy *et al.*	(BELLE Collab.)
HUANG	07	PR D75 012002	G.S. Huang *et al.*	(CLEO Collab.)
AQUINES	06	PRL 96 152001	O. Aquines *et al.*	(CLEO Collab.)
BONVICINI	06	PRL 96 022002	G. Bonvicini *et al.*	(CLEO Collab.)
PDG	06	JP G33 1	W.-M. Yao *et al.*	(PDG Collab.)
ARTUSO	05B	PRL 95 261801	M. Artuso *et al.*	(CLEO Collab.)
BESSON	85	PRL 54 381	D. Besson *et al.*	(CLEO Collab.)
LOVELOCK	85	PRL 54 377	D.M.J. Lovelock *et al.*	(CUSB Collab.)

$\Upsilon(11020)$

$I^G(J^{PC})=0^-(1^{--})$

$\Upsilon(11020)$ MASS

VALUE (MeV)	DOCUMENT ID		TECN	COMMENT
11019± 8 OUR AVERAGE				
11019± 5±7	BESSON	85	CLEO	$e^+e^-\to$ hadrons
11020±30	LOVELOCK	85	CUSB	$e^+e^-\to$ hadrons
• • • We do not use the following data for averages, fits, limits, etc. • • •				
10996± 2	[1] AUBERT	09E	BABR	$e^+e^-\to$ hadrons

[1] In a model where a flat non-resonant $b\overline{b}$-continuum is incoherently added to a second flat component interfering with two Breit-Wigner resonances. Systematic uncertainties not estimated.

$\Upsilon(11020)$ WIDTH

VALUE (MeV)	DOCUMENT ID		TECN	COMMENT
79±16 OUR AVERAGE				
61±13±22	BESSON	85	CLEO	$e^+e^-\to$ hadrons
90±20	LOVELOCK	85	CUSB	$e^+e^-\to$ hadrons
• • • We do not use the following data for averages, fits, limits, etc. • • •				
37± 3	[2] AUBERT	09E	BABR	$e^+e^-\to$ hadrons

[2] In a model where a flat non-resonant $b\overline{b}$-continuum is incoherently added to a second flat component interfering with two Breit-Wigner resonances. Systematic uncertainties not estimated.

$\Upsilon(11020)$ DECAY MODES

	Mode	Fraction (Γ_j/Γ)
Γ_1	e^+e^-	$(1.6\pm0.5)\times10^{-6}$

$\Upsilon(11020)$ PARTIAL WIDTHS

$\Gamma(e^+e^-)$ Γ_1

VALUE (keV)	DOCUMENT ID		TECN	COMMENT
0.130±0.030 OUR AVERAGE				
0.095±0.03 ±0.035	BESSON	85	CLEO	$e^+e^-\to$ hadrons
0.156±0.040	LOVELOCK	85	CUSB	$e^+e^-\to$ hadrons

See key on page 547

$\Upsilon(11020)$ REFERENCES

AUBERT	09E	PRL 102 012001	B. Aubert *et al.*	(BABAR Collab.)
BESSON	85	PRL 54 381	D. Besson *et al.*	(CLEO Collab.)
LOVELOCK	85	PRL 54 377	D.M.J. Lovelock *et al.*	(CUSB Collab.)

N BARYONS
(S = 0, I = 1/2)

p, $N^+ = uud$; n, $N^0 = udd$

p

$I(J^P) = \frac{1}{2}(\frac{1}{2}^+)$ Status: ****

p MASS (atomic mass units u)

The mass is known much more precisely in u (atomic mass units) than in MeV. See the next data block.

VALUE (u)	DOCUMENT ID		TECN	COMMENT
1.007276466812±0.000000000090	MOHR	12	RVUE	2010 CODATA value
• • • We do not use the following data for averages, fits, limits, etc. • • •				
1.00727646677 ±0.00000000010	MOHR	08	RVUE	2006 CODATA value
1.00727646688 ±0.00000000013	MOHR	05	RVUE	2002 CODATA value
1.00727646688 ±0.00000000013	MOHR	99	RVUE	1998 CODATA value
1.007276470 ±0.000000012	COHEN	87	RVUE	1986 CODATA value

p MASS (MeV)

The mass is known much more precisely in u (atomic mass units) than in MeV. The conversion from u to MeV, 1 u = 931.494 061(21) MeV/c^2 (MOHR 12, the 2010 CODATA value), involves the relatively poorly known electronic charge.

VALUE (MeV)	DOCUMENT ID		TECN	COMMENT
938.272046±0.000021	MOHR	12	RVUE	2010 CODATA value
• • • We do not use the following data for averages, fits, limits, etc. • • •				
938.272013±0.000023	MOHR	08	RVUE	2006 CODATA value
938.272029±0.000080	MOHR	05	RVUE	2002 CODATA value
938.271998±0.000038	MOHR	99	RVUE	1998 CODATA value
938.27231 ±0.00028	COHEN	87	RVUE	1986 CODATA value
938.2796 ±0.0027	COHEN	73	RVUE	1973 CODATA value

$|m_p - m_{\overline{p}}|/m_p$

A test of CPT invariance. Note that the comparison of the $\overline{p}$ and p charge-to-mass ratio, given in the next data block, is much better determined.

VALUE	CL%	DOCUMENT ID		TECN	COMMENT
<7 × 10^{-10}	90	[1] HORI	11	SPEC	$\overline{p}e^-$ He atom
• • • We do not use the following data for averages, fits, limits, etc. • • •					
<2 × 10^{-9}	90	[1] HORI	06	SPEC	$\overline{p}e^-$ He atom
<1.0 × 10^{-8}	90	[1] HORI	03	SPEC	$\overline{p}e^-$ ^{4}He, $\overline{p}e^-$ ^{3}He
<6 × 10^{-8}	90	[1] HORI	01	SPEC	$\overline{p}e^-$ He atom
<5 × 10^{-7}		[2] TORII	99	SPEC	$\overline{p}e^-$ He atom

[1] HORI 01, HORI 03, HORI 06, and HORI 11 use the more-precisely-known constraint on the $\overline{p}$ charge-to-mass ratio of GABRIELSE 99 (see below) to get their results. Their results are not independent of the HORI 01, HORI 03, HORI 06, and HORI 11 values for $|q_p+q_{\overline{p}}|/e$, below.

[2] TORII 99 uses the more-precisely-known constraint on the $\overline{p}$ charge-to-mass ratio of GABRIELSE 95 (see below) to get this result. This is not independent of the TORII 99 value for $|q_p+q_{\overline{p}}|/e$, below.

$\overline{p}/p$ CHARGE-TO-MASS RATIO, $|\frac{q_{\overline{p}}}{m_{\overline{p}}}|/(\frac{q_p}{m_p})$

A test of CPT invariance. Listed here are measurements involving the *inertial* masses. For a discussion of what may be inferred about the ratio of $\overline{p}$ and p *gravitational* masses, see ERICSON 90; they obtain an upper bound of 10^{-6}–10^{-7} for violation of the equivalence principle for $\overline{p}$'s.

VALUE	DOCUMENT ID		TECN	COMMENT
0.99999999991±0.00000000009	GABRIELSE	99	TRAP	Penning trap
• • • We do not use the following data for averages, fits, limits, etc. • • •				
1.0000000015 ±0.0000000011	[3] GABRIELSE	95	TRAP	Penning trap
1.000000023 ±0.000000042	[4] GABRIELSE	90	TRAP	Penning trap

[3] Equation (2) of GABRIELSE 95 should read $M(\overline{p})/M(p) = 0.999\,999\,9985\,(11)$ (G. Gabrielse, private communication).

[4] GABRIELSE 90 also measures $m_{\overline{p}}/m_{e^-} = 1836.152660 \pm 0.000083$ and $m_p/m_{e^-} = 1836.152680 \pm 0.000088$. Both are completely consistent with the 1986 CODATA (COHEN 87) value for m_p/m_{e^-} of 1836.152701 ± 0.000037.

$(|\frac{q_{\overline{p}}}{m_{\overline{p}}}|-\frac{q_p}{m_p})/\frac{q_p}{m_p}$

A test of CPT invariance. Taken from the $\overline{p}/p$ charge-to-mass ratio, above.

VALUE	DOCUMENT ID
(−9±9) × 10^{-11} OUR EVALUATION	

$|q_p + q_{\overline{p}}|/e$

A test of CPT invariance. Note that the comparison of the $\overline{p}$ and p charge-to-mass ratios given above is much better determined. See also a similar test involving the electron.

VALUE	CL%	DOCUMENT ID		TECN	COMMENT
<7 × 10^{-10}	90	[5] HORI	11	SPEC	$\overline{p}e^-$ He atom
• • • We do not use the following data for averages, fits, limits, etc. • • •					
<2 × 10^{-9}	90	[5] HORI	06	SPEC	$\overline{p}e^-$ He atom
<1.0 × 10^{-8}	90	[5] HORI	03	SPEC	$\overline{p}e^-$ ^{4}He, $\overline{p}e^-$ ^{3}He
<6 × 10^{-8}	90	[5] HORI	01	SPEC	$\overline{p}e^-$ He atom
<5 × 10^{-7}		[6] TORII	99	SPEC	$\overline{p}e^-$ He atom
<2 × 10^{-5}		[7] HUGHES	92	RVUE	

[5] HORI 01, HORI 03, HORI 06, and HORI 11 use the more-precisely-known constraint on the $\overline{p}$ charge-to-mass ratio of GABRIELSE 99 (see above) to get their results. Their results are not independent of the HORI 01, HORI 03, HORI 06, and HORI 11 values for $|m_p-m_{\overline{p}}|/m_p$, above.

[6] TORII 99 uses the more-precisely-known constraint on the $\overline{p}$ charge-to-mass ratio of GABRIELSE 95 (see above) to get this result. This is not independent of the TORII 99 value for $|m_p-m_{\overline{p}}|/m_p$, above.

[7] HUGHES 92 uses recent measurements of Rydberg-energy and cyclotron-frequency ratios.

$|q_p + q_e|/e$

See BRESSI 11 for a summary of experiments on the neutrality of matter.
See also "n CHARGE" in the neutron Listings.

VALUE	DOCUMENT ID		COMMENT
<1 × 10^{-21}	[8] BRESSI	11	Neutrality of SF_6
• • • We do not use the following data for averages, fits, limits, etc. • • •			
<3.2 × 10^{-20}	[9] SENGUPTA	00	binary pulsar
<0.8 × 10^{-21}	MARINELLI	84	Magnetic levitation
<1.0 × 10^{-21}	[8] DYLLA	73	Neutrality of SF_6

[8] BRESSI 11 uses the method of DYLLA 73 but finds serious errors in that experiment that greatly reduce its accuracy. The BRESSI 11 limit assumes that $n \rightarrow p e^- \nu_e$ conserves charge. Thus the limit applies equally to the charge of the neutron.

[9] SENGUPTA 00 uses the difference between the observed rate of of rotational energy loss by the binary pulsar PSR B1913+16 and the rate predicted by general relativity to set this limit. See the paper for assumptions.

p MAGNETIC MOMENT

See the "Note on Baryon Magnetic Moments" in the Λ Listings.

VALUE (μ_N)	DOCUMENT ID		TECN	COMMENT
2.792847356±0.000000023	MOHR	12	RVUE	2010 CODATA value
• • • We do not use the following data for averages, fits, limits, etc. • • •				
2.792847356±0.000000023	MOHR	08	RVUE	2006 CODATA value
2.792847351±0.000000028	MOHR	05	RVUE	2002 CODATA value
2.792847337±0.000000029	MOHR	99	RVUE	1998 CODATA value
2.792847386±0.000000063	COHEN	87	RVUE	1986 CODATA value
2.7928456 ±0.0000011	COHEN	73	RVUE	1973 CODATA value

$\overline{p}$ MAGNETIC MOMENT

A few early results have been omitted.

VALUE (μ_N)	DOCUMENT ID		TECN	COMMENT
−2.792845±0.000012	DISCIACCA	13	TRAP	Single $\overline{p}$, Penning trap
• • • We do not use the following data for averages, fits, limits, etc. • • •				
−2.7862 ±0.0083	PASK	09	CNTR	$\overline{p}$ He^+ hyperfine structure
−2.8005 ±0.0090	KREISSL	88	CNTR	$\overline{p}$ ^{208}Pb 11→ 10 X-ray
−2.817 ±0.048	ROBERTS	78	CNTR	
−2.791 ±0.021	HU	75	CNTR	Exotic atoms

$(\mu_p + \mu_{\overline{p}}) / \mu_p$

A test of CPT invariance.

VALUE (units 10^{-6})	DOCUMENT ID		TECN	COMMENT
0±5	DISCIACCA	13	TRAP	Single $\overline{p}$, Penning trap

p ELECTRIC DIPOLE MOMENT

A nonzero value is forbidden by both T invariance and P invariance.

VALUE (10^{-23} e cm)	EVTS	DOCUMENT ID		TECN	COMMENT
< 0.54		[10] DMITRIEV	03		Uses ^{199}Hg atom EDM
• • • We do not use the following data for averages, fits, limits, etc. • • •					
− 3.7 ± 6.3		CHO	89	NMR	Tl F molecules
< 400		DZUBA	85	THEO	Uses ^{129}Xe moment
130 ± 200		[11] WILKENING	84		
900 ±1400		[12] WILKENING	84		
700 ± 900	1G	HARRISON	69	MBR	Molecular beam

[10] DMITRIEV 03 calculates this limit from the limit on the electric dipole moment of the ^{199}Hg atom.

[11] This WILKENING 84 value includes a finite-size effect and a magnetic effect.

[12] This WILKENING 84 value is more cautious than the other and excludes the finite-size effect, which relies on uncertain nuclear integrals.

p ELECTRIC POLARIZABILITY α_p

For a very complete review of the "polarizability of the nucleon and Compton scattering," see SCHUMACHER 05. His recommended values for the proton are $\alpha_p = (12.0 \pm 0.6) \times 10^{-4}$ fm^3 and $\beta_p = (1.9 \mp 0.6) \times 10^{-4}$ fm^3, almost exactly our averages.

VALUE (10^{-4} fm^3)	DOCUMENT ID		TECN	COMMENT
11.2 ±0.4 OUR AVERAGE				
$10.65 \pm 0.35 \pm 0.36$	MCGOVERN	13	RVUE	χEFT + Compton scattering
12.1 ±1.1 ±0.5	[13] BEANE	03		EFT + γp
$11.82 \pm 0.98 ^{+0.52}_{-0.98}$	[14] BLANPIED	01	LEGS	$p(\vec{\gamma},\gamma)$, $p(\vec{\gamma},\pi^0)$, $p(\vec{\gamma},\pi^+)$
11.9 ±0.5 ±1.3	[15] OLMOSDEL...	01	CNTR	γp Compton scattering
12.1 ±0.8 ±0.5	[16] MACGIBBON	95	RVUE	global average
• • • We do not use the following data for averages, fits, limits, etc. • • •				
11.7 ±0.8 ±0.7	[17] BARANOV	01	RVUE	Global average
12.5 ±0.6 ±0.9	MACGIBBON	95	CNTR	γp Compton scattering
9.8 ±0.4 ±1.1	HALLIN	93	CNTR	γp Compton scattering
$10.62 ^{+1.25}_{-1.19} ^{+1.07}_{-1.03}$	ZIEGER	92	CNTR	γp Compton scattering
10.9 ±2.2 ±1.3	[18] FEDERSPIEL	91	CNTR	γp Compton scattering

[13] BEANE 03 uses effective field theory and low-energy γp and γd Compton-scattering data. It also gets for the isoscalar polarizabilities (see the erratum) $\alpha_N = (13.0 \pm 1.9 ^{+3.9}_{-1.5}) \times 10^{-4}$ fm^3 and $\beta_N = (-1.8 \pm 1.9 ^{+2.1}_{-0.9}) \times 10^{-4}$ fm^3.

[14] BLANPIED 01 gives $\alpha_p + \beta_p$ and $\alpha_p - \beta_p$. The separate α_p and β_p are provided to us by A. Sandorfi. The first error above is statistics plus systematics; the second is from the model.

[15] This OLMOSDELEON 01 result uses the TAPS data alone, and does not use the (re-evaluated) sum-rule constraint that $\alpha + \beta = (13.8 \pm 0.4) \times 10^{-4}$ fm^3. See the paper for a discussion.

[16] MACGIBBON 95 combine the results of ZIEGER 92, FEDERSPIEL 91, and their own experiment to get a "global average" in which model errors and systematic errors are treated in a consistent way. See MACGIBBON 95 for a discussion.

[17] BARANOV 01 combines the results of 10 experiments from 1958 through 1995 to get a global average that takes into account both systematic and model errors and does not use the theoretical constraint on the sum $\alpha_p + \beta_p$.

[18] FEDERSPIEL 91 obtains for the (static) electric polarizability α_p, defined in terms of the induced electric dipole moment by $\mathbf{D} = 4\pi\epsilon_0\alpha_p\mathbf{E}$, the value $(7.0 \pm 2.2 \pm 1.3) \times 10^{-4}$ fm^3.

p MAGNETIC POLARIZABILITY β_p

The electric and magnetic polarizabilities are subject to a dispersion sum-rule constraint $\overline{\alpha} + \overline{\beta} = (14.2 \pm 0.5) \times 10^{-4}$ fm^3. Errors here are anticorrelated with those on $\overline{\alpha}_p$ due to this constraint.

VALUE (10^{-4} fm^3)	DOCUMENT ID		TECN	COMMENT
2.5 ±0.4 OUR AVERAGE Error includes scale factor of 1.2.				
$3.15 \pm 0.35 \pm 0.36$	MCGOVERN	13	RVUE	χEFT + Compton scattering
3.4 ±1.1 ±0.1	[19] BEANE	03		EFT + γp
$1.43 \pm 0.98 ^{+0.52}_{-0.98}$	[20] BLANPIED	01	LEGS	$p(\vec{\gamma},\gamma)$, $p(\vec{\gamma},\pi^0)$, $p(\vec{\gamma},\pi^+)$
1.2 ±0.7 ±0.5	[21] OLMOSDEL...	01	CNTR	γp Compton scattering
2.1 ±0.8 ±0.5	[22] MACGIBBON	95	RVUE	global average
• • • We do not use the following data for averages, fits, limits, etc. • • •				
2.3 ±0.9 ±0.7	[23] BARANOV	01	RVUE	Global average
1.7 ±0.6 ±0.9	MACGIBBON	95	CNTR	γp Compton scattering
4.4 ±0.4 ±1.1	HALLIN	93	CNTR	γp Compton scattering
$3.58 ^{+1.19}_{-1.25} ^{+1.03}_{-1.07}$	ZIEGER	92	CNTR	γp Compton scattering
3.3 ±2.2 ±1.3	FEDERSPIEL	91	CNTR	γp Compton scattering

[19] BEANE 03 uses effective field theory and low-energy γp and γd Compton-scattering data. It also gets for the isoscalar polarizabilities (see the erratum) $\alpha_N = (13.0 \pm 1.9 ^{+3.9}_{-1.5}) \times 10^{-4}$ fm^3 and $\beta_N = (-1.8 \pm 1.9 ^{+2.1}_{-0.9}) \times 10^{-4}$ fm^3.

[20] BLANPIED 01 gives $\alpha_p + \beta_p$ and $\alpha_p - \beta_p$. The separate α_p and β_p are provided to us by A. Sandorfi. The first error above is statistics plus systematics; the second is from the model.

[21] This OLMOSDELEON 01 result uses the TAPS data alone, and does not use the (re-evaluated) sum-rule constraint that $\alpha + \beta = (13.8 \pm 0.4) \times 10^{-4}$ fm^3. See the paper for a discussion.

[22] MACGIBBON 95 combine the results of ZIEGER 92, FEDERSPIEL 91, and their own experiment to get a "global average" in which model errors and systematic errors are treated in a consistent way. See MACGIBBON 95 for a discussion.

[23] BARANOV 01 combines the results of 10 experiments from 1958 through 1995 to get a global average that takes into account both systematic and model errors and does not use the theoretical constraint on the sum $\alpha_p + \beta_p$.

p CHARGE RADIUS

This is the rms electric charge radius, $\sqrt{\langle r_E^2 \rangle}$.

Most measurements of the radius of the proton involve electron-proton interactions, and most of the more recent values agree with one another. The most precise of these is $r_p = 0.879(8)$ fm (BERNAUER 10). The CODATA 10 value (MOHR 12), obtained from the electronic results, is 0.8775(51). However, a measurement using muonic hydrogen finds $r_p = 0.84087(39)$ fm (ANTOGNINI 13), which is 13 times more precise and seven standard deviations (using the CODATA 10 error) from the electronic results.

Since POHL 10 (the first μp result), there has been a lot of discussion about the disagreement, especially concerning the modeling of muonic hydrogen. Here is an incomplete list of papers: DERUJULA 10, CLOET 11, DISTLER 11, DERUJULA 11, ARRINGTON 11, BERNAUER 11, and HILL 11.

Until the difference between the ep and μp values is understood, it does not make sense to average the values together. For the present, we give both values. It is up to workers in this field to solve this puzzle.

VALUE (fm)	DOCUMENT ID		TECN	COMMENT
0.84087 ±0.00026 ±0.00029	ANTOGNINI	13	LASR	μp-atom Lamb shift
0.8775 ±0.0051	MOHR	12	RVUE	2010 CODATA, ep data
• • • We do not use the following data for averages, fits, limits, etc. • • •				
0.879 ±0.005 ±0.006	BERNAUER	10	SPEC	$ep \to ep$ form factor
0.912 ±0.009 ±0.007	BORISYUK	10		reanalyzes old ep data
0.871 ±0.009 ±0.003	HILL	10		z-expansion reanalysis
$0.84184 \pm 0.00036 \pm 0.00056$	POHL	10	LASR	See ANTOGNINI 13
0.8768 ±0.0069	MOHR	08	RVUE	2006 CODATA value
$0.844 ^{+0.008}_{-0.004}$	BELUSHKIN	07		Dispersion analysis
0.897 ±0.018	BLUNDEN	05		SICK 03 + 2γ correction
0.8750 ±0.0068	MOHR	05	RVUE	2002 CODATA value
0.895 ±0.010 ±0.013	SICK	03		$ep \to ep$ reanalysis
0.830 ±0.040 ±0.040	[24] ESCHRICH	01		$ep \to ep$
0.883 ±0.014	MELNIKOV	00		1S Lamb Shift in H
0.880 ±0.015	ROSENFELDR...	00		ep + Coul. corrections
0.847 ±0.008	MERGELL	96		ep + disp. relations
0.877 ±0.024	WONG	94		reanalysis of Mainz ep data
0.865 ±0.020	MCCORD	91		$ep \to ep$
0.862 ±0.012	SIMON	80		$ep \to ep$
0.880 ±0.030	BORKOWSKI	74		$ep \to ep$
0.810 ±0.020	AKIMOV	72		$ep \to ep$
0.800 ±0.025	FREREJACQ...	66		$ep \to ep$ (CH_2 tgt.)
0.805 ±0.011	HAND	63		$ep \to ep$

[24] ESCHRICH 01 actually gives $\langle r^2 \rangle = (0.69 \pm 0.06 \pm 0.06)$ fm^2.

p MAGNETIC RADIUS

This is the rms magnetic radius, $\sqrt{\langle r_M^2 \rangle}$.

VALUE (fm)	DOCUMENT ID		TECN	COMMENT
0.777 ±0.013 ±0.010	BERNAUER	10	SPEC	$ep \to ep$ form factor
• • • We do not use the following data for averages, fits, limits, etc. • • •				
$0.876 \pm 0.010 \pm 0.016$	BORISYUK	10		reanalyzes old $ep \to ep$ data
0.854 ± 0.005	BELUSHKIN	07		Dispersion analysis

p MEAN LIFE

A test of baryon conservation. See the "p Partial Mean Lives" section below for limits for identified final states. The limits here are to "anything" or are for "disappearance" modes of a bound proton (p) or (n). See also the 3ν modes in the "Partial Mean Lives" section. Table 1 of BACK 03 is a nice summary.

LIMIT (years)	PARTICLE	CL%	DOCUMENT ID		TECN	COMMENT
$>5.8 \times 10^{29}$	***n***	90	[25] ARAKI	06	KLND	$n \to$ invisible
$>2.1 \times 10^{29}$	***p***	90	[26] AHMED	04	SNO	$p \to$ invisible
• • • We do not use the following data for averages, fits, limits, etc. • • •						
$>1.9 \times 10^{29}$	n	90	[26] AHMED	04	SNO	$n \to$ invisible
$>1.8 \times 10^{25}$	n	90	[27] BACK	03	BORX	
$>1.1 \times 10^{26}$	p	90	[27] BACK	03	BORX	
$>3.5 \times 10^{28}$	p	90	[28] ZDESENKO	03		$p \to$ invisible
$>1 \times 10^{28}$	p	90	[29] AHMAD	02	SNO	$p \to$ invisible
$>4 \times 10^{23}$	p	95	TRETYAK	01		$d \to n +$?
$>1.9 \times 10^{24}$	p	90	[30] BERNABEI	00B	DAMA	
$>1.6 \times 10^{25}$	p, n		[31,32] EVANS	77		
$>3 \times 10^{23}$	p		[32] DIX	70	CNTR	
$>3 \times 10^{23}$	p, n		[32,33] FLEROV	58		

[25] ARAKI 06 looks for signs of de-excitation of the residual nucleus after disappearance of a neutron from the s shell of ^{12}C.
[26] AHMED 04 looks for γ rays from the de-excitation of a residual ^{15}O* or ^{15}N* following the disappearance of a neutron or proton in ^{16}O.
[27] BACK 03 looks for decays of unstable nuclides left after N decays of parent ^{12}C, ^{13}C, ^{16}O nuclei. These are "invisible channel" limits.
[28] ZDESENKO 03 gets this limit on proton disappearance in deuterium by analyzing SNO data in AHMAD 02.
[29] AHMAD 02 (see its footnote 7) looks for neutrons left behind after the disappearance of the proton in deuterons.
[30] BERNABEI 00B looks for the decay of a $^{128}_{53}$I nucleus following the disappearance of a proton in the otherwise-stable $^{129}_{54}$Xe nucleus.
[31] EVANS 77 looks for the daughter nuclide ^{129}Xe from possible ^{130}Te decays in ancient Te ore samples.
[32] This mean-life limit has been obtained from a half-life limit by dividing the latter by ln(2) = 0.693.
[33] FLEROV 58 looks for the spontaneous fission of a ^{232}Th nucleus after the disappearance of one of its nucleons.

$\overline{p}$ MEAN LIFE

Of the two astrophysical limits here, that of GEER 00D involves considerably more refinements in its modeling. The other limits come from direct observations of stored antiprotons. See also "$\overline{p}$ Partial Mean Lives" after "p Partial Mean Lives," below, for exclusive-mode limits. The best (lifetime/branching fraction) limit there is 7×10^5 years, for $\overline{p} \to e^- \gamma$. We advance only the exclusive-mode limits to our Summary Tables.

LIMIT (years)	CL%	EVTS	DOCUMENT ID		TECN	COMMENT
• • • We do not use the following data for averages, fits, limits, etc. • • •						
$>8 \times 10^5$	90		[34] GEER	00D		$\overline{p}/p$ ratio, cosmic rays
>0.28			GABRIELSE	90	TRAP	Penning trap
>0.08	90	1	BELL	79	CNTR	Storage ring
$>1 \times 10^7$			GOLDEN	79	SPEC	$\overline{p}/p$ ratio, cosmic rays
$>3.7 \times 10^{-3}$			BREGMAN	78	CNTR	Storage ring

[34] GEER 00D uses agreement between a model of galactic $\overline{p}$ production and propagation and the observed $\overline{p}/p$ cosmic-ray spectrum to set this limit.

p DECAY MODES

See the "Note on Nucleon Decay" in our 1994 edition (Phys. Rev. **D50**, 1173) for a short review.

The "partial mean life" limits tabulated here are the limits on τ/B_i, where τ is the total mean life and B_i is the branching fraction for the mode in question. For N decays, p and n indicate proton and neutron partial lifetimes.

	Mode	Partial mean life (10^{30} years)	Confidence level
	Antilepton + meson		
τ_1	$N \to e^+ \pi$	> 2000 (n), > 8200 (p)	90%
τ_2	$N \to \mu^+ \pi$	> 1000 (n), > 6600 (p)	90%
τ_3	$N \to \nu \pi$	> 112 (n), > 16 (p)	90%
τ_4	$p \to e^+ \eta$	> 4200	90%
τ_5	$p \to \mu^+ \eta$	> 1300	90%
τ_6	$n \to \nu \eta$	> 158	90%
τ_7	$N \to e^+ \rho$	> 217 (n), > 710 (p)	90%
τ_8	$N \to \mu^+ \rho$	> 228 (n), > 160 (p)	90%
τ_9	$N \to \nu \rho$	> 19 (n), > 162 (p)	90%
τ_{10}	$p \to e^+ \omega$	> 320	90%
τ_{11}	$p \to \mu^+ \omega$	> 780	90%
τ_{12}	$n \to \nu \omega$	> 108	90%
τ_{13}	$N \to e^+ K$	> 17 (n), > 1000 (p)	90%
τ_{14}	$p \to e^+ K^0_S$		
τ_{15}	$p \to e^+ K^0_L$		
τ_{16}	$N \to \mu^+ K$	> 26 (n), > 1600 (p)	90%
τ_{17}	$p \to \mu^+ K^0_S$		
τ_{18}	$p \to \mu^+ K^0_L$		
τ_{19}	$N \to \nu K$	> 86 (n), > 2300 (p)	90%
τ_{20}	$n \to \nu K^0_S$	> 260	90%
τ_{21}	$p \to e^+ K^*(892)^0$	> 84	90%
τ_{22}	$N \to \nu K^*(892)$	> 78 (n), > 51 (p)	90%
	Antilepton + mesons		
τ_{23}	$p \to e^+ \pi^+ \pi^-$	> 82	90%
τ_{24}	$p \to e^+ \pi^0 \pi^0$	> 147	90%
τ_{25}	$n \to e^+ \pi^- \pi^0$	> 52	90%
τ_{26}	$p \to \mu^+ \pi^+ \pi^-$	> 133	90%
τ_{27}	$p \to \mu^+ \pi^0 \pi^0$	> 101	90%
τ_{28}	$n \to \mu^+ \pi^- \pi^0$	> 74	90%
τ_{29}	$n \to e^+ K^0 \pi^-$	> 18	90%
	Lepton + meson		
τ_{30}	$n \to e^- \pi^+$	> 65	90%
τ_{31}	$n \to \mu^- \pi^+$	> 49	90%
τ_{32}	$n \to e^- \rho^+$	> 62	90%
τ_{33}	$n \to \mu^- \rho^+$	> 7	90%
τ_{34}	$n \to e^- K^+$	> 32	90%
τ_{35}	$n \to \mu^- K^+$	> 57	90%
	Lepton + mesons		
τ_{36}	$p \to e^- \pi^+ \pi^+$	> 30	90%
τ_{37}	$n \to e^- \pi^+ \pi^0$	> 29	90%
τ_{38}	$p \to \mu^- \pi^+ \pi^+$	> 17	90%
τ_{39}	$n \to \mu^- \pi^+ \pi^0$	> 34	90%
τ_{40}	$p \to e^- \pi^+ K^+$	> 75	90%
τ_{41}	$p \to \mu^- \pi^+ K^+$	> 245	90%
	Antilepton + photon(s)		
τ_{42}	$p \to e^+ \gamma$	> 670	90%
τ_{43}	$p \to \mu^+ \gamma$	> 478	90%
τ_{44}	$n \to \nu \gamma$	> 28	90%
τ_{45}	$p \to e^+ \gamma \gamma$	> 100	90%
τ_{46}	$n \to \nu \gamma \gamma$	> 219	90%
	Three (or more) leptons		
τ_{47}	$p \to e^+ e^+ e^-$	> 793	90%
τ_{48}	$p \to e^+ \mu^+ \mu^-$	> 359	90%
τ_{49}	$p \to e^+ \nu \nu$	> 17	90%
τ_{50}	$n \to e^+ e^- \nu$	> 257	90%
τ_{51}	$n \to \mu^+ e^- \nu$	> 83	90%
τ_{52}	$n \to \mu^+ \mu^- \nu$	> 79	90%
τ_{53}	$p \to \mu^+ e^+ e^-$	> 529	90%
τ_{54}	$p \to \mu^+ \mu^+ \mu^-$	> 675	90%
τ_{55}	$p \to \mu^+ \nu \nu$	> 21	90%
τ_{56}	$p \to e^- \mu^+ \mu^+$	> 6	90%
τ_{57}	$n \to 3\nu$	> 0.0005	90%
τ_{58}	$n \to 5\nu$		
	Inclusive modes		
τ_{59}	$N \to e^+$ anything	> 0.6 (n, p)	90%
τ_{60}	$N \to \mu^+$ anything	> 12 (n, p)	90%
τ_{61}	$N \to \nu$ anything		
τ_{62}	$N \to e^+ \pi^0$ anything	> 0.6 (n, p)	90%
τ_{63}	$N \to$ 2 bodies, ν-free		

$\Delta B = 2$ dinucleon modes

The following are lifetime limits per iron nucleus.

τ_{64}	$pp \to \pi^+ \pi^+$	> 0.7	90%
τ_{65}	$pn \to \pi^+ \pi^0$	> 2	90%
τ_{66}	$nn \to \pi^+ \pi^-$	> 0.7	90%
τ_{67}	$nn \to \pi^0 \pi^0$	> 3.4	90%
τ_{68}	$pp \to e^+ e^+$	> 5.8	90%
τ_{69}	$pp \to e^+ \mu^+$	> 3.6	90%
τ_{70}	$pp \to \mu^+ \mu^+$	> 1.7	90%
τ_{71}	$pn \to e^+ \overline{\nu}$	> 2.8	90%
τ_{72}	$pn \to \mu^+ \overline{\nu}$	> 1.6	90%
τ_{73}	$nn \to \nu_e \overline{\nu}_e$	> 1.4	90%
τ_{74}	$nn \to \nu_\mu \overline{\nu}_\mu$	> 1.4	90%
τ_{75}	$pn \to$ invisible	> 0.000021	90%
τ_{76}	$pp \to$ invisible	> 0.00005	90%

$\overline{p}$ DECAY MODES

	Mode	Partial mean life (years)	Confidence level
τ_{77}	$\overline{p} \to e^- \gamma$	$> 7 \times 10^5$	90%
τ_{78}	$\overline{p} \to \mu^- \gamma$	$> 5 \times 10^4$	90%
τ_{79}	$\overline{p} \to e^- \pi^0$	$> 4 \times 10^5$	90%
τ_{80}	$\overline{p} \to \mu^- \pi^0$	$> 5 \times 10^4$	90%
τ_{81}	$\overline{p} \to e^- \eta$	$> 2 \times 10^4$	90%
τ_{82}	$\overline{p} \to \mu^- \eta$	$> 8 \times 10^3$	90%
τ_{83}	$\overline{p} \to e^- K^0_S$	> 900	90%
τ_{84}	$\overline{p} \to \mu^- K^0_S$	$> 4 \times 10^3$	90%
τ_{85}	$\overline{p} \to e^- K^0_L$	$> 9 \times 10^3$	90%
τ_{86}	$\overline{p} \to \mu^- K^0_L$	$> 7 \times 10^3$	90%
τ_{87}	$\overline{p} \to e^- \gamma \gamma$	$> 2 \times 10^4$	90%

Baryon Particle Listings

p

τ_{88}	$\overline{p} \rightarrow \mu^- \gamma\gamma$	$> 2 \times 10^4$	90%
τ_{89}	$\overline{p} \rightarrow e^- \rho$		
τ_{90}	$\overline{p} \rightarrow e^- \omega$	> 200	90%
τ_{91}	$\overline{p} \rightarrow e^- K^*(892)^0$		

p PARTIAL MEAN LIVES

The "partial mean life" limits tabulated here are the limits on τ/B_i, where τ is the total mean life for the proton and B_i is the branching fraction for the mode in question.

Decaying particle: p = proton, n = bound neutron. The same event may appear under more than one partial decay mode. Background estimates may be accurate to a factor of two.

Antilepton + meson

$\tau(N \rightarrow e^+ \pi)$ τ_1

LIMIT (10^{30} years)	PARTICLE	CL%	EVTS	BKGD EST	DOCUMENT ID		TECN
>2000	***n***	**90**	**0**	**0.27**	NISHINO	12	SKAM
>8200	***p***	**90**	**0**	**0.3**	NISHINO	09	SKAM
• • • We do not use the following data for averages, fits, limits, etc. • • •							
> 540	p	90	0	0.2	MCGREW	99	IMB3
> 158	n	90	3	5	MCGREW	99	IMB3
>1600	p	90	0	0.1	SHIOZAWA	98	SKAM
> 70	p	90	0	0.5	BERGER	91	FREJ
> 70	n	90	0	$\leq$ 0.1	BERGER	91	FREJ
> 550	p	90	0	0.7	[35] BECKER-SZ...	90	IMB3
> 260	p	90	0	<0.04	HIRATA	89C	KAMI
> 130	n	90	0	<0.2	HIRATA	89C	KAMI
> 310	p	90	0	0.6	SEIDEL	88	IMB
> 100	n	90	0	1.6	SEIDEL	88	IMB
> 1.3	n	90	0		BARTELT	87	SOUD
> 1.3	p	90	0		BARTELT	87	SOUD
> 250	p	90	0	0.3	HAINES	86	IMB
> 31	n	90	8	9	HAINES	86	IMB
> 64	p	90	0	<0.4	ARISAKA	85	KAMI
> 26	n	90	0	<0.7	ARISAKA	85	KAMI
> 82	p (free)	90	0	0.2	BLEWITT	85	IMB
> 250	p	90	0	0.2	BLEWITT	85	IMB
> 25	n	90	4	4	PARK	85	IMB
> 15	p, n	90	0		BATTISTONI	84	NUSX
> 0.5	p	90	1	0.3	[36] BARTELT	83	SOUD
> 0.5	n	90	1	0.3	[36] BARTELT	83	SOUD
> 5.8	p	90	2		[37] KRISHNA...	82	KOLR
> 5.8	n	90	2		[37] KRISHNA...	82	KOLR
> 0.1	n	90			[38] GURR	67	CNTR

[35] This BECKER-SZENDY 90 result includes data from SEIDEL 88.
[36] Limit based on zero events.
[37] We have calculated 90% CL limit from 1 confined event.
[38] We have converted half-life to 90% CL mean life.

$\tau(N \rightarrow \mu^+ \pi)$ τ_2

LIMIT (10^{30} years)	PARTICLE	CL%	EVTS	BKGD EST	DOCUMENT ID		TECN
>1000	***n***	**90**	**1**	**0.43**	NISHINO	12	SKAM
>6600	***p***	**90**	**0**	**0.3**	NISHINO	09	SKAM
• • • We do not use the following data for averages, fits, limits, etc. • • •							
> 473	p	90	0	0.6	MCGREW	99	IMB3
> 90	n	90	1	1.9	MCGREW	99	IMB3
> 81	p	90	0	0.2	BERGER	91	FREJ
> 35	n	90	1	1.0	BERGER	91	FREJ
> 230	p	90	0	<0.07	HIRATA	89C	KAMI
> 100	n	90	0	<0.2	HIRATA	89C	KAMI
> 270	p	90	0	0.5	SEIDEL	88	IMB
> 63	n	90	0	0.5	SEIDEL	88	IMB
> 76	p	90	2	1	HAINES	86	IMB
> 23	n	90	8	7	HAINES	86	IMB
> 46	p	90	0	<0.7	ARISAKA	85	KAMI
> 20	n	90	0	<0.4	ARISAKA	85	KAMI
> 59	p (free)	90	0	0.2	BLEWITT	85	IMB
> 100	p	90	1	0.4	BLEWITT	85	IMB
> 38	n	90	1	4	PARK	85	IMB
> 10	p, n	90	0		BATTISTONI	84	NUSX
> 1.3	p, n	90	0		ALEKSEEV	81	BAKS

$\tau(N \rightarrow \nu\pi)$ τ_3

LIMIT (10^{30} years)	PARTICLE	CL%	EVTS	BKGD EST	DOCUMENT ID		TECN
> 16	***p***	**90**	**6**	**6.7**	WALL	00B	SOU2
>112	***n***	**90**	**6**	**6.6**	MCGREW	99	IMB3
• • • We do not use the following data for averages, fits, limits, etc. • • •							
> 39	n	90	4	3.8	WALL	00B	SOU2
> 10	p	90	15	20.3	MCGREW	99	IMB3
> 13	n	90	1	1.2	BERGER	89	FREJ
> 10	p	90	11	14	BERGER	89	FREJ
> 25	p	90	32	32.8	[39] HIRATA	89C	KAMI
>100	n	90	1	3	HIRATA	89C	KAMI
> 6	n	90	73	60	HAINES	86	IMB
> 2	p	90	16	13	KAJITA	86	KAMI
> 40	n	90	0	1	KAJITA	86	KAMI
> 7	n	90	28	19	PARK	85	IMB
> 7	n	90	0		BATTISTONI	84	NUSX
> 2	p	90	$\leq$ 3		BATTISTONI	84	NUSX
> 5.8	p	90	1		[40] KRISHNA...	82	KOLR
> 0.3	p	90	2		[41] CHERRY	81	HOME
> 0.1	p	90			[42] GURR	67	CNTR

[39] In estimating the background, this HIRATA 89C limit (as opposed to the later limits of WALL 00B and MCGREW 99) does not take into account present understanding that the flux of ν_μ originating in the upper atmosphere is depleted. Doing so would reduce the background and thus also would reduce the limit here.
[40] We have calculated 90% CL limit from 1 confined event.
[41] We have converted 2 possible events to 90% CL limit.
[42] We have converted half-life to 90% CL mean life.

$\tau(p \rightarrow e^+ \eta)$ τ_4

LIMIT (10^{30} years)	PARTICLE	CL%	EVTS	BKGD EST	DOCUMENT ID		TECN
>4200	***p***	**90**	**0**	**0.44**	NISHINO	12	SKAM
• • • We do not use the following data for averages, fits, limits, etc. • • •							
> 81	p	90	1	1.7	WALL	00B	SOU2
> 313	p	90	0	0.2	MCGREW	99	IMB3
> 44	p	90	0	0.1	BERGER	91	FREJ
> 140	p	90	0	<0.04	HIRATA	89C	KAMI
> 100	p	90	0	0.6	SEIDEL	88	IMB
> 200	p	90	5	3.3	HAINES	86	IMB
> 64	p	90	0	<0.8	ARISAKA	85	KAMI
> 64	p (free)	90	5	6.5	BLEWITT	85	IMB
> 200	p	90	5	4.7	BLEWITT	85	IMB
> 1.2	p	90	2		[43] CHERRY	81	HOME

[43] We have converted 2 possible events to 90% CL limit.

$\tau(p \rightarrow \mu^+ \eta)$ τ_5

LIMIT (10^{30} years)	PARTICLE	CL%	EVTS	BKGD EST	DOCUMENT ID		TECN
>1300	***p***	**90**	**2**	**0.49**	NISHINO	12	SKAM
• • • We do not use the following data for averages, fits, limits, etc. • • •							
> 89	p	90	0	1.6	WALL	00B	SOU2
> 126	p	90	3	2.8	MCGREW	99	IMB3
> 26	p	90	1	0.8	BERGER	91	FREJ
> 69	p	90	1	<0.08	HIRATA	89C	KAMI
> 1.3	p	90	0	0.7	PHILLIPS	89	HPW
> 34	p	90	1	1.5	SEIDEL	88	IMB
> 46	p	90	7	6	HAINES	86	IMB
> 26	p	90	1	<0.8	ARISAKA	85	KAMI
> 17	p (free)	90	6	6	BLEWITT	85	IMB
> 46	p	90	7	8	BLEWITT	85	IMB

$\tau(n \rightarrow \nu\eta)$ τ_6

LIMIT (10^{30} years)	PARTICLE	CL%	EVTS	BKGD EST	DOCUMENT ID		TECN
>158	***n***	**90**	**0**	**1.2**	MCGREW	99	IMB3
• • • We do not use the following data for averages, fits, limits, etc. • • •							
> 71	n	90	2	3.7	WALL	00B	SOU2
> 29	n	90	0	0.9	BERGER	89	FREJ
> 54	n	90	2	0.9	HIRATA	89C	KAMI
> 16	n	90	3	2.1	SEIDEL	88	IMB
> 25	n	90	7	6	HAINES	86	IMB
> 30	n	90	0	0.4	KAJITA	86	KAMI
> 18	n	90	4	3	PARK	85	IMB
> 0.6	n	90	2		[44] CHERRY	81	HOME

[44] We have converted 2 possible events to 90% CL limit.

$\tau(N \rightarrow e^+ \rho)$ τ_7

LIMIT (10^{30} years)	PARTICLE	CL%	EVTS	BKGD EST	DOCUMENT ID		TECN
>710	***p***	**90**	**0**	**0.35**	NISHINO	12	SKAM
>217	***n***	**90**	**4**	**4.8**	MCGREW	99	IMB3
• • • We do not use the following data for averages, fits, limits, etc. • • •							
> 70	n	90	1	0.38	NISHINO	12	SKAM
> 29	p	90	0	2.2	BERGER	91	FREJ
> 41	n	90	0	1.4	BERGER	91	FREJ
> 75	p	90	2	2.7	HIRATA	89C	KAMI
> 58	n	90	0	1.9	HIRATA	89C	KAMI
> 38	n	90	2	4.1	SEIDEL	88	IMB
> 1.2	p	90	0		BARTELT	87	SOUD
> 1.5	n	90	0		BARTELT	87	SOUD
> 17	p	90	7	7	HAINES	86	IMB

See key on page 547

> 14	n	90	9	4	HAINES	86	IMB
> 12	p	90	0	<1.2	ARISAKA	85	KAMI
> 6	n	90	2	<1	ARISAKA	85	KAMI
> 6.7	p (free)	90	6	6	BLEWITT	85	IMB
> 17	p	90	7	7	BLEWITT	85	IMB
> 12	n	90	4	2	PARK	85	IMB
> 0.6	n	90	1	0.3	[45] BARTELT	83	SOUD
> 0.5	p	90	1	0.3	[45] BARTELT	83	SOUD
> 9.8	p	90	1		[46] KRISHNA...	82	KOLR
> 0.8	p	90	2		[47] CHERRY	81	HOME

[45] Limit based on zero events.
[46] We have calculated 90% CL limit from 0 confined events.
[47] We have converted 2 possible events to 90% CL limit.

$\tau(N \to \mu^+ \rho)$ τ_8

LIMIT (10^{30} years)	PARTICLE	CL%	EVTS	BKGD EST	DOCUMENT ID		TECN
>160	**p**	**90**	**1**	**0.42**	NISHINO	12	SKAM
>228	**n**	**90**	**3**	**9.5**	MCGREW	99	IMB3
• • • We do not use the following data for averages, fits, limits, etc. • • •							
> 36	n	90	0	0.29	NISHINO	12	SKAM
> 12	p	90	0	0.5	BERGER	91	FREJ
> 22	n	90	0	1.1	BERGER	91	FREJ
>110	p	90	0	1.7	HIRATA	89C	KAMI
> 23	n	90	1	1.8	HIRATA	89C	KAMI
> 4.3	p	90	0	0.7	PHILLIPS	89	HPW
> 30	p	90	0	0.5	SEIDEL	88	IMB
> 11	n	90	1	1.1	SEIDEL	88	IMB
> 16	p	90	4	4.5	HAINES	86	IMB
> 7	n	90	6	5	HAINES	86	IMB
> 12	p	90	0	<0.7	ARISAKA	85	KAMI
> 5	n	90	1	<1.2	ARISAKA	85	KAMI
> 5.5	p (free)	90	4	5	BLEWITT	85	IMB
> 16	p	90	4	5	BLEWITT	85	IMB
> 9	n	90	1	2	PARK	85	IMB

$\tau(N \to \nu \rho)$ τ_9

LIMIT (10^{30} years)	PARTICLE	CL%	EVTS	BKGD EST	DOCUMENT ID		TECN
>162	**p**	**90**	**18**	**21.7**	MCGREW	99	IMB3
> 19	**n**	**90**	**0**	**0.5**	SEIDEL	88	IMB
• • • We do not use the following data for averages, fits, limits, etc. • • •							
> 9	n	90	4	2.4	BERGER	89	FREJ
> 24	p	90	0	0.9	BERGER	89	FREJ
> 27	p	90	5	1.5	HIRATA	89C	KAMI
> 13	n	90	4	3.6	HIRATA	89C	KAMI
> 13	p	90	1	1.1	SEIDEL	88	IMB
> 8	p	90	6	5	HAINES	86	IMB
> 2	n	90	15	10	HAINES	86	IMB
> 11	p	90	2	1	KAJITA	86	KAMI
> 4	n	90	2	2	KAJITA	86	KAMI
> 4.1	p (free)	90	6	7	BLEWITT	85	IMB
> 8.4	p	90	6	5	BLEWITT	85	IMB
> 2	n	90	7	3	PARK	85	IMB
> 0.9	p	90	2		[48] CHERRY	81	HOME
> 0.6	n	90	2		[48] CHERRY	81	HOME

[48] We have converted 2 possible events to 90% CL limit.

$\tau(p \to e^+ \omega)$ τ_{10}

LIMIT (10^{30} years)	PARTICLE	CL%	EVTS	BKGD EST	DOCUMENT ID		TECN
>320	**p**	**90**	**1**	**0.53**	NISHINO	12	SKAM
• • • We do not use the following data for averages, fits, limits, etc. • • •							
>107	p	90	7	10.8	MCGREW	99	IMB3
> 17	p	90	0	1.1	BERGER	91	FREJ
> 45	p	90	2	1.45	HIRATA	89C	KAMI
> 26	p	90	1	1.0	SEIDEL	88	IMB
> 1.5	p	90	0		BARTELT	87	SOUD
> 37	p	90	6	5.3	HAINES	86	IMB
> 25	p	90	1	<1.4	ARISAKA	85	KAMI
> 12	p (free)	90	6	7.5	BLEWITT	85	IMB
> 37	p	90	6	5.7	BLEWITT	85	IMB
> 0.6	p	90	1	0.3	[49] BARTELT	83	SOUD
> 9.8	p	90	1		[50] KRISHNA...	82	KOLR
> 2.8	p	90	2		[51] CHERRY	81	HOME

[49] Limit based on zero events.
[50] We have calculated 90% CL limit from 0 confined events.
[51] We have converted 2 possible events to 90% CL limit.

$\tau(p \to \mu^+ \omega)$ τ_{11}

LIMIT (10^{30} years)	PARTICLE	CL%	EVTS	BKGD EST	DOCUMENT ID		TECN
>780	**p**	**90**	**0**	**0.48**	NISHINO	12	SKAM
• • • We do not use the following data for averages, fits, limits, etc. • • •							
>117	p	90	11	12.1	MCGREW	99	IMB3
> 11	p	90	0	1.0	BERGER	91	FREJ
> 57	p	90	2	1.9	HIRATA	89C	KAMI
> 4.4	p	90	0	0.7	PHILLIPS	89	HPW
> 10	p	90	2	1.3	SEIDEL	88	IMB
> 23	p	90	2	1	HAINES	86	IMB
> 6.5	p (free)	90	9	8.7	BLEWITT	85	IMB
> 23	p	90	8	7	BLEWITT	85	IMB

$\tau(n \to \nu\omega)$ τ_{12}

LIMIT (10^{30} years)	PARTICLE	CL%	EVTS	BKGD EST	DOCUMENT ID		TECN
>108	**n**	**90**	**12**	**22.5**	MCGREW	99	IMB3
• • • We do not use the following data for averages, fits, limits, etc. • • •							
> 17	n	90	1	0.7	BERGER	89	FREJ
> 43	n	90	3	2.7	HIRATA	89C	KAMI
> 6	n	90	2	1.3	SEIDEL	88	IMB
> 12	n	90	6	6	HAINES	86	IMB
> 18	n	90	2	2	KAJITA	86	KAMI
> 16	n	90	1	2	PARK	85	IMB
> 2.0	n	90	2		[52] CHERRY	81	HOME

[52] We have converted 2 possible events to 90% CL limit.

$\tau(N \to e^+ K)$ τ_{13}

LIMIT (10^{30} years)	PARTICLE	CL%	EVTS	BKGD EST	DOCUMENT ID		TECN
>1000	**p**	**90**	**6**	**4.7**	KOBAYASHI	05	SKAM
> 17	**n**	**90**	**35**	**29.4**	MCGREW	99	IMB3
• • • We do not use the following data for averages, fits, limits, etc. • • •							
> 85	p	90	3	4.9	WALL	00	SOU2
> 31	p	90	23	25.2	MCGREW	99	IMB3
> 60	p	90	0		BERGER	91	FREJ
> 150	p	90	0	<0.27	HIRATA	89C	KAMI
> 70	p	90	0	1.8	SEIDEL	88	IMB
> 77	p	90	5	4.5	HAINES	86	IMB
> 38	p	90	0	<0.8	ARISAKA	85	KAMI
> 24	p (free)	90	7	8.5	BLEWITT	85	IMB
> 77	p	90	5	4	BLEWITT	85	IMB
> 1.3	p	90	0		ALEKSEEV	81	BAKS
> 1.3	n	90	0		ALEKSEEV	81	BAKS

$\tau(p \to e^+ K^0_S)$ τ_{14}

LIMIT (10^{30} years)	PARTICLE	CL%	EVTS	BKGD EST	DOCUMENT ID		TECN
• • • We do not use the following data for averages, fits, limits, etc. • • •							
>120	p	90	1	1.3	WALL	00	SOU2
> 76	p	90	0	0.5	BERGER	91	FREJ

$\tau(p \to e^+ K^0_L)$ τ_{15}

LIMIT (10^{30} years)	PARTICLE	CL%	EVTS	BKGD EST	DOCUMENT ID		TECN
• • • We do not use the following data for averages, fits, limits, etc. • • •							
>51	p	90	2	3.5	WALL	00	SOU2
>44	p	90	0	$\leq$ 0.1	BERGER	91	FREJ

$\tau(N \to \mu^+ K)$ τ_{16}

LIMIT (10^{30} years)	PARTICLE	CL%	EVTS	BKGD EST	DOCUMENT ID		TECN
>1600	**p**	**90**	**13**	**13.2**	REGIS	12	SKAM
> 26	**n**	**90**	**20**	**28.4**	MCGREW	99	IMB3
• • • We do not use the following data for averages, fits, limits, etc. • • •							
>1300	p	90	3	3.9	KOBAYASHI	05	SKAM
> 120	p	90	0	<1.2	WALL	00	SOU2
> 120	p	90	4	7.2	MCGREW	99	IMB3
> 54	p	90	0		BERGER	91	FREJ
> 120	p	90	1	0.4	HIRATA	89C	KAMI
> 3.0	p	90	0	0.7	PHILLIPS	89	HPW
> 19	p	90	3	2.5	SEIDEL	88	IMB
> 1.5	p	90	0		[53] BARTELT	87	SOUD
> 1.1	n	90	0		BARTELT	87	SOUD
> 40	p	90	7	6	HAINES	86	IMB
> 19	p	90	1	<1.1	ARISAKA	85	KAMI
> 6.7	p (free)	90	11	13	BLEWITT	85	IMB
> 40	p	90	7	8	BLEWITT	85	IMB
> 6	p	90	1		BATTISTONI	84	NUSX
> 0.6	p	90	0		[54] BARTELT	83	SOUD
> 0.4	n	90	0		[54] BARTELT	83	SOUD
> 5.8	p	90	2		[55] KRISHNA...	82	KOLR
> 2.0	p	90	0		CHERRY	81	HOME
> 0.2	n	90			[56] GURR	67	CNTR

[53] BARTELT 87 limit applies to $p \to \mu^+ K^0_S$.
[54] Limit based on zero events.
[55] We have calculated 90% CL limit from 1 confined event.
[56] We have converted half-life to 90% CL mean life.

Baryon Particle Listings

p

$\tau(p \to \mu^+ K^0_S)$ τ_{17}

LIMIT (10^{30} years)	PARTICLE	CL%	EVTS	BKGD EST	DOCUMENT ID		TECN
• • • We do not use the following data for averages, fits, limits, etc. • • •							
>150	p	90	0	<0.8	WALL	00	SOU2
> 64	p	90	0	1.2	BERGER	91	FREJ

$\tau(p \to \mu^+ K^0_L)$ τ_{18}

LIMIT (10^{30} years)	PARTICLE	CL%	EVTS	BKGD EST	DOCUMENT ID		TECN
• • • We do not use the following data for averages, fits, limits, etc. • • •							
>83	p	90	0	0.4	WALL	00	SOU2
>44	p	90	0	$\leq$ 0.1	BERGER	91	FREJ

$\tau(N \to \nu K)$ τ_{19}

LIMIT (10^{30} years)	PARTICLE	CL%	EVTS	BKGD EST	DOCUMENT ID		TECN
>2300	**p**	**90**	**0**	**1.3**	KOBAYASHI	05	SKAM
> 86	**n**	**90**	**0**	**2.4**	HIRATA	89C	KAMI
• • • We do not use the following data for averages, fits, limits, etc. • • •							
> 26	n	90	16	9.1	WALL	00	SOU2
> 670	p	90			HAYATO	99	SKAM
> 151	p	90	15	21.4	MCGREW	99	IMB3
> 30	n	90	34	34.1	MCGREW	99	IMB3
> 43	p	90	1	1.54	[57] ALLISON	98	SOU2
> 15	n	90	1	1.8	BERGER	89	FREJ
> 15	p	90	1	1.8	BERGER	89	FREJ
> 100	p	90	9	7.3	HIRATA	89C	KAMI
> 0.28	p	90	0	0.7	PHILLIPS	89	HPW
> 0.3	p	90	0		BARTELT	87	SOUD
> 0.75	n	90	0		[58] BARTELT	87	SOUD
> 10	p	90	6	5	HAINES	86	IMB
> 15	n	90	3	5	HAINES	86	IMB
> 28	p	90	3	3	KAJITA	86	KAMI
> 32	n	90	0	1.4	KAJITA	86	KAMI
> 1.8	p (free)	90	6	11	BLEWITT	85	IMB
> 9.6	p	90	6	5	BLEWITT	85	IMB
> 10	n	90	2	2	PARK	85	IMB
> 5	n	90	0		BATTISTONI	84	NUSX
> 2	p	90	0		BATTISTONI	84	NUSX
> 0.3	n	90	0		[59] BARTELT	83	SOUD
> 0.1	p	90	0		[59] BARTELT	83	SOUD
> 5.8	p	90	1		[60] KRISHNA...	82	KOLR
> 0.3	n	90	2		[61] CHERRY	81	HOME

[57] This ALLISON 98 limit is with no background subtraction; with subtraction the limit becomes $> 46 \times 10^{30}$ years.
[58] BARTELT 87 limit applies to $n \to \nu K^0_S$.
[59] Limit based on zero events.
[60] We have calculated 90% CL limit from 1 confined event.
[61] We have converted 2 possible events to 90% CL limit.

$\tau(n \to \nu K^0_S)$ τ_{20}

LIMIT (10^{30} years)	PARTICLE	CL%	EVTS	BKGD EST	DOCUMENT ID		TECN
>260	**n**	**90**	**34**	**30**	[62] KOBAYASHI	05	SKAM
• • • We do not use the following data for averages, fits, limits, etc. • • •							
> 51	n	90	16	9.1	WALL	00	SOU2

[62] We have doubled the $n \to \nu K^0$ limit given in KOBAYASHI 05 to obtain this $n \to \nu K^0_S$ limit.

$\tau(p \to e^+ K^*(892)^0)$ τ_{21}

LIMIT (10^{30} years)	PARTICLE	CL%	EVTS	BKGD EST	DOCUMENT ID		TECN
>84	**p**	**90**	**38**	**52.0**	MCGREW	99	IMB3
• • • We do not use the following data for averages, fits, limits, etc. • • •							
>10	p	90	0	0.8	BERGER	91	FREJ
>52	p	90	2	1.55	HIRATA	89C	KAMI
>10	p	90	1	<1	ARISAKA	85	KAMI

$\tau(N \to \nu K^*(892))$ τ_{22}

LIMIT (10^{30} years)	PARTICLE	CL%	EVTS	BKGD EST	DOCUMENT ID		TECN
>51	**p**	**90**	**7**	**9.1**	MCGREW	99	IMB3
>78	**n**	**90**	**40**	**50**	MCGREW	99	IMB3
• • • We do not use the following data for averages, fits, limits, etc. • • •							
>22	n	90	0	2.1	BERGER	89	FREJ
>17	p	90	0	2.4	BERGER	89	FREJ
>20	p	90	5	2.1	HIRATA	89C	KAMI
>21	n	90	4	2.4	HIRATA	89C	KAMI
>10	p	90	7	6	HAINES	86	IMB
> 5	n	90	8	7	HAINES	86	IMB
> 8	p	90	3	2	KAJITA	86	KAMI
> 6	n	90	2	1.6	KAJITA	86	KAMI
> 5.8	p (free)	90	10	16	BLEWITT	85	IMB
> 9.6	p	90	7	6	BLEWITT	85	IMB
> 7	n	90	1	4	PARK	85	IMB
> 2.1	p	90	1		[63] BATTISTONI	82	NUSX

[63] We have converted 1 possible event to 90% CL limit.

Antilepton + mesons

$\tau(p \to e^+ \pi^+ \pi^-)$ τ_{23}

LIMIT (10^{30} years)	PARTICLE	CL%	EVTS	BKGD EST	DOCUMENT ID		TECN
>82	**p**	**90**	**16**	**23.1**	MCGREW	99	IMB3
• • • We do not use the following data for averages, fits, limits, etc. • • •							
>21	p	90	0	2.2	BERGER	91	FREJ

$\tau(p \to e^+ \pi^0 \pi^0)$ τ_{24}

LIMIT (10^{30} years)	PARTICLE	CL%	EVTS	BKGD EST	DOCUMENT ID		TECN
>147	**p**	**90**	**2**	**0.8**	MCGREW	99	IMB3
• • • We do not use the following data for averages, fits, limits, etc. • • •							
> 38	p	90	1	0.5	BERGER	91	FREJ

$\tau(n \to e^+ \pi^- \pi^0)$ τ_{25}

LIMIT (10^{30} years)	PARTICLE	CL%	EVTS	BKGD EST	DOCUMENT ID		TECN
>52	**n**	**90**	**38**	**34.2**	MCGREW	99	IMB3
• • • We do not use the following data for averages, fits, limits, etc. • • •							
>32	n	90	1	0.8	BERGER	91	FREJ

$\tau(p \to \mu^+ \pi^+ \pi^-)$ τ_{26}

LIMIT (10^{30} years)	PARTICLE	CL%	EVTS	BKGD EST	DOCUMENT ID		TECN
>133	**p**	**90**	**25**	**38.0**	MCGREW	99	IMB3
• • • We do not use the following data for averages, fits, limits, etc. • • •							
> 17	p	90	1	2.6	BERGER	91	FREJ
> 3.3	p	90	0	0.7	PHILLIPS	89	HPW

$\tau(p \to \mu^+ \pi^0 \pi^0)$ τ_{27}

LIMIT (10^{30} years)	PARTICLE	CL%	EVTS	BKGD EST	DOCUMENT ID		TECN
>101	**p**	**90**	**3**	**1.6**	MCGREW	99	IMB3
• • • We do not use the following data for averages, fits, limits, etc. • • •							
> 33	p	90	1	0.9	BERGER	91	FREJ

$\tau(n \to \mu^+ \pi^- \pi^0)$ τ_{28}

LIMIT (10^{30} years)	PARTICLE	CL%	EVTS	BKGD EST	DOCUMENT ID		TECN
>74	**n**	**90**	**17**	**20.8**	MCGREW	99	IMB3
• • • We do not use the following data for averages, fits, limits, etc. • • •							
>33	n	90	0	1.1	BERGER	91	FREJ

$\tau(n \to e^+ K^0 \pi^-)$ τ_{29}

LIMIT (10^{30} years)	PARTICLE	CL%	EVTS	BKGD EST	DOCUMENT ID		TECN
>18	**n**	**90**	**1**	**0.2**	BERGER	91	FREJ

Lepton + meson

$\tau(n \to e^- \pi^+)$ τ_{30}

LIMIT (10^{30} years)	PARTICLE	CL%	EVTS	BKGD EST	DOCUMENT ID		TECN
>65	**n**	**90**	**0**	**1.6**	SEIDEL	88	IMB
• • • We do not use the following data for averages, fits, limits, etc. • • •							
>55	n	90	0	1.09	BERGER	91B	FREJ
>16	n	90	9	7	HAINES	86	IMB
>25	n	90	2	4	PARK	85	IMB

$\tau(n \to \mu^- \pi^+)$ τ_{31}

LIMIT (10^{30} years)	PARTICLE	CL%	EVTS	BKGD EST	DOCUMENT ID		TECN
>49	**n**	**90**	**0**	**0.5**	SEIDEL	88	IMB
• • • We do not use the following data for averages, fits, limits, etc. • • •							
>33	n	90	0	1.40	BERGER	91B	FREJ
> 2.7	n	90	0	0.7	PHILLIPS	89	HPW
>25	n	90	7	6	HAINES	86	IMB
>27	n	90	2	3	PARK	85	IMB

$\tau(n \to e^- \rho^+)$ τ_{32}

LIMIT (10^{30} years)	PARTICLE	CL%	EVTS	BKGD EST	DOCUMENT ID		TECN
>62	**n**	**90**	**2**	**4.1**	SEIDEL	88	IMB
• • • We do not use the following data for averages, fits, limits, etc. • • •							
>12	n	90	13	6	HAINES	86	IMB
>12	n	90	5	3	PARK	85	IMB

$\tau(n \to \mu^- \rho^+)$ τ_{33}

LIMIT (10^{30} years)	PARTICLE	CL%	EVTS	BKGD EST	DOCUMENT ID		TECN
>7	**n**	**90**	**1**	**1.1**	SEIDEL	88	IMB
• • • We do not use the following data for averages, fits, limits, etc. • • •							
>2.6	n	90	0	0.7	PHILLIPS	89	HPW
>9	n	90	7	5	HAINES	86	IMB
>9	n	90	2	2	PARK	85	IMB

$\tau(n \to e^- K^+)$ τ_{34}

LIMIT (10^{30} years)	PARTICLE	CL%	EVTS	BKGD EST	DOCUMENT ID		TECN
>32	***n***	**90**	**3**	**2.96**	BERGER	91B	FREJ
• • • We do not use the following data for averages, fits, limits, etc. • • •							
> 0.23	*n*	90	0	0.7	PHILLIPS	89	HPW

$\tau(n \to \mu^- K^+)$ τ_{35}

LIMIT (10^{30} years)	PARTICLE	CL%	EVTS	BKGD EST	DOCUMENT ID		TECN
>57	***n***	**90**	**0**	**2.18**	BERGER	91B	FREJ
• • • We do not use the following data for averages, fits, limits, etc. • • •							
> 4.7	*n*	90	0	0.7	PHILLIPS	89	HPW

Lepton + mesons

$\tau(p \to e^- \pi^+ \pi^+)$ τ_{36}

LIMIT (10^{30} years)	PARTICLE	CL%	EVTS	BKGD EST	DOCUMENT ID		TECN
>30	***p***	**90**	**1**	**2.50**	BERGER	91B	FREJ
• • • We do not use the following data for averages, fits, limits, etc. • • •							
> 2.0	*p*	90	0	0.7	PHILLIPS	89	HPW

$\tau(n \to e^- \pi^+ \pi^0)$ τ_{37}

LIMIT (10^{30} years)	PARTICLE	CL%	EVTS	BKGD EST	DOCUMENT ID		TECN
>29	***n***	**90**	**1**	**0.78**	BERGER	91B	FREJ

$\tau(p \to \mu^- \pi^+ \pi^+)$ τ_{38}

LIMIT (10^{30} years)	PARTICLE	CL%	EVTS	BKGD EST	DOCUMENT ID		TECN
>17	***p***	**90**	**1**	**1.72**	BERGER	91B	FREJ
• • • We do not use the following data for averages, fits, limits, etc. • • •							
> 7.8	*p*	90	0	0.7	PHILLIPS	89	HPW

$\tau(n \to \mu^- \pi^+ \pi^0)$ τ_{39}

LIMIT (10^{30} years)	PARTICLE	CL%	EVTS	BKGD EST	DOCUMENT ID		TECN
>34	***n***	**90**	**0**	**0.78**	BERGER	91B	FREJ

$\tau(p \to e^- \pi^+ K^+)$ τ_{40}

LIMIT (10^{30} years)	PARTICLE	CL%	EVTS	BKGD EST	DOCUMENT ID		TECN
>75	***p***	**90**	**81**	**127.2**	MCGREW	99	IMB3
• • • We do not use the following data for averages, fits, limits, etc. • • •							
>20	*p*	90	3	2.50	BERGER	91B	FREJ

$\tau(p \to \mu^- \pi^+ K^+)$ τ_{41}

LIMIT (10^{30} years)	PARTICLE	CL%	EVTS	BKGD EST	DOCUMENT ID		TECN
>245	***p***	**90**	**3**	**4.0**	MCGREW	99	IMB3
• • • We do not use the following data for averages, fits, limits, etc. • • •							
> 5	*p*	90	2	0.78	BERGER	91B	FREJ

Antilepton + photon(s)

$\tau(p \to e^+ \gamma)$ τ_{42}

LIMIT (10^{30} years)	PARTICLE	CL%	EVTS	BKGD EST	DOCUMENT ID		TECN
>670	***p***	**90**	**0**	**0.1**	MCGREW	99	IMB3
• • • We do not use the following data for averages, fits, limits, etc. • • •							
>133	*p*	90	0	0.3	BERGER	91	FREJ
>460	*p*	90	0	0.6	SEIDEL	88	IMB
>360	*p*	90	0	0.3	HAINES	86	IMB
> 87	*p* (free)	90	0	0.2	BLEWITT	85	IMB
>360	*p*	90	0	0.2	BLEWITT	85	IMB
> 0.1	*p*	90			[64] GURR	67	CNTR

[64] We have converted half-life to 90% CL mean life.

$\tau(p \to \mu^+ \gamma)$ τ_{43}

LIMIT (10^{30} years)	PARTICLE	CL%	EVTS	BKGD EST	DOCUMENT ID		TECN
>478	***p***	**90**	**0**	**0.1**	MCGREW	99	IMB3
• • • We do not use the following data for averages, fits, limits, etc. • • •							
>155	*p*	90	0	0.1	BERGER	91	FREJ
>380	*p*	90	0	0.5	SEIDEL	88	IMB
> 97	*p*	90	3	2	HAINES	86	IMB
> 61	*p* (free)	90	0	0.2	BLEWITT	85	IMB
>280	*p*	90	0	0.6	BLEWITT	85	IMB
> 0.3	*p*	90			[65] GURR	67	CNTR

[65] We have converted half-life to 90% CL mean life.

$\tau(n \to \nu\gamma)$ τ_{44}

LIMIT (10^{30} years)	PARTICLE	CL%	EVTS	BKGD EST	DOCUMENT ID		TECN
>28	***n***	**90**	**163**	**144.7**	MCGREW	99	IMB3
• • • We do not use the following data for averages, fits, limits, etc. • • •							
>24	*n*	90	10	6.86	BERGER	91B	FREJ
> 9	*n*	90	73	60	HAINES	86	IMB
>11	*n*	90	28	19	PARK	85	IMB

$\tau(p \to e^+ \gamma\gamma)$ τ_{45}

LIMIT (10^{30} years)	PARTICLE	CL%	EVTS	BKGD EST	DOCUMENT ID		TECN
>100	***p***	**90**	**1**	**0.8**	BERGER	91	FREJ

$\tau(n \to \nu\gamma\gamma)$ τ_{46}

LIMIT (10^{30} years)	PARTICLE	CL%	EVTS	BKGD EST	DOCUMENT ID		TECN
>219	***n***	**90**	**5**	**7.5**	MCGREW	99	IMB3

Three (or more) leptons

$\tau(p \to e^+ e^+ e^-)$ τ_{47}

LIMIT (10^{30} years)	PARTICLE	CL%	EVTS	BKGD EST	DOCUMENT ID		TECN
>793	***p***	**90**	**0**	**0.5**	MCGREW	99	IMB3
• • • We do not use the following data for averages, fits, limits, etc. • • •							
>147	*p*	90	0	0.1	BERGER	91	FREJ
>510	*p*	90	0	0.3	HAINES	86	IMB
> 89	*p* (free)	90	0	0.5	BLEWITT	85	IMB
>510	*p*	90	0	0.7	BLEWITT	85	IMB

$\tau(p \to e^+ \mu^+ \mu^-)$ τ_{48}

LIMIT (10^{30} years)	PARTICLE	CL%	EVTS	BKGD EST	DOCUMENT ID		TECN
>359	***p***	**90**	**1**	**0.9**	MCGREW	99	IMB3
• • • We do not use the following data for averages, fits, limits, etc. • • •							
> 81	*p*	90	0	0.16	BERGER	91	FREJ
> 5.0	*p*	90	0	0.7	PHILLIPS	89	HPW

$\tau(p \to e^+ \nu\nu)$ τ_{49}

LIMIT (10^{30} years)	PARTICLE	CL%	EVTS	BKGD EST	DOCUMENT ID		TECN
>17	***p***	**90**	**152**	**153.7**	MCGREW	99	IMB3
• • • We do not use the following data for averages, fits, limits, etc. • • •							
>11	*p*	90	11	6.08	BERGER	91B	FREJ

$\tau(n \to e^+ e^- \nu)$ τ_{50}

LIMIT (10^{30} years)	PARTICLE	CL%	EVTS	BKGD EST	DOCUMENT ID		TECN
>257	***n***	**90**	**5**	**7.5**	MCGREW	99	IMB3
• • • We do not use the following data for averages, fits, limits, etc. • • •							
> 74	*n*	90	0	< 0.1	BERGER	91B	FREJ
> 45	*n*	90	5	5	HAINES	86	IMB
> 26	*n*	90	4	3	PARK	85	IMB

$\tau(n \to \mu^+ e^- \nu)$ τ_{51}

LIMIT (10^{30} years)	PARTICLE	CL%	EVTS	BKGD EST	DOCUMENT ID		TECN
>83	***n***	**90**	**25**	**29.4**	MCGREW	99	IMB3
• • • We do not use the following data for averages, fits, limits, etc. • • •							
>47	*n*	90	0	< 0.1	BERGER	91B	FREJ

$\tau(n \to \mu^+ \mu^- \nu)$ τ_{52}

LIMIT (10^{30} years)	PARTICLE	CL%	EVTS	BKGD EST	DOCUMENT ID		TECN
>79	***n***	**90**	**100**	**145**	MCGREW	99	IMB3
• • • We do not use the following data for averages, fits, limits, etc. • • •							
>42	*n*	90	0	1.4	BERGER	91B	FREJ
> 5.1	*n*	90	0	0.7	PHILLIPS	89	HPW
>16	*n*	90	14	7	HAINES	86	IMB
>19	*n*	90	4	7	PARK	85	IMB

$\tau(p \to \mu^+ e^+ e^-)$ τ_{53}

LIMIT (10^{30} years)	PARTICLE	CL%	EVTS	BKGD EST	DOCUMENT ID		TECN
>529	***p***	**90**	**0**	**1.0**	MCGREW	99	IMB3
• • • We do not use the following data for averages, fits, limits, etc. • • •							
> 91	*p*	90	0	≤ 0.1	BERGER	91	FREJ

Baryon Particle Listings

p

$\tau(p \to \mu^+\mu^+\mu^-)$ τ_{54}

LIMIT (10^{30} years)	PARTICLE	CL%	EVTS	BKGD EST	DOCUMENT ID		TECN
>675	**p**	**90**	**0**	**0.3**	MCGREW	99	IMB3
• • • We do not use the following data for averages, fits, limits, etc. • • •							
>119	p	90	0	0.2	BERGER	91	FREJ
> 10.5	p	90	0	0.7	PHILLIPS	89	HPW
>190	p	90	1	0.1	HAINES	86	IMB
> 44	p (free)	90	1	0.7	BLEWITT	85	IMB
>190	p	90	1	0.9	BLEWITT	85	IMB
> 2.1	p	90	1		[66] BATTISTONI	82	NUSX

[66] We have converted 1 possible event to 90% CL limit.

$\tau(p \to \mu^+\nu\nu)$ τ_{55}

LIMIT (10^{30} years)	PARTICLE	CL%	EVTS	BKGD EST	DOCUMENT ID		TECN
>21	**p**	**90**	**7**	**11.23**	BERGER	91B	FREJ

$\tau(p \to e^-\mu^+\mu^+)$ τ_{56}

LIMIT (10^{30} years)	PARTICLE	CL%	EVTS	BKGD EST	DOCUMENT ID		TECN
>6.0	**p**	**90**	**0**	**0.7**	PHILLIPS	89	HPW

$\tau(n \to 3\nu)$ τ_{57}

See also the "to anything" and "disappearance" limits for bound nucleons in the "p Mean Life" data block just in front of the list of possible p decay modes. Such modes could of course be to three (or five) neutrinos, and the limits are stronger, but we do not repeat them here.

LIMIT (10^{30} years)	PARTICLE	CL%	EVTS	BKGD EST	DOCUMENT ID		TECN
>0.00049	**n**	**90**	**2**	**2**	[67] SUZUKI	93B	KAMI
• • • We do not use the following data for averages, fits, limits, etc. • • •							
>0.0023	n	90			[68] GLICENSTEIN	97	KAMI
>0.00003	n	90	11	6.1	[69] BERGER	91B	FREJ
>0.00012	n	90	7	11.2	[69] BERGER	91B	FREJ
>0.0005	n	90	0		LEARNED	79	RVUE

[67] The SUZUKI 93B limit applies to any of $\nu_e\nu_e\overline{\nu}_e$, $\nu_\mu\nu_\mu\overline{\nu}_\mu$, or $\nu_\tau\nu_\tau\overline{\nu}_\tau$.

[68] GLICENSTEIN 97 uses Kamioka data and the idea that the disappearance of the neutron's magnetic moment should produce radiation.

[69] The first BERGER 91B limit is for $n \to \nu_e\nu_e\overline{\nu}_e$, the second is for $n \to \nu_\mu\nu_\mu\overline{\nu}_\mu$.

$\tau(n \to 5\nu)$ τ_{58}

See the note on $\tau(n \to 3\nu)$ on the previous data block.

LIMIT (10^{30} years)	PARTICLE	CL%	EVTS	BKGD EST	DOCUMENT ID		TECN
• • • We do not use the following data for averages, fits, limits, etc. • • •							
>0.0017	n	90			[70] GLICENSTEIN	97	KAMI

[70] GLICENSTEIN 97 uses Kamioka data and the idea that the disappearance of the neutron's magnetic moment should produce radiation.

Inclusive modes

$\tau(N \to e^+ \text{anything})$ τ_{59}

LIMIT (10^{30} years)	PARTICLE	CL%	EVTS	BKGD EST	DOCUMENT ID		TECN
>0.6	**p, n**	**90**			[71] LEARNED	79	RVUE

[71] The electron may be primary or secondary.

$\tau(N \to \mu^+ \text{anything})$ τ_{60}

LIMIT (10^{30} years)	PARTICLE	CL%	EVTS	BKGD EST	DOCUMENT ID		TECN
>12	**p, n**	**90**	**2**		[72,73] CHERRY	81	HOME
• • • We do not use the following data for averages, fits, limits, etc. • • •							
> 1.8	p, n	90			[73] COWSIK	80	CNTR
> 6	p, n	90			[73] LEARNED	79	RVUE

[72] We have converted 2 possible events to 90% CL limit.

[73] The muon may be primary or secondary.

$\tau(N \to \nu \text{anything})$ τ_{61}

Anything = π, ρ, K, etc.

LIMIT (10^{30} years)	PARTICLE	CL%	EVTS	BKGD EST	DOCUMENT ID		TECN
• • • We do not use the following data for averages, fits, limits, etc. • • •							
>0.0002	p, n	90	0		LEARNED	79	RVUE

$\tau(N \to e^+\pi^0 \text{anything})$ τ_{62}

LIMIT (10^{30} years)	PARTICLE	CL%	EVTS	BKGD EST	DOCUMENT ID		TECN
>0.6	**p, n**	**90**	**0**		LEARNED	79	RVUE

$\tau(N \to 2 \text{bodies}, \nu\text{-free})$ τ_{63}

LIMIT (10^{30} years)	PARTICLE	CL%	EVTS	BKGD EST	DOCUMENT ID		TECN
• • • We do not use the following data for averages, fits, limits, etc. • • •							
>1.3	p, n	90	0		ALEKSEEV	81	BAKS

$\Delta B = 2$ dinucleon modes

$\tau(pp \to \pi^+\pi^+)$ τ_{64}

LIMIT (10^{30} years)	CL%	EVTS	BKGD EST	DOCUMENT ID		TECN	COMMENT
>0.7	**90**	**4**	**2.34**	BERGER	91B	FREJ	τ per iron nucleus

$\tau(pn \to \pi^+\pi^0)$ τ_{65}

LIMIT (10^{30} years)	CL%	EVTS	BKGD EST	DOCUMENT ID		TECN	COMMENT
>2.0	**90**	**0**	**0.31**	BERGER	91B	FREJ	τ per iron nucleus

$\tau(nn \to \pi^+\pi^-)$ τ_{66}

LIMIT (10^{30} years)	CL%	EVTS	BKGD EST	DOCUMENT ID		TECN	COMMENT
>0.7	**90**	**4**	**2.18**	BERGER	91B	FREJ	τ per iron nucleus

$\tau(nn \to \pi^0\pi^0)$ τ_{67}

LIMIT (10^{30} years)	CL%	EVTS	BKGD EST	DOCUMENT ID		TECN	COMMENT
>3.4	**90**	**0**	**0.78**	BERGER	91B	FREJ	τ per iron nucleus

$\tau(pp \to e^+e^+)$ τ_{68}

LIMIT (10^{30} years)	CL%	EVTS	BKGD EST	DOCUMENT ID		TECN	COMMENT
>5.8	**90**	**0**	**<0.1**	BERGER	91B	FREJ	τ per iron nucleus

$\tau(pp \to e^+\mu^+)$ τ_{69}

LIMIT (10^{30} years)	CL%	EVTS	BKGD EST	DOCUMENT ID		TECN	COMMENT
>3.6	**90**	**0**	**<0.1**	BERGER	91B	FREJ	τ per iron nucleus

$\tau(pp \to \mu^+\mu^+)$ τ_{70}

LIMIT (10^{30} years)	CL%	EVTS	BKGD EST	DOCUMENT ID		TECN	COMMENT
>1.7	**90**	**0**	**0.62**	BERGER	91B	FREJ	τ per iron nucleus

$\tau(pn \to e^+\overline{\nu})$ τ_{71}

LIMIT (10^{30} years)	CL%	EVTS	BKGD EST	DOCUMENT ID		TECN	COMMENT
>2.8	**90**	**5**	**9.67**	BERGER	91B	FREJ	τ per iron nucleus

$\tau(pn \to \mu^+\overline{\nu})$ τ_{72}

LIMIT (10^{30} years)	CL%	EVTS	BKGD EST	DOCUMENT ID		TECN	COMMENT
>1.6	**90**	**4**	**4.37**	BERGER	91B	FREJ	τ per iron nucleus

$\tau(nn \to \nu_e\overline{\nu}_e)$ τ_{73}

We include "invisible" modes here.

LIMIT (10^{30} years)	CL%	EVTS	BKGD EST	DOCUMENT ID		TECN	COMMENT
>1.4	**90**			[74] ARAKI	06	KLND	$nn \to$ invisible
• • • We do not use the following data for averages, fits, limits, etc. • • •							
>0.000042	90			[75] TRETYAK	04	CNTR	$nn \to$ invisible
>0.000049	90			[76] BACK	03	BORX	$nn \to$ invisible
>0.000012	90			[77] BERNABEI	00B	DAMA	$nn \to$ invisible
>0.000012	90	5	9.7	BERGER	91B	FREJ	τ per iron nucleus

[74] ARAKI 06 looks for signs of de-excitation of the residual nucleus after disappearance of two neutrons from the s shell of ^{12}C.

[75] TRETYAK 04 uses data from an old Homestake-mine radiochemical experiment on limits for invisible decays of ^{39}K to ^{37}Ar.

[76] BACK 03 looks for decays of unstable nuclides left after NN decays of parent ^{12}C, ^{13}C, ^{16}O nuclei. These are "invisible channel" limits.

[77] BERNABEI 00B looks for the decay of a $^{127}_{54}$Xe nucleus following the disappearance of an nn pair in the otherwise-stable $^{129}_{54}$Xe nucleus. The limit here applies as well to $nn \to \nu_\mu\overline{\nu}_\mu$, $nn \to \nu_\tau\overline{\nu}_\tau$, or any "disappearance" mode.

$\tau(nn \to \nu_\mu\overline{\nu}_\mu)$ τ_{74}

See the proceeding data block. "Invisible modes" would include any multi-neutrino mode.

LIMIT (10^{30} years)	CL%	EVTS	BKGD EST	CL%	DOCUMENT ID		TECN	COMMENT
>1.4	**(CL = 90%) OUR LIMIT**							
• • • We do not use the following data for averages, fits, limits, etc. • • •								
>0.000006	90	4	4.4		BERGER	91B	FREJ	τ per iron nucleus

$\tau(pn \to \text{invisible})$ τ_{75}

This violates charge conservation as well as baryon number conservation.

VALUE (10^{30} years)	CL%	DOCUMENT ID		TECN
>0.000021	90	[78] TRETYAK	04	CNTR

[78] TRETYAK 04 uses data from an old Homestake-mine radiochemical experiment on limits for invisible decays of ^{39}K to ^{37}Ar.

$\tau(pp \rightarrow \text{invisible})$ τ_{76}

This violates charge conservation as well as baryon number conservation.

LIMIT (10^{30} years)	CL%	EVTS	BKGD EST	CL%	DOCUMENT ID		TECN
>0.00005				90	[79] BACK	03	BORX
• • • We do not use the following data for averages, fits, limits, etc. • • •							
>0.00000055	90				[80] BERNABEI	00B	DAMA

[79] BACK 03 looks for decays of unstable nuclides left after NN decays of parent ^{12}C, ^{13}C, ^{16}O nuclei. These are "invisible channel" limits.

[80] BERNABEI 00B looks for the decay of a $^{127}_{52}Te$ nucleus following the disappearance of a pp pair in the otherwise-stable $^{129}_{54}Xe$ nucleus.

$\overline{p}$ PARTIAL MEAN LIVES

The "partial mean life" limits tabulated here are the limits on $\overline{\tau}/B_i$, where $\overline{\tau}$ is the total mean life for the antiproton and B_i is the branching fraction for the mode in question.

$\tau(\overline{p} \rightarrow e^- \gamma)$ τ_{77}

VALUE (years)	CL%	DOCUMENT ID		TECN	COMMENT
> 7×10^5	90	GEER	00	APEX	8.9 GeV/c $\overline{p}$ beam
• • • We do not use the following data for averages, fits, limits, etc. • • •					
>1848	95	GEER	94	CALO	8.9 GeV/c $\overline{p}$ beam

$\tau(\overline{p} \rightarrow \mu^- \gamma)$ τ_{78}

VALUE (years)	CL%	DOCUMENT ID		TECN	COMMENT
> 5×10^4	90	GEER	00	APEX	8.9 GeV/c $\overline{p}$ beam
• • • We do not use the following data for averages, fits, limits, etc. • • •					
>5.0×10^4	90	HU	98B	APEX	8.9 GeV/c $\overline{p}$ beam

$\tau(\overline{p} \rightarrow e^- \pi^0)$ τ_{79}

VALUE (years)	CL%	DOCUMENT ID		TECN	COMMENT
> 4×10^5	90	GEER	00	APEX	8.9 GeV/c $\overline{p}$ beam
• • • We do not use the following data for averages, fits, limits, etc. • • •					
>554	95	GEER	94	CALO	8.9 GeV/c $\overline{p}$ beam

$\tau(\overline{p} \rightarrow \mu^- \pi^0)$ τ_{80}

VALUE (years)	CL%	DOCUMENT ID		TECN	COMMENT
> 5×10^4	90	GEER	00	APEX	8.9 GeV/c $\overline{p}$ beam
• • • We do not use the following data for averages, fits, limits, etc. • • •					
>4.8×10^4	90	HU	98B	APEX	8.9 GeV/c $\overline{p}$ beam

$\tau(\overline{p} \rightarrow e^- \eta)$ τ_{81}

VALUE (years)	CL%	DOCUMENT ID		TECN	COMMENT
> 2×10^4	90	GEER	00	APEX	8.9 GeV/c $\overline{p}$ beam
• • • We do not use the following data for averages, fits, limits, etc. • • •					
>171	95	GEER	94	CALO	8.9 GeV/c $\overline{p}$ beam

$\tau(\overline{p} \rightarrow \mu^- \eta)$ τ_{82}

VALUE (years)	CL%	DOCUMENT ID		TECN	COMMENT
> 8×10^3	90	GEER	00	APEX	8.9 GeV/c $\overline{p}$ beam
• • • We do not use the following data for averages, fits, limits, etc. • • •					
>7.9×10^3	90	HU	98B	APEX	8.9 GeV/c $\overline{p}$ beam

$\tau(\overline{p} \rightarrow e^- K_S^0)$ τ_{83}

VALUE (years)	CL%	DOCUMENT ID		TECN	COMMENT
>900	90	GEER	00	APEX	8.9 GeV/c $\overline{p}$ beam
• • • We do not use the following data for averages, fits, limits, etc. • • •					
> 29	95	GEER	94	CALO	8.9 GeV/c $\overline{p}$ beam

$\tau(\overline{p} \rightarrow \mu^- K_S^0)$ τ_{84}

VALUE (years)	CL%	DOCUMENT ID		TECN	COMMENT
> 4×10^3	90	GEER	00	APEX	8.9 GeV/c $\overline{p}$ beam
• • • We do not use the following data for averages, fits, limits, etc. • • •					
>4.3×10^3	90	HU	98B	APEX	8.9 GeV/c $\overline{p}$ beam

$\tau(\overline{p} \rightarrow e^- K_L^0)$ τ_{85}

VALUE (years)	CL%	DOCUMENT ID		TECN	COMMENT
> 9×10^3	90	GEER	00	APEX	8.9 GeV/c $\overline{p}$ beam
• • • We do not use the following data for averages, fits, limits, etc. • • •					
>9	95	GEER	94	CALO	8.9 GeV/c $\overline{p}$ beam

$\tau(\overline{p} \rightarrow \mu^- K_L^0)$ τ_{86}

VALUE (years)	CL%	DOCUMENT ID		TECN	COMMENT
> 7×10^3	90	GEER	00	APEX	8.9 GeV/c $\overline{p}$ beam
• • • We do not use the following data for averages, fits, limits, etc. • • •					
>6.5×10^3	90	HU	98B	APEX	8.9 GeV/c $\overline{p}$ beam

$\tau(\overline{p} \rightarrow e^- \gamma\gamma)$ τ_{87}

VALUE (years)	CL%	DOCUMENT ID		TECN	COMMENT
> 2×10^4	90	GEER	00	APEX	8.9 GeV/c $\overline{p}$ beam

$\tau(\overline{p} \rightarrow \mu^- \gamma\gamma)$ τ_{88}

VALUE (years)	CL%	DOCUMENT ID		TECN	COMMENT
> 2×10^4	90	GEER	00	APEX	8.9 GeV/c $\overline{p}$ beam
• • • We do not use the following data for averages, fits, limits, etc. • • •					
>2.3×10^4	90	HU	98B	APEX	8.9 GeV/c $\overline{p}$ beam

$\tau(\overline{p} \rightarrow e^- \rho)$ τ_{89}

VALUE (years)	CL%	DOCUMENT ID		TECN	COMMENT
• • • We do not use the following data for averages, fits, limits, etc. • • •					
>200	90	[81] GEER	00	APEX	8.9 GeV/c $\overline{p}$ beam

[81] This GEER 00 measurement has been withdrawn; see GEER 00C.

$\tau(\overline{p} \rightarrow e^- \omega)$ τ_{90}

VALUE (years)	CL%	DOCUMENT ID		TECN	COMMENT
>200	90	GEER	00	APEX	8.9 GeV/c $\overline{p}$ beam

$\tau(\overline{p} \rightarrow e^- K^*(892)^0)$ τ_{91}

VALUE (years)	CL%	DOCUMENT ID		TECN	COMMENT
• • • We do not use the following data for averages, fits, limits, etc. • • •					
>1×10^3	90	[82] GEER	00	APEX	8.9 GeV/c $\overline{p}$ beam

[82] This GEER 00 measurement has been withdrawn; see GEER 00C.

p REFERENCES

ANTOGNINI	13	SCI 339 417	A. Antognini *et al.* (MPIM, ETH, UPMC+)
DISCIACCA	13	PRL 110 130801	J. DiSciacca *et al.* (ATRAP Collab.)
MCGOVERN	13	EPJ A49 12	J.A. McGovern, D.R. Phillips, H.W. Griesshammer
MOHR	12	RMP 84 1527	P.J. Mohr, B.N. Taylor, D.B. Newell (NIST)
NISHINO	12	PR D85 112001	H. Nishino *et al.* (Super Kamiokande Collab.)
REGIS	12	PR D86 012006	C. Regis *et al.* (Super-Kamiokande Collab.)
ARRINGTON	11	PRL 107 119101	J. Arrington (ANL)
BERNAUER	11	PRL 107 119102	J.C. Bernauer *et al.* (MAMI A1 Collab.)
BRESSI	11	PR A83 052101	G. Bressi *et al.* (LEGN, PAVII, PADO, TRST+)
CLOET	11	PR C83 012201	I.C. Cloet, G.A. Miller (WASH)
DERUJULA	11	PL B697 26	A. de Rujula (MADE, BOST, CERN)
DISTLER	11	PL B696 343	M.O. Distler, J.C. Bernauer, T. Walcher (MANZ)
HILL	11	PRL 107 160402	R.J. Hill, G. Paz (EFI)
HORI	11	NAT 475 484	M. Hori *et al.* (MPIG, TOKY, BUDA, +)
BERNAUER	10	PRL 105 242001	J.C. Bernauer *et al.* (MAMI A1 Collab.)
BORISYUK	10	NP A843 59	D. Borisyuk (KIEV)
DERUJULA	10	PL B693 555	A. De Rujula (MADU, CERN)
HILL	10	PR D82 113005	R.J. Hill, G. Paz (CHIC)
POHL	10	NAT 466 213	R. Pohl *et al.* (MPIQ, ENSP, COIM, +)
NISHINO	09	PRL 102 141801	H. Nishino *et al.* (Super Kamiokande Collab.)
PASK	09	PL B678 55	T. Pask *et al.* (Stefan Meyer Inst., Vienna, TOKY+)
MOHR	08	RMP 80 633	P.J. Mohr, B.N. Taylor, D.B. Newell (NIST)
BELUSHKIN	07	PR C75 035202	M.A. Belushkin, H.W. Hammer, U.-G. Meissner (BONN+)
ARAKI	06	PRL 96 101802	T. Araki *et al.* (KamLAND Collab.)
HORI	06	PRL 96 243401	M. Hori *et al.* (CERN, TOKYO+)
BLUNDEN	05	PR C72 057601	P.G. Blunden, I. Sick (MANI, BASL)
KOBAYASHI	05	PR D72 052007	K. Kobayashi *et al.* (Super-Kamiokande Collab.)
MOHR	05	RMP 77 1	P.J. Mohr, B.N. Taylor (NIST)
SCHUMACHER	05	PPNP 55 567	M. Schumacher (GOET)
AHMED	04	PRL 92 102004	S.N. Ahmed *et al.* (SNO Collab.)
TRETYAK	04	JETPL 79 106	V.I. Tretyak, V.Yu. Denisov, Yu.G. Zdesenko (KIEV)
		Translated from ZETFP 79 136.	
BACK	03	PL B563 23	H.O. Back *et al.* (BOREXINO Collab.)
BEANE	03	PL B567 200	S.R. Beane *et al.*
Also		PL B607 320 (errat)	S.R. Beane *et al.*
DMITRIEV	03	PRL 91 212303	V.F. Dmitriev, R.A. Senkov (NOVO)
HORI	03	PRL 91 123401	M. Hori *et al.* (CERN ASACUSA Collab.)
SICK	03	PL B576 62	I. Sick (BASL)
ZDESENKO	03	PL B553 135	Yu.G. Zdesenko, V.I. Tretyak (KIEV)
AHMAD	02	PRL 89 011301	Q.R. Ahmad *et al.* (SNO Collab.)
BARANOV	01	PPN 32 376	P.S. Baranov *et al.*
		Translated from FECAY 32 699.	
BLANPIED	01	PR C64 025203	G. Blanpied *et al.* (BNL LEGS Collab.)
ESCHRICH	01	PL B522 233	I. Eschrich *et al.* (FNAL SELEX Collab.)
HORI	01	PRL 87 093401	M. Hori *et al.* (CERN ASACUSA Collab.)
OLMOSDEL...	01	EPJ A10 207	V. Olmos de Leon *et al.* (MAMI TAPS Collab.)
TRETYAK	01	PL B505 59	V.I. Tretyak, Yu.G. Zdesenko (KIEV)
BERNABEI	00B	PL B493 12	R. Bernabei *et al.* (Gran Sasso DAMA Collab.)
GEER	00	PRL 84 590	S. Geer *et al.* (FNAL APEX Collab.)
Also		PR D62 052004	S. Geer *et al.* (FNAL APEX Collab.)
Also		PRL 85 3546 (errat)	S. Geer *et al.* (FNAL APEX Collab.)
GEER	00C	PRL 85 3546 (errat)	S. Geer *et al.* (FNAL APEX Collab.)
GEER	00D	APJ 532 648	S.H. Geer, D.C. Kennedy
MELNIKOV	00	PRL 84 1673	K. Melnikov *et al.* (SLAC, KARL)
ROSENFELDR...	00	PL B479 381	R. Rosenfelder
SENGUPTA	00	PL B484 275	S. Sengupta
WALL	00	PR D61 072004	D. Wall *et al.* (Soudan-2 Collab.)
WALL	00B	PR D62 092003	D. Wall *et al.* (Soudan-2 Collab.)
GABRIELSE	99	PRL 82 3198	G. Gabrielse *et al.*
HAYATO	99	PRL 83 1529	Y. Hayato *et al.* (Super-Kamiokande Collab.)
MCGREW	99	PR D59 052004	C. McGrew *et al.* (IMB-3 Collab.)
MOHR	99	JPCRD 28 1713	P.J. Mohr, B.N. Taylor (NIST)
Also		RMP 72 351	P.J. Mohr, B.N. Taylor (NIST)
TORII	99	PR A59 223	H.A. Torii *et al.* (CERN PS-205 Collab.)
ALLISON	98	PL B427 217	W.W.M. Allison *et al.* (Soudan-2 Collab.)
HU	98B	PR D58 111101	M. Hu *et al.* (FNAL APEX Collab.)
SHIOZAWA	98	PRL 81 3319	M. Shiozawa *et al.* (Super-Kamiokande Collab.)
GLICENSTEIN	97	PL B411 326	J.F. Glicenstein (SACL)
MERGELL	96	NP A596 367	P. Mergell *et al.* (MANZ, BONN)
GABRIELSE	95	PRL 74 3544	G. Gabrielse *et al.* (HARV, MANZ, SEOUL)
MACGIBBON	95	PR C52 2097	B.E. MacGibbon *et al.* (ILL, SASK, INRM)
GEER	94	PRL 72 1596	S. Geer *et al.* (FNAL, UCLA, PSU)
WONG	94	IJMP E3 821	C.W. Wong (UCLA)
HALLIN	93	PR C48 1497	E.L. Hallin *et al.* (SASK, BOST, ILL)
SUZUKI	93B	PL B311 357	Y. Suzuki *et al.* (KAMIOKANDE Collab.)
HUGHES	92	PRL 69 578	R.J. Hughes, B.I. Deutch (LANL, AARH)
ZIEGER	92	PL B278 34	A. Zieger *et al.* (MPCM)
Also		PL B281 417 (erratum)	A. Zieger *et al.* (MPCM)
BERGER	91	ZPHY C50 385	C. Berger *et al.* (FREJUS Collab.)
BERGER	91B	PL B269 227	C. Berger *et al.* (FREJUS Collab.)
FEDERSPIEL	91	PRL 67 1511	F.J. Federspiel *et al.* (ILL)
MCCORD	91	NIM B56/57 496	M. McCord *et al.*
BECKER-SZ...	90	PR D42 2974	R.A. Becker-Szendy *et al.* (IMB-3 Collab.)
ERICSON	90	EPL 11 295	T.E.O. Ericson, A. Richter (CERN, DARM)
GABRIELSE	90	PRL 65 1317	G. Gabrielse *et al.* (HARV, MANZ, WASH+)

BERGER	89	NP B313 509	C. Berger *et al.* (FREJUS Collab.)
CHO	89	PRL 63 2559	D. Cho, K. Sangster, E.A. Hinds (YALE)
HIRATA	89C	PL B220 308	K.S. Hirata *et al.* (Kamiokande Collab.)
PHILLIPS	89	PL B224 348	T.J. Phillips *et al.* (HPW Collab.)
KREISSL	88	ZPHY C37 557	A. Kreissl *et al.* (CERN PS176 Collab.)
SEIDEL	88	PRL 61 2522	S. Seidel *et al.* (IMB Collab.)
BARTELT	87	PR D36 1990	J.E. Bartelt *et al.* (Soudan Collab.)
Also		PR D40 1701 (erratum)	J.E. Bartelt *et al.* (Soudan Collab.)
COHEN	87	RMP 59 1121	E.R. Cohen, B.N. Taylor (RISC, NBS)
HAINES	86	PRL 57 1986	T.J. Haines *et al.* (IMB Collab.)
KAJITA	86	JPSJ 55 711	T. Kajita *et al.* (Kamiokande Collab.)
ARISAKA	85	JPSJ 54 3213	K. Arisaka *et al.* (Kamiokande Collab.)
BLEWITT	85	PRL 55 2114	G.B. Blewitt *et al.* (IMB Collab.)
DZUBA	85	PL 154B 93	V.A. Dzuba, V.V. Flambaum, P.G. Silvestrov (NOVO)
PARK	85	PRL 54 22	H.S. Park *et al.* (IMB Collab.)
BATTISTONI	84	PL 133B 454	G. Battistoni *et al.* (NUSEX Collab.)
MARINELLI	84	PL 137B 439	M. Marinelli, G. Morpurgo (GENO)
WILKENING	84	PR A29 425	D.A. Wilkening, N.F. Ramsey, D.J. Larson (HARV+)
BARTELT	83	PRL 50 651	J.E. Bartelt *et al.* (MINN, ANL)
BATTISTONI	82	PL 118B 461	G. Battistoni *et al.* (NUSEX Collab.)
KRISHNA...	82	PL 115B 349	M.R. Krishnaswamy *et al.* (TATA, OSKC+)
ALEKSEEV	81	JETPL 33 651	E.N. Alekseev *et al.* (PNPI)
		Translated from ZETFP 33 664.	
CHERRY	81	PRL 47 1507	M.L. Cherry *et al.* (PENN, BNL)
COWSIK	80	PR D22 2204	R. Cowsik, V.S. Narasimham (TATA)
SIMON	80	NP A333 381	G.G. Simon *et al.*
BELL	79	PL 86B 215	M. Bell *et al.* (CERN)
GOLDEN	79	PRL 43 1196	R.L. Golden *et al.* (NASA, PSLL)
LEARNED	79	PRL 43 907	J.G. Learned, F. Reines, A. Soni (UCI)
BREGMAN	78	PL 78B 174	M. Bregman *et al.* (CERN)
ROBERTS	78	PR D17 358	B.L. Roberts (WILL, RHEL)
EVANS	77	SCI 197 989	J.C. Evans Jr., R.I. Steinberg (BNL, PENN)
HU	75	NP A254 403	E. Hu *et al.* (COLU, YALE)
BORKOWSKI	74	NP A222 269	F. Borkowski *et al.*
COHEN	73	JPCRD 2 664	E.R. Cohen, B.N. Taylor (RISC, NBS)
DYLLA	73	PR A7 1224	H.F. Dylla, J.G. King (MIT)
AKIMOV	72	JETP 35 651	Yu.K. Akimov *et al.* (YERE)
		Translated from ZETF 62 1231.	
DIX	70	Thesis Case	F.W. Dix (CASE)
HARRISON	69	PRL 22 1263	G.E. Harrison, P.G.H. Sandars, S.J. Wright (OXF)
GURR	67	PR 158 1321	H.S. Gurr *et al.* (CASE, WITW)
FREREJACQ...	66	PR 141 1308	D. Frerejacque *et al.*
HAND	63	RMP 35 335	L.N. Hand *et al.*
FLEROV	58	DOKL 3 79	G.N. Flerov *et al.* (ASCI)

n

$I(J^P) = \frac{1}{2}(\frac{1}{2}^+)$ Status: ****

We have omitted some results that have been superseded by later experiments. See our earlier editions.

Anyone interested in the neutron should look at these two new review articles: D. Dubbers and M.G. Schmidt, "The neutron and its role in cosmology and particle physics," Reviews of Modern Physics **83** 1111 (2011); and F.E. Wietfeldt and G.L. Greene, "The neutron lifetime," Reviews of Modern Physics **83** 1173 (2011).

n MASS (atomic mass units u)

The mass is known much more precisely in u (atomic mass units) than in MeV. See the next data block.

VALUE (u)	DOCUMENT ID		TECN	COMMENT
1.00866491600±0.00000000043	MOHR	12	RVUE	2010 CODATA value
• • • We do not use the following data for averages, fits, limits, etc. • • •				
1.00866491597±0.00000000043	MOHR	08	RVUE	2006 CODATA value
1.00866491560±0.00000000055	MOHR	05	RVUE	2002 CODATA value
1.00866491578±0.00000000055	MOHR	99	RVUE	1998 CODATA value
1.008665904 ±0.000000014	COHEN	87	RVUE	1986 CODATA value

n MASS (MeV)

The mass is known much more precisely in u (atomic mass units) than in MeV. The conversion from u to MeV, 1 u = 931.494 061(21) MeV/c^2 (MOHR 12, the 2010 CODATA value), involves the relatively poorly known electronic charge.

VALUE (MeV)	DOCUMENT ID		TECN	COMMENT
939.565379±0.000021	MOHR	12	RVUE	2010 CODATA value
• • • We do not use the following data for averages, fits, limits, etc. • • •				
939.565346±0.000023	MOHR	08	RVUE	2006 CODATA value
939.565360±0.000081	MOHR	05	RVUE	2002 CODATA value
939.565331±0.000037 [1]	KESSLER	99	SPEC	$np \to d\gamma$
939.565330±0.000038	MOHR	99	RVUE	1998 CODATA value
939.56565 ±0.00028 [2,3]	DIFILIPPO	94	TRAP	Penning trap
939.56563 ±0.00028	COHEN	87	RVUE	1986 CODATA value
939.56564 ±0.00028 [3,4]	GREENE	86	SPEC	$np \to d\gamma$
939.5731 ±0.0027 [3]	COHEN	73	RVUE	1973 CODATA value

[1] We use the 1998 CODATA u-to-MeV conversion factor (see the heading above) to get this mass in MeV from the much more precisely measured KESSLER 99 value of 1.00866491637 ± 0.00000000082 u.

[2] The mass is known much more precisely in u: m = 1.0086649235 ± 0.0000000023 u. We use the 1986 CODATA conversion factor to get the mass in MeV.

[3] These determinations are not independent of the $m_n - m_p$ measurements below.

[4] The mass is known much more precisely in u: m = 1.008664919 ± 0.000000014 u.

$\overline{n}$ MASS

VALUE (MeV)	EVTS	DOCUMENT ID		TECN	COMMENT
939.485±0.051	59	[5] CRESTI	86	HBC	$\overline{p}p \to \overline{n}n$

[5] This is a corrected result (see the erratum). The error is statistical. The maximum systematic error is 0.029 MeV.

$(m_n - m_{\overline{n}})/\, m_n$

A test of CPT invariance. Calculated from the n and $\overline{n}$ masses, above.

VALUE	DOCUMENT ID
(9±6) × 10^{-5} OUR EVALUATION	

$m_n - m_p$

VALUE (MeV)	DOCUMENT ID		TECN	COMMENT
1.29333217±0.00000042	[6] MOHR	12	RVUE	2010 CODATA value
• • • We do not use the following data for averages, fits, limits, etc. • • •				
1.29333214±0.00000043	[7] MOHR	08	RVUE	2006 CODATA value
1.2933317 ±0.0000005	[8] MOHR	05	RVUE	2002 CODATA value
1.2933318 ±0.0000005	[9] MOHR	99	RVUE	1998 CODATA value
1.293318 ±0.000009	[10] COHEN	87	RVUE	1986 CODATA value
1.2933328 ±0.0000072	GREENE	86	SPEC	$np \to d\gamma$
1.293429 ±0.000036	COHEN	73	RVUE	1973 CODATA value

[6] The 2010 CODATA mass difference in u is $m_n - m_p$ = 1.388 449 19(45) × $10^{-3}u$.

[7] Calculated by us from the MOHR 08 ratio m_n/m_p = 1.00137841918(46). In u, $m_n - m_p$ = 1.38844920(46) × 10^{-3} u.

[8] Calculated by us from the MOHR 05 ratio m_n/m_p = 1.00137841870 ± 0.00000000058. In u, $m_n - m_p$ = (1.3884487 ± 0.0000006) × 10^{-3} u.

[9] Calculated by us from the MOHR 99 ratio m_n/m_p = 1.00137841887 ± 0.00000000058. In u, $m_n - m_p$ = (1.3884489 ± 0.0000006) × 10^{-3} u.

[10] Calculated by us from the COHEN 87 ratio m_n/m_p = 1.001378404 ± 0.000000009. In u, $m_n - m_p$ = 0.001388434 ± 0.000000009 u.

n MEAN LIFE

Limits on lifetimes for *bound* neutrons are given in the section "p PARTIAL MEAN LIVES."

The mean life of the neutron, 878.5 ± 0.8 s, obtained by SEREBROV 05 (for a more detailed account, see SEREBROV 08A; and for comments on the systematic error for this result, see STEYERL 10) was so far from our average of seven other measurements, 885.7 ± 0.8 s, that it made no sense to include it in our average. Thus our 2006, 2008, and 2010 *Reviews* stayed with 885.7 ± 0.8 s; but we noted that in light of SEREBROV 05 our value should be regarded as suspect until further experiments clarified matters.

However, after our 2010 *Review*, PICHLMAIER 10 obtained a mean life of 880.7 ± 1.8 s, and we averaged the best seven results to get 881.5 ± 1.5 s for our 2011 off-year web update. Since then, ARZUMANOV 12, responding to comments of SEREBROV 10B, recalculated the systematic corrections to its 2000 measurement (ARZUMANOV 00) and lowered its value from 885.4 ± 0.9 ± 0.4 s to 881.6 ± 0.8 ± 1.9 s. And STEYERL 12 reanalyzed systematic corrections to MAMPE 89 and lowered its value from 887.6 ± 3.0 to 882.5 ± 1.4 ± 1.5 s. Thus the trend is definitely toward a shorter lifetime.

There seems little better to do than to again average the best seven measurements. The result, 880.3 ± 1.1 s (including a scale factor of 1.9), is 5.4 seconds lower than the value we gave in 2010—a drop of 6.8 old and 4.9 new standard deviations.

For a full review of all matters concerning the neutron lifetime, see F.E. Wietfeldt and G.L. Greene, "The neutron lifetime," Reviews of Modern Physics **83** 1173 (2011). In particular, there is a full discussion of the experimental methods and results; and an average lifetime is obtained making several different selections of those results. (The revised ARZUMANOV 12 mean life was not yet available.)

VALUE (s)	DOCUMENT ID		TECN	COMMENT
880.3± 1.1 OUR AVERAGE	Error includes scale factor of 1.9. See the ideogram below.			
887.7± 1.2± 1.9	[11] YUE	13	CNTR	In-beam n, trapped p
881.6± 0.8± 1.9	[12] ARZUMANOV	12	CNTR	UCN double bottle
882.5± 1.4± 1.5	[13] STEYERL	12	CNTR	UCN material bottle
880.7± 1.3± 1.2	PICHLMAIER	10	CNTR	UCN material bottle
878.5± 0.7± 0.3	SEREBROV	05	CNTR	UCN gravitational trap
889.2± 3.0± 3.8	BYRNE	96	CNTR	Penning trap
882.6± 2.7	[14] MAMPE	93	CNTR	UCN material bottle
• • • We do not use the following data for averages, fits, limits, etc. • • •				
886.3± 1.2± 3.2	NICO	05	CNTR	See YUE 13
886.8± 1.2± 3.2	DEWEY	03	CNTR	See NICO 05
885.4± 0.9± 0.4	ARZUMANOV	00	CNTR	See ARZUMANOV 12
888.4± 3.1± 1.1	[15] NESVIZHEV...	92	CNTR	UCN material bottle
888.4± 2.9	ALFIMENKOV	90	CNTR	See NESVIZHEVSKII 92
893.6± 3.8± 3.7	BYRNE	90	CNTR	See BYRNE 96

878 ±27 ±14	KOSSAKOW...	89	TPC	Pulsed beam
887.6± 3.0	MAMPE	89	CNTR	See STEYERL 12
877 ±10	PAUL	89	CNTR	Magnetic storage ring
876 ±10 ±19	LAST	88	SPEC	Pulsed beam
891 ± 9	SPIVAK	88	CNTR	Beam
903 ±13	KOSVINTSEV	86	CNTR	UCN material bottle
937 ±18	[16] BYRNE	80	CNTR	
875 ±95	KOSVINTSEV	80	CNTR	
881 ± 8	BONDAREN...	78	CNTR	See SPIVAK 88
918 ±14	CHRISTENSEN	72	CNTR	

[11] YUE 13 differs from NICO 05 in that a different and better method was used to measure the neutron density in the fiducial volume. This shifted the lifetime by +1.4 seconds and reduced the previously largest source of systematic uncertainty by a factor of five.

[12] ARZUMANOV 12 reanalyzes its systematic corrections in ARZUMANOV 00 and obtains this corrected value.

[13] STEYERL 12 is a detailed reanalysis of neutron storage loss corrections to the raw data of MAMPE 89, and it replaces that value.

[14] IGNATOVICH 95 calls into question some of the corrections and averaging procedures used by MAMPE 93. The response, BONDARENKO 96, denies the validity of the criticisms.

[15] The NESVIZHEVSKII 92 measurement has been withdrawn by A. Serebrov.

[16] The BYRNE 80 measurement has been withdrawn (J. Byrne, private communication, 1990).

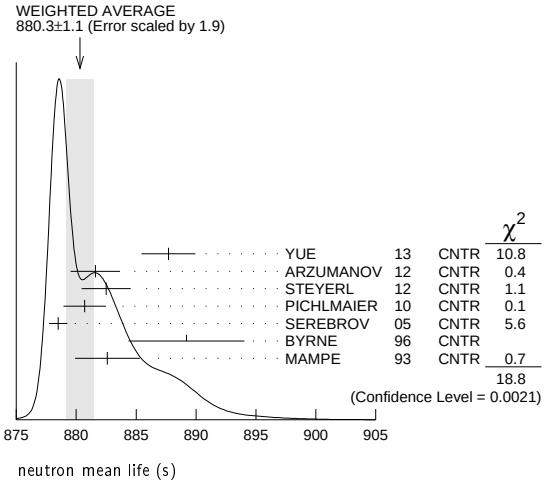

n MAGNETIC MOMENT

See the "Note on Baryon Magnetic Moments" in the Λ Listings.

VALUE (μ_N)	DOCUMENT ID		TECN	COMMENT
−1.91304272±0.00000045	MOHR	12	RVUE	2010 CODATA value
• • • We do not use the following data for averages, fits, limits, etc. • • •				
−1.91304273±0.00000045	MOHR	08	RVUE	2006 CODATA value
−1.91304273±0.00000045	MOHR	05	RVUE	2002 CODATA value
−1.91304272±0.00000045	MOHR	99	RVUE	1998 CODATA value
−1.91304275±0.00000045	COHEN	87	RVUE	1986 CODATA value
−1.91304277±0.00000048	[17] GREENE	82	MRS	

[17] GREENE 82 measures the moment to be $(1.04187564 \pm 0.00000026) \times 10^{-3}$ Bohr magnetons. The value above is obtained by multiplying this by $m_p/m_e = 1836.152701 \pm 0.000037$ (the 1986 CODATA value from COHEN 87).

n ELECTRIC DIPOLE MOMENT

A nonzero value is forbidden by both T invariance and P invariance. A number of early results have been omitted. See RAMSEY 90, GOLUB 94, and LAMOREAUX 09 for reviews.

VALUE (10^{-25} *e* cm)	CL%	DOCUMENT ID		TECN	COMMENT
< 0.29	90	[18] BAKER	06	MRS	UCN's, $h\nu = 2\mu_n B \pm 2d_n E$
• • • We do not use the following data for averages, fits, limits, etc. • • •					
< 0.63	90	[19] HARRIS	99	MRS	$d = (-0.1 \pm 0.36) \times 10^{-25}$
< 0.97	90	ALTAREV	96	MRS	$(+0.26 \pm 0.40 \pm 0.16) \times 10^{-25}$
< 1.1	95	ALTAREV	92	MRS	See ALTAREV 96
< 1.2	95	SMITH	90	MRS	See HARRIS 99
< 2.6	95	ALTAREV	86	MRS	$d = (-1.4 \pm 0.6) \times 10^{-25}$
0.3 ±4.8		PENDLEBURY	84	MRS	Ultracold neutrons
< 6	90	ALTAREV	81	MRS	$d = (2.1 \pm 2.4) \times 10^{-25}$
<16	90	ALTAREV	79	MRS	$d = (4.0 \pm 7.5) \times 10^{-25}$

[18] LAMOREAUX 07 faults BAKER 06 for not including in the estimate of systematic error an effect due to the Earth's rotation. BAKER 07 replies (1) that the effect was included implicitly in the analysis and (2) that further analysis confirms that the BAKER 06 limit is correct as is. See also SILENKO 07.

[19] This HARRIS 99 result includes the result of SMITH 90. However, the averaging of the results of these two experiments has been criticized by LAMOREAUX 00.

n MEAN-SQUARE CHARGE RADIUS

The mean-square charge radius of the neutron, $\langle r_n^2 \rangle$, is related to the neutron-electron scattering length b_{ne} by $\langle r_n^2 \rangle = 3(m_e a_0/m_n) b_{ne}$, where m_e and m_n are the masses of the electron and neutron, and a_0 is the Bohr radius. Numerically, $\langle r_n^2 \rangle = 86.34\, b_{ne}$, if we use a_0 for a nucleus with infinite mass.

VALUE (fm²)	DOCUMENT ID		COMMENT
−0.1161±0.0022 OUR AVERAGE	Error includes scale factor of 1.3. See the ideogram below.		
−0.115 ±0.002 ±0.003	KOPECKY	97	*ne* scattering (Pb)
−0.124 ±0.003 ±0.005	KOPECKY	97	*ne* scattering (Bi)
−0.114 ±0.003	KOESTER	95	*ne* scattering (Pb, Bi)
−0.134 ±0.009	ALEKSANDR...	86	*ne* scattering (Bi)
−0.115 ±0.003	[20] KROHN	73	*ne* scattering (Ne, Ar, Kr, Xe)
• • • We do not use the following data for averages, fits, limits, etc. • • •			
$-0.117\ ^{+0.007}_{-0.011}$	BELUSHKIN	07	Dispersion analysis
−0.113 ±0.003 ±0.004	KOPECKY	95	*ne* scattering (Pb)
−0.114 ±0.003	KOESTER	86	*ne* scattering (Pb, Bi)
−0.118 ±0.002	KOESTER	76	*ne* scattering (Pb)
−0.120 ±0.002	KOESTER	76	*ne* scattering (Bi)
−0.116 ±0.003	KROHN	66	*ne* scattering (Ne, Ar, Kr, Xe)

[20] This value is as corrected by KOESTER 76.

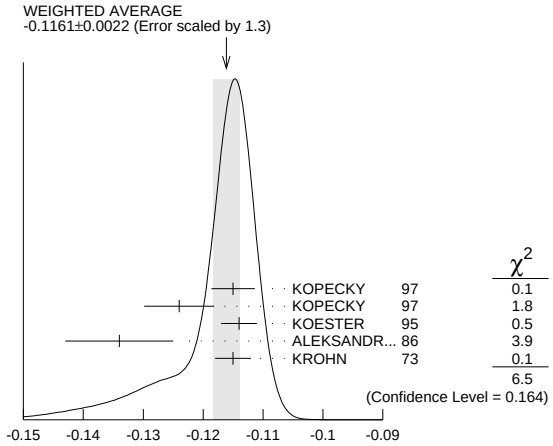

n MAGNETIC RADIUS

This is the rms magnetic radius, $\sqrt{\langle r_M^2 \rangle}$.

VALUE (fm)	DOCUMENT ID		COMMENT
$\mathbf{0.862\ ^{+0.009}_{-0.008}}$	BELUSHKIN	07	Dispersion analysis

n ELECTRIC POLARIZABILITY α_n

Following is the electric polarizability α_n defined in terms of the induced electric dipole moment by $\mathbf{D} = 4\pi\epsilon_0\alpha_n\mathbf{E}$. For a review, see SCHMIEDMAYER 89.

For a very complete review of the "polarizability of the nucleon and Compton scattering," see SCHUMACHER 05. His recommended values for the neutron are $\alpha_n = (12.5 \pm 1.7) \times 10^{-4}$ fm³ and $\beta_n = (2.7 \mp 1.8) \times 10^{-4}$ fm³, which agree with our averages within errors.

VALUE (10^{-4} fm³)	DOCUMENT ID		TECN	COMMENT
11.6± 1.5 OUR AVERAGE				
$12.5 \pm 1.8\ ^{+1.6}_{-1.3}$	[21] KOSSERT	03	CNTR	$\gamma d \to \gamma pn$
8.8± 2.4±3.0	[22] LUNDIN	03	CNTR	$\gamma d \to \gamma d$
12.0± 1.5±2.0	SCHMIEDM...	91	CNTR	*n* Pb transmission
$10.7\ ^{+\ 3.3}_{-10.7}$	ROSE	90B	CNTR	$\gamma d \to \gamma np$
• • • We do not use the following data for averages, fits, limits, etc. • • •				
13.6	[23] KOLB	00	CNTR	$\gamma d \to \gamma np$
0.0± 5.0	[24] KOESTER	95	CNTR	*n* Pb, *n* Bi transmission
$11.7\ ^{+\ 4.3}_{-11.7}$	ROSE	90	CNTR	See ROSE 90B
8 ±10	KOESTER	88	CNTR	*n* Pb, *n* Bi transmission
12 ±10	SCHMIEDM...	88	CNTR	*n* Pb, *n* C transmission

[21] KOSSERT 03 gets $\alpha_n - \beta_n = (9.8 \pm 3.6^{+2.1}_{-1.1} \pm 2.2) \times 10^{-4}$ fm^3, and uses $\alpha_n + \beta_n = (15.2 \pm 0.5) \times 10^{-4}$ fm^3 from LEVCHUK 00. Thus the errors on α_n and β_n are anti-correlated.
[22] LUNDIN 03 measures $\alpha_N - \beta_N = (6.4 \pm 2.4) \times 10^{-4}$ fm^3 and uses accurate values for α_p and α_p and a precise sum-rule result for $\alpha_n + \beta_n$. The second error is a model uncertainty, and errors on α_n and β_n are anticorrelated.
[23] KOLB 00 obtains this value with a lower limit of 7.6×10^{-4} fm^3 but no upper limit from this experiment alone. Combined with results of ROSE 90, the 1-σ range is (7.6–14.0) $\times 10^{-4}$ fm^3.
[24] KOESTER 95 uses natural Pb and the isotopes 208, 207, and 206. See this paper for a discussion of methods used by various groups to extract α_n from data.

n MAGNETIC POLARIZABILITY β_n

VALUE (10^{-4} fm^3)	DOCUMENT ID		TECN	COMMENT
3.7±2.0 OUR AVERAGE				
$2.7 \pm 1.8^{+1.3}_{-1.6}$	[25] KOSSERT	03	CNTR	$\gamma d \to \gamma p n$
$6.5 \pm 2.4 \pm 3.0$	[26] LUNDIN	03	CNTR	$\gamma d \to \gamma d$
• • • We do not use the following data for averages, fits, limits, etc. • • •				
1.6	[27] KOLB	00	CNTR	$\gamma d \to \gamma n p$

[25] KOSSERT 03 gets $\alpha_n - \beta_n = (9.8 \pm 3.6^{+2.1}_{-1.1} \pm 2.2) \times 10^{-4}$ fm^3, and uses $\alpha_n + \beta_n = (15.2 \pm 0.5) \times 10^{-4}$ fm^3 from LEVCHUK 00. Thus the errors on α_n and β_n are anti-correlated.
[26] LUNDIN 03 measures $\alpha_N - \beta_N = (6.4 \pm 2.4) \times 10^{-4}$ fm^3 and uses accurate values for α_p and α_p and a precise sum-rule result for $\alpha_n + \beta_n$. The second error is a model uncertainty, and errors on α_n and β_n are anticorrelated.
[27] KOLB 00 obtains this value with an upper limit of 7.6×10^{-4} fm^3 but no lower limit from this experiment alone. Combined with results of ROSE 90, the 1-σ range is (1.2–7.6) $\times 10^{-4}$ fm^3.

n CHARGE

See also "$|q_p + q_e|/e$" in the proton Listings.

VALUE (10^{-21} e)	DOCUMENT ID		TECN	COMMENT
− 0.2± 0.8 OUR AVERAGE				
− 0.1± 1.1	[28] BRESSI	11		Neutrality of SF_6
− 0.4± 1.1	[29] BAUMANN	88		Cold n deflection
• • • We do not use the following data for averages, fits, limits, etc. • • •				
−15 ±22	[30] GAEHLER	82	CNTR	Cold n deflection

[28] As a limit, this BRESSI 11 value is $< 1 \times 10^{-21}$ e.
[29] The BAUMANN 88 error ±1.1 gives the 68% CL limits about the the value −0.4.
[30] The GAEHLER 82 error ±22 gives the 90% CL limits about the the value −15.

LIMIT ON $n\overline{n}$ OSCILLATIONS

Mean Time for $n\overline{n}$ Transition in Vacuum

A test of ΔB=2 baryon number nonconservation. MOHAPATRA 80 and MOHAPATRA 89 discuss the theoretical motivations for looking for $n\overline{n}$ oscillations. DOVER 83 and DOVER 85 give phenomenological analyses. The best limits come from looking for the decay of neutrons bound in nuclei. However, these analyses require model-dependent corrections for nuclear effects. See KABIR 83, DOVER 89, ALBERICO 91, and GAL 00 for discussions. Direct searches for $n \to \overline{n}$ transitions using reactor neutrons are cleaner but give somewhat poorer limits. We include limits for both free and bound neutrons in the Summary Table. See MOHAPATRA 09 for a recent review.

VALUE (s)	CL%	DOCUMENT ID		TECN	COMMENT
$>1.3 \times 10^8$	90	CHUNG	02B	SOU2	n bound in iron
$>8.6 \times 10^7$	90	BALDO-...	94	CNTR	Reactor (free) neutrons
• • • We do not use the following data for averages, fits, limits, etc. • • •					
$>1 \times 10^7$	90	BALDO-...	90	CNTR	See BALDO-CEOLIN 94
$>1.2 \times 10^8$	90	BERGER	90	FREJ	n bound in iron
$>4.9 \times 10^5$	90	BRESSI	90	CNTR	Reactor neutrons
$>4.7 \times 10^5$	90	BRESSI	89	CNTR	See BRESSI 90
$>1.2 \times 10^8$	90	TAKITA	86	CNTR	n bound in oxygen
$>1 \times 10^6$	90	FIDECARO	85	CNTR	Reactor neutrons
$>8.8 \times 10^7$	90	PARK	85B	CNTR	
$>3 \times 10^7$		BATTISTONI	84	NUSX	
$> 2.7 \times 10^7$–1.1×10^8		JONES	84	CNTR	
$>2 \times 10^7$		CHERRY	83	CNTR	

LIMIT ON nn' OSCILLATIONS

Lee and Yang (LEE 56) proposed the existence of mirror world in an attempt to restore global parity symmetry. See BEREZHIANI 06 for a recent discussion.

VALUE (s)	CL%	DOCUMENT ID		TECN	COMMENT
>414	90	SEREBROV	08	CNTR	UCN, B field on & off
• • • We do not use the following data for averages, fits, limits, etc. • • •					
> 12	95	[31] ALTAREV	09A	CNTR	UCN, scan $0 \le B \le 12.5$ μT
>103	95	BAN	07	CNTR	UCN, B field on & off

[31] Losses of neutrons due to oscillations to mirror neutrons would be maximal when the magnetic fields B and B' in the two worlds were equal. Hence the scan over B by ALTAREV 09A: the limit applies for any B' over the given range. At $B' = 0$, the limit is 141 s (95% CL).

n DECAY MODES

	Mode	Fraction (Γ_i/Γ)	Confidence level
Γ_1	$p e^- \overline{\nu}_e$	100 %	
Γ_2	$p e^- \overline{\nu}_e \gamma$	[a] ($3.09 \pm 0.32) \times 10^{-3}$	
Γ_3	hydrogen-atom $\overline{\nu}_e$		
	Charge conservation (Q) violating mode		
Γ_4	$p \nu_e \overline{\nu}_e$	Q $< 8 \times 10^{-27}$	68%

[a] This limit is for γ energies between 15 and 340 keV.

n BRANCHING RATIOS

$\Gamma(p e^- \overline{\nu}_e \gamma)/\Gamma_{total}$ Γ_2/Γ

VALUE (units 10^{-3})	CL%	DOCUMENT ID		TECN	COMMENT
3.09±0.11±0.30		[32] COOPER	10	CNTR	γ, p, e^- coincidence
• • • We do not use the following data for averages, fits, limits, etc. • • •					
$3.13 \pm 0.11 \pm 0.33$		NICO	06	CNTR	See COOPER 10
<6.9	90	[33] BECK	02	CNTR	γ, p, e^- coincidence

[32] This COOPER 10 result is for γ energies between 15 and 340 keV.
[33] This BECK 02 limit is for γ energies between 35 and 100 keV.

Γ(hydrogen-atom $\overline{\nu}_e$)/Γ_{total} Γ_3/Γ

VALUE	CL%	DOCUMENT ID		TECN
• • • We do not use the following data for averages, fits, limits, etc. • • •				
$<3 \times 10^{-2}$	95	[34] GREEN	90	RVUE

[34] GREEN 90 infers that τ(hydrogen-atom$\overline{\nu}_e$) $> 3 \times 10^4$ s by comparing neutron lifetime measurements made in storage experiments with those made in β-decay experiments. However, the result depends sensitively on the lifetime measurements, and does not of course take into account more recent measurements of same.

$\Gamma(p \nu_e \overline{\nu}_e)/\Gamma_{total}$ Γ_4/Γ

Forbidden by charge conservation.

VALUE	CL%	DOCUMENT ID		TECN	COMMENT
<8 × 10^{-27}	68	[35] NORMAN	96	RVUE	^{71}Ga → ^{71}Ge neutrals
• • • We do not use the following data for averages, fits, limits, etc. • • •					
$<9.7 \times 10^{-18}$	90	ROY	83	CNTR	^{113}Cd → ^{113m}Inneut.
$<7.9 \times 10^{-21}$		VAIDYA	83	CNTR	^{87}Rb → ^{87m}Srneut.
$<9 \times 10^{-24}$	90	BARABANOV	80	CNTR	^{71}Ga → ^{71}GeX
$<3 \times 10^{-19}$		NORMAN	79	CNTR	^{87}Rb → ^{87m}Srneut.

[35] NORMAN 96 gets this limit by attributing SAGE and GALLEX counting rates to the charge-nonconserving transition ^{71}Ga → ^{71}Ge+neutrals rather than to solar-neutrino reactions.

BARYON DECAY PARAMETERS

Written 1996 by E.D. Commins (University of California, Berkeley).

Baryon semileptonic decays

The typical spin-1/2 baryon semileptonic decay is described by a matrix element, the hadronic part of which may be written as:

$$\overline{B}_f \left[f_1(q^2)\gamma_\lambda + i\, f_2(q^2)\sigma_{\lambda\mu}q^\mu + g_1(q^2)\gamma_\lambda\gamma_5 + g_3(q^2)\gamma_5 q_\lambda \right] B_i \ . \quad (1)$$

Here B_i and $\overline{B}_f$ are spinors describing the initial and final baryons, and $q = p_i - p_f$, while the terms in f_1, f_2, g_1, and g_3 account for vector, induced tensor ("weak magnetism"), axial vector, and induced pseudoscalar contributions [1]. Second-class current contributions are ignored here. In the limit of zero momentum transfer, f_1 reduces to the vector coupling constant g_V, and g_1 reduces to the axial-vector coupling constant g_A. The latter coefficients are related by Cabibbo's theory [2], generalized to six quarks (and three mixing angles) by Kobayashi and Maskawa [3]. The g_3 term is negligible for transitions in which an $e^\pm$ is emitted, and gives a very small correction, which can be estimated by PCAC [4], for $\mu^\pm$ modes. Recoil effects

include weak magnetism, and are taken into account adequately by considering terms of first order in

$$\delta = \frac{m_i - m_f}{m_i + m_f} \ , \tag{2}$$

where m_i and m_f are the masses of the initial and final baryons.

The experimental quantities of interest are the total decay rate, the lepton-neutrino angular correlation, the asymmetry coefficients in the decay of a polarized initial baryon, and the polarization of the decay baryon in its own rest frame for an unpolarized initial baryon. Formulae for these quantities are derived by standard means [5] and are analogous to formulae for nuclear beta decay [6]. We use the notation of Ref. 6 in the Listings for neutron beta decay. For comparison with experiments at higher q^2, it is necessary to modify the form factors at $q^2 = 0$ by a "dipole" q^2 dependence, and for high-precision comparisons to apply appropriate radiative corrections [7].

The ratio g_A/g_V may be written as

$$g_A/g_V = |\, g_A/g_V \,| \, e^{i\phi_{AV}} \ . \tag{3}$$

The presence of a "triple correlation" term in the transition probability, proportional to $\mathrm{Im}(g_A/g_V)$ and of the form

$$\boldsymbol{\sigma}_i \cdot (\mathbf{p}_\ell \times \mathbf{p}_\nu) \tag{4}$$

for initial baryon polarization or

$$\boldsymbol{\sigma}_f \cdot (\mathbf{p}_\ell \times \mathbf{p}_\nu) \tag{5}$$

for final baryon polarization, would indicate failure of time-reversal invariance. The phase angle ϕ has been measured precisely only in neutron decay (and in ^{19}Ne nuclear beta decay), and the results are consistent with T invariance.

Hyperon nonleptonic decays

The amplitude for a spin-1/2 hyperon decaying into a spin-1/2 baryon and a spin-0 meson may be written in the form

$$M = G_F \, m_\pi^2 \cdot \overline{B}_f \, (A - B\gamma_5) \, B_i \ , \tag{6}$$

where A and B are constants [1]. The transition rate is proportional to

$$\begin{aligned} R = 1 &+ \gamma \, \widehat{\boldsymbol{\omega}}_f \cdot \widehat{\boldsymbol{\omega}}_i + (1-\gamma)(\widehat{\boldsymbol{\omega}}_f \cdot \widehat{\mathbf{n}})(\widehat{\boldsymbol{\omega}}_i \cdot \widehat{\mathbf{n}}) \\ &+ \alpha(\widehat{\boldsymbol{\omega}}_f \cdot \widehat{\mathbf{n}} + \widehat{\boldsymbol{\omega}}_i \cdot \widehat{\mathbf{n}}) + \beta \widehat{\mathbf{n}} \cdot (\widehat{\boldsymbol{\omega}}_f \times \widehat{\boldsymbol{\omega}}_i) \ , \end{aligned} \tag{7}$$

where $\widehat{\mathbf{n}}$ is a unit vector in the direction of the final baryon momentum, and $\widehat{\boldsymbol{\omega}}_i$ and $\widehat{\boldsymbol{\omega}}_f$ are unit vectors in the directions of the initial and final baryon spins. (The sign of the last term in the above equation was incorrect in our 1988 and 1990 editions.) The parameters α, β, and γ are defined as

$$\begin{aligned} \alpha &= 2\,\mathrm{Re}(s^* p)/(\,|\,s\,|^2 + |\,p\,|^2) \ , \\ \beta &= 2\,\mathrm{Im}(s^* p)/(\,|\,s\,|^2 + |\,p\,|^2) \ , \\ \gamma &= (\,|\,s\,|^2 - |\,p\,|^2)/(\,|\,s\,|^2 + |\,p\,|^2) \ , \end{aligned} \tag{8}$$

where $s = A$ and $p = |\,\mathbf{p}_f\,| B/(E_f + m_f)$; here E_f and $\mathbf{p}_f$ are the energy and momentum of the final baryon. The parameters α, β, and γ satisfy

$$\alpha^2 + \beta^2 + \gamma^2 = 1 \ . \tag{9}$$

If the hyperon polarization is $\mathbf{P}_Y$, the polarization $\mathbf{P}_B$ of the decay baryons is

$$\mathbf{P}_B = \frac{(\alpha + \mathbf{P}_Y \cdot \widehat{\mathbf{n}})\widehat{\mathbf{n}} + \beta(\mathbf{P}_Y \times \widehat{\mathbf{n}}) + \gamma \widehat{\mathbf{n}} \times (\mathbf{P}_Y \times \widehat{\mathbf{n}})}{1 + \alpha \mathbf{P}_Y \cdot \widehat{\mathbf{n}}} \ . \tag{10}$$

Here $\mathbf{P}_B$ is defined in the rest system of the baryon, obtained by a Lorentz transformation along $\widehat{\mathbf{n}}$ from the hyperon rest frame, in which $\widehat{\mathbf{n}}$ and $\mathbf{P}_Y$ are defined.

An additional useful parameter ϕ is defined by

$$\beta = (1 - \alpha^2)^{1/2} \sin\phi \ . \tag{11}$$

In the Listings, we compile α and ϕ for each decay, since these quantities are most closely related to experiment and are essentially uncorrelated. When necessary, we have changed the signs of reported values to agree with our sign conventions. In the Baryon Summary Table, we give α, ϕ, and Δ (defined below) with errors, and also give the value of γ without error.

Time-reversal invariance requires, in the absence of final-state interactions, that s and p be relatively real, and therefore that $\beta = 0$. However, for the decays discussed here, the final-state interaction is strong. Thus

$$s = |\,s\,| \, e^{i\delta_s} \text{ and } p = |\,p\,| \, e^{i\delta_p} \ , \tag{12}$$

where δ_s and δ_p are the pion-baryon s- and p-wave strong interaction phase shifts. We then have

$$\beta = \frac{-2\,|\,s\,|\,|\,p\,|}{|\,s\,|^2 + |\,p\,|^2} \sin(\delta_s - \delta_p) \ . \tag{13}$$

One also defines $\Delta = -\tan^{-1}(\beta/\alpha)$. If T invariance holds, $\Delta = \delta_s - \delta_p$. For $\Lambda \to p\pi^-$ decay, the value of Δ may be compared with the s- and p-wave phase shifts in low-energy $\pi^- p$ scattering, and the results are consistent with T invariance.

See also the note on "Radiative Hyperon Decays" in the Ξ^0 Listings in this *Review*.

References

1. E.D. Commins and P.H. Bucksbaum, *Weak Interactions of Leptons and Quarks* (Cambridge University Press, Cambridge, England, 1983).
2. N. Cabibbo, Phys. Rev. Lett. **10**, 531 (1963).
3. M. Kobayashi and T. Maskawa, Prog. Theor. Phys. **49**, 652 (1973).
4. M.L. Goldberger and S.B. Treiman, Phys. Rev. **111**, 354 (1958).
5. P.H. Frampton and W.K. Tung, Phys. Rev. **D3**, 1114 (1971).
6. J.D. Jackson, S.B. Treiman, and H.W. Wyld, Jr., Phys. Rev. **106**, 517 (1957), and Nucl. Phys. **4**, 206 (1957).
7. Y. Yokoo, S. Suzuki, and M. Morita, Prog. Theor. Phys. **50**, 1894 (1973).

$n \to p e^- \bar{\nu}_e$ DECAY PARAMETERS

See the above "Note on Baryon Decay Parameters." For discussions of recent results, see the references cited at the beginning of the section on the neutron mean life. For discussions of the values of the weak coupling constants g_A and g_V obtained using the neutron lifetime and asymmetry parameter A, comparisons with other methods of obtaining these constants, and implications for particle physics and for astrophysics, see DUBBERS 91 and WOOLCOCK 91. For tests of the $V-A$ theory of neutron decay, see EROZOLIMSKII 91B, MOSTOVOI 96, NICO 05, SEVERIJNS 06, and ABELE 08.

$\lambda \equiv g_A / g_V$

VALUE			DOCUMENT ID		TECN	COMMENT
−1.2723 ±0.0023 OUR AVERAGE			Error includes scale factor of 2.2. See the ideogram below.			
−1.2755	±0.0030		[36] MENDENHALL	13	UCNA	Ultracold *n*, polarized
−1.2748	±0.0008	$^{+0.0010}_{-0.0011}$	[37] MUND	13	SPEC	Cold *n*, polarized
−1.275	±0.006	±0.015	SCHUMANN	08	CNTR	Cold *n*, polarized
−1.2686	±0.0046	±0.0007	[38] MOSTOVOI	01	CNTR	*A* and *B* × polarizations
−1.266	±0.004		LIAUD	97	TPC	Cold *n*, polarized, *A*
−1.2594	±0.0038		[39] YEROZLIM...	97	CNTR	Cold *n*, polarized, *A*
−1.262	±0.005		BOPP	86	SPEC	Cold *n*, polarized, *A*
• • • We do not use the following data for averages, fits, limits, etc. • • •						
−1.27590	±0.00239	$^{+0.00331}_{-0.00377}$	[40] PLASTER	12	UCNA	See MENDENHALL 13
−1.27590	$^{+0.00409}_{-0.00445}$		LIU	10	UCNA	See PLASTER 12
−1.2739	±0.0019		[41] ABELE	02	SPEC	See MUND 13
−1.274	±0.003		ABELE	97D	SPEC	Cold *n*, polarized, *A*
−1.266	±0.004		SCHRECK...	95	TPC	See LIAUD 97
−1.2544	±0.0036		EROZOLIM...	91	CNTR	See YEROZOLIMSKY 97
−1.226	±0.042		MOSTOVOY	83	RVUE	
−1.261	±0.012		EROZOLIM...	79	CNTR	Cold *n*, polarized, *A*
−1.259	±0.017		[42] STRATOWA	78	CNTR	*p* recoil spectrum, *a*
−1.263	±0.015		EROZOLIM...	77	CNTR	See EROZOLIMSKII 79
−1.250	±0.036		[42] DOBROZE...	75	CNTR	See STRATOWA 78
−1.258	±0.015		[43] KROHN	75	CNTR	Cold *n*, polarized, *A*
−1.263	±0.016		[44] KROPF	74	RVUE	*n* decay alone
−1.250	±0.009		[44] KROPF	74	RVUE	*n* decay + nuclear ft

[36] MENDENHALL 13 gets $A = -0.11954 \pm 0.00055 \pm 0.00098$ and $\lambda = -1.2756 \pm 0.0030$. We quote the nearly identical values that include the earlier UCNA measurement (PLASTER 12), with a correction to that result.
[37] This MUND 13 value includes earlier PERKEO II measurements (ABELE 02 and ABELE 97D).
[38] MOSTOVOI 01 measures the two *P*-odd correlations *A* and *B*, or rather *SA* and *SB*, where *S* is the *n* polarization, in free neutron decay.
[39] YEROZOLIMSKY 97 makes a correction to the EROZOLIMSKII 91 value.
[40] This PLASTER 12 value is identical with that given in LIU 10, but the experiment is now described in detail.
[41] This is the combined result of ABELE 02 and ABELE 97D.
[42] These experiments measure the absolute value of g_A/g_V only.
[43] KROHN 75 includes events of CHRISTENSEN 70.
[44] KROPF 74 reviews all data through 1972.

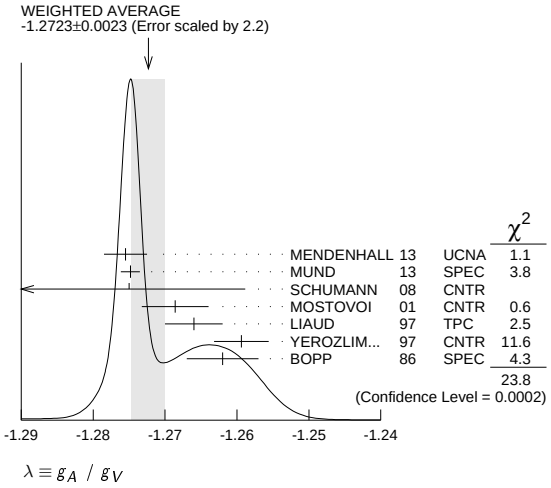

$\lambda \equiv g_A / g_V$

e^- ASYMMETRY PARAMETER *A*

This is the neutron-spin electron-momentum correlation coefficient. Unless otherwise noted, the values are corrected for radiative effects and weak magnetism. In the Standard Model, *A* is related to $\lambda \equiv g_A/g_V$ by $A = -2\lambda(\lambda+1)/(1+3\lambda^2)$; this assumes that g_A and g_V are real.

VALUE			DOCUMENT ID		TECN	COMMENT
−0.1184 ±0.0010 OUR AVERAGE			Error includes scale factor of 2.4. See the ideogram below.			
−0.11952	±0.00110		[45] MENDENHALL	13	UCNA	Ultracold *n*, polarized
−0.11926	±0.00031	$^{+0.00036}_{-0.00042}$	[46] MUND	13	SPEC	Cold *n*, polarized
−0.1160	±0.0009	±0.0012	LIAUD	97	TPC	Cold *n*, polarized
−0.1135	±0.0014		[47] YEROZLIM...	97	CNTR	Cold *n*, polarized
−0.1146	±0.0019		BOPP	86	SPEC	Cold *n*, polarized
• • • We do not use the following data for averages, fits, limits, etc. • • •						
−0.11966	±0.00089	$^{+0.00123}_{-0.00140}$	[48] PLASTER	12	UCNA	See MENDENHALL 13
−0.11966	±0.00089	$^{+0.00123}_{-0.00140}$	LIU	10	UCNA	See PLASTER 12
−0.1138	±0.0046	±0.0021	PATTIE	09	SPEC	Ultracold *n*, polarized
−0.1189	±0.0007		[49] ABELE	02	SPEC	See MUND 13
−0.1168	±0.0017		[50] MOSTOVOI	01	CNTR	Inferred
−0.1189	±0.0012		ABELE	97D	SPEC	Cold *n*, polarized
−0.1160	±0.0009	±0.0011	SCHRECK...	95	TPC	See LIAUD 97
−0.1116	±0.0014		EROZOLIM...	91	CNTR	See YEROZOLIMSKY 97
−0.114	±0.005		[51] EROZOLIM...	79	CNTR	Cold *n*, polarized
−0.113	±0.006		[51] KROHN	75	CNTR	Cold *n*, polarized

[45] MENDENHALL 13 gets $A = -0.11954 \pm 0.00055 \pm 0.00098$ and $\lambda = -1.2756 \pm 0.0030$. We quote the nearly identical values that include the earlier UCNA measurement (PLASTER 12), with a correction to that result.
[46] This MUND 13 value includes earlier PERKEO II measurements (ABELE 02 and ABELE 97D), with a correction to those results.
[47] YEROZOLIMSKY 97 makes a correction to the EROZOLIMSKII 91 value.
[48] This PLASTER 12 value is identical with that given in LIU 10, but the experiment is now described in detail.
[49] This is the combined result of ABELE 02 and ABELE 97D.
[50] MOSTOVOI 01 calculates this from its measurement of $\lambda = g_A/g_V$ above.
[51] These results are not corrected for radiative effects and weak magnetism, but the corrections are small compared to the errors.

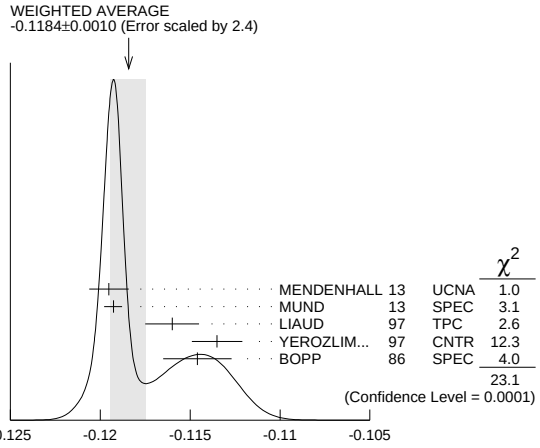

e^- asymmetry parameter *A*

$\bar{\nu}_e$ ASYMMETRY PARAMETER *B*

This is the neutron-spin antineutrino-momentum correlation coefficient. In the Standard Model, *B* is related to $\lambda \equiv g_A/g_V$ by $B = 2\lambda(\lambda-1)/(1+3\lambda^2)$; this assumes that g_A and g_V are real.

VALUE	DOCUMENT ID		TECN	COMMENT
0.9807±0.0030 OUR AVERAGE				
0.9802±0.0034±0.0036	SCHUMANN	07	CNTR	Cold *n*, polarized
0.967 ±0.006 ±0.010	KREUZ	05	CNTR	Cold *n*, polarized
0.9801±0.0046	SEREBROV	98	CNTR	Cold *n*, polarized
0.9894±0.0083	KUZNETSOV	95	CNTR	Cold *n*, polarized
1.00 ±0.05	CHRISTENSEN	70	CNTR	Cold *n*, polarized
0.995 ±0.034	EROZOLIM...	70C	CNTR	Cold *n*, polarized
• • • We do not use the following data for averages, fits, limits, etc. • • •				
0.9876±0.0004	[52] MOSTOVOI	01	CNTR	Inferred

[52] MOSTOVOI 01 calculates this from its measurement of $\lambda = g_A/g_V$ above.

PROTON ASYMMETRY PARAMETER *C*

Describes the correlation between the neutron spin and the proton momentum. In the Standard Model, *C* is related to $\lambda \equiv g_A/g_V$ by $C = -x_c(A+B) = x_c\, 4\lambda/(1+3\lambda^2)$, where $x_c = 0.27484$ is a kinematic factor; this assumes that g_A and g_V are real.

VALUE	DOCUMENT ID		TECN	COMMENT
−0.2377±0.0010±0.0024	SCHUMANN	08	CNTR	Cold *n*, polarized

e-$\bar{\nu}_e$ ANGULAR CORRELATION COEFFICIENT *a*

For a review of past experiments and plans for future measurements of the *a* parameter, see WIETFELDT 05. In the Standard Model, *a* is related to $\lambda \equiv g_A/g_V$ by $a = (1-\lambda^2)/(1+3\lambda^2)$; this assumes that g_A and g_V are real.

VALUE	DOCUMENT ID		TECN	COMMENT
−0.103 ±0.004 OUR AVERAGE				
−0.1054±0.0055	BYRNE	02	SPEC	Proton recoil spectrum
−0.1017±0.0051	STRATOWA	78	CNTR	Proton recoil spectrum
−0.091 ±0.039	GRIGOREV	68	SPEC	Proton recoil spectrum

• • • We do not use the following data for averages, fits, limits, etc. • • •

−0.1045±0.0014	[53]	MOSTOVOI	01	CNTR	Inferred

[53] MOSTOVOI 01 calculates this from its measurement of $\lambda=g_A/g_V$ above.

ϕ_{AV}, PHASE OF g_A RELATIVE TO g_V

Time reversal invariance requires this to be 0 or 180°. This is related to D given in the next data block and $\lambda \equiv g_A/g_V$ by $\sin(\phi_{AV}) \equiv D(1+3\lambda^2)/2|\lambda|$; this assumes that g_A and g_V are real.

VALUE (°)	CL%	DOCUMENT ID		TECN	COMMENT
180.017±0.026 OUR AVERAGE					
180.012±0.028	68	CHUPP	12	CNTR	Cold n, polarized > 91%
180.04 ±0.09		SOLDNER	04	CNTR	Cold n, polarized
180.08 ±0.13		LISING	00	CNTR	Polarized > 93%
• • • We do not use the following data for averages, fits, limits, etc. • • •					
180.013±0.028		MUMM	11	CNTR	See CHUPP 12
179.71 ±0.39		EROZOLIM...	78	CNTR	Cold n, polarized
180.35 ±0.43		EROZOLIM...	74	CNTR	Cold n, polarized
181.1 ±1.3	[54]	KROPF	74	RVUE	n decay
180.14 ±0.22		STEINBERG	74	CNTR	Cold n, polarized

[54] KROPF 74 reviews all data through 1972.

TRIPLE CORRELATION COEFFICIENT D

These are measurements of the component of n spin perpendicular to the decay plane in β decay. Should be zero if T invariance is not violated.

VALUE (units 10^{-4})	DOCUMENT ID		TECN	COMMENT
− 1.2 ± 2.0 OUR AVERAGE				
− 0.94± 1.89±0.97	CHUPP	12	CNTR	Cold n, polarized > 91%
− 2.8 ± 6.4 ±3.0	SOLDNER	04	CNTR	Cold n, polarized
− 6 ±12 ±5	LISING	00	CNTR	Polarized > 93%
• • • We do not use the following data for averages, fits, limits, etc. • • •				
− 0.96± 1.89±1.01	MUMM	11	CNTR	See CHUPP 12
+22 ±30	EROZOLIM...	78	CNTR	Cold n, polarized
−27 ±50	[55] EROZOLIM...	74	CNTR	Cold n, polarized
−11 ±17	STEINBERG	74	CNTR	Cold n, polarized

[55] EROZOLIMSKII 78 says asymmetric proton losses and nonuniform beam polarization may give a systematic error up to 30×10^{-4}, thus increasing the EROZOLIMSKII 74 error to 50×10^{-4}. STEINBERG 74 and STEINBERG 76 estimate these systematic errors to be insignificant in their experiment.

TRIPLE CORRELATION COEFFICIENT R

Another test of time-reversal invariance. R measures the polarization of the electron in the direction perpendicular to the plane defined by the neutron spin and the electron momentum. $R = 0$ for T invariance.

VALUE	DOCUMENT ID		TECN	COMMENT
+0.004±0.012±0.005	[56] KOZELA	12	CNTR	Mott polarimeter
• • • We do not use the following data for averages, fits, limits, etc. • • •				
+0.008±0.015±0.005	KOZELA	09	CNTR	See KOZELA 12

[56] KOZELA 12 also measures the polarization of the electron along the direction of the neutron spin. This is nonzero in the Standard Model; the correlation coefficient is $N = +0.067 \pm 0.011 \pm 0.004$.

n REFERENCES

We have omitted some papers that have been superseded by later experiments. See our earlier editions.

MENDENHALL 13 PR C87 032501 M.P. Mendenhall *et al.* (UCNA Collab.)
MUND 13 PRL 110 172502 D. Mund *et al.* (HEID, ILLG)
YUE 13 PRL 111 222501 A.T. Yue *et al.* (UMD, NIST, TENN, ORNL+)
ARZUMANOV 12 JETPL 95 224 S.S. Arzumanov *et al.* (KIAE)
Translated from ZETFP 95 248.
CHUPP 12 PR C86 035505 T.E. Chupp *et al.* (MICH, UCB, WASH+)
KOZELA 12 PR C85 045501 A. Kozela *et al.* (nTRV Collab.)
MOHR 12 RMP 84 1527 P.J. Mohr, B.N. Taylor, D.B. Newell (NIST)
PLASTER 12 PR C86 055501 B. Plaster *et al.* (UCNA Collab.)
STEYERL 12 PR C85 065503 A. Steyerl *et al.* (URI, SUSS)
BRESSI 11 PR A83 052101 G. Bressi *et al.* (LEGN, PAVI, PADO, TRST+)
DUBBERS 11 RMP 83 1111 D. Dubbers, M.G. Schmidt (HEID)
MUMM 11 PRL 107 102301 H.P. Mumm *et al.* (NIST, WASH, MICH, LBL+)
WIETFELDT 11 RMP 83 1173 F.E. Wietfeldt, G.L. Greene (TULA, TENN)
COOPER 10 PR C81 035503 R.L. Cooper *et al.* (MICH, NIST, TULA+)
LIU 10 PRL 105 181803 J. Liu *et al.* (UCNA Collab.)
Also PRL 105 219903 (errat) J. Liu *et al.* (UCNA Collab.)
PICHLMAIER 10 PL B693 221 A. Pichlmaier *et al.* (MUNT, PNPI, ILLG)
SEREBROV 10B PR C82 035501 A.P. Serebrov, A.K. Fomin (PNPI)
Also JETPL 92 271 A.P. Serebrov, A.K. Fomin (PNPI)
STEYERL 10 PR C81 055505 A. Steyerl *et al.* (URI)
ALTAREV 09A PR D80 032003 I. Altarev *et al.* (MUNT, RAL, CAEN+)
KOZELA 09 PRL 102 172301 A. Kozela *et al.* (JAGL, CRAC, PSI, CAEN+)
LAMOREAUX 09 JP G36 104002 S.K. Lamoreaux, R. Golub (YALE, NCSU)
MOHAPATRA 09 JP G36 104006 R.N. Mohapatra (UMD)
PATTIE 09 PRL 102 012301 R.W. Pattie Jr. *et al.* (Los Alamos UCNA Collab.)
ABELE 08 PPNP 60 1 H. Abele (HEID)
MOHR 08 RMP 80 633 P.J. Mohr, B.N. Taylor, D.B. Newell (NIST)
SCHUMANN 08 PRL 100 151801 M. Schumann *et al.* (HEID, ILLG, KARL+)
SEREBROV 08 PL B663 181 A.P. Serebrov *et al.* (PNPI, IOFF, ILLG+)
SEREBROV 08A PR C78 035505 A.P. Serebrov *et al.* (PNPI, JINR, ILLG)
BAKER 07 PRL 98 149102 C.A. Baker *et al.* (RAL, SUSS, ILLG)
BAN 07 PRL 99 161603 G. Ban *et al.* (CAEN, JAGL, PSI, JINR+)
BELUSHKIN 07 PR C75 035202 M.A. Belushkin, H.W. Hammer, U.-G. Meissner (BONN+)
LAMOREAUX 07 PRL 98 149101 S.K. Lamoreaux, R. Golub (YALE, NCSU)
SCHUMANN 07 PRL 99 191803 M. Schumann *et al.* (HEID, ILLG, KARL+)
SILENKO 07 PPNL 4 468 A.Ya. Silenko (Belarussian U.)
Translated from PFECAY 6 784.
BAKER 06 PRL 97 131801 C.A. Baker *et al.* (RAL, SUSS, ILLG)
BEREZHIANI 06 PRL 96 081801 Z. Berezhiani, L. Bento (Aguila U., LISB)
NICO 06 NAT 444 1059 J.S. Nico *et al.* (NIST, TULN, MICH, UMD+)
SEVERIJNS 06 RMP 78 991 N. Severijns, M. Beck, O. Naviliat-Cuncic (LEUV+)
KREUZ 05 PL B619 263 M. Kreuz *et al.* (HEID, ILLG, MANZ, KARL+)
MOHR 05 RMP 77 1 P.J. Mohr, B.N. Taylor (NIST)
NICO 05 PR C71 055502 J.S. Nico *et al.* (NIST, TULN, IND, TENN+)
SCHUMACHER 05 PPNP 55 567 M. Schumacher (GOET)
SEREBROV 05 PL B605 72 A. Serebrov *et al.* (PNPI, JINR, ILLG)
Also SPU 48 867 A.P. Serebrov *et al.* (PPNI, JINR, ILLG)
Translated from UFN 175 905.
WIETFELDT 05 MPLA 20 1783 F.E. Wietfeldt (TULN)
SOLDNER 04 PL B581 49 T. Soldner *et al.* (ILLG, MUNT)
DEWEY 03 PRL 91 152302 M.S. Dewey *et al.* (NIST, TULN, IND+)
KOSSERT 03 EPJ A16 259 K. Kossert *et al.* (Mainz MAMI Collab.)
Also PRL 88 162301 K. Kossert *et al.* (Mainz MAMI Collab.)
LUNDIN 03 PRL 90 192501 M. Lundin *et al.*
ABELE 02 PRL 88 211801 H. Abele *et al.* (PERKEO-II Collab.)
BECK 02 JETPL 76 332 M. Beck *et al.* (LEUV, SUSS, KIAE, PNPI)
Translated from ZETFP 76 392.
BYRNE 02 JP G28 1325 J. Byrne *et al.*
CHUNG 02B PR D66 032004 J. Chung *et al.* (SOUDAN-2 Collab.)
MOSTOVOI 01 PAN 64 1955 Yu.A. Mostovoi *et al.*
Translated from YAF 64 2040.
ARZUMANOV 00 PL B483 15 S. Arzumanov *et al.*
GAL 00 PR C61 028201 A. Gal
KOLB 00 PRL 85 1388 N.R. Kolb *et al.*
LAMOREAUX 00 PR D61 051301 S.K. Lamoreaux, R. Golub
LEVCHUK 00 NP A674 449 M.I. Levchuk, A.I. L'vov (BELA, LEBD)
LISING 00 PR C62 055501 L.J. Lising *et al.* (NIST emiT Collab.)
HARRIS 99 PRL 82 904 P.G. Harris *et al.*
KESSLER 99 PL A255 221 E.G. Kessler Jr *et al.*
MOHR 99 JPCRD 28 1713 P.J. Mohr, B.N. Taylor (NIST)
Also RMP 72 351 P.J. Mohr, B.N. Taylor (NIST)
SEREBROV 98 JETP 86 1074 A.P. Serebrov *et al.*
Translated from ZETF 113 1963.
ABELE 97D PL B407 212 H. Abele *et al.* (HEIDP, ILLG)
KOPECKY 97 PR C56 2229 S. Kopecky *et al.*
LIAUD 97 NP A612 53 P. Liaud *et al.* (ILLG, LAPP)
YEROZLIM... 97 PL B412 240 B.G. Erozolimsky *et al.* (HARV, PNPI, KIAE)
ALTAREV 96 PAN 59 1152 I.S. Altarev *et al.* (PNPI)
Translated from YAF 59 1204.
BONDAREN... 96 JETPL 64 416 L.N. Bondarenko *et al.* (KIAE)
Translated from ZETFP 64 382.
BYRNE 96 EPL 33 187 J. Byrne *et al.* (SUSS, ILLG)
MOSTOVOI 96 PAN 59 968 Y.A. Mostovoy (KIAE)
Translated from YAF 59 1013.
NORMAN 96 PR D53 4086 E.B. Norman, J.N. Bahcall, M. Goldhaber (LBL+)
IGNATOVICH 95 JETPL 62 1 V.K. Ignatovich (JINR)
Translated from ZETFP 62 3.
KOESTER 95 PR C51 3363 L. Koester *et al.* (+)
KOPECKY 95 PRL 74 2427 S. Kopecky *et al.*
KUZNETSOV 95 PRL 75 794 I.A. Kuznetsov *et al.* (PNPI, KIAE, HARV+)
SCHRECK... 95 PL B349 427 K. Schreckenbach *et al.* (MUNT, ILLG, LAPP)
BALDO-... 94 ZPHY C63 409 M. Baldo-Ceolin *et al.* (HEID, ILLG, PADO+)
DIFILIPPO 94 PRL 73 1481 F. DiFilippo *et al.* (MIT)
Also PRL 71 1998 V. Natarajan *et al.* (MIT)
GOLUB 94 PRPL 237C 1 R. Golub, K. Lamoreaux (HAHN, WASH)
MAMPE 93 JETPL 57 82 B. Mampe *et al.* (KIAE)
Translated from ZETFP 57 77.
ALTAREV 92 PL B276 242 I.S. Altarev *et al.* (PNPI)
NESVIZHEV... 92 JETP 75 405 V.V. Nesvizhevsky *et al.* (PNPI, JINR)
Translated from ZETF 102 740.
ALBERICO 91 NP A523 488 W.M. Alberico, A. de Pace, M. Pignone (TORI)
DUBBERS 91 NP A527 239c D. Dubbers (ILLG)
Also EPL 11 195 D. Dubbers, W. Mampe, J. Dohner (ILLG, HEID)
EROZOLIM... 91 PL B263 33 B.G. Erozolimsky *et al.* (PNPI, KIAE)
Also SJNP 52 999 B.G. Erozolimsky *et al.* (PNPI, KIAE)
Translated from YAF 52 1583.
EROZOLIM... 91B SJNP 53 260 B.G. Erozolimsky, Y.A. Mostovoy (KIAE)
Translated from YAF 53 418.
SCHMIEDM... 91 PRL 66 1015 J. Schmiedmayer *et al.* (TUW, ORNL)
WOOLCOCK 91 MPLA 6 2579 W.S. Woolcock (CANB)
ALFIMENKOV 90 JETPL 52 373 V.P. Alfimenkov *et al.* (PNPI, JINR)
Translated from ZETFP 52 984.
BALDO-... 90 PL B236 95 M. Baldo-Ceolin *et al.* (PADO, PAVI, HEIDP+)
BERGER 90 PL B240 237 C. Berger *et al.* (FREJUS Collab.)
BRESSI 90 NC 103A 731 G. Bressi *et al.* (PAVI, ROMA, MILA)
BYRNE 90 PRL 65 289 J. Byrne *et al.* (SUSS, NBS, SCOT, CBNM)
GREEN 90 JP G16 L75 K. Green, D. Thompson (RAL)
RAMSEY 90 ARNPS 40 1 N.F. Ramsey (HARV)
ROSE 90 PL B234 460 K.W. Rose *et al.* (GOET, MPCM, MANZ)
ROSE 90B NP A514 621 K.W. Rose *et al.* (GOET, MPCM)
SMITH 90 PL B234 191 K.F. Smith *et al.* (SUSS, RAL, HARV+)
BRESSI 89 ZPHY C43 175 G. Bressi *et al.* (INFN, MILA, PAVI, ROMA)
DOVER 89 NIM A284 13 C.B. Dover, A. Gal, J.M. Richard (BNL, HEBR+)
KOSSAKOW... 89 NP A503 473 R. Kossakowski *et al.* (LAPP, SAVO, ISNG+)
MAMPE 89 PRL 63 593 W. Mampe *et al.* (ILLG, RISL, SUSS, URI)
MOHAPATRA 89 NIM A284 1 R.N. Mohapatra (UMD)
PAUL 89 ZPHY C45 25 W. Paul *et al.* (BONN, WUPP, MPIH, ILLG)
SCHMIEDM... 89 NIM A284 137 J. Schmiedmayer, H. Rauch, P. Riehs (WIEN)
BAUMANN 88 PR D37 3107 J. Baumann *et al.* (BAYR, MUNI, ILLG)
KOESTER 88 ZPHY A329 229 L. Koester, W. Waschkowski, J. Meier (MUNI, MUNT)
LAST 88 PRL 60 995 I. Last *et al.* (HEIDP, ILLG, ANL)
SCHMIEDM... 88 PRL 61 1065 J. Schmiedmayer, H. Rauch, P. Riehs (TUW)
Also PRL 61 2509 (erratum) J. Schmiedmayer, H. Rauch, P. Riehs (TUW)
SPIVAK 88 JETP 67 1735 P.E. Spivak (KIAE)
Translated from ZETF 94 1.
COHEN 87 RMP 59 1121 E.R. Cohen, B.N. Taylor (RISC, NBS)
ALEKSANDR... 86 SJNP 44 900 Yu.A. Aleksandrov *et al.*
Translated from YAF 44 1384.
ALTAREV 86 JETPL 44 460 I.S. Altarev *et al.* (PNPI)
Translated from ZETFP 44 360.
BOPP 86 PR 56 919 P. Bopp *et al.* (HEIDP, ANL, ILLG)
Also ZPHY C37 179 E. Klempt *et al.* (HEIDP, ANL, ILLG)
CRESTI 86 PL B177 206 M. Cresti *et al.* (PADO)
Also PL B200 587 (erratum) M. Cresti *et al.* (PADO)
GREENE 86 PRL 56 819 G.L. Greene *et al.* (NBS, ILLG)
KOESTER 86 Physica B137 282 L. Koester *et al.*
KOSVINTSEV 86 JETPL 44 571 Y.Y. Kosvintsev, V.I. Morozov, G.I. Terekhov (KIAE)
Translated from ZETFP 44 444.
TAKITA 86 PR D34 902 M. Takita *et al.* (KEK, TOKY+)
DOVER 85 PR C31 1423 C.B. Dover, A. Gal, J.M. Richard (BNL)
FIDECARO 85 PL 156B 122 G. Fidecaro *et al.* (CERN, ILLG, PADO+)
PARK 85B NP B252 261 H.S. Park *et al.* (IMB Collab.)
BATTISTONI 84 PL 133B 454 G. Battistoni *et al.* (NUSEX Collab.)
JONES 84 PR 52 720 T.W. Jones *et al.* (IMB Collab.)
PENDLEBURY 84 PL 136B 327 J.M. Pendlebury *et al.* (SUSS, HARV, RAL+)
CHERRY 83 PR 50 1354 M.L. Cherry *et al.* (PENN, BNL)
DOVER 83 PR D27 1090 C.B. Dover, A. Gal, J.M. Richard (BNL)
KABIR 83 PR 51 231 P.K. Kabir (HARV)
MOSTOVOY 83 JETPL 37 196 Y.A. Mostovoy (KIAE)
Translated from ZETFP 37 162.

ROY	83	PR D28 1770	A. Roy *et al.*	(TATA)
VAIDYA	83	PR D27 486	S.C. Vaidya *et al.*	(TATA)
GAEHLER	82	PR D25 2887	R. Gahler, J. Kalus, W. Mampe	(BAYR, ILLG)
GREENE	82	Metrologia 18 93	G.L. Greene *et al.*	(YALE, HARV, ILLG+)
ALTAREV	81	PL 102B 13	I.S. Altarev *et al.*	(PNPI)
BARABANOV	80	JETPL 32 359	I.R. Barabanov *et al.*	(PNPI)
		Translated from ZETFP 32 384.		
BYRNE	80	PL 92B 274	J. Byrne *et al.*	(SUSS, RL)
KOSVINTSEV	80	JETPL 31 236	Y.Y. Kosvintsev *et al.*	(JINR)
		Translated from ZETFP 31 257.		
MOHAPATRA	80	PRL 44 1316	R.N. Mohapatra, R.E. Marshak	(CUNY, VPI)
ALTAREV	79	JETPL 29 730	I.S. Altarev *et al.*	(PNPI)
		Translated from ZETFP 29 794.		
EROZOLIM...	79	SJNP 30 356	B.G. Erozolimsky *et al.*	(KIAE)
		Translated from YAF 30 692.		
NORMAN	79	PRL 43 1226	E.B. Norman, A.G. Seamster	(WASH)
BONDAREN...	78	JETPL 28 303	L.N. Bondarenko *et al.*	(KIAE)
		Translated from ZETFP 28 328.		
Also		Smolenice Conf.	P.G. Bondarenko	(KIAE)
EROZOLIM...	78	SJNP 28 48	B.G. Erozolimsky *et al.*	(KIAE)
		Translated from YAF 28 98.		
STRATOWA	78	PR D18 3970	C. Stratowa, R. Dobrozemsky, P. Weinzierl	(SEIB)
EROZOLIM...	77	JETPL 23 663	B.G. Erozolimsky *et al.*	(KIAE)
		Translated from ZETFP 23 720.		
KOESTER	76	PRL 36 1021	L. Koester *et al.*	
STEINBERG	76	PR D13 2469	R.I. Steinberg *et al.*	(YALE, ISNG)
DOBROZE...	75	PR D11 510	R. Dobrozemsky *et al.*	(SEIB)
KROHN	75	PL 55B 175	V.E. Krohn, G.R. Ringo	(ANL)
EROZOLIM...	74	JETPL 20 345	B.G. Erozolimsky *et al.*	
		Translated from ZETFP 20 745.		
KROPF	74	ZPHY 267 129	H. Kropf, E. Paul	(LINZ)
Also		NP A154 160	H. Paul	(VIEN)
STEINBERG	74	PRL 33 41	R.I. Steinberg *et al.*	(YALE, ISNG)
COHEN	73	JPCRD 2 664	E.R. Cohen, B.N. Taylor	(RISC, NBS)
KROHN	73	PR D8 1305	V.E. Krohn, G.R. Ringo	
CHRISTENSEN	72	PR D5 1628	C.J. Christensen *et al.*	(RISO)
CHRISTENSEN	70	PR C1 1693	C.J. Christensen, V.E. Krohn, G.R. Ringo	(ANL)
EROZOLIM...	70C	PL 33B 351	B.G. Erozolimsky *et al.*	(KIAE)
GRIGOREV	68	SJNP 6 239	V.K. Grigoriev *et al.*	(ITEP)
		Translated from YAF 6 329.		
KROHN	66	PR 148 1303	V.E. Krohn, G.R. Ringo	
LEE	56	PR 104 254	T.D. Lee, C.N. Yang	(COLU, BNL)

N AND Δ RESONANCES

Revised Sept. 2013 by V. Burkert (Jefferson Lab), E. Klempt (University of Bonn), M.R. Pennington (Jefferson Lab), L. Tiator (University of Mainz), and R.L. Workman (George Washington University).

I. Introduction

The excited states of the nucleon have been studied in a large number of formation and production experiments. The Breit-Wigner masses and widths, the pole positions, and the elasticities of the N and Δ resonances in the Baryon Summary Table come largely from partial-wave analyses of πN total, elastic, and charge-exchange scattering data. The most comprehensive analyses were carried out by the Karlsruhe-Helsinki (KH80) [1], Carnegie Mellon-Berkeley (CMB80) [2], and George Washington U (GWU) [3] groups. Partial-wave analyses have also been performed on much smaller πN reaction data sets to get ηN, $K\Lambda$, and $K\Sigma$ branching fractions (see the Listings for references). Other branching fractions come from analyses of $\pi N \to \pi\pi N$ data.

In recent years, a large amount of data on photoproduction of many final states has been accumulated, and these data are beginning to tell us much about the properties of baryon resonances. A survey of data on photoproduction can be found in the proceedings of recent conferences [4] and workshops [5], and in recent reviews [6,7].

II. Naming scheme for baryon resonances

In the past, when nearly all resonance information came from elastic πN scattering, it was common to label resonances with the incoming partial wave $L_{2I,2J}$, as in $\Delta(1232)P_{33}$ and $N(1680)F_{15}$. However, most recent information has come from γN experiments. Therefore, we have replaced $L_{2I,2J}$ with the spin-parity J^P of the state, as in $\Delta(1232)3/2^+$ and $N(1680)5/2^+$; this name gives intrinsic properties of the resonance that are independent of the specific particles and reactions used to study them. This applies equally to all baryons, including Ξ resonances and charm baryons that are not produced in formation experiments. We do not, however, attach the mass or spin-parity to the names of the ground-state ("stable") baryons $N, \Lambda, \Sigma, \Xi, \Omega, \Lambda_c, \cdots$.

III. Using the *N* and Δ listings

Tables 1 and 2 list all the N and Δ entries in the Baryon Listings and give our evaluation of the overall status, the status from $\pi N \to \pi N$ scattering data and from photoproduction experiments, and the status channel by channel. Only the established resonances (overall status 3 or 4 stars) are promoted to the Baryon Summary Table. We long ago omitted from the Listings information from old analyses, prior to KH80 and CMB80, which can be found in earlier editions. A rather complete survey of older results was given in our 1982 edition [8].

As a rule, we award an overall status **** or *** only to those resonances which are derived from analyses of data sets that include precision differential cross sections and polarization observables, and are confirmed by independent analyses. All other signals are given ** or * status. We do not consider new results that are not accompanied by proper error evaluation. The following criteria are guidelines for future error analysis.

1. Uncertainties in resonance parameters: The publication must have a detailed discussion on how the uncertainties of parameters were estimated and why the author(s) believe that they approximately represent real uncertainties. This requires that the error estimates go beyond the simple fit error as e.g. given by MINUIT, and the robustness of the results must be demonstrated.

2. Fit quality: Concrete measures for the fit quality must be provided. The reduced global χ^2 value of the fit, while useful, is insufficient. Other possibilities include quoting variations of local χ^2 value in kinematic regions where evidence for new states or significantly improved information on resonance parameters is claimed.

3. Weight factors in observables: Analyses often use weight factors for certain data sets to either increase or reduce their impact on the results. This has been particularly important when polarization observables are involved, which usually are very sensitive to amplitude interferences but often have much poorer statistics than differential cross section data. To evaluate sensitivities, the resulting resonance parameters should be checked against variations of the specific weight factors.

In future, we intend to give – for **** and *** resonances – statistical *averages* and not only *our estimates*. This requires carefully determined statistical and systematic errors. The errors in Arndt 06 and Shrestha 12 in the Listings below are statistical errors only. They will hence not be used to define *averages* but may serve to establish the star ratings and to define *our estimates* of particle properties.

IV. Properties of resonances

Resonances are defined by poles of the S-matrix, whether in scattering, production or decay matrix elements. These are

poles in the complex plane in s, as discussed in the new review on *Resonances*. As traditional we quote here the pole positions in the complex energy $w = \sqrt{s}$ plane. Crucially, the position of the pole of the S-matrix is independent of the process, and the production and decay properties factorize. This is the rationale for listing the pole position first for each resonance.

Table 1. The status of the N resonances. Only those with an overall status of *** or **** are included in the main Baryon Summary Table.

					Status as seen in —						
Particle	J^P	Status overall	πN	γN	$N\eta$	$N\sigma$	$N\omega$	ΛK	ΣK	$N\rho$	$\Delta\pi$
N	$1/2^+$	****									
$N(1440)$	$1/2^+$	****	****	****		***				*	***
$N(1520)$	$3/2^-$	****	****	****	***					***	***
$N(1535)$	$1/2^-$	****	****	****	****					**	*
$N(1650)$	$1/2^-$	****	****	***	***			***	**	**	***
$N(1675)$	$5/2^-$	****	****	***	*			*		*	***
$N(1680)$	$5/2^+$	****	****	****	*	**				***	***
$N(1685)$	$?^?$	*									
$N(1700)$	$3/2^-$	***	***	**	*			*	*	*	***
$N(1710)$	$1/2^+$	***	***	***	***		**	***	**	*	**
$N(1720)$	$3/2^+$	****	****	***	***			**	**	**	*
$N(1860)$	$5/2^+$	**	**							*	*
$N(1875)$	$3/2^-$	***	*	***			**	***	**		***
$N(1880)$	$1/2^+$	**	*	*		**		*			
$N(1895)$	$1/2^-$	**	*	**	**			**	*		
$N(1900)$	$3/2^+$	***	**	***	**		**	***	**	*	**
$N(1990)$	$7/2^+$	**	**	**					*		
$N(2000)$	$5/2^+$	**	*	**	**			**	*	**	
$N(2040)$	$3/2^+$	*									
$N(2060)$	$5/2^-$	**	**	**	*				**		
$N(2100)$	$1/2^+$	*									
$N(2150)$	$3/2^-$	**	**	**				**			**
$N(2190)$	$7/2^-$	****	****	***			*	**		*	
$N(2220)$	$9/2^+$	****	****								
$N(2250)$	$9/2^-$	****	****								
$N(2600)$	$11/2^-$	***	***								
$N(2700)$	$13/2^+$	**	**								

**** Existence is certain, and properties are at least fairly well explored.
*** Existence is very likely but further confirmation of quantum numbers and branching fractions is required.
** Evidence of existence is only fair.
* Evidence of existence is poor.

These key properties of the S-matrix pole are in contrast to other quantities related to resonance phenomena, such as Breit-Wigner parameters or any K-matrix pole. Thus, Breit-Wigner parameters depend on the formalism used such as angular-momentum barrier factors, or cut-off parameters, and the assumed or modeled background. However, the accurate determination of pole parameters from the analysis of data on the real energy axis is not necessarily simple, or even straightforward. It requires the implementation of the correct analytic structure of the relevant (often coupled) channels. The example in the meson sector of the σ-pole highlights the need to incorporate right and left hand cut analyticity (and their relation imposed by crossing symmetry) into a dispersive analysis to obtain a robust determination of the pole position, for a very short-lived state close to the lowest threshold. The development of general methods that are simpler to implement in the baryon sector is a research problem of current interest, often exploiting techniques introduced long ago when the experimental data were far poorer than those presently available for reactions like $\gamma N \to \pi N$ [9]. No consensus yet exists for the use of any particular method, beyond the need to incorporate the general properties mentioned here and discussed more fully in the review of *Resonances*. This is an area we expect to be able to update in the next issue of the RPP.

To repeat: pole parameters appear first in the listings, then the Breit-Wigner mass and width parameters. Then we give "pole related quantities" like residues and phases of hadronic transition amplitudes and helicity amplitudes. Branching ratios and photoproduction amplitudes follow.

Table 2. The status of the Δ resonances. Only those with an overall status of *** or **** are included in the main Baryon Summary Table.

					Status as seen in —						
Particle	J^P	Status overall	πN	γN	$N\eta$	$N\sigma$	$N\omega$	ΛK	ΣK	$N\rho$	$\Delta\pi$
$\Delta(1232)$	$3/2^+$	****	****	****	F						
$\Delta(1600)$	$3/2^+$	***	***	***	o					*	***
$\Delta(1620)$	$1/2^-$	****	****	***	r					***	***
$\Delta(1700)$	$3/2^-$	****	****	****	b					**	***
$\Delta(1750)$	$1/2^+$	*	*		i						
$\Delta(1900)$	$1/2^-$	**	**	**			d		**	**	**
$\Delta(1905)$	$5/2^+$	****	****	****			d		***	**	**
$\Delta(1910)$	$1/2^+$	****	****	**			e		*	*	**
$\Delta(1920)$	$3/2^+$	***	***	**			n		***		**
$\Delta(1930)$	$5/2^-$	***	***								
$\Delta(1940)$	$3/2^-$	**	*	**	F				(seen	in	$\Delta\eta$)
$\Delta(1950)$	$7/2^+$	****	****	****	o				***	*	***
$\Delta(2000)$	$5/2^+$	**			r						**
$\Delta(2150)$	$1/2^-$	*	*		b						
$\Delta(2200)$	$7/2^-$	*	*		i						
$\Delta(2300)$	$9/2^+$	**	**				d				
$\Delta(2350)$	$5/2^-$	*	*				d				
$\Delta(2390)$	$7/2^+$	*	*				e				
$\Delta(2400)$	$9/2^-$	**	**				n				
$\Delta(2420)$	$11/2^+$	****	****	*							
$\Delta(2750)$	$13/2^-$	**	**								
$\Delta(2950)$	$15/2^+$	**	**								

**** Existence is certain, and properties are at least fairly well explored.
*** Existence is very likely but further confirmation of quantum numbers and branching fractions is required.
** Evidence of existence is only fair.
* Evidence of existence is poor.

V. Photoproduction

A new approach to the nucleon excitation spectrum is provided by dedicated facilities at the Universities of Bonn, Grenoble, and Mainz, and at the national laboratories Jefferson Lab in the US and SPring-8 in Japan. High-precision cross sections and polarization observables for the photoproduction of pseudoscalar mesons provide a data set that is nearly a "complete experiment," one that fully constrains the four complex amplitudes describing the spin-structure of the reaction [11]. A large number of photoproduction reactions has been studied.

In pseudo-scalar meson photoproduction, the four independent helicity amplitudes can be expressed in terms of the four

CGLN [12] amplitudes allowed by Lorentz and gauge invariance. These amplitudes can be expanded in a series of electric and magnetic multipoles. Except for J=1/2, one electric and one magnetic mulipole contributes to each J^P combination.

For a given state, these two amplitudes determine the resonance photo-decay helicity amplitudes $A_{1/2}$ and $A_{3/2}$. As described below, this resonance extraction has been carried out either assuming a Breit-Wigner resonance or at the pole.

If a Breit-Wigner parametrization is used, the $N\gamma$ partial width, Γ_γ, is given in terms of the helicity amplitudes $A_{1/2}$ and $A_{3/2}$ by

$$\Gamma_\gamma = \frac{k_{\rm BW}^2}{\pi}\frac{2m_N}{(2J+1)m_{\rm BW}}\left(|A_{1/2}|^2+|A_{3/2}|^2\right) \ . \qquad (1)$$

Here m_N and $m_{\rm BW}$ are the nucleon and resonance masses, J is the resonance spin, and $k_{\rm BW}$ is the photon c.m. decay momentum. Most earlier analyses have quoted these real quantities $A_{1/2}$ and $A_{3/2}$.

More recent studies have quoted related complex quantities, evaluated at the T-matrix pole. These complex helicity amplitudes, $\tilde{A}_{1/2}$ and $\tilde{A}_{3/2}$, can be cast onto the form

$$\tilde{A}_h = \sqrt{\frac{\pi(2J+1)w_{\rm pole}}{m_N k_{\rm pole}^2}}\frac{Res(T_h(\gamma N\to N\,b))}{\sqrt{Res(T\,(N\,b\to N\,b))}} \qquad (2)$$

where the residues (Res) are evaluated at the pole position, $w_{\rm pole}$, and $k_{\rm pole}^2=(w_{\rm pole}^2-m_N^2)^2/4w_{\rm pole}^2$ [13]. For Breit-Wigner amplitudes, $w_{\rm pole}=m_{\rm BW}$ and $\tilde{A}_h=A_h$. Similar relations for the photo- and electrocouplings at the pole position can be found in [14,15].

The determination of eight real numbers from four complex amplitudes (with one overall phase undetermined) requires at least seven independent measurements. At least one further measurement is required to resolve discrete ambiguities that result from the fact that data are proportional to squared amplitudes. Photon beams and nucleon targets can be polarized (with linear or circular polarization $P_\perp$, $P_\odot$ and $\vec{T}$, respectively); the recoil polarization of the outgoing baryon $\vec{R}$ can be measured. The experiments can be divided into three classes: (1) the beam and target are polarized (BT); (2) the beam is polarized and the recoil baryon polarization is measured (BR); (3) the target is polarized and the recoil polarization is measured (TR). Different sign conventions are used in the literature, as summarized in [16].

One of the best studied reactions is $\gamma p\to\Lambda K^+$. Published data include differential cross sections, the beam asymmetry Σ, the target asymmetry T, the recoil polarization P, and the BR double-polarization variables C_x', C_z', O_x', and O_z'. For the photoproduction of pions and etas, off proton and neutron targets, differential cross sections, single- and double-polarization asymmetries have been measured, mainly for pions.

VI. Electroproduction

Electro-production of mesons provides information on the internal structure of resonances. The helicity amplitudes are functions of the (squared) momentum transfer $Q^2=-(e-e')^2$, where e and e' are the 4-momenta of the incident and scattered electron, and a third amplitude, $S_{1/2}$, measures the resonance response to the longitudinal component of the virtual photon. Most data stem from the reactions $e^-p\to e^-\,n\pi^+$ and $e^-p\to e^-\,p\pi^0$ but also the reactions $e^-p\to e^-\,p\eta$, $e^-p\to e^-\,p\pi^+\pi^-$, and $e^-p\to e^-\,\Lambda(\Sigma^0)K^+$ have been studied. The data and their interpretation are reviewed in Refs. [18,19].

The transition to the $\Delta(1232)3/2^+$ is often quantified in terms of the magnetic dipole transition moment M_{1+} (or the magnetic transition form factor $G_{M,Ash}^*(Q^2)$) [20], and the electric and scalar quadrupole transition moments E_{1+} and S_{1+}. Fig. 1 shows the strength of the $p\to\Delta^+$ transition plotted versus the photon virtuality Q^2. At $Q^2=0$, M_{1+} dominates the resonance transition strength. The two amplitudes E_{1+} and S_{1+} imply a quadrupole deformation of the transition to the lowest excited state. The magnitude of $R_{EM}=E_{1+}/M_{1+}$ remains nearly constant, while the magnitude of $R_{SM}=S_{1+}/M_{1+}$ increases rapidly up to 25% at the highest Q^2 value. Dynamical models assign most of the quadrupole strength in the $p\Delta^+$ transition to the effect of a meson cloud around the bare Δ states.

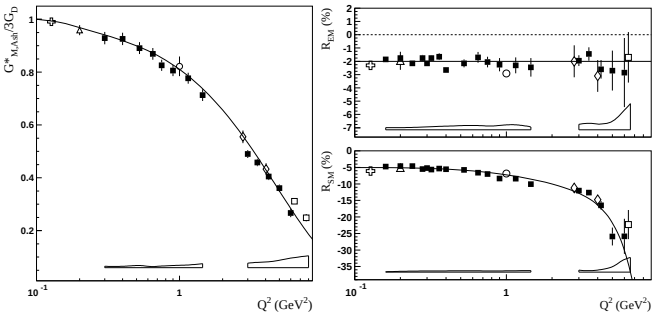

Figure 1: Left: The magnetic transition form factor for the $\gamma^*p\to\Delta^+(1232)$ transition versus the photon virtuality Q^2. Right: The electric and scalar quadrupole rations R_{EM} and R_{SM}. The different symbols are results from different experiments at JLab (squares, diamonds, circle) and MAMI (triangle, cross). The boxes near the horizontal axis indicate model uncertainties of the squares. Curves to guide the eyes. The figures are kindly provided by V. Burkert, JLab.

Fig. 2 shows the transverse and scalar helicity amplitudes for the $N(1440)1/2^+$, $N(1520)3/2^-$, and $N(1535)1/2^-$ resonances from JLab [18]. Similar results have been achieved at Mainz [19]. For the states $N(1440)1/2^+$ and $N(1520)3/2^-$, helicity amplitudes and $\pi\Delta$ and ρp decays were determined at JLab in an analysis of $\pi^+\pi^-p$ electroproduction [21]. The data show distinctly different Q^2 dependencies that indicate different internal structures.

The $N(1520)3/2^-$ helicity amplitudes reveal the dominance of its three-quark nature: the $A_{3/2}$ amplitude is large at the photon point and decreases rapidly $\sim Q^{-5}$ with increasing Q^2;

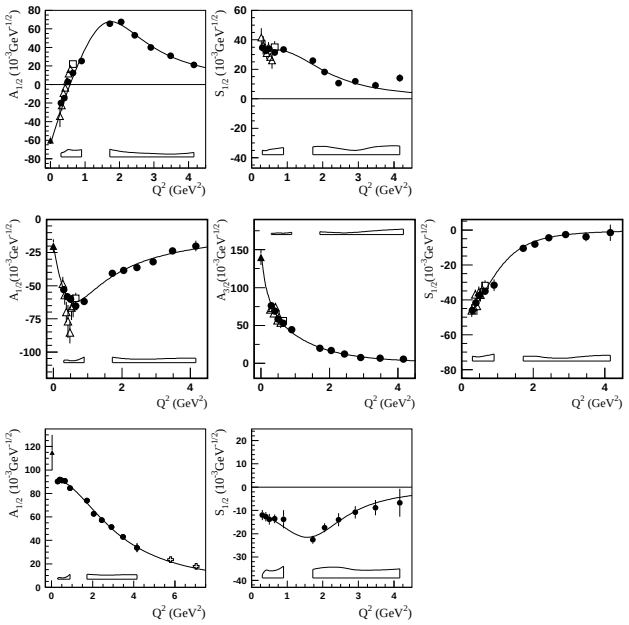

Figure 2: Transverse and scalar (longitudinal) helicity amplitudes for $\gamma p \to N(1440)1/2^+$ (top), $\gamma p \to N(1520)3/2^-$ (center), and $\gamma p \to N(1535)1/2^-$ (bottom) as extracted from the JLab/CLAS data in $n\pi^+$ production (full circles), in $p\pi^+\pi^-$ (open triangles), combined single and double pion production (open squares). The solid triangle is the PDG 2013 value at $Q^2 = 0$. The open boxes are the model uncertainties of the full circles. The figures are kindly provided by V. Burkert, JLab.

$A_{1/2}$ is small at the photon point, increases rapidly with Q^2 and then falls off with $\sim Q^{-3}$. Quantitative agreement with the data is, however, achieved only when meson cloud effects are included.

At high Q^2, both amplitudes for $N(1440)1/2^+$ are qualitatively described by light front quark models [22]: at short distances the resonance behaves as expected from a radial excitation of the nucleon. On the other hand, $A_{1/2}$ changes sign at about $0.6\,\mathrm{GeV}^2$. This remarkable behavior has not been observed before for any nucleon form factor or transition amplitude. Obviously, an important change in the structure occurs when the resonance is probed as a function of Q^2.

The Q^2 dependence of $A_{1/2}$ of the $N(1535)1/2^-$ resonance exhibits the expected $\sim Q^{-3}$ dependence, except for small Q^2 values where meson cloud effects set in.

VII. Partial wave analyses

Several PWA groups are now actively involved in the analysis of the new data. The GWU group maintains a nearly complete database covering reactions from πN and KN elastic scattering to $\gamma N \to N\pi$, $N\eta$, and $N\eta'$. It is presently the only group determining πN elastic amplitudes from scattering data in sliced energy bins. Given the high-precision of photoproduction data already or soon to be collected, the spectrum of N and Δ resonances will in the near future be better known.

Fits to the data are performed by various groups with the aim to understand the reaction dynamics and to identify N and Δ resonances. For practical reasons, approximations have to be made. We mention several analyses here: (1) The Mainz unitary isobar model [23] focusses on the correct treatment of the low-energy domain. Resonances are added to the unitary amplitude as a sum of Breit-Wigner amplitudes. This model also obtains resonance transition form factors and helicity amplitudes from electroproduction [19]. (2) For $N\pi$ electroproduction, the Yerevan/JLab group uses both the unitary isobar model and the dispersion relation approach developed in [22]. A phenomenological model was developed to extract resonance couplings and partial decay widths from exclusive $\pi^+\pi^- p$ electroproduction [21]. (3) Multichannel analyses using K-matrix parameterizations derive background terms from a chiral Lagrangian - providing a microscopical description of the background - (Giessen [24,25]) or from phenomenology (Bonn-Gatchina [26]) . (4.) Several groups (EBAC-Jlab [27,28], ANL-Osaka [29], Dubna-Mainz-Taipeh [30], Bonn-Jülich [31,32,33], Valencia [34]) use dynamical reaction models, driven by chiral Lagrangians, which take dispersive parts of intermediate states into account. Several other groups have made important contributions. The Giessen group pioneered multichannel analyses of large data sets on pion- and photo-induced reactions [24,25]. The Bonn-Gatchina group included recent high-statistics data and reported systematic searches for new baryon resonances in all relevant partial waves. A summary of their results can be found in Ref. [26].

References

1. G. Höhler, *Pion-Nucleon Scattering*, Landolt-Börnstein Vol. I/9b2 (1983), ed. H. Schopper, Springer Verlag.
2. R.E. Cutkosky *et al.*, Baryon 1980, *IV International Conference on Baryon Resonances*, Toronto, ed. N. Isgur, p. 19.
3. R.A. Arndt *et al.*, Phys. Rev. **C74**, 045205 (2006).
4. *Hadron 2011: 14th International Conference on Hadron Spectroscopy,* München, Germany, June, 13 - 17, 2011, published in eConf.
5. *NSTAR 2013: 9th International Workshop on the Physics of Excited Nucleons,* 27-30 May 2013, Peñíscola, Spain.
6. E. Klempt and J.M. Richard, Rev. Mod. Phys. **82**, 1095 (2010).
7. V. Credé and W. Roberts, Rept. Prog. Phys. **76**, 076301 (2013).
8. M. Roos *et al.*, Phys. Lett. **B111**, 1 (1982).
9. A. Svarc *et al.*, Phys. Rev. **C88**, 035206 (2013).
10. R.H. Dalitz and R.G. Moorhouse, Proc. Roy. Soc. Lond. **A318**, 279 (1970).
11. C. G. Fasano *et al.*, Phys. Rev. **C46**, 2430 (1992).
12. G.F. Chew *et al.*, Phys. Rev. **106**, 1345 (1957).
13. R. L. Workman, L. Tiator, and A. Sarantsev, Phys. Rev. **C87**, 068201 (2013).
14. N. Suzuki, T. Sato, and T. -S. H. Lee, Phys. Rev. **C82**, 045206 (2010).

15. H. Kamano, Phys. Rev. **C88**, 045203 (2013).
16. A.M. Sandorfi *et al.*, AIP Conf. Proc. **1432**, 219 (2012).
17. R. Beck and A. Thiel, J. Phys. Conf. Ser. **295**, 012023 (2011).
18. I. G. Aznauryan and V. D. Burkert, Prog. Part. Nucl. Phys. **67**, 1 (2012).
19. L. Tiator *et al.*, Eur. Phys. J. ST **198**, 141 (2011).
20. W.W. Ash, Phys. Lett. **B24**, 165 (1967).
21. V. I. Mokeev *et al.* [CLAS Collab.], Phys. Rev. **C86**, 035203 (2012).
22. I. G. Aznauryan, Phys. Rev. **C67**, 015209 (2003).
23. D. Drechsel, S. S. Kamalov, and L. Tiator, Eur. Phys. J. **A34**, 69 (2007).
24. G. Penner and U. Mosel, Phys. Rev. **C66**, 055211 (2002).
25. G. Penner and U. Mosel, Phys. Rev. **C66** (2002) 055212.
26. A.V. Anisovich *et al.*, EPJ **A48**, 15 (2012).
27. A. Matsuyama, T. Sato, and T.-S.H. Lee, Phys. Rept. **439**, 193 (2007).
28. T. Sato and T. -S. H. Lee, J. Phys. **G36**, 073001 (2009).
29. H. Kamano *et al.*, Phys. Rev. **C88**, 035209 (2013).
30. G. Y. Chen *et al.*, Phys. Rev. **C76**, 035206 (2007).
31. M. Döring *et al.*, Phys. Lett. **B681**, 26 (2009).
32. M. Döring *et al.*, Nucl. Phys. **A829**, 170 (2009).
33. D. Rönchen *et al.*, Eur. Phys. J. **A49**, 44 (2013).
34. S. Sarkar, E. Oset, and M. J. Vicente Vacas, Nucl. Phys. **A750**, 294 (2005); [Erratum-*ibid.*, **A780**, 78 (2006)].

$N(1440)\ 1/2^+$

$I(J^P) = \frac{1}{2}(\frac{1}{2}^+)$ Status: ****

Most of the results published before 1975 were last included in our 1982 edition, Physics Letters **111B** 1 (1982). Some further obsolete results published before 1984 were last included in our 2006 edition, Journal of Physics (generic for all A,B,E,G) **G33** 1 (2006).

$N(1440)$ BREIT-WIGNER MASS

VALUE (MeV)	DOCUMENT ID		TECN	COMMENT
1410 to 1450 (≈ 1430) OUR ESTIMATE				
1515 ±15	SHKLYAR	13	DPWA	Multichannel
1430 ± 8	ANISOVICH	12A	DPWA	Multichannel
1485.0± 1.2	ARNDT	06	DPWA	$\pi N \to \pi N, \eta N$
1440 ±30	CUTKOSKY	80	IPWA	$\pi N \to \pi N$
1410 ±12	HOEHLER	79	IPWA	$\pi N \to \pi N$
• • • We do not use the following data for averages, fits, limits, etc. • • •				
1412 ± 2	SHRESTHA	12A	DPWA	Multichannel
1440 ±12	ANISOVICH	10	DPWA	Multichannel
1439 ±19	BATINIC	10	DPWA	$\pi N \to N\pi, N\eta$
1436 ±15	SARANTSEV	08	DPWA	Multichannel
1468.0± 4.5	ARNDT	04	DPWA	$\pi N \to \pi N, \eta N$
1518 ± 5	PENNER	02C	DPWA	Multichannel
1479 ±80	VRANA	00	DPWA	Multichannel
1463 ± 7	ARNDT	96	IPWA	$\gamma N \to \pi N$
1467	ARNDT	95	DPWA	$\pi N \to N\pi$
1465	LI	93	IPWA	$\gamma N \to \pi N$
1462 ±10	MANLEY	92	IPWA	$\pi N \to \pi N$ & $N\pi\pi$
1471	CUTKOSKY	90	IPWA	$\pi N \to \pi N$
1380	[1] LONGACRE	77	IPWA	$\pi N \to N\pi\pi$
1390	[2] LONGACRE	75	IPWA	$\pi N \to N\pi\pi$

$N(1440)$ BREIT-WIGNER WIDTH

VALUE (MeV)	DOCUMENT ID		TECN	COMMENT
250 to 450 (≈ 350) OUR ESTIMATE				
605± 90	SHKLYAR	13	DPWA	Multichannel
365± 35	ANISOVICH	12A	DPWA	Multichannel
284± 18	ARNDT	06	DPWA	$\pi N \to \pi N, \eta N$
340± 70	CUTKOSKY	80	IPWA	$\pi N \to \pi N$
135± 10	HOEHLER	79	IPWA	$\pi N \to \pi N$
• • • We do not use the following data for averages, fits, limits, etc. • • •				
248± 5	SHRESTHA	12A	DPWA	Multichannel
335± 50	ANISOVICH	10	DPWA	Multichannel
437±141	BATINIC	10	DPWA	$\pi N \to N\pi, N\eta$
335± 40	SARANTSEV	08	DPWA	Multichannel
360± 26	ARNDT	04	DPWA	$\pi N \to \pi N, \eta N$
668± 41	PENNER	02C	DPWA	Multichannel
490±120	VRANA	00	DPWA	Multichannel
360± 20	ARNDT	96	IPWA	$\gamma N \to \pi N$
440	ARNDT	95	DPWA	$\pi N \to N\pi$
315	LI	93	IPWA	$\gamma N \to \pi N$
391± 34	MANLEY	92	IPWA	$\pi N \to \pi N$ & $N\pi\pi$
545±170	CUTKOSKY	90	IPWA	$\pi N \to \pi N$
200	[1] LONGACRE	77	IPWA	$\pi N \to N\pi\pi$
200	[2] LONGACRE	75	IPWA	$\pi N \to N\pi\pi$

$N(1440)$ POLE POSITION

REAL PART

VALUE (MeV)	DOCUMENT ID		TECN	COMMENT
1350 to 1380 (≈ 1365) OUR ESTIMATE				
1370± 4	ANISOVICH	12A	DPWA	Multichannel
1359	[3] ARNDT	06	DPWA	$\pi N \to \pi N, \eta N$
1385	[4] HOEHLER	93	SPED	$\pi N \to \pi N$
1375±30	CUTKOSKY	80	IPWA	$\pi N \to \pi N$
• • • We do not use the following data for averages, fits, limits, etc. • • •				
1386	SHKLYAR	13	DPWA	Multichannel
1370	SHRESTHA	12A	DPWA	Multichannel
1370± 4	ANISOVICH	10	DPWA	Multichannel
1363±11	BATINIC	10	DPWA	$\pi N \to N\pi, N\eta$
1371± 7	SARANTSEV	08	DPWA	Multichannel
1357	[5] ARNDT	04	DPWA	$\pi N \to \pi N, \eta N$
1383	VRANA	00	DPWA	Multichannel
1346	[6] ARNDT	95	DPWA	$\pi N \to N\pi$
1360	[7] ARNDT	91	DPWA	$\pi N \to \pi N$ Soln SM90
1370	CUTKOSKY	90	IPWA	$\pi N \to \pi N$
1381 or 1379	[8] LONGACRE	78	IPWA	$\pi N \to N\pi\pi$
1360 or 1333	[1] LONGACRE	77	IPWA	$\pi N \to N\pi\pi$

−2×IMAGINARY PART

VALUE (MeV)	DOCUMENT ID		TECN	COMMENT
160 to 220 (≈ 190) OUR ESTIMATE				
190± 7	ANISOVICH	12A	DPWA	Multichannel
162	[3] ARNDT	06	DPWA	$\pi N \to \pi N, \eta N$
164	[4] HOEHLER	93	SPED	$\pi N \to \pi N$
180±40	CUTKOSKY	80	IPWA	$\pi N \to \pi N$
• • • We do not use the following data for averages, fits, limits, etc. • • •				
277	SHKLYAR	13	DPWA	Multichannel
214	SHRESTHA	12A	DPWA	Multichannel
193± 7	ANISOVICH	10	DPWA	Multichannel
151±13	BATINIC	10	DPWA	$\pi N \to N\pi, N\eta$
192±20	SARANTSEV	08	DPWA	Multichannel
160	[5] ARNDT	04	DPWA	$\pi N \to \pi N, \eta N$
316	VRANA	00	DPWA	Multichannel
176	[6] ARNDT	95	DPWA	$\pi N \to N\pi$
252	[7] ARNDT	91	DPWA	$\pi N \to \pi N$ Soln SM90
228	CUTKOSKY	90	IPWA	$\pi N \to \pi N$
209 or 210	[8] LONGACRE	78	IPWA	$\pi N \to N\pi\pi$
167 or 234	[1] LONGACRE	77	IPWA	$\pi N \to N\pi\pi$

$N(1440)$ ELASTIC POLE RESIDUE

MODULUS $|r|$

VALUE (MeV)	DOCUMENT ID		TECN	COMMENT
40 to 52 (≈ 46) OUR ESTIMATE				
48±3	ANISOVICH	12A	DPWA	Multichannel
38	[3] ARNDT	06	DPWA	$\pi N \to \pi N, \eta N$
40	HOEHLER	93	SPED	$\pi N \to \pi N$
52±5	CUTKOSKY	80	IPWA	$\pi N \to \pi N$
• • • We do not use the following data for averages, fits, limits, etc. • • •				
126	SHKLYAR	13	DPWA	Multichannel
44	BATINIC	10	DPWA	$\pi N \to N\pi, N\eta$
36	[5] ARNDT	04	DPWA	$\pi N \to \pi N, \eta N$
42	[6] ARNDT	95	DPWA	$\pi N \to N\pi$
109	[7] ARNDT	91	DPWA	$\pi N \to \pi N$ Soln SM90
74	CUTKOSKY	90	IPWA	$\pi N \to \pi N$

PHASE θ

VALUE (°)	DOCUMENT ID		TECN	COMMENT
75 to 100 (≈ 85) OUR ESTIMATE				
− 78± 4	ANISOVICH	12A	DPWA	Multichannel
− 98	[3] ARNDT	06	DPWA	$\pi N \to \pi N, \eta N$
−100±35	CUTKOSKY	80	IPWA	$\pi N \to \pi N$

• • • We do not use the following data for averages, fits, limits, etc. • • •

− 60	SHKLYAR	13	DPWA	Multichannel
− 88	BATINIC	10	DPWA	$\pi N \to N\pi$, $N\eta$
−102	[5] ARNDT	04	DPWA	$\pi N \to \pi N$, ηN
−101	[6] ARNDT	95	DPWA	$\pi N \to N\pi$
− 93	[7] ARNDT	91	DPWA	$\pi N \to \pi N$ Soln SM90
− 84	CUTKOSKY	90	IPWA	$\pi N \to \pi N$

N(1440) INELASTIC POLE RESIDUE

The "normalized residue" is the residue divided by $\Gamma_{pole}/2$.

Normalized residue in $N\pi \to N(1440) \to \Delta\pi$, P-wave

MODULUS (%)	PHASE (°)	DOCUMENT ID		TECN	COMMENT
27±2	**40 ± 5**	ANISOVICH	12A	DPWA	Multichannel

Normalized residue in $N\pi \to N(1440) \to N\,(\pi\pi)^{I=0}_{S\text{-wave}}$

MODULUS (%)	PHASE (°)	DOCUMENT ID		TECN	COMMENT
21±5	**−135 ± 7**	ANISOVICH	12A	DPWA	Multichannel

N(1440) DECAY MODES

The following branching fractions are our estimates, not fits or averages.

	Mode	Fraction (Γ_j/Γ)
Γ_1	$N\pi$	55–75 %
Γ_2	$N\eta$	(0.0±1.0) %
Γ_3	$N\pi\pi$	30–40 %
Γ_4	$\Delta\pi$	20–30 %
Γ_5	$\Delta(1232)\pi$, P-wave	15–30 %
Γ_6	$N\rho$	<8 %
Γ_7	$N\rho$, S=1/2, P-wave	(0.0±1.0) %
Γ_8	$N\rho$, S=3/2, P-wave	
Γ_9	$N(\pi\pi)^{I=0}_{S\text{-wave}}$	10–20 %
Γ_{10}	$p\gamma$	0.035–0.048 %
Γ_{11}	$p\gamma$, helicity=1/2	0.035–0.048 %
Γ_{12}	$n\gamma$	0.02–0.04 %
Γ_{13}	$n\gamma$, helicity=1/2	0.02–0.04 %

N(1440) BRANCHING RATIOS

$\Gamma(N\pi)/\Gamma_{total}$ — Γ_1/Γ

VALUE (%)	DOCUMENT ID		TECN	COMMENT
55 to 75 OUR ESTIMATE				
56 ±2	SHKLYAR	13	DPWA	Multichannel
62 ±3	ANISOVICH	12A	DPWA	Multichannel
78.7±1.6	ARNDT	06	DPWA	$\pi N \to \pi N$, ηN
68 ±4	CUTKOSKY	80	IPWA	$\pi N \to \pi N$
51 ±5	HOEHLER	79	IPWA	$\pi N \to \pi N$
• • • We do not use the following data for averages, fits, limits, etc. • • •				
64.8±0.9	SHRESTHA	12A	DPWA	Multichannel
60 ±6	ANISOVICH	10	DPWA	Multichannel
62 ±4	BATINIC	10	DPWA	$\pi N \to N\pi$, $N\eta$
75.0±2.4	ARNDT	04	DPWA	$\pi N \to \pi N$, ηN
57 ±1	PENNER	02C	DPWA	Multichannel
72 ±5	VRANA	00	DPWA	Multichannel
68	ARNDT	95	DPWA	$\pi N \to N\pi$
69 ±3	MANLEY	92	IPWA	$\pi N \to \pi N$ & $N\pi\pi$

$\Gamma(N\eta)/\Gamma_{total}$ — Γ_2/Γ

VALUE (%)	DOCUMENT ID		TECN	COMMENT
0±1	VRANA	00	DPWA	Multichannel

Note: Signs of couplings from $\pi N \to N\pi\pi$ analyses were changed in the 1986 edition to agree with the baryon-first convention; the overall phase ambiguity is resolved by choosing a negative sign for the $\Delta(1620)$ S_{31} coupling to $\Delta(1232)\pi$.

$(\Gamma_i\Gamma_f)^{1/2}/\Gamma_{total}$ in $N\pi \to N(1440) \to \Delta(1232)\pi$, P-wave — $(\Gamma_1\Gamma_5)^{1/2}/\Gamma$

VALUE	DOCUMENT ID		TECN	COMMENT
+0.37 to +0.41 OUR ESTIMATE				
+0.41	[1,9] LONGACRE	77	IPWA	$\pi N \to N\pi\pi$
+0.37	[2] LONGACRE	75	IPWA	$\pi N \to N\pi\pi$
• • • We do not use the following data for averages, fits, limits, etc. • • •				
+0.39±0.02	MANLEY	92	IPWA	$\pi N \to \pi N$ & $N\pi\pi$

$\Gamma(\Delta(1232)\pi$, P-wave$)/\Gamma_{total}$ — Γ_5/Γ

VALUE (%)	DOCUMENT ID		TECN	COMMENT
15 to 30 (≈ 20) OUR ESTIMATE				
21 ±8	ANISOVICH	12A	DPWA	Multichannel
16 ±1	VRANA	00	DPWA	Multichannel
• • • We do not use the following data for averages, fits, limits, etc. • • •				
6.5±0.8	SHRESTHA	12A	DPWA	Multichannel

$(\Gamma_i\Gamma_f)^{1/2}/\Gamma_{total}$ in $N\pi \to N(1440) \to N\rho$, S=1/2, P-wave — $(\Gamma_1\Gamma_7)^{1/2}/\Gamma$

VALUE	DOCUMENT ID		TECN	COMMENT
±0.07 to ±0.25 OUR ESTIMATE				
−0.11	[1,9] LONGACRE	77	IPWA	$\pi N \to N\pi\pi$
+0.23	[2] LONGACRE	75	IPWA	$\pi N \to N\pi\pi$

$\Gamma(N\rho$, S=1/2, P-wave$)/\Gamma_{total}$ — Γ_7/Γ

VALUE (%)	DOCUMENT ID		TECN	COMMENT
0 ±1	VRANA	00	DPWA	Multichannel
• • • We do not use the following data for averages, fits, limits, etc. • • •				
1.3±0.4	SHRESTHA	12A	DPWA	Multichannel

$(\Gamma_i\Gamma_f)^{1/2}/\Gamma_{total}$ in $N\pi \to N(1440) \to N\rho$, S=3/2, P-wave — $(\Gamma_1\Gamma_8)^{1/2}/\Gamma$

VALUE	DOCUMENT ID		TECN	COMMENT
+0.18	[1,9] LONGACRE	77	IPWA	$\pi N \to N\pi\pi$

$(\Gamma_i\Gamma_f)^{1/2}/\Gamma_{total}$ in $N\pi \to N(1440) \to N(\pi\pi)^{I=0}_{S\text{-wave}}$ — $(\Gamma_1\Gamma_9)^{1/2}/\Gamma$

VALUE	DOCUMENT ID		TECN	COMMENT
±0.17 to ±0.25 OUR ESTIMATE				
−0.18	[1,9] LONGACRE	77	IPWA	$\pi N \to N\pi\pi$
−0.23	[2] LONGACRE	75	IPWA	$\pi N \to N\pi\pi$
• • • We do not use the following data for averages, fits, limits, etc. • • •				
+0.24±0.03	MANLEY	92	IPWA	$\pi N \to \pi N$ & $N\pi\pi$

$\Gamma(N(\pi\pi)^{I=0}_{S\text{-wave}})/\Gamma_{total}$ — Γ_9/Γ

VALUE (%)	DOCUMENT ID		TECN	COMMENT
10 to 20 (≈ 15) OUR ESTIMATE				
17±7	ANISOVICH	12A	DPWA	Multichannel
12±1	VRANA	00	DPWA	Multichannel
• • • We do not use the following data for averages, fits, limits, etc. • • •				
27±1	SHRESTHA	12A	DPWA	Multichannel

N(1440) PHOTON DECAY AMPLITUDES

Papers on γN amplitudes predating 1981 may be found in our 2006 edition, Journal of Physics (generic for all A,B,E,G) **G33** 1 (2006).

$N(1440) \to p\gamma$, helicity-1/2 amplitude $A_{1/2}$

VALUE ($GeV^{-1/2}$)	DOCUMENT ID		TECN	COMMENT
−0.060±0.004 OUR ESTIMATE				
−0.061±0.008	ANISOVICH	12A	DPWA	Multichannel
−0.056±0.001	WORKMAN	12A	DPWA	$\gamma N \to N\pi$
−0.051±0.002	DUGGER	07	DPWA	$\gamma N \to \pi N$
−0.069±0.018	CRAWFORD	83	IPWA	$\gamma N \to \pi N$
−0.063±0.008	AWAJI	81	DPWA	$\gamma N \to \pi N$
• • • We do not use the following data for averages, fits, limits, etc. • • •				
−0.085±0.003	SHKLYAR	13	DPWA	Multichannel
−0.084±0.003	SHRESTHA	12A	DPWA	Multichannel
−0.052±0.010	ANISOVICH	10	DPWA	Multichannel
−0.061	DRECHSEL	07	DPWA	$\gamma N \to \pi N$
−0.087	PENNER	02D	DPWA	Multichannel
−0.063±0.005	ARNDT	96	IPWA	$\gamma N \to \pi N$
−0.085±0.003	LI	93	IPWA	$\gamma N \to \pi N$
−0.129	[10] WADA	84	DPWA	Compton scattering

$N(1440) \to n\gamma$, helicity-1/2 amplitude $A_{1/2}$

VALUE ($GeV^{-1/2}$)	DOCUMENT ID		TECN	COMMENT
+0.040±0.010 OUR ESTIMATE				
0.048±0.004	CHEN	12A	DPWA	$\gamma N \to \pi N$
0.037±0.010	AWAJI	81	DPWA	$\gamma N \to \pi N$
0.030±0.003	FUJII	81	DPWA	$\gamma N \to \pi N$
• • • We do not use the following data for averages, fits, limits, etc. • • •				
0.040±0.005	SHRESTHA	12A	DPWA	Multichannel
0.054	DRECHSEL	07	DPWA	$\gamma N \to \pi N$
0.121	PENNER	02D	DPWA	Multichannel
0.045±0.015	ARNDT	96	IPWA	$\gamma N \to \pi N$
0.085±0.006	LI	93	IPWA	$\gamma N \to \pi N$

N(1440) FOOTNOTES

[1] LONGACRE 77 pole positions are from a search for poles in the unitarized T-matrix; the first (second) value uses, in addition to $\pi N \to N\pi\pi$ data, elastic amplitudes from a Saclay (CERN) partial-wave analysis. The other LONGACRE 77 values are from eyeball fits with Breit-Wigner circles to the T-matrix amplitudes.

[2] From method II of LONGACRE 75: eyeball fits with Breit-Wigner circles to the T-matrix amplitudes.

[3] ARNDT 06 also finds a second-sheet pole with real part = 1388 MeV, −2 × imaginary part = 165 MeV, and residue with modulus 86 MeV and phase = −46 degrees.

[4] See HOEHLER 93 for a detailed discussion of the evidence for and the pole parameters of N and Δ resonances as determined from Argand diagrams of πN elastic partial-wave amplitudes and from plots of the speeds with which the amplitudes traverse the diagrams.

[5] ARNDT 04 also finds a second-sheet pole with real part = 1385 MeV, −2 × imaginary part = 166 MeV, and residue with modulus 82 MeV and phase = −51°.

[6] ARNDT 95 also finds a second-sheet pole with real part = 1383 MeV, −2×imaginary part = 210 MeV, and residue with modulus 92 MeV and phase = −54°.

[7] ARNDT 91 (Soln SM90) also finds a second-sheet pole with real part = 1413 MeV, $-2\times$ imaginary part = 256 MeV, and residue = $(78-153i)$ MeV.
[8] LONGACRE 78 values are from a search for poles in the unitarized T-matrix. The first (second) value uses, in addition to $\pi N \to N\pi\pi$ data, elastic amplitudes from a Saclay (CERN) partial-wave analysis.
[9] LONGACRE 77 considers this coupling to be well determined.
[10] WADA 84 is inconsistent with other analyses; see the Note on N and Δ Resonances.

$N(1440)$ REFERENCES

For early references, see Physics Letters **111B** 1 (1982).

SHKLYAR	13	PR C87 015201	V. Shklyar, H. Lenske, U. Mosel	(GIES)
ANISOVICH	12A	EPJ A48 15	A.V. Anisovich *et al.*	(BONN, PNPI)
CHEN	12A	PR C86 015206	W. Chen *et al.*	(DUKE, GWU, MSST, ITEP+)
SHRESTHA	12A	PR C86 055203	M. Shrestha, D.M. Manley	(KSU)
WORKMAN	12A	PR C86 015202	R. Workman *et al.*	(GWU)
ANISOVICH	10	EPJ A44 203	A.V. Anisovich *et al.*	(BONN, PNPI)
BATINIC	10	PR C82 038203	M. Batinic *et al.*	(ZAGR)
SARANTSEV	08	PL B659 94	A.V. Sarantsev *et al.*	(CB-ELSA/A2-TAPS Collab.)
DRECHSEL	07	EPJ A34 69	D. Drechsel, S.S. Kamalov, L. Tiator	(MAINZ, JINR)
DUGGER	07	PR C76 025211	M. Dugger *et al.*	(Jefferson Lab CLAS Collab.)
ARNDT	06	PR C74 045205	R.A. Arndt *et al.*	(GWU)
PDG	06	JP G33 1	W.-M. Yao *et al.*	(PDG Collab.)
ARNDT	04	PR C69 035213	R.A. Arndt *et al.*	(GWU, TRIU)
PENNER	02C	PR C66 055211	G. Penner, U. Mosel	(GIES)
PENNER	02D	PR C66 055212	G. Penner, U. Mosel	(GIES)
VRANA	00	PRPL 328 181	T.P. Vrana, S.A. Dytman., T.-S.H. Lee	(PITT+)
ARNDT	96	PR C53 430	R.A. Arndt, I.I. Strakovsky, R.L. Workman	(VPI)
ARNDT	95	PR C52 2120	R.A. Arndt *et al.*	(VPI, BRCO)
HOEHLER	93	πN Newsletter 9 1	G. Hohler	(KARL)
LI	93	PR C47 2759	Z.J. Li *et al.*	(VPI)
MANLEY	92	PR D45 4002	D.M. Manley, E.M. Saleski	(KSA) IJP
Also		PR D30 904	D.M. Manley *et al.*	(VPI)
ARNDT	91	PR D43 2131	R.A. Arndt *et al.*	(VPI, TELE) IJP
CUTKOSKY	90	PR D42 235	R.E. Cutkosky, S. Wang	(CMU)
WADA	84	NP B247 313	Y. Wada *et al.*	(INUS)
CRAWFORD	83	NP B211 1	R.L. Crawford, W.T. Morton	(GLAS)
PDG	82	PL 111B 1	M. Roos *et al.*	(HELS, CIT, CERN)
AWAJI	81	Bonn Conf. 352	N. Awaji, R. Kajikawa	(NAGO)
Also		NP B197 365	K. Fujii *et al.*	(NAGO)
FUJII	81	NP B187 53	K. Fujii *et al.*	(NAGO, OSAK)
CUTKOSKY	80	Toronto Conf. 19	R.E. Cutkosky *et al.*	(CMU, LBL) IJP
Also		PR D20 2839	R.E. Cutkosky *et al.*	(CMU, LBL) IJP
HOEHLER	79	PDAT 12-1	G. Hohler *et al.*	(KARLT) IJP
Also		Toronto Conf. 3	R. Koch	(KARLT) IJP
LONGACRE	78	PR D17 1795	R.S. Longacre *et al.*	(LBL, SLAC)
LONGACRE	77	NP B122 493	R.S. Longacre, J. Dolbeau	(SACL) IJP
Also		NP B108 365	J. Dolbeau *et al.*	(SACL) IJP
LONGACRE	75	PL 55B 415	R.S. Longacre *et al.*	(LBL, SLAC) IJP

$N(1520)$ $3/2^-$

$I(J^P) = \frac{1}{2}(\frac{3}{2}^-)$ Status: ****

Most of the results published before 1975 were last included in our 1982 edition, Physics Letters **111B** 1 (1982). Some further obsolete results published before 1984 were last included in our 2006 edition, Journal of Physics (generic for all A,B,E,G) **G33** 1 (2006).

$N(1520)$ BREIT-WIGNER MASS

VALUE (MeV)	*DOCUMENT ID*		*TECN*	*COMMENT*
1510 to 1520 (≈ 1515) OUR ESTIMATE				
1505 ± 4	SHKLYAR	13	DPWA	Multichannel
1517 ± 3	ANISOVICH	12A	DPWA	Multichannel
1514.5 ± 0.2	ARNDT	06	DPWA	$\pi N \to \pi N$, ηN
1525 ±10	CUTKOSKY	80	IPWA	$\pi N \to \pi N$
1519 ± 4	HOEHLER	79	IPWA	$\pi N \to \pi N$
• • • We do not use the following data for averages, fits, limits, etc. • • •				
1512.6 ± 0.5	SHRESTHA	12A	DPWA	Multichannel
1524 ± 4	ANISOVICH	10	DPWA	Multichannel
1522 ± 8	BATINIC	10	DPWA	$\pi N \to N\pi$, $N\eta$
1520 ±10	THOMA	08	DPWA	Multichannel
1516.3 ± 0.8	ARNDT	04	DPWA	$\pi N \to \pi N$, ηN
1509 ± 1	PENNER	02C	DPWA	Multichannel
1518 ± 3	VRANA	00	DPWA	Multichannel
1516 ±10	ARNDT	96	IPWA	$\gamma N \to \pi N$
1515	ARNDT	95	DPWA	$\pi N \to N\pi$
1510	LI	93	IPWA	$\gamma N \to \pi N$
1524 ± 4	MANLEY	92	IPWA	$\pi N \to \pi N$ & $N\pi\pi$
1510	[1] LONGACRE	77	IPWA	$\pi N \to N\pi\pi$
1520	[2] LONGACRE	75	IPWA	$\pi N \to N\pi\pi$

$N(1520)$ BREIT-WIGNER WIDTH

VALUE (MeV)	*DOCUMENT ID*		*TECN*	*COMMENT*
100 to 125 (≈ 115) OUR ESTIMATE				
100 ± 2	SHKLYAR	13	DPWA	Multichannel
114 ± 5	ANISOVICH	12A	DPWA	Multichannel
103.6 ± 0.4	ARNDT	06	DPWA	$\pi N \to \pi N$, ηN
120 ±15	CUTKOSKY	80	IPWA	$\pi N \to \pi N$
114 ± 7	HOEHLER	79	IPWA	$\pi N \to \pi N$
• • • We do not use the following data for averages, fits, limits, etc. • • •				
117 ± 1	SHRESTHA	12A	DPWA	Multichannel
117 ± 6	ANISOVICH	10	DPWA	Multichannel
132 ±11	BATINIC	10	DPWA	$\pi N \to N\pi$, $N\eta$
125 ±15	THOMA	08	DPWA	Multichannel
98.6 ± 2.6	ARNDT	04	DPWA	$\pi N \to \pi N$, ηN
100 ± 2	PENNER	02C	DPWA	Multichannel
124 ± 4	VRANA	00	DPWA	Multichannel
106 ± 4	ARNDT	96	IPWA	$\gamma N \to \pi N$
106	ARNDT	95	DPWA	$\pi N \to N\pi$
120	LI	93	IPWA	$\gamma N \to \pi N$
124 ± 8	MANLEY	92	IPWA	$\pi N \to \pi N$ & $N\pi\pi$
110	[1] LONGACRE	77	IPWA	$\pi N \to N\pi\pi$
150	[2] LONGACRE	75	IPWA	$\pi N \to N\pi\pi$

$N(1520)$ POLE POSITION

REAL PART

VALUE (MeV)	*DOCUMENT ID*		*TECN*	*COMMENT*
1505 to 1515 (≈ 1510) OUR ESTIMATE				
1507 ± 3	ANISOVICH	12A	DPWA	Multichannel
1515	ARNDT	06	DPWA	$\pi N \to \pi N$, ηN
1510	[3] HOEHLER	93	ARGD	$\pi N \to \pi N$
1510 ± 5	CUTKOSKY	80	IPWA	$\pi N \to \pi N$
• • • We do not use the following data for averages, fits, limits, etc. • • •				
1492	SHKLYAR	13	DPWA	Multichannel
1501	SHRESTHA	12A	DPWA	Multichannel
1512 ± 3	ANISOVICH	10	DPWA	Multichannel
1506 ± 9	BATINIC	10	DPWA	$\pi N \to N\pi$, $N\eta$
1509 ± 7	THOMA	08	DPWA	Multichannel
1514	ARNDT	04	DPWA	$\pi N \to \pi N$, ηN
1504	VRANA	00	DPWA	Multichannel
1515	ARNDT	95	DPWA	$\pi N \to N\pi$
1511	ARNDT	91	DPWA	$\pi N \to \pi N$ Soln SM90
1514 or 1511	[4] LONGACRE	78	IPWA	$\pi N \to N\pi\pi$
1508 or 1505	[1] LONGACRE	77	IPWA	$\pi N \to N\pi\pi$

$-2\times$IMAGINARY PART

VALUE (MeV)	*DOCUMENT ID*		*TECN*	*COMMENT*
105 to 120 (≈ 110) OUR ESTIMATE				
111 ± 5	ANISOVICH	12A	DPWA	Multichannel
113	ARNDT	06	DPWA	$\pi N \to \pi N$, ηN
120	[3] HOEHLER	93	ARGD	$\pi N \to \pi N$
114 ±10	CUTKOSKY	80	IPWA	$\pi N \to \pi N$
• • • We do not use the following data for averages, fits, limits, etc. • • •				
94	SHKLYAR	13	DPWA	Multichannel
112	SHRESTHA	12A	DPWA	Multichannel
110 ± 6	ANISOVICH	10	DPWA	Multichannel
122 ± 9	BATINIC	10	DPWA	$\pi N \to N\pi$, $N\eta$
113 ±12	THOMA	08	DPWA	Multichannel
102	ARNDT	04	DPWA	$\pi N \to \pi N$, ηN
112	VRANA	00	DPWA	Multichannel
110	ARNDT	95	DPWA	$\pi N \to N\pi$
108	ARNDT	91	DPWA	$\pi N \to \pi N$ Soln SM90
146 or 137	[4] LONGACRE	78	IPWA	$\pi N \to N\pi\pi$
109 or 107	[1] LONGACRE	77	IPWA	$\pi N \to N\pi\pi$

$N(1520)$ ELASTIC POLE RESIDUE

MODULUS $|r|$

VALUE (MeV)	*DOCUMENT ID*		*TECN*	*COMMENT*
35 ± 3 OUR ESTIMATE				
36 ± 3	ANISOVICH	12A	DPWA	Multichannel
38	ARNDT	06	DPWA	$\pi N \to \pi N$, ηN
32	HOEHLER	93	ARGD	$\pi N \to \pi N$
35 ± 2	CUTKOSKY	80	IPWA	$\pi N \to \pi N$
• • • We do not use the following data for averages, fits, limits, etc. • • •				
27	SHKLYAR	13	DPWA	Multichannel
35	BATINIC	10	DPWA	$\pi N \to N\pi$, $N\eta$
35	ARNDT	04	DPWA	$\pi N \to \pi N$, ηN
34	ARNDT	95	DPWA	$\pi N \to N\pi$
33	ARNDT	91	DPWA	$\pi N \to \pi N$ Soln SM90

PHASE θ

VALUE (°)	*DOCUMENT ID*		*TECN*	*COMMENT*
−10 ± 5 OUR ESTIMATE				
−14 ± 3	ANISOVICH	12A	DPWA	Multichannel
− 5	ARNDT	06	DPWA	$\pi N \to \pi N$, ηN
− 8	HOEHLER	93	ARGD	$\pi N \to \pi N$
−12 ± 5	CUTKOSKY	80	IPWA	$\pi N \to \pi N$
• • • We do not use the following data for averages, fits, limits, etc. • • •				
−35	SHKLYAR	13	DPWA	Multichannel
− 7	BATINIC	10	DPWA	$\pi N \to N\pi$, $N\eta$
− 6	ARNDT	04	DPWA	$\pi N \to \pi N$, ηN
7	ARNDT	95	DPWA	$\pi N \to N\pi$
−10	ARNDT	91	DPWA	$\pi N \to \pi N$ Soln SM90

$N(1520)$ INELASTIC POLE RESIDUE

The "normalized residue" is the residue divided by $\Gamma_{pole}/2$.

Normalized residue in $N\pi \rightarrow N(1520) \rightarrow \Delta\pi$, S-wave

MODULUS (%)	PHASE (°)	DOCUMENT ID		TECN	COMMENT
33±5	**150 ± 20**	ANISOVICH	12A	DPWA	Multichannel

Normalized residue in $N\pi \rightarrow N(1520) \rightarrow \Delta\pi$, D-wave

MODULUS (%)	PHASE (°)	DOCUMENT ID		TECN	COMMENT
25±3	**100 ± 20**	ANISOVICH	12A	DPWA	Multichannel

$N(1520)$ DECAY MODES

The following branching fractions are our estimates, not fits or averages.

	Mode	Fraction (Γ_i/Γ)
Γ_1	$N\pi$	55–65 %
Γ_2	$N\eta$	$(2.3\pm0.4)\times10^{-3}$
Γ_3	$N\pi\pi$	20–30 %
Γ_4	$\Delta\pi$	15–25 %
Γ_5	$\Delta(1232)\pi$, S-wave	10–20 %
Γ_6	$\Delta(1232)\pi$, D-wave	10–15 %
Γ_7	$N\rho$	15–25 %
Γ_8	$N\rho$, S=3/2, S-wave	(9.0±1.0) %
Γ_9	$N(\pi\pi)^{I=0}_{S\text{-wave}}$	<8 %
Γ_{10}	$p\gamma$	0.31–0.52 %
Γ_{11}	$p\gamma$, helicity=1/2	0.01–0.02 %
Γ_{12}	$p\gamma$, helicity=3/2	0.30–0.50 %
Γ_{13}	$n\gamma$	0.30–0.53 %
Γ_{14}	$n\gamma$, helicity=1/2	0.04–0.10 %
Γ_{15}	$n\gamma$, helicity=3/2	0.25–0.45 %

$N(1520)$ BRANCHING RATIOS

$\Gamma(N\pi)/\Gamma_{total}$ Γ_1/Γ

VALUE (%)	DOCUMENT ID		TECN	COMMENT
55 to 65 OUR ESTIMATE				
57 ±2	SHKLYAR	13	DPWA	Multichannel
62 ±3	ANISOVICH	12A	DPWA	Multichannel
63.2±0.1	ARNDT	06	DPWA	$\pi N \rightarrow \pi N$, ηN
58 ±3	CUTKOSKY	80	IPWA	$\pi N \rightarrow \pi N$
54 ±3	HOEHLER	79	IPWA	$\pi N \rightarrow \pi N$
• • • We do not use the following data for averages, fits, limits, etc. • • •				
62.7±0.5	SHRESTHA	12A	DPWA	Multichannel
57 ±5	ANISOVICH	10	DPWA	Multichannel
55 ±5	BATINIC	10	DPWA	$\pi N \rightarrow N\pi$, $N\eta$
58 ±8	THOMA	08	DPWA	Multichannel
64.0±0.5	ARNDT	04	DPWA	$\pi N \rightarrow \pi N$, ηN
56 ±1	PENNER	02C	DPWA	Multichannel
63 ±2	VRANA	00	DPWA	Multichannel
61	ARNDT	95	DPWA	$\pi N \rightarrow N\pi$
59 ±3	MANLEY	92	IPWA	$\pi N \rightarrow \pi N$ & $N\pi\pi$

$\Gamma(N\eta)/\Gamma_{total}$ Γ_2/Γ

VALUE (%)	DOCUMENT ID		TECN	COMMENT
0.23±0.04 OUR AVERAGE				
0 ±1	SHKLYAR	13	DPWA	Multichannel
0.23±0.04	PENNER	02C	DPWA	Multichannel
0 ±1	VRANA	00	DPWA	Multichannel
• • • We do not use the following data for averages, fits, limits, etc. • • •				
0.1 ±0.1	BATINIC	10	DPWA	$\pi N \rightarrow N\pi$, $N\eta$
0.2 ±0.1	THOMA	08	DPWA	Multichannel
0.08 to 0.12	ARNDT	05	DPWA	Multichannel
0.08±0.01	TIATOR	99	DPWA	$\gamma p \rightarrow p\eta$

Note: Signs of couplings from $\pi N \rightarrow N\pi\pi$ analyses were changed in the 1986 edition to agree with the baryon-first convention; the overall phase ambiguity is resolved by choosing a negative sign for the $\Delta(1620)$ S_{31} coupling to $\Delta(1232)\pi$.

$(\Gamma_i\Gamma_f)^{1/2}/\Gamma_{total}$ in $N\pi \rightarrow N(1520) \rightarrow \Delta(1232)\pi$, S-wave $(\Gamma_1\Gamma_5)^{1/2}/\Gamma$

VALUE	DOCUMENT ID		TECN	COMMENT
−0.26 to −0.20 OUR ESTIMATE				
−0.26	[1,5] LONGACRE	77	IPWA	$\pi N \rightarrow N\pi\pi$
−0.24	[2] LONGACRE	75	IPWA	$\pi N \rightarrow N\pi\pi$
• • • We do not use the following data for averages, fits, limits, etc. • • •				
−0.18±0.05	MANLEY	92	IPWA	$\pi N \rightarrow \pi N$ & $N\pi\pi$

$\Gamma(\Delta(1232)\pi, S\text{-wave})/\Gamma_{total}$ Γ_5/Γ

VALUE (%)	DOCUMENT ID		TECN	COMMENT
10 to 20 OUR ESTIMATE				
19 ±4	ANISOVICH	12A	DPWA	Multichannel
15 ±2	VRANA	00	DPWA	Multichannel
• • • We do not use the following data for averages, fits, limits, etc. • • •				
9.3±0.7	SHRESTHA	12A	DPWA	Multichannel
12 ±4	THOMA	08	DPWA	Multichannel

$(\Gamma_i\Gamma_f)^{1/2}/\Gamma_{total}$ in $N\pi \rightarrow N(1520) \rightarrow \Delta(1232)\pi$, D-wave $(\Gamma_1\Gamma_6)^{1/2}/\Gamma$

VALUE	DOCUMENT ID		TECN	COMMENT
−0.28 to −0.24 OUR ESTIMATE				
−0.21	[1,5] LONGACRE	77	IPWA	$\pi N \rightarrow N\pi\pi$
−0.30	[2] LONGACRE	75	IPWA	$\pi N \rightarrow N\pi\pi$
• • • We do not use the following data for averages, fits, limits, etc. • • •				
−0.29±0.03	MANLEY	92	IPWA	$\pi N \rightarrow \pi N$ & $N\pi\pi$

$\Gamma(\Delta(1232)\pi, D\text{-wave})/\Gamma_{total}$ Γ_6/Γ

VALUE (%)	DOCUMENT ID		TECN	COMMENT
10 to 15 OUR ESTIMATE				
9 ±2	ANISOVICH	12A	DPWA	Multichannel
11 ±2	VRANA	00	DPWA	Multichannel
• • • We do not use the following data for averages, fits, limits, etc. • • •				
6.3±0.5	SHRESTHA	12A	DPWA	Multichannel
14 ±5	THOMA	08	DPWA	Multichannel

$(\Gamma_i\Gamma_f)^{1/2}/\Gamma_{total}$ in $N\pi \rightarrow N(1520) \rightarrow N\rho$, S=3/2, S-wave $(\Gamma_1\Gamma_8)^{1/2}/\Gamma$

VALUE	DOCUMENT ID		TECN	COMMENT
−0.35 to −0.31 OUR ESTIMATE				
−0.35	[1,5] LONGACRE	77	IPWA	$\pi N \rightarrow N\pi\pi$
−0.24	[2] LONGACRE	75	IPWA	$\pi N \rightarrow N\pi\pi$
• • • We do not use the following data for averages, fits, limits, etc. • • •				
−0.35±0.03	MANLEY	92	IPWA	$\pi N \rightarrow \pi N$ & $N\pi\pi$

$\Gamma(N\rho, S$=3/2, S-wave$)/\Gamma_{total}$ Γ_8/Γ

VALUE (%)	DOCUMENT ID		TECN	COMMENT
9 ±1	VRANA	00	DPWA	Multichannel
• • • We do not use the following data for averages, fits, limits, etc. • • •				
20.9±0.7	SHRESTHA	12A	DPWA	Multichannel

$(\Gamma_i\Gamma_f)^{1/2}/\Gamma_{total}$ in $N\pi \rightarrow N(1520) \rightarrow N(\pi\pi)^{I=0}_{S\text{-wave}}$ $(\Gamma_1\Gamma_9)^{1/2}/\Gamma$

VALUE	DOCUMENT ID		TECN	COMMENT
−0.22 to −0.06 OUR ESTIMATE				
−0.13	[1,5] LONGACRE	77	IPWA	$\pi N \rightarrow N\pi\pi$
−0.17	[2] LONGACRE	75	IPWA	$\pi N \rightarrow N\pi\pi$

$\Gamma(N(\pi\pi)^{I=0}_{S\text{-wave}})/\Gamma_{total}$ Γ_9/Γ

VALUE (%)	DOCUMENT ID		TECN	COMMENT
1±1	VRANA	00	DPWA	Multichannel
• • • We do not use the following data for averages, fits, limits, etc. • • •				
<1	SHRESTHA	12A	DPWA	Multichannel
<4	THOMA	08	DPWA	Multichannel

$N(1520)$ PHOTON DECAY AMPLITUDES

Papers on γN amplitudes predating 1981 may be found in our 2006 edition, Journal of Physics (generic for all A,B,E,G) **G33** 1 (2006).

$N(1520) \rightarrow p\gamma$, helicity-1/2 amplitude $A_{1/2}$

VALUE ($GeV^{-1/2}$)	DOCUMENT ID		TECN	COMMENT
−0.020±0.005 OUR ESTIMATE				
−0.022±0.004	ANISOVICH	12A	DPWA	Multichannel
−0.019±0.002	WORKMAN	12A	DPWA	$\gamma N \rightarrow N\pi$
−0.028±0.002	DUGGER	07	DPWA	$\gamma N \rightarrow \pi N$
−0.038±0.003	AHRENS	02	DPWA	$\gamma N \rightarrow \pi N$
−0.028±0.014	CRAWFORD	83	IPWA	$\gamma N \rightarrow \pi N$
−0.007±0.004	AWAJI	81	DPWA	$\gamma N \rightarrow \pi N$
• • • We do not use the following data for averages, fits, limits, etc. • • •				
−0.015±0.001	SHKLYAR	13	DPWA	Multichannel
−0.034±0.001	SHRESTHA	12A	DPWA	Multichannel
−0.032±0.006	ANISOVICH	10	DPWA	Multichannel
−0.027	DRECHSEL	07	DPWA	$\gamma N \rightarrow \pi N$
−0.003	PENNER	02D	DPWA	Multichannel
−0.052±0.010±0.007	[6] MUKHOPAD...	98		$\gamma p \rightarrow \eta p$
−0.020±0.007	ARNDT	96	IPWA	$\gamma N \rightarrow \pi N$
−0.020±0.002	LI	93	IPWA	$\gamma N \rightarrow \pi N$
−0.012	WADA	84	DPWA	Compton scattering

Baryon Particle Listings

$N(1520)$, $N(1535)$

$N(1520) \rightarrow p\gamma$, helicity-3/2 amplitude $A_{3/2}$

VALUE ($GeV^{-1/2}$)	DOCUMENT ID		TECN	COMMENT
0.140±0.010 OUR ESTIMATE				
0.131±0.010	ANISOVICH	12A	DPWA	Multichannel
0.141±0.002	WORKMAN	12A	DPWA	$\gamma N \rightarrow N\pi$
0.143±0.002	DUGGER	07	DPWA	$\gamma N \rightarrow \pi N$
0.147±0.010	AHRENS	02	DPWA	$\gamma N \rightarrow \pi N$
0.156±0.022	CRAWFORD	83	IPWA	$\gamma N \rightarrow \pi N$
0.168±0.013	AWAJI	81	DPWA	$\gamma N \rightarrow \pi N$
• • • We do not use the following data for averages, fits, limits, etc. • • •				
0.146±0.001	SHKLYAR	13	DPWA	Multichannel
0.127±0.003	SHRESTHA	12A	DPWA	Multichannel
0.138±0.008	ANISOVICH	10	DPWA	Multichannel
0.161	DRECHSEL	07	DPWA	$\gamma N \rightarrow \pi N$
0.151	PENNER	02D	DPWA	Multichannel
0.130±0.020±0.015	[6] MUKHOPAD...	98		$\gamma p \rightarrow \eta p$
0.167±0.005	ARNDT	96	IPWA	$\gamma N \rightarrow \pi N$
0.167±0.002	LI	93	IPWA	$\gamma N \rightarrow \pi N$
0.168	WADA	84	DPWA	Compton scattering

$N(1520) \rightarrow n\gamma$, helicity-1/2 amplitude $A_{1/2}$

VALUE ($GeV^{-1/2}$)	DOCUMENT ID		TECN	COMMENT
−0.050±0.010 OUR ESTIMATE				
−0.046±0.006	CHEN	12A	DPWA	$\gamma N \rightarrow \pi N$
−0.066±0.013	AWAJI	81	DPWA	$\gamma N \rightarrow \pi N$
−0.067±0.004	FUJII	81	DPWA	$\gamma N \rightarrow \pi N$
• • • We do not use the following data for averages, fits, limits, etc. • • •				
−0.038±0.003	SHRESTHA	12A	DPWA	Multichannel
−0.077	DRECHSEL	07	DPWA	$\gamma N \rightarrow \pi N$
−0.084	PENNER	02D	DPWA	Multichannel
−0.048±0.008	ARNDT	96	IPWA	$\gamma N \rightarrow \pi N$
−0.058±0.003	LI	93	IPWA	$\gamma N \rightarrow \pi N$

$N(1520) \rightarrow n\gamma$, helicity-3/2 amplitude $A_{3/2}$

VALUE ($GeV^{-1/2}$)	DOCUMENT ID		TECN	COMMENT
−0.115±0.010 OUR ESTIMATE				
−0.115±0.005	CHEN	12A	DPWA	$\gamma N \rightarrow \pi N$
−0.124±0.009	AWAJI	81	DPWA	$\gamma N \rightarrow \pi N$
−0.158±0.003	FUJII	81	DPWA	$\gamma N \rightarrow \pi N$
• • • We do not use the following data for averages, fits, limits, etc. • • •				
−0.101±0.004	SHRESTHA	12A	DPWA	Multichannel
−0.154	DRECHSEL	07	DPWA	$\gamma N \rightarrow \pi N$
−0.159	PENNER	02D	DPWA	Multichannel
−0.140±0.010	ARNDT	96	IPWA	$\gamma N \rightarrow \pi N$
−0.131±0.003	LI	93	IPWA	$\gamma N \rightarrow \pi N$

$N(1520)$ FOOTNOTES

[1] LONGACRE 77 pole positions are from a search for poles in the unitarized T-matrix; the first (second) value uses, in addition to $\pi N \rightarrow N\pi\pi$ data, elastic amplitudes from a Saclay (CERN) partial-wave analysis. The other LONGACRE 77 values are from eyeball fits with Breit-Wigner circles to the T-matrix amplitudes.

[2] From method II of LONGACRE 75: eyeball fits with Breit-Wigner circles to the T-matrix amplitudes.

[3] See HOEHLER 93 for a detailed discussion of the evidence for and the pole parameters of N and Δ resonances as determined from Argand diagrams of πN elastic partial-wave amplitudes and from plots of the speeds with which the amplitudes traverse the diagrams.

[4] LONGACRE 78 values are from a search for poles in the unitarized T-matrix. The first (second) value uses, in addition to $\pi N \rightarrow N\pi\pi$ data, elastic amplitudes from a Saclay (CERN) partial-wave analysis.

[5] LONGACRE 77 considers this coupling to be well determined.

[6] MUKHOPADHYAY 98 uses an effective Lagrangian approach to analyze η photoproduction data. The *ratio* of the $A_{3/2}$ and $A_{1/2}$ amplitudes is determined, with less model dependence than the amplitudes themselves, to be $A_{3/2}/A_{1/2} = -2.5 \pm 0.5 \pm 0.4$.

$N(1520)$ REFERENCES

For early references, see Physics Letters **111B** 1 (1982). For very early references, see Reviews of Modern Physics **37** 633 (1965).

SHKLYAR	13	PR C87 015201	V. Shklyar, H. Lenske, U. Mosel	(GIES)
ANISOVICH	12A	EPJ A48 15	A.V. Anisovich *et al.*	(BONN, PNPI)
CHEN	12A	PR C86 015206	W. Chen *et al.*	(DUKE, GWU, MSST, ITEP+)
SHRESTHA	12A	PR C86 055203	M. Shrestha, D.M. Manley	(KSU)
WORKMAN	12A	PR C86 015202	R. Workman *et al.*	(GWU)
ANISOVICH	10	EPJ A44 203	A.V. Anisovich *et al.*	(BONN, PNPI)
BATINIC	10	PR C82 038203	M. Batinic *et al.*	(ZAGR)
THOMA	08	PL B659 87	U. Thoma *et al.*	(CB-ELSA Collab.)
DRECHSEL	07	EPJ A34 69	D. Drechsel, S.S. Kamalov, L. Tiator	(MAINZ, JINR)
DUGGER	07	PR C76 025211	M. Dugger *et al.*	(Jefferson Lab CLAS Collab.)
ARNDT	06	PR C74 045205	R.A. Arndt *et al.*	(GWU)
PDG	06	JP G33 1	W.-M. Yao *et al.*	(PDG Collab.)
ARNDT	05	PR C72 045202	R.A. Arndt *et al.*	(GWU, PNPI)
ARNDT	04	PR C69 035213	R.A. Arndt *et al.*	(GWU, TRIU)
AHRENS	02	PRL 88 232002	J. Ahrens *et al.*	(Mainz MAMI GDH/A2 Collab.)
PENNER	02C	PR C66 055211	G. Penner, U. Mosel	(GIES)
PENNER	02D	PR C66 055212	G. Penner, U. Mosel	(GIES)
VRANA	00	PRPL 328 181	T.P. Vrana, S.A. Dytman,, T.-S.H. Lee	(PITT+)
TIATOR	99	PR C60 035210	L. Tiator *et al.*	
MUKHOPAD...	98	PL B444 7	N.C. Mukhopadhyay, N. Mathur	
ARNDT	96	PR C53 430	R.A. Arndt, I.I. Strakovsky, R.L. Workman	(VPI)
ARNDT	95	PR C52 2120	R.A. Arndt *et al.*	(VPI, BRCO)
HOEHLER	93	πN Newsletter 9 1	G. Hohler	(KARL)
LI	93	PR C47 2759	Z.J. Li *et al.*	(VPI)
MANLEY	92	PR D45 4002	D.M. Manley, E.M. Saleski	(KSA) IJP
Also		PR D30 904	D.M. Manley *et al.*	(VPI)
ARNDT	91	PR D43 2131	R.A. Arndt *et al.*	(VPI, TELE) IJP
WADA	84	NP B247 313	Y. Wada *et al.*	(INUS)
CRAWFORD	83	NP B211 1	R.L. Crawford, W.T. Morton	(GLAS)
PDG	82	PL 111B 1	M. Roos *et al.*	(HELS, CIT, CERN)
AWAJI	81	Bonn Conf. 352	N. Awaji, R. Kajikawa	(NAGO)
Also		NP B197 365	K. Fujii *et al.*	(NAGO)
FUJII	81	NP B187 53	K. Fujii *et al.*	(NAGO, OSAK)
CUTKOSKY	80	Toronto Conf. 19	R.E. Cutkosky *et al.*	(CMU, LBL) IJP
Also		PR D20 2839	R.E. Cutkosky *et al.*	(CMU, LBL) IJP
HOEHLER	79	PDAT 12-1	G. Hohler *et al.*	(KARLT) IJP
Also		Toronto Conf. 3	R. Koch	(KARLT) IJP
LONGACRE	78	PR D17 1795	R.S. Longacre *et al.*	(LBL, SLAC)
LONGACRE	77	NP B122 493	R.S. Longacre, J. Dolbeau	(SACL) IJP
Also		NP B108 365	J. Dolbeau *et al.*	(SACL) IJP
LONGACRE	75	PL 55B 415	R.S. Longacre *et al.*	(LBL, SLAC) IJP

$N(1535)$ $1/2^-$

$I(J^P) = \frac{1}{2}(\frac{1}{2}^-)$ Status: ****

Most of the results published before 1975 were last included in our 1982 edition, Physics Letters **111B** 1 (1982). Some further obsolete results published before 1984 were last included in our 2006 edition, Journal of Physics (generic for all A,B,E,G) **G33** 1 (2006).

$N(1535)$ BREIT-WIGNER MASS

VALUE (MeV)	DOCUMENT ID		TECN	COMMENT
1525 to 1545 (≈ 1535) OUR ESTIMATE				
1526 ± 2	SHKLYAR	13	DPWA	Multichannel
1519 ± 5	ANISOVICH	12A	DPWA	Multichannel
1547.0± 0.7	ARNDT	06	DPWA	$\pi N \rightarrow \pi N, \eta N$
1550 ±40	CUTKOSKY	80	IPWA	$\pi N \rightarrow \pi N$
1526 ± 7	HOEHLER	79	IPWA	$\pi N \rightarrow \pi N$
• • • We do not use the following data for averages, fits, limits, etc. • • •				
1538 ± 1	SHRESTHA	12A	DPWA	Multichannel
1535 ±20	ANISOVICH	10	DPWA	Multichannel
1553 ± 8	BATINIC	10	DPWA	$\pi N \rightarrow N\pi, N\eta$
1548 ±15	THOMA	08	DPWA	Multichannel
1546.7± 2.2	ARNDT	04	DPWA	$\pi N \rightarrow \pi N, \eta N$
1526 ± 2	PENNER	02C	DPWA	Multichannel
1530 ±10	BAI	01B	BES	$J/\psi \rightarrow p\bar{p}\eta$
1522 ±11	THOMPSON	01	CLAS	$\gamma^* p \rightarrow p\eta$
1542 ± 3	VRANA	00	DPWA	Multichannel
1532 ± 5	ARMSTRONG	99B	DPWA	$\gamma^* p \rightarrow p\eta$
1549.0± 2.1	ABAEV	96	DPWA	$\pi^- p \rightarrow \eta n$
1525 ±10	ARNDT	96	IPWA	$\gamma N \rightarrow \pi N$
1535	ARNDT	95	DPWA	$\pi N \rightarrow N\pi$
1544 ±13	KRUSCHE	95	DPWA	$\gamma p \rightarrow p\eta$
1518	LI	93	IPWA	$\gamma N \rightarrow \pi N$
1534 ± 7	MANLEY	92	IPWA	$\pi N \rightarrow \pi N$ & $N\pi\pi$
1520	[1] LONGACRE	77	IPWA	$\pi N \rightarrow N\pi\pi$
1510	[2] LONGACRE	75	IPWA	$\pi N \rightarrow N\pi\pi$

$N(1535)$ BREIT-WIGNER WIDTH

VALUE (MeV)	DOCUMENT ID		TECN	COMMENT
125 to 175 (≈ 150) OUR ESTIMATE				
131 ±12	SHKLYAR	13	DPWA	Multichannel
128 ±14	ANISOVICH	12A	DPWA	Multichannel
188.4± 3.8	ARNDT	06	DPWA	$\pi N \rightarrow \pi N, \eta N$
148.2± 8.1	GREEN	97	DPWA	$\pi N \rightarrow \pi N, \eta N$
240 ±80	CUTKOSKY	80	IPWA	$\pi N \rightarrow \pi N$
120 ±20	HOEHLER	79	IPWA	$\pi N \rightarrow \pi N$
• • • We do not use the following data for averages, fits, limits, etc. • • •				
141 ± 4	SHRESTHA	12A	DPWA	Multichannel
170 ±35	ANISOVICH	10	DPWA	Multichannel
182 ±25	BATINIC	10	DPWA	$\pi N \rightarrow N\pi, N\eta$
170 ±20	THOMA	08	DPWA	Multichannel
178.0±11.6	ARNDT	04	DPWA	$\pi N \rightarrow \pi N, \eta N$
129 ± 8	PENNER	02C	DPWA	Multichannel
95 ±25	BAI	01B	BES	$J/\psi \rightarrow p\bar{p}\eta$
143 ±18	THOMPSON	01	CLAS	$\gamma^* p \rightarrow p\eta$
112 ±19	VRANA	00	DPWA	Multichannel
154 ±20	ARMSTRONG	99B	DPWA	$\gamma^* p \rightarrow p\eta$
212 ±20	[3] KRUSCHE	97	DPWA	$\gamma N \rightarrow \eta N$
168.8±11.6	ABAEV	96	DPWA	$\pi^- p \rightarrow \eta n$
103 ± 5	ARNDT	96	IPWA	$\gamma N \rightarrow \pi N$
66	ARNDT	95	DPWA	$\pi N \rightarrow N\pi$
200 ±40	KRUSCHE	95	DPWA	$\gamma p \rightarrow p\eta$
84	LI	93	IPWA	$\gamma N \rightarrow \pi N$
151 ±27	MANLEY	92	IPWA	$\pi N \rightarrow \pi N$ & $N\pi\pi$
135	[1] LONGACRE	77	IPWA	$\pi N \rightarrow N\pi\pi$
100	[2] LONGACRE	75	IPWA	$\pi N \rightarrow N\pi\pi$

$N(1535)$ POLE POSITION

REAL PART

VALUE (MeV)	DOCUMENT ID		TECN	COMMENT
1490 to 1530 (≈ 1510) OUR ESTIMATE				
1501 ± 4	ANISOVICH	12A	DPWA	Multichannel
1502	ARNDT	06	DPWA	$\pi N \to \pi N$, ηN
1487	[4] HOEHLER	93	SPED	$\pi N \to \pi N$
1510 ± 50	CUTKOSKY	80	IPWA	$\pi N \to \pi N$
• • • We do not use the following data for averages, fits, limits, etc. • • •				
1490	SHKLYAR	13	DPWA	Multichannel
1515	SHRESTHA	12A	DPWA	Multichannel
1510 ± 25	ANISOVICH	10	DPWA	Multichannel
1521 ± 14	BATINIC	10	DPWA	$\pi N \to N\pi$, $N\eta$
1508^{+10}_{-30}	THOMA	08	DPWA	Multichannel
1526	ARNDT	04	DPWA	$\pi N \to \pi N$, ηN
1525	VRANA	00	DPWA	Multichannel
1510 ± 10	[5] ARNDT	98	DPWA	$\pi N \to \pi N$, ηN
1501	ARNDT	95	DPWA	$\pi N \to N\pi$
1499	ARNDT	91	DPWA	$\pi N \to \pi N$ Soln SM90
1496 or 1499	[6] LONGACRE	78	IPWA	$\pi N \to N\pi\pi$
1525 or 1527	[1] LONGACRE	77	IPWA	$\pi N \to N\pi\pi$

−2×IMAGINARY PART

VALUE (MeV)	DOCUMENT ID		TECN	COMMENT
90 to 250 (≈ 170) OUR ESTIMATE				
134 ± 11	ANISOVICH	12A	DPWA	Multichannel
95	ARNDT	06	DPWA	$\pi N \to \pi N$, ηN
260 ± 80	CUTKOSKY	80	IPWA	$\pi N \to \pi N$
• • • We do not use the following data for averages, fits, limits, etc. • • •				
100	SHKLYAR	13	DPWA	Multichannel
123	SHRESTHA	12A	DPWA	Multichannel
140 ± 30	ANISOVICH	10	DPWA	Multichannel
190 ± 28	BATINIC	10	DPWA	$\pi N \to N\pi$, $N\eta$
165 ± 15	THOMA	08	DPWA	Multichannel
130	ARNDT	04	DPWA	$\pi N \to \pi N$, ηN
102	VRANA	00	DPWA	Multichannel
170 ± 30	[5] ARNDT	98	DPWA	$\pi N \to \pi N$, ηN
124	ARNDT	95	DPWA	$\pi N \to N\pi$
110	ARNDT	91	DPWA	$\pi N \to \pi N$ Soln SM90
103 or 105	[6] LONGACRE	78	IPWA	$\pi N \to N\pi\pi$
135 or 123	[1] LONGACRE	77	IPWA	$\pi N \to N\pi\pi$

$N(1535)$ ELASTIC POLE RESIDUE

MODULUS $|r|$

VALUE (MeV)	DOCUMENT ID		TECN	COMMENT
50 ± 20 OUR ESTIMATE				
31 ± 4	ANISOVICH	12A	DPWA	Multichannel
16	ARNDT	06	DPWA	$\pi N \to \pi N$, ηN
120 ± 40	CUTKOSKY	80	IPWA	$\pi N \to \pi N$
• • • We do not use the following data for averages, fits, limits, etc. • • •				
15	SHKLYAR	13	DPWA	Multichannel
68	BATINIC	10	DPWA	$\pi N \to N\pi$, $N\eta$
33	ARNDT	04	DPWA	$\pi N \to \pi N$, ηN
31	ARNDT	95	DPWA	$\pi N \to N\pi$
23	ARNDT	91	DPWA	$\pi N \to \pi N$ Soln SM90

PHASE θ

VALUE (°)	DOCUMENT ID		TECN	COMMENT
−15 ± 15 OUR ESTIMATE				
−29 ± 5	ANISOVICH	12A	DPWA	Multichannel
−16	ARNDT	06	DPWA	$\pi N \to \pi N$, ηN
+15 ± 45	CUTKOSKY	80	IPWA	$\pi N \to \pi N$
• • • We do not use the following data for averages, fits, limits, etc. • • •				
−51	SHKLYAR	13	DPWA	Multichannel
12	BATINIC	10	DPWA	$\pi N \to N\pi$, $N\eta$
14	ARNDT	04	DPWA	$\pi N \to \pi N$, ηN
−12	ARNDT	95	DPWA	$\pi N \to N\pi$
−13	ARNDT	91	DPWA	$\pi N \to \pi N$ Soln SM90

$N(1535)$ INELASTIC POLE RESIDUE

The "normalized residue" is the residue divided by $\Gamma_{pole}/2$.

Normalized residue in $N\pi \to N(1535) \to N\eta$

MODULUS (%)	PHASE (°)	DOCUMENT ID		TECN	COMMENT
43 ± 3	**−76 ± 5**	ANISOVICH	12A	DPWA	Multichannel

Normalized residue in $N\pi \to N(1535) \to \Delta\pi$, D-wave

MODULUS (%)	PHASE (°)	DOCUMENT ID		TECN	COMMENT
12 ± 3	**145 ± 17**	ANISOVICH	12A	DPWA	Multichannel

$N(1535)$ DECAY MODES

The following branching fractions are our estimates, not fits or averages.

	Mode	Fraction (Γ_i/Γ)
Γ_1	$N\pi$	35–55 %
Γ_2	$N\eta$	(42 ±10) %
Γ_3	$N\pi\pi$	1–10 %
Γ_4	$\Delta\pi$	<1 %
Γ_5	$\Delta(1232)\pi$, D-wave	0–4 %
Γ_6	$N\rho$	<4 %
Γ_7	$N\rho$, S=1/2, S-wave	(2.0± 1.0) %
Γ_8	$N\rho$, S=3/2, D-wave	(0.0± 1.0) %
Γ_9	$N(\pi\pi)^{I=0}_{S\text{-wave}}$	(2 ± 1) %
Γ_{10}	$N(1440)\pi$	(8 ± 3) %
Γ_{11}	$p\gamma$	0.15–0.30 %
Γ_{12}	$p\gamma$, helicity=1/2	0.15–0.30 %
Γ_{13}	$n\gamma$	0.01–0.25 %
Γ_{14}	$n\gamma$, helicity=1/2	0.01–0.25 %

$N(1535)$ BRANCHING RATIOS

$\Gamma(N\pi)/\Gamma_{total}$ Γ_1/Γ

VALUE (%)	DOCUMENT ID		TECN	COMMENT
35 to 55 OUR ESTIMATE				
35 ± 3	SHKLYAR	13	DPWA	Multichannel
54 ± 5	ANISOVICH	12A	DPWA	Multichannel
35.5 ± 0.2	ARNDT	06	DPWA	$\pi N \to \pi N$, ηN
39.4 ± 0.9	GREEN	97	DPWA	$\pi N \to \pi N$, ηN
50 ±10	CUTKOSKY	80	IPWA	$\pi N \to \pi N$
38 ± 4	HOEHLER	79	IPWA	$\pi N \to \pi N$
• • • We do not use the following data for averages, fits, limits, etc. • • •				
37 ± 1	SHRESTHA	12A	DPWA	Multichannel
35 ±15	ANISOVICH	10	DPWA	Multichannel
46 ± 7	BATINIC	10	DPWA	$\pi N \to N\pi$, $N\eta$
37 ± 9	THOMA	08	DPWA	Multichannel
36.0 ± 0.9	ARNDT	04	DPWA	$\pi N \to \pi N$, ηN
36 ± 1	PENNER	02C	DPWA	Multichannel
35 ± 8	VRANA	00	DPWA	Multichannel
33.0 ± 1.1	ABAEV	96	DPWA	$\pi^- p \to \eta n$
31	ARNDT	95	DPWA	$\pi N \to N\pi$
51 ± 5	MANLEY	92	IPWA	$\pi N \to \pi N$ & $N\pi\pi$

$\Gamma(N\eta)/\Gamma_{total}$ Γ_2/Γ

VALUE (%)	CL%	DOCUMENT ID		TECN	COMMENT
42 ±10 OUR ESTIMATE					
58 ± 4		SHKLYAR	13	DPWA	Multichannel
33 ± 5		ANISOVICH	12A	DPWA	Multichannel
53 ± 1		PENNER	02C	DPWA	Multichannel
51 ± 5		VRANA	00	DPWA	Multichannel
• • • We do not use the following data for averages, fits, limits, etc. • • •					
41 ± 2		SHRESTHA	12A	DPWA	Multichannel
50 ± 7		BATINIC	10	DPWA	$\pi N \to N\pi$, $N\eta$
40 ±10		THOMA	08	DPWA	Multichannel
>45	95	[7] ARMSTRONG	99B	DPWA	$p\,(e,e'p)\,\eta$
56.8 ± 1.1		GREEN	97	DPWA	$\pi N \to \pi N$, ηN
59.1 ± 1.7		ABAEV	96	DPWA	$\pi^- p \to \eta n$

$\Gamma(N\eta)/\Gamma(N\pi)$ Γ_2/Γ_1

VALUE	DOCUMENT ID		TECN	COMMENT
• • • We do not use the following data for averages, fits, limits, etc. • • •				
0.95 ± 0.03	AZNAURYAN	09	CLAS	π, η electroproduction

$(\Gamma_i\Gamma_f)^{1/2}/\Gamma_{total}$ in $N\pi \to N(1535) \to N\eta$ $(\Gamma_1\Gamma_2)^{1/2}/\Gamma$

VALUE	DOCUMENT ID		TECN	COMMENT
+0.44 to +0.50 OUR ESTIMATE				
• • • We do not use the following data for averages, fits, limits, etc. • • •				
+0.47 ± 0.02	MANLEY	92	IPWA	$\pi N \to \pi N$ & $N\pi\pi$

Note: Signs of couplings from $\pi N \to N\pi\pi$ analyses were changed in the 1986 edition to agree with the baryon-first convention; the overall phase ambiguity is resolved by choosing a negative sign for the $\Delta(1620)$ S_{31} coupling to $\Delta(1232)\pi$.

$(\Gamma_i\Gamma_f)^{1/2}/\Gamma_{total}$ in $N\pi \to N(1535) \to \Delta(1232)\pi$, D-wave $(\Gamma_1\Gamma_5)^{1/2}/\Gamma$

VALUE	DOCUMENT ID		TECN	COMMENT
−0.04 to +0.06 OUR ESTIMATE				
0.00	[1] LONGACRE	77	IPWA	$\pi N \to N\pi\pi$
+0.06	[2] LONGACRE	75	IPWA	$\pi N \to N\pi\pi$
• • • We do not use the following data for averages, fits, limits, etc. • • •				
+0.00 ± 0.04	MANLEY	92	IPWA	$\pi N \to \pi N$ & $N\pi\pi$

$\Gamma(\Delta(1232)\pi, D\text{-wave})/\Gamma_{total}$ Γ_5/Γ

VALUE (%)	DOCUMENT ID		TECN	COMMENT
0 to 4 OUR ESTIMATE				
2.5±1.5	ANISOVICH	12A	DPWA	Multichannel
1 ±1	VRANA	00	DPWA	Multichannel
• • • We do not use the following data for averages, fits, limits, etc. • • •				
1.8±0.8	SHRESTHA	12A	DPWA	Multichannel
23 ±8	THOMA	08	DPWA	Multichannel

$(\Gamma_i\Gamma_f)^{1/2}/\Gamma_{total}$ in $N\pi \to N(1535) \to N\rho$, S=1/2, S-wave $(\Gamma_1\Gamma_7)^{1/2}/\Gamma$

VALUE	DOCUMENT ID		TECN	COMMENT
−0.14 to −0.06 OUR ESTIMATE				
−0.10	[1] LONGACRE	77	IPWA	$\pi N \to N\pi\pi$
−0.09	[2] LONGACRE	75	IPWA	$\pi N \to N\pi\pi$
• • • We do not use the following data for averages, fits, limits, etc. • • •				
−0.10±0.03	MANLEY	92	IPWA	$\pi N \to \pi N$ & $N\pi\pi$

$\Gamma(N\rho, S$=1/2, D-wave)/Γ_{total} Γ_7/Γ

VALUE (%)	DOCUMENT ID		TECN	COMMENT
2±1	VRANA	00	DPWA	Multichannel
• • • We do not use the following data for averages, fits, limits, etc. • • •				
10±1	SHRESTHA	12A	DPWA	Multichannel

$\Gamma(N\rho, S$=3/2, D-wave)/Γ_{total} Γ_8/Γ

VALUE (%)	DOCUMENT ID		TECN	COMMENT
0±1	VRANA	00	DPWA	Multichannel
• • • We do not use the following data for averages, fits, limits, etc. • • •				
8±1	SHRESTHA	12A	DPWA	Multichannel

$(\Gamma_i\Gamma_f)^{1/2}/\Gamma_{total}$ in $N\pi \to N(1535) \to N(\pi\pi)^{I=0}_{S\text{-wave}}$ $(\Gamma_1\Gamma_9)^{1/2}/\Gamma$

VALUE	DOCUMENT ID		TECN	COMMENT
+0.03 to +0.13 OUR ESTIMATE				
+0.08	[1] LONGACRE	77	IPWA	$\pi N \to N\pi\pi$
+0.09	[2] LONGACRE	75	IPWA	$\pi N \to N\pi\pi$
• • • We do not use the following data for averages, fits, limits, etc. • • •				
+0.07±0.04	MANLEY	92	IPWA	$\pi N \to \pi N$ & $N\pi\pi$

$\Gamma(N(\pi\pi)^{I=0}_{S\text{-wave}})/\Gamma_{total}$ Γ_9/Γ

VALUE (%)	DOCUMENT ID		TECN	COMMENT
2 ±1	VRANA	00	DPWA	Multichannel
• • • We do not use the following data for averages, fits, limits, etc. • • •				
1.5±0.5	SHRESTHA	12A	DPWA	Multichannel

$(\Gamma_i\Gamma_f)^{1/2}/\Gamma_{total}$ in $N\pi \to N(1535) \to N(1440)\pi$ $(\Gamma_1\Gamma_{10})^{1/2}/\Gamma$

VALUE	DOCUMENT ID		TECN	COMMENT
• • • We do not use the following data for averages, fits, limits, etc. • • •				
+0.10±0.05	MANLEY	92	IPWA	$\pi N \to \pi N$ & $N\pi\pi$

$\Gamma(N(1440)\pi)/\Gamma_{total}$ Γ_{10}/Γ

VALUE (%)	DOCUMENT ID		TECN	COMMENT
8±3 OUR ESTIMATE				
8±2	[8] STAROSTIN	03		$\pi^- p \to n3\pi^0$
10±9	VRANA	00	DPWA	Multichannel
• • • We do not use the following data for averages, fits, limits, etc. • • •				
< 1	SHRESTHA	12A	DPWA	Multichannel

$N(1535)$ PHOTON DECAY AMPLITUDES

Papers on γN amplitudes predating 1981 may be found in our 2006 edition, Journal of Physics (generic for all A,B,E,G) **G33** 1 (2006).

$N(1535) \to p\gamma$, helicity-1/2 amplitude $A_{1/2}$

VALUE (GeV$^{-1/2}$)	DOCUMENT ID		TECN	COMMENT
+0.115±0.015 OUR ESTIMATE				
0.105±0.010	ANISOVICH	12A	DPWA	Multichannel
0.128±0.004	WORKMAN	12A	DPWA	$\gamma N \to N\pi$
0.091±0.002	DUGGER	07	DPWA	$\gamma N \to \pi N$
0.120±0.011±0.015	[3] KRUSCHE	97	DPWA	$\gamma N \to \eta N$
0.097±0.006	BENMERROU...	95	DPWA	$\gamma N \to N\eta$
0.095±0.011	[9] BENMERROU...	91		$\gamma p \to p\eta$
0.053±0.015	CRAWFORD	83	IPWA	$\gamma N \to \pi N$
0.077±0.021	AWAJI	81	DPWA	$\gamma N \to \pi N$
• • • We do not use the following data for averages, fits, limits, etc. • • •				
0.091±0.004	SHKLYAR	13	DPWA	Multichannel
0.059±0.003	SHRESTHA	12A	DPWA	Multichannel
0.090±0.015	ANISOVICH	10	DPWA	Multichannel
0.090±0.025	[10] ANISOVICH	09A	DPWA	$\gamma d \to \eta N(N)$
0.066	DRECHSEL	07	DPWA	$\gamma N \to \pi N$
0.090	PENNER	02D	DPWA	Multichannel
0.060±0.015	ARNDT	96	IPWA	$\gamma N \to \pi N$
0.110 to 0.140	KRUSCHE	95	DPWA	$\gamma p \to p\eta$
0.125±0.025	KRUSCHE	95C	IPWA	$\gamma d \to \eta N(N)$
0.061±0.003	LI	93	IPWA	$\gamma N \to \pi N$
0.055	WADA	84	DPWA	Compton scattering

$N(1535) \to n\gamma$, helicity-1/2 amplitude $A_{1/2}$

VALUE (GeV$^{-1/2}$)	DOCUMENT ID		TECN	COMMENT
−0.075±0.020 OUR ESTIMATE				
−0.058±0.006	CHEN	12A	DPWA	$\gamma N \to \pi N$
−0.080±0.020	[11] ANISOVICH	09A	DPWA	$\gamma d \to \eta N(N)$
0.035±0.014	AWAJI	81	DPWA	$\gamma N \to \pi N$
−0.062±0.003	FUJII	81	DPWA	$\gamma N \to \pi N$
• • • We do not use the following data for averages, fits, limits, etc. • • •				
−0.049±0.003	SHRESTHA	12A	DPWA	Multichannel
−0.051	DRECHSEL	07	DPWA	$\gamma N \to \pi N$
−0.024	PENNER	02D	DPWA	Multichannel
−0.020±0.035	ARNDT	96	IPWA	$\gamma N \to \pi N$
−0.100±0.030	KRUSCHE	95C	IPWA	$\gamma d \to \eta N(N)$
−0.046±0.005	LI	93	IPWA	$\gamma N \to \pi N$

$N(1535) \to N\gamma$, ratio $A^n_{1/2}/A^p_{1/2}$

VALUE (GeV$^{-1/2}$)	DOCUMENT ID		TECN
• • • We do not use the following data for averages, fits, limits, etc. • • •			
−0.84±0.15	MUKHOPAD...	95B	IPWA

$N(1535)$ FOOTNOTES

[1] LONGACRE 77 pole positions are from a search for poles in the unitarized T-matrix; the first (second) value uses, in addition to $\pi N \to N\pi\pi$ data, elastic amplitudes from a Saclay (CERN) partial-wave analysis. The other LONGACRE 77 values are from eyeball fits with Breit-Wigner circles to the T-matrix amplitudes.

[2] From method II of LONGACRE 75: eyeball fits with Breit-Wigner circles to the T-matrix amplitudes.

[3] KRUSCHE 97 fits with the mass fixed at 1544 MeV.

[4] See HOEHLER 93 for a detailed discussion of the evidence for and the pole parameters of N and Δ resonances as determined from Argand diagrams of πN elastic partial-wave amplitudes and from plots of the speeds with which the amplitudes traverse the diagrams.

[5] ARNDT 98 also lists pole residues, which display more model dependence than do the associated pole positions.

[6] LONGACRE 78 values are from a search for poles in the unitarized T-matrix. The first (second) value uses, in addition to $\pi N \to N\pi\pi$ data, elastic amplitudes from a Saclay (CERN) partial-wave analysis.

[7] The best value ARMSTRONG 99B obtains is $\simeq 0.55$; this assumes S_{11} dominance in the reaction $p(e, e'p)\ \eta$ at $Q^2 = 4\ (\mathrm{GeV}/c)^2$.

[8] This STAROSTIN 03 value is an estimate made using simplest assumptions.

[9] BENMERROUCHE 91 uses an effective Lagrangian approach to analyze η photoproduction data.

[10] This ANISOVICH 09A amplitude is evaluated at the pole position; the phase is $(20\pm15)°$.

[11] This ANISOVICH 09A amplitude is evaluated at the pole position; the phase is $(20\pm20)°$.

$N(1535)$ REFERENCES

For early references, see Physics Letters **111B** 1 (1982).

SHKLYAR	13	PR C87 015201	V. Shklyar, H. Lenske, U. Mosel	(GIES)
ANISOVICH	12A	EPJ A48 15	A.V. Anisovich *et al.*	(BONN, PNPI)
CHEN	12A	PR C86 015206	W. Chen *et al.*	(DUKE, GWU, MSST, ITEP+)
SHRESTHA	12A	PR C86 055203	M. Shrestha, D.M. Manley	(KSU)
WORKMAN	12A	PR C86 015202	R. Workman *et al.*	(GWU)
ANISOVICH	10	EPJ A44 203	A.V. Anisovich *et al.*	(BONN, PNPI)
BATINIC	10	PR C82 038203	M. Batinic *et al.*	(ZAGR)
ANISOVICH	09A	EPJ A41 13	A.V. Anisovich *et al.*	(BONN, PNPI, BASL)
AZNAURYAN	09	PR C80 055203	I.G. Aznauryan *et al.*	(JLAB CLAS Collab.)
THOMA	08	PL B659 87	U. Thoma *et al.*	(CB-ELSA Collab.)
DRECHSEL	07	EPJ A34 69	D. Drechsel, S.S. Kamalov, L. Tiator	(MAINZ, JINR)
DUGGER	07	PR C76 025211	M. Dugger *et al.*	(Jefferson Lab CLAS Collab.)
ARNDT	06	PR C74 045205	R.A. Arndt *et al.*	(GWU)
PDG	06	JP G33 1	W.-M. Yao *et al.*	(PDG Collab.)
ARNDT	04	PR C69 035213	R.A. Arndt *et al.*	(GWU, TRIU)
STAROSTIN	03	PR C67 068201	A. Starostin *et al.*	(BNL Crystal Ball Collab.)
PENNER	02C	PR C66 055211	G. Penner, U. Mosel	(GIES)
PENNER	02D	PR C66 055212	G. Penner, U. Mosel	(GIES)
BAI	01B	PL B510 75	J.Z. Bai *et al.*	(BES Collab.)
THOMPSON	01	PRL 86 1702	R. Thompson *et al.*	(Jefferson CLAS Collab.)
VRANA	00	PRPL 328 181	T.P. Vrana, S.A. Dytman,, T.-S.H. Lee	(PITT+)
ARMSTRONG	99B	PR D60 052004	C.S. Armstrong *et al.*	
ARNDT	98	PR C58 3636	R.A. Arndt *et al.*	
GREEN	97	PR C55 R2167	A.M. Green, S. Wycech	(HELS, WINR)
KRUSCHE	97	PL B397 171	B. Krusche *et al.*	(GIES, RPI, SASK)
ABAEV	96	PR C53 385	V.V. Abaev, B.M.K. Nefkens	(UCLA)
ARNDT	96	PR C53 430	R.A. Arndt, I.I. Strakovsky, R.L. Workman	(VPI)
ARNDT	95	PR C52 2120	R.A. Arndt *et al.*	(VPI, BRCO)
BENMERROU...	95	PR D51 3237	M. Benmerrouche, N.C. Mukhopadhyay, J.F. Zhang	
KRUSCHE	95	PRL 74 3736	B. Krusche *et al.*	(GIES, MANZ, GLAS+)
KRUSCHE	95C	PL B358 40	B. Krusche *et al.*	(GIES, MANZ, GLAS+)
MUKHOPAD...	95B	PL B364 1	N.C. Mukhopadhyay, J.F. Zhang, M. Benmerrouche	
HOEHLER	93	πN Newsletter 9 1	G. Hohler	(KARL)
LI	93	PR C47 2759	Z.J. Li *et al.*	(VPI)
MANLEY	92	PR D45 4002	D.M. Manley, E.M. Saleski	(KSA) IJP
Also		PR D30 904	D.M. Manley *et al.*	(VPI)
ARNDT	91	PR D43 2131	R.A. Arndt *et al.*	(VPI, TELE) IJP
BENMERROU...	91	PRL 67 1070	M. Benmerrouche, N.C. Mukhopadhyay	(RPI)
WADA	84	NP B247 313	Y. Wada *et al.*	(INUS)
CRAWFORD	83	NP B211 1	R.L. Crawford, W.T. Morton	(GLAS)
PDG	82	PL 111B 1	M. Roos *et al.*	(HELS, CIT, CERN)
AWAJI	81	Bonn Conf. 352	N. Awaji, R. Kajikawa	(NAGO)
Also		NP B197 365	K. Fujii *et al.*	(NAGO)
FUJII	81	NP B187 53	K. Fujii *et al.*	(NAGO, OSAK)
CUTKOSKY	80	Toronto Conf. 19	R.E. Cutkosky *et al.*	(CMU, LBL) IJP
Also		PR D20 2839	R.E. Cutkosky *et al.*	(CMU, LBL) IJP
HOEHLER	79	PDAT 12-1	G. Hohler *et al.*	(KARLT) IJP
Also		Toronto Conf. 3	R. Koch	(KARLT) IJP
LONGACRE	78	PR D17 1795	R.S. Longacre *et al.*	(LBL, SLAC)
LONGACRE	77	NP B122 493	R.S. Longacre, J. Dolbeau	(SACL) IJP
Also		NP B108 365	J. Dolbeau *et al.*	(SACL) IJP
LONGACRE	75	PL 55B 415	R.S. Longacre *et al.*	(LBL, SLAC) IJP

$N(1650)\ 1/2^-$

$I(J^P) = \frac{1}{2}(\frac{1}{2}^-)$ Status: ****

Most of the results published before 1975 were last included in our 1982 edition, Physics Letters **111B** 1 (1982). Some further obsolete results published before 1984 were last included in our 2006 edition, Journal of Physics (generic for all A,B,E,G) **G33** 1 (2006).

$N(1650)$ BREIT-WIGNER MASS

VALUE (MeV)	DOCUMENT ID		TECN	COMMENT
1645 to 1670 (≈ 1655) OUR ESTIMATE				
1665 ± 2	SHKLYAR	13	DPWA	Multichannel
1651 ± 6	ANISOVICH	12A	DPWA	Multichannel
1634.7 ± 1.1	ARNDT	06	DPWA	$\pi N \to \pi N, \eta N$
1650 ±30	CUTKOSKY	80	IPWA	$\pi N \to \pi N$
1670 ± 8	HOEHLER	79	IPWA	$\pi N \to \pi N$
• • • We do not use the following data for averages, fits, limits, etc. • • •				
1664 ± 2	SHRESTHA	12A	DPWA	Multichannel
1680 ±40	ANISOVICH	10	DPWA	Multichannel
1652 ± 9	BATINIC	10	DPWA	$\pi N \to N\pi, N\eta$
1655 ±15	THOMA	08	DPWA	Multichannel
1651.2 ± 4.7	ARNDT	04	DPWA	$\pi N \to \pi N, \eta N$
1665 ± 2	PENNER	02C	DPWA	Multichannel
1647 ±20	BAI	01B	BES	$J/\psi \to p\bar{p}\eta$
1689 ±12	VRANA	00	DPWA	Multichannel
1677 ± 8	ARNDT	96	IPWA	$\gamma N \to \pi N$
1667	ARNDT	95	DPWA	$\pi N \to N\pi$
1712	[1] ARNDT	95	DPWA	$\pi N \to N\pi$
1674	LI	93	IPWA	$\gamma N \to \pi N$
1659 ± 9	MANLEY	92	IPWA	$\pi N \to \pi N$ & $N\pi\pi$
1672	MUSETTE	80	IPWA	$\pi^- p \to \Lambda K^0$
1680	SAXON	80	DPWA	$\pi^- p \to \Lambda K^0$
1700	[2] LONGACRE	77	IPWA	$\pi N \to N\pi\pi$
1660	[3] LONGACRE	75	IPWA	$\pi N \to N\pi\pi$

$N(1650)$ BREIT-WIGNER WIDTH

VALUE (MeV)	DOCUMENT ID		TECN	COMMENT
110 to 170 (≈ 140) OUR ESTIMATE				
147 ±14	SHKLYAR	13	DPWA	Multichannel
104 ±10	ANISOVICH	12A	DPWA	Multichannel
115.4 ± 2.8	ARNDT	06	DPWA	$\pi N \to \pi N, \eta N$
167.9 ± 9.4	GREEN	97	DPWA	$\pi N \to \pi N, \eta N$
150 ±40	CUTKOSKY	80	IPWA	$\pi N \to \pi N$
180 ±20	HOEHLER	79	IPWA	$\pi N \to \pi N$
• • • We do not use the following data for averages, fits, limits, etc. • • •				
126 ± 3	SHRESTHA	12A	DPWA	Multichannel
170 ±45	ANISOVICH	10	DPWA	Multichannel
202 ±16	BATINIC	10	DPWA	$\pi N \to N\pi, N\eta$
180 ±20	THOMA	08	DPWA	Multichannel
130.6 ± 7.0	ARNDT	04	DPWA	$\pi N \to \pi N, \eta N$
138 ± 7	PENNER	02C	DPWA	Multichannel
145 $^{+80}_{-45}$	BAI	01B	BES	$J/\psi \to p\bar{p}\eta$
202 ±40	VRANA	00	DPWA	Multichannel
160 ±12	ARNDT	96	IPWA	$\gamma N \to \pi N$
90	ARNDT	95	DPWA	$\pi N \to N\pi$
184	[1] ARNDT	95	DPWA	$\pi N \to N\pi$
225	LI	93	IPWA	$\gamma N \to \pi N$
173 ±12	MANLEY	92	IPWA	$\pi N \to \pi N$ & $N\pi\pi$
179	MUSETTE	80	IPWA	$\pi^- p \to \Lambda K^0$
120	SAXON	80	DPWA	$\pi^- p \to \Lambda K^0$
170	[2] LONGACRE	77	IPWA	$\pi N \to N\pi\pi$
130	[3] LONGACRE	75	IPWA	$\pi N \to N\pi\pi$

$N(1650)$ POLE POSITION

REAL PART

VALUE (MeV)	DOCUMENT ID		TECN	COMMENT
1640 to 1670 (≈ 1655) OUR ESTIMATE				
1647 ± 6	ANISOVICH	12A	DPWA	Multichannel
1648	ARNDT	06	DPWA	$\pi N \to \pi N, \eta N$
1670	[4] HOEHLER	93	ARGD	$\pi N \to \pi N$
1640 ±20	CUTKOSKY	80	IPWA	$\pi N \to \pi N$
• • • We do not use the following data for averages, fits, limits, etc. • • •				
1650	SHKLYAR	13	DPWA	Multichannel
1655	SHRESTHA	12A	DPWA	Multichannel
1670 ±35	ANISOVICH	10	DPWA	Multichannel
1646 ± 8	BATINIC	10	DPWA	$\pi N \to N\pi, N\eta$
1645 ±15	THOMA	08	DPWA	Multichannel
1653	ARNDT	04	DPWA	$\pi N \to \pi N, \eta N$
1663	VRANA	00	DPWA	Multichannel
1660 ±10	[5] ARNDT	98	DPWA	$\pi N \to \pi N, \eta N$
1673	ARNDT	95	DPWA	$\pi N \to N\pi$
1689	[1] ARNDT	95	DPWA	$\pi N \to N\pi$
1657	ARNDT	91	DPWA	$\pi N \to \pi N$ Soln SM90
1648 or 1651	[6] LONGACRE	78	IPWA	$\pi N \to N\pi\pi$
1699 or 1698	[2] LONGACRE	77	IPWA	$\pi N \to N\pi\pi$

−2×IMAGINARY PART

VALUE (MeV)	DOCUMENT ID		TECN	COMMENT
100 to 170 (≈ 135) OUR ESTIMATE				
103 ± 8	ANISOVICH	12A	DPWA	Multichannel
80	ARNDT	06	DPWA	$\pi N \to \pi N, \eta N$
163	[4] HOEHLER	93	ARGD	$\pi N \to \pi N$
150 ±30	CUTKOSKY	80	IPWA	$\pi N \to \pi N$
• • • We do not use the following data for averages, fits, limits, etc. • • •				
89	SHKLYAR	13	DPWA	Multichannel
123	SHRESTHA	12A	DPWA	Multichannel
170 ±40	ANISOVICH	10	DPWA	Multichannel
204 ±17	BATINIC	10	DPWA	$\pi N \to N\pi, N\eta$
187 ±20	THOMA	08	DPWA	Multichannel
182	ARNDT	04	DPWA	$\pi N \to \pi N, \eta N$
240	VRANA	00	DPWA	Multichannel
140 ±20	[5] ARNDT	98	DPWA	$\pi N \to \pi N, \eta N$
82	ARNDT	95	DPWA	$\pi N \to N\pi$
192	[1] ARNDT	95	DPWA	$\pi N \to N\pi$
160	ARNDT	91	DPWA	$\pi N \to \pi N$ Soln SM90
117 or 119	[6] LONGACRE	78	IPWA	$\pi N \to N\pi\pi$
174 or 173	[2] LONGACRE	77	IPWA	$\pi N \to N\pi\pi$

$N(1650)$ ELASTIC POLE RESIDUE

MODULUS $|r|$

VALUE (MeV)	DOCUMENT ID		TECN	COMMENT
20 to 50 (≈ 35) OUR ESTIMATE				
24 ± 3	ANISOVICH	12A	DPWA	Multichannel
14	ARNDT	06	DPWA	$\pi N \to \pi N, \eta N$
39	HOEHLER	93	ARGD	$\pi N \to \pi N$
60 ±10	CUTKOSKY	80	IPWA	$\pi N \to \pi N$
• • • We do not use the following data for averages, fits, limits, etc. • • •				
19	SHKLYAR	13	DPWA	Multichannel
100	BATINIC	10	DPWA	$\pi N \to N\pi, N\eta$
69	ARNDT	04	DPWA	$\pi N \to \pi N, \eta N$
22	ARNDT	95	DPWA	$\pi N \to N\pi$
72	[1] ARNDT	95	DPWA	$\pi N \to N\pi$
54	ARNDT	91	DPWA	$\pi N \to \pi N$ Soln SM90

PHASE θ

VALUE (°)	DOCUMENT ID		TECN	COMMENT
50 to 80 (≈ 70) OUR ESTIMATE				
−75 ±12	ANISOVICH	12A	DPWA	Multichannel
−69	ARNDT	06	DPWA	$\pi N \to \pi N, \eta N$
−37	HOEHLER	93	ARGD	$\pi N \to \pi N$
−75 ±25	CUTKOSKY	80	IPWA	$\pi N \to \pi N$
• • • We do not use the following data for averages, fits, limits, etc. • • •				
−46	SHKLYAR	13	DPWA	Multichannel
−65	BATINIC	10	DPWA	$\pi N \to N\pi, N\eta$
−55	ARNDT	04	DPWA	$\pi N \to \pi N, \eta N$
29	ARNDT	95	DPWA	$\pi N \to N\pi$
−85	[1] ARNDT	95	DPWA	$\pi N \to N\pi$
−38	ARNDT	91	DPWA	$\pi N \to \pi N$ Soln SM90

$N(1650)$ INELASTIC POLE RESIDUE

The "normalized residue" is the residue divided by $\Gamma_{pole}/2$.

Normalized residue in $N\pi \to N(1650) \to N\eta$

MODULUS (%)	PHASE (°)	DOCUMENT ID		TECN	COMMENT
29±3	**134 ± 10**	ANISOVICH	12A	DPWA	Multichannel

Normalized residue in $N\pi \to N(1650) \to \Lambda K$

MODULUS (%)	PHASE (°)	DOCUMENT ID		TECN	COMMENT
23±9	**85 ± 9**	ANISOVICH	12A	DPWA	Multichannel

Normalized residue in $N\pi \to N(1650) \to \Delta\pi$, D-wave

MODULUS (%)	PHASE (°)	DOCUMENT ID		TECN	COMMENT
23±4	**−30 ± 20**	ANISOVICH	12A	DPWA	Multichannel

$N(1650)$ DECAY MODES

The following branching fractions are our estimates, not fits or averages.

	Mode	Fraction (Γ_i/Γ)
Γ_1	$N\pi$	50–90 %
Γ_2	$N\eta$	5–15 %
Γ_3	ΛK	3–11 %
Γ_4	ΣK	
Γ_5	$N\pi\pi$	10–20 %
Γ_6	$\Delta\pi$	0–25 %
Γ_7	$\Delta(1232)\pi$, D-wave	0–25 %
Γ_8	$N\rho$	4–12 %
Γ_9	$N\rho$, S=1/2, S-wave	(1.0±1.0) %
Γ_{10}	$N\rho$, S=3/2, D-wave	(13.0±3.0) %
Γ_{11}	$N(\pi\pi)^{I=0}_{S\text{-wave}}$	<4 %
Γ_{12}	$N(1440)\pi$	<5 %
Γ_{13}	$p\gamma$	0.04–0.20 %
Γ_{14}	$p\gamma$, helicity=1/2	0.04–0.20 %
Γ_{15}	$n\gamma$	0.003–0.17 %
Γ_{16}	$n\gamma$, helicity=1/2	0.003–0.17 %

$N(1650)$ BRANCHING RATIOS

$\Gamma(N\pi)/\Gamma_{\text{total}}$ Γ_1/Γ

VALUE (%)	DOCUMENT ID		TECN	COMMENT
50 to 70 (≈ 60) OUR ESTIMATE				
74 ± 3	SHKLYAR	13	DPWA	Multichannel
51 ± 4	ANISOVICH	12A	DPWA	Multichannel
100	ARNDT	06	DPWA	$\pi N \to \pi N, \eta N$
73.5± 1.1	GREEN	97	DPWA	$\pi N \to \pi N, \eta N$
65 ±10	CUTKOSKY	80	IPWA	$\pi N \to \pi N$
61 ± 4	HOEHLER	79	IPWA	$\pi N \to \pi N$
• • • We do not use the following data for averages, fits, limits, etc. • • •				
57 ± 2	SHRESTHA	12A	DPWA	Multichannel
50 ±25	ANISOVICH	10	DPWA	Multichannel
79 ± 6	BATINIC	10	DPWA	$\pi N \to N\pi, N\eta$
70 ±15	THOMA	08	DPWA	Multichannel
100.0	ARNDT	04	DPWA	$\pi N \to \pi N, \eta N$
65 ± 4	PENNER	02C	DPWA	Multichannel
74 ± 2	VRANA	00	DPWA	Multichannel
99	ARNDT	95	DPWA	$\pi N \to N\pi$
27	[1] ARNDT	95	DPWA	$\pi N \to N\pi$
89 ± 7	MANLEY	92	IPWA	$\pi N \to \pi N$ & $N\pi\pi$

$\Gamma(N\eta)/\Gamma_{\text{total}}$ Γ_2/Γ

VALUE (%)	DOCUMENT ID		TECN	COMMENT
5 to 15 OUR ESTIMATE				
1 ±2	SHKLYAR	13	DPWA	Multichannel
18 ±4	ANISOVICH	12A	DPWA	Multichannel
1.0±0.6	PENNER	02C	DPWA	Multichannel
6 ±1	VRANA	00	DPWA	Multichannel
• • • We do not use the following data for averages, fits, limits, etc. • • •				
21 ±2	SHRESTHA	12A	DPWA	Multichannel
13 ±5	BATINIC	10	DPWA	$\pi N \to N\pi, N\eta$
15 ±6	THOMA	08	DPWA	Multichannel

$\Gamma(\Lambda K)/\Gamma_{\text{total}}$ Γ_3/Γ

VALUE (%)	DOCUMENT ID		TECN	COMMENT
2.9±0.4 OUR AVERAGE Error includes scale factor of 1.2.				
10 ±5	ANISOVICH	12A	DPWA	Multichannel
4 ±1	SHKLYAR	05	DPWA	Multichannel
2.7±0.4	PENNER	02C	DPWA	Multichannel
• • • We do not use the following data for averages, fits, limits, etc. • • •				
8 ±1	SHRESTHA	12A	DPWA	Multichannel

$(\Gamma_i\Gamma_f)^{1/2}/\Gamma_{\text{total}}$ in $N\pi \to N(1650) \to \Lambda K$ $(\Gamma_1\Gamma_3)^{1/2}/\Gamma$

VALUE	DOCUMENT ID		TECN	COMMENT
−0.27 to −0.17 OUR ESTIMATE				
−0.22	BELL	83	DPWA	$\pi^- p \to \Lambda K^0$
−0.22	SAXON	80	DPWA	$\pi^- p \to \Lambda K^0$

$(\Gamma_i\Gamma_f)^{1/2}/\Gamma_{\text{total}}$ in $N\pi \to N(1650) \to \Sigma K$ $(\Gamma_1\Gamma_4)^{1/2}/\Gamma$

VALUE	DOCUMENT ID		TECN	COMMENT
• • • We do not use the following data for averages, fits, limits, etc. • • •				
−0.254	LIVANOS	80	DPWA	$\pi p \to \Sigma K$

Note: Signs of couplings from $\pi N \to N\pi\pi$ analyses were changed in the 1986 edition to agree with the baryon-first convention; the overall phase ambiguity is resolved by choosing a negative sign for the $\Delta(1620)$ S_{31} coupling to $\Delta(1232)\pi$.

$(\Gamma_i\Gamma_f)^{1/2}/\Gamma_{\text{total}}$ in $N\pi \to N(1650) \to \Delta(1232)\pi$, D-wave $(\Gamma_1\Gamma_7)^{1/2}/\Gamma$

VALUE	DOCUMENT ID		TECN	COMMENT
+0.15 to 0.23 OUR ESTIMATE				
+0.29	[2,7] LONGACRE	77	IPWA	$\pi N \to N\pi\pi$
+0.15	[3] LONGACRE	75	IPWA	$\pi N \to N\pi\pi$
• • • We do not use the following data for averages, fits, limits, etc. • • •				
+0.26±0.14	THOMA	08	DPWA	Multichannel
+0.12±0.04	MANLEY	92	IPWA	$\pi N \to \pi N$ & $N\pi\pi$

$\Gamma(\Delta(1232)\pi, D\text{-wave})/\Gamma_{\text{total}}$ Γ_7/Γ

VALUE (%)	DOCUMENT ID		TECN	COMMENT
0 to 25 OUR ESTIMATE				
19±9	ANISOVICH	12A	DPWA	Multichannel
2±1	VRANA	00	DPWA	Multichannel
• • • We do not use the following data for averages, fits, limits, etc. • • •				
7±2	SHRESTHA	12A	DPWA	Multichannel
10±5	THOMA	08	DPWA	Multichannel

$(\Gamma_i\Gamma_f)^{1/2}/\Gamma_{\text{total}}$ in $N\pi \to N(1650) \to N\rho$, S=1/2, S-wave $(\Gamma_1\Gamma_9)^{1/2}/\Gamma$

VALUE	DOCUMENT ID		TECN	COMMENT
±0.03 to ±0.19 OUR ESTIMATE				
+0.17	[2,7] LONGACRE	77	IPWA	$\pi N \to N\pi\pi$
−0.16	[3] LONGACRE	75	IPWA	$\pi N \to N\pi\pi$
• • • We do not use the following data for averages, fits, limits, etc. • • •				
−0.01±0.09	MANLEY	92	IPWA	$\pi N \to \pi N$ & $N\pi\pi$

$\Gamma(N\rho, S\text{=}1/2, S\text{-wave})/\Gamma_{\text{total}}$ Γ_9/Γ

VALUE (%)	DOCUMENT ID		TECN	COMMENT
1±1	VRANA	00	DPWA	Multichannel
• • • We do not use the following data for averages, fits, limits, etc. • • •				
6±1	SHRESTHA	12A	DPWA	Multichannel

$(\Gamma_i\Gamma_f)^{1/2}/\Gamma_{\text{total}}$ in $N\pi \to N(1650) \to N\rho$, S=3/2, D-wave $(\Gamma_1\Gamma_{10})^{1/2}/\Gamma$

VALUE	DOCUMENT ID		TECN	COMMENT
+0.17 to +0.29 OUR ESTIMATE				
+0.29	[2,7] LONGACRE	77	IPWA	$\pi N \to N\pi\pi$
• • • We do not use the following data for averages, fits, limits, etc. • • •				
+0.16±0.06	MANLEY	92	IPWA	$\pi N \to \pi N$ & $N\pi\pi$

$\Gamma(N\rho, S\text{=}3/2, D\text{-wave})/\Gamma_{\text{total}}$ Γ_{10}/Γ

VALUE (%)	DOCUMENT ID		TECN	COMMENT
13±3	VRANA	00	DPWA	Multichannel
• • • We do not use the following data for averages, fits, limits, etc. • • •				
< 1	SHRESTHA	12A	DPWA	Multichannel

$(\Gamma_i\Gamma_f)^{1/2}/\Gamma_{\text{total}}$ in $N\pi \to N(1650) \to N(\pi\pi)^{I=0}_{S\text{-wave}}$ $(\Gamma_1\Gamma_{11})^{1/2}/\Gamma$

VALUE	DOCUMENT ID		TECN	COMMENT
+0.04 to +0.18 OUR ESTIMATE				
0.00	[2,7] LONGACRE	77	IPWA	$\pi N \to N\pi\pi$
+0.25	[3] LONGACRE	75	IPWA	$\pi N \to N\pi\pi$
• • • We do not use the following data for averages, fits, limits, etc. • • •				
+0.12±0.08	MANLEY	92	IPWA	$\pi N \to \pi N$ & $N\pi\pi$

$\Gamma(N(\pi\pi)^{I=0}_{S\text{-wave}})/\Gamma_{\text{total}}$ Γ_{11}/Γ

VALUE (%)	DOCUMENT ID		TECN	COMMENT
1±1	VRANA	00	DPWA	Multichannel
• • • We do not use the following data for averages, fits, limits, etc. • • •				
<1	SHRESTHA	12A	DPWA	Multichannel

$(\Gamma_i\Gamma_f)^{1/2}/\Gamma_{\text{total}}$ in $N\pi \to N(1650) \to N(1440)\pi$ $(\Gamma_1\Gamma_{12})^{1/2}/\Gamma$

VALUE	DOCUMENT ID		TECN	COMMENT
• • • We do not use the following data for averages, fits, limits, etc. • • •				
+0.11±0.06	MANLEY	92	IPWA	$\pi N \to \pi N$ & $N\pi\pi$

$\Gamma(N(1440)\pi)/\Gamma_{\text{total}}$ Γ_{12}/Γ

VALUE (%)	DOCUMENT ID		TECN	COMMENT
3±1	VRANA	00	DPWA	Multichannel
• • • We do not use the following data for averages, fits, limits, etc. • • •				
<1	SHRESTHA	12A	DPWA	Multichannel

$N(1650)$ PHOTON DECAY AMPLITUDES

Papers on γN amplitudes predating 1981 may be found in our 2006 edition, Journal of Physics (generic for all A,B,E,G) **G33** 1 (2006).

$N(1650) \rightarrow p\gamma$, helicity-1/2 amplitude $A_{1/2}$

VALUE ($GeV^{-1/2}$)	DOCUMENT ID		TECN	COMMENT
+0.045±0.010 OUR ESTIMATE				
0.033±0.007	ANISOVICH	12A	DPWA	Multichannel
0.055±0.030	WORKMAN	12A	DPWA	$\gamma N \rightarrow N\pi$
0.022±0.007	DUGGER	07	DPWA	$\gamma N \rightarrow \pi N$
0.033±0.015	CRAWFORD	83	IPWA	$\gamma N \rightarrow \pi N$
0.050±0.010	AWAJI	81	DPWA	$\gamma N \rightarrow \pi N$
• • • We do not use the following data for averages, fits, limits, etc. • • •				
0.063±0.006	SHKLYAR	13	DPWA	Multichannel
0.030±0.003	SHRESTHA	12A	DPWA	Multichannel
0.060±0.020	ANISOVICH	10	DPWA	Multichannel
0.100±0.035	[8] ANISOVICH	09A	DPWA	$\gamma d \rightarrow \eta N(N)$
0.033	DRECHSEL	07	DPWA	$\gamma N \rightarrow \pi N$
0.049	PENNER	02D	DPWA	Multichannel
0.069±0.005	ARNDT	96	IPWA	$\gamma N \rightarrow \pi N$
0.068±0.003	LI	93	IPWA	$\gamma N \rightarrow \pi N$
0.091	WADA	84	DPWA	Compton scattering

$N(1650) \rightarrow n\gamma$, helicity-1/2 amplitude $A_{1/2}$

VALUE ($GeV^{-1/2}$)	DOCUMENT ID		TECN	COMMENT
−0.050±0.020 OUR ESTIMATE				
−0.040±0.010	CHEN	12A	DPWA	$\gamma N \rightarrow \pi N$
−0.055±0.020	[9] ANISOVICH	09A	DPWA	$\gamma d \rightarrow \eta N(N)$
−0.008±0.004	AWAJI	81	DPWA	$\gamma N \rightarrow \pi N$
0.004±0.004	FUJII	81	DPWA	$\gamma N \rightarrow \pi N$
• • • We do not use the following data for averages, fits, limits, etc. • • •				
0.011±0.002	SHRESTHA	12A	DPWA	Multichannel
0.009	DRECHSEL	07	DPWA	$\gamma N \rightarrow \pi N$
−0.011	PENNER	02D	DPWA	Multichannel
−0.015±0.005	ARNDT	96	IPWA	$\gamma N \rightarrow \pi N$
−0.002±0.002	LI	93	IPWA	$\gamma N \rightarrow \pi N$

$N(1650)$ $\gamma p \rightarrow \Lambda K^+$ AMPLITUDES

$(\Gamma_i\Gamma_f)^{1/2}/\Gamma_{total}$ in $p\gamma \rightarrow N(1650) \rightarrow \Lambda K^+$ (E_{0+} amplitude)

VALUE (units 10^{-3})	DOCUMENT ID		TECN
• • • We do not use the following data for averages, fits, limits, etc. • • •			
7.8 ±0.3	WORKMAN	90	DPWA
8.13	TANABE	89	DPWA

$p\gamma \rightarrow N(1650) \rightarrow \Lambda K^+$ phase angle θ (E_{0+} amplitude)

VALUE (degrees)	DOCUMENT ID		TECN
• • • We do not use the following data for averages, fits, limits, etc. • • •			
−107 ±3	WORKMAN	90	DPWA
−107.8	TANABE	89	DPWA

$N(1650)$ FOOTNOTES

[1] ARNDT 95 finds two distinct states.
[2] LONGACRE 77 pole positions are from a search for poles in the unitarized T-matrix; the first (second) value uses, in addition to $\pi N \rightarrow N\pi\pi$ data, elastic amplitudes from a Saclay (CERN) partial-wave analysis. The other LONGACRE 77 values are from eyeball fits with Breit-Wigner circles to the T-matrix amplitudes.
[3] From method II of LONGACRE 75: eyeball fits with Breit-Wigner circles to the T-matrix amplitudes.
[4] See HOEHLER 93 for a detailed discussion of the evidence for and the pole parameters of N and Δ resonances as determined from Argand diagrams of πN elastic partial-wave amplitudes and from plots of the speeds with which the amplitudes traverse the diagrams.
[5] ARNDT 98 also lists pole residues, which display more model dependence than do the associated pole positions.
[6] LONGACRE 78 values are from a search for poles in the unitarized T-matrix. The first (second) value uses, in addition to $\pi N \rightarrow N\pi\pi$ data, elastic amplitudes from a Saclay (CERN) partial-wave analysis.
[7] LONGACRE 77 considers this coupling to be well determined.
[8] This ANISOVICH 09A amplitude is evaluated at the pole position; the phase is $(25\pm20)^\circ$.
[9] This ANISOVICH 09A amplitude is evaluated at the pole position; the phase is $(30\pm25)^\circ$.

$N(1650)$ REFERENCES

For early references, see Physics Letters **111B** 1 (1982).

SHKLYAR	13	PR C87 015201	V. Shklyar, H. Lenske, U. Mosel	(GIES)
ANISOVICH	12A	EPJ A48 15	A.V. Anisovich *et al.*	(BONN, PNPI)
CHEN	12A	PR C86 015206	W. Chen *et al.*	(DUKE, GWU, MSST, ITEP+)
SHRESTHA	12A	PR C86 055203	M. Shrestha, D.M. Manley	(KSU)
WORKMAN	12A	PR C86 015202	R. Workman *et al.*	(GWU)
ANISOVICH	10	EPJ A44 203	A.V. Anisovich *et al.*	(BONN, PNPI)
BATINIC	10	PR C82 038203	M. Batinic *et al.*	(ZAGR)
ANISOVICH	09A	EPJ A41 13	A.V. Anisovich *et al.*	(BONN, PNPI, BASL)
THOMA	08	PL B659 87	U. Thoma *et al.*	(CB-ELSA Collab.)
DRECHSEL	07	EPJ A34 69	D. Drechsel, S.S. Kamalov, L. Tiator	(MAINZ, JINR)
DUGGER	07	PR C76 025211	M. Dugger *et al.*	(Jefferson Lab CLAS Collab.)
ARNDT	06	PR C74 045205	R.A. Arndt *et al.*	(GWU)
PDG	06	JP G33 1	W.-M. Yao *et al.*	(PDG Collab.)
SHKLYAR	05	PR C72 015210	V. Shklyar, H. Lenske, U. Mosel	(GIES)
ARNDT	04	PR C69 035213	R.A. Arndt *et al.*	(GWU, TRIU)
PENNER	02C	PR C66 055211	G. Penner, U. Mosel	(GIES)
PENNER	02D	PR C66 055212	G. Penner, U. Mosel	(GIES)
BAI	01B	PL B510 75	J.Z. Bai *et al.*	(BES Collab.)
VRANA	00	PRPL 328 181	T.P. Vrana, S.A. Dytman,, T.-S.H. Lee	(PITT+)
ARNDT	98	PR C58 3636	R.A. Arndt *et al.*	
GREEN	97	PR C55 R2167	A.M. Green, S. Wycech	(HELS, WINR)
ARNDT	96	PR C53 430	R.A. Arndt, I.I. Strakovsky, R.L. Workman	(VPI)
ARNDT	95	PR C52 2120	R.A. Arndt *et al.*	(VPI, BRCO)
HOEHLER	93	πN Newsletter 9 1	G. Hohler	(KARL)
LI	93	PR C47 2759	Z.J. Li *et al.*	(VPI)
MANLEY	92	PR D45 4002	D.M. Manley, E.M. Saleski	(KSA) IJP
Also		PR D30 904	D.M. Manley *et al.*	(VPI)
ARNDT	91	PR D43 2131	R.A. Arndt *et al.*	(VPI, TELE) IJP
WORKMAN	90	PR C42 781	R.L. Workman	(VPI)
TANABE	89	PR C39 741	H. Tanabe, M. Kohno, C. Bennhold	(MANZ)
Also		NC 102A 193	M. Kohno, H. Tanabe, C. Bennhold	(MANZ)
WADA	84	NP B247 313	Y. Wada *et al.*	(INUS)
BELL	83	NP B222 389	K.W. Bell *et al.*	(RL) IJP
CRAWFORD	83	NP B211 1	R.L. Crawford, W.T. Morton	(GLAS)
PDG	82	PL 111B 1	M. Roos *et al.*	(HELS, CIT, CERN)
AWAJI	81	Bonn Conf. 352	N. Awaji, R. Kajikawa	(NAGO)
Also		NP B197 365	K. Fujii *et al.*	(NAGO)
FUJII	81	NP B187 53	K. Fujii *et al.*	(NAGO, OSAK)
CUTKOSKY	80	Toronto Conf. 19	R.E. Cutkosky *et al.*	(CMU, LBL) IJP
Also		PR D20 2839	R.E. Cutkosky *et al.*	(CMU, LBL) IJP
LIVANOS	80	Toronto Conf. 35	P. Livanos *et al.*	(SACL) IJP
MUSETTE	80	NC 57A 37	M. Musette	(BRUX) IJP
SAXON	80	NP B162 522	D.H. Saxon *et al.*	(RHEL, BRIS) IJP
HOEHLER	79	PDAT 12-1	G. Hohler *et al.*	(KARLT) IJP
Also		Toronto Conf. 3	R. Koch	(KARLT) IJP
LONGACRE	78	PR D17 1795	R.S. Longacre *et al.*	(LBL, SLAC)
LONGACRE	77	NP B122 493	R.S. Longacre, J. Dolbeau	(SACL) IJP
Also		NP B108 365	J. Dolbeau *et al.*	(SACL) IJP
LONGACRE	75	PL 55B 415	R.S. Longacre *et al.*	(LBL, SLAC) IJP

$N(1675)$ $5/2^-$

$I(J^P) = \frac{1}{2}(\frac{5}{2}^-)$ Status: ****

Most of the results published before 1975 were last included in our 1982 edition, Physics Letters **111B** 1 (1982). Some further obsolete results published before 1984 were last included in our 2006 edition, Journal of Physics (generic for all A,B,E,G) **G33** 1 (2006).

$N(1675)$ BREIT-WIGNER MASS

VALUE (MeV)	DOCUMENT ID		TECN	COMMENT
1670 to 1680 (≈ 1675) OUR ESTIMATE				
1666 ± 2	SHKLYAR	13	DPWA	Multichannel
1664 ± 5	ANISOVICH	12A	DPWA	Multichannel
1674.1± 0.2	ARNDT	06	DPWA	$\pi N \rightarrow \pi N, \eta N$
1675 ±10	CUTKOSKY	80	IPWA	$\pi N \rightarrow \pi N$
1679 ± 8	HOEHLER	79	IPWA	$\pi N \rightarrow \pi N$
• • • We do not use the following data for averages, fits, limits, etc. • • •				
1679 ± 1	SHRESTHA	12A	DPWA	Multichannel
1678 ± 5	ANISOVICH	10	DPWA	Multichannel
1679 ± 9	BATINIC	10	DPWA	$\pi N \rightarrow N\pi, N\eta$
1678 ±15	THOMA	08	DPWA	Multichannel
1676.2± 0.6	ARNDT	04	DPWA	$\pi N \rightarrow \pi N, \eta N$
1685 ± 4	VRANA	00	DPWA	Multichannel
1673 ± 5	ARNDT	96	IPWA	$\gamma N \rightarrow \pi N$
1673	ARNDT	95	DPWA	$\pi N \rightarrow N\pi$
1666	LI	93	IPWA	$\gamma N \rightarrow \pi N$
1676 ± 2	MANLEY	92	IPWA	$\pi N \rightarrow \pi N$ & $N\pi\pi$
1670	SAXON	80	DPWA	$\pi^- p \rightarrow \Lambda K^0$
1650	[1] LONGACRE	77	IPWA	$\pi N \rightarrow N\pi\pi$
1660	[2] LONGACRE	75	IPWA	$\pi N \rightarrow N\pi\pi$

$N(1675)$ BREIT-WIGNER WIDTH

VALUE (MeV)	DOCUMENT ID		TECN	COMMENT
130 to 165 (≈ 150) OUR ESTIMATE				
148 ± 1	SHKLYAR	13	DPWA	Multichannel
152 ± 7	ANISOVICH	12A	DPWA	Multichannel
146.5± 1.0	ARNDT	06	DPWA	$\pi N \rightarrow \pi N, \eta N$
160 ±20	CUTKOSKY	80	IPWA	$\pi N \rightarrow \pi N$
120 ±15	HOEHLER	79	IPWA	$\pi N \rightarrow \pi N$
• • • We do not use the following data for averages, fits, limits, etc. • • •				
145 ± 4	SHRESTHA	12A	DPWA	Multichannel
177 ±15	ANISOVICH	10	DPWA	Multichannel
152 ± 8	BATINIC	10	DPWA	$\pi N \rightarrow N\pi, N\eta$
220 ±25	THOMA	08	DPWA	Multichannel
151.8± 3.0	ARNDT	04	DPWA	$\pi N \rightarrow \pi N, \eta N$
131 ±10	VRANA	00	DPWA	Multichannel
154 ± 7	ARNDT	96	IPWA	$\gamma N \rightarrow \pi N$
154	ARNDT	95	DPWA	$\pi N \rightarrow N\pi$
136	LI	93	IPWA	$\gamma N \rightarrow \pi N$
159 ± 7	MANLEY	92	IPWA	$\pi N \rightarrow \pi N$ & $N\pi\pi$
40	SAXON	80	DPWA	$\pi^- p \rightarrow \Lambda K^0$
130	[1] LONGACRE	77	IPWA	$\pi N \rightarrow N\pi\pi$
150	[2] LONGACRE	75	IPWA	$\pi N \rightarrow N\pi\pi$

$N(1675)$ POLE POSITION

REAL PART

VALUE (MeV)	DOCUMENT ID		TECN	COMMENT
1655 to 1665 (≈ 1660) OUR ESTIMATE				
1654 ± 4	ANISOVICH	12A	DPWA	Multichannel
1657	ARNDT	06	DPWA	$\pi N \to \pi N, \eta N$
1656	[3] HOEHLER	93	ARGD	$\pi N \to \pi N$
1660 ± 10	CUTKOSKY	80	IPWA	$\pi N \to \pi N$
• • • We do not use the following data for averages, fits, limits, etc. • • •				
1640	SHKLYAR	13	DPWA	Multichannel
1656	SHRESTHA	12A	DPWA	Multichannel
1650 ± 5	ANISOVICH	10	DPWA	Multichannel
1658 ± 9	BATINIC	10	DPWA	$\pi N \to N\pi, N\eta$
1639 ± 10	THOMA	08	DPWA	Multichannel
1659	ARNDT	04	DPWA	$\pi N \to \pi N, \eta N$
1674	VRANA	00	DPWA	Multichannel
1663	ARNDT	95	DPWA	$\pi N \to N\pi$
1655	ARNDT	91	DPWA	$\pi N \to \pi N$ Soln SM90
1663 or 1668	[4] LONGACRE	78	IPWA	$\pi N \to N\pi\pi$
1649 or 1650	[1] LONGACRE	77	IPWA	$\pi N \to N\pi\pi$

−2×IMAGINARY PART

VALUE (MeV)	DOCUMENT ID		TECN	COMMENT
125 to 150 (≈ 135) OUR ESTIMATE				
151 ± 5	ANISOVICH	12A	DPWA	Multichannel
139	ARNDT	06	DPWA	$\pi N \to \pi N, \eta N$
126	[3] HOEHLER	93	ARGD	$\pi N \to \pi N$
140 ± 10	CUTKOSKY	80	IPWA	$\pi N \to \pi N$
• • • We do not use the following data for averages, fits, limits, etc. • • •				
108	SHKLYAR	13	DPWA	Multichannel
128	SHRESTHA	12A	DPWA	Multichannel
143 ± 7	ANISOVICH	10	DPWA	Multichannel
137 ± 7	BATINIC	10	DPWA	$\pi N \to N\pi, N\eta$
180 ± 20	THOMA	08	DPWA	Multichannel
146	ARNDT	04	DPWA	$\pi N \to \pi N, \eta N$
120	VRANA	00	DPWA	Multichannel
152	ARNDT	95	DPWA	$\pi N \to N\pi$
124	ARNDT	91	DPWA	$\pi N \to \pi N$ Soln SM90
146 or 171	[4] LONGACRE	78	IPWA	$\pi N \to N\pi\pi$
127 or 127	[1] LONGACRE	77	IPWA	$\pi N \to N\pi\pi$

$N(1675)$ ELASTIC POLE RESIDUE

MODULUS $|r|$

VALUE (MeV)	DOCUMENT ID		TECN	COMMENT
27 ± 5 OUR ESTIMATE				
28 ± 1	ANISOVICH	12A	DPWA	Multichannel
27	ARNDT	06	DPWA	$\pi N \to \pi N, \eta N$
23	HOEHLER	93	ARGD	$\pi N \to \pi N$
31 ± 5	CUTKOSKY	80	IPWA	$\pi N \to \pi N$
• • • We do not use the following data for averages, fits, limits, etc. • • •				
20	SHKLYAR	13	DPWA	Multichannel
25	BATINIC	10	DPWA	$\pi N \to N\pi, N\eta$
29	ARNDT	04	DPWA	$\pi N \to \pi N, \eta N$
29	ARNDT	95	DPWA	$\pi N \to N\pi$
28	ARNDT	91	DPWA	$\pi N \to \pi N$ Soln SM90

PHASE θ

VALUE (°)	DOCUMENT ID		TECN	COMMENT
−25 ± 6 OUR ESTIMATE				
−26 ± 4	ANISOVICH	12A	DPWA	Multichannel
−21	ARNDT	06	DPWA	$\pi N \to \pi N, \eta N$
−22	HOEHLER	93	ARGD	$\pi N \to \pi N$
−30 ± 10	CUTKOSKY	80	IPWA	$\pi N \to \pi N$
• • • We do not use the following data for averages, fits, limits, etc. • • •				
−49	SHKLYAR	13	DPWA	Multichannel
−16	BATINIC	10	DPWA	$\pi N \to N\pi, N\eta$
−22	ARNDT	04	DPWA	$\pi N \to \pi N, \eta N$
− 6	ARNDT	95	DPWA	$\pi N \to N\pi$
−17	ARNDT	91	DPWA	$\pi N \to \pi N$ Soln SM90

$N(1675)$ INELASTIC POLE RESIDUE

The "normalized residue" is the residue divided by $\Gamma_{pole}/2$.

Normalized residue in $N\pi \to N(1675) \to \Delta\pi$, D-wave

MODULUS (%)	PHASE (°)	DOCUMENT ID		TECN	COMMENT
33 ± 5	**82 ± 10**	ANISOVICH	12A	DPWA	Multichannel

Normalized residue in $N\pi \to N(1675) \to N\sigma$

MODULUS (%)	PHASE (°)	DOCUMENT ID		TECN	COMMENT
15 ± 4	**132 ± 18**	ANISOVICH	12A	DPWA	Multichannel

$N(1675)$ PHOTON DECAY AMPLITUDES

Papers on γN amplitudes predating 1981 may be found in our 2006 edition, Journal of Physics (generic for all A,B,E,G) **G33** 1 (2006).

$N(1675) \to p\gamma$, helicity-1/2 amplitude $A_{1/2}$

VALUE ($GeV^{-1/2}$)	DOCUMENT ID		TECN	COMMENT
+0.019 ± 0.008 OUR ESTIMATE				
0.024 ± 0.003	ANISOVICH	12A	DPWA	Multichannel
0.013 ± 0.001	WORKMAN	12A	DPWA	$\gamma N \to N\pi$
0.018 ± 0.002	DUGGER	07	DPWA	$\gamma N \to \pi N$
0.021 ± 0.011	CRAWFORD	83	IPWA	$\gamma N \to \pi N$
0.034 ± 0.005	AWAJI	81	DPWA	$\gamma N \to \pi N$
• • • We do not use the following data for averages, fits, limits, etc. • • •				
0.009 ± 0.001	SHKLYAR	13	DPWA	Multichannel
0.011 ± 0.001	SHRESTHA	12A	DPWA	Multichannel
0.021 ± 0.004	ANISOVICH	10	DPWA	Multichannel
0.015	DRECHSEL	07	DPWA	$\gamma N \to \pi N$
0.015 ± 0.010	ARNDT	96	IPWA	$\gamma N \to \pi N$
0.012 ± 0.002	LI	93	IPWA	$\gamma N \to \pi N$

$N(1675) \to p\gamma$, helicity-3/2 amplitude $A_{3/2}$

VALUE ($GeV^{-1/2}$)	DOCUMENT ID		TECN	COMMENT
+0.020 ± 0.005 OUR ESTIMATE				
0.025 ± 0.007	ANISOVICH	12A	DPWA	Multichannel
0.016 ± 0.001	WORKMAN	12A	DPWA	$\gamma N \to N\pi$
0.021 ± 0.001	DUGGER	07	DPWA	$\gamma N \to \pi N$
0.015 ± 0.009	CRAWFORD	83	IPWA	$\gamma N \to \pi N$
0.024 ± 0.008	AWAJI	81	DPWA	$\gamma N \to \pi N$
• • • We do not use the following data for averages, fits, limits, etc. • • •				
0.021 ± 0.001	SHKLYAR	13	DPWA	Multichannel
0.020 ± 0.001	SHRESTHA	12A	DPWA	Multichannel
0.024 ± 0.008	ANISOVICH	10	DPWA	Multichannel
0.022	DRECHSEL	07	DPWA	$\gamma N \to \pi N$
0.010 ± 0.007	ARNDT	96	IPWA	$\gamma N \to \pi N$
0.021 ± 0.002	LI	93	IPWA	$\gamma N \to \pi N$

$N(1675) \to n\gamma$, helicity-1/2 amplitude $A_{1/2}$

VALUE ($GeV^{-1/2}$)	DOCUMENT ID		TECN	COMMENT
−0.060 ± 0.005 OUR ESTIMATE				
−0.058 ± 0.002	CHEN	12A	DPWA	$\gamma N \to \pi N$
−0.057 ± 0.024	AWAJI	81	DPWA	$\gamma N \to \pi N$
−0.033 ± 0.004	FUJII	81	DPWA	$\gamma N \to \pi N$
• • • We do not use the following data for averages, fits, limits, etc. • • •				
−0.040 ± 0.004	SHRESTHA	12A	DPWA	Multichannel
−0.062	DRECHSEL	07	DPWA	$\gamma N \to \pi N$
−0.049 ± 0.010	ARNDT	96	IPWA	$\gamma N \to \pi N$
−0.060 ± 0.003	LI	93	IPWA	$\gamma N \to \pi N$

$N(1675) \to n\gamma$, helicity-3/2 amplitude $A_{3/2}$

VALUE ($GeV^{-1/2}$)	DOCUMENT ID		TECN	COMMENT
−0.085 ± 0.010 OUR ESTIMATE				
−0.080 ± 0.005	CHEN	12A	DPWA	$\gamma N \to \pi N$
−0.077 ± 0.018	AWAJI	81	DPWA	$\gamma N \to \pi N$
−0.069 ± 0.004	FUJII	81	DPWA	$\gamma N \to \pi N$
• • • We do not use the following data for averages, fits, limits, etc. • • •				
−0.068 ± 0.004	SHRESTHA	12A	DPWA	Multichannel
−0.084	DRECHSEL	07	DPWA	$\gamma N \to \pi N$
−0.051 ± 0.010	ARNDT	96	IPWA	$\gamma N \to \pi N$
−0.074 ± 0.003	LI	93	IPWA	$\gamma N \to \pi N$

$N(1675)$ DECAY MODES

The following branching fractions are our estimates, not fits or averages.

	Mode	Fraction (Γ_i/Γ)
Γ_1	$N\pi$	35–45 %
Γ_2	$N\eta$	(0 ± 7) × 10^{-3}
Γ_3	ΛK	<1 %
Γ_4	ΣK	
Γ_5	$N\pi\pi$	50–60 %
Γ_6	$\Delta\pi$	50–60 %
Γ_7	$\Delta(1232)\pi$, D-wave	(50 ±15) %
Γ_8	$\Delta(1232)\pi$, G-wave	
Γ_9	$N\rho$	< 1–3 %
Γ_{10}	$N\rho$, S=1/2, D-wave	(0.0 ± 1.0) %
Γ_{11}	$N\rho$, S=3/2, D-wave	(1.0 ± 1.0) %
Γ_{12}	$N\rho$, S=3/2, G-wave	
Γ_{13}	$N(\pi\pi)^{I=0}_{S\text{-wave}}$	(7.0 ± 3.0) %
Γ_{14}	$p\gamma$	0–0.02 %
Γ_{15}	$p\gamma$, helicity=1/2	0–0.01 %
Γ_{16}	$p\gamma$, helicity=3/2	0–0.01 %
Γ_{17}	$n\gamma$	0–0.15 %
Γ_{18}	$n\gamma$, helicity=1/2	0–0.05 %
Γ_{19}	$n\gamma$, helicity=3/2	0–0.10 %

$N(1675)$ BRANCHING RATIOS

$\Gamma(N\pi)/\Gamma_{total}$ Γ_1/Γ

VALUE (%)	DOCUMENT ID		TECN	COMMENT
35 to 45 OUR ESTIMATE				
41 ±1	SHKLYAR	13	DPWA	Multichannel
40 ±3	ANISOVICH	12A	DPWA	Multichannel
39.3±0.1	ARNDT	06	DPWA	$\pi N \to \pi N$, ηN
38 ±5	CUTKOSKY	80	IPWA	$\pi N \to \pi N$
38 ±3	HOEHLER	79	IPWA	$\pi N \to \pi N$
• • • We do not use the following data for averages, fits, limits, etc. • • •				
38.6±0.6	SHRESTHA	12A	DPWA	Multichannel
37 ±5	ANISOVICH	10	DPWA	Multichannel
35 ±4	BATINIC	10	DPWA	$\pi N \to N\pi$, $N\eta$
30 ±8	THOMA	08	DPWA	Multichannel
40.0±0.2	ARNDT	04	DPWA	$\pi N \to \pi N$, ηN
35 ±1	VRANA	00	DPWA	Multichannel
38	ARNDT	95	DPWA	$\pi N \to N\pi$
47 ±2	MANLEY	92	IPWA	$\pi N \to \pi N$ & $N\pi\pi$

$\Gamma(N\eta)/\Gamma_{total}$ Γ_2/Γ

VALUE (%)	DOCUMENT ID		TECN	COMMENT
0.0±0.7 OUR AVERAGE				
0 ±1	SHKLYAR	13	DPWA	Multichannel
0 ±1	VRANA	00	DPWA	Multichannel
• • • We do not use the following data for averages, fits, limits, etc. • • •				
<1	SHRESTHA	12A	DPWA	Multichannel
0.1±0.1	BATINIC	10	DPWA	$\pi N \to N\pi$, $N\eta$
3 ±3	THOMA	08	DPWA	Multichannel

$(\Gamma_i\Gamma_f)^{1/2}/\Gamma_{total}$ in $N\pi \to N(1675) \to \Lambda K$ $(\Gamma_1\Gamma_3)^{1/2}/\Gamma$

VALUE	DOCUMENT ID		TECN	COMMENT
±0.04 to ±0.08 OUR ESTIMATE				
−0.01	BELL	83	DPWA	$\pi^- p \to \Lambda K^0$
+0.036	[5] SAXON	80	DPWA	$\pi^- p \to \Lambda K^0$
• • • We do not use the following data for averages, fits, limits, etc. • • •				
−0.03 ±0.01	SHRESTHA	12A	DPWA	Multichannel

Note: Signs of couplings from $\pi N \to N\pi\pi$ analyses were changed in the 1986 edition to agree with the baryon-first convention; the overall phase ambiguity is resolved by choosing a negative sign for the $\Delta(1620)$ S_{31} coupling to $\Delta(1232)\pi$.

$(\Gamma_i\Gamma_f)^{1/2}/\Gamma_{total}$ in $N\pi \to N(1675) \to \Delta(1232)\pi$, D-wave $(\Gamma_1\Gamma_7)^{1/2}/\Gamma$

VALUE	DOCUMENT ID		TECN	COMMENT
+0.46 to +0.50 OUR ESTIMATE				
+0.46	[1,6] LONGACRE	77	IPWA	$\pi N \to N\pi\pi$
+0.50	[2] LONGACRE	75	IPWA	$\pi N \to N\pi\pi$
• • • We do not use the following data for averages, fits, limits, etc. • • •				
+0.496±0.003	MANLEY	92	IPWA	$\pi N \to \pi N$ & $N\pi\pi$

$\Gamma(\Delta(1232)\pi, D\text{-wave})/\Gamma_{total}$ Γ_7/Γ

VALUE (%)	DOCUMENT ID		TECN	COMMENT
50±15 OUR ESTIMATE				
33± 8	ANISOVICH	12A	DPWA	Multichannel
63± 2	VRANA	00	DPWA	Multichannel
• • • We do not use the following data for averages, fits, limits, etc. • • •				
46± 1	SHRESTHA	12A	DPWA	Multichannel
24± 8	THOMA	08	DPWA	Multichannel

$(\Gamma_i\Gamma_f)^{1/2}/\Gamma_{total}$ in $N\pi \to N(1675) \to N\rho$, S=1/2, D-wave $(\Gamma_1\Gamma_{10})^{1/2}/\Gamma$

VALUE	DOCUMENT ID		TECN	COMMENT
• • • We do not use the following data for averages, fits, limits, etc. • • •				
+0.04±0.02	MANLEY	92	IPWA	$\pi N \to \pi N$ & $N\pi\pi$

$\Gamma(N\rho, S$=1/2, D-wave$)/\Gamma_{total}$ Γ_{10}/Γ

VALUE (%)	DOCUMENT ID		TECN	COMMENT
0±1	VRANA	00	DPWA	Multichannel
• • • We do not use the following data for averages, fits, limits, etc. • • •				
<1	SHRESTHA	12A	DPWA	Multichannel

$(\Gamma_i\Gamma_f)^{1/2}/\Gamma_{total}$ in $N\pi \to N(1675) \to N\rho$, S=3/2, D-wave $(\Gamma_1\Gamma_{11})^{1/2}/\Gamma$

VALUE	DOCUMENT ID		TECN	COMMENT
−0.12 to −0.06 OUR ESTIMATE				
−0.15	[1,6] LONGACRE	77	IPWA	$\pi N \to N\pi\pi$
• • • We do not use the following data for averages, fits, limits, etc. • • •				
−0.03±0.02	MANLEY	92	IPWA	$\pi N \to \pi N$ & $N\pi\pi$

$\Gamma(N\rho, S$=3/2, D-wave$)/\Gamma_{total}$ Γ_{11}/Γ

VALUE (%)	DOCUMENT ID		TECN	COMMENT
1±1	VRANA	00	DPWA	Multichannel
• • • We do not use the following data for averages, fits, limits, etc. • • •				
<1	SHRESTHA	12A	DPWA	Multichannel

$(\Gamma_i\Gamma_f)^{1/2}/\Gamma_{total}$ in $N\pi \to N(1675) \to N(\pi\pi)^{I=0}_{S\text{-wave}}$ $(\Gamma_1\Gamma_{13})^{1/2}/\Gamma$

VALUE	DOCUMENT ID		TECN	COMMENT
+0.03	[1,6] LONGACRE	77	IPWA	$\pi N \to N\pi\pi$

$\Gamma(N(\pi\pi)^{I=0}_{S\text{-wave}})/\Gamma_{total}$ Γ_{13}/Γ

VALUE (%)	DOCUMENT ID		TECN	COMMENT
7±3	ANISOVICH	12A	DPWA	Multichannel

$N(1675)$ FOOTNOTES

[1] LONGACRE 77 pole positions are from a search for poles in the unitarized T-matrix; the first (second) value uses, in addition to $\pi N \to N\pi\pi$ data, elastic amplitudes from a Saclay (CERN) partial-wave analysis. The other LONGACRE 77 values are from eyeball fits with Breit-Wigner circles to the T-matrix amplitudes.

[2] From method II of LONGACRE 75: eyeball fits with Breit-Wigner circles to the T-matrix amplitudes.

[3] See HOEHLER 93 for a detailed discussion of the evidence for and the pole parameters of N and Δ resonances as determined from Argand diagrams of πN elastic partial-wave amplitudes and from plots of the speeds with which the amplitudes traverse the diagrams.

[4] LONGACRE 78 values are from a search for poles in the unitarized T-matrix. The first (second) value uses, in addition to $\pi N \to N\pi\pi$ data, elastic amplitudes from a Saclay (CERN) partial-wave analysis.

[5] SAXON 80 finds the coupling phase is near 90°.

[6] LONGACRE 77 considers this coupling to be well determined.

$N(1675)$ REFERENCES

For early references, see Physics Letters **111B** 1 (1982).

SHKLYAR	13	PR C87 015201	V. Shklyar, H. Lenske, U. Mosel	(GIES)
ANISOVICH	12A	EPJ A48 15	A.V. Anisovich *et al.*	(BONN, PNPI)
CHEN	12A	PR C86 015206	W. Chen *et al.*	(DUKE, GWU, MSST, ITEP+)
SHRESTHA	12A	PR C86 055203	M. Shrestha, D.M. Manley	(KSU)
WORKMAN	12A	PR C86 015202	R. Workman *et al.*	(GWU)
ANISOVICH	10	EPJ A44 203	A.V. Anisovich *et al.*	(BONN, PNPI)
BATINIC	10	PR C82 038203	M. Batinic *et al.*	(ZAGR)
THOMA	08	PL B659 87	U. Thoma *et al.*	(CB-ELSA Collab.)
DRECHSEL	07	EPJ A34 69	D. Drechsel, S.S. Kamalov, L. Tiator	(MAINZ, JINR)
DUGGER	07	PR C76 025211	M. Dugger *et al.*	(Jefferson Lab CLAS Collab.)
ARNDT	06	PR C74 045205	R.A. Arndt *et al.*	(GWU)
PDG	06	JP G33 1	W.-M. Yao *et al.*	(PDG Collab.)
ARNDT	04	PR C69 035213	R.A. Arndt *et al.*	(GWU, TRIU)
VRANA	00	PRPL 328 181	T.P. Vrana, S.A. Dytman,, T.-S.H. Lee	(PITT+)
ARNDT	96	PR C53 430	R.A. Arndt, I.I. Strakovsky, R.L. Workman	(VPI)
ARNDT	95	PR C52 2120	R.A. Arndt *et al.*	(VPI, BRCO)
HOEHLER	93	πN Newsletter 9 1	G. Hohler	(KARL)
LI	93	PR C47 2759	Z.J. Li *et al.*	(VPI)
MANLEY	92	PR D45 4002	D.M. Manley, E.M. Saleski	(KSA) IJP
Also		PR D30 904	D.M. Manley *et al.*	(VPI)
ARNDT	91	PR D43 2131	R.A. Arndt *et al.*	(VPI, TELE) IJP
BELL	83	NP B222 389	K.W. Bell *et al.*	(RL) IJP
CRAWFORD	83	NP B211 1	R.L. Crawford, W.T. Morton	(GLAS)
PDG	82	PL 111B 1	M. Roos *et al.*	(HELS, CIT, CERN)
AWAJI	81	Bonn Conf. 352	N. Awaji, R. Kajikawa	(NAGO)
Also		NP B197 365	K. Fujii *et al.*	(NAGO)
FUJII	81	NP B187 53	K. Fujii *et al.*	(NAGO, OSAK)
CUTKOSKY	80	Toronto Conf. 19	R.E. Cutkosky *et al.*	(CMU, LBL) IJP
Also		PR D20 2839	R.E. Cutkosky *et al.*	(CMU, LBL) IJP
SAXON	80	NP B162 522	D.H. Saxon *et al.*	(RHEL, BRIS) IJP
HOEHLER	79	PDAT 12-1	G. Hohler *et al.*	(KARLT) IJP
Also		Toronto Conf. 3	R. Koch	(KARLT) IJP
LONGACRE	78	PR D17 1795	R.S. Longacre *et al.*	(LBL, SLAC)
LONGACRE	77	NP B122 493	R.S. Longacre, J. Dolbeau	(SACL) IJP
Also		NP B108 365	J. Dolbeau *et al.*	(SACL) IJP
LONGACRE	75	PL 55B 415	R.S. Longacre *et al.*	(LBL, SLAC) IJP

$N(1680)$ $5/2^+$

$I(J^P) = \frac{1}{2}(\frac{5}{2}^+)$ Status: ****

Most of the results published before 1975 were last included in our 1982 edition, Physics Letters **111B** 1 (1982). Some further obsolete results published before 1984 were last included in our 2006 edition, Journal of Physics (generic for all A,B,E,G) **G33** 1 (2006).

$N(1680)$ BREIT-WIGNER MASS

VALUE (MeV)	DOCUMENT ID		TECN	COMMENT
1680 to 1690 (≈ 1685) OUR ESTIMATE				
1676 ± 2	SHKLYAR	13	DPWA	Multichannel
1689 ± 6	ANISOVICH	12A	DPWA	Multichannel
1680.1± 0.2	ARNDT	06	DPWA	$\pi N \to \pi N$, ηN
1680 ±10	CUTKOSKY	80	IPWA	$\pi N \to \pi N$
1684 ± 3	HOEHLER	79	IPWA	$\pi N \to \pi N$
• • • We do not use the following data for averages, fits, limits, etc. • • •				
1682.7± 0.5	SHRESTHA	12A	DPWA	Multichannel
1685 ± 5	ANISOVICH	10	DPWA	Multichannel
1680 ± 7	BATINIC	10	DPWA	$\pi N \to N\pi$, $N\eta$
1684 ± 8	THOMA	08	DPWA	Multichannel
1683.2± 0.7	ARNDT	04	DPWA	$\pi N \to \pi N$, ηN
1679 ± 3	VRANA	00	DPWA	Multichannel
1679 ± 5	ARNDT	96	IPWA	$\gamma N \to \pi N$
1678	ARNDT	95	DPWA	$\pi N \to N\pi$
1684 ± 4	MANLEY	92	IPWA	$\pi N \to \pi N$ & $N\pi\pi$
1660	[1] LONGACRE	77	IPWA	$\pi N \to N\pi\pi$
1670	[2] LONGACRE	75	IPWA	$\pi N \to N\pi\pi$

$N(1680)$ BREIT-WIGNER WIDTH

VALUE (MeV)	DOCUMENT ID		TECN	COMMENT
120 to 140 (≈ 130) OUR ESTIMATE				
115 ± 1	SHKLYAR	13	DPWA	Multichannel
118 ± 6	ANISOVICH	12A	DPWA	Multichannel
128.0± 1.1	ARNDT	06	DPWA	$\pi N \to \pi N, \eta N$
120 ±10	CUTKOSKY	80	IPWA	$\pi N \to \pi N$
128 ± 8	HOEHLER	79	IPWA	$\pi N \to \pi N$
• • • We do not use the following data for averages, fits, limits, etc. • • •				
126 ± 1	SHRESTHA	12A	DPWA	Multichannel
117 ±12	ANISOVICH	10	DPWA	Multichannel
142 ± 7	BATINIC	10	DPWA	$\pi N \to N\pi, N\eta$
105 ± 8	THOMA	08	DPWA	Multichannel
134.4± 3.8	ARNDT	04	DPWA	$\pi N \to \pi N, \eta N$
128 ± 9	VRANA	00	DPWA	Multichannel
124 ± 4	ARNDT	96	IPWA	$\gamma N \to \pi N$
126	ARNDT	95	DPWA	$\pi N \to N\pi$
139 ± 8	MANLEY	92	IPWA	$\pi N \to \pi N$ & $N\pi\pi$
150	[1] LONGACRE	77	IPWA	$\pi N \to N\pi\pi$
130	[2] LONGACRE	75	IPWA	$\pi N \to N\pi\pi$

$N(1680)$ POLE POSITION

REAL PART

VALUE (MeV)	DOCUMENT ID		TECN	COMMENT
1665 to 1680 (≈ 1675) OUR ESTIMATE				
1676±6	ANISOVICH	12A	DPWA	Multichannel
1674	ARNDT	06	DPWA	$\pi N \to \pi N, \eta N$
1673	[3] HOEHLER	93	ARGD	$\pi N \to \pi N$
1667±5	CUTKOSKY	80	IPWA	$\pi N \to \pi N$
• • • We do not use the following data for averages, fits, limits, etc. • • •				
1660	SHKLYAR	13	DPWA	Multichannel
1669	SHRESTHA	12A	DPWA	Multichannel
1672±4	ANISOVICH	10	DPWA	Multichannel
1666±8	BATINIC	10	DPWA	$\pi N \to N\pi, N\eta$
1674±5	THOMA	08	DPWA	Multichannel
1678	ARNDT	04	DPWA	$\pi N \to \pi N, \eta N$
1667	VRANA	00	DPWA	Multichannel
1670	ARNDT	95	DPWA	$\pi N \to N\pi$
1670	ARNDT	91	DPWA	$\pi N \to \pi N$ Soln SM90
1668 or 1674	[4] LONGACRE	78	IPWA	$\pi N \to N\pi\pi$
1656 or 1653	[1] LONGACRE	77	IPWA	$\pi N \to N\pi\pi$

−2×IMAGINARY PART

VALUE (MeV)	DOCUMENT ID		TECN	COMMENT
110 to 135 (≈ 120) OUR ESTIMATE				
113± 4	ANISOVICH	12A	DPWA	Multichannel
115	ARNDT	06	DPWA	$\pi N \to \pi N, \eta N$
135	[3] HOEHLER	93	ARGD	$\pi N \to \pi N$
110±10	CUTKOSKY	80	IPWA	$\pi N \to \pi N$
• • • We do not use the following data for averages, fits, limits, etc. • • •				
98	SHKLYAR	13	DPWA	Multichannel
119	SHRESTHA	12A	DPWA	Multichannel
114±12	ANISOVICH	10	DPWA	Multichannel
135± 6	BATINIC	10	DPWA	$\pi N \to N\pi, N\eta$
95±10	THOMA	08	DPWA	Multichannel
120	ARNDT	04	DPWA	$\pi N \to \pi N, \eta N$
122	VRANA	00	DPWA	Multichannel
120	ARNDT	95	DPWA	$\pi N \to N\pi$
116	ARNDT	91	DPWA	$\pi N \to \pi N$ Soln SM90
132 or 137	[4] LONGACRE	78	IPWA	$\pi N \to N\pi\pi$
145 or 143	[1] LONGACRE	77	IPWA	$\pi N \to N\pi\pi$

$N(1680)$ ELASTIC POLE RESIDUE

MODULUS $|r|$

VALUE (MeV)	DOCUMENT ID		TECN	COMMENT
40±5 OUR ESTIMATE				
43±4	ANISOVICH	12A	DPWA	Multichannel
42	ARNDT	06	DPWA	$\pi N \to \pi N, \eta N$
44	HOEHLER	93	ARGD	$\pi N \to \pi N$
34±2	CUTKOSKY	80	IPWA	$\pi N \to \pi N$
• • • We do not use the following data for averages, fits, limits, etc. • • •				
33	SHKLYAR	13	DPWA	Multichannel
44	BATINIC	10	DPWA	$\pi N \to N\pi, N\eta$
43	ARNDT	04	DPWA	$\pi N \to \pi N, \eta N$
40	ARNDT	95	DPWA	$\pi N \to N\pi$
37	ARNDT	91	DPWA	$\pi N \to \pi N$ Soln SM90

PHASE θ

VALUE (°)	DOCUMENT ID		TECN	COMMENT
−10±10 OUR ESTIMATE				
− 2±10	ANISOVICH	12A	DPWA	Multichannel
− 4	ARNDT	06	DPWA	$\pi N \to \pi N, \eta N$
−17	HOEHLER	93	ARGD	$\pi N \to \pi N$
−25± 5	CUTKOSKY	80	IPWA	$\pi N \to \pi N$
• • • We do not use the following data for averages, fits, limits, etc. • • •				
−32	SHKLYAR	13	DPWA	Multichannel
−19	BATINIC	10	DPWA	$\pi N \to N\pi, N\eta$
1	ARNDT	04	DPWA	$\pi N \to \pi N, \eta N$
+ 1	ARNDT	95	DPWA	$\pi N \to N\pi$
−14	ARNDT	91	DPWA	$\pi N \to \pi N$ Soln SM90

$N(1680)$ INELASTIC POLE RESIDUE

The "normalized residue" is the residue divided by $\Gamma_{pole}/2$.

Normalized residue in $N\pi \to N(1680) \to \Delta\pi$, P-wave

MODULUS (%)	PHASE (°)	DOCUMENT ID		TECN	COMMENT
15±3	**−70 ± 45**	ANISOVICH	12A	DPWA	Multichannel

Normalized residue in $N\pi \to N(1680) \to \Delta\pi$, F-wave

MODULUS (%)	PHASE (°)	DOCUMENT ID		TECN	COMMENT
23±4	**85 ± 15**	ANISOVICH	12A	DPWA	Multichannel

Normalized residue in $N\pi \to N(1680) \to N\,(\pi\pi)^{I=0}_{S-wave}$

MODULUS (%)	PHASE (°)	DOCUMENT ID		TECN	COMMENT
26±4	**−56 ± 15**	ANISOVICH	12A	DPWA	Multichannel

$N(1680)$ PHOTON DECAY AMPLITUDES

Papers on γN amplitudes predating 1981 may be found in our 2006 edition, Journal of Physics (generic for all A,B,E,G) **G33** 1 (2006).

$N(1680) \to p\gamma$, helicity-1/2 amplitude $A_{1/2}$

VALUE (GeV$^{-1/2}$)	DOCUMENT ID		TECN	COMMENT
−0.015±0.006 OUR ESTIMATE				
−0.013±0.003	ANISOVICH	12A	DPWA	Multichannel
−0.007±0.002	WORKMAN	12A	DPWA	$\gamma N \to N\pi$
−0.017±0.001	DUGGER	07	DPWA	$\gamma N \to \pi N$
−0.017±0.018	CRAWFORD	83	IPWA	$\gamma N \to \pi N$
−0.009±0.006	AWAJI	81	DPWA	$\gamma N \to \pi N$
• • • We do not use the following data for averages, fits, limits, etc. • • •				
0.003±0.001	SHKLYAR	13	DPWA	Multichannel
−0.017±0.001	SHRESTHA	12A	DPWA	Multichannel
−0.012±0.006	ANISOVICH	10	DPWA	Multichannel
−0.025	DRECHSEL	07	DPWA	$\gamma N \to \pi N$
−0.010±0.004	ARNDT	96	IPWA	$\gamma N \to \pi N$
−0.006±0.002	LI	93	IPWA	$\gamma N \to \pi N$

$N(1680) \to p\gamma$, helicity-3/2 amplitude $A_{3/2}$

VALUE (GeV$^{-1/2}$)	DOCUMENT ID		TECN	COMMENT
+0.133±0.012 OUR ESTIMATE				
0.135±0.006	ANISOVICH	12A	DPWA	Multichannel
0.140±0.002	WORKMAN	12A	DPWA	$\gamma N \to N\pi$
0.134±0.002	DUGGER	07	DPWA	$\gamma N \to \pi N$
0.132±0.010	CRAWFORD	83	IPWA	$\gamma N \to \pi N$
0.115±0.008	AWAJI	81	DPWA	$\gamma N \to \pi N$
• • • We do not use the following data for averages, fits, limits, etc. • • •				
0.116±0.001	SHKLYAR	13	DPWA	Multichannel
0.136±0.001	SHRESTHA	12A	DPWA	Multichannel
0.136±0.012	ANISOVICH	10	DPWA	Multichannel
0.134	DRECHSEL	07	DPWA	$\gamma N \to \pi N$
0.145±0.005	ARNDT	96	IPWA	$\gamma N \to \pi N$
0.154±0.002	LI	93	IPWA	$\gamma N \to \pi N$

$N(1680) \to n\gamma$, helicity-1/2 amplitude $A_{1/2}$

VALUE (GeV$^{-1/2}$)	DOCUMENT ID		TECN	COMMENT
+0.029±0.010 OUR ESTIMATE				
0.026±0.004	CHEN	12A	DPWA	$\gamma N \to \pi N$
0.017±0.014	AWAJI	81	DPWA	$\gamma N \to \pi N$
0.032±0.003	FUJII	81	DPWA	$\gamma N \to \pi N$
• • • We do not use the following data for averages, fits, limits, etc. • • •				
0.029±0.002	SHRESTHA	12A	DPWA	Multichannel
0.028	DRECHSEL	07	DPWA	$\gamma N \to \pi N$
0.030±0.005	ARNDT	96	IPWA	$\gamma N \to \pi N$
0.022±0.002	LI	93	IPWA	$\gamma N \to \pi N$

$N(1680) \rightarrow n\gamma$, helicity-3/2 amplitude $A_{3/2}$

VALUE ($GeV^{-1/2}$)	DOCUMENT ID		TECN	COMMENT
-0.033 ± 0.009 OUR ESTIMATE				
-0.029 ± 0.002	CHEN	12A	DPWA	$\gamma N \rightarrow \pi N$
-0.033 ± 0.013	AWAJI	81	DPWA	$\gamma N \rightarrow \pi N$
-0.023 ± 0.005	FUJII	81	DPWA	$\gamma N \rightarrow \pi N$
• • • We do not use the following data for averages, fits, limits, etc. • • •				
-0.059 ± 0.002	SHRESTHA	12A	DPWA	Multichannel
-0.038	DRECHSEL	07	DPWA	$\gamma N \rightarrow \pi N$
-0.040 ± 0.015	ARNDT	96	IPWA	$\gamma N \rightarrow \pi N$
-0.048 ± 0.002	LI	93	IPWA	$\gamma N \rightarrow \pi N$

$N(1680)$ DECAY MODES

The following branching fractions are our estimates, not fits or averages.

	Mode	Fraction (Γ_i/Γ)
Γ_1	$N\pi$	65–70 %
Γ_2	$N\eta$	$(\ 0\pm7)\times10^{-3}$
Γ_3	ΛK	
Γ_4	ΣK	
Γ_5	$N\pi\pi$	30–40 %
Γ_6	$\Delta\pi$	5–15 %
Γ_7	$\Delta(1232)\pi$, P-wave	(10±5) %
Γ_8	$\Delta(1232)\pi$, F-wave	0–12 %
Γ_9	$N\rho$	3–15 %
Γ_{10}	$N\rho$, $S=1/2$, F-wave	
Γ_{11}	$N\rho$, $S=3/2$, P-wave	<12;%
Γ_{12}	$N\rho$, $S=3/2$, F-wave	1–5 %
Γ_{13}	$N(\pi\pi)^{I=0}_{S\text{-wave}}$	(11±5) %
Γ_{14}	$p\gamma$	0.21–0.32 %
Γ_{15}	$p\gamma$, helicity=1/2	0.001–0.011 %
Γ_{16}	$p\gamma$, helicity=3/2	0.20–0.32 %
Γ_{17}	$n\gamma$	0.021–0.046 %
Γ_{18}	$n\gamma$, helicity=1/2	0.004–0.029 %
Γ_{19}	$n\gamma$, helicity=3/2	0.01–0.024 %

$N(1680)$ BRANCHING RATIOS

$\Gamma(N\pi)/\Gamma_{total}$ Γ_1/Γ

VALUE (%)	DOCUMENT ID		TECN	COMMENT
65 to 70 OUR ESTIMATE				
68 ± 1	SHKLYAR	13	DPWA	Multichannel
64 ± 5	ANISOVICH	12A	DPWA	Multichannel
70.1± 0.1	ARNDT	06	DPWA	$\pi N \rightarrow \pi N$, ηN
62 ± 5	CUTKOSKY	80	IPWA	$\pi N \rightarrow \pi N$
65 ± 2	HOEHLER	79	IPWA	$\pi N \rightarrow \pi N$
• • • We do not use the following data for averages, fits, limits, etc. • • •				
68.0± 0.5	SHRESTHA	12A	DPWA	Multichannel
66 ± 8	ANISOVICH	10	DPWA	Multichannel
67 ± 3	BATINIC	10	DPWA	$\pi N \rightarrow N\pi$, $N\eta$
72 ±15	THOMA	08	DPWA	Multichannel
67.0± 0.4	ARNDT	04	DPWA	$\pi N \rightarrow \pi N$, ηN
69 ± 2	VRANA	00	DPWA	Multichannel
68	ARNDT	95	DPWA	$\pi N \rightarrow N\pi$
70 ± 3	MANLEY	92	IPWA	$\pi N \rightarrow \pi N$ & $N\pi\pi$

$(\Gamma_i\Gamma_f)^{1/2}/\Gamma_{total}$ in $N\pi \rightarrow N(1680) \rightarrow N\eta$ $(\Gamma_1\Gamma_2)^{1/2}/\Gamma$

VALUE	DOCUMENT ID		TECN	COMMENT
• • • We do not use the following data for averages, fits, limits, etc. • • •				
not seen	BAKER	79	DPWA	$\pi^- p \rightarrow n\eta$

$\Gamma(N\eta)/\Gamma_{total}$ Γ_2/Γ

VALUE (%)	DOCUMENT ID		TECN	COMMENT
0.0 ±0.7 OUR AVERAGE				
0 ±1	SHKLYAR	13	DPWA	Multichannel
0 ±1	VRANA	00	DPWA	Multichannel
• • • We do not use the following data for averages, fits, limits, etc. • • •				
1.0 ±0.3	SHRESTHA	12A	DPWA	Multichannel
0.4 ±0.2	BATINIC	10	DPWA	$\pi N \rightarrow N\pi$, $N\eta$
<1	THOMA	08	DPWA	Multichannel
$0.15^{+0.35}_{-0.10}$	TIATOR	99	DPWA	$\gamma p \rightarrow p\eta$

$(\Gamma_i\Gamma_f)^{1/2}/\Gamma_{total}$ in $N\pi \rightarrow N(1680) \rightarrow \Lambda K$ $(\Gamma_1\Gamma_3)^{1/2}/\Gamma$

Coupling to ΛK not required in the analyses of SAXON 80 or BELL 83.

VALUE	DOCUMENT ID		TECN	COMMENT
• • • We do not use the following data for averages, fits, limits, etc. • • •				
−0.01	SHRESTHA	12A	DPWA	Multichannel

Note: Signs of couplings from $\pi N \rightarrow N\pi\pi$ analyses were changed in the 1986 edition to agree with the baryon-first convention; the overall phase ambiguity is resolved by choosing a negative sign for the $\Delta(1620)$ S_{31} coupling to $\Delta(1232)\pi$.

$(\Gamma_i\Gamma_f)^{1/2}/\Gamma_{total}$ in $N\pi \rightarrow N(1680) \rightarrow \Delta(1232)\pi$, P-wave $(\Gamma_1\Gamma_7)^{1/2}/\Gamma$

VALUE	DOCUMENT ID		TECN	COMMENT
−0.31 to −0.21 OUR ESTIMATE				
−0.27	[1,5] LONGACRE	77	IPWA	$\pi N \rightarrow N\pi\pi$
−0.25	[2] LONGACRE	75	IPWA	$\pi N \rightarrow N\pi\pi$
• • • We do not use the following data for averages, fits, limits, etc. • • •				
−0.26±0.04	MANLEY	92	IPWA	$\pi N \rightarrow \pi N$ & $N\pi\pi$

$\Gamma(\Delta(1232)\pi, P\text{-wave})/\Gamma_{total}$ Γ_7/Γ

VALUE (%)	DOCUMENT ID		TECN	COMMENT
10 ±5 OUR ESTIMATE				
5 ±3	ANISOVICH	12A	DPWA	Multichannel
14 ±3	VRANA	00	DPWA	Multichannel
• • • We do not use the following data for averages, fits, limits, etc. • • •				
10.5±0.9	SHRESTHA	12A	DPWA	Multichannel
8 ±3	THOMA	08	DPWA	Multichannel

$(\Gamma_i\Gamma_f)^{1/2}/\Gamma_{total}$ in $N\pi \rightarrow N(1680) \rightarrow \Delta(1232)\pi$, F-wave $(\Gamma_1\Gamma_8)^{1/2}/\Gamma$

VALUE	DOCUMENT ID		TECN	COMMENT
+0.03 to +0.11 OUR ESTIMATE				
+0.07	[1,5] LONGACRE	77	IPWA	$\pi N \rightarrow N\pi\pi$
+0.08	[2] LONGACRE	75	IPWA	$\pi N \rightarrow N\pi\pi$
• • • We do not use the following data for averages, fits, limits, etc. • • •				
+0.07±0.03	MANLEY	92	IPWA	$\pi N \rightarrow \pi N$ & $N\pi\pi$

$\Gamma(\Delta(1232)\pi, F\text{-wave})/\Gamma_{total}$ Γ_8/Γ

VALUE (%)	DOCUMENT ID		TECN	COMMENT
0 to 12 (≈5) OUR ESTIMATE				
10 ±3	ANISOVICH	12A	DPWA	Multichannel
1 ±1	VRANA	00	DPWA	Multichannel
• • • We do not use the following data for averages, fits, limits, etc. • • •				
1.0±0.1	SHRESTHA	12A	DPWA	Multichannel
4 ±3	THOMA	08	DPWA	Multichannel

$(\Gamma_i\Gamma_f)^{1/2}/\Gamma_{total}$ in $N\pi \rightarrow N(1680) \rightarrow N\rho$, $S=3/2$, P-wave $(\Gamma_1\Gamma_{11})^{1/2}/\Gamma$

VALUE	DOCUMENT ID		TECN	COMMENT
−0.30 to −0.10 OUR ESTIMATE				
−0.23	[1,5] LONGACRE	77	IPWA	$\pi N \rightarrow N\pi\pi$
−0.30	[2] LONGACRE	75	IPWA	$\pi N \rightarrow N\pi\pi$
• • • We do not use the following data for averages, fits, limits, etc. • • •				
−0.20±0.05	MANLEY	92	IPWA	$\pi N \rightarrow \pi N$ & $N\pi\pi$

$\Gamma(N\rho, S=3/2, P\text{-wave})/\Gamma_{total}$ Γ_{11}/Γ

VALUE (%)	DOCUMENT ID		TECN	COMMENT
5 ±1	VRANA	00	DPWA	Multichannel
• • • We do not use the following data for averages, fits, limits, etc. • • •				
7.4±0.7	SHRESTHA	12A	DPWA	Multichannel

$(\Gamma_i\Gamma_f)^{1/2}/\Gamma_{total}$ in $N\pi \rightarrow N(1680) \rightarrow N\rho$, $S=3/2$, F-wave $(\Gamma_1\Gamma_{12})^{1/2}/\Gamma$

VALUE	DOCUMENT ID		TECN	COMMENT
−0.18 to −0.10 OUR ESTIMATE				
−0.15	[1,5] LONGACRE	77	IPWA	$\pi N \rightarrow N\pi\pi$
• • • We do not use the following data for averages, fits, limits, etc. • • •				
−0.13±0.03	MANLEY	92	IPWA	$\pi N \rightarrow \pi N$ & $N\pi\pi$

$\Gamma(N\rho, S=3/2, F\text{-wave})/\Gamma_{total}$ Γ_{12}/Γ

VALUE (%)	DOCUMENT ID		TECN	COMMENT
3 ±1	VRANA	00	DPWA	Multichannel
• • • We do not use the following data for averages, fits, limits, etc. • • •				
2.4±0.3	SHRESTHA	12A	DPWA	Multichannel

$(\Gamma_i\Gamma_f)^{1/2}/\Gamma_{total}$ in $N\pi \rightarrow N(1680) \rightarrow N(\pi\pi)^{I=0}_{S\text{-wave}}$ $(\Gamma_1\Gamma_{13})^{1/2}/\Gamma$

VALUE	DOCUMENT ID		TECN	COMMENT
+0.25 to +0.35 OUR ESTIMATE				
+0.31	[1,5] LONGACRE	77	IPWA	$\pi N \rightarrow N\pi\pi$
+0.30	[2] LONGACRE	75	IPWA	$\pi N \rightarrow N\pi\pi$
• • • We do not use the following data for averages, fits, limits, etc. • • •				
+0.29±0.04	MANLEY	92	IPWA	$\pi N \rightarrow \pi N$ & $N\pi\pi$

Baryon Particle Listings

$N(1680)$, $N(1685)$, $N(1700)$

$\Gamma(N(\pi\pi)^{I=0}_{S\text{-wave}})/\Gamma_{\text{total}}$ Γ_{13}/Γ

VALUE (%)	DOCUMENT ID		TECN	COMMENT
11 ±5 OUR ESTIMATE				
14 ±7	ANISOVICH	12A	DPWA	Multichannel
9 ±1	VRANA	00	DPWA	Multichannel
• • • We do not use the following data for averages, fits, limits, etc. • • •				
9.4±0.8	SHRESTHA	12A	DPWA	Multichannel
11 ±5	THOMA	08	DPWA	Multichannel

$N(1680)$ FOOTNOTES

[1] LONGACRE 77 pole positions are from a search for poles in the unitarized T-matrix; the first (second) value uses, in addition to $\pi N \to N\pi\pi$ data, elastic amplitudes from a Saclay (CERN) partial-wave analysis. The other LONGACRE 77 values are from eyeball fits with Breit-Wigner circles to the T-matrix amplitudes.

[2] From method II of LONGACRE 75: eyeball fits with Breit-Wigner circles to the T-matrix amplitudes.

[3] See HOEHLER 93 for a detailed discussion of the evidence for and the pole parameters of N and Δ resonances as determined from Argand diagrams of πN elastic partial-wave amplitudes and from plots of the speeds with which the amplitudes traverse the diagrams.

[4] LONGACRE 78 values are from a search for poles in the unitarized T-matrix. The first (second) value uses, in addition to $\pi N \to N\pi\pi$ data, elastic amplitudes from a Saclay (CERN) partial-wave analysis.

[5] LONGACRE 77 considers this coupling to be well determined.

$N(1680)$ REFERENCES

For early references, see Physics Letters **111B** 1 (1982). For very early references, see Reviews of Modern Physics **37** 633 (1965).

SHKLYAR	13	PR C87 015201	V. Shklyar, H. Lenske, U. Mosel	(GIES)
ANISOVICH	12A	EPJ A48 15	A.V. Anisovich *et al.*	(BONN, PNPI)
CHEN	12A	PR C86 015206	W. Chen *et al.*	(DUKE, GWU, MSST, ITEP+)
SHRESTHA	12A	PR C86 055203	M. Shrestha, D.M. Manley	(KSU)
WORKMAN	12A	PR C86 015202	R. Workman *et al.*	(GWU)
ANISOVICH	10	EPJ A44 203	A.V. Anisovich *et al.*	(BONN, PNPI)
BATINIC	10	PR C82 038203	M. Batinic *et al.*	(ZAGR)
THOMA	08	PL B659 87	U. Thoma *et al.*	(CB-ELSA Collab.)
DRECHSEL	07	EPJ A34 69	D. Drechsel, S.S. Kamalov, L. Tiator	(MAINZ, JINR)
DUGGER	07	PR C76 025211	M. Dugger *et al.*	(Jefferson Lab CLAS Collab.)
ARNDT	06	PR C74 045205	R.A. Arndt *et al.*	(GWU)
PDG	06	JP G33 1	W.-M. Yao *et al.*	(PDG Collab.)
ARNDT	04	PR C69 035213	R.A. Arndt *et al.*	(GWU, TRIU)
VRANA	00	PRPL 328 181	T.P. Vrana, S.A. Dytman,, T.-S.H. Lee	(PITT+)
TIATOR	99	PR C60 035210	L. Tiator *et al.*	
ARNDT	96	PR C53 430	R.A. Arndt, I.I. Strakovsky, R.L. Workman	(VPI)
ARNDT	95	PR C52 2120	R.A. Arndt *et al.*	(VPI, BRCO)
HOEHLER	93	πN Newsletter 9 1	G. Hohler	(KARL)
LI	93	PR C47 2759	Z.J. Li *et al.*	(VPI)
MANLEY	92	PR D45 4002	D.M. Manley, E.M. Saleski	(KSA) IJP
Also		PR D30 904	D.M. Manley *et al.*	(VPI)
ARNDT	91	PR D43 2131	R.A. Arndt *et al.*	(VPI, TELE) IJP
BELL	83	NP B222 389	K.W. Bell *et al.*	(RL) IJP
CRAWFORD	83	NP B211 1	R.L. Crawford, W.T. Morton	(GLAS)
PDG	82	PL 111B 1	M. Roos *et al.*	(HELS, CIT, CERN)
AWAJI	81	Bonn Conf. 352	N. Awaji, R. Kajikawa	(NAGO)
Also		NP B197 365	K. Fujii *et al.*	(NAGO)
FUJII	81	NP B187 53	K. Fujii *et al.*	(NAGO, OSAK)
CUTKOSKY	80	Toronto Conf. 19	R.E. Cutkosky *et al.*	(CMU, LBL) IJP
Also		PR D20 2839	R.E. Cutkosky *et al.*	(CMU, LBL) IJP
SAXON	80	NP B162 522	D.H. Saxon *et al.*	(RHEL, BRIS) IJP
BAKER	79	NP B156 93	R.D. Baker *et al.*	(RHEL) IJP
HOEHLER	79	PDAT 12-1	G. Hohler *et al.*	(KARLT) IJP
Also		Toronto Conf. 3	R. Koch	(KARLT) IJP
LONGACRE	78	PR D17 1795	R.S. Longacre *et al.*	(LBL, SLAC)
LONGACRE	77	NP B122 493	R.S. Longacre, J. Dolbeau	(SACL) IJP
Also		NP B108 365	J. Dolbeau *et al.*	(SACL) IJP
LONGACRE	75	PL 55B 415	R.S. Longacre *et al.*	(LBL, SLAC) IJP

$N(1685)$ $?^?$

$I(J^P) = \frac{1}{2}(?^?)$ Status: *

OMITTED FROM SUMMARY TABLE

There is a small literature (which we do not try to cover) on this possible narrow state. See KUZNETSOV 11A, MART 11, and the other papers for further references. This state does not gain status by being a sought-after member of a baryon anti-decuplet.

$N(1685)$ MASS

VALUE (MeV)	DOCUMENT ID		TECN	COMMENT
• • • We do not use the following data for averages, fits, limits, etc. • • •				
1670±5	WERTHMUEL..13		CRBT	$\gamma d \to \eta n\,(p)$, $\gamma\,{}^3\mathrm{He} \to \eta n\,(pp)$
~ 1670	JAEGLE	11	CBTP	$\gamma d \to \eta n\,(p)$
~ 1685	KUZNETSOV	11	GRAL	$\gamma d \to \eta n\,(p)$
~ 1680	KUZNETSOV	07	GRAL	$\gamma d \to \eta n\,(p)$

$N(1685)$ WIDTH

VALUE (MeV)	DOCUMENT ID		TECN	COMMENT
• • • We do not use the following data for averages, fits, limits, etc. • • •				
30±15	WERTHMUEL..13		CRBT	$\gamma d \to \eta n\,(p)$, $\gamma\,{}^3\mathrm{He} \to \eta n\,(pp)$
~ 25	JAEGLE	11	CBTP	$\gamma d \to \eta n\,(p)$
<30	KUZNETSOV	11	GRAL	$\gamma d \to \eta n\,(p)$
<30	KUZNETSOV	07	GRAL	$\gamma d \to \eta n\,(p)$

$N(1685)$ REFERENCES

WERTHMUEL..13	PRL 111 232001	D. Werthmueller *et al.*	(Crystal Ball/TAPS Collab.)
JAEGLE 11	EPJ A47 89	I. Jaegle *et al.*	(CBELSA/TAPS Collab.)
Also	PRL 100 252002	I. Jaegle *et al.*	(CBELSA/TAPS Collab.)
KUZNETSOV 11	PR C83 022201	V. Kuznetsov *et al.*	(GRAAL Collab.)
KUZNETSOV 11A	JETPL 94 503	V. Kuznetsov, M.V. Polyakov, M. Thurmann	(INRM+)
MART 11	PR D83 094015	T. Mart	(U. Indonesia)
KUZNETSOV 07	PL B647 23	V. Kuznetsov *et al.*	(GRAAL Collab.)

$N(1700)$ $3/2^-$

$I(J^P) = \frac{1}{2}(\frac{3}{2}^-)$ Status: ***

Most of the results published before 1975 are now obsolete and have been omitted. They may be found in our 1982 edition, Physics Letters **111B** 1 (1982). Some further obsolete results published before 1984 were last included in our 2006 edition, Journal of Physics (generic for all A,B,E,G) **G33** 1 (2006).

The various partial-wave analyses do not agree very well.

The latest GWU analysis (ARNDT 06) finds no evidence for this resonance.

$N(1700)$ BREIT-WIGNER MASS

VALUE (MeV)	DOCUMENT ID		TECN	COMMENT
1650 to 1750 (≈ 1700) OUR ESTIMATE				
1790±40	ANISOVICH	12A	DPWA	Multichannel
1675±25	CUTKOSKY	80	IPWA	$\pi N \to \pi N$
1731±15	HOEHLER	79	IPWA	$\pi N \to \pi N$
• • • We do not use the following data for averages, fits, limits, etc. • • •				
1665± 3	SHRESTHA	12A	DPWA	Multichannel
1817±22	BATINIC	10	DPWA	$\pi N \to N\pi,\ N\eta$
1740±20	THOMA	08	DPWA	Multichannel
1736±33	VRANA	00	DPWA	Multichannel
1737±44	MANLEY	92	IPWA	$\pi N \to \pi N$ & $N\pi\pi$
1650	SAXON	80	DPWA	$\pi^- p \to \Lambda K^0$
1690 to 1710	BAKER	78	DPWA	$\pi^- p \to \Lambda K^0$
1719	BARBOUR	78	DPWA	$\gamma N \to \pi N$
1670±10	[1] BAKER	77	IPWA	$\pi^- p \to \Lambda K^0$
1690	[1] BAKER	77	DPWA	$\pi^- p \to \Lambda K^0$
1660	[2] LONGACRE	77	IPWA	$\pi N \to N\pi\pi$
1710	[3] LONGACRE	75	IPWA	$\pi N \to N\pi\pi$

$N(1700)$ BREIT-WIGNER WIDTH

VALUE (MeV)	DOCUMENT ID		TECN	COMMENT
100 to 250 (≈ 150) OUR ESTIMATE				
390±140	ANISOVICH	12A	DPWA	Multichannel
90± 40	CUTKOSKY	80	IPWA	$\pi N \to \pi N$
110± 30	HOEHLER	79	IPWA	$\pi N \to \pi N$
• • • We do not use the following data for averages, fits, limits, etc. • • •				
56± 8	SHRESTHA	12A	DPWA	Multichannel
134± 37	BATINIC	10	DPWA	$\pi N \to N\pi,\ N\eta$
180± 30	THOMA	08	DPWA	Multichannel
175±133	VRANA	00	DPWA	Multichannel
250±220	MANLEY	92	IPWA	$\pi N \to \pi N$ & $N\pi\pi$
70	SAXON	80	DPWA	$\pi^- p \to \Lambda K^0$
70 to 100	BAKER	78	DPWA	$\pi^- p \to \Lambda K^0$
126	BARBOUR	78	DPWA	$\gamma N \to \pi N$
90± 25	[1] BAKER	77	IPWA	$\pi^- p \to \Lambda K^0$
100	[1] BAKER	77	DPWA	$\pi^- p \to \Lambda K^0$
600	[2] LONGACRE	77	IPWA	$\pi N \to N\pi\pi$
300	[3] LONGACRE	75	IPWA	$\pi N \to N\pi\pi$

$N(1700)$ POLE POSITION

REAL PART

VALUE (MeV)	DOCUMENT ID		TECN	COMMENT
1650 to 1750 (≈ 1700) OUR ESTIMATE				
1770±40	ANISOVICH	12A	DPWA	Multichannel
1700	[4] HOEHLER	93	SPED	$\pi N \to \pi N$
1660±30	CUTKOSKY	80	IPWA	$\pi N \to \pi N$
• • • We do not use the following data for averages, fits, limits, etc. • • •				
1662	SHRESTHA	12A	DPWA	Multichannel
1806±23	BATINIC	10	DPWA	$\pi N \to N\pi,\ N\eta$
1710±15	THOMA	08	DPWA	Multichannel
1704	VRANA	00	DPWA	Multichannel
not seen	ARNDT	91	DPWA	$\pi N \to \pi N$ Soln SM90
1710 or 1678	[5] LONGACRE	78	IPWA	$\pi N \to N\pi\pi$
1616 or 1613	[2] LONGACRE	77	IPWA	$\pi N \to N\pi\pi$

−2×IMAGINARY PART

VALUE (MeV)	DOCUMENT ID		TECN	COMMENT
100 to 300 OUR ESTIMATE				
420±180	ANISOVICH	12A	DPWA	Multichannel
120	[4] HOEHLER	93	SPED	$\pi N \to \pi N$
90± 40	CUTKOSKY	80	IPWA	$\pi N \to \pi N$
• • • We do not use the following data for averages, fits, limits, etc. • • •				
55	SHRESTHA	12A	DPWA	Multichannel
129± 33	BATINIC	10	DPWA	$\pi N \to N\pi$, $N\eta$
155± 25	THOMA	08	DPWA	Multichannel
156	VRANA	00	DPWA	Multichannel
not seen	ARNDT	91	DPWA	$\pi N \to \pi N$ Soln SM90
607 or 567	[5] LONGACRE	78	IPWA	$\pi N \to N\pi\pi$
577 or 575	[2] LONGACRE	77	IPWA	$\pi N \to N\pi\pi$

N(1700) ELASTIC POLE RESIDUE

MODULUS |r|

VALUE (MeV)	DOCUMENT ID		TECN	COMMENT
5 to 50 OUR ESTIMATE				
50±40	ANISOVICH	12A	DPWA	Multichannel
5	HOEHLER	93	SPED	$\pi N \to \pi N$
6± 3	CUTKOSKY	80	IPWA	$\pi N \to \pi N$
• • • We do not use the following data for averages, fits, limits, etc. • • •				
7	BATINIC	10	DPWA	$\pi N \to N\pi$, $N\eta$

PHASE θ

VALUE (°)	DOCUMENT ID		TECN	COMMENT
−120 to 20 OUR ESTIMATE				
−100±40	ANISOVICH	12A	DPWA	Multichannel
0±50	CUTKOSKY	80	IPWA	$\pi N \to \pi N$
• • • We do not use the following data for averages, fits, limits, etc. • • •				
− 34	BATINIC	10	DPWA	$\pi N \to N\pi$, $N\eta$

N(1700) INELASTIC POLE RESIDUE

The "normalized residue" is the residue divided by $\Gamma_{pole}/2$.

Normalized residue in $N\pi \to N(1700) \to \Delta\pi$, S-wave

MODULUS (%)	PHASE (°)	DOCUMENT ID		TECN	COMMENT
34±21	**−60 ± 40**	ANISOVICH	12A	DPWA	Multichannel

Normalized residue in $N\pi \to N(1700) \to \Delta\pi$, D-wave

MODULUS (%)	PHASE (°)	DOCUMENT ID		TECN	COMMENT
8±6	**90 ± 35**	ANISOVICH	12A	DPWA	Multichannel

N(1700) DECAY MODES

The following branching fractions are our estimates, not fits or averages.

	Mode	Fraction (Γ_i/Γ)
Γ_1	$N\pi$	(12 ±5) %
Γ_2	$N\eta$	(0.0±1.0) %
Γ_3	ΛK	< 3 %
Γ_4	ΣK	
Γ_5	$N\pi\pi$	85–95 %
Γ_6	$\Delta\pi$	
Γ_7	$\Delta(1232)\pi$, S-wave	10–90 %
Γ_8	$\Delta(1232)\pi$, D-wave	< 20 %
Γ_9	$N\rho$	< 35 %
Γ_{10}	$N\rho$, S=1/2, D-wave	
Γ_{11}	$N\rho$, S=3/2, S-wave	(7.0±1.0) %
Γ_{12}	$N\rho$, S=3/2, D-wave	
Γ_{13}	$N(\pi\pi)^{I=0}_{S\text{-wave}}$	
Γ_{14}	$p\gamma$	0.01–0.05 %
Γ_{15}	$p\gamma$, helicity=1/2	0.0–0.024 %
Γ_{16}	$p\gamma$, helicity=3/2	0.002–0.026 %
Γ_{17}	$n\gamma$	0.01–0.13 %
Γ_{18}	$n\gamma$, helicity=1/2	0.0–0.09 %
Γ_{19}	$n\gamma$, helicity=3/2	0.01–0.05 %

N(1700) BRANCHING RATIOS

$\Gamma(N\pi)/\Gamma_{total}$ — Γ_1/Γ

VALUE (%)	DOCUMENT ID		TECN	COMMENT
12 ±5 OUR ESTIMATE				
12 ±5	ANISOVICH	12A	DPWA	Multichannel
11 ±5	CUTKOSKY	80	IPWA	$\pi N \to \pi N$
8 ±3	HOEHLER	79	IPWA	$\pi N \to \pi N$
• • • We do not use the following data for averages, fits, limits, etc. • • •				
2.8±0.5	SHRESTHA	12A	DPWA	Multichannel
9 ±6	BATINIC	10	DPWA	$\pi N \to N\pi$, $N\eta$
8 $^{+8}_{-4}$	THOMA	08	DPWA	Multichannel
4 ±2	VRANA	00	DPWA	Multichannel
1 ±2	MANLEY	92	IPWA	$\pi N \to \pi N$ & $N\pi\pi$

$\Gamma(N\eta)/\Gamma_{total}$ — Γ_2/Γ

VALUE (%)	DOCUMENT ID		TECN	COMMENT
0±1	VRANA	00	DPWA	Multichannel
• • • We do not use the following data for averages, fits, limits, etc. • • •				
14±5	BATINIC	10	DPWA	$\pi N \to N\pi$, $N\eta$
10±5	THOMA	08	DPWA	Multichannel

$(\Gamma_i\Gamma_f)^{1/2}/\Gamma_{total}$ in $N\pi \to N(1700) \to \Lambda K$ — $(\Gamma_1\Gamma_3)^{1/2}/\Gamma$

VALUE	DOCUMENT ID		TECN	COMMENT
−0.06 to +0.04 OUR ESTIMATE				
−0.012	BELL	83	DPWA	$\pi^- p \to \Lambda K^0$
−0.012	SAXON	80	DPWA	$\pi^- p \to \Lambda K^0$
• • • We do not use the following data for averages, fits, limits, etc. • • •				
−0.04	[6] BAKER	78	DPWA	See SAXON 80
−0.03 ±0.004	[1] BAKER	77	IPWA	$\pi^- p \to \Lambda K^0$
−0.03	[1] BAKER	77	DPWA	$\pi^- p \to \Lambda K^0$
+0.026±0.019	DEVENISH	74B		Fixed-t dispersion rel.

$(\Gamma_i\Gamma_f)^{1/2}/\Gamma_{total}$ in $N\pi \to N(1700) \to \Sigma K$ — $(\Gamma_1\Gamma_4)^{1/2}/\Gamma$

VALUE	DOCUMENT ID		TECN	COMMENT
• • • We do not use the following data for averages, fits, limits, etc. • • •				
not seen	LIVANOS	80	DPWA	$\pi p \to \Sigma K$
<0.017	[7] DEANS	75	DPWA	$\pi N \to \Sigma K$

Note: Signs of couplings from $\pi N \to N\pi\pi$ analyses were changed in the 1986 edition to agree with the baryon-first convention; the overall phase ambiguity is resolved by choosing a negative sign for the $\Delta(1620)$ S_{31} coupling to $\Delta(1232)\pi$.

$(\Gamma_i\Gamma_f)^{1/2}/\Gamma_{total}$ in $N\pi \to N(1700) \to \Delta(1232)\pi$, S-wave — $(\Gamma_1\Gamma_7)^{1/2}/\Gamma$

VALUE	DOCUMENT ID		TECN	COMMENT
0.00	[2] LONGACRE	77	IPWA	$\pi N \to N\pi\pi$
−0.16	[3] LONGACRE	75	IPWA	$\pi N \to N\pi\pi$
• • • We do not use the following data for averages, fits, limits, etc. • • •				
+0.02±0.03	MANLEY	92	IPWA	$\pi N \to \pi N$ & $N\pi\pi$

$\Gamma(\Delta(1232)\pi$, S-wave$)/\Gamma_{total}$ — Γ_7/Γ

VALUE (%)	DOCUMENT ID		TECN	COMMENT
10 to 90 OUR ESTIMATE				
72±23	ANISOVICH	12A	DPWA	Multichannel
11± 1	VRANA	00	DPWA	Multichannel
• • • We do not use the following data for averages, fits, limits, etc. • • •				
31± 9	SHRESTHA	12A	DPWA	Multichannel
10± 5	THOMA	08	DPWA	Multichannel

$(\Gamma_i\Gamma_f)^{1/2}/\Gamma_{total}$ in $N\pi \to N(1700) \to \Delta(1232)\pi$, D-wave — $(\Gamma_1\Gamma_8)^{1/2}/\Gamma$

VALUE	DOCUMENT ID		TECN	COMMENT
−0.12	[2] LONGACRE	77	IPWA	$\pi N \to N\pi\pi$
+0.14	[3] LONGACRE	75	IPWA	$\pi N \to N\pi\pi$
• • • We do not use the following data for averages, fits, limits, etc. • • •				
+0.10±0.09	MANLEY	92	IPWA	$\pi N \to \pi N$ & $N\pi\pi$

$\Gamma(\Delta(1232)\pi$, D-wave$)/\Gamma_{total}$ — Γ_8/Γ

VALUE (%)	DOCUMENT ID		TECN	COMMENT
<20 OUR ESTIMATE				
<10	ANISOVICH	12A	DPWA	Multichannel
79±56	VRANA	00	DPWA	Multichannel
• • • We do not use the following data for averages, fits, limits, etc. • • •				
3± 2	SHRESTHA	12A	DPWA	Multichannel
20±11	THOMA	08	DPWA	Multichannel

$(\Gamma_i\Gamma_f)^{1/2}/\Gamma_{total}$ in $N\pi \to N(1700) \to N\rho$, S=3/2, S-wave — $(\Gamma_1\Gamma_{11})^{1/2}/\Gamma$

VALUE	DOCUMENT ID		TECN	COMMENT
±0.01 to ±0.13 OUR ESTIMATE				
−0.07	[2] LONGACRE	77	IPWA	$\pi N \to N\pi\pi$
+0.07	[3] LONGACRE	75	IPWA	$\pi N \to N\pi\pi$
• • • We do not use the following data for averages, fits, limits, etc. • • •				
−0.04±0.06	MANLEY	92	IPWA	$\pi N \to \pi N$ & $N\pi\pi$

$\Gamma(N\rho$, S=3/2, S-wave$)/\Gamma_{total}$ — Γ_{11}/Γ

VALUE (%)	DOCUMENT ID		TECN	COMMENT
7±1	VRANA	00	DPWA	Multichannel
• • • We do not use the following data for averages, fits, limits, etc. • • •				
38±6	SHRESTHA	12A	DPWA	Multichannel

$(\Gamma_i\Gamma_f)^{1/2}/\Gamma_{total}$ in $N\pi \to N(1700) \to N(\pi\pi)^{I=0}_{S\text{-wave}}$ $(\Gamma_1\Gamma_{13})^{1/2}/\Gamma$

VALUE	DOCUMENT ID		TECN	COMMENT
±0.02 to ±0.28 OUR ESTIMATE				
0.00	[2] LONGACRE	77	IPWA	$\pi N \to N\pi\pi$
+0.2	[3] LONGACRE	75	IPWA	$\pi N \to N\pi\pi$
• • • We do not use the following data for averages, fits, limits, etc. • • •				
+0.02±0.02	MANLEY	92	IPWA	$\pi N \to \pi N$ & $N\pi\pi$

$\Gamma(N(\pi\pi)^{I=0}_{S\text{-wave}})/\Gamma_{total}$ Γ_{13}/Γ

VALUE (%)	DOCUMENT ID		TECN	COMMENT
0± 1	VRANA	00	DPWA	Multichannel
• • • We do not use the following data for averages, fits, limits, etc. • • •				
24± 6	SHRESTHA	12A	DPWA	Multichannel
18±12	THOMA	08	DPWA	Multichannel

$N(1700)$ PHOTON DECAY AMPLITUDES

Papers on γN amplitudes predating 1981 may be found in our 2006 edition, Journal of Physics (generic for all A,B,E,G) **G33** 1 (2006).

$N(1700) \to p\gamma$, helicity-1/2 amplitude $A_{1/2}$

VALUE ($GeV^{-1/2}$)	DOCUMENT ID		TECN	COMMENT
0.015±0.025 OUR ESTIMATE				
0.041±0.017	ANISOVICH	12A	DPWA	Multichannel
−0.016±0.014	CRAWFORD	83	IPWA	$\gamma N \to \pi N$
−0.002±0.013	AWAJI	81	DPWA	$\gamma N \to \pi N$
• • • We do not use the following data for averages, fits, limits, etc. • • •				
0.021±0.005	SHRESTHA	12A	DPWA	Multichannel
−0.033±0.021	BARBOUR	78	DPWA	$\gamma N \to \pi N$

$N(1700) \to p\gamma$, helicity-3/2 amplitude $A_{3/2}$

VALUE ($GeV^{-1/2}$)	DOCUMENT ID		TECN	COMMENT
−0.015±0.025 OUR ESTIMATE				
−0.034±0.013	ANISOVICH	12A	DPWA	Multichannel
−0.009±0.012	CRAWFORD	83	IPWA	$\gamma N \to \pi N$
0.029±0.014	AWAJI	81	DPWA	$\gamma N \to \pi N$
• • • We do not use the following data for averages, fits, limits, etc. • • •				
0.050±0.009	SHRESTHA	12A	DPWA	Multichannel
−0.014±0.025	BARBOUR	78	DPWA	$\gamma N \to \pi N$

$N(1700) \to n\gamma$, helicity-1/2 amplitude $A_{1/2}$

VALUE ($GeV^{-1/2}$)	DOCUMENT ID		TECN	COMMENT
0.020±0.015 OUR ESTIMATE				
0.006±0.024	AWAJI	81	DPWA	$\gamma N \to \pi N$
−0.002±0.013	FUJII	81	DPWA	$\gamma N \to \pi N$
• • • We do not use the following data for averages, fits, limits, etc. • • •				
−0.049±0.008	SHRESTHA	12A	DPWA	Multichannel
+0.050±0.042	BARBOUR	78	DPWA	$\gamma N \to \pi N$

$N(1700) \to n\gamma$, helicity-3/2 amplitude $A_{3/2}$

VALUE ($GeV^{-1/2}$)	DOCUMENT ID		TECN	COMMENT
−0.030±0.020 OUR ESTIMATE				
−0.033±0.017	AWAJI	81	DPWA	$\gamma N \to \pi N$
0.018±0.018	FUJII	81	DPWA	$\gamma N \to \pi N$
• • • We do not use the following data for averages, fits, limits, etc. • • •				
−0.092±0.014	SHRESTHA	12A	DPWA	Multichannel
+0.035±0.030	BARBOUR	78	DPWA	$\gamma N \to \pi N$

$N(1700)$ $\gamma p \to \Lambda K^+$ AMPLITUDES

$(\Gamma_i\Gamma_f)^{1/2}/\Gamma_{total}$ in $p\gamma \to N(1700) \to \Lambda K^+$ (E_{2-} amplitude)

VALUE (units 10^{-3})	DOCUMENT ID		TECN
• • • We do not use the following data for averages, fits, limits, etc. • • •			
4.09	TANABE	89	DPWA

$(\Gamma_i\Gamma_f)^{1/2}/\Gamma_{total}$ in $p\gamma \to N(1700) \to \Lambda K^+$ (M_{2-} amplitude)

VALUE (units 10^{-3})	DOCUMENT ID		TECN
• • • We do not use the following data for averages, fits, limits, etc. • • •			
−7.09	TANABE	89	DPWA

$p\gamma \to N(1700) \to \Lambda K^+$ phase angle θ (E_{2-} amplitude)

VALUE (degrees)	DOCUMENT ID		TECN
• • • We do not use the following data for averages, fits, limits, etc. • • •			
−35.9	TANABE	89	DPWA

$N(1700)$ FOOTNOTES

[1] The two BAKER 77 entries are from an IPWA using the Barrelet-zero method and from a conventional energy-dependent analysis.
[2] LONGACRE 77 pole positions are from a search for poles in the unitarized T-matrix; the first (second) value uses, in addition to $\pi N \to N\pi\pi$ data, elastic amplitudes from a Saclay (CERN) partial-wave analysis. The other LONGACRE 77 values are from eyeball fits with Breit-Wigner circles to the T-matrix amplitudes.
[3] From method II of LONGACRE 75: eyeball fits with Breit-Wigner circles to the T-matrix amplitudes.
[4] See HOEHLER 93 for a detailed discussion of the evidence for and the pole parameters of N and Δ resonances as determined from Argand diagrams of πN elastic partial-wave amplitudes and from plots of the speeds with which the amplitudes traverse the diagrams.
[5] LONGACRE 78 values are from a search for poles in the unitarized T-matrix. The first (second) value uses, in addition to $\pi N \to N\pi\pi$ data, elastic amplitudes from a Saclay (CERN) partial-wave analysis.
[6] The overall phase of BAKER 78 couplings has been changed to agree with previous conventions.
[7] The range given is from the four best solutions.

$N(1700)$ REFERENCES

For early references, see Physics Letters **111B** 1 (1982).

ANISOVICH	12A	EPJ A48 15	A.V. Anisovich *et al.*	(BONN, PNPI)
SHRESTHA	12A	PR C86 055203	M. Shrestha, D.M. Manley	(KSU)
BATINIC	10	PR C82 038203	M. Batinic *et al.*	(ZAGR)
THOMA	08	PL B659 87	U. Thoma *et al.*	(CB-ELSA Collab.)
ARNDT	06	PR C74 045205	R.A. Arndt *et al.*	(GWU)
PDG	06	JP G33 1	W.-M. Yao *et al.*	(PDG Collab.)
VRANA	00	PRPL 328 181	T.P. Vrana, S.A. Dytman,, T.-S.H. Lee	(PITT+)
HOEHLER	93	πN Newsletter 9 1	G. Hohler	(KARL)
MANLEY	92	PR D45 4002	D.M. Manley, E.M. Saleski	(KSA) IJP
Also		PR D30 904	D.M. Manley *et al.*	(VPI)
ARNDT	91	PR D43 2131	R.A. Arndt *et al.*	(VPI, TELE) IJP
TANABE	89	PR C39 741	H. Tanabe, M. Kohno, C. Bennhold	(MANZ)
Also		NC 102A 193	M. Kohno, H. Tanabe, C. Bennhold	(MANZ)
BELL	83	NP B222 389	K.W. Bell *et al.*	(RL) IJP
CRAWFORD	83	NP B211 1	R.L. Crawford, W.T. Morton	(GLAS)
PDG	82	PL 111B 1	M. Roos *et al.*	(HELS, CIT, CERN)
AWAJI	81	Bonn Conf. 352	N. Awaji, R. Kajikawa	(NAGO)
Also		NP B197 365	K. Fujii *et al.*	(NAGO)
FUJII	81	NP B187 53	K. Fujii *et al.*	(NAGO, OSAK)
CUTKOSKY	80	Toronto Conf. 19	R.E. Cutkosky *et al.*	(CMU, LBL) IJP
Also		PR D20 2839	R.E. Cutkosky *et al.*	(CMU, LBL) IJP
LIVANOS	80	Toronto Conf. 35	P. Livanos *et al.*	(SACL) IJP
SAXON	80	NP B162 522	D.H. Saxon *et al.*	(RHEL, BRIS) IJP
HOEHLER	79	PDAT 12-1	G. Hohler *et al.*	(KARLT) IJP
Also		Toronto Conf. 3	R. Koch	(KARLT) IJP
BAKER	78	NP B141 29	R.D. Baker *et al.*	(RL, CAVE) IJP
BARBOUR	78	NP B141 253	I.M. Barbour, R.L. Crawford, N.H. Parsons	(GLAS)
LONGACRE	78	PR D17 1795	R.S. Longacre *et al.*	(LBL, SLAC)
BAKER	77	NP B126 365	R.D. Baker *et al.*	(RHEL) IJP
LONGACRE	77	NP B122 493	R.S. Longacre, J. Dolbeau	(SACL) IJP
Also		NP B108 365	J. Dolbeau *et al.*	(SACL) IJP
DEANS	75	NP B96 90	S.R. Deans *et al.*	(SFLA, ALAH) IJP
LONGACRE	75	PL 55B 415	R.S. Longacre *et al.*	(LBL, SLAC) IJP
DEVENISH	74B	NP B81 330	R.C.E. Devenish, C.D. Froggatt, B.R. Martin	(DESY+)

$N(1710)$ $1/2^+$

$I(J^P) = \frac{1}{2}(\frac{1}{2}^+)$ Status: ***

Most of the results published before 1975 were last included in our 1982 edition, Physics Letters **111B** 1 (1982). Some further obsolete results published before 1984 were last included in our 2006 edition, Journal of Physics (generic for all A,B,E,G) **G33** 1 (2006).

The latest GWU analysis (ARNDT 06) finds no evidence for this resonance.

$N(1710)$ BREIT-WIGNER MASS

VALUE (MeV)	DOCUMENT ID		TECN	COMMENT
1680 to 1740 (≈ 1710) OUR ESTIMATE				
1737±17	SHKLYAR	13	DPWA	Multichannel
1710±20	ANISOVICH	12A	DPWA	Multichannel
1700±50	CUTKOSKY	80	IPWA	$\pi N \to \pi N$
1723± 9	HOEHLER	79	IPWA	$\pi N \to \pi N$
• • • We do not use the following data for averages, fits, limits, etc. • • •				
1662± 7	SHRESTHA	12A	DPWA	Multichannel
1725±25	ANISOVICH	10	DPWA	Multichannel
1729±16	[1] BATINIC	10	DPWA	$\pi N \to N\pi$, $N\eta$
1752± 3	PENNER	02C	DPWA	Multichannel
1699±65	VRANA	00	DPWA	Multichannel
1720±10	ARNDT	96	IPWA	$\gamma N \to \pi N$
1717±28	MANLEY	92	IPWA	$\pi N \to \pi N$ & $N\pi\pi$
1706	CUTKOSKY	90	IPWA	$\pi N \to \pi N$
1730	SAXON	80	DPWA	$\pi^- p \to \Lambda K^0$
1720	[2] LONGACRE	77	IPWA	$\pi N \to N\pi\pi$
1710	[3] LONGACRE	75	IPWA	$\pi N \to N\pi\pi$

$N(1710)$ BREIT-WIGNER WIDTH

VALUE (MeV)	DOCUMENT ID		TECN	COMMENT
50 to 250 (≈ 100) OUR ESTIMATE				
368±120	SHKLYAR	13	DPWA	Multichannel
200± 18	ANISOVICH	12A	DPWA	Multichannel
93± 30	CUTKOSKY	90	IPWA	$\pi N \to \pi N$
90± 30	CUTKOSKY	80	IPWA	$\pi N \to \pi N$
120± 15	HOEHLER	79	IPWA	$\pi N \to \pi N$

• • • We do not use the following data for averages, fits, limits, etc. • • •				
116± 17	SHRESTHA	12A	DPWA	Multichannel
200± 35	ANISOVICH	10	DPWA	Multichannel
180± 17	[1] BATINIC	10	DPWA	$\pi N \to N\pi$, $N\eta$
386± 59	PENNER	02C	DPWA	Multichannel
143±100	VRANA	00	DPWA	Multichannel
105± 10	ARNDT	96	IPWA	$\gamma N \to \pi N$
480±230	MANLEY	92	IPWA	$\pi N \to \pi N$ & $N\pi\pi$
540	BELL	83	DPWA	$\pi^- p \to \Lambda K^0$
550	SAXON	80	DPWA	$\pi^- p \to \Lambda K^0$
120	[2] LONGACRE	77	IPWA	$\pi N \to N\pi\pi$
75	[3] LONGACRE	75	IPWA	$\pi N \to N\pi\pi$

N(1710) POLE POSITION

REAL PART

VALUE (MeV)	DOCUMENT ID		TECN	COMMENT
1670 to 1770 (≈ 1720) OUR ESTIMATE				
1687±17	ANISOVICH	12A	DPWA	Multichannel
1690	[4] HOEHLER	93	SPED	$\pi N \to \pi N$
1698	CUTKOSKY	90	IPWA	$\pi N \to \pi N$
1690±20	CUTKOSKY	80	IPWA	$\pi N \to \pi N$
• • • We do not use the following data for averages, fits, limits, etc. • • •				
1670	SHKLYAR	13	DPWA	Multichannel
1644	SHRESTHA	12A	DPWA	Multichannel
1708±18	ANISOVICH	10	DPWA	Multichannel
1711±15	[1] BATINIC	10	DPWA	$\pi N \to N\pi$, $N\eta$
1679	VRANA	00	DPWA	Multichannel
1770	ARNDT	95	DPWA	$\pi N \to N\pi$
1636	ARNDT	91	DPWA	$\pi N \to \pi N$ Soln SM90
1708 or 1712	[5] LONGACRE	78	IPWA	$\pi N \to N\pi\pi$
1720 or 1711	[2] LONGACRE	77	IPWA	$\pi N \to N\pi\pi$

−2×IMAGINARY PART

VALUE (MeV)	DOCUMENT ID		TECN	COMMENT
80 to 380 (≈ 230) OUR ESTIMATE				
200±25	ANISOVICH	12A	DPWA	Multichannel
200	[4] HOEHLER	93	SPED	$\pi N \to \pi N$
88	CUTKOSKY	90	IPWA	$\pi N \to \pi N$
80±20	CUTKOSKY	80	IPWA	$\pi N \to \pi N$
• • • We do not use the following data for averages, fits, limits, etc. • • •				
159	SHKLYAR	13	DPWA	Multichannel
104	SHRESTHA	12A	DPWA	Multichannel
200±20	ANISOVICH	10	DPWA	Multichannel
174±16	[1] BATINIC	10	DPWA	$\pi N \to N\pi$, $N\eta$
132	VRANA	00	DPWA	Multichannel
378	ARNDT	95	DPWA	$\pi N \to N\pi$
544	ARNDT	91	DPWA	$\pi N \to \pi N$ Soln SM90
17 or 22	[5] LONGACRE	78	IPWA	$\pi N \to N\pi\pi$
123 or 115	[2] LONGACRE	77	IPWA	$\pi N \to N\pi\pi$

N(1710) ELASTIC POLE RESIDUE

MODULUS |r|

VALUE (MeV)	DOCUMENT ID		TECN	COMMENT
6±4	ANISOVICH	12A	DPWA	Multichannel
15	HOEHLER	93	SPED	$\pi N \to \pi N$
9	CUTKOSKY	90	IPWA	$\pi N \to \pi N$
8±2	CUTKOSKY	80	IPWA	$\pi N \to \pi N$
• • • We do not use the following data for averages, fits, limits, etc. • • •				
11	SHKLYAR	13	DPWA	Multichannel
24	[1] BATINIC	10	DPWA	$\pi N \to N\pi$, $N\eta$
37	ARNDT	95	DPWA	$\pi N \to N\pi$
149	ARNDT	91	DPWA	$\pi N \to \pi N$ Soln SM90

PHASE θ

VALUE (°)	DOCUMENT ID		TECN	COMMENT
120±70	ANISOVICH	12A	DPWA	Multichannel
−167	CUTKOSKY	90	IPWA	$\pi N \to \pi N$
175±35	CUTKOSKY	80	IPWA	$\pi N \to \pi N$
• • • We do not use the following data for averages, fits, limits, etc. • • •				
9	SHKLYAR	13	DPWA	Multichannel
20	[1] BATINIC	10	DPWA	$\pi N \to N\pi$, $N\eta$
−167	ARNDT	95	DPWA	$\pi N \to N\pi$
149	ARNDT	91	DPWA	$\pi N \to \pi N$ Soln SM90

N(1710) INELASTIC POLE RESIDUE

The "normalized residue" is the residue divided by $\Gamma_{pole}/2$.

Normalized residue in $N\pi \to N(1710) \to N\eta$

MODULUS (%)	PHASE (°)	DOCUMENT ID		TECN	COMMENT
12±4	**0 ± 45**	ANISOVICH	12A	DPWA	Multichannel

Normalized residue in $N\pi \to N(1710) \to \Lambda K$

MODULUS (%)	PHASE (°)	DOCUMENT ID		TECN	COMMENT
17±6	**−110 ± 20**	ANISOVICH	12A	DPWA	Multichannel

N(1710) DECAY MODES

The following branching fractions are our estimates, not fits or averages.

	Mode	Fraction (Γ_i/Γ)	Scale factor
Γ_1	$N\pi$	5–20 %	
Γ_2	$N\eta$	10–30 %	
Γ_3	$N\omega$	(8±5) %	3.5
Γ_4	ΛK	5–25 %	
Γ_5	ΣK		
Γ_6	$N\pi\pi$	40–90 %	
Γ_7	$\Delta\pi$	15–40 %	
Γ_8	$\Delta(1232)\pi$, P-wave		
Γ_9	$N\rho$	5–25 %	
Γ_{10}	$N\rho$, S=1/2, P-wave		
Γ_{11}	$N\rho$, S=3/2, P-wave		
Γ_{12}	$N(\pi\pi)^{I=0}_{S\text{-wave}}$	10–40 %	
Γ_{13}	$p\gamma$	0.002–0.08 %	
Γ_{14}	$p\gamma$, helicity=1/2	0.002–0.08 %	
Γ_{15}	$n\gamma$	0.0–0.02%	
Γ_{16}	$n\gamma$, helicity=1/2	0.0–0.02%	

N(1710) BRANCHING RATIOS

$\Gamma(N\pi)/\Gamma_{total}$ Γ_1/Γ

VALUE (%)	DOCUMENT ID		TECN	COMMENT
5 to 20 OUR ESTIMATE				
2± 2	SHKLYAR	13	PWA	Multichannel
5± 4	ANISOVICH	12A	DPWA	Multichannel
20± 4	CUTKOSKY	80	IPWA	$\pi N \to \pi N$
12± 4	HOEHLER	79	IPWA	$\pi N \to \pi N$
• • • We do not use the following data for averages, fits, limits, etc. • • •				
15± 4	SHRESTHA	12A	DPWA	Multichannel
12± 6	ANISOVICH	10	DPWA	Multichannel
22±24	[1] BATINIC	10	DPWA	$\pi N \to N\pi$, $N\eta$
14± 8	PENNER	02C	DPWA	Multichannel
27±13	VRANA	00	DPWA	Multichannel
9± 4	MANLEY	92	IPWA	$\pi N \to \pi N$ & $N\pi\pi$

$\Gamma(N\eta)/\Gamma_{total}$ Γ_2/Γ

VALUE (%)	DOCUMENT ID		TECN	COMMENT
10 to 30 OUR ESTIMATE				
45± 4	SHKLYAR	13	DPWA	Multichannel
17±10	ANISOVICH	12A	DPWA	Multichannel
36±11	PENNER	02C	DPWA	Multichannel
6± 1	VRANA	00	DPWA	Multichannel
• • • We do not use the following data for averages, fits, limits, etc. • • •				
11± 7	SHRESTHA	12A	DPWA	Multichannel
6± 8	[1] BATINIC	10	DPWA	$\pi N \to N\pi$, $N\eta$

$\Gamma(N\omega)/\Gamma_{total}$ Γ_3/Γ

VALUE (%)	DOCUMENT ID		TECN	COMMENT
8±5 OUR AVERAGE Error includes scale factor of 3.5.				
3±2	SHKLYAR	13	DPWA	Multichannel
13±2	PENNER	02C	DPWA	Multichannel

$(\Gamma_i\Gamma_f)^{1/2}/\Gamma_{total}$ in $N\pi \to N(1710) \to \Lambda K$ $(\Gamma_1\Gamma_4)^{1/2}/\Gamma$

VALUE	DOCUMENT ID		TECN	COMMENT
+0.12 to +0.18 OUR ESTIMATE				
+0.16	BELL	83	DPWA	$\pi^- p \to \Lambda K^0$
+0.14	SAXON	80	DPWA	$\pi^- p \to \Lambda K^0$

$\Gamma(\Lambda K)/\Gamma_{total}$ Γ_4/Γ

VALUE (%)	DOCUMENT ID		TECN	COMMENT
5 to 25 OUR ESTIMATE				
23± 7	ANISOVICH	12A	DPWA	Multichannel
5± 3	SHKLYAR	05	DPWA	Multichannel
5± 2	PENNER	02C	DPWA	Multichannel
10±10	VRANA	00	DPWA	Multichannel
• • • We do not use the following data for averages, fits, limits, etc. • • •				
8± 4	SHRESTHA	12A	DPWA	Multichannel

$\Gamma(\Sigma K)/\Gamma_{total}$ Γ_5/Γ

VALUE (%)	DOCUMENT ID		TECN	COMMENT
• • • We do not use the following data for averages, fits, limits, etc. • • •				
7±7	PENNER	02C	DPWA	Multichannel

$(\Gamma_i\Gamma_f)^{1/2}/\Gamma_{total}$ in $N\pi \to N(1710) \to \Sigma K$ $(\Gamma_1\Gamma_5)^{1/2}/\Gamma$

VALUE	DOCUMENT ID		TECN	COMMENT
• • • We do not use the following data for averages, fits, limits, etc. • • •				
−0.034	LIVANOS	80	DPWA	$\pi p \to \Sigma K$

Note: Signs of couplings from $\pi N \to N\pi\pi$ analyses were changed in the 1986 edition to agree with the baryon-first convention; the overall phase ambiguity is resolved by choosing a negative sign for the $\Delta(1620)$ S_{31} coupling to $\Delta(1232)\pi$.

$(\Gamma_i\Gamma_f)^{1/2}/\Gamma_{total}$ in $N\pi \to N(1710) \to \Delta(1232)\pi$, P-wave $(\Gamma_1\Gamma_8)^{1/2}/\Gamma$

VALUE	DOCUMENT ID		TECN	COMMENT
±0.16 to ±0.22 OUR ESTIMATE				
−0.17	[2] LONGACRE	77	IPWA	$\pi N \to N\pi\pi$
+0.20	[3] LONGACRE	75	IPWA	$\pi N \to N\pi\pi$
• • • We do not use the following data for averages, fits, limits, etc. • • •				
−0.21 ± 0.04	MANLEY	92	IPWA	$\pi N \to \pi N$ & $N\pi\pi$

$\Gamma(\Delta(1232)\pi, P\text{-wave})/\Gamma_{total}$ Γ_8/Γ

VALUE (%)	DOCUMENT ID		TECN	COMMENT
39 ± 8	VRANA	00	DPWA	Multichannel
• • • We do not use the following data for averages, fits, limits, etc. • • •				
6 ± 3	SHRESTHA	12A	DPWA	Multichannel

$(\Gamma_i\Gamma_f)^{1/2}/\Gamma_{total}$ in $N\pi \to N(1710) \to N\rho$, S=1/2, P-wave $(\Gamma_1\Gamma_{10})^{1/2}/\Gamma$

VALUE	DOCUMENT ID		TECN	COMMENT
±0.09 to ±0.19 OUR ESTIMATE				
+0.19	[2] LONGACRE	77	IPWA	$\pi N \to N\pi\pi$
−0.20	[3] LONGACRE	75	IPWA	$\pi N \to N\pi\pi$
• • • We do not use the following data for averages, fits, limits, etc. • • •				
+0.05 ± 0.06	MANLEY	92	IPWA	$\pi N \to \pi N$ & $N\pi\pi$

$\Gamma(N\rho, S$=1/2, P-wave$)/\Gamma_{total}$ Γ_{10}/Γ

VALUE (%)	DOCUMENT ID		TECN	COMMENT
17 ± 1	VRANA	00	DPWA	Multichannel
• • • We do not use the following data for averages, fits, limits, etc. • • •				
17 ± 6	SHRESTHA	12A	DPWA	Multichannel

$(\Gamma_i\Gamma_f)^{1/2}/\Gamma_{total}$ in $N\pi \to N(1710) \to N\rho$, S=3/2, P-wave $(\Gamma_1\Gamma_{11})^{1/2}/\Gamma$

VALUE	DOCUMENT ID		TECN	COMMENT
+0.31	[2] LONGACRE	77	IPWA	$\pi N \to N\pi\pi$

$(\Gamma_i\Gamma_f)^{1/2}/\Gamma_{total}$ in $N\pi \to N(\pi\pi)^{I=0}_{S\text{-wave}}$ $(\Gamma_1\Gamma_{12})^{1/2}/\Gamma$

VALUE	DOCUMENT ID		TECN	COMMENT
±0.14 to ±0.22 OUR ESTIMATE				
−0.26	[2] LONGACRE	77	IPWA	$\pi N \to N\pi\pi$
−0.28	[3] LONGACRE	75	IPWA	$\pi N \to N\pi\pi$
• • • We do not use the following data for averages, fits, limits, etc. • • •				
+0.04 ± 0.05	MANLEY	92	IPWA	$\pi N \to \pi N$ & $N\pi\pi$

$\Gamma(N(\pi\pi)^{I=0}_{S\text{-wave}})/\Gamma_{total}$ Γ_{12}/Γ

VALUE (%)	DOCUMENT ID		TECN	COMMENT
1 ± 1	VRANA	00	DPWA	Multichannel
• • • We do not use the following data for averages, fits, limits, etc. • • •				
<1	SHRESTHA	12A	DPWA	Multichannel

$N(1710)$ PHOTON DECAY AMPLITUDES

Papers on γN amplitudes predating 1981 may be found in our 2006 edition, Journal of Physics (generic for all A,B,E,G) **G33** 1 (2006).

$N(1710) \to p\gamma$, helicity-1/2 amplitude $A_{1/2}$

VALUE ($GeV^{-1/2}$)	DOCUMENT ID		TECN	COMMENT
0.040±0.020 OUR ESTIMATE				
0.052 ± 0.015	ANISOVICH	12A	DPWA	Multichannel
0.007 ± 0.015	ARNDT	96	IPWA	$\gamma N \to \pi N$
0.006 ± 0.018	CRAWFORD	83	IPWA	$\gamma N \to \pi N$
0.028 ± 0.009	AWAJI	81	DPWA	$\gamma N \to \pi N$
• • • We do not use the following data for averages, fits, limits, etc. • • •				
−0.050 ± 0.001	SHKLYAR	13	DPWA	Multichannel
−0.008 ± 0.003	SHRESTHA	12A	DPWA	Multichannel
0.025 ± 0.010	ANISOVICH	10	DPWA	Multichannel
0.044	PENNER	02D	DPWA	Multichannel
−0.037 ± 0.002	LI	93	IPWA	$\gamma N \to \pi N$

$N(1710) \to n\gamma$, helicity-1/2 amplitude $A_{1/2}$

VALUE ($GeV^{-1/2}$)	DOCUMENT ID		TECN	COMMENT
−0.040±0.020 OUR ESTIMATE				
−0.002 ± 0.015	ARNDT	96	IPWA	$\gamma N \to \pi N$
0.000 ± 0.018	AWAJI	81	DPWA	$\gamma N \to \pi N$
−0.001 ± 0.003	FUJII	81	DPWA	$\gamma N \to \pi N$
• • • We do not use the following data for averages, fits, limits, etc. • • •				
0.017 ± 0.003	SHRESTHA	12A	DPWA	Multichannel
−0.024	PENNER	02D	DPWA	Multichannel
0.052 ± 0.003	LI	93	IPWA	$\gamma N \to \pi N$

$N(1710)$ $\gamma p \to \Lambda K^+$ AMPLITUDES

$(\Gamma_i\Gamma_f)^{1/2}/\Gamma_{total}$ in $p\gamma \to N(1710) \to \Lambda K^+$ (M_{1-} amplitude)

VALUE (units 10^{-3})	DOCUMENT ID		TECN
• • • We do not use the following data for averages, fits, limits, etc. • • •			
−10.6 ±0.4	WORKMAN	90	DPWA
− 7.21	TANABE	89	DPWA

$p\gamma \to N(1710) \to \Lambda K^+$ phase angle θ (M_{1-} amplitude)

VALUE (degrees)	DOCUMENT ID		TECN
• • • We do not use the following data for averages, fits, limits, etc. • • •			
215 ±3	WORKMAN	90	DPWA
176.3	TANABE	89	DPWA

$N(1710)$ FOOTNOTES

[1] BATINIC 10 finds evidence for a second P_{11} state with all parameters except for the phase of the pole residue very similar to the parameters we give here.

[2] LONGACRE 77 pole positions are from a search for poles in the unitarized T-matrix; the first (second) value uses, in addition to $\pi N \to N\pi\pi$ data, elastic amplitudes from a Saclay (CERN) partial-wave analysis. The other LONGACRE 77 values are from eyeball fits with Breit-Wigner circles to the T-matrix amplitudes.

[3] From method II of LONGACRE 75: eyeball fits with Breit-Wigner circles to the T-matrix amplitudes.

[4] See HOEHLER 93 for a detailed discussion of the evidence for and the pole parameters of N and Δ resonances as determined from Argand diagrams of πN elastic partial-wave amplitudes and from plots of the speeds with which the amplitudes traverse the diagrams.

[5] LONGACRE 78 values are from a search for poles in the unitarized T-matrix. The first (second) value uses, in addition to $\pi N \to N\pi\pi$ data, elastic amplitudes from a Saclay (CERN) partial-wave analysis.

$N(1710)$ REFERENCES

For early references, see Physics Letters **111B** 1 (1982).

SHKLYAR	13	PR C87 015201	V. Shklyar, H. Lenske, U. Mosel	(GIES)
ANISOVICH	12A	EPJ A48 15	A.V. Anisovich *et al.*	(BONN, PNPI)
SHRESTHA	12A	PR C86 055203	M. Shrestha, D.M. Manley	(KSU)
ANISOVICH	10	EPJ A44 203	A.V. Anisovich *et al.*	(BONN, PNPI)
BATINIC	10	PR C82 038203	M. Batinic *et al.*	(ZAGR)
ARNDT	06	PR C74 045205	R.A. Arndt *et al.*	(GWU)
PDG	06	JP G33 1	W.-M. Yao *et al.*	(PDG Collab.)
SHKLYAR	05	PR C72 015210	V. Shklyar, H. Lenske, U. Mosel	(GIES)
PENNER	02C	PR C66 055211	G. Penner, U. Mosel	(GIES)
PENNER	02D	PR C66 055212	G. Penner, U. Mosel	(GIES)
VRANA	00	PRPL 328 181	T.P. Vrana, S.A. Dytman,, T.-S.H. Lee	(PITT+)
ARNDT	96	PR C53 430	R.A. Arndt, I.I. Strakovsky, R.L. Workman	(VPI)
ARNDT	95	PR C52 2120	R.A. Arndt *et al.*	(VPI, BRCO)
HOEHLER	93	πN Newsletter 9 1	G. Hohler	(KARL)
LI	93	PR C47 2759	Z.J. Li *et al.*	(VPI)
MANLEY	92	PR D45 4002	D.M. Manley, E.M. Saleski	(KSA) IJP
Also		PR D30 904	D.M. Manley *et al.*	(VPI)
ARNDT	91	PR D43 2131	R.A. Arndt *et al.*	(VPI, TELE) IJP
CUTKOSKY	90	PR D42 235	R.E. Cutkosky, S. Wang	(CMU)
WORKMAN	90	PR C42 781	R.L. Workman	(VPI)
TANABE	89	PR C39 741	H. Tanabe, M. Kohno, C. Bennhold	(MANZ)
Also		NC 102A 193	M. Kohno, H. Tanabe, C. Bennhold	(MANZ)
BELL	83	NP B222 389	K.W. Bell *et al.*	(RL) IJP
CRAWFORD	83	NP B211 1	R.L. Crawford, W.T. Morton	(GLAS)
PDG	82	PL 111B 1	M. Roos *et al.*	(HELS, CIT, CERN)
AWAJI	81	Bonn Conf. 352	N. Awaji, R. Kajikawa	(NAGO)
Also		NP B197 365	K. Fujii *et al.*	(NAGO)
FUJII	81	NP B187 53	K. Fujii *et al.*	(NAGO, OSAK)
CUTKOSKY	80	Toronto Conf. 19	R.E. Cutkosky *et al.*	(CMU, LBL) IJP
Also		PR D20 2839	R.E. Cutkosky *et al.*	(CMU, LBL) IJP
LIVANOS	80	Toronto Conf. 35	P. Livanos *et al.*	(SACL) IJP
SAXON	80	NP B162 522	D.H. Saxon *et al.*	(RHEL, BRIS) IJP
HOEHLER	79	PDAT 12-1	G. Hohler *et al.*	(KARLT) IJP
Also		Toronto Conf. 3	R. Koch	(KARLT) IJP
LONGACRE	78	PR D17 1795	R.S. Longacre *et al.*	(LBL, SLAC)
LONGACRE	77	NP B122 493	R.S. Longacre, J. Dolbeau	(SACL) IJP
Also		NP B108 365	J. Dolbeau *et al.*	(SACL) IJP
LONGACRE	75	PL 55B 415	R.S. Longacre *et al.*	(LBL, SLAC) IJP

$N(1720)\ 3/2^+$

$I(J^P) = \frac{1}{2}(\frac{3}{2}^+)$ Status: ****

Most of the results published before 1975 were last included in our 1982 edition, Physics Letters **111B** 1 (1982). Some further obsolete results published before 1984 were last included in our 2006 edition, Journal of Physics (generic for all A,B,E,G) **G33** 1 (2006).

$N(1720)$ BREIT-WIGNER MASS

VALUE (MeV)	DOCUMENT ID		TECN	COMMENT
1700 to 1750 (≈ 1720) OUR ESTIMATE				
1700 ± 10	SHKLYAR	13	DPWA	Multichannel
1690 $^{+70}_{-35}$	ANISOVICH	12A	DPWA	Multichannel
1763.8± 4.6	ARNDT	06	DPWA	$\pi N \to \pi N, \eta N$
1700 ± 50	CUTKOSKY	80	IPWA	$\pi N \to \pi N$
1710 ± 20	HOEHLER	79	IPWA	$\pi N \to \pi N$
• • • We do not use the following data for averages, fits, limits, etc. • • •				
1720 ± 5	SHRESTHA	12A	DPWA	Multichannel
1770 ±100	ANISOVICH	10	DPWA	Multichannel
1720 ± 18	BATINIC	10	DPWA	$\pi N \to N\pi, N\eta$
1790 ±100	THOMA	08	DPWA	Multichannel
1749.6± 4.5	ARNDT	04	DPWA	$\pi N \to \pi N, \eta N$
1705 ± 10	PENNER	02C	DPWA	Multichannel
1716 ±112	VRANA	00	DPWA	Multichannel
1713 ± 10	ARNDT	96	IPWA	$\gamma N \to \pi N$
1820	ARNDT	95	DPWA	$\pi N \to N\pi$
1720	LI	93	IPWA	$\gamma N \to \pi N$
1717 ± 31	MANLEY	92	IPWA	$\pi N \to \pi N$ & $N\pi\pi$
1690	SAXON	80	DPWA	$\pi^- p \to \Lambda K^0$
1750	[1] LONGACRE	77	IPWA	$\pi N \to N\pi\pi$
1720	[2] LONGACRE	75	IPWA	$\pi N \to N\pi\pi$

$N(1720)$ BREIT-WIGNER WIDTH

VALUE (MeV)	DOCUMENT ID		TECN	COMMENT
150 to 400 (≈ 250) OUR ESTIMATE				
152± 2	SHKLYAR	13	DPWA	Multichannel
420±100	ANISOVICH	12A	DPWA	Multichannel
210± 22	ARNDT	06	DPWA	$\pi N \to \pi N, \eta N$
125± 70	CUTKOSKY	80	IPWA	$\pi N \to \pi N$
190± 30	HOEHLER	79	IPWA	$\pi N \to \pi N$
• • • We do not use the following data for averages, fits, limits, etc. • • •				
200± 20	SHRESTHA	12A	DPWA	Multichannel
650±120	ANISOVICH	10	DPWA	Multichannel
244± 28	BATINIC	10	DPWA	$\pi N \to N\pi, N\eta$
690±100	THOMA	08	DPWA	Multichannel
256± 22	ARNDT	04	DPWA	$\pi N \to \pi N, \eta N$
237± 73	PENNER	02C	DPWA	Multichannel
121± 39	VRANA	00	DPWA	Multichannel
153± 15	ARNDT	96	IPWA	$\gamma N \to \pi N$
354	ARNDT	95	DPWA	$\pi N \to N\pi$
200	LI	93	IPWA	$\gamma N \to \pi N$
380±180	MANLEY	92	IPWA	$\pi N \to \pi N$ & $N\pi\pi$
120	SAXON	80	DPWA	$\pi^- p \to \Lambda K^0$
130	[1] LONGACRE	77	IPWA	$\pi N \to N\pi\pi$
150	[2] LONGACRE	75	IPWA	$\pi N \to N\pi\pi$

$N(1720)$ POLE POSITION

REAL PART

VALUE (MeV)	DOCUMENT ID		TECN	COMMENT
1660 to 1690 (≈ 1675) OUR ESTIMATE				
1660±30	ANISOVICH	12A	DPWA	Multichannel
1666	ARNDT	06	DPWA	$\pi N \to \pi N, \eta N$
1686	[3] HOEHLER	93	SPED	$\pi N \to \pi N$
1680±30	CUTKOSKY	80	IPWA	$\pi N \to \pi N$
• • • We do not use the following data for averages, fits, limits, etc. • • •				
1670	SHKLYAR	13	DPWA	Multichannel
1687	SHRESTHA	12A	DPWA	Multichannel
1660±35	ANISOVICH	10	DPWA	Multichannel
1691±23	BATINIC	10	DPWA	$\pi N \to N\pi, N\eta$
1630±90	THOMA	08	DPWA	Multichannel
1655	ARNDT	04	DPWA	$\pi N \to \pi N, \eta N$
1692	VRANA	00	DPWA	Multichannel
1717	ARNDT	95	DPWA	$\pi N \to N\pi$
1675	ARNDT	91	DPWA	$\pi N \to \pi N$ Soln SM90
1716 or 1716	[4] LONGACRE	78	IPWA	$\pi N \to N\pi\pi$
1745 or 1748	[1] LONGACRE	77	IPWA	$\pi N \to N\pi\pi$

−2×IMAGINARY PART

VALUE (MeV)	DOCUMENT ID		TECN	COMMENT
150 to 400 (≈ 250) OUR ESTIMATE				
450±100	ANISOVICH	12A	DPWA	Multichannel
355	ARNDT	06	DPWA	$\pi N \to \pi N, \eta N$
187	[3] HOEHLER	93	SPED	$\pi N \to \pi N$
120± 40	CUTKOSKY	80	IPWA	$\pi N \to \pi N$
• • • We do not use the following data for averages, fits, limits, etc. • • •				
118	SHKLYAR	13	DPWA	Multichannel
175	SHRESTHA	12A	DPWA	Multichannel
360± 80	ANISOVICH	10	DPWA	Multichannel
233± 23	BATINIC	10	DPWA	$\pi N \to N\pi, N\eta$
460± 80	THOMA	08	DPWA	Multichannel
278	ARNDT	04	DPWA	$\pi N \to \pi N, \eta N$
94	VRANA	00	DPWA	Multichannel
388	ARNDT	95	DPWA	$\pi N \to N\pi$
114	ARNDT	91	DPWA	$\pi N \to \pi N$ Soln SM90
124 or 126	[4] LONGACRE	78	IPWA	$\pi N \to N\pi\pi$
135 or 123	[1] LONGACRE	77	IPWA	$\pi N \to N\pi\pi$

$N(1720)$ ELASTIC POLE RESIDUE

MODULUS $|r|$

VALUE (MeV)	DOCUMENT ID		TECN	COMMENT
15±8 OUR ESTIMATE				
22±8	ANISOVICH	12A	DPWA	Multichannel
25	ARNDT	06	DPWA	$\pi N \to \pi N, \eta N$
15	HOEHLER	93	SPED	$\pi N \to \pi N$
8±2	CUTKOSKY	80	IPWA	$\pi N \to \pi N$
• • • We do not use the following data for averages, fits, limits, etc. • • •				
12	SHKLYAR	13	DPWA	Multichannel
20	BATINIC	10	DPWA	$\pi N \to N\pi, N\eta$
20	ARNDT	04	DPWA	$\pi N \to \pi N, \eta N$
39	ARNDT	95	DPWA	$\pi N \to N\pi$
11	ARNDT	91	DPWA	$\pi N \to \pi N$ Soln SM90

PHASE θ

VALUE (°)	DOCUMENT ID		TECN	COMMENT
−130±30 OUR ESTIMATE				
−115±30	ANISOVICH	12A	DPWA	Multichannel
− 94	ARNDT	06	DPWA	$\pi N \to \pi N, \eta N$
−160±30	CUTKOSKY	80	IPWA	$\pi N \to \pi N$
• • • We do not use the following data for averages, fits, limits, etc. • • •				
− 45	SHKLYAR	13	DPWA	Multichannel
−109	BATINIC	10	DPWA	$\pi N \to N\pi, N\eta$
− 88	ARNDT	04	DPWA	$\pi N \to \pi N, \eta N$
− 70	ARNDT	95	DPWA	$\pi N \to N\pi$
−130	ARNDT	91	DPWA	$\pi N \to \pi N$ Soln SM90

$N(1720)$ INELASTIC POLE RESIDUE

The "normalized residue" is the residue divided by $\Gamma_{pole}/2$.

Normalized residue in $N\pi \to N(1720) \to N\eta$

MODULUS (%)	DOCUMENT ID		TECN	COMMENT
3±2	ANISOVICH	12A	DPWA	Multichannel

Normalized residue in $N\pi \to N(1720) \to \Lambda K$

MODULUS (%)	PHASE (°)	DOCUMENT ID		TECN	COMMENT
6±4	**−150 ± 45**	ANISOVICH	12A	DPWA	Multichannel

Normalized residue in $N\pi \to N(1720) \to \Delta\pi$, P-wave

MODULUS (%)	PHASE (°)	DOCUMENT ID		TECN	COMMENT
29±8	**80 ± 40**	ANISOVICH	12A	DPWA	Multichannel

Normalized residue in $N\pi \to N(1720) \to \Delta\pi$, F-wave

MODULUS (%)	DOCUMENT ID		TECN	COMMENT
3±3	ANISOVICH	12A	DPWA	Multichannel

$N(1720)$ DECAY MODES

The following branching fractions are our estimates, not fits or averages.

	Mode	Fraction (Γ_i/Γ)
Γ_1	$N\pi$	(11± 3) %
Γ_2	$N\eta$	(4± 1) %
Γ_3	ΛK	1–15 %
Γ_4	ΣK	
Γ_5	$N\pi\pi$	>70 %
Γ_6	$\Delta\pi$	
Γ_7	$\Delta(1232)\pi$, P-wave	(75±15) %
Γ_8	$N\rho$	70–85 %

Γ_9	$N\rho$, S=1/2, P-wave	large
Γ_{10}	$N\rho$, S=3/2, P-wave	
Γ_{11}	$N(\pi\pi)^{I=0}_{S\text{-wave}}$	
Γ_{12}	$p\gamma$	0.05–0.25 %
Γ_{13}	$p\gamma$, helicity=1/2	0.05–0.15 %
Γ_{14}	$p\gamma$, helicity=3/2	0.002–0.16 %
Γ_{15}	$n\gamma$	0.0–0.016 %
Γ_{16}	$n\gamma$, helicity=1/2	0.0–0.01 %
Γ_{17}	$n\gamma$, helicity=3/2	0.0–0.015 %

N(1720) BRANCHING RATIOS

$\Gamma(N\pi)/\Gamma_{total}$ Γ_1/Γ

VALUE (%)	DOCUMENT ID		TECN	COMMENT
11 ±3 OUR ESTIMATE				
17 ±2	SHKLYAR	13	DPWA	Multichannel
10 ±5	ANISOVICH	12A	DPWA	Multichannel
9.4±0.5	ARNDT	06	DPWA	$\pi N \to \pi N$, ηN
10 ±4	CUTKOSKY	80	IPWA	$\pi N \to \pi N$
14 ±3	HOEHLER	79	IPWA	$\pi N \to \pi N$
• • • We do not use the following data for averages, fits, limits, etc. • • •				
13.6±0.6	SHRESTHA	12A	DPWA	Multichannel
14 ±5	ANISOVICH	10	DPWA	Multichannel
18 ±3	BATINIC	10	DPWA	$\pi N \to N\pi$, $N\eta$
9 ±6	THOMA	08	DPWA	Multichannel
19.0±0.4	ARNDT	04	DPWA	$\pi N \to \pi N$, ηN
17 ±2	PENNER	02C	DPWA	Multichannel
5 ±5	VRANA	00	DPWA	Multichannel
16	ARNDT	95	DPWA	$\pi N \to N\pi$
13 ±5	MANLEY	92	IPWA	$\pi N \to \pi N$ & $N\pi\pi$

$\Gamma(N\eta)/\Gamma_{total}$ Γ_2/Γ

VALUE (%)	DOCUMENT ID		TECN	COMMENT
2.1±1.4 OUR AVERAGE Error includes scale factor of 2.0. See the ideogram below.				
0 ±1	SHKLYAR	13	DPWA	Multichannel
3 ±2	ANISOVICH	12A	DPWA	Multichannel
4 ±1	VRANA	00	DPWA	Multichannel
• • • We do not use the following data for averages, fits, limits, etc. • • •				
< 1	SHRESTHA	12A	DPWA	Multichannel
0 ±1	BATINIC	10	DPWA	$\pi N \to N\pi$, $N\eta$
10 ±7	THOMA	08	DPWA	Multichannel
0.2±0.2	PENNER	02C	DPWA	Multichannel

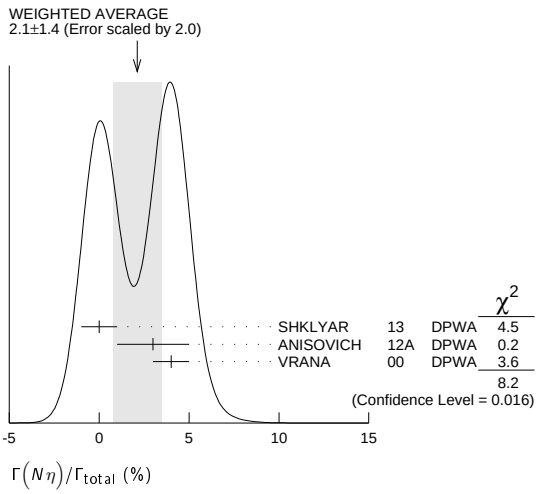

$\Gamma(\Lambda K)/\Gamma_{total}$ Γ_3/Γ

VALUE (%)	DOCUMENT ID		TECN	COMMENT
4.4±0.4 OUR AVERAGE				
4.3±0.4	SHKLYAR	05	DPWA	Multichannel
9 ±3	PENNER	02C	DPWA	Multichannel
• • • We do not use the following data for averages, fits, limits, etc. • • •				
2.8±0.4	SHRESTHA	12A	DPWA	Multichannel
12 ±9	THOMA	08	DPWA	Multichannel

$\Gamma(\Delta(1232)\pi, P\text{-wave})/\Gamma_{total}$ Γ_7/Γ

VALUE (%)	DOCUMENT ID		TECN	COMMENT
75±15	ANISOVICH	12A	DPWA	Multichannel

$(\Gamma_i\Gamma_f)^{1/2}/\Gamma_{total}$ in $N\pi \to N(1720) \to \Lambda K$ $(\Gamma_1\Gamma_3)^{1/2}/\Gamma$

VALUE	DOCUMENT ID		TECN	COMMENT
−0.14 to −0.06 OUR ESTIMATE				
−0.09	BELL	83	DPWA	$\pi^- p \to \Lambda K^0$
−0.11	SAXON	80	DPWA	$\pi^- p \to \Lambda K^0$

Note: Signs of couplings from $\pi N \to N\pi\pi$ analyses were changed in the 1986 edition to agree with the baryon-first convention; the overall phase ambiguity is resolved by choosing a negative sign for the $\Delta(1620)$ S_{31} coupling to $\Delta(1232)\pi$.

$(\Gamma_i\Gamma_f)^{1/2}/\Gamma_{total}$ in $N\pi \to N(1720) \to \Delta(1232)\pi$, P-wave $(\Gamma_1\Gamma_7)^{1/2}/\Gamma$

VALUE	DOCUMENT ID		TECN	COMMENT
−0.17	[1] LONGACRE	77	IPWA	$\pi N \to N\pi\pi$

$(\Gamma_i\Gamma_f)^{1/2}/\Gamma_{total}$ in $N\pi \to N(1720) \to N\rho$, S=1/2, P-wave $(\Gamma_1\Gamma_9)^{1/2}/\Gamma$

VALUE	DOCUMENT ID		TECN	COMMENT
−0.30 to +0.40 OUR ESTIMATE				
−0.26	[1] LONGACRE	77	IPWA	$\pi N \to N\pi\pi$
+0.40	[2] LONGACRE	75	IPWA	$\pi N \to N\pi\pi$
• • • We do not use the following data for averages, fits, limits, etc. • • •				
+0.34±0.05	MANLEY	92	IPWA	$\pi N \to \pi N$ & $N\pi\pi$

$\Gamma(N\rho, S$=1/2, P-wave$)/\Gamma_{total}$ Γ_9/Γ

VALUE (%)	DOCUMENT ID		TECN	COMMENT
91 ±1	VRANA	00	DPWA	Multichannel
• • • We do not use the following data for averages, fits, limits, etc. • • •				
1.4±0.5	SHRESTHA	12A	DPWA	Multichannel

$(\Gamma_i\Gamma_f)^{1/2}/\Gamma_{total}$ in $N\pi \to N(1720) \to N\rho$, S=3/2, P-wave $(\Gamma_1\Gamma_{10})^{1/2}/\Gamma$

VALUE	DOCUMENT ID		TECN	COMMENT
+0.15	[1] LONGACRE	77	IPWA	$\pi N \to N\pi\pi$

$(\Gamma_i\Gamma_f)^{1/2}/\Gamma_{total}$ in $N\pi \to N(1720) \to N(\pi\pi)^{I=0}_{S\text{-wave}}$ $(\Gamma_1\Gamma_{11})^{1/2}/\Gamma$

VALUE	DOCUMENT ID		TECN	COMMENT
−0.19	[1] LONGACRE	77	IPWA	$\pi N \to N\pi\pi$

N(1720) PHOTON DECAY AMPLITUDES

Papers on γN amplitudes predating 1981 may be found in our 2006 edition, Journal of Physics (generic for all A,B,E,G) **G33** 1 (2006).

$N(1720) \to p\gamma$, helicity-1/2 amplitude $A_{1/2}$

VALUE ($GeV^{-1/2}$)	DOCUMENT ID		TECN	COMMENT
0.100±0.020 OUR ESTIMATE				
0.110±0.045	ANISOVICH	12A	DPWA	Multichannel
0.095±0.002	WORKMAN	12A	DPWA	$\gamma N \to N\pi$
0.097±0.003	DUGGER	07	DPWA	$\gamma N \to \pi N$
0.044±0.066	CRAWFORD	83	IPWA	$\gamma N \to \pi N$
−0.004±0.007	AWAJI	81	DPWA	$\gamma N \to \pi N$
• • • We do not use the following data for averages, fits, limits, etc. • • •				
−0.065±0.002	SHKLYAR	13	DPWA	Multichannel
0.057±0.003	SHRESTHA	12A	DPWA	Multichannel
0.130±0.050	ANISOVICH	10	DPWA	Multichannel
0.073	DRECHSEL	07	DPWA	$\gamma N \to \pi N$
−0.053	PENNER	02D	DPWA	Multichannel
−0.015±0.015	ARNDT	96	IPWA	$\gamma N \to \pi N$
0.012±0.003	LI	93	IPWA	$\gamma N \to \pi N$

$N(1720) \to p\gamma$, helicity-3/2 amplitude $A_{3/2}$

VALUE ($GeV^{-1/2}$)	DOCUMENT ID		TECN	COMMENT
0.150±0.030	ANISOVICH	12A	DPWA	Multichannel
−0.048±0.002	WORKMAN	12A	DPWA	$\gamma N \to N\pi$
−0.039±0.003	DUGGER	07	DPWA	$\gamma N \to \pi N$
−0.024±0.006	CRAWFORD	83	IPWA	$\gamma N \to \pi N$
−0.040±0.016	AWAJI	81	DPWA	$\gamma N \to \pi N$
• • • We do not use the following data for averages, fits, limits, etc. • • •				
0.035±0.002	SHKLYAR	13	DPWA	Multichannel
−0.019±0.002	SHRESTHA	12A	DPWA	Multichannel
0.100±0.050	ANISOVICH	10	DPWA	Multichannel
−0.011	DRECHSEL	07	DPWA	$\gamma N \to \pi N$
0.027	PENNER	02D	DPWA	Multichannel
0.007±0.010	ARNDT	96	IPWA	$\gamma N \to \pi N$
−0.022±0.003	LI	93	IPWA	$\gamma N \to \pi N$

$N(1720) \to n\gamma$, helicity-1/2 amplitude $A_{1/2}$

VALUE ($GeV^{-1/2}$)	DOCUMENT ID		TECN	COMMENT
0.007±0.015	ARNDT	96	IPWA	$\gamma N \to \pi N$
0.002±0.005	AWAJI	81	DPWA	$\gamma N \to \pi N$
• • • We do not use the following data for averages, fits, limits, etc. • • •				
−0.002±0.001	SHRESTHA	12A	DPWA	Multichannel
−0.003	DRECHSEL	07	DPWA	$\gamma N \to \pi N$
−0.004	PENNER	02D	DPWA	Multichannel
0.050±0.004	LI	93	IPWA	$\gamma N \to \pi N$

$N(1720) \rightarrow n\gamma$, helicity-3/2 amplitude $A_{3/2}$

VALUE ($GeV^{-1/2}$)	DOCUMENT ID		TECN	COMMENT
-0.005 ± 0.025	ARNDT	96	IPWA	$\gamma N \rightarrow \pi N$
-0.015 ± 0.019	AWAJI	81	DPWA	$\gamma N \rightarrow \pi N$
• • • We do not use the following data for averages, fits, limits, etc. • • •				
-0.001 ± 0.002	SHRESTHA	12A	DPWA	Multichannel
-0.031	DRECHSEL	07	DPWA	$\gamma N \rightarrow \pi N$
0.003	PENNER	02D	DPWA	Multichannel
-0.017 ± 0.004	LI	93	IPWA	$\gamma N \rightarrow \pi N$

$N(1720)$ $\gamma p \rightarrow \Lambda K^+$ AMPLITUDES

$(\Gamma_i\Gamma_f)^{1/2}/\Gamma_{total}$ in $p\gamma \rightarrow N(1720) \rightarrow \Lambda K^+$ (E_{1+} amplitude)

VALUE (units 10^{-3})	DOCUMENT ID		TECN
• • • We do not use the following data for averages, fits, limits, etc. • • •			
10.2 ± 0.2	WORKMAN	90	DPWA
9.52	TANABE	89	DPWA

$p\gamma \rightarrow N(1720) \rightarrow \Lambda K^+$ phase angle θ (E_{1+} amplitude)

VALUE (degrees)	DOCUMENT ID		TECN
• • • We do not use the following data for averages, fits, limits, etc. • • •			
-124 ± 2	WORKMAN	90	DPWA
-103.4	TANABE	89	DPWA

$(\Gamma_i\Gamma_f)^{1/2}/\Gamma_{total}$ in $p\gamma \rightarrow N(1720) \rightarrow \Lambda K^+$ (M_{1+} amplitude)

VALUE (units 10^{-3})	DOCUMENT ID		TECN
• • • We do not use the following data for averages, fits, limits, etc. • • •			
-4.5 ± 0.2	WORKMAN	90	DPWA
3.18	TANABE	89	DPWA

$N(1720)$ FOOTNOTES

[1] LONGACRE 77 pole positions are from a search for poles in the unitarized T-matrix; the first (second) value uses, in addition to $\pi N \rightarrow N\pi\pi$ data, elastic amplitudes from a Saclay (CERN) partial-wave analysis. The other LONGACRE 77 values are from eyeball fits with Breit-Wigner circles to the T-matrix amplitudes.

[2] From method II of LONGACRE 75: eyeball fits with Breit-Wigner circles to the T-matrix amplitudes.

[3] See HOEHLER 93 for a detailed discussion of the evidence for and the pole parameters of N and Δ resonances as determined from Argand diagrams of πN elastic partial-wave amplitudes and from plots of the speeds with which the amplitudes traverse the diagrams.

[4] LONGACRE 78 values are from a search for poles in the unitarized T-matrix. The first (second) value uses, in addition to $\pi N \rightarrow N\pi\pi$ data, elastic amplitudes from a Saclay (CERN) partial-wave analysis.

$N(1720)$ REFERENCES

For early references, see Physics Letters **111B** 1 (1982).

SHKLYAR	13	PR C87 015201	V. Shklyar, H. Lenske, U. Mosel	(GIES)
ANISOVICH	12A	EPJ A48 15	A.V. Anisovich *et al.*	(BONN, PNPI)
SHRESTHA	12A	PR C86 055203	M. Shrestha, D.M. Manley	(KSU)
WORKMAN	12A	PR C86 015202	R. Workman *et al.*	(GWU)
ANISOVICH	10	EPJ A44 203	A.V. Anisovich *et al.*	(BONN, PNPI)
BATINIC	10	PR C82 038203	M. Batinic *et al.*	(ZAGR)
THOMA	08	PL B659 87	U. Thoma *et al.*	(CB-ELSA Collab.)
DRECHSEL	07	EPJ A34 69	D. Drechsel, S.S. Kamalov, L. Tiator	(MAINZ, JINR)
DUGGER	07	PR C76 025211	M. Dugger *et al.*	(Jefferson Lab CLAS Collab.)
ARNDT	06	PR C74 045205	R.A. Arndt *et al.*	(GWU)
PDG	06	JP G33 1	W.-M. Yao *et al.*	(PDG Collab.)
SHKLYAR	05	PR C72 015210	V. Shklyar, H. Lenske, U. Mosel	(GIES)
ARNDT	04	PR C69 035213	R.A. Arndt *et al.*	(GWU, TRIU)
PENNER	02C	PR C66 055211	G. Penner, U. Mosel	(GIES)
PENNER	02D	PR C66 055212	G. Penner, U. Mosel	(GIES)
VRANA	00	PRPL 328 181	T.P. Vrana, S.A. Dytman,, T.-S.H. Lee	(PITT+)
ARNDT	96	PR C53 430	R.A. Arndt, I.I. Strakovsky, R.L. Workman	(VPI)
ARNDT	95	PR C52 2120	R.A. Arndt *et al.*	(VPI, BRCO)
HOEHLER	93	πN Newsletter 9 1	G. Hohler	(KARL)
LI	93	PR C47 2759	Z.J. Li *et al.*	(VPI)
MANLEY	92	PR D45 4002	D.M. Manley, E.M. Saleski	(KSA) IJP
Also		PR D30 904	D.M. Manley *et al.*	(VPI)
ARNDT	91	PR D43 2131	R.A. Arndt *et al.*	(VPI, TELE) IJP
WORKMAN	90	PR C42 781	R.L. Workman	(VPI)
TANABE	89	PR C39 741	H. Tanabe, M. Kohno, C. Bennhold	(MANZ)
Also		NC 102A 193	M. Kohno, H. Tanabe, C. Bennhold	(MANZ)
BELL	83	NP B222 389	K.W. Bell *et al.*	(RL) IJP
CRAWFORD	83	NP B211 1	R.L. Crawford, W.T. Morton	(GLAS)
PDG	82	PL 111B 1	M. Roos *et al.*	(HELS, CIT, CERN)
AWAJI	81	Bonn Conf. 352	N. Awaji, R. Kajikawa	(NAGO)
Also		NP B197 365	K. Fujii *et al.*	(NAGO)
CUTKOSKY	80	Toronto Conf. 19	R.E. Cutkosky *et al.*	(CMU, LBL) IJP
Also		PR D20 2839	R.E. Cutkosky *et al.*	(CMU, LBL) IJP
SAXON	80	NP B162 522	D.H. Saxon *et al.*	(RHEL, BRIS) IJP
HOEHLER	79	PDAT 12-1	G. Hohler *et al.*	(KARLT) IJP
Also		Toronto Conf. 3	R. Koch	(KARLT) IJP
LONGACRE	78	PR D17 1795	R.S. Longacre *et al.*	(LBL, SLAC)
LONGACRE	77	NP B122 493	R.S. Longacre, J. Dolbeau	(SACL) IJP
Also		NP B108 365	J. Dolbeau *et al.*	(SACL) IJP
LONGACRE	75	PL 55B 415	R.S. Longacre *et al.*	(LBL, SLAC) IJP

$N(1860)$ $5/2^+$

$I(J^P) = \frac{1}{2}(\frac{5}{2}^+)$ Status: **

OMITTED FROM SUMMARY TABLE

Before the 2012 *Review*, all the evidence for a $J^P = 5/2^+$ state with a mass above 1800 MeV was filed under a two-star $N(2000)$. There is now some evidence from ANISOVICH 12A for two $5/2^+$ states in this region, so we have split the older data (according to mass) between two two-star $5/2^+$ states, an $N(1860)$ and an $N(2000)$.

$N(1860)$ BREIT-WIGNER MASS

VALUE (MeV)	DOCUMENT ID		TECN	COMMENT
1820 to 1960 ($\approx$ 1860) OUR ESTIMATE				
$1860 \ ^{+120}_{-\ 60}$	ANISOVICH	12A	DPWA	Multichannel
1817.7	ARNDT	06	DPWA	$\pi N \rightarrow \pi N, \eta N$
1882 ± 10	HOEHLER	79	IPWA	$\pi N \rightarrow \pi N$
• • • We do not use the following data for averages, fits, limits, etc. • • •				
1900 ± 7	SHRESTHA	12A	DPWA	Multichannel
1814	ARNDT	95	DPWA	$\pi N \rightarrow N\pi$
1903 ± 87	MANLEY	92	IPWA	$\pi N \rightarrow \pi N$ & $N\pi\pi$

$N(1860)$ BREIT-WIGNER WIDTH

VALUE (MeV)	DOCUMENT ID		TECN	COMMENT
$270 \ ^{+140}_{-\ 50}$	ANISOVICH	12A	DPWA	Multichannel
117.6	ARNDT	06	DPWA	$\pi N \rightarrow \pi N, \eta N$
95 ± 20	HOEHLER	79	IPWA	$\pi N \rightarrow \pi N$
• • • We do not use the following data for averages, fits, limits, etc. • • •				
219 ± 23	SHRESTHA	12A	DPWA	Multichannel
176	ARNDT	95	DPWA	$\pi N \rightarrow N\pi$
490 ± 310	MANLEY	92	IPWA	$\pi N \rightarrow \pi N$ & $N\pi\pi$

$N(1860)$ POLE POSITION

REAL PART

VALUE (MeV)	DOCUMENT ID		TECN	COMMENT
$1830^{+120}_{-\ 60}$	ANISOVICH	12A	DPWA	Multichannel
1807	ARNDT	06	DPWA	$\pi N \rightarrow \pi N, \eta N$
• • • We do not use the following data for averages, fits, limits, etc. • • •				
1863	SHRESTHA	12A	DPWA	Multichannel

$-2\times$IMAGINARY PART

VALUE (MeV)	DOCUMENT ID		TECN	COMMENT
$250^{+150}_{-\ 50}$	ANISOVICH	12A	DPWA	Multichannel
109	ARNDT	06	DPWA	$\pi N \rightarrow \pi N, \eta N$
• • • We do not use the following data for averages, fits, limits, etc. • • •				
189	SHRESTHA	12A	DPWA	Multichannel

$N(1860)$ ELASTIC POLE RESIDUE

MODULUS $|r|$

VALUE (MeV)	DOCUMENT ID		TECN	COMMENT
50 ± 20	ANISOVICH	12A	DPWA	Multichannel
60	ARNDT	06	DPWA	$\pi N \rightarrow \pi N, \eta N$

PHASE θ

VALUE (°)	DOCUMENT ID		TECN	COMMENT
-80 ± 40	ANISOVICH	12A	DPWA	Multichannel
-67	ARNDT	06	DPWA	$\pi N \rightarrow \pi N, \eta N$

$N(1860)$ DECAY MODES

	Mode
Γ_1	$N\pi$
Γ_2	$N\eta$
Γ_3	ΛK
Γ_4	$N\pi\pi$
Γ_5	$\Delta(1232)\pi$, P-wave
Γ_6	$\Delta(1232)\pi$, F-wave
Γ_7	$N\rho$, $S=3/2$, P-wave
Γ_8	$N\rho$, $S=3/2$, F-wave
Γ_9	$N(\pi\pi)^{I=0}_{S-wave}$
Γ_{10}	$p\gamma$
Γ_{11}	$p\gamma$, helicity=1/2
Γ_{12}	$p\gamma$, helicity=3/2
Γ_{13}	$n\gamma$
Γ_{14}	$n\gamma$, helicity=1/2
Γ_{15}	$n\gamma$, helicity=3/2

$N(1860)$ BRANCHING RATIOS

$\Gamma(N\pi)/\Gamma_{total}$ — **Γ_1/Γ**

VALUE (%)	DOCUMENT ID		TECN	COMMENT
20 ±6	ANISOVICH	12A	DPWA	Multichannel
12.7	ARNDT	06	DPWA	$\pi N \to \pi N$, ηN
4 ±2	HOEHLER	79	IPWA	$\pi N \to \pi N$
• • • We do not use the following data for averages, fits, limits, etc. • • •				
17 ±1	SHRESTHA	12A	DPWA	Multichannel
10	ARNDT	95	DPWA	$\pi N \to N\pi$
8 ±5	MANLEY	92	IPWA	$\pi N \to \pi N$ & $N\pi\pi$

$\Gamma(N\eta)/\Gamma_{total}$ — **Γ_2/Γ**

VALUE (%)	DOCUMENT ID		TECN	COMMENT
• • • We do not use the following data for averages, fits, limits, etc. • • •				
4±2	SHRESTHA	12A	DPWA	Multichannel

$\Gamma(\Lambda K)/\Gamma_{total}$ — **Γ_3/Γ**

VALUE (%)	DOCUMENT ID		TECN	COMMENT
• • • We do not use the following data for averages, fits, limits, etc. • • •				
<1	SHRESTHA	12A	DPWA	Multichannel

$(\Gamma_i\Gamma_f)^{1/2}/\Gamma_{total}$ in $N\pi \to N(1860) \to \Delta(1232)\pi$, P-wave — **$(\Gamma_1\Gamma_5)^{1/2}/\Gamma$**

VALUE	DOCUMENT ID		TECN	COMMENT
• • • We do not use the following data for averages, fits, limits, etc. • • •				
−0.03±0.03	SHRESTHA	12A	DPWA	Multichannel
+0.10±0.06	MANLEY	92	IPWA	$\pi N \to \pi N$ & $N\pi\pi$

$\Gamma(\Delta(1232)\pi$, F-wave$)/\Gamma_{total}$ — **Γ_6/Γ**

VALUE (%)	DOCUMENT ID		TECN	COMMENT
• • • We do not use the following data for averages, fits, limits, etc. • • •				
<1	SHRESTHA	12A	DPWA	Multichannel

$(\Gamma_i\Gamma_f)^{1/2}/\Gamma_{total}$ in $N\pi \to N(1860) \to N\rho$, S=3/2, P-wave — **$(\Gamma_1\Gamma_7)^{1/2}/\Gamma$**

VALUE	DOCUMENT ID		TECN	COMMENT
• • • We do not use the following data for averages, fits, limits, etc. • • •				
−0.07±0.03	SHRESTHA	12A	DPWA	Multichannel
−0.22±0.08	MANLEY	92	IPWA	$\pi N \to \pi N$ & $N\pi\pi$

$(\Gamma_i\Gamma_f)^{1/2}/\Gamma_{total}$ in $N\pi \to N(1860) \to N\rho$, S=3/2, F-wave — **$(\Gamma_1\Gamma_8)^{1/2}/\Gamma$**

VALUE	DOCUMENT ID		TECN	COMMENT
• • • We do not use the following data for averages, fits, limits, etc. • • •				
+0.11±0.06	MANLEY	92	IPWA	$\pi N \to \pi N$ & $N\pi\pi$

$\Gamma(N(\pi\pi)^{I=0}_{S-wave})/\Gamma_{total}$ — **Γ_9/Γ**

VALUE (%)	DOCUMENT ID		TECN	COMMENT
• • • We do not use the following data for averages, fits, limits, etc. • • •				
41±6	SHRESTHA	12A	DPWA	Multichannel

$N(1860)$ PHOTON DECAY AMPLITUDES

$N(1860) \to p\gamma$, helicity-1/2 amplitude $A_{1/2}$

VALUE ($GeV^{-1/2}$)	DOCUMENT ID		TECN	COMMENT
0.020±0.012	[1] ANISOVICH	12A	DPWA	Phase = (120 ± 50)°
• • • We do not use the following data for averages, fits, limits, etc. • • •				
−0.017±0.003	SHRESTHA	12A	DPWA	Multichannel

$N(1860) \to p\gamma$, helicity-3/2 amplitude $A_{3/2}$

VALUE	DOCUMENT ID		TECN	COMMENT
0.050±0.020	[1] ANISOVICH	12A	DPWA	Phase = (−80 ± 60)°
• • • We do not use the following data for averages, fits, limits, etc. • • •				
0.029±0.004	SHRESTHA	12A	DPWA	Multichannel

$N(1860) \to n\gamma$, helicity-1/2 amplitude $A_{1/2}$

VALUE ($GeV^{-1/2}$)	DOCUMENT ID		TECN	COMMENT
• • • We do not use the following data for averages, fits, limits, etc. • • •				
0.010±0.005	SHRESTHA	12A	DPWA	Multichannel

$N(1860) \to n\gamma$, helicity-3/2 amplitude $A_{3/2}$

VALUE ($GeV^{-1/2}$)	DOCUMENT ID		TECN	COMMENT
• • • We do not use the following data for averages, fits, limits, etc. • • •				
−0.009±0.005	SHRESTHA	12A	DPWA	Multichannel

$N(1860)$ FOOTNOTES

[1] This ANISOVICH 12A value is the complex helicity amplitude at the pole position.

$N(1860)$ REFERENCES

ANISOVICH	12A	EPJ A48 15	A.V. Anisovich *et al.*	(BONN, PNPI)
SHRESTHA	12A	PR C86 055203	M. Shrestha, D.M. Manley	(KSU)
ARNDT	06	PR C74 045205	R.A. Arndt *et al.*	(GWU)
ARNDT	95	PR C52 2120	R.A. Arndt *et al.*	(VPI, BRCO)
MANLEY	92	PR D45 4002	D.M. Manley, E.M. Saleski	(KSA)
Also		PR D30 904	D.M. Manley *et al.*	(VPI)
HOEHLER	79	PDAT 12-1	G. Hohler *et al.*	(KARLT)

$N(1875)$ $3/2^-$

$I(J^P) = \frac{1}{2}(\frac{3}{2}^-)$ Status: ***

Before the 2012 *Review*, all the evidence for a $J^P = 3/2^-$ state with a mass above 1800 MeV was filed under a two-star $N(2080)$. There is now evidence from ANISOVICH 12A for two $3/2^-$ states in this region, so we have split the older data (according to mass) between a three-star $N(1875)$ and a two-star $N(2120)$.

The latest GWU analysis (ARNDT 06) finds no evidence for this resonance.

$N(1875)$ BREIT-WIGNER MASS

VALUE (MeV)	DOCUMENT ID		TECN	COMMENT
1820 to 1920 (≈ 1875) OUR ESTIMATE				
1934± 10	SHKLYAR	13	DPWA	Multichannel
1880± 20	ANISOVICH	12A	DPWA	Multichannel
1920	BELL	83	DPWA	$\pi^- p \to \Lambda K^0$
1880±100	[1] CUTKOSKY	80	IPWA	$\pi N \to \pi N$
1900	SAXON	80	DPWA	$\pi^- p \to \Lambda K^0$
• • • We do not use the following data for averages, fits, limits, etc. • • •				
1951± 27	SHRESTHA	12A	DPWA	Multichannel
2048± 65	BATINIC	10	DPWA	$\pi N \to N\pi$, $N\eta$
1946± 1	PENNER	02C	DPWA	Multichannel
1895	MART	00	DPWA	$\gamma p \to \Lambda K^+$
2003± 18	VRANA	00	DPWA	Multichannel
1804± 55	MANLEY	92	IPWA	$\pi N \to \pi N$ & $N\pi\pi$
1880	BAKER	79	DPWA	$\pi^- p \to n\eta$

$N(1875)$ BREIT-WIGNER WIDTH

VALUE (MeV)	DOCUMENT ID		TECN	COMMENT
857±100	SHKLYAR	13	DPWA	Multichannel
200± 25	ANISOVICH	12A	DPWA	Multichannel
320	BELL	83	DPWA	$\pi^- p \to \Lambda K^0$
180± 60	[1] CUTKOSKY	80	IPWA	$\pi N \to \pi N$ (lower m)
240	SAXON	80	DPWA	$\pi^- p \to \Lambda K^0$
• • • We do not use the following data for averages, fits, limits, etc. • • •				
500± 45	SHRESTHA	12A	DPWA	Multichannel
529±128	BATINIC	10	DPWA	$\pi N \to N\pi$, $N\eta$
859± 7	PENNER	02C	DPWA	Multichannel
372	MART	00	DPWA	$\gamma p \to \Lambda K^+$
1070±858	VRANA	00	DPWA	Multichannel
450±185	MANLEY	92	IPWA	$\pi N \to \pi N$ & $N\pi\pi$
87	BAKER	79	DPWA	$\pi^- p \to n\eta$

$N(1875)$ POLE POSITION

REAL PART

VALUE (MeV)	DOCUMENT ID		TECN	COMMENT
1800 to 1950 OUR ESTIMATE				
1860± 25	ANISOVICH	12A	DPWA	Multichannel
1880±100	[1] CUTKOSKY	80	IPWA	$\pi N \to \pi N$ (lower m)
• • • We do not use the following data for averages, fits, limits, etc. • • •				
1810	SHKLYAR	13	DPWA	Multichannel
1975	SHRESTHA	12A	DPWA	Multichannel
1957± 49	BATINIC	10	DPWA	$\pi N \to N\pi$, $N\eta$
1824	VRANA	00	DPWA	Multichannel
not seen	ARNDT	91	DPWA	$\pi N \to \pi N$ Soln SM90

−2×IMAGINARY PART

VALUE (MeV)	DOCUMENT ID		TECN	COMMENT
150 to 250 OUR ESTIMATE				
200± 20	ANISOVICH	12A	DPWA	Multichannel
160± 80	[1] CUTKOSKY	80	IPWA	$\pi N \to \pi N$ (lower m)
• • • We do not use the following data for averages, fits, limits, etc. • • •				
98	SHKLYAR	13	DPWA	Multichannel
495	SHRESTHA	12A	DPWA	Multichannel
467±106	BATINIC	10	DPWA	$\pi N \to N\pi$, $N\eta$
614	VRANA	00	DPWA	Multichannel
not seen	ARNDT	91	DPWA	$\pi N \to \pi N$ Soln SM90

$N(1875)$ ELASTIC POLE RESIDUE

MODULUS $|r|$

VALUE (MeV)	DOCUMENT ID		TECN	COMMENT
2 to 10 OUR ESTIMATE				
2.5±1.0	ANISOVICH	12A	DPWA	Multichannel
10 ±5	[1] CUTKOSKY	80	IPWA	$\pi N \to \pi N$ (lower m)
• • • We do not use the following data for averages, fits, limits, etc. • • •				
3	SHKLYAR	13	DPWA	Multichannel
53	BATINIC	10	DPWA	$\pi N \to N\pi$, $N\eta$

PHASE θ

VALUE (°)	DOCUMENT ID		TECN	COMMENT
100±80	[1] CUTKOSKY	80	IPWA	$\pi N \to \pi N$ (lower m)
• • • We do not use the following data for averages, fits, limits, etc. • • •				
− 76	SHKLYAR	13	DPWA	Multichannel
− 65	BATINIC	10	DPWA	$\pi N \to N\pi$, $N\eta$

$N(1875)$ INELASTIC POLE RESIDUE

The "normalized residue" is the residue divided by $\Gamma_{pole}/2$.

Normalized residue in $N\pi \to N(1875) \to \Lambda K$

MODULUS (%)	DOCUMENT ID		TECN	COMMENT
1.5±0.5	ANISOVICH	12A	DPWA	Multichannel

Normalized residue in $N\pi \to N(1875) \to \Sigma K$

MODULUS (%)	DOCUMENT ID		TECN	COMMENT
4±2	ANISOVICH	12A	DPWA	Multichannel

Normalized residue in $N\pi \to N(1875) \to N\sigma$

MODULUS (%)	PHASE (°)	DOCUMENT ID		TECN	COMMENT
8±3	**−170 ± 65**	ANISOVICH	12A	DPWA	Multichannel

$N(1875)$ DECAY MODES

	Mode	Fraction (Γ_i/Γ)	Scale factor
Γ_1	$N\pi$	(7 ± 6) %	
Γ_2	$N\eta$	(1.2± 1.8) %	2.3
Γ_3	$N\omega$	(20 ± 4) %	
Γ_4	ΛK		
Γ_5	ΣK	(7 ± 4) $\times 10^{-3}$	
Γ_6	$N\pi\pi$		
Γ_7	$\Delta(1232)\pi$, S-wave	(40 ±10) %	
Γ_8	$\Delta(1232)\pi$, D-wave	(17 ±10) %	
Γ_9	$N\rho$, S=3/2, S-wave	(6 ± 6) %	
Γ_{10}	$N(\pi\pi)^{I=0}_{S\text{-wave}}$	(24 ±24) %	
Γ_{11}	$n\gamma$, helicity=1/2		
Γ_{12}	$n\gamma$, helicity=3/2		
Γ_{13}	$p\gamma$	0.008–0.016 %	
Γ_{14}	$p\gamma$, helicity=1/2	0.006–0.010 %	
Γ_{15}	$p\gamma$, helicity=3/2	0.002–0.006 %	

$N(1875)$ BRANCHING RATIOS

$\Gamma(N\pi)/\Gamma_{total}$ Γ_1/Γ

VALUE (%)	DOCUMENT ID		TECN	COMMENT
7±6 OUR ESTIMATE				
11±1	SHKLYAR	13	DPWA	Multichannel
3±2	ANISOVICH	12A	DPWA	Multichannel
10±4	[1] CUTKOSKY	80	IPWA	$\pi N \to \pi N$ (lower m)
• • • We do not use the following data for averages, fits, limits, etc. • • •				
7±2	SHRESTHA	12A	DPWA	Multichannel
17±7	BATINIC	10	DPWA	$\pi N \to N\pi$, $N\eta$
12±2	PENNER	02C	DPWA	Multichannel
13±3	VRANA	00	DPWA	Multichannel
23±3	MANLEY	92	IPWA	$\pi N \to \pi N$ & $N\pi\pi$

$\Gamma(N\eta)/\Gamma_{total}$ Γ_2/Γ

VALUE (%)	DOCUMENT ID		TECN	COMMENT
1.2±1.8 OUR AVERAGE Error includes scale factor of 2.3. See the ideogram below.				
0 ±1	SHKLYAR	13	DPWA	Multichannel
7 ±2	PENNER	02C	DPWA	Multichannel
0 ±2	VRANA	00	DPWA	Multichannel
• • • We do not use the following data for averages, fits, limits, etc. • • •				
8 ±3	BATINIC	10	DPWA	$\pi N \to N\pi$, $N\eta$

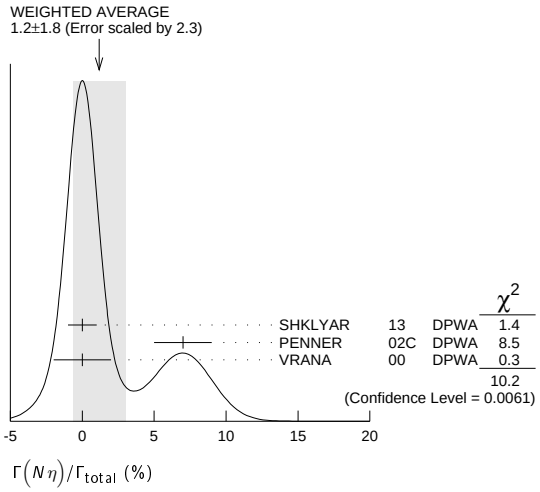

$(\Gamma_i\Gamma_f)^{1/2}/\Gamma_{total}$ in $N\pi \to N(1875) \to N\eta$ $(\Gamma_1\Gamma_2)^{1/2}/\Gamma$

VALUE (%)	DOCUMENT ID		TECN	COMMENT
6 ±4 OUR ESTIMATE				
5 ±2	ANISOVICH	12A	DPWA	Multichannel
6.5	BAKER	79	DPWA	$\pi^- p \to n\eta$

$\Gamma(N\omega)/\Gamma_{total}$ Γ_3/Γ

VALUE (%)	DOCUMENT ID		TECN	COMMENT
20±4 OUR AVERAGE				
20±5	SHKLYAR	13	DPWA	Multichannel
21±7	PENNER	02C	DPWA	Multichannel

$\Gamma(\Lambda K)/\Gamma_{total}$ Γ_4/Γ

VALUE (%)	DOCUMENT ID		TECN	COMMENT
• • • We do not use the following data for averages, fits, limits, etc. • • •				
0.2±0.2	PENNER	02C	DPWA	Multichannel

$(\Gamma_i\Gamma_f)^{1/2}/\Gamma_{total}$ in $N\pi \to N(1875) \to \Lambda K$ $(\Gamma_1\Gamma_4)^{1/2}/\Gamma$

VALUE (%)	DOCUMENT ID		TECN	COMMENT
4±2 OUR ESTIMATE				
4±2	ANISOVICH	12A	DPWA	Multichannel
4	BELL	83	DPWA	$\pi^- p \to \Lambda K^0$
3	SAXON	80	DPWA	$\pi^- p \to \Lambda K^0$

$\Gamma(\Sigma K)/\Gamma_{total}$ Γ_5/Γ

VALUE (%)	DOCUMENT ID		TECN	COMMENT
0.7±0.4	PENNER	02C	DPWA	Multichannel

$(\Gamma_i\Gamma_f)^{1/2}/\Gamma_{total}$ in $N\pi \to N(1875) \to \Sigma K$ $(\Gamma_1\Gamma_5)^{1/2}/\Gamma$

VALUE (%)	DOCUMENT ID		TECN	COMMENT
1 to 10 OUR ESTIMATE				
15 ±8	ANISOVICH	12A	DPWA	Multichannel
1.4 to 3.7	[2] DEANS	75	DPWA	$\pi N \to \Sigma K$

$(\Gamma_i\Gamma_f)^{1/2}/\Gamma_{total}$ in $N\pi \to N(1875) \to \Delta(1232)\pi$, S-wave $(\Gamma_1\Gamma_7)^{1/2}/\Gamma$

VALUE	DOCUMENT ID		TECN	COMMENT
• • • We do not use the following data for averages, fits, limits, etc. • • •				
−0.09±0.09	MANLEY	92	IPWA	$\pi N \to \pi N$ & $N\pi\pi$

$\Gamma(\Delta(1232)\pi$, S-wave$)/\Gamma_{total}$ Γ_7/Γ

VALUE (%)	DOCUMENT ID		TECN	COMMENT
40±10	VRANA	00	DPWA	Multichannel
• • • We do not use the following data for averages, fits, limits, etc. • • •				
87± 3	SHRESTHA	12A	DPWA	Multichannel

$(\Gamma_i\Gamma_f)^{1/2}/\Gamma_{total}$ in $N\pi \to N(1875) \to \Delta(1232)\pi$, D-wave $(\Gamma_1\Gamma_8)^{1/2}/\Gamma$

VALUE	DOCUMENT ID		TECN	COMMENT
• • • We do not use the following data for averages, fits, limits, etc. • • •				
+0.22±0.07	MANLEY	92	IPWA	$\pi N \to \pi N$ & $N\pi\pi$

$\Gamma(\Delta(1232)\pi$, D-wave$)/\Gamma_{total}$ Γ_8/Γ

VALUE (%)	DOCUMENT ID		TECN	COMMENT
17±10	VRANA	00	DPWA	Multichannel
• • • We do not use the following data for averages, fits, limits, etc. • • •				
< 6	SHRESTHA	12A	DPWA	Multichannel

$(\Gamma_i\Gamma_f)^{1/2}/\Gamma_{total}$ in $N\pi \to N(1875) \to N\rho$, S=3/2, S-wave $(\Gamma_1\Gamma_9)^{1/2}/\Gamma$

VALUE	DOCUMENT ID		TECN	COMMENT
• • • We do not use the following data for averages, fits, limits, etc. • • •				
-0.24 ± 0.06	MANLEY	92	IPWA	$\pi N \to \pi N$ & $N\pi\pi$

$\Gamma(N\rho, S$=3/2, S-wave)/Γ_{total} Γ_9/Γ

VALUE (%)	DOCUMENT ID		TECN	COMMENT
6±6	VRANA	00	DPWA	Multichannel
• • • We do not use the following data for averages, fits, limits, etc. • • •				
<5	SHRESTHA	12A	DPWA	Multichannel

$(\Gamma_i\Gamma_f)^{1/2}/\Gamma_{total}$ in $N\pi \to N(1875) \to N(\pi\pi)^{I=0}_{S\text{-wave}}$ $(\Gamma_1\Gamma_{10})^{1/2}/\Gamma$

VALUE	DOCUMENT ID		TECN	COMMENT
• • • We do not use the following data for averages, fits, limits, etc. • • •				
$+0.25\pm0.06$	MANLEY	92	IPWA	$\pi N \to \pi N$ & $N\pi\pi$

$\Gamma(N(\pi\pi)^{I=0}_{S\text{-wave}})/\Gamma_{total}$ Γ_{10}/Γ

VALUE (%)	DOCUMENT ID		TECN	COMMENT
24±24	VRANA	00	DPWA	Multichannel
• • • We do not use the following data for averages, fits, limits, etc. • • •				
< 4	SHRESTHA	12A	DPWA	Multichannel

$(\Gamma_i\Gamma_f)^{1/2}/\Gamma_{total}$ in $p\gamma \to N(1875) \to N\eta$ $(\Gamma_{13}\Gamma_2)^{1/2}/\Gamma$

VALUE (%)	DOCUMENT ID		TECN	COMMENT
60 ±12	ANISOVICH	12A	DPWA	Multichannel
0.37	HICKS	73	MPWA	$\gamma p \to p\eta$

$N(1875)$ PHOTON DECAY AMPLITUDES

Papers on γN amplitudes predating 1981 may be found in our 2006 edition, Journal of Physics (generic for all A,B,E,G) **G33** 1 (2006).

$N(1875) \to p\gamma$, helicity-1/2 amplitude $A_{1/2}$

VALUE (GeV$^{-1/2}$)	DOCUMENT ID		TECN	COMMENT
0.018 ± 0.010	ANISOVICH	12A	DPWA	Multichannel
-0.020 ± 0.008	AWAJI	81	DPWA	$\gamma N \to \pi N$
• • • We do not use the following data for averages, fits, limits, etc. • • •				
0.011 ± 0.001	SHKLYAR	13	DPWA	Multichannel
0.007 ± 0.008	SHRESTHA	12A	DPWA	Multichannel
0.012	PENNER	02D	DPWA	Multichannel
0.026 ± 0.052	DEVENISH	74	DPWA	$\gamma N \to \pi N$

$N(1875) \to p\gamma$, helicity-3/2 amplitude $A_{3/2}$

VALUE (GeV$^{-1/2}$)	DOCUMENT ID		TECN	COMMENT
-0.009 ± 0.005	ANISOVICH	12A	DPWA	Multichannel
0.017 ± 0.011	AWAJI	81	DPWA	$\gamma N \to \pi N$
• • • We do not use the following data for averages, fits, limits, etc. • • •				
0.026 ± 0.001	SHKLYAR	13	DPWA	Multichannel
0.043 ± 0.022	SHRESTHA	12A	DPWA	Multichannel
-0.010	PENNER	02D	DPWA	Multichannel
0.128 ± 0.057	DEVENISH	74	DPWA	$\gamma N \to \pi N$

$N(1875) \to n\gamma$, helicity-1/2 amplitude $A_{1/2}$

VALUE (GeV$^{-1/2}$)	DOCUMENT ID		TECN	COMMENT
0.010±0.010 OUR ESTIMATE				
0.007 ± 0.013	AWAJI	81	DPWA	$\gamma N \to \pi N$
• • • We do not use the following data for averages, fits, limits, etc. • • •				
0.055 ± 0.021	SHRESTHA	12A	DPWA	Multichannel
0.023	PENNER	02D	DPWA	Multichannel
0.053 ± 0.083	DEVENISH	74	DPWA	$\gamma N \to \pi N$

$N(1875) \to n\gamma$, helicity-3/2 amplitude $A_{3/2}$

VALUE (GeV$^{-1/2}$)	DOCUMENT ID		TECN	COMMENT
−0.020±0.015 OUR ESTIMATE				
-0.053 ± 0.034	AWAJI	81	DPWA	$\gamma N \to \pi N$
• • • We do not use the following data for averages, fits, limits, etc. • • •				
-0.085 ± 0.031	SHRESTHA	12A	DPWA	Multichannel
−0.009	PENNER	02D	DPWA	Multichannel
0.100 ± 0.141	DEVENISH	74	DPWA	$\gamma N \to \pi N$

$N(1875)$ $\gamma p \to \Lambda K^+$ AMPLITUDES

$(\Gamma_i\Gamma_f)^{1/2}/\Gamma_{total}$ in $p\gamma \to N(1875) \to \Lambda K^+$ (E_{2-} amplitude)

VALUE (units 10^{-3})	DOCUMENT ID		TECN	COMMENT
• • • We do not use the following data for averages, fits, limits, etc. • • •				
$2.29^{+0.7}_{-0.2}$	MART	00	DPWA	$\gamma p \to \Lambda K^+$
5.5 ±0.3	WORKMAN	90	DPWA	
4.09	TANABE	89	DPWA	

$p\gamma \to N(1875) \to \Lambda K^+$ phase angle θ (E_{2-} amplitude)

VALUE (degrees)	DOCUMENT ID		TECN
• • • We do not use the following data for averages, fits, limits, etc. • • •			
−48 ±5	WORKMAN	90	DPWA
−35.9	TANABE	89	DPWA

$(\Gamma_i\Gamma_f)^{1/2}/\Gamma_{total}$ in $p\gamma \to N(1875) \to \Lambda K^+$ (M_{2-} amplitude)

VALUE (units 10^{-3})	DOCUMENT ID		TECN
• • • We do not use the following data for averages, fits, limits, etc. • • •			
−6.7 ±0.2	WORKMAN	90	DPWA
−4.09	TANABE	89	DPWA

$N(1875)$ FOOTNOTES

[1] CUTKOSKY 80 finds a lower mass D_{13} resonance, as well as one in this region. Both are listed here.

[2] The range given for DEANS 75 is from the four best solutions. Disagrees with $\pi^+ p \to \Sigma^+ K^+$ data of WINNIK 77 around 1920 MeV.

$N(1875)$ REFERENCES

For early references, see Physics Letters **111B** 1 (1982).

SHKLYAR	13	PR C87 015201	V. Shklyar, H. Lenske, U. Mosel	(GIES)
ANISOVICH	12A	EPJ A48 15	A.V. Anisovich *et al.*	(BONN, PNPI)
SHRESTHA	12A	PR C86 055203	M. Shrestha, D.M. Manley	(KSU)
BATINIC	10	PR C82 038203	M. Batinic *et al.*	(ZAGR)
ARNDT	06	PR C74 045205	R.A. Arndt *et al.*	(GWU)
PDG	06	JP G33 1	W.-M. Yao *et al.*	(PDG Collab.)
PENNER	02C	PR C66 055211	G. Penner, U. Mosel	(GIES)
PENNER	02D	PR C66 055212	G. Penner, U. Mosel	(GIES)
MART	00	PR C61 012201	T. Mart, C. Bennhold	
VRANA	00	PRPL 328 181	T.P. Vrana, S.A. Dytman,, T.-S.H. Lee	(PITT+)
MANLEY	92	PR D45 4002	D.M. Manley, E.M. Saleski	(KSA) IJP
Also		PR D30 904	D.M. Manley *et al.*	(VPI)
ARNDT	91	PR D43 2131	R.A. Arndt *et al.*	(VPI, TELE) IJP
WORKMAN	90	PR C42 781	R.L. Workman	(VPI)
TANABE	89	PR C39 741	H. Tanabe, M. Kohno, C. Bennhold	(MANZ)
Also		NC 102A 193	M. Kohno, H. Tanabe, C. Bennhold	(MANZ)
BELL	83	NP B222 389	K.W. Bell *et al.*	(RL) IJP
AWAJI	81	Bonn Conf. 352	N. Awaji, R. Kajikawa	(NAGO)
Also		NP B197 365	K. Fujii *et al.*	(NAGO)
CUTKOSKY	80	Toronto Conf. 19	R.E. Cutkosky *et al.*	(CMU, LBL) IJP
Also		PR D20 2839	R.E. Cutkosky *et al.*	(CMU, LBL) IJP
SAXON	80	NP B162 522	D.H. Saxon *et al.*	(RHEL, BRIS) IJP
BAKER	79	NP B156 93	R.D. Baker *et al.*	(RHEL) IJP
WINNIK	77	NP B128 66	M. Winnik *et al.*	(HAIF) I
DEANS	75	NP B96 90	S.R. Deans *et al.*	(SFLA, ALAH) IJP
DEVENISH	74	PL 52B 227	R.C.E. Devenish, D.H. Lyth, W.A. Rankin	(DESY+) IJP
HICKS	73	PR D7 2614	H.R. Hicks *et al.*	(CMU, ORNL, SFLA) IJP

$N(1880)$ $1/2^+$

$I(J^P) = \frac{1}{2}(\frac{1}{2}^+)$ Status: **

OMITTED FROM SUMMARY TABLE

$N(1880)$ BREIT-WIGNER MASS

VALUE (MeV)	DOCUMENT ID		TECN	COMMENT
1870 ± 35	ANISOVICH	12A	DPWA	Multichannel
• • • We do not use the following data for averages, fits, limits, etc. • • •				
1900 ± 36	SHRESTHA	12A	DPWA	Multichannel
1885 ± 30	MANLEY	92	IPWA	$\pi N \to \pi N$ & $N\pi\pi$

$N(1880)$ BREIT-WIGNER WIDTH

VALUE (MeV)	DOCUMENT ID		TECN	COMMENT
235± 65	ANISOVICH	12A	DPWA	Multichannel
• • • We do not use the following data for averages, fits, limits, etc. • • •				
485 ± 142	SHRESTHA	12A	DPWA	Multichannel
113± 44	MANLEY	92	IPWA	$\pi N \to \pi N$ & $N\pi\pi$

$N(1880)$ POLE POSITION

REAL PART

VALUE (MeV)	DOCUMENT ID		TECN	COMMENT
1860 ± 35	ANISOVICH	12A	DPWA	Multichannel
• • • We do not use the following data for averages, fits, limits, etc. • • •				
1801	SHRESTHA	12A	DPWA	Multichannel

−2×IMAGINARY PART

VALUE (MeV)	DOCUMENT ID		TECN	COMMENT
250 ± 70	ANISOVICH	12A	DPWA	Multichannel
• • • We do not use the following data for averages, fits, limits, etc. • • •				
383	SHRESTHA	12A	DPWA	Multichannel

$N(1880)$ ELASTIC POLE RESIDUE

MODULUS $|r|$

VALUE (MeV)	DOCUMENT ID		TECN	COMMENT
6±4	ANISOVICH	12A	DPWA	Multichannel

PHASE θ

VALUE (°)	DOCUMENT ID		TECN	COMMENT
80±65	ANISOVICH	12A	DPWA	Multichannel

$N(1880)$ INELASTIC POLE RESIDUE

The "normalized residue" is the residue divided by $\Gamma_{pole}/2$.

Normalized residue in $N\pi \to N(1880) \to N\eta$

MODULUS (%)	PHASE (°)	DOCUMENT ID		TECN	COMMENT
11±7	−75 ± 55	ANISOVICH	12A	DPWA	Multichannel

Normalized residue in $N\pi \to N(1880) \to \Lambda K$

MODULUS (%)	PHASE (°)	DOCUMENT ID		TECN	COMMENT
3±2	40 ± 40	ANISOVICH	12A	DPWA	Multichannel

Normalized residue in $N\pi \to N(1880) \to \Sigma K$

MODULUS (%)	PHASE (°)	DOCUMENT ID		TECN	COMMENT
11±6	95 ± 40	ANISOVICH	12A	DPWA	Multichannel

Normalized residue in $N\pi \to N(1880) \to \Delta\pi$, P-wave

MODULUS (%)	PHASE (°)	DOCUMENT ID		TECN	COMMENT
20±8	−150 ± 50	ANISOVICH	12A	DPWA	Multichannel

$N(1880)$ DECAY MODES

	Mode
Γ_1	$N\pi$
Γ_2	$N\eta$
Γ_3	ΛK
Γ_4	ΣK
Γ_5	$\Delta(1232)\pi$
Γ_6	$N\rho$, S=1/2
Γ_7	$N(\pi\pi)^{I=0}_{S-wave}$
Γ_8	$p\gamma$
Γ_9	$n\gamma$

$N(1880)$ BRANCHING RATIOS

$\Gamma(N\pi)/\Gamma_{total}$ Γ_1/Γ

VALUE (%)	DOCUMENT ID		TECN	COMMENT
5±3	ANISOVICH	12A	DPWA	Multichannel
• • • We do not use the following data for averages, fits, limits, etc. • • •				
15±5	SHRESTHA	12A	DPWA	Multichannel
15±6	MANLEY	92	IPWA	$\pi N \to \pi N$ & $N\pi\pi$

$\Gamma(N\eta)/\Gamma_{total}$ Γ_2/Γ

VALUE (%)	DOCUMENT ID		TECN	COMMENT
25^{+30}_{-20}	ANISOVICH	12A	DPWA	Multichannel
• • • We do not use the following data for averages, fits, limits, etc. • • •				
16± 7	SHRESTHA	12A	DPWA	Multichannel

$\Gamma(\Lambda K)/\Gamma_{total}$ Γ_3/Γ

VALUE (%)	DOCUMENT ID		TECN	COMMENT
2± 1	ANISOVICH	12A	DPWA	Multichannel
• • • We do not use the following data for averages, fits, limits, etc. • • •				
32±10	SHRESTHA	12A	DPWA	Multichannel

$\Gamma(\Sigma K)/\Gamma_{total}$ Γ_4/Γ

VALUE (%)	DOCUMENT ID		TECN	COMMENT
17±7	ANISOVICH	12A	DPWA	Multichannel

$\Gamma(\Delta(1232)\pi)/\Gamma_{total}$ Γ_5/Γ

VALUE (%)	DOCUMENT ID		TECN	COMMENT
29±12	ANISOVICH	12A	DPWA	Multichannel
• • • We do not use the following data for averages, fits, limits, etc. • • •				
< 2	SHRESTHA	12A	DPWA	Multichannel

$\Gamma(N\rho, S=1/2)/\Gamma_{total}$ Γ_6/Γ

VALUE (%)	DOCUMENT ID		TECN	COMMENT
• • • We do not use the following data for averages, fits, limits, etc. • • •				
<1	SHRESTHA	12A	DPWA	Multichannel

$\Gamma(N(\pi\pi)^{I=0}_{S-wave})/\Gamma_{total}$ Γ_7/Γ

VALUE (%)	DOCUMENT ID		TECN	COMMENT
• • • We do not use the following data for averages, fits, limits, etc. • • •				
8±5	SHRESTHA	12A	DPWA	Multichannel

$N(1880)$ PHOTON DECAY AMPLITUDES

$N(1880) \to p\gamma$, helicity-1/2 amplitude $A_{1/2}$

VALUE ($GeV^{-1/2}$)	DOCUMENT ID		TECN	COMMENT
0.014±0.003	[1] ANISOVICH	12A	DPWA	Phase = (−130 ± 60)°
• • • We do not use the following data for averages, fits, limits, etc. • • •				
0.021±0.006	SHRESTHA	12A	DPWA	Multichannel

$N(1880) \to n\gamma$, helicity-1/2 amplitude $A_{1/2}$

VALUE ($GeV^{-1/2}$)	DOCUMENT ID		TECN	COMMENT
• • • We do not use the following data for averages, fits, limits, etc. • • •				
0.014±0.007	SHRESTHA	12A	DPWA	Multichannel

$N(1880)$ FOOTNOTES

[1] This ANISOVICH 12A value is the complex helicity amplitude at the pole position.

$N(1880)$ REFERENCES

ANISOVICH	12A	EPJ A48 15	A.V. Anisovich *et al.*	(BONN, PNPI)
SHRESTHA	12A	PR C86 055203	M. Shrestha, D.M. Manley	(KSU)
MANLEY	92	PR D45 4002	D.M. Manley, E.M. Saleski	(KSA)
Also		PR D30 904	D.M. Manley *et al.*	(VPI)

$N(1895)$ $1/2^-$

$I(J^P) = \frac{1}{2}(\frac{1}{2}^-)$ Status: **

OMITTED FROM SUMMARY TABLE

Before our 2012 *Review*, this state appeared in our Listings as the $N(2090)$. Any structure in the S_{11} wave above 1800 MeV is listed here. A few early results that are now obsolete have been omitted.

The latest GWU analysis (ARNDT 06) finds no evidence for this resonance.

$N(1895)$ BREIT-WIGNER MASS

VALUE (MeV)	DOCUMENT ID		TECN	COMMENT
1895±15	ANISOVICH	12A	DPWA	Multichannel
2180±80	CUTKOSKY	80	IPWA	$\pi N \to \pi N$
1880±20	HOEHLER	79	IPWA	$\pi N \to \pi N$
• • • We do not use the following data for averages, fits, limits, etc. • • •				
1910±15	SHRESTHA	12A	DPWA	Multichannel
1812±25	BATINIC	10	DPWA	$\pi N \to N\pi$, $N\eta$
1822±43	VRANA	00	DPWA	Multichannel
$1897\pm50^{+30}_{-2}$	PLOETZKE	98	SPEC	$\gamma p \to p\eta'(958)$
1928±59	MANLEY	92	IPWA	$\pi N \to \pi N$ & $N\pi\pi$

$N(1895)$ BREIT-WIGNER WIDTH

VALUE (MeV)	DOCUMENT ID		TECN	COMMENT
90^{+30}_{-15}	ANISOVICH	12A	DPWA	Multichannel
350±100	CUTKOSKY	80	IPWA	$\pi N \to \pi N$
95± 30	HOEHLER	79	IPWA	$\pi N \to \pi N$
• • • We do not use the following data for averages, fits, limits, etc. • • •				
502± 47	SHRESTHA	12A	DPWA	Multichannel
405± 40	BATINIC	10	DPWA	$\pi N \to N\pi$, $N\eta$
248±185	VRANA	00	DPWA	Multichannel
$396\pm155^{+35}_{-45}$	PLOETZKE	98	SPEC	$\gamma p \to p\eta'(958)$
414±157	MANLEY	92	IPWA	$\pi N \to \pi N$ & $N\pi\pi$

$N(1895)$ POLE POSITION

REAL PART

VALUE (MeV)	DOCUMENT ID		TECN	COMMENT
1900±15	ANISOVICH	12A	DPWA	Multichannel
2150±70	CUTKOSKY	80	IPWA	$\pi N \to \pi N$
1937 or 1949	[1] LONGACRE	78	IPWA	$\pi N \to N\pi\pi$
• • • We do not use the following data for averages, fits, limits, etc. • • •				
1858	SHRESTHA	12A	DPWA	Multichannel
1797±26	BATINIC	10	DPWA	$\pi N \to N\pi$, $N\eta$
1795	VRANA	00	DPWA	Multichannel

−2×IMAGINARY PART

VALUE (MeV)	DOCUMENT ID		TECN	COMMENT
90^{+30}_{-15}	ANISOVICH	12A	DPWA	Multichannel
350±100	CUTKOSKY	80	IPWA	$\pi N \to \pi N$
139 or 131	[1] LONGACRE	78	IPWA	$\pi N \to N\pi\pi$
• • • We do not use the following data for averages, fits, limits, etc. • • •				
479	SHRESTHA	12A	DPWA	Multichannel
420± 45	BATINIC	10	DPWA	$\pi N \to N\pi$, $N\eta$
220	VRANA	00	DPWA	Multichannel

Baryon Particle Listings

$N(1895)$

$N(1895)$ ELASTIC POLE RESIDUE

MODULUS $|r|$

VALUE (MeV)	DOCUMENT ID		TECN	COMMENT
1± 1	ANISOVICH	12A	DPWA	Multichannel
40±20	CUTKOSKY	80	IPWA	$\pi N \to \pi N$
• • • We do not use the following data for averages, fits, limits, etc. • • •				
60	BATINIC	10	DPWA	$\pi N \to N\pi,\ N\eta$

PHASE θ

VALUE (°)	DOCUMENT ID		TECN	COMMENT
0±90	CUTKOSKY	80	IPWA	$\pi N \to \pi N$
• • • We do not use the following data for averages, fits, limits, etc. • • •				
−164	BATINIC	10	DPWA	$\pi N \to N\pi,\ N\eta$

$N(1895)$ INELASTIC POLE RESIDUE

The "normalized residue" is the residue divided by $\Gamma_{pole}/2$.

Normalized residue in $N\pi \to N(1895) \to N\eta$

MODULUS (%)	PHASE (°)	DOCUMENT ID		TECN	COMMENT
6±2	40 ± 20	ANISOVICH	12A	DPWA	Multichannel

Normalized residue in $N\pi \to N(1895) \to \Lambda K$

MODULUS (%)	PHASE (°)	DOCUMENT ID		TECN	COMMENT
5±2	−90 ± 30	ANISOVICH	12A	DPWA	Multichannel

Normalized residue in $N\pi \to N(1895) \to \Sigma K$

MODULUS (%)	PHASE (°)	DOCUMENT ID		TECN	COMMENT
6±2	40 ± 30	ANISOVICH	12A	DPWA	Multichannel

$N(1895)$ DECAY MODES

	Mode
Γ_1	$N\pi$
Γ_2	$N\eta$
Γ_3	ΛK
Γ_4	ΣK
Γ_5	$N\pi\pi$
Γ_6	$\Delta\pi$
Γ_7	$\Delta(1232)\pi$, D-wave
Γ_8	$N\rho$
Γ_9	$N\rho$, S=1/2, S-wave
Γ_{10}	$N\rho$, S=3/2, D-wave
Γ_{11}	$N(\pi\pi)^{I=0}_{S\text{-wave}}$
Γ_{12}	$N(1440)\pi$
Γ_{13}	$p\gamma$, helicity=1/2
Γ_{14}	$n\gamma$, helicity=1/2

$N(1895)$ BRANCHING RATIOS

$\Gamma(N\pi)/\Gamma_{total}$ Γ_1/Γ

VALUE (%)	DOCUMENT ID		TECN	COMMENT
2± 1	ANISOVICH	12A	DPWA	Multichannel
18± 8	CUTKOSKY	80	IPWA	$\pi N \to \pi N$
9± 5	HOEHLER	79	IPWA	$\pi N \to \pi N$
• • • We do not use the following data for averages, fits, limits, etc. • • •				
17± 2	SHRESTHA	12A	DPWA	Multichannel
32± 6	BATINIC	10	DPWA	$\pi N \to N\pi,\ N\eta$
17± 3	VRANA	00	DPWA	Multichannel
10±10	MANLEY	92	IPWA	$\pi N \to \pi N$ & $N\pi\pi$

$\Gamma(N\eta)/\Gamma_{total}$ Γ_2/Γ

VALUE (%)	DOCUMENT ID		TECN	COMMENT
21± 6	ANISOVICH	12A	DPWA	Multichannel
41± 4	VRANA	00	DPWA	Multichannel
• • • We do not use the following data for averages, fits, limits, etc. • • •				
40± 4	SHRESTHA	12A	DPWA	Multichannel
22±10	BATINIC	10	DPWA	$\pi N \to N\pi,\ N\eta$

$\Gamma(\Lambda K)/\Gamma_{total}$ Γ_3/Γ

VALUE (%)	DOCUMENT ID		TECN	COMMENT
18 ±5	ANISOVICH	12A	DPWA	Multichannel
• • • We do not use the following data for averages, fits, limits, etc. • • •				
1.8±0.8	SHRESTHA	12A	DPWA	Multichannel

$(\Gamma_i\Gamma_f)^{1/2}/\Gamma_{total}$ in $N\pi \to N(1895) \to \Lambda K$ $(\Gamma_1\Gamma_3)^{1/2}/\Gamma$

VALUE	DOCUMENT ID		TECN	COMMENT
not seen	SAXON	80	DPWA	$\pi^- p \to \Lambda K^0$

$\Gamma(\Sigma K)/\Gamma_{total}$ Γ_4/Γ

VALUE (%)	DOCUMENT ID		TECN	COMMENT
13±7	ANISOVICH	12A	DPWA	Multichannel

$\Gamma(\Delta(1232)\pi, D\text{-wave})/\Gamma_{total}$ Γ_7/Γ

VALUE (%)	DOCUMENT ID		TECN	COMMENT
1±1	VRANA	00	DPWA	Multichannel
• • • We do not use the following data for averages, fits, limits, etc. • • •				
7±3	SHRESTHA	12A	DPWA	Multichannel

$\Gamma(N\rho, S\text{=}1/2, S\text{-wave})/\Gamma_{total}$ Γ_9/Γ

VALUE (%)	DOCUMENT ID		TECN	COMMENT
36±1	VRANA	00	DPWA	Multichannel
• • • We do not use the following data for averages, fits, limits, etc. • • •				
< 2	SHRESTHA	12A	DPWA	Multichannel

$\Gamma(N\rho, S\text{=}3/2, D\text{-wave})/\Gamma_{total}$ Γ_{10}/Γ

VALUE (%)	DOCUMENT ID		TECN	COMMENT
1±1	VRANA	00	DPWA	Multichannel
• • • We do not use the following data for averages, fits, limits, etc. • • •				
9±3	SHRESTHA	12A	DPWA	Multichannel

$\Gamma(N(\pi\pi)^{I=0}_{S\text{-wave}})/\Gamma_{total}$ Γ_{11}/Γ

VALUE (%)	DOCUMENT ID		TECN	COMMENT
2±1	VRANA	00	DPWA	Multichannel
• • • We do not use the following data for averages, fits, limits, etc. • • •				
<2	SHRESTHA	12A	DPWA	Multichannel

$\Gamma(N(1440)\pi)/\Gamma_{total}$ Γ_{12}/Γ

VALUE (%)	DOCUMENT ID		TECN	COMMENT
2±1	VRANA	00	DPWA	Multichannel
• • • We do not use the following data for averages, fits, limits, etc. • • •				
24±4	SHRESTHA	12A	DPWA	Multichannel

$N(1895)$ PHOTON DECAY AMPLITUDES

$N(1895) \to p\gamma$, helicity-1/2 amplitude $A_{1/2}$

VALUE ($GeV^{-1/2}$)	DOCUMENT ID		TECN	COMMENT
0.012±0.006	[2] ANISOVICH	12A	DPWA	Phase = (120 ±50)°
• • • We do not use the following data for averages, fits, limits, etc. • • •				
0.012±0.006	SHRESTHA	12A	DPWA	Multichannel

$N(1895) \to n\gamma$, helicity-1/2 amplitude $A_{1/2}$

VALUE ($GeV^{-1/2}$)	DOCUMENT ID		TECN	COMMENT
• • • We do not use the following data for averages, fits, limits, etc. • • •				
0.003±0.007	SHRESTHA	12A	DPWA	Multichannel

$N(1895)$ FOOTNOTES

[1] LONGACRE 78 values are from a search for poles in the unitarized T-matrix. The first (second) value uses, in addition to $\pi N \to N\pi\pi$ data, elastic amplitudes from a Saclay (CERN) partial-wave analysis.

[2] This ANISOVICH 12A value is the complex helicity amplitude at the pole position.

$N(1895)$ REFERENCES

ANISOVICH	12A	EPJ A48 15	A.V. Anisovich *et al.*	(BONN, PNPI)
SHRESTHA	12A	PR C86 055203	M. Shrestha, D.M. Manley	(KSU)
BATINIC	10	PR C82 038203	M. Batinic *et al.*	(ZAGR)
ARNDT	06	PR C74 045205	R.A. Arndt *et al.*	(GWU)
VRANA	00	PRPL 328 181	T.P. Vrana, S.A. Dytman,, T.-S.H. Lee	(PITT+)
PLOETZKE	98	PL B444 555	R. Ploetzke *et al.*	(Bonn SAPHIR Collab.)
MANLEY	92	PR D45 4002	D.M. Manley, E.M. Saleski	(KSA) IJP
Also		PR D30 904	D.M. Manley *et al.*	(VPI)
CUTKOSKY	80	Toronto Conf. 19	R.E. Cutkosky *et al.*	(CMU, LBL) IJP
Also		PR D20 2839	R.E. Cutkosky *et al.*	(CMU, LBL)
SAXON	80	NP B162 522	D.H. Saxon *et al.*	(RHEL, BRIS) IJP
HOEHLER	79	PDAT 12-1	G. Hohler *et al.*	(KARLT) IJP
Also		Toronto Conf. 3	R. Koch	(KARLT) IJP
LONGACRE	78	PR D17 1795	R.S. Longacre *et al.*	(LBL, SLAC)

N(1900) 3/2+

$I(J^P) = \frac{1}{2}(\frac{3}{2}^+)$ Status: ***

The latest GWU analysis (ARNDT 06) finds no evidence for this resonance.

N(1900) BREIT-WIGNER MASS

VALUE (MeV)	DOCUMENT ID		TECN	COMMENT
≈ 1900 OUR ESTIMATE				
1998± 3	SHKLYAR	13	DPWA	Multichannel
1905±30	ANISOVICH	12A	DPWA	Multichannel
1915±60	NIKONOV	08	DPWA	Multichannel
• • • We do not use the following data for averages, fits, limits, etc. • • •				
1900± 8	SHRESTHA	12A	DPWA	Multichannel
1951±53	PENNER	02C	DPWA	Multichannel
1879±17	MANLEY	92	IPWA	$\pi N \to \pi N$ & $N\pi\pi$

N(1900) BREIT-WIGNER WIDTH

VALUE (MeV)	DOCUMENT ID		TECN	COMMENT
~ 250 OUR ESTIMATE				
359± 10	SHKLYAR	13	DPWA	Multichannel
$250^{+120}_{-\ 50}$	ANISOVICH	12A	DPWA	Multichannel
180± 40	NIKONOV	08	DPWA	Multichannel
• • • We do not use the following data for averages, fits, limits, etc. • • •				
101± 15	SHRESTHA	12A	DPWA	Multichannel
622± 42	PENNER	02C	DPWA	Multichannel
498± 78	MANLEY	92	IPWA	$\pi N \to \pi N$ & $N\pi\pi$

N(1900) POLE POSITION

REAL PART

VALUE (MeV)	DOCUMENT ID		TECN	COMMENT
1900±30	ANISOVICH	12A	DPWA	Multichannel
• • • We do not use the following data for averages, fits, limits, etc. • • •				
1910	SHKLYAR	13	DPWA	Multichannel
1895	SHRESTHA	12A	DPWA	Multichannel

−2×IMAGINARY PART

VALUE (MeV)	DOCUMENT ID		TECN	COMMENT
$\mathbf{200^{+100}_{-\ 60}}$	ANISOVICH	12A	DPWA	Multichannel
• • • We do not use the following data for averages, fits, limits, etc. • • •				
173	SHKLYAR	13	DPWA	Multichannel
100	SHRESTHA	12A	DPWA	Multichannel

N(1900) ELASTIC POLE RESIDUE

MODULUS |r|

VALUE (MeV)	DOCUMENT ID		TECN	COMMENT
3±2	ANISOVICH	12A	DPWA	Multichannel
• • • We do not use the following data for averages, fits, limits, etc. • • •				
10	SHKLYAR	13	DPWA	Multichannel

PHASE θ

VALUE (°)	DOCUMENT ID		TECN	COMMENT
10±35	ANISOVICH	12A	DPWA	Multichannel
• • • We do not use the following data for averages, fits, limits, etc. • • •				
−64	SHKLYAR	13	DPWA	Multichannel

N(1900) INELASTIC POLE RESIDUE

The "normalized residue" is the residue divided by $\Gamma_{pole}/2$.

Normalized residue in $N\pi \to N(1900) \to N\eta$

MODULUS (%)	PHASE (°)	DOCUMENT ID		TECN	COMMENT
5±2	70 ± 60	ANISOVICH	12A	DPWA	Multichannel

Normalized residue in $N\pi \to N(1900) \to \Lambda K$

MODULUS (%)	PHASE (°)	DOCUMENT ID		TECN	COMMENT
7±3	135 ± 25	ANISOVICH	12A	DPWA	Multichannel

Normalized residue in $N\pi \to N(1900) \to \Sigma K$

MODULUS (%)	PHASE (°)	DOCUMENT ID		TECN	COMMENT
4±2	110 ± 30	ANISOVICH	12A	DPWA	Multichannel

N(1900) DECAY MODES

	Mode	Fraction (Γ_i/Γ)	Scale factor
Γ_1	$N\pi$	~ 5 %	
Γ_2	$N\pi\pi$		
Γ_3	$N\rho$, S=1/2, P-wave		
Γ_4	$N\eta$	~ 12 %	
Γ_5	$N\omega$	(13 ±9) %	3.1
Γ_6	ΛK	0–10 %	
Γ_7	ΣK	(5.0±2.0) %	
Γ_8	$p\gamma$		
Γ_9	$p\gamma$, helicity=1/2		
Γ_{10}	$p\gamma$, helicity=3/2		
Γ_{11}	$n\gamma$		
Γ_{12}	$n\gamma$, helicity=1/2		
Γ_{13}	$n\gamma$, helicity=3/2		

N(1900) BRANCHING RATIOS

$\Gamma(N\pi)/\Gamma_{total}$ Γ_1/Γ

VALUE (%)	DOCUMENT ID		TECN	COMMENT
~ 5 OUR ESTIMATE				
25±1	SHKLYAR	13	DPWA	Multichannel
3±2	ANISOVICH	12A	DPWA	Multichannel
• • • We do not use the following data for averages, fits, limits, etc. • • •				
7±4	SHRESTHA	12A	DPWA	Multichannel
2 to 9	NIKONOV	08	DPWA	Multichannel
16±2	PENNER	02C	DPWA	Multichannel
26±6	MANLEY	92	IPWA	$\pi N \to \pi N$ & $N\pi\pi$

$\Gamma(N\eta)/\Gamma_{total}$ Γ_4/Γ

VALUE (%)	DOCUMENT ID		TECN	COMMENT
~ 12 OUR ESTIMATE				
2±2	SHKLYAR	13	DPWA	Multichannel
10±4	ANISOVICH	12A	DPWA	Multichannel
14±5	PENNER	02C	DPWA	Multichannel
• • • We do not use the following data for averages, fits, limits, etc. • • •				
< 1	SHRESTHA	12A	DPWA	Multichannel

$\Gamma(N\omega)/\Gamma_{total}$ Γ_5/Γ

VALUE (%)	DOCUMENT ID		TECN	COMMENT
13±9 OUR AVERAGE Error includes scale factor of 3.1.				
10±3	SHKLYAR	13	DPWA	Multichannel
39±9	PENNER	02C	DPWA	Multichannel

$(\Gamma_i\Gamma_f)^{1/2}/\Gamma_{total}$ in $N\pi \to N(1900) \to N\rho$, S=1/2, P-wave $(\Gamma_1\Gamma_3)^{1/2}/\Gamma$

VALUE	DOCUMENT ID		TECN	COMMENT
• • • We do not use the following data for averages, fits, limits, etc. • • •				
0.21±0.08	SHRESTHA	12A	DPWA	Multichannel
−0.34±0.03	MANLEY	92	IPWA	$\pi N \to \pi N$ & $N\pi\pi$

$\Gamma(\Lambda K)/\Gamma_{total}$ Γ_6/Γ

VALUE (%)	DOCUMENT ID		TECN	COMMENT
0 to 10 OUR ESTIMATE				
16 ±5	ANISOVICH	12A	DPWA	Multichannel
2.4±0.3	SHKLYAR	05	DPWA	Multichannel
• • • We do not use the following data for averages, fits, limits, etc. • • •				
14 ±5	SHRESTHA	12A	DPWA	Multichannel
5 to 15	NIKONOV	08	DPWA	Multichannel
0.1±0.1	PENNER	02C	DPWA	Multichannel

$\Gamma(\Sigma K)/\Gamma_{total}$ Γ_7/Γ

VALUE (%)	DOCUMENT ID		TECN	COMMENT
5±2	ANISOVICH	12A	DPWA	Multichannel
• • • We do not use the following data for averages, fits, limits, etc. • • •				
1±1	PENNER	02C	DPWA	Multichannel

N(1900) PHOTON DECAY AMPLITUDES

Papers on γN amplitudes predating 1981 may be found in our 2006 edition, Journal of Physics (generic for all A,B,E,G) **G33** 1 (2006).

N(1900) → pγ, helicity-1/2 amplitude $A_{1/2}$

VALUE ($GeV^{-1/2}$)	DOCUMENT ID		TECN	COMMENT
0.026±0.015	ANISOVICH	12A	DPWA	Multichannel
• • • We do not use the following data for averages, fits, limits, etc. • • •				
−0.008±0.001	SHKLYAR	13	DPWA	Multichannel
0.041±0.008	SHRESTHA	12A	DPWA	Multichannel
−0.017	PENNER	02D	DPWA	Multichannel

$N(1900) \to p\gamma$, helicity-3/2 amplitude $A_{3/2}$

VALUE ($GeV^{-1/2}$)	DOCUMENT ID		TECN	COMMENT
-0.065 ± 0.030	ANISOVICH	12A	DPWA	Multichannel
• • • We do not use the following data for averages, fits, limits, etc. • • •				
$0. \pm 0.001$	SHKLYAR	13	DPWA	Multichannel
-0.004 ± 0.006	SHRESTHA	12A	DPWA	Multichannel
0.031	PENNER	02D	DPWA	Multichannel

$N(1900) \to n\gamma$, helicity-1/2 amplitude $A_{1/2}$

VALUE ($GeV^{-1/2}$)	DOCUMENT ID		TECN	COMMENT
• • • We do not use the following data for averages, fits, limits, etc. • • •				
-0.010 ± 0.004	SHRESTHA	12A	DPWA	Multichannel
-0.016	PENNER	02D	DPWA	Multichannel

$N(1900) \to n\gamma$, helicity-3/2 amplitude $A_{3/2}$

VALUE ($GeV^{-1/2}$)	DOCUMENT ID		TECN	COMMENT
• • • We do not use the following data for averages, fits, limits, etc. • • •				
-0.011 ± 0.007	SHRESTHA	12A	DPWA	Multichannel
-0.002	PENNER	02D	DPWA	Multichannel

$N(1900)$ REFERENCES

SHKLYAR	13	PR C87 015201	V. Shklyar, H. Lenske, U. Mosel	(GIES)
ANISOVICH	12A	EPJ A48 15	A.V. Anisovich *et al.*	(BONN, PNPI)
SHRESTHA	12A	PR C86 055203	M. Shrestha, D.M. Manley	(KSU)
NIKONOV	08	PL B662 245	V.A. Nikonov *et al.*	(Bonn, Gatchina)
ARNDT	06	PR C74 045205	R.A. Arndt *et al.*	(GWU)
PDG	06	JP G33 1	W.-M. Yao *et al.*	(PDG Collab.)
SHKLYAR	05	PR C72 015210	V. Shklyar, H. Lenske, U. Mosel	(GIES)
PENNER	02C	PR C66 055211	G. Penner, U. Mosel	(GIES)
PENNER	02D	PR C66 055212	G. Penner, U. Mosel	(GIES)
MANLEY	92	PR D45 4002	D.M. Manley, E.M. Saleski	(KSA)
Also		PR D30 904	D.M. Manley *et al.*	(VPI)

$N(1990)\ 7/2^+$

$I(J^P) = \frac{1}{2}(\frac{7}{2}^+)$ Status: **

OMITTED FROM SUMMARY TABLE

Most of the results published before 1975 are now obsolete and have been omitted. They may be found in our 1982 edition, Physics Letters **111B** 1 (1982). Some further obsolete results published before 1984 were last included in our 2006 edition, Journal of Physics (generic for all A,B,E,G) **G33** 1 (2006).

The various analyses do not agree very well with one another.

The latest GWU analysis (ARNDT 06) finds no evidence for this resonance.

$N(1990)$ BREIT-WIGNER MASS

VALUE (MeV)	DOCUMENT ID		TECN	COMMENT
≈ 1990 OUR ESTIMATE				
2060 ± 65	ANISOVICH	12A	DPWA	Multichannel
1970 ± 50	CUTKOSKY	80	IPWA	$\pi N \to \pi N$
2005 ± 150	HOEHLER	79	IPWA	$\pi N \to \pi N$
1999	BARBOUR	78	DPWA	$\gamma N \to \pi N$
• • • We do not use the following data for averages, fits, limits, etc. • • •				
1990 ± 45	SHRESTHA	12A	DPWA	Multichannel
2311 ± 16	VRANA	00	DPWA	Multichannel
2086 ± 28	MANLEY	92	IPWA	$\pi N \to \pi N$ & $N\pi\pi$

$N(1990)$ BREIT-WIGNER WIDTH

VALUE (MeV)	DOCUMENT ID		TECN	COMMENT
240 ± 50	ANISOVICH	12A	DPWA	Multichannel
350 ± 120	CUTKOSKY	80	IPWA	$\pi N \to \pi N$
350 ± 100	HOEHLER	79	IPWA	$\pi N \to \pi N$
216	BARBOUR	78	DPWA	$\gamma N \to \pi N$
• • • We do not use the following data for averages, fits, limits, etc. • • •				
203 ± 161	SHRESTHA	12A	DPWA	Multichannel
205 ± 72	VRANA	00	DPWA	Multichannel
535 ± 120	MANLEY	92	IPWA	$\pi N \to \pi N$ & $N\pi\pi$

$N(1990)$ POLE POSITION

REAL PART

VALUE (MeV)	DOCUMENT ID		TECN	COMMENT
2030 ± 65	ANISOVICH	12A	DPWA	Multichannel
1900 ± 30	CUTKOSKY	80	IPWA	$\pi N \to \pi N$
• • • We do not use the following data for averages, fits, limits, etc. • • •				
1941	SHRESTHA	12A	DPWA	Multichannel
2301	VRANA	00	DPWA	Multichannel
not seen	ARNDT	91	DPWA	$\pi N \to \pi N$ Soln SM90

$-2\times$IMAGINARY PART

VALUE (MeV)	DOCUMENT ID		TECN	COMMENT
240 ± 60	ANISOVICH	12A	DPWA	Multichannel
260 ± 60	CUTKOSKY	80	IPWA	$\pi N \to \pi N$
• • • We do not use the following data for averages, fits, limits, etc. • • •				
130	SHRESTHA	12A	DPWA	Multichannel
202	VRANA	00	DPWA	Multichannel
not seen	ARNDT	91	DPWA	$\pi N \to \pi N$ Soln SM90

$N(1990)$ ELASTIC POLE RESIDUE

MODULUS $|r|$

VALUE (MeV)	DOCUMENT ID		TECN	COMMENT
2 ± 1	ANISOVICH	12A	DPWA	Multichannel
9 ± 3	CUTKOSKY	80	IPWA	$\pi N \to \pi N$

PHASE θ

VALUE (°)	DOCUMENT ID		TECN	COMMENT
125 ± 65	ANISOVICH	12A	DPWA	Multichannel
-60 ± 30	CUTKOSKY	80	IPWA	$\pi N \to \pi N$

$N(1990)$ DECAY MODES

	Mode
Γ_1	$N\pi$
Γ_2	$N\eta$
Γ_3	ΛK
Γ_4	ΣK
Γ_5	$N\pi\pi$
Γ_6	$p\gamma$, helicity=1/2
Γ_7	$p\gamma$, helicity=3/2
Γ_8	$n\gamma$, helicity=1/2
Γ_9	$n\gamma$, helicity=3/2

$N(1990)$ BRANCHING RATIOS

$\Gamma(N\pi)/\Gamma_{total}$ Γ_1/Γ

VALUE (%)	DOCUMENT ID		TECN	COMMENT
2 ± 1	ANISOVICH	12A	DPWA	Multichannel
6 ± 2	CUTKOSKY	80	IPWA	$\pi N \to \pi N$
4 ± 2	HOEHLER	79	IPWA	$\pi N \to \pi N$
• • • We do not use the following data for averages, fits, limits, etc. • • •				
2 ± 1	SHRESTHA	12A	DPWA	Multichannel
22 ± 11	VRANA	00	DPWA	Multichannel
6 ± 2	MANLEY	92	IPWA	$\pi N \to \pi N$ & $N\pi\pi$

$(\Gamma_i\Gamma_f)^{1/2}/\Gamma_{total}$ in $N\pi \to N(1990) \to N\eta$ $(\Gamma_1\Gamma_2)^{1/2}/\Gamma$

VALUE	DOCUMENT ID		TECN	COMMENT
-0.043	BAKER	79	DPWA	$\pi^- p \to n\eta$

$\Gamma(N\eta)/\Gamma_{total}$ Γ_2/Γ

VALUE (%)	DOCUMENT ID		TECN	COMMENT
0 ± 1	VRANA	00	DPWA	Multichannel

$(\Gamma_i\Gamma_f)^{1/2}/\Gamma_{total}$ in $N\pi \to N(1990) \to \Lambda K$ $(\Gamma_1\Gamma_3)^{1/2}/\Gamma$

VALUE	DOCUMENT ID		TECN	COMMENT
$+0.01$	BELL	83	DPWA	$\pi^- p \to \Lambda K^0$
not seen	SAXON	80	DPWA	$\pi^- p \to \Lambda K^0$
-0.021 ± 0.033	DEVENISH	74B		Fixed-t dispersion rel.
• • • We do not use the following data for averages, fits, limits, etc. • • •				
-0.010 ± 0.003	SHRESTHA	12A	DPWA	Multichannel

$(\Gamma_i\Gamma_f)^{1/2}/\Gamma_{total}$ in $N\pi \to N(1990) \to \Sigma K$ $(\Gamma_1\Gamma_4)^{1/2}/\Gamma$

VALUE		DOCUMENT ID		TECN	COMMENT
0.010 to 0.023	[1]	DEANS	75	DPWA	$\pi N \to \Sigma K$
0.06		LANGBEIN	73	IPWA	$\pi N \to \Sigma K$ (sol. 1)

$(\Gamma_i\Gamma_f)^{1/2}/\Gamma_{total}$ in $N\pi \to N(1990) \to N\pi\pi$ $(\Gamma_1\Gamma_5)^{1/2}/\Gamma$

VALUE	DOCUMENT ID		TECN	COMMENT
not seen	LONGACRE	75	IPWA	$\pi N \to N\pi\pi$

$N(1990)$ PHOTON DECAY AMPLITUDES

Papers on γN amplitudes predating 1981 may be found in our 2006 edition, Journal of Physics (generic for all A,B,E,G) **G33** 1 (2006).

$N(1990) \to p\gamma$, helicity-1/2 amplitude $A_{1/2}$

VALUE ($GeV^{-1/2}$)		DOCUMENT ID		TECN	COMMENT
0.042 ± 0.014	[2]	ANISOVICH	12A	DPWA	Phase = $(-30 \pm 20)°$
0.030 ± 0.029		AWAJI	81	DPWA	$\gamma N \to \pi N$
• • • We do not use the following data for averages, fits, limits, etc. • • •					
0.040		BARBOUR	78	DPWA	$\gamma N \to \pi N$

$N(1990) \rightarrow p\gamma$, helicity-3/2 amplitude $A_{3/2}$

VALUE ($GeV^{-1/2}$)	DOCUMENT ID		TECN	COMMENT
0.058 ± 0.012	[2] ANISOVICH	12A	DPWA	Phase = $(-35 \pm 25)^\circ$
0.086 ± 0.060	AWAJI	81	DPWA	$\gamma N \rightarrow \pi N$
• • • We do not use the following data for averages, fits, limits, etc. • • •				
$+0.004$	BARBOUR	78	DPWA	$\gamma N \rightarrow \pi N$

$N(1990) \rightarrow n\gamma$, helicity-1/2 amplitude $A_{1/2}$

VALUE ($GeV^{-1/2}$)	DOCUMENT ID		TECN	COMMENT
-0.001	AWAJI	81	DPWA	$\gamma N \rightarrow \pi N$
• • • We do not use the following data for averages, fits, limits, etc. • • •				
-0.069	BARBOUR	78	DPWA	$\gamma N \rightarrow \pi N$

$N(1990) \rightarrow n\gamma$, helicity-3/2 amplitude $A_{3/2}$

VALUE ($GeV^{-1/2}$)	DOCUMENT ID		TECN	COMMENT
-0.178	AWAJI	81	DPWA	$\gamma N \rightarrow \pi N$
• • • We do not use the following data for averages, fits, limits, etc. • • •				
-0.072	BARBOUR	78	DPWA	$\gamma N \rightarrow \pi N$

$N(1990)$ FOOTNOTES

[1] The range given for DEANS 75 is from the four best solutions.
[2] This ANISOVICH 12A value is the complex helicity amplitude at the pole position.

$N(1990)$ REFERENCES

For early references, see Physics Letters **111B** 1 (1982).

ANISOVICH	12A	EPJ A48 15	A.V. Anisovich *et al.*	(BONN, PNPI)
SHRESTHA	12A	PR C86 055203	M. Shrestha, D.M. Manley	(KSU)
ARNDT	06	PR C74 045205	R.A. Arndt *et al.*	(GWU)
PDG	06	JP G33 1	W.-M. Yao *et al.*	(PDG Collab.)
VRANA	00	PRPL 328 181	T.P. Vrana, S.A. Dytman,, T.-S.H. Lee	(PITT+)
MANLEY	92	PR D45 4002	D.M. Manley, E.M. Saleski	(KSA) IJP
Also		PR D30 904	D.M. Manley *et al.*	(VPI)
ARNDT	91	PR D43 2131	R.A. Arndt *et al.*	(VPI, TELE) IJP
BELL	83	NP B222 389	K.W. Bell *et al.*	(RL) IJP
PDG	82	PL 111B 1	M. Roos *et al.*	(HELS, CIT, CERN)
AWAJI	81	Bonn Conf. 352	N. Awaji, R. Kajikawa	(NAGO)
Also		NP B197 365	K. Fujii *et al.*	(NAGO)
CUTKOSKY	80	Toronto Conf. 19	R.E. Cutkosky *et al.*	(CMU, LBL) IJP
Also		PR D20 2839	R.E. Cutkosky *et al.*	(CMU, LBL) IJP
SAXON	80	NP B162 522	D.H. Saxon *et al.*	(RHEL, BRIS) IJP
BAKER	79	NP B156 93	R.D. Baker *et al.*	(RHEL) IJP
HOEHLER	79	PDAT 12-1	G. Hohler *et al.*	(KARLT) IJP
Also		Toronto Conf. 3	R. Koch	(KARLT) IJP
BARBOUR	78	NP B141 253	I.M. Barbour, R.L. Crawford, N.H. Parsons	(GLAS)
DEANS	75	NP B96 90	S.R. Deans *et al.*	(SFLA, ALAH) IJP
LONGACRE	75	PL 55B 415	R.S. Longacre *et al.*	(LBL, SLAC) IJP
DEVENISH	74B	NP B81 330	R.C.E. Devenish, C.D. Froggatt, B.R. Martin	(DESY+)
LANGBEIN	73	NP B53 251	W. Langbein, F. Wagner	(MUNI) IJP

$N(2000)\ 5/2^+$

$I(J^P) = \frac{1}{2}(\frac{5}{2}^+)$ Status: **

OMITTED FROM SUMMARY TABLE

Before the 2012 *Review*, all the evidence for a $J^P = 5/2^+$ state with a mass above 1800 MeV was filed under a two-star $N(2000)$. There is now some evidence from ANISOVICH 12A for two $5/2^+$ states in this region, so we have split the older data (according to mass) between two two-star $5/2^+$ states, an $N(1860)$ and an $N(2000)$.

$N(2000)$ BREIT-WIGNER MASS

VALUE (MeV)	DOCUMENT ID		TECN	COMMENT
1950 to 2150 (≈ 2050) OUR ESTIMATE				
1946 ± 4	SHKLYAR	13	DPWA	Multichannel
2090 ± 120	ANISOVICH	12A	DPWA	Multichannel
• • • We do not use the following data for averages, fits, limits, etc. • • •				
2025	AYED	76	IPWA	$\pi N \rightarrow \pi N$
1970	[1] LANGBEIN	73	IPWA	$\pi N \rightarrow \Sigma K$ (sol. 2)
2175	ALMEHED	72	IPWA	$\pi N \rightarrow \pi N$
1930	DEANS	72	MPWA	$\gamma p \rightarrow \Lambda K$ (sol. D)

$N(2000)$ BREIT-WIGNER WIDTH

VALUE (MeV)	DOCUMENT ID		TECN	COMMENT
198 ± 2	SHKLYAR	13	DPWA	Multichannel
460 ± 100	ANISOVICH	12A	DPWA	Multichannel
• • • We do not use the following data for averages, fits, limits, etc. • • •				
157	AYED	76	IPWA	$\pi N \rightarrow \pi N$
170	[1] LANGBEIN	73	IPWA	$\pi N \rightarrow \Sigma K$ (sol. 2)
150	ALMEHED	72	IPWA	$\pi N \rightarrow \pi N$
112	DEANS	72	MPWA	$\gamma p \rightarrow \Lambda K$ (sol. D)

$N(2000)$ POLE POSITION

REAL PART

VALUE (MeV)	DOCUMENT ID		TECN	COMMENT
2030 ± 110	ANISOVICH	12A	DPWA	Multichannel
• • • We do not use the following data for averages, fits, limits, etc. • • •				
1900	SHKLYAR	13	DPWA	Multichannel
1779	ARNDT	04	DPWA	$\pi N \rightarrow \pi N, \eta N$

$-2\times$IMAGINARY PART

VALUE (MeV)	DOCUMENT ID		TECN	COMMENT
480 ± 100	ANISOVICH	12A	DPWA	Multichannel
• • • We do not use the following data for averages, fits, limits, etc. • • •				
123	SHKLYAR	13	DPWA	Multichannel
248	ARNDT	04	DPWA	$\pi N \rightarrow \pi N, \eta N$

$N(2000)$ ELASTIC POLE RESIDUE

MODULUS $|r|$

VALUE (MeV)	DOCUMENT ID		TECN	COMMENT
35^{+80}_{-15}	ANISOVICH	12A	DPWA	Multichannel
• • • We do not use the following data for averages, fits, limits, etc. • • •				
11	SHKLYAR	13	DPWA	Multichannel
47	ARNDT	04	DPWA	$\pi N \rightarrow \pi N, \eta N$

PHASE θ

VALUE ($^\circ$)	DOCUMENT ID		TECN	COMMENT
-100 ± 40	ANISOVICH	12A	DPWA	Multichannel
• • • We do not use the following data for averages, fits, limits, etc. • • •				
-6	SHKLYAR	13	DPWA	Multichannel
-61	ARNDT	04	DPWA	$\pi N \rightarrow \pi N, \eta N$

$N(2000)$ DECAY MODES

	Mode	Fraction (Γ_i/Γ)
Γ_1	$N\pi$	(9.9 ± 1.0) %
Γ_2	$N\eta$	(2.0 ± 2.0) %
Γ_3	$N\omega$	(1.0 ± 1.0) %
Γ_4	ΛK	
Γ_5	ΣK	
Γ_6	$p\gamma$	

$N(2000)$ BRANCHING RATIOS

$\Gamma(N\pi)/\Gamma_{total}$ Γ_1/Γ

VALUE (%)	DOCUMENT ID		TECN	COMMENT
9.9±1.0 OUR AVERAGE				
10 ±1	SHKLYAR	13	DPWA	Multichannel
9 ±4	ANISOVICH	12A	DPWA	Multichannel
• • • We do not use the following data for averages, fits, limits, etc. • • •				
8	AYED	76	IPWA	$\pi N \rightarrow \pi N$
25	ALMEHED	72	IPWA	$\pi N \rightarrow \pi N$

$\Gamma(N\eta)/\Gamma_{total}$ Γ_2/Γ

VALUE (%)	DOCUMENT ID		TECN	COMMENT
2±2	SHKLYAR	13	DWPA	Multichannel

$\Gamma(N\omega)/\Gamma_{total}$ Γ_3/Γ

VALUE (%)	DOCUMENT ID		TECN	COMMENT
1±1	SHKLYAR	13	DPWA	Multichannel

$(\Gamma_i\Gamma_f)^{1/2}/\Gamma_{total}$ in $N\pi \rightarrow N(2000) \rightarrow N\eta$ $(\Gamma_1\Gamma_2)^{1/2}/\Gamma$

VALUE	DOCUMENT ID		TECN	COMMENT
+0.03	BAKER	79	DPWA	$\pi^- p \rightarrow n\eta$

$(\Gamma_i\Gamma_f)^{1/2}/\Gamma_{total}$ in $N\pi \rightarrow N(2000) \rightarrow \Lambda K$ $(\Gamma_1\Gamma_4)^{1/2}/\Gamma$

VALUE	DOCUMENT ID		TECN	COMMENT
not seen	SAXON	80	DPWA	$\pi^- p \rightarrow \Lambda K^0$

$(\Gamma_i\Gamma_f)^{1/2}/\Gamma_{total}$ in $N\pi \rightarrow N(2000) \rightarrow \Sigma K$ $(\Gamma_1\Gamma_5)^{1/2}/\Gamma$

VALUE	DOCUMENT ID		TECN	COMMENT
0.022	[2] DEANS	75	DPWA	$\pi N \rightarrow \Sigma K$
0.05	[1] LANGBEIN	73	IPWA	$\pi N \rightarrow \Sigma K$ (sol. 2)

$(\Gamma_i\Gamma_f)^{1/2}/\Gamma_{total}$ in $p\gamma \rightarrow N(2000) \rightarrow \Lambda K$ $(\Gamma_6\Gamma_4)^{1/2}/\Gamma$

VALUE	DOCUMENT ID		TECN	COMMENT
0.0022	DEANS	72	MPWA	$\gamma p \rightarrow \Lambda K$ (sol. D)

$N(2000)$ PHOTON DECAY AMPLITUDES

Papers on γN amplitudes predating 1981 may be found in our 2006 edition, Journal of Physics (generic for all A,B,E,G) **G33** 1 (2006).

$N(2000) \rightarrow p\gamma$, helicity-1/2 amplitude $A_{1/2}$

VALUE ($GeV^{-1/2}$)	DOCUMENT ID		TECN	COMMENT
0.035 ± 0.015	[3] ANISOVICH	12A	DPWA	Phase = $(15 \pm 40)^\circ$
• • • We do not use the following data for averages, fits, limits, etc. • • •				
0.011 ± 0.001	SHKLYAR	13	DPWA	Multichannel

$N(2000) \rightarrow p\gamma$, helicity-3/2 amplitude $A_{3/2}$

VALUE ($GeV^{-1/2}$)	DOCUMENT ID		TECN	COMMENT
0.050 ± 0.014	[3] ANISOVICH	12A	DPWA	Phase = $(-130 \pm 40)^\circ$
• • • We do not use the following data for averages, fits, limits, etc. • • •				
0.025 ± 0.001	SHKLYAR	13	DPWA	Multichannel

$N(2000)$ FOOTNOTES

[1] Not seen in solution 1 of LANGBEIN 73.
[2] Value given is from solution 1 of DEANS 75; not present in solutions 2, 3, or 4.
[3] This ANISOVICH 12A value is the complex helicity amplitude at the pole position.

$N(2000)$ REFERENCES

SHKLYAR	13	PR C87 015201	V. Shklyar, H. Lenske, U. Mosel	(GIES)
ANISOVICH	12A	EPJ A48 15	A.V. Anisovich *et al.*	(BONN, PNPI)
PDG	06	JP G33 1	W.-M. Yao *et al.*	(PDG Collab.)
ARNDT	04	PR C69 035213	R.A. Arndt *et al.*	(GWU, TRIU)
SAXON	80	NP B162 522	D.H. Saxon *et al.*	(RHEL, BRIS) IJP
BAKER	79	NP B156 93	R.D. Baker *et al.*	(RHEL) IJP
AYED	76	Thesis CEA-N-1921	R. Ayed	(SACL) IJP
DEANS	75	NP B96 90	S.R. Deans *et al.*	(SFLA, ALAH) IJP
LANGBEIN	73	NP B53 251	W. Langbein, F. Wagner	(MUNI) IJP
ALMEHED	72	NP B40 157	S. Almehed, C. Lovelace	(LUND, RUTG) IJP
DEANS	72	PR D6 1906	S.R. Deans *et al.*	(SFLA) IJP

$N(2040)\ 3/2^+$

$J^P = \frac{3}{2}^+$ Status: *

OMITTED FROM SUMMARY TABLE

$N(2040)$ MASS

VALUE (MeV)	DOCUMENT ID		TECN	COMMENT
2052^{+13}_{-21} OUR AVERAGE				
$2040^{+\ 3}_{-\ 4} \pm 25$	ABLIKIM	09B	BES2	$J/\psi \rightarrow p\overline{p}\pi^0$
$2068 \pm\ 3^{+15}_{-40}$	ABLIKIM	06K	BES2	$J/\psi \rightarrow p\overline{n}\pi^-, n\overline{p}\pi^+$

$N(2040)$ WIDTH

VALUE (MeV)	DOCUMENT ID		TECN	COMMENT
191 ± 33 OUR AVERAGE				
$230 \pm\ 8 \pm 52$	ABLIKIM	09B	BES2	$J/\psi \rightarrow p\overline{p}\pi^0$
$165 \pm 14 \pm 40$	ABLIKIM	06K	BES2	$J/\psi \rightarrow p\overline{n}\pi^-, n\overline{p}\pi^+$

$N(2040)$ REFERENCES

ABLIKIM	09B	PR D80 052004	M. Ablikim *et al.*	(BES II Collab.)
ABLIKIM	06K	PRL 97 062001	M. Ablikim *et al.*	(BES II Collab.)

$N(2060)\ 5/2^-$

$I(J^P) = \frac{1}{2}(\frac{5}{2}^-)$ Status: **

OMITTED FROM SUMMARY TABLE

Before our 2012 *Review*, this state appeared in our Listings as the $N(2200)$.

The latest GWU analysis (ARNDT 06) finds no evidence for this resonance.

$N(2060)$ BREIT-WIGNER MASS

VALUE (MeV)	DOCUMENT ID		TECN	COMMENT
≈ 2060 OUR ESTIMATE				
2060 ± 15	ANISOVICH	12A	DPWA	Multichannel
1900	BELL	83	DPWA	$\pi^- p \rightarrow \Lambda K^0$
2180 ± 80	CUTKOSKY	80	IPWA	$\pi N \rightarrow \pi N$
1920	SAXON	80	DPWA	$\pi^- p \rightarrow \Lambda K^0$
2228 ± 30	HOEHLER	79	IPWA	$\pi N \rightarrow \pi N$
• • • We do not use the following data for averages, fits, limits, etc. • • •				
2116 ± 21	SHRESTHA	12A	DPWA	Multichannel
2217 ± 27	BATINIC	10	DPWA	$\pi N \rightarrow N\pi, N\eta$

$N(2060)$ BREIT-WIGNER WIDTH

VALUE (MeV)	DOCUMENT ID		TECN	COMMENT
$375 \pm\ 25$	ANISOVICH	12A	DPWA	Multichannel
130	BELL	83	DPWA	$\pi^- p \rightarrow \Lambda K^0$
400 ± 100	CUTKOSKY	80	IPWA	$\pi N \rightarrow \pi N$
220	SAXON	80	DPWA	$\pi^- p \rightarrow \Lambda K^0$
$310 \pm\ 50$	HOEHLER	79	IPWA	$\pi N \rightarrow \pi N$
• • • We do not use the following data for averages, fits, limits, etc. • • •				
307 ± 112	SHRESTHA	12A	DPWA	Multichannel
$481 \pm\ 17$	BATINIC	10	DPWA	$\pi N \rightarrow N\pi, N\eta$

$N(2060)$ POLE POSITION

REAL PART

VALUE (MeV)	DOCUMENT ID		TECN	COMMENT
2040 ± 15	ANISOVICH	12A	DPWA	Multichannel
2100 ± 60	CUTKOSKY	80	IPWA	$\pi N \rightarrow \pi N$
• • • We do not use the following data for averages, fits, limits, etc. • • •				
2064	SHRESTHA	12A	DPWA	Multichannel
2144 ± 31	BATINIC	10	DPWA	$\pi N \rightarrow N\pi, N\eta$

$-2\times$IMAGINARY PART

VALUE (MeV)	DOCUMENT ID		TECN	COMMENT
390 ± 25	ANISOVICH	12A	DPWA	Multichannel
360 ± 80	CUTKOSKY	80	IPWA	$\pi N \rightarrow \pi N$
• • • We do not use the following data for averages, fits, limits, etc. • • •				
267	SHRESTHA	12A	DPWA	Multichannel
438 ± 13	BATINIC	10	DPWA	$\pi N \rightarrow N\pi, N\eta$

$N(2060)$ ELASTIC POLE RESIDUE

MODULUS $|r|$

VALUE (MeV)	DOCUMENT ID		TECN	COMMENT
$19 \pm\ 5$	ANISOVICH	12A	DPWA	Multichannel
20 ± 10	CUTKOSKY	80	IPWA	$\pi N \rightarrow \pi N$
• • • We do not use the following data for averages, fits, limits, etc. • • •				
26	BATINIC	10	DPWA	$\pi N \rightarrow N\pi, N\eta$

PHASE θ

VALUE (°)	DOCUMENT ID		TECN	COMMENT
-125 ± 20	ANISOVICH	12A	DPWA	Multichannel
$-\ 90 \pm 50$	CUTKOSKY	80	IPWA	$\pi N \rightarrow \pi N$
• • • We do not use the following data for averages, fits, limits, etc. • • •				
$-\ 71$	BATINIC	10	DPWA	$\pi N \rightarrow N\pi, N\eta$

$N(2060)$ INELASTIC POLE RESIDUE

The "normalized residue" is the residue divided by $\Gamma_{pole}/2$.

Normalized residue in $N\pi \rightarrow N(2060) \rightarrow N\eta$

MODULUS (%)	PHASE (°)	DOCUMENT ID		TECN	COMMENT
5 ± 3	40 ± 25	ANISOVICH	12A	DPWA	Multichannel

Normalized residue in $N\pi \rightarrow N(2060) \rightarrow \Lambda K$

MODULUS (%)	DOCUMENT ID		TECN	COMMENT
1 ± 0.5	ANISOVICH	12A	DPWA	Multichannel

Normalized residue in $N\pi \rightarrow N(2060) \rightarrow \Sigma K$

MODULUS (%)	PHASE (°)	DOCUMENT ID		TECN	COMMENT
4 ± 2	-70 ± 30	ANISOVICH	12A	DPWA	Multichannel

$N(2060)$ DECAY MODES

	Mode
Γ_1	$N\pi$
Γ_2	$N\eta$
Γ_3	ΛK
Γ_4	ΣK
Γ_5	$N\pi\pi$
Γ_6	$\Delta\pi$
Γ_7	$\Delta(1232)\pi$, D-wave
Γ_8	$N\rho$
Γ_9	$N\rho$, S=1/2
Γ_{10}	$N\rho$, S=3/2, D-wave
Γ_{11}	$p\gamma$
Γ_{12}	$p\gamma$, helicity=1/2
Γ_{13}	$p\gamma$, helicity=3/2
Γ_{14}	$n\gamma$
Γ_{15}	$n\gamma$, helicity=1/2
Γ_{16}	$n\gamma$, helicity=3/2

$N(2060)$ BRANCHING RATIOS

$\Gamma(N\pi)/\Gamma_{total}$ — Γ_1/Γ

VALUE (%)	DOCUMENT ID		TECN	COMMENT
8±2	ANISOVICH	12A	DPWA	Multichannel
10±3	CUTKOSKY	80	IPWA	$\pi N \to \pi N$
7±2	HOEHLER	79	IPWA	$\pi N \to \pi N$
• • • We do not use the following data for averages, fits, limits, etc. • • •				
9±2	SHRESTHA	12A	DPWA	Multichannel
13±4	BATINIC	10	DPWA	$\pi N \to N\pi, N\eta$

$\Gamma(N\eta)/\Gamma_{total}$ — Γ_2/Γ

VALUE (%)	DOCUMENT ID		TECN	COMMENT
4 ±2	ANISOVICH	12A	DPWA	Multichannel
• • • We do not use the following data for averages, fits, limits, etc. • • •				
<1	SHRESTHA	12A	DPWA	Multichannel
0.2±1.0	BATINIC	10	DPWA	$\pi N \to N\pi, N\eta$

$(\Gamma_i\Gamma_f)^{1/2}/\Gamma_{total}$ in $N\pi \to N(2060) \to N\eta$ — $(\Gamma_1\Gamma_2)^{1/2}/\Gamma$

VALUE	DOCUMENT ID		TECN	COMMENT
0.066	BAKER	79	DPWA	$\pi^- p \to n\eta$

$(\Gamma_i\Gamma_f)^{1/2}/\Gamma_{total}$ in $N\pi \to N(2060) \to \Lambda K$ — $(\Gamma_1\Gamma_3)^{1/2}/\Gamma$

VALUE	DOCUMENT ID		TECN	COMMENT
−0.03	BELL	83	DPWA	$\pi^- p \to \Lambda K^0$
−0.05	SAXON	80	DPWA	$\pi^- p \to \Lambda K^0$
• • • We do not use the following data for averages, fits, limits, etc. • • •				
0.00±0.03	SHRESTHA	12A	DPWA	Multichannel

$\Gamma(\Sigma K)/\Gamma_{total}$ — Γ_4/Γ

VALUE (%)	DOCUMENT ID		TECN	COMMENT
3±2	ANISOVICH	12A	DPWA	Multichannel

$\Gamma(\Delta(1232)\pi, D\text{-wave})/\Gamma_{total}$ — Γ_7/Γ

VALUE (%)	DOCUMENT ID		TECN	COMMENT
• • • We do not use the following data for averages, fits, limits, etc. • • •				
40±13	SHRESTHA	12A	DPWA	Multichannel

$\Gamma(N\rho, S=1/2)/\Gamma_{total}$ — Γ_9/Γ

VALUE (%)	DOCUMENT ID		TECN	COMMENT
• • • We do not use the following data for averages, fits, limits, etc. • • •				
21±15	SHRESTHA	12A	DPWA	Multichannel

$\Gamma(N\rho, S=3/2, D\text{-wave})/\Gamma_{total}$ — Γ_{10}/Γ

VALUE (%)	DOCUMENT ID		TECN	COMMENT
• • • We do not use the following data for averages, fits, limits, etc. • • •				
<9	SHRESTHA	12A	DPWA	Multichannel

$N(2060)$ PHOTON DECAY AMPLITUDES

Papers on γN amplitudes predating 1981 may be found in our 2006 edition, Journal of Physics (generic for all A,B,E,G) **G33** 1 (2006).

$N(2060) \to p\gamma$, helicity-1/2 amplitude $A_{1/2}$

VALUE ($GeV^{-1/2}$)	DOCUMENT ID		TECN	COMMENT
0.065±0.012	[1] ANISOVICH	12A	DPWA	Phase = (15 ± 8)°
• • • We do not use the following data for averages, fits, limits, etc. • • •				
0.018±0.004	SHRESTHA	12A	DPWA	Multichannel

$N(2060) \to p\gamma$, helicity-3/2 amplitude $A_{3/2}$

VALUE ($GeV^{-1/2}$)	DOCUMENT ID		TECN	COMMENT
0.055^{+15}_{-35}	[1] ANISOVICH	12A	DPWA	Phase = (15 ± 10)°
• • • We do not use the following data for averages, fits, limits, etc. • • •				
0.010± 0.004	SHRESTHA	12A	DPWA	Multichannel

$N(2060) \to n\gamma$, helicity-1/2 amplitude $A_{1/2}$

VALUE ($GeV^{-1/2}$)	DOCUMENT ID		TECN	COMMENT
• • • We do not use the following data for averages, fits, limits, etc. • • •				
−0.012±0.017	SHRESTHA	12A	DPWA	Multichannel

$N(2060) \to n\gamma$, helicity-3/2 amplitude $A_{3/2}$

VALUE ($GeV^{-1/2}$)	DOCUMENT ID		TECN	COMMENT
• • • We do not use the following data for averages, fits, limits, etc. • • •				
−0.023±0.023	SHRESTHA	12A	DPWA	Multichannel

$N(2060)$ FOOTNOTES

[1] This ANISOVICH 12A value is the complex helicity amplitude at the pole position.

$N(2060)$ REFERENCES

ANISOVICH	12A	EPJ A48 15	A.V. Anisovich *et al.*	(BONN, PNPI)
SHRESTHA	12A	PR C86 055203	M. Shrestha, D.M. Manley	(KSU)
BATINIC	10	PR C82 038203	M. Batinic *et al.*	(ZAGR)
ARNDT	06	PR C74 045205	R.A. Arndt *et al.*	(GWU)
PDG	06	JP G33 1	W.-M. Yao *et al.*	(PDG Collab.)
BELL	83	NP B222 389	K.W. Bell *et al.*	(RL) IJP
CUTKOSKY	80	Toronto Conf. 19	R.E. Cutkosky *et al.*	(CMU, LBL) IJP
Also		PR D20 2839	R.E. Cutkosky *et al.*	(CMU, LBL)
SAXON	80	NP B162 522	D.H. Saxon *et al.*	(RHEL, BRIS) IJP
BAKER	79	NP B156 93	R.D. Baker *et al.*	(RHEL) IJP
HOEHLER	79	PDAT 12-1	G. Hohler *et al.*	(KARLT) IJP
Also		Toronto Conf. 3	R. Koch	(KARLT) IJP

$N(2100)$ $1/2^+$

$I(J^P) = \frac{1}{2}(\frac{1}{2}^+)$ Status: *

OMITTED FROM SUMMARY TABLE

The latest GWU analysis (ARNDT 06) finds no evidence for this resonance.

$N(2100)$ BREIT-WIGNER MASS

VALUE (MeV)	DOCUMENT ID		TECN	COMMENT
≈ 2100 OUR ESTIMATE				
2125±75	CUTKOSKY	80	IPWA	$\pi N \to \pi N$
2050±20	HOEHLER	79	IPWA	$\pi N \to \pi N$
• • • We do not use the following data for averages, fits, limits, etc. • • •				
2157±42	BATINIC	10	DPWA	$\pi N \to N\pi, N\eta$
$2068\pm\ 3^{+15}_{-40}$	ABLIKIM	06K	BES2	$J/\psi \to (p\pi^-)\overline{n}$
2084±93	VRANA	00	DPWA	Multichannel
$1986\pm26^{+10}_{-30}$	PLOETZKE	98	SPEC	$\gamma p \to p\eta'(958)$

$N(2100)$ BREIT-WIGNER WIDTH

VALUE (MeV)	DOCUMENT ID		TECN	COMMENT
260±100	CUTKOSKY	80	IPWA	$\pi N \to \pi N$
200± 30	HOEHLER	79	IPWA	$\pi N \to \pi N$
• • • We do not use the following data for averages, fits, limits, etc. • • •				
355± 88	BATINIC	10	DPWA	$\pi N \to N\pi, N\eta$
165± 14±40	ABLIKIM	06K	BES2	$J/\psi \to (p\pi^-)\overline{n}$
1077±643	VRANA	00	DPWA	Multichannel
$296\pm100^{+60}_{-10}$	PLOETZKE	98	SPEC	$\gamma p \to p\eta'(958)$

$N(2100)$ POLE POSITION

REAL PART

VALUE (MeV)	DOCUMENT ID		TECN	COMMENT
2120±40	CUTKOSKY	80	IPWA	$\pi N \to \pi N$
• • • We do not use the following data for averages, fits, limits, etc. • • •				
2120±47	BATINIC	10	DPWA	$\pi N \to N\pi, N\eta$
1810	VRANA	00	DPWA	Multichannel
not seen	ARNDT	91	DPWA	$\pi N \to \pi N$ Soln SM90

−2×IMAGINARY PART

VALUE (MeV)	DOCUMENT ID		TECN	COMMENT
240±80	CUTKOSKY	80	IPWA	$\pi N \to \pi N$
• • • We do not use the following data for averages, fits, limits, etc. • • •				
346±80	BATINIC	10	DPWA	$\pi N \to N\pi, N\eta$
622	VRANA	00	DPWA	Multichannel
not seen	ARNDT	91	DPWA	$\pi N \to \pi N$ Soln SM90

$N(2100)$ ELASTIC POLE RESIDUE

MODULUS $|r|$

VALUE (MeV)	DOCUMENT ID		TECN	COMMENT
14±7	CUTKOSKY	80	IPWA	$\pi N \to \pi N$
• • • We do not use the following data for averages, fits, limits, etc. • • •				
33	BATINIC	10	DPWA	$\pi N \to N\pi, N\eta$

PHASE θ

VALUE (°)	DOCUMENT ID		TECN	COMMENT
35±25	CUTKOSKY	80	IPWA	$\pi N \to \pi N$
• • • We do not use the following data for averages, fits, limits, etc. • • •				
−59	BATINIC	10	DPWA	$\pi N \to N\pi, N\eta$

$N(2100)$ DECAY MODES

	Mode	Fraction (Γ_i/Γ)
Γ_1	$N\pi$	
Γ_2	$N\eta$	(61±60) %
Γ_3	ΛK	
Γ_4	$N\pi\pi$	
Γ_5	$\Delta(1232)\pi$, P-wave	
Γ_6	$N\rho$, S=1/2, P-wave	
Γ_7	$N(\pi\pi)^{I=0}_{S\text{-wave}}$	

$N(2100)$ BRANCHING RATIOS

$\Gamma(N\pi)/\Gamma_{total}$ — Γ_1/Γ

VALUE (%)	DOCUMENT ID		TECN	COMMENT
12±3	CUTKOSKY	80	IPWA	$\pi N \to \pi N$
10±4	HOEHLER	79	IPWA	$\pi N \to \pi N$
• • • We do not use the following data for averages, fits, limits, etc. • • •				
16±5	BATINIC	10	DPWA	$\pi N \to N\pi, N\eta$
2±5	VRANA	00	DPWA	Multichannel

$\Gamma(N\eta)/\Gamma_{total}$ — Γ_2/Γ

VALUE (%)	DOCUMENT ID		TECN	COMMENT
61±61	VRANA	00	DPWA	Multichannel
• • • We do not use the following data for averages, fits, limits, etc. • • •				
83± 5	BATINIC	10	DPWA	$\pi N \to N\pi, N\eta$

$\Gamma(\Lambda K)/\Gamma_{total}$ — Γ_3/Γ

VALUE (%)	DOCUMENT ID		TECN	COMMENT
21±20	VRANA	00	DPWA	Multichannel

$(\Gamma_i\Gamma_f)^{1/2}/\Gamma_{total}$ in $N\pi \to N(2100) \to \Delta(1232)\pi$, P-wave — $(\Gamma_1\Gamma_5)^{1/2}/\Gamma$

$\Gamma(\Delta(1232)\pi, P\text{-wave})/\Gamma_{total}$ — Γ_5/Γ

VALUE (%)	DOCUMENT ID		TECN	COMMENT
2±1	VRANA	00	DPWA	Multichannel

$\Gamma(N\rho, S=1/2, P\text{-wave})/\Gamma_{total}$ — Γ_6/Γ

VALUE (%)	DOCUMENT ID		TECN	COMMENT
4±1	VRANA	00	DPWA	Multichannel

$\Gamma(N(\pi\pi)^{I=0}_{S\text{-wave}})/\Gamma_{total}$ — Γ_7/Γ

VALUE (%)	DOCUMENT ID		TECN	COMMENT
10±1	VRANA	00	DPWA	Multichannel

$N(2100)$ REFERENCES

BATINIC	10	PR C82 038203	M. Batinic *et al.*	(ZAGR)
ABLIKIM	06K	PRL 97 062001	M. Ablikim *et al.*	(BES II Collab.)
ARNDT	06	PR C74 045205	R.A. Arndt *et al.*	(GWU)
VRANA	00	PRPL 328 181	T.P. Vrana, S.A. Dytman,, T.-S.H. Lee	(PITT+)
PLOETZKE	98	PL B444 555	R. Ploetzke *et al.*	(Bonn SAPHIR Collab.)
ARNDT	91	PR D43 2131	R.A. Arndt *et al.*	(VPI, TELE) IJP
CUTKOSKY	80	Toronto Conf. 19	R.E. Cutkosky *et al.*	(CMU, LBL) IJP
Also		PR D20 2839	R.E. Cutkosky *et al.*	(CMU, LBL)
HOEHLER	79	PDAT 12-1	G. Hohler *et al.*	(KARLT) IJP
Also		Toronto Conf. 3	R. Koch	(KARLT) IJP

$N(2120)$ $3/2^-$

$I(J^P) = \frac{1}{2}(\frac{3}{2}^-)$ Status: **

OMITTED FROM SUMMARY TABLE

Before the 2012 *Review*, all the evidence for a $J^P = 3/2^-$ state with a mass above 1800 MeV was filed under a two-star $N(2080)$. There is now evidence from ANISOVICH 12A for two $3/2^-$ states in this region, so we have split the older data (according to mass) between a three-star $N(1875)$ and a two-star $N(2120)$.

$N(2120)$ BREIT-WIGNER MASS

VALUE (MeV)		DOCUMENT ID		TECN	COMMENT
2120 OUR ESTIMATE					
2150±60		ANISOVICH	12A	DPWA	Multichannel
2060±80	[1]	CUTKOSKY	80	IPWA	$\pi N \to \pi N$
2081±20		HOEHLER	79	IPWA	$\pi N \to \pi N$

$N(2120)$ BREIT-WIGNER WIDTH

VALUE (MeV)	DOCUMENT ID		TECN	COMMENT
330± 45	ANISOVICH	12A	DPWA	Multichannel
300±100	CUTKOSKY	80	IPWA	$\pi N \to \pi N$ (higher m)
265± 40	HOEHLER	79	IPWA	$\pi N \to \pi N$

$N(2120)$ POLE POSITION

REAL PART

VALUE (MeV)	DOCUMENT ID		TECN	COMMENT
2110±50	ANISOVICH	12A	DPWA	Multichannel
2050±70	CUTKOSKY	80	IPWA	$\pi N \to \pi N$ (higher m)

−2×IMAGINARY PART

VALUE (MeV)	DOCUMENT ID		TECN	COMMENT
340±45	ANISOVICH	12A	DPWA	Multichannel
200±80	CUTKOSKY	80	IPWA	$\pi N \to \pi N$ (higher m)

$N(2120)$ ELASTIC POLE RESIDUE

MODULUS $|r|$

VALUE (MeV)	DOCUMENT ID		TECN	COMMENT
13± 3	ANISOVICH	12A	DPWA	Multichannel
30±20	CUTKOSKY	80	IPWA	$\pi N \to \pi N$ (higher m)

PHASE θ

VALUE (°)	DOCUMENT ID		TECN	COMMENT
−20± 10	ANISOVICH	12A	DPWA	Multichannel
0±100	CUTKOSKY	80	IPWA	$\pi N \to \pi N$ (higher m)

$N(2120)$ INELASTIC POLE RESIDUE

The "normalized residue" is the residue divided by $\Gamma_{pole}/2$.

Normalized residue in $N\pi \to N(2120) \to \Lambda K$

MODULUS (%)	PHASE (°)	DOCUMENT ID		TECN	COMMENT
3±1	100 ± 30	ANISOVICH	12A	DPWA	Multichannel

Normalized residue in $N\pi \to N(2120) \to \Sigma K$

MODULUS (%)	PHASE (°)	DOCUMENT ID		TECN	COMMENT
2±1.5	−50 ± 40	ANISOVICH	12A	DPWA	Multichannel

$N(2120)$ DECAY MODES

	Mode
Γ_1	$N\pi$

$N(2120)$ BRANCHING RATIOS

$\Gamma(N\pi)/\Gamma_{total}$ — Γ_1/Γ

VALUE (%)	DOCUMENT ID		TECN	COMMENT
6±2	ANISOVICH	12A	DPWA	Multichannel
14±7	CUTKOSKY	80	IPWA	$\pi N \to \pi N$ (higher m)
6±2	HOEHLER	79	IPWA	$\pi N \to \pi N$

$N(2120)$ PHOTON DECAY AMPLITUDES

$N(2120) \to p\gamma$, helicity-1/2 amplitude $A_{1/2}$

VALUE		DOCUMENT ID		TECN	COMMENT
0.125±0.045	[2]	ANISOVICH	12A	DPWA	Phase = (−55 ± 20)°

$N(2120) \to p\gamma$, helicity-3/2 amplitude $A_{3/2}$

VALUE		DOCUMENT ID		TECN	COMMENT
0.150±0.060	[2]	ANISOVICH	12A	DPWA	Phase = (−35 ± 15)°

$N(2120)$ FOOTNOTES

[1] CUTKOSKY 80 finds a lower mass D_{13} resonance, as well as one in this region. Both are listed here.
[2] This ANISOVICH 12A value is the complex helicity amplitude at the pole position.

$N(2120)$ REFERENCES

ANISOVICH	12A	EPJ A48 15	A.V. Anisovich *et al.*	(BONN, PNPI)
CUTKOSKY	80	Toronto Conf. 19	R.E. Cutkosky *et al.*	(CMU, LBL)
HOEHLER	79	PDAT 12-1	G. Hohler *et al.*	(KARLT)

$N(2190)\ 7/2^-$

$I(J^P) = \frac{1}{2}(\frac{7}{2}^-)$ Status: ****

Most of the results published before 1975 were last included in our 1982 edition, Physics Letters **111B** 1 (1982). Some further obsolete results published before 1984 were last included in our 2006 edition, Journal of Physics (generic for all A,B,E,G) **G33** 1 (2006).

$N(2190)$ BREIT-WIGNER MASS

VALUE (MeV)	DOCUMENT ID		TECN	COMMENT
2100 to 2200 (≈ 2190) OUR ESTIMATE				
2180 ±20	ANISOVICH	12A	DPWA	Multichannel
2152.4± 1.4	ARNDT	06	DPWA	$\pi N \to \pi N, \eta N$
2200 ±70	CUTKOSKY	80	IPWA	$\pi N \to \pi N$
2140 ±12	HOEHLER	79	IPWA	$\pi N \to \pi N$
2140 ±40	HENDRY	78	MPWA	$\pi N \to \pi N$
• • • We do not use the following data for averages, fits, limits, etc. • • •				
2150 ±26	SHRESTHA	12A	DPWA	Multichannel
2125 ±61	BATINIC	10	DPWA	$\pi N \to N\pi, N\eta$
2192.1± 8.7	ARNDT	04	DPWA	$\pi N \to \pi N, \eta N$
2168 ±18	VRANA	00	DPWA	Multichannel
2131	ARNDT	95	DPWA	$\pi N \to N\pi$
2127 ± 9	MANLEY	92	IPWA	$\pi N \to \pi N$ & $N\pi\pi$
2180	SAXON	80	DPWA	$\pi^- p \to \Lambda K^0$

$N(2190)$ BREIT-WIGNER WIDTH

VALUE (MeV)	DOCUMENT ID		TECN	COMMENT
300 to 700 (≈ 500) OUR ESTIMATE				
335± 40	ANISOVICH	12A	DPWA	Multichannel
484± 13	ARNDT	06	DPWA	$\pi N \to \pi N, \eta N$
500±150	CUTKOSKY	80	IPWA	$\pi N \to \pi N$
390± 30	HOEHLER	79	IPWA	$\pi N \to \pi N$
270± 50	HENDRY	78	MPWA	$\pi N \to \pi N$
• • • We do not use the following data for averages, fits, limits, etc. • • •				
500± 74	SHRESTHA	12A	DPWA	Multichannel
381±160	BATINIC	10	DPWA	$\pi N \to N\pi, N\eta$
726± 62	ARNDT	04	DPWA	$\pi N \to \pi N, \eta N$
453±101	VRANA	00	DPWA	Multichannel
476	ARNDT	95	DPWA	$\pi N \to N\pi$
550± 50	MANLEY	92	IPWA	$\pi N \to \pi N$ & $N\pi\pi$
80	SAXON	80	DPWA	$\pi^- p \to \Lambda K^0$

$N(2190)$ POLE POSITION

REAL PART

VALUE (MeV)	DOCUMENT ID		TECN	COMMENT
2050 to 2100 (≈ 2075) OUR ESTIMATE				
2150±25	ANISOVICH	12A	DPWA	Multichannel
2070	ARNDT	06	DPWA	$\pi N \to \pi N, \eta N$
2042	[1] HOEHLER	93	SPED	$\pi N \to \pi N$
2100±50	CUTKOSKY	80	IPWA	$\pi N \to \pi N$
• • • We do not use the following data for averages, fits, limits, etc. • • •				
2062	SHRESTHA	12A	DPWA	Multichannel
2063±32	BATINIC	10	DPWA	$\pi N \to N\pi, N\eta$
2076	ARNDT	04	DPWA	$\pi N \to \pi N, \eta N$
2107	VRANA	00	DPWA	Multichannel
2030	ARNDT	95	DPWA	$\pi N \to N\pi$
2060	ARNDT	91	DPWA	$\pi N \to \pi N$ Soln SM90

−2×IMAGINARY PART

VALUE (MeV)	DOCUMENT ID		TECN	COMMENT
400 to 520 (≈ 450) OUR ESTIMATE				
330± 30	ANISOVICH	12A	DPWA	Multichannel
520	ARNDT	06	DPWA	$\pi N \to \pi N, \eta N$
482	[1] HOEHLER	93	SPED	$\pi N \to \pi N$
400±160	CUTKOSKY	80	IPWA	$\pi N \to \pi N$
• • • We do not use the following data for averages, fits, limits, etc. • • •				
428	SHRESTHA	12A	DPWA	Multichannel
330±101	BATINIC	10	DPWA	$\pi N \to N\pi, N\eta$
502	ARNDT	04	DPWA	$\pi N \to \pi N, \eta N$
380	VRANA	00	DPWA	Multichannel
460	ARNDT	95	DPWA	$\pi N \to N\pi$
464	ARNDT	91	DPWA	$\pi N \to \pi N$ Soln SM90

$N(2190)$ ELASTIC POLE RESIDUE

MODULUS $|r|$

VALUE (MeV)	DOCUMENT ID		TECN	COMMENT
30± 5	ANISOVICH	12A	DPWA	Multichannel
72	ARNDT	06	DPWA	$\pi N \to \pi N, \eta N$
45	HOEHLER	93	SPED	$\pi N \to \pi N$
25±10	CUTKOSKY	80	IPWA	$\pi N \to \pi N$
• • • We do not use the following data for averages, fits, limits, etc. • • •				
34	BATINIC	10	DPWA	$\pi N \to N\pi, N\eta$
68	ARNDT	04	DPWA	$\pi N \to \pi N, \eta N$
46	ARNDT	95	DPWA	$\pi N \to N\pi$
54	ARNDT	91	DPWA	$\pi N \to \pi N$ Soln SM90

PHASE θ

VALUE (°)	DOCUMENT ID		TECN	COMMENT
30±10	ANISOVICH	12A	DPWA	Multichannel
−32	ARNDT	06	DPWA	$\pi N \to \pi N, \eta N$
−30±50	CUTKOSKY	80	IPWA	$\pi N \to \pi N$
• • • We do not use the following data for averages, fits, limits, etc. • • •				
−19	BATINIC	10	DPWA	$\pi N \to N\pi, N\eta$
−32	ARNDT	04	DPWA	$\pi N \to \pi N, \eta N$
−23	ARNDT	95	DPWA	$\pi N \to N\pi$
−44	ARNDT	91	DPWA	$\pi N \to \pi N$ Soln SM90

$N(2190)$ INELASTIC POLE RESIDUE

The "normalized residue" is the residue divided by $\Gamma_{pole}/2$.

Normalized residue in $N\pi \to N(2190) \to \Lambda K$

MODULUS (%)	PHASE (°)	DOCUMENT ID		TECN	COMMENT
3±1	**20 ± 15**	ANISOVICH	12A	DPWA	Multichannel

$N(2190)$ DECAY MODES

The following branching fractions are our estimates, not fits or averages.

	Mode	Fraction (Γ_i/Γ)
Γ_1	$N\pi$	10–20 %
Γ_2	$N\eta$	(0.0±1.0) %
Γ_3	$N\omega$	seen
Γ_4	ΛK	seen
Γ_5	ΣK	
Γ_6	$N\pi\pi$	seen
Γ_7	$N\rho$	seen
Γ_8	$p\gamma$	0.02–0.06 %
Γ_9	$p\gamma$, helicity=1/2	0.02–0.04 %
Γ_{10}	$p\gamma$, helicity=3/2	0.002–0.02 %

$N(2190)$ BRANCHING RATIOS

$\Gamma(N\pi)/\Gamma_{total}$ Γ_1/Γ

VALUE (%)	DOCUMENT ID		TECN	COMMENT
10 to 20 OUR ESTIMATE				
16 ± 2	ANISOVICH	12A	DPWA	Multichannel
23.8± 0.1	ARNDT	06	DPWA	$\pi N \to \pi N, \eta N$
12 ± 6	CUTKOSKY	80	IPWA	$\pi N \to \pi N$
14 ± 2	HOEHLER	79	IPWA	$\pi N \to \pi N$
16 ± 4	HENDRY	78	MPWA	$\pi N \to \pi N$
• • • We do not use the following data for averages, fits, limits, etc. • • •				
20 ± 1	SHRESTHA	12A	DPWA	Multichannel
18 ±12	BATINIC	10	DPWA	$\pi N \to N\pi, N\eta$
23.0± 0.2	ARNDT	04	DPWA	$\pi N \to \pi N, \eta N$
20 ± 4	VRANA	00	DPWA	Multichannel
23	ARNDT	95	DPWA	$\pi N \to N\pi$
22 ± 1	MANLEY	92	IPWA	$\pi N \to \pi N$ & $N\pi\pi$

$\Gamma(N\eta)/\Gamma_{total}$ Γ_2/Γ

VALUE (%)	DOCUMENT ID		TECN	COMMENT
0 ±1	VRANA	00	DPWA	Multichannel
• • • We do not use the following data for averages, fits, limits, etc. • • •				
2 ±1	SHRESTHA	12A	DPWA	Multichannel
0.1±0.3	BATINIC	10	DPWA	$\pi N \to N\pi, N\eta$

$\Gamma(N\omega)/\Gamma_{total}$ Γ_3/Γ

VALUE (%)	DOCUMENT ID		TECN	COMMENT
seen	WILLIAMS	09	IPWA	$\gamma p \to p\omega$

$\Gamma(\Lambda K)/\Gamma_{total}$ Γ_4/Γ

VALUE (%)	DOCUMENT ID		TECN	COMMENT
0.5 ± 0.3	ANISOVICH	12A	DPWA	Multichannel
• • • We do not use the following data for averages, fits, limits, etc. • • •				
<1	SHRESTHA	12A	DPWA	Multichannel

$(\Gamma_i\Gamma_f)^{1/2}/\Gamma_{total}$ in $N\pi \to N(2190) \to \Lambda K$ $(\Gamma_1\Gamma_4)^{1/2}/\Gamma$

VALUE	DOCUMENT ID		TECN	COMMENT
−0.02	BELL	83	DPWA	$\pi^- p \to \Lambda K^0$
−0.02	SAXON	80	DPWA	$\pi^- p \to \Lambda K^0$

$(\Gamma_i\Gamma_f)^{1/2}/\Gamma_{total}$ in $N\pi \to N(2190) \to N\rho$, S=3/2, D-wave $(\Gamma_1\Gamma_0)^{1/2}/\Gamma$

VALUE	DOCUMENT ID		TECN	COMMENT
• • • We do not use the following data for averages, fits, limits, etc. • • •				
−0.13±0.05	SHRESTHA	12A	DPWA	Multichannel
−0.25±0.03	MANLEY	92	IPWA	$\pi N \to \pi N$ & $N\pi\pi$

$\Gamma(N\rho, S$=3/2, D-wave$)/\Gamma_{total}$ Γ_0/Γ

VALUE (%)	DOCUMENT ID		TECN	COMMENT
29±28	VRANA	00	DPWA	Multichannel

$N(2190)$ PHOTON DECAY AMPLITUDES

Papers on γN amplitudes predating 1981 may be found in our 2006 edition, Journal of Physics (generic for all A,B,E,G) **G33** 1 (2006).

$N(2190) \to p\gamma$, helicity-1/2 amplitude $A_{1/2}$

VALUE ($GeV^{-1/2}$)	DOCUMENT ID		TECN	COMMENT
−0.065±0.008	ANISOVICH	12A	DPWA	Multichannel

$N(2190) \to p\gamma$, helicity-3/2 amplitude $A_{3/2}$

VALUE ($GeV^{-1/2}$)	DOCUMENT ID		TECN	COMMENT
0.035±0.017	ANISOVICH	12A	DPWA	Multichannel

$N(2190) \to p\gamma$, ratio of helicity amplitudes $A_{3/2}/A_{1/2}$

VALUE	DOCUMENT ID		TECN	COMMENT
• • • We do not use the following data for averages, fits, limits, etc. • • •				
−0.17±0.15	WILLIAMS	09	IPWA	$\gamma p \to p\omega$

$N(2190)$ $\gamma p \to \Lambda K^+$ AMPLITUDES

$(\Gamma_i\Gamma_f)^{1/2}/\Gamma_{total}$ in $p\gamma \to N(2190) \to \Lambda K^+$ (E_{4-} amplitude)

VALUE (units 10^{-3})	DOCUMENT ID		TECN
• • • We do not use the following data for averages, fits, limits, etc. • • •			
2.5 ±1.0	WORKMAN	90	DPWA
2.04	TANABE	89	DPWA

$p\gamma \to N(2190) \to \Lambda K^+$ phase angle θ (E_{4-} amplitude)

VALUE (degrees)	DOCUMENT ID		TECN
• • • We do not use the following data for averages, fits, limits, etc. • • •			
− 4 ±9	WORKMAN	90	DPWA
−27.5	TANABE	89	DPWA

$(\Gamma_i\Gamma_f)^{1/2}/\Gamma_{total}$ in $p\gamma \to N(2190) \to \Lambda K^+$ (M_{4-} amplitude)

VALUE (units 10^{-3})	DOCUMENT ID		TECN
• • • We do not use the following data for averages, fits, limits, etc. • • •			
−7.0 ±0.7	WORKMAN	90	DPWA
−5.78	TANABE	89	DPWA

$N(2190)$ FOOTNOTES

[1] See HOEHLER 93 for a detailed discussion of the evidence for and the pole parameters of N and Δ resonances as determined from Argand diagrams of πN elastic partial-wave amplitudes and from plots of the speeds with which the amplitudes traverse the diagrams.

$N(2190)$ REFERENCES

For early references, see Physics Letters **111B** 1 (1982).

ANISOVICH	12A	EPJ A48 15	A.V. Anisovich *et al.*	(BONN, PNPI)
SHRESTHA	12A	PR C86 055203	M. Shrestha, D.M. Manley	(KSU)
BATINIC	10	PR C82 038203	M. Batinic *et al.*	(ZAGR)
WILLIAMS	09	PR C80 065209	M. Williams *et al.*	(CEBAF CLAS Collab.)
ARNDT	06	PR C74 045205	R.A. Arndt *et al.*	(GWU)
PDG	06	JP G33 1	W.-M. Yao *et al.*	(PDG Collab.)
ARNDT	04	PR C69 035213	R.A. Arndt *et al.*	(GWU, TRIU)
VRANA	00	PRPL 328 181	T.P. Vrana, S.A. Dytman,, T.-S.H. Lee	(PITT+)
ARNDT	95	PR C52 2120	R.A. Arndt *et al.*	(VPI, BRCO)
HOEHLER	93	πN Newsletter 9 1	G. Hohler	(KARL)
MANLEY	92	PR D45 4002	D.M. Manley, E.M. Saleski	(KSA) IJP
Also		PR D30 904	D.M. Manley *et al.*	(VPI)
ARNDT	91	PR D43 2131	R.A. Arndt *et al.*	(VPI, TELE) IJP
WORKMAN	90	PR C42 781	R.L. Workman	(VPI)
TANABE	89	PR C39 741	H. Tanabe, M. Kohno, C. Bennhold	(MANZ)
Also		NC 102A 193	M. Kohno, H. Tanabe, C. Bennhold	(MANZ)
BELL	83	NP B222 389	K.W. Bell *et al.*	(RL) IJP
PDG	82	PL 111B 1	M. Roos *et al.*	(HELS, CIT, CERN)
CUTKOSKY	80	Toronto Conf. 19	R.E. Cutkosky *et al.*	(CMU, LBL) IJP
Also		PR D20 2839	R.E. Cutkosky *et al.*	(CMU, LBL) IJP
SAXON	80	NP B162 522	D.H. Saxon *et al.*	(RHEL, BRIS) IJP
HOEHLER	79	PDAT 12-1	G. Hohler *et al.*	(KARLT) IJP
Also		Toronto Conf. 3	R. Koch	(KARLT) IJP
HENDRY	78	PRL 41 222	A.W. Hendry	(IND, LBL) IJP
Also		ANP 136 1	A.W. Hendry	(IND)

$N(2220)$ $9/2^+$

$I(J^P) = \frac{1}{2}(\frac{9}{2}^+)$ Status: ****

Most of the results published before 1975 were last included in our 1982 edition, Physics Letters **111B** 1 (1982). Some further obsolete results published before 1980 were last included in our 2006 edition, Journal of Physics (generic for all A,B,E,G) **G33** 1 (2006).

$N(2220)$ BREIT-WIGNER MASS

VALUE (MeV)	DOCUMENT ID		TECN	COMMENT
2200 to 2300 (≈ 2250) OUR ESTIMATE				
2316.3± 2.9	ARNDT	06	DPWA	$\pi N \to \pi N, \eta N$
2230 ± 80	CUTKOSKY	80	IPWA	$\pi N \to \pi N$
2205 ± 10	HOEHLER	79	IPWA	$\pi N \to \pi N$
2300 ±100	HENDRY	78	MPWA	$\pi N \to \pi N$
• • • We do not use the following data for averages, fits, limits, etc. • • •				
2270 ± 11	ARNDT	04	DPWA	$\pi N \to \pi N, \eta N$
2258	ARNDT	95	DPWA	$\pi N \to N\pi$

$N(2220)$ BREIT-WIGNER WIDTH

VALUE (MeV)	DOCUMENT ID		TECN	COMMENT
350 to 500 (≈ 400) OUR ESTIMATE				
633± 17	ARNDT	06	DPWA	$\pi N \to \pi N, \eta N$
500±150	CUTKOSKY	80	IPWA	$\pi N \to \pi N$
365± 30	HOEHLER	79	IPWA	$\pi N \to \pi N$
450±150	HENDRY	78	MPWA	$\pi N \to \pi N$
• • • We do not use the following data for averages, fits, limits, etc. • • •				
366± 42	ARNDT	04	DPWA	$\pi N \to \pi N, \eta N$
334	ARNDT	95	DPWA	$\pi N \to N\pi$

$N(2220)$ POLE POSITION

REAL PART

VALUE (MeV)	DOCUMENT ID		TECN	COMMENT
2130 to 2200 (≈ 2170) OUR ESTIMATE				
2150±35	ANISOVICH	12A	DPWA	Multichannel
2199	ARNDT	06	DPWA	$\pi N \to \pi N, \eta N$
2135	[1] HOEHLER	93	ARGD	$\pi N \to \pi N$
2160±80	CUTKOSKY	80	IPWA	$\pi N \to \pi N$
• • • We do not use the following data for averages, fits, limits, etc. • • •				
2209	ARNDT	04	DPWA	$\pi N \to \pi N, \eta N$
2203	ARNDT	95	DPWA	$\pi N \to N\pi$
2253	ARNDT	91	DPWA	$\pi N \to \pi N$ Soln SM90

−2×IMAGINARY PART

VALUE (MeV)	DOCUMENT ID		TECN	COMMENT
400 to 560 (≈ 480) OUR ESTIMATE				
440± 40	ANISOVICH	12A	DPWA	Multichannel
372	ARNDT	06	DPWA	$\pi N \to \pi N, \eta N$
400	[2] HOEHLER	93	ARGD	$\pi N \to \pi N$
480±100	CUTKOSKY	80	IPWA	$\pi N \to \pi N$
• • • We do not use the following data for averages, fits, limits, etc. • • •				
564	ARNDT	04	DPWA	$\pi N \to \pi N, \eta N$
536	ARNDT	95	DPWA	$\pi N \to N\pi$
640	ARNDT	91	DPWA	$\pi N \to \pi N$ Soln SM90

$N(2220)$ ELASTIC POLE RESIDUE

MODULUS $|r|$

VALUE (MeV)	DOCUMENT ID		TECN	COMMENT
60±12	ANISOVICH	12A	DPWA	Multichannel
33	ARNDT	06	DPWA	$\pi N \to \pi N, \eta N$
40	HOEHLER	93	ARGD	$\pi N \to \pi N$
45±20	CUTKOSKY	80	IPWA	$\pi N \to \pi N$
• • • We do not use the following data for averages, fits, limits, etc. • • •				
96	ARNDT	04	DPWA	$\pi N \to \pi N, \eta N$
68	ARNDT	95	DPWA	$\pi N \to N\pi$
85	ARNDT	91	DPWA	$\pi N \to \pi N$ Soln SM90

PHASE θ

VALUE (°)	DOCUMENT ID		TECN	COMMENT
−58±12	ANISOVICH	12A	DPWA	Multichannel
−33	ARNDT	06	DPWA	$\pi N \to \pi N, \eta N$
−50	HOEHLER	93	ARGD	$\pi N \to \pi N$
−45±25	CUTKOSKY	80	IPWA	$\pi N \to \pi N$
• • • We do not use the following data for averages, fits, limits, etc. • • •				
−71	ARNDT	04	DPWA	$\pi N \to \pi N, \eta N$
−43	ARNDT	95	DPWA	$\pi N \to N\pi$
−62	ARNDT	91	DPWA	$\pi N \to \pi N$ Soln SM90

$N(2220)$ DECAY MODES

The following branching fractions are our estimates, not fits or averages.

	Mode	Fraction (Γ_i/Γ)
Γ_1	$N\pi$	15–25 %
Γ_2	$N\eta$	
Γ_3	ΛK	

$N(2220)$ BRANCHING RATIOS

$\Gamma(N\pi)/\Gamma_{total}$ Γ_1/Γ

VALUE (%)	DOCUMENT ID		TECN	COMMENT
15 to 25 OUR ESTIMATE				
24 ±5	ANISOVICH	12A	DPWA	Multichannel
24.6±0.1	ARNDT	06	DPWA	$\pi N \to \pi N, \eta N$
15 ±3	CUTKOSKY	80	IPWA	$\pi N \to \pi N$
18.0±1.5	HOEHLER	79	IPWA	$\pi N \to \pi N$
12 ±4	HENDRY	78	MPWA	$\pi N \to \pi N$
• • • We do not use the following data for averages, fits, limits, etc. • • •				
20.0±0.6	ARNDT	04	DPWA	$\pi N \to \pi N, \eta N$
26	ARNDT	95	DPWA	$\pi N \to N\pi$

$(\Gamma_i\Gamma_f)^{1/2}/\Gamma_{total}$ in $N\pi \to N(2220) \to \Lambda K$ $(\Gamma_1\Gamma_3)^{1/2}/\Gamma$

VALUE	DOCUMENT ID		TECN	COMMENT
not required	BELL	83	DPWA	$\pi^- p \to \Lambda K^0$
not seen	SAXON	80	DPWA	$\pi^- p \to \Lambda K^0$

$N(2220)$ PHOTON DECAY AMPLITUDES

Papers on γN amplitudes predating 1981 may be found in our 2006 edition, Journal of Physics (generic for all A,B,E,G) **G33** 1 (2006).

$N(2220) \to p\gamma$, helicity-1/2 amplitude $A_{1/2}$

VALUE (GeV$^{-1/2}$)	DOCUMENT ID		TECN	COMMENT
<0.01	[3] ANISOVICH	12A	DPWA	Multichannel

$N(2220) \to p\gamma$, helicity-3/2 amplitude $A_{3/2}$

VALUE (GeV$^{-1/2}$)	DOCUMENT ID		TECN	COMMENT
<0.01	[3] ANISOVICH	12A	DPWA	Multichannel

$N(2220)$ FOOTNOTES

[1] See HOEHLER 93 for a detailed discussion of the evidence for and the pole parameters of N and Δ resonances as determined from Argand diagrams of πN elastic partial-wave amplitudes and from plots of the speeds with which the amplitudes traverse the diagrams.

[2] See HOEHLER 93 for a detailed discussion of the evidence for and the pole parameters of N and Δ resonances as determined from Argand diagrams of πN elastic partial-wave amplitudes and from plots of the speeds with which the amplitudes traverse the diagrams.

[3] This ANISOVICH 12A value is the complex helicity amplitude at the pole position.

$N(2220)$ REFERENCES

For early references, see Physics Letters **111B** 1 (1982).

ANISOVICH	12A	EPJ A48 15	A.V. Anisovich *et al.*	(BONN, PNPI)
ARNDT	06	PR C74 045205	R.A. Arndt *et al.*	(GWU)
PDG	06	JP G33 1	W.-M. Yao *et al.*	(PDG Collab.)
ARNDT	04	PR C69 035213	R.A. Arndt *et al.*	(GWU, TRIU)
ARNDT	95	PR C52 2120	R.A. Arndt *et al.*	(VPI, BRCO)
HOEHLER	93	πN Newsletter 9 1	G. Hohler	(KARL)
ARNDT	91	PR D43 2131	R.A. Arndt *et al.*	(VPI, TELE) IJP
BELL	83	NP B222 389	K.W. Bell *et al.*	(RL) IJP
PDG	82	PL 111B 1	M. Roos *et al.*	(HELS, CIT, CERN)
CUTKOSKY	80	Toronto Conf. 19	R.E. Cutkosky *et al.*	(CMU, LBL) IJP
Also		PR D20 2839	R.E. Cutkosky *et al.*	(CMU, LBL) IJP
SAXON	80	NP B162 522	D.H. Saxon *et al.*	(RHEL, BRIS) IJP
HOEHLER	79	PDAT 12-1	G. Hohler *et al.*	(KARLT) IJP
Also		Toronto Conf. 3	R. Koch	(KARLT) IJP
HENDRY	78	PRL 41 222	A.W. Hendry	(IND, LBL) IJP
Also		ANP 136 1	A.W. Hendry	(IND)

$N(2250)$ $9/2^-$

$I(J^P) = \frac{1}{2}(\frac{9}{2}^-)$ Status: ****

Some obsolete results published before 1980 were last included in our 2006 edition, Journal of Physics (generic for all A,B,E,G) **G33** 1 (2006).

$N(2250)$ BREIT-WIGNER MASS

VALUE (MeV)	DOCUMENT ID		TECN	COMMENT
2200 to 2350 (≈ 2275) OUR ESTIMATE				
2280± 40	ANISOVICH	12A	DPWA	Multichannel
2302± 6	ARNDT	06	DPWA	$\pi N \to \pi N, \eta N$
2250± 80	CUTKOSKY	80	IPWA	$\pi N \to \pi N$
2268± 15	HOEHLER	79	IPWA	$\pi N \to \pi N$
2200±100	HENDRY	78	MPWA	$\pi N \to \pi N$
• • • We do not use the following data for averages, fits, limits, etc. • • •				
2376± 43	ARNDT	04	DPWA	$\pi N \to \pi N, \eta N$
2291	ARNDT	95	DPWA	$\pi N \to N\pi$

$N(2250)$ BREIT-WIGNER WIDTH

VALUE (MeV)	DOCUMENT ID		TECN	COMMENT
230 to 800 (≈ 500) OUR ESTIMATE				
520± 50	ANISOVICH	12A	DPWA	Multichannel
628± 28	ARNDT	06	DPWA	$\pi N \to \pi N, \eta N$
480±120	CUTKOSKY	80	IPWA	$\pi N \to \pi N$
300± 40	HOEHLER	79	IPWA	$\pi N \to \pi N$
350±100	HENDRY	78	MPWA	$\pi N \to \pi N$
• • • We do not use the following data for averages, fits, limits, etc. • • •				
924±178	ARNDT	04	DPWA	$\pi N \to \pi N, \eta N$
772	ARNDT	95	DPWA	$\pi N \to N\pi$

$N(2250)$ POLE POSITION

REAL PART

VALUE (MeV)	DOCUMENT ID		TECN	COMMENT
2150 to 2250 (≈ 2200) OUR ESTIMATE				
2195±45	ANISOVICH	12A	DPWA	Multichannel
2217	ARNDT	06	DPWA	$\pi N \to \pi N, \eta N$
2187	[1] HOEHLER	93	SPED	$\pi N \to \pi N$
2150±50	CUTKOSKY	80	IPWA	$\pi N \to \pi N$
• • • We do not use the following data for averages, fits, limits, etc. • • •				
2238	ARNDT	04	DPWA	$\pi N \to \pi N, \eta N$
2087	ARNDT	95	DPWA	$\pi N \to N\pi$
2243	ARNDT	91	DPWA	$\pi N \to \pi N$ Soln SM90

$-2\times$IMAGINARY PART

VALUE (MeV)	DOCUMENT ID		TECN	COMMENT
350 to 550 (≈ 450) OUR ESTIMATE				
470± 50	ANISOVICH	12A	DPWA	Multichannel
431	ARNDT	06	DPWA	$\pi N \to \pi N, \eta N$
388	[1] HOEHLER	93	SPED	$\pi N \to \pi N$
360±100	CUTKOSKY	80	IPWA	$\pi N \to \pi N$
• • • We do not use the following data for averages, fits, limits, etc. • • •				
536	ARNDT	04	DPWA	$\pi N \to \pi N, \eta N$
680	ARNDT	95	DPWA	$\pi N \to N\pi$
650	ARNDT	91	DPWA	$\pi N \to \pi N$ Soln SM90

$N(2250)$ ELASTIC POLE RESIDUE

MODULUS $|r|$

VALUE (MeV)	DOCUMENT ID		TECN	COMMENT
26±5	ANISOVICH	12A	DPWA	Multichannel
21	ARNDT	06	DPWA	$\pi N \to \pi N, \eta N$
21	HOEHLER	93	SPED	$\pi N \to \pi N$
20±6	CUTKOSKY	80	IPWA	$\pi N \to \pi N$
• • • We do not use the following data for averages, fits, limits, etc. • • •				
33	ARNDT	04	DPWA	$\pi N \to \pi N, \eta N$
24	ARNDT	95	DPWA	$\pi N \to N\pi$
47	ARNDT	91	DPWA	$\pi N \to \pi N$ Soln SM90

PHASE θ

VALUE (°)	DOCUMENT ID		TECN	COMMENT
−38±25	ANISOVICH	12A	DPWA	Multichannel
−20	ARNDT	06	DPWA	$\pi N \to \pi N, \eta N$
−50±20	CUTKOSKY	80	IPWA	$\pi N \to \pi N$
• • • We do not use the following data for averages, fits, limits, etc. • • •				
−25	ARNDT	04	DPWA	$\pi N \to \pi N, \eta N$
−44	ARNDT	95	DPWA	$\pi N \to N\pi$
−37	ARNDT	91	DPWA	$\pi N \to \pi N$ Soln SM90

$N(2250)$ DECAY MODES

The following branching fractions are our estimates, not fits or averages.

	Mode	Fraction (Γ_i/Γ)
Γ_1	$N\pi$	5–15 %
Γ_2	$N\eta$	
Γ_3	ΛK	

$N(2250)$ BRANCHING RATIOS

$\Gamma(N\pi)/\Gamma_{total}$ **Γ_1/Γ**

VALUE (%)	DOCUMENT ID		TECN	COMMENT
5 to 15 OUR ESTIMATE				
12 ±4	ANISOVICH	12A	DPWA	Multichannel
8.9±0.1	ARNDT	06	DPWA	$\pi N \to \pi N, \eta N$
10 ±2	CUTKOSKY	80	IPWA	$\pi N \to \pi N$
10 ±2	HOEHLER	79	IPWA	$\pi N \to \pi N$
9 ±2	HENDRY	78	MPWA	$\pi N \to \pi N$
• • • We do not use the following data for averages, fits, limits, etc. • • •				
11.0±0.4	ARNDT	04	DPWA	$\pi N \to \pi N, \eta N$
10	ARNDT	95	DPWA	$\pi N \to N\pi$

$(\Gamma_i\Gamma_f)^{1/2}/\Gamma_{total}$ in $N\pi \to N(2250) \to \Lambda K$ **$(\Gamma_1\Gamma_3)^{1/2}/\Gamma$**

VALUE	DOCUMENT ID		TECN	COMMENT
−0.02	BELL	83	DPWA	$\pi^- p \to \Lambda K^0$
not seen	SAXON	80	DPWA	$\pi^- p \to \Lambda K^0$

$N(2250)$ PHOTON DECAY AMPLITUDES

Papers on γN amplitudes predating 1981 may be found in our 2006 edition, Journal of Physics (generic for all A,B,E,G) **G33** 1 (2006).

$N(2250) \to p\gamma$, helicity-1/2 amplitude $A_{1/2}$

VALUE ($GeV^{-1/2}$)	DOCUMENT ID		TECN	COMMENT
<0.01	[2] ANISOVICH	12A	DPWA	Multichannel

$N(2250) \to p\gamma$, helicity-3/2 amplitude $A_{3/2}$

VALUE ($GeV^{-1/2}$)	DOCUMENT ID		TECN	COMMENT
<0.01	[2] ANISOVICH	12A	DPWA	Multichannel

$N(2250)$ FOOTNOTES

[1] See HOEHLER 93 for a detailed discussion of the evidence for and the pole parameters of N and Δ resonances as determined from Argand diagrams of πN elastic partial-wave amplitudes and from plots of the speeds with which the amplitudes traverse the diagrams.
[2] This ANISOVICH 12A value is the complex helicity amplitude at the pole position.

$N(2250)$ REFERENCES

ANISOVICH	12A	EPJ A48 15	A.V. Anisovich *et al.*	(BONN, PNPI)
ARNDT	06	PR C74 045205	R.A. Arndt *et al.*	(GWU)
PDG	06	JP G33 1	W.-M. Yao *et al.*	(PDG Collab.)
ARNDT	04	PR C69 035213	R.A. Arndt *et al.*	(GWU, TRIU)
ARNDT	95	PR C52 2120	R.A. Arndt *et al.*	(VPI, BRCO)
HOEHLER	93	πN Newsletter 9 1	G. Hohler	(KARL)
ARNDT	91	PR D43 2131	R.A. Arndt *et al.*	(VPI, TELE) IJP
BELL	83	NP B222 389	K.W. Bell *et al.*	(RL) IJP
CUTKOSKY	80	Toronto Conf. 19	R.E. Cutkosky *et al.*	(CMU, LBL) IJP
Also		PR D20 2839	R.E. Cutkosky *et al.*	(CMU, LBL) IJP
SAXON	80	NP B162 522	D.H. Saxon *et al.*	(RHEL, BRIS) IJP
HOEHLER	79	PDAT 12-1	G. Hohler *et al.*	(KARLT) IJP
Also		Toronto Conf. 3	R. Koch	(KARLT) IJP
HENDRY	78	PRL 41 222	A.W. Hendry	(IND, LBL) IJP
Also		ANP 136 1	A.W. Hendry	(IND)

$N(2300)$ $1/2^+$

$I(J^P) = \frac{1}{2}(\frac{1}{2}^+)$ Status: **

OMITTED FROM SUMMARY TABLE

$N(2300)$ MASS

VALUE (MeV)	DOCUMENT ID		TECN	COMMENT
$2300^{+40}_{-30}{}^{+109}_{-0}$	ABLIKIM	13A	BES3	$\psi(2S) \to p\overline{p}\pi^0$

$N(2300)$ WIDTH

VALUE (MeV)	DOCUMENT ID		TECN	COMMENT
$340\pm30^{+110}_{-58}$	ABLIKIM	13A	BES3	$\psi(2S) \to p\overline{p}\pi^0$

$N(2300)$ REFERENCES

ABLIKIM	13A	PRL 110 022001	M. Ablikim *et al.*	(BES III Collab.)

$N(2570)$ $5/2^-$

$I(J^P) = \frac{1}{2}(\frac{5}{2}^-)$ Status: **

OMITTED FROM SUMMARY TABLE

$N(2570)$ MASS

VALUE (MeV)	DOCUMENT ID		TECN	COMMENT
$2570^{+19}_{-10}{}^{+34}_{-10}$	ABLIKIM	13A	BES3	$\psi(2S) \to p\overline{p}\pi^0$

$N(2570)$ WIDTH

VALUE (MeV)	DOCUMENT ID		TECN	COMMENT
$250^{+14}_{-24}{}^{+69}_{-21}$	ABLIKIM	13A	BES3	$\psi(2S) \to p\overline{p}\pi^0$

$N(2570)$ REFERENCES

ABLIKIM	13A	PRL 110 022001	M. Ablikim *et al.*	(BES III Collab.)

$N(2600)$ $11/2^-$

$I(J^P) = \frac{1}{2}(\frac{11}{2}^-)$ Status: ***

$N(2600)$ BREIT-WIGNER MASS

VALUE (MeV)	DOCUMENT ID		TECN	COMMENT
2550 to 2750 (≈ 2600) OUR ESTIMATE				
2623±197	ARNDT	06	DPWA	$\pi N \to \pi N, \eta N$
2577± 50	HOEHLER	79	IPWA	$\pi N \to \pi N$
2700±100	HENDRY	78	MPWA	$\pi N \to \pi N$

$N(2600)$ BREIT-WIGNER WIDTH

VALUE (MeV)	DOCUMENT ID		TECN	COMMENT
500 to 800 (≈ 650) OUR ESTIMATE				
1311±996	ARNDT	06	DPWA	$\pi N \to \pi N, \eta N$
400±100	HOEHLER	79	IPWA	$\pi N \to \pi N$
900±100	HENDRY	78	MPWA	$\pi N \to \pi N$

$N(2600)$ DECAY MODES

	Mode	Fraction (Γ_i/Γ)
Γ_1	$N\pi$	5–10 %

$N(2600)$ BRANCHING RATIOS

$\Gamma(N\pi)/\Gamma_{total}$ **Γ_1/Γ**

VALUE (%)	DOCUMENT ID		TECN	COMMENT
5 to 10 OUR ESTIMATE				
5.0±1.8	ARNDT	06	DPWA	$\pi N \to \pi N, \eta N$
5 ±1	HOEHLER	79	IPWA	$\pi N \to \pi N$
8 ±2	HENDRY	78	MPWA	$\pi N \to \pi N$

$N(2600)$ REFERENCES

ARNDT	06	PR C74 045205	R.A. Arndt *et al.*	(GWU)
HOEHLER	79	PDAT 12-1	G. Hohler *et al.*	(KARLT) IJP
Also		Toronto Conf. 3	R. Koch	(KARLT) IJP
HENDRY	78	PRL 41 222	A.W. Hendry	(IND, LBL) IJP
Also		ANP 136 1	A.W. Hendry	(IND)

$N(2700)$ $13/2^+$

$I(J^P) = \frac{1}{2}(\frac{13}{2}^+)$ Status: **

OMITTED FROM SUMMARY TABLE

The latest GWU analysis (ARNDT 06) finds no evidence for this resonance.

$N(2700)$ BREIT-WIGNER MASS

VALUE (MeV)	DOCUMENT ID		TECN	COMMENT
≈ 2700 OUR ESTIMATE				
2612± 45	HOEHLER	79	IPWA	$\pi N \rightarrow \pi N$
3000±100	HENDRY	78	MPWA	$\pi N \rightarrow \pi N$

$N(2700)$ BREIT-WIGNER WIDTH

VALUE (MeV)	DOCUMENT ID		TECN	COMMENT
350± 50	HOEHLER	79	IPWA	$\pi N \rightarrow \pi N$
900±150	HENDRY	78	MPWA	$\pi N \rightarrow \pi N$

$N(2700)$ DECAY MODES

	Mode
Γ_1	$N\pi$

$N(2700)$ BRANCHING RATIOS

$\Gamma(N\pi)/\Gamma_{total}$ **Γ_1/Γ**

VALUE (%)	DOCUMENT ID		TECN	COMMENT
4±1	HOEHLER	79	IPWA	$\pi N \rightarrow \pi N$
7±2	HENDRY	78	MPWA	$\pi N \rightarrow \pi N$

$N(2700)$ REFERENCES

ARNDT	06	PR C74 045205	R.A. Arndt *et al.*	(GWU)
HOEHLER	79	PDAT 12-1	G. Hohler *et al.*	(KARLT) IJP
Also		Toronto Conf. 3	R. Koch	(KARLT) IJP
HENDRY	78	PRL 41 222	A.W. Hendry	(IND, LBL) IJP
Also		ANP 136 1	A.W. Hendry	(IND)

$N(\sim 3000$ Region) Partial-Wave Analyses

OMITTED FROM SUMMARY TABLE

We list here miscellaneous high-mass candidates for isospin-1/2 resonances found in partial-wave analyses.

Our 1982 edition had an $N(3245)$, an $N(3690)$, and an $N(3755)$, each a narrow peak seen in a production experiment. Since nothing has been heard from them since the 1960's, we declare them to be dead. There was also an $N(3030)$, deduced from total cross-section and 180° elastic cross-section measurements; it is the KOCH 80 $L_{1,15}$ state below.

$N(\sim 3000)$ BREIT-WIGNER MASS

VALUE (MeV)	DOCUMENT ID		TECN	COMMENT
≈ 3000 OUR ESTIMATE				
2600	KOCH	80	IPWA	$\pi N \rightarrow \pi N\ D_{13}$
3100	KOCH	80	IPWA	$\pi N \rightarrow \pi N\ L_{1,15}$ wave
3500	KOCH	80	IPWA	$\pi N \rightarrow \pi N\ M_{1,17}$ wave
3500 to 4000	KOCH	80	IPWA	$\pi N \rightarrow \pi N\ N_{1,19}$ wave
3500±200	HENDRY	78	MPWA	$\pi N \rightarrow \pi N\ L_{1,15}$ wave
3800±200	HENDRY	78	MPWA	$\pi N \rightarrow \pi N\ M_{1,17}$ wave
4100±200	HENDRY	78	MPWA	$\pi N \rightarrow \pi N\ N_{1,19}$ wave

$N(\sim 3000)$ BREIT-WIGNER WIDTH

VALUE (MeV)	DOCUMENT ID		TECN	COMMENT
1300±200	HENDRY	78	MPWA	$\pi N \rightarrow \pi N\ L_{1,15}$ wave
1600±200	HENDRY	78	MPWA	$\pi N \rightarrow \pi N\ M_{1,17}$ wave
1900±300	HENDRY	78	MPWA	$\pi N \rightarrow \pi N\ N_{1,19}$ wave

$N(\sim 3000)$ DECAY MODES

	Mode
Γ_1	$N\pi$

$N(\sim 3000)$ BRANCHING RATIOS

$\Gamma(N\pi)/\Gamma_{total}$ **Γ_1/Γ**

VALUE (%)	DOCUMENT ID		TECN	COMMENT
6 ±2	HENDRY	78	MPWA	$\pi N \rightarrow \pi N\ L_{1,15}$ wave
4.0±1.5	HENDRY	78	MPWA	$\pi N \rightarrow \pi N\ M_{1,17}$ wave
3.0±1.5	HENDRY	78	MPWA	$\pi N \rightarrow \pi N\ N_{1,19}$ wave

$N(\sim 3000)$ REFERENCES

KOCH	80	Toronto Conf. 3	R. Koch	(KARLT) IJP
HENDRY	78	PRL 41 222	A.W. Hendry	(IND, LBL) IJP
Also		ANP 136 1	A.W. Hendry	(IND) IJP

Δ BARYONS
(S = 0, I = 3/2)

$\Delta^{++} = uuu$, $\Delta^{+} = uud$, $\Delta^{0} = udd$, $\Delta^{-} = ddd$

Δ(1232) 3/2+

$I(J^P) = \frac{3}{2}(\frac{3}{2}^+)$ Status: ****

Most of the results published before 1975 were last included in our 1982 edition, Physics Letters **111B** 1 (1982). Some further obsolete results published before 1984 were last included in our 2006 edition, Journal of Physics (generic for all A,B,E,G) **G33** 1 (2006).

Δ(1232) BREIT-WIGNER MASSES

MIXED CHARGES

VALUE (MeV)	DOCUMENT ID		TECN	COMMENT
1230 to 1234 (≈ 1232) OUR ESTIMATE				
1228 ±2	ANISOVICH	12A	DPWA	Multichannel
1233.4±0.4	ARNDT	06	DPWA	$\pi N \to \pi N, \eta N$
1232 ±3	CUTKOSKY	80	IPWA	$\pi N \to \pi N$
1233 ±2	HOEHLER	79	IPWA	$\pi N \to \pi N$
• • • We do not use the following data for averages, fits, limits, etc. • • •				
1231.1±0.2	SHRESTHA	12A	DPWA	Multichannel
1230 ±2	ANISOVICH	10	DPWA	Multichannel
1232.9±1.2	ARNDT	04	DPWA	$\pi N \to \pi N, \eta N$
1228 ±1	PENNER	02C	DPWA	Multichannel
1234 ±5	VRANA	00	DPWA	Multichannel
1233	ARNDT	95	DPWA	$\pi N \to N\pi$
1231 ±1	MANLEY	92	IPWA	$\pi N \to \pi N$ & $N\pi\pi$

Δ(1232)++ MASS

VALUE (MeV)	DOCUMENT ID		TECN	COMMENT
• • • We do not use the following data for averages, fits, limits, etc. • • •				
1230.55±0.20	GRIDNEV	06	DPWA	$\pi N \to \pi N$
1231.88±0.29	BERNICHA	96		Fit to PEDRONI 78
1230.5 ±0.2	ABAEV	95	IPWA	$\pi N \to \pi N$
1230.9 ±0.3	KOCH	80B	IPWA	$\pi N \to \pi N$
1231.1 ±0.2	PEDRONI	78		$\pi N \to \pi N$ 70–370 MeV

Δ(1232)+ MASS

VALUE (MeV)	DOCUMENT ID		COMMENT
• • • We do not use the following data for averages, fits, limits, etc. • • •			
1234.9±1.4	MIROSHNIC...	79	Fit photoproduction

Δ(1232)0 MASS

VALUE (MeV)	DOCUMENT ID		TECN	COMMENT
• • • We do not use the following data for averages, fits, limits, etc. • • •				
1231.3 ±0.6	BREITSCHOP...06		CNTR	Using new CHEX data
1233.40±0.22	GRIDNEV	06	DPWA	$\pi N \to \pi N$
1234.35±0.75	BERNICHA	96		Fit to PEDRONI 78
1233.1 ±0.3	ABAEV	95	IPWA	$\pi N \to \pi N$
1233.6 ±0.5	KOCH	80B	IPWA	$\pi N \to \pi N$
1233.8 ±0.2	PEDRONI	78		$\pi N \to \pi N$ 70–370 MeV

$m_{\Delta^0} - m_{\Delta^{++}}$

VALUE (MeV)	DOCUMENT ID		TECN	COMMENT
• • • We do not use the following data for averages, fits, limits, etc. • • •				
2.86±0.30	GRIDNEV	06	DPWA	$\pi N \to \pi N$
2.25±0.68	BERNICHA	96		Fit to PEDRONI 78
2.6 ±0.4	ABAEV	95	IPWA	$\pi N \to \pi N$
2.7 ±0.3	[1] PEDRONI	78		See the masses

[1] Using $\pi^{\pm}d$ as well, PEDRONI 78 determine $(M^- - M^{++}) + (M^0 - M^+)/3 = 4.6 \pm 0.2$ MeV.

Δ(1232) BREIT-WIGNER WIDTHS

MIXED CHARGES

VALUE (MeV)	DOCUMENT ID		TECN	COMMENT
114 to 120 (≈ 117) OUR ESTIMATE				
110 ± 3	ANISOVICH	12A	DPWA	Multichannel
118.7± 0.6	ARNDT	06	DPWA	$\pi N \to \pi N, \eta N$
120 ± 5	CUTKOSKY	80	IPWA	$\pi N \to \pi N$
116 ± 5	HOEHLER	79	IPWA	$\pi N \to \pi N$
• • • We do not use the following data for averages, fits, limits, etc. • • •				
113.0± 0.5	SHRESTHA	12A	DPWA	Multichannel
112 ± 4	ANISOVICH	10	DPWA	Multichannel
118.0± 2.2	ARNDT	04	DPWA	$\pi N \to \pi N, \eta N$
106 ± 1	PENNER	02C	DPWA	Multichannel
112 ±18	VRANA	00	DPWA	Multichannel
114	ARNDT	95	DPWA	$\pi N \to N\pi$
118 ± 4	MANLEY	92	IPWA	$\pi N \to \pi N$ & $N\pi\pi$

Δ(1232)++ WIDTH

VALUE (MeV)	DOCUMENT ID		TECN	COMMENT
• • • We do not use the following data for averages, fits, limits, etc. • • •				
112.2 ±0.7	GRIDNEV	06	DPWA	$\pi N \to \pi N$
109.07±0.48	BERNICHA	96		Fit to PEDRONI 78
111.0 ±1.0	KOCH	80B	IPWA	$\pi N \to \pi N$
111.3 ±0.5	PEDRONI	78		$\pi N \to \pi N$ 70–370 MeV

Δ(1232)+ WIDTH

VALUE (MeV)	DOCUMENT ID		COMMENT
• • • We do not use the following data for averages, fits, limits, etc. • • •			
131.1±2.4	MIROSHNIC...	79	Fit photoproduction

Δ(1232)0 WIDTH

VALUE (MeV)	DOCUMENT ID		TECN	COMMENT
• • • We do not use the following data for averages, fits, limits, etc. • • •				
112.5 ±1.9	BREITSCHOP...06		CNTR	Using new CHEX data
116.9 ±0.7	GRIDNEV	06	DPWA	$\pi N \to \pi N$
117.58±1.16	BERNICHA	96		Fit to PEDRONI 78
113.0 ±1.5	KOCH	80B	IPWA	$\pi N \to \pi N$
117.9 ±0.9	PEDRONI	78		$\pi N \to \pi N$ 70–370 MeV

Δ^0-Δ^{++} WIDTH DIFFERENCE

VALUE (MeV)	DOCUMENT ID		TECN	COMMENT
• • • We do not use the following data for averages, fits, limits, etc. • • •				
4.66±1.0	GRIDNEV	06	DPWA	$\pi N \to \pi N$
8.45±1.11	BERNICHA	96		Fit to PEDRONI 78
5.1 ±1.0	ABAEV	95	IPWA	$\pi N \to \pi N$
6.6 ±1.0	PEDRONI	78		See the widths

Δ(1232) POLE POSITIONS

REAL PART, MIXED CHARGES

VALUE (MeV)	DOCUMENT ID		TECN	COMMENT
1209 to 1211 (≈ 1210) OUR ESTIMATE				
1210.5±1.0	ANISOVICH	12A	DPWA	Multichannel
1211	ARNDT	06	DPWA	$\pi N \to \pi N, \eta N$
1209	[2] HOEHLER	93	ARGD	$\pi N \to \pi N$
1210 ±1	CUTKOSKY	80	IPWA	$\pi N \to \pi N$
• • • We do not use the following data for averages, fits, limits, etc. • • •				
1212	SHRESTHA	12A	DPWA	Multichannel
1211 ±1	ANISOVICH	10	DPWA	Multichannel
1210	ARNDT	04	DPWA	$\pi N \to \pi N, \eta N$
1217	VRANA	00	DPWA	Multichannel
1211	ARNDT	95	DPWA	$\pi N \to N\pi$
1210	ARNDT	91	DPWA	$\pi N \to \pi N$ Soln SM90

−2×IMAGINARY PART, MIXED CHARGES

VALUE (MeV)	DOCUMENT ID		TECN	COMMENT
98 to 102 (≈ 100) OUR ESTIMATE				
99±2	ANISOVICH	12A	DPWA	Multichannel
99	ARNDT	06	DPWA	$\pi N \to \pi N, \eta N$
100	[2] HOEHLER	93	ARGD	$\pi N \to \pi N$
100±2	CUTKOSKY	80	IPWA	$\pi N \to \pi N$
• • • We do not use the following data for averages, fits, limits, etc. • • •				
98	SHRESTHA	12A	DPWA	Multichannel
100±2	ANISOVICH	10	DPWA	Multichannel
100	ARNDT	04	DPWA	$\pi N \to \pi N, \eta N$
96	VRANA	00	DPWA	Multichannel
100	ARNDT	95	DPWA	$\pi N \to N\pi$
100	ARNDT	91	DPWA	$\pi N \to \pi N$ Soln SM90

REAL PART, Δ(1232)++

VALUE (MeV)	DOCUMENT ID		COMMENT
• • • We do not use the following data for averages, fits, limits, etc. • • •			
1212.50±0.24	BERNICHA	96	Fit to PEDRONI 78

−2×IMAGINARY PART, Δ(1232)++

VALUE (MeV)	DOCUMENT ID		COMMENT
• • • We do not use the following data for averages, fits, limits, etc. • • •			
97.37±0.42	BERNICHA	96	Fit to PEDRONI 78

REAL PART, Δ(1232)+

VALUE (MeV)	DOCUMENT ID		TECN	COMMENT
• • • We do not use the following data for averages, fits, limits, etc. • • •				
1211 ±1 to 1212 ± 1	HANSTEIN	96	DPWA	$\gamma N \to \pi N$
1206.9±0.9 to 1210.5 ± 1.8	MIROSHNIC...	79		Fit photoproduction

−2×IMAGINARY PART, Δ(1232)+

VALUE (MeV)	DOCUMENT ID		TECN	COMMENT
• • • We do not use the following data for averages, fits, limits, etc. • • •				
102 ±2 to 99 ± 2	[3] HANSTEIN	96	DPWA	$\gamma N \to \pi N$
111.2±2.0 to 116.6 ± 2.2	MIROSHNIC...	79		Fit photoproduction

REAL PART, Δ(1232)⁰

VALUE (MeV)	DOCUMENT ID		COMMENT
• • • We do not use the following data for averages, fits, limits, etc. • • •			
1213.20±0.66	BERNICHA	96	Fit to PEDRONI 78

−2×IMAGINARY PART, Δ(1232)⁰

VALUE (MeV)	DOCUMENT ID		COMMENT
• • • We do not use the following data for averages, fits, limits, etc. • • •			
104.10±1.01	BERNICHA	96	Fit to PEDRONI 78

[2] See HOEHLER 93 for a detailed discussion of the evidence for and the pole parameters of N and Δ resonances as determined from Argand diagrams of πN elastic partial-wave amplitudes and from plots of the speeds with which the amplitudes traverse the diagrams.

[3] The second (lower) value of HANSTEIN 96 here goes with the second (higher) value of the real part in the preceding data block.

Δ(1232) ELASTIC POLE RESIDUES

ABSOLUTE VALUE, MIXED CHARGES

VALUE (MeV)	DOCUMENT ID		TECN	COMMENT
51.6±0.6	ANISOVICH	12A	DPWA	Multichannel
52	ARNDT	06	DPWA	$\pi N \to \pi N, \eta N$
50	HOEHLER	93	ARGD	$\pi N \to \pi N$
53 ±2	CUTKOSKY	80	IPWA	$\pi N \to \pi N$
• • • We do not use the following data for averages, fits, limits, etc. • • •				
53	ARNDT	04	DPWA	$\pi N \to \pi N, \eta N$
38	[4] ARNDT	95	DPWA	$\pi N \to N\pi$
52	ARNDT	91	DPWA	$\pi N \to \pi N$ Soln SM90

PHASE, MIXED CHARGES

VALUE (°)	DOCUMENT ID		TECN	COMMENT
−46±1	ANISOVICH	12A	DPWA	Multichannel
−47	ARNDT	06	DPWA	$\pi N \to \pi N, \eta N$
−48	HOEHLER	93	ARGD	$\pi N \to \pi N$
−47±1	CUTKOSKY	80	IPWA	$\pi N \to \pi N$
• • • We do not use the following data for averages, fits, limits, etc. • • •				
−47	ARNDT	04	DPWA	$\pi N \to \pi N, \eta N$
−22	[4] ARNDT	95	DPWA	$\pi N \to N\pi$
−31	ARNDT	91	DPWA	$\pi N \to \pi N$ Soln SM90

[4] This ARNDT 95 value is in error, as pointed out by HOHLER 01. The corrected value is in line with the ARNDT 91 value (R.A. Arndt, private communication).

Δ(1232) DECAY MODES

The following branching fractions are our estimates, not fits or averages.

	Mode	Fraction (Γ_i/Γ)
Γ_1	$N\pi$	100 %
Γ_2	$N\gamma$	0.55–0.65 %
Γ_3	$N\gamma$, helicity=1/2	0.11–0.13 %
Γ_4	$N\gamma$, helicity=3/2	0.44–0.52 %

Δ(1232) BRANCHING RATIOS

$\Gamma(N\pi)/\Gamma_{total}$ Γ_1/Γ

VALUE	DOCUMENT ID		TECN	COMMENT
1.0 OUR ESTIMATE				
1.00	ARNDT	06	DPWA	$\pi N \to \pi N, \eta N$
1.0	CUTKOSKY	80	IPWA	$\pi N \to \pi N$
1.0	HOEHLER	79	IPWA	$\pi N \to \pi N$
• • • We do not use the following data for averages, fits, limits, etc. • • •				
0.994	SHRESTHA	12A	DPWA	Multichannel
1.0	ANISOVICH	10	DPWA	Multichannel
1.000	ARNDT	04	DPWA	$\pi N \to \pi N, \eta N$
1.00	PENNER	02C	DPWA	Multichannel
1.00 ±0.01	VRANA	00	DPWA	Multichannel
1.0	ARNDT	95	DPWA	$\pi N \to N\pi$
1.0	MANLEY	92	IPWA	$\pi N \to \pi N$ & $N\pi\pi$

Δ(1232) PHOTON DECAY AMPLITUDES

Papers on γN amplitudes predating 1981 may be found in our 2006 edition, Journal of Physics (generic for all A,B,E,G) **G33** 1 (2006).

Δ(1232) → $N\gamma$, helicity-1/2 amplitude $A_{1/2}$

VALUE ($GeV^{-1/2}$)	DOCUMENT ID		TECN	COMMENT
−0.135 ±0.006 OUR ESTIMATE				
−0.131 ±0.004	ANISOVICH	12A	DPWA	Multichannel
−0.139 ±0.002	WORKMAN	12A	DPWA	$\gamma N \to N\pi$
−0.139 ±0.004	DUGGER	07	DPWA	$\gamma N \to \pi N$
−0.137 ±0.005	AHRENS	04A	DPWA	$\vec{\gamma}\vec{p} \to N\pi$
−0.1357±0.0013±0.0037	BLANPIED	01	LEGS	$\gamma p \to p\gamma, p\pi^0, n\pi^+$
−0.131 ±0.001	BECK	00	IPWA	$\vec{\gamma}p \to p\pi^0, n\pi^+$
−0.140 ±0.005	KAMALOV	99	DPWA	$\gamma N \to \pi N$
−0.1294±0.0013	HANSTEIN	98	IPWA	$\gamma N \to \pi N$
−0.1278±0.0012	DAVIDSON	97	DPWA	$\gamma N \to \pi N$
−0.135 ±0.016	DAVIDSON	91B	FIT	$\gamma N \to \pi N$
−0.145 ±0.015	CRAWFORD	83	IPWA	$\gamma N \to \pi N$
−0.138 ±0.004	AWAJI	81	DPWA	$\gamma N \to \pi N$
• • • We do not use the following data for averages, fits, limits, etc. • • •				
−0.137 ±0.001	SHRESTHA	12A	DPWA	Multichannel
−0.136 ±0.005	ANISOVICH	10	DPWA	Multichannel
−0.140	DRECHSEL	07	DPWA	$\gamma N \to \pi N$
−0.129 ±0.001	ARNDT	02	DPWA	$\gamma p \to N\pi$
−0.128	PENNER	02D	DPWA	Multichannel
−0.1312	HANSTEIN	98	DPWA	$\gamma N \to \pi N$
−0.135 ±0.005	ARNDT	97	IPWA	$\gamma N \to \pi N$
−0.141 ±0.005	ARNDT	96	IPWA	$\gamma N \to \pi N$
−0.143 ±0.004	LI	93	IPWA	$\gamma N \to \pi N$
−0.140 ±0.007	DAVIDSON	90	FIT	See DAVIDSON 91B

Δ(1232) → $N\gamma$, helicity-3/2 amplitude $A_{3/2}$

VALUE ($GeV^{-1/2}$)	DOCUMENT ID		TECN	COMMENT
−0.255 ±0.005 OUR ESTIMATE				
−0.254 ±0.005	ANISOVICH	12A	DPWA	Multichannel
−0.262 ±0.003	WORKMAN	12A	DPWA	$\gamma N \to N\pi$
−0.258 ±0.005	DUGGER	07	DPWA	$\gamma N \to \pi N$
−0.256 ±0.003	AHRENS	04A	DPWA	$\vec{\gamma}\vec{p} \to N\pi$
−0.2669±0.0016±0.0078	BLANPIED	01	LEGS	$\gamma p \to p\gamma, p\pi^0, n\pi^+$
−0.251 ±0.001	BECK	00	IPWA	$\vec{\gamma}p \to p\pi^0, n\pi^+$
−0.258 ±0.006	KAMALOV	99	DPWA	$\gamma N \to \pi N$
−0.2466±0.0013	HANSTEIN	98	IPWA	$\gamma N \to \pi N$
−0.2524±0.0013	DAVIDSON	97	DPWA	$\gamma N \to \pi N$
−0.251 ±0.033	DAVIDSON	91B	FIT	$\gamma N \to \pi N$
−0.263 ±0.026	CRAWFORD	83	IPWA	$\gamma N \to \pi N$
−0.259 ±0.006	AWAJI	81	DPWA	$\gamma N \to \pi N$
• • • We do not use the following data for averages, fits, limits, etc. • • •				
−0.251 ±0.001	SHRESTHA	12A	DPWA	Multichannel
−0.267 ±0.008	ANISOVICH	10	DPWA	Multichannel
−0.265	DRECHSEL	07	DPWA	$\gamma N \to \pi N$
−0.243 ±0.001	ARNDT	02	DPWA	$\gamma p \to N\pi$
−0.247	PENNER	02D	DPWA	Multichannel
−0.2522	HANSTEIN	98	DPWA	$\gamma N \to \pi N$
−0.250 ±0.008	ARNDT	97	IPWA	$\gamma N \to \pi N$
−0.261 ±0.005	ARNDT	96	IPWA	$\gamma N \to \pi N$
−0.262 ±0.004	LI	93	IPWA	$\gamma N \to \pi N$
−0.254 ±0.011	DAVIDSON	90	FIT	See DAVIDSON 91B

Δ(1232) → $N\gamma$, E_2/M_1 ratio

VALUE	DOCUMENT ID		TECN	COMMENT
−0.025 ±0.005 OUR ESTIMATE				
−0.0274±0.0003±0.0030	AHRENS	04A	DPWA	$\vec{\gamma}\vec{p} \to N\pi$
−0.020 ±0.002	ARNDT	02	DPWA	$\gamma p \to N\pi$
−0.0307±0.0026±0.0024	BLANPIED	01	LEGS	$\gamma p \to p\gamma, p\pi^0, n\pi^+$
−0.016 ±0.004 ±0.002	GALLER	01	DPWA	$\gamma p \to \gamma p$
−0.025 ±0.001 ±0.002	BECK	00	IPWA	$\vec{\gamma}p \to p\pi^0, n\pi^+$
−0.0233±0.0017	HANSTEIN	98	IPWA	$\gamma N \to \pi N$
−0.015 ±0.005	[5] ARNDT	97	IPWA	$\gamma N \to \pi N$
−0.0319±0.0024	DAVIDSON	97	DPWA	$\gamma N \to \pi N$
• • • We do not use the following data for averages, fits, limits, etc. • • •				
−0.022	DRECHSEL	07	DPWA	$\gamma N \to \pi N$
−0.026	PENNER	02D	DPWA	Multichannel
−0.0254±0.0010	HANSTEIN	98	DPWA	$\gamma N \to \pi N$
−0.025 ±0.002 ±0.002	BECK	97	IPWA	$\gamma N \to \pi N$
−0.030 ±0.003 ±0.002	BLANPIED	97	DPWA	$\gamma N \to \pi N, \gamma N$
−0.027 ±0.003 ±0.001	KHANDAKER	95	DPWA	$\gamma N \to \pi N$
−0.015 ±0.005	WORKMAN	92	IPWA	$\gamma N \to \pi N$
−0.0157±0.0072	DAVIDSON	91B	FIT	$\gamma N \to \pi N$
−0.0107±0.0037	DAVIDSON	90	FIT	$\gamma N \to \pi N$
−0.015 ±0.002	DAVIDSON	86	FIT	$\gamma N \to \pi N$
+0.037 ±0.004	TANABE	85	FIT	$\gamma N \to \pi N$

Δ(1232) → $N\gamma$, absolute value of E_2/M_1 ratio at pole

VALUE	DOCUMENT ID		TECN	COMMENT
• • • We do not use the following data for averages, fits, limits, etc. • • •				
0.065±0.007	ARNDT	97	DPWA	$\gamma N \to \pi N$
0.058	HANSTEIN	96	DPWA	$\gamma N \to \pi N$

Δ(1232) → $N\gamma$, phase of E_2/M_1 ratio at pole

VALUE	DOCUMENT ID		TECN	COMMENT
• • • We do not use the following data for averages, fits, limits, etc. • • •				
−122 ±5	ARNDT	97	DPWA	$\gamma N \to \pi N$
−127.2	HANSTEIN	96	DPWA	$\gamma N \to \pi N$

[5] This ARNDT 97 value is very sensitive to the database being fitted. The result is from a fit to the full pion photoproduction database, apart from the BLANPIED 97 cross-section measurements.

Δ(1232) MAGNETIC MOMENTS

Δ(1232)++ MAGNETIC MOMENT

The values are extracted from UCLA and SIN data on $\pi^+ p$ bremsstrahlung using a variety of different theoretical approximations and methods. Our estimate is *only* a rough guess of the range we expect the moment to lie within.

VALUE (μ_N)	DOCUMENT ID		TECN	COMMENT
3.7 to 7.5 OUR ESTIMATE				
• • • We do not use the following data for averages, fits, limits, etc. • • •				
6.14 ± 0.51	LOPEZCAST...	01	DPWA	$\pi^+ p \to \pi^+ p\gamma$
$4.52 \pm 0.50 \pm 0.45$	BOSSHARD	91		$\pi^+ p \to \pi^+ p\gamma$ (SIN data)
3.7 to 4.2	LIN	91B		$\pi^+ p \to \pi^+ p\gamma$ (from UCLA data)
4.6 to 4.9	LIN	91B		$\pi^+ p \to \pi^+ p\gamma$ (from SIN data)
5.6 to 7.5	WITTMAN	88		$\pi^+ p \to \pi^+ p\gamma$ (from UCLA data)
6.9 to 9.8	HELLER	87		$\pi^+ p \to \pi^+ p\gamma$ (from UCLA data)
4.7 to 6.7	NEFKENS	78		$\pi^+ p \to \pi^+ p\gamma$ (UCLA data)

Δ(1232)+ MAGNETIC MOMENT

VALUE (μ_N)	DOCUMENT ID		COMMENT
• • • We do not use the following data for averages, fits, limits, etc. • • •			
$2.7^{+1.0}_{-1.3} \pm 1.5 \pm 3$	[6] KOTULLA	02	$\gamma p \to p\pi^0\gamma'$

[6] The second error is systematic, the third is an estimate of theoretical uncertainties.

Δ(1232) REFERENCES

For early references, see Physics Letters **111B** 1 (1982).

ANISOVICH	12A	EPJ A48 15	A.V. Anisovich *et al.*	(BONN, PNPI)
SHRESTHA	12A	PR C86 055203	M. Shrestha, D.M. Manley	(KSU)
WORKMAN	12A	PR C86 015202	R. Workman *et al.*	(GWU)
ANISOVICH	10	EPJ A44 203	A.V. Anisovich *et al.*	(BONN, PNPI)
DRECHSEL	07	EPJ A34 69	D. Drechsel, S.S. Kamalov, L. Tiator	(MAINZ, JINR)
DUGGER	07	PR C76 025211	M. Dugger *et al.*	(Jefferson Lab CLAS Collab.)
ARNDT	06	PR C74 045205	R.A. Arndt *et al.*	(GWU)
BREITSCHOP...	06	PL B639 424	J. Breitschopf *et al.*	(TUBIN, HEBR, CSUS)
GRIDNEV	06	PAN 69 1542	A.B. Gridnev *et al.*	(PNPI, BONN, GWU)
PDG	06	JP G33 1	W.-M. Yao *et al.*	(PDG Collab.)
AHRENS	04A	EPJ A21 323	J. Ahrens *et al.*	(Mainz GDH, A2 Collab.)
ARNDT	04	PR C69 035213	R.A. Arndt *et al.*	(GWU, TRIU)
ARNDT	02	PR C66 055213	R. A. Arndt *et al.*	(GWU)
KOTULLA	02	PRL 89 272001	M. Kotulla *et al.*	(MAMI TAPS Collab.)
PENNER	02C	PR C66 055211	G. Penner, U. Mosel	(GIES)
PENNER	02D	PR C66 055212	G. Penner, U. Mosel	(GIES)
BLANPIED	01	PR C64 025203	G. Blanpied *et al.*	(BNL LEGS Collab.)
GALLER	01	PL B503 245	G. Galler *et al.*	(Mainz LARA Collab.)
HOHLER	01	NSTAR 2001 185	G. Hohler	(KARL)
LOPEZCAST...	01	PL B517 339	G. Lopez Castro, A. Mariano	
Also		NP A697 440	G. Lopez Castro, A. Mariano	
BECK	00	PR C61 035204	R. Beck *et al.*	(Mainz Microtron DAPHNE Col.)
VRANA	00	PRPL 328 181	T.P. Vrana, S.A. Dytman, T.-S.H. Lee	(PITT+)
KAMALOV	99	PRL 83 4494	S.S. Kamalov, S.N. Yang	(Taiwan U.)
HANSTEIN	98	NP A632 561	O. Hanstein, D. Drechsel, L. Tiator	
ARNDT	97	PR C56 577	R.A. Arndt, I.I. Strakovsky, R.L. Workman	(VPI)
BECK	97	PRL 78 606	R. Beck *et al.*	(MANZ, SACL, PAVI, GLAS)
Also		PRL 79 4510	R.L. Beck, H.P. Krahn	(MANZ)
Also		PRL 79 4512	R.L. Beck, H.P. Krahn	(MANZ)
Also		PRL 79 4515 (erratum)	R.L. Beck *et al.*	(MANZ, SACL, PAVI, GLAS)
BLANPIED	97	PRL 79 4337	G.S. Blanpied *et al.*	(LEGS Collab.)
DAVIDSON	97	PRL 79 4509	R.M. Davidson, N.C.A. Mukhopadhyay	(RPI)
ARNDT	96	PR C53 430	R.A. Arndt, I.I. Strakovsky, R.L. Workman	(VPI)
BERNICHA	96	NP A597 623	A. Bernicha, G. Lopez Castro, J. Pestieau	(LOUV+)
HANSTEIN	96	PL B385 45	O. Hanstein, D. Drechsel, L. Tiator	(MANZ)
ABAEV	95	ZPHY A352 85	V.V. Abaev, S.P. Kruglov	(PNPI)
ARNDT	95	PR C52 2120	R.A. Arndt *et al.*	(VPI, BRCO)
KHANDAKER	95	PR D51 3966	M. Khandaker, A.M. Sandorfi	(BNL, VPI)
HOEHLER	93	πN Newsletter 9 1	G. Hohler	(KARL)
LI	93	PR C47 2759	Z.J. Li *et al.*	(VPI)
MANLEY	92	PR D45 4002	D.M. Manley, E.M. Saleski	(KSA) IJP
Also		PR D30 904	D.M. Manley *et al.*	(VPI)
WORKMAN	92	PR C46 1546	R.L. Workman, R.A. Arndt, Z.J. Li	(VPI)
ARNDT	91	PR D43 2131	R.A. Arndt *et al.*	(VPI, TELE) IJP
BOSSHARD	91	PR D44 1962	A. Bosshard *et al.*	(ZURI, LBL, VILL+)
Also		PRL 64 2619	A. Bosshard *et al.*	(CATH, LAUS, LBL+)
DAVIDSON	91B	PR D43 71	R.M. Davidson, N.C. Mukhopadhyay, R.S. Wittman	
LIN	91B	PR C44 1819	D.H. Lin, M.K. Liou, Z.M. Ding	(CUNY, CSOK)
Also		PR C43 R930	D. Lin, M.K. Liou	(CUNY)
DAVIDSON	90	PR D42 20	R.M. Davidson, N.C. Mukhopadhyay	(RPI)
WITTMAN	88	PR C37 2075	R. Wittman	(TRIU)
HELLER	87	PR C35 718	L. Heller *et al.*	(LANL, MIT, ILL)
DAVIDSON	86	PRL 56 804	R.M. Davidson, N.C. Mukhopadhyay, R. Wittman	(RPI)
TANABE	85	PR C31 1876	H. Tanabe, K. Ohta	(KOMAB)
CRAWFORD	83	NP B211 1	R.L. Crawford, W.T. Morton	(GLAS)
PDG	82	PL 111B 1	M. Roos *et al.*	(HELS, CIT, CERN)
AWAJI	81	Bonn Conf. 352	N. Awaji, R. Kajikawa	(NAGO)
Also		NP B197 365	K. Fujii *et al.*	(NAGO)
CUTKOSKY	80	Toronto Conf. 19	R.E. Cutkosky *et al.*	(CMU, LBL) IJP
Also		PR D20 2839	R.E. Cutkosky *et al.*	(CMU, LBL)
KOCH	80B	NP A336 331	R. Koch, E. Pietarinen	(KARLT) IJP
HOEHLER	79	PDAT 12-1	G. Hohler *et al.*	(KARLT) IJP
Also		Toronto Conf. 3	R. Koch	(KARLT) IJP
MIROSHNIC...	79	SJNP 29 94	I.I. Miroshnichenko *et al.*	(KFTI) IJP
		Translated from YAF 29 188.		
NEFKENS	78	PR D18 3911	B.M.K. Nefkens *et al.*	(UCLA, CATH) IJP
PEDRONI	78	NP A300 321	E. Pedroni *et al.*	(SIN, ISNG, KARLE+) IJP

Δ(1600) 3/2+

$I(J^P) = \frac{3}{2}(\frac{3}{2}^+)$ Status: ***

Most of the results published before 1975 are now obsolete and have been omitted. They may be found in our 1982 edition, Physics Letters **111B** 1 (1982). Some further obsolete results published before 1984 were last included in our 2006 edition, Journal of Physics (generic for all A,B,E,G) **G33** 1 (2006).

The various analyses are not in good agreement.

Δ(1600) BREIT-WIGNER MASS

VALUE (MeV)	DOCUMENT ID		TECN	COMMENT
1500 to 1700 (≈ 1600) OUR ESTIMATE				
1510 ± 20	ANISOVICH	12A	DPWA	Multichannel
1600 ± 50	CUTKOSKY	80	IPWA	$\pi N \to \pi N$
1522 ± 13	HOEHLER	79	IPWA	$\pi N \to \pi N$
• • • We do not use the following data for averages, fits, limits, etc. • • •				
1626 ± 8	SHRESTHA	12A	DPWA	Multichannel
1650 ± 40	HORN	08A	DPWA	Multichannel
1667 ± 1	PENNER	02C	DPWA	Multichannel
1687 ± 44	VRANA	00	DPWA	Multichannel
1672 ± 15	ARNDT	96	IPWA	$\gamma N \to \pi N$
1706	LI	93	IPWA	$\gamma N \to \pi N$
1706 ± 10	MANLEY	92	IPWA	$\pi N \to \pi N$ & $N\pi\pi$
1690	BARNHAM	80	IPWA	$\pi N \to N\pi\pi$
1560	[1] LONGACRE	77	IPWA	$\pi N \to N\pi\pi$
1640	[2] LONGACRE	75	IPWA	$\pi N \to N\pi\pi$

Δ(1600) BREIT-WIGNER WIDTH

VALUE (MeV)	DOCUMENT ID		TECN	COMMENT
220 to 420 (≈ 320) OUR ESTIMATE				
220 ± 45	ANISOVICH	12A	DPWA	Multichannel
300 ± 100	CUTKOSKY	80	IPWA	$\pi N \to \pi N$
220 ± 40	HOEHLER	79	IPWA	$\pi N \to \pi N$
• • • We do not use the following data for averages, fits, limits, etc. • • •				
225 ± 18	SHRESTHA	12A	DPWA	Multichannel
530 ± 60	HORN	08A	DPWA	Multichannel
397 ± 10	PENNER	02C	DPWA	Multichannel
493 ± 75	VRANA	00	DPWA	Multichannel
315 ± 20	ARNDT	96	IPWA	$\gamma N \to \pi N$
215	LI	93	IPWA	$\gamma N \to \pi N$
430 ± 73	MANLEY	92	IPWA	$\pi N \to \pi N$ & $N\pi\pi$
250	BARNHAM	80	IPWA	$\pi N \to N\pi\pi$
180	[1] LONGACRE	77	IPWA	$\pi N \to N\pi\pi$
300	[2] LONGACRE	75	IPWA	$\pi N \to N\pi\pi$

Δ(1600) POLE POSITION

REAL PART

VALUE (MeV)	DOCUMENT ID		TECN	COMMENT
1460 to 1560 (≈ 1510) OUR ESTIMATE				
1498 ± 25	ANISOVICH	12A	DPWA	Multichannel
1457	ARNDT	06	DPWA	$\pi N \to \pi N, \eta N$
1550	[3] HOEHLER	93	SPED	$\pi N \to \pi N$
1550 ± 40	CUTKOSKY	80	IPWA	$\pi N \to \pi N$
• • • We do not use the following data for averages, fits, limits, etc. • • •				
1599	SHRESTHA	12A	DPWA	Multichannel
1510^{+20}_{-50}	HORN	08A	DPWA	Multichannel
1599	VRANA	00	DPWA	Multichannel
1675	ARNDT	95	DPWA	$\pi N \to N\pi$
1612	ARNDT	91	DPWA	$\pi N \to \pi N$ Soln SM90
1609 or 1610	[4] LONGACRE	78	IPWA	$\pi N \to N\pi\pi$
1541 or 1542	[1] LONGACRE	77	IPWA	$\pi N \to N\pi\pi$

−2×IMAGINARY PART

VALUE (MeV)	DOCUMENT ID		TECN	COMMENT
200 to 350 (≈ 275) OUR ESTIMATE				
230 ± 50	ANISOVICH	12A	DPWA	Multichannel
400	ARNDT	06	DPWA	$\pi N \to \pi N, \eta N$
200 ± 60	CUTKOSKY	80	IPWA	$\pi N \to \pi N$
• • • We do not use the following data for averages, fits, limits, etc. • • •				
211	SHRESTHA	12A	DPWA	Multichannel
230 ± 40	HORN	08A	DPWA	Multichannel
312	VRANA	00	DPWA	Multichannel
386	ARNDT	95	DPWA	$\pi N \to N\pi$
230	ARNDT	91	DPWA	$\pi N \to \pi N$ Soln SM90
323 or 325	[4] LONGACRE	78	IPWA	$\pi N \to N\pi\pi$
178 or 178	[1] LONGACRE	77	IPWA	$\pi N \to N\pi\pi$

Δ(1600) ELASTIC POLE RESIDUE

MODULUS |r|

VALUE (MeV)	DOCUMENT ID		TECN	COMMENT
11±6	ANISOVICH	12A	DPWA	Multichannel
44	ARNDT	06	DPWA	$\pi N \to \pi N, \eta N$
17±4	CUTKOSKY	80	IPWA	$\pi N \to \pi N$
• • • We do not use the following data for averages, fits, limits, etc. • • •				
52	ARNDT	95	DPWA	$\pi N \to N\pi$
16	ARNDT	91	DPWA	$\pi N \to \pi N$ Soln SM90

PHASE θ

VALUE (°)	DOCUMENT ID		TECN	COMMENT
−160±33	ANISOVICH	12A	DPWA	Multichannel
+147	ARNDT	06	DPWA	$\pi N \to \pi N, \eta N$
−150±30	CUTKOSKY	80	IPWA	$\pi N \to \pi N$
• • • We do not use the following data for averages, fits, limits, etc. • • •				
+ 14	ARNDT	95	DPWA	$\pi N \to N\pi$
− 73	ARNDT	91	DPWA	$\pi N \to \pi N$ Soln SM90

Δ(1600) INELASTIC POLE RESIDUE

The "normalized residue" is the residue divided by $\Gamma_{pole}/2$.

Normalized residue in $N\pi \to \Delta(1600) \to \Delta\pi$, P-wave

MODULUS (%)	PHASE (°)	DOCUMENT ID		TECN	COMMENT
14±10	**154 ± 40**	ANISOVICH	12A	DPWA	Multichannel

Normalized residue in $N\pi \to \Delta(1600) \to \Delta\pi$, F-wave

MODULUS (%)	DOCUMENT ID		TECN	COMMENT
1.0±0.5	ANISOVICH	12A	DPWA	Multichannel

Δ(1600) DECAY MODES

The following branching fractions are our estimates, not fits or averages.

	Mode	Fraction (Γ_i/Γ)
Γ_1	$N\pi$	10–25 %
Γ_2	ΣK	
Γ_3	$N\pi\pi$	75–90 %
Γ_4	$\Delta\pi$	40–70 %
Γ_5	$\Delta(1232)\pi$, P-wave	
Γ_6	$\Delta(1232)\pi$, F-wave	
Γ_7	$N\rho$	<25 %
Γ_8	$N\rho$, S=1/2, P-wave	
Γ_9	$N\rho$, S=3/2, P-wave	
Γ_{10}	$N\rho$, S=3/2, F-wave	
Γ_{11}	$N(1440)\pi$	10–35 %
Γ_{12}	$N(1440)\pi$, P-wave	
Γ_{13}	$N\gamma$	0.001–0.035 %
Γ_{14}	$N\gamma$, helicity=1/2	0.0–0.02 %
Γ_{15}	$N\gamma$, helicity=3/2	0.001–0.015 %

Δ(1600) BRANCHING RATIOS

$\Gamma(N\pi)/\Gamma_{total}$ Γ_1/Γ

VALUE (%)	DOCUMENT ID		TECN	COMMENT
10 to 25 OUR ESTIMATE				
12±5	ANISOVICH	12A	DPWA	Multichannel
18±4	CUTKOSKY	80	IPWA	$\pi N \to \pi N$
21±6	HOEHLER	79	IPWA	$\pi N \to \pi N$
• • • We do not use the following data for averages, fits, limits, etc. • • •				
8±2	SHRESTHA	12A	DPWA	Multichannel
10±3	HORN	08A	DPWA	Multichannel
13±1	PENNER	02C	DPWA	Multichannel
28±5	VRANA	00	DPWA	Multichannel
12±2	MANLEY	92	IPWA	$\pi N \to \pi N$ & $N\pi\pi$

$(\Gamma_i\Gamma_f)^{1/2}/\Gamma_{total}$ in $N\pi \to \Delta(1600) \to \Sigma K$ $(\Gamma_1\Gamma_2)^{1/2}/\Gamma$

VALUE	DOCUMENT ID		TECN	COMMENT
−0.36 to −0.28 OUR ESTIMATE				
• • • We do not use the following data for averages, fits, limits, etc. • • •				
0.006 to 0.042	[5] DEANS	75	DPWA	$\pi N \to \Sigma K$

Note: Signs of couplings from $\pi N \to N\pi\pi$ analyses were changed in the 1986 edition to agree with the baryon-first convention; the overall phase ambiguity is resolved by choosing a negative sign for the Δ(1620) S_{31} coupling to Δ(1232)π.

$(\Gamma_i\Gamma_f)^{1/2}/\Gamma_{total}$ in $N\pi \to \Delta(1600) \to \Delta(1232)\pi$, P-wave $(\Gamma_1\Gamma_5)^{1/2}/\Gamma$

VALUE	DOCUMENT ID		TECN	COMMENT
+0.27 to +0.33 OUR ESTIMATE				
+0.24±0.05	BARNHAM	80	IPWA	$\pi N \to N\pi\pi$
+0.34	[1,6] LONGACRE	77	IPWA	$\pi N \to N\pi\pi$
+0.30	[2] LONGACRE	75	IPWA	$\pi N \to N\pi\pi$
• • • We do not use the following data for averages, fits, limits, etc. • • •				
+0.29±0.02	MANLEY	92	IPWA	$\pi N \to \pi N$ & $N\pi\pi$

$\Gamma(\Delta(1232)\pi$, P-wave$)/\Gamma_{total}$ Γ_5/Γ

VALUE (%)	DOCUMENT ID		TECN	COMMENT
78± 6	ANISOVICH	12A	DPWA	Multichannel
59±10	VRANA	00	DPWA	Multichannel
• • • We do not use the following data for averages, fits, limits, etc. • • •				
70± 3	SHRESTHA	12A	DPWA	Multichannel

$(\Gamma_i\Gamma_f)^{1/2}/\Gamma_{total}$ in $N\pi \to \Delta(1600) \to \Delta(1232)\pi$, F-wave $(\Gamma_1\Gamma_6)^{1/2}/\Gamma$

VALUE	DOCUMENT ID		TECN	COMMENT
−0.15 to −0.03 OUR ESTIMATE				
−0.07	[1,6] LONGACRE	77	IPWA	$\pi N \to N\pi\pi$

$(\Gamma_i\Gamma_f)^{1/2}/\Gamma_{total}$ in $N\pi \to \Delta(1600) \to N\rho$, S=1/2, P-wave $(\Gamma_1\Gamma_8)^{1/2}/\Gamma$

VALUE	DOCUMENT ID		TECN	COMMENT
+0.10	[1,6] LONGACRE	77	IPWA	$\pi N \to N\pi\pi$

$(\Gamma_i\Gamma_f)^{1/2}/\Gamma_{total}$ in $N\pi \to \Delta(1600) \to N\rho$, S=3/2, P-wave $(\Gamma_1\Gamma_9)^{1/2}/\Gamma$

VALUE	DOCUMENT ID		TECN	COMMENT
+0.10	[1,6] LONGACRE	77	IPWA	$\pi N \to N\pi\pi$

$(\Gamma_i\Gamma_f)^{1/2}/\Gamma_{total}$ in $N\pi \to \Delta(1600) \to N(1440)\pi$, P-wave $(\Gamma_1\Gamma_{12})^{1/2}/\Gamma$

VALUE	DOCUMENT ID		TECN	COMMENT
+0.15 to +0.23 OUR ESTIMATE				
+0.23±0.04	BARNHAM	80	IPWA	$\pi N \to N\pi\pi$
• • • We do not use the following data for averages, fits, limits, etc. • • •				
+0.16±0.02	MANLEY	92	IPWA	$\pi N \to \pi N$ & $N\pi\pi$

$\Gamma(N(1440)\pi)/\Gamma_{total}$ Γ_{11}/Γ

VALUE (%)	DOCUMENT ID		TECN	COMMENT
13±4	VRANA	00	DPWA	Multichannel
• • • We do not use the following data for averages, fits, limits, etc. • • •				
22±3	SHRESTHA	12A	DPWA	Multichannel

Δ(1600) PHOTON DECAY AMPLITUDES

Papers on γN amplitudes predating 1981 may be found in our 2006 edition, Journal of Physics (generic for all A,B,E,G) **G33** 1 (2006).

Δ(1600) → Nγ, helicity-1/2 amplitude $A_{1/2}$

VALUE ($GeV^{-1/2}$)	DOCUMENT ID		TECN	COMMENT
−0.045±0.015 OUR ESTIMATE				
−0.050±0.009	ANISOVICH	12A	DPWA	Multichannel
−0.018±0.015	ARNDT	96	IPWA	$\gamma N \to \pi N$
−0.039±0.030	CRAWFORD	83	IPWA	$\gamma N \to \pi N$
−0.046±0.013	AWAJI	81	DPWA	$\gamma N \to \pi N$
• • • We do not use the following data for averages, fits, limits, etc. • • •				
0.006±0.005	SHRESTHA	12A	DPWA	Multichannel
0.0	PENNER	02D	DPWA	Multichannel
−0.026±0.002	LI	93	IPWA	$\gamma N \to \pi N$
−0.200	[7] WADA	84	DPWA	Compton scattering
0.000±0.030	BARBOUR	78	DPWA	$\gamma N \to \pi N$

Δ(1600) → Nγ, helicity-3/2 amplitude $A_{3/2}$

VALUE ($GeV^{-1/2}$)	DOCUMENT ID		TECN	COMMENT
−0.035±0.015 OUR ESTIMATE				
−0.040±0.012	ANISOVICH	12A	DPWA	Multichannel
−0.025±0.015	ARNDT	96	IPWA	$\gamma N \to \pi N$
−0.013±0.014	CRAWFORD	83	IPWA	$\gamma N \to \pi N$
0.025±0.031	AWAJI	81	DPWA	$\gamma N \to \pi N$
• • • We do not use the following data for averages, fits, limits, etc. • • •				
0.052±0.008	SHRESTHA	12A	DPWA	Multichannel
−0.024	PENNER	02D	DPWA	Multichannel
−0.016±0.002	LI	93	IPWA	$\gamma N \to \pi N$
0.023	WADA	84	DPWA	Compton scattering
0.000±0.045	BARBOUR	78	DPWA	$\gamma N \to \pi N$

Baryon Particle Listings

Δ(1600), Δ(1620)

Δ(1600) FOOTNOTES

[1] LONGACRE 77 pole positions are from a search for poles in the unitarized T-matrix; the first (second) value uses, in addition to $\pi N \to N\pi\pi$ data, elastic amplitudes from a Saclay (CERN) partial-wave analysis. The other LONGACRE 77 values are from eyeball fits with Breit-Wigner circles to the T-matrix amplitudes.
[2] From method II of LONGACRE 75: eyeball fits with Breit-Wigner circles to the T-matrix amplitudes.
[3] See HOEHLER 93 for a detailed discussion of the evidence for and the pole parameters of N and Δ resonances as determined from Argand diagrams of πN elastic partial-wave amplitudes and from plots of the speeds with which the amplitudes traverse the diagrams.
[4] LONGACRE 78 values are from a search for poles in the unitarized T-matrix. The first (second) value uses, in addition to $\pi N \to N\pi\pi$ data, elastic amplitudes from a Saclay (CERN) partial-wave analysis.
[5] The range given is from the four best solutions. DEANS 75 disagrees with $\pi^+ p \to \Sigma^+ K^+$ data of WINNIK 77 around 1920 MeV.
[6] LONGACRE 77 considers this coupling to be well determined.
[7] WADA 84 is inconsistent with other analyses — see the Note on N and Δ Resonances.

Δ(1600) REFERENCES

For early references, see Physics Letters **111B** 1 (1982).

ANISOVICH	12A	EPJ A48 15	A.V. Anisovich *et al.*	(BONN, PNPI)
SHRESTHA	12A	PR C86 055203	M. Shrestha, D.M. Manley	(KSU)
HORN	08A	EPJ A38 173	I. Horn *et al.*	(CB-ELSA Collab.)
Also		PRL 101 202002	I. Horn *et al.*	(CB-ELSA Collab.)
ARNDT	06	PR C74 045205	R.A. Arndt *et al.*	(GWU)
PDG	06	JP G33 1	W.-M. Yao *et al.*	(PDG Collab.)
PENNER	02C	PR C66 055211	G. Penner, U. Mosel	(GIES)
PENNER	02D	PR C66 055212	G. Penner, U. Mosel	(GIES)
VRANA	00	PRPL 328 181	T.P. Vrana, S.A. Dytman,, T.-S.H. Lee	(PITT+)
ARNDT	96	PR C53 430	R.A. Arndt, I.I. Strakovsky, R.L. Workman	(VPI)
ARNDT	95	PR C52 2120	R.A. Arndt *et al.*	(VPI, BRCO)
HOEHLER	93	πN Newsletter 9 1	G. Hohler	(KARL)
LI	93	PR C47 2759	Z.J. Li *et al.*	(VPI)
MANLEY	92	PR D45 4002	D.M. Manley, E.M. Saleski	(KSA) IJP
Also		PR D30 904	D.M. Manley *et al.*	(VPI)
ARNDT	91	PR D43 2131	R.A. Arndt *et al.*	(VPI, TELE) IJP
WADA	84	NP B247 313	Y. Wada *et al.*	(INUS)
CRAWFORD	83	NP B211 1	R.L. Crawford, W.T. Morton	(GLAS)
PDG	82	PL 111B 1	M. Roos *et al.*	(HELS, CIT, CERN)
AWAJI	81	Bonn Conf. 352	N. Awaji, R. Kajikawa	(NAGO)
Also		NP B197 365	K. Fujii *et al.*	(NAGO)
BARNHAM	80	NP B168 243	K.W.J. Barnham *et al.*	(LOIC)
CUTKOSKY	80	Toronto Conf. 19	R.E. Cutkosky *et al.*	(CMU, LBL) IJP
Also		PR D20 2839	R.E. Cutkosky *et al.*	(CMU, LBL) IJP
HOEHLER	79	PDAT 12-1	G. Hohler *et al.*	(KARLT) IJP
Also		Toronto Conf. 3	R. Koch	(KARLT) IJP
BARBOUR	78	NP B141 253	I.M. Barbour, R.L. Crawford, N.H. Parsons	(GLAS)
LONGACRE	78	PR D17 1795	R.S. Longacre *et al.*	(LBL, SLAC)
LONGACRE	77	NP B122 493	R.S. Longacre, J. Dolbeau	(SACL) IJP
Also		NP B108 365	J. Dolbeau *et al.*	(SACL) IJP
WINNIK	77	NP B128 66	M. Winnik *et al.*	(HAIF) I
DEANS	75	NP B96 90	S.R. Deans *et al.*	(SFLA, ALAH) IJP
LONGACRE	75	PL 55B 415	R.S. Longacre *et al.*	(LBL, SLAC) IJP

Δ(1620) 1/2⁻

$I(J^P) = \frac{3}{2}(\frac{1}{2}^-)$ Status: ****

Most of the results published before 1975 were last included in our 1982 edition, Physics Letters **111B** 1 (1982). Some further obsolete results published before 1984 were last included in our 2006 edition, Journal of Physics (generic for all A,B,E,G) **G33** 1 (2006).

Δ(1620) BREIT-WIGNER MASS

VALUE (MeV)	*DOCUMENT ID*		*TECN*	*COMMENT*
1600 to 1660 (≈ 1630) OUR ESTIMATE				
1600 ± 8	ANISOVICH	12A	DPWA	Multichannel
1615.2± 0.4	ARNDT	06	DPWA	$\pi N \to \pi N, \eta N$
1620 ±20	CUTKOSKY	80	IPWA	$\pi N \to \pi N$
1610 ± 7	HOEHLER	79	IPWA	$\pi N \to \pi N$
• • • We do not use the following data for averages, fits, limits, etc. • • •				
1600 ± 1	SHRESTHA	12A	DPWA	Multichannel
1625 ±10	ANISOVICH	10	DPWA	Multichannel
1650 ±25	THOMA	08	DPWA	Multichannel
1614.1± 1.1	ARNDT	04	DPWA	$\pi N \to \pi N, \eta N$
1612 ± 2	PENNER	02C	DPWA	Multichannel
1617 ±15	VRANA	00	DPWA	Multichannel
1672 ± 5	ARNDT	96	IPWA	$\gamma N \to \pi N$
1617	ARNDT	95	DPWA	$\pi N \to N\pi$
1669	LI	93	IPWA	$\gamma N \to \pi N$
1672 ± 7	MANLEY	92	IPWA	$\pi N \to \pi N$ & $N\pi\pi$
1620	BARNHAM	80	IPWA	$\pi N \to N\pi\pi$
1712.8± 6.0	[1] CHEW	80	BPWA	$\pi^+ p \to \pi^+ p$
1786.7± 2.0	[1] CHEW	80	BPWA	$\pi^+ p \to \pi^+ p$
1580	[2] LONGACRE	77	IPWA	$\pi N \to N\pi\pi$
1600	[3] LONGACRE	75	IPWA	$\pi N \to N\pi\pi$

Δ(1620) BREIT-WIGNER WIDTH

VALUE (MeV)	*DOCUMENT ID*		*TECN*	*COMMENT*
130 to 150 (≈ 140) OUR ESTIMATE				
130 ±11	ANISOVICH	12A	DPWA	Multichannel
146.9± 1.9	ARNDT	06	DPWA	$\pi N \to \pi N, \eta N$
140 ±20	CUTKOSKY	80	IPWA	$\pi N \to \pi N$
139 ±18	HOEHLER	79	IPWA	$\pi N \to \pi N$
• • • We do not use the following data for averages, fits, limits, etc. • • •				
112 ± 2	SHRESTHA	12A	DPWA	Multichannel
148 ±15	ANISOVICH	10	DPWA	Multichannel
250 ±60	THOMA	08	DPWA	Multichannel
141.0± 6.0	ARNDT	04	DPWA	$\pi N \to \pi N, \eta N$
202 ± 7	PENNER	02C	DPWA	Multichannel
143 ±42	VRANA	00	DPWA	Multichannel
147 ± 8	ARNDT	96	IPWA	$\gamma N \to \pi N$
108	ARNDT	95	DPWA	$\pi N \to N\pi$
184	LI	93	IPWA	$\gamma N \to \pi N$
154 ±37	MANLEY	92	IPWA	$\pi N \to \pi N$ & $N\pi\pi$
120	BARNHAM	80	IPWA	$\pi N \to N\pi\pi$
228.3±18.0	[1] CHEW	80	BPWA	$\pi^+ p \to \pi^+ p$ (lower mass)
30.0± 6.4	[1] CHEW	80	BPWA	$\pi^+ p \to \pi^+ p$ (higher mass)
120	[2] LONGACRE	77	IPWA	$\pi N \to N\pi\pi$
150	[3] LONGACRE	75	IPWA	$\pi N \to N\pi\pi$

Δ(1620) POLE POSITION

REAL PART

VALUE (MeV)	*DOCUMENT ID*		*TECN*	*COMMENT*
1590 to 1610 (≈ 1600) OUR ESTIMATE				
1597± 4	ANISOVICH	12A	DPWA	Multichannel
1595	ARNDT	06	DPWA	$\pi N \to \pi N, \eta N$
1608	[4] HOEHLER	93	SPED	$\pi N \to \pi N$
1600±15	CUTKOSKY	80	IPWA	$\pi N \to \pi N$
• • • We do not use the following data for averages, fits, limits, etc. • • •				
1587	SHRESTHA	12A	DPWA	Multichannel
1596± 7	ANISOVICH	10	DPWA	Multichannel
1615±25	THOMA	08	DPWA	Multichannel
1594	ARNDT	04	DPWA	$\pi N \to \pi N, \eta N$
1607	VRANA	00	DPWA	Multichannel
1585	ARNDT	95	DPWA	$\pi N \to N\pi$
1587	ARNDT	91	DPWA	$\pi N \to \pi N$ Soln SM90
1583 or 1583	[5] LONGACRE	78	IPWA	$\pi N \to N\pi\pi$
1575 or 1572	[2] LONGACRE	77	IPWA	$\pi N \to N\pi\pi$

−2×IMAGINARY PART

VALUE (MeV)	*DOCUMENT ID*		*TECN*	*COMMENT*
120 to 140 (≈ 130) OUR ESTIMATE				
130± 9	ANISOVICH	12A	DPWA	Multichannel
135	ARNDT	06	DPWA	$\pi N \to \pi N, \eta N$
116	[4] HOEHLER	93	SPED	$\pi N \to \pi N$
120±20	CUTKOSKY	80	IPWA	$\pi N \to \pi N$
• • • We do not use the following data for averages, fits, limits, etc. • • •				
107	SHRESTHA	12A	DPWA	Multichannel
130±10	ANISOVICH	10	DPWA	Multichannel
180±35	THOMA	08	DPWA	Multichannel
118	ARNDT	04	DPWA	$\pi N \to \pi N, \eta N$
148	VRANA	00	DPWA	Multichannel
104	ARNDT	95	DPWA	$\pi N \to N\pi$
120	ARNDT	91	DPWA	$\pi N \to \pi N$ Soln SM90
143 or 149	[5] LONGACRE	78	IPWA	$\pi N \to N\pi\pi$
119 or 128	[2] LONGACRE	77	IPWA	$\pi N \to N\pi\pi$

Δ(1620) ELASTIC POLE RESIDUE

MODULUS |r|

VALUE (MeV)	*DOCUMENT ID*		*TECN*	*COMMENT*
18±2	ANISOVICH	12A	DPWA	Multichannel
15	ARNDT	06	DPWA	$\pi N \to \pi N, \eta N$
19	HOEHLER	93	SPED	$\pi N \to \pi N$
15±2	CUTKOSKY	80	IPWA	$\pi N \to \pi N$
• • • We do not use the following data for averages, fits, limits, etc. • • •				
17	ARNDT	04	DPWA	$\pi N \to \pi N, \eta N$
14	ARNDT	95	DPWA	$\pi N \to N\pi$
15	ARNDT	91	DPWA	$\pi N \to \pi N$ Soln SM90

PHASE θ

VALUE (°)	*DOCUMENT ID*		*TECN*	*COMMENT*
−100± 5	ANISOVICH	12A	DPWA	Multichannel
− 92	ARNDT	06	DPWA	$\pi N \to \pi N, \eta N$
− 95	HOEHLER	93	SPED	$\pi N \to \pi N$
−110±20	CUTKOSKY	80	IPWA	$\pi N \to \pi N$
• • • We do not use the following data for averages, fits, limits, etc. • • •				
−104	ARNDT	04	DPWA	$\pi N \to \pi N, \eta N$
−121	ARNDT	95	DPWA	$\pi N \to N\pi$
−125	ARNDT	91	DPWA	$\pi N \to \pi N$ Soln SM90

Δ(1620) INELASTIC POLE RESIDUE

The "normalized residue" is the residue divided by $\Gamma_{pole}/2$.

Normalized residue in $N\pi \to \Delta(1620) \to \Delta\pi$, D-wave

MODULUS (%)	*PHASE* (°)	*DOCUMENT ID*		*TECN*	*COMMENT*
38±9	**−85 ± 30**	ANISOVICH	12A	DPWA	Multichannel

$\Delta(1620)$ DECAY MODES

The following branching fractions are our estimates, not fits or averages.

	Mode	Fraction (Γ_i/Γ)
Γ_1	$N\pi$	20–30 %
Γ_2	$N\pi\pi$	70–80 %
Γ_3	$\Delta\pi$	30–60 %
Γ_4	$\Delta(1232)\pi$, D-wave	
Γ_5	$N\rho$	7–25 %
Γ_6	$N\rho$, S=1/2, S-wave	
Γ_7	$N\rho$, S=3/2, D-wave	
Γ_8	$N(1440)\pi$	
Γ_9	$N\gamma$	0.03–0.10 %
Γ_{10}	$N\gamma$, helicity=1/2	0.03–0.10 %

$\Delta(1620)$ BRANCHING RATIOS

$\Gamma(N\pi)/\Gamma_{\text{total}}$ Γ_1/Γ

VALUE (%)	DOCUMENT ID		TECN	COMMENT
20 to 30 OUR ESTIMATE				
28 ± 3	ANISOVICH	12A	DPWA	Multichannel
31.5 ± 0.1	ARNDT	06	DPWA	$\pi N \to \pi N$, ηN
25 ± 3	CUTKOSKY	80	IPWA	$\pi N \to \pi N$
35 ± 6	HOEHLER	79	IPWA	$\pi N \to \pi N$
• • • We do not use the following data for averages, fits, limits, etc. • • •				
33 ± 2	SHRESTHA	12A	DPWA	Multichannel
23 ± 5	ANISOVICH	10	DPWA	Multichannel
22 ±12	THOMA	08	DPWA	Multichannel
31.0 ± 0.4	ARNDT	04	DPWA	$\pi N \to \pi N$, ηN
34 ± 1	PENNER	02C	DPWA	Multichannel
45 ± 5	VRANA	00	DPWA	Multichannel
29	ARNDT	95	DPWA	$\pi N \to N\pi$
9 ± 2	MANLEY	92	IPWA	$\pi N \to \pi N$ & $N\pi\pi$
60	[1] CHEW	80	BPWA	$\pi^+ p \to \pi^+ p$ (lower mass)
36	[1] CHEW	80	BPWA	$\pi^+ p \to \pi^+ p$ (higher mass)

Note: Signs of couplings from $\pi N \to N\pi\pi$ analyses were changed in the 1986 edition to agree with the baryon-first convention; the overall phase ambiguity is resolved by choosing a negative sign for the $\Delta(1620)$ S_{31} coupling to $\Delta(1232)\pi$.

$(\Gamma_i\Gamma_f)^{1/2}/\Gamma_{\text{total}}$ in $N\pi \to \Delta(1620) \to \Delta(1232)\pi$, D-wave $(\Gamma_1\Gamma_4)^{1/2}/\Gamma$

VALUE	DOCUMENT ID		TECN	COMMENT
−0.36 to −0.28 OUR ESTIMATE				
−0.33 ± 0.06	BARNHAM	80	IPWA	$\pi N \to N\pi\pi$
−0.39	[2,6] LONGACRE	77	IPWA	$\pi N \to N\pi\pi$
−0.40	[3] LONGACRE	75	IPWA	$\pi N \to N\pi\pi$
• • • We do not use the following data for averages, fits, limits, etc. • • •				
−0.24 ± 0.03	MANLEY	92	IPWA	$\pi N \to \pi N$ & $N\pi\pi$

$\Gamma(\Delta(1232)\pi$, D-wave$)/\Gamma_{\text{total}}$ Γ_4/Γ

VALUE (%)	DOCUMENT ID		TECN	COMMENT
60 ± 17	ANISOVICH	12A	DPWA	Multichannel
39 ± 2	VRANA	00	DPWA	Multichannel
• • • We do not use the following data for averages, fits, limits, etc. • • •				
32 ± 2	SHRESTHA	12A	DPWA	Multichannel
48 ±25	THOMA	08	DPWA	Multichannel

$(\Gamma_i\Gamma_f)^{1/2}/\Gamma_{\text{total}}$ in $N\pi \to \Delta(1620) \to N\rho$, S=1/2, S-wave $(\Gamma_1\Gamma_6)^{1/2}/\Gamma$

VALUE	DOCUMENT ID		TECN	COMMENT
+0.12 to +0.22 OUR ESTIMATE				
+0.40 ± 0.10	BARNHAM	80	IPWA	$\pi N \to N\pi\pi$
+0.08	[2,6] LONGACRE	77	IPWA	$\pi N \to N\pi\pi$
+0.28	[3] LONGACRE	75	IPWA	$\pi N \to N\pi\pi$
• • • We do not use the following data for averages, fits, limits, etc. • • •				
+0.15 ± 0.02	MANLEY	92	IPWA	$\pi N \to \pi N$ & $N\pi\pi$

$\Gamma(N\rho$, S=1/2, S-wave$)/\Gamma_{\text{total}}$ Γ_6/Γ

VALUE (%)	DOCUMENT ID		TECN	COMMENT
14 ± 3	VRANA	00	DPWA	Multichannel
• • • We do not use the following data for averages, fits, limits, etc. • • •				
26 ± 2	SHRESTHA	12A	DPWA	Multichannel

$(\Gamma_i\Gamma_f)^{1/2}/\Gamma_{\text{total}}$ in $N\pi \to \Delta(1620) \to N\rho$, S=3/2, D-wave $(\Gamma_1\Gamma_7)^{1/2}/\Gamma$

VALUE	DOCUMENT ID		TECN	COMMENT
−0.15 to −0.03 OUR ESTIMATE				
−0.13	[2,6] LONGACRE	77	IPWA	$\pi N \to N\pi\pi$
• • • We do not use the following data for averages, fits, limits, etc. • • •				
−0.03 ± 0.01	SHRESTHA	12A	DPWA	Multichannel
−0.06 ± 0.02	MANLEY	92	IPWA	$\pi N \to \pi N$ & $N\pi\pi$

$\Gamma(N\rho$, S=3/2, D-wave$)/\Gamma_{\text{total}}$ Γ_7/Γ

VALUE (%)	DOCUMENT ID		TECN	COMMENT
2 ± 1	VRANA	00	DPWA	Multichannel

$(\Gamma_i\Gamma_f)^{1/2}/\Gamma_{\text{total}}$ in $N\pi \to \Delta(1620) \to N(1440)\pi$ $(\Gamma_1\Gamma_8)^{1/2}/\Gamma$

VALUE	DOCUMENT ID		TECN	COMMENT
0.11 ± 0.05	BARNHAM	80	IPWA	$\pi N \to N\pi\pi$

$\Gamma(N(1440)\pi)/\Gamma_{\text{total}}$ Γ_8/Γ

VALUE (%)	DOCUMENT ID		TECN	COMMENT
0 ± 1	VRANA	00	DPWA	Multichannel
• • • We do not use the following data for averages, fits, limits, etc. • • •				
9 ± 1	SHRESTHA	12A	DPWA	Multichannel
19 ±12	THOMA	08	DPWA	Multichannel

$\Delta(1620)$ PHOTON DECAY AMPLITUDES

Papers on γN amplitudes predating 1981 may be found in our 2006 edition, Journal of Physics (generic for all A,B,E,G) **G33** 1 (2006).

$\Delta(1620) \to N\gamma$, helicity-1/2 amplitude $A_{1/2}$

VALUE (GeV$^{-1/2}$)	DOCUMENT ID		TECN	COMMENT
+0.040 ± 0.015 OUR ESTIMATE				
0.052 ± 0.005	ANISOVICH	12A	DPWA	Multichannel
0.029 ± 0.003	WORKMAN	12A	DPWA	$\gamma N \to N\pi$
0.050 ± 0.002	DUGGER	07	DPWA	$\gamma N \to \pi N$
0.035 ± 0.010	CRAWFORD	83	IPWA	$\gamma N \to \pi N$
0.010 ± 0.015	AWAJI	81	DPWA	$\gamma N \to \pi N$
• • • We do not use the following data for averages, fits, limits, etc. • • •				
−0.003 ± 0.003	SHRESTHA	12A	DPWA	Multichannel
0.063 ± 0.012	ANISOVICH	10	DPWA	Multichannel
0.066	DRECHSEL	07	DPWA	$\gamma N \to \pi N$
−0.050	PENNER	02D	DPWA	Multichannel
0.035 ± 0.020	ARNDT	96	IPWA	$\gamma N \to \pi N$
0.042 ± 0.003	LI	93	IPWA	$\gamma N \to \pi N$
0.066	WADA	84	DPWA	Compton scattering

$\Delta(1620)$ FOOTNOTES

[1] CHEW 80 reports two S_{31} resonances at somewhat higher masses than other analyses. Problems with this analysis are discussed in section 2.1.11 of HOEHLER 83.

[2] LONGACRE 77 pole positions are from a search for poles in the unitarized T-matrix; the first (second) value uses, in addition to $\pi N \to N\pi\pi$ data, elastic amplitudes from a Saclay (CERN) partial-wave analysis. The other LONGACRE 77 values are from eyeball fits with Breit-Wigner circles to the T-matrix amplitudes.

[3] From method II of LONGACRE 75: eyeball fits with Breit-Wigner circles to the T-matrix amplitudes.

[4] See HOEHLER 93 for a detailed discussion of the evidence for and the pole parameters of N and Δ resonances as determined from Argand diagrams of πN elastic partial-wave amplitudes and from plots of the speeds with which the amplitudes traverse the diagrams.

[5] LONGACRE 78 values are from a search for poles in the unitarized T-matrix. The first (second) value uses, in addition to $\pi N \to N\pi\pi$ data, elastic amplitudes from a Saclay (CERN) partial-wave analysis.

[6] LONGACRE 77 considers this coupling to be well determined.

$\Delta(1620)$ REFERENCES

For early references, see Physics Letters **111B** 1 (1982).

ANISOVICH	12A	EPJ A48 15	A.V. Anisovich *et al.*	(BONN, PNPI)
SHRESTHA	12A	PR C86 055203	M. Shrestha, D.M. Manley	(KSU)
WORKMAN	12A	PR C86 015202	R. Workman *et al.*	(GWU)
ANISOVICH	10	EPJ A44 203	A.V. Anisovich *et al.*	(BONN, PNPI)
THOMA	08	PL B659 87	U. Thoma *et al.*	(CB-ELSA Collab.)
DRECHSEL	07	EPJ A34 69	D. Drechsel, S.S. Kamalov, L. Tiator	(MAINZ, JINR)
DUGGER	07	PR C76 025211	M. Dugger *et al.*	(Jefferson Lab CLAS Collab.)
ARNDT	06	PR C74 045205	R.A. Arndt *et al.*	(GWU)
PDG	06	JP G33 1	W.-M. Yao *et al.*	(PDG Collab.)
ARNDT	04	PR C69 035213	R.A. Arndt *et al.*	(GWU, TRIU)
PENNER	02C	PR C66 055211	G. Penner, U. Mosel	(GIES)
PENNER	02D	PR C66 055212	G. Penner, U. Mosel	(GIES)
VRANA	00	PRPL 328 181	T.P. Vrana, S.A. Dytman,, T.-S.H. Lee	(PITT+)
ARNDT	96	PR C53 430	R.A. Arndt, I.I. Strakovsky, R.L. Workman	(VPI)
ARNDT	95	PR C52 2120	R.A. Arndt *et al.*	(VPI, BRCO)
HOEHLER	93	πN Newsletter 9 1	G. Hohler	(KARL)
LI	93	PR C47 2759	Z.J. Li *et al.*	(VPI)
MANLEY	92	PR D45 4002	D.M. Manley, E.M. Saleski	(KSA) IJP
Also		PR D30 904	D.M. Manley *et al.*	(VPI)
ARNDT	91	PR D43 2131	R.A. Arndt *et al.*	(VPI, TELE) IJP
WADA	84	NP B247 313	Y. Wada *et al.*	(INUS)
CRAWFORD	83	NP B211 1	R.L. Crawford, W.T. Morton	(GLAS)
HOEHLER	83	Landolt-Boernstein 1/9B2	G. Hohler	(KARLT)
PDG	82	PL 111B 1	M. Roos *et al.*	(HELS, CIT, CERN)
AWAJI	81	Bonn Conf. 352	N. Awaji, R. Kajikawa	(NAGO)
Also		NP B197 365	K. Fujii *et al.*	(NAGO)
BARNHAM	80	NP B168 243	K.W.J. Barnham *et al.*	(LOIC)
CHEW	80	Toronto Conf. 123	D.M. Chew	(LBL) IJP
CUTKOSKY	80	Toronto Conf. 19	R.E. Cutkosky *et al.*	(CMU, LBL) IJP
Also		PR D20 2839	R.E. Cutkosky *et al.*	(CMU, LBL) IJP
HOEHLER	79	PDAT 12-1	G. Hohler *et al.*	(KARLT) IJP
Also		Toronto Conf. 3	R. Koch	(KARLT) IJP
LONGACRE	78	PR D17 1795	R.S. Longacre *et al.*	(LBL, SLAC)
LONGACRE	77	NP B122 493	R.S. Longacre, J. Dolbeau	(SACL) IJP
Also		NP B108 365	J. Dolbeau *et al.*	(SACL) IJP
LONGACRE	75	PL 55B 415	R.S. Longacre *et al.*	(LBL, SLAC) IJP

Δ(1700) 3/2⁻

$I(J^P) = \frac{3}{2}(\frac{3}{2}^-)$ Status: ****

Most of the results published before 1975 were last included in our 1982 edition, Physics Letters **111B** 1 (1982). Some further obsolete results published before 1984 were last included in our 2006 edition, Journal of Physics (generic for all A,B,E,G) **G33** 1 (2006).

Δ(1700) BREIT-WIGNER MASS

VALUE (MeV)	DOCUMENT ID		TECN	COMMENT
1670 to 1750 (≈ 1700) OUR ESTIMATE				
1715^{+30}_{-15}	ANISOVICH	12A	DPWA	Multichannel
1695.0 ± 1.3	ARNDT	06	DPWA	$\pi N \to \pi N, \eta N$
1710 ±30	CUTKOSKY	80	IPWA	$\pi N \to \pi N$
1680 ±70	HOEHLER	79	IPWA	$\pi N \to \pi N$
• • • We do not use the following data for averages, fits, limits, etc. • • •				
1691 ± 4	SHRESTHA	12A	DPWA	Multichannel
1780 ±40	ANISOVICH	10	DPWA	Multichannel
1790 ±30	HORN	08A	DPWA	Multichannel
1770 ±40	THOMA	08	DPWA	Multichannel
1687.9 ± 2.5	ARNDT	04	DPWA	$\pi N \to \pi N, \eta N$
1678 ± 1	PENNER	02C	DPWA	Multichannel
1732 ±23	VRANA	00	DPWA	Multichannel
1690 ±15	ARNDT	96	IPWA	$\gamma N \to \pi N$
1680	ARNDT	95	DPWA	$\pi N \to N\pi$
1655	LI	93	IPWA	$\gamma N \to \pi N$
1762 ±44	MANLEY	92	IPWA	$\pi N \to \pi N$ & $N\pi\pi$
1650	BARNHAM	80	IPWA	$\pi N \to N\pi\pi$
$1718.4^{+13.1}_{-13.0}$	[1] CHEW	80	BPWA	$\pi^+ p \to \pi^+ p$
1600	[2] LONGACRE	77	IPWA	$\pi N \to N\pi\pi$
1680	[3] LONGACRE	75	IPWA	$\pi N \to N\pi\pi$

Δ(1700) BREIT-WIGNER WIDTH

VALUE (MeV)	DOCUMENT ID		TECN	COMMENT
200 to 400 (≈ 300) OUR ESTIMATE				
310^{+40}_{-15}	ANISOVICH	12A	DPWA	Multichannel
375.5 ± 7.0	ARNDT	06	DPWA	$\pi N \to \pi N, \eta N$
280 ± 80	CUTKOSKY	80	IPWA	$\pi N \to \pi N$
230 ± 80	HOEHLER	79	IPWA	$\pi N \to \pi N$
• • • We do not use the following data for averages, fits, limits, etc. • • •				
248 ± 9	SHRESTHA	12A	DPWA	Multichannel
580 ±120	ANISOVICH	10	DPWA	Multichannel
580 ± 60	HORN	08A	DPWA	Multichannel
630 ±150	THOMA	08	DPWA	Multichannel
364.8 ± 16.6	ARNDT	04	DPWA	$\pi N \to \pi N, \eta N$
606 ± 15	PENNER	02C	DPWA	Multichannel
119 ± 70	VRANA	00	DPWA	Multichannel
285 ± 20	ARNDT	96	IPWA	$\gamma N \to \pi N$
272	ARNDT	95	DPWA	$\pi N \to N\pi$
348	LI	93	IPWA	$\gamma N \to \pi N$
600 ±250	MANLEY	92	IPWA	$\pi N \to \pi N$ & $N\pi\pi$
160	BARNHAM	80	IPWA	$\pi N \to N\pi\pi$
193.3 ± 26.0	[1] CHEW	80	BPWA	$\pi^+ p \to \pi^+ p$
200	[2] LONGACRE	77	IPWA	$\pi N \to N\pi\pi$
240	[3] LONGACRE	75	IPWA	$\pi N \to N\pi\pi$

Δ(1700) POLE POSITION

REAL PART

VALUE (MeV)	DOCUMENT ID		TECN	COMMENT
1620 to 1680 (≈ 1650) OUR ESTIMATE				
1680 ± 10	ANISOVICH	12A	DPWA	Multichannel
1632	ARNDT	06	DPWA	$\pi N \to \pi N, \eta N$
1651	[4] HOEHLER	93	SPED	$\pi N \to \pi N$
1675 ± 25	CUTKOSKY	80	IPWA	$\pi N \to \pi N$
• • • We do not use the following data for averages, fits, limits, etc. • • •				
1656	SHRESTHA	12A	DPWA	Multichannel
1650 ± 30	ANISOVICH	10	DPWA	Multichannel
1640 ± 25	HORN	08A	DPWA	Multichannel
1610 ± 35	THOMA	08	DPWA	Multichannel
1617	ARNDT	04	DPWA	$\pi N \to \pi N, \eta N$
1726	VRANA	00	DPWA	Multichannel
1655	ARNDT	95	DPWA	$\pi N \to N\pi$
1646	ARNDT	91	DPWA	$\pi N \to \pi N$ Soln SM90
1681 or 1672	[5] LONGACRE	78	IPWA	$\pi N \to N\pi\pi$
1600 or 1594	[2] LONGACRE	77	IPWA	$\pi N \to N\pi\pi$

−2×IMAGINARY PART

VALUE (MeV)	DOCUMENT ID		TECN	COMMENT
160 to 300 (≈ 230) OUR ESTIMATE				
305 ± 15	ANISOVICH	12A	DPWA	Multichannel
253	ARNDT	06	DPWA	$\pi N \to \pi N, \eta N$
159	[4] HOEHLER	93	SPED	$\pi N \to \pi N$
220 ± 40	CUTKOSKY	80	IPWA	$\pi N \to \pi N$
• • • We do not use the following data for averages, fits, limits, etc. • • •				
226	SHRESTHA	12A	DPWA	Multichannel
275 ± 35	ANISOVICH	10	DPWA	Multichannel
325 ± 35	HORN	08A	DPWA	Multichannel
320 ± 60	THOMA	08	DPWA	Multichannel
226	ARNDT	04	DPWA	$\pi N \to \pi N, \eta N$
118	VRANA	00	DPWA	Multichannel
242	ARNDT	95	DPWA	$\pi N \to N\pi$
208	ARNDT	91	DPWA	$\pi N \to \pi N$ Soln SM90
245 or 241	[5] LONGACRE	78	IPWA	$\pi N \to N\pi\pi$
208 or 201	[2] LONGACRE	77	IPWA	$\pi N \to N\pi\pi$

Δ(1700) ELASTIC POLE RESIDUE

MODULUS |r|

VALUE (MeV)	DOCUMENT ID		TECN	COMMENT
42 ± 7	ANISOVICH	12A	DPWA	Multichannel
18	ARNDT	06	DPWA	$\pi N \to \pi N, \eta N$
10	HOEHLER	93	SPED	$\pi N \to \pi N$
13 ± 3	CUTKOSKY	80	IPWA	$\pi N \to \pi N$
• • • We do not use the following data for averages, fits, limits, etc. • • •				
16	ARNDT	04	DPWA	$\pi N \to \pi N, \eta N$
16	ARNDT	95	DPWA	$\pi N \to N\pi$
13	ARNDT	91	DPWA	$\pi N \to \pi N$ Soln SM90

PHASE θ

VALUE (°)	DOCUMENT ID		TECN	COMMENT
− 3 ± 15	ANISOVICH	12A	DPWA	Multichannel
−40	ARNDT	06	DPWA	$\pi N \to \pi N, \eta N$
−20 ± 25	CUTKOSKY	80	IPWA	$\pi N \to \pi N$
• • • We do not use the following data for averages, fits, limits, etc. • • •				
−47	ARNDT	04	DPWA	$\pi N \to \pi N, \eta N$
−12	ARNDT	95	DPWA	$\pi N \to N\pi$
−22	ARNDT	91	DPWA	$\pi N \to \pi N$ Soln SM90

Δ(1700) INELASTIC POLE RESIDUE

The "normalized residue" is the residue divided by $\Gamma_{pole}/2$.

Normalized residue in $N\pi \to \Delta(1700) \to \Delta\eta$

MODULUS (%)	PHASE (°)	DOCUMENT ID		TECN	COMMENT
12 ± 3	**−60 ± 15**	ANISOVICH	12A	DPWA	Multichannel

Δ(1700) DECAY MODES

The following branching fractions are our estimates, not fits or averages.

	Mode	Fraction (Γ_i/Γ)
Γ_1	$N\pi$	10–20 %
Γ_2	ΣK	
Γ_3	$N\pi\pi$	80–90 %
Γ_4	$\Delta\pi$	30–60 %
Γ_5	$\Delta(1232)\pi$, S-wave	25–50 %
Γ_6	$\Delta(1232)\pi$, D-wave	5–15 %
Γ_7	$N\rho$	30–55 %
Γ_8	$N\rho$, S=1/2, D-wave	
Γ_9	$N\rho$, S=3/2, S-wave	5–20 %
Γ_{10}	$N\rho$, S=3/2, D-wave	
Γ_{11}	$N(1535)\pi$	
Γ_{12}	$\Delta(1232)\eta$	(5.0 ± 2.0) %
Γ_{13}	$N\gamma$	0.22–0.60 %
Γ_{14}	$N\gamma$, helicity=1/2	0.12–0.30 %
Γ_{15}	$N\gamma$, helicity=3/2	0.10–0.30 %

Δ(1700) BRANCHING RATIOS

$\Gamma(N\pi)/\Gamma_{total}$ Γ_1/Γ

VALUE (%)	DOCUMENT ID		TECN	COMMENT
10 to 20 OUR ESTIMATE				
22 ±4	ANISOVICH	12A	DPWA	Multichannel
15.6 ± 0.1	ARNDT	06	DPWA	$\pi N \to \pi N, \eta N$
12 ±3	CUTKOSKY	80	IPWA	$\pi N \to \pi N$
20 ±3	HOEHLER	79	IPWA	$\pi N \to \pi N$

• • • We do not use the following data for averages, fits, limits, etc. • • •

14 ±1		SHRESTHA	12A	DPWA	Multichannel
16 ±7		ANISOVICH	10	DPWA	Multichannel
20 ±7		HORN	08A	DPWA	Multichannel
15 ±8		THOMA	08	DPWA	Multichannel
15.0±0.1		ARNDT	04	DPWA	$\pi N \to \pi N, \eta N$
14 ±1		PENNER	02C	DPWA	Multichannel
5 ±1		VRANA	00	DPWA	Multichannel
16		ARNDT	95	DPWA	$\pi N \to N\pi$
14 ±6		MANLEY	92	IPWA	$\pi N \to \pi N$ & $N\pi\pi$
16	[1]	CHEW	80	BPWA	$\pi^+ p \to \pi^+ p$

Note: Signs of couplings from $\pi N \to N\pi\pi$ analyses were changed in the 1986 edition to agree with the baryon-first convention; the overall phase ambiguity is resolved by choosing a negative sign for the Δ(1620) S_{31} coupling to Δ(1232)π.

$(\Gamma_i\Gamma_f)^{1/2}/\Gamma_{total}$ in $N\pi \to \Delta(1700) \to \Delta(1232)\pi$, S-wave $(\Gamma_1\Gamma_5)^{1/2}/\Gamma$

VALUE	DOCUMENT ID		TECN	COMMENT
+0.21 to +0.29 OUR ESTIMATE				
+0.18±0.04	BARNHAM	80	IPWA	$\pi N \to N\pi\pi$
+0.30	[2,6] LONGACRE	77	IPWA	$\pi N \to N\pi\pi$
+0.24	[3] LONGACRE	75	IPWA	$\pi N \to N\pi\pi$
• • • We do not use the following data for averages, fits, limits, etc. • • •				
+0.32±0.06	MANLEY	92	IPWA	$\pi N \to \pi N$ & $N\pi\pi$

$\Gamma(\Delta(1232)\pi$, S-wave$)/\Gamma_{total}$ Γ_5/Γ

VALUE (%)	DOCUMENT ID		TECN	COMMENT
20^{+25}_{-13}	ANISOVICH	12A	DPWA	Multichannel
90± 2	VRANA	00	DPWA	Multichannel
• • • We do not use the following data for averages, fits, limits, etc. • • •				
54± 3	SHRESTHA	12A	DPWA	Multichannel

$(\Gamma_i\Gamma_f)^{1/2}/\Gamma_{total}$ in $N\pi \to \Delta(1700) \to \Delta(1232)\pi$, D-wave $(\Gamma_1\Gamma_6)^{1/2}/\Gamma$

VALUE	DOCUMENT ID		TECN	COMMENT
+0.05 to +0.11 OUR ESTIMATE				
0.14±0.04	BARNHAM	80	IPWA	$\pi N \to N\pi\pi$
+0.05	[2,6] LONGACRE	77	IPWA	$\pi N \to N\pi\pi$
+0.10	[3] LONGACRE	75	IPWA	$\pi N \to N\pi\pi$
• • • We do not use the following data for averages, fits, limits, etc. • • •				
+0.08±0.03	MANLEY	92	IPWA	$\pi N \to \pi N$ & $N\pi\pi$

$\Gamma(\Delta(1232)\pi$, D-wave$)/\Gamma_{total}$ Γ_6/Γ

VALUE (%)	DOCUMENT ID		TECN	COMMENT
5 to 15 OUR ESTIMATE				
12^{+14}_{-7}	ANISOVICH	12A	DPWA	Multichannel
4± 1	VRANA	00	DPWA	Multichannel
• • • We do not use the following data for averages, fits, limits, etc. • • •				
1± 1	SHRESTHA	12A	DPWA	Multichannel

$(\Gamma_i\Gamma_f)^{1/2}/\Gamma_{total}$ in $N\pi \to \Delta(1700) \to N\rho$, S=1/2, D-wave $(\Gamma_1\Gamma_8)^{1/2}/\Gamma$

VALUE	DOCUMENT ID		TECN	COMMENT
+0.17±0.05	BARNHAM	80	IPWA	$\pi N \to N\pi\pi$

$(\Gamma_i\Gamma_f)^{1/2}/\Gamma_{total}$ in $N\pi \to \Delta(1700) \to N\rho$, S=3/2, S-wave $(\Gamma_1\Gamma_9)^{1/2}/\Gamma$

VALUE	DOCUMENT ID		TECN	COMMENT
±0.11 to ±0.19 OUR ESTIMATE				
+0.04	[2,6] LONGACRE	77	IPWA	$\pi N \to N\pi\pi$
−0.30	[3] LONGACRE	75	IPWA	$\pi N \to N\pi\pi$
• • • We do not use the following data for averages, fits, limits, etc. • • •				
+0.10±0.03	MANLEY	92	IPWA	$\pi N \to \pi N$ & $N\pi\pi$

$\Gamma(N\rho$, S=3/2, S-wave$)/\Gamma_{total}$ Γ_9/Γ

VALUE (%)	DOCUMENT ID		TECN	COMMENT
1±1	VRANA	00	DPWA	Multichannel
• • • We do not use the following data for averages, fits, limits, etc. • • •				
30±3	SHRESTHA	12A	DPWA	Multichannel

$(\Gamma_i\Gamma_f)^{1/2}/\Gamma_{total}$ in $N\pi \to \Delta(1700) \to N\rho$, S=3/2, D-wave $(\Gamma_1\Gamma_{10})^{1/2}/\Gamma$

VALUE	DOCUMENT ID		TECN	COMMENT
0.18±0.07	BARNHAM	80	IPWA	$\pi N \to N\pi\pi$

$\Gamma(N(1535)\pi)/\Gamma_{total}$ Γ_{11}/Γ

VALUE (%)	DOCUMENT ID		TECN	COMMENT
• • • We do not use the following data for averages, fits, limits, etc. • • •				
4±2	HORN	08A	DPWA	Multichannel

$\Gamma(\Delta(1232)\eta)/\Gamma_{total}$ Γ_{12}/Γ

VALUE (%)	DOCUMENT ID		TECN	COMMENT
5±2	ANISOVICH	12A	DPWA	Multichannel
• • • We do not use the following data for averages, fits, limits, etc. • • •				
2±1	HORN	08A	DPWA	Multichannel

$\Gamma(N(1535)\pi)/\Gamma(\Delta(1232)\eta)$ Γ_{11}/Γ_{12}

VALUE	DOCUMENT ID		TECN	COMMENT
• • • We do not use the following data for averages, fits, limits, etc. • • •				
0.67	KASHEVAROV	09	CBAL	$\gamma p \to p\pi^0\eta$

Δ(1700) PHOTON DECAY AMPLITUDES

Papers on γN amplitudes predating 1981 may be found in our 2006 edition, Journal of Physics (generic for all A,B,E,G) **G33** 1 (2006).

Δ(1700) → Nγ, helicity-1/2 amplitude $A_{1/2}$

VALUE ($GeV^{-1/2}$)	DOCUMENT ID		TECN	COMMENT
0.140±0.030 OUR ESTIMATE				
0.132±0.005	DUGGER	13	DPWA	$\gamma N \to \pi N$
0.160±0.020	ANISOVICH	12A	DPWA	Multichannel
0.105±0.005	WORKMAN	12A	DPWA	$\gamma N \to \pi N$
0.125±0.003	DUGGER	07	DPWA	$\gamma N \to \pi N$
0.111±0.017	CRAWFORD	83	IPWA	$\gamma N \to \pi N$
0.089±0.033	AWAJI	81	DPWA	$\gamma N \to \pi N$
• • • We do not use the following data for averages, fits, limits, etc. • • •				
0.058±0.010	SHRESTHA	12A	DPWA	Multichannel
0.160±0.045	ANISOVICH	10	DPWA	Multichannel
0.160±0.040	HORN	08A	DPWA	Multichannel
0.226	DRECHSEL	07	DPWA	$\gamma N \to \pi N$
0.096	PENNER	02D	DPWA	Multichannel
0.090±0.025	ARNDT	96	IPWA	$\gamma N \to \pi N$
0.121±0.004	LI	93	IPWA	$\gamma N \to \pi N$

Δ(1700) → Nγ, helicity-3/2 amplitude $A_{3/2}$

VALUE ($GeV^{-1/2}$)	DOCUMENT ID		TECN	COMMENT
0.140±0.030 OUR ESTIMATE				
0.108±0.005	DUGGER	13	DPWA	$\gamma N \to \pi N$
0.165±0.025	ANISOVICH	12A	DPWA	Multichannel
0.092±0.004	WORKMAN	12A	DPWA	$\gamma N \to \pi N$
0.105±0.003	DUGGER	07	DPWA	$\gamma N \to \pi N$
0.107±0.015	CRAWFORD	83	IPWA	$\gamma N \to \pi N$
0.060±0.015	AWAJI	81	DPWA	$\gamma N \to \pi N$
• • • We do not use the following data for averages, fits, limits, etc. • • •				
0.097±0.008	SHRESTHA	12A	DPWA	Multichannel
0.160±0.040	ANISOVICH	10	DPWA	Multichannel
0.150±0.030	HORN	08A	DPWA	Multichannel
0.210	DRECHSEL	07	DPWA	$\gamma N \to \pi N$
0.154	PENNER	02D	DPWA	Multichannel
0.097±0.020	ARNDT	96	IPWA	$\gamma N \to \pi N$
0.115±0.004	LI	93	IPWA	$\gamma N \to \pi N$

Δ(1700) FOOTNOTES

[1] Problems with CHEW 80 are discussed in section 2.1.11 of HOEHLER 83.

[2] LONGACRE 77 pole positions are from a search for poles in the unitarized T-matrix; the first (second) value uses, in addition to $\pi N \to N\pi\pi$ data, elastic amplitudes from a Saclay (CERN) partial-wave analysis. The other LONGACRE 77 values are from eyeball fits with Breit-Wigner circles to the T-matrix amplitudes.

[3] From method II of LONGACRE 75: eyeball fits with Breit-Wigner circles to the T-matrix amplitudes.

[4] See HOEHLER 93 for a detailed discussion of the evidence for and the pole parameters of N and Δ resonances as determined from Argand diagrams of πN elastic partial-wave amplitudes and from plots of the speeds with which the amplitudes traverse the diagrams.

[5] LONGACRE 78 values are from a search for poles in the unitarized T-matrix. The first (second) value uses, in addition to $\pi N \to N\pi\pi$ data, elastic amplitudes from a Saclay (CERN) partial-wave analysis.

[6] LONGACRE 77 considers this coupling to be well determined.

Δ(1700) REFERENCES

For early references, see Physics Letters **111B** 1 (1982).

DUGGER	13	PR C88 065203	M. Dugger *et al.*	(CLAS Collab.)
ANISOVICH	12A	EPJ A48 15	A.V. Anisovich *et al.*	(BONN, PNPI)
SHRESTHA	12A	PR C86 055203	M. Shrestha, D.M. Manley	(KSU)
WORKMAN	12A	PR C86 015202	R. Workman *et al.*	(GWU)
ANISOVICH	10	EPJ A44 203	A.V. Anisovich *et al.*	(BONN, PNPI)
KASHEVAROV	09	EPJ A42 141	V.L. Kashevarov *et al.*	(MAMI Crystal Ball/TAPS)
HORN	08A	EPJ A38 173	I. Horn *et al.*	(CB-ELSA Collab.)
Also		PRL 101 202002	I. Horn *et al.*	(CB-ELSA Collab.)
THOMA	08	PL B659 87	U. Thoma *et al.*	(CB-ELSA Collab.)
DRECHSEL	07	EPJ A34 69	D. Drechsel, S.S. Kamalov, L. Tiator	(MAINZ, JINR)
DUGGER	07	PR C76 025211	M. Dugger *et al.*	(Jefferson Lab CLAS Collab.)
ARNDT	06	PR C74 045205	R.A. Arndt *et al.*	(GWU)
PDG	06	JP G33 1	W.-M. Yao *et al.*	(PDG Collab.)
ARNDT	04	PR C69 035213	R.A. Arndt *et al.*	(GWU, TRIU)
PENNER	02C	PR C66 055211	G. Penner, U. Mosel	(GIES)
PENNER	02D	PR C66 055212	G. Penner, U. Mosel	(GIES)
VRANA	00	PRPL 328 181	T.P. Vrana, S.A. Dytman,, T.-S.H. Lee	(PITT+)
ARNDT	96	PR C53 430	R.A. Arndt, I.I. Strakovsky, R.L. Workman	(VPI)
ARNDT	95	PR C52 2120	R.A. Arndt *et al.*	(VPI, BRCO)
HOEHLER	93	πN Newsletter 9 1	G. Hohler	(KARL)
LI	93	PR C47 2759	Z.J. Li *et al.*	(VPI)
MANLEY	92	PR D45 4002	D.M. Manley, E.M. Saleski	(KSA) IJP
Also		PR D30 904	D.M. Manley *et al.*	(VPI)
ARNDT	91	PR D43 2131	R.A. Arndt *et al.*	(VPI, TELE) IJP
CRAWFORD	83	NP B211 1	R.L. Crawford, W.T. Morton	(GLAS)

Baryon Particle Listings

Δ(1700), Δ(1750), Δ(1900)

HOEHLER	83	Landolt-Boernstein 1/9B2	G. Hohler	(KARLT)
PDG	82	PL 111B 1	M. Roos *et al.*	(HELS, CIT, CERN)
AWAJI	81	Bonn Conf. 352	N. Awaji, R. Kajikawa	(NAGO)
Also		NP B197 365	K. Fujii *et al.*	(NAGO)
BARNHAM	80	NP B168 243	K.W.J. Barnham *et al.*	(LOIC)
CHEW	80	Toronto Conf. 123	D.M. Chew	(LBL) IJP
CUTKOSKY	80	Toronto Conf. 19	R.E. Cutkosky *et al.*	(CMU, LBL) IJP
Also		PR D20 2839	R.E. Cutkosky *et al.*	(CMU, LBL) IJP
HOEHLER	79	PDAT 12-1	G. Hohler *et al.*	(KARLT) IJP
Also		Toronto Conf. 3	R. Koch	(KARLT) IJP
LONGACRE	78	PR D17 1795	R.S. Longacre *et al.*	(LBL, SLAC)
LONGACRE	77	NP B122 493	R.S. Longacre, J. Dolbeau	(SACL) IJP
Also		NP B108 365	J. Dolbeau *et al.*	(SACL) IJP
LONGACRE	75	PL 55B 415	R.S. Longacre *et al.*	(LBL, SLAC) IJP

Δ(1750) 1/2+

$I(J^P) = \frac{3}{2}(\frac{1}{2}^+)$ Status: *

OMITTED FROM SUMMARY TABLE

Neither ARNDT 06 nor ANISOVICH 12A finds any evidence for this resonance.

Δ(1750) BREIT-WIGNER MASS

VALUE (MeV)	DOCUMENT ID		TECN	COMMENT
≈ 1750 OUR ESTIMATE				
• • • We do not use the following data for averages, fits, limits, etc. • • •				
1712 ± 1	PENNER	02C	DPWA	Multichannel
1721 ±61	VRANA	00	DPWA	Multichannel
1744 ±36	MANLEY	92	IPWA	$\pi N \to \pi N$ & $N\pi\pi$
1715.2±21.0	[1] CHEW	80	BPWA	$\pi^+ p \to \pi^+ p$
1778.4± 9.0	[1] CHEW	80	BPWA	$\pi^+ p \to \pi^+ p$

Δ(1750) BREIT-WIGNER WIDTH

VALUE (MeV)	DOCUMENT ID		TECN	COMMENT
• • • We do not use the following data for averages, fits, limits, etc. • • •				
643 ± 17	PENNER	02C	DPWA	Multichannel
70 ± 50	VRANA	00	DPWA	Multichannel
300 ±120	MANLEY	92	IPWA	$\pi N \to \pi N$ & $N\pi\pi$
93.3± 55.0	[1] CHEW	80	BPWA	$\pi^+ p \to \pi^+ p$
23.0± 29.0	[1] CHEW	80	BPWA	$\pi^+ p \to \pi^+ p$

Δ(1750) POLE POSITION

REAL PART

VALUE (MeV)	DOCUMENT ID		TECN	COMMENT
1748	[2] ARNDT	04	DPWA	$\pi N \to \pi N, \eta N$
• • • We do not use the following data for averages, fits, limits, etc. • • •				
1714	VRANA	00	DPWA	Multichannel

−2×IMAGINARY PART

VALUE (MeV)	DOCUMENT ID		TECN	COMMENT
524	[2] ARNDT	04	DPWA	$\pi N \to \pi N, \eta N$
• • • We do not use the following data for averages, fits, limits, etc. • • •				
68	VRANA	00	DPWA	Multichannel

Δ(1750) ELASTIC POLE RESIDUE

MODULUS |r|

VALUE (MeV)	DOCUMENT ID		TECN	COMMENT
48	[2] ARNDT	04	DPWA	$\pi N \to \pi N, \eta N$

PHASE θ

VALUE (°)	DOCUMENT ID		TECN	COMMENT
158	[2] ARNDT	04	DPWA	$\pi N \to \pi N, \eta N$

Δ(1750) DECAY MODES

	Mode
Γ_1	$N\pi$
Γ_2	$N\pi\pi$
Γ_3	$N(1440)\pi$
Γ_4	ΣK

Δ(1750) BRANCHING RATIOS

$\Gamma(N\pi)/\Gamma_{total}$ Γ_1/Γ

VALUE (%)	DOCUMENT ID		TECN	COMMENT
• • • We do not use the following data for averages, fits, limits, etc. • • •				
1±1	PENNER	02C	DPWA	Multichannel
6±9	VRANA	00	DPWA	Multichannel
8±3	MANLEY	92	IPWA	$\pi N \to \pi N$ & $N\pi\pi$
18	[1] CHEW	80	BPWA	$\pi^+ p \to \pi^+ p$
20	[1] CHEW	80	BPWA	$\pi^+ p \to \pi^+ p$

$(\Gamma_i\Gamma_f)^{1/2}/\Gamma_{total}$ in $N\pi \to \Delta(1700) \to N(1440)\pi$ $(\Gamma_1\Gamma_3)^{1/2}/\Gamma$

VALUE	DOCUMENT ID		TECN	COMMENT
• • • We do not use the following data for averages, fits, limits, etc. • • •				
+0.15 ±0.03	MANLEY	92	IPWA	$\pi N \to \pi N$ & $N\pi\pi$

$\Gamma(N(1440)\pi)/\Gamma_{total}$ Γ_3/Γ

VALUE (%)	DOCUMENT ID		TECN	COMMENT
83±1	VRANA	00	DPWA	Multichannel

$\Gamma(\Sigma K)/\Gamma_{total}$ Γ_4/Γ

VALUE (%)	DOCUMENT ID		TECN	COMMENT
• • • We do not use the following data for averages, fits, limits, etc. • • •				
0.1±0.1	PENNER	02C	DPWA	Multichannel

Δ(1750) PHOTON DECAY AMPLITUDES

Papers on γN amplitudes predating 1981 may be found in our 2006 edition, Journal of Physics (generic for all A,B,E,G) **G33** 1 (2006).

$\Delta(1750) \to N\gamma$, helicity-1/2 amplitude $A_{1/2}$

VALUE ($GeV^{-1/2}$)	DOCUMENT ID		TECN	COMMENT
• • • We do not use the following data for averages, fits, limits, etc. • • •				
0.053	PENNER	02D	DPWA	Multichannel

Δ(1750) FOOTNOTES

[1] CHEW 80 reports four resonances in the P_{31} wave — see also the Δ(1910). Problems with this analysis are discussed in section 2.1.11 of HOEHLER 83.

[2] ARNDT 04 gives no corresponding Breit-Wigner parameters for this state, because the mass so obtained is about 500 MeV higher than that suggested by the position of the pole.

Δ(1750) REFERENCES

ANISOVICH	12A	EPJ A48 15	A.V. Anisovich *et al.*	(BONN, PNPI)
ARNDT	06	PR C74 045205	R.A. Arndt *et al.*	(GWU)
PDG	06	JP G33 1	W.-M. Yao *et al.*	(PDG Collab.)
ARNDT	04	PR C69 035213	R.A. Arndt *et al.*	(GWU, TRIU)
PENNER	02C	PR C66 055211	G. Penner, U. Mosel	(GIES)
PENNER	02D	PR C66 055212	G. Penner, U. Mosel	(GIES)
VRANA	00	PRPL 328 181	T.P. Vrana, S.A. Dytman,, T.-S.H. Lee	(PITT+)
MANLEY	92	PR D45 4002	D.M. Manley, E.M. Saleski	(KSA)
Also		PR D30 904	D.M. Manley *et al.*	(VPI)
HOEHLER	83	Landolt-Boernstein 1/9B2	G. Hohler	(KARLT)
CHEW	80	Toronto Conf. 123	D.M. Chew	(LBL)

Δ(1900) 1/2−

$I(J^P) = \frac{3}{2}(\frac{1}{2}^-)$ Status: **

OMITTED FROM SUMMARY TABLE

Some obsolete results published before 1980 were last included in our 2006 edition, Journal of Physics (generic for all A,B,E,G) **G33** 1 (2006). Some further obsolete results published before 1984 were last included in our 2006 edition, Journal of Physics (generic for all A,B,E,G) **G33** 1 (2006).

The latest GWU analysis (ARNDT 06) finds no evidence for this resonance.

Δ(1900) BREIT-WIGNER MASS

VALUE (MeV)	DOCUMENT ID		TECN	COMMENT
1840 to 1920 (≈ 1860) OUR ESTIMATE				
1840 ±30	ANISOVICH	12A	DPWA	Multichannel
1890 ±50	CUTKOSKY	80	IPWA	$\pi N \to \pi N$
1908 ±30	HOEHLER	79	IPWA	$\pi N \to \pi N$
• • • We do not use the following data for averages, fits, limits, etc. • • •				
1868 ±12	SHRESTHA	12A	DPWA	Multichannel
1802 ±87	VRANA	00	DPWA	Multichannel
1920 ±24	MANLEY	92	IPWA	$\pi N \to \pi N$ & $N\pi\pi$
1918.5±23.0	CHEW	80	BPWA	$\pi^+ p \to \pi^+ p$

Δ(1900) BREIT-WIGNER WIDTH

VALUE (MeV)	DOCUMENT ID		TECN	COMMENT
300 ±45	ANISOVICH	12A	DPWA	Multichannel
170 ±50	CUTKOSKY	80	IPWA	$\pi N \to \pi N$
140 ±40	HOEHLER	79	IPWA	$\pi N \to \pi N$
• • • We do not use the following data for averages, fits, limits, etc. • • •				
234 ±27	SHRESTHA	12A	DPWA	Multichannel
48 ±45	VRANA	00	DPWA	Multichannel
263 ±39	MANLEY	92	IPWA	$\pi N \to \pi N$ & $N\pi\pi$
93.5±54.0	CHEW	80	BPWA	$\pi^+ p \to \pi^+ p$

Δ(1900) POLE POSITION

REAL PART

VALUE (MeV)	DOCUMENT ID		TECN	COMMENT
1845 ± 25	ANISOVICH	12A	DPWA	Multichannel
1780	[1] HOEHLER	93	SPED	$\pi N \to \pi N$
1870 ± 40	CUTKOSKY	80	IPWA	$\pi N \to \pi N$
• • • We do not use the following data for averages, fits, limits, etc. • • •				
1844	SHRESTHA	12A	DPWA	Multichannel
1795	VRANA	00	DPWA	Multichannel
not seen	ARNDT	91	DPWA	$\pi N \to \pi N$ Soln SM90
2029 or 2025	[2] LONGACRE	78	IPWA	$\pi N \to N\pi\pi$

−2×IMAGINARY PART

VALUE (MeV)	DOCUMENT ID		TECN	COMMENT
300 ± 45	ANISOVICH	12A	DPWA	Multichannel
180 ± 50	CUTKOSKY	80	IPWA	$\pi N \to \pi N$
• • • We do not use the following data for averages, fits, limits, etc. • • •				
223	SHRESTHA	12A	DPWA	Multichannel
58	VRANA	00	DPWA	Multichannel
not seen	ARNDT	91	DPWA	$\pi N \to \pi N$ Soln SM90
164 or 163	[2] LONGACRE	78	IPWA	$\pi N \to N\pi\pi$

Δ(1900) ELASTIC POLE RESIDUE

MODULUS |r|

VALUE (MeV)	DOCUMENT ID		TECN	COMMENT
10 ± 3	ANISOVICH	12A	DPWA	Multichannel
10 ± 3	CUTKOSKY	80	IPWA	$\pi N \to \pi N$

PHASE θ

VALUE (°)	DOCUMENT ID		TECN	COMMENT
−125 ± 20	ANISOVICH	12A	DPWA	Multichannel
+ 20 ± 40	CUTKOSKY	80	IPWA	$\pi N \to \pi N$

Δ(1900) INELASTIC POLE RESIDUE

The "normalized residue" is the residue divided by $\Gamma_{pole}/2$.

Normalized residue in $N\pi \to \Delta(1900) \to \Sigma K$

MODULUS (%)	PHASE (°)	DOCUMENT ID		TECN	COMMENT
7 ± 2	−50 ± 30	ANISOVICH	12A	DPWA	Multichannel

Normalized residue in $N\pi \to \Delta(1900) \to \Delta\pi$, D-wave

MODULUS (%)	PHASE (°)	DOCUMENT ID		TECN	COMMENT
12^{+8}_{-5}	110 ± 20	ANISOVICH	12A	DPWA	Multichannel

Δ(1900) DECAY MODES

The following branching fractions are our estimates, not fits or averages.

	Mode	Fraction (Γ_i/Γ)
Γ_1	$N\pi$	10–30 %
Γ_2	ΣK	
Γ_3	$N\pi\pi$	
Γ_4	$\Delta\pi$	
Γ_5	$\Delta(1232)\pi$, D-wave	
Γ_6	$N\rho$	
Γ_7	$N\rho$, S=1/2, S-wave	
Γ_8	$N\rho$, S=3/2, D-wave	
Γ_9	$N(1440)\pi$, S-wave	
Γ_{10}	$N\gamma$, helicity=1/2	

Δ(1900) BRANCHING RATIOS

$\Gamma(N\pi)/\Gamma_{total}$ Γ_1/Γ

VALUE (%)	DOCUMENT ID		TECN	COMMENT
7 ± 3	ANISOVICH	12A	DPWA	Multichannel
10 ± 3	CUTKOSKY	80	IPWA	$\pi N \to \pi N$
8 ± 4	HOEHLER	79	IPWA	$\pi N \to \pi N$
• • • We do not use the following data for averages, fits, limits, etc. • • •				
8 ± 1	SHRESTHA	12A	DPWA	Multichannel
33 ± 10	VRANA	00	DPWA	Multichannel
41 ± 4	MANLEY	92	IPWA	$\pi N \to \pi N$ & $N\pi\pi$
28	CHEW	80	BPWA	$\pi^+ p \to \pi^+ p$

$(\Gamma_i\Gamma_f)^{1/2}/\Gamma_{total}$ in $N\pi \to \Delta(1900) \to \Sigma K$ $(\Gamma_1\Gamma_2)^{1/2}/\Gamma$

VALUE	DOCUMENT ID		TECN	COMMENT
<0.03	CANDLIN	84	DPWA	$\pi^+ p \to \Sigma^+ K^+$

$(\Gamma_i\Gamma_f)^{1/2}/\Gamma_{total}$ in $N\pi \to \Delta(1900) \to \Delta(1232)\pi$, D-wave $(\Gamma_1\Gamma_5)^{1/2}/\Gamma$

VALUE	DOCUMENT ID		TECN	COMMENT
• • • We do not use the following data for averages, fits, limits, etc. • • •				
+0.25 ± 0.07	MANLEY	92	IPWA	$\pi N \to \pi N$ & $N\pi\pi$

$\Gamma(\Delta(1232)\pi$, D-wave$)/\Gamma_{total}$ Γ_5/Γ

VALUE (%)	DOCUMENT ID		TECN	COMMENT
15^{+50}_{-10}	ANISOVICH	12A	DPWA	Multichannel
28 ± 1	VRANA	00	DPWA	Multichannel
• • • We do not use the following data for averages, fits, limits, etc. • • •				
56 ± 6	SHRESTHA	12A	DPWA	Multichannel

$(\Gamma_i\Gamma_f)^{1/2}/\Gamma_{total}$ in $N\pi \to \Delta(1900) \to N\rho$, S=1/2, S-wave $(\Gamma_1\Gamma_7)^{1/2}/\Gamma$

VALUE	DOCUMENT ID		TECN	COMMENT
• • • We do not use the following data for averages, fits, limits, etc. • • •				
−0.14 ± 0.11	MANLEY	92	IPWA	$\pi N \to \pi N$ & $N\pi\pi$

$\Gamma(N\rho$, S=1/2, S-wave$)/\Gamma_{total}$ Γ_7/Γ

VALUE (%)	DOCUMENT ID		TECN	COMMENT
30 ± 2	VRANA	00	DPWA	Multichannel
• • • We do not use the following data for averages, fits, limits, etc. • • •				
12 ± 4	SHRESTHA	12A	DPWA	Multichannel

$(\Gamma_i\Gamma_f)^{1/2}/\Gamma_{total}$ in $N\pi \to \Delta(1900) \to N\rho$, S=3/2, D-wave $(\Gamma_1\Gamma_8)^{1/2}/\Gamma$

VALUE	DOCUMENT ID		TECN	COMMENT
• • • We do not use the following data for averages, fits, limits, etc. • • •				
−0.37 ± 0.07	MANLEY	92	IPWA	$\pi N \to \pi N$ & $N\pi\pi$

$\Gamma(N\rho$, S=3/2, D-wave$)/\Gamma_{total}$ Γ_8/Γ

VALUE (%)	DOCUMENT ID		TECN	COMMENT
5 ± 1	VRANA	00	DPWA	Multichannel
• • • We do not use the following data for averages, fits, limits, etc. • • •				
23 ± 5	SHRESTHA	12A	DPWA	Multichannel

$(\Gamma_i\Gamma_f)^{1/2}/\Gamma_{total}$ in $N\pi \to \Delta(1900) \to N(1440)\pi$, S-wave $(\Gamma_1\Gamma_9)^{1/2}/\Gamma$

VALUE	DOCUMENT ID		TECN	COMMENT
• • • We do not use the following data for averages, fits, limits, etc. • • •				
−0.16 ± 0.11	MANLEY	92	IPWA	$\pi N \to \pi N$ & $N\pi\pi$

$\Gamma(N(1440)\pi$, S-wave$)/\Gamma_{total}$ Γ_9/Γ

VALUE (%)	DOCUMENT ID		TECN	COMMENT
4 ± 1	VRANA	00	DPWA	Multichannel
• • • We do not use the following data for averages, fits, limits, etc. • • •				
<1	SHRESTHA	12A	DPWA	Multichannel

Δ(1900) PHOTON DECAY AMPLITUDES

Papers on γN amplitudes predating 1981 may be found in our 2006 edition, Journal of Physics (generic for all A,B,E,G) **G33** 1 (2006).

Δ(1900) → Nγ, helicity-1/2 amplitude $A_{1/2}$

VALUE ($GeV^{-1/2}$)	DOCUMENT ID		TECN	COMMENT
0.059 ± 0.016	[3] ANISOVICH	12A	DPWA	Phase = (60 ± 25)°
−0.004 ± 0.016	CRAWFORD	83	IPWA	$\gamma N \to \pi N$
0.029 ± 0.008	AWAJI	81	DPWA	$\gamma N \to \pi N$
• • • We do not use the following data for averages, fits, limits, etc. • • •				
−0.082 ± 0.009	SHRESTHA	12A	DPWA	Multichannel

Δ(1900) FOOTNOTES

[1] See HOEHLER 93 for a detailed discussion of the evidence for and the pole parameters of N and Δ resonances as determined from Argand diagrams of πN elastic partial-wave amplitudes and from plots of the speeds with which the amplitudes traverse the diagrams.
[2] LONGACRE 78 values are from a search for poles in the unitarized T-matrix. The first (second) value uses, in addition to $\pi N \to N\pi\pi$ data, elastic amplitudes from a Saclay (CERN) partial-wave analysis.
[3] This ANISOVICH 12A value is the complex helicity amplitude at the pole position.

Δ(1900) REFERENCES

For early references, see Physics Letters **111B** 1 (1982).

ANISOVICH	12A	EPJ A48 15	A.V. Anisovich *et al.*	(BONN, PNPI)
SHRESTHA	12A	PR C86 055203	M. Shrestha, D.M. Manley	(KSU)
ARNDT	06	PR C74 045205	R.A. Arndt *et al.*	(GWU)
PDG	06	JP G33 1	W.-M. Yao *et al.*	(PDG Collab.)
VRANA	00	PRPL 328 181	T.P. Vrana, S.A. Dytman,, T.-S.H. Lee	(PITT+)
HOEHLER	93	πN Newsletter 9 1	G. Hohler	(KARL)
MANLEY	92	PR D45 4002	D.M. Manley, E.M. Saleski	(KSA) IJP
Also		PR D30 904	D.M. Manley *et al.*	(VPI)
ARNDT	91	PR D43 2131	R.A. Arndt *et al.*	(VPI, TELE) IJP
CANDLIN	84	NP B238 477	D.J. Candlin *et al.*	(EDIN, RAL, LOWC)
CRAWFORD	83	NP B211 1	R.L. Crawford, W.T. Morton	(GLAS)
AWAJI	81	Bonn Conf. 352	N. Awaji, R. Kajikawa	(NAGO)
Also		NP B197 365	K. Fujii *et al.*	(NAGO)
CHEW	80	Toronto Conf. 123	D.M. Chew	(LBL) IJP
CUTKOSKY	80	Toronto Conf. 19	R.E. Cutkosky *et al.*	(CMU, LBL) IJP
Also		PR D20 2839	R.E. Cutkosky *et al.*	(CMU, LBL) IJP
HOEHLER	79	PDAT 12-1	G. Hohler *et al.*	(KARLT) IJP
Also		Toronto Conf. 3	R. Koch	(KARLT) IJP
LONGACRE	78	PR D17 1795	R.S. Longacre *et al.*	(LBL, SLAC)

Δ(1905) 5/2+

$I(J^P) = \frac{3}{2}(\frac{5}{2}^+)$ Status: ****

Most of the results published before 1975 were last included in our 1982 edition, Physics Letters **111B** 1 (1982). Some further obsolete results published before 1984 were last included in our 2006 edition, Journal of Physics (generic for all A,B,E,G) **G33** 1 (2006).

Δ(1905) BREIT-WIGNER MASS

VALUE (MeV)	DOCUMENT ID		TECN	COMMENT
1855 to 1910 (≈ 1880) OUR ESTIMATE				
1861 ± 6	ANISOVICH	12A	DPWA	Multichannel
1857.8± 1.6	ARNDT	06	DPWA	$\pi N \to \pi N, \eta N$
1910 ±30	CUTKOSKY	80	IPWA	$\pi N \to \pi N$
1905 ±20	HOEHLER	79	IPWA	$\pi N \to \pi N$
• • • We do not use the following data for averages, fits, limits, etc. • • •				
1818 ± 8	SHRESTHA	12A	DPWA	Multichannel
1890 ±25	[1] ANISOVICH	10	DPWA	Multichannel
1855.7± 4.2	ARNDT	04	DPWA	$\pi N \to \pi N, \eta N$
1873 ±77	VRANA	00	DPWA	Multichannel
1895 ± 8	ARNDT	96	IPWA	$\gamma N \to \pi N$
1850	ARNDT	95	DPWA	$\pi N \to N\pi$
1881 ±18	MANLEY	92	IPWA	$\pi N \to \pi N$ & $N\pi\pi$
1960 ±40	CANDLIN	84	DPWA	$\pi^+ p \to \Sigma^+ K^+$
$1787.0^{+\ 6.0}_{-\ 5.7}$	CHEW	80	BPWA	$\pi^+ p \to \pi^+ p$
1830	[2] LONGACRE	75	IPWA	$\pi N \to N\pi\pi$

Δ(1905) BREIT-WIGNER WIDTH

VALUE (MeV)	DOCUMENT ID		TECN	COMMENT
270 to 400 (≈ 330) OUR ESTIMATE				
335 ± 18	ANISOVICH	12A	DPWA	Multichannel
320.6± 8.6	ARNDT	06	DPWA	$\pi N \to \pi N, \eta N$
400 ±100	CUTKOSKY	80	IPWA	$\pi N \to \pi N$
260 ± 20	HOEHLER	79	IPWA	$\pi N \to \pi N$
• • • We do not use the following data for averages, fits, limits, etc. • • •				
278 ± 18	SHRESTHA	12A	DPWA	Multichannel
335 ± 30	ANISOVICH	10	DPWA	Multichannel
334 ± 22	ARNDT	04	DPWA	$\pi N \to \pi N, \eta N$
461 ±111	VRANA	00	DPWA	Multichannel
354 ± 10	ARNDT	96	IPWA	$\gamma N \to \pi N$
294	ARNDT	95	DPWA	$\pi N \to N\pi$
327 ± 51	MANLEY	92	IPWA	$\pi N \to \pi N$ & $N\pi\pi$
270 ± 40	CANDLIN	84	DPWA	$\pi^+ p \to \Sigma^+ K^+$
$66.0^{+\ 24.0}_{-\ 16.0}$	CHEW	80	BPWA	$\pi^+ p \to \pi^+ p$
220	[2] LONGACRE	75	IPWA	$\pi N \to N\pi\pi$

Δ(1905) POLE POSITION

REAL PART

VALUE (MeV)	DOCUMENT ID		TECN	COMMENT
1805 to 1835 (≈ 1820) OUR ESTIMATE				
1805±10	ANISOVICH	12A	DPWA	Multichannel
1819	ARNDT	06	DPWA	$\pi N \to \pi N, \eta N$
1829	[3] HOEHLER	93	SPED	$\pi N \to \pi N$
1830±40	CUTKOSKY	80	IPWA	$\pi N \to \pi N$
• • • We do not use the following data for averages, fits, limits, etc. • • •				
1769	SHRESTHA	12A	DPWA	Multichannel
1800±15	ANISOVICH	10	DPWA	Multichannel
1825	ARNDT	04	DPWA	$\pi N \to \pi N, \eta N$
1793	VRANA	00	DPWA	Multichannel
1832	ARNDT	95	DPWA	$\pi N \to N\pi$
1794	ARNDT	91	DPWA	$\pi N \to \pi N$ Soln SM90
1813 or 1808	[4] LONGACRE	78	IPWA	$\pi N \to N\pi\pi$

−2×IMAGINARY PART

VALUE (MeV)	DOCUMENT ID		TECN	COMMENT
265 to 300 (≈ 280) OUR ESTIMATE				
300±15	ANISOVICH	12A	DPWA	Multichannel
247	ARNDT	06	DPWA	$\pi N \to \pi N, \eta N$
303	[3] HOEHLER	93	SPED	$\pi N \to \pi N$
280±60	CUTKOSKY	80	IPWA	$\pi N \to \pi N$
• • • We do not use the following data for averages, fits, limits, etc. • • •				
239	SHRESTHA	12A	DPWA	Multichannel
300±20	ANISOVICH	10	DPWA	Multichannel
270	ARNDT	04	DPWA	$\pi N \to \pi N, \eta N$
302	VRANA	00	DPWA	Multichannel
254	ARNDT	95	DPWA	$\pi N \to N\pi$
230	ARNDT	91	DPWA	$\pi N \to \pi N$ Soln SM90
193 or 187	[4] LONGACRE	78	IPWA	$\pi N \to N\pi\pi$

Δ(1905) ELASTIC POLE RESIDUE

MODULUS |r|

VALUE (MeV)	DOCUMENT ID		TECN	COMMENT
20±2	ANISOVICH	12A	DPWA	Multichannel
15	ARNDT	06	DPWA	$\pi N \to \pi N, \eta N$
25	HOEHLER	93	SPED	$\pi N \to \pi N$
25±8	CUTKOSKY	80	IPWA	$\pi N \to \pi N$
• • • We do not use the following data for averages, fits, limits, etc. • • •				
16	ARNDT	04	DPWA	$\pi N \to \pi N, \eta N$
12	ARNDT	95	DPWA	$\pi N \to N\pi$
14	ARNDT	91	DPWA	$\pi N \to \pi N$ Soln SM90

PHASE θ

VALUE (°)	DOCUMENT ID		TECN	COMMENT
−44± 5	ANISOVICH	12A	DPWA	Multichannel
−30	ARNDT	06	DPWA	$\pi N \to \pi N, \eta N$
−50±20	CUTKOSKY	80	IPWA	$\pi N \to \pi N$
• • • We do not use the following data for averages, fits, limits, etc. • • •				
−25	ARNDT	04	DPWA	$\pi N \to \pi N, \eta N$
− 4	ARNDT	95	DPWA	$\pi N \to N\pi$
−40	ARNDT	91	DPWA	$\pi N \to \pi N$ Soln SM90

Δ(1905) INELASTIC POLE RESIDUE

The "normalized residue" is the residue divided by $\Gamma_{pole}/2$.

Normalized residue in $N\pi \to \Delta(1905) \to \Delta\pi$, P-wave

MODULUS (%)	PHASE (°)	DOCUMENT ID		TECN	COMMENT
25±6	**0 ± 15**	ANISOVICH	12A	DPWA	Multichannel

Δ(1905) DECAY MODES

The following branching fractions are our estimates, not fits or averages.

	Mode	Fraction (Γ_i/Γ)
Γ_1	$N\pi$	9–15 %
Γ_2	ΣK	
Γ_3	$N\pi\pi$	85–95 %
Γ_4	$\Delta\pi$	<25 %
Γ_5	$\Delta(1232)\pi$, P-wave	
Γ_6	$\Delta(1232)\pi$, F-wave	
Γ_7	$N\rho$	>60 %
Γ_8	$N\rho$, S=3/2, P-wave	
Γ_9	$N\rho$, S=3/2, F-wave	
Γ_{10}	$N\rho$, S=1/2, F-wave	
Γ_{11}	$N\gamma$	0.012–0.036 %
Γ_{12}	$N\gamma$, helicity=1/2	0.002–0.006 %
Γ_{13}	$N\gamma$, helicity=3/2	0.01–0.03 %

Δ(1905) BRANCHING RATIOS

$\Gamma(N\pi)/\Gamma_{total}$ Γ_1/Γ

VALUE (%)	DOCUMENT ID		TECN	COMMENT
9 to 15 OUR ESTIMATE				
13 ±2	ANISOVICH	12A	DPWA	Multichannel
12.2±0.1	ARNDT	06	DPWA	$\pi N \to \pi N, \eta N$
8 ±3	CUTKOSKY	80	IPWA	$\pi N \to \pi N$
15 ±2	HOEHLER	79	IPWA	$\pi N \to \pi N$
• • • We do not use the following data for averages, fits, limits, etc. • • •				
6 ±1	SHRESTHA	12A	DPWA	Multichannel
12 ±3	ANISOVICH	10	DPWA	Multichannel
12.0±0.2	ARNDT	04	DPWA	$\pi N \to \pi N, \eta N$
9 ±1	VRANA	00	DPWA	Multichannel
12	ARNDT	95	DPWA	$\pi N \to N\pi$
12 ±3	MANLEY	92	IPWA	$\pi N \to \pi N$ & $N\pi\pi$
11	CHEW	80	BPWA	$\pi^+ p \to \pi^+ p$

$(\Gamma_i\Gamma_f)^{1/2}/\Gamma_{total}$ in $N\pi \to \Delta(1905) \to \Sigma K$ $(\Gamma_1\Gamma_2)^{1/2}/\Gamma$

VALUE	DOCUMENT ID		TECN	COMMENT
−0.015±0.003	CANDLIN	84	DPWA	$\pi^+ p \to \Sigma^+ K^+$

Note: Signs of couplings from $\pi N \to N\pi\pi$ analyses were changed in the 1986 edition to agree with the baryon-first convention; the overall phase ambiguity is resolved by choosing a negative sign for the Δ(1620) S_{31} coupling to $\Delta(1232)\pi$.

$(\Gamma_i\Gamma_f)^{1/2}/\Gamma_{total}$ in $N\pi \to \Delta(1905) \to \Delta(1232)\pi$, P-wave $(\Gamma_1\Gamma_5)^{1/2}/\Gamma$

VALUE	DOCUMENT ID		TECN	COMMENT
• • • We do not use the following data for averages, fits, limits, etc. • • •				
−0.04±0.05	MANLEY	92	IPWA	$\pi N \to \pi N$ & $N\pi\pi$

$\Gamma(\Delta(1232)\pi, P\text{-wave})/\Gamma_{total}$ Γ_5/Γ

VALUE (%)	DOCUMENT ID		TECN	COMMENT
45 ± 14	ANISOVICH	12A	DPWA	Multichannel
23 ± 1	VRANA	00	DPWA	Multichannel
• • • We do not use the following data for averages, fits, limits, etc. • • •				
28 ± 7	SHRESTHA	12A	DPWA	Multichannel

$(\Gamma_i\Gamma_f)^{1/2}/\Gamma_{total}$ in $N\pi \to \Delta(1905) \to \Delta(1232)\pi$, F-wave $(\Gamma_1\Gamma_6)^{1/2}/\Gamma$

VALUE	DOCUMENT ID		TECN	COMMENT
+0.20	[2] LONGACRE	75	IPWA	$\pi N \to N\pi\pi$
• • • We do not use the following data for averages, fits, limits, etc. • • •				
+0.02 ± 0.03	MANLEY	92	IPWA	$\pi N \to \pi N$ & $N\pi\pi$

$\Gamma(\Delta(1232)\pi, F\text{-wave})/\Gamma_{total}$ Γ_6/Γ

VALUE (%)	DOCUMENT ID		TECN	COMMENT
44 ± 1	VRANA	00	DPWA	Multichannel
• • • We do not use the following data for averages, fits, limits, etc. • • •				
64 ± 8	SHRESTHA	12A	DPWA	Multichannel

$(\Gamma_i\Gamma_f)^{1/2}/\Gamma_{total}$ in $N\pi \to \Delta(1905) \to N\rho, S{=}3/2, P\text{-wave}$ $(\Gamma_1\Gamma_8)^{1/2}/\Gamma$

VALUE	DOCUMENT ID		TECN	COMMENT
+0.30 to +0.36 OUR ESTIMATE				
+0.33	[2] LONGACRE	75	IPWA	$\pi N \to N\pi\pi$
• • • We do not use the following data for averages, fits, limits, etc. • • •				
+0.33 ± 0.03	MANLEY	92	IPWA	$\pi N \to \pi N$ & $N\pi\pi$

$\Gamma(N\rho, S{=}3/2, P\text{-wave})/\Gamma_{total}$ Γ_8/Γ

VALUE (%)	DOCUMENT ID		TECN	COMMENT
24 ± 1	VRANA	00	DPWA	Multichannel
• • • We do not use the following data for averages, fits, limits, etc. • • •				
< 6	SHRESTHA	12A	DPWA	Multichannel

$\Delta(1905)$ PHOTON DECAY AMPLITUDES

Papers on γN amplitudes predating 1981 may be found in our 2006 edition, Journal of Physics (generic for all A,B,E,G) **G33** 1 (2006).

$\Delta(1905) \to N\gamma$, helicity-1/2 amplitude $A_{1/2}$

VALUE (GeV$^{-1/2}$)	DOCUMENT ID		TECN	COMMENT
+0.022 ± 0.005 OUR ESTIMATE				
0.020 ± 0.002	DUGGER	13	DPWA	$\gamma N \to \pi N$
0.025 ± 0.004	ANISOVICH	12A	DPWA	Multichannel
0.019 ± 0.002	WORKMAN	12A	DPWA	$\gamma N \to \pi N$
0.021 ± 0.004	DUGGER	07	DPWA	$\gamma N \to \pi N$
0.021 ± 0.010	CRAWFORD	83	IPWA	$\gamma N \to \pi N$
0.043 ± 0.020	AWAJI	81	DPWA	$\gamma N \to \pi N$
• • • We do not use the following data for averages, fits, limits, etc. • • •				
0.066 ± 0.018	SHRESTHA	12A	DPWA	Multichannel
0.028 ± 0.012	[1] ANISOVICH	10	DPWA	Multichannel
0.018	DRECHSEL	07	DPWA	$\gamma N \to \pi N$
0.022 ± 0.005	ARNDT	96	IPWA	$\gamma N \to \pi N$
0.055 ± 0.004	LI	93	IPWA	$\gamma N \to \pi N$

$\Delta(1905) \to N\gamma$, helicity-3/2 amplitude $A_{3/2}$

VALUE (GeV$^{-1/2}$)	DOCUMENT ID		TECN	COMMENT
−0.045 ± 0.010 OUR ESTIMATE				
−0.049 ± 0.005	DUGGER	13	DPWA	$\gamma N \to \pi N$
−0.049 ± 0.004	ANISOVICH	12A	DPWA	Multichannel
−0.038 ± 0.004	WORKMAN	12A	DPWA	$\gamma N \to \pi N$
−0.046 ± 0.005	DUGGER	07	DPWA	$\gamma N \to \pi N$
−0.056 ± 0.028	CRAWFORD	83	IPWA	$\gamma N \to \pi N$
−0.025 ± 0.023	AWAJI	81	DPWA	$\gamma N \to \pi N$
• • • We do not use the following data for averages, fits, limits, etc. • • •				
−0.223 ± 0.029	SHRESTHA	12A	DPWA	Multichannel
−0.042 ± 0.015	[1] ANISOVICH	10	DPWA	Multichannel
−0.028	DRECHSEL	07	DPWA	$\gamma N \to \pi N$
−0.045 ± 0.005	ARNDT	96	IPWA	$\gamma N \to \pi N$
0.002 ± 0.003	LI	93	IPWA	$\gamma N \to \pi N$

$\Delta(1905)$ FOOTNOTES

[1] ANISOVICH 10 finds an alternate solution for this resonance. The only statistically significant differences are in the Breit-Wigner mass and γp couplings.

[2] From method II of LONGACRE 75: eyeball fits with Breit-Wigner circles to the T-matrix amplitudes.

[3] See HOEHLER 93 for a detailed discussion of the evidence for and the pole parameters of N and Δ resonances as determined from Argand diagrams of πN elastic partial-wave amplitudes and from plots of the speeds with which the amplitudes traverse the diagrams.

[4] LONGACRE 78 values are from a search for poles in the unitarized T-matrix. The first (second) value uses, in addition to $\pi N \to N\pi\pi$ data, elastic amplitudes from a Saclay (CERN) partial-wave analysis.

$\Delta(1905)$ REFERENCES

For early references, see Physics Letters **111B** 1 (1982).

DUGGER	13	PR C88 065203	M. Dugger *et al.*	(CLAS Collab.)
ANISOVICH	12A	EPJ A48 15	A.V. Anisovich *et al.*	(BONN, PNPI)
SHRESTHA	12A	PR C86 055203	M. Shrestha, D.M. Manley	(KSU)
WORKMAN	12A	PR C86 015202	R. Workman *et al.*	(GWU)
ANISOVICH	10	EPJ A44 203	A.V. Anisovich *et al.*	(BONN, PNPI)
DRECHSEL	07	EPJ A34 69	D. Drechsel, S.S. Kamalov, L. Tiator	(MAINZ, JINR)
DUGGER	07	PR C76 025211	M. Dugger *et al.*	(Jefferson Lab CLAS Collab.)
ARNDT	06	PR C74 045205	R.A. Arndt *et al.*	(GWU)
PDG	06	JP G33 1	W.-M. Yao *et al.*	(PDG Collab.)
ARNDT	04	PR C69 035213	R.A. Arndt *et al.*	(GWU, TRIU)
VRANA	00	PRPL 328 181	T.P. Vrana, S.A. Dytman,, T.-S.H. Lee	(PITT+)
ARNDT	96	PR C53 430	R.A. Arndt, I.I. Strakovsky, R.L. Workman	(VPI)
ARNDT	95	PR C52 2120	R.A. Arndt *et al.*	(VPI, BRCO)
HOEHLER	93	πN Newsletter 9 1	G. Hohler	(KARL)
LI	93	PR C47 2759	Z.J. Li *et al.*	(VPI)
MANLEY	92	PR D45 4002	D.M. Manley, E.M. Saleski	(KSA) IJP
Also		PR D30 904	D.M. Manley *et al.*	(VPI)
ARNDT	91	PR D43 2131	R.A. Arndt *et al.*	(VPI, TELE) IJP
CANDLIN	84	NP B238 477	D.J. Candlin *et al.*	(EDIN, RAL, LOWC)
CRAWFORD	83	NP B211 1	R.L. Crawford, W.T. Morton	(GLAS)
PDG	82	PL 111B 1	M. Roos *et al.*	(HELS, CIT, CERN)
AWAJI	81	Bonn Conf. 352	N. Awaji, R. Kajikawa	(NAGO)
Also		NP B197 365	K. Fujii *et al.*	(NAGO)
CHEW	80	Toronto Conf. 123	D.M. Chew	(LBL) IJP
CUTKOSKY	80	Toronto Conf. 19	R.E. Cutkosky *et al.*	(CMU, LBL) IJP
Also		PR D20 2839	R.E. Cutkosky *et al.*	(CMU, LBL) IJP
HOEHLER	79	PDAT 12-1	G. Hohler *et al.*	(KARLT) IJP
Also		Toronto Conf. 3	R. Koch	(KARLT) IJP
LONGACRE	78	PR D17 1795	R.S. Longacre *et al.*	(LBL, SLAC)
LONGACRE	75	PL 55B 415	R.S. Longacre *et al.*	(LBL, SLAC) IJP

$\Delta(1910)$ $1/2^+$

$I(J^P) = \frac{3}{2}(\frac{1}{2}^+)$ Status: ****

Most of the results published before 1975 were last included in our 1982 edition, Physics Letters **111B** 1 (1982). Some further obsolete results published before 1984 were last included in our 2006 edition, Journal of Physics (generic for all A,B,E,G) **G33** 1 (2006).

$\Delta(1910)$ BREIT-WIGNER MASS

VALUE (MeV)	DOCUMENT ID		TECN	COMMENT
1860 to 1910 (≈ 1890) OUR ESTIMATE				
1860 ±40	ANISOVICH	12A	DPWA	Multichannel
2067.9 ± 1.7	ARNDT	06	DPWA	$\pi N \to \pi N, \eta N$
1910 ±40	CUTKOSKY	80	IPWA	$\pi N \to \pi N$
1888 ±20	HOEHLER	79	IPWA	$\pi N \to \pi N$
• • • We do not use the following data for averages, fits, limits, etc. • • •				
1934 ± 5	SHRESTHA	12A	DPWA	Multichannel
1995 ±12	VRANA	00	DPWA	Multichannel
2152	ARNDT	95	DPWA	$\pi N \to N\pi$
1882 ±10	MANLEY	92	IPWA	$\pi N \to \pi N$ & $N\pi\pi$
1960.1 ± 21.0	[1] CHEW	80	BPWA	$\pi^+ p \to \pi^+ p$
$2121.4^{+13.0}_{-14.3}$	[1] CHEW	80	BPWA	$\pi^+ p \to \pi^+ p$
1790	[2] LONGACRE	77	IPWA	$\pi N \to N\pi\pi$

$\Delta(1910)$ BREIT-WIGNER WIDTH

VALUE (MeV)	DOCUMENT ID		TECN	COMMENT
220 to 340 (≈ 280) OUR ESTIMATE				
350 ± 55	ANISOVICH	12A	DPWA	Multichannel
543 ± 10	ARNDT	06	DPWA	$\pi N \to \pi N, \eta N$
225 ± 50	CUTKOSKY	80	IPWA	$\pi N \to \pi N$
280 ± 50	HOEHLER	79	IPWA	$\pi N \to \pi N$
• • • We do not use the following data for averages, fits, limits, etc. • • •				
211 ± 11	SHRESTHA	12A	DPWA	Multichannel
713 ±465	VRANA	00	DPWA	Multichannel
760	ARNDT	95	DPWA	$\pi N \to N\pi$
239 ± 25	MANLEY	92	IPWA	$\pi N \to \pi N$ & $N\pi\pi$
152.9 ± 60.0	[1] CHEW	80	BPWA	$\pi^+ p \to \pi^+ p$
172.2 ± 37.0	[1] CHEW	80	BPWA	$\pi^+ p \to \pi^+ p$
170	[2] LONGACRE	77	IPWA	$\pi N \to N\pi\pi$

$\Delta(1910)$ POLE POSITION

REAL PART

VALUE (MeV)	DOCUMENT ID		TECN	COMMENT
1830 to 1880 (≈ 1855) OUR ESTIMATE				
1850 ±40	ANISOVICH	12A	DPWA	Multichannel
1771	ARNDT	06	DPWA	$\pi N \to \pi N, \eta N$
1874	[3] HOEHLER	93	SPED	$\pi N \to \pi N$
1880 ±30	CUTKOSKY	80	IPWA	$\pi N \to \pi N$
• • • We do not use the following data for averages, fits, limits, etc. • • •				
1910	SHRESTHA	12A	DPWA	Multichannel
1880	VRANA	00	DPWA	Multichannel
1810	ARNDT	95	DPWA	$\pi N \to N\pi$
1950	ARNDT	91	DPWA	$\pi N \to \pi N$ Soln SM90
1792 or 1801	[2] LONGACRE	77	IPWA	$\pi N \to N\pi\pi$

Baryon Particle Listings

Δ(1910)

−2×IMAGINARY PART

VALUE (MeV)	DOCUMENT ID		TECN	COMMENT
200 to 500 (≈ 350) OUR ESTIMATE				
350±45	ANISOVICH	12A	DPWA	Multichannel
479	ARNDT	06	DPWA	$\pi N \to \pi N$, ηN
283	[3] HOEHLER	93	SPED	$\pi N \to \pi N$
200±40	CUTKOSKY	80	IPWA	$\pi N \to \pi N$
• • • We do not use the following data for averages, fits, limits, etc. • • •				
199	SHRESTHA	12A	DPWA	Multichannel
496	VRANA	00	DPWA	Multichannel
494	ARNDT	95	DPWA	$\pi N \to N\pi$
398	ARNDT	91	DPWA	$\pi N \to \pi N$ Soln SM90
172 or 165	[2] LONGACRE	77	IPWA	$\pi N \to N\pi\pi$

Δ(1910) ELASTIC POLE RESIDUE

MODULUS |r|

VALUE (MeV)	DOCUMENT ID		TECN	COMMENT
24±6	ANISOVICH	12A	DPWA	Multichannel
45	ARNDT	06	DPWA	$\pi N \to \pi N$, ηN
38	HOEHLER	93	SPED	$\pi N \to \pi N$
20±4	CUTKOSKY	80	IPWA	$\pi N \to \pi N$
• • • We do not use the following data for averages, fits, limits, etc. • • •				
53	ARNDT	95	DPWA	$\pi N \to N\pi$
37	ARNDT	91	DPWA	$\pi N \to \pi N$ Soln SM90

PHASE θ

VALUE (°)	DOCUMENT ID		TECN	COMMENT
−145±30	ANISOVICH	12A	DPWA	Multichannel
+172	ARNDT	06	DPWA	$\pi N \to \pi N$, ηN
− 90±30	CUTKOSKY	80	IPWA	$\pi N \to \pi N$
• • • We do not use the following data for averages, fits, limits, etc. • • •				
−176	ARNDT	95	DPWA	$\pi N \to N\pi$
− 91	ARNDT	91	DPWA	$\pi N \to \pi N$ Soln SM90

Δ(1910) INELASTIC POLE RESIDUE

The "normalized residue" is the residue divided by $\Gamma_{pole}/2$.

Normalized residue in $N\pi \to \Delta(1910) \to \Sigma K$

MODULUS (%)	PHASE (°)	DOCUMENT ID		TECN	COMMENT
7±2	**−110 ± 30**	ANISOVICH	12A	DPWA	Multichannel

Normalized residue in $N\pi \to \Delta(1910) \to \Delta\pi$, P-wave

MODULUS (%)	PHASE (°)	DOCUMENT ID		TECN	COMMENT
16±9	**95 ± 40**	ANISOVICH	12A	DPWA	Multichannel

Δ(1910) DECAY MODES

The following branching fractions are our estimates, not fits or averages.

	Mode	Fraction (Γ_i/Γ)
Γ_1	$N\pi$	15–30 %
Γ_2	ΣK	(9± 5) %
Γ_3	$N\pi\pi$	
Γ_4	$\Delta\pi$	(60±28) %
Γ_5	$\Delta(1232)\pi$, P-wave	
Γ_6	$N\rho$	
Γ_7	$N\rho$, S=3/2, P-wave	
Γ_8	$N(1440)\pi$	
Γ_9	$N(1440)\pi$, P-wave	
Γ_{10}	$N\gamma$	0.0–0.02 %
Γ_{11}	$N\gamma$, helicity=1/2	0.0–0.02 %

Δ(1910) BRANCHING RATIOS

$\Gamma(N\pi)/\Gamma_{total}$ Γ_1/Γ

VALUE (%)	DOCUMENT ID		TECN	COMMENT
15 to 30 OUR ESTIMATE				
12 ± 3	ANISOVICH	12A	DPWA	Multichannel
23.9± 0.1	ARNDT	06	DPWA	$\pi N \to \pi N$, ηN
19 ± 3	CUTKOSKY	80	IPWA	$\pi N \to \pi N$
24 ± 6	HOEHLER	79	IPWA	$\pi N \to \pi N$
• • • We do not use the following data for averages, fits, limits, etc. • • •				
17 ± 1	SHRESTHA	12A	DPWA	Multichannel
29 ±21	VRANA	00	DPWA	Multichannel
26	ARNDT	95	DPWA	$\pi N \to N\pi$
23 ± 8	MANLEY	92	IPWA	$\pi N \to \pi N$ & $N\pi\pi$
17	[1] CHEW	80	BPWA	$\pi^+ p \to \pi^+ p$
40	[1] CHEW	80	BPWA	$\pi^+ p \to \pi^+ p$

$(\Gamma_i\Gamma_f)^{1/2}/\Gamma_{total}$ in $N\pi \to \Delta(1910) \to \Sigma K$ $(\Gamma_1\Gamma_2)^{1/2}/\Gamma$

VALUE	DOCUMENT ID		TECN	COMMENT
< 0.03	CANDLIN	84	DPWA	$\pi^+ p \to \Sigma^+ K^+$
• • • We do not use the following data for averages, fits, limits, etc. • • •				
−0.019	LIVANOS	80	DPWA	$\pi p \to \Sigma K$

$\Gamma(\Sigma K)/\Gamma_{total}$ Γ_2/Γ

VALUE (%)	DOCUMENT ID		TECN	COMMENT
9±5	ANISOVICH	12A	DPWA	Multichannel

Note: Signs of couplings from $\pi N \to N\pi\pi$ analyses were changed in the 1986 edition to agree with the baryon-first convention; the overall phase ambiguity is resolved by choosing a negative sign for the Δ(1620) S_{31} coupling to $\Delta(1232)\pi$.

$(\Gamma_i\Gamma_f)^{1/2}/\Gamma_{total}$ in $N\pi \to \Delta(1910) \to \Delta(1232)\pi$, P-wave $(\Gamma_1\Gamma_5)^{1/2}/\Gamma$

VALUE	DOCUMENT ID		TECN	COMMENT
+0.06	[2] LONGACRE	77	IPWA	$\pi N \to N\pi\pi$

$\Gamma(\Delta\pi)/\Gamma_{total}$ Γ_4/Γ

VALUE (%)	DOCUMENT ID		TECN	COMMENT
60±28	ANISOVICH	12A	DPWA	Multichannel

$(\Gamma_i\Gamma_f)^{1/2}/\Gamma_{total}$ in $N\pi \to \Delta(1910) \to N\rho$, S=3/2, P-wave $(\Gamma_1\Gamma_7)^{1/2}/\Gamma$

VALUE	DOCUMENT ID		TECN	COMMENT
+0.29	[2] LONGACRE	77	IPWA	$\pi N \to N\pi\pi$

$(\Gamma_i\Gamma_f)^{1/2}/\Gamma_{total}$ in $N\pi \to \Delta(1910) \to N(1440)\pi$, P-wave $(\Gamma_1\Gamma_9)^{1/2}/\Gamma$

VALUE	DOCUMENT ID		TECN	COMMENT
• • • We do not use the following data for averages, fits, limits, etc. • • •				
−0.39±0.04	MANLEY	92	IPWA	$\pi N \to \pi N$ & $N\pi\pi$

$\Gamma(N(1440)\pi)/\Gamma_{total}$ Γ_8/Γ

VALUE (%)	DOCUMENT ID		TECN	COMMENT
56±7	VRANA	00	DPWA	Multichannel
• • • We do not use the following data for averages, fits, limits, etc. • • •				
47±6	SHRESTHA	12A	DPWA	Multichannel

Δ(1910) PHOTON DECAY AMPLITUDES

Papers on γN amplitudes predating 1981 may be found in our 2006 edition, Journal of Physics (generic for all A,B,E,G) **G33** 1 (2006).

Δ(1910) → $N\gamma$, helicity-1/2 amplitude $A_{1/2}$

VALUE ($GeV^{-1/2}$)	DOCUMENT ID		TECN	COMMENT
+0.020±0.010 OUR ESTIMATE				
0.022±0.009	ANISOVICH	12A	DPWA	Multichannel
−0.002±0.008	ARNDT	96	IPWA	$\gamma N \to \pi N$
0.014±0.030	CRAWFORD	83	IPWA	$\gamma N \to \pi N$
0.025±0.011	AWAJI	81	DPWA	$\gamma N \to \pi N$
• • • We do not use the following data for averages, fits, limits, etc. • • •				
0.030±0.002	SHRESTHA	12A	DPWA	Multichannel
0.032±0.003	LI	93	IPWA	$\gamma N \to \pi N$

Δ(1910) FOOTNOTES

[1] CHEW 80 reports four resonances in the P_{31} wave — see also the Δ(1750). Problems with this analysis are discussed in section 2.1.11 of HOEHLER 83.

[2] LONGACRE 77 pole positions are from a search for poles in the unitarized T-matrix; the first (second) value uses, in addition to $\pi N \to N\pi\pi$ data, elastic amplitudes from a Saclay (CERN) partial-wave analysis. The other LONGACRE 77 values are from eyeball fits with Breit-Wigner circles to the T-matrix amplitudes.

[3] See HOEHLER 93 for a detailed discussion of the evidence for and the pole parameters of N and Δ resonances as determined from Argand diagrams of πN elastic partial-wave amplitudes and from plots of the speeds with which the amplitudes traverse the diagrams.

Δ(1910) REFERENCES

For early references, see Physics Letters **111B** 1 (1982).

ANISOVICH	12A	EPJ A48 15	A.V. Anisovich *et al.*	(BONN, PNPI)
SHRESTHA	12A	PR C86 055203	M. Shrestha, D.M. Manley	(KSU)
ARNDT	06	PR C74 045205	R.A. Arndt *et al.*	(GWU)
PDG	06	JP G33 1	W.-M. Yao *et al.*	(PDG Collab.)
VRANA	00	PRPL 328 181	T.P. Vrana, S.A. Dytman,, T.-S.H. Lee	(PITT+)
ARNDT	96	PR C53 430	R.A. Arndt, I.I. Strakovsky, R.L. Workman	(VPI)
ARNDT	95	PR C52 2120	R.A. Arndt *et al.*	(VPI, BRCO)
HOEHLER	93	πN Newsletter 9 1	G. Hoehler	(KARL)
LI	93	PR C47 2759	Z.J. Li *et al.*	(VPI)
MANLEY	92	PR D45 4002	D.M. Manley, E.M. Saleski	(KSA) IJP
Also		PR D30 904	D.M. Manley *et al.*	(VPI)
ARNDT	91	PR D43 2131	R.A. Arndt *et al.*	(VPI, TELE) IJP

CANDLIN	84	NP B238 477	D.J. Candlin *et al.*	(EDIN, RAL, LOWC)
CRAWFORD	83	NP B211 1	R.L. Crawford, W.T. Morton	(GLAS)
HOEHLER	83	Landolt-Boernstein 1/9B2	G. Hohler	(KARLT)
PDG	82	PL 111B 1	M. Roos *et al.*	(HELS, CIT, CERN)
AWAJI	81	Bonn Conf. 352	N. Awaji, R. Kajikawa	(NAGO)
Also		NP B197 365	K. Fujii *et al.*	(NAGO)
CHEW	80	Toronto Conf. 123	D.M. Chew	(LBL) IJP
CUTKOSKY	80	Toronto Conf. 19	R.E. Cutkosky *et al.*	(CMU, LBL) IJP
Also		PR D20 2839	R.E. Cutkosky *et al.*	(CMU, LBL) IJP
LIVANOS	80	Toronto Conf. 35	P. Livanos *et al.*	(SACL) IJP
HOEHLER	79	PDAT 12-1	G. Hohler *et al.*	(KARLT) IJP
Also		Toronto Conf. 3	R. Koch	(KARLT) IJP
LONGACRE	77	NP B122 493	R.S. Longacre, J. Dolbeau	(SACL) IJP
Also		NP B108 365	J. Dolbeau *et al.*	(SACL) IJP

$\Delta(1920)\ 3/2^+$

$I(J^P) = \frac{3}{2}(\frac{3}{2}^+)$ Status: ***

Most of the results published before 1975 were last included in our 1982 edition, Physics Letters **111B** 1 (1982). Some further obsolete results published before 1984 were last included in our 2006 edition, Journal of Physics (generic for all A,B,E,G) **G33** 1 (2006).

The latest GWU analysis (ARNDT 06) finds no evidence for this resonance.

$\Delta(1920)$ BREIT-WIGNER MASS

VALUE (MeV)	DOCUMENT ID		TECN	COMMENT
1900 to 1970 (≈ 1920) OUR ESTIMATE				
1900 ± 30	ANISOVICH	12A	DPWA	Multichannel
1920 ± 80	CUTKOSKY	80	IPWA	$\pi N \to \pi N$
1868 ± 10	HOEHLER	79	IPWA	$\pi N \to \pi N$
• • • We do not use the following data for averages, fits, limits, etc. • • •				
2146 ± 32	SHRESTHA	12A	DPWA	Multichannel
1990 ± 35	HORN	08A	DPWA	Multichannel
2057 ± 1	PENNER	02C	DPWA	Multichannel
1889 ±100	VRANA	00	DPWA	Multichannel
2014 ± 16	MANLEY	92	IPWA	$\pi N \to \pi N$ & $N\pi\pi$
1840 ± 40	CANDLIN	84	DPWA	$\pi^+ p \to \Sigma^+ K^+$
1955.0± 13.0	[1] CHEW	80	BPWA	$\pi^+ p \to \pi^+ p$
$2065.0^{+13.6}_{-12.9}$	[1] CHEW	80	BPWA	$\pi^+ p \to \pi^+ p$

$\Delta(1920)$ BREIT-WIGNER WIDTH

VALUE (MeV)	DOCUMENT ID		TECN	COMMENT
180 to 300 (≈ 260) OUR ESTIMATE				
310 ± 60	ANISOVICH	12A	DPWA	Multichannel
300 ±100	CUTKOSKY	80	IPWA	$\pi N \to \pi N$
220 ± 80	HOEHLER	79	IPWA	$\pi N \to \pi N$
• • • We do not use the following data for averages, fits, limits, etc. • • •				
400 ± 80	SHRESTHA	12A	DPWA	Multichannel
330 ± 60	HORN	08A	DPWA	Multichannel
525 ± 32	PENNER	02C	DPWA	Multichannel
123 ± 53	VRANA	00	DPWA	Multichannel
152 ± 55	MANLEY	92	IPWA	$\pi N \to \pi N$ & $N\pi\pi$
200 ± 40	CANDLIN	84	DPWA	$\pi^+ p \to \Sigma^+ K^+$
88.3± 35.0	[1] CHEW	80	BPWA	$\pi^+ p \to \pi^+ p$
62.0± 44.0	[1] CHEW	80	BPWA	$\pi^+ p \to \pi^+ p$

$\Delta(1920)$ POLE POSITION

REAL PART

VALUE (MeV)	DOCUMENT ID		TECN	COMMENT
1850 to 1950 (≈ 1900) OUR ESTIMATE				
1890±30	ANISOVICH	12A	DPWA	Multichannel
1900	[2] HOEHLER	93	SPED	$\pi N \to \pi N$
1900±80	CUTKOSKY	80	IPWA	$\pi N \to \pi N$
• • • We do not use the following data for averages, fits, limits, etc. • • •				
2110	SHRESTHA	12A	DPWA	Multichannel
1980^{+25}_{-45}	HORN	08A	DPWA	Multichannel
1880	VRANA	00	DPWA	Multichannel
not seen	ARNDT	91	DPWA	$\pi N \to \pi N$ Soln SM90

−2×IMAGINARY PART

VALUE (MeV)	DOCUMENT ID		TECN	COMMENT
200 to 400 (≈ 300) OUR ESTIMATE				
300± 60	ANISOVICH	12A	DPWA	Multichannel
300±100	CUTKOSKY	80	IPWA	$\pi N \to \pi N$
• • • We do not use the following data for averages, fits, limits, etc. • • •				
386	SHRESTHA	12A	DPWA	Multichannel
310^{+40}_{-60}	HORN	08A	DPWA	Multichannel
120	VRANA	00	DPWA	Multichannel
not seen	ARNDT	91	DPWA	$\pi N \to \pi N$ Soln SM90

$\Delta(1920)$ ELASTIC POLE RESIDUE

MODULUS $|r|$

VALUE (MeV)	DOCUMENT ID		TECN	COMMENT
17±8	ANISOVICH	12A	DPWA	Multichannel
24±4	CUTKOSKY	80	IPWA	$\pi N \to \pi N$

PHASE θ

VALUE (°)	DOCUMENT ID		TECN	COMMENT
− 40±20	ANISOVICH	12A	DPWA	Multichannel
−150±30	CUTKOSKY	80	IPWA	$\pi N \to \pi N$

$\Delta(1920)$ INELASTIC POLE RESIDUE

The "normalized residue" is the residue divided by $\Gamma_{pole}/2$.

Normalized residue in $N\pi \to \Delta(1920) \to \Delta\eta$

MODULUS (%)	PHASE (°)	DOCUMENT ID		TECN	COMMENT
17±8	**70 ± 20**	ANISOVICH	12A	DPWA	Multichannel

Normalized residue in $N\pi \to \Delta(1920) \to \Sigma K$

MODULUS (%)	PHASE (°)	DOCUMENT ID		TECN	COMMENT
9±3	**80 ± 40**	ANISOVICH	12A	DPWA	Multichannel

Normalized residue in $N\pi \to \Delta(1920) \to \Delta\pi$, P-wave

MODULUS (%)	PHASE (°)	DOCUMENT ID		TECN	COMMENT
20±12	**−120 ± 30**	ANISOVICH	12A	DPWA	Multichannel

Normalized residue in $N\pi \to \Delta(1920) \to \Delta\pi$, F-wave

MODULUS (%)	PHASE (°)	DOCUMENT ID		TECN	COMMENT
28±7	**−95 ± 35**	ANISOVICH	12A	DPWA	Multichannel

$\Delta(1920)$ DECAY MODES

The following branching fractions are our estimates, not fits or averages.

	Mode	Fraction (Γ_i/Γ)
Γ_1	$N\pi$	5–20 %
Γ_2	ΣK	(2.14±0.30) %
Γ_3	$N\pi\pi$	
Γ_4	$\Delta(1232)\pi$, P-wave	
Γ_5	$\Delta(1232)\pi$, F-wave	
Γ_6	$N(1440)\pi$, P-wave	
Γ_7	$N(1535)\pi$	
Γ_8	$N a_0(980)$	
Γ_9	$\Delta(1232)\eta$	(15 ±8) %
Γ_{10}	$N\gamma$	0.0–0.4 %
Γ_{11}	$N\gamma$, helicity=1/2	0.0–0.2 %
Γ_{12}	$N\gamma$, helicity=3/2	0.0–0.2 %

$\Delta(1920)$ BRANCHING RATIOS

$\Gamma(N\pi)/\Gamma_{total}$ Γ_1/Γ

VALUE (%)	DOCUMENT ID		TECN	COMMENT
5 to 20 OUR ESTIMATE				
8±4	ANISOVICH	12A	DPWA	Multichannel
20±5	CUTKOSKY	80	IPWA	$\pi N \to \pi N$
14±4	HOEHLER	79	IPWA	$\pi N \to \pi N$
• • • We do not use the following data for averages, fits, limits, etc. • • •				
16±4	SHRESTHA	12A	DPWA	Multichannel
15±8	HORN	08A	DPWA	Multichannel
15±1	PENNER	02C	DPWA	Multichannel
5±4	VRANA	00	DPWA	Multichannel
2±2	MANLEY	92	IPWA	$\pi N \to \pi N$ & $N\pi\pi$
24	[1] CHEW	80	BPWA	$\pi^+ p \to \pi^+ p$
18	[1] CHEW	80	BPWA	$\pi^+ p \to \pi^+ p$

$(\Gamma_i\Gamma_f)^{1/2}/\Gamma_{total}$ in $N\pi \to \Delta(1920) \to \Sigma K$ $(\Gamma_1\Gamma_2)^{1/2}/\Gamma$

VALUE	DOCUMENT ID		TECN	COMMENT
−0.052±0.015	CANDLIN	84	DPWA	$\pi^+ p \to \Sigma^+ K^+$
• • • We do not use the following data for averages, fits, limits, etc. • • •				
−0.049	LIVANOS	80	DPWA	$\pi p \to \Sigma K$

$\Gamma(\Sigma K)/\Gamma_{total}$ Γ_2/Γ

VALUE (%)	DOCUMENT ID		TECN	COMMENT
2.14±0.30 OUR AVERAGE				
4 ±2	ANISOVICH	12A	DPWA	Multichannel
2.1 ±0.3	PENNER	02C	DPWA	Multichannel

$(\Gamma_i\Gamma_f)^{1/2}/\Gamma_{total}$ in $N\pi \to \Delta(1920) \to \Delta(1232)\pi$, P-wave $(\Gamma_1\Gamma_4)^{1/2}/\Gamma$

VALUE	DOCUMENT ID		TECN	COMMENT
• • • We do not use the following data for averages, fits, limits, etc. • • •				
−0.13±0.04	MANLEY	92	IPWA	$\pi N \to \pi N$ & $N\pi\pi$

$\Gamma(\Delta(1232)\pi$, P-wave$)/\Gamma_{total}$ Γ_4/Γ

VALUE (%)	DOCUMENT ID		TECN	COMMENT
22±12	ANISOVICH	12A	DPWA	Multichannel
41± 3	VRANA	00	DPWA	Multichannel
• • • We do not use the following data for averages, fits, limits, etc. • • •				
7± 5	SHRESTHA	12A	DPWA	Multichannel

$\Gamma(\Delta(1232)\pi$, F-wave$)/\Gamma_{total}$ Γ_5/Γ

VALUE (%)	DOCUMENT ID		TECN	COMMENT
45±20	ANISOVICH	12A	DPWA	Multichannel

$(\Gamma_i\Gamma_f)^{1/2}/\Gamma_{total}$ in $N\pi \to \Delta(1920) \to N(1440)\pi$, P-wave $(\Gamma_1\Gamma_6)^{1/2}/\Gamma$

VALUE	DOCUMENT ID		TECN	COMMENT
• • • We do not use the following data for averages, fits, limits, etc. • • •				
+0.06±0.07	MANLEY	92	IPWA	$\pi N \to \pi N$ & $N\pi\pi$

$\Gamma(N(1440)\pi$, P-wave$)/\Gamma_{total}$ Γ_6/Γ

VALUE (%)	DOCUMENT ID		TECN	COMMENT
53±8	VRANA	00	DPWA	Multichannel
• • • We do not use the following data for averages, fits, limits, etc. • • •				
<20	SHRESTHA	12A	DPWA	Multichannel

$\Gamma(N(1535)\pi)/\Gamma_{total}$ Γ_7/Γ

VALUE (%)	DOCUMENT ID		TECN	COMMENT
• • • We do not use the following data for averages, fits, limits, etc. • • •				
6±4	HORN	08A	DPWA	Multichannel

$\Gamma(Na_0(980))/\Gamma_{total}$ Γ_8/Γ

VALUE (%)	DOCUMENT ID		TECN	COMMENT
• • • We do not use the following data for averages, fits, limits, etc. • • •				
4±2	HORN	08A	DPWA	Multichannel

$\Gamma(\Delta(1232)\eta)/\Gamma_{total}$ Γ_9/Γ

VALUE (%)	DOCUMENT ID		TECN	COMMENT
15±8	ANISOVICH	12A	DPWA	Multichannel
• • • We do not use the following data for averages, fits, limits, etc. • • •				
10±5	HORN	08A	DPWA	Multichannel

$\Delta(1920)$ PHOTON DECAY AMPLITUDES

Papers on γN amplitudes predating 1981 may be found in our 2006 edition, Journal of Physics (generic for all A,B,E,G) **G33** 1 (2006).

$\Delta(1920) \to N\gamma$, helicity-1/2 amplitude $A_{1/2}$

VALUE (GeV$^{-1/2}$)	DOCUMENT ID		TECN	COMMENT
$0.130^{+0.030}_{-0.060}$	ANISOVICH	12A	DPWA	Multichannel
0.040±0.014	AWAJI	81	DPWA	$\gamma N \to \pi N$
• • • We do not use the following data for averages, fits, limits, etc. • • •				
0.051±0.010	SHRESTHA	12A	DPWA	Multichannel
0.022±0.008	HORN	08A	DPWA	Multichannel
−0.007	PENNER	02D	DPWA	Multichannel

$\Delta(1920) \to N\gamma$, helicity-3/2 amplitude $A_{3/2}$

VALUE (GeV$^{-1/2}$)	DOCUMENT ID		TECN	COMMENT
$-0.115^{+0.025}_{-0.050}$	ANISOVICH	12A	DPWA	Multichannel
0.023±0.017	AWAJI	81	DPWA	$\gamma N \to \pi N$
• • • We do not use the following data for averages, fits, limits, etc. • • •				
0.017±0.015	SHRESTHA	12A	DPWA	Multichannel
0.042±0.012	HORN	08A	DPWA	Multichannel
−0.001	PENNER	02D	DPWA	Multichannel

$\Delta(1920)$ FOOTNOTES

[1] CHEW 80 reports two P_{33} resonances in this mass region. Problems with this analysis are discussed in section 2.1.11 of HOEHLER 83.
[2] See HOEHLER 93 for a detailed discussion of the evidence for and the pole parameters of N and Δ resonances as determined from Argand diagrams of πN elastic partial-wave amplitudes and from plots of the speeds with which the amplitudes traverse the diagrams.

$\Delta(1920)$ REFERENCES

For early references, see Physics Letters **111B** 1 (1982).

ANISOVICH	12A	EPJ A48 15	A.V. Anisovich *et al.*	(BONN, PNPI)
SHRESTHA	12A	PR C86 055203	M. Shrestha, D.M. Manley	(KSU)
HORN	08A	EPJ A38 173	I. Horn *et al.*	(CB-ELSA Collab.)
Also		PRL 101 202002	I. Horn *et al.*	(CB-ELSA Collab.)
ARNDT	06	PR C74 045205	R.A. Arndt *et al.*	(GWU)
PDG	06	JP G33 1	W.-M. Yao *et al.*	(PDG Collab.)
PENNER	02C	PR C66 055211	G. Penner, U. Mosel	(GIES)
PENNER	02D	PR C66 055212	G. Penner, U. Mosel	(GIES)
VRANA	00	PRPL 328 181	T.P. Vrana, S.A. Dytman,, T.-S.H. Lee	(PITT+)
HOEHLER	93	πN Newsletter 9 1	G. Hohler	(KARL)
MANLEY	92	PR D45 4002	D.M. Manley, E.M. Saleski	(KSA) IJP
Also		PR D30 904	D.M. Manley *et al.*	(VPI)
ARNDT	91	PR D43 2131	R.A. Arndt *et al.*	(VPI, TELE) IJP
CANDLIN	84	NP B238 477	D.J. Candlin *et al.*	(EDIN, RAL, LOWC)
HOEHLER	83	Landolt-Boernstein 1/9B2	G. Hohler	(KARLT)
PDG	82	PL 111B 1	M. Roos *et al.*	(HELS, CIT, CERN)
AWAJI	81	Bonn Conf. 352	N. Awaji, R. Kajikawa	(NAGO)
Also		NP B197 365	K. Fujii *et al.*	(NAGO)
CHEW	80	Toronto Conf. 123	D.M. Chew	(LBL) IJP
CUTKOSKY	80	Toronto Conf. 19	R.E. Cutkosky *et al.*	(CMU, LBL) IJP
Also		PR D20 2839	R.E. Cutkosky *et al.*	(CMU, LBL) IJP
LIVANOS	80	Toronto Conf. 35	P. Livanos *et al.*	(SACL) IJP
HOEHLER	79	PDAT 12-1	G. Hohler *et al.*	(KARLT) IJP
Also		Toronto Conf. 3	R. Koch	(KARLT) IJP

$\Delta(1930)$ $5/2^-$

$I(J^P) = \frac{3}{2}(\frac{5}{2}^-)$ Status: ***

Most of the results published before 1975 were last included in our 1982 edition, Physics Letters **111B** 1 (1982). Some further obsolete results published before 1984 were last included in our 2006 edition, Journal of Physics (generic for all A,B,E,G) **G33** 1 (2006).

$\Delta(1930)$ BREIT-WIGNER MASS

VALUE (MeV)	DOCUMENT ID		TECN	COMMENT
1900 to 2000 (≈ 1950) OUR ESTIMATE				
2233 ± 53	ARNDT	06	DPWA	$\pi N \to \pi N, \eta N$
1940 ± 30	CUTKOSKY	80	IPWA	$\pi N \to \pi N$
1901 ± 15	HOEHLER	79	IPWA	$\pi N \to \pi N$
• • • We do not use the following data for averages, fits, limits, etc. • • •				
1930 ± 12	SHRESTHA	12A	DPWA	Multichannel
2046 ± 45	ARNDT	04	DPWA	$\pi N \to \pi N, \eta N$
1932 ±100	VRANA	00	DPWA	Multichannel
1955 ± 15	ARNDT	96	IPWA	$\gamma N \to \pi N$
2056	ARNDT	95	DPWA	$\pi N \to N\pi$
1963	LI	93	IPWA	$\gamma N \to \pi N$
1956 ± 22	MANLEY	92	IPWA	$\pi N \to \pi N$ & $N\pi\pi$
$1910.0^{+15.0}_{-17.2}$	CHEW	80	BPWA	$\pi^+ p \to \pi^+ p$

$\Delta(1930)$ BREIT-WIGNER WIDTH

VALUE (MeV)	DOCUMENT ID		TECN	COMMENT
220 to 500 (≈ 360) OUR ESTIMATE				
773 ±187	ARNDT	06	DPWA	$\pi N \to \pi N, \eta N$
320 ± 60	CUTKOSKY	80	IPWA	$\pi N \to \pi N$
195 ± 60	HOEHLER	79	IPWA	$\pi N \to \pi N$
• • • We do not use the following data for averages, fits, limits, etc. • • •				
235 ± 39	SHRESTHA	12A	DPWA	Multichannel
402 ±198	ARNDT	04	DPWA	$\pi N \to \pi N, \eta N$
316 ±237	VRANA	00	DPWA	Multichannel
350 ± 20	ARNDT	96	IPWA	$\gamma N \to \pi N$
590	ARNDT	95	DPWA	$\pi N \to N\pi$
260	LI	93	IPWA	$\gamma N \to \pi N$
530 ±140	MANLEY	92	IPWA	$\pi N \to \pi N$ & $N\pi\pi$
$74.8^{+17.0}_{-16.0}$	CHEW	80	BPWA	$\pi^+ p \to \pi^+ p$

$\Delta(1930)$ POLE POSITION

REAL PART

VALUE (MeV)	DOCUMENT ID		TECN	COMMENT
1840 to 1960 (≈ 1900) OUR ESTIMATE				
2001	ARNDT	06	DPWA	$\pi N \to \pi N, \eta N$
1850	[1] HOEHLER	93	SPED	$\pi N \to \pi N$
1890±50	CUTKOSKY	80	IPWA	$\pi N \to \pi N$
• • • We do not use the following data for averages, fits, limits, etc. • • •				
1882	SHRESTHA	12A	DPWA	Multichannel
1966	ARNDT	04	DPWA	$\pi N \to \pi N, \eta N$
1883	VRANA	00	DPWA	Multichannel
1913	ARNDT	95	DPWA	$\pi N \to N\pi$
2018	ARNDT	91	DPWA	$\pi N \to \pi N$ Soln SM90

−2×IMAGINARY PART

VALUE (MeV)	DOCUMENT ID		TECN	COMMENT
175 to 360 (≈ 270) OUR ESTIMATE				
387	ARNDT	06	DPWA	$\pi N \to \pi N, \eta N$
180	[1] HOEHLER	93	SPED	$\pi N \to \pi N$
260±60	CUTKOSKY	80	IPWA	$\pi N \to \pi N$
• • • We do not use the following data for averages, fits, limits, etc. • • •				
187	SHRESTHA	12A	DPWA	Multichannel
364	ARNDT	04	DPWA	$\pi N \to \pi N, \eta N$
250	VRANA	00	DPWA	Multichannel
246	ARNDT	95	DPWA	$\pi N \to N\pi$
398	ARNDT	91	DPWA	$\pi N \to \pi N$ Soln SM90

Δ(1930) ELASTIC POLE RESIDUE

MODULUS |r|

VALUE (MeV)	DOCUMENT ID		TECN	COMMENT
7	ARNDT	06	DPWA	$\pi N \to \pi N, \eta N$
20	HOEHLER	93	SPED	$\pi N \to \pi N$
18±6	CUTKOSKY	80	IPWA	$\pi N \to \pi N$
• • • We do not use the following data for averages, fits, limits, etc. • • •				
16	ARNDT	04	DPWA	$\pi N \to \pi N, \eta N$
8	ARNDT	95	DPWA	$\pi N \to N\pi$
15	ARNDT	91	DPWA	$\pi N \to \pi N$ Soln SM90

PHASE θ

VALUE (°)	DOCUMENT ID		TECN	COMMENT
−12	ARNDT	06	DPWA	$\pi N \to \pi N, \eta N$
−20±40	CUTKOSKY	80	IPWA	$\pi N \to \pi N$
• • • We do not use the following data for averages, fits, limits, etc. • • •				
−21	ARNDT	04	DPWA	$\pi N \to \pi N, \eta N$
−47	ARNDT	95	DPWA	$\pi N \to N\pi$
−24	ARNDT	91	DPWA	$\pi N \to \pi N$ Soln SM90

Δ(1930) DECAY MODES

The following branching fractions are our estimates, not fits or averages.

	Mode	Fraction (Γ_i/Γ)
Γ_1	$N\pi$	5–15 %
Γ_2	ΣK	
Γ_3	$N\pi\pi$	
Γ_4	$N\gamma$	0.0–0.02 %
Γ_5	$N\gamma$, helicity=1/2	0.0–0.01 %
Γ_6	$N\gamma$, helicity=3/2	0.0–0.01 %

Δ(1930) BRANCHING RATIOS

$\Gamma(N\pi)/\Gamma_{total}$ Γ_1/Γ

VALUE (%)	DOCUMENT ID		TECN	COMMENT
5 to 15 OUR ESTIMATE				
8.1±1.2	ARNDT	06	DPWA	$\pi N \to \pi N, \eta N$
14 ±4	CUTKOSKY	80	IPWA	$\pi N \to \pi N$
4 ±3	HOEHLER	79	IPWA	$\pi N \to \pi N$
• • • We do not use the following data for averages, fits, limits, etc. • • •				
7.9±0.4	SHRESTHA	12A	DPWA	Multichannel
4.0±1.4	ARNDT	04	DPWA	$\pi N \to \pi N, \eta N$
9 ±8	VRANA	00	DPWA	Multichannel
11	ARNDT	95	DPWA	$\pi N \to N\pi$
18 ±2	MANLEY	92	IPWA	$\pi N \to \pi N$ & $N\pi\pi$
11	CHEW	80	BPWA	$\pi^+ p \to \pi^+ p$

$(\Gamma_i\Gamma_f)^{1/2}/\Gamma_{total}$ in $N\pi \to \Delta(1930) \to \Sigma K$ $(\Gamma_1\Gamma_2)^{1/2}/\Gamma$

VALUE	DOCUMENT ID		TECN	COMMENT
< 0.015	CANDLIN	84	DPWA	$\pi^+ p \to \Sigma^+ K^+$
• • • We do not use the following data for averages, fits, limits, etc. • • •				
−0.031	LIVANOS	80	DPWA	$\pi p \to \Sigma K$

$(\Gamma_i\Gamma_f)^{1/2}/\Gamma_{total}$ in $N\pi \to \Delta(1930) \to N\pi\pi$ $(\Gamma_1\Gamma_3)^{1/2}/\Gamma$

VALUE	DOCUMENT ID		TECN	COMMENT
not seen	LONGACRE	75	IPWA	$\pi N \to N\pi\pi$

Δ(1930) PHOTON DECAY AMPLITUDES

Papers on γN amplitudes predating 1981 may be found in our 2006 edition, Journal of Physics (generic for all A,B,E,G) **G33** 1 (2006).

Δ(1930) → $N\gamma$, helicity-1/2 amplitude $A_{1/2}$

VALUE ($GeV^{-1/2}$)	DOCUMENT ID		TECN	COMMENT
−0.009±0.028 OUR ESTIMATE				
−0.007±0.010	ARNDT	96	IPWA	$\gamma N \to \pi N$
0.009±0.009	AWAJI	81	DPWA	$\gamma N \to \pi N$
• • • We do not use the following data for averages, fits, limits, etc. • • •				
0.011±0.003	SHRESTHA	12A	DPWA	Multichannel
−0.019±0.001	LI	93	IPWA	$\gamma N \to \pi N$

Δ(1930) → $N\gamma$, helicity-3/2 amplitude $A_{3/2}$

VALUE ($GeV^{-1/2}$)	DOCUMENT ID		TECN	COMMENT
−0.018±0.028 OUR ESTIMATE				
0.005±0.010	ARNDT	96	IPWA	$\gamma N \to \pi N$
−0.025±0.011	AWAJI	81	DPWA	$\gamma N \to \pi N$
• • • We do not use the following data for averages, fits, limits, etc. • • •				
0.002±0.002	SHRESTHA	12A	DPWA	Multichannel
0.009±0.001	LI	93	IPWA	$\gamma N \to \pi N$

Δ(1930) FOOTNOTES

[1] See HOEHLER 93 for a detailed discussion of the evidence for and the pole parameters of N and Δ resonances as determined from Argand diagrams of πN elastic partial-wave amplitudes and from plots of the speeds with which the amplitudes traverse the diagrams.

Δ(1930) REFERENCES

For early references, see Physics Letters **111B** 1 (1982).

SHRESTHA	12A	PR C86 055203	M. Shrestha, D.M. Manley	(KSU)
ARNDT	06	PR C74 045205	R.A. Arndt *et al.*	(GWU)
PDG	06	JP G33 1	W.-M. Yao *et al.*	(PDG Collab.)
ARNDT	04	PR C69 035213	R.A. Arndt *et al.*	(GWU, TRIU)
VRANA	00	PRPL 328 181	T.P. Vrana, S.A. Dytman,, T.-S.H. Lee	(PITT+)
ARNDT	96	PR C53 430	R.A. Arndt, I.I. Strakovsky, R.L. Workman	(VPI)
ARNDT	95	PR C52 2120	R.A. Arndt *et al.*	(VPI, BRCO)
HOEHLER	93	πN Newsletter 9 1	G. Hohler	(KARL)
LI	93	PR C47 2759	Z.J. Li *et al.*	(VPI)
MANLEY	92	PR D45 4002	D.M. Manley, E.M. Saleski	(KSA) IJP
Also		PR D30 904	D.M. Manley *et al.*	(VPI)
ARNDT	91	PR D43 2131	R.A. Arndt *et al.*	(VPI, TELE) IJP
CANDLIN	84	NP B238 477	D.J. Candlin *et al.*	(EDIN, RAL, LOWC)
PDG	82	PL 111B 1	M. Roos *et al.*	(HELS, CIT, CERN)
AWAJI	81	Bonn Conf. 352	N. Awaji, R. Kajikawa	(NAGO)
Also		NP B197 365	K. Fujii *et al.*	(NAGO)
CHEW	80	Toronto Conf. 123	D.M. Chew	(LBL) IJP
CUTKOSKY	80	Toronto Conf. 19	R.E. Cutkosky *et al.*	(CMU, LBL) IJP
Also		PR D20 2839	R.E. Cutkosky *et al.*	(CMU, LBL) IJP
LIVANOS	80	Toronto Conf. 35	P. Livanos *et al.*	(SACL) IJP
HOEHLER	79	PDAT 12-1	G. Hohler *et al.*	(KARLT) IJP
Also		Toronto Conf. 3	R. Koch	(KARLT) IJP
LONGACRE	75	PL 55B 415	R.S. Longacre *et al.*	(LBL, SLAC) IJP

Δ(1940) 3/2⁻

$I(J^P) = \frac{3}{2}(\frac{3}{2}^-)$ Status: **

OMITTED FROM SUMMARY TABLE

The latest GWU analysis (ARNDT 06) finds no evidence for this resonance.

Δ(1940) BREIT-WIGNER MASS

VALUE (MeV)	DOCUMENT ID		TECN	COMMENT
1940 to 2060 (≈ 2000) OUR ESTIMATE				
1995 $^{+105}_{-60}$	ANISOVICH	12A	DPWA	Multichannel
2058.1± 34.5	CHEW	80	BPWA	$\pi^+ p \to \pi^+ p$
1940 ±100	CUTKOSKY	80	IPWA	$\pi N \to \pi N$
• • • We do not use the following data for averages, fits, limits, etc. • • •				
1990 ± 40	HORN	08A	DPWA	Multichannel
2057 ±110	MANLEY	92	IPWA	$\pi N \to \pi N$ & $N\pi\pi$

Δ(1940) BREIT-WIGNER WIDTH

VALUE (MeV)	DOCUMENT ID		TECN	COMMENT
450 ±100	ANISOVICH	12A	DPWA	Multichannel
198.4± 45.5	CHEW	80	BPWA	$\pi^+ p \to \pi^+ p$
200 ±100	CUTKOSKY	80	IPWA	$\pi N \to \pi N$
• • • We do not use the following data for averages, fits, limits, etc. • • •				
410 ± 70	HORN	08A	DPWA	Multichannel
460 ±320	MANLEY	92	IPWA	$\pi N \to \pi N$ & $N\pi\pi$

Δ(1940) POLE POSITION

REAL PART

VALUE (MeV)	DOCUMENT ID		TECN	COMMENT
1990 $^{+100}_{-50}$	ANISOVICH	12A	DPWA	Multichannel
1900±100	CUTKOSKY	80	IPWA	$\pi N \to \pi N$
1915 or 1926	[1] LONGACRE	78	IPWA	$\pi N \to N\pi\pi$
• • • We do not use the following data for averages, fits, limits, etc. • • •				
1985± 30	HORN	08A	DPWA	Multichannel

−2×IMAGINARY PART

VALUE (MeV)	DOCUMENT ID		TECN	COMMENT
450±90	ANISOVICH	12A	DPWA	Multichannel
200±60	CUTKOSKY	80	IPWA	$\pi N \to \pi N$
190 or 186	[1] LONGACRE	78	IPWA	$\pi N \to N\pi\pi$
• • • We do not use the following data for averages, fits, limits, etc. • • •				
390±50	HORN	08A	DPWA	Multichannel

Δ(1940) ELASTIC POLE RESIDUE

MODULUS |r|

VALUE (MeV)	DOCUMENT ID		TECN	COMMENT
4±4	ANISOVICH	12A	DPWA	Multichannel
8±3	CUTKOSKY	80	IPWA	$\pi N \to \pi N$

PHASE θ

VALUE (°)	DOCUMENT ID		TECN	COMMENT
135±45	CUTKOSKY	80	IPWA	$\pi N \to \pi N$

Baryon Particle Listings

$\Delta(1940)$, $\Delta(1950)$

$\Delta(1940)$ DECAY MODES

	Mode
Γ_1	$N\pi$
Γ_2	ΣK
Γ_3	$N\pi\pi$
Γ_4	$\Delta(1232)\pi$, S-wave
Γ_5	$\Delta(1232)\pi$, D-wave
Γ_6	$N\rho$, S=3/2, S-wave
Γ_7	$N(1535)\pi$
Γ_8	$Na_0(980)$
Γ_9	$\Delta(1232)\eta$
Γ_{10}	$N\gamma$, helicity=1/2
Γ_{11}	$N\gamma$, helicity=3/2

$\Delta(1940)$ BRANCHING RATIOS

$\Gamma(N\pi)/\Gamma_{total}$ Γ_1/Γ

VALUE (%)	DOCUMENT ID		TECN	COMMENT
18	CHEW	80	BPWA	$\pi^+ p \to \pi^+ p$
5 ± 2	CUTKOSKY	80	IPWA	$\pi N \to \pi N$
• • • We do not use the following data for averages, fits, limits, etc. • • •				
9 ± 4	HORN	08A	DPWA	Multichannel
18 ± 12	MANLEY	92	IPWA	$\pi N \to \pi N$ & $N\pi\pi$

$(\Gamma_i\Gamma_f)^{1/2}/\Gamma_{total}$ in $N\pi \to \Delta(1940) \to \Sigma K$ $(\Gamma_1\Gamma_2)^{1/2}/\Gamma$

VALUE	DOCUMENT ID		TECN	COMMENT
<0.015	CANDLIN	84	DPWA	$\pi^+ p \to \Sigma^+ K^+$

$(\Gamma_i\Gamma_f)^{1/2}/\Gamma_{total}$ in $N\pi \to \Delta(1940) \to \Delta(1232)\pi$, S-wave $(\Gamma_1\Gamma_4)^{1/2}/\Gamma$

VALUE	DOCUMENT ID		TECN	COMMENT
• • • We do not use the following data for averages, fits, limits, etc. • • •				
+0.11 ± 0.10	MANLEY	92	IPWA	$\pi N \to \pi N$ & $N\pi\pi$

$(\Gamma_i\Gamma_f)^{1/2}/\Gamma_{total}$ in $N\pi \to \Delta(1940) \to \Delta(1232)\pi$, D-wave $(\Gamma_1\Gamma_5)^{1/2}/\Gamma$

VALUE	DOCUMENT ID		TECN	COMMENT
• • • We do not use the following data for averages, fits, limits, etc. • • •				
+0.27 ± 0.16	MANLEY	92	IPWA	$\pi N \to \pi N$ & $N\pi\pi$

$(\Gamma_i\Gamma_f)^{1/2}/\Gamma_{total}$ in $N\pi \to \Delta(1940) \to N\rho$, S=3/2, S-wave $(\Gamma_1\Gamma_6)^{1/2}/\Gamma$

VALUE	DOCUMENT ID		TECN	COMMENT
• • • We do not use the following data for averages, fits, limits, etc. • • •				
+0.25 ± 0.10	MANLEY	92	IPWA	$\pi N \to \pi N$ & $N\pi\pi$

$\Gamma(N(1535)\pi)/\Gamma_{total}$ Γ_7/Γ

VALUE (%)	DOCUMENT ID		TECN	COMMENT
• • • We do not use the following data for averages, fits, limits, etc. • • •				
2 ± 1	HORN	08A	DPWA	Multichannel

$\Gamma(Na_0(980))/\Gamma_{total}$ Γ_8/Γ

VALUE (%)	DOCUMENT ID		TECN	COMMENT
• • • We do not use the following data for averages, fits, limits, etc. • • •				
2 ± 1	HORN	08A	DPWA	Multichannel

$\Gamma(\Delta(1232)\eta)/\Gamma_{total}$ Γ_9/Γ

VALUE (%)	DOCUMENT ID		TECN	COMMENT
• • • We do not use the following data for averages, fits, limits, etc. • • •				
4 ± 2	HORN	08A	DPWA	Multichannel

$\Delta(1940)$ PHOTON DECAY AMPLITUDES

Papers on γN amplitudes predating 1981 may be found in our 2006 edition, Journal of Physics (generic for all A,B,E,G) **G33** 1 (2006).

$\Delta(1940) \to N\gamma$, helicity-1/2 amplitude $A_{1/2}$

VALUE (GeV$^{-1/2}$)	DOCUMENT ID		TECN	COMMENT
−0.036 ± 0.058	AWAJI	81	DPWA	$\gamma N \to \pi N$
• • • We do not use the following data for averages, fits, limits, etc. • • •				
0.160 ± 0.040	HORN	08A	DPWA	Multichannel

$\Delta(1940) \to N\gamma$, helicity-3/2 amplitude $A_{3/2}$

VALUE (GeV$^{-1/2}$)	DOCUMENT ID		TECN	COMMENT
−0.031 ± 0.012	AWAJI	81	DPWA	$\gamma N \to \pi N$
• • • We do not use the following data for averages, fits, limits, etc. • • •				
0.110 ± 0.030	HORN	08A	DPWA	Multichannel

$\Delta(1940)$ FOOTNOTES

[1] LONGACRE 78 values are from a search for poles in the unitarized T-matrix. The first (second) value uses, in addition to $\pi N \to N\pi\pi$ data, elastic amplitudes from a Saclay (CERN) partial-wave analysis.

$\Delta(1940)$ REFERENCES

ANISOVICH	12A	EPJ A48 15	A.V. Anisovich *et al.*	(BONN, PNPI)
HORN	08A	EPJ A38 173	I. Horn *et al.*	(CB-ELSA Collab.)
Also		PRL 101 202002	I. Horn *et al.*	(CB-ELSA Collab.)
ARNDT	06	PR C74 045205	R.A. Arndt *et al.*	(GWU)
PDG	06	JP G33 1	W.-M. Yao *et al.*	(PDG Collab.)
MANLEY	92	PR D45 4002	D.M. Manley, E.M. Saleski	(KSA) IJP
Also		PR D30 904	D.M. Manley *et al.*	(VPI)
CANDLIN	84	NP B238 477	D.J. Candlin *et al.*	(EDIN, RAL, LOWC)
AWAJI	81	Bonn Conf. 352	N. Awaji, R. Kajikawa	(NAGO)
Also		NP B197 365	K. Fujii *et al.*	(NAGO)
CHEW	80	Toronto Conf. 123	D.M. Chew	(LBL) IJP
CUTKOSKY	80	Toronto Conf. 19	R.E. Cutkosky *et al.*	(CMU, LBL) IJP
Also		PR D20 2839	R.E. Cutkosky *et al.*	(CMU, LBL)
LONGACRE	78	PR D17 1795	R.S. Longacre *et al.*	(LBL, SLAC)

$\Delta(1950)$ $7/2^+$

$I(J^P) = \frac{3}{2}(\frac{7}{2}^+)$ Status: ****

Most of the results published before 1975 were last included in our 1982 edition, Physics Letters **111B** 1 (1982). Some further obsolete results published before 1984 were last included in our 2006 edition, Journal of Physics (generic for all A,B,E,G) **G33** 1 (2006).

$\Delta(1950)$ BREIT-WIGNER MASS

VALUE (MeV)	DOCUMENT ID		TECN	COMMENT
1915 to 1950 (≈ 1930) OUR ESTIMATE				
1915 ± 6	ANISOVICH	12A	DPWA	Multichannel
1921.3 ± 0.2	ARNDT	06	DPWA	$\pi N \to \pi N$, ηN
1950 ±15	CUTKOSKY	80	IPWA	$\pi N \to \pi N$
1913 ± 8	HOEHLER	79	IPWA	$\pi N \to \pi N$
• • • We do not use the following data for averages, fits, limits, etc. • • •				
1918 ± 1	SHRESTHA	12A	DPWA	Multichannel
1928 ± 8	ANISOVICH	10	DPWA	Multichannel
1923.3 ± 0.5	ARNDT	04	DPWA	$\pi N \to \pi N$, ηN
1936 ± 5	VRANA	00	DPWA	Multichannel
1947 ± 9	ARNDT	96	IPWA	$\gamma N \to \pi N$
1921	ARNDT	95	DPWA	$\pi N \to N\pi$
1940	LI	93	IPWA	$\gamma N \to \pi N$
1945 ± 2	MANLEY	92	IPWA	$\pi N \to \pi N$ & $N\pi\pi$
1925 ±20	CANDLIN	84	DPWA	$\pi^+ p \to \Sigma^+ K^+$
$1855.0^{+11.0}_{-10.0}$	CHEW	80	BPWA	$\pi^+ p \to \pi^+ p$
1925	[1] LONGACRE	75	IPWA	$\pi N \to N\pi\pi$

$\Delta(1950)$ BREIT-WIGNER WIDTH

VALUE (MeV)	DOCUMENT ID		TECN	COMMENT
235 to 335 (≈ 285) OUR ESTIMATE				
246 ±10	ANISOVICH	12A	DPWA	Multichannel
271.1 ± 1.1	ARNDT	06	DPWA	$\pi N \to \pi N$, ηN
340 ±50	CUTKOSKY	80	IPWA	$\pi N \to \pi N$
224 ±10	HOEHLER	79	IPWA	$\pi N \to \pi N$
• • • We do not use the following data for averages, fits, limits, etc. • • •				
259 ± 4	SHRESTHA	12A	DPWA	Multichannel
290 ±14	ANISOVICH	10	DPWA	Multichannel
278.2 ± 3.0	ARNDT	04	DPWA	$\pi N \to \pi N$, ηN
245 ±12	VRANA	00	DPWA	Multichannel
302 ± 9	ARNDT	96	IPWA	$\gamma N \to \pi N$
232	ARNDT	95	DPWA	$\pi N \to N\pi$
306	LI	93	IPWA	$\gamma N \to \pi N$
300 ± 7	MANLEY	92	IPWA	$\pi N \to \pi N$ & $N\pi\pi$
330 ±40	CANDLIN	84	DPWA	$\pi^+ p \to \Sigma^+ K^+$
$157.2^{+22.0}_{-19.0}$	CHEW	80	BPWA	$\pi^+ p \to \pi^+ p$
240	[1] LONGACRE	75	IPWA	$\pi N \to N\pi\pi$

$\Delta(1950)$ POLE POSITION

REAL PART

VALUE (MeV)	DOCUMENT ID		TECN	COMMENT
1870 to 1890 (≈ 1880) OUR ESTIMATE				
1890 ± 4	ANISOVICH	12A	DPWA	Multichannel
1876	ARNDT	06	DPWA	$\pi N \to \pi N$, ηN
1878	[2] HOEHLER	93	ARGD	$\pi N \to \pi N$
1890 ±15	CUTKOSKY	80	IPWA	$\pi N \to \pi N$
• • • We do not use the following data for averages, fits, limits, etc. • • •				
1871	SHRESTHA	12A	DPWA	Multichannel
1882 ± 8	ANISOVICH	10	DPWA	Multichannel
1874	ARNDT	04	DPWA	$\pi N \to \pi N$, ηN
1910	VRANA	00	DPWA	Multichannel
1880	ARNDT	95	DPWA	$\pi N \to N\pi$
1884	ARNDT	91	DPWA	$\pi N \to \pi N$ Soln SM90
1924 or 1924	[3] LONGACRE	78	IPWA	$\pi N \to N\pi\pi$

−2×IMAGINARY PART

VALUE (MeV)	DOCUMENT ID		TECN	COMMENT
220 to 260 (≈ 240) OUR ESTIMATE				
243 ± 8	ANISOVICH	12A	DPWA	Multichannel
227	ARNDT	06	DPWA	$\pi N \to \pi N, \eta N$
230	[2] HOEHLER	93	ARGD	$\pi N \to \pi N$
260 ± 40	CUTKOSKY	80	IPWA	$\pi N \to \pi N$
• • • We do not use the following data for averages, fits, limits, etc. • • •				
220	SHRESTHA	12A	DPWA	Multichannel
262 ± 12	ANISOVICH	10	DPWA	Multichannel
236	ARNDT	04	DPWA	$\pi N \to \pi N, \eta N$
230	VRANA	00	DPWA	Multichannel
236	ARNDT	95	DPWA	$\pi N \to N\pi$
238	ARNDT	91	DPWA	$\pi N \to \pi N$ Soln SM90
258 or 258	[3] LONGACRE	78	IPWA	$\pi N \to N\pi\pi$

Δ(1950) ELASTIC POLE RESIDUE

MODULUS |r|

VALUE (MeV)	DOCUMENT ID		TECN	COMMENT
58 ± 2	ANISOVICH	12A	DPWA	Multichannel
53	ARNDT	06	DPWA	$\pi N \to \pi N, \eta N$
47	HOEHLER	93	ARGD	$\pi N \to \pi N$
50 ± 7	CUTKOSKY	80	IPWA	$\pi N \to \pi N$
• • • We do not use the following data for averages, fits, limits, etc. • • •				
57	ARNDT	04	DPWA	$\pi N \to \pi N, \eta N$
54	ARNDT	95	DPWA	$\pi N \to N\pi$
61	ARNDT	91	DPWA	$\pi N \to \pi N$ Soln SM90

PHASE θ

VALUE (°)	DOCUMENT ID		TECN	COMMENT
−24 ± 3	ANISOVICH	12A	DPWA	Multichannel
−31	ARNDT	06	DPWA	$\pi N \to \pi N, \eta N$
−32	HOEHLER	93	ARGD	$\pi N \to \pi N$
−33 ± 8	CUTKOSKY	80	IPWA	$\pi N \to \pi N$
• • • We do not use the following data for averages, fits, limits, etc. • • •				
−34	ARNDT	04	DPWA	$\pi N \to \pi N, \eta N$
−17	ARNDT	95	DPWA	$\pi N \to N\pi$
−23	ARNDT	91	DPWA	$\pi N \to \pi N$ Soln SM90

Δ(1950) INELASTIC POLE RESIDUE

The "normalized residue" is the residue divided by $\Gamma_{pole}/2$.

Normalized residue in $N\pi \to \Delta(1950) \to \Sigma K$

MODULUS (%)	PHASE (°)	DOCUMENT ID		TECN	COMMENT
5 ± 1	**−65 ± 25**	ANISOVICH	12A	DPWA	Multichannel

Normalized residue in $N\pi \to \Delta(1950) \to \Delta\pi$, F-wave

MODULUS (%)	PHASE (°)	DOCUMENT ID		TECN	COMMENT
12 ± 4	**12 ± 10**	ANISOVICH	12A	DPWA	Multichannel

Δ(1950) DECAY MODES

The following branching fractions are our estimates, not fits or averages.

	Mode	Fraction (Γ_i/Γ)
Γ_1	$N\pi$	35–45 %
Γ_2	ΣK	
Γ_3	$N\pi\pi$	
Γ_4	$\Delta\pi$	20–30 %
Γ_5	$\Delta(1232)\pi$, F-wave	
Γ_6	$\Delta(1232)\pi$, H-wave	
Γ_7	$N\rho$	<10 %
Γ_8	$N\rho$, S=1/2, F-wave	
Γ_9	$N\rho$, S=3/2, F-wave	
Γ_{10}	$N\gamma$	0.08–0.13 %
Γ_{11}	$N\gamma$, helicity=1/2	0.03–0.055 %
Γ_{12}	$N\gamma$, helicity=3/2	0.05–0.075 %

Δ(1950) BRANCHING RATIOS

$\Gamma(N\pi)/\Gamma_{total}$ — Γ_1/Γ

VALUE (%)	DOCUMENT ID		TECN	COMMENT
35 to 45 OUR ESTIMATE				
45 ± 2	ANISOVICH	12A	DPWA	Multichannel
47.1 ± 0.1	ARNDT	06	DPWA	$\pi N \to \pi N, \eta N$
39 ± 4	CUTKOSKY	80	IPWA	$\pi N \to \pi N$
38 ± 2	HOEHLER	79	IPWA	$\pi N \to \pi N$
• • • We do not use the following data for averages, fits, limits, etc. • • •				
45.6 ± 0.4	SHRESTHA	12A	DPWA	Multichannel
44 ± 8	ANISOVICH	10	DPWA	Multichannel
48.0 ± 0.2	ARNDT	04	DPWA	$\pi N \to \pi N, \eta N$
44 ± 1	VRANA	00	DPWA	Multichannel
49	ARNDT	95	DPWA	$\pi N \to N\pi$
38 ± 1	MANLEY	92	IPWA	$\pi N \to \pi N$ & $N\pi\pi$
44	CHEW	80	BPWA	$\pi^+ p \to \pi^+ p$

$(\Gamma_i\Gamma_f)^{1/2}/\Gamma_{total}$ in $N\pi \to \Delta(1950) \to \Sigma K$ — $(\Gamma_1\Gamma_2)^{1/2}/\Gamma$

VALUE	DOCUMENT ID		TECN	COMMENT
−0.053 ± 0.005	CANDLIN	84	DPWA	$\pi^+ p \to \Sigma^+ K^+$

$\Gamma(\Sigma K)/\Gamma_{total}$ — Γ_2/Γ

VALUE (%)	DOCUMENT ID		TECN	COMMENT
0.4 ± 0.1	ANISOVICH	12A	DPWA	Multichannel

Note: Signs of couplings from $\pi N \to N\pi\pi$ analyses were changed in the 1986 edition to agree with the baryon-first convention; the overall phase ambiguity is resolved by choosing a negative sign for the Δ(1620) S_{31} coupling to $\Delta(1232)\pi$.

$(\Gamma_i\Gamma_f)^{1/2}/\Gamma_{total}$ in $N\pi \to \Delta(1950) \to \Delta(1232)\pi$, F-wave — $(\Gamma_1\Gamma_5)^{1/2}/\Gamma$

VALUE	DOCUMENT ID		TECN	COMMENT
+0.28 to +0.32 OUR ESTIMATE				
+0.32	[1] LONGACRE	75	IPWA	$\pi N \to N\pi\pi$
• • • We do not use the following data for averages, fits, limits, etc. • • •				
+0.27 ± 0.02	MANLEY	92	IPWA	$\pi N \to \pi N$ & $N\pi\pi$

$\Gamma(\Delta(1232)\pi$, F-wave$)/\Gamma_{total}$ — Γ_5/Γ

VALUE (%)	DOCUMENT ID		TECN	COMMENT
2.8 ± 1.4	ANISOVICH	12A	DPWA	Multichannel
36 ± 1	VRANA	00	DPWA	Multichannel
• • • We do not use the following data for averages, fits, limits, etc. • • •				
8 ± 1	SHRESTHA	12A	DPWA	Multichannel

$(\Gamma_i\Gamma_f)^{1/2}/\Gamma_{total}$ in $N\pi \to \Delta(1950) \to N\rho$, S=3/2, F-wave — $(\Gamma_1\Gamma_9)^{1/2}/\Gamma$

VALUE	DOCUMENT ID		TECN	COMMENT
+0.24	[1] LONGACRE	75	IPWA	$\pi N \to N\pi\pi$

Δ(1950) PHOTON DECAY AMPLITUDES

Papers on γN amplitudes predating 1981 may be found in our 2006 edition, Journal of Physics (generic for all A,B,E,G) **G33** 1 (2006).

Δ(1950) → Nγ, helicity-1/2 amplitude $A_{1/2}$

VALUE ($GeV^{-1/2}$)	DOCUMENT ID		TECN	COMMENT
−0.076 ± 0.012 OUR ESTIMATE				
−0.071 ± 0.004	ANISOVICH	12A	DPWA	Multichannel
−0.083 ± 0.004	WORKMAN	12A	DPWA	$\gamma N \to N\pi$
−0.068 ± 0.007	AWAJI	81	DPWA	$\gamma N \to \pi N$
• • • We do not use the following data for averages, fits, limits, etc. • • •				
−0.065 ± 0.001	SHRESTHA	12A	DPWA	Multichannel
−0.083 ± 0.008	ANISOVICH	10	DPWA	Multichannel
−0.094	DRECHSEL	07	DPWA	$\gamma N \to \pi N$
−0.079 ± 0.006	ARNDT	96	IPWA	$\gamma N \to \pi N$
−0.102 ± 0.003	LI	93	IPWA	$\gamma N \to \pi N$

Δ(1950) → Nγ, helicity-3/2 amplitude $A_{3/2}$

VALUE ($GeV^{-1/2}$)	DOCUMENT ID		TECN	COMMENT
−0.097 ± 0.010 OUR ESTIMATE				
−0.094 ± 0.005	ANISOVICH	12A	DPWA	Multichannel
−0.096 ± 0.004	WORKMAN	12A	DPWA	$\gamma N \to N\pi$
−0.094 ± 0.016	AWAJI	81	DPWA	$\gamma N \to \pi N$
• • • We do not use the following data for averages, fits, limits, etc. • • •				
−0.083 ± 0.001	SHRESTHA	12A	DPWA	Multichannel
−0.092 ± 0.008	ANISOVICH	10	DPWA	Multichannel
−0.121	DRECHSEL	07	DPWA	$\gamma N \to \pi N$
−0.103 ± 0.006	ARNDT	96	IPWA	$\gamma N \to \pi N$
−0.115 ± 0.003	LI	93	IPWA	$\gamma N \to \pi N$

Δ(1950) FOOTNOTES

[1] From method II of LONGACRE 75: eyeball fits with Breit-Wigner circles to the T-matrix amplitudes.

[2] See HOEHLER 93 for a detailed discussion of the evidence for and the pole parameters of N and Δ resonances as determined from Argand diagrams of πN elastic partial-wave amplitudes and from plots of the speeds with which the amplitudes traverse the diagrams.

[3] LONGACRE 78 values are from a search for poles in the unitarized T-matrix. The first (second) value uses, in addition to $\pi N \to N\pi\pi$ data, elastic amplitudes from a Saclay (CERN) partial-wave analysis.

$\Delta(1950)$ REFERENCES

ANISOVICH	12A	EPJ A48 15	A.V. Anisovich *et al.*	(BONN, PNPI)
SHRESTHA	12A	PR C86 055203	M. Shrestha, D.M. Manley	(KSU)
WORKMAN	12A	PR C86 015202	R. Workman *et al.*	(GWU)
ANISOVICH	10	EPJ A44 203	A.V. Anisovich *et al.*	(BONN, PNPI)
DRECHSEL	07	EPJ A34 69	D. Drechsel, S.S. Kamalov, L. Tiator	(MAINZ, JINR)
ARNDT	06	PR C74 045205	R.A. Arndt *et al.*	(GWU)
PDG	06	JP G33 1	W.-M. Yao *et al.*	(PDG Collab.)
ARNDT	04	PR C69 035213	R.A. Arndt *et al.*	(GWU, TRIU)
VRANA	00	PRPL 328 181	T.P. Vrana, S.A. Dytman,, T.-S.H. Lee	(PITT+)
ARNDT	96	PR C53 430	R.A. Arndt, I.I. Strakovsky, R.L. Workman	(VPI)
ARNDT	95	PR C52 2120	R.A. Arndt *et al.*	(VPI, BRCO)
HOEHLER	93	πN Newsletter 9 1	G. Hohler	(KARL)
LI	93	PR C47 2759	Z.J. Li *et al.*	(VPI)
MANLEY	92	PR D45 4002	D.M. Manley, E.M. Saleski	(KSA) IJP
Also		PR D30 904	D.M. Manley *et al.*	(VPI)
ARNDT	91	PR D43 2131	R.A. Arndt *et al.*	(VPI, TELE) IJP
CANDLIN	84	NP B238 477	D.J. Candlin *et al.*	(EDIN, RAL, LOWC)
PDG	82	PL 111B 1	M. Roos *et al.*	(HELS, CIT, CERN)
AWAJI	81	Bonn Conf. 352	N. Awaji, R. Kajikawa	(NAGO)
Also		NP B197 365	K. Fujii *et al.*	(NAGO)
CHEW	80	Toronto Conf. 123	D.M. Chew	(LBL) IJP
CUTKOSKY	80	Toronto Conf. 19	R.E. Cutkosky *et al.*	(CMU, LBL) IJP
Also		PR D20 2839	R.E. Cutkosky *et al.*	(CMU, LBL) IJP
HOEHLER	79	PDAT 12-1	G. Hohler *et al.*	(KARLT) IJP
Also		Toronto Conf. 3	R. Koch	(KARLT) IJP
LONGACRE	78	PR D17 1795	R.S. Longacre *et al.*	(LBL, SLAC)
LONGACRE	75	PL 55B 415	R.S. Longacre *et al.*	(LBL, SLAC) IJP

$\Delta(2000)\ 5/2^+$

$I(J^P) = \frac{3}{2}(\frac{5}{2}^+)$ Status: **

OMITTED FROM SUMMARY TABLE

The latest GWU analysis (ARNDT 06) finds no evidence for this resonance.

$\Delta(2000)$ BREIT-WIGNER MASS

VALUE (MeV)	DOCUMENT ID		TECN	COMMENT
≈ 2000 OUR ESTIMATE				
1724± 61	VRANA	00	DPWA	Multichannel
2200±125	CUTKOSKY	80	IPWA	$\pi N \to \pi N$
• • • We do not use the following data for averages, fits, limits, etc. • • •				
2015± 24	SHRESTHA	12A	DPWA	Multichannel
1752± 32	MANLEY	92	IPWA	$\pi N \to \pi N$ & $N\pi\pi$

$\Delta(2000)$ BREIT-WIGNER WIDTH

VALUE (MeV)	DOCUMENT ID		TECN	COMMENT
138± 68	VRANA	00	DPWA	Multichannel
400±125	CUTKOSKY	80	IPWA	$\pi N \to \pi N$
• • • We do not use the following data for averages, fits, limits, etc. • • •				
500± 52	SHRESTHA	12A	DPWA	Multichannel
251± 93	MANLEY	92	IPWA	$\pi N \to \pi N$ & $N\pi\pi$

$\Delta(2000)$ POLE POSITION

REAL PART

VALUE (MeV)	DOCUMENT ID		TECN	COMMENT
1697	VRANA	00	DPWA	Multichannel
2150±100	CUTKOSKY	80	IPWA	$\pi N \to \pi N$
• • • We do not use the following data for averages, fits, limits, etc. • • •				
1976	SHRESTHA	12A	DPWA	Multichannel

$-2\times$IMAGINARY PART

VALUE (MeV)	DOCUMENT ID		TECN	COMMENT
112	VRANA	00	DPWA	Multichannel
350±100	CUTKOSKY	80	IPWA	$\pi N \to \pi N$
• • • We do not use the following data for averages, fits, limits, etc. • • •				
488	SHRESTHA	12A	DPWA	Multichannel

$\Delta(2000)$ ELASTIC POLE RESIDUE

MODULUS $|r|$

VALUE (MeV)	DOCUMENT ID		TECN	COMMENT
16±5	CUTKOSKY	80	IPWA	$\pi N \to \pi N$

PHASE θ

VALUE (°)	DOCUMENT ID		TECN	COMMENT
150±90	CUTKOSKY	80	IPWA	$\pi N \to \pi N$

$\Delta(2000)$ DECAY MODES

	Mode
Γ_1	$N\pi$
Γ_2	$N\pi\pi$
Γ_3	$\Delta(1232)\pi$, P-wave
Γ_4	$\Delta(1232)\pi$, F-wave
Γ_5	$N\rho$, $S=3/2$, P-wave
Γ_6	$p\gamma$
Γ_7	$p\gamma$, helicity=1/2
Γ_8	$p\gamma$, helicity=3/2

$\Delta(2000)$ BRANCHING RATIOS

$\Gamma(N\pi)/\Gamma_{total}$ Γ_1/Γ

VALUE (%)	DOCUMENT ID		TECN	COMMENT
0±1	VRANA	00	DPWA	Multichannel
7±4	CUTKOSKY	80	IPWA	$\pi N \to \pi N$
• • • We do not use the following data for averages, fits, limits, etc. • • •				
7±1	SHRESTHA	12A	DPWA	Multichannel
2±1	MANLEY	92	IPWA	$\pi N \to \pi N$ & $N\pi\pi$

$(\Gamma_i\Gamma_f)^{1/2}/\Gamma_{total}$ in $N\pi \to \Delta(2000) \to \Delta(1232)\pi$, P-wave $(\Gamma_1\Gamma_3)^{1/2}/\Gamma$

VALUE	DOCUMENT ID		TECN	COMMENT
• • • We do not use the following data for averages, fits, limits, etc. • • •				
+0.07±0.03	MANLEY	92	IPWA	$\pi N \to \pi N$ & $N\pi\pi$

$\Gamma(\Delta(1232)\pi, P\text{-wave})/\Gamma_{total}$ Γ_3/Γ

VALUE (%)	DOCUMENT ID		TECN	COMMENT
0±1	VRANA	00	DPWA	Multichannel
• • • We do not use the following data for averages, fits, limits, etc. • • •				
3±3	SHRESTHA	12A	DPWA	Multichannel

$(\Gamma_i\Gamma_f)^{1/2}/\Gamma_{total}$ in $N\pi \to \Delta(2000) \to \Delta(1232)\pi$, F-wave $(\Gamma_1\Gamma_4)^{1/2}/\Gamma$

VALUE	DOCUMENT ID		TECN	COMMENT
• • • We do not use the following data for averages, fits, limits, etc. • • •				
+0.09±0.04	MANLEY	92	IPWA	$\pi N \to \pi N$ & $N\pi\pi$

$\Gamma(\Delta(1232)\pi, F\text{-wave})/\Gamma_{total}$ Γ_4/Γ

VALUE (%)	DOCUMENT ID		TECN	COMMENT
40±1	VRANA	00	DPWA	Multichannel
• • • We do not use the following data for averages, fits, limits, etc. • • •				
< 3	SHRESTHA	12A	DPWA	Multichannel

$(\Gamma_i\Gamma_f)^{1/2}/\Gamma_{total}$ in $N\pi \to \Delta(2000) \to N\rho$, $S=3/2$, P-wave $(\Gamma_1\Gamma_5)^{1/2}/\Gamma$

VALUE	DOCUMENT ID		TECN	COMMENT
• • • We do not use the following data for averages, fits, limits, etc. • • •				
−0.06±0.01	MANLEY	92	IPWA	$\pi N \to \pi N$ & $N\pi\pi$

$\Gamma(N\rho, S=3/2, P\text{-wave})/\Gamma_{total}$ Γ_5/Γ

VALUE (%)	DOCUMENT ID		TECN	COMMENT
60±60	VRANA	00	DPWA	Multichannel
• • • We do not use the following data for averages, fits, limits, etc. • • •				
90± 3	SHRESTHA	12A	DPWA	Multichannel

$\Delta(2000)$ PHOTON DECAY AMPLITUDES

$\Delta(2000) \to p\gamma$, helicity-1/2 amplitude $A_{1/2}$

VALUE (GeV$^{-1/2}$)	DOCUMENT ID		TECN	COMMENT
• • • We do not use the following data for averages, fits, limits, etc. • • •				
−0.061±0.018	SHRESTHA	12A	DPWA	Multichannel

$\Delta(2000) \to p\gamma$, helicity-3/2 amplitude $A_{3/2}$

VALUE (GeV$^{-1/2}$)	DOCUMENT ID		TECN	COMMENT
• • • We do not use the following data for averages, fits, limits, etc. • • •				
0.158±0.032	SHRESTHA	12A	DPWA	Multichannel

$\Delta(2000)$ REFERENCES

SHRESTHA	12A	PR C86 055203	M. Shrestha, D.M. Manley	(KSU)
ARNDT	06	PR C74 045205	R.A. Arndt *et al.*	(GWU)
VRANA	00	PRPL 328 181	T.P. Vrana, S.A. Dytman,, T.-S.H. Lee	(PITT+)
MANLEY	92	PR D45 4002	D.M. Manley, E.M. Saleski	(KSA) IJP
Also		PR D30 904	D.M. Manley *et al.*	(VPI)
CUTKOSKY	80	Toronto Conf. 19	R.E. Cutkosky *et al.*	(CMU, LBL)
Also		PR D20 2839	R.E. Cutkosky *et al.*	(CMU, LBL)

$\Delta(2150)\ 1/2^-$

$I(J^P) = \frac{3}{2}(\frac{1}{2}^-)$ Status: *

OMITTED FROM SUMMARY TABLE

The latest GWU analysis (ARNDT 06) finds no evidence for this resonance.

$\Delta(2150)$ BREIT-WIGNER MASS

VALUE (MeV)	DOCUMENT ID		TECN	COMMENT
≈ 2150 OUR ESTIMATE				
2047.4± 27.0	[1] CHEW	80	BPWA	$\pi^+ p \to \pi^+ p$
2203.2± 8.4	[1] CHEW	80	BPWA	$\pi^+ p \to \pi^+ p$
2150 ±100	CUTKOSKY	80	IPWA	$\pi N \to \pi N$

$\Delta(2150)$ BREIT-WIGNER WIDTH

VALUE (MeV)	DOCUMENT ID		TECN	COMMENT
121.6± 62.0	[1] CHEW	80	BPWA	$\pi^+ p \to \pi^+ p$
120.5± 45.0	[1] CHEW	80	BPWA	$\pi^+ p \to \pi^+ p$
200 ±100	CUTKOSKY	80	IPWA	$\pi N \to \pi N$

$\Delta(2150)$ POLE POSITION

REAL PART

VALUE (MeV)	DOCUMENT ID		TECN	COMMENT
2140±80	CUTKOSKY	80	IPWA	$\pi N \to \pi N$

−2×IMAGINARY PART

VALUE (MeV)	DOCUMENT ID		TECN	COMMENT
200±80	CUTKOSKY	80	IPWA	$\pi N \to \pi N$

$\Delta(2150)$ ELASTIC POLE RESIDUE

MODULUS $|r|$

VALUE (MeV)	DOCUMENT ID		TECN	COMMENT
7±2	CUTKOSKY	80	IPWA	$\pi N \to \pi N$

PHASE θ

VALUE (°)	DOCUMENT ID		TECN	COMMENT
−60±90	CUTKOSKY	80	IPWA	$\pi N \to \pi N$

$\Delta(2150)$ DECAY MODES

	Mode
Γ_1	$N\pi$
Γ_2	ΣK

$\Delta(2150)$ BRANCHING RATIOS

$\Gamma(N\pi)/\Gamma_{total}$ — **Γ_1/Γ**

VALUE (%)	DOCUMENT ID		TECN	COMMENT
41	[1] CHEW	80	BPWA	$\pi^+ p \to \pi^+ p$
37	[1] CHEW	80	BPWA	$\pi^+ p \to \pi^+ p$
8±2	CUTKOSKY	80	IPWA	$\pi N \to \pi N$

$(\Gamma_i\Gamma_f)^{1/2}/\Gamma_{total}$ in $N\pi \to \Delta(2150) \to \Sigma K$ — **$(\Gamma_1\Gamma_2)^{1/2}/\Gamma$**

VALUE	DOCUMENT ID		TECN	COMMENT
<0.03	CANDLIN	84	DPWA	$\pi^+ p \to \Sigma^+ K^+$

$\Delta(2150)$ FOOTNOTES

[1] CHEW 80 reports two S_{31} resonances in this mass region. Problems with this analysis are discussed in section 2.1.11 of HOEHLER 83.

$\Delta(2150)$ REFERENCES

ARNDT	06	PR C74 045205	R.A. Arndt *et al.*	(GWU)
CANDLIN	84	NP B238 477	D.J. Candlin *et al.*	(EDIN, RAL, LOWC)
HOEHLER	83	Landolt-Boernstein 1/9B2	G. Hohler	(KARLT)
CHEW	80	Toronto Conf. 123	D.M. Chew	(LBL) IJP
CUTKOSKY	80	Toronto Conf. 19	R.E. Cutkosky *et al.*	(CMU, LBL) IJP
Also		PR D20 2839	R.E. Cutkosky *et al.*	(CMU, LBL)

$\Delta(2200)\ 7/2^-$

$I(J^P) = \frac{3}{2}(\frac{7}{2}^-)$ Status: *

OMITTED FROM SUMMARY TABLE

The various analyses are not in good agreement.

The latest GWU analysis (ARNDT 06) finds no evidence for this resonance.

$\Delta(2200)$ BREIT-WIGNER MASS

VALUE (MeV)	DOCUMENT ID		TECN	COMMENT
≈ 2200 OUR ESTIMATE				
2200±80	CUTKOSKY	80	IPWA	$\pi N \to \pi N$
2215±60	HOEHLER	79	IPWA	$\pi N \to \pi N$
2280±80	HENDRY	78	MPWA	$\pi N \to \pi N$
• • • We do not use the following data for averages, fits, limits, etc. • • •				
2280±40	CANDLIN	84	DPWA	$\pi^+ p \to \Sigma^+ K^+$

$\Delta(2200)$ BREIT-WIGNER WIDTH

VALUE (MeV)	DOCUMENT ID		TECN	COMMENT
450±100	CUTKOSKY	80	IPWA	$\pi N \to \pi N$
400±100	HOEHLER	79	IPWA	$\pi N \to \pi N$
400±150	HENDRY	78	MPWA	$\pi N \to \pi N$
• • • We do not use the following data for averages, fits, limits, etc. • • •				
400± 50	CANDLIN	84	DPWA	$\pi^+ p \to \Sigma^+ K^+$

$\Delta(2200)$ POLE POSITION

REAL PART

VALUE (MeV)	DOCUMENT ID		TECN	COMMENT
2100±50	CUTKOSKY	80	IPWA	$\pi N \to \pi N$

−2×IMAGINARY PART

VALUE (MeV)	DOCUMENT ID		TECN	COMMENT
340±80	CUTKOSKY	80	IPWA	$\pi N \to \pi N$

$\Delta(2200)$ ELASTIC POLE RESIDUE

MODULUS $|r|$

VALUE (MeV)	DOCUMENT ID		TECN	COMMENT
8±3	CUTKOSKY	80	IPWA	$\pi N \to \pi N$

PHASE θ

VALUE (°)	DOCUMENT ID		TECN	COMMENT
−70±40	CUTKOSKY	80	IPWA	$\pi N \to \pi N$

$\Delta(2200)$ DECAY MODES

	Mode
Γ_1	$N\pi$
Γ_2	ΣK

$\Delta(2200)$ BRANCHING RATIOS

$\Gamma(N\pi)/\Gamma_{total}$ — **Γ_1/Γ**

VALUE (%)	DOCUMENT ID		TECN	COMMENT
6±2	CUTKOSKY	80	IPWA	$\pi N \to \pi N$
5±2	HOEHLER	79	IPWA	$\pi N \to \pi N$
9±2	HENDRY	78	MPWA	$\pi N \to \pi N$

$(\Gamma_i\Gamma_f)^{1/2}/\Gamma_{total}$ in $N\pi \to \Delta(2200) \to \Sigma K$ — **$(\Gamma_1\Gamma_2)^{1/2}/\Gamma$**

VALUE	DOCUMENT ID		TECN	COMMENT
−0.014±0.005	CANDLIN	84	DPWA	$\pi^+ p \to \Sigma^+ K^+$

$\Delta(2200)$ REFERENCES

ARNDT	06	PR C74 045205	R.A. Arndt *et al.*	(GWU)
CANDLIN	84	NP B238 477	D.J. Candlin *et al.*	(EDIN, RAL, LOWC)
CUTKOSKY	80	Toronto Conf. 19	R.E. Cutkosky *et al.*	(CMU, LBL) IJP
Also		PR D20 2839	R.E. Cutkosky *et al.*	(CMU, LBL) IJP
HOEHLER	79	PDAT 12-1	G. Hohler *et al.*	(KARLT) IJP
Also		Toronto Conf. 3	R. Koch	(KARLT) IJP
HENDRY	78	PRL 41 222	A.W. Hendry	(IND, LBL) IJP
Also		ANP 136 1	A.W. Hendry	(IND)

$\Delta(2300)\ 9/2^+$

$I(J^P) = \frac{3}{2}(\frac{9}{2}^+)$ Status: **

OMITTED FROM SUMMARY TABLE

The latest GWU analysis (ARNDT 06) finds no evidence for this resonance.

$\Delta(2300)$ BREIT-WIGNER MASS

VALUE (MeV)	DOCUMENT ID		TECN	COMMENT
≈ 2300 OUR ESTIMATE				
2204.5± 3.4	CHEW	80	BPWA	$\pi^+ p \rightarrow \pi^+ p$
2400 ±125	CUTKOSKY	80	IPWA	$\pi N \rightarrow \pi N$
2217 ± 80	HOEHLER	79	IPWA	$\pi N \rightarrow \pi N$
2450 ±100	HENDRY	78	MPWA	$\pi N \rightarrow \pi N$
• • • We do not use the following data for averages, fits, limits, etc. • • •				
2400	CANDLIN	84	DPWA	$\pi^+ p \rightarrow \Sigma^+ K^+$

$\Delta(2300)$ BREIT-WIGNER WIDTH

VALUE (MeV)	DOCUMENT ID		TECN	COMMENT
32.3± 1.0	CHEW	80	BPWA	$\pi^+ p \rightarrow \pi^+ p$
425 ±150	CUTKOSKY	80	IPWA	$\pi N \rightarrow \pi N$
300 ±100	HOEHLER	79	IPWA	$\pi N \rightarrow \pi N$
500 ±200	HENDRY	78	MPWA	$\pi N \rightarrow \pi N$
• • • We do not use the following data for averages, fits, limits, etc. • • •				
200	CANDLIN	84	DPWA	$\pi^+ p \rightarrow \Sigma^+ K^+$

$\Delta(2300)$ POLE POSITION

REAL PART

VALUE (MeV)	DOCUMENT ID		TECN	COMMENT
2370±80	CUTKOSKY	80	IPWA	$\pi N \rightarrow \pi N$

−2×IMAGINARY PART

VALUE (MeV)	DOCUMENT ID		TECN	COMMENT
420±160	CUTKOSKY	80	IPWA	$\pi N \rightarrow \pi N$

$\Delta(2300)$ ELASTIC POLE RESIDUE

MODULUS $|r|$

VALUE (MeV)	DOCUMENT ID		TECN	COMMENT
10±4	CUTKOSKY	80	IPWA	$\pi N \rightarrow \pi N$

PHASE θ

VALUE (°)	DOCUMENT ID		TECN	COMMENT
−20±30	CUTKOSKY	80	IPWA	$\pi N \rightarrow \pi N$

$\Delta(2300)$ DECAY MODES

	Mode
Γ_1	$N\pi$
Γ_2	ΣK

$\Delta(2300)$ BRANCHING RATIOS

$\Gamma(N\pi)/\Gamma_{total}$ Γ_1/Γ

VALUE (%)	DOCUMENT ID		TECN	COMMENT
5	CHEW	80	BPWA	$\pi^+ p \rightarrow \pi^+ p$
6±2	CUTKOSKY	80	IPWA	$\pi N \rightarrow \pi N$
3±2	HOEHLER	79	IPWA	$\pi N \rightarrow \pi N$
8±2	HENDRY	78	MPWA	$\pi N \rightarrow \pi N$

$(\Gamma_i\Gamma_f)^{1/2}/\Gamma_{total}$ in $N\pi \rightarrow \Delta(2300) \rightarrow \Sigma K$ $(\Gamma_1\Gamma_2)^{1/2}/\Gamma$

VALUE	DOCUMENT ID		TECN	COMMENT
−0.017	CANDLIN	84	DPWA	$\pi^+ p \rightarrow \Sigma^+ K^+$

$\Delta(2300)$ REFERENCES

ARNDT	06	PR C74 045205	R.A. Arndt *et al.* (GWU)
CANDLIN	84	NP B238 477	D.J. Candlin *et al.* (EDIN, RAL, LOWC)
CHEW	80	Toronto Conf. 123	D.M. Chew (LBL) IJP
CUTKOSKY	80	Toronto Conf. 19	R.E. Cutkosky *et al.* (CMU, LBL) IJP
Also		PR D20 2839	R.E. Cutkosky *et al.* (CMU, LBL)
HOEHLER	79	PDAT 12-1	G. Hohler *et al.* (KARLT) IJP
Also		Toronto Conf. 3	R. Koch (KARLT) IJP
HENDRY	78	PRL 41 222	A.W. Hendry (IND, LBL) IJP
Also		ANP 136 1	A.W. Hendry (IND)

$\Delta(2350)\ 5/2^-$

$I(J^P) = \frac{3}{2}(\frac{5}{2}^-)$ Status: *

OMITTED FROM SUMMARY TABLE

The latest GWU analysis (ARNDT 06) finds no evidence for this resonance.

$\Delta(2350)$ BREIT-WIGNER MASS

VALUE (MeV)	DOCUMENT ID		TECN	COMMENT
≈ 2350 OUR ESTIMATE				
2400±125	CUTKOSKY	80	IPWA	$\pi N \rightarrow \pi N$
2305± 26	HOEHLER	79	IPWA	$\pi N \rightarrow \pi N$
• • • We do not use the following data for averages, fits, limits, etc. • • •				
2459±100	VRANA	00	DPWA	Multichannel
2171± 18	MANLEY	92	IPWA	$\pi N \rightarrow \pi N$ & $N\pi\pi$

$\Delta(2350)$ BREIT-WIGNER WIDTH

VALUE (MeV)	DOCUMENT ID		TECN	COMMENT
400±150	CUTKOSKY	80	IPWA	$\pi N \rightarrow \pi N$
300± 70	HOEHLER	79	IPWA	$\pi N \rightarrow \pi N$
• • • We do not use the following data for averages, fits, limits, etc. • • •				
480±360	VRANA	00	DPWA	Multichannel
264± 51	MANLEY	92	IPWA	$\pi N \rightarrow \pi N$ & $N\pi\pi$

$\Delta(2350)$ POLE POSITION

REAL PART

VALUE (MeV)	DOCUMENT ID		TECN	COMMENT
2400±125	CUTKOSKY	80	IPWA	$\pi N \rightarrow \pi N$
• • • We do not use the following data for averages, fits, limits, etc. • • •				
2427	VRANA	00	DPWA	Multichannel

−2×IMAGINARY PART

VALUE (MeV)	DOCUMENT ID		TECN	COMMENT
400±150	CUTKOSKY	80	IPWA	$\pi N \rightarrow \pi N$
• • • We do not use the following data for averages, fits, limits, etc. • • •				
458	VRANA	00	DPWA	Multichannel

$\Delta(2350)$ ELASTIC POLE RESIDUE

MODULUS $|r|$

VALUE (MeV)	DOCUMENT ID		TECN	COMMENT
15±8	CUTKOSKY	80	IPWA	$\pi N \rightarrow \pi N$

PHASE θ

VALUE (°)	DOCUMENT ID		TECN	COMMENT
−70±70	CUTKOSKY	80	IPWA	$\pi N \rightarrow \pi N$

$\Delta(2350)$ DECAY MODES

	Mode
Γ_1	$N\pi$
Γ_2	ΣK

$\Delta(2350)$ BRANCHING RATIOS

$\Gamma(N\pi)/\Gamma_{total}$ Γ_1/Γ

VALUE (%)	DOCUMENT ID		TECN	COMMENT
20 ±10	CUTKOSKY	80	IPWA	$\pi N \rightarrow \pi N$
4 ± 2	HOEHLER	79	IPWA	$\pi N \rightarrow \pi N$
• • • We do not use the following data for averages, fits, limits, etc. • • •				
7 ±14	VRANA	00	DPWA	Multichannel
2.0± 0.3	MANLEY	92	IPWA	$\pi N \rightarrow \pi N$ & $N\pi\pi$

$(\Gamma_i\Gamma_f)^{1/2}/\Gamma_{total}$ in $N\pi \rightarrow \Delta(2350) \rightarrow \Sigma K$ $(\Gamma_1\Gamma_2)^{1/2}/\Gamma$

VALUE	DOCUMENT ID		TECN	COMMENT
<0.015	CANDLIN	84	DPWA	$\pi^+ p \rightarrow \Sigma^+ K^+$

$\Delta(2350)$ REFERENCES

ARNDT	06	PR C74 045205	R.A. Arndt *et al.* (GWU)
VRANA	00	PRPL 328 181	T.P. Vrana, S.A. Dytman,, T.-S.H. Lee (PITT+)
MANLEY	92	PR D45 4002	D.M. Manley, E.M. Saleski (KSA) IJP
Also		PR D30 904	D.M. Manley *et al.* (VPI)
CANDLIN	84	NP B238 477	D.J. Candlin *et al.* (EDIN, RAL, LOWC)
CUTKOSKY	80	Toronto Conf. 19	R.E. Cutkosky *et al.* (CMU, LBL) IJP
Also		PR D20 2839	R.E. Cutkosky *et al.* (CMU, LBL)
HOEHLER	79	PDAT 12-1	G. Hohler *et al.* (KARLT) IJP
Also		Toronto Conf. 3	R. Koch (KARLT) IJP

See key on page 547

$\Delta(2390)\ 7/2^+$

$I(J^P) = \frac{3}{2}(\frac{7}{2}^+)$ Status: *

OMITTED FROM SUMMARY TABLE

The latest GWU analysis (ARNDT 06) finds no evidence for this resonance.

$\Delta(2390)$ BREIT-WIGNER MASS

VALUE (MeV)	DOCUMENT ID		TECN	COMMENT
≈ 2390 OUR ESTIMATE				
2350±100	CUTKOSKY	80	IPWA	$\pi N \to \pi N$
2425± 60	HOEHLER	79	IPWA	$\pi N \to \pi N$

$\Delta(2390)$ BREIT-WIGNER WIDTH

VALUE (MeV)	DOCUMENT ID		TECN	COMMENT
300±100	CUTKOSKY	80	IPWA	$\pi N \to \pi N$
300± 80	HOEHLER	79	IPWA	$\pi N \to \pi N$

$\Delta(2390)$ POLE POSITION

REAL PART

VALUE (MeV)	DOCUMENT ID		TECN	COMMENT
2350±100	CUTKOSKY	80	IPWA	$\pi N \to \pi N$

−2×IMAGINARY PART

VALUE (MeV)	DOCUMENT ID		TECN	COMMENT
260±100	CUTKOSKY	80	IPWA	$\pi N \to \pi N$

$\Delta(2390)$ ELASTIC POLE RESIDUE

MODULUS $|r|$

VALUE (MeV)	DOCUMENT ID		TECN	COMMENT
12±6	CUTKOSKY	80	IPWA	$\pi N \to \pi N$

PHASE θ

VALUE (°)	DOCUMENT ID		TECN	COMMENT
−90±60	CUTKOSKY	80	IPWA	$\pi N \to \pi N$

$\Delta(2390)$ DECAY MODES

	Mode
Γ_1	$N\pi$
Γ_2	ΣK

$\Delta(2390)$ BRANCHING RATIOS

$\Gamma(N\pi)/\Gamma_{total}$ — **Γ_1/Γ**

VALUE (%)	DOCUMENT ID		TECN	COMMENT
8±4	CUTKOSKY	80	IPWA	$\pi N \to \pi N$
7±4	HOEHLER	79	IPWA	$\pi N \to \pi N$

$(\Gamma_i\Gamma_f)^{1/2}/\Gamma_{total}$ in $N\pi \to \Delta(2390) \to \Sigma K$ — **$(\Gamma_1\Gamma_2)^{1/2}/\Gamma$**

VALUE	DOCUMENT ID		TECN	COMMENT
<0.015	CANDLIN	84	DPWA	$\pi^+ p \to \Sigma^+ K^+$

$\Delta(2390)$ REFERENCES

ARNDT	06	PR C74 045205	R.A. Arndt *et al.*	(GWU)
CANDLIN	84	NP B238 477	D.J. Candlin *et al.*	(EDIN, RAL, LOWC)
CUTKOSKY	80	Toronto Conf. 19	R.E. Cutkosky *et al.*	(CMU, LBL) IJP
Also		PR D20 2839	R.E. Cutkosky *et al.*	(CMU, LBL)
HOEHLER	79	PDAT 12-1	G. Hohler *et al.*	(KARLT) IJP
Also		Toronto Conf. 3	R. Koch	(KARLT) IJP

$\Delta(2400)\ 9/2^-$

$I(J^P) = \frac{3}{2}(\frac{9}{2}^-)$ Status: **

OMITTED FROM SUMMARY TABLE

$\Delta(2400)$ BREIT-WIGNER MASS

VALUE (MeV)	DOCUMENT ID		TECN	COMMENT
≈ 2400 OUR ESTIMATE				
2643±141	ARNDT	06	DPWA	$\pi N \to \pi N, \eta N$
2300±100	CUTKOSKY	80	IPWA	$\pi N \to \pi N$
2468± 50	HOEHLER	79	IPWA	$\pi N \to \pi N$
2200±100	HENDRY	78	MPWA	$\pi N \to \pi N$

$\Delta(2400)$ BREIT-WIGNER WIDTH

VALUE (MeV)	DOCUMENT ID		TECN	COMMENT
895±432	ARNDT	06	DPWA	$\pi N \to \pi N, \eta N$
330±100	CUTKOSKY	80	IPWA	$\pi N \to \pi N$
480±100	HOEHLER	79	IPWA	$\pi N \to \pi N$
450±200	HENDRY	78	MPWA	$\pi N \to \pi N$

$\Delta(2400)$ POLE POSITION

REAL PART

VALUE (MeV)	DOCUMENT ID		TECN	COMMENT
1983	ARNDT	06	DPWA	$\pi N \to \pi N, \eta N$
2260±60	CUTKOSKY	80	IPWA	$\pi N \to \pi N$

−2×IMAGINARY PART

VALUE (MeV)	DOCUMENT ID		TECN	COMMENT
878	ARNDT	06	DPWA	$\pi N \to \pi N, \eta N$
320±160	CUTKOSKY	80	IPWA	$\pi N \to \pi N$

$\Delta(2400)$ ELASTIC POLE RESIDUE

MODULUS $|r|$

VALUE (MeV)	DOCUMENT ID		TECN	COMMENT
24	ARNDT	06	DPWA	$\pi N \to \pi N, \eta N$
8±4	CUTKOSKY	80	IPWA	$\pi N \to \pi N$

PHASE θ

VALUE (°)	DOCUMENT ID		TECN	COMMENT
−139	ARNDT	06	DPWA	$\pi N \to \pi N, \eta N$
− 25±15	CUTKOSKY	80	IPWA	$\pi N \to \pi N$

$\Delta(2400)$ DECAY MODES

	Mode
Γ_1	$N\pi$
Γ_2	ΣK

$\Delta(2400)$ BRANCHING RATIOS

$\Gamma(N\pi)/\Gamma_{total}$ — **Γ_1/Γ**

VALUE (%)	DOCUMENT ID		TECN	COMMENT
6.4±2.2	ARNDT	06	DPWA	$\pi N \to \pi N, \eta N$
5 ±2	CUTKOSKY	80	IPWA	$\pi N \to \pi N$
6 ±3	HOEHLER	79	IPWA	$\pi N \to \pi N$
10 ±3	HENDRY	78	MPWA	$\pi N \to \pi N$

$(\Gamma_i\Gamma_f)^{1/2}/\Gamma_{total}$ in $N\pi \to \Delta(2400) \to \Sigma K$ — **$(\Gamma_1\Gamma_2)^{1/2}/\Gamma$**

VALUE	DOCUMENT ID		TECN	COMMENT
<0.015	CANDLIN	84	DPWA	$\pi^+ p \to \Sigma^+ K^+$

$\Delta(2400)$ REFERENCES

ARNDT	06	PR C74 045205	R.A. Arndt *et al.*	(GWU)
CANDLIN	84	NP B238 477	D.J. Candlin *et al.*	(EDIN, RAL, LOWC)
CUTKOSKY	80	Toronto Conf. 19	R.E. Cutkosky *et al.*	(CMU, LBL) IJP
Also		PR D20 2839	R.E. Cutkosky *et al.*	(CMU, LBL)
HOEHLER	79	PDAT 12-1	G. Hohler *et al.*	(KARLT) IJP
Also		Toronto Conf. 3	R. Koch	(KARLT) IJP
HENDRY	78	PRL 41 222	A.W. Hendry	(IND, LBL) IJP
Also		ANP 136 1	A.W. Hendry	(IND)

Δ(2420) 11/2+

$I(J^P) = \frac{3}{2}(\frac{11}{2}^+)$ Status: ****

Most of the results published before 1975 are now obsolete and have been omitted. They may be found in our 1982 edition, Physics Letters **111B** 1 (1982).

Δ(2420) BREIT-WIGNER MASS

VALUE (MeV)	DOCUMENT ID		TECN	COMMENT
2300 to 2500 (≈ 2420) OUR ESTIMATE				
2633 ± 29	ARNDT	06	DPWA	$\pi N \to \pi N, \eta N$
2400 ±125	CUTKOSKY	80	IPWA	$\pi N \to \pi N$
2416 ± 17	HOEHLER	79	IPWA	$\pi N \to \pi N$
2400 ± 60	HENDRY	78	MPWA	$\pi N \to \pi N$
• • • We do not use the following data for averages, fits, limits, etc. • • •				
2400	CANDLIN	84	DPWA	$\pi^+ p \to \Sigma^+ K^+$
2358.0± 9.0	CHEW	80	BPWA	$\pi^+ p \to \pi^+ p$

Δ(2420) BREIT-WIGNER WIDTH

VALUE (MeV)	DOCUMENT ID		TECN	COMMENT
300 to 500 (≈ 400) OUR ESTIMATE				
692 ± 47	ARNDT	06	DPWA	$\pi N \to \pi N, \eta N$
450 ±150	CUTKOSKY	80	IPWA	$\pi N \to \pi N$
340 ± 28	HOEHLER	79	IPWA	$\pi N \to \pi N$
460 ±100	HENDRY	78	MPWA	$\pi N \to \pi N$
• • • We do not use the following data for averages, fits, limits, etc. • • •				
400	CANDLIN	84	DPWA	$\pi^+ p \to \Sigma^+ K^+$
202.2± 45.0	CHEW	80	BPWA	$\pi^+ p \to \pi^+ p$

Δ(2420) POLE POSITION

REAL PART

VALUE (MeV)	DOCUMENT ID		TECN	COMMENT
2260 to 2400 (≈ 2330) OUR ESTIMATE				
2529	ARNDT	06	DPWA	$\pi N \to \pi N, \eta N$
2300	[1] HOEHLER	93	ARGD	$\pi N \to \pi N$
2360±100	CUTKOSKY	80	IPWA	$\pi N \to \pi N$

−2×IMAGINARY PART

VALUE (MeV)	DOCUMENT ID		TECN	COMMENT
350 to 750 (≈ 550) OUR ESTIMATE				
621	ARNDT	06	DPWA	$\pi N \to \pi N, \eta N$
620	[1] HOEHLER	93	ARGD	$\pi N \to \pi N$
420±100	CUTKOSKY	80	IPWA	$\pi N \to \pi N$

Δ(2420) ELASTIC POLE RESIDUE

MODULUS |r|

VALUE (MeV)	DOCUMENT ID		TECN	COMMENT
33	ARNDT	06	DPWA	$\pi N \to \pi N, \eta N$
39	HOEHLER	93	ARGD	$\pi N \to \pi N$
18±6	CUTKOSKY	80	IPWA	$\pi N \to \pi N$

PHASE θ

VALUE (°)	DOCUMENT ID		TECN	COMMENT
−45	ARNDT	06	DPWA	$\pi N \to \pi N, \eta N$
−60	HOEHLER	93	ARGD	$\pi N \to \pi N$
−30±40	CUTKOSKY	80	IPWA	$\pi N \to \pi N$

Δ(2420) DECAY MODES

The following branching fractions are our estimates, not fits or averages.

	Mode	Fraction (Γ_i/Γ)
Γ_1	$N\pi$	5–15 %
Γ_2	ΣK	

Δ(2420) BRANCHING RATIOS

$\Gamma(N\pi)/\Gamma_{total}$ Γ_1/Γ

VALUE (%)	DOCUMENT ID		TECN	COMMENT
5 to 15 OUR ESTIMATE				
8.5±0.8	ARNDT	06	DPWA	$\pi N \to \pi N, \eta N$
8 ±3	CUTKOSKY	80	IPWA	$\pi N \to \pi N$
8.0±1.5	HOEHLER	79	IPWA	$\pi N \to \pi N$
11 ±2	HENDRY	78	MPWA	$\pi N \to \pi N$
• • • We do not use the following data for averages, fits, limits, etc. • • •				
22	CHEW	80	BPWA	$\pi^+ p \to \pi^+ p$

$(\Gamma_i\Gamma_f)^{1/2}/\Gamma_{total}$ in $N\pi \to \Delta(2420) \to \Sigma K$ $(\Gamma_1\Gamma_2)^{1/2}/\Gamma$

VALUE	DOCUMENT ID		TECN	COMMENT
−0.016	CANDLIN	84	DPWA	$\pi^+ p \to \Sigma^+ K^+$

Δ(2420) FOOTNOTES

[1] See HOEHLER 93 for a detailed discussion of the evidence for and the pole parameters of N and Δ resonances as determined from Argand diagrams of πN elastic partial-wave amplitudes and from plots of the speeds with which the amplitudes traverse the diagrams.

Δ(2420) REFERENCES

ARNDT	06	PR C74 045205	R.A. Arndt *et al.*	(GWU)
HOEHLER	93	πN Newsletter 9 1	G. Hohler	(KARL)
CANDLIN	84	NP B238 477	D.J. Candlin *et al.*	(EDIN, RAL, LOWC)
PDG	82	PL 111B 1	M. Roos *et al.*	(HELS, CIT, CERN)
CHEW	80	Toronto Conf. 123	D.M. Chew	(LBL) IJP
CUTKOSKY	80	Toronto Conf. 19	R.E. Cutkosky *et al.*	(CMU, LBL) IJP
Also		PR D20 2839	R.E. Cutkosky *et al.*	(CMU, LBL)
HOEHLER	79	PDAT 12-1	G. Hohler *et al.*	(KARLT) IJP
Also		Toronto Conf. 3	R. Koch	(KARLT) IJP
HENDRY	78	PRL 41 222	A.W. Hendry	(IND, LBL) IJP
Also		ANP 136 1	A.W. Hendry	(IND)

Δ(2750) 13/2−

$I(J^P) = \frac{3}{2}(\frac{13}{2}^-)$ Status: **

OMITTED FROM SUMMARY TABLE

The latest GWU analysis (ARNDT 06) finds no evidence for this resonance.

Δ(2750) BREIT-WIGNER MASS

VALUE (MeV)	DOCUMENT ID		TECN	COMMENT
≈ 2750 OUR ESTIMATE				
2794± 80	HOEHLER	79	IPWA	$\pi N \to \pi N$
2650±100	HENDRY	78	MPWA	$\pi N \to \pi N$

Δ(2750) BREIT-WIGNER WIDTH

VALUE (MeV)	DOCUMENT ID		TECN	COMMENT
350±100	HOEHLER	79	IPWA	$\pi N \to \pi N$
500±100	HENDRY	78	MPWA	$\pi N \to \pi N$

Δ(2750) DECAY MODES

	Mode
Γ_1	$N\pi$

Δ(2750) BRANCHING RATIOS

$\Gamma(N\pi)/\Gamma_{total}$ Γ_1/Γ

VALUE (%)	DOCUMENT ID		TECN	COMMENT
4.0±1.5	HOEHLER	79	IPWA	$\pi N \to \pi N$
5 ±1	HENDRY	78	MPWA	$\pi N \to \pi N$

Δ(2750) REFERENCES

ARNDT	06	PR C74 045205	R.A. Arndt *et al.*	(GWU)
HOEHLER	79	PDAT 12-1	G. Hohler *et al.*	(KARLT) IJP
Also		Toronto Conf. 3	R. Koch	(KARLT) IJP
HENDRY	78	PRL 41 222	A.W. Hendry	(IND, LBL) IJP
Also		ANP 136 1	A.W. Hendry	(IND)

$\Delta(2950)\ 15/2^+$

$I(J^P) = \frac{3}{2}(\frac{15}{2}^+)$ Status: **

OMITTED FROM SUMMARY TABLE

$\Delta(2950)$ BREIT-WIGNER MASS

VALUE (MeV)	DOCUMENT ID		TECN	COMMENT
≈ 2950 OUR ESTIMATE				
2990±100	HOEHLER	79	IPWA	$\pi N \to \pi N$
2850±100	HENDRY	78	MPWA	$\pi N \to \pi N$

$\Delta(2950)$ BREIT-WIGNER WIDTH

VALUE (MeV)	DOCUMENT ID		TECN	COMMENT
330±100	HOEHLER	79	IPWA	$\pi N \to \pi N$
700±200	HENDRY	78	MPWA	$\pi N \to \pi N$

$\Delta(2950)$ DECAY MODES

	Mode
Γ_1	$N\pi$

$\Delta(2950)$ BRANCHING RATIOS

$\Gamma(N\pi)/\Gamma_{total}$ Γ_1/Γ

VALUE (%)	DOCUMENT ID		TECN	COMMENT
4±2	HOEHLER	79	IPWA	$\pi N \to \pi N$
3±1	HENDRY	78	MPWA	$\pi N \to \pi N$

$\Delta(2950)$ REFERENCES

HOEHLER	79	PDAT 12-1	G. Hohler *et al.*	(KARLT) IJP
Also		Toronto Conf. 3	R. Koch	(KARLT) IJP
HENDRY	78	PRL 41 222	A.W. Hendry	(IND, LBL) IJP
Also		ANP 136 1	A.W. Hendry	(IND)

$\Delta(\sim 3000$ Region) Partial-Wave Analyses

OMITTED FROM SUMMARY TABLE

We list here miscellaneous high-mass candidates for isospin-3/2 resonances found in partial-wave analyses.

Our 1982 edition also had a $\Delta(2850)$ and a $\Delta(3230)$. The evidence for them was deduced from total cross-section and 180° elastic cross-section measurements. The $\Delta(2850)$ has been resolved into the $\Delta(2750)$ $I_{3,13}$ and $\Delta(2950)$ $K_{3,15}$. The $\Delta(3230)$ is perhaps related to the $K_{3,13}$ of HENDRY 78 and to the $L_{3,17}$ of KOCH 80.

$\Delta(\sim 3000)$ BREIT-WIGNER MASS

VALUE (MeV)	DOCUMENT ID		TECN	COMMENT
≈ 3000 OUR ESTIMATE				
3300	[1] KOCH	80	IPWA	$\pi N \to \pi N\ L_{3,17}$ wave
3500	[1] KOCH	80	IPWA	$\pi N \to \pi N\ M_{3,19}$ wave
2850±150	HENDRY	78	MPWA	$\pi N \to \pi N\ I_{3,11}$ wave
3200±200	HENDRY	78	MPWA	$\pi N \to \pi N\ K_{3,13}$ wave
3300±200	HENDRY	78	MPWA	$\pi N \to \pi N\ L_{3,17}$ wave
3700±200	HENDRY	78	MPWA	$\pi N \to \pi N\ M_{3,19}$ wave
4100±300	HENDRY	78	MPWA	$\pi N \to \pi N\ N_{3,21}$ wave

$\Delta(\sim 3000)$ BREIT-WIGNER WIDTH

VALUE (MeV)	DOCUMENT ID		TECN	COMMENT
700±200	HENDRY	78	MPWA	$\pi N \to \pi N\ I_{3,11}$ wave
1000±300	HENDRY	78	MPWA	$\pi N \to \pi N\ K_{3,13}$ wave
1100±300	HENDRY	78	MPWA	$\pi N \to \pi N\ L_{3,17}$ wave
1300±400	HENDRY	78	MPWA	$\pi N \to \pi N\ M_{3,19}$ wave
1600±500	HENDRY	78	MPWA	$\pi N \to \pi N\ N_{3,21}$ wave

$\Delta(\sim 3000)$ DECAY MODES

	Mode
Γ_1	$N\pi$

$\Delta(\sim 3000)$ BRANCHING RATIOS

$\Gamma(N\pi)/\Gamma_{total}$ Γ_1/Γ

VALUE (%)	DOCUMENT ID		TECN	COMMENT
6±2	HENDRY	78	MPWA	$\pi N \to \pi N\ I_{3,11}$ wave
5±2	HENDRY	78	MPWA	$\pi N \to \pi N\ K_{3,13}$ wave
3±1	HENDRY	78	MPWA	$\pi N \to \pi N\ L_{3,17}$ wave
3±1	HENDRY	78	MPWA	$\pi N \to \pi N\ M_{3,19}$ wave
2±1	HENDRY	78	MPWA	$\pi N \to \pi N\ N_{3,21}$ wave

$\Delta(\sim 3000)$ FOOTNOTES

[1] In addition, KOCH 80 reports some evidence for an S_{31} $\Delta(2700)$ and a P_{33} $\Delta(2800)$.

$\Delta(\sim 3000)$ REFERENCES

KOCH	80	Toronto Conf. 3	R. Koch	(KARLT) IJP
HENDRY	78	PRL 41 222	A.W. Hendry	(IND, LBL) IJP
Also		ANP 136 1	A.W. Hendry	(IND)

Λ BARYONS
(S = −1, I = 0)

$\Lambda^0 = uds$

Λ $I(J^P) = 0(\frac{1}{2}^+)$ Status: ****

We have omitted some results that have been superseded by later experiments. See our earlier editions.

Λ MASS

The fit uses Λ, Σ^+, Σ^0, Σ^- mass and mass-difference measurements.

VALUE (MeV)	EVTS	DOCUMENT ID		TECN	COMMENT
1115.683±0.006 OUR FIT					
1115.683±0.006 OUR AVERAGE					
1115.678±0.006±0.006	20k	HARTOUNI	94	SPEC	pp 27.5 GeV/c
1115.690±0.008±0.006	18k	[1] HARTOUNI	94	SPEC	pp 27.5 GeV/c
• • • We do not use the following data for averages, fits, limits, etc. • • •					
1115.59 ±0.08	935	HYMAN	72	HEBC	
1115.39 ±0.12	195	MAYEUR	67	EMUL	
1115.6 ±0.4		LONDON	66	HBC	
1115.65 ±0.07	488	[2] SCHMIDT	65	HBC	
1115.44 ±0.12		[3] BHOWMIK	63	RVUE	

[1] We assume CPT invariance: this is the $\overline{\Lambda}$ mass as measured by HARTOUNI 94. See below for the fractional mass difference, testing CPT.
[2] The SCHMIDT 65 masses have been reevaluated using our April 1973 proton and $K^\pm$ and $\pi^\pm$ masses. P. Schmidt, private communication (1974).
[3] The mass has been raised 35 keV to take into account a 46 keV increase in the proton mass and an 11 keV decrease in the $\pi^\pm$ mass (note added Reviews of Modern Physics **39** 1 (1967)).

$(m_\Lambda - m_{\overline{\Lambda}}) / m_\Lambda$

A test of CPT invariance.

VALUE (units 10^{-5})	EVTS	DOCUMENT ID		TECN	COMMENT
− 0.1 ± 1.1 OUR AVERAGE		Error includes scale factor of 1.6.			
+ 1.3 ± 1.2	31k	[4] RYBICKI	96	NA32	π^- Cu, 230 GeV
− 1.08± 0.90		HARTOUNI	94	SPEC	pp 27.5 GeV/c
4.5 ± 5.4		CHIEN	66	HBC	6.9 GeV/c $\overline{p}p$
• • • We do not use the following data for averages, fits, limits, etc. • • •					
−26 ±13		BADIER	67	HBC	2.4 GeV/c $\overline{p}p$

[4] RYBICKI 96 is an analysis of old ACCMOR (NA32) data.

Λ MEAN LIFE

Measurements with an error $\geq 0.1 \times 10^{-10}$ s have been omitted altogether, and only the latest high-statistics measurements are used for the average.

VALUE (10^{-10} s)	EVTS	DOCUMENT ID		TECN	COMMENT
2.632±0.020 OUR AVERAGE		Error includes scale factor of 1.6.			See the ideogram below.
2.69 ±0.03	53k	ZECH	77	SPEC	Neutral hyperon beam
2.611±0.020	34k	CLAYTON	75	HBC	0.96–1.4 GeV/c K^-p
2.626±0.020	36k	POULARD	73	HBC	0.4–2.3 GeV/c K^-p
• • • We do not use the following data for averages, fits, limits, etc. • • •					
2.69 ±0.05	6582	ALTHOFF	73B	OSPK	$\pi^+ n \to \Lambda K^+$
2.54 ±0.04	4572	BALTAY	71B	HBC	K^-p at rest
2.535±0.035	8342	GRIMM	68	HBC	
2.47 ±0.08	2600	HEPP	68	HBC	
2.35 ±0.09	916	BURAN	66	HLBC	
$2.452^{+0.056}_{-0.054}$	2213	ENGELMANN	66	HBC	
2.59 ±0.09	794	HUBBARD	64	HBC	
2.59 ±0.07	1378	SCHWARTZ	64	HBC	
2.36 ±0.06	2239	BLOCK	63	HEBC	

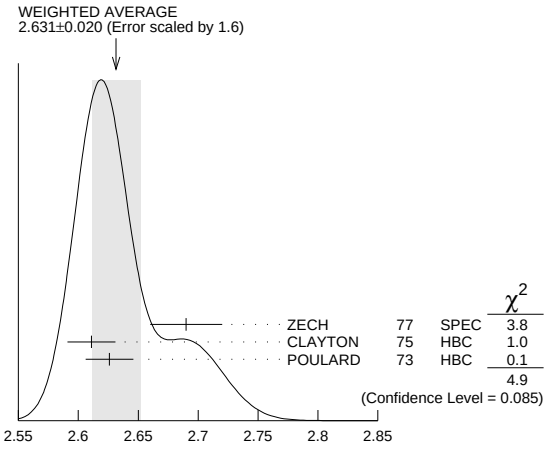

$(\tau_\Lambda - \tau_{\overline{\Lambda}}) / \tau_\Lambda$

A test of CPT invariance.

VALUE	DOCUMENT ID		TECN	COMMENT
−0.001 ±0.009 OUR AVERAGE				
−0.0018±0.0066±0.0056	BARNES	96	CNTR	LEAR $\overline{p}p \to \overline{\Lambda}\Lambda$
0.044 ±0.085	BADIER	67	HBC	2.4 GeV/c $\overline{p}p$

BARYON MAGNETIC MOMENTS

Written 1994 by C.G. Wohl (LBNL).

The figure below shows the measured magnetic moments of the stable baryons. It also shows the predictions of the simplest quark model, using the measured p, n, and Λ moments as input. In this model, the moments are [1]

$$\mu_p = (4\mu_u - \mu_d)/3 \qquad \mu_n = (4\mu_d - \mu_u)/3$$
$$\mu_{\Sigma^+} = (4\mu_u - \mu_s)/3 \qquad \mu_{\Sigma^-} = (4\mu_d - \mu_s)/3$$
$$\mu_{\Xi^0} = (4\mu_s - \mu_u)/3 \qquad \mu_{\Xi^-} = (4\mu_s - \mu_d)/3$$
$$\mu_\Lambda = \mu_s \qquad \mu_{\Sigma^0} = (2\mu_u + 2\mu_d - \mu_s)/3$$
$$\mu_{\Omega^-} = 3\mu_s$$

and the $\Sigma^0 \to \Lambda$ transition moment is

$$\mu_{\Sigma^0\Lambda} = (\mu_d - \mu_u)/\sqrt{3}\,.$$

The quark moments that result from this model are $\mu_u = +1.852\,\mu_N$, $\mu_d = -0.972\,\mu_N$, and $\mu_s = -0.613\,\mu_N$. The corresponding effective quark masses, taking the quarks to be Dirac point particles, where $\mu = q\hbar/2m$, are 338, 322, and 510 MeV. As the figure shows, the model gives a good first approximation to the experimental moments. For efforts to make a better model, we refer to the literature [2].

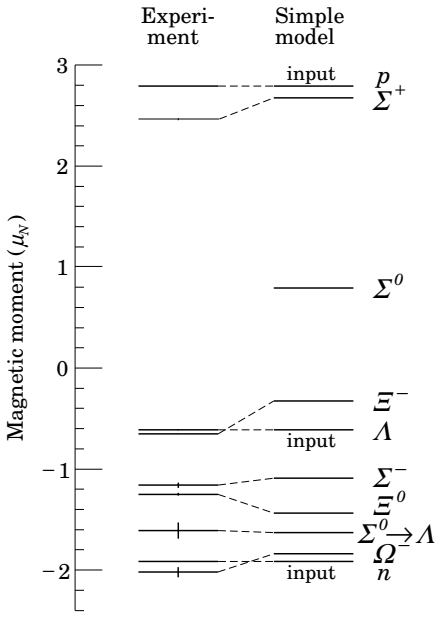

References

1. See, for example, D.H. Perkins, *Introduction to High Energy Physics* (Addison-Wesley, Reading, MA, 1987), or D. Griffiths, *Introduction to Elementary Particles* (Harper & Row, New York, 1987).
2. See, for example, J. Franklin, Phys. Rev. **D29**, 2648 (1984); H.J. Lipkin, Nucl. Phys. **B241**, 477 (1984); K. Suzuki, H. Kumagai, and Y. Tanaka, Europhys. Lett. **2**, 109 (1986); S.K. Gupta and S.B. Khadkikar, Phys. Rev. **D36**, 307 (1987); M.I. Krivoruchenko, Sov. J. Nucl. Phys. **45**, 109 (1987); L. Brekke and J.L. Rosner, Comm. Nucl. Part. Phys. **18**, 83 (1988); K.-T. Chao, Phys. Rev. **D41**, 920 (1990) and references cited therein Also, see references cited in discussions of results in the experimental papers..

Λ MAGNETIC MOMENT

See the "Note on Baryon Magnetic Moments" above. Measurements with an error $\geq 0.15\ \mu_N$ have been omitted.

VALUE (μ_N)	EVTS	DOCUMENT ID		TECN	COMMENT
−0.613 ±0.004 OUR AVERAGE					
−0.606 ±0.015	200k	COX	81	SPEC	
−0.6138±0.0047	3M	SCHACHIN...	78	SPEC	
−0.59 ±0.07	350k	HELLER	77	SPEC	
−0.57 ±0.05	1.2M	BUNCE	76	SPEC	
−0.66 ±0.07	1300	DAHL-JENSEN	71	EMUL	200 kG field

Λ ELECTRIC DIPOLE MOMENT

A nonzero value is forbidden by both T invariance and P invariance.

VALUE (10^{-16} e cm)	CL%	DOCUMENT ID		TECN
< 1.5	95	[5] PONDROM	81	SPEC
• • • We do not use the following data for averages, fits, limits, etc. • • •				
<100	95	[6] BARONI	71	EMUL
<500	95	GIBSON	66	EMUL

[5] PONDROM 81 measures $(-3.0 \pm 7.4) \times 10^{-17}$ e-cm.
[6] BARONI 71 measures $(-5.9 \pm 2.9) \times 10^{-15}$ e-cm.

Λ DECAY MODES

	Mode	Fraction (Γ_i/Γ)
Γ_1	$p\pi^-$	(63.9 ±0.5) %
Γ_2	$n\pi^0$	(35.8 ±0.5) %
Γ_3	$n\gamma$	(1.75±0.15) × 10^{-3}
Γ_4	$p\pi^-\gamma$	[a] (8.4 ±1.4) × 10^{-4}
Γ_5	$pe^-\overline{\nu}_e$	(8.32±0.14) × 10^{-4}
Γ_6	$p\mu^-\overline{\nu}_\mu$	(1.57±0.35) × 10^{-4}

[a] See the Listings below for the pion momentum range used in this measurement.

CONSTRAINED FIT INFORMATION

An overall fit to 5 branching ratios uses 20 measurements and one constraint to determine 5 parameters. The overall fit has a $\chi^2 = 10.5$ for 16 degrees of freedom.

The following *off-diagonal* array elements are the correlation coefficients $\langle \delta x_i \delta x_j \rangle / (\delta x_i \cdot \delta x_j)$, in percent, from the fit to the branching fractions, $x_i \equiv \Gamma_i/\Gamma_{total}$. The fit constrains the x_i whose labels appear in this array to sum to one.

	x_1	x_2	x_3	x_5
x_2	−100			
x_3	−2	−1		
x_5	46	−46	−1	
x_6	0	0	0	0

Λ BRANCHING RATIOS

$\Gamma(p\pi^-)/\Gamma(N\pi)$ — $\Gamma_1/(\Gamma_1+\Gamma_2)$

VALUE	EVTS	DOCUMENT ID		TECN	COMMENT
0.641±0.005 OUR FIT					
0.640±0.005 OUR AVERAGE					
0.646±0.008	4572	BALTAY	71B	HBC	K^-p at rest
0.635±0.007	6736	DOYLE	69	HBC	$\pi^-p \rightarrow \Lambda K^0$
0.643±0.016	903	HUMPHREY	62	HBC	
0.624±0.030		CRAWFORD	59B	HBC	$\pi^-p \rightarrow \Lambda K^0$

$\Gamma(n\pi^0)/\Gamma(N\pi)$ — $\Gamma_2/(\Gamma_1+\Gamma_2)$

VALUE	EVTS	DOCUMENT ID		TECN
0.359±0.005 OUR FIT				
0.310±0.028 OUR AVERAGE				
0.35 ±0.05		BROWN	63	HLBC
0.291±0.034	75	CHRETIEN	63	HLBC

$\Gamma(n\gamma)/\Gamma_{total}$ — Γ_3/Γ

VALUE (units 10^{-3})	EVTS	DOCUMENT ID		TECN	COMMENT
1.75±0.15 OUR FIT					
1.75±0.15	1816	LARSON	93	SPEC	K^-p at rest
• • • We do not use the following data for averages, fits, limits, etc. • • •					
$1.78\pm0.24^{+0.14}_{-0.16}$	287	NOBLE	92	SPEC	See LARSON 93

$\Gamma(n\gamma)/\Gamma(n\pi^0)$ — Γ_3/Γ_2

VALUE (units 10^{-3})	EVTS	DOCUMENT ID		TECN	COMMENT
• • • We do not use the following data for averages, fits, limits, etc. • • •					
2.86±0.74±0.57	24	BIAGI	86	SPEC	SPS hyperon beam

$\Gamma(p\pi^-\gamma)/\Gamma(p\pi^-)$ — Γ_4/Γ_1

VALUE (units 10^{-3})	EVTS	DOCUMENT ID		TECN	COMMENT
1.32±0.22	72	BAGGETT	72C	HBC	π^- < 95 MeV/c

$\Gamma(pe^-\overline{\nu}_e)/\Gamma(p\pi^-)$ — Γ_5/Γ_1

VALUE (units 10^{-3})	EVTS	DOCUMENT ID		TECN	COMMENT
1.301±0.019 OUR FIT					
1.301±0.019 OUR AVERAGE					
1.335±0.056	7111	BOURQUIN	83	SPEC	SPS hyperon beam
1.313±0.024	10k	WISE	80	SPEC	
1.23 ±0.11	544	LINDQUIST	77	SPEC	$\pi^-p \rightarrow K^0\Lambda$
1.27 ±0.07	1089	KATZ	73	HBC	
1.31 ±0.06	1078	ALTHOFF	71	OSPK	
1.17 ±0.13	86	[7] CANTER	71	HBC	K^-p at rest
1.20 ±0.12	143	[8] MALONEY	69	HBC	
1.17 ±0.18	120	[8] BAGLIN	64	FBC	K^- freon 1.45 GeV/c
1.23 ±0.20	150	[8] ELY	63	FBC	
• • • We do not use the following data for averages, fits, limits, etc. • • •					
1.32 ±0.15	218	[7] LINDQUIST	71	OSPK	See LINDQUIST 77

[7] Changed by us from $\Gamma(pe^-\overline{\nu}_e)/\Gamma(N\pi)$ assuming the authors used $\Gamma(p\pi^-)/\Gamma_{total} = 2/3$.
[8] Changed by us from $\Gamma(pe^-\overline{\nu}_e)/\Gamma(N\pi)$ because $\Gamma(pe^-\nu)/\Gamma(p\pi^-)$ is the directly measured quantity.

Baryon Particle Listings

Λ

$\Gamma(p\mu^-\overline{\nu}_\mu)/\Gamma(N\pi)$ $\Gamma_6/(\Gamma_1+\Gamma_2)$

VALUE (units 10^{-4})	EVTS	DOCUMENT ID		TECN	COMMENT
1.57±0.35 OUR FIT					
1.57±0.35 OUR AVERAGE					
1.4 ±0.5	14	BAGGETT	72B	HBC	K^-p at rest
2.4 ±0.8	9	CANTER	71B	HBC	K^-p at rest
1.3 ±0.7	3	LIND	64	RVUE	
1.5 ±1.2	2	RONNE	64	FBC	

Λ DECAY PARAMETERS

See the "Note on Baryon Decay Parameters" in the neutron Listings. Some early results have been omitted.

α_- FOR $\Lambda \to p\pi^-$

VALUE	EVTS	DOCUMENT ID		TECN	COMMENT
0.642±0.013 OUR AVERAGE					
0.584±0.046	8500	ASTBURY	75	SPEC	
0.649±0.023	10325	CLELAND	72	OSPK	
0.67 ±0.06	3520	DAUBER	69	HBC	From Ξ decay
0.645±0.017	10130	OVERSETH	67	OSPK	Λ from π^-p
0.62 ±0.07	1156	CRONIN	63	CNTR	Λ from π^-p

α_+ FOR $\overline{\Lambda} \to \overline{p}\pi^+$

VALUE	EVTS	DOCUMENT ID		TECN	COMMENT
−0.71 ±0.08 OUR AVERAGE					
−0.755±0.083±0.063	≈ 8.7k	ABLIKIM	10	BES	$J/\psi \to \Lambda\overline{\Lambda}$
−0.63 ±0.13	770	TIXIER	88	DM2	$J/\psi \to \Lambda\overline{\Lambda}$

ϕ ANGLE FOR $\Lambda \to p\pi^-$ $(\tan\phi = \beta/\gamma)$

VALUE (°)	EVTS	DOCUMENT ID	TECN	COMMENT
− 6.5± 3.5 OUR AVERAGE				
− 7.0± 4.5	10325	CLELAND 72	OSPK	Λ from π^-p
− 8.0± 6.0	10130	OVERSETH 67	OSPK	Λ from π^-p
13.0±17.0	1156	CRONIN 63	OSPK	Λ from π^-p

α_0 / α_- = $\alpha(\Lambda \to n\pi^0)$ / $\alpha(\Lambda \to p\pi^-)$

VALUE	EVTS	DOCUMENT ID		TECN	COMMENT
1.01 ±0.07 OUR AVERAGE					
1.000±0.068	4760	[9] OLSEN	70	OSPK	$\pi^+n \to \Lambda K^+$
1.10 ±0.27		CORK	60	CNTR	

[9] OLSEN 70 compares proton and neutron distributions from Λ decay.

$(\alpha+\overline{\alpha})/(\alpha-\overline{\alpha})$ in $\Lambda \to p\pi^-$, $\overline{\Lambda} \to \overline{p}\pi^+$

Zero if *CP* is conserved; α_- and α_+ are the asymmetry parameters for $\Lambda \to p\pi^-$ and $\overline{\Lambda} \to \overline{p}\pi^+$ decay. See also the Ξ^- for a similar test involving the decay chain $\Xi^- \to \Lambda\pi^-$, $\Lambda \to p\pi^-$ and the corresponding antiparticle chain.

VALUE	EVTS	DOCUMENT ID		TECN	COMMENT
0.006±0.021 OUR AVERAGE					
−0.081±0.055±0.059	≈ 8.7k	ABLIKIM	10	BES	$J/\psi \to \Lambda\overline{\Lambda}$
+0.013±0.022	96k	BARNES	96	CNTR	LEAR $\overline{p}p \to \overline{\Lambda}\Lambda$
+0.01 ±0.10	770	TIXIER	88	DM2	$J/\psi \to \Lambda\overline{\Lambda}$
−0.02 ±0.14	10k	[10] CHAUVAT	85	CNTR	pp, $\overline{p}p$ ISR
• • • We do not use the following data for averages, fits, limits, etc. • • •					
−0.07 ±0.09	4063	BARNES	87	CNTR	See BARNES 96

[10] CHAUVAT 85 actually gives $\alpha_+(\overline{\Lambda})/\alpha_-(\Lambda) = -1.04 \pm 0.29$. Assumes polarization is same in $\overline{p}p \to \overline{\Lambda}X$ and $pp \to \Lambda X$. Tests of this assumption, based on *C*-invariance and fragmentation, are satisfied by the data.

g_A / g_V FOR $\Lambda \to pe^-\overline{\nu}_e$

Measurements with fewer than 500 events have been omitted. Where necessary, signs have been changed to agree with our conventions, which are given in the "Note on Baryon Decay Parameters" in the neutron Listings. The measurements all assume that the form factor $g_2 = 0$. See also the footnote on DWORKIN 90.

VALUE	EVTS	DOCUMENT ID		TECN	COMMENT
−0.718±0.015 OUR AVERAGE					
−0.719±0.016±0.012	37k	[11] DWORKIN	90	SPEC	$e\nu$ angular corr.
−0.70 ±0.03	7111	BOURQUIN	83	SPEC	$\Xi \to \Lambda\pi^-$
−0.734±0.031	10k	[12] WISE	81	SPEC	$e\nu$ angular correl.
• • • We do not use the following data for averages, fits, limits, etc. • • •					
−0.63 ±0.06	817	ALTHOFF	73	OSPK	Polarized Λ

[11] The tabulated result assumes the weak-magnetism coupling $w \equiv g_W(0)/g_V(0)$ to be 0.97, as given by the CVC hypothesis and as assumed by the other listed measurements. However, DWORKIN 90 *measures* w to be 0.15 ± 0.30, and then $g_A/g_V = -0.731 \pm 0.016$.

[12] This experiment measures only the absolute value of g_A/g_V.

Λ REFERENCES

We have omitted some papers that have been superseded by later experiments. See our earlier editions.

ABLIKIM	10	PR D81 012003	M. Ablikim *et al.*	(BES Collab.)
BARNES	96	PR C54 1877	P.D. Barnes *et al.*	(CERN PS-185 Collab.)
RYBICKI	96	APP B27 2155	K. Rybicki	
HARTOUNI	94	PRL 72 1322	E.P. Hartouni *et al.*	(BNL E766 Collab.)
Also		PRL 72 2821 (erratum)	E.P. Hartouni *et al.*	(BNL E766 Collab.)
LARSON	93	PR D47 799	K.D. Larson *et al.*	(BNL-811 Collab.)
NOBLE	92	PRL 69 414	A.J. Noble *et al.*	(BIRM, BOST, BRCO+)
DWORKIN	90	PR D41 780	J. Dworkin *et al.*	(MICH, WISC, RUTG+)
TIXIER	88	PL B212 523	M.H. Tixier *et al.*	(DM2 Collab.)
BARNES	87	PL B199 147	P.D. Barnes *et al.*	(CMU, SACL, LANL+)
BIAGI	86	ZPHY C30 201	S.F. Biagi *et al.*	(BRIS, CERN, GEVA+)
CHAUVAT	85	PL 163B 273	P. Chauvat *et al.*	(CERN, CLER, UCLA+)
BOURQUIN	83	ZPHY C21 1	M.H. Bourquin *et al.*	(BRIS, GEVA, HEIDP+)
COX	81	PRL 46 877	P.T. Cox *et al.*	(MICH, WISC, RUTG, MINN+)
PONDROM	81	PR D23 814	L. Pondrom *et al.*	(WISC, MICH, RUTG+)
WISE	81	PL 98B 123	J.E. Wise *et al.*	(MASA, BNL)
WISE	80	PL 91B 165	J.E. Wise *et al.*	(MASA, BNL)
SCHACHIN...	78	PRL 41 1348	L. Schachinger *et al.*	(MICH, RUTG, WISC)
HELLER	77	PL 68B 480	K. Heller *et al.*	(MICH, WISC, HEIDH)
LINDQUIST	77	PR D16 2104	J. Lindquist *et al.*	(EFI, OSU, ANL)
Also		JP G2 L211	J. Lindquist *et al.*	(EFI, WUSL, OSU+)
ZECH	77	NP B124 413	G. Zech *et al.*	(SIEG, CERN, DORT, HEIDH)
BUNCE	76	PRL 36 1113	G.R.M. Bunce *et al.*	(WISC, MICH, RUTG)
ASTBURY	75	NP B99 30	P. Astbury *et al.*	(LOIC, CERN, ETH+)
CLAYTON	75	NP B95 130	E.F. Clayton *et al.*	(LOIC, RHEL)
ALTHOFF	73	PL 43B 237	K.H. Althoff *et al.*	(CERN, HEID)
ALTHOFF	73B	NP B66 29	K.H. Althoff *et al.*	(CERN, HEID)
KATZ	73	Thesis MDDP-TR-74-044	C.N. Katz	(UMD)
POULARD	73	PL 46B 135	G. Poulard, A. Givernaud, A.C. Borg	(SACL)
BAGGETT	72B	ZPHY 252 362	M.J. Baggett *et al.*	(HEID)
BAGGETT	72C	PL 42B 379	M.J. Baggett *et al.*	(HEID)
CLELAND	72	NP B40 221	W.E. Cleland *et al.*	(CERN, GEVA, LUND)
HYMAN	72	PR D5 1063	L.G. Hyman *et al.*	(ANL, CMU)
ALTHOFF	71	PL 37B 531	K.H. Althoff *et al.*	(CERN, HEID)
BALTAY	71B	PR D4 670	C. Baltay *et al.*	(COLU, BING)
BARONI	71	LNC 2 1256	G. Baroni, S. Petrera, G. Romano	(ROMA)
CANTER	71	PRL 26 868	J. Canter *et al.*	(STON, COLU)
CANTER	71B	PRL 27 59	J. Canter *et al.*	(STON, COLU)
DAHL-JENSEN	71	NC 3A 1	E. Dahl-Jensen *et al.*	(CERN, ANKA, LAUS+)
LINDQUIST	71	PRL 27 612	J. Lindquist *et al.*	(EFI, WUSL, OSU+)
OLSEN	70	PRL 24 843	S.L. Olsen *et al.*	(WISC, MICH)
DAUBER	69	PR 179 1262	P.M. Dauber *et al.*	(LRL)
DOYLE	69	Thesis UCRL 18139	J.C. Doyle	(LRL)
MALONEY	69	PRL 23 425	J.E. Maloney, B. Sechi-Zorn	(UMD)
GRIMM	68	NC 54A 187	H.J. Grimm	(HEID)
HEPP	68	ZPHY 214 71	V. Hepp, H. Schleich	(HEID)
BADIER	67	PL 25B 152	J. Badier *et al.*	(EPOL)
MAYEUR	67	U.Libr.Brux.Bul. 32	C. Mayeur, E. Tompa, J.H. Wickens	(BELG, LOUC)
OVERSETH	67	PRL 19 391	O.E. Overseth, R.F. Roth	(MICH, PRIN)
PDG	67	RMP 39 1	A.H. Rosenfeld *et al.*	(LRL, CERN, YALE)
BURAN	66	PL 20 318	T. Buran *et al.*	(OSLO)
CHIEN	66	PR 152 1171	C.Y. Chien *et al.*	(YALE, BNL)
ENGELMANN	66	NC 45A 1038	R. Engelmann *et al.*	(HEID, REHO)
GIBSON	66	NC 45A 882	W.M. Gibson, K. Green	(BRIS)
LONDON	66	PR 143 1034	G.W. London *et al.*	(BNL, SYRA)
SCHMIDT	65	PR 140B 1328	P. Schmidt	(COLU)
BAGLIN	64	NC 35 977	C. Baglin *et al.*	(EPOL, CERN, LOUC, RHEL+)
HUBBARD	64	PR 135 B183	J.R. Hubbard *et al.*	(LRL)
LIND	64	PR 135 B1483	V.G. Lind *et al.*	(WISC)
RONNE	64	PL 11 357	B.E. Ronne *et al.*	(CERN, EPOL, LOUC+)
SCHWARTZ	64	Thesis UCRL 11360	J.A. Schwartz	(LRL)
BHOWMIK	63	NC 28 1494	B. Bhowmik, D.P. Goyal	(DELH)
BLOCK	63	PR 130 766	M.M. Block *et al.*	(NWES, BGNA, SYRA+)
BROWN	63	PR 130 769	J.L. Brown *et al.*	(LRL, MICH)
CHRETIEN	63	PR 131 2208	M. Chretien *et al.*	(BRAN, BROW, HARV+)
CRONIN	63	PR 129 1795	J.W. Cronin, O.E. Overseth	(PRIN)
ELY	63	PR 131 868	R.P. Ely *et al.*	(LRL)
HUMPHREY	62	PR 127 1305	W.E. Humphrey, R.R. Ross	(LRL)
CORK	60	PR 120 1000	B. Cork *et al.*	(LRL, PRIN, BNL)
CRAWFORD	59B	PRL 2 266	F.S. Crawford *et al.*	(LRL)

Λ AND Σ RESONANCES

Introduction: Since our last edition, there have been a few measurements of properties of the lowest Λ and Σ resonances—mostly of masses and widths. But the field remains at a standstill. What follows is a much abbreviated version of the note on Λ and Σ Resonances from our 1990 edition [1]. In particular, see that edition for some representative Argand plots from partial-wave analyses.

Table 1 is an attempt to evaluate the status, both overall and channel by channel, of each Λ and Σ resonance in the Particle Listings. The evaluations are of course partly subjective. A blank indicates there is no evidence at all: either the relevant couplings are small or the resonance does not really exist. The main Baryon Summary Table includes only the established resonances (overall status 3 or 4 stars). A number of the 1- and 2-star entries may eventually disappear, but there are certainly many resonances yet to be discovered underlying the established ones.

Sign conventions for resonance couplings: In terms of the isospin-0 and -1 elastic scattering amplitudes A_0 and A_1, the amplitude for $K^- p \to \overline{K}^0 n$ scattering is $\pm(A_1 - A_0)/2$, where the sign depends on conventions used in conjunction with the Clebsch-Gordan coefficients (such as, is the baryon or the meson the "first" particle). If this reaction is partial-wave analyzed and if the overall phase is chosen so that, say, the $\Sigma(1775)D_{15}$ amplitude at resonance points along the positive imaginary axis (points "up"), then any Σ at resonance will point "up" and any Λ at resonance will point "down" (along the negative imaginary axis). Thus the phase at resonance determines the isospin. The above ignores background amplitudes in the resonating partial waves.

That is the basic idea. In a similar but somewhat more complicated way, the phases of the $\overline{K}N \to \Lambda\pi$ and $\overline{K}N \to \Sigma\pi$ amplitudes for a resonating wave help determine the SU(3) multiplet to which the resonance belongs. Again, a convention has to be adopted for some overall arbitrary phases: which way is "up"? Our convention is that of Levi-Setti [2] and is shown in Fig. 1, which also compares experimental results with theoretical predictions for the signs of several resonances. In the Listings, a + or − sign in front of a measurement of an inelastic resonance coupling indicates the sign (the *absence* of a sign means that the sign is not determined, *not* that it is positive). For more details, see Appendix II of our 1982 edition [3].

Errors on masses and widths: The errors quoted on resonance parameters from partial-wave analyses are often only statistical, and the parameters can change by more than these errors when a different parametrization of the waves is used. Furthermore, the different analyses use more or less the same data, so it is not really appropriate to treat the different determinations of the resonance parameters as independent or to average them together. In any case, the spread of the masses, widths, and branching fractions from the different analyses is certainly a better indication of the uncertainties than are the quoted errors. In the Baryon Summary Table, we usually give a range reflecting the spread of the values rather than a particular value with error.

For three states, the Λ(1520), the Λ(1820), and the Σ(1775), there is enough information to make an overall fit to the various branching fractions. It is then necessary to use the quoted errors, but the errors obtained from the fit should not be taken seriously.

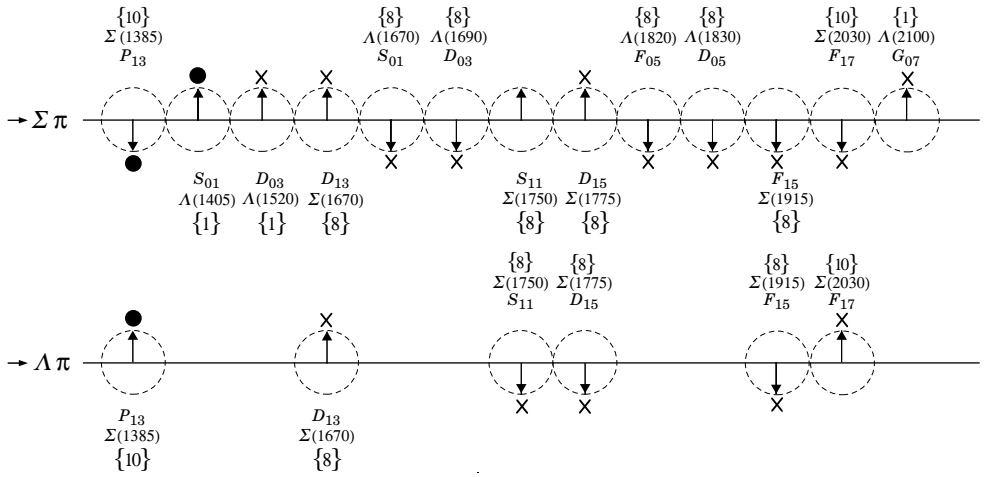

Figure 1. The signs of the imaginary parts of resonating amplitudes in the $\overline{K}N \to \Lambda\pi$ and $\Sigma\pi$ channels. The signs of the $\Sigma(1385)$ and $\Lambda(1405)$, marked with a •, are set by convention, and then the others are determined relative to them. The signs required by the SU(3) assignments of the resonances are shown with an arrow, and the experimentally determined signs are shown with an ×.

Table 1. The status of the Λ and Σ resonances. Only those with an overall status of *** or **** are included in the main Baryon Summary Table.

Particle	J^P	Overall status	Status as seen in — $N\overline{K}$	$\Lambda\pi$	$\Sigma\pi$	Other channels
Λ(1116)	1/2+	****		F		$N\pi$(weakly)
Λ(1405)	1/2−	****	****	o	****	
Λ(1520)	3/2−	****	****	r	****	$\Lambda\pi\pi, \Lambda\gamma$
Λ(1600)	1/2+	***	***	b	**	
Λ(1670)	1/2−	****	****	i	****	$\Lambda\eta$
Λ(1690)	3/2−	****	****	d	****	$\Lambda\pi\pi, \Sigma\pi\pi$
Λ(1800)	1/2−	***	***	d	**	$N\overline{K}^*, \Sigma(1385)\pi$
Λ(1810)	1/2+	***	***	e	**	$N\overline{K}^*$
Λ(1820)	5/2+	****	****	n	****	$\Sigma(1385)\pi$
Λ(1830)	5/2−	****	***	F	****	$\Sigma(1385)\pi$
Λ(1890)	3/2+	****	****	o	**	$N\overline{K}^*, \Sigma(1385)\pi$
Λ(2000)		*		r	*	$\Lambda\omega, N\overline{K}^*$
Λ(2020)	7/2+	*	*	b	*	
Λ(2100)	7/2−	****	****	i	***	$\Lambda\omega, N\overline{K}^*$
Λ(2110)	5/2+	***	**	d	*	$\Lambda\omega, N\overline{K}^*$
Λ(2325)	3/2−	*	*	d		$\Lambda\omega$
Λ(2350)		***	***	e	*	
Λ(2585)		**	**	n		
Σ(1193)	1/2+	****				$N\pi$(weakly)
Σ(1385)	3/2+	****		****	****	
Σ(1480)		*	*	*	*	
Σ(1560)		**		**	**	
Σ(1580)	3/2−	*	*	*		
Σ(1620)	1/2−	**	**	*	*	
Σ(1660)	1/2+	***	***	*	**	
Σ(1670)	3/2−	****	****	****	****	several others
Σ(1690)		**	*	**	*	$\Lambda\pi\pi$
Σ(1750)	1/2−	***	***	**	*	$\Sigma\eta$
Σ(1770)	1/2+	*				
Σ(1775)	5/2−	****	****	****	***	several others
Σ(1840)	3/2+	*	*	**	*	
Σ(1880)	1/2+	**	**	**		$N\overline{K}^*$
Σ(1915)	5/2+	****	***	****	***	$\Sigma(1385)\pi$
Σ(1940)	3/2−	***	*	***	**	quasi-2-body
Σ(2000)	1/2−	*		*		$N\overline{K}^*, \Lambda(1520)\pi$
Σ(2030)	7/2+	****	****	****	**	several others
Σ(2070)	5/2+	*	*		*	
Σ(2080)	3/2+	**		**		
Σ(2100)	7/2−	*		*	*	
Σ(2250)		***	***	*	*	
Σ(2455)		**	*			
Σ(2620)		**	*			
Σ(3000)		*	*	*		
Σ(3170)		*				multi-body

**** Existence is certain, and properties are at least fairly well explored.
*** Existence ranges from very likely to certain, but further confirmation is desirable and/or quantum numbers, branching fractions, *etc.* are not well determined.
** Evidence of existence is only fair.
* Evidence of existence is poor.

Production experiments: Partial-wave analyses of course separate partial waves, whereas a peak in a cross section or an invariant mass distribution usually cannot be disentangled from background and analyzed for its quantum numbers; and more than one resonance may be contributing to the peak. Results from partial-wave analyses and from production experiments are generally kept separate in the Listings, and in the Baryon Summary Table results from production experiments are used only for the low-mass states. The Σ(1385) and Λ(1405) of course lie below the $\overline{K}N$ threshold and nearly everything about them is learned from production experiments; and production and formation experiments agree quite well in the case of Λ(1520) and results have been combined. There is some disagreement between production and formation experiments in the 1600–1700 MeV region: see the note on the Σ(1670).

References

1. Particle Data Group, Phys. Lett. **B239**, VIII.64 (1990).
2. R. Levi-Setti, in *Proceedings of the Lund International Conference on Elementary Particles* (Lund, 1969), p. 339.
3. Particle Data Group, Phys. Lett. **111B** (1982).

Λ(1405) 1/2−

$I(J^P) = 0(\frac{1}{2}^-)$ Status: ****

The nature of the Λ(1405) has been a puzzle for decades: three-quark state or hybrid; two poles or one. We cannot here survey the rather extensive literature. See, for example, CIEPLY 10, KISSLINGER 11, SEKIHARA 11, and SHEVCHENKO 12A for discussions and earlier references.

It seems to be the universal opinion of the chiral-unitary community that there are two poles in the 1400-MeV region. ZYCHOR 08 presents experimental evidence against the two-pole model, but this is disputed by GENG 07A. See also REVAI 09, which finds little basis for choosing between one- and two-pole models; and IKEDA 12, which favors the two-pole model.

A single, ordinary three-quark Λ(1405) fits nicely into a $J^P = 1/2^-$ SU(4) $\overline{4}$ multiplet, whose other members are the $\Lambda_c(2595)^+$, $\Xi_c(2790)^+$, and $\Xi_c(2790)^0$; see Fig. 1 of our note on "Charmed Baryons."

Λ(1405) MASS

PRODUCTION EXPERIMENTS

VALUE (MeV)	EVTS	DOCUMENT ID		TECN	COMMENT
$1405.1^{+1.3}_{-1.0}$ OUR AVERAGE					
1405 $^{+11}_{-9}$		HASSANVAND	13	SPEC	$pp \to p\Lambda(1405)K^+$
1405 $^{+1.4}_{-1.0}$		ESMAILI	10	RVUE	^{4}He $K^- \to \Sigma^\pm\pi^\mp X$ at rest
1406.5 ± 4.0		[1] DALITZ	91		M-matrix fit
• • • We do not use the following data for averages, fits, limits, etc. • • •					
1391 ± 1	700	[1] HEMINGWAY	85	HBC	K^-p 4.2 GeV/c
~ 1405	400	[2] THOMAS	73	HBC	π^-p 1.69 GeV/c
1405	120	BARBARO-...	68B	DBC	K^-d 2.1–2.7 GeV/c
1400 ± 5	67	BIRMINGHAM	66	HBC	K^-p 3.5 GeV/c
1382 ± 8		ENGLER	65	HDBC	π^-p, π^+d 1.68 GeV/c
1400 ±24		MUSGRAVE	65	HBC	$\overline{p}p$ 3–4 GeV/c
1410		ALEXANDER	62	HBC	π^-p 2.1 GeV/c
1405		ALSTON	62	HBC	K^-p 1.2–0.5 GeV/c
1405		ALSTON	61B	HBC	K^-p 1.15 GeV/c

EXTRAPOLATIONS BELOW $N\overline{K}$ THRESHOLD

VALUE (MeV)	DOCUMENT ID		TECN	COMMENT
• • • We do not use the following data for averages, fits, limits, etc. • • •				
1407.56 or 1407.50	[3] KIMURA	00		potential model
1411	[4] MARTIN	81		K-matrix fit
1406	[5] CHAO	73	DPWA	0–range fit (sol. B)
1421	MARTIN	70	RVUE	Constant K-matrix
1416 ±4	MARTIN	69	HBC	Constant K-matrix
1403 ±3	KIM	67	HBC	K-matrix fit
1407.5±1.2	[6] KITTEL	66	HBC	0–effective-range fit
1410.7±1.0	KIM	65	HBC	0–effective-range fit
1409.6±1.7	[6] SAKITT	65	HBC	0–effective-range fit

Λ(1405) WIDTH

PRODUCTION EXPERIMENTS

VALUE (MeV)	EVTS	DOCUMENT ID		TECN	COMMENT
50.5± 2.0 OUR AVERAGE					
62 ±10		HASSANVAND	13	SPEC	$pp \to p\Lambda(1405)K^+$
50 ± 2		[1] DALITZ	91		M-matrix fit

• • • We do not use the following data for averages, fits, limits, etc. • • •

24	$^{+4}_{-3}$		ESMAILI	10	RVUE	^{4}He $K^- \to \Sigma^\pm\pi^\mp X$ at rest
32	± 1	700	[1] HEMINGWAY	85	HBC	$K^- p$ 4.2 GeV/c
45	to 55	400	[2] THOMAS	73	HBC	$\pi^- p$ 1.69 GeV/c
35		120	BARBARO-...	68B	DBC	$K^- d$ 2.1–2.7 GeV/c
50	±10	67	BIRMINGHAM	66	HBC	$K^- p$ 3.5 GeV/c
89	±20		ENGLER	65	HDBC	
60	±20		MUSGRAVE	65	HBC	
35	± 5		ALEXANDER	62	HBC	
50			ALSTON	62	HBC	
20			ALSTON	61B	HBC	

EXTRAPOLATIONS BELOW $N\overline{K}$ THRESHOLD

VALUE (MeV)		DOCUMENT ID		TECN	COMMENT
• • • We do not use the following data for averages, fits, limits, etc. • • •					
50.24 or 50.26	[3]	KIMURA	00		potential model
30	[4]	MARTIN	81		K-matrix fit
55	[5,7]	CHAO	73	DPWA	0–range fit (sol. B)
20		MARTIN	70	RVUE	Constant K-matrix
29 ±6		MARTIN	69	HBC	Constant K-matrix
50 ±5		KIM	67	HBC	K-matrix fit
34.1±4.1	[6]	KITTEL	66	HBC	
37.0±3.2		KIM	65	HBC	
28.2±4.1	[6]	SAKITT	65	HBC	

$\Lambda(1405)$ DECAY MODES

	Mode	Fraction (Γ_i/Γ)
Γ_1	$\Sigma\pi$	100 %
Γ_2	$\Lambda\gamma$	
Γ_3	$\Sigma^0\gamma$	
Γ_4	$N\overline{K}$	

$\Lambda(1405)$ PARTIAL WIDTHS

$\Gamma(\Lambda\gamma)$ Γ_2

VALUE (keV)	DOCUMENT ID		COMMENT
• • • We do not use the following data for averages, fits, limits, etc. • • •			
27±8	BURKHARDT	91	Isobar model fit

$\Gamma(\Sigma^0\gamma)$ Γ_3

VALUE (keV)	DOCUMENT ID		COMMENT
• • • We do not use the following data for averages, fits, limits, etc. • • •			
10 ± 4 or 23 ± 7	BURKHARDT	91	Isobar model fit

$\Lambda(1405)$ BRANCHING RATIOS

$\Gamma(N\overline{K})/\Gamma(\Sigma\pi)$ Γ_4/Γ_1

VALUE	CL%	DOCUMENT ID		TECN	COMMENT
• • • We do not use the following data for averages, fits, limits, etc. • • •					
<3	95	HEMINGWAY	85	HBC	$K^- p$ 4.2 GeV/c

$\Lambda(1405)$ FOOTNOTES

[1] DALITZ 91 fits the HEMINGWAY 85 data.
[2] THOMAS 73 data is fit by CHAO 73 (see next section).
[3] The KIMURA 00 values are from fits A and B from a coupled-channel potential model using low-energy $\overline{K}N$ and $\Sigma\pi$ data, kaonic-hydrogen x-ray measurements, and our $\Lambda(1405)$ mass and width. The results bear mainly on the *nature* of the $\Lambda(1405)$: three-quark state or $\overline{K}N$ bound state.
[4] The MARTIN 81 fit includes the $K^\pm p$ forward scattering amplitudes and the dispersion relations they must satisfy.
[5] See also the accompanying paper of THOMAS 73.
[6] Data of SAKITT 65 are used in the fit by KITTEL 66.
[7] An asymmetric shape, with $\Gamma/2 = 41$ MeV below resonance, 14 MeV above.

$\Lambda(1405)$ REFERENCES

HASSANVAND	13	PR C87 055202	M. Hassanvand *et al.*	
Also		PR C88 019905 (errat.)	M. Hassanvand *et al.*	
IKEDA	12	NP A881 98	Y. Ikeda, T. Hyodo, W. Weise	(TINT, RIKEN, MUNT)
SHEVCHENKO	12A	PR C85 034001	N.V. Shevchenko	(REZ)
KISSLINGER	11	EPJ A47 8	L.S. Kisslinger, E.M. Henley	(CMU, WASH)
SEKIHARA	11	PR C83 055202	T. Sekihara, T. Hyodo, D. Jido	(KYOT, KYOTU+)
CIEPLY	10	EPJ A43 191	A. Cieply, J. Smejkal	(NPI, Tech. U, Czech Rep.)
ESMAILI	10	PL B686 23	J. Esmaili, Y. Akaishi, T. Yamazaki	(RIKEN, ISUT+)
REVAI	09	PR C79 035202	J. Revai, N.V. Shevchenko	(BUDA, NPI Czech Rep.)
ZYCHOR	08	PL B660 167	I. Zychor *et al.*	(COSY-ANKE Collab.)
GENG	07A	EPJ A34 405	L.S. Geng, E. Oset	(VALE)
KIMURA	00	PR C62 015206	M. Kimura *et al.*	
BURKHARDT	91	PR C44 607	H. Burkhardt, J. Lowe	(NOTT, UNM, BIRM)
DALITZ	91	JP G17 289	R.H. Dalitz, A. Deloff	(OXFTP, WINR)
HEMINGWAY	85	NP B253 742	R.J. Hemingway	(CERN) J
MARTIN	81	NP B179 33	A.D. Martin	(DURH)
CHAO	73	NP B56 46	Y.A. Chao *et al.*	(RHEL, CMU, LOUC)
THOMAS	73	NP B56 15	D.W. Thomas *et al.*	(CMU) J
MARTIN	70	NP B16 479	A.D. Martin, G.G. Ross	(DURH)
MARTIN	69	PR 183 1352	B.R. Martin, M. Sakitt	(LOUC, BNL)
Also		PR 183 1345	B.R. Martin, M. Sakitt	(LOUC, BNL)
BARBARO-...	68B	PRL 21 573	A. Barbaro-Galtieri *et al.*	(LRL, SLAC)
KIM	67	PRL 19 1074	J.K. Kim	(YALE)
BIRMINGHAM	66	PR 152 1148	M. Haque *et al.*	(BIRM, GLAS, LOIC, OXF+)
KITTEL	66	PL 21 349	W. Kittel, G. Otter, I. Wacek	(VIEN)
ENGLER	65	PRL 15 224	A. Engler *et al.*	(CMU, BNL) IJ
KIM	65	PRL 14 29	J.K. Kim	(COLU)
MUSGRAVE	65	NC 35 735	B. Musgrave *et al.*	(BIRM, CERN, EPOL+)
SAKITT	65	PR 139 B719	M. Sakitt *et al.*	(UMD, LRL)
ALEXANDER	62	PRL 8 447	G. Alexander *et al.*	(LRL) I
ALSTON	62	CERN Conf. 311	M.H. Alston *et al.*	(LRL) I
ALSTON	61B	PRL 6 698	M.H. Alston *et al.*	(LRL) I

OTHER RELATED PAPERS

IWASAKI	97	PRL 78 3067	M. Iwasaki *et al.*	(KEK 228 Collab.)
FINK	90	PR C41 2720	P.J.Jr. Fink *et al.*	(IBMY, ORST, ANSM)
LEINWEBER	90	ANP 198 203	D.B. Leinweber	(MCMS)
MUELLER-GR...	90	NP A513 557	A. Mueller-Groeling, K. Holinde, J. Speth	(JULI)
BARRETT	89	NC 102A 179	R.C. Barrett	(SURR)
BATTY	89	NC 102A 255	C.J. Batty, A. Gal	(RAL, HEBR)
CAPSTICK	89	Excited Baryons 88, p.32	S. Capstick	(GUEL)
LOWE	89	NC 102A 167	J. Lowe	(BIRM)
WHITEHOUSE	89	PRL 63 1352	D.A. Whitehouse *et al.*	(BIRM, BOST, BRCO+)
SIEGEL	88	PR C38 2221	P.B. Siegel, W. Weise	(REGE)
WORKMAN	88	PR D37 3117	R.L. Workman, H.W. Fearing	(TRIU)
SCHNICK	87	PRL 58 1719	J. Schnick, R.H. Landau	(ORST)
CAPSTICK	86	PR D34 2809	S. Capstick, N. Isgur	(TNTO)
JENNINGS	86	PL B176 229	B.K. Jennings	(TRIU)
MALTMAN	86	PR D34 1372	K. Maltman, N. Isgur	(LANL, TNTO)
ZHONG	86	PL B171 471	Y.S. Zhong *et al.*	(ADLD, TRIU, SURR)
BURKHARDT	85	NP A440 653	H. Burkhardt, J. Lowe, A.S. Rosenthal	(NOTT+)
DAREWYCH	85	PR D32 1765	J.W. Darewych, R. Koniuk, N. Isgur	(YORKC, TNTO)
VEIT	85	PR D31 1033	E.A. Veit *et al.*	(TRIU, ADLD, SURR)
KIANG	84	PR C30 1638	D. Kiang *et al.*	(DALH, MCMS)
MILLER	84	Conference paper	D.J. Miller	(LOUC)
Conf. Intersections between Particle and Nuclear Physics, p. 783				
VANDIJK	84	PR D30 937	W. van Dijk	(MCMS)
VEIT	84	PL 137B 415	E.A. Veit *et al.*	(TRIU, SURR, CERN)
DALITZ	82	Heid. Conf.	R.H. Dalitz *et al.*	(OXFTP)
Heidelberg Conf., p. 201				
DALITZ	81	Kaon Conf.	R.H. Dalitz, J.G. McGinley	(OXFTP)
Low and Intermediate Energy Kaon-Nucleon Physics, p.381				
MARTIN	81B	Kaon Conf.	A.D. Martin	(DURH)
Low and Intermediate Energy Kaon-Nucelon Physics, p. 97				
OADES	77	NC 42A 462	G.C. Oades, G. Rasche	(AARH, ZURI)
SHAW	73	Purdue Conf. 417	G.L. Shaw	(UCI)
BARBARO-...	72	LBL-555	A. Barbaro-Galtieri	(LBL)
DOBSON	72	PR D6 3256	P.N. Dobson, R. McElhaney	(HAWA)
RAJASEKA...	72	PR D5 610	G. Rajasekaran	(TATA)
Earlier papers also cited in RAJASEKARAN 72.				
CLINE	71	PRL 26 1194	D. Cline, R. Laumann, J. Mapp	(WISC)
MARTIN	71	PL 35B 62	A.D. Martin, A.D. Martin, G.G. Ross	(DURH, LOUC+)
DALITZ	67	PR 153 1617	R.H. Dalitz, T.C. Wong, G. Rajasekaran	(OXFTP+)
DONALD	66	PL 22 711	R.A. Donald *et al.*	(LIVP)
KADYK	66	PRL 17 599	J.A. Kadyk *et al.*	(LRL)
ABRAMS	65	PR 139 B454	G.S. Abrams, B. Sechi-Zorn	(UMD)

$\Lambda(1520)$ $3/2^-$

$I(J^P) = 0(\frac{3}{2}^-)$ Status: ****

Discovered by FERRO-LUZZI 62; the elaboration in WATSON 63 is the classic paper on the Breit-Wigner analysis of a multichannel resonance.

The measurements of the mass, width, and elasticity published before 1975 are now obsolete and have been omitted. They were last listed in our 1982 edition Physics Letters **111B** 1 (1982).

Production and formation experiments agree quite well, so they are listed together here.

$\Lambda(1520)$ MASS

VALUE (MeV)	EVTS	DOCUMENT ID		TECN	COMMENT
1519.5 ±1.0 OUR ESTIMATE					
1519.54±0.17 OUR AVERAGE					
1519.6 ±0.5		ZHANG	13A	DPWA	Multichannel
1520.4 ±0.6 ±1.5		[1] QIANG	10	SPEC	$ep \to e'K^+X$ (fit to X)
1517.3 ±1.5	300	BARBER	80D	SPEC	$\gamma p \to \Lambda(1520)K^+$
1517.8 ±1.2	5k	BARLAG	79	HBC	$K^- p$ 4.2 GeV/c
1520.0 ±0.5		ALSTON-...	78	DPWA	$\overline{K}N \to \overline{K}N$
1519.7 ±0.3	4k	CAMERON	77	HBC	$K^- p$ 0.96–1.36 GeV/c
1519 ±1		GOPAL	77	DPWA	$\overline{K}N$ multichannel
1519.4 ±0.3	2000	CORDEN	75	DBC	$K^- d$ 1.4–1.8 GeV/c

[1] QIANG 10 gets 1518.8 MeV for the pole mass (no errors given).

$\Lambda(1520)$ WIDTH

VALUE (MeV)	EVTS	DOCUMENT ID		TECN	COMMENT
15.6 ±1.0 OUR ESTIMATE					
15.73±0.29 OUR AVERAGE Error includes scale factor of 1.1.					
17 ±1		ZHANG	13A	DPWA	Multichannel
18.6 ±1.9 ±1.0		[2] QIANG	10	SPEC	$ep \to e'K^+X$ (fit to X)
16.3 ±3.3	300	BARBER	80D	SPEC	$\gamma p \to \Lambda(1520)K^+$
16 ±1		GOPAL	80	DPWA	$\overline{K}N \to \overline{K}N$
14 ±3	677	[3] BARLAG	79	HBC	$K^- p$ 4.2 GeV/c
15.4 ±0.5		ALSTON-...	78	DPWA	$\overline{K}N \to \overline{K}N$
16.3 ±0.5	4k	CAMERON	77	HBC	$K^- p$ 0.96–1.36 GeV/c
15.0 ±0.5		GOPAL	77	DPWA	$\overline{K}N$ multichannel
15.5 ±1.6	2000	CORDEN	75	DBC	$K^- d$ 1.4–1.8 GeV/c

[2] QIANG 10 gets 17.2 MeV for the pole width (no errors given).
[3] From the best-resolution sample of $\Lambda\pi\pi$ events only.

Baryon Particle Listings

Λ(1520)

Λ(1520) POLE POSITION

REAL PART

VALUE (MeV)	DOCUMENT ID		TECN	COMMENT
• • • We do not use the following data for averages, fits, limits, etc. • • •				
1518	ZHANG	13A	DPWA	Multichannel

−2×IMAGINARY PART

VALUE (MeV)	DOCUMENT ID		TECN	COMMENT
• • • We do not use the following data for averages, fits, limits, etc. • • •				
16	ZHANG	13A	DPWA	Multichannel

Λ(1520) DECAY MODES

	Mode	Fraction (Γ_i/Γ)
Γ_1	$N\overline{K}$	45 ± 1%
Γ_2	$\Sigma\pi$	42 ± 1%
Γ_3	$\Lambda\pi\pi$	10 ± 1%
Γ_4	$\Sigma(1385)\pi$	
Γ_5	$\Sigma(1385)\pi(\rightarrow \Lambda\pi\pi)$	
Γ_6	$\Lambda(\pi\pi)_{S\text{-wave}}$	
Γ_7	$\Sigma\pi\pi$	0.9 ± 0.1%
Γ_8	$\Lambda\gamma$	0.85 ± 0.15%
Γ_9	$\Sigma^0\gamma$	

CONSTRAINED FIT INFORMATION

An overall fit to 9 branching ratios uses 28 measurements and one constraint to determine 6 parameters. The overall fit has a $\chi^2 = 18.9$ for 23 degrees of freedom.

The following *off-diagonal* array elements are the correlation coefficients $\langle \delta x_i \delta x_j \rangle / (\delta x_i \cdot \delta x_j)$, in percent, from the fit to the branching fractions, $x_i \equiv \Gamma_i/\Gamma_{\text{total}}$. The fit constrains the x_i whose labels appear in this array to sum to one.

x_2	−63				
x_3	−32	−34			
x_7	−4	−3	−1		
x_8	−8	−7	−3	0	
x_9	−24	−21	−10	−1	−1
	x_1	x_2	x_3	x_7	x_8

Λ(1520) BRANCHING RATIOS

See "Sign conventions for resonance couplings" in the Note on Λ and Σ Resonances.

$\Gamma(N\overline{K})/\Gamma_{\text{total}}$ — Γ_1/Γ

VALUE	DOCUMENT ID		TECN	COMMENT
0.45 ±0.01 OUR ESTIMATE				
0.448±0.007 OUR FIT Error includes scale factor of 1.2.				
0.456±0.010 OUR AVERAGE				
0.47 ±0.04	ZHANG	13A	DPWA	Multichannel
0.47 ±0.02	GOPAL	80	DPWA	$\overline{K}N \rightarrow \overline{K}N$
0.45 ±0.03	ALSTON-...	78	DPWA	$\overline{K}N \rightarrow \overline{K}N$
0.448±0.014	CORDEN	75	DBC	K^-d 1.4–1.8 GeV/c
• • • We do not use the following data for averages, fits, limits, etc. • • •				
0.47 ±0.01	GOPAL	77	DPWA	See GOPAL 80
0.42	MAST	76	HBC	$K^-p \rightarrow \overline{K}^0 n$

$\Gamma(\Sigma\pi)/\Gamma_{\text{total}}$ — Γ_2/Γ

VALUE	DOCUMENT ID		TECN	COMMENT
0.42 ±0.01 OUR ESTIMATE				
0.421±0.007 OUR FIT Error includes scale factor of 1.2.				
0.425±0.011 OUR AVERAGE				
0.47 ±0.05	ZHANG	13A	DPWA	Multichannel
0.426±0.014	CORDEN	75	DBC	K^-d 1.4–1.8 GeV/c
0.418±0.017	BARBARO-...	69B	HBC	K^-p 0.28–0.45 GeV/c
• • • We do not use the following data for averages, fits, limits, etc. • • •				
0.46	KIM	71	DPWA	K-matrix analysis

$\Gamma(\Sigma\pi)/\Gamma(N\overline{K})$ — Γ_2/Γ_1

VALUE	DOCUMENT ID		TECN	COMMENT
0.940±0.026 OUR FIT Error includes scale factor of 1.3.				
0.95 ±0.04 OUR AVERAGE Error includes scale factor of 1.7. See the ideogram below.				
0.98 ±0.03	[4] GOPAL	77	DPWA	$\overline{K}N$ multichannel
0.82 ±0.08	BURKHARDT	69	HBC	K^-p 0.8–1.2 GeV/c
1.06 ±0.14	SCHEUER	68	DBC	K^-N 3 GeV/c
0.96 ±0.20	DAHL	67	HBC	π^-p 1.6–4 GeV/c
0.73 ±0.11	DAUBER	67	HBC	K^-p 2 GeV/c
• • • We do not use the following data for averages, fits, limits, etc. • • •				
1.06 ±0.12	BERTHON	74	HBC	Quasi-2-body σ
1.72 ±0.78	MUSGRAVE	65	HBC	

[4] The $\overline{K}N \rightarrow \Sigma\pi$ amplitude at resonance is $+0.46 \pm 0.01$.

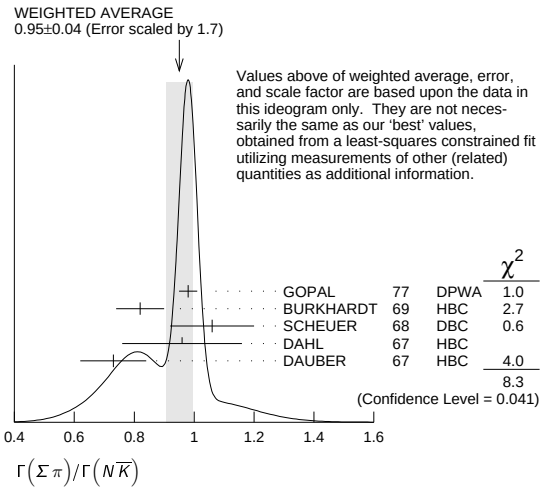

$\Gamma(\Lambda\pi\pi)/\Gamma_{\text{total}}$ — Γ_3/Γ

VALUE	DOCUMENT ID		TECN	COMMENT
0.10 ±0.01 OUR ESTIMATE				
0.095±0.005 OUR FIT Error includes scale factor of 1.2.				
0.096±0.008 OUR AVERAGE Error includes scale factor of 1.6.				
0.091±0.006	CORDEN	75	DBC	K^-d 1.4–1.8 GeV/c
0.11 ±0.01	[5] MAST	73B	IPWA	$K^-p \rightarrow \Lambda\pi\pi$

[5] Assumes $\Gamma(N\overline{K})/\Gamma_{\text{total}} = 0.46 \pm 0.02$.

$\Gamma(\Lambda\pi\pi)/\Gamma(N\overline{K})$ — Γ_3/Γ_1

VALUE	DOCUMENT ID		TECN	COMMENT
0.212±0.012 OUR FIT Error includes scale factor of 1.2.				
0.202±0.021 OUR AVERAGE				
0.22 ±0.03	BURKHARDT	69	HBC	K^-p 0.8–1.2 GeV/c
0.19 ±0.04	SCHEUER	68	DBC	K^-N 3 GeV/c
0.17 ±0.05	DAHL	67	HBC	π^-p 1.6–4 GeV/c
0.21 ±0.18	DAUBER	67	HBC	K^-p 2 GeV/c
• • • We do not use the following data for averages, fits, limits, etc. • • •				
0.27 ±0.13	BERTHON	74	HBC	Quasi-2-body σ
0.2	KIM	71	DPWA	K-matrix analysis

$\Gamma(\Sigma\pi)/\Gamma(\Lambda\pi\pi)$ — Γ_2/Γ_3

VALUE	DOCUMENT ID		TECN	COMMENT
4.43±0.25 OUR FIT Error includes scale factor of 1.2.				
3.9 ±0.6 OUR AVERAGE				
3.9 ±1.0	UHLIG	67	HBC	K^-p 0.9–1.0 GeV/c
3.3 ±1.1	BIRMINGHAM	66	HBC	K^-p 3.5 GeV/c
4.5 ±1.0	ARMENTEROS	65C	HBC	

$\Gamma(\Sigma(1385)\pi)/\Gamma_{\text{total}}$ — Γ_4/Γ

VALUE	DOCUMENT ID		TECN	COMMENT
0.041±0.005	CHAN	72	HBC	$K^-p \rightarrow \Lambda\pi\pi$

$\Gamma(\Sigma(1385)\pi(\rightarrow \Lambda\pi\pi))/\Gamma(\Lambda\pi\pi)$ — Γ_5/Γ_3

The $\Lambda\pi\pi$ mode is largely due to $\Sigma(1385)\pi$. Only the values of $(\Sigma(1385)\pi)\ /\ (\Lambda 2\pi)$ given by MAST 73B and CORDEN 75 are based on real 3-body partial-wave analyses. The discrepancy between the two results is essentially due to the different hypotheses made concerning the shape of the $(\pi\pi)_{S\text{-wave}}$ state.

VALUE	CL%	DOCUMENT ID		TECN	COMMENT
0.58±0.22		CORDEN	75	DBC	K^-d 1.4–1.8 GeV/c
0.82±0.10		[6] MAST	73B	IPWA	$K^-p \rightarrow \Lambda\pi\pi$
• • • We do not use the following data for averages, fits, limits, etc. • • •					
<0.44	90	WIELAND	11	SPHR	$\gamma p \rightarrow K^+\Lambda(1520)$
0.39±0.10		[7] BURKHARDT	71	HBC	$K^-p \rightarrow (\Lambda\pi\pi)\pi$

[6] Both $\Sigma(1385)\pi$ DS_{03} and $\Sigma(\pi\pi)$ DP_{03} contribute.
[7] The central bin (1514–1524 MeV) gives 0.74 ± 0.10; other bins are lower by 2-to-5 standard deviations.

$\Gamma(\Lambda(\pi\pi)_{S\text{-wave}})/\Gamma(\Lambda\pi\pi)$ — Γ_6/Γ_3

VALUE	DOCUMENT ID		TECN	COMMENT
0.20±0.08	CORDEN	75	DBC	K^-d 1.4–1.8 GeV/c

$\Gamma(\Sigma\pi\pi)/\Gamma_{\text{total}}$ — Γ_7/Γ

VALUE	DOCUMENT ID		TECN	COMMENT
0.009 ±0.001 OUR ESTIMATE				
0.0086±0.0005 OUR FIT				
0.0086±0.0005 OUR AVERAGE				
0.007 ±0.002	[8] CORDEN	75	DBC	K^-d 1.4–1.8 GeV/c
0.0085±0.0006	[9] MAST	73	MPWA	$K^-p \rightarrow \Sigma\pi\pi$
0.010 ±0.0015	BARBARO-...	69B	HBC	K^-p 0.28–0.45 GeV/c

[8] Much of the $\Sigma\pi\pi$ decay proceeds via $\Sigma(1385)\pi$.
[9] Assumes $\Gamma(N\overline{K})/\Gamma_{\text{total}} = 0.46$.

$\Gamma(\Lambda\gamma)/\Gamma_{\text{total}}$ Γ_8/Γ

VALUE (units 10^{-3})	EVTS	DOCUMENT ID		TECN	COMMENT
8.5±1.5 OUR ESTIMATE					
8.8±1.1 OUR FIT					
8.8±1.1 OUR AVERAGE					
$10.7\pm2.9^{+1.5}_{-0.4}$	32	TAYLOR	05	CLAS	$\gamma p \to K^+\Lambda\gamma$
10.2±2.1±1.5	290	ANTIPOV	04A	SPNX	$p N(C) \to \Lambda(1520) K^+ N(C)$
8.0±1.4	238	MAST	68B	HBC	Using $\Gamma(N\overline{K})/\Gamma_{\text{total}} = 0.45$

$\Gamma(\Sigma^0\gamma)/\Gamma_{\text{total}}$ Γ_9/Γ

VALUE	DOCUMENT ID		TECN	COMMENT
0.0193±0.0034 OUR FIT				
0.02 ±0.0035	[10] MAST	68B	HBC	Not measured; see note

[10] Calculated from $\Gamma(\Lambda\gamma)/\Gamma_{\text{total}}$, assuming SU(3). Needed to constrain the sum of all the branching ratios to be unity.

$\Lambda(1520)$ REFERENCES

ZHANG	13A	PR C88 035205	H. Zhang *et al.*	(KSU)
WIELAND	11	EPJ A47 47	F. Wieland *et al.*	(ELSA SAPHIR Collab.)
QIANG	10	PL B694 123	Y. Qiang *et al.*	(DUKE, JEFF, PNPI, GWU+)
TAYLOR	05	PR C71 054609	S. Taylor *et al.*	(JLab CLAS Collab.)
Also		PR C72 039902 (errat.)	S. Taylor *et al.*	(JLab CLAS Collab.)
ANTIPOV	04A	PL B604 22	Yu.M. Antipov *et al.*	(IHEP SPHINX Collab.)
PDG	82	PL 111B 1	M. Roos *et al.*	(HELS, CIT, CERN)
BARBER	80D	ZPHY C7 17	D.P. Barber *et al.*	(DARE, LANC, SHEF)
GOPAL	80	Toronto Conf. 159	G.P. Gopal	(RHEL) IJP
BARLAG	79	NP B149 220	S.J.M. Barlag *et al.*	(AMST, CERN, NIJM+)
ALSTON-...	78	PR D18 182	M. Alston-Garnjost *et al.*	(LBL, MTHO+) IJP
Also		PRL 38 1007	M. Alston-Garnjost *et al.*	(LBL, MTHO+) IJP
CAMERON	77	NP B131 399	W. Cameron *et al.*	(RHEL, LOIC) IJP
GOPAL	77	NP B119 362	G.P. Gopal *et al.*	(LOIC, RHEL) IJP
MAST	76	PR D14 13	T.S. Mast *et al.*	(LBL)
CORDEN	75	NP B84 306	M.J. Corden *et al.*	(BIRM)
BERTHON	74	NC 21A 146	A. Berthon *et al.*	(CDEF, RHEL, SACL+)
MAST	73	PR D7 3212	T.S. Mast *et al.*	(LBL) IJP
MAST	73B	PR D7 5	T.S. Mast *et al.*	(LBL) IJP
CHAN	72	PRL 28 256	S.B. Chan *et al.*	(MASA, YALE)
BURKHARDT	71	NP B27 64	E. Burkhardt *et al.*	(HEID, CERN, SACL)
KIM	71	PRL 27 356	J.K. Kim	(HARV) IJP
Also		Duke Conf. 161 Hyperon Resonances, 1970	J.K. Kim	(HARV) IJP
BARBARO-...	69B	Lund Conf. 352	A. Barbaro-Galtieri *et al.*	(LRL)
Also		Duke Conf. 95 Hyperon Resonances 1970	R.D. Tripp	(LRL)
BURKHARDT	69	NP B14 106	E. Burkhardt *et al.*	(HEID, EFI, CERN+)
MAST	68B	PRL 21 1715	T.S. Mast *et al.*	(LRL)
SCHEUER	68	NP B8 503	J.C. Scheuer *et al.*	(SABRE Collab.)
DAHL	67	PR 163 1377	O.I. Dahl *et al.*	(LRL)
DAUBER	67	PL 24B 525	P.M. Dauber *et al.*	(UCLA)
UHLIG	67	PR 155 1448	R.P. Uhlig *et al.*	(UMD, NRL)
BIRMINGHAM	66	PR 152 1148	M. Haque *et al.*	(BIRM, GLAS, LOIC, OXF+)
ARMENTEROS	65C	PL 19 338	R. Armenteros *et al.*	(CERN, HEID, SACL)
MUSGRAVE	65	NC 35 735	B. Musgrave *et al.*	(BIRM, CERN, EPOL+)
WATSON	63	PR 131 2248	M.B. Watson, M. Ferro-Luzzi, R.D. Tripp	(LRL) IJP
FERRO-LUZZI	62	PRL 8 28	M. Ferro-Luzzi, R.D. Tripp, M.B. Watson	(LRL) IJP

$\Lambda(1600)$ $1/2^+$

$I(J^P) = 0(\frac{1}{2}^+)$ Status: ***

See also the $\Lambda(1810)$ P_{01}. There are quite possibly two P_{01} states in this region.

$\Lambda(1600)$ MASS

VALUE (MeV)	DOCUMENT ID		TECN	COMMENT
1560 to 1700 (≈ 1600) OUR ESTIMATE				
1592± 10	ZHANG	13A	DPWA	Multichannel
1568± 20	GOPAL	80	DPWA	$\overline{K}N \to \overline{K}N$
1703±100	ALSTON-...	78	DPWA	$\overline{K}N \to \overline{K}N$
1573± 25	GOPAL	77	DPWA	$\overline{K}N$ multichannel
1596± 6	KANE	74	DPWA	$K^-p \to \Sigma\pi$
1620± 10	LANGBEIN	72	IPWA	$\overline{K}N$ multichannel
• • • We do not use the following data for averages, fits, limits, etc. • • •				
1572 or 1617	[1] MARTIN	77	DPWA	$\overline{K}N$ multichannel
1646± 7	[2] CARROLL	76	DPWA	Isospin-0 total σ
1570	KIM	71	DPWA	K-matrix analysis

$\Lambda(1600)$ WIDTH

VALUE (MeV)	DOCUMENT ID		TECN	COMMENT
50 to 250 (≈ 150) OUR ESTIMATE				
150± 28	ZHANG	13A	DPWA	Multichannel
116± 20	GOPAL	80	DPWA	$\overline{K}N \to \overline{K}N$
593±200	ALSTON-...	78	DPWA	$\overline{K}N \to \overline{K}N$
147± 50	GOPAL	77	DPWA	$\overline{K}N$ multichannel
175± 20	KANE	74	DPWA	$K^-p \to \Sigma\pi$
60± 10	LANGBEIN	72	IPWA	$\overline{K}N$ multichannel
• • • We do not use the following data for averages, fits, limits, etc. • • •				
247 or 271	[1] MARTIN	77	DPWA	$\overline{K}N$ multichannel
20	[2] CARROLL	76	DPWA	Isospin-0 total σ
50	KIM	71	DPWA	K-matrix analysis

$\Lambda(1600)$ POLE POSITION

REAL PART

VALUE (MeV)	DOCUMENT ID		TECN	COMMENT
• • • We do not use the following data for averages, fits, limits, etc. • • •				
1572	ZHANG	13A	DPWA	Multichannel

−2×IMAGINARY PART

VALUE (MeV)	DOCUMENT ID		TECN	COMMENT
• • • We do not use the following data for averages, fits, limits, etc. • • •				
138	ZHANG	13A	DPWA	Multichannel

$\Lambda(1600)$ DECAY MODES

	Mode	Fraction (Γ_i/Γ)
Γ_1	$N\overline{K}$	15–30 %
Γ_2	$\Sigma\pi$	10–60 %

The above branching fractions are our estimates, not fits or averages.

$\Lambda(1600)$ BRANCHING RATIOS

See "Sign conventions for resonance couplings" in the Note on Λ and Σ Resonances.

$\Gamma(N\overline{K})/\Gamma_{\text{total}}$ Γ_1/Γ

VALUE	DOCUMENT ID		TECN	COMMENT
0.15 to 0.30 OUR ESTIMATE				
0.14±0.04	ZHANG	13A	DPWA	Multichannel
0.23±0.04	GOPAL	80	DPWA	$\overline{K}N \to \overline{K}N$
0.14±0.05	ALSTON-...	78	DPWA	$\overline{K}N \to \overline{K}N$
0.25±0.15	LANGBEIN	72	IPWA	$\overline{K}N$ multichannel
• • • We do not use the following data for averages, fits, limits, etc. • • •				
0.24±0.04	GOPAL	77	DPWA	See GOPAL 80
0.30 or 0.29	[1] MARTIN	77	DPWA	$\overline{K}N$ multichannel

$(\Gamma_i\Gamma_f)^{1/2}/\Gamma_{\text{total}}$ in $N\overline{K} \to \Lambda(1600) \to \Sigma\pi$ $(\Gamma_1\Gamma_2)^{1/2}/\Gamma$

VALUE	DOCUMENT ID		TECN	COMMENT
−0.23±0.03	ZHANG	13A	DPWA	Multichannel
−0.16±0.04	GOPAL	77	DPWA	$\overline{K}N$ multichannel
−0.33±0.11	KANE	74	DPWA	$K^-p \to \Sigma\pi$
0.28±0.09	LANGBEIN	72	IPWA	$\overline{K}N$ multichannel
• • • We do not use the following data for averages, fits, limits, etc. • • •				
−0.39 or −0.39	[1] MARTIN	77	DPWA	$\overline{K}N$ multichannel
not seen	HEPP	76B	DPWA	$K^-N \to \Sigma\pi$

$\Lambda(1600)$ FOOTNOTES

[1] The two MARTIN 77 values are from a T-matrix pole and from a Breit-Wigner fit.
[2] A total cross-section bump with $(J+1/2)\,\Gamma_{el}\,/\,\Gamma_{\text{total}} = 0.04$.

$\Lambda(1600)$ REFERENCES

ZHANG	13A	PR C88 035205	H. Zhang *et al.*	(KSU)
GOPAL	80	Toronto Conf. 159	G.P. Gopal	(RHEL) IJP
ALSTON-...	78	PR D18 182	M. Alston-Garnjost *et al.*	(LBL, MTHO+) IJP
Also		PRL 38 1007	M. Alston-Garnjost *et al.*	(LBL, MTHO+) IJP
GOPAL	77	NP B119 362	G.P. Gopal *et al.*	(LOIC, RHEL) IJP
MARTIN	77	NP B127 349	B.R. Martin, M.K. Pidcock, R.G. Moorhouse	(LOUC+) IJP
Also		NP B126 266	B.R. Martin, M.K. Pidcock	(LOUC)
Also		NP B126 285	B.R. Martin, M.K. Pidcock	(LOUC) IJP
CARROLL	76	PRL 37 806	A.S. Carroll *et al.*	(BNL) I
HEPP	76B	PL 65B 487	V. Hepp *et al.*	(CERN, HEIDH, MPIM) IJP
KANE	74	LBL-2452	D.F. Kane	(LBL) IJP
LANGBEIN	72	NP B47 477	W. Langbein, F. Wagner	(MPIM) IJP
KIM	71	PRL 27 356	J.K. Kim	(HARV) IJP

Baryon Particle Listings

$\Lambda(1670)$

$\Lambda(1670)\ 1/2^-$

$I(J^P) = 0(\frac{1}{2}^-)$ Status: ****

The measurements of the mass, width, and elasticity published before 1974 are now obsolete and have been omitted. They were last listed in our 1982 edition Physics Letters **111B** 1 (1982).

$\Lambda(1670)$ MASS

VALUE (MeV)		DOCUMENT ID		TECN	COMMENT
1660 to 1680 (≈ 1670) OUR ESTIMATE					
1672 ±3		ZHANG	13A	DPWA	Multichannel
1677.5±0.8	[1]	GARCIA-REC...	03	DPWA	$\overline{K}N$ multichannel
1673 ±2		MANLEY	02	DPWA	$\overline{K}N$ multichannel
1670.8±1.7		KOISO	85	DPWA	$K^-p \to \Sigma\pi$
1667 ±5		GOPAL	80	DPWA	$\overline{K}N \to \overline{K}N$
1671 ±3		ALSTON-...	78	DPWA	$\overline{K}N \to \overline{K}N$
1670 ±5		GOPAL	77	DPWA	$\overline{K}N$ multichannel
1675 ±2		HEPP	76B	DPWA	$K^-N \to \Sigma\pi$
1679 ±1		KANE	74	DPWA	$K^-p \to \Sigma\pi$
1665 ±5		PREVOST	74	DPWA	$K^-N \to \Sigma(1385)\pi$
• • • We do not use the following data for averages, fits, limits, etc. • • •					
1668.9±2.0		ABAEV	96	DPWA	$K^-p \to \Lambda\eta$
1664	[2]	MARTIN	77	DPWA	$\overline{K}N$ multichannel

$\Lambda(1670)$ WIDTH

VALUE (MeV)		DOCUMENT ID		TECN	COMMENT
25 to 50 (≈ 35) OUR ESTIMATE					
29 ± 5		ZHANG	13A	DPWA	Multichannel
29.2± 1.4	[1]	GARCIA-REC...	03	DPWA	$\overline{K}N$ multichannel
23 ± 6		MANLEY	02	DPWA	$\overline{K}N$ multichannel
34.1± 3.7		KOISO	85	DPWA	$K^-p \to \Sigma\pi$
29 ± 5		GOPAL	80	DPWA	$\overline{K}N \to \overline{K}N$
29 ± 5		ALSTON-...	78	DPWA	$\overline{K}N \to \overline{K}N$
45 ±10		GOPAL	77	DPWA	$\overline{K}N$ multichannel
46 ± 5		HEPP	76B	DPWA	$K^-N \to \Sigma\pi$
40 ± 3		KANE	74	DPWA	$K^-p \to \Sigma\pi$
19 ± 5		PREVOST	74	DPWA	$K^-N \to \Sigma(1385)\pi$
• • • We do not use the following data for averages, fits, limits, etc. • • •					
21.1± 3.6		ABAEV	96	DPWA	$K^-p \to \Lambda\eta$
12	[2]	MARTIN	77	DPWA	$\overline{K}N$ multichannel

$\Lambda(1670)$ POLE POSITIONS

REAL PART

VALUE (MeV)	DOCUMENT ID		TECN	COMMENT
• • • We do not use the following data for averages, fits, limits, etc. • • •				
1667	ZHANG	13A	DPWA	Multichannel

$-2\times$IMAGINARY PART

VALUE (MeV)	DOCUMENT ID		TECN	COMMENT
• • • We do not use the following data for averages, fits, limits, etc. • • •				
26	ZHANG	13A	DPWA	Multichannel

$\Lambda(1670)$ DECAY MODES

	Mode	Fraction (Γ_i/Γ)
Γ_1	$N\overline{K}$	20–30 %
Γ_2	$\Sigma\pi$	25–55 %
Γ_3	$\Lambda\eta$	10–25 %
Γ_4	$\Sigma(1385)\pi$	
	The above branching fractions are our estimates, not fits or averages.	
Γ_5	$N\overline{K}^*(892)$, S=3/2, D-wave	(5±4) %

$\Lambda(1670)$ BRANCHING RATIOS

See "Sign conventions for resonance couplings" in the Note on Λ and Σ Resonances.

$\Gamma(N\overline{K})/\Gamma_{total}$ Γ_1/Γ

VALUE	DOCUMENT ID		TECN	COMMENT
0.20 to 0.30 OUR ESTIMATE				
0.26±0.25	ZHANG	13A	DPWA	Multichannel
0.37±0.07	MANLEY	02	DPWA	$\overline{K}N$ multichannel
0.18±0.03	GOPAL	80	DPWA	$\overline{K}N \to \overline{K}N$
0.17±0.03	ALSTON-...	78	DPWA	$\overline{K}N \to \overline{K}N$
• • • We do not use the following data for averages, fits, limits, etc. • • •				
0.20±0.03	GOPAL	77	DPWA	See GOPAL 80
0.15	[2] MARTIN	77	DPWA	$\overline{K}N$ multichannel

$\Gamma(\Lambda\eta)/\Gamma_{total}$ Γ_3/Γ

VALUE	DOCUMENT ID		TECN	COMMENT
• • • We do not use the following data for averages, fits, limits, etc. • • •				
0.30±0.08	ABAEV	96	DPWA	$K^-p \to \Lambda\eta$

$(\Gamma_i\Gamma_f)^{1/2}/\Gamma_{total}$ in $N\overline{K} \to \Lambda(1670) \to \Sigma\pi$ $(\Gamma_1\Gamma_2)^{1/2}/\Gamma$

VALUE	DOCUMENT ID		TECN	COMMENT
−0.29±0.06	ZHANG	13A	DPWA	Multichannel
−0.38±0.03	MANLEY	02	DPWA	$\overline{K}N$ multichannel
−0.26±0.02	KOISO	85	DPWA	$K^-p \to \Sigma\pi$
−0.31±0.03	GOPAL	77	DPWA	$\overline{K}N$ multichannel
−0.29±0.03	HEPP	76B	DPWA	$K^-N \to \Sigma\pi$
−0.23±0.03	LONDON	75	HLBC	$K^-p \to \Sigma^0\pi^0$
−0.27±0.02	KANE	74	DPWA	$K^-p \to \Sigma\pi$
• • • We do not use the following data for averages, fits, limits, etc. • • •				
−0.13	[2] MARTIN	77	DPWA	$\overline{K}N$ multichannel

$(\Gamma_i\Gamma_f)^{1/2}/\Gamma_{total}$ in $N\overline{K} \to \Lambda(1670) \to \Lambda\eta$ $(\Gamma_1\Gamma_3)^{1/2}/\Gamma$

VALUE	DOCUMENT ID		TECN	COMMENT
−0.30±0.10	ZHANG	13A	DPWA	Multichannel
+0.24±0.04	MANLEY	02	DPWA	$\overline{K}N$ multichannel
+0.20±0.05	BAXTER	73	DPWA	$K^-p \to$ neutrals
• • • We do not use the following data for averages, fits, limits, etc. • • •				
0.24	KIM	71	DPWA	K-matrix analysis
0.26	ARMENTEROS	69C	HBC	
0.20 or 0.23	BERLEY	65	HBC	

$(\Gamma_i\Gamma_f)^{1/2}/\Gamma_{total}$ in $N\overline{K} \to \Lambda(1670) \to \Sigma(1385)\pi$ $(\Gamma_1\Gamma_4)^{1/2}/\Gamma$

VALUE	DOCUMENT ID		TECN	COMMENT
−0.17±0.06	MANLEY	02	DPWA	$\overline{K}N$ multichannel
−0.18±0.05	PREVOST	74	DPWA	$K^-N \to \Sigma(1385)\pi$

$\Gamma(N\overline{K}^*(892), S$=3/2, D-wave$)/\Gamma_{total}$ Γ_5/Γ

VALUE	DOCUMENT ID		TECN	COMMENT
0.05±0.04	ZHANG	13A	DPWA	Multichannel

$\Lambda(1670)$ FOOTNOTES

[1] GARCIA-RECIO 03 gives pole, not Breit-Wigner, parameters, but the narrow width of the $\Lambda(1670)$ means there will be little difference.

[2] MARTIN 77 obtains identical resonance parameters from a T-matrix pole and from a Breit-Wigner fit.

$\Lambda(1670)$ REFERENCES

ZHANG	13A	PR C88 035205	H. Zhang *et al.*	(KSU)
GARCIA-REC...	03	PR D67 076009	C. Garcia-Recio *et al.*	(GRAN, VALE)
MANLEY	02	PRL 88 012002	D.M. Manley *et al.*	(BNL Crystal Ball Collab.)
ABAEV	96	PR C53 385	V.V. Abaev, B.M.K. Nefkens	(UCLA)
KOISO	85	NP A433 619	H. Koiso *et al.*	(TOKY, MASA)
PDG	82	PL 111B 1	M. Roos *et al.*	(HELS, CIT, CERN)
GOPAL	80	Toronto Conf. 159	G.P. Gopal	(RHEL) IJP
ALSTON-...	78	PR D18 182	M. Alston-Garnjost *et al.*	(LBL, MTHO+) IJP
Also		PRL 38 1007	M. Alston-Garnjost *et al.*	(LBL, MTHO+) IJP
GOPAL	77	NP B119 362	G.P. Gopal *et al.*	(LOIC, RHEL) IJP
MARTIN	77	NP B127 349	B.R. Martin, M.K. Pidcock, R.G. Moorhouse	(LOUC+) IJP
Also		NP B126 266	B.R. Martin, M.K. Pidcock	(LOUC)
Also		NP B126 285	B.R. Martin, M.K. Pidcock	(LOUC) IJP
HEPP	76B	PL 65B 487	V. Hepp *et al.*	(CERN, HEIDH, MPIM) IJP
LONDON	75	NP B85 289	G.W. London *et al.*	(BNL, CERN, EPOL+)
KANE	74	LBL-2452	D.F. Kane	(LBL) IJP
PREVOST	74	NP B69 246	J. Prevost *et al.*	(SACL, CERN, HEID)
BAXTER	73	NP B67 125	D.F. Baxter *et al.*	(OXF) IJP
KIM	71	PRL 27 356	J.K. Kim	(HARV) IJP
Also		Duke Conf. 161 Hyperon Resonances, 1970	J.K. Kim	(HARV) IJP
ARMENTEROS	69C	Lund Paper 229 Values are quoted in LEVI-SETTI 69.	R. Armenteros *et al.*	(CERN, HEID, SACL) IJP
BERLEY	65	PRL 15 641	D. Berley *et al.*	(BNL) IJP

$\Lambda(1690)\ 3/2^-$

$I(J^P) = 0(\frac{3}{2}^-)$ Status: ****

The measurements of the mass, width, and elasticity published before 1974 are now obsolete and have been omitted. They were last listed in our 1982 edition Physics Letters **111B** 1 (1982).

$\Lambda(1690)$ MASS

VALUE (MeV)	DOCUMENT ID		TECN	COMMENT
1685 to 1695 (≈ 1690) OUR ESTIMATE				
1691 ±3	ZHANG	13A	DPWA	Multichannel
1695.7±2.6	KOISO	85	DPWA	$K^-p \to \Sigma\pi$
1690 ±5	GOPAL	80	DPWA	$\overline{K}N \to \overline{K}N$
1692 ±5	ALSTON-...	78	DPWA	$\overline{K}N \to \overline{K}N$
1690 ±5	GOPAL	77	DPWA	$\overline{K}N$ multichannel
1690 ±3	HEPP	76B	DPWA	$K^-N \to \Sigma\pi$
1689 ±1	KANE	74	DPWA	$K^-p \to \Sigma\pi$
• • • We do not use the following data for averages, fits, limits, etc. • • •				
1687 or 1689	[1] MARTIN	77	DPWA	$\overline{K}N$ multichannel
1692 ±4	CARROLL	76	DPWA	Isospin-0 total σ

$\Lambda(1690)$ WIDTH

VALUE (MeV)	DOCUMENT ID		TECN	COMMENT
50 to 70 (≈ 60) OUR ESTIMATE				
54 ± 5	ZHANG	13A	DPWA	Multichannel
67.2± 5.6	KOISO	85	DPWA	$K^-p \to \Sigma\pi$
61 ± 5	GOPAL	80	DPWA	$\overline{K}N \to \overline{K}N$
64 ±10	ALSTON-...	78	DPWA	$\overline{K}N \to \overline{K}N$
60 ± 5	GOPAL	77	DPWA	$\overline{K}N$ multichannel
82 ± 8	HEPP	76B	DPWA	$K^-N \to \Sigma\pi$
60 ± 4	KANE	74	DPWA	$K^-p \to \Sigma\pi$
• • • We do not use the following data for averages, fits, limits, etc. • • •				
62 or 62	[1] MARTIN	77	DPWA	$\overline{K}N$ multichannel
38	CARROLL	76	DPWA	Isospin-0 total σ

$\Lambda(1690)$ POLE POSITION

REAL PART

VALUE (MeV)	DOCUMENT ID	TECN	COMMENT
• • • We do not use the following data for averages, fits, limits, etc. • • •			
1689	ZHANG 13A	DPWA	Multichannel

$-2\times$IMAGINARY PART

VALUE (MeV)	DOCUMENT ID	TECN	COMMENT
• • • We do not use the following data for averages, fits, limits, etc. • • •			
53	ZHANG 13A	DPWA	Multichannel

$\Lambda(1690)$ DECAY MODES

	Mode	Fraction (Γ_i/Γ)
Γ_1	$N\overline{K}$	20–30 %
Γ_2	$\Sigma\pi$	20–40 %
Γ_3	$\Lambda\pi\pi$	∼ 25 %
Γ_4	$\Sigma\pi\pi$	∼ 20 %
Γ_5	$\Lambda\eta$	
Γ_6	$\Sigma(1385)\pi$, S-wave	

The above branching fractions are our estimates, not fits or averages.

$\Lambda(1690)$ BRANCHING RATIOS

The sum of all the quoted branching ratios is more than 1.0. The two-body ratios are from partial-wave analyses, and thus probably are more reliable than the three-body ratios, which are determined from bumps in cross sections. Of the latter, the $\Sigma\pi\pi$ bump looks more significant. (The error given for the $\Lambda\pi\pi$ ratio looks unreasonably small.) Hardly any of the $\Sigma\pi\pi$ decay can be via $\Sigma(1385)$, for then seven times as much $\Lambda\pi\pi$ decay would be required. See "Sign conventions for resonance couplings" in the Note on Λ and Σ Resonances.

$\Gamma(N\overline{K})/\Gamma_{total}$ Γ_1/Γ

VALUE	DOCUMENT ID		TECN	COMMENT
0.2 to 0.3 OUR ESTIMATE				
0.25±0.04	ZHANG	13A	DPWA	Multichannel
0.23±0.03	GOPAL	80	DPWA	$\overline{K}N \to \overline{K}N$
0.22±0.03	ALSTON-...	78	DPWA	$\overline{K}N \to \overline{K}N$
• • • We do not use the following data for averages, fits, limits, etc. • • •				
0.24±0.03	GOPAL	77	DPWA	See GOPAL 80
0.28 or 0.26	[1] MARTIN	77	DPWA	$\overline{K}N$ multichannel

$(\Gamma_i\Gamma_f)^{1/2}/\Gamma_{total}$ in $N\overline{K} \to \Lambda(1690) \to \Sigma\pi$ $(\Gamma_1\Gamma_2)^{1/2}/\Gamma$

VALUE	DOCUMENT ID		TECN	COMMENT
−0.27±0.03	ZHANG	13A	DPWA	Multichannel
−0.34±0.02	KOISO	85	DPWA	$K^-p \to \Sigma\pi$
−0.25±0.03	GOPAL	77	DPWA	$\overline{K}N$ multichannel
−0.29±0.03	HEPP	76B	DPWA	$K^-N \to \Sigma\pi$
−0.28±0.03	LONDON	75	HLBC	$K^-p \to \Sigma^0\pi^0$
−0.28±0.02	KANE	74	DPWA	$K^-p \to \Sigma\pi$
• • • We do not use the following data for averages, fits, limits, etc. • • •				
−0.30 or −0.28	[1] MARTIN	77	DPWA	$\overline{K}N$ multichannel

$(\Gamma_i\Gamma_f)^{1/2}/\Gamma_{total}$ in $N\overline{K} \to \Lambda(1690) \to \Lambda\pi\pi$ $(\Gamma_1\Gamma_3)^{1/2}/\Gamma$

VALUE	DOCUMENT ID		TECN	COMMENT
• • • We do not use the following data for averages, fits, limits, etc. • • •				
0.25±0.02	[2] BARTLEY	68	HDBC	$K^-p \to \Lambda\pi\pi$

$(\Gamma_i\Gamma_f)^{1/2}/\Gamma_{total}$ in $N\overline{K} \to \Lambda(1690) \to \Sigma\pi\pi$ $(\Gamma_1\Gamma_4)^{1/2}/\Gamma$

VALUE	DOCUMENT ID	TECN	COMMENT
0.21	ARMENTEROS68C	HDBC	$K^-N \to \Sigma\pi\pi$

$(\Gamma_i\Gamma_f)^{1/2}/\Gamma_{total}$ in $N\overline{K} \to \Lambda(1690) \to \Lambda\eta$ $(\Gamma_1\Gamma_5)^{1/2}/\Gamma$

VALUE	DOCUMENT ID		TECN	COMMENT
0.00±0.03	BAXTER	73	DPWA	$K^-p \to$ neutrals

$(\Gamma_i\Gamma_f)^{1/2}/\Gamma_{total}$ in $N\overline{K} \to \Lambda(1690) \to \Sigma(1385)\pi$, S-wave $(\Gamma_1\Gamma_6)^{1/2}/\Gamma$

VALUE	DOCUMENT ID		TECN	COMMENT
−0.28±0.06	ZHANG	13A	DPWA	Multichannel
+0.27±0.04	PREVOST	74	DPWA	$K^-N \to \Sigma(1385)\pi$

$\Lambda(1690)$ FOOTNOTES

[1] The two MARTIN 77 values are from a T-matrix pole and from a Breit-Wigner fit. Another D_{03} Λ at 1966 MeV is also suggested by MARTIN 77, but is very uncertain.

[2] BARTLEY 68 uses only cross-section data. The enhancement is not seen by PREVOST 71.

$\Lambda(1690)$ REFERENCES

ZHANG	13A	PR C88 035205	H. Zhang *et al.*	(KSU)
KOISO	85	NP A433 619	H. Koiso *et al.*	(TOKY, MASA)
PDG	82	PL 111B 1	M. Roos *et al.*	(HELS, CIT, CERN)
GOPAL	80	Toronto Conf. 159	G.P. Gopal	(RHEL) IJP
ALSTON-...	78	PR D18 182	M. Alston-Garnjost *et al.*	(LBL, MTHO+) IJP
Also		PRL 38 1007	M. Alston-Garnjost *et al.*	(LBL, MTHO+) IJP
GOPAL	77	NP B119 362	G.P. Gopal *et al.*	(LOIC, RHEL) IJP
MARTIN	77	NP B127 349	B.R. Martin, M.K. Pidcock, R.G. Moorhouse	(LOUC+) IJP
Also		NP B126 266	B.R. Martin, M.K. Pidcock	(LOUC)
Also		NP B126 285	B.R. Martin, M.K. Pidcock	(LOUC) IJP
CARROLL	76	PRL 37 806	A.S. Carroll *et al.*	(BNL) I
HEPP	76B	PL 65B 487	V. Hepp *et al.*	(CERN, HEIDH, MPIM) IJP
LONDON	75	NP B85 289	G.W. London *et al.*	(BNL, CERN, EPOL+)
KANE	74	LBL-2452	D.F. Kane	(LBL) IJP
PREVOST	74	NP B69 246	J. Prevost *et al.*	(SACL, CERN, HEID)
BAXTER	73	NP B67 125	D.F. Baxter *et al.*	(OXF) IJP
PREVOST	71	Amsterdam Conf.	J. Prevost	(CERN, HEID, SACL)
ARMENTEROS	68C	NP B8 216	R. Armenteros *et al.*	(CERN, HEID, SACL) I
BARTLEY	68	PRL 21 1111	J.H. Bartley *et al.*	(TUFTS, FSU, BRAN) I

$\Lambda(1710)\ 1/2^+$

$I(J^P) = 0(\frac{1}{2}^+)$ Status: *

OMITTED FROM SUMMARY TABLE

$\Lambda(1710)$ MASS

VALUE (MeV)	DOCUMENT ID	TECN	COMMENT
1713±13	ZHANG 13A	DPWA	Multichannel

$\Lambda(1710)$ WIDTH

VALUE (MeV)	DOCUMENT ID	TECN	COMMENT
180±42	ZHANG 13A	DPWA	Multichannel

$\Lambda(1710)$ DECAY MODES

	Mode	Fraction (Γ_i/Γ)
Γ_1	$N\overline{K}$	(43±4) %
Γ_2	$\Sigma\pi$	(21±5) %
Γ_3	$\Sigma^*(1385)\pi$, P-wave	(20±8) %
Γ_4	$N\overline{K}^*(892)$	
Γ_5	$N\overline{K}^*(892)$, S=1/2	(5±4) %
Γ_6	$N\overline{K}^*(892)$, S=3/2, P-wave	(10±8) %

Baryon Particle Listings

$\Lambda(1710)$, $\Lambda(1800)$

$\Lambda(1710)$ BRANCHING RATIOS

$\Gamma(N\overline{K})/\Gamma_{total}$ — Γ_1/Γ

VALUE	DOCUMENT ID		TECN	COMMENT
0.43±0.04	ZHANG	13A	DPWA	Multichannel

$\Gamma(\Sigma\pi)/\Gamma_{total}$ — Γ_2/Γ

VALUE	DOCUMENT ID		TECN	COMMENT
0.21±0.05	ZHANG	13A	DPWA	Multichannel

$\Gamma(\Sigma^*(1385)\pi$, P-wave$)/\Gamma_{total}$ — Γ_3/Γ

VALUE	DOCUMENT ID		TECN	COMMENT
0.20±0.08	ZHANG	13A	DPWA	Multichannel

$\Gamma(N\overline{K}^*(892)$, S=1/2$)/\Gamma_{total}$ — Γ_5/Γ

VALUE	DOCUMENT ID		TECN	COMMENT
0.05±0.04	ZHANG	13A	DPWA	Multichannel

$\Gamma(N\overline{K}^*(892)$, S=3/2, P-wave$)/\Gamma_{total}$ — Γ_6/Γ

VALUE	DOCUMENT ID		TECN	COMMENT
0.10±0.08	ZHANG	13A	DPWA	Multichannel

$\Lambda(1710)$ REFERENCES

ZHANG 13A PR C88 035205 H. Zhang *et al.* (KSU)

$\Lambda(1800)$ $1/2^-$

$I(J^P) = 0(\frac{1}{2}^-)$ Status: ***

This is the second resonance in the S_{01} wave, the first being the $\Lambda(1670)$.

$\Lambda(1800)$ MASS

VALUE (MeV)	DOCUMENT ID		TECN	COMMENT
1720 to 1850 (≈ 1800) OUR ESTIMATE				
1783±19	ZHANG	13A	DPWA	Multichannel
1845±10	MANLEY	02	DPWA	$\overline{K}N$ multichannel
1841±10	GOPAL	80	DPWA	$\overline{K}N \to \overline{K}N$
1725±20	ALSTON-...	78	DPWA	$\overline{K}N \to \overline{K}N$
1825±20	GOPAL	77	DPWA	$\overline{K}N$ multichannel
1830±20	LANGBEIN	72	IPWA	$\overline{K}N$ multichannel
• • • We do not use the following data for averages, fits, limits, etc. • • •				
1767 or 1842	[1] MARTIN	77	DPWA	$\overline{K}N$ multichannel
1780	KIM	71	DPWA	K-matrix analysis
1872±10	BRICMAN	70B	DPWA	$\overline{K}N \to \overline{K}N$

$\Lambda(1800)$ WIDTH

VALUE (MeV)	DOCUMENT ID		TECN	COMMENT
200 to 400 (≈ 300) OUR ESTIMATE				
256±35	ZHANG	13A	DPWA	Multichannel
518±84	MANLEY	02	DPWA	$\overline{K}N$ multichannel
228±20	GOPAL	80	DPWA	$\overline{K}N \to \overline{K}N$
185±20	ALSTON-...	78	DPWA	$\overline{K}N \to \overline{K}N$
230±20	GOPAL	77	DPWA	$\overline{K}N$ multichannel
70±15	LANGBEIN	72	IPWA	$\overline{K}N$ multichannel
• • • We do not use the following data for averages, fits, limits, etc. • • •				
435 or 473	[1] MARTIN	77	DPWA	$\overline{K}N$ multichannel
40	KIM	71	DPWA	K-matrix analysis
100±20	BRICMAN	70B	DPWA	$\overline{K}N \to \overline{K}N$

$\Lambda(1800)$ POLE POSITION

REAL PART

VALUE (MeV)	DOCUMENT ID		TECN	COMMENT
• • • We do not use the following data for averages, fits, limits, etc. • • •				
1729	ZHANG	13A	DPWA	Multichannel

−2×IMAGINARY PART

VALUE (MeV)	DOCUMENT ID		TECN	COMMENT
• • • We do not use the following data for averages, fits, limits, etc. • • •				
198	ZHANG	13A	DPWA	Multichannel

$\Lambda(1800)$ DECAY MODES

	Mode	Fraction (Γ_i/Γ)
Γ_1	$N\overline{K}$	25–40 %
Γ_2	$\Sigma\pi$	seen
Γ_3	$\Sigma(1385)\pi$	seen
	The above branching fractions are our estimates, not fits or averages.	
Γ_4	$\Lambda\eta$	(6±5) %
Γ_5	$N\overline{K}^*(892)$	seen
Γ_6	$N\overline{K}^*(892)$, S=1/2, S-wave	
Γ_7	$N\overline{K}^*(892)$, S=3/2, D-wave	

$\Lambda(1800)$ BRANCHING RATIOS

See "Sign conventions for resonance couplings" in the Note on Λ and Σ Resonances.

$\Gamma(N\overline{K})/\Gamma_{total}$ — Γ_1/Γ

VALUE	DOCUMENT ID		TECN	COMMENT
0.25 to 0.40 OUR ESTIMATE				
0.13±0.06	ZHANG	13A	DPWA	Multichannel
0.24±0.10	MANLEY	02	DPWA	$\overline{K}N$ multichannel
0.36±0.04	GOPAL	80	DPWA	$\overline{K}N \to \overline{K}N$
0.28±0.05	ALSTON-...	78	DPWA	$\overline{K}N \to \overline{K}N$
0.35±0.15	LANGBEIN	72	IPWA	$\overline{K}N$ multichannel
• • • We do not use the following data for averages, fits, limits, etc. • • •				
0.37±0.05	GOPAL	77	DPWA	See GOPAL 80
1.21 or 0.70	[1] MARTIN	77	DPWA	$\overline{K}N$ multichannel
0.80	KIM	71	DPWA	K-matrix analysis
0.18±0.02	BRICMAN	70B	DPWA	$\overline{K}N \to \overline{K}N$

$(\Gamma_i\Gamma_f)^{1/2}/\Gamma_{total}$ in $N\overline{K} \to \Lambda(1800) \to \Sigma\pi$ — $(\Gamma_1\Gamma_2)^{1/2}/\Gamma$

VALUE	DOCUMENT ID		TECN	COMMENT
−0.07±0.02	ZHANG	13A	DPWA	Multichannel
−0.08±0.05	GOPAL	77	DPWA	$\overline{K}N$ multichannel
• • • We do not use the following data for averages, fits, limits, etc. • • •				
−0.74 or −0.43	[1] MARTIN	77	DPWA	$\overline{K}N$ multichannel
0.24	KIM	71	DPWA	K-matrix analysis

$(\Gamma_i\Gamma_f)^{1/2}/\Gamma_{total}$ in $N\overline{K} \to \Lambda(1800) \to \Sigma(1385)\pi$ — $(\Gamma_1\Gamma_3)^{1/2}/\Gamma$

VALUE	DOCUMENT ID		TECN	COMMENT
−0.09 ±0.05	ZHANG	13A	DPWA	Multichannel
+0.056±0.028	[2] CAMERON	78	DPWA	$K^-p \to \Sigma(1385)\pi$

$\Gamma(\Lambda\eta)/\Gamma_{total}$ — Γ_4/Γ

VALUE	DOCUMENT ID		TECN	COMMENT
0.06±0.05	ZHANG	13A	DPWA	Multichannel

$(\Gamma_i\Gamma_f)^{1/2}/\Gamma_{total}$ in $N\overline{K} \to \Lambda(1800) \to N\overline{K}^*(892)$, S=1/2, S-wave $(\Gamma_1\Gamma_6)^{1/2}/\Gamma$

VALUE	DOCUMENT ID		TECN	COMMENT
−0.13±0.02	ZHANG	13A	DPWA	Multichannel
−0.17±0.03	[2] CAMERON	78B	DPWA	$K^-p \to N\overline{K}^*$

$(\Gamma_i\Gamma_f)^{1/2}/\Gamma_{total}$ in $N\overline{K} \to \Lambda(1800) \to N\overline{K}^*(892)$, S=3/2, D-wave $(\Gamma_1\Gamma_7)^{1/2}/\Gamma$

VALUE	DOCUMENT ID		TECN	COMMENT
−0.13±0.04	CAMERON	78B	DPWA	$K^-p \to N\overline{K}^*$

$\Lambda(1800)$ FOOTNOTES

[1] The two MARTIN 77 values are from a T-matrix pole and from a Breit-Wigner fit.
[2] The published sign has been changed to be in accord with the baryon-first convention.

$\Lambda(1800)$ REFERENCES

ZHANG 13A PR C88 035205 H. Zhang *et al.* (KSU)
MANLEY 02 PRL 88 012002 D.M. Manley *et al.* (BNL Crystal Ball Collab.)
GOPAL 80 Toronto Conf. 159 G.P. Gopal (RHEL) IJP
ALSTON-... 78 PR D18 182 M. Alston-Garnjost *et al.* (LBL, MTHO+) IJP
Also PRL 38 1007 M. Alston-Garnjost *et al.* (LBL, MTHO+) IJP
CAMERON 78 NP B143 189 W. Cameron *et al.* (RHEL, LOIC) IJP
CAMERON 78B NP B146 327 W. Cameron *et al.* (RHEL, LOIC) IJP
GOPAL 77 NP B119 362 G.P. Gopal *et al.* (LOIC, RHEL) IJP
MARTIN 77 NP B127 349 B.R. Martin, M.K. Pidcock, R.G. Moorhouse (LOUC+) IJP
Also NP B126 266 B.R. Martin, M.K. Pidcock (LOUC) IJP
Also NP B126 285 B.R. Martin, M.K. Pidcock (LOUC) IJP
LANGBEIN 72 NP B47 477 W. Langbein, F. Wagner (MPIM) IJP
KIM 71 PRL 27 356 J.K. Kim (HARV) IJP
Also Duke Conf. 161 J.K. Kim (HARV) IJP
Hyperon Resonances, 1970
BRICMAN 70B PL 33B 511 C. Bricman, M. Ferro-Luzzi, J.P. Lagnaux (CERN) IJP

Λ(1810) 1/2+

$I(J^P) = 0(\frac{1}{2}^+)$ Status: ***

Almost all the recent analyses contain a P_{01} state, and sometimes two of them, but the masses, widths, and branching ratios vary greatly. See also the Λ(1600) P_{01}.

Λ(1810) MASS

VALUE (MeV)	DOCUMENT ID		TECN	COMMENT
1750 to 1850 (≈ 1810) OUR ESTIMATE				
1821±10	ZHANG	13A	DPWA	Multichannel
1841±20	GOPAL	80	DPWA	$\overline{K}N \to \overline{K}N$
1853±20	GOPAL	77	DPWA	$\overline{K}N$ multichannel
1735± 5	CARROLL	76	DPWA	Isospin-0 total σ
1746±10	PREVOST	74	DPWA	$K^-N \to \Sigma(1385)\pi$
1780±20	LANGBEIN	72	IPWA	$\overline{K}N$ multichannel
• • • We do not use the following data for averages, fits, limits, etc. • • •				
1861 or 1953	[1] MARTIN	77	DPWA	$\overline{K}N$ multichannel
1755	KIM	71	DPWA	K-matrix analysis
1800	ARMENTEROS	70	HBC	$\overline{K}N \to \overline{K}N$
1750	ARMENTEROS	70	HBC	$\overline{K}N \to \Sigma\pi$
1690±10	BARBARO-...	70	HBC	$\overline{K}N \to \Sigma\pi$
1740	BAILEY	69	DPWA	$\overline{K}N \to \overline{K}N$
1745	ARMENTEROS	68B	HBC	$\overline{K}N \to \overline{K}N$

Λ(1810) WIDTH

VALUE (MeV)	DOCUMENT ID		TECN	COMMENT
50 to 250 (≈ 150) OUR ESTIMATE				
174±50	ZHANG	13A	DPWA	Multichannel
164±20	GOPAL	80	DPWA	$\overline{K}N \to \overline{K}N$
90±20	CAMERON	78B	DPWA	$K^-p \to N\overline{K}^*$
166±20	GOPAL	77	DPWA	$\overline{K}N$ multichannel
46±20	PREVOST	74	DPWA	$K^-N \to \Sigma(1385)\pi$
120±10	LANGBEIN	72	IPWA	$\overline{K}N$ multichannel
• • • We do not use the following data for averages, fits, limits, etc. • • •				
535 or 585	[1] MARTIN	77	DPWA	$\overline{K}N$ multichannel
28	CARROLL	76	DPWA	Isospin-0 total σ
35	KIM	71	DPWA	K-matrix analysis
30	ARMENTEROS	70	HBC	$\overline{K}N \to \overline{K}N$
70	ARMENTEROS	70	HBC	$\overline{K}N \to \Sigma\pi$
22	BARBARO-...	70	HBC	$\overline{K}N \to \Sigma\pi$
300	BAILEY	69	DPWA	$\overline{K}N \to \overline{K}N$
147	ARMENTEROS	68B	HBC	

Λ(1810) POLE POSITION

REAL PART

VALUE (MeV)	DOCUMENT ID		TECN	COMMENT
• • • We do not use the following data for averages, fits, limits, etc. • • •				
1780	ZHANG	13A	DPWA	Multichannel

−2×IMAGINARY PART

VALUE (MeV)	DOCUMENT ID		TECN	COMMENT
• • • We do not use the following data for averages, fits, limits, etc. • • •				
64	ZHANG	13A	DPWA	Multichannel

Λ(1810) DECAY MODES

	Mode	Fraction (Γ_i/Γ)
Γ_1	$N\overline{K}$	20–50 %
Γ_2	$\Sigma\pi$	10–40 %
Γ_3	$\Sigma(1385)\pi$	seen
Γ_4	$N\overline{K}^*(892)$	30–60 %
Γ_5	$N\overline{K}^*(892)$, S=1/2, P-wave	
Γ_6	$N\overline{K}^*(892)$, S=3/2, P-wave	

The above branching fractions are our estimates, not fits or averages.

Λ(1810) BRANCHING RATIOS

See "Sign conventions for resonance couplings" in the Note on Λ and Σ Resonances.

$\Gamma(N\overline{K})/\Gamma_{total}$ Γ_1/Γ

VALUE	DOCUMENT ID		TECN	COMMENT
0.2 to 0.5 OUR ESTIMATE				
0.19±0.08	ZHANG	13A	DPWA	Multichannel
0.24±0.04	GOPAL	80	DPWA	$\overline{K}N \to \overline{K}N$
0.36±0.05	LANGBEIN	72	IPWA	$\overline{K}N$ multichannel
• • • We do not use the following data for averages, fits, limits, etc. • • •				
0.21±0.04	GOPAL	77	DPWA	See GOPAL 80
0.52 or 0.49	[1] MARTIN	77	DPWA	$\overline{K}N$ multichannel
0.30	KIM	71	DPWA	K-matrix analysis
0.15	ARMENTEROS	70	DPWA	$\overline{K}N \to \overline{K}N$
0.55	BAILEY	69	DPWA	$\overline{K}N \to \overline{K}N$
0.4	ARMENTEROS	68B	DPWA	$\overline{K}N \to \overline{K}N$

$(\Gamma_i\Gamma_f)^{1/2}/\Gamma_{total}$ in $N\overline{K} \to \Lambda(1810) \to \Sigma\pi$ $(\Gamma_1\Gamma_2)^{1/2}/\Gamma$

VALUE	DOCUMENT ID		TECN	COMMENT
−0.08±0.05	ZHANG	13A	DPWA	Multichannel
−0.24±0.04	GOPAL	77	DPWA	$\overline{K}N$ multichannel
• • • We do not use the following data for averages, fits, limits, etc. • • •				
+0.25 or +0.23	[1] MARTIN	77	DPWA	$\overline{K}N$ multichannel
< 0.01	LANGBEIN	72	IPWA	$\overline{K}N$ multichannel
0.17	KIM	71	DPWA	K-matrix analysis
+0.20	[2] ARMENTEROS	70	DPWA	$\overline{K}N \to \Sigma\pi$
−0.13±0.03	BARBARO-...	70	DPWA	$\overline{K}N \to \Sigma\pi$

$(\Gamma_i\Gamma_f)^{1/2}/\Gamma_{total}$ in $N\overline{K} \to \Lambda(1810) \to \Sigma(1385)\pi$ $(\Gamma_1\Gamma_3)^{1/2}/\Gamma$

VALUE	DOCUMENT ID		TECN	COMMENT
+0.18±0.10	PREVOST	74	DPWA	$K^-N \to \Sigma(1385)\pi$

$(\Gamma_i\Gamma_f)^{1/2}/\Gamma_{total}$ in $N\overline{K} \to \Lambda(1810) \to N\overline{K}^*(892)$, S=1/2, P-wave $(\Gamma_1\Gamma_5)^{1/2}/\Gamma$

VALUE	DOCUMENT ID		TECN	COMMENT
−0.14±0.03	[2] CAMERON	78B	DPWA	$K^-p \to N\overline{K}^*$

$(\Gamma_i\Gamma_f)^{1/2}/\Gamma_{total}$ in $N\overline{K} \to \Lambda(1810) \to N\overline{K}^*(892)$, S=3/2, P-wave $(\Gamma_1\Gamma_6)^{1/2}/\Gamma$

VALUE	DOCUMENT ID		TECN	COMMENT
+0.38±0.06	ZHANG	13A	DPWA	Multichannel
+0.35±0.06	CAMERON	78B	DPWA	$K^-p \to N\overline{K}^*$

Λ(1810) FOOTNOTES

[1] The two MARTIN 77 values are from a T-matrix pole and from a Breit-Wigner fit.
[2] The published sign has been changed to be in accord with the baryon-first convention.

Λ(1810) REFERENCES

ZHANG	13A	PR C88 035205	H. Zhang *et al.*	(KSU)
GOPAL	80	Toronto Conf. 159	G.P. Gopal	(RHEL) IJP
CAMERON	78B	NP B146 327	W. Cameron *et al.*	(RHEL, LOIC) IJP
GOPAL	77	NP B119 362	G.P. Gopal *et al.*	(LOIC, RHEL) IJP
MARTIN	77	NP B127 349	B.R. Martin, M.K. Pidcock, R.G. Moorhouse	(LOUC+) IJP
Also		NP B126 266	B.R. Martin, M.K. Pidcock	(LOUC)
Also		NP B126 285	B.R. Martin, M.K. Pidcock	(LOUC) IJP
CARROLL	76	PRL 37 806	A.S. Carroll *et al.*	(BNL) I
PREVOST	74	NP B69 246	J. Prevost *et al.*	(SACL, CERN, HEID)
LANGBEIN	72	NP B47 477	W. Langbein, F. Wagner	(MPIM) IJP
KIM	71	PRL 27 356	J.K. Kim	(HARV) IJP
Also		Duke Conf. 161 Hyperon Resonances, 1970	J.K. Kim	(HARV) IJP
ARMENTEROS	70	Duke Conf. 123 Hyperon Resonances, 1970	R. Armenteros *et al.*	(CERN, HEID, SACL) IJP
BARBARO-...	70	Duke Conf. 173 Hyperon Resonances, 1970	A. Barbaro-Galtieri	(LRL) IJP
BAILEY	69	Thesis UCRL 50617	J.M. Bailey	(LLL) IJP
ARMENTEROS	68B	NP B8 195	R. Armenteros *et al.*	(CERN, HEID, SACL) IJP

Λ(1820) 5/2+

$I(J^P) = 0(\frac{5}{2}^+)$ Status: ****

This resonance is the cornerstone for all partial-wave analyses in this region. Most of the results published before 1973 are now obsolete and have been omitted. They may be found in our 1982 edition Physics Letters **111B** 1 (1982).

Most of the quoted errors are statistical only; the systematic errors due to the particular parametrizations used in the partial-wave analyses are not included. For this reason we do not calculate weighted averages for the mass and width.

Λ(1820) MASS

VALUE (MeV)	DOCUMENT ID		TECN	COMMENT
1815 to 1825 (≈ 1820) OUR ESTIMATE				
1823.5±0.8	ZHANG	13A	DPWA	Multichannel
1823 ±3	GOPAL	80	DPWA	$\overline{K}N \to \overline{K}N$
1819 ±2	ALSTON-...	78	DPWA	$\overline{K}N \to \overline{K}N$
1822 ±2	GOPAL	77	DPWA	$\overline{K}N$ multichannel
1821 ±2	KANE	74	DPWA	$K^-p \to \Sigma\pi$
• • • We do not use the following data for averages, fits, limits, etc. • • •				
1830	DECLAIS	77	DPWA	$\overline{K}N \to \overline{K}N$
1817 or 1819	[1] MARTIN	77	DPWA	$\overline{K}N$ multichannel

Λ(1820) WIDTH

VALUE (MeV)	DOCUMENT ID		TECN	COMMENT
70 to 90 (≈ 80) OUR ESTIMATE				
89±2	ZHANG	13A	DPWA	Multichannel
77±5	GOPAL	80	DPWA	$\overline{K}N \rightarrow \overline{K}N$
72±5	ALSTON-...	78	DPWA	$\overline{K}N \rightarrow \overline{K}N$
81±5	GOPAL	77	DPWA	$\overline{K}N$ multichannel
87±3	KANE	74	DPWA	$K^-p \rightarrow \Sigma\pi$
• • • We do not use the following data for averages, fits, limits, etc. • • •				
82	DECLAIS	77	DPWA	$\overline{K}N \rightarrow \overline{K}N$
76 or 76	[1] MARTIN	77	DPWA	$\overline{K}N$ multichannel

Λ(1820) POLE POSITION

REAL PART

VALUE (MeV)	DOCUMENT ID		TECN	COMMENT
• • • We do not use the following data for averages, fits, limits, etc. • • •				
1814	ZHANG	13A	DPWA	Multichannel

−2×IMAGINARY PART

VALUE (MeV)	DOCUMENT ID		TECN	COMMENT
• • • We do not use the following data for averages, fits, limits, etc. • • •				
85	ZHANG	13A	DPWA	Multichannel

Λ(1820) DECAY MODES

	Mode	Fraction (Γ_i/Γ)
Γ_1	$N\overline{K}$	55–65 %
Γ_2	$\Sigma\pi$	8–14 %
Γ_3	$\Sigma(1385)\pi$	5–10 %
Γ_4	$\Sigma(1385)\pi$, *P*-wave	
Γ_5	$\Sigma(1385)\pi$, *F*-wave	
Γ_6	$\Lambda\eta$	
Γ_7	$\Sigma\pi\pi$	
	The above branching fractions are our estimates, not fits or averages.	
Γ_8	$N\overline{K}^*(892)$, S=3/2, *P*-wave	(3.0±1.0) %

Λ(1820) BRANCHING RATIOS

Errors quoted do not include uncertainties in the parametrizations used in the partial-wave analyses and are thus too small. See also "Sign conventions for resonance couplings" in the Note on Λ and Σ Resonances.

$\Gamma(N\overline{K})/\Gamma_{total}$ Γ_1/Γ

VALUE	DOCUMENT ID		TECN	COMMENT
0.55 to 0.65 OUR ESTIMATE				
0.54±0.01	ZHANG	13A	DPWA	Multichannel
0.58±0.02	GOPAL	80	DPWA	$\overline{K}N \rightarrow \overline{K}N$
0.60±0.03	ALSTON-...	78	DPWA	$\overline{K}N \rightarrow \overline{K}N$
• • • We do not use the following data for averages, fits, limits, etc. • • •				
0.51	DECLAIS	77	DPWA	$\overline{K}N \rightarrow \overline{K}N$
0.57±0.02	GOPAL	77	DPWA	See GOPAL 80
0.59 or 0.58	[1] MARTIN	77	DPWA	$\overline{K}N$ multichannel

$(\Gamma_i\Gamma_f)^{1/2}/\Gamma_{total}$ in $N\overline{K} \rightarrow \Lambda(1820) \rightarrow \Sigma\pi$ $(\Gamma_1\Gamma_2)^{1/2}/\Gamma$

VALUE	DOCUMENT ID		TECN	COMMENT
−0.28±0.01	ZHANG	13A	DPWA	Multichannel
−0.28±0.03	GOPAL	77	DPWA	$\overline{K}N$ multichannel
−0.28±0.01	KANE	74	DPWA	$K^-p \rightarrow \Sigma\pi$
• • • We do not use the following data for averages, fits, limits, etc. • • •				
−0.25 or −0.25	[1] MARTIN	77	DPWA	$\overline{K}N$ multichannel

$\Gamma(\Sigma\pi\pi)/\Gamma_{total}$ Γ_7/Γ

VALUE	DOCUMENT ID		TECN	COMMENT
no clear signal	[2] ARMENTEROS	68C	HDBC	$K^-N \rightarrow \Sigma\pi\pi$

$(\Gamma_i\Gamma_f)^{1/2}/\Gamma_{total}$ in $N\overline{K} \rightarrow \Lambda(1820) \rightarrow \Sigma(1385)\pi$, *P*-wave $(\Gamma_1\Gamma_4)^{1/2}/\Gamma$

VALUE	DOCUMENT ID		TECN	COMMENT
−0.20 ±0.02	ZHANG	13A	DPWA	Multichannel
−0.167±0.054	[3] CAMERON	78	DPWA	$K^-p \rightarrow \Sigma(1385)\pi$
+0.27 ±0.03	PREVOST	74	DPWA	$K^-N \rightarrow \Sigma(1385)\pi$

$(\Gamma_i\Gamma_f)^{1/2}/\Gamma_{total}$ in $N\overline{K} \rightarrow \Lambda(1820) \rightarrow \Sigma(1385)\pi$, *F*-wave $(\Gamma_1\Gamma_5)^{1/2}/\Gamma$

VALUE	DOCUMENT ID		TECN	COMMENT
+0.065±0.029	[3] CAMERON	78	DPWA	$K^-p \rightarrow \Sigma(1385)\pi$

$(\Gamma_i\Gamma_f)^{1/2}/\Gamma_{total}$ in $N\overline{K} \rightarrow \Lambda(1820) \rightarrow \Lambda\eta$ $(\Gamma_1\Gamma_6)^{1/2}/\Gamma$

VALUE	DOCUMENT ID		TECN
$-0.096^{+0.040}_{-0.020}$	RADER	73	MPWA

$\Gamma(N\overline{K}^*(892), S=3/2, P\text{-wave})/\Gamma_{total}$ Γ_8/Γ

VALUE	DOCUMENT ID		TECN	COMMENT
0.03±0.01	ZHANG	13A	DPWA	Multichannel

Λ(1820) FOOTNOTES

[1] The two MARTIN 77 values are from a T-matrix pole and from a Breit-Wigner fit.
[2] There is a suggestion of a bump, enough to be consistent with what is expected from $\Sigma(1385) \rightarrow \Sigma\pi$ decay.
[3] The published sign has been changed to be in accord with the baryon-first convention.

Λ(1820) REFERENCES

ZHANG	13A	PR C88 035205	H. Zhang *et al.*	(KSU)
PDG	82	PL 111B 1	M. Roos *et al.*	(HELS, CIT, CERN)
GOPAL	80	Toronto Conf. 159	G.P. Gopal	(RHEL) IJP
ALSTON-...	78	PR D18 182	M. Alston-Garnjost *et al.*	(LBL, MTHO+) IJP
Also		PRL 38 1007	M. Alston-Garnjost *et al.*	(LBL, MTHO+) IJP
CAMERON	78	NP B143 189	W. Cameron *et al.*	(RHEL, LOIC) IJP
DECLAIS	77	CERN 77-16	Y. Declais *et al.*	(CAEN, CERN) IJP
GOPAL	77	NP B119 362	G.P. Gopal *et al.*	(LOIC, RHEL) IJP
MARTIN	77	NP B127 349	B.R. Martin, M.K. Pidcock, R.G. Moorhouse	(LOUC+) IJP
Also		NP B126 266	B.R. Martin, M.K. Pidcock	(LOUC)
Also		NP B126 285	B.R. Martin, M.K. Pidcock	(LOUC) IJP
KANE	74	LBL-2452	D.F. Kane	(LBL) IJP
PREVOST	74	NP B69 246	J. Prevost *et al.*	(SACL, CERN, HEID)
RADER	73	NC 16A 178	R.K. Rader *et al.*	(SACL, HEID, CERN+)
ARMENTEROS	68C	NP B8 216	R. Armenteros *et al.*	(CERN, HEID, SACL) I

Λ(1830) 5/2⁻

$I(J^P) = 0(\frac{5}{2}^-)$ Status: ****

For results published before 1973 (they are now obsolete), see our 1982 edition Physics Letters **111B** 1 (1982).

The best evidence for this resonance is in the $\Sigma\pi$ channel.

Λ(1830) MASS

VALUE (MeV)	DOCUMENT ID		TECN	COMMENT
1810 to 1830 (≈ 1830) OUR ESTIMATE				
1820± 4	ZHANG	13A	DPWA	Multichannel
1831±10	GOPAL	80	DPWA	$\overline{K}N \rightarrow \overline{K}N$
1825±10	GOPAL	77	DPWA	$\overline{K}N$ multichannel
1825± 1	KANE	74	DPWA	$K^-p \rightarrow \Sigma\pi$
• • • We do not use the following data for averages, fits, limits, etc. • • •				
1817 or 1818	[1] MARTIN	77	DPWA	$\overline{K}N$ multichannel

Λ(1830) WIDTH

VALUE (MeV)	DOCUMENT ID		TECN	COMMENT
60 to 110 (≈ 95) OUR ESTIMATE				
114±10	ZHANG	13A	DPWA	Multichannel
100±10	GOPAL	80	DPWA	$\overline{K}N \rightarrow \overline{K}N$
94±10	GOPAL	77	DPWA	$\overline{K}N$ multichannel
119± 3	KANE	74	DPWA	$K^-p \rightarrow \Sigma\pi$
• • • We do not use the following data for averages, fits, limits, etc. • • •				
56 or 56	[1] MARTIN	77	DPWA	$\overline{K}N$ multichannel

Λ(1830) POLE POSITION

REAL PART

VALUE (MeV)	DOCUMENT ID		TECN	COMMENT
• • • We do not use the following data for averages, fits, limits, etc. • • •				
1809	ZHANG	13A	DPWA	Multichannel

−2×IMAGINARY PART

VALUE (MeV)	DOCUMENT ID		TECN	COMMENT
• • • We do not use the following data for averages, fits, limits, etc. • • •				
109	ZHANG	13A	DPWA	Multichannel

Λ(1830) DECAY MODES

	Mode	Fraction (Γ_i/Γ)
Γ_1	$N\overline{K}$	3–10 %
Γ_2	$\Sigma\pi$	35–75 %
Γ_3	$\Sigma(1385)\pi$	>15 %
	The above branching fractions are our estimates, not fits or averages.	
Γ_4	$\Sigma(1385)\pi$, *D*-wave	(52±6) %
Γ_5	$\Lambda\eta$	

$\Lambda(1830)$ BRANCHING RATIOS

See "Sign conventions for resonance couplings" in the Note on Λ and Σ Resonances.

$\Gamma(N\overline{K})/\Gamma_{total}$ Γ_1/Γ

VALUE	DOCUMENT ID		TECN	COMMENT
0.03 to 0.10 OUR ESTIMATE				
0.041±0.005	ZHANG	13A	DPWA	Multichannel
0.08 ±0.03	GOPAL	80	DPWA	$\overline{K}N \to \overline{K}N$
0.02 ±0.02	ALSTON-...	78	DPWA	$\overline{K}N \to \overline{K}N$
• • • We do not use the following data for averages, fits, limits, etc. • • •				
0.04 ±0.03	GOPAL	77	DPWA	See GOPAL 80
0.04 or 0.04	[1] MARTIN	77	DPWA	$\overline{K}N$ multichannel

$(\Gamma_i\Gamma_f)^{1/2}/\Gamma_{total}$ in $N\overline{K} \to \Lambda(1830) \to \Sigma\pi$ $(\Gamma_1\Gamma_2)^{1/2}/\Gamma$

VALUE	DOCUMENT ID		TECN	COMMENT
−0.13±0.01	ZHANG	13A	DPWA	Multichannel
−0.17±0.03	GOPAL	77	DPWA	$\overline{K}N$ multichannel
−0.15±0.01	KANE	74	DPWA	$K^-p \to \Sigma\pi$
• • • We do not use the following data for averages, fits, limits, etc. • • •				
−0.17 or −0.17	[1] MARTIN	77	DPWA	$\overline{K}N$ multichannel

$(\Gamma_i\Gamma_f)^{1/2}/\Gamma_{total}$ in $N\overline{K} \to \Lambda(1830) \to \Sigma(1385)\pi$ $(\Gamma_1\Gamma_3)^{1/2}/\Gamma$

VALUE	DOCUMENT ID		TECN	COMMENT
+0.141±0.014	[2] CAMERON	78	DPWA	$K^-p \to \Sigma(1385)\pi$
+0.13 ±0.03	PREVOST	74	DPWA	$K^-N \to \Sigma(1385)\pi$

$\Gamma(\Sigma(1385)\pi$, D-wave$)/\Gamma_{total}$ Γ_4/Γ

VALUE	DOCUMENT ID		TECN	COMMENT
0.52±0.06	ZHANG	13A	DPWA	Multichannel

$(\Gamma_i\Gamma_f)^{1/2}/\Gamma_{total}$ in $N\overline{K} \to \Lambda(1830) \to \Lambda\eta$ $(\Gamma_1\Gamma_5)^{1/2}/\Gamma$

VALUE	DOCUMENT ID		TECN
−0.044±0.020	RADER	73	MPWA

$\Lambda(1830)$ FOOTNOTES

[1] The two MARTIN 77 values are from a T-matrix pole and from a Breit-Wigner fit.
[2] The CAMERON 78 upper limit on G-wave decay is 0.03. The published sign has been changed to be in accord with the baryon-first convention.

$\Lambda(1830)$ REFERENCES

ZHANG	13A	PR C88 035205	H. Zhang *et al.*	(KSU)
PDG	82	PL 111B 1	M. Roos *et al.*	(HELS, CIT, CERN)
GOPAL	80	Toronto Conf. 159	G.P. Gopal	(RHEL) IJP
ALSTON-...	78	PR D18 182	M. Alston-Garnjost *et al.*	(LBL, MTHO+) IJP
Also		PRL 38 1007	M. Alston-Garnjost *et al.*	(LBL, MTHO+) IJP
CAMERON	78	NP B143 189	W. Cameron *et al.*	(RHEL, LOIC) IJP
GOPAL	77	NP B119 362	G.P. Gopal *et al.*	(LOIC, RHEL) IJP
MARTIN	77	NP B127 349	B.R. Martin, M.K. Pidcock, R.G. Moorhouse	(LOUC+) IJP
Also		NP B126 266	B.R. Martin, M.K. Pidcock	(LOUC)
Also		NP B126 285	B.R. Martin, M.K. Pidcock	(LOUC) IJP
KANE	74	LBL-2452	D.F. Kane	(LBL) IJP
PREVOST	74	NP B69 246	J. Prevost *et al.*	(SACL, CERN, HEID)
RADER	73	NC 16A 178	R.K. Rader *et al.*	(SACL, HEID, CERN+)

$\Lambda(1890)$ $3/2^+$

$I(J^P) = 0(\frac{3}{2}^+)$ Status: ****

For results published before 1974 (they are now obsolete), see our 1982 edition Physics Letters **111B** 1 (1982).

The $J^P = 3/2^+$ assignment is consistent with all available data (including polarization) and recent partial-wave analyses. The dominant inelastic modes remain unknown.

$\Lambda(1890)$ MASS

VALUE (MeV)	DOCUMENT ID		TECN	COMMENT
1850 to 1910 (≈ 1890) OUR ESTIMATE				
1900± 5	ZHANG	13A	DPWA	Multichannel
1897± 5	GOPAL	80	DPWA	$\overline{K}N \to \overline{K}N$
1908±10	ALSTON-...	78	DPWA	$\overline{K}N \to \overline{K}N$
1900± 5	GOPAL	77	DPWA	$\overline{K}N$ multichannel
1894±10	HEMINGWAY	75	DPWA	$K^-p \to \overline{K}N$
• • • We do not use the following data for averages, fits, limits, etc. • • •				
1856 or 1868	[1] MARTIN	77	DPWA	$\overline{K}N$ multichannel
1900	[2] NAKKASYAN	75	DPWA	$K^-p \to \Lambda\omega$

$\Lambda(1890)$ WIDTH

VALUE (MeV)	DOCUMENT ID		TECN	COMMENT
60 to 200 (≈ 100) OUR ESTIMATE				
161±15	ZHANG	13A	DPWA	Multichannel
74±10	GOPAL	80	DPWA	$\overline{K}N \to \overline{K}N$
119±20	ALSTON-...	78	DPWA	$\overline{K}N \to \overline{K}N$
72±10	GOPAL	77	DPWA	$\overline{K}N$ multichannel
107±10	HEMINGWAY	75	DPWA	$K^-p \to \overline{K}N$
• • • We do not use the following data for averages, fits, limits, etc. • • •				
191 or 193	[1] MARTIN	77	DPWA	$\overline{K}N$ multichannel
100	[2] NAKKASYAN	75	DPWA	$K^-p \to \Lambda\omega$

$\Lambda(1890)$ POLE POSITION

REAL PART

VALUE (MeV)	DOCUMENT ID		TECN	COMMENT
• • • We do not use the following data for averages, fits, limits, etc. • • •				
1876	ZHANG	13A	DPWA	Multichannel

−2×IMAGINARY PART

VALUE (MeV)	DOCUMENT ID		TECN	COMMENT
• • • We do not use the following data for averages, fits, limits, etc. • • •				
145	ZHANG	13A	DPWA	Multichannel

$\Lambda(1890)$ DECAY MODES

	Mode	Fraction (Γ_i/Γ)
Γ_1	$N\overline{K}$	20–35 %
Γ_2	$\Sigma\pi$	3–10 %
Γ_3	$\Sigma(1385)\pi$	seen
Γ_4	$\Sigma(1385)\pi$, P-wave	
Γ_5	$\Sigma(1385)\pi$, F-wave	
Γ_6	$N\overline{K}^*(892)$	seen
Γ_7	$N\overline{K}^*(892)$, S=1/2	
Γ_8	$N\overline{K}^*(892)$, S=3/2, F-wave	
Γ_9	$\Lambda\omega$	

The above branching fractions are our estimates, not fits or averages.

$\Lambda(1890)$ BRANCHING RATIOS

See "Sign conventions for resonance couplings" in the Note on Λ and Σ Resonances.

$\Gamma(N\overline{K})/\Gamma_{total}$ Γ_1/Γ

VALUE	DOCUMENT ID		TECN	COMMENT
0.20 to 0.35 OUR ESTIMATE				
0.37±0.03	ZHANG	13A	DPWA	Multichannel
0.20±0.02	GOPAL	80	DPWA	$\overline{K}N \to \overline{K}N$
0.34±0.05	ALSTON-...	78	DPWA	$\overline{K}N \to \overline{K}N$
0.24±0.04	HEMINGWAY	75	DPWA	$K^-p \to \overline{K}N$
• • • We do not use the following data for averages, fits, limits, etc. • • •				
0.18±0.02	GOPAL	77	DPWA	See GOPAL 80
0.36 or 0.34	[1] MARTIN	77	DPWA	$\overline{K}N$ multichannel

$(\Gamma_i\Gamma_f)^{1/2}/\Gamma_{total}$ in $N\overline{K} \to \Lambda(1890) \to \Sigma\pi$ $(\Gamma_1\Gamma_2)^{1/2}/\Gamma$

VALUE	DOCUMENT ID		TECN	COMMENT
−0.09±0.02	ZHANG	13A	DPWA	Multichannel
−0.09±0.03	GOPAL	77	DPWA	$\overline{K}N$ multichannel
• • • We do not use the following data for averages, fits, limits, etc. • • •				
+0.15 or +0.14	[1] MARTIN	77	DPWA	$\overline{K}N$ multichannel

$(\Gamma_i\Gamma_f)^{1/2}/\Gamma_{total}$ in $N\overline{K} \to \Lambda(1890) \to \Sigma(1385)\pi$, P-wave $(\Gamma_1\Gamma_4)^{1/2}/\Gamma$

VALUE	DOCUMENT ID		TECN	COMMENT
<0.03	CAMERON	78	DPWA	$K^-p \to \Sigma(1385)\pi$

$(\Gamma_i\Gamma_f)^{1/2}/\Gamma_{total}$ in $N\overline{K} \to \Lambda(1890) \to \Sigma(1385)\pi$, F-wave $(\Gamma_1\Gamma_5)^{1/2}/\Gamma$

VALUE	DOCUMENT ID		TECN	COMMENT
−0.31 ±0.04	ZHANG	13A	DPWA	Multichannel
−0.126±0.055	[3] CAMERON	78	DPWA	$K^-p \to \Sigma(1385)\pi$

$(\Gamma_i\Gamma_f)^{1/2}/\Gamma_{total}$ in $N\overline{K} \to \Lambda(1890) \to N\overline{K}^*(892)$, S=1/2 $(\Gamma_1\Gamma_7)^{1/2}/\Gamma$

VALUE	DOCUMENT ID		TECN	COMMENT
−0.17±0.05	ZHANG	13A	DPWA	Multichannel
−0.07±0.03	[3,4] CAMERON	78B	DPWA	$K^-p \to N\overline{K}^*$

$(\Gamma_i\Gamma_f)^{1/2}/\Gamma_{total}$ in $N\overline{K} \to \Lambda(1890) \to N\overline{K}^*(892)$, S=3/2, F-wave $(\Gamma_1\Gamma_8)^{1/2}/\Gamma$

VALUE	DOCUMENT ID		TECN	COMMENT
−0.11±0.03	ZHANG	13A	DPWA	Multichannel

$(\Gamma_i\Gamma_f)^{1/2}/\Gamma_{total}$ in $N\overline{K} \to \Lambda(1890) \to \Lambda\omega$ $(\Gamma_1\Gamma_9)^{1/2}/\Gamma$

VALUE	DOCUMENT ID		TECN	COMMENT
seen	BACCARI	77	IPWA	$K^-p \to \Lambda\omega$
0.032	[2] NAKKASYAN	75	DPWA	$K^-p \to \Lambda\omega$

Λ(1890) FOOTNOTES

[1] The two MARTIN 77 values are from a T-matrix pole and from a Breit-Wigner fit.
[2] Found in one of two best solutions.
[3] The published sign has been changed to be in accord with the baryon-first convention.
[4] Upper limits on the P_3 and F_3 waves are each 0.03.

Λ(1890) REFERENCES

ZHANG	13A	PR C88 035205	H. Zhang *et al.*	(KSU)
PDG	82	PL 111B 1	M. Roos *et al.*	(HELS, CIT, CERN)
GOPAL	80	Toronto Conf. 159	G.P. Gopal	(RHEL) IJP
ALSTON-...	78	PR D18 182	M. Alston-Garnjost *et al.*	(LBL, MTHO+) IJP
Also		PRL 38 1007	M. Alston-Garnjost *et al.*	(LBL, MTHO+) IJP
CAMERON	78	NP B143 189	W. Cameron *et al.*	(RHEL, LOIC) IJP
CAMERON	78B	NP B146 327	W. Cameron *et al.*	(RHEL, LOIC) IJP
BACCARI	77	NC 41A 96	B. Baccari *et al.*	(SACL, CDEF) IJP
GOPAL	77	NP B119 362	G.P. Gopal *et al.*	(LOIC, RHEL) IJP
MARTIN	77	NP B127 349	B.R. Martin, M.K. Pidcock, R.G. Moorhouse	(LOUC+) IJP
Also		NP B126 266	B.R. Martin, M.K. Pidcock	(LOUC)
Also		NP B126 285	B.R. Martin, M.K. Pidcock	(LOUC) IJP
HEMINGWAY	75	NP B91 12	R.J. Hemingway *et al.*	(CERN, HEIDH, MPIM) IJP
NAKKASYAN	75	NP B93 85	A. Nakkasyan	(CERN) IJP

Λ(2000) $I(J^P) = 0(?^?)$ Status: *

OMITTED FROM SUMMARY TABLE

ZHANG 13A claims a $J^P = 1/2^-$ state.

We list here all the ambiguous resonance possibilities with a mass around 2 GeV. The proposed quantum numbers are D_3 (BARBARO-GALTIERI 70 in $\Sigma\pi$), D_3+F_5, P_3+D_5, or P_1+D_3 (BRANDSTETTER 72 in $\Lambda\omega$), and S_1 (CAMERON 78B in $N\overline{K}^*$). The first two of the above analyses should now be considered obsolete. See also NAKKASYAN 75.

Λ(2000) MASS

VALUE (MeV)	DOCUMENT ID		TECN	COMMENT
≈ 2000 OUR ESTIMATE				
2020±16	ZHANG	13A	DPWA	Multichannel
2030±30	CAMERON	78B	DPWA	$K^-p \to N\overline{K}^*$
1935 to 1971	[1] BRANDSTET...	72	DPWA	$K^-p \to \Lambda\omega$
1951 to 2034	[1] BRANDSTET...	72	DPWA	$K^-p \to \Lambda\omega$
2010±30	BARBARO-...	70	DPWA	$K^-p \to \Sigma\pi$

Λ(2000) WIDTH

VALUE (MeV)	DOCUMENT ID		TECN	COMMENT
255±63	ZHANG	13A	DPWA	Multichannel
125±25	CAMERON	78B	DPWA	$K^-p \to N\overline{K}^*$
180 to 240	[1] BRANDSTET...	72	DPWA	(lower mass)
73 to 154	[1] BRANDSTET...	72	DPWA	(higher mass)
130±50	BARBARO-...	70	DPWA	$K^-p \to \Sigma\pi$

Λ(2000) DECAY MODES

	Mode	Fraction (Γ_i/Γ)
Γ_1	$N\overline{K}$	(27±6) %
Γ_2	$\Sigma\pi$	
Γ_3	$\Lambda\eta$	(16±7) %
Γ_4	$\Lambda\omega$	
Γ_5	$N\overline{K}^*(892)$, S=1/2, S-wave	
Γ_6	$N\overline{K}^*(892)$, S=3/2, D-wave	

Λ(2000) BRANCHING RATIOS

See "Sign conventions for resonance couplings" in the Note on Λ and Σ Resonances.

$\Gamma(N\overline{K})/\Gamma_{total}$ Γ_1/Γ

VALUE	DOCUMENT ID		TECN	COMMENT
0.27±0.06	ZHANG	13A	DPWA	Multichannel

$(\Gamma_i\Gamma_f)^{1/2}/\Gamma_{total}$ in $N\overline{K} \to \Lambda(2000) \to \Sigma\pi$ $(\Gamma_1\Gamma_2)^{1/2}/\Gamma$

VALUE	DOCUMENT ID		TECN	COMMENT
−0.07±0.03	ZHANG	13A	DPWA	Multichannel
−0.20±0.04	BARBARO-...	70	DPWA	$K^-p \to \Sigma\pi$

$\Gamma(\Lambda\eta)/\Gamma_{total}$ Γ_3/Γ

VALUE	DOCUMENT ID		TECN	COMMENT
0.16±0.07	ZHANG	13A	DPWA	Multichannel

$(\Gamma_i\Gamma_f)^{1/2}/\Gamma_{total}$ in $N\overline{K} \to \Lambda(2000) \to \Lambda\omega$ $(\Gamma_1\Gamma_4)^{1/2}/\Gamma$

VALUE	DOCUMENT ID		TECN	COMMENT
0.17 to 0.25	[1] BRANDSTET...	72	DPWA	(lower mass)
0.04 to 0.15	[1] BRANDSTET...	72	DPWA	(higher mass)

$(\Gamma_i\Gamma_f)^{1/2}/\Gamma_{total}$ in $N\overline{K} \to \Lambda(2000) \to N\overline{K}^*(892)$, S=1/2, S-wave $(\Gamma_1\Gamma_5)^{1/2}/\Gamma$

VALUE	DOCUMENT ID		TECN	COMMENT
−0.12±0.03	[2] CAMERON	78B	DPWA	$K^-p \to N\overline{K}^*$

$(\Gamma_i\Gamma_f)^{1/2}/\Gamma_{total}$ in $N\overline{K} \to \Lambda(2000) \to N\overline{K}^*(892)$, S=3/2, D-wave $(\Gamma_1\Gamma_6)^{1/2}/\Gamma$

VALUE	DOCUMENT ID		TECN	COMMENT
+0.34±0.05	ZHANG	13A	DPWA	Multichannel
+0.09±0.03	CAMERON	78B	DPWA	$K^-p \to N\overline{K}^*$

Λ(2000) FOOTNOTES

[1] The parameters quoted here are ranges from the three best fits; the lower state probably has $J \leq 3/2$, and the higher one probably has $J \leq 5/2$.
[2] The published sign has been changed to be in accord with the baryon-first convention.

Λ(2000) REFERENCES

ZHANG	13A	PR C88 035205	H. Zhang *et al.*	(KSU)
CAMERON	78B	NP B146 327	W. Cameron *et al.*	(RHEL, LOIC) IJP
NAKKASYAN	75	NP B93 85	A. Nakkasyan	(CERN) IJP
BRANDSTET...	72	NP B39 13	A.A. Brandstetter *et al.*	(RHEL, CDEF+)
BARBARO-...	70	Duke Conf. 173 Hyperon Resonances, 1970	A. Barbaro-Galtieri	(LRL) IJP

Λ(2020) 7/2+ $I(J^P) = 0(\frac{7}{2}^+)$ Status: *

OMITTED FROM SUMMARY TABLE

In LITCHFIELD 71, need for the state rests solely on a possibly inconsistent polarization measurement at 1.784 GeV/c. HEMINGWAY 75 does not require this state. GOPAL 77 does not need it in either $N\overline{K}$ or $\Sigma\pi$. With new K^-n angular distributions included, DECLAIS 77 sees it. However, this and other new data are included in GOPAL 80 and the state is not required. BACCARI 77 weakly supports it.

Λ(2020) MASS

VALUE (MeV)	DOCUMENT ID		TECN	COMMENT
≈ 2020 OUR ESTIMATE				
2043±22	ZHANG	13A	DPWA	Multichannel
2140	BACCARI	77	DPWA	$K^-p \to \Lambda\omega$
2117	DECLAIS	77	DPWA	$\overline{K}N \to \overline{K}N$
2100±30	LITCHFIELD	71	DPWA	$K^-p \to \overline{K}N$
2020±20	BARBARO-...	70	DPWA	$K^-p \to \Sigma\pi$

Λ(2020) WIDTH

VALUE (MeV)	DOCUMENT ID		TECN	COMMENT
200±75	ZHANG	13A	DPWA	Multichannel
128	BACCARI	77	DPWA	$K^-p \to \Lambda\omega$
167	DECLAIS	77	DPWA	$\overline{K}N \to \overline{K}N$
120±30	LITCHFIELD	71	DPWA	$K^-p \to \overline{K}N$
160±30	BARBARO-...	70	DPWA	$K^-p \to \Sigma\pi$

Λ(2020) DECAY MODES

	Mode	Fraction (Γ_i/Γ)
Γ_1	$N\overline{K}$	
Γ_2	$\Sigma\pi$	
Γ_3	$\Lambda\omega$	
Γ_4	$N\overline{K}^*(892)$, S=1/2	(30±9) %

Λ(2020) BRANCHING RATIOS

See "Sign conventions for resonance couplings" in the Note on Λ and Σ Resonances.

$\Gamma(N\overline{K})/\Gamma_{total}$ Γ_1/Γ

VALUE	DOCUMENT ID		TECN	COMMENT
0.028±0.005	ZHANG	13A	DPWA	Multichannel
0.05	DECLAIS	77	DPWA	$\overline{K}N \to \overline{K}N$
0.05 ±0.02	LITCHFIELD	71	DPWA	$K^-p \to \overline{K}N$

$(\Gamma_i\Gamma_f)^{1/2}/\Gamma_{total}$ in $N\overline{K} \to \Lambda(2020) \to \Sigma\pi$ $(\Gamma_1\Gamma_2)^{1/2}/\Gamma$

VALUE	DOCUMENT ID		TECN	COMMENT
$+0.02\pm0.01$	ZHANG	13A	DPWA	Multichannel
-0.15 ± 0.02	BARBARO-...	70	DPWA	$K^-p \to \Sigma\pi$

$(\Gamma_i\Gamma_f)^{1/2}/\Gamma_{total}$ in $N\overline{K} \to \Lambda(2020) \to \Lambda\omega$ $(\Gamma_1\Gamma_3)^{1/2}/\Gamma$

VALUE	DOCUMENT ID		TECN	COMMENT
<0.05	BACCARI	77	DPWA	$K^-p \to \Lambda\omega$

$\Gamma(N\overline{K}^*(892), S=1/2)/\Gamma_{total}$ Γ_4/Γ

VALUE	DOCUMENT ID		TECN	COMMENT
0.30±0.09	ZHANG	13A	DPWA	Multichannel

Λ(2020) REFERENCES

ZHANG	13A	PR C88 035205	H. Zhang *et al.*	(KSU)
GOPAL	80	Toronto Conf. 159	G.P. Gopal	(RHEL)
BACCARI	77	NC 41A 96	B. Baccari *et al.*	(SACL, CDEF) IJP
DECLAIS	77	CERN 77-16	Y. Declais *et al.*	(CAEN, CERN) IJP
GOPAL	77	NP B119 362	G.P. Gopal *et al.*	(LOIC, RHEL)
HEMINGWAY	75	NP B91 12	R.J. Hemingway *et al.*	(CERN, HEIDH, MPIM) IJP
LITCHFIELD	71	NP B30 125	P.J. Litchfield *et al.*	(RHEL, CDEF, SACL) IJP
BARBARO-...	70	Duke Conf. 173	A. Barbaro-Galtieri	(LRL) IJP

Hyperon Resonances, 1970

Λ(2050) 3/2⁻

$I(J^P) = 0(\frac{3}{2}^-)$ Status: *

OMITTED FROM SUMMARY TABLE

Λ(2050) MASS

VALUE (MeV)	DOCUMENT ID		TECN	COMMENT
2056±22	ZHANG	13A	DPWA	Multichannel

Λ(2050) WIDTH

VALUE (MeV)	DOCUMENT ID		TECN	COMMENT
493±61	ZHANG	13A	DPWA	Multichannel

Λ(2050) DECAY MODES

	Mode	Fraction (Γ_i/Γ)
Γ_1	$N\overline{K}$	(19 ±4) %
Γ_2	$\Sigma\pi$	(6.0±3.0) %
Γ_3	$\Sigma^*(1385)\pi$, *S*-wave	(8 ±6) %
Γ_4	$\Sigma^*(1385)\pi$, *D*-wave	(4.0±3.0) %
Γ_5	$N\overline{K}^*(892)$, S=1/2	(23 ±7) %

Λ(2050) BRANCHING RATIOS

$\Gamma(N\overline{K})/\Gamma_{total}$ Γ_1/Γ

VALUE	DOCUMENT ID		TECN	COMMENT
0.19±0.04	ZHANG	13A	DPWA	Multichannel

$\Gamma(\Sigma\pi)/\Gamma_{total}$ Γ_2/Γ

VALUE	DOCUMENT ID		TECN	COMMENT
0.06±0.03	ZHANG	13A	DPWA	Multichannel

$\Gamma(\Sigma^*(1385)\pi, S\text{-wave})/\Gamma_{total}$ Γ_3/Γ

VALUE	DOCUMENT ID		TECN	COMMENT
0.08±0.06	ZHANG	13A	DPWA	Multichannel

$\Gamma(\Sigma^*(1385)\pi, D\text{-wave})/\Gamma_{total}$ Γ_4/Γ

VALUE	DOCUMENT ID		TECN	COMMENT
0.04±0.03	ZHANG	13A	DPWA	Multichannel

$\Gamma(N\overline{K}^*(892), S=1/2)/\Gamma_{total}$ Γ_5/Γ

VALUE	DOCUMENT ID		TECN	COMMENT
0.23±0.07	ZHANG	13A	DPWA	Multichannel

Λ(2050) REFERENCES

ZHANG	13A	PR C88 035205	H. Zhang *et al.*	(KSU)

Λ(2100) 7/2⁻

$I(J^P) = 0(\frac{7}{2}^-)$ Status: ****

Most of the results published before 1973 are now obsolete and have been omitted. They may be found in our 1982 edition Physics Letters **111B** 1 (1982).

This entry only includes results from partial-wave analyses. Parameters of peaks seen in cross sections and in invariant-mass distributions around 2100 MeV used to be listed in a separate entry immediately following. It may be found in our 1986 edition Physics Letters **170B** 1 (1986).

Λ(2100) MASS

VALUE (MeV)	DOCUMENT ID		TECN	COMMENT
2090 to 2110 (≈ 2100) OUR ESTIMATE				
2086± 6	ZHANG	13A	DPWA	Multichannel
2104±10	GOPAL	80	DPWA	$\overline{K}N \to \overline{K}N$
2106±30	DEBELLEFON	78	DPWA	$\overline{K}N \to \overline{K}N$
2110±10	GOPAL	77	DPWA	$\overline{K}N$ multichannel
2105±10	HEMINGWAY	75	DPWA	$K^-p \to \overline{K}N$
2115±10	KANE	74	DPWA	$K^-p \to \Sigma\pi$
• • • We do not use the following data for averages, fits, limits, etc. • • •				
2094	BACCARI	77	DPWA	$K^-p \to \Lambda\omega$
2094	DECLAIS	77	DPWA	$\overline{K}N \to \overline{K}N$
2110 or 2089	[1] NAKKASYAN	75	DPWA	$K^-p \to \Lambda\omega$

Λ(2100) WIDTH

VALUE (MeV)	DOCUMENT ID		TECN	COMMENT
100 to 250 (≈ 200) OUR ESTIMATE				
305±16	ZHANG	13A	DPWA	Multichannel
157±40	DEBELLEFON	78	DPWA	$\overline{K}N \to \overline{K}N$
250±30	GOPAL	77	DPWA	$\overline{K}N$ multichannel
241±30	HEMINGWAY	75	DPWA	$K^-p \to \overline{K}N$
152±15	KANE	74	DPWA	$K^-p \to \Sigma\pi$
• • • We do not use the following data for averages, fits, limits, etc. • • •				
98	BACCARI	77	DPWA	$K^-p \to \Lambda\omega$
250	DECLAIS	77	DPWA	$\overline{K}N \to \overline{K}N$
244 or 302	[1] NAKKASYAN	75	DPWA	$K^-p \to \Lambda\omega$

Λ(2100) POLE POSITION

REAL PART

VALUE (MeV)	DOCUMENT ID		TECN	COMMENT
• • • We do not use the following data for averages, fits, limits, etc. • • •				
2023	ZHANG	13A	DPWA	Multichannel

−2×IMAGINARY PART

VALUE (MeV)	DOCUMENT ID		TECN	COMMENT
• • • We do not use the following data for averages, fits, limits, etc. • • •				
239	ZHANG	13A	DPWA	Multichannel

Λ(2100) DECAY MODES

	Mode	Fraction (Γ_i/Γ)
Γ_1	$N\overline{K}$	25–35 %
Γ_2	$\Sigma\pi$	∼ 5 %
Γ_3	$\Lambda\eta$	<3 %
Γ_4	ΞK	<3 %
Γ_5	$\Lambda\omega$	<8 %
Γ_6	$N\overline{K}^*(892)$	10–20 %
Γ_7	$N\overline{K}^*(892)$, $S=3/2$, *D*-wave	
Γ_8	$N\overline{K}^*(892)$, $S=1/2$, *G*-wave	
Γ_9	$N\overline{K}^*(892)$, $S=3/2$, *G*-wave	

The above branching fractions are our estimates, not fits or averages.

Λ(2100) BRANCHING RATIOS

See "Sign conventions for resonance couplings" in the Note on Λ and Σ Resonances.

$\Gamma(N\overline{K})/\Gamma_{total}$ Γ_1/Γ

VALUE	DOCUMENT ID		TECN	COMMENT
0.25 to 0.35 OUR ESTIMATE				
0.23±0.01	ZHANG	13A	DPWA	Multichannel
0.34±0.03	GOPAL	80	DPWA	$\overline{K}N \to \overline{K}N$
0.24±0.06	DEBELLEFON	78	DPWA	$\overline{K}N \to \overline{K}N$
0.31±0.03	HEMINGWAY	75	DPWA	$K^-p \to \overline{K}N$
• • • We do not use the following data for averages, fits, limits, etc. • • •				
0.29	DECLAIS	77	DPWA	$\overline{K}N \to \overline{K}N$
0.30±0.03	GOPAL	77	DPWA	See GOPAL 80

$(\Gamma_i\Gamma_f)^{1/2}/\Gamma_{total}$ in $N\overline{K} \to \Lambda(2100) \to \Sigma\pi$ $(\Gamma_1\Gamma_2)^{1/2}/\Gamma$

VALUE	DOCUMENT ID		TECN	COMMENT
$+0.03\pm0.01$	ZHANG	13A	DPWA	Multichannel
$+0.12\pm0.04$	GOPAL	77	DPWA	$\overline{K}N$ multichannel
$+0.11\pm0.01$	KANE	74	DPWA	$K^-p \to \Sigma\pi$

$(\Gamma_i\Gamma_f)^{1/2}/\Gamma_{total}$ in $N\overline{K} \to \Lambda(2100) \to \Lambda\eta$ $(\Gamma_1\Gamma_3)^{1/2}/\Gamma$

VALUE	DOCUMENT ID		TECN	COMMENT
-0.050 ± 0.020	RADER	73	MPWA	$K^-p \to \Lambda\eta$

$(\Gamma_i\Gamma_f)^{1/2}/\Gamma_{total}$ in $N\overline{K} \to \Lambda(2100) \to \Xi K$ $(\Gamma_1\Gamma_4)^{1/2}/\Gamma$

VALUE	DOCUMENT ID		TECN	COMMENT
0.035 ± 0.018	LITCHFIELD	71	DPWA	$K^-p \to \Xi K$
• • • We do not use the following data for averages, fits, limits, etc. • • •				
0.003	MULLER	69B	DPWA	$K^-p \to \Xi K$
0.05	TRIPP	67	RVUE	$K^-p \to \Xi K$

$(\Gamma_i\Gamma_f)^{1/2}/\Gamma_{total}$ in $N\overline{K} \to \Lambda(2100) \to \Lambda\omega$ $(\Gamma_1\Gamma_5)^{1/2}/\Gamma$

VALUE	DOCUMENT ID		TECN	COMMENT
-0.070	[2] BACCARI	77	DPWA	GD_{37} wave
$+0.011$	[2] BACCARI	77	DPWA	GG_{17} wave
$+0.008$	[2] BACCARI	77	DPWA	GG_{37} wave
0.122 or 0.154	[1] NAKKASYAN	75	DPWA	$K^-p \to \Lambda\omega$

$(\Gamma_i\Gamma_f)^{1/2}/\Gamma_{total}$ in $N\overline{K} \to \Lambda(2100) \to N\overline{K}^*(892)$, S=3/2, D-wave $(\Gamma_1\Gamma_7)^{1/2}/\Gamma$

VALUE	DOCUMENT ID		TECN	COMMENT
$+0.16\pm0.02$	ZHANG	13A	DPWA	Multichannel
$+0.21\pm0.04$	CAMERON	78B	DPWA	$K^-p \to N\overline{K}^*$

$(\Gamma_i\Gamma_f)^{1/2}/\Gamma_{total}$ in $N\overline{K} \to \Lambda(2100) \to N\overline{K}^*(892)$, S=1/2, G-wave $(\Gamma_1\Gamma_8)^{1/2}/\Gamma$

VALUE	DOCUMENT ID		TECN	COMMENT
-0.03 ± 0.02	ZHANG	13A	DPWA	Multichannel
-0.04 ± 0.03	[3] CAMERON	78B	DPWA	$K^-p \to N\overline{K}^*$

$(\Gamma_i\Gamma_f)^{1/2}/\Gamma_{total}$ in $N\overline{K} \to \Lambda(2100) \to N\overline{K}^*(892)$, S=3/2, G-wave $(\Gamma_1\Gamma_9)^{1/2}/\Gamma$

VALUE	DOCUMENT ID		TECN	COMMENT
$+0.08\pm0.02$	ZHANG	13A	DPWA	Multichannel

Λ(2100) FOOTNOTES

[1] The NAKKASYAN 75 values are from the two best solutions found. Each has the Λ(2100) and one additional resonance (P_3 or F_5).
[2] Note that the three for BACCARI 77 entries are for three different waves.
[3] The published sign has been changed to be in accord with the baryon-first convention. The upper limit on the G_3 wave is 0.03.

Λ(2100) REFERENCES

ZHANG	13A	PR C88 035205	H. Zhang *et al.*	(KSU)
PDG	86	PL 170B 1	M. Aguilar-Benitez *et al.*	(CERN, CIT+)
PDG	82	PL 111B 1	M. Roos *et al.*	(HELS, CIT, CERN)
GOPAL	80	Toronto Conf. 159	G.P. Gopal	(RHEL) IJP
CAMERON	78B	NP B146 327	W. Cameron *et al.*	(RHEL, LOIC) IJP
DEBELLEFON	78	NC 42A 403	A. de Bellefon *et al.*	(CDEF, SACL) IJP
BACCARI	77	NC 41A 96	B. Baccari *et al.*	(SACL, CDEF) IJP
DECLAIS	77	CERN 77-16	Y. Declais *et al.*	(CAEN, CERN) IJP
GOPAL	77	NP B119 362	G.P. Gopal *et al.*	(LOIC, RHEL) IJP
HEMINGWAY	75	NP B91 12	R.J. Hemingway *et al.*	(CERN, HEIDH, MPIM) IJP
NAKKASYAN	75	NP B93 85	A. Nakkasyan	(CERN) IJP
KANE	74	LBL-2452	D.F. Kane	(LBL) IJP
RADER	73	NC 16A 178	R.K. Rader *et al.*	(SACL, HEID, CERN+)
LITCHFIELD	71	NP B30 125	P.J. Litchfield *et al.*	(RHEL, CDEF, SACL) IJP
MULLER	69B	Thesis UCRL 19372	R.A. Muller	(LRL)
TRIPP	67	NP B3 10	R.D. Tripp *et al.*	(LRL, SLAC, CERN+)

Λ(2110) 5/2+

$I(J^P) = 0(\frac{5}{2}^+)$ Status: ***

For results published before 1974 (they are now obsolete), see our 1982 edition Physics Letters **111B** 1 (1982). All the references have been retained.

This resonance is in the Baryon Summary Table, but the evidence for it could be better.

Λ(2110) MASS

VALUE (MeV)	DOCUMENT ID		TECN	COMMENT
2090 to 2140 (≈ 2110) OUR ESTIMATE				
2036 ± 13	ZHANG	13A	DPWA	Multichannel
2092 ± 25	GOPAL	80	DPWA	$\overline{K}N \to \overline{K}N$
2125 ± 25	CAMERON	78B	DPWA	$K^-p \to N\overline{K}^*$
2106 ± 50	DEBELLEFON	78	DPWA	$\overline{K}N \to \overline{K}N$
2140 ± 20	DEBELLEFON	77	DPWA	$K^-p \to \Sigma\pi$
2100 ± 50	GOPAL	77	DPWA	$\overline{K}N$ multichannel
2112 ± 7	KANE	74	DPWA	$K^-p \to \Sigma\pi$
• • • We do not use the following data for averages, fits, limits, etc. • • •				
2137	BACCARI	77	DPWA	$K^-p \to \Lambda\omega$
2103	[1] NAKKASYAN	75	DPWA	$K^-p \to \Lambda\omega$

Λ(2110) WIDTH

VALUE (MeV)	DOCUMENT ID		TECN	COMMENT
150 to 250 (≈ 200) OUR ESTIMATE				
400 ± 38	ZHANG	13A	DPWA	Multichannel
245 ± 25	GOPAL	80	DPWA	$\overline{K}N \to \overline{K}N$
160 ± 30	CAMERON	78B	DPWA	$K^-p \to N\overline{K}^*$
251 ± 50	DEBELLEFON	78	DPWA	$\overline{K}N \to \overline{K}N$
140 ± 20	DEBELLEFON	77	DPWA	$K^-p \to \Sigma\pi$
200 ± 50	GOPAL	77	DPWA	$\overline{K}N$ multichannel
190 ± 30	KANE	74	DPWA	$K^-p \to \Sigma\pi$
• • • We do not use the following data for averages, fits, limits, etc. • • •				
132	BACCARI	77	DPWA	$K^-p \to \Lambda\omega$
391	[1] NAKKASYAN	75	DPWA	$K^-p \to \Lambda\omega$

Λ(2110) POLE POSITION

REAL PART

VALUE (MeV)	DOCUMENT ID		TECN	COMMENT
• • • We do not use the following data for averages, fits, limits, etc. • • •				
1970	ZHANG	13A	DPWA	Multichannel

−2×IMAGINARY PART

VALUE (MeV)	DOCUMENT ID		TECN	COMMENT
• • • We do not use the following data for averages, fits, limits, etc. • • •				
350	ZHANG	13A	DPWA	Multichannel

Λ(2110) DECAY MODES

	Mode	Fraction (Γ_i/Γ)
Γ_1	$N\overline{K}$	5–25 %
Γ_2	$\Sigma\pi$	10–40 %
Γ_3	$\Lambda\omega$	seen
Γ_4	$\Sigma(1385)\pi$	seen
Γ_5	$\Sigma(1385)\pi$, P-wave	
Γ_6	$N\overline{K}^*(892)$	10–60 %
Γ_7	$N\overline{K}^*(892)$, S=1/2	
Γ_8	$N\overline{K}^*(892)$, S=3/2, P-wave	

The above branching fractions are our estimates, not fits or averages.

Λ(2110) BRANCHING RATIOS

See "Sign conventions for resonance couplings" in the Note on Λ and Σ Resonances.

$\Gamma(N\overline{K})/\Gamma_{total}$ Γ_1/Γ

VALUE	DOCUMENT ID		TECN	COMMENT
0.05 to 0.25 OUR ESTIMATE				
0.083 ± 0.005	ZHANG	13A	DPWA	Multichannel
0.07 ± 0.03	GOPAL	80	DPWA	$\overline{K}N \to \overline{K}N$
0.27 ± 0.06	[2] DEBELLEFON	78	DPWA	$\overline{K}N \to \overline{K}N$
• • • We do not use the following data for averages, fits, limits, etc. • • •				
0.07 ± 0.03	GOPAL	77	DPWA	See GOPAL 80

$(\Gamma_i\Gamma_f)^{1/2}/\Gamma_{total}$ in $N\overline{K} \to \Lambda(2110) \to \Sigma\pi$ $(\Gamma_1\Gamma_2)^{1/2}/\Gamma$

VALUE	DOCUMENT ID		TECN	COMMENT
$+0.04 \pm 0.01$	ZHANG	13A	DPWA	Multichannel
$+0.14 \pm 0.01$	DEBELLEFON	77	DPWA	$K^- p \to \Sigma\pi$
$+0.20 \pm 0.03$	KANE	74	DPWA	$K^- p \to \Sigma\pi$
• • • We do not use the following data for averages, fits, limits, etc. • • •				
$+0.10 \pm 0.03$	GOPAL	77	DPWA	$\overline{K}N$ multichannel

$(\Gamma_i\Gamma_f)^{1/2}/\Gamma_{total}$ in $N\overline{K} \to \Lambda(2110) \to \Lambda\omega$ $(\Gamma_1\Gamma_3)^{1/2}/\Gamma$

VALUE	DOCUMENT ID		TECN	COMMENT
<0.05	BACCARI	77	DPWA	$K^- p \to \Lambda\omega$
0.112	[1] NAKKASYAN	75	DPWA	$K^- p \to \Lambda\omega$

$(\Gamma_i\Gamma_f)^{1/2}/\Gamma_{total}$ in $N\overline{K} \to \Lambda(2110) \to \Sigma(1385)\pi$, P-wave $(\Gamma_1\Gamma_5)^{1/2}/\Gamma$

VALUE	DOCUMENT ID		TECN	COMMENT
$+0.04 \pm 0.01$	ZHANG	13A	DPWA	Multichannel
$+0.071 \pm 0.025$	[3] CAMERON	78	DPWA	$K^- p \to \Sigma(1385)\pi$

$(\Gamma_i\Gamma_f)^{1/2}/\Gamma_{total}$ in $N\overline{K} \to \Lambda(2110) \to N\overline{K}^*(892)$, S=1/2 $(\Gamma_1\Gamma_7)^{1/2}/\Gamma$

VALUE	DOCUMENT ID		TECN	COMMENT
-0.09 ± 0.01	ZHANG	13A	DPWA	Multichannel
-0.17 ± 0.04	[4] CAMERON	78B	DPWA	$K^- p \to N\overline{K}^*$

$(\Gamma_i\Gamma_f)^{1/2}/\Gamma_{total}$ in $N\overline{K} \to \Lambda(2110) \to N\overline{K}^*(892)$, S=3/2, P-wave $(\Gamma_1\Gamma_8)^{1/2}/\Gamma$

VALUE	DOCUMENT ID		TECN	COMMENT
0.24 ± 0.01	ZHANG	13A	DPWA	Multichannel

Λ(2110) FOOTNOTES

[1] Found in one of two best solutions.
[2] The published error of 0.6 was a misprint.
[3] The CAMERON 78 upper limit on F-wave decay is 0.03. The sign here has been changed to be in accord with the baryon-first convention.
[4] The published sign has been changed to be in accord with the baryon-first convention. The CAMERON 78B upper limits on the P_3 and F_3 waves are each 0.03.

Λ(2110) REFERENCES

ZHANG	13A	PR C88 035205	H. Zhang *et al.*	(KSU)
PDG	82	PL 111B 1	M. Roos *et al.*	(HELS, CIT, CERN)
GOPAL	80	Toronto Conf. 159	G.P. Gopal	(RHEL) IJP
CAMERON	78	NP B143 189	W. Cameron *et al.*	(RHEL, LOIC) IJP
CAMERON	78B	NP B146 327	W. Cameron *et al.*	(RHEL, LOIC) IJP
DEBELLEFON	78	NC 42A 403	A. de Bellefon *et al.*	(CDEF, SACL) IJP
BACCARI	77	NC 41A 96	B. Baccari *et al.*	(SACL, CDEF) IJP
DEBELLEFON	77	NC 37A 175	A. de Bellefon *et al.*	(CDEF, SACL) IJP
GOPAL	77	NP B119 362	G.P. Gopal *et al.*	(LOIC, RHEL) IJP
NAKKASYAN	75	NP B93 85	A. Nakkasyan	(CERN) IJP
KANE	74	LBL-2452	D.F. Kane	(LBL) IJP

Λ(2325) 3/2⁻

$I(J^P) = 0(\frac{3}{2}^-)$ Status: *

OMITTED FROM SUMMARY TABLE

BACCARI 77 finds this state with either $J^P = 3/2^-$ or $3/2^+$ in a energy-dependent partial-wave analyses of $K^- p \to \Lambda\omega$ from 2070 to 2436 MeV. A subsequent semi-energy-independent analysis from threshold to 2436 MeV selects $3/2^-$. DEBELLEFON 78 (same group) also sees this state in an energy-dependent partial-wave analysis of $K^- p \to \overline{K}N$ data, and finds $J^P = 3/2^-$ or $3/2^+$. They again prefer $J^P = 3/2^-$, but only on the basis of model-dependent considerations.

Λ(2325) MASS

VALUE (MeV)	DOCUMENT ID		TECN	COMMENT
≈ 2325 OUR ESTIMATE				
2342±30	DEBELLEFON	78	DPWA	$\overline{K}N \to \overline{K}N$
2327±20	BACCARI	77	DPWA	$K^- p \to \Lambda\omega$

Λ(2325) WIDTH

VALUE (MeV)	DOCUMENT ID		TECN	COMMENT
177±40	DEBELLEFON	78	DPWA	$\overline{K}N \to \overline{K}N$
160±40	BACCARI	77	IPWA	$K^- p \to \Lambda\omega$

Λ(2325) DECAY MODES

	Mode
Γ_1	$N\overline{K}$
Γ_2	$\Lambda\omega$

Λ(2325) BRANCHING RATIOS

$\Gamma(N\overline{K})/\Gamma_{total}$ Γ_1/Γ

VALUE	DOCUMENT ID		TECN	COMMENT
0.19±0.06	DEBELLEFON	78	DPWA	$\overline{K}N \to \overline{K}N$

$(\Gamma_i\Gamma_f)^{1/2}/\Gamma_{total}$ in $N\overline{K} \to \Lambda(2325) \to \Lambda\omega$ $(\Gamma_1\Gamma_2)^{1/2}/\Gamma$

VALUE	DOCUMENT ID		TECN	COMMENT
0.06±0.02	[1] BACCARI	77	IPWA	DS_{33} wave
0.05±0.02	[1] BACCARI	77	DPWA	DD_{13} wave
0.08±0.03	[1] BACCARI	77	DPWA	DD_{33} wave

Λ(2325) FOOTNOTES

[1] Note that the three BACCARI 77 entries are for three different waves.

Λ(2325) REFERENCES

DEBELLEFON	78	NC 42A 403	A. de Bellefon *et al.*	(CDEF, SACL) IJP
BACCARI	77	NC 41A 96	B. Baccari *et al.*	(SACL, CDEF) IJP

Λ(2350) 9/2⁺

$I(J^P) = 0(\frac{9}{2}^+)$ Status: ***

DAUM 68 favors $J^P = 7/2^-$ or $9/2^+$. BRICMAN 70 favors $9/2^+$. LASINSKI 71 suggests three states in this region using a Pomeron + resonances model. There are now also three formation experiments from the College de France-Saclay group, DEBELLEFON 77, BACCARI 77, and DEBELLEFON 78, which find $9/2^+$ in energy-dependent partial-wave analyses of $\overline{K}N \to \Sigma\pi$, $\Lambda\omega$, and $N\overline{K}$.

Λ(2350) MASS

VALUE (MeV)	DOCUMENT ID		TECN	COMMENT
2340 to 2370 (≈ 2350) OUR ESTIMATE				
2370±50	DEBELLEFON	78	DPWA	$\overline{K}N \to \overline{K}N$
2365±20	DEBELLEFON	77	DPWA	$K^- p \to \Sigma\pi$
2358± 6	BRICMAN	70	CNTR	Total, charge exchange
• • • We do not use the following data for averages, fits, limits, etc. • • •				
2372	BACCARI	77	DPWA	$K^- p \to \Lambda\omega$
2344±15	COOL	70	CNTR	$K^- p$, $K^- d$ total
2360±20	LU	70	CNTR	$\gamma p \to K^+ Y^*$
2340± 7	BUGG	68	CNTR	$K^- p$, $K^- d$ total

Λ(2350) WIDTH

VALUE (MeV)	DOCUMENT ID		TECN	COMMENT
100 to 250 (≈ 150) OUR ESTIMATE				
204±50	DEBELLEFON	78	DPWA	$\overline{K}N \to \overline{K}N$
110±20	DEBELLEFON	77	DPWA	$K^- p \to \Sigma\pi$
324±30	BRICMAN	70	CNTR	Total, charge exchange
• • • We do not use the following data for averages, fits, limits, etc. • • •				
257	BACCARI	77	DPWA	$K^- p \to \Lambda\omega$
190	COOL	70	CNTR	$K^- p$, $K^- d$ total
55	LU	70	CNTR	$\gamma p \to K^+ Y^*$
140±20	BUGG	68	CNTR	$K^- p$, $K^- d$ total

Λ(2350) DECAY MODES

	Mode	Fraction (Γ_i/Γ)
Γ_1	$N\overline{K}$	~ 12 %
Γ_2	$\Sigma\pi$	~ 10 %
Γ_3	$\Lambda\omega$	

The above branching fractions are our estimates, not fits or averages.

Λ(2350) BRANCHING RATIOS

See "Sign conventions for resonance couplings" in the Note on Λ and Σ Resonances.

$\Gamma(N\overline{K})/\Gamma_{total}$ Γ_1/Γ

VALUE	DOCUMENT ID		TECN	COMMENT
~ 0.12 OUR ESTIMATE				
0.12±0.04	DEBELLEFON	78	DPWA	$\overline{K}N \to \overline{K}N$

$(\Gamma_i\Gamma_f)^{1/2}/\Gamma_{total}$ in $N\overline{K} \to \Lambda(2350) \to \Sigma\pi$ $(\Gamma_1\Gamma_2)^{1/2}/\Gamma$

VALUE	DOCUMENT ID		TECN	COMMENT
−0.11±0.02	DEBELLEFON	77	DPWA	$K^- p \to \Sigma\pi$

$(\Gamma_i\Gamma_f)^{1/2}/\Gamma_{total}$ in $N\overline{K} \to \Lambda(2350) \to \Lambda\omega$ $(\Gamma_1\Gamma_3)^{1/2}/\Gamma$

VALUE	DOCUMENT ID		TECN	COMMENT
<0.05	BACCARI	77	DPWA	$K^- p \to \Lambda\omega$

Baryon Particle Listings

Λ(2350), Λ(2585) Bumps

Λ(2350) REFERENCES

DEBELLEFON	78	NC 42A 403	A. de Bellefon *et al.*	(CDEF, SACL) IJP
BACCARI	77	NC 41A 96	B. Baccari *et al.*	(SACL, CDEF) IJP
DEBELLEFON	77	NC 37A 175	A. de Bellefon *et al.*	(CDEF, SACL) IJP
LASINSKI	71	NP B29 125	T.A. Lasinski	(EFI) IJP
BRICMAN	70	PL 31B 152	C. Bricman *et al.*	(CERN, CAEN, SACL)
COOL	70	PR D1 1887	R.L. Cool *et al.*	(BNL) I
Also		PRL 16 1228	R.L. Cool *et al.*	(BNL) I
LU	70	PR D2 1846	D.C. Lu *et al.*	(YALE)
BUGG	68	PR 168 1466	D.V. Bugg *et al.*	(RHEL, BIRM, CAVE) I
DAUM	68	NP B7 19	C. Daum *et al.*	(CERN) JP

Λ(2585) Bumps

$I(J^P) = 0(?^?)$ Status: **

OMITTED FROM SUMMARY TABLE

Λ(2585) MASS (BUMPS)

VALUE (MeV)	DOCUMENT ID		TECN	COMMENT
≈ 2585 OUR ESTIMATE				
2585 ± 45	ABRAMS	70	CNTR	K^-p, K^-d total
2530 ± 25	LU	70	CNTR	$\gamma p \rightarrow K^+ Y^*$

Λ(2585) WIDTH (BUMPS)

VALUE (MeV)	DOCUMENT ID		TECN	COMMENT
300	ABRAMS	70	CNTR	K^-p, K^-d total
150	LU	70	CNTR	$\gamma p \rightarrow K^+ Y^*$

Λ(2585) DECAY MODES (BUMPS)

	Mode
Γ_1	$N\overline{K}$

Λ(2585) BRANCHING RATIOS (BUMPS)

$(J+\frac{1}{2})\times\Gamma(N\overline{K})/\Gamma_{total}$ Γ_1/Γ

J is not known, so only $(J+\frac{1}{2}) \times \Gamma(N\overline{K})/\Gamma_{total}$ can be given.

VALUE	DOCUMENT ID		TECN	COMMENT
1	ABRAMS	70	CNTR	K^-p, K^-d total
0.12 ± 0.12	[1] BRICMAN	70	CNTR	Total, charge exchange

Λ(2585) FOOTNOTES (BUMPS)

[1] The resonance is at the end of the region analyzed — no clear signal.

Λ(2585) REFERENCES (BUMPS)

ABRAMS	70	PR D1 1917	R.J. Abrams *et al.*	(BNL) I
Also		PRL 16 1228	R.L. Cool *et al.*	(BNL) I
BRICMAN	70	PL 31B 152	C. Bricman *et al.*	(CERN, CAEN, SACL)
LU	70	PR D2 1846	D.C. Lu *et al.*	(YALE)

Σ BARYONS
($S = -1$, $I = 1$)

$\Sigma^+ = uus$, $\Sigma^0 = uds$, $\Sigma^- = dds$

Σ^+

$I(J^P) = 1(\frac{1}{2}^+)$ Status: ****

We have omitted some results that have been superseded by later experiments. See our earlier editions.

Σ^+ MASS

The fit uses Σ^+, Σ^0, Σ^-, and Λ mass and mass-difference measurements.

VALUE (MeV)	EVTS	DOCUMENT ID		TECN	COMMENT
1189.37±0.07 OUR FIT Error includes scale factor of 2.2.					
1189.37±0.06 OUR AVERAGE Error includes scale factor of 1.8. See the ideogram below.					
1189.33±0.04	607	[1] BOHM	72	EMUL	
1189.16±0.12		HYMAN	67	HEBC	
1189.61±0.08	4205	SCHMIDT	65	HBC	See note with Λ mass
1189.48±0.22	58	[2] BHOWMIK	64	EMUL	
1189.38±0.15	144	[2] BARKAS	63	EMUL	

[1] BOHM 72 is updated with our 1973 K^-, π^-, and π^0 masses (Reviews of Modern Physics **45** S1 (1973)).

[2] These masses have been raised 30 keV to take into account a 46 keV increase in the proton mass and a 21 keV decrease in the π^0 mass (note added 1967 edition, Reviews of Modern Physics **39** 1 (1967)).

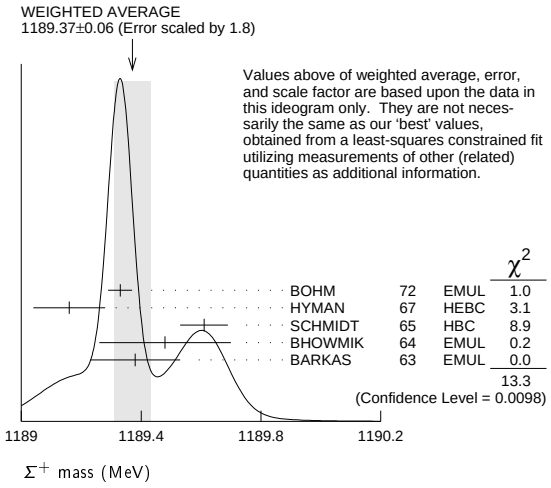

Σ^+ MEAN LIFE

Measurements with fewer than 1000 events have been omitted.

VALUE (10^{-10} s)	EVTS	DOCUMENT ID		TECN	COMMENT
0.8018±0.0026 OUR AVERAGE					
0.8038±0.0040±0.0014		BARBOSA	00	E761	hyperons, 375 GeV
0.8043±0.0080±0.0014		[3] BARBOSA	00	E761	hyperons, 375 GeV
0.798 ±0.005	30k	MARRAFFINO	80	HBC	K^-p 0.42–0.5 GeV/c
0.807 ±0.013	5719	CONFORTO	76	HBC	K^-p 1–1.4 GeV/c
0.795 ±0.010	20k	EISELE	70	HBC	K^-p at rest
0.803 ±0.008	10664	BARLOUTAUD	69	HBC	K^-p 0.4–1.2 GeV/c
0.83 ±0.032	1300	[4] CHANG	66	HBC	

[3] This is a measurement of the $\overline{\Sigma}^-$ lifetime. Here we assume CPT invariance; see below for the fractional Σ^+-$\overline{\Sigma}^-$ lifetime difference obtained by BARBOSA 00.

[4] We have increased the CHANG 66 error of 0.018; see our 1970 edition, Reviews of Modern Physics **42** 87 (1970).

$(\tau_{\Sigma^+} - \tau_{\overline{\Sigma}^-}) / \tau_{\Sigma^+}$

A test of CPT invariance.

VALUE	DOCUMENT ID		TECN	COMMENT
$(-6\pm12)\times10^{-4}$	BARBOSA	00	E761	hyperons, 375 GeV

Σ^+ MAGNETIC MOMENT

See the "Note on Baryon Magnetic Moments" in the Λ Listings. Measurements with an error $\geq 0.1\ \mu_N$ have been omitted.

VALUE (μ_N)	EVTS	DOCUMENT ID		TECN	COMMENT
2.458 ±0.010 OUR AVERAGE Error includes scale factor of 2.1. See the ideogram below.					
2.4613±0.0034±0.0040	250k	MORELOS	93	SPEC	pCu 800 GeV
2.428 ±0.036 ±0.007	12k	[5] MORELOS	93	SPEC	pCu 800 GeV
2.479 ±0.012 ±0.022	137k	WILKINSON	87	SPEC	pBe 400 GeV
2.4040±0.0198	44k	[6] ANKENBRA...	83	CNTR	pCu 400 GeV

[5] We assume CPT invariance: this is (minus) the $\overline{\Sigma}^-$ magnetic moment as measured by MORELOS 93. See below for the moment difference testing CPT.

[6] ANKENBRANDT 83 gives the value 2.38 ± 0.02μ_N. MORELOS 93 uses the same hyperon magnet and channel and claims to determine the field integral better, leading to the revised value given here.

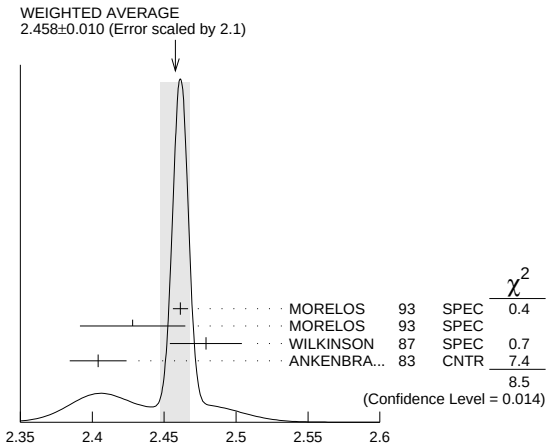

$(\mu_{\Sigma^+} + \mu_{\overline{\Sigma}^-}) / \mu_{\Sigma^+}$

A test of CPT invariance.

VALUE	DOCUMENT ID		TECN	COMMENT
0.014±0.015	[7] MORELOS	93	SPEC	pCu 800 GeV

[7] This is our calculation from the MORELOS 93 measurements of the Σ^+ and $\overline{\Sigma}^-$ magnetic moments given above. The statistical error on $\mu_{\overline{\Sigma}^-}$ dominates the error here.

Σ^+ DECAY MODES

	Mode		Fraction (Γ_i/Γ)		Confidence level
Γ_1	$p\pi^0$		(51.57±0.30) %		
Γ_2	$n\pi^+$		(48.31±0.30) %		
Γ_3	$p\gamma$		(1.23±0.05)	$\times10^{-3}$	
Γ_4	$n\pi^+\gamma$	[a]	(4.5 ±0.5)	$\times10^{-4}$	
Γ_5	$\Lambda e^+\nu_e$		(2.0 ±0.5)	$\times10^{-5}$	
	$\Delta S = \Delta Q$ (SQ) violating modes or $\Delta S = 1$ weak neutral current ($S1$) modes				
Γ_6	$ne^+\nu_e$	SQ	< 5	$\times10^{-6}$	90%
Γ_7	$n\mu^+\nu_\mu$	SQ	< 3.0	$\times10^{-5}$	90%
Γ_8	pe^+e^-	$S1$	< 7	$\times10^{-6}$	
Γ_9	$p\mu^+\mu^-$	$S1$	(9 $^{+9}_{-8}$)	$\times10^{-8}$	

[a] See the Listings below for the pion momentum range used in this measurement.

CONSTRAINED FIT INFORMATION

An overall fit to 2 branching ratios uses 14 measurements and one constraint to determine 3 parameters. The overall fit has a $\chi^2 = 7.7$ for 12 degrees of freedom.

The following *off-diagonal* array elements are the correlation coefficients $\langle \delta x_i \delta x_j \rangle / (\delta x_i \cdot \delta x_j)$, in percent, from the fit to the branching fractions, $x_i \equiv \Gamma_i/\Gamma_{\text{total}}$. The fit constrains the x_i whose labels appear in this array to sum to one.

x_2	−100	
x_3	12	−14
	x_1	x_2

Baryon Particle Listings

Σ^+

Σ^+ BRANCHING RATIOS

$\Gamma(n\pi^+)/\Gamma(N\pi)$ $\Gamma_2/(\Gamma_1+\Gamma_2)$

VALUE	EVTS	DOCUMENT ID		TECN	COMMENT
0.4836±0.0030 OUR FIT					
0.4836±0.0030 OUR AVERAGE					
0.4828±0.0036	10k	[8] MARRAFFINO	80	HBC	K^-p 0.42–0.5 GeV/c
0.488 ±0.008	1861	NOWAK	78	HBC	
0.484 ±0.015	537	TOVEE	71	EMUL	
0.488 ±0.010	1331	BARLOUTAUD	69	HBC	K^-p 0.4–1.2 GeV/c
0.46 ±0.02	534	CHANG	66	HBC	
0.490 ±0.024	308	HUMPHREY	62	HBC	

[8] MARRAFFINO 80 actually gives $\Gamma(p\pi^0)/\Gamma(\text{total}) = 0.5172 \pm 0.0036$.

$\Gamma(p\gamma)/\Gamma(p\pi^0)$ Γ_3/Γ_1

VALUE (units 10^{-3})	EVTS	DOCUMENT ID		TECN	COMMENT
2.38±0.10 OUR FIT					
2.38±0.10 OUR AVERAGE					
2.32±0.11±0.10	32k	TIMM	95	E761	Σ^+ 375 GeV
$2.81\pm0.39^{+0.21}_{-0.43}$	408	HESSEY	89	CNTR	$K^-p \to \Sigma^+\pi^-$ at rest
2.52±0.28	190	[9] KOBAYASHI	87	CNTR	$\pi^+p \to \Sigma^+K^+$
$2.46^{+0.30}_{-0.35}$	155	BIAGI	85	CNTR	CERN hyperon beam
2.11±0.38	46	MANZ	80	HBC	$K^-p \to \Sigma^+\pi^-$
2.1 ±0.3	45	ANG	69B	HBC	K^-p at rest
2.76±0.51	31	GERSHWIN	69B	HBC	$K^-p \to \Sigma^+\pi^-$
3.7 ±0.8	24	BAZIN	65	HBC	K^-p at rest

[9] KOBAYASHI 87 actually gives $\Gamma(p\gamma)/\Gamma(\text{total}) = (1.30 \pm 0.15) \times 10^{-3}$.

$\Gamma(n\pi^+\gamma)/\Gamma(n\pi^+)$ Γ_4/Γ_2

The π^+ momentum cuts differ, so we do not average the results but simply use the latest value in the Summary Table.

VALUE (units 10^{-3})	EVTS	DOCUMENT ID		TECN	COMMENT
0.93±0.10	180	EBENHOH	73	HBC	$\pi^+ < 150$ MeV/c
• • • We do not use the following data for averages, fits, limits, etc. • • •					
0.27±0.05	29	ANG	69B	HBC	$\pi^+ < 110$ MeV/c
~ 1.8		BAZIN	65B	HBC	$\pi^+ < 116$ MeV/c

$\Gamma(\Lambda e^+\nu_e)/\Gamma_{\text{total}}$ Γ_5/Γ

VALUE (units 10^{-5})	EVTS	DOCUMENT ID		TECN	COMMENT
2.0±0.5 OUR AVERAGE					
1.6±0.7	5	BALTAY	69	HBC	K^-p at rest
2.9±1.0	10	EISELE	69	HBC	K^-p at rest
2.0±0.8	6	BARASH	67	HBC	K^-p at rest

$\Gamma(ne^+\nu_e)/\Gamma(n\pi^+)$ Γ_6/Γ_2

Test of $\Delta S = \Delta Q$ rule. Experiments with an effective denominator less than 100,000 have been omitted.

EFFECTIVE DENOM.	EVTS	DOCUMENT ID		TECN	COMMENT
$< 1.1 \times 10^{-5}$ OUR LIMIT Our 90% CL limit = (2.3 events)/(effective denominator sum). [Number of events increased to 2.3 for a 90% confidence level.]					
111000	0	[10] EBENHOH	74	HBC	K^-p at rest
105000	0	[10] SECHI-ZORN	73	HBC	K^-p at rest

[10] Effective denominator calculated by us.

$\Gamma(n\mu^+\nu_\mu)/\Gamma(n\pi^+)$ Γ_7/Γ_2

Test of $\Delta S = \Delta Q$ rule.

EFFECTIVE DENOM.	EVTS	DOCUMENT ID		TECN
$< 6.2 \times 10^{-5}$ OUR LIMIT Our 90% CL limit = (6.7 events)/(effective denominator sum). [Number of events increased to 6.7 for a 90% confidence level.]				
33800	0	BAGGETT	69B	HBC
62000	2	[11] EISELE	69B	HBC
10150	0	[12] COURANT	64	HBC
1710	0	[12] NAUENBERG	64	HBC
120	1	GALTIERI	62	EMUL

[11] Effective denominator calculated by us.
[12] Effective denominator taken from EISELE 67.

$\Gamma(pe^+e^-)/\Gamma_{\text{total}}$ Γ_8/Γ

VALUE (units 10^{-6})	DOCUMENT ID		TECN	COMMENT
<7	[13] ANG	69B	HBC	K^-p at rest

[13] ANG 69B found three pe^+e^- events in agreement with $\gamma \to e^+e^-$ conversion from $\Sigma^+ \to p\gamma$. The limit given here is for neutral currents.

$\Gamma(p\mu^+\mu^-)/\Gamma_{\text{total}}$ Γ_9/Γ

A test for a $\Delta S = 1$ weak neutral current, but also allowed by higher-order electroweak interactions.

VALUE (units 10^{-8})	EVTS	DOCUMENT ID		TECN	COMMENT
$\mathbf{8.6^{+6.6}_{-5.4}\pm5.5}$	3	[14] PARK	05	HYCP	p Cu, 800 GeV

[14] The masses of the three dimuons of PARK 05 are within 1 MeV of one another, perhaps indicating the existence of a new state P^0 with mass 214.3 ± 0.5 MeV. In that case, the decay is $\Sigma^+ \to pP^0$, $P^0 \to \mu^+\mu^-$, with a branching fraction of $(3.1^{+2.4}_{-1.9} \pm 1.5) \times 10^{-8}$.

$\Gamma(\Sigma^+ \to ne^+\nu_e)/\Gamma(\Sigma^- \to ne^-\overline{\nu}_e)$ $\Gamma_6/\Gamma_3^{\Sigma^-}$

VALUE	CL%	EVTS	DOCUMENT ID		TECN	COMMENT
<0.009 OUR LIMIT Our 90% CL limit, using $\Gamma(ne^+\nu_e)/\Gamma(n\pi^+)$ above.						
• • • We do not use the following data for averages, fits, limits, etc. • • •						
<0.019	90	0	EBENHOH	74	HBC	K^-p at rest
<0.018	90	0	SECHI-ZORN	73	HBC	K^-p at rest
<0.12	95	0	COLE	71	HBC	K^-p at rest
<0.03	90	0	EISELE	69B	HBC	See EBENHOH 74

$\Gamma(\Sigma^+ \to n\mu^+\nu_\mu)/\Gamma(\Sigma^- \to n\mu^-\overline{\nu}_\mu)$ $\Gamma_7/\Gamma_4^{\Sigma^-}$

VALUE	EVTS	DOCUMENT ID		TECN	COMMENT
<0.12 OUR LIMIT Our 90% CL limit, using $\Gamma(n\mu^+\nu_\mu)/\Gamma(n\pi^+)$ above.					
• • • We do not use the following data for averages, fits, limits, etc. • • •					
$0.06^{+0.045}_{-0.03}$	2	EISELE	69B	HBC	K^-p at rest

$\Gamma(\Sigma^+ \to n\ell^+\nu)/\Gamma(\Sigma^- \to n\ell^-\overline{\nu})$ $(\Gamma_6+\Gamma_7)/(\Gamma_3^{\Sigma^-}+\Gamma_4^{\Sigma^-})$

Test of $\Delta S = \Delta Q$ rule.

VALUE	EVTS	DOCUMENT ID		TECN
<0.043 OUR LIMIT Our 90% CL limit, using $\left[\Gamma(ne^+\nu_e) + \Gamma(n\mu^+\nu_\mu)\right]/\Gamma(n\pi^+)$.				
• • • We do not use the following data for averages, fits, limits, etc. • • •				
<0.08	1	NORTON	69	HBC
<0.034	0	BAGGETT	67	HBC

Σ^+ DECAY PARAMETERS

See the "Note on Baryon Decay Parameters" in the neutron Listings. A few early results have been omitted.

α_0 FOR $\Sigma^+ \to p\pi^0$

VALUE	EVTS	DOCUMENT ID		TECN	COMMENT
$\mathbf{-0.980^{+0.017}_{-0.015}}$ **OUR FIT**					
$\mathbf{-0.980^{+0.017}_{-0.013}}$ **OUR AVERAGE**					
$-0.945^{+0.055}_{-0.042}$	1259	[15] LIPMAN	73	OSPK	$\pi^+p \to \Sigma^+$
−0.940±0.045	16k	BELLAMY	72	ASPK	$\pi^+p \to \Sigma^+K^+$
$-0.98^{+0.05}_{-0.02}$	1335	[16] HARRIS	70	OSPK	$\pi^+p \to \Sigma^+K^+$
−0.999±0.022	32k	BANGERTER	69	HBC	K^-p 0.4 GeV/c

[15] Decay protons scattered off aluminum.
[16] Decay protons scattered off carbon.

ϕ_0 ANGLE FOR $\Sigma^+ \to p\pi^0$ $(\tan\phi_0 = \beta/\gamma)$

VALUE (°)	EVTS	DOCUMENT ID		TECN	COMMENT
36 ±34 OUR AVERAGE					
$38.1^{+35.7}_{-37.1}$	1259	[17] LIPMAN	73	OSPK	$\pi^+p \to \Sigma^+K^+$
22 ±90		[18] HARRIS	70	OSPK	$\pi^+p \to \Sigma^+K^+$

[17] Decay proton scattered off aluminum.
[18] Decay protons scattered off carbon.

α_+ / α_0

Older results have been omitted.

VALUE	EVTS	DOCUMENT ID		TECN	COMMENT
−0.069±0.013 OUR FIT					
−0.073±0.021	23k	MARRAFFINO	80	HBC	K^-p 0.42–0.5 GeV/c

α_+ FOR $\Sigma^+ \to n\pi^+$

VALUE	EVTS	DOCUMENT ID		TECN	COMMENT
0.068±0.013 OUR FIT					
0.066±0.016 OUR AVERAGE					
0.037±0.049	4101	BERLEY	70B	HBC	
0.069±0.017	35k	BANGERTER	69	HBC	K^-p 0.4 GeV/c

ϕ_+ ANGLE FOR $\Sigma^+ \to n\pi^+$ $(\tan\phi_+ = \beta/\gamma)$

VALUE (°)	EVTS	DOCUMENT ID		TECN	COMMENT
167±20 OUR AVERAGE Error includes scale factor of 1.1.					
184±24	1054	[19] BERLEY	70B	HBC	
143±29	560	BANGERTER	69B	HBC	K^-p 0.4 GeV/c

[19] Changed from 176 to 184° to agree with our sign convention.

α_γ FOR $\Sigma^+ \to p\gamma$

VALUE	EVTS	DOCUMENT ID		TECN	COMMENT
−0.76 ±0.08 OUR AVERAGE					
−0.720±0.086±0.045	35k	[20] FOUCHER	92	SPEC	Σ^+ 375 GeV
−0.86 ±0.13 ±0.04	190	KOBAYASHI	87	CNTR	$\pi^+p \to \Sigma^+K^+$
$-0.53^{+0.38}_{-0.36}$	46	MANZ	80	HBC	$K^-p \to \Sigma^+\pi^-$
$-1.03^{+0.52}_{-0.42}$	61	GERSHWIN	69B	HBC	$K^-p \to \Sigma^+\pi^-$

[20] See TIMM 95 for a detailed description of the analysis.

Σ^+ REFERENCES

We have omitted some papers that have been superseded by later experiments. See our earlier editions.

PARK	05	PRL 94 021801	H.K. Park *et al.*	(FNAL HyperCP Collab.)
BARBOSA	00	PR D61 031101	R.F. Barbosa *et al.*	(FNAL E761 Collab.)
TIMM	95	PR D51 4638	S. Timm *et al.*	(FNAL E761 Collab.)
MORELOS	93	PRL 71 3417	A. Morelos *et al.*	(FNAL E761 Collab.)
FOUCHER	92	PRL 68 3004	M. Foucher *et al.*	(FNAL E761 Collab.)
HESSEY	89	ZPHY C42 175	N.P. Hessey *et al.*	(BNL-811 Collab.)
KOBAYASHI	87	PRL 59 868	M. Kobayashi *et al.*	(KYOT)
WILKINSON	87	PRL 58 855	C.A. Wilkinson *et al.*	(WISC, MICH, RUTG+)
BIAGI	85	ZPHY C28 495	S.F. Biagi *et al.*	(CERN WA62 Collab.)
ANKENBRA...	83	PRL 51 863	C.M. Ankenbrandt *et al.*	(FNAL, IOWA, ISU+)
MANZ	80	PL 96B 217	A. Manz *et al.*	(MPIM, VAND)
MARRAFFINO	80	PR D21 2501	J. Marraffino *et al.*	(VAND, MPIM)
NOWAK	78	NP B139 61	R.J. Nowak *et al.*	(LOUC, BELG, DURH+)
CONFORTO	76	NP B105 189	B. Conforto *et al.*	(RHEL, LOIC)
EBENHOH	74	ZPHY 266 367	H. Ebenhoh *et al.*	(HEIDT)
EBENHOH	73	ZPHY 264 413	W. Ebenhoh *et al.*	(HEIDT)
LIPMAN	73	PL 43B 89	N.H. Lipman *et al.*	(RHEL, SUSS, LOWC)
PDG	73	RMP 45 S1	T.A. Lasinski *et al.*	(LBL, BRAN, CERN+)
SECHI-ZORN	73	PR D8 12	B. Sechi-Zorn, G.A. Snow	(UMD)
BELLAMY	72	PL 39B 299	E.H. Bellamy *et al.*	(LOWC, RHEL, SUSS)
BOHM	72	NP B48 1	G. Bohm *et al.*	(BERL, KIDR, BRUX, IASD+)
Also		IIHE-73.2 Nov	G. Bohm	(BERL, KIDR, BRUX, IASD, DUUC+)
COLE	71	PR D4 631	J. Cole *et al.*	(STON, COLU)
TOVEE	71	NP B33 493	D.N. Tovee *et al.*	(LOUC, KIDR, BERL+)
BERLEY	70B	PR D1 2015	D. Berley *et al.*	(BNL, MASA, YALE)
EISELE	70	ZPHY 238 372	F. Eisele *et al.*	(HEID)
HARRIS	70	PRL 24 165	F. Harris *et al.*	(MICH, WISC)
PDG	70	RMP 42 87	A. Barbaro-Galtieri *et al.*	(LRL, BRAN+)
ANG	69B	ZPHY 228 151	G. Ang *et al.*	(HEID)
BAGGETT	69B	Thesis MDDP-TR-973	N.V. Baggett	(UMD)
BALTAY	69	PRL 22 615	C. Baltay *et al.*	(COLU, STON)
BANGERTER	69	Thesis UCRL 19244	R.O. Bangerter	(LRL)
BANGERTER	69B	PR 187 1821	R.O. Bangerter *et al.*	(LRL)
BARLOUTAUD	69	NP B14 153	R. Barloutaud *et al.*	(SACL, CERN, HEID)
EISELE	69	ZPHY 221 1	F. Eisele *et al.*	(HEID)
Also		PRL 13 291	W. Willis *et al.*	(BNL, CERN, HEID, UMD)
EISELE	69B	ZPHY 221 401	F. Eisele *et al.*	(HEID)
GERSHWIN	69B	PR 188 2077	L.K. Gershwin *et al.*	(LRL)
Also		Thesis UCRL 19246	L.K. Gershwin	(LRL)
NORTON	69	Thesis Nevis 175	H. Norton	(COLU)
BAGGETT	67	PRL 19 1458	N. Baggett *et al.*	(UMD)
Also		Vienna Abs. 374	N.V. Baggett, B. Kehoe	(UMD)
Also		Private Comm.	N.V. Baggett	(UMD)
BARASH	67	PRL 19 181	N. Barash *et al.*	(UMD)
EISELE	67	ZPHY 205 409	F. Eisele *et al.*	(HEID)
HYMAN	67	PL 25B 376	L.G. Hyman *et al.*	(ANL, CMU, NWES)
PDG	67	RMP 39 1	A.H. Rosenfeld *et al.*	(LRL, CERN, YALE)
CHANG	66	PR 151 1081	C.Y. Chang	(COLU)
Also		Thesis Nevis 145	C.Y. Chang	(COLU)
BAZIN	65	PRL 14 154	M. Bazin *et al.*	(PRIN, COLU)
BAZIN	65B	PR 140B 1358	M. Bazin *et al.*	(PRIN, RUTG, COLU)
SCHMIDT	65	PR 140B 1328	P. Schmidt	(COLU)
BHOWMIK	64	NP 53 22	B. Bhowmik *et al.*	(DELH)
COURANT	64	PR 136 B1791	H. Courant *et al.*	(CERN, HEID, UMD+)
NAUENBERG	64	PRL 12 679	U. Nauenberg *et al.*	(COLU, RUTG, PRIN)
BARKAS	63	PRL 11 26	W.H. Barkas, J.N. Dyer, H.H. Heckman	(LRL)
Also		Thesis UCRL 9450	J.N. Dyer	(LRL)
GALTIERI	62	PRL 9 26	A. Barbaro-Galtieri *et al.*	(LRL)
HUMPHREY	62	PR 127 1305	W.E. Humphrey, R.R. Ross	(LRL)

Σ^0

$I(J^P) = 1(\frac{1}{2}^+)$ Status: ****

COURANT 63 and ALFF 65, using $\Sigma^0 \to \Lambda e^+ e^-$ decays (Dalitz decays), determined the Σ^0 parity to be positive, given that $J = 1/2$ and that certain very reasonable assumptions about form factors are true. The results of experiments involving the Primakoff effect, from which the Σ^0 mean life and $\Sigma^0 \to \Lambda$ transition magnetic moment come (see below), strongly support $J = 1/2$.

Σ^0 MASS

The fit uses Σ^+, Σ^0, Σ^-, and Λ mass and mass-difference measurements.

VALUE (MeV)	EVTS	DOCUMENT ID		TECN	COMMENT
1192.642±0.024 OUR FIT					
• • • We do not use the following data for averages, fits, limits, etc. • • •					
1192.65 ±0.020±0.014	3327	[1] WANG	97	SPEC	$\Sigma^0 \to \Lambda\gamma \to (p\pi^-)(e^+e^-)$

[1] This WANG 97 result is redundant with the Σ^0-Λ mass-difference measurement below.

$m_{\Sigma^-} - m_{\Sigma^0}$

VALUE (MeV)	EVTS	DOCUMENT ID		TECN	COMMENT
4.807±0.035 OUR FIT	Error includes scale factor of 1.1.				
4.86 ±0.08 OUR AVERAGE	Error includes scale factor of 1.2.				
4.87 ±0.12	37	DOSCH	65	HBC	
5.01 ±0.12	12	SCHMIDT	65	HBC	See note with Λ mass
4.75 ±0.1	18	BURNSTEIN	64	HBC	

$m_{\Sigma^0} - m_{\Lambda}$

VALUE (MeV)	EVTS	DOCUMENT ID		TECN	COMMENT
76.959±0.023 OUR FIT					
76.966±0.020±0.013	3327	WANG	97	SPEC	$\Sigma^0 \to \Lambda\gamma \to (p\pi^-)(e^+e^-)$
• • • We do not use the following data for averages, fits, limits, etc. • • •					
76.23 ±0.55	109	COLAS	75	HLBC	$\Sigma^0 \to \Lambda\gamma$
76.63 ±0.28	208	SCHMIDT	65	HBC	See note with Λ mass

Σ^0 MEAN LIFE

These lifetimes are deduced from measurements of the cross sections for the Primakoff process $\Lambda \to \Sigma^0$ in nuclear Coulomb fields. An alternative expression of the same information is the Σ^0-Λ transition magnetic moment given in the following section. The relation is $(\mu_{\Sigma\Lambda}/\mu_N)^2\ \tau = 1.92951 \times 10^{-19}$ s (see DEVLIN 86).

VALUE (10^{-20} s)	DOCUMENT ID		TECN	COMMENT
7.4±0.7 OUR EVALUATION	Using $\mu_{\Sigma\Lambda}$ (see the above note).			
$6.5^{+1.7}_{-1.1}$	[2] DEVLIN	86	SPEC	Primakoff effect
7.6±0.5±0.7	[3] PETERSEN	86	SPEC	Primakoff effect
• • • We do not use the following data for averages, fits, limits, etc. • • •				
5.8±1.3	[2] DYDAK	77	SPEC	See DEVLIN 86

[2] DEVLIN 86 is a recalculation of the results of DYDAK 77 removing a numerical approximation made in that work.
[3] An additional uncertainty of the Primakoff formalism is estimated to be $< 5\%$.

$|\mu(\Sigma^0 \to \Lambda)|$ TRANSITION MAGNETIC MOMENT

See the note in the Σ^0 mean-life section above. Also, see the "Note on Baryon Magnetic Moments" in the Λ Listings.

VALUE (μ_N)	DOCUMENT ID		TECN	COMMENT
1.61±0.08 OUR AVERAGE				
$1.72^{+0.17}_{-0.19}$	[4] DEVLIN	86	SPEC	Primakoff effect
1.59±0.05±0.07	[5] PETERSEN	86	SPEC	Primakoff effect
• • • We do not use the following data for averages, fits, limits, etc. • • •				
$1.82^{+0.25}_{-0.18}$	[4] DYDAK	77	SPEC	See DEVLIN 86

[4] DEVLIN 86 is a recalculation of the results of DYDAK 77 removing a numerical approximation made in that work.
[5] An additional uncertainty of the Primakoff formalism is estimated to be $< 2.5\%$.

Σ^0 DECAY MODES

	Mode	Fraction (Γ_i/Γ)	Confidence level
Γ_1	$\Lambda\gamma$	100 %	
Γ_2	$\Lambda\gamma\gamma$	< 3 %	90%
Γ_3	$\Lambda e^+ e^-$	[a] 5×10^{-3}	

[a] A theoretical value using QED.

Σ^0 BRANCHING RATIOS

$\Gamma(\Lambda\gamma\gamma)/\Gamma_{total}$ Γ_2/Γ

VALUE	CL%	DOCUMENT ID		TECN
<0.03	90	COLAS	75	HLBC

$\Gamma(\Lambda e^+ e^-)/\Gamma_{total}$ Γ_3/Γ

See COURANT 63 and ALFF 65 for measurements of the invariant-mass spectrum of the Dalitz pairs.

VALUE	DOCUMENT ID		COMMENT
0.00545	FEINBERG	58	Theoretical QED calculation

Σ^0 REFERENCES

WANG	97	PR D56 2544	M.H.L.S. Wang *et al.*	(BNL-E766 Collab.)
DEVLIN	86	PR D34 1626	T. Devlin, P.C. Petersen, A. Beretvas	(RUTG)
PETERSEN	86	PRL 57 949	P.C. Petersen *et al.*	(RUTG, WISC, MICH+)
DYDAK	77	NP B118 1	F. Dydak *et al.*	(CERN, DORT, HEIDH)
COLAS	75	NP B91 253	J. Colas *et al.*	(ORSAY)
ALFF	65	PR 137 B1105	C. Alff *et al.*	(COLU, RUTG, BNL) P
DOSCH	65	PL 14 239	H.C. Dosch *et al.*	(HEID)
SCHMIDT	65	PR 140B 1328	P. Schmidt	(COLU)
BURNSTEIN	64	PRL 13 66	R.A. Burnstein *et al.*	(UMD)
COURANT	63	PRL 10 409	H. Courant *et al.*	(CERN, UMD) P
FEINBERG	58	PR 109 1019	G. Feinberg	(BNL)

Baryon Particle Listings

Σ^-

Σ^- $I(J^P) = 1(\frac{1}{2}^+)$ Status: ****

We have omitted some results that have been superseded by later experiments. See our earlier editions.

Σ^- MASS

The fit uses Σ^+, Σ^0, Σ^-, and Λ mass and mass-difference measurements.

VALUE (MeV)	EVTS	DOCUMENT ID		TECN	COMMENT
1197.449±0.030 OUR FIT		Error includes scale factor of 1.2.			
1197.45 ±0.04 OUR AVERAGE		Error includes scale factor of 1.2.			
1197.417±0.040		GUREV	93	SPEC	Σ^- C atom, crystal diff.
1197.532±0.057		GALL	88	CNTR	Σ^- Pb, Σ^- W atoms
1197.43 ±0.08	3000	SCHMIDT	65	HBC	See note with Λ mass
• • • We do not use the following data for averages, fits, limits, etc. • • •					
1197.24 ±0.15		[1] DUGAN	75	CNTR	Exotic atoms

[1] GALL 88 concludes that the DUGAN 75 mass needs to be reevaluated.

$m_{\Sigma^-} - m_{\Sigma^+}$

VALUE (MeV)	EVTS	DOCUMENT ID		TECN
8.08±0.08 OUR FIT	Error includes scale factor of 1.9.			
8.09±0.16 OUR AVERAGE				
7.91±0.23	86	BOHM	72	EMUL
8.25±0.25	2500	DOSCH	65	HBC
8.25±0.40	87	BARKAS	63	EMUL

$m_{\Sigma^-} - m_{\Lambda}$

VALUE (MeV)	EVTS	DOCUMENT ID		TECN	COMMENT
81.766±0.030 OUR FIT	Error includes scale factor of 1.2.				
81.69 ±0.07 OUR AVERAGE					
81.64 ±0.09	2279	HEPP	68	HBC	
81.80 ±0.13	85	SCHMIDT	65	HBC	See note with Λ mass
81.70 ±0.19		BURNSTEIN	64	HBC	

Σ^- MEAN LIFE

Measurements with an error $\geq 0.2 \times 10^{-10}$ s have been omitted.

VALUE (10^{-10} s)	EVTS	DOCUMENT ID		TECN	COMMENT
1.479±0.011 OUR AVERAGE	Error includes scale factor of 1.3.				See the ideogram below.
1.480±0.014	16k	MARRAFFINO	80	HBC	K^-p 0.42–0.5 GeV/c
1.49 ±0.03	8437	CONFORTO	76	HBC	K^-p 1–1.4 GeV/c
1.463±0.039	2400	ROBERTSON	72	HBC	K^-p 0.25 GeV/c
1.42 ±0.05	1383	BAKKER	71	DBC	$K^-N \rightarrow \Sigma^-\pi\pi$
$1.41\ ^{+0.09}_{-0.08}$		TOVEE	71	EMUL	
1.485±0.022	100k	EISELE	70	HBC	K^-p at rest
1.472±0.016	10k	BARLOUTAUD	69	HBC	K^-p 0.4–1.2 GeV/c
1.38 ±0.07	506	WHITESIDE	68	HBC	K^-p at rest
1.666±0.075	3267	[2] CHANG	66	HBC	K^-p at rest
1.58 ±0.06	1208	HUMPHREY	62	HBC	K^-p at rest

[2] We have increased the CHANG 66 error of 0.026; see our 1970 edition, Reviews of Modern Physics **42** 87 (1970).

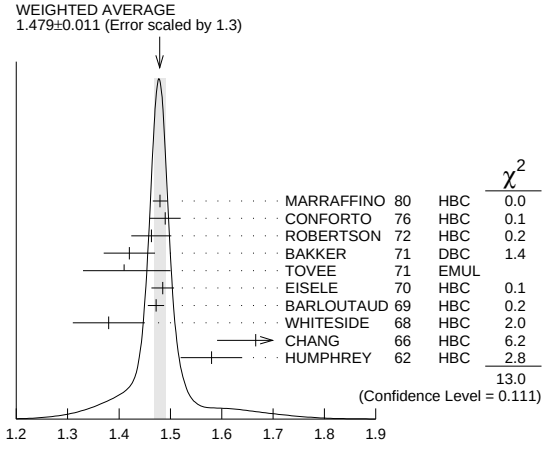

Σ^- MAGNETIC MOMENT

See the "Note on Baryon Magnetic Moments" in the Λ Listings. Measurements with an error $\geq 0.3\ \mu_N$ have been omitted.

VALUE (μ_N)	EVTS	DOCUMENT ID		TECN	COMMENT
−1.160±0.025 OUR AVERAGE	Error includes scale factor of 1.7. See the ideogram below.				
−1.105±0.029±0.010		HERTZOG	88	CNTR	Σ^- Pb, Σ^- W atoms
−1.166±0.014±0.010	671k	ZAPALAC	86	SPEC	$ne^-\nu$, $n\pi^-$ decays
−1.23 ±0.03 ±0.03		WAH	85	CNTR	pCu → Σ^-X
• • • We do not use the following data for averages, fits, limits, etc. • • •					
−0.89 ±0.14	516k	DECK	83	SPEC	pBe → Σ^-X

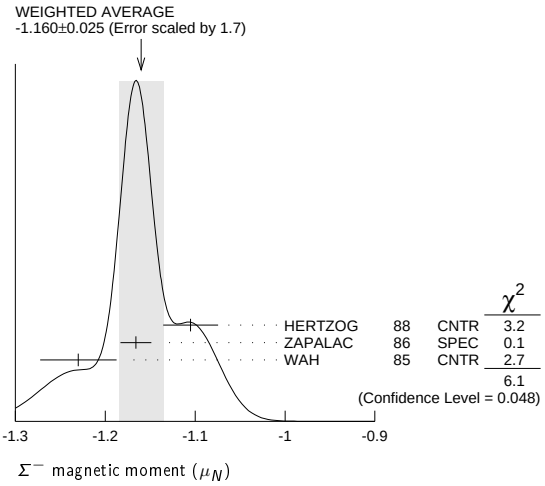

Σ^- CHARGE RADIUS

VALUE (fm)	DOCUMENT ID		TECN	COMMENT
0.780±0.080±0.060	[3] ESCHRICH	01	SELX	$\Sigma^-e \rightarrow \Sigma^-e$

[3] ESCHRICH 01 actually gives $\langle r^2 \rangle = (0.61 \pm 0.12 \pm 0.09)$ fm^2.

Σ^- DECAY MODES

	Mode	Fraction (Γ_i/Γ)
Γ_1	$n\pi^-$	(99.848±0.005) %
Γ_2	$n\pi^-\gamma$	[a] (4.6 ±0.6) × 10^{-4}
Γ_3	$ne^-\overline{\nu}_e$	(1.017±0.034) × 10^{-3}
Γ_4	$n\mu^-\overline{\nu}_\mu$	(4.5 ±0.4) × 10^{-4}
Γ_5	$\Lambda e^-\overline{\nu}_e$	(5.73 ±0.27) × 10^{-5}

[a] See the Listings below for the pion momentum range used in this measurement.

CONSTRAINED FIT INFORMATION

An overall fit to 3 branching ratios uses 16 measurements and one constraint to determine 4 parameters. The overall fit has a $\chi^2 = 8.7$ for 13 degrees of freedom.

The following *off-diagonal* array elements are the correlation coefficients $\langle \delta x_i \delta x_j \rangle / (\delta x_i \cdot \delta x_j)$, in percent, from the fit to the branching fractions, $x_i \equiv \Gamma_i/\Gamma_{\text{total}}$. The fit constrains the x_i whose labels appear in this array to sum to one.

	x_1	x_3	x_4
x_3	−64		
x_4	−77	0	
x_5	−5	0	0

Σ^- BRANCHING RATIOS

$\Gamma(n\pi^-\gamma)/\Gamma(n\pi^-)$ Γ_2/Γ_1

The π^+ momentum cuts differ, so we do not average the results but simply use the latest value for the Summary Table.

VALUE (units 10^{-3})	EVTS	DOCUMENT ID		TECN	COMMENT
0.46±0.06	292	EBENHOH	73	HBC	$\pi^+ < 150$ MeV/c
• • • We do not use the following data for averages, fits, limits, etc. • • •					
0.10±0.02	23	ANG	69B	HBC	$\pi^- < 110$ MeV/c
~ 1.1		BAZIN	65B	HBC	$\pi^- < 166$ MeV/c

$\Gamma(ne^-\overline{\nu}_e)/\Gamma(n\pi^-)$ Γ_3/Γ_1

Measurements with an error $\geq 0.2\times10^{-3}$ have been omitted.

VALUE (units 10^{-3})	EVTS	DOCUMENT ID		TECN	COMMENT
1.019±0.035 OUR FIT					
$1.019^{+0.031}_{-0.040}$ OUR AVERAGE					
0.96 ±0.05	2847	BOURQUIN	83C	SPEC	SPS hyperon beam
$1.09\ ^{+0.06}_{-0.08}$	601	[4] EBENHOH	74	HBC	K^-p at rest
$1.05\ ^{+0.07}_{-0.13}$	455	[4] SECHI-ZORN	73	HBC	K^-p at rest
0.97 ±0.15	57	COLE	71	HBC	K^-p at rest
1.11 ±0.09	180	BIERMAN	68	HBC	

[4] An additional negative systematic error is included for internal radiative corrections and latest form factors; see BOURQUIN 83C.

$\Gamma(n\mu^-\overline{\nu}_\mu)/\Gamma(n\pi^-)$ Γ_4/Γ_1

VALUE (units 10^{-3})	EVTS	DOCUMENT ID		TECN	COMMENT
0.45±0.04 OUR FIT					
0.45±0.04 OUR AVERAGE					
0.38±0.11	13	COLE	71	HBC	K^-p at rest
0.43±0.06	72	ANG	69	HBC	K^-p at rest
0.43±0.09	56	BAGGETT	69	HBC	K^-p at rest
0.56±0.20	11	BAZIN	65B	HBC	K^-p at rest
0.66±0.15	22	COURANT	64	HBC	

$\Gamma(\Lambda e^-\overline{\nu}_e)/\Gamma(n\pi^-)$ Γ_5/Γ_1

VALUE (units 10^{-4})	EVTS	DOCUMENT ID		TECN	COMMENT
0.574±0.027 OUR FIT					
0.574±0.027 OUR AVERAGE					
0.561±0.031	1620	[5] BOURQUIN	82	SPEC	SPS hyperon beam
0.63 ±0.11	114	THOMPSON	80	ASPK	Hyperon beam
0.52 ±0.09	31	BALTAY	69	HBC	K^-p at rest
0.69 ±0.12	31	EISELE	69	HBC	K^-p at rest
0.64 ±0.12	35	BARASH	67	HBC	K^-p at rest
0.75 ±0.28	11	COURANT	64	HBC	K^-p at rest

[5] The value is from BOURQUIN 83B, and includes radiation corrections and new acceptance.

Σ^- DECAY PARAMETERS

See the "Note on Baryon Decay Parameters" in the neutron Listings. Older, outdated results have been omitted.

α_- FOR $\Sigma^- \to n\pi^-$

VALUE	EVTS	DOCUMENT ID		TECN	COMMENT
−0.068±0.008 OUR AVERAGE					
−0.062±0.024	28k	HANSL	78	HBC	$K^-p \to \Sigma^-\pi^+$
−0.067±0.011	60k	BOGERT	70	HBC	K^-p 0.4 GeV/c
−0.071±0.012	51k	BANGERTER	69	HBC	K^-p 0.4 GeV/c

ϕ ANGLE FOR $\Sigma^- \to n\pi^-$ $(\tan\phi = \beta\,/\,\gamma)$

VALUE (°)	EVTS	DOCUMENT ID		TECN	COMMENT
10±15 OUR AVERAGE					
+ 5±23	1092	[6] BERLEY	70B	HBC	n rescattering
14±19	1385	BANGERTER	69B	HBC	K^-p 0.4 GeV/c

[6] BERLEY 70B changed from −5 to +5° to agree with our sign convention.

g_A/g_V FOR $\Sigma^- \to ne^-\overline{\nu}_e$

Measurements with fewer than 500 events have been omitted. Where necessary, signs have been changed to agree with our conventions, which are given in the "Note on Baryon Decay Parameters" in the neutron Listings. What is actually listed is $|g_1/f_1 - 0.237 g_2/f_1|$. This reduces to $g_A/g_V \equiv g_1(0)/f_1(0)$ on making the usual assumption that $g_2 = 0$. See also the note on HSUEH 88.

VALUE	EVTS	DOCUMENT ID		TECN	COMMENT
0.340±0.017 OUR AVERAGE					
+0.327±0.007±0.019	50k	[7] HSUEH	88	SPEC	Σ^- 250 GeV
+0.34 ±0.05	4456	[8] BOURQUIN	83C	SPEC	SPS hyperon beam
0.385±0.037	3507	[9] TANENBAUM	74	ASPK	
• • • We do not use the following data for averages, fits, limits, etc. • • •					
0.29 ±0.07	25k	HSUEH	85	SPEC	See HSUEH 88
$0.17\ ^{+0.07}_{-0.09}$	519	DECAMP	77	ELEC	Hyperon beam

[7] The sign is, *with our conventions*, unambiguously positive. The value assumes, as usual, that $g_2 = 0$. If g_2 is included in the fit, than (with our sign convention) $g_2 = -0.56 \pm 0.37$, with a corresponding reduction of g_A/g_V to $+0.20 \pm 0.08$.

[8] BOURQUIN 83C favors the positive sign by at least 2.6 standard deviations.

[9] TANENBAUM 74 gives 0.435 ± 0.035, assuming no q^2 dependence in g_A and g_V. The listed result allows q^2 dependence, and is taken from HSUEH 88.

$f_2(0)/f_1(0)$ FOR $\Sigma^- \to ne^-\overline{\nu}_e$

The signs have been changed to be in accord with our conventions, given in the "Note on Baryon Decay Parameters" in the neutron Listings.

VALUE	EVTS	DOCUMENT ID		TECN	COMMENT
0.97±0.14 OUR AVERAGE					
+0.96±0.07±0.13	50k	HSUEH	88	SPEC	Σ^- 250 GeV
+1.02±0.34	4456	BOURQUIN	83C	SPEC	SPS hyperon beam

TRIPLE CORRELATION COEFFICIENT D for $\Sigma^- \to ne^-\overline{\nu}_e$

The coefficient D of the term $D\,\mathbf{P}\cdot(\hat{\mathbf{p}}_e\times\hat{\mathbf{p}}_\nu)$ in the $\Sigma^- \to ne^-\overline{\nu}$ decay angular distribution. A nonzero value would indicate a violation of time-reversal invariance.

VALUE	EVTS	DOCUMENT ID		TECN	COMMENT
0.11±0.10	50k	HSUEH	88	SPEC	Σ^- 250 GeV

g_V/g_A FOR $\Sigma^- \to \Lambda e^-\overline{\nu}_e$

For the sign convention, see the "Note on Baryon Decay Parameters" in the neutron Listings. The value is predicted to be zero by conserved vector current theory. The values averaged assume CVC-SU(3) weak magnetism term.

VALUE	EVTS	DOCUMENT ID		TECN	COMMENT
0.01 ±0.10 OUR AVERAGE Error includes scale factor of 1.5. See the ideogram below.					
−0.034±0.080	1620	[10] BOURQUIN	82	SPEC	SPS hyperon beam
−0.29 ±0.29	114	THOMPSON	80	ASPK	BNL hyperon beam
−0.17 ±0.35	55	TANENBAUM	75B	SPEC	BNL hyperon beam
+0.45 ±0.20	186	[10,11] FRANZINI	72	HBC	

[10] The sign has been changed to agree with our convention.

[11] The FRANZINI 72 value includes the events of earlier papers.

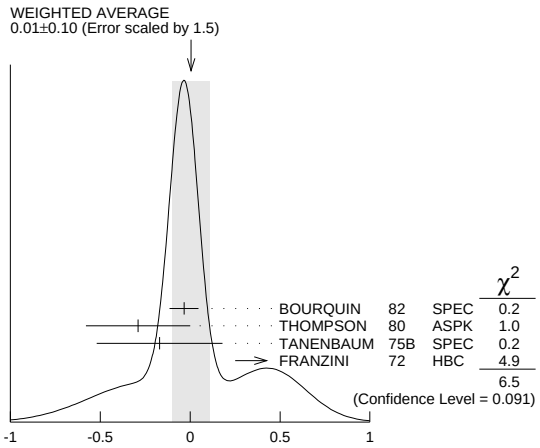

g_V/g_A for $\Sigma^- \to \Lambda e^-\overline{\nu}_e$

g_{WM}/g_A FOR $\Sigma^- \to \Lambda e^-\overline{\nu}_e$

The values quoted assume the CVC prediction $g_V = 0$.

VALUE	EVTS	DOCUMENT ID		TECN	COMMENT
2.4 ±1.7 OUR AVERAGE					
1.75±3.5	114	THOMPSON	80	ASPK	BNL hyperon beam
3.5 ±4.5	55	TANENBAUM	75B	SPEC	BNL hyperon beam
2.4 ±2.1	186	FRANZINI	72	HBC	

Σ^- REFERENCES

We have omitted some papers that have been superseded by later experiments. See our earlier editions.

ESCHRICH	01	PL B522 233	I. Eschrich *et al.* (FNAL SELEX Collab.)
GUREV	93	JETPL 57 400 Translated from ZETFP 57 389.	M.P. Gurev *et al.* (PNPI)
GALL	88	PRL 60 186	K.P. Gall *et al.* (BOST, MIT, WILL, CIT+)
HERTZOG	88	PR D37 1142	D.W. Hertzog *et al.* (WILL, BOST, MIT+)
HSUEH	88	PR D38 2056	S.Y. Hsueh *et al.* (CHIC, ELMT, FNAL+)
ZAPALAC	86	PRL 57 1526	G. Zapalac *et al.* (EFI, ELMT, FNAL+)
HSUEH	85	PRL 54 2399	S.Y. Hsueh *et al.* (CHIC, ELMT, FNAL+)
WAH	85	PRL 55 2551	Y.W. Wah *et al.* (FNAL, IOWA, ISU)
BOURQUIN	83B	ZPHY C21 27	M.H. Bourquin *et al.* (BRIS, GEVA, HEIDP+)
BOURQUIN	83C	ZPHY C21 17	M.H. Bourquin *et al.* (BRIS, GEVA, HEIDP+)
DECK	83	PR D28 1	L. Deck *et al.* (RUTG, WISC, MICH, MINN)
BOURQUIN	82	ZPHY C12 307	M.H. Bourquin *et al.* (BRIS, GEVA, HEIDP+)
MARRAFFINO	80	PR D21 2501	J. Marraffino *et al.* (VAND, MPIM)
THOMPSON	80	PR D21 25	J.A. Thompson *et al.* (PITT, BNL)
HANSL	78	NP B132 45	T. Hansl *et al.* (MPIM, VAND)
DECAMP	77	PL 66B 295	D. Decamp *et al.* (LALO, EPOL)
CONFORTO	76	NP B105 189	B. Conforto *et al.* (RHEL, LOIC)
DUGAN	75	NP A254 396	G. Dugan *et al.* (COLU, YALE)
TANENBAUM	75B	PR D12 1871	W. Tanenbaum *et al.* (YALE, FNAL, BNL)
EBENHOH	74	ZPHY 266 367	H. Ebenhoh *et al.* (HEIDT)
TANENBAUM	74	PRL 33 175	W. Tanenbaum *et al.* (YALE, FNAL, BNL)
EBENHOH	73	ZPHY 264 413	W. Ebenhoh *et al.* (HEIDT)
SECHI-ZORN	73	PR D8 12	B. Sechi-Zorn, G.A. Snow (UMD)
BOHM	72	NP B48 1	G. Bohm *et al.* (BERL, KIDR, BRUX, IASD+)
FRANZINI	72	PR D6 2417	P. Franzini *et al.* (COLU, HEID, UMD+)
ROBERTSON	72	Thesis UMI 78-00877	R.M. Robertson (IIT)
BAKKER	71	LNC 1 37	A.M. Bakker *et al.* (SABRE Collab.)
COLE	71	PR D4 631	J. Cole *et al.* (STON, COLU)
Also		Thesis Nevis 175	H. Norton (COLU)
TOVEE	71	NP B33 493	D.N. Tovee *et al.* (LOUC, KIDR, BERL+)
BERLEY	70B	PR D1 2015	D. Berley *et al.* (BNL, MASA, YALE)
BOGERT	70	PR D2 6	D.V. Bogert *et al.* (BNL, MASA, YALE)
EISELE	70	ZPHY 238 372	F. Eisele *et al.* (HEID)
PDG	70	RMP 42 87	A. Barbaro-Galtieri *et al.* (LRL, BRAN+)
ANG	69	ZPHY 223 103	G. Ang *et al.* (HEID)
ANG	69B	ZPHY 228 151	G. Ang *et al.* (HEID)

BAGGETT	69	PRL 23 249	N.V. Baggett, B. Kehoe, G.A. Snow	(UMD)
BALTAY	69	PRL 22 615	C. Baltay *et al.*	(COLU, STON)
BANGERTER	69	Thesis UCRL 19244	R.O. Bangerter	(LRL)
BANGERTER	69B	PR 187 1821	R.O. Bangerter *et al.*	(LRL)
BARLOUTAUD	69	NP B14 153	R. Barloutaud *et al.*	(SACL, CERN, HEID)
EISELE	69	ZPHY 221 1	F. Eisele *et al.*	(HEID)
BIERMAN	68	PRL 20 1459	E. Bierman *et al.*	(PRIN)
HEPP	68	ZPHY 214 71	V. Hepp, H. Schleich	(HEID)
WHITESIDE	68	NC 54A 537	H. Whiteside, J. Gollub	(OBER)
BARASH	67	PRL 19 181	N. Barash *et al.*	(UMD)
CHANG	66	PR 151 1081	C.Y. Chang	(COLU)
BAZIN	65B	PR 140B 1358	M. Bazin *et al.*	(PRIN, RUTG, COLU)
DOSCH	65	PL 14 239	H.C. Dosch *et al.*	(HEID)
Also		PR 151 1081	C.Y. Chang	(COLU)
SCHMIDT	65	PR 140B 1328	P. Schmidt	(COLU)
BURNSTEIN	64	PRL 13 66	R.A. Burnstein *et al.*	(UMD)
COURANT	64	PR 136 B1791	H. Courant *et al.*	(CERN, HEID, UMD+)
BARKAS	63	PRL 11 26	W.H. Barkas, J.N. Dyer, H.H. Heckman	(LRL)
HUMPHREY	62	PR 127 1305	W.E. Humphrey, R.R. Ross	(LRL)

$\Sigma(1385)\ 3/2^+$

$I(J^P) = 1(\frac{3}{2}^+)$ Status: ****

Discovered by ALSTON 60. Early measurements of the mass and width for combined charge states have been omitted. They may be found in our 1984 edition Reviews of Modern Physics **56** S1 (1984).

We average only the most significant determinations. We do not average results from inclusive experiments with large backgrounds or results which are not accompanied by some discussion of experimental resolution. Nevertheless systematic differences between experiments remain. (See the ideograms in the Listings below.) These differences could arise from interference effects that change with production mechanism and/or beam momentum. They can also be accounted for in part by differences in the parametrizations employed. (See BORENSTEIN 74 for a discussion on this point.) Thus BORENSTEIN 74 uses a Breit-Wigner with energy-independent width, since a P-wave was found to give unsatisfactory fits. CAMERON 78 uses the same form. On the other hand HOLMGREN 77 obtains a good fit to their $\Lambda\pi$ spectrum with a P-wave Breit-Wigner, but includes the partial width for the $\Sigma\pi$ decay mode in the parametrization. AGUILAR-BENITEZ 81D gives masses and widths for five different Breit-Wigner shapes. The results vary considerably. Only the best-fit S-wave results are given here.

$\Sigma(1385)$ MASSES

$\Sigma(1385)^+$ MASS

VALUE (MeV)	EVTS	DOCUMENT ID		TECN	COMMENT
1382.80±0.35 OUR AVERAGE		Error includes scale factor of 1.9. See the ideogram below.			
1383.2 ±0.9 $^{+0.1}_{-1.5}$		AGAKISHIEV	12	SPEC	$pp \to \Sigma(1385)^+ K^+ n$, 3.5 GeV
1384.1 ±0.7	1897	BAUBILLIER	84	HBC	$K^- p \to$ 8.25 GeV/c
1384.5 ±0.5	5256	AGUILAR-...	81D	HBC	$K^- p \to \Lambda\pi\pi$ 4.2 GeV/c
1383.0 ±0.4	9361	AGUILAR-...	81D	HBC	$K^- p \to \Lambda 3\pi$ 4.2 GeV/c
1381.9 ±0.3	6900	CAMERON	78	HBC	$K^- p$ 0.96–1.36 GeV/c
1381 ±1	6846	BORENSTEIN	74	HBC	$K^- p$ 2.18 GeV/c
1383.5 ±0.85	2300	HABIBI	73	HBC	$K^- p \to \Lambda\pi\pi$
1382 ±2	400	AGUILAR-...	72B	HBC	$K^- p \to \Lambda\pi$'s
1384.4 ±1.0	1260	SIEGEL	67	HBC	$K^- p$ 2.1 GeV/c
1382 ±1	750	ARMENTEROS	65B	HBC	$K^- p$ 0.9–1.2 GeV/c
1381.0 ±1.6	859	HUWE	64	HBC	$K^- p$ 1.22 GeV/c
• • • We do not use the following data for averages, fits, limits, etc. • • •					
1385.1 ±1.2	600	BAKER	80	HYBR	$\pi^+ p$ 7 GeV/c
1383.2 ±1.0	750	BAKER	80	HYBR	$K^- p$ 7 GeV/c
1381 ±2	7k	[1] BAUBILLIER	79B	HBC	$K^- p$ 8.25 GeV/c
1391 ±2	2k	CAUTIS	79	HYBR	$\pi^+ p/K^- p$ 11.5 GeV
1390 ±2	100	[1] SUGAHARA	79B	HBC	$\pi^- p$ 6 GeV/c
1385 ±3	22k	[1,2] BARREIRO	77B	HBC	$K^- p$ 4.2 GeV/c
1385 ±1	2594	HOLMGREN	77	HBC	See AGUILAR-BENITEZ 81D
1380 ±2		[1] BARDADIN-...	75	HBC	$K^- p$ 14.3 GeV/c
1382 ±1	3740	[3] BERTHON	74	HBC	$K^- p$ 1263–1843 MeV/c
1390 ±6	46	AGUILAR-...	70B	HBC	$K^- p \to \Sigma\pi$'s 4 GeV/c
1383 ±8	62	[4] BIRMINGHAM	66	HBC	$K^- p$ 3.5 GeV/c
1378 ±5	135	LONDON	66	HBC	$K^- p$ 2.24 GeV/c
1384.3 ±1.9	250	[4] SMITH	65	HBC	$K^- p$ 1.8 GeV/c
1382.6 ±2.1	250	[4] SMITH	65	HBC	$K^- p$ 1.95 GeV/c
1375.0 ±3.9	170	COOPER	64	HBC	$K^- p$ 1.45 GeV/c
1376.0 ±3.9	154	[4] ELY	61	HLBC	$K^- p$ 1.11 GeV/c

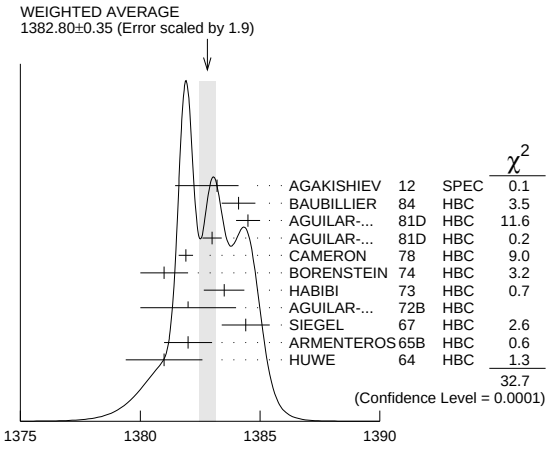

$\Sigma(1385)^0$ MASS

VALUE (MeV)	EVTS	DOCUMENT ID		TECN	COMMENT
1383.7±1.0 OUR AVERAGE		Error includes scale factor of 1.4. See the ideogram below.			
1384.1±0.8	5722	AGUILAR-...	81D	HBC	$K^- p \to \Lambda 3\pi$ 4.2 GeV/c
1380 ±2	3100	[5] BORENSTEIN	74	HBC	$K^- p \to \Lambda 3\pi$ 2.18 GeV/c
1385.1±2.5	240	[4] THOMAS	73	HBC	$\pi^- p \to \Lambda\pi^0 K^0$
• • • We do not use the following data for averages, fits, limits, etc. • • •					
1389 ±3	500	[6] BAUBILLIER	79B	HBC	$K^- p$ 8.25 GeV/c

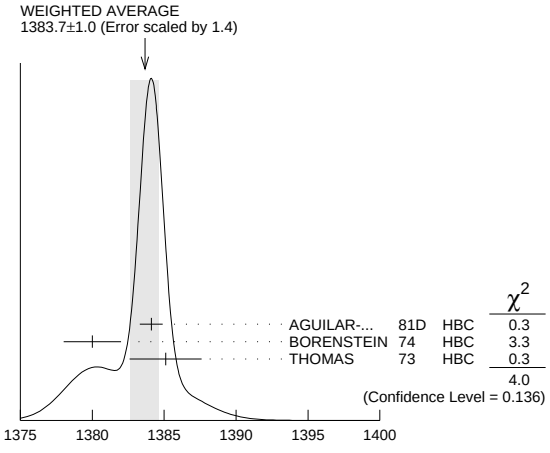

$\Sigma(1385)^-$ MASS

VALUE (MeV)	EVTS	DOCUMENT ID		TECN	COMMENT
1387.2±0.5 OUR AVERAGE		Error includes scale factor of 2.2. See the ideogram below.			
1388.3±1.7	620	AGUILAR-...	81D	HBC	$K^- p \to \Lambda\pi\pi$ 4.2 GeV/c
1384.9±0.8	3346	AGUILAR-...	81D	HBC	$K^- p \to \Lambda 3\pi$ 4.2 GeV/c
1387.6±0.3	9720	CAMERON	78	HBC	$K^- p$ 0.96–1.36 GeV/c
1383 ±2	2303	BORENSTEIN	74	HBC	$K^- p$ 2.18 GeV/c
1390.7±1.2	1900	HABIBI	73	HBC	$K^- p \to \Lambda\pi\pi$
1387.1±1.9	630	[4] THOMAS	73	HBC	$\pi^- p \to \Lambda\pi^- K^+$
1390.7±2.0	370	SIEGEL	67	HBC	$K^- p$ 2.1 GeV/c
1384 ±1	1380	ARMENTEROS	65B	HBC	$K^- p$ 0.9–1.2 GeV/c
1385.3±1.9	1086	[4] HUWE	64	HBC	$K^- p$ 1.15–1.30 GeV/c
• • • We do not use the following data for averages, fits, limits, etc. • • •					
1383 ±1	4.5k	[1] BAUBILLIER	79B	HBC	$K^- p$ 8.25 GeV/c
1380 ±6	150	[1] SUGAHARA	79B	HBC	$\pi^- p$ 6 GeV/c
1387 ±3	12k	[1,2] BARREIRO	77B	HBC	$K^- p$ 4.2 GeV/c
1391 ±3	193	HOLMGREN	77	HBC	See AGUILAR-BENITEZ 81D
1383 ±2		[1] BARDADIN-...	75	HBC	$K^- p$ 14.3 GeV/c
1389 ±1	3060	[3] BERTHON	74	HBC	$K^- p$ 1263–1843 MeV/c
1389 ±9	15	LONDON	66	HBC	$K^- p$ 2.24 GeV/c
1391.5±2.6	120	[4] SMITH	65	HBC	$K^- p$ 1.8 GeV/c
1399.8±2.2	58	[4] SMITH	65	HBC	$K^- p$ 1.95 GeV/c
1392.0±6.2	200	COOPER	64	HBC	$K^- p$ 1.45 GeV/c
1382 ±3	93	DAHL	61	DBC	$K^- d$ 0.45 GeV/c
1376.0±4.4	224	[4] ELY	61	HLBC	$K^- p$ 1.11 GeV/c

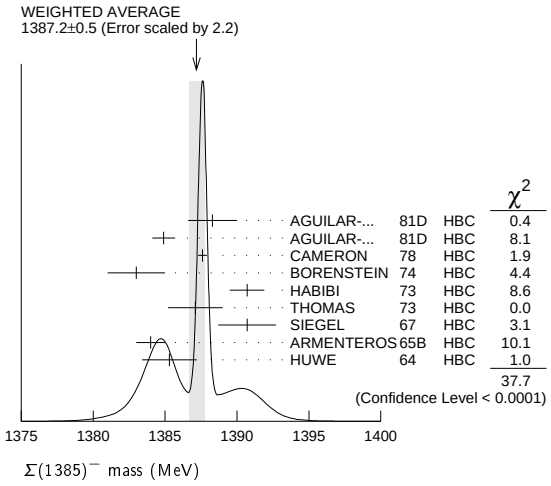

$m_{\Sigma(1385)^-} - m_{\Sigma(1385)^+}$

VALUE (MeV)	CL%	DOCUMENT ID		TECN	COMMENT
• • • We do not use the following data for averages, fits, limits, etc. • • •					
−2 to +6	95	[7] BORENSTEIN	74	HBC	$K^- p$ 2.18 GeV/c
7.2±1.4		[7] HABIBI	73	HBC	$K^- p \to \Lambda\pi\pi$
6.3±2.0		[7] SIEGEL	67	HBC	$K^- p$ 2.1 GeV/c
11 ±9		[7] LONDON	66	HBC	$K^- p$ 2.24 GeV/c
9 ±6		LONDON	66	HBC	$\Lambda 3\pi$ events
2.0±1.5		[7] ARMENTEROS	65B	HBC	$K^- p$ 0.9–1.2 GeV/c
7.2±2.1		[7] SMITH	65	HBC	$K^- p$ 1.8 GeV/c
17.2±2.0		[7] SMITH	65	HBC	$K^- p$ 1.95 GeV/c
17 ±7		[7] COOPER	64	HBC	$K^- p$ 1.45 GeV/c
4.3±2.2		[7] HUWE	64	HBC	$K^- p$ 1.22 GeV/c
0.0±4.2		[7] ELY	61	HLBC	$K^- p$ 1.11 GeV/c

$m_{\Sigma(1385)^0} - m_{\Sigma(1385)^+}$

VALUE (MeV)	CL%	DOCUMENT ID		TECN	COMMENT
• • • We do not use the following data for averages, fits, limits, etc. • • •					
−4 to +4	95	[7] BORENSTEIN	74	HBC	$K^- p$ 2.18 GeV/c

$m_{\Sigma(1385)^-} - m_{\Sigma(1385)^0}$

VALUE (MeV)	DOCUMENT ID		TECN	COMMENT
• • • We do not use the following data for averages, fits, limits, etc. • • •				
2.0±2.4	[7] THOMAS	73	HBC	$\pi^- p \to \Lambda\pi^- K^+$

$\Sigma(1385)$ WIDTHS

$\Sigma(1385)^+$ WIDTH

VALUE (MeV)	EVTS	DOCUMENT ID		TECN	COMMENT
36.0± 0.7 OUR AVERAGE					
40.2± 2.1 $^{+1.2}_{-2.8}$		AGAKISHIEV	12	SPEC	$pp \to \Sigma(1385)^+ K^+ n$, 3.5 GeV
37.2± 2.0	1897	BAUBILLIER	84	HBC	$K^- p$ 8.25 GeV/c
35.1± 1.7	5256	AGUILAR-...	81D	HBC	$K^- p \to \Lambda\pi\pi$ 4.2 GeV/c
37.5± 2.0	9361	AGUILAR-...	81D	HBC	$K^- p \to \Lambda 3\pi$ 4.2 GeV/c
35.5± 1.9	6900	CAMERON	78	HBC	$K^- p$ 0.96–1.36 GeV/c
34.0± 1.6	6846	[8] BORENSTEIN	74	HBC	$K^- p$ 2.18 GeV/c
38.3± 3.2	2300	[9] HABIBI	73	HBC	$K^- p \to \Lambda\pi\pi$
32.5± 6.0	400	AGUILAR-...	72B	HBC	$K^- p \to \Lambda\pi$'s
36 ± 4	1260	[9] SIEGEL	67	HBC	$K^- p$ 2.1 GeV/c
32.0± 4.7	750	[9] ARMENTEROS	65B	HBC	$K^- p$ 0.95–1.20 GeV/c
46.5± 6.4	859	[9] HUWE	64	HBC	$K^- p$ 1.15–1.30 GeV/c
• • • We do not use the following data for averages, fits, limits, etc. • • •					
40 ± 3	600	BAKER	80	HYBR	$\pi^+ p$ 7 GeV/c
37 ± 2	750	BAKER	80	HYBR	$K^- p$ 7 GeV/c
37 ± 2	7k	[1] BAUBILLIER	79B	HBC	$K^- p$ 8.25 GeV/c
30 ± 4	2k	CAUTIS	79	HYBR	$\pi^+ p/K^- p$ 11.5 GeV
30 ± 6	100	[1] SUGAHARA	79B	HBC	$\pi^- p$ 6 GeV/c
43 ± 5	22k	[1,2] BARREIRO	77B	HBC	$K^- p$ 4.2 GeV/c
34 ± 2	2594	HOLMGREN	77	HBC	See AGUILAR-BENITEZ 81D
40.0± 3.2		[1] BARDADIN-...	75	HBC	$K^- p$ 14.3 GeV/c
48 ± 3	3740	[3] BERTHON	74	HBC	$K^- p$ 1263–1843 MeV/c
33 ±20	46	[9] AGUILAR-...	70B	HBC	$K^- p \to \Sigma\pi$'s 4 GeV/c
25 ±32	62	[9] BIRMINGHAM	66	HBC	$K^- p$ 3.5 GeV/c
30.3± 7.5	250	[9] SMITH	65	HBC	$K^- p$ 1.8 GeV/c
33.1± 8.3	250	[9] SMITH	65	HBC	$K^- p$ 1.95 GeV/c
51 ±16	170	[9] COOPER	64	HBC	$K^- p$ 1.45 GeV/c
48 ±16	154	[9] ELY	61	HLBC	$K^- p$ 1.11 GeV/c

$\Sigma(1385)^0$ WIDTH

VALUE (MeV)	EVTS	DOCUMENT ID		TECN	COMMENT
36 ± 5 OUR AVERAGE					
34.8± 5.6	5722	AGUILAR-...	81D	HBC	$K^- p \to \Lambda 3\pi$ 4.2 GeV/c
39.3±10.2	240	[9] THOMAS	73	HBC	$\pi^- p \to \Lambda\pi^0 K^0$
• • • We do not use the following data for averages, fits, limits, etc. • • •					
53 ± 8	3100	[10] BORENSTEIN	74	HBC	$K^- p \to \Lambda 3\pi$ 2.18 GeV/c
30 ± 9	106	CURTIS	63	OSPK	$\pi^- p$ 1.5 GeV/c

$\Sigma(1385)^-$ WIDTH

VALUE (MeV)	EVTS	DOCUMENT ID		TECN	COMMENT
39.4± 2.1 OUR AVERAGE		Error includes scale factor of 1.7.			See the ideogram below.
38.4±10.7	620	AGUILAR-...	81D	HBC	$K^- p \to \Lambda\pi\pi$ 4.2 GeV/c
34.6± 4.2	3346	AGUILAR-...	81D	HBC	$K^- p \to \Lambda 3\pi$ 4.2 GeV/c
39.2± 1.7	9720	CAMERON	78	HBC	$K^- p$ 0.96–1.36 GeV/c
35 ± 3	2303	[8] BORENSTEIN	74	HBC	$K^- p$ 2.18 GeV/c
51.9± 4.8	1900	[9] HABIBI	73	HBC	$K^- p \to \Lambda\pi\pi$
48.2± 7.7	630	[9] THOMAS	73	HBC	$\pi^- p \to \Lambda\pi^- K^0$
31.0± 6.5	370	[9] SIEGEL	67	HBC	$K^- p$ 2.1 GeV/c
38.0± 4.1	1382	[9] ARMENTEROS	65B	HBC	$K^- p$ 0.95–1.20 GeV/c
62 ± 7	1086	HUWE	64	HBC	$K^- p$ 1.15–1.30 GeV/c
• • • We do not use the following data for averages, fits, limits, etc. • • •					
44 ± 4	4.5k	[1] BAUBILLIER	79B	HBC	$K^- p$ 8.25 GeV/c
58 ± 4	150	[1] SUGAHARA	79B	HBC	$\pi^- p$ 6 GeV/c
45 ± 5	12k	[1,2] BARREIRO	77B	HBC	$K^- p$ 4.2 GeV/c
35 ±10	193	HOLMGREN	77	HBC	See AGUILAR-BENITEZ 81D
47 ± 6		[1] BARDADIN-...	75	HBC	$K^- p$ 14.3 GeV/c
40 ± 3	3060	[3] BERTHON	74	HBC	$K^- p$ 1263–1843 MeV/c
29.2±10.6	120	[9] SMITH	65	HBC	$K^- p$ 1.80 GeV/c
17.1± 8.9	58	[9] SMITH	65	HBC	$K^- p$ 1.95 GeV/c
88 ±24	200	[9] COOPER	64	HBC	$K^- p$ 1.45 GeV/c
40		DAHL	61	DBC	$K^- d$ 0.45 GeV/c
66 ±18	224	[9] ELY	61	HLBC	$K^- p$ 1.11 GeV/c

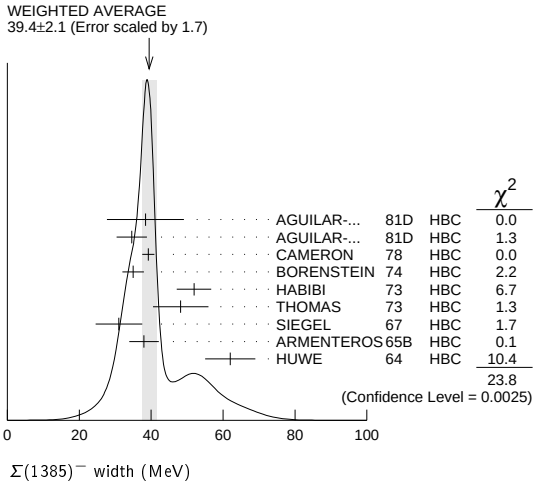

$\Sigma(1385)$ POLE POSITIONS

$\Sigma(1385)^+$ REAL PART

VALUE	DOCUMENT ID	COMMENT
1379±1	LICHTENBERG74	Extrapolates HABIBI 73

$\Sigma(1385)^+$ −IMAGINARY PART

VALUE	DOCUMENT ID	COMMENT
17.5±1.5	LICHTENBERG74	Extrapolates HABIBI 73

$\Sigma(1385)^-$ REAL PART

VALUE	DOCUMENT ID	COMMENT
1383±1	LICHTENBERG74	Extrapolates HABIBI 73

$\Sigma(1385)^-$ −IMAGINARY PART

VALUE	DOCUMENT ID	COMMENT
22.5±1.5	LICHTENBERG74	Extrapolates HABIBI 73

Baryon Particle Listings

$\Sigma(1385)$, $\Sigma(1480)$ Bumps

$\Sigma(1385)$ DECAY MODES

	Mode	Fraction (Γ_i/Γ)	Confidence level
Γ_1	$\Lambda\pi$	(87.0 ±1.5) %	
Γ_2	$\Sigma\pi$	(11.7 ±1.5) %	
Γ_3	$\Lambda\gamma$	($1.25^{+0.13}_{-0.12}$) %	
Γ_4	$\Sigma^+\gamma$	(7.0 ±1.7) $\times 10^{-3}$	
Γ_5	$\Sigma^-\gamma$	< 2.4 $\times 10^{-4}$	90%
Γ_6	$N\overline{K}$		

The above branching fractions are our estimates, not fits or averages.

$\Sigma(1385)$ BRANCHING RATIOS

$\Gamma(\Sigma\pi)/\Gamma(\Lambda\pi)$ Γ_2/Γ_1

VALUE	DOCUMENT ID		TECN	CHG	COMMENT
0.135±0.011 OUR AVERAGE					
0.20 ±0.06	DIONISI	78B	HBC	±	$K^- p \to Y^* K\overline{K}$
0.16 ±0.03	BERTHON	74	HBC	+	$K^- p$ 1.26–1.84 GeV/c
0.11 ±0.02	BERTHON	74	HBC	−	$K^- p$ 1.26–1.84 GeV/c
0.21 ±0.05	BORENSTEIN	74	HBC	+	$K^- p \to \Lambda\pi^+\pi^-$, $\Sigma^0\pi^+\pi^-$
0.18 ±0.04	MAST	73	MPWA	±	$K^- p \to \Lambda\pi^+\pi^-$, $\Sigma^0\pi^+\pi^-$
0.10 ±0.05	THOMAS	73	HBC	−	$\pi^- p \to \Lambda K\pi$, $\Sigma K\pi$
0.16 ±0.07	AGUILAR-...	72B	HBC	+	$K^- p$ 3.9, 4.6 GeV/c
0.13 ±0.04	COLLEY	71B	DBC	−0	K^- N 1.5 GeV/c
0.13 ±0.04	PAN	69	HBC	+	$\pi^+ p \to \Lambda K\pi$, $\Sigma K\pi$
0.08 ±0.06	LONDON	66	HBC	+	$K^- p$ 2.24 GeV/c
0.163±0.041	ARMENTEROS	65B	HBC	±	$K^- p$ 0.95–1.20 GeV/c
0.09 ±0.04	HUWE	64	HBC	±	$K^- p$ 1.2–1.7 GeV
• • • We do not use the following data for averages, fits, limits, etc. • • •					
<0.04	ALSTON	62	HBC	±0	$K^- p$ 1.15 GeV/c
0.04 ±0.04	BASTIEN	61	HBC	±	

$\Gamma(\Lambda\gamma)/\Gamma(\Lambda\pi)$ Γ_3/Γ_1

This ratio is of course for $\Sigma(1385)^0 \to \Lambda\gamma$ and $\Lambda\pi^0$.

VALUE (units 10^{-2})	EVTS	DOCUMENT ID		TECN	COMMENT
$1.43^{+0.15}_{-0.13}$ OUR AVERAGE					
$1.42\pm0.12^{+0.11}_{-0.07}$	624 ± 25	KELLER	11	CLAS	$\gamma p \to K^+\Lambda$, E_γ 1.6–3.8 GeV
$1.53\pm0.39^{+0.15}_{-0.24}$	61	TAYLOR	05	CLAS	$\gamma p \to K^+\Lambda\gamma$

$\Gamma(\Sigma^+\gamma)/\Gamma(\Sigma\pi)$ Γ_4/Γ_2

This ratio is for $\Sigma(1385)^+ \to \Sigma^+\gamma$ over $\Sigma(1385)^+ \to \Sigma\pi$.

VALUE (%)	DOCUMENT ID		TECN	COMMENT
$5.98\pm1.11^{+0.27}_{-0.61}$	[11] KELLER	12	CLAS	$\gamma p \to K^0\Sigma(1385)^+$

$\Gamma(\Sigma^-\gamma)/\Gamma_{total}$ Γ_5/Γ

VALUE	CL%	DOCUMENT ID		TECN	CHG	COMMENT
<2.4 × 10⁻⁴	90	[12] MOLCHANOV	04	SELX	−	Σ^- Pb → $\Sigma(1385)^-$ Pb, 600 GeV
• • • We do not use the following data for averages, fits, limits, etc. • • •						
$<6.1\times10^{-4}$	90	[13] ARIK	77	SPEC	−	Σ^- Pb → $\Sigma(1385)^-$ Pb, 23 GeV

$(\Gamma_i\Gamma_f)^{1/2}/\Gamma_{total}$ in $N\overline{K} \to \Sigma(1385) \to \Lambda\pi$ $(\Gamma_6\Gamma_1)^{1/2}/\Gamma$

VALUE	DOCUMENT ID		CHG	COMMENT
+0.586±0.319	[14] DEVENISH	74B	0	Fixed-t dispersion rel.

$\Sigma(1385)$ FOOTNOTES

[1] From fit to inclusive $\Lambda\pi$ spectrum.
[2] Includes data of HOLMGREN 77.
[3] The errors are statistical only. The resolution is not unfolded.
[4] The error is enlarged to $\Gamma/\sqrt{N}$. See the note on the $K^*(892)$ mass in the 1984 edition.
[5] From a fit to $\Lambda\pi^0$ with the width fixed at 34 MeV.
[6] From fit to inclusive $\Lambda\pi^0$ spectrum with the width fixed at 40 MeV.
[7] Redundant with data in the mass Listings.
[8] Results from $\Lambda\pi^+\pi^-$ and $\Lambda\pi^+\pi^-\pi^0$ combined by us.
[9] The error is enlarged to $4\Gamma/\sqrt{N}$. See the note on the $K^*(892)$ mass in the 1984 edition.
[10] Consistent with +, 0, and − widths equal.
[11] KELLER 12 gives $\Gamma(\Sigma^+\gamma)/\Gamma(\Sigma^+\pi^0) = (11.95 \pm 2.21^{+0.53}_{-1.21})\%$, using 1/2 our total $\Sigma(1385) \to \Sigma\pi$ fraction for $\Sigma^+\pi^0$. We divide the KELLER 12 value by two.
[12] We calculate this from the MOLCHANOV 04 upper limit of 9.5 keV on the $\Sigma^-\gamma$ width.
[13] We calculate this from the ARIK 77 upper limit of 24 keV on the $\Sigma^-\gamma$ width.
[14] An extrapolation of the parametrized amplitude below threshold.

$\Sigma(1385)$ REFERENCES

AGAKISHIEV	12	PR C85 035203	G. Agakishiev *et al.* (HADES Collab.)
KELLER	12	PR D85 052004	D. Keller *et al.* (JLab CLAS Collab.)
KELLER	11	PR D83 072004	D. Keller *et al.* (CLAS Collab.)
TAYLOR	05	PR C71 054609	S. Taylor *et al.* (JLab CLAS Collab.)
Also		PR C72 039902 (errat.)	S. Taylor *et al.* (JLab CLAS Collab.)
MOLCHANOV	04	PL B590 161	V.V. Molchanov *et al.* (FNAL SELEX Collab.)
BAUBILLIER	84	ZPHY C23 213	M. Baubillier *et al.* (BIRM, CERN, GLAS+)
PDG	84	RMP 56 S1	C.G. Wohl *et al.* (LBL, CIT, CERN)
AGUILAR-...	81D	AFIS A77 144	M. Aguilar-Benitez, J. Salicio (MADR)
BAKER	80	NP B166 207	P.A. Baker *et al.* (LOIC)
BAUBILLIER	79B	NP B148 18	M. Baubillier *et al.* (BIRM, CERN, GLAS+)
CAUTIS	79	NP B156 507	C.V. Cautis *et al.* (SLAC)
SUGAHARA	79B	NP B156 237	R. Sugahara *et al.* (KEK, OSKC, KINK)
CAMERON	78	NP B143 189	W. Cameron *et al.* (RHEL, LOIC)
DIONISI	78B	PL 78B 154	C. Dionisi, R. Armenteros, J. Diaz (CERN, AMST+)
ARIK	77	PRL 38 1000	E. Arik *et al.* (PITT, BNL, MASA)
BARREIRO	77B	NP B126 319	F. Barreiro *et al.* (CERN, AMST, NIJM)
HOLMGREN	77	NP B119 261	S.O. Holmgren *et al.* (CERN, AMST, NIJM)
BARDADIN-...	75	NP B98 418	M. Bardadin-Otwinowska *et al.* (SACL, EPOL+)
BERTHON	74	NC 21A 146	A. Berthon *et al.* (CDEF, RHEL, SACL+)
BORENSTEIN	74	PR D9 3006	S.R. Borenstein *et al.* (BNL, MICH)
DEVENISH	74B	NP B81 330	R.C.E. Devenish, C.D. Froggatt, B.R. Martin (DESY+)
LICHTENBERG	74	PR D10 3865	D.B. Lichtenberg (IND)
Also		Private Comm.	D.B. Lichtenberg (IND)
HABIBI	73	Thesis Nevis 199	M. Habibi (COLU)
Also		Purdue Conf. 387	C. Baltay *et al.* (COLU, BING)
MAST	73	PR D7 3212	T.S. Mast *et al.* (LBL) IJP
Also		PR D7 5	T.S. Mast *et al.* (LBL) IJP
THOMAS	73	NP B56 15	D.W. Thomas *et al.* (CMU) JP
AGUILAR-...	72B	PR D6 29	M. Aguilar-Benitez *et al.* (BNL)
COLLEY	71B	NP B31 61	D.C. Colley *et al.* (BIRM, EDIN, GLAS+)
AGUILAR-...	70B	PRL 25 58	M. Aguilar-Benitez *et al.* (BNL, SYRA)
PAN	69	PRL 23 808	Y.L. Pan, F.L. Forman (PENN) I
SIEGEL	67	Thesis UCRL 18041	D.M. Siegel (LRL)
BIRMINGHAM	66	PR 152 1148	M. Haque *et al.* (BIRM, GLAS, LOIC, OXF+)
LONDON	66	PR 143 1034	G.W. London *et al.* (BNL, SYRA) J
ARMENTEROS	65B	PL 19 75	R. Armenteros *et al.* (CERN, HEID, SACL)
SMITH	65	Thesis UCLA	L.T. Smith (UCLA)
COOPER	64	PL 8 365	W.A. Cooper *et al.* (CERN, AMST)
HUWE	64	Thesis UCRL 11291	D.O. Huwe (LRL) JP
Also		PR 181 1824	D.O. Huwe (LRL)
CURTIS	63	PR 132 1771	L.J. Curtis *et al.* (MICH) J
ALSTON	62	CERN Conf. 311	M.H. Alston *et al.* (LRL)
BASTIEN	61	PRL 6 702	P.L. Bastien, M. Ferro-Luzzi, A.H. Rosenfeld (LRL)
DAHL	61	PRL 6 142	O.I. Dahl *et al.* (LRL)
ELY	61	PRL 7 461	R.P. Ely *et al.* (LRL) J
ALSTON	60	PRL 5 520	M.H. Alston *et al.* (LRL) I

$\Sigma(1480)$ Bumps

$I(J^P) = 1(?^?)$ Status: *

OMITTED FROM SUMMARY TABLE

These are peaks seen in $\Lambda\pi$ and $\Sigma\pi$ spectra in the reaction $\pi^+ p \to (Y\pi)K^+$ at 1.7 GeV/c. Also, the Y polarization oscillates in the same region.

MILLER 70 suggests a possible alternate explanation in terms of a reflection of $N(1675) \to \Lambda K$ decay. However, such an explanation for the $(\Sigma^+\pi^0)K^+$ channel in terms of $\Delta(1650) \to \Sigma K$ decay seems unlikely (see PAN 70). In addition such reflections would also have to account for the oscillation of the Y polarization in the 1480 MeV region.

HANSON 71, with less data than PAN 70, can neither confirm nor deny the existence of this state. MAST 75 sees no structure in this region in $K^- p \to \Lambda\pi^0$.

ENGELEN 80 performs a multichannel analysis of $K^- p \to p\overline{K}^0\pi^-$ at 4.2 GeV/c. They observe a 3.5 standard-deviation signal at 1480 MeV in $p\overline{K}^0$ which cannot be explained as a reflection of any competing channel.

PRAKHOV 04 sees no evidence for this or other light Σ resonances, aside from the $\Sigma(1385)$, in $K^- p \to \Lambda\pi^0\pi^0$.

ZYCHOR 06 finds peaks in $pp \to pK^+(\pi^\pm X^\mp)$ at p_{beam} = 3.65 GeV/c.

$\Sigma(1480)$ MASS (PRODUCTION EXPERIMENTS)

VALUE (MeV)	EVTS	DOCUMENT ID		TECN	COMMENT
≈ 1480 OUR ESTIMATE					
1480±15	365 ± 60	ZYCHOR	06	SPEC	$pp \to pK^+(\pi^\pm X^\mp)$
1480	120	ENGELEN	80	HBC	$K^- p \to (p\overline{K}^0)\pi^-$
1485±10		CLINE	73	MPWA	$K^- d \to (\Lambda\pi^-)p$
1479±10		PAN	70	HBC	$\pi^+ p \to (\Lambda\pi^+)K^+$
1465±15		PAN	70	HBC	$\pi^+ p \to (\Sigma\pi)K^+$

$\Sigma(1480)$ WIDTH (PRODUCTION EXPERIMENTS)

VALUE (MeV)	EVTS	DOCUMENT ID		TECN	COMMENT
60±15	365 ± 60	ZYCHOR	06	SPEC	$pp \to pK^+(\pi^\pm X^\mp)$
80±20	120	ENGELEN	80	HBC	$K^- p \to (p\overline{K}^0)\pi^-$
40±20		CLINE	73	MPWA	$K^- d \to (\Lambda\pi^-)p$
31±15		PAN	70	HBC	$\pi^+ p \to (\Lambda\pi^+)K^+$
30±20		PAN	70	HBC	$\pi^+ p \to (\Sigma\pi)K^+$

$\Sigma(1480)$ DECAY MODES (PRODUCTION EXPERIMENTS)

	Mode
Γ_1	$N\overline{K}$
Γ_2	$\Lambda\pi$
Γ_3	$\Sigma\pi$

$\Sigma(1480)$ BRANCHING RATIOS (PRODUCTION EXPERIMENTS)

$\Gamma(\Sigma\pi)/\Gamma(\Lambda\pi)$ Γ_3/Γ_2

VALUE	DOCUMENT ID		TECN	CHG
0.82 ± 0.51	PAN	70	HBC	+

$\Gamma(N\overline{K})/\Gamma(\Lambda\pi)$ Γ_1/Γ_2

VALUE	DOCUMENT ID		TECN	CHG
0.72 ± 0.50	PAN	70	HBC	+

$\Gamma(N\overline{K})/\Gamma_{\text{total}}$ Γ_1/Γ

VALUE	DOCUMENT ID		TECN	COMMENT
small	CLINE	73	MPWA	$K^-d \rightarrow (\Lambda\pi^-)p$

$\Sigma(1480)$ REFERENCES (PRODUCTION EXPERIMENTS)

ZYCHOR	06	PRL 96 012002	I. Zychor *et al.*	(ANKE Collab.)
PRAKHOV	04	PR C69 042202	S. Prakhov *et al.*	(BNL Crystal Ball Collab.)
ENGELEN	80	NP B167 61	J.J. Engelen *et al.*	(NIJM, AMST, CERN+)
MAST	75	PR D11 3078	T.S. Mast *et al.*	(LBL)
CLINE	73	LNC 6 205	D. Cline, R. Laumann, J. Mapp	(WISC) IJP
HANSON	71	PR D4 1296	P. Hanson, G.E. Kalmus, J. Louie	(LBL) I
MILLER	70	Duke Conf. 229	D.H. Miller	(PURD)
Hyperon Resonances, 1970				
PAN	70	PR D2 449	Y.L. Pan *et al.*	(PENN)
Also		PRL 23 808	Y.L. Pan, F.L. Forman	(PENN) I
Also		PRL 23 806	Y.L. Pan, F.L. Forman	(PENN) I

$\Sigma(1560)$ Bumps

$I(J^P) = 1(?^?)$ Status: **

OMITTED FROM SUMMARY TABLE

This entry lists peaks reported in mass spectra around 1560 MeV without implying that they are necessarily related.

DIONISI 78B observes a 6 standard-deviation enhancement at 1553 MeV in the charged $\Lambda/\Sigma\pi$ mass spectra from $K^-p \rightarrow (\Lambda/\Sigma)\pi K\overline{K}$ at 4.2 GeV/c. In a CERN ISR experiment, LOCKMAN 78 reports a narrow 6 standard-deviation enhancement at 1572 MeV in $\Lambda\pi^{\pm}$ from the reaction $pp \rightarrow \Lambda\pi^+\pi^-X$. These enhancements are unlikely to be associated with the $\Sigma(1580)$ (which has not been confirmed by several recent experiments – see the next entry in the Listings).

CARROLL 76 observes a bump at 1550 MeV (as well as one at 1580 MeV) in the isospin-1 $\overline{K}N$ total cross section, but uncertainties in cross section measurements outside the mass range of the experiment preclude estimating its significance.

See also MEADOWS 80 for a review of this state.

$\Sigma(1560)$ MASS (PRODUCTION EXPERIMENTS)

VALUE (MeV)	EVTS	DOCUMENT ID		TECN	CHG	COMMENT
≈ 1560 OUR ESTIMATE						
1553 ± 7	121	DIONISI	78B	HBC	±	$K^-p \rightarrow (Y\pi)K\overline{K}$
1572 ± 4	40	LOCKMAN	78	SPEC	±	$pp \rightarrow \Lambda\pi^+\pi^-X$

$\Sigma(1560)$ WIDTH (PRODUCTION EXPERIMENTS)

VALUE (MeV)	EVTS	DOCUMENT ID		TECN	CHG	COMMENT
79 ± 30	121	DIONISI	78B	HBC	±	$K^-p \rightarrow (Y\pi)K\overline{K}$
15 ± 6	40	[1] LOCKMAN	78	SPEC	±	$pp \rightarrow \Lambda\pi^+\pi^-X$

$\Sigma(1560)$ DECAY MODES (PRODUCTION EXPERIMENTS)

	Mode	Fraction (Γ_i/Γ)
Γ_1	$\Lambda\pi$	seen
Γ_2	$\Sigma\pi$	

$\Sigma(1560)$ BRANCHING RATIOS (PRODUCTION EXPERIMENTS)

$\Gamma(\Sigma\pi)/[\Gamma(\Lambda\pi)+\Gamma(\Sigma\pi)]$ $\Gamma_2/(\Gamma_1+\Gamma_2)$

VALUE	DOCUMENT ID		TECN	CHG	COMMENT
0.35 ± 0.12	DIONISI	78B	HBC	±	$K^-p \rightarrow (Y\pi)K\overline{K}$

$\Gamma(\Lambda\pi)/\Gamma_{\text{total}}$ Γ_1/Γ

VALUE	DOCUMENT ID		TECN	CHG	COMMENT
seen	LOCKMAN	78	SPEC	±	$pp \rightarrow \Lambda\pi^+\pi^-X$

$\Sigma(1560)$ FOOTNOTES (PRODUCTION EXPERIMENTS)

[1] The width observed by LOCKMAN 78 is consistent with experimental resolution.

$\Sigma(1560)$ REFERENCES (PRODUCTION EXPERIMENTS)

MEADOWS	80	Toronto Conf. 283	B.T. Meadows	(CINC)
DIONISI	78B	PL 78B 154	C. Dionisi, R. Armenteros, J. Diaz	(CERN, AMST+) I
LOCKMAN	78	Saclay DPHPE 78-01	W. Lockman *et al.*	(UCLA, SACL)
CARROLL	76	PRL 37 806	A.S. Carroll *et al.*	(BNL) I

$\Sigma(1580)$ $3/2^-$

$I(J^P) = 1(\frac{3}{2}^-)$ Status: *

OMITTED FROM SUMMARY TABLE

Seen in the isospin-1 $\overline{K}N$ cross section at BNL (LI 73, CARROLL 76) and in a partial-wave analysis of $K^-p \rightarrow \Lambda\pi^0$ for c.m. energies 1560–1600 MeV by LITCHFIELD 74. LITCHFIELD 74 finds $J^P = 3/2^-$. Not seen by ENGLER 78 or by CAMERON 78C (with larger statistics in $K^0_Lp \rightarrow \Lambda\pi^+$ and $\Sigma^0\pi^+$).

Neither OLMSTED 04 (in $K^-p \rightarrow \Lambda\pi^0$) nor PRAKHOV 04 (in $K^-p \rightarrow \Lambda\pi^0\pi^0$) see any evidence for this state.

$\Sigma(1580)$ MASS

VALUE (MeV)	DOCUMENT ID		TECN	COMMENT
≈ 1580 OUR ESTIMATE				
1583 ± 4	[1] CARROLL	76	DPWA	Isospin-1 total σ
1582 ± 4	[2] LITCHFIELD	74	DPWA	$K^-p \rightarrow \Lambda\pi^0$

$\Sigma(1580)$ WIDTH

VALUE (MeV)	DOCUMENT ID		TECN	COMMENT
15	[1] CARROLL	76	DPWA	Isospin-1 total σ
11 ± 4	[2] LITCHFIELD	74	DPWA	$K^-p \rightarrow \Lambda\pi^0$

$\Sigma(1580)$ DECAY MODES

	Mode
Γ_1	$N\overline{K}$
Γ_2	$\Lambda\pi$
Γ_3	$\Sigma\pi$

$\Sigma(1580)$ BRANCHING RATIOS

See "Sign conventions for resonance couplings" in the Note on Λ and Σ Resonances.

$\Gamma(N\overline{K})/\Gamma_{\text{total}}$ Γ_1/Γ

VALUE	DOCUMENT ID		TECN	COMMENT
$+0.03\pm0.01$	[2] LITCHFIELD	74	DPWA	$\overline{K}N$ multichannel

$(\Gamma_i\Gamma_f)^{1/2}/\Gamma_{\text{total}}$ in $N\overline{K} \rightarrow \Sigma(1580) \rightarrow \Lambda\pi$ $(\Gamma_1\Gamma_2)^{1/2}/\Gamma$

VALUE	DOCUMENT ID		TECN	COMMENT
not seen	CAMERON	78C	HBC	$K^0_Lp \rightarrow \Lambda\pi^+$
not seen	ENGLER	78	HBC	$K^0_Lp \rightarrow \Lambda\pi^+$
$+0.10\pm0.02$	[2] LITCHFIELD	74	DPWA	$K^-p \rightarrow \Lambda\pi^0$

$(\Gamma_i\Gamma_f)^{1/2}/\Gamma_{\text{total}}$ in $N\overline{K} \rightarrow \Sigma(1580) \rightarrow \Sigma\pi$ $(\Gamma_1\Gamma_3)^{1/2}/\Gamma$

VALUE	DOCUMENT ID		TECN	COMMENT
not seen	CAMERON	78C	HBC	$K^0_Lp \rightarrow \Sigma^0\pi^+$
not seen	ENGLER	78	HBC	$K^0_Lp \rightarrow \Sigma^0\pi^+$
$+0.03\pm0.04$	[2] LITCHFIELD	74	DPWA	$\overline{K}N$ multichannel

Baryon Particle Listings

$\Sigma(1580)$, $\Sigma(1620)$, $\Sigma(1620)$ Production Experiments

$\Sigma(1580)$ FOOTNOTES

[1] CARROLL 76 sees a total-cross-section bump with $(J+1/2)\ \Gamma_{el}\ /\ \Gamma_{total} = 0.06$.

[2] The main effect observed by LITCHFIELD 74 is in the $\Lambda\pi$ final state; the $\overline{K}N$ and $\Sigma\pi$ couplings are estimated from a multichannel fit including total-cross-section data of LI 73.

$\Sigma(1580)$ REFERENCES

OLMSTED	04	PL B588 29	J. Olmsted *et al.*	(BNL Crystal Ball Collab.)
PRAKHOV	04	PR C69 042202	S. Prakhov *et al.*	(BNL Crystal Ball Collab.)
CAMERON	78C	NP B132 189	W. Cameron *et al.*	(BGNA, EDIN, GLAS+) I
ENGLER	78	PR D18 3061	A. Engler *et al.*	(CMU, ANL)
CARROLL	76	PRL 37 806	A.S. Carroll *et al.*	(BNL) I
LITCHFIELD	74	PL 51B 509	P.J. Litchfield	(CERN) IJP
LI	73	Purdue Conf. 283	K.K. Li	(BNL) I

$\Sigma(1620)\ 1/2^-$

$I(J^P) = 1(\frac{1}{2}^-)$ Status: *

OMITTED FROM SUMMARY TABLE

The S_{11} state at 1697 MeV reported by VANHORN 75 is tentatively listed under the $\Sigma(1750)$. CARROLL 76 sees two bumps in the isospin-1 total cross section near this mass. GAO 12 sees no evidence for this resonance.

Production experiments are listed separately in the next entry.

$\Sigma(1620)$ MASS

VALUE (MeV)		DOCUMENT ID		TECN	COMMENT
≈ 1620 OUR ESTIMATE					
1600±15		ZHANG	13A	DPWA	Multichannel
1600± 6	[1]	MORRIS	78	DPWA	$K^-n \to \Lambda\pi^-$
1608± 5	[2]	CARROLL	76	DPWA	Isospin-1 total σ
1633±10	[3]	CARROLL	76	DPWA	Isospin-1 total σ
1630±10		LANGBEIN	72	IPWA	$\overline{K}N$ multichannel
1620		KIM	71	DPWA	K-matrix analysis

$\Sigma(1620)$ WIDTH

VALUE (MeV)		DOCUMENT ID		TECN	COMMENT
400±152		ZHANG	13A	DPWA	Multichannel
87± 19	[1]	MORRIS	78	DPWA	$K^-n \to \Lambda\pi^-$
15	[2]	CARROLL	76	DPWA	Isospin-1 total σ
10	[3]	CARROLL	76	DPWA	Isospin-1 total σ
65± 20		LANGBEIN	72	IPWA	$\overline{K}N$ multichannel
40		KIM	71	DPWA	K-matrix analysis

$\Sigma(1620)$ POLE POSITION

REAL PART

VALUE (MeV)	DOCUMENT ID		TECN	COMMENT
• • • We do not use the following data for averages, fits, limits, etc. • • •				
1501	ZHANG	13A	DPWA	Multichannel

$-2\times$IMAGINARY PART

VALUE (MeV)	DOCUMENT ID		TECN	COMMENT
• • • We do not use the following data for averages, fits, limits, etc. • • •				
171	ZHANG	13A	DPWA	Multichannel

$\Sigma(1620)$ DECAY MODES

	Mode
Γ_1	$N\overline{K}$
Γ_2	$\Lambda\pi$
Γ_3	$\Sigma\pi$

$\Sigma(1620)$ BRANCHING RATIOS

$\Gamma(N\overline{K})/\Gamma_{total}$ Γ_1/Γ

VALUE	DOCUMENT ID		TECN	COMMENT
0.59±0.10	ZHANG	13A	DPWA	Multichannel
0.22±0.02	LANGBEIN	72	IPWA	$\overline{K}N$ multichannel
0.05	KIM	71	DPWA	K-matrix analysis

$(\Gamma_i\Gamma_f)^{1/2}/\Gamma_{total}$ in $N\overline{K} \to \Sigma(1620) \to \Lambda\pi$ $(\Gamma_1\Gamma_2)^{1/2}/\Gamma$

VALUE	DOCUMENT ID		TECN	COMMENT
0.12±0.02	[1] MORRIS	78	DPWA	$K^-n \to \Lambda\pi^-$
not seen	BAILLON	75	IPWA	$\overline{K}N \to \Lambda\pi$
0.15	KIM	71	DPWA	K-matrix analysis

$(\Gamma_i\Gamma_f)^{1/2}/\Gamma_{total}$ in $N\overline{K} \to \Sigma(1620) \to \Sigma\pi$ $(\Gamma_1\Gamma_3)^{1/2}/\Gamma$

VALUE	DOCUMENT ID		TECN	COMMENT
+0.32±0.03	ZHANG	13A	DPWA	Multichannel
not seen	HEPP	76B	DPWA	$K^-N \to \Sigma\pi$
+0.40±0.06	LANGBEIN	72	IPWA	$\overline{K}N$ multichannel
+0.08	KIM	71	DPWA	K-matrix analysis

$\Sigma(1620)$ FOOTNOTES

[1] MORRIS 78 obtains an equally good fit without including this resonance.

[2] Total cross-section bump with $(J+1/2)\ \Gamma_{el}\ /\ \Gamma_{total}$ is 0.06 seen by CARROLL 76.

[3] Total cross-section bump with $(J+1/2)\ \Gamma_{el}\ /\ \Gamma_{total}$ is 0.04 seen by CARROLL 76.

$\Sigma(1620)$ REFERENCES

ZHANG	13A	PR C88 035205	H. Zhang *et al.*	(KSU)
GAO	12	PR C86 025201	P. Gao, J. Shi, B.S. Zou	(BHEP, BEIJT)
Also		NP A867 41	P. Gao, B.S. Zou, A. Sibirtsev	(BHEP, BEIJT+)
MORRIS	78	PR D17 55	W.A. Morris *et al.*	(FSU) IJP
CARROLL	76	PRL 37 806	A.S. Carroll *et al.*	(BNL) I
HEPP	76B	PL 65B 487	V. Hepp *et al.*	(CERN, HEIDH, MPIM) IJP
BAILLON	75	NP B94 39	P.H. Baillon, P.J. Litchfield	(CERN, RHEL) IJP
VANHORN	75	NP B87 145	A.J. van Horn	(LBL) IJP
Also		NP B87 157	A.J. van Horn	(LBL) IJP
LANGBEIN	72	NP B47 477	W. Langbein, F. Wagner	(MPIM) IJP
KIM	71	PRL 27 356	J.K. Kim	(HARV) IJP
Also		Duke Conf. 161 Hyperon Resonances, 1970	J.K. Kim	(HARV) IJP

$\Sigma(1620)$ Production Experiments

$I(J^P) = 1(?^?)$

OMITTED FROM SUMMARY TABLE

Formation experiments are listed separately in the previous entry.

The results of CRENNELL 69B at 3.9 GeV/c are not confirmed by SABRE 70 at 3.0 GeV/c. However, at 4.5 GeV/c, AMMANN 70 sees a peak at 1642 MeV which on the basis of branching ratios they do not associate with the $\Sigma(1670)$. See MILLER 70 for a review of these conflicts.

$\Sigma(1620)$ MASS (PRODUCTION EXPERIMENTS)

VALUE (MeV)	EVTS	DOCUMENT ID		TECN	CHG	COMMENT
≈ 1620 OUR ESTIMATE						
1642±12		AMMANN	70	DBC		K^-N 4.5 GeV/c
1618± 3	20	BLUMENFELD	69	HBC	+	$K^0_L p$
1619± 8		CRENNELL	69B	DBC	±	$K^-N \to \Lambda\pi\pi\pi$
• • • We do not use the following data for averages, fits, limits, etc. • • •						
1616± 8		CRENNELL	68	DBC	±	See CRENNELL 69B

$\Sigma(1620)$ WIDTH (PRODUCTION EXPERIMENTS)

VALUE (MeV)	EVTS	DOCUMENT ID		TECN	CHG	COMMENT
55±24		AMMANN	70	DBC		K^-N 4.5 GeV/c
30±10	20	BLUMENFELD	69	HBC	+	
72^{+22}_{-15}		CRENNELL	69B	DBC	±	
• • • We do not use the following data for averages, fits, limits, etc. • • •						
66±16		CRENNELL	68	DBC	±	See CRENNELL 69B

$\Sigma(1620)$ DECAY MODES (PRODUCTION EXPERIMENTS)

	Mode
Γ_1	$N\overline{K}$
Γ_2	$\Lambda\pi$
Γ_3	$\Sigma\pi$
Γ_4	$\Lambda\pi\pi$
Γ_5	$\Sigma(1385)\pi$
Γ_6	$\Lambda(1405)\pi$

$\Sigma(1620)$ BRANCHING RATIOS (PRODUCTION EXPERIMENTS)

$\Gamma(\Lambda\pi\pi)/\Gamma(\Lambda\pi)$ Γ_4/Γ_2

VALUE	EVTS	DOCUMENT ID	TECN	CHG
~ 2.5	14	BLUMENFELD 69	HBC	+

$\Gamma(N\overline{K})/\Gamma(\Lambda\pi)$ Γ_1/Γ_2

VALUE	DOCUMENT ID		TECN	CHG	COMMENT
0.4±0.4	AMMANN	70	DBC		K^-p 4.5 GeV/c
0.0±0.1	CRENNELL	68	DBC	+	See CRENNELL 69B

$\Gamma(\Lambda\pi)/\Gamma_{total}$ Γ_2/Γ

VALUE	DOCUMENT ID		TECN	CHG
large	CRENNELL	68	DBC	±

$\Gamma(\Sigma(1385)\pi)/\Gamma(\Lambda\pi)$ Γ_5/Γ_2

VALUE	CL%	DOCUMENT ID		TECN	CHG	COMMENT
<0.3	95	AMMANN	70	DBC		K^-p 4.5 GeV/c
0.2±0.1		CRENNELL	68	DBC	±	

$\Gamma(\Sigma\pi)/\Gamma(\Lambda\pi)$ Γ_3/Γ_2

VALUE	CL%	DOCUMENT ID		TECN	COMMENT
<1.1	95	AMMANN	70	DBC	K^-N 4.5 GeV/c

$\Gamma(\Lambda(1405)\pi)/\Gamma(\Lambda\pi)$ Γ_6/Γ_2

VALUE	DOCUMENT ID		TECN	COMMENT
0.7±0.4	AMMANN	70	DBC	K^-p 4.5 GeV/c

$\Sigma(1620)$ REFERENCES (PRODUCTION EXPERIMENTS)

AMMANN	70	PRL 24 327	A.C. Ammann *et al.*	(PURD, IND)
Also		PR D7 1345	A.C. Ammann *et al.*	(PURD, IUPU)
MILLER	70	Duke Conf. 229 Hyperon Resonances, 1970	D.H. Miller	(PURD)
SABRE	70	NP B16 201	R. Barloutaud *et al.*	(SABRE Collab.)
BLUMENFELD	69	PL 29B 58	B.J. Blumenfeld, G.R. Kalbfleisch	(BNL) I
CRENNELL	69B	Lund Paper 183 Results are quoted in LEVI-SETTI 69C.	D.J. Crennell *et al.*	(BNL, CUNY) I
Also		Lund Conf.	R. Levi-Setti	(EFI)
CRENNELL	68	PRL 21 648	D.J. Crennell *et al.*	(BNL, CUNY) I

$\Sigma(1660)$ $1/2^+$

$I(J^P) = 1(\frac{1}{2}^+)$ Status: ***

For results published before 1974 (they are now obsolete), see our 1982 edition Physics Letters **111B** 1 (1982).

$\Sigma(1660)$ MASS

VALUE (MeV)	DOCUMENT ID		TECN	COMMENT
1630 to 1690 (≈ 1660) OUR ESTIMATE				
1633 ± 3	GAO	12	DPWA	$\overline{K}N \to \Lambda\pi$
1665.1±11.2	[1] KOISO	85	DPWA	$K^-p \to \Sigma\pi$
1670 ±10	GOPAL	80	DPWA	$\overline{K}N \to \overline{K}N$
1679 ±10	ALSTON-...	78	DPWA	$\overline{K}N \to \overline{K}N$
1676 ±15	GOPAL	77	DPWA	$\overline{K}N$ multichannel
1668 ±25	VANHORN	75	DPWA	$K^-p \to \Lambda\pi^0$
1670 ±20	KANE	74	DPWA	$K^-p \to \Sigma\pi$
• • • We do not use the following data for averages, fits, limits, etc. • • •				
1565 or 1597	[2] MARTIN	77	DPWA	$\overline{K}N$ multichannel
1660 ±30	[3] BAILLON	75	IPWA	$\overline{K}N \to \Lambda\pi$
1671 ± 2	[4] PONTE	75	DPWA	$K^-p \to \Lambda\pi^0$

$\Sigma(1660)$ WIDTH

VALUE (MeV)	DOCUMENT ID		TECN	COMMENT
40 to 200 (≈ 100) OUR ESTIMATE				
$121 \pm {4 \atop 7}$	GAO	12	DPWA	$\overline{K}N \to \Lambda\pi$
81.5± 22.2	[1] KOISO	85	DPWA	$K^-p \to \Sigma\pi$
152 ± 20	GOPAL	80	DPWA	$\overline{K}N \to \overline{K}N$
38 ± 10	ALSTON-...	78	DPWA	$\overline{K}N \to \overline{K}N$
120 ± 20	GOPAL	77	DPWA	$\overline{K}N$ multichannel
$230 \pm {165 \atop 60}$	VANHORN	75	DPWA	$K^-p \to \Lambda\pi^0$
250 ±110	KANE	74	DPWA	$K^-p \to \Sigma\pi$
• • • We do not use the following data for averages, fits, limits, etc. • • •				
202 or 217	[2] MARTIN	77	DPWA	$\overline{K}N$ multichannel
80 ± 40	[3] BAILLON	75	IPWA	$\overline{K}N \to \Lambda\pi$
81 ± 10	[4] PONTE	75	DPWA	$K^-p \to \Lambda\pi^0$

$\Sigma(1660)$ DECAY MODES

	Mode	Fraction (Γ_i/Γ)
Γ_1	$N\overline{K}$	10–30 %
Γ_2	$\Lambda\pi$	seen
Γ_3	$\Sigma\pi$	seen

$\Sigma(1660)$ BRANCHING RATIOS

See "Sign conventions for resonance couplings" in the Note on Λ and Σ Resonances.

$\Gamma(N\overline{K})/\Gamma_{total}$ Γ_1/Γ

VALUE	DOCUMENT ID		TECN	COMMENT
0.1 to 0.3 OUR ESTIMATE				
0.12±0.03	GOPAL	80	DPWA	$\overline{K}N \to \overline{K}N$
0.10±0.05	ALSTON-...	78	DPWA	$\overline{K}N \to \overline{K}N$
• • • We do not use the following data for averages, fits, limits, etc. • • •				
<0.04	GOPAL	77	DPWA	See GOPAL 80
0.27 or 0.29	[2] MARTIN	77	DPWA	$\overline{K}N$ multichannel

$(\Gamma_i\Gamma_f)^{1/2}/\Gamma_{total}$ in $N\overline{K} \to \Sigma(1660) \to \Lambda\pi$ $(\Gamma_1\Gamma_2)^{1/2}/\Gamma$

VALUE	DOCUMENT ID		TECN	COMMENT
$-0.064 {+0.005 \atop -0.003}$	GAO	12	DPWA	$\overline{K}N \to \Lambda\pi$
< 0.04	GOPAL	77	DPWA	$\overline{K}N$ multichannel
$0.12 {+0.12 \atop -0.04}$	VANHORN	75	DPWA	$K^-p \to \Lambda\pi^0$
• • • We do not use the following data for averages, fits, limits, etc. • • •				
−0.10 or −0.11	[2] MARTIN	77	DPWA	$\overline{K}N$ multichannel
−0.04 ±0.02	[3] BAILLON	75	IPWA	$\overline{K}N \to \Lambda\pi$
+0.16 ±0.01	[4] PONTE	75	DPWA	$K^-p \to \Lambda\pi^0$

$(\Gamma_i\Gamma_f)^{1/2}/\Gamma_{total}$ in $N\overline{K} \to \Sigma(1660) \to \Sigma\pi$ $(\Gamma_1\Gamma_3)^{1/2}/\Gamma$

VALUE	DOCUMENT ID		TECN	COMMENT
−0.13±0.04	[1] KOISO	85	DPWA	$K^-p \to \Sigma\pi$
−0.16±0.03	GOPAL	77	DPWA	$\overline{K}N$ multichannel
−0.11±0.01	KANE	74	DPWA	$K^-p \to \Sigma\pi$
• • • We do not use the following data for averages, fits, limits, etc. • • •				
−0.34 or −0.37	[2] MARTIN	77	DPWA	$\overline{K}N$ multichannel
not seen	HEPP	76B	DPWA	$K^-N \to \Sigma\pi$

$\Sigma(1660)$ FOOTNOTES

[1] The evidence of KOISO 85 is weak.
[2] The two MARTIN 77 values are from a T-matrix pole and from a Breit-Wigner fit.
[3] From solution 1 of BAILLON 75; not present in solution 2.
[4] From solution 2 of PONTE 75; not present in solution 1.

$\Sigma(1660)$ REFERENCES

GAO	12	PR C86 025201	P. Gao, J. Shi, B.S. Zou	(BHEP, BEIJT)
Also		NP A867 41	P. Gao, B.S. Zou, A. Sibirtsev	(BHEP, BEIJT+)
KOISO	85	NP A433 619	H. Koiso *et al.*	(TOKY, MASA)
PDG	82	PL 111B 1	M. Roos *et al.*	(HELS, CIT, CERN)
GOPAL	80	Toronto Conf. 159	G.P. Gopal	(RHEL) IJP
ALSTON-...	78	PR D18 182	M. Alston-Garnjost *et al.*	(LBL, MTHO+) IJP
Also		PRL 38 1007	M. Alston-Garnjost *et al.*	(LBL, MTHO+) IJP
GOPAL	77	NP B119 362	G.P. Gopal *et al.*	(LOIC, RHEL) IJP
MARTIN	77	NP B127 349	B.R. Martin, M.K. Pidcock, R.G. Moorhouse	(LOUC+) IJP
Also		NP B126 266	B.R. Martin, M.K. Pidcock	(LOUC)
Also		NP B126 285	B.R. Martin, M.K. Pidcock	(LOUC) IJP
HEPP	76B	PL 65B 487	V. Hepp *et al.*	(CERN, HEIDH, MPIM) IJP
BAILLON	75	NP B94 39	P.H. Baillon, P.J. Litchfield	(CERN, RHEL) IJP
PONTE	75	PR D12 2597	R.A. Ponte *et al.*	(MASA, TENN, UCR) IJP
VANHORN	75	NP B87 145	A.J. van Horn	(LBL) IJP
Also		NP B87 157	A.J. van Horn	(LBL) IJP
KANE	74	LBL-2452	D.F. Kane	(LBL) IJP

THE $\Sigma(1670)$ REGION

Production experiments: The measured $\Sigma\pi/\Sigma\pi\pi$ branching ratio for the $\Sigma(1670)$ produced in the reaction $K^-p \to \pi^-\Sigma(1670)^+$ is strongly dependent on momentum transfer. This was first discovered by EBERHARD 69, who suggested that there exist two Σ resonances with the same mass and quantum numbers: one with a large $\Sigma\pi\pi$ (mainly $\Lambda(1405)\pi$) branching fraction produced peripherally, and the other with a large $\Sigma\pi$ branching fraction produced at larger angles. The experimental results have been confirmed by AGUILAR-BENITEZ 70, ASPELL 74, ESTES 74, and TIMMERMANS 76. If, in fact, there are two resonances, the most likely quantum numbers for both the $\Sigma\pi$ and the $\Lambda(1405)\pi$ states are D_{13}. There is also possibly a third Σ in this region, the $\Sigma(1690)$ in the Listings, the main evidence for which is a large $\Lambda\pi/\Sigma\pi$ branching ratio. These topics have been reviewed by EBERHARD 73 and by MILLER 70.

Formation experiments: Two states are also observed near this mass in formation experiments. One of these, the $\Sigma(1670)D_{13}$, has the same quantum numbers as those observed in production and has a large $\Sigma\pi/\Sigma\pi\pi$ branching ratio; it may well be the $\Sigma(1670)$ produced at larger angles (see TIMMERMANS 76). The other state, the $\Sigma(1660)P_{11}$, has different quantum numbers, its $\Sigma\pi/\Sigma\pi\pi$ branching ratio is unknown, and its relation to the produced $\Sigma(1670)$ states is obscure.

$\Sigma(1670)$ $3/2^-$

$I(J^P) = 1(\frac{3}{2}^-)$ Status: ****

For most results published before 1974 (they are now obsolete), see our 1982 edition Physics Letters **111B** 1 (1982).

Results from production experiments are listed separately in the next entry.

$\Sigma(1670)$ MASS

VALUE (MeV)	DOCUMENT ID		TECN	COMMENT
1665 to 1685 (≈ 1670) OUR ESTIMATE				
1678 ± 2	ZHANG	13A	DPWA	Multichannel
1673 ± 1	GAO	12	DPWA	$\overline{K}N \to \Lambda\pi$
1665.1 ± 4.1	KOISO	85	DPWA	$K^-p \to \Sigma\pi$
1682 ± 5	GOPAL	80	DPWA	$\overline{K}N \to \overline{K}N$
1679 ±10	ALSTON-...	78	DPWA	$\overline{K}N \to \overline{K}N$
1670 ± 5	GOPAL	77	DPWA	$\overline{K}N$ multichannel
1670 ± 6	HEPP	76B	DPWA	$K^-N \to \Sigma\pi$
1685 ±20	BAILLON	75	IPWA	$\overline{K}N \to \Lambda\pi$
1659 $^{+12}_{-5}$	VANHORN	75	DPWA	$K^-p \to \Lambda\pi^0$
1670 ± 2	KANE	74	DPWA	$K^-p \to \Sigma\pi$
• • • We do not use the following data for averages, fits, limits, etc. • • •				
1667 or 1668	[1] MARTIN	77	DPWA	$\overline{K}N$ multichannel
1650	DEBELLEFON	76	IPWA	$K^-p \to \Lambda\pi^0$
1671 ± 3	PONTE	75	DPWA	$K^-p \to \Lambda\pi^0$ (sol. 1)
1655 ± 2	PONTE	75	DPWA	$K^-p \to \Lambda\pi^0$ (sol. 2)

$\Sigma(1670)$ WIDTH

VALUE (MeV)	DOCUMENT ID		TECN	COMMENT
40 to 80 (≈ 60) OUR ESTIMATE				
55 ± 4	ZHANG	13A	DPWA	Multichannel
52 $^{+5}_{-2}$	GAO	12	DPWA	$\overline{K}N \to \Lambda\pi$
65.0 ± 7.3	KOISO	85	DPWA	$K^-p \to \Sigma\pi$
79 ±10	GOPAL	80	DPWA	$\overline{K}N \to \overline{K}N$
56 ±20	ALSTON-...	78	DPWA	$\overline{K}N \to \overline{K}N$
50 ± 5	GOPAL	77	DPWA	$\overline{K}N$ multichannel
56 ± 3	HEPP	76B	DPWA	$K^-N \to \Sigma\pi$
85 ±25	BAILLON	75	IPWA	$\overline{K}N \to \Lambda\pi$
32 ±11	VANHORN	75	DPWA	$K^-p \to \Lambda\pi^0$
79 ± 6	KANE	74	DPWA	$K^-p \to \Sigma\pi$
• • • We do not use the following data for averages, fits, limits, etc. • • •				
46 or 46	[1] MARTIN	77	DPWA	$\overline{K}N$ multichannel
80	DEBELLEFON	76	IPWA	$K^-p \to \Lambda\pi^0$
44 ±11	PONTE	75	DPWA	$K^-p \to \Lambda\pi^0$ (sol. 1)
76 ± 5	PONTE	75	DPWA	$K^-p \to \Lambda\pi^0$ (sol. 2)

$\Sigma(1670)$ POLE POSITION

REAL PART

VALUE (MeV)	DOCUMENT ID		TECN	COMMENT
• • • We do not use the following data for averages, fits, limits, etc. • • •				
1674	ZHANG	13A	DPWA	Multichannel

−2×IMAGINARY PART

VALUE (MeV)	DOCUMENT ID		TECN	COMMENT
• • • We do not use the following data for averages, fits, limits, etc. • • •				
54	ZHANG	13A	DPWA	Multichannel

$\Sigma(1670)$ DECAY MODES

	Mode	Fraction (Γ_i/Γ)
Γ_1	$N\overline{K}$	7–13 %
Γ_2	$\Lambda\pi$	5–15 %
Γ_3	$\Sigma\pi$	30–60 %
Γ_4	$\Lambda\pi\pi$	
Γ_5	$\Sigma\pi\pi$	
Γ_6	$\Sigma(1385)\pi$	
Γ_7	$\Sigma(1385)\pi$, S-wave	
Γ_8	$\Lambda(1405)\pi$	
Γ_9	$\Lambda(1520)\pi$	

The above branching fractions are our estimates, not fits or averages.

$\Sigma(1670)$ BRANCHING RATIOS

See "Sign conventions for resonance couplings" in the Note on Λ and Σ Resonances.

$\Gamma(N\overline{K})/\Gamma_{total}$ Γ_1/Γ

VALUE	DOCUMENT ID		TECN	COMMENT
0.07 to 0.13 OUR ESTIMATE				
0.062 ± 0.007	ZHANG	13A	DPWA	Multichannel
0.10 ± 0.03	GOPAL	80	DPWA	$\overline{K}N \to \overline{K}N$
0.11 ± 0.03	ALSTON-...	78	DPWA	$\overline{K}N \to \overline{K}N$
• • • We do not use the following data for averages, fits, limits, etc. • • •				
0.08 ± 0.03	GOPAL	77	DPWA	See GOPAL 80
0.07 or 0.07	[1] MARTIN	77	DPWA	$\overline{K}N$ multichannel

$(\Gamma_i\Gamma_f)^{1/2}/\Gamma_{total}$ in $N\overline{K} \to \Sigma(1670) \to \Lambda\pi$ $(\Gamma_1\Gamma_2)^{1/2}/\Gamma$

VALUE	DOCUMENT ID		TECN	COMMENT
+0.08 ± 0.01	ZHANG	13A	DPWA	Multichannel
+0.081 $^{+0.002}_{-0.004}$	GAO	12	DPWA	$\overline{K}N \to \Lambda\pi$
+0.17 ± 0.03	[2] MORRIS	78	DPWA	$K^-n \to \Lambda\pi^-$
+0.13 ± 0.02	[2] MORRIS	78	DPWA	$K^-n \to \Lambda\pi^-$
+0.10 ± 0.02	GOPAL	77	DPWA	$\overline{K}N$ multichannel
+0.06 ± 0.02	BAILLON	75	IPWA	$\overline{K}N \to \Lambda\pi$
+0.09 ± 0.02	VANHORN	75	DPWA	$K^-p \to \Lambda\pi^0$
+0.018 ± 0.060	DEVENISH	74B		Fixed-t dispersion rel.
• • • We do not use the following data for averages, fits, limits, etc. • • •				
+0.08 or +0.08	[1] MARTIN	77	DPWA	$\overline{K}N$ multichannel
+0.05	DEBELLEFON	76	IPWA	$K^-p \to \Lambda\pi^0$
+0.08 ± 0.01	PONTE	75	DPWA	$K^-p \to \Lambda\pi^0$ (sol. 1)
+0.17 ± 0.01	PONTE	75	DPWA	$K^-p \to \Lambda\pi^0$ (sol. 2)

$(\Gamma_i\Gamma_f)^{1/2}/\Gamma_{total}$ in $N\overline{K} \to \Sigma(1670) \to \Sigma\pi$ $(\Gamma_1\Gamma_3)^{1/2}/\Gamma$

VALUE	DOCUMENT ID		TECN	COMMENT
+0.20 ± 0.01	ZHANG	13A	DPWA	Multichannel
+0.20 ± 0.02	KOISO	85	DPWA	$K^-p \to \Sigma\pi$
+0.21 ± 0.02	GOPAL	77	DPWA	$\overline{K}N$ multichannel
+0.20 ± 0.01	HEPP	76B	DPWA	$K^-N \to \Sigma\pi$
+0.21 ± 0.03	KANE	74	DPWA	$K^-p \to \Sigma\pi$
• • • We do not use the following data for averages, fits, limits, etc. • • •				
+0.18 or +0.17	[1] MARTIN	77	DPWA	$\overline{K}N$ multichannel

$\Gamma(\Lambda\pi\pi)/\Gamma_{total}$ Γ_4/Γ

VALUE	DOCUMENT ID		TECN	COMMENT
• • • We do not use the following data for averages, fits, limits, etc. • • •				
<0.11	ARMENTEROS68E		HBC	K^-p (Γ_1=0.09)

$\Gamma(\Sigma\pi\pi)/\Gamma_{total}$ Γ_5/Γ

VALUE	DOCUMENT ID		TECN	COMMENT
• • • We do not use the following data for averages, fits, limits, etc. • • •				
<0.14	[3] ARMENTEROS68E		HBC	K^-p, K^-d (Γ_1=0.09)

$(\Gamma_i\Gamma_f)^{1/2}/\Gamma_{total}$ in $N\overline{K} \to \Sigma(1670) \to \Sigma(1385)\pi$, S-wave $(\Gamma_1\Gamma_7)^{1/2}/\Gamma$

VALUE	DOCUMENT ID		TECN	COMMENT
+0.11 ± 0.03	PREVOST	74	DPWA	$K^-N \to \Sigma(1385)\pi$
• • • We do not use the following data for averages, fits, limits, etc. • • •				
0.17 ± 0.02	[4] SIMS	68	DBC	$K^-N \to \Lambda\pi\pi$

$\Gamma(\Lambda(1405)\pi)/\Gamma_{total}$ Γ_8/Γ

VALUE	DOCUMENT ID		TECN	COMMENT
• • • We do not use the following data for averages, fits, limits, etc. • • •				
<0.06	ARMENTEROS68E		HBC	K^-p, K^-d (Γ_1=0.09)

$\Gamma_i\Gamma_f/\Gamma^2_{total}$ in $N\overline{K} \to \Sigma(1670) \to \Lambda(1405)\pi$ $\Gamma_1\Gamma_8/\Gamma^2$

VALUE	DOCUMENT ID		TECN	COMMENT
0.007 ± 0.002	[5] BRUCKER	70	DBC	$K^-N \to \Sigma\pi\pi$
• • • We do not use the following data for averages, fits, limits, etc. • • •				
<0.03	BERLEY	69	HBC	K^-p 0.6–0.82 GeV/c

$\Gamma(\Lambda(1405)\pi)/\Gamma(\Sigma(1385)\pi)$ Γ_8/Γ_6

VALUE	DOCUMENT ID		TECN	COMMENT
0.23±0.08	BRUCKER	70	DBC	$K^- N \to \Sigma\pi\pi$

$(\Gamma_i\Gamma_f)^{1/2}/\Gamma_{total}$ in $N\overline{K} \to \Sigma(1670) \to \Lambda(1520)\pi$ $(\Gamma_1\Gamma_9)^{1/2}/\Gamma$

VALUE	DOCUMENT ID		TECN	COMMENT
0.081±0.016	[6] CAMERON	77	DPWA	P-wave decay

$\Sigma(1670)$ FOOTNOTES

[1] The two MARTIN 77 values are from a T-matrix pole and from a Breit-Wigner fit.
[2] Results are with and without an S_{11} $\Sigma(1620)$ in the fit.
[3] Ratio only for $\Sigma 2\pi$ system in $I = 1$, which cannot be $\Sigma(1385)$.
[4] SIMS 68 uses only cross-section data. Result used as upper limit only.
[5] Assuming the $\Lambda(1405)\pi$ cross-section bump is due only to $3/2^-$ resonance.
[6] The CAMERON 77 upper limit on F-wave decay is 0.03.

$\Sigma(1670)$ REFERENCES

ZHANG	13A	PR C88 035205	H. Zhang *et al.*	(KSU)
GAO	12	PR C86 025201	P. Gao, J. Shi, B.S. Zou	(BHEP, BEIJT)
Also		NP A867 41	P. Gao, B.S. Zou, A. Sibirtsev	(BHEP, BEIJT+)
KOISO	85	NP A433 619	H. Koiso *et al.*	(TOKY, MASA)
PDG	82	PL 111B 1	M. Roos *et al.*	(HELS, CIT, CERN)
GOPAL	80	Toronto Conf. 159	G.P. Gopal	(RHEL) IJP
ALSTON-...	78	PR D18 182	M. Alston-Garnjost *et al.*	(LBL, MTHO+) IJP
Also		PRL 38 1007	M. Alston-Garnjost *et al.*	(LBL, MTHO+) IJP
MORRIS	78	PR D17 55	W.A. Morris *et al.*	(FSU) IJP
CAMERON	77	NP B131 399	W. Cameron *et al.*	(RHEL, LOIC) IJP
GOPAL	77	NP B119 362	G.P. Gopal *et al.*	(LOIC, RHEL) IJP
MARTIN	77	NP B127 349	B.R. Martin, M.K. Pidcock, R.G. Moorhouse	(LOUC+) IJP
Also		NP B126 266	B.R. Martin, M.K. Pidcock	(LOUC)
Also		NP B126 285	B.R. Martin, M.K. Pidcock	(LOUC) IJP
DEBELLEFON	76	NP B109 129	A. de Bellefon, A. Berthon	(CDEF) IJP
HEPP	76B	PL 65B 487	V. Hepp *et al.*	(CERN, HEIDH, MPIM) IJP
BAILLON	75	NP B94 39	P.H. Baillon, P.J. Litchfield	(CERN, RHEL) IJP
PONTE	75	PR D12 2597	R.A. Ponte *et al.*	(MASA, TENN, UCR) IJP
VANHORN	75	NP B87 145	A.J. van Horn	(LBL) IJP
Also		NP B87 157	A.J. van Horn	(LBL) IJP
DEVENISH	74B	NP B81 330	R.C.E. Devenish, C.D. Froggatt, B.R. Martin	(DESY+)
KANE	74	LBL-2452	D.F. Kane	(LBL) IJP
PREVOST	74	NP B69 246	J. Prevost *et al.*	(SACL, CERN, HEID)
BRUCKER	70	Duke Conf. 155 Hyperon Resonances, 1970	E.B. Brucker *et al.*	(FSU) I
BERLEY	69	PL 30B 430	D. Berley *et al.*	(BNL)
ARMENTEROS	68E	PL 28B 521	R. Armenteros *et al.*	(CERN, HEID, SACL) I
SIMS	68	PRL 21 1413	W.H. Sims *et al.*	(FSU, TUFTS, BRAN)

$\Sigma(1670)$ Bumps

$I(J^P) = 1(?^?)$

OMITTED FROM SUMMARY TABLE

Formation experiments are listed separately in the preceding entry.

Probably there are two states at the same mass with the same quantum numbers, one decaying to $\Sigma\pi$ and $\Lambda\pi$, the other to $\Lambda(1405)\pi$. See the note in front of the preceding entry.

$\Sigma(1670)$ MASS (PRODUCTION EXPERIMENTS)

VALUE (MeV)	EVTS	DOCUMENT ID		TECN	CHG	COMMENT
≈ 1670 OUR ESTIMATE						
1670± 4		[1] CARROLL	76	DPWA		Isospin-1 total σ
1675±10		[2] HEPP	76	DBC	−	$K^- N$ 1.6–1.75 GeV/c
1665± 1		APSELL	74	HBC		$K^- p$ 2.87 GeV/c
1688± 2 or 1683 ± 5	1.2k	BERTHON	74	HBC	0	Quasi-2-body σ
1670± 6		AGUILAR-...	70B	HBC		$K^- p \to \Sigma\pi\pi$ 4 GeV
1668±10		AGUILAR-...	70B	HBC		$K^- p \to \Sigma 3\pi$ 4 GeV
1660±10		ALVAREZ	63	HBC	+	$K^- p$ 1.51 GeV/c
• • • We do not use the following data for averages, fits, limits, etc. • • •						
1668±10	150	[3] FERRERSORIA	81	OMEG	−	$\pi^- p$ 9,12 GeV/c
1655 to 1677		TIMMERMANS	76	HBC	+	$K^- p$ 4.2 GeV/c
1665± 5		BUGG	68	CNTR		$K^- p$, d total σ
1661± 9	70	PRIMER	68	HBC	+	See BARNES 69E
1685		ALEXANDER	62C	HBC	−0	$\pi^- p$ 2–2.2 GeV/c

$\Sigma(1670)$ WIDTH (PRODUCTION EXPERIMENTS)

VALUE (MeV)	EVTS	DOCUMENT ID		TECN	CHG	COMMENT
67.0± 2.4		APSELL	74	HBC		$K^- p$ 2.87 GeV/c
110 ±12		AGUILAR-...	70B	HBC		$K^- p \to \Sigma\pi\pi$ 4 GeV
135 $^{+40}_{-30}$		AGUILAR-...	70B	HBC		$K^- p \to \Sigma 3\pi$ 4 GeV
40 ±10		ALVAREZ	63	HBC	+	
• • • We do not use the following data for averages, fits, limits, etc. • • •						
90 ±20	150	[3] FERRERSORIA	81	OMEG	−	$\pi^- p$ 9,12 GeV/c
52		[1] CARROLL	76	DPWA		Isospin-1 total σ
48 to 63		TIMMERMANS	76	HBC	+	$K^- p$ 4.2 GeV/c
30 ±15		BUGG	68	CNTR		
60 ±20	70	PRIMER	68	HBC	+	See BARNES 69E
45		ALEXANDER	62C	HBC	−0	

$\Sigma(1670)$ DECAY MODES (PRODUCTION EXPERIMENTS)

	Mode
Γ_1	$N\overline{K}$
Γ_2	$\Lambda\pi$
Γ_3	$\Sigma\pi$
Γ_4	$\Lambda\pi\pi$
Γ_5	$\Sigma\pi\pi$
Γ_6	$\Sigma(1385)\pi$
Γ_7	$\Lambda(1405)\pi$

$\Sigma(1670)$ BRANCHING RATIOS (PRODUCTION EXPERIMENTS)

$\Gamma(N\overline{K})/\Gamma(\Sigma\pi)$ Γ_1/Γ_3

VALUE	EVTS	DOCUMENT ID		TECN	CHG	COMMENT
<0.03		TIMMERMANS	76	HBC	+	$K^- p$ 4.2 GeV/c
<0.10		BERTHON	74	HBC	0	Quasi-2-body σ
<0.2		AGUILAR-...	70B	HBC		
<0.26		BARNES	69E	HBC	+	$K^- p$ 3.9–5 GeV/c
0.025		BUGG	68	CNTR	0	Assuming $J = 3/2$
<0.24	0	PRIMER	68	HBC	+	$K^- p$ 4.6–5 GeV/c
<0.6		LONDON	66	HBC	+	$K^- p$ 2.25 GeV/c
<0.19	0	ALVAREZ	63	HBC	+	$K^- p$ 1.15 GeV/c
≥ 0.5 ±0.25		SMITH	63	HBC	−0	

$\Gamma(\Lambda\pi)/\Gamma(\Sigma\pi)$ Γ_2/Γ_3

VALUE	EVTS	DOCUMENT ID		TECN	CHG	COMMENT
0.76±0.09		ESTES	74	HBC	0	$K^- p$ 2.1,2.6 GeV/c
0.45±0.15		BARNES	69E	HBC	+	$K^- p$ 3.9–5 GeV/c
0.15±0.07		HUWE	69	HBC	+	
0.11±0.06	33	BUTTON-...	68	HBC	+	$K^- p$ 1.7 GeV/c
• • • We do not use the following data for averages, fits, limits, etc. • • •						
≤ 0.45±0.07		TIMMERMANS	76	HBC	+	$K^- p$ 4.2 GeV/c
0.55±0.11		BERTHON	74	HBC	0	Quasi-2-body σ
0	0	PRIMER	68	HBC	+	See BARNES 69E
<0.6		LONDON	66	HBC	+	$K^- p$ 2.25 GeV/c
1.2	130	ALVAREZ	63	HBC	+	$K^- p$ 1.15 GeV/c
1.2		SMITH	63	HBC	−0	

$\Gamma(\Lambda\pi\pi)/\Gamma(\Sigma\pi)$ Γ_4/Γ_3

VALUE	EVTS	DOCUMENT ID		TECN	CHG	COMMENT
<0.6		LONDON	66	HBC	+	$K^- p$ 2.25 GeV/c
0.56	90	ALVAREZ	63	HBC	+	$K^- p$ 1.15 GeV/c
0.17		SMITH	63	HBC	−0	

$\Gamma(\Sigma\pi\pi)/\Gamma(\Sigma\pi)$ Γ_5/Γ_3

VALUE	EVTS	DOCUMENT ID		TECN	CHG	COMMENT
largest at small angles		ESTES	74	HBC	0	$K^- p$ 2.1,2.6 GeV/c
• • • We do not use the following data for averages, fits, limits, etc. • • •						
<0.2		[2] HEPP	76	DBC	−	$K^- N$ 1.6–1.75 GeV/c
0.56	180	ALVAREZ	63	HBC	+	$K^- p$ 1.15 GeV/c

$\Gamma(\Lambda(1405)\pi)/\Gamma(\Sigma\pi)$ Γ_7/Γ_3

VALUE	EVTS	DOCUMENT ID		TECN	CHG	COMMENT
1.8 ±0.3 to 0.02 ± 0.07		[3,4] TIMMERMANS	76	HBC	+	$K^- p$ 4.2 GeV/c
largest at small angles		ESTES	74	HBC	±	$K^- p$ 2.1,2.6 GeV/c
3.0 ±1.6	50	LONDON	66	HBC	+	$K^- p$ 2.25 GeV/c
• • • We do not use the following data for averages, fits, limits, etc. • • •						
0.58±0.20	17	PRIMER	68	HBC	+	See BARNES 69E

Baryon Particle Listings

$\Sigma(1670)$ Bumps, $\Sigma(1690)$ Bumps

$\Gamma(\Sigma\pi)/\Gamma(\Sigma\pi\pi)$ Γ_3/Γ_5

VALUE	DOCUMENT ID		TECN	CHG	COMMENT
varies with prod. angle	[5] APSELL	74	HBC	+	K^-p 2.87 GeV/c
1.39±0.16	BERTHON	74	HBC	0	Quasi-2-body σ
2.5 to 0.24	[4] EBERHARD	69	HBC		K^-p 2.6 GeV/c
<0.4	BIRMINGHAM	66	HBC	+	K^-p 3.5 GeV/c
0.30±0.15	LONDON	66	HBC	+	K^-p 2.25 GeV/c

$\Gamma(\Lambda(1405)\pi)/\Gamma(\Sigma\pi\pi)$ Γ_7/Γ_5

VALUE	DOCUMENT ID		TECN	CHG	COMMENT
0.97±0.08	TIMMERMANS	76	HBC		K^-p 4.2 GeV/c
1.00±0.02	APSELL	74	HBC		K^-p 2.87 GeV/c
$0.90^{+0.10}_{-0.16}$	EBERHARD	65	HBC	+	K^-p 2.45 GeV/c

$\Gamma(\Lambda(1405)\pi)/\Gamma(\Sigma(1385)\pi)$ Γ_7/Γ_6

VALUE	DOCUMENT ID		TECN	CHG	COMMENT
<0.8	EBERHARD	65	HBC	+	K^-p 2.45 GeV/c

$\Gamma(\Lambda\pi\pi)/\Gamma(\Sigma\pi\pi)$ Γ_4/Γ_5

VALUE	DOCUMENT ID		TECN	CHG	COMMENT
0.35±0.2	BIRMINGHAM	66	HBC	+	K^-p 3.5 GeV/c

$\Gamma(\Lambda\pi)/\Gamma(\Sigma\pi\pi)$ Γ_2/Γ_5

VALUE	DOCUMENT ID		TECN	CHG	COMMENT
<0.2	BIRMINGHAM	66	HBC	+	K^-p 3.5 GeV/c

$\Gamma(\Lambda\pi)/[\Gamma(\Lambda\pi)+\Gamma(\Sigma\pi)]$ $\Gamma_2/(\Gamma_2+\Gamma_3)$

VALUE	DOCUMENT ID		TECN
<0.6	AGUILAR-...	70B	HBC

$\Gamma(\Sigma(1385)\pi)/\Gamma(\Sigma\pi)$ Γ_6/Γ_3

VALUE	DOCUMENT ID		TECN	COMMENT
≤ 0.21±0.05	TIMMERMANS	76	HBC	K^-p 4.2 GeV/c

$\Sigma(1670)$ QUANTUM NUMBERS (PRODUCTION EXPERIMENTS)

VALUE	EVTS	DOCUMENT ID		TECN	CHG	COMMENT
$J^P = 3/2^-$	400	BUTTON-...	68	HBC	±	$\Sigma^0\pi$
$J^P = 3/2^-$		EBERHARD	67	HBC	+	$\Lambda(1405)\pi$
$J^P = 3/2^+$		LEVEQUE	65	HBC		$\Lambda(1405)\pi$

$\Sigma(1670)$ FOOTNOTES

[1] Total cross-section bump with $(J+1/2)\ \Gamma_{el}\ /\ \Gamma_{total} = 0.23$.
[2] Enhancements in $\Sigma\pi$ and $\Sigma\pi\pi$ cross sections.
[3] Backward production in the $\Lambda\pi^-K^+$ final state.
[4] Depending on production angle.
[5] APSELL 74, ESTES 74, and TIMMERMANS 76 find strong branching ratio dependence on production angle, as in earlier production experiments.

$\Sigma(1670)$ REFERENCES (PRODUCTION EXPERIMENTS)

FERRERSORIA	81	NP B178 373	A. Ferrer Soria *et al.* (CERN, CDEF, EPOL+)
CARROLL	76	PRL 37 806	A.S. Carroll *et al.* (BNL) I
HEPP	76	NP B115 82	V. Hepp *et al.* (CERN, HEID, MPIM) I
TIMMERMANS	76	NP B112 77	J.J.M. Timmermans *et al.* (NIJM, CERN+) JP
APSELL	74	PR D10 1419	S.P. Apsell *et al.* (BRAN, UMD, SYRA+) I
BERTHON	74	NC 21A 146	A. Berthon *et al.* (CDEF, RHEL, SACL+)
ESTES	74	Thesis LBL-3827	R.D. Estes (LBL)
AGUILAR-...	70B	PRL 25 58	M. Aguilar-Benitez *et al.* (BNL, SYRA)
BARNES	69E	BNL 13823	V.E. Barnes *et al.* (BNL, SYRA)
EBERHARD	69	PRL 22 200	P.H. Eberhard *et al.* (LRL)
HUWE	69	PR 181 1824	D.O. Huwe (LRL)
BUGG	68	PR 168 1466	D.V. Bugg *et al.* (RHEL, BIRM, CAVE) I
BUTTON-...	68	PRL 21 1123	J. Button-Shafer (MASA, LRL) JP
PRIMER	68	PRL 20 610	M. Primer *et al.* (SYRA, BNL)
EBERHARD	67	PR 163 1446	P. Eberhard *et al.* (LRL, ILL) IJP
BIRMINGHAM	66	PR 152 1148	M. Haque *et al.* (BIRM, GLAS, LOIC, OXF+)
LONDON	66	PR 143 1034	G.W. London *et al.* (BNL, SYRA) IJ
EBERHARD	65	PRL 14 466	P.H. Eberhard *et al.* (LRL, ILL) I
LEVEQUE	65	PL 18 69	A. Leveque *et al.* (SACL, EPOL, GLAS+) JP
ALVAREZ	63	PRL 10 184	L.W. Alvarez *et al.* (LRL) I
SMITH	63	Athens Conf. 67	G.A. Smith (LRL)
ALEXANDER	62C	CERN Conf. 320	G. Alexander *et al.* (LRL) I

$\Sigma(1690)$ Bumps

$I(J^P) = 1(?^?)$ Status: **

OMITTED FROM SUMMARY TABLE

See the note preceding the $\Sigma(1670)$ Listings. Seen in production experiments only, mainly in $\Lambda\pi$.

$\Sigma(1690)$ MASS (PRODUCTION EXPERIMENTS)

VALUE (MeV)	EVTS	DOCUMENT ID		TECN	CHG	COMMENT
≈ 1690 OUR ESTIMATE						
1698±20	70	[1] GODDARD	79	HBC	+	π^+p 10.3 GeV/c
1707±20	40	[2] GODDARD	79	HBC	+	π^+p 10.3 GeV/c
1698±20	15	ADERHOLZ	69	HBC	+	π^+p 8 GeV/c
1682± 2	46	BLUMENFELD	69	HBC	+	K^0_Lp
1700±20		MOTT	69	HBC	+	K^-p 5.5 GeV/c
1694±24	60	[3] PRIMER	68	HBC	+	K^-p 4.6–5 GeV/c
1700± 6		[4] SIMS	68	HBC	−	$K^-N \rightarrow \Lambda\pi\pi$
1715±12	30	COLLEY	67	HBC	+	K^-p 6 GeV/c

$\Sigma(1690)$ WIDTH (PRODUCTION EXPERIMENTS)

VALUE (MeV)	EVTS	DOCUMENT ID		TECN	CHG	COMMENT
240± 60	70	[1] GODDARD	79	HBC	+	π^+p 10.3 GeV/c
$130^{+100}_{-\ 60}$	40	[2] GODDARD	79	HBC	+	π^+p 10.3 GeV/c
142± 40	15	ADERHOLZ	69	HBC	+	π^+p 8 GeV/c
25± 10	46	BLUMENFELD	69	HBC	+	K^0_Lp
130± 25		MOTT	69	HBC	+	K^-p 5.5 GeV/c
105± 35	60	[3] PRIMER	68	HBC	+	K^-p 4.6–5 GeV/c
62± 14		[4] SIMS	68	HBC	−	$K^-N \rightarrow \Lambda\pi\pi$
100± 35	30	COLLEY	67	HBC	+	K^-p 6 GeV/c

$\Sigma(1690)$ DECAY MODES (PRODUCTION EXPERIMENTS)

	Mode
Γ_1	$N\overline{K}$
Γ_2	$\Lambda\pi$
Γ_3	$\Sigma\pi$
Γ_4	$\Sigma(1385)\pi$
Γ_5	$\Lambda\pi\pi$ (including $\Sigma(1385)\pi$)

$\Sigma(1690)$ BRANCHING RATIOS (PRODUCTION EXPERIMENTS)

$\Gamma(N\overline{K})/\Gamma(\Lambda\pi)$ Γ_1/Γ_2

VALUE	EVTS	DOCUMENT ID		TECN	CHG	COMMENT
small		GODDARD	79	HBC	+	π^+p 10.2 GeV/c
<0.2		MOTT	69	HBC	+	K^-p 5.5 GeV/c
0.4±0.25	18	COLLEY	67	HBC	+	6/30 events

$\Gamma(\Sigma\pi)/\Gamma(\Lambda\pi)$ Γ_3/Γ_2

VALUE	CL%	DOCUMENT ID		TECN	CHG	COMMENT
small		GODDARD	79	HBC	+	π^+p 10.2 GeV/c
<0.4	90	MOTT	69	HBC	+	K^-p 5.5 GeV/c
0.3±0.3		COLLEY	67	HBC	+	4/30 events

$\Gamma(\Sigma(1385)\pi)/\Gamma(\Lambda\pi)$ Γ_4/Γ_2

VALUE	DOCUMENT ID		TECN	CHG	COMMENT
<0.5	MOTT	69	HBC	+	K^-p 5.5 GeV/c

$\Gamma(\Lambda\pi\pi(\text{including }\Sigma(1385)\pi))/\Gamma(\Lambda\pi)$ Γ_5/Γ_2

VALUE	DOCUMENT ID		TECN	CHG	COMMENT
2.0±0.6	BLUMENFELD	69	HBC	+	31/15 events
0.5±0.25	COLLEY	67	HBC	+	15/30 events

$\Gamma(\Sigma(1385)\pi)/\Gamma(\Lambda\pi\pi(\text{including }\Sigma(1385)\pi))$ Γ_4/Γ_5

VALUE	DOCUMENT ID		TECN	CHG	COMMENT
large	SIMS	68	HBC	−	$K^-N \rightarrow \Lambda\pi\pi$
small	COLLEY	67	HBC	+	K^-p 6 GeV/c

$\Sigma(1690)$ FOOTNOTES (PRODUCTION EXPERIMENTS)

[1] From $\pi^+ p \rightarrow (\Lambda\pi^+) K^+$. $J > 1/2$ is not required by the data.
[2] From $\pi^+ p \rightarrow (\Lambda\pi^+)(K\pi)^+$. $J > 1/2$ is indicated, but large background precludes a definite conclusion.
[3] See the $\Sigma(1670)$ Listings. AGUILAR-BENITEZ 70B with three times the data of PRIMER 68 find no evidence for the $\Sigma(1690)$.
[4] This analysis, which is difficult and requires several assumptions and shows no unambiguous $\Sigma(1690)$ signal, suggests $J^P = 5/2^+$. Such a state would lead all previously known Y^* trajectories.

$\Sigma(1690)$ REFERENCES (PRODUCTION EXPERIMENTS)

GODDARD	79	PR D19 1350	M.C. Goddard *et al.*	(TNTO, BNL) IJ
AGUILAR-...	70B	PRL 25 58	M. Aguilar-Benitez *et al.*	(BNL, SYRA)
ADERHOLZ	69	NP B11 259	M. Aderholz *et al.*	(AACH3, BERL, CERN+) I
BLUMENFELD	69	PL 29B 58	B.J. Blumenfeld, G.R. Kalbfleisch	(BNL) I
MOTT	69	PR 177 1966	J. Mott *et al.*	(NWES, ANL) I
Also		PRL 18 266	M. Derrick *et al.*	(ANL, NWES) I
PRIMER	68	PRL 20 610	M. Primer *et al.*	(SYRA, BNL) I
SIMS	68	PRL 21 1413	W.H. Sims *et al.*	(FSU, TUFTS, BRAN) I
COLLEY	67	PL 24B 489	D.C. Colley	(BIRM, GLAS, LOIC, MUNI, OXF+) I

$\Sigma(1730)$ 3/2$^+$

$I(J^P) = 1(\frac{3}{2}^+)$ Status: *

OMITTED FROM SUMMARY TABLE

$\Sigma(1730)$ MASS

VALUE (MeV)	DOCUMENT ID		TECN	COMMENT
1727±27	ZHANG	13A	DPWA	Multichannel

$\Lambda(1730)$ WIDTH

VALUE (MeV)	DOCUMENT ID		TECN	COMMENT
276±87	ZHANG	13A	DPWA	Multichannel

$\Sigma(1730)$ DECAY MODES

	Mode	Fraction (Γ_i/Γ)
Γ_1	$N\overline{K}$	(2.0± 1.0) %
Γ_2	$\Lambda\pi$	(70 ±17) %
Γ_3	$\Sigma\pi$	(12 ± 6) %

$\Sigma(1730)$ BRANCHING RATIOS

$\Gamma(N\overline{K})/\Gamma_{total}$ — **Γ_1/Γ**

VALUE	DOCUMENT ID		TECN	COMMENT
0.02±0.01	ZHANG	13A	DPWA	Multichannel

$\Gamma(\Lambda\pi)/\Gamma_{total}$ — **Γ_2/Γ**

VALUE	DOCUMENT ID		TECN	COMMENT
0.70±0.17	ZHANG	13A	DPWA	Multichannel

$\Gamma(\Sigma\pi)/\Gamma_{total}$ — **Γ_3/Γ**

VALUE	DOCUMENT ID		TECN	COMMENT
0.12±0.06	ZHANG	13A	DPWA	Multichannel

$\Sigma(1730)$ REFERENCES

ZHANG	13A	PR C88 035205	H. Zhang *et al.*	(KSU)

$\Sigma(1750)$ 1/2$^-$

$I(J^P) = 1(\frac{1}{2}^-)$ Status: ***

For most results published before 1974 (they are now obsolete), see our 1982 edition Physics Letters **111B** 1 (1982).

There is evidence for this state in many partial-wave analyses, but with wide variations in the mass, width, and couplings. The latest analyses indicated significant couplings to $N\overline{K}$ and $\Lambda\pi$, as well as to $\Sigma\eta$ whose threshold is at 1746 MeV (JONES 74).

$\Sigma(1750)$ MASS

VALUE (MeV)	DOCUMENT ID		TECN	COMMENT
1730 to 1800 (≈ 1750) OUR ESTIMATE				
1739± 8	ZHANG	13A	DPWA	Multichannel
1756±10	GOPAL	80	DPWA	$\overline{K}N \rightarrow \overline{K}N$
1770±10	ALSTON-...	78	DPWA	$\overline{K}N \rightarrow \overline{K}N$
1770±15	GOPAL	77	DPWA	$\overline{K}N$ multichannel
• • • We do not use the following data for averages, fits, limits, etc. • • •				
1800 or 1813	[1] MARTIN	77	DPWA	$\overline{K}N$ multichannel
1715±10	[2] CARROLL	76	DPWA	Isospin-1 total σ
1730	DEBELLEFON	76	IPWA	$K^- p \rightarrow \Lambda\pi^0$
1780±30	BAILLON	75	IPWA	$\overline{K}N \rightarrow \Lambda\pi$ (sol. 1)
1700±30	BAILLON	75	IPWA	$\overline{K}N \rightarrow \Lambda\pi$ (sol. 2)
1697^{+20}_{-10}	VANHORN	75	DPWA	$K^- p \rightarrow \Lambda\pi^0$
1785±12	CHU	74	DBC	Fits $\sigma(K^- n \rightarrow \Sigma^- \eta)$
1760± 5	[3] JONES	74	HBC	Fits $\sigma(K^- p \rightarrow \Sigma^0 \eta)$
1739±10	PREVOST	74	DPWA	$K^- N \rightarrow \Sigma(1385)\pi$

$\Sigma(1750)$ WIDTH

VALUE (MeV)	DOCUMENT ID		TECN	COMMENT
60 to 160 (≈ 90) OUR ESTIMATE				
182±60	ZHANG	13A	DPWA	Multichannel
64±10	GOPAL	80	DPWA	$\overline{K}N \rightarrow \overline{K}N$
161±20	ALSTON-...	78	DPWA	$\overline{K}N \rightarrow \overline{K}N$
60±10	GOPAL	77	DPWA	$\overline{K}N$ multichannel
• • • We do not use the following data for averages, fits, limits, etc. • • •				
117 or 119	[1] MARTIN	77	DPWA	$\overline{K}N$ multichannel
10	[2] CARROLL	76	DPWA	Isospin-1 total σ
110	DEBELLEFON	76	IPWA	$K^- p \rightarrow \Lambda\pi^0$
140±30	BAILLON	75	IPWA	$\overline{K}N \rightarrow \Lambda\pi$ (sol. 1)
160±50	BAILLON	75	IPWA	$\overline{K}N \rightarrow \Lambda\pi$ (sol. 2)
66^{+14}_{-12}	VANHORN	75	DPWA	$K^- p \rightarrow \Lambda\pi^0$
89±33	CHU	74	DBC	Fits $\sigma(K^- n \rightarrow \Sigma^- \eta)$
92± 7	[3] JONES	74	HBC	Fits $\sigma(K^- p \rightarrow \Sigma^0 \eta)$
108±20	PREVOST	74	DPWA	$K^- N \rightarrow \Sigma(1385)\pi$

$\Sigma(1750)$ POLE POSITION

REAL PART

VALUE (MeV)	DOCUMENT ID		TECN	COMMENT
• • • We do not use the following data for averages, fits, limits, etc. • • •				
1708	ZHANG	13A	DPWA	Multichannel

−2×IMAGINARY PART

VALUE (MeV)	DOCUMENT ID		TECN	COMMENT
• • • We do not use the following data for averages, fits, limits, etc. • • •				
158	ZHANG	13A	DPWA	Multichannel

$\Sigma(1750)$ DECAY MODES

	Mode	Fraction (Γ_i/Γ)
Γ_1	$N\overline{K}$	10–40 %
Γ_2	$\Lambda\pi$	seen
Γ_3	$\Sigma\pi$	<8 %
Γ_4	$\Sigma\eta$	15–55 %
Γ_5	$\Sigma(1385)\pi$, D-wave	
Γ_6	$\Lambda(1520)\pi$	
	The above branching fractions are our estimates, not fits or averages.	
Γ_7	$N\overline{K}^*(892)$, S=1/2	(8±4) %

Baryon Particle Listings

$\Sigma(1750)$, $\Sigma(1770)$

$\Sigma(1750)$ BRANCHING RATIOS

See "Sign conventions for resonance couplings" in the Note on Λ and Σ Resonances.

$\Gamma(N\overline{K})/\Gamma_{total}$ — **Γ_1/Γ**

VALUE	DOCUMENT ID		TECN	COMMENT
0.1 to 0.4 OUR ESTIMATE				
0.09 ± 0.07	ZHANG	13A	DPWA	Multichannel
0.14 ± 0.03	GOPAL	80	DPWA	$\overline{K}N\to\overline{K}N$
0.33 ± 0.05	ALSTON-...	78	DPWA	$\overline{K}N\to\overline{K}N$
• • • We do not use the following data for averages, fits, limits, etc. • • •				
0.15 ± 0.03	GOPAL	77	DPWA	See GOPAL 80
0.06 or 0.05	[1] MARTIN	77	DPWA	$\overline{K}N$ multichannel

$(\Gamma_i\Gamma_f)^{1/2}/\Gamma_{total}$ in $N\overline{K}\to\Sigma(1750)\to\Lambda\pi$ — **$(\Gamma_1\Gamma_2)^{1/2}/\Gamma$**

VALUE	DOCUMENT ID		TECN	COMMENT
$+0.10\ \pm0.04$	ZHANG	13A	DPWA	Multichannel
$0.04\ \pm0.03$	GOPAL	77	DPWA	$\overline{K}N$ multichannel
• • • We do not use the following data for averages, fits, limits, etc. • • •				
-0.10 or -0.09	[1] MARTIN	77	DPWA	$\overline{K}N$ multichannel
-0.12	DEBELLEFON	76	IPWA	$K^-p\to\Lambda\pi^0$
$-0.12\ \pm0.02$	BAILLON	75	IPWA	$\overline{K}N\to\Lambda\pi$ (sol. 1)
$-0.13\ \pm0.03$	BAILLON	75	IPWA	$\overline{K}N\to\Lambda\pi$ (sol. 2)
$-0.13\ \pm0.04$	VANHORN	75	DPWA	$K^-p\to\Lambda\pi^0$
-0.120 ± 0.077	DEVENISH	74B		Fixed-t dispersion rel.

$(\Gamma_i\Gamma_f)^{1/2}/\Gamma_{total}$ in $N\overline{K}\to\Sigma(1750)\to\Sigma\pi$ — **$(\Gamma_1\Gamma_3)^{1/2}/\Gamma$**

VALUE	DOCUMENT ID		TECN	COMMENT
$+0.17\pm0.07$	ZHANG	13A	DPWA	Multichannel
-0.09 ± 0.05	GOPAL	77	DPWA	$\overline{K}N$ multichannel
• • • We do not use the following data for averages, fits, limits, etc. • • •				
$+0.06$ or $+0.06$	[1] MARTIN	77	DPWA	$\overline{K}N$ multichannel
0.13 ± 0.02	LANGBEIN	72	IPWA	$\overline{K}N$ multichannel

$(\Gamma_i\Gamma_f)^{1/2}/\Gamma_{total}$ in $N\overline{K}\to\Sigma(1750)\to\Sigma\eta$ — **$(\Gamma_1\Gamma_4)^{1/2}/\Gamma$**

VALUE	DOCUMENT ID		TECN	COMMENT
0.23 ± 0.01	[3] JONES	74	HBC	Fits $\sigma(K^-p\to\Sigma^0\eta)$
• • • We do not use the following data for averages, fits, limits, etc. • • •				
seen	CLINE	69	DBC	Threshold bump

$(\Gamma_i\Gamma_f)^{1/2}/\Gamma_{total}$ in $N\overline{K}\to\Sigma(1750)\to\Sigma(1385)\pi$, D-wave — **$(\Gamma_1\Gamma_5)^{1/2}/\Gamma$**

VALUE	DOCUMENT ID		TECN	COMMENT
$+0.17\pm0.07$	ZHANG	13A	DPWA	Multichannel
$+0.18\pm0.15$	PREVOST	74	DPWA	$K^-N\to\Sigma(1385)\pi$

$(\Gamma_i\Gamma_f)^{1/2}/\Gamma_{total}$ in $N\overline{K}\to\Sigma(1750)\to\Lambda(1520)\pi$ — **$(\Gamma_1\Gamma_6)^{1/2}/\Gamma$**

VALUE	DOCUMENT ID		TECN	COMMENT
• • • We do not use the following data for averages, fits, limits, etc. • • •				
0.032 ± 0.021	CAMERON	77	DPWA	P-wave decay

$\Gamma(N\overline{K}^*(892),S=1/2)/\Gamma_{total}$ — **Γ_7/Γ**

VALUE	DOCUMENT ID		TECN	COMMENT
0.08 ± 0.04	ZHANG	13A	DPWA	Multichannel

$\Sigma(1750)$ FOOTNOTES

[1] The two MARTIN 77 values are from a T-matrix pole and from a Breit-Wigner fit.
[2] A total cross-section bump with $(J+1/2)\ \Gamma_{el}\ /\ \Gamma_{total} = 0.30$.
[3] An S-wave Breit-Wigner fit to the threshold cross section with no background and errors statistical only.

$\Sigma(1750)$ REFERENCES

ZHANG	13A	PR C88 035205	H. Zhang *et al.*	(KSU)
PDG	82	PL 111B 1	M. Roos *et al.*	(HELS, CIT, CERN)
GOPAL	80	Toronto Conf. 159	G.P. Gopal	(RHEL) IJP
ALSTON-...	78	PR D18 182	M. Alston-Garnjost *et al.*	(LBL, MTHO+) IJP
Also		PRL 38 1007	M. Alston-Garnjost *et al.*	(LBL, MTHO+) IJP
CAMERON	77	NP B131 399	W. Cameron *et al.*	(RHEL, LOIC) IJP
GOPAL	77	NP B119 362	G.P. Gopal *et al.*	(LOIC, RHEL) IJP
MARTIN	77	NP B127 349	B.R. Martin, M.K. Pidcock, R.G. Moorhouse	(LOUC+) IJP
Also		NP B126 266	B.R. Martin, M.K. Pidcock	(LOUC)
Also		NP B126 285	B.R. Martin, M.K. Pidcock	(LOUC) IJP
CARROLL	76	PRL 37 806	A.S. Carroll *et al.*	(BNL) I
DEBELLEFON	76	NP B109 129	A. de Bellefon, A. Berthon	(CDEF) IJP
BAILLON	75	NP B94 39	P.H. Baillon, P.J. Litchfield	(CERN, RHEL) IJP
VANHORN	75	NP B87 145	A.J. van Horn	(LBL) IJP
Also		NP B87 157	A.J. van Horn	(LBL) IJP
CHU	74	NC 20A 35	R.Y.L. Chu *et al.*	(PLAT, TUFTS, BRAN) IJP
DEVENISH	74B	NP B81 330	R.C.E. Devenish, C.D. Froggatt, B.R. Martin	(DESY+)
JONES	74	NP B73 141	M.D. Jones	(CHIC) IJP
PREVOST	74	NP B69 246	J. Prevost *et al.*	(SACL, CERN, HEID)
LANGBEIN	72	NP B47 477	W. Langbein, F. Wagner	(MPIM) IJP
CLINE	69	LNC 2 407	D. Cline, R. Laumann, J. Mapp	(WISC)

$\Sigma(1770)\ 1/2^+$

$I(J^P) = 1(\frac{1}{2}^+)$ Status: *

OMITTED FROM SUMMARY TABLE

Evidence for this state now rests solely on solution 1 of BAILLON 75, (see the footnotes) but the $\Lambda\pi$ partial-wave amplitudes of this solution are in disagreement with amplitudes from most other $\Lambda\pi$ analyses. ZHANG 13A finds no evidence for this state.

$\Sigma(1770)$ MASS

VALUE (MeV)	DOCUMENT ID		TECN	COMMENT
≈ 1770 OUR ESTIMATE				
1738 ± 10	[1] GOPAL	77	DPWA	$\overline{K}N$ multichannel
1770 ± 20	[2] BAILLON	75	IPWA	$\overline{K}N\to\Lambda\pi$
1772	[3] KANE	72	DPWA	$K^-p\to\Sigma\pi$

$\Sigma(1770)$ WIDTH

VALUE (MeV)	DOCUMENT ID		TECN	COMMENT
72 ± 10	[1] GOPAL	77	DPWA	$\overline{K}N$ multichannel
80 ± 30	[2] BAILLON	75	IPWA	$\overline{K}N\to\Lambda\pi$
80	[3] KANE	72	DPWA	$K^-p\to\Sigma\pi$

$\Sigma(1770)$ DECAY MODES

	Mode
Γ_1	$N\overline{K}$
Γ_2	$\Lambda\pi$
Γ_3	$\Sigma\pi$

$\Sigma(1770)$ BRANCHING RATIOS

See "Sign conventions for resonance couplings" in the Note on Λ and Σ Resonances.

$\Gamma(N\overline{K})/\Gamma_{total}$ — **Γ_1/Γ**

VALUE	DOCUMENT ID		TECN	COMMENT
0.14 ± 0.04	[1] GOPAL	77	DPWA	$\overline{K}N$ multichannel

$(\Gamma_i\Gamma_f)^{1/2}/\Gamma_{total}$ in $N\overline{K}\to\Sigma(1770)\to\Lambda\pi$ — **$(\Gamma_1\Gamma_2)^{1/2}/\Gamma$**

VALUE	DOCUMENT ID		TECN	COMMENT
$<\ 0.04$	GOPAL	77	DPWA	$\overline{K}N$ multichannel
-0.08 ± 0.02	[2] BAILLON	75	IPWA	$\overline{K}N\to\Lambda\pi$

$(\Gamma_i\Gamma_f)^{1/2}/\Gamma_{total}$ in $N\overline{K}\to\Sigma(1770)\to\Sigma\pi$ — **$(\Gamma_1\Gamma_3)^{1/2}/\Gamma$**

VALUE	DOCUMENT ID		TECN	COMMENT
$<\ 0.04$	GOPAL	77	DPWA	$\overline{K}N$ multichannel
-0.108	[3] KANE	72	DPWA	$K^-p\to\Sigma\pi$

$\Sigma(1770)$ FOOTNOTES

[1] Required to fit the isospin-1 total cross section of CARROLL 76 in the $\overline{K}N$ channel. The addition of new K^-p polarization and K^-n differential cross-section data in GOPAL 80 find it to be more consistent with the $\Sigma(1660)$ P_{11}.
[2] From solution 1 of BAILLON 75; not present in solution 2.
[3] Not required in KANE 74, which supersedes KANE 72.

$\Sigma(1770)$ REFERENCES

ZHANG	13A	PR C88 035205	H. Zhang *et al.*	(KSU)
GOPAL	80	Toronto Conf. 159	G.P. Gopal	(RHEL)
GOPAL	77	NP B119 362	G.P. Gopal *et al.*	(LOIC, RHEL) IJP
CARROLL	76	PRL 37 806	A.S. Carroll *et al.*	(BNL) I
BAILLON	75	NP B94 39	P.H. Baillon, P.J. Litchfield	(CERN, RHEL) IJP
KANE	74	LBL-2452	D.F. Kane	(LBL) IJP
KANE	72	PR D5 1583	D.F.J. Kane	(LBL)

$\Sigma(1775)\ 5/2^-$

$I(J^P) = 1(\frac{5}{2}^-)$ Status: ****

Discovered by GALTIERI 63, this resonance plays the same role as cornerstone for isospin-1 analyses in this region as the $\Lambda(1820)F_{05}$ does in the isospin-0 channel.

For most results published before 1974 (they are now obsolete), see our 1982 edition Physics Letters **111B** 1 (1982).

$\Sigma(1775)$ MASS

VALUE (MeV)	DOCUMENT ID		TECN	COMMENT
1770 to 1780 (≈ 1775) OUR ESTIMATE				
1778 ± 1	ZHANG	13A	DPWA	Multichannel
1778 ± 5	GOPAL	80	DPWA	$\overline{K}N \to \overline{K}N$
1777 ± 5	ALSTON-...	78	DPWA	$\overline{K}N \to \overline{K}N$
1774 ± 5	GOPAL	77	DPWA	$\overline{K}N$ multichannel
1775 ± 10	BAILLON	75	IPWA	$\overline{K}N \to \Lambda\pi$
1774 ± 10	VANHORN	75	DPWA	$K^-p \to \Lambda\pi^0$
1772 ± 6	KANE	74	DPWA	$K^-p \to \Sigma\pi$
• • • We do not use the following data for averages, fits, limits, etc. • • •				
1772 or 1777	[1] MARTIN	77	DPWA	$\overline{K}N$ multichannel
1765	DEBELLEFON	76	IPWA	$K^-p \to \Lambda\pi^0$

$\Sigma(1775)$ WIDTH

VALUE (MeV)	DOCUMENT ID		TECN	COMMENT
105 to 135 (≈ 120) OUR ESTIMATE				
131 ± 3	ZHANG	13A	DPWA	Multichannel
137 ± 10	GOPAL	80	DPWA	$\overline{K}N \to \overline{K}N$
116 ± 10	ALSTON-...	78	DPWA	$\overline{K}N \to \overline{K}N$
130 ± 10	GOPAL	77	DPWA	$\overline{K}N$ multichannel
125 ± 15	BAILLON	75	IPWA	$\overline{K}N \to \Lambda\pi$
146 ± 18	VANHORN	75	DPWA	$K^-p \to \Lambda\pi^0$
154 ± 10	KANE	74	DPWA	$K^-p \to \Sigma\pi$
• • • We do not use the following data for averages, fits, limits, etc. • • •				
102 or 103	[1] MARTIN	77	DPWA	$\overline{K}N$ multichannel
120	DEBELLEFON	76	IPWA	$K^-p \to \Lambda\pi^0$

$\Sigma(1775)$ POLE POSITION

REAL PART

VALUE (MeV)	DOCUMENT ID		TECN	COMMENT
• • • We do not use the following data for averages, fits, limits, etc. • • •				
1759	ZHANG	13A	DPWA	Multichannel

−2×IMAGINARY PART

VALUE (MeV)	DOCUMENT ID		TECN	COMMENT
• • • We do not use the following data for averages, fits, limits, etc. • • •				
118	ZHANG	13A	DPWA	Multichannel

$\Sigma(1775)$ DECAY MODES

	Mode	Fraction (Γ_i/Γ)
Γ_1	$N\overline{K}$	37–43%
Γ_2	$\Lambda\pi$	14–20%
Γ_3	$\Sigma\pi$	2–5%
Γ_4	$\Sigma(1385)\pi$	8–12%
Γ_5	$\Sigma(1385)\pi$, D-wave	
Γ_6	$\Lambda(1520)\pi$, P-wave	17–23%
Γ_7	$\Sigma\pi\pi$	
Γ_8	$\Delta(1232)\overline{K}$, D-wave	
Γ_9	$N\overline{K}^*(892)$, S=1/2	
Γ_{10}	$N\overline{K}^*(892)$, S=3/2, D-wave	

The above branching fractions are our estimates, not fits or averages.

CONSTRAINED FIT INFORMATION

An overall fit to 7 branching ratios uses 18 measurements and one constraint to determine 5 parameters. The overall fit has a $\chi^2 = 363.4$ for 14 degrees of freedom.

The following *off-diagonal* array elements are the correlation coefficients $\langle \delta x_i \delta x_j \rangle / (\delta x_i \cdot \delta x_j)$, in percent, from the fit to the branching fractions, $x_i \equiv \Gamma_i/\Gamma_{\text{total}}$. The fit constrains the x_i whose labels appear in this array to sum to one.

x_2	−44			
x_3	−23	10		
x_4	−23	−32	−4	
x_6	−3	1	1	−84
	x_1	x_2	x_3	x_4

$\Sigma(1775)$ BRANCHING RATIOS

See "Sign conventions for resonance couplings" in the Note on Λ and Σ Resonances. Also, the errors quoted do not include uncertainties due to the parametrization used in the partial-wave analyses and are thus too small.

$\Gamma(N\overline{K})/\Gamma_{\text{total}}$ Γ_1/Γ

VALUE	DOCUMENT ID		TECN	COMMENT
0.37 to 0.43 OUR ESTIMATE				
0.421 ± 0.020 OUR FIT Error includes scale factor of 2.5.				
0.398 ± 0.009 OUR AVERAGE				
0.40 ± 0.01	ZHANG	13A	DPWA	Multichannel
0.40 ± 0.02	GOPAL	80	DPWA	$\overline{K}N \to \overline{K}N$
0.37 ± 0.03	ALSTON-...	78	DPWA	$\overline{K}N \to \overline{K}N$
• • • We do not use the following data for averages, fits, limits, etc. • • •				
0.41 ± 0.03	GOPAL	77	DPWA	See GOPAL 80
0.37 or 0.36	[1] MARTIN	77	DPWA	$\overline{K}N$ multichannel

$\Gamma(\Lambda\pi)/\Gamma(N\overline{K})$ Γ_2/Γ_1

VALUE	DOCUMENT ID		TECN	COMMENT
0.48 ± 0.06 OUR FIT Error includes scale factor of 2.3.				
0.33 ± 0.05	UHLIG	67	HBC	K^-p 0.9 GeV/c

$(\Gamma_i\Gamma_f)^{1/2}/\Gamma_{\text{total}}$ in $N\overline{K} \to \Sigma(1775) \to \Lambda\pi$ $(\Gamma_1\Gamma_2)^{1/2}/\Gamma$

VALUE	DOCUMENT ID		TECN	COMMENT
0.293 ± 0.013 OUR FIT Error includes scale factor of 1.8.				
0.295 ± 0.012 OUR AVERAGE Signs on measurements were ignored. Error includes scale factor of 1.4. See the ideogram below.				
−0.31 ± 0.01	ZHANG	13A	DPWA	Multichannel
−0.28 ± 0.03	GOPAL	77	DPWA	$\overline{K}N$ multichannel
−0.25 ± 0.02	BAILLON	75	IPWA	$\overline{K}N \to \Lambda\pi$
$-0.28\ ^{+0.04}_{-0.05}$	VANHORN	75	DPWA	$K^-p \to \Lambda\pi^0$
−0.259 ± 0.048	DEVENISH	74B		Fixed-t dispersion rel.
• • • We do not use the following data for averages, fits, limits, etc. • • •				
−0.29 or −0.28	[1] MARTIN	77	DPWA	$\overline{K}N$ multichannel
−0.30	DEBELLEFON	76	IPWA	$K^-p \to \Lambda\pi^0$

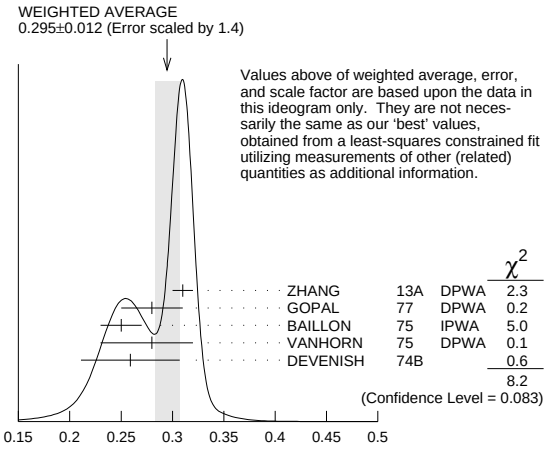

$(\Gamma_i\Gamma_f)^{1/2}/\Gamma_{\text{total}}$ in $N\overline{K} \to \Sigma(1775) \to \Lambda\pi$

$(\Gamma_i\Gamma_f)^{1/2}/\Gamma_{\text{total}}$ in $N\overline{K} \to \Sigma(1775) \to \Sigma\pi$ $(\Gamma_1\Gamma_3)^{1/2}/\Gamma$

VALUE	DOCUMENT ID		TECN	COMMENT
0.090 ± 0.009 OUR FIT Error includes scale factor of 1.4.				
0.090 ± 0.011 OUR AVERAGE Signs on measurements were ignored. Error includes scale factor of 1.6. See the ideogram below.				
+0.08 ± 0.01	ZHANG	13A	DPWA	Multichannel
+0.13 ± 0.02	GOPAL	77	DPWA	$\overline{K}N$ multichannel
0.09 ± 0.01	KANE	74	DPWA	$K^-p \to \Sigma\pi$
• • • We do not use the following data for averages, fits, limits, etc. • • •				
+0.08 or +0.08	[1] MARTIN	77	DPWA	$\overline{K}N$ multichannel

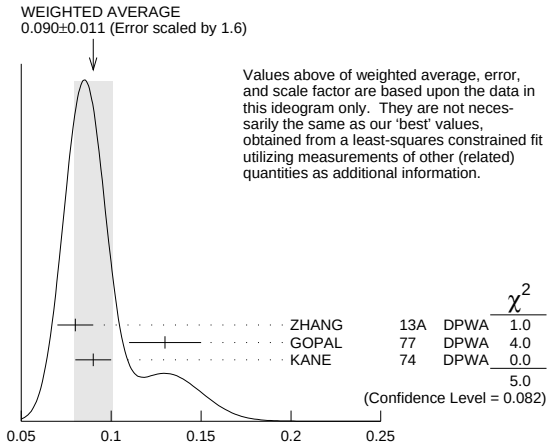

$(\Gamma_i\Gamma_f)^{1/2}/\Gamma_{total}$ in $N\overline{K} \to \Sigma(1775) \to \Sigma\pi$

$\Gamma(\Sigma(1385)\pi)/\Gamma(N\overline{K})$ Γ_4/Γ_1

VALUE	DOCUMENT ID		TECN	COMMENT
0.79±0.11 OUR FIT Error includes scale factor of 3.2.				
0.25±0.09	UHLIG	67	HBC	K^-p 0.9 GeV/c

$(\Gamma_i\Gamma_f)^{1/2}/\Gamma_{total}$ in $N\overline{K} \to \Sigma(1775) \to \Sigma(1385)\pi$, D-wave $(\Gamma_1\Gamma_5)^{1/2}/\Gamma$

VALUE	DOCUMENT ID		TECN	COMMENT
0.155±0.024 OUR AVERAGE Signs on measurements were ignored. Error includes scale factor of 3.5. See the ideogram below.				
−0.12 ±0.01	ZHANG	13A	DPWA	Multichannel
−0.184±0.011	[2] CAMERON	78	DPWA	$K^-p \to \Sigma(1385)\pi$
+0.20 ±0.02	PREVOST	74	DPWA	$K^-N \to \Sigma(1385)\pi$
• • • We do not use the following data for averages, fits, limits, etc. • • •				
0.32 ±0.06	SIMS	68	DBC	$K^-N \to \Lambda\pi\pi$
0.24 ±0.03	ARMENTEROS	67C	HBC	$K^-p \to \Lambda\pi\pi$

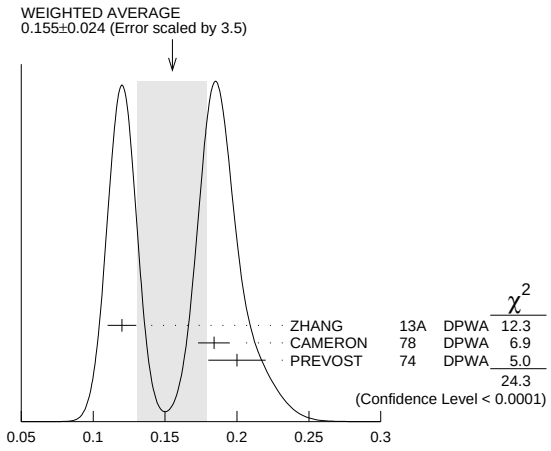

$(\Gamma_i\Gamma_f)^{1/2}/\Gamma_{total}$ in $N\overline{K} \to \Sigma(1775) \to \Sigma(1385)\pi$, D-wave

$\Gamma(\Lambda(1520)\pi, P\text{-wave})/\Gamma(N\overline{K})$ Γ_6/Γ_1

VALUE	DOCUMENT ID		TECN	COMMENT
$0.053^{+0.080}_{-0.035}$ OUR FIT Error includes scale factor of 11.8.				
0.28 ±0.05	UHLIG	67	HBC	K^-p 0.9 GeV/c

$(\Gamma_i\Gamma_f)^{1/2}/\Gamma_{total}$ in $N\overline{K} \to \Sigma(1775) \to \Lambda(1520)\pi$, P-wave $(\Gamma_1\Gamma_6)^{1/2}/\Gamma$

VALUE	DOCUMENT ID		TECN	COMMENT
0.10 ±0.06 OUR FIT Error includes scale factor of 11.5.				
0.20 ±0.07 OUR AVERAGE Signs on measurements were ignored. Error includes scale factor of 10.7. See the ideogram below.				
−0.06 ±0.01	ZHANG	13A	DPWA	Multichannel
−0.305±0.010	[3] CAMERON	77	DPWA	$K^-p \to \Lambda(1520)\pi^0$
0.31 ±0.02	BARLETTA	72	DPWA	$K^-p \to \Lambda(1520)\pi^0$
0.27 ±0.03	ARMENTEROS	65C	HBC	$K^-p \to \Lambda(1520)\pi^0$

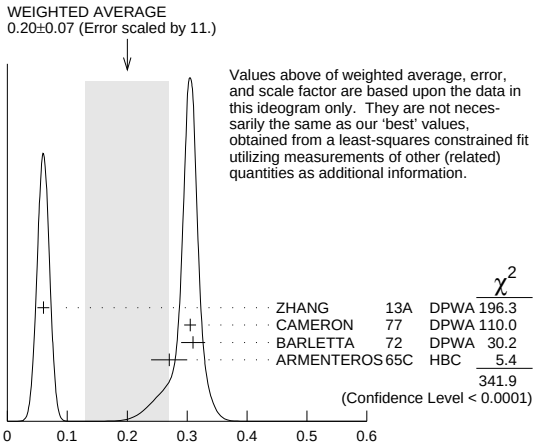

$(\Gamma_i\Gamma_f)^{1/2}/\Gamma_{total}$ in $N\overline{K} \to \Sigma(1775) \to \Lambda(1520)\pi$, P-wave

$\Gamma(\Sigma\pi\pi)/\Gamma_{total}$ Γ_7/Γ

VALUE	DOCUMENT ID		TECN	COMMENT
• • • We do not use the following data for averages, fits, limits, etc. • • •				
0.12	[4] ARMENTEROS	68C	HDBC	$K^-N \to \Sigma\pi\pi$

$(\Gamma_i\Gamma_f)^{1/2}/\Gamma_{total}$ in $N\overline{K} \to \Sigma(1775) \to \Delta(1232)\overline{K}$, D-wave $(\Gamma_1\Gamma_8)^{1/2}/\Gamma$

VALUE	DOCUMENT ID		TECN	COMMENT
+0.06±0.03	ZHANG	13A	DPWA	Multichannel

$(\Gamma_i\Gamma_f)^{1/2}/\Gamma_{total}$ in $N\overline{K} \to \Sigma(1775) \to N\overline{K}^*(892)$, S=1/2 $(\Gamma_1\Gamma_9)^{1/2}/\Gamma$

VALUE	DOCUMENT ID		TECN	COMMENT
+0.04±0.01	ZHANG	13A	DPWA	Multichannel

$(\Gamma_i\Gamma_f)^{1/2}/\Gamma_{total}$ in $N\overline{K} \to \Sigma(1775) \to N\overline{K}^*(892)$, S=3/2, D-wave $(\Gamma_1\Gamma_{10})^{1/2}/\Gamma$

VALUE	DOCUMENT ID		TECN	COMMENT
+0.04±0.01	ZHANG	13A	DPWA	Multichannel

$\Sigma(1775)$ FOOTNOTES

[1] The two MARTIN 77 values are from a T-matrix pole and from a Breit-Wigner fit.
[2] The CAMERON 78 upper limit on G-wave decay is 0.03.
[3] This rate combines P-wave- and F-wave decays. The CAMERON 77 results for the separate P-wave- and F-wave decays are -0.303 ± 0.010 and -0.037 ± 0.014. The published signs have been changed here to be in accord with the baryon-first convention.
[4] For about 3/4 of this, the $\Sigma\pi$ system has $I = 0$ and is almost entirely $\Lambda(1520)$. For the rest, the $\Sigma\pi$ has $I = 1$, which is about what is expected from the known $\Sigma(1775) \to \Sigma(1385)\pi$ rate, as seen in $\Lambda\pi\pi$.

$\Sigma(1775)$ REFERENCES

ZHANG	13A	PR C88 035205	H. Zhang *et al.*	(KSU)
PDG	82	PL 111B 1	M. Roos *et al.*	(HELS, CIT, CERN)
GOPAL	80	Toronto Conf. 159	G.P. Gopal	(RHEL) IJP
ALSTON-...	78	PR D18 182	M. Alston-Garnjost *et al.*	(LBL, MTHO+) IJP
Also		PRL 38 1007	M. Alston-Garnjost *et al.*	(LBL, MTHO+) IJP
CAMERON	78	NP B143 189	W. Cameron *et al.*	(RHEL, LOIC) IJP
CAMERON	77	NP B131 399	W. Cameron *et al.*	(RHEL, LOIC) IJP
GOPAL	77	NP B119 362	G.P. Gopal *et al.*	(LOIC, RHEL) IJP
MARTIN	77	NP B127 349	B.R. Martin, M.K. Pidcock, R.G. Moorhouse	(LOUC+) IJP
Also		NP B126 266	B.R. Martin, M.K. Pidcock	(LOUC)
Also		NP B126 285	B.R. Martin, M.K. Pidcock	(LOUC) IJP
DEBELLEFON	76	NP B109 129	A. de Bellefon, A. Berthon	(CDEF) IJP
BAILLON	75	NP B94 39	P.H. Baillon, P.J. Litchfield	(CERN, RHEL) IJP
VANHORN	75	NP B87 145	A.J. van Horn	(LBL) IJP
Also		NP B87 157	A.J. van Horn	(LBL) IJP
DEVENISH	74B	NP B81 330	R.C.E. Devenish, C.D. Froggatt, B.R. Martin	(DESY+)
KANE	74	LBL-2452	D.F. Kane	(LBL) IJP
PREVOST	74	NP B69 246	J. Prevost *et al.*	(SACL, CERN, HEID)
BARLETTA	72	NP B40 45	W.A. Barletta	(EFI) IJP
Also		PRL 17 841	S. Fenster *et al.*	(CHIC, ANL, CERN) IJP
ARMENTEROS	68C	NP B8 216	R. Armenteros *et al.*	(CERN, HEID, SACL) I
SIMS	68	PRL 21 1413	W.H. Sims *et al.*	(FSU, TUFTS, BRAN)
ARMENTEROS	67C	ZPHY 202 486	R. Armenteros *et al.*	(CERN, HEID, SACL)
UHLIG	67	PR 155 1448	R.P. Uhlig *et al.*	(UMD, NRL)
ARMENTEROS	65C	PL 19 338	R. Armenteros *et al.*	(CERN, HEID, SACL) IJP
GALTIERI	63	PL 6 296	A. Galtieri, A. Hussain, R. Tripp	(LRL) IJ

See key on page 547

$\Sigma(1840)\ 3/2^+$

$I(J^P) = 1(\frac{3}{2}^+)$ Status: *

OMITTED FROM SUMMARY TABLE

For the time being, we list together here all resonance claims in the P_{13} wave between 1700 and 1900 MeV.

$\Sigma(1840)$ MASS

VALUE (MeV)	DOCUMENT ID		TECN	COMMENT
≈ 1840 OUR ESTIMATE				
1798 or 1802	[1] MARTIN	77	DPWA	$\overline{K}N$ multichannel
1720 ± 30	[2] BAILLON	75	IPWA	$\overline{K}N \to \Lambda\pi$
1925 ± 200	VANHORN	75	DPWA	$K^-p \to \Lambda\pi^0$
1840 ± 10	LANGBEIN	72	IPWA	$\overline{K}N$ multichannel

$\Sigma(1840)$ WIDTH

VALUE (MeV)	DOCUMENT ID		TECN	COMMENT
93 or 93	[1] MARTIN	77	DPWA	$\overline{K}N$ multichannel
120 ± 30	[2] BAILLON	75	IPWA	$\overline{K}N \to \Lambda\pi$
65^{+50}_{-20}	VANHORN	75	DPWA	$K^-p \to \Lambda\pi^0$
120 ± 10	LANGBEIN	72	IPWA	$\overline{K}N$ multichannel

$\Sigma(1840)$ DECAY MODES

	Mode
Γ_1	$N\overline{K}$
Γ_2	$\Lambda\pi$
Γ_3	$\Sigma\pi$

$\Sigma(1840)$ BRANCHING RATIOS

See "Sign conventions for resonance couplings" in the Note on Λ and Σ Resonances.

$\Gamma(N\overline{K})/\Gamma_{total}$ Γ_1/Γ

VALUE	DOCUMENT ID		TECN	COMMENT
0 or 0	[1] MARTIN	77	DPWA	$\overline{K}N$ multichannel
0.37 ± 0.13	LANGBEIN	72	IPWA	$\overline{K}N$ multichannel

$(\Gamma_i\Gamma_f)^{1/2}/\Gamma_{total}$ in $N\overline{K} \to \Sigma(1840) \to \Lambda\pi$ $(\Gamma_1\Gamma_2)^{1/2}/\Gamma$

VALUE	DOCUMENT ID		TECN	COMMENT
+0.03 or +0.03	[1] MARTIN	77	DPWA	$\overline{K}N$ multichannel
+0.11 ±0.02	[2] BAILLON	75	IPWA	$\overline{K}N \to \Lambda\pi$
+0.06 ±0.04	VANHORN	75	DPWA	$K^-p \to \Lambda\pi^0$
+0.122 ± 0.078	DEVENISH	74B		Fixed-t dispersion rel.
0.20 ±0.04	LANGBEIN	72	IPWA	$\overline{K}N$ multichannel

$(\Gamma_i\Gamma_f)^{1/2}/\Gamma_{total}$ in $N\overline{K} \to \Sigma(1840) \to \Sigma\pi$ $(\Gamma_1\Gamma_3)^{1/2}/\Gamma$

VALUE	DOCUMENT ID		TECN	COMMENT
−0.04 or −0.04	[1] MARTIN	77	DPWA	$\overline{K}N$ multichannel
0.15 ± 0.04	LANGBEIN	72	IPWA	$\overline{K}N$ multichannel

$\Sigma(1840)$ FOOTNOTES

[1] The two MARTIN 77 values are from a T-matrix pole and from a Breit-Wigner fit.

[2] From solution 1 of BAILLON 75; not present in solution 2.

$\Sigma(1840)$ REFERENCES

MARTIN	77	NP B127 349	B.R. Martin, M.K. Pidcock, R.G. Moorhouse	(LOUC+) IJP
Also		NP B126 266	B.R. Martin, M.K. Pidcock	(LOUC)
Also		NP B126 285	B.R. Martin, M.K. Pidcock	(LOUC) IJP
BAILLON	75	NP B94 39	P.H. Baillon, P.J. Litchfield	(CERN, RHEL) IJP
VANHORN	75	NP B87 145	A.J. van Horn	(LBL) IJP
Also		NP B87 157	A.J. van Horn	(LBL) IJP
DEVENISH	74B	NP B81 330	R.C.E. Devenish, C.D. Froggatt, B.R. Martin	(DESY+)
LANGBEIN	72	NP B47 477	W. Langbein, F. Wagner	(MPIM) IJP

$\Sigma(1880)\ 1/2^+$

$I(J^P) = 1(\frac{1}{2}^+)$ Status: **

OMITTED FROM SUMMARY TABLE

A P_{11} resonance is suggested by several partial-wave analyses, but with wide variations in the mass and other parameters. We list here all claims which lie well above the P_{11} $\Sigma(1770)$.

$\Sigma(1880)$ MASS

VALUE (MeV)	DOCUMENT ID		TECN	COMMENT
≈ 1880 OUR ESTIMATE				
1821 ± 17	ZHANG	13A	DPWA	Multichannel
1826 ± 20	GOPAL	80	DPWA	$\overline{K}N \to \overline{K}N$
1870 ± 10	CAMERON	78B	DPWA	$K^-p \to N\overline{K}^*$
1847 or 1863	[1] MARTIN	77	DPWA	$\overline{K}N$ multichannel
1960 ± 30	[2] BAILLON	75	IPWA	$\overline{K}N \to \Lambda\pi$
1985 ± 50	VANHORN	75	DPWA	$K^-p \to \Lambda\pi^0$
1898	[3] LEA	73	DPWA	Multichannel K-matrix
~ 1850	ARMENTEROS	70	IPWA	$\overline{K}N \to \overline{K}N$
1950 ± 50	BARBARO-...	70	DPWA	$K^-N \to \Lambda\pi$
1920 ± 30	LITCHFIELD	70	DPWA	$K^-N \to \Lambda\pi$
1850	BAILEY	69	DPWA	$\overline{K}N \to \overline{K}N$
1882 ± 40	SMART	68	DPWA	$K^-N \to \Lambda\pi$

$\Sigma(1880)$ WIDTH

VALUE (MeV)	DOCUMENT ID		TECN	COMMENT
300 ± 59	ZHANG	13A	DPWA	Multichannel
86 ± 15	GOPAL	80	DPWA	$\overline{K}N \to \overline{K}N$
80 ± 10	CAMERON	78B	DPWA	$K^-p \to N\overline{K}^*$
216 or 220	[1] MARTIN	77	DPWA	$\overline{K}N$ multichannel
260 ± 40	[2] BAILLON	75	IPWA	$\overline{K}N \to \Lambda\pi$
220 ± 140	VANHORN	75	DPWA	$K^-p \to \Lambda\pi^0$
222	[3] LEA	73	DPWA	Multichannel K-matrix
~ 30	ARMENTEROS	70	IPWA	$\overline{K}N \to \overline{K}N$
200 ± 50	BARBARO-...	70	DPWA	$K^-N \to \Lambda\pi$
170 ± 40	LITCHFIELD	70	DPWA	$K^-N \to \Lambda\pi$
200	BAILEY	69	DPWA	$\overline{K}N \to \overline{K}N$
222 ± 150	SMART	68	DPWA	$K^-N \to \Lambda\pi$

$\Sigma(1880)$ POLE POSITION

REAL PART

VALUE (MeV)	DOCUMENT ID	TECN	COMMENT
• • • We do not use the following data for averages, fits, limits, etc. • • •			
1776	ZHANG 13A	DPWA	Multichannel

−2×IMAGINARY PART

VALUE (MeV)	DOCUMENT ID	TECN	COMMENT
• • • We do not use the following data for averages, fits, limits, etc. • • •			
270	ZHANG 13A	DPWA	Multichannel

$\Sigma(1880)$ DECAY MODES

	Mode	Fraction (Γ_i/Γ)
Γ_1	$N\overline{K}$	
Γ_2	$\Lambda\pi$	
Γ_3	$\Sigma\pi$	
Γ_4	$\Lambda(1520)\pi$, D-wave	(2.0 ± 1.0) %
Γ_5	$N\overline{K}^*(892)$, S=1/2, P-wave	
Γ_6	$N\overline{K}^*(892)$, S=3/2, P-wave	
Γ_7	$\Delta(1232)\overline{K}$, P-wave	(39 ± 8) %

$\Sigma(1880)$ BRANCHING RATIOS

See "Sign conventions for resonance couplings" in the Note on Λ and Σ Resonances.

$\Gamma(N\overline{K})/\Gamma_{total}$ Γ_1/Γ

VALUE	DOCUMENT ID		TECN	COMMENT
0.10 ± 0.03	ZHANG	13A	DPWA	Multichannel
0.06 ± 0.02	GOPAL	80	DPWA	$\overline{K}N \to \overline{K}N$
0.27 or 0.27	[1] MARTIN	77	DPWA	$\overline{K}N$ multichannel
0.31	[3] LEA	73	DPWA	Multichannel K-matrix
0.20	ARMENTEROS	70	IPWA	$\overline{K}N \to \overline{K}N$
0.22	BAILEY	69	DPWA	$\overline{K}N \to \overline{K}N$

$(\Gamma_i\Gamma_f)^{1/2}/\Gamma_{total}$ in $N\overline{K}\to\Sigma(1880)\to\Lambda\pi$ $(\Gamma_1\Gamma_2)^{1/2}/\Gamma$

VALUE	DOCUMENT ID		TECN	COMMENT
-0.24 or -0.24	[1] MARTIN	77	DPWA	$\overline{K}N$ multichannel
-0.12 ± 0.02	[2] BAILLON	75	IPWA	$\overline{K}N\to\Lambda\pi$
$+0.05\ ^{+0.07}_{-0.02}$	VANHORN	75	DPWA	$K^-p\to\Lambda\pi^0$
-0.169 ± 0.119	DEVENISH	74B		Fixed-t dispersion rel.
-0.30	[3] LEA	73	DPWA	Multichannel K-matrix
-0.09 ± 0.04	BARBARO-...	70	DPWA	$K^-N\to\Lambda\pi$
-0.14 ± 0.03	LITCHFIELD	70	DPWA	$K^-N\to\Lambda\pi$
-0.11 ± 0.03	SMART	68	DPWA	$K^-N\to\Lambda\pi$

$(\Gamma_i\Gamma_f)^{1/2}/\Gamma_{total}$ in $N\overline{K}\to\Sigma(1880)\to\Sigma\pi$ $(\Gamma_1\Gamma_3)^{1/2}/\Gamma$

VALUE	DOCUMENT ID		TECN	COMMENT
$+0.30$ or $+0.29$	[1] MARTIN	77	DPWA	$\overline{K}N$ multichannel
not seen	[3] LEA	73	DPWA	Multichannel K-matrix

$\Gamma(\Lambda(1520)\pi, D\text{-wave})/\Gamma_{total}$ Γ_4/Γ

VALUE	DOCUMENT ID		TECN	COMMENT
0.02 ± 0.01	ZHANG	13A	DPWA	Multichannel

$(\Gamma_i\Gamma_f)^{1/2}/\Gamma_{total}$ in $N\overline{K}\to\Sigma(1880)\to N\overline{K}^*(892)$, $S=1/2$, P-wave $(\Gamma_1\Gamma_5)^{1/2}/\Gamma$

VALUE	DOCUMENT ID		TECN	COMMENT
-0.05 ± 0.03	[4] CAMERON	78B	DPWA	$K^-p\to N\overline{K}^*$

$(\Gamma_i\Gamma_f)^{1/2}/\Gamma_{total}$ in $N\overline{K}\to\Sigma(1880)\to N\overline{K}^*(892)$, $S=3/2$, P-wave $(\Gamma_1\Gamma_6)^{1/2}/\Gamma$

VALUE	DOCUMENT ID		TECN	COMMENT
$+0.11\pm0.03$	CAMERON	78B	DPWA	$K^-p\to N\overline{K}^*$

$\Gamma(\Delta(1232)\overline{K}, P\text{-wave})/\Gamma_{total}$ Γ_7/Γ

VALUE	DOCUMENT ID		TECN	COMMENT
0.39 ± 0.08	ZHANG	13A	DPWA	Multichannel

$\Sigma(1880)$ FOOTNOTES

[1] The two MARTIN 77 values are from a T-matrix pole and from a Breit-Wigner fit.
[2] From solution 1 of BAILLON 75; not present in solution 2.
[3] Only unconstrained states from table 1 of LEA 73 are listed.
[4] The published sign has been changed to be in accord with the baryon-first convention.

$\Sigma(1880)$ REFERENCES

ZHANG	13A	PR C88 035205	H. Zhang *et al.*	(KSU)
GOPAL	80	Toronto Conf. 159	G.P. Gopal	(RHEL) IJP
CAMERON	78B	NP B146 327	W. Cameron *et al.*	(RHEL, LOIC) IJP
MARTIN	77	NP B127 349	B.R. Martin, M.K. Pidcock, R.G. Moorhouse	(LOUC+) IJP
Also		NP B126 266	B.R. Martin, M.K. Pidcock	(LOUC)
Also		NP B126 285	B.R. Martin, M.K. Pidcock	(LOUC) IJP
BAILLON	75	NP B94 39	P.H. Baillon, P.J. Litchfield	(CERN, RHEL) IJP
VANHORN	75	NP B87 145	A.J. van Horn	(LBL) IJP
Also		NP B87 157	A.J. van Horn	(LBL) IJP
DEVENISH	74B	NP B81 330	R.C.E. Devenish, C.D. Froggatt, B.R. Martin	(DESY+)
LEA	73	NP B56 77	A.T. Lea *et al.*	(RHEL, LOUC, GLAS, AARH) IJP
ARMENTEROS	70	Duke Conf. 123 Hyperon Resonances, 1970	R. Armenteros *et al.*	(CERN, HEID, SACL) IJP
BARBARO-...	70	Duke Conf. 173 Hyperon Resonances, 1970	A. Barbaro-Galtieri	(LRL) IJP
LITCHFIELD	70	NP B22 269	P.J. Litchfield	(RHEL) IJP
BAILEY	69	Thesis UCRL 50617	J.M. Bailey	(LLL) IJP
SMART	68	PR 169 1330	W.M. Smart	(LRL) IJP

$\Sigma(1900)\ 1/2^-$

$I(J^P) = 1(\frac{1}{2}^-)$ Status: *

OMITTED FROM SUMMARY TABLE

$\Sigma(1900)$ MASS

VALUE (MeV)	DOCUMENT ID		TECN	COMMENT
1900 ± 21	ZHANG	13A	DPWA	Multichannel

$\Lambda(1900)$ WIDTH

VALUE (MeV)	DOCUMENT ID		TECN	COMMENT
191 ± 47	ZHANG	13A	DPWA	Multichannel

$\Sigma(1900)$ DECAY MODES

	Mode	Fraction (Γ_i/Γ)
Γ_1	$N\overline{K}$	(67±17) %
Γ_2	$\Sigma\pi$	(10± 5) %

$\Sigma(1900)$ BRANCHING RATIOS

$\Gamma(N\overline{K})/\Gamma_{total}$ Γ_1/Γ

VALUE	DOCUMENT ID		TECN	COMMENT
0.67 ± 0.17	ZHANG	13A	DPWA	Multichannel

$\Gamma(\Sigma\pi)/\Gamma_{total}$ Γ_2/Γ

VALUE	DOCUMENT ID		TECN	COMMENT
0.10 ± 0.05	ZHANG	13A	DPWA	Multichannel

$\Sigma(1900)$ REFERENCES

ZHANG	13A	PR C88 035205	H. Zhang *et al.*	(KSU)

$\Sigma(1915)\ 5/2^+$

$I(J^P) = 1(\frac{5}{2}^+)$ Status: ****

Discovered by COOL 66. For results published before 1974 (they are now obsolete), see our 1982 edition Physics Letters **111B** 1 (1982).

This entry only includes results from partial-wave analyses. Parameters of peaks seen in cross sections and invariant-mass distributions in this region used to be listed in in a separate entry immediately following. They may be found in our 1986 edition Physics Letters **170B** 1 (1986).

$\Sigma(1915)$ MASS

VALUE (MeV)	DOCUMENT ID		TECN	COMMENT
1900 to 1935 ($\approx$ 1915) OUR ESTIMATE				
1920 ± 7	ZHANG	13A	DPWA	Multichannel
1937 ± 20	ALSTON-...	78	DPWA	$\overline{K}N\to\overline{K}N$
1894 ± 5	[1] CORDEN	77C		$K^-n\to\Sigma\pi$
1909 ± 5	[1] CORDEN	77C		$K^-n\to\Sigma\pi$
1920 ± 10	GOPAL	77	DPWA	$\overline{K}N$ multichannel
1900 ± 4	[2] CORDEN	76	DPWA	$K^-n\to\Lambda\pi^-$
1920 ± 30	BAILLON	75	IPWA	$\overline{K}N\to\Lambda\pi$
1914 ± 10	HEMINGWAY	75	DPWA	$K^-p\to\overline{K}N$
$1920\ ^{+15}_{-20}$	VANHORN	75	DPWA	$K^-p\to\Lambda\pi^0$
1920 ± 5	KANE	74	DPWA	$K^-p\to\Sigma\pi$
• • • We do not use the following data for averages, fits, limits, etc. • • •				
not seen	DECLAIS	77	DPWA	$\overline{K}N\to\overline{K}N$
1925 or 1933	[3] MARTIN	77	DPWA	$\overline{K}N$ multichannel
1915	DEBELLEFON	76	IPWA	$K^-p\to\Lambda\pi^0$

$\Sigma(1915)$ WIDTH

VALUE (MeV)	DOCUMENT ID		TECN	COMMENT
80 to 160 ($\approx$ 120) OUR ESTIMATE				
149 ± 17	ZHANG	13A	DPWA	Multichannel
161 ± 20	ALSTON-...	78	DPWA	$\overline{K}N\to\overline{K}N$
107 ± 14	[1] CORDEN	77C		$K^-n\to\Sigma\pi$
85 ± 13	[1] CORDEN	77C		$K^-n\to\Sigma\pi$
130 ± 10	GOPAL	77	DPWA	$\overline{K}N$ multichannel
75 ± 14	[2] CORDEN	76	DPWA	$K^-n\to\Lambda\pi^-$
70 ± 20	BAILLON	75	IPWA	$\overline{K}N\to\Lambda\pi$
85 ± 15	HEMINGWAY	75	DPWA	$K^-p\to\overline{K}N$
102 ± 18	VANHORN	75	DPWA	$K^-p\to\Lambda\pi^0$
162 ± 25	KANE	74	DPWA	$K^-p\to\Sigma\pi$
• • • We do not use the following data for averages, fits, limits, etc. • • •				
171 or 173	[3] MARTIN	77	DPWA	$\overline{K}N$ multichannel
60	DEBELLEFON	76	IPWA	$K^-p\to\Lambda\pi^0$

$\Sigma(1915)$ POLE POSITION

REAL PART

VALUE (MeV)	DOCUMENT ID		TECN	COMMENT
• • • We do not use the following data for averages, fits, limits, etc. • • •				
1897	ZHANG	13A	DPWA	Multichannel

$-2\times$IMAGINARY PART

VALUE (MeV)	DOCUMENT ID		TECN	COMMENT
• • • We do not use the following data for averages, fits, limits, etc. • • •				
133	ZHANG	13A	DPWA	Multichannel

$\Sigma(1915)$ DECAY MODES

	Mode	Fraction (Γ_i/Γ)
Γ_1	$N\overline{K}$	5–15 %
Γ_2	$\Lambda\pi$	seen
Γ_3	$\Sigma\pi$	seen
Γ_4	$\Sigma(1385)\pi$	<5 %
Γ_5	$\Sigma(1385)\pi$, P-wave	
Γ_6	$\Sigma(1385)\pi$, F-wave	

The above branching fractions are our estimates, not fits or averages.

$\Sigma(1915)$ BRANCHING RATIOS

See "Sign conventions for resonance couplings" in the Note on Λ and Σ Resonances.

$\Gamma(N\overline{K})/\Gamma_{total}$ Γ_1/Γ

VALUE	DOCUMENT ID		TECN	COMMENT
0.05 to 0.15 OUR ESTIMATE				
0.026±0.004	ZHANG	13A	DPWA	Multichannel
0.03 ±0.02	[4] GOPAL	80	DPWA	$\overline{K}N \to \overline{K}N$
0.14 ±0.05	ALSTON-...	78	DPWA	$\overline{K}N \to \overline{K}N$
0.11 ±0.04	HEMINGWAY	75	DPWA	$K^-p \to \overline{K}N$
• • • We do not use the following data for averages, fits, limits, etc. • • •				
0.05 ±0.03	GOPAL	77	DPWA	See GOPAL 80
0.08 or 0.08	[3] MARTIN	77	DPWA	$\overline{K}N$ multichannel

$(\Gamma_i\Gamma_f)^{1/2}/\Gamma_{total}$ in $N\overline{K} \to \Sigma(1915) \to \Lambda\pi$ $(\Gamma_1\Gamma_2)^{1/2}/\Gamma$

VALUE	DOCUMENT ID		TECN	COMMENT
−0.09 ±0.03	GOPAL	77	DPWA	$\overline{K}N$ multichannel
−0.10 ±0.01	[2] CORDEN	76	DPWA	$K^-n \to \Lambda\pi^-$
−0.06 ±0.02	BAILLON	75	IPWA	$\overline{K}N \to \Lambda\pi$
−0.09 ±0.02	VANHORN	75	DPWA	$K^-p \to \Lambda\pi^0$
−0.087±0.056	DEVENISH	74B		Fixed-t dispersion rel.
• • • We do not use the following data for averages, fits, limits, etc. • • •				
−0.09 or −0.09	[3] MARTIN	77	DPWA	$\overline{K}N$ multichannel
−0.10	DEBELLEFON	76	IPWA	$K^-p \to \Lambda\pi^0$

$(\Gamma_i\Gamma_f)^{1/2}/\Gamma_{total}$ in $N\overline{K} \to \Sigma(1915) \to \Sigma\pi$ $(\Gamma_1\Gamma_3)^{1/2}/\Gamma$

VALUE	DOCUMENT ID		TECN	COMMENT
−0.14±0.01	ZHANG	13A	DPWA	Multichannel
−0.17±0.01	[1] CORDEN	77C		$K^-n \to \Sigma\pi$
−0.15±0.02	[1] CORDEN	77C		$K^-n \to \Sigma\pi$
−0.19±0.03	GOPAL	77	DPWA	$\overline{K}N$ multichannel
−0.16±0.03	KANE	74	DPWA	$K^-p \to \Sigma\pi$
• • • We do not use the following data for averages, fits, limits, etc. • • •				
−0.05 or −0.05	[3] MARTIN	77	DPWA	$\overline{K}N$ multichannel

$(\Gamma_i\Gamma_f)^{1/2}/\Gamma_{total}$ in $N\overline{K} \to \Sigma(1915) \to \Sigma(1385)\pi$, P-wave $(\Gamma_1\Gamma_5)^{1/2}/\Gamma$

VALUE	DOCUMENT ID		TECN	COMMENT
<0.01	CAMERON	78	DPWA	$K^-p \to \Sigma(1385)\pi$

$(\Gamma_i\Gamma_f)^{1/2}/\Gamma_{total}$ in $N\overline{K} \to \Sigma(1915) \to \Sigma(1385)\pi$, F-wave $(\Gamma_1\Gamma_6)^{1/2}/\Gamma$

VALUE	DOCUMENT ID		TECN	COMMENT
+0.06 ±0.02	ZHANG	13A	DPWA	Multichannel
+0.039±0.009	[5] CAMERON	78	DPWA	$K^-p \to \Sigma(1385)\pi$

$\Sigma(1915)$ FOOTNOTES

[1] The two entries for CORDEN 77C are from two different acceptable solutions.
[2] Preferred solution 3; see CORDEN 76 for other possibilities.
[3] The two MARTIN 77 values are from a T-matrix pole and from a Breit-Wigner fit.
[4] The mass and width are fixed to the GOPAL 77 values due to the low elasticity.
[5] The published sign has been changed to be in accord with the baryon-first convention.

$\Sigma(1915)$ REFERENCES

ZHANG	13A	PR C88 035205	H. Zhang *et al.*	(KSU)
PDG	86	PL 170B 1	M. Aguilar-Benitez *et al.*	(CERN, CIT+)
PDG	82	PL 111B 1	M. Roos *et al.*	(HELS, CIT, CERN)
GOPAL	80	Toronto Conf. 159	G.P. Gopal	(RHEL) IJP
ALSTON-...	78	PR D18 182	M. Alston-Garnjost *et al.*	(LBL, MTHO+) IJP
Also		PRL 38 1007	M. Alston-Garnjost *et al.*	(LBL, MTHO+) IJP
CAMERON	78	NP B143 189	W. Cameron *et al.*	(RHEL, LOIC) IJP
CORDEN	77C	NP B125 61	M.J. Corden *et al.*	(BIRM) IJP
DECLAIS	77	CERN 77-16	Y. Declais *et al.*	(CAEN, CERN) IJP
GOPAL	77	NP B119 362	G.P. Gopal *et al.*	(LOIC, RHEL) IJP
MARTIN	77	NP B127 349	B.R. Martin, M.K. Pidcock, R.G. Moorhouse	(LOUC+) IJP
Also		NP B126 266	B.R. Martin, M.K. Pidcock	(LOUC)
Also		NP B126 285	B.R. Martin, M.K. Pidcock	(LOUC) IJP
CORDEN	76	NP B104 382	M.J. Corden *et al.*	(BIRM) IJP
DEBELLEFON	76	NP B109 129	A. de Bellefon, A. Berthon	(CDEF) IJP
BAILLON	75	NP B94 39	P.H. Baillon, P.J. Litchfield	(CERN, RHEL) IJP
HEMINGWAY	75	NP B91 12	R.J. Hemingway *et al.*	(CERN, HEIDH, MPIM) IJP
VANHORN	75	NP B87 145	A.J. van Horn	(LBL) IJP
Also		NP B87 157	A.J. van Horn	(LBL) IJP
DEVENISH	74B	NP B81 330	R.C.E. Devenish, C.D. Froggatt, B.R. Martin	(DESY+)
KANE	74	LBL-2452	D.F. Kane	(LBL) IJP
COOL	66	PRL 16 1228	R.L. Cool *et al.*	(BNL)

$\Sigma(1940)\ 3/2^+$

$I(J^P) = 1(\frac{3}{2}^+)$ Status: *

OMITTED FROM SUMMARY TABLE

$\Sigma(1940)$ MASS

VALUE (MeV)	DOCUMENT ID		TECN	COMMENT
1941±18	ZHANG	13A	DPWA	Multichannel

$\Lambda(1945)$ WIDTH

VALUE (MeV)	DOCUMENT ID		TECN	COMMENT
400±49	ZHANG	13A	DPWA	Multichannel

$\Sigma(1940)$ DECAY MODES

	Mode	Fraction (Γ_i/Γ)
Γ_1	$N\overline{K}$	(13.0±2.0) %
Γ_2	$\Sigma\pi$	(4.0±2.0) %
Γ_3	$\Sigma(1385)\pi$, P-wave	(22 ±7) %
Γ_4	$\Lambda(1520)\pi$, S-wave	(5.0±2.0) %

$\Sigma(1940)$ BRANCHING RATIOS

$\Gamma(N\overline{K})/\Gamma_{total}$ Γ_1/Γ

VALUE	DOCUMENT ID		TECN	COMMENT
0.13±0.02	ZHANG	13A	DPWA	Multichannel

$\Gamma(\Sigma\pi)/\Gamma_{total}$ Γ_2/Γ

VALUE	DOCUMENT ID		TECN	COMMENT
0.04±0.02	ZHANG	13A	DPWA	Multichannel

$\Gamma(\Sigma(1385)\pi$, P-wave$)/\Gamma_{total}$ Γ_3/Γ

VALUE	DOCUMENT ID		TECN	COMMENT
0.22±0.07	ZHANG	13A	DPWA	Multichannel

$\Gamma(\Lambda(1520)\pi$, S-wave$)/\Gamma_{total}$ Γ_4/Γ

VALUE	DOCUMENT ID		TECN	COMMENT
0.05±0.02	ZHANG	13A	DPWA	Multichannel

$\Sigma(1940)$ REFERENCES

ZHANG	13A	PR C88 035205	H. Zhang *et al.*	(KSU)

$\Sigma(1940)\ 3/2^-$

$I(J^P) = 1(\frac{3}{2}^-)$ Status: ***

For results published before 1974 (they are now obsolete), see our 1982 edition Physics Letters **111B** 1 (1982).

Not all analyses require this state. It is not required by the GOYAL 77 analysis of $K^-n \to (\Sigma\pi)^-$ nor by the GOPAL 80 analysis of $K^-n \to K^-n$. See also HEMINGWAY 75.

$\Sigma(1940)$ MASS

VALUE (MeV)	DOCUMENT ID		TECN	COMMENT
1900 to 1950 (≈ 1940) OUR ESTIMATE				
1920±50	GOPAL	77	DPWA	$\overline{K}N$ multichannel
1950±30	BAILLON	75	IPWA	$\overline{K}N \to \Lambda\pi$
1949^{+40}_{-60}	VANHORN	75	DPWA	$K^-p \to \Lambda\pi^0$
1935±80	KANE	74	DPWA	$K^-p \to \Sigma\pi$
1940±20	LITCHFIELD	74B	DPWA	$K^-p \to \Lambda(1520)\pi^0$
1950±20	LITCHFIELD	74C	DPWA	$K^-p \to \Delta(1232)\overline{K}$
• • • We do not use the following data for averages, fits, limits, etc. • • •				
1886 or 1893	[1] MARTIN	77	DPWA	$\overline{K}N$ multichannel
1940	DEBELLEFON	76	IPWA	$K^-p \to \Lambda\pi^0$, F_{17} wave

$\Sigma(1940)$ WIDTH

VALUE (MeV)	DOCUMENT ID		TECN	COMMENT
150 to 300 (≈ 220) OUR ESTIMATE				
170±25	CAMERON	78B	DPWA	$K^-p \to N\overline{K}^*$
300±80	GOPAL	77	DPWA	$\overline{K}N$ multichannel
150±75	BAILLON	75	IPWA	$\overline{K}N \to \Lambda\pi$
160^{+70}_{-40}	VANHORN	75	DPWA	$K^-p \to \Lambda\pi^0$
330±80	KANE	74	DPWA	$K^-p \to \Sigma\pi$
60±20	LITCHFIELD	74B	DPWA	$K^-p \to \Lambda(1520)\pi^0$
70^{+30}_{-20}	LITCHFIELD	74C	DPWA	$K^-p \to \Delta(1232)\overline{K}$
• • • We do not use the following data for averages, fits, limits, etc. • • •				

157 or 159 [1] MARTIN 77 DPWA $\overline{K}N$ multichannel

$\Sigma(1940)$ DECAY MODES

	Mode	Fraction (Γ_i/Γ)
Γ_1	$N\overline{K}$	<20 %
Γ_2	$\Lambda\pi$	seen
Γ_3	$\Sigma\pi$	seen
Γ_4	$\Sigma(1385)\pi$	seen
Γ_5	$\Sigma(1385)\pi$, S-wave	
Γ_6	$\Lambda(1520)\pi$	seen
Γ_7	$\Lambda(1520)\pi$, P-wave	
Γ_8	$\Lambda(1520)\pi$, F-wave	
Γ_9	$\Delta(1232)\overline{K}$	seen
Γ_{10}	$\Delta(1232)\overline{K}$, S-wave	
Γ_{11}	$\Delta(1232)\overline{K}$, D-wave	
Γ_{12}	$N\overline{K}^*(892)$	seen
Γ_{13}	$N\overline{K}^*(892)$, S=3/2, S-wave	

$\Sigma(1940)$ BRANCHING RATIOS

See "Sign conventions for resonance couplings" in the Note on Λ and Σ Resonances.

$\Gamma(N\overline{K})/\Gamma_{total}$ Γ_1/Γ

VALUE	DOCUMENT ID		TECN	COMMENT
<0.2 OUR ESTIMATE				
<0.04	GOPAL	77	DPWA	$\overline{K}N$ multichannel
0.14 or 0.13	[1] MARTIN	77	DPWA	$\overline{K}N$ multichannel

$(\Gamma_i\Gamma_f)^{1/2}/\Gamma_{total}$ in $N\overline{K} \to \Sigma(1940) \to \Lambda\pi$ $(\Gamma_1\Gamma_2)^{1/2}/\Gamma$

VALUE	DOCUMENT ID		TECN	COMMENT
-0.06 ± 0.03	GOPAL	77	DPWA	$\overline{K}N$ multichannel
-0.04 ± 0.02	BAILLON	75	IPWA	$\overline{K}N \to \Lambda\pi$
$-0.05\ ^{+0.03}_{-0.02}$	VANHORN	75	DPWA	$K^-p \to \Lambda\pi^0$
-0.153 ± 0.070	DEVENISH	74B		Fixed-t dispersion rel.
• • • We do not use the following data for averages, fits, limits, etc. • • •				
-0.15 or -0.14	[1] MARTIN	77	DPWA	$\overline{K}N$ multichannel

$(\Gamma_i\Gamma_f)^{1/2}/\Gamma_{total}$ in $N\overline{K} \to \Sigma(1940) \to \Sigma\pi$ $(\Gamma_1\Gamma_3)^{1/2}/\Gamma$

VALUE	DOCUMENT ID		TECN	COMMENT
-0.08 ± 0.04	GOPAL	77	DPWA	$\overline{K}N$ multichannel
-0.14 ± 0.04	KANE	74	DPWA	$K^-p \to \Sigma\pi$
• • • We do not use the following data for averages, fits, limits, etc. • • •				
$+0.16$ or $+0.16$	[1] MARTIN	77	DPWA	$\overline{K}N$ multichannel

$(\Gamma_i\Gamma_f)^{1/2}/\Gamma_{total}$ in $N\overline{K} \to \Sigma(1940) \to \Lambda(1520)\pi$, P-wave $(\Gamma_1\Gamma_7)^{1/2}/\Gamma$

VALUE	DOCUMENT ID		TECN	COMMENT
< 0.03	CAMERON	77	DPWA	$K^-p \to \Lambda(1520)\pi^0$
-0.11 ± 0.04	LITCHFIELD	74B	DPWA	$K^-p \to \Lambda(1520)\pi^0$

$(\Gamma_i\Gamma_f)^{1/2}/\Gamma_{total}$ in $N\overline{K} \to \Sigma(1940) \to \Lambda(1520)\pi$, F-wave $(\Gamma_1\Gamma_8)^{1/2}/\Gamma$

VALUE	DOCUMENT ID		TECN	COMMENT
0.062 ± 0.021	CAMERON	77	DPWA	$K^-p \to \Lambda(1520)\pi^0$
-0.08 ± 0.04	LITCHFIELD	74B	DPWA	$K^-p \to \Lambda(1520)\pi^0$

$(\Gamma_i\Gamma_f)^{1/2}/\Gamma_{total}$ in $N\overline{K} \to \Sigma(1940) \to \Delta(1232)\overline{K}$, S-wave $(\Gamma_1\Gamma_{10})^{1/2}/\Gamma$

VALUE	DOCUMENT ID		TECN	COMMENT
-0.16 ± 0.05	LITCHFIELD	74C	DPWA	$K^-p \to \Delta(1232)\overline{K}$

$(\Gamma_i\Gamma_f)^{1/2}/\Gamma_{total}$ in $N\overline{K} \to \Sigma(1940) \to \Delta(1232)\overline{K}$, D-wave $(\Gamma_1\Gamma_{11})^{1/2}/\Gamma$

VALUE	DOCUMENT ID		TECN	COMMENT
-0.14 ± 0.05	LITCHFIELD	74C	DPWA	$K^-p \to \Delta(1232)\overline{K}$

$(\Gamma_i\Gamma_f)^{1/2}/\Gamma_{total}$ in $N\overline{K} \to \Sigma(1940) \to \Sigma(1385)\pi$ $(\Gamma_1\Gamma_4)^{1/2}/\Gamma$

VALUE	DOCUMENT ID		TECN	COMMENT
$+0.066 \pm 0.025$	[2] CAMERON	78	DPWA	$K^-p \to \Sigma(1385)\pi$

$(\Gamma_i\Gamma_f)^{1/2}/\Gamma_{total}$ in $N\overline{K} \to \Sigma(1940) \to N\overline{K}^*(892)$ $(\Gamma_1\Gamma_{12})^{1/2}/\Gamma$

VALUE	DOCUMENT ID		TECN	COMMENT
-0.09 ± 0.02	[3] CAMERON	78B	DPWA	$K^-p \to N\overline{K}^*$

$\Sigma(1940)$ FOOTNOTES

[1] The two MARTIN 77 values are from a T-matrix pole and from a Breit-Wigner fit.
[2] The published sign has been changed to be in accord with the baryon-first convention.
[3] Upper limits on the D_1 and D_3 waves are each 0.03.

$\Sigma(1940)$ REFERENCES

PDG	82	PL 111B 1	M. Roos *et al.*	(HELS, CIT, CERN)
GOPAL	80	Toronto Conf. 159	G.P. Gopal	(RHEL)
CAMERON	78	NP B143 189	W. Cameron *et al.*	(RHEL, LOIC) IJP
CAMERON	78B	NP B146 327	W. Cameron *et al.*	(RHEL, LOIC) IJP
CAMERON	77	NP B131 399	W. Cameron *et al.*	(RHEL, LOIC) IJP
GOPAL	77	NP B119 362	G.P. Gopal *et al.*	(LOIC, RHEL) IJP
GOYAL	77	PR D16 2746	D.P. Goyal, A.V. Sodhi	(DELH)
MARTIN	77	NP B127 349	B.R. Martin, M.K. Pidcock, R.G. Moorhouse	(LOUC+) IJP
Also		NP B126 266	B.R. Martin, M.K. Pidcock	(LOUC)
Also		NP B126 285	B.R. Martin, M.K. Pidcock	(LOUC) IJP
DEBELLEFON	76	NP B109 129	A. de Bellefon, A. Berthon	(CDEF) IJP
BAILLON	75	NP B94 39	P.H. Baillon, P.J. Litchfield	(CERN, RHEL) IJP
HEMINGWAY	75	NP B91 12	R.J. Hemingway *et al.*	(CERN, HEIDH, MPIM) IJP
VANHORN	75	NP B87 145	A.J. van Horn	(LBL) IJP
Also		NP B87 157	A.J. van Horn	(LBL) IJP
DEVENISH	74B	NP B81 330	R.C.E. Devenish, C.D. Froggatt, B.R. Martin	(DESY+)
KANE	74	LBL-2452	D.F. Kane	(LBL) IJP
LITCHFIELD	74B	NP B74 19	P.J. Litchfield *et al.*	(CERN, HEIDH) IJP
LITCHFIELD	74C	NP B74 39	P.J. Litchfield *et al.*	(CERN, HEIDH) IJP

$\Sigma(2000)$ $1/2^-$

$I(J^P) = 1(\frac{1}{2}^-)$ Status: *

OMITTED FROM SUMMARY TABLE

We list here all reported S_{11} states lying above the $\Sigma(1750)$ S_{11}. ZHANG 13A finds no evidence for those states.

$\Sigma(2000)$ MASS

VALUE (MeV)	DOCUMENT ID		TECN	COMMENT
≈ 2000 OUR ESTIMATE				
1944±15	GOPAL	80	DPWA	$\overline{K}N \to \overline{K}N$
1955±15	GOPAL	77	DPWA	$\overline{K}N$ multichannel
1755 or 1834	[1] MARTIN	77	DPWA	$\overline{K}N$ multichannel
2004±40	VANHORN	75	DPWA	$K^-p \to \Lambda\pi^0$

$\Sigma(2000)$ WIDTH

VALUE (MeV)	DOCUMENT ID		TECN	COMMENT
215±25	GOPAL	80	DPWA	$\overline{K}N \to \overline{K}N$
170±40	GOPAL	77	DPWA	$\overline{K}N$ multichannel
413 or 450	[1] MARTIN	77	DPWA	$\overline{K}N$ multichannel
116±40	VANHORN	75	DPWA	$K^-p \to \Lambda\pi^0$

$\Sigma(2000)$ DECAY MODES

	Mode
Γ_1	$N\overline{K}$
Γ_2	$\Lambda\pi$
Γ_3	$\Sigma\pi$
Γ_4	$\Lambda(1520)\pi$
Γ_5	$N\overline{K}^*(892)$, S=1/2, S-wave
Γ_6	$N\overline{K}^*(892)$, S=3/2, D-wave

$\Sigma(2000)$ BRANCHING RATIOS

See "Sign conventions for resonance couplings" in the Note on Λ and Σ Resonances.

$\Gamma(N\overline{K})/\Gamma_{total}$ Γ_1/Γ

VALUE	DOCUMENT ID		TECN	COMMENT
0.51±0.05	GOPAL	80	DPWA	$\overline{K}N \to \overline{K}N$
0.44±0.05	GOPAL	77	DPWA	See GOPAL 80
0.62 or 0.57	[1] MARTIN	77	DPWA	$\overline{K}N$ multichannel

$(\Gamma_i\Gamma_f)^{1/2}/\Gamma_{total}$ in $N\overline{K} \to \Sigma(2000) \to \Lambda\pi$ $(\Gamma_1\Gamma_2)^{1/2}/\Gamma$

VALUE	DOCUMENT ID		TECN	COMMENT
0.08 ± 0.03	GOPAL	77	DPWA	$\overline{K}N$ multichannel
-0.19 or -0.18	[1] MARTIN	77	DPWA	$\overline{K}N$ multichannel
not seen	BAILLON	75	IPWA	$\overline{K}N \to \Lambda\pi$
$+0.07\ ^{+0.02}_{-0.01}$	VANHORN	75	DPWA	$K^-p \to \Lambda\pi^0$

$(\Gamma_i\Gamma_f)^{1/2}/\Gamma_{total}$ in $N\overline{K} \to \Sigma(2000) \to \Sigma\pi$ $(\Gamma_1\Gamma_3)^{1/2}/\Gamma$

VALUE	DOCUMENT ID		TECN	COMMENT
$+0.20 \pm 0.04$	GOPAL	77	DPWA	$\overline{K}N$ multichannel
$+0.26$ or $+0.24$	[1] MARTIN	77	DPWA	$\overline{K}N$ multichannel

$(\Gamma_i\Gamma_f)^{1/2}/\Gamma_{total}$ in $N\overline{K} \to \Sigma(2000) \to \Lambda(1520)\pi$ $(\Gamma_1\Gamma_4)^{1/2}/\Gamma$

VALUE	DOCUMENT ID		TECN	COMMENT
$+0.081 \pm 0.021$	[2] CAMERON	77	DPWA	P-wave decay

$(\Gamma_i\Gamma_f)^{1/2}/\Gamma_{total}$ in $N\overline{K} \to \Sigma(2000) \to N\overline{K}^*(892)$, S=1/2, S-wave $(\Gamma_1\Gamma_5)^{1/2}/\Gamma$

VALUE	DOCUMENT ID		TECN	COMMENT
$+0.10 \pm 0.02$	[2] CAMERON	78B	DPWA	$K^-p \to N\overline{K}^*$

$(\Gamma_i\Gamma_f)^{1/2}/\Gamma_{total}$ in $N\overline{K} \to \Sigma(2000) \to N\overline{K}^*(892)$, S=3/2, D-wave

$(\Gamma_1\Gamma_6)^{1/2}/\Gamma$

VALUE	DOCUMENT ID		TECN	COMMENT
-0.07 ± 0.03	CAMERON	78B	DPWA	$K^-p \to N\overline{K}^*$

$\Sigma(2000)$ FOOTNOTES

[1] The two MARTIN 77 values are from a T-matrix pole and from a Breit-Wigner fit.
[2] The published sign has been changed to be in accord with the baryon-first convention.

$\Sigma(2000)$ REFERENCES

ZHANG	13A	PR C88 035205	H. Zhang *et al.*	(KSU)
GOPAL	80	Toronto Conf. 159	G.P. Gopal	(RHEL) IJP
CAMERON	78B	NP B146 327	W. Cameron *et al.*	(RHEL, LOIC) IJP
CAMERON	77	NP B131 399	W. Cameron *et al.*	(RHEL, LOIC) IJP
GOPAL	77	NP B119 362	G.P. Gopal *et al.*	(LOIC, RHEL) IJP
MARTIN	77	NP B127 349	B.R. Martin, M.K. Pidcock, R.G. Moorhouse	(LOUC+) IJP
Also		NP B126 266	B.R. Martin, M.K. Pidcock	(LOUC)
Also		NP B126 285	B.R. Martin, M.K. Pidcock	(LOUC) IJP
BAILLON	75	NP B94 39	P.H. Baillon, P.J. Litchfield	(CERN, RHEL) IJP
VANHORN	75	NP B87 145	A.J. van Horn	(LBL) IJP
Also		NP B87 157	A.J. van Horn	(LBL) IJP

$\Sigma(2030)$ $7/2^+$

$I(J^P) = 1(\frac{7}{2}^+)$ Status: ****

Discovered by COOL 66 and by WOHL 66. For most results published before 1974 (they are now obsolete), see our 1982 edition Physics Letters **111B** 1 (1982).

This entry only includes results from partial-wave analyses. Parameters of peaks seen in cross sections and invariant-mass distributions around 2030 MeV may be found in our 1984 edition, Reviews of Modern Physics **56** S1 (1984).

$\Sigma(2030)$ MASS

VALUE (MeV)	DOCUMENT ID		TECN	COMMENT
2025 to 2040 ($\approx$ 2030) OUR ESTIMATE				
2030 ± 5	ZHANG	13A	DPWA	Multichannel
2036 ± 5	GOPAL	80	DPWA	$\overline{K}N \to \overline{K}N$
2038 ± 10	CORDEN	77B		$K^-N \to N\overline{K}^*$
2040 ± 5	GOPAL	77	DPWA	$\overline{K}N$ multichannel
2030 ± 3	[1] CORDEN	76	DPWA	$K^-n \to \Lambda\pi^-$
2035 ± 15	BAILLON	75	IPWA	$\overline{K}N \to \Lambda\pi$
2038 ± 10	HEMINGWAY	75	DPWA	$K^-p \to \overline{K}N$
2042 ± 11	VANHORN	75	DPWA	$K^-p \to \Lambda\pi^0$
2020 ± 6	KANE	74	DPWA	$K^-p \to \Sigma\pi$
2035 ± 10	LITCHFIELD	74B	DPWA	$K^-p \to \Lambda(1520)\pi^0$
2020 ± 30	LITCHFIELD	74C	DPWA	$K^-p \to \Delta(1232)\overline{K}$
2025 ± 10	LITCHFIELD	74D	DPWA	$K^-p \to \Lambda(1820)\pi^0$
• • • We do not use the following data for averages, fits, limits, etc. • • •				
2027 to 2057	GOYAL	77	DPWA	$K^-N \to \Sigma\pi$
2030	DEBELLEFON	76	IPWA	$K^-p \to \Lambda\pi^0$

$\Sigma(2030)$ WIDTH

VALUE (MeV)	DOCUMENT ID		TECN	COMMENT
150 to 200 ($\approx$ 180) OUR ESTIMATE				
207 ± 17	ZHANG	13A	DPWA	Multichannel
172 ± 10	GOPAL	80	DPWA	$\overline{K}N \to \overline{K}N$
137 ± 40	CORDEN	77B		$K^-N \to N\overline{K}^*$
190 ± 10	GOPAL	77	DPWA	$\overline{K}N$ multichannel
201 ± 9	[1] CORDEN	76	DPWA	$K^-n \to \Lambda\pi^-$
180 ± 20	BAILLON	75	IPWA	$\overline{K}N \to \Lambda\pi$
172 ± 15	HEMINGWAY	75	DPWA	$K^-p \to \overline{K}N$
178 ± 13	VANHORN	75	DPWA	$K^-p \to \Lambda\pi^0$
111 ± 5	KANE	74	DPWA	$K^-p \to \Sigma\pi$
160 ± 20	LITCHFIELD	74B	DPWA	$K^-p \to \Lambda(1520)\pi^0$
200 ± 30	LITCHFIELD	74C	DPWA	$K^-p \to \Delta(1232)\overline{K}$
• • • We do not use the following data for averages, fits, limits, etc. • • •				
260	DECLAIS	77	DPWA	$\overline{K}N \to \overline{K}N$
126 to 195	GOYAL	77	DPWA	$K^-N \to \Sigma\pi$
160	DEBELLEFON	76	IPWA	$K^-p \to \Lambda\pi^0$
70 to 125	LITCHFIELD	74D	DPWA	$K^-p \to \Lambda(1820)\pi^0$

$\Sigma(2030)$ POLE POSITION

REAL PART

VALUE (MeV)	DOCUMENT ID		TECN	COMMENT
• • • We do not use the following data for averages, fits, limits, etc. • • •				
1993	ZHANG	13A	DPWA	Multichannel

$-2\times$IMAGINARY PART

VALUE (MeV)	DOCUMENT ID		TECN	COMMENT
• • • We do not use the following data for averages, fits, limits, etc. • • •				
176	ZHANG	13A	DPWA	Multichannel

$\Sigma(2030)$ DECAY MODES

	Mode	Fraction (Γ_i/Γ)
Γ_1	$N\overline{K}$	17–23 %
Γ_2	$\Lambda\pi$	17–23 %
Γ_3	$\Sigma\pi$	5–10 %
Γ_4	ΞK	<2 %
Γ_5	$\Sigma(1385)\pi$	5–15 %
Γ_6	$\Sigma(1385)\pi$, F-wave	
Γ_7	$\Lambda(1520)\pi$	10–20 %
Γ_8	$\Lambda(1520)\pi$, D-wave	
Γ_9	$\Lambda(1520)\pi$, G-wave	
Γ_{10}	$\Delta(1232)\overline{K}$	10–20 %
Γ_{11}	$\Delta(1232)\overline{K}$, F-wave	
Γ_{12}	$\Delta(1232)\overline{K}$, H-wave	
Γ_{13}	$N\overline{K}^*(892)$	<5 %
Γ_{14}	$N\overline{K}^*(892)$, S=1/2, F-wave	
Γ_{15}	$N\overline{K}^*(892)$, S=3/2, F-wave	
Γ_{16}	$\Lambda(1820)\pi$, P-wave	

The above branching fractions are our estimates, not fits or averages.

$\Sigma(2030)$ BRANCHING RATIOS

See "Sign conventions for resonance couplings" in the Note on Λ and Σ Resonances.

$\Gamma(N\overline{K})/\Gamma_{total}$ Γ_1/Γ

VALUE	DOCUMENT ID		TECN	COMMENT
0.17 to 0.23 OUR ESTIMATE				
0.13 ± 0.01	ZHANG	13A	DPWA	Multichannel
0.19 ± 0.03	GOPAL	80	DPWA	$\overline{K}N \to \overline{K}N$
0.18 ± 0.03	HEMINGWAY	75	DPWA	$K^-p \to \overline{K}N$
• • • We do not use the following data for averages, fits, limits, etc. • • •				
0.15	DECLAIS	77	DPWA	$\overline{K}N \to \overline{K}N$
0.24 ± 0.02	GOPAL	77	DPWA	See GOPAL 80

$(\Gamma_i\Gamma_f)^{1/2}/\Gamma_{total}$ in $N\overline{K} \to \Sigma(2030) \to \Lambda\pi$ $(\Gamma_1\Gamma_2)^{1/2}/\Gamma$

VALUE	DOCUMENT ID		TECN	COMMENT
$+0.15\ \pm0.01$	ZHANG	13A	DPWA	Multichannel
$+0.18\ \pm0.02$	GOPAL	77	DPWA	$\overline{K}N$ multichannel
$+0.20\ \pm0.01$	[1] CORDEN	76	DPWA	$K^-n \to \Lambda\pi^-$
$+0.18\ \pm0.02$	BAILLON	75	IPWA	$\overline{K}N \to \Lambda\pi$
$+0.20\ \pm0.01$	VANHORN	75	DPWA	$K^-p \to \Lambda\pi^0$
$+0.195\pm0.053$	DEVENISH	74B		Fixed-t dispersion rel.
• • • We do not use the following data for averages, fits, limits, etc. • • •				
0.20	DEBELLEFON	76	IPWA	$K^-p \to \Lambda\pi^0$

$(\Gamma_i\Gamma_f)^{1/2}/\Gamma_{total}$ in $N\overline{K} \to \Sigma(2030) \to \Sigma\pi$ $(\Gamma_1\Gamma_3)^{1/2}/\Gamma$

VALUE	DOCUMENT ID		TECN	COMMENT
$-0.08\ \pm0.01$	ZHANG	13A	DPWA	Multichannel
$-0.09\ \pm0.01$	[2] CORDEN	77C		$K^-n \to \Sigma\pi$
$-0.06\ \pm0.01$	[2] CORDEN	77C		$K^-n \to \Sigma\pi$
$-0.15\ \pm0.03$	GOPAL	77	DPWA	$\overline{K}N$ multichannel
$-0.10\ \pm0.01$	KANE	74	DPWA	$K^-p \to \Sigma\pi$
• • • We do not use the following data for averages, fits, limits, etc. • • •				
-0.085 ± 0.02	[3] GOYAL	77	DPWA	$K^-N \to \Sigma\pi$

$(\Gamma_i\Gamma_f)^{1/2}/\Gamma_{total}$ in $N\overline{K} \to \Sigma(2030) \to \Xi K$ $(\Gamma_1\Gamma_4)^{1/2}/\Gamma$

VALUE	DOCUMENT ID		TECN	COMMENT
0.023	MULLER	69B	DPWA	$K^-p \to \Xi K$
<0.05	BURGUN	68	DPWA	$K^-p \to \Xi K$
<0.05	TRIPP	67	RVUE	$K^-p \to \Xi K$

$(\Gamma_i\Gamma_f)^{1/2}/\Gamma_{total}$ in $N\overline{K} \to \Sigma(2030) \to \Sigma(1385)\pi$, F-wave $(\Gamma_1\Gamma_6)^{1/2}/\Gamma$

VALUE	DOCUMENT ID		TECN	COMMENT
$+0.16\ \pm0.01$	ZHANG	13A	DPWA	Multichannel
$+0.153\pm0.026$	[4] CAMERON	78	DPWA	$K^-p \to \Sigma(1385)\pi$

$(\Gamma_i\Gamma_f)^{1/2}/\Gamma_{total}$ in $N\overline{K} \to \Sigma(2030) \to \Lambda(1520)\pi$, D-wave $(\Gamma_1\Gamma_8)^{1/2}/\Gamma$

VALUE	DOCUMENT ID		TECN	COMMENT
$+0.114\pm0.010$	[4] CAMERON	77	DPWA	$K^-p \to \Lambda(1520)\pi^0$
$0.14\ \pm0.03$	LITCHFIELD	74B	DPWA	$K^-p \to \Lambda(1520)\pi^0$
• • • We do not use the following data for averages, fits, limits, etc. • • •				
$0.10\ \pm0.03$	[5] CORDEN	75B	DBC	$K^-n \to N\overline{K}\pi^-$

Baryon Particle Listings

$\Sigma(2030)$, $\Sigma(2070)$, $\Sigma(2080)$

$(\Gamma_i\Gamma_f)^{1/2}/\Gamma_{total}$ in $N\overline{K} \to \Sigma(2030) \to \Lambda(1520)\pi$, G-wave $(\Gamma_1\Gamma_9)^{1/2}/\Gamma$

VALUE	DOCUMENT ID		TECN	COMMENT
$+0.146\pm0.010$	[4] CAMERON	77	DPWA	$K^-p \to \Lambda(1520)\pi^0$
$0.02\ \pm0.02$	LITCHFIELD	74B	DPWA	$K^-p \to \Lambda(1520)\pi^0$

$(\Gamma_i\Gamma_f)^{1/2}/\Gamma_{total}$ in $N\overline{K} \to \Sigma(2030) \to \Delta(1232)\overline{K}$, F-wave $(\Gamma_1\Gamma_{11})^{1/2}/\Gamma$

VALUE	DOCUMENT ID		TECN	COMMENT
$+0.12\pm0.02$	ZHANG	13A	DPWA	Multichannel
0.16 ± 0.03	LITCHFIELD	74C	DPWA	$K^-p \to \Delta(1232)\overline{K}$
• • • We do not use the following data for averages, fits, limits, etc. • • •				
0.17 ± 0.03	[5] CORDEN	75B	DBC	$K^-n \to N\overline{K}\pi^-$

$(\Gamma_i\Gamma_f)^{1/2}/\Gamma_{total}$ in $N\overline{K} \to \Sigma(2030) \to \Delta(1232)\overline{K}$, H-wave $(\Gamma_1\Gamma_{12})^{1/2}/\Gamma$

VALUE	DOCUMENT ID		TECN	COMMENT
0.00 ± 0.02	LITCHFIELD	74C	DPWA	$K^-p \to \Delta(1232)\overline{K}$

$(\Gamma_i\Gamma_f)^{1/2}/\Gamma_{total}$ in $N\overline{K} \to \Sigma(2030) \to N\overline{K}^*(892)$, S=1/2, F-wave $(\Gamma_1\Gamma_{14})^{1/2}/\Gamma$

VALUE	DOCUMENT ID		TECN	COMMENT
$+0.06\pm0.02$	ZHANG	13A	DPWA	Multichannel
$+0.06\pm0.03$	[4] CAMERON	78B	DPWA	$K^-p \to N\overline{K}^*$
-0.02 ± 0.01	CORDEN	77B		$K^-d \to NN\overline{K}^*$

$(\Gamma_i\Gamma_f)^{1/2}/\Gamma_{total}$ in $N\overline{K} \to \Sigma(2030) \to N\overline{K}^*(892)$, S=3/2, F-wave $(\Gamma_1\Gamma_{15})^{1/2}/\Gamma$

VALUE	DOCUMENT ID		TECN	COMMENT
$+0.05\pm0.01$	ZHANG	13A	DPWA	Multichannel
$+0.04\pm0.03$	[6] CAMERON	78B	DPWA	$K^-p \to N\overline{K}^*$
-0.12 ± 0.02	CORDEN	77B		$K^-d \to NN\overline{K}^*$

$(\Gamma_i\Gamma_f)^{1/2}/\Gamma_{total}$ in $N\overline{K} \to \Sigma(2030) \to \Lambda(1820)\pi$, P-wave $(\Gamma_1\Gamma_{16})^{1/2}/\Gamma$

VALUE	DOCUMENT ID		TECN	COMMENT
0.14 ± 0.02	CORDEN	75B	DBC	$K^-n \to N\overline{K}\pi^-$
0.18 ± 0.04	LITCHFIELD	74D	DPWA	$K^-p \to \Lambda(1820)\pi^0$

$\Sigma(2030)$ FOOTNOTES

[1] Preferred solution 3; see CORDEN 76 for other possibilities.
[2] The two entries for CORDEN 77C are from two different acceptable solutions.
[3] This coupling is extracted from unnormalized data.
[4] The published sign has been changed to be in accord with the baryon-first convention.
[5] An upper limit.
[6] The upper limit on the G_3 wave is 0.03.

$\Sigma(2030)$ REFERENCES

ZHANG	13A	PR C88 035205	H. Zhang *et al.*	(KSU)
PDG	84	RMP 56 S1	C.G. Wohl *et al.*	(LBL, CIT, CERN)
PDG	82	PL 111B 1	M. Roos *et al.*	(HELS, CIT, CERN)
GOPAL	80	Toronto Conf. 159	G.P. Gopal	(RHEL) IJP
CAMERON	78	NP B143 189	W. Cameron *et al.*	(RHEL, LOIC) IJP
CAMERON	78B	NP B146 327	W. Cameron *et al.*	(RHEL, LOIC) IJP
CAMERON	77	NP B131 399	W. Cameron *et al.*	(RHEL, LOIC) IJP
CORDEN	77B	NP B121 365	M.J. Corden *et al.*	(BIRM) IJP
CORDEN	77C	NP B125 61	M.J. Corden *et al.*	(BIRM) IJP
DECLAIS	77	CERN 77-16	Y. Declais *et al.*	(CAEN, CERN) IJP
GOPAL	77	NP B119 362	G.P. Gopal *et al.*	(LOIC, RHEL) IJP
GOYAL	77	PR D16 2746	D.P. Goyal, A.V. Sodhi	(DELH) IJP
CORDEN	76	NP B104 382	M.J. Corden *et al.*	(BIRM) IJP
DEBELLEFON	76	NP B109 129	A. de Bellefon, A. Berthon	(CDEF) IJP
BAILLON	75	NP B94 39	P.H. Baillon, P.J. Litchfield	(CERN, RHEL) IJP
CORDEN	75B	NP B92 365	M.J. Corden *et al.*	(BIRM) IJP
HEMINGWAY	75	NP B91 12	R.J. Hemingway *et al.*	(CERN, HEIDH, MPIM) IJP
VANHORN	75	NP B87 145	A.J. van Horn	(LBL) IJP
Also		NP B87 157	A.J. van Horn	(LBL) IJP
DEVENISH	74B	NP B81 330	R.C.E. Devenish, C.D. Froggatt, B.R. Martin	(DESY+)
KANE	74	LBL-2452	D.F. Kane	(LBL) IJP
LITCHFIELD	74B	NP B74 19	P.J. Litchfield *et al.*	(CERN, HEIDH) IJP
LITCHFIELD	74C	NP B74 39	P.J. Litchfield *et al.*	(CERN, HEIDH) IJP
LITCHFIELD	74D	NP B74 12	P.J. Litchfield *et al.*	(CERN, HEIDH) IJP
MULLER	69B	Thesis UCRL 19372	R.A. Muller	(LRL)
BURGUN	68	NP B8 447	G. Burgun *et al.*	(SACL, CDEF, RHEL)
TRIPP	67	NP B3 10	R.D. Tripp *et al.*	(LRL, SLAC, CERN+)
COOL	66	PRL 16 1228	R.L. Cool *et al.*	(BNL)
WOHL	66	PRL 17 107	C.G. Wohl, F.T. Solmitz, M.L. Stevenson	(LRL) IJP

$\Sigma(2070)\ 5/2^+$

$I(J^P) = 1(\frac{5}{2}^+)$ Status: *

OMITTED FROM SUMMARY TABLE

This state suggested by BERTHON 70B finds support in GOPAL 80 with new K^-p polarization and K^-n angular distributions. The very broad state seen in KANE 72 is not required in the later (KANE 74) analysis of $\overline{K}N \to \Sigma\pi$.

$\Sigma(2070)$ MASS

VALUE (MeV)	DOCUMENT ID		TECN	COMMENT
≈ 2070 OUR ESTIMATE				
2051 ± 25	GOPAL	80	DPWA	$\overline{K}N \to \overline{K}N$
2057	KANE	72	DPWA	$K^-p \to \Sigma\pi$
2070 ± 10	BERTHON	70B	DPWA	$K^-p \to \Sigma\pi$

$\Sigma(2070)$ WIDTH

VALUE (MeV)	DOCUMENT ID		TECN	COMMENT
300 ± 30	GOPAL	80	DPWA	$\overline{K}N \to \overline{K}N$
906	KANE	72	DPWA	$K^-p \to \Sigma\pi$
140 ± 20	BERTHON	70B	DPWA	$K^-p \to \Sigma\pi$

$\Sigma(2070)$ DECAY MODES

	Mode
Γ_1	$N\overline{K}$
Γ_2	$\Sigma\pi$

$\Sigma(2070)$ BRANCHING RATIOS

See "Sign conventions for resonance couplings" in the Note on Λ and Σ Resonances.

$\Gamma(N\overline{K})/\Gamma_{total}$ Γ_1/Γ

VALUE	DOCUMENT ID		TECN	COMMENT
0.08 ± 0.03	GOPAL	80	DPWA	$\overline{K}N \to \overline{K}N$

$(\Gamma_i\Gamma_f)^{1/2}/\Gamma_{total}$ in $N\overline{K} \to \Sigma(2070) \to \Sigma\pi$ $(\Gamma_1\Gamma_2)^{1/2}/\Gamma$

VALUE	DOCUMENT ID		TECN	COMMENT
$+0.104$	KANE	72	DPWA	$K^-p \to \Sigma\pi$
$+0.12\ \pm0.02$	BERTHON	70B	DPWA	$K^-p \to \Sigma\pi$

$\Sigma(2070)$ REFERENCES

GOPAL	80	Toronto Conf. 159	G.P. Gopal	(RHEL) IJP
KANE	74	LBL-2452	D.F. Kane	(LBL)
KANE	72	PR D5 1583	D.F.J. Kane	(LBL)
BERTHON	70B	NP B24 417	A. Berthon *et al.*	(CDEF, RHEL, SACL) IJP

$\Sigma(2080)\ 3/2^+$

$I(J^P) = 1(\frac{3}{2}^+)$ Status: **

OMITTED FROM SUMMARY TABLE

Suggested by some but not all partial-wave analyses across this region.

$\Sigma(2080)$ MASS

VALUE (MeV)	DOCUMENT ID		TECN	COMMENT
≈ 2080 OUR ESTIMATE				
$2091\pm\ 7$	[1] CORDEN	76	DPWA	$K^-n \to \Lambda\pi^-$
2070 to 2120	DEBELLEFON	76	IPWA	$K^-p \to \Lambda\pi^0$
2120 ± 40	BAILLON	75	IPWA	$\overline{K}N \to \Lambda\pi$ (sol. 1)
2140 ± 40	BAILLON	75	IPWA	$\overline{K}N \to \Lambda\pi$ (sol. 2)
$2082\pm\ 4$	COX	70	DPWA	See CORDEN 76
2070 ± 30	LITCHFIELD	70	DPWA	$K^-N \to \Lambda\pi$

$\Sigma(2080)$ WIDTH

VALUE (MeV)	DOCUMENT ID		TECN	COMMENT
186 ± 48	[1] CORDEN	76	DPWA	$K^-n \to \Lambda\pi^-$
100	DEBELLEFON	76	IPWA	$K^-p \to \Lambda\pi^0$
240 ± 50	BAILLON	75	IPWA	$\overline{K}N \to \Lambda\pi$ (sol. 1)
200 ± 50	BAILLON	75	IPWA	$\overline{K}N \to \Lambda\pi$ (sol. 2)
87 ± 20	COX	70	DPWA	See CORDEN 76
250 ± 40	LITCHFIELD	70	DPWA	$K^-N \to \Lambda\pi$

$\Sigma(2080)$ DECAY MODES

	Mode
Γ_1	$N\overline{K}$
Γ_2	$\Lambda\pi$

$\Sigma(2080)$ BRANCHING RATIOS

See "Sign conventions for resonance couplings" in the Note on Λ and Σ Resonances.

$(\Gamma_i\Gamma_f)^{1/2}/\Gamma_{total}$ in $N\overline{K} \to \Sigma(2080) \to \Lambda\pi$ **$(\Gamma_1\Gamma_2)^{1/2}/\Gamma$**

VALUE	DOCUMENT ID		TECN	COMMENT
-0.10 ± 0.03	[1] CORDEN	76	DPWA	$K^-n \to \Lambda\pi^-$
-0.10	DEBELLEFON	76	IPWA	$K^-p \to \Lambda\pi^0$
-0.13 ± 0.04	BAILLON	75	IPWA	$\overline{K}N \to \Lambda\pi$ (sol. 1 and 2)
-0.16 ± 0.03	COX	70	DPWA	See CORDEN 76
-0.09 ± 0.03	LITCHFIELD	70	DPWA	$K^-N \to \Lambda\pi$

$\Sigma(2080)$ FOOTNOTES

[1] Preferred solution 3; see CORDEN 76 for other possibilities, including a D_{15} at this mass.

$\Sigma(2080)$ REFERENCES

CORDEN	76	NP B104 382	M.J. Corden *et al.*	(BIRM) IJP
DEBELLEFON	76	NP B109 129	A. de Bellefon, A. Berthon	(CDEF) IJP
Also		NP B90 1	A. de Bellefon *et al.*	(CDEF, SACL) IJP
BAILLON	75	NP B94 39	P.H. Baillon, P.J. Litchfield	(CERN, RHEL) IJP
COX	70	NP B19 61	G.F. Cox *et al.*	(BIRM, EDIN, GLAS, LOIC) IJP
LITCHFIELD	70	NP B22 269	P.J. Litchfield	(RHEL) IJP

$\Sigma(2100)\ 7/2^-$

$I(J^P) = 1(\frac{7}{2}^-)$ Status: *

OMITTED FROM SUMMARY TABLE

$\Sigma(2100)$ MASS

VALUE (MeV)	DOCUMENT ID		TECN	COMMENT
≈ 2100 OUR ESTIMATE				
2060±20	BARBARO-...	70	DPWA	$K^-p \to \Lambda\pi^0$
2120±30	BARBARO-...	70	DPWA	$K^-p \to \Sigma\pi$

$\Sigma(2100)$ WIDTH

VALUE (MeV)	DOCUMENT ID		TECN	COMMENT
70±30	BARBARO-...	70	DPWA	$K^-p \to \Lambda\pi^0$
135±30	BARBARO-...	70	DPWA	$K^-p \to \Sigma\pi$

$\Sigma(2100)$ DECAY MODES

	Mode
Γ_1	$N\overline{K}$
Γ_2	$\Lambda\pi$
Γ_3	$\Sigma\pi$

$\Sigma(2100)$ BRANCHING RATIOS

See "Sign conventions for resonance couplings" in the Note on Λ and Σ Resonances.

$(\Gamma_i\Gamma_f)^{1/2}/\Gamma_{total}$ in $N\overline{K} \to \Sigma(2100) \to \Lambda\pi$ **$(\Gamma_1\Gamma_2)^{1/2}/\Gamma$**

VALUE	DOCUMENT ID		TECN	COMMENT
-0.07 ± 0.02	BARBARO-...	70	DPWA	$K^-p \to \Lambda\pi^0$

$(\Gamma_i\Gamma_f)^{1/2}/\Gamma_{total}$ in $N\overline{K} \to \Sigma(2100) \to \Sigma\pi$ **$(\Gamma_1\Gamma_3)^{1/2}/\Gamma$**

VALUE	DOCUMENT ID		TECN	COMMENT
$+0.13\pm0.02$	BARBARO-...	70	DPWA	$K^-p \to \Sigma\pi$

$\Sigma(2100)$ REFERENCES

BARBARO-...	70	Duke Conf. 173 Hyperon Resonances, 1970	A. Barbaro-Galtieri	(LRL) IJP

$\Sigma(2250)$

$I(J^P) = 1(?^?)$ Status: ***

Results from partial-wave analyses are too weak to warrant separating them from the production and cross-section experiments. LASINSKI 71 in $\overline{K}N$ using a Pomeron + resonances model, and DEBELLEFON 76, DEBELLEFON 77, and DEBELLEFON 78 in energy-dependent partial-wave analyses of $\overline{K}N \to \Lambda\pi$, $\Sigma\pi$, and $N\overline{K}$, respectively, suggest two resonances around this mass.

$\Sigma(2250)$ MASS

VALUE (MeV)	DOCUMENT ID		TECN	COMMENT
2210 to 2280 (≈ 2250) OUR ESTIMATE				
2270±50	DEBELLEFON	78	DPWA	D_5 wave
2210±30	DEBELLEFON	78	DPWA	G_9 wave
2275±20	DEBELLEFON	77	DPWA	D_5 wave
2215±20	DEBELLEFON	77	DPWA	G_9 wave
2300±30	[1] DEBELLEFON	75B	HBC	$K^-p \to \Xi^{*0}K^0$
2251^{+30}_{-20}	VANHORN	75	DPWA	$K^-p \to \Lambda\pi^0$, F_5 wave
2280±14	AGUILAR-...	70B	HBC	K^-p 3.9, 4.6 GeV/c
2237±11	BRICMAN	70	CNTR	Total, charge exchange
2255±10	COOL	70	CNTR	K^-p, K^-d total
2250± 7	BUGG	68	CNTR	K^-p, K^-d total
• • • We do not use the following data for averages, fits, limits, etc. • • •				
2260	DEBELLEFON	76	IPWA	D_5 wave
2215	DEBELLEFON	76	IPWA	G_9 wave
2250±20	LU	70	CNTR	$\gamma p \to K^+Y^*$
2245	BLANPIED	65	CNTR	$\gamma p \to K^+Y^*$
2299± 6	BOCK	65	HBC	$\overline{p}p$ 5.7 GeV/c

$\Sigma(2250)$ WIDTH

VALUE (MeV)	DOCUMENT ID		TECN	COMMENT
60 to 150 (≈ 100) OUR ESTIMATE				
120±40	DEBELLEFON	78	DPWA	D_5 wave
80±20	DEBELLEFON	78	DPWA	G_9 wave
70±20	DEBELLEFON	77	DPWA	D_5 wave
60±20	DEBELLEFON	77	DPWA	G_9 wave
130±20	[1] DEBELLEFON	75B	HBC	$K^-p \to \Xi^{*0}K^0$
192±30	VANHORN	75	DPWA	$K^-p \to \Lambda\pi^0$, F_5 wave
100±20	AGUILAR-...	70B	HBC	K^-p 3.9, 4.6 GeV/c
164±50	BRICMAN	70	CNTR	Total, charge exchange
230±20	BUGG	68	CNTR	K^-p, K^-d total
• • • We do not use the following data for averages, fits, limits, etc. • • •				
100	DEBELLEFON	76	IPWA	D_5 wave
140	DEBELLEFON	76	IPWA	G_9 wave
170	COOL	70	CNTR	K^-p, K^-d total
125	LU	70	CNTR	$\gamma p \to K^+Y^*$
150	BLANPIED	65	CNTR	$\gamma p \to K^+Y^*$
21^{+17}_{-21}	BOCK	65	HBC	$\overline{p}p$ 5.7 GeV/c

$\Sigma(2250)$ DECAY MODES

	Mode	Fraction (Γ_i/Γ)
Γ_1	$N\overline{K}$	<10 %
Γ_2	$\Lambda\pi$	seen
Γ_3	$\Sigma\pi$	seen
Γ_4	$N\overline{K}\pi$	
Γ_5	$\Xi(1530)K$	

The above branching fractions are our estimates, not fits or averages.

$\Sigma(2250)$ BRANCHING RATIOS

See "Sign conventions for resonance couplings" in the Note on Λ and Σ Resonances.

$\Gamma(N\overline{K})/\Gamma_{total}$ **Γ_1/Γ**

VALUE	DOCUMENT ID		TECN	COMMENT
<0.1 OUR ESTIMATE				
0.08±0.02	DEBELLEFON	78	DPWA	D_5 wave
0.02±0.01	DEBELLEFON	78	DPWA	G_9 wave

$(J+\frac{1}{2})\times\Gamma(N\overline{K})/\Gamma_{total}$ **Γ_1/Γ**

VALUE	DOCUMENT ID		TECN	COMMENT
• • • We do not use the following data for averages, fits, limits, etc. • • •				
0.16±0.12	BRICMAN	70	CNTR	Total, charge exchange
0.42	COOL	70	CNTR	K^-p, K^-d total
0.47	BUGG	68	CNTR	

Baryon Particle Listings

$\Sigma(2250)$, $\Sigma(2455)$ Bumps, $\Sigma(2620)$ Bumps, $\Sigma(3000)$ Bumps

$(\Gamma_i\Gamma_f)^{1/2}/\Gamma_{total}$ in $N\overline{K} \to \Sigma(2250) \to \Lambda\pi$ $(\Gamma_1\Gamma_2)^{1/2}/\Gamma$

VALUE	DOCUMENT ID		TECN	COMMENT
-0.16 ± 0.03	VANHORN	75	DPWA	$K^-p \to \Lambda\pi^0$, F_5 wave
• • • We do not use the following data for averages, fits, limits, etc. • • •				
$+0.11$	DEBELLEFON	76	IPWA	D_5 wave
-0.10	DEBELLEFON	76	IPWA	G_9 wave
-0.18	BARBARO-...	70	DPWA	$K^-p \to \Lambda\pi^0$, G_9 wave

$(\Gamma_i\Gamma_f)^{1/2}/\Gamma_{total}$ in $N\overline{K} \to \Sigma(2250) \to \Sigma\pi$ $(\Gamma_1\Gamma_3)^{1/2}/\Gamma$

VALUE	DOCUMENT ID		TECN	COMMENT
$+0.06\pm0.02$	DEBELLEFON	77	DPWA	D_5 wave
-0.03 ± 0.02	DEBELLEFON	77	DPWA	G_9 wave
$+0.07$	BARBARO-...	70	DPWA	$K^-p \to \Sigma\pi$, G_9 wave

$\Gamma(N\overline{K})/\Gamma(\Sigma\pi)$ Γ_1/Γ_3

VALUE	DOCUMENT ID		TECN	COMMENT
• • • We do not use the following data for averages, fits, limits, etc. • • •				
<0.18	BARNES	69	HBC	1 standard dev. limit

$\Gamma(\Lambda\pi)/\Gamma(\Sigma\pi)$ Γ_2/Γ_3

VALUE	DOCUMENT ID		TECN	COMMENT
• • • We do not use the following data for averages, fits, limits, etc. • • •				
<0.18	BARNES	69	HBC	1 standard dev. limit

$(\Gamma_i\Gamma_f)^{1/2}/\Gamma_{total}$ in $N\overline{K} \to \Sigma(2250) \to \Xi(1530)K$ $(\Gamma_1\Gamma_5)^{1/2}/\Gamma$

VALUE	DOCUMENT ID		TECN	COMMENT
0.18 ± 0.04	[1] DEBELLEFON	75B	HBC	$K^-p \to \Xi^{*0}K^0$

$\Sigma(2250)$ FOOTNOTES

[1] Seen in the (initial and final state) D_5 wave. Isospin not determined.

$\Sigma(2250)$ REFERENCES

DEBELLEFON	78	NC 42A 403	A. de Bellefon *et al.*	(CDEF, SACL) IJP
DEBELLEFON	77	NC 37A 175	A. de Bellefon *et al.*	(CDEF, SACL) IJP
DEBELLEFON	76	NP B109 129	A. de Bellefon, A. Berthon	(CDEF) IJP
Also		NP B90 1	A. de Bellefon *et al.*	(CDEF, SACL) IJP
DEBELLEFON	75B	NC 28A 289	A. de Bellefon *et al.*	(CDEF, SACL)
VANHORN	75	NP B87 145	A.J. van Horn	(LBL) IJP
Also		NP B87 157	A.J. van Horn	(LBL) IJP
LASINSKI	71	NP B29 125	T.A. Lasinski	(EFI) IJP
AGUILAR-...	70B	PRL 25 58	M. Aguilar-Benitez *et al.*	(BNL, SYRA)
BARBARO-...	70	Duke Conf. 173 Hyperon Resonances, 1970	A. Barbaro-Galtieri	(LRL) IJP
BRICMAN	70	PL 31B 152	C. Bricman *et al.*	(CERN, CAEN, SACL)
COOL	70	PR D1 1887	R.L. Cool *et al.*	(BNL) I
Also		PRL 16 1228	R.L. Cool *et al.*	(BNL) I
LU	70	PR D2 1846	D.C. Lu *et al.*	(YALE)
BARNES	69	PRL 22 479	V.E. Barnes *et al.*	(BNL, SYRA)
BUGG	68	PR 168 1466	D.V. Bugg *et al.*	(RHEL, BIRM, CAVE) I
BLANPIED	65	PRL 14 741	W.A. Blanpied *et al.*	(YALE, CEA)
BOCK	65	PL 17 166	R.K. Bock *et al.*	(CERN, SACL)

$\Sigma(2455)$ Bumps

$I(J^P) = 1(?^?)$ Status: **

OMITTED FROM SUMMARY TABLE

There is also some slight evidence for Y^* states in this mass region from the reaction $\gamma p \to K^+X$ — see GREENBERG 68.

$\Sigma(2455)$ MASS

VALUE (MeV)	DOCUMENT ID		TECN	COMMENT
≈ 2455 OUR ESTIMATE				
2455 ± 10	ABRAMS	70	CNTR	K^-p, K^-d total
2455 ± 7	BUGG	68	CNTR	K^-p, K^-d total

$\Sigma(2455)$ WIDTH

VALUE (MeV)	DOCUMENT ID		TECN	COMMENT
140	ABRAMS	70	CNTR	K^-p, K^-d total
100 ± 20	BUGG	68	CNTR	

$\Sigma(2455)$ DECAY MODES

	Mode
Γ_1	$N\overline{K}$

$\Sigma(2455)$ BRANCHING RATIOS

$(J+\frac{1}{2})\times\Gamma(N\overline{K})/\Gamma_{total}$ Γ_1/Γ

VALUE	DOCUMENT ID		TECN	COMMENT
0.39	ABRAMS	70	CNTR	K^-p, K^-d total
0.05 ± 0.05	[1] BRICMAN	70	CNTR	Total, charge exchange
0.3	BUGG	68	CNTR	

$\Sigma(2455)$ FOOTNOTES

[1] Fit of total cross section given by BRICMAN 70 is poor in this region.

$\Sigma(2455)$ REFERENCES

ABRAMS	70	PR D1 1917	R.J. Abrams *et al.*	(BNL) I
Also		PRL 19 678	R.J. Abrams *et al.*	(BNL)
BRICMAN	70	PL 31B 152	C. Bricman *et al.*	(CERN, CAEN, SACL)
BUGG	68	PR 168 1466	D.V. Bugg *et al.*	(RHEL, BIRM, CAVE) I
GREENBERG	68	PRL 20 221	J.S. Greenberg *et al.*	(YALE)

$\Sigma(2620)$ Bumps

$I(J^P) = 1(?^?)$ Status: **

OMITTED FROM SUMMARY TABLE

$\Sigma(2620)$ MASS

VALUE (MeV)	DOCUMENT ID		TECN	COMMENT
≈ 2620 OUR ESTIMATE				
2542 ± 22	DIBIANCA	75	DBC	$K^-N \to \Xi K\pi$
2620 ± 15	ABRAMS	70	CNTR	K^-p, K^-d total

$\Sigma(2620)$ WIDTH

VALUE (MeV)	DOCUMENT ID		TECN	COMMENT
221 ± 81	DIBIANCA	75	DBC	$K^-N \to \Xi K\pi$
175	ABRAMS	70	CNTR	K^-p, K^-d total

$\Sigma(2620)$ DECAY MODES

	Mode
Γ_1	$N\overline{K}$

$\Sigma(2620)$ BRANCHING RATIOS

$(J+\frac{1}{2})\times\Gamma(N\overline{K})/\Gamma_{total}$ Γ_1/Γ

VALUE	DOCUMENT ID		TECN	COMMENT
0.32	ABRAMS	70	CNTR	K^-p, K^-d total
0.36 ± 0.12	BRICMAN	70	CNTR	Total, charge exchange

$\Sigma(2620)$ REFERENCES

DIBIANCA	75	NP B98 137	F.A. Dibianca, R.J. Endorf	(CMU)
ABRAMS	70	PR D1 1917	R.J. Abrams *et al.*	(BNL) I
Also		PRL 19 678	R.J. Abrams *et al.*	(BNL)
BRICMAN	70	PL 31B 152	C. Bricman *et al.*	(CERN, CAEN, SACL)

$\Sigma(3000)$ Bumps

$I(J^P) = 1(?^?)$ Status: *

OMITTED FROM SUMMARY TABLE

Seen as an enhancement in $\Lambda\pi$ and $\overline{K}N$ invariant mass spectra and in the missing mass of neutrals recoiling against a K^0.

$\Sigma(3000)$ MASS

VALUE (MeV)	DOCUMENT ID		TECN	CHG	COMMENT
≈ 3000 OUR ESTIMATE					
3000	EHRLICH	66	HBC	0	π^-p 7.91 GeV/c

$\Sigma(3000)$ DECAY MODES

	Mode
Γ_1	$N\overline{K}$
Γ_2	$\Lambda\pi$

$\Sigma(3000)$ REFERENCES

EHRLICH	66	PR 152 1194	R. Ehrlich, W. Selove, H. Yuta	(PENN) I

$\Sigma(3170)$ Bumps

$I(J^P) = 1(?^?)$ Status: *

OMITTED FROM SUMMARY TABLE

Seen by AMIRZADEH 79 as a narrow 6.5-standard-deviation enhancement in the reaction $K^- p \rightarrow Y^{*+}\pi^-$ using data from independent high statistics bubble chamber experiments at 8.25 and 6.5 GeV/c. The dominant decay modes are multibody, multistrange final states and the production is via isospin-3/2 baryon exchange. Isospin 1 is favored.

Not seen in a $K^- p$ experiment in LASS at 11 GeV/c (ASTON 85B).

$\Sigma(3170)$ MASS (PRODUCTION EXPERIMENTS)

VALUE (MeV)	EVTS	DOCUMENT ID		TECN	COMMENT
≈ 3170 OUR ESTIMATE					
3170±5	35	AMIRZADEH	79	HBC	$K^- p \rightarrow Y^{*+}\pi^-$

$\Sigma(3170)$ WIDTH (PRODUCTION EXPERIMENTS)

VALUE (MeV)	EVTS	DOCUMENT ID		TECN	COMMENT
<20	35	[1] AMIRZADEH	79	HBC	$K^- p \rightarrow Y^{*+}\pi^-$

$\Sigma(3170)$ DECAY MODES (PRODUCTION EXPERIMENTS)

	Mode	Fraction (Γ_i/Γ)
Γ_1	$\Lambda K\overline{K}\pi$'s	seen
Γ_2	$\Sigma K\overline{K}\pi$'s	seen
Γ_3	$\Xi K\pi$'s	seen

$\Sigma(3170)$ BRANCHING RATIOS (PRODUCTION EXPERIMENTS)

$\Gamma(\Lambda K\overline{K}\pi$'s$)/\Gamma_{total}$ **Γ_1/Γ**

VALUE	DOCUMENT ID		TECN	COMMENT
seen	AMIRZADEH	79	HBC	$K^- p \rightarrow Y^{*+}\pi^-$

$\Gamma(\Sigma K\overline{K}\pi$'s$)/\Gamma_{total}$ **Γ_2/Γ**

VALUE	DOCUMENT ID		TECN	COMMENT
seen	AMIRZADEH	79	HBC	$K^- p \rightarrow Y^{*+}\pi^-$

$\Gamma(\Xi K\pi$'s$)/\Gamma_{total}$ **Γ_3/Γ**

VALUE	DOCUMENT ID		TECN	COMMENT
seen	AMIRZADEH	79	HBC	$K^- p \rightarrow Y^{*+}\pi^-$

$\Sigma(3170)$ FOOTNOTES (PRODUCTION EXPERIMENTS)

[1] Observed width consistent with experimental resolution.

$\Sigma(3170)$ REFERENCES (PRODUCTION EXPERIMENTS)

ASTON	85B	PR D32 2270	D. Aston *et al.*	(SLAC, CARL, CNRC, CINC)
AMIRZADEH	79	PL 89B 125	J. Amirzadeh *et al.*	(BIRM, CERN, GLAS+) I
Also		Toronto Conf. 263	J.B. Kinson *et al.*	(BIRM, CERN, GLAS+) I

Ξ BARYONS
($S = -2$, $I = 1/2$)

$\Xi^0 = uss$, $\Xi^- = dss$

Ξ^0

$I(J^P) = \frac{1}{2}(\frac{1}{2}^+)$ Status: ****

The parity has not actually been measured, but + is of course expected.

Ξ^0 MASS

The fit uses the Ξ^0, Ξ^-, and $\overline{\Xi}^+$ masses and the $\Xi^- - \Xi^0$ mass difference. It assumes that the Ξ^- and $\overline{\Xi}^+$ masses are the same.

VALUE (MeV)	EVTS	DOCUMENT ID		TECN	COMMENT
1314.86±0.20 OUR FIT					
1314.82±0.06±0.20	3120	FANTI	00	NA48	p Be, 450 GeV
• • • We do not use the following data for averages, fits, limits, etc. • • •					
1315.2 ±0.92	49	WILQUET	72	HLBC	
1313.4 ±1.8	1	PALMER	68	HBC	

$m_{\Xi^-} - m_{\Xi^0}$

The fit uses the Ξ^0, Ξ^-, and $\overline{\Xi}^+$ masses and the $\Xi^- - \Xi^0$ mass difference. It assumes that the Ξ^- and $\overline{\Xi}^+$ masses are the same.

VALUE (MeV)	EVTS	DOCUMENT ID		TECN	COMMENT
6.85±0.21 OUR FIT					
6.3 ±0.7 OUR AVERAGE					
6.9 ±2.2	29	LONDON	66	HBC	
6.1 ±0.9	88	PJERROU	65B	HBC	
6.8 ±1.6	23	JAUNEAU	63	FBC	
• • • We do not use the following data for averages, fits, limits, etc. • • •					
6.1 ±1.6	45	CARMONY	64B	HBC	See PJERROU 65B

Ξ^0 MEAN LIFE

VALUE (10^{-10} s)	EVTS	DOCUMENT ID		TECN	COMMENT
2.90±0.09 OUR AVERAGE					
2.83±0.16	6300	[1] ZECH	77	SPEC	Neutral hyperon beam
$2.88^{+0.21}_{-0.19}$	652	BALTAY	74	HBC	1.75 GeV/c K^-p
$2.90^{+0.32}_{-0.27}$	157	[2] MAYEUR	72	HLBC	2.1 GeV/c K^-
$3.07^{+0.22}_{-0.20}$	340	DAUBER	69	HBC	
3.0 ±0.5	80	PJERROU	65B	HBC	
$2.5\ ^{+0.4}_{-0.3}$	101	HUBBARD	64	HBC	
$3.9\ ^{+1.4}_{-0.8}$	24	JAUNEAU	63	FBC	
• • • We do not use the following data for averages, fits, limits, etc. • • •					
$3.5\ ^{+1.0}_{-0.8}$	45	CARMONY	64B	HBC	See PJERROU 65B

[1] The ZECH 77 result is $\tau_{\Xi^0} = [2.77-(\tau_\Lambda - 2.69)] \times 10^{-10}$ s, in which we use $\tau_\Lambda = 2.63 \times 10^{-10}$ s.
[2] The MAYEUR 72 value is modified by the erratum.

Ξ^0 MAGNETIC MOMENT

See the "Note on Baryon Magnetic Moments" in the Λ Listings.

VALUE (μ_N)	EVTS	DOCUMENT ID		TECN
−1.250±0.014 OUR AVERAGE				
−1.253±0.014	270k	COX	81	SPEC
−1.20 ±0.06	42k	BUNCE	79	SPEC

Ξ^0 DECAY MODES

	Mode	Fraction (Γ_i/Γ)	Confidence level
Γ_1	$\Lambda\pi^0$	(99.524±0.012) %	
Γ_2	$\Lambda\gamma$	(1.17 ±0.07) $\times 10^{-3}$	
Γ_3	$\Lambda e^+ e^-$	(7.6 ±0.6) $\times 10^{-6}$	
Γ_4	$\Sigma^0\gamma$	(3.33 ±0.10) $\times 10^{-3}$	
Γ_5	$\Sigma^+ e^- \overline{\nu}_e$	(2.52 ±0.08) $\times 10^{-4}$	
Γ_6	$\Sigma^+ \mu^- \overline{\nu}_\mu$	(2.33 ±0.35) $\times 10^{-6}$	

$\Delta S = \Delta Q$ (SQ) violating modes or $\Delta S = 2$ forbidden ($S2$) modes

Γ_7	$\Sigma^- e^+ \nu_e$	SQ	<	9	$\times 10^{-4}$	90%
Γ_8	$\Sigma^- \mu^+ \nu_\mu$	SQ	<	9	$\times 10^{-4}$	90%
Γ_9	$p\pi^-$	$S2$	<	8	$\times 10^{-6}$	90%
Γ_{10}	$p e^- \overline{\nu}_e$	$S2$	<	1.3	$\times 10^{-3}$	
Γ_{11}	$p \mu^- \overline{\nu}_\mu$	$S2$	<	1.3	$\times 10^{-3}$	

CONSTRAINED FIT INFORMATION

An overall fit to 5 branching ratios uses 11 measurements and one constraint to determine 5 parameters. The overall fit has a $\chi^2 = 7.5$ for 7 degrees of freedom.

The following *off-diagonal* array elements are the correlation coefficients $\langle \delta x_i \delta x_j \rangle / (\delta x_i \cdot \delta x_j)$, in percent, from the fit to the branching fractions, $x_i \equiv \Gamma_i/\Gamma_{\rm total}$. The fit constrains the x_i whose labels appear in this array to sum to one.

	x_1	x_2	x_4	x_5
x_2	−57			
x_4	−82	0		
x_5	−7	0	0	
x_6	0	0	0	1

Ξ^0 BRANCHING RATIOS

$\Gamma(\Lambda\gamma)/\Gamma(\Lambda\pi^0)$ Γ_2/Γ_1

VALUE (units 10^{-3})	EVTS	DOCUMENT ID		TECN	COMMENT
1.17±0.07 OUR FIT					
1.17±0.07 OUR AVERAGE					
1.17±0.05±0.06	672	[3] LAI	04A	NA48	p Be, 450 GeV
1.91±0.34±0.19	31	[4] FANTI	00	NA48	p Be, 450 GeV
1.06±0.12±0.11	116	JAMES	90	SPEC	FNAL hyperons

[3] LAI 04A used our 2002 value of 99.5% for the $\Xi^0 \to \Lambda\pi^0$ branching fraction to get $\Gamma(\Xi^0 \to \Lambda\gamma)/\Gamma_{\rm total} = (1.16 \pm 0.05 \pm 0.06) \times 10^{-3}$. We adjust slightly to go back to what was directly measured.
[4] FANTI 00 used our 1998 value of 99.5% for the $\Xi^0 \to \Lambda\pi^0$ branching fraction to get $\Gamma(\Xi^0 \to \Lambda\gamma)/\Gamma_{\rm total} = (1.90 \pm 0.34 \pm 0.19) \times 10^{-3}$. We adjust slightly to go back to what was directly measured.

$\Gamma(\Lambda e^+ e^-)/\Gamma_{\rm total}$ Γ_3/Γ

VALUE (units 10^{-6})	EVTS	DOCUMENT ID		TECN	COMMENT
7.6±0.4±0.5	397 ± 21	[5] BATLEY	07C	NA48	p Be, 400 GeV

[5] This BATLEY 07C result is consistent with internal bremsstrahlung.

$\Gamma(\Sigma^0\gamma)/\Gamma(\Lambda\pi^0)$ Γ_4/Γ_1

VALUE (units 10^{-3})	EVTS	DOCUMENT ID		TECN	COMMENT
3.35±0.10 OUR FIT					
3.35±0.10 OUR AVERAGE					
3.34±0.05±0.09	4045	ALAVI-HARATI	01C	KTEV	p nucleus, 800 GeV
3.16±0.76±0.32	17	[6] FANTI	00	NA48	p Be, 450 GeV
3.56±0.42±0.10	85	TEIGE	89	SPEC	FNAL hyperons

[6] FANTI 00 used our 1998 value of 99.5% for the $\Xi^0 \to \Lambda\pi^0$ branching fraction to get $\Gamma(\Xi^0 \to \Sigma^0\gamma)/\Gamma_{\rm total} = (3.14 \pm 0.76 \pm 0.32) \times 10^{-3}$. We adjust slightly to go back to what was directly measured.

$\Gamma(\Sigma^+ e^- \overline{\nu}_e)/\Gamma_{\rm total}$ Γ_5/Γ

VALUE (units 10^{-4})	EVTS	DOCUMENT ID		TECN	COMMENT
2.52±0.08 OUR FIT					
2.53±0.08 OUR AVERAGE					
2.51±0.03±0.09	6101	BATLEY	07	NA48	p Be, 400 GeV
2.55±0.14±0.10	419	[7] BATLEY	07	NA48	p Be, 400 GeV
2.71±0.22±0.31	176	AFFOLDER	99	KTEV	p nucleus, 800 GeV

[7] This BATLEY 07 result is for $\overline{\Xi}^0 \to \overline{\Sigma}^- e^+ \nu_e$ events.

$\Gamma(\Sigma^+ \mu^- \overline{\nu}_\mu)/\Gamma_{\rm total}$ Γ_6/Γ

VALUE (units 10^{-6})	EVTS	DOCUMENT ID		TECN	COMMENT
2.3 ±0.4 OUR FIT					
2.17±0.32±0.17	66	[8] BATLEY	13	NA48	p Be, 400 GeV

[8] BATLEY 13 used $\Xi^0 \to \Sigma^+ e^- \overline{\nu}_e$ decay as a normalization mode and its branching fraction value of $(2.51 \pm 0.03 \pm 0.09) \times 10^{-4}$ from BATLEY 07.

$\Gamma(\Sigma^+ \mu^- \overline{\nu}_\mu)/\Gamma(\Sigma^+ e^- \overline{\nu}_e)$ Γ_6/Γ_5

VALUE	EVTS	DOCUMENT ID		TECN	COMMENT
0.0092±0.0015 OUR FIT					
0.018 $^{+0.007}_{-0.005}$ ±0.002	9	ABOUZAID	05	KTEV	p nucleus 800 GeV

$\Gamma(\Sigma^- e^+ \nu_e)/\Gamma(\Lambda\pi^0)$ Γ_7/Γ_1

Test of $\Delta S = \Delta Q$ rule.

VALUE (units 10^{-3})	CL%	EVTS	DOCUMENT ID		TECN	COMMENT
<0.9	90	0	YEH	74	HBC	Effective denom.=2500
• • • We do not use the following data for averages, fits, limits, etc. • • •						
<1.5			DAUBER	69	HBC	
<6			HUBBARD	66	HBC	

$\Gamma(\Sigma^- \mu^+ \nu_\mu)/\Gamma(\Lambda\pi^0)$ Γ_8/Γ_1

Test of $\Delta S = \Delta Q$ rule.

VALUE (units 10^{-3})	CL%	EVTS	DOCUMENT ID		TECN	COMMENT
<0.9	90	0	YEH	74	HBC	Effective denom.=2500
• • • We do not use the following data for averages, fits, limits, etc. • • •						
<1.5			DAUBER	69	HBC	
<6			HUBBARD	66	HBC	

$\Gamma(p\pi^-)/\Gamma(\Lambda\pi^0)$ Γ_9/Γ_1

ΔS=2. Forbidden in first-order weak interaction.

VALUE (units 10^{-6})	CL%	EVTS	DOCUMENT ID		TECN	COMMENT
< 8.2	90		WHITE	05	HYCP	p Cu, 800 GeV
• • • We do not use the following data for averages, fits, limits, etc. • • •						
< 36	90		GEWENIGER	75	SPEC	
<1800	90	0	YEH	74	HBC	Effective denom.=1300
< 900			DAUBER	69	HBC	
<5000			HUBBARD	66	HBC	

$\Gamma(pe^-\overline{\nu}_e)/\Gamma(\Lambda\pi^0)$ Γ_{10}/Γ_1

ΔS=2. Forbidden in first-order weak interaction.

VALUE (units 10^{-3})	CL%	EVTS	DOCUMENT ID		TECN	COMMENT
<1.3			DAUBER	69	HBC	
• • • We do not use the following data for averages, fits, limits, etc. • • •						
<3.4	90	0	YEH	74	HBC	Effective denom.=670
<6			HUBBARD	66	HBC	

$\Gamma(p\mu^-\overline{\nu}_\mu)/\Gamma(\Lambda\pi^0)$ Γ_{11}/Γ_1

ΔS=2. Forbidden in first-order weak interaction.

VALUE (units 10^{-3})	CL%	EVTS	DOCUMENT ID		TECN	COMMENT
<1.3			DAUBER	69	HBC	
• • • We do not use the following data for averages, fits, limits, etc. • • •						
<3.5	90	0	YEH	74	HBC	Effective denom.=664
<6			HUBBARD	66	HBC	

Ξ^0 DECAY PARAMETERS

See the "Note on Baryon Decay Parameters" in the neutron Listings.

$\alpha(\Xi^0)\ \alpha_-(\Lambda)$

This is a product of the $\Xi^0 \to \Lambda\pi^0$ and $\Lambda \to p\pi^-$ asymmetries.

VALUE	EVTS	DOCUMENT ID		TECN	COMMENT
-0.261 ± 0.006 OUR AVERAGE					
$-0.276\pm0.001\pm0.035$	4M	BATLEY	10B	NA48	p Be, 400 GeV
$-0.260\pm0.004\pm0.005$	300k	HANDLER	82	SPEC	FNAL hyperons
• • • We do not use the following data for averages, fits, limits, etc. • • •					
-0.317 ± 0.027	6075	BUNCE	78	SPEC	FNAL hyperons
$-0.35\ \pm0.06$	505	BALTAY	74	HBC	K^-p 1.75 GeV/c
$-0.28\ \pm0.06$	739	DAUBER	69	HBC	K^-p 1.7–2.6 GeV/c

α FOR $\Xi^0 \to \Lambda\pi^0$

The above average, $\alpha(\Xi^0)\alpha_-(\Lambda) = -0.261 \pm 0.006$, divided by our current average $\alpha_-(\Lambda) = 0.642 \pm 0.013$, gives the following value for $\alpha(\Xi^0)$.

VALUE	DOCUMENT ID
-0.406 ± 0.013 OUR EVALUATION	

ϕ ANGLE FOR $\Xi^0 \to \Lambda\pi^0$ $(\tan\phi = \beta/\gamma)$

VALUE (°)	EVTS	DOCUMENT ID		TECN	COMMENT
21±12 OUR AVERAGE					
16±17	652	BALTAY	74	HBC	1.75 GeV/c K^-p
38±19	739	[9] DAUBER	69	HBC	
− 8±30	146	[10] BERGE	66	HBC	

[9] DAUBER 69 uses $\alpha_\Lambda = 0.647 \pm 0.020$.

[10] The errors have been multiplied by 1.2 due to approximations used for the Ξ polarization; see DAUBER 69 for a discussion.

RADIATIVE HYPERON DECAYS

Revised July 2011 by J.D. Jackson (LBNL).

The weak radiative decays of spin-1/2 hyperons, $B_i \to B_f\gamma$, yield information about matrix elements (form factors) similar to that gained from weak hadronic decays. For a polarized spin-1/2 hyperon decaying radiatively via a $\Delta Q = 0$, $\Delta S = 1$ transition, the angular distribution of the direction $\hat{\mathbf{p}}$ of the final spin-1/2 baryon in the hyperon rest frame is

$$\frac{dN}{d\Omega} = \frac{N}{4\pi}\,(1 + \alpha_\gamma\,\mathbf{P}_i\cdot\hat{\mathbf{p}})\ . \qquad (1)$$

Here $\mathbf{P}_i$ is the polarization of the decaying hyperon, and α_γ is the asymmetry parameter. In terms of the form factors $F_1(q^2)$, $F_2(q^2)$, and $G(q^2)$ of the effective hadronic weak electromagnetic vertex,

$$F_1(q^2)\gamma_\lambda + iF_2(q^2)\sigma_{\lambda\mu}q^\mu + G(q^2)\gamma_\lambda\gamma_5\ ,$$

α_γ is

$$\alpha_\gamma = \frac{2\,\mathrm{Re}[G(0)F_M^*(0)]}{|G(0)|^2 + |F_M(0)|^2}\ , \qquad (2)$$

where $F_M = (m_i - m_f)[F_2 - F_1/(m_i + m_f)]$. If the decaying hyperon is unpolarized, the decay baryon has a longitudinal polarization given by $P_f = -\alpha_\gamma$ [1].

The angular distribution for the weak hadronic decay, $B_i \to B_f\pi$, has the same form as Eq. (1), but of course with a different asymmetry parameter, α_π. Now, however, if the decaying hyperon is unpolarized, the decay baryon has a longitudinal polarization given by $P_f = +\alpha_\pi$ [2,3]. The difference of sign is because the spins of the pion and photon are different.

$\Xi^0 \to \Lambda\gamma$ *decay*—The radiative decay $\Xi^0 \to \Lambda\gamma$ of an unpolarized Ξ^0 uses the hadronic decay $\Lambda \to p\pi^-$ as the analyzer. As noted above, the longitudinal polarization of the Λ will be $P_\Lambda = -\alpha_{\Xi\Lambda\gamma}$. Let α_- be the $\Lambda \to p\pi^-$ asymmetry parameter and $\theta_{\Lambda p}$ be the angle, as seen in the Λ rest frame, between the Λ line of flight and the proton momentum. Then the hadronic version of Eq. (1) applied to the $\Lambda \to p\pi^-$ decay gives

$$\frac{dN}{d\cos\theta_{\Lambda p}} = \frac{N}{2}\,(1 - \alpha_{\Xi\Lambda\gamma}\,\alpha_-\cos\theta_{\Lambda p}) \qquad (3)$$

for the angular distribution of the proton in the Λ frame. Our current value, from the CERN NA48/1 experiment [4], is $\alpha_{\Xi\Lambda\gamma} = -0.704 \pm 0.019 \pm 0.064$.

$\Xi^0 \to \Sigma^0\gamma$ *decay*—The asymmetry parameter here, $\alpha_{\Xi\Sigma\gamma}$, is measured by following the decay chain $\Xi^0 \to \Sigma^0\gamma$, $\Sigma^0 \to \Lambda\gamma$, $\Lambda \to p\pi^-$. Again, for an unpolarized Ξ^0, the longitudinal polarization of the Σ^0 will be $P_\Sigma = -\alpha_{\Xi\Sigma\gamma}$. In the $\Sigma^0 \to \Lambda\gamma$ decay, a parity-conserving magnetic-dipole transition, the polarization of the Σ^0 is transferred to the Λ, as may be seen as follows. Let $\theta_{\Sigma\Lambda}$ be the angle seen in the Σ^0 rest frame between the Σ^0 line of flight and the Λ momentum. For Σ^0 helicity $+1/2$, the probability amplitudes for positive and negative spin states of the Σ^0 *along the* Λ *momentum* are $\cos(\theta_{\Sigma\Lambda}/2)$ and $\sin(\theta_{\Sigma\Lambda}/2)$. Then the amplitude for a negative helicity photon and a negative helicity Λ is $\cos(\theta_{\Sigma\Lambda}/2)$, while the amplitude for positive helicities for the photon and Λ is $\sin(\theta_{\Sigma\Lambda}/2)$. For Σ^0 helicity $-1/2$, the amplitudes are interchanged. If the Σ^0 has longitudinal polarization P_Σ, the probabilities for Λ helicities $\pm1/2$ are therefore

$$p(\pm1/2) = \frac{1}{2}(1 \mp P_\Sigma)\cos^2(\theta_{\Sigma\Lambda}/2) + \frac{1}{2}(1 \pm P_\Sigma)\sin^2(\theta_{\Sigma\Lambda}/2)\ , \qquad (4)$$

and the longitudinal polarization of the Λ is

$$P_\Lambda = -P_\Sigma \cos\theta_{\Sigma\Lambda} = +\alpha_{\Xi\Sigma\gamma} \cos\theta_{\Sigma\Lambda} \ . \qquad (5)$$

Using Eq. (1) for the $\Lambda \to p\pi^-$ decay again, we get for the joint angular distribution of the $\Sigma^0 \to \Lambda\gamma$, $\Lambda \to p\pi^-$ chain,

$$\frac{d^2N}{d\cos\theta_{\Sigma\Lambda}\, d\cos\theta_{\Lambda p}} = \frac{N}{4}\left(1 + \alpha_{\Xi\Sigma\gamma}\cos\theta_{\Sigma\Lambda}\,\alpha_-\cos\theta_{\Lambda p}\right) . \qquad (6)$$

Our current average for $\alpha_{\Xi\Sigma\gamma}$ is -0.69 ± 0.06 [4,5].

References

1. R.E. Behrends, Phys. Rev. **111**, 1691 (1958); see Eq. (7) or (8).
2. In ancient times, the signs of the asymmetry term in the angular distributions of radiative and hadronic decays of polarized hyperons were sometimes opposite. For roughly 50 years, however, the overwhelming convention has been to make them the same. The aim, not always achieved, is to remove ambiguities.
3. For the definition of α_π, see the note on "Baryon Decay Parameters" in the Neutron Listings.
4. J.R. Batley *et al.*, Phys. Lett. **B693**, 241 (2010).
5. A. Alavi-Harati *et al.*, Phys. Rev. Lett. **86**, 3239 (2001).

α FOR $\Xi^0 \to \Lambda\gamma$

See the note above on "Radiative Hyperon Decays."

VALUE	EVTS	DOCUMENT ID		TECN	COMMENT
$-0.704 \pm 0.019 \pm 0.064$	52k	[11] BATLEY	10B	NA48	p Be, 400 GeV
• • • We do not use the following data for averages, fits, limits, etc. • • •					
$-0.78 \pm 0.18 \pm 0.06$	672	LAI	04A	NA48	See BATLEY 10B
-0.43 ± 0.44	87	[12] JAMES	90	SPEC	FNAL hyperons

[11] BATLEY 10B also measured the $\overline{\Xi}^0 \to \overline{\Lambda}\gamma$ asymmetry to be -0.798 ± 0.064 (no systematic error given) with 4769 events.
[12] The sign has been changed; see the erratum, JAMES 02.

α FOR $\Xi^0 \to \Lambda e^+ e^-$

VALUE	EVTS	DOCUMENT ID		TECN	COMMENT
-0.8 ± 0.2	397 ± 21	[13] BATLEY	07C	NA48	p Be, 400 GeV

[13] This BATLEY 07C result is consistent with the asymmetry α for $\Xi^0 \to \Lambda\gamma$, as expected if the mechanism is internal bremsstrahlung.

α FOR $\Xi^0 \to \Sigma^0\gamma$

See the note above on "Radiative Hyperon Decays."

VALUE	EVTS	DOCUMENT ID		TECN	COMMENT
-0.69 ± 0.06 OUR AVERAGE					
$-0.729 \pm 0.030 \pm 0.076$	15k	[14] BATLEY	10B	NA48	p Be, 400 GeV
$-0.63 \pm 0.08 \pm 0.05$	4045	ALAVI-HARATI	01C	KTEV	p nucleus, 800 GeV
• • • We do not use the following data for averages, fits, limits, etc. • • •					
$+0.20 \pm 0.32 \pm 0.05$	85	[15] TEIGE	89	SPEC	FNAL hyperons

[14] BATLEY 10B also measured the $\overline{\Xi}^0 \to \overline{\Sigma}^0\gamma$ asymmetry to be -0.786 ± 0.104 (no systematic error given) with 1404 events.
[15] This result has been withdrawn, due to an error. See the erratum, TEIGE 02.

$g_1(0)/f_1(0)$ FOR $\Xi^0 \to \Sigma^+ e^- \overline{\nu}_e$

VALUE	EVTS	DOCUMENT ID		TECN	COMMENT
1.22±0.05 OUR AVERAGE					
1.21 ± 0.05		BATLEY	13	NA48	p Be, 400 GeV
$1.32^{+0.21}_{-0.17} \pm 0.05$	487	[16] ALAVI-HARATI	01I	KTEV	p nucleus, 800 GeV
• • • We do not use the following data for averages, fits, limits, etc. • • •					
$1.20 \pm 0.04 \pm 0.03$	6520	[17] BATLEY	07	NA48	See BATLEY 13

[16] ALAVI-HARATI 01I assumes here that the second-class current is zero and that the weak-magnetism term takes its exact SU(3) value.
[17] This BATLEY 07 result uses our 2006 value of V_{US} from semileptonic kaon decays as input.

$g_2(0)/f_1(0))$ FOR $\Xi^0 \to \Sigma^+ e^- \overline{\nu}_e$

VALUE	EVTS	DOCUMENT ID		TECN	COMMENT
$-1.7^{+2.1}_{-2.0} \pm 0.5$	487	[18] ALAVI-HARATI	01I	KTEV	p nucleus, 800 GeV

[18] ALAVI-HARATI 01I thus assumes that $g_2 = 0$ in calculating g_1/f_1, above.

$f_2(0)/f_1(0)$ FOR $\Xi^0 \to \Sigma^+ e^- \overline{\nu}_e$

VALUE	EVTS	DOCUMENT ID		TECN	COMMENT
2.0±0.9 OUR AVERAGE					
2.0 ± 1.3		BATLEY	13	NA48	p Be, 400 GeV
$2.0 \pm 1.2 \pm 0.5$	487	ALAVI-HARATI	01I	KTEV	p nucleus, 800 GeV

Ξ^0 REFERENCES

BATLEY	13	PL B720 105	J.R. Batley *et al.*	(CERN NA48/1 Collab.)
BATLEY	10B	PL B693 241	J.R. Batley *et al.*	(CERN NA48/1 Collab.)
BATLEY	07	PL B645 36	J.R. Batley *et al.*	(CERN NA48/1 Collab.)
BATLEY	07C	PL B650 1	J.R. Batley *et al.*	(CERN NA48 Collab.)
ABOUZAID	05	PRL 95 081801	E. Abouzaid *et al.*	(FNAL KTeV Collab.)
WHITE	05	PRL 94 101804	C.G. White *et al.*	(FNAL HyperCP Collab.)
LAI	04A	PL B584 251	A. Lai *et al.*	(CERN NA48 Collab.)
JAMES	02	PRL 89 169901 (errat)	C. James *et al.*	(MINN, MICH, WISC, RUTG)
TEIGE	02	PRL 89 169902 (errat)	S. Teige *et al.*	(RUTG, MICH, MINN)
ALAVI-HARATI	01C	PRL 86 3239	A. Alavi-Harati *et al.*	(FNAL KTeV Collab.)
ALAVI-HARATI	01I	PRL 87 132001	A. Alavi-Harati *et al.*	(FNAL KTeV Collab.)
FANTI	00	EPJ C12 69	V. Fanti *et al.*	(CERN NA48 Collab.)
AFFOLDER	99	PRL 82 3751	A. Affolder *et al.*	(FNAL KTeV Collab.)
JAMES	90	PRL 64 843	C. James *et al.*	(MINN, MICH, WISC, RUTG)
TEIGE	89	PRL 63 2717	S. Teige *et al.*	(RUTG, MICH, MINN)
HANDLER	82	PR D25 639	R. Handler *et al.*	(WISC, MICH, MINN+)
COX	81	PRL 46 877	P.T. Cox *et al.*	(MICH, WISC, RUTG, MINN+)
BUNCE	79	PL 86B 386	G.R.M. Bunce *et al.*	(BNL, MICH, RUTG+)
BUNCE	78	PR D18 633	G.R.M. Bunce *et al.*	(WISC, MICH, RUTG)
ZECH	77	NP B124 413	G. Zech *et al.*	(SIEG, CERN, DORT, HEIDH)
GEWENIGER	75	PL 57B 193	C. Geweniger *et al.*	(CERN, HEIDH)
BALTAY	74	PR D9 49	C. Baltay *et al.*	(COLU, BING) J
YEH	74	PR D10 3545	N. Yeh *et al.*	(BING, COLU)
MAYEUR	72	NP B47 333	C. Mayeur *et al.*	(BRUX, CERN, TUFTS, LOUC)
Also		NP B53 268 (erratum)	C. Mayeur	
WILQUET	72	PL 42B 372	G. Wilquet *et al.*	(BRUX, CERN, TUFTS+)
DAUBER	69	PR 179 1262	P.M. Dauber *et al.*	(LRL)
PALMER	68	PL 26B 323	R.B. Palmer *et al.*	(BNL, SYRA)
BERGE	66	PR 147 945	J.P. Berge *et al.*	(LRL)
HUBBARD	66	Thesis UCRL 11510	J.R. Hubbard	(LRL)
LONDON	66	PR 143 1034	G.W. London *et al.*	(BNL, SYRA)
PJERROU	65B	PRL 14 275	G.M. Pjerrou *et al.*	(UCLA)
Also		Thesis	G.M. Pjerrou	(UCLA)
CARMONY	64B	PRL 12 482	D.D. Carmony *et al.*	(UCLA)
HUBBARD	64	PR 135 B183	J.R. Hubbard *et al.*	(LRL)
JAUNEAU	63	PL 4 49	L. Jauneau *et al.*	(EPOL, CERN, LOUC+)
Also		Siena Conf. 1 1	L. Jauneau *et al.*	(EPOL, CERN, LOUC+)

Ξ^-

$I(J^P) = \frac{1}{2}(\frac{1}{2}^+)$ Status: ****

The parity has not actually been measured, but + is of course expected.

We have omitted some results that have been superseded by later experiments. See our earlier editions.

Ξ^- MASS

The fit uses the Ξ^-, $\overline{\Xi}^+$, and Ξ^0 masses and the $\Xi^- - \overline{\Xi}^+$ mass difference. It assumes that the Ξ^- and $\overline{\Xi}^+$ masses are the same.

VALUE (MeV)	EVTS	DOCUMENT ID		TECN	COMMENT
1321.71±0.07 OUR FIT					
1321.70±0.08±0.05	2478 ± 68	ABDALLAH	06E	DLPH	from Z decays
• • • We do not use the following data for averages, fits, limits, etc. • • •					
1321.46 ± 0.34	632	DIBIANCA	75	DBC	4.9 GeV/c $K^- d$
1321.12 ± 0.41	268	WILQUET	72	HLBC	
1321.87 ± 0.51	195	[1] GOLDWASSER	70	HBC	5.5 GeV/c $K^- p$
1321.67 ± 0.52	6	CHIEN	66	HBC	6.9 GeV/c $\overline{p}p$
1321.4 ± 1.1	299	LONDON	66	HBC	
1321.3 ± 0.4	149	PJERROU	65B	HBC	
1321.1 ± 0.3	241	[2] BADIER	64	HBC	
1321.4 ± 0.4	517	[2] JAUNEAU	63D	FBC	
1321.1 ± 0.65	62	[2] SCHNEIDER	63	HBC	

[1] GOLDWASSER 70 uses $m_\Lambda = 1115.58$ MeV.
[2] These masses have been increased 0.09 MeV because the Λ mass increased.

$\overline{\Xi}^+$ MASS

The fit uses the Ξ^-, $\overline{\Xi}^+$, and Ξ^0 masses and the $\Xi^- - \overline{\Xi}^+$ mass difference. It assumes that the Ξ^- and $\overline{\Xi}^+$ masses are the same.

VALUE (MeV)	EVTS	DOCUMENT ID		TECN	COMMENT
1321.71±0.07 OUR FIT					
1321.73±0.08±0.05	2256 ± 63	ABDALLAH	06E	DLPH	from Z decays
• • • We do not use the following data for averages, fits, limits, etc. • • •					
1321.6 ± 0.8	35	VOTRUBA	72	HBC	10 GeV/c $K^+ p$
1321.2 ± 0.4	34	STONE	70	HBC	
1320.69 ± 0.93	5	CHIEN	66	HBC	6.9 GeV/c $\overline{p}p$

$(m_{\Xi^-} - m_{\overline{\Xi}^+}) / m_{\Xi^-}$

A test of CPT invariance.

VALUE	DOCUMENT ID	TECN	COMMENT
$(-2.5 \pm 8.7) \times 10^{-5}$	ABDALLAH 06E	DLPH	from Z decays

Ξ^- MEAN LIFE

Measurements with an error $> 0.2 \times 10^{-10}$ s or with systematic errors not included have been omitted.

VALUE (10^{-10} s)	EVTS	DOCUMENT ID		TECN	COMMENT
1.639±0.015 OUR AVERAGE					
1.65 ±0.07 ±0.12	2478 ± 68	ABDALLAH	06E	DLPH	from Z decays
1.652±0.051	32k	BOURQUIN	84	SPEC	Hyperon beam
1.665±0.065	41k	BOURQUIN	79	SPEC	Hyperon beam
1.609±0.028	4286	HEMINGWAY	78	HBC	4.2 GeV/c K^-p
1.67 ±0.08		DIBIANCA	75	DBC	4.9 GeV/c K^-d
1.63 ±0.03	4303	BALTAY	74	HBC	1.75 GeV/c K^-p
$1.73\ ^{+0.08}_{-0.07}$	680	MAYEUR	72	HLBC	2.1 GeV/c K^-
1.61 ±0.04	2610	DAUBER	69	HBC	
1.80 ±0.16	299	LONDON	66	HBC	
1.70 ±0.12	246	PJERROU	65B	HBC	
1.69 ±0.07	794	HUBBARD	64	HBC	
$1.86\ ^{+0.15}_{-0.14}$	517	JAUNEAU	63D	FBC	

$\overline{\Xi}^+$ MEAN LIFE

VALUE (10^{-10} s)	EVTS	DOCUMENT ID		TECN	COMMENT
1.70±0.08±0.12	2256 ± 63	ABDALLAH	06E	DLPH	from Z decays
• • • We do not use the following data for averages, fits, limits, etc. • • •					
$1.55\ ^{+0.35}_{-0.20}$	35	[3] VOTRUBA	72	HBC	10 GeV/c K^+p
1.6 ±0.3	34	STONE	70	HBC	
$1.9\ ^{+0.7}_{-0.5}$	12	[3] SHEN	67	HBC	
1.51±0.55	5	[3] CHIEN	66	HBC	6.9 GeV/c $\overline{p}p$

[3] The error is statistical only.

$(\tau_{\Xi^-} - \tau_{\overline{\Xi}^+}) / \tau_{\Xi^-}$

A test of CPT invariance.

VALUE	DOCUMENT ID		TECN	COMMENT
−0.01±0.07	ABDALLAH	06E	DLPH	from Z decays

Ξ^- MAGNETIC MOMENT

See the "Note on Baryon Magnetic Moments" in the Λ Listings.

VALUE (μ_N)	EVTS	DOCUMENT ID		TECN	COMMENT
−0.6507±0.0025 OUR AVERAGE					
−0.6505±0.0025	4.36M	DURYEA	92	SPEC	800 GeV p Be
−0.661 ±0.036 ±0.036	44k	TROST	89	SPEC	Ξ^- ∼ 250 GeV
−0.69 ±0.04	218k	RAMEIKA	84	SPEC	400 GeV pBe
• • • We do not use the following data for averages, fits, limits, etc. • • •					
−0.674 ±0.021 ±0.020	122k	HO	90	SPEC	See DURYEA 92
−2.1 ±0.8	2436	COOL	74	OSPK	1.8 GeV/c K^-p
−0.1 ±2.1	2724	BINGHAM	70B	OSPK	1.8 GeV/c K^-p

$\overline{\Xi}^+$ MAGNETIC MOMENT

See the "Note on Baryon Magnetic Moments" in the Λ Listings.

VALUE (μ_N)	EVTS	DOCUMENT ID		TECN	COMMENT
+0.657±0.028±0.020	70k	HO	90	SPEC	800 GeV pBe

$(\mu_{\Xi^-} + \mu_{\overline{\Xi}^+}) / |\mu_{\Xi^-}|$

A test of CPT invariance. We calculate this from the Ξ^- and $\overline{\Xi}^+$ magnetic moments above.

VALUE	DOCUMENT ID
+0.01±0.05 OUR EVALUATION	

Ξ^- DECAY MODES

	Mode	Fraction (Γ_i/Γ)	Confidence level
Γ_1	$\Lambda\pi^-$	(99.887±0.035) %	
Γ_2	$\Sigma^-\gamma$	(1.27 ±0.23) × 10^{-4}	
Γ_3	$\Lambda e^-\overline{\nu}_e$	(5.63 ±0.31) × 10^{-4}	
Γ_4	$\Lambda\mu^-\overline{\nu}_\mu$	$(3.5\ ^{+3.5}_{-2.2}) \times 10^{-4}$	
Γ_5	$\Sigma^0 e^-\overline{\nu}_e$	(8.7 ±1.7) × 10^{-5}	
Γ_6	$\Sigma^0\mu^-\overline{\nu}_\mu$	< 8 × 10^{-4}	90%
Γ_7	$\Xi^0 e^-\overline{\nu}_e$	< 2.3 × 10^{-3}	90%

$\Delta S = 2$ forbidden ($S2$) modes

Γ_8	$n\pi^-$	$S2$	<	1.9	× 10^{-5}	90%
Γ_9	$n e^-\overline{\nu}_e$	$S2$	<	3.2	× 10^{-3}	90%
Γ_{10}	$n\mu^-\overline{\nu}_\mu$	$S2$	<	1.5	%	90%
Γ_{11}	$p\pi^-\pi^-$	$S2$	<	4	× 10^{-4}	90%
Γ_{12}	$p\pi^- e^-\overline{\nu}_e$	$S2$	<	4	× 10^{-4}	90%
Γ_{13}	$p\pi^-\mu^-\overline{\nu}_\mu$	$S2$	<	4	× 10^{-4}	90%
Γ_{14}	$p\mu^-\mu^-$	L	<	4	× 10^{-8}	90%

CONSTRAINED FIT INFORMATION

An overall fit to 4 branching ratios uses 5 measurements and one constraint to determine 5 parameters. The overall fit has a $\chi^2 = 1.0$ for 1 degrees of freedom.

The following *off-diagonal* array elements are the correlation coefficients $\langle \delta x_i \delta x_j \rangle / (\delta x_i \cdot \delta x_j)$, in percent, from the fit to the branching fractions, $x_i \equiv \Gamma_i/\Gamma_{\text{total}}$. The fit constrains the x_i whose labels appear in this array to sum to one.

	x_1	x_2	x_3	x_4
x_2	−6			
x_3	−8	0		
x_4	−99	0	−1	
x_5	−5	0	0	0

Ξ^- BRANCHING RATIOS

A number of early results have been omitted.

$\Gamma(\Sigma^-\gamma)/\Gamma(\Lambda\pi^-)$ Γ_2/Γ_1

VALUE (units 10^{-4})	EVTS	DOCUMENT ID		TECN	COMMENT
1.27±0.24 OUR FIT					
1.27±0.23 OUR AVERAGE					
1.22±0.23±0.06	211	[4] DUBBS	94	E761	Ξ^- 375 GeV
2.27±1.02	9	BIAGI	87B	SPEC	SPS hyperon beam

[4] DUBBS 94 also finds weak evidence that the asymmetry parameter α_γ is positive ($\alpha_\gamma = 1.0 \pm 1.3$).

$\Gamma(\Lambda e^-\overline{\nu}_e)/\Gamma(\Lambda\pi^-)$ Γ_3/Γ_1

VALUE (units 10^{-3})	EVTS	DOCUMENT ID		TECN	COMMENT
0.564±0.031 OUR FIT					
0.564±0.031	2857	BOURQUIN	83	SPEC	SPS hyperon beam
• • • We do not use the following data for averages, fits, limits, etc. • • •					
0.30 ±0.13	11	THOMPSON	80	ASPK	Hyperon beam

$\Gamma(\Lambda\mu^-\overline{\nu}_\mu)/\Gamma(\Lambda\pi^-)$ Γ_4/Γ_1

VALUE (units 10^{-3})	CL%	EVTS	DOCUMENT ID		TECN	COMMENT
$\mathbf{0.35\ ^{+0.35}_{-0.22}}$ **OUR FIT**						
0.35±0.35		1	YEH	74	HBC	Effective denom.=2859
• • • We do not use the following data for averages, fits, limits, etc. • • •						
< 2.3	90	0	THOMPSON	80	ASPK	Effective denom.=1017
< 1.3			DAUBER	69	HBC	
<12			BERGE	66	HBC	

$\Gamma(\Sigma^0 e^-\overline{\nu}_e)/\Gamma(\Lambda\pi^-)$ Γ_5/Γ_1

VALUE (units 10^{-3})	EVTS	DOCUMENT ID		TECN	COMMENT
0.087±0.017 OUR FIT					
0.087±0.017	154	BOURQUIN	83	SPEC	SPS hyperon beam

$[\Gamma(\Lambda e^-\overline{\nu}_e) + \Gamma(\Sigma^0 e^-\overline{\nu}_e)]/\Gamma(\Lambda\pi^-)$ $(\Gamma_3+\Gamma_5)/\Gamma_1$

VALUE (units 10^{-3})	EVTS	DOCUMENT ID		TECN	COMMENT
• • • We do not use the following data for averages, fits, limits, etc. • • •					
0.651±0.031	3011	[5] BOURQUIN	83	SPEC	SPS hyperon beam
0.68 ±0.22	17	[6] DUCLOS	71	OSPK	

[5] See the separate BOURQUIN 83 values for $\Gamma(\Lambda e^-\overline{\nu}_e)/\Gamma(\Lambda\pi^-)$ and $\Gamma(\Sigma^0 e^-\overline{\nu}_e)/\Gamma(\Lambda\pi^-)$ above.

[6] DUCLOS 71 cannot distinguish Σ^0's from Λ's. The Cabibbo theory predicts the Σ^0 rate is about a factor 6 smaller than the Λ rate.

$\Gamma(\Sigma^0\mu^-\overline{\nu}_\mu)/\Gamma(\Lambda\pi^-)$ Γ_6/Γ_1

VALUE (units 10^{-3})	CL%	EVTS	DOCUMENT ID		TECN	COMMENT
<0.76	90	0	YEH	74	HBC	Effective denom.=3026
• • • We do not use the following data for averages, fits, limits, etc. • • •						
<5			BERGE	66	HBC	

$\Gamma(\Xi^0 e^-\overline{\nu}_e)/\Gamma(\Lambda\pi^-)$ Γ_7/Γ_1

VALUE (units 10^{-3})	CL%	EVTS	DOCUMENT ID		TECN	COMMENT
<2.3	90	0	YEH	74	HBC	Effective denom.=1000

Baryon Particle Listings

Ξ^-

$\Gamma(n\pi^-)/\Gamma(\Lambda\pi^-)$ Γ_8/Γ_1

ΔS=2. Forbidden in first-order weak interaction.

VALUE (units 10^{-3})	CL%	EVTS	DOCUMENT ID		TECN	COMMENT
<0.019	90		BIAGI	82B	SPEC	SPS hyperon beam
• • • We do not use the following data for averages, fits, limits, etc. • • •						
<3.0	90	0	YEH	74	HBC	Effective denom.=760
<1.1			DAUBER	69	HBC	
<5.0			FERRO-LUZZI	63	HBC	

$\Gamma(ne^-\overline{\nu}_e)/\Gamma(\Lambda\pi^-)$ Γ_9/Γ_1

ΔS=2. Forbidden in first-order weak interaction.

VALUE (units 10^{-3})	CL%	EVTS	DOCUMENT ID		TECN	COMMENT
< 3.2	90	0	YEH	74	HBC	Effective denom.=715
• • • We do not use the following data for averages, fits, limits, etc. • • •						
<10	90		BINGHAM	65	RVUE	

$\Gamma(n\mu^-\overline{\nu}_\mu)/\Gamma(\Lambda\pi^-)$ Γ_{10}/Γ_1

ΔS=2. Forbidden in first-order weak interaction.

VALUE (units 10^{-3})	CL%	EVTS	DOCUMENT ID		TECN	COMMENT
<15.3	90	0	YEH	74	HBC	Effective denom.=150

$\Gamma(p\pi^-\pi^-)/\Gamma(\Lambda\pi^-)$ Γ_{11}/Γ_1

ΔS=2. Forbidden in first-order weak interaction.

VALUE (units 10^{-4})	CL%	EVTS	DOCUMENT ID		TECN	COMMENT
<3.7	90	0	YEH	74	HBC	Effective denom.=6200

$\Gamma(p\pi^-e^-\overline{\nu}_e)/\Gamma(\Lambda\pi^-)$ Γ_{12}/Γ_1

ΔS=2. Forbidden in first-order weak interaction.

VALUE (units 10^{-4})	CL%	EVTS	DOCUMENT ID		TECN	COMMENT
<3.7	90	0	YEH	74	HBC	Effective denom.=6200

$\Gamma(p\pi^-\mu^-\overline{\nu}_\mu)/\Gamma(\Lambda\pi^-)$ Γ_{13}/Γ_1

ΔS=2. Forbidden in first-order weak interaction.

VALUE (units 10^{-4})	CL%	EVTS	DOCUMENT ID		TECN	COMMENT
<3.7	90	0	YEH	74	HBC	Effective denom.=6200

$\Gamma(p\mu^-\mu^-)/\Gamma(\Lambda\pi^-)$ Γ_{14}/Γ_1

A ΔL=2 decay, forbidden by total lepton number conservation.

VALUE (units 10^{-8})	CL%	DOCUMENT ID		TECN	COMMENT
<4.0	90	RAJARAM	05	HYCP	p Cu, 800 GeV
• • • We do not use the following data for averages, fits, limits, etc. • • •					
$<3.7\times10^4$	90	[7] LITTENBERG	92B	HBC	Uses YEH 74 data

[7] This LITTENBERG 92B limit and the identical YEH 74 limits for the preceding three modes all result from nonobservance of any 3-prong decays of the Ξ^-. One could as well apply the limit to the *sum* of the four modes.

Ξ^- DECAY PARAMETERS

See the "Note on Baryon Decay Parameters" in the neutron Listings.

$\alpha(\Xi^-)\alpha_-(\Lambda)$

VALUE	EVTS	DOCUMENT ID		TECN	COMMENT
−0.294 ±0.005 OUR AVERAGE		Error includes scale factor of 1.7. See the ideogram below.			
−0.2963±0.0042	189k	LUK	00	E756	p Be, 800 GeV
−0.2894±0.0073	63k	[8] LUK	00	E756	p Be, 800 GeV
−0.303 ±0.004 ±0.004	192k	RAMEIKA	86	SPEC	400 GeV pBe
−0.257 ±0.020	11k	ASTON	85B	LASS	11 GeV/c K^-p
−0.260 ±0.017	21k	BENSINGER	85	MPS	5 GeV/c K^-p
−0.299 ±0.007	150k	BIAGI	82	SPEC	SPS hyperon beam
−0.315 ±0.026	9046	CLELAND	80C	ASPK	BNL hyperon beam
−0.239 ±0.021	6599	HEMINGWAY	78	HBC	4.2 GeV/c K^-p
−0.243 ±0.025	4303	BALTAY	74	HBC	1.75 GeV/c K^-p
−0.252 ±0.032	2436	COOL	74	OSPK	1.8 GeV/c K^-p
−0.253 ±0.028	2781	DAUBER	69	HBC	

[8] This LUK 00 value is for $\alpha(\overline{\Xi}^+)\ \alpha_+(\overline{\Lambda})$. We assume *CP* conservation here by including it in the average for $\alpha(\Xi^-)\ \alpha_-(\Lambda)$. But see the second data block below for the *CP* test.

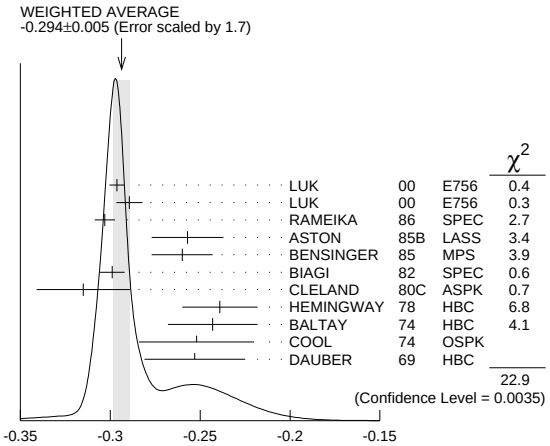

α FOR $\Xi^-\to\Lambda\pi^-$

The above average, $\alpha(\Xi^-)\ \alpha_-(\Lambda) = -0.294 \pm 0.005$, where the error includes a scale factor of 1.7, divided by our current average $\alpha_-(\Lambda) = 0.642 \pm 0.013$, gives the following value for $\alpha(\Xi^-)$.

VALUE	DOCUMENT ID
−0.458±0.012 OUR EVALUATION	Error includes scale factor of 1.8.

$\frac{[\alpha(\Xi^-)\alpha_-(\Lambda)-\alpha(\overline{\Xi}^+)\alpha_+(\overline{\Lambda})]}{[\alpha(\Xi^-)\alpha_-(\Lambda)+\alpha(\overline{\Xi}^+)\alpha_+(\overline{\Lambda})]}$

This is zero if *CP* is conserved. The α's are the decay-asymmetry parameters for $\Xi^-\to\Lambda\pi^-$ and $\Lambda\to p\pi^-$ and for $\overline{\Xi}^+\to\overline{\Lambda}\pi^+$ and $\overline{\Lambda}\to\overline{p}\pi^+$.

VALUE (units 10^{-4})	EVTS	DOCUMENT ID		TECN	COMMENT
0.0± 5.1±4.4	158M	HOLMSTROM	04	HYCP	p Cu, 800 GeV
• • • We do not use the following data for averages, fits, limits, etc. • • •					
+120 ±140	252k	LUK	00	E756	p Be, 800 GeV

ϕ ANGLE FOR $\Xi^-\to\Lambda\pi^-$ $(\tan\phi=\beta/\gamma)$

VALUE (°)	EVTS	DOCUMENT ID		TECN	COMMENT
− 2.1 ± 0.8 OUR AVERAGE					
− 2.39± 0.64±0.64	144M	[9] HUANG	04	HYCP	p Cu, 800 GeV
− 1.61± 2.66±0.37	1.35M	[10] CHAKRAVO...	03	E756	p Be, 800 GeV
5 ±10	11k	ASTON	85B	LASS	K^-p
14.7 ±16.0	21k	[11] BENSINGER	85	MPS	5 GeV/c K^-p
11 ± 9	4303	BALTAY	74	HBC	1.75 GeV/c K^-p
5 ±16	2436	COOL	74	OSPK	1.8 GeV/c K^-p
−14 ±11	2781	DAUBER	69	HBC	Uses $\alpha_\Lambda = 0.647 \pm 0.020$
0 ±12	1004	[12] BERGE	66	HBC	
• • • We do not use the following data for averages, fits, limits, etc. • • •					
−26 ±30	2724	BINGHAM	70B	OSPK	
0 ±20.4	364	[12] LONDON	66	HBC	Using $\alpha_\Lambda = 0.62$
54 ±30	356	[12] CARMONY	64B	HBC	

[9] From this result and α_Ξ, HUANG 04 gets $\beta_\Xi = -0.037 \pm 0.011 \pm 0.010$ and $\gamma_\Xi = 0.888 \pm 0.0004 \pm 0.006$. And the strong p–s phase difference for $\Lambda\pi^-$ scattering is $(4.6 \pm 1.4 \pm 1.2)^\circ$.

[10] From this result and α_Ξ, CHAKRAVORTY 03 obtains $\beta_\Xi = -0.025 \pm 0.042 \pm 0.006$ and $\gamma_\Xi = 0.889\pm0.001\pm0.007$. And the strong p–s phase difference for $\Lambda\pi^-$ scattering is $(3.17 \pm 5.28 \pm 0.73)^\circ$.

[11] BENSINGER 85 used $\alpha_\Lambda = 0.642 \pm 0.013$.

[12] The errors have been multiplied by 1.2 due to approximations used for the Ξ polarization; see DAUBER 69 for a discussion.

g_A / g_V FOR $\Xi^-\to\Lambda e^-\overline{\nu}_e$

VALUE	EVTS	DOCUMENT ID		TECN	COMMENT
−0.25±0.05	1992	[13] BOURQUIN	83	SPEC	SPS hyperon beam

[13] BOURQUIN 83 assumes that $g_2 = 0$. Also, the sign has been changed to agree with our conventions, given in the "Note on Baryon Decay Parameters" in the neutron Listings.

Ξ^- REFERENCES

We have omitted some papers that have been superseded by later experiments. See our earlier editions.

ABDALLAH	06E	PL B639 179	J. Abdallah *et al.*	(DELPHI Collab.)
RAJARAM	05	PRL 94 181801	D. Rajaram *et al.*	(FNAL HyperCP Collab.)
HOLMSTROM	04	PRL 93 262001	T. Holmstrom *et al.*	(FNAL HyperCP Collab.)
HUANG	04	PRL 93 011802	M. Huang *et al.*	(FNAL HyperCP Collab.)
CHAKRAVO...	03	PRL 91 031601	A. Chakravorty *et al.*	(FNAL E756 Collab.)
LUK	00	PRL 85 4860	K.B. Luk *et al.*	(FNAL E756 Collab.)
DUBBS	94	PRL 72 808	T. Dubbs *et al.*	(FNAL E761 Collab.)
DURYEA	92	PRL 68 768	J. Duryea *et al.*	(MINN, FNAL, MICH, RUTG)
LITTENBERG	92B	PR D46 R892	L.S. Littenberg, R.E. Shrock	(BNL, STON)
HO	90	PRL 65 1713	P.M. Ho *et al.*	(MICH, FNAL, MINN, RUTG)
Also		PR D44 3402	P.M. Ho *et al.*	(MICH, FNAL, MINN, RUTG)
TROST	89	PR D40 1703	L.H. Trost *et al.*	(FNAL-715 Collab.)
BIAGI	87B	ZPHY C35 143	S.F. Biagi *et al.*	(BRIS, CERN, GEVA+)

RAMEIKA	86	PR D33 3172	R. Rameika *et al.*	(RUTG, MICH, WISC+)
ASTON	85B	PR D32 2270	D. Aston *et al.*	(SLAC, CARL, CNRC, CINC)
BENSINGER	85	NP B252 561	J.R. Bensinger *et al.*	(CHIC, ELMT, FNAL+)
BOURQUIN	84	NP B241 1	M.H. Bourquin *et al.*	(BRIS, GEVA, HEIDP+)
RAMEIKA	84	PRL 52 581	R. Rameika *et al.*	(RUTG, MICH, WISC+)
BOURQUIN	83	ZPHY C21 1	M.H. Bourquin *et al.*	(BRIS, GEVA, HEIDP+)
BIAGI	82	PL 112B 265	S.F. Biagi *et al.*	(BRIS, CAVE, GEVA+)
BIAGI	82B	PL 112B 277	S.F. Biagi *et al.*	(LOQM, GEVA, RL+)
CLELAND	80C	PR D21 12	W.E. Cleland *et al.*	(PITT, BNL)
THOMPSON	80	PR D21 25	J.A. Thompson *et al.*	(PITT, BNL)
BOURQUIN	79	PL 87B 297	M.H. Bourquin *et al.*	(BRIS, GEVA, HEIDP+)
HEMINGWAY	78	NP B142 205	R.J. Hemingway *et al.*	(CERN, ZEEM, NIJM+)
DIBIANCA	75	NP B98 137	F.A. Dibianca, R.J. Endorf	(CMU)
BALTAY	74	PR D9 49	C. Baltay *et al.*	(COLU, BING) J
COOL	74	PR D10 792	R.L. Cool *et al.*	(BNL)
Also		PRL 29 1630	R.L. Cool *et al.*	(BNL)
YEH	74	PR D10 3545	N. Yeh *et al.*	(BING, COLU)
MAYEUR	72	NP B47 333	C. Mayeur *et al.*	(BRUX, CERN, TUFTS, LOUC)
VOTRUBA	72	NP B45 77	M.F. Votruba, A. Safder, T.M. Ratcliffe	(BIRM+)
WILQUET	72	PL 42B 372	G. Wilquet *et al.*	(BRUX, CERN, TUFTS+)
DUCLOS	71	NP B32 493	J. Duclos *et al.*	(CERN)
BINGHAM	70B	PR D1 3010	G.M. Bingham *et al.*	(UCSD, WASH)
GOLDWASSER	70	PR D1 1960	E.L. Goldwasser, P.F. Schultz	(ILL)
STONE	70	PL 32B 515	S.L. Stone *et al.*	(ROCH)
DAUBER	69	PR 179 1262	P.M. Dauber *et al.*	(LRL) J
SHEN	67	PL 25B 443	B.C. Shen, A. Firestone, G. Goldhaber	(UCB+)
BERGE	66	PR 147 945	J.P. Berge *et al.*	(LRL)
CHIEN	66	PR 152 1171	C.Y. Chien *et al.*	(YALE, BNL)
LONDON	66	PR 143 1034	G.W. London *et al.*	(BNL, SYRA)
BINGHAM	65	PRSL 285 202	H.H. Bingham	(CERN)
PJERROU	65B	PRL 14 275	G.M. Pjerrou *et al.*	(UCLA)
Also		Thesis	G.M. Pjerrou	(UCLA)
BADIER	64	Dubna Conf. 1 593	J. Badier *et al.*	(EPOL, SACL, ZEEM)
CARMONY	64B	PRL 12 482	D.D. Carmony *et al.*	(UCLA) J
HUBBARD	64	PR 135 B183	J.R. Hubbard *et al.*	(LRL)
FERRO-LUZZI	63	PR 130 1568	M. Ferro-Luzzi *et al.*	(LRL)
JAUNEAU	63D	Siena Conf. 4	L. Jauneau *et al.*	(EPOL, CERN, LOUC+)
Also		PL 5 261	L. Jauneau *et al.*	(EPOL, CERN, LOUC+)
SCHNEIDER	63	PL 4 360	J. Schneider	(CERN)

Ξ RESONANCES

The accompanying table gives our evaluation of the present status of the Ξ resonances. Not much is known about Ξ resonances. This is because (1) they can only be produced as a part of a final state, and so the analysis is more complicated than if direct formation were possible, (2) the production cross sections are small (typically a few μb), and (3) the final states are topologically complicated and difficult to study with electronic techniques. Thus early information about Ξ resonances came entirely from bubble chamber experiments, where the numbers of events are small, and only in the 1980's did electronic experiments make any significant contributions. However, nothing of significance on Ξ resonances has been added since our 1988 edition.

For a detailed earlier review, see Meadows [1].

Table 1. The status of the Ξ resonances. Only those with an overall status of *** or **** are included in the Baryon Summary Table.

Particle	J^P	Overall status	Status as seen in — $\Xi\pi$	ΛK	ΣK	$\Xi(1530)\pi$	Other channels
Ξ(1318)	1/2+	****					Decays weakly
Ξ(1530)	3/2+	****	****				
Ξ(1620)		*	*				
Ξ(1690)		***		***	**		
Ξ(1820)	3/2−	***	**	***	**	**	
Ξ(1950)		***	**	**		*	
Ξ(2030)		***		**	***		
Ξ(2120)		*		*			
Ξ(2250)		**					3-body decays
Ξ(2370)		**					3-body decays
Ξ(2500)		*		*	*		3-body decays

**** Existence is certain, and properties are at least fairly well explored.
*** Existence ranges from very likely to certain, but further confirmation is desirable and/or quantum numbers, branching fractions, *etc.* are not well determined.
** Evidence of existence is only fair.
* Evidence of existence is poor.

Reference

1. B.T. Meadows, in *Proceedings of the IVth International Conference on Baryon Resonances* (Toronto, 1980), ed. N. Isgur, p. 283.

Ξ(1530) 3/2+

$I(J^P) = \frac{1}{2}(\frac{3}{2}^+)$ Status: ****

This is the only Ξ resonance whose properties are all reasonably well known. Assuming that the Λ_c^+ has $J^P = 1/2^+$, AUBERT 08AK, in a study of $\Lambda_c^+ \to \Xi^-\pi^+K^+$, finds conclusively that the spin of the $\Xi(1530)^0$ is 3/2. In conjunction with SCHLEIN 63B and BUTTON-SHAFER 66, this proves also that the parity is +.

We use only those determinations of the mass and width that are accompanied by some discussion of systematics and resolution.

Ξ(1530) MASSES

$\Xi(1530)^0$ MASS

VALUE (MeV)	EVTS	DOCUMENT ID		TECN	COMMENT
1531.80±0.32 OUR FIT Error includes scale factor of 1.3.					
1531.78±0.34 OUR AVERAGE Error includes scale factor of 1.4. See the ideogram below.					
1532.2 ±0.7		DEBELLEFON	75B	HBC	$K^-p \to \Xi^-\overline{K}\pi$
1533 ±1		ROSS	73B	HBC	$K^-p \to \Xi\overline{K}\pi(\pi)$
1531.4 ±0.8	59	BADIER	72	HBC	K^-p 3.95 GeV/c
1532.0 ±0.4	1262	BALTAY	72	HBC	K^-p 1.75 GeV/c
1531.3 ±0.6	324	BORENSTEIN	72	HBC	K^-p 2.2 GeV/c
1532.3 ±0.7	286	KIRSCH	72	HBC	K^-p 2.87 GeV/c
1528.7 ±1.1	76	LONDON	66	HBC	K^-p 2.24 GeV/c
• • • We do not use the following data for averages, fits, limits, etc. • • •					
1532.1 ±0.4	1244	ASTON	85B	LASS	K^-p 11 GeV/c
1532.1 ±0.6	2700	[1] BAUBILLIER	81B	HBC	K^-p 8.25 GeV/c
1530 ±1	450	BIAGI	81	SPEC	SPS hyperon beam
1527 ±6	80	SIXEL	79	HBC	K^-p 10 GeV/c
1535 ±4	100	SIXEL	79	HBC	K^-p 16 GeV/c
1533.6 ±1.4	97	BERTHON	74	HBC	Quasi-2-body σ

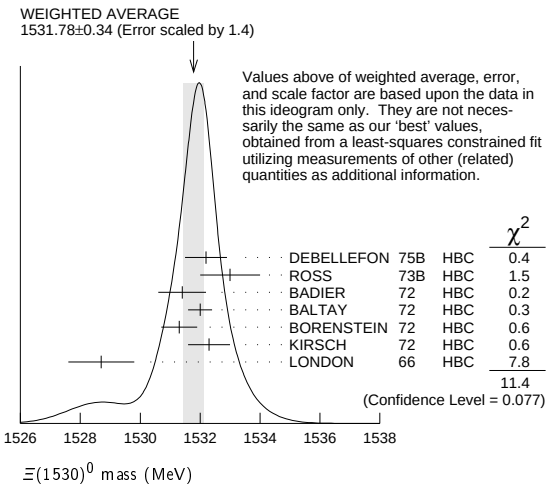

$\Xi(1530)^-$ MASS

VALUE (MeV)	EVTS	DOCUMENT ID		TECN	COMMENT
1535.0±0.6 OUR FIT					
1535.2±0.8 OUR AVERAGE					
1534.5±1.2		DEBELLEFON	75B	HBC	$K^-p \to \Xi^-\overline{K}\pi$
1535.3±2.0		ROSS	73B	HBC	$K^-p \to \Xi\overline{K}\pi(\pi)$
1536.2±1.6	185	KIRSCH	72	HBC	K^-p 2.87 GeV/c
1535.7±3.2	38	LONDON	66	HBC	K^-p 2.24 GeV/c
• • • We do not use the following data for averages, fits, limits, etc. • • •					
1540 ±3	48	BERTHON	74	HBC	Quasi-2-body σ
1534.7±1.1	334	BALTAY	72	HBC	K^-p 1.75 GeV/c

$m_{\Xi(1530)^-} - m_{\Xi(1530)}$

VALUE (MeV)	DOCUMENT ID		TECN	COMMENT
3.2±0.6 OUR FIT				
2.9±0.9 OUR AVERAGE				
2.7±1.0	BALTAY	72	HBC	K^-p 1.75 GeV/c
2.0±3.2	MERRILL	66	HBC	K^-p 1.7–2.7 GeV/c
5.7±3.0	PJERROU	65B	HBC	K^-p 1.8–1.95 GeV/c
• • • We do not use the following data for averages, fits, limits, etc. • • •				
3.9±1.8	[2] KIRSCH	72	HBC	K^-p 2.87 GeV/c
7 ±4	[2] LONDON	66	HBC	K^-p 2.24 GeV/c

Baryon Particle Listings

$\Xi(1530)$, $\Xi(1620)$, $\Xi(1690)$

$\Xi(1530)$ WIDTHS

$\Xi(1530)^0$ WIDTH

VALUE (MeV)	EVTS	DOCUMENT ID		TECN	COMMENT
9.1±0.5 OUR AVERAGE					
9.5±1.2		DEBELLEFON	75B	HBC	$K^- p \to \Xi^- \overline{K}\pi$
9.1±2.4		ROSS	73B	HBC	$K^- p \to \Xi \overline{K}\pi(\pi)$
11 ±2		BADIER	72	HBC	$K^- p$ 3.95 GeV/c
9.0±0.7		BALTAY	72	HBC	$K^- p$ 1.75 GeV/c
8.4±1.4		BORENSTEIN	72	HBC	$\Xi^- \pi^+$
11.0±1.8		KIRSCH	72	HBC	$\Xi^- \pi^+$
7 ±7		BERGE	66	HBC	$K^- p$ 1.5–1.7 GeV/c
8.5±3.5		LONDON	66	HBC	$K^- p$ 2.24 GeV/c
7 ±2		SCHLEIN	63B	HBC	$K^- p$ 1.8, 1.95 GeV/c
• • • We do not use the following data for averages, fits, limits, etc. • • •					
12.8±1.0	2700	[1] BAUBILLIER	81B	HBC	$K^- p$ 8.25 GeV/c
19 ±6	80	[3] SIXEL	79	HBC	$K^- p$ 10 GeV/c
14 ±5	100	[3] SIXEL	79	HBC	$K^- p$ 16 GeV/c

$\Xi(1530)^-$ WIDTH

VALUE (MeV)	DOCUMENT ID		TECN	COMMENT
$9.9^{+1.7}_{-1.9}$ OUR AVERAGE				
9.6±2.8	DEBELLEFON	75B	HBC	$K^- p \to \Xi^- \overline{K}\pi$
8.3±3.6	ROSS	73B	HBC	$K^- p \to \Xi \overline{K}\pi(\pi)$
$7.8^{+3.5}_{-7.8}$	BALTAY	72	HBC	$K^- p$ 1.75 GeV/c
16.2±4.6	KIRSCH	72	HBC	$\Xi^- \pi^0$, $\Xi^0 \pi^-$

$\Xi(1530)$ POLE POSITIONS

$\Xi(1530)^0$ REAL PART

VALUE	DOCUMENT ID	COMMENT
1531.6±0.4	LICHTENBERG74	Using HABIBI 73

$\Xi(1530)^0$ IMAGINARY PART

VALUE	DOCUMENT ID	COMMENT
4.45±0.35	LICHTENBERG74	Using HABIBI 73

$\Xi(1530)^-$ REAL PART

VALUE	DOCUMENT ID	COMMENT
1534.4±1.1	LICHTENBERG74	Using HABIBI 73

$\Xi(1530)^-$ IMAGINARY PART

VALUE	DOCUMENT ID	COMMENT
$3.9^{+1.75}_{-3.9}$	LICHTENBERG74	Using HABIBI 73

$\Xi(1530)$ DECAY MODES

	Mode	Fraction (Γ_i/Γ)	Confidence level
Γ_1	$\Xi\pi$	100 %	
Γ_2	$\Xi\gamma$	<4 %	90%

$\Xi(1530)$ BRANCHING RATIOS

$\Gamma(\Xi\gamma)/\Gamma_{total}$ Γ_2/Γ

VALUE	CL%	DOCUMENT ID		TECN	COMMENT
<0.04	90	KALBFLEISCH	75	HBC	$K^- p$ 2.18 GeV/c

$\Xi(1530)$ FOOTNOTES

[1] BAUBILLIER 81B is a fit to the inclusive spectrum. The resolution (5 MeV) is not unfolded.
[2] Redundant with data in the mass Listings.
[3] SIXEL 79 doesn't unfold the experimental resolution of 15 MeV.

$\Xi(1530)$ REFERENCES

AUBERT	08AK	PR D78 034008	B. Aubert *et al.*	(BABAR Collab.)
ASTON	85B	PR D32 2270	D. Aston *et al.*	(SLAC, CARL, CNRC, CINC)
BAUBILLIER	81B	NP B192 1	M. Baubillier *et al.*	(BIRM, CERN, GLAS+)
BIAGI	81	ZPHY C9 305	S.F. Biagi *et al.*	(BRIS, CAVE, GEVA+)
SIXEL	79	NP B159 125	P. Sixel *et al.*	(AACH3, BERL, CERN, LOIC+)
DEBELLEFON	75B	NC 28A 289	A. de Bellefon *et al.*	(CDEF, SACL)
KALBFLEISCH	75	PR D11 987	G.R. Kalbfleisch, R.C. Strand, J.W. Chapman	(BNL+)
BERTHON	74	NC 21A 146	A. Berthon *et al.*	(CDEF, RHEL, SACL+)
LICHTENBERG	74	PR D10 3865	D.B. Lichtenberg	(IND)
Also		Private Comm.	D.B. Lichtenberg	(IND)
HABIBI	73	Thesis Nevis 199	M. Habibi	(COLU)
ROSS	73B	Purdue Conf. 355	R.T. Ross, J.L. Lloyd, D. Radojicic	(OXF)
BADIER	72	NP B37 429	J. Badier *et al.*	(EPOL)
BALTAY	72	PL 42B 129	C. Baltay *et al.*	(COLU, BING)
BORENSTEIN	72	PR D5 1559	S.R. Borenstein *et al.*	(BNL, MICH) I
KIRSCH	72	NP B40 349	L.E. Kirsch *et al.*	(BRAN, UMD, SYRA+) I
BERGE	66	PR 147 945	J.P. Berge *et al.*	(LRL) I
BUTTON-...	66	PR 142 883	J. Button-Shafer *et al.*	(LRL) JP
LONDON	66	PR 143 1034	G.W. London *et al.*	(BNL, SYRA) IJ
MERRILL	66	Thesis UCRL 16455	D.W. Merrill	(LRL) JP
PJERROU	65B	PRL 14 275	G.M. Pjerrou *et al.*	(UCLA)
SCHLEIN	63B	PRL 11 167	P.E. Schlein *et al.*	(UCLA) IJP

OTHER RELATED PAPERS

MAZZUCATO	81	NP B178 1	M. Mazzucato *et al.*	(AMST, CERN, NIJM+)
BRIEFEL	77	PR D16 2706	E. Briefel *et al.*	(BRAN, UMD, SYRA+)
BRIEFEL	75	PR D12 1859	E. Briefel *et al.*	(BRAN, UMD, SYRA+)
HUNGERBU...	74	PR D10 2051	V. Hungerbuhler *et al.*	(YALE, FNAL, BNL+)
BUTTON-...	66	PR 142 883	J. Button-Shafer *et al.*	(LRL) JP

$\Xi(1620)$

$I(J^P) = \frac{1}{2}(?^?)$ Status: *

J, P need confirmation.

OMITTED FROM SUMMARY TABLE

What little evidence there is consists of weak signals in the $\Xi\pi$ channel. A number of other experiments (e.g., BORENSTEIN 72 and HASSALL 81) have looked for but not seen any effect.

$\Xi(1620)$ MASS

VALUE (MeV)	EVTS	DOCUMENT ID		TECN	COMMENT
≈ 1620 OUR ESTIMATE					
1624± 3	31	BRIEFEL	77	HBC	$K^- p$ 2.87 GeV/c
1633±12	34	DEBELLEFON	75B	HBC	$K^- p \to \Xi^- \overline{K}\pi$
1606± 6	29	ROSS	72	HBC	$K^- p$ 3.1–3.7 GeV/c

$\Xi(1620)$ WIDTH

VALUE (MeV)	EVTS	DOCUMENT ID		TECN	COMMENT
22.5	31	[1] BRIEFEL	77	HBC	$K^- p$ 2.87 GeV/c
40 ±15	34	DEBELLEFON	75B	HBC	$K^- p \to \Xi^- \overline{K}\pi$
21 ± 7	29	ROSS	72	HBC	$K^- p \to \Xi^- \pi^+ K^{*0}(892)$

$\Xi(1620)$ DECAY MODES

	Mode
Γ_1	$\Xi\pi$

$\Xi(1620)$ FOOTNOTES

[1] The fit is insensitive to values between 15 and 30 MeV.

$\Xi(1620)$ REFERENCES

HASSALL	81	NP B189 397	J.K. Hassall *et al.*	(CAVE, MSU)
BRIEFEL	77	PR D16 2706	E. Briefel *et al.*	(BRAN, UMD, SYRA+)
Also		Duke Conf. 317 Hyperon Resonances, 1970	E. Briefel *et al.*	(BRAN, UMD, SYRA+)
Also		PR D12 1859	E. Briefel *et al.*	(BRAN, UMD, SYRA+)
DEBELLEFON	75B	NC 28A 289	A. de Bellefon *et al.*	(CDEF, SACL)
BORENSTEIN	72	PR D5 1559	S.R. Borenstein *et al.*	(BNL, MICH) I
ROSS	72	PL 38B 177	R.T. Ross *et al.*	(OXF) I

OTHER RELATED PAPERS

HUNGERBU...	74	PR D10 2051	V. Hungerbuhler *et al.*	(YALE, FNAL, BNL+)
SCHMIDT	73	Purdue Conf. 363	P.E. Schmidt	(BRAN)
KALBFLEISCH	70	Duke Conf. 331 Hyperon Resonances 1970	G.R. Kalbfleisch	(BNL) I
APSELL	69	PRL 23 884	S.P. Apsell *et al.*	(BRAN, UMD, SYRA+)
BARTSCH	69	PL 28B 439	J. Bartsch *et al.*	(AACH, BERL, CERN+)

$\Xi(1690)$

$I(J^P) = \frac{1}{2}(?^?)$ Status: ***

AUBERT 08AK, in a study of $\Lambda_c^+ \to \Xi^- \pi^+ K^+$, finds some evidence that the $\Xi(1690)$ has $J^P = 1/2^-$.

DIONISI 78 sees a threshold enhancement in both the neutral and negatively charged $\Sigma\overline{K}$ mass spectra in $K^- p \to (\Sigma\overline{K})K\pi$ at 4.2 GeV/c. The data from the $\Sigma\overline{K}$ channels alone cannot distinguish between a resonance and a large scattering length. Weaker evidence at the same mass is seen in the corresponding $\Lambda\overline{K}$ channels, and a coupled-channel analysis yields results consistent with a new Ξ.

BIAGI 81 sees an enhancement at 1700 MeV in the diffractively produced ΛK^- system. A peak is also observed in the $\Lambda\overline{K}^0$ mass spectrum at 1660 MeV that is consistent with a 1720 MeV resonance decaying to $\Sigma^0\overline{K}^0$, with the γ from the Σ^0 decay not detected.

BIAGI 87 provides further confirmation of this state in diffractive dissociation of Ξ^- into ΛK^-. The significance claimed is 6.7 standard deviations.

ADAMOVICH 98 sees a peak of 1400 ± 300 events in the $\Xi^-\pi^+$ spectrum produced by 345 GeV/c Σ^--nucleus interactions.

$\Xi(1690)$ MASSES

MIXED CHARGES

VALUE (MeV)	DOCUMENT ID
1690±10 OUR ESTIMATE	This is only an educated guess; the error given is larger than the error on the average of the published values.

$\Xi(1690)^0$ MASS

VALUE (MeV)	EVTS	DOCUMENT ID		TECN	COMMENT
1686±4	1400	ADAMOVICH	98	WA89	Σ^- nucleus, 345 GeV/c
1699±5	175	[1] DIONISI	78	HBC	K^-p 4.2 GeV/c
1684±5	183	[2] DIONISI	78	HBC	K^-p 4.2 GeV/c

$\Xi(1690)^-$ MASS

VALUE (MeV)	EVTS	DOCUMENT ID		TECN	COMMENT
1691.1± 1.9±2.0	104	BIAGI	87	SPEC	Ξ^-Be 116 GeV
1700 ±10	150	[3] BIAGI	81	SPEC	Ξ^-H 100, 135 GeV
1694 ± 6	45	[4] DIONISI	78	HBC	K^-p 4.2 GeV/c

$\Xi(1690)$ WIDTHS

MIXED CHARGES

VALUE (MeV)	DOCUMENT ID
<30 OUR ESTIMATE	

$\Xi(1690)^0$ WIDTH

VALUE (MeV)	EVTS	DOCUMENT ID		TECN	COMMENT
10± 6	1400	ADAMOVICH	98	WA89	Σ^- nucleus, 345 GeV/c
44±23	175	[1] DIONISI	78	HBC	K^-p 4.2 GeV/c
20± 4	183	[2] DIONISI	78	HBC	K^-p 4.2 GeV/c

$\Xi(1690)^-$ WIDTH

VALUE (MeV)	CL%	EVTS	DOCUMENT ID		TECN	COMMENT
< 8	90	104	BIAGI	87	SPEC	Ξ^-Be 116 GeV
47±14		150	[3] BIAGI	81	SPEC	Ξ^-H 100, 135 GeV
26± 6		45	[4] DIONISI	78	HBC	K^-p 4.2 GeV/c

$\Xi(1690)$ DECAY MODES

	Mode	Fraction (Γ_i/Γ)
Γ_1	$\Lambda\overline{K}$	seen
Γ_2	$\Sigma\overline{K}$	seen
Γ_3	$\Xi\pi$	seen
Γ_4	$\Xi^-\pi^+\pi^0$	
Γ_5	$\Xi^-\pi^+\pi^-$	possibly seen
Γ_6	$\Xi(1530)\pi$	

$\Xi(1690)$ BRANCHING RATIOS

$\Gamma(\Lambda\overline{K})/\Gamma_{total}$ Γ_1/Γ

VALUE	EVTS	DOCUMENT ID		TECN	CHG	COMMENT
seen	104	BIAGI	87	SPEC	–	Ξ^-Be 116 GeV

$\Gamma(\Sigma\overline{K})/\Gamma(\Lambda\overline{K})$ Γ_2/Γ_1

VALUE	EVTS	DOCUMENT ID		TECN	CHG	COMMENT
0.75±0.39	75	ABE	02C	BELL		$e^+e^- \approx \Upsilon(4S)$
2.7 ±0.9		DIONISI	78	HBC	0	K^-p 4.2 GeV/c
3.1 ±1.4		DIONISI	78	HBC	–	K^-p 4.2 GeV/c

$\Gamma(\Xi\pi)/\Gamma(\Sigma\overline{K})$ Γ_3/Γ_2

VALUE	DOCUMENT ID		TECN	CHG	COMMENT
<0.09	DIONISI	78	HBC	0	K^-p 4.2 GeV/c

$\Gamma(\Xi\pi)/\Gamma_{total}$ Γ_3/Γ

VALUE	DOCUMENT ID		TECN	COMMENT
seen	ADAMOVICH	98	WA89	Σ^- nucleus, 345 GeV/c

$\Gamma(\Xi^-\pi^+\pi^0)/\Gamma(\Sigma\overline{K})$ Γ_4/Γ_2

VALUE	DOCUMENT ID		TECN	CHG	COMMENT
<0.04	DIONISI	78	HBC	0	K^-p 4.2 GeV/c

$\Gamma(\Xi^-\pi^+\pi^-)/\Gamma_{total}$ Γ_5/Γ

VALUE	EVTS	DOCUMENT ID		TECN	CHG	COMMENT
possibly seen	4	BIAGI	87	SPEC	–	Ξ^-Be 116 GeV

$\Gamma(\Xi^-\pi^+\pi^-)/\Gamma(\Sigma\overline{K})$ Γ_5/Γ_2

VALUE	DOCUMENT ID		TECN	CHG	COMMENT
<0.03	DIONISI	78	HBC	–	K^-p 4.2 GeV/c

$\Gamma(\Xi(1530)\pi)/\Gamma(\Sigma\overline{K})$ Γ_6/Γ_2

VALUE	DOCUMENT ID		TECN	CHG	COMMENT
<0.06	DIONISI	78	HBC	–	K^-p 4.2 GeV/c

$\Xi(1690)$ FOOTNOTES

[1] From a fit to the Σ^+K^- spectrum.
[2] From a coupled-channel analysis of the Σ^+K^- and $\Lambda\overline{K}^0$ spectra.
[3] A fit to the inclusive spectrum from $\Xi^-N \to \Lambda K^-X$.
[4] From a coupled-channel analysis of the Σ^0K^- and ΛK^- spectra.

$\Xi(1690)$ REFERENCES

AUBERT	08AK	PR D78 034008	B. Aubert *et al.*	(BABAR Collab.)
ABE	02C	PL B524 33	K. Abe *et al.*	(KEK BELLE Collab.)
ADAMOVICH	98	EPJ C5 621	M.I. Adamovich *et al.*	(CERN WA89 Collab.)
BIAGI	87	ZPHY C34 15	S.F. Biagi *et al.*	(BRIS, CERN, GEVA+) I
BIAGI	81	ZPHY C9 305	S.F. Biagi *et al.*	(BRIS, CAVE, GEVA+)
DIONISI	78	PL 80B 145	C. Dionisi *et al.*	(CERN, AMST, NIJM+) I

$\Xi(1820)$ $3/2^-$

$I(J^P) = \frac{1}{2}(\frac{3}{2}^-)$ Status: ***

The clearest evidence is an 8-standard-deviation peak in ΛK^- seen by GAY 76C. TEODORO 78 favors $J = 3/2$, but cannot make a parity discrimination. BIAGI 87C is consistent with $J = 3/2$ and favors negative parity for this J value.

$\Xi(1820)$ MASS

We only average the measurements that appear to us to be most significant and best determined.

VALUE (MeV)	EVTS	DOCUMENT ID		TECN	CHG	COMMENT
1823 ± 5 OUR ESTIMATE						
1823.4± 1.4 OUR AVERAGE						
1819.4± 3.1±2.0	280	[1] BIAGI	87	SPEC	0	Ξ^-Be → (ΛK^-) X
1826 ± 3 ±1	54	BIAGI	87C	SPEC	0	Ξ^-Be → $(\Lambda\overline{K}^0)$ X
1822 ± 6		JENKINS	83	MPS	–	$K^-p \to K^+$ (MM)
1830 ± 6	300	BIAGI	81	SPEC	–	SPS hyperon beam
1823 ± 2	130	GAY	76C	HBC	–	K^-p 4.2 GeV/c
• • • We do not use the following data for averages, fits, limits, etc. • • •						
1817 ± 3		ADAMOVICH	99B	WA89		Σ^- nucleus, 345 GeV
1797 ±19	74	BRIEFEL	77	HBC	0	K^-p 2.87 GeV/c
1829 ± 9	68	BRIEFEL	77	HBC	−0	$\Xi(1530)\pi$
1860 ±14	39	BRIEFEL	77	HBC	–	$\Sigma^-\overline{K}^0$
1870 ± 9	44	BRIEFEL	77	HBC	0	$\Lambda\overline{K}^0$
1813 ± 4	57	BRIEFEL	77	HBC	–	ΛK^-
1807 ±27		DIBIANCA	75	DBC	−0	$\Xi\pi\pi$, $\Xi^*\pi$
1762 ± 8	28	[2] BADIER	72	HBC	−0	$\Xi\pi$, $\Xi\pi\pi$, YK
1838 ± 5	38	[2] BADIER	72	HBC	−0	$\Xi\pi$, $\Xi\pi\pi$, YK
1830 ±10	25	[3] CRENNELL	70B	DBC	−0	3.6, 3.9 GeV/c
1826 ±12		[4] CRENNELL	70B	DBC	−0	3.6, 3.9 GeV/c
1830 ±10	40	ALITTI	69	HBC	–	Λ, $\Sigma\overline{K}$
1814 ± 4	30	BADIER	65	HBC	0	$\Lambda\overline{K}^0$
1817 ± 7	29	SMITH	65C	HBC	−0	$\Lambda\overline{K}^0$, ΛK^-
1770		HALSTEINSLID	63	FBC	−0	K^-freon 3.5 GeV/c

$\Xi(1820)$ WIDTH

VALUE (MeV)	EVTS	DOCUMENT ID		TECN	CHG	COMMENT
24 $^{+15}_{-10}$ OUR ESTIMATE						
24 ± 6 OUR AVERAGE Error includes scale factor of 1.5. See the ideogram below.						
24.6± 5.3	280	[1] BIAGI	87	SPEC	0	Ξ^-Be → (ΛK^-) X
12 ±14 ±1.7	54	BIAGI	87C	SPEC	0	Ξ^-Be → $(\Lambda\overline{K}^0)$ X
72 ±20	300	BIAGI	81	SPEC	–	SPS hyperon beam
21 ± 7	130	GAY	76C	HBC	–	K^-p 4.2 GeV/c
• • • We do not use the following data for averages, fits, limits, etc. • • •						
23 ±13		ADAMOVICH	99B	WA89		Σ^- nucleus, 345 GeV
99 ±57	74	BRIEFEL	77	HBC	0	K^-p 2.87 GeV/c
52 ±34	68	BRIEFEL	77	HBC	−0	$\Xi(1530)\pi$
72 ±17	39	BRIEFEL	77	HBC	–	$\Sigma^-\overline{K}^0$
44 ±11	44	BRIEFEL	77	HBC	0	$\Lambda\overline{K}^0$
26 ±11	57	BRIEFEL	77	HBC	–	ΛK^-
85 ±58		DIBIANCA	75	DBC	−0	$\Xi\pi\pi$, $\Xi^*\pi$
51 ±13		[2] BADIER	72	HBC	−0	Lower mass

58	±13	[2] BADIER	72	HBC	−0	Higher mass
103	$^{+38}_{-24}$	[3] CRENNELL	70B	DBC	−0	3.6, 3.9 GeV/c
48	$^{+36}_{-19}$	[4] CRENNELL	70B	DBC	−0	3.6, 3.9 GeV/c
55	$^{+40}_{-20}$	ALITTI	69	HBC	−	Λ, $\Sigma\overline{K}$
12	± 4	BADIER	65	HBC	0	$\Lambda\overline{K}^0$
30	± 7	SMITH	65B	HBC	−0	$\Lambda\overline{K}$
< 80		HALSTEINSLID	63	FBC	−0	K^-freon 3.5 GeV/c

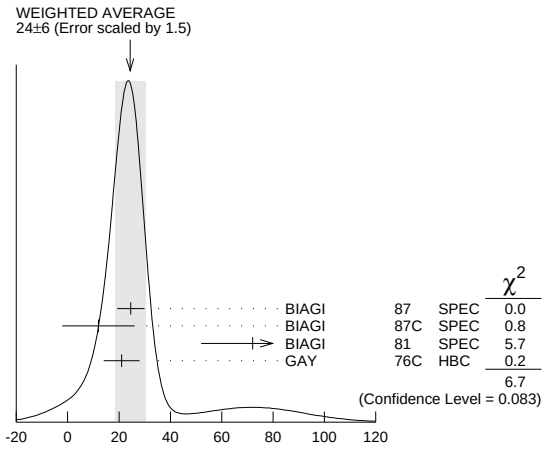

Ξ(1820) DECAY MODES

	Mode	Fraction (Γ_i/Γ)
Γ_1	$\Lambda\overline{K}$	large
Γ_2	$\Sigma\overline{K}$	small
Γ_3	$\Xi\pi$	small
Γ_4	$\Xi(1530)\pi$	small
Γ_5	$\Xi\pi\pi$(not $\Xi(1530)\pi$)	

Ξ(1820) BRANCHING RATIOS

The dominant modes seem to be $\Lambda\overline{K}$ and (perhaps) $\Xi(1530)\pi$, but the branching fractions are very poorly determined.

$\Gamma(\Lambda\overline{K})/\Gamma_{total}$ Γ_1/Γ

VALUE	DOCUMENT ID		TECN	CHG	COMMENT
0.25±0.05 OUR AVERAGE					
0.24±0.05	ANISOVICH	12A	DPWA		Multichannel
0.30±0.15	ALITTI	69	HBC	−	K^-p 3.9–5 GeV/c

$\Gamma(\Xi\pi)/\Gamma_{total}$ Γ_3/Γ

VALUE	DOCUMENT ID		TECN	CHG	COMMENT
0.10±0.10	ALITTI	69	HBC	−	K^-p 3.9–5 GeV/c

$\Gamma(\Xi\pi)/\Gamma(\Lambda\overline{K})$ Γ_3/Γ_1

VALUE	CL%	DOCUMENT ID		TECN	CHG	COMMENT
<0.36	95	GAY	76C	HBC	−	K^-p 4.2 GeV/c
0.20±0.20		BADIER	65	HBC	0	K^-p 3 GeV/c

$\Gamma(\Xi\pi)/\Gamma(\Xi(1530)\pi)$ Γ_3/Γ_4

VALUE	DOCUMENT ID		TECN	CHG	COMMENT
$\mathbf{1.5^{+0.6}_{-0.4}}$	APSELL	70	HBC	0	K^-p 2.87 GeV/c

$\Gamma(\Sigma\overline{K})/\Gamma_{total}$ Γ_2/Γ

VALUE	DOCUMENT ID		TECN	CHG	COMMENT
0.30±0.15	ALITTI	69	HBC	−	K^-p 3.9–5 GeV/c
• • • We do not use the following data for averages, fits, limits, etc. • • •					
<0.02	TRIPP	67	RVUE		Use SMITH 65C

$\Gamma(\Sigma\overline{K})/\Gamma(\Lambda\overline{K})$ Γ_2/Γ_1

VALUE	DOCUMENT ID		TECN	CHG	COMMENT
0.24±0.10	GAY	76C	HBC	−	K^-p 4.2 GeV/c

$\Gamma(\Xi(1530)\pi)/\Gamma_{total}$ Γ_4/Γ

VALUE	DOCUMENT ID		TECN	CHG	COMMENT
0.30±0.15	ALITTI	69	HBC	−	K^-p 3.9–5 GeV/c
• • • We do not use the following data for averages, fits, limits, etc. • • •					
seen	ASTON	85B	LASS		K^-p 11 GeV/c
not seen	[5] HASSALL	81	HBC		K^-p 6.5 GeV/c
<0.25	[6] DAUBER	69	HBC		K^-p 2.7 GeV/c

$\Gamma(\Xi(1530)\pi)/\Gamma(\Lambda\overline{K})$ Γ_4/Γ_1

VALUE	DOCUMENT ID		TECN	CHG	COMMENT
0.38±0.27 OUR AVERAGE Error includes scale factor of 2.3.					
1.0 ±0.3	GAY	76C	HBC	−	K^-p 4.2 GeV/c
0.26±0.13	SMITH	65C	HBC	−0	K^-p 2.45–2.7 GeV/c

$\Gamma(\Xi\pi\pi(\text{not }\Xi(1530)\pi))/\Gamma(\Lambda\overline{K})$ Γ_5/Γ_1

VALUE	DOCUMENT ID		TECN	CHG	COMMENT
0.30±0.20	BIAGI	87	SPEC	−	Ξ^- Be 116 GeV
• • • We do not use the following data for averages, fits, limits, etc. • • •					
<0.14	[7] BADIER	65	HBC	0	1 st. dev. limit
>0.1	SMITH	65C	HBC	−0	K^-p 2.45–2.7 GeV/c

$\Gamma(\Xi\pi\pi(\text{not }\Xi(1530)\pi))/\Gamma(\Xi(1530)\pi)$ Γ_5/Γ_4

VALUE	DOCUMENT ID		TECN	CHG	COMMENT
consistent with zero	GAY	76C	HBC	−	K^-p 4.2 GeV/c
• • • We do not use the following data for averages, fits, limits, etc. • • •					
0.3±0.5	[8] APSELL	70	HBC	0	K^-p 2.87 GeV/c

Ξ(1820) FOOTNOTES

[1] BIAGI 87 also sees weak signals in the in the $\Xi^-\pi^+\pi^-$ channel at 1782.6 ± 1.4 MeV (Γ = 6.0 ± 1.5 MeV) and 1831.9 ± 2.8 MeV (Γ = 9.6 ± 9.9 MeV).
[2] BADIER 72 adds all channels and divides the peak into lower and higher mass regions. The data can also be fitted with a single Breit-Wigner of mass 1800 MeV and width 150 MeV.
[3] From a fit to inclusive $\Xi\pi$, $\Xi\pi\pi$, and ΛK^- spectra.
[4] From a fit to inclusive $\Xi\pi$ and $\Xi\pi\pi$ spectra only.
[5] Including $\Xi\pi\pi$.
[6] DAUBER 69 uses in part the same data as SMITH 65C.
[7] For the decay mode $\Xi^-\pi^+\pi^0$ only. This limit includes $\Xi(1530)\pi$.
[8] Or less. Upper limit for the 3-body decay.

Ξ(1820) REFERENCES

ANISOVICH	12A	EPJ A48 15	A.V. Anisovich *et al.*	(BONN, PNPI)
ADAMOVICH	99B	EPJ C11 271	M.I. Adamovich *et al.*	(CERN WA89 Collab.)
BIAGI	87	ZPHY C34 15	S.F. Biagi *et al.*	(BRIS, CERN, GEVA+)
BIAGI	87C	ZPHY C34 175	S.F. Biagi *et al.*	(BRIS, CERN, GEVA+) JP
ASTON	85B	PR D32 2270	D. Aston *et al.*	(SLAC, CARL, CNRC, CINC)
JENKINS	83	PRL 51 951	C.M. Jenkins *et al.*	(FSU, BRAN, LBL+)
BIAGI	81	ZPHY C9 305	S.F. Biagi *et al.*	(BRIS, CAVE, GEVA+)
HASSALL	81	NP B189 397	J.K. Hassall *et al.*	(CAVE, MSU)
TEODORO	78	PL 77B 451	D. Teodoro *et al.*	(AMST, CERN, NIJM+) JP
BRIEFEL	77	PR D16 2706	E. Briefel *et al.*	(BRAN, UMD, SYRA+)
Also		PRL 23 884	S.P. Apsell *et al.*	(BRAN, UMD, SYRA+)
GAY	76C	PL 62B 477	J.B. Gay *et al.*	(AMST, CERN, NIJM) IJ
DIBIANCA	75	NP B98 137	F.A. Dibianca, R.J. Endorf	(CMU)
BADIER	72	NP B37 429	J. Badier *et al.*	(EPOL)
APSELL	70	PRL 24 777	S.P. Apsell *et al.*	(BRAN, UMD, SYRA+) I
CRENNELL	70B	PR D1 847	D.J. Crennell *et al.*	(BNL)
ALITTI	69	PRL 22 79	J. Alitti *et al.*	(BNL, SYRA) I
DAUBER	69	PR 179 1262	P.M. Dauber *et al.*	(LRL)
TRIPP	67	NP B3 10	R.D. Tripp *et al.*	(LRL, SLAC, CERN+)
BADIER	65	PL 16 171	J. Badier *et al.*	(EPOL, SACL, AMST) I
SMITH	65B	Athens Conf. 251	G.A. Smith, J.S. Lindsey	(LRL)
SMITH	65C	PRL 14 25	G.A. Smith *et al.*	(LRL) IJP
HALSTEINSLID	63	Siena Conf. 1 73	A. Halsteinslid *et al.*	(BERG, CERN, EPOL+) I

OTHER RELATED PAPERS

TEODORO	78	PL 77B 451	D. Teodoro *et al.*	(AMST, CERN, NIJM+) JP
BRIEFEL	75	PR D12 1859	E. Briefel *et al.*	(BRAN, UMD, SYRA+)
SCHMIDT	73	Purdue Conf. 363	P.E. Schmidt	(BRAN)
MERRILL	68	PR 167 1202	D.W. Merrill, J. Button-Shafer	(LRL)
SMITH	64	PRL 13 61	G.A. Smith *et al.*	(LRL) IJP

Ξ(1950)

$I(J^P) = \frac{1}{2}(?^?)$ Status: ***

We list here everything reported between 1875 and 2000 MeV. The accumulated evidence for a Ξ near 1950 MeV seems strong enough to include a Ξ(1950) in the main Baryon Table, but not much can be said about its properties. In fact, there may be more than one Ξ near this mass.

Ξ(1950) MASS

VALUE (MeV)	EVTS	DOCUMENT ID		TECN	COMMENT
1950±15 OUR ESTIMATE					
1955± 6		ADAMOVICH	99B	WA89	Σ^- nucleus, 345 GeV
1944± 9	129	BIAGI	87	SPEC	Ξ^-Be → $(\Xi^-\pi^+)\pi^-$X
1963± 5±2	63	BIAGI	87C	SPEC	Ξ^-Be → $(\Lambda\overline{K}^0)$ X
1937± 7	150	BIAGI	81	SPEC	SPS hyperon beam
1961±18	139	BRIEFEL	77	HBC	2.87 K^-p → $\Xi^-\pi^+$X
1936±22	44	BRIEFEL	77	HBC	2.87 K^-p → $\Xi^0\pi^-$X
1964±10	56	BRIEFEL	77	HBC	$\Xi(1530)\pi$
1900±12		DIBIANCA	75	DBC	$\Xi\pi$
1952±11	25	ROSS	73C		$(\Xi\pi)^-$
1956± 6	29	BADIER	72	HBC	$\Xi\pi$, $\Xi\pi\pi$, YK
1955±14	21	GOLDWASSER	70	HBC	$\Xi\pi$
1894±18	66	DAUBER	69	HBC	$\Xi\pi$
1930±20	27	ALITTI	68	HBC	$\Xi^-\pi^+$
1933±16	35	BADIER	65	HBC	$\Xi^-\pi^+$

Ξ(1950) WIDTH

VALUE (MeV)	EVTS	DOCUMENT ID		TECN	COMMENT
60±20 OUR ESTIMATE					
68±22		ADAMOVICH	99B	WA89	Σ^- nucleus, 345 GeV
100±31	129	BIAGI	87	SPEC	Ξ^-Be → $(\Xi^-\pi^+)\pi^-$X
25±15±1.2	63	BIAGI	87C	SPEC	Ξ^-Be → $(\Lambda\overline{K}^0)$ X
60± 8	150	BIAGI	81	SPEC	SPS hyperon beam
159±57	139	BRIEFEL	77	HBC	2.87 K^-p → $\Xi^-\pi^+$X
87±26	44	BRIEFEL	77	HBC	2.87 K^-p → $\Xi^0\pi^-$X
60±39	56	BRIEFEL	77	HBC	$\Xi(1530)\pi$
63±78		DIBIANCA	75	DBC	$\Xi\pi$
38±10		ROSS	73C		$(\Xi\pi)^-$
35±11	29	BADIER	72	HBC	$\Xi\pi$, $\Xi\pi\pi$, YK
56±26	21	GOLDWASSER	70	HBC	$\Xi\pi$
98±23	66	DAUBER	69	HBC	$\Xi\pi$
80±40	27	ALITTI	68	HBC	$\Xi^-\pi^+$
140±35	35	BADIER	65	HBC	$\Xi^-\pi^+$

Ξ(1950) DECAY MODES

	Mode	Fraction (Γ_i/Γ)
Γ_1	$\Lambda\overline{K}$	seen
Γ_2	$\Sigma\overline{K}$	possibly seen
Γ_3	$\Xi\pi$	seen
Γ_4	$\Xi(1530)\pi$	
Γ_5	$\Xi\pi\pi$(not $\Xi(1530)\pi$)	

Ξ(1950) BRANCHING RATIOS

$\Gamma(\Sigma\overline{K})/\Gamma(\Lambda\overline{K})$ Γ_2/Γ_1

VALUE	CL%	EVTS	DOCUMENT ID		TECN	COMMENT
<2.3	90	0	BIAGI	87C	SPEC	Ξ^-Be 116 GeV

$\Gamma(\Sigma\overline{K})/\Gamma_{total}$ Γ_2/Γ

VALUE	EVTS	DOCUMENT ID		TECN	COMMENT
possibly seen	17	HASSALL	81	HBC	K^-p 6.5 GeV/c

$\Gamma(\Xi\pi)/\Gamma(\Xi(1530)\pi)$ Γ_3/Γ_4

VALUE	DOCUMENT ID		TECN
$2.8^{+0.7}_{-0.6}$	APSELL	70	HBC

$\Gamma(\Xi\pi\pi(\text{not }\Xi(1530)\pi))/\Gamma(\Xi(1530)\pi)$ Γ_5/Γ_4

VALUE	DOCUMENT ID		TECN
0.0±0.3	APSELL	70	HBC

Ξ(1950) REFERENCES

ADAMOVICH	99B	EPJ C11 271	M.I. Adamovich *et al.*	(CERN WA89 Collab.)
BIAGI	87	ZPHY C34 15	S.F. Biagi *et al.*	(BRIS, CERN, GEVA+)
BIAGI	87C	ZPHY C34 175	S.F. Biagi *et al.*	(BRIS, CERN, GEVA+)
BIAGI	81	ZPHY C9 305	S.F. Biagi *et al.*	(BRIS, CAVE, GEVA+)
HASSALL	81	NP B189 397	J.K. Hassall *et al.*	(CAVE, MSU)
BRIEFEL	77	PR D16 2706	E. Briefel *et al.*	(BRAN, UMD, SYRA+)
Also		Duke Conf. 317 Hyperon Resonances, 1970	E. Briefel *et al.*	(BRAN, UMD, SYRA+)
DIBIANCA	75	NP B98 137	F.A. Dibianca, R.J. Endorf	(CMU)
ROSS	73C	Purdue Conf. 345	R.T. Ross, J.L. Lloyd, D. Radojicic	(OXF)
BADIER	72	NP B37 429	J. Badier *et al.*	(EPOL)
APSELL	70	PRL 24 777	S.P. Apsell *et al.*	(BRAN, UMD, SYRA+) I
GOLDWASSER	70	PR D1 1960	E.L. Goldwasser, P.F. Schultz	(ILL)
DAUBER	69	PR 179 1262	P.M. Dauber *et al.*	(LRL) I
ALITTI	68	PRL 21 1119	J. Alitti *et al.*	(BNL, SYRA) I
BADIER	65	PL 16 171	J. Badier *et al.*	(EPOL, SACL, AMST) I

Ξ(2030)

$I(J^P) = \frac{1}{2}(\geq \frac{5}{2}^?)$ Status: ***

The evidence for this state has been much improved by HEMINGWAY 77, who see an eight standard deviation enhancement in $\Sigma\overline{K}$ and a weaker coupling to $\Lambda\overline{K}$. ALITTI 68 and HEMINGWAY 77 observe no signals in the $\Xi\pi\pi$ (or $\Xi(1530)\pi$) channel, in contrast to DIBIANCA 75. The decay $(\Lambda/\Sigma)\overline{K}\pi$ reported by BARTSCH 69 is also not confirmed by HEMINGWAY 77.

A moments analysis of the HEMINGWAY 77 data indicates at a level of three standard deviations that $J \geq 5/2$.

Ξ(2030) MASS

VALUE (MeV)	EVTS	DOCUMENT ID		TECN	CHG	COMMENT
2025 ± 5 OUR ESTIMATE						
2025.1± 2.4 OUR AVERAGE		Error includes scale factor of 1.3. See the ideogram below.				
2022 ± 7		JENKINS	83	MPS	–	K^-p → K^+ MM
2024 ± 2	200	HEMINGWAY	77	HBC	–	K^-p 4.2 GeV/c
2044 ± 8		DIBIANCA	75	DBC	−0	$\Xi\pi\pi$, $\Xi^*\pi$
2019 ± 7	15	ROSS	73C	HBC	−0	$\Sigma\overline{K}$
2030 ±10	42	ALITTI	69	HBC	–	K^-p 3.9–5 GeV/c
2058 ±17	40	BARTSCH	69	HBC	−0	K^-p 10 GeV/c

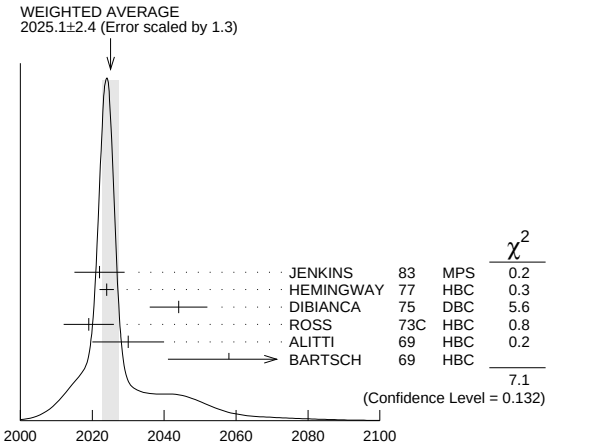

Ξ(2030) WIDTH

VALUE (MeV)	EVTS	DOCUMENT ID		TECN	CHG	COMMENT
$\mathbf{20^{+15}_{-5}}$ **OUR ESTIMATE**						
21± 6 OUR AVERAGE		Error includes scale factor of 1.3. See the ideogram below.				
16± 5	200	HEMINGWAY	77	HBC	–	K^-p 4.2 GeV/c
60±24		DIBIANCA	75	DBC	−0	$\Xi\pi\pi$, $\Xi^*\pi$
33±17	15	ROSS	73C	HBC	−0	$\Sigma\overline{K}$
45^{+40}_{-20}		ALITTI	69	HBC	–	K^-p 3.9–5 GeV/c
57±30		BARTSCH	69	HBC	−0	K^-p 10 GeV/c

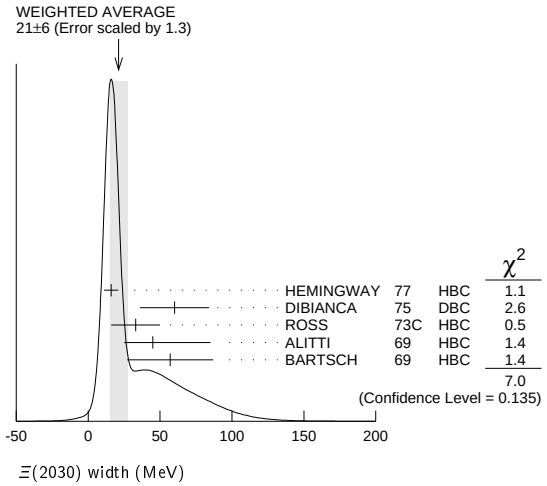

Ξ(2030) DECAY MODES

	Mode	Fraction (Γ_i/Γ)
Γ_1	$\Lambda\overline{K}$	~ 20 %
Γ_2	$\Sigma\overline{K}$	~ 80 %
Γ_3	$\Xi\pi$	small
Γ_4	$\Xi(1530)\pi$	small
Γ_5	$\Xi\pi\pi$(not $\Xi(1530)\pi$)	small
Γ_6	$\Lambda\overline{K}\pi$	small
Γ_7	$\Sigma\overline{K}\pi$	small

Ξ(2030) BRANCHING RATIOS

$\Gamma(\Xi\pi)/[\Gamma(\Lambda\overline{K})+\Gamma(\Sigma\overline{K})+\Gamma(\Xi\pi)+\Gamma(\Xi(1530)\pi)]$ $\Gamma_3/(\Gamma_1+\Gamma_2+\Gamma_3+\Gamma_4)$

VALUE	DOCUMENT ID	TECN	CHG	COMMENT
• • • We do not use the following data for averages, fits, limits, etc. • • •				
<0.30	ALITTI 69	HBC	–	1 standard dev. limit

$\Gamma(\Xi\pi)/\Gamma(\Sigma\overline{K})$ Γ_3/Γ_2

VALUE	CL%	DOCUMENT ID	TECN	CHG	COMMENT
<0.19	95	HEMINGWAY 77	HBC	–	K^-p 4.2 GeV/c

$\Gamma(\Lambda\overline{K})/[\Gamma(\Lambda\overline{K})+\Gamma(\Sigma\overline{K})+\Gamma(\Xi\pi)+\Gamma(\Xi(1530)\pi)]$ $\Gamma_1/(\Gamma_1+\Gamma_2+\Gamma_3+\Gamma_4)$

VALUE	DOCUMENT ID	TECN	CHG	COMMENT
0.25±0.15	ALITTI 69	HBC	–	K^-p 3.9–5 GeV/c

$\Gamma(\Lambda\overline{K})/\Gamma(\Sigma\overline{K})$ Γ_1/Γ_2

VALUE	DOCUMENT ID	TECN	CHG	COMMENT
0.22±0.09	HEMINGWAY 77	HBC	–	K^-p 4.2 GeV/c

$\Gamma(\Sigma\overline{K})/[\Gamma(\Lambda\overline{K})+\Gamma(\Sigma\overline{K})+\Gamma(\Xi\pi)+\Gamma(\Xi(1530)\pi)]$ $\Gamma_2/(\Gamma_1+\Gamma_2+\Gamma_3+\Gamma_4)$

VALUE	DOCUMENT ID	TECN	CHG	COMMENT
0.75±0.20	ALITTI 69	HBC	–	K^-p 3.9–5 GeV/c

$\Gamma(\Xi(1530)\pi)/[\Gamma(\Lambda\overline{K})+\Gamma(\Sigma\overline{K})+\Gamma(\Xi\pi)+\Gamma(\Xi(1530)\pi)]$ $\Gamma_4/(\Gamma_1+\Gamma_2+\Gamma_3+\Gamma_4)$

VALUE	DOCUMENT ID	TECN	CHG	COMMENT
• • • We do not use the following data for averages, fits, limits, etc. • • •				
<0.15	ALITTI 69	HBC	–	1 standard dev. limit

$[\Gamma(\Xi(1530)\pi)+\Gamma(\Xi\pi\pi$(not $\Xi(1530)\pi))]/\Gamma(\Sigma\overline{K})$ $(\Gamma_4+\Gamma_5)/\Gamma_2$

VALUE	CL%	DOCUMENT ID	TECN	CHG	COMMENT
<0.11	95	[1] HEMINGWAY 77	HBC	–	K^-p 4.2 GeV/c

$\Gamma(\Lambda\overline{K}\pi)/\Gamma_{total}$ Γ_6/Γ

VALUE	DOCUMENT ID	TECN	COMMENT
• • • We do not use the following data for averages, fits, limits, etc. • • •			
seen	BARTSCH 69	HBC	K^-p 10 GeV

$\Gamma(\Lambda\overline{K}\pi)/\Gamma(\Sigma\overline{K})$ Γ_6/Γ_2

VALUE	CL%	DOCUMENT ID	TECN	CHG	COMMENT
<0.32	95	HEMINGWAY 77	HBC	–	K^-p 4.2 GeV/c

$\Gamma(\Sigma\overline{K}\pi)/\Gamma_{total}$ Γ_7/Γ

VALUE	DOCUMENT ID	TECN	COMMENT
• • • We do not use the following data for averages, fits, limits, etc. • • •			
seen	BARTSCH 69	HBC	K^-p 10 GeV

$\Gamma(\Sigma\overline{K}\pi)/\Gamma(\Sigma\overline{K})$ Γ_7/Γ_2

VALUE	CL%	DOCUMENT ID	TECN	CHG	COMMENT
<0.04	95	[2] HEMINGWAY 77	HBC	–	K^-p 4.2 GeV/c

Ξ(2030) FOOTNOTES

[1] For the decay mode $\Xi^-\pi^+\pi^-$ only.
[2] For the decay mode $\Sigma^\pm K^-\pi^\mp$ only.

Ξ(2030) REFERENCES

JENKINS	83	PRL 51 951	C.M. Jenkins *et al.*	(FSU, BRAN, LBL+)
HEMINGWAY	77	PL 68B 197	R.J. Hemingway *et al.*	(AMST, CERN, NIJM+) IJ
Also		PL 62B 477	J.B. Gay *et al.*	(AMST, CERN, NIJM)
DIBIANCA	75	NP B98 137	F.A. Dibianca, R.J. Endorf	(CMU)
ROSS	73C	Purdue Conf. 345	R.T. Ross, J.L. Lloyd, D. Radojicic	(OXF)
ALITTI	69	PRL 22 79	J. Alitti *et al.*	(BNL, SYRA) I
BARTSCH	69	PL 28B 439	J. Bartsch *et al.*	(AACH, BERL, CERN+)
ALITTI	68	PRL 21 1119	J. Alitti *et al.*	(BNL, SYRA)

Ξ(2120)

$I(J^P) = \frac{1}{2}(?^?)$ Status: *
J, P need confirmation.

OMITTED FROM SUMMARY TABLE

Ξ(2120) MASS

VALUE (MeV)	EVTS	DOCUMENT ID	TECN	COMMENT
≈ 2120 OUR ESTIMATE				
2137±4	18	[1] CHLIAPNIK... 79	HBC	K^+p 32 GeV/c
2123±7		[2] GAY 76C	HBC	K^-p 4.2 GeV/c

Ξ(2120) WIDTH

VALUE (MeV)	EVTS	DOCUMENT ID	TECN	COMMENT
<20	18	[1] CHLIAPNIK... 79	HBC	K^+p 32 GeV/c
25±12		[2] GAY 76C	HBC	K^-p 4.2 GeV/c

Ξ(2120) DECAY MODES

	Mode	Fraction (Γ_i/Γ)
Γ_1	$\Lambda\overline{K}$	seen

Ξ(2120) BRANCHING RATIOS

$\Gamma(\Lambda\overline{K})/\Gamma_{total}$ Γ_1/Γ

VALUE	DOCUMENT ID	TECN	COMMENT
seen	[1] CHLIAPNIK... 79	HBC	$K^+p \to (\overline{\Lambda}K^+)$ X
seen	[2] GAY 76C	HBC	K^-p 4.2 GeV/c

Ξ(2120) FOOTNOTES

[1] CHLIAPNIKOV 79 does not uniquely identify the K^+ in the $(\overline{\Lambda}K^+)$ X final state. It also reports bumps with fewer events at 2240, 2540, and 2830 MeV.
[2] GAY 76C sees a 4-standard deviation signal. However, HEMINGWAY 77, with more events from the same experiment points out that the signal is greatly reduced if a cut is made on the 4-momentum u. This suggests an anomalous production mechanism if the $\Xi(2120)$ is real.

Ξ(2120) REFERENCES

CHLIAPNIK...	79	NP B158 253	P.V. Chliapnikov *et al.*	(CERN, BELG, MONS)
HEMINGWAY	77	PL 68B 197	R.J. Hemingway *et al.*	(AMST, CERN, NIJM+)
GAY	76C	PL 62B 477	J.B. Gay *et al.*	(AMST, CERN, NIJM)

$\Xi(2250)$

$I(J^P) = \frac{1}{2}(?^?)$ Status: **
J, P need confirmation.

OMITTED FROM SUMMARY TABLE

The evidence for this state is mixed. BARTSCH 69 sees a bump of not much statistical significance in $\Lambda\overline{K}\pi$, $\Sigma\overline{K}\pi$, and $\Xi\pi\pi$ mass spectra. GOLDWASSER 70 sees a narrower bump in $\Xi\pi\pi$ at a higher mass. Not seen by HASSALL 81 with 45 events/μb at 6.5 GeV/c. Seen by JENKINS 83. Perhaps seen by BIAGI 87.

$\Xi(2250)$ MASS

VALUE (MeV)	EVTS	DOCUMENT ID		TECN	CHG	COMMENT
≈ 2250 OUR ESTIMATE						
2189± 7	66	BIAGI	87	SPEC	–	Ξ^-Be → ($\Xi^-\pi^+\pi^-$) X
2214± 5		JENKINS	83	MPS	–	$K^-p \to K^+$ MM
2295±15	18	GOLDWASSER	70	HBC	–	K^-p 5.5 GeV/c
2244±52	35	BARTSCH	69	HBC		K^-p 10 GeV/c

$\Xi(2250)$ WIDTH

VALUE (MeV)	EVTS	DOCUMENT ID		TECN	CHG	COMMENT
46±27	66	BIAGI	87	SPEC	–	Ξ^-Be → ($\Xi^-\pi^+\pi^-$) X
< 30		GOLDWASSER	70	HBC	–	K^-p 5.5 GeV/c
130±80		BARTSCH	69	HBC		

$\Xi(2250)$ DECAY MODES

	Mode
Γ_1	$\Xi\pi\pi$
Γ_2	$\Lambda\overline{K}\pi$
Γ_3	$\Sigma\overline{K}\pi$

$\Xi(2250)$ REFERENCES

BIAGI	87	ZPHY C34 15	S.F. Biagi *et al.*	(BRIS, CERN, GEVA+)
JENKINS	83	PRL 51 951	C.M. Jenkins *et al.*	(FSU, BRAN, LBL+)
HASSALL	81	NP B189 397	J.K. Hassall *et al.*	(CAVE, MSU)
GOLDWASSER	70	PR D1 1960	E.L. Goldwasser, P.F. Schultz	(ILL)
BARTSCH	69	PL 28B 439	J. Bartsch *et al.*	(AACH, BERL, CERN+)

$\Xi(2370)$

$I(J^P) = \frac{1}{2}(?^?)$ Status: **
J, P need confirmation.

OMITTED FROM SUMMARY TABLE

$\Xi(2370)$ MASS

VALUE (MeV)	EVTS	DOCUMENT ID		TECN	CHG	COMMENT
≈ 2370 OUR ESTIMATE						
2356±10		JENKINS	83	MPS	–	$K^-p \to K^+$ MM
2370	50	HASSALL	81	HBC	−0	K^-p 6.5 GeV/c
2373± 8	94	AMIRZADEH	80	HBC	−0	K^-p 8.25 GeV/c
2392±27		DIBIANCA	75	DBC		$\Xi 2\pi$

$\Xi(2370)$ WIDTH

VALUE (MeV)	EVTS	DOCUMENT ID		TECN	CHG	COMMENT
80	50	HASSALL	81	HBC	−0	K^-p 6.5 GeV/c
80±25	94	AMIRZADEH	80	HBC	−0	K^-p 8.25 GeV/c
75±69		DIBIANCA	75	DBC		$\Xi 2\pi$

$\Xi(2370)$ DECAY MODES

	Mode	Fraction (Γ_i/Γ)
Γ_1	$\Lambda\overline{K}\pi$ Includes $\Gamma_4 + \Gamma_6$.	seen
Γ_2	$\Sigma\overline{K}\pi$ Includes $\Gamma_5 + \Gamma_6$.	seen
Γ_3	$\Omega^- K$	
Γ_4	$\Lambda\overline{K}^*(892)$	
Γ_5	$\Sigma\overline{K}^*(892)$	
Γ_6	$\Sigma(1385)\overline{K}$	

$\Xi(2370)$ BRANCHING RATIOS

$\Gamma(\Lambda\overline{K}\pi)/\Gamma_{total}$ Γ_1/Γ

VALUE	DOCUMENT ID		TECN	CHG	COMMENT
seen	AMIRZADEH	80	HBC	−0	K^-p 8.25 GeV/c

$\Gamma(\Sigma\overline{K}\pi)/\Gamma_{total}$ Γ_2/Γ

VALUE	DOCUMENT ID		TECN	CHG	COMMENT
seen	AMIRZADEH	80	HBC	−0	K^-p 8.25 GeV/c

$[\Gamma(\Lambda\overline{K}\pi) + \Gamma(\Sigma\overline{K}\pi)]/\Gamma_{total}$ $(\Gamma_1+\Gamma_2)/\Gamma$

VALUE	EVTS	DOCUMENT ID		TECN	CHG	COMMENT
seen	50	HASSALL	81	HBC	−0	K^-p 6.5 GeV/c

$\Gamma(\Omega^- K)/\Gamma_{total}$ Γ_3/Γ

VALUE	DOCUMENT ID		TECN	CHG	COMMENT
0.09±0.04	[1] KINSON	80	HBC	–	K^-p 8.25 GeV/c

$[\Gamma(\Lambda\overline{K}^*(892)) + \Gamma(\Sigma\overline{K}^*(892))]/\Gamma_{total}$ $(\Gamma_4+\Gamma_5)/\Gamma$

VALUE	DOCUMENT ID		TECN	CHG	COMMENT
0.22±0.13	[1] KINSON	80	HBC	–	K^-p 8.25 GeV/c

$\Gamma(\Sigma(1385)\overline{K})/\Gamma_{total}$ Γ_6/Γ

VALUE	DOCUMENT ID		TECN	CHG	COMMENT
0.12±0.08	[1] KINSON	80	HBC	–	K^-p 8.25 GeV/c

$\Xi(2370)$ FOOTNOTES

[1] KINSON 80 is a reanalysis of AMIRZADEH 80 with 50% more events.

$\Xi(2370)$ REFERENCES

JENKINS	83	PRL 51 951	C.M. Jenkins *et al.*	(FSU, BRAN, LBL+)
HASSALL	81	NP B189 397	J.K. Hassall *et al.*	(CAVE, MSU)
AMIRZADEH	80	PL 90B 324	J. Amirzadeh *et al.*	(BIRM, CERN, GLAS+) I
KINSON	80	Toronto Conf. 263	J.B. Kinson *et al.*	(BIRM, CERN, GLAS+) I
DIBIANCA	75	NP B98 137	F.A. Dibianca, R.J. Endorf	(CMU)

$\Xi(2500)$

$I(J^P) = \frac{1}{2}(?^?)$ Status: *
J, P need confirmation.

OMITTED FROM SUMMARY TABLE

The ALITTI 69 peak might be instead the $\Xi(2370)$ or might be neither the $\Xi(2370)$ nor the $\Xi(2500)$.

$\Xi(2500)$ MASS

VALUE (MeV)	EVTS	DOCUMENT ID		TECN	CHG	COMMENT
≈ 2500 OUR ESTIMATE						
2505±10		JENKINS	83	MPS	–	$K^-p \to K^+$ MM
2430±20	30	ALITTI	69	HBC	–	K^-p 4.6–5 GeV/c
2500±10	45	BARTSCH	69	HBC	−0	K^-p 10 GeV/c

$\Xi(2500)$ WIDTH

VALUE (MeV)	DOCUMENT ID		TECN	CHG
150^{+60}_{-40}	ALITTI	69	HBC	–
59±27	BARTSCH	69	HBC	−0

$\Xi(2500)$ DECAY MODES

	Mode	Fraction (Γ_i/Γ)
Γ_1	$\Xi\pi$	
Γ_2	$\Lambda\overline{K}$	
Γ_3	$\Sigma\overline{K}$	
Γ_4	$\Xi\pi\pi$	seen
Γ_5	$\Xi(1530)\pi$	
Γ_6	$\Lambda\overline{K}\pi + \Sigma\overline{K}\pi$	seen

$\Xi(2500)$ BRANCHING RATIOS

$\Gamma(\Xi\pi)/[\Gamma(\Xi\pi) + \Gamma(\Lambda\overline{K}) + \Gamma(\Sigma\overline{K}) + \Gamma(\Xi(1530)\pi)]$ $\Gamma_1/(\Gamma_1+\Gamma_2+\Gamma_3+\Gamma_5)$

VALUE	DOCUMENT ID		TECN	COMMENT
<0.5	ALITTI	69	HBC	1 standard dev. limit

$\Gamma(\Lambda\overline{K})/[\Gamma(\Xi\pi) + \Gamma(\Lambda\overline{K}) + \Gamma(\Sigma\overline{K}) + \Gamma(\Xi(1530)\pi)]$ $\Gamma_2/(\Gamma_1+\Gamma_2+\Gamma_3+\Gamma_5)$

VALUE	DOCUMENT ID		TECN	CHG
0.5±0.2	ALITTI	69	HBC	–

Baryon Particle Listings

$\Xi(2500)$

$\Gamma(\Sigma\overline{K})/[\Gamma(\Xi\pi)+\Gamma(\Lambda\overline{K})+\Gamma(\Sigma\overline{K})+\Gamma(\Xi(1530)\pi)]$ $\Gamma_3/(\Gamma_1+\Gamma_2+\Gamma_3+\Gamma_5)$

VALUE	DOCUMENT ID		TECN	CHG
0.5 ± 0.2	ALITTI	69	HBC	–

$\Gamma(\Xi(1530)\pi)/[\Gamma(\Xi\pi)+\Gamma(\Lambda\overline{K})+\Gamma(\Sigma\overline{K})+\Gamma(\Xi(1530)\pi)]$ $\Gamma_5/(\Gamma_1+\Gamma_2+\Gamma_3+\Gamma_5)$

VALUE	DOCUMENT ID		TECN	COMMENT
<0.2	ALITTI	69	HBC	1 standard dev. limit

$\Gamma(\Xi\pi\pi)/\Gamma_{total}$ Γ_4/Γ

VALUE	DOCUMENT ID		TECN	CHG
seen	BARTSCH	69	HBC	–0

$[\Gamma(\Lambda\overline{K}\pi)+\Gamma(\Sigma\overline{K}\pi)]/\Gamma_{total}$ Γ_6/Γ

VALUE	DOCUMENT ID		TECN	CHG
seen	BARTSCH	69	HBC	–0

$\Xi(2500)$ REFERENCES

JENKINS	83	PRL 51 951	C.M. Jenkins *et al.*	(FSU, BRAN, LBL+)
ALITTI	69	PRL 22 79	J. Alitti *et al.*	(BNL, SYRA) I
BARTSCH	69	PL 28B 439	J. Bartsch *et al.*	(AACH, BERL, CERN+)

Ω BARYONS
($S = -3$, $I = 0$)

$\Omega^- = sss$

Ω^-

$I(J^P) = 0(\frac{3}{2}^+)$ Status: ****

The unambiguous discovery in both production and decay was by BARNES 64. The quantum numbers follow from the assignment of the particle to the baryon decuplet. DEUTSCHMANN 78 and BAUBILLIER 78 rule out $J = 1/2$ and find consistency with $J = 3/2$. AUBERT,BE 06 finds from the decay angular distributions of $\Xi_c^0 \to \Omega^- K^+$ and $\Omega_c^0 \to \Omega^- K^+$ that $J = 3/2$; this depends on the spins of the Ξ_c^0 and Ω_c^0 being $J = 1/2$, their supposed values.

We have omitted some results that have been superseded by later experiments. See our earlier editions.

Ω^- MASS

The fit assumes the Ω^- and $\overline{\Omega}^+$ masses are the same, and averages them together.

VALUE (MeV)	EVTS	DOCUMENT ID		TECN	COMMENT
1672.45±0.29 OUR FIT					
1672.43±0.32 OUR AVERAGE					
1673 ±1	100	HARTOUNI	85	SPEC	80–280 GeV K_L^0C
1673.0 ±0.8	41	BAUBILLIER	78	HBC	8.25 GeV/c K^-p
1671.7 ±0.6	27	HEMINGWAY	78	HBC	4.2 GeV/c K^-p
1673.4 ±1.7	4	[1] DIBIANCA	75	DBC	4.9 GeV/c K^-d
1673.3 ±1.0	3	PALMER	68	HBC	K^-p 4.6, 5 GeV/c
1671.8 ±0.8	3	SCHULTZ	68	HBC	K^-p 5.5 GeV/c
1674.2 ±1.6	5	SCOTTER	68	HBC	K^-p 6 GeV/c
1672.1 ±1.0	1	[2] FRY	55	EMUL	
• • • We do not use the following data for averages, fits, limits, etc. • • •					
1671.43±0.78	13	[3] DEUTSCH...	73	HBC	K^-p 10 GeV/c
1671.9 ±1.2	6	[3] SPETH	69	HBC	See DEUTSCHMANN 73
1673.0 ±8.0	1	ABRAMS	64	HBC	$\to \Xi^-\pi^0$
1670.6 ±1.0	1	[2] FRY	55B	EMUL	
1615	1	[4] EISENBERG	54	EMUL	

[1] DIBIANCA 75 gives a mass for each event. We quote the average.

[2] The FRY 55 and FRY 55B events were identified as Ω^- by ALVAREZ 73. The masses assume decay to ΛK^- at rest. For FRY 55B, decay from an atomic orbit could Doppler shift the K^- energy and the resulting Ω^- mass by several MeV. This shift is negligible for FRY 55 because the Ω decay is approximately perpendicular to its orbital velocity, as is known because the Λ strikes the nucleus (L.Alvarez, private communication 1973). We have calculated the error assuming that the orbital n is 4 or larger.

[3] Excluded from the average; the Ω^- lifetimes measured by the experiments differ significantly from other measurements.

[4] The EISENBERG 54 mass was calculated for decay in flight. ALVAREZ 73 has shown that the Ω interacted with an Ag nucleus to give $K^-\,\Xi$Ag.

$\overline{\Omega}^+$ MASS

The fit assumes the Ω^- and $\overline{\Omega}^+$ masses are the same, and averages them together.

VALUE (MeV)	EVTS	DOCUMENT ID		TECN	COMMENT
1672.45±0.29 OUR FIT					
1672.5 ±0.7 OUR AVERAGE					
1672 ±1	72	HARTOUNI	85	SPEC	80–280 GeV K_L^0C
1673.1 ±1.0	1	FIRESTONE	71B	HBC	12 GeV/c K^+d

$(m_{\Omega^-} - m_{\overline{\Omega}^+}) / m_{\Omega^-}$

A test of CPT invariance.

VALUE	DOCUMENT ID		TECN	COMMENT
$(-1.44\pm7.98)\times10^{-5}$	CHAN	98	E756	p Be, 800 GeV

Ω^- MEAN LIFE

Measurements with an error $> 0.1\times10^{-10}$ s have been omitted. The fit assumes the Ω^- and $\overline{\Omega}^+$ mean lives are the same, and averages them together.

VALUE (10^{-10} s)	EVTS	DOCUMENT ID		TECN	COMMENT
0.821±0.011 OUR FIT					
0.821±0.011 OUR AVERAGE					
0.817±0.013±0.018	6934	CHAN	98	E756	p Be, 800 GeV
0.811±0.037	1096	LUK	88	SPEC	pBe 400 GeV
0.823±0.013	12k	BOURQUIN	84	SPEC	SPS hyperon beam
• • • We do not use the following data for averages, fits, limits, etc. • • •					
0.822±0.028	2437	BOURQUIN	79B	SPEC	See BOURQUIN 84

$\overline{\Omega}^+$ MEAN LIFE

The fit assumes the Ω^- and $\overline{\Omega}^+$ mean lives are the same, and averages them together.

VALUE (10^{-10} s)	EVTS	DOCUMENT ID		TECN	COMMENT
0.821±0.011 OUR FIT					
0.823±0.031±0.022	1801	CHAN	98	E756	p Be, 800 GeV

$(\tau_{\Omega^-} - \tau_{\overline{\Omega}^+}) / \tau_{\Omega^-}$

A test of CPT invariance. Our calculation, from the averages in the preceding two data blocks.

VALUE	DOCUMENT ID
0.00±0.05 OUR ESTIMATE	

Ω^- MAGNETIC MOMENT

VALUE (μ_N)	EVTS	DOCUMENT ID		TECN	COMMENT
−2.02 ±0.05 OUR AVERAGE					
−2.024±0.056	235k	WALLACE	95	SPEC	Ω^- 300–550 GeV
−1.94 ±0.17 ±0.14	25k	DIEHL	91	SPEC	Spin-transfer production

Ω^- DECAY MODES

	Mode	Fraction (Γ_i/Γ)		Confidence level
Γ_1	ΛK^-	(67.8±0.7) %		
Γ_2	$\Xi^0\pi^-$	(23.6±0.7) %		
Γ_3	$\Xi^-\pi^0$	(8.6±0.4) %		
Γ_4	$\Xi^-\pi^+\pi^-$	$(3.7^{+0.7}_{-0.6})\times10^{-4}$		
Γ_5	$\Xi(1530)^0\pi^-$	< 7	$\times10^{-5}$	90%
Γ_6	$\Xi^0 e^-\overline{\nu}_e$	(5.6±2.8)	$\times10^{-3}$	
Γ_7	$\Xi^-\gamma$	< 4.6	$\times10^{-4}$	90%
	$\Delta S = 2$ forbidden ($S2$) modes			
Γ_8	$\Lambda\pi^-$	$S2$ < 2.9	$\times10^{-6}$	90%

Ω^- BRANCHING RATIOS

The BOURQUIN 84 values (which include results of BOURQUIN 79B, a separate experiment) are much more accurate than any other results, and so the other results have been omitted.

$\Gamma(\Lambda K^-)/\Gamma_{total}$ Γ_1/Γ

VALUE	EVTS	DOCUMENT ID		TECN	COMMENT
0.678±0.007	14k	BOURQUIN	84	SPEC	SPS hyperon beam
• • • We do not use the following data for averages, fits, limits, etc. • • •					
0.686±0.013	1920	BOURQUIN	79B	SPEC	See BOURQUIN 84

$\Gamma(\Xi^0\pi^-)/\Gamma_{total}$ Γ_2/Γ

VALUE	EVTS	DOCUMENT ID		TECN	COMMENT
0.236±0.007	1947	BOURQUIN	84	SPEC	SPS hyperon beam
• • • We do not use the following data for averages, fits, limits, etc. • • •					
0.234±0.013	317	BOURQUIN	79B	SPEC	See BOURQUIN 84

$\Gamma(\Xi^-\pi^0)/\Gamma_{total}$ Γ_3/Γ

VALUE	EVTS	DOCUMENT ID		TECN	COMMENT
0.086±0.004	759	BOURQUIN	84	SPEC	SPS hyperon beam
• • • We do not use the following data for averages, fits, limits, etc. • • •					
0.080±0.008	145	BOURQUIN	79B	SPEC	See BOURQUIN 84

$\Gamma(\Xi^-\pi^+\pi^-)/\Gamma_{total}$ Γ_4/Γ

VALUE (units 10^{-4})	EVTS	DOCUMENT ID		TECN	COMMENT
$3.74^{+0.67}_{-0.56}$	100	[5] KAMAEV	10	HYCP	p Cu, 800 GeV
• • • We do not use the following data for averages, fits, limits, etc. • • •					
$4.3\ ^{+3.4}_{-1.3}$	4	BOURQUIN	84	SPEC	SPS hyperon beam

[5] This KAMAEV 10 value uses 76 $\Omega^- \to \Xi^-\pi^+\pi^-$ and 24 $\overline{\Omega}^+ \to \overline{\Xi}^+\pi^-\pi^+$ decays. The Ω^- and $\overline{\Omega}^+$ branching fractions measurements are statistically equal. The errors given combine statistical and systematic contributions. The *CP* branching-fraction asymmetry, $(\Omega^- - \overline{\Omega}^+)$/sum, is $+0.12 \pm 0.20$.

$\Gamma(\Xi(1530)^0\pi^-)/\Gamma_{total}$ Γ_5/Γ

VALUE (units 10^{-4})	CL%	EVTS	DOCUMENT ID		TECN	COMMENT
<0.7	90		KAMAEV	10	HYCP	p Cu, 800 GeV
• • • We do not use the following data for averages, fits, limits, etc. • • •						
$6.4^{+5.1}_{-2.0}$		4	[6] BOURQUIN	84	SPEC	SPS hyperon beam

[6] The same 4 events as in the previous mode, with the isospin factor to take into account $\Xi(1530)^0 \to \Xi^0\pi^0$ decays included. BOURQUIN 84 adopted a theoretical assumption that $\Xi(1530)^0\pi^-$ would dominate $\Xi^-\pi^+\pi^-$ decay.

$\Gamma(\Xi^0 e^-\overline{\nu}_e)/\Gamma_{total}$ Γ_6/Γ

VALUE (units 10^{-3})	EVTS	DOCUMENT ID		TECN	COMMENT
5.6±2.8	14	BOURQUIN	84	SPEC	SPS hyperon beam
• • • We do not use the following data for averages, fits, limits, etc. • • •					
~ 10	3	BOURQUIN	79B	SPEC	See BOURQUIN 84

$\Gamma(\Xi^-\gamma)/\Gamma_{total}$ Γ_7/Γ

VALUE (units 10^{-4})	CL%	EVTS	DOCUMENT ID		TECN	COMMENT
< 4.6	90	0	ALBUQUERQ...94		E761	Ω^- 375 GeV
• • • We do not use the following data for averages, fits, limits, etc. • • •						
<22	90	9	BOURQUIN	84	SPEC	SPS hyperon beam
<31	90	0	BOURQUIN	79B	SPEC	See BOURQUIN 84

$\Gamma(\Lambda\pi^-)/\Gamma_{total}$ Γ_8/Γ

ΔS=2. Forbidden in first-order weak interaction.

VALUE (units 10^{-6})	CL%	DOCUMENT ID		TECN	COMMENT
< 2.9	90	WHITE	05	HYCP	p Cu, 800 GeV
• • • We do not use the following data for averages, fits, limits, etc. • • •					
< 190	90	BOURQUIN	84	SPEC	SPS hyperon beam
<1300	90	BOURQUIN	79B	SPEC	See BOURQUIN 84

Ω^- DECAY PARAMETERS

α FOR $\Omega^- \to \Lambda K^-$

Some early results have been omitted.

VALUE	EVTS	DOCUMENT ID		TECN	COMMENT
0.0180±0.0024 OUR AVERAGE					
$+0.0207\pm0.0051\pm0.0081$	960k	[7] CHEN	05	HYCP	p Cu, 800 GeV
$+0.0178\pm0.0019\pm0.0016$	4.5M	[7] LU	05A	HYCP	p Cu, 800 GeV
• • • We do not use the following data for averages, fits, limits, etc. • • •					
$-0.028\ \pm0.047$	6953	CHAN	98	E756	p Be, 800 GeV
$-0.034\ \pm0.079$	1743	LUK	88	SPEC	p Be 400 GeV
$-0.025\ \pm0.028$	12k	BOURQUIN	84	SPEC	SPS hyperon beam

[7] The results of CHEN 05 and LU 05A are from different experimental runs.

$\overline{\alpha}$ FOR $\overline{\Omega}^+ \to \overline{\Lambda}K^+$

VALUE	EVTS	DOCUMENT ID		TECN	COMMENT
$-0.0181\pm0.0028\pm0.0026$	1.89M	LU	06	HYCP	p Cu, 800 GeV
• • • We do not use the following data for averages, fits, limits, etc. • • •					
$+0.017\ \pm0.077$	1823	CHAN	98	E756	p Be, 800 GeV

$(\alpha + \overline{\alpha})/(\alpha - \overline{\alpha})$ in $\Omega^- \to \Lambda K^-$, $\overline{\Omega}^+ \to \overline{\Lambda}K^+$

Zero if *CP* is conserved.

VALUE	DOCUMENT ID		TECN	COMMENT
$-0.016\pm0.092\pm0.089$	[8] LU	06	HYCP	p Cu, 800 GeV

[8] This value uses the results of CHEN 05, LU 05A, and LU 06.

α FOR $\Omega^- \to \Xi^0\pi^-$

VALUE	EVTS	DOCUMENT ID		TECN	COMMENT
+0.09±0.14	1630	BOURQUIN	84	SPEC	SPS hyperon beam

α FOR $\Omega^- \to \Xi^-\pi^0$

VALUE	EVTS	DOCUMENT ID		TECN	COMMENT
+0.05±0.21	614	BOURQUIN	84	SPEC	SPS hyperon beam

Ω^- REFERENCES

We have omitted some papers that have been superseded by later experiments. See our earlier editions.

KAMAEV	10	PL B693 236	O. Kamaev *et al.*	(FNAL HyperCP Collab.)
AUBERT,BE	06	PRL 97 112001	B. Aubert *et al.*	(BABAR Collab.)
LU	06	PRL 96 242001	L.C. Lu *et al.*	(FNAL HyperCP Collab.)
CHEN	05	PR D71 051102	Y.C. Chen *et al.*	(FNAL HyperCP Collab.)
LU	05A	PL B617 11	L.C. Lu *et al.*	(FNAL HyperCP Collab.)
WHITE	05	PRL 94 101804	C.G. White *et al.*	(FNAL HyperCP Collab.)
CHAN	98	PR D58 072002	A.W. Chan *et al.*	(FNAL E756 Collab.)
WALLACE	95	PRL 74 3732	N.B. Wallace *et al.*	(MINN, ARIZ, MICH+)
ALBUQUERQ...	94	PR D50 R18	I.F. Albuquerque *et al.*	(FNAL E761 Collab.)
DIEHL	91	PRL 67 804	H.T. Diehl *et al.*	(RUTG, FNAL, MICH+)
LUK	88	PR D38 19	K.B. Luk *et al.*	(RUTG, WISC, MICH, MINN)
HARTOUNI	85	PRL 54 628	E.P. Hartouni *et al.*	(COLU, ILL, FNAL)
BOURQUIN	84	NP B241 1	M.H. Bourquin *et al.*	(BRIS, GEVA, HEIDP+)
Also		PL 87B 297	M.H. Bourquin *et al.*	(BRIS, GEVA, HEIDP+)
BOURQUIN	79B	PL 88B 192	M.H. Bourquin *et al.*	(BRIS, GEVA, HEIDP+)
BAUBILLIER	78	PL 78B 342	M. Baubillier *et al.*	(BIRM, CERN, GLAS+) J
DEUTSCH...	78	PL 73B 96	M. Deutschmann *et al.*	(AACH3, BERL, CERN+) J
HEMINGWAY	78	NP B142 205	R.J. Hemingway *et al.*	(CERN, ZEEM, NIJM+)
DIBIANCA	75	NP B98 137	F.A. Dibianca, R.J. Endorf	(CMU)
ALVAREZ	73	PR D8 702	L.W. Alvarez	(LBL)
DEUTSCH...	73	NP B61 102	M. Deutschmann *et al.*	(ABCLV Collab.)
FIRESTONE	71B	PRL 26 410	I. Firestone *et al.*	(LRL)
SPETH	69	PL 29B 252	R. Speth *et al.*	(AACH, BERL, CERN, LOIC+)
PALMER	68	PL 26B 323	R.B. Palmer *et al.*	(BNL, SYRA)
SCHULTZ	68	PR 168 1509	P.F. Schultz *et al.*	(ILL, ANL, NWES+)
SCOTTER	68	PL 26B 474	D. Scotter *et al.*	(BIRM, GLAS, LOIC+)
ABRAMS	64	PRL 13 670	G.S. Abrams *et al.*	(UMD, NRL)
BARNES	64	PRL 12 204	V.E. Barnes *et al.*	(BNL)
FRY	55	PR 97 1189	W.F. Fry, J. Schneps, M.S. Swami	(WISC)
FRY	55B	NC 2 346	W.F. Fry, J. Schneps, M.S. Swami	(WISC)
EISENBERG	54	PR 96 541	Y. Eisenberg	(CORN)

$\Omega(2250)^-$

$I(J^P) = 0(?^?)$ Status: ***

$\Omega(2250)^-$ MASS

VALUE (MeV)	EVTS	DOCUMENT ID		TECN	COMMENT
2252± 9 OUR AVERAGE					
2253±13	44	ASTON	87B	LASS	K^-p 11 GeV/c
2251± 9±8	78	BIAGI	86B	SPEC	SPS Ξ^- beam

$\Omega(2250)^-$ WIDTH

VALUE (MeV)	EVTS	DOCUMENT ID		TECN	COMMENT
55±18 OUR AVERAGE					
81±38	44	ASTON	87B	LASS	K^-p 11 GeV/c
48±20	78	BIAGI	86B	SPEC	SPS Ξ^- beam

$\Omega(2250)^-$ DECAY MODES

	Mode	Fraction (Γ_i/Γ)
Γ_1	$\Xi^-\pi^+K^-$	seen
Γ_2	$\Xi(1530)^0K^-$	seen

$\Omega(2250)^-$ BRANCHING RATIOS

$\Gamma(\Xi(1530)^0K^-)/\Gamma(\Xi^-\pi^+K^-)$ Γ_2/Γ_1

VALUE	EVTS	DOCUMENT ID		TECN	COMMENT
~ 1.0	44	ASTON	87B	LASS	K^-p 11 GeV/c
0.70±0.20	49	BIAGI	86B	SPEC	Ξ^- Be 116 GeV/c

$\Omega(2250)^-$ REFERENCES

ASTON	87B	PL B194 579	D. Aston *et al.*	(SLAC, NAGO, CINC, INUS)
BIAGI	86B	ZPHY C31 33	S.F. Biagi *et al.*	(LOQM, GEVA, RAL+)

See key on page 547

$\Omega(2380)^-$

Status: **

OMITTED FROM SUMMARY TABLE

$\Omega(2380)^-$ MASS

VALUE (MeV)	EVTS	DOCUMENT ID		TECN	COMMENT
≈ 2380 OUR ESTIMATE					
2384±9±8	45	BIAGI	86B	SPEC	SPS Ξ^- beam

$\Omega(2380)^-$ WIDTH

VALUE (MeV)	EVTS	DOCUMENT ID		TECN	COMMENT
26±23	45	BIAGI	86B	SPEC	SPS Ξ^- beam

$\Omega(2380)^-$ DECAY MODES

	Mode	Fraction (Γ_i/Γ)
Γ_1	$\Xi^-\pi^+K^-$	
Γ_2	$\Xi(1530)^0K^-$	seen
Γ_3	$\Xi^-\overline{K}^*(892)^0$	

$\Omega(2380)^-$ BRANCHING RATIOS

$\Gamma(\Xi(1530)^0K^-)/\Gamma(\Xi^-\pi^+K^-)$ Γ_2/Γ_1

VALUE	CL%	EVTS	DOCUMENT ID		TECN	COMMENT
<0.44	90	9	BIAGI	86B	SPEC	Ξ^- Be 116 GeV/c

$\Gamma(\Xi^-\overline{K}^*(892)^0)/\Gamma(\Xi^-\pi^+K^-)$ Γ_3/Γ_1

VALUE	EVTS	DOCUMENT ID		TECN	COMMENT
0.5±0.3	21	BIAGI	86B	SPEC	Ξ^- Be 116 GeV/c

$\Omega(2380)^-$ REFERENCES

BIAGI 86B ZPHY C31 33 S.F. Biagi *et al.* (LOQM, GEVA, RAL+)

$\Omega(2470)^-$

Status: **

OMITTED FROM SUMMARY TABLE

A peak in the $\Omega^-\pi^+\pi^-$ mass spectrum with a signal significance claimed to be at least 5.5 standard deviations. There is no reason to seriously doubt the existence of this state, but unless the evidence is overwhelming we usually wait for confirmation from a second experiment before elevating peaks to the Summary Table.

$\Omega(2470)^-$ MASS

VALUE (MeV)	EVTS	DOCUMENT ID		TECN	COMMENT
2474±12	59	ASTON	88G	LASS	K^-p 11 GeV/c

$\Omega(2470)^-$ WIDTH

VALUE (MeV)	EVTS	DOCUMENT ID		TECN	COMMENT
72±33	59	ASTON	88G	LASS	K^-p 11 GeV/c

$\Omega(2470)^-$ DECAY MODES

	Mode
Γ_1	$\Omega^-\pi^+\pi^-$

$\Omega(2470)^-$ REFERENCES

ASTON 88G PL B215 799 D. Aston *et al.* (SLAC, NAGO, CINC, INUS)

CHARMED BARYONS
($C = +1$)

$\Lambda_c^+ = udc$, $\Sigma_c^{++} = uuc$, $\Sigma_c^+ = udc$, $\Sigma_c^0 = ddc$,
$\Xi_c^+ = usc$, $\Xi_c^0 = dsc$, $\Omega_c^0 = ssc$

CHARMED BARYONS

Revised March 2012 by C.G. Wohl (LBNL).

There are 17 known charmed baryons, and four other candidates not well enough established to be promoted to the Summary Tables.* Fig. 1(a) shows the mass spectrum, and for comparison Fig. 1(b) shows the spectrum of the lightest strange baryons. The Λ_c and Σ_c spectra ought to look much like the Λ and Σ spectra, since a Λ_c or a Σ_c differs from a Λ or a Σ only by the replacement of the s quark with a c quark. However, a Ξ or an Ω has more than one s quark, only *one* of which is changed to a c quark to make a Ξ_c or an Ω_c. Thus the Ξ_c and Ω_c spectra ought to be richer than the Ξ and Ω spectra.**

Before discussing the observed spectra, we review the theory of SU(4) multiplets, which tells what charmed baryons to expect; this is essential, because few of the spin-parity values given in Fig. 1(a) have been measured. Rather, they have been assigned in accord with expectations of the theory. However, they are all very likely as shown (see below).

SU(4) multiplets—Baryons made from u, d, s, and c quarks belong to SU(4) multiplets. The multiplet numerology, analogous to $3\times3\times3 = 10+8_1+8_2+1$ for the subset of baryons made from just u, d, and s quarks, is $4\times4\times4 = 20+20'_1+20'_2+\bar{4}$. Figure 2(a) shows the 20-plet whose bottom level is an SU(3) decuplet, such as the decuplet that includes the $\Delta(1232)$. Figure 2(b) shows the $20'$-plet whose bottom level is an SU(3) octet, such as the octet that includes the nucleon. Figure 2(c) shows the $\bar{4}$ multiplet, an inverted tetrahedron. One level up from the bottom level of each multiplet are the baryons with one c quark. All the baryons in a given multiplet have the same spin and parity. Each N or Δ or SU(3)-singlet-Λ resonance calls for another $20'$- or 20- or $\bar{4}$-plet, respectively.

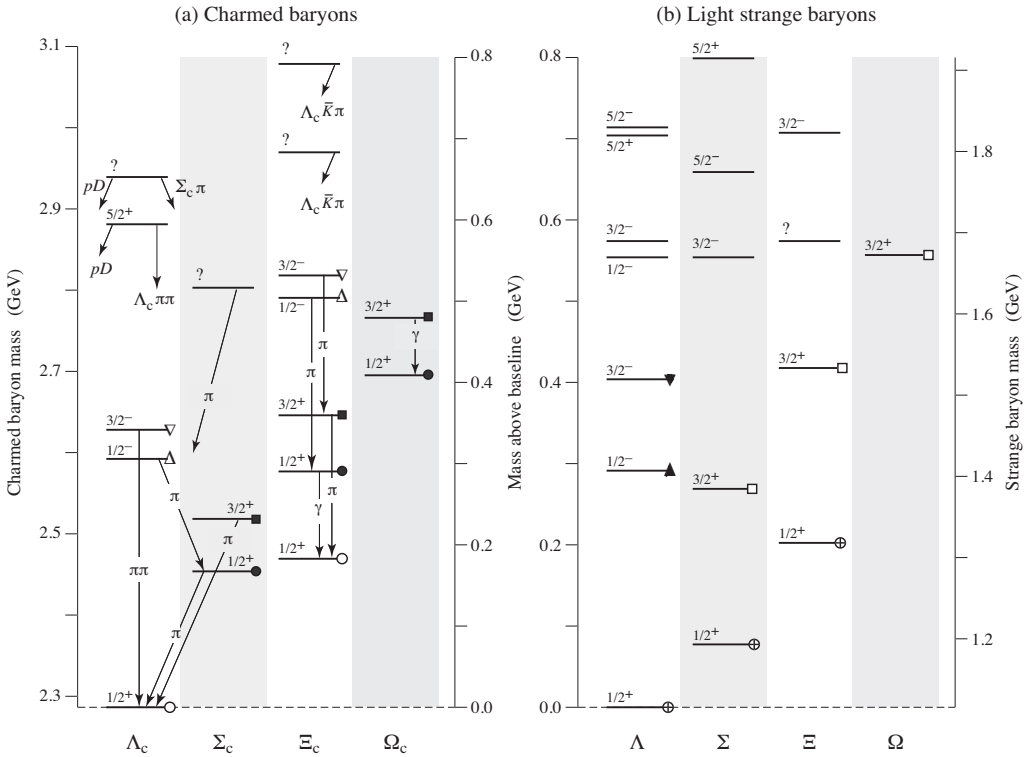

Fig. 1. (a) The known charmed baryons, and (b) the lightest "4-star" strange baryons. Note that there are two $J^P = 1/2^+$ Ξ_c states, and that the lightest Ω_c does not have $J = 3/2$. The $J^P = 1/2^+$ states, all tabbed with a circle, belong to the SU(4) multiplet that includes the nucleon; states with a circle with the same *fill* belong to the same SU(3) multiplet within that SU(4) multiplet. Similar remarks apply to the other states: same shape of tab, same SU(4) multiplet; same fill of that shape, same SU(3) multiplet. The $J^P = 1/2^-$ and $3/2^-$ states tabbed with triangles complete two SU(4) $\bar{4}$ multiplets.

The flavor symmetries shown in Fig. 2 are of course badly broken, but the figure is the simplest way to see what charmed baryons should exist. For example, from Fig. 2(b), we expect to find, in the same $J^P = 1/2^+$ 20′-plet as the nucleon, a Λ_c, a Σ_c, *two* Ξ_c's, and an Ω_c. Note that this Ω_c has $J^P = 1/2^+$ and is not in the same SU(4) multiplet as the famous $J^P = 3/2^+$ Ω^-.

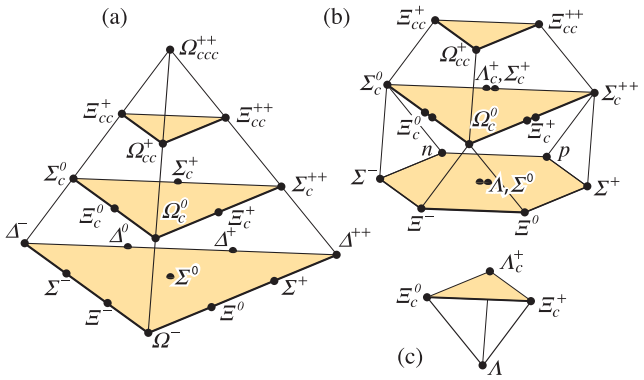

Figure 2: SU(4) multiplets of baryons made of u, d, s, and c quarks. (a) The 20-plet with an SU(3) decuplet on the lowest level. (b) The 20′-plet with an SU(3) octet on the lowest level. (c) The $\overline{4}$-plet. Note that here and in Fig. 3, but not in Fig. 1, each charge state is shown separately.

Figure 3 shows in more detail the middle level of the 20′-plet of Fig. 2(b); it splits apart into two SU(3) multiplets, a $\bar{3}$ and a 6. The states of the $\bar{3}$ are antisymmetric under the interchange of the two light quarks (the u, d, and s quarks), whereas the states of the 6 are symmetric under this interchange. We use a prime to distinguish the Ξ_c in the 6 from the one in the $\bar{3}$.

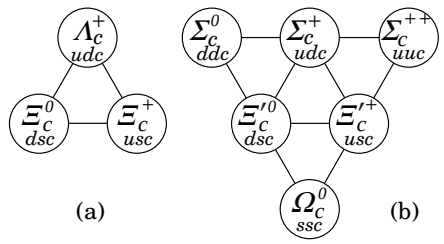

Figure 3: The SU(3) multiplets on the second level of the SU(4) multiplet of Fig. 2(b). The Λ_c and Ξ_c tabbed with open circles in Fig. 1(a) complete a $J^P = 1/2^+$ SU(3) $\overline{3}$-plet, as in (a) here. The Σ_c, Ξ_c, and Ω_c tabbed with closed circles in Fig. 1(a) complete a $J^P = 1/2^+$ SU(3) 6-plet, as in (b) here. Together the nine particles complete the charm = +1 level of a $J^P = 1/2^+$ SU(4) 20′-plet, as in Fig. 2(b).

The observed spectra—(1) The parity of the lightest Λ_c is defined to be positive (as are the parities of the p, n, and Λ); the limited evidence about its spin is consistent with $J = 1/2$. However, few of the J^P quantum numbers given in Fig. 1(a) have been measured. Models using spin-spin and spin-orbit interactions between the quarks, with parameters determined using a few of the masses as input, lead to the J^P assignments shown.† There are no surprises: the $J^P = 1/2^+$ states come first, then the $J^P = 3/2^+$ states ...

(2) There is, however, evidence that many of the J^P assignments in Fig. 1(a) must be correct. As is well known, the successive mass differences between the $J^P = 3/2^+$ particles, the $\Delta(1232)^-$, $\Sigma(1385)^-$, $\Xi(1535)^-$, and Ω^-, which lie along the lower left edge of the 20-plet in Fig. 2(a), should according to SU(3) be about equal; and indeed experimentally they nearly are. In the same way, the mass differences between the $J^P = 1/2^+$ $\Sigma_c(2455)^0$, $\Xi_c'^0$, and Ω_c^0,‡ the particles along the left edge of Fig. 3(b), should be about equal—assuming, of course, that they *do* all have the same J^P. The measured differences are 125.0 ± 2.9 MeV and 117.3 ± 3.4 MeV—not perfect, but close. Similarly, the mass differences between the presumed $J^P = 3/2^+$ $\Sigma_c(2520)^0$, $\Xi_c(2645)^0$, and $\Omega_c(2770)^0$ are 127.1 ± 0.8 MeV and 120.0 ± 2.1 MeV. In Fig. 1(a), these two sets of charm particles are tabbed with solid circles and solid squares.

(3) Other evidence comes from the decay of the $\Lambda_c(2593)$. The only allowed strong decay is $\Lambda_c(2593)^+ \to \Lambda_c^+ \pi\pi$, and this appears to be dominated by the submode $\Sigma_c(2455)\pi$, despite little available phase space for the latter (the "Q" is about 2 MeV, the c.m. decay momentum about 20 MeV/c). Thus the decay is almost certainly s-wave, which, assuming that the $\Sigma_c(2455)$ does indeed have $J^P = 1/2^+$, makes $J^P = 1/2^-$ for the $\Lambda_c(2593)$.

Footnotes:

* The unpromoted states are a $\Lambda_c(2765)^+$, a $\Xi_c(2930)$, a $\Xi_c(3055)$, and a $\Xi_c(3123)$. There is also very weak evidence for a baryon with *two* c quarks, a Ξ_{cc}^+ at 3519 MeV. See the Particle Listings.

** For example, there are three Ω_c^0 states (properly symmetrized states of ssc, scs, and css) corresponding to each Ω^- (sss) state.

† This is not the place to discuss the details of the models, nor to attempt a guide to the literature. See the discovery papers of the various charmed baryons for references to the models that lead to the quantum-number assignments.

‡ A reminder about the Particle Data Group naming scheme: A particle has its mass as part of its name if and only if it decays strongly. Thus $\Sigma(1385)$ and $\Sigma_c(2455)$ but Ω^- and Ξ_c'.

Baryon Particle Listings

Λ_c^+

Λ_c^+ $I(J^P) = 0(\frac{1}{2}^+)$ Status: ****

The parity of the Λ_c^+ is defined to be positive (as are the parities of the proton, neutron, and Λ). The quark content is udc. Results of an analysis of $pK^-\pi^+$ decays (JEZABEK 92) are consistent with $J = 1/2$. Nobody doubts that the spin is indeed 1/2.

The only new measurements since our 2010 Review are of limits on rare or forbidden $\Lambda_c^+ \to p\ell^+\ell^-$ and $\overline{p}\ell^+\ell^+$ modes.

We have omitted some results that have been superseded by later experiments. The omitted results may be found in earlier editions.

Λ_c^+ MASS

Our value in 2004, 2284.9±0.6 MeV, was the average of the measurements now filed below as "not used." The BABAR measurement is so much better that we use it alone. Note that it is about 2.6 (old) standard deviations above the 2004 value.

The fit also includes Σ_c–Λ_c^+ and Λ_c^{*+}–Λ_c^+ mass-difference measurements, but this doesn't affect the Λ_c^+ mass. The new (in 2006) Λ_c^+ mass simply pushes all those other masses higher.

VALUE (MeV)	EVTS	DOCUMENT ID		TECN	COMMENT
2286.46±0.14 OUR FIT					
2286.46±0.14	4891	[1] AUBERT,B	05S	BABR	$\Lambda K_S^0 K^+$ and $\Sigma^0 K_S^0 K^+$
• • • We do not use the following data for averages, fits, limits, etc. • • •					
2284.7 ±0.6 ±0.7	1134	AVERY	91	CLEO	Six modes
2281.7 ±2.7 ±2.6	29	ALVAREZ	90B	NA14	$pK^-\pi^+$
2285.8 ±0.6 ±1.2	101	BARLAG	89	NA32	$pK^-\pi^+$
2284.7 ±2.3 ±0.5	5	AGUILAR-...	88B	LEBC	$pK^-\pi^+$
2283.1 ±1.7 ±2.0	628	ALBRECHT	88C	ARG	$pK^-\pi^+$, $p\overline{K}^0$, $\Lambda 3\pi$
2286.2 ±1.7 ±0.7	97	ANJOS	88B	E691	$pK^-\pi^+$
2281 ±3	2	JONES	87	HBC	$pK^-\pi^+$
2283 ±3	3	BOSETTI	82	HBC	$pK^-\pi^+$
2290 ±3	1	CALICCHIO	80	HYBR	$pK^-\pi^+$

[1] AUBERT,B 05S uses low-Q $\Lambda K_S^0 K^+$ and $\Sigma^0 K_S^0 K^+$ decays to minimize systematic errors. The error above includes systematic as well as statistical errors. Many cross checks and adjustments to properties of the BABAR detector, as well as the large number of clean events, make this by far the best measurement of the Λ_c^+ mass.

Λ_c^+ MEAN LIFE

Measurements with an error $\geq 100 \times 10^{-15}$ s or with fewer than 20 events have been omitted from the Listings.

VALUE (10^{-15} s)	EVTS	DOCUMENT ID		TECN	COMMENT
200 ± 6 OUR AVERAGE Error includes scale factor of 1.6. See the ideogram below.					
204.6± 3.4± 2.5	8034	LINK	02C	FOCS	$pK^-\pi^+$
198.1± 7.0± 5.6	1630	KUSHNIR...	01	SELX	$\Lambda_c^+ \to pK^-\pi^+$
179.6± 6.9± 4.4	4749	MAHMOOD	01	CLE2	$e^+e^- \approx \Upsilon(4S)$
215 ±16 ± 8	1340	FRABETTI	93D	E687	γBe, $\Lambda_c^+ \to pK^-\pi^+$
• • • We do not use the following data for averages, fits, limits, etc. • • •					
180 ±30 ±30	29	ALVAREZ	90	NA14	γ, $\Lambda_c^+ \to pK^-\pi^+$
200 ±30 ±30	90	FRABETTI	90	E687	γBe, $\Lambda_c^+ \to pK^-\pi^+$
196 $^{+23}_{-20}$	101	BARLAG	89	NA32	$pK^-\pi^+$ + c.c.
220 ±30 ±20	97	ANJOS	88B	E691	$pK^-\pi^+$ + c.c.

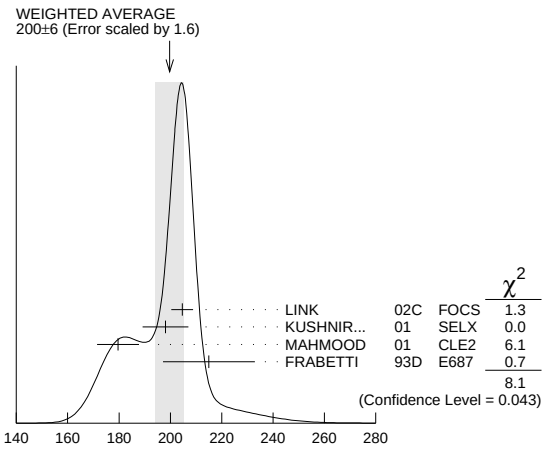

Λ_c^+ DECAY MODES

Nearly all branching fractions of the Λ_c^+ are measured relative to the $pK^-\pi^+$ mode, but there are no model-independent measurements of this branching fraction. We explain how we arrive at our value of B($\Lambda_c^+ \to pK^-\pi^+$) in a Note at the beginning of the branching-ratio measurements, below. When this branching fraction is eventually well determined, all the other branching fractions will slide up or down proportionally as the true value differs from the value we use here.

	Mode		Fraction (Γ_i/Γ)	Scale factor/ Confidence level
	Hadronic modes with a p: $S = -1$ final states			
Γ_1	$p\overline{K}^0$		(2.3 ± 0.6) %	
Γ_2	$pK^-\pi^+$	[a]	(5.0 ± 1.3) %	
Γ_3	$p\overline{K}^*(892)^0$	[b]	(1.6 ± 0.5) %	
Γ_4	$\Delta(1232)^{++}K^-$		(8.6 ± 3.0) $\times 10^{-3}$	
Γ_5	$\Lambda(1520)\pi^+$	[b]	(1.8 ± 0.6) %	
Γ_6	$pK^-\pi^+$ nonresonant		(2.8 ± 0.8) %	
Γ_7	$p\overline{K}^0\pi^0$		(3.3 ± 1.0) %	
Γ_8	$p\overline{K}^0\eta$		(1.2 ± 0.4) %	
Γ_9	$p\overline{K}^0\pi^+\pi^-$		(2.6 ± 0.7) %	
Γ_{10}	$pK^-\pi^+\pi^0$		(3.4 ± 1.0) %	
Γ_{11}	$pK^*(892)^-\pi^+$	[b]	(1.1 ± 0.5) %	
Γ_{12}	$p(K^-\pi^+)_{\text{nonresonant}}\pi^0$		(3.6 ± 1.2) %	
Γ_{13}	$\Delta(1232)\overline{K}^*(892)$		seen	
Γ_{14}	$pK^-\pi^+\pi^+\pi^-$		(1.1 ± 0.8) $\times 10^{-3}$	
Γ_{15}	$pK^-\pi^+\pi^0\pi^0$		(8 ± 4) $\times 10^{-3}$	
Γ_{16}	$pK^-\pi^+3\pi^0$			
	Hadronic modes with a p: $S = 0$ final states			
Γ_{17}	$p\pi^+\pi^-$		(3.5 ± 2.0) $\times 10^{-3}$	
Γ_{18}	$pf_0(980)$	[b]	(2.8 ± 1.9) $\times 10^{-3}$	
Γ_{19}	$p\pi^+\pi^+\pi^-\pi^-$		(1.8 ± 1.2) $\times 10^{-3}$	
Γ_{20}	pK^+K^-		(7.7 ± 3.5) $\times 10^{-4}$	
Γ_{21}	$p\phi$	[b]	(8.2 ± 2.7) $\times 10^{-4}$	
Γ_{22}	pK^+K^- non-ϕ		(3.5 ± 1.7) $\times 10^{-4}$	
	Hadronic modes with a hyperon: $S = -1$ final states			
Γ_{23}	$\Lambda\pi^+$		(1.07± 0.28) %	
Γ_{24}	$\Lambda\pi^+\pi^0$		(3.6 ± 1.3) %	
Γ_{25}	$\Lambda\rho^+$		< 5 %	CL=95%
Γ_{26}	$\Lambda\pi^+\pi^+\pi^-$		(2.6 ± 0.7) %	
Γ_{27}	$\Sigma(1385)^+\pi^+\pi^-$, $\Sigma^{*+} \to \Lambda\pi^+$		(7 ± 4) $\times 10^{-3}$	
Γ_{28}	$\Sigma(1385)^-\pi^+\pi^+$, $\Sigma^{*-} \to \Lambda\pi^-$		(5.5 ± 1.7) $\times 10^{-3}$	
Γ_{29}	$\Lambda\pi^+\rho^0$		(1.1 ± 0.5) %	
Γ_{30}	$\Sigma(1385)^+\rho^0$, $\Sigma^{*+} \to \Lambda\pi^+$		(3.7 ± 3.1) $\times 10^{-3}$	
Γ_{31}	$\Lambda\pi^+\pi^+\pi^-$ nonresonant		< 8 $\times 10^{-3}$	CL=90%
Γ_{32}	$\Lambda\pi^+\pi^+\pi^-\pi^0$ total		(1.8 ± 0.8) %	
Γ_{33}	$\Lambda\pi^+\eta$	[b]	(1.8 ± 0.6) %	
Γ_{34}	$\Sigma(1385)^+\eta$	[b]	(8.5 ± 3.3) $\times 10^{-3}$	
Γ_{35}	$\Lambda\pi^+\omega$	[b]	(1.2 ± 0.5) %	
Γ_{36}	$\Lambda\pi^+\pi^+\pi^-\pi^0$, no η or ω		< 7 $\times 10^{-3}$	CL=90%
Γ_{37}	$\Lambda K^+\overline{K}^0$		(4.7 ± 1.5) $\times 10^{-3}$	S=1.2
Γ_{38}	$\Xi(1690)^0K^+$, $\Xi^{*0} \to \Lambda\overline{K}^0$		(1.3 ± 0.5) $\times 10^{-3}$	
Γ_{39}	$\Sigma^0\pi^+$		(1.05± 0.28) %	
Γ_{40}	$\Sigma^+\pi^0$		(1.00± 0.34) %	
Γ_{41}	$\Sigma^+\eta$		(5.5 ± 2.3) $\times 10^{-3}$	
Γ_{42}	$\Sigma^+\pi^+\pi^-$		(3.6 ± 1.0) %	
Γ_{43}	$\Sigma^+\rho^0$		< 1.4 %	CL=95%
Γ_{44}	$\Sigma^-\pi^+\pi^+$		(1.7 ± 0.5) %	
Γ_{45}	$\Sigma^0\pi^+\pi^0$		(1.8 ± 0.8) %	
Γ_{46}	$\Sigma^0\pi^+\pi^+\pi^-$		(8.3 ± 3.1) $\times 10^{-3}$	
Γ_{47}	$\Sigma^+\pi^+\pi^-\pi^0$		—	
Γ_{48}	$\Sigma^+\omega$	[b]	(2.7 ± 1.0) %	
Γ_{49}	$\Sigma^+K^+K^-$		(2.8 ± 0.8) $\times 10^{-3}$	
Γ_{50}	$\Sigma^+\phi$	[b]	(3.1 ± 0.9) $\times 10^{-3}$	
Γ_{51}	$\Xi(1690)^0K^+$, $\Xi^{*0} \to \Sigma^+K^-$		(8.1 ± 3.0) $\times 10^{-4}$	
Γ_{52}	$\Sigma^+K^+K^-$ nonresonant		< 6 $\times 10^{-4}$	CL=90%
Γ_{53}	Ξ^0K^+		(3.9 ± 1.4) $\times 10^{-3}$	
Γ_{54}	$\Xi^-K^+\pi^+$		(5.1 ± 1.4) $\times 10^{-3}$	
Γ_{55}	$\Xi(1530)^0K^+$	[b]	(2.6 ± 1.0) $\times 10^{-3}$	

Hadronic modes with a hyperon: $S = 0$ final states

Γ_{56}	ΛK^+		(5.0 ± 1.6)	$\times 10^{-4}$	
Γ_{57}	$\Lambda K^+ \pi^+ \pi^-$		< 4	$\times 10^{-4}$	CL=90%
Γ_{58}	$\Sigma^0 K^+$		(4.2 ± 1.3)	$\times 10^{-4}$	
Γ_{59}	$\Sigma^0 K^+ \pi^+ \pi^-$		< 2.1	$\times 10^{-4}$	CL=90%
Γ_{60}	$\Sigma^+ K^+ \pi^-$		(1.7 ± 0.7)	$\times 10^{-3}$	
Γ_{61}	$\Sigma^+ K^*(892)^0$	[b]	(2.8 ± 1.1)	$\times 10^{-3}$	
Γ_{62}	$\Sigma^- K^+ \pi^+$		< 1.0	$\times 10^{-3}$	CL=90%

Doubly Cabibbo-suppressed modes

Γ_{63}	$p K^+ \pi^-$		< 2.3	$\times 10^{-4}$	CL=90%

Semileptonic modes

Γ_{64}	$\Lambda \ell^+ \nu_\ell$	[c]	(2.0 ± 0.6)	%
Γ_{65}	$\Lambda e^+ \nu_e$		(2.1 ± 0.6)	%
Γ_{66}	$\Lambda \mu^+ \nu_\mu$		(2.0 ± 0.7)	%

Inclusive modes

Γ_{67}	e^+ anything		(4.5 ± 1.7)	%	
Γ_{68}	$p e^+$ anything		(1.8 ± 0.9)	%	
Γ_{69}	Λe^+ anything				
Γ_{70}	p anything		(50 ±16)	%	
Γ_{71}	p anything (no Λ)		(12 ±19)	%	
Γ_{72}	p hadrons				
Γ_{73}	n anything		(50 ±16)	%	
Γ_{74}	n anything (no Λ)		(29 ±17)	%	
Γ_{75}	Λ anything		(35 ±11)	%	S=1.4
Γ_{76}	$\Sigma^\pm$ anything	[d]	(10 ± 5)	%	
Γ_{77}	3prongs		(24 ± 8)	%	

$\Delta C = 1$ weak neutral current ($C1$) modes, or Lepton Family number (LF), or Lepton number (L), or Baryon number (B) violating modes

Γ_{78}	$p e^+ e^-$	$C1$	< 5.5	$\times 10^{-6}$	CL=90%
Γ_{79}	$p \mu^+ \mu^-$	$C1$	< 4.4	$\times 10^{-5}$	CL=90%
Γ_{80}	$p e^+ \mu^-$	LF	< 9.9	$\times 10^{-6}$	CL=90%
Γ_{81}	$p e^- \mu^+$	LF	< 1.9	$\times 10^{-5}$	CL=90%
Γ_{82}	$\overline{p} 2e^+$	L,B	< 2.7	$\times 10^{-6}$	CL=90%
Γ_{83}	$\overline{p} 2\mu^+$	L,B	< 9.4	$\times 10^{-6}$	CL=90%
Γ_{84}	$\overline{p} e^+ \mu^+$	L,B	< 1.6	$\times 10^{-5}$	CL=90%
Γ_{85}	$\Sigma^- \mu^+ \mu^+$	L	< 7.0	$\times 10^{-4}$	CL=90%

[a] See the note on "Λ_c^+ Branching Fractions" below.

[b] This branching fraction includes all the decay modes of the final-state resonance.

[c] An ℓ indicates an e or a μ mode, not a sum over these modes.

[d] The value is for the sum of the charge states or particle/antiparticle states indicated.

CONSTRAINED FIT INFORMATION

An overall fit to 18 branching ratios uses 33 measurements and one constraint to determine 12 parameters. The overall fit has a $\chi^2 = 15.5$ for 22 degrees of freedom.

The following *off-diagonal* array elements are the correlation coefficients $\langle \delta x_i \delta x_j \rangle / (\delta x_i \cdot \delta x_j)$, in percent, from the fit to the branching fractions, $x_i \equiv \Gamma_i / \Gamma_{\rm total}$. The fit constrains the x_i whose labels appear in this array to sum to one.

x_{23}	96									
x_{26}	97	93								
x_{37}	82	83	80							
x_{39}	95	98	92	82						
x_{42}	93	90	91	77	88					
x_{44}	82	79	80	68	78	80				
x_{46}	69	66	70	57	66	65	57			
x_{49}	88	85	86	72	84	93	75	61		
x_{50}	85	82	83	70	81	90	72	59	84	
x_{54}	93	96	90	80	94	87	77	64	82	79
	x_2	x_{23}	x_{26}	x_{37}	x_{39}	x_{42}	x_{44}	x_{46}	x_{49}	x_{50}

Λ_c^+ BRANCHING FRACTIONS

Revised 2002 by P.R. Burchat (Stanford University).

Most Λ_c^+ branching fractions are measured relative to the decay mode $\Lambda_c^+ \to pK^-\pi^+$. However, there are no completely model-independent measurements of the absolute branching fraction for $\Lambda_c^+ \to pK^-\pi^+$. Here we describe the measurements that have been used to extract $\mathrm{B}(\Lambda_c^+ \to pK^-\pi^+)$, the model-dependence of the results, and the method we have used to average the results.

ARGUS (ALBRECHT 88C) and CLEO (CRAWFORD 92) measure $\mathrm{B}(\overline{B} \to \Lambda_c^+ \mathrm{X}) \cdot \mathrm{B}(\Lambda_c^+ \to pK^-\pi^+)$ to be $(0.30 \pm 0.12 \pm 0.06)\%$ and $(0.273 \pm 0.051 \pm 0.039)\%$. Under the assumptions that decays of $\overline{B}$ mesons to baryons are dominated by $\overline{B} \to \Lambda_c^+ \mathrm{X}$ and that $\Lambda_c^+ \mathrm{X}$ final states other than $\Lambda_c^+ \overline{N} \mathrm{X}$ can be neglected, they also measure $\mathrm{B}(\overline{B} \to \Lambda_c^+ \mathrm{X})$ to be $(6.8 \pm 0.5 \pm 0.3)\%$ (ALBRECHT 92O) and $(6.4 \pm 0.8 \pm 0.8)\%$ (CRAWFORD 92). Combining these results, we get $\mathrm{B}(\Lambda_c^+ \to pK^-\pi^+) = (4.14 \pm 0.91)\%$. However, the assumption that $\overline{B}$ decay modes to baryons other than $\Lambda_c^+ \overline{N} \mathrm{X}$ are negligible is not on solid ground experimentally or theoretically [2]. Therefore, the branching fraction for $\Lambda_c^+ \to pK^-\pi^+$ given above may be low by some undetermined amount.

A second type of model-dependent determination of $\mathrm{B}(\Lambda_c^+ \to pK^-\pi^+)$ is based on measurements by ARGUS (ALBRECHT 91G) and CLEO (BERGFELD 94) of $\sigma(e^+e^- \to \Lambda_c^+ \mathrm{X}) \cdot \mathrm{B}(\Lambda_c^+ \to \Lambda \ell^+ \nu_\ell) = (4.15 \pm 1.03 \pm 1.18)$ pb and $(4.77 \pm 0.25 \pm 0.66)$ pb. ARGUS (ALBRECHT 96E) and CLEO (AVERY 91) have also measured $\sigma(e^+e^- \to \Lambda_c^+ \mathrm{X}) \cdot \mathrm{B}(\Lambda_c^+ \to pK^-\pi^+)$. The weighted average is (11.2 ± 1.3) pb.

From these measurements, we extract $R \equiv \mathrm{B}(\Lambda_c^+ \to pK^-\pi^+)/\mathrm{B}(\Lambda_c^+ \to \Lambda \ell^+ \nu_\ell) = 2.40 \pm 0.43$. We estimate the $\Lambda_c^+ \to pK^-\pi^+$ branching fraction from the equation

$$\mathrm{B}(\Lambda_c^+ \to pK^-\pi^+) = R\, f\, F\, \frac{\Gamma(D \to \mathrm{X} \ell^+ \nu_\ell)}{1 + |V_{cd}/V_{cs}|^2} \cdot \tau(\Lambda_c^+) \ , \quad (1)$$

where $f = \mathrm{B}(\Lambda_c^+ \to \Lambda \ell^+ \nu_\ell)/\mathrm{B}(\Lambda_c^+ \to X_s \ell^+ \nu_\ell)$ and $F = \Gamma(\Lambda_c^+ \to X_s \ell^+ \nu_\ell)/\Gamma(D^0 \to X_s \ell^+ \nu_\ell)$. When we use $1 + |V_{cd}/V_{cs}|^2 = 1.05$ and the world averages $\Gamma(D \to \mathrm{X} \ell^+ \nu_\ell) = (0.166 \pm 0.006) \times 10^{12}\ \mathrm{s}^{-1}$ and $\tau(\Lambda_c^+) = (0.192 \pm 0.005) \times 10^{-12}$ s, we calculate $\mathrm{B}(\Lambda_c^+ \to pK^-\pi^+) = (7.3 \pm 1.4)\% \cdot f\, F$. Theoretical estimates for f and F are near 1.0 with significant uncertainties.

So, we have two results with significant model-dependence: $\mathrm{B}(\Lambda_c^+ \to pK^-\pi^+) = (4.14 \pm 0.91)\%$ from $\overline{B}$ decays, and $\mathrm{B}(\Lambda_c^+ \to pK^-\pi^+) = (7.3 \pm 1.4)\% \cdot f\, F$ from semileptonic Λ_c^+ decays. If we set $f\, F = 1.0$ in the second result, and assign an uncertainty of 30% to each result to account for the unknown model-dependence, we get the consistent results $\mathrm{B}(\Lambda_c^+ \to pK^-\pi^+) = (4.14 \pm 0.91 \pm 1.24)\%$ and $\mathrm{B}(\Lambda_c^+ \to pK^-\pi^+) = (7.3 \pm 1.4 \pm 2.2)\%$. The weighted average of these two results is $\mathrm{B}(\Lambda_c^+ \to pK^-\pi^+) = (5.0 \pm 1.3)\%$, where the uncertainty contains both the experimental uncertainty and the 30% estimate of model dependence in each result. We assigned the value $(5.0 \pm 1.3)\%$ to the $\Lambda_c^+ \to pK^-\pi^+$ branching fraction in our 2000 *Review* [1].

A third type of measurement of $B(\Lambda_c^+ \to pK^-\pi^+)$ has been published by CLEO (JAFFE 00). Under the assumption that a $\overline{D}$ meson and an antiproton in opposite hemispheres is evidence for a Λ_c^+ in the hemisphere of the $\overline{p}$, the fraction of such $\overline{D}\,\overline{p}$ events with a $\Lambda_c^+ \to pK^-\pi^+$ decay can be used to determine the $\Lambda_c^+ \to pK^-\pi^+$ branching fraction. CLEO measures $B(\Lambda_c^+ \to pK^-\pi^+) = (5.0 \pm 1.3)\%$, which is coincidentally exactly the same value as our PDG 00 average given above. The quoted uncertainty includes significant contributions from model-dependent effects (*e.g.,* differences between the $\overline{p}$ momentum spectrum in events with a Λ_c^+ and $\overline{p}$ in the same hemisphere, and with a $\overline{D}$ and $\overline{p}$ in opposite hemispheres; extrapolation of the Λ_c^+ and $\overline{D}$ momentum spectrum below the minimum value used for rejecting B decay products; and our limited understanding of backgrounds such as $D\overline{D}N\overline{p}$ events).

We have chosen to continue to assign the value $(5.0 \pm 1.3)\%$ to the $\Lambda_c^+ \to pK^-\pi^+$ branching fraction (given as PDG 02 below). As was noted earlier, most of the other Λ_c^+ decay modes are measured relative to this mode.

New methods for measuring the Λ_c^+ absolute branching fractions have been proposed [2,3].

References

1. D.E. Groom *et al.* (Particle Data Group), *Review of Particle Physics*, Eur. Phys. J. **C15**, 1 (2000).
2. I. Dunietz, Phys. Rev. **D58**, 094010 (1998).
3. P. Migliozzi *et al.*, Phys. Lett. **B462**, 217 (1999).

Λ_c^+ BRANCHING RATIOS

Hadronic modes with a p: $S = -1$ final states

$\Gamma(p\overline{K}^0)/\Gamma(pK^-\pi^+)$ Γ_1/Γ_2

VALUE	EVTS	DOCUMENT ID		TECN	COMMENT
0.47±0.04 OUR AVERAGE					
0.46±0.02±0.04	1025	ALAM	98	CLE2	$e^+e^- \approx \Upsilon(4S)$
0.44±0.07±0.05	133	AVERY	91	CLEO	e^+e^- 10.5 GeV
0.55±0.17±0.14	45	ANJOS	90	E691	γBe 70–260 GeV
0.62±0.15±0.03	73	ALBRECHT	88C	ARG	e^+e^- 10 GeV

$\Gamma(pK^-\pi^+)/\Gamma_{total}$ Γ_2/Γ

See the note on "Λ_c^+ Branching Fractions" above.

VALUE	EVTS	DOCUMENT ID		TECN	COMMENT
0.050±0.013 OUR FIT					
0.050±0.013		PDG	02		See note at top of ratios
• • • We do not use the following data for averages, fits, limits, etc. • • •					
0.050±0.005±0.012	1205	[2] JAFFE	00	CLE2	e^+e^- 10.52–10.58 GeV
0.041±0.010		[3,4] ALBRECHT	92O	ARG	$e^+e^- \approx \Upsilon(4S)$
0.044±0.012		[3,5] CRAWFORD	92	CLEO	e^+e^- 10.5 GeV

[2] JAFFE 00 assumes that a $\overline{D}$ meson and an antiproton in opposite hemispheres tags for a Λ_c^+ in the hemisphere of the $\overline{p}$. The fraction of such $\overline{D}\,\overline{p}$ events with a $\Lambda_c^+ \to pK^-\pi^+$ decay then gives the $pK^-\pi^+$ branching fraction. See the paper for assumptions, caveats, etc.

[3] To extract $\Gamma(pK^-\pi^+)/\Gamma_{total}$, we use $B(\overline{B} \to \Lambda_c^+ X)\cdot B(\Lambda_c^+ \to pK^-\pi^+) = (0.28 \pm 0.06)\%$, which is the average of measurements from ARGUS (ALBRECHT 88C) and CLEO (CRAWFORD 92).

[4] ALBRECHT 92O measures $B(\overline{B} \to \Lambda_c^+ X) = (6.8 \pm 0.5 \pm 0.3)\%$.

[5] CRAWFORD 92 measures $B(\overline{B} \to \Lambda_c^+ X) = (6.4 \pm 0.8 \pm 0.8)\%$.

$\Gamma(p\overline{K}^*(892)^0)/\Gamma(pK^-\pi^+)$ Γ_3/Γ_2

Unseen decay modes of the $\overline{K}^*(892)^0$ are included.

VALUE	EVTS	DOCUMENT ID		TECN	COMMENT
0.31±0.04 OUR AVERAGE					
0.29±0.04±0.03		[6] AITALA	00	E791	π^- N, 500 GeV
$0.35^{+0.06}_{-0.07}$±0.03	39	BOZEK	93	NA32	π^- Cu 230 GeV
0.42±0.24	12	BASILE	81B	CNTR	$pp \to \Lambda_c^+ e^- X$
• • • We do not use the following data for averages, fits, limits, etc. • • •					
0.35±0.11		BARLAG	90D	NA32	See BOZEK 93

[6] AITALA 00 makes a coherent 5-dimensional amplitude analysis of 946 ± 38 $\Lambda_c^+ \to pK^-\pi^+$ decays.

$\Gamma(\Delta(1232)^{++}K^-)/\Gamma(pK^-\pi^+)$ Γ_4/Γ_2

VALUE	EVTS	DOCUMENT ID		TECN	COMMENT
0.17±0.04 OUR AVERAGE Error includes scale factor of 1.1.					
0.18±0.03±0.03		[7] AITALA	00	E791	π^- N, 500 GeV
$0.12^{+0.04}_{-0.05}$±0.05	14	BOZEK	93	NA32	π^- Cu 230 GeV
0.40±0.17	17	BASILE	81B	CNTR	$pp \to \Lambda_c^+ e^- X$

[7] AITALA 00 makes a coherent 5-dimensional amplitude analysis of 946 ± 38 $\Lambda_c^+ \to pK^-\pi^+$ decays.

$\Gamma(\Lambda(1520)\pi^+)/\Gamma(pK^-\pi^+)$ Γ_5/Γ_2

Unseen decay modes of the $\Lambda(1520)$ are included.

VALUE	EVTS	DOCUMENT ID		TECN	COMMENT
0.35±0.08 OUR AVERAGE					
0.34±0.08±0.05		[8] AITALA	00	E791	π^- N, 500 GeV
$0.40^{+0.18}_{-0.13}$±0.09	12	BOZEK	93	NA32	π^- Cu 230 GeV

[8] AITALA 00 makes a coherent 5-dimensional amplitude analysis of 946 ± 38 $\Lambda_c^+ \to pK^-\pi^+$ decays.

$\Gamma(pK^-\pi^+ \text{nonresonant})/\Gamma(pK^-\pi^+)$ Γ_6/Γ_2

VALUE	EVTS	DOCUMENT ID		TECN	COMMENT
0.55±0.06 OUR AVERAGE					
0.55±0.06±0.04		[9] AITALA	00	E791	π^- N, 500 GeV
$0.56^{+0.07}_{-0.09}$±0.05	71	BOZEK	93	NA32	π^- Cu 230 GeV

[9] AITALA 00 makes a coherent 5-dimensional amplitude analysis of 946 ± 38 $\Lambda_c^+ \to pK^-\pi^+$ decays.

$\Gamma(p\overline{K}^0\pi^0)/\Gamma(pK^-\pi^+)$ Γ_7/Γ_2

VALUE	EVTS	DOCUMENT ID		TECN	COMMENT
0.66±0.05±0.07	774	ALAM	98	CLE2	$e^+e^- \approx \Upsilon(4S)$

$\Gamma(p\overline{K}^0\eta)/\Gamma(pK^-\pi^+)$ Γ_8/Γ_2

Unseen decay modes of the η are included.

VALUE	EVTS	DOCUMENT ID		TECN	COMMENT
0.25±0.04±0.04	57	AMMAR	95	CLE2	$e^+e^- \approx \Upsilon(4S)$

$\Gamma(p\overline{K}^0\pi^+\pi^-)/\Gamma(pK^-\pi^+)$ Γ_9/Γ_2

VALUE	EVTS	DOCUMENT ID		TECN	COMMENT
0.51±0.06 OUR AVERAGE					
0.52±0.04±0.05	985	ALAM	98	CLE2	$e^+e^- \approx \Upsilon(4S)$
0.43±0.12±0.04	83	AVERY	91	CLEO	e^+e^- 10.5 GeV
0.98±0.36±0.08	12	BARLAG	90D	NA32	π^- 230 GeV

$\Gamma(pK^-\pi^+\pi^0)/\Gamma(pK^-\pi^+)$ Γ_{10}/Γ_2

VALUE	EVTS	DOCUMENT ID		TECN	COMMENT
0.67±0.04±0.11	2606	ALAM	98	CLE2	$e^+e^- \approx \Upsilon(4S)$

$\Gamma(pK^*(892)^-\pi^+)/\Gamma(p\overline{K}^0\pi^+\pi^-)$ Γ_{11}/Γ_9

Unseen decay modes of the $K^*(892)^-$ are included.

VALUE	EVTS	DOCUMENT ID		TECN	COMMENT
0.44±0.14	17	ALEEV	94	BIS2	nN 20–70 GeV

$\Gamma(p(K^-\pi^+)_{\text{nonresonant}}\pi^0)/\Gamma(pK^-\pi^+)$ Γ_{12}/Γ_2

VALUE	EVTS	DOCUMENT ID		TECN	COMMENT
0.73±0.12±0.05	67	BOZEK	93	NA32	π^- Cu 230 GeV

$\Gamma(\Delta(1232)\overline{K}^*(892))/\Gamma_{total}$ Γ_{13}/Γ

VALUE	EVTS	DOCUMENT ID		TECN	COMMENT
seen	35	AMENDOLIA	87	SPEC	γGe-Si

$\Gamma(pK^-\pi^+\pi^+\pi^-)/\Gamma(pK^-\pi^+)$ Γ_{14}/Γ_2

VALUE	DOCUMENT ID		TECN	COMMENT
0.022±0.015	BARLAG	90D	NA32	π^- 230 GeV

$\Gamma(pK^-\pi^+\pi^0\pi^0)/\Gamma(pK^-\pi^+)$ Γ_{15}/Γ_2

VALUE	EVTS	DOCUMENT ID		TECN	COMMENT
0.16±0.07±0.03	15	BOZEK	93	NA32	π^- Cu 230 GeV

$\Gamma(pK^-\pi^+3\pi^0)/\Gamma(pK^-\pi^+)$ Γ_{16}/Γ_2

VALUE	EVTS	DOCUMENT ID		TECN	COMMENT
• • • We do not use the following data for averages, fits, limits, etc. • • •					
0.10±0.06±0.02	8	BOZEK	93	NA32	π^- Cu 230 GeV

Hadronic modes with a p: $S = 0$ final states

$\Gamma(p\pi^+\pi^-)/\Gamma(pK^-\pi^+)$ Γ_{17}/Γ_2

VALUE	DOCUMENT ID		TECN	COMMENT
0.069±0.036	BARLAG	90D	NA32	π^- 230 GeV

$\Gamma(p f_0(980))/\Gamma(p K^-\pi^+)$ Γ_{18}/Γ_2

Unseen decay modes of the $f_0(980)$ are included.

VALUE	DOCUMENT ID		TECN	COMMENT
0.055±0.036	BARLAG	90D	NA32	π^- 230 GeV

$\Gamma(p\pi^+\pi^+\pi^-\pi^-)/\Gamma(p K^-\pi^+)$ Γ_{19}/Γ_2

VALUE	DOCUMENT ID		TECN	COMMENT
0.036±0.023	BARLAG	90D	NA32	π^- 230 GeV

$\Gamma(p K^+ K^-)/\Gamma(p K^-\pi^+)$ Γ_{20}/Γ_2

VALUE	EVTS	DOCUMENT ID		TECN	COMMENT
0.015±0.006 OUR AVERAGE		Error includes scale factor of 2.1.			
0.014±0.002±0.002	676	ABE	02C	BELL	$e^+e^- \approx \Upsilon(4S)$
0.039±0.009±0.007	214	ALEXANDER	96C	CLE2	$e^+e^- \approx \Upsilon(4S)$
• • • We do not use the following data for averages, fits, limits, etc. • • •					
0.096±0.029±0.010	30	FRABETTI	93H	E687	γBe, $\overline{E}_\gamma$ 220 GeV
0.048±0.027		BARLAG	90D	NA32	π^- 230 GeV

$\Gamma(p\phi)/\Gamma(p K^-\pi^+)$ Γ_{21}/Γ_2

Unseen decay modes of the ϕ are included.

VALUE	EVTS	DOCUMENT ID		TECN	COMMENT
0.0164±0.0032 OUR AVERAGE		Error includes scale factor of 1.2.			
0.015 ±0.002 ±0.002	345	ABE	02C	BELL	$e^+e^- \approx \Upsilon(4S)$
0.024 ±0.006 ±0.003	54	ALEXANDER	96C	CLE2	$e^+e^- \approx \Upsilon(4S)$
• • • We do not use the following data for averages, fits, limits, etc. • • •					
0.040 ±0.027		BARLAG	90D	NA32	π^- 230 GeV

$\Gamma(p K^+ K^-\text{non-}\phi)/\Gamma(p K^-\pi^+)$ Γ_{22}/Γ_2

VALUE	EVTS	DOCUMENT ID		TECN	COMMENT
0.007±0.002±0.002	344	ABE	02C	BELL	$e^+e^- \approx \Upsilon(4S)$

Hadronic modes with a hyperon: $S = -1$ final states

$\Gamma(\Lambda\pi^+)/\Gamma(p K^-\pi^+)$ Γ_{23}/Γ_2

VALUE	CL%	EVTS	DOCUMENT ID		TECN	COMMENT
0.214±0.016 OUR FIT			Error includes scale factor of 1.1.			
0.204±0.019 OUR AVERAGE						
0.217±0.013±0.020		750	LINK	05F	FOCS	γ nucleus, $\overline{E}_\gamma \approx 180$ GeV
0.18 ±0.03 ±0.04			ALBRECHT	92	ARG	$e^+e^- \approx 10.4$ GeV
0.18 ±0.03 ±0.03		87	AVERY	91	CLEO	e^+e^- 10.5 GeV
• • • We do not use the following data for averages, fits, limits, etc. • • •						
<0.33	90		ANJOS	90	E691	γBe 70–260 GeV
<0.16	90		ALBRECHT	88C	ARG	e^+e^- 10 GeV

$\Gamma(\Lambda\pi^+\pi^0)/\Gamma(p K^-\pi^+)$ Γ_{24}/Γ_2

VALUE	EVTS	DOCUMENT ID		TECN	COMMENT
0.73±0.09±0.16	464	AVERY	94	CLE2	$e^+e^- \approx \Upsilon(3S), \Upsilon(4S)$

$\Gamma(\Lambda\rho^+)/\Gamma(p K^-\pi^+)$ Γ_{25}/Γ_2

VALUE	CL%	DOCUMENT ID		TECN	COMMENT
<0.95	95	AVERY	94	CLE2	$e^+e^- \approx \Upsilon(3S), \Upsilon(4S)$

$\Gamma(\Lambda\pi^+\pi^+\pi^-)/\Gamma(p K^-\pi^+)$ Γ_{26}/Γ_2

VALUE	EVTS	DOCUMENT ID		TECN	COMMENT
0.525±0.032 OUR FIT					
0.522±0.032 OUR AVERAGE					
0.508±0.024±0.024	1356	LINK	05F	FOCS	γ nucleus, $\overline{E}_\gamma \approx 180$ GeV
0.65 ±0.11 ±0.12	289	AVERY	91	CLEO	e^+e^- 10.5 GeV
0.82 ±0.29 ±0.27	44	ANJOS	90	E691	γBe 70–260 GeV
0.94 ±0.41 ±0.13	10	BARLAG	90D	NA32	π^- 230 GeV
0.61 ±0.16 ±0.04	105	ALBRECHT	88C	ARG	e^+e^- 10 GeV

$\Gamma(\Sigma(1385)^+\pi^+\pi^-, \Sigma^{*+} \to \Lambda\pi^+)/\Gamma(\Lambda\pi^+\pi^+\pi^-)$ Γ_{27}/Γ_{26}

VALUE	DOCUMENT ID		TECN	COMMENT
0.28±0.10±0.08	LINK	05F	FOCS	γ nucleus, $\overline{E}_\gamma \approx 180$ GeV

$\Gamma(\Sigma(1385)^-\pi^+\pi^+, \Sigma^{*-} \to \Lambda\pi^-)/\Gamma(\Lambda\pi^+\pi^+\pi^-)$ Γ_{28}/Γ_{26}

VALUE	DOCUMENT ID		TECN	COMMENT
0.21±0.03±0.02	LINK	05F	FOCS	γ nucleus, $\overline{E}_\gamma \approx 180$ GeV

$\Gamma(\Lambda\pi^+\rho^0)/\Gamma(\Lambda\pi^+\pi^+\pi^-)$ Γ_{29}/Γ_{26}

VALUE	DOCUMENT ID		TECN	COMMENT
0.40±0.12±0.12	LINK	05F	FOCS	γ nucleus, $\overline{E}_\gamma \approx 180$ GeV

$\Gamma(\Sigma(1385)^+\rho^0, \Sigma^{*+} \to \Lambda\pi^+)/\Gamma(\Lambda\pi^+\pi^+\pi^-)$ Γ_{30}/Γ_{26}

VALUE	DOCUMENT ID		TECN	COMMENT
0.14±0.09±0.07	LINK	05F	FOCS	γ nucleus, $\overline{E}_\gamma \approx 180$ GeV

$\Gamma(\Lambda\pi^+\pi^+\pi^-\text{nonresonant})/\Gamma(\Lambda\pi^+\pi^+\pi^-)$ Γ_{31}/Γ_{26}

VALUE	CL%	DOCUMENT ID		TECN	COMMENT
<0.3	90	LINK	05F	FOCS	γ nucleus, $\overline{E}_\gamma \approx 180$ GeV

$\Gamma(p\overline{K}^0\pi^+\pi^-)/\Gamma(\Lambda\pi^+\pi^+\pi^-)$ Γ_9/Γ_{26}

VALUE	EVTS	DOCUMENT ID		TECN	COMMENT
• • • We do not use the following data for averages, fits, limits, etc. • • •					
2.6±1.2		ALEEV	96	SPEC	n nucleus, 50 GeV/c
4.3±1.2	130	ALEEV	84	BIS2	nC 40–70 GeV

$\Gamma(\Lambda\pi^+\pi^+\pi^-\pi^0\text{total})/\Gamma(p K^-\pi^+)$ Γ_{32}/Γ_2

VALUE	EVTS	DOCUMENT ID		TECN	COMMENT
0.36±0.09±0.09	50	[10] CRONIN-HEN...03		CLE3	$e^+e^- \approx \Upsilon(4S)$

[10] CRONIN-HENNESSY 03 finds this channel to be dominantly $\Lambda\eta\pi^+$ and $\Lambda\omega\pi^+$; see below.

$\Gamma(\Lambda\pi^+\eta)/\Gamma(p K^-\pi^+)$ Γ_{33}/Γ_2

Unseen decay modes of the η are included.

VALUE	EVTS	DOCUMENT ID		TECN	COMMENT
0.36±0.07 OUR AVERAGE					
0.41±0.17±0.10	11	CRONIN-HEN...03		CLE3	$e^+e^- \approx \Upsilon(4S)$
0.35±0.05±0.06	116	AMMAR	95	CLE2	$e^+e^- \approx \Upsilon(4S)$

$\Gamma(\Sigma(1385)^+\eta)/\Gamma(p K^-\pi^+)$ Γ_{34}/Γ_2

Unseen decay modes of the $\Sigma(1385)^+$ and η are included.

VALUE	EVTS	DOCUMENT ID		TECN	COMMENT
0.17±0.04±0.03	54	AMMAR	95	CLE2	$e^+e^- \approx \Upsilon(4S)$

$\Gamma(\Lambda\pi^+\omega)/\Gamma(p K^-\pi^+)$ Γ_{35}/Γ_2

Unseen decay modes of the ω are included.

VALUE	EVTS	DOCUMENT ID		TECN	COMMENT
0.24±0.06±0.06	32	CRONIN-HEN...03		CLE3	$e^+e^- \approx \Upsilon(4S)$

$\Gamma(\Lambda\pi^+\pi^+\pi^-\pi^0, \text{no } \eta \text{ or } \omega)/\Gamma(p K^-\pi^+)$ Γ_{36}/Γ_2

VALUE	CL%	DOCUMENT ID		TECN	COMMENT
<0.13	90	CRONIN-HEN...03		CLE3	$e^+e^- \approx \Upsilon(4S)$

$\Gamma(\Lambda K^+\overline{K}^0)/\Gamma(p K^-\pi^+)$ Γ_{37}/Γ_2

VALUE	EVTS	DOCUMENT ID		TECN	COMMENT
0.093±0.018 OUR FIT		Error includes scale factor of 1.7.			
0.131±0.020 OUR AVERAGE					
0.142±0.018±0.022	251	LINK	05F	FOCS	γ nucleus, $\overline{E}_\gamma \approx 180$ GeV
0.12 ±0.02 ±0.02	59	AMMAR	95	CLE2	$e^+e^- \approx \Upsilon(4S)$

$\Gamma(\Xi(1690)^0 K^+, \Xi^{*0} \to \Lambda\overline{K}^0)/\Gamma(\Lambda K^+\overline{K}^0)$ Γ_{38}/Γ_{37}

VALUE	EVTS	DOCUMENT ID		TECN	COMMENT
0.28±0.07 OUR AVERAGE					
0.32±0.10±0.04	84±24	LINK	05F	FOCS	γ nucleus, $\overline{E}_\gamma \approx 180$ GeV
0.26±0.08±0.03	93	ABE	02C	BELL	$e^+e^- \approx \Upsilon(4S)$

$\Gamma(\Lambda K^+\overline{K}^0)/\Gamma(\Lambda\pi^+)$ Γ_{37}/Γ_{23}

VALUE	EVTS	DOCUMENT ID		TECN	COMMENT
0.43 ±0.08 OUR FIT		Error includes scale factor of 2.0.			
0.395±0.026±0.036	460 ± 30	AUBERT	07U	BABR	$e^+e^- \approx \Upsilon(4S)$

$\Gamma(\Sigma^0\pi^+)/\Gamma(p K^-\pi^+)$ Γ_{39}/Γ_2

VALUE	EVTS	DOCUMENT ID		TECN	COMMENT
0.210±0.018 OUR FIT					
0.20 ±0.04 OUR AVERAGE					
0.21 ±0.02 ±0.04	196	AVERY	94	CLE2	$e^+e^- \approx \Upsilon(3S), \Upsilon(4S)$
0.17 ±0.06 ±0.04		ALBRECHT	92	ARG	$e^+e^- \approx 10.4$ GeV

$\Gamma(\Sigma^0\pi^+)/\Gamma(\Lambda\pi^+)$ Γ_{39}/Γ_{23}

VALUE	EVTS	DOCUMENT ID		TECN	COMMENT
0.98 ±0.05 OUR FIT					
0.98 ±0.05 OUR AVERAGE					
0.977±0.015±0.051	33k	AUBERT	07U	BABR	$e^+e^- \approx \Upsilon(4S)$
1.09 ±0.11 ±0.19	750	LINK	05F	FOCS	γ nucleus, $\overline{E}_\gamma \approx 180$ GeV

$\Gamma(\Sigma^+\pi^0)/\Gamma(p K^-\pi^+)$ Γ_{40}/Γ_2

VALUE	EVTS	DOCUMENT ID		TECN	COMMENT
0.20±0.03±0.03	93	KUBOTA	93	CLE2	$e^+e^- \approx \Upsilon(4S)$

$\Gamma(\Sigma^+\eta)/\Gamma(p K^-\pi^+)$ Γ_{41}/Γ_2

Unseen decay modes of the η are included.

VALUE	EVTS	DOCUMENT ID		TECN	COMMENT
0.11±0.03±0.02	26	AMMAR	95	CLE2	$e^+e^- \approx \Upsilon(4S)$

$\Gamma(\Sigma^+\pi^+\pi^-)/\Gamma(p K^-\pi^+)$ Γ_{42}/Γ_2

VALUE	EVTS	DOCUMENT ID		TECN	COMMENT
0.72±0.07 OUR FIT					
0.69±0.08 OUR AVERAGE					
0.72±0.14	47 ± 9	VAZQUEZ-JA...08		SELX	Σ^- nucleus, 600 GeV
0.74±0.07±0.09	487	KUBOTA	93	CLE2	$e^+e^- \approx \Upsilon(4S)$
$0.54^{+0.18}_{-0.15}$	11	BARLAG	92	NA32	π^- Cu 230 GeV

$\Gamma(\Sigma^+\rho^0)/\Gamma(p K^-\pi^+)$ Γ_{43}/Γ_2

VALUE	CL%	DOCUMENT ID		TECN	COMMENT
<0.27	95	KUBOTA	93	CLE2	$e^+e^- \approx \Upsilon(4S)$

$\Gamma(\Sigma^-\pi^+\pi^+)/\Gamma(pK^-\pi^+)$ Γ_{44}/Γ_2

VALUE	EVTS	DOCUMENT ID		TECN	COMMENT
0.33 ±0.06 OUR FIT					
0.314±0.067	30 ± 6	VAZQUEZ-JA...08		SELX	Σ^- nucleus, 600 GeV

$\Gamma(\Sigma^-\pi^+\pi^+)/\Gamma(\Sigma^+\pi^+\pi^-)$ Γ_{44}/Γ_{42}

VALUE	EVTS	DOCUMENT ID		TECN	COMMENT
0.46±0.09 OUR FIT					
0.53±0.15±0.07	56	FRABETTI	94E	E687	γBe, $\overline{E}_\gamma$ 220 GeV

$\Gamma(\Sigma^0\pi^+\pi^0)/\Gamma(pK^-\pi^+)$ Γ_{45}/Γ_2

VALUE	EVTS	DOCUMENT ID		TECN	COMMENT
0.36±0.09±0.10	117	AVERY	94	CLE2	$e^+e^- \approx \Upsilon(3S), \Upsilon(4S)$

$\Gamma(\Sigma^0\pi^+\pi^+\pi^-)/\Gamma(pK^-\pi^+)$ Γ_{46}/Γ_2

VALUE	EVTS	DOCUMENT ID		TECN	COMMENT
0.17±0.04 OUR FIT					
0.21±0.05±0.05	90	AVERY	94	CLE2	$e^+e^- \approx \Upsilon(3S), \Upsilon(4S)$

$\Gamma(\Sigma^0\pi^+\pi^+\pi^-)/\Gamma(\Lambda\pi^+\pi^+\pi^-)$ Γ_{46}/Γ_{26}

VALUE	EVTS	DOCUMENT ID		TECN	COMMENT
0.31±0.08 OUR FIT					
0.26±0.06±0.09	480	LINK	05F	FOCS	γ nucleus, $\overline{E}_\gamma \approx 180$ GeV

$\Gamma(\Sigma^+\omega)/\Gamma(pK^-\pi^+)$ Γ_{48}/Γ_2

Unseen decay modes of the ω are included.

VALUE	EVTS	DOCUMENT ID		TECN	COMMENT
0.54±0.13±0.06	107	KUBOTA	93	CLE2	$e^+e^- \approx \Upsilon(4S)$

$\Gamma(\Sigma^+K^+K^-)/\Gamma(pK^-\pi^+)$ Γ_{49}/Γ_2

VALUE	EVTS	DOCUMENT ID		TECN	COMMENT
0.056±0.008 OUR FIT					
0.070±0.011±0.011	59	AVERY	93	CLE2	$e^+e^- \approx 10.5$ GeV

$\Gamma(\Sigma^+K^+K^-)/\Gamma(\Sigma^+\pi^+\pi^-)$ Γ_{49}/Γ_{42}

VALUE	EVTS	DOCUMENT ID		TECN	COMMENT
0.078±0.009 OUR FIT					
0.074±0.009 OUR AVERAGE					
0.076±0.007±0.009	246	ABE	02C	BELL	$e^+e^- \approx \Upsilon(4S)$
0.071±0.011±0.011	103	LINK	02G	FOCS	γ nucleus, ≈ 180 GeV

$\Gamma(\Sigma^+\phi)/\Gamma(pK^-\pi^+)$ Γ_{50}/Γ_2

Unseen decay modes of the ϕ are included.

VALUE	EVTS	DOCUMENT ID		TECN	COMMENT
0.062±0.010 OUR FIT					
0.069±0.023±0.016	26	AVERY	93	CLE2	$e^+e^- \approx 10.5$ GeV

$\Gamma(\Sigma^+\phi)/\Gamma(\Sigma^+\pi^+\pi^-)$ Γ_{50}/Γ_{42}

Unseen decay modes of the ϕ are included.

VALUE	EVTS	DOCUMENT ID		TECN	COMMENT
0.087±0.012 OUR FIT					
0.086±0.012 OUR AVERAGE					
0.085±0.012±0.012	129	ABE	02C	BELL	$e^+e^- \approx \Upsilon(4S)$
0.087±0.016±0.006	57	LINK	02G	FOCS	γ nucleus, ≈ 180 GeV

$\Gamma(\Xi(1690)^0K^+, \Xi^{*0}\to\Sigma^+K^-)/\Gamma(\Sigma^+\pi^+\pi^-)$ Γ_{51}/Γ_{42}

VALUE	EVTS	DOCUMENT ID		TECN	COMMENT
0.023±0.005 OUR AVERAGE					
0.023±0.005±0.005	75	ABE	02C	BELL	$e^+e^- \approx \Upsilon(4S)$
0.022±0.006±0.006	34	LINK	02G	FOCS	γ nucleus, ≈ 180 GeV

$\Gamma(\Sigma^+K^+K^-$ nonresonant$)/\Gamma(\Sigma^+\pi^+\pi^-)$ Γ_{52}/Γ_{42}

VALUE	CL%	DOCUMENT ID		TECN	COMMENT
<0.018	90	ABE	02C	BELL	$e^+e^- \approx \Upsilon(4S)$
• • • We do not use the following data for averages, fits, limits, etc. • • •					
<0.028	90	LINK	02G	FOCS	γ nucleus, ≈ 180 GeV

$\Gamma(\Xi^0K^+)/\Gamma(pK^-\pi^+)$ Γ_{53}/Γ_2

VALUE	EVTS	DOCUMENT ID		TECN	COMMENT
0.078±0.013±0.013	56	AVERY	93	CLE2	$e^+e^- \approx 10.5$ GeV

$\Gamma(\Xi^-K^+\pi^+)/\Gamma(pK^-\pi^+)$ Γ_{54}/Γ_2

VALUE	EVTS	DOCUMENT ID		TECN	COMMENT
0.102±0.010 OUR FIT Error includes scale factor of 1.1.					
0.098±0.021 OUR AVERAGE Error includes scale factor of 1.3. See the ideogram below.					
0.14 ±0.03 ±0.02	34	ALBRECHT	95B	ARG	$e^+e^- \approx 10.4$ GeV
0.079±0.013±0.014	60	AVERY	93	CLE2	$e^+e^- \approx 10.5$ GeV
0.15 ±0.04 ±0.03	30	AVERY	91	CLEO	e^+e^- 10.5 GeV

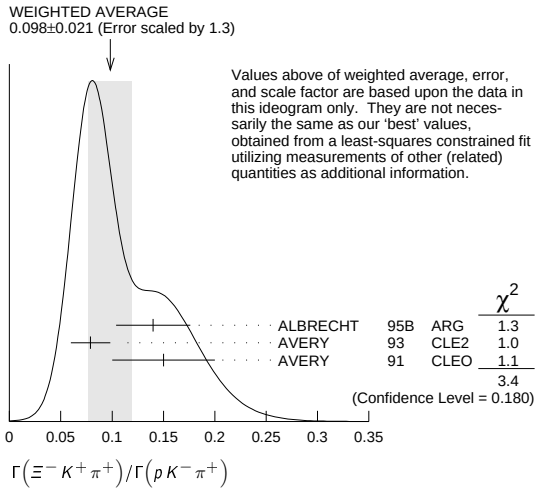

$\Gamma(\Xi(1530)^0K^+)/\Gamma(pK^-\pi^+)$ Γ_{55}/Γ_2

Unseen decay modes of the $\Xi(1530)^0$ are included.

VALUE	EVTS	DOCUMENT ID		TECN	COMMENT
0.052±0.014 OUR AVERAGE					
0.05 ±0.02 ±0.01	11	ALBRECHT	95B	ARG	$e^+e^- \approx 10.4$ GeV
0.053±0.016±0.010	24	AVERY	93	CLE2	$e^+e^- \approx 10.5$ GeV

$\Gamma(\Xi^-K^+\pi^+)/\Gamma(\Lambda\pi^+)$ Γ_{54}/Γ_{23}

VALUE	EVTS	DOCUMENT ID		TECN	COMMENT
0.47 ±0.04 OUR FIT					
0.480±0.016±0.039	2665 ± 84	AUBERT	07U	BABR	$e^+e^- \approx \Upsilon(4S)$

Hadronic modes with a hyperon: $S = 0$ final states

$\Gamma(\Lambda K^+)/\Gamma(\Lambda\pi^+)$ Γ_{56}/Γ_{23}

VALUE	EVTS	DOCUMENT ID		TECN	COMMENT
0.047±0.009 OUR AVERAGE Error includes scale factor of 1.8.					
0.044±0.004±0.003	1162±101	AUBERT	07U	BABR	$e^+e^- \approx \Upsilon(4S)$
0.074±0.010±0.012	265	ABE	02C	BELL	$e^+e^- \approx \Upsilon(4S)$

$\Gamma(\Lambda K^+\pi^+\pi^-)/\Gamma(\Lambda\pi^+)$ Γ_{57}/Γ_{23}

VALUE	CL%	DOCUMENT ID		TECN	COMMENT
<4.1 × 10⁻²	90	AUBERT	07U	BABR	$e^+e^- \approx \Upsilon(4S)$

$\Gamma(\Sigma^0K^+)/\Gamma(\Sigma^0\pi^+)$ Γ_{58}/Γ_{39}

VALUE	EVTS	DOCUMENT ID		TECN	COMMENT
0.040±0.006 OUR AVERAGE					
0.038±0.005±0.003	366 ± 52	AUBERT	07U	BABR	$e^+e^- \approx \Upsilon(4S)$
0.056±0.014±0.008	75	ABE	02C	BELL	$e^+e^- \approx \Upsilon(4S)$

$\Gamma(\Sigma^0K^+\pi^+\pi^-)/\Gamma(\Sigma^0\pi^+)$ Γ_{59}/Γ_{39}

VALUE	CL%	DOCUMENT ID		TECN	COMMENT
<2.0 × 10⁻²	90	AUBERT	07U	BABR	$e^+e^- \approx \Upsilon(4S)$

$\Gamma(\Sigma^+K^+\pi^-)/\Gamma(\Sigma^+\pi^+\pi^-)$ Γ_{60}/Γ_{42}

VALUE	EVTS	DOCUMENT ID		TECN	COMMENT
0.047±0.011±0.008	105	ABE	02C	BELL	$e^+e^- \approx \Upsilon(4S)$

$\Gamma(\Sigma^+K^*(892)^0)/\Gamma(\Sigma^+\pi^+\pi^-)$ Γ_{61}/Γ_{42}

Unseen decay modes of the $K^*(892)^0$ are included.

VALUE	EVTS	DOCUMENT ID		TECN	COMMENT
0.078±0.018±0.013	49	LINK	02G	FOCS	γ nucleus, ≈ 180 GeV

$\Gamma(\Sigma^-K^+\pi^+)/\Gamma(\Sigma^+K^*(892)^0)$ Γ_{62}/Γ_{61}

VALUE	CL%	DOCUMENT ID		TECN	COMMENT
<0.35	90	LINK	02G	FOCS	γ nucleus, ≈ 180 GeV

Doubly Cabibbo-suppressed modes

$\Gamma(pK^+\pi^-)/\Gamma(pK^-\pi^+)$ Γ_{63}/Γ_2

VALUE	CL%	DOCUMENT ID		TECN	COMMENT
<0.0046	90	LINK	05K	FOCS	R = (0.05 ± 0.26 ± 0.02)%

Semileptonic modes

$\Gamma(\Lambda\ell^+\nu_\ell)/\Gamma(pK^-\pi^+)$ Γ_{64}/Γ_2

We average here the averages of the next two data blocks.

VALUE	DOCUMENT ID		COMMENT
0.41±0.05 OUR AVERAGE			
0.42±0.07	PDG	02	Our $\Gamma(\Lambda e^+\nu_e)/\Gamma(pK^-\pi^+)$
0.39±0.08	PDG	02	Our $\Gamma(\Lambda\mu^+\nu_\mu)/\Gamma(pK^-\pi^+)$

$\Gamma(\Lambda e^+ \nu_e)/\Gamma(p K^- \pi^+)$ Γ_{65}/Γ_2

VALUE	DOCUMENT ID		TECN	COMMENT
0.42±0.07 OUR AVERAGE				
0.43±0.08	[11,12] BERGFELD	94	CLE2	$e^+e^- \approx \Upsilon(4S)$
0.38±0.14	[12,13] ALBRECHT	91G	ARG	$e^+e^- \approx 10.4$ GeV

[11] BERGFELD 94 measures $\sigma(e^+e^- \to \Lambda_c^+ X)\cdot B(\Lambda_c^+ \to \Lambda e^+ \nu_e) = (4.87 \pm 0.28 \pm 0.69)$ pb.

[12] To extract $\Gamma(\Lambda_c^+ \to \Lambda e^+ \nu_e)/\Gamma(\Lambda_c^+ \to p K^- \pi^+)$, we use $\sigma(e^+e^- \to \Lambda_c^+ X)\cdot B(\Lambda_c \to p K^- \pi^+) = (11.2 \pm 1.3)$ pb, which is the weighted average of measurements from ARGUS (ALBRECHT 96E) and CLEO (AVERY 91).

[13] ALBRECHT 91G measures $\sigma(e^+e^- \to \Lambda_c^+ X)\cdot B(\Lambda_c^+ \to \Lambda e^+ \nu_e) = (4.20 \pm 1.28 \pm 0.71)$ pb.

$\Gamma(\Lambda \mu^+ \nu_\mu)/\Gamma(p K^- \pi^+)$ Γ_{66}/Γ_2

VALUE	DOCUMENT ID		TECN	COMMENT
0.39±0.08 OUR AVERAGE				
0.40±0.09	[14,15] BERGFELD	94	CLE2	$e^+e^- \approx \Upsilon(4S)$
0.35±0.20	[15,16] ALBRECHT	91G	ARG	$e^+e^- \approx 10.4$ GeV

[14] BERGFELD 94 measures $\sigma(e^+e^- \to \Lambda_c^+ X)\cdot B(\Lambda_c^+ \to \Lambda \mu^+ \nu_\mu) = (4.43 \pm 0.51 \pm 0.64)$ pb.

[15] To extract $\Gamma(\Lambda_c^+ \to \Lambda \mu^+ \nu_\mu)/\Gamma(\Lambda_c^+ \to p K^- \pi^+)$, we use $\sigma(e^+e^- \to \Lambda_c^+ X)\cdot B(\Lambda_c \to p K^- \pi^+) = (11.2 \pm 1.3)$ pb, which is the weighted average of measurements from ARGUS (ALBRECHT 96E) and CLEO (AVERY 91).

[16] ALBRECHT 91G measures $\sigma(e^+e^- \to \Lambda_c^+ X)\cdot B(\Lambda_c^+ \to \Lambda \mu^+ \nu_\mu) = (3.91 \pm 2.02 \pm 0.90)$ pb.

Inclusive modes

$\Gamma(e^+ \text{anything})/\Gamma_{\text{total}}$ Γ_{67}/Γ

VALUE	DOCUMENT ID		TECN	COMMENT
0.045±0.017	VELLA	82	MRK2	e^+e^- 4.5–6.8 GeV

$\Gamma(p e^+ \text{anything})/\Gamma_{\text{total}}$ Γ_{68}/Γ

VALUE	DOCUMENT ID		TECN	COMMENT
0.018±0.009	[17] VELLA	82	MRK2	e^+e^- 4.5–6.8 GeV

[17] VELLA 82 includes protons from Λ decay.

$\Gamma(\Lambda e^+ \text{anything})/\Gamma_{\text{total}}$ Γ_{69}/Γ

VALUE	DOCUMENT ID		TECN	COMMENT
• • • We do not use the following data for averages, fits, limits, etc. • • •				
0.011±0.008	[18] VELLA	82	MRK2	e^+e^- 4.5–6.8 GeV

[18] VELLA 82 includes Λ's from Σ^0 decay.

$\Gamma(p \text{ anything})/\Gamma_{\text{total}}$ Γ_{70}/Γ

VALUE	DOCUMENT ID		TECN	COMMENT
0.50±0.08±0.14	[19] CRAWFORD	92	CLEO	e^+e^- 10.5 GeV

[19] This CRAWFORD 92 value includes protons from Λ decay. The value is model dependent, but account is taken of this in the systematic error.

$\Gamma(p \text{ anything (no } \Lambda))/\Gamma_{\text{total}}$ Γ_{71}/Γ

VALUE	DOCUMENT ID		TECN	COMMENT
0.12±0.10±0.16	CRAWFORD	92	CLEO	e^+e^- 10.5 GeV

$\Gamma(n \text{ anything})/\Gamma_{\text{total}}$ Γ_{73}/Γ

VALUE	DOCUMENT ID		TECN	COMMENT
0.50±0.08±0.14	[20] CRAWFORD	92	CLEO	e^+e^- 10.5 GeV

[20] This CRAWFORD 92 value includes neutrons from Λ decay. The value is model dependent, but account is taken of this in the systematic error.

$\Gamma(n \text{ anything (no } \Lambda))/\Gamma_{\text{total}}$ Γ_{74}/Γ

VALUE	DOCUMENT ID		TECN	COMMENT
0.29±0.09±0.15	CRAWFORD	92	CLEO	e^+e^- 10.5 GeV

$\Gamma(p \text{ hadrons})/\Gamma_{\text{total}}$ Γ_{72}/Γ

VALUE	DOCUMENT ID		TECN	COMMENT
• • • We do not use the following data for averages, fits, limits, etc. • • •				
0.41±0.24	ADAMOVICH	87	EMUL	γA 20–70 GeV/c

$\Gamma(\Lambda \text{ anything})/\Gamma_{\text{total}}$ Γ_{75}/Γ

VALUE	EVTS	DOCUMENT ID		TECN	COMMENT
0.35±0.11 OUR AVERAGE		Error includes scale factor of 1.4. See the ideogram below.			
0.59±0.10±0.12		CRAWFORD	92	CLEO	e^+e^- 10.5 GeV
0.49±0.24		ADAMOVICH	87	EMUL	γA 20–70 GeV/c
0.23±0.10	8	[21] ABE	86	HYBR	20 GeV γp

[21] ABE 86 includes Λ's from Σ^0 decay.

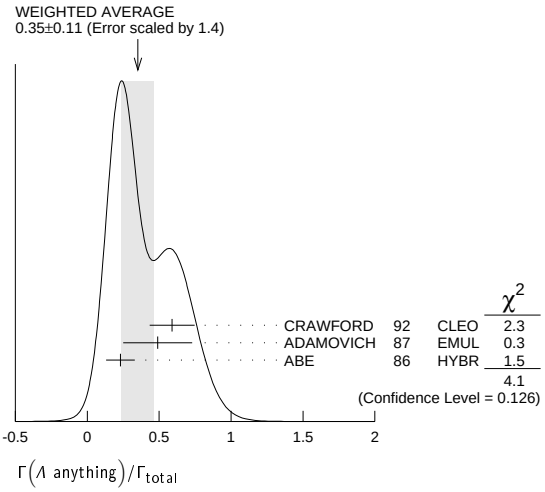

$\Gamma(\Sigma^\pm \text{anything})/\Gamma_{\text{total}}$ Γ_{76}/Γ

VALUE	EVTS	DOCUMENT ID		TECN	COMMENT
0.1±0.05	5	ABE	86	HYBR	20 GeV γp

$\Gamma(3\text{prongs})/\Gamma_{\text{total}}$ Γ_{77}/Γ

VALUE	DOCUMENT ID	TECN	COMMENT
0.24±0.07±0.04	KAYIS-TOPAK.03	CHRS	ν_μ emulsion, $\overline{E}$=27 GeV

Rare or forbidden modes

$\Gamma(p e^+ e^-)/\Gamma_{\text{total}}$ Γ_{78}/Γ

A test for the ΔC=1 weak neutral current. Allowed by higher-order electroweak interactions.

VALUE	CL%	EVTS	DOCUMENT ID		TECN	COMMENT
<5.5 × 10^{-6}	90	4.0±7.1	LEES	11G	BABR	$e^+e^- \approx \Upsilon(4S)$

$\Gamma(p \mu^+ \mu^-)/\Gamma_{\text{total}}$ Γ_{79}/Γ

A test for the ΔC=1 weak neutral current. Allowed by higher-order electroweak interactions.

VALUE	CL%	EVTS	DOCUMENT ID		TECN	COMMENT
<44 × 10^{-6}	90	11.1±5.6	LEES	11G	BABR	$e^+e^- \approx \Upsilon(4S)$
• • • We do not use the following data for averages, fits, limits, etc. • • •						
< 3.4 × 10^{-4}	90	0	KODAMA	95	E653	π^- emulsion 600 GeV

$\Gamma(p e^+ \mu^-)/\Gamma_{\text{total}}$ Γ_{80}/Γ

A test of lepton family-number conservation.

VALUE	CL%	EVTS	DOCUMENT ID		TECN	COMMENT
<9.9 × 10^{-6}	90	−0.7±3.0	LEES	11G	BABR	$e^+e^- \approx \Upsilon(4S)$

$\Gamma(p e^- \mu^+)/\Gamma_{\text{total}}$ Γ_{81}/Γ

A test of lepton family-number conservation.

VALUE	CL%	EVTS	DOCUMENT ID		TECN	COMMENT
<19 × 10^{-6}	90	6.2±4.9	LEES	11G	BABR	$e^+e^- \approx \Upsilon(4S)$

$\Gamma(\overline{p} 2e^+)/\Gamma_{\text{total}}$ Γ_{82}/Γ

A test of lepton- and baryon-number conservation.

VALUE	CL%	EVTS	DOCUMENT ID		TECN	COMMENT
<2.7 × 10^{-6}	90	−1.5±4.5	LEES	11G	BABR	$e^+e^- \approx \Upsilon(4S)$

$\Gamma(\overline{p} 2\mu^+)/\Gamma_{\text{total}}$ Γ_{83}/Γ

A test of lepton- and baryon-number conservation and of lepton family-number conservation.

VALUE	CL%	EVTS	DOCUMENT ID		TECN	COMMENT
<9.4 × 10^{-6}	90	0.0±2.2	LEES	11G	BABR	$e^+e^- \approx \Upsilon(4S)$

$\Gamma(\overline{p} e^+ \mu^+)/\Gamma_{\text{total}}$ Γ_{84}/Γ

A test of lepton- and baryon-number conservation and of lepton family-number conservation.

VALUE	CL%	EVTS	DOCUMENT ID		TECN	COMMENT
<16 × 10^{-6}	90	10.1±6.8	LEES	11G	BABR	$e^+e^- \approx \Upsilon(4S)$

$\Gamma(\Sigma^- \mu^+ \mu^+)/\Gamma_{\text{total}}$ Γ_{85}/Γ

A test of lepton-number conservation.

VALUE	CL%	EVTS	DOCUMENT ID		TECN	COMMENT
<7.0 × 10^{-4}	90	0	KODAMA	95	E653	π^- emulsion 600 GeV

Baryon Particle Listings

Λ_c^+, $\Lambda_c(2595)^+$

Λ_c^+ DECAY PARAMETERS

See the note on "Baryon Decay Parameters" in the neutron Listings.

α FOR $\Lambda_c^+ \to \Lambda\pi^+$

VALUE	EVTS	DOCUMENT ID		TECN	COMMENT
−0.91±0.15 OUR AVERAGE					
−0.78±0.16±0.19		LINK	06A	FOCS	γ A, $\overline{E}_\gamma \approx$ 180 GeV
−0.94±0.21±0.12	414	[22] BISHAI	95	CLE2	$e^+e^- \approx \Upsilon(4S)$
−0.96±0.42		ALBRECHT	92	ARG	$e^+e^- \approx$ 10.4 GeV
−1.1 ±0.4	86	AVERY	90B	CLEO	$e^+e^- \approx$ 10.6 GeV

[22] BISHAI 95 actually gives $\alpha = -0.94^{+0.21}_{-0.06}{}^{+0.12}_{-0.06}$, chopping the errors at the physical limit −1.0. However, for $\alpha \approx -1.0$, some experiments should *get* unphysical values ($\alpha < -1.0$), and for averaging with other measurements such values (or errors that extend below −1.0) should *not* be chopped.

α FOR $\Lambda_c^+ \to \Sigma^+\pi^0$

VALUE	EVTS	DOCUMENT ID		TECN	COMMENT
−0.45±0.31±0.06	89	BISHAI	95	CLE2	$e^+e^- \approx \Upsilon(4S)$

α FOR $\Lambda_c^+ \to \Lambda\ell^+\nu_\ell$

The experiments don't cover the complete (or same incomplete) $M(\Lambda\ell^+)$ range, but we average them together anyway.

VALUE	EVTS	DOCUMENT ID		TECN	COMMENT
−0.86±0.04 OUR AVERAGE					
−0.86±0.03±0.02	3201	[23] HINSON	05	CLEO	$e^+e^- \approx \Upsilon(4S)$
−0.91±0.42±0.25		[24] ALBRECHT	94B	ARG	$e^+e^- \approx$ 10 GeV
• • • We do not use the following data for averages, fits, limits, etc. • • •					
$-0.82^{+0.09}_{-0.06}{}^{+0.06}_{-0.03}$	700	[25] CRAWFORD	95	CLE2	See HINSON 05
$-0.89^{+0.17}_{-0.11}{}^{+0.09}_{-0.05}$	350	[26] BERGFELD	94	CLE2	See CRAWFORD 95

[23] HINSON 05 measures the form-factor ratio $R \equiv f_2/f_1$ for $\Lambda_c^+ \to \Lambda e^+\nu_e$ events to be $-0.31 \pm 0.05 \pm 0.04$ and the pole mass to be $2.21 \pm 0.08 \pm 0.14$ GeV/c^2, and from these calculates α, averaged over q^2, where $\langle q^2\rangle = 0.67$ (GeV/c)^2.

[24] ALBRECHT 94B uses Λe^+ and $\Lambda\mu^+$ events in the mass range $1.85 < M(\Lambda\ell^+) < 2.20$ GeV.

[25] CRAWFORD 95 measures the form-factor ratio $R \equiv f_2/f_1$ for $\Lambda_c^+ \to \Lambda e^+\nu_e$ events to be $-0.25 \pm 0.14 \pm 0.08$ and from this calculates α, averaged over q^2, to be the above.

[26] BERGFELD 94 uses Λe^+ events.

Λ_c^+, $\overline{\Lambda}_c^-$ *CP*-VIOLATING DECAY ASYMMETRIES

$(\alpha + \overline{\alpha})/(\alpha - \overline{\alpha})$ in $\Lambda_c^+ \to \Lambda\pi^+$, $\overline{\Lambda}_c^- \to \overline{\Lambda}\pi^-$

This is zero if *CP* is conserved.

VALUE	DOCUMENT ID		TECN	COMMENT
−0.07±0.19±0.24	LINK	06A	FOCS	γ A, $\overline{E}_\gamma \approx$ 180 GeV

$(\alpha + \overline{\alpha})/(\alpha - \overline{\alpha})$ in $\Lambda_c^+ \to \Lambda e^+\nu_e$, $\overline{\Lambda}_c^- \to \overline{\Lambda}e^-\overline{\nu}_e$

This is zero if *CP* is conserved.

VALUE	DOCUMENT ID		TECN	COMMENT
0.00±0.03±0.02	HINSON	05	CLEO	$e^+e^- \approx \Upsilon(4S)$

Λ_c^+ REFERENCES

We have omitted some papers that have been superseded by later experiments. The omitted papers may be found in our 1992 edition (Physical Review **D45**, 1 June, Part II) or in earlier editions.

LEES	11G	PR D84 072006	J.P. Lees *et al.*	(BABAR Collab.)
VAZQUEZ-JA...	08	PL B666 299	E. Vazquez-Jauregui *et al.*	(SELEX Collab.)
AUBERT	07U	PR D75 052002	B. Aubert *et al.*	(BABAR Collab.)
LINK	06A	PL B634 165	J.M. Link *et al.*	(FNAL FOCUS Collab.)
AUBERT,B	05S	PR D72 052006	B. Aubert *et al.*	(BABAR Collab.)
HINSON	05	PRL 94 191801	J.W. Hinson *et al.*	(CLEO Collab.)
LINK	05F	PL B624 22	J.M. Link *et al.*	(FNAL FOCUS Collab.)
LINK	05K	PL B624 166	J.M. Link *et al.*	(FNAL FOCUS Collab.)
CRONIN-HEN...	03	PR D67 012001	D. Cronin-Hennessy *et al.*	(CLEO Collab.)
KAYIS-TOPAK...	03	PL B555 156	A. Kayis-Topaksu *et al.*	(CERN CHORUS Collab.)
ABE	02C	PL B524 33	K. Abe *et al.*	(KEK BELLE Collab.)
LINK	02C	PRL 88 161801	J.M. Link *et al.*	(FNAL FOCUS Collab.)
LINK	02G	PL B540 25	J.M. Link *et al.*	(FNAL FOCUS Collab.)
PDG	02	PR D66 010001	K. Hagiwara *et al.*	
KUSHNIR...	01	PRL 86 5243	A. Kushnirenko *et al.*	(FNAL SELEX Collab.)
MAHMOOD	01	PRL 86 2232	A.H. Mahmood *et al.*	(CLEO Collab.)
AITALA	00	PL B471 449	E.M. Aitala *et al.*	(FNAL E791 Collab.)
JAFFE	00	PR D62 072005	D.E. Jaffe *et al.*	(CLEO Collab.)
ALAM	98	PR D57 4467	M.S. Alam *et al.*	(CLEO Collab.)
ALBRECHT	96E	PRPL 276 223	H. Albrecht *et al.*	(ARGUS Collab.)
ALEEV	96	JINRRC 3-77 31	A.N. Aleev *et al.*	(Serpukhov EXCHARM Collab.)
ALEXANDER	96C	PR D53 R1013	J.P. Alexander *et al.*	(CLEO Collab.)
ALBRECHT	95B	PL B342 397	H. Albrecht *et al.*	(ARGUS Collab.)
AMMAR	95	PRL 74 3534	R. Ammar *et al.*	(CLEO Collab.)
BISHAI	95	PL B350 256	M. Bishai *et al.*	(CLEO Collab.)
CRAWFORD	95	PRL 75 624	G. Crawford *et al.*	(CLEO Collab.)
KODAMA	95	PL B345 85	K. Kodama *et al.*	(FNAL E653 Collab.)
ALBRECHT	94B	PL B326 320	H. Albrecht *et al.*	(ARGUS Collab.)
ALEEV	94	PAN 57 1370	A.N. Aleev *et al.*	(Serpukhov BIS-2 Collab.)
		Translated from YF 57 1443.		
AVERY	94	PL B325 257	P. Avery *et al.*	(CLEO Collab.)
BERGFELD	94	PL B323 219	T. Bergfeld *et al.*	(CLEO Collab.)
FRABETTI	94E	PL B328 193	P.L. Frabetti *et al.*	(FNAL E687 Collab.)
AVERY	93	PRL 71 2391	P. Avery *et al.*	(CLEO Collab.)
BOZEK	93	PL B312 247	A. Bozek *et al.*	(CERN NA32 Collab.)
FRABETTI	93D	PRL 70 1755	P.L. Frabetti *et al.*	(FNAL E687 Collab.)
FRABETTI	93H	PL B314 477	P.L. Frabetti *et al.*	(FNAL E687 Collab.)
KUBOTA	93	PRL 71 3255	Y. Kubota *et al.*	(CLEO Collab.)
ALBRECHT	92	PL B274 239	H. Albrecht *et al.*	(ARGUS Collab.)
ALBRECHT	92O	ZPHY C56 1	H. Albrecht *et al.*	(ARGUS Collab.)
BARLAG	92	PL B283 465	S. Barlag *et al.*	(ACCMOR Collab.)
CRAWFORD	92	PR D45 752	G. Crawford *et al.*	(CLEO Collab.)
JEZABEK	92	PL B286 175	M. Jezabek, K. Rybicki, R. Rylko	(CRAC)
ALBRECHT	91G	PL B269 234	H. Albrecht *et al.*	(ARGUS Collab.)
AVERY	91	PR D43 3599	P. Avery *et al.*	(CLEO Collab.)
ALVAREZ	90	ZPHY C47 539	M.P. Alvarez *et al.*	(CERN NA14/2 Collab.)
ALVAREZ	90B	PL B246 256	M.P. Alvarez *et al.*	(CERN NA14/2 Collab.)
ANJOS	90	PR D41 801	J.C. Anjos *et al.*	(FNAL E691 Collab.)
AVERY	90B	PRL 65 2842	P. Avery *et al.*	(CLEO Collab.)
BARLAG	90D	ZPHY C48 29	S. Barlag *et al.*	(ACCMOR Collab.)
FRABETTI	90	PL B251 639	P.L. Frabetti *et al.*	(FNAL E687 Collab.)
BARLAG	89	PL B218 374	S. Barlag *et al.*	(ACCMOR Collab.)
AGUILAR-...	88B	ZPHY C40 321	M. Aguilar-Benitez *et al.*	(LEBC-EHS Collab.)
Also		PL B189 254	M. Aguilar-Benitez *et al.*	(LEBC-EHS Collab.)
Also		PL B199 462	M. Aguilar-Benitez *et al.*	(LEBC-EHS Collab.)
Also		SJNP 48 833	M. Begalli *et al.*	(LEBC-EHS Collab.)
		Translated from YAF 48 1310.		
ALBRECHT	88C	PL B207 109	H. Albrecht *et al.*	(ARGUS Collab.)
ANJOS	88B	PRL 60 1379	J.C. Anjos *et al.*	(FNAL E691 Collab.)
ADAMOVICH	87	EPL 4 887	M.I. Adamovich *et al.*	(Photon Emulsion Collab.)
Also		SJNP 46 447	F. Viaggi *et al.*	(Photon Emulsion Collab.)
		Translated from YAF 46 799.		
AMENDOLIA	87	ZPHY C36 513	S.R. Amendolia *et al.*	(CERN NA1 Collab.)
JONES	87	ZPHY C36 593	G.T. Jones *et al.*	(CERN WA21 Collab.)
ABE	86	PR D33 1	K. Abe *et al.*	
ALEEV	84	ZPHY C23 333	A.N. Aleev *et al.*	(BIS-2 Collab.)
BOSETTI	82	PL 109B 234	P.C. Bosetti *et al.*	(AACH3, BONN, CERN+)
VELLA	82	PRL 48 1515	E. Vella *et al.*	(SLAC, LBL, UCB)
BASILE	81B	NC 62A 14	M. Basile *et al.*	(CERN, BGNA, PGIA, FRAS)
CALICCHIO	80	PL 93B 521	M. Calicchio *et al.*	(BARI, BIRM, BRUX+)

OTHER RELATED PAPERS

MIGLIOZZI	99	PL B462 217	P. Migliozzi *et al.*	
DUNIETZ	98	PR D58 094010	I. Dunietz	

$\Lambda_c(2595)^+$

$I(J^P) = 0(\frac{1}{2}^-)$ Status: ***

The $\Lambda_c^+\pi^+\pi^-$ mode is largely, and perhaps entirely, $\Sigma_c\pi$, which is just at threshold; since the Σ_c has $J^P = 1/2^+$, the J^P here is almost certainly $1/2^-$. This result is in accord with the theoretical expectation that this is the charm counterpart of the strange $\Lambda(1405)$.

$\Lambda_c(2595)^+$ MASS

The mass is obtained from the $\Lambda_c(2595)^+ - \Lambda_c^+$ mass-difference measurements below.

VALUE (MeV)	DOCUMENT ID
2592.25±0.28 OUR FIT	

$\Lambda_c(2595)^+ - \Lambda_c^+$ MASS DIFFERENCE

VALUE (MeV)	EVTS	DOCUMENT ID		TECN	COMMENT
305.79±0.24 OUR FIT					
305.79±0.14±0.20	3.5k	AALTONEN	11H	CDF	$p\overline{p}$ at 1.96 TeV
• • • We do not use the following data for averages, fits, limits, etc. • • •					
305.6 ±0.3		[1] BLECHMAN	03		Threshold shift
309.7 ±0.9 ±0.4	19	ALBRECHT	97	ARG	$e^+e^- \approx$ 10 GeV
309.2 ±0.7 ±0.3	14 ± 4.5	FRABETTI	96	E687	γBe, $\overline{E}_\gamma \approx$ 220 GeV
307.5 ±0.4 ±1.0	112 ± 17	EDWARDS	95	CLE2	$e^+e^- \approx$ 10.5 GeV

[1] BLECHMAN 03 finds that a more sophisticated treatment than a simple Breit-Wigner for the proximity of the threshold of the dominant decay, $\Sigma_c(2455)\pi$, lowers the $\Lambda_c(2595)^+ - \Lambda_c^+$ mass difference by 2 or 3 MeV. The analysis of AALTONEN 11H bears this out.

$\Lambda_c(2595)^+$ WIDTH

VALUE (MeV)	EVTS	DOCUMENT ID		TECN	COMMENT
2.59±0.30±0.47	3.5k	[2] AALTONEN	11H	CDF	$p\overline{p}$ at 1.96 TeV
• • • We do not use the following data for averages, fits, limits, etc. • • •					
$2.9\ ^{+2.9}_{-2.1}\ ^{+1.8}_{-1.4}$	19	ALBRECHT	97	ARG	$e^+e^- \approx$ 10 GeV
$3.9\ ^{+1.4}_{-1.2}\ ^{+2.0}_{-1.0}$	112 ± 17	EDWARDS	95	CLE2	$e^+e^- \approx$ 10.5 GeV

[2] AALTONEN 11H treats the three charged modes $\Lambda_c(2595)^+ \to \Sigma_c(2455)^{++}\pi^-$, $\Sigma_c(2455)^+\pi^0$, $\Sigma_c(2455)^0\pi^+$ separately in terms of a common coupling constant h_2 and obtains $h_2^2 = 0.36 \pm 0.08$. From this the width is determined.

$\Lambda_c(2595)^+$ DECAY MODES

$\Lambda_c^+\pi\pi$ and its submode $\Sigma_c(2455)\pi$ — the latter just barely — are the only strong decays allowed to an excited Λ_c^+ having this mass; and the submode seems to dominate.

	Mode	Fraction (Γ_i/Γ)
Γ_1	$\Lambda_c^+\pi^+\pi^-$	[a] $\approx$ 67 %
Γ_2	$\Sigma_c(2455)^{++}\pi^-$	24 $\pm$ 7 %
Γ_3	$\Sigma_c(2455)^0\pi^+$	24 $\pm$ 7 %
Γ_4	$\Lambda_c^+\pi^+\pi^-$ 3-body	18 $\pm$ 10 %
Γ_5	$\Lambda_c^+\pi^0$	[b] not seen
Γ_6	$\Lambda_c^+\gamma$	not seen

[a] Assuming isospin conservation, so that the other third is $\Lambda_c^+\pi^0\pi^0$.

[b] A test that the isospin is indeed 0, so that the particle is indeed a Λ_c^+.

$\Lambda_c(2595)^+$ BRANCHING RATIOS

$\Gamma(\Sigma_c(2455)^{++}\pi^-)/\Gamma(\Lambda_c^+\pi^+\pi^-)$ Γ_2/Γ_1

VALUE	DOCUMENT ID		TECN	COMMENT
0.36±0.10 OUR AVERAGE				
0.37±0.12±0.13	ALBRECHT	97	ARG	$e^+e^-\approx$ 10 GeV
0.36±0.09±0.09	EDWARDS	95	CLE2	$e^+e^-\approx$ 10.5 GeV

$\Gamma(\Sigma_c(2455)^0\pi^+)/\Gamma(\Lambda_c^+\pi^+\pi^-)$ Γ_3/Γ_1

VALUE	DOCUMENT ID		TECN	COMMENT
0.37±0.10 OUR AVERAGE				
0.29±0.10±0.11	ALBRECHT	97	ARG	$e^+e^-\approx$ 10 GeV
0.42±0.09±0.09	EDWARDS	95	CLE2	$e^+e^-\approx$ 10.5 GeV

$[\Gamma(\Sigma_c(2455)^{++}\pi^-)+\Gamma(\Sigma_c(2455)^0\pi^+)]/\Gamma(\Lambda_c^+\pi^+\pi^-)$ $(\Gamma_2+\Gamma_3)/\Gamma_1$

VALUE	CL%	DOCUMENT ID		TECN	COMMENT
• • • We do not use the following data for averages, fits, limits, etc. • • •					
$0.66^{+0.13}_{-0.16}\pm0.07$		ALBRECHT	97	ARG	$e^+e^-\approx$ 10 GeV
>0.51	90	[3] FRABETTI	96	E687	γBe, $\overline{E}_\gamma\approx$ 220 GeV

[3] The results of FRABETTI 96 are consistent with this ratio being 100%.

$\Gamma(\Lambda_c^+\pi^0)/\Gamma(\Lambda_c^+\pi^+\pi^-)$ Γ_5/Γ_1

$\Lambda_c^+\pi^0$ decay is forbidden by isospin conservation if this state is in fact a Λ_c.

VALUE	CL%	DOCUMENT ID		TECN	COMMENT
<3.53	90	EDWARDS	95	CLE2	$e^+e^-\approx$ 10.5 GeV

$\Gamma(\Lambda_c^+\gamma)/\Gamma(\Lambda_c^+\pi^+\pi^-)$ Γ_6/Γ_1

VALUE	CL%	DOCUMENT ID		TECN	COMMENT
<0.98	90	EDWARDS	95	CLE2	$e^+e^-\approx$ 10.5 GeV

$\Lambda_c(2595)^+$ REFERENCES

AALTONEN	11H	PR D84 012003	T. Aaltonen *et al.*	(CDF Collab.)
BLECHMAN	03	PR D67 074033	A.E. Blechman *et al.*	(JHU, FLOR)
ALBRECHT	97	PL B402 207	H. Albrecht *et al.*	(ARGUS Collab.)
FRABETTI	96	PL B365 461	P.L. Frabetti *et al.*	(FNAL E687 Collab.)
EDWARDS	95	PRL 74 3331	K.W. Edwards *et al.*	(CLEO Collab.)

$\Lambda_c(2625)^+$

$I(J^P) = 0(\frac{3}{2}^-)$ Status: ***

The spin-parity has not been measured but is expected to be $3/2^-$: this is presumably the charm counterpart of the strange $\Lambda(1520)$.

$\Lambda_c(2625)^+$ MASS

The mass is obtained from the $\Lambda_c(2625)^+$–Λ_c^+ mass-difference measurements below.

VALUE (MeV)	EVTS	DOCUMENT ID		TECN	COMMENT
2628.11±0.19 OUR FIT Error includes scale factor of 1.1.					
• • • We do not use the following data for averages, fits, limits, etc. • • •					
2626.6 ±0.5 ±1.5	42 ± 9	ALBRECHT	93F	ARG	See ALBRECHT 97

$\Lambda_c(2625)^+ - \Lambda_c^+$ MASS DIFFERENCE

VALUE (MeV)	EVTS	DOCUMENT ID		TECN	COMMENT
341.65±0.13 OUR FIT Error includes scale factor of 1.1.					
341.65±0.15 OUR AVERAGE Error includes scale factor of 1.3. See the ideogram below.					
341.65±0.04±0.12	6.2k	AALTONEN	11H	CDF	$p\overline{p}$ at 1.96 TeV
342.1 ±0.5 ±0.5	51	ALBRECHT	97	ARG	$e^+e^-\approx$ 10 GeV
342.2 ±0.2 ±0.5	245 ± 19	EDWARDS	95	CLE2	$e^+e^-\approx$ 10.5 GeV
340.4 ±0.6 ±0.3	40 ± 9	FRABETTI	94	E687	γBe, $\overline{E}_\gamma$ = 220 GeV

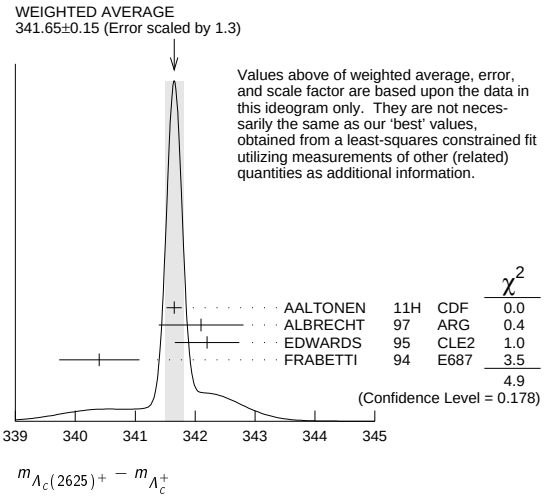

$\Lambda_c(2625)^+$ WIDTH

VALUE (MeV)	CL%	EVTS	DOCUMENT ID		TECN	COMMENT
<0.97	90	6.2k	AALTONEN	11H	CDF	$p\overline{p}$ at 1.96 TeV
• • • We do not use the following data for averages, fits, limits, etc. • • •						
<1.9	90	245 ± 19	EDWARDS	95	CLE2	$e^+e^-\approx$ 10.5 GeV
<3.2	90		ALBRECHT	93F	ARG	$e^+e^-\approx\Upsilon(4S)$

$\Lambda_c(2625)^+$ DECAY MODES

$\Lambda_c^+\pi\pi$ and its submode $\Sigma(2455)\pi$ are the only strong decays allowed to an excited Λ_c^+ having this mass.

	Mode	Fraction (Γ_i/Γ)	Confidence level
Γ_1	$\Lambda_c^+\pi^+\pi^-$	[a] $\approx$67%	
Γ_2	$\Sigma_c(2455)^{++}\pi^-$	<5	90%
Γ_3	$\Sigma_c(2455)^0\pi^+$	<5	90%
Γ_4	$\Lambda_c^+\pi^+\pi^-$ 3-body	large	
Γ_5	$\Lambda_c^+\pi^0$	[b] not seen	
Γ_6	$\Lambda_c^+\gamma$	not seen	

[a] Assuming isospin conservation, so that the other third is $\Lambda_c^+\pi^0\pi^0$.

[b] A test that the isospin is indeed 0, so that the particle is indeed a Λ_c^+.

$\Lambda_c(2625)^+$ BRANCHING RATIOS

$\Gamma(\Sigma_c(2455)^{++}\pi^-)/\Gamma(\Lambda_c^+\pi^+\pi^-)$ Γ_2/Γ_1

VALUE	CL%	DOCUMENT ID		TECN	COMMENT
<0.08	90	EDWARDS	95	CLE2	$e^+e^-\approx$ 10.5 GeV

$\Gamma(\Sigma_c(2455)^0\pi^+)/\Gamma(\Lambda_c^+\pi^+\pi^-)$ Γ_3/Γ_1

VALUE	CL%	DOCUMENT ID		TECN	COMMENT
<0.07	90	EDWARDS	95	CLE2	$e^+e^-\approx$ 10.5 GeV

$[\Gamma(\Sigma_c(2455)^{++}\pi^-)+\Gamma(\Sigma_c(2455)^0\pi^+)]/\Gamma(\Lambda_c^+\pi^+\pi^-)$ $(\Gamma_2+\Gamma_3)/\Gamma_1$

VALUE	CL%	EVTS	DOCUMENT ID		TECN	COMMENT
• • • We do not use the following data for averages, fits, limits, etc. • • •						
<0.36	90		FRABETTI	94	E687	γBe, $\overline{E}_\gamma$ = 220 GeV
0.46±0.14		21	ALBRECHT	93F	ARG	$e^+e^-\approx\Upsilon(4S)$

$\Gamma(\Lambda_c^+\pi^+\pi^-$ 3-body$)/\Gamma(\Lambda_c^+\pi^+\pi^-)$ Γ_4/Γ_1

VALUE	EVTS	DOCUMENT ID		TECN	COMMENT
• • • We do not use the following data for averages, fits, limits, etc. • • •					
0.54±0.14	16	ALBRECHT	93F	ARG	$e^+e^-\approx\Upsilon(4S)$

$\Gamma(\Lambda_c^+\pi^0)/\Gamma(\Lambda_c^+\pi^+\pi^-)$ Γ_5/Γ_1

$\Lambda_c^+\pi^0$ decay is forbidden by isospin conservation if this state is in fact a Λ_c.

VALUE	CL%	DOCUMENT ID		TECN	COMMENT
<0.91	90	EDWARDS	95	CLE2	$e^+e^-\approx$ 10.5 GeV

$\Gamma(\Lambda_c^+\gamma)/\Gamma(\Lambda_c^+\pi^+\pi^-)$ Γ_6/Γ_1

VALUE	CL%	DOCUMENT ID		TECN	COMMENT
<0.52	90	EDWARDS	95	CLE2	$e^+e^-\approx$ 10.5 GeV

Baryon Particle Listings

$\Lambda_c(2625)^+$, $\Lambda_c(2765)^+$, $\Lambda_c(2880)^+$, $\Lambda_c(2940)^+$

$\Lambda_c(2625)^+$ REFERENCES

AALTONEN	11H	PR D84 012003	T. Aaltonen *et al.*	(CDF Collab.)
ALBRECHT	97	PL B402 207	H. Albrecht *et al.*	(ARGUS Collab.)
EDWARDS	95	PRL 74 3331	K.W. Edwards *et al.*	(CLEO Collab.)
FRABETTI	94	PRL 72 961	P.L. Frabetti *et al.*	(FNAL E687 Collab.)
ALBRECHT	93F	PL B317 227	H. Albrecht *et al.*	(ARGUS Collab.)

$\Lambda_c(2765)^+$ or $\Sigma_c(2765)$

$I(J^P) = ?(?^?)$ Status: *

OMITTED FROM SUMMARY TABLE

A broad, statistically significant peak (997^{+141}_{-129} events) seen in $\Lambda_c^+\pi^+\pi^-$. However, nothing at all is known about its quantum numbers, including whether it is a Λ_c^+ or a Σ_c, or whether the width might be due to overlapping states.

$\Lambda_c(2765)^+$ MASS

The mass is obtained from the $\Lambda_c(2765)^+ - \Lambda_c^+$ mass-difference measurement below.

VALUE (MeV)	DOCUMENT ID
2766.6±2.4 OUR FIT	

$\Lambda_c(2765)^+ - \Lambda_c^+$ MASS DIFFERENCE

VALUE (MeV)	EVTS	DOCUMENT ID		TECN	COMMENT
480.1±2.4 OUR FIT					
480.1±2.4	997^{+141}_{-129}	ARTUSO	01	CLE2	$e^+e^- \approx \Upsilon(4S)$

$\Lambda_c(2765)^+$ WIDTH

VALUE (MeV)	DOCUMENT ID		TECN	COMMENT
50	ARTUSO	01	CLE2	$e^+e^- \approx \Upsilon(4S)$

$\Lambda_c(2765)^+$ DECAY MODES

	Mode	Fraction (Γ_i/Γ)
Γ_1	$\Lambda_c^+\pi^+\pi^-$	seen

$\Lambda_c(2765)^+$ REFERENCES

ARTUSO	01	PRL 86 4479	M. Artuso *et al.*	(CLEO Collab.)

$\Lambda_c(2880)^+$

$I(J^P) = 0(\frac{5}{2}^+)$ Status: ***

A narrow peak seen in $\Lambda_c^+\pi^+\pi^-$ and in pD^0. It is not seen in pD^+, and therefore it is probably a Λ_c^+ and not a Σ_c. The evidence for spin 5/2 comes from the $\Sigma_c(2455)\pi$ decay angular distribution, and the evidence for parity + comes from agreement of the $\Sigma_c(2520)/\Sigma_c(2455)$ branching ratio with a prediction of heavy quark symmetry (see MIZUK 07).

$\Lambda_c(2880)^+$ MASS

VALUE (MeV)	EVTS	DOCUMENT ID		TECN	COMMENT
2881.53±0.35 OUR FIT					
2881.50±0.35 OUR AVERAGE					
2881.9 ±0.1 ±0.5	2.8k±190	AUBERT	07	BABR	in pD^0
2881.2 ±0.2 ±0.4	690 ± 50	MIZUK	07	BELL	in $\Sigma_c(2455)^{0,++}\pi^\pm$

$\Lambda_c(2880)^+ - \Lambda_c^+$ MASS DIFFERENCE

VALUE (MeV)	EVTS	DOCUMENT ID		TECN	COMMENT
595.1±0.4 OUR FIT					
596 ±1 ±2	350^{+57}_{-55}	ARTUSO	01	CLE2	in $\Lambda_c^+\pi^+\pi^-$

$\Lambda_c(2880)^+$ WIDTH

VALUE (MeV)	CL%	EVTS	DOCUMENT ID		TECN	COMMENT
5.8±1.1 OUR AVERAGE						
5.8±1.5±1.1		2.8k±190	AUBERT	07	BABR	in pD^0
5.8±0.7±1.1		690 ± 50	MIZUK	07	BELL	in $\Sigma_c(2455)^{0,++}\pi^\pm$
• • • We do not use the following data for averages, fits, limits, etc. • • •						
<8	90		ARTUSO	01	CLEO	in $\Lambda_c^+\pi^+\pi^-$

$\Lambda_c(2880)^+$ DECAY MODES

	Mode	Fraction (Γ_i/Γ)
Γ_1	$\Lambda_c^+\pi^+\pi^-$	seen
Γ_2	$\Sigma_c(2455)^{0,++}\pi^\pm$	seen
Γ_3	$\Sigma_c(2520)^{0,++}\pi^\pm$	seen
Γ_4	pD^0	seen

$\Lambda_c(2880)^+$ BRANCHING RATIOS

$\Gamma(\Sigma_c(2455)^{0,++}\pi^\pm)/\Gamma(\Lambda_c^+\pi^+\pi^-)$ Γ_2/Γ_1

VALUE	EVTS	DOCUMENT ID		TECN	COMMENT
0.392±0.031 OUR AVERAGE Error includes scale factor of 1.3.					
0.404±0.021±0.014		MIZUK	07	BELL	in $\Sigma_c(2455)^{0,++}\pi^\pm$
0.31 ±0.06 ±0.03	96	ARTUSO	01	CLE2	$e^+e^- \approx \Upsilon(4S)$

$\Gamma(\Sigma_c(2520)^{0,++}\pi^\pm)/\Gamma(\Lambda_c^+\pi^+\pi^-)$ Γ_3/Γ_1

VALUE	CL%	DOCUMENT ID		TECN	COMMENT
0.091±0.025±0.010		MIZUK	07	BELL	in $\Sigma_c(2455)^{0,++}\pi^\pm$
• • • We do not use the following data for averages, fits, limits, etc. • • •					
<0.11	90	ARTUSO	01	CLE2	$e^+e^- \approx \Upsilon(4S)$

$\Gamma(\Sigma_c(2520)^{0,++}\pi^\pm)/\Gamma(\Sigma_c(2455)^{0,++}\pi^\pm)$ Γ_3/Γ_2

VALUE	DOCUMENT ID		TECN	COMMENT
• • • We do not use the following data for averages, fits, limits, etc. • • •				
0.225±0.062±0.025	[1] MIZUK	07	BELL	in $\Sigma_c(2455)^{0,++}\pi^\pm$

[1] This MIZUK 07 ratio is redundant with MIZUK 07 ratios given above.

$\Lambda_c(2880)^+$ REFERENCES

AUBERT	07	PRL 98 012001	B. Aubert *et al.*	(BABAR Collab.)
MIZUK	07	PRL 98 262001	R. Mizuk *et al.*	(BELLE Collab.)
ARTUSO	01	PRL 86 4479	M. Artuso *et al.*	(CLEO Collab.)

$\Lambda_c(2940)^+$

$I(J^P) = 0(?^?)$ Status: ***

A fairly narrow peak of good statistical significance first seen in the pD^0 mass spectrum. It is not seen in pD^+, and thus it is probably a Λ_c^+ and not a Σ_c. It is also seen in $\Sigma_c(2455)^{0,++}\pi^\pm$.

$\Lambda_c(2940)^+$ MASS

VALUE (MeV)	EVTS	DOCUMENT ID		TECN	COMMENT
$2939.3^{+1.4}_{-1.5}$ OUR AVERAGE					
2939.8±1.3±1.0	2280±310	AUBERT	07	BABR	in pD^0
$2938.0\pm1.3^{+2.0}_{-4.0}$	220^{+80}_{-60}	MIZUK	07	BELL	in $\Sigma_c(2455)^{0,++}\pi^\pm$

$\Lambda_c(2940)^+$ WIDTH

VALUE (MeV)	EVTS	DOCUMENT ID		TECN	COMMENT
$17\ ^{+8}_{-6}$ OUR AVERAGE					
17.5±5.2± 5.9	2280±310	AUBERT	07	BABR	in pD^0
$13\ ^{+8}_{-5}\ ^{+27}_{-\ 7}$	220^{+80}_{-60}	MIZUK	07	BELL	in $\Sigma_c(2455)^{0,++}\pi^\pm$

$\Lambda_c(2940)^+$ DECAY MODES

	Mode	Fraction (Γ_i/Γ)
Γ_1	pD^0	seen
Γ_2	$\Sigma_c(2455)^{0,++}\pi^\pm$	seen

$\Lambda_c(2940)^+$ REFERENCES

AUBERT	07	PRL 98 012001	B. Aubert *et al.*	(BABAR Collab.)
MIZUK	07	PRL 98 262001	R. Mizuk *et al.*	(BELLE Collab.)

$\Sigma_c(2455)$

$I(J^P) = 1(\frac{1}{2}^+)$ Status: ****

The angular distribution of $B^- \to \Sigma_c(2455)^0 \overline{p}$ favors $J = 1/2$ (as the quark model predicts). $J = 3/2$ is excluded by more than four σ see AUBERT 08BN.

$\Sigma_c(2455)$ MASSES

The masses are obtained from the mass-difference measurements that follow.

$\Sigma_c(2455)^{++}$ MASS

VALUE (MeV)	DOCUMENT ID
2453.98±0.16 OUR FIT	

$\Sigma_c(2455)^+$ MASS

VALUE (MeV)	DOCUMENT ID
2452.9±0.4 OUR FIT	

$\Sigma_c(2455)^0$ MASS

VALUE (MeV)	DOCUMENT ID
2453.74±0.16 OUR FIT	

$\Sigma_c(2455) - \Lambda_c^+$ MASS DIFFERENCES

$m_{\Sigma_c^{++}} - m_{\Lambda_c^+}$

VALUE (MeV)	EVTS	DOCUMENT ID		TECN	COMMENT
167.52± 0.08 OUR FIT					
167.51± 0.09 OUR AVERAGE	Error includes scale factor of 1.1.				
167.44± 0.04±0.12	13.8k	AALTONEN	11H	CDF	$p\overline{p}$ at 1.96 TeV
167.4 ± 0.1 ±0.2	2k	ARTUSO	02	CLE2	$e^+e^- \approx \Upsilon(4S)$
167.35± 0.19±0.12	461	LINK	00C	FOCS	γ A, $\overline{E}_\gamma$ 180 GeV
167.76± 0.29±0.15	122	AITALA	96B	E791	π^- N, 500 GeV
167.6 ± 0.6 ±0.6	56	FRABETTI	96	E687	γBe, $\overline{E}_\gamma \approx$ 220 GeV
168.2 ± 0.3 ±0.2	126	CRAWFORD	93	CLE2	$e^+e^- \approx \Upsilon(4S)$
167.8 ± 0.4 ±0.3	54	BOWCOCK	89	CLEO	e^+e^- 10 GeV
168.2 ± 0.5 ±1.6	92	ALBRECHT	88D	ARG	e^+e^- 10 GeV
167.4 ± 0.5 ±2.0	46	DIESBURG	87	SPEC	nA ~ 600 GeV
• • • We do not use the following data for averages, fits, limits, etc. • • •					
167 ± 1	2	JONES	87	HBC	νp in BEBC
166 ± 1	1	BOSETTI	82	HBC	See JONES 87
168 ± 3	6	BALTAY	79	HLBC	ν Ne-H in 15-ft
166 ±15	1	CAZZOLI	75	HBC	νp in BNL 7-ft

$m_{\Sigma_c^+} - m_{\Lambda_c^+}$

VALUE (MeV)	EVTS	DOCUMENT ID		TECN	COMMENT
166.4±0.4 OUR FIT					
166.4±0.2±0.3	661	AMMAR	01	CLE2	$e^+e^- \approx \Upsilon(4S)$
• • • We do not use the following data for averages, fits, limits, etc. • • •					
168.5±0.4±0.2	111	CRAWFORD	93	CLE2	See AMMAR 01
168 ±3	1	CALICCHIO	80	HBC	νp in BEBC-TST

$m_{\Sigma_c^0} - m_{\Lambda_c^+}$

VALUE (MeV)	EVTS	DOCUMENT ID		TECN	COMMENT
167.27±0.08 OUR FIT					
167.29±0.09 OUR AVERAGE					
167.28±0.03±0.12	15.9k	AALTONEN	11H	CDF	$p\overline{p}$ at 1.96 TeV
167.2 ±0.1 ±0.2	2k	ARTUSO	02	CLE2	$e^+e^- \approx \Upsilon(4S)$
167.38±0.21±0.13	362	LINK	00C	FOCS	γ A, $\overline{E}_\gamma$ 180 GeV
167.38±0.29±0.15	143	AITALA	96B	E791	π^- N, 500 GeV
167.8 ±0.6 ±0.2		ALEEV	96	SPEC	n nucleus, 50 GeV/c
166.6 ±0.5 ±0.6	69	FRABETTI	96	E687	γBe, $\overline{E}_\gamma \approx$ 220 GeV
167.1 ±0.3 ±0.2	124	CRAWFORD	93	CLE2	$e^+e^- \approx \Upsilon(4S)$
168.4 ±1.0 ±0.3	14	ANJOS	89D	E691	γBe 90–260 GeV
• • • We do not use the following data for averages, fits, limits, etc. • • •					
167.9 ±0.5 ±0.3	48	[1] BOWCOCK	89	CLEO	e^+e^- 10 GeV
167.0 ±0.5 ±1.6	70	[1] ALBRECHT	88D	ARG	e^+e^- 10 GeV
178.2 ±0.4 ±2.0	85	[2] DIESBURG	87	SPEC	nA ~ 600 GeV
163 ±2	1	AMMAR	86	EMUL	νA

[1] This result enters the fit through $m_{\Sigma_c^{++}} - m_{\Sigma_c^0}$ given below.

[2] See the note on DIESBURG 87 in the $m_{\Sigma_c^{++}} - m_{\Sigma_c^0}$ section below.

$\Sigma_c(2455)$ MASS DIFFERENCES

$m_{\Sigma_c^{++}} - m_{\Sigma_c^0}$

VALUE (MeV)	DOCUMENT ID		TECN	COMMENT
0.24±0.09 OUR FIT Error includes scale factor of 1.1.				
0.26±0.14 OUR AVERAGE Error includes scale factor of 1.2.				
+ 0.2 ±0.1 ±0.1	ARTUSO	02	CLE2	$e^+e^- \approx \Upsilon(4S)$
− 0.03±0.28±0.11	LINK	00C	FOCS	γ A, $\overline{E}_\gamma$ 180 GeV
+ 0.38±0.40±0.15	AITALA	96B	E791	π^- N, 500 GeV
+ 1.1 ±0.4 ±0.1	CRAWFORD	93	CLE2	$e^+e^- \approx \Upsilon(4S)$
− 0.1 ±0.6 ±0.1	BOWCOCK	89	CLEO	e^+e^- 10 GeV
+ 1.2 ±0.7 ±0.3	ALBRECHT	88D	ARG	e^+e^- ~ 10 GeV
• • • We do not use the following data for averages, fits, limits, etc. • • •				
−10.8 ±2.9	[3] DIESBURG	87	SPEC	nA ~ 600 GeV

[3] DIESBURG 87 is completely incompatible with the other experiments, which is surprising since it agrees with them about $m_{\Sigma_c(2455)^{++}} - m_{\Lambda_c^+}$. We go with the majority here.

$m_{\Sigma_c^+} - m_{\Sigma_c^0}$

VALUE (MeV)	DOCUMENT ID		TECN	COMMENT
−0.9±0.4 OUR FIT				
• • • We do not use the following data for averages, fits, limits, etc. • • •				
1.4±0.5±0.3	CRAWFORD	93	CLE2	See AMMAR 01

$\Sigma_c(2455)$ WIDTHS

$\Sigma_c(2455)^{++}$ WIDTH

VALUE (MeV)	EVTS	DOCUMENT ID		TECN	COMMENT
2.26±0.25 OUR AVERAGE					
2.34±0.13±0.45	13.8k	AALTONEN	11H	CDF	$p\overline{p}$ at 1.96 TeV
2.3 ±0.2 ±0.3	2k	ARTUSO	02	CLE2	$e^+e^- \approx \Upsilon(4S)$
$2.05^{+0.41}_{-0.38}$±0.38	1110	LINK	02	FOCS	γ A, $\overline{E}_\gamma \approx$ 180 GeV

$\Sigma_c(2455)^+$ WIDTH

VALUE (MeV)	CL%	EVTS	DOCUMENT ID		TECN	COMMENT
<4.6	90	661	AMMAR	01	CLE2	$e^+e^- \approx \Upsilon(4S)$

$\Sigma_c(2455)^0$ WIDTH

VALUE (MeV)	EVTS	DOCUMENT ID		TECN	COMMENT
2.16±0.26 OUR AVERAGE Error includes scale factor of 1.1.					
1.65±0.11±0.49	15.9k	AALTONEN	11H	CDF	$p\overline{p}$ at 1.96 TeV
2.6 ±0.5 ±0.3		AUBERT	08BN	BABR	$B^- \to \overline{p}\Lambda_c^+\pi^-$
2.5 ±0.2 ±0.3	2k	ARTUSO	02	CLE2	$e^+e^- \approx \Upsilon(4S)$
$1.55^{+0.41}_{-0.37}$±0.38	913	LINK	02	FOCS	γ A, $\overline{E}_\gamma \approx$ 180 GeV

$\Sigma_c(2455)$ DECAY MODES

$\Lambda_c^+\pi$ is the only strong decay allowed to a Σ_c having this mass.

	Mode	Fraction (Γ_i/Γ)
Γ_1	$\Lambda_c^+\pi$	≈ 100 %

$\Sigma_c(2455)$ REFERENCES

AALTONEN	11H	PR D84 012003	T. Aaltonen *et al.*	(CDF Collab.)
AUBERT	08BN	PR D78 112003	B. Aubert *et al.*	(BABAR Collab.)
ARTUSO	02	PR D65 071101	M. Artuso *et al.*	(CLEO Collab.)
LINK	02	PL B525 205	J.M. Link *et al.*	(FNAL FOCUS Collab.)
AMMAR	01	PRL 86 1167	R. Ammar *et al.*	(CLEO Collab.)
LINK	00C	PL B488 218	J.M. Link *et al.*	(FNAL FOCUS Collab.)
AITALA	96B	PL B379 292	E.M. Aitala *et al.*	(FNAL E791 Collab.)
ALEEV	96	JINRRC 3-77 31	A.N. Aleev *et al.*	(Serpukhov EXCHARM Collab.)
FRABETTI	96	PL B365 461	P.L. Frabetti *et al.*	(FNAL E687 Collab.)
CRAWFORD	93	PRL 71 3259	G. Crawford *et al.*	(CLEO Collab.)
ANJOS	89D	PRL 62 1721	J.C. Anjos *et al.*	(FNAL E691 Collab.)
BOWCOCK	89	PRL 62 1240	T.J.V. Bowcock *et al.*	(CLEO Collab.)
ALBRECHT	88D	PL B211 489	H. Albrecht *et al.*	(ARGUS Collab.)
DIESBURG	87	PRL 59 2711	M. Diesburg *et al.*	(FNAL E400 Collab.)
JONES	87	ZPHY C36 593	G.T. Jones *et al.*	(CERN WA21 Collab.)
AMMAR	86	JETPL 43 515 Translated from ZETFP 43 401.	R. Ammar *et al.*	(ITEP)
BOSETTI	82	PL 109B 234	P.C. Bosetti *et al.*	(AACH3, BONN, CERN+)
CALICCHIO	80	PL 93B 521	M. Calicchio *et al.*	(BARI, BIRM, BRUX+)
BALTAY	79	PRL 42 1721	C. Baltay *et al.*	(COLU, BNL) I
CAZZOLI	75	PRL 34 1125	E.G. Cazzoli *et al.*	(BNL)

$\Sigma_c(2520)$

$I(J^P) = 1(\frac{3}{2}^+)$ Status: ***

Seen in the $\Lambda_c^+ \pi^\pm$ mass spectrum. The natural assignment is that this is the $J^P = 3/2^+$ excitation of the $\Sigma_c(2455)$, the charm counterpart of the $\Sigma(1385)$, but neither J nor P has been measured.

$\Sigma_c(2520)$ MASSES

The masses are obtained from the mass-difference measurements that follow.

$\Sigma_c(2520)^{++}$ MASS

VALUE (MeV)	EVTS	DOCUMENT ID	TECN	COMMENT
2517.9±0.6 OUR FIT	Error includes scale factor of 1.6.			
• • • We do not use the following data for averages, fits, limits, etc. • • •				
2530 ±5 ±5	6	[1] AMMOSOV 93	HLBC	$\nu p \to \mu^- \Sigma_c(2530)^{++}$

[1] AMMOSOV 93 sees a cluster of 6 events and estimates the background to be 1 event.

$\Sigma_c(2520)^{+}$ MASS

VALUE (MeV)	DOCUMENT ID
2517.5±2.3 OUR FIT	

$\Sigma_c(2520)^{0}$ MASS

VALUE (MeV)	DOCUMENT ID
2518.8±0.6 OUR FIT Error includes scale factor of 1.5.	

$\Sigma_c(2520)$ MASS DIFFERENCES

$m_{\Sigma_c(2520)^{++}} - m_{\Lambda_c^+}$

VALUE (MeV)	EVTS	DOCUMENT ID	TECN	COMMENT
231.4 ±0.6 OUR FIT Error includes scale factor of 1.6.				
231.4 ±0.7 OUR AVERAGE Error includes scale factor of 1.8. See the ideogram below.				
230.73±0.56±0.16	8.8k	AALTONEN 11H	CDF	$p\overline{p}$ at 1.96 TeV
231.5 ±0.4 ±0.3	1330 ± 110	ATHAR 05	CLEO	e^+e^-, 9.4–11.5 GeV
234.5 ±1.1 ±0.8	677	BRANDENB... 97	CLE2	$e^+e^- \approx \Upsilon(4S)$

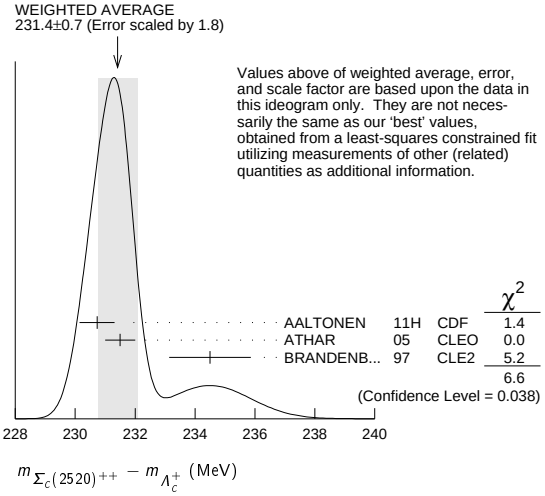

$m_{\Sigma_c(2520)^{+}} - m_{\Lambda_c^+}$

VALUE (MeV)	EVTS	DOCUMENT ID	TECN	COMMENT
231.0±2.3 OUR FIT				
231.0±1.1±2.0	327	AMMAR 01	CLE2	$e^+e^- \approx \Upsilon(4S)$

$m_{\Sigma_c(2520)^{0}} - m_{\Lambda_c^+}$

VALUE (MeV)	EVTS	DOCUMENT ID	TECN	COMMENT
232.3 ±0.5 OUR FIT Error includes scale factor of 1.6.				
232.3 ±0.5 OUR AVERAGE Error includes scale factor of 1.4. See the ideogram below.				
232.88±0.43±0.16	9.0k	AALTONEN 11H	CDF	$p\overline{p}$ at 1.96 TeV
231.4 ±0.5 ±0.3	1350 ± 120	ATHAR 05	CLEO	e^+e^-, 9.4–11.5 GeV
232.6 ±1.0 ±0.8	504	BRANDENB... 97	CLE2	$e^+e^- \approx \Upsilon(4S)$

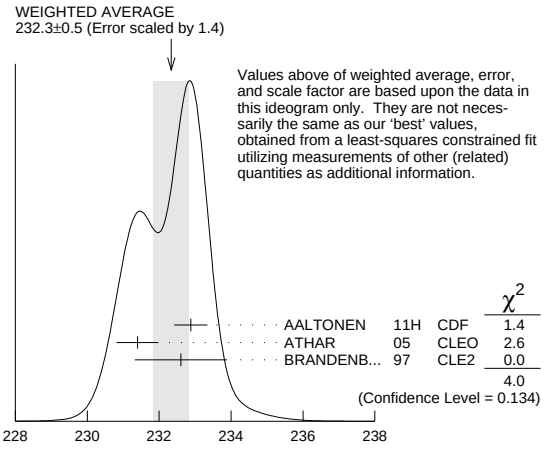

$m_{\Sigma_c(2520)^{++}} - m_{\Sigma_c(2520)^{0}}$

VALUE (MeV)	DOCUMENT ID	TECN	COMMENT
• • • We do not use the following data for averages, fits, limits, etc. • • •			
+0.1±0.8±0.3	[2] ATHAR 05	CLEO	e^+e^-, 9.4–11.5 GeV
1.9±1.4±1.0	[3] BRANDENB... 97	CLE2	$e^+e^- \approx \Upsilon(4S)$

[2] This ATHAR 05 result is redundant with measurements in earlier entries.
[3] This BRANDENBURG 97 result is redundant with measurements in earlier entries.

$\Sigma_c(2520)$ WIDTHS

$\Sigma_c(2520)^{++}$ WIDTH

VALUE (MeV)	EVTS	DOCUMENT ID	TECN	COMMENT
14.9 ±1.5 OUR AVERAGE				
15.03±2.12±1.36	8.8k	AALTONEN 11H	CDF	$p\overline{p}$ at 1.96 TeV
$14.4\ ^{+1.6}_{-1.5}$ ±1.4	1330 ± 110	ATHAR 05	CLEO	e^+e^-, 9.4–11.5 GeV
$17.9\ ^{+3.8}_{-3.2}$ ±4.0	677	BRANDENB... 97	CLE2	$e^+e^- \approx \Upsilon(4S)$

$\Sigma_c(2520)^{+}$ WIDTH

VALUE (MeV)	CL%	EVTS	DOCUMENT ID	TECN	COMMENT
<17	90	327	AMMAR 01	CLE2	$e^+e^- \approx \Upsilon(4S)$

$\Sigma_c(2520)^{0}$ WIDTH

VALUE (MeV)	EVTS	DOCUMENT ID	TECN	COMMENT
14.5 ±1.5 OUR AVERAGE				
12.51±1.82±1.37	9.0k	AALTONEN 11H	CDF	$p\overline{p}$ at 1.96 TeV
$16.6\ ^{+1.9}_{-1.7}$ ±1.4	1350 ± 120	ATHAR 05	CLEO	e^+e^-, 9.4–11.5 GeV
$13.0\ ^{+3.7}_{-3.0}$ ±4.0	504	BRANDENB... 97	CLE2	$e^+e^- \approx \Upsilon(4S)$

$\Sigma_c(2520)$ DECAY MODES

$\Lambda_c^+ \pi$ is the only strong decay allowed to a Σ_c having this mass.

	Mode	Fraction (Γ_i/Γ)
Γ_1	$\Lambda_c^+ \pi$	≈ 100 %

$\Sigma_c(2520)$ REFERENCES

AALTONEN	11H	PR D84 012003	T. Aaltonen *et al.*	(CDF Collab.)
ATHAR	05	PR D71 051101	S.B. Athar *et al.*	(CLEO Collab.)
AMMAR	01	PRL 86 1167	R. Ammar *et al.*	(CLEO Collab.)
BRANDENB...	97	PRL 78 2304	G. Brandenburg *et al.*	(CLEO Collab.)
AMMOSOV	93	JETPL 58 247	V.V. Ammosov *et al.*	(SERP)

Translated from ZETFP 58 241.

$\Sigma_c(2800)$

$I(J^P) = 1(?^?)$ Status: ***

Seen in the $\Lambda_c^+\pi^+$, $\Lambda_c^+\pi^0$, and $\Lambda_c^+\pi^-$ mass spectra.

$\Sigma_c(2800)$ MASSES

The charged ++ and + masses are obtained from the mass-difference measurements that follow. The neutral mass is dominated by the mass-difference measurement, but is pulled up somewhat by the less well-determined but considerably higher direct-mass measurement. It is possible, in fact, that AUBERT 08BN is seeing a different Σ_c.

$\Sigma_c(2800)^{++}$ MASS

VALUE (MeV)	DOCUMENT ID
2801^{+4}_{-6} OUR FIT	

$\Sigma_c(2800)^{+}$ MASS

VALUE (MeV)	DOCUMENT ID
2792^{+14}_{-5} OUR FIT	

$\Sigma_c(2800)^{0}$ MASS

VALUE (MeV)	DOCUMENT ID	TECN	COMMENT
2806^{+5}_{-7} OUR FIT Error includes scale factor of 1.3.			
$2846 \pm 8 \pm 10$	AUBERT	08BN BABR	$B^- \to \overline{p}\Lambda_c^+\pi^-$

$\Sigma_c(2800)$ MASS DIFFERENCES

$m_{\Sigma_c(2800)^{++}} - m_{\Lambda_c^+}$

VALUE (MeV)	EVTS	DOCUMENT ID	TECN	COMMENT
514^{+4}_{-6} OUR FIT				
$514.5^{+3.4+2.8}_{-3.1-4.9}$	2810^{+1090}_{-775}	MIZUK 05	BELL	$e^+e^- \approx \Upsilon(4S)$

$m_{\Sigma_c(2800)^{+}} - m_{\Lambda_c^+}$

VALUE (MeV)	EVTS	DOCUMENT ID	TECN	COMMENT
505^{+14}_{-5} OUR FIT				
$505.4^{+5.8+12.4}_{-4.6-2.0}$	1540^{+1750}_{-1050}	MIZUK 05	BELL	$e^+e^- \approx \Upsilon(4S)$

$m_{\Sigma_c(2800)^{0}} - m_{\Lambda_c^+}$

VALUE (MeV)	EVTS	DOCUMENT ID	TECN	COMMENT
519^{+5}_{-7} OUR FIT Error includes scale factor of 1.3.				
$515.4^{+3.2+2.1}_{-3.1-6.0}$	2240^{+1300}_{-740}	MIZUK 05	BELL	$e^+e^- \approx \Upsilon(4S)$

$\Sigma_c(2800)$ WIDTHS

$\Sigma_c(2800)^{++}$ WIDTH

VALUE (MeV)	EVTS	DOCUMENT ID	TECN	COMMENT
75^{+18+12}_{-13-11}	2810^{+1090}_{-775}	MIZUK 05	BELL	$e^+e^- \approx \Upsilon(4S)$

$\Sigma_c(2800)^{+}$ WIDTH

VALUE (MeV)	EVTS	DOCUMENT ID	TECN	COMMENT
62^{+37+52}_{-23-38}	1540^{+1750}_{-1050}	MIZUK 05	BELL	$e^+e^- \approx \Upsilon(4S)$

$\Sigma_c(2800)^{0}$ WIDTH

VALUE (MeV)	EVTS	DOCUMENT ID	TECN	COMMENT
72^{+22}_{-15} OUR AVERAGE				
$86^{+33}_{-22} \pm 12$		AUBERT 08BN	BABR	$B^- \to \overline{p}\Lambda_c^+\pi^-$
61^{+18+22}_{-13-13}	2240^{+1300}_{-740}	MIZUK 05	BELL	$e^+e^- \approx \Upsilon(4S)$

$\Sigma_c(2800)$ DECAY MODES

	Mode	Fraction (Γ_i/Γ)
Γ_1	$\Lambda_c^+\pi$	seen

$\Sigma_c(2800)$ REFERENCES

AUBERT 08BN PR D78 112003 B. Aubert *et al.* (BABAR Collab.)
MIZUK 05 PRL 94 122002 R. Mizuk *et al.* (BELLE Collab.)

Ξ_c^+

$I(J^P) = \frac{1}{2}(\frac{1}{2}^+)$ Status: ***

According to the quark model, the Ξ_c^+ (quark content usc) and Ξ_c^0 form an isospin doublet, and the spin-parity ought to be $J^P = 1/2^+$. None of I, J, or P has actually been measured.

Ξ_c^+ MASS

The fit uses the Ξ_c^+ and Ξ_c^0 mass and mass-difference measurements.

VALUE (MeV)	EVTS	DOCUMENT ID		TECN	COMMENT
$2467.8^{+0.4}_{-0.6}$ OUR FIT					
$2467.6^{+0.4}_{-1.0}$ OUR AVERAGE					
$2468.1 \pm 0.4^{+0.2}_{-1.4}$	4950 ± 286	[1] LESIAK	05	BELL	e^+e^-, $\Upsilon(4S)$
$2465.8 \pm 1.9 \pm 2.5$	90	FRABETTI	98	E687	γ Be, $\overline{E}_\gamma$= 220 GeV
$2467.0 \pm 1.6 \pm 2.0$	147	EDWARDS	96	CLE2	$e^+e^- \approx \Upsilon(4S)$
$2465.1 \pm 3.6 \pm 1.9$	30	ALBRECHT	90F	ARG	e^+e^- at $\Upsilon(4S)$
$2467 \pm 3 \pm 4$	23	ALAM	89	CLEO	e^+e^- 10.6 GeV
$2466.5 \pm 2.7 \pm 1.2$	5	BARLAG	89C	ACCM	π^- Cu 230 GeV
• • • We do not use the following data for averages, fits, limits, etc. • • •					
$2464.4 \pm 2.0 \pm 1.4$	30	FRABETTI	93B	E687	See FRABETTI 98
$2459 \pm 5 \pm 30$	56	[2] COTEUS	87	SPEC	nA $\simeq$ 600 GeV
2460 ± 25	82	BIAGI	83	SPEC	Σ^-Be 135 GeV

[1] The systematic error was (wrongly) given the other way round in LESIAK 05; see the erratum.

[2] Although COTEUS 87 claims to agree well with BIAGI 83 on the mass and width, there appears to be a discrepancy between the two experiments. BIAGI 83 sees a single peak (stated significance about 6 standard deviations) in the $\Lambda K^-\pi^+\pi^+$ mass spectrum. COTEUS 87 sees *two* peaks in the same spectrum, one at the Ξ_c^+ mass, the other 75 MeV lower. The latter is attributed to $\Xi_c^+ \to \Sigma^0 K^-\pi^+\pi^+ \to (\Lambda\gamma)K^-\pi^+\pi^+$, with the γ unseen. The *combined* significance of the double peak is stated to be 5.5 standard deviations. But the absence of any trace of a lower peak in BIAGI 83 seems to us to throw into question the interpretation of the lower peak of COTEUS 87.

Ξ_c^+ MEAN LIFE

VALUE (10^{-15} s)	EVTS	DOCUMENT ID	TECN	COMMENT
442 ± 26 OUR AVERAGE Error includes scale factor of 1.3. See the ideogram below.				
$503 \pm 47 \pm 18$	250	MAHMOOD 02	CLE2	$e^+e^- \approx \Upsilon(4S)$
$439 \pm 22 \pm 9$	532	LINK 01D	FOCS	γ nucleus, $\overline{E}_\gamma \approx$ 180 GeV
$340^{+70}_{-50} \pm 20$	56	FRABETTI 98	E687	γ Be, $\overline{E}_\gamma$= 220 GeV
$400^{+180}_{-120} \pm 100$	102	COTEUS 87	SPEC	nA $\simeq$ 600 GeV
$480^{+210}_{-150} {}^{+200}_{-100}$	53	BIAGI 85C	SPEC	Σ^-Be 135 GeV
• • • We do not use the following data for averages, fits, limits, etc. • • •				
$410^{+110}_{-80} \pm 20$	30	FRABETTI 93B	E687	See FRABETTI 98
200^{+110}_{-60}	6	BARLAG 89C	ACCM	π^- (K^-) Cu 230 GeV

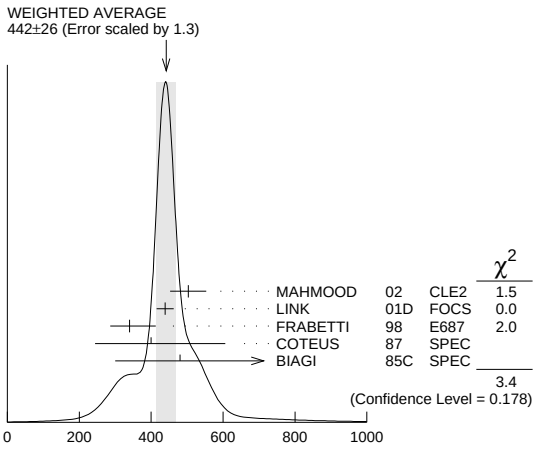

Ξ_c^+ mean life

Ξ_c^+

Ξ_c^+ DECAY MODES

	Mode		Fraction (Γ_i/Γ)	Confidence level
	No absolute branching fractions have been measured. The following are branching *ratios* relative to $\Xi^-2\pi^+$.			
	Cabibbo-favored ($S=-2$) decays — relative to $\Xi^-2\pi^+$			
Γ_1	$p2K_S^0$		0.087 ± 0.021	
Γ_2	$\Lambda\overline{K}^0\pi^+$		—	
Γ_3	$\Sigma(1385)^+\overline{K}^0$	[a]	$1.0\ \pm0.5$	
Γ_4	$\Lambda K^-2\pi^+$		0.323 ± 0.033	
Γ_5	$\Lambda\overline{K}^*(892)^0\pi^+$	[a]	<0.16	90%
Γ_6	$\Sigma(1385)^+K^-\pi^+$	[a]	<0.23	90%
Γ_7	$\Sigma^+K^-\pi^+$		$0.94\ \pm0.10$	
Γ_8	$\Sigma^+\overline{K}^*(892)^0$	[a]	$0.81\ \pm0.15$	
Γ_9	$\Sigma^0K^-2\pi^+$		$0.27\ \pm0.12$	
Γ_{10}	$\Xi^0\pi^+$		$0.55\ \pm0.16$	
Γ_{11}	$\Xi^-2\pi^+$		**DEFINED AS 1**	
Γ_{12}	$\Xi(1530)^0\pi^+$	[a]	<0.10	90%
Γ_{13}	$\Xi^0\pi^+\pi^0$		$2.3\ \pm0.7$	
Γ_{14}	$\Xi^0\pi^-2\pi^+$		$1.7\ \pm0.5$	
Γ_{15}	$\Xi^0e^+\nu_e$		$2.3\ ^{+0.7}_{-0.8}$	
Γ_{16}	$\Omega^-K^+\pi^+$		$0.07\ \pm0.04$	
	Cabibbo-suppressed decays — relative to $\Xi^-2\pi^+$			
Γ_{17}	$pK^-\pi^+$		$0.21\ \pm0.04$	
Γ_{18}	$p\overline{K}^*(892)^0$	[a]	0.116 ± 0.030	
Γ_{19}	$\Sigma^+\pi^+\pi^-$		$0.48\ \pm0.20$	
Γ_{20}	$\Sigma^-2\pi^+$		$0.18\ \pm0.09$	
Γ_{21}	$\Sigma^+K^+K^-$		$0.15\ \pm0.06$	
Γ_{22}	$\Sigma^+\phi$	[a]	<0.11	90%
Γ_{23}	$\Xi(1690)^0K^+$, $\Xi(1690)^0\to\Sigma^+K^-$		<0.05	90%

[a] This branching fraction includes all the decay modes of the final-state resonance.

Ξ_c^+ BRANCHING RATIOS

Cabibbo-favored ($S=-2$) decays

$\Gamma(p2K_S^0)/\Gamma(\Xi^-2\pi^+)$ Γ_1/Γ_{11}

VALUE	EVTS	DOCUMENT ID		TECN	COMMENT
$0.087\pm0.016\pm0.014$	168 ± 27	LESIAK	05	BELL	e^+e^-, $\Upsilon(4S)$

$\Gamma(\Sigma(1385)^+\overline{K}^0)/\Gamma(\Xi^-2\pi^+)$ Γ_3/Γ_{11}

Unseen decay modes of the $\Sigma(1385)^+$ are included.

VALUE	EVTS	DOCUMENT ID		TECN	COMMENT
$1.00\pm0.49\pm0.24$	20	LINK	03E	FOCS	<1.72, 90% CL

$\Gamma(\Lambda K^-2\pi^+)/\Gamma(\Xi^-2\pi^+)$ Γ_4/Γ_{11}

VALUE	EVTS	DOCUMENT ID		TECN	COMMENT
0.323 ± 0.033 OUR AVERAGE					
$0.32\ \pm0.03\ \pm0.02$	1177 ± 55	LESIAK	05	BELL	e^+e^-, $\Upsilon(4S)$
$0.28\ \pm0.06\ \pm0.06$	58	LINK	03E	FOCS	γ nucleus, $\overline{E}_\gamma\approx180$ GeV
$0.58\ \pm0.16\ \pm0.07$	61	BERGFELD	96	CLE2	$e^+e^-\approx\ \Upsilon(4S)$

$\Gamma(\Lambda\overline{K}^*(892)^0\pi^+)/\Gamma(\Lambda K^-2\pi^+)$ Γ_5/Γ_4

Unseen decay modes of the $\overline{K}^*(892)^0$ are included.

VALUE	CL%	DOCUMENT ID		TECN	COMMENT
<0.5	90	BERGFELD	96	CLE2	$e^+e^-\approx\ \Upsilon(4S)$

$\Gamma(\Sigma(1385)^+K^-\pi^+)/\Gamma(\Lambda K^-2\pi^+)$ Γ_6/Γ_4

Unseen decay modes of the $\Sigma(1385)^+$ are included.

VALUE	CL%	DOCUMENT ID		TECN	COMMENT
<0.7	90	BERGFELD	96	CLE2	$e^+e^-\approx\ \Upsilon(4S)$

$\Gamma(\Sigma^+K^-\pi^+)/\Gamma(\Xi^-2\pi^+)$ Γ_7/Γ_{11}

VALUE	EVTS	DOCUMENT ID		TECN	COMMENT
0.94 ± 0.10 OUR AVERAGE					
$0.91\pm0.11\pm0.04$	251	LINK	03E	FOCS	γ nucleus, $\overline{E}_\gamma\approx180$ GeV
$0.92\pm0.20\pm0.07$		[3] JUN	00	SELX	Σ^- nucleus, 600 GeV
$1.18\pm0.26\pm0.17$	119	BERGFELD	96	CLE2	$e^+e^-\approx\ \Upsilon(4S)$

[3] This JUN 00 result is redundant with other results given below.

$\Gamma(\Sigma^+\overline{K}^*(892)^0)/\Gamma(\Xi^-2\pi^+)$ Γ_8/Γ_{11}

Unseen decay modes of the $\overline{K}^*(892)^0$ are included.

VALUE	EVTS	DOCUMENT ID		TECN	COMMENT
0.81 ± 0.15 OUR AVERAGE					
$0.78\pm0.16\pm0.06$	119	LINK	03E	FOCS	γ nucleus, $\overline{E}_\gamma\approx180$ GeV
$0.92\pm0.27\pm0.14$	61	BERGFELD	96	CLE2	$e^+e^-\approx\ \Upsilon(4S)$

$\Gamma(\Sigma^0K^-2\pi^+)/\Gamma(\Lambda K^-2\pi^+)$ Γ_9/Γ_4

VALUE	EVTS	DOCUMENT ID		TECN	COMMENT
0.84 ± 0.36	47	[4] COTEUS	87	SPEC	$nA\simeq600$ GeV

[4] See, however, the note on the COTEUS 87 Ξ_c^+ mass measurement.

$\Gamma(\Xi^0\pi^+)/\Gamma(\Xi^-2\pi^+)$ Γ_{10}/Γ_{11}

VALUE	EVTS	DOCUMENT ID		TECN	COMMENT
$0.55\pm0.13\pm0.09$	39	EDWARDS	96	CLE2	$e^+e^-\approx\ \Upsilon(4S)$

$\Gamma(\Xi^-2\pi^+)/\Gamma_{\text{total}}$ Γ_{11}/Γ

VALUE	EVTS	DOCUMENT ID		TECN	COMMENT
• • • We do not use the following data for averages, fits, limits, etc. • • •					
seen	131	BERGFELD	96	CLE2	$e^+e^-\approx\ \Upsilon(4S)$
seen	160	AVERY	95	CLE2	$e^+e^-\approx\ \Upsilon(4S)$
seen	30	FRABETTI	93B	E687	γBe, $\overline{E}_\gamma=220$ GeV
seen	30	ALBRECHT	90F	ARG	e^+e^- at $\Upsilon(4S)$
seen	23	ALAM	89	CLEO	e^+e^- 10.6 GeV

$\Gamma(\Xi(1530)^0\pi^+)/\Gamma(\Xi^-2\pi^+)$ Γ_{12}/Γ_{11}

Unseen decay modes of the $\Xi(1530)^0$ are included.

VALUE	CL%	DOCUMENT ID		TECN	COMMENT
<0.1	90	LINK	03E	FOCS	γ nucleus, $\overline{E}_\gamma\approx180$ GeV
• • • We do not use the following data for averages, fits, limits, etc. • • •					
<0.2	90	BERGFELD	96	CLE2	$e^+e^-\approx\ \Upsilon(4S)$

$\Gamma(\Xi^0\pi^+\pi^0)/\Gamma(\Xi^-2\pi^+)$ Γ_{13}/Γ_{11}

VALUE	EVTS	DOCUMENT ID		TECN	COMMENT
$2.34\pm0.57\pm0.37$	81	EDWARDS	96	CLE2	$e^+e^-\approx\ \Upsilon(4S)$

$\Gamma(\Xi(1530)^0\pi^+)/\Gamma(\Xi^0\pi^+\pi^0)$ Γ_{12}/Γ_{13}

VALUE	CL%	DOCUMENT ID		TECN	COMMENT
• • • We do not use the following data for averages, fits, limits, etc. • • •					
<0.3	90	EDWARDS	96	CLE2	$e^+e^-\approx\ \Upsilon(4S)$

$\Gamma(\Xi^0\pi^-2\pi^+)/\Gamma(\Xi^-2\pi^+)$ Γ_{14}/Γ_{11}

VALUE	EVTS	DOCUMENT ID		TECN	COMMENT
$1.74\pm0.42\pm0.27$	57	EDWARDS	96	CLE2	$e^+e^-\approx\ \Upsilon(4S)$

$\Gamma(\Xi^0e^+\nu_e)/\Gamma(\Xi^-2\pi^+)$ Γ_{15}/Γ_{11}

VALUE	EVTS	DOCUMENT ID		TECN	COMMENT
$2.3\pm0.6^{+0.3}_{-0.6}$	41	ALEXANDER	95B	CLE2	$e^+e^-\approx\ \Upsilon(4S)$

$\Gamma(\Omega^-K^+\pi^+)/\Gamma(\Xi^-2\pi^+)$ Γ_{16}/Γ_{11}

VALUE	EVTS	DOCUMENT ID		TECN	COMMENT
$0.07\pm0.03\pm0.03$	14	LINK	03E	FOCS	<0.12, 90% CL

Cabibbo-suppressed decays

$\Gamma(pK^-\pi^+)/\Gamma(\Xi^-2\pi^+)$ Γ_{17}/Γ_{11}

VALUE	EVTS	DOCUMENT ID		TECN	COMMENT
$0.21\ \pm0.04$ OUR AVERAGE					
0.194 ± 0.054	47 ± 11	VAZQUEZ-JA...08		SELX	Σ^- nucleus, 600 GeV
$0.234\pm0.047\pm0.022$	202	LINK	01B	FOCS	γ nucleus
• • • We do not use the following data for averages, fits, limits, etc. • • •					
$0.20\ \pm0.04\ \pm0.02$	76	JUN	00	SELX	See VAZQUEZ-JAUREGUI 08

$\Gamma(p\overline{K}^*(892)^0)/\Gamma(pK^-\pi^+)$ Γ_{18}/Γ_{17}

Unseen decay modes of the $\overline{K}^*(892)^0$ are included.

VALUE	DOCUMENT ID		TECN	COMMENT
$0.54\pm0.09\pm0.05$	LINK	01B	FOCS	γ nucleus

$\Gamma(\Sigma^+\pi^+\pi^-)/\Gamma(\Xi^-2\pi^+)$ Γ_{19}/Γ_{11}

VALUE	EVTS	DOCUMENT ID		TECN	COMMENT
0.48 ± 0.20	21 ± 8	VAZQUEZ-JA...08		SELX	Σ^- nucleus, 600 GeV

$\Gamma(\Sigma^-2\pi^+)/\Gamma(\Xi^-2\pi^+)$ Γ_{20}/Γ_{11}

VALUE	EVTS	DOCUMENT ID		TECN	COMMENT
0.18 ± 0.09	10 ± 4	VAZQUEZ-JA...08		SELX	Σ^- nucleus, 600 GeV

$\Gamma(\Sigma^+K^+K^-)/\Gamma(\Sigma^+K^-\pi^+)$ Γ_{21}/Γ_7

VALUE	EVTS	DOCUMENT ID		TECN	COMMENT
$0.16\pm0.06\pm0.01$	17	LINK	03E	FOCS	γ nucleus, $\overline{E}_\gamma\approx180$ GeV

$\Gamma(\Sigma^+\phi)/\Gamma(\Sigma^+K^-\pi^+)$ Γ_{22}/Γ_7

Unseen decay modes of the ϕ are included.

VALUE	CL%	DOCUMENT ID		TECN	COMMENT
<0.12	90	LINK	03E	FOCS	γ nucleus, $\overline{E}_\gamma \approx 180$ GeV

$\Gamma(\Xi(1690)^0K^+\times B(\Xi(1690)^0 \to \Sigma^+K^-))/\Gamma(\Sigma^+K^-\pi^+)$ Γ_{23}/Γ_7

VALUE	CL%	DOCUMENT ID		TECN	COMMENT
<0.05	90	LINK	03E	FOCS	γ nucleus, $\overline{E}_\gamma \approx 180$ GeV

Ξ_c^+ REFERENCES

VAZQUEZ-JA...	08	PL B666 299	E. Vazquez-Jauregui *et al.*	(SELEX Collab.)
LESIAK	05	PL B605 237	T. Lesiak *et al.*	(BELLE Collab.)
Also		PL B617 198 (errat)	T. Lesiak *et al.*	(BELLE Collab.)
LINK	03E	PL B571 139	J.M. Link *et al.*	(FNAL FOCUS Collab.)
MAHMOOD	02	PR D65 031102	A.H. Mahmood *et al.*	(CLEO Collab.)
LINK	01B	PL B512 277	J.M. Link *et al.*	(FNAL FOCUS Collab.)
LINK	01D	PL B523 53	J.M. Link *et al.*	(FNAL FOCUS Collab.)
JUN	00	PRL 84 1857	S.Y. Jun *et al.*	(FNAL SELEX Collab.)
FRABETTI	98	PL B427 211	P.L. Frabetti *et al.*	(FNAL E687 Collab.)
BERGFELD	96	PL B365 431	T. Bergfeld *et al.*	(CLEO Collab.)
EDWARDS	96	PL B373 261	K.W. Edwards *et al.*	(CLEO Collab.)
ALEXANDER	95B	PRL 74 3113	J. Alexander *et al.*	(CLEO Collab.)
Also		PRL 75 4155 (erratum)	J. Alexander *et al.*	(CLEO Collab.)
AVERY	95	PRL 75 4364	P. Avery *et al.*	(CLEO Collab.)
FRABETTI	93B	PRL 70 1381	P.L. Frabetti *et al.*	(FNAL E687 Collab.)
ALBRECHT	90F	PL B247 121	H. Albrecht *et al.*	(ARGUS Collab.)
ALAM	89	PL B226 401	M.S. Alam *et al.*	(CLEO Collab.)
BARLAG	89C	PL B233 522	S. Barlag *et al.*	(ACCMOR Collab.)
COTEUS	87	PRL 59 1530	P. Coteus *et al.*	(FNAL E400 Collab.)
BIAGI	85C	PL 150B 230	S.F. Biagi *et al.*	(CERN WA62 Collab.)
BIAGI	83	PL 122B 455	S.F. Biagi *et al.*	(CERN WA62 Collab.)

Ξ_c^0

$I(J^P) = \frac{1}{2}(\frac{1}{2}^+)$ Status: ***

According to the quark model, the Ξ_c^0 (quark content dsc) and Ξ_c^+ form an isospin doublet, and the spin-parity ought to be $J^P = 1/2^+$. None of I, J, or P has actually been measured.

Ξ_c^0 MASS

The fit uses the Ξ_c^0 and Ξ_c^+ mass and mass-difference measurements.

VALUE (MeV)	EVTS	DOCUMENT ID		TECN	COMMENT
$2470.88^{+0.34}_{-0.80}$ OUR FIT Error includes scale factor of 1.1.					
$2471.09^{+0.35}_{-1.00}$ OUR AVERAGE					
$2471.0 \pm 0.3\ ^{+0.2}_{-1.4}$	8620 ± 355	[1] LESIAK	05	BELL	e^+e^-, $\Upsilon(4S)$
$2470.0 \pm 2.8 \pm 2.6$	85	FRABETTI	98B	E687	γ Be, $\overline{E}_\gamma = 220$ GeV
$2469 \pm 2 \pm 3$	9	HENDERSON	92B	CLEO	Ω^-K^+
$2472.1 \pm 2.7 \pm 1.6$	54	ALBRECHT	90F	ARG	e^+e^- at $\Upsilon(4S)$
$2473.3 \pm 1.9 \pm 1.2$	4	BARLAG	90	ACCM	π^- (K^-) Cu 230 GeV
$2472 \pm 3 \pm 4$	19	ALAM	89	CLEO	e^+e^- 10.6 GeV
• • • We do not use the following data for averages, fits, limits, etc. • • •					
$2462.1 \pm 3.1 \pm 1.4$	42	[2] FRABETTI	93C	E687	See FRABETTI 98B
$2471 \pm 3 \pm 4$	14	AVERY	89	CLEO	See ALAM 89

[1] The systematic error was (wrongly) given the other way round in LESIAK 05.
[2] The FRABETTI 93C mass is well below the other measurements.

$\Xi_c^0 - \Xi_c^+$ MASS DIFFERENCE

VALUE (MeV)	DOCUMENT ID		TECN	COMMENT
$3.1^{+0.4}_{-0.5}$ OUR FIT				
3.1 ± 0.5 OUR AVERAGE				
$+2.9 \pm 0.5$	LESIAK	05	BELL	e^+e^-, $\Upsilon(4S)$
$+7.0 \pm 4.5 \pm 2.2$	ALBRECHT	90F	ARG	e^+e^- at $\Upsilon(4S)$
$+6.8 \pm 3.3 \pm 0.5$	BARLAG	90	ACCM	π^- (K^-) Cu 230 GeV
$+5 \pm 4 \pm 1$	ALAM	89	CLEO	$\Xi_c^0 \to \Xi^-\pi^+$, $\Xi_c^+ \to \Xi^-\pi^+\pi^+$

Ξ_c^0 MEAN LIFE

VALUE (10^{-15} s)	EVTS	DOCUMENT ID		TECN	COMMENT
112^{+13}_{-10} OUR AVERAGE					
$118^{+14}_{-12} \pm 5$	110	LINK	02H	FOCS	γ nucleus, ≈ 180 GeV
$101^{+25}_{-17} \pm 5$	42	FRABETTI	93C	E687	γBe, $\overline{E}_\gamma = 220$ GeV
82^{+59}_{-30}	4	BARLAG	90	ACCM	π^- (K^-) Cu 230 GeV

Ξ_c^0 DECAY MODES

No absolute branching fractions have been measured. Several measurements of ratios of fractions may be found in the Listings that follow.

Mode	Fraction (Γ_i/Γ)
No absolute branching fractions have been measured. The following are branching *ratios* relative to $\Xi^-\pi^+$.	
Cabibbo-favored (S = −2) decays — relative to $\Xi^-\pi^+$	
Γ_1 $pK^-K^-\pi^+$	0.34 ±0.04
Γ_2 $pK^-\overline{K}^*(892)^0$	0.21 ±0.05
Γ_3 $pK^-K^-\pi^+$ (no $\overline{K}^{*0}$)	0.21 ±0.04
Γ_4 ΛK_S^0	0.210±0.028
Γ_5 $\Lambda K^-\pi^+$	1.07 ±0.14
Γ_6 $\Lambda\overline{K}^0\pi^+\pi^-$	seen
Γ_7 $\Lambda K^-\pi^+\pi^+\pi^-$	seen
Γ_8 $\Xi^-\pi^+$	**DEFINED AS 1**
Γ_9 $\Xi^-\pi^+\pi^+\pi^-$	3.3 ±1.4
Γ_{10} Ω^-K^+	0.297±0.024
Γ_{11} $\Xi^-e^+\nu_e$	3.1 ±1.1
Γ_{12} $\Xi^-\ell^+$ anything	1.0 ±0.5
Cabibbo-suppressed decays — relative to $\Xi^-\pi^+$	
Γ_{13} Ξ^-K^+	0.028±0.006
Γ_{14} ΛK^+K^- (no ϕ)	0.029±0.007
Γ_{15} $\Lambda\phi$	0.034±0.007

Ξ_c^0 BRANCHING RATIOS

Cabibbo-favored (S = −2) decays

$\Gamma(pK^-K^-\pi^+)/\Gamma(\Xi^-\pi^+)$ Γ_1/Γ_8

VALUE	EVTS	DOCUMENT ID		TECN	COMMENT
0.34±0.04 OUR AVERAGE					
$0.33 \pm 0.03 \pm 0.03$	1908 ± 62	LESIAK	05	BELL	e^+e^-, $\Upsilon(4S)$
$0.35 \pm 0.06 \pm 0.03$	148 ± 18	DANKO	04	CLEO	e^+e^-

$\Gamma(pK^-\overline{K}^*(892)^0)/\Gamma(\Xi^-\pi^+)$ Γ_2/Γ_8

Unseen decay modes of the $\overline{K}^*(892)^0$ are included.

VALUE	DOCUMENT ID		TECN	COMMENT
0.210±0.045±0.015	DANKO	04	CLEO	e^+e^-
• • • We do not use the following data for averages, fits, limits, etc. • • •				
seen	BARLAG	90	ACCM	π^- (K^-) Cu 230 GeV

$\Gamma(pK^-K^-\pi^+(\text{no }\overline{K}^{*0}))/\Gamma(\Xi^-\pi^+)$ Γ_3/Γ_8

VALUE	DOCUMENT ID		TECN	COMMENT
0.21±0.04±0.02	DANKO	04	CLEO	e^+e^-

$\Gamma(\Lambda K_S^0)/\Gamma(\Xi^-\pi^+)$ Γ_4/Γ_8

VALUE	EVTS	DOCUMENT ID		TECN	COMMENT
0.21±0.02±0.02	465 ± 37	LESIAK	05	BELL	e^+e^-, $\Upsilon(4S)$
• • • We do not use the following data for averages, fits, limits, etc. • • •					
seen	7	ALBRECHT	95B	ARG	$e^+e^- \approx 10.4$ GeV

$\Gamma(\Lambda K^-\pi^+)/\Gamma(\Xi^-\pi^+)$ Γ_5/Γ_8

VALUE	EVTS	DOCUMENT ID		TECN	COMMENT
1.07±0.12±0.07	2979 ± 211	LESIAK	05	BELL	e^+e^-, $\Upsilon(4S)$

$\Gamma(\Lambda\overline{K}^0\pi^+\pi^-)/\Gamma_{\text{total}}$ Γ_6/Γ

VALUE	DOCUMENT ID		TECN	COMMENT
seen	FRABETTI	98B	E687	γ Be, $\overline{E}_\gamma = 220$ GeV

$\Gamma(\Lambda K^-\pi^+\pi^+\pi^-)/\Gamma_{\text{total}}$ Γ_7/Γ

VALUE	DOCUMENT ID		TECN	COMMENT
seen	FRABETTI	98B	E687	γ Be, $\overline{E}_\gamma = 220$ GeV

$\Gamma(\Xi^-\pi^+)/\Gamma(\Xi^-\pi^+\pi^+\pi^-)$ Γ_8/Γ_9

VALUE	DOCUMENT ID		TECN	COMMENT
0.30±0.12±0.05	ALBRECHT	90F	ARG	e^+e^- at $\Upsilon(4S)$

$\Gamma(\Omega^-K^+)/\Gamma(\Xi^-\pi^+)$ Γ_{10}/Γ_8

VALUE	EVTS	DOCUMENT ID		TECN	COMMENT
0.297±0.024 OUR AVERAGE					
$0.294 \pm 0.018 \pm 0.016$	650	AUBERT,B	05M	BABR	$e^+e^- \approx \Upsilon(4S)$
$0.50 \pm 0.21 \pm 0.05$	9	HENDERSON	92B	CLEO	$e^+e^- \approx 10.6$ GeV

$\Gamma(\Xi^-e^+\nu_e)/\Gamma(\Xi^-\pi^+)$ Γ_{11}/Γ_8

VALUE	EVTS	DOCUMENT ID		TECN	COMMENT
$3.1 \pm 1.0^{+0.3}_{-0.5}$	54	ALEXANDER	95B	CLE2	$e^+e^- \approx \Upsilon(4S)$

Baryon Particle Listings

Ξ_c^0, $\Xi_c'^+$, $\Xi_c'^0$, $\Xi_c(2645)$

$\Gamma(\Xi^-\ell^+\text{anything})/\Gamma(\Xi^-\pi^+)$ Γ_{12}/Γ_8

The ratio is for the *average* (not the sum) of the Ξ^-e^+ anything and $\Xi^-\mu^+$ anything modes.

VALUE	EVTS	DOCUMENT ID		TECN	COMMENT
0.96±0.43±0.18	18	ALBRECHT	93B	ARG	$e^+e^-\approx 10.4$ GeV

$\Gamma(\Xi^-\ell^+\text{anything})/\Gamma(\Xi^-\pi^+\pi^+\pi^-)$ Γ_{12}/Γ_9

The ratio is for the *average* (not the sum) of the Ξ^-e^+ anything and $\Xi^-\mu^+$ anything modes.

VALUE	EVTS	DOCUMENT ID		TECN	COMMENT
0.29±0.12±0.04	18	ALBRECHT	93B	ARG	$e^+e^-\approx 10.4$ GeV

Cabibbo-suppressed decays

$\Gamma(\Xi^-K^+)/\Gamma(\Xi^-\pi^+)$ Γ_{13}/Γ_8

VALUE (units 10^{-2})	EVTS	DOCUMENT ID		TECN	COMMENT
2.75±0.51±0.25	314 ± 58	CHISTOV	13	BELL	$e^+e^-\approx \Upsilon(4S)$

$\Gamma(\Lambda K^+K^-(\text{no}\,\phi))/\Gamma(\Xi^-\pi^+)$ Γ_{14}/Γ_8

VALUE (units 10^{-2})	EVTS	DOCUMENT ID		TECN	COMMENT
2.86±0.61±0.37	510 ± 110	CHISTOV	13	BELL	$e^+e^-\approx \Upsilon(4S)$

$\Gamma(\Lambda\phi)/\Gamma(\Xi^-\pi^+)$ Γ_{15}/Γ_8

VALUE (units 10^{-2})	EVTS	DOCUMENT ID		TECN	COMMENT
3.43±0.58±0.32	316 ± 54	CHISTOV	13	BELL	$e^+e^-\approx \Upsilon(4S)$

Ξ_c^0 DECAY PARAMETERS

See the note on "Baryon Decay Parameters" in the neutron Listings.

α FOR $\Xi_c^0\to\Xi^-\pi^+$

VALUE	EVTS	DOCUMENT ID		TECN	COMMENT
$\mathbf{-0.56\pm0.39^{+0.10}_{-0.09}}$	138	CHAN	01	CLE2	$e^+e^-\approx \Upsilon(4S)$

Ξ_c^0 REFERENCES

CHISTOV	13	PR D88 071103	R. Chistov *et al.*	(BELLE Collab.)
AUBERT,B	05M	PRL 95 142003	B. Aubert *et al.*	(BABAR Collab.)
LESIAK	05	PL B605 237	T. Lesiak *et al.*	(BELLE Collab.)
Also		PL B617 198 (errat)	T. Lesiak *et al.*	(BELLE Collab.)
DANKO	04	PR D69 052004	I. Danko *et al.*	(CLEO Collab.)
LINK	02H	PL B541 211	J.M. Link *et al.*	(FNAL FOCUS Collab.)
CHAN	01	PR D63 111102	S. Chan *et al.*	(CLEO Collab.)
FRABETTI	98B	PL B426 403	P.L. Frabetti *et al.*	(FNAL E687 Collab.)
ALBRECHT	95B	PL B342 397	H. Albrecht *et al.*	(ARGUS Collab.)
ALEXANDER	95B	PRL 74 3113	J. Alexander *et al.*	(CLEO Collab.)
Also		PRL 75 4155 (erratum)	J. Alexander *et al.*	(CLEO Collab.)
ALBRECHT	93B	PL B303 368	H. Albrecht *et al.*	(ARGUS Collab.)
FRABETTI	93C	PRL 70 2058	P.L. Frabetti *et al.*	(FNAL E687 Collab.)
HENDERSON	92B	PL B283 161	S. Henderson *et al.*	(CLEO Collab.)
ALBRECHT	90F	PL B247 121	H. Albrecht *et al.*	(ARGUS Collab.)
BARLAG	90	PL B236 495	S. Barlag *et al.*	(ACCMOR Collab.)
ALAM	89	PL B226 401	M.S. Alam *et al.*	(CLEO Collab.)
AVERY	89	PRL 62 863	P. Avery *et al.*	(CLEO Collab.)

$\Xi_c'^+$

$I(J^P) = \frac{1}{2}(\frac{1}{2}^+)$ Status: ***

The $\Xi_c'^+$ and $\Xi_c'^0$ presumably complete the SU(3) sextet whose other members are the Σ_c^{++}, Σ_c^+, Σ_c^0, and Ω_c^0: see Fig. 3 in the Note on Charmed Baryons just before the Λ_c^+ Listings. The quantum numbers given above come from this presumption but have not been measured.

$\Xi_c'^+$ MASS

The mass is obtained from the mass-difference measurement that follows.

VALUE (MeV)	DOCUMENT ID
2575.6±3.1 OUR FIT	

$\Xi_c'^+ - \Xi_c^+$ MASS DIFFERENCE

VALUE (MeV)	EVTS	DOCUMENT ID		TECN	COMMENT
107.8±3.0 OUR FIT					
107.8±1.7±2.5	25	JESSOP	99	CLE2	$e^+e^-\approx \Upsilon(4S)$

$\Xi_c'^+$ DECAY MODES

The $\Xi_c'^+ - \Xi_c^+$ mass difference is too small for any strong decay to occur.

	Mode	Fraction (Γ_i/Γ)
Γ_1	$\Xi_c^+\gamma$	seen

$\Xi_c'^+$ REFERENCES

JESSOP	99	PRL 82 492	C.P. Jessop *et al.*	(CLEO Collab.)

$\Xi_c'^0$

$I(J^P) = \frac{1}{2}(\frac{1}{2}^+)$ Status: ***

See the note in the Listing for the $\Xi_c'^+$, above.

$\Xi_c'^0$ MASS

The mass is obtained from the mass-difference measurement that follows.

VALUE (MeV)	DOCUMENT ID
2577.9±2.9 OUR FIT	

$\Xi_c'^0 - \Xi_c^0$ MASS DIFFERENCE

VALUE (MeV)	EVTS	DOCUMENT ID		TECN	COMMENT
107.0±2.9 OUR FIT					
107.0±1.4±2.5	28	JESSOP	99	CLE2	$e^+e^-\approx \Upsilon(4S)$

$\Xi_c'^0$ DECAY MODES

The $\Xi_c'^0 - \Xi_c^0$ mass difference is too small for any strong decay to occur.

	Mode	Fraction (Γ_i/Γ)
Γ_1	$\Xi_c^0\gamma$	seen

$\Xi_c'^0$ REFERENCES

JESSOP	99	PRL 82 492	C.P. Jessop *et al.*	(CLEO Collab.)

$\Xi_c(2645)$

$I(J^P) = \frac{1}{2}(\frac{3}{2}^+)$ Status: ***

A narrow peak seen in the $\Xi_c\pi$ mass spectrum. The natural assignment is that this is the $J^P = 3/2^+$ excitation of the Ξ_c in the same SU(4) multiplet as the $\Delta(1232)$, but the quantum numbers have not been measured.

$\Xi_c(2645)$ MASSES

The masses are obtained from the mass-difference measurements that follow.

$\Xi_c(2645)^+$ MASS

VALUE (MeV)	EVTS	DOCUMENT ID		TECN	COMMENT
$\mathbf{2645.9^{+0.5}_{-0.6}}$ **OUR FIT**	Error includes scale factor of 1.1.				
$\mathbf{2645.6\pm0.2^{+0.6}_{-0.8}}$	578 ± 32	LESIAK	08	BELL	$e^+e^-\approx \Upsilon(4S)$

$\Xi_c(2645)^0$ MASS

VALUE (MeV)	EVTS	DOCUMENT ID		TECN	COMMENT
2645.9±0.5 OUR FIT					
$\mathbf{2645.7\pm0.2^{+0.6}_{-0.7}}$	611 ± 32	LESIAK	08	BELL	$e^+e^-\approx \Upsilon(4S)$

$\Xi_c(2645) - \Xi_c$ MASS DIFFERENCES

$m_{\Xi_c(2645)^+} - m_{\Xi_c^0}$

VALUE (MeV)	EVTS	DOCUMENT ID		TECN	COMMENT
$\mathbf{175.0^{+0.8}_{-0.6}}$ **OUR FIT**	Error includes scale factor of 1.2.				
175.6±1.4 OUR AVERAGE	Error includes scale factor of 1.7.				
177.1±0.5±1.1	47	FRABETTI	98B	E687	γ Be, $\overline{E}_\gamma = 220$ GeV
174.3±0.5±1.0	34	GIBBONS	96	CLE2	$e^+e^-\approx \Upsilon(4S)$

$m_{\Xi_c(2645)^0} - m_{\Xi_c^+}$

VALUE (MeV)	EVTS	DOCUMENT ID		TECN	COMMENT
178.1±0.6 OUR FIT					
178.2±0.5±1.0	55	AVERY	95	CLE2	$e^+e^-\approx \Upsilon(4S)$

$\Xi_c(2645)^+ - \Xi_c(2645)^0$ MASS DIFFERENCE

$m_{\Xi_c(2645)^+} - m_{\Xi_c(2645)^0}$

VALUE (MeV)	DOCUMENT ID		TECN	COMMENT
0.0±0.5 OUR FIT				
−0.1±0.3±0.6	LESIAK	08	BELL	≈ 600 evts each

$\Xi_c(2645)$ WIDTHS

$\Xi_c(2645)^+$ WIDTH

VALUE (MeV)	CL%	DOCUMENT ID		TECN	COMMENT
<3.1	90	GIBBONS	96	CLE2	$e^+e^-\approx \Upsilon(4S)$

$\Xi_c(2645)^0$ WIDTH

VALUE (MeV)	CL%	EVTS	DOCUMENT ID		TECN	COMMENT
<5.5	90	55	AVERY	95	CLE2	$e^+e^- \approx \Upsilon(4S)$

$\Xi_c(2645)$ DECAY MODES

$\Xi_c\pi$ is the only strong decay allowed to a Ξ_c resonance having this mass.

	Mode	Fraction (Γ_i/Γ)
Γ_1	$\Xi_c^0\pi^+$	seen
Γ_2	$\Xi_c^+\pi^-$	seen

$\Xi_c(2645)$ REFERENCES

LESIAK	08	PL B665 9	T. Lesiak *et al.*	(BELLE Collab.)
FRABETTI	98B	PL B426 403	P.L. Frabetti *et al.*	(FNAL E687 Collab.)
GIBBONS	96	PRL 77 810	L.K. Gibbons *et al.*	(CLEO Collab.)
AVERY	95	PRL 75 4364	P. Avery *et al.*	(CLEO Collab.)

$\Xi_c(2790)$

$I(J^P) = \frac{1}{2}(\frac{1}{2}^-)$ Status: ***

A peak seen in the $\Xi_c'\pi$ mass spectrum. The simplest assignment, based on the mass, width, and decay mode, is that this belongs in the same SU(4) multiplet as the $\Lambda(1405)$ and the $\Lambda_c(2595)^+$, but the spin and parity have not been measured.

$\Xi_c(2790)$ MASSES

The masses are obtained from the mass-difference measurements that follow.

$\Xi_c(2790)^+$ MASS

VALUE (MeV)	DOCUMENT ID
2789.1±3.2 OUR FIT	

$\Xi_c(2790)^0$ MASS

VALUE (MeV)	DOCUMENT ID
2791.8±3.3 OUR FIT	

$\Xi_c(2790) - \Xi_c$ MASS DIFFERENCES

$m_{\Xi_c(2790)^+} - m_{\Xi_c^0}$

VALUE (MeV)	EVTS	DOCUMENT ID		TECN	COMMENT
318.2±3.2 OUR FIT					
318.2±1.3±2.9	18	CSORNA	01	CLEO	$e^+e^- \approx \Upsilon(4S)$

$m_{\Xi_c(2790)^0} - m_{\Xi_c^+}$

VALUE (MeV)	EVTS	DOCUMENT ID		TECN	COMMENT
324.0±3.3 OUR FIT					
324.0±1.3±3.0	14	CSORNA	01	CLEO	$e^+e^- \approx \Upsilon(4S)$

$\Xi_c(2790)$ WIDTHS

$\Xi_c(2790)^+$ WIDTH

VALUE (MeV)	CL%	DOCUMENT ID		TECN	COMMENT
<15	90	CSORNA	01	CLEO	$e^+e^- \approx \Upsilon(4S)$

$\Xi_c(2790)^0$ WIDTH

VALUE (MeV)	CL%	DOCUMENT ID		TECN	COMMENT
<12	90	CSORNA	01	CLEO	$e^+e^- \approx \Upsilon(4S)$

$\Xi_c(2790)$ DECAY MODES

	Mode	Fraction (Γ_i/Γ)
Γ_1	$\Xi_c'\pi$	seen

$\Xi_c(2790)$ REFERENCES

CSORNA	01	PRL 86 4243	S.E. Csorna *et al.*	(CLEO Collab.)

$\Xi_c(2815)$

$I(J^P) = \frac{1}{2}(\frac{3}{2}^-)$ Status: ***

A narrow peak seen in the $\Xi_c\pi\pi$ mass spectrum. The simplest assignment is that this belongs to the same SU(4) multiplet as the $\Lambda(1520)$ and the $\Lambda_c(2625)$, but the spin and parity have not been measured.

$\Xi_c(2815)$ MASSES

The masses are obtained from the mass-difference measurements that follow.

$\Xi_c(2815)^+$ MASS

VALUE (MeV)	EVTS	DOCUMENT ID		TECN	COMMENT
2816.6±0.9 OUR FIT					
$2817.0\pm1.2^{+0.7}_{-0.8}$	73 ± 10	LESIAK	08	BELL	$e^+e^- \approx \Upsilon(4S)$

$\Xi_c(2815)^0$ MASS

VALUE (MeV)	EVTS	DOCUMENT ID		TECN	COMMENT
2819.6±1.2 OUR FIT					
$2820.4\pm1.4^{+0.9}_{-1.0}$	48 ± 8	LESIAK	08	BELL	$e^+e^- \approx \Upsilon(4S)$

$\Xi_c(2815) - \Xi_c$ MASS DIFFERENCES

$m_{\Xi_c(2815)^+} - m_{\Xi_c^+}$

VALUE (MeV)	EVTS	DOCUMENT ID		TECN	COMMENT
348.8±0.9 OUR FIT					
348.6±0.6±1.0	20	ALEXANDER	99B	CLE2	$e^+e^- \approx \Upsilon(4S)$

$m_{\Xi_c(2815)^0} - m_{\Xi_c^0}$

VALUE (MeV)	EVTS	DOCUMENT ID		TECN	COMMENT
348.7±1.2 OUR FIT					
347.2±0.7±2.0	9	ALEXANDER	99B	CLE2	$e^+e^- \approx \Upsilon(4S)$

$\Xi_c(2815)^+ - \Xi_c(2815)^0$ MASS DIFFERENCE

$m_{\Xi_c(2815)^+} - m_{\Xi_c(2815)^0}$

VALUE (MeV)	DOCUMENT ID		TECN	COMMENT
−3.1±1.3 OUR FIT				
−3.4±1.9±0.9	LESIAK	08	BELL	73 & 48 events

$\Xi_c(2815)$ WIDTHS

$\Xi_c(2815)^+$ WIDTH

VALUE (MeV)	CL%	DOCUMENT ID		TECN	COMMENT
<3.5	90	ALEXANDER	99B	CLE2	$e^+e^- \approx \Upsilon(4S)$

$\Xi_c(2815)^0$ WIDTH

VALUE (MeV)	CL%	DOCUMENT ID		TECN	COMMENT
<6.5	90	ALEXANDER	99B	CLE2	$e^+e^- \approx \Upsilon(4S)$

$\Xi_c(2815)$ DECAY MODES

The $\Xi_c\pi\pi$ modes are consistent with being entirely via $\Xi_c(2645)\pi$.

	Mode	Fraction (Γ_i/Γ)
Γ_1	$\Xi_c^+\pi^+\pi^-$	seen
Γ_2	$\Xi_c^0\pi^+\pi^-$	seen

$\Xi_c(2815)$ REFERENCES

LESIAK	08	PL B665 9	T. Lesiak *et al.*	(BELLE Collab.)
ALEXANDER	99B	PRL 83 3390	J.P. Alexander *et al.*	(CLEO Collab.)

Baryon Particle Listings

$\Xi_c(2930)$, $\Xi_c(2980)$, $\Xi_c(3055)$

$\Xi_c(2930)$

$I(J^P) = ?(?^?)$ Status: *

OMITTED FROM SUMMARY TABLE

A peak seen in the $\Lambda_c^+ K^-$ mass projection of $B^- \to \Lambda_c^+ \overline{\Lambda}_c^- K^-$ events.

$\Xi_c(2930)$ MASS

VALUE (MeV)	EVTS	DOCUMENT ID		TECN	COMMENT
2931 ± 3 ± 5	≈ 34	AUBERT	08H	BABR	$\Upsilon(4S) \to B\overline{B}$

$\Xi_c(2930)$ WIDTH

VALUE (MeV)	EVTS	DOCUMENT ID		TECN	COMMENT
36 ± 7 ± 11	≈ 34	AUBERT	08H	BABR	$\Upsilon(4S) \to B\overline{B}$

$\Xi_c(2930)$ REFERENCES

AUBERT 08H PR D77 031101 B. Aubert *et al.* (BABAR Collab.)

$\Xi_c(2980)$

$I(J^P) = \frac{1}{2}(?^?)$ Status: ***

$\Xi_c(2980)$ MASSES

$\Xi_c(2980)^+$ MASS

VALUE (MeV)	EVTS	DOCUMENT ID		TECN	COMMENT
2971.4 ± 3.3 OUR AVERAGE Error includes scale factor of 2.1. See the ideogram below.					
2969.3 ± 2.2 ± 1.7	756 ± 206	AUBERT	08J	BABR	$e^+e^- \approx$ 10.58 GeV
$2967.7 \pm 2.3 ^{+1.1}_{-1.2}$	78 ± 13	LESIAK	08	BELL	$e^+e^- \approx \Upsilon(4S)$
2978.5 ± 2.1 ± 2.0	405 ± 51	CHISTOV	06	BELL	$e^+e^- \approx \Upsilon(4S)$

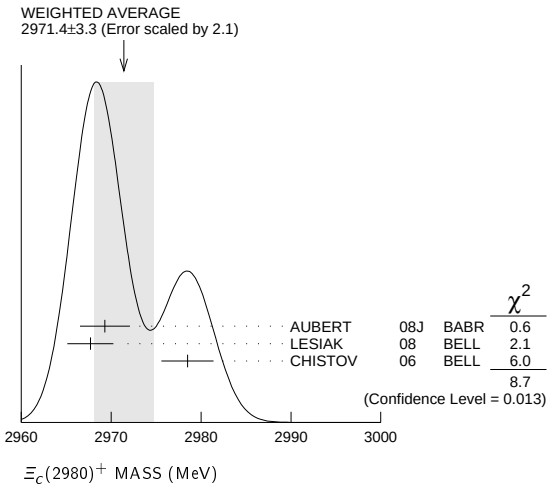

$\Xi_c(2980)^+$ MASS (MeV)

$\Xi_c(2980)^0$ MASS

The evidence is statistically weaker for this charge state.

VALUE (MeV)	EVTS	DOCUMENT ID		TECN	COMMENT
2968.0 ± 2.6 OUR AVERAGE Error includes scale factor of 1.2.					
2972.9 ± 4.4 ± 1.6	67 ± 44	AUBERT	08J	BABR	$e^+e^- \approx$ 10.58 GeV
$2965.7 \pm 2.4 ^{+1.1}_{-1.2}$	57 ± 13	LESIAK	08	BELL	$e^+e^- \approx \Upsilon(4S)$
2977.1 ± 8.8 ± 3.5	42 ± 24	CHISTOV	06	BELL	$e^+e^- \approx \Upsilon(4S)$

$\Xi_c(2980)$ WIDTHS

$\Xi_c(2980)^+$ WIDTH

VALUE (MeV)	EVTS	DOCUMENT ID		TECN	COMMENT
26 ± 7 OUR AVERAGE Error includes scale factor of 1.5. See the ideogram below.					
27 ± 8 ± 2	756 ± 206	AUBERT	08J	BABR	$e^+e^- \approx$ 10.58 GeV
18 ± 6 ± 3	78 ± 13	LESIAK	08	BELL	$e^+e^- \approx \Upsilon(4S)$
43.5 ± 7.5 ± 7.0	405 ± 51	CHISTOV	06	BELL	$e^+e^- \approx \Upsilon(4S)$

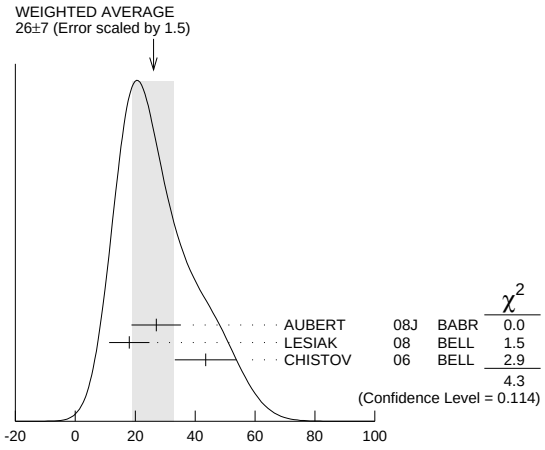

$\Xi_c(2980)^+$ WIDTH (MeV)

$\Xi_c(2980)^0$ WIDTH

VALUE (MeV)	EVTS	DOCUMENT ID		TECN	COMMENT
20 ± 7 OUR AVERAGE Error includes scale factor of 1.3.					
31 ± 7 ± 8	67 ± 44	AUBERT	08J	BABR	$e^+e^- \approx$ 10.58 GeV
15 ± 6 ± 3	57 ± 13	LESIAK	08	BELL	$e^+e^- \approx \Upsilon(4S)$

$\Xi_c(2980)$ DECAY MODES

	Mode	Fraction (Γ_i/Γ)
Γ_1	$\Lambda_c^+ \overline{K}\pi$	seen
Γ_2	$\Sigma_c(2455)\overline{K}$	seen
Γ_3	$\Lambda_c^+ \overline{K}$	not seen
Γ_4	$\Xi_c 2\pi$	seen
Γ_5	$\Xi_c(2645)\pi$	seen

$\Xi_c(2980)$ BRANCHING RATIOS

$\Gamma(\Lambda_c^+ \overline{K}\pi)/\Gamma_{total}$ Γ_1/Γ

VALUE	DOCUMENT ID		TECN	COMMENT
seen	AUBERT	08J	BABR	$e^+e^- \approx \Upsilon(4S)$
seen	CHISTOV	06	BELL	$e^+e^- \approx \Upsilon(4S)$

$\Gamma(\Sigma_c(2455)\overline{K})/\Gamma(\Lambda_c^+ \overline{K}\pi)$ Γ_2/Γ_1

VALUE	DOCUMENT ID		TECN	COMMENT
0.55 ± 0.07 ± 0.13	AUBERT	08J	BABR	$e^+e^- \approx \Upsilon(4S)$

$\Gamma(\Xi_c(2645)\pi)/\Gamma_{total}$ Γ_5/Γ

VALUE	DOCUMENT ID		TECN	COMMENT
seen	LESIAK	08	BELL	$e^+e^- \approx \Upsilon(4S)$

$\Xi_c(2980)$ REFERENCES

AUBERT 08J PR D77 012002 B. Aubert *et al.* (BABAR Collab.)
LESIAK 08 PL B665 9 T. Lesiak *et al.* (BELLE Collab.)
CHISTOV 06 PRL 97 162001 R. Chistov *et al.* (BELLE Collab.)

$\Xi_c(3055)$

$I(J^P) = ?(?^?)$ Status: **

OMITTED FROM SUMMARY TABLE

A peak in the $\Sigma_c(2455)^{++} K^- \to \Lambda_c^+ K^- \pi^+$ mass spectrum with a claimed significance of 6.4 standard deviations.

$\Xi_c(3055)$ MASSES

$\Xi_c(3055)^+$ MASS

VALUE (MeV)	EVTS	DOCUMENT ID		TECN	COMMENT
3054.2 ± 1.2 ± 0.5	218 ± 95	AUBERT	08J	BABR	$e^+e^- \approx$ 10.58 GeV

$\Xi_c(3055)$ WIDTHS

$\Xi_c(3055)^+$ WIDTH

VALUE (MeV)	EVTS	DOCUMENT ID		TECN	COMMENT
17 ± 6 ± 11	218 ± 95	AUBERT	08J	BABR	$e^+e^- \approx$ 10.58 GeV

$\Xi_c(3055)$ REFERENCES

AUBERT 08J PR D77 012002 B. Aubert *et al.* (BABAR Collab.)

$\Xi_c(3080)$

$I(J^P) = \frac{1}{2}(?^?)$ Status: ***

A narrow peak seen in the $\Lambda_c^+ K^- \pi^+$ and $\Lambda_c^+ K_S^0 \pi^-$ mass spectra.

$\Xi_c(3080)$ MASSES

$\Xi_c(3080)^+$ MASS

VALUE (MeV)	EVTS	DOCUMENT ID		TECN	COMMENT
3077.0±0.4 OUR AVERAGE					
3077.0±0.4±0.2	403 ± 60	AUBERT	08J	BABR	$e^+e^- \approx$ 10.58 GeV
3076.7±0.9±0.5	326 ± 40	CHISTOV	06	BELL	$e^+e^- \approx \Upsilon(4S)$

$\Xi_c(3080)^0$ MASS

VALUE (MeV)	EVTS	DOCUMENT ID		TECN	COMMENT
3079.9±1.4 OUR AVERAGE Error includes scale factor of 1.3.					
3079.3±1.1±0.2	90 ± 27	AUBERT	08J	BABR	$e^+e^- \approx$ 10.58 GeV
3082.8±1.8±1.5	67 ± 20	CHISTOV	06	BELL	$e^+e^- \approx \Upsilon(4S)$

$\Xi_c(3080)$ WIDTHS

$\Xi_c(3080)^+$ WIDTH

VALUE (MeV)	EVTS	DOCUMENT ID		TECN	COMMENT
5.8±1.0 OUR AVERAGE					
5.5±1.3±0.6	403 ± 60	AUBERT	08J	BABR	$e^+e^- \approx$ 10.58 GeV
6.2±1.2±0.8	326 ± 40	CHISTOV	06	BELL	$e^+e^- \approx \Upsilon(4S)$

$\Xi_c(3080)^0$ WIDTH

VALUE (MeV)	EVTS	DOCUMENT ID		TECN	COMMENT
5.6±2.2 OUR AVERAGE					
5.9±2.3±1.5	90 ± 27	AUBERT	08J	BABR	$e^+e^- \approx$ 10.58 GeV
5.2±3.1±1.8	67 ± 20	CHISTOV	06	BELL	$e^+e^- \approx \Upsilon(4S)$

$\Xi_c(3080)$ DECAY MODES

	Mode	Fraction (Γ_i/Γ)
Γ_1	$\Lambda_c^+ \overline{K} \pi$	seen
Γ_2	$\Sigma_c(2455)\overline{K}$	seen
Γ_3	$\Sigma_c(2455)\overline{K} + \Sigma_c(2520)\overline{K}$	seen
Γ_4	$\Lambda_c^+ \overline{K}$	not seen
Γ_5	$\Lambda_c^+ \overline{K} \pi^+ \pi^-$	not seen

$\Xi_c(3080)$ BRANCHING RATIOS

$\Gamma(\Sigma_c(2455)\overline{K})/\Gamma(\Lambda_c^+ \overline{K}\pi)$ Γ_2/Γ_1

VALUE	DOCUMENT ID		TECN	COMMENT
0.45±0.06 OUR AVERAGE				
0.45±0.05±0.05	AUBERT	08J	BABR	in $\Lambda_c^+ K^- \pi^+$
0.44±0.12±0.07	AUBERT	08J	BABR	in $\Lambda_c^+ K_S^0 \pi^-$

$[\Gamma(\Sigma_c(2455)\overline{K}) + \Gamma(\Sigma_c(2520)\overline{K})]/\Gamma(\Lambda_c^+ \overline{K}\pi)$ Γ_3/Γ_1

VALUE	DOCUMENT ID		TECN	COMMENT
0.89±0.12 OUR AVERAGE				
0.95±0.14±0.06	AUBERT	08J	BABR	in $\Lambda_c^+ K^- \pi^+$
0.78±0.21±0.05	AUBERT	08J	BABR	in $\Lambda_c^+ K_S^0 \pi^-$

$\Xi_c(3080)$ REFERENCES

AUBERT 08J PR D77 012002 B. Aubert *et al.* (BABAR Collab.)
CHISTOV 06 PRL 97 162001 R. Chistov *et al.* (BELLE Collab.)

$\Xi_c(3123)$

$I(J^P) = ?(?^?)$ Status: *

OMITTED FROM SUMMARY TABLE

A peak in the $\Sigma_c(2520)^{++} K^- \rightarrow \Lambda_c^+ K^- \pi^+$ mass spectrum with a significance of 3.6 standard deviations.

$\Xi_c(3123)$ MASSES

$\Xi_c(3123)^+$ MASS

VALUE (MeV)	EVTS	DOCUMENT ID		TECN	COMMENT
3122.9±1.3±0.3	101 ± 35	AUBERT	08J	BABR	$e^+e^- \approx$ 10.58 GeV

$\Xi_c(3123)$ WIDTHS

$\Xi_c(3123)^+$ WIDTH

VALUE (MeV)	EVTS	DOCUMENT ID		TECN	COMMENT
4.4±3.4±1.7	101 ± 35	AUBERT	08J	BABR	$e^+e^- \approx$ 10.58 GeV

$\Xi_c(3123)$ REFERENCES

AUBERT 08J PR D77 012002 B. Aubert *et al.* (BABAR Collab.)

Ω_c^0

$I(J^P) = 0(\frac{1}{2}^+)$ Status: ***

The quantum numbers have not been measured, but are simply assigned in accord with the quark model, in which the Ω_c^0 is the *ssc* ground state.

Ω_c^0 MASS

VALUE (MeV)	EVTS	DOCUMENT ID		TECN	COMMENT
2695.2± 1.7 OUR FIT Error includes scale factor of 1.3.					
2695.2$^{+\ 1.8}_{-\ 1.6}$ OUR AVERAGE Error includes scale factor of 1.3. See the ideogram below.					
2693.6± 0.3$^{+1.8}_{-1.5}$	725 ± 45	SOLOVIEVA	09	BELL	$\Omega^-\pi^+$ in $e^+e^- \rightarrow \Upsilon(4S)$
2694.6± 2.6±1.9	40	[1] CRONIN-HEN..01		CLE2	$e^+e^- \approx$ 10.6 GeV
2699.9± 1.5±2.5	42	[2] FRABETTI	94H	E687	γBe, $\overline{E}_\gamma$= 221 GeV
• • • We do not use the following data for averages, fits, limits, etc. • • •					
2705.9± 3.3±2.0	10	[3] FRABETTI	93	E687	γBe, $\overline{E}_\gamma$= 221 GeV
2719.0± 7.0±2.5	11	[4] ALBRECHT	92H	ARG	$e^+e^- \approx$ 10.6 GeV
2740 ±20	3	BIAGI	85B	SPEC	Σ^-Be 135 GeV/c

[1] CRONIN-HENNESSY 01 sees 40.4 ± 9.0 events in a sum over five channels.
[2] FRABETTI 94H claims a signal of 42.5 ± 8.8 $\Sigma^+ K^- K^- \pi^+$ events. The background is about 24 events.
[3] FRABETTI 93 claims a signal of 10.3 ± 3.9 $\Omega^-\pi^+$ events above a background of 5.8 events.
[4] ALBRECHT 92H claims a signal of 11.5 ± 4.3 $\Xi^- K^- \pi^+ \pi^+$ events. The background is about 5 events.

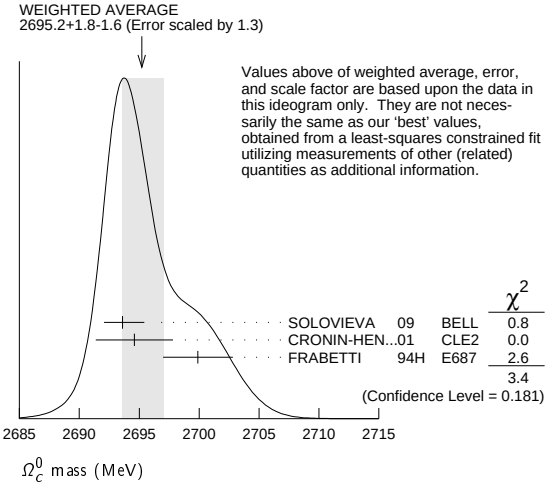

Ω_c^0 MEAN LIFE

VALUE (10^{-15} s)	EVTS	DOCUMENT ID		TECN	COMMENT
69±12 OUR AVERAGE					
72±11±11	64	LINK	03C	FOCS	$\Omega^-\pi^+$, $\Xi^- K^-\pi^+\pi^+$
55$^{+13+18}_{-11-23}$	86	ADAMOVICH	95B	WA89	$\Omega^-\pi^-\pi^+\pi^+$, $\Xi^- K^-\pi^+\pi^+$
86$^{+27}_{-20}$±28	25	FRABETTI	95D	E687	$\Sigma^+ K^- K^-\pi^+$

Ω_c^0 DECAY MODES

No absolute branching fractions have been measured.

	Mode	Fraction (Γ_i/Γ)
Γ_1	$\Sigma^+ K^- K^- \pi^+$	seen
Γ_2	$\Xi^0 K^- \pi^+$	seen
Γ_3	$\Xi^- K^- \pi^+ \pi^+$	seen
Γ_4	$\Omega^- e^+ \nu_e$	seen
Γ_5	$\Omega^- \pi^+$	seen
Γ_6	$\Omega^- \pi^+ \pi^0$	seen
Γ_7	$\Omega^- \pi^- \pi^+ \pi^+$	seen

Ω_c^0 BRANCHING RATIOS

$\Gamma(\Sigma^+ K^- K^- \pi^+)/\Gamma_{\text{total}}$ Γ_1/Γ

VALUE	EVTS	DOCUMENT ID		TECN	COMMENT
seen	42	FRABETTI	94H	E687	γBe, $\overline{E}_\gamma$= 221 GeV

Baryon Particle Listings

Ω_c^0, $\Omega_c(2770)^0$

$\Gamma(\Sigma^+ K^- K^- \pi^+)/\Gamma(\Omega^- \pi^+)$ Γ_1/Γ_5

VALUE	CL%	DOCUMENT ID		TECN	COMMENT
• • • We do not use the following data for averages, fits, limits, etc. • • •					
<4.8	90	CRONIN-HEN...01		CLE2	$e^+e^- \approx$ 10.6 GeV

$\Gamma(\Xi^0 K^- \pi^+)/\Gamma(\Omega^- \pi^+)$ Γ_2/Γ_5

VALUE	EVTS	DOCUMENT ID		TECN	COMMENT
4.0±2.5±0.4	9	CRONIN-HEN...01		CLE2	$e^+e^- \approx$ 10.6 GeV

$\Gamma(\Xi^- K^- \pi^+ \pi^+)/\Gamma_{total}$ Γ_3/Γ

VALUE	EVTS	DOCUMENT ID		TECN	COMMENT
seen	11	ALBRECHT	92H	ARG	$e^+e^- \approx$ 10.6 GeV
seen	3	BIAGI	85B	SPEC	Σ^- Be 135 GeV/c

$\Gamma(\Xi^- K^- \pi^+ \pi^+)/\Gamma(\Omega^- \pi^+)$ Γ_3/Γ_5

VALUE	CL%	EVTS	DOCUMENT ID		TECN	COMMENT
0.46±0.13±0.03		45 ± 12	AUBERT	07AH	BABR	$e^+e^- \approx \Upsilon(4S)$
• • • We do not use the following data for averages, fits, limits, etc. • • •						
1.6 ±1.1 ±0.4		7	CRONIN-HEN...01		CLE2	$e^+e^- \approx$ 10.6 GeV
<2.8	90		FRABETTI	93	E687	γBe, $\overline{E}_\gamma$= 221 GeV

$\Gamma(\Omega^- \pi^+)/\Gamma(\Omega^- e^+ \nu_e)$ Γ_5/Γ_4

VALUE	EVTS	DOCUMENT ID		TECN	COMMENT
0.41±0.19±0.04	11	AMMAR	02	CLE2	$e^+e^- \approx \Upsilon(4S)$

$\Gamma(\Omega^- \pi^+ \pi^0)/\Gamma(\Omega^- \pi^+)$ Γ_6/Γ_5

VALUE	EVTS	DOCUMENT ID		TECN	COMMENT
1.27±0.31±0.11	64 ± 15	AUBERT	07AH	BABR	$e^+e^- \approx \Upsilon(4S)$
• • • We do not use the following data for averages, fits, limits, etc. • • •					
4.2 ±2.2 ±0.9	12	CRONIN-HEN...01		CLE2	$e^+e^- \approx$ 10.6 GeV

$\Gamma(\Omega^- \pi^- \pi^+ \pi^+)/\Gamma(\Omega^- \pi^+)$ Γ_7/Γ_5

VALUE	CL%	EVTS	DOCUMENT ID		TECN	COMMENT
0.28±0.09±0.01		25 ± 8	AUBERT	07AH	BABR	$e^+e^- \approx \Upsilon(4S)$
• • • We do not use the following data for averages, fits, limits, etc. • • •						
<0.56	90		CRONIN-HEN...01		CLE2	$e^+e^- \approx$ 10.6 GeV
seen			ADAMOVICH	95B	WA89	Σ^- 340 GeV
<1.6	90		FRABETTI	93	E687	γBe, $\overline{E}_\gamma$= 221 GeV

Ω_c^0 REFERENCES

SOLOVIEVA	09	PL B672 1	E. Solovieva *et al.*	(BELLE Collab.)
AUBERT	07AH	PRL 99 062001	B. Aubert *et al.*	(BABAR Collab.)
LINK	03C	PL B561 41	J.M. Link *et al.*	(FNAL FOCUS Collab.)
AMMAR	02	PRL 89 171803	R. Ammar *et al.*	(CLEO Collab.)
CRONIN-HEN...	01	PRL 86 3730	D. Cronin-Hennessy *et al.*	(CLEO Collab.)
ADAMOVICH	95B	PL B358 151	M.I. Adamovich *et al.*	(CERN WA89 Collab.)
FRABETTI	95D	PL B357 678	P.L. Frabetti *et al.*	(FNAL E687 Collab.)
FRABETTI	94H	PL B338 106	P.L. Frabetti *et al.*	(FNAL E687 Collab.)
FRABETTI	93	PL B300 190	P.L. Frabetti *et al.*	(FNAL E687 Collab.)
ALBRECHT	92H	PL B288 367	H. Albrecht *et al.*	(ARGUS Collab.)
BIAGI	85B	ZPHY C28 175	S.F. Biagi *et al.*	(CERN WA62 Collab.)

$\Omega_c(2770)^0$

$I(J^P) = 0(\frac{3}{2}^+)$ Status: ***

The natural assignment is that this goes with the $\Sigma_c(2520)$ and $\Xi_c(2645)$ to complete the lowest mass $J^P = \frac{3}{2}^+$ SU(3) sextet, part of the SU(4) 20-plet that includes the $\Delta(1232)$. But J and P have not been measured.

$\Omega_c(2770)^0$ MASS

The mass is obtained from the mass-difference measurement that follows.

VALUE (MeV)	DOCUMENT ID
2765.9±2.0 OUR FIT Error includes scale factor of 1.2.	

$\Omega_c(2770)^0 - \Omega_c^0$ MASS DIFFERENCE

VALUE (MeV)	EVTS	DOCUMENT ID		TECN	COMMENT
$70.7^{+0.8}_{-0.9}$ OUR FIT					
$70.7^{+0.8}_{-1.0}$ OUR AVERAGE					
$70.7\pm0.9^{+0.1}_{-0.9}$	54 ± 9	SOLOVIEVA	09	BELL	$\Omega_c^0\gamma$ in $e^+e^- \rightarrow \Upsilon(4S)$
70.8±1.0±1.1	105 ± 22	AUBERT,BE	06I	BABR	$e^+e^- \approx \Upsilon(4S)$

$\Omega_c(2770)^0$ DECAY MODES

The $\Omega_c(2770)^0 - \Omega_c^0$ mass difference is too small for any strong decay to occur.

	Mode	Fraction (Γ_i/Γ)
Γ_1	$\Omega_c^0\gamma$	presumably 100%

$\Omega_c(2770)^0$ REFERENCES

SOLOVIEVA	09	PL B672 1	E. Solovieva *et al.*	(BELLE Collab.)
AUBERT,BE	06I	PRL 97 232001	B. Aubert *et al.*	(BABAR Collab.)

DOUBLY CHARMED BARYONS ($C = +2$)

$\Xi_{cc}^{++} = ucc$, $\Xi_{cc}^{+} = dcc$, $\Omega_{cc}^{+} = scc$

Ξ_{cc}^{+}

$I(J^P) = ?(?^?)$ Status: *

OMITTED FROM SUMMARY TABLE

This would presumably be an isospin-1/2 particle, a ccu Ξ_{cc}^{++} and a ccd Ξ_{cc}^{+}. However, opposed to the evidence cited below, the BABAR experiment has found no evidence for a Ξ_{cc}^{+} in a search in $\Lambda_c^+ K^- \pi^+$ and $\Xi_c^0 \pi^+$ modes, and no evidence of a Ξ_{cc}^{++} in $\Lambda_c^+ K^- \pi^+ \pi^+$ and $\Xi_c^0 \pi^+ \pi^+$ modes (AUBERT,B 06D). Nor have the BELLE and LHCb experiments found any evidence for a Ξ_{cc}^{+} in the $\Lambda_c^+ K^- \pi^+$ mode (CHISTOV 06 and AAIJ 13CD).

Ξ_{cc}^{+} MASS

VALUE (MeV)	EVTS	DOCUMENT ID		TECN	COMMENT
3518.9±0.9 OUR AVERAGE					
3518 ±3	6	[1] OCHERASHVI...05		SELX	Σ^- nucleus ≈ 600 GeV
3519 ±1	16	[2] MATTSON	02	SELX	Σ^- nucleus ≈ 600 GeV

[1] OCHERASHVILI 05 claims "an excess of 5.62 events over ... 1.38 ± 0.13 events" for a significance of 4.8 σ in pD^+K^- events.

[2] MATTSON 02 claims "an excess of 15.9 events over an expected background of 6.1 ± 0.5 events, a statistical significance of 6.3 σ" in the $\Lambda_c^+ K^- \pi^+$ invariant-mass spectrum. The probability that the peak is a fluctuation increases from 1.0×10^{-6} to 1.1×10^{-4} when the number of bins searched is considered.

Ξ_{cc}^{+} MEAN LIFE

VALUE (10^{-15} s)	CL%	DOCUMENT ID		TECN	COMMENT
<33	90	MATTSON	02	SELX	Σ^- nucleus, ≈ 600 GeV

Ξ_{cc}^{+} DECAY MODES

	Mode
Γ_1	$\Lambda_c^+ K^- \pi^+$
Γ_2	pD^+K^-

$\Gamma(pD^+K^-)/\Gamma(\Lambda_c^+ K^- \pi^+)$ Γ_2/Γ_1

VALUE	EVTS	DOCUMENT ID		TECN	COMMENT
0.36±0.21	6	OCHERASHVI...05		SELX	Σ^- ≈ 600 GeV

Ξ_{cc}^{+} REFERENCES

AAIJ	13CD	JHEP 1312 090	R. Aaij *et al.*	(LHCb Collab.)
AUBERT,B	06D	PR D74 011103	B. Aubert *et al.*	(BABAR Collab.)
CHISTOV	06	PRL 97 162001	R. Chistov *et al.*	(BELLE Collab.)
OCHERASHVI...05		PL B628 18	A. Ocherashvili *et al.*	(FNAL SELEX Collab.)
MATTSON	02	PRL 89 112001	M. Mattson *et al.*	(FNAL SELEX Collab.)

BOTTOM BARYONS ($B = -1$)

$\Lambda_b^0 = udb$, $\Xi_b^0 = usb$, $\Xi_b^- = dsb$, $\Omega_b^- = ssb$

Λ_b^0

$I(J^P) = 0(\frac{1}{2}^+)$ Status: ***

In the quark model, a Λ_b^0 is an isospin-0 udb state. The lowest Λ_b^0 ought to have $J^P = 1/2^+$. None of I, J, or P have actually been measured.

Λ_b^0 MASS

$m_{\Lambda_b^0}$

VALUE (MeV)	EVTS	DOCUMENT ID		TECN	COMMENT
5619.5 ± 0.4 OUR AVERAGE					
5619.7 ± 0.7 ± 1.1		[1] AAD	13U	ATLS	pp at 7 TeV
5619.44 ± 0.13 ± 0.38		[2] AAIJ	13AV	LHCB	pp at 7 TeV
5619.7 ± 1.2 ± 1.2		[3] ACOSTA	06	CDF	$p\overline{p}$ at 1.96 TeV
5621 ± 4 ± 3		[4] ABE	97B	CDF	$p\overline{p}$ at 1.8 TeV
5668 ± 16 ± 8	4	[5] ABREU	96N	DLPH	$e^+e^- \to Z$
5614 ± 21 ± 4	4	[5] BUSKULIC	96L	ALEP	$e^+e^- \to Z$
• • • We do not use the following data for averages, fits, limits, etc. • • •					
5619.19 ± 0.70 ± 0.30		[1] AAIJ	12E	LHCB	Repl. by AAIJ 13AV
not seen		[6] ABE	93B	CDF	Sup. by ABE 97B
5640 ± 50 ± 30	16	[7] ALBAJAR	91E	UA1	$p\overline{p}$ 630 GeV
5640 $^{+100}_{-210}$	52	BARI	91	SFM	$\Lambda_b^0 \to pD^0\pi^-$
5650 $^{+150}_{-200}$	90	BARI	91	SFM	$\Lambda_b^0 \to \Lambda_c^+\pi^+\pi^-\pi^-$

[1] Uses $\Lambda_b^0 \to J/\psi\Lambda$ fully reconstructed decays.

[2] Uses $\Lambda_b^0 \to J/\psi\Lambda$ fully reconstructed decays.

[3] Uses exclusively reconstructed final states containing a $J/\psi \to \mu^+\mu^-$ decays.

[4] ABE 97B observed 38 events with a background of 18 ± 1.6 events in the mass range 5.60–5.65 GeV/c^2, a significance of > 3.4 standard deviations.

[5] Uses 4 fully reconstructed Λ_b events.

[6] ABE 93B states that, based on the signal claimed by ALBAJAR 91E, CDF should have found 30 ± 23 $\Lambda_b^0 \to J/\psi(1S)\Lambda$ events. Instead, CDF found not more than 2 events.

[7] ALBAJAR 91E claims 16 ± 5 events above a background of 9 ± 1 events, a significance of about 5 standard deviations.

$m_{\Lambda_b^0} - m_{B^0}$

VALUE (MeV)	DOCUMENT ID		TECN	COMMENT
339.2±1.4±0.1	[8] ACOSTA	06	CDF	$p\overline{p}$ at 1.96 TeV

[8] Uses exclusively reconstructed final states containing $J/\psi \to \mu^+\mu^-$ decays.

$m_{\Lambda_b^0} - m_{B^+}$

VALUE (MeV)	DOCUMENT ID		TECN	COMMENT
339.71±0.71±0.09	[9] AAIJ	12E	LHCB	pp at 7 TeV

[9] Uses exclusively reconstructed final states containing $J/\psi \to \mu^+\mu^-$ decays.

Λ_b^0 MEAN LIFE

See b-baryon Admixture section for data on b-baryon mean life average over species of b-baryon particles.

"OUR EVALUATION" is an average using rescaled values of the data listed below. The average and rescaling were performed by the Heavy Flavor Averaging Group (HFAG) and are described at http://www.slac.stanford.edu/xorg/hfag/. The averaging/rescaling procedure takes into account correlations between the measurements and asymmetric lifetime errors.

VALUE (10^{-12} s)	EVTS	DOCUMENT ID		TECN	COMMENT
1.451±0.013 OUR EVALUATION					
1.415±0.027±0.006		[10] AAIJ	14E	LHCB	pp at 7 TeV
1.449±0.036±0.017		[10] AAD	13U	ATLS	pp at 7 TeV
1.503±0.052±0.031		[10] CHATRCHYAN	13AC	CMS	pp at 7 TeV
1.303±0.075±0.035		[10] ABAZOV	12U	D0	$p\overline{p}$ at 1.96 TeV
1.537±0.045±0.014		[10] AALTONEN	11	CDF	$p\overline{p}$ at 1.96 TeV
1.401±0.046±0.035		[11] AALTONEN	10B	CDF	$p\overline{p}$ at 1.96 TeV
1.290 $^{+0.119}_{-0.110}$ $^{+0.087}_{-0.091}$		[12] ABAZOV	07U	D0	$p\overline{p}$ at 1.96 TeV
1.11 $^{+0.19}_{-0.18}$ ±0.05		[13] ABREU	99W	DLPH	$e^+e^- \to Z$
1.29 $^{+0.24}_{-0.22}$ ±0.06		[13] ACKERSTAFF	98G	OPAL	$e^+e^- \to Z$
1.21 ±0.11		[13] BARATE	98D	ALEP	$e^+e^- \to Z$
1.32 ±0.15 ±0.07		[14] ABE	96M	CDF	$p\overline{p}$ at 1.8 TeV
• • • We do not use the following data for averages, fits, limits, etc. • • •					
1.218 $^{+0.130}_{-0.115}$ ±0.042		[10] ABAZOV	07S	D0	Repl. by ABAZOV 12U
1.593 $^{+0.083}_{-0.078}$ ±0.033		[10] ABULENCIA	07A	CDF	Repl. by AALTONEN 11
1.22 $^{+0.22}_{-0.18}$ ±0.04		[10] ABAZOV	05C	D0	Repl. by ABAZOV 07S
1.19 $^{+0.21}_{-0.18}$ $^{+0.07}_{-0.08}$		ABREU	96D	DLPH	Repl. by ABREU 99W
1.14 $^{+0.22}_{-0.19}$ ±0.07	69	AKERS	95K	OPAL	Repl. by ACKERSTAFF 98G
1.02 $^{+0.23}_{-0.18}$ ±0.06	44	BUSKULIC	95L	ALEP	Repl. by BARATE 98D

[10] Measured mean life using fully reconstructed $\Lambda_b^0 \to J/\psi\Lambda$ decays.

[11] Measured mean life using fully reconstructed $\Lambda_b^0 \to \Lambda_c^+\pi^-$ decays.

[12] Measured using semileptonic decays $\Lambda_b^0 \to \Lambda_c^+\mu\nu X$ and $\Lambda_c^+ \to K_S^0 p$.

[13] Measured using $\Lambda_c\ell^-$ and $\Lambda\ell^+\ell^-$.

[14] Excess $\Lambda_c\ell^-$, decay lengths.

$\tau_{\Lambda_b^0}/\tau_{\overline{\Lambda}_b^0}$

VALUE	DOCUMENT ID		TECN	COMMENT
0.940±0.035±0.006	[15] AAIJ	14E	LHCB	pp at 7 TeV

[15] Measured using $\Lambda_b^0 \to J/\psi\Lambda$ decays.

$\tau_{\Lambda_b^0}/\tau_{B^0}$ MEAN LIFE RATIO

$\tau_{\Lambda_b^0}/\tau_{B^0}$ (direct measurements)

"OUR EVALUATION" has been obtained by the Heavy Flavor Averaging Group (HFAG) by including both B^0 and B^+ decays.

VALUE	DOCUMENT ID		TECN	COMMENT
0.955±0.009 OUR EVALUATION				
0.950±0.023 OUR AVERAGE Error includes scale factor of 1.7. See the ideogram below.				
0.929±0.018±0.004	[16] AAIJ	14E	LHCB	pp at 7 TeV
0.960±0.025±0.016	[17] AAD	13U	ATLS	pp at 7 TeV
0.864±0.052±0.033	[18,19] ABAZOV	12U	D0	$p\overline{p}$ at 1.96 TeV
1.020±0.030±0.008	[18] AALTONEN	11	CDF	$p\overline{p}$ at 1.96 TeV
• • • We do not use the following data for averages, fits, limits, etc. • • •				
0.976±0.012±0.006	[20] AAIJ	13BB	LHCB	pp at 7 TeV
0.811 $^{+0.096}_{-0.087}$ ±0.034	[18,19] ABAZOV	07S	D0	Repl. by ABAZOV 12U
1.041±0.057	[21] ABULENCIA	07A	CDF	Repl. by AALTONEN 11
0.87 $^{+0.17}_{-0.14}$ ±0.03	[21] ABAZOV	05C	D0	Repl. by ABAZOV 07S

[16] Measured using $\Lambda_b^0 \to J/\psi\Lambda$ and $B^0 \to J/\psi K^{*0}$ decays.

[17] Measured with $\Lambda_b^0 \to J/\psi(\mu^+\mu^-)\,\Lambda^0(p\pi^-)$ decays.

[18] Uses fully reconstructed $\Lambda_b \to J/\psi\Lambda$ decays.

[19] Uses $B^0 \to J/\psi K_S^0$ decays for denominator.

[20] Measures $1/\tau_{\Lambda_b^0} - 1/\tau_{B^0}$ and uses $\tau_{B^0} = 1.519 \pm 0.007$ ps to extract lifetime ratio.

[21] Measured mean life ratio using fully reconstructed decays.

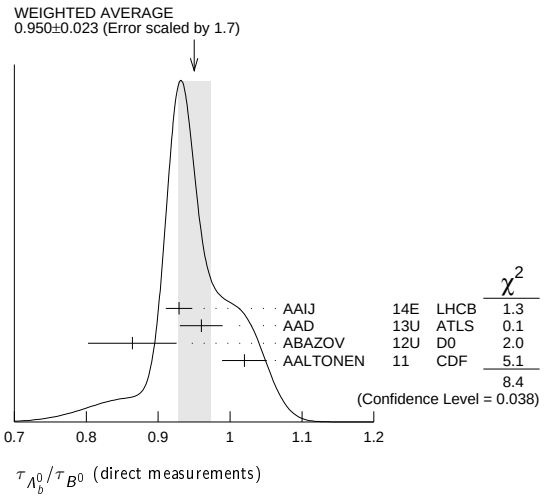

Λ_b^0 DECAY MODES

The branching fractions B(b-baryon $\to \Lambda \ell^- \overline{\nu}_\ell$ anything) and B($\Lambda_b^0 \to \Lambda_c^+ \ell^- \overline{\nu}_\ell$ anything) are not pure measurements because the underlying measured products of these with B($b \to b$-baryon) were used to determine B($b \to b$-baryon), as described in the note "Production and Decay of b-Flavored Hadrons."

For inclusive branching fractions, *e.g.*, $\Lambda_b \to \overline{\Lambda}_c$ anything, the values usually are multiplicities, not branching fractions. They can be greater than one.

	Mode	Fraction (Γ_i/Γ)	Scale factor/ Confidence level
Γ_1	$J/\psi(1S)\Lambda \times$ B($b \to \Lambda_b^0$)	$(5.8 \pm 0.8) \times 10^{-5}$	
Γ_2	$pD^0\pi^-$	$(5.9\ ^{+4.0}_{-3.2}) \times 10^{-4}$	
Γ_3	pD^0K^-	$(4.3\ ^{+3.0}_{-2.4}) \times 10^{-5}$	
Γ_4	$\Lambda_c^+\pi^-$	$(5.7\ ^{+4.0}_{-2.6}) \times 10^{-3}$	S=1.6
Γ_5	$\Lambda_c^+K^-$	$(4.2\ ^{+2.6}_{-1.9}) \times 10^{-4}$	
Γ_6	$\Lambda_c^+ a_1(1260)^-$	seen	
Γ_7	$\Lambda_c^+\pi^+\pi^-\pi^-$	$(8\ ^{+5}_{-4}) \times 10^{-3}$	S=1.6
Γ_8	$\Lambda_c(2595)^+\pi^-$, $\Lambda_c(2595)^+ \to \Lambda_c^+\pi^+\pi^-$	$(3.7\ ^{+2.8}_{-2.3}) \times 10^{-4}$	
Γ_9	$\Lambda_c(2625)^+\pi^-$, $\Lambda_c(2625)^+ \to \Lambda_c^+\pi^+\pi^-$	$(3.6\ ^{+2.7}_{-2.1}) \times 10^{-4}$	
Γ_{10}	$\Sigma_c(2455)^0\pi^+\pi^-$, $\Sigma_c^0 \to \Lambda_c^+\pi^-$	$(6\ ^{+5}_{-4}) \times 10^{-4}$	
Γ_{11}	$\Sigma_c(2455)^{++}\pi^-\pi^-$, $\Sigma_c^{++} \to \Lambda_c^+\pi^+$	$(3.5\ ^{+2.8}_{-2.3}) \times 10^{-4}$	
Γ_{12}	$\Lambda K^0 2\pi^+ 2\pi^-$		
Γ_{13}	$\Lambda_c^+\ell^-\overline{\nu}_\ell$ anything [a]	$(9.9 \pm 2.2)\ \%$	
Γ_{14}	$\Lambda_c^+\ell^-\overline{\nu}_\ell$	$(6.5\ ^{+3.2}_{-2.5})\ \%$	S=1.8
Γ_{15}	$\Lambda_c^+\pi^+\pi^-\ell^-\overline{\nu}_\ell$	$(5.6 \pm 3.1)\ \%$	
Γ_{16}	$\Lambda_c(2595)^+\ell^-\overline{\nu}_\ell$	$(8 \pm 5) \times 10^{-3}$	
Γ_{17}	$\Lambda_c(2625)^+\ell^-\overline{\nu}_\ell$	$(1.4\ ^{+0.9}_{-0.7})\ \%$	
Γ_{18}	$\Sigma_c(2455)^0\pi^+\ell^-\overline{\nu}_\ell$		
Γ_{19}	$\Sigma_c(2455)^{++}\pi^-\ell^-\overline{\nu}_\ell$		
Γ_{20}	ph^- [b]	$< 2.3 \times 10^{-5}$	CL=90%
Γ_{21}	$p\pi^-$	$(4.1 \pm 0.8) \times 10^{-6}$	
Γ_{22}	pK^-	$(4.9 \pm 0.9) \times 10^{-6}$	
Γ_{23}	$\Lambda\mu^+\mu^-$	$(1.08 \pm 0.28) \times 10^{-6}$	
Γ_{24}	$\Lambda\gamma$	$< 1.3 \times 10^{-3}$	CL=90%

[a] Not a pure measurement. See note at head of Λ_b^0 Decay Modes.

[b] Here h^- means π^- or K^-.

CONSTRAINED FIT INFORMATION

An overall fit to 8 branching ratios uses 8 measurements and one constraint to determine 6 parameters. The overall fit has a $\chi^2 = 4.5$ for 3 degrees of freedom.

The following *off-diagonal* array elements are the correlation coefficients $\langle \delta x_i \delta x_j \rangle / (\delta x_i \cdot \delta x_j)$, in percent, from the fit to the branching fractions, $x_i \equiv \Gamma_i/\Gamma_{\text{total}}$. The fit constrains the x_i whose labels appear in this array to sum to one.

x_7	93			
x_{14}	14	13		
x_{21}	0	0	0	
x_{22}	0	0	0	84
	x_4	x_7	x_{14}	x_{21}

Λ_b^0 BRANCHING RATIOS

$\Gamma(J/\psi(1S)\Lambda \times \text{B}(b \to \Lambda_b^0))/\Gamma_{\text{total}}$ Γ_1/Γ

VALUE (units 10^{-5})	EVTS	DOCUMENT ID		TECN	COMMENT
5.8 ± 0.8 OUR AVERAGE					
$6.01 \pm 0.60 \pm 0.58 \pm 0.28$		[22] ABAZOV	11O	D0	$p\overline{p}$ at 1.96 TeV
$4.7 \pm 2.3 \pm 0.2$		[23] ABE	97B	CDF	$p\overline{p}$ at 1.8 TeV
• • • We do not use the following data for averages, fits, limits, etc. • • •					
$180 \pm 60 \pm 90$	16	ALBAJAR	91E	UA1	$p\overline{p}$ at 630 GeV

[22] ABAZOV 11O uses B($B^0 \to J/\psi K_S^0$) × B($b \to B^0$) = $(1.74 \pm 0.08) \times 10^{-4}$ to obtain the result. The $(\pm 0.08) \times 10^{-4}$ uncertainty of this product is listed as the last uncertainty of the measurement, $(\pm 0.28) \times 10^{-5}$.

[23] ABE 97B reports [B($\Lambda_b^0 \to J/\psi\Lambda$) × B($b \to \Lambda_b^0$)] / [B($B^0 \to J/\psi K_S^0$) × B($b \to B^0$)] = $0.27 \pm 0.12 \pm 0.05$. We multiply by our best value B($B^0 \to J/\psi K_S^0$) × B($b \to B^0$) = $(1.74 \pm 0.08) \times 10^{-4}$. Our first error is their experiment error and our second error is the systematic error from using our best value.

$\Gamma(pD^0\pi^-)/\Gamma_{\text{total}}$ Γ_2/Γ

VALUE	EVTS	DOCUMENT ID		TECN	COMMENT
• • • We do not use the following data for averages, fits, limits, etc. • • •					
seen	52	BARI	91	SFM	$D^0 \to K^-\pi^+$
seen		BASILE	81	SFM	$D^0 \to K^-\pi^+$

$\Gamma(pD^0K^-)/\Gamma(pD^0\pi^-)$ Γ_3/Γ_2

VALUE (units 10^{-2})	DOCUMENT ID		TECN	COMMENT
$7.3 \pm 0.8^{+0.5}_{-0.6}$	AAIJ	14H	LHCB	pp at 7 TeV

$\Gamma(\Lambda_c^+\pi^-)/\Gamma_{\text{total}}$ Γ_4/Γ

VALUE (units 10^{-3})	EVTS	DOCUMENT ID		TECN	COMMENT
$5.7^{+4.0}_{-2.6}$ **OUR FIT** Error includes scale factor of 1.6.					
$8.8 \pm 2.8 \pm 1.5$		[24] ABULENCIA	07B	CDF	$p\overline{p}$ at 1.96 TeV
• • • We do not use the following data for averages, fits, limits, etc. • • •					
seen	3	ABREU	96N	DLPH	$\Lambda_c^+ \to pK^-\pi^+$
seen	4	BUSKULIC	96L	ALEP	$\Lambda_c^+ \to pK^-\pi^+$, $p\overline{K}^0$, $\Lambda\pi^+\pi^+\pi^-$

[24] The result is obtained from ($f_{\text{baryon}}/f_{\text{d}}$) (B($\Lambda_b^0 \to \Lambda_c^+\pi^-$)/B($\overline{B}^0 \to D^+\pi^-$)) = $0.82 \pm 0.08 \pm 0.11 \pm 0.22$, assuming $f_{\text{baryon}}/f_{\text{d}} = 0.25 \pm 0.04$ and B($\overline{B}^0 \to D^+\pi^-$) = $(2.68 \pm 0.13) \times 10^{-3}$.

$\Gamma(pD^0\pi^-)/\Gamma(\Lambda_c^+\pi^-)$ Γ_2/Γ_4

VALUE	DOCUMENT ID		TECN	COMMENT
0.104 ± 0.005 ± 0.027	[25] AAIJ	14H	LHCB	pp at 7 TeV

[25] AAIJ 14H reports [$\Gamma(\Lambda_b^0 \to pD^0\pi^-)/\Gamma(\Lambda_b^0 \to \Lambda_c^+\pi^-)$] × [B($D^0 \to K^-\pi^+$)] / [B($\Lambda_c^+ \to pK^-\pi^+$)] = $(8.06 \pm 0.23 \pm 0.35) \times 10^{-2}$ which we multiply or divide by our best values B($D^0 \to K^-\pi^+$) = $(3.88 \pm 0.05) \times 10^{-2}$, B($\Lambda_c^+ \to pK^-\pi^+$) = $(5.0 \pm 1.3) \times 10^{-2}$. Our first error is their experiment's error and our second error is the systematic error from using our best values.

$\Gamma(\Lambda_c^+K^-)/\Gamma(\Lambda_c^+\pi^-)$ Γ_5/Γ_4

VALUE (units 10^{-2})	DOCUMENT ID		TECN	COMMENT
7.31 ± 0.16 ± 0.16	AAIJ	14H	LHCB	pp at 7 TeV

$\Gamma(\Lambda_c^+ a_1(1260)^-)/\Gamma_{\text{total}}$ Γ_6/Γ

VALUE	EVTS	DOCUMENT ID		TECN	COMMENT
seen	1	ABREU	96N	DLPH	$\Lambda_c^+ \to pK^-\pi^+$, $a_1^- \to \rho^0\pi^- \to \pi^+\pi^-\pi^-$

$\Gamma(\Lambda_c^+\pi^+\pi^-\pi^-)/\Gamma_{\text{total}}$ Γ_7/Γ

VALUE (units 10^{-3})	EVTS	DOCUMENT ID		TECN	COMMENT
8^{+5}_{-4} **OUR FIT** Error includes scale factor of 1.6.					
$17 \pm 4^{+11}_{-8}$		[26] AALTONEN	12A	CDF	$p\overline{p}$ at 1.96 TeV
• • • We do not use the following data for averages, fits, limits, etc. • • •					
seen	90	BARI	91	SFM	$\Lambda_c^+ \to pK^-\pi^+$

[26] AALTONEN 12A reports [$\Gamma(\Lambda_b^0 \to \Lambda_c^+\pi^+\pi^-\pi^-)/\Gamma_{\text{total}}$] / [B($\Lambda_b^0 \to \Lambda_c^+\pi^-$)] = $3.04 \pm 0.33^{+0.70}_{-0.55}$ which we multiply by our best value B($\Lambda_b^0 \to \Lambda_c^+\pi^-$) = $(5.7^{+4.0}_{-2.6}) \times 10^{-3}$. Our first error is their experiment's error and our second error is the systematic error from using our best value.

$\Gamma(\Lambda_c^+\pi^+\pi^-\pi^-)/\Gamma(\Lambda_c^+\pi^-)$ Γ_7/Γ_4

VALUE	DOCUMENT ID		TECN	COMMENT
1.46 ± 0.22 OUR FIT Error includes scale factor of 1.1.				
1.43 ± 0.16 ± 0.13	AAIJ	11E	LHCB	pp at 7 TeV

$\Gamma(\Lambda_c(2595)^+\pi^-, \Lambda_c(2595)^+ \to \Lambda_c^+\pi^+\pi^-)/\Gamma(\Lambda_c^+\pi^+\pi^-\pi^-)$ Γ_8/Γ_7

VALUE (units 10^{-2})	DOCUMENT ID		TECN	COMMENT
$4.4 \pm 1.7^{+0.6}_{-0.4}$	AAIJ	11E	LHCB	pp at 7 TeV

$\Gamma(\Lambda_c(2625)^+\pi^-, \Lambda_c(2625)^+ \to \Lambda_c^+\pi^+\pi^-)/\Gamma(\Lambda_c^+\pi^+\pi^-\pi^-)$ Γ_9/Γ_7

VALUE (units 10^{-2})	DOCUMENT ID		TECN	COMMENT
4.3 ± 1.5 ± 0.4	AAIJ	11E	LHCB	pp at 7 TeV

$\Gamma(\Sigma_c(2455)^0\pi^+\pi^-, \Sigma_c^0 \to \Lambda_c^+\pi^-)/\Gamma(\Lambda_c^+\pi^+\pi^-\pi^-)$ Γ_{10}/Γ_7

VALUE (units 10^{-2})	DOCUMENT ID		TECN	COMMENT
7.4 ± 2.4 ± 1.2	AAIJ	11E	LHCB	pp at 7 TeV

Baryon Particle Listings

Λ_b^0

$\Gamma(\Sigma_c(2455)^{++}\pi^-\pi^-, \Sigma_c^{++} \to \Lambda_c^+\pi^+)/\Gamma(\Lambda_c^+\pi^+\pi^-\pi^-)$ Γ_{11}/Γ_7

VALUE (units 10^{-2})	DOCUMENT ID		TECN	COMMENT
4.2±1.8±0.7	AAIJ	11E	LHCB	pp at 7 TeV

$\Gamma(\Lambda K^0 2\pi^+ 2\pi^-)/\Gamma_{total}$ Γ_{12}/Γ

VALUE	EVTS	DOCUMENT ID		TECN	COMMENT
• • • We do not use the following data for averages, fits, limits, etc. • • •					
seen	4	[27] ARENTON	86	FMPS	$\Lambda K_S^0 2\pi^+ 2\pi^-$

[27] See the footnote to the ARENTON 86 mass value.

$\Gamma(\Lambda_c^+\ell^-\overline{\nu}_\ell \text{anything})/\Gamma_{total}$ Γ_{13}/Γ

The values and averages in this section serve only to show what values result if one assumes our B(b → b-baryon). They cannot be thought of as measurements since the underlying product branching fractions were also used to determine B(b → b-baryon) as described in the note on "Production and Decay of b-Flavored Hadrons."

VALUE	EVTS	DOCUMENT ID		TECN	COMMENT
0.099±0.022 OUR AVERAGE					
0.093±0.017±0.015		[28] BARATE	98D	ALEP	e^+e^- → Z
0.13 ±0.04 ±0.02	29	[29] ABREU	95S	DLPH	e^+e^- → Z
• • • We do not use the following data for averages, fits, limits, etc. • • •					
0.082±0.020±0.013	55	[30] BUSKULIC	95L	ALEP	Repl. by BARATE 98D
0.16 ±0.06 ±0.03	21	[31] BUSKULIC	92E	ALEP	Λ_c^+ → $pK^-\pi^+$

[28] BARATE 98D reports $[\Gamma(\Lambda_b^0 \to \Lambda_c^+\ell^-\overline{\nu}_\ell \text{anything})/\Gamma_{total}] \times [B(\overline{b} \to b\text{-baryon})] = 0.0086 \pm 0.0007 \pm 0.0014$ which we divide by our best value $B(\overline{b} \to b\text{-baryon}) = (9.2 \pm 1.5) \times 10^{-2}$. Our first error is their experiment's error and our second error is the systematic error from using our best value. Measured using $\Lambda_c\ell^-$ and $\Lambda\ell^+\ell^-$.

[29] ABREU 95S reports $[\Gamma(\Lambda_b^0 \to \Lambda_c^+\ell^-\overline{\nu}_\ell \text{anything})/\Gamma_{total}] \times [B(\overline{b} \to b\text{-baryon})] = 0.0118 \pm 0.0026^{+0.0031}_{-0.0021}$ which we divide by our best value $B(\overline{b} \to b\text{-baryon}) = (9.2 \pm 1.5) \times 10^{-2}$. Our first error is their experiment's error and our second error is the systematic error from using our best value.

[30] BUSKULIC 95L reports $[\Gamma(\Lambda_b^0 \to \Lambda_c^+\ell^-\overline{\nu}_\ell \text{anything})/\Gamma_{total}] \times [B(\overline{b} \to b\text{-baryon})] = 0.00755 \pm 0.0014 \pm 0.0012$ which we divide by our best value $B(\overline{b} \to b\text{-baryon}) = (9.2 \pm 1.5) \times 10^{-2}$. Our first error is their experiment's error and our second error is the systematic error from using our best value.

[31] BUSKULIC 92E reports $[\Gamma(\Lambda_b^0 \to \Lambda_c^+\ell^-\overline{\nu}_\ell \text{anything})/\Gamma_{total}] \times [B(\overline{b} \to b\text{-baryon})] = 0.015 \pm 0.0035 \pm 0.0045$ which we divide by our best value $B(\overline{b} \to b\text{-baryon}) = (9.2 \pm 1.5) \times 10^{-2}$. Our first error is their experiment's error and our second error is the systematic error from using our best value. Superseded by BUSKULIC 95L.

$\Gamma(\Lambda_c^+\ell^-\overline{\nu}_\ell)/\Gamma_{total}$ Γ_{14}/Γ

VALUE	DOCUMENT ID		TECN	COMMENT
$0.065^{+0.032}_{-0.025}$ OUR FIT Error includes scale factor of 1.8.				
$0.050^{+0.011}_{-0.008}{}^{+0.016}_{-0.012}$	[32] ABDALLAH	04A	DLPH	e^+e^- → Z^0

[32] Derived from a combined likelihood and event rate fit to the distribution of the Isgur-Wise variable and using HQET. The slope of the form factor is measured to be $\rho^2 = 2.03 \pm 0.46^{+0.72}_{-1.00}$.

$\Gamma(\Lambda_c^+\ell^-\overline{\nu}_\ell)/\Gamma(\Lambda_c^+\pi^-)$ Γ_{14}/Γ_4

VALUE	DOCUMENT ID		TECN	COMMENT
11 $^{+4}_{-5}$ OUR FIT Error includes scale factor of 1.2.				
16.6±3.0$^{+2.8}_{-3.6}$	AALTONEN	09E	CDF	$p\overline{p}$ at 1.96 TeV

$\Gamma(\Lambda_c^+\pi^+\pi^-\ell^-\overline{\nu}_\ell)/\Gamma_{total}$ Γ_{15}/Γ

VALUE	DOCUMENT ID		TECN	COMMENT
$0.056^{+0.031}_{-0.030}$	[33] ABDALLAH	04A	DLPH	e^+e^- → Z^0

[33] Derived from the fraction of $\Gamma(\Lambda_b^0 \to \Lambda_c^+\ell^-\overline{\nu}_\ell)$ / ($\Gamma(\Lambda_b^0 \to \Lambda_c^+\ell^-\overline{\nu}_\ell) + \Gamma(\Lambda_b^0 \to \Lambda_c^+\pi^+\pi^-\ell^-\overline{\nu}_\ell)$) $= 0.47^{+0.10}_{-0.08}{}^{+0.07}_{-0.06}$.

$\Gamma(\Lambda_c^+\ell^-\overline{\nu}_\ell)/[\Gamma(\Lambda_c^+\ell^-\overline{\nu}_\ell) + \Gamma(\Lambda_c^+\pi^+\pi^-\ell^-\overline{\nu}_\ell)]$ $\Gamma_{14}/(\Gamma_{14}+\Gamma_{15})$

VALUE	DOCUMENT ID		TECN	COMMENT
$0.47^{+0.10}_{-0.08}{}^{+0.07}_{-0.06}$	ABDALLAH	04A	DLPH	e^+e^- → Z^0

$\Gamma(\Lambda_c(2595)^+\ell^-\overline{\nu}_\ell)/\Gamma(\Lambda_c^+\ell^-\overline{\nu}_\ell)$ Γ_{16}/Γ_{14}

VALUE	DOCUMENT ID		TECN	COMMENT
0.126±0.033$^{+0.047}_{-0.038}$	AALTONEN	09E	CDF	$p\overline{p}$ at 1.96 TeV

$\Gamma(\Lambda_c(2625)^+\ell^-\overline{\nu}_\ell)/\Gamma(\Lambda_c^+\ell^-\overline{\nu}_\ell)$ Γ_{17}/Γ_{14}

VALUE	DOCUMENT ID		TECN	COMMENT
0.210±0.042$^{+0.071}_{-0.050}$	AALTONEN	09E	CDF	$p\overline{p}$ at 1.96 TeV

$[\frac{1}{2}\Gamma(\Sigma_c(2455)^0\pi^+\ell^-\overline{\nu}_\ell) + \frac{1}{2}\Gamma(\Sigma_c(2455)^{++}\pi^-\ell^-\overline{\nu}_\ell)]/\Gamma(\Lambda_c^+\ell^-\overline{\nu}_\ell)$ $(\frac{1}{2}\Gamma_{18}+\frac{1}{2}\Gamma_{19})/\Gamma_{14}$

VALUE	DOCUMENT ID		TECN	COMMENT
$0.054\pm0.022^{+0.021}_{-0.018}$	AALTONEN	09E	CDF	$p\overline{p}$ at 1.96 TeV

$\Gamma(ph^-)/\Gamma_{total}$ Γ_{20}/Γ

VALUE	CL%	DOCUMENT ID		TECN	COMMENT
$<2.3 \times 10^{-5}$	90	[34] ACOSTA	05O	CDF	$p\overline{p}$ at 1.96 TeV

[34] Assumes f_Λ / f_d = 0.25, and equal momentum distribution for Λ_b and B mesons.

$\Gamma(p\pi^-)/\Gamma_{total}$ Γ_{21}/Γ

VALUE (units 10^{-6})	CL%	DOCUMENT ID		TECN	COMMENT
4.1±0.8 OUR FIT					
3.6±0.8±0.6		[35] AALTONEN	09C	CDF	$p\overline{p}$ at 1.96 TeV
• • • We do not use the following data for averages, fits, limits, etc. • • •					
<5.0	90	[36] BUSKULIC	96V	ALEP	e^+e^- → Z

[35] AALTONEN 09C reports $[\Gamma(\Lambda_b^0 \to p\pi^-)/\Gamma_{total}] / [B(B^0 \to K^+\pi^-)] \times [B(\overline{b} \to b\text{-baryon})] / [B(\overline{b} \to B^0)] = 0.042 \pm 0.007 \pm 0.006$ which we multiply or divide by our best values $B(B^0 \to K^+\pi^-) = (1.96 \pm 0.05) \times 10^{-5}$, $B(\overline{b} \to b\text{-baryon}) = (9.2 \pm 1.5) \times 10^{-2}$, $B(\overline{b} \to B^0) = (40.2 \pm 0.7) \times 10^{-2}$. Our first error is their experiment's error and our second error is the systematic error from using our best values.

[36] BUSKULIC 96V assumes PDG 96 production fractions for B^0, B^+, B_s, b baryons.

$\Gamma(pK^-)/\Gamma_{total}$ Γ_{22}/Γ

VALUE (units 10^{-6})	CL%	DOCUMENT ID		TECN	COMMENT
4.9±0.9 OUR FIT					
5.6±1.0±0.9		[37] AALTONEN	09C	CDF	$p\overline{p}$ at 1.96 TeV
• • • We do not use the following data for averages, fits, limits, etc. • • •					
<360	90	[38] ADAM	96D	DLPH	e^+e^- → Z
< 50	90	[39] BUSKULIC	96V	ALEP	e^+e^- → Z

[37] AALTONEN 09C reports $[\Gamma(\Lambda_b^0 \to pK^-)/\Gamma_{total}] / [B(B^0 \to K^+\pi^-)] \times [B(\overline{b} \to b\text{-baryon})] / [B(\overline{b} \to B^0)] = 0.066 \pm 0.009 \pm 0.008$ which we multiply or divide by our best values $B(B^0 \to K^+\pi^-) = (1.96 \pm 0.05) \times 10^{-5}$, $B(\overline{b} \to b\text{-baryon}) = (9.2 \pm 1.5) \times 10^{-2}$, $B(\overline{b} \to B^0) = (40.2 \pm 0.7) \times 10^{-2}$. Our first error is their experiment's error and our second error is the systematic error from using our best values.

[38] ADAM 96D assumes $f_{B^0} = f_{B^-} = 0.39$ and $f_{B_s} = 0.12$.

[39] BUSKULIC 96V assumes PDG 96 production fractions for B^0, B^+, B_s, b baryons.

$\Gamma(p\pi^-)/\Gamma(pK^-)$ Γ_{21}/Γ_{22}

VALUE	DOCUMENT ID		TECN	COMMENT
0.84±0.09 OUR FIT				
0.86±0.08±0.05	AAIJ	12AR	LHCB	pp at 7 TeV

$\Gamma(\Lambda\mu^+\mu^-)/\Gamma_{total}$ Γ_{23}/Γ

VALUE (units 10^{-7})	DOCUMENT ID		TECN	COMMENT
10.8±2.8 OUR AVERAGE				
9.6±1.6±2.5	[40] AAIJ	13AJ	LHCB	pp at 7 TeV
17.3±4.2±5.5	AALTONEN	11AI	CDF	$p\overline{p}$ at 1.96 TeV

[40] Uses $B(\Lambda_b^0 \to J/\psi\Lambda) = (6.2 \pm 1.4) \times 10^{-4}$.

$\Gamma(\Lambda\gamma)/\Gamma_{total}$ Γ_{24}/Γ

VALUE	CL%	DOCUMENT ID		TECN	COMMENT
$<1.3 \times 10^{-3}$	90	ACOSTA	02G	CDF	$p\overline{p}$ at 1.8 TeV

PARTIAL BRANCHING FRACTIONS IN $\Lambda_b \to \Lambda\mu^+\mu^-$

B($\Lambda_b \to \Lambda\mu^+\mu^-$) ($q^2 < 2.0$ GeV$^2/c^4$)

VALUE (units 10^{-7})	DOCUMENT ID		TECN	COMMENT
0.3 ±0.5 OUR AVERAGE				
0.28±0.38±0.40	[41] AAIJ	13AJ	LHCB	pp at 7 TeV
0.15±2.01±0.05	AALTONEN	11AI	CDF	$p\overline{p}$ at 1.96 TeV

[41] Uses $B(\Lambda_b^0 \to J/\psi\Lambda) = (6.2 \pm 1.4) \times 10^{-4}$.

B($\Lambda_b \to \Lambda\mu^+\mu^-$) ($2.0 < q^2 < 4.3$ GeV$^2/c^4$)

VALUE (units 10^{-7})	DOCUMENT ID		TECN	COMMENT
0.34±0.28 OUR AVERAGE				
0.31±0.26±0.10	[42] AAIJ	13AJ	LHCB	pp at 7 TeV
1.8 ±1.7 ±0.6	AALTONEN	11AI	CDF	$p\overline{p}$ at 1.96 TeV

[42] Uses $B(\Lambda_b^0 \to J/\psi\Lambda) = (6.2 \pm 1.4) \times 10^{-4}$.

B($\Lambda_b \to \Lambda\mu^+\mu^-$) ($4.3 < q^2 < 8.68$ GeV$^2/c^4$)

VALUE (units 10^{-7})	DOCUMENT ID		TECN	COMMENT
0.15±0.17 OUR AVERAGE				
0.15±0.17±0.04	[43] AAIJ	13AJ	LHCB	pp at 7 TeV
−0.2 ±1.6 ±0.1	AALTONEN	11AI	CDF	$p\overline{p}$ at 1.96 TeV

[43] Uses $B(\Lambda_b^0 \to J/\psi\Lambda) = (6.2 \pm 1.4) \times 10^{-4}$.

B($\Lambda_b \to \Lambda\mu^+\mu^-$) ($10.09 < q^2 < 12.86$ GeV$^2/c^4$)

VALUE (units 10^{-7})	DOCUMENT ID		TECN	COMMENT
0.62±0.29 OUR AVERAGE				
0.56±0.21±0.20	[44] AAIJ	13AJ	LHCB	pp at 7 TeV
3.0 ±1.5 ±1.0	AALTONEN	11AI	CDF	$p\overline{p}$ at 1.96 TeV

[44] Uses $B(\Lambda_b^0 \to J/\psi\Lambda) = (6.2 \pm 1.4) \times 10^{-4}$.

B($\Lambda_b \to \Lambda\mu^+\mu^-$) ($14.18 < q^2 < 16.0$ GeV$^2/c^4$)

VALUE (units 10^{-7})		DOCUMENT ID		TECN	COMMENT
0.82±0.30 OUR AVERAGE					
0.79±0.24±0.23	[45]	AAIJ	13AJ	LHCB	pp at 7 TeV
1.0 ±0.7 ±0.3		AALTONEN	11AI	CDF	$p\overline{p}$ at 1.96 TeV

[45] Uses B($\Lambda_b^0 \to J/\psi\Lambda$) = (6.2 ± 1.4) × 10^{-4}.

B($\Lambda_b \to \Lambda\mu^+\mu^-$) ($16.0 < q^2$ GeV$^2/c^4$)

VALUE (units 10^{-7})		DOCUMENT ID		TECN	COMMENT
1.18±0.34 OUR AVERAGE					
1.10±0.18±0.29	[46,47]	AAIJ	13AJ	LHCB	pp at 7 TeV
7.0 ±1.9 ±2.2		AALTONEN	11AI	CDF	$p\overline{p}$ at 1.96 TeV

[46] Uses B($\Lambda_b^0 \to J/\psi\Lambda$) = (6.2 ± 1.4) × 10^{-4}.

[47] Requires $16.00 < q^2 < 20.30$ GeV$^2/c^4$.

B($\Lambda_b \to \Lambda\mu^+\mu^-$) ($1.0 < q^2 < 6.0$ GeV$^2/c^4$)

VALUE (units 10^{-7})	DOCUMENT ID		TECN	COMMENT
1.3±2.1±0.4	AALTONEN	11AI	CDF	$p\overline{p}$ at 1.96 TeV

B($\Lambda_b \to \Lambda\mu^+\mu^-$) ($0.0 < q^2 < 4.3$ GeV$^2/c^4$)

VALUE (units 10^{-7})	DOCUMENT ID		TECN	COMMENT
2.7±2.5±0.9	AALTONEN	11AI	CDF	$p\overline{p}$ at 1.96 TeV

CP VIOLATION

A_{CP} is defined as

$$A_{CP} = \frac{B(\Lambda_b^0 \to f) - B(\overline{\Lambda}_b^0 \to \overline{f})}{B(\Lambda_b^0 \to f) + B(\overline{\Lambda}_b^0 \to \overline{f})},$$

the *CP*-violation asymmetry of exclusive Λ_b^0 and $\overline{\Lambda}_b^0$ decay.

$A_{CP}(\Lambda_b \to p\pi^-)$

VALUE	DOCUMENT ID		TECN	COMMENT
0.03±0.17±0.05	AALTONEN	11N	CDF	$p\overline{p}$ at 1.96 TeV

$A_{CP}(\Lambda_b \to pK^-)$

VALUE	DOCUMENT ID		TECN	COMMENT
0.37±0.17±0.03	AALTONEN	11N	CDF	$p\overline{p}$ at 1.96 TeV

Λ_b^0 DECAY PARAMETERS

See the note on "Baryon Decay Parameters" in the neutron Listings.

α decay parameter for $\Lambda_b \to J/\psi\Lambda$

VALUE		DOCUMENT ID		TECN	COMMENT
0.05±0.17±0.07	[48]	AAIJ	13AG	LHCB	pp at 7 TeV

[48] An angular analysis of $\Lambda_b \to J/\psi\Lambda$ decay is performed and a Λ_b transverse production polarization of 0.06 ± 0.07 ± 0.02 is also reported.

Λ_b^0 REFERENCES

AAIJ	14E	JHEP 1404 114	R. Aaij *et al.*	(LHCb Collab.)
AAIJ	14H	PR D89 032001	R. Aaij *et al.*	(LHCb Collab.)
AAD	13U	PR D87 032002	G. Aad *et al.*	(ATLAS Collab.)
AAIJ	13AG	PL B724 27	R. Aaij *et al.*	(LHCb Collab.)
AAIJ	13AJ	PL B725 25	R. Aaij *et al.*	(LHCb Collab.)
AAIJ	13AV	PRL 110 182001	R. Aaij *et al.*	(LHCb Collab.)
AAIJ	13BB	PRL 111 102003	R. Aaij *et al.*	(LHCb Collab.)
CHATRCHYAN	13AC	JHEP 1307 163	S. Chatrchyan *et al.*	(CMS Collab.)
AAIJ	12AR	JHEP 1210 037	R. Aaij *et al.*	(LHCb Collab.)
AAIJ	12E	PL B708 241	R. Aaij *et al.*	(LHCb Collab.)
AALTONEN	12A	PR D85 032003	T. Aaltonen *et al.*	(CDF Collab.)
ABAZOV	12U	PR D85 112003	V.M. Abazov *et al.*	(D0 Collab.)
AAIJ	11E	PR D84 092001	R. Aaij *et al.*	(LHCb Collab.)
Also		PR D85 039904 (errat.)	R. Aaij *et al.*	(LHCb Collab.)
AALTONEN	11	PRL 106 121804	T. Aaltonen *et al.*	(CDF Collab.)
AALTONEN	11AI	PRL 107 201802	T. Aaltonen *et al.*	(CDF Collab.)
AALTONEN	11N	PRL 106 181802	T. Aaltonen *et al.*	(CDF Collab.)
ABAZOV	11O	PR D84 031102	V.M. Abazov *et al.*	(D0 Collab.)
AALTONEN	10B	PRL 104 102002	T. Aaltonen *et al.*	(CDF Collab.)
AALTONEN	09C	PRL 103 031801	T. Aaltonen *et al.*	(CDF Collab.)
AALTONEN	09E	PR D79 032001	T. Aaltonen *et al.*	(CDF Collab.)
ABAZOV	07S	PRL 99 142001	V.M. Abazov *et al.*	(D0 Collab.)
ABAZOV	07U	PRL 99 182001	V.M. Abazov *et al.*	(D0 Collab.)
ABULENCIA	07A	PRL 98 122001	A. Abulencia *et al.*	(FNAL CDF Collab.)
ABULENCIA	07B	PRL 98 122002	A. Abulencia *et al.*	(FNAL CDF Collab.)
ACOSTA	06	PRL 96 202001	D. Acosta *et al.*	(CDF Collab.)
ABAZOV	05C	PRL 94 102001	V.M. Abazov *et al.*	(D0 Collab.)
ACOSTA	05O	PR D72 051104	D. Acosta *et al.*	(CDF Collab.)
ABDALLAH	04A	PL B585 63	J. Abdallah *et al.*	(DELPHI Collab.)
ACOSTA	02G	PR D66 112002	D. Acosta *et al.*	(CDF Collab.)
ABREU	99W	EPJ C10 185	P. Abreu *et al.*	(DELPHI Collab.)
ACKERSTAFF	98G	PL B426 161	K. Ackerstaff *et al.*	(OPAL Collab.)
BARATE	98D	EPJ C2 197	R. Barate *et al.*	(ALEPH Collab.)
ABE	97B	PR D55 1142	F. Abe *et al.*	(CDF Collab.)
ABE	96M	PRL 77 1439	F. Abe *et al.*	(CDF Collab.)
ABREU	96D	ZPHY C71 199	P. Abreu *et al.*	(DELPHI Collab.)
ABREU	96N	PL B374 351	P. Abreu *et al.*	(DELPHI Collab.)
ADAM	96D	ZPHY C72 207	W. Adam *et al.*	(DELPHI Collab.)
BUSKULIC	96L	PL B380 442	D. Buskulic *et al.*	(ALEPH Collab.)
BUSKULIC	96V	PL B384 471	D. Buskulic *et al.*	(ALEPH Collab.)
PDG	96	PR D54 1	R. M. Barnett *et al.*	(PDG Collab.)
ABREU	95S	ZPHY C68 375	P. Abreu *et al.*	(DELPHI Collab.)
AKERS	95K	PL B353 402	R. Akers *et al.*	(OPAL Collab.)
BUSKULIC	95L	PL B357 685	D. Buskulic *et al.*	(ALEPH Collab.)
ABE	93B	PR D47 R2639	F. Abe *et al.*	(CDF Collab.)
BUSKULIC	92E	PL B294 145	D. Buskulic *et al.*	(ALEPH Collab.)
ALBAJAR	91E	PL B273 540	C. Albajar *et al.*	(UA1 Collab.)
BARI	91	NC 104A 1787	G. Bari *et al.*	(CERN R422 Collab.)
ARENTON	86	NP B274 707	M.W. Arenton *et al.*	(ARIZ, NDAM, VAND)
BASILE	81	LNC 31 97	M. Basile *et al.*	(CERN R415 Collab.)

$\Lambda_b(5912)^0$

$J^P = \frac{1}{2}^-$ Status: ***

Quantum numbers are based on quark model expectations.

$\Lambda_b(5912)^0$ MASS

VALUE (MeV)		DOCUMENT ID		TECN	COMMENT
5912.1±0.1±0.4	[1,2]	AAIJ	12AL	LHCB	pp at 7 TeV

[1] Observed in $\Lambda_b(5912)^0 \to \Lambda_b^0\pi^+\pi^-$ decays with 17.6 ± 4.8 candidates with a significance of 5.2 sigma.

[2] AAIJ 12AL measures $m(\Lambda_b(5912)^0) - m(\Lambda_b^0) = 292.60 \pm 0.12 \pm 0.04$ MeV. We have adjusted the measurement to our best value of $m(\Lambda_b^0) = 5619.5 \pm 0.4$ MeV. Our first error is their experiment's error and our second error is the systematic error from using our best values.

$\Lambda_b(5912)^0$ WIDTH

VALUE (MeV)	CL%	DOCUMENT ID		TECN	COMMENT
<0.66	90	AAIJ	12AL	LHCB	pp at 7 TeV

$\Lambda_b(5912)^0$ DECAY MODES

	Mode	Fraction (Γ_i/Γ)
Γ_1	$\Lambda_b^0\pi^+\pi^-$	seen

$\Lambda_b(5912)^0$ BRANCHING RATIOS

$\Gamma(\Lambda_b^0\pi^+\pi^-)/\Gamma_{total}$ Γ_1/Γ

VALUE	DOCUMENT ID		TECN	COMMENT
seen	AAIJ	12AL	LHCB	pp at 7 TeV

$\Lambda_b(5912)^0$ REFERENCES

AAIJ	12AL	PRL 109 172003	R. Aaij *et al.*	(LHCb Collab.)

$\Lambda_b(5920)^0$

$J^P = \frac{3}{2}^-$ Status: ***

Quantum numbers are based on quark model expectations.

$\Lambda_b(5920)^0$ MASS

VALUE (MeV)		DOCUMENT ID		TECN	COMMENT
5919.73±0.32 OUR AVERAGE					
5919.3 ±0.5 ±0.4	[1,2]	AALTONEN	13V	CDF	$p\overline{p}$ at 1.96 TeV
5919.9 ±0.1 ±0.4	[3,4]	AAIJ	12AL	LHCB	pp at 7 TeV

[1] Measured in $\Lambda_b(5920)^0 \to \Lambda_b^0\pi^+\pi^-$ decays with $17.3^{+5.3}_{-4.6}$ events, with a significance of 3.5 sigma.

[2] AALTONEN 13V measures $m(\Lambda_b(5920)^0) - m(\Lambda_b^0) - 2m(\pi) = 20.68 \pm 0.35 \pm 0.30$ MeV. We have adjusted the measurement to our best values of $m(\Lambda_b^0) = 5619.5 \pm 0.4$ MeV and $m(\pi) = 139.57018 \pm 0.00035$ MeV. Our first error is their experiment's error and our second error is the systematic error from using our best values.

[3] Observed in $\Lambda_b(5920)^0 \to \Lambda_b^0\pi^+\pi^-$ decays with 52.5 ± 8.1 candidates with a significance of 10.2 sigma.

[4] AAIJ 12AL measures $m(\Lambda_b(5920)^0) - m(\Lambda_b^0) = 300.40 \pm 0.08 \pm 0.04$ MeV. We have adjusted the measurement to our best value of $m(\Lambda_b^0) = 5619.5 \pm 0.4$ MeV. Our first error is their experiment's error and our second error is the systematic error from using our best values.

$\Lambda_b(5920)^0$ WIDTH

VALUE (MeV)	CL%	DOCUMENT ID		TECN	COMMENT
<0.63	90	AAIJ	12AL	LHCB	pp at 7 TeV

$\Lambda_b(5920)^0$ DECAY MODES

	Mode	Fraction (Γ_i/Γ)
Γ_1	$\Lambda_b^0\pi^+\pi^-$	seen

Baryon Particle Listings

$\Lambda_b(5920)^0$, Σ_b, Σ_b^*

$\Lambda_b(5920)^0$ BRANCHING RATIOS

$\Gamma(\Lambda_b^0\pi^+\pi^-)/\Gamma_{\text{total}}$ — Γ_1/Γ

VALUE	DOCUMENT ID	TECN	COMMENT
seen	AAIJ	12AL LHCB	pp at 7 TeV

$\Lambda_b(5920)^0$ REFERENCES

AALTONEN	13V	PR D88 071101	T. Aaltonen *et al.*	(CDF Collab.)
AAIJ	12AL	PRL 109 172003	R. Aaij *et al.*	(LHCb Collab.)

Σ_b

$I(J^P) = 1(\frac{1}{2}^+)$ Status: ***

I, J, P need confirmation.

In the quark model Σ_b^+, Σ_b^0, Σ_b^- are an isotriplet (uub, udb, ddb) state. The lowest Σ_b ought to have $J^P = 1/2^+$. None of I, J, or P have actually been measured.

Σ_b MASS

Σ_b^+ MASS

VALUE (MeV)	DOCUMENT ID		TECN	COMMENT
$5811.3^{+0.9}_{-0.8}\pm1.7$	[1] AALTONEN	12F	CDF	$p\overline{p}$ at 1.96 TeV
• • • We do not use the following data for averages, fits, limits, etc. • • •				
$5807.8^{+2.0}_{-2.2}\pm1.7$	[2] AALTONEN	07K	CDF	Repl. by AALTONEN 12F

Σ_b^- MASS

VALUE (MeV)	DOCUMENT ID		TECN	COMMENT
$5815.5^{+0.6}_{-0.5}\pm1.7$	[1] AALTONEN	12F	CDF	$p\overline{p}$ at 1.96 TeV
• • • We do not use the following data for averages, fits, limits, etc. • • •				
$5815.2\pm1.0\pm1.7$	[2] AALTONEN	07K	CDF	Repl. by AALTONEN 12F

$m_{\Sigma_b^+} - m_{\Sigma_b^-}$

VALUE (MeV)	DOCUMENT ID		TECN	COMMENT
$-4.2^{+1.1}_{-1.0}\pm0.1$	[1] AALTONEN	12F	CDF	$p\overline{p}$ at 1.96 TeV

[1] Measured using the fully reconstructed $\Lambda_b^0 \to \Lambda_c^+\pi^-$ and $\Lambda_c^+ \to K^-\pi^+$ decays.

[2] Observed four $\Lambda_b^0\pi^\pm$ resonances in the fully reconstructed decay mode $\Lambda_b^0 \to \Lambda_c^+\pi^-$, where $\Lambda_c^+ \to pK^-\pi^+$.

Σ_b WIDTH

Σ_b^+ WIDTH

VALUE (MeV)	DOCUMENT ID		TECN	COMMENT
$9.7^{+3.8+1.2}_{-2.8-1.1}$	[3] AALTONEN	12F	CDF	$p\overline{p}$ at 1.96 TeV

Σ_b^- WIDTH

VALUE (MeV)	DOCUMENT ID		TECN	COMMENT
$4.9^{+3.1}_{-2.1}\pm1.1$	[3] AALTONEN	12F	CDF	$p\overline{p}$ at 1.96 TeV

[3] Measured using the fully reconstructed $\Lambda_b^0 \to \Lambda_c^+\pi^-$ and $\Lambda_c^+ \to K^-\pi^+$ decays.

Σ_b DECAY MODES

	Mode	Fraction (Γ_i/Γ)
Γ_1	$\Lambda_b^0\pi$	dominant

Σ_b BRANCHING RATIOS

$\Gamma(\Lambda_b^0\pi)/\Gamma_{\text{total}}$ — Γ_1/Γ

VALUE	DOCUMENT ID	TECN	COMMENT
dominant	AALTONEN	07K CDF	$p\overline{p}$ at 1.96 TeV

Σ_b REFERENCES

AALTONEN	12F	PR D85 092011	T. Aaltonen *et al.*	(CDF Collab.)
AALTONEN	07K	PRL 99 202001	T. Aaltonen *et al.*	(CDF Collab.)

Σ_b^*

$I(J^P) = 1(\frac{3}{2}^+)$ Status: ***

I, J, P need confirmation.

I, J, P need confirmation. Quantum numbers shown are quark-model predictions.

Σ_b^* MASS

Σ_b^{*+} MASS

VALUE (MeV)	DOCUMENT ID		TECN	COMMENT
$5832.1\pm0.7^{+1.7}_{-1.8}$	[1] AALTONEN	12F	CDF	$p\overline{p}$ at 1.96 TeV

Σ_b^{*-} MASS

VALUE (MeV)	DOCUMENT ID		TECN	COMMENT
$5835.1\pm0.6^{+1.7}_{-1.8}$	[1] AALTONEN	12F	CDF	$p\overline{p}$ at 1.96 TeV

$m_{\Sigma_b^{*+}} - m_{\Sigma_b^{*-}}$

VALUE (MeV)	DOCUMENT ID		TECN	COMMENT
$-3.0^{+1.0}_{-0.9}\pm0.1$	[1] AALTONEN	12F	CDF	$p\overline{p}$ at 1.96 TeV

[1] Measured using the fully reconstructed $\Lambda_b^0 \to \Lambda_c^+\pi^-$ and $\Lambda_c^+ \to K^-\pi^+$ decays.

Σ_b^* WIDTH

Σ_b^{*+} WIDTH

VALUE (MeV)	DOCUMENT ID		TECN	COMMENT
$11.5^{+2.7+1.0}_{-2.2-1.5}$	[2] AALTONEN	12F	CDF	$p\overline{p}$ at 1.96 TeV

Σ_b^{*-} WIDTH

VALUE (MeV)	DOCUMENT ID		TECN	COMMENT
$7.5^{+2.2+0.9}_{-1.8-1.4}$	[2] AALTONEN	12F	CDF	$p\overline{p}$ at 1.96 TeV

[2] Measured using the fully reconstructed $\Lambda_b^0 \to \Lambda_c^+\pi^-$ and $\Lambda_c^+ \to K^-\pi^+$ decays.

$m_{\Sigma_b^*} - m_{\Sigma_b}$

VALUE (MeV)	DOCUMENT ID		TECN	COMMENT
$21.2^{+2.0+0.4}_{-1.9-0.3}$	[3] AALTONEN	07K	CDF	$p\overline{p}$ at 1.96 TeV

[3] Observed four $\Lambda_b^0\pi^\pm$ resonances in the fully reconstructed decay mode $\Lambda_b^0 \to \Lambda_c^+\pi^-$, where $\Lambda_c^+ \to pK^-\pi^+$. Assumes $m_{\Sigma_b^{*+}} - m_{\Sigma_b^+} = m_{\Sigma_b^{*-}} - m_{\Sigma_b^-}$

Σ_b^* DECAY MODES

	Mode	Fraction (Γ_i/Γ)
Γ_1	$\Lambda_b^0\pi$	dominant

Σ_b^* BRANCHING RATIOS

$\Gamma(\Lambda_b^0\pi)/\Gamma_{\text{total}}$ — Γ_1/Γ

VALUE	DOCUMENT ID	TECN	COMMENT
dominant	AALTONEN	07K CDF	$p\overline{p}$ at 1.96 TeV

Σ_b^* REFERENCES

AALTONEN	12F	PR D85 092011	T. Aaltonen *et al.*	(CDF Collab.)
AALTONEN	07K	PRL 99 202001	T. Aaltonen *et al.*	(CDF Collab.)

Ξ_b^0, Ξ_b^-

$I(J^P) = \frac{1}{2}(\frac{1}{2}^+)$ Status: ***

I, *J*, *P* need confirmation.

In the quark model, Ξ_b^0 and Ξ_b^- are an isodoublet (*usb*, *dsb*) state; the lowest Ξ_b^0 and Ξ_b^- ought to have $J^P = 1/2^+$. None of *I*, *J*, or *P* have actually been measured.

Ξ_b MASSES

Ξ_b^- MASS

VALUE (MeV)	DOCUMENT ID		TECN	COMMENT
5794.9± 0.9 OUR AVERAGE	Includes data from the datablock that follows this one. Error includes scale factor of 1.1.			
5795.8± 0.9± 0.4	[1] AAIJ	13AV	LHCB	pp at 7 TeV
5796.7± 5.1± 1.4	[2] AALTONEN	11X	CDF	$p\overline{p}$ at 1.96 TeV
5790.9± 2.6± 0.8	[3] AALTONEN	09AP	CDF	$p\overline{p}$ at 1.96 TeV
5774 ±11 ±15	[4] ABAZOV	07K	D0	$p\overline{p}$ at 1.96 TeV
• • • We do not use the following data for averages, fits, limits, etc. • • •				
5792.9± 2.5± 1.7	[5] AALTONEN	07A	CDF	Repl. by AALTONEN 09AP

[1] Measured in $\Xi_b^- \to J/\psi\Xi^-$ decays.

[2] Measured in $\Xi_b^- \to \Xi_c^0\pi^-$ with $25.8^{+5.5}_{-5.2}$ candidates.

[3] Measured in $\Xi_b^- \to J/\psi\Xi^-$ decays with 66^{+14}_{-9} candidates.

[4] Observed in $\Xi_b^- \to J/\psi\Xi^-$ decays with $15.2 \pm 4.4^{+1.9}_{-0.4}$ candidates, a significance of 5.5 sigma.

[5] Observed in $\Xi_b^- \to J/\psi\Xi^-$ decays with 17.5 ± 4.3 candidates, a significance of 7.7 sigma.

Ξ_b^0 MASS

VALUE (MeV)	DOCUMENT ID		TECN	COMMENT
The data in this block is included in the average printed for a previous datablock.				
5793.1±2.5 OUR AVERAGE	Error includes scale factor of 1.1.			
5794.3±2.4±0.7	AAIJ	14H	LHCB	pp at 7 TeV
5787.8±5.0±1.3	[6] AALTONEN	11X	CDF	$p\overline{p}$ at 1.96 TeV

[6] Measured in $\Xi_b^0 \to \Xi_c^+\pi^-$ with $25.3^{+5.6}_{-5.4}$ candidates.

$m_{\Xi_b^-} - m_{\Lambda_b^0}$

VALUE (MeV)	DOCUMENT ID		TECN	COMMENT
176.2±0.9±0.1	AAIJ	13AV	LHCB	pp at 7 TeV

$m_{\Xi_b^0} - m_{\Lambda_b^0}$

VALUE (MeV)	DOCUMENT ID		TECN	COMMENT
174.8±2.4±0.5	AAIJ	14H	LHCB	pp at 7 TeV

$m_{\Xi_b^-} - m_{\Xi_b^0}$

VALUE (MeV)	DOCUMENT ID		TECN	COMMENT
3.1±5.6±1.3	[7] AALTONEN	11X	CDF	$p\overline{p}$ at 1.96 TeV

[7] Derived from measurements in $\Xi_b^0 \to \Xi_c^+\pi^-$ and $\Xi_b^- \to J/\psi\Xi^-$ from AALTONEN 09AP taking correlated systematic uncertainties into account.

Ξ_b^- MEAN LIFE

VALUE (10^{-12} s)	DOCUMENT ID		TECN	COMMENT
1.56$^{+0.27}_{-0.25}$ OUR EVALUATION				
1.56$^{+0.27}_{-0.25}$±0.02	[8] AALTONEN	09AP	CDF	$p\overline{p}$ at 1.96 TeV

[8] Measured in $\Xi_b^- \to J/\psi\Xi^-$ decays with 66^{+14}_{-9} candidates.

Ξ_b MEAN LIFE

"OUR EVALUATION" is an average using rescaled values of the data listed below. The average and rescaling were performed by the Heavy Flavor Averaging Group (HFAG) and are described at http://www.slac.stanford.edu/xorg/hfag/. The averaging/rescaling procedure takes into account correlations between the measurements and asymmetric lifetime errors.

VALUE (10^{-12} s)	EVTS	DOCUMENT ID		TECN	COMMENT
1.49$^{+0.19}_{-0.18}$ OUR EVALUATION					
1.56$^{+0.27}_{-0.25}$±0.02		[9] AALTONEN	09AP	CDF	$p\overline{p}$ at 1.96 TeV
1.48$^{+0.40}_{-0.31}$±0.12		[10] ABDALLAH	05C	DLPH	$e^+e^- \to Z^0$
1.35$^{+0.37}_{-0.28}$$^{+0.15}_{-0.17}$		[11] BUSKULIC	96T	ALEP	$e^+e^- \to Z$
• • • We do not use the following data for averages, fits, limits, etc. • • •					
1.5 $^{+0.7}_{-0.4}$ ±0.3	8	[12] ABREU	95V	DLPH	Repl. by ABDALLAH 05C

[9] Measured in $\Xi_b^- \to J/\psi\Xi^-$ decays with 66^{+14}_{-9} candidates.

[10] Used the decay length of Ξ^- accompanied by a lepton of the same sign.

[11] Excess $\Xi^-\ell^-$, impact parameters.

[12] Excess $\Xi^-\ell^-$, decay lengths.

Ξ_b DECAY MODES

	Mode	Fraction (Γ_i/Γ)	Scale factor
Γ_1	$\Xi_b \to \Xi^-\ell^-\overline{\nu}_\ell X \times$ B($\overline{b} \to \Xi_b$)	(3.9 ±1.2) × 10^{-4}	1.4
Γ_2	$\Xi_b^- \to J/\psi\Xi^- \times$ B($b \to \Xi_b^-$)	(1.02$^{+0.26}_{-0.21}$) × 10^{-5}	
Γ_3	$\Xi_b^0 \to p D^0 K^- \times$ B($\overline{b} \to \Xi_b$)	(1.8 $^{+1.3}_{-1.1}$) × 10^{-6}	
Γ_4	$\Xi_b^0 \to \Lambda_c^+ K^- \times$ B($\overline{b} \to \Xi_b$)	(8 ±7) × 10^{-7}	

Ξ_b BRANCHING RATIOS

$\Gamma(\Xi^-\ell^-\overline{\nu}_\ell X \times$ B($\overline{b} \to \Xi_b$)$)/\Gamma_{total}$ Γ_1/Γ

VALUE (units 10^{-4})	DOCUMENT ID		TECN	COMMENT
3.9±1.2 OUR AVERAGE	Error includes scale factor of 1.4.			
3.0±1.0±0.3	ABDALLAH	05C	DLPH	$e^+e^- \to Z^0$
5.4±1.1±0.8	BUSKULIC	96T	ALEP	Excess $\Xi^-\ell^-$ over $\Xi^-\ell^+$
• • • We do not use the following data for averages, fits, limits, etc. • • •				
5.9±2.1±1.0	ABREU	95V	DLPH	Repl. by ABDALLAH 05C

$\Gamma(J/\psi\Xi^- \times$ B($b \to \Xi_b^-$)$)/\Gamma_{total}$ Γ_2/Γ

VALUE (units 10^{-4})	DOCUMENT ID		TECN	COMMENT
0.102$^{+0.026}_{-0.021}$ OUR AVERAGE				
0.098$^{+0.023}_{-0.016}$±0.014	[13] AALTONEN	09AP	CDF	$p\overline{p}$ at 1.96 TeV
0.16 ±0.07 ±0.02	[14] ABAZOV	07K	D0	$p\overline{p}$ at 1.96 TeV

[13] AALTONEN 09AP reports [$\Gamma(\Xi_b^- \to J/\psi\Xi^- \times$ B($b \to \Xi_b^-$))/Γ_{total}] / [B($\Lambda_b^0 \to J/\psi(1S)\Lambda \times$ B($b \to \Lambda_b^0$))] = $0.167^{+0.037}_{-0.025} \pm 0.012$ which we multiply by our best value B($\Lambda_b^0 \to J/\psi(1S)\Lambda \times$ B($b \to \Lambda_b^0$)) = (5.8 ± 0.8) × 10^{-5}. Our first error is their experiment's error and our second error is the systematic error from using our best value.

[14] ABAZOV 07K reports [$\Gamma(\Xi_b^- \to J/\psi\Xi^- \times$ B($b \to \Xi_b^-$))/Γ_{total}] / [B($\Lambda_b^0 \to J/\psi(1S)\Lambda \times$ B($b \to \Lambda_b^0$))] = $0.28 \pm 0.09^{+0.09}_{-0.08}$ which we multiply by our best value B($\Lambda_b^0 \to J/\psi(1S)\Lambda \times$ B($b \to \Lambda_b^0$)) = (5.8 ± 0.8) × 10^{-5}. Our first error is their experiment's error and our second error is the systematic error from using our best value.

$\Gamma(p D^0 K^- \times$ B($\overline{b} \to \Xi_b$)$)/\Gamma_{total}$ Γ_3/Γ

VALUE	DOCUMENT ID		TECN	COMMENT
(1.8±0.4$^{+1.2}_{-1.0}$) × 10^{-6}	[15] AAIJ	14H	LHCB	pp at 7 TeV

[15] AAIJ 14H reports [$\Gamma(\Xi_b^0 \to p D^0 K^- \times$ B($\overline{b} \to \Xi_b$))/Γ_{total}] / [B($\overline{b} \to b$-baryon)] / [B($\Lambda_b^0 \to p D^0 K^-$)] = 0.44 ± 0.09 ± 0.06 which we multiply by our best values B($\overline{b} \to b$-baryon) = (9.2 ± 1.5) × 10^{-2}, B($\Lambda_b^0 \to p D^0 K^-$) = (4.3$^{+3.0}_{-2.4}$) × 10^{-5}. Our first error is their experiment's error and our second error is the systematic error from using our best values.

$\Gamma(\Lambda_c^+ K^- \times$ B($\overline{b} \to \Xi_b$)$)/\Gamma(p D^0 K^- \times$ B($\overline{b} \to \Xi_b$)$)$ Γ_4/Γ_3

VALUE	DOCUMENT ID		TECN	COMMENT
0.44±0.24±0.12	[16] AAIJ	14H	LHCB	pp at 7 TeV

[16] AAIJ 14H reports [$\Gamma(\Xi_b^0 \to \Lambda_c^+ K^- \times$ B($\overline{b} \to \Xi_b$))/$\Gamma(\Xi_b^0 \to p D^0 K^- \times$ B($\overline{b} \to \Xi_b$))] × [B($\Lambda_c^+ \to p K^-\pi^+$)] / [B($D^0 \to K^-\pi^+$)] = 0.57 ± 0.22 ± 0.21 which we multiply or divide by our best values B($\Lambda_c^+ \to p K^-\pi^+$) = (5.0 ± 1.3) × 10^{-2}, B($D^0 \to K^-\pi^+$) = (3.88 ± 0.05) × 10^{-2}. Our first error is their experiment's error and our second error is the systematic error from using our best values.

Ξ_b REFERENCES

AAIJ	14H	PR D89 032001	R. Aaij *et al.*	(LHCb Collab.)
AAIJ	13AV	PRL 110 182001	R. Aaij *et al.*	(LHCb Collab.)
AALTONEN	11X	PRL 107 102001	T. Aaltonen *et al.*	(CDF Collab.)
AALTONEN	09AP	PR D80 072003	T. Aaltonen *et al.*	(CDF Collab.)
AALTONEN	07A	PRL 99 052002	T. Aaltonen *et al.*	(CDF Collab.)
ABAZOV	07K	PRL 99 052001	V.M. Abazov *et al.*	(D0 Collab.)
ABDALLAH	05C	EPJ C44 299	J. Abdallah *et al.*	(DELPHI Collab.)
BUSKULIC	96T	PL B384 449	D. Buskulic *et al.*	(ALEPH Collab.)
ABREU	95V	ZPHY C68 541	P. Abreu *et al.*	(DELPHI Collab.)

Baryon Particle Listings

$\Xi_b(5945)^0$, Ω_b^-, b-baryon ADMIXTURE (Λ_b, Ξ_b, Σ_b, Ω_b)

$\Xi_b(5945)^0$

$J^P = \frac{3}{2}^+$ Status: ***

Quantum numbers are based on quark model expectations.

$\Xi_b(5945)^0$ MASS

VALUE (MeV)	DOCUMENT ID		TECN	COMMENT
5949.3±0.8±0.9	[1] CHATRCHYAN	12S	CMS	pp at 7 TeV, 5.3 fb^{-1}

[1] CHATRCHYAN 12S measures $m(\Xi_b(5945)^0) - m(\Xi_b^-) - m(\pi^+) = 14.84 \pm 0.74 \pm 0.28$ MeV. We have adjusted the measurement to our best values of $m(\Xi_b^-) = 5794.9 \pm 0.9$ MeV, $m(\pi^+) = 139.57018 \pm 0.00035$ MeV. Our first error is their experiment's error and our second error is the systematic error from using our best values.

$\Xi_b(5945)^0$ WIDTH

VALUE (MeV)	DOCUMENT ID		TECN	COMMENT
2.1±1.7	[2] CHATRCHYAN	12S	CMS	pp at 7 TeV, 5.3 fb^{-1}

[2] Systematic uncertainty not evaluated.

$\Xi_b(5945)^0$ DECAY MODES

	Mode	Fraction (Γ_i/Γ)
Γ_1	$\Xi_b^- \pi^+$	seen

$\Xi_b(5945)^0$ BRANCHING RATIOS

$\Gamma(\Xi_b^- \pi^+)/\Gamma_{total}$ **Γ_1/Γ**

VALUE	DOCUMENT ID		TECN	COMMENT
seen	CHATRCHYAN	12S	CMS	pp at 7 TeV, 5.3 fb^{-1}

$\Xi_b(5945)^0$ REFERENCES

CHATRCHYAN 12S PRL 108 252002 S. Chatrchyan *et al.* (CMS Collab.)

Ω_b^-

$I(J^P) = 0(\frac{1}{2}^+)$ Status: ***

I, J, P need confirmation.

In the quark model Ω_b^- is ssb ground state. None of its quantum numbers has been measured.

Ω_b^- MASS

VALUE (MeV)	DOCUMENT ID		TECN	COMMENT
6048.8± 3.2 OUR AVERAGE	Error includes scale factor of 1.5.			
6046.0± 2.2± 0.5	[1] AAIJ	13AV	LHCB	pp at 7 TeV
6054.4± 6.8± 0.9	[2] AALTONEN	09AP	CDF	$p\overline{p}$ at 1.96 TeV
6165 ±10 ±13	[3] ABAZOV	08AL	D0	$p\overline{p}$ at 1.96 TeV

[1] Measured in $\Omega_b^- \to J/\psi\Omega^-$ with 19 ± 5 events.

[2] Observed in $\Omega_b^- \to J/\psi\Omega^-$ decays with 16^{+6}_{-4} candidates, a significance of 5.5 sigma from a combined mass-lifetime fit.

[3] Observed in $\Omega_b^- \to J/\psi\Omega^-$ decays with 17.8 ± 4.9 ± 0.8 candidates, a significance of 5.4 sigma.

$m_{\Omega_b^-} - m_{\Lambda_b^0}$

VALUE (MeV)	DOCUMENT ID		TECN	COMMENT
426.4±2.2±0.4	AAIJ	13AV	LHCB	pp at 7 TeV

Ω_b MEAN LIFE

VALUE (10^{-12} s)	DOCUMENT ID		TECN	COMMENT
$1.13^{+0.53}_{-0.40}\pm0.02$	[4] AALTONEN	09AP	CDF	$p\overline{p}$ at 1.96 TeV

[4] Observed in $\Omega_b^- \to J/\psi\Omega^-$ decays with 16^{+6}_{-4} candidates, a significance of 5.5 sigma from a combined mass-lifetime fit.

Ω_b^- DECAY MODES

	Mode	Fraction (Γ_i/Γ)
Γ_1	$J/\psi\Omega^- \times B(b \to \Omega_b)$	$(2.9^{+1.1}_{-0.8}) \times 10^{-6}$

Ω_b^- BRANCHING RATIOS

$\Gamma(J/\psi\Omega^- \times B(b \to \Omega_b))/\Gamma_{total}$ **Γ_1/Γ**

VALUE (units 10^{-4})	DOCUMENT ID		TECN	COMMENT
$0.029^{+0.011}_{-0.008}$ OUR AVERAGE				
$0.026^{+0.010}_{-0.007}\pm0.004$	[5] AALTONEN	09AP	CDF	$p\overline{p}$ at 1.96 TeV
0.08 ±0.04 ±0.02	[6] ABAZOV	08AL	D0	$p\overline{p}$ at 1.96 TeV

[5] AALTONEN 09AP reports $[\Gamma(\Omega_b^- \to J/\psi\Omega^- \times B(b \to \Omega_b))/\Gamma_{total}] / [B(\Lambda_b^0 \to J/\psi(1S)\Lambda \times B(b \to \Lambda_b^0))] = 0.045^{+0.017}_{-0.012} \pm 0.004$ which we multiply by our best value $B(\Lambda_b^0 \to J/\psi(1S)\Lambda \times B(b \to \Lambda_b^0)) = (5.8 \pm 0.8) \times 10^{-5}$. Our first error is their experiment's error and our second error is the systematic error from using our best value.

[6] ABAZOV 08AL reports $[\Gamma(\Omega_b^- \to J/\psi\Omega^- \times B(b \to \Omega_b))/\Gamma_{total}] / [B(\Xi_b^- \to J/\psi\Xi^- \times B(b \to \Xi_b^-))] = 0.80 \pm 0.32^{+0.14}_{-0.22}$ which we multiply by our best value $B(\Xi_b^- \to J/\psi\Xi^- \times B(b \to \Xi_b^-)) = (1.02^{+0.26}_{-0.21}) \times 10^{-5}$. Our first error is their experiment's error and our second error is the systematic error from using our best value.

Ω_b^- REFERENCES

AAIJ 13AV PRL 110 182001 R. Aaij *et al.* (LHCb Collab.)
AALTONEN 09AP PR D80 072003 T. Aaltonen *et al.* (CDF Collab.)
ABAZOV 08AL PRL 101 232002 V.M. Abazov *et al.* (D0 Collab.)

b-baryon ADMIXTURE (Λ_b, Ξ_b, Σ_b, Ω_b)

b-baryon ADMIXTURE MEAN LIFE

Each measurement of the b-baryon mean life is an average over an admixture of various b baryons which decay weakly. Different techniques emphasize different admixtures of produced particles, which could result in a different b-baryon mean life. More b-baryon flavor specific channels are not included in the measurement.

"OUR EVALUATION" is an average using rescaled values of the data listed below. The average and rescaling were performed by the Heavy Flavor Averaging Group (HFAG) and are described at http://www.slac.stanford.edu/xorg/hfag/. The averaging/rescaling procedure takes into account correlations between the measurements and asymmetric lifetime errors.

VALUE (10^{-12} s)	EVTS	DOCUMENT ID		TECN	COMMENT
1.449±0.015 OUR EVALUATION					
1.415±0.027±0.006		AAIJ	14E	LHCB	pp at 7 TeV
1.449±0.036±0.017		[1] AAD	13U	ATLS	pp at 7 TeV
1.303±0.075±0.035		[2] ABAZOV	12U	D0	$p\overline{p}$ at 1.96 TeV
1.401±0.046±0.035		[3] AALTONEN	10B	CDF	$p\overline{p}$ at 1.96 TeV
$1.290^{+0.119}_{-0.110}{}^{+0.087}_{-0.091}$		[4] ABAZOV	07U	D0	$p\overline{p}$ at 1.96 TeV
$1.593^{+0.083}_{-0.078}\pm0.033$		[2] ABULENCIA	07A	CDF	$p\overline{p}$ at 1.96 TeV
1.16 ±0.20 ±0.08		[5] ABREU	99W	DLPH	$e^+e^- \to Z$
1.19 ±0.14 ±0.07		[6] ABREU	99W	DLPH	$e^+e^- \to Z$
$1.11\ ^{+0.19}_{-0.18}$ ±0.05		[7] ABREU	99W	DLPH	$e^+e^- \to Z$
$1.29\ ^{+0.24}_{-0.22}$ ±0.06		[7] ACKERSTAFF	98G	OPAL	$e^+e^- \to Z$
1.20 ±0.08 ±0.06		[8] BARATE	98D	ALEP	$e^+e^- \to Z$
1.21 ±0.11		[7] BARATE	98D	ALEP	$e^+e^- \to Z$
1.32 ±0.15 ±0.07		[9] ABE	96M	CDF	$p\overline{p}$ at 1.8 TeV
$1.10\ ^{+0.19}_{-0.17}$ ±0.09		[7] ABREU	96D	DLPH	$e^+e^- \to Z$
1.16 ±0.11 ±0.06		[7] AKERS	96	OPAL	$e^+e^- \to Z$
• • • We do not use the following data for averages, fits, limits, etc. • • •					
$1.218^{+0.130}_{-0.115}\pm0.042$		[2] ABAZOV	07S	D0	Repl. by ABAZOV 12U
$1.22\ ^{+0.22}_{-0.18}$ ±0.04		[2] ABAZOV	05C	D0	Repl. by ABAZOV 07S
1.14 ±0.08 ±0.04		[10] ABREU	99W	DLPH	$e^+e^- \to Z$
$1.46\ ^{+0.22}_{-0.21}\ ^{+0.07}_{-0.09}$		ABREU	96D	DLPH	Repl. by ABREU 99W
$1.27\ ^{+0.35}_{-0.29}$ ±0.09		ABREU	95S	DLPH	Repl. by ABREU 99W
$1.05\ ^{+0.12}_{-0.11}$ ±0.09	290	BUSKULIC	95L	ALEP	Repl. by BARATE 98D
$1.04\ ^{+0.48}_{-0.38}$ ±0.10	11	[11] ABREU	93F	DLPH	Excess $\Lambda\mu^-$, decay lengths
$1.05\ ^{+0.23}_{-0.20}$ ±0.08	157	[12] AKERS	93	OPAL	Excess $\Lambda\ell^-$, decay lengths
$1.12\ ^{+0.32}_{-0.29}$ ±0.16	101	[13] BUSKULIC	92I	ALEP	Excess $\Lambda\ell^-$, impact parameters

[1] Measured with $\Lambda_b^0 \to J/\psi(\mu^+\mu^-)\,\Lambda^0(p\pi^-)$ decays.
[2] Measured mean life using fully reconstructed $\Lambda_b^0 \to J/\psi\Lambda$ decays.
[3] Measured mean life using fully reconstructed $\Lambda_b^0 \to \Lambda_c^+\pi^-$ decays.
[4] Measured using semileptonic decays $\Lambda_b(0) \to \Lambda_c^+\mu\nu X$, $\Lambda_c^+ \to K_S^0 p$.
[5] Measured using $\Lambda\ell^-$ decay length.
[6] Measured using $p\ell^-$ decay length.
[7] Measured using $\Lambda_c\ell^-$ and $\Lambda\ell^+\ell^-$.
[8] Measured using the excess of $\Lambda\ell^-$, lepton impact parameter.
[9] Measured using $\Lambda_c\ell^-$.
[10] This ABREU 99W result is the combined result of the $\Lambda\ell^-$, $p\ell^-$, and excess $\Lambda\mu^-$ impact parameter measurements.
[11] ABREU 93F superseded by ABREU 96D.
[12] AKERS 93 superseded by AKERS 96.
[13] BUSKULIC 92I superseded by BUSKULIC 95L.

b-baryon ADMIXTURE DECAY MODES (Λ_b,Ξ_b,Σ_b,Ω_b)

These branching fractions are actually an average over weakly decaying *b*-baryons weighted by their production rates at the LHC, LEP, and Tevatron, branching ratios, and detection efficiencies. They scale with the *b*-baryon production fraction B($b \to$ *b*-baryon).

The branching fractions B(*b*-baryon $\to \Lambda\ell^-\overline{\nu}_\ell$anything) and B($\Lambda_b^0 \to \Lambda_c^+\ell^-\overline{\nu}_\ell$anything) are not pure measurements because the underlying measured products of these with B($b \to$ *b*-baryon) were used to determine B($b \to$ *b*-baryon), as described in the note "Production and Decay of *b*-Flavored Hadrons."

For inclusive branching fractions, *e.g.*, $B \to D^\pm$anything, the values usually are multiplicities, not branching fractions. They can be greater than one.

	Mode	Fraction (Γ_i/Γ)
Γ_1	$p\mu^-\overline{\nu}$anything	($5.3^{+\ 2.2}_{-\ 1.9}$) %
Γ_2	$p\ell\overline{\nu}_\ell$anything	(5.1± 1.2) %
Γ_3	$p$anything	(64 ±21) %
Γ_4	$\Lambda\ell^-\overline{\nu}_\ell$anything	(3.5± 0.6) %
Γ_5	$\Lambda\ell^+\nu_\ell$anything	
Γ_6	Λanything	
Γ_7	$\Lambda_c^+\ell^-\overline{\nu}_\ell$anything	
Γ_8	$\Lambda/\overline{\Lambda}$anything	(36 ± 7) %
Γ_9	$\Xi^-\ell^-\overline{\nu}_\ell$anything	(6.0± 1.6) $\times 10^{-3}$

b-baryon ADMIXTURE (Λ_b, Ξ_b, Σ_b, Ω_b) BRANCHING RATIOS

$\Gamma(p\mu^-\overline{\nu}$anything$)/\Gamma_{total}$ Γ_1/Γ

VALUE	EVTS	DOCUMENT ID		TECN	COMMENT
$0.053^{+0.020}_{-0.017}\pm0.009$	125	[14] ABREU	95S	DLPH	$e^+e^- \to Z$

[14] ABREU 95S reports $[\Gamma(b\text{-baryon} \to p\mu^-\overline{\nu}\text{anything})/\Gamma_{total}] \times [B(\overline{b} \to b\text{-baryon})] = 0.0049 \pm 0.0011^{+0.0015}_{-0.0011}$ which we divide by our best value B($\overline{b} \to$ *b*-baryon) = (9.2 ± 1.5) $\times 10^{-2}$. Our first error is their experiment's error and our second error is the systematic error from using our best value.

$\Gamma(p\ell\overline{\nu}_\ell$anything$)/\Gamma_{total}$ Γ_2/Γ

VALUE	DOCUMENT ID		TECN	COMMENT
0.051±0.009±0.008	[15] BARATE	98V	ALEP	$e^+e^- \to Z$

[15] BARATE 98V reports $[\Gamma(b\text{-baryon} \to p\ell\overline{\nu}_\ell\text{anything})/\Gamma_{total}] \times [B(\overline{b} \to b\text{-baryon})] = (4.72 \pm 0.66 \pm 0.44) \times 10^{-3}$ which we divide by our best value B($\overline{b} \to$ *b*-baryon) = (9.2 ± 1.5) $\times 10^{-2}$. Our first error is their experiment's error and our second error is the systematic error from using our best value.

$\Gamma(p\ell\overline{\nu}_\ell$anything$)/\Gamma(p$anything$)$ Γ_2/Γ_3

VALUE	DOCUMENT ID		TECN	COMMENT
0.080±0.012±0.014	BARATE	98V	ALEP	$e^+e^- \to Z$

$\Gamma(\Lambda\ell^-\overline{\nu}_\ell$anything$)/\Gamma_{total}$ Γ_4/Γ

The values and averages in this section serve only to show what values result if one assumes our B($b \to$ *b*-baryon). They cannot be thought of as measurements since the underlying product branching fractions were also used to determine B($b \to$ *b*-baryon) as described in the note on "Production and Decay of *b*-Flavored Hadrons."

VALUE	EVTS	DOCUMENT ID		TECN	COMMENT
0.035±0.006 OUR AVERAGE					
0.035±0.005±0.006		[16] BARATE	98D	ALEP	$e^+e^- \to Z$
0.032±0.004±0.005		[17] AKERS	96	OPAL	Excess of $\Lambda\ell^-$ over $\Lambda\ell^+$
0.033±0.008±0.005	262	[18] ABREU	95S	DLPH	Excess of $\Lambda\ell^-$ over $\Lambda\ell^+$
0.066±0.013±0.011	290	[19] BUSKULIC	95L	ALEP	Excess of $\Lambda\ell^-$ over $\Lambda\ell^+$
• • • We do not use the following data for averages, fits, limits, etc. • • •					
seen	157	[20] AKERS	93	OPAL	Excess of $\Lambda\ell^-$ over $\Lambda\ell^+$
0.076±0.022±0.012	101	[21] BUSKULIC	92I	ALEP	Excess of $\Lambda\ell^-$ over $\Lambda\ell^+$

[16] BARATE 98D reports $[\Gamma(b\text{-baryon} \to \Lambda\ell^-\overline{\nu}_\ell\text{anything})/\Gamma_{total}] \times [B(\overline{b} \to b\text{-baryon})] = 0.00326 \pm 0.00016 \pm 0.00039$ which we divide by our best value B($\overline{b} \to$ *b*-baryon) = (9.2 ± 1.5) $\times 10^{-2}$. Our first error is their experiment's error and our second error is the systematic error from using our best value. Measured using the excess of $\Lambda\ell^-$, lepton impact parameter.
[17] AKERS 96 reports $[\Gamma(b\text{-baryon} \to \Lambda\ell^-\overline{\nu}_\ell\text{anything})/\Gamma_{total}] \times [B(\overline{b} \to b\text{-baryon})] = 0.00291 \pm 0.00023 \pm 0.00025$ which we divide by our best value B($\overline{b} \to$ *b*-baryon) = (9.2 ± 1.5) $\times 10^{-2}$. Our first error is their experiment's error and our second error is the systematic error from using our best value.
[18] ABREU 95S reports $[\Gamma(b\text{-baryon} \to \Lambda\ell^-\overline{\nu}_\ell\text{anything})/\Gamma_{total}] \times [B(\overline{b} \to b\text{-baryon})] = 0.0030 \pm 0.0006 \pm 0.0004$ which we divide by our best value B($\overline{b} \to$ *b*-baryon) = (9.2 ± 1.5) $\times 10^{-2}$. Our first error is their experiment's error and our second error is the systematic error from using our best value.
[19] BUSKULIC 95L reports $[\Gamma(b\text{-baryon} \to \Lambda\ell^-\overline{\nu}_\ell\text{anything})/\Gamma_{total}] \times [B(\overline{b} \to b\text{-baryon})] = 0.0061 \pm 0.0006 \pm 0.0010$ which we divide by our best value B($\overline{b} \to$ *b*-baryon) = (9.2 ± 1.5) $\times 10^{-2}$. Our first error is their experiment's error and our second error is the systematic error from using our best value.
[20] AKERS 93 superseded by AKERS 96.
[21] BUSKULIC 92I reports $[\Gamma(b\text{-baryon} \to \Lambda\ell^-\overline{\nu}_\ell\text{anything})/\Gamma_{total}] \times [B(\overline{b} \to b\text{-baryon})] = 0.0070 \pm 0.0010 \pm 0.0018$ which we divide by our best value B($\overline{b} \to$ *b*-baryon) = (9.2 ± 1.5) $\times 10^{-2}$. Our first error is their experiment's error and our second error is the systematic error from using our best value. Superseded by BUSKULIC 95L.

$\Gamma(\Lambda\ell^+\nu_\ell$anything$)/\Gamma(\Lambda$anything$)$ Γ_5/Γ_6

VALUE	DOCUMENT ID		TECN	COMMENT
0.080±0.012±0.008	ABBIENDI	99L	OPAL	$e^+e^- \to Z$
• • • We do not use the following data for averages, fits, limits, etc. • • •				
0.070±0.012±0.007	ACKERSTAFF	97N	OPAL	Repl. by ABBIENDI 99L

$\Gamma(\Lambda/\overline{\Lambda}$anything$)/\Gamma_{total}$ Γ_8/Γ

VALUE	DOCUMENT ID		TECN	COMMENT
0.36±0.07 OUR AVERAGE				
0.38±0.05±0.06	[22] ABBIENDI	99L	OPAL	$e^+e^- \to Z$
$0.24^{+0.13}_{-0.08}\pm0.04$	[23] ABREU	95C	DLPH	$e^+e^- \to Z$
• • • We do not use the following data for averages, fits, limits, etc. • • •				
0.43±0.06±0.07	[24] ACKERSTAFF	97N	OPAL	Repl. by ABBIENDI 99L

[22] ABBIENDI 99L reports $[\Gamma(b\text{-baryon} \to \Lambda/\overline{\Lambda}\text{anything})/\Gamma_{total}] \times [B(\overline{b} \to b\text{-baryon})] = 0.035 \pm 0.0032 \pm 0.0035$ which we divide by our best value B($\overline{b} \to$ *b*-baryon) = (9.2 ± 1.5) $\times 10^{-2}$. Our first error is their experiment's error and our second error is the systematic error from using our best value.
[23] ABREU 95C reports $0.28^{+0.17}_{-0.12}$ from a measurement of $[\Gamma(b\text{-baryon} \to \Lambda/\overline{\Lambda}\text{anything})/\Gamma_{total}] \times [B(\overline{b} \to b\text{-baryon})]$ assuming B($\overline{b} \to$ *b*-baryon) = 0.08 ± 0.02, which we rescale to our best value B($\overline{b} \to$ *b*-baryon) = (9.2 ± 1.5) $\times 10^{-2}$. Our first error is their experiment's error and our second error is the systematic error from using our best value.
[24] ACKERSTAFF 97N reports $[\Gamma(b\text{-baryon} \to \Lambda/\overline{\Lambda}\text{anything})/\Gamma_{total}] \times [B(\overline{b} \to b\text{-baryon})] = 0.0393 \pm 0.0046 \pm 0.0037$ which we divide by our best value B($\overline{b} \to$ *b*-baryon) = (9.2 ± 1.5) $\times 10^{-2}$. Our first error is their experiment's error and our second error is the systematic error from using our best value.

$\Gamma(\Xi^-\ell^-\overline{\nu}_\ell$anything$)/\Gamma_{total}$ Γ_9/Γ

VALUE	DOCUMENT ID		TECN	COMMENT
0.0060±0.0016 OUR AVERAGE				
0.0059±0.0015±0.0010	[25] BUSKULIC	96T	ALEP	Excess $\Xi^-\ell^-$ over $\Xi^-\ell^+$
0.0064±0.0025±0.0010	[26] ABREU	95V	DLPH	Excess $\Xi^-\ell^-$ over $\Xi^-\ell^+$

[25] BUSKULIC 96T reports $[\Gamma(b\text{-baryon} \to \Xi^-\ell^-\overline{\nu}_\ell\text{anything})/\Gamma_{total}] \times [B(\overline{b} \to b\text{-baryon})] = 0.00054 \pm 0.00011 \pm 0.00008$ which we divide by our best value B($\overline{b} \to$ *b*-baryon) = (9.2 ± 1.5) $\times 10^{-2}$. Our first error is their experiment's error and our second error is the systematic error from using our best value.
[26] ABREU 95V reports $[\Gamma(b\text{-baryon} \to \Xi^-\ell^-\overline{\nu}_\ell\text{anything})/\Gamma_{total}] \times [B(\overline{b} \to b\text{-baryon})] = 0.00059 \pm 0.00021 \pm 0.0001$ which we divide by our best value B($\overline{b} \to$ *b*-baryon) = (9.2 ± 1.5) $\times 10^{-2}$. Our first error is their experiment's error and our second error is the systematic error from using our best value.

b-baryon ADMIXTURE (Λ_b, Ξ_b, Σ_b, Ω_b) REFERENCES

AAIJ	14E	JHEP 1404 114	R. Aaij *et al.*	(LHCb Collab.)
AAD	13U	PR D87 032002	G. Aad *et al.*	(ATLAS Collab.)
ABAZOV	12U	PR D85 112003	V.M. Abazov *et al.*	(D0 Collab.)
AALTONEN	10B	PRL 104 102002	T. Aaltonen *et al.*	(CDF Collab.)
ABAZOV	07S	PRL 99 142001	V.M. Abazov *et al.*	(D0 Collab.)
ABAZOV	07U	PRL 99 182001	V.M. Abazov *et al.*	(D0 Collab.)
ABULENCIA	07A	PRL 98 122001	A. Abulencia *et al.*	(FNAL CDF Collab.)
ABAZOV	05C	PRL 94 102001	V.M. Abazov *et al.*	(D0 Collab.)
ABBIENDI	99L	EPJ C9 1	G. Abbiendi *et al.*	(OPAL Collab.)
ABREU	99W	EPJ C10 185	P. Abreu *et al.*	(DELPHI Collab.)
ACKERSTAFF	98G	PL B426 161	K. Ackerstaff *et al.*	(OPAL Collab.)
BARATE	98D	EPJ C2 197	R. Barate *et al.*	(ALEPH Collab.)
BARATE	98V	EPJ C5 205	R. Barate *et al.*	(ALEPH Collab.)
ACKERSTAFF	97N	ZPHY C74 423	K. Ackerstaff *et al.*	(OPAL Collab.)
ABE	96M	PRL 77 1439	F. Abe *et al.*	(CDF Collab.)
ABREU	96D	ZPHY C71 199	P. Abreu *et al.*	(DELPHI Collab.)
AKERS	96	ZPHY C69 195	R. Akers *et al.*	(OPAL Collab.)
BUSKULIC	96T	PL B384 449	D. Buskulic *et al.*	(ALEPH Collab.)
ABREU	95C	PL B347 447	P. Abreu *et al.*	(DELPHI Collab.)
ABREU	95S	ZPHY C68 375	P. Abreu *et al.*	(DELPHI Collab.)
ABREU	95V	ZPHY C68 541	P. Abreu *et al.*	(DELPHI Collab.)
BUSKULIC	95L	PL B357 685	D. Buskulic *et al.*	(ALEPH Collab.)
ABREU	93F	PL B311 379	P. Abreu *et al.*	(DELPHI Collab.)
AKERS	93	PL B316 435	R. Akers *et al.*	(OPAL Collab.)
BUSKULIC	92I	PL B297 449	D. Buskulic *et al.*	(ALEPH Collab.)

MISCELLANEOUS SEARCHES

Notes in the Search Listings

SEARCHES IN OTHER SECTIONS

SEARCHES FOR MONOPOLES, SUPERSYMMETRY, TECHNICOLOR, COMPOSITENESS, EXTRA DIMENSIONS, etc.

Magnetic Monopole Searches

MAGNETIC MONOPOLES

Updated August 2013 by D. Milstead (Stockholm Univ.) and E.J. Weinberg (Columbia Univ.).

The symmetry between electric and magnetic fields in the sourcefree Maxwell's equations naturally suggests that electric charges might have magnetic counterparts, known as magnetic monopoles. Although the greatest interest has been in the supermassive monopoles that are a firm prediction of all grand unified theories, one cannot exclude the possibility of lighter monopoles, even though there is at present no strong theoretical motivation for these.

In either case, the magnetic charge is constrained by a quantization condition first found by Dirac [1]. Consider a monopole with magnetic charge Q_M and a Coulomb magnetic field

$$\mathbf{B} = \frac{Q_M}{4\pi}\frac{\hat{\mathbf{r}}}{r^2}\,. \tag{1}$$

Any vector potential $\mathbf{A}$ whose curl is equal to $\mathbf{B}$ must be singular along some line running from the origin to spatial infinity. This Dirac string singularity could potentially be detected through the extra phase that the wavefunction of a particle with electric charge Q_E would acquire if it moved along a loop encircling the string. For the string to be unobservable, this phase must be a multiple of 2π. Requiring that this be the case for any pair of electric and magnetic charges gives the condition that all charges be integer multiples of minimum charges $Q_E^{\rm min}$ and $Q_M^{\rm min}$ obeying

$$Q_E^{\rm min} Q_M^{\rm min} = 2\pi\,. \tag{2}$$

(For monopoles which also carry an electric charge, called dyons, the quantization conditions on their electric charges can be modified. However, the constraints on magnetic charges, as well as those on all purely electric particles, will be unchanged.)

Another way to understand this result is to note that the conserved orbital angular momentum of a point electric charge moving in the field of a magnetic monopole has an additional component, with

$$\mathbf{L} = m\mathbf{r}\times\mathbf{v} - 4\pi Q_E Q_M \hat{\mathbf{r}} \tag{3}$$

Requiring the radial component of $\mathbf{L}$ to be quantized in half-integer units yields Eq. (2).

If there are unbroken gauge symmetries in addition to the U(1) of electromagnetism, the above analysis must be modified [2,3]. For example, a monopole could have both a U(1) magnetic charge and a color magnetic charge. The latter could combine with the color charge of a quark to give an additional contribution to the phase factor associated with a loop around the Dirac string, so that the U(1) charge could be the Dirac charge $Q_M^D \equiv 2\pi/e$, the result that would be obtained by substituting the electron charge into Eq. (2). On the other hand, for monopoles without color-magnetic charge, one would simply insert the quark electric charges into Eq. (2) and conclude that Q_M must be a multiple of $6\pi/e$.

The prediction of GUT monopoles arises from the work of 't Hooft [4] and Polyakov [5], who showed that certain spontaneously broken gauge theories have nonsingular classical solutions that lead to magnetic monopoles in the quantum theory. The simplest example occurs in a theory where the vacuum expectation value of a triplet Higgs field ϕ breaks an SU(2) gauge symmetry down to the U(1) of electromagnetism and gives a mass M_V to two of the gauge bosons. In order to have finite energy, ϕ must approach a vacuum value at infinity. However, there is a continuous family of possible vacua, since the scalar field potential determines only the magnitude v of $\langle\phi\rangle$, but not its orientation in the internal SU(2) space. In the monopole solution, the direction of ϕ in internal space is correlated with the position in physical space; *i.e.*, $\phi^a \sim v\hat{r}^a$. The stability of the solution follows from the fact that this twisting Higgs field cannot be smoothly deformed to a spatially uniform vacuum configuration. Reducing the energetic cost of the spatial variation of ϕ requires a nonzero gauge potential, which turns out to yield the magnetic field corresponding to a charge $Q_M = 4\pi/e$. Numerical solution of the classical field equations shows that the mass of this monopole is

$$M_{\rm mon} \sim \frac{4\pi M_V}{e^2}\,. \tag{4}$$

The essential ingredient here was the fact that the Higgs fields at spatial infinity could be arranged in a topologically nontrivial configuration. A discussion of the general conditions under which this is possible is beyond the scope of this review, so we restrict ourselves to the two phenomenologically most important cases.

The first is the electroweak theory, with SU(2)×U(1) broken to U(1). There are no topologically nontrivial configurations of the Higgs field, and hence no topologically stable monopole solutions.

The second is when any simple Lie group is broken to a subgroup with a U(1) factor, a case that includes all grand unified theories. The monopole mass is determined by the mass scale of the symmetry breaking that allows nontrivial topology. For example, an SU(5) model with

$$\mathrm{SU(5)} \xrightarrow{M_X} \mathrm{SU(3)\times SU(2)\times U(1)} \xrightarrow{M_W} \mathrm{SU(3)\times U(1)} \tag{5}$$

has a monopole [6] with $Q_M = 2\pi/e$ and mass

$$M_{\rm mon} \sim \frac{4\pi M_{\rm X}}{g^2}\,, \tag{6}$$

where g is the SU(5) gauge coupling. For a unification scale of 10^{16} GeV, these monopoles would have a mass $M_{\rm mon} \sim 10^{17}$ – 10^{18} GeV.

In theories with several stages of symmetry breaking, monopoles of different mass scales can arise. In an SO(10) theory with

$$\mathrm{SO(10)} \xrightarrow{M_1} \mathrm{SU(4)} \times \mathrm{SU(2)} \times \mathrm{SU(2)} \xrightarrow{M_2} \mathrm{SU(3)} \times \mathrm{SU(2)} \times \mathrm{U(1)} \tag{7}$$

there is monopole with $Q_M = 2\pi/e$ and mass $\sim 4\pi M_1/g^2$ and a much lighter monopole with $Q_M = 4\pi/e$ and mass $\sim 4\pi M_2/g^2$ [7].

The central core of a GUT monopole contains the fields of the superheavy gauge bosons that mediate baryon number violation, so one might expect that baryon number conservation could be violated in baryon–monopole scattering. The surprising feature, pointed out by Callan [8] and Rubakov [9], is that these processes are not suppressed by powers of the gauge boson mass. Instead, the cross-sections for catalysis processes such as $p + \text{monopole} \to e^+ + \pi^0 + \text{monopole}$ are essentially geometric; *i.e.*, $\sigma_{\Delta B}\beta \sim 10^{-27}$ cm^2, where $\beta = v/c$. Note, however, that intermediate mass monopoles arising at later stages of symmetry breakings, such as the doubly charged monopoles of the SO(10) theory, do not catalyze baryon number violation.

Production and Annihilation: GUT monopoles are far too massive to be produced in any foreseeable accelerator. However, they could have been produced in the early universe as topological defects arising via the Kibble mechanism [10] in a symmetry-breaking phase transition. Estimates of the initial monopole abundance, and of the degree to which it can be reduced by monopole-antimonopole annihilation, predict a present-day monopole abundance that exceeds by many orders of magnitude the astrophysical and experimental bounds described below [11]. Cosmological inflation and other proposed solutions to this primordial monopole problem generically lead to present-day abundances exponentially smaller than could be plausibly detected, although potentially observable abundances can be obtained in scenarios with carefully tuned parameters.

If monopoles light enough to be produced at colliders exist, one would expect that these could be produced by analogs of the electromagnetic processes that produce pairs of electrically charged particles. Because of the large size of the magnetic charge, this is a strong coupling problem for which perturbation theory cannot be trusted. Indeed, the problem of obtaining reliable quantitative estimates of the production cross-sections remains an open one, on which there is no clear consensus.

Astrophysical and Cosmological Bounds: If there were no galactic magnetic field, one would expect monopoles in the galaxy to have typical velocities of the order of $10^{-3}c$, comparable to the virial velocity in the galaxy (relevant if the monopoles cluster with the galaxy) and the peculiar velocity of the galaxy with respect to the CMB rest frame (relevant if the monopoles are not bound to the galaxy). This situation is modified by the existence of a galactic magnetic field $B \sim 3\mu$G. A monopole with the Dirac charge and mass M would be accelerated by this field to a velocity

$$v_{\rm mag} \sim \begin{cases} c, & M \lesssim 10^{11}\mathrm{GeV}\ , \\ 10^{-3}c\left(\frac{10^{17}\,\mathrm{GeV}}{M}\right)^{1/2}, & M \gtrsim 10^{11}\mathrm{GeV}\ . \end{cases} \tag{8}$$

Accelerating these monopoles drains energy from the magnetic field. Parker [12] obtained an upper bound on the flux of monopoles in the galaxy by requiring that the rate of this energy loss be small compared to the time scale on which the galactic field can be regenerated. With reasonable choices for the astrophysical parameters (see Ref. 13 for details), this Parker bound is

$$F < \begin{cases} 10^{-15}\,\mathrm{cm^{-2}\,sr^{-1}\,sec^{-1}}, & M \lesssim 10^{17}\,\mathrm{GeV}\ , \\ 10^{-15}\left(\frac{M}{10^{17}\,\mathrm{GeV}}\right)\mathrm{cm^{-2}\,sr^{-1}\,sec^{-1}}, & M \gtrsim 10^{17}\,\mathrm{GeV}\ . \end{cases} \tag{9}$$

Applying similar arguments to an earlier seed field that was the progenitor of the current galactic field leads to a tighter bound [14],

$$F < \left[\frac{M}{10^{17}\mathrm{GeV}} + (3\times 10^{-6})\right] 10^{-16}\,\mathrm{cm^{-2}sr^{-1}sec^{-1}}. \tag{10}$$

Considering magnetic fields in galactic clusters gives a bound [15] which, although less secure, is about three orders of magnitude lower than the Parker bound.

A flux bound can also be inferred from the total mass of monopoles in the universe. If the monopole mass density is a fraction Ω_M of the critical density, and the monopoles were uniformly distributed throughout the universe, there would be a monopole flux

$$F_{\rm uniform} = 1.3\times 10^{-16}\Omega_M \left(\frac{10^{17}\,\mathrm{GeV}}{M}\right)\left(\frac{v}{10^{-3}c}\right)\mathrm{cm^{-2}sr^{-1}sec^{-1}}. \tag{11}$$

If we assume that $\Omega_M \sim 0.1$, this gives a stronger constraint than the Parker bound for $M \sim 10^{15}$ GeV. However, monopoles with masses $\sim 10^{17}$ GeV are not ejected by the galactic field and can be gravitationally bound to the galaxy. In this case their flux within the galaxy is increased by about five orders of magnitude for a given value of Ω_M, and the mass density bound only becomes stronger than the Parker bound for $M \sim 10^{18}$ GeV.

A much more stringent flux bound applies to GUT monopoles that catalyze baryon number violation. The essential idea is that compact astrophysical objects would capture monopoles at a rate proportional to the galactic flux. These monopoles would then catalyze proton decay, with the energy released in the decay leading to an observable increase in the luminosity of the object. A variety of bounds, based on neutron stars [16–20], white dwarfs [21], and Jovian planets [22] have been obtained. These depend in the obvious manner on the catalysis cross section, but also on the details of the astrophysical scenarios; *e.g.*, on how much the accumulated density is reduced by monopole-antimonopole annihilation, and

on whether monopoles accumulated in the progenitor star survive its collapse to a white dwarf or neutron star. The bounds obtained in this manner lie in the range

$$F\Big(\frac{\sigma_{\Delta B}\beta}{10^{-27}\mathrm{cm}^2}\Big) \sim (10^{-18} - 10^{-29})\mathrm{cm}^{-2}\mathrm{sr}^{-1}\mathrm{sec}^{-1}. \qquad (12)$$

It is important to remember that not all GUT monopoles catalyze baryon number nonconservation. In particular, the intermediate mass monopoles that arise in some GUTs at later stages of symmetry-breaking are examples of theoretically motivated monopoles that are exempt from the bound of Eq. (12).

Searches for Magnetic Monopoles: To date there have been no confirmed observations of exotic particles possessing magnetic charge. Precision measurements of the properties of known particles have led to tight limits on the values of magnetic charge they may possess. Using the induction method (see below), the electron's magnetic charge has been found to be $Q_e^m < 10^{-24}Q_M^D$ [23](where Q_M^D is the Dirac charge). Furthermore, measurements of the anomalous magnetic moment of the muon have been used to place a model dependent lower limit of 120 GeV on the monopole mass [1] [24]. Nevertheless, guided mainly by Dirac's argument and the predicted existence of monopoles from spontaneous symmetry breaking mechanisms, searches have been routinely made for monopoles produced at accelerators, in cosmic rays, and bound in matter [25]. Although the resultant limits from such searches are usually made under the assumption of a particle possessing only magnetic charge, most of the searches are also sensitive to dyons.

Search Techniques: Search strategies are determined by the expected interactions of monopoles as they pass through matter. These would give rise to a number of striking characteristic signatures. Since a complete description of monopole search techniques falls outside of the scope of this minireview, only the most common methods are described below. More comprehensive descriptions of search techniques can be found in Refs. [26,27].

The induction method exploits the long-ranged electromagnetic interaction of the monopole with the quantum state of a superconducting ring which would lead to a monopole which passes through such a ring inducing a permanent current. The induction technique typically uses Superconducting Quantum Interference Devices (SQUID) technology for detection and is employed for searches for monopoles in cosmic rays and matter. Another approach is to exploit the electromagnetic energy loss of monopoles. Monopoles with Dirac charge would typically lose energy at a rate which is several thousand times larger than that expected from particles possessing the elementary electric charge. Consequently, scintillators, gas chambers and nuclear track detectors (NTDs) have been used in cosmic ray and collider experiments. A further approach, which has been used at colliders, is to search for particles describing a non-helical path in a uniform magnetic field.

Searches for Monopoles Bound in Matter: Monopoles have been sought in a range of bulk materials which it is assumed would have absorbed incident cosmic ray monopoles over a long exposure time of order million years. Materials which have been studied include moon rock, meteorites, manganese modules, and sea water [28]. A stringent upper limit on the monopoles per nucleon ratio of $\sim 10^{-29}$ has been obtained [28].

Searches in Cosmic Rays: Direct searches for monopoles in cosmic rays refer to those experiments in which the passage of the monopole is measured by an active detector. Catalysis processes in which GUT monopoles could induce nucleon decay are discussed in the next section. To interpret the results of the non-catalysis searches, the cross section for the catalysis process is typically either set to zero [29] or assigned a modest value (1mb) [30]. Searches which explicitly exploit the expected catalysed decays are discussed in the next section.

Although early cosmic ray searches using the induction technique [31] and NTDs [32] observed monopole candidates, none of these apparent observations have been confirmed. Recent experiments have typically employed large scale detectors. The MACRO experiment at the Gran Sasso underground laboratory comprised three different types of detector: liquid scintillator, limited stream tubes, and NTDs, which provided a total acceptance of $\sim 10000\mathrm{m}^2$ for an isotropic flux. As shown in Fig. 1, this experiment has so far provided the most extensive β-dependent flux limits for GUT monopoles with Dirac charge [30]. Also shown are limits from an experiment at the OHYA mine in Japan [29], which used a $2000\mathrm{m}^2$ array of NTDs.

In Fig. 1, upper flux limits are also shown as a function of mass for monopole speed $\beta > 0.05$. In addition to MACRO and OYHA flux limits, results from the SLIM [33] high-altitude experiment are shown. The SLIM experiment provided a good sensitivity to intermediate mass monopoles ($10^5 \lesssim M \lesssim 10^{12}$ GeV). In addition to the results shown in Fig. 1, limits as low as $\sim 3 \times 10^{-18}$ $\mathrm{cm}^{-2}\mathrm{s}^{-1}\mathrm{sr}^{-1}$ and $\sim 10^{-17}$ $\mathrm{cm}^{-2}\mathrm{s}^{-1}\mathrm{sr}^{-1}$ were obtained for monopoles with $\beta > 0.8$ and $\beta > 0.625$ by the IceCube [34] and Antares [35] experiments, respectively. The most stringent constraints on the flux of ultra-relativistic monopoles have been obtained by the RICE [36] and ANITA-II experiments [37] at the South Pole which were sensitive to monopoles with γ values of $10^7 \lesssim \gamma \lesssim 10^{12}$ and $10^9 \lesssim \gamma \lesssim 10^{13}$, respectively, and which produced flux limits as low as 10^{-19} $\mathrm{cm}^{-2}\mathrm{s}^{-1}\mathrm{sr}^{-1}$.

Searches via the Catalysis of Nucleon-Decay: Searches have been performed for evidence of the catalysed decay of a nucleon by a monopole, as predicted by the Callan-Rubakov mechanism. The searches are thus sensitive to the assumed value of the catalysis decay cross section. Searches have been made with the Soudan [38] and Macro [39] experiments, using

[1] Where no ambiguity is likely to arise, a reference to a monopole implies a particle possessing Dirac charge.

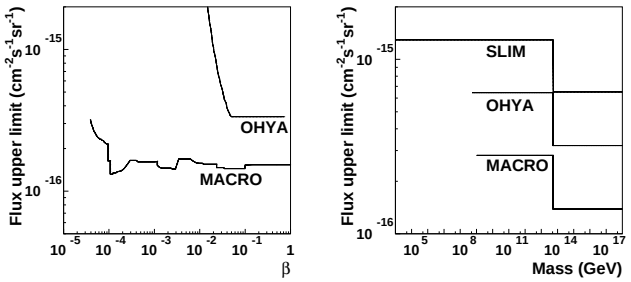

Figure 1: Upper flux limits for (a) GUT monopoles as a function of β (b) Monopoles as a function of mass for $\beta > 0.05$.

tracking detectors. Searches at IMB [40] and the underwater Lake Baikal experiment [41] which exploit the Cerenkov effect have also been made. The resulting β-dependent flux limits from these experiments typically vary between $\sim 10^{-16}$ and $\sim 10^{-14}\mathrm{cm}^{-2}\mathrm{sr}^{-1}\mathrm{s}^{-1}$ [25]. A recent search for low energy neutrinos (assumed to be produced from induced proton decay in the sun) was made at Super-Kamiokande [42]. A β-dependent of limit of $6.3 \times 10^{-24}(\frac{\beta}{10^{-3}})^2\mathrm{cm}^{-2}\mathrm{sr}^{-1}\mathrm{s}^{-1}$ was obtained.

Searches at Colliders: Searches have been performed at hadron-hadron, electron-positron and lepton-hadron experiments. Collider searches can be broadly classed as being direct or indirect. In a direct search, evidence of the passage of a monopole through material, such as a charged particle track, is sought. In indirect searches, virtual monopole processes are assumed to influence the production rates of certain final states.

Direct Searches at Colliders: Collider experiments typically express their results in terms of upper limits on a production cross section and/or monopole mass. To calculate these limits, ansatzes are used to model the kinematics of monopole-antimonopole pair production processes since perturbative field theory cannot be used to calculate the rate and kinematic properties of produced monopoles. Limits therefore suffer from a degree of model-dependence, implying that a comparison between the results of different experiments can be problematic, in particular when this concerns excluded mass regions. A conservative approach with as little model-dependence as possible is thus to present the upper cross-section limits as a function of one half the centre-of-mass energy of the collisions, as shown in Fig. 2 for recent results from high energy colliders.

Searches for monopoles produced at the highest available energies in hadron-hadron collisions were made in pp collisions at the LHC by the ATLAS experiment [43]. In this search, highly ionising particles leaving characteristic energy deposition profiles were sought. Tevatron searches have also been carried out by the CDF [44] and E882 [45] experiments. The CDF experiment used a dedicated time-of-flight system whereas the E882 experiment employed the induction technique to search for stopped monopoles in discarded detector material which had been part of the CDF and D0 detectors using periods of luminosity. Earlier searches at the Tevatron, such as [46], used

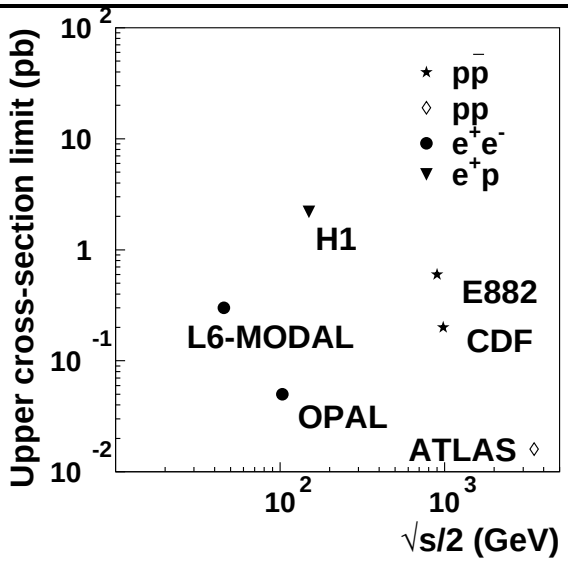

Figure 2: Upper limits on the production cross sections of monopoles from various collider-based experiments.

NTDs and were based on comparatively modest amounts of integrated luminosity. Lower energy hadron-hadron experiments have employed a variety of search techniques including plastic track detectors [47] and searches for trapped monopoles [48].

The only LEP-2 search was made by OPAL [49] which quoted cross section limits for the production of monopoles possessing masses up to around 103 GeV. At LEP-1, searches were made with NTDs deployed around an interaction region. This allowed a range of charges to be sought for masses up to $\sim$ 45 GeV. The L6-MODAL experiment [50] gave limits for monopoles with charges in the range $0.9Q_M^D$ and $3.6Q_M^D$, whilst an earlier search by the MODAL experiment was sensitive to monopoles with charges as low as $0.1Q_M^D$ [51]. The deployment of NTDs around the beam interaction point was also used at earlier e^+e^- colliders such as KEK [52] and PETRA [53]. Searches at e^+e^- facilities have also been made for particles following non-helical trajectories [54,55].

There has so far been one search for monopole production in lepton-hadron scattering. Using the induction method, monopoles were sought which could have stopped in the aluminium beampipe which had been used by the H1 experiment at HERA [56]. Cross section limits were set for monopoles with charges in the range $Q_M^D - 6Q_M^D$ for masses up to around 140 GeV.

Indirect Searches at Colliders: It has been proposed that virtual monopoles can mediate processes which give rise to multi-photon final-states [57,58]. Photon-based searches were made by the D0 [59] and L3 [60] experiments. The D0 work led to spin-dependent lower mass limits of between 610 and 1580 GeV, while L3 reported a lower mass limit of 510 GeV. However, it should be stressed that uncertainties on the theoretical calculations which were used to derive these limits are difficult to estimate.

References

1. P.A.M.Dirac, Proc. Roy. Soc. Lond. **A133**, 60 (1931).
2. F. Englert and P. Windey, Phys. Rev. **D14**, 2728 (1976).
3. P. Goddard, J. Nuyts, and D. I. Olive, Nucl. Phys. **B125**, 1 (1977).
4. G.'t Hooft, Nucl. Phys. **B79**, 276 (1974).
5. A.M. Polyakov, JETP Lett. **20**, 194 (1974) [Pisma Zh. Eksp. Teor. Fiz. **20**, 430 (1974)].
6. C.P. Dokos and T.N. Tomaras, Phys. Rev. **D21**, 2940 (1980).
7. G. Lazarides and Q. Shafi, Phys. Lett. **B94**, 149 (1980).
8. C.G. Callan, Phys. Rev. **D26**, 2058 (1982).
9. V.A. Rubakov, Nucl. Phys. **B203**, 311 (1982).
10. T.W.B. Kibble, J. Phys. **A9**, 1387 (1976).
11. J. Preskill, Phys. Rev. Lett. **43**, 1365 (1979).
12. E.N. Parker, Astrophys. J. **160**, 383 (1970).
13. M.S. Turner, E.N. Parker, and T.J. Bogdan, Phys. Rev. **D26**, 1296 (1982).
14. F.C. Adams *et al.*, Phys. Rev. Lett. **70**, 2511 (1993).
15. Y. Rephaeli and M.S. Turner, Phys. Lett. **B121**, 115 (1983).
16. E.W. Kolb, S.A. Colgate, and J.A. Harvey, Phys. Rev. Lett. **49**, 1373 (1982).
17. S. Dimopoulos, J. Preskill, and F. Wilczek, Phys. Lett. **B119**, 320 (1982).
18. K. Freese, M.S. Turner, and D.N. Schramm, Phys. Rev. Lett. **51**, 1625 (1983).
19. E.W. Kolb and M.S. Turner, Astrophys. J. **286**, 702 (1984).
20. J.A. Harvey, Nucl. Phys. **B236**, 255 (1984).
21. K. Freese and E. Krasteva, Phys. Rev. **D59**, 063007 (1999).
22. J. Arafune, M. Fukugita, and S. Yanagita, Phys. Rev. **D32**, 2586 (1985).
23. L.L. Vant-Hull, Phys. Rev. **173**, 1412 (1968).
24. S. Graf, A. Schaefer, and W. Greiner, Phys. Lett. **B262**, 463 (1991).
25. Review of Particle Physics 2012 (*this Review*), listing on *Searches for Magnetic Monopoles*.
26. G. Giacomelli and L. Patrizii, arXiv:hep-ex/0506014.
27. M. Fairbairn *et al.*, Phys. Rept. **438**, 1 (2007).
28. J.M. Kovalik and J.L. Kirschvink, Phys. Rev. **A33**, 1183 (1986) ; H. Jeon and M. J. Longo, Phys. Rev. Lett. **75**, 1443 (1995) [Erratum-ibid. **76**, 159 (1996)].
29. S. Orito *et al.*, Phys. Rev. Lett. **66**, 1951 (1991).
30. M. Ambrosio *et al.*, [MACRO Collab.], Eur. Phys. J. **C25**, 511 (2002).
31. B. Cabrera, Phys. Rev. Lett. **48**, 1378 (1982).
32. P.B. Price *et al.*, Phys. Rev. Lett. **35**, 487 (1975).
33. S. Balestra *et al.*, Eur. Phys. J. **C55**, 57 (2008).
34. R. Abbasi *et al.* [IceCube Collab.], Phys. Rev. D **87**, 022001 (2013).
35. S. Adrian-Martinez *et al.* [ANTARES Collab.], Astropart. Phys. **35**, 634 (2012).
36. D.P. Hogan *et al.*, Phys. Rev. **D78**, 075031 (2008).
37. M. Detrixhe *et al.*, Phys. Rev. **D83**, 023513 (2011).
38. J.E. Bartelt *et al.*, Phys. Rev. **D36**, 1990 (1987) [Erratum-ibid. **D40**, 1701 (1989)].
39. M. Ambrosio *et al.*, Eur. Phys. J. C **26**, 163 (2002).
40. R. Becker-Szendy *et al.*, Phys. Rev. **D49**, 2169 (1994).
41. V. A. Balkanov *et al.*, Prog. Part. Nucl. Phys. **40**, 391 (1998).
42. K. Ueno *et al.* [Super-Kamiokande Collab.], Astropart. Phys. **36**, 131 (2012).
43. G. Aad *et al.* [ATLAS Collab.], Phys. Rev. Lett. **109**, 261803 (2012).
44. A. Abulencia *et al.*, [CDF Collab.], Phys. Rev. Lett. **96**, 201801 (2006).
45. G.R. Kalbfleisch *et al.*, Phys. Rev. **D69**, 052002 (2004).
46. P.B. Price, G.X. Ren, and K. Kinoshita, Phys. Rev. Lett. **59**, 2523 (1987).
47. B. Aubert *et al.*, Phys. Lett. **B120**, 465 (1983).
48. R.A. Carrigan, F.A. Nezrick, and B.P. Strauss, Phys. Rev. **D8**, 3717 (1973).
49. G. Abbiendi *et al.*, [OPAL Collab.], Phys. Lett. **B663**, 37 (2008).
50. J.L. Pinfold *et al.*, Phys. Lett. **B316**, 407 (1993).
51. K. Kinoshita *et al.*, Phys. Rev. **D46**, 881 (1992).
52. K. Kinoshita *et al.*, Phys. Lett. **B228**, 543 (1989).
53. P. Musset *et al.*, Phys. Lett. **B128**, 333 (1983).
54. T. Gentile *et al.*, [Cleo Collab.], Phys. Rev. **D35**, 1081 (1987).
55. W. Braunschweig *et al.*, [TASSO Collab.], Z. Phys. **C38**, 543 (1988).
56. A. Aktas *et al.*, [H1 Collab.], Eur. Phys. J. **C41**, 133 (2005).
57. A. De Rujula, Nucl. Phys. **B435**, 257 (1995).
58. I.F. Ginzburg and A. Schiller, Phys. Rev. **D60**, 075016 (1999).
59. B. Abbott *et al.*, [D0 Collab.], Phys. Rev. Lett. **81**, 524 (1998).
60. M. Acciarri *et al.*, [L3 Collab.], Phys. Lett. **B345**, 609 (1995).

Monopole Production Cross Section — Accelerator Searches

X-SECT (cm^2)	MASS (GeV)	CHG (g)	ENERGY (GeV)	BEAM	DOCUMENT ID		TECN
$<1.6E-38$	200–1200	1	7000	pp	[1] AAD	12CS	ATLS
$<5E-38$	45–102	1	206	e^+e^-	[2] ABBIENDI	08	OPAL
$<0.2E-36$	200–700	1	1960	$p\overline{p}$	[3] ABULENCIA	06K	CNTR
$<2.E-36$		1	300	e^+p	[4,5] AKTAS	05A	INDU
$<0.2E-36$		2	300	e^+p	[4,5] AKTAS	05A	INDU
$<0.09E-36$		3	300	e^+p	[4,5] AKTAS	05A	INDU
$<0.05E-36$		≥ 6	300	e^+p	[4,5] AKTAS	05A	INDU
$<2.E-36$		1	300	e^+p	[4,6] AKTAS	05A	INDU
$<0.2E-36$		2	300	e^+p	[4,6] AKTAS	05A	INDU
$<0.07E-36$		3	300	e^+p	[4,6] AKTAS	05A	INDU
$<0.06E-36$		≥ 6	300	e^+p	[4,6] AKTAS	05A	INDU
$<0.6E-36$	>265	1	1800	$p\overline{p}$	[7] KALBFLEISCH	04	INDU
$<0.2E-36$	>355	2	1800	$p\overline{p}$	[7] KALBFLEISCH	04	INDU
$<0.07E-36$	>410	3	1800	$p\overline{p}$	[7] KALBFLEISCH	04	INDU
$<0.2E-36$	>375	6	1800	$p\overline{p}$	[7] KALBFLEISCH	04	INDU
$<0.7E-36$	>295	1	1800	$p\overline{p}$	[8,9] KALBFLEISCH	00	INDU
$<7.8E-36$	>260	2	1800	$p\overline{p}$	[8,9] KALBFLEISCH	00	INDU
$<2.3E-36$	>325	3	1800	$p\overline{p}$	[8,10] KALBFLEISCH	00	INDU
$<0.11E-36$	>420	6	1800	$p\overline{p}$	[8,10] KALBFLEISCH	00	INDU
$<0.65E-33$	<3.3	≥ 2	11A	^{197}Au	[11] HE	97	
$<1.90E-33$	<8.1	≥ 2	160A	^{208}Pb	[11] HE	97	
$<3.E-37$	<45.0	1.0	88–94	e^+e^-	PINFOLD	93	PLAS
$<3.E-37$	<41.6	2.0	88–94	e^+e^-	PINFOLD	93	PLAS
$<7.E-35$	<44.9	0.2–1.0	89–93	e^+e^-	KINOSHITA	92	PLAS
$<2.E-34$	<850	≥ 0.5	1800	$p\overline{p}$	BERTANI	90	PLAS
$<1.2E-33$	<800	≥ 1	1800	$p\overline{p}$	PRICE	90	PLAS
$<1.E-37$	<29	1	50–61	e^+e^-	KINOSHITA	89	PLAS

<1.E−37	<18	2	50–61	e^+e^-	KINOSHITA	89	PLAS	
<1.E−38	<17	<1	35	e^+e^-	BRAUNSCH...	88B	CNTR	
<8.E−37	<24	1	50–52	e^+e^-	KINOSHITA	88	PLAS	
<1.3E−35	<22	2	50–52	e^+e^-	KINOSHITA	88	PLAS	
<9.E−37	<4	<0.15	10.6	e^+e^-	GENTILE	87	CLEO	
<3.E−32	<800	≥1	1800	$p\overline{p}$	PRICE	87	PLAS	
<3.E−38		<3	29	e^+e^-	FRYBERGER	84	PLAS	
<1.E−31		1,3	540	$p\overline{p}$	AUBERT	83B	PLAS	
<4.E−38	<10	<6	34	e^+e^-	MUSSET	83	PLAS	
<8.E−36	<20		52	pp	[12] DELL	82	CNTR	
<9.E−37	<30	<3	29	e^+e^-	KINOSHITA	82	PLAS	
<1.E−37	<20	<24	63	pp	CARRIGAN	78	CNTR	
<1.E−37	<30	<3	56	pp	HOFFMANN	78	PLAS	
			62	pp	[12] DELL	76	SPRK	
<4.E−33			300	p	[12] STEVENS	76B	SPRK	
<1.E−40	<5	<2	70	p	[13] ZRELOV	76	CNTR	
<2.E−30			300	n	[12] BURKE	75	OSPK	
<1.E−38			8	ν	[14] CARRIGAN	75	HLBC	
<5.E−43	<12	<10	400	p	EBERHARD	75B	INDU	
<2.E−36	<30	<3	60	pp	GIACOMELLI	75	PLAS	
<5.E−42	<13	<24	400	p	CARRIGAN	74	CNTR	
<6.E−42	<12	<24	300	p	CARRIGAN	73	CNTR	
<2.E−36		1	0.001	γ	[13] BARTLETT	72	CNTR	
<1.E−41	<5		70	p	GUREVICH	72	EMUL	
<1.E−40	<3	<2	28	p	AMALDI	63	EMUL	
<2.E−40	<3	<2	30	p	PURCELL	63	CNTR	
<1.E−35	<3	<4	28	p	FIDECARO	61	CNTR	
<2.E−35	<1	1	6	p	BRADNER	59	EMUL	

[1] AAD 12CS searched for monopoles as highly ionising objects. The cross section limits are based on an assumed Drell Yan-like production process for spin 1/2 monopoles. The limits are mass- and scenario-dependent.

[2] ABBIENDI 08 assume production of spin 1/2 monopoles with effective charge $g\beta$ (n=1), via $e^+e^- \rightarrow \gamma^* \rightarrow M\overline{M}$, so that the cross section is proportional to $(1 + \cos^2\theta)$. There is no z information for such highly saturated tracks, so a parabolic track in the jet chamber is projected onto the xy plane. Charge per hit in the chamber produces a clean separation of signal and background.

[3] ABULENCIA 06K searches for high-ionizing signals in CDF central outer tracker and time-of-flight detector. For Drell-Yan $M\overline{M}$ production, the cross section limit implies $M > 360$ GeV at 95% CL.

[4] AKTAS 05A model-dependent limits as a function of monopole mass shown for arbitrary mass of 60 GeV. Based on search for stopped monopoles in the H1 Al beam pipe.

[5] AKTAS 05A limits with assumed elastic spin 0 monopole pair production.

[6] AKTAS 05A limits with assumed inelastic spin 1/2 monopole pair production.

[7] KALBFLEISCH 04 reports searches for stopped magnetic monopoles in Be, Al, and Pb samples obtained from discarded material from the upgrading of DØ and CDF. A large-aperture warm-bore cryogenic detector was used. The approach was an extension of the methods of KALBFLEISCH 00. Cross section results moderately model dependent; interpretation as a mass lower limit depends on possibly invalid perturbation expansion.

[8] KALBFLEISCH 00 used an induction method to search for stopped monopoles in pieces of the DØ (FNAL) beryllium beam pipe and in extensions to the drift chamber aluminum support cylinder. Results are model dependent.

[9] KALBFLEISCH 00 result is for aluminum.

[10] KALBFLEISCH 00 result is for beryllium.

[11] HE 97 used a lead target and barium phosphate glass detectors. Cross-section limits are well below those predicted via the Drell-Yan mechanism.

[12] Multiphoton events.

[13] Cherenkov radiation polarization.

[14] Re-examines CERN neutrino experiments.

Monopole Production — Other Accelerator Searches

MASS (GeV)	CHG (g)	SPIN	ENERGY (GeV)	BEAM	DOCUMENT ID		TECN
> 610	≥1	0	1800	$p\overline{p}$	[1] ABBOTT	98K	D0
> 870	≥1	1/2	1800	$p\overline{p}$	[1] ABBOTT	98K	D0
>1580	≥1	1	1800	$p\overline{p}$	[1] ABBOTT	98K	D0
> 510			88–94	e^+e^-	[2] ACCIARRI	95C	L3

[1] ABBOTT 98K search for heavy pointlike Dirac monopoles via central production of a pair of photons with high transverse energies.

[2] ACCIARRI 95C finds a limit $B(Z \rightarrow \gamma\gamma\gamma) < 0.8 \times 10^{-5}$ (which is possible via a monopole loop) at 95% CL and sets the mass limit via a cross section model.

Monopole Flux — Cosmic Ray Searches

"Caty" in the charge column indicates a search for monopole-catalyzed nucleon decay.

FLUX ($cm^{-2}sr^{-1}s^{-1}$)	MASS (GeV)	CHG (g)	COMMENTS ($\beta = v/c$)	EVTS	DOCUMENT ID		TECN
<3E-18		1	$\beta > 0.8$	0	[1] ABBASI	13	ICCB
<1.3E-17		1	$\beta > 0.625$	0	[2] ADRIAN-MAR...	12A	ANTR
<6E-28	<1E17	Caty	1E-5< β <0.04	0	[3] UENO	12	SKAM
<1E-19		**1**	**γ >1E10**	0	[4] DETRIXHE	11	ANIT
<3.8E-17		1	$\beta > 0.76$	0	[1] ABBASI	10A	ICCB
<1.3E−15	1E4<M<5E13	1	$\beta > 0.05$	0	[5] BALESTRA	08	PLAS
<0.65E−15	>5E13	1	$\beta > 0.05$	0	[5] BALESTRA	08	PLAS
<1E−18		**1**	**γ >1 E8**	0	[4] HOGAN	08	RICE
<1.4E−16		**1**	**1.1E−4 < β <1**	0	[6] AMBROSIO	02B	MCRO
<3E−16		Caty	1.1E−4 < β <5E−3	0	[7] AMBROSIO	02C	MCRO
<1.5E−15		1	5E−3 < β < 0.99	0	[8] AMBROSIO	02D	MCRO
<1E−15		1	1.1×10^{-4}–0.1	0	[9] AMBROSIO	97	MCRO
<5.6E−15		1	(0.18–3.0)E−3	0	[10] AHLEN	94	MCRO
<2.7E−15		Caty	$\beta \sim 1 \times 10^{-3}$	0	[11] BECKER-SZ...	94	IMB
<8.7E−15		1	>2.E−3	0	THRON	92	SOUD
<4.4E−12		1	all β	0	GARDNER	91	INDU
<7.2E−13		1	all β	0	HUBER	91	INDU
<3.7E−15	>E12	1	β=1.E−4	0	[12] ORITO	91	PLAS
<3.2E−16	>E10	1	$\beta > 0.05$	0	[12] ORITO	91	PLAS
<3.2E−16	>E10–E12	2,3		0	[12] ORITO	91	PLAS
<3.8E−13		1	all β	0	BERMON	90	INDU
<5.E−16		Caty	β <1.E−3	0	[11] BEZRUKOV	90	CHER
<1.8E−14		1	β >1.1E−4	0	[13] BUCKLAND	90	HEPT
<1E−18			3.E−4 < β <1.5E−3	0	[14] GHOSH	90	MICA
<7.2E−13		1	all β	0	HUBER	90	INDU
<5.E−12	>E7	1	3.E−4 < β <5.E−3	0	BARISH	87	CNTR
<1.E−13		Caty	1.E−5 < β <1	0	[11] BARTELT	87	SOUD
<1.E−10		1	all β	0	EBISU	87	INDU
<2.E−13			1.E−4 < β <6.E−4	0	MASEK	87	HEPT
<2.E−14			4.E−5 < β <2.E−4	0	NAKAMURA	87	PLAS
<2.E−14			1.E−3 < β <1	0	NAKAMURA	87	PLAS
<5.E−14			9.E−4 < β <1.E−2	0	SHEPKO	87	CNTR
<2.E−13			4.E−4 < β <1	0	TSUKAMOTO	87	CNTR
<5.E−14		1	all β	1	[15] CAPLIN	86	INDU
<5.E−12		1		0	CROMAR	86	INDU
<1.E−13		1	7.E−4 < β	0	HARA	86	CNTR
<7.E−11		1	all β	0	INCANDELA	86	INDU
<1.E−18			4.E−4 < β <1.E−3	0	[14] PRICE	86	MICA
<5.E−12		1		0	BERMON	85	INDU
<6.E−12		1		0	CAPLIN	85	INDU
<6.E−10		1		0	EBISU	85	INDU
<3.E−15		Caty	5.E−5 ≤ β ≤ 1.E−3	0	[11] KAJITA	85	KAMI
<2.E−21		Caty	β <1.E−3	0	[11,16] KAJITA	85	KAMI
<3.E−15		Caty	1.E−3 < β <1.E−1	0	[11] PARK	85B	CNTR
<5.E−12		1	1.E−4 < β <1	0	BATTISTONI	84	NUSX
<7.E−12		1		0	INCANDELA	84	INDU
<7.E−13		1	3.E−4 < β	0	[13] KAJINO	84	CNTR
<2.E−12		1	3.E−4 < β <1.E−1	0	KAJINO	84B	CNTR
<6.E−13		1	5.E−4 < β <1	0	KAWAGOE	84	CNTR
<2.E−14			1.E−3 < β	0	[11] KRISHNA...	84	CNTR
<4.E−13		1	6.E−4 < β <2.E−3	0	LISS	84	CNTR
<1.E−16			3.E−4 < β <1.E−3	0	[14] PRICE	84	MICA
<1.E−13		1	1.E−4 < β	0	PRICE	84B	PLAS
<4.E−13		1	6.E−4 < β <2.E−3	0	TARLE	84	CNTR
				7	[17] ANDERSON	83	EMUL
<4.E−13		1	1.E−2 < β <1.E−3	0	BARTELT	83B	CNTR
<1.E−12		1	7.E−3 < β <1	0	BARWICK	83	PLAS
<3.E−13		1	1.E−3 < β <4.E−1	0	BONARELLI	83	CNTR
<3.E−12		Caty	5.E−4 < β <5.E−2	0	[11] BOSETTI	83	CNTR
<4.E−11		1		0	CABRERA	83	INDU
<5.E−15		1	1.E−2 < β <1	0	DOKE	83	PLAS
<8.E−15		Caty	1.E−4 < β <1.E−1	0	[11] ERREDE	83	IMB
<5.E−12		1	1.E−4 < β <3.E−2	0	GROOM	83	CNTR
<2.E−12			6.E−4 < β <1	0	MASHIMO	83	CNTR
<1.E−13		1	β=3.E−3	0	ALEXEYEV	82	CNTR
<2.E−12		1	7.E−3 < β <6.E−1	0	BONARELLI	82	CNTR
6.E−10		1	all β	1	[18] CABRERA	82	INDU
<2.E−11			1.E−2 < β <1.E−1	0	MASHIMO	82	CNTR
<2.E−15			concentrator	0	BARTLETT	81	PLAS
<1.E−13	>1		1.E−3 < β	0	KINOSHITA	81B	PLAS
<5.E−11	<E17		3.E−4 < β <1.E−3	0	ULLMAN	81	CNTR
<2.E−11			concentrator	0	BARTLETT	78	PLAS
1.E−1	>200	2		1	[19] PRICE	75	PLAS
<2.E−13		>2		0	FLEISCHER	71	PLAS
<1.E−19		>2	obsidian, mica	0	FLEISCHER	69C	PLAS
<5.E−15	<15	<3	concentrator	0	CARITHERS	66	ELEC
<2.E−11		<1–3	concentrator	0	MALKUS	51	EMUL

[1] ABBASI 13 and ABBASI 10A were based on a Cherenkov signature in an array of optical modules which were sunk in the Antarctic ice cap. Limits are speed-dependent.

[2] ADRIAN-MARTINEZ 12A measurements were based on a Cherenkov signature in an underwater telescope in the Western Mediterranean Sea. Limits are speed-dependent.

[3] The limits from UENO 12 depend on the monopole speed and are also sensitive to assumed values of monopole mass and the catalysis cross section.

[4] HOGAN 08 and DETRIXHE 11 limits on relativistic monopoles are based on nonobservation of radio Cherenkov signals at the South Pole. Limits are speed-dependent.

[5] BALESTRA 08 exposed of nuclear track detector modules totaling 400 m^2 for 4 years at the Chacaltaya Laboratory (5230 m) in search for intermediate-mass monopoles with $\beta > 0.05$. The analysis is mainly based on three CR39 modules. For $M > 5 \times 10^{13}$ GeV there can be upward-going monopoles as well, hence the flux limit is half that obtained for less massive monopoles. Previous experiments (e.g. MACRO and OHYA (ORITO 91)) had set limits only for $M > 1 \times 10^9$ GeV.

[6] AMBROSIO 02B direct search final result for $m \geq 10^{17}$ GeV, based upon 4.2 to 9.5 years of running, depending upon the subsystem. Limit with CR39 track-etch detector extends the limit from β=4 $\times 10^{-5}$ (3.1×10^{-16} cm^{-2} sr^{-1} s^{-1}) to $\beta = 1 \times 10^{-4}$ (2.1×10^{-16} cm^{-2} sr^{-1} s^{-1}). Limit curve in paper is piecewise continuous due to different detection techniques for different β ranges.

[7] AMBROSIO 02C limit for catalysis of nucleon decay with catalysis cross section of $\approx$ 1 mb. The flux limit increases by $\sim$ 3 at the higher β limit, and increases to 1×10^{-14} cm^{-2} sr^{-1} s^{-1} if the catalysis cross section is 0.01 mb. Based upon 71193 hr of data with the streamer detector, with an acceptance of 4250 m^2 sr.

[8] AMBROSIO 02D result for "more than two years of data." Ionization search using several subsystems. Limit curve as a function of β not given. Included in AMBROSIO 02B.

[9] AMBROSIO 97 global MACRO 90%CL is 0.78×10^{-15} at β=1.1×10^{-4}, goes through a minimum at 0.61×10^{-15} near β=(1.1–2.7) $\times10^{-3}$, then rises to 0.84×10^{-15} at β=0.1. The global limit in this region is below the Parker bound at 10^{-15}. Less stringent limits are established for $4\times10^{-5}<\beta<1\times10^{-4}$. Limits set by various triggers and different subdetectors are given in the paper. All limits assume a catalysis cross section smaller than a few mb.

[10] AHLEN 94 limit for dyons extends down to β=0.9E−4 and a limit of 1.3E−14 extends to β = 0.8E−4. Also see comment by PRICE 94 and reply of BARISH 94. One loophole in the AHLEN 94 result is that in the case of monopoles catalyzing nucleon decay, relativistic particles could veto the events. See AMBROSIO 97 for additional results.

[11] Catalysis of nucleon decay; sensitive to assumed catalysis cross section.

[12] ORITO 91 limits are functions of velocity. Lowest limits are given here.

[13] Used DKMPR mechanism and Penning effect.

[14] Assumes monopole attaches fermion nucleus.

[15] Limit from combining data of CAPLIN 86, BERMON 85, INCANDELA 84, and CABRERA 83. For a discussion of controversy about CAPLIN 86 observed event, see GUY 87. Also see SCHOUTEN 87.

[16] Based on lack of high-energy solar neutrinos from catalysis in the sun.

[17] Anomalous long-range α (^{4}He) tracks.

[18] CABRERA 82 candidate event has single Dirac charge within ±5%.

[19] ALVAREZ 75, FLEISCHER 75, and FRIEDLANDER 75 explain as fragmenting nucleus. EBERHARD 75 and ROSS 76 discuss conflict with other experiments. HAGSTROM 77 reinterprets as antinucleus. PRICE 78 reassesses.

Monopole Flux — Astrophysics

FLUX ($cm^{-2}sr^{-1}s^{-1}$)	MASS (GeV)	CHG (g)	COMMENTS (β = v/c)	EVTS	DOCUMENT ID		TECN
<1.3E−20			faint white dwarf		[1] FREESE	99	ASTR
<1.E−16	E17	1	galactic field	0	[2] ADAMS	93	COSM
<1.E−23			Jovian planets		[1] ARAFUNE	85	ASTR
<1.E−16	E15		solar trapping	0	BRACCI	85B	ASTR
<1.E−18		1		0	[1] HARVEY	84	COSM
<3.E−23			neutron stars		KOLB	84	ASTR
<7.E−22			pulsars	0	[1] FREESE	83B	ASTR
<1.E−18	<E18	1	intergalactic field	0	[1] REPHAELI	83	COSM
<1.E−23			neutron stars	0	[1] DIMOPOUL...	82	COSM
<5.E−22			neutron stars	0	[1] KOLB	82	COSM
<5.E−15	>E21		galactic halo		SALPETER	82	COSM
<1.E−12	E19	1	β=3.E−3	0	[3] TURNER	82	COSM
<1.E−16		1	galactic field	0	PARKER	70	COSM

[1] Catalysis of nucleon decay.

[2] ADAMS 93 limit based on "survival and growth of a small galactic seed field" is 10^{-16} ($m/10^{17}$ GeV) $cm^{-2}s^{-1}sr^{-1}$. Above 10^{17} GeV, limit 10^{-16} (10^{17} GeV/m) $cm^{-2}s^{-1}sr^{-1}$ (from requirement that monopole density does not overclose the universe) is more stringent.

[3] Re-evaluates PARKER 70 limit for GUT monopoles.

Monopole Density — Matter Searches

DENSITY	CHG (g)	MATERIAL	EVTS	DOCUMENT ID		TECN
<9.8E−5/gram	≥ 1	Polar rock	0	BENDTZ	13	INDU
<6.9E−6/gram	>1/3	Meteorites and other	0	JEON	95	INDU
<2.E−7/gram	>0.6	Fe ore	0	[1] EBISU	87	INDU
<4.6E−6/gram	> 0.5	deep schist	0	KOVALIK	86	INDU
<1.6E−6/gram	> 0.5	manganese nodules	0	[2] KOVALIK	86	INDU
<1.3E−6/gram	> 0.5	seawater	0	KOVALIK	86	INDU
>1.E+14/gram	>1/3	iron aerosols	>1	MIKHAILOV	83	SPEC
<6.E−4/gram		air, seawater	0	CARRIGAN	76	CNTR
<5.E−1/gram	>0.04	11 materials	0	CABRERA	75	INDU
<2.E−4/gram	>0.05	moon rock	0	ROSS	73	INDU
<6.E−7/gram	<140	seawater	0	KOLM	71	CNTR
<1.E−2/gram	<120	manganese nodules	0	FLEISCHER	69	PLAS
<1.E−4/gram	>0	manganese	0	FLEISCHER	69B	PLAS
<2.E−3/gram	<1–3	magnetite, meteor	0	GOTO	63	EMUL
<2.E−2/gram		meteorite	0	PETUKHOV	63	CNTR

[1] Mass 1×10^{14}–1×10^{17} GeV.

[2] KOVALIK 86 examined 498 kg of schist from two sites which exhibited clear mineralogical evidence of having been buried at least 20 km deep and held below the Curie temperature.

Monopole Density — Astrophysics

DENSITY	CHG (g)	MATERIAL	EVTS	DOCUMENT ID		TECN
<1.E−9/gram	1	sun, catalysis	0	[1] ARAFUNE	83	COSM
<6.E−33/nucl	1	moon wake	0	SCHATTEN	83	ELEC
<2.E−28/nucl		earth heat	0	CARRIGAN	80	COSM
<2.E−4/prot		42cm absorption	0	BRODERICK	79	COSM
<2.E−13/m^3		moon wake	0	SCHATTEN	70	ELEC

[1] Catalysis of nucleon decay.

REFERENCES FOR Magnetic Monopole Searches

ABBASI	13	PR D87 022001	R. Abbasi *et al.* (IceCube Collab.)
BENDTZ	13	PRL 110 121803	K. Bendtz *et al.*
AAD	12CS	PRL 109 261803	G. Aad *et al.* (ATLAS Collab.)
ADRIAN-MAR...	12A	ASP 35 634	S. Adrian-Martinez *et al.* (ANTARES Collab.)
UENO	12	ASP 36 131	K. Ueno *et al.* (Super-Kamiokande Collab.)
DETRIXHE	11	PR D83 023513	M. Detrixhe *et al.* (ANITA Collab.)
ABBASI	10A	EPJ C69 361	R. Abbasi *et al.* (IceCube Collab.)
ABBIENDI	08	PL B663 37	G. Abbiendi *et al.* (OPAL Collab.)
BALESTRA	08	EPJ C55 57	S. Balestra *et al.* (SLIM Collab.)
HOGAN	08	PR D78 075031	D.P. Hogan *et al.* (KANS, NEBR, DELA)
ABULENCIA	06K	PRL 96 201801	A. Abulencia *et al.* (CDF Collab.)
AKTAS	05A	EPJ C41 133	A. Aktas *et al.* (H1 Collab.)
KALBFLEISCH	04	PR D69 052002	G.R. Kalbfleisch *et al.* (OKLA)
AMBROSIO	02B	EPJ C25 511	M. Ambrosio *et al.* (MACRO Collab.)
AMBROSIO	02C	EPJ C26 163	M. Ambrosio *et al.* (MACRO Collab.)
AMBROSIO	02D	ASP 18 27	M. Ambrosio *et al.* (MACRO Collab.)
KALBFLEISCH	00	PRL 85 5292	G.R. Kalbfleisch *et al.*
FREESE	99	PR D59 063007	K. Freese, E. Krasteva
ABBOTT	98K	PRL 81 524	B. Abbott *et al.* (D0 Collab.)
AMBROSIO	97	PL B406 249	M. Ambrosio *et al.* (MACRO Collab.)
HE	97	PRL 79 3134	Y.D. He (UCB)
ACCIARRI	95C	PL B345 609	M. Acciarri *et al.* (L3 Collab.)
JEON	95	PRL 75 1443	H. Jeon, M.J. Longo (MICH)
Also		PRL 76 159 (erratum)	H. Jeon, M.J. Longo
AHLEN	94	PRL 72 608	S.P. Ahlen *et al.* (MACRO Collab.)
BARISH	94	PRL 73 1306	B.C. Barish, G. Giacomelli, J.T. Hong (CIT+)
BECKER-SZ...	94	PR D49 2169	R.A. Becker-Szendy *et al.* (IMB Collab.)
PRICE	94	PRL 73 1305	P.B. Price (UCB)
ADAMS	93	PRL 70 2511	F.C. Adams *et al.* (MICH, FNAL)
PINFOLD	93	PL B316 407	J.L. Pinfold *et al.* (ALBE, HARV, MONT+)
KINOSHITA	92	PR D46 R881	K. Kinoshita *et al.* (HARV, BGNA, REHO)
THRON	92	PR D46 4846	J.L. Thron *et al.* (SOUDAN-2 Collab.)
GARDNER	91	PR D44 622	R.D. Gardner *et al.* (STAN)
HUBER	91	PR D44 636	M.E. Huber *et al.* (STAN)
ORITO	91	PRL 66 1951	S. Orito *et al.* (ICEPP, WASCR, NIHO, ICRR)
BERMON	90	PRL 64 839	S. Bermon *et al.* (IBM, BNL)
BERTANI	90	EPL 12 613	M. Bertani *et al.* (BGNA, INFN)
BEZRUKOV	90	SJNP 52 54	L.B. Bezrukov *et al.* (INRM)
		Translated from YAF 52 86.	
BUCKLAND	90	PR D41 2726	K.N. Buckland *et al.* (UCSD)
GHOSH	90	EPL 12 25	D.C. Ghosh, S. Chatterjea (JADA)
HUBER	90	PRL 64 835	M.E. Huber *et al.* (STAN)
PRICE	90	PRL 65 149	P.B. Price, J. Guiru, K. Kinoshita (UCB, HARV)
KINOSHITA	89	PL B228 543	K. Kinoshita *et al.* (HARV, TISA, KEK+)
BRAUNSCH...	88B	ZPHY C38 543	R. Braunschweig *et al.* (TASSO Collab.)
KINOSHITA	88	PRL 60 1610	K. Kinoshita *et al.* (HARV, TISA, KEK+)
BARISH	87	PR D36 2641	B.C. Barish, G. Liu, C. Lane (CIT)
BARTELT	87	PR D36 1990	J.E. Bartelt *et al.* (Soudan Collab.)
Also		PR D40 1701 (erratum)	J.E. Bartelt *et al.* (Soudan Collab.)
EBISU	87	PR D36 3359	T. Ebisu, T. Watanabe (KOBE)
Also		JP G11 883	T. Ebisu, T. Watanabe (KOBE)
GENTILE	87	PR D35 1081	T. Gentile *et al.* (CLEO Collab.)
GUY	87	NAT 325 463	J. Guy (LOIC)
MASEK	87	PR D35 2758	G.E. Masek *et al.* (UCSD)
NAKAMURA	87	PL B183 395	S. Nakamura *et al.* (INUS, WASCR, NIHO)
PRICE	87	PRL 59 2523	P.B. Price, R. Guoxiao, K. Kinoshita (UCB, HARV)
SCHOUTEN	87	JP E20 850	J.C. Schouten *et al.* (LOIC)
SHEPKO	87	PR D35 2917	M.J. Shepko *et al.* (TAMU)
TSUKAMOTO	87	EPL 3 39	T. Tsukamoto *et al.* (ICRR)
CAPLIN	86	NAT 321 402	A.D. Caplin *et al.* (LOIC)
Also		JP E20 850	J.C. Schouten *et al.* (LOIC)
Also		NAT 325 463	J. Guy (LOIC)
CROMAR	86	PRL 56 2561	M.W. Cromar, A.F. Clark, F.R. Fickett (NBSB)
HARA	86	PRL 56 553	T. Hara *et al.* (ICRR, KYOT, KEK, KOBE+)
INCANDELA	86	PR D34 2637	J. Incandela *et al.* (CHIC, FNAL, MICH)
KOVALIK	86	PR A33 1183	J.M. Kovalik, J.L. Kirschvink (CIT)
PRICE	86	PRL 56 1226	P.B. Price, M.H. Salamon (UCB)
ARAFUNE	85	PR D32 2586	J. Arafune, M. Fukugita, S. Yanagita (ICRR, KYOTU+)
BERMON	85	PRL 55 1850	S. Bermon *et al.* (IBM)
BRACCI	85B	NP B258 726	L. Bracci, G. Fiorentini, G. Mezzorani (PISA+)
Also		LNC 42 123	L. Bracci, G. Fiorentini (PISA)
CAPLIN	85	NAT 317 234	A.D. Caplin *et al.* (LOIC)
EBISU	85	JP G11 883	T. Ebisu, T. Watanabe (KOBE)
KAJITA	85	JPSJ 54 4065	T. Kajita *et al.* (ICRR, KEK, NIIG)
PARK	85B	NP B252 261	H.S. Park *et al.* (IMB Collab.)
BATTISTONI	84	PL 133B 454	G. Battistoni *et al.* (NUSEX Collab.)
FRYBERGER	84	PR D29 1524	D. Fryberger *et al.* (SLAC, UCB)
HARVEY	84	NP B236 255	J.A. Harvey (PRIN)
INCANDELA	84	PRL 53 2067	J. Incandela *et al.* (CHIC, FNAL, MICH)
KAJINO	84	PRL 52 1373	F. Kajino *et al.* (ICRR)
KAJINO	84B	JP G10 447	F. Kajino *et al.* (ICRR)
KAWAGOE	84	LNC 41 315	K. Kawagoe *et al.* (TOKY)
KOLB	84	APJ 286 702	E.W. Kolb, M.S. Turner (FNAL, CHIC)
KRISHNA...	84	PL 142B 99	M.R. Krishnaswamy *et al.* (TATA, OSKC+)
LISS	84	PR D30 884	T.M. Liss, S.P. Ahlen, G. Tarle (UCB, IND+)
PRICE	84	PRL 52 1265	P.B. Price *et al.* (ROMA, UCB, IND+)
PRICE	84B	PL 140B 112	P.B. Price (CERN)
TARLE	84	PRL 52 90	G. Tarle, S.P. Ahlen, T.M. Liss (UCB, MICH+)
ANDERSON	83	PR D28 2308	S.N. Anderson *et al.* (WASH)
ARAFUNE	83	PL 133B 380	J. Arafune, M. Fukugita (ICRR, KYOTU)
AUBERT	83B	PL 120B 465	B. Aubert *et al.* (CERN, LAPP)
BARTELT	83B	PRL 50 655	J.E. Bartelt *et al.* (MINN, ANL)
BARWICK	83	PR D28 2338	S.W. Barwick, K. Kinoshita, P.B. Price (UCB)
BONARELLI	83	PL 126B 137	R. Bonarelli, P. Capiluppi, I. d'Antone (BGNA)
BOSETTI	83	PL 133B 265	P.C. Bosetti *et al.* (AACH3, HAWA, TOKY)
CABRERA	83	PRL 51 1933	B. Cabrera *et al.* (STAN)
DOKE	83	PL 129B 370	T. Doke *et al.* (WASU, RIKK, TTAM, RIKEN)
ERREDE	83	PRL 51 245	S.M. Errede *et al.* (IMB Collab.)
FREESE	83B	PRL 51 1625	K. Freese, M.S. Turner, D.N. Schramm (CHIC)
GROOM	83	PRL 50 573	D.E. Groom *et al.* (UTAH, STAN)
MASHIMO	83	PL 128B 327	T. Mashimo *et al.* (ICEPP)
MIKHAILOV	83	PL 130B 331	V.F. Mikhailov (KAZA)
MUSSET	83	PL 128B 333	P. Musset, M. Price, E. Lohrmann (CERN, HAMB)
REPHAELI	83	PL 121B 115	Y. Rephaeli, M.S. Turner (CHIC)
SCHATTEN	83	PR D27 1525	K.H. Schatten (NASA)
ALEXEYEV	82	LNC 35 413	E.N. Alekseev *et al.* (INRM)
BONARELLI	82	PL 112B 100	R. Bonarelli *et al.* (BGNA)
CABRERA	82	PRL 48 1378	B. Cabrera (STAN)
DELL	82	NP B209 45	G.F. Dell *et al.* (BNL, ADEL, ROMA)
DIMOPOUL...	82	PL 119B 320	S. Dimopoulos, J. Preskill, F. Wilczek (HARV+)
KINOSHITA	82	PRL 48 77	K. Kinoshita, P.B. Price, D. Fryberger (UCB+)
KOLB	82	PRL 49 1373	E.W. Kolb, S.A. Colgate, J.A. Harvey (LASL, PRIN)
MASHIMO	82	JPSJ 51 3067	T. Mashimo, K. Kawagoe, M. Koshiba (INUS)
SALPETER	82	PRL 49 1114	E.E. Salpeter, S.L. Shapiro, I. Wasserman (CORN)
TURNER	82	PR D26 1296	M.S. Turner, E.N. Parker, T.J. Bogdan (CHIC)
BARTLETT	81	PR D24 612	D.F. Bartlett *et al.* (COLO, GESC)
KINOSHITA	81B	PR D24 1707	K. Kinoshita, P.B. Price (UCB)
ULLMAN	81	PRL 47 289	J.D. Ullman (LEHM, BNL)
CARRIGAN	80	NAT 288 348	R.A. Carrigan (FNAL)

BRODERICK	79	PR D19 1046	J.J. Broderick *et al.*	(VPI)
BARTLETT	78	PR D18 2253	D.F. Bartlett, D. Soo, M.G. White	(COLO, PRIN)
CARRIGAN	78	PR D17 1754	R.A. Carrigan, B.P. Strauss, G. Giacomelli	(FNAL+)
HOFFMANN	78	LNC 23 357	H. Hoffmann *et al.*	(CERN, ROMA)
PRICE	78	PR D18 1382	P.B. Price *et al.*	(UCB, HOUS)
HAGSTROM	77	PRL 38 729	R. Hagstrom	(LBL)
CARRIGAN	76	PR D13 1823	R.A. Carrigan, F.A. Nezrick, B.P. Strauss	(FNAL)
DELL	76	LNC 15 269	G.F. Dell *et al.*	(CERN, BNL, ROMA, ADEL)
ROSS	76	LBL-4665	R.R. Ross	(LBL)
STEVENS	76B	PR D14 2207	D.M. Stevens *et al.*	(VPI, BNL)
ZRELOV	76	CZJP B26 1306	V.P. Zrelov *et al.*	(JINR)
ALVAREZ	75	LBL-4260	L.W. Alvarez	(LBL)
BURKE	75	PL 60B 113	D.L. Burke *et al.*	(MICH)
CABRERA	75	Thesis	B. Cabrera	(STAN)
CARRIGAN	75	NP B91 279	R.A. Carrigan, F.A. Nezrick	(FNAL)
Also		PR D3 56	R.A. Carrigan, F.A. Nezrick	(FNAL)
EBERHARD	75	PR D11 3099	P.H. Eberhard *et al.*	(LBL, MPIM)
EBERHARD	75B	LBL-4289	P.H. Eberhard	(LBL)
FLEISCHER	75	PRL 35 1412	R.L. Fleischer, R.N.F. Walker	(GESC, WUSL)
FRIEDLANDER	75	PRL 35 1167	M.W. Friedlander	(WUSL)
GIACOMELLI	75	NC 28A 21	G. Giacomelli *et al.*	(BGNA, CERN, SACL+)
PRICE	75	PRL 35 487	P.B. Price *et al.*	(UCB, HOUS)
CARRIGAN	74	PR D10 3867	R.A. Carrigan, F.A. Nezrick, B.P. Strauss	(FNAL)
CARRIGAN	73	PR D8 3717	R.A. Carrigan, F.A. Nezrick, B.P. Strauss	(FNAL)
ROSS	73	PR D8 698	R.R. Ross *et al.*	(LBL, SLAC)
Also		PR D4 3260	P.H. Eberhard *et al.*	(LBL, SLAC)
Also		SCI 167 701	L.W. Alvarez *et al.*	(LBL, SLAC)
BARTLETT	72	PR D6 1817	D.F. Bartlett, M.D. Lahana	(COLO)
GUREVICH	72	PL 38B 549	I.I. Gurevich *et al.*	(KIAE, NOVO, SERP)
Also		JETP 34 917 Translated from ZETF 61 1721.	L.M. Barkov, I.I. Gurevich, M.S. Zolotorev	(KIAE+)
Also		PL 31B 394	I.I. Gurevich *et al.*	(KIAE, NOVO, SERP)
FLEISCHER	71	PR D4 24	R.L. Fleischer *et al.*	(GESC)
KOLM	71	PR D4 1285	H.H. Kolm, F. Villa, A. Odian	(MIT, SLAC)
PARKER	70	APJ 160 383	E.N. Parker	(CHIC)
SCHATTEN	70	PR D1 2245	K.H. Schatten	(NASA)
FLEISCHER	69	PR 177 2029	R.L. Fleischer *et al.*	(GESC, FSU)
FLEISCHER	69B	PR 184 1393	R.L. Fleischer *et al.*	(GESC, UNCS, GSCO)
FLEISCHER	69C	PR 184 1398	R.L. Fleischer, P.B. Price, R.T. Woods	(GESC)
Also		JAP 41 958	R.L. Fleischer *et al.*	(GESC)
CARITHERS	66	PR 149 1070	W.C.J. Carithers, R.J. Stefanski, R.K. Adair	
AMALDI	63	NC 28 773	E. Amaldi *et al.*	(ROMA, UCSD, CERN)
GOTO	63	PR 132 387	E. Goto, H.H. Kolm, K.W. Ford	(TOKY, MIT, BRAN)
PETUKHOV	63	NP 49 87	V.A. Petukhov, M.N. Yakimenko	(LEBD)
PURCELL	63	PR 129 2326	E.M. Purcell *et al.*	(HARV, BNL)
FIDECARO	61	NC 22 657	M. Fidecaro, G. Finocchiaro, G. Giacomelli	(CERN)
BRADNER	59	PR 114 603	H. Bradner, W.M. Isbell	(LBL)
MALKUS	51	PR 83 899	W.V.R. Malkus	(CHIC)

OTHER RELATED PAPERS

GROOM	86	PRPL 140 323	D.E. Groom	(UTAH)
Review				

Supersymmetric Particle Searches

SUPERSYMMETRY, PART I (THEORY)

Revised October 2013 by Howard E. Haber (UC Santa Cruz).

I.1. Introduction: Supersymmetry (SUSY) is a generalization of the space-time symmetries of quantum field theory that transforms fermions into bosons and vice versa [1]. The existence of such a non-trivial extension of the Poincaré symmetry of ordinary quantum field theory was initially surprising, and its form is highly constrained by theoretical principles [2]. Supersymmetry also provides a framework for the unification of particle physics and gravity [3–6] at the Planck energy scale, $M_{\rm P} \approx 10^{19}$ GeV, where the gravitational interactions become comparable in magnitude to the gauge interactions. Moreover, supersymmetry can provide an explanation of the large hierarchy between the energy scale that characterizes electroweak symmetry breaking (of order 100 GeV) and the Planck scale [7–10]. The stability of this large *gauge hierarchy* with respect to radiative quantum corrections is not possible to maintain in the Standard Model without an *unnatural* fine-tuning of the parameters of the fundamental theory at the Planck scale. In contrast, in a supersymmetric extension of the Standard Model, it is possible to maintain the gauge hierarchy with no fine-tuning of parameters, and provide a natural framework for elementary scalar fields.

If supersymmetry were an exact symmetry of nature, then particles and their *superpartners*, which differ in spin by half a unit, would be degenerate in mass. Since superpartners have not (yet) been observed, supersymmetry must be a broken symmetry. Nevertheless, the stability of the gauge hierarchy can still be maintained if the supersymmetry breaking is *soft* [11,12], and the corresponding supersymmetry-breaking mass parameters are no larger than a few TeV. Whether this is still plausible in light of recent supersymmetry searches at the LHC [13] will be discussed in Section I.7.

In particular, soft-supersymmetry-breaking terms of the Lagrangian involve combinations of fields with total mass dimension of three or less, with some restrictions on the dimension-three terms as elucidated in Ref. 11. The impact of the soft terms becomes negligible at energy scales much larger than the size of the supersymmetry-breaking masses. Thus, a theory of *weak-scale supersymmetry*, where the effective scale of supersymmetry breaking is tied to the scale of electroweak symmetry breaking, provides a *natural* framework for the origin and the stability of the gauge hierarchy [7–10].

The Standard Model cannot be the correct theory of fundamental particles and their interactions (applicable at all energy scales). However, no unambiguous experimental results currently exist that imply that the Standard Model breaks down at the TeV scale. The expectations of new physics beyond

the Standard Model at the TeV scale are based primarily on three theoretical arguments. First, a natural explanation of the gauge hierarchy demands new physics at the TeV scale [10]. Second, the unification of the three Standard Model gauge couplings at a very high energy close to the Planck scale is possible if new physics beyond the Standard Model (which modifies the running of the gauge couplings above the electroweak scale) is present. The minimal supersymmetric extension of the Standard Model (MSSM), where superpartner masses lie below a few TeV, provides an example of successful gauge coupling unification [14]. Third, the existence of dark matter, which makes up approximately one quarter of the energy density of the universe, cannot be explained within the Standard Model of particle physics [15]. Remarkably, a stable weakly-interacting massive particle (WIMP) whose mass and interaction rate are governed by new physics associated with the TeV-scale can be consistent with the observed density of dark matter (this is the so-called *WIMP miracle*, which is reviewed in Ref. 16). The lightest supersymmetric particle is a promising (although not the unique) candidate for the dark matter [17–21]. Further aspects of dark matter can be found in Ref. 22.

Another phenomenon not explained by the Standard Model is the origin of the matter–antimatter asymmetry of the universe [23]. Models of baryogenesis must satisfy the three Sakharov conditions [24]: C and CP violation, baryon number violation and a departure from thermal equilibrium. For example, the matter–antimatter asymmetry in the early universe can be generated at the electroweak phase transition if the transition is sufficiently first-order [25]. These conditions are not satisfied in the Standard Model, since the CP violation is too small and the phase transition is not strongly first-order [25]. In contrast, it is possible to satisfy these conditions in supersymmetric extensions of the Standard Model, where new sources of CP-violation exist and supersymmetric loops provide corrections to the temperature-dependent effective potential that can render the transition sufficiently first-order. The MSSM parameter space in which electroweak baryogenesis occurs is strongly constrained by LHC data [26]. However, extended supersymmetric models provide new opportunities for successful electroweak baryogenesis [27].

I.2. Structure of the MSSM: The minimal supersymmetric extension of the Standard Model consists of the fields of the two-Higgs-doublet extension of the Standard Model and the corresponding supersymmetric partners [28,29]. A particle and its superpartner together form a supermultiplet. The corresponding field content of the supermultiplets of the MSSM and their gauge quantum numbers are shown in Table 1. The electric charge $Q = T_3 + \frac{1}{2}Y$ is determined in terms of the third component of the weak isospin (T_3) and the U(1) weak hypercharge (Y).

Table 1: The fields of the MSSM and their SU(3)×SU(2)×U(1) quantum numbers are listed. For simplicity, only one generation of quarks and leptons is exhibited. For each lepton, quark, and Higgs super-multiplet, there is a corresponding anti-particle multiplet of charge-conjugated fermions and their associated scalar partners.

Field Content of the MSSM						
Super-multiplets	Super-field	Bosonic fields	Fermionic partners	SU(3)	SU(2)	U(1)
gluon/gluino	$\widehat{V}_8$	g	$\widetilde{g}$	8	1	0
gauge/	$\widehat{V}$	$W^{\pm}$, W^0	$\widetilde{W}^{\pm}$, $\widetilde{W}^0$	1	3	0
gaugino	$\widehat{V}'$	B	$\widetilde{B}$	1	1	0
slepton/	$\widehat{L}$	$(\widetilde{\nu}_L, \widetilde{e}_L^-)$	$(\nu, e^-)_L$	1	2	-1
lepton	$\widehat{E}^c$	$\widetilde{e}_R^-$	e_R^-	1	1	-2
squark/	$\widehat{Q}$	$(\widetilde{u}_L, \widetilde{d}_L)$	$(u, d)_L$	3	2	1/3
quark	$\widehat{U}^c$	$\widetilde{u}_R$	u_R	3	1	4/3
	$\widehat{D}^c$	$\widetilde{d}_R$	d_R	3	1	$-2/3$
Higgs/	$\widehat{H}_d$	(H_d^0, H_d^-)	$(\widetilde{H}_d^0, \widetilde{H}_d^-)$	1	2	-1
higgsino	$\widehat{H}_u$	(H_u^+, H_u^0)	$(\widetilde{H}_u^+, \widetilde{H}_u^0)$	1	2	1

The gauge supermultiplets consist of the gluons and their *gluino* fermionic superpartners and the SU(2)×U(1) gauge bosons and their *gaugino* fermionic superpartners. The matter supermultiplets consist of three generations of left-handed and right-handed quarks and leptons, their scalar superpartners (*squarks* and *sleptons*), and the corresponding antiparticles. The Higgs supermultiplets consist of two complex Higgs doublets, their *higgsino* fermionic superpartners, and the corresponding antiparticles. The enlarged Higgs sector of the MSSM constitutes the minimal structure needed to guarantee the cancellation of anomalies from the introduction of the higgsino superpartners. Moreover, without a second Higgs doublet, one cannot generate mass for both "up"-type and "down"-type quarks (and charged leptons) in a way consistent with the underlying supersymmetry [30–32].

The fields of a given supermultiplet are components of a *superfield*. Vector superfields contain the gauge boson fields and their gaugino partners. Chiral superfields contain the spin-0 and spin-1/2 fields of the matter or Higgs supermultiplets. A general supersymmetric Lagrangian is determined by three functions of the chiral superfields [6]: the superpotential, the Kähler potential, and the gauge kinetic function (which can be appropriately generalized to accommodate higher derivative terms [33]). Minimal forms for the Kähler potential and gauge kinetic function, which generate canonical kinetic energy terms for all the fields, are required for *renormalizable* globally supersymmetric theories. A renormalizable superpotential, which is at most cubic in the chiral superfields, yields supersymmetric Yukawa couplings and mass terms. A combination of gauge invariance and supersymmetry produces couplings of gaugino fields to matter (or Higgs) fields and their corresponding superpartners. The (renormalizable) MSSM Lagrangian is then constructed by including all possible supersymmetric interaction terms (of dimension four or less) that satisfy

SU(3)×SU(2)×U(1) gauge invariance and B–L conservation (where B = baryon number and L = lepton number). Finally, the most general soft-supersymmetry-breaking terms consistent with these symmetries are added [11,12,34].

Although the MSSM is the focus of much of this review, there is some motivation for considering non-minimal supersymmetric extensions of the Standard Model. For example, extra structure is needed to generate non-zero neutrino masses as discussed in Section I.8. In addition, in order to address some theoretical issues and tensions associated with the MSSM, it has been fruitful to introduce one additional singlet Higgs superfield. The resulting next-to-minimal supersymmetric extension of the Standard Model (NMSSM) [35] is considered further in Sections I.5, I.7 and I.9. Finally, one is always free to add additional fields to the Standard Model along with the corresponding superpartners. However, only certain choices for the new fields (*e.g.*, the addition of complete SU(5) multiplets) will preserve the successful gauge coupling unification. Some examples will be briefly mentioned in Section I.9.

I.2.1. R-parity and the lightest supersymmetric particle: As a consequence of B–L invariance, the MSSM possesses a multiplicative R-parity invariance, where $R = (-1)^{3(B-L)+2S}$ for a particle of spin S [36]. This implies that all the ordinary Standard Model particles have even R-parity, whereas the corresponding supersymmetric partners have odd R-parity. The conservation of R-parity in scattering and decay processes has a crucial impact on supersymmetric phenomenology. For example, any initial state in a scattering experiment will involve ordinary (R-even) particles. Consequently, it follows that supersymmetric particles must be produced in pairs. In general, these particles are highly unstable and decay into lighter states. Moreover, R-parity invariance also implies that the lightest supersymmetric particle (LSP) is absolutely stable, and must eventually be produced at the end of a decay chain initiated by the decay of a heavy unstable supersymmetric particle.

In order to be consistent with cosmological constraints, a stable LSP is almost certainly electrically and color neutral [19]. Consequently, the LSP in an R-parity-conserving theory is weakly interacting with ordinary matter, *i.e.*, it behaves like a stable heavy neutrino and will escape collider detectors without being directly observed. Thus, the canonical signature for conventional R-parity-conserving supersymmetric theories is missing (transverse) energy, due to the escape of the LSP. Moreover, as noted in Section I.1 and reviewed in Refs. [20,21], the stability of the LSP in R-parity-conserving supersymmetry makes it a promising candidate for dark matter.

I.2.2. The goldstino and gravitino: In the MSSM, supersymmetry breaking is accomplished by including the most general renormalizable soft-supersymmetry-breaking terms consistent with the SU(3)×SU(2)×U(1) gauge symmetry and R-parity invariance. These terms parameterize our ignorance of the fundamental mechanism of supersymmetry breaking. If supersymmetry breaking occurs spontaneously, then a massless Goldstone fermion called the *goldstino* ($\widetilde{G}_{1/2}$) must exist. The goldstino would then be the LSP, and could play an important role in supersymmetric phenomenology [37].

However, the goldstino degrees of freedom are physical only in models of spontaneously-broken global supersymmetry. If supersymmetry is a local symmetry, then the theory must incorporate gravity; the resulting theory is called supergravity [38]. In models of spontaneously-broken supergravity, the goldstino is "absorbed" by the *gravitino* ($\widetilde{G}$) [sometimes called $\widetilde{g}_{3/2}$ in the older literature], the spin-3/2 superpartner of the graviton [39]. By this super-Higgs mechanism, the goldstino is removed from the physical spectrum and the gravitino acquires a mass ($m_{3/2}$). In processes with center-of-mass energy $E \gg m_{3/2}$, the goldstino–gravitino equivalence theorem [40] states that the interactions of the helicity $\pm\frac{1}{2}$ gravitino (whose properties approximate those of the goldstino) dominate those of the helicity $\pm\frac{3}{2}$ gravitino. The interactions of gravitinos with other light fields can be described by a low-energy effective Lagrangian that is determined by fundamental principles [41].

I.2.3. Hidden sectors and the structure of supersymmetry breaking: It is very difficult (perhaps impossible) to construct a realistic model of spontaneously-broken low-energy supersymmetry where the supersymmetry breaking arises solely as a consequence of the interactions of the particles of the MSSM. An alternative scheme posits a theory consisting of at least two distinct sectors: a *hidden* sector consisting of particles that are completely neutral with respect to the Standard Model gauge group, and a *visible* sector consisting of the particles of the MSSM [34]. There are no renormalizable tree-level interactions between particles of the visible and hidden sectors. Supersymmetry breaking is assumed to originate in the hidden sector, and its effects are transmitted to the MSSM by some mechanism (often involving the mediation by particles that comprise an additional *messenger* sector). Two theoretical scenarios that exhibit this structure are gravity mediated and gauge mediated supersymmetry breaking.

Supergravity models provide a natural mechanism for transmitting the supersymmetry breaking of the hidden sector to the particle spectrum of the MSSM. In models of *gravity mediated* supersymmetry breaking, gravity is the messenger of supersymmetry breaking [42–46]. More precisely, supersymmetry breaking is mediated by effects of gravitational strength (suppressed by inverse powers of the Planck mass). In this scenario, the gravitino mass is of order the electroweak-symmetry-breaking scale, while its couplings are roughly gravitational in strength [3,47]. Such a gravitino typically plays no role in supersymmetric phenomenology at colliders (except perhaps indirectly in the case where the gravitino is the LSP [48]).

Under certain theoretical assumptions on the structure of the Kähler potential (the so-called sequestered form introduced in Ref. 49), supersymmetry breaking is due entirely to the super-conformal (super-Weyl) anomaly, which is common to all supergravity models [49]. In this case, gaugino masses are radiatively generated at one-loop and squark and slepton masses are flavor-diagonal. This approach is called *anomaly-mediated*

supersymmetry breaking (AMSB). Indeed, anomaly mediation is more generic than originally conceived, and provides a ubiquitous source of supersymmetry breaking [50]. However in the simplest formulation of AMSB as applied to the MSSM, the squared-masses of the sleptons are negative. This is the so-called tachyonic slepton problem. It may be possible to cure this fatal flaw in approaches beyond the minimal supersymmetric model [51]. Alternatively, one can assert that anomaly mediation is not the sole source of supersymmetry breaking, at least in the slepton sector.

In *gauge mediated* supersymmetry breaking (GMSB), gauge forces transmit the supersymmetry breaking to the MSSM. A typical structure of such models involves a hidden sector where supersymmetry is broken, a messenger sector consisting of particles (messengers) with nontrivial SU(3)×SU(2)×U(1) quantum numbers, and the visible sector consisting of the fields of the MSSM [52–54]. The direct coupling of the messengers to the hidden sector generates a supersymmetry-breaking spectrum in the messenger sector. Supersymmetry breaking is then transmitted to the MSSM via the virtual exchange of the messengers. In models of *direct gauge mediation*, there is no hidden sector. In particular, the sector in which the supersymmetry breaking originates includes fields that carry nontrivial Standard Model quantum numbers, which allows for the direct transmission of supersymmetry breaking to the MSSM [55]. In this case, no separate messenger sector distinct from the fundamental supersymmetry-breaking sector is required.

The gravitino mass in models of gauge mediated supersymmetry breaking is typically in the eV range (although in some cases it can be as large as a few GeV), which implies that $\widetilde{G}$ is the LSP [17]. In particular, the gravitino is a potential dark matter candidate (for a review and guide to the literature, see Ref. 21). Big bang nucleosynthesis also provides some interesting constraints on the gravitino and the properties of the next-to-lightest supersymmetric particle that decays into the gravitino LSP [56]. The couplings of the helicity $\pm\frac{1}{2}$ components of $\widetilde{G}$ to the particles of the MSSM (which approximate those of the goldstino as previously noted in Section I.2.2) are significantly stronger than gravitational strength and amenable to experimental collider analyses.

The concept of a hidden sector is more general than supersymmetry. *Hidden valley* models [57] posit the existence of a hidden sector of new particles and interactions that are very weakly coupled to particles of the Standard Model. The impact of a hidden valley on supersymmetric phenomenology at colliders can be significant if the LSP lies in the hidden sector [58].

I.2.4. Supersymmetry and extra dimensions:
Approaches to supersymmetry breaking have also been developed in the context of theories in which the number of space dimensions is greater than three. In particular, a number of supersymmetry-breaking mechanisms have been proposed that are inherently extra-dimensional [59]. The size of the extra dimensions can be significantly larger than $M_{\rm P}^{-1}$; in some cases of order $(\text{TeV})^{-1}$ or even larger [60,61].

For example, in one approach the fields of the MSSM live on some brane (a lower-dimensional manifold embedded in a higher-dimensional spacetime), while the sector of the theory that breaks supersymmetry lives on a second spatially-separated brane. Two examples of this approach are anomaly-mediated supersymmetry breaking [49] and gaugino-mediated supersymmetry breaking [62]. In both cases, supersymmetry breaking is transmitted through fields that live in the bulk (the higher-dimensional space between the two branes). This setup has some features in common with both gravity mediated and gauge mediated supersymmetry breaking (*e.g.*, a hidden and visible sector and messengers).

Alternatively, one can consider a higher-dimensional theory that is compactified to four spacetime dimensions. In this approach, supersymmetry is broken by boundary conditions on the compactified space that distinguish between fermions and bosons. This is the so-called Scherk-Schwarz mechanism [63]. The phenomenology of such models can be strikingly different from that of the usual MSSM [64].

I.2.5. Split-supersymmetry: If supersymmetry is not connected with the origin of the electroweak scale, it may still be possible that some remnant of the superparticle spectrum survives down to the TeV-scale or below. This is the idea of *split-supersymmetry* [65], in which scalar superpartners of the quarks and leptons are significantly heavier (perhaps by many orders of magnitude) than 1 TeV, whereas the fermionic superpartners of the gauge and Higgs bosons have masses on the order of 1 TeV or below (protected by some chiral symmetry). With the exception of a single light neutral scalar whose properties are practically indistinguishable from those of the Standard Model Higgs boson, all other Higgs bosons are also assumed to be very heavy.

The recent observation of a Higgs boson at a mass of 126 GeV [66,67] implies that there is an upper bound in the MSSM on the mass scale that characterizes the top squarks in the range of 10 to 10^6 TeV [69,70]. It is not difficult to formulate models in which gaugino masses are one-loop suppressed relative to the masses of the squarks and sleptons. The higgsino mass scale may or may not be likewise suppressed depending on the details of the model [71]. Recently, a number of authors have considered a supersymmetric spectrum with the squarks, slepton and the heavy Higgs masses around 10^3 TeV, whereas gaugino masses are around 1 TeV [70,71]. In this scenario, only the lighter gaugino states are kinematically accessible at the LHC. The one light Higgs scalar of the model (identified with the observed scalar state at 126 GeV) is indistinguishable from the Standard Model Higgs boson.

The supersymmetry breaking required to produce such a split-supersymmetry spectrum would destabilize the gauge hierarchy, and thus yield no natural explanation for the scale of electroweak symmetry breaking. Nevertheless, models of split-supersymmetry can account for the dark matter (which is

assumed to be the LSP gaugino or higgsino) and gauge coupling unification, thereby preserving two of the good features of weak-scale supersymmetry.

I.3. Parameters of the MSSM: The parameters of the MSSM are conveniently described by considering separately the supersymmetry-conserving and the supersymmetry-breaking sectors. A careful discussion of the conventions used here in defining the tree-level MSSM parameters can be found in Ref. 72. For simplicity, consider first the case of one generation of quarks, leptons, and their scalar superpartners.

I.3.1. The supersymmetric-conserving parameters: The parameters of the supersymmetry-conserving sector consist of: (i) gauge couplings, g_s, g, and g', corresponding to the Standard Model gauge group SU(3)×SU(2)×U(1) respectively; (ii) a supersymmetry-conserving higgsino mass parameter μ; and (iii) Higgs-fermion Yukawa coupling constants, λ_u, λ_d, and λ_e, corresponding to the coupling of one generation of left- and right-handed quarks and leptons, and their superpartners to the Higgs bosons and higgsinos. Because there is no right-handed neutrino (and its superpartner) in the MSSM as defined here, a Yukawa coupling λ_ν is not included here. The complex μ parameter and Yukawa couplings enter via the most general renormalizable R-parity-conserving superpotential,

$$W = \lambda_d \widehat{H}_d \widehat{Q} \widehat{D}^c - \lambda_u \widehat{H}_u \widehat{Q} \widehat{U}^c + \lambda_e \widehat{H}_d \widehat{L} \widehat{E}^c + \mu \widehat{H}_u \widehat{H}_d \,, \qquad (1)$$

where the superfields are defined in Table 1 and the gauge group indices are suppressed. The reader is warned that in the literature, μ is sometimes defined with the opposite sign to the one given in Eq. (1).

I.3.2. The supersymmetry-breaking parameters: The supersymmetry-breaking sector contains the following sets of parameters: (i) three complex gaugino Majorana mass parameters, M_3, M_2, and M_1, associated with the SU(3), SU(2), and U(1) subgroups of the Standard Model; (ii) five diagonal scalar squared-mass parameters for the squarks and sleptons, $M^2_{\widetilde{Q}}$, $M^2_{\widetilde{U}}$, $M^2_{\widetilde{D}}$, $M^2_{\widetilde{L}}$, and $M^2_{\widetilde{E}}$ [corresponding to the five electroweak gauge multiplets, *i.e.*, superpartners of $(u,d)_L$, u^c_L, d^c_L, $(\nu,\, e^-)_L$, and e^c_L, where the superscript c indicates a charge-conjugated fermion]; and (iii) three Higgs-squark-squark and Higgs-slepton-slepton trilinear interaction terms, with complex coefficients $\lambda_u A_U$, $\lambda_d A_D$, and $\lambda_e A_E$ (which define the so-called "A-parameters"). It is traditional to factor out the Yukawa couplings in the definition of the A-parameters (originally motivated by a simple class of gravity mediated supersymmetry-breaking models [3,5]). If the A-parameters defined as above are parametrically of the same order (or smaller) relative to other supersymmetry-breaking mass parameters, then only the third generation A-parameters are phenomenologically relevant. The reader is warned that the convention for the overall sign of the A-parameters varies in the literature.

Finally, we have (iv) three scalar squared-mass parameters: two of which (m_1^2 and m_2^2) are real parameters that contribute to the diagonal Higgs squared-masses, given by $m_1^2 + |\mu|^2$ and $m_2^2 + |\mu|^2$, and a third that contributes to the off-diagonal Higgs squared-mass term, $m_{12}^2 \equiv B\mu$ (which defines the complex "B-parameter"). The breaking of the electroweak symmetry SU(2)×U(1) to $\mathrm{U(1)_{EM}}$ is only possible after introducing the supersymmetry-breaking Higgs squared-mass parameters. Minimizing the resulting tree-level Higgs scalar potential, these three squared-mass parameters can be re-expressed in terms of the two Higgs vacuum expectation values, v_d and v_u (also called v_1 and v_2, respectively, in the literature), and the CP-odd Higgs mass m_A (cf. Section I.5). Here, v_d [v_u] is the vacuum expectation value of the neutral component of the Higgs field H_d [H_u] that couples exclusively to down-type (up-type) quarks and leptons.

Note that $v_d^2 + v_u^2 = 2m_W^2/g^2 \simeq (174\ \mathrm{GeV})^2$ is fixed by the W mass and the SU(2) gauge coupling, whereas the ratio

$$\tan\beta = v_u/v_d \qquad (2)$$

is a free parameter. It is convenient to choose the phases of the Higgs fields such that m_{12}^2 is real and non-negative. In this case, we can adopt a convention where $0 \leq \beta \leq \pi/2$. The tree-level conditions for the scalar potential minimum relate the diagonal and off-diagonal Higgs squared-masses in terms of $m_Z^2 = \frac{1}{4}(g^2 + g'^2)(v_d^2 + v_u^2)$, the angle β and the CP-odd Higgs mass m_A:

$$\sin 2\beta = \frac{2m_{12}^2}{m_1^2 + m_2^2 + 2|\mu|^2} = \frac{2m_{12}^2}{m_A^2}\,, \qquad (3)$$

$$\tfrac{1}{2}m_Z^2 = -|\mu|^2 + \frac{m_1^2 - m_2^2\tan^2\beta}{\tan^2\beta - 1}\,. \qquad (4)$$

One must also guard against the existence of charge and/or color breaking global minima due to non-zero vacuum expectation values for the squark and charged slepton fields. This possibility can be avoided if the A-parameters are not unduly large [43,73].

Note that supersymmetry-breaking mass terms for the fermionic superpartners of scalar fields and non-holomorphic trilinear scalar interactions (*i.e.*, interactions that mix scalar fields and their complex conjugates) have not been included above in the soft-supersymmetry-breaking sector. These terms can potentially destabilize the gauge hierarchy [11] in models with gauge-singlet superfields. The latter are not present in the MSSM; hence as noted in Ref. 12, these so-called non-standard soft-supersymmetry-breaking terms are benign. However, the coefficients of these terms (which have dimensions of mass) are expected to be significantly suppressed compared to the TeV-scale in a fundamental theory of supersymmetry-breaking [74]. Consequently, we follow the usual approach and omit these terms from further consideration.

I.3.3. MSSM-124: The total number of independent physical parameters that define the MSSM (in its most general form) is quite large, primarily due to the soft-supersymmetry-breaking sector. In particular, in the case of three generations of quarks, leptons, and their superpartners, $M^2_{\widetilde{Q}}$, $M^2_{\widetilde{U}}$, $M^2_{\widetilde{D}}$, $M^2_{\widetilde{L}}$,

and $M^2_{\widetilde{E}}$ are hermitian 3×3 matrices, and A_U, A_D, and A_E are complex 3×3 matrices. In addition, M_1, M_2, M_3, B, and μ are in general complex parameters. Finally, as in the Standard Model, the Higgs-fermion Yukawa couplings, λ_f ($f=u$, d, and e), are complex 3×3 matrices that are related to the quark and lepton mass matrices via: $M_f=\lambda_f v_f$, where $v_e\equiv v_d$ [with v_u and v_d as defined above Eq. (2)].

However, not all these parameters are physical. Some of the MSSM parameters can be eliminated by expressing interaction eigenstates in terms of the mass eigenstates, with an appropriate redefinition of the MSSM fields to remove unphysical degrees of freedom. The analysis of Ref. 75 shows that the MSSM possesses 124 independent parameters. Of these, 18 correspond to Standard Model parameters (including the QCD vacuum angle $\theta_{\rm QCD}$), one corresponds to a Higgs sector parameter (the analogue of the Standard Model Higgs mass), and 105 are genuinely new parameters of the model. The latter include: five real parameters and three CP-violating phases in the gaugino/higgsino sector, 21 squark and slepton masses, 36 real mixing angles to define the squark and slepton mass eigenstates, and 40 CP-violating phases that can appear in squark and slepton interactions. The most general R-parity-conserving minimal supersymmetric extension of the Standard Model (without additional theoretical assumptions) will be denoted henceforth as MSSM-124 [76].

I.4. The supersymmetric-particle spectrum: The supersymmetric particles (*sparticles*) differ in spin by half a unit from their Standard Model partners. The supersymmetric partners of the gauge and Higgs bosons are fermions, whose names are obtained by appending "ino" to the end of the corresponding Standard Model particle name. The gluino is the color-octet Majorana fermion partner of the gluon with mass $M_{\widetilde{g}}=|M_3|$. The supersymmetric partners of the electroweak gauge and Higgs bosons (the gauginos and higgsinos) can mix due to SU(2)×U(1) breaking effects. As a result, the physical states of definite mass are model-dependent linear combinations of the charged and neutral gauginos and higgsinos, called *charginos* and *neutralinos*, respectively. Like the gluino, the neutralinos are also Majorana fermions, which provide for some distinctive phenomenological signatures [77,78]. The supersymmetric partners of the quarks and leptons are spin-zero bosons: the *squarks*, charged *sleptons*, and *sneutrinos*, respectively. A complete set of Feynman rules for the sparticles of the MSSM can be found in Ref. 79. The MSSM Feynman rules also are implicitly contained in a number of Feynman diagram and amplitude generation software packages (see *e.g.*, Refs. [80–82]).

It should be noted that all mass formulae quoted in this section are tree-level results. Radiative loop corrections will modify these results and must be included in any precision study of supersymmetric phenomenology [83]. Beyond tree level, the definition of the supersymmetric parameters becomes convention-dependent. For example, one can define physical couplings or running couplings, which differ beyond the tree level. This provides a challenge to any effort that attempts to extract supersymmetric parameters from data. The Supersymmetry Les Houches Accord (SLHA) [84] has been adopted, which establishes a set of conventions for specifying generic file structures for supersymmetric model specifications and input parameters, supersymmetric mass and coupling spectra, and decay tables. These provide a universal interface between spectrum calculation programs, decay packages, and high energy physics event generators. Ultimately, these efforts will facilitate the reconstruction of the fundamental supersymmetric theory (and its breaking mechanism) from high-precision studies of supersymmetric phenomena at future colliders.

I.4.1. The charginos and neutralinos: The mixing of the charged gauginos ($\widetilde{W}^\pm$) and charged higgsinos (H_u^+ and H_d^-) is described (at tree-level) by a 2×2 complex mass matrix [85–87]:

$$M_C\equiv\begin{pmatrix} M_2 & \frac{1}{\sqrt{2}}gv_u \\ \frac{1}{\sqrt{2}}gv_d & \mu \end{pmatrix}. \qquad (5)$$

To determine the physical chargino states and their masses, one must perform a singular value decomposition [88,89] of the complex matrix M_C:

$$U^*M_CV^{-1}=\mathrm{diag}(M_{\widetilde{\chi}_1^+},M_{\widetilde{\chi}_2^+}), \qquad (6)$$

where U and V are unitary matrices, and the right-hand side of Eq. (6) is the diagonal matrix of (non-negative) chargino masses. The physical chargino states are denoted by $\widetilde{\chi}_1^\pm$ and $\widetilde{\chi}_2^\pm$. These are linear combinations of the charged gaugino and higgsino states determined by the matrix elements of U and V [85–87]. The chargino masses correspond to the *singular values* [88] of M_C, *i.e.*, the positive square roots of the eigenvalues of $M_C^\dagger M_C$:

$$M^2_{\widetilde{\chi}_1^+,\widetilde{\chi}_2^+}=\tfrac{1}{2}\Big\{|\mu|^2+|M_2|^2+2m_W^2\mp\Big[\big(|\mu|^2+|M_2|^2+2m_W^2\big)^2 - 4|\mu|^2|M_2|^2-4m_W^4\sin^2 2\beta+8m_W^2\sin2\beta\,\mathrm{Re}(\mu M_2)\Big]^{1/2}\Big\}, \qquad (7)$$

where the states are ordered such that $M_{\widetilde{\chi}_1^+}\le M_{\widetilde{\chi}_2^+}$. Note that the relative phase of M_2 and μ is meaningful.

The mixing of the neutral gauginos ($\widetilde{B}$ and $\widetilde{W}^0$) and neutral higgsinos ($\widetilde{H}_d^0$ and $\widetilde{H}_u^0$) is described (at tree-level) by a 4×4 complex symmetric mass matrix [85,86,90,91]:

$$M_N\equiv\begin{pmatrix} M_1 & 0 & -\frac{1}{2}g'v_d & \frac{1}{2}g'v_u \\ 0 & M_2 & \frac{1}{2}gv_d & -\frac{1}{2}gv_u \\ -\frac{1}{2}g'v_d & \frac{1}{2}gv_d & 0 & -\mu \\ \frac{1}{2}g'v_u & -\frac{1}{2}gv_u & -\mu & 0 \end{pmatrix}. \qquad (8)$$

To determine the physical neutralino states and their masses, one must perform a Takagi-diagonalization [88,89,92,93] of the complex symmetric matrix M_N:

$$W^TM_NW=\mathrm{diag}(M_{\widetilde{\chi}_1^0},M_{\widetilde{\chi}_2^0},M_{\widetilde{\chi}_3^0},M_{\widetilde{\chi}_4^0}), \qquad (9)$$

where W is a unitary matrix and the right-hand side of Eq. (9) is the diagonal matrix of (non-negative) neutralino masses. The

physical neutralino states are denoted by $\widetilde{\chi}_i^0$ ($i = 1, \ldots 4$), where the states are ordered such that $M_{\widetilde{\chi}_1^0} \leq M_{\widetilde{\chi}_2^0} \leq M_{\widetilde{\chi}_3^0} \leq M_{\widetilde{\chi}_4^0}$. The $\widetilde{\chi}_i^0$ are the linear combinations of the neutral gaugino and higgsino states determined by the matrix elements of W (which is denoted by N^{-1} in Ref. 85). The neutralino masses correspond to the singular values of M_N, *i.e.*, the positive square roots of the eigenvalues of $M_N^\dagger M_N$. Exact formulae for these masses can be found in Refs. [90] and [94]. A numerical algorithm for determining the mixing matrix W has been given by Ref. 95.

If a chargino or neutralino state approximates a particular gaugino or higgsino state, it is convenient to employ the corresponding nomenclature. Specifically, if $|M_1|$ and $|M_2|$ are small compared to m_Z and $|\mu|$, then the lightest neutralino $\widetilde{\chi}_1^0$ would be nearly a pure *photino*, $\widetilde{\gamma}$, the supersymmetric partner of the photon. If $|M_1|$ and m_Z are small compared to $|M_2|$ and $|\mu|$, then the lightest neutralino would be nearly a pure *bino*, $\widetilde{B}$, the supersymmetric partner of the weak hypercharge gauge boson. If $|M_2|$ and m_Z are small compared to $|M_1|$ and $|\mu|$, then the lightest chargino pair and neutralino would constitute a triplet of roughly mass-degenerate pure *winos*, $\widetilde{W}^\pm$, and $\widetilde{W}_3^0$, the supersymmetric partners of the weak SU(2) gauge bosons. Finally, if $|\mu|$ and m_Z are small compared to $|M_1|$ and $|M_2|$, then the lightest chargino pair and neutralino would be nearly pure *higgsino* states, the supersymmetric partners of the Higgs bosons. Each of the above cases leads to a strikingly different phenomenology.

In the NMSSM, an additional Higgs singlet superfield is added to the MSSM. This superfield comprises two real Higgs scalar degrees of freedom and an associated neutral higgsino degree of freedom. Consequently, there are five neutralino mass eigenstates that are obtained by a Takagi-diagonalization of the 5×5 neutralino mass matrix. In many cases, the fifth neutralino state is dominated by its SU(2)×U(1) singlet component, and thus is very weakly coupled to the Standard Model particles and their superpartners.

I.4.2. The squarks, sleptons and sneutrinos: For a given fermion f, there are two supersymmetric partners, $\widetilde{f}_L$ and $\widetilde{f}_R$, which are scalar partners of the corresponding left-handed and right-handed fermion. (There is no $\widetilde{\nu}_R$ in the MSSM.) However, in general $\widetilde{f}_L$–$\widetilde{f}_R$ mixing is possible, in which case $\widetilde{f}_L$ and $\widetilde{f}_R$ are not mass eigenstates. For three generations of squarks, one must diagonalize 6×6 matrices corresponding to the basis $(\widetilde{q}_{iL}, \widetilde{q}_{iR})$, where $i = 1, 2, 3$ are the generation labels. For simplicity, only the one-generation case is illustrated in detail below. (The effects of second and third generation squark mixing can be significant and is treated in Ref. 96.)

Using the notation of the third family, the one-generation tree-level squark squared-mass matrix is given by [97]

$$\mathcal{M}^2 = \begin{pmatrix} M_{\widetilde{Q}}^2 + m_q^2 + L_q & m_q X_q^* \\ m_q X_q & M_{\widetilde{R}}^2 + m_q^2 + R_q \end{pmatrix}, \qquad (10)$$

where

$$X_q \equiv A_q - \mu^* (\cot\beta)^{2T_{3q}}, \qquad (11)$$

and $T_{3q} = \frac{1}{2}$ [$-\frac{1}{2}$] for $q = t$ [b]. The diagonal squared-masses are governed by soft-supersymmetry-breaking squared-masses $M_{\widetilde{Q}}^2$ and $M_{\widetilde{R}}^2 \equiv M_{\widetilde{U}}^2$ [$M_{\widetilde{D}}^2$] for $q = t$ [b], the corresponding quark masses m_t [m_b], and electroweak correction terms:

$$L_q \equiv (T_{3q} - e_q \sin^2\theta_W) m_Z^2 \cos 2\beta\,, \quad R_q \equiv e_q \sin^2\theta_W\, m_Z^2 \cos 2\beta\,, \qquad (12)$$

where $e_q = \frac{2}{3}$ [$-\frac{1}{3}$] for $q = t$ [b]. The off-diagonal squark squared-masses are proportional to the corresponding quark masses and depend on $\tan\beta$, the soft-supersymmetry-breaking A-parameters and the higgsino mass parameter μ. Assuming that the A-parameters are parametrically of the same order (or smaller) relative to other supersymmetry-breaking mass parameters, it then follows that $\widetilde{q}_L$–$\widetilde{q}_R$ mixing effects are small, with the possible exception of the third generation, where mixing can be enhanced by factors of m_t and $m_b \tan\beta$.

In the case of third generation $\widetilde{q}_L$–$\widetilde{q}_R$ mixing, the mass eigenstates (usually denoted by $\widetilde{q}_1$ and $\widetilde{q}_2$, with $m_{\widetilde{q}_1} < m_{\widetilde{q}_2}$) are determined by diagonalizing the 2×2 matrix $\mathcal{M}^2$ given by Eq. (10). The corresponding squared-masses and mixing angle are given by [97]:

$$m_{\widetilde{q}_{1,2}}^2 = \frac{1}{2}\left[\mathrm{Tr}\,\mathcal{M}^2 \mp \sqrt{(\mathrm{Tr}\mathcal{M}^2)^2 - 4\det\mathcal{M}^2}\right],$$

$$\sin 2\theta_{\tilde{q}} = \frac{2m_q|X_q|}{m_{\widetilde{q}_2}^2 - m_{\widetilde{q}_1}^2}\,. \qquad (13)$$

The one-generation results above also apply to the charged sleptons, with the obvious substitutions: $q \to \tau$ with $T_{3\tau} = -\frac{1}{2}$ and $e_\tau = -1$, and the replacement of the supersymmetry-breaking parameters: $M_{\widetilde{Q}}^2 \to M_{\widetilde{L}}^2$, $M_{\widetilde{D}}^2 \to M_{\widetilde{E}}^2$, and $A_q \to A_\tau$. For the neutral sleptons, $\widetilde{\nu}_R$ does not exist in the MSSM, so $\widetilde{\nu}_L$ is a mass eigenstate.

In the case of three generations, the supersymmetry-breaking scalar-squared masses [$M_{\widetilde{Q}}^2$, $M_{\widetilde{U}}^2$, $M_{\widetilde{D}}^2$, $M_{\widetilde{L}}^2$, and $M_{\widetilde{E}}^2$] and the A-parameters [A_U, A_D, and A_E] are now 3×3 matrices as noted in Section I.3.3. The diagonalization of the 6×6 squark mass matrices yields $\widetilde{f}_{iL}$–$\widetilde{f}_{jR}$ mixing (for $i \neq j$). In practice, since the $\widetilde{f}_L$–$\widetilde{f}_R$ mixing is appreciable only for the third generation, this additional complication can often be neglected (although see Ref. 96 for examples in which the mixing between the second and third generation squarks is relevant).

I.5. The supersymmetric Higgs sector: Consider first the MSSM Higgs sector [31,32,98]. Despite the large number of potential CP-violating phases among the MSSM-124 parameters, the tree-level MSSM Higgs sector is automatically CP-conserving. This follows from the fact that the only potentially complex parameter (m_{12}^2) of the MSSM Higgs potential can be chosen real and positive by rephasing the Higgs fields, in which case $\tan\beta$ is a real positive parameter. Consequently, the physical neutral Higgs scalars are CP-eigenstates. The MSSM Higgs sector contains five physical spin-zero particles: a charged Higgs boson pair ($H^\pm$), two CP-even neutral Higgs bosons (denoted by h^0 and H^0 where $m_h < m_H$), and one

CP-odd neutral Higgs boson (A^0). The recent discovery of a Standard Model-like Higgs boson at the LHC with a mass of 126 GeV [66,67] strongly suggests that this state should be identified with h^0, although the possibility that the 126 GeV state should be identified with H^0 cannot be completely ruled out [99].

In the NMSSM [35], the scalar component of the singlet Higgs superfield adds two additional neutral states to the Higgs sector. In this model, the tree-level Higgs sector can exhibit explicit CP-violation. If CP is conserved, then the two extra neutral scalar states are CP-even and CP-odd, respectively. These states can potentially mix with the neutral Higgs states of the MSSM. If scalar states exist that are dominantly singlet, then they are weakly coupled to Standard Model gauge bosons and fermions through their small mixing with the MSSM Higgs scalars. Consequently, it is possible that one (or both) of the singlet-dominated states is considerably lighter than the Higgs boson that was observed at the LHC.

I.5.1 The Tree-level Higgs sector: The properties of the Higgs sector are determined by the Higgs potential, which is made up of quadratic terms [whose squared-mass coefficients were specified above Eq. (2)] and quartic interaction terms governed by dimensionless couplings. The quartic interaction terms are manifestly supersymmetric at tree level (although these are modified by supersymmetry-breaking effects at the loop level). In general, the quartic couplings arise from two sources: (i) the supersymmetric generalization of the scalar potential (the so-called "F-terms"), and (ii) interaction terms related by supersymmetry to the coupling of the scalar fields and the gauge fields, whose coefficients are proportional to the corresponding gauge couplings (the so-called "D-terms").

In the MSSM, F-term contributions to the quartic couplings are absent. As a result, the strengths of the MSSM quartic Higgs interactions are fixed in terms of the gauge couplings. Due to the resulting constraint on the form of the two-Higgs-doublet scalar potential, all the tree-level MSSM Higgs-sector parameters depend only on two quantities: $\tan\beta$ [defined in Eq. (2)] and one Higgs mass usually taken to be m_A. From these two quantities, one can predict the values of the remaining Higgs boson masses, an angle α (which measures the mixture of the original $Y = \pm 1$ Higgs doublet states in the physical CP-even neutral scalars), and the Higgs boson self-couplings. Moreover, the tree-level mass of the lighter CP-even Higgs boson is bounded, $m_h \leq m_Z|\cos 2\beta| \leq m_Z$ [31,32]. This bound can be substantially modified when radiative corrections are included, as discussed in Section I.5.2.

In the NMSSM, the superpotential contains a trilinear term that couples the two $Y = \pm 1$ Higgs doublet superfields and the singlet Higgs superfield. The coefficient of this term is denoted by λ. Consequently, the tree-level bound for the mass of the lightest CP-even MSSM Higgs boson is modified [100],

$$m_h^2 \leq m_Z^2 \cos^2 2\beta + \lambda^2 v^2 \sin^2 2\beta\,, \qquad (14)$$

where $v \equiv (v_u^2 + v_d^2)^{1/2} = 174$ GeV. If one demands that λ should stay finite below the Planck scale, then λ is constrained to lie below about 0.7. However, in light of the observed Higgs mass of 126 GeV, there is some phenomenological motivation for considering larger values of λ [101].

I.5.2 The radiatively-corrected Higgs sector: When radiative corrections are incorporated, additional parameters of the supersymmetric model enter via virtual supersymmetric particles that can appear in loops. The impact of these corrections can be significant [102]. The qualitative behavior of these radiative corrections can be most easily seen in the large top-squark mass limit, where in addition, both the splitting of the two diagonal entries and the off-diagonal entries of the top-squark squared-mass matrix [Eq. (10)] are small in comparison to the geometric mean of the two top-squark squared-masses, $M_{\rm S}^2 \equiv M_{\tilde{t}_1} M_{\tilde{t}_2}$. In this case (assuming $m_A > m_Z$), the predicted upper bound for m_h is approximately given by

$$m_h^2 \lesssim m_Z^2 \cos^2 2\beta + \frac{3g^2 m_t^4}{8\pi^2 m_W^2}\left[\ln\left(\frac{M_{\rm S}^2}{m_t^2}\right) + \frac{X_t^2}{M_{\rm S}^2}\left(1 - \frac{X_t^2}{12 M_{\rm S}^2}\right)\right], \qquad (15)$$

where $X_t \equiv A_t - \mu\cot\beta$ is proportional to the off-diagonal entry of the top-squark squared-mass matrix (which for simplicity is taken here to be real). The Higgs mass upper limit is saturated when $\tan\beta$ is large (*i.e.*, $\cos^2 2\beta \sim 1$) and $X_t = \sqrt{6}\, M_S$. This value of X_t defines the so-called *maximal mixing* scenario.

A more complete treatment of the radiative corrections [103] shows that Eq. (15) somewhat overestimates the true upper bound of m_h. These more refined computations, which incorporate renormalization group improvement and the leading two-loop contributions, yield $m_h \lesssim 135$ GeV in the large $\tan\beta$ regime (with an accuracy of a few GeV) for $m_t = 175$ GeV and $M_S \lesssim 2$ TeV [103].

In addition, one-loop radiative corrections can introduce CP-violating effects in the Higgs sector, which depend on some of the CP-violating phases among the MSSM-124 parameters [104]. Although these effects are more model-dependent, they can have a non-trivial impact on the Higgs searches at LHC and at future colliders. A summary of the MSSM Higgs mass limits based on searches at LEP, Tevatron and LHC and the corresponding references to the literature can be found in Ref. 67.

In the NMSSM, the dominant radiative correction to Eq. (14) is the same as the one given in Eq. (15). However, in contrast to the MSSM, one does not need as large a boost from the radiative corrections to achieve a Higgs mass of 126 GeV. For example, the observed Higgs mass is easily achieved in the NMSSM parameter regime where $\tan\beta \sim 2$ and $\lambda \sim 0.7$.

I.6. Restricting the MSSM parameter freedom: In Sections I.4 and I.5, we surveyed the parameters that comprise the MSSM-124. However, in its most general form, the MSSM-124 is not a phenomenologically-viable theory over most of its parameter space. This conclusion follows from the observation

that a generic point in the MSSM-124 parameter space exhibits: (i) no conservation of the separate lepton numbers L_e, L_μ, and L_τ; (ii) unsuppressed flavor-changing neutral currents (FCNCs); and (iii) new sources of CP violation that are inconsistent with the experimental bounds.

For example, the MSSM contains many new sources of CP violation [68]. In particular, in weak-scale supersymmetry some combinations of the complex phases of the gaugino-mass parameters, the A-parameters, and μ must be less than on the order of 10^{-2}–10^{-3} to avoid generating electric dipole moments for the neutron, electron, and atoms in conflict with observed data [105–107]. The non-observation of FCNCs [108–110] places additional strong constraints on the off-diagonal matrix elements of the squark and slepton soft-supersymmetry-breaking squared-masses and A-parameters (see Section I.3.3). As a result of the phenomenological deficiencies listed above, almost the entire MSSM-124 parameter space is ruled out! This theory is viable only at very special "exceptional" regions of the full parameter space.

The MSSM-124 is also theoretically incomplete as it provides no explanation for the origin of the supersymmetry-breaking parameters (and in particular, why these parameters should conform to the exceptional regions of the parameter space mentioned above). Moreover, there is no understanding of the choice of parameters that leads to the breaking of the electroweak symmetry. What is needed ultimately is a fundamental theory of supersymmetry breaking, which would provide a rationale for a set of soft-supersymmetry-breaking terms that is consistent with all phenomenological constraints.

The successful unification of the SU(3)×SU(2)×U(1) gauge couplings in supersymmetric grand unified theories [8,65,111,112] suggests that the high-energy structure of the theory may be considerably simpler than its low-energy realization. In a top-down approach, the dynamics that governs the more fundamental theory at high energies is used to derive the effective broken-supersymmetric theory at the TeV scale. A suitable choice for the high energy dynamics is one that yields a TeV-scale theory that satisfies all relevant phenomenological constraints.

In this Section, we examine a number of theoretical frameworks that potentially yield phenomenologically viable regions of the MSSM-124 parameter space. The resulting supersymmetric particle spectrum is then a function of a relatively small number of input parameters. This is accomplished by imposing a simple structure on the soft-supersymmetry-breaking terms at a common high-energy scale M_X (typically chosen to be the Planck scale, $M_{\rm P}$, the grand unification scale, $M_{\rm GUT}$, or the messenger scale, $M_{\rm mess}$). Using the renormalization group equations, one can then derive the low-energy MSSM parameters relevant for collider physics. The initial conditions (at the appropriate high-energy scale) for the renormalization group equations depend on the mechanism by which supersymmetry breaking is communicated to the effective low energy theory.

Examples of this scenario are provided by models of gravity mediated, anomaly mediated and gauge mediated supersymmetry breaking, to be discussed in more detail below. In some of these approaches, one of the diagonal Higgs squared-mass parameters is driven negative by renormalization group evolution [113]. In such models, electroweak symmetry breaking is generated radiatively, and the resulting electroweak symmetry-breaking scale is intimately tied to the scale of low-energy supersymmetry breaking.

I.6.1. Gaugino mass unification:

One prediction that arises in many grand unified supergravity models and gauge mediated supersymmetry-breaking models is the unification of the (tree-level) gaugino mass parameters at some high-energy scale $M_{\rm X}$:

$$M_1(M_X) = M_2(M_X) = M_3(M_X) = m_{1/2}\,. \tag{16}$$

Due to renormalization group running, the effective low-energy gaugino mass parameters (at the electroweak scale) are related:

$$M_3 = (g_s^2/g^2)M_2 \simeq 3.5M_2\,, \qquad M_1 = (5g'^2/3g^2)M_2 \simeq 0.5M_2. \tag{17}$$

In this case, the chargino and neutralino masses and mixing angles depend only on three unknown parameters: the gluino mass, μ, and $\tan\beta$. It then follows that the lightest neutralino must be heavier than 46 GeV due to the non-observation of charginos at LEP [114]. If in addition $|\mu| \gg |M_1| \gtrsim m_Z$, then the lightest neutralino is nearly a pure bino, an assumption often made in supersymmetric particle searches at colliders.

Although Eqs. (16) and (17) are often assumed in many phenomenological studies, a truly model-independent approach would take the gaugino mass parameters, M_i, to be independent parameters to be determined by experiment. Indeed, an approximately massless neutralino *cannot* be ruled out at present by a model-independent analysis [115].

It is possible that the tree-level masses for the gauginos are absent. In this case, the gaugino mass parameters arise at one-loop and do not satisfy Eq. (17). For example, the gaugino masses in AMSB models arise entirely from a model-independent contribution derived from the super-conformal anomaly [49,116]. In this case, Eq. (17) is replaced (in the one-loop approximation) by:

$$M_i \simeq \frac{b_i g_i^2}{16\pi^2} m_{3/2}\,, \tag{18}$$

where $m_{3/2}$ is the gravitino mass and the b_i are the coefficients of the MSSM gauge beta-functions corresponding to the corresponding U(1), SU(2), and SU(3) gauge groups, $(b_1, b_2, b_3) = (\frac{33}{5}, 1, -3)$. Eq. (18) yields $M_1 \simeq 2.8M_2$ and $M_3 \simeq -8.3M_2$, which implies that the lightest chargino pair and neutralino comprise a nearly mass-degenerate triplet of winos, $\widetilde{W}^\pm$, $\widetilde{W}^0$ (cf. Table 1), over most of the MSSM parameter space. For example, if $|\mu| \gg m_Z$, then Eq. (18) implies that $M_{\widetilde{\chi}_1^\pm} \simeq M_{\widetilde{\chi}_1^0} \simeq M_2$ [117]. The corresponding supersymmetric phenomenology differs significantly from the standard phenomenology based on Eq. (17) [118,119].

Finally, it should be noted that the unification of gaugino masses (and scalar masses) can be accidental. In particular, the energy scale where unification takes place may not be directly related to any physical scale. One version of this phenomenon has been called *mirage unification* and can occur in certain theories of fundamental supersymmetry breaking [120].

I.6.2. The constrained MSSM: mSUGRA, CMSSM, ... In the *minimal* supergravity (mSUGRA) framework [3–5,42–44], a form of the Kähler potential is employed that yields minimal kinetic energy terms for the MSSM fields [46]. As a result, the soft-supersymmetry-breaking parameters at the high-energy scale M_X take a particularly simple form in which the scalar squared-masses and the A-parameters are flavor-diagonal and universal [44]:

$$\begin{aligned} &M_{\widetilde{Q}}^2(M_X) = M_{\widetilde{U}}^2(M_X) = M_{\widetilde{D}}^2(M_X) = m_0^2\mathbf{1}\,, \\ &M_{\widetilde{L}}^2(M_X) = M_{\widetilde{E}}^2(M_X) = m_0^2\mathbf{1}\,, \\ &m_1^2(M_X) = m_2^2(M_X) = m_0^2\,, \\ &A_U(M_X) = A_D(M_X) = A_E(M_X) = A_0\mathbf{1}\,, \end{aligned} \tag{19}$$

where $\mathbf{1}$ is a 3×3 identity matrix in generation space. As in the Standard Model, this approach exhibits minimal flavor violation [121,122], whose unique source is the nontrivial flavor structure of the Higgs-fermion Yukawa couplings. The gaugino masses are also unified according to Eq. (16).

Renormalization group evolution is then used to derive the values of the supersymmetric parameters at the low-energy (electroweak) scale. For example, to compute squark masses, one must use the *low-energy* values for $M_{\widetilde{Q}}^2$, $M_{\widetilde{U}}^2$, and $M_{\widetilde{D}}^2$ in Eq. (10). Through the renormalization group running with boundary conditions specified in Eqs. (17) and (19), one can show that the low-energy values of $M_{\widetilde{Q}}^2$, $M_{\widetilde{U}}^2$, and $M_{\widetilde{D}}^2$ depend primarily on m_0^2 and $m_{1/2}^2$. A number of useful approximate analytic expressions for superpartner masses in terms of the mSUGRA parameters can be found in Ref. 123.

In the mSUGRA approach, four flavors of squarks (with two squark eigenstates per flavor) are nearly mass-degenerate. If $\tan\beta$ is not very large, $\widetilde{b}_R$ is also approximately degenerate in mass with the first two generations of squarks. The $\widetilde{b}_L$ mass and the diagonal $\widetilde{t}_L$ and $\widetilde{t}_R$ masses are typically reduced relative to the common squark mass of the first two generations. In addition, there are six flavors of nearly mass-degenerate sleptons (with two slepton eigenstates per flavor for the charged sleptons and one per flavor for the sneutrinos); the sleptons are expected to be somewhat lighter than the mass-degenerate squarks. As noted below Eq. (10), third-generation squark masses and tau-slepton masses are sensitive to the strength of the respective $\widetilde{f}_L$–$\widetilde{f}_R$ mixing. The LSP is typically the lightest neutralino, $\widetilde{\chi}_1^0$, which is dominated by its bino component. Regions of the mSUGRA parameter space in which the LSP is electrically charged do exist but are not phenomenologically viable [19].

One can count the number of independent parameters in the mSUGRA framework. In addition to 18 Standard Model parameters (excluding the Higgs mass), one must specify m_0, $m_{1/2}$, A_0, the Planck-scale values for μ and B-parameters (denoted by μ_0 and B_0), and the gravitino mass $m_{3/2}$. Without additional model assumptions, $m_{3/2}$ is independent of the parameters that govern the mass spectrum of the superpartners of the Standard Model [44]. In principle, A_0, B_0, μ_0, and $m_{3/2}$ can be complex, although in the mSUGRA approach, these parameters are taken (arbitrarily) to be real.

As previously noted, renormalization group evolution is used to compute the low-energy values of the mSUGRA parameters, which then fixes all the parameters of the low-energy MSSM. In particular, the two Higgs vacuum expectation values (or equivalently, m_Z and $\tan\beta$) can be expressed as a function of the Planck-scale supergravity parameters. The simplest procedure is to remove μ_0 and B_0 in favor of m_Z and $\tan\beta$ [the sign of μ_0, denoted $\mathrm{sgn}(\mu_0)$ below, is not fixed in this process]. In this case, the MSSM spectrum and its interaction strengths are determined by five parameters:

$$m_0\,,\ A_0\,,\ m_{1/2}\,,\ \tan\beta\,,\ \text{and}\ \ \mathrm{sgn}(\mu_0)\,, \tag{20}$$

and an independent gravitino mass $m_{3/2}$ (in addition to the 18 parameters of the Standard Model). This framework is conventionally called the *constrained minimal supersymmetric extension of the Standard Model* (CMSSM).

In the early literature, additional conditions were obtained by assuming a simplified form for the hidden sector that provides the fundamental source of supersymmetry breaking. Two additional relations emerged among the mSUGRA parameters [42,46]: $B_0 = A_0 - m_0$ and $m_{3/2} = m_0$. These relations characterize a theory that was called minimal supergravity when first proposed. In the more recent literature, it has been more common to omit these extra conditions in defining the mSUGRA model (in which case the mSUGRA model and the CMSSM are synonymous). The authors of Ref. 124 advocate restoring the original nomenclature in which the mSUGRA model is defined with the extra conditions as originally proposed. Additional mSUGRA variations can be considered where different relations among the CMSSM parameters are imposed.

One can also relax the universality of scalar masses by decoupling the squared-masses of the Higgs bosons and the squarks/sleptons. This leads to the non-universal Higgs mass models (NUHMs), thereby adding one or two new parameters to the CMSSM depending on whether the diagonal Higgs scalar squared-mass parameters (m_1^2 and m_2^2) are set equal (NUHM1) or taken to be independent (NUHM2) at the high energy scale M_X^2. Clearly, this modification preserves the minimal flavor violation of the mSUGRA approach. Nevertheless, the mSUGRA approach and its NUHM generalizations are probably too simplistic. Theoretical considerations suggest that the universality of Planck-scale soft-supersymmetry-breaking parameters is not generic [125]. In particular, effective operators at the Planck scale exist that do not respect flavor universality, and it is difficult to find a theoretical principle that would forbid them.

In the framework of supergravity, if anomaly mediation is the sole source of supersymmetry breaking, then the gaugino mass parameters, diagonal scalar squared-mass parameters, and the supersymmetry-breaking trilinear scalar interaction terms (proportional to $\lambda_f A_F$) are determined in terms of the beta functions of the gauge and Yukawa couplings and the anomalous dimensions of the squark and slepton fields [49,116,119]. As noted in Section I.2.3, this approach yields tachyonic sleptons in the MSSM unless additional sources of supersymmetry breaking are present. In the *minimal* AMSB (mAMSB) scenario, a universal squared-mass parameter, m_0^2, is added to the AMSB expressions for the diagonal scalar squared-masses [119]. Thus, the mAMSB spectrum and its interaction strengths are determined by four parameters, m_0^2, $m_{3/2}$, $\tan\beta$ and $\mathrm{sgn}(\mu_0)$.

The mAMSB scenario appears to be ruled out based on the observed value of the Higgs boson mass, assuming an upper limit on M_S of a few TeV, since the mAMSB constraint on A_F implies that the maximal mixing scenario cannot be achieved [cf. Eq. (15)]. Indeed, under the stated assumptions, the mAMSB Higgs mass upper bound lies below the observed Higgs mass value [126]. Thus within the AMSB scenario, either an additional supersymmetry-breaking contribution to $\lambda_f A_F$ and/or new ingredients beyond the MSSM are required.

I.6.3. Gauge mediated supersymmetry breaking: In contrast to models of gravity mediated supersymmetry breaking, the universality of the fundamental soft-supersymmetry-breaking squark and slepton squared-mass parameters is guaranteed in gauge mediated supersymmetry breaking (GMSB) because the supersymmetry breaking is communicated to the sector of MSSM fields via gauge interactions [53,54]. In GMSB models, the mass scale of the messenger sector (or its equivalent) is sufficiently below the Planck scale such that the additional supersymmetry-breaking effects mediated by supergravity can be neglected.

In the minimal GMSB approach, there is one effective mass scale, Λ, that determines all low-energy scalar and gaugino mass parameters through loop effects, while the resulting A-parameters are suppressed. In order that the resulting superpartner masses be of order 1 TeV or less, one must have $\Lambda \sim 100$ TeV. The origin of the μ and B-parameters is quite model-dependent, and lies somewhat outside the ansatz of gauge mediated supersymmetry breaking.

The simplest GMSB models appear to be ruled out based on the observed value of the Higgs boson mass. Due to suppressed A parameters, it is difficult to boost the contributions of the radiative corrections in Eq. (15) to obtain a Higgs mass as large as 126 GeV. However, this conflict can be alleviated in more complicated GMSB models [127]. To analyze these generalized GMSB models, it has been especially fruitful to develop model-independent techniques that encompass all known GMSB models [128]. These techniques are well-suited for a comprehensive analysis [129] of the phenomenological profile of gauge mediated supersymmetry breaking.

The gravitino is the LSP in GMSB models, as noted in Section I.2.3. As a result, the next-to-lightest supersymmetric particle (NLSP) now plays a crucial role in the phenomenology of supersymmetric particle production and decays. Note that unlike the LSP, the NLSP can be charged. In GMSB models, the most likely candidates for the NLSP are $\widetilde{\chi}_1^0$ and $\widetilde{\tau}_R^{\pm}$. The NLSP will decay into its superpartner plus a gravitino (*e.g.*, $\widetilde{\chi}_1^0 \to \gamma\widetilde{G}$, $\widetilde{\chi}_1^0 \to Z\widetilde{G}$, $\widetilde{\chi}_1^0 \to h^0\widetilde{G}$ or $\widetilde{\tau}_R^{\pm} \to \tau^{\pm}\widetilde{G}$), with lifetimes and branching ratios that depend on the model parameters. There are also GMSB scenarios in which there are several nearly degenerate so-called co-NLSP's, any one of which can be produced at the penultimate step of a supersymmetric decay chain [130]. For example, in the slepton co-NLSP case, all three right-handed sleptons are close enough in mass and thus can each play the role of the NLSP.

Different choices for the identity of the NLSP and its decay rate lead to a variety of distinctive supersymmetric phenomenologies [54,131]. For example, a long-lived $\widetilde{\chi}_1^0$-NLSP that decays outside collider detectors leads to supersymmetric decay chains with missing energy in association with leptons and/or hadronic jets (this case is indistinguishable from the standard phenomenology of the $\widetilde{\chi}_1^0$-LSP). On the other hand, if $\widetilde{\chi}_1^0 \to \gamma\widetilde{G}$ is the dominant decay mode, and the decay occurs inside the detector, then nearly *all* supersymmetric particle decay chains would contain a photon. In contrast, in the case of a $\widetilde{\tau}_R^{\pm}$-NLSP, the $\widetilde{\tau}_R^{\pm}$ would either be long-lived or would decay inside the detector into a τ-lepton plus missing energy.

I.6.4. The phenomenological MSSM: Of course, any of the theoretical assumptions described in this Section could be wrong and must eventually be tested experimentally. To facilitate the exploration of MSSM phenomena in a more model-independent way while respecting the constraints noted at the beginning of this Section, the phenomenological MSSM (pMSSM) has been introduced [132].

The pMSSM is governed by 19 independent real parameters beyond the Standard Model, which include the three gaugino mass parameters M_1, M_2 and M_3, the Higgs sector parameters m_A and $\tan\beta$, the Higgsino mass parameter μ, five squark and slepton squared-mass parameters for the degenerate first and second generations ($M_{\widetilde{Q}}^2$, $M_{\widetilde{U}}^2$, $M_{\widetilde{D}}^2$, $M_{\widetilde{L}}^2$ and $M_{\widetilde{E}}^2$), the five corresponding squark and slepton squared-mass parameters for the third generation, and three third-generation A-parameters (A_t, A_b and A_τ). As previously noted, the first and second generation A-parameters can be neglected as their phenomenological consequences are negligible.

I.7. Experimental data confronts the MSSM:

At present, there is no evidence for weak-scale supersymmetry from the data analyzed by the LHC experiments. Recent LHC data has been especially effective in ruling out the existence of colored supersymmetric particles (primarily the gluino and the first generation of squarks) with masses below about 1 TeV [13,133]. The precise mass limits are model dependent. For example, higher mass colored superpartners have been ruled out in the context of the CMSSM. In more generic frameworks

of the MSSM, regions of parameter space can be identified in which lighter squarks and gluinos below 1 TeV cannot be definitely ruled out. Details of these constraints can be found in Ref. 13. Additional constraints arise from limits on the contributions of virtual supersymmetric particle exchange to a variety of Standard Model processes [108–110].

In light of the negative results in the search for supersymmetry, one must confront the tension that exists between the theoretical expectations for the magnitude of the supersymmetry-breaking parameters and the non-observation of supersymmetric phenomena.

I.7.1 Naturalness constraints and the little hierarchy:

In Section I, weak-scale supersymmetry was motivated as a natural solution to the hierarchy problem, which could provide an understanding of the origin of the electroweak symmetry-breaking scale without a significant fine-tuning of the fundamental parameters that govern the MSSM. In this context, the soft-supersymmetry-breaking masses must be generally of the order of 1 TeV or below [134]. This requirement is most easily seen in the determination of m_Z by the scalar potential minimum condition. In light of Eq. (4), to avoid the fine-tuning of MSSM parameters, the soft-supersymmetry-breaking squared-masses m_1^2 and m_2^2 and the higgsino squared-mass $|\mu|^2$ should all be roughly of $\mathcal{O}(m_Z^2)$. Many authors have proposed quantitative measures of fine-tuning [134–136]. One of the simplest measures is the one given by Barbieri and Giudice [134],

$$\Delta_i \equiv \left| \frac{\partial \ln m_Z^2}{\partial \ln p_i} \right| , \qquad \Delta \equiv \max\ \Delta_i \, , \tag{21}$$

where the p_i are the MSSM parameters at the high-energy scale M_X, which are set by the fundamental supersymmetry-breaking dynamics. The theory is more fine-tuned as Δ becomes larger.

One can apply the fine-tuning measure to any explicit model of supersymmetry breaking. For example, in the approaches discussed in Section I.6, the p_i are parameters of the model at the energy scale M_X where the soft-supersymmetry-breaking operators are generated by the dynamics of supersymmetry breaking. Renormalization group evolution then determines the values of the parameters appearing in Eq. (4) at the electroweak scale. In this way, Δ is sensitive to all the supersymmetry-breaking parameters of the model (see e.g. Ref. 137).

As anticipated, there is a tension between the present experimental lower limits on the masses of colored supersymmetric particles [138] and the expectation that supersymmetry-breaking is associated with the electroweak symmetry-breaking scale. Moreover, this tension is exacerbated by the observed value of the Higgs mass ($m_h \simeq 126$ GeV), which is not far from the the MSSM upper bound ($m_h \lesssim 135$ GeV) [which depends on the top-squark mass and mixing as noted in Section I.5.2]. If $M_{\rm SUSY}$ characterizes the scale of supersymmetric particle masses, then one would crudely expect $\Delta \sim M_{\rm SUSY}^2/m_Z^2$. For example, if $M_{\rm SUSY} \sim 1$ TeV then there must be at least a $\Delta^{-1} \sim 1\%$ fine-tuning of the MSSM parameters to achieve the observed value of m_Z. This separation of the electroweak symmetry-breaking and supersymmetry-breaking scales is an example of the *little hierarchy problem* [140,141].

However, one must be very cautious when drawing conclusions about the viability of weak-scale supersymmetry to explain the origin of electroweak symmetry breaking [142]. First, one must decide the largest tolerable value of Δ within the framework of weak-scale supersymmetry (should it be $\Delta \sim 10$? 100? 1000?). Second, the fine-tuning parameter Δ depends quite sensitively on the structure of the supersymmetry-breaking dynamics, such as the value of M_X and relations among supersymmetry-breaking parameters in the fundamental high energy theory [143]. For example, in so-called focus point supersymmetry models [144], all squark masses can be as heavy as 5 TeV *without* significant fine-tuning. This can be attributed to a focusing behavior of the renormalization group evolution where certain relations hold among the high-energy values of the scalar squared-mass supersymmetry-breaking parameters.

Among the colored superpartners, the third generation squarks generically have the most significant impact on the naturalness constraints [145], while their masses are the least constrained by the LHC data. Hence, in the absence of any relation between third generation squarks and those of the first two generations, the naturalness constraints due to present LHC data can be considerably weaker than those obtained in the CMSSM. Indeed, models with first and second generation squark masses in the multi-TeV range do not generically require significant fine tuning. Such models have the added benefit that undesirable FCNCs mediated by squark exchange are naturally suppressed [146]. Other MSSM mass spectra that are compatible with moderate fine tuning have been considered in Refs. [133,143,147].

The lower bounds on squark and gluino masses may not be as large as suggested by the experimental analyses based on the CMSSM or simplified models [148]. For example, mass bounds for the gluino and the first and second generation squarks based on the CMSSM can often be evaded in alternative or extended MSSM models, *e.g.*, compressed supersymmetry [149] and stealth supersymmetry [150]. Moreover, experimental limits on the masses for the third generation squarks (which enter the fine-tuning considerations more directly) and color-neutral supersymmetric particles are less constrained than the masses of other colored supersymmetric states.

Finally, one can also consider extensions of the MSSM in which the degree of fine-tuning is relaxed. For example, it has already been noted in Section I.5.2 that it is possible to accommodate the observed Higgs mass more easily in the NMSSM due to contributions to m_h^2 proportional to the parameter λ. This means that we do not have to rely on a contribution to the Higgs mass from the radiative corrections to boost the Higgs mass sufficiently above its tree-level bound. In turn, this allows for smaller top squark masses, which are more consistent with the demands of naturalness. The reduction of the fine-tuning in various NMSSM models was initially advocated in Ref. 151, and

more recently has been exhibited in Refs. [101,152]. Naturalness can also be relaxed in extended supersymmetric models with vector-like quarks [153] and in gauge extensions of the MSSM [154].

Thus, it is premature to conclude, after the first few years of LHC operation at just above half the design energy and with less than a quarter of the design luminosity, that weak-scale supersymmetry is on the verge of exclusion.

I.7.2 Constraints from virtual exchange of supersymmetric particles

There are a number of low-energy measurements that are sensitive to the effects of new physics through indirect searches via supersymmetric loop effects. For example, the virtual exchange of supersymmetric particles can contribute to the muon anomalous magnetic moment, $a_\mu \equiv \frac{1}{2}(g-2)_\mu$, as reviewed in Ref. 155. The Standard Model prediction for a_μ exhibits a 3.6σ deviation from the experimentally observed value [156]. This discrepancy is difficult to accommodate in the constrained supersymmetry models of Section I.6.2 and I.6.3 given the present sparticle mass bounds. Nevertheless, there are regions of the more general pMSSM parameter space that are consistent with the observed value of a_μ [157].

The rare inclusive decay $b \to s\gamma$ also provides a sensitive probe to the virtual effects of new physics beyond the Standard Model. Recent experimental measurements of $B \to X_s+\gamma$ [159] are in very good agreement with the theoretical Standard Model predictions of Ref. 160. Since supersymmetric loop corrections can contribute an observable shift from the Standard Model predictions, the absence of any significant deviations places useful constraints on the MSSM parameter space [161].

The rare decay $B_s \to \mu^+\mu^-$ is especially sensitive to supersymmetric loop effects, with some loop contributions scaling as $\tan^6\beta$ when $\tan\beta \gg 1$ [162]. The recent observation of this rare decay mode by the LHCb Collab. [163] is consistent with the predicted Standard Model rate. The absence of a *significant* deviation in these and other B-physics observables from their Standard Model predictions also places useful constraints on the MSSM parameter space [110,139,164].

Finally, we note that the constraints from precision electroweak observables [165] are easily accommodated in models of weak-scale supersymmetry [166]. Thus, robust regions of the MSSM parameter space, compatible with the results of direct and indirect searches for supersymmetry, remain unconstrained.

I.8. Massive neutrinos in low-energy supersymmetry: In the minimal Standard Model and its supersymmetric extension, there are no right-handed neutrinos, and Majorana mass terms for the left-handed neutrinos are absent. However, given the overwhelming evidence for neutrino masses and mixing [167,168], any viable model of fundamental particles must provide a mechanism for generating neutrino masses [169]. In extended supersymmetric models, various mechanisms exist for producing massive neutrinos [170]. Although one can devise models for generating massive Dirac neutrinos [171], the most common approaches for incorporating neutrino masses are based on L-violating supersymmetric extensions of the MSSM, which generate massive Majorana neutrinos. Two classes of L-violating supersymmetric models will now be considered.

I.8.1. The supersymmetric seesaw: Neutrino masses can be incorporated into the Standard Model by introducing SU(3)×SU(2)×U(1) singlet right-handed neutrinos (ν_R) and super-heavy Majorana masses (typically near the grand unification mass scale) for the ν_R. In addition, one must also include a standard Yukawa couplings between the lepton doublets, the Higgs doublet, and the ν_R. The Higgs vacuum expectation value then induces an off-diagonal ν_L–ν_R masses on the order of the electroweak scale. Diagonalizing the neutrino mass matrix (in the three-generation model) yields three superheavy neutrino states, and three very light neutrino states that are identified with the light neutrinos observed in nature. This is the seesaw mechanism [172].

It is straightforward to construct a supersymmetric generalization of the seesaw model of neutrino masses [173,174]. In the seesaw-extended Standard Model, lepton number is broken due to the presence of $\Delta L = 2$ terms in the Lagrangian (which include the Majorana mass terms for the superheavy neutrinos). Consequently, the seesaw-extended MSSM conserves R-parity. The supersymmetric analogue of the Majorana neutrino mass term in the sneutrino sector leads to sneutrino–antisneutrino mixing phenomena [174,175].

I.8.2. R-parity-violating supersymmetry: In order to incorporate massive neutrinos in supersymmetric models while retaining the minimal particle content of the MSSM, one must relax the assumption of R-parity invariance. The most general R-parity-violating (RPV) model involving the MSSM spectrum introduces many new parameters to both the supersymmetry-conserving and the supersymmetry-breaking sectors [176]. Each new interaction term violates either B or L conservation. For example, starting from the MSSM superpotential previously given in Eq. (1) [suitably generalized to three generations of quarks, leptons and their superpartners], consider the effect of adding the following new terms:

$$(\lambda_L)_{pmn}\widehat{L}_p\widehat{L}_m\widehat{E}^c_n + (\lambda'_L)_{pmn}\widehat{L}_p\widehat{Q}_m\widehat{D}^c_n + (\lambda_B)_{pmn}\widehat{U}^c_p\widehat{D}^c_m\widehat{D}^c_n\,, \quad (22)$$

where p, m, and n are generation indices, and gauge group indices are suppressed. Eq. (22) yields new scalar-fermion Yukawa couplings consisting of all possible combinations involving two Standard Model fermions and one scalar superpartner.

Note that the term in Eq. (22) proportional to λ_B violates B, while the other two terms violate L. Even if all the terms of Eq. (22) are absent, there is one more possible supersymmetric source of R-parity violation. Namely, one can add a term to the superpotential, $(\mu_L)_p\widehat{H}_u\widehat{L}_p$, where $\widehat{H}_u$ is the $Y = 1$ Higgs doublet superfield given in Table 1. This term is the RPV generalization of the higgsino mass parameter μ of the MSSM, in which the $Y = -1$ Higgs/higgsino supermultiplet $\widehat{H}_d$ is replaced by the slepton/lepton supermultiplet $\widehat{L}_p$. The RPV-parameters $(\mu_L)_p$ also violate L.

Phenomenological constraints derived from data on various low-energy B- and L-violating processes can be used to establish limits on each of the coefficients $(\lambda_L)_{pmn}$, $(\lambda'_L)_{pmn}$, and $(\lambda_B)_{pmn}$ taken one at a time [176,177]. If more than one coefficient is simultaneously non-zero, then the limits are in general more complicated [178]. All possible RPV terms cannot be simultaneously present and unsuppressed; otherwise the proton decay rate would be many orders of magnitude larger than the present experimental bound. One way to avoid proton decay is to impose B or L invariance (either one alone would suffice). Otherwise, one must accept the requirement that certain RPV coefficients must be extremely suppressed.

One particularly interesting class of RPV models is one in which B is conserved, but L is violated. It is possible to enforce baryon number conservation (and the stability of the proton), while allowing for lepton-number-violating interactions by imposing a discrete $\mathbf{Z_3}$ baryon *triality* symmetry on the low-energy theory [179], in place of the standard $\mathbf{Z_2}$ R-parity. Since the distinction between the Higgs and matter supermultiplets is lost in RPV models where L is violated, the mixing of sleptons and Higgs bosons, the mixing of neutrinos and neutralinos, and the mixing of charged leptons and charginos are now possible, leading to more complicated mass matrices and mass eigenstates than in the MSSM. Recent attempts to fit neutrino masses and mixing in this framework can be found in Ref. 180.

Alternatively, one can consider imposing a lepton parity such that all lepton superfields are odd [181,182]. In this case, only the B-violating term in Eq. (22) survives, and L is conserved. Models of this type have been considered in Ref. 183. Since L is conserved, the mixing of the lepton and Higgs superfields is forbidden. However, one expects that lepton parity cannot be exact due to quantum gravity effects. Remarkably, the standard $\mathbf{Z_2}$ R-parity and the $\mathbf{Z_3}$ baryon triality are stable with respect to quantum gravity effects, as they can be identified as residual discrete symmetries that arise from broken non-anomalous gauge symmetries [181].

The supersymmetric phenomenology of the RPV models exhibits features that are distinct from that of the MSSM [176]. The LSP is no longer stable, which implies that not all supersymmetric decay chains must yield missing-energy events at colliders. Indeed, the sparticle mass bounds obtained in searches for R-parity-conserving supersymmetry can be considerably relaxed in certain RPV models due to the absence of large missing transverse energy signatures [184]. This can alleviate some of the tension with naturalness discussed in Section I.7.1.

Nevertheless, the loss of the missing-energy signature is often compensated by other striking signals (which depend on which R-parity-violating parameters are dominant). For example, supersymmetric particles in RPV models can be singly produced (in contrast to R-parity-conserving models where supersymmetric particles must be produced in pairs). The phenomenology of pair-produced supersymmetric particles is also modified in RPV models due to new decay chains not present in R-parity-conserving supersymmetry models [176].

In RPV models with lepton number violation (these include low-energy supersymmetry models with baryon triality mentioned above), both $\Delta L=1$ and $\Delta L=2$ phenomena are allowed, leading to neutrino masses and mixing [185], neutrinoless double-beta decay [186], sneutrino-antisneutrino mixing [187], and resonant s-channel production of sneutrinos in e^+e^- collisions [188] and charged sleptons in $p\bar{p}$ and pp collisions [189].

I.9. Extensions beyond the MSSM: Extensions of the MSSM have been proposed to solve a variety of theoretical problems. One such problem involves the μ parameter of the MSSM. Although μ is a supersymmetric-*preserving* parameter, it must be of order the effective supersymmetry-breaking scale of the MSSM to yield a consistent supersymmetric phenomenology [190]. Any natural solution to the so-called μ-problem must incorporate a symmetry that enforces $\mu = 0$ and a small symmetry-breaking parameter that generates a value of μ that is not parametrically larger than the effective supersymmetry-breaking scale [191]. A number of proposed mechanisms in the literature (*e.g.*, see Refs. [190–193]) provide concrete examples of a natural solution to the μ-problem of the MSSM.

In extensions of the MSSM, new compelling solutions to the μ-problem are possible. For example, one can replace μ by the vacuum expectation value of a new SU(3)×SU(2)×U(1) singlet scalar field. This is the NMSSM, which yields phenomena that were briefly discussed in Sections I.4, I.5 and I.7. The NMSSM superpotential consists only of trilinear terms whose coefficients are dimensionless. There are some advantages to extending the NMSSM further to the USSM [93] by adding a new broken U(1) gauge symmetry [194], under which the singlet field is charged.

Alternatively, one can consider a generalized version of the NMSSM (called the GNMSSM in Ref. 152), where all possible renormalizable terms in the superpotential are allowed, which yields new supersymmetric mass terms (analogous to the μ term of the MSSM). Although the GNMSSM does not solve the μ-problem, it does exhibit regions of parameter space in which the degree of fine-tuning is relaxed, as discussed in Section I.7.1.

It is also possible to add higher dimensional Higgs multiplets, such as Higgs triplet superfields [195], provided a custodial-symmetric model (in which the ρ-parameter of precision electroweak physics is close to 1 [165]) can be formulated. Such models can provide a rich phenomenology of new signals for future LHC studies.

All supersymmetric models discussed in this review possess self-conjugate fermions—the Majorana gluinos and neutralinos. However, it is possible to add additional chiral superfields in the adjoint representation. The spin-1/2 components of these new superfields can pair up with the gauginos to form Dirac gauginos [196,197]. Such states appear in models of so-called supersoft supersymmetry breaking [198], in some generalized GMSB models [199] and in R-symmetric supersymmetry [27,200]. Such approaches often lead to improved naturalness and/or significantly relaxed flavor constraints. The

implications of models of Dirac gauginos on the observed Higgs boson mass and its properties is addressed in Ref. 201.

For completeness, we briefly note other MSSM extensions considered in the literature. These include an enlarged electroweak gauge group beyond SU(2)×U(1) [202]; and/or the addition of new (possibly exotic) matter supermultiplets such as vector-like fermions and their superpartners [153,203].

References

1. The early history of supersymmetry and a guide to the original literature can be found in *The Supersymmetric World—The Beginnings of the Theory*, edited by G. Kane and M. Shifman (World Scientific, Singapore, 2000).
2. R. Haag, J.T. Lopuszanski, and M. Sohnius, Nucl. Phys. **B88**, 257 (1975);
S.R. Coleman and J. Mandula, Phys. Rev. **159** (1967) 1251.
3. H.P. Nilles, Phys. Reports **110**, 1 (1984).
4. P. Nath, R. Arnowitt, and A.H. Chamseddine, *Applied $N = 1$ Supergravity* (World Scientific, Singapore, 1984).
5. S.P. Martin, in *Perspectives on Supersymmetry II*, edited by G.L. Kane (World Scientific, Singapore, 2010) pp. 1–153; see `http://zippy.physics.niu.edu/primer.html` for the latest version and errata.
6. S. Weinberg, *The Quantum Theory of Fields, Volume III: Supersymmetry* (Cambridge University Press, Cambridge, UK, 2000);
P. Binétruy, *Supersymmetry : Theory, Experiment, and Cosmology* (Oxford University Press, Oxford, UK, 2006).
7. E. Witten, Nucl. Phys. **B188**, 513 (1981).
8. S. Dimopoulos and H. Georgi, Nucl. Phys. **B193**, 150 (1981).
9. N. Sakai, Z. Phys. **C11**, 153 (1981);
R.K. Kaul, Phys. Lett. **109B**, 19 (1982);
R.K. Kaul and M. Parthasarathi, Nucl. Phys. **B199**, 36 (1982).
10. L. Susskind, Phys. Reports **104**, 181 (1984).
11. L. Girardello and M. Grisaru, Nucl. Phys. **B194**, 65 (1982).
12. L.J. Hall and L. Randall, Phys. Rev. Lett. **65**, 2939 (1990);
I. Jack and D.R.T. Jones, Phys. Lett. **B457**, 101 (1999).
13. O. Buchmüller and P. de Jong, "Supersymmetry Part II (Experiment)," in the 2013 web edition of the *Review of Particle Physics* at `http://pdg.lbl.gov`. See also there *Particle Listings: Other Searches–Supersymmetric Particles* .
14. For a review, see N. Polonsky, *Supersymmetry: Structure and phenomena. Extensions of the standard model*, Lect. Notes Phys. **M68**, 1 (2001).
15. G. Bertone, D. Hooper, and J. Silk, Phys. Reports **405**, 279 (2005).
16. D. Hooper, "TASI 2008 Lectures on Dark Matter," in *The Dawn of the LHC Era, Proceedings of the 2008 Theoretical and Advanced Study Institute in Elementary Particle Physics,* Boulder, Colorado, 2–27 June 2008, edited by Tao Han (World Scientific, Singapore, 2009).
17. H. Pagels and J.R. Primack, Phys. Rev. Lett. **48**, 223 (1982).
18. H. Goldberg, Phys. Rev. Lett. **50**, 1419 (1983) [erratum: **103**, 099905 (2009)].
19. J. Ellis *et al.*, Nucl. Phys. **B238**, 453 (1984).
20. G. Jungman, M. Kamionkowski, and K. Griest, Phys. Reports **267**, 195 (1996);
K. Griest and M. Kamionkowski, Phys. Reports **333**, 167 (2000).
21. F.D. Steffen, Eur. Phys. J. **C59**, 557 (2009).
22. M. Drees and G. Gerbier, "Dark Matter," in the 2013 web edition of the *Review of Particle Physics* at `pdg.lbl.gov`.
23. For a review, see J.M. Cline, in *Particle Physics and Cosmology: the Fabric of Spacetime*, edited by F. Bernardeau, C. Grojean and J. Dalibard, Proceedings of Les Houches Summer School **86**, 53–116 (2007).
24. A.D. Sakharov, JETP Lett. **5**, 24 (1967); Sov. Phys. JETP **49**, 594 (1979).
25. Reviews of electroweak baryogyenesis can be found in A.G. Cohen, D. Kaplan, and A. Nelson, Ann. Rev. Nucl. Part. Sci. **43**, 27 (1993);
D.E. Morrissey and M.J. Ramsey-Musolf, New J. Phys. **14**, 125003 (2012).
26. T. Cohen, D.E. Morrissey, and A. Pierce, Phys. Rev. **D86**, 013009 (2012);
D. Curtin, P. Jaiswal, and P. Meade, JHEP **1208**, 005 (2012);
M. Carena *et al.*, JHEP **1302**, 001 (2013).
27. U. Sarkar and R. Adhikari, Phys. Rev. **D55**, 3836 (1997);
R. Fok *et al.*, Phys. Rev. **D87**, 055018 (2013).
28. H.E. Haber and G.L. Kane, Phys. Reports **117**, 75 (1985).
29. M. Drees, R. Godbole, and P. Roy, *Theory and Phenomenology of Sparticles* (World Scientific, Singapore, 2005);
H. Baer and X. Tata, *Weak Scale Supersymmetry: from Superfields to Scattering Events* (Cambridge University Press, Cambridge, UK, 2006);
I.J.R. Aitchison, *Supersymmetry in Particle Physics: an elementary introduction* (Cambridge University Press, Cambridge, UK, 2007).
30. P. Fayet, Nucl. Phys. **B90**, 104 (1975).
31. K. Inoue *et al.*, Prog. Theor. Phys. **67**, 1889 (1982);
R. Flores and M. Sher, Ann. Phys. (NY) **148**, 95 (1983).
32. J.F. Gunion and H.E. Haber, Nucl. Phys. **B272**, 1 (1986) [erratum: **B402**, 567 (1993)].
33. I. Buchbinder, S. Kuzenko, and J. Yarevskaya, Nucl. Phys. **B411**, 665 (1994);
I. Antoniadis, E. Dudas, and D.M. Ghilencea, JHEP **0803**, 045 (2008).
34. For an overview of the theory and models of the soft-supersymmetry-breaking Lagrangian, see D.J.H. Chung *et al.*, Phys. Reports **407**, 1 (2005).
35. J. Ellis *et al.*, Phys. Rev. **D39**, 844 (1989);
U. Ellwanger and C. Hugonie, Eur. J. Phys. **C25**, 297 (2002);
U. Ellwanger, C. Hugonie, and A.M. Teixeira, Phys. Reports **496**, 1 (2010);
M. Maniatis, Int. J. Mod. Phys. A **25**, 3505 (2010).
36. P. Fayet, Phys. Lett. **69B**, 489 (1977);
G. Farrar and P. Fayet, Phys. Lett. **76B**, 575 (1978).
37. P. Fayet, Phys. Lett. **84B**, 421 (1979); Phys. Lett. **86B**, 272 (1979).

38. D.Z. Freedman and A. Van Proeyen, *Supergravity* (Cambridge University Press, Cambridge, UK, 2012).
39. S. Deser and B. Zumino, Phys. Rev. Lett. **38**, 1433 (1977);
E. Cremmer *et al.*, Phys. Lett. **79B**, 231 (1978).
40. R. Casalbuoni *et al.*, Phys. Lett. **B215**, 313 (1988); Phys. Rev. **D39**, 2281 (1989);
A.L. Maroto and J.R. Pelaez, Phys. Rev. **D62**, 023518 (2000).
41. Z. Komargodski and N. Seiberg, JHEP **0909**, 066 (2009);
I. Antoniadis *et al.*, Theor. Math. Phys. **170**, 26 (2012).
42. A.H. Chamseddine, R. Arnowitt, and P. Nath, Phys. Rev. Lett. **49**, 970 (1982);
R. Barbieri, S. Ferrara, and C.A. Savoy, Phys. Lett. **119B**, 343 (1982);
L. Ibáñez, Nucl. Phys. **B218**, 514 (1982);
H.-P. Nilles, M. Srednicki, and D. Wyler, Phys. Lett. **120B**, 346 (1983); **124B**, 337 (1983);
E. Cremmer, P. Fayet, and L. Girardello, Phys. Lett. **122B**, 41 (1983);
N. Ohta, Prog. Theor. Phys. **70**, 542 (1983).
43. L. Alvarez-Gaumé, J. Polchinski, and M.B. Wise, Nucl. Phys. **B221**, 495 (1983).
44. L.J. Hall, J. Lykken, and S. Weinberg, Phys. Rev. **D27**, 2359 (1983).
45. S.K. Soni and H.A. Weldon, Phys. Lett. **126B**, 215 (1983);
Y. Kawamura, H. Murayama, and M. Yamaguchi, Phys. Rev. **D51**, 1337 (1995).
46. See, *e.g.*, A. Brignole, L.E. Ibáñez, and C. Munoz, in *Perspectives on Supersymmetry II*, edited by G.L. Kane (World Scientific, Singapore, 2010) pp. 244–268.
47. A.B. Lahanas and D.V. Nanopoulos, Phys. Reports **145**, 1 (1987).
48. J.L. Feng, A. Rajaraman, and F. Takayama, Phys. Rev. Lett. **91**, 011302 (2003); Phys. Rev. **D68**, 063504 (2003); Gen. Rel. Grav. **36**, 2575 (2004).
49. L. Randall and R. Sundrum, Nucl. Phys. **B557**, 79 (1999).
50. F. D'Eramo, J. Thaler, and Z. Thomas, JHEP **1206**, 151 (2012); JHEP **1309**, 125 (2013);
S.P. de Alwis, Phys. Rev. **D77**, 105020 (2008); JHEP **1301**, 006 (2013).
51. See *e.g.*, I. Jack, D.R.T. Jones, and R. Wild, Phys. Lett. **B535**, 193 (2002);
B. Murakami and J.D. Wells, Phys. Rev. **D68**, 035006 (2003);
R. Kitano, G.D. Kribs, and H. Murayama, Phys. Rev. **D70**, 035001 (2004);
R. Hodgson *et al.*, Nucl. Phys. **B728**, 192 (2005);
D.R.T. Jones and G.G. Ross, Phys. Lett. **B642**, 540 (2006).
52. M. Dine, W. Fischler, and M. Srednicki, Nucl. Phys. **B189**, 575 (1981);
S. Dimopoulos and S. Raby, Nucl. Phys. **B192**, 353 (1982); **B219**, 479 (1983);
M. Dine and W. Fischler, Phys. Lett. **110B**, 227 (1982);
C. Nappi and B. Ovrut, Phys. Lett. **113B**, 175 (1982);
L. Alvarez-Gaumé, M. Claudson, and M. Wise, Nucl. Phys. **B207**, 96 (1982).
53. M. Dine and A.E. Nelson, Phys. Rev. **D48**, 1277 (1993);
M. Dine, A.E. Nelson, and Y. Shirman, Phys. Rev. **D51**, 1362 (1995);
M. Dine *et al.*, Phys. Rev. **D53**, 2658 (1996).
54. G.F. Giudice and R. Rattazzi, Phys. Reports **322**, 419 (1999).
55. E. Poppitz and S.P. Trivedi, Phys. Rev. **D55**, 5508 (1997);
H. Murayama, Phys. Rev. Lett. **79**, 18 (1997);
M.A. Luty and J. Terning, Phys. Rev. **D57**, 6799 (1998);
K. Agashe, Phys. Lett. **B435**, 83 (1998);
N. Arkani-Hamed, J. March-Russell, and H. Murayama, Nucl. Phys. **B509**, 3 (1998);
C. Csaki, Y. Shirman, and J. Terning, JHEP **0705**, 099 (2007);
M. Ibe and R. Kitano, Phys. Rev. **D77**, 075003 (2008).
56. M. Kawasaki *et al.*, Phys. Rev. **D78**, 065011 (2008).
57. M.J. Strassler and K. M. Zurek, Phys. Lett. **B651**, 374 (2007);
T. Han *et al.*, JHEP **0807**, 008 (2008).
58. M.J. Strassler, `arXiv:hep-ph/0607160`;
K.M. Zurek, Phys. Rev. **D79**, 115002 (2009).
59. See *e.g.*, M. Quiros, in *Particle Physics and Cosmology: The Quest for Physics Beyond the Standard Model(s), Proceedings of the 2002 Theoretical Advanced Study Institute in Elementary Particle Physics (TASI 2002),* edited by H.E. Haber and A.E. Nelson (World Scientific, Singapore, 2004) pp. 549–601;
C. Csaki, in *ibid.*, pp. 605–698.
60. See, *e.g.*, J. Parsons and A. Pomarol, "Extra Dimensions," in the 2013 web edition of the *Review of Particle Physics* at `http://pdg.lbl.gov`.
61. See *e.g.*, V.A. Rubakov, Phys. Usp. **44**, 871 (2001);
J. Hewett and M. Spiropulu, Ann. Rev. Nucl. Part. Sci. **52**, 397 (2002).
62. Z. Chacko, M.A. Luty, and E. Ponton, JHEP **0007**, 036 (2000);
D.E. Kaplan, G.D. Kribs, and M. Schmaltz, Phys. Rev. **D62**, 035010 (2000);
Z. Chacko *et al.*, JHEP **0001**, 003 (2000).
63. J. Scherk and J.H. Schwarz, Phys. Lett. **82B**, 60 (1979); Nucl. Phys. **B153**, 61 (1979).
64. See, *e.g.*, R. Barbieri, L.J. Hall, and Y. Nomura, Phys. Rev. **D66**, 045025 (2002); Nucl. Phys. **B624**, 63 (2002).
65. N. Arkani-Hamed and S. Dimopoulos, JHEP **0506**, 073 (2005);
G.F. Giudice and A. Romanino, Nucl. Phys. **B699**, 65 (2004) [erratum: **B706**, 487 (2005)].
66. G. Aad *et al.* [ATLAS Collab.], Phys. Lett. **B716**, 1 (2012);
S. Chatrchyan *et al.* [CMS Collab.], Phys. Lett. **B716**, 30 (2012).
67. M. Carena, *et al.*, "The Higgs Boson H^0," in the 2013 web edition of the *Review of Particle Physics* at `pdg.lbl.gov`.
68. S. Khalil, Int. J. Mod. Phys. **A18**, 1697 (2003).
69. G.F. Giudice and A. Strumia, Nucl. Phys. **B858**, 63 (2012).
70. A. Arvanitaki *et al.*, JHEP **1302**, 126 (2013);
N. Arkani-Hamed *et al.*, `arXiv:1212.6971 [hep-ph]`.
71. L.J. Hall and Y. Nomura, JHEP **1201**, 082 (2012);
M. Ibe and T.T. Yanagida, Phys. Lett. **B709**, 374 (2012).
72. H.E. Haber, in *Recent Directions in Particle Theory, Proceedings of the 1992 Theoretical Advanced Study Institute*

in Particle Physics, edited by J. Harvey and J. Polchinski (World Scientific, Singapore, 1993) pp. 589–686.

73. J.M. Frere, D.R.T. Jones, and S. Raby, Nucl. Phys. **B222**, 11 (1983);
J.P. Derendinger and C.A. Savoy, Nucl. Phys. **B237**, 307 (1984);
J.F. Gunion, H.E. Haber, and M. Sher, Nucl. Phys. **B306**, 1 (1988);
J.A. Casas, A. Lleyda, and C. Munoz, Nucl. Phys. **B471**, 3 (1996).
74. S.P. Martin, Phys. Rev. **D61**, 035004 (2000).
75. S. Dimopoulos and D. Sutter, Nucl. Phys. **B452**, 496 (1995);
D.W. Sutter, Stanford Ph. D. thesis, `hep-ph/9704390`.
76. H.E. Haber, Nucl. Phys. B (Proc. Suppl.) **62A-C**, 469 (1998).
77. R.M. Barnett, J.F. Gunion, and H.E. Haber, Phys. Lett. **B315**, 349 (1993);
H. Baer, X. Tata, and J. Woodside, Phys. Rev. **D41**, 906 (1990).
78. S.M. Bilenky, E.Kh. Khristova, and N.P. Nedelcheva, Phys. Lett. **B161**, 397 (1985); Bulg. J. Phys. **13**, 283 (1986);
G. Moortgat-Pick and H. Fraas, Eur. Phys. J. **C25**, 189 (2002).
79. J. Rosiek, Phys. Rev. **D41**, 3464 (1990) [erratum: `hep-ph/9511250`]. The most recent corrected version of this manuscript can be found on the author's webpage, `www.fuw.edu.pl/~rosiek/physics/prd41.html`.
80. J. Alwall *et al.*, JHEP **0709**, 028 (2007). The MadGraph homepage is located at `madgraph.hep.uiuc.edu/`.
81. T. Hahn, Comput. Phys. Commun. **140**, 418 (2001);
T. Hahn and C. Schappacher, Comput. Phys. Commun. **143**, 54 (2002). The FeynArts homepage is located at `www.feynarts.de/`.
82. A. Pukhov *et al.*, INP MSU report 98-41/542 (`arXiv: hep-ph/9908288`);
E. Boos *et al.* [CompHEP Collab.], Nucl. Instrum. Meth. A534, 250 (2004). The CompHEP homepage is located at `http://comphep.sinp.msu.ru`.
83. D.M. Pierce *et al.*, Nucl. Phys. **B491**, 3 (1997).
84. P. Skands *et al.*, JHEP **07** 036 (2004);
B.C. Allanach *et al.*, Comput. Phys. Commun. **180**, 8 (2009). The Supersymmetry Les Houches Accord homepage is located at `home.fnal.gov/~skands/slha/`.
85. For further details, see *e.g.*, Appendix C of Ref. 28 and Appendix A of Ref. 32.
86. J.L. Kneur and G. Moultaka, Phys. Rev. **D59**, 015005 (1999).
87. S.Y. Choi *et al.*, Eur. Phys. J. **C14**, 535 (2000).
88. R.A. Horn and C.R. Johnson, *Matrix Analysis*, 2nd Edition (Cambridge University Press, Cambridge, UK, 2003).
89. H.K. Dreiner, H.E. Haber, and S.P. Martin, Phys. Reports **494**, 1 (2010).
90. S.Y. Choi *et al.*, Eur. Phys. J. **C22**, 563 (2001); **C23**, 769 (2002).
91. G.J. Gounaris, C. Le Mouel, and P.I. Porfyriadis, Phys. Rev. **D65**, 035002 (2002);
G.J. Gounaris and C. Le Mouel, Phys. Rev. **D66**, 055007 (2002).
92. T. Takagi, Japan J. Math. **1**, 83 (1925).
93. S.Y. Choi *et al.*, Nucl. Phys. **B778**, 85 (2007).
94. M.M. El Kheishen, A.A. Aboshousha, and A.A. Shafik, Phys. Rev. **D45**, 4345 (1992);
M. Guchait, Z. Phys. **C57**, 157 (1993) [erratum: **C61**, 178 (1994)].
95. T. Hahn, preprint MPP-2006-85, `physics/0607103`.
96. K. Hikasa and M. Kobayashi, Phys. Rev. **D36**, 724 (1987);
F. Gabbiani and A. Masiero, Nucl. Phys. **B322**, 235 (1989);
Ph. Brax and C.A. Savoy, Nucl. Phys. **B447**, 227 (1995).
97. J. Ellis and S. Rudaz, Phys. Lett. **128B**, 248 (1983);
F. Browning, D. Chang, and W.Y. Keung, Phys. Rev. **D64**, 015010 (2001);
A. Bartl *et al.*, Phys. Lett. **B573**, 153 (2003); Phys. Rev. **D70**, 035003 (2004).
98. J.F. Gunion *et al.*, *The Higgs Hunter's Guide* (Westview Press, Boulder, CO, 2000);
M. Carena and H.E. Haber, Prog. Part. Nucl. Phys. **50**, 63 (2003);
A. Djouadi, Phys. Reports **459**, 1 (2008).
99. P. Bechtle *et al.*, Eur. Phys. J. **C73**, 2354 (2013); M. Carena *et al.*, Eur. Phys. J. **C73**, 2552 (2013).
100. H.E. Haber and M. Sher, Phys. Rev. **D35**, 2206 (1987).
101. L.J. Hall, D. Pinner, and J.T. Ruderman, JHEP **1204**, 131 (2012).
102. H.E. Haber and R. Hempfling, Phys. Rev. Lett. **66**, 1815 (1991);
Y. Okada, M. Yamaguchi, and T. Yanagida, Prog. Theor. Phys. **85**, 1 (1991);
J. Ellis, G. Ridolfi, and F. Zwirner, Phys. Lett. **B257**, 83 (1991).
103. See, *e.g.*, G. Degrassi *et al.*, Eur. Phys. J. **C28**, 133 (2003);
S.P. Martin, Phys. Rev. **D75**, 055005 (2007);
P. Kant *et al.*, JHEP **1008**, 104 (2010).
104. A. Pilaftsis and C.E.M. Wagner, Nucl. Phys. **B553**, 3 (1999);
D.A. Demir, Phys. Rev. **D60**, 055006 (1999);
S.Y. Choi, M. Drees, and J.S. Lee, Phys. Lett. **B481**, 57 (2000);
M. Carena *et al.*, Nucl. Phys. **B586**, 92 (2000); Phys. Lett. **B495**, 155 (2000); Nucl. Phys. **B625**, 345 (2002);
M. Frank *et al.*, JHEP **0702**, 047 (2007);
S. Heinemeyer *et al.*, Phys. Lett. **B652**, 300 (2007).
105. W. Fischler, S. Paban, and S. Thomas, Phys. Lett. **B289**, 373 (1992);
S.M. Barr, Int. J. Mod. Phys. **A8**, 209 (1993);
T. Ibrahim and P. Nath, Phys. Rev. **D58**, 111301 (1998) [erratum: **D60**, 099902 (1999)];
M. Brhlik, G.J. Good, and G.L. Kane, Phys. Rev. **D59**, 115004 (1999);
V.D. Barger *et al.*, Phys. Rev. **D64**, 056007 (2001);
S. Abel, S. Khalil, and O. Lebedev, Nucl. Phys. **B606**, 151 (2001);
K.A. Olive *et al.*, Phys. Rev. **D72**, 075001 (2005);
G.F. Giudice and A. Romanino, Phys. Lett. **B634**, 307 (2006).
106. A. Masiero and L. Silvestrini, in *Perspectives on Supersymmetry*, edited by G.L. Kane (World Scientific, Singapore, 1998) pp. 423–441.

107. M. Pospelov and A. Ritz, Annals Phys. **318**, 119 (2005).
108. See, *e.g.*, F. Gabbiani *et al.*, Nucl. Phys. **B477**, 321 (1996);
A. Masiero, and O. Vives, New J. Phys. **4**, 1 (2002).
109. For a review and references to the original literature, see: M.J. Ramsey-Musolf and S. Su, Phys. Reports **456**, 1 (2008).
110. M. Carena, A. Menon and C.E.M. Wagner, Phys. Rev. **D79**, 075025 (2009);
S. Jager, Eur. Phys. J. **C59**, 497 (2009);
W. Altmannshofer *et al.*, Nucl. Phys. **B830**, 17 (2010).
111. M.B. Einhorn and D.R.T. Jones, Nucl. Phys. **B196**, 475 (1982).
112. For a review, see R.N. Mohapatra, in *Particle Physics 1999*, ICTP Summer School in Particle Physics, Trieste, Italy, edited by G. Senjanovic and A.Yu. Smirnov (World Scientific, Singapore, 2000) pp. 336–394;
W.J. Marciano and G. Senjanovic, Phys. Rev. **D25**, 3092 (1982).
113. L.E. Ibáñez and G.G. Ross, Phys. Lett. **B110**, 215 (1982).
114. J. Abdullah *et al.* [DELPHI Collab.], Eur. Phys. J. **C31**, 421 (2004).
115. H.K. Dreiner *et al.*, Eur. Phys. J. **C62**, 547 (2009).
116. G.F. Giudice *et al.*, JHEP **9812**, 027 (1998);
A. Pomarol and R. Rattazzi, JHEP **9905**, 013 (1999);
D.W. Jung and J.Y. Lee, JHEP **0903**, 123 (2009).
117. J.F. Gunion and H.E. Haber, Phys. Rev. **D37**, 2515 (1988);
S.Y. Choi, M. Drees, and B. Gaissmaier, Phys. Rev. **D70**, 014010 (2004).
118. J.L. Feng *et al.*, Phys. Rev. Lett. **83**, 1731 (1999);
J.F. Gunion and S. Mrenna, Phys. Rev. **D62**, 015002 (2000).
119. T. Gherghetta, G.F. Giudice, and J.D. Wells, Nucl. Phys. **B559**, 27 (1999).
120. M. Endo, M. Yamaguchi, and K. Yoshioka, Phys. Rev. **D72**, 015004 (2005);
K. Choi, K.S. Jeong, and K.-I. Okumura, JHEP **0509**, 039 (2005);
O. Loaiza-Brito *et al.*, AIP Conf. Proc. **805**, 198 (2006).
121. See *e.g.*, G. D'Ambrosio *et al.*, Nucl. Phys. **B465**, 155 (2002).
122. For a review of minimal flavor violation in supersymmetric theories, see C. Smith, Acta Phys. Polon. Supp. **3**, 53 (2010).
123. M. Drees and S.P. Martin, in *Electroweak Symmetry Breaking and New Physics at the TeV Scale*, edited by T. Barklow *et al.* (World Scientific, Singapore, 1996) pp. 146–215.
124. J.R. Ellis *et al.*, Phys. Lett. **B573**, 162 (2003); Phys. Rev. **D70**, 055005 (2004).
125. L.E. Ibáñez and D. Lüst, Nucl. Phys. **B382**, 305 (1992);
B. de Carlos, J.A. Casas, and C. Munoz, Phys. Lett. **B299**, 234 (1993);
V. Kaplunovsky and J. Louis, Phys. Lett. **B306**, 269 (1993);
A. Brignole, L.E. Ibáñez, and C. Munoz, Nucl. Phys. **B422**, 125 (1994) [erratum: **B436**, 747 (1995)].
126. A. Arbey *et al.*, Phys. Rev. **D87**, 115020 (2013).
127. P. Draper *et al.*, Phys. Rev. **D85**, 095007 (2012).
128. P. Meade, N. Seiberg, and D. Shih, Prog. Theor. Phys. Suppl. **177**, 143 (2009);
M. Buican *et al.*, JHEP **0903**, 016 (2009).
129. A. Rajaraman *et al.*, Phys. Lett. **B678**, 367 (2009);
L.M. Carpenter *et al.*, Phys. Rev. **D79**, 035002 (2009).
130. S. Ambrosanio, G.D. Kribs, and S.P. Martin, Nucl. Phys. **B516**, 55 (1998).
131. For a review and guide to the literature, see J.F. Gunion and H.E. Haber, in *Perspectives on Supersymmetry II*, edited by G.L. Kane (World Scientific, Singapore, 2010) pp. 420–445.
132. A. Djouadi, J.L. Kneur, and G. Moultaka, Comput. Phys. Commun. **176**, 426-455 (2007);
C.F. Berger *et al.*, JHEP **0902**, 023 (2009).
133. H. Baer *et al.*, JHEP **1205**, 109 (2012).
134. R. Barbieri and G.F. Giudice, Nucl. Phys. **B305**, 63 (1988).
135. G.W. Anderson and D.J. Castano, Phys. Lett. **B347**, 300 (1995); Phys. Rev. **D52**, 1693 (1995); Phys. Rev. **D53**, 2403 (1996);
J.L. Feng, K.T. Matchev, and T. Moroi, Phys. Rev. **D61**, 075005 (2000);
P. Athron and D.J. Miller, Phys. Rev. **D76**, 075010 (2007);
M.E. Cabrera, J.A. Casas, and R.R. de Austri, JHEP **0903**, 075 (2009).
136. D.M. Ghilencea and G.G. Ross, Nucl. Phys. **B868**, 65 (2013).
137. G.L. Kane and S.F. King, Phys. Lett. **B451**, 113 (1999);
M. Bastero-Gil, G.L. Kane, and S.F. King, Phys. Lett. **B474**, 103 (2000);
J.A. Casas, J.R. Espinosa, and I, Hidalgo, JHEP **0401**, 008 (2004);
J. Abe, T. Kobayashi, and Y. Omura, Phys. Rev. **D76**, 015002 (2007);
R. Essig and J.-F. Fortin, JHEP **0804**, 073 (2008).
138. P. Bechtle *et al.*, JHEP **1206**, 098 (2012).
139. O. Buchmüller *et al.*, Eur. Phys. J. **C72**, 2243 (2012).
140. R. Barbieri and A. Strumia, `hep-ph/0007265`.
141. L. Giusti, A. Romanino, and A. Strumia, Nucl. Phys. **B550**, 3 (1999);
H.C. Cheng and I. Low, JHEP **0309**, 051 (2003); **0408**, 061 (2004).
142. H. Baer, V. Barger, and D. Mickelson, Phys. Rev. **D88**, 095013 (2013).
143. H. Baer *et al.*, Phys. Rev. **D87**, 035017 (2013); 115028 (2013);
J.L. Feng, Ann. Rev. Nucl. Part. Sci. **63**, 351 (2013).
144. J. Feng, K. Matchev, and T. Moroi, Phys. Rev. Lett. **84**, 2322 (2000); Phys. Rev. **D61**, 075005 (2000);
J. Feng and F. Wilczek, Phys. Lett. **B631**, 170 (2005);
D. Horton and G.G. Ross, Nucl. Phys. **B830**, 221 (2010).
145. M. Drees, Phys. Rev. **D33**, 1468 (1986);
S. Dimopoulos and G.F. Giudice, Phys. Lett. **B357**, 573 (1995);
A. Pomarol and D. Tommasini, Nucl. Phys. **B466**, 3 (1996).
146. M. Dine, A. Kagan, and S. Samuel, Phys. Lett. **B243**, 250 (1990);
A.G. Cohen, D.B. Kaplan, and A.E. Nelson, Phys. Lett. **B388**, 588 (1996).

147. K.L. Chan, U. Chattopadhyay, and P. Nath, Phys. Rev. **D58**, 096004 (1998);
R. Kitano and Y. Nomura, Phys. Rev. **D73**, 095004 (2006);
M. Perelstein and C. Spethmann, JHEP **0704**, 070 (2007);
H. Abe, T. Kobayashi, and Y. Omura, Phys. Rev. **D76**, 015002 (2007);
D. Horton and G.G. Ross, Nucl. Phys. **B830**, 221 (2010);
H. Baer *et al.*, JHEP **1010**, 018 (2010);
M. Asano *et al.*, JHEP **1012**, 019 (2010);
H. Baer, V. Barger, and P. Huang, JHEP **1111**, 031 (2011);
C. Brust *et al.*, JHEP **1203**, 103 (2012);
M. Papucci, J.T. Ruderman, and A. Weiler, JHEP **1209**, 035 (2012);
H.K. Dreiner, M. Kramer, and J. Tattersall, Europhys. Lett. **99**, 61001 (2012).

148. N. Arkani-Hamed *et al.*, `hep-ph/0703088`;
J. Alwall *et al.*, Phys. Rev. D **79**, 015005 (2009);
J. Alwall, P. Schuster, and N. Toro, Phys. Rev. **D79**, 075020 (2009);
D.S.M. Alves, E. Izaguirre, and J.G. Wacker, Phys. Lett. **B702**, 64 (2011); JHEP **1110**, 012 (2011);
D. Alves *et al.*, J. Phys. G **39**, 105005 (2012).

149. S.P. Martin, Phys. Rev. **D75**, 115005 (2007); Phys. Rev. **D78**, 055019 (2009);
T.J. LeCompte and S.P. Martin, Phys. Rev. **D85**, 035023 (2012).

150. J. Fan, M. Reece, and J.T. Ruderman, JHEP **1111**, 012 (2011).

151. R. Dermisek and J.F. Gunion, Phys. Rev. Lett. **95**, 041801 (2005); Phys. Rev. **D75**, 095019 (2007); Phys. Rev. **D76**, 095006 (2007).

152. G.G. Ross and K. Schmidt-Hoberg, Nucl. Phys. **B862**, 710 (2012); JHEP **1208**, 074 (2012);
A. Kaminska, G.G. Ross, and K. Schmidt-Hoberg, JHEP **1311**, 209 (2013).

153. S.P. Martin and J.D. Wells, Phys. Rev. **D86**, 035017 (2012).

154. B. Bellazzini *et al.*, Phys. Rev. **D79**, 095003 (2009).

155. D. Stockinger, J. Phys. **G34**, R45 (2007).

156. J.P. Miller *et al.*, Ann. Rev. Nucl. Part. Sci. **62**, 237 (2012);
E. de Rafael, Nucl. Phys. Proc. Suppl. **234**, 193 (2013).

157. M. Ibe, T. T. Yanagida, and N. Yokozaki, JHEP **1308**, 067 (2013).

158. M. Benayoun *et al.*, Eur. Phys. J. **C72**, 1848 (2012).

159. A. Limosani *et al.* [Belle Collab.], Phys. Rev. Lett. **103**, 241801 (2009);
J.P. Lees *et al.* [BaBar Collab.], Phys. Rev. Lett. **109**, 191801 (2012); Phys. Rev. **D86**, 112008 (2012).

160. M. Misiak *et al.*, Phys. Rev. Lett. **98**, 022002 (2007);
T. Becher and M. Neubert, Phys. Rev. Lett. **98**, 022003 (2007).

161. See, *e.g.*, M. Ciuchini *et al.*, Phys. Rev. **D67**, 075016 (2003);
T. Hurth, Rev. Mod. Phys. **75**, 1159 (2003);
F. Mahmoudi, JHEP **0712**, 026 (2007);
K.A. Olive and L. Velasco-Sevilla, JHEP **0805**, 052 (2008).

162. S.R. Choudhury and N. Gaur, Phys. Lett. **B451**, 86 (1999);
K.S. Babu and C.F. Kolda, Phys. Rev. Lett. **84**, 228 (2000);
G. Isidori and A. Retico, JHEP **0111**, 001 (2001); JHEP **0209**, 063 (2002).

163. R. Aaij *et al.* [LHCb Collab.], Phys. Rev. Lett. **110**, 021801 (2013); **111**, 101805 (2013).

164. F. Mahmoudi, S. Neshatpour, and J. Orloff, JHEP **1208**, 092 (2012);
A. Arbey *et al.*, Phys. Rev. **D87**, 035026 (2013).

165. J. Erler and A. Freitas, "Electroweak Model and Constraints on New Physics," in this *Review*.

166. J.R. Ellis *et al.*, JHEP **0708**, 083 (2007);
S. Heinemeyer *et al.*, JHEP **0808**, 087 (2008);
G.-C. Cho *et al.*, JHEP **1111**, 068 (2011).

167. For the current status of neutrino masses and mixing, see:
M.C. Gonzalez-Garcia *et al.*, JHEP **1212**, 123 (2012);
D.V. Forero, M. Tortola, and J.W.F. Valle, Phys. Rev. **D86**, 073012 (2012);
G.L. Fogli *et al.*, Phys. Rev. **D86**, 013012 (2012).

168. See the section on neutrinos in "Particle Listings—Leptons" in the 2013 web edition of the *Review of Particle Physics* at `http://pdg.lbl.gov`.

169. K. Zuber, Phys. Reports **305**, 295 (1998).

170. For a review of neutrino masses in supersymmetry, see *e.g.*, B. Mukhopadhyaya, *Proc. Indian National Science Academy* **A70**, 239 (2004);
M. Hirsch and J.W.F. Valle, New J. Phys. **6**, 76 (2004).

171. F. Borzumati and Y. Nomura, Phys. Rev. **D64**, 053005 (2001).

172. P. Minkowski, Phys. Lett. **67B**, 421 (1977);
M. Gell-Mann, P. Ramond, and R. Slansky, in *Supergravity*, edited by D. Freedman and P. van Nieuwenhuizen (North Holland, Amsterdam, 1979) p. 315;
T. Yanagida, Prog. Theor. Phys. **64**, 1103 (1980);
R. Mohapatra and G. Senjanovic, Phys. Rev. Lett. **44**, 912 (1980); Phys. Rev. **D23**, 165 (1981).

173. J. Hisano *et al.*, Phys. Lett. **B357**, 579 (1995);
J. Hisano *et al.*, Phys. Rev. **D53**, 2442 (1996);
J.A. Casas and A. Ibarra, Nucl. Phys. **B618**, 171 (2001);
J. Ellis *et al.*, Phys. Rev. **D66**, 115013 (2002);
A. Masiero, S.K. Vempati, and O. Vives, New J. Phys. **6**, 202 (2004);
E. Arganda *et al.*, Phys. Rev. **D71**, 035011 (2005);
F.R. Joaquim and A. Rossi, Phys. Rev. Lett. **97**, 181801 (2006);
J.R. Ellis and O. Lebedev, Phys. Lett. **B653**, 411 (2007).

174. Y. Grossman and H.E. Haber, Phys. Rev. Lett. **78**, 3438 (1997);
A. Dedes, H.E. Haber, and J. Rosiek, JHEP **0711**, 059 (2007).

175. M. Hirsch, H.V. Klapdor-Kleingrothaus, and S.G. Kovalenko, Phys. Lett. **B398**, 311 (1997);
L.J. Hall, T. Moroi, and H. Murayama, Phys. Lett. **B424**, 305 (1998);
K. Choi, K. Hwang, and W.Y. Song, Phys. Rev. Lett. **88**, 141801 (2002);
T. Honkavaara, K. Huitu, and S. Roy, Phys. Rev. **D73**, 055011 (2006).

176. M. Chemtob, Prog. Part. Nucl. Phys. **54**, 71 (2005);
R. Barbier *et al.*, Phys. Reports **420**, 1 (2005).

177. H. Dreiner, in *Perspectives on Supersymmetry II*, edited by G.L. Kane (World Scientific, Singapore, 2010) pp. 565–583.
178. B.C. Allanach, A. Dedes, and H.K. Dreiner, Phys. Rev. **D60**, 075014 (1999).
179. L.E. Ibáñez and G.G. Ross, Nucl. Phys. **B368**, 3 (1992); L.E. Ibáñez, Nucl. Phys. **B398**, 301 (1993).
180. A. Dedes, S. Rimmer, and J. Rosiek, JHEP **0608**, 005 (2006); B.C. Allanach and C.H. Kom, JHEP **0804**, 081 (2008); H.K. Dreiner *et al.*, Phys. Rev. **D84**, 113005 (2011).
181. L.E. Ibáñez and G.G. Ross, Nucl. Phys. **B368**, 3 (1992).
182. H.K. Dreiner, C. Luhn, and M. Thormeier Phys. Rev. **D73**, 075007 (2006).
183. K. Tamvakis, Phys. Lett. **B382**, 251 (1996); G. Eyal and Y. Nir, JHEP, **06**, 024 (1999); A. Florex *et al.*, Phys. Rev. **D87**, 095010 (2013).
184. B.C. Allanach and B. Gripaios, JHEP **1205**, 062 (2012); M. Asano, K. Rolbiecki, and K. Sakurai, JHEP **1301**, 128 (2013).
185. See *e.g.*, J.C. Romao, Nucl. Phys. Proc. Suppl. **81**, 231 (2000); Y. Grossman and S. Rakshit, Phys. Rev. **D69**, 093002 (2004).
186. R.N. Mohapatra, Phys. Rev. **D34**, 3457 (1986); K.S. Babu and R.N. Mohapatra, Phys. Rev. Lett. **75**, 2276 (1995); M. Hirsch, H.V. Klapdor-Kleingrothaus, and S.G. Kovalenko, Phys. Rev. Lett. **75**, 17 (1995); Phys. Rev. **D53**, 1329 (1996).
187. Y. Grossman and H.E. Haber, Phys. Rev. **D59**, 093008 (1999).
188. S. Dimopoulos and L.J. Hall, Phys. Lett. **B207**, 210 (1988); J. Kalinowski *et al.*, Phys. Lett. **B406**, 314 (1997); J. Erler, J.L. Feng, and N. Polonsky, Phys. Rev. Lett. **78**, 3063 (1997).
189. H.K. Dreiner, P. Richardson, and M.H. Seymour, Phys. Rev. **D63**, 055008 (2001).
190. J.E. Kim and H.P. Nilles, Phys. Lett. **B138**, 150 (1984).
191. J.E. Kim and H.P. Nilles, Mod. Phys. Lett. **A9**, 3575 (1994).
192. G.F. Giudice and A. Masiero, Phys. Lett. **B206**, 480 (1988).
193. J.A. Casas and C. Munoz, Phys. Lett. **B306**, 288 (1993).
194. M. Cvetič *et al.*, Phys. Rev. **D56**, 2861 (1997) [erratum: **D58**, 119905 (1998)].
195. A. Delgado, G. Nardini, and M. Quiros, Phys. Rev. **D86**, 115010 (2012).
196. P. Fayet, Phys. Lett. **78B**, 417 (1978).
197. For a recent review, see K. Benakli, Fortsch. Phys. **59**, 1079 (2011).
198. P.J. Fox, A.E. Nelson, and N. Weiner, JHEP **0208**, 035 (2002).
199. K. Benakli and M.D. Goodsell, Nucl. Phys. **B816**, 185 (2009); **B840**, 1 (2010).
200. G.D. Kribs, E. Poppitz, and N. Weiner, Phys. Rev. **D78**, 055010 (2008).
201. K. Benakli, M.D. Goodsell, and F. Staub, JHEP **1306**, 073 (2013).
202. See *e.g.*, J.L. Hewett and T.G. Rizzo, Phys. Reports **183**, 193 (1989).
203. S.F. King, S. Moretti, and R. Nevzorov, Phys. Lett. **B634**, 278 (2006); Phys. Rev. **D73**, 035009 (2006).

SUPERSYMMETRY, PART II (EXPERIMENT)

Written September 2013 by O. Buchmueller (Imperial College London) and P. de Jong (Nikhef).

II.1. Introduction

Supersymmetry (SUSY), a transformation relating fermions to bosons and vice versa [1–9], is one of the most compelling possible extensions of the Standard Model of particle physics (SM) that could be discovered at high-energy colliders such as the Large Hadron Collider (LHC) at CERN.

On theoretical grounds SUSY is motivated as a generalization of space-time symmetries. A low-energy realization of SUSY, *i.e.*, SUSY at the TeV scale, is, however, not a necessary consequence. Instead, low-energy SUSY is motivated by the possible cancellation of quadratic divergences in radiative corrections to the Higgs boson mass [10–15]. Furthermore, it is intriguing that a weakly interacting, (meta)stable supersymmetric particle might make up some or all of the dark matter in the universe [16–18]. In addition, SUSY predicts that gauge couplings, as measured experimentally at the electroweak scale, unify at an energy scale $\mathcal{O}(10^{16})$GeV ("GUT scale") near the Planck scale [19–25].

In the minimal supersymmetric extension to the Standard Model, the so called MSSM [26,27,11], a supersymmetry transformation relates every fermion and gauge boson in the SM to a supersymmetric partner with half a unit of spin difference, but otherwise with the same properties and quantum numbers. These are the "sfermions": squarks ($\tilde{q}$) and sleptons ($\tilde{\ell}$, $\tilde{\nu}$), and the "gauginos". The MSSM Higgs sector contains two doublets, for up-type quarks and for down-type quarks and charged leptons respectively, and the partners of the Higgs doublets are known as "higgsinos." The charged weak gauginos

and higgsinos mix to "charginos" ($\tilde{\chi}^{\pm}$), and the neutral ones mix to "neutralinos" ($\tilde{\chi}^0$). The SUSY partners of the gluons are known as "gluinos" ($\tilde{g}$). The fact that such particles are not yet observed leads to the conclusion that, if supersymmetry is realized, it is a broken symmetry. A description of SUSY in the form of an effective Lagrangian with only "soft" SUSY breaking terms and SUSY masses at the TeV scale maintains cancellation of quadratic divergences in particle physics models.

The phenomenology of SUSY is to a large extent determined by the SUSY breaking mechanism and the SUSY breaking scale. This determines the SUSY particle masses, the mass hierarchy, the field contents of physical particles, and their decay modes. In addition, phenomenology crucially depends on whether the multiplicative quantum number of R-parity [27], $R = (-1)^{3(B-L)+2S}$, where B and L are baryon and lepton numbers and S is the spin, is conserved or violated. If R-parity is conserved, SUSY particles (sparticles), which have odd R-parity, are produced in pairs and the decays of each SUSY particle must involve an odd number of lighter SUSY particles. The lightest SUSY particle (LSP) is then stable and often assumed to be a weakly interacting massive particle (WIMP). If R-parity is violated, new terms λ_{ijk}, λ'_{ijk} and λ''_{ijk} appear in the superpotential, where ijk are generation indices; λ-type couplings appear between lepton superfields only, λ''-type are between quark superfields only, and λ'-type couplings connect the two. R-parity violation implies lepton and/or baryon number violation. More details of the theoretical framework of SUSY are discussed elsewhere in this volume [28].

Today low-energy data from flavor physics experiments, high-precision electroweak observables as well as astrophysical data impose strong constraints on the allowed SUSY parameter space. Recent examples of such data include measurements of the rare B-meson decay $B_s \to \mu^+\mu^-$ [29,30], and accurate determinations of the cosmological dark matter relic density constraint [31,32].

These indirect constraints are often more sensitive to higher SUSY mass scales than experiments searching for direct sparticle production at colliders, but the interpretation of these results is often strongly model dependent. In contrast, direct searches for sparticle production at collider experiments are less subject to interpretation ambiguities and therefore they play a crucial role in the search for SUSY.

The discovery of a new scalar boson with a mass around 126 GeV compatible with a Higgs boson imposes constraints on SUSY, which are discussed elsewhere [28,33].

In this review we limit ourselves to direct searches, covering data analyses at LEP, HERA, the Tevatron and the LHC. With the advent of the LHC, the experimental situation is changing rapidly. Compared to earlier PDG reviews, more emphasis is given to LHC results; for more details on LEP and Tevatron constraints, see earlier PDG reviews [34].

II.2. Experimental search program

The electron-positron collider LEP was operational at CERN between 1989 and 2000. In the initial phase, center-of-mass energies around the Z-peak were probed, but after 1995 the LEP experiments collected a significant amount of luminosity at higher center-of-mass energies, some 235 pb^{-1} per experiment at $\sqrt{s} \geq 204$ GeV, with a maximum $\sqrt{s}$ of 209 GeV.

Searches for new physics at e^+e^- colliders benefit from the clean experimental environment and the fact that momentum balance can be measured not only in the plane transverse to the beam, but also in the direction along the beam (up to the beam pipe holes), defined as the longitudinal direction. Searches at LEP are dominated by the data samples taken at the highest center-of-mass energies.

Significant constraints on SUSY have been set by the CDF and D0 experiments at the Tevatron, a proton-antiproton collider at a center-of-mass energy of up to 1.96 TeV. CDF and D0 have collected integrated luminosities between 10 and 11 fb^{-1} each up to the end of collider operations in 2011.

The electron-proton collider HERA provided collisions to the H1 and ZEUS experiments between 1992 and 2007, at a center-of-mass energy up to 318 GeV. A total integrated luminosity of approximately 0.5 fb^{-1} has been collected by each experiment. Since in ep collisions no annihilation process takes place, SUSY searches at HERA typically look for R-parity violating production of single SUSY particles.

The landscape of SUSY searches, however, has significantly changed since the LHC has started proton-proton operation at a center-of-mass energy of 7 TeV in 2010. By the end of 2011 the experiments ATLAS and CMS had collected about 5 fb^{-1} of integrated luminosity each, and the LHCb experiment had collected approximately 1 fb^{-1}. In 2012, the LHC operated at a center-of-mass energy of 8 TeV, and ATLAS and CMS collected approximately 20 fb^{-1} each, whereas LHCb collected 2 fb^{-1}.

Proton-(anti)proton colliders produce interactions at higher center-of-mass energies than those available at LEP, and cross sections of QCD-mediated processes are larger, which is reflected in the higher sensitivity for SUSY particles carrying color charge: squarks and gluinos. Large background contributions from Standard Model processes, however, pose challenges to trigger and analysis. Such backgrounds are dominated by multijet production processes, including, particularly at the LHC, those of top quark production, as well as jet production in association with vector bosons. The proton momentum is shared between its parton constituents, and in each collision only a fraction of the total center-of-mass energy is available in the hard parton-parton scattering. Since the parton momenta in the longitudinal direction are not known on an event-by-event basis, use of momentum conservation constraints in an analysis is restricted to the transverse plane, leading to the definition of transverse variables, such as the missing transverse momentum, and the transverse mass. Proton-proton collisions at the LHC differ from proton-antiproton collisions at the Tevatron in the

sense that there are no valence anti-quarks in the proton, and that gluon-initiated processes play a more dominant role. The increased center-of-mass energy of the LHC compared to the Tevatron significantly extends the kinematic reach for SUSY searches. This is reflected foremost in the sensitivity for squarks and gluinos, but also for other SUSY particles.

The main production mechanisms of massive colored sparticles at hadron colliders are squark-squark, squark-gluino and gluino-gluino production; when "squark" is used "antisquark" is also implied. The typical SUSY search signature at hadron colliders contains high-p_{T} jets, which are produced in the decay chains of heavy squarks and gluinos, and significant missing momentum originating from the two LSPs produced at the end of the decay chain. Assuming R-parity conservation, the LSPs are neutral and weakly interacting massive particles which escape detection.

Selection variables designed to separate the SUSY signal from the Standard Model backgrounds include H_{T}, $E_{\mathrm{T}}^{\mathrm{miss}}$, and m_{eff}. The quantities H_{T} and $E_{\mathrm{T}}^{\mathrm{miss}}$ refer to the measured transverse energy and missing transverse momentum in the event, respectively. They are usually defined as the scalar (H_{T}) and negative vector sum ($E_{\mathrm{T}}^{\mathrm{miss}}$) of the transverse jet energies or transverse calorimeter clusters energies measured in the event. The quantity m_{eff} is referred to as the effective mass of the event and is defined as $m_{\mathrm{eff}} = H_{\mathrm{T}} + |E_{\mathrm{T}}^{\mathrm{miss}}|$. The peak of the m_{eff} distribution for SUSY signal events correlates with the SUSY mass scale, in particular with the mass difference between the primary produced SUSY particle and the LSP [35], whereas the Standard Model backgrounds dominate at low m_{eff}. Additional reduction of multijet backgrounds can be achieved by demanding isolated leptons or photons in the final states.

In the past few years alternative approaches have been developed to increase the sensitivity to pair production of heavy sparticles with masses around 1 TeV focusing on the kinematics of their decays, and to further suppress the background from multijet production. Prominent examples of these new approaches are searches using the α_{T} [36–40], *razor* [41], *stransverse mass* (m_{T2}) [42], and *contransverse mass* (m_{CT}) [43] variables.

II.3. Interpretation of results

Since the mechanism by which SUSY is broken is unknown, a general approach to SUSY via the most general soft SUSY breaking Lagrangian adds a significant number of new free parameters. For the minimal supersymmetric standard model, MSSM, *i.e.*, the model with the minimal particle content, these comprise 105 new parameters. A phenomenological analysis of SUSY searches leaving all these parameters free is not feasible. For the practical interpretation of SUSY searches at colliders several approaches are taken to reduce the number of free parameters.

One approach is to assume a SUSY breaking mechanism and lower the number of free parameters through the assumption of additional constraints. In particular in past years, interpretations of experimental results were predominately performed in constrained models of gravity mediated [44,45], gauge mediated [46,47], and anomaly mediated [48,49] SUSY breaking. Before the start of the LHC and even during its first year of operation, the most popular model for interpretation of collider based SUSY searches was the constrained MSSM (CMSSM) [44,50,51], which in the literature is also referred to as minimal supergravity, or MSUGRA. The CMSSM is described by five parameters: the common sfermion mass m_0, the common gaugino mass $m_{1/2}$, and the common trilinear coupling parameter A_0, all expressed at the GUT scale, the ratio of the vacuum expectation values of the Higgs fields for up-type and down-type fermions $\tan\beta$, and the sign of the higgsino mass parameter μ, defined at the electroweak scale. In gauge mediation models, the paradigm of general gauge mediation (GGM) [52] is slowly replacing minimal gauge mediation, denoted traditionally as GMSB (gauge mediated SUSY breaking).

These constrained SUSY models are theoretically well motivated and provide a rich spectrum of experimental signatures. Therefore, they represent a useful framework to benchmark performance, compare limits or reaches and assess the expected sensitivity of different search strategies. However, with universality relations imposed on the soft SUSY breaking parameters, they do not cover all possible kinematic signatures and mass relations of SUSY. In such scenarios the squarks are often nearly degenerate in mass, in particular for the first and second generation. The exclusion of parameter space in the CMSSM and in CMSSM-inspired models is mainly driven by first and second generation squark production together with gluino production.

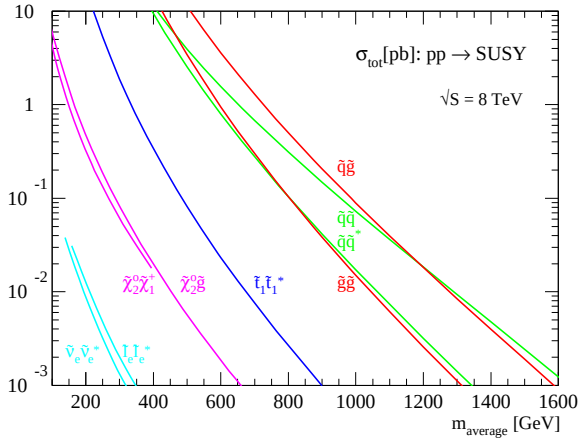

Figure 1: Cross sections for pair production of different sparticles as a function of their mass at the LHC for a center-of-mass energy of 8 TeV [53]. Typically the production cross section of colored squarks and gluinos is several orders of magnitude larger than the one for leptons or charginos. Except for the explicitly shown pair production of stops, production cross sections for squarks assumes mass degeneracy of left- and right-handed u, d, s, c and b squarks.

As shown in Fig. 1 [53] these processes possess the largest production cross sections in proton-proton collisions, and thus the LHC searches typically provide the tightest mass limits on these colored sparticles. This, however, implies that the allowed parameter space of constrained SUSY models today has been restrained significantly by searches from ATLAS and CMS. Furthermore, confronting the remaining allowed parameter space with other collider and non-collider measurements, which are directly or indirectly sensitive to contributions from SUSY, the overall compatibility of these models with all data is significantly worse than in the pre-LHC era (see section II.7 for further discussion), indicating that very constrained models like the CMSSM might no longer be good benchmark scenarios to solely characterize the results of SUSY searches at the LHC.

For this reasons, an effort has been made in the past years to complement the traditional constrained models with more flexible interpretation approaches.

One answer to study a broader and more comprehensive subset of the MSSM is via the phenomenological-MSSM, or pMSSM [54–56]. It is derived from the MSSM, using experimental data to eliminate parameters that are free in principle but have already been highly constrained by measurements of *e.g.*, flavor mixing and CP-violation. This effective approach reduces the number of free parameters in the MSSM to typically 19, making it a practical compromise between the full MSSM and highly constrained models such as the CMSSM.

Even less dependent on fundamental assumptions are interpretations in terms of so-called simplified models [57–60]. Such models assume a limited set of SUSY particle production and decay modes and leave open the possibility to vary masses and other parameters freely. Therefore, simplified models enable comprehensive studies of individual SUSY topologies, and are useful for optimization of the experimental searches over a wide parameter space. As a consequence, since 2011 ATLAS and CMS have adopted simplified models as the primary framework to provide interpretations of their searches. Today, almost every individual search provides interpretations of their results in one or even several simplified models that are characteristic of SUSY topologies probed by the analysis.

However, while these models are very convenient for the interpretation of individual SUSY production and decay topologies, care must be taken when applying these limits to more complex SUSY spectra. Therefore, in practise, simplified model limits are often used as an approximation of the constraints that can be placed on sparticle masses in more complex SUSY spectra. Yet, depending on the assumed SUSY spectrum, the sparticle of interest, and the considered simplified model limit, this approximation can lead to a significant mistake, typically an overestimation, in the assumed constraint on the sparticle mass (see for example [61]) . Only on a case-by-case basis can it be determined whether the limit of a given simplified model represents a good approximation of the true underlying constraint that can be applied on a sparticle mass in a complex SUSY spectrum. In the following, we will always point out explicitly the assumptions that have entered the limits when quoting interpretations from simplified models.

This review covers results up to September 2013 and since none of the searches performed so far have shown significant excess above the SM background prediction, the interpretation of the presented results are exclusion limits on SUSY parameter space.

II.4. Exclusion limits on gluino and squark masses

Gluinos and squarks are the SUSY partners of gluons and quarks, and thus carry color charge. Limits on squark masses of the order 100 GeV have been set by the LEP experiments [62]. However, due to the colored production of this particles at hadron colliders (see e.g. Fig. 1), hadron collider experiments are able to set much tighter mass limits.

Today, the results of the LHC experiments dominate the search for direct squark and gluino production. Pair production of these massive colored sparticles at hadron colliders generally involve both s-channel and t-channel parton-parton interactions. Since there is a negligible amount of bottom and top quark content in the proton, top- and bottom squark production proceeds through s-channel diagrams only with smaller cross sections. In the past, experimental analyses of squark and/or gluino production typically assumed the first and second generation squarks to be approximately degenerate in mass. However, in order to have even less model dependent interpretations of the searches, the experiments have started to also provide simplified model limits on individual first or second generation squarks.

Assuming R-parity conservation and assuming gluinos to be heavier than squarks, squarks will predominantly decay to a quark and a neutralino or chargino, if kinematically allowed. The decay may involve the lightest neutralino (typically the LSP) or chargino, but, depending on the masses of the gauginos, may involve heavier neutralinos or charginos. For pair production of first and second generation squarks, the simplest decay modes involve two jets and missing momentum, with potential extra jets stemming from initial state or final state radiation (ISR/FSR) or from decay modes with longer cascades. Similarly, gluino pair production leads to four jets and missing momentum, and possibly additional jets from ISR/FSR or cascades. Associated production of a gluino and a (anti-)squark is also possible, in particular if squarks and gluinos have similar masses, typically leading to three or more jets in the final state. In cascades, isolated photons or leptons may appear from the decays of sparticles such as neutralinos or charginos. Final states are thus characterized by significant missing transverse momentum, and at least two, and possibly many more high p_{T} jets, which can be accompanied by one or more isolated objects like photons or leptons, including τ leptons, in the final state. Table 1 shows a schematic overview of characteristic final state signatures of gluino and squark production for different mass hierarchy hypotheses and assuming decays involving the lightest neutralino.

Table 1: Typical search signatures at hadron colliders for direct gluino and first- and second-generation squark production assuming different mass hierarchies.

Mass Hierarchy	Main Production	Dominant Decay	Typical Signature
$m_{\tilde{q}} << m_{\tilde{g}}$	$\tilde{q}\bar{\tilde{q}}, \tilde{q}\tilde{q}$	$\tilde{q} \to q\tilde{\chi}_1^0$	≥ 2 jets + $E_{\mathrm{T}}^{\mathrm{miss}}$ + X
$m_{\tilde{q}} \approx m_{\tilde{g}}$	$\tilde{q}\tilde{g}, \bar{\tilde{q}}\tilde{g}$	$\tilde{q} \to q\tilde{\chi}_1^0$	≥ 3 jets + $E_{\mathrm{T}}^{\mathrm{miss}}$ + X
		$\tilde{g} \to q\bar{q}\tilde{\chi}_1^0$	
$m_{\tilde{q}} >> m_{\tilde{g}}$	$\tilde{g}\tilde{g}$	$\tilde{g} \to q\bar{q}\tilde{\chi}_1^0$	≥ 4 jets + $E_{\mathrm{T}}^{\mathrm{miss}}$ + X

II.4.1 Exclusion limits on the gluino mass

Limits set by the Tevatron experiments on the gluino mass assume the framework of the CMSSM, with $\tan\beta = 5$ (CDF) or $\tan\beta = 3$ (D0), $A_0 = 0$ and $\mu < 0$, and amount to lower limits of about 310 GeV for all squark masses, or 390 GeV for the case $m_{\tilde{q}} = m_{\tilde{g}}$ [63,64]. During the first year of physics operation of the LHC in 2010, these limits have been superseded by those provided by ATLAS and CMS.

Today, limits on the gluino mass have been set using up to approximately 20 fb^{-1} of data recorded at a center-of-mass energy of 8 TeV. As shown in Fig. 2, the ATLAS collaboration places limits for several searches in the framework of the CMSSM, assuming $\tan\beta = 30$, $A_0 = -2m_0$, and $\mu > 0$ For low m_0 the inclusive all-hadronic search considering at least two to six jets [65] provides the most stringent limit, while for values of m_0 above $\approx$ 1600 GeV a more dedicated search [66] requiring zero or one isolated lepton accompanied with at least three jets identified to originate from bottom quarks (b-jets) takes over. The limits at low m_0 are mainly driven by squark-gluino and squark-squark production and at high m_0 gluino pair production dominates. As also indicated in Fig. 1, all other particle production modes do not play a significant role for limits in the CMSSM. In this constrained model gluino masses below around 1300 GeV [66] are excluded by the ATLAS collaboration for all squark masses, while for equal squark and gluino masses, the limit is about 1700 GeV [65]. The CMS collaboration has not yet provided an interpretation of their 8 TeV searches in the CMSSM but based on the performance reported for simplified models it is expected that the limits are similar to those shown in Fig. 2.

Limits on the gluino mass have also been established in the framework of simplified models. Assuming only gluino pair production, in particular three primary decay chains of the gluino have been considered by the LHC experiments for interpretations of their search results. The first decay chain $\tilde{g} \to q\bar{q}\tilde{\chi}_1^0$ assumes gluino mediated production of first and second generation squarks which leads to four light flavor quarks in the final state. Therefore, inclusive all-hadronic analyses searching for multijet plus $E_{\mathrm{T}}^{\mathrm{miss}}$ final states are utilized to put limits on this simplified model. These limits are derived as a function of the gluino and neutralino (LSP) mass. As shown

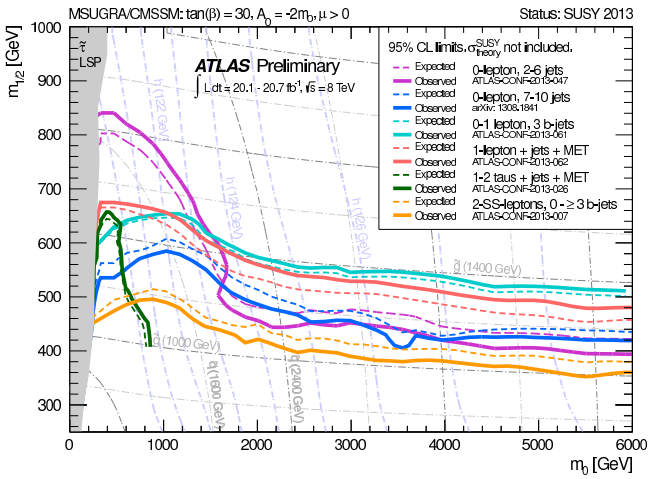

Figure 2: Limits, at 95% C.L., derived from several different ATLAS searches in the CMSSM parameters m_0 and $m_{1/2}$, assuming $\tan\beta = 30$, $A_0 = -2m_0$ and $\mu > 0$.

in Fig. 3 (left), using the cross section from next-to-leading order QCD corrections and the resummation of soft gluon emission at next-to-leading-logarithmic accuracy as reference, the CMS collaboration [67] excludes in this simplified model gluino masses below approximately 1200 GeV, for a massless neutralino. In scenarios where neutralinos are not very light, the efficiency of the analyses is reduced by the fact that jets are less energetic, and there is less missing transverse momentum in the event. This leads to weaker limits when the mass difference $\Delta m = m_{\tilde{g}} - m_{\tilde{\chi}_1^0}$ is reduced. For example, for neutralino masses above about 450 GeV no limit on the gluino mass can be set for this decay chain. Therefore, limits on gluino masses are strongly affected by the assumption of the neutralino mass. Similar results for this simplified model have been obtained by ATLAS [65].

The second important decay chain of the gluino considered for interpretation in a simplified model is $\tilde{g} \to b\bar{b}\tilde{\chi}_1^0$. Here the decay is mediated via bottom squarks and thus leads to four jets from b quarks and $E_{\mathrm{T}}^{\mathrm{miss}}$ in the final state. Also for this topology inclusive all-hadronic searches provide the highest sensitivity. However, with four b quarks in the final state, the use of secondary vertex reconstruction for the identification of jets originating from b quarks provides a powerful handle on the SM background. Therefore, in addition to a multijet plus $E_{\mathrm{T}}^{\mathrm{miss}}$ signature these searches also require several jets to be tagged as b-jets. As shown in Fig. 3 (middle), for this simplified model CMS [68] excludes gluino masses below $\approx$ 1200 GeV for a massless neutralino, while for neutralino masses above $\approx$ 650 GeV no limit on the gluino mass can be set. Comparable limits for this simplified model are provided by a search from ATLAS [66].

Not only first and second generation squarks or bottom squarks may be the product of gluino decays but also, if

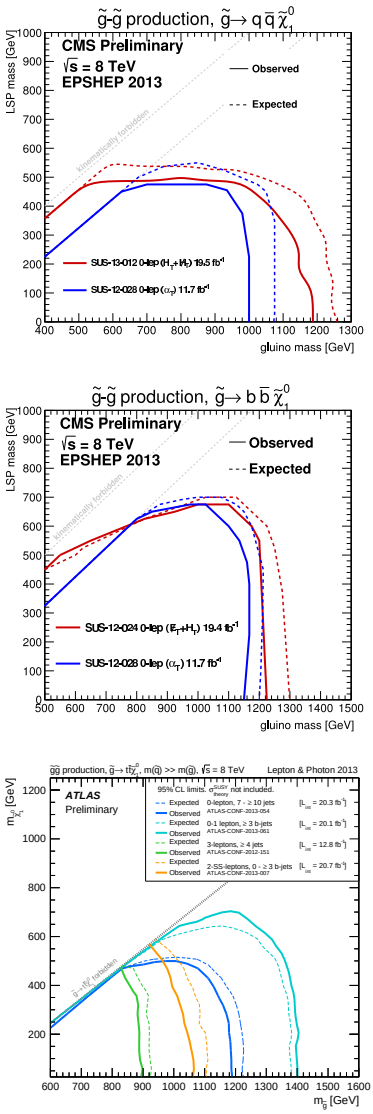

Figure 3: Upper mass limits, at 95% C.L., on gluino pair production for the decay chains $\tilde{g} \to q\bar{q}\tilde{\chi}_1^0$ (left), $\tilde{g} \to b\bar{b}\tilde{\chi}_1^0$ (middle), and $\tilde{g} \to t\bar{t}\tilde{\chi}_1^0$ (right). The limits are defined in the framework of simplified models assuming a single decay chain, (i.e. 100% branching fraction). The left and middle plot show limits from the CMS collaboration, while the displayed limits for $\tilde{g} \to t\bar{t}\tilde{\chi}_1^0$ are obtained from ATLAS searches.

kinematically allowed, top squarks via the decay $\tilde{g} \to \tilde{t}t$. This leads to a "four tops" final state $ttttt\tilde{\chi}_1^0\tilde{\chi}_1^0$ and defines the third important simplified model, $\tilde{g} \to t\bar{t}\tilde{\chi}_1^0$, characterizing gluino pair production. The topology of this decay is very rich in different experimental signatures: as many as four isolated leptons, four b-jets, several light flavor quark jets, and significant missing momentum from the neutrinos in the W decay and from the two neutralinos. Therefore, in contrast to the other two simplified models, dedicated searches optimized for this particular final state provide the best mass limit on the gluino for this simplified model. As shown in Fig. 3 (right), the ATLAS search [66] requiring significant $E_{\mathrm{T}}^{\mathrm{miss}}$, zero or one isolated lepton, and at least three jets identified as b-jets provides the strongest limit on the gluino mass. At 95% C.L. it rules out a gluino mass below $\approx$ 1400 GeV for $m_{\tilde{\chi}_1^0} < 300$ GeV. For neutralino masses above $\approx$ 700 GeV, no limit can be placed on the gluino mass for this simplified model. A CMS search [69] also especially optimized for this decay topology by requiring one isolated lepton and high jet multiplicity obtains similar limits.

When comparing the limits in Fig. 3 for the three different simplified models it becomes apparent that more parameter space can be excluded when the gluino decay chain is mediated via third generation squarks. The reason for this is the better control of the SM background by means of identification of b-jets as well as dedicated topology requirements like high jet multiplicity or isolated leptons for these special signatures. However, this variation in sensitivity of the searches for different gluino decay chains is also a clear indication that care must be taken when limits from these simplified models are applied to SUSY models possessing more complex underlying spectra.

If the gluino decay is suppressed, for example if squark masses are high, gluinos may live longer than typical hadronization times. It is expected that such gluinos will hadronize to semi-stable strongly interacting particles known as R-hadrons. Searches for R-hadrons exploit the typical signature of stable charged massive particles in the detector. As shown in Fig. 4, the CMS experiment excludes semi-stable gluino R-hadrons with masses below approximately 1.3 TeV [70]. The limits depend on the probability for gluinos to form bound states known as gluinoballs, as these are neutral and not observed in the tracking detectors. Similar limits are obtained by the ATLAS experiment [71].

Alternatively, since such R-hadrons are strongly interacting, they may be stopped in the calorimeter or in other material, and decay later into energetic jets. These decays are searched for by identifying the jets outside the time window associated with bunch-bunch collisions [72–74]. The latest ATLAS analysis [73] based on the full 2011 and 2012 data set combined (28 fb^{-1}) places limits at 95% C.L. on gluino production over almost 16 orders of magnitude in gluino lifetime. For $m_{\tilde{\chi}_1^0} > 100$ GeV, assuming a 100% branching fraction for gluino decay to gluon (or $q\bar{q}$) + neutralino, gluinos with lifetimes from 10 μs to 1000 s and $m_{\tilde{g}} < 857$ GeV are excluded. When SUSY spectra are compressed, this limits weakens to $m_{\tilde{g}} < 572$ GeV for $m_{\tilde{g}} - m_{\tilde{\chi}_1^0} < 100$ GeV .

In summary, for interpretations in the CMSSM, simplified models, and semi-stable R-hadrons, the best limits on the gluino mass range from around 1200 GeV to about 1400 GeV, while for interpretations in the context of stopped R-hadrons the limit on $m_{\tilde{g}}$ is around 850 GeV. All these limits weaken significantly for compressed SUSY spectra when the mass difference $m_{\tilde{g}} - m_{\tilde{\chi}_1^0}$ is reduced.

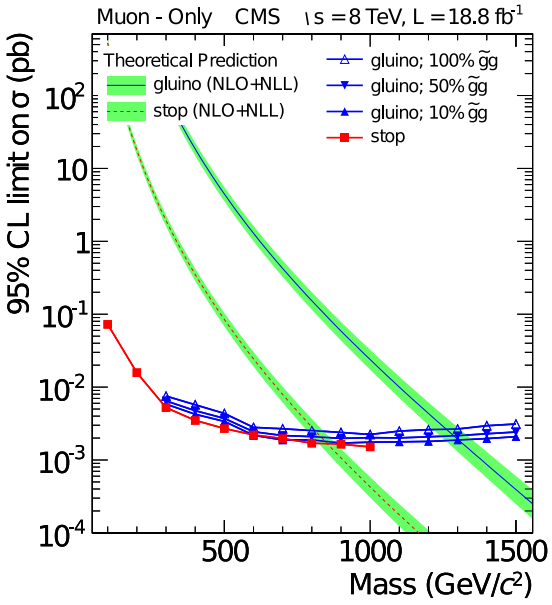

Figure 4: Observed 95% C.L. upper limits on the cross section for (semi-)stable top squarks or gluinos. For gluinos, different fractions of gluinoball states produced after hadronization scenarios are indicated. The observed limits are compared with the predicted theoretical cross sections where the bands represent the theoretical uncertainties on the cross section values.

R-parity violating gluino decays are searched for in multijet final states without missing transverse momentum. CDF [75], ATLAS [76] and CMS [77] put limits on the cross section for such decays.

II.4.2. Exclusion limits on first and second generation squark masses

Limits on first and second generation squark masses set by the Tevatron experiments assume the CMSSM model, and amount to lower limits of about 380 GeV for all gluino masses, or 390 GeV for the case $m_{\tilde{q}} = m_{\tilde{g}}$ [63,64].

At the LHC, limits on squark masses have been set using up to approximately 20 fb^{-1} of data at 8 TeV. As shown in Fig. 2, the ATLAS collaboration [65] excludes in the framework of the CMSSM squark masses below $\approx$ 1600 GeV for all gluino masses. For equal squark and gluino masses, the limit is about 1700 GeV.

Interpretations in simplified models are typically characterizing squark pair production with only one decay chain of $\tilde{q} \to q\tilde{\chi}_1^0$. Here it is assumed that the left and right-handed $\tilde{u}$, $\tilde{d}$, $\tilde{s}$ and $\tilde{c}$ squarks are degenerate in mass. Furthermore, it is assumed that the mass of the gluino is very high and thus contributions of the corresponding t-channel diagrams to squark pair production are negligible. Therefore, the total production cross section for this simplified model is eight times the production cross section of an individual squark (e.g. $\tilde{u}_L$). The CMS collaboration provides interpretations of two all-hadronic searches [67,78] for this simplified model. As displayed in Fig. 5, best observed exclusion of squark masses is just below 800 GeV for a light neutralino. The effects of heavy neutralinos on squark limits are similar to those discussed in the gluino case (see section II.4.1) and only for neutralino masses below $\approx$ 300 GeV squark masses can be excluded. Results from the ATLAS collaboration [65] for this simplified model are similar.

For the same analysis ATLAS also provides an interpretation of their search result in a simplified model assuming strong production of first and second generation squarks in association with gluinos. This interpretation excludes squark masses below $\approx$ 1400 GeV for all gluino masses as well as gluino masses below $\approx$ 1400 GeV for all squark masses. For equal squark and gluino masses, the limit is about 1700 GeV and therefore very similar to limits provided in the CMSSM.

If the assumption of mass degenerate first and second generation squarks is dropped and only the production of a single light squark is assumed, the limits weaken significantly. This is shown as the much smaller exclusion region in Fig. 5, which represents the 95% C.L. upper limit of pair production of a single light squark, with the gluino and all other squarks decoupled to very high masses. With a best observed limit of only $\approx$ 450 GeV for a massless neutralino and a neutralino mass of $\approx$ 100 GeV above which no limit can be placed, the exclusion reach of the LHC experiments for single light squark is rather weak. It should be noted that this limit is not a result of a simple scaling of the above mentioned mass limits assuming eightfold mass degeneracy but it also takes into account that for an eight times lower production cross section the analyses must probe kinematic regions of phase space that are closer to the ones of SM background production. Since signal acceptance and the ratio of expected signal to SM background events of the analyses are typically worse in this region of phase space not only the 1/8 reduction in production cross section but also a worse analysis sensitivity are responsible for the much weaker limit on single squark pair production.

R-parity violating production of single squarks via a λ'-type coupling has been studied at HERA. In such models, a lower limit on the squark mass of the order of 275 GeV has been set for electromagnetic-strength-like couplings $\lambda' = 0.3$ [79].

II.4.3. Exclusion limits on third generation squark masses

SUSY at the TeV-scale is often motivated by naturalness arguments, most notably as a solution to stabilize quadratic divergences in radiative corrections to the Higgs boson mass. In this context, the most relevant terms for SUSY phenomenology arise from the interplay between the masses of the third generation squarks and the Yukawa coupling of the top quark to the Higgs boson. This motivates a potential constraint on the masses of the top squarks and the left-handed bottom squark. Due to the large top quark mass, significant mixing between

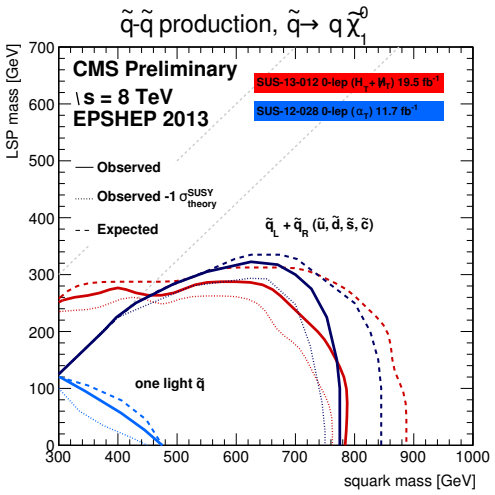

Figure 5: 95% C.L. exclusion contours in the squark-neutralino mass plane defined in the framework of simplified models assuming a single decay chain of $\tilde{q} \to q\tilde{\chi}_1^0$. Two assumptions for the squark pair production cross sections are displayed; a) eightfold degeneracy for the masses of the first and second generation squarks (red and dark blue contours) and b) only one light flavor squark (light blue contours). For the α_T based CMS analysis [78](light and dark blue contours), the diagonal part of $m_{\tilde{q}} - m_{\tilde{\chi}_1^0} < 200$ GeV is not directly kinematically accessible and therefore no limit is provided. The other CMS analysis [67] (red limit contours) shown in this plot provides a limit beyond this mass difference by allowing significant contributions from signal events with hard ISR jets in the interpretation of the result.

$\tilde{t}_L$ and $\tilde{t}_R$ is expected, leading to a lighter mass state $\tilde{t}_1$ and a heavier mass state $\tilde{t}_2$. In the MSSM, the lightest top squark ($\tilde{t}_1$) can be the lightest squark.

The discovery of a Higgs boson at a mass around 126 GeV has consequences for third generation squarks in the MSSM, which are discussed elsewhere [28]. As a consequence, and in the absence of a SUSY discovery so far, searches for third generation squark production have become a major focus of the SUSY search program at the LHC. For this reason direct and gluino mediated top and/or bottom squark production processes, leading to experimental signatures that are rich in jets originating from bottom quarks, are either subject of reinterpretation of inclusive analyses or targets for dedicated searches. The latter ones have become especially important for searches of direct top squark production.

Direct production of top and bottom squark pairs at hadron colliders is suppressed with respect to first generation squarks, due to the absence of t and b quarks in the proton (see e.g. the example of direct top squark production in Fig. 1). At the LHC, assuming eightfold mass degeneracy for light flavor squarks as reference, this suppression is at the level of two orders of magnitude for top and bottom squark masses of around 600 GeV. Moreover, at the LHC, there is a very large background of top quark pair production, making especially the experimental analysis of top squark pair production a challenge.

Bottom squarks are expected to decay predominantly to $b\tilde{\chi}^0$ giving raise to the characteristic multi b-jet and $E_{\mathrm{T}}^{\mathrm{miss}}$ signature. Direct production of bottom squark pairs has been studied at the Tevatron and at the LHC. Limits from the Tevatron are $m_{\tilde{b}} > 247$ GeV for a massless neutralino [80,81](see also Fig. 6). Using the 2011 data the LHC experiments were able to surpass these limits and based on the full 2012 data set, as shown in Fig. 6, using an all-hadronic search requiring significant $E_{\mathrm{T}}^{\mathrm{miss}}$ and two jets reconstructed as b-jets, ATLAS has set a limit of $m_{\tilde{b}} >\approx 650$ GeV for the same scenario. For $m_{\tilde{\chi}_1^0} \approx 280$ GeV or higher no limit can be placed on direct bottom squark pair production in this simplified model [82]. The latest CMS results for this simplified model are featured in [78] and exhibit a similar reach.

Further bottom squark decay modes have also been studied by ATLAS and CMS. For example, in a simplified model for the $\tilde{b} \to t\tilde{\chi}^{\pm}$ decay mode, bottom squark quark masses below approximately 450 GeV are excluded [83,84].

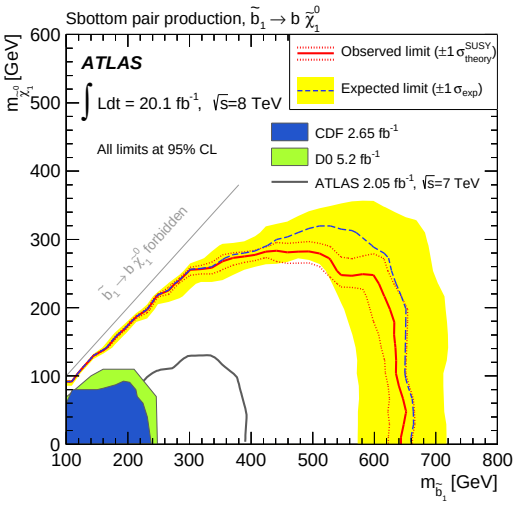

Figure 6: 95% C.L. exclusion contours in the sbottom-neutralino mass plane defined in the framework of a simplified model assuming a single decay chain of $\tilde{b} \to b\tilde{\chi}_1^0$.

The top squark decay modes depend on the SUSY mass spectrum, and on the $\tilde{t}_L$-$\tilde{t}_R$ mixture of the top squark mass eigenstate. If kinematically allowed, the two-body decays $\tilde{t} \to t\tilde{\chi}^0$ (requires $m_{\tilde{t}} - m_{\tilde{\chi}^0} > m_t$) and $\tilde{t} \to b\tilde{\chi}^{\pm}$ (requires $m_{\tilde{t}} - m_{\tilde{\chi}^{\pm}} > m_b$) are expected to dominate. If not, the top squark decay may proceed either via the two-body decay $\tilde{t} \to c\tilde{\chi}^0$ or through $\tilde{t} \to bf\bar{f}'\tilde{\chi}^0$ (where f and $\bar{f}'$ denote a fermion-antifermion pair with appropriate quantum numbers). For $m_{\tilde{t}} - m_{\tilde{\chi}^0} > m_b$ the latter decay chain represents a four-body decay with a W boson, charged Higgs H, slepton $\tilde{\ell}$, or light flavor squark

$\tilde{q}$, exchange. If the exchanged W boson and/or sleptons are kinematically allowed to be on-shell ($m_{\tilde{t}} - m_{\tilde{\chi}^\pm} > m_b + m_W$ and/or $m_{\tilde{t}} - m_{\tilde{\ell}} > m_b$), the three-body decays $\tilde{t} \to Wb\tilde{\chi}^0$ and/or $\tilde{t} \to bl\tilde{\ell}$ will become dominant. For further discussion on top squark decays see for example [85].

Limits from LEP on the $\tilde{t}_1$ mass are $m_{\tilde{t}} > 96$ GeV in the charm plus neutralino final state, and > 93 GeV in the lepton, b-quark and sneutrino final state [62].

The Tevatron experiments have performed a number of searches for top squarks, often assuming direct pair production. In the $b\ell\tilde{\nu}$ decay channel, and assuming a 100% branching fraction, limits are set as $m_{\tilde{t}} > 210$ GeV for $m_{\tilde{\nu}} < 110$ GeV and $m_{\tilde{t}} - m_{\tilde{\nu}} > 30$ GeV, or $m_{\tilde{t}} > 235$ GeV for $m_{\tilde{\nu}} < 50$ GeV [86,87]. In the $\tilde{t} \to c\tilde{\chi}^0$ decay mode, a top squark with a mass below 180 GeV is excluded for a neutralino lighter than 95 GeV [88,89]. In both analyses, no limits on the top squark can be set for heavy sneutrinos or neutralinos. In the $\tilde{t} \to b\tilde{\chi}_1^\pm$ decay channel, searches for a relatively light top squark have been performed in the dilepton final state [90,91]. The CDF experiment sets limits in the $\tilde{t} - \tilde{\chi}_1^0$ mass plane for various branching fractions of the chargino decay to leptons and for two value of $m_{\tilde{\chi}_1^\pm}$. For $m_{\tilde{\chi}_1^\pm} = 105.8$ GeV and $m_{\tilde{\chi}_1^0} = 47.6$ GeV, top squarks between 128 and 135 GeV are excluded for W-like leptonic branching fractions of the chargino.

Today the LHC experiments have improved these limits substantially. As shown in the right plot of Fig. 7, limits on the top squark mass assuming a simplified model with a single decay chain of $\tilde{t} \to t\tilde{\chi}_1^0$ reach up to almost 700 GeV for light neutralinos, while for $m_{\tilde{\chi}_1^0} > 240$ GeV no limits can be provided. The most important searches for this top squark decay topology are dedicated searches requiring zero or one isolated lepton, modest $E_{\rm T}^{\rm miss}$, and four or more jets out of which at least one jet must be reconstructed as b-jet [92–93]. To increase the sensitivity to this decay topology different signal regions are considered in these ATLAS analyses. A search of the CMS collaboration requiring one isolated lepton and using a boosted decision tree for a dedicated optimization in the $m_{\tilde{t}} - m_{\tilde{\chi}_1^0}$ plane [94] provides a comparable limit for this simplified model.

Assuming that the top squark decay exclusively proceeds via the chargino mediated decay chain $\tilde{t} \to b\tilde{\chi}_1^\pm$, $\tilde{\chi}_1^\pm \to W^{\pm(*)}\tilde{\chi}_1^0$ yields stop mass exclusion limits that vary strongly with the assumptions made on the $\tilde{t} - \tilde{\chi}_1^\pm - \tilde{\chi}_1^0$ mass hierarchy (see Fig. 7 left plot). Above the universal chargino mass limit of $m_{\tilde{\chi}_1^\pm} > 103.5$ GeV from LEP (see section II.5.1) the strongest limits are placed for nearly mass degenerate chargino and neutralinos. For $m_{\tilde{\chi}_1^\pm} - m_{\tilde{\chi}_1^0} > 5$ GeV, a stop mass of ≈ 650 GeV for a light $\tilde{\chi}_1^0$ is excluded, while no limit can be placed for $m_{\tilde{\chi}_1^0} > 280$ GeV [82]. These limits, however, can weaken significantly when other assumptions about the mass hierarchy are imposed. For example, as also shown in Fig. 7, if the chargino becomes nearly mass degenerate with the top squark the key experimental signature turns from an all-hadronic final state with b-jets and $E_{\rm T}^{\rm miss}$ into a multi-lepton and $E_{\rm T}^{\rm miss}$

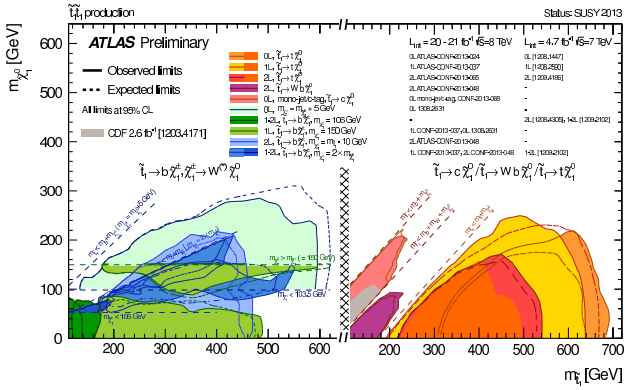

Figure 7: 95% C.L. exclusion contours in the $m_{\tilde{t}} - m_{\tilde{\chi}_1^0}$ plane for different top squark decay chains and different searches from the ATLAS collaboration. The plot on the right shows simplified model limits for three different decay chains; $\tilde{t} \to c\tilde{\chi}_1^0$ (W and t forbidden), $\tilde{t} \to Wb\tilde{\chi}_1^0$ (t forbidden), and $\tilde{t} \to t\tilde{\chi}_1^0$ (t allowed), which represent three different kinematic regions of the top squark decay. The plot to the left shows simplified model limits for the top decay chain via a chargino: $\tilde{t} \to b\tilde{\chi}_1^\pm$, $\tilde{\chi}_1^\pm \to W^{\pm(*)}\tilde{\chi}_1^0$. For this case, several exemplary hypotheses on the $\tilde{t} - \tilde{\chi}_1^\pm - \tilde{\chi}_1^0$ mass hierarchy are assumed.

topology. Assuming $m_{\tilde{\chi}_1^\pm} = m_{\tilde{t}} - 10$ GeV provides a best limit of $m_{\tilde{t}} = 470$ GeV for neutralino masses below 100 GeV, whereas for $m_{\tilde{\chi}_1^0} > 200$ GeV no limit can be obtained [95]. As for the decay with top quarks in the final state, the CMS analysis [94] also provides comparable limits for this decay chain.

If the decays $\tilde{t} \to t\tilde{\chi}_1^0$ and $\tilde{t} \to b\tilde{\chi}_1^\pm$, $\tilde{\chi}_1^\pm \to W^{\pm(*)}\tilde{\chi}_1^0$ are kinematically forbidden, the decay chains $\tilde{t} \to Wb\tilde{\chi}^0$ and $\tilde{t} \to c\tilde{\chi}^0$ can become important. As shown in the right plot of Fig. 7, ATLAS provides for the kinematic region $m_{\tilde{t}} - m_{\tilde{\chi}^\pm} > m_b + m_W$ upper limits on top squark mass of ≈ 230 GeV for a neutralino lighter than ≈ 100 GeV [95], while the boosted decision tree based CMS analysis pushes this limit to about 320 GeV for neutralino masses below ≈ 200 GeV [94]. For the kinematic region in which even the production of real W bosons is not allowed, ATLAS improves the Tevatron limit on $\tilde{t} \to c\tilde{\chi}^0$ substantially. Based on a combination of a monojet analysis and a dedicated charm quark identification algorithm, a top squark with a mass below 240 GeV is excluded for a neutralino lighter than 200 GeV [96].

R-parity violating production of single top squarks has been searched for at LEP, HERA, and the Tevatron. For example, an analysis from the ZEUS collaboration [97] makes an interpretation of its search result assuming top squarks to be produced via a λ' coupling and decay either to $b\tilde{\chi}_1^\pm$ or R-parity-violating to a lepton and a jet. Limits are set on λ'_{131} as a function of the top squark mass in an MSSM framework with gaugino mass unification at the GUT scale. The search for top squark pair production in the context of R-parity violating supersymmetry has now also become a focus

point for searches at the LHC. Recently the CMS collaboration has performed a search for top squarks using a variety of multilepton final states [98]. It provides lower limits on the top squark mass in models with non-zero leptonic R-parity violating couplings λ_{122} and λ_{233}. For a bino mass of 200 GeV, these limits are 1020 GeV and 820 GeV, respectively. The analysis also provides limits in a model with the semileptonic R-parity violating coupling λ'_{233}.

Top squarks can also be long-lived and hadronize to a R-hadron, for example in the scenario where the top squark is the next-to-lightest SUSY particle (NLSP), with a small mass difference to the LSP. Searches for massive stable charged particles are sensitive to such top squarks. As shown in Fig. 4 for the CMS analysis [70], the LHC experiments have set limits $m_{\tilde{t}} > 800$ GeV in such scenarios, surpassing significantly the earlier Tevatron limits of about 300 GeV [99,100].

It should be noted that limits discussed in this section belong to different top and bottom squark decay channels, different sparticle mass hierarchies, and different simplified decay scenarios. Therefore, care must be taken when interpreting these limits in the context of more complete SUSY models.

II.4.4. Summary of exclusion limits on squarks and gluinos assuming R-Parity conservation

A summary of the most important squark and gluino mass limits for different interpretation approaches assuming R-parity conservation is shown in Table 2.

For gluino masses rather similar limits, ranging from 1.2 TeV to 1.4 TeV, are obtained from different model assumptions indicating that the LHC is indeed probing for a large region in SUSY parameter space direct gluino production at the 1 TeV scale and beyond. However, for neutralino masses above approximately 700 GeV in the best case, ATLAS and CMS searches cannot place any limits on the gluino mass.

Limits on direct squark production, on the other hand, depend strongly on the chosen model. Especially for direct production of top squarks there are still large regions in parameter space where masses below 0.5 TeV cannot be excluded. This is also true for first and second generation squarks when only one single squark is considered. Furthermore, for neutralino masses above $\approx$ 300 GeV no limit on any direct squark production scenario can be placed by the LHC.

Table 2: Summary of squark mass and gluino mass limits using different interpretation approaches assuming R-parity conservation. Masses in this table are provided in GeV. Further details about assumption and analyses from which these limits are obtained are discussed in the corresponding sections of the text.

Model	Assumption	$m_{\tilde{q}}$	$m_{\tilde{g}}$
CMSSM	$m_{\tilde{q}} \approx m_{\tilde{g}}$	$\approx$ 1700	$\approx$ 1700
	all $m_{\tilde{q}}$	-	$\approx$ 1300
	all $m_{\tilde{g}}$	$\approx$ 1600	-
Simplified model $\tilde{g}\tilde{q}, \tilde{g}\bar{\tilde{q}}$	$m_{\tilde{\chi}^0_1}$= 0, $m_{\tilde{q}} \approx m_{\tilde{g}}$	$\approx$ 1700	$\approx$ 1700
	$m_{\tilde{\chi}^0_1}$= 0, all $m_{\tilde{q}}$	-	$\approx$ 1400
	$m_{\tilde{\chi}^0_1}$= 0, all $m_{\tilde{g}}$	$\approx$ 1400	-
Simplified models $\tilde{g}\tilde{g}$			
$\tilde{g} \to q\bar{q}\tilde{\chi}^0_1$	$m_{\tilde{\chi}^0_1}$ =0	-	$\approx$ 1200
	$m_{\tilde{\chi}^0_1} > \approx$ 450	-	no limit
$\tilde{g} \to b\bar{b}\tilde{\chi}^0_1$	$m_{\tilde{\chi}^0_1}$ =0	-	$\approx$ 1200
	$m_{\tilde{\chi}^0_1} > \approx$ 650	-	no limit
$\tilde{g} \to t\bar{t}\tilde{\chi}^0_1$	$m_{\tilde{\chi}^0_1}$ =0	-	$\approx$ 1400
	$m_{\tilde{\chi}^0_1} > \approx$ 700	-	no limit
Simplified models $\tilde{q}\tilde{q}$			
$\tilde{q} \to q\tilde{\chi}^0_1$	$m_{\tilde{\chi}^0_1}$ =0	$\approx$ 800	-
	$m_{\tilde{\chi}^0_1} > \approx$ 300	no limit	-
$\tilde{u}_L \to q\tilde{\chi}^0_1$	$m_{\tilde{\chi}^0_1}$ =0	$\approx$ 450	-
	$m_{\tilde{\chi}^0_1} > \approx$ 100	no limit	-
$\tilde{b} \to b\tilde{\chi}^0_1$	$m_{\tilde{\chi}^0_1}$ =0	$\approx$ 650	-
	$m_{\tilde{\chi}^0_1} > \approx$ 300	no limit	-
$\tilde{t} \to t\tilde{\chi}^0_1$	$m_{\tilde{\chi}^0_1}$ =0	$\approx$ 700	-
	$m_{\tilde{\chi}^0_1} > \approx$ 250	no limit	-
$\tilde{t} \to b\tilde{\chi}^\pm_1$	$m_{\tilde{\chi}^0_1}$ =0	$\approx$ 700	-
$[m_{\tilde{\chi}^\pm_1} - m_{\tilde{\chi}^0} > 5$ GeV]	$m_{\tilde{\chi}^0_1} > \approx$ 300	no limit	-
$\tilde{t} \to b\tilde{\chi}^\pm_1$	$m_{\tilde{\chi}^0_1}$ =0	$\approx$ 500	-
$[m_{\tilde{t}} - m_{\tilde{\chi}^\pm_1} > 10$ GeV]	$m_{\tilde{\chi}^0_1} > \approx$ 200	no limit	-
$\tilde{t} \to Wb\tilde{\chi}^0_1$	$m_{\tilde{\chi}^0_1} < \approx$ 200	$\approx$ 300	-
$[m_{\tilde{t}} - m_{\tilde{\chi}^0} > m_b + m_W]$			
$\tilde{t} \to c\tilde{\chi}^0_1$	$m_{\tilde{\chi}^0_1} < \approx$ 200	$\approx$ 250	-
$[m_{\tilde{t}} - m_{\tilde{\chi}^0} > m_c]$			

II.5. Exclusion limits on the masses of charginos and neutralinos

Charginos and neutralinos result from mixing of the charged wino and higgsino states, and the neutral bino, wino and higgsino states, respectively. The mixing is determined by a limited number of parameters. For charginos these are the wino mass parameter M_2, the higgsino mass parameter μ, and $\tan\beta$, and for neutralinos these are the same parameters plus the bino mass parameter M_1. The mass states are four charginos $\tilde{\chi}^+_1$, $\tilde{\chi}^-_1$, $\tilde{\chi}^+_2$ and $\tilde{\chi}^-_2$, and four neutralinos $\tilde{\chi}^0_1$, $\tilde{\chi}^0_2$, $\tilde{\chi}^0_3$ and $\tilde{\chi}^0_4$, ordered in increasing mass. Depending on the mixing, the chargino and neutralino composition is dominated by specific states, which are referred to as bino-like ($M_1 << M_2, \mu$), wino-like ($M_2 << M_1, \mu$), or higgsino-like ($\mu << M_1, M_2$). If gaugino mass unification at the GUT scale is assumed, a relation between M_1 and M_2 at the electroweak scale follows: $M_1 = 5/3 \tan^2\theta_W M_2 \approx 0.5 M_2$, with θ_W the weak mixing angle. Charginos and neutralinos carry no color charge, and only have electroweak couplings (neglecting gravity).

II.5.1. Exclusion limits on chargino masses

If kinematically allowed, two body decay modes such as $\tilde{\chi}^\pm \to \tilde{f}\bar{f}'$ (including $\ell\tilde{\nu}$ and $\tilde{\ell}\nu$) are dominant. If not, three body decay $\tilde{\chi}^\pm \to f\bar{f}'\tilde{\chi}^0$ are mediated through virtual W

bosons or sfermions. If sfermions are heavy, the W mediation dominates, and $f\bar{f}'$ are distributed with branching fractions similar to W decay products. If, on the other hand, sleptons are light enough to play a significant role in the decay mediation, leptonic final states will be enhanced.

At LEP, charginos have been searched for in fully-hadronic, semi-leptonic and fully leptonic decay modes [101,102]. A general lower limit on the lightest chargino mass of 103.5 GeV is derived, except in corners of phase space with low electron sneutrino mass, where destructive interference in chargino production, or two-body decay modes, play a role. The limit is also affected if the mass difference between $\tilde{\chi}_1^\pm$ and $\tilde{\chi}_1^0$ is small; dedicated searches for such scenarios set a lower limit of 92 GeV.

At the Tevatron, charginos are searched for via associated production of $\tilde{\chi}_1^\pm\tilde{\chi}_2^0$ [103,104]. Decay modes involving multi-lepton final states provide the best discrimination against the large multijet background. Analyses look for at least three charged isolated leptons, for two leptons with missing transverse momentum, or for two leptons with the same charge. Depending on the $(\tilde{\chi}_1^\pm - \tilde{\chi}_1^0)$ and/or $(\tilde{\chi}_2^0 - \tilde{\chi}_1^0)$ mass differences, leptons may be soft.

At the LHC, the search strategy is similar to that at the Tevatron. As shown in Fig. 1, pair production of chargino and neutralinos at the LHC, for masses of several hundreds of GeV, is at least two orders of magnitude smaller than for colored SUSY particles (e.g. top squark pair production). For this reason a high statistics data sample is required to improve the sensitivity of LEP and Tevatron searches for direct chargino/neutralino production. With the data collected in 2012, ATLAS and CMS have now started to surpass in regions of SUSY parameter space the limits from LEP and Tevatron. Chargino pair production is searched for in the dilepton plus missing momentum final state. In the interpretation of the results, both ATLAS [105] and CMS [106] assume mediation through light sleptons; the analyses do not yet place limits on charginos decaying via a W boson. In the light slepton scenario, chargino mass limits up to 550 GeV are set for massless LSPs, but no limits on the chargino mass can be set for $\tilde{\chi}_1^0$ heavier than 150 GeV. The trilepton plus missing momentum final state is used to set limits on $\tilde{\chi}_1^\pm\tilde{\chi}_2^0$ production, assuming wino-like $\tilde{\chi}^\pm$ and $\tilde{\chi}_2^0$, bino-like $\tilde{\chi}_1^0$, and $m_{\tilde{\chi}^\pm} = m_{\tilde{\chi}_2^0}$, leaving $m_{\tilde{\chi}^\pm}$ and $m_{\tilde{\chi}_1^0}$ free. Again, the branching fraction of leptonic final states is determined by the slepton masses. If the decay is predominantly mediated by a light $\tilde{\ell}_\mathrm{L}$, i.e. $\tilde{\ell}_\mathrm{R}$ is assumed to be heavy, the three lepton flavors will be produced in equal amounts. It is assumed that $\tilde{\ell}_\mathrm{L}$ and sneutrino masses are equal, and diagrams with sneutrinos are included. In this scenario, ATLAS [107] and CMS [106] exclude chargino masses below 730 GeV for massless LSPs; no limits are set for LSPs above 350 GeV. If the decay is dominated by a light $\tilde{\ell}_\mathrm{R}$, the chargino cannot be a pure wino but needs to have a large higgsino component, preferring the decays to tau leptons. Assuming that also the $\tilde{\chi}_2^0$ decay leads to two tau leptons in the final state, CMS sets limits of 350 GeV on the chargino mass for massless LSPs [106]. ATLAS assumes a simplified model in which staus are significantly lighter than the other sleptons in order to search for a similar multi-tau final state, and sets a similar limit on the chargino mass [108]. If sleptons are heavy, the chargino is assumed to decay to a W boson plus LSP, and the $\tilde{\chi}_2^0$ into either Z plus LSP, or Higgs plus LSP. In the WZ channel, ATLAS [107] and CMS [106] limits on the chargino mass reach 300 GeV for massless LSPs, but no limits are set for LSPs heavier than 100 GeV. The WH channel is also investigated, for $m_H = 126$ GeV and using Higgs decays to $b\bar{b}$ (ATLAS [109]) or Higgs decays to $b\bar{b}$, WW, ZZ and $\tau^+\tau^-$ (CMS [110]) , assuming a SM-like branching fraction in these final states. Chargino mass limits extend up to 287 GeV for massless LSPs, but vanish for LSPs above 50 GeV. The CMS results on electroweak gaugino searches are summarized in Fig. 8, the ATLAS results are similar.

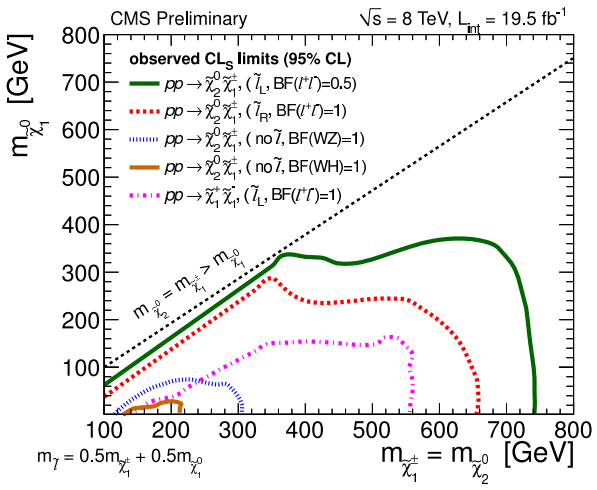

Figure 8: A summary of limits on chargino and neutralino masses as obtained by CMS.

In both the wino region (a characteristic of anomaly-mediated SUSY breaking models) and the higgsino region of the MSSM, the mass splitting between $\tilde{\chi}_1^\pm$ and $\tilde{\chi}_1^0$ is small. In such scenarios, charginos may be long-lived. Charginos decaying in the detectors away from the primary vertex could lead to signatures such as kinked-tracks, or apparently disappearing tracks, since, for example, the pion in $\tilde{\chi}_1^\pm \to \pi^\pm\tilde{\chi}_1^0$ might be too soft to be reconstructed. At the LHC, a search has been performed for such disappearing tracks, and interpreted within anomaly-mediated SUSY breaking models. Charginos with lifetimes between 0.1 and 10 ns are excluded for chargino masses up to 500 GeV [111]. Within AMSB models, a lower limit on the chargino mass of 270 GeV is set, for a mass difference with the LSP of 160 MeV and a lifetime of 0.2 ns.

Charginos with a lifetime longer than the time needed to pass through the detector appear as charged stable massive particles. Limits have been derived by the LEP experiments [112]

and by D0 at the Tevatron [100]. D0 results exclude higgsino-like stable charginos below 244 GeV, and gaugino-like stable charginos below 278 GeV.

II.5.2. Exclusion limits on neutralino masses

In a considerable part of the MSSM parameter space, and in particular when demanding that the LSP carries no electric or color charge, the lightest neutralino $\tilde{\chi}_1^0$ is the LSP. If R-parity is conserved, such a $\tilde{\chi}_1^0$ is stable. Since it is weakly interacting, it will typically escape detectors unseen. Limits on the invisible width of the Z boson apply to neutralinos with a mass below 45.5 GeV, but depend on the Z-neutralino coupling. Such a coupling could be small or even absent; in such a scenario there is no general lower limit on the mass of the lightest neutralino [113]. In models with gaugino mass unification and sfermion mass unification at the GUT scale, a lower limit on the neutralino mass is derived from limits from direct searches, notably for charginos and sleptons, and amounts to 47 GeV [114]. Assuming a constraining model like the CMSSM, this limit increases to 50 GeV at LEP; however the strong constraints now set by the LHC increase such CMSSM-derived $\tilde{\chi}_1^0$ mass limits to well above 200 GeV [115].

Even though a LSP neutralino is only weakly interacting, collider experiments are not totally blind to neutralino pair production. Pair production of neutralinos accompanied by initial state radiation could lead to an observable final state. At LEP, final states with only a single isolated photon were studied, but backgrounds from neutrino pair production were too large. At hadron colliders, monojet final states have been used to set limits on dark matter properties using an effective Lagrangian approach [116–118].

In gauge-mediated models, the LSP is typically a gravitino, and the phenomenology is determined by the nature of the NLSP. A NLSP neutralino will decay to a gravitino and a SM particle whose nature is determined by the neutralino composition. Final states with two high p_{T} photons and missing momentum are searched for, and interpreted in gauge mediation models with bino-like neutralinos [119–123]. Assuming only gluino pair production and a bino-like neutralino produced in gluino decay, limits on gluino masses of about 1 TeV are set for all neutralino masses, as shown in Fig. 9 for the CMS diphoton analysis.

Assuming the production of at least two neutralinos per event, neutralinos with large non-bino components can also be searched for in final states with missing momentum plus any two bosons out of the collection γ, Z, Higgs. Searches for final states with Z ($\rightarrow \ell^+\ell^-$) bosons and missing transverse momentum have been performed at the Tevatron [124] and at the LHC [125,126], and are interpreted in such models.

In gauge mediation models, NLSP neutralino decays need not be prompt, and experiments have searched for late decays. CDF have searched for delayed $\tilde{\chi}_1^0 \rightarrow \gamma\tilde{G}$ decays using the timing of photon signals in the calorimeter [127]. CMS has used the same technique at the LHC [128]. Results are given as upper limits on the neutralino production cross section as a function of neutralino mass and lifetime. D0 has looked at the direction of showers in the electromagnetic calorimeter with a similar goal [129], and ATLAS has searched for photon candidates that do not point back to the primary vertex [130].

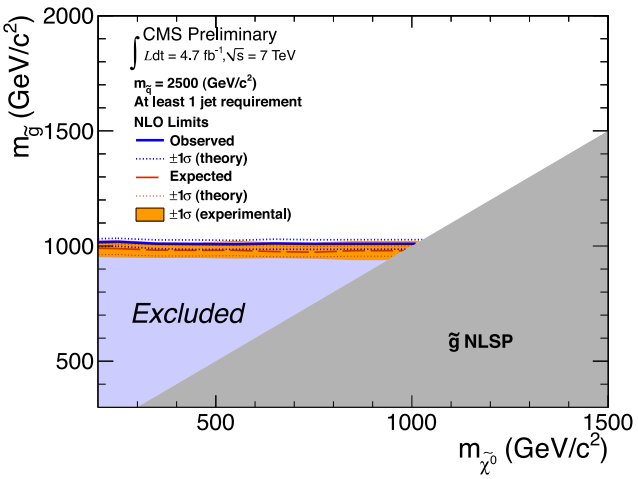

Figure 9: Observed 95% C.L. limits on the gluino mass as a function of the neutralino mass, in general gauge mediation models assuming only gluino pair production, with a bino-like neutralino produced in gluino decay, and a neutralino decay to photon plus gravitino.

Heavier neutralinos, in particular $\tilde{\chi}_2^0$, have been searched for in their decays to the lightest neutralino plus a γ, a Z boson or a Higgs boson. Limits on electroweak production of $\tilde{\chi}_2^0$ plus $\tilde{\chi}_1^\pm$ from trilepton analyses have been discussed in the section on charginos; the assumption of equal mass of $\tilde{\chi}_2^0$ and $\tilde{\chi}_1^\pm$ make the limits on chargino masses apply to $\tilde{\chi}_2^0$ as well. Heavier neutralinos in the decay chains of colored particles are searched for by the presence of missing momentum plus an isolated high-energy photon [123] or leptons [129,131–132]. In $\tilde{\chi}_2^0$ decays to $\tilde{\chi}_1^0$ and a lepton pair, the lepton pair invariant mass distribution may show a structure that can be used to measure the $\tilde{\chi}_2^0 - \tilde{\chi}_1^0$ mass difference in case of a signal [133], but it can also be used in the search itself, in order to suppress background [134].

The lightest neutralino can decay in models with R-parity violation. If the decay involves a non-zero λ coupling, the final state will be a multi-lepton one. Searches for events with four or more isolated charged leptons by ATLAS [135] and CMS [136] are interpreted in such models. An ATLAS search for events with isolated muons and a displaced vertex is interpreted in a model with R-parity violating neutralino decay involving a non-zero λ' coupling [137].

Table 3: Summary of weak gaugino mass limits, assuming R-parity conservation. Masses in the table are provided in GeV. Further details about assumptions and analyses from which these limits are obtained are discussed in the text.

Assumption	m_χ
$\tilde{\chi}_1^\pm$, all $\Delta m(\tilde{\chi}_1^\pm, \tilde{\chi}_1^0)$	> 92
$\tilde{\chi}_1^\pm$ $\Delta m > 5$, $m_{\tilde{\nu}} > 300$	> 103.5
$\tilde{\chi}_1^\pm$, $m_{(\tilde{\ell},\tilde{\nu})} = (m_{\tilde{\chi}_1^\pm} + m_{\tilde{\chi}_1^0})/2$	
$m_{\tilde{\chi}_1^0} \approx 0$	$103.5 - 115, > 550$
$\tilde{\chi}_1^\pm$, $m_{\tilde{\chi}_1^0} > 150$	no LHC limit
$\tilde{\chi}_1^\pm$, $m_{\tilde{\ell}} > m_{\tilde{\chi}_1^\pm}$	no LHC limit
$m_{\tilde{\chi}_1^\pm} = m_{\tilde{\chi}_2^0}$, $m_{\tilde{\ell}_L} = (m_{\tilde{\chi}_1^\pm} + m_{\tilde{\chi}_1^0})/2$	
$m_{\tilde{\chi}_1^0} \approx 0$	> 730
$m_{\tilde{\chi}_1^0} > 350$	no LHC limit
$m_{\tilde{\chi}_1^\pm} = m_{\tilde{\chi}_2^0}$, $m_{\tilde{\ell}_R} = (m_{\tilde{\chi}_1^\pm} + m_{\tilde{\chi}_1^0})/2$	
$m_{\tilde{\chi}_1^0} \approx 0$	> 350
$m_{\tilde{\chi}_1^0} > 100$	no LHC limit
$m_{\tilde{\chi}_1^\pm} = m_{\tilde{\chi}_2^0}$, $m_{\tilde{\ell}} > m_{\tilde{\chi}_1^\pm}$, BF$(WZ) = 1$	
$m_{\tilde{\chi}_1^0} \approx 0$	> 300
$m_{\tilde{\chi}_1^0} > 100$	no LHC limit
$m_{\tilde{\chi}_1^\pm} = m_{\tilde{\chi}_2^0}$, $m_{\tilde{\ell}} > m_{\tilde{\chi}_1^\pm}$, BF$(WH) = 1$	
$m_{\tilde{\chi}_1^0} \approx 0$	> 280
$m_{\tilde{\chi}_1^0} > 50$	no LHC limit

II.6. Exclusion limits on slepton masses

In models with slepton and gaugino mass unification at the GUT scale, the right-handed slepton, $\tilde{\ell}_R$, is expected to be lighter than the left-handed slepton, $\tilde{\ell}_L$. For tau sleptons there may be considerable mixing between the L and R states, leading to a significant mass difference between the lighter $\tilde{\tau}_1$ and the heavier $\tilde{\tau}_2$.

II.6.1. Exclusion limits on the masses of charged sleptons

The most model-independent searches for selectrons, smuons and staus originate from the LEP experiments [138]. Smuon production only takes place via s-channel γ^*/Z exchange. Search results are often quoted for $\tilde{\mu}_R$, since it is typically lighter than $\tilde{\mu}_L$ and has a weaker coupling to the Z boson; limits are therefore conservative. Decays are expected to be dominated by $\tilde{\mu}_R \to \mu\tilde{\chi}_1^0$, leading to two non-back-to-back muons and missing momentum. Limits are calculated in the MSSM under the assumption of gaugino mass unification at the GUT scale, and depend on the mass difference between the smuon and $\tilde{\chi}_1^0$. A $\tilde{\mu}_R$ with a mass below 94 GeV is excluded for $m_{\tilde{\mu}_R} - m_{\tilde{\chi}_1^0} > 10$ GeV. The selectron case is similar to the smuon case, except that an additional production mechanism is provided by t-channel neutralino exchange. The $\tilde{e}_R$ lower mass limit is 100 GeV for $m_{\tilde{\chi}_1^0} < 85$ GeV. Due to the t-channel neutralino exchange, $\tilde{e}_R\tilde{e}_L$ pair production was possible at LEP, and a lower limit of 73 GeV was set on the selectron mass regardless of the neutralino mass by scanning over MSSM parameter space [139]. The potentially large mixing between $\tilde{\tau}_L$ and $\tilde{\tau}_R$ not only makes the $\tilde{\tau}_1$ light, but can also make its coupling to the Z boson small. LEP lower limits on the $\tilde{\tau}$ mass range between 87 and 93 GeV depending on the $\tilde{\chi}_1^0$ mass, for $m_{\tilde{\tau}} - m_{\tilde{\chi}_1^0} > 7$ GeV [138].

As shown in Fig. 1, at the LHC pair production of sleptons is not only heavily suppressed with respect to pair production of colored SUSY particles but is also almost two orders of magnitude smaller than pair production of chargino and neutralinos. Therefore, only with the 2012 LHC data ATLAS and CMS are starting to surpass the sensitivity of the LEP analyses.

ATLAS and CMS have searched for direct production of selectron pairs and smuon pairs at the LHC, with each slepton decaying to its corresponding SM partner lepton and the $\tilde{\chi}_1^0$ LSP. ATLAS [105] and CMS [106] set limits in this model of 220 GeV for $\tilde{\ell}_R$, and 290 GeV for $\tilde{\ell}_L$, for a massless $\tilde{\chi}_1^0$ and assuming equal selectron and smuon masses, as shown in Fig. 10. The limits deteriorate with increasing $\tilde{\chi}_1^0$ mass due to decreasing missing momentum and lepton momentum. As a consequence, there is a gap between LEP and LHC limits for $\tilde{\chi}_1^0$ masses above 20 GeV, and no limits are set for $\tilde{\chi}_1^0$ masses above 90 GeV ($\tilde{\ell}_R$) or above 150 GeV ($\tilde{\ell}_L$).

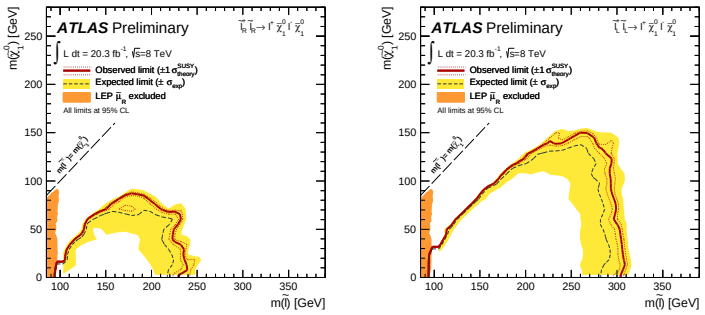

Figure 10: Exclusion limits on $\tilde{\ell}_R$ masses (left) and $\tilde{\ell}_L$ masses (right), assuming equal selectron and smuon masses in both scenarios, and assuming a 100% branching fraction for $\tilde{\ell} \to \ell\tilde{\chi}_1^0$.

In gauge-mediated SUSY breaking models, sleptons can be (co-)NLSPs, *i.e.*, the next-to-lightest SUSY particles and almost degenerate in mass, decaying to a lepton and a gravitino. This decay can either be prompt, or the slepton can have a non-zero lifetime. Combining several analyses, lower mass limits on $\tilde{\mu}_R$ of 96.3 GeV and on $\tilde{e}_R$ of 66 GeV are set for all slepton lifetimes at LEP [140]. In a considerable part of parameter space in these models, the $\tilde{\tau}$ is the NLSP. The LEP experiments have set lower limits on the mass of such a $\tilde{\tau}$ between 87 and 97 GeV, depending on the $\tilde{\tau}$ lifetime. ATLAS has searched for final states with τs, jets and missing transverse momentum, and has interpreted the results in GMSB

models setting limits on the model parameters [141]. CMS has interpreted a multilepton analysis in terms of limits on gauge mediation models with slepton (co-)NLSP [142]. CDF has put limits on gauge mediation models at high $\tan\beta$ and slepton (co-)NLSP using an analysis searching for like-charge light leptons and taus [143].

Limits also exist on sleptons in R-parity violating models, both from LEP and the Tevatron experiments. From LEP, lower limits on $\tilde{\mu}_{\rm R}$ and $\tilde{e}_{\rm R}$ masses in such models are 97 GeV, and the limits on the stau mass are very close: 96 GeV [144].

Charged slepton decays may be kinematically suppressed, for example in the scenario of a NLSP slepton with a very small mass difference to the LSP. Such a slepton may appear to be a stable charged massive particle. Interpretation of searches at LEP for such signatures within GMSB models with stau NLSP or slepton co-NLSP exclude masses up to 99 GeV [112]. Searches of stable charged particles at the Tevatron [99,100] and at the LHC [145,70] are also interpreted in terms of limits on stable charged sleptons. The limits obtained at the LHC exclude stable staus with masses below 339 GeV when produced directly in pairs, and below 500 GeV when staus are produced both directly and indirectly in the decay of other particles in a GMSB model. Drell-Yan production of $q = 1$ stable lepton-like particles is excluded for masses below 574 GeV [70].

II.6.2. Exclusion limits on sneutrino masses

The invisible width of the Z boson puts a lower limit on the sneutrino mass of about 45 GeV. Tighter limits are derived from other searches, notably for gauginos and sleptons, under the assumption of gaugino and sfermion mass universality at the GUT scale, and amount to approximately 94 GeV in the MSSM [146]. It is possible that the lightest sneutrino is the LSP; however, a left-handed sneutrino LSP is ruled out as a cold dark matter candidate [147,148].

Production of pairs of sneutrinos in R-parity violating models has been searched for at LEP [144]. Assuming fully leptonic decays via λ-type couplings, lower mass limits between 85 and 100 GeV are set. At the Tevatron [149,150] and at the LHC [151], searches have focused on scenarios with resonant production of a sneutrino, decaying to $e\mu$, $\mu\tau$ and $e\mu$ final states. No signal has been seen, and limits have been set on sneutrino masses as a function of the value of relevant RPV couplings. As an example, the ATLAS analysis excludes a resonant tau sneutrino with a mass below 800 GeV for $\lambda_{312} > 0.01$ and $\lambda'_{311} > 0.01$ [151].

II.7. Global interpretations

Apart from the interpretation of direct searches for sparticle production at colliders in terms of limits on masses of individual SUSY particles, model-dependent interpretations of allowed SUSY parameter space are derived from global SUSY fits. Typically these fits combine the results from collider experiments with indirect constraints on SUSY as obtained from low-energy experiments, flavor physics, high-precision electroweak results, and astrophysical data.

Table 4: Summary of slepton mass limits from LEP and LHC, assuming R-parity conservation and 100% branching fraction for $\tilde{\ell} \to \ell\tilde{\chi}^0_1$. Masses in this table are provided in GeV.

Assumption	$m_{\tilde{\ell}}$
$\tilde{\mu}_{\rm R}$, $\Delta m(\tilde{\mu}_{\rm R}, \tilde{\chi}^0_1) > 10$	> 94
$\tilde{e}_{\rm R}$, $\Delta m(\tilde{e}_{\rm R}, \tilde{\chi}^0_1) > 10$	> 94
$\tilde{e}_{\rm R}$, any Δm	> 73
$\tilde{\tau}_{\rm R}$, $\Delta m((\tilde{\tau}_{\rm R}, \tilde{\chi}^0_1) > 7$	> 87
$\tilde{\nu}_e$, $\Delta m(\tilde{e}_{\rm R}, \tilde{\chi}^0_1) > 10$	> 94
$m_{\tilde{e}_{\rm R}} = m_{\tilde{\mu}_{\rm R}}$, $m_{\tilde{\chi}^0_1} \approx 0$	> 220
$m_{\tilde{\chi}^0_1} > \approx 90$	no LHC limit
$m_{\tilde{e}_{\rm L}} = m_{\tilde{\mu}_{\rm L}}$, $m_{\tilde{\chi}^0_1} \approx 0$	> 290
$m_{\tilde{\chi}^0_1} > \approx 150$	no LHC limit

In the pre-LHC era these fits were mainly dominated by indirect constraints. Even for very constrained models like the CMSSM, the allowed parameter space, in terms of squark and gluino masses, ranged from several hundreds of GeV to a few TeV. Furthermore, these global fits indicated that squarks and gluino masses in the range of 500 to 1000 GeV were the preferred region of parameter space, although values as high as few TeV were allowed with lower probabilities [152].

With ATLAS and CMS now probing mass scales around 1 TeV and even beyond, the importance of the direct searches for global analyses of allowed SUSY parameter space has strongly increased. For example, imposing the new experimental limits on constrained supergravity models pushes the most likely values of first generation squark and gluino masses significantly beyond 1 TeV, typically resulting in overall values of fit quality much worse than those in the pre-LHC era [115]. Although these constrained models are not yet ruled out, the extended experimental limits impose tight constraints on the allowed parameter space.

For this reason, the emphasis of global SUSY fits has shifted towards less-constrained SUSY models. Especially interpretations in the pMSSM [153] but also in simplified models have been useful to generalize SUSY searches, for example to redesign experimental analyses in order to increase their sensitivity for compressed spectra, where the mass of the LSP is much closer to squark and gluino masses than predicted, for example, by the CMSSM. As shown in Table 2, for neutralino masses above a few hundred GeV the current set of ATLAS and CMS searches cannot exclude the existence of light squarks and also gluinos above approximately 1 TeV are not yet fully excluded.

Furthermore, the discovery of a Higgs boson with a mass around 126 GeV has triggered many studies regarding the compatibility of SUSY parameter space with this new particle. Much of it is still work in progress and it will be interesting to see how the interplay between the results from direct SUSY searches and more precise measurements of the properties of the

See key on page 547

Higgs boson will unfold in the forthcoming era of high-energy running of the LHC.

II.8. Summary and Outlook

Direct searches for SUSY, combined with limits from high-precision experiments that look for new physics in loops, put SUSY under considerable scrutiny. In particular the absence of any observation of new phenomena at the first run of the LHC, at $\sqrt{s} = 7$ and 8 TeV, place significant constraints on SUSY parameter space. Today, inclusive searches probe production of gluinos in the rage of $1.0 - 1.4$ TeV, first and second generation squarks to about 1.0 TeV , third generation squarks at scales around 600 GeV, electroweak gauginos at scales around $300 - 500$ GeV, and sleptons around 200 GeV. However, depending on the assumptions made of the underlying SUSY spectrum these limits can also weaken considerably. An overview of the current landscape of SUSY searches and corresponding exclusion limits at the LHC is shown in Fig. 11 from the ATLAS experiment [154]. The corresponding results of the CMS experiment are similar [155].

The interpretation of results at the LHC has moved away from constrained models like the CMSSM towards a large set of simplified models, or the pMSSM. On the one hand this move is because the LHC limits have put constrained models like the CMSSM under severe pressure, while on the other hand simplified models leave more freedom to vary parameters and form a better representation of the underlying sensitivity of analyses. However, these interpretations in simplified models do not come without a price: the decomposition of a potentially complicated reality in a limited set of individual decay chains can be significantly incomplete. Therefore, quoted limits in simplified models are only valid under the explicit assumptions made in these models, assumptions that are usually stated on the plots, and in the relevant LHC papers. Interpretations of simplified models in generic cases, ignoring the assumptions made, can lead to overestimation of limits on SUSY parameter space. In this context, the limit range of $1.0 - 1.4$ TeV on generic colored SUSY particles only hold for light neutralinos, in the R-parity conserving MSSM. Limits on third generation squarks and electroweak gauginos also only hold for light neutralinos, and under specific assumptions for decay modes and slepton masses. In general, SUSY below the 1 TeV scale is not yet ruled out.

The next run of the LHC, at $\sqrt{s} = 13$ TeV or higher, with significantly larger integrated luminosities, will present again a great opportunity for SUSY searches. The operation at higher energy will increase the production cross section for SUSY particles, shown in Fig. 1, substantially. While typically for masses around 500 GeV the increase is about 3 to 5 times the production cross section at 8 TeV, this becomes an increase of almost two orders of magnitude for a SUSY mass scale of 1.5 to 2 TeV. Apart from pushing the sensitivity of LHC searches to higher mass scales, further LHC data will also help to reduce holes and gaps that are left behind in today's SUSY limits. These could be, for example, due to compressed particle spectra, stealth SUSY, or the violation of R-parity.

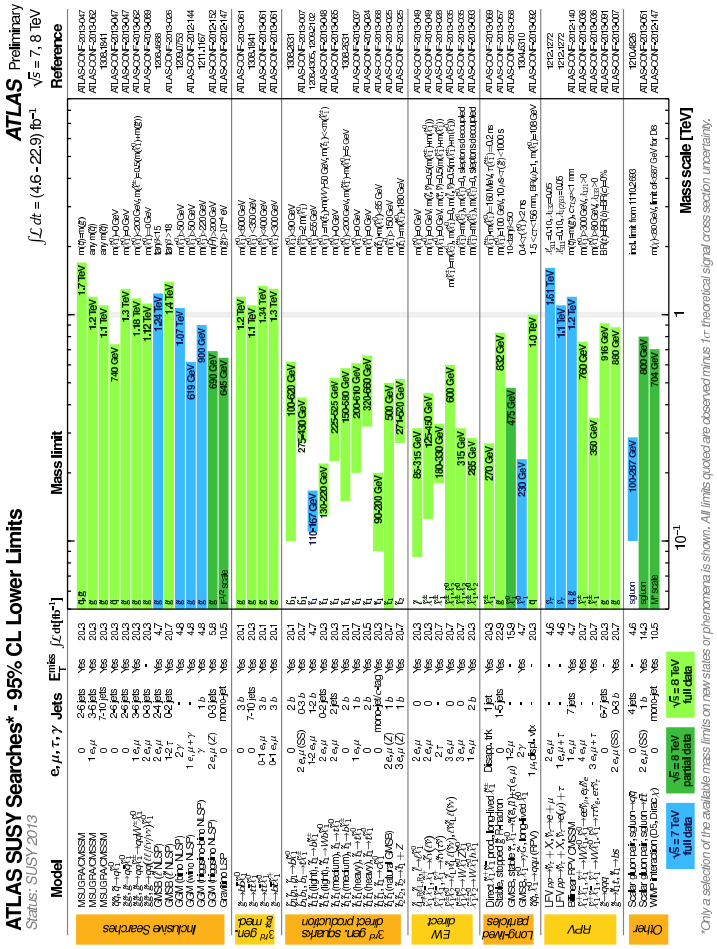

Figure 11: Overview of the current landscape of SUSY searches at the LHC. The plot shows exclusion mass limits of ATLAS for different searches and interpretation assumptions. The corresponding results of CMS are comparable.

References

1. H. Miyazawa, Prog. Theor. Phys. **36**, 1266 (1966).
2. Yu. A. Golfand and E.P. Likhtman, Sov. Phys. JETP Lett. **13**, 323 (1971).
3. J.L. Gervais and B. Sakita, Nucl. Phys. **B34**, 632 (1971).
4. D.V. Volkov and V.P. Akulov, Phys. Lett. **B46**, 109 (1973).
5. J. Wess and B. Zumino, Phys. Lett. **B49**, 52 (1974).
6. J. Wess and B. Zumino, Nucl. Phys. **B70**, 39 (1974).
7. A. Salam and J.A. Strathdee, Nucl. Phys. **B76**, 477 (1974).
8. H.P. Nilles, Phys. Reports **110**, 1 (1984).
9. H.E. Haber and G.L. Kane, Phys. Reports **117**, 75 (1987).
10. E. Witten, Nucl. Phys. **B188**, 513 (1981).
11. S. Dimopoulos and H. Georgi, Nucl. Phys. **B193**, 150 (1981).
12. M. Dine, W. Fischler, and M. Srednicki, Nucl. Phys. **B189**, 575 (1981).

13. S. Dimopoulos and S. Raby, Nucl. Phys. **B192**, 353 (1981).
14. N. Sakai, Z. Phys. **C11**, 153 (1981).
15. R.K. Kaul and P. Majumdar, Nucl. Phys. **B199**, 36 (1982).
16. H. Goldberg, Phys. Rev. Lett. **50**, 1419 (1983).
17. J.R. Ellis *et al.*, Nucl. Phys. **B238**, 453 (1984).
18. G. Jungman and M. Kamionkowski, Phys. Reports **267**, 195 (1996).
19. S. Dimopoulos, S. Raby, and F. Wilczek, Phys. Rev. **D24**, 1681 (1981).
20. W. J. Marciano and G. Senjanović, Phys. Rev. **D25**, 3092 (1982).
21. M.B. Einhorn and D.R.T. Jones, Nucl. Phys. **B196**, 475 (1982).
22. L.E. Ibanez and G.G. Ross, Phys. Lett. **B105**, 439 (1981).
23. N. Sakai, Z. Phys. **C11**, 153 (1981).
24. U. Amaldi, W. de Boer, and H. Furstenau, Phys. Lett. **B260**, 447 (1991).
25. P. Langacker and N. Polonsky, Phys. Rev. **D52**, 3081 (1995).
26. P. Fayet, Phys. Lett. **B64**, 159 (1976).
27. G.R. Farrar and P. Fayet, Phys. Lett. **B76**, 575 (1978).
28. H.E. Haber, *Supersymmetry, Part I (Theory)*, this volume.
29. CMS Collab., Phys. Rev. Lett. **111**, 101804 (2013).
30. LHCb Collab., Phys. Rev. Lett. **111**, 101805 (2013).
31. G. Hinshaw *et al.*, Astrophys. J. Supp. **208**, 19H (2013).
32. Planck Collab, *Planck 2013 results. XVI. Cosmological parameters*, arXiv:1303.5076 [astro-ph.CO].
33. M. Carena *et al.*, *Higgs Bosons: Theory and Searches*, this volume.
34. J.-F. Grivaz, *Supersymmetry, Part II (Experiment)*, in: 2010 Review of Particle Physics, K. Nakamura *et al.*, (Particle Data Group), J. Phys. **G37**, 075021 (2010).
35. I. Hinchliffe *et al.*, Phys. Rev. **D55**, 5520 (1997).
36. L. Randall and D. Tucker-Smith, Phys. Rev. Lett. **101**, 221803 (2008).
37. CMS Collab., Phys. Lett. **B698**, 196 (2011).
38. CMS Collab., Phys. Rev. Lett. **107**, 221804 (2011).
39. CMS Collab., JHEP **1301**, 077 (2013).
40. CMS Collab., Eur. Phys. J. **C73**, 2568 (2013).
41. CMS Collab., Phys. Rev. **D85**, 012004 (2012).
42. C.G. Lester and D.J. Summers, Phys. Lett. **B463**, 99 (1999).
43. D.R. Tovey, JHEP **04**, 034 (2008).
44. A.H. Chamseddine, R. Arnowitt, and P Nath, Phys. Rev. Lett. **49**, 970 (1982).
45. E. Cremmer *et al.*, Nucl. Phys. **B212**, 413 (1983).
46. P. Fayet, Phys. Lett. **B70**, 461 (1977).
47. M. Dine, A.E. Nelson, and Yu. Shirman, Phys. Rev. **D51**, 1362 (1995).
48. G.F. Giudice *et al.*, JHEP **9812**, 027 (1998).
49. L. Randall and R. Sundrum, Nucl. Phys. **B557**, 79 (1999).
50. R. Arnowitt and P Nath, Phys. Rev. Lett. **69**, 725 (1992).
51. G.L. Kane *et al.*, Phys. Rev. **D49**, 6173 (1994).
52. P. Meade, N. Seiberg, and D. Shih, Prog. Theor. Phys. Supp. **177**, 143 (2009).
53. W. Beenakker *et al.*, Nucl. Phys. **B492**, 51 (1997); W. Beenakker *et al.*, Nucl. Phys. **B515**, 3 (1998); W. Beenakker *et al.*, Phys. Rev. Lett. **83**, 3780 (1999), Erratum *ibid.*, **100**, 029901 (2008); M. Spira, hep-ph/0211145 (2002);T. Plehn, Czech. J. Phys. 55, B213 (2005).
54. A. Djouadi, J-L. Kneur, and G. Moultaka, Comp. Phys. Comm. **176**, 426 (2007).
55. C.F. Berger *et al.*, JHEP **02**, 023 (2009).
56. H. Baer *et al.*, hep-ph/9305342, 1993.
57. R.M. Barnett, H.E. Haber, and G.L. Kane, Nucl. Phys. **B267**, 625 (1986).
58. H. Baer, D. Karatas, and X. Tata, Phys. Lett. **B183**, 220 (1987).
59. J. Alwall, Ph.C. Schuster, and N. Toro, Phys. Rev. **D79**, 075020 (2009).
60. J. Alwall *et al.*, Phys. Rev. **D79**, 015005 (2009).
61. O. Buchmueller and J. Marrouche, *Universal mass limits on gluino and third-generation squarks in the context of Natural-like SUSY spectra*, arXiv:1304.2185 [hep-ph].
62. LEP2 SUSY Working Group, ALEPH, DELPHI, L3 and OPAL experiments, note LEPSUSYWG/04-02.1, http://lepsusy.web.cern.ch/lepsusy.
63. CDF Collab., Phys. Rev. Lett. **102**, 121801 (2009).
64. D0 Collab., Phys. Lett. **B660**, 449 (2008).
65. ATLAS Collab., *Search for squarks and gluinos with the ATLAS detector in final states with jets and missing transverse momentum and 20.3 fb^{-1} of $\sqrt{s}$=8 TeV proton-proton collision data*, ATLAS-CONF-2013-047 (2013).
66. ATLAS Collab., *Search for strong production of supersymmetric particles in final states with missing transverse momentum and at least three b-jets using 20.1 fb^{-1} of pp collisions at $\sqrt{s}$=8 TeV with the ATLAS Detector* , ATLAS-CONF-2013-061 (2013).
67. CMS Collab., *Search for New Physics in the Multijets and Missing Momentum Final State in Proton-Proton Collisions at $\sqrt{s} = 8$ TeV*, CMS-PAS-SUS-13-012 (2013).
68. CMS Collab., Phys. Lett. **B725**, 243 (2013).
69. CMS Collab., *Search for Supersymmetry in pp collisions at 8 TeV in events with a single lepton, multiple jets and b-tags* , CMS-PAS-SUS-13-007 (2013).
70. CMS Collab., JHEP **07**, 122 (2013).
71. ATLAS Collab., Phys. Lett. **B720**, 277 (2013).
72. D0 Collab., Phys. Rev. Lett. **99**, 131801 (2007).
73. ATLAS Collab., *Search for long-lived stopped gluino R-hadrons decaying out-of-time with LHC collisions in 2011 and 2012 using the ATLAS detector*, ATLAS-CONF-2013-057 (2013).
74. CMS Collab., *Search for Stopped Heavy Stable Charged Particles in pp collisions at $\sqrt{s} = 7$ TeV*, CMS-PAS-EXO-11-020 (2011).
75. CDF Collab., Phys. Rev. Lett. **107**, 042001 (2011).
76. ATLAS Collab., *Search for massive particles in multijet signatures with the ATLAS detector in $\sqrt{s} = 8$ TeV pp collisions at the LHC*, ATLAS-CONF-2013-091 (2013).

77. CMS Collab., *Search for light- and heavy-flavor three-jet resonances in multijet final states at 8 TeV*, CMS-PAS-EXO-12-049 (2012).
78. CMS Collab., Eur. Phys. J. **C73**, 2568 (2013).
79. H1 Collab., Eur. Phys. J. **C71**, 1572 (2011).
80. CDF Collab., Phys. Rev. Lett. **105**, 081802 (2010).
81. D0 Collab., Phys. Lett. **B693**, 95 (2010).
82. ATLAS Collab., JHEP **10**, 189 (2013).
83. ATLAS Collab., *Search for strongly produced supersymmetric particles in final states with two same-sign leptons and jets with the ATLAS detector using 21 fb^{-1} of proton-proton collisions at $\sqrt{s} = 8$ TeV*, ATLAS-CONF-2013-007 (2013).
84. CMS Collab., JHEP **03**, 037 (2013), JHEP **07**, 041 (2013).
85. C. Boehm, A. Djouadi, and Y. Mambrini, Phys. Rev. **D61**, 095006 (2000).
86. CDF Collab., Phys. Rev. **D82**, 092001 (2010).
87. D0 Collab., Phys. Lett. **B696**, 321 (2011).
88. CDF Collab., JHEP **10**, 158 (2012).
89. D0 Collab., Phys. Lett. **B665**, 1 (2008).
90. CDF Collab., Phys. Rev. Lett. **104**, 251801 (2010).
91. D0 Collab., Phys. Lett. **B674**, 4 (2009).
92. ATLAS Collab., *Search for direct production of the top squark in the all-hadronic ttbar + etmiss final state in 21 fb^{-1} of p-p collisions at $\sqrt{s} = 8$ TeV with the ATLAS detector*, ATLAS-CONF-2013-024 (2013).
93. ATLAS Collab., *Search for direct top squark pair production in final states with one isolated lepton, jets, and missing transverse momentum in $\sqrt{s} = 8$ TeV pp collisions using 21 fb^{-1} of ATLAS data* , ATLAS-CONF-2013-037 (2013).
94. CMS Collab., *Search for direct top squark pair production in the single lepton final state at $\sqrt{s} = 8$ TeV* , CMS-PAS-SUS-13-011, (2013), arXiv:1308.1586 [hep-ex], submitted to Eur. Phys. J. C.
95. ATLAS Collab., *Search for direct top squark pair production in final states with two leptons in $\sqrt{s} = 8$ TeV pp collisions using 20 fb^{-1} of ATLAS data* , ATLAS-CONF-2013-048 (2013).
96. ATLAS Collab., *Search for pair-produced top squarks decaying into a charm quark and the lightest neutralinos with 20.3 fb^{-1} of pp collisions at $\sqrt{s} = 8$ TeV with the ATLAS detector at the LHC* , ATLAS-CONF-2013-068 (2013).
97. ZEUS Collab., Eur. Phys. J. **C50**, 269 (2007).
98. CMS Collab., *Search for top squarks in R-parity-violating supersymmetry using three or more leptons and b-tagged jets*, CMS-PAS-SUS-13-003 (2013), arXiv:1306.6643 [hep-ex], accepted by Phys. Rev. Lett.
99. CDF Collab., Phys. Rev. Lett. **103**, 021802 (2009).
100. D0 Collab., Phys. Rev. **D87**, 052011 (2013).
101. LEP2 SUSY Working Group, ALEPH, DELPHI, L3 and OPAL experiments, note LEPSUSYWG/01-03.1, http://lepsusy.web.cern.ch/lepsusy.
102. LEP2 SUSY Working Group, ALEPH, DELPHI, L3 and OPAL experiments, note LEPSUSYWG/02-04.1, http://lepsusy.web.cern.ch/lepsusy.
103. CDF Collab., *Search for trilepton new physics and chargino-neutralino production at the Collider Detector at Fermilab*, CDF Note 10636 (2011).
104. D0 Collab., Phys. Lett. **B680**, 34 (2009).
105. ATLAS Collab., *Search for direct-slepton and direct-chargino production in final states with two opposite-sign leptons, missing transverse momentum and no jets in 20 fb^{-1} of pp collisions at $\sqrt{s} = 8$ TeV with the ATLAS detector*, ATLAS-CONF-2013-049 (2013).
106. CMS Collab., *Search for electroweak production of charginos, neutralinos, and sleptons using leptonic final states in pp collisions at 8 TeV*, CMS-PAS-SUS-13-006 (2013).
107. ATLAS Collab., *Search for direct production of charginos and neutralinos in events with three leptons and missing transverse momentum in 21 fb^{-1} of pp collisions at $\sqrt{s} = 8$ TeV with the ATLAS detector*, ATLAS-CONF-2013-035 (2013).
108. ATLAS Collab., *Search for electroweak production of supersymmetric particles in final states with at least two hadronically decaying taus and missing transverse momentum with the ATLAS detector in proton-proton collisions at $\sqrt{s} = 8$ TeV*, ATLAS-CONF-2013-028 (2013).
109. ATLAS Collab., *Search for chargino and neutralino production in final states with one lepton, two b-jets consistent with a Higgs boson, and missing transverse momentum with the ATLAS detector in 20.3 fb^{-1} of $\sqrt{s} = 8$ TeV pp collisions*, ATLAS-CONF-2013-093 (2013).
110. CMS Collab., *Search for electroweak production of charginos and neutralinos in final states with a Higgs boson in pp collisions at 8 TeV*, CMS-PAS-SUS-13-017 (2013).
111. ATLAS Collab., *Search for charginos nearly mass-degenerate with the lightest neutralino based on a disappearing-track signature in pp collisions at $\sqrt{s} = 8$ TeV with the ATLAS detector*, ATLAS-CONF-2013-069 (2013).
112. LEP2 SUSY Working Group, ALEPH, DELPHI, L3 and OPAL experiments, note LEPSUSYWG/02-05.1, http://lepsusy.web.cern.ch/lepsusy.
113. H. Dreiner *et al.*, Eur. Phys. J. **C62**, 547 (2009).
114. LEP2 SUSY Working Group, ALEPH, DELPHI, L3 and OPAL experiments, note LEPSUSYWG/04-07.1, http://lepsusy.web.cern.ch/lepsusy.
115. For a sampling of recent post-LHC global analyses, see: M. Citron *et al.*, Phys. Rev. **D87**, 036012 (2013); C. Strege *et al.*, JCAP 1304 (2013) 013; A. Fowlie *et al.*, Phys. Rev. **D86**, 075010 (2012); P. Bechtle *et al.*, JHEP **1206**, 098 (2012); O. Buchmueller *et al.*, Eur. Phys. J. **C72**, 2243 (2012).
116. CDF Collab., Phys. Rev. Lett. **108**, 211804 (2012).
117. CMS Collab., *Search for new physics in monojet events in pp collisions at $\sqrt{s} = 8$ TeV*, CMS-PAS-EXO-12-048 (2012).
118. ATLAS Collab., *Search for New Phenomena in Monojet plus Missing Transverse Momentum Final States using 10 fb^{-1} of pp Collisions at $\sqrt{s} = 8$ TeV with the ATLAS detector at the LHC*, ATLAS-CONF-2012-147 (2012).
119. LEP2 SUSY Working Group, ALEPH, DELPHI, L3 and OPAL experiments, note LEPSUSYWG/04-09.1, http://lepsusy.web.cern.ch/lepsusy.
120. CDF Collab., Phys. Rev. Lett. **104**, 011801 (2010).

121. D0 Collab., Phys. Rev. Lett. **105**, 221802 (2010).
122. ATLAS Collab., Phys. Lett. **B718**, 411 (2012).
123. CMS Collab., JHEP **03**, 111 (2013).
124. D0 Collab., Phys. Rev. **D86**, 071701 (2012).
125. CMS Collab., Phys. Lett. **B716**, 260 (2012).
126. ATLAS Collab., *Search for supersymmetry in final states with jets, missing transverse momentum and a Z boson at* $\sqrt{s} = 8$ *TeV with the ATLAS detector*, ATLAS-CONF-2012-152 (2012).
127. CDF Collab., Phys. Rev. **D88**, 031103 (2013).
128. CMS Collab., Phys. Lett. **B722**, 273 (2013).
129. D0 Collab., Phys. Rev. Lett. **101**, 111802 (2008).
130. ATLAS Collab, Phys. Rev. **D88**, 012001 (2013).
131. CDF Collab., Phys. Rev. **D85**, 011104 (2012).
132. ATLAS Collab., Phys. Lett. **B709**, 137 (2012).
133. ATLAS Collab., *Expected Performance of the ATLAS experiment, Detector, Trigger and Physics*, CERN-OPEN-2008-020 (2008).
134. CMS Collab., *Search for New Physics in Events with Opposite-sign Leptons, Jets and Missing Transverse Energy*, CMS-PAS-SUS-11-011 (2011).
135. ATLAS Collab., *Search for supersymmetry in events with four or more leptons in 21* fb^{-1} *of pp collisions at* $\sqrt{s} = 8$ *TeV with the ATLAS detector*, ATLAS-CONF-2013-036 (2013).
136. CMS Collab., *Search for RPV SUSY in the four-lepton final state*, CMS-PAS-SUS-13-010 (2013).
137. ATLAS Collab., *Search for long-lived, heavy particles in final states with a muon and a multi-track displaced vertex in proton-proton collisions at* $\sqrt{s} = 8$ *TeV with the ATLAS detector*, ATLAS-CONF-2013-092 (2013).
138. LEP2 SUSY Working Group, ALEPH, DELPHI, L3 and OPAL experiments, note LEPSUSYWG/04-01.1, `http://lepsusy.web.cern.ch/lepsusy`.
139. ALEPH Collab., Phys. Lett. **B544**, 73 (2002).
140. LEP2 SUSY Working Group, ALEPH, DELPHI, L3 and OPAL experiments, note LEPSUSYWG/02-09.2, `http://lepsusy.web.cern.ch/lepsusy`.
141. ATLAS Collab., *Search for Supersymmetry in Events with Large Missing Transverse Momentum, Jets, and at Least One Tau Lepton in 21* fb^{-1} *of* $\sqrt{s} = 8$ *TeV Proton-Proton Collision Data with the ATLAS Detector*, ATLAS-CONF-2013-026 (2013).
142. CMS Collab., *A Search for Anomalous Production of Events with three or more leptons using* 9.2 fb^{-1} *of* $\sqrt{s} = 8$ *TeV CMS data*, CMS-PAS-SUS-12-026 (2012).
143. CDF Collab., Phys. Rev. Lett. **110**, 201802 (2013).
144. LEP2 SUSY Working Group, ALEPH, DELPHI, L3 and OPAL experiments, note LEPSUSYWG/02-10.1, `http://lepsusy.web.cern.ch/lepsusy`.
145. ATLAS Collab., *A search for heavy long-lived sleptons using 16* fb^{-1} *of pp collisions at* $\sqrt{s} = 8$ *TeV with the ATLAS detector*, ATLAS-CONF-2013-058 (2013).
146. DELPHI Collab., Eur. Phys. J. **C31**, 412 (2003).
147. T. Falk, K.A. Olive, and M. Srednicki, Phys. Lett. **B339**, 248 (1994).
148. C. Arina and N. Fornengo, JHEP **11**, 029 (2007).
149. CDF Collab., Phys. Rev. Lett. **105**, 191801 (2010).
150. D0 Collab., Phys. Rev. Lett. **105**, 191802 (2010).
151. ATLAS Collab., Phys. Lett. **B723**, 15 (2013).
152. For a sampling of pre-LHC global analyses, see: O. Buchmueller *et al.*, Eur. Phys. J. **C71**, 1722 (2011); E.A. Baltz and P. Gondolo, JHEP **0410**, 052 (2004); B.C. Allanach and C.G. Lester, Phys. Rev. **D73**, 015013 (2006); R.R. de Austri *et al.*, JHEP **0605**, 002 (2006); R. Lafaye *et al.*, Eur. Phys. J. **C54**, 617 (2008); S. Heinemeyer *et al.*, JHEP **0808**, 08 (2008); R. Trotta *et al.*, JHEP **0812**, 024 (2008); P. Bechtle *et al.*, Eur. Phys. J. **C66**, 215 (2010).
153. For a sampling of recent pMSSM analyses, see: M. Cahill-Rowley *et al.*, Phys. Rev. **D88**, 035002 (2013) `(arXiv:1211.1981 [hep-ph])`;C. Boehm *et al.*, JHEP **1306**, 113, (2013); S AbdusSalam, Phys. Rev. **D87**, 115012 (2013); A. Arbey *et al.*, Eur. Phys. J. **C72**, 2169 (2012); M. Carena *et al.*, Phys. Rev. **D86**, 075025 (2012); S. Sekmen *et al.*, JHEP **1202**, 075 (2012);.
154. Physics Summary Plots, ATLAS experiment, `http://twiki.cern.ch/twiki/bin/view/AtlasPublic/CombinedSummaryPlots`.
155. Supersymmetry Physics Results, CMS experiment, `http://twiki.cern.ch/twiki/bin/view/CMSPUBlic/PhysicsResultsSUS`.

SUPERSYMMETRIC MODEL ASSUMPTIONS

The exclusion of particle masses within a mass range (m_1, m_2) will be denoted with the notation "none m_1–m_2" in the VALUE column of the following Listings. The latest unpublished results are described in the "Supersymmetry: Experiment" review.

Most of the results shown below, unless stated otherwise, are based on the Minimal Supersymmetric Standard Model (MSSM), as described in the Note on Supersymmetry. Unless otherwise indicated, this includes the assumption of common gaugino and scalar masses at the scale of Grand Unification (GUT), and use of the resulting relations in the spectrum and decay branching ratios. It is also assumed that R-parity (R) is conserved. Unless otherwise indicated, the results also assume that:

1) The $\widetilde{\chi}_1^0$ is the lighest supersymmetric particle (LSP)
2) $m_{\widetilde{f}_L} = m_{\widetilde{f}_R}$, where $\widetilde{f}_{L,R}$ refer to the scalar partners of left- and right-handed fermions.

Limits involving different assumptions are identified in the Comments or in the Footnotes. We summarize here the notations used in this Chapter to characterize some of the most common deviations from the MSSM (for further details, see the Note on Supersymmetry).

Theories with R-parity violation ($\not{R}$) are characterized by a superpotential of the form: $\lambda_{ijk} L_i L_j e^c_k + \lambda'_{ijk} L_i Q_j d^c_k + \lambda''_{ijk} u^c_i d^c_j d^c_k$, where i, j, k are generation indices. The presence of any of these couplings is often identified in the following by the symbols $LL\overline{E}$, $LQ\overline{D}$, and $\overline{UDD}$. Mass limits in the presence of $\not{R}$ will often refer to "direct" and "indirect" decays. Direct refers to $\not{R}$ decays of the particle in consideration. Indirect refers to cases where $\not{R}$ appears in the decays of the LSP.

In several models, most notably in theories with so-called Gauge Mediated Supersymmetry Breaking (GMSB), the gravitino ($\widetilde{G}$) is the LSP. It is usually much lighter than any other massive particle in the spectrum, and $m_{\widetilde{G}}$ is then neglected

in all decay processes involving gravitinos. In these scenarios, particles other than the neutralino are sometimes considered as the next-to-lighest supersymmetric particle (NLSP), and are assumed to decay to their even-R partner plus $\widetilde{G}$. If the lifetime is short enough for the decay to take place within the detector, $\widetilde{G}$ is assumed to be undetected and to give rise to missing energy ($\not{E}$) or missing transverse energy ($\not{E}_T$) signatures.

When needed, specific assumptions on the eigenstate content of $\widetilde{\chi}^0$ and $\widetilde{\chi}^\pm$ states are indicated, using the notation $\widetilde{\gamma}$ (photino), $\widetilde{H}$ (higgsino), $\widetilde{W}$ (wino), and $\widetilde{Z}$ (zino) to signal that the limit of pure states was used. The terms gaugino is also used, to generically indicate wino-like charginos and zino-like neutralinos.

CONTENTS:

$\widetilde{\chi}_1^0$ (Lightest Neutralino) MASS LIMIT

$\widetilde{\chi}_1^0$ is often assumed to be the lightest supersymmetric particle (LSP). See also the $\widetilde{\chi}_2^0$, $\widetilde{\chi}_3^0$, $\widetilde{\chi}_4^0$ section below.

We have divided the $\widetilde{\chi}_1^0$ listings below into five sections:

1) Accelerator limits for stable $\widetilde{\chi}_1^0$,
2) Bounds on $\widetilde{\chi}_1^0$ from dark matter searches,
3) $\widetilde{\chi}_1^0 - p$ elastic cross section (spin-dependent, spin-independent interactions),
4) Other bounds on $\widetilde{\chi}_1^0$ from astrophysics and cosmology, and
5) Unstable $\widetilde{\chi}_1^0$ (Lightest Neutralino) mass limit.

Accelerator limits for stable $\widetilde{\chi}_1^0$

Unless otherwise stated, results in this section assume spectra, production rates, decay modes, and branching ratios as evaluated in the MSSM, with gaugino and sfermion mass unification at the GUT scale. These papers generally study production of $\widetilde{\chi}_i^0\widetilde{\chi}_j^0$ ($i \geq 1$, $j \geq 2$), $\widetilde{\chi}_1^+\widetilde{\chi}_1^-$, and (in the case of hadronic collisions) $\widetilde{\chi}_1^+\widetilde{\chi}_2^0$ pairs. The mass limits on $\widetilde{\chi}_1^0$ are either direct, or follow indirectly from the constraints set by the non-observation of $\widetilde{\chi}_1^\pm$ and $\widetilde{\chi}_2^0$ states on the gaugino and higgsino MSSM parameters M_2 and μ. In some cases, information is used from the nonobservation of slepton decays.

Obsolete limits obtained from e^+e^- collisions up to $\sqrt{s}$=184 GeV have been removed from this compilation and can be found in the 2000 Edition (The European Physical Journal **C15** 1 (2000)) of this Review. $\Delta m = m_{\widetilde{\chi}_2^0} - m_{\widetilde{\chi}_1^0}$.

VALUE (GeV)	CL%	DOCUMENT ID		TECN	COMMENT
>40	95	[1] ABBIENDI	04H	OPAL	all tanβ, Δm >5 GeV, m_0 >500 GeV, $A_0 = 0$
>42.4	95	[2] HEISTER	04	ALEP	all tanβ, all Δm, all m_0
>39.2	95	[3] ABDALLAH	03M	DLPH	all tanβ, $m_{\widetilde{\nu}}$ >500 GeV
>46	95	[4] ABDALLAH	03M	DLPH	all tanβ, all Δm, all m_0
>32.5	95	[5] ACCIARRI	00D	L3	tanβ > 0.7, Δm > 3 GeV, all m_0
• • • We do not use the following data for averages, fits, limits, etc. • • •					
		[6] DREINER	09	THEO	

[1] ABBIENDI 04H search for charginos and neutralinos in events with acoplanar leptons+jets and multi-jet final states in the 192–209 GeV data, combined with the results on leptonic final states from ABBIENDI 04. The results hold for a scan over the parameter space covering the region $0 < M_2 <$5000 GeV, $-1000 < \mu <$1000 GeV and tanβ from 1 to 40. This limit supersedes ABBIENDI 00H.

[2] HEISTER 04 data collected up to 209 GeV. Updates earlier analysis of selectrons from HEISTER 02E, includes a new analysis of charginos and neutralinos decaying into stau and uses results on charginos with initial state radiation from HEISTER 02J. The limit is based on the direct search for charginos and neutralinos, the constraints from the slepton search and the Higgs mass limits from HEISTER 02 using a top mass of 175 GeV, interpreted in a framework with universal gaugino and sfermion masses. Assuming the mixing in the stau sector to be negligible, the limit improves to 43.1 GeV. Under the assumption of MSUGRA with unification of the Higgs and sfermion masses, the limit improves to 50 GeV, and reaches 53 GeV for $A_0 = 0$. These limits include and update the results of BARATE 01.

[3] ABDALLAH 03M uses data from $\sqrt{s} =$ 192–208 GeV. A limit on the mass of $\widetilde{\chi}_1^0$ is derived from direct searches for neutralinos combined with the chargino search. Neutralinos are searched in the production of $\widetilde{\chi}_1^0\widetilde{\chi}_2^0$, $\widetilde{\chi}_1^0\widetilde{\chi}_3^0$, as well as $\widetilde{\chi}_2^0\widetilde{\chi}_3^0$ and $\widetilde{\chi}_2^0\widetilde{\chi}_4^0$ giving rise to cascade decays, and $\widetilde{\chi}_1^0\widetilde{\chi}_2^0$ and $\widetilde{\chi}_1^0\widetilde{\chi}_2^0$, followed by the decay $\widetilde{\chi}_2^0 \rightarrow \widetilde{\tau}\tau$. The results hold for the parameter space defined by values of $M_2 <$ 1 TeV, $|\mu| \leq$ 2 TeV with the $\widetilde{\chi}_1^0$ as LSP. The limit is obtained for tan$\beta = 1$ and large m_0, where $\widetilde{\chi}_2^0\widetilde{\chi}_4^0$ and chargino pair production are important. If the constraint from Higgs searches is also imposed, the limit improves to 49.0 GeV in the $m_h^{\max}$ scenario with m_t=174.3 GeV. These limits update the results of ABREU 00J.

[4] ABDALLAH 03M uses data from $\sqrt{s} =$ 192–208 GeV. An indirect limit on the mass of $\widetilde{\chi}_1^0$ is derived by constraining the MSSM parameter space by the results from direct searches for neutralinos (including cascade decays and $\widetilde{\tau}\tau$ final states), for charginos (for all Δm_+) and for sleptons, stop and sbottom. The results hold for the full parameter space defined by values of $M_2 <$ 1 TeV, $|\mu| \leq$ 2 TeV with the $\widetilde{\chi}_1^0$ as LSP. Constraints from the Higgs search in the $m_h^{\max}$ scenario assuming m_t=174.3 GeV are included. The limit is obtained for tan$\beta \geq$ 5 when stau mixing leads to mass degeneracy between $\widetilde{\tau}_1$ and $\widetilde{\chi}_1^0$ and the limit is based on $\widetilde{\chi}_2^0$ production followed by its decay to $\widetilde{\tau}_1\tau$. In the pathological scenario where m_0 and $|\mu|$ are large, so that the $\widetilde{\chi}_2^0$ production cross section is negligible, and where there is mixing in the stau sector but not in stop nor sbottom, the limit is based on charginos with soft decay products and an ISR photon. The limit then degrades to 39 GeV. See Figs 40–42 for the dependence of the limit on tanβ and $m_{\widetilde{\nu}}$. These limits update the results of ABREU 00W.

[5] ACCIARRI 00D data collected at $\sqrt{s}$=189 GeV. The results hold over the full parameter space defined by $0.7 \leq$ tan$\beta \leq$ 60, $0 \leq M_2 \leq$ 2 TeV, $m_0 \leq$ 500 GeV, $|\mu| \leq$ 2 TeV The minimum mass limit is reached for tanβ=1 and large m_0. The results of slepton searches from ACCIARRI 99W are used to help set constraints in the region of small m_0. The limit improves to 48 GeV for $m_0 \gtrsim$ 200 GeV and tan$\beta \gtrsim$ 10. See their Figs. 6–8 for the tanβ and m_0 dependence of the limits. Updates ACCIARRI 98F.

[6] DREINER 09 show that in the general MSSM with non-universal gaugino masses there exists no model-independent laboratory bound on the mass of the lightest neutralino. An essentially massless χ_1^0 is allowed by the experimental and observational data, imposing some constraints on other MSSM parameters, including M_2, μ and the slepton and squark masses.

Bounds on $\widetilde{\chi}_1^0$ from dark matter searches

These papers generally exclude regions in the $M_2 - \mu$ parameter plane assuming that $\widetilde{\chi}_1^0$ is the dominant form of dark matter in the galactic halo. These limits are based on the lack of detection in laboratory experiments, telescopes, or by the absence of a signal in underground neutrino detectors. The latter signal is expected if $\widetilde{\chi}_1^0$ accumulates in the Sun or the Earth and annihilates into high-energy ν's.

VALUE	DOCUMENT ID		TECN
• • • We do not use the following data for averages, fits, limits, etc. • • •			
	[1] AARTSEN	13	ICCB
	[2] AARTSEN	13C	ICCB
	[3] ABRAMOWSKI	13	HESS
	[4] ACKERMANN	13A	FRMI
	[5] ADRIAN-MAR.	13	ANTR
	[6] BERGSTROM	13	COSM
	[7] BOLIEV	13	BAKS
	[6] JIN	13	ASTR
	[6] KOPP	13	COSM
	[8] ABBASI	12	ICCB
	[9] ABRAMOWSKI	11	HESS
	[10] ABDO	10	FRMI
	[11] ACKERMANN	10	FRMI
	[12] ABBASI	09B	ICCB
	[13] ACHTERBERG	06	AMND
	[14] ACKERMANN	06	AMND

[15] DEBOER	06	RVUE	
[16] DESAI	04	SKAM	
[16] AMBROSIO	99	MCRO	
[17] LOSECCO	95	RVUE	
[18] MORI	93	KAMI	
[19] BOTTINO	92	COSM	
[20] BOTTINO	91	RVUE	
[21] GELMINI	91	COSM	
[22] KAMIONKOW..91		RVUE	
[23] MORI	91B	KAMI	
[24] OLIVE	88	COSM	

none 4–15 GeV

[1] AARTSEN 13 is based on data collected during 317 effective days with the IceCube 79-string detector including the DeepCore sub-array. They looked for interactions of ν_μ's from neutralino annihilations in the Sun over a background of atmospheric neutrinos and set 90% CL limits on the muon flux. They also obtain limits on the spin dependent and spin independent neutralino-proton cross section for neutralino masses in the range 20–5000 GeV.

[2] AARTSEN 13C is based on data collected during 339.8 effective days with the IceCube 59-string detector. They looked for interactions of ν_μ's from neutralino annihilations in nearby galaxies and galaxy clusters. They obtain limits on the neutralino annihilation cross section for neutralino masses in the range 30–100, 000 GeV.

[3] ABRAMOWSKI 13 place upper limits on the annihilation cross section with $\gamma\gamma$ final states in the energy range of 0.5–25 TeV.

[4] ACKERMANN 13A is based on 3.7 years of data with Fermi-LAT and search for monochromatic gamma-rays in the energy range of 5–300 GeV from dark matter annihilations. No globally significant lines are reported.

[5] ADRIAN-MARTINEZ 13 is based on data from the ANTARES neutrino telescope. They looked for interactions of ν_μ's from neutralino annihilations in the Sun over a background of atmospheric neutrinos and set 90% CL limits on the muon flux. They also obtain limits on the spin dependent and spin independent neutralino-proton cross section for neutralino masses in the range 50–10, 000 GeV.

[6] BERGSTROM 13, JIN 13, and KOPP 13 derive limits on the mass and annihilation cross section using AMS-02 data. JIN 13 also sets a limit on the lifetime of the dark matter particle.

[7] BOLIEV 13 is based on data collected during 24.12 years of live time with the Bakson Underground Scintillator Telescope. They looked for interactions of ν_μ's from neutralino annihilations in the Sun over a background of atmospheric neutrinos and set 90% CL limits on the muon flux. They also obtain limits on the spin dependent and spin independent neutralino-proton cross section for neutralino masses in the range 10–1000 GeV.

[8] ABBASI 12 is based on data collected during 812 effective days with AMANDA II and 149 days of the IceCube 40-string detector combined with the data of ABBASI 09B. They looked for interactions of ν_μ's from neutralino annihilations in the Sun over a background of atmospheric neutrinos and set 90% CL limits on the muon flux. No excess is observed. They also obtain limits on the spin dependent neutralino-proton cross section for neutralino masses in the range 50–5000 GeV.

[9] ABRAMOWSKI 11 place upper limits on the annihilation cross section with $\gamma\gamma$ final states.

[10] ABDO 10 place upper limits on the annihilation cross section with $\gamma\gamma$ or $\mu^+\mu^-$ final states.

[11] ACKERMANN 10 place upper limits on the annihilation cross section with $b\overline{b}$ or $\mu^+\mu^-$ final states.

[12] ABBASI 09B is based on data collected during 104.3 effective days with the IceCube 22-string detector. They looked for interactions of ν_μ's from neutralino annihilations in the Sun over a background of atmospheric neutrinos and set 90% CL limits on the muon flux. They also obtain limits on the spin dependent neutralino–proton cross section for neutralino masses in the range 250–5000 GeV.

[13] ACHTERBERG 06 is based on data collected during 421.9 effective days with the AMANDA detector. They looked for interactions of ν_μs from the centre of the Earth over a background of atmospheric neutrinos and set 90 % CL limits on the muon flux. Their limit is compared with the muon flux expected from neutralino annihilations into W^+W^- and $b\overline{b}$ at the centre of the Earth for MSSM parameters compatible with the relic dark matter density, see their Fig. 7.

[14] ACKERMANN 06 is based on data collected during 143.7 days with the AMANDA-II detector. They looked for interactions of ν_μs from the Sun over a background of atmospheric neutrinos and set 90 % CL limits on the muon flux. Their limit is compared with the muon flux expected from neutralino annihilations into W^+W^- in the Sun for SUSY model parameters compatible with the relic dark matter density, see their Fig. 3.

[15] DEBOER 06 interpret an excess of diffuse Galactic gamma rays observed with the EGRET satellite as originating from π^0 decays from the annihilation of neutralinos into quark jets. They analyze the corresponding parameter space in a supergravity inspired MSSM model with radiative electroweak symmetry breaking, see their Fig. 3 for the preferred region in the $(m_0, m_{1/2})$ plane of a scenario with large $\tan\beta$.

[16] AMBROSIO 99 and DESAI 04 set new neutrino flux limits which can be used to limit the parameter space in supersymmetric models based on neutralino annihilation in the Sun and the Earth.

[17] LOSECCO 95 reanalyzed the IMB data and places lower limit on $m_{\widetilde{\chi}^0_1}$ of 18 GeV if the LSP is a photino and 10 GeV if the LSP is a higgsino based on LSP annihilation in the sun producing high-energy neutrinos and the limits on neutrino fluxes from the IMB detector.

[18] MORI 93 excludes some region in M_2–μ parameter space depending on $\tan\beta$ and lightest scalar Higgs mass for neutralino dark matter $m_{\widetilde{\chi}^0} > m_W$, using limits on upgoing muons produced by energetic neutrinos from neutralino annihilation in the Sun and the Earth.

[19] BOTTINO 92 excludes some region M_2-μ parameter space assuming that the lightest neutralino is the dark matter, using upgoing muons at Kamiokande, direct searches by Ge detectors, and by LEP experiments. The analysis includes top radiative corrections on Higgs parameters and employs two different hypotheses for nucleon-Higgs coupling. Effects of rescaling in the local neutralino density according to the neutralino relic abundance are taken into account.

[20] BOTTINO 91 excluded a region in $M_2-\mu$ plane using upgoing muon data from Kamioka experiment, assuming that the dark matter surrounding us is composed of neutralinos and that the Higgs boson is not too heavy.

[21] GELMINI 91 exclude a region in $M_2-\mu$ plane using dark matter searches.

[22] KAMIONKOWSKI 91 excludes a region in the M_2–μ plane using IMB limit on upgoing muons originated by energetic neutrinos from neutralino annihilation in the sun, assuming that the dark matter is composed of neutralinos and that $m_{H_1^0} \lesssim 50$ GeV. See Fig. 8 in the paper.

[23] MORI 91B exclude a part of the region in the M_2–μ plane with $m_{\widetilde{\chi}^0_1} \lesssim 80$ GeV using a limit on upgoing muons originated by energetic neutrinos from neutralino annihilation in the earth, assuming that the dark matter surrounding us is composed of neutralinos and that $m_{H_1^0} \lesssim 80$ GeV.

[24] OLIVE 88 result assumes that photinos make up the dark matter in the galactic halo. Limit is based on annihilations in the sun and is due to an absence of high energy neutrinos detected in underground experiments. The limit is model dependent.

$\widetilde{\chi}^0_1$-p elastic cross section

Experimental results on the $\widetilde{\chi}^0_1$-p elastic cross section are evaluated at $m_{\widetilde{\chi}^0_1}$=100 GeV. The experimental results on the cross section are often mass dependent. Therefore, the mass and cross section results are also given where the limit is strongest, when appropriate. Results are quoted separately for spin-dependent interactions (based on an effective 4-Fermi Lagrangian of the form $\overline{\chi}\gamma^\mu\gamma^5\chi\overline{q}\gamma_\mu\gamma^5 q$) and spin-independent interactions ($\overline{\chi}\chi\overline{q}q$). For calculational details see GRIEST 88B, ELLIS 88D, BARBIERI 89C, DREES 93B, ARNOWITT 96, BERGSTROM 96, and BAER 97 in addition to the theory papers listed in the Tables. For a description of the theoretical assumptions and experimental techniques underlying most of the listed papers, see the review on "Dark matter" in this "Review of Particle Physics," and references therein. Most of the following papers use galactic halo and nuclear interaction assumptions from (LEWIN 96).

Spin-dependent interactions

VALUE (pb)	CL%	DOCUMENT ID		TECN	COMMENT
• • • We do not use the following data for averages, fits, limits, etc. • • •					
< 0.01	90	[1] APRILE	13	X100	Xe
< 0.01	90	[2] AKIMOV	12	ZEP3	Xe
< 0.07	90	[3] ARCHAMBAU..	12	PICA	F
$< 7 \times 10^{-3}$		[4] BEHNKE	12	COUP	CF_3I
< 1.8	90	[5] DAW	12	DRFT	CS_2; CF_4
$< 8.5 \times 10^{-3}$		[6] FELIZARDO	12	SMPL	C_2ClF_5
< 0.016	90	[7] KIM	12	KIMS	CsI
5×10^{-10} to 10^{-5}	95	[8] BUCHMUEL...	11B	THEO	
< 1	90	[9] ANGLE	08A	XE10	Xe
< 0.055		[10] BEDNYAKOV	08	HDMS	Ge
< 0.33	90	BEHNKE	08	COUP	CF_3I
< 5		[11] AKERIB	06	CDMS	Ge
< 2		[12] SHIMIZU	06A	CNTR	CaF_2
< 0.4		ALNER	05	NAIA	NaI Spin Dep.
< 2		[13] BARNABE-HE..	05	PICA	C
2×10^{-11} to 1×10^{-4}		[14] ELLIS	04	THEO	$\mu > 0$
< 0.8		[15] AHMED	03	NAIA	NaI Spin Dep.
< 40		[16] TAKEDA	03	BOLO	NaF Spin Dep.
< 10		[17] ANGLOHER	02	CRES	Saphire
8×10^{-7} to 2×10^{-5}		[18] ELLIS	01C	THEO	$\tan\beta \leq 10$
< 3.8		[19] BERNABEI	00D	DAMA	Xe
< 0.8		SPOONER	00	UKDM	NaI
< 4.8		BELLI	99C	DAMA	F
<100		[20] OOTANI	99	BOLO	LiF
< 0.6		BERNABEI	98C	DAMA	Xe
< 5		[21] BERNABEI	97	DAMA	F

[1] The strongest limit is 0.006 pb and occurs at $m_\chi = 60$ GeV. APRILE 13 also presents limits for the scattering on neutrons. At 100 GeV, the upper limit is 4×10^{-4} pb and the strongest limit is 3.5×10^{-4} pb at 45 GeV.

[2] This result updates LEBEDENKO 09A. The strongest limit is 8×10^{-3} pb at $m_\chi = 50$ GeV. Limit applies to the neutralino neutron elastic cross section.

[3] This result updates ARCHAMBAULT 09. The strongest limit is 0.032 pb at $m_\chi = 20$ GeV.

[4] The strongest limit is 6×10^{-3} at $m_\chi = 60$ GeV.

[5] The strongest limit is 1.8 pb and occurs at $m_\chi = 100$ GeV.

[6] The strongest limit is 5.7×10^{-3} at $m_\chi = 35$ GeV.

[7] This result updates LEE 07A. The strongest limit is at $m_\chi = 80$ GeV.

[8] Predictions for the spin-dependent elastic cross section based on a frequentist approach to electroweak observables in the framework of $N = 1$ supergravity models with radiative breaking of the electroweak gauge symmetry.

[9] The strongest limit is 0.6 pb and occurs at m_χ= 30 GeV. The limit for scattering on neutrons is 0.01 pb at m_χ= 100 GeV, and the strongest limit is 0.0045 pb at m_χ= 30 GeV.

[10] Limit applies to neutron elastic cross section.

[11] The strongest upper limit is 0.25 pb and occurs at $m_\chi \simeq 40$ GeV.

[12] The strongest upper limit is 4 pb and occurs at $m_\chi \simeq 60$ GeV. The limit on the neutron spin-dependent elastic cross section is 0.07 pb. This latter limit is improved in AHMED 09, where a limit of 0.02 pb is obtained at $m_\chi = 100$ GeV. The strongest limit in AHMED 09 is 0.018 pb and occurs at $m_\chi = 60$ GeV.

[13] The strongest upper limit is 1.2 pb and occurs at $m_\chi \simeq 40$ GeV. The limit on the neutron spin-dependent cross section is 35 pb.

[14] The strongest upper limit is 0.35 pb and occurs at $m_\chi \simeq 60$ GeV.

[15] The strongest upper limit is 1.2 pb and occurs $m_\chi \simeq 30$ GeV.

[16] ELLIS 04 calculates the χp elastic scattering cross section in the framework of N=1 supergravity models with radiative breaking of the electroweak gauge symmetry, but without universal scalar masses. In the case of universal squark and slepton masses, but non-universal Higgs masses, the limit becomes 2×10^{-4}, see ELLIS 03E.

[17] The strongest upper limit is 0.75 pb and occurs at $m_\chi \approx 70$ GeV.

[18] The strongest upper limit is 30 pb and occurs at $m_\chi \approx 20$ GeV.

[19] The strongest upper limit is 8 pb and occurs at $m_\chi \simeq 30$ GeV.

[20] ELLIS 01C calculates the χ-p elastic scattering cross section in the framework of N=1 supergravity models with radiative breaking of the electroweak gauge symmetry. In models with nonuniversal Higgs masses, the upper limit to the cross section is 6×10^{-4}.

[21] The strongest upper limit is 3 pb and occurs at $m_\chi \simeq 60$ GeV. The limits are for inelastic scattering $X^0 + {}^{129}\mathrm{Xe} \rightarrow X^0 + {}^{129}\mathrm{Xe}^*$ (39.58 keV).

[22] The strongest upper limit is 4.4 pb and occurs at $m_\chi \simeq 60$ GeV.

[23] The strongest upper limit is about 35 pb and occurs at $m_\chi \simeq 15$ GeV.

Spin-independent interactions

VALUE (pb)	CL%	DOCUMENT ID		TECN	COMMENT
• • • We do not use the following data for averages, fits, limits, etc. • • •					
$< 2.2\times10^{-6}$	90	[1] AALSETH	13	CGNT	Ge
		[2] AGNESE	13	CDMS	Si
$< 5 \times10^{-8}$	90	[3] LI	13B	TEXO	Ge
1.6×10^{-6}; 3.7×10^{-5}		[4] AKIMOV	12	ZEP3	Xe
$< 2.6\times10^{-9}$	90	[5] ANGLOHER	12	CRES	$CaWO_4$
	90	[6] APRILE	12	X100	Xe
3×10^{-12} to 3×10^{-9}	95	[7] ARCHAMBAU..	12	PICA	C_4F_{10}
$< 1.6\times10^{-7}$		[8] BECHTLE	12	THEO	
$<10^{-9}$	95	[9] BEHNKE	12	COUP	CF_3I
$< 6.5\times10^{-6}$		[10] BUCHMUEL...	12A	THEO	
$<10^{-9}$	95	[11] FELIZARDO	12	SMPL	C_2ClF_5
$< 2.3\times10^{-7}$	90	[12] FOWLIE	12A	THEO	
$< 3.3\times10^{-8}$	90	[13] KIM	12	KIMS	CsI
$< 4.4\times10^{-8}$	90	[14] AHMED	11A		Ge
$< 4 \times10^{-8}$	90	[15] ARMENGAUD	11	EDE2	Ge
$< 7 \times10^{-7}$	90	[16] AHMED	10	CDMS	Ge
$< 1 \times10^{-7}$	90	[17] ANGLOHER	09	CRES	$CaWO_4$
$< 1 \times10^{-6}$	90	[18] ANGLE	08	XE10	Xe
$< 7.5\times10^{-7}$	90	BENETTI	08	WARP	Ar
$< 2 \times10^{-7}$		[19] ALNER	07A	ZEP2	Xe
$<90 \times10^{-7}$		[20] AKERIB	06A	CDMS	Ge
$<12 \times10^{-7}$		ALNER	05	NAIA	NaI Spin Indep.
$<20 \times10^{-7}$		[21] ALNER	05A	ZEPL	
$<14 \times10^{-7}$		[22] ANGLOHER	05	CRES	$CaWO_4$
$< 4 \times10^{-7}$		SANGLARD	05	EDEL	Ge
2×10^{-11} to 1.5×10^{-7}	95	[23] AKERIB	04	CDMS	Ge
2×10^{-11} to 8×10^{-6}		[24] BALTZ	04	THEO	
$< 5 \times10^{-8}$		[25,26] ELLIS	04	THEO	$\mu > 0$
$< 2 \times10^{-5}$		[27] PIERCE	04A	THEO	
$< 3 \times10^{-6}$		[28] AHMED	03	NAIA	NaI Spin Indep.
2×10^{-13} to 2×10^{-7}		[29] AKERIB	03	CDMS	Ge
$< 1.4\times10^{-5}$		[30] BAER	03A	THEO	
$< 6 \times10^{-6}$		[31] KLAPDOR-K...	03	HDMS	Ge
$< 1.4\times10^{-6}$		[32] ABRAMS	02	CDMS	Ge
1×10^{-12} to 7×10^{-6}		[33] BENOIT	02	EDEL	Ge
$< 3 \times10^{-5}$		[25] KIM	02B	THEO	
$< 1 \times10^{-5}$		[34] MORALES	02B	CSME	Ge
$< 1 \times10^{-6}$		[35] MORALES	02C	IGEX	Ge
$< 3 \times10^{-5}$		BALTZ	01	THEO	
$< 4.5\times10^{-6}$		[36] BAUDIS	01	HDMS	Ge
$< 7 \times10^{-6}$		BENOIT	01	EDEL	Ge
$< 1 \times10^{-8}$		[37] BOTTINO	01	THEO	
5×10^{-10} to 1.5×10^{-8}		[38] CORSETTI	01	THEO	$\tan\beta \leq 25$
$< 4 \times10^{-6}$		[39] ELLIS	01C	THEO	$\tan\beta \leq 10$
2×10^{-10} to 1×10^{-7}		[38] GOMEZ	01	THEO	
$< 3 \times10^{-6}$		[38] LAHANAS	01	THEO	
$< 6 \times10^{-7}$		ABUSAIDI	00	CDMS	Ge, Si
		[40] ACCOMANDO	00	THEO	
2.5×10^{-9} to 3.5×10^{-8}		[41] BERNABEI	00	DAMA	NaI
$< 1.5\times10^{-5}$		[42] FENG	00	THEO	$\tan\beta$=10
$< 4 \times10^{-5}$		MORALES	00	IGEX	Ge
$< 7 \times10^{-6}$		SPOONER	00	UKDM	NaI
		BAUDIS	99	HDMO	^{76}Ge
		[43] BERNABEI	99	DAMA	NaI
		[44] BERNABEI	98	DAMA	NaI
$< 7 \times10^{-6}$		BERNABEI	98C	DAMA	Xe

[1] AALSETH 13 presents 90% CL limits on the elastic cross section for masses in the range 4–25 GeV in addition to a region of interest at about 8 GeV. The strongest upper limit is 2×10^{-5} pb at $m_\chi = 14$ GeV.

[2] AGNESE 13 presents 90% CL limits on the elastic cross section for masses in the range 7–100 GeV using the Si based detector. The strongest upper limit is 1.8×10^{-6} pb at $m_\chi = 50$ GeV. This limit is improved to 7×10^{-7} pb in AGNESE 13A.

[3] LI 13B presents 90% CL limits on the elastic cross section for masses in the range 4–40 GeV. The strongest upper limit is 4×10^{-5} pb at $m_\chi = 14$ GeV.

[4] This result updates LEBEDENKO 09. The strongest limit is 3.9×10^{-8} pb at $m_\chi = 52$ GeV.

[5] ANGLOHER 12 presents results of 730 kg days from the CRESST-II dark matter detector. They find two maxima in the likelihood function corresponding to best fit WIMP masses of 25.3 and 11.6 GeV with elastic cross sections of 1.6×10^{-6} and 3.7×10^{-5} pb respectively, see their Table 4. The statistical significance is more than 4σ.

[6] APRILE 12 updates the result of APRILE 11B. The strongest upper limit is $< 2.0\times10^{-9}$ pb and occurs at $m_\chi \simeq 50$ GeV.

[7] The strongest limit is 6.1×10^{-5} pb at $m_\chi = 20$ GeV.

[8] Predictions for the spin-independent elastic cross section based on a frequentist approach to electroweak observables in the framework of $N = 1$ supergravity models with radiative breaking of the electroweak gauge symmetry using the 5 fb^{-1} LHC data and XENON100.

[9] The strongest limit is 1.4×10^{-7} at $m_\chi = 60$ GeV.

[10] Predictions for the spin-independent elastic cross section based on a frequentist approach to electroweak observables in the framework of $N = 1$ supergravity models with radiative breaking of the electroweak gauge symmetry using the 5 fb^{-1} LHC data and XENON100.

[11] The strongest limit is 4.7×10^{-6} at $m_\chi = 35$ GeV.

[12] Predictions for the spin-independent elastic cross section based on a Bayesian approach to electroweak observables in the framework of $N = 1$ supergravity models with radiative breaking of the electroweak gauge symmetry using the 5 fb^{-1} LHC data and XENON100.

[13] This result updates LEE 07A. The strongest limit is 2.1×10^{-7} at $m_\chi = 70$ GeV.

[14] AHMED 11A gives combined results from CDMS and EDELWEISS. The strongest limit is at $m_\chi = 90$ GeV.

[15] ARMENGAUD 11 updates result of ARMENGAUD 10. Strongest limit at $m_\chi = 85$ GeV.

[16] The strongest upper limit is $< 3.8\times10^{-8}$ pb and occurs at $m_\chi \simeq 70$ GeV. AHMED 10 updates the results of AHMED 09.

[17] The strongest upper limit is 4.8×10^{-7} pb and occurs at $m_\chi = 50$ GeV.

[18] The strongest upper limit is 5.1×10^{-8} pb and occurs at $m_\chi \simeq 30$ GeV. The values quoted here are based on the analysis performed in ANGLE 08 with the update from SORENSEN 09.

[19] The strongest upper limit is 6.6×10^{-7} pb and occurs at $m_\chi \simeq 65$ GeV.

[20] AKERIB 06A updates the results of AKERIB 05. The strongest upper limit is 1.6×10^{-7} pb and occurs at $m_\chi \approx 60$ GeV.

[21] The strongest upper limit is also close to 1.0×10^{-6} pb and occurs at $m_\chi \simeq 70$ GeV. BENOIT 06 claim that the discrimination power of ZEPLIN-I measurement (ALNER 05A) is not reliable enough to obtain a limit better than 1×10^{-3} pb. However, SMITH 06 do not agree with the criticisms of BENOIT 06.

[22] The strongest upper limit is also close to 1.4×10^{-6} pb and occurs at $m_\chi \simeq 70$ GeV.

[23] AKERIB 04 is incompatible with BERNABEI 00 most likely value, under the assumption of standard WIMP-halo interactions. The strongest upper limit is 4×10^{-7} pb and occurs at $m_\chi \simeq 60$ GeV.

[24] Predictions for the spin-independent elastic cross section in the framework of $N = 1$ supergravity models with radiative breaking of the electroweak gauge symmetry.

[25] KIM 02 and ELLIS 04 calculate the χp elastic scattering cross section in the framework of N=1 supergravity models with radiative breaking of the electroweak gauge symmetry, but without universal scalar masses.

[26] In the case of universal squark and slepton masses, but non-universal Higgs masses, the limit becomes 2×10^{-6} (2×10^{-11} when constraint from the BNL g–2 experiment are included), see ELLIS 03E. ELLIS 05 display the sensitivity of the elastic scattering cross section to the π-Nucleon Σ term.

[27] PIERCE 04A calculates the χp elastic scattering cross section in the framework of models with very heavy scalar masses. See Fig. 2 of the paper.

[28] The strongest upper limit is 1.8×10^{-5} pb and occurs at $m_\chi \approx 80$ GeV.

[29] Under the assumption of standard WIMP-halo interactions, Akerib 03 is incompatible with BERNABEI 00 most likely value at the 99.98% CL. See Fig. 4.

[30] BAER 03A calculates the χp elastic scattering cross section in several models including the framework of N=1 supergravity models with radiative breaking of the electroweak gauge symmetry.

[31] The strongest upper limit is 7×10^{-6} pb and occurs at $m_\chi \simeq 30$ GeV.

[32] ABRAMS 02 is incompatible with the DAMA most likely value at the 99.9% CL. The strongest upper limit is 3×10^{-6} pb and occurs at $m_\chi \simeq 30$ GeV.

[33] BENOIT 02 excludes the central result of DAMA at the 99.8%CL.

[34] The strongest upper limit is 2×10^{-5} pb and occurs at $m_\chi \simeq 40$ GeV.

[35] The strongest upper limit is 7×10^{-6} pb and occurs at $m_\chi \simeq 46$ GeV.

[36] The strongest upper limit is 1.8×10^{-5} pb and occurs at $m_\chi \simeq 32$ GeV

[37] BOTTINO 01 calculates the χ-p elastic scattering cross section in the framework of the following supersymmetric models: N=1 supergravity with the radiative breaking of the electroweak gauge symmetry, N=1 supergravity with nonuniversal scalar masses and an effective MSSM model at the electroweak scale.

[38] Calculates the χ-p elastic scattering cross section in the framework of N=1 supergravity models with radiative breaking of the electroweak gauge symmetry.

[39] ELLIS 01C calculates the χ-p elastic scattering cross section in the framework of N=1 supergravity models with radiative breaking of the electroweak gauge symmetry. ELLIS 02B find a range 2×10^{-8}–1.5×10^{-7} at $\tan\beta$=50. In models with nonuniversal Higgs masses, the upper limit to the cross section is 4×10^{-7}.

[40] ACCOMANDO 00 calculate the χ-p elastic scattering cross section in the framework of minimal N=1 supergravity models with radiative breaking of the electroweak gauge symmetry. The limit is relaxed by at least an order of magnitude when models with nonuniversal scalar masses are considered. A subset of the authors in ARNOWITT 02 updated the limit to $< 9\times10^{-8}$ ($\tan\beta < 55$).

[41] BERNABEI 00 search for annual modulation of the WIMP signal. The data favor the hypothesis of annual modulation at 4σ and are consistent, for a particular model framework quoted there, with m_{X^0}=44^{+12}_{-9} GeV and a spin-independent X^0-proton cross section of $(5.4 \pm 1.0)\times10^{-6}$ pb. See also BERNABEI 01 and BERNABEI 00C.

[42] FENG 00 calculate the χ-p elastic scattering cross section in the framework of N=1 supergravity models with radiative breaking of the electroweak gauge symmetry with a particular emphasis on focus point models. At $\tan\beta$=50, the range is 8×10^{-8}–4×10^{-7}.

[43] BERNABEI 99 search for annual modulation of the WIMP signal. The data favor the hypothesis of annual modulation at 99.6%CL and are consistent, for the particular model

framework considered there, with m_{X^0}=59 $^{+17}_{-14}$ GeV and spin-independent X^0-proton cross section of $(7.0^{+0.4}_{-1.2}) \times 10^{-6}$ pb (1 σ errors).

[44] BERNABEI 98 search for annual modulation of the WIMP signal. The data are consistent, for the particular model framework considered there, with m_{X^0}=59 $^{+36}_{-19}$ GeV and spin-independent X^0-proton cross section of $(1.0^{+0.1}_{-0.4}) \times 10^{-5}$ pb (1 σ errors).

Other bounds on $\tilde{\chi}_1^0$ from astrophysics and cosmology

Most of these papers generally exclude regions in the $M_2 - \mu$ parameter plane by requiring that the $\tilde{\chi}_1^0$ contribution to the overall cosmological density is less than some maximal value to avoid overclosure of the Universe. Those not based on the cosmological density are indicated. Many of these papers also include LEP and/or other bounds.

VALUE	DOCUMENT ID		TECN	COMMENT
>46 GeV	[1] ELLIS	00	RVUE	
• • • We do not use the following data for averages, fits, limits, etc. • • •				
	[2] CABRERA	13	COSM	
	[3] ELLIS	13B	COSM	
	[2] STREGE	13	COSM	
	[4] AKULA	12	COSM	
	[4] ARBEY	12A	COSM	
	[4] BAER	12	COSM	
	[5] BALAZS	12	COSM	
	[6] BECHTLE	12	COSM	
	[7] BESKIDT	12	COSM	
> 18 GeV	[8] BOTTINO	12	COSM	
	[4] BUCHMUEL...	12	COSM	
	[9] BUCHMUEL...	12A	COSM	
	[4] CAO	12A	COSM	
	[4] ELLIS	12B	COSM	
	[10] FENG	12B	COSM	
	[11] FOWLIE	12A	COSM	
	[4] KADASTIK	12	COSM	
	[5] STREGE	12	COSM	
	[12] BUCHMUEL...	11	COSM	
	[13] ROSZKOWSKI	11	COSM	
	[14] ELLIS	10	COSM	
	[15] BUCHMUEL...	09	COSM	
	[16] DREINER	09	THEO	
	[17] BUCHMUEL...	08	COSM	
	[13] ELLIS	08	COSM	
	[18] CALIBBI	07	COSM	
	[19] ELLIS	07	COSM	
	[20] ALLANACH	06	COSM	
	[21] DE-AUSTRI	06	COSM	
	[13] BAER	05	COSM	
	[22] BALTZ	04	COSM	
> 6 GeV	[8,23] BELANGER	04	THEO	
	[24] ELLIS	04B	COSM	
	[25] PIERCE	04A	COSM	
	[26] BAER	03	COSM	
> 6 GeV	[8] BOTTINO	03	COSM	
	[26] CHATTOPAD...	03	COSM	
	[27] ELLIS	03	COSM	
	[13] ELLIS	03B	COSM	
	[26] ELLIS	03C	COSM	
	[26] LAHANAS	03	COSM	
	[28] LAHANAS	02	COSM	
	[29] BARGER	01C	COSM	
	[30] ELLIS	01B	COSM	
	[27] BOEHM	00B	COSM	
	[31] FENG	00	COSM	
< 600 GeV	[32] ELLIS	98B	COSM	
	[33] EDSJO	97	COSM	Co-annihilation
	[34] BAER	96	COSM	
	[13] BEREZINSKY	95	COSM	
	[35] FALK	95	COSM	*CP*-violating phases
	[36] DREES	93	COSM	Minimal supergravity
	[37] FALK	93	COSM	Sfermion mixing
	[36] KELLEY	93	COSM	Minimal supergravity
	[38] MIZUTA	93	COSM	Co-annihilation
	[39] LOPEZ	92	COSM	Minimal supergravity, m_0=A=0
	[40] MCDONALD	92	COSM	
	[41] GRIEST	91	COSM	
	[42] NOJIRI	91	COSM	Minimal supergravity
	[43] OLIVE	91	COSM	
	[44] ROSZKOWSKI	91	COSM	
	[45] GRIEST	90	COSM	
	[43] OLIVE	89	COSM	
none 100 eV – 15 GeV	SREDNICKI	88	COSM	$\tilde{\gamma}$; $m_{\tilde{f}}$=100 GeV
none 100 eV–5 GeV	ELLIS	84	COSM	$\tilde{\gamma}$; for $m_{\tilde{f}}$=100 GeV
	GOLDBERG	83	COSM	$\tilde{\gamma}$
	[46] KRAUSS	83	COSM	$\tilde{\gamma}$
	VYSOTSKII	83	COSM	$\tilde{\gamma}$

[1] ELLIS 00 updates ELLIS 98. Uses LEP e^+e^- data at $\sqrt{s}$=202 and 204 GeV to improve bound on neutralino mass to 51 GeV when scalar mass universality is assumed and 46 GeV when Higgs mass universality is relaxed. Limits on tanβ improve to > 2.7 ($\mu > 0$), > 2.2 ($\mu < 0$) when scalar mass universality is assumed and > 1.9 (both signs of μ) when Higgs mass universality is relaxed.

[2] CABRERA 13 and STREGE 13 place constraints on the SUSY parameter space in the framework of $N = 1$ supergravity models with radiative breaking of the electroweak gauge symmetry with and without non-universal Higgs masses using the 5.8 fb^{-1}, $\sqrt{s} = 7$ TeV ATLAS supersymmetry searches and XENON100 results.

[3] ELLIS 13B place constraints on the SUSY parameter space in the framework of $N = 1$ supergravity models with radiative breaking of the electroweak gauge symmetry with and without Higgs mass universality. Models with universality below the GUT scale are also considered.

[4] Implications of the LHC result on the Higgs mass and on the SUSY parameter space in the framework of $N = 1$ supergravity models with radiative breaking of the electroweak gauge symmetry.

[5] BALAZS 12 and STREGE 12 place constraints on the SUSY parameter space in the framework of $N = 1$ supergravity models with radiative breaking of the electroweak gauge symmetry using the 1 fb^{-1} LHC supersymmetry searches, the 5 fb^{-1} Higgs mass constraints, both with $\sqrt{s} = 7$ TeV, and XENON100 results.

[6] BECHTLE 12 places constraints on the SUSY parameter space in the framework of $N = 1$ supergravity models with radiative breaking of the electroweak gauge symmetry using indirect experimental searches, using the 5 fb^{-1} LHC and XENON100 data.

[7] BESKIDT 12 places constraints on the SUSY parameter space in the framework of $N = 1$ supergravity models with radiative breaking of the electroweak gauge symmetry using indirect experimental searches, the 5 fb^{-1} LHC and the XENON100 data.

[8] BELANGER 04 and BOTTINO 12 (see also BOTTINO 03, BOTTINO 03A and BOTTINO 04) do not assume gaugino or scalar mass unification.

[9] BUCHMUELLER 12A places constraints on the SUSY parameter space in the framework of $N = 1$ supergravity models with radiative breaking of the electroweak gauge symmetry using indirect experimental searches, using the 5 fb^{-1} LHC and XENON100 data.

[10] FENG 12B places constraints on the SUSY parameter space in the framework of $N = 1$ supergravity models with radiative breaking of the electroweak gauge symmetry and large sfermion masses using the 1 fb^{-1} LHC supersymmetry searches, the 5 fb^{-1} LHC Higgs mass constraints both with $\sqrt{s} = 7$ TeV, and XENON100 results.

[11] FOWLIE 12A places constraints on the SUSY parameter space in the framework of $N = 1$ supergravity models with radiative breaking of the electroweak gauge symmetry using indirect experimental searches, using the 5 fb^{-1} LHC and XENON100 data.

[12] BUCHMUELLER 11 places constraints on the SUSY parameter space in the framework of $N = 1$ supergravity models with radiative breaking of the electroweak gauge symmetry using indirect experimental searches and including supersymmetry breaking relations between A and B parameters.

[13] Places constraints on the SUSY parameter space in the framework of N=1 supergravity models with radiative breaking of the electroweak gauge symmetry but non-Universal Higgs masses.

[14] ELLIS 10 places constraints on the SUSY parameter space in the framework of $N = 1$ supergravity models with radiative breaking of the electroweak gauge symmetry with universality above the GUT scale.

[15] BUCHMUELLER 09 places constraints on the SUSY parameter space in the framework of $N = 1$ supergravity models with radiative breaking of the electroweak gauge symmetry using indirect experimental searches.

[16] DREINER 09 show that in the general MSSM with non-universal gaugino masses there exists no model-independent laboratory bound on the mass of the lightest neutralino. An essentially massless χ_1^0 is allowed by the experimental and observational data, imposing some constraints on other MSSM parameters, including M_2, μ and the slepton and squark masses.

[17] BUCHMUELLER 08 places constraints on the SUSY parameter space in the framework of $N = 1$ supergravity models with radiative breaking of the electroweak gauge symmetry using indirect experimental searches.

[18] CALIBBI 07 places constraints on the SUSY parameter space in the framework of $N = 1$ supergravity models with radiative breaking of the electroweak gauge symmetry with universality above the GUT scale including the effects of right-handed neutrinos.

[19] ELLIS 07 places constraints on the SUSY parameter space in the framework of $N = 1$ supergravity models with radiative breaking of the electroweak gauge symmetry with universality below the GUT scale.

[20] ALLANACH 06 places constraints on the SUSY parameter space in the framework of $N = 1$ supergravity models with radiative breaking of the electroweak gauge symmetry.

[21] DE-AUSTRI 06 places constraints on the SUSY parameter space in the framework of $N = 1$ supergravity models with radiative breaking of the electroweak gauge symmetry.

[22] BALTZ 04 places constraints on the SUSY parameter space in the framework of $N = 1$ supergravity models with radiative breaking of the electroweak gauge symmetry.

[23] Limit assumes a pseudo scalar mass < 200 GeV. For larger pseudo scalar masses, $m_\chi >$ 18(29) GeV for tan$\beta = 50(10)$. Bounds from WMAP, $(g-2)_\mu$, $b \to s\gamma$, LEP.

[24] ELLIS 04B places constraints on the SUSY parameter space in the framework of N=1 supergravity models with radiative breaking of the electroweak gauge symmetry including supersymmetry breaking relations between A and B parameters. See also ELLIS 03D.

[25] PIERCE 04A places constraints on the SUSY parameter space in the framework of models with very heavy scalar masses.

[26] BAER 03, CHATTOPADHYAY 03, ELLIS 03C and LAHANAS 03 place constraints on the SUSY parameter space in the framework of N=1 supergravity models with radiative breaking of the electroweak gauge symmetry based on WMAP results for the cold dark matter density.

[27] BOEHM 00B and ELLIS 03 place constraints on the SUSY parameter space in the framework of minimal N=1 supergravity models with radiative breaking of the electroweak gauge symmetry. Includes the effect of χ-$\tilde{t}$ co-annihilations.

[28] LAHANAS 02 places constraints on the SUSY parameter space in the framework of minimal N=1 supergravity models with radiative breaking of the electroweak gauge symmetry. Focuses on the role of pseudo-scalar Higgs exchange.

[29] BARGER 01C use the cosmic relic density inferred from recent CMB measurements to constrain the parameter space in the framework of minimal N=1 supergravity models with radiative breaking of the electroweak gauge symmetry.

[30] ELLIS 01B places constraints on the SUSY parameter space in the framework of minimal N=1 supergravity models with radiative breaking of the electroweak gauge symmetry. Focuses on models with large tanβ.

[31] FENG 00 explores cosmologically allowed regions of MSSM parameter space with multi-TeV masses.

[32] ELLIS 98B assumes a universal scalar mass and radiative supersymmetry breaking with universal gaugino masses. The upper limit to the LSP mass is increased due to the inclusion of $\chi - \tilde{\tau}_R$ coannihilations.

[33] EDSJO 97 included all coannihilation processes between neutralinos and charginos for any neutralino mass and composition.

[34] Notes the location of the neutralino Z resonance and h resonance annihilation corridors in minimal supergravity models with radiative electroweak breaking.

[35] Mass of the bino (=LSP) is limited to $m_{\widetilde{B}} \lesssim$ 350 GeV for m_t = 174 GeV.

[36] DREES 93, KELLEY 93 compute the cosmic relic density of the LSP in the framework of minimal N=1 supergravity models with radiative breaking of the electroweak gauge symmetry.

[37] FALK 93 relax the upper limit to the LSP mass by considering sfermion mixing in the MSSM.

[38] MIZUTA 93 include coannihilations to compute the relic density of Higgsino dark matter.

[39] LOPEZ 92 calculate the relic LSP density in a minimal SUSY GUT model.

[40] MCDONALD 92 calculate the relic LSP density in the MSSM including exact tree-level annihilation cross sections for all two-body final states.

[41] GRIEST 91 improve relic density calculations to account for coannihilations, pole effects, and threshold effects.

[42] NOJIRI 91 uses minimal supergravity mass relations between squarks and sleptons to narrow cosmologically allowed parameter space.

[43] Mass of the bino (=LSP) is limited to $m_{\widetilde{B}} \lesssim$ 350 GeV for $m_t \leq 200$ GeV. Mass of the higgsino (=LSP) is limited to $m_{\widetilde{H}} \lesssim$ 1 TeV for $m_t \leq 200$ GeV.

[44] ROSZKOWSKI 91 calculates LSP relic density in mixed gaugino/higgsino region.

[45] Mass of the bino (=LSP) is limited to $m_{\widetilde{B}} \lesssim$ 550 GeV. Mass of the higgsino (=LSP) is limited to $m_{\widetilde{H}} \lesssim$ 3.2 TeV.

[46] KRAUSS 83 finds $m_{\widetilde{\gamma}}$ not 30 eV to 2.5 GeV. KRAUSS 83 takes into account the gravitino decay. Find that limits depend strongly on reheated temperature. For example a new allowed region $m_{\widetilde{\gamma}}$ = 4–20 MeV exists if $m_{\text{gravitino}}$ <40 TeV. See figure 2.

Unstable $\widetilde{\chi}_1^0$ (Lightest Neutralino) MASS LIMIT

Unless otherwise stated, results in this section assume spectra and production rates as evaluated in the MSSM. Unless otherwise stated, the goldstino or gravitino mass $m_{\widetilde{G}}$ is assumed to be negligible relative to all other masses. In the following, $\widetilde{G}$ is assumed to be undetected and to give rise to a missing energy ($\not{E}$) signature.

VALUE (GeV)	CL%	DOCUMENT ID		TECN	COMMENT
• • • We do not use the following data for averages, fits, limits, etc. • • •					
		[1] AAD	13AP	ATLS	$2\gamma + \not{E}_T$, GMSB, SPS8
none 220–380	95	[2] AAD	13Q	ATLS	$\gamma + b + \not{E}_T$, higgsino-like neutralino, GMSB
		[3] AAD	13R	ATLS	$\widetilde{\chi}_1^0 \rightarrow \mu jj$, $\not{R}$, $\lambda'_{211} \neq 0$
		[4] AALTONEN	13I	CDF	$\widetilde{\chi}_1^0 \rightarrow \gamma\widetilde{G}$, $\not{E}_T$, GMSB
>220	95	[5] CHATRCHYAN	13AH	CMS	$\widetilde{\chi}_1^0 \rightarrow \gamma\widetilde{G}$, GMSB, SPS8, $c\tau$ < 500 mm
		[6] AAD	12CP	ATLS	$2\gamma + \not{E}_T$, GMSB
		[7] AAD	12CT	ATLS	$\geq 4\ell^{\pm}$, $\not{R}$
		[8] AAD	12R	ATLS	$\widetilde{\chi}_1^0 \rightarrow \mu jj$, $\not{R}$, $\lambda'_{211} \neq 0$
		[9] ABAZOV	12AD	D0	$\widetilde{\chi}_1^0\widetilde{\chi}_1^0 \rightarrow \gamma Z\widetilde{G}\widetilde{G}$, GMSB
		[10] CHATRCHYAN	12BK	CMS	$2\gamma + \not{E}_T$, GMSB
		[11] CHATRCHYAN	11B	CMS	$\widetilde{W}^0 \rightarrow \gamma\widetilde{G}$, $\widetilde{W}^{\pm} \rightarrow \ell^{\pm}\widetilde{G}$, GMSB
>149	95	[12] AALTONEN	10	CDF	$p\overline{p} \rightarrow \widetilde{\chi}\widetilde{\chi}$, $\widetilde{\chi}=\widetilde{\chi}_2^0$, $\widetilde{\chi}_1^{\pm}$, $\widetilde{\chi}_1^0 \rightarrow \gamma\widetilde{G}$, GMSB
>175	95	[13] ABAZOV	10P	D0	$\widetilde{\chi}_1^0 \rightarrow \gamma\widetilde{G}$, GMSB
		[14] AALTONEN	08U	CDF	$\widetilde{\chi}_1^0 \rightarrow \gamma\widetilde{G}$, GMSB
>125	95	[15] ABAZOV	08F	D0	$p\overline{p} \rightarrow \widetilde{\chi}\widetilde{\chi}$, $\widetilde{\chi}=\widetilde{\chi}_2^0$, $\widetilde{\chi}_1^{\pm}$, $\widetilde{\chi}_1^0 \rightarrow \gamma\widetilde{G}$, GMSB
		[16] ABAZOV	08X	D0	$\widetilde{\chi}_1^0 \rightarrow Z^0\widetilde{G}$, GMSB
		[17] ABULENCIA	07H	CDF	$\not{R}$, $LL\overline{E}$
		[18] ABAZOV	06D	D0	$\not{R}$, $LL\overline{E}$
		[19] ABAZOV	06P	D0	$\not{R}$, λ_{122}
> 96.8	95	[20] ABBIENDI	06B	OPAL	$e^+e^- \rightarrow \widetilde{B}\widetilde{B}$, $(\widetilde{B} \rightarrow \widetilde{G}\gamma)$
		[21] ABDALLAH	05B	DLPH	$e^+e^- \rightarrow \widetilde{G}\widetilde{\chi}_1^0$, $(\widetilde{\chi}_1^0 \rightarrow \widetilde{G}\gamma)$
> 96	95	[22] ABDALLAH	05B	DLPH	$e^+e^- \rightarrow \widetilde{B}\widetilde{B}$, $(\widetilde{B} \rightarrow \widetilde{G}\gamma)$
> 93	95	[23] ACOSTA	05E	CDF	$p\overline{p} \rightarrow \widetilde{\chi}\widetilde{\chi}$, $\widetilde{\chi}=\widetilde{\chi}_2^0$, $\widetilde{\chi}_1^{\pm}$,$\widetilde{\chi}_1^0 \rightarrow \gamma\widetilde{G}$, GMSB
		[24] AKTAS	05	H1	$e^{\pm}p \rightarrow q\widetilde{\chi}_1^0$, $\widetilde{\chi}_1^0 \rightarrow \gamma\widetilde{G}$, GMSB+$\not{R}$ $LQ\overline{D}$
		[25] ABBIENDI	04N	OPAL	$e^+e^- \rightarrow \gamma\gamma\not{E}$
> 66	95	[26,27] ABDALLAH	04H	DLPH	AMSB, $\mu > 0$
> 38.0	95	[28,29] ABDALLAH	04M	DLPH	$\not{R}(\overline{U}\overline{D}\overline{D})$
		[30] ACHARD	04E	L3	$e^+e^- \rightarrow \widetilde{G}\widetilde{\chi}_1^0$, $\widetilde{\chi}_1^0 \rightarrow \widetilde{G}\gamma$
> 99.5	95	[31] ACHARD	04E	L3	$e^+e^- \rightarrow \widetilde{B}\widetilde{B}$, $(\widetilde{B} \rightarrow \widetilde{G}\gamma)$
> 89		[32] ABDALLAH	03D	DLPH	$e^+e^- \rightarrow \widetilde{\chi}_1^0\widetilde{\chi}_1^0$, GMSB, $m(\widetilde{G})$<1eV
		[33] HEISTER	03C	ALEP	$e^+e^- \rightarrow \widetilde{B}\widetilde{B}$, $(\widetilde{B} \rightarrow \gamma\widetilde{G})$
		[34] HEISTER	03C	ALEP	$e^+e^- \rightarrow \widetilde{G}\widetilde{\chi}_1^0$, $(\widetilde{\chi}_1^0 \rightarrow \widetilde{G}\gamma)$
> 39.9	95	[35] ACHARD	02	L3	$\not{R}$, MSUGRA
> 92	95	[36] HEISTER	02R	ALEP	short lifetime
> 54	95	[36] HEISTER	02R	ALEP	any lifetime
> 85	95	[37] ABBIENDI	01	OPAL	$e^+e^- \rightarrow \widetilde{\chi}_1^0\widetilde{\chi}_1^0$, GMSB, tan$\beta$=2
> 76	95	[37] ABBIENDI	01	OPAL	$e^+e^- \rightarrow \widetilde{\chi}_1^0\widetilde{\chi}_1^0$, GMSB, tan$\beta$=20
> 32.5	95	[38] ACCIARRI	01	L3	$\not{R}$, all m_0, $0.7 \leq \tan\beta \leq 40$
		[39] ADAMS	01	NTEV	$\widetilde{\chi}^0 \rightarrow \mu\mu\nu$, $\not{R}$, $LL\overline{E}$
> 29	95	[40] ABBIENDI	99T	OPAL	$e^+e^- \rightarrow \widetilde{\chi}_1^0\widetilde{\chi}_1^0$, $\not{R}$, m_0=500 GeV, tan$\beta > 1.2$
> 29	95	[41] BARATE	99E	ALEP	$\not{R}$, $L\overline{Q}\overline{D}$, tan$\beta$=1.41, m_0=500 GeV
		[42] ABREU	98	DLPH	$e^+e^- \rightarrow \widetilde{\chi}_1^0\widetilde{\chi}_1^0$ $(\widetilde{\chi}_1^0 \rightarrow \gamma\widetilde{G})$
> 23	95	[43] BARATE	98S	ALEP	$\not{R}$, $LL\overline{E}$
		[44] ELLIS	97	THEO	$e^+e^- \rightarrow \widetilde{\chi}_1^0\widetilde{\chi}_1^0$, $\widetilde{\chi}_1^0 \rightarrow \gamma\widetilde{G}$
		[45] CABIBBO	81	COSM	

[1] AAD 13AP searched in 4.8 fb^{-1} of pp collisions at $\sqrt{s}$ = 7 TeV for events containing non-pointing photons in a diphoton plus missing transverse energy final state. No excess is observed above the background expected from Standard Model processes. The results are used to set 95% C.L. exclusion limits in the context of gauge-mediated supersymmetric breaking models, with the lightest neutralino being the next-to-lightest supersymmetric particle and decaying with a lifetime in excess of 0.25 ns into a photon and a gravitino. For limits in the NLSP lifetime versus Λ plane, for the SPS8 model, see their Fig. 8.

[2] AAD 13Q searched in 4.7 fb^{-1} of pp collisions at $\sqrt{s}$ = 7 TeV for events containing a high-p_T isolated photon, at least one jet identified as originating from a bottom quark, and high missing transverse momentum. Such signatures may originate from supersymmetric models with gauge-mediated supersymmetry breaking in events in which one of a pair of higgsino-like neutralinos decays into a photon and a gravitino while the other decays into a Higgs boson and a gravitino. No significant excess above the expected background was found and limits were set on the neutralino mass in a generalized GMSB model (GGM) with a higgsino-like neutralino NLSP, see their Fig. 4. Intermediate neutralino masses between 220 and 380 GeV are excluded at 95% C.L, regardless of the squark and gluino masses, purely on the basis of the expected weak production.

[3] AAD 13R looked in 4.4 fb^{-1} of pp collisions at $\sqrt{s}$ = 7 TeV for events containing new, heavy particles that decay at a significant distance from their production point into a final state containing a high-momentum muon and charged hadrons. No excess over the expected background is observed and limits are placed on the production cross-section of neutralinos via squarks for various $m_{\widetilde{q}}$, $m_{\widetilde{\chi}_1^0}$ in an R-parity violating scenario with $\lambda'_{211} \neq 0$, as a function of the neutralino lifetime, see their Fig. 6.

[4] AALTONEN 13I searched in 6.3 fb^{-1} of $p\overline{p}$ collisions at $\sqrt{s}$ = 1.96 TeV for events containing $\not{E}_T$ and a delayed photon that arrives late in the detector relative to the time expected from prompt production. No evidence of delayed photon production is observed.

[5] CHATRCHYAN 13AH searched in 4.9 fb^{-1} of pp collisions at $\sqrt{s}$ = 7 TeV for events containing $\not{E}_T$ and a delayed photon that arrives late in the detector relative to the time expected from prompt production. No significant excess above the expected background was found and limits were set on the pair production of $\widetilde{\chi}_1^0$ depending on the neutralino proper decay length, see Fig. 8. Supersedes CHATRCHYAN 12BK.

[6] AAD 12CP searched in 4.8 fb^{-1} of pp collisions at $\sqrt{s}$ = 7 TeV for events with two photons and large $\not{E}_T$ due to $\widetilde{\chi}_1^0 \rightarrow \gamma\widetilde{G}$ decays in a GMSB framework. No significant excess above the expected background was found and limits were set on the neutralino mass in a generalized GMSB model (GGM) with a bino-like neutralino NLSP, see Figs. 6 and 7. The other sparticle masses were decoupled, tanβ = 2 and $c\tau_{NLSP}$ < 0.1 mm. Also, in the framework of the SPS8 model, limits are presented in Fig. 8.

[7] AAD 12CT searched in 4.7 fb^{-1} of pp collisions at $\sqrt{s}$ = 7 TeV for events containing four or more leptons (electrons or muons) and either moderate values of missing transverse momentum or large effective mass. No significant excess is found in the data. Limits are presented in a simplified model of R-parity violating supersymmetry in which charginos are pair-produced and then decay into a W-boson and a $\widetilde{\chi}_1^0$, which in turn decays through an RPV coupling into two charged leptons ($e^{\pm}e^{\mp}$ or $\mu^{\pm}\mu^{\mp}$) and a neutrino. In this model, limits are set on the neutralino mass as a function of the chargino mass, see Fig. 3a. Limits are also set in an R-parity violating mSUGRA model, see Fig. 3b.

[8] AAD 12R looked in 33 pb^{-1} of pp collisions at $\sqrt{s}$ = 7 TeV for events containing new, heavy particles that decay at a significant distance from their production point into a final state containing a high-momentum muon and charged hadrons. No excess over the expected background is observed and limits are placed on the production cross-section of neutralinos via squarks for various ($m_{\widetilde{q}}$, $m_{\widetilde{\chi}_1^0}$) in an R-parity violating scenario with $\lambda'_{211} \neq 0$, as a function of the neutralino lifetime, see their Fig. 8. Superseded by AAD 13R.

[9] ABAZOV 12AD looked in 6.2 fb^{-1} of pp collisions at $\sqrt{s}$ = 1.96 TeV for events with a photon, a Z-boson, and large $\not{E}_T$ in the final state. This topology corresponds to a GMSB model where pairs of neutralino NLSPs are either pair produced promptly or from decays of other supersymmetric particles and then decay to either $Z\widetilde{G}$ or $\gamma\widetilde{G}$. No significant excess over the SM expectation is observed and a limit at 95% C.L. on the cross section is derived as a function of the effective SUSY breaking scale Λ, see Fig. 3. Assuming N_{mes} = 2, M_{mes} = 3 Λ, tanβ = 3, μ = 0.75 M_1, and C_{grav} = 1, the model is excluded at 95% C.L. for values of Λ < 87 TeV.

[10] CHATRCHYAN 12BK searched in 2.23 fb^{-1} of pp collisions at $\sqrt{s}$ = 7 TeV for events with two photons and large $\not{E}_T$ due to $\widetilde{\chi}_1^0 \rightarrow \gamma\widetilde{G}$ decays in a GMSB framework. No significant excess above the expected background was found and limits were set on the pair production of $\widetilde{\chi}_1^0$ depending on the neutralino lifetime, see Fig. 6.

[11] CHATRCHYAN 11B looked in 35 pb^{-1} of pp collisions at $\sqrt{s}$=7 TeV for events with an isolated lepton (e or μ), a photon and $\not{E}_T$ which may arise in a generalized gauge mediated model from the decay of Wino-like NLSPs. No evidence for an excess over the expected background is observed. Limits are derived in the plane of squark/gluino mass versus Wino mass (see Fig. 4). Mass degeneracy of the produced squarks and gluinos is assumed.

[12] AALTONEN 10 searched in 2.6 fb^{-1} of $p\overline{p}$ collisions at $\sqrt{s}$ = 1.96 TeV for diphoton events with large $\not{E}_T$. They may originate from the production of $\widetilde{\chi}^{\pm}$ in pairs or associated to a $\widetilde{\chi}_2^0$, decaying into $\widetilde{\chi}_1^0$ which itself decays in GMSB to $\gamma\widetilde{G}$. There is no excess of events beyond expectation. An upper limit on the cross section is calculated in the GMSB model as a function of the $\widetilde{\chi}_1^0$ mass and lifetime, see their Fig. 2. A limit

is derived on the $\tilde{\chi}_1^0$ mass of 149 GeV for $\tau_{\tilde{\chi}_1^0} \ll 1$ ns, which improves the results of previous searches.

[13] ABAZOV 10P looked in 6.3 fb^{-1} of $p\overline{p}$ collisions at $\sqrt{s} = 1.96$ TeV for events with at least two isolated γs and large $\not{E}_T$. These could be the signature of $\tilde{\chi}_2^0$ and $\tilde{\chi}_1^\pm$ production, decaying to $\tilde{\chi}_1^0$ and finally $\tilde{\chi}_1^0 \to \gamma\tilde{G}$ in a GMSB framework. No significant excess over the SM expectation is observed, and a limit at 95% C.L. on the cross section is derived for $N_{mes} = 1$, $\tan\beta = 15$ and $\mu > 0$, see their Fig. 2. This allows them to set a limit on the effective SUSY breaking scale $\Lambda > 124$ TeV, from which the excluded $\tilde{\chi}_1^0$ mass range is obtained.

[14] AALTONEN 08U searched in 570 pb^{-1} of $p\overline{p}$ collisions at $\sqrt{s} = 1.96$ TeV for events that contain a time-delayed photon, at least one jet, and large $\not{E}_T$. The time-of-arrival is measured for each electromagnetic tower with a resolution of 0.50 ns. The number of observed events in the signal region is consistent with the background estimation. An upper limit on the cross section is derived as a function of the $\tilde{\chi}_1^0$ mass and lifetime, shown in their Fig. 24. The comparison with the NLO cross section for GMSB yields an exclusion of the $\tilde{\chi}_1^0$ mass as a function of its lifetime, see Fig. 25. See ABULENCIA 07P for a previous analysis of the same data set.

[15] ABAZOV 08F looked in 1.1 fb^{-1} of $p\overline{p}$ collisions at $\sqrt{s} = 1.96$ TeV for diphoton events with large $\not{E}_T$. They may originate from the production of $\tilde{\chi}^\pm$ in pairs or associated to a $\tilde{\chi}_2^0$, decaying to a $\tilde{\chi}_1^0$ which itself decays promptly in GMSB to $\tilde{\chi}_1^0 \to \gamma\tilde{G}$. No significant excess was found compared to the background expectation. A limit is derived on the masses of SUSY particles in the GMSB framework for $M = 2\Lambda$, $N = 1$, $\tan\beta = 15$ and $\mu > 0$, see Figure 2. It also excludes $\Lambda < 91.5$ TeV. Supersedes the results of ABAZOV 05A. Superseded by ABAZOV 10P.

[16] ABAZOV 08X searched in 1.1 fb^{-1} of $p\overline{p}$ collisions at $\sqrt{s} = 1.96$ TeV for an excess of events with electron pairs. Their vertex, reconstructed from the directions measured in the segmented electromagnetic calorimeter, is required to be away from the primary interaction point. Such delayed decays might be expected for a Higgsino-like $\tilde{\chi}_1^0$ in GMSB. No significant excess was found compared to the background expectation. Upper limits on the cross-section times branching ratio are extracted as a function of the lifetime for several ranges of dielectron invariant masses, see their Fig. 3.

[17] ABULENCIA 07H searched in 346 pb^{-1} of $p\overline{p}$ collisions at $\sqrt{s} = 1.96$ TeV for events with at least three leptons (e or μ) from the decay of $\tilde{\chi}_1^0$ via $LL\overline{E}$ couplings. The results are consistent with the hypothesis of no signal. Upper limits on the cross-section are extracted and a limit is derived in the framework of mSUGRA on the masses of $\tilde{\chi}_1^0$ and $\tilde{\chi}_1^\pm$, see e.g. their Fig. 3 and Tab. II.

[18] ABAZOV 06D looked in 360 pb^{-1} of $p\overline{p}$ collisions at $\sqrt{s} = 1.96$ TeV for events with three leptons originating from the pair production of charginos and neutralinos, followed by $R\!\!\!/$ decays mediated by $LL\overline{E}$ couplings. One coupling is assumed to be dominant at a time. No significant excess was found compared to the background expectation in the $ee\ell$, $\mu\mu\ell$ nor $ee\tau$ ($\ell = e, \mu$) final states. Upper limits on the cross-section are extracted in a specific MSUGRA model and a MSSM model without unification of M_1 and M_2 at the GUT scale. A limit is derived on the masses of charginos and neutralinos for both scenarios assuming λ_{ijk} couplings such that the decay length is less than 1 cm, see their Table III and Fig. 4.

[19] ABAZOV 06P looked in 380 pb^{-1} of $p\overline{p}$ collisions at $\sqrt{s} = 1.96$ TeV for events with at least 2 opposite sign isolated muons which might arise from the decays of neutralinos into $\mu\mu\nu$ via $R\!\!\!/$ couplings $LL\overline{E}$. No events are observed in the decay region defined by a radius between 5 and 20 cm, in agreement with the SM expectation. Limits are set on the cross-section times branching ratio as a function of lifetime, shown in their Fig. 3. This limit excludes the SUSY interpretation of the NuTeV excess of dimuon events reported in ADAMS 01.

[20] ABBIENDI 06B use 600 pb^{-1} of data from $\sqrt{s} = 189$–209 GeV. They look for events with diphotons + $\not{E}$ final states originating from prompt decays of pair-produced neutralinos in a GMSB scenario with $\tilde{\chi}_1^0$ NLSP. Limits on the cross-section are computed as a function of m($\tilde{\chi}_1^0$), see their Fig. 14. The limit on the $\tilde{\chi}_1^0$ mass is for a pure Bino state assuming a prompt decay, with lifetimes up to 10^{-9}s. Supersedes the results of ABBIENDI 04N.

[21] ABDALLAH 05B use data from $\sqrt{s} = 180$–209 GeV. They look for events with single photons + $\not{E}$ final states. Limits are computed in the plane (m($\tilde{G}$) , m($\tilde{\chi}_1^0$)), shown in their Fig. 9b for a pure Bino state in the GMSB framework and in Fig. 9c for a no-scale supergravity model. Supersedes the results of ABREU 00Z.

[22] ABDALLAH 05B use data from $\sqrt{s} = 130$–209 GeV. They look for events with diphotons + $\not{E}$ final states and single photons not pointing to the vertex, expected in GMSB when the $\tilde{\chi}_1^0$ is the NLSP. Limits are computed in the plane (m($\tilde{G}$), m($\tilde{\chi}_1^0$)), see their Fig. 10. The lower limit is derived on the $\tilde{\chi}_1^0$ mass for a pure Bino state assuming a prompt decay and $m_{\tilde{e}_R} = m_{\tilde{e}_L} = 2\, m_{\tilde{\chi}_1^0}$. It improves to 100 GeV for $m_{\tilde{e}_R} = m_{\tilde{e}_L} = 1.1\, m_{\tilde{\chi}_1^0}$. and the limit in the plane (m($\tilde{\chi}_1^0$), m($\tilde{e}_R$)) is shown in Fig. 10b. For long-lived neutralinos, cross-section limits are displayed in their Fig 11. Supersedes the results of ABREU 00Z.

[23] ACOSTA 05E looked in 202 pb^{-1} of $p\overline{p}$ collisions at $\sqrt{s}$=1.96 TeV for diphoton events with large $\not{E}_T$. They may originate from the production of $\tilde{\chi}^\pm$ in pairs or associated to a $\tilde{\chi}_2^0$, decaying to a $\tilde{\chi}_1^0$ which itself decays promptly in GMSB to $\gamma\tilde{G}$. No events are selected at large $\not{E}_T$ compared to the background expectation. A limit is derived on the masses of SUSY particles in the GMSB framework for $M = 2\,\Lambda$, $N = 1$, $\tan\beta = 15$ and $\mu > 0$, see Figure 2. It also excludes $\Lambda < 69$ TeV. Supersedes the results of ABE 99I.

[24] AKTAS 05 data collected at 319 GeV with 64.3 pb^{-1} of e^+p and 13.5 pb^{-1} of e^-p. They look for $R\!\!\!/$ resonant $\tilde{\chi}_1^0$ production via t-channel exchange of a $\tilde{e}$, followed by prompt GMSB decay of the $\tilde{\chi}_1^0$ to $\gamma\tilde{G}$. Upper limits at 95% on the cross section are derived, see their Figure 4, and compared to two example scenarios. In Figure 5, they display 95% exclusion limits in the plane of $M(\tilde{\chi}_1^0)$ versus $M(\tilde{e}_L) - M(\tilde{\chi}_1^0)$ for the two scenarios and several values of the λ' Yukawa coupling.

[25] ABBIENDI 04N use data from $\sqrt{s} = 189$–209 GeV, setting limits on $\sigma(e^+e^- \to XX) \times B^2(X \to Y\gamma)$, with Y invisible (see their Fig. 4). Limits on $\tilde{\chi}_1^0$ masses for a specific model are given. Supersedes the results of ABBIENDI,G 00D.

[26] ABDALLAH 04H use data from LEP 1 and $\sqrt{s} = 192$–208 GeV. They re-use results or re-analyze the data from ABDALLAH 03M to put limits on the parameter space of anomaly-mediated supersymmetry breaking (AMSB), which is scanned in the region $1 < m_{3/2} < 50$ TeV, $0 < m_0 < 1000$ GeV, $1.5 < \tan\beta < 35$, both signs of μ. The constraints are obtained from the searches for mass degenerate chargino and neutralino, for SM-like and invisible Higgs, for leptonically decaying charginos and from the limit on non-SM Z width of 3.2 MeV. The limit is for $m_t = 174.3$ GeV (see Table 2 for other m_t values).

[27] The limit improves to 73 GeV for $\mu < 0$.

[28] ABDALLAH 04M use data from $\sqrt{s} = 192$–208 GeV to derive limits on sparticle masses under the assumption of $R\!\!\!/$ with $LL\overline{E}$ or $\overline{UDD}$ couplings. The results are valid in the ranges $90 < m_0 < 500$ GeV, $0.7 < \tan\beta < 30$, $-200 < \mu < 200$ GeV, $0 < M_2 < 400$ GeV. Supersedes the result of ABREU 01D and ABREU 00U.

[29] The limit improves to 39.5 GeV for $LL\overline{E}$ couplings.

[30] ACHARD 04E use data from $\sqrt{s} = 189$–209 GeV. They look for events with single photons + $\not{E}$ final states. Limits are computed in the plane (m($\tilde{G}$), m($\tilde{\chi}_1^0$)), shown in their Fig. 8c for a no-scale supergravity model, excluding, e.g., Gravitino masses below 10^{-5} eV for neutralino masses below 172 GeV. Supersedes the results of ACCIARRI 99R.

[31] ACHARD 04E use data from $\sqrt{s} = 189$–209 GeV. They look for events with diphotons + $\not{E}$ final states. Limits are computed in the plane (m($\tilde{\chi}_1^0$), m($\tilde{e}_R$)), see their Fig. 8d. The limit on the $\tilde{\chi}_1^0$ mass is for a pure Bino state assuming a prompt decay, with $m_{\tilde{e}_L} = 1.1\, m_{\tilde{\chi}_1^0}$ and $m_{\tilde{e}_R} = 2.5\, m_{\tilde{\chi}_1^0}$. Supersedes the results of ACCIARRI 99R.

[32] ABDALLAH 03D use data from $\sqrt{s} = 161$–208 GeV. They look for 4-tau + $\not{E}$ final states, expected in GMSB when the $\tilde{\tau}_1$ is the NLSP, and 4-lepton + $\not{E}$ final states, expected in the co-NLSP scenario, and assuming a short-lived $\tilde{\chi}_1^0$ (m($\tilde{G}$)<1 eV). Limits are computed in the plane (m($\tilde{\tau}_1$), m($\tilde{\chi}_1^0$)) from a scan of the GMSB parameters space, after combining these results with the search for slepton pair production from the same paper to cover prompt decays and for the case of $\tilde{\chi}_1^0$ NLSP from ABREU 00Z. The limit above is reached for a single generation of messengers and when the $\tilde{\tau}_1$ is the NLSP. Stronger limits are obtained when more messenger generations are assumed or when the other sleptons are co-NLSP, see their Fig. 10. Supersedes the results of ABREU 01G.

[33] HEISTER 03C use the data from $\sqrt{s} = 189$–209 GeV to search for $\gamma\,\not{E}_T$ final states with non-pointing photons and $\gamma\gamma\,\not{E}_T$ events. Interpreted in the framework of Minimal GMSB, a lower bound on the $\tilde{\chi}_1^0$ mass is obtained as function of its lifetime. For a laboratory lifetime of less than 3 ns, the limit at 95% CL is 98.8 GeV. For other lifetimes, see their Fig. 5. These results are interpreted in a more general GMSB framework in HEISTER 02R.

[34] HEISTER 03C use the data from $\sqrt{s} = 189$–209 GeV to search for $\gamma\,\not{E}_T$ final states. They obtained an upper bound on the cross section for the process $e^+e^- \to \tilde{G}\tilde{\chi}_1^0$, followed by the prompt decay $\tilde{\chi}_1^0 \to \gamma\tilde{G}$, shown in their Fig. 4. These results supersede BARATE 98H.

[35] ACHARD 02 searches for the production of sparticles in the case of $R\!\!\!/$ prompt decays with $LL\overline{E}$ or $\overline{UDD}$ couplings at $\sqrt{s}$=189–208 GeV. The search is performed for direct and indirect decays, assuming one coupling at the time to be nonzero. The MSUGRA limit results from a scan over the MSSM parameter space with the assumption of gaugino and scalar mass unification at the GUT scale, imposing simultaneously the exclusions from neutralino, chargino, sleptons, and squarks analyses. The limit holds for $\overline{UDD}$ couplings and increases to 40.2 GeV for $LL\overline{E}$ couplings. For L3 limits from $LQ\overline{D}$ couplings, see ACCIARRI 01.

[36] HEISTER 02R search for signals of GMSB in the 189–209 GeV data. For the $\tilde{\chi}_1^0$ NLSP scenario, they looked for topologies consisting of $\gamma\gamma\not{E}$ or a single γ not pointing to the interaction vertex. For the $\tilde{\ell}$ NLSP case, the topologies consist of $\ell\ell\not{E}$ or $4\ell\not{E}$ (from $\tilde{\chi}_1^0\tilde{\chi}_1^0$) production), including leptons with large impact parameters, kinks, or stable particles. Limits are derived from a scan over the GMSB parameters (see their Table 5 for the ranges). The limits are valid whichever is the NLSP. The absolute mass bound on the $\tilde{\chi}_1^0$ for any lifetime includes indirect limits from the chargino search, and from the slepton search HEISTER 02E preformed within the MSUGRA framework. A bound for any NLSP and any lifetime of 77 GeV has also been derived by using the constraints from the neutral Higgs search in HEISTER 02. Limits on the universal SUSY mass scale Λ are also derived in the paper. Supersedes the results from BARATE 00G.

[37] ABBIENDI 01 looked for final states with $\gamma\gamma\not{E}$, $\ell\ell\not{E}$, with possibly additional activity and four leptons + $\not{E}$ to search for prompt decays of $\tilde{\chi}_1^0$ or $\tilde{\ell}_1$ in GMSB. They derive limits in the plane ($m_{\tilde{\chi}_1^0}$,$m_{\tilde{\tau}_1}$), see Fig. 6, allowing either the $\tilde{\chi}_1^0$ or a $\tilde{\ell}_1$ to be the NLSP. Two scenarios are considered: $\tan\beta$=2 with the 3 sleptons degenerate in mass and $\tan\beta$=20 where the $\tilde{\tau}_1$ is lighter than the other sleptons. Data taken at $\sqrt{s}$=189 GeV.

[38] ACCIARRI 01 searches for multi-lepton and/or multi-jet final states from $R\!\!\!/$ prompt decays with $LL\overline{E}$, $LQ\overline{D}$, or $\overline{UDD}$ couplings at $\sqrt{s}$=189 GeV. The search is performed for direct and indirect decays of neutralinos, charginos, and scalar leptons, with the $\tilde{\chi}_1^0$ or a $\tilde{\ell}$ as LSP and assuming one coupling to be nonzero at a time. Mass limits are derived using simultaneously the constraints from the neutralino, chargino, and slepton analyses; and the Z^0 width measurements from ACCIARRI 00C in a scan of the parameter space assuming MSUGRA with gaugino and scalar mass universality. Updates and supersedes the results from ACCIARRI 99I.

[39] ADAMS 01 looked for neutral particles with mass > 2.2 GeV, produced by 900 GeV protons incident on a Beryllium oxide target and decaying through weak interactions into $\mu\mu$, μe, or $\mu\pi$ final states in the decay channel of the NuTeV detector (E815) at Fermilab. The number of observed events is $3\,\mu\mu$, $0\,\mu e$, and $0\,\mu\pi$ with an expected background of 0.069 ± 0.010, 0.13 ± 0.02, and 0.14 ± 0.02, respectively. The $\mu\mu$ events are consistent with the $R\!\!\!/$ decay of a neutralino with mass around 5 GeV. However, they share several aspects with ν-interaction backgrounds. An upper limit on the differential production cross section of neutralinos in pp interactions as function of the decay length is given in Fig. 3.

[40] ABBIENDI 99T searches for the production of neutralinos in the case of R-parity violation with $LL\overline{E}$, $LQ\overline{D}$, or $\overline{UDD}$ couplings using data from $\sqrt{s}$=183 GeV. They investigate topologies with multiple leptons, jets plus leptons, or multiple jets, assuming one coupling at the time to be non-zero and giving rise to direct or indirect decays. Mixed decays (where one particle has a direct, the other an indirect decay) are also considered for the $\overline{UDD}$ couplings. Upper limits on the cross section are derived which, combined with the constraint from the Z^0 width, allow to exclude regions in the M_2 versus μ plane for any coupling. Limits on the neutralino mass are obtained for non-zero $LL\overline{E}$ couplings $> 10^{-5}$. The limit disappears for $\tan\beta < 1.2$ and it improves to 50 GeV for $\tan\beta > 20$.

[41] BARATE 99E looked for the decay of gauginos via R-violating couplings $LQ\overline{D}$. The bound is significantly reduced for smaller values of m_0. Data collected at $\sqrt{s}$=130–172 GeV.

[42] ABREU 98 uses data at $\sqrt{s}$=161 and 172 GeV. Upper bounds on $\gamma\gamma\not{E}$ cross section are obtained. Similar limits on $\gamma\not{E}$ are also given, relevant for $e^+e^- \to \tilde{\chi}_1^0\tilde{G}$ production.

[43] BARATE 98S looked for the decay of gauginos via R-violating coupling $LL\overline{E}$. The bound improves to 25 GeV if the chargino decays into neutralino which further decays into lepton pairs. Data collected at $\sqrt{s}$=130–172 GeV.

[44] ELLIS 97 reanalyzed the LEP2 ($\sqrt{s}$=161 GeV) limits of $\sigma(\gamma\gamma+E_{\rm miss})<0.2$ pb to exclude $m_{\tilde{\chi}_1^0}<63$ GeV if $m_{\tilde{e}_L}=m_{\tilde{e}_R}<150$ GeV and $\tilde{\chi}_1^0$ decays to $\gamma\tilde{G}$ inside detector.

[45] CABIBBO 81 consider $\tilde{\gamma} \to \gamma+$ goldstino. Photino must be either light enough (<30 eV) to satisfy cosmology bound, or heavy enough (>0.3 MeV) to have disappeared at early universe.

$\tilde{\chi}_2^0$, $\tilde{\chi}_3^0$, $\tilde{\chi}_4^0$ (Neutralinos) MASS LIMITS

Neutralinos are unknown mixtures of photinos, z-inos, and neutral higgsinos (the supersymmetric partners of photons and of Z and Higgs bosons). The limits here apply only to $\tilde{\chi}_2^0$, $\tilde{\chi}_3^0$, and $\tilde{\chi}_4^0$. $\tilde{\chi}_1^0$ is the lightest supersymmetric particle (LSP); see $\tilde{\chi}_1^0$ Mass Limits. It is not possible to quote rigorous mass limits because they are extremely model dependent; i.e. they depend on branching ratios of various $\tilde{\chi}^0$ decay modes, on the masses of decay products ($\tilde{e}$, $\tilde{\gamma}$, $\tilde{q}$, $\tilde{g}$), and on the $\tilde{e}$ mass exchanged in $e^+e^- \to \tilde{\chi}_i^0\tilde{\chi}_j^0$. Limits arise either from direct searches, or from the MSSM constraints set on the gaugino and higgsino mass parameters M_2 and μ through searches for lighter charginos and neutralinos. Often limits are given as contour plots in the $m_{\tilde{\chi}^0} - m_{\tilde{e}}$ plane vs other parameters. When specific assumptions are made, e.g, the neutralino is a pure photino ($\tilde{\gamma}$), pure z-ino ($\tilde{Z}$), or pure neutral higgsino ($\tilde{H}^0$), the neutralinos will be labelled as such.

Limits obtained from e^+e^- collisions at energies up to 136 GeV, as well as other limits from different techniques, are now superseded and have not been included in this compilation. They can be found in the 1998 Edition (The European Physical Journal **C3** 1 (1998)) of this Review. $\Delta m = m_{\tilde{\chi}_2^0} - m_{\tilde{\chi}_1^0}$.

VALUE (GeV)	CL%	DOCUMENT ID		TECN	COMMENT
		[1] AAD	13	ATLS	$3\ell^\pm + \not{E}_T$, pMSSM, SMS
		[2] CHATRCHYAN	12BJ	CMS	$\geq 2\,\ell$, jets + $\not{E}_T$, $pp \to \tilde{\chi}_1^\pm\tilde{\chi}_2^0$
> 78	95	[3] ABBIENDI	04H	OPAL	$\tilde{\chi}_2^0$, all tanβ, Δm>5 GeV, m_0 >500 GeV, $A_0=0$
> 62.4	95	[4] ABREU	00W	DLPH	$\tilde{\chi}_2^0$, $1 \leq \tan\beta \leq 40$, all Δm, all m_0
> 99.9	95	[4] ABREU	00W	DLPH	$\tilde{\chi}_3^0$, $1 \leq \tan\beta \leq 40$, all Δm, all m_0
>116.0	95	[4] ABREU	00W	DLPH	$\tilde{\chi}_4^0$, $1 \leq \tan\beta \leq 40$, all Δm, all m_0
• • • We do not use the following data for averages, fits, limits, etc. • • •					
		[5] AAD	12AS	ATLS	$3\ell^\pm + \not{E}_T$, pMSSM
		[6] AAD	12T	ATLS	$\ell^\pm\ell^\pm + \not{E}_T$, $pp \to \tilde{\chi}_1^\pm\tilde{\chi}_2^0$
		[7] ABULENCIA	07N	CDF	$p\overline{p} \to \tilde{\chi}_1^\pm\tilde{\chi}_2^0$
		[8] ABDALLAH	05B	DLPH	$e^+e^- \to \tilde{\chi}_2^0\tilde{\chi}_2^0$, $(\tilde{\chi}_2^0 \to \tilde{\chi}_1^0\gamma)$
		[9] ACHARD	04E	L3	$e^+e^- \to \tilde{\chi}_2^0\tilde{\chi}_2^0$, $(\tilde{\chi}_2^0 \to \tilde{\chi}_1^0\gamma)$
> 80.0	95	[10] ACHARD	02	L3	$\tilde{\chi}_2^0$, $\not{R}$, MSUGRA
>107.2	95	[10] ACHARD	02	L3	$\tilde{\chi}_3^0$, $\not{R}$, MSUGRA
		[11] ABREU	01B	DLPH	$e^+e^- \to \tilde{\chi}_i^0\tilde{\chi}_j^0$
> 68.0	95	[12] ACCIARRI	01	L3	$\tilde{\chi}_2^0$, $\not{R}$, all m_0, $0.7 \leq \tan\beta \leq 40$
> 99.0	95	[12] ACCIARRI	01	L3	$\tilde{\chi}_3^0$, $\not{R}$, all m_0, $0.7 \leq \tan\beta \leq 40$
> 50	95	[13] ABREU	00U	DLPH	$\tilde{\chi}_2^0$, $\not{R}$ ($LL\overline{E}$), all Δm, $1 \leq \tan\beta \leq 30$
		[14] ABBIENDI	99F	OPAL	$e^+e^- \to \tilde{\chi}_2^0\tilde{\chi}_1^0$ $(\tilde{\chi}_2^0 \to \gamma\tilde{\chi}_1^0)$
		[15] ABBIENDI	99F	OPAL	$e^+e^- \to \tilde{\chi}_2^0\tilde{\chi}_2^0$ $(\tilde{\chi}_2^0 \to \gamma\tilde{\chi}_1^0)$
		[16] ABBOTT	98C	D0	$p\overline{p} \to \tilde{\chi}_1^\pm\tilde{\chi}_2^0$
> 82.2	95	[17] ABE	98J	CDF	$p\overline{p} \to \tilde{\chi}_1^\pm\tilde{\chi}_2^0$
> 92	95	[18] ACCIARRI	98F	L3	$\tilde{H}_2^0$, tanβ=1.41, $M_2<500$ GeV
		[19] ACCIARRI	98V	L3	$e^+e^- \to \tilde{\chi}_2^0\tilde{\chi}_{1,2}^0$ $(\tilde{\chi}_2^0 \to \gamma\tilde{\chi}_1^0)$
> 53	95	[20] BARATE	98H	ALEP	$e^+e^- \to \tilde{\gamma}\tilde{\gamma}$ $(\tilde{\gamma} \to \gamma\tilde{H}^0)$
> 74	95	[21] BARATE	98J	ALEP	$e^+e^- \to \tilde{\gamma}\tilde{\gamma}$ $(\tilde{\gamma} \to \gamma\tilde{H}^0)$
		[22] ABACHI	96	D0	$p\overline{p} \to \tilde{\chi}_1^\pm\tilde{\chi}_2^0$
		[23] ABE	96K	CDF	$p\overline{p} \to \tilde{\chi}_1^\pm\tilde{\chi}_2^0$

[1] AAD 13 searched in 4.7 fb^{-1} of pp collisions at $\sqrt{s}=7$ TeV for charginos and neutralinos decaying to a final state with three leptons (e and μ) and missing transverse energy. No excess beyond the Standard Model expectation is observed. Exclusion limits are derived in the phenomenological MSSM, see Fig. 2 and 3, and in simplified models, see Fig. 4. For the simplified models with intermediate slepton decays, degenerate $\tilde{\chi}_1^\pm$ and $\tilde{\chi}_2^0$ masses up to 500 GeV are excluded at 95% C.L. for very large mass differences with the $\tilde{\chi}_1^0$. Supersedes AAD 12AS.

[2] CHATRCHYAN 12BJ searched in 4.98 fb^{-1} of pp collisions at $\sqrt{s}=7$ TeV for direct electroweak production of charginos and neutralinos in events with at least two leptons, jets and missing transverse momentum. No significant excesses over the expected SM backgrounds are observed and 95% C.L. limits on the production cross section of $\tilde{\chi}_1^\pm\tilde{\chi}_2^0$ pair production were set in a number of simplified models, see Figs. 7 to 12. Most limits are for exactly 3 jets.

[3] ABBIENDI 04H search for charginos and neutralinos in events with acoplanar leptons+jets and multi-jet final states in the 192–209 GeV data, combined with the results on leptonic final states from ABBIENDI 04. The results hold for a scan over the parameter space covering the region $0 < M_2 <$5000 GeV, $-1000 < \mu <$1000 GeV and tanβ from 1 to 40. This limit supersedes ABBIENDI 00H.

[4] ABREU 00W combines data collected at $\sqrt{s}$=189 GeV with results from lower energies. The mass limit is obtained by constraining the MSSM parameter space with gaugino and sfermion mass universality at the GUT scale, using the results of negative direct searches for neutralinos (including cascade decays and $\tilde{\tau}\tau$ final states) from ABREU 01, for charginos from ABREU 00J and ABREU 00T (for all Δm_+), and for charged sleptons from ABREU 01B. The results hold for the full parameter space defined by all values of M_2 and $|\mu| \leq 2$ TeV with the $\tilde{\chi}_1^0$ as LSP.

[5] AAD 12AS searched in 2.06 fb^{-1} of pp collisions at $\sqrt{s}=7$ TeV for charginos and neutralinos decaying to a final state with three leptons (e and μ) and missing transverse energy. No excess beyond the Standard Model expectation is observed. Exclusion limits are derived in the phenomenological MSSM, see Fig. 2 (top), and in simplified models, see Fig. 2 (bottom).

[6] AAD 12T looked in 1 fb^{-1} of pp collisions at $\sqrt{s}=7$ TeV for the production of supersymmetric particles decaying into final states with missing transverse momentum and exactly two isolated leptons (e or μ). Same-sign dilepton events were separately studied. Additionally, in opposite-sign events, a search was made for an excess of same-flavor over different-flavor lepton pairs. No excess over the expected background is observed and limits are placed on the effective production cross section of opposite-sign dilepton events with $\not{E}_T > 250$ GeV and on same-sign dilepton events with $\not{E}_T > 100$ GeV. The latter limit is interpreted in a simplified electroweak gaugino production model.

[7] ABULENCIA 07N searched in 1 fb^{-1} of $p\overline{p}$ collisions at $\sqrt{s}=1.96$ TeV for events with two same sign leptons (e or μ) from the decay of $\tilde{\chi}_1^\pm\tilde{\chi}_2^0 X$ and large $\not{E}_T$. A slight excess of 13 events is observed over a SM background expectation of 7.8 ± 1.1. However, the kinematic distributions do not show any anomalous deviation from expectations in any particular region of parameter space.

[8] ABDALLAH 05B use data from $\sqrt{s}$ = 130–209 GeV, looking for events with diphotons + $\not{E}$. Limits on the cross-section are computed in the plane (m($\tilde{\chi}_2^0$), m($\tilde{\chi}_1^0$)), see Fig. 12. Supersedes the results of ABREU 00Z.

[9] ACHARD 04E use data from $\sqrt{s}$ = 189–209 GeV, looking for events with diphotons + $\not{E}$. Limits are computed in the plane (m($\tilde{\chi}_2^0$), m($\tilde{e}_R$)), for $\Delta m > 10$ GeV, see Fig. 7. Supersedes the results of ACCIARRI 99R.

[10] ACHARD 02 searches for the production of sparticles in the case of $\not{R}$ prompt decays with $LL\overline{E}$ or $\overline{UDD}$ couplings at $\sqrt{s}$=189–208 GeV. The search is performed for direct and indirect decays, assuming one coupling at the time to be nonzero. The MSUGRA limit results from a scan over the MSSM parameter space with the assumption of gaugino and scalar mass unification at the GUT scale, imposing simultaneously the exclusions from neutralino, chargino, sleptons, and squarks analyses. The limit of $\tilde{\chi}_2^0$ holds for $\overline{UDD}$ couplings and increases to 84.0 GeV for $LL\overline{E}$ couplings. The same $\tilde{\chi}_3^0$ limit holds for both $LL\overline{E}$ and $\overline{UDD}$ couplings. For L3 limits from $LQ\overline{D}$ couplings, see ACCIARRI 01.

[11] ABREU 01B used data from $\sqrt{s}$=189 GeV to search for the production of $\tilde{\chi}_i^0\tilde{\chi}_j^0$. They looked for di-jet and di-lepton pairs with $\not{E}$ for events from $\tilde{\chi}_i^0\tilde{\chi}_j^0$ with the decay $\tilde{\chi}_j^0 \to f\overline{f}\tilde{\chi}_1^0$; multi-jet and multi-lepton pairs with or without additional photons to cover the cascade decays $\tilde{\chi}_j^0 \to f\overline{f}\tilde{\chi}_2^0$, followed by $\tilde{\chi}_j^0 \to f\overline{f}\tilde{\chi}_1^0$ or $\tilde{\chi}_j^0 \to \gamma\tilde{\chi}_1^0$; multi-tau final states from $\tilde{\chi}_2^0 \to \tilde{\tau}\tau$ with $\tilde{\tau} \to \tau\tilde{\chi}_1^0$. See Figs. 9 and 10 for limits on the (μ,M_2) plane for tanβ=1.0 and different values of m_0.

[12] ACCIARRI 01 searches for multi-lepton and/or multi-jet final states from $\not{R}$ prompt decays with $LL\overline{E}$, $LQ\overline{D}$, or $\overline{UDD}$ couplings at $\sqrt{s}$=189 GeV. The search is performed for direct and indirect decays of neutralinos, charginos, and scalar leptons, with the $\tilde{\chi}_1^0$ or a $\tilde{\ell}$ as LSP and assuming one coupling to be nonzero at a time. Mass limits are derived using simultaneously the constraints from the neutralino, chargino, and slepton analyses; and the Z^0 width measurements from ACCIARRI 00C in a scan of the parameter space assuming MSUGRA with gaugino and scalar mass universality. Updates and supersedes the results from ACCIARRI 99I.

[13] ABREU 00U searches for the production of charginos and neutralinos in the case of R-parity violation with $LL\overline{E}$ couplings, using data from $\sqrt{s}$=189 GeV. They investigate topologies with multiple leptons or jets plus leptons, assuming one coupling to be nonzero at the time and giving rise to direct or indirect decays. Limits are obtained in the M_2 versus μ plane and a limit on the neutralino mass is derived from a scan over the parameters m_0 and tanβ.

[14] ABBIENDI 99F looked for $\gamma\not{E}$ final states at $\sqrt{s}$=183 GeV. They obtained an upper bound on the cross section for the production $e^+e^- \to \tilde{\chi}_2^0\tilde{\chi}_1^0$ followed by the prompt decay $\tilde{\chi}_2^0 \to \gamma\tilde{\chi}_1^0$ of 0.075–0.80 pb in the region $m_{\tilde{\chi}_2^0}+m_{\tilde{\chi}_1^0} > m_Z$, $m_{\tilde{\chi}_2^0}$=91–183 GeV, and $\Delta m > 5$ GeV. See Fig. 7 for explicit limits in the $(m_{\tilde{\chi}_2^0}, m_{\tilde{\chi}_1^0})$ plane.

[15] ABBIENDI 99F looked for $\gamma\gamma\not{E}$ final states at $\sqrt{s}$=183 GeV. They obtained an upper bound on the cross section for the production $e^+e^- \to \tilde{\chi}_2^0\tilde{\chi}_2^0$ followed by the prompt decay $\tilde{\chi}_2^0 \to \gamma\tilde{\chi}_1^0$ of 0.08–0.37 pb for $m_{\tilde{\chi}_2^0}$=45–81.5 GeV, and $\Delta m > 5$ GeV. See Fig. 11 for explicit limits in the $(m_{\tilde{\chi}_2^0}, m_{\tilde{\chi}_1^0})$ plane.

[16] ABBOTT 98C searches for trilepton final states (ℓ=e,μ). See footnote to ABBOTT 98C in the Chargino Section for details on the assumptions. Assuming a negligible decay rate of $\tilde{\chi}_1^\pm$ and $\tilde{\chi}_2^0$ to quarks, they obtain $m_{\tilde{\chi}_2^0} \gtrsim 103$ GeV.

[17] ABE 98J searches for trilepton final states (ℓ=e,μ). See footnote to ABE 98J in the Chargino Section for details on the assumptions. The quoted result for $m_{\tilde{\chi}_2^0}$ corresponds to the best limit within the selected range of parameters, obtained for $m_{\tilde{q}} > m_{\tilde{g}}$, tan$\beta$=2, and μ=−600 GeV.

[18] ACCIARRI 98F is obtained from direct searches in the $e^+e^- \to \tilde{\chi}_{1,2}^0\tilde{\chi}_2^0$ production channels, and indirectly from $\tilde{\chi}_1^\pm$ and $\tilde{\chi}_1^0$ searches within the MSSM. See footnote to ACCIARRI 98F in the chargino Section for further details on the assumptions. Data taken at $\sqrt{s}$ = 130–172 GeV.

[19] ACCIARRI 98V looked for $\gamma(\gamma)\not{E}$ final states at $\sqrt{s}$=183 GeV. They obtained an upper bound on the cross section for the production $e^+e^- \to \tilde{\chi}_2^0\tilde{\chi}_{1,2}^0$ followed by the prompt decay $\tilde{\chi}_2^0 \to \gamma\tilde{\chi}_1^0$. See Figs. 4a and 6a for explicit limits in the $(m_{\tilde{\chi}_2^0}, m_{\tilde{\chi}_1^0})$ plane.

[20] BARATE 98H looked for $\gamma\gamma$ $\not{E}$ final states at $\sqrt{s}$ = 161,172 GeV. They obtained an upper bound on the cross section for the production $e^+e^- \to \tilde{\chi}_2^0\tilde{\chi}_2^0$ followed by the prompt decay $\tilde{\chi}_2^0 \to \gamma\tilde{\chi}_1^0$ of 0.4–0.8 pb for $m_{\tilde{\chi}_2^0}$ = 10–80 GeV. The bound above is for the specific case of $\tilde{\chi}_1^0 = \tilde{H}^0$ and $\tilde{\chi}_2^0 = \tilde{\gamma}$ and $m_{\tilde{e}_R}$ = 100 GeV. See Fig. 6 and 7 for explicit limits in the $(\tilde{\chi}_2^0,\tilde{\chi}_1^0)$ plane and in the $(\tilde{\chi}_2^0,\tilde{e}_R)$ plane.

[21] BARATE 98J looked for $\gamma\gamma$ $\not{E}$ final states at $\sqrt{s}$ = 161–183 GeV. They obtained an upper bound on the cross section for the production $e^+e^- \to \tilde{\chi}_2^0\tilde{\chi}_2^0$ followed by the prompt decay $\tilde{\chi}_2^0 \to \gamma\tilde{\chi}_1^0$ of 0.08–0.24 pb for $m_{\tilde{\chi}_2^0} < 91$ GeV. The bound above is for the specific case of $\tilde{\chi}_1^0 = \tilde{H}^0$ and $\tilde{\chi}_2^0 = \tilde{\gamma}$ and $m_{\tilde{e}_R}$ = 100 GeV.

[22] ABACHI 96 searches for 3-lepton final states. Efficiencies are calculated using mass relations and branching ratios in the Minimal Supergravity scenario. Results are presented as lower bounds on $\sigma(\tilde{\chi}_1^\pm\tilde{\chi}_2^0) \times B(\tilde{\chi}_1^\pm \to \ell\nu_\ell\tilde{\chi}_1^0) \times B(\tilde{\chi}_2^0 \to \ell^+\ell^-\tilde{\chi}_1^0)$ as a function of $m_{\tilde{\chi}_1^0}$. Limits range from 3.1 pb ($m_{\tilde{\chi}_1^0}$ = 45 GeV) to 0.6 pb ($m_{\tilde{\chi}_1^0}$ = 100 GeV).

[23] ABE 96K looked for trilepton events from chargino-neutralino production. They obtained lower bounds on $m_{\tilde{\chi}_2^0}$ as a function of μ. The lower bounds are in the 45–50 GeV range for gaugino-dominant $\tilde{\chi}_2^0$ with negative μ, if tanβ <10. See paper for more details of the assumptions.

$\tilde{\chi}_1^\pm$, $\tilde{\chi}_2^\pm$ (Charginos) MASS LIMITS

Charginos are unknown mixtures of w-inos and charged higgsinos (the supersymmetric partners of W and Higgs bosons). A lower mass limit for the lightest chargino ($\tilde{\chi}_1^\pm$) of approximately 45 GeV, independent of the field composition and of the decay mode, has been obtained by the LEP experiments from the analysis of the Z width and decays. These results, as well as other now superseded limits from e^+e^- collisions at energies below 136 GeV, and from hadronic collisions, can be found in the 1998 Edition (The European Physical Journal **C3** 1 (1998)) of this Review.

Unless otherwise stated, results in this section assume spectra, production rates, decay modes and branching ratios as evaluated in the MSSM, with gaugino and sfermion mass unification at the GUT scale. These papers generally study production of $\tilde{\chi}_1^0\tilde{\chi}_2^0$, $\tilde{\chi}_1^+\tilde{\chi}_1^-$ and (in the case of hadronic collisions) $\tilde{\chi}_1^\pm\tilde{\chi}_2^0$ pairs, including the effects of cascade decays. The mass limits on $\tilde{\chi}_1^\pm$ are either direct, or follow indirectly from the constraints set by the non-observation of $\tilde{\chi}_2^0$ states on the gaugino and higgsino MSSM parameters M_2 and μ. For generic values of the MSSM parameters, limits from high-energy e^+e^- collisions coincide with the highest value of the mass allowed by phase-space, namely $m_{\tilde{\chi}_1^\pm} \lesssim \sqrt{s}/2$. The still unpublished combination of the results of the four LEP collaborations from the 2000 run of LEP2 at $\sqrt{s}$ up to $\simeq$ 209 GeV yields a lower mass limit of 103.5 GeV valid for general MSSM models. The limits become however weaker in certain regions of the MSSM parameter space where the detection efficiencies or production cross sections are suppressed. For example, this may happen when: (i) the mass differences $\Delta m_+ = m_{\tilde{\chi}_1^\pm} - m_{\tilde{\chi}_1^0}$ or $\Delta m_\nu = m_{\tilde{\chi}_1^\pm} - m_{\tilde{\nu}}$ are very small, and the detection efficiency is reduced; (ii) the electron sneutrino mass is small, and the $\tilde{\chi}_1^\pm$ production rate is suppressed due to a destructive interference between s and t channel exchange diagrams. The regions of MSSM parameter space where the following limits are valid are indicated in the comment lines or in the footnotes.

VALUE (GeV)	CL%	DOCUMENT ID		TECN	COMMENT
		[1] AAD	13	ATLS	$3\ell^\pm + \not{E}_T$, pMSSM, SMS
		[2] AAD	13B	ATLS	$2\ell^\pm + \not{E}_T$, pMSSM, SMS
>540	95	[3] AAD	12CT	ATLS	$\geq 4\ell^\pm$, $\not{R}$, $m_{\tilde{\chi}_1^0}$ > 300 GeV
		[4] CHATRCHYAN	12BJ	CMS	$\geq 2\,\ell$, jets + $\not{E}_T$, $pp \to \tilde{\chi}_1^\pm\tilde{\chi}_2^0$
>101	95	[5] ABBIENDI	04H	OPAL	all tanβ, Δm_+ >5 GeV, m_0 >500 GeV, $A_0 = 0$
> 89		[6] ABBIENDI	03H	OPAL	$0.5 \leq \Delta m_+ \leq 5$ GeV, higgsino-like, tanβ=1.5
> 97.1	95	[7] ABDALLAH	03M	DLPH	$\tilde{\chi}_1^\pm$, $\Delta m_+ \geq 3$ GeV, $m_{\tilde{\nu}} > m_{\tilde{\chi}^\pm}$
> 75	95	[7] ABDALLAH	03M	DLPH	$\tilde{\chi}_1^\pm$,higgsino,all Δm_+,$m_{\tilde{f}} > m_{\tilde{\chi}^\pm}$
> 70	95	[7] ABDALLAH	03M	DLPH	$\tilde{\chi}_1^\pm$, all Δm_+, $m_{\tilde{\nu}}$ >500 GeV, $M_2 \leq 2M_1 \leq 10M_2$
> 94	95	[8] ABDALLAH	03M	DLPH	$\tilde{\chi}_1^\pm$, tan$\beta \leq 40$, Δm_+ >3 GeV,all m_0
> 88	95	[9] HEISTER	02J	ALEP	$\tilde{\chi}_1^\pm$, all Δm_+, large m_0
> 67.7	95	[10] ACCIARRI	00D	L3	tan$\beta > 0.7$, all Δm_+, all m_0
> 69.4	95	[11] ACCIARRI	00K	L3	$e^+e^- \to \tilde{\chi}^\pm\tilde{\chi}^\mp$, all Δm_+, heavy scalars
• • • We do not use the following data for averages, fits, limits, etc. • • •					
		[12] AALTONEN	13Q	CDF	$\tilde{\chi}_1^\pm \to \tau X$, simplified gravity- and gauge-mediated models
		[13] AAD	12AS	ATLS	$3\ell^\pm + \not{E}_T$, pMSSM
		[14] AAD	12T	ATLS	$\ell^\pm\ell^\mp + \not{E}_T$, $\ell^\pm\ell^\pm + \not{E}_T$, $pp \to \tilde{\chi}_1^\pm\tilde{\chi}_2^0$
		[15] CHATRCHYAN	11B	CMS	$\widetilde{W}^0 \to \gamma\tilde{G}$,$\widetilde{W}^\pm \to \ell^\pm\tilde{G}$,GMSB
>163	95	[16] CHATRCHYAN	11V	CMS	tanβ=3, m_0=60 GeV, A_0=0, μ >0
>129	95	[17] AALTONEN	09G	CDF	$p\overline{p} \to \tilde{\chi}_1^\pm\tilde{\chi}_2^0$
>138	95	[18] ABAZOV	09T	D0	$p\overline{p} \to \tilde{\chi}_1^\pm\tilde{\chi}_2^0$
		[19] AALTONEN	08AE	CDF	$p\overline{p} \to \tilde{\chi}_1^\pm\tilde{\chi}_2^0$
		[20] AALTONEN	08L	CDF	$p\overline{p} \to \tilde{\chi}_1^\pm\tilde{\chi}_2^0$
>229	95	[21] ABAZOV	08F	D0	$p\overline{p} \to \tilde{\chi}\tilde{\chi}$, $\tilde{\chi}=\tilde{\chi}_2^0$, $\tilde{\chi}_1^\pm$, $\tilde{\chi}_1^0 \to \gamma\tilde{G}$, GMSB
		[22] AALTONEN	07J	CDF	$p\overline{p} \to \tilde{\chi}_1^\pm\tilde{\chi}_2^0$
		[23] ABULENCIA	07H	CDF	$\not{R}$, $LL\overline{E}$
		[24] ABULENCIA	07N	CDF	$p\overline{p} \to \tilde{\chi}_1^\pm\tilde{\chi}_2^0$
		[25] ABAZOV	06D	D0	$\not{R}$, $LL\overline{E}$
>195	95	[26] ABAZOV	05A	D0	$p\overline{p} \to \tilde{\chi}\tilde{\chi}$, $\tilde{\chi}=\tilde{\chi}_2^0$, $\tilde{\chi}_1^\pm$,$\tilde{\chi}_1^0 \to \gamma\tilde{G}$, GMSB
>167	95	[27] ACOSTA	05E	CDF	$p\overline{p} \to \tilde{\chi}\tilde{\chi}$, $\tilde{\chi}=\tilde{\chi}_2^0$, $\tilde{\chi}_1^\pm$,$\tilde{\chi}_1^0 \to \gamma\tilde{G}$, GMSB
> 66	95	[28,29] ABDALLAH	04H	DLPH	AMSB, $\mu > 0$
>102.5	95	[30,31] ABDALLAH	04M	DLPH	$\not{R}(\overline{UDD})$
>100		[32] ABDALLAH	03D	DLPH	$e^+e^- \to \tilde{\chi}_1^\pm\tilde{\chi}_1^\mp$ ($\tilde{\chi}_1^\pm \to \tilde{\tau}_1\nu_\tau$, $\tilde{\tau}_1 \to \tau\tilde{G}$)
>103		[33] HEISTER	03G	ALEP	$\not{R}$ decays, m_0 > 500 GeV
>102.7	95	[34] ACHARD	02	L3	$\not{R}$, MSUGRA
		[35] GHODBANE	02	THEO	
> 94.3	95	[36] ABREU	01C	DLPH	$\tilde{\chi}^\pm \to \tau J$
> 93.8	95	[37] ACCIARRI	01	L3	$\not{R}$, all m_0, $0.7 \leq \tan\beta \leq 40$
>100	95	[38] BARATE	01B	ALEP	$\not{R}$ decays, $m_0 > 500$ GeV
> 91.8	95	[39] ABREU	00V	DLPH	$e^+e^- \to \tilde{\chi}_1^\pm\tilde{\chi}_1^\pm$ ($\tilde{\chi}_1^\pm \to \tilde{\tau}_1\nu_\tau$, $\tilde{\tau}_1 \to \tau\tilde{G}$)
		[40] CHO	00B	THEO	EW analysis
> 76	95	[41] ABBIENDI	99T	OPAL	$\not{R}$, m_0=500 GeV
> 51	95	[42] MALTONI	99B	THEO	EW analysis, $\Delta m_+ \sim 1$ GeV
> 81.5	95	[43] ABE	98J	CDF	$p\overline{p} \to \tilde{\chi}_1^\pm\tilde{\chi}_2^0$
		[44] ACKERSTAFF	98K	OPAL	$\tilde{\chi}^+ \to \ell^+\not{E}$
> 65.7	95	[45] ACKERSTAFF	98L	OPAL	$\Delta m_+ > 3$ GeV, $\Delta m_\nu > 2$ GeV
		[46] ACKERSTAFF	98V	OPAL	light gluino
		[47] CARENA	97	THEO	$g_\mu - 2$
		[48] KALINOWSKI	97	THEO	$W \to \tilde{\chi}_1^\pm\tilde{\chi}_1^0$
		[49] ABE	96K	CDF	$p\overline{p} \to \tilde{\chi}_1^\pm\tilde{\chi}_2^0$

[1] AAD 13 searched in 4.7 fb^{-1} of pp collisions at $\sqrt{s}$ = 7 TeV for charginos and neutralinos decaying to a final state with three leptons (e and μ) and missing transverse energy. No excess beyond the Standard Model expectation is observed. Exclusion limits are derived in the phenomenological MSSM, see Fig. 2 and 3, and in simplified models, see Fig. 4. For the simplified models with intermediate slepton decays, degenerate $\tilde{\chi}_1^\pm$ and $\tilde{\chi}_2^0$ masses up to 500 GeV are excluded at 95% C.L. for very large mass differences with the $\tilde{\chi}_1^0$. Supersedes AAD 12AS.

[2] AAD 13B searched in 4.7 fb^{-1} of pp collisions at $\sqrt{s}$ = 7 TeV for gauginos decaying to a final state with two leptons (e and μ) and missing transverse energy. No excess beyond the Standard Model expectation is observed. Limits are derived in a simplified model of wino-like chargino pair production, where the chargino always decays to the lightest neutralino via an intermediate on-shell charged slepton, see Fig. 2(b). Chargino masses between 110 and 340 GeV are excluded at 95% C.L. for $m_{\tilde{\chi}_1^0}$ = 10 GeV. Exclusion limits are also derived in the phenomenological MSSM, see Fig. 3.

[3] AAD 12CT searched in 4.7 fb^{-1} of pp collisions at $\sqrt{s}$ = 7 TeV for events containing four or more leptons (electrons or muons) and either moderate values of missing transverse momentum or large effective mass. No significant excess is found in the data. Limits are presented in a simplified model of R-parity violating supersymmetry in which charginos are pair-produced and then decay into a W-boson and a $\tilde{\chi}_1^0$, which in turn decays through an RPV coupling into two charged leptons ($e^\pm e^\mp$ or $e^\pm\mu^\mp$) and a neutrino. In this model, chargino masses up to 540 GeV are excluded at 95% C.L. for $m_{\tilde{\chi}_1^0}$ above 300 GeV, see Fig. 3a. The limit deteriorates for lighter $\tilde{\chi}_1^0$. Limits are also set in an R-parity violating mSUGRA model, see Fig. 3b.

[4] CHATRCHYAN 12BJ searched in 4.98 fb^{-1} of pp collisions at $\sqrt{s}$ = 7 TeV for direct electroweak production of charginos and neutralinos in events with at least two leptons, jets and missing transverse momentum. No significant excesses over the expected SM backgrounds are observed and 95% C.L. limits on the production cross section of $\tilde{\chi}_1^\pm\tilde{\chi}_2^0$ pair production were set in a number of simplified models, see Figs. 7 to 12.

[5] ABBIENDI 04H search for charginos and neutralinos in events with acoplanar leptons+jets and multi-jet final states in the 192–209 GeV data, combined with the results on leptonic final states from ABBIENDI 04. The results hold for a scan over the parameter space covering the region $0 < M_2 <$5000 GeV, $-1000 < \mu <$1000 GeV and tanβ from 1 to 40. This limit supersedes ABBIENDI 00H.

[6] ABBIENDI 03H used e^+e^- data at $\sqrt{s}$ = 188–209 GeV to search for chargino pair production in the case of small Δm_+. They select events with an energetic photon, large $\not{E}$ and little hadronic or leptonic activity. The bound applies to higgsino-like charginos with zero lifetime and a 100% branching ratio $\tilde{\chi}_1^\pm \to \tilde{\chi}_1^0 W^*$. The mass limit for gaugino-like charginos, in case of non-universal gaugino masses, is of 92 GeV for $m_{\tilde{\nu}}$ = 1000 GeV and is lowered to 74 GeV for $m_{\tilde{\nu}} \geq$ 100 GeV. Limits in the plane ($m_{\tilde{\chi}_1^\pm}$, Δm_+) are shown in Fig. 7. Exclusion regions are also derived for the AMSB scenario in the ($m_{3/2}$, tanβ) plane, see their Fig. 9.

[7] ABDALLAH 03M searches for the production of charginos using data from $\sqrt{s}$ = 192 to 208 GeV to investigate topologies with multiple leptons, jets plus leptons, multi-jets, or isolated photons. The first limit holds for tan$\beta \geq$ 1 and is obtained at Δm_+= 3 GeV in the higgsino region. For $\Delta m_+ \geq$ 10 (5) GeV and large m_0, the limit improves to 102.7 (101.7) GeV. For the region of small Δm_+, all data from $\sqrt{s}$ = 130 to 208 GeV are used to investigate final states with heavy stable charged particles, decay vertices inside the detector and soft topologies with a photon from initial state radiation. The second limit is obtained in the higgsino region, assuming gaugino mass universality at the GUT scale and 1<tanβ <50. For the case of non-universality of gaugino masses, the parameter space is scanned in the domain 1<tanβ <50 and, for $\Delta m_+ <$ 3 GeV, for

values of M_1, M_2 and μ such that $M_2 \leq 2M_1 \leq 10\,M_2$ and $|\mu| \geq M_2$. The third limit is obtained in the gaugino region. See Fig. 36 for the dependence of the low Δm_+ limits on Δm_+. These limits include and update the results of ABREU 00J and ABREU 00T.

[8] ABDALLAH 03M uses data from $\sqrt{s}$ = 192–208 GeV to obtain limits in the framework of the MSSM with gaugino and sfermion mass universality at the GUT scale. An indirect limit on the mass of charginos is derived by constraining the MSSM parameter space by the results from direct searches for neutralinos (including cascade decays), for charginos and for sleptons. These limits are valid for values of $M_2 < 1$ TeV, $|\mu| \leq 2$ TeV with the $\widetilde{\chi}_1^0$ as LSP. Constraints from the Higgs search in the $m_h^{\max}$ scenario assuming m_t= 174.3 GeV are included. The quoted limit applies if there is no mixing in the third family or when $m_{\widetilde{\tau}_1} - m_{\widetilde{\chi}_1^0} > 6$ GeV. If mixing is included the limit degrades to 90 GeV. See Fig. 43 for the mass limits as a function of tanβ. These limits update the results of ABREU 00W.

[9] HEISTER 02J search for chargino production with small Δm_+ in final states with a hard isolated initial state radiation photon and few low-momentum particles, using 189–208 GeV data. This search is sensitive in the intermediate Δm_+ region. Combined with searches for $\not{E}$ topologies and for stable charged particles, the above bound is obtained for m_0 larger than few hundred GeV, 1<tanβ < 300 and holds for any chargino field contents. For light scalars, the general limit reduces to the one from the Z^0, but under the assumption of gaugino and sfermion mass unification the above bound is recovered. See Figs. 4–6 for the more general dependence of the limits on Δm_+. Updates BARATE 98X.

[10] ACCIARRI 00D data collected at $\sqrt{s}$=189 GeV. The results hold over the full parameter space defined by $0.7 \leq \tan\beta \leq 60$, $0 \leq M_2 \leq 2$ TeV, $|\mu| \leq 2$ TeV $m_0 \leq 500$ GeV. The results of slepton searches from ACCIARRI 99W are used to help set constraints in the region of small m_0. See their Figs. 5 for the tanβ and M_2 dependence on the limits. See the text for the impact of a large B($\widetilde{\chi}^\pm \to \tau\widetilde{\nu}_\tau$) on the result. The region of small Δm_+ is excluded by the analysis of ACCIARRI 00K. Updates ACCIARRI 98F.

[11] ACCIARRI 00K searches for the production of charginos with small Δm_+ using data from $\sqrt{s}$=189 GeV. They investigate soft final states with a photon from initial state radiation. The results are combined with the limits on prompt decays from ACCIARRI 00D and from heavy stable charged particles from ACCIARRI 99L (see Heavy Charged Lepton Searches). The production and decay branching ratios are evaluated within the MSSM, assuming heavy sfermions. The parameter space is scanned in the domain 1<tanβ <50, 0.3 <M_1/M_2 <50, and 0< $|\mu|$ <2 TeV. The limit is obtained in the higgsino region and improves to 78.6 GeV for gaugino-like charginos. The limit is unchanged for light scalar quarks. For light $\widetilde{\tau}$ or $\widetilde{\nu}_\tau$, the limit is unchanged in the gaugino-like region and is lowered by 0.8 GeV in the higgsino-like case. For light $\widetilde{\mu}$ or $\widetilde{\nu}_\mu$, the limit is unchanged in the higgsino-like region and is lowered by 0.9 GeV in the gaugino-like region. No direct mass limits are obtained for light $\widetilde{e}$ or $\widetilde{\nu}_e$.

[12] AALTONEN 13Q searched in 6.0 fb^{-1} of $p\overline{p}$ collisions at $\sqrt{s} = 1.96$ TeV for evidence of chargino-neutralino associated production in like-sign dilepton final states. One lepton is identified as the hadronic decay of a tau lepton, while the other is an electron or muon. Good agreement with the Standard Model predictions is observed and limits are set on the chargino-neutralino cross section for simplified gravity- and gauge-mediated models, see their Figs 2 and 3.

[13] AAD 12AS searched in 2.06 fb^{-1} of pp collisions at $\sqrt{s} = 7$ TeV for charginos and neutralinos decaying to a final state with three leptons (e and μ) and missing transverse energy. No excess beyond the Standard Model expectation is observed. Exclusion limits are derived in the phenomenological MSSM, see Fig. 2 (top), and in simplified models, see Fig. 2 (bottom).

[14] AAD 12T looked in 1 fb^{-1} of pp collisions at $\sqrt{s} = 7$ TeV for the production of supersymmetric particles decaying into final states with missing transverse momentum and exactly two isolated leptons (e or μ). Opposite-sign and same-sign dilepton events were separately studied. Additionally, in opposite-sign events, a search was made for an excess of same-flavor over different-flavor lepton pairs. No excess over the expected background is observed and limits are placed on the effective production cross section of opposite-sign dilepton events with $\not{E}_T > 250$ GeV and on same-sign dilepton events with $\not{E}_T > 100$ GeV. The latter limit is interpreted in a simplified electroweak gaugino production model as a lower chargino mass limit.

[15] CHATRCHYAN 11B looked in 35 pb^{-1} of pp collisions at $\sqrt{s}$=7 TeV for events with an isolated lepton (e or μ), a photon and $\not{E}_T$ which may arise in a generalized gauge mediated model from the decay of Wino-like NLSPs. No evidence for an excess over the expected background is observed. Limits are derived in the plane of squark/gluino mass versus Wino mass (see Fig. 4). Mass degeneracy of the produced squarks and gluinos is assumed.

[16] CHATRCHYAN 11V looked in 35 pb^{-1} of pp collisions at $\sqrt{s} = 7$ TeV for events with ≥ 3 isolated leptons (e, μ or τ), with or without jets and $\not{E}_T$. No evidence for an excess over the expected background is observed. Limits are derived in the CMSSM (m_0, $m_{1/2}$) plane for tan$\beta = 3$ (see Fig. 5).

[17] AALTONEN 09G searched in 976 pb^{-1} of $p\overline{p}$ collisions at $\sqrt{s} = 1.96$ TeV for events with trileptons ($\mu\mu\mu$ or $\mu\mu e$) with a low, 5 GeV, p_T threshold, and large $\not{E}_T$ from the decay of $\widetilde{\chi}_1^\pm \widetilde{\chi}_2^0 X$. The selected number of events is consistent with the SM background expectation. The results are combined with the analysis of AALTONEN 07J to set a limit on the $\widetilde{\chi}_1^\pm$ mass for a mSUGRA scenario with no slepton mixing.

[18] ABAZOV 09T searched in 2.3 fb^{-1} of $p\overline{p}$ collisions at $\sqrt{s} = 1.96$ TeV for events with trileptons (e, μ or hadronically decaying τ) from the decay of $\widetilde{\chi}_1^\pm \widetilde{\chi}_2^0 X$ and large $\not{E}_T$. No evidence for a signal is observed. The data are used to constrain the cross section times branching ratio as a function of the $\widetilde{\chi}_1^\pm$ mass under the assumption that $m_{\widetilde{\chi}_1^\pm} = m_{\widetilde{\chi}_2^0}$ = 2 $m_{\widetilde{\chi}_1^0}$, tanβ = 3, $\mu > 0$ and that the sleptons are heavier than the $\widetilde{\chi}_1^\pm$, see their Fig. 8. A chargino lighter than 138 GeV is excluded in the "3l-max" scenario. Exclusion regions in the (m_0, $m_{1/2}$) plane are shown in their Fig. 9 for a mSUGRA scenario with tanβ = 3, $A_0 = 0$ and $\mu > 0$. The tanβ dependence of this exclusion is illustrated in Fig. 10. Supersedes the results of ABAZOV 05U.

[19] AALTONEN 08AE searched in 2.0 fb^{-1} of $p\overline{p}$ collisions at $\sqrt{s} = 1.96$ TeV for events with trileptons (e, μ or a charged isolated track from τ) from the decay of $p\overline{p} \to \widetilde{\chi}_1^\pm \widetilde{\chi}_2^0 X$ and large $\not{E}_T$. The selected number of events is consistent with the SM background expectation. The data are used to constrain the cross section times branching ratio as a function of the $\widetilde{\chi}_1^\pm$ mass. Exclusion regions in the (m_0, $m_{1/2}$) plane are shown in their Fig. 2 for a mSUGRA scenario. When the $\widetilde{\chi}_1^\pm$ is nearly mass degenerate with the $\widetilde{\tau}_1$ the leptons are too soft and no limit is obtained. For the case $m_0 = 60$ GeV a lower limit of 145 GeV on the chargino mass is obtained in this mSUGRA scenario.

[20] AALTONEN 08L searched in 0.7 to 1.0 fb^{-1} of $p\overline{p}$ collisions at $\sqrt{s} = 1.96$ TeV for events with one high-p_T electron or muon and two additional leptons (e or μ) from the decay of $\widetilde{\chi}_1^\pm \widetilde{\chi}_2^0 X$. The selected number of events is consistent with the SM background expectation. The data are used to constrain the cross section times branching ratio as a function of the $\widetilde{\chi}_1^\pm$ mass. The results are compared to three MSSM scenarios. An exclusion on chargino and neutralino production is only obtained in a scenario of no mixing between sleptons, yielding nearly equal branching ratios to all three lepton flavors. It amounts to $m_{\widetilde{\chi}_1^\pm} > 151$ GeV, while the analysis is not sensitive to chargino masses below about 110 GeV. The analyses have been combined with the analyses of AALTONEN 07J and ABULENCIA 07N. The observed limits for the combination are less stringent than the one obtained for the high-p_T analysis due to slight excesses in the other channels.

[21] ABAZOV 08F looked in 1.1 fb^{-1} of $p\overline{p}$ collisions at $\sqrt{s} = 1.96$ TeV for diphoton events with large $\not{E}_T$. They may originate from the production of $\widetilde{\chi}^\pm$ in pairs or associated to a $\widetilde{\chi}_2^0$, decaying to a $\widetilde{\chi}_1^0$ which itself decays promptly in GMSB to $\widetilde{\chi}_1^0 \to \gamma\widetilde{G}$. No significant excess was found compared to the background expectation. A limit is derived on the masses of SUSY particles in the GMSB framework for $M = 2\Lambda$, $N = 1$, tanβ = 15 and $\mu > 0$, see Figure 2. It also excludes $\Lambda < 91.5$ TeV. Supersedes the results of ABAZOV 05A.

[22] AALTONEN 07J searched in 0.7 to 1.1 fb^{-1} of $p\overline{p}$ collisions at $\sqrt{s} = 1.96$ TeV for events with either two same sign leptons (e or μ) or trileptons from the decay of $\widetilde{\chi}_1^\pm \widetilde{\chi}_2^0 X$ and large $\not{E}_T$. The selected number of events is consistent with the SM background expectation. The data are used to constrain the cross section times branching ratio as a function of the $\widetilde{\chi}_1^\pm$ mass. The results, shown in their Fig. 2, are compared to several MSSM scenarios. The strongest exclusion is in the case of no mixing between sleptons, yielding nearly equal branching ratios to all three lepton flavors, and amounting to $m_{\widetilde{\chi}_1^\pm} > 129$ GeV. This analysis includes the same sign dilepton analysis of ABULENCIA 07N.

[23] ABULENCIA 07H searched in 346 pb^{-1} of $p\overline{p}$ collisions at $\sqrt{s} = 1.96$ TeV for events with at least three leptons (e or μ) from the decay of $\widetilde{\chi}_1^0$ via $LL\overline{E}$ couplings. The results are consistent with the hypothesis of no signal. Upper limits on the cross-section are extracted and a limit is derived in the framework of mSUGRA on the masses of $\widetilde{\chi}_1^0$ and $\widetilde{\chi}_1^\pm$, see e.g. their Fig. 3 and Tab. II.

[24] ABULENCIA 07N searched in 1 fb^{-1} of $p\overline{p}$ collisions at $\sqrt{s} = 1.96$ TeV for events with two same sign leptons (e or μ) from the decay of $\widetilde{\chi}_1^\pm \widetilde{\chi}_2^0 X$ and large $\not{E}_T$. A slight excess of 13 events is observed over a SM background expectation of 7.8 ± 1.1. However, the kinematic distributions do not show any anomalous deviation from expectations in any particular region of parameter space.

[25] ABAZOV 06D looked in 360 pb^{-1} of $p\overline{p}$ collisions at $\sqrt{s} = 1.96$ TeV for events with three leptons originating from the pair production of charginos and neutralinos, followed by $\not{R}$ decays mediated by $LL\overline{E}$ couplings. One coupling is assumed to be dominant at a time. No significant excess was found compared to the background expectation in the $ee\ell$, $\mu\mu\ell$ nor $ee\tau$ ($\ell = e, \mu$) final states. Upper limits on the cross-section are extracted in a specific MSUGRA model and a MSSM model without unification of M_1 and M_2 at the GUT scale. A limit is derived on the masses of charginos and neutralinos for both scenarios assuming λ_{ijk} couplings such that the decay length is less than 1 cm, see their Table III and Fig. 4.

[26] ABAZOV 05A looked in 263 pb^{-1} of $p\overline{p}$ collisions at $\sqrt{s} = 1.96$ TeV for diphoton events with large $\not{E}_T$. They may originate from the production of $\widetilde{\chi}^\pm$ in pairs or associated to a $\widetilde{\chi}_2^0$, decaying to a $\widetilde{\chi}_1^0$ which itself decays promptly in GMSB to $\widetilde{\chi}_1^0 \to \gamma\widetilde{G}$. No significant excess was found at large $\not{E}_T$ compared to the background expectation. A limit is derived on the masses of SUSY particles in the GMSB framework for $M = 2\,\Lambda$, $N = 1$, tanβ = 15 and $\mu > 0$, see Figure 2. It also excludes $\Lambda < 79.6$ TeV. Very similar results are obtained for different choices of parameters, see their Table 2. Supersedes the results of ABBOTT 98.

[27] ACOSTA 05E looked in 202 pb^{-1} of $p\overline{p}$ collisions at $\sqrt{s}$=1.96 TeV for diphoton events with large $\not{E}_T$. They may originate from the production of $\widetilde{\chi}^\pm$ in pairs or associated to a $\widetilde{\chi}_2^0$, decaying to a $\widetilde{\chi}_1^0$ which itself decays promptly in GMSB to $\gamma\widetilde{G}$. No events are selected at large $\not{E}_T$ compared to the background expectation. A limit is derived on the masses of SUSY particles in the GMSB framework for $M = 2\,\Lambda$, $N = 1$, tanβ = 15 and $\mu > 0$, see Figure 2. It also excludes $\Lambda < 69$ TeV. Supersedes the results of ABE 99I.

[28] ABDALLAH 04H use data from LEP 1 and $\sqrt{s}$ = 192–208 GeV. They re-use results or re-analyze the data from ABDALLAH 03M to put limits on the parameter space of anomaly-mediated supersymmetry breaking (AMSB), which is scanned in the region 1< $m_{3/2}$ <50 TeV, 0< m_0 <1000 GeV, 1.5<tanβ <35, both signs of μ. The constraints are obtained from the searches for mass degenerate chargino and neutralino, for SM-like and invisible Higgs, for leptonically decaying charginos and from the limit on non-SM Z width of 3.2 MeV. The limit is for m_t = 174.3 GeV (see Table 2 for other m_t values).

[29] The limit improves to 73 GeV for $\mu < 0$.

[30] ABDALLAH 04M use data from $\sqrt{s}$ = 192–208 GeV to derive limits on sparticle masses under the assumption of $\not{R}$ with $LL\overline{E}$ or $\overline{UDD}$ couplings. The results are valid in the ranges 90< m_0 <500 GeV, 0.7<tanβ <30, $-200 < \mu <$200 GeV, 0< M_2 <400 GeV. Supersedes the result of ABREU 01D and ABREU 00U.

[31] The limit improves to 103 GeV for $LL\overline{E}$ couplings.

[32] ABDALLAH 03D use data from $\sqrt{s}$ = 183–208 GeV. They look for final states with two acoplanar leptons, expected in GMSB when the $\widetilde{\tau}_1$ is the NLSP and assuming a short-lived $\widetilde{\chi}_1^\pm$. Limits are obtained in the plane (m($\widetilde{\tau}$),m($\widetilde{\chi}_1^\pm$)) for different domains of m($\widetilde{G}$), after combining these results with the search for slepton pair production from the same paper. The limit above is valid if the $\widetilde{\tau}_1$ is the NLSP for all values of m($\widetilde{G}$) provided m($\widetilde{\chi}_1^\pm$) − m($\widetilde{\tau}_1$) $\geq$ 0.3 GeV. For larger m($\widetilde{G}$) > 100 eV the limit improves to 102 GeV, see their Fig. 11. In the co-NLSP scenario, the limits are 96 and 102 GeV for all m($\widetilde{G}$) and m($\widetilde{G}$) > 100 eV, respectively. Supersedes the results of ABREU 01G.

[33] HEISTER 03G searches for the production of charginos prompt decays. in the case of $\not{R}$ prompt decays with $LL\overline{E}$, $LQ\overline{D}$ or $\overline{UDD}$ couplings at $\sqrt{s}$=189–209 GeV. The search is performed for indirect decays, assuming one coupling at a time to be non-zero. The limit holds for tanβ=1.41. Excluded regions in the (μ,M_2) plane are shown in their Fig. 3.

[34] ACHARD 02 searches for the production of sparticles in the case of $\not{R}$ prompt decays with $LL\overline{E}$ or $\overline{UDD}$ couplings at $\sqrt{s}$=189–208 GeV. The search is performed for direct and

indirect decays, assuming one coupling at the time to be nonzero. The MSUGRA limit results from a scan over the MSSM parameter space with the assumption of gaugino and scalar mass unification at the GUT scale, imposing simultaneously the exclusions from neutralino, chargino, sleptons, and squarks analyses. The limit of $\widetilde{\chi}_1^\pm$ holds for $\overline{UDD}$ couplings and increases to 103.0 GeV for $LL\overline{E}$ couplings. For L3 limits from $LQ\overline{D}$ couplings, see ACCIARRI 01.

[35] GHODBANE 02 reanalyzes DELPHI data at $\sqrt{s}$=189 GeV in the presence of complex phases for the MSSM parameters.

[36] ABREU 01C looked for τ pairs with $\not{E}$ at $\sqrt{s}$=183–189 GeV to search for the associated production of charginos, followed by the decay $\widetilde{\chi}^\pm \to \tau J$, J being an invisible massless particle. See Fig. 6 for the regions excluded in the (μ, M_2) plane.

[37] ACCIARRI 01 searches for multi-lepton and/or multi-jet final states from R prompt decays with $LL\overline{E}$, $LQ\overline{D}$, or $\overline{UDD}$ couplings at $\sqrt{s}$=189 GeV. The search is performed for direct and indirect decays of neutralinos, charginos, and scalar leptons, with the $\widetilde{\chi}_1^0$ or a $\widetilde{\ell}$ as LSP and assuming one coupling to be nonzero at a time. Mass limits are derived using simultaneously the constraints from the neutralino, chargino, and slepton analyses; and the Z^0 width measurements from ACCIARRI 00C in a scan of the parameter space assuming MSUGRA with gaugino and scalar mass universality. Updates and supersedes the results from ACCIARRI 99I.

[38] BARATE 01B searches for the production of charginos in the case of R prompt decays with $LL\overline{E}$, $LQ\overline{D}$, or $\overline{UDD}$ couplings at $\sqrt{s}$=189–202 GeV. The search is performed for indirect decays, assuming one coupling at a time to be nonzero. Updates BARATE 00H.

[39] ABREU 00V use data from $\sqrt{s}$= 183–189 GeV. They look for final states with two acoplanar leptons, expected in GMSB when the $\widetilde{\tau}_1$ is the NLSP and assuming a short-lived $\widetilde{\chi}_1^\pm$. Limits are obtained in the plane $(m_{\widetilde{\tau}}, m_{\widetilde{\chi}_1^\pm})$ for different domains of $m_{\widetilde{G}}$, after combining these results with the search for slepton pair production in the SUGRA framework from ABREU 01 to cover prompt decays and on stable particle searches from ABREU 00Q. The limit above is valid for all values of $m_{\widetilde{G}}$.

[40] CHO 00B studied constraints on the MSSM spectrum from precision EW observables. Global fits favour charginos with masses at the lower bounds allowed by direct searches. Allowing for variations of the squark and slepton masses does not improve the fits.

[41] ABBIENDI 99T searches for the production of neutralinos in the case of R-parity violation with $LL\overline{E}$, $LQ\overline{D}$, or $\overline{UDD}$ couplings using data from $\sqrt{s}$=183 GeV. They investigate topologies with multiple leptons, jets plus leptons, or multiple jets, assuming one coupling at the time to be non-zero and giving rise to direct or indirect decays. Mixed decays (where one particle has a direct, the other an indirect decay) are also considered for the $\overline{UDD}$ couplings. Upper limits on the cross section are derived which, combined with the constraint from the Z^0 width, allow to exclude regions in the M_2 versus μ plane for any coupling. Limits on the chargino mass are obtained for non-zero $LL\overline{E}$ couplings $> 10^{-5}$ and assuming decays via a W^*.

[42] MALTONI 99B studied the effect of light chargino-neutralino to the electroweak precision data with a particular focus on the case where they are nearly degenerate ($\Delta m_\pm \sim 1$ GeV) which is difficult to exclude from direct collider searches. The quoted limit is for higgsino-like case while the bound improves to 56 GeV for wino-like case. The values of the limits presented here are obtained in an update to MALTONI 99B, as described in MALTONI 00.

[43] ABE 98J searches for trilepton final states (ℓ=e,μ). Efficiencies are calculated using mass relations in the Minimal Supergravity scenario, exploring the domain of parameter space defined by 1.1 $<\tan\beta <$ 8, $-1000 < \mu$(GeV)< -200, and $m_{\widetilde{q}}/m_{\widetilde{g}}$=1–2. In this region $m_{\widetilde{\chi}_1^\pm} \sim m_{\widetilde{\chi}_2^0}$ and $m_{\widetilde{\chi}_1^\pm} \sim 2m_{\widetilde{\chi}_1^0}$. Results are presented in Fig. 1 as upper bounds on $\sigma(p\overline{p} \to \widetilde{\chi}_1^\pm \widetilde{\chi}_2^0)\times$B($3\ell$). Limits range from 0.8 pb ($m_{\widetilde{\chi}_1^\pm}$=50 GeV) to 0.23 pb ($m_{\widetilde{\chi}_1^\pm}$=100 GeV) at 95%CL. The gaugino mass unification hypothesis and the assumed mass relation between squarks and gluinos define the value of the leptonic branching ratios. The quoted result corresponds to the best limit within the selected range of parameters, obtained for $m_{\widetilde{q}} > m_{\widetilde{g}}$, $\tan\beta$=2, and μ=$-$600 GeV. Mass limits for different values of $\tan\beta$ and μ are given in Fig. 2.

[44] ACKERSTAFF 98K looked for dilepton+$\not{E}_T$ final states at $\sqrt{s}$=130–172 GeV. Limits on $\sigma(e^+e^- \to \widetilde{\chi}_1^+\widetilde{\chi}_1^-)\times$B$^2(\ell)$, with B($\ell$)=B($\chi^+ \to \ell^+\nu_\ell\chi_1^0$) (B($\ell$)=B($\chi^+ \to \ell^+\overline{\nu}_\ell$)), are given in Fig. 16 (Fig. 17).

[45] ACKERSTAFF 98L limit is obtained for $0 < M_2 < 1500$, $|\mu| < 500$ and $\tan\beta > 1$, but remains valid outside this domain. The dependence on the trilinear-coupling parameter A is studied, and found negligible. The limit holds for the smallest value of m_0 consistent with scalar lepton constraints (ACKERSTAFF 97H) and for all values of m_0 where the condition $\Delta m_{\widetilde{\nu}} > 2.0$ GeV is satisfied. $\Delta m_\nu > 10$ GeV if $\widetilde{\chi}^\pm \to \ell\overline{\nu}_\ell$. The limit improves to 84.5 GeV for m_0=1 TeV. Data taken at $\sqrt{s}$=130–172 GeV.

[46] ACKERSTAFF 98V excludes the light gluino with universal gaugino mass where charginos, neutralinos decay as $\widetilde{\chi}_1^\pm, \widetilde{\chi}_2^0 \to q\overline{q}\widetilde{g}$ from total hadronic cross sections at $\sqrt{s}$=130–172 GeV. See paper for the case of nonuniversal gaugino mass.

[47] CARENA 97 studied the constraints on chargino and sneutrino masses from muon $g-2$. The bound can be important for large $\tan\beta$.

[48] KALINOWSKI 97 studies the constraints on the chargino-neutralino parameter space from limits on $\Gamma(W \to \widetilde{\chi}_1^\pm\widetilde{\chi}_1^0)$ achievable at LEP2. This is relevant when $\widetilde{\chi}_1^\pm$ is "invisible," i.e., if $\widetilde{\chi}_1^\pm$ dominantly decays into $\widetilde{\nu}_\ell\ell^\pm$ with little energy for the lepton. Small otherwise allowed regions could be excluded.

[49] ABE 96K looked for trilepton events from chargino-neutralino production. The bound on $m_{\widetilde{\chi}_1^\pm}$ can reach up to 47 GeV for specific choices of parameters. The limits on the combined production cross section times 3-lepton branching ratios range between 1.4 and 0.4 pb, for 45$<m_{\widetilde{\chi}_1^\pm}(GeV)<$100. See the paper for more details on the parameter dependence of the results.

Long-lived $\widetilde{\chi}^\pm$ (Chargino) MASS LIMITS

Limits on charginos which leave the detector before decaying.

VALUE (GeV)	CL%	DOCUMENT ID		TECN	COMMENT
>103	95	[1] AAD	13H	ATLS	long-lived $\widetilde{\chi}^\pm \to \widetilde{\chi}_1^0\pi^\pm$, mAMSB, $\Delta m_{\widetilde{\chi}_1^0}$ = 160 MeV
> 92	95	[2] AAD	12BJ	ATLS	long-lived $\widetilde{\chi}^\pm \to \pi^\pm\widetilde{\chi}_1^0$, mAMSB
>171	95	[3] ABAZOV	09M	D0	$\widetilde{H}$
>102	95	[4] ABBIENDI	03L	OPAL	$m_{\widetilde{\nu}}$ >500 GeV
none 2–93.0	95	[5] ABREU	00T	DLPH	$\widetilde{H}^\pm$ or $m_{\widetilde{\nu}} > m_{\widetilde{\chi}^\pm}$
• • • We do not use the following data for averages, fits, limits, etc. • • •					
>270	95	[6] AAD	13BD	ATLS	disappearing-track signature, AMSB
>278	95	[7] ABAZOV	13B	D0	long-lived $\widetilde{\chi}^\pm$, gaugino-like
>244	95	[7] ABAZOV	13B	D0	long-lived $\widetilde{\chi}^\pm$, higgsino-like
	95	[8] ABAZOV	12L	D0	long-lived $\widetilde{\chi}^\pm$, gaugino-like
	95	[9] ABAZOV	12L	D0	long-lived $\widetilde{\chi}^\pm$, higgsino-like
> 83	95	[10] BARATE	97K	ALEP	
> 28.2	95	ADACHI	90C	TOPZ	

[1] AAD 13H searched in 4.7 fb^{-1} of pp collisions at $\sqrt{s}$ = 7 TeV for direct electroweak production of long-lived charginos in the context of AMSB scenarios. The search is based on the signature of a high-momentum isolated track with few associated hits in the outer part of the tracking system, arising from a chargino decay into a neutralino and a low-momentum pion. The p_T spectrum of the tracks was found to be consistent with the SM expectations. Constraints on the lifetime and the production cross section were obtained, see Fig. 6. In the minimal AMSB framework with $\tan\beta$ = 5, and $\mu > 0$, a chargino having a mass below 103 (85) GeV for a chargino-neutralino mass splitting $\Delta m_{\widetilde{\chi}_1^0}$ of 160 (170) MeV is excluded at the 95% C.L. See Fig. 7 for more precise bounds.

[2] AAD 12BJ looked in 1.02 fb^{-1} of pp collisions at $\sqrt{s}$ = 7 TeV for signatures of decaying charginos resulting in isolated tracks with few associated hits in the outer region of the tracking system. The p_T spectrum of the tracks was found to be consistent with the SM expectations. Constraints on the lifetime and the production cross section were obtained. In the minimal AMSB framework with $m_{3/2} < 32$ TeV, $m_0 < 1.5$ TeV, $\tan\beta$ = 5, and $\mu > 0$, a chargino having a mass below 92 GeV and a lifetime between 0.5 ns and 2 ns is excluded at the 95% C.L. See their Fig. 8 for more precise bounds.

[3] ABAZOV 09M searched in 1.1 fb^{-1} of $p\overline{p}$ collisions at $\sqrt{s}$ = 1.96 TeV for events with direct production of a pair of charged massive stable particles identified by their TOF. The number of the observed events is consistent with the predicted background. The data are used to constrain the production cross section as a function of the $\widetilde{\chi}_1^\pm$ mass, see their Fig. 2. The quoted limit improves to 206 GeV for gaugino-like charginos.

[4] ABBIENDI 03L used e^+e^- data at $\sqrt{s}$ = 130–209 GeV to select events with two high momentum tracks with anomalous dE/dx. The excluded cross section is compared to the theoretical expectation as a function of the heavy particle mass in their Fig. 3. The bounds are valid for colorless fermions with lifetime longer than 10^{-6} s. Supersedes the results from ACKERSTAFF 98P.

[5] ABREU 00T searches for the production of heavy stable charged particles, identified by their ionization or Cherenkov radiation, using data from $\sqrt{s}$= 130 to 189 GeV. These limits include and update the results of ABREU 98P.

[6] AAD 13BD searched in 20.3 fb^{-1} of pp collisions at $\sqrt{s}$ = 8 TeV for events containing tracks with no associated hits in the outer region of the tracking system resulting from the decay of charginos that are nearly mass degenerate with the lightest neutralino, as is often the case in AMSB scenarios. No significant excess above the background expectation is observed for candidate tracks with large transverse momentum. Constraints on chargino properties are obtained and in the minimal AMSB model, a chargino mass below 270 GeV is excluded at 95% C.L., see their Fig. 7.

[7] ABAZOV 13B looked in 6.3 fb^{-1} of $p\overline{p}$ collisions at $\sqrt{s}$ = 1.96 TeV for charged massive long-lived particles in events with muon-like particles that have both speed and ionization energy loss inconsistent with muons produced in beam collisions. In the absence of an excess, limits are set at 95% C.L. on gaugino- and higgsino-like charginos, see their Table 20 and Fig. 23.

[8] ABAZOV 12L looked in 5.2 fb^{-1} of $p\overline{p}$ collisions at $\sqrt{s}$ = 1.96 TeV for charged massive long-lived particles in events in which one or more particles are reconstructed as muons but have speed and ionization energy loss inconsistent with muons produced in beam collisions. Long-lived pair-produced gaugino-like charginos are excluded below 267 GeV at 95% C.L. using the nominal value of the NLO production cross section.

[9] ABAZOV 12L looked in 5.2 fb^{-1} of $p\overline{p}$ collisions at $\sqrt{s}$ = 1.96 TeV for charged massive long-lived particles in events in which one or more particles are reconstructed as muons but have speed and ionization energy loss inconsistent with muons produced in beam collisions. Long-lived pair-produced Higgsino-like charginos are excluded below 217 GeV at 95% C.L. using the nominal value of the NLO production cross section.

[10] BARATE 97K uses e^+e^- data collected at $\sqrt{s}$ = 130–172 GeV. Limit valid for $\tan\beta = \sqrt{2}$ and $m_{\widetilde{\nu}} > 100$ GeV. The limit improves to 86 GeV for $m_{\widetilde{\nu}} > 250$ GeV.

$\widetilde{\nu}$ (Sneutrino) MASS LIMIT

The limits may depend on the number, $N(\widetilde{\nu})$, of sneutrinos assumed to be degenerate in mass. Only $\widetilde{\nu}_L$ (not $\widetilde{\nu}_R$) is assumed to exist. It is possible that $\widetilde{\nu}$ could be the lightest supersymmetric particle (LSP).

We report here, but do not include in the Listings, the limits obtained from the fit of the final results obtained by the LEP Collaborations on the invisible width of the Z boson ($\Delta\Gamma_{\rm inv.} < 2.0$ MeV, LEP-SLC 06): $m_{\widetilde{\nu}} > 43.7$ GeV ($N(\widetilde{\nu})$=1) and $m_{\widetilde{\nu}} > 44.7$ GeV ($N(\widetilde{\nu})$=3) .

VALUE (GeV)	CL%	DOCUMENT ID		TECN	COMMENT
		[1] AAD	11Z	ATLS	$\widetilde{\nu}_\tau \to e\mu$, $\not{R}$
> 94	95	[2] ABDALLAH	03M	DLPH	$1 \le \tan\beta \le 40$, $m_{\widetilde{e}_R} - m_{\widetilde{\chi}_1^0} >$10 GeV
> 84	95	[3] HEISTER	02N	ALEP	$\widetilde{\nu}_e$, any Δm
> 37.1	95	[4] ADRIANI	93M	L3	$\Gamma(Z \to$ invisible); $N(\widetilde{\nu})$=1
> 41	95	[5] DECAMP	92	ALEP	$\Gamma(Z \to$ invisible); $N(\widetilde{\nu})$=3
> 36	95	ABREU	91F	DLPH	$\Gamma(Z \to$ invisible); $N(\widetilde{\nu})$=1
> 31.2	95	[6] ALEXANDER	91F	OPAL	$\Gamma(Z \to$ invisible); $N(\widetilde{\nu})$=1

• • • We do not use the following data for averages, fits, limits, etc. • • •

		[7] AAD	13AI	ATLS	$\tilde{\nu}_\tau \to e\mu$, $e\tau$, $\mu\tau$, $\not{R}$
		[8] AAD	11H	ATLS	$\tilde{\nu}_\tau \to e\mu$, $\not{R}$
		[9] AALTONEN	10Z	CDF	$\tilde{\nu}_\tau \to e\mu$, $e\tau$, $\mu\tau$, $\not{R}$
		[10] ABAZOV	10M	D0	$\tilde{\nu}_\tau \to e\mu$, $\not{R}$
		[11] AALTONEN	09V	CDF	$\tilde{\nu} \to \mu\mu$, $\not{R}$ $LQ\overline{D}$
		[12] ABAZOV	08Q	D0	$\tilde{\nu}_\tau \to e\mu$, $\not{R}$
		[13] SCHAEL	07A	ALEP	$\tilde{\nu}_{\mu,\tau}$, $\not{R}$, (s+t)-channel
		[14] ABAZOV	06I	D0	$\not{R}$, λ'_{211}
		[15] ABDALLAH	06C	DLPH	$\tilde{\nu}_\ell$, $\not{R}$, (s+t)-channel
		[16] ABULENCIA	06M	CDF	$\tilde{\nu}_\tau \to e\mu$, $\not{R}$
		[17] ABULENCIA	05A	CDF	$\tilde{\nu} \to ee$, $\mu\mu$, $\not{R}$ $LQ\overline{D}$
		[18] ACOSTA	05R	CDF	$\tilde{\nu} \to \tau\tau$, $\not{R}$, $LQ\overline{D}$
		[19] ABBIENDI	04F	OPAL	$\not{R}$, $\tilde{\nu}_{e,\mu,\tau}$
> 95	95	[20,21] ABDALLAH	04H	DLPH	AMSB, $\mu > 0$
> 98	95	[22] ABDALLAH	04M	DLPH	$\not{R}(LL\overline{E})$,$\tilde{\nu}_e$,indirect,$\Delta m > 5$ GeV
> 85	95	[22] ABDALLAH	04M	DLPH	$\not{R}(LL\overline{E})$,$\tilde{\nu}_\mu$,indirect,$\Delta m > 5$ GeV
> 85	95	[22] ABDALLAH	04M	DLPH	$\not{R}(LL\overline{E})$,$\tilde{\nu}_\tau$,indirect,$\Delta m > 5$ GeV
		[23] ABDALLAH	03F	DLPH	$\tilde{\nu}_{\mu,\tau}$, $\not{R}$ $LL\overline{E}$ decays
		[24] ACOSTA	03E	CDF	$\tilde{\nu}$, $\not{R}$, $LQ\overline{D}$ production and $LL\overline{E}$ decays
> 88	95	[25] HEISTER	03G	ALEP	$\tilde{\nu}_e$, $\not{R}$ decays, $\mu=-200$ GeV, $\tan\beta=2$
> 65	95	[25] HEISTER	03G	ALEP	$\tilde{\nu}_{\mu,\tau}$, $\not{R}$ decays
		[26] ABAZOV	02H	D0	$\not{R}$, λ'_{211}
> 95	95	[27] ACHARD	02	L3	$\tilde{\nu}_e$, $\not{R}$ decays, $\mu=-200$ GeV, $\tan\beta=\sqrt{2}$
> 65	95	[27] ACHARD	02	L3	$\tilde{\nu}_{\nu,\tau}$, $\not{R}$ decays
>149	95	[27] ACHARD	02	L3	$\tilde{\nu}$, $\not{R}$ decays, MSUGRA
		[28] HEISTER	02F	ALEP	$e\gamma \to \tilde{\nu}_{\mu,\tau}\ell_k$, $\not{R}$ $LL\overline{E}$
none 100–264	95	[29] ABBIENDI	00R	OPAL	$\tilde{\nu}_{\mu,\tau}$, $\not{R}$, $(s+t)$-channel
none 100–200	95	[30] ABBIENDI	00R	OPAL	$\tilde{\nu}_\tau$, $\not{R}$, s-channel
		[31] ABREU	00S	DLPH	$\tilde{\nu}_\ell$, $\not{R}$, $(s+t)$-channel
none 50–210	95	[32] ACCIARRI	00P	L3	$\tilde{\nu}_{\mu,\tau}$, $\not{R}$, s-channel
none 50–210	95	[33] BARATE	00I	ALEP	$\tilde{\nu}_{\mu,\tau}$, $\not{R}$, $(s+t)$-channel
none 90–210	95	[34] BARATE	00I	ALEP	$\tilde{\nu}_{\mu,\tau}$, $\not{R}$, s-channel
none 100–160	95	[35] ABBIENDI	99	OPAL	$\tilde{\nu}_e$, $\not{R}$, t-channel
$\neq m_Z$	95	[36] ACCIARRI	97U	L3	$\tilde{\nu}_\tau$, $\not{R}$, s-channel
none 125–180	95	[36] ACCIARRI	97U	L3	$\tilde{\nu}_\tau$, $\not{R}$, s-channel
		[37] CARENA	97	THEO	$g_\mu - 2$
> 46.0	95	[38] BUSKULIC	95E	ALEP	$N(\tilde{\nu})$=1, $\tilde{\nu} \to \nu\nu\ell\overline{\ell}'$
none 20–25000		[39] BECK	94	COSM	Stable $\tilde{\nu}$, dark matter
<600		[40] FALK	94	COSM	$\tilde{\nu}$ LSP, cosmic abundance
none 3–90	90	[41] SATO	91	KAMI	Stable $\tilde{\nu}_e$ or $\tilde{\nu}_\mu$, dark matter
none 4–90	90	[41] SATO	91	KAMI	Stable $\tilde{\nu}_\tau$, dark matter

[1] AAD 11Z looked in 1.07 fb^{-1} of pp collisions at $\sqrt{s} = 7$ TeV for events with one electron and one muon of opposite charge from the production of $\tilde{\nu}_\tau$ via an $\not{R}$ λ'_{311} coupling and followed by a decay via λ_{312} into $e + \mu$. No evidence for an (e, μ) resonance over the SM expectation is observed, and a limit is derived in the plane of λ'_{311} versus $m_{\tilde{\nu}}$ for three values of λ_{312}, see their Fig. 2. Masses $m_{\tilde{\nu}} < 1.32$ (1.45) TeV are excluded for $\lambda'_{311} = 0.10$ and $\lambda_{312} = 0.05$ ($\lambda'_{311} = 0.11$ and $\lambda_{312} = 0.07$).

[2] ABDALLAH 03M uses data from $\sqrt{s} = 192$–208 GeV to obtain limits in the framework of the MSSM with gaugino and sfermion mass universality at the GUT scale. An indirect limit on the mass is derived by constraining the MSSM parameter space by the results from direct searches for neutralinos (including cascade decays) and for sleptons. These limits are valid for values of $M_2 < 1$ TeV, $|\mu| \leq 1$ TeV with the $\tilde{\chi}^0_1$ as LSP. The quoted limit is obtained when there is no mixing in the third family. See Fig. 43 for the mass limits as a function of $\tan\beta$. These limits update the results of ABREU 00W.

[3] HEISTER 02N derives a bound on $m_{\tilde{\nu}_e}$ by exploiting the mass relation between the $\tilde{\nu}_e$ and $\tilde{e}$, based on the assumption of universal GUT scale gaugino and scalar masses $m_{1/2}$ and m_0 and the search described in the $\tilde{e}$ section. In the MSUGRA framework with radiative electroweak symmetry breaking, the limit improves to $m_{\tilde{\nu}_e} > 130$ GeV, assuming a trilinear coupling A_0=0 at the GUT scale. See Figs. 5 and 7 for the dependence of the limits on $\tan\beta$.

[4] ADRIANI 93M limit from $\Delta\Gamma(Z)$(invisible)< 16.2 MeV.

[5] DECAMP 92 limit is from Γ(invisible)/$\Gamma(\ell\ell) = 5.91 \pm 0.15$ ($N_\nu = 2.97 \pm 0.07$).

[6] ALEXANDER 91F limit is for one species of $\tilde{\nu}$ and is derived from Γ(invisible, new)/$\Gamma(\ell\ell)$ < 0.38.

[7] AAD 13AI searched in 4.6 fb^{-1} of pp collisions at $\sqrt{s} = 7$ TeV for evidence of heavy particles decaying into $e\mu$, $e\tau$ or $\mu\tau$ final states. No significant excess above the Standard Model expectation is observed, and 95% C.L. exclusions are placed on the cross section times branching ratio for the production of an R-parity-violating supersymmetric tau sneutrino, see their Fig. 2. For couplings $\lambda'_{311} = 0.10$ and $\lambda_{i3k} = 0.05$, the lower limits on the $\tilde{\nu}_\tau$ mass are 1610, 1110, 1100 GeV in the $e\mu$, $e\tau$, and $\mu\tau$ channels, respectively.

[8] AAD 11H looked in 35 pb^{-1} of pp collisions at $\sqrt{s} = 7$ TeV for events with one electron and one muon of opposite charge from the production of $\tilde{\nu}_\tau$ via an $\not{R}$ λ'_{311} coupling and followed by a decay via λ_{312} into $e + \mu$. No evidence for an excess over the SM expectation is observed, and a limit is derived in the plane of λ'_{311} versus $m_{\tilde{\nu}}$ for several values of λ_{312}, see their Fig. 2. Superseded by AAD 11Z.

[9] AALTONEN 10Z searched in 1 fb^{-1} of $p\overline{p}$ collisions at $\sqrt{s} = 1.96$ TeV for events from the production $d\overline{d} \to \tilde{\nu}_\tau$ with the subsequent decays $\tilde{\nu}_\tau \to e\mu$, $\mu\tau$, $e\tau$ in the MSSM framework with $\not{R}$. Two isolated leptons of different flavor and opposite charges are required, with τs identified by their hadronic decay. No statistically significant excesses are observed over the SM background. Upper limits on λ'^2_{311} times the branching ratio are listed in their Table III for various $\tilde{\nu}_\tau$ masses. Limits on the cross section times branching ratio for $\lambda'_{311} = 0.10$ and $\lambda_{i3k} = 0.05$, displayed in Fig. 2, are used to set limits on the $\tilde{\nu}_\tau$ mass of 558 GeV for the $e\mu$, 441 GeV for the $\mu\tau$ and 442 GeV for the $e\tau$ channels.

[10] ABAZOV 10M looked in 5.3 fb^{-1} of $p\overline{p}$ collisions at $\sqrt{s} = 1.96$ TeV for events with exactly one pair of high p_T isolated $e\mu$ and a veto against hard jets. No evidence for an excess over the SM expectation is observed, and a limit at 95% C.L. on the cross section times branching ratio is derived, see their Fig. 3. These limits are translated into limits on couplings as a function of $m_{\tilde{\nu}_\tau}$ as shown on their Fig. 4. As an example, for $m_{\tilde{\nu}_\tau} =$ 100 GeV and $\lambda_{312} \leq 0.07$, couplings $\lambda'_{311} > 7.7 \times 10^{-4}$ are excluded.

[11] AALTONEN 09V searched in 2.3 fb^{-1} of $p\overline{p}$ collisions at $\sqrt{s} = 1.96$ TeV for events with an oppositely charged pair originating from the $\not{R}$ production of a sneutrino decaying to dimuons. A limit is derived on the cross section times branching ratio, B, of $\tilde{\nu} \to \mu\mu$ for several values of the coupling λ', see their Fig. 3. For λ'^2B = 0.01, the range 100 GeV $\leq m_{\tilde{\nu}} \leq$ 810 GeV is excluded.

[12] ABAZOV 08Q searched in 1.04 fb^{-1} of $p\overline{p}$ collisions at $\sqrt{s} = 1.96$ TeV for an excess of events with oppositely charged $e\mu$ pairs. They might be expected in a SUSY model with $\not{R}$ where a sneutrino is produced by $LQ\overline{D}$ couplings and decays via $LL\overline{E}$ couplings, focusing on $\tilde{\nu}_\tau$, hence on the λ'_{311} and λ_{312} constants. No significant excess was found compared to the background expectation. Upper limits on the cross-section times branching ratio are extracted and displayed in their Fig. 2. Exclusion regions are determined for the $\tilde{\nu}_\tau$ mass as a function of both couplings, see their Fig. 3. As an indication, for $\tilde{\nu}_\tau$ masses of 100 GeV and $\lambda_{312} = 0.01$, values of $\lambda'_{311} \geq 1.6 \times 10^{-3}$ are excluded at the 95% C.L. Superseded by ABAZOV 10M.

[13] SCHAEL 07A searches for the s- or t-channel exchange of sneutrinos in the case of $\not{R}$ with $LL\overline{E}$ couplings by studying di-lepton production at $\sqrt{s} = 189$–209 GeV. Limits are obtained on the couplings as a function of the $\tilde{\nu}$ mass, see their Figs. 22-24. The results of this analysis are combined with BARATE 00I.

[14] ABAZOV 06I looked in 380 pb^{-1} of $p\overline{p}$ collisions at $\sqrt{s} = 1.96$ TeV for events with at least 2 muons and 2 jets for s-channel production of $\tilde{\mu}$ or $\tilde{\nu}$ and subsequent decay via $\not{R}$ couplings $LQ\overline{D}$. The data are in agreement with the SM expectation. They set limits on resonant slepton production and derive exclusion contours on λ'_{211} in the mass plane of $\tilde{\ell}$ versus $\tilde{\chi}^0_1$ assuming a MSUGRA model with $\tan\beta = 5$, $\mu < 0$ and $A_0 = 0$, see their Fig. 3. For $\lambda'_{211} \geq 0.09$ slepton masses up to 358 GeV are excluded. Supersedes the results of ABAZOV 02H.

[15] ABDALLAH 06C searches for anomalies in the production cross sections and forward-backward asymmetries of the $\ell^+\ell^-(\gamma)$ final states (ℓ=e,μ,τ) from 675 pb^{-1} of e^+e^- data at $\sqrt{s}$=130–207 GeV. Limits are set on the s- and t-channel exchange of sneutrinos in the presence of $\not{R}$ with $\lambda LL\overline{E}$ couplings. For points between the energies at which data were taken, information is obtained from events in which a photon was radiated. Exclusion limits in the (λ,$m_{\tilde{\nu}}$) plane are given in Fig. 16. These limits include and update the results of ABREU 00S.

[16] ABULENCIA 06M searched in 344 pb^{-1} of $p\overline{p}$ collisions at $\sqrt{s} = 1.96$ TeV for an excess of events with oppositely charged $e\mu$ pairs. They might be expected in a SUSY model with $\not{R}$ where a sneutrino is produced by $LQ\overline{D}$ couplings and decays via $LL\overline{E}$ couplings, focusing on $\tilde{\nu}_\tau$, hence on the λ'_{311} and λ_{132} constants. No significant excess was found compared to the background expectation. Upper limits on the cross-section times branching ratio are extracted and exclusion regions determined for the $\tilde{\nu}_\tau$ mass as a function of both couplings, see their Fig. 3. As an indication, $\tilde{\nu}_\tau$ masses are excluded up to 300 GeV for $\lambda'_{311} \geq 0.01$ and $\lambda_{132} \geq 0.02$. Superseded by AALTONEN 10Z.

[17] ABULENCIA 05A looked in $\sim$ 200 pb^{-1} of $p\overline{p}$ collisions at $\sqrt{s} = 1.96$ TeV for dimuon and dielectron events. They may originate from the $\not{R}$ production of a sneutrino decaying to dileptons. No significant excess rate was found compared to the background expectation. A limit is derived on the cross section times branching ratio, B, of $\tilde{\nu} \to ee$, $\mu\mu$ of 25 fb at high mass, see their Figure 2. Sneutrino masses are excluded at 95% CL below 680, 620, 460 GeV (ee channel) and 665, 590, 450 GeV ($\mu\mu$ channel) for a λ' coupling and branching ratio such that $\lambda'^2 B = 0.01$, 0.005, 0.001, respectively.

[18] ACOSTA 05R looked in 195 pb^{-1} of $p\overline{p}$ collisions at $\sqrt{s} = 1.96$ TeV for ditau events with one identified hadronic tau decay and one other tau decay. They may originate from the $\not{R}$ production of a sneutrino decaying to $\tau\tau$. No significant excess rate was found compared to the background expectation, dominated by Drell-Yan. A limit is derived on the cross section times branching ratio, B, of $\tilde{\nu} \to \tau\tau$, see their Figure 3. Sneutrino masses below 377 GeV are excluded at 95% CL for a λ' coupling to $d\overline{d}$ and branching ratio such that $\lambda'^2 B = 0.01$.

[19] ABBIENDI 04F use data from $\sqrt{s} = 189$–209 GeV. They derive limits on sparticle masses under the assumption of $\not{R}$ with $LL\overline{E}$ or $LQ\overline{D}$ couplings. The results are valid for $\tan\beta = 1.5$, $\mu = -200$ GeV, and a BR for the decay given by CMSSM, assuming no sensitivity to other decays. Limits are quoted for $m_{\tilde{\chi}^0} = 60$ GeV and degrade for low-mass $\tilde{\chi}^0_1$. For $\tilde{\nu}_e$ the direct (indirect) limits with $LL\overline{E}$ couplings are 89 (95) GeV and with $LQ\overline{D}$ they are 89 (88) GeV. For $\tilde{\nu}_{\mu,\tau}$ the direct (indirect) limits with $LL\overline{E}$ couplings are 79 (81) GeV and with $LQ\overline{D}$ they are 74 (no limit) GeV. Supersedes the results of ABBIENDI 00.

[20] ABDALLAH 04H use data from LEP 1 and $\sqrt{s} = 192$–208 GeV. They re-use results or re-analyze the data from ABDALLAH 03M to put limits on the parameter space of anomaly-mediated supersymmetry breaking (AMSB), which is scanned in the region $1 < m_{3/2} < 50$ TeV, $0 < m_0 < 1000$ GeV, $1.5 < \tan\beta < 35$, both signs of μ. The constraints are obtained from the searches for mass degenerate chargino and neutralino, for SM-like and invisible Higgs, for leptonically decaying charginos and from the limit on non-SM Z width of 3.2 MeV. The limit is for $m_t = 174.3$ GeV (see Table 2 for other m_t values).

[21] The limit improves to 114 GeV for $\mu < 0$.

[22] ABDALLAH 04M use data from $\sqrt{s} = 189$–208 GeV. The results are valid for $\mu = -200$ GeV, $\tan\beta = 1.5$, $\Delta m > 5$ GeV and assuming a BR of 1 for the given decay. The limit quoted is for indirect decays using the neutralino constraint of 39.5 GeV, also derived in ABDALLAH 04M. For indirect decays the limit on $\tilde{\nu}_e$ decreases to 96 GeV if the constraint from the neutralino is not used and for direct decays it remains 96 GeV. For indirect decays the limit on $\tilde{\nu}_\mu$ decreases to 82 GeV if the constraint from the neutralino is not used and to 83 GeV for direct decays. For indirect decays the limit on $\tilde{\nu}_\tau$ decreases to 82 GeV if the constraint from the neutralino is not used and improves to 91 GeV for direct decays. Supersedes the results of ABREU 00U.

[23] ABDALLAH 03F looked for events of the type $e^+e^- \to \tilde{\nu} \to \tilde{\chi}^0\nu$, $\tilde{\chi}^\pm\ell^\mp$ followed by $\not{R}$ decays of the $\tilde{\chi}^0$ via λ_{1j1} (j = 2,3) couplings in the data at $\sqrt{s} = 183$–208 GeV.

From a scan over the SUGRA parameters, they derive upper limits on the λ_{1j1} couplings as a function of the sneutrino mass, see their Figs. 5–8.

[24] ACOSTA 03E search for $e\mu$, $e\tau$ and $\mu\tau$ final states, and sets limits on the product of production cross-section and decay branching ratio for a $\tilde{\nu}$ in RPV models (see Fig. 3).

[25] HEISTER 03G searches for the production of sneutrinos in the case of $\not{R}$ prompt decays with $LL\overline{E}$, $LQ\overline{D}$ or $\overline{UDD}$ couplings at $\sqrt{s}$ = 189–209 GeV. The search is performed for direct and indirect decays, assuming one coupling at a time to be non-zero. The limit holds for indirect $\overline{\nu}$ decays via $\overline{UDD}$ couplings and $\Delta m > 10$ GeV. Stronger limits are reached for ($\overline{\nu}_e$,$\overline{\nu}_{\mu,\tau}$) for $LL\overline{E}$ direct (100,90) GeV or indirect (98,89) GeV and for $LQ\overline{D}$ direct (–,79) GeV or indirect (91,78) GeV couplings. For $LL\overline{E}$ indirect decays, use is made of the bound $m(\tilde{\chi}^0_1) > 23$ GeV from BARATE 98S. Supersedes the results from BARATE 01B.

[26] ABAZOV 02H looked in 94 pb^{-1} of $p\overline{p}$ collisions at $\sqrt{s}$=1.8 TeV for events with at least 2 muons and 2 jets for s-channel production of $\tilde{\mu}$ or $\tilde{\nu}$ and subsequent decay via $\not{R}$ couplings $LQ\overline{D}$. A scan over the MSUGRA parameters is performed to exclude regions of the (m_0,$m_{1/2}$) plane, examples being shown in Fig. 2.

[27] ACHARD 02 searches for the associated production of sneutrinos in the case of $\not{R}$ prompt decays with $LL\overline{E}$ or $\overline{UDD}$ couplings at $\sqrt{s}$=189–208 GeV. The search is performed for direct and indirect decays, assuming one coupling at the time to be nonzero. The limit holds for direct decays via $LL\overline{E}$ couplings. Stronger limits are reached for ($\tilde{\nu}_e$,$\tilde{\nu}_{\mu,\tau}$) for $LL\overline{E}$ indirect (99,78) GeV and for $\overline{UDD}$ direct or indirect (99,70) GeV decays. The MSUGRA limit results from a scan over the MSSM parameter space with the assumption of gaugino and scalar mass unification at the GUT scale, imposing simultaneously the exclusions from neutralino, chargino, sleptons, and squarks analyses. The limit holds for $\overline{UDD}$ couplings and increases to 152.7 GeV for $LL\overline{E}$ couplings.

[28] HEISTER 02F searched for single sneutrino production via $e\gamma \to \tilde{\nu}_j \ell_k$ mediated by $\not{R}$ $LL\overline{E}$ couplings, decaying directly or indirectly via a $\tilde{\chi}^0_1$ and assuming a single coupling to be nonzero at a time. Final states with three leptons and possible $\not{E}_T$ due to neutrinos were selected in the 189–209 GeV data. Limits on the couplings λ_{1jk} as function of the sneutrino mass are shown in Figs. 10–14. The couplings λ_{232} and λ_{233} are not accessible and λ_{121} and λ_{131} are measured with better accuracy in sneutrino resonant production. For all tested couplings, except λ_{133}, the limits are significantly improved compared to the low-energy limits.

[29] ABBIENDI 00R studied the effect of s- and t-channel τ or μ sneutrino exchange in $e^+e^- \to e^+e^-$ at $\sqrt{s}$=130–189 GeV, via the R-parity violating coupling $\lambda_{1i1}L_1L_ie_1$ (i=2 or 3). The limits quoted here hold for $\lambda_{1j1} >$0.13, and supersede the results of ABBIENDI 99. See Fig. 11 for limits on $m_{\tilde{\nu}}$ versus coupling.

[30] ABBIENDI 00R studied the effect of s-channel τ sneutrino exchange in $e^+e^- \to \mu^+\mu^-$ at $\sqrt{s}$=130–189 GeV, in presence of the R-parity violating couplings $\lambda_{i3j}L_iL_3e_j$ (i=1 and 2), with λ_{131}=λ_{232}. The limits quoted here hold for $\lambda_{131} > 0.09$, and supersede the results of ABBIENDI 99. See Fig. 12 for limits on $m_{\tilde{\nu}}$ versus coupling.

[31] ABREU 00S searches for anomalies in the production cross sections and forward-backward asymmetries of the $\ell^+\ell^-(\gamma)$ final states (ℓ=e,μ,τ) from e^+e^- collisions at $\sqrt{s}$=130–189 GeV. Limits are set on the s- and t-channel exchange of sneutrinos in the presence of $\not{R}$ with $\lambda LL\overline{E}$ couplings. For points between the energies at which data were taken, information is obtained from events in which a photon was radiated. Exclusion limits in the (λ,$m_{\tilde{\nu}}$) plane are given in Fig. 5. These limits include and update the results of ABREU 99A.

[32] ACCIARRI 00P use the dilepton total cross sections and asymmetries at $\sqrt{s}$=m_Z and $\sqrt{s}$=130–189 GeV data to set limits on the effect of $\not{R}$ $LL\overline{E}$ couplings giving rise to μ or τ sneutrino exchange. See their Fig. 5 for limits on the sneutrino mass versus couplings.

[33] BARATE 00I studied the effect of s-channel and t-channel τ or μ sneutrino exchange in $e^+e^- \to e^+e^-$ at $\sqrt{s}$= 130–183 GeV, via the R-parity violating coupling $\lambda_{1i1}L_1L_ie^c_1$ (i=2 or 3). The limits quoted here hold for $\lambda_{1j1} > 0.1$. See their Fig. 15 for limits as a function of the coupling. Superseded by SCHAEL 07A.

[34] BARATE 00I studied the effect of s-channel τ sneutrino exchange in $e^+e^- \to \mu^+\mu^-$ at $\sqrt{s}$= 130–183 GeV, in presence of the R-parity violating coupling $\lambda_{i3j}L_iL_3e^c_j$ (i=1 and 2). The limits quoted here hold for $\sqrt{|\lambda_{131}\lambda_{232}|} > 0.2$. See their Fig. 16 for limits as a function of the coupling. Superseded by SCHAEL 07A.

[35] ABBIENDI 99 studied the effect of t-channel electron sneutrino exchange in $e^+e^- \to \tau^+\tau^-$ at $\sqrt{s}$=130–183 GeV, in presence of the R-parity violating couplings $\lambda_{131}L_1L_3e^c_1$. The limits quoted here hold for $\lambda_{131} > 0.6$.

[36] ACCIARRI 97U studied the effect of the s-channel tau-sneutrino exchange in $e^+e^- \to e^+e^-$ at $\sqrt{s}$=m_Z and $\sqrt{s}$=130–172 GeV, via the R-parity violating coupling $\lambda_{131}L_1L_ie^c_1$. The limits quoted here hold for $\lambda_{131} > 0.05$. Similar limits were studied in $e^+e^- \to \mu^+\mu^-$ together with $\lambda_{232}L_2L_3e^c_2$ coupling.

[37] CARENA 97 studied the constraints on chargino and sneutrino masses from muon $g-2$. The bound can be important for large tanβ.

[38] BUSKULIC 95E looked for $Z \to \tilde{\nu}\overline{\tilde{\nu}}$, where $\tilde{\nu} \to \nu\chi^0_1$ and χ^0_1 decays via R-parity violating interactions into two leptons and a neutrino.

[39] BECK 94 limit can be inferred from limit on Dirac neutrino using $\sigma(\tilde{\nu}) = 4\sigma(\nu)$. Also private communication with H.V. Klapdor-Kleingrothaus.

[40] FALK 94 puts an upper bound on $m_{\tilde{\nu}}$ when $\tilde{\nu}$ is LSP by requiring its relic density does not overclose the Universe.

[41] SATO 91 search for high-energy neutrinos from the sun produced by annihilation of sneutrinos in the sun. Sneutrinos are assumed to be stable and to constitute dark matter in our galaxy. SATO 91 follow the analysis of NG 87, OLIVE 88, and GAISSER 86.

CHARGED SLEPTONS

This section contains limits on charged scalar leptons ($\tilde{\ell}$, with ℓ=e,μ,τ). Studies of width and decays of the Z boson (use is made here of $\Delta\Gamma_{\rm inv} < 2.0$ MeV, LEP 00) conclusively rule out $m_{\tilde{\ell}_R} < 40$ GeV (41 GeV for $\tilde{\ell}_L$) , independently of decay modes, for each individual slepton. The limits improve to 43 GeV (43.5 GeV for $\tilde{\ell}_L$) assuming all 3 flavors to be degenerate. Limits on higher mass sleptons depend on model assumptions and on the mass splitting Δm= $m_{\tilde{\ell}} - m_{\tilde{\chi}^0_1}$. The mass and composition of $\tilde{\chi}^0_1$ may affect the selectron production rate in e^+e^- collisions through t-channel exchange diagrams. Production rates are also affected by the potentially large mixing angle of the lightest mass eigenstate $\tilde{\ell}_1$=$\tilde{\ell}_R$ sinθ_ℓ + $\tilde{\ell}_L$ cosθ_ℓ. It is generally assumed that only $\tilde{\tau}$ may have significant mixing. The coupling to the Z vanishes for θ_ℓ=0.82. In the high-energy limit of e^+e^- collisions the interference between γ and Z exchange leads to a minimal cross section for θ_ℓ=0.91, a value which is sometimes used in the following entries relative to data taken at LEP2. When limits on $m_{\tilde{\ell}_R}$ are quoted, it is understood that limits on $m_{\tilde{\ell}_L}$ are usually at least as strong.

Possibly open decays involving gauginos other than $\tilde{\chi}^0_1$ will affect the detection efficiencies. Unless otherwise stated, the limits presented here result from the study of $\tilde{\ell}^+\tilde{\ell}^-$ production, with production rates and decay properties derived from the MSSM. Limits made obsolete by the recent analyses of e^+e^- collisions at high energies can be found in previous Editions of this Review.

For decays with final state gravitinos ($\tilde{G}$), $m_{\tilde{G}}$ is assumed to be negligible relative to all other masses.

$\tilde{e}$ (Selectron) MASS LIMIT

VALUE (GeV)	CL%	DOCUMENT ID		TECN	COMMENT
		[1] AAD	13B	ATLS	$2\ell^\pm + \not{E}_T$, SMS, pMSSM
> 97.5		[2] ABBIENDI	04	OPAL	$\tilde{e}_R$,$\Delta m > 11$ GeV, $|\mu| >$100 GeV, tanβ=1.5
> 94.4		[3] ACHARD	04	L3	$\tilde{e}_R$,$\Delta m > 10$ GeV, $|\mu| >$200 GeV, tan$\beta \geq 2$
> 71.3		[3] ACHARD	04	L3	$\tilde{e}_R$, all Δm
none 30–94	95	[4] ABDALLAH	03M	DLPH	$\Delta m >$15 GeV, $\tilde{e}^+_R\tilde{e}^-_R$
> 94	95	[5] ABDALLAH	03M	DLPH	$\tilde{e}_R$,$1 \leq$ tan$\beta \leq 40$, $\Delta m >$10 GeV
> 95	95	[6] HEISTER	02E	ALEP	$\Delta m >$ 15 GeV, $\tilde{e}^+_R\tilde{e}^-_R$
> 73	95	[7] HEISTER	02N	ALEP	$\tilde{e}_R$, any Δm
>107	95	[7] HEISTER	02N	ALEP	$\tilde{e}_L$, any Δm
• • • We do not use the following data for averages, fits, limits, etc. • • •					
> 89	95	[8] ABBIENDI	04F	OPAL	$\not{R}$, $\tilde{e}_L$
> 92	95	[9] ABDALLAH	04M	DLPH	$\not{R}$, $\tilde{e}_R$, indirect, $\Delta m >$5 GeV
> 93	95	[10] HEISTER	03G	ALEP	$\tilde{e}_R$,$\not{R}$ decays,μ=$-$200 GeV, tanβ=2
> 69	95	[11] ACHARD	02	L3	$\tilde{e}_R$, $\not{R}$ decays, μ=$-$200 GeV, tanβ=$\sqrt{2}$
> 92	95	[12] BARATE	01	ALEP	$\Delta m >$ 10 GeV, $\tilde{e}^+_R\tilde{e}^-_R$
> 77	95	[13] ABBIENDI	00J	OPAL	$\Delta m >$5 GeV, $\tilde{e}^+_R\tilde{e}^-_R$
> 83	95	[14] ABREU	00U	DLPH	$\tilde{e}_R$, $\not{R}$ ($LL\overline{E}$)
> 67	95	[15] ABREU	00V	DLPH	$\tilde{e}_R\tilde{e}_R$ ($\tilde{e}_R \to e\tilde{G}$), $m_{\tilde{G}} >$10 eV
> 85	95	[16] BARATE	00G	ALEP	$\tilde{\ell}_R \to \ell\tilde{G}$, any $\tau(\tilde{\ell}_R)$
> 29.5	95	[17] ACCIARRI	99I	L3	$\tilde{e}_R$, $\not{R}$, tan$\beta \geq 2$
> 56	95	[18] ACCIARRI	98F	L3	$\Delta m >$ 5 GeV, $\tilde{e}^+_R\tilde{e}^-_R$, tan$\beta \geq$ 1.41
> 77	95	[19] BARATE	98K	ALEP	Any Δm, $\tilde{e}^+_R\tilde{e}^-_R$, $\tilde{e}_R \to e\gamma\tilde{G}$
> 77	95	[20] BREITWEG	98	ZEUS	$m_{\tilde{q}}$=$m_{\tilde{e}}$, $m(\tilde{\chi}^0_1)$= 40 GeV
> 63	95	[21] AID	96C	H1	$m_{\tilde{q}}$=$m_{\tilde{e}}$, $m_{\tilde{\chi}^0_1}$=35 GeV

[1] AAD 13B searched in 4.7 fb^{-1} of pp collisions at $\sqrt{s}$ = 7 TeV for sleptons decaying to a final state with two leptons (e and μ) and missing transverse energy. No excess beyond the Standard Model expectation is observed. Limits are derived in a simplified model of direct left-handed slepton pair production, where left-handed slepton masses between 85 and 195 GeV are excluded at 95% C.L. for $m_{\tilde{\chi}^0_1} = 20$ GeV. See also Fig. 2(a). Exclusion limits are also derived in the phenomenological MSSM, see Fig. 3.

[2] ABBIENDI 04 search for $\tilde{e}_R\tilde{e}_R$ production in acoplanar di-electron final states in the 183–208 GeV data. See Fig. 13 for the dependence of the limits on $m_{\tilde{\chi}^0_1}$ and for the limit at tanβ=35 This limit supersedes ABBIENDI 00G.

[3] ACHARD 04 search for $\tilde{e}_R\tilde{e}_L$ and $\tilde{e}_R\tilde{e}_R$ production in single- and acoplanar di-electron final states in the 192–209 GeV data. Absolute limits on $m_{\tilde{e}_R}$ are derived from a scan over the MSSM parameter space with universal GUT scale gaugino and scalar masses $m_{1/2}$ and m_0, $1 \leq$ tan$\beta \leq 60$ and $-2 \leq \mu \leq 2$ TeV. See Fig. 4 for the dependence of the limits on $m_{\tilde{\chi}^0_1}$. This limit supersedes ACCIARRI 99W.

[4] ABDALLAH 03M looked for acoplanar dielectron + $\not{E}$ final states at $\sqrt{s}$ = 189–208 GeV. The limit assumes μ=$-$200 GeV and tanβ=1.5 in the calculation of the production cross section and B($\tilde{e} \to e\tilde{\chi}^0_1$). See Fig. 15 for limits in the ($m_{\tilde{e}_R}$, $m_{\tilde{\chi}^0_1}$) plane. These limits include and update the results of ABREU 01

[5] ABDALLAH 03M uses data from $\sqrt{s}$ = 192–208 GeV to obtain limits in the framework of the MSSM with gaugino and sfermion mass universality at the GUT scale. An indirect limit on the mass is derived by constraining the MSSM parameter space by the results from direct searches for neutralinos (including cascade decays) and for sleptons. These limits are valid for values of $M_2 <$1 TeV, $|\mu| \leq$ 1 TeV with the $\tilde{\chi}^0_1$ as LSP. The quoted limit is obtained when there is no mixing in the third family. See Fig. 43 for the mass limits as a function of tanβ. These limits update the results of ABREU 00W.

[6] HEISTER 02E looked for acoplanar dielectron + $\not{E}_T$ final states from e^+e^- interactions between 183 and 209 GeV. The mass limit assumes $\mu < -200$ GeV and tanβ=2 for the production cross section and B($\tilde{e} \to e\tilde{\chi}^0_1$)=1. See their Fig. 4 for the dependence of the limit on Δm. These limits include and update the results of BARATE 01.

[7] HEISTER 02N search for $\tilde{e}_R\tilde{e}_L$ and $\tilde{e}_R\tilde{e}_R$ production in single- and acoplanar di-electron final states in the 183–208 GeV data. Absolute limits on $m_{\tilde{e}_R}$ are derived from a scan over the MSSM parameter space with universal GUT scale gaugino and scalar masses $m_{1/2}$ and m_0, $1 \leq$ tan$\beta \leq 50$ and $-10 \leq \mu \leq 10$ TeV. The region of small $|\mu|$, where cascade decays are important, is covered by a search for $\tilde{\chi}^0_1\tilde{\chi}^0_3$ in final states with

leptons and possibly photons. Limits on $m_{\tilde{e}_L}$ are derived by exploiting the mass relation between the $\tilde{e}_L$ and $\tilde{e}_R$, based on universal m_0 and $m_{1/2}$. When the constraint from the mass limit of the lightest Higgs from HEISTER 02 is included, the bounds improve to $m_{\tilde{e}_R}$ >77(75) GeV and $m_{\tilde{e}_L}$ >115(115) GeV for a top mass of 175(180) GeV. In the MSUGRA framework with radiative electroweak symmetry breaking, the limits improve further to $m_{\tilde{e}_R}$ >95 GeV and $m_{\tilde{e}_L}$ >152 GeV, assuming a trilinear coupling A_0=0 at the GUT scale. See Figs. 4, 5, 7 for the dependence of the limits on tanβ.

[8] ABBIENDI 04F use data from $\sqrt{s}$ = 189–209 GeV. They derive limits on sparticle masses under the assumption of $\not{R}$ with $LL\overline{E}$ or $LQ\overline{D}$ couplings. The results are valid for tanβ = 1.5, $\mu = -200$ GeV, with, in addition, $\Delta m \geq 5$ GeV for indirect decays via $LQ\overline{D}$. The limit quoted applies to direct decays via $LL\overline{E}$ or $LQ\overline{D}$ couplings. For indirect decays, the limits on the $\tilde{e}_R$ mass are respectively 99 and 92 GeV for $LL\overline{E}$ and $LQ\overline{D}$ couplings and $m_{\tilde{\chi}^0} = 10$ GeV and degrade slightly for larger $\tilde{\chi}^0_1$ mass. Supersedes the results of ABBIENDI 00.

[9] ABDALLAH 04M use data from $\sqrt{s}$ = 192–208 GeV to derive limits on sparticle masses under the assumption of $\not{R}$ with $LL\overline{E}$ or $\overline{UDD}$ couplings. The results are valid for $\mu = -200$ GeV, tanβ = 1.5, $\Delta m > 5$ GeV and assuming a BR of 1 for the given decay. The limit quoted is for indirect $UD\overline{D}$ decays using the neutralino constraint of 39.5 GeV for $LL\overline{E}$ and of 38.0 GeV for $\overline{UDD}$ couplings, also derived in ABDALLAH 04M. For indirect decays via $LL\overline{E}$ the limit improves to 95 GeV if the constraint from the neutralino is used and to 94 GeV if it is not used. For indirect decays via $\overline{UDD}$ couplings it remains unchanged when the neutralino constraint is not used. Supersedes the result of ABREU 00U.

[10] HEISTER 03G searches for the production of selectrons in the case of $\not{R}$ prompt decays with $LL\overline{E}$, $LQ\overline{D}$ or $\overline{UDD}$ couplings at $\sqrt{s}$ = 189–209 GeV. The search is performed for direct and indirect decays, assuming one coupling at a time to be non-zero. The limit holds for indirect decays mediated by $LQ\overline{D}$ couplings with $\Delta m > 10$ GeV. Limits are also given for $LL\overline{E}$ direct ($m_{\tilde{e},R} > 96$ GeV) and indirect decays ($m_{\tilde{e},R} > 96$ GeV for $m(\tilde{\chi}^0_1) > 23$ GeV from BARATE 98S) and for $\overline{UDD}$ indirect decays ($m_{\tilde{e},R} > 94$ GeV with $\Delta m > 10$ GeV). Supersedes the results from BARATE 01B.

[11] ACHARD 02 searches for the production of selectrons in the case of $\not{R}$ prompt decays with $LL\overline{E}$ or $\overline{UDD}$ couplings at $\sqrt{s}$=189–208 GeV. The search is performed for direct and indirect decays, assuming one coupling at the time to be nonzero. The limit holds for direct decays via $LL\overline{E}$ couplings. Stronger limits are reached for $LL\overline{E}$ indirect (79 GeV) and for $\overline{UDD}$ direct or indirect (96 GeV) decays.

[12] BARATE 01 looked for acoplanar dielectron + $\not{E}_T$ final states at 189 to 202 GeV. The limit assumes μ=−200 GeV and tanβ=2 for the production cross section and 100% branching ratio for $\tilde{e} \rightarrow e\tilde{\chi}^0_1$. See their Fig. 1 for the dependence of the limit on Δm. These limits include and update the results of BARATE 99Q.

[13] ABBIENDI 00J looked for acoplanar dielectron + $\not{E}_T$ final states at $\sqrt{s}$= 161–183 GeV. The limit assumes $\mu < -100$ GeV and tanβ=1.5 for the production cross section and decay branching ratios, evaluated within the MSSM, and zero efficiency for decays other than $\tilde{e} \rightarrow e\tilde{\chi}^0_1$. See their Fig. 12 for the dependence of the limit on Δm and tanβ.

[14] ABREU 00U studies decays induced by R-parity violating $LL\overline{E}$ couplings, using data from $\sqrt{s}$=189 GeV. They investigate topologies with multiple leptons, assuming one coupling at the time to be nonzero and giving rise to indirect decays. The limits assume a neutralino mass limit of 30 GeV, also derived in ABREU 00U. Updates ABREU 00I. Superseded by ABDALLAH 04M.

[15] ABREU 00V use data from $\sqrt{s}$= 130–189 GeV to search for tracks with large impact parameter or visible decay vertices. Limits are obtained as a function of $m_{\tilde{G}}$, from a scan of the GMSB parameters space, after combining these results with the search for slepton pair production in the SUGRA framework from ABREU 01 to cover prompt decays and on stable particle searches from ABREU 00Q. For limits at different $m_{\tilde{G}}$, see their Fig. 12.

[16] BARATE 00G combines the search for acoplanar dileptons, leptons with large impact parameters, kinks, and stable heavy-charged tracks, assuming 3 flavors of degenerate sleptons, produced in the schannel. Data collected at $\sqrt{s}$=189 GeV.

[17] ACCIARRI 99I establish indirect limits on $m_{\tilde{e}_R}$ from the regions excluded in the M_2 versus m_0 plane by their chargino and neutralino searches at $\sqrt{s}$=130–183 GeV. The situations where the $\tilde{\chi}^0_1$ is the LSP (indirect decays) and where a $\tilde{\ell}$ is the LSP (direct decays) were both considered. The weakest limit, quoted above, comes from direct decays with $\overline{UDD}$ couplings; $LL\overline{E}$ couplings or indirect decays lead to a stronger limit.

[18] ACCIARRI 98F looked for acoplanar dielectron+$\not{E}_T$ final states at $\sqrt{s}$=130–172 GeV. The limit assumes μ=−200 GeV, and zero efficiency for decays other than $\tilde{e}_R \rightarrow e\tilde{\chi}^0_1$. See their Fig. 6 for the dependence of the limit on Δm.

[19] BARATE 98K looked for $e^+e^-\gamma\gamma + \not{E}$ final states at $\sqrt{s}$= 161–184 GeV. The limit assumes μ=−200 GeV and tanβ=2 for the evaluation of the production cross section. See Fig. 4 for limits on the ($m_{\tilde{e}_R}$,$m_{\tilde{\chi}^0_1}$) plane and for the effect of cascade decays.

[20] BREITWEG 98 used positron+jet events with missing energy and momentum to look for $e^+q \rightarrow \tilde{e}\tilde{q}$ via gaugino-like neutralino exchange with decays into $(e\tilde{\chi}^0_1)(q\tilde{\chi}^0_1)$. See paper for dependences in $m(\tilde{q})$, $m(\tilde{\chi}^0_1)$.

[21] AID 96C used positron+jet events with missing energy and momentum to look for $e^+q \rightarrow \tilde{e}\tilde{q}$ via neutralino exchange with decays into $(e\tilde{\chi}^0_1)(q\tilde{\chi}^0_1)$. See the paper for dependences on $m_{\tilde{q}}$, $m_{\tilde{\chi}^0_1}$.

$\tilde{\mu}$ (Smuon) MASS LIMIT

VALUE (GeV)	CL%	DOCUMENT ID		TECN	COMMENT
		[1] AAD	13B	ATLS	$2\ell^{\pm} + \not{E}_T$, SMS, pMSSM
>91.0		[2] ABBIENDI	04	OPAL	Δm >3 GeV, $\tilde{\mu}^+_R\tilde{\mu}^-_R$, $\lvert\mu\rvert$ >100 GeV, tanβ=1.5
>86.7		[3] ACHARD	04	L3	Δm >10 GeV, $\tilde{\mu}^+_R\tilde{\mu}^-_R$, $\lvert\mu\rvert$ >200 GeV, tan$\beta \geq 2$
none 30–88	95	[4] ABDALLAH	03M	DLPH	Δm >5 GeV, $\tilde{\mu}^+_R\tilde{\mu}^-_R$
>94	95	[5] ABDALLAH	03M	DLPH	$\tilde{\mu}_R$,1 $\leq$ tanβ $\leq$ 40, Δm >10 GeV
>88	95	[6] HEISTER	02E	ALEP	$\Delta m > 15$ GeV, $\tilde{\mu}^+_R\tilde{\mu}^-_R$

• • • We do not use the following data for averages, fits, limits, etc. • • •

		[7] ABAZOV	06I	D0	$\not{R}$, λ'_{211}
>74	95	[8] ABBIENDI	04F	OPAL	$\not{R}$, $\tilde{\mu}_L$
>87	95	[9] ABDALLAH	04M	DLPH	$\not{R}$, $\tilde{\mu}_R$, indirect, Δm >5 GeV
>81	95	[10] HEISTER	03G	ALEP	$\tilde{\mu}_L$,$\not{R}$ decays
		[11] ABAZOV	02H	D0	$\not{R}$, λ'_{211}
>61	95	[12] ACHARD	02	L3	$\tilde{\mu}_R$, $\not{R}$ decays
>85	95	[13] BARATE	01	ALEP	$\Delta m > 10$ GeV, $\tilde{\mu}^+_R\tilde{\mu}^-_R$
>65	95	[14] ABBIENDI	00J	OPAL	Δm >2 GeV, $\tilde{\mu}^+_R\tilde{\mu}^-_R$
>80	95	[15] ABREU	00V	DLPH	$\tilde{\mu}_R\tilde{\mu}_R$ ($\tilde{\mu}_R \rightarrow \mu\tilde{G}$), $m_{\tilde{G}}$ >8 eV
>77	95	[16] BARATE	98K	ALEP	Any Δm, $\tilde{\mu}^+_R\tilde{\mu}^-_R$, $\tilde{\mu}_R \rightarrow \mu\gamma\tilde{G}$

[1] AAD 13B searched in 4.7 fb^{-1} of pp collisions at $\sqrt{s}$ = 7 TeV for sleptons decaying to a final state with two leptons (e and μ) and missing transverse energy. No excess beyond the Standard Model expectation is observed. Limits are derived in a simplified model of direct left-handed slepton pair production, where left-handed slepton masses between 85 and 195 GeV are excluded at 95% C.L. for $m_{\tilde{\chi}^0_1} = 20$ GeV. See also Fig. 2(a). Exclusion limits are also derived in the phenomenological MSSM, see Fig. 3.

[2] ABBIENDI 04 search for $\tilde{\mu}_R\tilde{\mu}_R$ production in acoplanar di-muon final states in the 183–208 GeV data. See Fig. 14 for the dependence of the limits on $m_{\tilde{\chi}^0_1}$ and for the limit at tanβ=35. Under the assumption of 100% branching ratio for $\tilde{\mu}_R \rightarrow \mu\tilde{\chi}^0_1$, the limit improves to 94.0 GeV for $\Delta m > 4$ GeV. See Fig. 11 for the dependence of the limits on $m_{\tilde{\chi}^0_1}$ at several values of the branching ratio. This limit supersedes ABBIENDI 00G.

[3] ACHARD 04 search for $\tilde{\mu}_R\tilde{\mu}_R$ production in acoplanar di-muon final states in the 192–209 GeV data. Limits on $m_{\tilde{\mu}_R}$ are derived from a scan over the MSSM parameter space with universal GUT scale gaugino and scalar masses $m_{1/2}$ and m_0, $1 \leq$ tan$\beta \leq 60$ and $-2 \leq \mu \leq 2$ TeV. See Fig. 4 for the dependence of the limits on $m_{\tilde{\chi}^0_1}$. This limit supersedes ACCIARRI 99W.

[4] ABDALLAH 03M looked for acoplanar dimuon + $\not{E}$ final states at $\sqrt{s}$ = 189–208 GeV. The limit assumes B($\tilde{\mu} \rightarrow \mu\tilde{\chi}^0_1$) = 100%. See Fig. 16 for limits on the ($m_{\tilde{\mu}_R}$, $m_{\tilde{\chi}^0_1}$) plane. These limits include and update the results of ABREU 01.

[5] ABDALLAH 03M uses data from $\sqrt{s}$ = 192–208 GeV to obtain limits in the framework of the MSSM with gaugino and sfermion mass universality at the GUT scale. An indirect limit on the mass is derived by constraining the MSSM parameter space by the results from direct searches for neutralinos (including cascade decays) and for sleptons. These limits are valid for values of $M_2 < 1$ TeV, $\lvert\mu\rvert \leq 1$ TeV with the $\tilde{\chi}^0_1$ as LSP. The quoted limit is obtained when there is no mixing in the third family. See Fig. 43 for the mass limits as a function of tanβ. These limits update the results of ABREU 00W.

[6] HEISTER 02E looked for acoplanar dimuon + $\not{E}_T$ final states from e^+e^- interactions between 183 and 209 GeV. The mass limit assumes B($\tilde{\mu} \rightarrow \mu\tilde{\chi}^0_1$)=1. See their Fig. 4 for the dependence of the limit on Δm. These limits include and update the results of BARATE 01.

[7] ABAZOV 06I looked in 380 pb^{-1} of $p\overline{p}$ collisions at $\sqrt{s}$ = 1.96 TeV for events with at least 2 muons and 2 jets for s-channel production of $\tilde{\mu}$ or $\tilde{\nu}$ and subsequent decay via $\not{R}$ couplings $LQ\overline{D}$. The data are in agreement with the SM expectation. They set limits on resonant slepton production and derive exclusion contours on λ'_{211} in the mass plane of $\tilde{\ell}$ versus $\tilde{\chi}^0_1$ assuming a MSUGRA model with tan$\beta = 5$, $\mu < 0$ and $A_0 = 0$, see their Fig. 3. For $\lambda'_{211} \geq 0.09$ slepton masses up to 358 GeV are excluded. Supersedes the results of ABAZOV 02H.

[8] ABBIENDI 04F use data from $\sqrt{s}$ = 189–209 GeV. They derive limits on sparticle masses under the assumption of $\not{R}$ with $LL\overline{E}$ or $LQ\overline{D}$ couplings. The results are valid for tanβ = 1.5, $\mu = -200$ GeV, with, in addition, $\Delta m > 5$ GeV for indirect decays via $LQ\overline{D}$. The limit quoted applies to direct decays with $LL\overline{E}$ couplings and improves to 75 GeV for $LQ\overline{D}$ couplings. The limits on the $\tilde{\mu}_R$ mass for indirect decays are respectively 94 and 87 GeV for $LL\overline{E}$ and $LQ\overline{D}$ couplings and $m_{\tilde{\chi}^0} = 10$ GeV. Supersedes the results of ABBIENDI 00.

[9] ABDALLAH 04M use data from $\sqrt{s}$ = 192–208 GeV to derive limits on sparticle masses under the assumption of $\not{R}$ with $LL\overline{E}$ or $\overline{UDD}$ couplings. The results are valid for $\mu = -200$ GeV, tanβ = 1.5, $\Delta m > 5$ GeV and assuming a BR of 1 for the given decay. The limit quoted is for indirect $UD\overline{D}$ decays using the neutralino constraint of 39.5 GeV for $LL\overline{E}$ and of 38.0 GeV for $\overline{UDD}$ couplings, also derived in ABDALLAH 04M. For indirect decays via $LL\overline{E}$ the limit improves to 90 GeV if the constraint from the neutralino is used and remains at 87 GeV if it is not used. For indirect decays via $\overline{UDD}$ couplings it degrades to 85 GeV when the neutralino constraint is not used. Supersedes the result of ABREU 00U.

[10] HEISTER 03G searches for the production of smuons in the case of $\not{R}$ prompt decays with $LL\overline{E}$, $LQ\overline{D}$ or $\overline{UDD}$ couplings at $\sqrt{s}$ = 189–209 GeV. The search is performed for direct and indirect decays, assuming one coupling at a time to be non-zero. The limit holds for direct decays mediated by $\not{R}$ $LQ\overline{D}$ couplings and improves to 90 GeV for indirect decays (for $\Delta m > 10$ GeV). Limits are also given for $LL\overline{E}$ direct ($m_{\tilde{\mu}R} > 87$ GeV) and indirect decays ($m_{\tilde{\mu}R} > 96$ GeV for $m(\tilde{\chi}^0_1) > 23$ GeV from BARATE 98S) and for $\overline{UDD}$ indirect decays ($m_{\tilde{\mu}R} > 85$ GeV for $\Delta m > 10$ GeV). Supersedes the results from BARATE 01B.

[11] ABAZOV 02H looked in 94 pb^{-1} of $p\overline{p}$ collisions at $\sqrt{s}$=1.8 TeV for events with at least 2 muons and 2 jets for s-channel production of $\tilde{\mu}$ or $\tilde{\nu}$ and subsequent decay via $\not{R}$ couplings $LQ\overline{D}$. A scan over the MSUGRA parameters is performed to exclude regions of the (m_0,$m_{1/2}$) plane, examples being shown in Fig. 2.

[12] ACHARD 02 searches for the production of smuons in the case of $\not{R}$ prompt decays with $LL\overline{E}$ or $\overline{UDD}$ couplings at $\sqrt{s}$=189–208 GeV. The search is performed for direct and indirect decays, assuming one coupling at the time to be nonzero. The limit holds for direct decays via $LL\overline{E}$ couplings. Stronger limits are reached for $LL\overline{E}$ indirect (87 GeV) and for $\overline{UDD}$ direct or indirect (86 GeV) decays.

[13] BARATE 01 looked for acoplanar dimuon + $\not{E}_T$ final states at 189 to 202 GeV. The limit assumes 100% branching ratio for $\tilde{\mu} \rightarrow \mu\tilde{\chi}^0_1$. See their Fig. 1 for the dependence of the limit on Δm. These limits include and update the results of BARATE 99Q.

[14] ABBIENDI 00J looked for acoplanar dimuon + $\not{E}_T$ final states at $\sqrt{s}$= 161–183 GeV. The limit assumes B($\tilde{\mu} \rightarrow \mu\tilde{\chi}^0_1$)=1. Using decay branching ratios derived from the

MSSM, a lower limit of 65 GeV is obtained for $\mu < -100$ GeV and tanβ=1.5. See their Figs. 10 and 13 for the dependence of the limit on the branching ratio and on Δm.

[15] ABREU 00V use data from $\sqrt{s}$= 130–189 GeV to search for tracks with large impact parameter or visible decay vertices. Limits are obtained as function of $m_{\widetilde{G}}$, after combining these results with the search for slepton pair production in the SUGRA framework from ABREU 01 to cover prompt decays and on stable particle searches from ABREU 00Q. For limits at different $m_{\widetilde{G}}$, see their Fig. 12.

[16] BARATE 98K looked for $\mu^+\mu^-\gamma\gamma + \not{E}$ final states at $\sqrt{s}$= 161–184 GeV. See Fig. 4 for limits on the $(m_{\widetilde{\mu}_R}, m_{\widetilde{\chi}^0_1})$ plane and for the effect of cascade decays.

$\widetilde{\tau}$ (Stau) MASS LIMIT

VALUE (GeV)	CL%	DOCUMENT ID		TECN	COMMENT
>85.2		[1] ABBIENDI	04	OPAL	$\Delta m > 6$ GeV, θ_τ=π/2, $\|\mu\| >$ 100 GeV, tanβ=1.5
>78.3		[2] ACHARD	04	L3	$\Delta m > 15$ GeV, θ_τ=π/2, $|\mu| >$200 GeV,tan$\beta \geq 2$
>81.9	95	[3] ABDALLAH	03M	DLPH	$\Delta m >$15 GeV, all θ_τ
none m_τ – 26.3	95	[3] ABDALLAH	03M	DLPH	$\Delta m > m_\tau$, all θ_τ
>79	95	[4] HEISTER	02E	ALEP	$\Delta m > 15$ GeV, θ_τ=π/2
>76	95	[4] HEISTER	02E	ALEP	$\Delta m > 15$ GeV, θ_τ=0.91
• • • We do not use the following data for averages, fits, limits, etc. • • •					
		[5] AAD	12AF	ATLS	2τ + jets + $\not{E}_T$, GMSB
		[6] AAD	12AG	ATLS	$\geq 1\tau_h$ + jets + $\not{E}_T$, GMSB
		[7] AAD	12CM	ATLS	$\geq 1\tau$ + jets + $\not{E}_T$, GMSB
>87.4	95	[8] ABBIENDI	06B	OPAL	$\widetilde{\tau}_R \rightarrow \tau\widetilde{G}$, all $\tau(\widetilde{\tau}_R)$
>74	95	[9] ABBIENDI	04F	OPAL	$\not{R}$, $\widetilde{\tau}_L$
>68	95	[10,11] ABDALLAH	04H	DLPH	AMSB, $\mu > 0$
>90	95	[12] ABDALLAH	04M	DLPH	$\not{R}$, $\widetilde{\tau}_R$, indirect, Δm >5 GeV
>82.5		[13] ABDALLAH	03D	DLPH	$\widetilde{\tau}_R \rightarrow \tau\widetilde{G}$, all $\tau(\widetilde{\tau}_R)$
>70	95	[14] HEISTER	03G	ALEP	$\widetilde{\tau}_R$,$\not{R}$ decay
>61	95	[15] ACHARD	02	L3	$\widetilde{\tau}_R$, $\not{R}$ decays
>77	95	[16] HEISTER	02R	ALEP	τ_1, any lifetime
>70	95	[17] BARATE	01	ALEP	$\Delta m > 10$ GeV, θ_τ=π/2
>68	95	[17] BARATE	01	ALEP	$\Delta m > 10$ GeV, θ_τ=0.91
>64	95	[18] ABBIENDI	00J	OPAL	Δm >10 GeV, $\widetilde{\tau}^+_R\widetilde{\tau}^-_R$
>84	95	[19] ABREU	00V	DLPH	$\widetilde{\ell}_R\widetilde{\ell}_R$ ($\widetilde{\ell}_R \rightarrow \ell\widetilde{G}$), $m_{\widetilde{G}}$ >9 eV
>73	95	[20] ABREU	00V	DLPH	$\widetilde{\tau}_1\widetilde{\tau}_1$ ($\widetilde{\tau}_1 \rightarrow \tau\widetilde{G}$), all $\tau(\widetilde{\tau}_1)$
>52		[21] BARATE	98K	ALEP	Any Δm,θ_τ=π/2,$\widetilde{\tau}_R \rightarrow \tau\gamma\widetilde{G}$

[1] ABBIENDI 04 search for $\widetilde{\tau}\widetilde{\tau}$ production in acoplanar di-tau final states in the 183–208 GeV data. See Fig. 15 for the dependence of the limits on $m_{\widetilde{\chi}^0_1}$ and for the limit at tanβ=35. Under the assumption of 100% branching ratio for $\widetilde{\tau}_R \rightarrow \tau\widetilde{\chi}^0_1$, the limit improves to 89.8 GeV for $\Delta m > 8$ GeV. See Fig. 12 for the dependence of the limits on $m_{\widetilde{\chi}^0_1}$ at several values of the branching ratio and for their dependence on θ_τ. This limit supersedes ABBIENDI 00G.

[2] ACHARD 04 search for $\widetilde{\tau}\widetilde{\tau}$ production in acoplanar di-tau final states in the 192–209 GeV data. Limits on $m_{\widetilde{\tau}_R}$ are derived from a scan over the MSSM parameter space with universal GUT scale gaugino and scalar masses $m_{1/2}$ and m_0, $1 \leq$ tan$\beta \leq 60$ and $-2 \leq \mu \leq 2$ TeV. See Fig. 4 for the dependence of the limits on $m_{\widetilde{\chi}^0_1}$.

[3] ABDALLAH 03M looked for acoplanar ditaus + $\not{E}$ final states at $\sqrt{s}$ = 130–208 GeV. A dedicated search was made for low mass $\widetilde{\tau}$s decoupling from the Z^0. The limit assumes B($\widetilde{\tau} \rightarrow \tau\widetilde{\chi}^0_1$) = 100%. See Fig. 20 for limits on the $(m_{\widetilde{\tau}}, m_{\widetilde{\chi}^0_1})$ plane and as function of the $\widetilde{\chi}^0_1$ mass and of the branching ratio. The limit in the low-mass region improves to 29.6 and 31.1 GeV for $\widetilde{\tau}_R$ and $\widetilde{\tau}_L$, respectively, at $\Delta m > m_\tau$. The limit in the high-mass region improves to 84.7 GeV for $\widetilde{\tau}_R$ and $\Delta m > 15$ GeV. These limits include and update the results of ABREU 01.

[4] HEISTER 02E looked for acoplanar ditau + $\not{E}_T$ final states from e^+e^- interactions between 183 and 209 GeV. The mass limit assumes B($\widetilde{\tau} \rightarrow \tau\widetilde{\chi}^0_1$)=1. See their Fig. 4 for the dependence of the limit on Δm. These limits include and update the results of BARATE 01.

[5] AAD 12AF searched in 2 fb^{-1} of pp collisions at $\sqrt{s}$ = 7 TeV for events with two tau leptons, jets and large $\not{E}_T$ in a GMSB framework. No significant excess above the expected background was found and an upper limit on the visible cross section for new phenomena is set. A 95% C.L. lower limit of 32 TeV on the mGMSB breaking scale Λ is set for M_{mess} = 250 TeV, N_5 = 3, $\mu > 0$ and C_{grav} = 1, independent of tanβ.

[6] AAD 12AG searched in 2.05 fb^{-1} of pp collisions at $\sqrt{s}$ = 7 TeV for events with at least one hadronically decaying tau lepton, jets, and large $\not{E}_T$ in a GMSB framework. No significant excess above the expected background was found and an upper limit on the visible cross section for new phenomena is set. A 95% C.L. lower limit of 30 TeV on the mGMSB breaking scale Λ is set for M_{mess} = 250 TeV, N_5 = 3, $\mu > 0$ and C_{grav} = 1, independent of tanβ. For large values of tanβ, the limit on Λ increases to 43 TeV.

[7] AAD 12CM searched in 4.7 fb^{-1} of pp collisions at $\sqrt{s}$=7 TeV for events with at least one tau lepton, zero or one additional light lepton (e/μ) jets, and large $\not{E}_T$ in a GMSB framework. No significant excess above the expected background was found and an upper limit on the visible cross section for new phenomena is set. A 95% C. L. lower limit of 54 TeV on the mGMSB breaking scale Λ is set for M_{mess} = 250 TeV, N_5 = 3, $\mu > 0$ and C_{grav} = 1, for tan$\beta > 20$. Here the $\widetilde{\tau}_1$ is the NLSP.

[8] ABBIENDI 06B use 600 pb^{-1} of data from $\sqrt{s}$ = 189–209 GeV. They look for events from pair-produced staus in a GMSB scenario with $\widetilde{\tau}$ NLSP including prompt $\widetilde{\tau}$ decays to ditaus + $\not{E}$ final states, large impact parameters, kinked tracks and heavy stable charged particles. Limits on the cross-section are computed as a function of m($\widetilde{\tau}$) and the lifetime, see their Fig. 7. The limit is compared to the $\sigma \cdot BR^2$ from a scan over the GMSB parameter space.

[9] ABBIENDI 04F use data from $\sqrt{s}$ = 189–209 GeV. They derive limits on sparticle masses under the assumption of $\not{R}$ with $LL\overline{E}$ or $LQ\overline{D}$ couplings. The results are valid for tanβ = 1.5, $\mu = -200$ GeV, with, in addition, $\Delta m > 5$ GeV for indirect decays via $LQ\overline{D}$. The limit quoted applies to direct decays with $LL\overline{E}$ couplings and improves to 75 GeV for $LQ\overline{D}$ couplings. The limit on the $\widetilde{\tau}_R$ mass for indirect decays is 92 GeV for $LL\overline{E}$ couplings at $m_{\widetilde{\chi}^0} = 10$ GeV and no exclusion is obtained for $LQ\overline{D}$ couplings. Supersedes the results of ABBIENDI 00.

[10] ABDALLAH 04H use data from LEP 1 and $\sqrt{s}$ = 192–208 GeV. They re-use results or re-analyze the data from ABDALLAH 03M to put limits on the parameter space of anomaly-mediated supersymmetry breaking (AMSB), which is scanned in the region $1 < m_{3/2} < 50$ TeV, $0 < m_0 < 1000$ GeV, $1.5 <$ tan$\beta < 35$, both signs of μ. The constraints are obtained from the searches for mass degenerate chargino and neutralino, for SM-like and invisible Higgs, for leptonically decaying charginos and from the limit on non-SM Z width of 3.2 MeV. The limit is for m_t = 174.3 GeV (see Table 2 for other m_t values).

[11] The limit improves to 75 GeV for $\mu < 0$.

[12] ABDALLAH 04M use data from $\sqrt{s}$ = 192–208 GeV to derive limits on sparticle masses under the assumption of $\not{R}$ with $LL\overline{E}$ couplings. The results are valid for $\mu = -200$ GeV, tanβ = 1.5, $\Delta m > 5$ GeV and assuming a BR of 1 for the given decay. The limit quoted is for indirect decays using the neutralino constraint of 39.5 GeV, also derived in ABDALLAH 04M. For indirect decays via $LL\overline{E}$ the limit decreases to 86 GeV if the constraint from the neutralino is not used. Supersedes the result of ABREU 00U.

[13] ABDALLAH 03D use data from $\sqrt{s}$ = 130–208 GeV to search for tracks with large impact parameter or visible decay vertices and for heavy charged stable particles. Limits are obtained as function of m($\widetilde{G}$), after combining these results with the search for slepton pair production in the SUGRA framework from ABDALLAH 03M to cover prompt decays. The above limit is reached for the stau decaying promptly, m($\widetilde{G}$) < 6 eV, and is computed for stau mixing yielding the minimal cross section. Stronger limits are obtained for longer lifetimes, See their Fig. 9. Supersedes the results of ABREU 01G.

[14] HEISTER 03G searches for the production of stau in the case of $\not{R}$ prompt decays with $LL\overline{E}$, $LQ\overline{D}$ or $\overline{UDD}$ couplings at $\sqrt{s}$ = 189–209 GeV. The search is performed for direct and indirect decays, assuming one coupling at a time to be non-zero. The limit holds for indirect decays mediated by $\not{R}$ $\overline{UDD}$ couplings with $\Delta m > 10$ GeV. Limits are also given for $LL\overline{E}$ direct ($m_{\widetilde{\tau}_R} > 87$ GeV) and indirect decays ($m_{\widetilde{\tau}_R} > 95$ GeV for $m(\widetilde{\chi}^0_1) > 23$ GeV from BARATE 98S) and for $LQ\overline{D}$ indirect decays ($m_{\widetilde{\tau}_R} > 76$ GeV). Supersedes the results from BARATE 01B.

[15] ACHARD 02 searches for the production of staus in the case of $\not{R}$ prompt decays with $LL\overline{E}$ or $\overline{UDD}$ couplings at $\sqrt{s}$=189–208 GeV. The search is performed for direct and indirect decays, assuming one coupling at the time to be nonzero. The limit holds for direct decays via $LL\overline{E}$ couplings. Stronger limits are reached for $LL\overline{E}$ indirect (86 GeV) and for $\overline{UDD}$ direct or indirect (75 GeV) decays.

[16] HEISTER 02R search for signals of GMSB in the 189–209 GeV data. For the $\widetilde{\chi}^0_1$ NLSP scenario, they looked for topologies consisting of $\gamma\gamma\not{E}$ or a single γ not pointing to the interaction vertex. For the $\widetilde{\ell}$ NLSP case, the topologies consist of $\ell\ell\not{E}$, including leptons with large impact parameters, kinks, or stable particles. Limits are derived from a scan over the GMSB parameters (see their Table 5 for the ranges). The limit remains valid whichever is the NLSP. The absolute mass bound on the $\widetilde{\chi}^0_1$ for any lifetime includes indirect limits from the slepton search HEISTER 02E preformed within the MSUGRA framework. A bound for any NLSP and any lifetime of 77 GeV has also been derived by using the constraints from the neutral Higgs search in HEISTER 02. In the co-NLSP scenario, limits $m_{\widetilde{e}_R} > 83$ GeV (neglecting t-channel exchange) and $m_{\widetilde{\mu}_R} > 88$ GeV are obtained independent of the lifetime. Supersedes the results from BARATE 00G.

[17] BARATE 01 looked for acoplanar ditau + $\not{E}_T$ final states at 189 to 202 GeV. A slight excess (with 1.2% probability) of events is observed relative to the expected SM background. The limit assumes 100% branching ratio for $\widetilde{\tau} \rightarrow \tau\widetilde{\chi}^0_1$. See their Fig. 1 for the dependence of the limit on Δm. These limits include and update the results of BARATE 99Q.

[18] ABBIENDI 00J looked for acoplanar ditau + $\not{E}_T$ final states at $\sqrt{s}$= 161–183 GeV. The limit assumes B($\widetilde{\tau} \rightarrow \tau\widetilde{\chi}^0_1$)=1. Using decay branching ratios derived from the MSSM, a lower limit of 60 GeV at Δm >9 GeV is obtained for $\mu < -100$ GeV and tanβ=1.5. See their Figs. 11 and 14 for the dependence of the limit on the branching ratio and on Δm.

[19] ABREU 00V use data from $\sqrt{s}$= 130–189 GeV to search for tracks with large impact parameter or visible decay vertices. Limits are obtained as function of $m_{\widetilde{G}}$, after combining these results with the search for slepton pair production in the SUGRA framework from ABREU 01 to cover prompt decays and on stable particle searches from ABREU 00Q. The above limit assumes the degeneracy of stau and smuon. For limits at different $m_{\widetilde{G}}$, see their Fig. 12.

[20] ABREU 00V use data from $\sqrt{s}$= 130–189 GeV to search for tracks with large impact parameter or visible decay vertices. Limits are obtained as function of $m_{\widetilde{G}}$, after combining these results with the search for slepton pair production in the SUGRA framework from ABREU 01 to cover prompt decays and on stable particle searches from ABREU 00Q. The above limit is reached for the stau mixing yielding the minimal cross section and decaying promptly. Stronger limits are obtained for longer lifetimes or for $\widetilde{\tau}_R$; see their Fig. 11. For $10 \leq m_{\widetilde{G}} \leq 310$ eV, the whole range $2 \leq m_{\widetilde{\tau}_1} \leq 80$ GeV is excluded. Supersedes the results of ABREU 99C and ABREU 99F.

[21] BARATE 98K looked for $\tau^+\tau^-\gamma\gamma + \not{E}$ final states at $\sqrt{s}$= 161–184 GeV. See Fig. 4 for limits on the $(m_{\widetilde{\tau}_R}, m_{\widetilde{\chi}^0_1})$ plane and for the effect of cascade decays.

Degenerate Charged Sleptons

Unless stated otherwise in the comment lines or in the footnotes, the following limits assume 3 families of degenerate charged sleptons.

VALUE (GeV)	CL%	DOCUMENT ID		TECN	COMMENT
>93	95	[1] BARATE	01	ALEP	$\Delta m > 10$ GeV, $\widetilde{\ell}^+_R\widetilde{\ell}^-_R$
>70	95	[1] BARATE	01	ALEP	all Δm, $\widetilde{\ell}^+_R\widetilde{\ell}^-_R$
• • • We do not use the following data for averages, fits, limits, etc. • • •					
>91.9	95	[2] ABBIENDI	06B	OPAL	$\widetilde{\ell}_R \rightarrow \ell\widetilde{G}$, all $\ell(\widetilde{\ell}_R)$
>88		[3] ABDALLAH	03D	DLPH	$\widetilde{\ell}_R \rightarrow \ell\widetilde{G}$, all $\ell(\widetilde{\ell}_R)$
>82.7	95	[4] ACHARD	02	L3	$\widetilde{\ell}_R$, $\not{R}$ decays, MSUGRA
>83	95	[5] ABBIENDI	01	OPAL	$e^+e^- \rightarrow \widetilde{\ell}_1\widetilde{\ell}_1$, GMSB, tan$\beta$=2
		[6] ABREU	01	DLPH	$\widetilde{\ell} \rightarrow \ell\widetilde{\chi}^0_2$, $\widetilde{\chi}^0_2 \rightarrow \gamma\widetilde{\chi}^0_1$, ℓ=e,μ
>68.8	95	[7] ACCIARRI	01	L3	$\widetilde{\ell}_R$, $\not{R}$, 0.7 $\leq$ tan$\beta \leq$ 40
>84	95	[8,9] ABREU	00V	DLPH	$\widetilde{\ell}_R\widetilde{\ell}_R$ ($\widetilde{\ell}_R \rightarrow \ell\widetilde{G}$), $m_{\widetilde{G}}$ >9 eV

[1] BARATE 01 looked for acoplanar dilepton + $\not{E}_T$ and single electron (for $\tilde{e}_R\tilde{e}_L$) final states at 189 to 202 GeV. The limit assumes μ=−200 GeV and tanβ=2 for the production cross section and decay branching ratios, evaluated within the MSSM, and zero efficiency for decays other than $\tilde{\ell} \to \ell\tilde{\chi}_1^0$. The slepton masses are determined from the GUT relations without stau mixing. See their Fig. 1 for the dependence of the limit on Δm.

[2] ABBIENDI 06B use 600 pb^{-1} of data from $\sqrt{s}$ = 189–209 GeV. They look for events from pair-produced staus in a GMSB scenario with $\tilde{\ell}$ co-NLSP including prompt $\tilde{\ell}$ decays to dileptons + $\not{E}$ final states, large impact parameters, kinked tracks and heavy stable charged particles. Limits on the cross-section are computed as a function of m($\tilde{\ell}$) and the lifetime, see their Fig. 7. The limit is compared to the $\sigma \cdot BR^2$ from a scan over the GMSB parameter space. The highest mass limit is reached for $\tilde{\mu}_R$, from which the quoted mass limit is derived by subtracting m_τ.

[3] ABDALLAH 03D use data from $\sqrt{s}$ = 130–208 GeV to search for tracks with large impact parameter or visible decay vertices and for heavy charged stable particles. Limits are obtained as function of m($\tilde{G}$), after combining these results with the search for slepton pair production in the SUGRA framework from ABDALLAH 03M to cover prompt decays The above limit is reached for prompt decays and assumes the degeneracy of the sleptons. For limits at different m($\tilde{G}$), see their Fig. 9. Supersedes the results of ABREU 01G.

[4] ACHARD 02 searches for the production of sparticles in the case of $R\!\!\!/$ prompt decays with $LL\overline{E}$ or $\overline{UDD}$ couplings at $\sqrt{s}$=189–208 GeV. The search is performed for direct and indirect decays, assuming one coupling at the time to be nonzero. The MSUGRA limit results from a scan over the MSSM parameter space with the assumption of gaugino and scalar mass unification at the GUT scale and no mixing in the slepton sector, imposing simultaneously the exclusions from neutralino, chargino, sleptons, and squarks analyses. The limit holds for $LL\overline{E}$ couplings and increases to 88.7 GeV for $\overline{UDD}$ couplings. For L3 limits from $LQ\overline{D}$ couplings, see ACCIARRI 01.

[5] ABBIENDI 01 looked for final states with $\gamma\gamma\not{E}$, $\ell\ell\not{E}$, with possibly additional activity and four leptons + $\not{E}$ to search for prompt decays of $\tilde{\chi}_1^0$ or $\tilde{\ell}_1$ in GMSB. They derive limits in the plane ($m_{\tilde{\chi}_1^0}$,$m_{\tilde{\tau}_1}$), see Fig. 6, allowing either the $\tilde{\chi}_1^0$ or a $\tilde{\ell}_1$ to be the NLSP. Two scenarios are considered: tanβ=2 with the 3 sleptons degenerate in mass and tanβ=20 where the $\tilde{\tau}_1$ is lighter than the other sleptons. Data taken at $\sqrt{s}$=189 GeV. For tanβ=20, the obtained limits are $m_{\tilde{\tau}_1} > 69$ GeV and $m_{\tilde{e}_1,\tilde{\mu}_1} > 88$ GeV.

[6] ABREU 01 looked for acoplanar dilepton + diphoton + $\not{E}$ final states from $\tilde{\ell}$ cascade decays at $\sqrt{s}$=130–189 GeV. See Fig. 9 for limits on the (μ,M_2) plane for $m_{\tilde{\ell}}$=80 GeV, tanβ=1.0, and assuming degeneracy of $\tilde{\mu}$ and $\tilde{e}$.

[7] ACCIARRI 01 searches for multi-lepton and/or multi-jet final states from $R\!\!\!/$ prompt decays with $LL\overline{E}$, $LQ\overline{D}$, or $\overline{UDD}$ couplings at $\sqrt{s}$=189 GeV. The search is performed for direct and indirect decays of neutralinos, charginos, and scalar leptons, with the $\tilde{\chi}_1^0$ or a $\tilde{\ell}$ as LSP and assuming one coupling to be nonzero at a time. Mass limits are derived using simultaneously the constraints from the neutralino, chargino, and slepton analyses; and the Z^0 width measurements from ACCIARRI 00C in a scan of the parameter space assuming MSUGRA with gaugino and scalar mass universality. Updates and supersedes the results from ACCIARRI 99I.

[8] ABREU 00V use data from $\sqrt{s}$= 130–189 GeV to search for tracks with large impact parameter or visible decay vertices. Limits are obtained as function of $m_{\tilde{G}}$, after combining these results with the search for slepton pair production in the SUGRA framework from ABREU 01 to cover prompt decays and on stable particle searches from ABREU 00Q. For limits at different $m_{\tilde{G}}$, see their Fig. 12.

[9] The above limit assumes the degeneracy of stau and smuon.

Long-lived $\tilde{\ell}$ (Slepton) MASS LIMIT

Limits on scalar leptons which leave detector before decaying. Limits from Z decays are independent of lepton flavor. Limits from continuum e^+e^- annihilation are also independent of flavor for smuons and staus. Selectron limits from e^+e^- collisions in the continuum depend on MSSM parameters because of the additional neutralino exchange contribution.

VALUE (GeV)	CL%	DOCUMENT ID		TECN	COMMENT
> 98	95	[1] ABBIENDI	03L	OPAL	$\tilde{\mu}_R$, $\tilde{\tau}_R$
none 2–87.5	95	[2] ABREU	00Q	DLPH	$\tilde{\mu}_R$, $\tilde{\tau}_R$
> 81.2	95	[3] ACCIARRI	99H	L3	$\tilde{\mu}_R$, $\tilde{\tau}_R$
> 81	95	[4] BARATE	98K	ALEP	$\tilde{\mu}_R$, $\tilde{\tau}_R$
• • • We do not use the following data for averages, fits, limits, etc. • • •					
>300	95	[5] AAD	13AA	ATLS	long-lived $\tilde{\tau}$, GMSB, tanβ = 5–20
		[6] ABAZOV	13B	D0	long-lived $\tilde{\tau}$, 100 <$m_{\tilde{\tau}}$ <300 GeV
>339	95	[7,8] CHATRCHYAN	13AB	CMS	long-lived $\tilde{\tau}$, direct $\tilde{\tau}_1$ pair prod., minimal GMSB, SPS line 7
>500	95	[7,9] CHATRCHYAN	13AB	CMS	long-lived $\tilde{\tau}$, $\tilde{\tau}_1$ from direct pair prod. and from decay of heavier SUSY particles, minimal GMSB, SPS line 7
>314	95	[10] CHATRCHYAN	12L	CMS	long-lived $\tilde{\tau}$, $\tilde{\tau}_1$ from decay of heavier SUSY particles, minimal GMSB, SPS line 7
>136	95	[11] AAD	11P	ATLS	stable $\tilde{\tau}$, GMSB scenario, tanβ=5

[1] ABBIENDI 03L used e^+e^- data at $\sqrt{s}$ = 130–209 GeV to select events with two high momentum tracks with anomalous dE/dx. The excluded cross section is compared to the theoretical expectation as a function of the heavy particle mass in their Fig. 3. The limit improves to 98.5 GeV for $\tilde{\mu}_L$ and $\tilde{\tau}_L$. The bounds are valid for colorless spin 0 particles with lifetimes longer than 10^{-6} s. Supersedes the results from ACKERSTAFF 98P.

[2] ABREU 00Q searches for the production of pairs of heavy, charged stable particles in e^+e^- annihilation at $\sqrt{s}$= 130–189 GeV. The upper bound improves to 88 GeV for $\tilde{\mu}_L$, $\tilde{\tau}_L$. These limits include and update the results of ABREU 98P.

[3] ACCIARRI 99H searched for production of pairs of back-to-back heavy charged particles at $\sqrt{s}$=130–183 GeV. The upper bound improves to 82.2 GeV for $\tilde{\mu}_L$, $\tilde{\tau}_L$.

[4] The BARATE 98K mass limit improves to 82 GeV for $\tilde{\mu}_L$,$\tilde{\tau}_L$. Data collected at $\sqrt{s}$=161–184 GeV.

[5] AAD 13AA searched in 4.7 fb^{-1} of pp collisions at $\sqrt{s}$ = 7 TeV for events containing long-lived massive particles in a GMSB framework. No significant excess above the expected background was found. A 95% C.L. lower limit of 300 GeV is placed on long-lived $\tilde{\tau}$'s in the GMSB model with $M_{mess} = 250$ TeV, $N_S = 3$, $\mu > 0$, for tanβ = 5–20. The lower limit on the GMSB breaking scale Λ was found to be 99–110 TeV, for tanβ values between 5 and 40, see Fig. 4 (top). Also, directly produced long-lived sleptons, or sleptons decaying to long-lived ones, are excluded at 95% C.L. up to a $\tilde{\tau}$ mass of 278 GeV for models with slepton splittings smaller than 50 GeV.

[6] ABAZOV 13B looked in 6.3 fb^{-1} of $p\overline{p}$ collisions at $\sqrt{s}$ = 1.96 TeV for charged massive long-lived particles in events with muon-like particles that have both speed and ionization energy loss inconsistent with muons produced in beam collisions. In the absence of an excess, limits are set at 95% C.L. on the production cross section of stau leptons in the mass range 100–300 GeV, see their Table 20 and Fig. 23.

[7] CHATRCHYAN 13AB looked in 5.0 fb^{-1} of pp collisions at $\sqrt{s}$ = 7 TeV and in 18.8 fb^{-1} of pp collisions at $\sqrt{s}$ = 8 TeV for events with heavy stable particles, identified by their anomalous dE/dx in the tracker or additionally requiring that it be identified as muon in the muon chambers, from pair production of $\tilde{\tau}_1$'s. No evidence for an excess over the expected background is observed. Supersedes CHATRCHYAN 12L.

[8] CHATRCHYAN 13AB limits are derived for pair production of $\tilde{\tau}_1$ as a function of mass in minimal GMSB scenarios along the Snowmass Points and Slopes (SPS) line 7 (see Fig. 8 and Table 7). The limit given here is valid for direct pair $\tilde{\tau}_1$ production.

[9] CHATRCHYAN 13AB limits are derived for the production of $\tilde{\tau}_1$ as a function of mass in minimal GMSB scenarios along the Snowmass Points and Slopes (SPS) line 7 (see Fig. 8 and Table 7). The limit given here is valid for the production of $\tilde{\tau}_1$ from both direct pair production and from the decay of heavier supersymmetric particles.

[10] CHATRCHYAN 12L looked in 5.0 fb^{-1} of pp collisions at $\sqrt{s}$ = 7 TeV for events with heavy stable particles, identified by their anomalous dE/dx in the tracker or additionally requiring that it be identified as muon in the muon chambers, from pair production of $\tilde{\tau}_1$'s. No evidence for an excess over the expected background is observed. Limits are derived for the production of $\tilde{\tau}_1$ as a function of mass in minimal GMSB scenarios along the Snowmass Points and Slopes (SPS) line 7 (see Fig. 3). The limit given here is valid for the production of $\tilde{\tau}_1$ in the decay of heavier supersymmetric particles.

[11] AAD 11P looked in 37 pb^{-1} of pp collisions at $\sqrt{s}$ = 7 TeV for events with two heavy stable particles, reconstructed in the Inner tracker and the Muon System and identified by their time of flight in the Muon System. No evidence for an excess over the SM expectation is observed. Limits on the mass are derived, see Fig. 3, for $\tilde{\tau}$ in a GMSB scenario and for sleptons produced by electroweak processes only, in which case the limit degrades to 110 GeV.

$\tilde{q}$ (Squark) MASS LIMIT

For $m_{\tilde{q}} > 60$–70 GeV, it is expected that squarks would undergo a cascade decay via a number of neutralinos and/or charginos rather than undergo a direct decay to photinos as assumed by some papers. Limits obtained when direct decay is assumed are usually higher than limits when cascade decays are included.

Limits from e^+e^- collisions depend on the mixing angle of the lightest mass eigenstate $\tilde{q}_1 = \tilde{q}_R \sin\theta_q + \tilde{q}_L \cos\theta_q$. It is usually assumed that only the sbottom and stop squarks have non-trivial mixing angles (see the stop and sbottom sections). Here, unless otherwise noted, squarks are always taken to be either left/right degenerate, or purely of left or right type. Data from Z decays have set squark mass limits above 40 GeV, in the case of $\tilde{q} \to q\tilde{\chi}_1$ decays if $\Delta m = m_{\tilde{q}} - m_{\tilde{\chi}_1^0} \gtrsim 5$ GeV. For smaller values of Δm, current constraints on the invisible width of the Z ($\Delta\Gamma_{\rm inv} < 2.0$ MeV, LEP 00) exclude $m_{\tilde{u}_{L,R}}$ <44 GeV, $m_{\tilde{d}_R}$ <33 GeV, $m_{\tilde{d}_L}$ <44 GeV and, assuming all squarks degenerate, $m_{\tilde{q}}$ <45 GeV.

Limits made obsolete by the most recent analyses of e^+e^-, $p\overline{p}$, and ep collisions can be found in previous Editions of this *Review*.

VALUE (GeV)	CL%	DOCUMENT ID		TECN	COMMENT
>1110	**(CL = 95%) OUR EVALUATION**				
>1360	95	[1] AAD	13L	ATLS	jets + $\not{E}_T$, CMSSM, $m_{\tilde{g}} = m_{\tilde{q}}$
>1200	95	[2] AAD	13Q	ATLS	γ+b+$\not{E}_T$,higgsino-like neutralino, $m_{\tilde{\chi}_1^0}$ > 220 GeV, GMSB
		[3] CHATRCHYAN	13	CMS	$\ell^\pm\ell^\mp$ + jets + $\not{E}_T$, CMSSM
>1250	95	[4] CHATRCHYAN	13G	CMS	0,1,2, ≥ 3 b-jets + $\not{E}_T$, CMSSM, $m_{\tilde{q}} = m_{\tilde{g}}$
>1430	95	[5] CHATRCHYAN	13H	CMS	2γ + ≥ 4 jets + low $\not{E}_T$, stealth SUSY model
> 750	95	[6] CHATRCHYAN	13T	CMS	jets + $\not{E}_T$, $\tilde{q} \to q\tilde{\chi}_1^0$ simplified model, $m_{\tilde{\chi}_1^0}$= 0 GeV
> 820	95	[7] AAD	12AX	ATLS	ℓ +jets +$\not{E}_T$, CMSSM, $m_{\tilde{q}}$=$m_{\tilde{g}}$
>1200	95	[8] AAD	12CJ	ATLS	$\ell^\pm$+jets+$\not{E}_T$, CMSSM, $m_{\tilde{q}}$=$m_{\tilde{g}}$
> 870	95	[9] AAD	12CP	ATLS	2γ +$\not{E}_T$, GMSB, bino NLSP, $m_{\tilde{\chi}_1^0}$ > 50 GeV
> 950	95	[10] AAD	12W	ATLS	jets + $\not{E}_T$, CMSSM, $m_{\tilde{q}} = m_{\tilde{g}}$
		[11] CHATRCHYAN	12	CMS	e, μ, jets, razor, CMSSM
> 760	95	[12] CHATRCHYAN	12AE	CMS	jets + $\not{E}_T$, $\tilde{q} \to q\tilde{\chi}_1^0$, $m_{\tilde{\chi}_1^0}$ < 200 GeV
		[13] CHATRCHYAN	12AL	CMS	≥ 3$\ell^\pm$, $R\!\!\!/$
>1110	95	[14] CHATRCHYAN	12AT	CMS	jets + $\not{E}_T$, CMSSM
>1180	95	[14] CHATRCHYAN	12AT	CMS	jets + $\not{E}_T$, CMSSM, $m_{\tilde{q}}$=$m_{\tilde{g}}$
> 690	95	[15] AAD	11B	ATLS	$\ell^\pm\ell^\pm$+$\not{E}_T$, $m_{\tilde{g}}$=$m_{\tilde{q}}$+10GeV, $m_{\tilde{\chi}_1^0}$=100GeV, tanβ=4
> 550	95	[15] AAD	11B	ATLS	$\ell^+\ell^-$+$\not{E}_T$, $m_{\tilde{g}}$=$m_{\tilde{q}}$+10GeV, $m_{\tilde{\chi}_1^0}$=100GeV, tanβ=4

> 558	95	[16] AAD	11C	ATLS	$\ell^+\ell^-$+jets+$\not{E}_T$, $m_{\widetilde{g}}=m_{\widetilde{q}}$+10GeV, $m_{\widetilde{\chi}^0_1}$=100GeV, tanβ=4	
> 700	95	[17] AAD	11G	ATLS	ℓ+jets+$\not{E}_T$, tanβ=3, A_0=0, $\mu>0$, $m_{\widetilde{g}}=m_{\widetilde{q}}$	
> 870	95	[18] AAD	11N	ATLS	jets+$\not{E}_T$, degenerate $m_{\widetilde{q}}$ of first two generations, $m_{\widetilde{\chi}^0_1}$=0, all other supersymmetric particles heavy, $m_{\widetilde{q}}=m_{\widetilde{g}}$	
> 775	95	[18] AAD	11N	ATLS	jets+$\not{E}_T$, CMSSM, $m_{\widetilde{q}}=m_{\widetilde{g}}$	
>1100	95	[19] CHATRCHYAN	11W	CMS	jets + $\not{E}_T$, CMSSM	
> 392	95	[20] AALTONEN	09S	CDF	jets+$\not{E}_T$, $m_{\widetilde{q}}=m_{\widetilde{g}}$	
> 379	95	[21] ABAZOV	08G	D0	jets+$\not{E}_T$, tanβ=3, μ<0, A_0=0, any $m_{\widetilde{g}}$	
> 99.5		[22] ACHARD	04	L3	Δm >10 GeV, $e^+e^-\to \widetilde{q}_{L,R}\overline{\widetilde{q}}_{L,R}$	
> 97		[22] ACHARD	04	L3	Δm >10 GeV, $e^+e^-\to \widetilde{q}_R\overline{\widetilde{q}}_R$	
> 138	95	[23] ABBOTT	01D	D0	$\ell\ell$+jets+$\not{E}_T$, tanβ < 10, m_0 < 300 GeV, μ < 0, A_0=0	
> 255	95	[23] ABBOTT	01D	D0	tanβ=2, $m_{\widetilde{g}}=m_{\widetilde{q}}$, μ <0, A_0=0, $\ell\ell$+jets+$\not{E}_T$	
> 97	95	[24] BARATE	01	ALEP	$e^+e^-\to \widetilde{q}\overline{\widetilde{q}}$, Δm > 6 GeV	
> 224	95	[25] ABE	96D	CDF	$m_{\widetilde{g}} \le m_{\widetilde{q}}$; with cascade decays, $\ell\ell$+jets+$\not{E}_T$	

• • • We do not use the following data for averages, fits, limits, etc. • • •

> 700	95	[26] CHATRCHYAN	13AO	CMS	$\ell^\pm\ell^\mp$ + jets + $\not{E}_T$, CMSSM, m_0 < 700 GeV	
>1350	95	[27] CHATRCHYAN	13AV	CMS	jets (+ leptons) + $\not{E}_T$, CMSSM, $m_{\widetilde{g}}=m_{\widetilde{q}}$	
> 800	95	[28] CHATRCHYAN	13W	CMS	$\ge$ 1 photons + jets + $\not{E}_T$, GGM, wino-like NLSP, $m_{\widetilde{\chi}^0_1}$ = 375 GeV	
>1000	95	[28] CHATRCHYAN	13W	CMS	$\ge$ 2 photons + jets + $\not{E}_T$, GGM, bino-like NLSP, $m_{\widetilde{\chi}^0_1}$ = 375 GeV	
> 340	95	[29] DREINER	12A	THEO	$m_{\widetilde{q}} \sim m_{\widetilde{\chi}^0_1}$	
> 650	95	[30] DREINER	12A	THEO	$m_{\widetilde{q}}=m_{\widetilde{g}} \sim m_{\widetilde{\chi}^0_1}$	
		[31] AAD	11AE	ATLS	$\ell^\pm\ell^\pm$	
		[32] AAD	11AF	ATLS	$\ge$ 6 jets + $\not{E}_T$, CMSSM	
> 290	95	[33] AARON	11	H1	$e^-p\to \widetilde{d}_R$, $\not{R}$, $L\,Q\overline{D}$,λ'=0.3	
> 275	95	[33] AARON	11	H1	$e^+p\to \widetilde{u}_L$, $\not{R}$, $L\,Q\overline{D}$, λ'=0.3	
> 330	95	[34] AARON	11C	H1	$\widetilde{u}$, $\not{R}$, $L\,Q\overline{D}$, λ'=0.3	
		[35] CHATRCHYAN	11AC	CMS	jets + $\not{E}_T$, CMSSM	
		[36] CHATRCHYAN	11C	CMS	$\widetilde{q}\to X\widetilde{\chi}^0_2\to X\ell^+\ell^-\widetilde{\chi}^0_1$	
		[37] CHATRCHYAN	11G	CMS	$\widetilde{\chi}^0_1\to \gamma\widetilde{G}$	
		[38] CHATRCHYAN	11Q	CMS	ℓ + jets + $\not{E}_T$	
> 830	95	[39] CHATRCHYAN	11V	CMS	GMSB scenario, $\overline{\ell}$ co-NLSP	
		[40] CHATRCHYAN	11V	CMS	$\not{R}$	
		[41] KHACHATRY...	11I	CMS	jets + $\not{E}_T$	
		[42] ABAZOV	09S	D0	jets+τ+$\not{E}_T$, tanβ=15, μ <0, A_0=$-2m_0$	
> 490	95	[43] SCHAEL	07A	ALEP	$\widetilde{d}_R$, $\not{R}$, λ=0.3	
> 544	95	[43] SCHAEL	07A	ALEP	$\widetilde{s}_R$, $\not{R}$, λ=0.3	
> 273	95	[44] CHEKANOV	05A	ZEUS	$\widetilde{q}\to \mu q$, $\not{R}$, $L\,Q\overline{D}$, λ=0.3	
> 270	95	[44] CHEKANOV	05A	ZEUS	$\widetilde{q}\to \tau q$, $\not{R}$, $L\,Q\overline{D}$, λ=0.3	
> 275		[45] AKTAS	04D	H1	$e^\pm p\to \widetilde{U}_L$, $\not{R}$, $L\,Q\overline{D}$	
> 280		[45] AKTAS	04D	H1	$e^\pm p\to \widetilde{D}_R$, $\not{R}$, $L\,Q\overline{D}$	
		[46] ADLOFF	03	H1	$e^\pm p\to \widetilde{q}$, $\not{R}$, $L\,Q\overline{D}$	
> 276	95	[47] CHEKANOV	03B	ZEUS	$\widetilde{d}\to e^-u,\nu d$,$\not{R}$,$L\,Q\overline{D}$,$\lambda$ >0.1	
> 260	95	[47] CHEKANOV	03B	ZEUS	$\widetilde{u}\to e^+d$,$\not{R}$,$L\,Q\overline{D}$,λ >0.1	
> 82.5	95	[48] HEISTER	03G	ALEP	$\widetilde{u}_R$,$\not{R}$ decay	
> 77	95	[48] HEISTER	03G	ALEP	$\widetilde{d}_R$,$\not{R}$ decay	
> 240	95	[49] ABAZOV	02F	D0	$\widetilde{q}$, $\not{R}$ λ'_{2jk} indirect decays, tanβ=2, any $m_{\widetilde{g}}$	
> 265	95	[49] ABAZOV	02F	D0	$\widetilde{q}$, $\not{R}$ λ'_{2jk} indirect decays, tanβ=2, $m_{\widetilde{q}}=m_{\widetilde{g}}$	
		[50] ABAZOV	02G	D0	$p\overline{p}\to \widetilde{g}\widetilde{g}$, $\widetilde{g}\widetilde{q}$	
none 80–121	95	[51] ABBIENDI	02	OPAL	$e\gamma\to \widetilde{u}_L$, $\not{R}$ $L\,Q\overline{D}$, λ=0.3	
none 80–158	95	[51] ABBIENDI	02	OPAL	$e\gamma\to \widetilde{d}_R$, $\not{R}$ $L\,Q\overline{D}$, λ=0.3	
none 80–185	95	[52] ABBIENDI	02B	OPAL	$e\gamma\to \widetilde{u}_L$, $\not{R}$ $L\,Q\overline{D}$, λ=0.3	
none 80–196	95	[52] ABBIENDI	02B	OPAL	$e\gamma\to \widetilde{d}_R$, $\not{R}$ $L\,Q\overline{D}$, λ=0.3	
> 79	95	[53] ACHARD	02	L3	$\widetilde{u}_R$, $\not{R}$ decays	
> 55	95	[53] ACHARD	02	L3	$\widetilde{d}_R$, $\not{R}$ decays	
> 263	95	[54] CHEKANOV	02	ZEUS	$\widetilde{u}_L\to \mu q$, $\not{R}$, $L\,Q\overline{D}$, λ=0.3	
> 258	95	[54] CHEKANOV	02	ZEUS	$\widetilde{u}_L\to \tau q$, $\not{R}$, $L\,Q\overline{D}$, λ=0.3	
> 82	95	[55] BARATE	01B	ALEP	$\widetilde{u}_R$, $\not{R}$ decays	
> 68	95	[55] BARATE	01B	ALEP	$\widetilde{d}_R$, $\not{R}$ decays	
none 150–204	95	[56] BREITWEG	01	ZEUS	$e^+p\to \widetilde{d}_R$, $\not{R}$ $L\,Q\overline{D}$, λ=0.3	
> 200	95	[57] ABBOTT	00C	D0	$\widetilde{u}_L$, $\not{R}$, λ'_{2jk} decays	
> 180	95	[57] ABBOTT	00C	D0	$\widetilde{d}_R$, $\not{R}$, λ'_{2jk} decays	
> 390	95	[58] ACCIARRI	00P	L3	$e^+e^-\to q\overline{q}$, $\not{R}$, λ=0.3	
> 148	95	[59] AFFOLDER	00K	CDF	$\widetilde{d}_L$, $\not{R}$ λ'_{ij3} decays	
> 200	95	[60] BARATE	00I	ALEP	$e^+e^-\to q\overline{q}$, $\not{R}$, λ=0.3	
none 150–269	95	[61] BREITWEG	00E	ZEUS	$e^+p\to \widetilde{u}_L$, $\not{R}$, $L\,Q\overline{D}$, λ=0.3	
> 240	95	[62] ABBOTT	99	D0	$\widetilde{q}\to \widetilde{\chi}^0_2X\to \widetilde{\chi}^0_1\gamma X$, $m_{\widetilde{\chi}^0_2}-m_{\widetilde{\chi}^0_1}$ > 20 GeV	
> 320	95	[62] ABBOTT	99	D0	$\widetilde{q}\to \widetilde{\chi}^0_1X\to \widetilde{G}\gamma X$	
> 243	95	[63] ABBOTT	99K	D0	any $m_{\widetilde{g}}$, $\not{R}$, tanβ=2, μ < 0	
> 250	95	[64] ABBOTT	99L	D0	tanβ=2, μ <0, A=0, jets+$\not{E}_T$	
> 200	95	[65] ABE	99M	CDF	$p\overline{p}\to \widetilde{q}\overline{q}$, $\not{R}$	
none 80–134	95	[66] ABREU	99G	DLPH	$e\gamma\to \widetilde{u}_L$, $\not{R}$ $L\,Q\overline{D}$, λ=0.3	
none 80–161	95	[66] ABREU	99G	DLPH	$e\gamma\to \widetilde{d}_R$, $\not{R}$ $L\,Q\overline{D}$, λ=0.3	
> 225	95	[67] ABBOTT	98E	D0	$\widetilde{u}_L$, $\not{R}$, λ'_{1jk} decays	
> 204	95	[67] ABBOTT	98E	D0	$\widetilde{d}_R$, $\not{R}$, λ'_{1jk} decays	
> 79	95	[67] ABBOTT	98E	D0	$\widetilde{d}_L$, $\not{R}$, λ'_{ijk} decays	
> 202	95	[68] ABE	98S	CDF	$\widetilde{u}_L$, $\not{R}$ λ'_{2jk} decays	
> 160	95	[68] ABE	98S	CDF	$\widetilde{d}_R$, $\not{R}$ λ'_{2jk} decays	
> 140	95	[69] ACKERSTAFF	98V	OPAL	$e^+e^-\to q\overline{q}$, $\not{R}$, λ=0.3	
> 77	95	[70] BREITWEG	98	ZEUS	$m_{\widetilde{q}}=m_{\widetilde{e}}$, $m(\widetilde{\chi}^0_1)$= 40 GeV	
		[71] DATTA	97	THEO	$\widetilde{\nu}$'s lighter than $\widetilde{\chi}^\pm_1$, $\widetilde{\chi}^0_2$	
> 216	95	[72] DERRICK	97	ZEUS	$ep\to \widetilde{q}$, $\widetilde{q}\to \mu j$ or τj, $\not{R}$	
none 130–573	95	[73] HEWETT	97	THEO	$q\widetilde{g}\to \widetilde{q}$, $\widetilde{q}\to q\widetilde{g}$, with a light gluino	
none 190–650	95	[74] TEREKHOV	97	THEO	$qg\to \widetilde{q}\widetilde{g}$, $\widetilde{q}\to q\widetilde{g}$, with a light gluino	
> 63	95	[75] AID	96C	H1	$m_{\widetilde{q}}=m_{\widetilde{e}}$, $m_{\widetilde{\chi}^0_1}$=35 GeV	
none 330–400	95	[76] TEREKHOV	96	THEO	$ug\to \widetilde{u}\widetilde{g}$, $\widetilde{u}\to u\widetilde{g}$ with a light gluino	
> 176	95	[77] ABACHI	95C	D0	Any $m_{\widetilde{g}}$ <300 GeV; with cascade decays	
		[78] ABE	95T	CDF	$\widetilde{q}\to \widetilde{\chi}^0_2\to \widetilde{\chi}^0_1\gamma$	
> 90	90	[79] ABE	92L	CDF	Any $m_{\widetilde{g}}$ <410 GeV; with cascade decay	
> 100		[80] ROY	92	RVUE	$p\overline{p}\to \widetilde{q}\overline{q}$; $\not{R}$	
		[81] NOJIRI	91	COSM		

[1] AAD 13L searched in 4.7 fb^{-1} of pp collisions at $\sqrt{s}$ = 7 TeV for the production of squarks and gluinos in events containing jets, missing transverse momentum and no high-p_T electrons or muons. No excess over the expected SM background is observed. In mSUGRA/CMSSM models with tanβ = 10, A_0 = 0 and μ > 0, squarks and gluinos of equal mass are excluded for masses below 1360 GeV at 95% C.L. In a simplified model containing only squarks of the first two generations, a gluino octet and a massless neutralino, squark masses below 1320 GeV are excluded at 95% C.L. for gluino masses below 2 TeV. See Figures 10–15 for more precise bounds.

[2] AAD 13Q searched in 4.7 fb^{-1} of pp collisions at $\sqrt{s}$ = 7 TeV for events containing a high-p_T isolated photon, at least one jet identified as originating from a bottom quark, and high missing transverse momentum. Such signatures may originate from supersymmetric models with gauge-mediated supersymmetry breaking in events in which one of a pair of higgsino-like neutralinos decays into a photon and a gravitino while the other decays into a Higgs boson and a gravitino. No significant excess above the expected background was found and limits were set on the squark mass as a function of the neutralino mass in a generalized GMSB model (GGM) with a higgsino-like neutralino NLSP, see their Fig. 4. For neutralino masses greater than 220 GeV, squark masses below 1020 GeV are excluded at 95% C.L.

[3] CHATRCHYAN 13 looked in 4.98 fb^{-1} of pp collisions at $\sqrt{s}$ = 7 TeV for events with two opposite-sign leptons (e, μ, τ), jets and missing transverse energy. No excess beyond the Standard Model expectation is observed. Exclusion limits are derived in the mSUGRA/CMSSM model with tanβ = 10, A_0 = 0 and μ > 0, see Fig. 6.

[4] CHATRCHYAN 13G searched in 4.98 fb^{-1} of pp collisions at $\sqrt{s}$ = 7 TeV for the production of squarks and gluinos in events containing 0,1,2, $\ge$ 3 b-jets, missing transverse momentum and no electrons or muons. No excess over the expected SM background is observed. In mSUGRA/CMSSM models with tanβ = 10, A_0 = 0, and μ > 0, squarks and gluinos of equal mass are excluded for masses below 1250 GeV at 95% C.L. Exclusions are also derived in various simplified models, see Fig. 7.

[5] CHATRCHYAN 13H searched in 4.96 fb^{-1} of pp collisions at $\sqrt{s}$ = 7 TeV for events with two photons, $\ge$ 4 jets and low $\not{E}_T$ due to $\widetilde{q}\to \gamma\widetilde{\chi}^0_1$ decays in a stealth SUSY framework, where the $\widetilde{\chi}^0_1$ decays through a singlino ($\widetilde{S}$) intermediate state to $\gamma S\,\widetilde{G}$, with the singlet state S decaying to two jets. No significant excess above the expected background was found and limits were set in a particular R-parity conserving stealth SUSY model. The model assumes $m_{\widetilde{\chi}^0_1}$ = 0.5 $m_{\widetilde{q}}$, $m_{\widetilde{S}}$ = 100 GeV and m_S = 90 GeV. Under these assumptions, squark masses less than 1430 GeV were excluded at the 95% C.L.

[6] CHATRCHYAN 13T searched in 11.7 fb^{-1} of pp collisions at $\sqrt{s}$ = 8 TeV for events with at least two energetic jets and significant $\not{E}_T$, using the α_T variable to discriminate between processes with genuine and misreconstructed $\not{E}_T$. No significant excess above the Standard Model expectations is observed. Limits are set on squark masses in simplified models where the decay $\widetilde{q}\to q\widetilde{\chi}^0_1$ takes place with a branching ratio of 100%, assuming an eightfold degeneracy of the masses of the first two generation squarks, see Fig. 8 and Table 9. Also limits in the case of a single light squark are given.

[7] AAD 12AX searched in 1.04 fb^{-1} of pp collisions at $\sqrt{s}$ = 7 TeV for supersymmetry in events containing jets, missing transverse momentum and one isolated electron or muon. No excess over the expected SM background is observed and model-independent limits are set on the cross section of new physics contributions to the signal regions. In mSUGRA/CMSSM models with tanβ = 10, A_0 = 0 and μ > 0, squarks and gluinos of equal mass are excluded for masses below 820 GeV at 95% C.L. Limits are also set on simplified models for squark production and decay via an intermediate chargino and on supersymmetric models with bilinear R-parity violation. Supersedes AAD 11G.

[8] AAD 12CJ searched in 4.7 fb^{-1} of pp collisions at $\sqrt{s}$ = 7 TeV for events containing one or more isolated leptons (electrons or muons), jets and $\not{E}_T$. The observations are in good agreement with the SM expectations and exclusion limits have been set in number of SUSY models. In the mSUGRA/CMSSM model with tanβ = 10, A_0 = 0, and μ > 0, 95% C.L. exclusion limits have been derived for $m_{\widetilde{q}}$ < 1200 GeV, assuming equal squark and gluino masses. In minimal GMSB, values of the effective SUSY breaking scale Λ < 50 TeV are excluded at 95% C.L. for tanβ < 45. Also exclusion limits in a number of simplified models have been presented, see Figs. 10 and 12.

[9] AAD 12CP searched in 4.8 fb^{-1} of pp collisions at $\sqrt{s}$ = 7 TeV for events with two photons and large $\not{E}_T$ due to $\widetilde{\chi}^0_1 \rightarrow \gamma\widetilde{G}$ decays in a GMSB framework. No significant excess above the expected background was found and limits were set on the squark mass as a function of the neutralino mass in a generalized GMSB model (GGM) with a bino-like neutralino NLSP. The other sparticle masses were decoupled, tanβ = 2 and $c\tau_{NLSP}$ < 0.1 mm. Also, in the framework of the SPS8 model, a 95% C.L. lower limit was set on the breaking scale Λ of 196 TeV.

[10] AAD 12W searched in 1.04 fb^{-1} of pp collisions at $\sqrt{s}$ = 7 TeV for the production of squarks and gluinos in events containing jets, missing transverse momentum and no electrons or muons. No excess over the expected SM background is observed. In mSUGRA/CMSSM models with tanβ = 10, A_0 = 0 and μ > 0, squarks and gluinos of equal mass are excluded for masses below 950 GeV at 95% C.L. In a simplified model containing only squarks of the first two generations, a gluino octet and a massless neutralino, squark masses below 875 GeV are excluded at 95% C.L.

[11] CHATRCHYAN 12 looked in 35 pb^{-1} of pp collisions at $\sqrt{s}$ = 7 TeV for events with e and/or μ and/or jets, a large total transverse energy, and $\not{E}_T$. The event selection is based on the dimensionless razor variable R, related to the $\not{E}_T$ and M_R, an indicator of the heavy particle mass scale. No evidence for an excess over the expected background is observed. Limits are derived in the CMSSM (m_0, $m_{1/2}$) plane for tanβ = 3, 10 and 50 (see Fig. 7 and 8). Limits are also obtained for Simplified Model Spectra.

[12] CHATRCHYAN 12AE searched in 4.98 fb^{-1} of pp collisions at $\sqrt{s}$ = 7 TeV for events with at least three jets and large missing transverse momentum. No significant excesses over the expected SM backgrounds are observed and 95% C.L. limits on the production cross section of squarks in a scenario where $\widetilde{q} \rightarrow q\widetilde{\chi}^0_1$ with a 100% branching ratio, see Fig. 3. For $m_{\widetilde{\chi}^0_1}$ < 200 GeV, values of $m_{\widetilde{q}}$ below 760 GeV are excluded at 95% C.L. Also limits in the CMSSM are presented, see Fig. 2.

[13] CHATRCHYAN 12AL looked in 4.98 fb^{-1} of pp collisions at $\sqrt{s}$ = 7 TeV for anomalous production of events with three or more isolated leptons. Limits on squark and gluino masses are set in $R\!\!\!/$ SUSY models with leptonic $LL\overline{E}$ couplings, λ_{123} > 0.05, and hadronic $\overline{UDD}$ couplings, λ''_{112} > 0.05 , see their Fig. 5. In the $\overline{UDD}$ case the leptons arise from supersymmetric cascade decays. A very specific supersymmetric spectrum is assumed. All decays are prompt.

[14] CHATRCHYAN 12AT searched in 4.73 fb^{-1} of pp collisions at $\sqrt{s}$ = 7 TeV for the production of squarks and gluinos in events containing jets, missing transverse momentum and no electrons or muons. No excess over the expected SM background is observed. In mSUGRA/CMSSM models with tanβ = 10, A_0 = 0 and μ > 0, squarks with masses below 1110 GeV are excluded at 95% C.L. Squarks and gluinos of equal mass are excluded for masses below 1180 GeV at 95% C.L. Exclusions are also derived in various simplified models, see Fig. 6.

[15] AAD 11B looked in 35 pb^{-1} of pp collisions at $\sqrt{s}$ = 7 TeV for events with same or opposite charge dileptons (e or μ) and $\not{E}_T$ from the production of squarks and gluinos with leptonic decays from $\widetilde{\chi}^\pm_1$ or $\widetilde{\chi}^0_2$. No evidence for an excess over the SM expectation is observed, and limits are derived in the CMSSM (m_0, $m_{1/2}$) plane (see Fig. 2) and in the ($m_{\widetilde{g}}$, $m_{\widetilde{q}}$) plane under the assumptions tanβ = 4, μ = 1.5 M, $m_{\widetilde{\chi}^0_2}$ = M - 100 GeV, $m_{\widetilde{\ell}_L}$ = M/2, $m_{\widetilde{\chi}^0_1}$ = 100 GeV, where M = min($m_{\widetilde{g}}$, $m_{\widetilde{q}}$) (see Fig. 3). The exclusion limit for a compressed spectrum is 590 GeV for the same charge and 450 GeV for the opposite charge events.

[16] AAD 11C looked in 35 pb^{-1} of pp collisions at $\sqrt{s}$ = 7 TeV for events with jets, same flavor opposite charge dileptons (e or μ) and $\not{E}_T$ from the production of squarks and gluinos with decays $\widetilde{q} \rightarrow q\widetilde{\chi}^0_2$ and $\widetilde{\chi}^0_2 \rightarrow \ell^+\ell^-\widetilde{\chi}^0_1$. No evidence for an excess over the SM expectation is observed, and a limit is derived in the ($m_{\widetilde{g}}$, $m_{\widetilde{q}}$) plane under the assumptions tanβ = 4, μ = 1.5 M, $m_{\widetilde{\chi}^0_2}$ = M - 100 GeV, $m_{\widetilde{\ell}_L}$ = M/2, $m_{\widetilde{\chi}^0_1}$ = 100 GeV, where M = min($m_{\widetilde{g}}$, $m_{\widetilde{q}}$). The excluded mass region is shown in a plane of ($m_{\widetilde{g}}$, $m_{\widetilde{q}}$), see their Fig. 3. The exclusion limit for a compressed spectrum is 503 GeV.

[17] AAD 11G looked in 35 pb^{-1} of pp collisions at $\sqrt{s}$ = 7 TeV for events with a single lepton (e or μ), jets and $\not{E}_T$ from the production of squarks and gluinos. No evidence for an excess over the SM expectation is observed, and a limit is derived in the CMSSM (m_0, $m_{1/2}$) plane for tanβ = 3, see Fig. 2.

[18] AAD 11N looked in 35 pb^{-1} of pp collisions at $\sqrt{s}$ = 7 TeV for events with $\geq$ 2 jets and $\not{E}_T$. Four signal regions were defined, and the background model was found to be in good agreement with the data. Limits are derived in the ($m_{\widetilde{g}}$, $m_{\widetilde{q}}$) plane (see Fig. 2) for a simplified model where degenerate masses of the squarks of the first two generations are assumed, $m_{\widetilde{\chi}^0_1}$ = 0, and all other masses including third generation squarks are set to 5 TeV. Limits are also derived in the CMSSM (m_0, $m_{1/2}$) plane (see Fig. 3) for tanβ = 3.

[19] CHATRCHYAN 11W looked in 1.14 fb^{-1} of pp collisions at $\sqrt{s}$ = 7 TeV for events with $\geq$ 2 jets, large total jet energy, and $\not{E}_T$. After combining multi-jet events into two pseudo-jets signal events are selected by a cut on $\alpha_T = E_T^{j_2}/M_T$, the transverse energy of the less energetic jet over the transverse mass. Given the lack of an excess over the SM backgrounds, limits are derived in the CMSSM (m_0, $m_{1/2}$) plane (see Fig. 4) for tanβ = 10. The limits are only weakly dependent on tanβ and A_0.

[20] AALTONEN 09S searched in 2 fb^{-1} of $p\overline{p}$ collisions at $\sqrt{s}$ = 1.96 TeV for events with at least 2 jets and $\not{E}_T$. No evidence for a signal is observed. A limit is derived for a mSUGRA scenario in the $m_{\widetilde{q}}$ versus $m_{\widetilde{g}}$ plane, see their Fig. 2. For $m_{\widetilde{g}}$ < 340 GeV the bound increases to 400 GeV.

[21] ABAZOV 08G looked in 2.1 fb^{-1} of $p\overline{p}$ collisions at $\sqrt{s}$=1.96 TeV for events with acoplanar jets or multijets with large $\not{E}_T$. No significant excess was found compared to the background expectation. A limit is derived on the masses of squarks and gluinos for specific MSUGRA parameter values, see Figure 3. Similar results would be obtained for a large class of parameter sets. Supersedes the results of ABAZOV 06C.

[22] ACHARD 04 search for the production of $\widetilde{q}\widetilde{q}$ of the first two generations in acoplanar di-jet final states in the 192–209 GeV data. Degeneracy of the squark masses is assumed either for both left and right squarks or for right squarks only, as well as B($\widetilde{q} \rightarrow q\widetilde{\chi}^0_1$) = 1 See Fig. 7 for the dependence of the limits on $m_{\widetilde{\chi}^0_1}$. This limit supersedes ACCIARRI 99V.

[23] ABBOTT 01D looked in $\sim$ 108 pb^{-1} of $p\overline{p}$ collisions at $\sqrt{s}$=1.8 TeV for events with ee, $\mu\mu$, or $e\mu$ accompanied by at least 2 jets and $\not{E}_T$. Excluded regions are obtained in the MSUGRA framework from a scan over the parameters 0<m_0 <300 GeV, 10<$m_{1/2}$ <110 GeV, and 1.2 <tanβ <10.

[24] BARATE 01 looked for acoplanar dijets + $\not{E}_T$ final states at 189 to 202 GeV. The limit assumes B($\widetilde{q} \rightarrow q\widetilde{\chi}^0_1$)=1, with $\Delta m = m_{\widetilde{q}} - m_{\widetilde{\chi}^0_1}$. It applies to tan$\beta$=4, μ=−400 GeV. See their Fig. 2 for the exclusion in the ($m_{\widetilde{q}}$,$m_{\widetilde{g}}$) plane. These limits include and update the results of BARATE 99Q.

[25] ABE 96D searched for production of gluinos and five degenerate squarks in final states containing a pair of leptons, two jets, and missing E_T. The two leptons arise from the semileptonic decays of charginos produced in the cascade decays. The limit is derived for fixed tanβ = 4.0, μ = −400 GeV, and m_{H^+} = 500 GeV, and with the cascade decays of the squarks and gluinos calculated within the framework of the Minimal Supergravity scenario.

[26] CHATRCHYAN 2013AO searched in 4.98 fb^{-1} of pp collisions at $\sqrt{s}$ = 7 TeV for events with two opposite-sign isolated leptons accompanied by hadronic jets and $\not{E}_T$. No significant excesses over the expected SM backgrounds are observed and 95% C.L. exclusion limits are derived in the mSUGRA/CMSSM model with tanβ = 10, A_0 = 0 and μ > 0, see Fig. 8.

[27] CHATRCHYAN 13AV searched in 4.7 fb^{-1} of pp collisions at $\sqrt{s}$ = 7 TeV for new heavy particle pairs decaying into jets (possibly b-tagged), leptons and $\not{E}_T$ using the Razor variables. No significant excesses over the expected SM backgrounds are observed and 95% C.L. exclusion limits are derived in the mSUGRA/CMSSM model with tanβ = 10, A_0 = 0 and μ > 0, see Fig. 3. The results are also interpreted in various simplified models, see Fig. 4.

[28] CHATRCHYAN 13W searched in 4.93 fb^{-1} of pp collisions at $\sqrt{s}$ = 7 TeV for events with one or more photons, hadronic jets and $\not{E}_T$. No significant excess above the Standard Model expectations is observed. Limits are set on squark masses in the general gauge-mediated SUSY breaking model (GGM), for both a wino-like and bino-like neutralino NLSP scenario, see Fig. 5.

[29] DREINER 12A reassesses constraints from CMS (at 7 TeV, $\sim$ 4.4 fb^{-1}) under the assumption that the fist and second generation squarks and the lightest SUSY particle are quasi-degenerate in mass (compressed spectrum).

[30] DREINER 12A reassesses constraints from CMS (at 7 TeV, $\sim$ 4.4 fb^{-1}) under the assumption that the first and second generation squarks, the gluino, and the lightest SUSY particle are quasi-degenerate in mass (compressed spectrum).

[31] AAD 11AE looked in 34 pb^{-1} of pp collisions at $\sqrt{s}$ = 7 TeV for events with $\geq$ 2 same charge isolated leptons (e, μ) and $\geq$ 1 jet. They are assumed to come from $\widetilde{q}\widetilde{q}$ production, where the $\widetilde{q}$ decays to $\widetilde{\chi}^\pm_1$ or $\widetilde{\chi}^0_2$ with equal branching ratios, followed by the decays $\widetilde{\chi}^\pm_1 \rightarrow W^\pm\widetilde{\chi}^0_1$ and $\widetilde{\chi}^0_2 \rightarrow Z^0\widetilde{\chi}^0_1$. No evidence for an excess over the expected background is observed. Limits are derived on the cross sections as a function of the masses of the $\widetilde{q}$, $\widetilde{\chi}^\pm_1/\widetilde{\chi}^0_2$ and $\widetilde{\chi}^0_1$ (see Fig. 9 and 10).

[32] AAD 11AF looked in 1.34 fb^{-1} of pp collisions at $\sqrt{s}$ = 7 TeV for events with 6 up to 8 jets and $\not{E}_T$. No evidence for an excess over the expected background is observed. Limits are derived in the CMSSM (m_0, $m_{1/2}$) plane for tanβ = 10 (see Fig. 5). The limit improves to $m_{\widetilde{g}}$ > 680 GeV for $m_{\widetilde{q}}$ = 2 $m_{\widetilde{g}}$.

[33] AARON 11 looked in 255 pb^{-1} of e^+p and 183 pb^{-1} of e^-p collisions at $\sqrt{s}$ = 319 GeV for events with at least 1 lepton and jets from R_p violation with $LQ\overline{D}$ couplings, assuming dominance of a single λ'_{ijk} coupling. No evidence for an excess over the SM expectation is observed, and limits are derived in the (λ', $m_{\widetilde{q}}$) plane for the MSSM with tanβ = 6, see their Figs. 7 and 8. Limits are also derived in a CMSSM-type scenario.

[34] AARON 11C looked in 281 pb^{-1} of e^+p and 165 pb^{-1} of e^-p collisions at $\sqrt{s}$ =319 GeV and $\sqrt{s}$ =301 GeV for contact interactions measured from deviations of the dσ/dQ^2 of neutral current events. They are interpreted in the framework of R-parity violation with $LQ\overline{D}$ couplings. No evidence for an excess over the SM expectation is observed, and limits are derived for $m_{\widetilde{q}}/\lambda'$, see Table 4.

[35] CHATRCHYAN 11AC looked in 36 pb^{-1} of pp collisions at $\sqrt{s}$ = 7 TeV for events with $\geq$ 3 jets, a large total transverse energy, and $\not{E}_T$. No evidence for an excess over the expected background is observed. Limits are derived in the CMSSM (m_0, $m_{1/2}$) plane and the ($m_{\widetilde{g}}$, $m_{\widetilde{q}}$) plane for tanβ = 10 (see Fig. 10). Limits are also obtained for Simplified Model Spectra.

[36] CHATRCHYAN 11C looked in 34 pb^{-1} of pp collisions at $\sqrt{s}$=7 TeV for events with opposite charge isolated dileptons (e or μ), jets and $\not{E}_T$ from pair production of $\widetilde{g}$ and $\widetilde{q}$. No evidence for an excess over the expected background is observed. Limits are derived in the CMSSM (m_0, $m_{1/2}$) plane for tanβ = 3 (see Fig. 4).

[37] CHATRCHYAN 11G looked in 36 pb^{-1} of pp collisions at $\sqrt{s}$ = 7 TeV for events with $\geq$ 2 isolated photons, $\geq$ 1 jet and $\not{E}_T$, which may arise in a generalized gauge mediated model from the decay of a $\widetilde{\chi}^0_1$ NLSP. No evidence for an excess over the expected background is observed. Limits are derived in the plane of squark versus gluino mass (see Fig. 4) for several values of $m_{\widetilde{\chi}^0_1}$.

[38] CHATRCHYAN 11Q looked in 36 pb^{-1} of pp collisions at $\sqrt{s}$ = 7 TeV for events with a single isolated lepton (e or μ), $\geq$ 4 jets and $\not{E}_T$. No evidence for an excess over the expected background is observed. Limits are derived in the CMSSM (m_0, $m_{1/2}$) plane for tanβ = 10 (see Fig. 7).

[39] CHATRCHYAN 11V looked in 35 pb^{-1} of pp collisions at $\sqrt{s}$ = 7 TeV for events with $\geq$ 3 isolated leptons (e, μ or τ), with or without jets and $\not{E}_T$. Multi-lepton final states originate from $\widetilde{q} \rightarrow \widetilde{\chi}^0 + X$, followed by $\widetilde{\chi}^0 \rightarrow \widetilde{\ell}^\pm\ell^\mp$ and $\widetilde{\ell} \rightarrow \ell\widetilde{G}$. No evidence for an excess over the expected background is observed. Limits are derived (see Fig. 4) for a GMSB-type scenario with mass-degenerate right-handed sleptons (slepton co-NLSP scenario).

[40] CHATRCHYAN 11V looked in 35 pb^{-1} of pp collisions at $\sqrt{s}$ = 7 TeV for events with $\geq$ 3 isolated leptons (e, μ or τ), with or without jets and $\not{E}_T$. No evidence for an excess over the expected background is observed. Limits are derived in the $R\!\!\!/$ framework (see

Fig. 4) in the ($m_{\widetilde{g}}$, $m_{\widetilde{q}}$) plane assuming the dominance of a λ_{122} or λ_{123} coupling, $m_{\widetilde{\chi}^0_1}$ = 300 GeV, $m_{\widetilde{\ell}}$ = 1000 GeV, and decoupled wino and Higgsino.

[41] KHACHATRYAN 11I looked in 35 pb^{-1} of pp collisions at $\sqrt{s}$ = 7 TeV for events with $\geq$ 2 jets and $\not\!\!E_T$. After combining multi-jet events into two pseudo-jets signal events are selected by a cut on $\alpha_T = E_T^{j_2}/M_T$, the transverse energy of the less energetic jet over the transverse mass. No evidence for an excess over the expected background is observed. Limits are derived in the CMSSM (m_0, $m_{1/2}$) plane (see Fig. 5) for tanβ = 3. Superseded by CHATRCHYAN 11W.

[42] ABAZOV 09S looked in 0.96 fb^{-1} of $p\overline{p}$ collisions at $\sqrt{s}$ = 1.96 TeV for events with at least 2 jets, a tau decaying hadronically and $\not\!\!E_T$ from the production $\widetilde{q}_L\,\widetilde{q}_R$, with the taus originating from the decay of a $\widetilde{\chi}^0_2$ or $\widetilde{\chi}^\pm_1$. The results were combined with ABAZOV 08G which searched for events with jets and $\not\!\!E_T$ without requiring taus. No evidence for an excess over the SM expectation is observed. The excluded region is shown for an mSUGRA model in a plane of $m_{1/2}$ versus m_0 in the "tau corridor," see their Figs. 5 and 6. The largest excluded squark mass in the corridor is 340 GeV for the tau analysis only and 410 GeV for the combined analysis.

[43] SCHAEL 07A studied the effect on hadronic cross sections and charge asymmetries of t-channel down-type squark exchange via R-parity violating couplings $LQ\overline{D}$ at $\sqrt{s}$ = 189–209 GeV. The limit here refers to the case j = 1, 2 and holds for λ'_{1jk} of electromagnetic strength. The results of this analysis are combined with BARATE 00I.

[44] CHEKANOV 05A search for lepton flavor violating processes $e^\pm p \to \ell X$, where $\ell = \mu$ or τ with high p_T, in 130 pb^{-1} at 300 and 318 GeV. Such final states may originate from LQD couplings with simultaneously non-zero λ'_{1jk} and λ'_{ijk} (i=2 or 3). The quoted mass bounds hold for a u-type squark, assume a λ' of electromagnetic strength and contributions from only direct squark decays. For d-type squarks the bounds are strengthened to 278 and 275 GeV for the μ and τ final states, respectively. Supersedes the results of CHEKANOV 02.

[45] AKTAS 04D looked in 77.8 pb^{-1} of $e^\pm p$ collisions at $\sqrt{s}$ = 319 GeV for resonant production of $\widetilde{q}$ by R-parity violating $LQ\overline{D}$ couplings assuming that one of the λ' couplings dominates over all others. They consider final states with or without leptons and/or jets and/or $\not\!\!p_T$ resulting from direct and indirect decays. They combine the channels to derive limits on λ'_{1j1} and λ'_{11k} as a function of the squark mass, see their Figs. 8 and 9, from a scan over the parameters 70 $< M_2 <$ 350 GeV, $-300 < \mu < 300$ GeV, tanβ = 6, for a fixed mass of 90 GeV for degenerate sleptons and an LSP mass $>$ 30 GeV. The quoted limits refer to $\lambda' = 0.3$, with U=u,c,t and D=d,s,b. Supersedes the results of ADLOFF 01B. Superseded by AARON 11.

[46] ADLOFF 03 looked for the s-channel production of squarks via $R\!\!\!/\ LQ\overline{D}$ couplings in 117.2 pb^{-1} of e^+p data at $\sqrt{s}$ = 301 and 319 GeV and of e^-p data at $\sqrt{s}$ = 319 GeV. The comparison of the data with the SM differential cross section allows limits to be set on couplings for processes mediated through contact interactions. They obtain lower bounds on the value of $m_{\widetilde{q}}/\lambda'$ of 710 GeV for the process $e^+\overline{u} \to \overline{\widetilde{d}}^k$ (and charge conjugate), mediated by λ'_{11k}, and of 430 GeV for the process $e^+d \to \widetilde{u}^j$ (and charge conjugate), mediated by λ'_{1j1}. Superseded by AARON 11C.

[47] CHEKANOV 03B used 131.5 pb^{-1} of e^+p and e^-p data taken at 300 and 318 GeV to look for narrow resonances in the eq or νq final states. Such final states may originate from $LQ\overline{D}$ couplings with non-zero λ'_{1j1} (leading to $\widetilde{u}_j$) or λ'_{11k} (leading to $\widetilde{d}_k$). See their Fig. 8 and explanations in the text for limits. The quoted mass bound assumes that only direct squark decays contribute.

[48] HEISTER 03G searches for the production of squarks in the case of $R\!\!\!/$ prompt decays with $\overline{UDD}$ direct couplings at at $\sqrt{s}$ = 189–209 GeV.

[49] ABAZOV 02F looked in 77.5 pb^{-1} of $p\overline{p}$ collisions at 1.8 TeV for events with $\geq 2\mu + \geq$ 4jets, originating from associated production of squarks followed by an indirect $R\!\!\!/$ decay (of the $\widetilde{\chi}^0_1$) via $LQ\overline{D}$ couplings of the type λ'_{2jk} where j=1,2 and k=1,2,3. Bounds are obtained in the MSUGRA scenario by a scan in the range $0 \leq M_0 \leq$ 400 GeV, $60 \leq m_{1/2} \leq$ 120 GeV for fixed values A_0=0, μ <0, and tanβ=2 or 6. The bounds are weaker for tanβ=6. See Figs. 2,3 for the exclusion contours in $m_{1/2}$ versus m_0 for tanβ=2 and 6, respectively.

[50] ABAZOV 02G search for associated production of gluinos and squarks in 92.7 pb^{-1} of $p\overline{p}$ collisions at $\sqrt{s}$=1.8 TeV, using events with one electron, $\geq$ 4 jets, and large $\not\!\!E_T$. The results are compared to a MSUGRA scenario with μ <0, A_0=0, and tanβ=3 and allow to exclude a region of the (m_0,$m_{1/2}$) shown in Fig. 11.

[51] ABBIENDI 02 looked for events with an electron or neutrino and a jet in e^+e^- at 189 GeV. Squarks (or leptoquarks) could originate from a $LQ\overline{D}$ coupling of an electron with a quark from the fluctuation of a virtual photon. Limits on the couplings λ'_{1jk} as a function of the squark mass are shown in Figs. 8–9, assuming that only direct squark decays contribute.

[52] ABBIENDI 02B looked for events with an electron or neutrino and a jet in e^+e^- at 189–209 GeV. Squarks (or leptoquarks) could originate from a $LQ\overline{D}$ coupling of an electron with a quark from the fluctuation of a virtual photon. Limits on the couplings λ'_{1jk} as a function of the squark mass are shown in Fig. 4, assuming that only direct squark decays contribute. The quoted limits are read off from Fig. 4. Supersedes the results of ABBIENDI 02.

[53] ACHARD 02 searches for the production of squarks in the case of $R\!\!\!/$ prompt decays with $\overline{UDD}$ couplings at $\sqrt{s}$=189–208 GeV. The search is performed for direct and indirect decays, assuming one coupling at the time to be nonzero. The limit holds for indirect decays. Stronger limits are reached for ($\widetilde{u}_R$,$\widetilde{d}_R$) direct (80,56) GeV and ($\widetilde{u}_L$,$\widetilde{d}_L$) direct or indirect (87,86) GeV decays.

[54] CHEKANOV 02 search for lepton flavor violating processes $e^+p \to \ell X$, where $\ell = \mu$ or τ with high p_T, in 47.7 pb^{-1} of e^+p collisions at 300 GeV. Such final states may originate from $LQ\overline{D}$ couplings with simultaneously nonzero λ'_{1jk} and λ'_{ijk} (i=2 or 3). The quoted mass bound assumes that only direct squark decays contribute.

[55] BARATE 01B searches for the production of squarks in the case of $R\!\!\!/$ prompt decays with $LL\overline{E}$ indirect or $\overline{UDD}$ direct couplings at $\sqrt{s}$=189–202 GeV. The limit holds for direct decays mediated by $R\!\!\!/\ \overline{UDD}$ couplings. Limits are also given for $LL\overline{E}$ indirect decays ($m_{\widetilde{u}_R} >$ 90 GeV and $m_{\widetilde{d}_R} >$ 89 GeV). Supersedes the results from BARATE 00H.

[56] BREITWEG 01 searches for squark production in 47.7 pb^{-1} of e^+p collisions, mediated by $R\!\!\!/$ couplings $LQ\overline{D}$ and leading to final states with $\not\!\!\nu$ and $\geq$ 1 jet, complementing the e^+X final states of BREITWEG 00E. Limits are derived on $\lambda'\sqrt{\beta}$, where β is the branching fraction of the squarks into e^+q+$\overline{\nu}q$, as function of the squark mass, see their Fig. 15. The quoted mass limit assumes that only direct squark decays contribute.

[57] ABBOTT 00C searched in $\sim$ 94 pb^{-1} of $p\overline{p}$ collisions for events with $\mu\mu$+jets, originating from associated production of leptoquarks. The results can be interpreted as limits on production of squarks followed by direct $R\!\!\!/$ decay via $\lambda'_{2jk}L_2Q_jd^c_k$ couplings. Bounds are obtained on the cross section for branching ratios of 1 and of 1/2, see their Fig. 4. The former yields the limit on the $\widetilde{u}_L$. The latter is combined with the bound of ABBOTT 99J from the $\mu\nu$+jets channel and of ABBOTT 98E and ABBOTT 98J from the $\nu\nu$+jets channel to yield the limit on $\widetilde{d}_R$.

[58] ACCIARRI 00P studied the effect on hadronic cross sections of t-channel down-type squark exchange via R-parity violating coupling $\lambda'_{1jk}L_1Q_jd^c_k$. The limit here refers to the case j=1,2, and holds for λ'_{1jk}=0.3. Data collected at $\sqrt{s}$=130–189 GeV, superseding the results of ACCIARRI 98J.

[59] AFFOLDER 00K searched in $\sim$ 88 pb^{-1} of $p\overline{p}$ collisions for events with 2–3 jets, at least one being b-tagged, large $\not\!\!E_T$ and no high p_T leptons. Such $\nu\nu$+b-jets events would originate from associated production of squarks followed by direct $R\!\!\!/$ decay via $\lambda'_{ij3}L_iQ_jd^c_3$ couplings. Bounds are obtained on the production cross section assuming zero branching ratio to charged leptons.

[60] BARATE 00I studied the effect on hadronic cross sections and charge asymmetries of t-channel down-type squark exchange via R-parity violating coupling $\lambda'_{1jk}L_1Q_jd^c_k$. The limit here refers to the case j=1,2, and holds for λ'_{1jk}=0.3. A 50 GeV limit is found for up-type squarks with k=3. Data collected at $\sqrt{s}$= 130–183 GeV. Superseded by SCHAEL 07A.

[61] BREITWEG 00E searches for squark exchange in e^+p collisions, mediated by $R\!\!\!/$ couplings $LQ\overline{D}$ and leading to final states with an identified e^+ and $\geq$ 1 jet. The limit applies to up-type squarks of all generations, and assumes B($\widetilde{q} \to qe$)=1.

[62] ABBOTT 99 searched for $\gamma\not\!\!E_T$ + $\geq$ 2 jet final states, and set limits on $\sigma(p\overline{p} \to \widetilde{q}$+X)·B($\widetilde{q} \to \gamma\not\!\!E_T$X). The quoted limits correspond to $m_{\widetilde{g}} \geq m_{\widetilde{q}}$, with B($\widetilde{\chi}^0_2 \to \widetilde{\chi}^0_1\gamma$)=1 and B($\widetilde{\chi}^0_1 \to \widetilde{G}\gamma$)=1, respectively. They improve to 310 GeV (360 GeV in the case of $\gamma\widetilde{G}$ decay) for $m_{\widetilde{g}}$=$m_{\widetilde{q}}$.

[63] ABBOTT 99K uses events with an electron pair and four jets to search for the decay of the $\widetilde{\chi}^0_1$ LSP via $R\!\!\!/\ LQ\overline{D}$ couplings. The particle spectrum and decay branching ratios are taken in the framework of minimal supergravity. An excluded region at 95% CL is obtained in the (m_0,$m_{1/2}$) plane under the assumption that A_0=0, μ < 0, tanβ=2 and any one of the couplings $\lambda'_{1jk} > 10^{-3}$ (j=1,2 and k=1,2,3) and from which the above limit is computed. For equal mass squarks and gluinos, the corresponding limit is 277 GeV. The results are essentially independent of A_0, but the limit deteriorates rapidly with increasing tanβ or μ >0.

[64] ABBOTT 99L consider events with three or more jets and large $\not\!\!E_T$. Spectra and decay rates are evaluated in the framework of minimal Supergravity, assuming five flavors of degenerate squarks, and scanning the space of the universal gaugino ($m_{1/2}$) and scalar (m_0) masses. See their Figs. 2–3 for the dependence of the limit on the relative value of $m_{\widetilde{q}}$ and $m_{\widetilde{g}}$.

[65] ABE 99M looked in 107 pb^{-1} of $p\overline{p}$ collisions at $\sqrt{s}$=1.8 TeV for events with like sign dielectrons and two or more jets from the sequential decays $\widetilde{q} \to q\widetilde{\chi}^0_1$ and $\widetilde{\chi}^0_1 \to eq\overline{q}'$, assuming $R\!\!\!/$ coupling $L_1Q_jD^c_k$, with j=2,3 and k=1,2,3. They assume five degenerate squark flavors, B($\widetilde{q} \to q\widetilde{\chi}^0_1$)=1, B($\widetilde{\chi}^0_1 \to eq\overline{q}'$)=0.25 for both e^+ and e^-, and $m_{\widetilde{g}} \geq$ 200 GeV. The limit is obtained for $m_{\widetilde{\chi}^0_1} \geq m_{\widetilde{q}}/2$ and improves for heavier gluinos or heavier χ^0_1.

[66] ABREU 99G looked for events with an electron or neutrino and a jet in e^+e^- at 183 GeV. Squarks (or leptoquarks) could originate from a $LQ\overline{D}$ coupling of an electron with a quark from the fluctuation of a virtual photon. Limits on the couplings λ'_{1jk} as a function of the squark mass are shown in Fig. 4, assuming that only direct squark decays contribute.

[67] ABBOTT 98E searched in $\sim$ 115 pb^{-1} of $p\overline{p}$ collisions for events with $e\nu$+jets, originating from associated production of squarks followed by direct $R\!\!\!/$ decay via $\lambda'_{1jk}L_1Q_jd^c_k$ couplings. Bounds are obtained by combining these results with the previous bound of ABBOTT 97B from the ee+jets channel and with a reinterpretation of ABACHI 96B $\nu\nu$+jets channel.

[68] ABE 98S looked in $\sim$ 110 pb^{-1} of $p\overline{p}$ collisions at $\sqrt{s}$=1.8 TeV for events with $\mu\mu$+jets originating from associated production of squarks followed by direct $R\!\!\!/$ decay via $\lambda'_{2jk}L_2Q_jd^c_k$ couplings. Bounds are obtained on the production cross section times the square of the branching ratio, see Fig. 2. Mass limits result from the comparison with theoretical cross sections and branching ratio equal to 1 for $\widetilde{u}_L$ and 1/2 for $\widetilde{d}_R$.

[69] ACKERSTAFF 98V and ACCIARRI 98J studied the interference of t-channel squark ($\widetilde{d}_R$) exchange via R-parity violating $\lambda'_{1jk}L_1Q_jd^c_k$ coupling in $e^+e^- \to q\overline{q}$. The limit is for λ'_{1jk}=0.3. See paper for related limits on $\widetilde{u}_L$ exchange. Data collected at $\sqrt{s}$=130–172 GeV.

[70] BREITWEG 98 used positron+jet events with missing energy and momentum to look for $e^+q \to \bar{e}\bar{q}$ via gaugino-like neutralino exchange with decays into ($e\widetilde{\chi}^0_1$)($q\widetilde{\chi}^0_1$). See paper for dependences in $m_{\widetilde{e}}$, $m_{\widetilde{\chi}^0_1}$.

[71] DATTA 97 argues that the squark mass bound by ABACHI 95C can be weakened by 10–20 GeV if one relaxes the assumption of the universal scalar mass at the GUT-scale so that the $\widetilde{\chi}^\pm_1$,$\widetilde{\chi}^0_2$ in the squark cascade decays have dominant and invisible decays to $\widetilde{\nu}$.

[72] DERRICK 97 looked for lepton-number violating final states via R-parity violating couplings $\lambda'_{ijk}L_iQ_jd_k$. When $\lambda'_{11k}\lambda'_{ijk} \neq 0$, the process $eu \to \widetilde{d}^*_k \to \ell_i u_j$ is possible. When $\lambda'_{1j1}\lambda'_{ijk} \neq 0$, the process $e\overline{d} \to \widetilde{u}^*_j \to \ell_i\overline{d}_k$ is possible. 100% branching

fraction $\tilde{q} \to \ell j$ is assumed. The limit quoted here corresponds to $\tilde{t} \to \tau q$ decay, with λ'=0.3. For different channels, limits are slightly better. See Table 6 in their paper.

[73] HEWETT 97 reanalyzed the limits on possible resonances in di-jet mode ($\tilde{q} \to q\tilde{g}$) from ALITTI 93 quoted in "Limits for Excited q (q^*) from Single Production," ABE 96 in "SCALE LIMITS for Contact Interactions: $\Lambda(qqqq)$," and unpublished CDF, DØ bounds. The bound applies to the gluino mass of 5 GeV, and improves for lighter gluino. The analysis has gluinos in parton distribution function.

[74] TEREKHOV 97 improved the analysis of TEREKHOV 96 by including di-jet angular distributions in the analysis.

[75] AID 96C used positron+jet events with missing energy and momentum to look for $e^+q \to \tilde{e}\tilde{q}$ via neutralino exchange with decays into $(e\tilde{\chi}_1^0)(q\tilde{\chi}_1^0)$. See the paper for dependences on $m_{\tilde{e}}$, $m_{\tilde{\chi}_1^0}$.

[76] TEREKHOV 96 reanalyzed the limits on possible resonances in di-jet mode ($\tilde{u} \to u\tilde{g}$) from ABE 95N quoted in "MASS LIMITS for g_A (axigluon)." The bound applies only to the case with a light gluino.

[77] ABACHI 95C assume five degenerate squark flavors with $m_{\tilde{q}_L} = m_{\tilde{q}_R}$. Sleptons are assumed to be heavier than squarks. The limits are derived for fixed $\tan\beta = 2.0$ $\mu = -250$ GeV, and m_{H^+}=500 GeV, and with the cascade decays of the squarks and gluinos calculated within the framework of the Minimal Supergravity scenario. The bounds are weakly sensitive to the three fixed parameters for a large fraction of parameter space. No limit is given for m_{gluino} >547 GeV.

[78] ABE 95T looked for a cascade decay of five degenerate squarks into $\tilde{\chi}_2^0$ which further decays into $\tilde{\chi}_1^0$ and a photon. No signal is observed. Limits vary widely depending on the choice of parameters. For $\mu = -40$ GeV, $\tan\beta = 1.5$, and heavy gluinos, the range 50<$m_{\tilde{q}}$ (GeV)<110 is excluded at 90% CL. See the paper for details.

[79] ABE 92L assume five degenerate squark flavors and $m_{\tilde{q}_L} = m_{\tilde{q}_R}$. ABE 92L includes the effect of cascade decay, for a particular choice of parameters, $\mu = -250$ GeV, $\tan\beta = 2$. Results are weakly sensitive to these parameters over much of parameter space. No limit for $m_{\tilde{q}} \leq 50$ GeV (but other experiments rule out that region). Limits are 10–20 GeV higher if $B(\tilde{q} \to q\tilde{\gamma}) = 1$. Limit assumes GUT relations between gaugino masses and the gauge coupling; in particular that for $|\mu|$ not small, $m_{\tilde{\chi}_1^0} \approx m_{\tilde{g}}/6$. This last relation implies that as $m_{\tilde{g}}$ increases, the mass of $\tilde{\chi}_1^0$ will eventually exceed $m_{\tilde{q}}$ so that no decay is possible. Even before that occurs, the signal will disappear; in particular no bounds can be obtained for $m_{\tilde{g}}$ >410 GeV. m_{H^+}=500 GeV.

[80] ROY 92 reanalyzed CDF limits on di-lepton events to obtain limits on squark production in R-parity violating models. The 100% decay $\tilde{q} \to q\tilde{\chi}$ where $\tilde{\chi}$ is the LSP, and the LSP decays either into $\ell q\overline{d}$ or $\ell\ell\overline{e}$ is assumed.

[81] NOJIRI 91 argues that a heavy squark should be nearly degenerate with the gluino in minimal supergravity not to overclose the universe.

Long-lived $\tilde{q}$ (Squark) MASS LIMIT

The following are bounds on long-lived scalar quarks, assumed to hadronise into hadrons with lifetime long enough to escape the detector prior to a possible decay. Limits may depend on the mixing angle of mass eigenstates: $\tilde{q}_1 = \tilde{q}_L\cos\theta_q + \tilde{q}_R\sin\theta_q$.

The coupling to the Z^0 boson vanishes for up-type squarks when θ_u=0.98, and for down type squarks when θ_d=1.17.

VALUE (GeV)	CL%	DOCUMENT ID		TECN	COMMENT
• • • We do not use the following data for averages, fits, limits, etc. • • •					
>683	95	[1] AAD	13AA	ATLS	$\tilde{t}$, R-hadrons, generic interaction model
>612	95	[2] AAD	13AA	ATLS	$\tilde{b}$, R-hadrons, generic interaction model
>344	95	[3] AAD	13BC	ATLS	R-hadrons, $\tilde{t} \to b\tilde{\chi}_1^0$, Regge model, lifetime between 10^{-5} and 10^3 s, $m_{\tilde{\chi}_1^0}$ = 100 GeV
>379	95	[4] AAD	13BC	ATLS	R-hadrons, $\tilde{t} \to t\tilde{\chi}_1^0$, Regge model, lifetime between 10^{-5} and 10^3 s, $m_{\tilde{\chi}_1^0}$ = 100 GeV
>935	95	[5] CHATRCHYAN	13AB	CMS	long-lived $\tilde{t}$ forming R-hadrons, cloud interaction model
>249	95	[6] AALTONEN	09Z	CDF	$\tilde{t}$
> 95	95	[7] HEISTER	03H	ALEP	$\tilde{u}$
> 92	95	[7] HEISTER	03H	ALEP	$\tilde{d}$
none 2–85	95	[8] ABREU	98P	DLPH	$\tilde{u}_L$
none 2–81	95	[8] ABREU	98P	DLPH	$\tilde{u}_R$
none 2–80	95	[8] ABREU	98P	DLPH	$\tilde{u}$, θ_u=0.98
none 2–83	95	[8] ABREU	98P	DLPH	$\tilde{d}_L$
none 5–40	95	[8] ABREU	98P	DLPH	$\tilde{d}_R$
none 5–38	95	[8] ABREU	98P	DLPH	$\tilde{d}$, θ_d=1.17

[1] AAD 13AA searched in 4.7 fb^{-1} of pp collisions at $\sqrt{s}$ = 7 TeV for events containing colored long-lived particles that hadronize forming R-hadrons. No significant excess above the expected background was found. Long-lived R-hadrons containing a $\tilde{t}$ are excluded for masses up to 683 GeV at 95% C.L in a general interaction model. Also, limits independent of the fraction of R-hadrons that arrive charged in the muon system were derived, see Fig. 6.

[2] AAD 13AA searched in 4.7 fb^{-1} of pp collisions at $\sqrt{s}$ = 7 TeV for events containing colored long-lived particles that hadronize forming R-hadrons. No significant excess above the expected background was found. Long-lived R-hadrons containing a $\tilde{b}$ are excluded for masses up to 612 GeV at 95% C.L in a general interaction model. Also, limits independent of the fraction of R-hadrons that arrive charged in the muon system were derived, see Fig. 6.

[3] AAD 13BC searched in 5.0 fb^{-1} of pp collisions at $\sqrt{s}$ = 7 TeV and in 22.9 fb^{-1} of pp collisions at $\sqrt{s}$ = 8 TeV for bottom squark R-hadrons that have come to rest within the ATLAS calorimeter and decay at some later time to hadronic jets and a neutralino. In absence of an excess of events above the expected backgrounds, limits are set on sbottom masses for the decay $\tilde{b} \to b\tilde{\chi}_1^0$, for different lifetimes, and for a neutralino mass of 100 GeV, see their Table 6 and Fig 10.

[4] AAD 13BC searched in 5.0 fb^{-1} of pp collisions at $\sqrt{s}$ = 7 TeV and in 22.9 fb^{-1} of pp collisions at $\sqrt{s}$ = 8 TeV for bottom squark R-hadrons that have come to rest within the ATLAS calorimeter and decay at some later time to hadronic jets and a neutralino. In absence of an excess of events above the expected backgrounds, limits are set on stop masses for the decay $\tilde{t} \to t\tilde{\chi}_1^0$, for different lifetimes, and for a neutralino mass of 100 GeV, see their Table 6 and Fig 10.

[5] CHATRCHYAN 13AB looked in 5.0 fb^{-1} of pp collisions at $\sqrt{s}$ = 7 TeV and in 18.8 fb^{-1} of pp collisions at $\sqrt{s}$ = 8 TeV for events with heavy stable particles, identified by their anomalous dE/dx in the tracker or additionally requiring that it be identified as muon in the muon chambers, from pair production of $\tilde{t}_1$'s. No evidence for an excess over the expected background is observed. Limits are derived for pair production of stops as a function of mass in the cloud interaction model (see Fig. 8 and Table 6). In the charge-suppressed model, the limit decreases to 818 GeV.

[6] AALTONEN 09Z searched in 1 fb^{-1} of $p\overline{p}$ collisions at $\sqrt{s}$ = 1.96 TeV for events with direct production of a pair of charged massive stable particles identified by their TOF. No excess of events is observed over the expected background. The data are used to set a bound on the production cross section, and the result is compared with the pair production cross section of stable stops as a function of the $\tilde{t}$ mass, see their Fig. 2.

[7] HEISTER 03H use e^+e^- data at and around the Z^0 peak to look for hadronizing stable squarks. Combining their results on searches for charged and neutral R-hadrons with JANOT 03, a lower limit of 15.7 GeV on the mass is obtained. Combining this further with the results of searches for tracks with anomalous ionization in data from 183 to 208 GeV yields the quoted bounds.

[8] ABREU 98P assumes that 40% of the squarks will hadronize into a charged hadron, and 60% into a neutral hadron which deposits most of its energy in hadron calorimeter. Data collected at $\sqrt{s}$=130–183 GeV.

$\tilde{b}$ (Sbottom) MASS LIMIT

Limits in e^+e^- depend on the mixing angle of the mass eigenstate $\tilde{b}_1 = \tilde{b}_L\cos\theta_b + \tilde{b}_R\sin\theta_b$. Coupling to the Z vanishes for $\theta_b \sim 1.17$. As a consequence, no absolute constraint in the mass region $\lesssim$40 GeV is available in the literature at this time from e^+e^- collisions. In the Listings below, we use $\Delta m = m_{\tilde{b}_1} - m_{\tilde{\chi}_1^0}$.

VALUE (GeV)	CL%	DOCUMENT ID		TECN	COMMENT
>600	95	[1] CHATRCHYAN	13T	CMS	jets + $\not{E}_T$, $\tilde{b} \to b\tilde{\chi}_1^0$ simplified model, $m_{\tilde{\chi}_1^0}$= 0 GeV
>450	95	[2] CHATRCHYAN	13V	CMS	same-sign $\ell^\pm\ell^\pm$ + ≥ 2 b-jets, $\tilde{b} \to t\tilde{\chi}_1^\pm$, $\tilde{\chi}_1^\pm \to W^\pm\tilde{\chi}_1^0$ simplified model, $m_{\tilde{\chi}_1^0}$ = 50 GeV
>390		[3] AAD	12AN	ATLS	$\tilde{b}_1 \to b\tilde{\chi}_1^0$, simplified model, $m_{\tilde{\chi}_1^0}$ < 60 GeV
		[4] CHATRCHYAN	12AI	CMS	$\ell^\pm\ell^\pm$ + b-jets + $\not{E}_T$
>410	95	[5] CHATRCHYAN	12BO	CMS	$\tilde{b}_1 \to b\tilde{\chi}_1^0$, simplified model, $m_{\tilde{\chi}_1^0}$ = 50 GeV
>230	95	[6] AALTONEN	10R	CDF	$\tilde{b}_1 \to b\tilde{\chi}_1^0$, $m_{\tilde{\chi}_1^0}$ < 70 GeV
>247	95	[7] ABAZOV	10L	D0	$\tilde{b}_1 \to b\tilde{\chi}_1^0$, $m_{\tilde{\chi}_1^0}$ = 0 GeV
>220	95	[8] ABULENCIA	06I	CDF	$\tilde{g} \to \tilde{b}b$, Δm >6 GeV, $\tilde{b}_1 \to b\tilde{\chi}_1^0$, $m_{\tilde{g}}$ <270 GeV
> 95		[9] ACHARD	04	L3	$\tilde{b} \to b\tilde{\chi}_1^0$, θ_b=0, Δm > 15–25 GeV
> 81		[9] ACHARD	04	L3	$\tilde{b} \to b\tilde{\chi}_1^0$, all θ_b, Δm > 15–25 GeV
> 7.5	95	[10] JANOT	04	THEO	unstable $\tilde{b}_1$, $e^+e^- \to$ hadrons
> 93	95	[11] ABDALLAH	03M	DLPH	$\tilde{b} \to b\tilde{\chi}_1^0$, θ_b=0, Δm >7 GeV
> 76	95	[11] ABDALLAH	03M	DLPH	$\tilde{b} \to b\tilde{\chi}_1^0$, all θ_b, Δm >7 GeV
> 85.1	95	[12] ABBIENDI	02H	OPAL	$\tilde{b} \to b\tilde{\chi}_1^0$, all θ_b, Δm >10 GeV, CDF
> 89	95	[13] HEISTER	02K	ALEP	$\tilde{b} \to b\tilde{\chi}_1^0$, all θ_b, Δm >8 GeV, CDF
none 3.5–4.5	95	[14] SAVINOV	01	CLEO	$\tilde{B}$ meson
none 80–145		[15] AFFOLDER	00D	CDF	$\tilde{b} \to b\tilde{\chi}_1^0$, $m_{\tilde{\chi}_1^0}$ <50 GeV
• • • We do not use the following data for averages, fits, limits, etc. • • •					
>620	95	[16] AAD	13AU	ATLS	2 b-jets + $\not{E}_T$, $\tilde{b}_1 \to b\tilde{\chi}_1^0$, $m_{\tilde{\chi}_1^0}$ < 120 GeV
>550	95	[17] CHATRCHYAN	13AT	CMS	jets + $\not{E}_T$, $\tilde{b} \to b\tilde{\chi}_1^0$ simplified model, $m_{\tilde{\chi}_1^0}$= 50 GeV
>294	95	[18] AAD	11K	ATLS	stable $\tilde{b}$
		[19] AAD	11O	ATLS	$\tilde{g} \to \tilde{b}_1 b$, $\tilde{b}_1 \to b\tilde{\chi}_1^0$, $m_{\tilde{\chi}_1^0}$=60 GeV
		[20] CHATRCHYAN	11D	CMS	$\tilde{b}, \tilde{t} \to b$
		[21] AALTONEN	09R	CDF	$\tilde{g} \to b\tilde{b}$, $\tilde{b} \to b\tilde{\chi}_1^0$
>193	95	[22] AALTONEN	07E	CDF	$\tilde{b}_1 \to b\tilde{\chi}_1^0$, $m_{\tilde{\chi}_1^0}$=40 GeV
none 35–222	95	[23] ABAZOV	06R	D0	$\tilde{b} \to b\tilde{\chi}_1^0$, $m_{\tilde{\chi}_1^0}$=50 GeV
> 78	95	[24] ABDALLAH	04M	DLPH	R, $\tilde{b}_L$, indirect, Δm >5 GeV
none 50–82	95	[25] ABDALLAH	03C	DLPH	$\tilde{b} \to b\tilde{g}$, stable $\tilde{g}$, all θ_b, Δm >10 GeV
		[26] BERGER	03	THEO	
> 71.5	95	[27] HEISTER	03G	ALEP	$\tilde{b}_L$, R decay
> 27.4	95	[28] HEISTER	03H	ALEP	$\tilde{b} \to b\tilde{g}$, stable $\tilde{g}$ or $\tilde{b}$
> 48	95	[29] ACHARD	02	L3	$\tilde{b}_1$, R decays

	[30] BAEK	02	THEO		
	[31] BECHER	02	THEO		
	[32] CHEUNG	02B	THEO		
	[33] CHO	02	THEO		
	[34] BERGER	01	THEO	$p\overline{p} \rightarrow$ X+b-quark	
none 52–115 95	[35] ABBOTT	99F	D0	$\tilde{b} \rightarrow b\tilde{\chi}_1^0$, $m_{\tilde{\chi}_1^0}$ <20 GeV	

[1] CHATRCHYAN 13T searched in 11.7 fb^{-1} of pp collisions at $\sqrt{s}$ = 8 TeV for events with at least two energetic jets and significant $\not\!\!E_T$, using the α_T variable to discriminate between processes with genuine and misreconstructed $\not\!\!E_T$. No significant excess above the Standard Model expectations is observed. Limits are set on sbottom masses in simplified models where the decay $\tilde{b} \rightarrow b\tilde{\chi}_1^0$ takes place with a branching ratio of 100%, see Fig. 8 and Table 9.

[2] CHATRCHYAN 13V searched in 10.5 fb^{-1} of pp collisions at $\sqrt{s}$ = 8 TeV for events with two isolated same-sign dileptons and at least two b-jets in the final state. No significant excess above the Standard Model expectations is observed. Limits are set on the bottom mass in a simplified models where the decay $\tilde{b} \rightarrow t\tilde{\chi}_1^{\pm}$, $\tilde{\chi}_1^{\pm} \rightarrow W^{\pm}\tilde{\chi}_1^0$ takes place with a branching ratio of 100%, with varying mass of the $\tilde{\chi}_1^{\pm}$, for $m_{\tilde{\chi}_1^0}$ = 50 GeV, see Fig. 4.

[3] AAD 12AN searched in 2.05 fb^{-1} of pp collisions at $\sqrt{s}$ = 7 TeV for scalar bottom quarks in events with large missing transverse momentum and two b-jets in the final state. The data are found to be consistent with the Standard Model expectations. Limits are set in an R-parity conserving minimal supersymmetric scenario, assuming B($\tilde{b}_1 \rightarrow b\tilde{\chi}_1^0$) = 100%, see their Fig. 2.

[4] CHATRCHYAN 12AI looked in 4.98 fb^{-1} of pp collisions at $\sqrt{s}$ = 7 TeV for events with two same-sign leptons (e, μ), but not necessarily same flavor, at least 2 b-jets and missing transverse energy. No excess beyond the Standard Model expectation is observed. Exclusion limits are derived in a simplified model for sbottom pair production, where the sbottom decays through $\tilde{b}_1 \rightarrow t\tilde{\chi}_1 W$, see Fig. 8.

[5] CHATRCHYAN 12BO searched in 4.7 fb^{-1} of pp collisions at $\sqrt{s}$ = 7 TeV for scalar bottom quarks in events with large missing transverse momentum and two b-jets in the final state. The data are found to be consistent with the Standard Model expectations. Limits are set in an R-parity conserving minimal supersymmetric scenario, assuming B($\tilde{b}_1 \rightarrow b\tilde{\chi}_1^0$) = 100%, see their Fig. 2.

[6] AALTONEN 10R searched in 2.65 fb^{-1} of $p\overline{p}$ collisions at $\sqrt{s}$ = 1.96 TeV for events with $\not\!\!E_T$ and exactly two jets, at least one of which is b-tagged. The results are in agreement with the SM prediction, and a limit on the cross section of 0.1 pb is obtained for the range of masses 80 < $m_{\tilde{b}_1}$ < 280 GeV assuming that the sbottom decays exclusively to $b\tilde{\chi}_1^0$. The excluded mass region in the framework of conserved R_p is shown in a plane of ($m_{\tilde{b}_1}$, $m_{\tilde{\chi}_1^0}$), see their Fig.2.

[7] ABAZOV 10L looked in 5.2 fb^{-1} of $p\overline{p}$ collisions at $\sqrt{s}$ = 1.96 TeV for events with at least 2 b-jets and $\not\!\!E_T$ from the production of $\tilde{b}_1\tilde{b}_1$. No evidence for an excess over the SM expectation is observed, and a limit on the cross section is derived under the assumption of 100% branching ratio. The excluded mass region in the framework of conserved R_p is shown in a plane of ($m_{\tilde{b}_1}$,$m_{\tilde{\chi}_1^0}$), see their Fig. 3b. The exclusion also extends to $m_{\tilde{\chi}_1^0}$ = 110 GeV for 160< $m_{\tilde{b}_1}$ < 200 GeV.

[8] ABULENCIA 06I searched in 156 pb^{-1} of $p\overline{p}$ collisions at $\sqrt{s}$ = 1.96 TeV for multijet events with large $\not\!\!E_T$. They request at least 2 b-tagged jets and no isolated leptons. They investigate the production of gluinos decaying into $\tilde{b}_1 b$ followed by $\tilde{b}_1 \rightarrow b\tilde{\chi}_1^0$. Both branching fractions are assumed to be 100% and the LSP mass to be 60 GeV. No significant excess was found compared to the background expectation. Upper limits on the cross-section are extracted and a limit is derived on the masses of sbottom and gluinos, see their Fig.3.

[9] ACHARD 04 search for the production of $\tilde{b}\overline{\tilde{b}}$ in acoplanar b-tagged di-jet final states in the 192–209 GeV data. See Fig. 6 for the dependence of the limits on $m_{\tilde{\chi}_1^0}$. This limit supersedes ACCIARRI 99V.

[10] JANOT 04 reanalyzes $e^+e^- \rightarrow$ hadrons total cross section data with $\sqrt{s}$ = 20–209 GeV from PEP, PETRA, TRISTAN, SLC, and LEP and constrains the mass of $\tilde{b}_1$ assuming it decays quickly to hadrons.

[11] ABDALLAH 03M looked for $\tilde{b}$ pair production in events with acoplanar jets and $\not\!\!E$ at $\sqrt{s}$ = 189–208 GeV. The limit improves to 87 (98) GeV for all θ_b (θ_b = 0) for Δm > 10 GeV. See Fig. 24 and Table 11 for other choices of Δm. These limits include and update the results of ABREU,P 00D.

[12] ABBIENDI 02H search for events with two acoplanar jets and $\not\!\!p_T$ in the 161–209 GeV data. The limit assumes 100% branching ratio and uses the exclusion at large Δm from CDF (AFFOLDER 00D). For θ_b=0, the bound improves to > 96.9 GeV. See Fig. 4 and Table 6 for the more general dependence on the limits on Δm. These results supersede ABBIENDI 99M.

[13] HEISTER 02K search for bottom squarks in final states with acoplanar jets with b tagging, using 183–209 GeV data. The mass bound uses the CDF results from AFFOLDER 00D. See Fig. 5 for the more general dependence of the limits on Δm. Updates BARATE 01.

[14] SAVINOV 01 use data taken at $\sqrt{s}$=10.52 GeV, below the $B\overline{B}$ threshold. They look for events with a pair of leptons with opposite charge and a fully reconstructed hadronic D or D^* decay. These could originate from production of a light-sbottom hadron followed by $\bar{B} \rightarrow D^{(*)}\ell^-\bar{\nu}$, in case the $\tilde{\nu}$ is the LSP, or $\bar{B} \rightarrow D^{(*)}\pi\ell^-$, in case of $\not{R}$. The mass range 3.5 ≤ $M(\bar{B})$ ≤ 4.5 GeV was explored, assuming 100% branching ratio for either of the decays. In the $\tilde{\nu}$LSP scenario, the limit holds only for $M(\tilde{\nu})$ less than about 1 GeV and for the D^* decays it is reduced to the range 3.9–4.5 GeV. For the $\not{R}$ decay, the whole range is excluded.

[15] AFFOLDER 00D search for final states with 2 or 3 jets and $\not\!\!E_T$, one jet with a b tag. See their Fig. 3 for the mass exclusion in the $m_{\tilde{t}}$, $m_{\tilde{\chi}_1^0}$ plane.

[16] AAD 13AU searched in 20.1 fb^{-1} of pp collisions at $\sqrt{s}$ = 8 TeV for events containing two jets identified as originating from b-quarks and large missing transverse momentum. No excess of events above the expected level of Standard Model background was found. Exclusion limits at 95% C.L. are set on the masses of third-generation squarks. Assuming that the decay $\tilde{b}_1 \rightarrow b\tilde{\chi}_1^0$ takes place 100% of the time, a $\tilde{b}_1$ mass below 620 GeV is excluded for $m_{\tilde{\chi}_1^0}$ < 120 GeV. For more details, see their Fig. 5.

[17] CHATRCHYAN 13AT provides interpretations of various searches for supersymmetry by the CMS experiment based on 4.73–4.98 fb^{-1} of pp collisions at $\sqrt{s}$ = 7 TeV in the framework of simplified models. Limits are set on the sbottom mass in a simplified models where sbottom quarks are pair-produced and the decay $\tilde{b} \rightarrow b\tilde{\chi}_1^0$ takes place with a branching ratio of 100%, see Fig. 4.

[18] AAD 11K looked in 34 pb^{-1} of pp collisions at $\sqrt{s}$ = 7 TeV for events with heavy stable particles, identified by their anomalous dE/dx in the tracker or time of flight in the tile calorimeter, from pair production of $\tilde{b}$. No evidence for an excess over the SM expectation is observed and limits on the mass are derived for pair production of sbottom, see Fig. 4.

[19] AAD 11O looked in 35 pb^{-1} of pp collisions at $\sqrt{s}$ = 7 TeV for events with jets, of which at least one is a b-jet, and $\not\!\!E_T$. No excess above the Standard Model was found. Limits are derived in the ($m_{\tilde{g}}$, $m_{\tilde{b}_1}$) plane (see Fig. 2) under the assumption of 100% branching ratios and $\tilde{b}_1$ being the lightest squark. The quoted limit is valid for $m_{\tilde{b}_1}$ < 500 GeV. A similar approach for $\tilde{t}_1$ as the lightest squark with $\tilde{g} \rightarrow \tilde{t}_1 t$ and $\tilde{t}_1 \rightarrow b\tilde{\chi}_1^{\pm}$ with 100% branching ratios leads to a gluino mass limit of 520 GeV for 130 < $m_{\tilde{t}_1}$ < 300 GeV. Limits are also derived in the CMSSM (m_0, $m_{1/2}$) plane for tanβ = 40, see Fig. 4, and in scenarios based on the gauge group SO(10).

[20] CHATRCHYAN 11D looked in 35 pb^{-1} of pp collisions at $\sqrt{s}$ = 7 TeV for events with ≥ 2 jets, at least one of which is b-tagged, and $\not\!\!E_T$, where the b-jets are decay products of $\tilde{t}$ or $\tilde{b}$. No evidence for an excess over the expected background is observed. Limits are derived in the CMSSM (m_0, $m_{1/2}$) plane for tanβ = 50 (see Fig. 2).

[21] AALTONEN 09R searched in 2.5 fb^{-1} of $p\overline{p}$ collisions at $\sqrt{s}$ = 1.96 TeV for events with at least 2 b-tagged jets and $\not\!\!E_T$, originating from the decay $\tilde{g} \rightarrow b\tilde{b}$ followed by $\tilde{b} \rightarrow b\tilde{\chi}_1^0$. Both decays are assumed to have 100% branching ratio. No significant deviation from the SM prediction is observed. An upper limit on the gluino pair production cross section is calculated as a function of the gluino mass, see their Fig. 2. A limit is derived in the $m_{\tilde{b}}$ versus $m_{\tilde{g}}$ plane which improves the results of previous searches, see their Fig. 3.

[22] AALTONEN 07E searched in 295 pb^{-1} of $p\overline{p}$ collisions at $\sqrt{s}$ = 1.96 TeV for multijet events with large $\not\!\!E_T$. They request at least one heavy flavor-tagged jet and no identified leptons. The branching ratio $\tilde{b}_1 \rightarrow b\tilde{\chi}_1^0$ is assumed to be 100%. No significant excess was found compared to the background expectation. Upper limits on the cross-section are extracted and a limit is derived on the masses of sbottom versus $\tilde{\chi}_1^0$, see their Fig. 5. Superseded by AALTONEN 10R.

[23] ABAZOV 06R looked in 310 pb^{-1} of $p\overline{p}$ collisions at $\sqrt{s}$ = 1.96 TeV for events with 2 or 3 jets and large $\not\!\!E_T$ with at least 1 b-tagged jet and a veto against isolated leptons. No excess is observed relative to the SM background expectations. Limits are set on the sbottom pair production cross-section under the assumption that the only decay mode is into $b\tilde{\chi}_1^0$. Exclusion contours are derived in the plane of sbottom versus neutralino masses, shown in their Fig. 2. The observed limit is more constraining than the expected one due to a lack of events corresponding to large sbottom masses. Superseded by ABAZOV 10L.

[24] ABDALLAH 04M use data from $\sqrt{s}$ = 192–208 GeV to derive limits on sparticle masses under the assumption of $\not{R}$ with $\overline{UDD}$ couplings. The results are valid for μ = −200 GeV, tanβ = 1.5, Δm > 5 GeV and assuming a BR of 1 for the given decay. The limit quoted is for indirect $\overline{UDD}$ decays using the neutralino constraint of 38.0 GeV, also derived in ABDALLAH 04M, and assumes no mixing. For indirect decays it remains at 78 GeV when the neutralino constraint is not used. Supersedes the result of ABREU 01D.

[25] ABDALLAH 03C looked for events of the type $q\overline{q}R^{\pm}R^{\pm}$, $q\overline{q}R^{\pm}R^0$, or $q\overline{q}R^0R^0$ in e^+e^- interactions at $\sqrt{s}$ = 189–208 GeV. The $R^{\pm}$ bound states are identified by anomalous dE/dx in the tracking chambers and the R^0 by missing energy due to their reduced energy loss in the calorimeters. Excluded mass regions in the (m($\tilde{b}$), m($\tilde{g}$)) plane for m($\tilde{g}$) > 2 GeV are obtained for several values of the probability for the gluino to fragment into $R^{\pm}$ or R^0, as shown in their Fig. 19. The limit improves to 94 GeV for θ_b=0.

[26] BERGER 03 studies the constraints on a $\tilde{b}_1$ with mass in the 2.2–5.5 GeV region coming from radiative decays of Υ(nS) into sbottomonium. The constraints apply only if $\tilde{b}_1$ lives long enough to permit formation of the sbottomonium bound state. A small region of mass in the $m_{\tilde{b}_1} - m_{\tilde{g}}$ plane survives current experimental constraints from CLEO.

[27] HEISTER 03G searches for the production of $\tilde{b}$ pairs in the case of $\not{R}$ prompt decays with $LL\overline{E}$, $LQ\overline{D}$ or $\overline{UDD}$ couplings at $\sqrt{s}$ = 189–209 GeV. The limit holds for indirect decays mediated by $\not{R}$ $\overline{UDD}$ couplings. It improves to 90 GeV for indirect decays mediated by $\not{R}$ $LL\overline{E}$ couplings and to 80 GeV for indirect decays mediated by $\not{R}$ $LQ\overline{D}$ couplings. Supersedes the results from BARATE 01B.

[28] HEISTER 03H use their results on bounds on stable squarks, on stable gluinos and on squarks decaying to a stable gluino from the same paper to derive a mass limit on $\tilde{b}$, see their Fig. 13. The limit for a long-lived $\tilde{b}_1$ is 92 GeV.

[29] ACHARD 02 searches for the production of squarks in the case of $\not{R}$ prompt decays with $\overline{UDD}$ couplings at $\sqrt{s}$=189–208 GeV. The search is performed for direct and indirect decays, assuming one coupling at the time to be nonzero. The limit is computed for the minimal cross section and holds for indirect decays and reaches 55 GeV for direct decays.

[30] BAEK 02 studies the constraints on a $\tilde{b}_1$ with mass in the 2.2–5.5 GeV region coming from precision measurements of Z^0 decays. It is noted that CP-violating couplings in the MSSM parameters relax the strong constraints otherwised derived from CP conservation.

[31] BECHER 02 studies the constraints on a $\tilde{b}_1$ with mass in the 2.2–5.5 GeV region coming from radiative B meson decays, and sets limits on the off-diagonal flavor-changing couplings $qb\tilde{g}$ (q=d,s).

[32] CHEUNG 02B studies the constraints on a $\tilde{b}_1$ with mass in the 2.2–5.5 GeV region and a gluino in the mass range 12–16 GeV, using precision measurements of Z^0 decays and e^+e^- annihilations at LEP2. Few detectable events are predicted in the LEP2 data for the model proposed by BERGER 01.

[33] CHO 02 studies the constraints on a $\tilde{b}_1$ with mass in the 2.2–5.5 GeV region coming from precision measurements of Z^0 decays. Strong constraints are obtained for CP-conserving MSSM couplings.

[34] BERGER 01 reanalyzed interpretation of Tevatron data on bottom-quark production. Argues that pair production of light gluinos (m∼ 12–16 GeV) with subsequent 2-body decay into a light sbottom (m∼ 2–5.5 GeV) and bottom can reconcile Tevatron data with predictions of perturbative QCD for the bottom production rate. The sbottom must

either decay hadronically via a R-parity- and B-violating interaction, or be long-lived. Constraints on the mass spectrum are derived from the measurements of time-averaged B^0-$\overline{B}^0$ mixing.

[35] ABBOTT 99F looked for events with two jets, with or without an associated muon from b decay, and $\not{E}_T$. See Fig. 2 for the dependence of the limit on $m_{\widetilde{\chi}^0_1}$. No limit for $m_{\widetilde{\chi}^0_1} > 47$ GeV. Superseded by ABAZOV 06R.

$\widetilde{t}$ (Stop) MASS LIMIT

Limits depend on the decay mode. In e^+e^- collisions they also depend on the mixing angle of the mass eigenstate $\widetilde{t}_1 = \widetilde{t}_L \cos\theta_t + \widetilde{t}_R \sin\theta_t$. The coupling to the Z vanishes when $\theta_t = 0.98$. In the Listings below, we use $\Delta m \equiv m_{\widetilde{t}_1} - m_{\widetilde{\chi}^0_1}$ or $\Delta m \equiv m_{\widetilde{t}_1} - m_{\widetilde{\nu}}$, depending on relevant decay mode. See also bounds in "$\widetilde{q}$ (Squark) MASS LIMIT." Limits made obsolete by the most recent analyses of e^+e^- and $p\overline{p}$ collisions can be found in previous Editions of this *Review*.

VALUE (GeV)	CL%	DOCUMENT ID		TECN	COMMENT
none 123–167	95	[1] AAD	13T	ATLS	1 or 2 $\ell^\pm$ + b-jets + $\not{E}_T$, $\widetilde{t}_1 \to b\widetilde{\chi}^\pm_1$, $m_{\widetilde{\chi}^0_1}=55$ GeV, $m_{\widetilde{\chi}^\pm_1}=106$ GeV
> 650	95	[2] CHATRCHYAN	13BS	CMS	1 $\ell^\pm$ + jets + $\not{E}_T$, $\widetilde{t} \to t\widetilde{\chi}^0_1$ simplified model, $m_{\widetilde{\chi}^0_1}=0$ GeV
> 240	95	[3] AAD	12AH	ATLS	Z+jets+$\not{E}_T$, GMSB, $m_{\widetilde{\chi}^0_1} > m_Z$
none 300	95	[4] AAD	12CB	ATLS	$\ell^\pm\ell^\mp$ + jets + $\not{E}_T$, $\widetilde{t}_1 \to t\widetilde{\chi}^0_1$, $m_{\widetilde{\chi}^0_1}=0$ GeV
none 370–465	95	[5] AAD	12CE	ATLS	$\widetilde{t}_1 \to t\widetilde{\chi}^0_1$, hadronic t decays, $m_{\widetilde{\chi}^0_1}=0$ GeV
none 230–440	95	[6] AAD	12CF	ATLS	$\ell^\pm$ + jets + $\not{E}_T$, $\widetilde{t}_1 \to t\widetilde{\chi}^0_1$, $m_{\widetilde{\chi}^0_1}=0$ GeV
> 130	95	[7] AAD	12CL	ATLS	$\ell^\pm\ell^\mp$ + jets + $\not{E}_T$, $\widetilde{t}_1 \to b\widetilde{\chi}^\pm_1$, $m_{\widetilde{\chi}^\pm_1}=106$ GeV
		[8] AAD	12J	ATLS	$pp \to e\mu + X$, $\not{R}$
> 180	95	[9] AALTONEN	12AO	CDF	$\widetilde{t}_1 \to c\widetilde{\chi}^0_1$, $m_{\widetilde{\chi}^0_1}=90$ GeV
> 200	95	[10] ABAZOV	12H	D0	$\widetilde{t}_1\overline{\widetilde{t}}_1 \to b\overline{b}\mu\tau\widetilde{\nu}\overline{\widetilde{\nu}}$, $m_{\widetilde{\nu}}$=45GeV
	95	[11] ABAZOV	12L	D0	long-lived $\widetilde{q}$ forming R-hadrons
> 210	95	[12] ABAZOV	11N	D0	$\widetilde{t}_1 \to b\ell\widetilde{\nu}$, $m_{\widetilde{\nu}}$ <110 GeV, $m_{\widetilde{t}_1} - m_{\widetilde{\nu}} > 30$ GeV
none 60–180	95	[13] AALTONEN	10Y	CDF	$\widetilde{t}_1 \to b\ell\widetilde{\nu}$, $m_{\widetilde{\nu}}=45$ GeV
none 95–150	95	[14] ABAZOV	08Z	D0	$\widetilde{t} \to c\widetilde{\chi}^0_1$, $m_c < \Delta m < m_W + m_b$
none 80–120	95	[15] ABAZOV	04	D0	$\widetilde{t} \to b\ell\nu\widetilde{\chi}^0$, $m_{\widetilde{\chi}^0}=50$ GeV
> 90		[16] ACHARD	04	L3	$\widetilde{t} \to c\widetilde{\chi}^0_1$, all θ_t, Δm > 15–25 GeV
> 93		[16] ACHARD	04	L3	$\widetilde{b} \to b\ell\widetilde{\nu}$, all θ_t, Δm >15 GeV
> 88		[16] ACHARD	04	L3	$\widetilde{b} \to b\tau\widetilde{\nu}$, all θ_t, Δm >15 GeV
> 75	95	[17] ABDALLAH	03M	DLPH	$\widetilde{t} \to c\widetilde{\chi}^0$, θ_t=0, Δm >2 GeV
> 71	95	[17] ABDALLAH	03M	DLPH	$\widetilde{t} \to c\widetilde{\chi}^0$, all θ_t, Δm >2 GeV
> 96	95	[17] ABDALLAH	03M	DLPH	$\widetilde{t} \to c\widetilde{\chi}^0$, θ_t=0, Δm >10 GeV
> 92	95	[17] ABDALLAH	03M	DLPH	$\widetilde{t} \to c\widetilde{\chi}^0$, all θ_t, Δm >10 GeV
> 95.7	95	[18] ABBIENDI	02H	OPAL	$c\widetilde{\chi}^0_1$, all θ_t, Δm >10 GeV
> 92.6	95	[18] ABBIENDI	02H	OPAL	$b\ell\widetilde{\nu}$, all θ_t, Δm >10 GeV
> 91.5	95	[18] ABBIENDI	02H	OPAL	$b\tau\widetilde{\nu}$, all θ_t, Δm >10 GeV
> 63	95	[19] HEISTER	02K	ALEP	any decay, any lifetime, all θ_t
> 92	95	[19] HEISTER	02K	ALEP	$\widetilde{t} \to c\widetilde{\chi}^0_1$, all θ_t, Δm >8 GeV, CDF
> 97	95	[19] HEISTER	02K	ALEP	$\widetilde{t} \to b\ell\widetilde{\nu}$, all θ_t, Δm >8 GeV, DØ
> 78	95	[19] HEISTER	02K	ALEP	$\widetilde{t} \to b\widetilde{\chi}^0_1 W^*$, all θ_t, Δm >8 GeV
• • • We do not use the following data for averages, fits, limits, etc. • • •					
> 580	95	[20] AAD	13AU	ATLS	2 b-jets + $\not{E}_T$, $\widetilde{t}_1 \to b\widetilde{\chi}^\pm_1$, $m_{\widetilde{\chi}^\pm_1} - m_{\widetilde{\chi}^0_1}=5$ GeV, $m_{\widetilde{\chi}^0_1}=100$ GeV
>1020		[21] CHATRCHYAN	13BN	CMS	$\geq$ 3 leptons + b-jets, $\not{R}$, $LL\overline{E}$, $\lambda_{123} \neq 0$, $m_{\widetilde{\chi}^0_1}=200$ GeV
> 820		[21] CHATRCHYAN	13BN	CMS	$\geq$ 3 leptons + b-jets, $\not{R}$, $LL\overline{E}$, $\lambda_{233} \neq 0$, $m_{\widetilde{\chi}^0_1}=200$ GeV
> 525	95	[22] CHATRCHYAN	13M	CMS	τ lepton + b-jet, $\not{R}$, $L_3Q_3D_3$, $\widetilde{t}_1 \to \tau b$ simplified model
> 600	95	[23] HAN	13	RVUE	natural SUSY, combination of $\widetilde{t}_1 \to t\widetilde{\chi}^0_1$ and $\widetilde{t}_1 \to b\widetilde{\chi}^\pm_1$
> 340	95	[24] CHATRCHYAN	12AN	CMS	long-lived $\widetilde{t} \to t\widetilde{\chi}^0_1$
> 737	95	[25] CHATRCHYAN	12L	CMS	long-lived $\widetilde{t}$ forming R-hadrons
> 309	95	[26] AAD	11K	ATLS	stable $\widetilde{t}$
> 202	95	[27] KHACHATRY...	11C	CMS	stable $\widetilde{t}_1$
none 128–135	95	[28] AALTONEN	10O	CDF	$\widetilde{t}_1 \to b\widetilde{\chi}^\pm_1 \to b\ell\widetilde{\chi}^0_1\nu$, $m_{\widetilde{\chi}^\pm_1}$ =106 GeV, $m_{\widetilde{\chi}^0_1}=48$ GeV
		[29] ABAZOV	09N	D0	$\widetilde{t} \to b\widetilde{\chi}^\pm_1$
		[30] ABAZOV	09O	D0	$\widetilde{t} \to b\ell\widetilde{\nu}$
> 153	95	[31] AALTONEN	08Z	CDF	$\not{R}$, $\widetilde{t}_1 \to b\tau$
> 185	95	[32] ABAZOV	08	D0	$\widetilde{t} \to b\ell\widetilde{\nu}$, $m_{\widetilde{\nu}}$=70 GeV
> 132		[33] AALTONEN	07E	CDF	$\widetilde{t}_1 \to c\widetilde{\chi}^0_1$, $m_{\widetilde{\chi}^0_1}$=48 GeV
none 80–134	95	[34] ABAZOV	07B	D0	$\widetilde{t} \to c\widetilde{\chi}^0_1$, $m_{\widetilde{\chi}^0_1} < 48$ GeV
		[35] CHEKANOV	07	ZEUS	$e^+p \to \widetilde{t}_1$, $\not{R}$, $LQ\overline{D}$
> 77	95	[36] ABBIENDI	04F	OPAL	$\not{R}$, direct, all θ_t
> 77	95	[37] ABDALLAH	04M	DLPH	$\not{R}$, indirect, all θ_t, Δm >5 GeV
		[38] AKTAS	04B	H1	$\not{R}$, $\widetilde{t}_1$
> 74.5		[39] DAS	04	THEO	$\widetilde{t}\overline{\widetilde{t}} \to b\ell\nu_\ell\chi^0\overline{b}q\overline{q}'\chi^0$, $m_{\chi^0_1}$ = 15 GeV, no $\overline{t} \to c\chi^0$
none 50–87	95	[40] ABDALLAH	03C	DLPH	$\widetilde{t} \to c\widetilde{g}$, stable $\widetilde{g}$, all θ_t, $\Delta M > 10$ GeV
none 80–131	95	[41] ACOSTA	03C	CDF	$\widetilde{t} \to b\ell\widetilde{\nu}$, $m_{\widetilde{\nu}} \leq 63$ GeV
		[42] CHAKRAB...	03	THEO	$p\overline{p} \to \widetilde{t}\overline{t}t^*$, RPV
> 71.5	95	[43] HEISTER	03G	ALEP	$\widetilde{t}_L$, $\not{R}$ decay
> 80	95	[44] HEISTER	03H	ALEP	$\widetilde{t} \to c\widetilde{g}$, stable $\widetilde{g}$ or $\widetilde{t}$, all θ_t, all ΔM
> 144	95	[45] ABAZOV	02C	D0	$\widetilde{t} \to b\ell\widetilde{\nu}$, $m_{\widetilde{\nu}}$=45 GeV
> 77	95	[46] ACHARD	02	L3	$\widetilde{t}_1$, $\not{R}$ decays
		[47] AFFOLDER	01B	CDF	$t \to \widetilde{t}\chi^0_1$
> 61	95	[48] ABREU	00I	DLPH	$\not{R}$ ($LL\overline{E}$), θ_t=0.98, $\Delta m > 4$GeV
none 68–119	95	[49] AFFOLDER	00D	CDF	$\widetilde{t} \to c\widetilde{\chi}^0_1$, $m_{\widetilde{\chi}^0_1}$ <40 GeV
none 84–120	95	[50] AFFOLDER	00G	CDF	$\widetilde{t}_1 \to b\ell\widetilde{\nu}$, $m_{\widetilde{\nu}}$ <45 GeV
> 120	95	[51] ABE	99M	CDF	$p\overline{p} \to \widetilde{t}_1\overline{\widetilde{t}}_1$, $\not{R}$
none 9–24.4	95	[52] AID	96	H1	$ep \to \widetilde{t}\overline{t}$, $\not{R}$ decays
> 138	95	[53] AID	96	H1	$ep \to \widetilde{t}$, $\not{R}$, $\lambda\cos\theta_t > 0.03$
> 45		[54] CHO	96	RVUE	B^0-$\overline{B}^0$ and ϵ, θ_t=0.98, $\tan\beta$ <2
none 11–41	95	[55] BUSKULIC	95E	ALEP	$\not{R}$ ($LL\overline{E}$), θ_t=0.98
none 6.0–41.2	95	AKERS	94K	OPAL	$\widetilde{t} \to c\widetilde{\chi}^0_1$, θ_t=0, Δm >2 GeV
none 5.0–46.0	95	AKERS	94K	OPAL	$\widetilde{t} \to c\widetilde{\chi}^0_1$, θ_t=0, Δm >5 GeV
none 11.2–25.5	95	AKERS	94K	OPAL	$\widetilde{t} \to c\widetilde{\chi}^0_1$, θ_t=0.98, Δm >2GeV
none 7.9–41.2	95	AKERS	94K	OPAL	$\widetilde{t} \to c\widetilde{\chi}^0_1$, θ_t=0.98, Δm >5GeV
none 7.6–28.0	95	[56] SHIRAI	94	VNS	$\widetilde{t} \to c\widetilde{\chi}^0_1$, any θ_t, Δm >10GeV
none 10–20	95	[56] SHIRAI	94	VNS	$\widetilde{t} \to c\widetilde{\chi}^0_1$, any θ_t, $\Delta m > 2.5$ GeV

[1] AAD 13T searched in 4.7 fb^{-1} of pp collisions at $\sqrt{s} = 7$ TeV for pair production of light $\widetilde{t}_1$ squarks with masses similar to, or lighter than, the top quark mass. Final states containing exclusively one or two leptons (electrons or muons), large missing transverse momentum, light jets and b-jets are used to reconstruct the top squark pair system. The $\widetilde{t}_1$ is assumed to decay through $\widetilde{t}_1 \to b\widetilde{\chi}^\pm_1$ with a 100 % branching ratio. The chargino is then assumed to decay through a virtual W boson, $\widetilde{\chi}^\pm_1 \to W^*\widetilde{\chi}^0_1$. The data are found to be consistent with the Standard Model expectations. The results are interpreted in a simplified model as a function of $m_{\widetilde{t}_1}$ and $m_{\widetilde{\chi}^0_1}$, for either $m_{\widetilde{\chi}^\pm_1} = 2\, m_{\widetilde{\chi}^0_1}$ or for a fixed choice of $m_{\widetilde{\chi}^\pm_1} = 106$ GeV, see Fig. 2. Assuming $m_{\widetilde{\chi}^\pm_1} = 106$ GeV, $\widetilde{t}_1$ masses between 123 and 167 GeV are excluded at 95% C.L for $m_{\widetilde{\chi}^0_1} = 55$ GeV.

[2] CHATRCHYAN 13BS searched in 19.5 fb^{-1} of pp collisions at $\sqrt{s} = 8$ TeV for events with a single isolated lepton, hadronic jets, large $\not{E}_T$, and large transverse mass. No significant excess above the Standard Model expectations is observed. Limits are set on stop masses in simplified models where the decay $\widetilde{t} \to t\widetilde{\chi}^0_1$ takes place with a branching ratio which has been varied between 50% and 100%, see Fig. 12, and where the decay $\widetilde{t} \to b\widetilde{\chi}^\pm_1$, $\widetilde{\chi}^\pm_1 \to W^\pm\widetilde{\chi}^0_1$ takes place with a branching ratio of 100%, with varying intermediate mass of the $\widetilde{\chi}^\pm_1$, see Fig. 11.

[3] AAD 12AH searched in 2.05 fb^{-1} of pp collisions at $\sqrt{s} = 7$ TeV for pair production of $\widetilde{t}_1$ in events with two same-flavor, opposite-sign leptons (e or μ) with invariant mass consistent with the Z boson, large missing transverse momentum and jets in the final state. At least one of the jets is identified as originating from a b-quark. The data are found to be consistent with the Standard Model expectations. The results are interpreted in a GMSB scenario where the $\widetilde{\chi}^0_1$ is the NLSP and is purely higgsino-like. Other model parameters are $\tan\beta = 10$, $m_{\widetilde{u}_3} = m_{\widetilde{q}_3} = -A_t/2$. Scalar top masses below 240 GeV are excluded for all values of $m_{\widetilde{\chi}^0_1} > m_Z$.

[4] AAD 12CB searched in 4.7 fb^{-1} of pp collisions at $\sqrt{s} = 7$ TeV for pair production of $\widetilde{t}_1$ in events with two opposite-sign leptons (electrons or muons), jets, and $\not{E}_T$. The $\widetilde{t}_1$ is assumed to decay through $\widetilde{t}_1 \to t\widetilde{\chi}^0_1$ with a 100% branching ratio. The data are found to be consistent with the Standard Model expectations. The results are interpreted in a simplified model as a function of $m_{\widetilde{t}_1}$ and $m_{\widetilde{\chi}^0_1}$, see Fig. 2. Assuming a massless $\widetilde{\chi}^0_1$, a $\widetilde{t}_1$ with a mass of 300 GeV is excluded at 95% C.L.

[5] AAD 12CE searched in 4.7 fb^{-1} of pp collisions at $\sqrt{s}$ = 7 TeV for pair production of $\tilde{t}_1$ where $\tilde{t}_1 \to t\tilde{\chi}_1^0$ with a 100 % branching ratio and where both tops decay hadronically. The data are found to be consistent with the Standard Model expectations. The results are interpreted in a simplified model as a function of $m_{\tilde{t}_1}$ and $m_{\tilde{\chi}_1^0}$, see Fig. 4. For a massless $\tilde{\chi}_1^0$, masses of $\tilde{t}_1$ between 370 GeV and 465 GeV are excluded at 95% C.L. The upper limit deteriorates to 445 GeV for $m_{\tilde{\chi}_1^0} < 50$ GeV.

[6] AAD 12CF searched in 4.7 fb^{-1} of pp collisions at $\sqrt{s}$ = 7 TeV for pair production of $\tilde{t}_1$ in events with one isolated electron or muon, jets, and $\not{E}_T$. The $\tilde{t}_1$ is assumed to decay through $\tilde{t}_1 \to t\tilde{\chi}_1^0$ a 100 % branching ratio. The data are found to be consistent with the Standard Model expectations. The results are interpreted in a simplified model as a function of $m_{\tilde{t}_1}$ and $m_{\tilde{\chi}_1^0}$, see Fig. 2. For a massless $\tilde{\chi}_1^0$, masses of $\tilde{t}_1$ between 230 GeV and 440 GeV are excluded at 95% C.L. The upper limit deteriorates to 400 GeV for $m_{\tilde{\chi}_1^0} < 125$ GeV and the lower limit is increased to about 330 GeV.

[7] AAD 12CL searched in 4.7 fb^{-1} of pp collisions at $\sqrt{s}$ = 7 TeV for pair production of $\tilde{t}_1$ in events with two opposite-sign leptons (electrons or muons), jets, and $\not{E}_T$. The $\tilde{t}_1$ is assumed to decay through $\tilde{t}_1 \to b\tilde{\chi}_1^\pm$ with a 100 % branching ratio. The chargino is then assumed to decay through a virtual W boson, $\tilde{\chi}_1^\pm \to W^*\tilde{\chi}_1^0$. The data are found to be consistent with the Standard Model expectations. The results are interpreted in a simplified model as a function of $m_{\tilde{t}_1}$ and $m_{\tilde{\chi}_1^0}$ for a fixed choice of $m_{\tilde{\chi}_1^\pm} = 106$ GeV, see Fig. 2. Assuming $m_{\tilde{\chi}_1^\pm}$=106 GeV, $\tilde{t}_1$ masses below 130 GeV are excluded at 95% C.L. for $m_{\tilde{\chi}_1^0} < 70$ GeV.

[8] AAD 12J looked in 2.1 fb^{-1} of pp collisions at $\sqrt{s}$ = 7 TeV for evidence of lepton flavor violating interactions in the $e\mu$ continuum due to a t-channel exchange of an R-parity violating scalar top quark. No deviations from the SM expectations were found. Limits on R-parity violating couplings are calculated as a function of the scalar stop mass, see their Fig. 4b.

[9] AALTONEN 12AO searched in 2.6 fb^{-1} of $p\overline{p}$ collisions at $\sqrt{s}$ = 1.96 TeV for events containing $\not{E}_T$ and at least two jets, of which at least one is identified as originating from a charm quark. No excess over the expected SM background is observed. Limits are set on the production of $\tilde{t}_1$ in the assumption that the only decay model is into $c\tilde{\chi}_1^0$ and for $m_{\tilde{\chi}_1^0}$ = 90 GeV, see Fig. 2. According to Fig. 2 there is an exclusion gap from 100–130 GeV.

[10] ABAZOV 12H looked in 7.3 fb^{-1} of $p\overline{p}$ collisions at $\sqrt{s}$ = 1.96 TeV for events containing one muon, one tau decaying hadronically, at least one jet, and missing transverse energy. No evidence for an excess over the SM expectation is observed and 95% C.L. limits are set in the plane ($m_{\tilde{t}_1}$, $m_{\tilde{\nu}}$), see their Fig. 5 (where B($\tilde{t}_1 \to b\mu\tilde{\nu}$) = B($\tilde{t}_1 \to b\tau\tilde{\nu}$) = 1/3) and Fig. 6 (where B($\tilde{t}_1 \to b\mu\tilde{\nu}$) = 0.1 and B($\tilde{t}_1 \to b\tau\tilde{\nu}$) = 0.8).

[11] ABAZOV 12L looked in 5.2 fb^{-1} of $p\overline{p}$ collisions at $\sqrt{s}$ = 1.96 TeV for charged massive long-lived particles in events in which one or more particles are reconstructed as muons but have speed and ionization energy loss inconsistent with muons produced in beam collisions. Long-lived stops with mass below 285 GeV are excluded at 95% C.L, using the nominal value of the NLO production cross section. For the latter, a charge survival probability of 38% has been assumed

[12] ABAZOV 11N looked in 5.4 fb^{-1} of $p\overline{p}$ collisions at $\sqrt{s}$ = 1.96 TeV for events with exactly one e and μ and $\not{E}_T$ from the production of $\tilde{t}_1\tilde{t}_1$. No evidence for an excess over the SM expectation is observed, and a limit is derived in a plane of ($m_{\tilde{t}_1}$, $m_{\tilde{\nu}}$), see their Fig. 4, under the assumption of 100% branching ratio for $\tilde{t}_1 \to b\ell\tilde{\nu}$.

[13] AALTONEN 10Y searched in 1 fb^{-1} of $p\overline{p}$ collisions at $\sqrt{s}$ = 1.96 TeV for events with an oppositely charged lepton pair (e or μ), $\not{E}_T$ and at least one jet. A limit is derived on the cross section assuming 100% branching ratio of $\tilde{t}_1 \to b\ell\tilde{\nu}$ and an invisible $\tilde{\nu}$, see their Fig. 10. In Fig. 11, the exclusion contour is shown in the plane of ($m_{\tilde{t}_1}$,$m_{\tilde{\nu}}$).

[14] ABAZOV 08Z looked in 995 pb^{-1} of $p\overline{p}$ collisions at $\sqrt{s}$ = 1.96 TeV for events with exactly 2 jets, at least one being tagged as heavy quark, and $\not{E}_T$, originating from stop pair production. Branching ratios are assumed to be 100% for $\tilde{t}_1 \to c\tilde{\chi}_1^0$. No evidence for an excess over the SM expectation is observed. The excluded region is shown in a plane of $m_{\tilde{t}}$ versus $m_{\tilde{\chi}_1^0}$, see their Fig. 5. No limit can be obtained for $m_{\tilde{\chi}_1^0} > 70$ GeV. Supersedes the results of ABAZOV 07B.

[15] ABAZOV 04 looked at 108.3pb^{-1} of $p\overline{p}$ collisions at $\sqrt{s}$ = 1.8 TeV for events with e+μ+$\not{E}_T$ as signature for the 3- and 4-body decays of stop into $b\ell\nu\tilde{\chi}^0$ final states. For the $b\ell\tilde{\nu}$ channel they use the results from ABAZOV 02C. No significant excess is observed compared to the Standard Model expectation and limits are derived on the mass of $\tilde{t}_1$ for the 3- and 4-body decays in the ($m_{\tilde{t}}$, $m_{\tilde{\chi}^0}$) plane, see their Figure 4.

[16] ACHARD 04 search in the 192–209 GeV data for the production of $\tilde{t}\,\overline{\tilde{t}}$ in acoplanar di-jet final states and, in case of $b\ell\tilde{\nu}$ ($b\tau\tilde{\nu}$) final states, two leptons (taus). The limits for θ_t= 0 improve to 95, 96 and 93 GeV, respectively. All limits assume 100% branching ratio for the respective decay modes. See Fig. 6 for the dependence of the limits on $m_{\tilde{\chi}_1^0}$. These limits supersede ACCIARRI 99V.

[17] ABDALLAH 03M looked for $\tilde{t}$ pair production in events with acoplanar jets and $\not{E}$ at $\sqrt{s}$ = 189–208 GeV. See Fig. 23 and Table 11 for other choices of Δm. These limits include and update the results of ABREU,P 00D.

[18] ABBIENDI 02H looked for events with two acoplanar jets, $\not{p}_T$, and, in the case of $b\ell\tilde{\nu}$ final states, two leptons, in the 161–209 GeV data. The bound for $c\tilde{\chi}_1^0$ applies to the region where $\Delta m < m_W + m_b$, else the decay $\tilde{t}_1 \to b\tilde{\chi}_1^0 W^+$ becomes dominant. The limit for $b\ell\tilde{\nu}$ assumes equal branching ratios for the three lepton flavors and for $b\tau\tilde{\nu}$ 100% for this channel. For θ_t=0, the bounds improve to > 97.6 GeV ($c\tilde{\chi}_1^0$), > 96.0 GeV ($b\ell\tilde{\nu}$), and > 95.5 ($b\tau\tilde{\nu}$). See Figs. 5–6 and Table 5 for the more general dependence of the limits on Δm. These results supersede ABBIENDI 99M.

[19] HEISTER 02K search for top squarks in final states with jets (with/without b tagging or leptons) or long-lived hadrons, using 183–209 GeV data. The absolute mass bound is obtained by varying the branching ratio of $\tilde{t} \to c\tilde{\chi}_1^0$ and the lepton fraction in $\tilde{t} \to b\tilde{\chi}_1^0 f\overline{f}'$ decays. The mass bound for $\tilde{t} \to c\tilde{\chi}_1^0$ uses the CDF results from AFFOLDER 00D and for $\tilde{t} \to b\ell\tilde{\nu}$ the DØ results from ABAZOV 02C. See Figs. 2–5 for the more general dependence of the limits on Δm. Updates BARATE 01 and BARATE 00P.

[20] AAD 13AU searched in 20.1 fb^{-1} of pp collisions at $\sqrt{s}$ = 8 TeV for events containing two jets identified as originating from b-quarks and large missing transverse momentum. No excess of events above the expected level of Standard Model background was found. Exclusion limits at 95% C.L. are set on the masses of third-generation squarks. Assuming that the decay $\tilde{t}_1 \to b\tilde{\chi}_1^\pm$ takes place 100% of the time, a $\tilde{t}_1$ mass below 580 GeV (440 GeV) is excluded for Δm = $m_{\tilde{\chi}_1^\pm} - m_{\tilde{\chi}_1^0}$ = 5 GeV (20 GeV) and for $m_{\tilde{\chi}_1^0}$ = 100 GeV. For more details, see their Fig. 6.

[21] CHATRCHYAN 13BN searched in 19.5 fb^{-1} of pp collisions at $\sqrt{s}$ = 8 TeV for events with three or more isolated leptons and b-quark jets. No excess above the Standard Model expectations is observed. Limits are set on stop masses in $R\!\!\!/$ SUSY models with leptonic $LL\overline{E}$ couplings, see Fig. 2. Also limits have been set in a model with $LQ\overline{D}$ couplings.

[22] CHATRCHYAN 13M searched in 4.8 fb^{-1} of pp collisions at $\sqrt{s}$ = 7 TeV for events containing an isolated electron or muon, a hadronically decaying τ lepton and two b-quark jets. No excess above the Standard Model expectations is observed. Limits are set on stop masses in $R\!\!\!/$ SUSY models with $L_3Q_3D_3$ couplings, see Fig. 2. In a simplified model where the decay $\tilde{t}_1 \to \tau b$ takes place with a branching ratio of 100%, stop masses below 525 GeV are excluded at 95% C.L.

[23] HAN 13 used combined ATLAS results based on 20.1 fb^{-1} of pp collisions at $\sqrt{s}$ = 8 TeV to derive 95% C.L. exclusion limits on the stop mass in the framework of natural SUSY in the MSSM, after considering the constraints from the Higgs mass, B-physics, and electroweak precision measurements.

[24] CHATRCHYAN 12AN looked in 4.0 fb^{-1} of pp collisions at $\sqrt{s}$ = 7 TeV for events with pair production of long-lived stops. The hadronization of the stops leads to R-hadrons which may stop inside the detector and later decay via $\tilde{t} \to t\tilde{\chi}_1^0$ during gaps between the proton bunches. No significant excess over the expected background is observed. From a counting experiment, a limit at 95% C.L. on the cross section as a function of $m_{\tilde{t}}$ is derived, see Fig. 4. The mass limit is valid for lifetimes between 10^{-5} and 10^3 seconds, for what they call "the daughter top energy E_t >" 125 GeV and assuming the *cloud* interaction model for R-hadrons. Supersedes KHACHATRYAN 11.

[25] CHATRCHYAN 12L looked in 5.0 fb^{-1} of pp collisions at $\sqrt{s}$ = 7 TeV for events with heavy stable particles, identified by their anomalous dE/dx in the tracker or additionally requiring that it be identified as muon in the muon chambers, from pair production of $\tilde{t}_1$'s. No evidence for an excess over the expected background is observed. Limits are derived for pair production of stops as a function of mass (see Fig. 3). In the conservative scenario where every hadronic interaction causes it to become neutral, the limit decreases to 626 GeV. Supersedes KHACHATRYAN 11C.

[26] AAD 11K looked in 34 pb^{-1} of pp collisions at $\sqrt{s}$ = 7 TeV for events with heavy stable particles, identified by their anomalous dE/dx in the tracker or time of flight in the tile calorimeter, from pair production of $\tilde{t}$. No evidence for an excess over the SM expectation is observed and limits on the mass are derived for pair production of stop, see Fig. 4.

[27] KHACHATRYAN 11C looked in 3.1 pb^{-1} of pp collisions at $\sqrt{s}$ = 7 TeV for events with heavy stable particles, identified by their anomalous dE/dx in the tracker or time of flight in the muon chambers, from pair production of $\tilde{t}_1$. No evidence for an excess over the expected background is observed. Limits are derived for pair production of stop as a function of mass, see Fig. 3, and compared to the production cross section in a benchmark scenario.

[28] AALTONEN 10O searched in 2.7 fb^{-1} of $p\overline{p}$ collisions at $\sqrt{s}$ = 1.96 TeV for events with a charged lepton pair (e or μ), $\not{E}_T$ and at least two jets. A fit of the data is made to the $\tilde{t}_1\,\overline{\tilde{t}}_1$ hypothesis. Assuming a 100% branching ratio of $\tilde{t}_1 \to b\tilde{\chi}_1^\pm$, the exclusion is independent of the value of the $\tilde{\chi}_1^\pm \to \ell\tilde{\chi}_1^0\nu$ branching ratio.

[29] ABAZOV 09N looked in 0.9 fb^{-1} of $p\overline{p}$ collisions at $\sqrt{s}$ = 1.96 TeV for events with $\geq$ 3 jets, at least one being b-tagged, one electron or muon and $\not{E}_T$ originating from associated production $\tilde{t}\,\overline{\tilde{t}}$, with one $\tilde{t}$ decaying leptonically, the other hadronically. The branching ratios for $\tilde{t}_1 \to b\tilde{\chi}_1^\pm$ and $\tilde{\chi}_1^\pm \to \tilde{\chi}_1^0 W^\pm$ are assumed to be 100%. The separation from the dominant $t\overline{t}$ background is based on a multivariate likelihood discriminant analysis. The tested mass range is 130 GeV $\leq m_{\tilde{t}} \leq$ 190 GeV, 90 GeV $\leq m_{\tilde{\chi}_1^\pm} \leq$ 150 GeV and $m_{\tilde{\chi}_1^0}$ = 50 GeV fixed. The excluded cross section is a factor 2–13 larger than the theoretical expectation in the considered MSSM scenarios, see their Fig. 3.

[30] ABAZOV 09O looked in 1 fb^{-1} of $p\overline{p}$ collisions at $\sqrt{s}$ = 1.96 TeV for events with two electrons or one electron and one muon and $\not{E}_T$ originating from associated production $\tilde{t}\,\overline{\tilde{t}}$, followed by the three-body decays $\tilde{t} \to b\ell\tilde{\nu}$. No evidence for an excess over the SM expectation is observed. The excluded region is shown in a plane of $m_{\tilde{\nu}}$ versus $m_{\tilde{t}}$, see their Fig. 3. The largest excluded $\tilde{t}$ mass is 175 GeV for a $\tilde{\nu}$ mass of 45 GeV, and the largest excluded $\tilde{\nu}$ mass is 96 GeV for a $\tilde{t}$ mass of 140 GeV. Superseded by ABAZOV 11N.

[31] AALTONEN 08Z searched in 322 pb^{-1} of $p\overline{p}$ collisions at $\sqrt{s}$ = 1.96 TeV for dijet events with a lepton (e or μ) and a hadronic τ decay produced via R-parity violating couplings $LQ\overline{D}$. No heavy flavour-tagged jets are requested. No significant excess was found compared to the background expectation. Upper limits on the cross-section times the square of the branching ratio B($\tilde{t}_1 \to b\tau$) are extracted, and a limit is derived on the stop mass assuming B($\tilde{t}_1 \to b\tau$) = 1, see their Fig. 2. Supersedes the results of ACOSTA 04B.

[32] ABAZOV 08 looked at approximately 400 pb^{-1} of $p\overline{p}$ collisions at $\sqrt{s}$ = 1.96 TeV for events with $b\overline{b}\ell\ell'\not{E}_T$ with $\ell\ell' = e^\pm\mu^\mp$ or $\ell\ell' = \mu^+\mu^-$, originating from associated production $\tilde{t}\,\overline{\tilde{t}}$. Branching ratios are assumed to be 100% for both $\tilde{\chi}_1^\pm \to \ell\tilde{\nu}$ and $\tilde{\nu} \to \nu\tilde{\chi}_1^0$. No evidence for an excess over the SM expectation is observed. The excluded region is shown in a plane of $m_{\tilde{\nu}}$ versus $m_{\tilde{t}}$, see their Fig.3. Superseded by ABAZOV 09O.

[33] AALTONEN 07E searched in 295 pb^{-1} of $p\overline{p}$ collisions at $\sqrt{s}$ = 1.96 TeV for multijet events with large $\not{E}_T$. They request at least one heavy flavor-tagged jet and no identified leptons. The branching ratio $\tilde{t}_1 \to c\tilde{\chi}_1^0$ is assumed to be 100%. No significant excess was found compared to the background expectation. Upper limits on the cross-section are extracted and a limit is derived on the masses of stop versus $\tilde{\chi}_1^0$, see their Fig. 4.

[34] ABAZOV 07B looked in 360 pb^{-1} of $p\overline{p}$ collisions at $\sqrt{s}$ = 1.96 TeV for events with a pair of acoplanar heavy-flavor jets with $\not{E}_T$. No excess is observed relative to the SM background expectations. Limits are set on the production of $\tilde{t}_1$ under the assumption that the only decay mode is into $c\tilde{\chi}_1^0$, see their Fig. 4 for the limit in the ($m_{\tilde{t}}$,

$m_{\widetilde{\chi}^0_1}$) plane. No limit can be obtained for $m_{\widetilde{\chi}^0_1} > 54$ GeV. Supersedes the results of ABAZOV 04B.

[35] CHEKANOV 07 search for the $LQ\overline{D}$ R-parity violating process $e^+p \to \widetilde{t}_1$ in 65 pb^{-1} at 318 GeV. Final states may originate from $LQ\overline{D}$ couplings $\widetilde{t} \to e^+d$ and from the R-parity conserving decay $\widetilde{t} \to \widetilde{\chi}^+b$, giving rise to e + jet, e + multi-jet, and ν + multi-jet. The excluded region in an MSSM scenario is presented for λ'_{131} as a function of the stop mass in Fig. 6. Other excluded regions in a more restricted mSUGRA model are shown in Fig. 7 and 8.

[36] ABBIENDI 04F use data from $\sqrt{s} = 189$–209 GeV. They derive limits on the stop mass under the assumption of $\not{R}$ with $LQ\overline{D}$ or $\overline{UDD}$ couplings. The limit quoted applies to direct decays with $\overline{UDD}$ couplings when the stop decouples from the Z^0 and improves to 88 GeV for $\theta_t = 0$. For $LQ\overline{D}$ couplings, the limit improves to 98 (100) GeV for λ'_{13k} or λ'_{23k} couplings and all θ_t ($\theta_t = 0$). For λ'_{33k} couplings it is 96 (98) GeV for all θ_t ($\theta_t = 0$). Supersedes the results of ABBIENDI 00.

[37] ABDALLAH 04M use data from $\sqrt{s} = 192$–208 GeV to derive limits on sparticle masses under the assumption of $\not{R}$ with $LL\overline{E}$ or $\overline{UDD}$ couplings. The results are valid for $\mu = -200$ GeV, $\tan\beta = 1.5$, $\Delta m > 5$ GeV and assuming a BR of 1 for the given decay. The limit quoted is for decoupling of the stop from the Z^0 and indirect $\overline{UDD}$ decays using the neutralino constraint of 39.5 GeV for $LL\overline{E}$ and of 38.0 GeV for $\overline{UDD}$ couplings, also derived in ABDALLAH 04M. For no mixing (decoupling) and indirect decays via $LL\overline{E}$ the limit improves to 92 (87) GeV if the constraint from the neutralino is used and to 88 (81) GeV if it is not used. For indirect decays via $\overline{UDD}$ couplings it improves to 87 GeV for no mixing and using the constraint from the neutralino, whereas it becomes 81 GeV (67) GeV for no mixing (decoupling) if the neutralino constraint is not used. Supersedes the result of ABREU 01D.

[38] AKTAS 04B looked in 106 pb^{-1} of $e^\pm p$ collisions at $\sqrt{s} = 319$ GeV and 301 GeV for resonant production of $\widetilde{t}_1$ by R-parity violating $LQ\overline{D}$ couplings couplings with λ'_{131}, others being zero. They consider the decays $\widetilde{t}_1 \to e^+d$ and $\widetilde{t}_1 \to W\widetilde{b}$ followed by $\widetilde{b} \to \overline{\nu}_e d$ and assume gauginos too heavy to participate in the decays. They combine the channels $je\not{p}_T$, $j\mu\not{p}_T$, $jj\not{p}_T$ to derive limits in the plane ($m_{\widetilde{t}}$, λ'_{131}), see their Fig. 5.

[39] DAS 04 reanalyzes AFFOLDER 00G data and obtains constraints on $m_{\widetilde{t}_1}$ as a function of B($\widetilde{t} \to b\ell\nu\chi^0$)×B($\widetilde{t} \to b\overline{q}q'\chi^0$), B($\widetilde{t} \to c\chi^0$) and m_{χ^0}. Bound weakens for larger B($\widetilde{t} \to c\chi^0$) and m_{χ^0}.

[40] ABDALLAH 03C looked for events of the type $q\overline{q}R^\pm R^\pm$, $q\overline{q}R^\pm R^0$ or $q\overline{q}R^0R^0$ in e^+e^- interactions at $\sqrt{s} = 189$–208 GeV. The $R^\pm$ bound states are identified by anomalous dE/dx in the tracking chambers and the R^0 by missing energy, due to their reduced energy loss in the calorimeters. Excluded mass regions in the ($m(\widetilde{t})$, $m(\widetilde{g})$) plane for $m(\widetilde{g}) > 2$ GeV are obtained for several values of the probability for the gluino to fragment into $R^\pm$ or R^0, as shown in their Fig. 18. The limit improves to 90 GeV for $\theta_t = 0$.

[41] ACOSTA 03C searched in 107 pb^{-1} of $p\overline{p}$ collisions at $\sqrt{s}$=1.8 TeV for pair production of $\widetilde{t}$ followed by the decay $\widetilde{t} \to b\ell\widetilde{\nu}$. They looked for events with two isolated leptons (e or μ), at least one jet and $\not{E}_T$. The excluded mass range is reduced for larger $m_{\widetilde{\nu}}$, and no limit is set for $m_{\widetilde{\nu}} > 88.4$ GeV (see Fig. 2). Superseded by AALTONEN 10Y.

[42] Theoretical analysis of e^+e^-+2 jet final states from the RPV decay of $t\overline{t}^*$ pairs produced in $p\overline{p}$ collisions at $\sqrt{s}$=1.8 TeV. 95%CL limits of 220 (165) GeV are derived for B($\widetilde{t} \to eq$)=1 (0.5).

[43] HEISTER 03G searches for the production of $\widetilde{t}$ pairs in the case of $\not{R}$ prompt decays with $LL\overline{E}$, $LQ\overline{D}$ or $\overline{UDD}$ couplings at $\sqrt{s} = 189$–209 GeV. The limit holds for indirect decays mediated by $\not{R}$ $\overline{UDD}$ couplings. It improves to 91 GeV for indirect decays mediated by $\not{R}$ $LL\overline{E}$ couplings, to 97 GeV for direct (assuming B($\widetilde{t}_L \to q\tau$) = 100%) and to 85 GeV for indirect decays mediated by $\not{R}$ $LQ\overline{D}$ couplings. Supersedes the results from BARATE 01B.

[44] HEISTER 03H use e^+e^- data from 183–208 GeV to look for the production of stop decaying into a c quark and a stable gluino hadronizing into charged or neutral R-hadrons. Combining these results with bounds on stable squarks and on a stable gluino LSP from the same paper yields the quoted limit. See their Fig. 13 for the dependence of the mass limit on the gluino mass and on θ_t.

[45] ABAZOV 02C looked in 108.3pb^{-1} of $p\overline{p}$ collisions at $\sqrt{s}$=1.8 TeV for events with $e\mu\not{E}_T$, originating from associated production $\widetilde{t}\,\overline{\widetilde{t}}$. Branching ratios are assumed to be 100%. The bound for the $b\ell\widetilde{\nu}$ decay weakens for large $\widetilde{\nu}$ mass (see Fig. 3), and no limit is set when $m_{\widetilde{\nu}} > 85$ GeV. See Fig. 4 for the limits in case of decays to a real $\widetilde{\chi}^\pm_1$, followed by $\widetilde{\chi}^\pm_1 \to \ell\widetilde{\nu}$, as a function of $m_{\widetilde{\chi}^\pm_1}$.

[46] ACHARD 02 searches for the production of squarks in the case of $\not{R}$ prompt decays with $\overline{UDD}$ couplings at $\sqrt{s}$=189–208 GeV. The search is performed for direct and indirect decays, assuming one coupling at the time to be nonzero. The limit is computed for the minimal cross section and holds for both direct and indirect decays.

[47] AFFOLDER 01B searches for decays of the top quark into stop and LSP, in $t\overline{t}$ events. Limits on the stop mass as a function of the LSP mass and of the decay branching ratio are shown in Fig. 3. They exclude branching ratios in excess of 45% for SLP masses up to 40 GeV.

[48] ABREU 00I searches for the production of stop in the case of R-parity violation with $LL\overline{E}$ couplings, for which only indirect decays are allowed. They investigate topologies with jets plus leptons in data from $\sqrt{s}$=183 GeV. The lower bound on the stop mass assumes a neutralino mass limit of 27 GeV, also derived in ABREU 00I.

[49] AFFOLDER 00D search for final states with 2 or 3 jets and $\not{E}_T$, one jet with a c tag. See their Fig. 2 for the mass exclusion in the ($m_{\widetilde{t}}$,$m_{\widetilde{\chi}^0_1}$) plane. The maximum excluded $m_{\widetilde{t}}$ value is 119 GeV, for $m_{\widetilde{\chi}^0_1}$= 40 GeV.

[50] AFFOLDER 00G searches for $\widetilde{t}_1\,\overline{\widetilde{t}}^*_1$ production, with $\widetilde{t}_1 \to b\ell\widetilde{\nu}$, leading to topologies with ≥ 1 isolated lepton (e or μ), $\not{E}_T$, and ≥ 2 jets with ≥ 1 tagged as b quark by a secondary vertex. See Fig. 4 for the excluded mass range as a function of $m_{\widetilde{\nu}}$. Cross-section limits for $\widetilde{t}_1\,\overline{\widetilde{t}}^*_1$, with $\widetilde{t}_1 \to b\chi^\pm_1$ ($\chi^\pm_1 \to \ell^\pm\nu\widetilde{\chi}^0_1$), are given in Fig. 2. Superseded by AALTONEN 10Y.

[51] ABE 99M looked in 107 pb^{-1} of $p\overline{p}$ collisions at $\sqrt{s}$=1.8 TeV for events with like sign dielectrons and two or more jets from the sequential decays $\widetilde{q} \to q\widetilde{\chi}^0_1$ and $\widetilde{\chi}^0_1 \to eq\overline{q}'$, assuming $\not{R}$ coupling $L_1Q_jD^c_k$, with j=2,3 and k=1,2,3. They assume B($\widetilde{t}_1 \to c\widetilde{\chi}^0_1$)=1, B($\widetilde{\chi}^0_1 \to eq\overline{q}'$)=0.25 for both e^+ and e^-, and $m_{\widetilde{\chi}^0_1} \geq m_{\widetilde{t}_1}/2$. The limit improves for heavier $\widetilde{\chi}^0_1$.

[52] AID 96 considers photoproduction of $\widetilde{t}\,\overline{\widetilde{t}}$ pairs, with 100% R-parity violating decays of $\widetilde{t}$ to eq, with q=d, s, or b quarks.

[53] AID 96 considers production and decay of $\widetilde{t}$ via the R-parity violating coupling $\lambda' L_1 Q_3 d^c_1$.

[54] CHO 96 studied the consistency among the B^0-$\overline{B}^0$ mixing, ϵ in K^0-$\overline{K}^0$ mixing, and the measurements of V_{cb}, V_{ub}/V_{cb}. For the range 25.5 GeV<$m_{\widetilde{t}_1}$ <$m_Z/2$ left by AKERS 94K for $\theta_t = 0.98$, and within the allowed range in M_2-μ parameter space from chargino, neutralino searches by ACCIARRI 95E, they found the scalar top contribution to B^0-$\overline{B}^0$ mixing and ϵ to be too large if $\tan\beta$ <2. For more on their assumptions, see the paper and their reference 10.

[55] BUSKULIC 95E looked for $Z \to \widetilde{t}\,\overline{\widetilde{t}}$, where $\widetilde{t} \to c\chi^0_1$ and χ^0_1 decays via R-parity violating interactions into two leptons and a neutrino.

[56] SHIRAI 94 bound assumes the cross section without the s-channel Z-exchange and the QCD correction, underestimating the cross section up to 20% and 30%, respectively. They assume m_c=1.5 GeV.

Heavy $\widetilde{g}$ (Gluino) MASS LIMIT

For $m_{\widetilde{g}} > 60$–70 GeV, it is expected that gluinos would undergo a cascade decay via a number of neutralinos and/or charginos rather than undergo a direct decay to photinos as assumed by some papers. Limits obtained when direct decay is assumed are usually higher than limits when cascade decays are included. Limits made obsolete by the most recent analyses of $p\overline{p}$ collisions can be found in previous Editions of this *Review*.

VALUE (GeV)	CL%	DOCUMENT ID		TECN	COMMENT
>1100	95	[1,2] AAD	13AV	ATLS	$\geq$ 7jets + $\not{E}_T$, $\widetilde{g} \to t\overline{t}\widetilde{\chi}^0_1$, $m_{\widetilde{\chi}^0_1} < 350$ GeV
>1150	95	[1,3] AAD	13AV	ATLS	$\geq$ 7jets + $\not{E}_T$, $\widetilde{g} \to t\overline{t}\widetilde{\chi}^0_1$, $\widetilde{t} \to t\widetilde{\chi}^0_1$, $m_{\widetilde{t}} < 750$ GeV, $m_{\widetilde{\chi}^0_1}$ = 60 GeV
> 900	95	[1,4] AAD	13AV	ATLS	$\geq$ 7jets + $\not{E}_T$, $\widetilde{g} \to t\overline{t}\widetilde{\chi}^0_1$, $\widetilde{t} \to \overline{s}\overline{b}$ (RPV), 400 GeV < $m_{\widetilde{t}}$ < 1000 GeV
>1000	95	[1,5] AAD	13AV	ATLS	$\geq$ 7jets + $\not{E}_T$, $\widetilde{g} \to \overline{q}q'\widetilde{\chi}^\pm_1$, $\widetilde{\chi}^\pm_1 \to W^\pm\widetilde{\chi}^0_1$, ($m_{\widetilde{\chi}^\pm_1}$-$m_{\widetilde{\chi}^0_1}$) / ($m_{\widetilde{g}}$-$m_{\widetilde{\chi}^0_1}$) = 0.5, $m_{\widetilde{\chi}^0_1}$ < 200 GeV
>1100	95	[1,6] AAD	13AV	ATLS	$\geq$ 7jets + $\not{E}_T$, mSUGRA/CMSSM, large m_0
> 700	95	[7] CHATRCHYAN	13G	CMS	0,1,2, $\geq$ 3 b-jets + $\not{E}_T$, CMSSM
>1250	95	[7] CHATRCHYAN	13G	CMS	0,1,2, $\geq$ 3 b-jets + $\not{E}_T$, CMSSM, $m_{\widetilde{g}} = m_{\widetilde{q}}$
>1300	95	[8] CHATRCHYAN	13P	CMS	1 $\ell^\pm$ + jets + $\not{E}_T$, CMSSM, $m_0 < 800$ GeV
>1150	95	[9] CHATRCHYAN	13R	CMS	$\geq$ 1 τ + jets + $\not{E}_T$, CMSSM, $m_0 < 440$ GeV
>1125	95	[10,11] CHATRCHYAN	13T	CMS	jets + $\not{E}_T$, $\widetilde{g} \to b\overline{b}\widetilde{\chi}^0_1$ simplified model, $m_{\widetilde{\chi}^0_1}$= 0 GeV
> 950	95	[10,12] CHATRCHYAN	13T	CMS	jets + $\not{E}_T$, $\widetilde{g} \to q\overline{q}\widetilde{\chi}^0_1$ simplified model, $m_{\widetilde{\chi}^0_1}$= 0 GeV
> 950	95	[10,13] CHATRCHYAN	13T	CMS	jets + $\not{E}_T$, $\widetilde{g} \to t\overline{t}\widetilde{\chi}^0_1$ simplified model, $m_{\widetilde{\chi}^0_1}$= 0 GeV
>1000	95	[14] CHATRCHYAN	13V	CMS	same-sign $\ell^\pm\ell^\pm$ + $\geq$ 2 b-jets, $\widetilde{g} \to t\overline{t}\widetilde{\chi}^0_1$ simplified model, $m_{\widetilde{\chi}^0_1}$ < 400 GeV
> 550	95	[15] AAD	12AP	ATLS	$\ell^\pm\ell^\pm$ + jets + $\not{E}_T$, $\widetilde{g} \to \widetilde{t}_1 t$, CMSSM
> 820	95	[16] AAD	12AX	ATLS	ℓ +jets +$\not{E}_T$, CMSSM, $m_{\widetilde{g}}$=$m_{\widetilde{q}}$
> 840	95	[17] AAD	12BI	ATLS	$\geq$ 6–9 jets + $\not{E}_T$, CMSSM, high m_0
>1020	95	[18] AAD	12BY	ATLS	$\widetilde{g} \to bb\widetilde{\chi}^0_1$, $m_{\widetilde{\chi}^0_1} < 400$ GeV
> 940	95	[18] AAD	12BY	ATLS	$\widetilde{g} \to tt\widetilde{\chi}^0_1$, $m_{\widetilde{\chi}^0_1} < 50$ GeV
>1200	95	[19] AAD	12CJ	ATLS	$\ell^\pm$+jets+$\not{E}_T$, CMSSM, $m_{\widetilde{g}}$=$m_{\widetilde{q}}$
> 666	95	[20] AAD	12CU	ATLS	$\widetilde{g} \to jjj$, $\not{R}$
> 800	95	[21] CHATRCHYAN	12AT	CMS	jets + $\not{E}_T$, CMSSM
>1180	95	[21] CHATRCHYAN	12AT	CMS	jets + $\not{E}_T$, CMSSM, $m_{\widetilde{g}}$=$m_{\widetilde{q}}$
> 710	95	[22] CHATRCHYAN	12U	CMS	$\ell^\pm\ell^\pm$ + jets + $\not{E}_T$, CMSSM
> 700	95	[23] AAD	11G	ATLS	ℓ+jets+$\not{E}_T$, $\tan\beta$=3, A_0=0, $\mu > 0$, $m_{\widetilde{g}}$=$m_{\widetilde{q}}$
> 500	95	[24] AAD	11N	ATLS	jets+$\not{E}_T$, degenerate $m_{\widetilde{q}}$ of first two generations,$m_{\widetilde{\chi}^0_1}$=0, all other supersymmetric particles heavy, any $m_{\widetilde{q}}$
> 870	95	[24] AAD	11N	ATLS	jets+$\not{E}_T$, degenerate $m_{\widetilde{q}}$ of first two generations,$m_{\widetilde{\chi}^0_1}$=0, all other supersymmetric particles heavy, $m_{\widetilde{q}}$=$m_{\widetilde{g}}$

> 775	95	[24] AAD	11N	ATLS	jets+$\not{E}_T$, CMSSM, $m_{\widetilde{q}}=m_{\widetilde{g}}$	
> 590	95	[25] AAD	11O	ATLS	$\widetilde{g}\to b\bar{b}_1\, b$, $\bar{b}_1\to b\widetilde{\chi}_1^0$, $m_{\widetilde{\chi}_1^0}$=60 GeV	
> 500	95	[26] CHATRCHYAN	11AC	CMS	jets + $\not{E}_T$, CMSSM, $m_{\widetilde{q}}$ <1000 GeV	
> 280	95	[27] AALTONEN	09S	CDF	jets+$\not{E}_T$, tanβ=5, μ<0, A_0=0, any $m_{\widetilde{q}}$	
> 392	95	[27] AALTONEN	09S	CDF	jets+$\not{E}_T$, tanβ=5, μ<0, A_0=0, $m_{\widetilde{q}}=m_{\widetilde{g}}$	
> 308	95	[28] ABAZOV	08G	D0	jets+$\not{E}_T$, tanβ=3, μ<0, A_0=0, any $m_{\widetilde{q}}$	
> 390	95	[28] ABAZOV	08G	D0	jets+$\not{E}_T$, tanβ=3, μ<0, A_0=0, $m_{\widetilde{q}}=m_{\widetilde{g}}$	
> 270	95	[29] ABULENCIA	06I	CDF	$\widetilde{g}\to\bar{b}\,b$, Δm >6 GeV, $\bar{b}_1\to b\widetilde{\chi}_1^0$, $m_{\bar{b}_1}$ <220 GeV	
> 195	95	[30] AFFOLDER	02	CDF	Jets+$\not{E}_T$, any $m_{\widetilde{q}}$	
> 300	95	[30] AFFOLDER	02	CDF	Jets+$\not{E}_T$, $m_{\widetilde{q}}=m_{\widetilde{g}}$	
> 129	95	[31] ABBOTT	01D	D0	$\ell\ell$+jets+$\not{E}_T$, tanβ < 10, m_0 < 300 GeV, μ < 0, A_0=0	
> 175	95	[31] ABBOTT	01D	D0	$\ell\ell$+jets+$\not{E}_T$, tanβ=2, large m_0, μ < 0, A_0=0	
> 255	95	[31] ABBOTT	01D	D0	$\ell\ell$+jets+$\not{E}_T$, tanβ=2, $m_{\widetilde{g}}=m_{\widetilde{q}}$, μ < 0, A_0=0	
> 168	95	[32] AFFOLDER	01J	CDF	$\ell\ell$+Jets+$\not{E}_T$, tanβ=2, μ=−800 GeV, $m_{\widetilde{q}}\gg m_{\widetilde{g}}$	
> 221	95	[32] AFFOLDER	01J	CDF	$\ell\ell$+Jets+$\not{E}_T$, tanβ=2, μ=−800 GeV, $m_{\widetilde{q}}=m_{\widetilde{g}}$	
> 190	95	[33] ABBOTT	99L	D0	Jets+$\not{E}_T$, tanβ=2, μ <0, A=0	
> 260	95	[33] ABBOTT	99L	D0	Jets+$\not{E}_T$, $m_{\widetilde{g}}=m_{\widetilde{q}}$	
• • • We do not use the following data for averages, fits, limits, etc. • • •						
		[34] AAD	13AB	ATLS	jets + 0,1,2 $\ell^\pm$, CMSSM	
>1360	95	[35] AAD	13L	ATLS	jets + $\not{E}_T$, CMSSM, $m_{\widetilde{g}}=m_{\widetilde{q}}$	
> 900	95	[36] AAD	13Q	ATLS	γ+b+$\not{E}_T$,higgsino-like neutralino, $m_{\widetilde{\chi}_1^0}$ > 220 GeV, GMSB	
		[37] CHATRCHYAN	13	CMS	$\ell^\pm\ell^\mp$ + jets + $\not{E}_T$, CMSSM	
>1170	95	[38] CHATRCHYAN	13AK	CMS	b-jets + $\not{E}_T$, $\widetilde{g}\to b\bar{b}\widetilde{\chi}_1^0$ simplified model, $m_{\widetilde{\chi}_1^0}$= 0 GeV	
>1020	95	[38] CHATRCHYAN	13AK	CMS	b-jets + $\not{E}_T$, $\widetilde{g}\to t\bar{t}\widetilde{\chi}_1^0$ simplified model, $m_{\widetilde{\chi}_1^0}$= 0 GeV	
> 870	95	[39,40] CHATRCHYAN	13AM	CMS	$1\ell^\pm$ + b-jets + $\not{E}_T$, $\widetilde{g}\to t\bar{t}\widetilde{\chi}_1^0$ simplified model, $m_{\widetilde{\chi}_1^0}$= 0 GeV	
		[39,41] CHATRCHYAN	13AM	CMS	1 $\ell^\pm$ + b-jets + $\not{E}_T$, CMSSM	
> 700	95	[42] CHATRCHYAN	13AO	CMS	$e^\pm e^\mp$ + jets + $\not{E}_T$, CMSSM, m_0 < 700 GeV	
>1000	95	[43] CHATRCHYAN	13AT	CMS	jets + $\not{E}_T$, $\widetilde{g}\to q\bar{q}\widetilde{\chi}_1^0$ simplified model, $m_{\widetilde{\chi}_1^0}$= 50 GeV	
>1350	95	[44] CHATRCHYAN	13AV	CMS	jets (+ leptons) + $\not{E}_T$, CMSSM, $m_{\widetilde{g}}=m_{\widetilde{q}}$	
> 800	95	[45] CHATRCHYAN	13W	CMS	$\geq$ 1 photons + jets + $\not{E}_T$, GGM, wino-like NLSP, $m_{\widetilde{\chi}_1^0}$ = 375 GeV	
>1000	95	[45] CHATRCHYAN	13W	CMS	$\geq$ 2 photons + jets + $\not{E}_T$, GGM, bino-like NLSP, $m_{\widetilde{\chi}_1^0}$ = 375 GeV	
		[46] AAD	12BA	CDF	b-jets + $\not{E}_T$	
>1070	95	[47] AAD	12CP	ATLS	2γ +$\not{E}_T$, GMSB, bino NLSP, $m_{\widetilde{\chi}_1^0}$ > 50 GeV	
> 950	95	[48] AAD	12W	ATLS	jets + $\not{E}_T$, CMSSM, $m_{\widetilde{g}}=m_{\widetilde{q}}$	
> 805	95	[49] AAD	12X	ATLS	2γ + $\not{E}_T$, GMSB, bino NLSP, $m_{\widetilde{\chi}_1^0}$ > 50 GeV	
		[50] CHATRCHYAN	12	CMS	e, μ, jets, razor, CMSSM	
>1000	95	[51] CHATRCHYAN	12AE	CMS	jets + $\not{E}_T$, $\widetilde{g}\to qq\widetilde{\chi}_1^0$, $m_{\widetilde{\chi}_1^0}$ < 200 GeV	
		[52] CHATRCHYAN	12AH	CMS	b-jets, + $\not{E}_T$, $\widetilde{g}\to b\bar{b}\widetilde{\chi}_1^0$	
		[52] CHATRCHYAN	12AH	CMS	b-jets, + $\not{E}_T$, $\widetilde{g}\to t\bar{t}\widetilde{\chi}_1^0$	
		[53] CHATRCHYAN	12AI	CMS	$\ell^\pm\ell^\pm$ + b-jets + $\not{E}_T$	
		[54] CHATRCHYAN	12AL	CMS	$\geq 3\ell^\pm$, $\not{R}$	
none 280–460	95	[55] CHATRCHYAN	12BD	CMS	$\widetilde{g}\to jjj$, $\not{R}$	
		[56] CHATRCHYAN	12Q	CMS	$\widetilde{g}\to q\bar{q}\widetilde{\chi}_2^0$, $\widetilde{\chi}_2^0\to Z\widetilde{\chi}_1^0$	
> 500	95	[57] DREINER	12A	THEO	$m_{\widetilde{g}}\sim m_{\widetilde{\chi}_1^0}$	
> 650	95	[58] DREINER	12A	THEO	$m_{\widetilde{g}}=m_{\widetilde{q}}\sim m_{\widetilde{\chi}_1^0}$	
> 520	95	[59] AAD	11AF	ATLS	$\geq$ 6 jets + $\not{E}_T$, CMSSM	
> 560	95	[60] AAD	11X	ATLS	$\widetilde{g}\to\widetilde{\chi}_1^0 X\to\gamma\widetilde{G}X$	
> 155	95	[61] AALTONEN	11Q	CDF	$\not{R}$, $\overline{UDD}$, $m_{\widetilde{q}}=m_{\widetilde{g}}$ + 10 GeV	
		[62] CHATRCHYAN	11AB	CMS	$\ell^\pm\ell^\pm$	
		[63] CHATRCHYAN	11G	CMS	$\widetilde{\chi}_1^0\to\gamma\widetilde{G}$	
		[64] CHATRCHYAN	11Q	CMS	ℓ + jets + $\not{E}_T$	
>1040	95	[65] CHATRCHYAN	11V	CMS	GMSB scenario, $\bar{\ell}$ co-NLSP	
		[66] CHATRCHYAN	11W	CMS	jets + $\not{E}_T$, CMSSM	
		[67] KHACHATRY...11I		CMS	jets + $\not{E}_T$	
> 224	95	[68] ABAZOV	02F	D0	$\not{R}$ λ'_{2jk} indirect decays, tanβ=2, any $m_{\widetilde{q}}$	
> 265	95	[68] ABAZOV	02F	D0	$\not{R}$ λ'_{2jk} indirect decays, tanβ=2, $m_{\widetilde{q}}=m_{\widetilde{g}}$	
		[69] ABAZOV	02G	D0	$p\bar{p}\to\widetilde{g}\widetilde{g}$, $\widetilde{g}\widetilde{q}$	
		[70] CHEUNG	02B	THEO		
		[71] BERGER	01	THEO	$p\bar{p}\to$ X+b-quark	
> 240	95	[72] ABBOTT	99	D0	$\widetilde{g}\to\widetilde{\chi}_2^0 X\to\widetilde{\chi}_1^0\gamma X$, $m_{\widetilde{\chi}_2^0}-m_{\widetilde{\chi}_1^0}>20$ GeV	
> 320	95	[72] ABBOTT	99	D0	$\widetilde{g}\to\widetilde{\chi}_1^0 X\to\widetilde{G}\gamma X$	
> 227	95	[73] ABBOTT	99K	D0	any $m_{\widetilde{q}}$, $\not{R}$, tanβ=2, μ < 0	
> 212	95	[74] ABACHI	95C	D0	$m_{\widetilde{g}}\geq m_{\widetilde{q}}$; with cascade decays	
> 144	95	[74] ABACHI	95C	D0	Any $m_{\widetilde{q}}$; with cascade decays	
		[75] ABE	95T	CDF	$\widetilde{g}\to\widetilde{\chi}_2^0\to\widetilde{\chi}_1^0\gamma$	
		[76] HEBBEKER	93	RVUE	e^+e^- jet analyses	
> 218	90	[77] ABE	92L	CDF	$m_{\widetilde{q}}\leq m_{\widetilde{g}}$; with cascade decay	
> 100		[78] ROY	92	RVUE	$p\bar{p}\to\widetilde{g}\widetilde{g}$; $\not{R}$	
		[79] NOJIRI	91	COSM		
none 4–53	90	[80] ALBAJAR	87D	UA1	Any $m_{\widetilde{q}}>m_{\widetilde{g}}$	
none 4–75	90	[80] ALBAJAR	87D	UA1	$m_{\widetilde{q}}=m_{\widetilde{g}}$	
none 16–58	90	[81] ANSARI	87D	UA2	$m_{\widetilde{q}}\lesssim$ 100 GeV	

[1] AAD 13AV searched in 20.3 fb^{-1} of pp collisions at $\sqrt{s}$ = 8 TeV for events containing large number of jets (7 or more), with missing transverse momentum and no isolated electrons or muons. The sensitivity of the search is enhanced by considering the number of b-tagged jets and the scalar sum of masses of large-radius jets in an event. No evidence was found for excesses above the expected level of Standard Model background.

[2] Exclusion limits at 95% C.L. are set on the gluino mass assuming the gluino decays exclusively via an off-shell top squark, $\widetilde{g}\to t\bar{t}\widetilde{\chi}_1^0$, see their Fig. 9.

[3] Exclusion limits at 95% C.L. are set on the gluino mass assuming the gluino decays exclusively via an on-shell top quark, $\widetilde{g}\to\bar{t}\,t$, with consecutively $t\to t\widetilde{\chi}_1^0$, assuming $m_{\widetilde{\chi}_1^0}$ = 60 GeV, see their Fig. 10.

[4] Exclusion limits at 95% C.L. are set on the gluino mass assuming the gluino decays exclusively via an on-shell top quark, $\widetilde{g}\to\bar{t}\,t$, with the stop consecutively decaying via the R-parity- and baryon-number-violating decay $\bar{t}\to\bar{s}\bar{b}$, see Fig. 14.

[5] Exclusion limits at 95% C.L. are set on the gluino mass assuming the gluino decays exclusively via an on-shell quark and a chargino, $\widetilde{g}\to\overline{q}q'\widetilde{\chi}_1^\pm$, with consecutively $\widetilde{\chi}_1^\pm\to W^\pm\widetilde{\chi}_1^0$, see their Fig. 11. An alternative interpretation in the case where the gluino can decay via $\widetilde{\chi}_1^\pm$ or $\widetilde{\chi}_2^0$ is given in Fig. 12.

[6] Exclusion limits at the 95% C.L. are derived in the mSUGRA/CMSSM model with parameters tanβ = 30, $A_0=-2\,m_0$ and μ > 0, see their Fig. 13. For large universal scalar masses m_0, gluino masses smaller than 1.1 TeV are excluded at 95% C.L.

[7] CHATRCHYAN 13G searched in 4.98 fb^{-1} of pp collisions at $\sqrt{s}$ = 7 TeV for the production of squarks and gluinos in events containing 0,1,2, $\geq$ 3 b-jets, missing transverse momentum and no electrons or muons. No excess over the expected SM background is observed. In mSUGRA/CMSSM models with tanβ = 10, A_0 = 0, and μ > 0, gluinos with masses below 700 GeV are excluded at 95% C.L. Squarks and gluinos of equal mass are excluded for masses below 1250 GeV at 95% C.L. Exclusions are also derived in various simplified models, see Fig. 7.

[8] CHATRCHYAN 13P searched in 4.98 fb^{-1} of pp collisions at $\sqrt{s}$ = 7 TeV for events containing a single isolated electron or muon, energetic jets and large $\not{E}_T$. No significant excesses over the expected SM backgrounds are observed and 95% C.L. exclusion limits are derived in the mSUGRA/CMSSM model with tanβ = 10, A_0 = 0 and μ > 0, see Fig. 17. The results are also interpreted in a simplified model, see Fig. 19.

[9] CHATRCHYAN 13R searched in 4.98 fb^{-1} of pp collisions at $\sqrt{s}$ = 7 TeV for events containing one or more hadronically decaying τ leptons, energetic jets and large $\not{E}_T$. No significant excesses over the expected SM backgrounds are observed and 95% C.L. exclusion limits are derived in the mSUGRA/CMSSM model with tanβ=10, A_0=0 and μ >0, see Fig. 7. The results are also interpreted in various simplified models, see Fig. 9.

[10] CHATRCHYAN 13T searched in 11.7 fb^{-1} of pp collisions at $\sqrt{s}$ = 8 TeV for events with at least two energetic jets and significant $\not{E}_T$, using the α_T variable to discriminate between processes with genuine and misreconstructed $\not{E}_T$. No significant excess above the Standard Model expectations is observed.

[11] CHATRCHYAN 13T limits are set on gluino masses in simplified models where the decay $\widetilde{g}\to b\bar{b}\widetilde{\chi}_1^0$ takes place with a branching ratio of 100%, see Fig. 8 and Table 9.

[12] CHATRCHYAN 13T limits are set on gluino masses in simplified models where the decay $\widetilde{g}\to q\bar{q}\widetilde{\chi}_1^0$ takes place with a branching ratio of 100%, see Fig. 8 and Table 9.

[13] CHATRCHYAN 13T limits are set on gluino masses in simplified models where the decay $\widetilde{g}\to t\bar{t}\widetilde{\chi}_1^0$ takes place with a branching ratio of 100%, see Fig. 8 and Table 9.

[14] CHATRCHYAN 13V searched in 10.5 fb^{-1} of pp collisions at $\sqrt{s}$ = 8 TeV for events with two isolated same-sign dileptons and at least two b-jets in the final state. No significant excess above the Standard Model expectations is observed. Limits are set on the gluino mass in simplified models where the decay $\widetilde{g}\to t\bar{t}\widetilde{\chi}_1^0$ takes place with a branching ratio of 100%, or where the decay $\widetilde{g}\to\bar{t}\,t$, $\bar{t}\to t\widetilde{\chi}_1^0$ takes place with a branching ratio of 100%, with varying mass of the $\widetilde{\chi}_1^0$, or where the decay $\widetilde{g}\to\bar{b}b$, $\bar{b}\to t\widetilde{\chi}_1^\pm$, $\widetilde{\chi}_1^\pm\to W^\pm\widetilde{\chi}_1^0$ takes place with a branching ratio of 100%, with varying mass of the $\widetilde{\chi}_1^\pm$, see Fig. 4.

[15] AAD 12AP searched in 2.05 fb^{-1} of pp collisions at $\sqrt{s}$ = 7 TeV for gluinos decaying via the scalar partner of the top quark into events with two same-sign leptons, jets and missing transverse energy. No excess beyond the Standard Model expectation is observed. Exclusion limits are derived in the mSUGRA/CMSSM model with tanβ = 10, A_0 = 0 and μ > 0, see Fig. 4, and in simplified models, see Figs. 2 and 3.

[16] AAD 12AX searched in 1.04 fb^{-1} of pp collisions at $\sqrt{s}$ = 7 TeV for supersymmetry in events containing jets, missing transverse momentum and one isolated electron or muon. No excess over the expected SM background is observed and model-independent limits are set on the cross section of new physics contributions to the signal regions. In mSUGRA/CMSSM models with tanβ = 10, A_0 = 0 and μ > 0, squarks and gluinos of equal mass are excluded for masses below 820 GeV at 95% C.L. Limits are also set on simplified models for gluino production and decay via an intermediate chargino and on supersymmetric models with bilinear R-parity violation. Supersedes AAD 11G.

[17] AAD 12BI looked in 4.7 fb^{-1} of pp collisions at $\sqrt{s}$ = 7 TeV for events with $\geq$ 6 to $\geq$ 9 jets plus $\not{E}_T$. No excess over the expected background is observed. Limits are derived in the CMSSM (m_0, $m_{1/2}$) plane for tanβ = 10, A_0 = 0 and μ > 0, see their Fig. 7. Limits are also set in the ($m_{\widetilde{g}}$,$m_{\widetilde{\chi}^0_1}$) plane in a simplified supersymmetric model with four tops + $\not{E}_T$ in the final state. Supersedes AAD 11AF.

[18] AAD 12BY searched in 4.7 fb^{-1} of pp collisions at $\sqrt{s}$ = 7 TeV for events with large missing transverse momentum and at least three b-jets in the final state. The data are found to be consistent with the Standard Model expectations. In a simplified supersymmetric scenario where $\widetilde{g} \rightarrow \widetilde{b}_1 b$ and $\widetilde{b}_1 \rightarrow b\widetilde{\chi}^0_1$, with branching ratios of 100% for both decays, a 95% C.L. limit on the gluino mass of 1000 GeV is set for $m_{\widetilde{b}_1} < 870$ GeV and $m_{\widetilde{\chi}^0_1} = 60$ GeV. In a scenario where the sbottom is heavier than the gluino and the gluino decays through a three-body decay into bottom quarks 100% of the time, $\widetilde{g} \rightarrow bb\widetilde{\chi}^0_1$, the limit on the gluino mass becomes 1020 GeV, provided $m_{\widetilde{\chi}^0_1} < 400$ GeV. In a scenario where $\widetilde{g} \rightarrow \widetilde{t}_1 t$ and $\widetilde{t}_1 \rightarrow t\widetilde{\chi}^0_1$, with branching ratios of 100% for both decays, a 95% C.L. limit on the gluino mass of 820 GeV is set for $m_{\widetilde{t}_1} < 640$ GeV and $m_{\widetilde{\chi}^0_1} = 60$ GeV. In a scenario where the stop is heavier than the gluino and the gluino decays through a three-body decay into top quarks 100% of the time, $\widetilde{g} \rightarrow tt\widetilde{\chi}^0_1$, the limit on the gluino mass becomes 940 GeV, provided $m_{\widetilde{\chi}^0_1} < 50$ GeV.

[19] AAD 12CJ searched in 4.7 fb^{-1} of pp collisions at $\sqrt{s}$ = 7 TeV for events containing one or more isolated leptons (electrons or muons), jets and $\not{E}_T$. The observations are in good agreement with the SM expectations and exclusion limits have been set in number of SUSY models. In the mSUGRA/CMSSM model with tanβ = 10, A_0 = 0, and μ > 0, 95% C.L. exclusion limits have been derived for $m_{\widetilde{g}} < 1200$ GeV, assuming equal squark and gluino masses. In minimal GMSB, values of the effective SUSY breaking scale Λ < 50 TeV are excluded at 95% C.L. for tanβ < 45. Also exclusion limits in a number of simplified models have been presented, see Figs. 10 and 11.

[20] AAD 12CU searched in 4.6 fb^{-1} of pp collisions at $\sqrt{s}$ = 7 TeV for pair production of gluinos decaying into six-quark final states in an R-parity violating supersymmetric model. The data are found to be consistent with the Standard Model expectations. Based on an analysis where all six jets in the final state are resolved, a 95% C.L. limit of 666 GeV is placed on the gluino mass. The gluino decay is assumed to be prompt.

[21] CHATRCHYAN 12AT searched in 4.73 fb^{-1} of pp collisions at $\sqrt{s}$ = 7 TeV for the production of squarks and gluinos in events containing jets, missing transverse momentum and no electrons or muons. No excess over the expected SM background is observed. In mSUGRA/CMSSM models with tanβ = 10, A_0 = 0 and μ > 0, gluinos with masses below 800 GeV are excluded at 95% C.L. Squarks and gluinos of equal mass are excluded for masses below 1180 GeV at 95% C.L. Exclusions are also derived in various simplified models, see Fig. 6.

[22] CHATRCHYAN 12U looked in 4.98 fb^{-1} of pp collisions at $\sqrt{s}$ = 7 TeV for events with two same-sign leptons (e, μ, τ) not necessarily the same flavor, jets and missing transverse energy. No excess beyond the Standard Model expectation is observed. Exclusion limits are derived in the mSUGRA/CMSSM model with tanβ = 10, A_0 = 0, and μ > 0, see Fig. 3. The limit is independent of the squark masses. The exclusion includes a $-$ 1 σ_{th} reduction to account for the theory uncertainty on the cross section.

[23] AAD 11G looked in 35 pb^{-1} of pp collisions at $\sqrt{s}$ = 7 TeV for events with a single lepton (e or μ), jets and $\not{E}_T$ from the production of squarks and gluinos. No evidence for an excess over the SM expectation is observed, and a limit is derived in the CMSSM (m_0, $m_{1/2}$) plane for tanβ = 3, see Fig. 2.

[24] AAD 11N looked in 35 pb^{-1} of pp collisions at $\sqrt{s}$ = 7 TeV for events with $\geq$ 2 jets and $\not{E}_T$. Four signal regions were defined, and the background model was found to be in good agreement with the data. Limits are derived in the ($m_{\widetilde{g}}$, $m_{\widetilde{q}}$) plane (see Fig. 2) for a simplified model where degenerate masses of the squarks of the first two generations are assumed, $m_{\widetilde{\chi}^0_1} = 0$, and all other masses including third generation squarks are set to 5 TeV. Limits are also derived in the CMSSM (m_0, $m_{1/2}$) plane (see Fig. 3) for tanβ = 3.

[25] AAD 11O looked in 35 pb^{-1} of pp collisions at $\sqrt{s}$ = 7 TeV for events with jets, of which at least one is a b-jet, and $\not{E}_T$. No excess above the Standard Model was found. Limits are derived in the ($m_{\widetilde{g}}$, $m_{\widetilde{b}_1}$) plane (see Fig. 2) under the assumption of 100% branching ratios and $\widetilde{b}_1$ being the lightest squark. The quoted limit is valid for $m_{\widetilde{b}_1} <$ 500 GeV. A similar approach for $\widetilde{t}_1$ as the lightest squark with $\widetilde{g} \rightarrow \widetilde{t}_1 t$ and $\widetilde{t}_1 \rightarrow b\widetilde{\chi}^{\pm}_1$ with 100% branching ratios leads to a gluino mass limit of 520 GeV for 130 < $m_{\widetilde{t}_1}$ < 300 GeV. Limits are also derived in the CMSSM (m_0, $m_{1/2}$) plane for tanβ = 40, see Fig. 4, and in scenarios based on the gauge group SO(10).

[26] CHATRCHYAN 11AC looked in 36 pb^{-1} of pp collisions at $\sqrt{s}$ = 7 TeV for events with $\geq$ 3 jets, a large total transverse energy, and $\not{E}_T$. No evidence for an excess over the expected background is observed. Limits are derived in the CMSSM (m_0, $m_{1/2}$) plane and the ($m_{\widetilde{g}}$, $m_{\widetilde{q}}$) plane for tanβ = 10 (see Fig. 10). Limits are also obtained for Simplified Model Spectra.

[27] AALTONEN 09S searched in 2 fb^{-1} of $p\overline{p}$ collisions at $\sqrt{s}$ = 1.96 TeV for events with at least 2 jets and $\not{E}_T$. No evidence for a signal is observed. A limit is derived for a mSUGRA scenario in the $m_{\widetilde{q}}$ versus $m_{\widetilde{g}}$ plane, see their Fig. 2.

[28] ABAZOV 08G looked in 2.1 fb^{-1} of $p\overline{p}$ collisions at $\sqrt{s}$=1.96 TeV for events with acoplanar jets or multijets with large $\not{E}_T$. No significant excess was found compared to the background expectation. A limit is derived on the masses of squarks and gluinos for specific MSUGRA parameter values, see Figure 3. Similar results would be obtained for a large class of parameter sets. Supersedes the results of ABAZOV 06C.

[29] ABULENCIA 06I searched in 156 pb^{-1} of $p\overline{p}$ collisions at $\sqrt{s}$ = 1.96 TeV for multijet events with large $\not{E}_T$. They request at least 2 b-tagged jets and no isolated leptons. They investigate the production of gluinos decaying into $\widetilde{b}_1 b$ followed by $\widetilde{b}_1 \rightarrow b\widetilde{\chi}^0_1$. Both branching fractions are assumed to be 100% and the LSP mass to be 60 GeV. No significant excess was found compared to the background expectation. Upper limits on the cross-section are extracted and a limit is derived on the masses of sbottom and gluinos, see their Fig.3.

[30] AFFOLDER 02 searched in $\sim$ 84 pb^{-1} of $p\overline{p}$ collisions for events with $\geq$ 3 jets and $\not{E}_T$, arising from the production of gluinos and/or squarks. Limits are derived by scanning the parameter space, for $m_{\widetilde{q}} \geq m_{\widetilde{g}}$ in the framework of minimal Supergravity, assuming five flavors of degenerate squarks, and for $m_{\widetilde{q}} < m_{\widetilde{g}}$ in the framework of constrained MSSM, assuming conservatively four flavors of degenerate squarks. See Fig. 3 for the variation of the limit as function of the squark mass. Supersedes the results of ABE 97K.

[31] ABBOTT 01D looked in $\sim$ 108 pb^{-1} of $p\overline{p}$ collisions at $\sqrt{s}$=1.8 TeV for events with ee, $\mu\mu$, or $e\mu$ accompanied by at least 2 jets and $\not{E}_T$. Excluded regions are obtained in the MSUGRA framework from a scan over the parameters 0<m_0 <300 GeV, 10<$m_{1/2}$ <110 GeV, and 1.2 <tanβ <10.

[32] AFFOLDER 01J searched in $\sim$ 106 pb^{-1} of $p\overline{p}$ collisions for events with 2 like-sign leptons (e or μ), $\geq$ 2 jets and $\not{E}_T$, expected to arise from the production of gluinos and/or squarks with cascade decays into $\widetilde{\chi}^{\pm}$ or $\widetilde{\chi}^0_2$. Spectra and decay rates are evaluated in the framework of minimal Supergravity, assuming five flavors of degenerate squarks and a pseudoscalar Higgs mass m_A=500 GeV. The limits are derived for tanβ=2, μ=$-$800 GeV, and scanning over $m_{\widetilde{g}}$ and $m_{\widetilde{q}}$. See Fig. 2 for the variation of the limit as function of the squark mass. These limits supersede the results of ABE 96D.

[33] ABBOTT 99L consider events with three or more jets and large $\not{E}_T$. Spectra and decay rates are evaluated in the framework of minimal Supergravity, assuming five flavors of degenerate squarks, and scanning the space of the universal gaugino ($m_{1/2}$) and scalar (m_0) masses See their Figs. 2–3 for the dependence of the limit on the relative value of $m_{\widetilde{q}}$ and $m_{\widetilde{g}}$.

[34] AAD 13AB searched in 4.7 fb^{-1} of pp collisions at $\sqrt{s}$ = 7 TeV for the production of squarks and gluinos in events containing 0,1 or 2 high-p_T leptons and with or without jets identified as originating from b-quarks. No excess over the expected SM background is observed. Limits are derived in mSUGRA/CMSSM models with tanβ = 10, A_0 = 0 and μ > 0, see their Fig. 12. Also, exclusion limits in simplified models containing gluinos, squarks, charginos, and stops are set, see their Figures 10 and 11.

[35] AAD 13L searched in 4.7 fb^{-1} of pp collisions at $\sqrt{s}$ = 7 TeV for the production of squarks and gluinos in events containing jets, missing transverse momentum and no high-p_T electrons or muons. No excess over the expected SM background is observed. In mSUGRA/CMSSM models with tanβ = 10, A_0 = 0 and μ > 0, squarks and gluinos of equal mass are excluded for masses below 1360 GeV at 95% C.L. In a simplified model containing only squarks of the first two generations, a gluino octet and a massless neutralino, gluino masses below 860 GeV are excluded at 95% C.L, for squark masses below 2 TeV. See their Figures 10–15 for more precise bounds.

[36] AAD 13Q searched in 4.7 fb^{-1} of pp collisions at $\sqrt{s}$ = 7 TeV for events containing a high-p_T isolated photon, at least one jet identified as originating from a bottom quark, and high missing transverse momentum. Such signatures may originate from supersymmetric models with gauge-mediated supersymmetry breaking in events in which one of a pair of higgsino-like neutralinos decays into a photon and a gravitino while the other decays into a Higgs boson and a gravitino. No significant excess above the expected background was found and limits were set on the gluino mass as a function of the neutralino mass in a generalized GMSB model (GGM) with a higgsino-like neutralino NLSP, see their Fig. 4. For neutralino masses greater than 220 GeV, gluino masses below 900 GeV are excluded at 95% C.L.

[37] CHATRCHYAN 13 looked in 4.98 fb^{-1} of pp collisions at $\sqrt{s}$ = 7 TeV for events with two opposite-sign leptons (e, μ, τ), jets and missing transverse energy. No excess beyond the Standard Model expectation is observed. Exclusion limits are derived in the mSUGRA/CMSSM model with tanβ = 10, A_0 = 0 and μ > 0, see Fig. 6.

[38] CHATRCHYAN 13AK searched in 19.4 fb^{-1} of pp collisions at $\sqrt{s}$ = 8 TeV for events with large $\not{E}_T$, no isolated electron or muon, and at least three jets with one or more identified as a b-quark jet. No significant excesses over the expected SM backgrounds are observed and 95% C.L. limits on the production cross section of gluinos are set as a function of the gluino and neutralino mass in a scenario where $\widetilde{g} \rightarrow b\overline{b}\widetilde{\chi}^0_1$ with a 100% branching ratio, see Fig. 7 left, and in a scenario where $\widetilde{g} \rightarrow t\overline{t}\widetilde{\chi}^0_1$ with a 100% branching ratio, see Fig. 7, right. Supersedes CHATRCHYAN 12AH.

[39] CHATRCHYAN 13AM searched in 4.98 fb^{-1} of pp collisions at $\sqrt{s}$ = 7 TeV for events with large $\not{E}_T$, a single isolated electron or muon, and multiple jets including some identified as a b-quark jet. No significant excesses over the expected SM backgrounds are observed and 95% C.L.

[40] CHATRCHYAN 13AM limits on the production cross section of gluinos are set as a function of the gluino and neutralino mass in a scenario where $\widetilde{g} \rightarrow t\overline{t}\widetilde{\chi}^0_1$ with a 100% branching ratio, see Fig. 10.

[41] CHATRCHYAN 13AM exclusion limits are derived in the mSUGRA/CMSSM model with tanβ = 10, A_0 = 0 and μ > 0, see Fig. 8.

[42] CHATRCHYAN 2013AO searched in 4.98 fb^{-1} of pp collisions at $\sqrt{s}$ = 7 TeV for events with two opposite-sign isolated leptons accompanied by hadronic jets and $\not{E}_T$. No significant excesses over the expected SM backgrounds are observed and 95% C.L. exclusion limits are derived in the mSUGRA/CMSSM model with tanβ = 10, A_0 = 0 and μ > 0, see Fig. 8. The results are also interpreted in an asymmetric simplified model of gluino pair production, see Fig. 7.

[43] CHATRCHYAN 13AT provides interpretations of various searches for supersymmetry by the CMS experiment based on 4.73–4.98 fb^{-1} of pp collisions at $\sqrt{s}$ = 7 TeV in the framework of simplified models. Limits are set on the gluino mass in a simplified models where gluinos are pair-produced and the decay $\widetilde{g} \rightarrow q\overline{q}\widetilde{\chi}^0_1$ takes place with a branching ratio of 100%, see Fig. 4.

[44] CHATRCHYAN 13AV searched in 4.7 fb^{-1} of pp collisions at $\sqrt{s}$ = 7 TeV for new heavy particle pairs decaying into jets (possibly b-tagged), leptons and $\not{E}_T$ using the Razor variables. No significant excesses over the expected SM backgrounds are observed and 95% C.L. exclusion limits are derived in the mSUGRA/CMSSM model with tanβ = 10, A_0 = 0 and μ > 0, see Fig. 3. The results are also interpreted in various simplified models, see Fig. 4.

[45] CHATRCHYAN 13W searched in 4.93 fb^{-1} of pp collisions at $\sqrt{s}=7$ TeV for events with one or more photons, hadronic jets and $\not{E}_T$. No significant excess above the Standard Model expectations is observed. Limits are set on gluino masses in the general gauge-mediated SUSY breaking model (GGM), for both a wino-like and bino-like neutralino NLSP scenario, see Fig. 5.

[46] AAD 12BA searched in 2.05 fb^{-1} of pp collisions at $\sqrt{s}=7$ TeV for events with heavy flavor jets and large $\not{E}_T$ due to $\tilde{g}\to\tilde{t}_1 b$ or $\tilde{g}\to\tilde{t}_1 t$ decays. No significant excess above the expected background was found and limits were set on the gluino mass in simplified R-parity conserving models in which only scalar bottoms and tops appear in the gluino decay and in an SO(10) model framework.

[47] AAD 12CP searched in 4.8 fb^{-1} of pp collisions at $\sqrt{s}=7$ TeV for events with two photons and large $\not{E}_T$ due to $\tilde{\chi}_1^0\to\gamma\tilde{G}$ decays in a GMSB framework. No significant excess above the expected background was found and limits were set on the gluino mass as a function of the neutralino mass in a generalized GMSB model (GGM) with a bino-like neutralino NLSP. The other sparticle masses were decoupled, $\tan\beta=2$ and $c\tau_{NLSP}<0.1$ mm. Also, in the framework of the SPS8 model, a 95% C.L. lower limit was set on the breaking scale Λ of 196 TeV.

[48] AAD 12W searched in 1.04 fb^{-1} of pp collisions at $\sqrt{s}=7$ TeV for the production of squarks and gluinos in events containing jets, missing transverse momentum and no electrons or muons. No excess over the expected SM background is observed. In mSUGRA/CMSSM models with $\tan\beta=10$, $A_0=0$ and $\mu>0$, squarks and gluinos of equal mass are excluded for masses below 950 GeV at 95% C.L. In a simplified model containing only squarks of the first two generations, a gluino octet and a massless neutralino, gluino masses below 700 GeV are excluded at 95% C.L.

[49] AAD 12X searched in 1.07 fb^{-1} of pp collisions at $\sqrt{s}=7$ TeV for events with two photons and large $\not{E}_T$ due to $\tilde{\chi}_1^0\to\gamma\tilde{G}$ decays in a GMSB framework. No significant excess above the expected background was found and limits were set on the gluino mass as a function of the neutralino mass in a generalized GMSB model (GGM) with a bino-like neutralino NLSP. The other sparticle masses were set to 1.5 TeV, $\tan\beta=2$ and $c\tau_{NLSP}<0.1$ mm. Also, in the framework of the SPS8 model, a 95% C.L. lower limit was set on the breaking scale Λ of 145 TeV. Superseded by AAD 12CP.

[50] CHATRCHYAN 12 looked in 35 pb^{-1} of pp collisions at $\sqrt{s}=7$ TeV for events with e and/or μ and/or jets, a large total transverse energy, and $\not{E}_T$. The event selection is based on the dimensionless razor variable R, related to the $\not{E}_T$ and M_R, an indicator of the heavy particle mass scale. No evidence for an excess over the expected background is observed. Limits are derived in the CMSSM (m_0, $m_{1/2}$) plane for $\tan\beta=3$, 10 and 50 (see Fig. 7 and 8). Limits are also obtained for Simplified Model Spectra.

[51] CHATRCHYAN 12AE searched in 4.98 fb^{-1} of pp collisions at $\sqrt{s}=7$ TeV for events with at least three jets and large missing transverse momentum. No significant excesses over the expected SM backgrounds are observed and 95% C.L. limits on the production cross section of gluinos in a scenario where $\tilde{g}\to q q\tilde{\chi}_1^0$ with a 100% branching ratio, see Fig. 3. For $m_{\tilde{\chi}_1^0}<200$ GeV, values of $m_{\tilde{g}}$ below 1000 GeV are excluded at 95% C.L. Also limits in the CMSSM are presented, see Fig. 2.

[52] CHATRCHYAN 12AH searched in 4.98 fb^{-1} of pp collisions at $\sqrt{s}=7$ TeV for events with large $\not{E}_T$, at least three jets, and at least one, two or three b-quark jets. No significant excesses over the expected SM backgrounds are observed and 95% C.L. limits on the production cross section of gluinos are set as a function of the gluino and neutralino mass in a scenario where $\tilde{g}\to b b\tilde{\chi}_1^0$ with a 100% branching ratio, see Fig. 14, and in a scenario where $\tilde{g}\to t t\tilde{\chi}_1^0$ with a 100% branching ratio, see Fig. 15.

[53] CHATRCHYAN 12AI looked in 4.98 fb^{-1} of pp collisions at $\sqrt{s}=7$ TeV for events with two same-sign leptons (e, μ), but not necessarily same flavor, at least 2 b-jets and missing transverse energy. No excess beyond the Standard Model expectation is observed. Exclusion limits are derived in simplified models where gluinos are pair produced and decay through $\tilde{g}\to t\bar{t}\tilde{\chi}_1$ (intermediate stop, real or virtual), see Fig. 6, or through $\tilde{g}\to b\bar{t}W^+\tilde{\chi}_1$ (intermediate sbottom), see Fig. 8.

[54] CHATRCHYAN 12AL looked in 4.98 fb^{-1} of pp collisions at $\sqrt{s}=7$ TeV for anomalous production of events with three or more isolated leptons. Limits on squark and gluino masses are set in $R\!\!\!/$ SUSY models with leptonic $LL\bar{E}$ couplings, $\lambda_{123}>0.05$, and hadronic $\overline{UDD}$ couplings, $\lambda''_{112}>0.05$, see their Fig. 5. In the $\overline{UDD}$ case the leptons arise from supersymmetric cascade decays. A very specific supersymmetric spectrum is assumed. All decays are prompt.

[55] CHATRCHYAN 12BD searched in 5.0 fb^{-1} of pp collisions at $\sqrt{s}=7$ TeV for three-jet resonances produced in the decay of a gluino in R-parity violating supersymmetric models. No excess over the expected SM background is observed. Assuming a branching ratio for gluino decay into three jets of 100%, limits are set on the cross section of gluino pair production, see Fig. 4. Gluino masses between 280 GeV and 460 GeV are excluded at 95% C.L.

[56] CHATRCHYAN 12Q looked in 4.98 fb^{-1} of pp collisions at $\sqrt{s}=7$ TeV for anomalous production of events with a Z-boson, jets and significant $\not{E}_T$. No evidence for an excess over the expected background is observed. Limits are set in a simplified supersymmetric model where the $\tilde{\chi}_2^0\to Z\tilde{\chi}_1^0$ decay is dominant, see Figs. 5 and 6.

[57] DREINER 12A reassesses constraints from CMS (at 7 TeV, $\sim$ 4.4 fb^{-1}) under the assumption that the gluino and the lightest SUSY particle are quasi-degenerate in mass (compressed spectrum).

[58] DREINER 12A reassesses constraints from CMS (at 7 TeV, $\sim$ 4.4 fb^{-1}) under the assumption that the first and second generation squarks, the gluino, and the lightest SUSY particle are quasi-degenerate in mass (compressed spectrum).

[59] AAD 11AF looked in 1.34 fb^{-1} of pp collisions at $\sqrt{s}=7$ TeV for events with 6 up to 8 jets and $\not{E}_T$. No evidence for an excess over the expected background is observed. Limits are derived in the CMSSM (m_0, $m_{1/2}$) plane for $\tan\beta=10$ (see Fig. 5). The limit improves to $m_{\tilde{g}}>680$ GeV for $m_{\tilde{q}}=2\,m_{\tilde{g}}$.

[60] AAD 11X looked in 36 pb^{-1} of pp collisions at $\sqrt{s}=7$ TeV for events with ≥ 2 photons and $\not{E}_T$ from the pair production of gluinos with cascade decays to $\tilde{\chi}_1^0$ followed by $\tilde{\chi}_1^0\to\gamma\tilde{G}$ prompt decay. No evidence for an excess over the SM expectation is observed, and a limit on the number of new physics events is set. Limits are derived in a Generalized Gauge Mediated model in the ($m_{\tilde{g}}$, $m_{\tilde{\chi}_1^0}$) plane (see Fig. 5) under the assumptions $\tan\beta=2$ and all sparticle masses at 1.5 TeV, except the $\tilde{g}$, $\tilde{\chi}_1^0$, and $\tilde{G}$. Superseded by AAD 12X.

[61] AALTONEN 11Q searched in 3.2 fb^{-1} of $p\bar{p}$ collisions at $\sqrt{s}=1.96$ TeV for events with at least 6 jets from the pair production of gluinos and squarks with the subsequent decays $\tilde{g}\to$ 3jets in the MSSM framework with $R\!\!\!/$. No statistically significant bumps in the 3-jet systems are observed over the SM background. Limits on the cross section times branching ratio are derived as a function of the gluino mass, displayed in Fig. 3. For decoupled squarks in the range $0.5<m_{\tilde{q}}<0.7$ TeV gluinos are excluded below 144 GeV. The quoted limit is for near degeneracy of squark and gluino masses.

[62] CHATRCHYAN 11AB looked in 35 pb^{-1} of pp collisions at $\sqrt{s}=7$ TeV for events with ≥ 2 same charge isolated leptons (e, μ or τ), jets and $\not{E}_T$. Such events might be produced from $\tilde{g}\tilde{g}$ or $\tilde{g}\tilde{q}$ decaying via charginos into leptons. No evidence for an excess over the expected background is observed. Limits are derived in the CMSSM (m_0, $m_{1/2}$) plane for $\tan\beta=3$ (see Fig. 10).

[63] CHATRCHYAN 11G looked in 36 pb^{-1} of pp collisions at $\sqrt{s}=7$ TeV for events with ≥ 2 isolated photons, ≥ 1 jet and $\not{E}_T$, which may arise in a generalized gauge mediated model from the decay of a $\tilde{\chi}_1^0$ NLSP. No evidence for an excess over the expected background is observed. Limits are derived in the plane of squark versus gluino mass (see Fig. 4) for several values of $m_{\tilde{\chi}_1^0}$.

[64] CHATRCHYAN 11Q looked in 36 pb^{-1} of pp collisions at $\sqrt{s}=7$ TeV for events with a single isolated lepton (e or μ), ≥ 4 jets and $\not{E}_T$. No evidence for an excess over the expected background is observed. Limits are derived in the CMSSM (m_0, $m_{1/2}$) plane for $\tan\beta=10$ (see Fig. 7).

[65] CHATRCHYAN 11V looked in 35 pb^{-1} of pp collisions at $\sqrt{s}=7$ TeV for events with ≥ 3 isolated leptons (e, μ or τ), with or without jets and $\not{E}_T$. Multi-lepton final states originate from $\tilde{q}\to\tilde{\chi}^0+X$, followed by $\tilde{\chi}^0\to\tilde{\ell}^{\pm}\ell^{\mp}$ and $\tilde{\ell}\to\ell\tilde{G}$. No evidence for an excess over the expected background is observed. Limits are derived (see Fig. 4) for a GMSB-type scenario with mass-degenerate right-handed sleptons (slepton co-NLSP scenario).

[66] CHATRCHYAN 11W looked in 1.14 fb^{-1} of pp collisions at $\sqrt{s}=7$ TeV for events with ≥ 2 jets, large total jet energy, and $\not{E}_T$. After combining multi-jet events into two pseudo-jets signal events are selected by a cut on $\alpha_T=E_T^{j_2}/M_T$, the transverse energy of the less energetic jet over the transverse mass. Given the lack of an excess over the SM backgrounds, limits are derived in the CMSSM (m_0, $m_{1/2}$) plane (see Fig. 4) for $\tan\beta=10$. The limits are only weakly dependent on $\tan\beta$ and A_0.

[67] KHACHATRYAN 11I looked in 35 pb^{-1} of pp collisions at $\sqrt{s}=7$ TeV for events with ≥ 2 jets and $\not{E}_T$. After combining multi-jet events into two pseudo-jets signal events are selected by a cut on $\alpha_T=E_T^{j_2}/M_T$, the transverse energy of the less energetic jet over the transverse mass. No evidence for an excess over the expected background is observed. Limits are derived in the CMSSM (m_0, $m_{1/2}$) plane (see Fig. 5) for $\tan\beta=3$. Superseded by CHATRCHYAN 11W.

[68] ABAZOV 02F looked in 77.5 pb^{-1} of $p\bar{p}$ collisions at 1.8 TeV for events with $\geq 2\mu+\geq$ 4jets, originating from associated production of squarks followed by an indirect R decay (of the $\tilde{\chi}_1^0$) via $LQ\overline{D}$ couplings of the type λ'_{2jk} where j=1,2 and k=1,2,3. Bounds are obtained in the MSUGRA scenario by a scan in the range $0\leq M_0\leq 400$ GeV, $60\leq m_{1/2}\leq 120$ GeV for fixed values A_0=0, $\mu<0$, and $\tan\beta$=2 or 6. The bounds are weaker for $\tan\beta$=6. See Figs. 2,3 for the exclusion contours in $m_{1/2}$ versus m_0 for $\tan\beta$=2 and 6, respectively.

[69] ABAZOV 02G search for associated production of gluinos and squarks in 92.7 pb^{-1} of $p\bar{p}$ collisions at $\sqrt{s}$=1.8 TeV, using events with one electron, ≥ 4 jets, and large $\not{E}_T$. The results are compared to a MSUGRA scenario with $\mu<0$, A_0=0, and $\tan\beta$=3 and allow to exclude a region of the (m_0,$m_{1/2}$) shown in Fig. 11.

[70] CHEUNG 02B studies the constraints on a $\tilde{b}_1$ with mass in the 2.2–5.5 GeV region and a gluino in the mass range 12–16 GeV, using precision measurements of Z^0 decays and e^+e^- annihilations at LEP2. Few detectable events are predicted in the LEP2 data for the model proposed by BERGER 01.

[71] BERGER 01 reanalyzed interpretation of Tevatron data on bottom-quark production. Argues that pair production of light gluinos ($m\sim$ 12–16 GeV) with subsequent 2-body decay into a light sbottom ($m\sim$ 2–5.5 GeV) and bottom can reconcile Tevatron data with predictions of perturbative QCD for the bottom production rate. The sbottom must either decay hadronically via a R-parity- and B-violating interaction, or be long-lived.

[72] ABBOTT 99 searched for $\gamma\not{E}_T+\geq 2$ jet final states, and set limits on $\sigma(p\bar{p}\to\tilde{g}\tilde{g}+X)\cdot B(\tilde{g}\to\gamma\not{E}_T X)$. The quoted limits correspond to $m_{\tilde{q}}\geq m_{\tilde{g}}$, with $B(\tilde{\chi}_2^0\to\tilde{\chi}_1^0\gamma)$=1 and $B(\tilde{\chi}_1^0\to\tilde{G}\gamma)$=1, respectively. They improve to 310 GeV (360 GeV in the case of $\gamma\tilde{G}$ decay) for $m_{\tilde{g}}=m_{\tilde{q}}$.

[73] ABBOTT 99K uses events with an electron pair and four jets to search for the decay of the $\tilde{\chi}_1^0$ LSP via $R\!\!\!/\,LQ\overline{D}$ couplings. The particle spectrum and decay branching ratios are taken in the framework of minimal supergravity. An excluded region at 95% CL is obtained in the (m_0,$m_{1/2}$) plane under the assumption that A_0=0, $\mu<0$, $\tan\beta$=2 and any one of the couplings $\lambda'_{1jk}>10^{-3}$ (j=1,2 and k=1,2,3) and from which the above limit is computed. For equal mass squarks and gluinos, the corresponding limit is 277 GeV. The results are essentially independent of A_0, but the limit deteriorates rapidly with increasing $\tan\beta$ or $\mu>0$.

[74] ABACHI 95C assume five degenerate squark flavors with with $m_{\tilde{q}_L}=m_{\tilde{q}_R}$. Sleptons are assumed to be heavier than squarks. The limits are derived for fixed $\tan\beta=2.0$ $\mu=-250$ GeV, and m_{H^+}=500 GeV, and with the cascade decays of the squarks and gluinos calculated within the framework of the Minimal Supergravity scenario. The bounds are weakly sensitive to the three fixed parameters for a large fraction of parameter space.

[75] ABE 95T looked for a cascade decay of gluino into $\tilde{\chi}_2^0$ which further decays into $\tilde{\chi}_1^0$ and a photon. No signal is observed. Limits vary widely depending on the choice of parameters. For $\mu=-40$ GeV, $\tan\beta=1.5$, and heavy squarks, the range $50<m_{\tilde{g}}$ (GeV)<140 is excluded at 90% CL. See the paper for details.

[76] HEBBEKER 93 combined jet analyses at various e^+e^- colliders. The 4-jet analyses at TRISTAN/LEP and the measured α_s at PEP/PETRA/TRISTAN/LEP are used. A constraint on effective number of quarks $N=6.3\pm1.1$ is obtained, which is compared to that with a light gluino, N=8.

[77] ABE 92L bounds are based on similar assumptions as ABACHI 95C. Not sensitive to $m_{\text{gluino}}<40$ GeV (but other experiments rule out that region).

[78] ROY 92 reanalyzed CDF limits on di-lepton events to obtain limits on gluino production in R-parity violating models. The 100% decay $\tilde{g}\to q\bar{q}\tilde{\chi}$ where $\tilde{\chi}$ is the LSP, and the LSP decays either into $\ell q\overline{d}$ or $\ell\ell\overline{e}$ is assumed.

[79] NOJIRI 91 argues that a heavy gluino should be nearly degenerate with squarks in minimal supergravity not to overclose the universe.

[80] The limits of ALBAJAR 87D are from $p\overline{p} \to \tilde{g}\tilde{g}X$ ($\tilde{g} \to q\overline{q}\tilde{\gamma}$) and assume $m_{\tilde{q}} > m_{\tilde{g}}$. These limits apply for $m_{\tilde{\gamma}} \lesssim 20$ GeV and $\tau(\tilde{g}) < 10^{-10}$ s.

[81] The limit of ANSARI 87D assumes $m_{\tilde{q}} > m_{\tilde{g}}$ and $m_{\tilde{\gamma}} \approx 0$.

Long-lived/light $\tilde{g}$ (Gluino) MASS LIMIT

Limits on light gluinos ($m_{\tilde{g}} < 5$ GeV), or gluinos which leave the detector before decaying.

VALUE (GeV)	CL%	DOCUMENT ID		TECN	COMMENT
• • • We do not use the following data for averages, fits, limits, etc. • • •					
> 985	95	[1] AAD	13AA	ATLS	$\tilde{g}$, R-hadrons, generic interaction model
> 832	95	[2] AAD	13BC	ATLS	R-hadrons, $\tilde{g} \to g/q\overline{q}\tilde{\chi}_1^0$, generic R-hadron model, lifetime between 10^{-5} and 10^3 s, $m_{\tilde{\chi}_1^0} = 100$ GeV
>1322	95	[3] CHATRCHYAN	13AB	CMS	long-lived $\tilde{g}$ forming R-hadrons, f = 0.1, cloud interaction model
none 200–341	95	[4] AAD	12P	ATLS	long-lived $\tilde{g} \to g\tilde{\chi}_1^0$, $m_{\tilde{\chi}_1^0} =$ 100 GeV
> 640	95	[5] CHATRCHYAN	12AN	CMS	long-lived $\tilde{g} \to g\tilde{\chi}_1^0$
>1098	95	[6] CHATRCHYAN	12L	CMS	long-lived $\tilde{g}$ forming R-hadrons, f = 0.1
> 586	95	[7] AAD	11K	ATLS	stable $\tilde{g}$
> 544	95	[8] AAD	11P	ATLS	stable $\tilde{g}$, GMSB scenario, $\tan\beta$=5
> 370	95	[9] KHACHATRY...	11	CMS	long lived $\tilde{g}$
> 398	95	[10] KHACHATRY...	11C	CMS	stable $\tilde{g}$
> 15	90	[11] BERGER	10	THEO	hadron scattering data, α_s
> 51	95	[12] KAPLAN	08	THEO	event shapes at LEP
		[13] ABAZOV	07L	D0	long-lived $\tilde{g}$
> 12		[14] BERGER	05	THEO	hadron scattering data
none 2–18	95	[15] ABDALLAH	03C	DLPH	$e^+e^- \to q\overline{q}\tilde{g}\tilde{g}$, stable $\tilde{g}$
> 5		[16] ABDALLAH	03G	DLPH	QCD beta function
		[17] HEISTER	03	ALEP	Color factors
> 26.9	95	[18] HEISTER	03H	ALEP	$e^+e^- \to q\overline{q}\tilde{g}\tilde{g}$
> 6.3		[19] JANOT	03	RVUE	$\Delta\Gamma_{had}$ <3.9 MeV
		[20] MAFI	00	THEO	$pp \to$ jets + $\not{p}_T$
		[21] ALAVI-HARATI	99E	KTEV	$pN \to R^0$, with $R^0 \to \rho^0\tilde{\gamma}$ and $R^0 \to \pi^0\tilde{\gamma}$
		[22] BAER	99	RVUE	Stable $\tilde{g}$ hadrons
		[23] FANTI	99	NA48	pBe $\to R^0 \to \eta\tilde{\gamma}$
		[24] ACKERSTAFF	98V	OPAL	$e^+e^- \to \tilde{\chi}_1^+\tilde{\chi}_1^-$
		[25] ADAMS	97B	KTEV	$pN \to R^0 \to \rho^0\tilde{\gamma}$
		[26] ALBUQUERQ...	97	E761	$R^+(uud\tilde{g}) \to S^0(uds\tilde{g})\pi^+$, $X^-(ssd\tilde{g}) \to S^0\pi^-$
> 6.3	95	[27] BARATE	97L	ALEP	Color factors
> 5	99	[28] CSIKOR	97	RVUE	β function, $Z \to$ jets
> 1.5	90	[29] DEGOUVEA	97	THEO	$Z \to jjj\tilde{g}$
		[30] FARRAR	96	RVUE	$R^0 \to \pi^0\tilde{\gamma}$
none 1.9–13.6	95	[31] AKERS	95R	OPAL	Z decay into a long-lived $(\tilde{g}q\overline{q})^{\pm}$
< 0.7		[32] CLAVELLI	95	RVUE	quarkonia
none 1.5–3.5		[33] CAKIR	94	RVUE	$\Upsilon(1S) \to \gamma+$ gluinonium
not 3–5		[34] LOPEZ	93C	RVUE	LEP
≈ 4		[35] CLAVELLI	92	RVUE	α_s running
		[36] ANTONIADIS	91	RVUE	α_s running
> 1		[37] ANTONIADIS	91	RVUE	$pN \to$ missing energy
		[38] NAKAMURA	89	SPEC	R-Δ^{++}
> 3.8	90	[39] ARNOLD	87	EMUL	π^- (350 GeV). $\sigma \simeq A^1$
> 3.2	90	[39] ARNOLD	87	EMUL	π^- (350 GeV). $\sigma \simeq A^{0.72}$
none 0.6–2.2	90	[40] TUTS	87	CUSB	$\Upsilon(1S) \to \gamma+$ gluinonium
none 1 –4.5	90	[41] ALBRECHT	86C	ARG	$1\times10^{-11} \lesssim \tau \lesssim 1\times10^{-9}$ s
none 1–4	90	[42] BADIER	86	BDMP	$1\times10^{-10} < \tau < 1\times10^{-7}$ s
none 3–5		[43] BARNETT	86	RVUE	$p\overline{p} \to$ gluino gluino gluon
none		[44] VOLOSHIN	86	RVUE	If (quasi) stable; $\tilde{g}uud$
none 0.5–2		[45] COOPER-...	85B	BDMP	For $m_{\tilde{q}}$=300 GeV
none 0.5–4		[45] COOPER-...	85B	BDMP	For $m_{\tilde{q}}$ <65 GeV
none 0.5–3		[45] COOPER-...	85B	BDMP	For $m_{\tilde{q}}$=150 GeV
none 2–4		[46] DAWSON	85	RVUE	$\tau > 10^{-7}$ s
none 1–2.5		[46] DAWSON	85	RVUE	For $m_{\tilde{q}}$=100 GeV
none 0.5–4.1	90	[47] FARRAR	85	RVUE	FNAL beam dump
> 1		[48] GOLDMAN	85	RVUE	Gluinonium
>1–2		[49] HABER	85	RVUE	
		[50] BALL	84	CALO	
		[51] BRICK	84	RVUE	
		[52] FARRAR	84	RVUE	
> 2		[53] BERGSMA	83C	RVUE	For $m_{\tilde{q}}$ <100 GeV
		[54] CHANOWITZ	83	RVUE	$\tilde{g}u\overline{d}$, $\tilde{g}uud$
>2–3		[55] KANE	82	RVUE	Beam dump
>1.5–2		FARRAR	78	RVUE	R-hadron

[1] AAD 13AA searched in 4.7 fb^{-1} of pp collisions at $\sqrt{s} = 7$ TeV for events containing colored long-lived particles that hadronize forming R-hadrons. No significant excess above the expected background was found. Long-lived R-hadrons containing a $\tilde{g}$ are excluded for masses up to 985 GeV at 95% C.L in a general interaction model. Also, limits independent of the fraction of R-hadrons that arrive charged in the muon system were derived, see Fig. 6.

[2] AAD 13BC searched in 5.0 fb^{-1} of pp collisions at $\sqrt{s} = 7$ TeV and in 22.9 fb^{-1} of pp collisions at $\sqrt{s} = 8$ TeV for bottom squark R-hadrons that have come to rest within the ATLAS calorimeter and decay at some later time to hadronic jets and a neutralino. In absence of an excess of events above the expected backgrounds, limits are set on gluino masses for different decays, lifetimes, and neutralino masses, see their Table 6 and Fig. 10.

[3] CHATRCHYAN 13AB looked in 5.0 fb^{-1} of pp collisions at $\sqrt{s} = 7$ TeV and in 18.8 fb^{-1} of pp collisions at $\sqrt{s} = 8$ TeV for events with heavy stable particles, identified by their anomalous dE/dx in the tracker or additionally requiring that it be identified as muon in the muon chambers, from pair production of $\tilde{g}$'s. No evidence for an excess over the expected background is observed. Limits are derived for pair production of gluinos as a function of mass (see Fig. 8 and Table 5), depending on the fraction, f, of formation of $\tilde{g}$–g (R-gluonball) states. The quoted limit is for f = 0.1, while for f = 0.5 it degrades to 1276 GeV. In the conservative scenario where every hadronic interaction causes it to become neutral, the limit decreases to 928 GeV for f = 0.1.

[4] AAD 12P looked in 31 pb^{-1} of pp collisions at $\sqrt{s} = 7$ TeV for events with pair production of long-lived gluinos. The hadronization of the gluinos leads to R-hadrons which may stop inside the detector and later decay via $\tilde{g} \to g\tilde{\chi}_1^0$ during gaps between the proton bunches. No significant excess over the expected background is observed. From a counting experiment, a limit at 95% C.L. on the cross section as a function of $m_{\tilde{g}}$ is derived for $m_{\tilde{\chi}_1^0} = 100$ GeV, see Fig. 4. The limit is valid for lifetimes between 10^{-5} and 10^3 seconds and assumes the *Generic* matter interaction model for the production cross section.

[5] CHATRCHYAN 12AN looked in 4.0 fb^{-1} of pp collisions at $\sqrt{s} = 7$ TeV for events with pair production of long-lived gluinos. The hadronization of the gluinos leads to R-hadrons which may stop inside the detector and later decay via $\tilde{g} \to g\tilde{\chi}_1^0$ during gaps between the proton bunches. No significant excess over the expected background is observed. From a counting experiment, a limit at 95% C.L. on the cross section as a function of $m_{\tilde{g}}$ is derived, see Fig. 3. The mass limit is valid for lifetimes between 10^{-5} and 10^3 seconds, for what they call "the daughter gluon energy $E_g >$" 100 GeV and assuming the *cloud* interaction model for R-hadrons. Supersedes KHACHATRYAN 11.

[6] CHATRCHYAN 12L looked in 5.0 fb^{-1} of pp collisions at $\sqrt{s} = 7$ TeV for events with heavy stable particles, identified by their anomalous dE/dx in the tracker or additionally requiring that it be identified as muon in the muon chambers, from pair production of $\tilde{g}$'s. No evidence for an excess over the expected background is observed. Limits are derived for pair production of gluinos as a function of mass (see Fig. 3), depending on the fraction, f, of formation of $\tilde{g}$–g (R-glueball) states. The quoted limit is for f = 0.1, while for f = 0.5 it degrades to 1046 GeV. In the conservative scenario where every hadronic interaction causes it to become neutral, the limit decreases to 928 GeV for f=0.1. Supersedes KHACHATRYAN 11C.

[7] AAD 11K looked in 34 pb^{-1} of pp collisions at $\sqrt{s} = 7$ TeV for events with heavy stable particles, identified by their anomalous dE/dx in the tracker or time of flight in the tile calorimeter, from pair production of $\tilde{g}$. No evidence for an excess over the SM expectation is observed. Limits are derived for pair production of gluinos as a function of mass (see Fig. 4), for a fraction, f = 10%, of formation of $\tilde{g} - g$ (R-gluonball). If instead of a phase space driven approach for the hadronic scattering of the R-hadrons, a triple-Regge model or a bag-model is used, the limit degrades to 566 and 562 GeV, respectively.

[8] AAD 11P looked in 37 pb^{-1} of pp collisions at $\sqrt{s} = 7$ TeV for events with heavy stable particles, reconstructed and identified by their time of flight in the Muon System. There is no requirement on their observation in the tracker to increase the sensitivity to cases where gluinos have a large fraction, f, of formation of neutral $\tilde{g} - g$ (R-gluonball). No evidence for an excess over the SM expectation is observed. Limits are derived as a function of mass (see Fig. 4), for f=0.1. For fractions f = 0.5 and 1.0 the limit degrades to 537 and 530 GeV, respectively.

[9] KHACHATRYAN 11 looked in 10 pb^{-1} of pp collisions at $\sqrt{s} = 7$ TeV for events with pair production of long-lived gluinos. The hadronization of the gluinos leads to R-hadrons which may stop inside the detector and later decay via $\tilde{g} \to g\tilde{\chi}_1^0$ during gaps between the proton bunches. No significant excess over the expected background is observed. From a counting experiment, a limit at 95% C.L. on the cross section times branching ratio is derived for $m_{\tilde{g}} - m_{\tilde{\chi}_1^0} > 100$ GeV, see their Fig. 2. Assuming 100% branching ratio, lifetimes between 75 ns and 3×10^5 s are excluded for $m_{\tilde{g}} = 300$ GeV. The $\tilde{g}$ mass exclusion is obtained with the same assumptions for lifetimes between 10 μs and 1000 s, but shows some dependence on the model for R-hadron interactions with matter, illustrated in Fig. 3. From a time-profile analysis, the mass exclusion is 382 GeV for a lifetime of 10 μs under the same assumptions as above.

[10] KHACHATRYAN 11C looked in 3.1 pb^{-1} of pp collisions at $\sqrt{s} = 7$ TeV for events with heavy stable particles, identified by their anomalous dE/dx in the tracker or additionally requiring that it be identified as muon in the muon chambers, from pair production of $\tilde{g}$. No evidence for an excess over the expected background is observed. Limits are derived for pair production of gluinos as a function of mass (see Fig. 3), depending on the fraction, f, of formation of $\tilde{g} - g$ (R-gluonball). The quoted limit is for f=0.1, while for f=0.5 it degrades to 357 GeV. In the conservative scenario where every hadronic interaction causes it to become neutral, the limit decreases to 311 GeV for f=0.1.

[11] BERGER 10 updated the results of BERGER 05. They fit parton distribution functions including the effects of a light gluino as an extra parton. Different data on α_s is also included. A fit for $\alpha_s(M_Z)$ is performed as a function of the gluino mass. The bound is determined by comparing the quality of the fit to the CT10 fit, and the CT10 tolerance criterion is used to define the significance. The lower bound is 25 GeV for fixed $\alpha_s(M_Z) = 0.118$.

[12] KAPLAN 08 reanalysed jet event shape data from LEP 1 and LEP 2 using soft collinear effective theory methods. These data are sensitive to the effects of new degrees of freedoms, including a relatively light gluino, at different energy scales, roughly between 5 and 50 GeV. The analysis relies on theoretical modeling of and approximations for non-perturbative effects and matching between different scales.

[13] ABAZOV 07L looked in approximately 410 pb^{-1} of $p\overline{p}$ collisions at $\sqrt{s} = 1.96$ TeV for events with a long-lived gluino from split supersymmetry, decaying after stopping in the detector into $g\tilde{\chi}_1^0$ with lifetimes from 30 μs to 100 h. The signal signature is a largely empty event with a single large transverse energy deposit in the calorimeter. The main

background is due to cosmic muons interacting in the calorimeter. The data agree with the estimated background and allow the authors to estimate a limit on the rate of an out-of-time monojet signal of a given energy. Assuming the branching ratios $\tilde{g} \to g\tilde{\chi}_1^0$ to be 100% the results can be translated to limits on the gluino cross section versus the gluino mass for fixed $\tilde{\chi}_1^0$ mass. After comparing to the expected gluino cross sections, the excluded region of gluino masses can be obtained, see examples in their Fig. 3.

[14] BERGER 05 include the light gluino in proton PDF and perform global analysis of hadronic data. Effects on the running of α_s also included. Strong dependency on $\alpha_s(m_Z)$. Bound quoted for $\alpha_s(m_Z) = 0.118$. Superseded by BERGER 10.

[15] ABDALLAH 03C looked for events of the type $q\overline{q}R^{\pm}R^{\pm}$, $q\overline{q}R^{\pm}R^{0}$ or $q\overline{q}R^{0}R^{0}$ in e^+e^- interactions at 91.2 GeV collected in 1994. The $R^{\pm}$ bound states are identified by anomalous dE/dx in the tracking chambers and the R^0 by missing energy, due to their reduced energy loss in the calorimeters. The upper value of the excluded range depends on the probability for the gluino to fragment into $R^{\pm}$ or R^0, see their Fig. 17. It improves to 23 GeV for 100% fragmentation to $R^{\pm}$.

[16] ABDALLAH 03G used e^+e^- data at and around the Z^0 peak, above the Z^0 up to $\sqrt{s}$ = 202 GeV and events from radiative return to cover the low energy region. They perform a direct measurement of the QCD beta-function from the means of fully inclusive event observables. Compared to the energy range, gluinos below 5 GeV can be considered massless and are firmly excluded by the measurement.

[17] HEISTER 03 use e^+e^- data from 1994 and 1995 at and around the Z^0 peak to measure the 4-jet rate and angular correlations. The comparison with QCD NLO calculations allow $\alpha_S(M_Z)$ and the color factor ratios to be extracted and the results are in agreement with the expectations from QCD. The inclusion of a massless gluino in the beta functions yields T_R / C_F = 0.15 ± 0.06 ± 0.06 (expectation is T_R / C_F = 3/8), excluding a massless gluino at more than 95% CL. As no NLO calculations are available for massive gluinos, the earlier LO results from BARATE 97L for massive gluinos remain valid.

[18] HEISTER 03H use e^+e^- data at and around the Z^0 peak to look for stable gluinos hadronizing into charged or neutral R-hadrons with arbitrary branching ratios. Combining these results with bounds on the Z^0 hadronic width from electroweak measurements (JANOT 03) to cover the low mass region the quoted lower limit on the mass of a long-lived gluino is obtained.

[19] JANOT 03 excludes a light gluino from the upper limit on an additional contribution to the Z hadronic width. At higher confidence levels, $m_{\tilde{g}} > 5.3(4.2)$ GeV at $3\sigma(5\sigma)$ level.

[20] MAFI 00 reanalyzed CDF data assuming a stable heavy gluino as the LSP, with model for R-hadron-nucleon scattering. Gluino masses between 35 GeV and 115 GeV are excluded based on the CDF Run I data. Combined with the analysis of BAER 99, this allows a LSP gluino mass between 25 and 35 GeV if the probability of fragmentation into charged R-hadron P>1/2. The cosmological exclusion of such a gluino LSP are assumed to be avoided as in BAER 99. Gluino could be NLSP with $\tau_{\tilde{g}} \sim 100$ yrs, and decay to gluon gravitino.

[21] ALAVI-HARATI 99E looked for R^0 bound states, yielding $\pi^+\pi^-$ or π^0 in the final state. The experiment is sensitive to values of $\Delta m = m_{R^0} - m_{\tilde{\gamma}}$ larger than 280 MeV and 140 MeV for the two decay modes, respectively, and to R^0 mass and lifetime in the ranges 0.8–5 GeV and 10^{-10}–10^{-3} s. The limits obtained depend on B($R^0 \to \pi^+\pi^-$photino) and B($R^0 \to \pi^0$photino) on the value of $m_{R^0}/m_{\tilde{\gamma}}$, and on the ratio of production rates $\sigma(R^0)/\sigma(K_L^0)$. See Figures in the paper for the excluded R^0 production rates as a function of Δm, R^0 mass and lifetime. Using the production rates expected from perturbative QCD, and assuming dominance of the above decay channels over the suitable phase space, R^0 masses in the range 0.8–5 GeV are excluded at 90%CL for a large fraction of the sensitive lifetime region. ALAVI-HARATI 99E updates and supersedes the results of ADAMS 97B.

[22] BAER 99 set constraints on the existence of stable $\tilde{g}$ hadrons, in the mass range $m_{\tilde{g}} > 3$ GeV. They argue that strong-interaction effects in the low-energy annihilation rates could leave small enough relic densities to evade cosmological constraints up to $m_{\tilde{g}} < 10$ TeV. They consider jet+$\not{E}_T$ as well as heavy-ionizing charged-particle signatures from production of stable $\tilde{g}$ hadrons at LEP and Tevatron, developing modes for the energy loss of $\tilde{g}$ hadrons inside the detectors. Results are obtained as a function of the fragmentation probability P of the $\tilde{g}$ into a charged hadron. For P< 1/2, and for various energy-loss models, OPAL and CDF data exclude gluinos in the 3 <$m_{\tilde{g}}$(GeV)< 130 mass range. For P> 1/2, gluinos are excluded in the mass ranges 3 <$m_{\tilde{g}}$(GeV)< 23 and 50 <$m_{\tilde{g}}$(GeV)< 200.

[23] FANTI 99 looked for R^0 bound states yielding high P_T $\eta \to 3\pi^0$ decays. The experiment is sensitive to a region of R^0 mass and lifetime in the ranges of 1–5 GeV and 10^{-10}–10^{-3} s. The limits obtained depend on B($R^0 \to \eta\tilde{\gamma}$), on the value of $m_{R^0}/m_{\tilde{\gamma}}$, and on the ratio of production rates $\sigma(R^0)/\sigma(K_L^0)$. See Fig. 6–7 for the excluded production rates as a function of R^0 mass and lifetime.

[24] ACKERSTAFF 98V excludes the light gluino with universal gaugino mass where charginos, neutralinos decay as $\tilde{\chi}_1^{\pm}$,$\tilde{\chi}_2^0 \to q\overline{q}\tilde{g}$ from total hadronic cross sections at $\sqrt{s}$=130–172 GeV. See paper for the case of nonuniversal gaugino mass.

[25] ADAMS 97B looked for $\rho^0 \to \pi^+\pi^-$ as a signature of R^0=($\tilde{g}g$) bound states. The experiment is sensitive to an R^0 mass range of 1.2–4.5 GeV and to a lifetime range of 10^{-10}–10^{-3} sec. Precise limits depend on the assumed value of $m_{R^0}/m_{\tilde{\gamma}}$. See Fig. 7 for the excluded mass and lifetime region.

[26] ALBUQUERQUE 97 looked for weakly decaying baryon-like states which contain a light gluino, following the suggestions in FARRAR 96. See their Table 1 for limits on the production fraction. These limits exclude gluino masses in the range 100–600 MeV for the predicted lifetimes (FARRAR 96) and production rates, which are assumed to be comparable to those of strange or charmed baryons.

[27] BARATE 97L studied the QCD color factors from four-jet angular correlations and the differential two-jet rate in Z decay. Limit obtained from the determination of n_f = 4.24 ± 0.29 ± 1.15, assuming T_F/C_F=3/8 and C_A/C_F=9/4.

[28] CSIKOR 97 combined the α_s from $\sigma(e^+e^- \to$ hadron), τ decay, and jet analysis in Z decay. They exclude a light gluino below 5 GeV at more than 99.7%CL.

[29] DEGOUVEA 97 reanalyzed AKERS 95A data on Z decay into four jets to place constraints on a light stable gluino. The mass limit corresponds to the pole mass of 2.8 GeV. The analysis, however, is limited to the leading-order QCD calculation.

[30] FARRAR 96 studied the possible R^0=($\tilde{g}g$) component in Fermilab E799 experiment and used its bound B($K_L^0 \to \pi^0\nu\overline{\nu}$) $\leq 5.8 \times 10^{-5}$ to place constraints on the combination of R^0 production cross section and its lifetime.

[31] AKERS 95R looked for Z decay into $q\overline{q}\tilde{g}\tilde{g}$, by searching for charged particles with dE/dx consistent with $\tilde{g}$ fragmentation into a state $(\tilde{g}q\overline{q})^{\pm}$ with lifetime $\tau > 10^{-7}$ sec. The fragmentation probability into a charged state is assumed to be 25%.

[32] CLAVELLI 95 updates the analysis of CLAVELLI 93, based on a comparison of the hadronic widths of charmonium and bottomonium S-wave states. The analysis includes a parametrization of relativistic corrections. Claims that the presence of a light gluino improves agreement with the data by slowing down the running of α_s.

[33] CAKIR 94 reanalyzed TUTS 87 and later unpublished data from CUSB to exclude pseudo-scalar gluinonium $\eta_{\tilde{g}}(\tilde{g}\tilde{g})$ of mass below 7 GeV. it was argued, however, that the perturbative QCD calculation of the branching fraction $\Upsilon \to \eta_{\tilde{g}}\gamma$ is unreliable for $m_{\eta_{\tilde{g}}} < 3$ GeV. The gluino mass is defined by $m_{\tilde{g}}$=($m_{\eta_{\tilde{q}}}$)/2. The limit holds for any gluino lifetime.

[34] LOPEZ 93C uses combined restraint from the radiative symmetry breaking scenario within the minimal supergravity model, and the LEP bounds on the (M_2,μ) plane. Claims that the light gluino window is strongly disfavored.

[35] CLAVELLI 92 claims that a light gluino mass around 4 GeV should exist to explain the discrepancy between α_s at LEP and at quarkonia (Υ), since a light gluino slows the running of the QCD coupling.

[36] ANTONIADIS 91 argue that possible light gluinos (< 5 GeV) contradict the observed running of α_s between 5 GeV and m_Z. The significance is less than 2 s.d.

[37] ANTONIADIS 91 interpret the search for missing energy events in 450 GeV/c pN collisions, AKESSON 91, in terms of light gluinos.

[38] NAKAMURA 89 searched for a long-lived ($\tau \gtrsim 10^{-7}$ s) charge-(±2) particle with mass $\lesssim$ 1.6 GeV in proton-Pt interactions at 12 GeV and found that the yield is less than 10^{-8} times that of the pion. This excludes R-Δ^{++} (a $\tilde{g}uuu$ state) lighter than 1.6 GeV.

[39] The limits assume $m_{\tilde{q}} = 100$ GeV. See their figure 3 for limits vs. $m_{\tilde{q}}$.

[40] The gluino mass is defined by half the bound $\tilde{g}\tilde{g}$ mass. If zero gluino mass gives a $\tilde{g}\tilde{g}$ of mass about 1 GeV as suggested by various glueball mass estimates, then the low-mass bound can be replaced by zero. The high-mass bound is obtained by comparing the data with nonrelativistic potential-model estimates.

[41] ALBRECHT 86C search for secondary decay vertices from $\chi_{b1}(1P) \to \tilde{g}\tilde{g}g$ where $\tilde{g}$'s make long-lived hadrons. See their figure 4 for excluded region in the $m_{\tilde{g}} - m_{\tilde{g}}$ and $m_{\tilde{g}} - m_{\tilde{q}}$ plane. The lower $m_{\tilde{g}}$ region below $\sim$ 2 GeV may be sensitive to fragmentation effects. Remark that the $\tilde{g}$-hadron mass is expected to be $\sim$ 1 GeV (glueball mass) in the zero $\tilde{g}$ mass limit.

[42] BADIER 86 looked for secondary decay vertices from long-lived $\tilde{g}$-hadrons produced at 300 GeV π^- beam dump. The quoted bound assumes $\tilde{g}$-hadron nucleon total cross section of 10μb. See their figure 7 for excluded region in the $m_{\tilde{g}} - m_{\tilde{q}}$ plane for several assumed total cross-section values.

[43] BARNETT 86 rule out light gluinos (m = 3–5 GeV) by calculating the monojet rate from gluino gluino gluon events (and from gluino gluino events) and by using UA1 data from $p\overline{p}$ collisions at CERN.

[44] VOLOSHIN 86 rules out stable gluino based on the cosmological argument that predicts too much hydrogen consisting of the charged stable hadron $\tilde{g}uud$. Quasi-stable ($\tau > 1.\times10^{-7}$s) light gluino of $m_{\tilde{g}}$ <3 GeV is also ruled out by nonobservation of the stable charged particles, $\tilde{g}uud$, in high energy hadron collisions.

[45] COOPER-SARKAR 85B is BEBC beam-dump. Gluinos decaying in dump would yield $\tilde{\gamma}$'s in the detector giving neutral-current-like interactions. For $m_{\tilde{q}}$ >330 GeV, no limit is set.

[46] DAWSON 85 first limit from neutral particle search. Second limit based on FNAL beam dump experiment.

[47] FARRAR 85 points out that BALL 84 analysis applies only if the $\tilde{g}$'s decay before interacting, i.e. $m_{\tilde{q}}$ <80$m_{\tilde{g}}^{1.5}$. FARRAR 85 finds $m_{\tilde{g}}$ <0.5 not excluded for $m_{\tilde{q}}$ = 30–1000 GeV and $m_{\tilde{g}}$ <1.0 not excluded for $m_{\tilde{q}}$ = 100–500 GeV by BALL 84 experiment.

[48] GOLDMAN 85 use nonobservation of a pseudoscalar $\tilde{g}$-$\tilde{g}$ bound state in radiative ψ decay.

[49] HABER 85 is based on survey of all previous searches sensitive to low mass $\tilde{g}$'s. Limit makes assumptions regarding the lifetime and electric charge of the lightest supersymmetric particle.

[50] BALL 84 is FNAL beam dump experiment. Observed no interactions of $\tilde{\gamma}$ in the calorimeter, where $\tilde{\gamma}$'s are expected to come from pair-produced $\tilde{g}$'s. Search for long-lived $\tilde{\gamma}$ interacting in calorimeter 56m from target. Limit is for $m_{\tilde{q}}$ = 40 GeV and production cross section proportional to A$^{0.72}$. BALL 84 find no $\tilde{g}$ allowed below 4.1 GeV at CL = 90%. Their figure 1 shows dependence on $m_{\tilde{q}}$ and A. See also KANE 82.

[51] BRICK 84 reanalyzed FNAL 147 GeV HBC data for R-$\Delta(1232)^{++}$ with $\tau > 10^{-9}$ s and p_{lab} >2 GeV. Set CL = 90% upper limits 6.1, 4.4, and 29 microbarns in pp, π^+p, K^+p collisions respectively. R-Δ^{++} is defined as being $\tilde{g}$ and 3 up quarks. If mass = 1.2–1.5 GeV, then limits may be lower than theory predictions.

[52] FARRAR 84 argues that $m_{\tilde{g}}$ <100 MeV is not ruled out if the lightest R-hadrons are long-lived. A long lifetime would occur if R-hadrons are lighter than $\tilde{\gamma}$'s or if $m_{\tilde{q}}$ >100 GeV.

[53] BERGSMA 83C is reanalysis of CERN-SPS beam-dump data. See their figure 1.

[54] CHANOWITZ 83 find in bag-model that charged s-hadron exists which is stable against strong decay if $m_{\tilde{g}}$ <1 GeV. This is important since tracks from decay of neutral s-hadron cannot be reconstructed to primary vertex because of missed $\tilde{\gamma}$. Charged s-hadron leaves track from vertex.

[55] KANE 82 inferred above $\tilde{g}$ mass limit from retroactive analysis of hadronic collision and beam dump experiments. Limits valid if $\tilde{g}$ decays inside detector.

LIGHT $\tilde{G}$ (Gravitino) MASS LIMITS FROM COLLIDER EXPERIMENTS

The following are bounds on light ($\ll$ 1 eV) gravitino indirectly inferred from its coupling to matter suppressed by the gravitino decay constant.

Unless otherwise stated, all limits assume that other supersymmetric particles besides the gravitino are too heavy to be produced. The gravitino is assumed to be undetected and to give rise to a missing energy ($\not{E}$) signature.

VALUE (eV)	CL%	DOCUMENT ID		TECN	COMMENT
• • • We do not use the following data for averages, fits, limits, etc. • • •					
$> 1.09 \times 10^{-5}$	95	[1] ABDALLAH	05B	DLPH	$e^+e^- \to \widetilde{G}\widetilde{G}\gamma$
$> 1.35 \times 10^{-5}$	95	[2] ACHARD	04E	L3	$e^+e^- \to \widetilde{G}\widetilde{G}\gamma$
$> 1.3 \times 10^{-5}$		[3] HEISTER	03C	ALEP	$e^+e^- \to \widetilde{G}\widetilde{G}\gamma$
$>11.7 \times 10^{-6}$	95	[4] ACOSTA	02H	CDF	$p\overline{p} \to \widetilde{G}\widetilde{G}\gamma$
$> 8.7 \times 10^{-6}$	95	[5] ABBIENDI,G	00D	OPAL	$e^+e^- \to \widetilde{G}\widetilde{G}\gamma$
$>10.0 \times 10^{-6}$	95	[6] ABREU	00Z	DLPH	$e^+e^- \to \widetilde{G}\widetilde{G}\gamma$
$>11 \times 10^{-6}$	95	[7] AFFOLDER	00J	CDF	$p\overline{p} \to \widetilde{G}\widetilde{G}$ +jet
$> 8.9 \times 10^{-6}$	95	[8] ACCIARRI	99R	L3	$e^+e^- \to \widetilde{G}\widetilde{G}\gamma$
$> 7.9 \times 10^{-6}$	95	[9] ACCIARRI	98V	L3	$e^+e^- \to \widetilde{G}\widetilde{G}\gamma$
$> 8.3 \times 10^{-6}$	95	[9] BARATE	98J	ALEP	$e^+e^- \to \widetilde{G}\widetilde{G}\gamma$

[1] ABDALLAH 05B use data from $\sqrt{s} = 180$–208 GeV. They look for events with a single photon + $\not{E}$ final states from which a cross section limit of $\sigma < 0.18$ pb at 208 GeV is obtained, allowing a limit on the mass to be set. Supersedes the results of ABREU 00Z.

[2] ACHARD 04E use data from $\sqrt{s} = 189$–209 GeV. They look for events with a single photon + $\not{E}$ final states from which a limit on the Gravitino mass is set corresponding to $\sqrt{F} > 238$ GeV. Supersedes the results of ACCIARRI 99R.

[3] HEISTER 03C use the data from $\sqrt{s} = 189$–209 GeV to search for $\gamma\not{E}_T$ final states.

[4] ACOSTA 02H looked in 87 pb^{-1} of $p\overline{p}$ collisions at $\sqrt{s}$=1.8 TeV for events with a high-E_T photon and $\not{E}_T$. They compared the data with a GMSB model where the final state could arise from $q\overline{q} \to \widetilde{G}\widetilde{G}\gamma$. Since the cross section for this process scales as $1/|F|^4$, a limit at 95% CL is derived on $|F|^{1/2} > 221$ GeV. A model independent limit for the above topology is also given in the paper.

[5] ABBIENDI,G 00D searches for $\gamma\not{E}$ final states from $\sqrt{s}$=189 GeV.

[6] ABREU 00Z search for $\gamma\not{E}$ final states using data from $\sqrt{s}$=189 GeV. Superseded by ABDALLAH 05B.

[7] AFFOLDER 00J searches for final states with an energetic jet (from quark or gluon) and large $\not{E}_T$ from undetected gravitinos.

[8] ACCIARRI 99R search for $\gamma\not{E}$ final states using data from $\sqrt{s}$=189 GeV. Superseded by ACHARD 04E.

[9] Searches for $\gamma\not{E}$ final states at $\sqrt{s}$=183 GeV.

Supersymmetry Miscellaneous Results

Results that do not appear under other headings or that make nonminimal assumptions.

VALUE	CL%	DOCUMENT ID		TECN	COMMENT
• • • We do not use the following data for averages, fits, limits, etc. • • •					
		[1] AAD	13P	ATLS	dark γ, hidden valley
		[2] AALTONEN	12AB	CDF	hidden-valley Higgs
none 100–185	95	[3] AAD	11AA	ATLS	scalar gluons
		[4] CHATRCHYAN	11E	CMS	$\mu\mu$ resonances
		[5] ABAZOV	10N	D0	γ_D, hidden valley
		[6] LOVE	08A	CLEO	$\not{R}$, $Y \to \mu\tau$
		[7] ABULENCIA	06P	CDF	$\ell\gamma\not{E}_T$, $\ell\ell\gamma$, GMSB
		[8] ACOSTA	04E	CDF	
		[9] TCHIKILEV	04	ISTR	$K^- \to \pi^-\pi^0 P$
		[10] AFFOLDER	02D	CDF	$p\overline{p} \to \gamma b$ ($\not{E}_T$)
		[11] AFFOLDER	01H	CDF	$p\overline{p} \to \gamma\gamma$X
		[12] ABBOTT	00G	D0	$p\overline{p} \to 3\ell + \not{E}_T$, $\not{R}$, $LL\overline{E}$
		[13] ABREU,P	00C	DLPH	$e^+e^- \to \gamma + S/P$
		[14] ABACHI	97	D0	$\gamma\gamma X$
		[15] BARBER	84B	RVUE	
		[16] HOFFMAN	83	CNTR	$\pi p \to n(e^+e^-)$

[1] AAD 13P searched in 5 fb^{-1} of pp collisions at $\sqrt{s} = 7$ TeV for single lepton-jets with at least four muons; pairs of lepton-jets, each with two or more muons; and pairs of lepton-jets with two or more electrons. All of these could be signatures of Hidden Valley supersymmetric models. No statistically significant deviations from the Standard Model expectations are found. 95% C.L. limits are placed on the production cross section times branching ratio of dark photons for several parameter sets of a Hidden Valley model.

[2] AALTONEN 12AB looked in 5.1 fb^{-1} of $p\overline{p}$ collisions at $\sqrt{s} = 1.96$ TeV for anomalous production of multiple low-energy leptons in association with a W or Z boson. Such events may occur in hidden valley models in which a supersymmetric Higgs boson is produced in association with a W or Z boson, with $H \to \widetilde{\chi}_1^0\widetilde{\chi}_1^0$ pair and with the $\widetilde{\chi}_1^0$ further decaying into a dark photon (γ_D) and the unobservable lightest SUSY particle of the hidden sector. As the γ_D is expected to be light, it may decay into a lepton pair. No significant excess over the SM expectation is observed and a limit at 95% C.L. is set on the cross section for a benchmark model of supersymmetric hidden-valley Higgs production.

[3] AAD 11AA looked in 34 pb^{-1} of pp collisions at $\sqrt{s} = 7$ TeV for events with ≥ 4 jets originating from pair production of scalar gluons, each decaying to two gluons. No two-jet resonances are observed over the SM background. Limits are derived on the cross section times branching ratio (see Fig. 3). Assuming 100% branching ratio for the decay to two gluons, the quoted exclusion range is obtained, except for a 5 GeV mass window around 140 GeV.

[4] CHATRCHYAN 11E looked in 35 pb^{-1} of pp collisions at $\sqrt{s} = 7$ TeV for events with collimated μ pairs (leptonic jets) from the decay of hidden sector states. No evidence for new resonance production is found. Limits are derived and compared to various SUSY models (see Fig. 4) where the LSP, either the $\widetilde{\chi}_1^0$ or a $\widetilde{q}$, decays to dark sector particles.

[5] ABAZOV 10N looked in 5.8 fb^{-1} of $p\overline{p}$ collisions at $\sqrt{s} = 1.96$ TeV for events from hidden valley models in which a $\widetilde{\chi}_1^0$ decays into a dark photon, γ_D, and the unobservable lightest SUSY particle of the hidden sector. As the γ_D is expected to be light, it may decay into a tightly collimated lepton pair, called lepton jet. They searched for events with $\not{E}_T$ and two isolated lepton jets observable by an opposite charged lepton pair ee, $e\mu$ or $\mu\mu$. No significant excess over the SM expectation is observed, and a limit at 95% C.L. on the cross section times branching ratio is derived, see their Table I. They also examined the invariant mass of the lepton jets for a narrow resonance, see their Fig. 4, but found no evidence for a signal.

[6] LOVE 08A searched for decays of Y(nS) with n = 1, 2, 3 into $\mu\tau$ in 1.1, 1.3, 1.4 fb^{-1}, respectively, in the CLEO III detector at CESR. The signature is a muon with ≈ 97 % of the beam energy and an electron from the decay of τ. No evidence for lepton flavour violation is found and 95% CL limits on the branching ratio are estimated to be 6.0, 14.4 and 20.3×10^{-6} for n = 1, 2, 3, respectively.

[7] ABULENCIA 06P searched in 305 pb^{-1} of $p\overline{p}$ collisions at $\sqrt{s} = 1.96$ TeV for an excess of events with $\ell\gamma\not{E}_T$ and $\ell\ell\gamma$ ($\ell = e, \mu$). No significant excess was found compared to the background expectation. No events are found such as the $ee\gamma\gamma\not{E}_T$ event observed in ABE 99I.

[8] ACOSTA 04E looked in 107 pb^{-1} of $p\overline{p}$ collisions at $\sqrt{s} = 1.8$ TeV for events with two same sign leptons without selection of other objects nor $\not{E}_T$. No significant excess is observed compared to the Standard Model expectation and constraints are derived on the parameter space of MSUGRA models, see Figure 4.

[9] Looked for the scalar partner of a goldstino in decays $K^- \to \pi^-\pi^0 P$ from a 25 GeV K^- beam produced at the IHEP 70 GeV proton synchrotron. The sgoldstino is assumed to be sufficiently long-lived to be invisible. A 90% CL upper limit on the decay branching ratio is set at $\sim 9.0 \times 10^{-6}$ for a sgoldstino mass range from 0 to 200 MeV, excluding the interval near $m(\pi^0)$, where the limit is $\sim 3.5 \times 10^{-5}$.

[10] AFFOLDER 02D looked in 85 pb^{-1} of $p\overline{p}$ collisions at $\sqrt{s}$=1.8 TeV for events with a high-E_T photon, and a b-tagged jet with or without $\not{E}_T$. They compared the data with models where the final state could arise from cascade decays of gluinos and/or squarks into $\widetilde{\chi}^\pm$ and $\widetilde{\chi}_2^0$ or direct associated production of $\widetilde{\chi}_2^0\widetilde{\chi}_2^\pm$, followed by $\widetilde{\chi}_2^0 \to \gamma\widetilde{\chi}_1^0$ or a GMSB model where $\widetilde{\chi}_1^0 \to \gamma\widetilde{G}$. It is concluded that the experimental sensitivity is insufficient to detect the associated production or the GMSB model, but some sensitivity may exist to the cascade decays. A model independent limit for the above topology is also given in the paper.

[11] AFFOLDER 01H searches for $p\overline{p} \to \gamma\gamma$X events, where the di-photon system originates from sgoldstino production, in 100 pb^{-1} of data. Upper limits on the cross section times branching ratio are shown as function of the di-photon mass >70 GeV in Fig. 5. Excluded regions are derived in the plane of the sgoldstino mass versus the supersymmetry breaking scale for two representative sets of parameter values, as shown in Figs. 6 and 7.

[12] ABBOTT 00G searches for trilepton final states (ℓ=e,μ) with $\not{E}_T$ from the indirect decay of gauginos via $LL\overline{E}$ couplings. Efficiencies are computed for all possible production and decay modes of SUSY particles in the framework of the Minimal Supergravity scenario. See Figs. 1–4 for excluded regions in the $m_{1/2}$ versus m_0 plane.

[13] ABREU,P 00C look for the CP-even (S) and CP-odd (P) scalar partners of the goldstino, expected to be produced in association with a photon. The S/P decay into two photons or into two gluons and both the tri-photon and the photon + two jets topologies are investigated. Upper limits on the production cross section are shown in Fig. 5 and the excluded regions in Fig. 6. Data collected at $\sqrt{s}$= 189–202 GeV.

[14] ABACHI 97 searched for $p\overline{p} \to \gamma\gamma\not{E}_T + X$ as supersymmetry signature. It can be caused by selectron, sneutrino, or neutralino production with a radiative decay of their decay products. They placed limits on cross sections.

[15] BARBER 84B consider that $\widetilde{\mu}$ and $\widetilde{e}$ may mix leading to $\mu \to e\widetilde{\gamma}\widetilde{\gamma}$. They discuss mass-mixing limits from decay dist. asym. in LBL-TRIUMF data and e^+ polarization in SIN data.

[16] HOFFMAN 83 set CL = 90% limit $d\sigma/dt$ B$(e^+e^-) < 3.5 \times 10^{-32}$ cm^2/GeV^2 for spin-1 partner of Goldstone fermions with 140 $< m <$160 MeV decaying $\to e^+e^-$ pair.

REFERENCES FOR Supersymmetric Particle Searches

AAD	13	PL B718 841	G. Aad *et al.*	(ATLAS Collab.)
AAD	13AA	PL B720 277	G. Aad *et al.*	(ATLAS Collab.)
AAD	13AB	EPJ C73 2362	G. Aad *et al.*	(ATLAS Collab.)
AAD	13AI	PL B723 15	G. Aad *et al.*	(ATLAS Collab.)
AAD	13AP	PR D88 012001	G. Aad *et al.*	(ATLAS Collab.)
AAD	13AU	JHEP 1310 189	G. Aad *et al.*	(ATLAS Collab.)
AAD	13AV	JHEP 1310 130	G. Aad *et al.*	(ATLAS Collab.)
AAD	13B	PL B718 879	G. Aad *et al.*	(ATLAS Collab.)
AAD	13BC	PR D88 112003	G. Aad *et al.*	(ATLAS Collab.)
AAD	13BD	PR D88 112006	G. Aad *et al.*	(ATLAS Collab.)
AAD	13H	JHEP 1301 131	G. Aad *et al.*	(ATLAS Collab.)
AAD	13L	PR D87 012008	G. Aad *et al.*	(ATLAS Collab.)
AAD	13P	PL B719 299	G. Aad *et al.*	(ATLAS Collab.)
AAD	13Q	PL B719 261	G. Aad *et al.*	(ATLAS Collab.)
AAD	13R	PL B719 280	G. Aad *et al.*	(ATLAS Collab.)
AAD	13T	PL B720 13	G. Aad *et al.*	(ATLAS Collab.)
AALSETH	13	PR D88 012002	C.E. Aalseth *et al.*	(CoGeNT Collab.)
AALTONEN	13I	PR D88 031103	T. Aaltonen *et al.*	(CDF Collab.)
AALTONEN	13Q	PRL 110 201802	T. Aaltonen *et al.*	(CDF Collab.)
AARTSEN	13	PRL 110 131302	M.G. Aartsen *et al.*	(IceCube Collab.)
AARTSEN	13C	PR D88 122001	M.G. Aartsen *et al.*	(IceCube Collab.)
ABAZOV	13B	PR D87 052011	V.M. Abazov *et al.*	(D0 Collab.)
ABRAMOWSKI	13	PRL 110 041301	A. Abramowski *et al.*	(H.E.S.S. Collab.)
ACKERMANN	13A	PR D88 082002	M. Ackermann *et al.*	(Fermi-LAT Collab.)
ADRIAN-MAR...	13	JCAP 1311 032	S. Adrian-Martinez *et al.*	(ANTARES Collab.)
AGNESE	13	PR D88 031104	R. Agnese *et al.*	(CDMS Collab.)
AGNESE	13A	PRL 111 251301	R. Agnese *et al.*	(CDMS Collab.)
APRILE	13	PRL 111 021301	E. Aprile *et al.*	(XENON100 Collab.)
BERGSTROM	13	PRL 111 171101	L. Bergstrom *et al.*	
BOLIEV	13	JCAP 1309 019	M. Boliev *et al.*	
CABRERA	13	JHEP 1307 182	M. Cabrera, J. Casas, R. de Austri	
CHATRCHYAN	13	PL B718 815	S. Chatrchyan *et al.*	(CMS Collab.)
CHATRCHYAN	13AB	JHEP 1307 122	S. Chatrchyan *et al.*	(CMS Collab.)
CHATRCHYAN	13AH	PL B722 273	S. Chatrchyan *et al.*	(CMS Collab.)
CHATRCHYAN	13AK	PL B725 243	S. Chatrchyan *et al.*	(CMS Collab.)
CHATRCHYAN	13AM	PR D87 052006	S. Chatrchyan *et al.*	(CMS Collab.)
CHATRCHYAN	13AO	PR D87 072001	S. Chatrchyan *et al.*	(CMS Collab.)
CHATRCHYAN	13AT	PR D88 052017	S. Chatrchyan *et al.*	(CMS Collab.)
CHATRCHYAN	13AV	PRL 111 081802	S. Chatrchyan *et al.*	(CMS Collab.)
CHATRCHYAN	13BN	PRL 111 221801	S. Chatrchyan *et al.*	(CMS Collab.)
CHATRCHYAN	13BS	EPJ C73 2677	S. Chatrchyan *et al.*	(CMS Collab.)
CHATRCHYAN	13G	JHEP 1301 077	S. Chatrchyan *et al.*	(CMS Collab.)
CHATRCHYAN	13H	PL B719 42	S. Chatrchyan *et al.*	(CMS Collab.)
CHATRCHYAN	13M	PRL 110 081801	S. Chatrchyan *et al.*	(CMS Collab.)
CHATRCHYAN	13P	EPJ C73 2404	S. Chatrchyan *et al.*	(CMS Collab.)
CHATRCHYAN	13R	EPJ C73 2493	S. Chatrchyan *et al.*	(CMS Collab.)
CHATRCHYAN	13T	EPJ C73 2568	S. Chatrchyan *et al.*	(CMS Collab.)
CHATRCHYAN	13V	JHEP 1303 037	S. Chatrchyan *et al.*	(CMS Collab.)
Also		JHEP 1307 041 (errat.)	S. Chatrchyan *et al.*	(CMS Collab.)
CHATRCHYAN	13W	JHEP 1303 111	S. Chatrchyan *et al.*	(CMS Collab.)
ELLIS	13B	EPJ C73 2403	J. Ellis *et al.*	
HAN	13	JHEP 1310 216	C. Han *et al.*	
JIN	13	JCAP 1311 026	H.-B. Jin, Y.-L. Wu, Y.-F. Zhou	
KOPP	13	PR D88 076013	J. Kopp	
LI	13B	PRL 110 261301	H.B. Li *et al.*	(TEXONO Collab.)

Searches Particle Listings

Supersymmetric Particle Searches

STREGE 13 JCAP 1304 013 C. Strege *et al.*
AAD 12AF PL B714 180 G. Aad *et al.* (ATLAS Collab.)
AAD 12AG PL B714 197 G. Aad *et al.* (ATLAS Collab.)
AAD 12AH PL B715 44 G. Aad *et al.* (ATLAS Collab.)
AAD 12AN PRL 108 181802 G. Aad *et al.* (ATLAS Collab.)
AAD 12AP PRL 108 241802 G. Aad *et al.* (ATLAS Collab.)
AAD 12AS PRL 108 261804 G. Aad *et al.* (ATLAS Collab.)
AAD 12AX PR D85 012006 G. Aad *et al.* (ATLAS Collab.)
Also PR D87 099903 (errat.) G. Aad *et al.* (ATLAS Collab.)
AAD 12BA PR D85 112006 G. Aad *et al.* (ATLAS Collab.)
AAD 12BI JHEP 1207 167 G. Aad *et al.* (ATLAS Collab.)
AAD 12BJ EPJ C72 1993 G. Aad *et al.* (ATLAS Collab.)
AAD 12BY EPJ C72 2174 G. Aad *et al.* (ATLAS Collab.)
AAD 12CB JHEP 1211 094 G. Aad *et al.* (ATLAS Collab.)
AAD 12CE PRL 109 211802 G. Aad *et al.* (ATLAS Collab.)
AAD 12CF PRL 109 211803 G. Aad *et al.* (ATLAS Collab.)
AAD 12CJ PR D86 092002 G. Aad *et al.* (ATLAS Collab.)
AAD 12CL EPJ C72 2237 G. Aad *et al.* (ATLAS Collab.)
AAD 12CM EPJ C72 2215 G. Aad *et al.* (ATLAS Collab.)
AAD 12CP PL B718 411 G. Aad *et al.* (ATLAS Collab.)
AAD 12CT JHEP 1212 124 G. Aad *et al.* (ATLAS Collab.)
AAD 12CU JHEP 1212 086 G. Aad *et al.* (ATLAS Collab.)
AAD 12J EPJ C72 2040 G. Aad *et al.* (ATLAS Collab.)
AAD 12P EPJ C72 1965 G. Aad *et al.* (ATLAS Collab.)
AAD 12R PL B707 478 G. Aad *et al.* (ATLAS Collab.)
AAD 12T PL B709 137 G. Aad *et al.* (ATLAS Collab.)
AAD 12W PL B710 67 G. Aad *et al.* (ATLAS Collab.)
AAD 12X PL B710 519 G. Aad *et al.* (ATLAS Collab.)
AALTONEN 12AB PR D85 092001 T. Aaltonen *et al.* (CDF Collab.)
AALTONEN 12AO JHEP 1210 158 T. Aaltonen *et al.* (CDF Collab.)
ABAZOV 12AD PR D86 071701 V.M. Abazov *et al.* (D0 Collab.)
ABAZOV 12H PL B710 578 V.M. Abazov *et al.* (D0 Collab.)
ABAZOV 12L PRL 108 121802 V.M. Abazov *et al.* (D0 Collab.)
ABBASI 12 PR D85 042002 R. Abbasi *et al.* (IceCube Collab.)
AKIMOV 12 PL B709 14 D.Yu. Akimov *et al.* (ZEPLIN-III Collab.)
AKULA 12 PR D85 075001 S. Akula *et al.* (NEAS, MICH)
ANGLOHER 12 EPJ C72 1971 G. Angloher *et al.* (CRESST-II Collab.)
APRILE 12 PRL 109 181301 E. Aprile *et al.* (XENON100 Collab.)
ARBEY 12A PL B708 162 A. Arbey *et al.*
ARCHAMBAU... 12 PL B711 153 S. Archambault *et al.* (PICASSO Collab.)
BAER 12 JHEP 1205 091 H. Baer, V. Barger, A. Mustafayev (OKLA, WISC+)
BALAZS 12 EPJ C73 2563 C. Balazs *et al.*
BECHTLE 12 JHEP 1206 098 P. Bechtle *et al.*
BEHNKE 12 PR D86 052001 E. Behnke *et al.* (COUPP Collab.)
BESKIDT 12 EPJ C72 2166 C. Beskidt *et al.* (KARLE, JINR, ITEP)
BOTTINO 12 PR D85 095013 A. Bottino, N. Fornengo, S. Scopel (TORI, SOGA)
BUCHMUEL... 12 EPJ C72 2020 O. Buchmueller *et al.*
BUCHMUEL... 12A EPJ C72 2243 O. Buchmueller *et al.*
CAO 12A PL B710 665 J. Cao *et al.*
CHATRCHYAN 12 PR D85 012004 S. Chatrchyan *et al.* (CMS Collab.)
CHATRCHYAN 12AE PRL 109 171803 S. Chatrchyan *et al.* (CMS Collab.)
CHATRCHYAN 12AH PR D86 072010 S. Chatrchyan *et al.* (CMS Collab.)
CHATRCHYAN 12AI JHEP 1208 110 S. Chatrchyan *et al.* (CMS Collab.)
CHATRCHYAN 12AL JHEP 1206 169 S. Chatrchyan *et al.* (CMS Collab.)
CHATRCHYAN 12AN JHEP 1208 026 S. Chatrchyan *et al.* (CMS Collab.)
CHATRCHYAN 12AT JHEP 1210 018 S. Chatrchyan *et al.* (CMS Collab.)
CHATRCHYAN 12BD PL B718 329 S. Chatrchyan *et al.* (CMS Collab.)
CHATRCHYAN 12BJ JHEP 1211 147 S. Chatrchyan *et al.* (CMS Collab.)
CHATRCHYAN 12BK JHEP 1211 172 S. Chatrchyan *et al.* (CMS Collab.)
CHATRCHYAN 12BO JHEP 1212 055 S. Chatrchyan *et al.* (CMS Collab.)
CHATRCHYAN 12L PL B713 408 S. Chatrchyan *et al.* (CMS Collab.)
CHATRCHYAN 12Q PL B716 260 S. Chatrchyan *et al.* (CMS Collab.)
CHATRCHYAN 12U PRL 109 071803 S. Chatrchyan *et al.* (CMS Collab.)
DAW 12 ASP 35 397 E. Daw *et al.* (DRIFT-IId Collab)
DREINER 12A EPL 99 61001 H.K. Dreiner, M. Kramer, J. Tattersall (BONN+)
ELLIS 12B EPJ C72 2005 J. Ellis, K. Olive
FELIZARDO 12 PRL 108 201302 M. Felizardo *et al.* (SIMPLE Collab.)
FENG 12B PR D85 075007 J. Feng, K. Matchev, D. Sanford
FOWLIE 12A PR D86 075010 A. Fowlie *et al.*
KADASTIK 12 JHEP 1205 061 M. Kadastik *et al.*
KIM 12 PRL 108 181301 S.C. Kim *et al.* (KIMS Collab.)
STREGE 12 JCAP 1203 030 C. Strege *et al.* (LOIC, AMST, MADU, GRAN+)
AAD 11AA EPJ C71 1828 G. Aad *et al.* (ATLAS Collab.)
AAD 11AE JHEP 1110 107 G. Aad *et al.* (ATLAS Collab.)
AAD 11AF JHEP 1111 099 G. Aad *et al.* (ATLAS Collab.)
AAD 11B EPJ C71 1682 G. Aad *et al.* (ATLAS Collab.)
AAD 11C EPJ C71 1647 G. Aad *et al.* (ATLAS Collab.)
AAD 11G PRL 106 131802 G. Aad *et al.* (ATLAS Collab.)
AAD 11H PRL 106 251801 G. Aad *et al.* (ATLAS Collab.)
AAD 11K PL B701 1 G. Aad *et al.* (ATLAS Collab.)
AAD 11N PL B701 186 G. Aad *et al.* (ATLAS Collab.)
AAD 11O PL B701 398 G. Aad *et al.* (ATLAS Collab.)
AAD 11P PL B703 428 G. Aad *et al.* (ATLAS Collab.)
AAD 11X EPJ C71 1744 G. Aad *et al.* (ATLAS Collab.)
AAD 11Z EPJ C71 1809 G. Aad *et al.* (ATLAS Collab.)
AALTONEN 11Q PRL 107 042001 T. Aaltonen *et al.* (CDF Collab.)
AARON 11 EPJ C71 1572 E.D. Aaron *et al.* (H1 Collab.)
AARON 11C PL B705 52 F. D. Aaron *et al.* (H1 Collab.)
ABAZOV 11N PL B696 321 V.M. Abazov *et al.* (D0 Collab.)
ABRAMOWSKI 11 PRL 106 161301 A. Abramowski *et al.* (H.E.S.S. Collab.)
AHMED 11A PR D84 011102 Z. Ahmed *et al.* (CDMS and EDELWEISS Collabs.)
APRILE 11B PRL 107 131302 E. Aprile *et al.* (XENON100 Collab.)
ARMENGAUD 11 PL B702 329 E. Armengaud *et al.* (EDELWEISS II Collab.)
BUCHMUEL... 11 EPJ C71 1583 O. Buchmueller *et al.*
BUCHMUEL... 11B EPJ C71 1722 O. Buchmueller *et al.*
CHATRCHYAN 11AB JHEP 1106 077 S. Chatrchyan *et al.* (CMS Collab.)
CHATRCHYAN 11AC JHEP 1108 155 S. Chatrchyan *et al.* (CMS Collab.)
CHATRCHYAN 11B JHEP 1106 093 S. Chatrchyan *et al.* (CMS Collab.)
CHATRCHYAN 11C JHEP 1106 026 S. Chatychyan *et al.* (CMS Collab.)
CHATRCHYAN 11D JHEP 1107 113 S. Chatrchyan *et al.* (CMS Collab.)
CHATRCHYAN 11E JHEP 1107 098 S. Chatrchyan *et al.* (CMS Collab.)
CHATRCHYAN 11G PRL 106 211802 S. Chatrchyan *et al.* (CMS Collab.)
CHATRCHYAN 11Q JHEP 1108 156 S. Chatrchyan *et al.* (CMS Collab.)
CHATRCHYAN 11V PL B704 411 S. Chatrchyan *et al.* (CMS Collab.)
CHATRCHYAN 11W PRL 107 221804 S. Chatrchyan *et al.* (CMS Collab.)
KHACHATRY... 11 PRL 106 011801 V. Khachatryan *et al.* (CMS Collab.)
KHACHATRY... 11C JHEP 1103 024 V. Khachatryan *et al.* (CMS Collab.)
KHACHATRY... 11I PL B698 196 V. Khachatryan *et al.* (CMS Collab.)
ROSZKOWSKI 11 PR D83 015014 L. Roszkowski *et al.*
AALTONEN 10 PRL 104 011801 T. Aaltonen *et al.* (CDF Collab.)
AALTONEN 10O PRL 104 251801 T. Aaltonen *et al.* (CDF Collab.)
AALTONEN 10R PRL 105 081802 T. Aaltonen *et al.* (CDF Collab.)
AALTONEN 10Y PR D82 092001 T. Aaltonen *et al.* (CDF Collab.)
AALTONEN 10Z PRL 105 191801 T. Aaltonen *et al.* (CDF Collab.)
ABAZOV 10L PL B693 95 V.M. Abazov *et al.* (D0 Collab.)
ABAZOV 10M PRL 105 191802 V.M. Abazov *et al.* (D0 Collab.)
ABAZOV 10N PRL 105 211802 V.M. Abazov *et al.* (D0 Collab.)
ABAZOV 10P PRL 105 221802 V.M. Abazov *et al.* (D0 Collab.)
ABDO 10 JCAP 1004 014 A.A. Abdo *et al.* (Fermi-LAT Collab.)
ACKERMANN 10 JCAP 1005 025 M. Ackermann (Fermi-LAT Collab.)
AHMED 10 SCI 327 1619 Z. Ahmed *et al.* (CDMS II Collab.)
ARMENGAUD 10 PL B687 294 E. Armengaud *et al.* (EDELWEISS II Collab.)
BERGER 10 PR D82 114023 E.L. Berger *et al.*
ELLIS 10 EPJ C69 201 J. Ellis, A. Mustafayev, K. Olive
AALTONEN 09G PR D79 052004 T. Aaltonen *et al.* (CDF Collab.)
AALTONEN 09R PRL 102 221801 T. Aaltonen *et al.* (CDF Collab.)
AALTONEN 09S PRL 102 121801 T. Aaltonen *et al.* (CDF Collab.)
AALTONEN 09V PRL 102 091805 T. Aaltonen *et al.* (CDF Collab.)
AALTONEN 09Z PRL 103 021802 T. Aaltonen *et al.* (CDF Collab.)
ABAZOV 09M PRL 102 161802 V.M. Abazov *et al.* (D0 Collab.)
ABAZOV 09N PL B674 4 V.M. Abazov *et al.* (D0 Collab.)
ABAZOV 09O PL B675 289 V.M. Abazov *et al.* (D0 Collab.)
ABAZOV 09S PL B680 24 V.M. Abazov *et al.* (D0 Collab.)
ABAZOV 09T PL B680 34 V.M. Abazov *et al.* (D0 Collab.)
ABBASI 09B PRL 102 201302 R. Abbasi *et al.* (IceCube Collab.)
AHMED 09 PRL 102 011301 Z. Ahmed *et al.* (CDMS Collab.)
ANGLOHER 09 ASP 31 270 G. Angloher *et al.* (CRESST Collab.)
ARCHAMBAU...09 PL B682 185 S. Archambault *et al.* (PICASSO Collab.)
BUCHMUEL... 09 EPJ C64 391 O. Buchmueller *et al.* (LOIC, FNAL, CERN+)
DREINER 09 EPJ C62 547 H. Dreiner *et al.*
LEBEDENKO 09 PR D80 052010 V.N. Lebedenko *et al.* (ZEPLIN-III Collab.)
LEBEDENKO 09A PRL 103 151302 V.N. Lebedenko *et al.* (ZEPLIN-III Collab.)
SORENSEN 09 NIM A601 339 P. Sorensen *et al.* (XENON10 Collab.)
AALTONEN 08AE PRL 101 251801 T. Aaltonen *et al.* (CDF Collab.)
AALTONEN 08L PR D77 052002 T. Aaltonen *et al.* (CDF Collab.)
AALTONEN 08U PR D78 032015 T. Aaltonen *et al.* (CDF Collab.)
AALTONEN 08Z PRL 101 071802 T. Aaltonen *et al.* (CDF Collab.)
ABAZOV 08 PL B659 500 V.M. Abazov *et al.* (D0 Collab.)
ABAZOV 08F PL B659 856 V.M. Abazov *et al.* (D0 Collab.)
ABAZOV 08G PL B660 449 V.M. Abazov *et al.* (D0 Collab.)
ABAZOV 08Q PRL 100 241803 V.M. Abazov *et al.* (D0 Collab.)
ABAZOV 08X PRL 101 111802 V.M. Abazov *et al.* (D0 Collab.)
ABAZOV 08Z PL B665 1 V.M. Abazov *et al.* (D0 Collab.)
ANGLE 08 PRL 100 021303 J. Angle *et al.* (XENON10 Collab.)
ANGLE 08A PRL 101 091301 J. Angle *et al.* (XENON10 Collab.)
BEDNYAKOV 08 PAN 71 111 V.A. Bednyakov, H.P. Klapdor-Kleingrothaus, I.V. Krivosheina
Translated from YAF 71 112.
BEHNKE 08 SCI 319 933 E. Behnke (COUPP Collab.)
BENETTI 08 ASP 28 495 P. Benetti *et al.* (WARP Collab.)
BUCHMUEL... 08 JHEP 0809 117 O. Buchmueller *et al.*
ELLIS 08 PR D78 075012 J. Ellis, K. Olive, P. Sandick (CERN, MINN)
KAPLAN 08 PRL 101 022002 D.E. Kaplan, M.D. Schwartz
LOVE 08A PRL 101 201601 W. Love *et al.* (CLEO Collab.)
AALTONEN 07E PR D76 072010 T. Aaltonen *et al.* (CDF Collab.)
AALTONEN 07J PRL 99 191806 T. Aaltonen *et al.* (CDF Collab.)
ABAZOV 07B PL B645 119 V.M. Abazov *et al.* (D0 Collab.)
ABAZOV 07L PRL 99 131801 V.M. Abazov *et al.* (D0 Collab.)
ABULENCIA 07H PRL 98 131804 A. Abulencia *et al.* (CDF Collab.)
ABULENCIA 07N PRL 98 221803 A. Abulencia *et al.* (CDF Collab.)
ABULENCIA 07P PRL 99 121801 A. Abulencia *et al.* (CDF Collab.)
ALNER 07A ASP 28 287 G.J. Alner *et al.* (ZEPLIN-II Collab.)
CALIBBI 07 JHEP 0709 081 L. Calibbi *et al.*
CHEKANOV 07 EPJ C50 269 S. Chekanov *et al.* (ZEUS Collab.)
ELLIS 07 JHEP 0706 079 J. Ellis, K. Olive, P. Sandick (CERN, MINN)
LEE 07A PRL 99 091301 H.S. Lee *et al.* (KIMS Collab.)
SCHAEL 07A EPJ C49 411 S. Schael *et al.* (ALEPH Collab.)
ABAZOV 06C PL B638 119 V.M. Abazov *et al.* (D0 Collab.)
ABAZOV 06D PL B638 441 V.M. Abazov *et al.* (D0 Collab.)
ABAZOV 06I PRL 97 111801 V.M. Abazov *et al.* (D0 Collab.)
ABAZOV 06P PRL 97 161802 V.M. Abazov *et al.* (D0 Collab.)
ABAZOV 06R PRL 97 171806 V.M. Abazov *et al.* (D0 Collab.)
ABBIENDI 06B EPJ C46 307 G. Abbiendi *et al.* (OPAL Collab.)
ABDALLAH 06C EPJ C45 589 J. Abdallah *et al.* (DELPHI Collab.)
ABULENCIA 06I PRL 96 171802 A. Abulencia *et al.* (CDF Collab.)
ABULENCIA 06M PRL 96 211802 A. Abulencia *et al.* (CDF Collab.)
ABULENCIA 06P PRL 97 031801 A. Abulencia *et al.* (CDF Collab.)
ACHTERBERG 06 ASP 26 129 A. Achterberg *et al.* (AMANDA Collab.)
ACKERMANN 06 ASP 24 459 M. Ackermann *et al.* (AMANDA Collab.)
AKERIB 06 PR D73 011102 D.S. Akerib *et al.* (CDMS Collab.)
AKERIB 06A PRL 96 011302 D.S. Akerib *et al.* (CDMS Collab.)
ALLANACH 06 PR D73 015013 B.C. Allanach *et al.*
BENOIT 06 PL B637 156 A. Benoit *et al.*
DE-AUSTRI 06 JHEP 0605 002 R.R. de Austri, R. Trotta, L. Roszkowski
DEBOER 06 PL B636 13 W. de Boer *et al.*
LEP-SLC 06 PRPL 427 257 ALEPH, DELPHI, L3, OPAL, SLD and working groups
SHIMIZU 06A PL B633 195 Y. Shimizu *et al.*
SMITH 06 PL B642 567 N.J.T. Smith, A.S. Murphy, T.J. Summer
ABAZOV 05A PRL 94 041801 V.M. Abazov *et al.* (D0 Collab.)
ABAZOV 05U PRL 95 151805 V.M. Abazov *et al.* (D0 Collab.)
ABDALLAH 05B EPJ C38 395 J. Abdallah *et al.* (DELPHI Collab.)
ABULENCIA 05A PRL 95 252001 A. Abulencia *et al.* (CDF Collab.)
ACOSTA 05E PR D71 031104 D. Acosta *et al.* (CDF Collab.)
ACOSTA 05R PRL 95 131801 D. Acosta *et al.* (CDF Collab.)
AKERIB 05 PR D72 052009 D.S. Akerib *et al.* (CDMS Collab.)
AKTAS 05 PL B616 31 A. Aktas *et al.* (H1 Collab.)
ALNER 05 PL B616 17 G.J. Alner *et al.* (UK Dark Matter Collab.)
ALNER 05A ASP 23 444 G.J. Alner *et al.* (UK Dark Matter Collab.)
ANGLOHER 05 ASP 23 325 G. Angloher *et al.* (CRESST-II Collab.)
BAER 05 JHEP 0507 065 H. Baer *et al.* (FSU, MSU, HAWA)
BARNABE-HE...05 PL B624 186 M. Barnabe-Heider *et al.* (PICASSO Collab.)
BERGER 05 PR D71 014007 E.L. Berger *et al.*
CHEKANOV 05A EPJ C44 463 S. Chekanov *et al.* (ZEUS Collab.)
ELLIS 05 PR D71 095007 J. Ellis *et al.*
SANGLARD 05 PR D71 122002 V. Sanglard *et al.* (EDELWEISS Collab.)
ABAZOV 04 PL B581 147 V.M. Abazov *et al.* (D0 Collab.)
ABAZOV 04B PRL 93 011801 V.M. Abazov *et al.* (D0 Collab.)
ABBIENDI 04 EPJ C32 453 G. Abbiendi *et al.* (OPAL Collab.)
ABBIENDI 04F EPJ C33 149 G. Abbiendi *et al.* (OPAL Collab.)
ABBIENDI 04H EPJ C35 1 G. Abbiendi *et al.* (OPAL Collab.)
ABBIENDI 04N PL B602 167 G. Abbiendi *et al.* (OPAL Collab.)
ABDALLAH 04H EPJ C34 145 J. Abdallah *et al.* (DELPHI Collab.)
ABDALLAH 04M EPJ C36 1 J. Abdallah *et al.* (DELPHI Collab.)
Also EPJ C37 129 (errat) J. Abdallah *et al.* (DELPHI Collab.)
ACHARD 04 PL B580 37 P. Achard *et al.* (L3 Collab.)
ACHARD 04E PL B587 16 P. Achard *et al.* (L3 Collab.)
ACOSTA 04B PRL 92 051803 D. Acosta *et al.* (CDF Collab.)
ACOSTA 04E PRL 93 061802 D. Acosta *et al.* (CDF Collab.)
AKERIB 04 PRL 93 211301 D. Akerib *et al.* (CDMSII Collab.)
AKTAS 04B PL B599 159 A. Aktas *et al.* (H1 Collab.)
AKTAS 04D EPJ C36 425 A. Aktas *et al.* (H1 Collab.)
BALTZ 04 JHEP 0410 052 E. Baltz, P. Gondolo
BELANGER 04 JHEP 0403 012 G. Belanger *et al.*
BOTTINO 04 PR D69 037302 A. Bottino *et al.*
DAS 04 PL B596 293 S.P. Das, A. Datta, M. Maity
DESAI 04 PR D70 083523 S. Desai *et al.* (Super-Kamiokande Collab.)
ELLIS 04 PR D69 015005 J. Ellis *et al.*
ELLIS 04B PR D70 055005 J. Ellis *et al.*
HEISTER 04 PL B583 247 A. Heister *et al.* (ALEPH Collab.)
JANOT 04 PL B594 23 P. Janot
PIERCE 04A PR D70 075006 A. Pierce
TCHIKILEV 04 PL B602 149 O.G. Tchikilev *et al.* (ISTRA+ Coolab.)
ABBIENDI 03H EPJ C29 479 G. Abbiendi *et al.* (OPAL Collab.)
ABBIENDI 03L PL B572 8 G. Abbiendi *et al.* (OPAL Collab.)
ABDALLAH 03C EPJ C26 505 J. Abdallah *et al.* (DELPHI Collab.)

ABDALLAH 03D EPJ C27 153 J. Abdallah *et al.* (DELPHI Collab.)
ABDALLAH 03F EPJ C28 15 J. Abdallah *et al.* (DELPHI Collab.)
ABDALLAH 03G EPJ C29 285 J. Abdallah *et al.* (DELPHI Collab.)
ABDALLAH 03M EPJ C31 421 J. Abdallah *et al.* (DELPHI Collab.)
ACOSTA 03C PRL 90 251801 D. Acosta *et al.* (CDF Collab.)
ACOSTA 03E PRL 91 171602 D. Acosta *et al.* (CDF Collab.)
ADLOFF 03 PL B568 35 C. Adloff *et al.* (H1 Collab.)
AHMED 03 ASP 19 691 B. Ahmed *et al.* (UK Dark Matter Collab.)
AKERIB 03 PR D68 082002 D. Akerib *et al.* (CDMS Collab.)
BAER 03 JCAP 0305 006 H. Baer, C. Balazs
BAER 03A JCAP 0309 007 H. Baer *et al.*
BERGER 03 PL B552 223 E. Berger *et al.*
BOTTINO 03 PR D68 043506 A. Bottino *et al.*
BOTTINO 03A PR D67 063519 A. Bottino, N. Fornengo, S. Scopel
CHAKRAB... 03 PR D68 015005 S. Chakrabarti, M. Guchait, N.K. Mondal
CHATTOPAD... 03 PR D68 035005 U. Chattopadhyay, A. Corsetti, P. Nath
CHEKANOV 03B PR D68 052004 S. Chekanov *et al.* (ZEUS Collab.)
ELLIS 03 ASP 18 395 J. Ellis, K.A. Olive, Y. Santoso
ELLIS 03B NP B652 259 J. Ellis *et al.*
ELLIS 03C PL B565 176 J. Ellis *et al.*
ELLIS 03D PL B573 162 J. Ellis *et al.*
ELLIS 03E PR D67 123502 J. Ellis *et al.*
HEISTER 03 EPJ C27 1 A. Heister *et al.* (ALEPH)
HEISTER 03C EPJ C28 1 A. Heister *et al.* (ALEPH Collab.)
HEISTER 03G EPJ C31 1 A. Heister *et al.* (ALEPH Collab.)
HEISTER 03H EPJ C31 327 A. Heister *et al.* (ALEPH Collab.)
JANOT 03 PL B564 183 P. Janot
KLAPDOR-K... 03 ASP 18 525 H.V. Klapdor-Kleingrothaus *et al.*
LAHANAS 03 PL B568 55 A. Lahanas, D. Nanopoulos
TAKEDA 03 PL B572 145 A. Takeda *et al.*
ABAZOV 02C PRL 88 171802 V.M. Abazov *et al.* (D0 Collab.)
ABAZOV 02F PRL 89 171801 V.M. Abazov *et al.* (D0 Collab.)
ABAZOV 02G PR D66 112001 V.M. Abazov *et al.* (D0 Collab.)
ABAZOV 02H PRL 89 261801 V.M. Abazov *et al.* (D0 Collab.)
ABBIENDI 02 EPJ C23 1 G. Abbiendi *et al.* (OPAL Collab.)
ABBIENDI 02B PL B526 233 G. Abbiendi *et al.* (OPAL Collab.)
ABBIENDI 02H PL B545 272 G. Abbiendi *et al.* (OPAL Collab.)
Also PL B548 258 (errat) G. Abbiendi *et al.* (OPAL Collab.)
ABRAMS 02 PR D66 122003 D. Abrams *et al.* (CDMS Collab.)
ACHARD 02 PL B524 65 P. Achard *et al.* (L3 Collab.)
ACOSTA 02H PRL 89 281801 D. Acosta *et al.* (CDF Collab.)
AFFOLDER 02 PRL 88 041801 T. Affolder *et al.* (CDF Collab.)
AFFOLDER 02D PR D65 052006 T. Affolder *et al.* (CDF Collab.)
ANGLOHER 02 ASP 18 43 G. Angloher *et al.* (CRESST Collab.)
ARNOWITT 02 hep-ph/0211417 R. Arnowitt, B. Dutta
BAEK 02 PL B541 161 S. Baek
BECHER 02 PL B540 278 T. Becher *et al.*
BENOIT 02 PL B545 43 A. Benoit *et al.* (EDELWEISS Collab.)
CHEKANOV 02 PR D65 092004 S. Chekanov *et al.* (ZEUS Collab.)
CHEUNG 02B PRL 89 221801 K. Cheung, W.-Y. Keung
CHO 02 PRL 89 091801 G.-C. Cho
ELLIS 02B PL B532 318 J. Ellis, A. Ferstl, K.A. Olive
GHODBANE 02 NP B647 190 N. Ghodbane *et al.*
HEISTER 02 PL B526 191 A. Heister *et al.* (ALEPH Collab.)
HEISTER 02E PL B526 206 A. Heister *et al.* (ALEPH Collab.)
HEISTER 02F EPJ C25 1 A. Heister *et al.* (ALEPH Collab.)
HEISTER 02J PL B533 223 A. Heister *et al.* (ALEPH Collab.)
HEISTER 02K PL B537 5 A. Heister *et al.* (ALEPH Collab.)
HEISTER 02N PL B544 73 A. Heister *et al.* (ALEPH Collab.)
HEISTER 02R EPJ C25 339 A. Heister *et al.* (ALEPH Collab.)
KIM 02 PL B527 18 H.B. Kim *et al.*
KIM 02B JHEP 0212 034 Y.G. Kim *et al.*
LAHANAS 02 EPJ C23 185 A. Lahanas, V.C. Spanos
MORALES 02B ASP 16 325 A. Morales *et al.* (COSME Collab.)
MORALES 02C PL B532 8 A. Morales *et al.* (IGEX Collab.)
ABBIENDI 01 PL B501 12 G. Abbiendi *et al.* (OPAL Collab.)
ABBOTT 01D PR D63 091102 B. Abbott *et al.* (D0 Collab.)
ABREU 01 EPJ C19 29 P. Abreu *et al.* (DELPHI Collab.)
ABREU 01B EPJ C19 201 P. Abreu *et al.* (DELPHI Collab.)
ABREU 01C PL B502 24 P. Abreu *et al.* (DELPHI Collab.)
ABREU 01D PL B500 22 P. Abreu *et al.* (DELPHI Collab.)
ABREU 01G PL B503 34 P. Abreu *et al.* (DELPHI Collab.)
ACCIARRI 01 EPJ C19 397 M. Acciarri *et al.* (L3 Collab.)
ADAMS 01 PRL 87 041801 T. Adams *et al.* (NuTeV Collab.)
ADLOFF 01B EPJ C20 639 C. Adloff *et al.* (H1 Collab.)
AFFOLDER 01B PR D63 091101 T. Affolder *et al.* (CDF Collab.)
AFFOLDER 01H PR D64 092002 T. Affolder *et al.* (CDF Collab.)
AFFOLDER 01J PRL 87 251803 T. Affolder *et al.* (CDF Collab.)
BALTZ 01 PRL 86 5004 E. Baltz, P. Gondolo
BARATE 01 PL B499 67 R. Barate *et al.* (ALEPH Collab.)
BARATE 01B EPJ C19 415 R. Barate *et al.* (ALEPH Collab.)
BARGER 01C PL B518 117 V. Barger, C. Kao
BAUDIS 01 PR D63 022001 L. Baudis *et al.* (Heidelberg-Moscow Collab.)
BENOIT 01 PL B513 15 A. Benoit *et al.* (EDELWEISS Collab.)
BERGER 01 PRL 86 4231 E. Berger *et al.*
BERNABEI 01 PL B509 197 R. Bernabei *et al.* (DAMA Collab.)
BOTTINO 01 PR D63 125003 A. Bottino *et al.*
BREITWEG 01 PR D63 052002 J. Breitweg *et al.* (ZEUS Collab.)
CORSETTI 01 PR D64 125010 A. Corsetti, P. Nath
ELLIS 01B PL B510 236 J. Ellis *et al.*
ELLIS 01C PR D63 065016 J. Ellis, A. Ferstl, K.A. Olive
GOMEZ 01 PL B512 252 M.E. Gomez, J.D. Vergados
LAHANAS 01 PL B518 94 A. Lahanas, D.V. Nanopoulos, V. Spanos
SAVINOV 01 PR D63 051101 V. Savinov *et al.* (CLEO Collab.)
ABBIENDI 00 EPJ C12 1 G. Abbiendi *et al.* (OPAL Collab.)
ABBIENDI 00G EPJ C14 51 G. Abbiendi *et al.* (OPAL Collab.)
ABBIENDI 00H EPJ C14 187 G. Abbiendi *et al.* (OPAL Collab.)
Also EPJ C16 707 (errat) G. Abbiendi *et al.* (OPAL Collab.)
ABBIENDI 00J EPJ C12 551 G. Abbiendi *et al.* (OPAL Collab.)
ABBIENDI 00R EPJ C13 553 G. Abbiendi *et al.* (OPAL Collab.)
ABBIENDI,G 00D EPJ C18 253 G. Abbiendi *et al.* (OPAL Collab.)
ABBOTT 00C PRL 84 2088 B. Abbott *et al.* (D0 Collab.)
ABBOTT 00G PR D62 071701 B. Abbott *et al.* (D0 Collab.)
ABREU 00I EPJ C13 591 P. Abreu *et al.* (DELPHI Collab.)
ABREU 00J PL B479 129 P. Abreu *et al.* (DELPHI Collab.)
ABREU 00Q PL B478 65 P. Abreu *et al.* (DELPHI Collab.)
ABREU 00S PL B485 45 P. Abreu *et al.* (DELPHI Collab.)
ABREU 00T PL B485 95 P. Abreu *et al.* (DELPHI Collab.)
ABREU 00U PL B487 36 P. Abreu *et al.* (DELPHI Collab.)
ABREU 00V EPJ C16 211 P. Abreu *et al.* (DELPHI Collab.)
ABREU 00W PL B489 38 P. Abreu *et al.* (DELPHI Collab.)
ABREU 00Z EPJ C17 53 P. Abreu *et al.* (DELPHI Collab.)
ABREU,P 00C PL B494 203 P. Abreu *et al.* (DELPHI Collab.)
ABREU,P 00D PL B496 59 P. Abreu *et al.* (DELPHI Collab.)
ABUSAIDI 00 PRL 84 5699 R. Abusaidi *et al.* (CDMS Collab.)
ACCIARRI 00C EPJ C16 1 M. Acciarri *et al.* (L3 Collab.)
ACCIARRI 00D PL B472 420 M. Acciarri *et al.* (L3 Collab.)
ACCIARRI 00K PL B482 31 M. Acciarri *et al.* (L3 Collab.)
ACCIARRI 00P PL B489 81 M. Acciarri *et al.* (L3 Collab.)
ACCOMANDO 00 NP B585 124 E. Accomando *et al.*
AFFOLDER 00D PRL 84 5704 T. Affolder *et al.* (CDF Collab.)
AFFOLDER 00G PRL 84 5273 T. Affolder *et al.* (CDF Collab.)
AFFOLDER 00J PRL 85 1378 T. Affolder *et al.* (CDF Collab.)
AFFOLDER 00K PRL 85 2056 T. Affolder *et al.* (CDF Collab.)
BARATE 00G EPJ C16 71 R. Barate *et al.* (ALEPH Collab.)
BARATE 00H EPJ C13 29 R. Barate *et al.* (ALEPH Collab.)
BARATE 00I EPJ C12 183 R. Barate *et al.* (ALEPH Collab.)
BARATE 00P PL B488 234 R. Barate *et al.* (ALEPH Collab.)
BERNABEI 00 PL B480 23 R. Bernabei *et al.* (DAMA Collab.)
BERNABEI 00C EPJ C18 283 R. Bernabei *et al.* (DAMA Collab.)
BERNABEI 00D NJP 2 15 R. Bernabei *et al.* (DAMA Collab.)
BOEHM 00B PR D62 035012 C. Boehm, A. Djouadi, M. Drees
BREITWEG 00E EPJ C16 253 J. Breitweg *et al.* (ZEUS Collab.)
CHO 00B NP B574 623 G.-C. Cho, K. Hagiwara
ELLIS 00 PR D62 075010 J. Ellis *et al.*
FENG 00 PL B482 388 J.L. Feng, K.T. Matchev, F. Wilczek
LEP 00 CERN-EP-2000-016 LEP Collabs. (ALEPH, DELPHI, L3, OPAL, SLD+)
MAFI 00 PR D62 035003 A. Mafi, S. Raby
MALTONI 00 PL B476 107 M. Maltoni *et al.*
MORALES 00 PL B489 268 A. Morales *et al.* (IGEX Collab.)
PDG 00 EPJ C15 1 D.E. Groom *et al.* (PDG Collab.)
SPOONER 00 PL B473 330 N.J.C. Spooner *et al.* (UK Dark Matter Col.)
ABBIENDI 99 EPJ C6 1 G. Abbiendi *et al.* (OPAL Collab.)
ABBIENDI 99F EPJ C8 23 G. Abbiendi *et al.* (OPAL Collab.)
ABBIENDI 99M PL B456 95 G. Abbiendi *et al.* (OPAL Collab.)
ABBIENDI 99T EPJ C11 619 G. Abbiendi *et al.* (OPAL Collab.)
ABBOTT 99 PRL 82 29 B. Abbott *et al.* (D0 Collab.)
ABBOTT 99F PR D60 031101 B. Abbott *et al.* (D0 Collab.)
ABBOTT 99J PRL 83 2896 B. Abbott *et al.* (D0 Collab.)
ABBOTT 99K PRL 83 4476 B. Abbott *et al.* (D0 Collab.)
ABBOTT 99L PRL 83 4937 B. Abbott *et al.* (D0 Collab.)
ABE 99I PR D59 092002 F. Abe *et al.* (CDF Collab.)
ABE 99M PRL 83 2133 F. Abe *et al.* (CDF Collab.)
ABREU 99A EPJ C11 383 P. Abreu *et al.* (DELPHI Collab.)
ABREU 99C EPJ C6 385 P. Abreu *et al.* (DELPHI Collab.)
ABREU 99F EPJ C7 595 P. Abreu *et al.* (DELPHI Collab.)
ABREU 99G PL B446 62 P. Abreu *et al.* (DELPHI Collab.)
ACCIARRI 99H PL B456 283 M. Acciarri *et al.* (L3 Collab.)
ACCIARRI 99I PL B459 354 M. Acciarri *et al.* (L3 Collab.)
ACCIARRI 99L PL B462 354 M. Acciarri *et al.* (L3 Collab.)
ACCIARRI 99R PL B470 268 M. Acciarri *et al.* (L3 Collab.)
ACCIARRI 99V PL B471 308 M. Acciarri *et al.* (L3 Collab.)
ACCIARRI 99W PL B471 280 M. Acciarri *et al.* (L3 Collab.)
ALAVI-HARATI 99E PRL 83 2128 A. Alavi-Harati *et al.* (FNAL KTeV Collab.)
AMBROSIO 99 PR D60 082002 M. Ambrosio *et al.* (Macro Collab.)
BAER 99 PR D59 075002 H. Baer, K. Cheung, J.F. Gunion
BARATE 99E EPJ C7 383 R. Barate *et al.* (ALEPH Collab.)
BARATE 99Q PL B469 303 R. Barate *et al.* (ALEPH Collab.)
BAUDIS 99 PR D59 022001 L. Baudis *et al.* (Heidelberg-Moscow Collab.)
BELLI 99C NP B563 97 P. Belli *et al.* (DAMA Collab.)
BERNABEI 99 PL B450 448 R. Bernabei *et al.* (DAMA Collab.)
FANTI 99 PL B446 117 V. Fanti *et al.* (CERN NA48 Collab.)
MALTONI 99B PL B463 230 M. Maltoni, M.I. Vysotsky
OOTANI 99 PL B461 371 W. Ootani *et al.*
ABBOTT 98 PRL 80 442 B. Abbott *et al.* (D0 Collab.)
ABBOTT 98C PRL 80 1591 B. Abbott *et al.* (D0 Collab.)
ABBOTT 98E PRL 80 2051 B. Abbott *et al.* (D0 Collab.)
ABBOTT 98J PRL 81 38 B. Abbott *et al.* (D0 Collab.)
ABE 98J PRL 80 5275 F. Abe *et al.* (CDF Collab.)
ABE 98S PRL 81 4806 F. Abe *et al.* (CDF Collab.)
ABREU 98 EPJ C1 1 P. Abreu *et al.* (DELPHI Collab.)
ABREU 98P PL B444 491 P. Abreu *et al.* (DELPHI Collab.)
ACCIARRI 98F EPJ C4 207 M. Acciarri *et al.* (L3 Collab.)
ACCIARRI 98J PL B433 163 M. Acciarri *et al.* (L3 Collab.)
ACCIARRI 98V PL B444 503 M. Acciarri *et al.* (L3 Collab.)
ACKERSTAFF 98K EPJ C4 47 K. Ackerstaff *et al.* (OPAL Collab.)
ACKERSTAFF 98L EPJ C2 213 K. Ackerstaff *et al.* (OPAL Collab.)
ACKERSTAFF 98P PL B433 195 K. Ackerstaff *et al.* (OPAL Collab.)
ACKERSTAFF 98V EPJ C2 441 K. Ackerstaff *et al.* (OPAL Collab.)
BARATE 98H PL B420 127 R. Barate *et al.* (ALEPH Collab.)
BARATE 98J PL B429 201 R. Barate *et al.* (ALEPH Collab.)
BARATE 98K PL B433 176 R. Barate *et al.* (ALEPH Collab.)
BARATE 98S EPJ C4 433 R. Barate *et al.* (ALEPH Collab.)
BARATE 98X EPJ C2 417 R. Barate *et al.* (ALEPH Collab.)
BERNABEI 98 PL B424 195 R. Bernabei *et al.* (DAMA Collab.)
BERNABEI 98C PL B436 379 R. Bernabei *et al.* (DAMA Collab.)
BREITWEG 98 PL B434 214 J. Breitweg *et al.* (ZEUS Collab.)
ELLIS 98 PR D58 095002 J. Ellis *et al.*
ELLIS 98B PL B444 367 J. Ellis, T. Falk, K. Olive
PDG 98 EPJ C3 1 C. Caso *et al.* (PDG Collab.)
ABACHI 97 PRL 78 2070 S. Abachi *et al.* (D0 Collab.)
ABBOTT 97B PRL 79 4321 B. Abbott *et al.* (D0 Collab.)
ABE 97K PR D56 R1357 F. Abe *et al.* (CDF Collab.)
ACCIARRI 97U PL B414 373 M. Acciarri *et al.* (L3 Collab.)
ACKERSTAFF 97H PL B396 301 K. Ackerstaff *et al.* (OPAL Collab.)
ADAMS 97B PRL 79 4083 J. Adams *et al.* (FNAL KTeV Collab.)
ALBUQUERQ... 97 PRL 78 3252 I.F. Albuquerque *et al.* (FNAL E761 Collab.)
BAER 97 PR D57 567 H. Baer, M. Brhlik
BARATE 97K PL B405 379 R. Barate *et al.* (ALEPH Collab.)
BARATE 97L ZPHY C76 1 R. Barate *et al.* (ALEPH Collab.)
BERNABEI 97 ASP 7 73 R. Bernabei *et al.* (DAMA Collab.)
CARENA 97 PL B390 234 M. Carena, G.F. Giudice, C.E.M. Wagner
CSIKOR 97 PRL 78 4335 F. Csikor, Z. Fodor (EOTV, CERN)
DATTA 97 PL B395 54 A. Datta, M. Guchait, N. Parua (ICTP, TATA)
DEGOUVEA 97 PL B400 117 A. de Gouvea, H. Murayama
DERRICK 97 ZPHY C73 613 M. Derrick *et al.* (ZEUS Collab.)
EDSJO 97 PR D56 1879 J. Edsjo, P. Gondolo
ELLIS 97 PL B394 354 J. Ellis, J.L. Lopez, D.V. Nanopoulos
HEWETT 97 PR D56 5703 J.L. Hewett, T.G. Rizzo, M.A. Doncheski
KALINOWSKI 97 PL B400 112 J. Kalinowski, P. Zerwas
TEREKHOV 97 PL B412 86 I. Terekhov (ALAT)
ABACHI 96 PRL 76 2228 S. Abachi *et al.* (D0 Collab.)
ABACHI 96B PRL 76 2222 S. Abachi *et al.* (D0 Collab.)
ABE 96 PRL 77 438 F. Abe *et al.* (CDF Collab.)
ABE 96D PRL 76 2006 F. Abe *et al.* (CDF Collab.)
ABE 96K PRL 76 4307 F. Abe *et al.* (CDF Collab.)
AID 96 ZPHY C71 211 S. Aid *et al.* (H1 Collab.)
AID 96C PL B380 461 S. Aid *et al.* (H1 Collab.)
ARNOWITT 96 PR D54 2374 R. Arnowitt, P. Nath
BAER 96 PR D53 597 H. Baer, M. Brhlik
BERGSTROM 96 ASP 5 263 L. Bergstrom, P. Gondolo
CHO 96 PL B372 101 G.C. Cho, Y. Kizukuri, N. Oshimo (TOKAH, OCH)
FARRAR 96 PRL 76 4111 G.R. Farrar (RUTG)
LEWIN 96 ASP 6 87 J.D. Lewin, P.F. Smith
TEREKHOV 96 PL B385 139 I. Terkhov, L. Clavelli (ALAT)
ABACHI 95C PRL 75 618 S. Abachi *et al.* (D0 Collab.)
ABE 95N PRL 74 3538 F. Abe *et al.* (CDF Collab.)
ABE 95T PRL 75 613 F. Abe *et al.* (CDF Collab.)
ACCIARRI 95E PL B350 109 M. Acciarri *et al.* (L3 Collab.)
AKERS 95A ZPHY C65 367 R. Akers *et al.* (OPAL Collab.)
AKERS 95R ZPHY C67 203 R. Akers *et al.* (OPAL Collab.)
BEREZINSKY 95 ASP 5 1 V. Berezinsky *et al.*
BUSKULIC 95E PL B349 238 D. Buskulic *et al.* (ALEPH Collab.)
CLAVELLI 95 PR D51 1117 L. Clavelli, P.W. Coulter (ALAT)

FALK	95	PL B354 99	T. Falk, K.A. Olive, M. Srednicki	(MINN, UCSB)
LOSECCO	95	PL B342 392	J.M. LoSecco	(NDAM)
AKERS	94K	PL B337 207	R. Akers *et al.*	(OPAL Collab.)
BECK	94	PL B336 141	M. Beck *et al.*	(MPIH, KIAE, SASSO)
CAKIR	94	PR D50 3268	M.B. Cakir, G.R. Farrar	(RUTG)
FALK	94	PL B339 248	T. Falk, K.A. Olive, M. Srednicki	(UCSB, MINN)
SHIRAI	94	PRL 72 3313	J. Shirai *et al.*	(VENUS Collab.)
ADRIANI	93M	PRPL 236 1	O. Adriani *et al.*	(L3 Collab.)
ALITTI	93	NP B400 3	J. Alitti *et al.*	(UA2 Collab.)
CLAVELLI	93	PR D47 1973	L. Clavelli, P.W. Coulter, K.J. Yuan	(ALAT)
DREES	93	PR D47 376	M. Drees, M.M. Nojiri	(DESY, SLAC)
DREES	93B	PR D48 3483	M. Drees, M.M. Nojiri	
FALK	93	PL B318 354	T. Falk *et al.*	(UCB, UCSB, MINN)
HEBBEKER	93	ZPHY C60 63	T. Hebbeker	(CERN)
KELLEY	93	PR D47 2461	S. Kelley *et al.*	(TAMU, ALAH)
LOPEZ	93C	PL B313 241	J.L. Lopez, D.V. Nanopoulos, X. Wang	(TAMU, HARC+)
MIZUTA	93	PL B298 120	S. Mizuta, M. Yamaguchi	(TOHO)
MORI	93	PR D48 5505	M. Mori *et al.*	(KEK, NIIG, TOKY, TOKA+)
ABE	92L	PRL 69 3439	F. Abe *et al.*	(CDF Collab.)
BOTTINO	92	MPL A7 733	A. Bottino *et al.*	(TORI, ZARA)
Also		PL B265 57	A. Bottino *et al.*	(TORI, INFN)
CLAVELLI	92	PR D46 2112	L. Clavelli	(ALAT)
DECAMP	92	PRPL 216 253	D. Decamp *et al.*	(ALEPH Collab.)
LOPEZ	92	NP B370 445	J.L. Lopez, D.V. Nanopoulos, K.J. Yuan	(TAMU)
MCDONALD	92	PL B283 80	J. McDonald, K.A. Olive, M. Srednicki	(LISB+)
ROY	92	PL B283 270	D.P. Roy	(CERN)
ABREU	91F	NP B367 511	P. Abreu *et al.*	(DELPHI Collab.)
AKESSON	91	ZPHY C52 219	T. Akesson *et al.*	(HELIOS Collab.)
ALEXANDER	91F	ZPHY C52 175	G. Alexander *et al.*	(OPAL Collab.)
ANTONIADIS	91	PL B262 109	I. Antoniadis, J. Ellis, D.V. Nanopoulos	(EPOL+)
BOTTINO	91	PL B265 57	A. Bottino *et al.*	(TORI, INFN)
GELMINI	91	NP B351 623	G.B. Gelmini, P. Gondolo, E. Roulet	(UCLA, TRST)
GRIEST	91	PR D43 3191	K. Griest, D. Seckel	
KAMIONKOW...	91	PR D44 3021	M. Kamionkowski	(CHIC, FNAL)
MORI	91B	PL B270 89	M. Mori *et al.*	(Kamiokande Collab.)
NOJIRI	91	PL B261 76	M.M. Nojiri	(KEK)
OLIVE	91	NP B355 208	K.A. Olive, M. Srednicki	(MINN, UCSB)
ROSZKOWSKI	91	PL B262 59	L. Roszkowski	(CERN)
SATO	91	PR D44 2220	N. Sato *et al.*	(Kamiokande Collab.)
ADACHI	90C	PL B244 352	I. Adachi *et al.*	(TOPAZ Collab.)
GRIEST	90	PR D41 3565	K. Griest, M. Kamionkowski, M.S. Turner	(UCB+)
BARBIERI	89C	NP B313 725	R. Barbieri, M. Frigeni, G. Giudice	
NAKAMURA	89	PR D39 1261	T.T. Nakamura *et al.*	(KYOT, TMTC)
OLIVE	89	PL B230 78	K.A. Olive, M. Srednicki	(MINN, UCSB)
ELLIS	88D	NP B307 883	J. Ellis, R. Flores	
GRIEST	88B	PR D38 2357	K. Griest	
OLIVE	88	PL B205 553	K.A. Olive, M. Srednicki	(MINN, UCSB)
SREDNICKI	88	NP B310 693	M. Srednicki, R. Watkins, K.A. Olive	(MINN, UCSB)
ALBAJAR	87D	PL B198 261	C. Albajar *et al.*	(UA1 Collab.)
ANSARI	87D	PL B195 613	R. Ansari *et al.*	(UA2 Collab.)
ARNOLD	87	PL B186 435	R.G. Arnold *et al.*	(BRUX, DUUC, LOUC+)
NG	87	PL B188 138	K.W. Ng, K.A. Olive, M. Srednicki	(MINN, UCSB)
TUTS	87	PL B186 233	P.M. Tuts *et al.*	(CUSB Collab.)
ALBRECHT	86C	PL 167B 360	H. Albrecht *et al.*	(ARGUS Collab.)
BADIER	86	ZPHY C31 21	J. Badier *et al.*	(NA3 Collab.)
BARNETT	86	NP B267 625	R.M. Barnett, H.E. Haber, G.L. Kane	(LBL, UCSC+)
GAISSER	86	PR D34 2206	T.K. Gaisser, G. Steigman, S. Tilav	(BART, DELA)
VOLOSHIN	86	SJNP 43 495	M.B. Voloshin, L.B. Okun	(ITEP)
		Translated from YAF 43 779.		
COOPER-...	85B	PL 160B 212	A.M. Cooper-Sarkar *et al.*	(WA66 Collab.)
DAWSON	85	PR D31 1581	S. Dawson, E. Eichten, C. Quigg	(LBL, FNAL)
FARRAR	85	PRL 55 895	G.R. Farrar	(RUTG)
GOLDMAN	85	Physica 15D 181	T. Goldman, H.E. Haber	(LANL, UCSC)
HABER	85	PRPL 117 75	H.E. Haber, G.L. Kane	(UCSC, MICH)
BALL	84	PRL 53 1314	R.C. Ball *et al.*	(MICH, FIRZ, OSU, FNAL+)
BARBER	84B	PL 139B 427	J.S. Barber, R.E. Shrock	(STON)
BRICK	84	PR D30 1134	D.H. Brick *et al.*	(BROW, CAVE, IIT+)
ELLIS	84	NP B238 453	J. Ellis *et al.*	(CERN)
FARRAR	84	PRL 53 1029	G.R. Farrar	(RUTG)
BERGSMA	83C	PL 121B 429	F. Bergsma *et al.*	(CHARM Collab.)
CHANOWITZ	83	PL 126B 225	M.S. Chanowitz, S. Sharpe	(UCB, LBL)
GOLDBERG	83	PRL 50 1419	H. Goldberg	(NEAS)
HOFFMAN	83	PR D28 660	C.M. Hoffman *et al.*	(LANL, ARZS)
KRAUSS	83	NP B227 556	L.M. Krauss	(HARV)
VYSOTSKII	83	SJNP 37 948	M.I. Vysotsky	(ITEP)
		Translated from YAF 37 1597.		
KANE	82	PL 112B 227	G.L. Kane, J.P. Leveille	(MICH)
CABIBBO	81	PL 105B 155	N. Cabibbo, G.R. Farrar, L. Maiani	(ROMA, RUTG)
FARRAR	78	PL 76B 575	G.R. Farrar, P. Fayet	(CIT)
Also		PL 79B 442	G.R. Farrar, P. Fayet	(CIT)

Technicolor

DYNAMICAL ELECTROWEAK SYMMETRY BREAKING: IMPLICATIONS OF THE H

Written October 2013 by R.S. Chivukula (Michigan State University), M. Narain (Brown University), and J. Womersley (STFC, Rutherford Appleton Laboratory).

1. Introduction and Phenomenology

In theories of dynamical electroweak symmetry breaking, the electroweak interactions are broken to electromagnetism by the vacuum expectation value of a composite operator, typically a fermion bilinear. In these theories, the longitudinal components of the massive weak bosons are identified with composite Nambu-Goldstone bosons arising from dynamical symmetry breaking in a strongly-coupled extension of the standard model. Viable theories of dynamical electroweak symmetry breaking must also explain (or at least accommodate) the presence of an additional composite scalar state to be identified with the H scalar boson [1,2] – a state unlike any other observed to date.

Theories of dynamical electroweak symmetry breaking can be classified by the nature of the composite singlet state to be associated with the H, and the corresponding dimensional scales f, the analog of the pion decay-constant in QCD, and Λ, the scale of the underlying strong dynamics.[1] Of particular importance is the ratio v/f, where $v^2 = 1/(\sqrt{2}G_F) \approx (246\,\mathrm{GeV})^2$, since this ratio measures the expected size of the deviations of the couplings of a composite Higgs boson from those expected in the standard model. The basic possibilities, and the additional states that they predict, are described below.

1.1 Technicolor, $v/f \simeq 1$, $\Lambda \simeq 1$ TeV:

Technicolor models [8–10] incorporate a new asymptotically free gauge theory ("technnicolor") and additional massless fermions ("technifermions" transforming under a vectorial representation of the gauge group). The global chiral symmetry of the fermions is spontaneously broken by the formation of a technifermion condensate, just as the approximate chiral symmetry in QCD is broken down to isospin by the formation of a quark condensate. The $SU(2)_W \times U(1)_Y$ interactions are embedded in the global technifermion chiral symmetries in such a way that the only unbroken gauge symmetry after chiral symmetry breaking is $U(1)_{em}$.[2] These theories naturally provide the Nambu-Goldstone bosons "eaten" by the W and Z boson, and there are various possibilities for the scalar H as described below.

In these theories there would typically be additional states (e.g. vector mesons, analogous to the ρ and ω mesons in QCD) with TeV masses [14,15], and the WW and ZZ scattering amplitudes would expected to be strong at energies of order 1 TeV. In all of these cases, however, to the extent that the H has couplings consistent with those of the standard model, these theories are very highly constrained.

a) **H as a singlet scalar resonance:** The strongly-interacting fermions which make up the Nambu-Goldstone bosons eaten by the weak bosons would naturally be expected to also form an isoscalar neutral bound state, analogous to the σ particle expected in pion-scattering in QCD [16]. However, in this case, there is no symmetry protecting the mass of such a particle – which would therefore generically be of order the energy scale of the underlying strong dynamics Λ. In the simplest theories of this kind – those with a global $SU(2)_L \times SU(2)_R$ chiral symmetry which is spontaneously broken to $SU(2)_V$ – the natural dynamical scale Λ would be of order a TeV, resulting in a particle too heavy to be identified with the H. The scale of

[1] In a strongly interacting theory "Naive Dimensional Analysis" [3,4] implies that, in the absence of fine-tuning, $\Lambda \simeq g^* f$ where $g^* \simeq 4\pi$ is the typical size of a strong coupling in the low-energy theory [5,6]. This estimate is modified in the presence of multiple flavors or colors [7].

[2] For a review of technicolor models, see [11–13].

the underlying interactions could naturally be smaller than 1 TeV if the global symmetries of the theory are larger than $SU(2)_L \times SU(2)_R$, but in this case there would be additional (pseudo-)Nambu-Goldstone bosons (more on this below). A theory of this kind would only be viable, therefore, if some choice of the parameters of the high energy theory could give rise to sufficiently light state without the appearance of additional particles that should have already been observed. Furthermore, while a particle with these quantum numbers could have Higgs-like couplings to any electrically neutral spin-zero state made of quarks, leptons, or gauge-bosons, there is no symmetry insuring that the coupling strengths of such a composite singlet scalar state would be precisely the same as those of the standard model Higgs.

b) **H as a dilaton:** It is possible that the underlying strong dynamics is approximately scale-invariant, as inspired by theories of "walking technicolor" [17–21], and that both the scale and electroweak symmetries are spontaneously broken at the TeV energy scale [22]. In this case, due to the spontaneous breaking of approximate scale invariance, one might expect a corresponding (pseudo-) Nambu-Goldstone boson with a mass less than a TeV, the dilaton [18]. [3] A dilaton couples to the trace of the energy momentum tensor, which leads to a simllar pattern of two-body couplings as the couplings of the standard model Higgs boson [27–29]. Scale-invariance is a space-time symmetry, however, and by the Coleman-Mandula theorem [30], we know that space-time symmetries cannot be embedded in a larger symmetry which includes the global symmetries that we can identify with the electroweak group. Therefore the decay-constants associated with the breaking of the scale and electroweak symmetries will not, in general, be precisely the same.[4] In other words, if there are no large anomalous dimensions associated with the W- and Z-bosons or the top- or bottom-quarks, the ratios of the couplings of the dilaton to these particles would be the same as the ratios of the same couplings for the standard model Higgs boson, but the overall strength of the dilaton couplings would be expected to be different [31,32]. Furthermore, the couplings of the dilaton to gluon- and photon-pairs can be related to the beta functions of the corresponding gauge interactions in the underlying high-energy theory, and will not in general yield couplings with the exactly the same strengths as the standard model.

c) **H as a singlet Pseudo-Nambu-Goldstone Boson:** If the global symmetries of the technicolor theory are larger than $SU(2)_L \times SU(2)_R$, there can be extra singlet (pseudo-) Nambu-Goldstone bosons which could be identified with the H. In this case, however, the coupling strength of the singlet state to WW and ZZ pairs would be comparable to the couplings to gluon and photon pairs, and these would all arise from loop-level couplings in the underlying technicolor theory [33]. This pattern of couplings is not supported by the data.

1.2 The Higgs doublet as a pseudo-Nambu-Goldstone Boson, $v/f < 1$, $\Lambda > 1$ TeV:

In technicolor models, the symmetry-breaking properties of the underlying strong dynamics necessarily breaks the electroweak gauge symmetries. An alternative possibility is that the underlying strong dynamics itself does not break the electroweak interactions, and that the entire quartet of bosons in the Higgs doublet (including the state associated with the H) are composite (pseudo-) Nambu-Goldstone particles [34–37]. In this case, the underlying dynamics can occur at energies larger than 1 TeV and additional interactions with the top-quark mass generating sector (and possibly with additional weakly-coupled gauge bosons) cause the vacuum energy to be minimized when the composite Higgs doublet gains a vacuum expectation value [38]. In these theories, the couplings of the remaining singlet scalar state would naturally be equal to that of the standard model Higgs boson up to corrections of order $(v/f)^2$ and, therefore, constraints on the size of deviations of the H couplings from that of the standard model Higgs give rise to lower bounds on the scales f and Λ.

The electroweak gauge interactions, as well as the interactions responsible for the top-quark mass, explicitly break the chiral symmetries of the composite Higgs model, and lead generically to sizable corrections to the mass-squared of the Higgs-doublet – the so-called "Little Hierarchy Problem" [39]. "Little Higgs" theories [40–43] are examples of composite Higgs models in which the (collective) symmetry-breaking structure is selected so as to suppress these contributions to the Higgs mass-squared, while allowing for a sufficiently large Higgs-boson self-coupling. The collective symmetry breaking required in Little Higgs models typically requires a larger global symmetry of the underlying theory, and hence additional relatively light (compared to Λ) scalar particles, extra electroweak vector bosons (e.g. an additional $SU(2) \times U(1)$ gauge group), and vector-like partners of the top-quark of charge $+2/3$ and possibly also $+5/3$ [44]. Finally, in addition to these states, one would expect the underlying dynamics to yield additional scalar and vector resonances with masses of order Λ.

[3] Even in this case, however, a dilaton associated with electroweak symmetry breaking will likely not *generically* be as light as the H [23–26].

[4] If both the electroweak symmetry and the approximate scale symmetry are broken only by electroweak doublet condensate(s), then the decay-constants for scale and electroweak symmetry breaking may be approximately equal – differing only by terms formally proportional to the amount of explicit scale-symmetry breaking.

1.3 Top-Condensate, Top-Color, Top-Seesaw and related theories, $v/f < 1$, $\Lambda > 1$ TeV:

A final alternative is to consider a strongly interacting theory with a high (compared to a TeV) underlying dynamical scale that *would* naturally break the electroweak interactions, but whose strength is adjusted ("fine-tuned") to produce electroweak symmetry breaking at 1 TeV. This alternative is possible if the electroweak (quantum) phase transition is continuous (second order) in the strength of the strong dynamics [45]. If the fine tuning can be achieved, the underlying strong interactions will produce a light composite Higgs bound state with couplings equal to that of the standard model Higgs boson up to corrections of order $(1\ \mathrm{TeV}/\Lambda)^2$. As in theories in which electroweak symmetry breaking occurs through vacuum alignment, therefore, constraints on the size of deviations of the H couplings from that of the standard model Higgs give rise to lower bounds on the scale Λ. Formally, in the limit $\Lambda \to \infty$ (a limit which requires arbitrarily fine adjustment of the strength of the high-energy interactions), these theories are equivalent to a theory with a fundamental Higgs boson – and the fine adjustment of the coupling strength is a manifestation of the hierarchy problem of theories with a fundamental scalar particle.

In many of these theories the top-quark itself interacts strongly (at high energies), potentially through an extended color gauge sector [46–49]. In these theories, top-quark condensation (or the condensation of an admixture of the top with additional vector-like quarks) is responsible for electroweak symmetry breaking, and the H is identified with a bound state involving the third generation of quarks. These theories typically include an extra set of massive color-octet vector bosons (top-gluons), and an extra $U(1)$ interaction (giving rise to a top-color Z') which couple preferentially to the third generation and whose masses define the scale Λ of the underlying physics.

In addition to the electroweak symmetry breaking dynamics described above, which gives rise to the masses of the W and Z particles, additional interactions must be introduced to produce the masses of the standard model fermions. Two general avenues have been suggested for these new interactions. In one case, e.g. "extended technicolor" theories [50,51], the gauge interactions in the underlying strongly interacting theory are extended to incorporate flavor. This extended gauge symmetry is broken down (possibly sequentially, at several different mass scales) to the residual strongly-interacting interaction responsible for electroweak symmetry breaking. The massive gauge-bosons corresponding to the broken symmetries then mediate interactions between mass operators for the quarks/leptons and the corresponding bilinears of the strongly-interacting fermions, giving rise to the masses of the ordinary fermions after electroweak symmetry breaking. An alternative proposal, "partial compositeness" [52], postulates additional interactions giving rise to mixing between the ordinary quarks and leptons and massive composite fermions in the strongly-interacting underlying theory. Theories incorporating partial compositeness include additional vector-like partners of the ordinary quarks and leptons, typically with masses of order a TeV or less.

In both cases, the effects of these flavor interactions on the electroweak properties of the ordinary quarks and leptons are likely to be most pronounced in the third generation of fermions.[5] The additional particles present, especially the additional scalars, often couple more strongly to heavier fermions. Moreover, since the flavor interactions must give rise to quark mixing, we expect that a generic theory of this kind could give rise to large flavor-changing neutral-currents [51]- - though these constraints are typically somewhat relaxed if the theory "walks" [17–21] or if $\Lambda > 1$ TeV [53]. For these reasons, most authors assume that the underlying flavor dynamics respects flavor symmetries ("minimal" [54,55] or "next-to-minimal" [56] flavor violation) which suppress flavor-changing neutral currents in the two light generations.[6] Additional considerations apply when extending these considerations to potential explanation of neutrino masses (see, for example, [59,60]) .

Since the underlying high-energy dynamics in these theories are strongly coupled, there are no reliable calculation techniques that can be applied to analyze their properties. Instead, most phenomenological studies depend on the construction of a "low-energy" effective theory describing additional scalar, fermion, or vector boson degrees of freedom, which incorporates the relevant symmetries and, when available, dynamical principles. In some cases, motivated by the AdS/CFT correspondence [61], the strongly-interacting theories described above have been investigated by analyzing a dual compactified five-dimensional gauge theory. In these cases, the AdS/CFT "dictionary" is used to map the features of the underlying strongly coupled high-energy dynamics onto the low-energy weakly coupled dual theory [62].

More recently, progress has been made in investigating strongly-coupled models using lattice gauge theory [63,64]. These calculations offer the prospect of establishing which strongly coupled theories of electroweak symmetry breaking have a particle with properties consistent with those observed for the H – and for establishing concrete predictions for these theories at the LHC [65].

2. Experimental Searches

As discussed above, the extent to which the couplings of the H conform to the expectations for a standard model Higgs boson constrains the viability of each of these models.

[5] Indeed, from this point of view, the vector-like partners of the top-quark in top-seesaw and little Higgs models can be viewed as incorporating partial compositeness to explain the origin of the top quark's large mass.

[6] In theories of partial compositeness, the masses of the ordinary fermions depend on the scaling-dimension of the operators corresponding to the composite fermions with which they mix. This leads to a new mechanism for generating the mass-hierarchy of the observed quarks and leptons that, potentially, incorporates minimal or next-to-minimal flavor violation [57,58].

Measurements of the H couplings, and their interpretation in terms of effective field theory, are summarized in the H review in this volume. In what follows, we will focus on searches for the additional particles that might be expected to accompany the singlet scalar: extra scalars, fermions, and vector bosons. In some cases, detailed model-specific searches have been made for the particles described above (though generally not yet taking account of the demonstrated existence of the H boson).

In most cases, however, generic searches (e.g. for extra W' or Z' particles, extra scalars in the context of multi-Higgs models, or for fourth-generation quarks) are quoted that can be used – when appropriately translated – to derive bounds on a specific model of interest.

The mass scale of the new particles implied by the interpretations of the low mass of H discussed above, and existing studies from the Tevatron and lower-energy colliders, suggests that only the Large Hadron Collider has any real sensitivity. A number of analyses already carried out by ATLAS and CMS use relevant final states and might have been expected to observe a deviation from standard model expectations – in no case so far has any such deviation been reported. The detailed implications of these searches in various model frameworks are described below.

2.1 W' or Z' Bosons

Massive vector bosons or particles with similar decay channels would be expected to arise in Little Higgs theories, in theories of Technicolor, or models involving a dilaton, adjusted to produce a light Higgs boson, consistent with the observed H. These particles would be expected to decay to pairs of vector bosons, to third generation quarks, or to leptons. The generic searches for W' and Z' vector bosons listed below can, therefore, be used to constrain models incorporating a composite Higgs-like boson. ATLAS [74] and CMS [75] have searched for Z' production with $Z' \to ee$ or $\mu\mu$ in collision data recorded at $\sqrt{s} = 8$ TeV during the 2012 run of the LHC. These searches are carried out using a integrated luminosity of 20 fb^{-1} and 20.6 fb^{-1} by ATLAS and CMS respectively. The main backgrounds to these analyses arise from Drell-Yan, $t\bar{t}$, and diboson production and are estimated using Monte Carlo, with the cross sections scaled by next-to-next-to-leading-order k-factors. Instrumental backgrounds from QCD multijet and W+jet events are estimated using control data samples. One of the challenges of this analysis is the modeling of the dilepton pair invariant mass resolution. The dielectron channel has higher sensitivity due to the superior mass resolution compared to the dimuon channel. No deviation from the standard model prediction is seen in the dielectron and dimuon invariant mass spectra, by either the ATLAS or the CMS analysis, and lower limits on possible Z' boson masses are set. A $Z'_{\rm SSM}$ with couplings equal to the standard model Z (a "sequential standard model" Z') and a mass below 2.86 TeV is excluded by ATLAS, while CMS sets a 95% C.L. lower mass limit of 2.96 TeV. The ATLAS analysis rules out various $E6$-motivated bosons (Z'_ψ, Z'_χ) with masses lower than $2.38 - 2.54$ TeV. A Z'_ψ with a mass below 2.6 TeV is excluded by CMS. ATLAS searches are also interpreted to obtain a lower mass limit of 2.47 TeV for a Randall-Sundrum graviton with coupling parameter $k/\overline{M}_{Pl} = 0.1$. In addition, ATLAS has performed a search for Z' decaying to a ditau final state [76]. An excess in this signature could have interesting implications for models in which lepton universality is not a necessary requirement and enhanced couplings to the third generation are allowed. This analysis leads to a lower limit on the mass of $Z'_{\rm SSM}$ of 1.9 TeV.

ATLAS [77] has also searched for Z' bosons decaying into top quark pairs using 14 fb^{-1} of collision data collected at $\sqrt{s} = 8$ TeV. The lepton plus jets final state is used, where the top quark pair decays as $t\bar{t} \to WbWb$ with one W boson decaying leptonically and the other hadronically. CMS [70] has carried out a similar search for Z' resonances decaying to $t\bar{t}$ pairs, using "semi-leptonic" and "all-hadronic" decays of the top quarks. The data sample analyzed corresponds to an integrated luminosity of 19.7 fb^{-1}. Both analyses consider $t\bar{t}$ events at the kinematic production threshold, and those produced with high Lorentz boosts. In addition to a conventional resolved-jet analysis, large radius jet-substructure identification techniques are used to reconstruct the $t\bar{t}$ resonance. The $t\bar{t}$ invariant mass spectrum is analyzed for any local excess, and no evidence for any resonance is seen.

Upper limits are set by ATLAS on the cross section times branching ratio of a narrow Z' boson decaying to top quark pairs ranging from 5.3 pb for a Z' mass of 0.5 TeV to 0.08 pb for a mass of 3 TeV. A narrow leptophobic topcolor Z' boson, with $\Gamma/m = 1.2\%$, and a mass below 1.8 TeV is excluded, and upper limits are also set on the cross section times branching ratio for a broad Kaluza Klein excitation of the gluon (g_{KK}) with $\Gamma/m = 15.3\%$ decaying to $t\bar{t}$ which range from 9.6 pb for a mass of 0.5 TeV to 0.152 pb for a mass of 2.5 TeV.

CMS sets upper limits on the production cross section times branching ratio for narrow (wide) resonances at 1.94(1.71) pb for a mass of 0.5 TeV, and 0.029(0.045) pb for a mass of 2 TeV. Topcolor Z' bosons with masses below 2.1 TeV and 2.7 TeV are excluded for $\Gamma/m = 1.2\%$ and 10%, respectively. In the Randall-Sundrum model, g_{KK} masses below 2.5 TeV are excluded.

The semi-leptonic analysis is sensitive to a spin-zero resonance with narrow width, produced via gluon fusion without interference with the standard model background. For heavy Higgs-like particles decaying into $t\bar{t}$, CMS obtains upper limits on the cross sections of 0.8 pb and 0.3 pb for spin-zero resonances with masses of 500 and 750 GeV, respectively [70].

CMS [94] has additionally searched for heavy Z' resonances decaying to the $b\bar{b}$ final state by selecting event with dijets with one or both of the jets tagged as a b-jet. The search is performed using 19.6 fb^{-1} of data collected at $\sqrt{s}$=8 TeV and excludes a sequential standard model Z' with a mass between 1.20 and 1.68 TeV, when the decay branching ratio of $Z' \to b\bar{b}$ relative to $Z' \to jj$ is taken to be 0.22.

Both ATLAS and CMS have also searched for massive charged vector bosons. ATLAS [88] and CMS [89] have searched for a resonant W' state decaying to WZ in the fully-leptonic channel, $\ell\nu\ell'\ell'$ (where $\ell, \ell' = e, \mu$). The WZ invariant mass distribution reconstructed from the observed lepton and neutrino momenta and L_T, the scalar sum of the charged lepton p_Ts, are used as the discriminating variables to identify the W' signal and reject the backgrounds. The backgrounds are mainly from standard model WZ production. No significant localized excess is observed in the reconstructed WZ invariant mass distribution. Using a sample of 19.6 fb^{-1} of data recorded at $\sqrt{s} = 8$ TeV, CMS excludes a W' with masses between 0.17 and 1.45 TeV. The analysis by ATLAS, based on 13 fb^{-1} collected at $\sqrt{s} = 8$ TeV, derives upper limits on the production cross section times branching ratio and obtains a bound on the W' mass of 1.18 TeV in the context of benchmark Extended Gauge models.

CMS [90] also performed a search for $W' \to WZ$ using dijet events, with one or both of the jets identified as a W or a Z boson using jet-substructure techniques. In the absence of any excess, a W' decaying into WZ is excluded up to 1.73 TeV at 95% C.L.

Searches by CMS [91] for a heavy W' decaying to $e\nu$ or $\mu\nu$ again yield a null signal, allowing a standard model-like W' with masses up to 3.35 TeV to be excluded. This result can be re-interpreted to rule out a split UED Kaluza-Klein W^2_{KK} excitation below 3.7 TeV for the mass parameter μ=10 TeV, and in addition set a limit on the scale of a new helicity non-conserving four-fermion contact interaction Λ of 13.0 (10.9) TeV for the electron (muon) channel.

Heavy new gauge bosons can couple to left-handed fermions like the W boson or to right-handed fermions. W' bosons that couple only to right-handed fermions may not have leptonic decay modes, depending on the mass of the right-handed neutrino. For these W' bosons, the tb decay mode is especially important because it is the hadronic decay mode with the best signal-to-background. CMS [92] has carried out a search for $W' \to tb$ decays followed by $t \to bW$ and $W \to \ell\nu$. The analysis relies on the invariant mass of the W', using $\ell\nu$+jets events with one or more b-tags and uses multivariate techniques to improve signal to background separation. The measurement is carried out for arbitrary combinations of the coupling strengths of the W' to left- and right-handed fermions. Based on an analysis of 19.6 fb^{-1} of data, W' bosons with purely left-handed (right-handed) couplings to fermions are excluded for masses below 2.09 (2.03) TeV. ATLAS [93] has also searched for W' bosons in single-top quark production, using 14.3 fb^{-1} of data recorded at $\sqrt{s} = 8$ TeV. The analysis looks at the $\ell\nu b\bar{b}$ final state ($\ell = e, \mu$) again using a multivariate method. No significant deviation from the standard model expectation is observed and for a left-handed (right-handed) W' boson, masses below 1.74 (1.84) TeV are excluded at the 95% confidence level.

2.2 Technicolor Resonances

While the W' and Z' searches listed above have not been interpreted in terms of specific technicolor models, the technicolor-inspired searches listed here have been carried out at the LHC.

ATLAS has searched for a dijet resonance [86] with an invariant mass in the range $130 - 300$ GeV, produced in association with a W or a Z boson. The analysis used 20.3 fb^{-1} of data recorded at $\sqrt{s} = 8$ TeV. The W or Z boson is required to decay leptonically ($\ell = e, \mu$). No significant deviation from the standard model prediction is observed and limits are set on the production cross section times branching ratio for a hypothetical technipion produced in association with a W or Z boson from the decay of a technirho particle in the context of Low Scale Technicolor models.

Both ATLAS and CMS searches for a resonant W' state decaying to WZ in the fully-leptonic channel, $\ell\nu\ell'\ell'(\ell, \ell' = e, \mu)$, described earlier [88,89], have also been used to place limits on a technirho decaying to WZ in similar models.

2.3 Vector-like third generation quarks

Vector-like quarks have non-chiral couplings to W bosons, i.e. their left- and right-handed components couple in the same way. They therefore have vectorial couplings to W bosons. Vector-like quarks arise in Little Higgs theories and theories of a composite Higgs with partial compositeness. In the following the notation T quark refers to a vector-like quark with charge 2/3 and the notation B quark refers to a vector-like quark with charge $-1/3$. T quarks can decay to bW, tZ, or tH. Weak isospin singlets are expected to decay to all three final states with branching fractions of 50%, 25%, 25%, respectively. Weak isospin doublets are expected to decay exclusively to tZ and to tH [67]. Analogously, B quarks can decay to tW, bZ, or bH. All limits in this section are quoted at a confidence level of 95%.

Searches for T quarks that decay to W bosons

CMS has searched for pair production of heavy T quarks that decay exclusively to bW [71] based on the data collected at $\sqrt{s} = 7$ TeV in 2011 with an integrated luminosity of 5 fb^{-1}. The analysis selects events with exactly one charged lepton, assuming that the W boson from the second T quark decays hadronically. Under this hypothesis, a 2C kinematic fit can be performed to reconstruct the mass of the T quark. The two-dimensional distribution of reconstructed mass vs H_T is used to test for the signal. H_T is the scalar sum of the missing p_T and the transverse momenta of the lepton and the leading four jets. No excess over standard model backgrounds is observed. This analysis excludes new quarks that decay 100% to bW for masses below 570 GeV.

A search by ATLAS for the production of a heavy T quark together with its antiparticle, assumes a significant branching ratio for subsequent decay into a W boson and a b quark [78]. The search is based on 14.3 fb^{-1} of data recorded at $\sqrt{s} = 8$ TeV. It uses the lepton+jets final state with an isolated electron or muon and at least four jets, at least one of which

must be tagged as a b-jet. The selection is optimized for T quark masses above about 400 GeV by requiring a high boost of the W decay products. No significant excess of events above standard model expectation is observed. For a chiral fourth generation quark with branching ratio $BR(T \to Wb) = 1$, masses lower than 740 GeV are excluded.

Searches for T and B quarks that decay to Z bosons

CMS has performed a search targeted on T quarks that decay exclusively to tZ based on an integrated luminosity of 1.1 fb^{-1} from pp collisions at $\sqrt{s} = 7$ TeV [68]. Selected events must have three isolated charged leptons, two of which must be consistent with a leptonic Z-boson decay. No significant excess was observed. T quark masses below 485 GeV are excluded.

CMS has also searched for the pair-production of a heavy B quark and its antiparticle, one of which decays to bZ based on 19.6 fb^{-1} of data collected at $\sqrt{s} = 8$ TeV. Events with a Z-boson decay to e^+e^- or $\mu^+\mu^-$ and a jet identified as originating from a b quark are selected. The signal from $B \to bZ$ decays would appear as a local enhancement in the bZ mass distribution. No such enhancement is found and B quarks that decay 100% into bZ are excluded below 700 GeV. This analysis also sets upper limits on the branching fraction for $B \to bZ$ decays of 30-100% in the B quark mass range 450-700 GeV.

A complementary search has been carried out by ATLAS for new heavy quarks decaying into a Z boson and a third generation quark [79]. The analysis targets both a new charge +2/3 quark T, with $T \to Zt$, and a new charge -1/3 quark B, with $B \to bZ$. The search uses 14.3 fb^{-1} of data recorded at $\sqrt{s}$=8 TeV. Selected events contain a high transverse momentum Z boson that decays leptonically, together with two b-jets. No significant excess of events above the standard model expectation is observed, and mass limits are set depending on the assumed branching ratios, see Fig. 1. In a weak-isospin singlet scenario, a T (B) quark with mass lower than 585 (645) GeV is excluded, while for a particular weak-isospin doublet scenario, a T (B) quark with mass lower than 680 (725) GeV is excluded.

Searches for T quarks that decay to H bosons

ATLAS has performed a search for $T\overline{T}$ production with an appreciable T quark branching fraction into tH, followed by $H \to b\overline{b}$. These events are characterized by a large number of jets, many of which are b-jets. Thus the event selection requires one isolated electron or muon and at least six jets, two of which must be tagged as b-jets. The data are classified according to their b-jet multiplicity and the distribution of H_T, the scalar sum of the lepton and jet p_Ts and the missing p_T, is used to search for the signal. No excess of events is found. Weak isospin doublet T quarks are excluded below 790 GeV and weak isospin singlet T quarks are excluded below 640 GeV. This search is orthogonal to the search for T quarks that decay to bW and the results of the two searches are combined.

Searches for T and B quarks in multiple final states

Pair-production of T or B quarks with their antiparticles can result in events with like-sign leptons, for example if the decay $T \to tH \to bWW^+W^-$ is present, followed by leptonic decays of two same-sign W bosons. ATLAS and CMS have searched for this final state. The CMS search is part of the analysis described in the following paragraph. The ATLAS search [73] requires exactly two leptons, both with the same electric charge, at least two jets of which at least one must be tagged as a b-jet, and missing p_T. ATLAS quotes exclusions of some possible branching fraction combinations depending on the mass of the new quarks. T quarks that are electroweak singlets are excluded below 540 GeV and the sensitivity is largest for T quarks that decay exclusively to tH. B quarks that are electroweak singlets are excluded below 590 GeV and the sensitivity for B quarks is maximal if they exclusively decay to tW. The limits set by all the ATLAS searches are superimposed in Fig. 1 and Fig. 2.

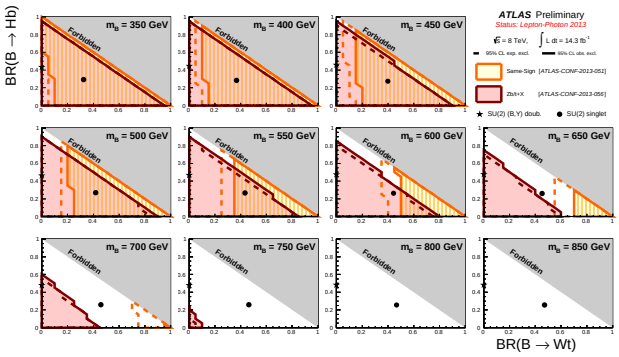

Figure 1: Exclusion limits for BB pair production in the $BR(B \to Wt)$ versus $BR(B \to Ht)$ plane. The limits of the two ATLAS searches are superimposed on the plots. The circle and star symbols denote the default branching ratios for the weak-isospin singlet and doublet cases.

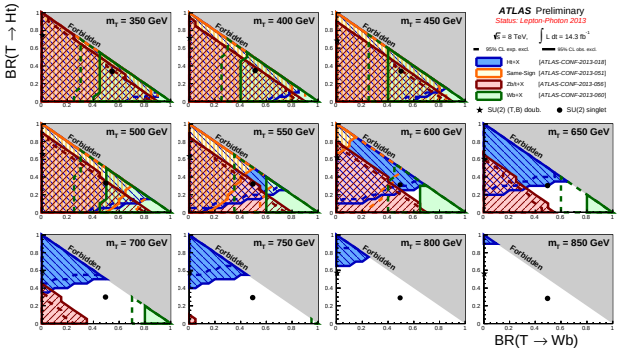

Figure 2: Exclusion limits for TT pair production in the $B(T \to Wb)$ versus $B(T \to Ht)$ plane. The limits of the four ATLAS searches are superimposed on the plots. The circle and star symbols denote the default branching ratios for the weak-isospin singlet and doublet cases.

An inclusive search by CMS targeted at heavy T quarks decaying to any combination of bW, tZ, or tH is described in Ref. [80]. This analysis is based on the data collected at $\sqrt{s}$ = 8 TeV in 2012 with an integrated luminosity of 19.5 fb^{-1}. Selected events have at least one isolated charged lepton. Events are categorized according to number and flavour of the leptons, the number of jets, and the presence of hadronic vector boson and top quark decays that are merged into a single jet. The use of jet substructure to identify hadronic decays significantly increases the acceptance for high T quark masses. The analysis of the high-background single lepton channels is based on a multivariate algorithm using Boosted Decision Trees. The analysis of the low background multilepton channels is based on the event counts in the individual channels. No excess above standard model backgrounds is observed. Limits on the pair production cross section of the new quarks are set, combining all event categories, for all combinations of branching fractions into the three final states. For T quarks that exclusively decay to $bW/tZ/tH$, masses below 700/782/706 GeV are excluded. Electroweak singlet vector-like T quarks which decay 50% to bW, 25% to tZ, and 25% to tH are excluded for masses below 696 GeV. The CMS analysis also quotes limits between 690 and 782 GeV on the mass of the T quark for all possible values of the branching fractions into the three different final states bW, tZ and tH. The observed limit for all combination of the three branching fractions is shown in Fig. 3 (left panel). Every point in the triangle corresponds to a particular set of branching fraction values for $T \to bW$, tZ and tH, such that all three add up to one. In Fig. 3 (right panel) the cross section limit is plotted for the nominal combination of branching fractions (50% to bW, 25% to tZ, and 25% to tH).

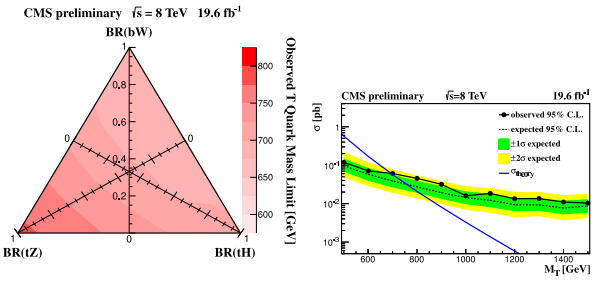

Figure 3: The branching fraction triangle with observed limits for the T quark mass are shown in the left panel. The upper limit on the T quark production cross section for branching fractions into bW, tH, tZ of 50%, 25%, 25% is shown in the right panel [80].

CMS has also carried out a similar inclusive search for the pair production of B quarks that decay into tW, bZ, or bH based on 19.8 fb^{-1} of data collected at $\sqrt{s}$ = 8 TeV [81]. Events must have one isolated electron or muon, at least four jets of which at least one is tagged as a b-jet, and missing p_T. Events are classified according to the number of highly boosted W, Z, or H boson decays. No significant excess of events is observed and B quarks below 582 and 732 GeV are excluded, depending on the B quark decay branching fractions. B quarks that decay exclusively into tW are excluded below 732 GeV. The observed limits for all combinations of branching fractions are shown in Fig. 4, together with the cross section limit plotted for the nominal combination of branching fractions (50% to tW, 25% to bZ, and 25% to bH).

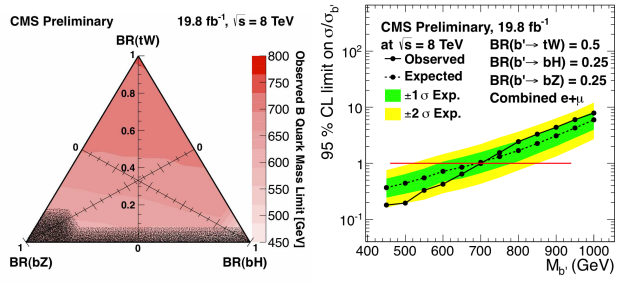

Figure 4: The branching fraction triangle with observed limits for the B quark mass is shown in the left panel. The shaded area at the bottom was not probed by the analysis. The upper limit on the B quark production cross section for branching fractions into mtW, bH, bZ modes of 50%, 25%, 25% respectively, is shown in the right panel [81].

2.4 A charge +5/3 top-partner quark

In models of dynamical electroweak symmetry breaking, the same interactions which give rise to the mass of the top-quark can give unacceptably large corrections to the branching ratio of the Z boson to $b\bar{b}$ [66]. These corrections can be substantially reduced, however, in theories with an extended "custodial symmetry" [44]. This symmetry requires the existence of a charge +5/3 vector-like partner of the top quark.

CMS has performed a search for heavy top with exotic charge 5/3, $T_{5/3}$ vector-like quark following the models in Refs. [82,83]. CMS has searched for the pair-production of $T_{5/3}$ with $T_{5/3}$ decays to tW with a 100% branching fraction. It is assumed that $T_{5/3}$ is heavier than the B quark. The analysis is based on searching for same-sign leptons, from the two W bosons from one of the $T_{5/3}$. Requiring same-sign leptons eliminates most of the standard model background processes, leaving those with smaller cross sections: $t\bar{t}$, W, $t\bar{t}Z$, WWW, and same-sign WW. In addition backgrounds from instrumental effects due to charge misidentification are considered. The CMS search also utilizes jet substructure techniques to identify boosted $T_{5/3}$ topologies. These searches restrict the $T_{5/3}$ mass to be higher than 770 GeV [84].

The single $T_{5/3}$ production cross section depends on the coupling constant λ of the $tWT_{5/3}$ vertex. ATLAS has performed an analysis of same-sign dileptons for the cases where $\lambda = 1$, $\lambda = 3$ which includes both the single and pair production, and for $\lambda \ll 1$, which corresponds to pair production only. This

analysis leads to a 95% C.L. lower limit on the mass of the $T_{5/3}$ of 680, 700, and 670 GeV for $\lambda = 1, 3$ and $\ll 1$, respectively.

2.5 Colorons, Z' and Colored Scalars

These particles are associated with top-condensate and top-seesaw models, which involve an enlarged color gauge group. The new particles decay to dijets, $t\bar{t}$, and $b\bar{b}$.

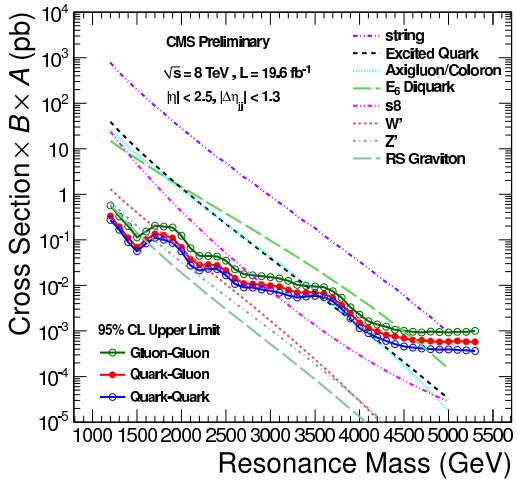

Figure 5: Observed 95% C.L. limits on $\sigma \times B \times A$ for string resonances, excited quarks, axigluons, colorons, E6 diquarks, s8 resonances, W' and Z' bosons, and Randall-Sundrum gravitons [85].

Direct searches for colorons, W', Z', color-octect scalars and other heavy objects decaying to $q\overline{q}$, qg, qq, or gg has been performed using LHC data from pp collisions at $\sqrt{s}$ =7 and 8 TeV. Based on the analysis of dijet events from a data sample corresponding to a luminosity of 19.6 fb^{-1}, the CMS experiment excludes pair production of colorons with mass between $1.20 - 3.60$ and $3.90 - 4.08$ TeV at 95% C.L., color-octet scalars (s8) with masses between $1.20 - 2.79$ TeV, W' bosons with masses below 2.29 TeV, and Z' Boson with masses below 1.68 TeV, as shown in Fig. 5 [85].

A search for pair-produced colorons based on an integrated luminosity of 5.0 fb^{-1} at $\sqrt{s} = 7$ TeV by CMS excludes colorons with masses between 250 GeV and 740 GeV, assuming colorons decay 100% into $q\overline{q}$ [87]. This analysis is based on events with at least four jets and two dijet combinations with similar dijet mass.

3. Conclusions

As the above analyses have demonstrated, there is already substantial sensitivity to possible new particles predicted to accompany the H in dynamical frameworks of electroweak symmetry breaking. No hints of any deviations from the standard model have been observed, and limits typically at the scale of a few hundred GeV to 1 TeV are set.

Given the need to better understand the H and to pin down how it behaves, we expect that such analyses will be a major theme of the next run of the LHC, and we look forward to increased sensitivity as a result of the higher luminosity and increased centre of mass energy of collisions.

References

1. G. Aad *et al.* [ATLAS Collab.], Phys. Lett. B **716**, 1 (2012) [arXiv:1207.7214 [hep-ex]].
2. S. Chatrchyan *et al.* [CMS Collab.], Phys. Lett. B **716**, 30 (2012) [arXiv:1207.7235 [hep-ex]].
3. S. Weinberg, Physica A **96**, 327 (1979).
4. A. Manohar and H. Georgi, Nucl. Phys. B **234**, 189 (1984).
5. H. Georgi, Nucl. Phys. B **266**, 274 (1986).
6. R. S. Chivukula, hep-ph/0011264.
7. R. S. Chivukula, M. J. Dugan and M. Golden, Phys. Rev. D **47**, 2930 (1993) [hep-ph/9206222].
8. S. Weinberg, Phys. Rev. D **13**, 974 (1976).
9. S. Weinberg, Phys. Rev. D **19**, 1277 (1979).
10. L. Susskind, Phys. Rev. D **20**, 2619 (1979).
11. K. Lane, hep-ph/0202255.
12. C. T. Hill and E. H. Simmons, Phys. Rept. **381**, 235 (2003), [Erratum-*ibid.,* **390**, 553 (2004)] [hep-ph/0203079.
13. R. Shrock, hep-ph/0703050 [HEP-PH].
14. E. Eichten *et al.*, Rev. Mod. Phys. **56**, 579 (1984) [Addendum-*ibid.,* **58**, 1065 (1986)].
15. E. Eichten *et al.*, Phys. Rev. D **34**, 1547 (1986).
16. R. S. Chivukula and V. Koulovassilopoulos, Phys. Lett. B **309**, 371 (1993) [hep-ph/9304293].
17. B. Holdom, Phys. Lett. B **150**, 301 (1985).
18. K. Yamawaki, M. Bando, and K. -i. Matumoto, Phys. Rev. Lett. **56**, 1335 (1986).
19. T. W. Appelquist, D. Karabali, and L. C. R. Wijewardhana, Phys. Rev. Lett. **57**, 957 (1986).
20. T. Appelquist and L. C. R. Wijewardhana, Phys. Rev. D **35**, 774 (1987).
21. T. Appelquist and L. C. R. Wijewardhana, Phys. Rev. D **36**, 568 (1987).
22. E. Gildener and S. Weinberg, Phys. Rev. D **13**, 3333 (1976).
23. Z. Chacko, R. Franceschini, and R. K. Mishra, JHEP **1304**, 015 (2013) [arXiv:1209.3259 [hep-ph]].
24. B. Bellazzini *et al.*, Eur. Phys. J. C **73**, 2333 (2013) [arXiv:1209.3299 [hep-ph]].
25. B. Bellazzini *et al.*, arXiv:1305.3919 [hep-th].
26. Z. Chacko, R. K. Mishra, and D. Stolarski, arXiv:1304.1795 [hep-ph].
27. J. R. Ellis, M. K. Gaillard, and D. V. Nanopoulos, Nucl. Phys. B **106**, 292 (1976).
28. M. A. Shifman *et al.*, Sov. J. Nucl. Phys. **30**, 711 (1979) [Yad. Fiz. **30**, 1368 (1979)].
29. A. I. Vainshtein, V. I. Zakharov, and M. A. Shifman, Sov. Phys. Usp. **23**, 429 (1980) [Usp. Fiz. Nauk **131**, 537 (1980)].
30. S. R. Coleman and J. Mandula, Phys. Rev. **159**, 1251 (1967).
31. M. Bando, K. -i. Matumoto, and K. Yamawaki, Phys. Lett. B **178**, 308 (1986).
32. W. D. Goldberger, B. Grinstein, and W. Skiba, Phys. Rev. Lett. **100**, 111802 (2008) [arXiv:0708.1463 [hep-ph]].

33. E. Eichten, K. Lane, and A. Martin, arXiv:1210.5462 [hep-ph].
34. D. B. Kaplan and H. Georgi, Phys. Lett. B **136**, 183 (1984).
35. D. B. Kaplan, H. Georgi, and S. Dimopoulos, Phys. Lett. B **136**, 187 (1984).
36. K. Agashe, R. Contino, and A. Pomarol, Nucl. Phys. B **719**, 165 (2005).
37. G. F. Giudice *et al.*, JHEP **0706**, 045 (2007) [hep-ph/0703164].
38. M. E. Peskin, Nucl. Phys. B **175**, 197 (1980).
39. R. Barbieri and A. Strumia, hep-ph/0007265.
40. N. Arkani-Hamed, A. G. Cohen, and H. Georgi, Phys. Lett. B **513**, 232 (2001) [hep-ph/0105239].
41. N. Arkani-Hamed *et al.*, JHEP **0208**, 020 (2002) [hep-ph/0202089].
42. N. Arkani-Hamed *et al.*, JHEP **0207**, 034 (2002) [hep-ph/0206021].
43. M. Schmaltz and D. Tucker-Smith, Ann. Rev. Nucl. Part. Sci. **55**, 229 (2005) [hep-ph/0502182].
44. K. Agashe *et al.*, Phys. Lett. B **641**, 62 (2006) [hep-ph/0605341].
45. R. S. Chivukula, A. G. Cohen, and K. D. Lane, Nucl. Phys. B **343**, 554 (1990).
46. V.A. Miransky, M. Tanabashi, and K.Yamawaki, Phys. Lett. **B221**, 177 (1989) and Mod. Phys. Lett. **A4**, 1043 (1989);
W. A. Bardeen, C. T. Hill, and M. Lindner, Phys. Rev. D **41**, 1647 (1990).
47. C. T. Hill, Phys. Lett. B **266**, 419 (1991).
48. B. A. Dobrescu and C. T. Hill, Phys. Rev. Lett. **81**, 2634 (1998) [hep-ph/9712319].
49. R. S. Chivukula *et al.*, Phys. Rev. D **59**, 075003 (1999) [hep-ph/9809470].
50. S. Dimopoulos and L. Susskind, Nucl. Phys. B **155**, 237 (1979).
51. E. Eichten and K. D. Lane, Phys. Lett. B **90**, 125 (1980).
52. D. B. Kaplan, Nucl. Phys. B **365**, 259 (1991).
53. R. S. Chivukula, B. A. Dobrescu, and E. H. Simmons, Phys. Lett. B **401**, 74 (1997) [hep-ph/9702416].
54. R. S. Chivukula and H. Georgi, Phys. Lett. B **188**, 99 (1987).
55. G. D'Ambrosio *et al.*, Nucl. Phys. B **645**, 155 (2002) [hep-ph/0207036].
56. K. Agashe *et al.*, hep-ph/0509117.
57. Y. Grossman and M. Neubert, Phys. Lett. B **474**, 361 (2000).
58. T. Gherghetta and A. Pomarol, Nucl. Phys. B **586**, 141 (2000).
59. T. Appelquist and R. Shrock, Phys. Lett. B **548**, 204 (2002) [hep-ph/0204141].
60. B. Keren-Zur *et al.*, Nucl. Phys. B **867**, 429 (2013) [arXiv:1205.5803 [hep-ph]].
61. J. M. Maldacena, Adv. Theor. Math. Phys. **2**, 231 (1998) [hep-th/9711200].
62. For a review, see C. Csaki, J. Hubisz, and P. Meade, hep-ph/0510275;
See also J. Parsons, A. Pomarol, *'Extra Dimensions'* review, section *III.2*, in this volume.
63. E. T. Neil, PoS LATTICE **2011**, 009 (2011) [arXiv:1205.4706 [hep-lat]].
64. J. Giedt, PoS LATTICE **2012**, 006 (2012).
65. T. Appelquist *et al.*, arXiv:1309.1206 [hep-lat].
66. R. S. Chivukula, S. B. Selipsky, and E. H. Simmons, Phys. Rev. Lett. **69**, 575 (1992) [hep-ph/9204214].
67. F. del Aguila *et al.*, Nucl. Phys. B **334**, 1 (1990).
68. S. Chatrchyan *et al.*, [CMS Collab.], Phys. Rev. Lett. **107**, 271802 (2011) [arXiv:1109.4985 [hep-ex]].
69. CMS-PAS-B2G-12-021, CERN, Geneva (2013).
70. S. Chatrchyan *et al.*, [CMS Collab.], accepted by PRL (2013) [arXiv:1309.2030 [hep-ex]].
71. S. Chatrchyan *et al.*, [CMS Collab.], Phys. Lett. **B718**, 307 (2012) arXiv:1209.0471 [hep-ex].
72. S. Chatrchyan *et al.*, [CMS Collab.], Phys. Rev. **D86**, 112003 (2012) arXiv:1209.1062 [hep-ex].
73. ATLAS-CONF-2013-051, CERN, Geneva (2013).
74. ATLAS-CONF-2013-017, CERN, Geneva (2013).
75. CMS-PAS-EXO-12-061, CERN, Geneva (2012).
76. ATLAS-CONF-2013-066, CERN, Geneva (2013).
77. ATLAS-CONF-2013-052, CERN, Geneva (2013).
78. ATLAS-CONF-2013-060, CERN, Geneva (2013).
79. ATLAS-CONF-2013-056, CERN, Geneva (2013).
80. CMS-PAS-B2G-12-015, CERN, Geneva (2013).
81. CMS-PAS-B2G-12-019, CERN, Geneva (2013).
82. R. Contino and G. Servant, JHEP **0806**, 026 (2008) arXiv:0801.1679 [hep-ex].
83. J. Mrazek and A. Wulzer, Phys. Rev. **D81**, 075006 (2010) arXiv:0909.3977 [hep-ph].
84. CMS-PAS-B2G-12-012, CERN, Geneva (2013).
85. CMS-PAS-EXO-12-059, CERN, Geneva (2013).
86. ATLAS-CONF-2013-074, CERN, Geneva (2013).
87. S. Chatrchyan *et al.*, [CMS Collab.], Phys. Rev. Lett. **110**, 141802 (2013).
88. ATLAS-CONF-2013-015, CERN, Geneva (2013).
89. CMS-PAS-EXO-12-025, CERN, Geneva (2013).
90. CMS-PAS-EXO-12-024, CERN, Geneva (2013).
91. CMS-PAS-EXO-12-025, CERN, Geneva (2013).
92. CMS-PAS-B2G-12-010, CERN, Geneva (2013).
93. ATLAS-CONF-2013-050, CERN, Geneva (2013).
94. CMS-PAS-EXO-12-023, CERN, Geneva (2013).

The latest unpublished results are described in "Dynamical Electroweak Symmetry Breaking" review.

MASS LIMITS for Resonances in Models of Dynamical Electroweak Symmetry Breaking

VALUE (GeV)	CL%	DOCUMENT ID		TECN	COMMENT
• • • We do not use the following data for averages, fits, limits, etc. • • •					
> 703		[1] AAD	13AN	ATLS	$pp \to a_T \to W\gamma$
> 494		[2] AAD	13AN	ATLS	$pp \to \omega_T \to Z\gamma$
none 500–1740	95	[3] AAD	13AQ	ATLS	top-color Z'
>1300	95	[4] CHATRCHYAN	13AP	CMS	top-color Z'
>2100	95	[3] CHATRCHYAN	13BM	CMS	top-color Z'
		[5] BAAK	12	RVUE	QCD-like technicolor
none 167–687	95	[6] CHATRCHYAN	12AF	CMS	$\rho_T \to WZ$
> 805	95	[3] AALTONEN	11AD	CDF	top-color Z'
> 805	95	[3] AALTONEN	11AE	CDF	top-color Z'
		[7] CHIVUKULA	11	RVUE	top-Higgs
		[8] CHIVUKULA	11A	RVUE	techini-π
		[9] AALTONEN	10I	CDF	$p\overline{p} \to \rho_T/\omega_T \to W\pi_T$

none 208–408	95	[10] ABAZOV	10A	D0	$\rho_T \to WZ$
		[11] ABAZOV	07I	D0	$p\overline{p} \to \rho_T/\omega_T \to W\pi_T$
> 280	95	[12] ABULENCIA	05A	CDF	$\rho_T \to e^+e^-, \mu^+\mu^-$
		[13] CHEKANOV	02B	ZEUS	color octet techni-π
> 207	95	[14] ABAZOV	01B	D0	$\rho_T \to e^+e^-$
none 90–206.7	95	[15] ABDALLAH	01	DLPH	$e^+e^- \to \rho_T$
		[16] AFFOLDER	00F	CDF	color-singlet techni-ρ, $\rho_T \to W\pi_T, 2\pi_T$
> 600	95	[17] AFFOLDER	00K	CDF	color-octet techni-ρ, $\rho_{T8} \to 2\pi_{LQ}$
none 350–440	95	[18] ABE	99F	CDF	color-octet techni-ρ, $\rho_{T8} \to \overline{b}b$
		[19] ABE	99N	CDF	techni-ω, $\omega_T \to \gamma\overline{b}b$
none 260–480	95	[20] ABE	97G	CDF	color-octet techni-ρ, $\rho_{T8} \to$ 2jets

[1] AAD 13AN search for vector techni-resonance a_T decaying into $W\gamma$.

[2] AAD 13AN search for vector techni-resonance ω_T decaying into $Z\gamma$.

[3] Search for top-color Z' decaying to $t\overline{t}$. The quoted limit is for $\Gamma_{Z'}/m_{Z'} = 0.012$.

[4] CHATRCHYAN 13AP search for top-color leptophobic Z' decaying to $t\overline{t}$. The quoted limit is for $\Gamma_{Z'}/m_{Z'} = 0.012$.

[5] BAAK 12 give electroweak oblique parameter constraints on the QCD-like technicolor models. See their Fig. 28.

[6] CHATRCHYAN 12AF search for a vector techni-resonance decaying to WZ. The limit assumes $M_{\pi_T} = (3/4)\ M_{\rho_T} - 25$ GeV. See their Fig. 3 for the limit in $M_{\pi_T} - M_{\rho_T}$ plane of the low scale technicolor model.

[7] Using the LHC limit on the Higgs boson production cross section, CHIVUKULA 11 obtain a limit on the top-Higgs mass > 300 GeV at 95% CL assuming 150 GeV top-pion mass.

[8] Using the LHC limit on the Higgs boson production cross section, CHIVUKULA 11A obtain a limit on the techinipion mass ruling out the region 110 GeV $< m_P < 2m_t$. Existence of color techni-fermions, top-color mechanism, and $N_{TC} \geq 3$ are assumed.

[9] AALTONEN 10I search for the vector techni-resonances (ρ_T, ω_T) decaying into $W\pi_T$ with $W \to \ell\nu$ and $\pi_T \to b\overline{b}$, $b\overline{c}$, or $b\overline{u}$. See their Fig. 3 for the exclusion plot in $M_{\pi_T} - M_{\rho_T}$ plane.

[10] ABAZOV 10A search for a vector techni-resonance decaying into WZ. The limit assumes $M_{\rho_T} < M_{\pi_T} + M_W$.

[11] ABAZOV 07I search for the vector techni-resonances (ρ_T, ω_T) decaying into $W\pi_T$ with $W \to e\nu$ and $\pi_T \to b\overline{b}$ or $b\overline{c}$. See their Fig. 2 for the exclusion plot in $M_{\pi_T} - M_{\rho_T}$ plane.

[12] ABULENCIA 05A search for resonances decaying to electron or muon pairs in $p\overline{p}$ collisions. at $\sqrt{s} = 1.96$ TeV. The limit assumes Technicolor-scale mass parameters $M_V = M_A = 500$ GeV.

[13] CHEKANOV 02B search for color octet techni-π P decaying into dijets in ep collisions. See their Fig. 5 for the limit on $\sigma(ep \to ePX)\cdot B(P \to 2j)$.

[14] ABAZOV 01B searches for vector techni-resonances (ρ_T,ω_T) decaying to e^+e^-. The limit assumes $M_{\rho_T} = M_{\omega_T} < M_{\pi_T} + M_W$.

[15] The limit is independent of the π_T mass. See their Fig. 9 and Fig. 10 for the exclusion plot in the M_{ρ_T}–M_{π_T} plane. ABDALLAH 01 limit on the techni-pion mass is $M_{\pi_T} > 79.8$ GeV for N_D=2, assuming its point-like coupling to gauge bosons.

[16] AFFOLDER 00F search for ρ_T decaying into $W\pi_T$ or $\pi_T\pi_T$ with $W \to \ell\nu$ and $\pi_T \to \overline{b}b$, $\overline{b}c$. See Fig. 1 in the above Note on "Dynamical Electroweak Symmetry Breaking" for the exclusion plot in the M_{ρ_T}–M_{π_T} plane.

[17] AFFOLDER 00K search for the ρ_{T8} decaying into $\pi_{LQ}\pi_{LQ}$ with $\pi_{LQ} \to b\nu$. For $\pi_{LQ} \to c\nu$, the limit is $M_{\rho_{T8}}$ >510 GeV. See their Fig. 2 and Fig. 3 for the exclusion plot in the $M_{\rho_{T8}}$–$M_{\pi_{LQ}}$ plane.

[18] ABE 99F search for a new particle X decaying into $b\overline{b}$ in $p\overline{p}$ collisions at E_{cm}= 1.8 TeV. See Fig. 7 in the above Note on "Dynamical Electroweak Symmetry Breaking" for the upper limit on $\sigma(p\overline{p} \to X)\times B(X \to b\overline{b})$. ABE 99F also exclude top gluons of width Γ=0.3M in the mass interval 280 <M< 670 GeV, of width Γ=0.5M in the mass interval 340 <M< 640 GeV, and of width Γ=0.7M in the mass interval 375 <M< 560 GeV.

[19] ABE 99N search for the techni-ω decaying into $\gamma\pi_T$. The technipion is assumed to decay $\pi_T \to b\overline{b}$. See Fig. 2 in the above Note on "Dynamical Electroweak Symmetry Breaking" for the exclusion plot in the M_{ω_T}–M_{π_T} plane.

[20] ABE 97G search for a new particle X decaying into dijets in $p\overline{p}$ collisions at E_{cm}= 1.8 TeV. See Fig. 5 in the above Note on "Dynamical Electroweak Symmetry Breaking" for the upper limit on $\sigma(p\overline{p} \to X)\times B(X \to 2j)$.

REFERENCES FOR Technicolor

AAD	13AN	PR D87 112003	G. Aad *et al.*	(ATLAS Collab.)
AAD	13AQ	PR D88 012004	G. Aad *et al.*	(ATLAS Collab.)
CHATRCHYAN	13AP	PR D87 072002	S. Chatrchyan *et al.*	(CMS Collab.)
CHATRCHYAN	13BM	PRL 111 211804	S. Chatrchyan *et al.*	(CMS Collab.)
BAAK	12	EPJ C72 2003	M. Baak *et al.*	(Gfitter Group)
CHATRCHYAN	12AF	PRL 109 141801	S. Chatrchyan *et al.*	(CMS Collab.)
AALTONEN	11AD	PR D84 072003	T. Aaltonen *et al.*	(CDF Collab.)
AALTONEN	11AE	PR D84 072004	T. Aaltonen *et al.*	(CDF Collab.)
CHIVUKULA	11	PR D84 095022	R.S. Chivukula *et al.*	
CHIVUKULA	11A	PR D84 115025	R. S. Chivukula *et al.*	
AALTONEN	10I	PRL 104 111802	T. Aaltonen *et al.*	(CDF Collab.)
ABAZOV	10A	PRL 104 061801	V.M. Abazov *et al.*	(D0 Collab.)
ABAZOV	07I	PRL 98 221801	V.M. Abazov *et al.*	(D0 Collab.)
ABULENCIA	05A	PRL 95 252001	A. Abulencia *et al.*	(CDF Collab.)
CHEKANOV	02B	PL B531 9	S. Chekanov *et al.*	(ZEUS Collab.)
ABAZOV	01B	PRL 87 061802	V.M. Abazov *et al.*	(D0 Collab.)
ABDALLAH	01	EPJ C22 17	J. Abdallah *et al.*	(DELPHI Collab.)
AFFOLDER	00F	PRL 84 1110	T. Affolder *et al.*	(CDF Collab.)
AFFOLDER	00K	PRL 85 2056	T. Affolder *et al.*	(CDF Collab.)
ABE	99F	PRL 82 2038	F. Abe *et al.*	(CDF Collab.)
ABE	99N	PRL 83 3124	F. Abe *et al.*	(CDF Collab.)
ABE	97G	PR D55 R5263	F. Abe *et al.*	(CDF Collab.)

Quark and Lepton Compositeness, Searches for

The latest unpublished results are described in the "Quark and Lepton Compositeness" review.

SEARCHES FOR QUARK AND LEPTON COMPOSITENESS

Revised 2001 by K. Hagiwara (KEK), and K. Hikasa and M. Tanabashi (Tohoku University).

If quarks and leptons are made of constituents, then at the scale of constituent binding energies, there should appear new interactions among quarks and leptons. At energies much below the compositeness scale (Λ), these interactions are suppressed by inverse powers of Λ. The dominant effect should come from the lowest dimensional interactions with four fermions (contact terms), whose most general chirally invariant form reads [1]

$$L = \frac{g^2}{2\Lambda^2}\Big[\eta_{LL}\,\overline{\psi}_L\gamma_\mu\psi_L\,\overline{\psi}_L\gamma^\mu\psi_L + \eta_{RR}\,\overline{\psi}_R\gamma_\mu\psi_R\,\overline{\psi}_R\gamma^\mu\psi_R + 2\eta_{LR}\,\overline{\psi}_L\gamma_\mu\psi_L\,\overline{\psi}_R\gamma^\mu\psi_R\Big]\ . \tag{1}$$

Chiral invariance provides a natural explanation why quark and lepton masses are much smaller than their inverse size Λ. We may determine the scale Λ unambiguously by using the above form of the effective interactions; the conventional method [1] is to fix its scale by setting $g^2/4\pi = g^2(\Lambda)/4\pi = 1$ for the new strong interaction coupling and by setting the largest magnitude of the coefficients $\eta_{\alpha\beta}$ to be unity. In the following, we denote

$$\begin{aligned}
&\Lambda = \Lambda^\pm_{LL} \ \text{ for } \ (\eta_{LL}, \eta_{RR}, \eta_{LR}) = (\pm1, 0, 0)\ ,\\
&\Lambda = \Lambda^\pm_{RR} \ \text{ for } \ (\eta_{LL}, \eta_{RR}, \eta_{LR}) = (0, \pm1, 0)\ ,\\
&\Lambda = \Lambda^\pm_{VV} \ \text{ for } \ (\eta_{LL}, \eta_{RR}, \eta_{LR}) = (\pm1, \pm1, \pm1)\ ,\\
&\Lambda = \Lambda^\pm_{AA} \ \text{ for } \ (\eta_{LL}, \eta_{RR}, \eta_{LR}) = (\pm1, \pm1, \mp1)\ ,
\end{aligned} \tag{2}$$

as typical examples. Such interactions can arise by constituent interchange (when the fermions have common constituents, *e.g.*, for $ee \to ee$) and/or by exchange of the binding quanta (whenever binding quanta couple to constituents of both particles).

Another typical consequence of compositeness is the appearance of excited leptons and quarks (ℓ^* and q^*). Phenomenologically, an excited lepton is defined to be a heavy lepton which shares leptonic quantum number with one of the existing leptons (an excited quark is defined similarly). For example, an excited electron e^* is characterized by a nonzero transition-magnetic coupling with electrons. Smallness of the lepton mass and the success of QED prediction for g–2 suggest chirality conservation, *i.e.*, an excited lepton should not couple to both left- and right-handed components of the corresponding lepton.

Excited leptons may be classified by SU(2)×U(1) quantum numbers. Typical examples are:

1. Sequential type

$$\begin{pmatrix}\nu^*\\ \ell^*\end{pmatrix}_L\ , \qquad [\nu^*_R]\ , \qquad \ell^*_R\ .$$

ν^*_R is necessary unless ν^* has a Majorana mass.

2. Mirror type

$$[\nu_L^*]\,, \qquad \ell_L^*\,, \qquad \begin{pmatrix}\nu^*\\ \ell^*\end{pmatrix}_R\,.$$

3. Homodoublet type

$$\begin{pmatrix}\nu^*\\ \ell^*\end{pmatrix}_L\,, \qquad \begin{pmatrix}\nu^*\\ \ell^*\end{pmatrix}_R\,.$$

Similar classification can be made for excited quarks.

Excited fermions can be pair produced via their gauge couplings. The couplings of excited leptons with Z are listed in the following table (for notation see Eq. (1) in "Standard Model of Electroweak Interactions"):

	Sequential type	Mirror type	Homodoublet type
V^{ℓ^*}	$-\frac{1}{2}+2\sin^2\theta_W$	$-\frac{1}{2}+2\sin^2\theta_W$	$-1+2\sin^2\theta_W$
A^{ℓ^*}	$-\frac{1}{2}$	$+\frac{1}{2}$	0
$V^{\nu_D^*}$	$+\frac{1}{2}$	$+\frac{1}{2}$	$+1$
$A^{\nu_D^*}$	$+\frac{1}{2}$	$-\frac{1}{2}$	0
$V^{\nu_M^*}$	0	0	—
$A^{\nu_M^*}$	$+1$	-1	—

Here ν_D^* (ν_M^*) stands for Dirac (Majorana) excited neutrino. The corresponding couplings of excited quarks can be easily obtained. Although form factor effects can be present for the gauge couplings at $q^2 \neq 0$, they are usually neglected.

In addition, transition magnetic type couplings with a gauge boson are expected. These couplings can be generally parameterized as follows:

$$\begin{aligned}\mathcal{L} = &\frac{\lambda_\gamma^{(f^*)} e}{2m_{f^*}}\,\overline{f}^*\sigma^{\mu\nu}(\eta_L\tfrac{1-\gamma_5}{2}+\eta_R\tfrac{1+\gamma_5}{2})f F_{\mu\nu}\\ &+\frac{\lambda_Z^{(f^*)} e}{2m_{f^*}}\,\overline{f}^*\sigma^{\mu\nu}(\eta_L\tfrac{1-\gamma_5}{2}+\eta_R\tfrac{1+\gamma_5}{2})f Z_{\mu\nu}\\ &+\frac{\lambda_W^{(\ell^*)} g}{2m_{\ell^*}}\,\overline{\ell}^*\sigma^{\mu\nu}\tfrac{1-\gamma_5}{2}\nu W_{\mu\nu}\\ &+\frac{\lambda_W^{(\nu^*)} g}{2m_{\nu^*}}\,\overline{\nu}^*\sigma^{\mu\nu}(\eta_L\tfrac{1-\gamma_5}{2}+\eta_R\tfrac{1+\gamma_5}{2})\ell\, W^\dagger_{\mu\nu}\\ &+\text{h.c.}\,, \end{aligned} \tag{3}$$

where $g = e/\sin\theta_W$, $F_{\mu\nu} = \partial_\mu A_\nu - \partial_\nu A_\mu$ is the photon field strength, $Z_{\mu\nu} = \partial_\mu Z_\nu - \partial_\nu Z_\mu$, *etc.* The normalization of the coupling is chosen such that

$$\max(|\eta_L|, |\eta_R|) = 1\,.$$

Chirality conservation requires

$$\eta_L \eta_R = 0\,. \tag{4}$$

Some experimental analyses assume the relation $\eta_L = \eta_R = 1$, which violates chiral symmetry. We encode the results of such analyses if the crucial part of the cross section is proportional to the factor $\eta_L^2 + \eta_R^2$ and the limits can be reinterpreted as those for chirality conserving cases $(\eta_L, \eta_R) = (1, 0)$ or $(0, 1)$ after rescaling λ.

These couplings in Eq. (3) can arise from SU(2)×U(1)-invariant higher-dimensional interactions. A well-studied model is the interaction of homodoublet type ℓ^* with the Lagrangian [2,3]

$$\mathcal{L} = \frac{1}{2\Lambda}\overline{L}^*\sigma^{\mu\nu}(g f\tfrac{\tau^a}{2}W^a_{\mu\nu} + g' f' Y B_{\mu\nu})\tfrac{1-\gamma_5}{2}L + \text{h.c.}\,, \tag{5}$$

where L denotes the lepton doublet (ν, ℓ), Λ is the compositeness scale, g, g' are SU(2) and $\mathrm{U}(1)_Y$ gauge couplings, and $W^a_{\mu\nu}$ and $B_{\mu\nu}$ are the field strengths for SU(2) and $\mathrm{U}(1)_Y$ gauge fields. The same interaction occurs for mirror-type excited leptons. For sequential-type excited leptons, the ℓ^* and ν^* couplings become unrelated, and the couplings receive the extra suppression of $(250\,\text{GeV})/\Lambda$ or m_{L^*}/Λ. In any case, these couplings satisfy the relation

$$\lambda_W = -\sqrt{2}\sin^2\theta_W(\lambda_Z\cot\theta_W + \lambda_\gamma)\,. \tag{6}$$

Additional coupling with gluons is possible for excited quarks:

$$\begin{aligned}\mathcal{L} = &\frac{1}{2\Lambda}\overline{Q}^*\sigma^{\mu\nu}\left(g_s f_s\tfrac{\lambda^a}{2}G^a_{\mu\nu} + g\, f\tfrac{\tau^a}{2}W^a_{\mu\nu} + g'\, f' Y B_{\mu\nu}\right)\\ &\times\tfrac{1-\gamma_5}{2}Q + \text{h.c.}\,, \end{aligned} \tag{7}$$

where Q denotes a quark doublet, g_s is the QCD gauge coupling, and $G^a_{\mu\nu}$ the gluon field strength.

It should be noted that the electromagnetic radiative decay of $\ell^*(\nu^*)$ is forbidden if $f = -f'$ ($f = f'$). These two possibilities ($f = f'$ and $f = -f'$) are investigated in many analyses of the LEP experiments above the Z pole.

Several different conventions are used by LEP experiments on Z pole to express the transition magnetic couplings. To facilitate comparison, we re-express these in terms of λ_Z and λ_γ using the following relations and taking $\sin^2\theta_W = 0.23$. We assume chiral couplings, *i.e.*, $|c| = |d|$ in the notation of Ref. 2.

1. ALEPH (charged lepton and neutrino)

$$\lambda_Z^{\text{ALEPH}} = \frac{1}{2}\lambda_Z \quad (1990\text{ papers}) \tag{8a}$$

$$\frac{2c}{\Lambda} = \frac{\lambda_Z}{m_{\ell^*}[\text{or } m_{\nu^*}]} \quad (\text{for } |c| = |d|) \tag{8b}$$

2. ALEPH (quark)

$$\lambda_u^{\text{ALEPH}} = \frac{\sin\theta_W\cos\theta_W}{\sqrt{\frac{1}{4}-\frac{2}{3}\sin^2\theta_W+\frac{8}{9}\sin^4\theta_W}}\,\lambda_Z = 1.11\lambda_Z \tag{9}$$

3. L3 and DELPHI (charged lepton)

$$\lambda^{\text{L3}} = \lambda_Z^{\text{DELPHI}} = -\frac{\sqrt{2}}{\cot\theta_W - \tan\theta_W}\,\lambda_Z = -1.10\lambda_Z \tag{10}$$

4. L3 (neutrino)

$$f_Z^{\text{L3}} = \sqrt{2}\lambda_Z \tag{11}$$

5. OPAL (charged lepton)

$$\frac{f^{\rm OPAL}}{\Lambda} = -\frac{2}{\cot\theta_W - \tan\theta_W}\,\frac{\lambda_Z}{m_{\ell^*}} = -1.56\,\frac{\lambda_Z}{m_{\ell^*}} \qquad (12)$$

6. OPAL (quark)

$$\frac{f^{\rm OPAL}c}{\Lambda} = \frac{\lambda_Z}{2m_{q^*}} \quad (\text{for } |c| = |d|) \qquad (13)$$

7. DELPHI (charged lepton)

$$\lambda_\gamma^{\rm DELPHI} = -\frac{1}{\sqrt{2}}\,\lambda_\gamma \qquad (14)$$

If leptons are made of color triplet and antitriplet constituents, we may expect their color-octet partners. Transitions between the octet leptons (ℓ_8) and the ordinary lepton (ℓ) may take place via the dimension-five interactions

$$\mathcal{L} = \frac{1}{2\Lambda}\sum_\ell \left\{ \overline{\ell}_8^{\,\alpha}\; g_S\, F_{\mu\nu}^{\alpha}\, \sigma^{\mu\nu}\left(\eta_L\, \ell_L + \eta_R\, \ell_R\right) + h.c. \right\} \qquad (15)$$

where the summation is over charged leptons and neutrinos. The leptonic chiral invariance implies $\eta_L\, \eta_R = 0$ as before.

References

1. E.J. Eichten, K.D. Lane, and M.E. Peskin, Phys. Rev. Lett. **50**, 811 (1983).
2. K. Hagiwara, S. Komamiya, and D. Zeppenfeld, Z. Phys. **C29**, 115 (1985).
3. N. Cabibbo, L. Maiani, and Y. Srivastava, Phys. Lett. **139B**, 459 (1984).

CONTENTS:

SCALE LIMITS for Contact Interactions: $\Lambda(eeee)$

Limits are for $\Lambda_{LL}^{\pm}$ only. For other cases, see each reference.

Λ_{LL}^{+}(TeV)	Λ_{LL}^{-}(TeV)	CL%	DOCUMENT ID		TECN	COMMENT
>8.3	**>10.3**	95	[1] BOURILKOV	01	RVUE	$E_{\rm cm}$= 192–208 GeV
• • • We do not use the following data for averages, fits, limits, etc. • • •						
>4.5	>7.0	95	[2] SCHAEL	07A	ALEP	$E_{\rm cm}$= 189–209 GeV
>5.3	>6.8	95	ABDALLAH	06C	DLPH	$E_{\rm cm}$= 130–207 GeV
>4.7	>6.1	95	[3] ABBIENDI	04G	OPAL	$E_{\rm cm}$= 130–207 GeV
>4.3	>4.9	95	ACCIARRI	00P	L3	$E_{\rm cm}$= 130–189 GeV

[1] A combined analysis of the data from ALEPH, DELPHI, L3, and OPAL.
[2] SCHAEL 07A limits are from R_c, Q_{FB}^{depl}, and hadronic cross section measurements.
[3] ABBIENDI 04G limits are from $e^+e^- \to e^+e^-$ cross section at $\sqrt{s}$ = 130–207 GeV.

SCALE LIMITS for Contact Interactions: $\Lambda(ee\mu\mu)$

Limits are for $\Lambda_{LL}^{\pm}$ only. For other cases, see each reference.

Λ_{LL}^{+}(TeV)	Λ_{LL}^{-}(TeV)	CL%	DOCUMENT ID		TECN	COMMENT
>6.6	**>9.5**	95	[1] SCHAEL	07A	ALEP	$E_{\rm cm}$= 189–209 GeV
> 8.5	>3.8	95	ACCIARRI	00P	L3	$E_{\rm cm}$= 130–189 GeV
• • • We do not use the following data for averages, fits, limits, etc. • • •						
>7.3	>7.6	95	ABDALLAH	06C	DLPH	$E_{\rm cm}$= 130–207 GeV
>8.1	>7.3	95	[2] ABBIENDI	04G	OPAL	$E_{\rm cm}$= 130–207 GeV

[1] SCHAEL 07A limits are from R_c, Q_{FB}^{depl}, and hadronic cross section measurements.
[2] ABBIENDI 04G limits are from $e^+e^- \to \mu\mu$ cross section at $\sqrt{s}$ = 130–207 GeV.

SCALE LIMITS for Contact Interactions: $\Lambda(ee\tau\tau)$

Limits are for $\Lambda_{LL}^{\pm}$ only. For other cases, see each reference.

Λ_{LL}^{+}(TeV)	Λ_{LL}^{-}(TeV)	CL%	DOCUMENT ID		TECN	COMMENT
>7.9	>5.8	95	[1] SCHAEL	07A	ALEP	$E_{\rm cm}$= 189–209 GeV
>7.9	>4.6	95	ABDALLAH	06C	DLPH	$E_{\rm cm}$= 130–207 GeV
>4.9	**>7.2**	95	[2] ABBIENDI	04G	OPAL	$E_{\rm cm}$= 130–207 GeV
• • • We do not use the following data for averages, fits, limits, etc. • • •						
>5.4	>4.7	95	ACCIARRI	00P	L3	$E_{\rm cm}$= 130–189 GeV

[1] SCHAEL 07A limits are from R_c, Q_{FB}^{depl}, and hadronic cross section measurements.
[2] ABBIENDI 04G limits are from $e^+e^- \to \tau\tau$ cross section at $\sqrt{s}$ = 130–207 GeV.

SCALE LIMITS for Contact Interactions: $\Lambda(\ell\ell\ell\ell)$

Lepton universality assumed. Limits are for $\Lambda_{LL}^{\pm}$ only. For other cases, see each reference.

Λ_{LL}^{+}(TeV)	Λ_{LL}^{-}(TeV)	CL%	DOCUMENT ID		TECN	COMMENT
>7.9	**> 10.3**	95	[1] SCHAEL	07A	ALEP	$E_{\rm cm}$= 189–209 GeV
>9.1	>8.2	95	ABDALLAH	06C	DLPH	$E_{\rm cm}$= 130–207 GeV
• • • We do not use the following data for averages, fits, limits, etc. • • •						
>7.7	>9.5	95	[2] ABBIENDI	04G	OPAL	$E_{\rm cm}$= 130–207 GeV
			[3] BABICH	03	RVUE	
>9.0	>5.2	95	ACCIARRI	00P	L3	$E_{\rm cm}$= 130–189 GeV

[1] SCHAEL 07A limits are from R_c, Q_{FB}^{depl}, and hadronic cross section measurements.
[2] ABBIENDI 04G limits are from $e^+e^- \to \ell^+\ell^-$ cross section at $\sqrt{s}$ = 130–207 GeV.
[3] BABICH 03 obtain a bound -0.175 TeV^{-2} $< 1/\Lambda_{LL}^2 <$ 0.095 TeV^{-2} (95%CL) in a model independent analysis allowing all of Λ_{LL}, Λ_{LR}, Λ_{RL}, Λ_{RR} to coexist.

SCALE LIMITS for Contact Interactions: $\Lambda(eeqq)$

Limits are for $\Lambda_{LL}^{\pm}$ only. For other cases, see each reference.

Λ_{LL}^{+}(TeV)	Λ_{LL}^{-}(TeV)	CL%	DOCUMENT ID		TECN	COMMENT
> 9.5	**>12.1**	95	[1] AAD	13E	ATLS	$(eeqq)$
> **10.1**	>9.4	95	[2] AAD	12AB	ATLS	$(eeqq)$
> 8.4	**>10.2**	95	[3] ABDALLAH	09	DLPH	$(eebb)$
> 9.4	**>5.6**	95	[4] SCHAEL	07A	ALEP	$(eecc)$
> 9.4	>4.9	95	[3] SCHAEL	07A	ALEP	$(eebb)$
>23.3	**>12.5**	95	[5] CHEUNG	01B	RVUE	$(eeuu)$
>11.1	**>26.4**	95	[5] CHEUNG	01B	RVUE	$(eedd)$
• • • We do not use the following data for averages, fits, limits, etc. • • •						
> 4.2	>4.0	95	[6] AARON	11C	H1	$(eeqq)$
> 3.8	>3.8	95	[7] ABDALLAH	11	DLPH	$(eetc)$
>12.9	>7.2	95	[8] SCHAEL	07A	ALEP	$(eeqq)$
> 3.7	>5.9	95	[9] ABULENCIA	06L	CDF	$(eeqq)$

[1] AAD 13E limis are from e^+e^- mass distribution in pp collisions at $E_{\rm cm}$ = 7 TeV.
[2] AAD 12AB limis are from e^+e^- mass distribution in pp collisions at $E_{\rm cm}$ = 7 TeV.
[3] ABDALLAH 09 and SCHAEL 07A limits are from R_b, A_{FB}^b.
[4] SCHAEL 07A limits are from R_c, Q_{FB}^{depl}, and hadronic cross section measurements.
[5] CHEUNG 01B is an update of BARGER 98E.
[6] AARON 11C limits are from Q^2 spectrum measurements of $e^\pm p \to e^\pm X$.
[7] ABDALLAH 11 limit is from $e^+e^- \to t\overline{c}$ cross section. $\Lambda_{LL} = \Lambda_{LR} = \Lambda_{RL} = \Lambda_{RR}$ is assumed.
[8] SCHAEL 07A limit assumes quark flavor universality of the contact interactions.
[9] ABULENCIA 06L limits are from $p\overline{p}$ collisions at $\sqrt{s}$ = 1.96 TeV.

Searches Particle Listings

Quark and Lepton Compositeness

SCALE LIMITS for Contact Interactions: Λ(μμqq)

Λ^+_{LL}(TeV)	Λ^-_{LL}(TeV)	CL%	DOCUMENT ID		TECN	COMMENT
>9.6	>12.9	95	[1] AAD	13E	ATLS	$(\mu\mu qq)$ (isosinglet)
>9.5	**> 13.1**	95	[2] CHATRCHYAN	13K	CMS	$(\mu\mu qq)$ (isosinglet)
• • • We do not use the following data for averages, fits, limits, etc. • • •						
>8.0	>7.0	95	[3] AAD	12AB	ATLS	$(\mu\mu qq)$ (isosinglet)

[1] AAD 13E limis are from $\mu^+\mu^-$ mass distribution in pp collisions at E_{cm} = 7 TeV.
[2] CHATRCHYAN 13K limis are from $\mu^+\mu^-$ mass distribution in pp collisions at E_{cm} = 7 TeV.
[3] AAD 12AB limis are from $\mu^+\mu^-$ mass distribution in pp collisions at E_{cm} = 7 TeV.

SCALE LIMITS for Contact Interactions: Λ(ℓνℓν)

VALUE (TeV)	CL%	DOCUMENT ID		TECN	COMMENT
>3.10	90	[1] JODIDIO	86	SPEC	$\Lambda^\pm_{LR}(\nu_\mu\nu_e\mu e)$
• • • We do not use the following data for averages, fits, limits, etc. • • •					
>3.8		[2] DIAZCRUZ	94	RVUE	$\Lambda^+_{LL}(\tau\nu_\tau e\nu_e)$
>8.1		[2] DIAZCRUZ	94	RVUE	$\Lambda^-_{LL}(\tau\nu_\tau e\nu_e)$
>4.1		[3] DIAZCRUZ	94	RVUE	$\Lambda^+_{LL}(\tau\nu_\tau\mu\nu_\mu)$
>6.5		[3] DIAZCRUZ	94	RVUE	$\Lambda^-_{LL}(\tau\nu_\tau\mu\nu_\mu)$

[1] JODIDIO 86 limit is from $\mu^+ \to \overline{\nu}_\mu e^+\nu_e$. Chirality invariant interactions $L = (g^2/\Lambda^2)$ $[\eta_{LL}\ (\overline{\nu}_{\mu L}\gamma^\alpha\mu_L)\ (\overline{e}_L\gamma_\alpha\nu_{eL}) + \eta_{LR}\ (\overline{\nu}_{\mu L}\gamma^\alpha\nu_{eL}\ (\overline{e}_R\gamma_\alpha\mu_R)]$ with $g^2/4\pi = 1$ and $(\eta_{LL},\eta_{LR}) = (0,\pm1)$ are taken. No limits are given for $\Lambda^\pm_{LL}$ with $(\eta_{LL},\eta_{LR}) = (\pm1,0)$. For more general constraints with right-handed neutrinos and chirality nonconserving contact interactions, see their text.
[2] DIAZCRUZ 94 limits are from $\Gamma(\tau \to e\nu\nu)$ and assume flavor-dependent contact interactions with $\Lambda(\tau\nu_\tau e\nu_e) \ll \Lambda(\mu\nu_\mu e\nu_e)$.
[3] DIAZCRUZ 94 limits are from $\Gamma(\tau \to \mu\nu\nu)$ and assume flavor-dependent contact interactions with $\Lambda(\tau\nu_\tau\mu\nu_\mu) \ll \Lambda(\mu\nu_\mu e\nu_e)$.

SCALE LIMITS for Contact Interactions: Λ(eνqq)

VALUE (TeV)	CL%	DOCUMENT ID		TECN
>2.81	95	[1] AFFOLDER	01I	CDF

[1] AFFOLDER 00I bound is for a scalar interaction $\overline{q}_R\, q_L\, \overline{\nu}e_L$.

SCALE LIMITS for Contact Interactions: Λ(qqqq)

Limits are for $\Lambda^\pm_{LL}$ with color-singlet isoscalar exchanges among u_L's and d_L's only, unless otherwise noted. See EICHTEN 84 for details.

VALUE (TeV)	CL%	DOCUMENT ID		TECN	COMMENT
>9.9	95	[1] CHATRCHYAN	13AN	CMS	$pp \to$ dijet.; Λ^+_{LL}
• • • We do not use the following data for averages, fits, limits, etc. • • •					
>7.6	95	[2] AAD	13D	ATLS	$pp \to$ dijet angl.
>7.5	95	[3] CHATRCHYAN	12Z	CMS	$pp \to$ dijet angl.; Λ^+_{LL}
>3.4	95	[4] AAD	11	ATLS	$pp \to$ dijet; Λ^+_{LL}
>5.6	95	[5] KHACHATRY...11F		CMS	$pp \to$ dijet angl.; Λ^+_{LL}

[1] CHATRCHYAN 13AN limit is from inclusive jet p_T spectrum in pp collisions at E_{cm} = 7 TeV. They also obtain $\Lambda^-_{LL} > 14.3$ TeV.
[2] AAD 13D limit is from dijet angular distribution in pp collisions at E_{cm} = 7 TeV. The constant prior in $1/\Lambda^4$ is applied.
[3] CHATRCHYAN 12Z limit is from dijet angular distribution in pp collisions at E_{cm} = 7 TeV. They also obtain $\Lambda^-_{LL} > 10.5$ TeV.
[4] AAD 11 limit is from dijet angular distribution and dijet centrality ratio in pp collisions at E_{cm} = 7 TeV.
[5] KHACHATRYAN 11F limit is from dijet angular distribution in pp collisions at E_{cm} = 7 TeV. They also obtain $\Lambda^-_{LL} > 6.7$ TeV.

SCALE LIMITS for Contact Interactions: Λ(ννqq)

Limits are for $\Lambda^\pm_{LL}$ only. For other cases, see each reference.

Λ^+_{LL}(TeV)	Λ^-_{LL}(TeV)	CL%	DOCUMENT ID		TECN	COMMENT
>5.0	**>5.4**	95	[1] MCFARLAND	98	CCFR	νN scattering

[1] MCFARLAND 98 assumed a flavor universal interaction. Neutrinos were mostly of muon type.

MASS LIMITS for Excited e (e*)

Most e^+e^- experiments assume one-photon or Z exchange. The limits from some e^+e^- experiments which depend on λ have assumed transition couplings which are chirality violating ($\eta_L = \eta_R$). However they can be interpreted as limits for chirality-conserving interactions after multiplying the coupling value λ by $\sqrt{2}$; see Note.

Excited leptons have the same quantum numbers as other ortholeptons. See also the searches for ortholeptons in the "Searches for Heavy Leptons" section.

Limits for Excited e (e*) from Pair Production

These limits are obtained from $e^+e^- \to e^{*+}e^{*-}$ and thus rely only on the (electroweak) charge of e^*. Form factor effects are ignored unless noted. For the case of limits from Z decay, the e^* coupling is assumed to be of sequential type. Possible t channel contribution from transition magnetic coupling is neglected. All limits assume a dominant $e^* \to e\gamma$ decay except the limits from $\Gamma(Z)$.

For limits prior to 1987, see our 1992 edition (Physical Review **D45** S1 (1992)).

VALUE (GeV)	CL%	DOCUMENT ID		TECN	COMMENT
>103.2	95	[1] ABBIENDI	02G	OPAL	$e^+e^- \to e^*e^*$ Homodoublet type
• • • We do not use the following data for averages, fits, limits, etc. • • •					
>102.8	95	[2] ACHARD	03B	L3	$e^+e^- \to e^*e^*$ Homodoublet type

[1] From e^+e^- collisions at $\sqrt{s}$ = 183–209 GeV. $f = f'$ is assumed.
[2] From e^+e^- collisions at $\sqrt{s}$ = 189–209 GeV. $f = f'$ is assumed. ACHARD 03B also obtain limit for $f = -f'$: $m_{e^*} > 96.6$ GeV.

Limits for Excited e (e*) from Single Production

These limits are from $e^+e^- \to e^*e$, $W \to e^*\nu$, or $ep \to e^*X$ and depend on transition magnetic coupling between e and e^*. All limits assume $e^* \to e\gamma$ decay except as noted. Limits from LEP, UA2, and H1 are for chiral coupling, whereas all other limits are for nonchiral coupling, $\eta_L = \eta_R = 1$. In most papers, the limit is expressed in the form of an excluded region in the λ–m_{e^*} plane. See the original papers.

For limits prior to 1987, see our 1992 edition (Physical Review **D45** S1 (1992)).

VALUE (GeV)	CL%	DOCUMENT ID		TECN	COMMENT
>2200	95	[1] AAD	13BB	ATLS	$pp \to e e^* X$
• • • We do not use the following data for averages, fits, limits, etc. • • •					
>1900	95	[2] CHATRCHYAN	13AE	CMS	$pp \to e e^* X$
>1870	95	[3] AAD	12AZ	ATLS	$pp \to e^{(*)} e^* X$
>1070	95	[4] CHATRCHYAN	11X	CMS	$pp \to e e^* X$
> 272	95	[5] AARON	08A	H1	$ep \to e^* X$
		[6] ABAZOV	08H	D0	$p\overline{p} \to e^* e$
> 209	95	[7] ACOSTA	05B	CDF	$p\overline{p} \to e^* X$
> 206	95	[8] ACHARD	03B	L3	$e^+e^- \to e e^*$
> 208	95	[9] ABBIENDI	02G	OPAL	$e^+e^- \to e e^*$
> 228	95	[10] CHEKANOV	02D	ZEUS	$ep \to e^* X$

[1] AAD 13BB search for single e^* production in pp collisions with $e^* \to e\gamma$ decay. $f = f' = 1$, and e^* production via contact interaction with $\Lambda = m_{e^*}$ are assumed.
[2] CHATRCHYAN 13AE search for single e^* production in pp collisions with $e^* \to e\gamma$ decay. $f = f' = 1$, and e^* production via contact interaction with $\Lambda = m_{e^*}$ are assumed.
[3] AAD 12AZ search for e^* production via four-fermion contact interaction in pp collisions with $e^* \to e\gamma$ decay. The quoted limit assumes $\Lambda = m_{e^*}$. See their Fig. 8 for the exclusion plot in the mass-coupling plane.
[4] CHATRCHYAN 11X search for single e^* production in pp collisions with the decay $e^* \to e\gamma$. $f = f' = \Lambda/m_{e^*}$ is assumed. See their Fig. 2 for the exclusion plot in the mass-coupling plane.
[5] AARON 08A search for single e^* production in ep collisions with the decays $e^* \to e\gamma$, eZ, νW. The quoted limit assumes $f = f' = \Lambda/m_{e^*}$. See their Fig. 3 and Fig. 4 for the exclusion plots in the mass-coupling plane.
[6] ABAZOV 08H search for single e^* production in $p\overline{p}$ collisions with the decays $e^* \to e\gamma$. The e^* production is assumed to be described by an effective four-fermion interaction. See their Fig. 5 for the exclusion plot in the mass-coupling plane.
[7] ACOSTA 05B search for single e^* production in $p\overline{p}$ collisions with the decays $e^* \to e\gamma$. $f = f' = \Lambda/m_{e^*}$ is assumed for the e^* coupling. See their Fig.3 for the exclusion limit in the mass-coupling plane.
[8] ACHARD 03B result is from e^+e^- collisions at $\sqrt{s}$ = 189–209 GeV. See their Fig. 4 for the exclusion plot in the mass-coupling plane.
[9] ABBIENDI 02G result is from e^+e^- collisions at $\sqrt{s}$ = 183–209 GeV. $f = f' = \Lambda/m_{e^*}$ is assumed for e^* coupling. See their Fig. 4c for the exclusion limit in the mass-coupling plane.
[10] CHEKANOV 02D search for single e^* production in ep collisions with the decays $e^* \to e\gamma$, eZ, νW. $f = f' = \Lambda/m_{e^*}$ is assumed for the e^* coupling. See their Fig. 5a for the exclusion plot in the mass-coupling plane.

Limits for Excited e (e*) from $e^+e^- \to \gamma\gamma$

These limits are derived from indirect effects due to e^* exchange in the t channel and depend on transition magnetic coupling between e and e^*. All limits are for $\lambda_\gamma = 1$. All limits except ABE 89J and ACHARD 02D are for nonchiral coupling with $\eta_L = \eta_R = 1$. We choose the chiral coupling limit as the best limit and list it in the Summary Table.

For limits prior to 1987, see our 1992 edition (Physical Review **D45** S1 (1992)).

VALUE (GeV)	CL%	DOCUMENT ID		TECN	COMMENT
>356	95	[1] ABDALLAH	04N	DLPH	$\sqrt{s}$= 161–208 GeV
• • • We do not use the following data for averages, fits, limits, etc. • • •					
>310	95	ACHARD	02D	L3	$\sqrt{s}$= 192–209 GeV

[1] ABDALLAH 04N also obtain a limit on the excited electron mass with ee^* chiral coupling, $m_{e^*} > 295$ GeV at 95% CL.

Indirect Limits for Excited e (e^*)

These limits make use of loop effects involving e^* and are therefore subject to theoretical uncertainty.

VALUE (GeV)	DOCUMENT ID		TECN	COMMENT
• • • We do not use the following data for averages, fits, limits, etc. • • •				
	[1] DORENBOS...	89	CHRM	$\overline{\nu}_\mu e \to \overline{\nu}_\mu e$, $\nu_\mu e \to \nu_\mu e$
	[2] GRIFOLS	86	THEO	$\nu_\mu e \to \nu_\mu e$
	[3] RENARD	82	THEO	$g-2$ of electron

[1] DORENBOSCH 89 obtain the limit $\lambda_\gamma^2 \Lambda_{cut}^2 / m_{e^*}^2 < 2.6$ (95% CL), where Λ_{cut} is the cutoff scale, based on the one-loop calculation by GRIFOLS 86. If one assumes that $\Lambda_{cut} = 1$ TeV and $\lambda_\gamma = 1$, one obtains $m_{e^*} > 620$ GeV. However, one generally expects $\lambda_\gamma \approx m_{e^*}/\Lambda_{cut}$ in composite models.

[2] GRIFOLS 86 uses $\nu_\mu e \to \nu_\mu e$ and $\overline{\nu}_\mu e \to \overline{\nu}_\mu e$ data from CHARM Collaboration to derive mass limits which depend on the scale of compositeness.

[3] RENARD 82 derived from $g-2$ data limits on mass and couplings of e^* and μ^*. See figures 2 and 3 of the paper.

MASS LIMITS for Excited μ (μ^*)

Limits for Excited μ (μ^*) from Pair Production

These limits are obtained from $e^+e^- \to \mu^{*+}\mu^{*-}$ and thus rely only on the (electroweak) charge of μ^*. Form factor effects are ignored unless noted. For the case of limits from Z decay, the μ^* coupling is assumed to be of sequential type. All limits assume a dominant $\mu^* \to \mu\gamma$ decay except the limits from $\Gamma(Z)$.

For limits prior to 1987, see our 1992 edition (Physical Review **D45** S1 (1992)).

VALUE (GeV)	CL%	DOCUMENT ID		TECN	COMMENT
>103.2	95	[1] ABBIENDI	02G	OPAL	$e^+e^- \to \mu^*\mu^*$ Homodoublet type
• • • We do not use the following data for averages, fits, limits, etc. • • •					
>102.8	95	[2] ACHARD	03B	L3	$e^+e^- \to \mu^*\mu^*$ Homodoublet type

[1] From e^+e^- collisions at $\sqrt{s} = 183$–209 GeV. $f = f'$ is assumed.

[2] From e^+e^- collisions at $\sqrt{s} = 189$–209 GeV. $f = f'$ is assumed. ACHARD 03B also obtain limit for $f = -f'$: $m_{\mu^*} > 96.6$ GeV.

Limits for Excited μ (μ^*) from Single Production

These limits are from $e^+e^- \to \mu^*\mu$ and depend on transition magnetic coupling between μ and μ^*. All limits assume $\mu^* \to \mu\gamma$ decay. Limits from LEP are for chiral coupling, whereas all other limits are for nonchiral coupling, $\eta_L = \eta_R = 1$. In most papers, the limit is expressed in the form of an excluded region in the λ–m_{μ^*} plane. See the original papers.

For limits prior to 1987, see our 1992 edition (Physical Review **D45** S1 (1992)).

VALUE (GeV)	CL%	DOCUMENT ID		TECN	COMMENT
>2200	95	[1] AAD	13BB	ATLS	$pp \to \mu\mu^* X$
• • • We do not use the following data for averages, fits, limits, etc. • • •					
>1900	95	[2] CHATRCHYAN	13AE	CMS	$pp \to \mu\mu^* X$
>1750	95	[3] AAD	12AZ	ATLS	$pp \to \mu^{(*)}\mu^* X$
>1090	95	[4] CHATRCHYAN	11X	CMS	$pp \to \mu\mu^* X$
> 180	95	[5] ACHARD	03B	L3	$e^+e^- \to \mu\mu^*$
> 190	95	[6] ABBIENDI	02G	OPAL	$e^+e^- \to \mu\mu^*$

[1] AAD 13BB search for single μ^* production in pp collisions with $\mu^* \to \mu\gamma$ decay. $f = f' = 1$, and μ^* production via contact interaction with $\Lambda = m_{\mu^*}$ are assumed.

[2] CHATRCHYAN 13AE search for single μ^* production in pp collisions with $\mu^* \to \mu\gamma$ decay. $f = f' = 1$, and μ^* production via contact interaction with $\Lambda = m_{\mu^*}$ are assumed.

[3] AAD 12AZ search for μ^* production via four-fermion contact interaction in pp collisions with $\mu^* \to \mu\gamma$ decay. The quoted limit assumes $\Lambda = m_{\mu^*}$. See their Fig. 8 for the exclusion plot in the mass-coupling plane.

[4] CHATRCHYAN 11X search for single μ^* production in pp collisions with the decay $\mu^* \to \mu\gamma$. $f = f' = \Lambda/m_{\mu^*}$ is assumed. See their Fig. 2 for the exclusion plot in the mass-coupling plane.

[5] ACHARD 03B result is from e^+e^- collisions at $\sqrt{s} = 189$–209 GeV. $f = f' = \Lambda/m_{\mu^*}$ is assumed. See their Fig. 4 for the exclusion plot in the mass-coupling plane.

[6] ABBIENDI 02G result is from e^+e^- collisions at $\sqrt{s} = 183$–209 GeV. $f = f' = \Lambda/m_{\mu^*}$ is assumed for μ^* coupling. See their Fig. 4c for the exclusion limit in the mass-coupling plane.

Indirect Limits for Excited μ (μ^*)

These limits make use of loop effects involving μ^* and are therefore subject to theoretical uncertainty.

VALUE (GeV)	DOCUMENT ID		TECN	COMMENT
• • • We do not use the following data for averages, fits, limits, etc. • • •				
	[1] RENARD	82	THEO	$g-2$ of muon

[1] RENARD 82 derived from $g-2$ data limits on mass and couplings of e^* and μ^*. See figures 2 and 3 of the paper.

MASS LIMITS for Excited τ (τ^*)

Limits for Excited τ (τ^*) from Pair Production

These limits are obtained from $e^+e^- \to \tau^{*+}\tau^{*-}$ and thus rely only on the (electroweak) charge of τ^*. Form factor effects are ignored unless noted. For the case of limits from Z decay, the τ^* coupling is assumed to be of sequential type. All limits assume a dominant $\tau^* \to \tau\gamma$ decay except the limits from $\Gamma(Z)$.

For limits prior to 1987, see our 1992 edition (Physical Review **D45** S1 (1992)).

VALUE (GeV)	CL%	DOCUMENT ID		TECN	COMMENT
>103.2	95	[1] ABBIENDI	02G	OPAL	$e^+e^- \to \tau^*\tau^*$ Homodoublet type
• • • We do not use the following data for averages, fits, limits, etc. • • •					
>102.8	95	[2] ACHARD	03B	L3	$e^+e^- \to \tau^*\tau^*$ Homodoublet type

[1] From e^+e^- collisions at $\sqrt{s} = 183$–209 GeV. $f = f'$ is assumed.

[2] From e^+e^- collisions at $\sqrt{s} = 189$–209 GeV. $f = f'$ is assumed. ACHARD 03B also obtain limit for $f = -f'$: $m_{\tau^*} > 96.6$ GeV.

Limits for Excited τ (τ^*) from Single Production

These limits are from $e^+e^- \to \tau^*\tau$ and depend on transition magnetic coupling between τ and τ^*. All limits assume $\tau^* \to \tau\gamma$ decay. Limits from LEP are for chiral coupling, whereas all other limits are for nonchiral coupling, $\eta_L = \eta_R = 1$. In most papers, the limit is expressed in the form of an excluded region in the λ–m_{τ^*} plane. See the original papers.

VALUE (GeV)	CL%	DOCUMENT ID		TECN	COMMENT
>185	95	[1] ABBIENDI	02G	OPAL	$e^+e^- \to \tau\tau^*$
• • • We do not use the following data for averages, fits, limits, etc. • • •					
>180	95	[2] ACHARD	03B	L3	$e^+e^- \to \tau\tau^*$

[1] ABBIENDI 02G result is from e^+e^- collisions at $\sqrt{s} = 183$–209 GeV. $f = f' = \Lambda/m_{\tau^*}$ is assumed for τ^* coupling. See their Fig. 4c for the exclusion limit in the mass-coupling plane.

[2] ACHARD 03B result is from e^+e^- collisions at $\sqrt{s} = 189$–209 GeV. $f = f' = \Lambda/m_{\tau^*}$ is assumed. See their Fig. 4 for the exclusion plot in the mass-coupling plane.

MASS LIMITS for Excited Neutrino (ν^*)

Limits for Excited ν (ν^*) from Pair Production

These limits are obtained from $e^+e^- \to \nu^*\nu^*$ and thus rely only on the (electroweak) charge of ν^*. Form factor effects are ignored unless noted. The ν^* coupling is assumed to be of sequential type unless otherwise noted. All limits assume a dominant $\nu^* \to \nu\gamma$ decay except the limits from $\Gamma(Z)$.

VALUE (GeV)	CL%	DOCUMENT ID		TECN	COMMENT
>102.6	95	[1] ACHARD	03B	L3	$e^+e^- \to \nu^*\nu^*$ Homodoublet type
• • • We do not use the following data for averages, fits, limits, etc. • • •					
	[2] ABBIENDI	04N	OPAL		

[1] From e^+e^- collisions at $\sqrt{s} = 189$–209 GeV. $f = -f'$ is assumed. ACHARD 03B also obtain limit for $f = f'$: $m_{\nu_e^*} > 101.7$ GeV, $m_{\nu_\mu^*} > 101.8$ GeV, and $m_{\nu_\tau^*} > 92.9$ GeV. See their Fig. 4 for the exclusion plot in the mass-coupling plane.

[2] From e^+e^- collisions at $\sqrt{s} = 192$–209 GeV, ABBIENDI 04N obtain limit on $\sigma(e^+e^- \to \nu^*\nu^*)\ B^2(\nu^* \to \nu\gamma)$. See their Fig.2. The limit ranges from 20 to 45 fb for $m_{\nu^*} > 45$ GeV.

Limits for Excited ν (ν^*) from Single Production

These limits are from $e^+e^- \to \nu\nu^*$, $Z \to \nu\nu^*$, or $ep \to \nu^* X$ and depend on transition magnetic coupling between ν/e and ν^*. Assumptions about ν^* decay mode are given in footnotes.

VALUE (GeV)	CL%	DOCUMENT ID		TECN	COMMENT
>213	95	[1] AARON	08	H1	$ep \to \nu^* X$
• • • We do not use the following data for averages, fits, limits, etc. • • •					
>190	95	[2] ACHARD	03B	L3	$e^+e^- \to \nu\nu^*$
none 50–150	95	[3] ADLOFF	02	H1	$ep \to \nu^* X$
>158	95	[4] CHEKANOV	02D	ZEUS	$ep \to \nu^* X$

[1] AARON 08 search for single ν^* production in ep collisions with the decays $\nu^* \to \nu\gamma$, νZ, eW. The quoted limit assumes $f = -f' = \Lambda/m_{\nu^*}$. See their Fig. 3 and Fig. 4 for the exclusion plots in the mass-coupling plane.

[2] ACHARD 03B result is from e^+e^- collisions at $\sqrt{s} = 189$–209 GeV. The quoted limit is for ν_e^*. $f = -f' = \Lambda/m_{\nu^*}$ is assumed. See their Fig. 4 for the exclusion plot in the mass-coupling plane.

[3] ADLOFF 02 search for single ν^* production in ep collisions with the decays $\nu^* \to \nu\gamma$, νZ, eW. The quoted limit assumes $f = -f' = \Lambda/m_{\nu^*}$. See their Fig. 1 for the exclusion plots in the mass-coupling plane.

[4] CHEKANOV 02D search for single ν^* production in ep collisions with the decays $\nu^* \to \nu\gamma$, νZ, eW. $f = -f' = \Lambda/m_{\nu^*}$ is assumed for the e^* coupling. CHEKANOV 02D also obtain limit for $f = f' = \Lambda/m_{\nu^*}$: $m_{\nu^*} > 135$ GeV. See their Fig. 5c and Fig. 5d for the exclusion plot in the mass-coupling plane.

MASS LIMITS for Excited q (q^*)

Limits for Excited q (q^*) from Pair Production

These limits are mostly obtained from $e^+e^- \to q^*\overline{q}^*$ and thus rely only on the (electroweak) charge of the q^*. Form factor effects are ignored unless noted. Assumptions about the q^* decay are given in the comments and footnotes.

VALUE (GeV)	CL%	DOCUMENT ID		TECN	COMMENT
>338	95	[1] AALTONEN	10H	CDF	$q^* \to t W^-$
• • • We do not use the following data for averages, fits, limits, etc. • • •					
		[2] BARATE	98U	ALEP	$Z \to q^* q^*$
> 45.6	95	[3] ADRIANI	93M	L3	u or d type, $Z \to q^* q^*$
> 41.7	95	[4] BARDADIN-...	92	RVUE	u-type, $\Gamma(Z)$
> 44.7	95	[4] BARDADIN-...	92	RVUE	d-type, $\Gamma(Z)$
> 40.6	95	[5] DECAMP	92	ALEP	u-type, $\Gamma(Z)$
> 44.2	95	[5] DECAMP	92	ALEP	d-type, $\Gamma(Z)$
> 45	95	[6] DECAMP	92	ALEP	u or d type, $Z \to q^* q^*$
> 45	95	[5] ABREU	91F	DLPH	u-type, $\Gamma(Z)$
> 45	95	[5] ABREU	91F	DLPH	d-type, $\Gamma(Z)$

[1] AALTONEN 10H obtain limits on the q^*q^* production cross section in $p\overline{p}$ collisions. See their Fig. 3.

[2] BARATE 98U obtain limits on the form factor. See their Fig. 16 for limits in mass-form factor plane.

[3] ADRIANI 93M limit is valid for $B(q^* \to qg) > 0.25$ (0.17) for up (down) type.

[4] BARDADIN-OTWINOWSKA 92 limit based on $\Delta\Gamma(Z)<36$ MeV.

[5] These limits are independent of decay modes.

[6] Limit is for $B(q^* \to qg)+B(q^* \to q\gamma)=1$.

Limits for Excited q (q^*) from Single Production

These limits are from $e^+e^- \to q^*\overline{q}$, $p\overline{p} \to q^*X$, or $pp \to q^*X$ and depend on transition magnetic couplings between q and q^*. Assumptions about q^* decay mode are given in the footnotes and comments.

VALUE (GeV)	CL%	DOCUMENT ID		TECN	COMMENT
>3500	95	[1] AAD	14A	ATLS	$pp \to q^*X,\ q^* \to q\gamma$
• • • We do not use the following data for averages, fits, limits, etc. • • •					
> 870	95	[2] AAD	13AF	ATLS	$pp \to b^*X,\ b^* \to tW$
>3320	95	[3] CHATRCHYAN	13A	CMS	$pp \to q^*X,\ q^* \to qg$
>1940	95	[4] CHATRCHYAN	13AI	CMS	$pp \to q^*X,\ q^* \to qZ,qW$
>2380	95	[5] CHATRCHYAN	13AJ	CMS	$pp \to q^*X,\ q^* \to qW$
>2150	95	[6] CHATRCHYAN	13AJ	CMS	$pp \to q^*X,\ q^* \to qZ$
none 1000–3190	95	[7] CHATRCHYAN	13AS	CMS	$pp \to q^*X,\ q^* \to qg$
>2460	95	[8] AAD	12AO	ATLS	$pp \to q^*X,\ q^* \to q\gamma$
>2990	95	[9] AAD	12S	ATLS	$pp \to q^*X,\ q^* \to qg$
		[10] ABAZOV	11F	D0	$p\overline{p} \to q^*X,\ q^* \to qZ,qW$
>2490	95	[11] CHATRCHYAN	11Y	CMS	$pp \to q^*X,\ q^* \to qg$

[1] AAD 14A assume $\Lambda = m_{q^*}$, $f_s = f = f' = 1$.

[2] AAD 13AF search for b^* decaying to tW in pp collisions at $\sqrt{s} = 7$ TeV. $\kappa_L^b = g_L = 1$, $\kappa_R^b = g_R = 0$ are assumed. See their Fig.6 for limits on $\sigma \cdot B$.

[3] CHATRCHYAN 13A assume $\Lambda = m_{q^*}$.

[4] CHATRCHYAN 13AI assume q^* production via qg fusion and $\Lambda = m_{q^*}$, $f_s = f = f' = 1$. For q^* production via qg fusion and via contact interactions, the limit becomes $m_{q^*} > 2220$ GeV.

[5] CHATRCHYAN 13AJ use the hadronic decay of W.

[6] CHATRCHYAN 13AJ use the hadronic decay of Z.

[7] CHATRCHYAN 13AS assume $\Lambda = m_{q^*}$.

[8] AAD 12AO assume $\Lambda = m_{q^*}$, $f_s = f = f' = 1$.

[9] AAD 12S assume $\Lambda = m_{q^*}$.

[10] ABAZOV 11F search for vectorlike quarks decaying to W+jet and Z+jet in $p\overline{p}$ collisions. See their Fig. 3 and Fig. 4 for the limits on $\sigma \cdot B$.

[11] CHATRCHYAN 11Y assume degenerate q^* with $f_s = \Lambda/m_{q^*}$.

MASS LIMITS for Color Sextet Quarks (q_6)

VALUE (GeV)	CL%	DOCUMENT ID		TECN	COMMENT
>84	95	[1] ABE	89D	CDF	$p\overline{p} \to q_6\overline{q}_6$

[1] ABE 89D look for pair production of unit-charged particles which leave the detector before decaying. In the above limit the color sextet quark is assumed to fragment into a unit-charged or neutral hadron with equal probability and to have long enough lifetime not to decay within the detector. A limit of 121 GeV is obtained for a color decuplet.

MASS LIMITS for Color Octet Charged Leptons (ℓ_8)

$\lambda \equiv m_{\ell_8}/\Lambda$

VALUE (GeV)	CL%	DOCUMENT ID		TECN	COMMENT
>86	95	[1] ABE	89D	CDF	Stable ℓ_8: $p\overline{p} \to \ell_8\overline{\ell}_8$
• • • We do not use the following data for averages, fits, limits, etc. • • •					
		[2] ABT	93	H1	e_8: $ep \to e_8X$

[1] ABE 89D look for pair production of unit-charged particles which leave the detector before decaying. In the above limit the color octet lepton is assumed to fragment into a unit-charged or neutral hadron with equal probability and to have long enough lifetime not to decay within the detector. The limit improves to 99 GeV if it always fragments into a unit-charged hadron.

[2] ABT 93 search for e_8 production via e-gluon fusion in ep collisions with $e_8 \to eg$. See their Fig. 3 for exclusion plot in the m_{e_8}–Λ plane for m_{e_8} = 35–220 GeV.

MASS LIMITS for Color Octet Neutrinos (ν_8)

$\lambda \equiv m_{\ell_8}/\Lambda$

VALUE (GeV)	CL%	DOCUMENT ID		TECN	COMMENT
>110	90	[1] BARGER	89	RVUE	ν_8: $p\overline{p} \to \nu_8\overline{\nu}_8$
• • • We do not use the following data for averages, fits, limits, etc. • • •					
none 3.8–29.8	95	[2] KIM	90	AMY	ν_8: $e^+e^- \to$ acoplanar jets
none 9–21.9	95	[3] BARTEL	87B	JADE	ν_8: $e^+e^- \to$ acoplanar jets

[1] BARGER 89 used ABE 89B limit for events with large missing transverse momentum. Two-body decay $\nu_8 \to \nu g$ is assumed.

[2] KIM 90 is at E_{cm} = 50–60.8 GeV. The same assumptions as in BARTEL 87B are used.

[3] BARTEL 87B is at E_{cm} = 46.3–46.78 GeV. The limit assumes the ν_8 pair production cross section to be eight times larger than that of the corresponding heavy neutrino pair production. This assumption is not valid in general for the weak couplings, and the limit can be sensitive to its $SU(2)_L \times U(1)_Y$ quantum numbers.

MASS LIMITS for W_8 (Color Octet W Boson)

VALUE (GeV)	DOCUMENT ID		TECN	COMMENT
• • • We do not use the following data for averages, fits, limits, etc. • • •				
	[1] ALBAJAR	89	UA1	$p\overline{p} \to W_8X,\ W_8 \to Wg$

[1] ALBAJAR 89 give $\sigma(W_8 \to W+\text{jet})/\sigma(W) < 0.019$ (90% CL) for $m_{W_8} > 220$ GeV.

REFERENCES FOR Searches for Quark and Lepton Compositeness

AAD	14A	PL B728 562	G. Aad *et al.*	(ATLAS Collab.)
AAD	13AF	PL B721 171	G. Aad *et al.*	(ATLAS Collab.)
AAD	13BB	NJP 15 093011	G. Aad *et al.*	(ATLAS Collab.)
AAD	13D	JHEP 1301 029	G. Aad *et al.*	(ATLAS Collab.)
AAD	13E	PR D87 015010	G. Aad *et al.*	(ATLAS Collab.)
CHATRCHYAN	13A	JHEP 1301 013	S. Chatrchyan *et al.*	(CMS Collab.)
CHATRCHYAN	13AE	PL B720 309	S. Chatrchyan *et al.*	(CMS Collab.)
CHATRCHYAN	13AI	PL B722 28	S. Chatrchyan *et al.*	(CMS Collab.)
CHATRCHYAN	13AJ	PL B723 280	S. Chatrchyan *et al.*	(CMS Collab.)
CHATRCHYAN	13AN	PR D87 052017	S. Chatrchyan *et al.*	(CMS Collab.)
CHATRCHYAN	13AS	PR D87 114015	S. Chatrchyan *et al.*	(CMS Collab.)
CHATRCHYAN	13K	PR D87 032001	S. Chatrchyan *et al.*	(CMS Collab.)
AAD	12AB	PL B712 40	G. Aad *et al.*	(ATLAS Collab.)
AAD	12AO	PRL 108 211802	G. Aad *et al.*	(ATLAS Collab.)
AAD	12AZ	PR D85 072003	G. Aad *et al.*	(ATLAS Collab.)
AAD	12S	PL B708 37	G. Aad *et al.*	(ATLAS Collab.)
CHATRCHYAN	12Z	JHEP 1205 055	S. Chatrchyan *et al.*	(CMS Collab.)
AAD	11	PL B694 327	G. Aad *et al.*	(ATLAS Collab.)
AARON	11C	PL B705 52	F. D. Aaron *et al.*	(H1 Collab.)
ABAZOV	11F	PRL 106 081801	V.M. Abazov *et al.*	(D0 Collab.)
ABDALLAH	11	EPJ C71 1555	J. Abdallah *et al.*	(DELPHI Collab.)
CHATRCHYAN	11X	PL B704 143	S. Chatrchyan *et al.*	(CMS Collab.)
CHATRCHYAN	11Y	PL B704 123	S. Chatrchyan *et al.*	(CMS Collab.)
KHACHATRY...	11F	PRL 106 201804	V. Khachatryan *et al.*	(CMS Collab.)
AALTONEN	10H	PRL 104 091801	T. Aaltonen *et al.*	(CDF Collab.)
ABDALLAH	09	EPJ C60 1	J. Abdallah *et al.*	(DELPHI Collab.)
AARON	08	PL B663 382	F.D. Aaron *et al.*	(H1 Collab.)
AARON	08A	PL B666 131	F.D. Aaron *et al.*	(H1 Collab.)
ABAZOV	08H	PR D77 091102	V.M. Abazov *et al.*	(D0 Collab.)
SCHAEL	07A	EPJ C49 411	S. Schael *et al.*	(ALEPH Collab.)
ABDALLAH	06C	EPJ C45 589	J. Abdallah *et al.*	(DELPHI Collab.)
ABULENCIA	06L	PRL 96 211801	A. Abulencia *et al.*	(CDF Collab.)
ACOSTA	05B	PRL 94 101802	D. Acosta *et al.*	(CDF Collab.)
ABBIENDI	04G	EPJ C33 173	G. Abbiendi *et al.*	(OPAL Collab.)
ABBIENDI	04N	PL B602 167	G. Abbiendi *et al.*	(OPAL Collab.)
ABDALLAH	04N	EPJ C37 405	J. Abdallah *et al.*	(DELPHI Collab.)
ACHARD	03B	PL B568 23	P. Achard *et al.*	(L3 Collab.)
BABICH	03	EPJ C29 103	A.A. Babich *et al.*	
ABBIENDI	02G	PL B544 57	G. Abbiendi *et al.*	(OPAL Collab.)
ACHARD	02D	PL B531 28	P. Achard *et al.*	(L3 Collab.)
ADLOFF	02	PL B525 9	C. Adloff *et al.*	(H1 Collab.)
CHEKANOV	02D	PL B549 32	S. Chekanov *et al.*	(ZEUS Collab.)
AFFOLDER	01I	PRL 87 231803	T. Affolder *et al.*	(CDF Collab.)
BOURILKOV	01	PR D64 071701	D. Bourilkov	
CHEUNG	01B	PL B517 167	K. Cheung	
ACCIARRI	00P	PL B489 81	M. Acciarri *et al.*	(L3 Collab.)
AFFOLDER	00I	PR D62 012004	T. Affolder *et al.*	(CDF Collab.)
BARATE	98U	EPJ C4 571	R. Barate *et al.*	(ALEPH Collab.)
BARGER	98E	PR D57 391	V. Barger *et al.*	
MCFARLAND	98	EPJ C1 509	K.S. McFarland *et al.*	(CCFR/NuTeV Collab.)
DIAZCRUZ	94	PR D49 R2149	J.L. Diaz Cruz, O.A. Sampayo	(CINV)
ABT	93	NP B396 3	I. Abt *et al.*	(H1 Collab.)
ADRIANI	93M	PRPL 236 1	O. Adriani *et al.*	(L3 Collab.)
BARDADIN-...	92	ZPHY C55 163	M. Bardadin-Otwinowska	(CLER)
DECAMP	92	PRPL 216 253	D. Decamp *et al.*	(ALEPH Collab.)
PDG	92	PR D45 S1	K. Hikasa *et al.*	(KEK, LBL, BOST+)
ABREU	91F	NP B367 511	P. Abreu *et al.*	(DELPHI Collab.)
KIM	90	PL B240 243	G.N. Kim *et al.*	(AMY Collab.)
ABE	89B	PRL 62 1825	F. Abe *et al.*	(CDF Collab.)
ABE	89D	PRL 63 1447	F. Abe *et al.*	(CDF Collab.)
ABE	89J	ZPHY C45 175	K. Abe *et al.*	(VENUS Collab.)
ALBAJAR	89	ZPHY C44 15	C. Albajar *et al.*	(UA1 Collab.)
BARGER	89	PL B220 464	V. Barger *et al.*	(WISC, KEK)
DORENBOS...	89	ZPHY C41 567	J. Dorenbosch *et al.*	(CHARM Collab.)
BARTEL	87B	ZPHY C36 15	W. Bartel *et al.*	(JADE Collab.)
GRIFOLS	86	PL 168B 264	J.A. Grifols, S. Peris	(BARC)
JODIDIO	86	PR D34 1967	A. Jodidio *et al.*	(LBL, NWES, TRIU)
Also		PR D37 237 (erratum)	A. Jodidio *et al.*	(LBL, NWES, TRIU)
EICHTEN	84	RMP 56 579	E. Eichten *et al.*	(FNAL, LBL, OSU)
RENARD	82	PL 116B 264	F.M. Renard	(CERN)

Extra Dimensions

For explanation of terms used and discussion of significant model dependence of following limits, see the "Extra Dimensions" review. Footnotes describe originally quoted limit. δ indicates the number of extra dimensions.

Limits not encoded here are summarized in the "Extra Dimensions" review, where the latest unpublished results are also described.

EXTRA DIMENSIONS

Updated October 2013 by John Parsons (Columbia University) and Alex Pomarol (Universitat Autònoma de Barcelona)

I Introduction

Proposals for a spacetime with more than three spatial dimensions date back to the 1920's, mainly through the work of Kaluza and Klein, in an attempt to unify the forces of nature [1]. Although their initial idea failed, the formalism that they and others developed is still useful nowadays. Around 1980, string theory proposed again to enlarge the number of space dimensions, this time as a requirement for describing a consistent theory of quantum gravity. The extra dimensions were supposed to be compactified at a scale close to the Planck scale, and thus not testable experimentally in the near future.

A different approach was given by Arkani-Hamed, Dimopoulos and Dvali (ADD) in their seminal paper in 1998 [2], where they showed that the weakness of gravity could be explained by postulating two or more extra dimensions in which only gravity could propagate. The size of these extra dimensions should range between roughly a millimeter and $\sim$1/TeV, leading to possible observable consequences in current and future experiments. A year later, Randall and Sundrum (RS) [3] found a new possibility using a warped geometry, postulating a five-dimensional Anti-de Sitter (AdS) spacetime with a compactification scale of order TeV. The origin of the smallness of the electroweak scale versus the Planck scale was explained by the gravitational redshift factor present in the warped AdS metric. As in the ADD model, originally only gravity was assumed to propagate in the extra dimensions, although it was soon clear that this was not necessary in warped extra-dimensions and also the SM gauge fields [4] and SM fermions [5,6] could propagate in the five-dimensional space.

The physics of warped extra-dimensional models has an alternative interpretation by means of the AdS/CFT correspondence [7]. Models with warped extra dimensions are related to four-dimensional strongly-interacting theories, allowing an understanding of the properties of five-dimensional fields as those of four-dimensional composite states [8]. This approach has opened new directions for tackling outstanding questions in particle physics, such as the flavor problem, grand unification, and the origin of electroweak symmetry breaking or supersymmetry breaking.

Kaluza-Klein Theories: Field theories with compact extra dimensions can be written as theories in ordinary four dimensions (4D) by performing a Kaluza-Klein (KK) reduction. As an illustration, consider a simple example, namely a field theory of a complex scalar in flat five-dimensional (5D) spacetime. The action will be given by †

$$S_5 = -\int d^4x\, dy\, M_5 \left[|\partial_\mu \phi|^2 + |\partial_y \phi|^2 + \lambda_5 |\phi|^4\right] , \qquad (1)$$

where y refers to the extra (fifth) dimension. A universal scale M_5 has been extracted in front of the action in order to keep the 5D field with the same mass-dimension as in 4D. This theory is perturbative for energies $E \lesssim \ell_5 M_5/\lambda_5$ where $\ell_5 = 24\pi^3$ [9].

Let us now consider that the fifth dimension is compact with the topology of a circle S^1 of radius R, which corresponds to the identification of y with $y + 2\pi R$. In such a case, the 5D complex scalar field can be expanded in a Fourier series:

$$\phi(x,y) = \frac{1}{\sqrt{2\pi R M_5}} \sum_{n=-\infty}^{\infty} e^{iny/R} \phi^{(n)}(x) ,$$

that, inserted in Eq. (1) and integrating over y, gives

$$S_5 = S_4^{(0)} + S_4^{(n)} ,$$

where

$$S_4^{(0)} = -\int d^4x \left[|\partial_\mu \phi^{(0)}|^2 + \lambda_4 |\phi^{(0)}|^4\right] , \text{ and} \qquad (2)$$

$$S_4^{(n)} = -\int d^4x \sum_{n\neq 0} \left[|\partial_\mu \phi^{(n)}|^2 + \left(\frac{n}{R}\right)^2 |\phi^{(n)}|^2\right] + \text{quartic int.}$$

The $n = 0$ mode self-coupling is given by

$$\lambda_4 = \frac{\lambda_5}{2\pi R M_5} . \qquad (3)$$

The above action corresponds to a 4D theory with a massless scalar $\phi^{(0)}$, referred to as the zero-mode, and an infinite tower of massive modes $\phi^{(n)}$, known as KK modes. The KK reduction thus allows a treatment of 5D theories as 4D field theories with an infinite number of fields. At energies smaller than $1/R$, the KK modes can be neglected, leaving the zero-mode action of Eq. (2). The strength of the interaction of the zero-mode, given by Eq. (3), decreases as R increases. Thus, for a large extra dimension $R \gg 1/M_5$, the massless scalar is weakly coupled.

II Large Extra Dimensions for Gravity

II.1 The ADD Scenario

The ADD scenario [2,10,11] assumes a $D = 4 + \delta$ dimensional spacetime, with δ compactified spatial dimensions. The weakness of gravity arises since it propagates in the higher-dimensional space. The SM is assumed to be localized in a 4D subspace, a 3-brane, as can be found in certain string constructions [12]. Gravity is described by the Einstein-Hilbert action in $D = 4 + \delta$ spacetime dimensions

$$S_D = -\frac{\bar{M}_D^{2+\delta}}{2} \int d^4x d^\delta y \sqrt{-g}\mathcal{R} + \int d^4x \sqrt{-g_{\rm ind}}\, \mathcal{L}_{\rm SM} , \qquad (4)$$

where x labels the ordinary four coordinates, y the δ extra coordinates, g refers to the determinant of the D-dimensional

† Our convention for the metric is $\eta_{MN} = \text{Diag}(-1,1,1,1,1)$.

metric whose Ricci scalar is defined by $\mathcal{R}$, and $\bar{M}_D$ is the reduced Planck scale of the D-dimensional theory. In the second term of Eq. (4), which gives the gravitational interactions of SM fields, the D-dimensional metric reduces to the induced metric on the 3-brane where the SM fields propagate. The extra dimensions are assumed to be flat and compactified in a volume V_δ. As an example, consider a toroidal compactification of equal radii R and volume $V_\delta = (2\pi R)^\delta$. After a KK reduction, one finds that the fields that couple to the SM are the spin-2 gravitational field $G_{\mu\nu}(x,y)$ and a tower of spin-1 KK graviscalars [13]. The graviscalars, however, only couple to SM fields through the trace of the energy-momentum tensor, resulting in weaker couplings to the SM fields. The Fourier expansion of the spin-2 field is given by

$$G_{\mu\nu}(x,y) = G^{(0)}_{\mu\nu}(x) + \frac{1}{\sqrt{V_\delta}} \sum_{\vec{n}\neq 0} e^{i\vec{n}\cdot\vec{y}/R} G^{(\vec{n})}_{\mu\nu}(x)\,, \qquad (5)$$

where $\vec{y} = (y_1, y_2, ..., y_\delta)$ are the extra-dimensional coordinates and $\vec{n} = (n_1, n_2, ..., n_\delta)$. Eq. (5) contains a massless state, the 4D graviton, and its KK tower with masses $m^2_{\vec{n}} = |\vec{n}|^2/R^2$. At energies below $1/R$ the action is that of the zero-mode

$$S^{(0)}_4 = -\frac{\bar{M}_D^{2+\delta}}{2} \int d^4x\, V_\delta \sqrt{-g^{(0)}}\mathcal{R}^{(0)} + \int d^4x \sqrt{-g^{(0)}_{\rm ind}}\,\mathcal{L}_{\rm SM}\,,$$

where we can identify the 4D reduced Planck mass, $M_P \equiv G_N/\sqrt{8\pi} \simeq 2.4\times 10^{18}$ GeV, as a function of the D-dimensional parameters:

$$M_P^2 = V^\delta \bar{M}_D^{2+\delta} \equiv R^\delta M_D^{2+\delta}\,. \qquad (6)$$

Fixing M_D at around the electroweak scale $M_D \sim$ TeV to avoid introducing a new mass-scale in the model, Eq. (6) gives a prediction for R:

$$\delta = 1, 2, ..., 6 \;\rightarrow\; R \sim 10^9 \text{ km}\,, 0.5 \text{ mm}\,, ...\,, 0.1 \text{ MeV}^{-1}\,. \qquad (7)$$

The option $\delta = 1$ is clearly ruled out. However this is not the case for $\delta \geq 2$, and possible observable consequences can be sought in present and future experiments.

Consistency of the model requires a stabilization mechanism for the radii of the extra dimensions, to the values shown in Eq. (7). The fact that we need $R \gg 1/M_D$ leads to a new hierarchy problem, the solution of which might require imposing supersymmetry in the extra-dimensional bulk [14].

II.2 Tests of the Gravitational Force Law at Sub-mm Distances

The KK modes of the graviton give rise to deviations from Newton's law of gravitation for distances $\gtrsim 1/R$. Such deviations are usually parametrized by a modified Newtonian potential of the form

$$V(r) = -G_N \frac{m_1 m_2}{r}\left[1 + \alpha\, e^{-r/\lambda}\right]\,. \qquad (8)$$

For a 2-torus compactification, $\alpha = 16/3$ and $\lambda = R$. Searches for deviations from Newton's law of gravitation have been performed in several experiments. Ref. [15] gives the present constraints: $R < 37\mu$m at 95% CL for $\delta = 2$, corresponding to $M_D > 3.6$ TeV.

II.3 Astrophysical and Cosmological Constraints

The light KK gravitons could be copiously produced in stars, carrying away energy. Ensuring that the graviton luminosity is low enough to preserve the agreement of stellar models with observations provides powerful bounds on the scale M_D. The most stringent arises from supernova SN1987A, giving $M_D > 27$ (2.4) TeV for $\delta = 2$ (3) [16]. After a supernova explosion, most of the KK gravitons stay gravitationally trapped in the remnant neutron star. The requirement that neutron stars are not excessively heated by KK decays into photons leads to $M_D > 1700$ (76) TeV for $\delta = 2$ (3) [17].

Cosmological constraints are also quite stringent [18]. To avoid overclosure of the universe by relic gravitons one needs $M_D > 7$ TeV for $\delta = 2$. Relic KK gravitons decaying into photons contribute to the cosmic diffuse gamma radiation, from which one can derive the bound $M_D > 100$ TeV for $\delta = 2$.

We must mention however that bounds coming from the decays of KK gravitons into photons can be reduced if we assume that KK gravitons decay mainly into other non-SM states. This could happen, for example, if there were other 3-branes with hidden sectors residing on them [10].

II.4 Collider Signals

Collider limits on extra-dimensional models are dominated by Run I LHC results, which are based on total integrated luminosities of $\sim$5 fb^{-1} ($\sim$20 fb^{-1}) collected in 2011 (2012) at a center-of-mass energy of 7 (8) TeV. This review focuses on the most recent limits, most of which are 8 TeV preliminary results which can be found on the WWW pages of public results of the ATLAS [19] and CMS [20] experiments; a more complete record of published results can be found in the PDG Listings.

II.4a Graviton and Other Particle Production

Although each KK graviton has a purely gravitational coupling, suppressed by $1/M_P$, inclusive processes in which one sums over the almost continuous spectrum of available gravitons have cross sections suppressed only by powers of M_D. Processes involving gravitons are therefore detectable in collider experiments if $M_D \sim$ TeV. A number of experimental searches for evidence of large extra dimensions have been performed at colliders, and interpreted in the context of the ADD model.

One signature arises from direct graviton emission. By making a derivative expansion of Einstein gravity, one can construct an effective theory, valid for energies much lower than M_D, and use it to make predictions for graviton-emission processes at colliders [13,21,22]. Gravitons produced in the final state would escape detection, giving rise to missing transverse energy ($\not\!\!E_T$). The results quoted below are 95% CL lower limits on M_D for a range of values of δ between 2 and 6, with more stringent limits corresponding to lower δ values.

At hadron colliders, experimentally sensitive channels include the $j + \not\!\!E_T$ and $\gamma + \not\!\!E_T$ final states. At the LHC, using the full 20 fb^{-1} dataset at 8 TeV and assuming k-factors of

1.5 (1.4) for $\delta = 2, 3$ ($\delta = 4 - 6$) to account for next-to-leading order (NLO) contributions to the signal cross sections, CMS sets limits of $M_D > 3.12 - 5.67$ TeV [23] from analyzing the $j + \not{E}_T$ final state. ATLAS $j + \not{E}_T$ results with 10 fb^{-1} of 8 TeV data provide limits of $M_D > 2.58 - 3.88$ TeV [24], using leading order (LO) cross sections. For these $j + \not{E}_T$ analyses, the LHC experiments handle somewhat differently the issue that the effective theory is only valid for energies much less than M_D: CMS suppresses the graviton cross section by a factor $M_D^4/\hat{s}^2$ for $\sqrt{\hat{s}} > M_D$, where $\sqrt{\hat{s}}$ is the parton-level center-of-mass energy of the hard collision. ATLAS considers the impact of simply truncating the differential cross section to remove the contribution from events where $\sqrt{\hat{s}} > M_D$, and shows that the effect of the truncation grows from a negligible impact for $\delta = 2$ up to a 50% reduction in the total cross section for $\delta = 6$. The ATLAS limits are quoted using the full phase space. Less stringent limits are obtained from analyses of the $\gamma + \not{E}_T$ final state, where both ATLAS [25] and CMS [26] have published results using their full 7 TeV datasets of $\sim$5 fb^{-1}.

In models in which the ADD scenario is embedded in a string theory at the TeV scale [12], we expect the string scale M_s to be smaller than M_D, and therefore expect production of string resonances at the LHC [27]. Analysis of the dijet invariant mass distribution has been interpreted by CMS for their 8 TeV data to exclude at 95% CL string excitations of quarks and gluons that decay predominantly to $q + g$ with masses in the range from 1.20 to 5.08 TeV [28]. An ATLAS dijet analysis [29] using a 13 fb^{-1} dataset of 8 TeV collisions provides its results in the context of model-independent limits on the cross section times acceptance for generic resonances of a variety of possible widths.

II.4b Virtual graviton effects

One can also search for virtual graviton effects, the calculation of which however depends on the ultraviolet cut-off of the theory and is therefore very model dependent. In the literature, several different formulations exist [13,22,30] for the dimension-eight operator for gravity exchange at tree level:

$$\mathcal{L}_8 = \pm\frac{4}{M_{TT}^4}\left(T_{\mu\nu}T^{\mu\nu} - \frac{1}{\delta+2}T^{\mu}_{\mu}T^{\nu}_{\nu}\right), \qquad (9)$$

where $T_{\mu\nu}$ is the energy-momentum tensor and M_{TT} is related to M_D by some model-dependent coefficient [31]. The relations with the parametrizations of Refs. [30] and [13] are, respectively, $M_{TT} = M_S$ and $M_{TT} = (2/\pi)^{1/4}\Lambda_T$. The experimental results below are given as 95% CL lower limits on M_{TT}, including in some cases the possibility of both constructive or destructive interference, depending on the sign chosen in Eq. (9).

The most stringent limits arise from the CMS analysis of the dielectron [32] and dimuon [33] final states, using their full sample of 8 TeV collisions; the combined result corresponds to an approximate limit of $M_{TT} > 3.7$ TeV, assuming constructive interference. Using its full dataset at 7 TeV to analyse the $\gamma\gamma$ final state, ATLAS provides limits [34] of $M_{TT} > 2.94$ TeV (2.52 TeV) for constructive (destructive) interference; the ATLAS limit improves to $M_{TT} > 3.14$ TeV for constructive interference when they combine this diphoton result with their 7 TeV dilepton analysis [35].

At the one-loop level, gravitons can also generate dimension-six operators with coefficients that are also model dependent. Experimental bounds on these operators can also give stringent constraints on M_D [31].

II.4c Black Hole Production

The physics at energies $\sqrt{s} \sim M_D$ is sensitive to the details of the unknown quantum theory of gravity. Nevertheless, in the transplanckian regime, $\sqrt{s} \gg M_D$, one can rely on a semiclassical description of gravity to obtain predictions. An interesting feature of transplanckian physics is the creation of black holes [36]. A black hole is expected to be formed in a collision in which the impact parameter is smaller than the Schwarzschild radius [37]:

$$R_S = \frac{1}{M_D}\left[\frac{2^{\delta}\pi^{(\delta-3)/2}}{\delta+2}\Gamma\left(\frac{\delta+3}{2}\right)\frac{M_{BH}}{M_D}\right]^{1/(\delta+1)}, \qquad (10)$$

where M_{BH} is the mass of the black hole, which would roughly correspond to the total energy in the collision. The cross section for black hole production can be estimated to be of the same order as the geometric area $\sigma \sim \pi R_S^2$. For $M_D \sim$ TeV, this gives a production of $\sim 10^7$ black holes at the $\sqrt{s} = 14$ TeV LHC with an integrated luminosity of 30 fb^{-1} [36]. A black hole would provide a striking experimental signature since it is expected to thermally radiate with a Hawking temperature $T_H = (\delta + 1)/(4\pi R_S)$, and therefore would evaporate democratically into all SM states. Nevertheless, given the present constraints on M_D, the LHC will not be able to reach energies much above M_D. This implies that predictions based on the semiclassical approximation could receive sizable modifications from model-dependent quantum-gravity effects.

The most stringent limits on microscopic black holes arise from LHC searches which observed no excesses above the SM background in high-multiplicity final states. The results are usually quoted as model-independent limits on the cross section for new physics in the final state and kinematic region analyzed. These results can then be used to provide constraints of models of low-scale gravity and weakly-coupled string theory. In addition, limits are sometimes quoted on particular implementations of models, which are used as benchmarks to illustrate the sensitivity. For example, the ATLAS analysis [38] of the track multiplicity in same-sign dimuon events, using their full 20 fb^{-1} sample at 8 TeV, excludes semiclassical black holes below masses in the range of 5.1 - 5.7 TeV, fixing $M_D = 1.5$ TeV and depending on details of the model and also the number of extra dimensions. A CMS analysis [39] of multi-object final states using 12 fb^{-1} of 8 TeV data provides similar limits, but extending out to values of $M_D \sim 5$ TeV.

For black hole masses near M_D, the semi-classical approximation is not valid, and one instead expects quantum black

holes that decay primarily into two-body final states [40]. LHC results provide lower limits on quantum black hole masses of order 5 TeV, depending on the details of the model, including from the CMS multi-object analysis [39] and from an ATLAS search in the photon+jet final state [41] using their full 8 TeV dataset.

In weakly-coupled string models the semiclassical description of gravity fails in the energy range between M_s and M_s/g_s^2 where stringy effects are important. In this regime one expects, instead of black holes, the formation of string balls, made of highly excited long strings, that could be copiously produced at the LHC for $M_s \sim$ TeV [42], and would evaporate thermally at the Hagedorn temperature giving rise to high-multiplicity events. The same analyses used to search for black holes can be interpreted in the context of string balls. For example, the ATLAS same-sign dimuon analysis [38] excludes string balls with minimal masses below 5.3 TeV, for the case of $\delta = 6$ and with model parameters fixed to values of $g_s = 0.4$, $M_D = 1.5$ TeV, and $M_s = M_D/1.26 = 1.2$ TeV. The CMS multi-object [39] analysis excludes the production of string balls with a minimum mass below ~ 5.5 TeV for $g_s = 0.4$, M_D in the range of $1.4 - 2.1$ TeV, and $M_s = M_D/1.25$.

III TeV-Scale Extra Dimensions

III.1 Warped Extra Dimensions

The RS model [3] is the most attractive setup of warped extra dimensions at the TeV scale, since it provides an alternative solution to the hierarchy problem. The RS model is based on a 5D theory with the extra dimension compactified in an orbifold, S^1/Z_2, a circle S^1 with the extra identification of y with $-y$. This corresponds to the segment $y \in [0, \pi R]$, a manifold with boundaries at $y = 0$ and $y = \pi R$. Let us now assume that this 5D theory has a cosmological constant in the bulk Λ, and on the two boundaries Λ_0 and $\Lambda_{\pi R}$:

$$S_5 = -\int d^4x\, dy \Big\{ \sqrt{-g} \left[\frac{1}{2} M_5^3 \mathcal{R} + \Lambda \right] + \sqrt{-g_0}\delta(y)\Lambda_0 + \sqrt{-g_{\pi \mathrm{R}}}\delta(y - \pi R)\Lambda_{\pi R} \Big\}, \tag{11}$$

where g_0 and $g_{\pi R}$ are the values of the determinant of the induced metric on the two respective boundaries. Einstein's equations can be solved, giving in this case the metric

$$ds^2 = a(y)^2 dx^\mu dx^\nu \eta_{\mu\nu} + dy^2 \,, \quad a(y) = e^{-ky} \,, \tag{12}$$

where $k = \sqrt{-\Lambda/6M_5^3}$. Consistency of the solution requires $\Lambda_0 = -\Lambda_{\pi R} = -\Lambda/k$. The metric in Eq. (12) corresponds to a 5D AdS space. The factor $a(y)$ is called the "warp" factor and determines how 4D scales change as a function of the position in the extra dimension. In particular, this implies that energy scales for 4D fields localized at the boundary at $y = \pi R$ are red-shifted by a factor $e^{-k\pi R}$ with respect to those localized at $y = 0$. For this reason, the boundaries at $y = 0$ and $y = \pi R$ are usually referred to as the ultraviolet (UV) and infrared (IR) boundaries, respectively.

As in the ADD case, we can perform a KK reduction and obtain the low-energy effective theory of the 4D massless graviton. In this case we obtain

$$M_P^2 = \int_0^{\pi R} dy\, e^{-2ky} M_5^3 = \frac{M_5^3}{2k} \left(1 - e^{-2k\pi R} \right) . \tag{13}$$

Taking $M_5 \sim k \sim M_P$, we can generate an IR-boundary scale of order $ke^{-k\pi R} \sim$ TeV for an extra dimension of radius $R \simeq 11/k$. Mechanisms to stabilize R to this value have been proposed [43] that, contrary to the ADD case, do not require introducing any new small or large parameter. Therefore a natural solution to the hierarchy problem can be achieved in this framework if the Higgs field, whose vacuum expectation value (VEV) is responsible for electroweak symmetry breaking, is localized at the IR-boundary where the effective mass scales are of order TeV.

In the RS model [3], all the SM fields were assumed to be localized on the IR-boundary. Nevertheless, for the hierarchy problem, only the Higgs field has to be localized there. SM gauge bosons and fermions can propagate in the 5D bulk [4,5,6,44]. By performing a KK reduction from the 5D action of a gauge boson, we find [4]

$$\frac{1}{g_4^2} = \int_0^{\pi R} dy\, \frac{1}{g_5^2} = \frac{\pi R}{g_5^2} \,,$$

where g_D ($D = 4, 5$) is the gauge coupling in D-dimensions. Therefore the 4D gauge couplings can be of order one, as is the case of the SM, if one demands $g_5^2 \sim \pi R$. Using $kR \sim 10$ and $g_4 \sim 0.5$, one obtains the 5D gauge coupling

$$g_5 \sim 4/\sqrt{k} \,. \tag{14}$$

Boundary kinetic terms for the gauge bosons can modify this relation, allowing for larger values of $g_5\sqrt{k}$.

Fermions propagating in a warped extra-dimension have 4D massless zero-modes with wavefunctions which vary as $f_0 \sim Exp[(1/2 - c_f)ky]$, where $c_f k$ is their 5D mass [45,6]. Depending on the free parameter $c_f k$, fermions can be localized either towards the UV-boundary ($c_f > 1/2$) or IR-boundary ($c_f < 1/2$). Since the Higgs is localized on the IR-boundary, one can generate exponentially suppressed Yukawa couplings by having the fermion zero-modes localized towards the UV-boundary, generating naturally the light SM fermion spectrum [6]. A large overlap with the wavefunction of the Higgs is needed for the top quark, in order to generate its large mass, thus requiring it to be localized towards the IR-boundary. In conclusion, the large mass hierarchies present in the SM fermion spectrum can be easily obtained in warped models via suitable choices of the order-one parameters c_f [46]. In these scenarios, deviations in flavor physics from the SM predictions are expected to arise from flavor-changing KK gluon couplings [47], putting certain constraints on the parameters of the models and predicting new physics effects to be observed in B-physics processes [48].

The masses of the KK states can also be calculated. One finds [6]

$$m_n \simeq \left(n + \frac{\alpha}{2} - \frac{1}{4}\right) \pi k e^{-\pi k R}, \qquad (15)$$

where $n = 1, 2, ...$ and $\alpha = \{|c_f - 1/2|, 0, 1\}$ for KK fermions, KK gauge bosons and KK gravitons, respectively. Their masses are of order $ke^{-\pi kR} \sim$ TeV; the first KK state of the gauge bosons would be the lightest, while gravitons are expected to be the heaviest.

III.1a Models of Electroweak Symmetry Breaking

Theories in warped extra dimensions can be used to implement symmetry breaking at low energies by boundary conditions [49]. For example, for a $U(1)$ gauge symmetry in the 5D bulk, this can be easily achieved by imposing a Dirichlet boundary condition on the IR-boundary for the gauge-boson field, $A_\mu|_{y=\pi R} = 0$. This makes the zero-mode gauge boson get a mass, given by $m_A = g_4\sqrt{2k/g_5^2}e^{-\pi kR}$. A very different situation occurs if the Dirichlet boundary condition is imposed on the UV-boundary, $A_\mu|_{y=0} = 0$. In this case the zero-mode gauge boson disappears from the spectrum. Finally, if a Dirichlet boundary condition is imposed on the two boundaries, one obtains a massless 4D scalar corresponding to the fifth component of the 5D gauge boson, A_5. Thus, different scenarios can be implemented by appropriately choosing the 5D bulk gauge symmetry, $\mathcal{G}_5$, and the symmetries to which it reduces on the UV and IR-boundary, $\mathcal{H}_{UV}$ and $\mathcal{H}_{IR}$ respectively. In all cases the KK spectrum comes in representations of the group $\mathcal{G}_5$.

The recent discovery of a light Higgs with $m_H \sim 125$ GeV [50] rules out Higgsless 5D models for electroweak symmetry breaking [51]. This discovery however is consistent with 5D composite Higgs model where a light Higgs is present in the spectrum.

Composite Higgs models: Warped extra dimensions can give rise to scenarios, often called gauge-Higgs unified models, where the Higgs appears as the fifth component of a 5D gauge boson, A_5. The Higgs mass is protected by the 5D gauge invariance and can only get a nonzero value from non-local one-loop effects [52]. To guarantee the relation $M_W^2 \simeq M_Z^2 \cos^2\theta_W$, a custodial $SU(2)_V$ symmetry is needed in the bulk and IR-boundary [53]. The simplest realization [54] has

$$\mathcal{G}_5 = SU(3)_c \times SO(5) \times U(1)_X\,,$$
$$\mathcal{H}_{IR} = SU(3)_c \times SO(4) \times U(1)_X\,,$$
$$\mathcal{H}_{UV} = G_{SM}\,.$$

The Higgs gets a potential at the one-loop level that triggers a VEV, breaking the electroweak symmetry. In these models there is a light Higgs whose mass can be around 125 GeV, as required by the recently discovered Higgs boson [50]. This state, as will be explained in Sec. III.2, behaves as a composite pseudo-Goldstone boson with couplings that deviate from the SM Higgs [55]. The lightest KK modes of the model are color fermions with charges $Q = -1/3, 2/3$ and $5/3$ [56].

III.1b Constraints from Electroweak Precision Tests

Models in which the SM gauge bosons propagate in 1/TeV-sized extra dimensions give generically large corrections to electroweak observables. When the SM fermions are confined on a boundary these corrections are universal and can be parametrized by four quantities: $\widehat{S}$, $\widehat{T}$, W and Y, as defined in Ref. [57]. For warped models, where the 5D gauge coupling of Eq. (14) is large, the most relevant parameter is $\widehat{T}$, which gives the bound $m_{KK} \gtrsim 10$ TeV [44]. When a custodial symmetry is imposed [53], the main constraint comes from the $\widehat{S}$ parameter, requiring $m_{KK} \gtrsim 3$ TeV, independent of the value of g_5. Corrections to the $Zb_L\bar{b}_L$ coupling can also be important [44], especially in warped models for electroweak symmetry breaking as the ones described above.

III.1c Kaluza-Klein Searches

The main prediction of 1/TeV-sized extra dimensions is the presence of a discretized KK spectrum, with masses around the TeV scale, associated with the SM fields that propagate in the extra dimension.

In the RS model [3], only gravity propagates in the 5D bulk. Experimental searches have been performed for the lightest KK graviton through its decay to a variety of SM particle-antiparticle pairs. The results are usually interpreted in the plane of the dimensionless coupling k/M_P versus m_1, where M_P is the reduced Planck mass defined previously and m_1 is the mass of the lightest KK excitation of the graviton. Since the AdS curvature $\sim k$ cannot exceed the cut-off scale of the model, which is estimated to be $\ell_5^{1/3}M_5$ [31], one must demand $k \ll \sqrt{2\ell_5}M_P$. The results quoted below are 95% CL lower limits on the KK graviton mass for a coupling $k/M_P = 0.1$.

The most stringent limits currently arise from searches for dilepton resonances, combining results from the ee and $\mu\mu$ final states. The ATLAS dilepton analysis [58] uses their full sample of 8 TeV collisions and excludes gravitons with masses below 2.47 TeV. The CMS dilepton analysis [59] combines the full 7 TeV dataset with the first 4 fb^{-1} of 8 TeV data to exclude graviton masses below 2.39 TeV. The $\gamma\gamma$ final state is quite powerful, with a branching ratio twice that of any individual lepton flavor, plus lower backgrounds. The ATLAS $\gamma\gamma$ analysis [34] using the full dataset at 7 TeV provides, in combination with $ee/\mu\mu$ results of the same 7 TeV dataset, a lower limit on the graviton mass of 2.23 TeV; this result is dominated by the $\gamma\gamma$ channel, which on its own provides a limit of 2.06 TeV. Less stringent limits on the KK graviton mass come from the WW [60,61] and ZZ [62] final states.

In warped extra-dimensional models in which the SM fields propagate in the 5D bulk, the couplings of the KK graviton to $ee/\mu\mu/\gamma\gamma$ are suppressed [63], and the above bounds do not apply. Furthermore, the KK graviton is the heaviest KK state (see Eq. (15)), and therefore experimental searches for KK gauge bosons and fermions are more appropriate discovery channels in these scenarios. For the scenarios discussed above in which only the Higgs and the top quark are localized close to the IR-boundary, the KK gauge bosons mainly decay

into top quarks, longitudinal W/Z bosons, and Higgs bosons. Couplings to light SM fermions are suppressed by a factor $g/\sqrt{g_5^2 k} \sim 0.2$ [6] for the value of Eq. (14) that is considered from now on. Searches have been made for evidence of the lightest KK excitation of the gluon, through its decay to $t\bar{t}$ pairs. The searches need to take into account the natural KK gluon width, which is typically $\sim 15\%$ of its mass. The decay of a heavy particle to $t\bar{t}$ would tend to produce highly boosted (anti-)top quarks in the final state. Products of the subsequent top decays would therefore tend to be close to each other in the detector. In the case of $t \to Wb \to jjb$ decays, the three jets could overlap one another and not be individually reconstructed with the standard jet algorithms, while $t \to Wb \to \ell\nu b$ decays could result in the lepton failing standard isolation cuts due to its proximity to the b-jet; in both cases, the efficiency for properly reconstructing the final state would fall as the mass of the original particle increases. To avoid the loss in sensitivity which would result, a number of techniques, known generally as "top tagging", have been developed to reconstruct and identify highly boosted top quarks, for example by using a single "fat" jet to contain all the decay products of a hadronic top decay. The large backgrounds from QCD jets can then be reduced by requiring the "jet mass" be consistent with that of a top quark, and also by examining the substructure of the large jet for indication that it resulted from the hadronic decay of a top quark. These techniques are key to extending to very high masses the range of accessible resonances decaying to $t\bar{t}$ pairs. The most stringent current limits result from analyses of the lepton-plus-jets channel, with less stringent limits from analyses of the fully hadronic channel. CMS analyses of the lepton-plus-jets [64](fully hadronic [65]) final state using the full 8 TeV dataset of 20 fb^{-1} exclude KK gluons with masses below 2.54 TeV (1.8 TeV), assuming a k-factor of 1.3 (without using the techniques for boosted top reconstruction, the lepton-plus-jets limit would be 1.7 TeV). An ATLAS analysis [66] of the lepton-plus-jets final state, using 14 fb^{-1} of 8 TeV data, excludes KK gluon masses below 2.0 TeV, whereas the ATLAS fully hadronic analysis [67], using the full 7 TeV dataset, yields a lower limit of 1.62 TeV; both of the ATLAS analyses assume LO cross section values. The results are not directly comparable between the two experiments, since they employ in their respective analyses different implementations of the theoretical model.

A gauge boson KK excitation could be also sought through its decay to longitudinal W/Z bosons. While searches for WZ resonances have been used to set limits on sequential SM W' bosons [68] or other models, as yet no WZ experimental results have been interpreted in the context of warped extra dimensions. The decay to a pair of intermediate vector bosons has, however, been exploited to search for KK gravitons in models in which the SM fields propagate in the 5D bulk. ATLAS analyses of the full 5 fb^{-1} dataset at 7 TeV searching for $G^* \to WW \to \ell\nu\ell\nu$ ($\ell\nu qq'$) [60]([61]) exclude gravitons with masses below 0.84 (0.71) TeV, both for $k/M_P = 1.0$ and using LO cross sections. Results from searches for $G^* \to ZZ \to \ell\ell\bar{q}q$ include CMS [69](ATLAS [70]) lower limits on the graviton mass of 0.71 TeV (0.85 TeV) for $k/M_P = 0.5$ (1.0), using 20 fb^{-1} (7 fb^{-1}) of 8 TeV data. CMS has searched, using their full 8 TeV dataset, for $G^* \to WW/ZZ$ in the fully hadronic decay mode [71], reconstructing each hadronic W/Z decay using the boosted techniques mentioned previously; the results, which are approximate since the finite graviton width is not taken into account, are exclusions of the graviton mass in the range between 1 TeV and 1.59 TeV (1.17 TeV) for decays to WW (ZZ), for $k/M_P = 0.1$.

The lightest KK states are, in certain models, the partners of the top quark. For example, in 5D composite Higgs models these are colored states with charges $Q = -1/3, 2/3$ and $5/3$, and masses expected to be below the TeV [56]. They can be either singly- or pair-produced, and mainly decay into a combination of W/Z with top/bottom [72]. Of particular note, the $Q = 5/3$ state decays mainly into $W^+t \to W^+W^+b$, giving a pair of same-sign leptons in the final state. CMS has used a same-sign dilepton analysis [73] of their full 20 fb^{-1} dataset at 8 TeV to search for pair-production of the $Q = 5/3$ state, excluding masses below 770 GeV. A search by ATLAS, using their full 7 TeV dataset and requiring in addition to a pair of same-sign leptons at least one b-tagged jet in the event [74], provides a lower mass limit on the $Q = 5/3$ state of 670 GeV from pair production, and up to 700 GeV from single production, the cross section for which is model-dependent [75]. Both LHC experiments have searched for pair-production of vector-like quarks T and B of charges $Q = 2/3$ and $-1/3$ respectively, assuming the allowable decays are $T \to Wb/Zt/Ht$ and $B \to Wt/Zb/Hb$. In each case, it is assumed the branching ratios of the three decay modes sum to unity, but the individual branching ratios, which are model-dependent, are allowed to vary within this constraint. CMS has performed inclusive searches, using their full 8 TeV data sample, for T [76] and B [77] pair-production, providing lower limits on the masses in the range of $687 - 782$ GeV ($582 - 732$ GeV) for T (B) vector-like quarks, depending on the values of the individual branching ratios. ATLAS has presented results from searches for pair-production of vector-like quarks, with 14 fb^{-1} of 8 TeV data, using same-sign dileptons with b-jets [78] as well as analyses targeting final states that include $Z + b/t$ [79], $H + t$ [80], and $W + b$ [81]; the first two analyses are relevant for both T and B searches, while the latter two apply only for T. The ATLAS results are similar to the CMS limits quoted above, though ATLAS does not provide a statistical combination of their results but has presented summary plots [19] which show the overlap of the separate results as a function of the individual branching ratio values.

III.2 Connection with Strongly-Coupled Models via the AdS/CFT Correspondence

The AdS/CFT correspondence [7] provides a connection between warped extra-dimensional models and strongly-coupled

theories in ordinary 4D. Although the exact connection is only known for certain cases, the AdS/CFT techniques have been very useful to obtain, at the qualitative level, a 4D holographic description of the various phenomena in warped extra-dimensional models [8].

The connection goes as follows. The physics of the bulk AdS_5 models can be interpreted as that of a 4D conformal field theory (CFT) which is strongly-coupled. The extra-dimensional coordinate y plays the role of the renormalization scale μ of the CFT by means of the identification $\mu \equiv ke^{-ky}$. Therefore the UV-boundary corresponds in the CFT to a UV cut-off scale at $\Lambda_{UV} = k \sim M_P$, breaking explicitly conformal invariance, while the IR-boundary can be interpreted as a spontaneous breaking of the conformal symmetry at energies $ke^{-k\pi R} \sim$ TeV. Fields localized on the UV-boundary are elementary fields external to the CFT, while fields localized on the IR-boundary and KK states corresponds to composite resonances of the CFT. Furthermore, local gauge symmetries in the 5D models, $\mathcal{G}_5$, correspond to global symmetries of the CFT, while the UV-boundary symmetry can be interpreted as a gauging of the subgroup $\mathcal{H}_{UV}$ of $\mathcal{G}_5$ in the CFT. Breaking gauge symmetries by IR-boundary conditions corresponds to the spontaneous breaking $\mathcal{G}_5 \to \mathcal{H}_{IR}$ in the CFT at energies $\sim ke^{-k\pi R}$. Using this correspondence one can easily derive the 4D massless spectrum of the compactified AdS_5 models. One also has the identification $k^3/M_5^3 \approx 16\pi^2/N^2$ and $g_5^2 k \approx 16\pi^2/N^r$ ($r = 1$ or 2 for CFT fields in the fundamental or adjoint representation of the gauge group), where N plays the role of the number of colors of the CFT. Therefore the weak-coupling limit in AdS_5 corresponds to a large-N expansion in the CFT.

Following the above AdS/CFT dictionary one can understand the RS solution to the hierarchy problem from a 4D viewpoint. The equivalent 4D model is a CFT with a TeV mass-gap and a Higgs emerging as a composite state. In the particular case where the Higgs is the fifth-component of the gauge-boson, A_5, this corresponds to models, similar to those proposed in Ref. [82], where the Higgs is a composite pseudo-Goldstone boson arising from the spontaneous breaking $\mathcal{G}_5 \to \mathcal{H}_{IR}$ in the CFT. The AdS/CFT dictionary tells us that KK states must behave as composite resonances. For example, if the SM gauge bosons propagate in the 5D bulk, the lowest KK $SU(2)_L$-gauge boson must have properties similar to those of the Techni-rho ρ_T [83] with a coupling to longitudinal W/Z bosons given by $g_5\sqrt{k} \approx g_{\rho_T}$, while the coupling to elementary fermions is $g^2/\sqrt{g_5^2 k} \approx g^2 F_{\rho_T}/M_{\rho_T}$.

Fermions in compactified AdS_5 also have a simple 4D holographic interpretation. The 4D massless mode described in Sec. III.1 corresponds to an external fermion ψ_i linearly coupled to a fermionic CFT operator $\mathcal{O}_i$: $\mathcal{L}_{\rm int} = \lambda_i \bar{\psi}_i \mathcal{O}_i + h.c.$. The dimension of the operator $\mathcal{O}_i$ is related to the 5D fermion mass according to $\mathrm{Dim}[\mathcal{O}_i] = |c_f + 1/2| - 1$. Therefore, by varying c_f one varies $\mathrm{Dim}[\mathcal{O}_i]$, making the coupling λ_i irrelevant ($c_f > 1/2$), marginal ($c_f = 1/2$) or relevant ($c_f < 1/2$). When irrelevant, the coupling is exponentially suppressed at low energies, and then the coupling of ψ_i to the CFT (and eventually to the composite Higgs) is very small. When relevant, the coupling grows in the IR and become as large as g_5 (in units of k), meaning that the fermion is as strongly coupled as the CFT states [54]. In this latter case ψ_i behaves as a composite fermion.

III.3 Flat Extra Dimensions

Models with quantum-gravity at the TeV scale, as in the ADD scenario, can have extra (flat) dimensions of 1/TeV size, as happens in string scenarios [84]. All SM fields may propagate in these extra dimensions, leading to the possibility of observing their corresponding KK states.

A simple example is to assume that the SM gauge bosons propagate in a flat five-dimensional orbifold S^1/Z_2 of radius R, with the fermions localized on a 4D boundary. The KK gauge bosons behave as sequential SM gauge bosons with a coupling to fermions enhanced by a factor $\sqrt{2}$ [84]. The experimental limits on such sequential gauge bosons could therefore be recast as limits on KK gauge bosons. Such an interpretation of the ATLAS 7 TeV dilepton analysis [85] yielded the bound $1/R > 4.16$ TeV. Indirect bounds from LEP2 require however $1/R \gtrsim 6$ TeV [57].

An alternative scenario, known as Universal Extra Dimensions (UED) [86], assumes that all SM fields propagate universally in a flat orbifold S^1/Z_2 with an extra Z_2 parity, called KK-parity, that interchanges the two boundaries. In this case, the lowest KK state is stable and is a Dark Matter candidate. At colliders, KK particles would have to be created in pairs, and would then cascade decay to the lightest KK particle (LKP), which would be stable and escape detection. Experimental signatures, such as jets or leptons and $\not{E}_T$, would be similar to those of typical R-parity conserving SUSY searches. Theoretical studies of the trilepton final state [87] suggest a potential bound from the LHC at 8 TeV with 20 fb^{-1} of $1/R \gtrsim 1.3$ TeV for $\Lambda R = 10$, where Λ is the cut-off scale of the model. The experimental searches have not yet been interpreted in the general UED scenario; for example, the ATLAS trilepton analysis [88] of their full 8 TeV dataset provides upper limits on the visible cross section for new physics that could be utilized to determine UED limits.

Experimental limits have been provided on two specific UED models which include KK parity violation. In one case, KK parity is violated by gravitational interactions [89], and the LKP can decay via $\gamma^* \to \gamma + G$. Beginning with strong production of a pair of KK quarks and/or gluons [90,91], the final state would be $\gamma\gamma + \not{E}_T + X$. Using their full 7 TeV datasets, ATLAS [92] and CMS [93] each determine a limit of $1/R \gtrsim 1.4$ TeV for $\Lambda R = 20$. In a second model, that involves two UEDs, the breaking of the KK parity allows the decay of the KK photon to $t\bar{t}$ [94]. The ATLAS same-sign lepton plus b-jet analysis [74], applied for searches of pair-produced KK photons, excludes KK masses below 0.9 TeV in this model.

Finally, realistic models of electroweak symmetry breaking can also be constructed with flat extra spatial dimensions,

similarly to those in the warped case, requiring, however, the presence of sizeable boundary kinetic terms [95]. There is also the possibility of breaking supersymmetry by boundary conditions [96]. Models of this type could explain naturally the presence of a Higgs boson lighter than $M_D \sim$ TeV [97].

References

1. For a comprehensive collection of the original papers see, "Modern Kaluza-Klein Theories", edited by T. Appelquist *et al.*, Addison-Wesley (1987).
2. N. Arkani-Hamed *et al.*, Phys. Lett. **B429**, 263 (1998).
3. L. Randall and R. Sundrum, Phys. Rev. Lett. **83**, 3370 (1999).
4. H. Davoudiasl *et al.*, Phys. Lett. **B473**, 43 (2000); A. Pomarol, Phys. Lett. **B486**, 153 (2000).
5. S. Chang *et al.*, Phys. Rev. **D62**, 084025 (2000).
6. T. Gherghetta and A. Pomarol, Nucl. Phys. **B586**, 141 (2000).
7. J.M. Maldacena, Adv. Theor. Math. Phys. **2**, 231 (1998); E. Witten, Adv. Theor. Math. Phys. **2**, 253 (1998); S.S. Gubser *et al.*, Phys. Lett. **B428**, 105 (1998).
8. N. Arkani-Hamed *et al.*, JHEP **0108**, 017 (2001).
9. Z. Chacko *et al.*, JHEP **0007**, 036 (2000).
10. N. Arkani-Hamed *et al.*, Phys. Rev. **D59**, 086004 (1999).
11. For a review see for example, R. Rattazzi, hep-ph/0607055 (2006); I. Antoniadis, Yellow report CERN-2002-002 (2002).
12. I. Antoniadis *et al.*, Phys. Lett. **B436**, 257 (1998).
13. G.F. Giudice *et al.*, Nucl. Phys. **B544**, 3 (1999).
14. For the case of two extra dimensions, see for example, N. Arkani-Hamed *et al.*, Phys. Rev. **D62**, 105002 (2000).
15. E.G. Adelberger *et al.*, Prog. Part. Nucl. Phys. **62**, 102 (2009).
16. C. Hanhart *et al.*, Phys. Lett. **B509**, 1 (2001).
17. S. Hannestad and G.G. Raffelt, Phys. Rev. **D67**, 125008 (2003).
18. L.J. Hall and D. Tucker-Smith, Phys. Rev. **D60**, 085008 (1999).
19. ATLAS public results are available on WWW at https://twiki.cern.ch/twiki/bin/view/AtlasPublic.
20. CMS public results are available on WWW at https://twiki.cern.ch/twiki/bin/view/CMSPublic/PhysicsResults.
21. E.A. Mirabelli *et al.*, Phys. Rev. Lett. **82**, 2236 (1999).
22. T. Han *et al.*, Phys. Rev. **D59**, 105006 (1999).
23. CMS Collab., CMS Note PAS-EXO-12-048.
24. ATLAS Collab., ATLAS Note CONF-2012-147.
25. ATLAS Collab., Phys. Rev. Lett. **110**, 011802 (2012).
26. CMS Collab., Phys. Rev. Lett. **108**, 261803 (2012).
27. See for example S. Cullen *et al.*, Phys. Rev. **D62**, 055012 (2000).
28. CMS Collab., CMS Note PAS-EXO-12-059.
29. ATLAS Collab., ATLAS Note CONF-2012-148.
30. J.L. Hewett, Phys. Rev. Lett. **82**, 4765 (1999).
31. G.F. Giudice and A. Strumia, Nucl. Phys. **B663**, 377 (2003).
32. CMS Collab., CMS Note PAS-EXO-12-031.
33. CMS Collab., CMS Note PAS-EXO-12-027.
34. ATLAS Collab., NJP **15**, 043007 (2013).
35. ATLAS Collab. Phys. Rev. **D87**, 015010 (2013).
36. S.B. Giddings and S. Thomas, Phys. Rev. **D65**, 056010 (2002); S. Dimopoulos and G. Landsberg, Phys. Rev. Lett. **87**, 161602 (2001); for a review see for example, P. Kanti, Int. J. Mod. Phys. **A19**, 4899 (2004).
37. R.C. Myers and M.J. Perry, Annals Phys. **172**, 304 (1986).
38. ATLAS Collab., Phys. Rev. **D88**, 072001 (2013).
39. CMS Collab., JHEP **07**, 178 (2013).
40. P. Meade and L. Randall, JHEP **0805**, 003 (2008).
41. ATLAS Collab., arXiv:1309.3230, submitted to PLB.
42. S. Dimopoulos and R. Emparan, Phys. Lett. **B526**, 393 (2002).
43. W.D. Goldberger and M.B. Wise, Phys. Rev. Lett. **83**, 4922 (1999); J. Garriga, A. Pomarol, Phys. Lett. **B560**, 91 (2003).
44. For a review see for example, H. Davoudiasl *et al.*, New J. Phys. **12**, 075011 (2010); T. Gherghetta, arXiv:1008.2570.
45. Y. Grossman and M. Neubert, Phys. Lett. **B474**, 361 (2000).
46. S.J. Huber and Q. Shafi, Phys. Lett. **B498**, 256 (2001).
47. A. Delgado *et al.*, JHEP **0001**, 030 (2000).
48. K. Agashe *et al.*, Phys. Rev. **D71**, 016002 (2005); for a recent analysis see for example, M. Bauer *et al.*, JHEP **1009**, 017 (2010).
49. For a review see for example, A. Pomarol, Int. J. Mod. Phys. **A24**, 61 (2009).
50. See, for example, PDG review of Higgs boson in this volume.
51. C. Csaki *et al.*, Phys. Rev. Lett. **92**, 101802 (2004); for a review see for example, C. Csaki *et al.*, hep-ph/0510275.
52. Y. Hosotani, Phys. Lett. **B126**, 309 (1983).
53. K. Agashe *et al.*, JHEP **0308**, 050 (2003).
54. K. Agashe *et al.*, Nucl. Phys. **B719**, 165 (2005); for a review see for example, R. Contino, arXiv:1005.4269.
55. G. F. Giudice *et al.*, JHEP **0706** (2007) 045.
56. R. Contino *et al.*, Phys. Rev. **D75**, 055014 (2007).
57. R. Barbieri *et al.*, Nucl. Phys. **B703**, 127 (2004).
58. ATLAS Collab., ATLAS Note CONF-2013-017.
59. CMS Collab., Phys. Lett. **B720**, 63 (2013).
60. ATLAS Collab., Phys. Lett. **B718**, 860 (2013).
61. ATLAS Collab., Phys. Rev. **D87**, 112006 (2013).
62. ATLAS Collab., Phys. Lett. **B712**, 331 (2012).
63. K. Agashe *et al.*, Phys. Rev. **D76**, 036006 (2007).
64. CMS Collab., CMS Note PAS-B2G-12-006.
65. CMS Collab., CMS Note PAS-B2G-12-005.
66. ATLAS Collab., ATLAS Note CONF-2013-052.
67. ATLAS Collab., JHEP **1301**, 116 (2013).
68. See, for example, PDG review of W' boson searches in this volume.
69. CMS Collab., CMS Note EXO-12-022.
70. ATLAS Collab., ATLAS Note CONF-2012-150.
71. CMS Collab., CMS Note EXO-12-024.
72. R. Contino and G. Servant, JHEP **0806**, 026 (2008); J.A. Aguilar-Saavedra, JHEP **0911**, 030 (2009); J. Mrazek and A. Wulzer, Phys. Rev. **D81**, 075006 (2010); G. Dissertori *et al.*, JHEP **1009**, 019 (2010).

73. CMS Collab., CMS Note PAS-B2G-12-012.
74. ATLAS Collab., ATLAS Note CONF-2012-130.
75. A. De Simone *et al.*, JHEP **1304**, 004 (2013).
76. CMS Collab., CMS Note PAS-B2G-12-015.
77. CMS Collab., CMS Note PAS-B2G-12-019.
78. ATLAS Collab., ATLAS Note CONF-2013-051.
79. ATLAS Collab., ATLAS Note CONF-2013-056.
80. ATLAS Collab., ATLAS Note CONF-2013-018.
81. ATLAS Collab., ATLAS Note CONF-2013-060.
82. H. Georgi *et al.*, Phys. Lett. **B143**, 152 (1984); D.B. Kaplan *et al.*, Phys. Lett. **B136**, 183 (1984).
83. See, for example, PDG review on *'Dynamical Electroweak Symmetry Breaking'* in this volume.
84. See for example, I. Antoniadis and K. Benakli, Int. J. Mod. Phys. **A15**, 4237 (2000).
85. ATLAS Collab., JHEP **1211**, 138 (2012).
86. T. Appelquist *et al.*, Phys. Rev. **D64**, 035002 (2001); for a review see for example, A. Datta *et al.*, New J. Phys. **12**, 075017 (2010).
87. A. Belyaev *et al.*, JHEP **1306**, 080 (2013).
88. ATLAS Collab., ATLAS Note CONF-2013-070.
89. C. Macesanu, *et al.*, Phys. Lett. **B546**, 253 (2002).
90. C. Macesanu *et al.*, Phys. Rev. **D66**, 015009 (2002).
91. H.C. Cheng *et al.*, Phys. Rev. **D66**, 036005 (2002).
92. ATLAS Collab., Phys. Lett. **B718**, 411 (2012).
93. CMS Collab., JHEP **03**, 111 (2013).
94. G. Burdman *et al.*, Phys. Rev. **D74**, 075008 (2006).
95. For a review see for example, G. Panico *et al.*, JHEP **1102**, 103 (2011).
96. J. Scherk and J.H. Schwarz, Phys. Lett. **B82**, 60 (1979).
97. See for example, A. Pomarol and M. Quiros, Phys. Lett. **B438**, 255 (1998); I. Antoniadis *et al.*, Nucl. Phys. **B544**, 503 (1999); R. Barbieri *et al.*, Phys. Rev. **D63**, 105007 (2001).

CONTENTS:

Limits on R from Deviations in Gravitational Force Law

This section includes limits on the size of extra dimensions from deviations in the Newtonian ($1/r^2$) gravitational force law at short distances. Deviations are parametrized by a gravitational potential of the form $V = -(G\ m\ m'/r)\ [1 + \alpha\ \exp(-r/R)]$. For δ toroidal extra dimensions of equal size, $\alpha = 8\delta/3$. Quoted bounds are for $\delta = 2$ unless otherwise noted.

VALUE (μm)	CL%	DOCUMENT ID		COMMENT
< 30	95	[1] KAPNER	07	Torsion pendulum
• • • We do not use the following data for averages, fits, limits, etc. • • •				
		[2] XU	13	Nuclei properties
		[3] BEZERRA	11	Torsion oscillator
		[4] SUSHKOV	11	Torsion pendulum
		[5] BEZERRA	10	Microcantilever
		[6] MASUDA	09	Torsion pendulum
		[7] GERACI	08	Microcantilever
		[8] TRENKEL	08	Newton's constant
		[9] DECCA	07A	Torsion oscillator
< 47	95	[10] TU	07	Torsion pendulum
		[11] SMULLIN	05	Microcantilever
<130	95	[12] HOYLE	04	Torsion pendulum
		[13] CHIAVERINI	03	Microcantilever
$\lesssim$200	95	[14] LONG	03	Microcantilever
<190	95	[15] HOYLE	01	Torsion pendulum
		[16] HOSKINS	85	Torsion pendulum

[1] KAPNER 07 search for new forces, probing a range of $\alpha \simeq 10^{-3}$–10^{5} and length scales $R \simeq$ 10–1000 μm. For $\delta = 1$ the bound on R is 44 μm. For $\delta = 2$, the bound is expressed in terms of M_*, here translated to a bound on the radius. See their Fig. 6 for details on the bound.

[2] XU 13 obtain constraints on non-Newtonian forces with strengths $|\alpha| \simeq 10^{34}$–10^{36} and length scales $R \simeq$ 1–10 fm. See their Fig. 4 for more details. These constraints do not place limits on the size of extra flat dimensions.

[3] BEZERRA 11 obtain constraints on non-Newtonian forces with strengths $10^{11} \lesssim |\alpha| \lesssim 10^{18}$ and length scales $R =$ 30–1260 nm. See their Fig. 2 for more details. These constraints do not place limits on the size of extra flat dimensions.

[4] SUSHKOV 11 obtain improved limits on non-Newtonian forces with strengths $10^{7} \lesssim |\alpha| \lesssim 10^{11}$ and length scales 0.4 μm $< R <$ 4 μm (95% CL). See their Fig. 2. These bounds do not place limits on the size of extra flat dimensions. However, a model dependent bound of $M_* > 70$ TeV is obtained assuming gauge bosons that couple to baryon number also propagate in $(4 + \delta)$ dimensions.

[5] BEZERRA 10 obtain improved constraints on non-Newtonian forces with strengths $10^{19} \lesssim |\alpha| \lesssim 10^{29}$ and length scales $R =$ 1.6–14 nm (95% CL). See their Fig. 1. This bound does not place limits on the size of extra flat dimensions.

[6] MASUDA 09 obtain improved constraints on non-Newtonian forces with strengths $10^{9} \lesssim |\alpha| \lesssim 10^{11}$ and length scales $R =$ 1.0–2.9 μm (95% CL). See their Fig. 3. This bound does not place limits on the size of extra flat dimensions.

[7] GERACI 08 obtain improved constraints on non-Newtonian forces with strengths $|\alpha| >$ 14,000 and length scales $R =$ 5–15 μm. See their Fig. 9. This bound does not place limits on the size of extra flat dimensions.

[8] TRENKEL 08 uses two independent measurements of Newton's constant G to constrain new forces with strength $|\alpha| \simeq 10^{-4}$ and length scales $R =$ 0.02–1 m. See their Fig. 1. This bound does not place limits on the size of extra flat dimensions.

[9] DECCA 07A search for new forces and obtain bounds in the region with strengths $|\alpha| \simeq 10^{13}$–10^{18} and length scales $R =$ 20–86 nm. See their Fig. 6. This bound does not place limits on the size of extra flat dimensions.

[10] TU 07 search for new forces probing a range of $|\alpha| \simeq 10^{-1}$–10^{5} and length scales $R \simeq$ 20–1000 μm. For $\delta = 1$ the bound on R is 53 μm. See their Fig. 3 for details on the bound.

[11] SMULLIN 05 search for new forces, and obtain bounds in the region with strengths $\alpha \simeq 10^{3}$–10^{8} and length scales $R =$ 6–20 μm. See their Figs. 1 and 16 for details on the bound. This work does not place limits on the size of extra flat dimensions.

[12] HOYLE 04 search for new forces, probing α down to 10^{-2} and distances down to 10μm. Quoted bound on R is for $\delta = 2$. For $\delta = 1$, bound goes to 160 μm. See their Fig. 34 for details on the bound.

[13] CHIAVERINI 03 search for new forces, probing α above 10^{4} and λ down to 3μm, finding no signal. See their Fig. 4 for details on the bound. This bound does not place limits on the size of extra flat dimensions.

[14] LONG 03 search for new forces, probing α down to 3, and distances down to about 10μm. See their Fig. 4 for details on the bound.

[15] HOYLE 01 search for new forces, probing α down to 10^{-2} and distances down to 20μm. See their Fig. 4 for details on the bound. The quoted bound is for $\alpha \geq 3$.

[16] HOSKINS 85 search for new forces, probing distances down to 4 mm. See their Fig. 13 for details on the bound. This bound does not place limits on the size of extra flat dimensions.

Limits on R from On-Shell Production of Gravitons: $\delta = 2$

This section includes limits on on-shell production of gravitons in collider and astrophysical processes. Bounds quoted are on R, the assumed common radius of the flat extra dimensions, for $\delta = 2$ extra dimensions. Studies often quote bounds in terms of derived parameter; experiments are actually sensitive to the masses of the KK gravitons: $m_{\vec{n}} = |\vec{n}|/R$. See the Review on "Extra Dimensions" for details. Bounds are given in μm for $\delta = 2$.

VALUE (μm)	CL%	DOCUMENT ID		TECN	COMMENT
< 23	95	[1] CHATRCHYAN	12AP	CMS	$pp \to jG$
• • • We do not use the following data for averages, fits, limits, etc. • • •					
< 25	95	[2] AAD	13AD	ATLS	$pp \to jG$
< 127	95	[3] AAD	13C	ATLS	$pp \to \gamma G$
< 34.4	95	[4] AAD	13D	ATLS	$pp \to jj$
< 0.0087	95	[5] AJELLO	12	FRMI	Neutron star γ sources
< 92	95	[6] AAD	11S	ATLS	$pp \to jG$
< 72	95	[7] CHATRCHYAN	11U	CMS	$pp \to jG$
< 245	95	[8] AALTONEN	08AC	CDF	$p\overline{p} \to \gamma G, jG$
< 615	95	[9] ABAZOV	08S	D0	$p\overline{p} \to \gamma G$
< 0.916	95	[10] DAS	08		Supernova cooling
< 350	95	[11] ABULENCIA,A	06	CDF	$p\overline{p} \to jG$
< 270	95	[12] ABDALLAH	05B	DLPH	$e^+e^- \to \gamma G$
< 210	95	[13] ACHARD	04E	L3	$e^+e^- \to \gamma G$
< 480	95	[14] ACOSTA	04C	CDF	$\overline{p}p \to jG$
< 0.00038	95	[15] CASSE	04		Neutron star γ sources
< 610	95	[16] ABAZOV	03	D0	$\overline{p}p \to jG$
< 0.96	95	[17] HANNESTAD	03		Supernova cooling
< 0.096	95	[18] HANNESTAD	03		Diffuse γ background
< 0.051	95	[19] HANNESTAD	03		Neutron star γ sources
< 0.00016	95	[20] HANNESTAD	03		Neutron star heating
< 300	95	[21] HEISTER	03C	ALEP	$e^+e^- \to \gamma G$
		[22] FAIRBAIRN	01		Cosmology
< 0.66	95	[23] HANHART	01		Supernova cooling
		[24] CASSISI	00		Red giants
<1300	95	[25] ACCIARRI	99S	L3	$e^+e^- \to ZG$

[1] CHATRCHYAN 12AP search for $pp \to jG$, using 5.0 fb^{-1} of data at $\sqrt{s} = 7$ TeV to place bounds on M_D for two to six extra dimensions, from which this bound on R is derived. See their Table 7 for bounds on all $\delta \leq 6$.

[2] AAD 13AD search for $pp \to jG$, using 4.7 fb^{-1} of data at $\sqrt{s} = 7$ TeV to place bounds on M_D for two to six extra dimensions, from which this bound on R is derived. See their Table 8 for bounds on all $\delta \leq 6$.

[3] AAD 13C search for $pp \to \gamma G$, using 4.6 fb^{-1} of data at $\sqrt{s} = 7$ TeV to place bounds on M_D for two to six extra dimensions, from which this bound on R is derived.

[4] AAD 13D search for the dijet decay of quantum black holes in 4.8 fb^{-1} of data produced in pp collisions at $\sqrt{s} = 7$ TeV to place bounds on M_D for two to seven extra dimensions, from which these bounds on R are derived. Limits on M_D for all $\delta \leq 7$ are given in their Table 3.

[5] AJELLO 12 obtain a limit on R from the gamma-ray emission of point γ sources that arise from the photon decay of KK gravitons which are gravitationally bound around neutron stars. Limits for all $\delta \leq 7$ are given in their Table 7.

[6] AAD 11S search for $pp \to jG$, using 33 pb^{-1} of data at $\sqrt{s} = 7$ TeV, to place bounds on M_D for two to four extra dimensions, from which these bounds on R are derived. See their Table 3 for bounds on all $\delta \leq 4$.

[7] CHATRCHYAN 11U search for $pp \to jG$, using 36 pb^{-1} of data at $\sqrt{s} = 7$ TeV, to place bounds on M_D for two to six extra dimensions, from which these bounds on R are derived. See their Table 3 for bounds on all $\delta \leq 6$.

[8] AALTONEN 08AC search for $p\overline{p} \to \gamma G$ and $p\overline{p} \to jG$ at $\sqrt{s} = 1.96$ TeV with 2.0 fb^{-1} and 1.1 fb^{-1} respectively, in order to place bounds on the fundamental scale and size of the extra dimensions. See their Table III for limits on all $\delta \leq 6$.

[9] ABAZOV 08S search for $p\overline{p} \to \gamma G$, using 1 fb^{-1} of data at $\sqrt{s} = 1.96$ TeV to place bounds on M_D for two to eight extra dimensions, from which these bounds on R are derived. See their paper for intermediate values of δ.

[10] DAS 08 obtain a limit on R from Kaluza-Klein graviton cooling of SN1987A due to plasmon-plasmon annihilation.

[11] ABULENCIA,A 06 search for $p\overline{p} \to jG$ using 368 pb^{-1} of data at $\sqrt{s} = 1.96$ TeV. See their Table II for bounds for all $\delta \leq 6$.

[12] ABDALLAH 05B search for $e^+e^- \to \gamma G$ at $\sqrt{s} = 180$–209 GeV to place bounds on the size of extra dimensions and the fundamental scale. Limits for all $\delta \leq 6$ are given in their Table 6. These limits supersede those in ABREU 00Z.

[13] ACHARD 04E search for $e^+e^- \to \gamma G$ at $\sqrt{s} = 189$–209 GeV to place bounds on the size of extra dimensions and the fundamental scale. See their Table 8 for limits with $\delta \leq 8$. These limits supersede those in ACCIARRI 99R.

[14] ACOSTA 04C search for $\overline{p}p \to jG$ at $\sqrt{s} = 1.8$ TeV to place bounds on the size of extra dimensions and the fundamental scale. See their paper for bounds on $\delta = 4, 6$.

[15] CASSE 04 obtain a limit on R from the gamma-ray emission of point γ sources that arises from the photon decay of gravitons around newly born neutron stars, applying the technique of HANNESTAD 03 to neutron stars in the galactic bulge. Limits for all $\delta \leq 7$ are given in their Table I.

[16] ABAZOV 03 search for $p\overline{p} \to jG$ at $\sqrt{s}$=1.8 TeV to place bounds on M_D for 2 to 7 extra dimensions, from which these bounds on R are derived. See their paper for bounds on intermediate values of δ. We quote results without the approximate NLO scaling introduced in the paper.

[17] HANNESTAD 03 obtain a limit on R from graviton cooling of supernova SN1987a. Limits for all $\delta \leq 7$ are given in their Tables V and VI.

[18] HANNESTAD 03 obtain a limit on R from gravitons emitted in supernovae and which subsequently decay, contaminating the diffuse cosmic γ background. Limits for all $\delta \leq 7$ are given in their Tables V and VI. These limits supersede those in HANNESTAD 02.

[19] HANNESTAD 03 obtain a limit on R from gravitons emitted in two recent supernovae and which subsequently decay, creating point γ sources. Limits for all $\delta \leq 7$ are given in their Tables V and VI. These limits are corrected in the published erratum.

[20] HANNESTAD 03 obtain a limit on R from the heating of old neutron stars by the surrounding cloud of trapped KK gravitons. Limits for all $\delta \leq 7$ are given in their Tables V and VI. These limits supersede those in HANNESTAD 02.

[21] HEISTER 03C use the process $e^+e^- \to \gamma G$ at $\sqrt{s} = 189$–209 GeV to place bounds on the size of extra dimensions and the scale of gravity. See their Table 4 for limits with $\delta \leq 6$ for derived limits on M_D.

[22] FAIRBAIRN 01 obtains bounds on R from over production of KK gravitons in the early universe. Bounds are quoted in paper in terms of fundamental scale of gravity. Bounds depend strongly on temperature of QCD phase transition and range from $R < 0.13\ \mu$m to 0.001 μm for δ=2; bounds for δ=3,4 can be derived from Table 1 in the paper.

[23] HANHART 01 obtain bounds on R from limits on graviton cooling of supernova SN 1987a using numerical simulations of proto-neutron star neutrino emission.

[24] CASSISI 00 obtain rough bounds on M_D (and thus R) from red giant cooling for δ=2,3. See their paper for details.

[25] ACCIARRI 99S search for $e^+e^- \to ZG$ at $\sqrt{s}$=189 GeV. Limits on the gravity scale are found in their Table 2, for $\delta \leq 4$.

Mass Limits on M_{TT}

This section includes limits on the cut-off mass scale, M_{TT}, of dimension-8 operators from KK graviton exchange in models of large extra dimensions. Ambiguities in the UV-divergent summation are absorbed into the parameter λ, which is taken to be $\lambda = \pm 1$ in the following analyses. Bounds for $\lambda = -1$ are shown in parenthesis after the bound for $\lambda = +1$, if appropriate. Different papers use slightly different definitions of the mass scale. The definition used here is related to another popular convention by $M_{TT}^4 = (2/\pi)\,\Lambda_T^4$, as discussed in the above Review on "Extra Dimensions."

VALUE (TeV)		CL%	DOCUMENT ID		TECN	COMMENT
> 3.2		95	[1] AAD	13E	ATLS	$pp \to e^+e^-, \mu^+\mu^-, \gamma\gamma$
• • • We do not use the following data for averages, fits, limits, etc. • • •						
> 2.94	(>2.52)	95	[2] AAD	13AS	ATLS	$pp \to \gamma\gamma$
> 2.66	(>2.27)	95	[3] AAD	12Y	ATLS	$pp \to \gamma\gamma$
			[4] BAAK	12	RVUE	Electroweak
> 2.86		95	[5] CHATRCHYAN	12J	CMS	$pp \to e^+e^-, \mu^+\mu^-$
> 2.84	(>2.41)	95	[6] CHATRCHYAN	12R	CMS	$pp \to \gamma\gamma$
> 0.90	(>0.92)	95	[7] AARON	11C	H1	$e^\pm p \to e^\pm X$
> 1.74	(>1.71)	95	[8] CHATRCHYAN	11A	CMS	$pp \to \gamma\gamma$
> 1.48		95	[9] ABAZOV	09AE	D0	$p\overline{p} \to$ dijet, ang. distrib.
> 1.45		95	[10] ABAZOV	09D	D0	$p\overline{p} \to e^+e^-, \gamma\gamma$
> 1.1	(> 1.0)	95	[11] SCHAEL	07A	ALEP	$e^+e^- \to e^+e^-$
> 0.898	(> 0.998)	95	[12] ABDALLAH	06C	DLPH	$e^+e^- \to \ell^+\ell^-$
> 0.853	(> 0.939)	95	[13] GERDES	06		$p\overline{p} \to e^+e^-, \gamma\gamma$
> 0.96	(> 0.93)	95	[14] ABAZOV	05V	D0	$p\overline{p} \to \mu^+\mu^-$
> 0.78	(> 0.79)	95	[15] CHEKANOV	04B	ZEUS	$e^\pm p \to e^\pm X$
> 0.805	(> 0.956)	95	[16] ABBIENDI	03D	OPAL	$e^+e^- \to \gamma\gamma$
> 0.7	(> 0.7)	95	[17] ACHARD	03D	L3	$e^+e^- \to ZZ$
> 0.82	(> 0.78)	95	[18] ADLOFF	03	H1	$e^\pm p \to e^\pm X$
> 1.28	(> 1.25)	95	[19] GIUDICE	03	RVUE	
>20.6	(> 15.7)	95	[20] GIUDICE	03	RVUE	Dim-6 operators
> 0.80	(> 0.85)	95	[21] HEISTER	03C	ALEP	$e^+e^- \to \gamma\gamma$
> 0.84	(> 0.99)	95	[22] ACHARD	02D	L3	$e^+e^- \to \gamma\gamma$
> 1.2	(> 1.1)	95	[23] ABBOTT	01	D0	$p\overline{p} \to e^+e^-, \gamma\gamma$
> 0.60	(> 0.63)	95	[24] ABBIENDI	00R	OPAL	$e^+e^- \to \mu^+\mu^-$
> 0.63	(> 0.50)	95	[24] ABBIENDI	00R	OPAL	$e^+e^- \to \tau^+\tau^-$
> 0.68	(> 0.61)	95	[24] ABBIENDI	00R	OPAL	$e^+e^- \to \mu^+\mu^-, \tau^+\tau^-$
			[25] ABREU	00A	DLPH	$e^+e^- \to \gamma\gamma$
> 0.680	(> 0.542)	95	[26] ABREU	00S	DLPH	$e^+e^- \to \mu^+\mu^-, \tau^+\tau^-$
> 15–28		99.7	[27] CHANG	00B	RVUE	Electroweak
> 0.98		95	[28] CHEUNG	00	RVUE	$e^+e^- \to \gamma\gamma$
> 0.29–0.38		95	[29] GRAESSER	00	RVUE	$(g-2)_\mu$
> 0.50–1.1		95	[30] HAN	00	RVUE	Electroweak
> 2.0	(> 2.0)	95	[31] MATHEWS	00	RVUE	$\overline{p}p \to jj$
> 1.0	(> 1.1)	95	[32] MELE	00	RVUE	$e^+e^- \to VV$
			[33] ABBIENDI	99P	OPAL	
			[34] ACCIARRI	99M	L3	
			[35] ACCIARRI	99S	L3	
> 1.412	(> 1.077)	95	[36] BOURILKOV	99		$e^+e^- \to e^+e^-$

[1] AAD 13E use 4.9 and 5.0 fb^{-1} of data from pp collisions at $\sqrt{s} = 7$ TeV in the dielectron and dimuon channels, respectively, to place lower limits on M_{TT} (equivalent to their M_S). The dielectron and dimuon channels are combined with previous results in the diphoton channel to set the best limit. Bounds on individual channels and different priors can be found in their Table VIII.

[2] AAD 13AS use 4.9 fb^{-1} of data from pp collisions at $\sqrt{s} = 7$ TeV to place lower limits on M_{TT} (equivalent to their M_S).

[3] AAD 12Y use 2.12 fb^{-1} of data from pp collisions at $\sqrt{s} = 7$ TeV to place lower limits on M_{TT} (equivalent to their M_S).

[4] BAAK 12 use electroweak precision observables to place bounds on the ratio Λ_T/M_D as a function of M_D. See their Fig. 22 for constraints with a Higgs mass of 120 GeV.

[5] CHATRCHYAN 12J use approximately 2 fb^{-1} of data from pp collisions at $\sqrt{s} = 7$ TeV in the dielectron and dimuon channels to place lower limits on Λ_T, here converted to M_{TT}.

[6] CHATRCHYAN 12R use 2.2 fb^{-1} of data from pp collisions at $\sqrt{s} = 7$ TeV to place lower limits on M_{TT} (equivalent to their M_S).

[7] AARON 11C search for deviations in the differential cross section of $e^\pm p \to e^\pm X$ in 446 pb^{-1} of data taken at $\sqrt{s} = 301$ and 319 GeV to place a bound on M_{TT}.

[8] CHATRCHYAN 11A use 36 pb^{-1} of data from pp collisions at $\sqrt{s} = 7$ TeV to place lower limits on Λ_T, here converted to M_{TT}.

[9] ABAZOV 09AE use dijet angular distributions in 0.7 fb^{-1} of data from $p\overline{p}$ collisions at $\sqrt{s} = 1.96$ TeV to place lower bounds on Λ_T (equivalent to their M_S), here converted to M_{TT}.

[10] ABAZOV 09D use 1.05 fb^{-1} of data from $p\overline{p}$ collisions at $\sqrt{s} = 1.96$ TeV to place lower bounds on Λ_T (equivalent to their M_s), here converted to M_{TT}.

[11] SCHAEL 07A use e^+e^- collisions at $\sqrt{s} = 189$–209 GeV to place lower limits on Λ_T, here converted to limits on M_{TT}.

[12] ABDALLAH 06C use e^+e^- collisions at $\sqrt{s} \sim 130$–207 GeV to place lower limits on M_{TT}, which is equivalent to their definition of M_S. Bound shown includes all possible final state leptons, $\ell = e, \mu, \tau$. Bounds on individual leptonic final states can be found in their Table 31.

[13] GERDES 06 use 100 to 110 pb^{-1} of data from $p\overline{p}$ collisions at $\sqrt{s} = 1.8$ TeV, as recorded by the CDF Collaboration during Run I of the Tevatron. Bound shown includes a K-factor of 1.3. Bounds on individual e^+e^- and $\gamma\gamma$ final states are found in their Table I.

[14] ABAZOV 05V use 246 pb^{-1} of data from $p\overline{p}$ collisions at $\sqrt{s} = 1.96$ TeV to search for deviations in the differential cross section to $\mu^+\mu^-$ from graviton exchange.

[15] CHEKANOV 04B search for deviations in the differential cross section of $e^\pm p \to e^\pm X$ with 130 pb^{-1} of combined data and Q^2 values up to 40,000 GeV^2 to place a bound on M_{TT}.

[16] ABBIENDI 03D use e^+e^- collisions at $\sqrt{s}$=181–209 GeV to place bounds on the ultraviolet scale M_{TT}, which is equivalent to their definition of M_s.

[17] ACHARD 03D look for deviations in the cross section for $e^+e^- \to ZZ$ from $\sqrt{s} =$ 200–209 GeV to place a bound on M_{TT}.

[18] ADLOFF 03 search for deviations in the differential cross section of $e^\pm p \to e^\pm X$ at $\sqrt{s}$=301 and 319 GeV to place bounds on M_{TT}.

[19] GIUDICE 03 review existing experimental bounds on M_{TT} and derive a combined limit.

[20] GIUDICE 03 place bounds on Λ_6, the coefficient of the gravitationally-induced dimension-6 operator $(2\pi\lambda/\Lambda_6^2)(\sum \overline{f}\gamma_\mu\gamma^5 f)(\sum \overline{f}\gamma^\mu\gamma^5 f)$, using data from a variety of experiments. Results are quoted for $\lambda = \pm 1$ and are independent of δ.

[21] HEISTER 03C use e^+e^- collisions at $\sqrt{s}$= 189–209 GeV to place bounds on the scale of dim-8 gravitational interactions. Their $M_s^\pm$ is equivalent to our M_{TT} with $\lambda = \pm 1$.

[22] ACHARD 02 search for s-channel graviton exchange effects in $e^+e^- \to \gamma\gamma$ at E_{cm} = 192–209 GeV.
[23] ABBOTT 01 search for variations in differential cross sections to e^+e^- and $\gamma\gamma$ final states at the Tevatron.
[24] ABBIENDI 00R uses e^+e^- collisions at $\sqrt{s}$= 189 GeV.
[25] ABREU 00A search for s-channel graviton exchange effects in $e^+e^- \to \gamma\gamma$ at E_{cm}= 189–202 GeV.
[26] ABREU 00S uses e^+e^- collisions at $\sqrt{s}$=183 and 189 GeV. Bounds on μ and τ individual final states given in paper.
[27] CHANG 00B derive 3σ limit on M_{TT} of (28,19,15) TeV for δ=(2,4,6) respectively assuming the presence of a torsional coupling in the gravitational action. Highly model dependent.
[28] CHEUNG 00 obtains limits from anomalous diphoton production at OPAL due to graviton exchange. Original limit for δ=4. However, unknown UV theory renders δ dependence unreliable. Original paper works in HLZ convention.
[29] GRAESSER 00 obtains a bound from graviton contributions to $g-2$ of the muon through loops of 0.29 TeV for δ=2 and 0.38 TeV for δ=4,6. Limits scale as $\lambda^{1/2}$. However calculational scheme not well-defined without specification of high-scale theory. See the "Extra Dimensions Review."
[30] HAN 00 calculates corrections to gauge boson self-energies from KK graviton loops and constrain them using S and T. Bounds on M_{TT} range from 0.5 TeV (δ=6) to 1.1 TeV (δ=2); see text. Limits have strong dependence, $\lambda^{\delta+2}$, on unknown λ coefficient.
[31] MATHEWS 00 search for evidence of graviton exchange in CDF and DØ dijet production data. See their Table 2 for slightly stronger δ-dependent bounds. Limits expressed in terms of $\tilde{M}_S^4 = M_{TT}^4/8$.
[32] MELE 00 obtains bound from KK graviton contributions to $e^+e^- \to VV$ (V=γ,W,Z) at LEP. Authors use Hewett conventions.
[33] ABBIENDI 99P search for s-channel graviton exchange effects in $e^+e^- \to \gamma\gamma$ at E_{cm}=189 GeV. The limits $G_+ > 660$ GeV and $G_- > 634$ GeV are obtained from combined E_{cm}=183 and 189 GeV data, where $G_\pm$ is a scale related to the fundamental gravity scale.
[34] ACCIARRI 99M search for the reaction $e^+e^- \to \gamma G$ and s-channel graviton exchange effects in $e^+e^- \to \gamma\gamma$, W^+W^-, ZZ, e^+e^-, $\mu^+\mu^-$, $\tau^+\tau^-$, $q\overline{q}$ at E_{cm}=183 GeV. Limits on the gravity scale are listed in their Tables 1 and 2.
[35] ACCIARRI 99S search for the reaction $e^+e^- \to ZG$ and s-channel graviton exchange effects in $e^+e^- \to \gamma\gamma$, W^+W^-, ZZ, e^+e^-, $\mu^+\mu^-$, $\tau^+\tau^-$, $q\overline{q}$ at E_{cm}=189 GeV. Limits on the gravity scale are listed in their Tables 1 and 2.
[36] BOURILKOV 99 performs global analysis of LEP data on e^+e^- collisions at $\sqrt{s}$=183 and 189 GeV. Bound is on Λ_T.

Limits on $1/R = M_c$

This section includes limits on $1/R = M_c$, the compactification scale in models with one TeV-sized extra dimension, due to exchange of Standard Model KK excitations. Bounds assume fermions are not in the bulk, unless stated otherwise. See the "Extra Dimensions" review for discussion of model dependence.

VALUE (TeV)	CL%	DOCUMENT ID		TECN	COMMENT
>4.16	95	[1] AAD	12CC	ATLS	$pp \to \ell\overline{\ell}$
>6.1		[2] BARBIERI	04	RVUE	Electroweak
• • • We do not use the following data for averages, fits, limits, etc. • • •					
	95	[3] CHATRCHYAN	13AQ	CMS	$pp \to \ell X$
>1.38	95	[4] CHATRCHYAN	13W	CMS	$pp \to \gamma\gamma$, δ=6, M_D=5 TeV
>0.715	95	[5] EDELHAUSER	13	RVUE	$pp \to \ell\overline{\ell} + X$
>1.40	95	[6] AAD	12CP	ATLS	$pp \to \gamma\gamma$, δ=6, M_D=5 TeV
>1.23	95	[7] AAD	12X	ATLS	$pp \to \gamma\gamma$, δ=6, M_D=5 TeV
>0.26	95	[8] ABAZOV	12M	D0	$p\overline{p} \to \mu\mu$
>0.75	95	[9] BAAK	12	RVUE	Electroweak
		[10] FLACKE	12	RVUE	Electroweak
>0.43	95	[11] NISHIWAKI	12	RVUE	$H \to WW, \gamma\gamma$
>0.729	95	[12] AAD	11F	ATLS	$pp \to \gamma\gamma$, δ=6, M_D=5 TeV
>0.961	95	[13] AAD	11X	ATLS	$pp \to \gamma\gamma$, δ=6, M_D=5 TeV
>0.477	95	[14] ABAZOV	10P	D0	$p\overline{p} \to \gamma\gamma$, δ=6, M_D=5 TeV
>1.59	95	[15] ABAZOV	09AE	D0	$p\overline{p} \to$ dijet, angular dist.
>0.6	95	[16] HAISCH	07	RVUE	$\overline{B} \to X_s\gamma$
>0.6	90	[17] GOGOLADZE	06	RVUE	Electroweak
>3.3	95	[18] CORNET	00	RVUE	Electroweak
> 3.3–3.8	95	[19] RIZZO	00	RVUE	Electroweak

[1] AAD 12CC use 4.9 and 5.0 fb^{-1} of data from pp collisions at $\sqrt{s}$ = 7 TeV in the dielectron and dimuon channels, respectively, to place a lower bound on the mass of the lightest KK Z/γ boson (equivalent to $1/R = M_c$). The limit quoted here assumes a flat prior corresponding to when the pure Z/γ KK cross section term dominates. See their Section 15 for more details.
[2] BARBIERI 04 use electroweak precision observables to place a lower bound on the compactification scale $1/R$. Both the gauge bosons and the Higgs boson are assumed to propagate in the bulk.
[3] CHATRCHYAN 13AQ use 5.0 fb^{-1} of data from pp collisions at $\sqrt{s}$ = 7 TeV and a further 3.7 fb^{-1} of data at $\sqrt{s}$ = 8 TeV to place a lower bound on the compactification scale $1/R$, in models with universal extra dimensions and Standard Model fields propagating in the bulk. See their Fig. 5 for the bound as a function of the universal bulk fermion mass parameter μ.
[4] CHATRCHYAN 13W use diphoton events with large missing transverse momentum in 4.93 fb^{-1} of data produced from pp collisions at $\sqrt{s}$ = 7 TeV to place a lower bound on the compactification scale in a universal extra dimension model with gravitational decays. The bound assumes that the cutoff scale Λ, for the radiative corrections to the Kaluza-Klein masses, satisfies $\Lambda/M_c = 20$. The model parameters are chosen such that the decay $\gamma^* \to G\gamma$ occurs with an appreciable branching fraction.
[5] EDELHAUSER 13 use 19.6 and 20.6 fb^{-1} of data from pp collisions at $\sqrt{s}$ = 8 TeV analyzed by the CMS Collaboration in the dielectron and dimuon channels, respectively, to place a lower bound on the mass of the second lightest Kaluza-Klein Z/γ boson (converted to a limit on $1/R = M_c$). The bound assumes Standard Model fields propagating in the bulk and that the cutoff scale Λ, for the radiative corrections to the Kaluza-Klein masses, satisfies $\Lambda/M_c = 20$.
[6] AAD 12CP use diphoton events with large missing transverse momentum in 4.8 fb^{-1} of data produced from pp collisions at $\sqrt{s}$ = 7 TeV to place a lower bound on the compactification scale in a universal extra dimension model with gravitational decays. The bound assumes that the cutoff scale Λ, for the radiative corrections to the Kaluza-Klein masses, satisfies $\Lambda/M_c = 20$. The model parameters are chosen such that the decay $\gamma^* \to G\gamma$ occurs with an appreciable branching fraction.
[7] AAD 12X use diphoton events with large missing transverse momentum in 1.07 fb^{-1} of data produced from pp collisions at $\sqrt{s}$ = 7 TeV to place a lower bound on the compactification scale in a universal extra dimension model with gravitational decays. The bound assumes that the cutoff scale Λ, for the radiative corrections to the Kaluza-Klein masses, satisfies $\Lambda/M_c = 20$. The model parameters are chosen such that the decay $\gamma^* \to G\gamma$ occurs with an appreciable branching fraction.
[8] ABAZOV 12M use same-sign dimuon events in 7.3 fb^{-1} of data from $p\overline{p}$ collisions at $\sqrt{s}$ = 1.96 TeV to place a lower bound on the compactification scale $1/R$, in models with universal extra dimensions where all Standard Model fields propagate in the bulk.
[9] BAAK 12 use electroweak precision observables to place a lower bound on the compactification scale $1/R$, in models with universal extra dimensions and Standard Model fields propagating in the bulk. Bound assumes a 125 GeV Higgs mass. See their Fig. 25 for the bound as a function of the Higgs mass.
[10] FLACKE 12 use electroweak precision observables to place a lower bound on the compactification scale $1/R$, in models with universal extra dimensions and Standard Model fields propagating in the bulk. See their Fig. 1 for the bound as a function of the universal bulk fermion mass parameter μ.
[11] NISHIWAKI 12 use up to 2 fb^{-1} of data from the ATLAS and CMS experiments that constrains the production cross section of a Higgs-like particle to place a lower bound on the compactification scale $1/R$ in universal extra dimension models. The quoted bound assumes Standard Model fields propagating in the bulk and a 125 GeV Higgs mass. See their Fig. 1 for the bound as a function of the Higgs mass.
[12] AAD 11F use diphoton events with large missing transverse energy in 3.1 pb^{-1} of data produced from pp collisions at $\sqrt{s}$ = 7 TeV to place a lower bound on the compactification scale in a universal extra dimension model with gravitational decays. The bound assumes that the cutoff scale Λ, for the radiative corrections to the Kaluza-Klein masses, satisfies $\Lambda/M_c = 20$. The model parameters are chosen such that the decay $\gamma^* \to G\gamma$ occurs with an appreciable branching fraction.
[13] AAD 11X use diphoton events with large missing transverse energy in 36 pb^{-1} of data produced from pp collisions at $\sqrt{s}$ = 7 TeV to place a lower bound on the compactification scale in a universal extra dimension model with gravitational decays. The bound assumes that the cutoff scale Λ, for the radiative corrections to the Kaluza-Klein masses, satisfies $\Lambda/M_c = 20$. The model parameters are chosen such that the decay $\gamma^* \to G\gamma$ occurs with an appreciable branching fraction.
[14] ABAZOV 10P use diphoton events with large missing transverse energy in 6.3 fb^{-1} of data produced from $p\overline{p}$ collisions at $\sqrt{s}$ = 1.96 TeV to place a lower bound on the compactification scale in a universal extra dimension model with gravitational decays. The bound assumes that the cutoff scale Λ, for the radiative corrections to the Kaluza-Klein masses, satisfies Λ/M_c=20. The model parameters are chosen such that the decay $\gamma^* \to G\gamma$ occurs with an appreciable branching fraction.
[15] ABAZOV 09AE use dijet angular distributions in 0.7 fb^{-1} of data from $p\overline{p}$ collisions at $\sqrt{s}$ = 1.96 TeV to place a lower bound on the compactification scale.
[16] HAISCH 07 use inclusive $\overline{B}$-meson decays to place a Higgs mass independent bound on the compactification scale $1/R$ in the minimal universal extra dimension model.
[17] GOGOLADZE 06 use electroweak precision observables to place a lower bound on the compactification scale in models with universal extra dimensions. Bound assumes a 115 GeV Higgs mass. See their Fig. 3 for the bound as a function of the Higgs mass.
[18] CORNET 00 translates a bound on the coefficient of the 4-fermion operator $(\overline{\ell}\gamma_\mu\tau^a\ell)(\overline{\ell}\gamma^\mu\tau^a\ell)$ derived by Hagiwara and Matsumoto into a limit on the mass scale of KK W bosons.
[19] RIZZO 00 obtains limits from global electroweak fits in models with a Higgs in the bulk (3.8 TeV) or on the standard brane (3.3 TeV).

Limits on Kaluza-Klein Gravitons in Warped Extra Dimensions

This sections places limits on the mass of the first Kaluza-Klein (KK) excitation of the graviton in the warped extra dimension model of Randall and Sundrum. Bounds in parenthesis assume Standard Model fields propagate in the bulk. Experimental bounds depend strongly on the warp parameter, k. See the "Extra Dimensions" review for a full discussion.

Here we list limits for the value of the warp parameter $k/\overline{M}_P = 0.1$.

VALUE (GeV)		CL%	DOCUMENT ID		TECN	COMMENT
>2160		95	[1] AAD	12CC	ATLS	$pp \to G \to \ell\overline{\ell}$
• • • We do not use the following data for averages, fits, limits, etc. • • •						
>1230	(>840)	95	[2] AAD	13A	ATLS	$pp \to G \to WW$
>2230		95	[3] AAD	13AS	ATLS	$pp \to \gamma\gamma$, e^+e^-, $\mu^+\mu^-$
>2390		95	[4] CHATRCHYAN	13AF	CMS	$pp \to e^+e^-$, $\mu^+\mu^-$
			[5] CHATRCHYAN	13U	CMS	$pp \to G \to ZZ$
> 845		95	[6] AAD	12AD	ATLS	$pp \to G \to ZZ$
>1950		95	[7] AAD	12Y	ATLS	$pp \to \gamma\gamma$, e^+e^-, $\mu^+\mu^-$
			[8] AALTONEN	12V	CDF	$p\overline{p} \to G \to ZZ$
			[9] BAAK	12	RVUE	Electroweak
>1840		95	[10] CHATRCHYAN	12R	CMS	$pp \to G \to \gamma\gamma$
>1630		95	[11] AAD	11AD	ATLS	$pp \to G \to \ell\overline{\ell}$
			[12] AALTONEN	11G	CDF	$p\overline{p} \to G \to ZZ$
>1058		95	[13] AALTONEN	11R	CDF	$p\overline{p} \to G \to e^+e^-, \gamma\gamma$
> 754		95	[14] ABAZOV	11H	D0	$p\overline{p} \to G \to WW$
>1079		95	[15] CHATRCHYAN	11	CMS	$pp \to G \to \ell\overline{\ell}$
> 607			[16] AALTONEN	10N	CDF	$p\overline{p} \to G \to WW$
>1050			[17] ABAZOV	10F	D0	$p\overline{p} \to G \to e^+e^-, \gamma\gamma$
			[18] AALTONEN	08S	CDF	$p\overline{p} \to G \to ZZ$
> 900			[19] ABAZOV	08J	D0	$p\overline{p} \to G \to e^+e^-, \gamma\gamma$
			[20] AALTONEN	07G	CDF	$p\overline{p} \to G \to \gamma\gamma$
> 889			[21] AALTONEN	07H	CDF	$p\overline{p} \to G \to e\overline{e}$
> 785			[22] ABAZOV	05N	D0	$p\overline{p} \to G \to \ell\ell, \gamma\gamma$
> 710			[23] ABULENCIA	05A	CDF	$p\overline{p} \to G \to \ell\overline{\ell}$

[1] AAD 12CC use 4.9 and 5.0 fb^{-1} of data from pp collisions at $\sqrt{s}$ = 7 TeV in the dielectron and dimuon channels, respectively, to place a lower bound on the mass of the lightest KK graviton. See their Figure 5 for limits on the lightest KK graviton mass as a function of $k/\overline{M}_P$.

[2] AAD 13A use 4.7 fb^{-1} of data from pp collisions at $\sqrt{s}$ = 7 TeV to place a lower bound on the mass of the lightest KK graviton.

[3] AAD 13AS use 4.9 fb^{-1} of data from pp collisions at $\sqrt{s}$ = 7 TeV in the diphoton channel to place lower limits on the mass of the lightest KK graviton. The diphoton channel is combined with previous results in the dielectron and dimuon channels to set the best limit. See their Table 2 for warp parameter values $k/\overline{M}_P$ between 0.01 and 0.1.

[4] CHATRCHYAN 13AF use 5.3 and 4.1 fb^{-1} of data from pp collisions at $\sqrt{s}$ = 7 TeV and 8 TeV, respectively, in the dielectron and dimuon channels, to place a lower bound on the mass of the lightest KK graviton.

[5] CHATRCHYAN 13U use 5 fb^{-1} of data from pp collisions at $\sqrt{s}$ = 7 TeV to search for KK gravitons in a warped extra dimension decaying to ZZ dibosons. See their Figure 5 for limits on the lightest KK graviton mass as a function of $k/\overline{M}_P$.

[6] AAD 12AD use 1.02 fb^{-1} of data from pp collisions at $\sqrt{s}$ = 7 TeV to search for KK gravitons in a warped extra dimension decaying to ZZ dibosons in the $lljj$ and $llll$ channels (ℓ=e, μ). The limit is quoted for the combined $lljj + llll$ channels. See their Figure 5 for limits on the cross section $\sigma(G \rightarrow ZZ)$ as a function of the graviton mass.

[7] AAD 12Y use 2.12 fb^{-1} of data from pp collisions at $\sqrt{s}$ = 7 TeV in the diphoton channel to place lower limits on the mass of the lightest KK graviton. The diphoton channel is combined with previous results in the dielectron and dimuon channels to set the best limit. See their Table 3 for warp parameter values $k/\overline{M}_P$ between 0.01 and 0.1.

[8] AALTONEN 12V use 6 fb^{-1} of data from $p\overline{p}$ collisions at $\sqrt{s}$ = 1.96 TeV to search for KK gravitons in a warped extra dimension decaying to ZZ dibosons in the $lljj$ and $llll$ channels (ℓ=e, μ). It provides improved limits over the previous analysis in AALTONEN 11G. See their Figure 16 for limits from all channels combined on the cross section times branching ratio $\sigma(p\overline{p} \rightarrow G^* \rightarrow ZZ)$ as a function of the graviton mass.

[9] BAAK 12 use electroweak precision observables to place a lower bound on the compactification scale $k\, e^{-\pi k R}$, assuming Standard Model fields propagate in the bulk and the Higgs is confined to the IR brane. See their Fig. 27 for more details.

[10] CHATRCHYAN 12R use 2.2 fb^{-1} of data from pp collisions at $\sqrt{s}$ = 7 TeV in the diphoton channel to place lower limits on the mass of the lightest KK graviton. See their Table III for warp parameter values $k/\overline{M}_P$ between 0.01 and 0.1.

[11] AAD 11AD use 1.08 and 1.21 fb^{-1} of data from pp collisions at $\sqrt{s}$ = 7 TeV in the dielectron and dimuon channels, respectively, to place a lower bound on the mass of the lightest graviton. For warp parameter values $k/\overline{M}_P$ between 0.01 to 0.1 the lower limit on the mass of the lightest graviton is between 0.71 and 1.63 TeV. See their Table IV for more details.

[12] AALTONEN 11G use 2.5–2.9 fb^{-1} of data from $p\overline{p}$ collisions at $\sqrt{s}$ = 1.96 TeV to search for KK gravitons in a warped extra dimension decaying to ZZ dibosons via the $eeee$, $ee\mu\mu$, $\mu\mu\mu\mu$, $eejj$, and $\mu\mu jj$ channels. See their Fig. 20 for limits on the cross section $\sigma(G \rightarrow ZZ)$ as a function of the graviton mass.

[13] AALTONEN 11R uses 5.7 fb^{-1} of data from $p\overline{p}$ collisions at $\sqrt{s}$ = 1.96 TeV in the dielectron channel to place a lower bound on the mass of the lightest graviton. It provides combined limits with the diphoton channel analysis of AALTONEN 11U. For warp parameter values $k/\overline{M}_P$ between 0.01 to 0.1 the lower limit on the mass of the lightest graviton is between 612 and 1058 GeV. See their Table I for more details.

[14] ABAZOV 11H use 5.4 fb^{-1} of data from $p\overline{p}$ collisions at $\sqrt{s}$ = 1.96 TeV to place a lower bound on the mass of the lightest graviton. Their 95% C.L. exclusion limit does not include masses less than 300 GeV.

[15] CHATRCHYAN 11 use 35 and 40 pb^{-1} of data from pp collisions at $\sqrt{s}$ = 7 TeV in the dielectron and dimuon channels, respectively, to place a lower bound on the mass of the lightest graviton. For a warp parameter value $k/\overline{M}_P$ = 0.05, the lower limit on the mass of the lightest graviton is 0.855 TeV.

[16] AALTONEN 10N use 2.9 fb^{-1} of data from $p\overline{p}$ collisions at $\sqrt{s}$ = 1.96 TeV to place a lower bound on the mass of the lightest graviton.

[17] ABAZOV 10F use 5.4 fb^{-1} of data from $p\overline{p}$ collisions at $\sqrt{s}$ = 1.96 TeV to place a lower bound on the mass of the lightest graviton. For warp parameter values of $k/\overline{M}_P$ between 0.01 and 0.1 the lower limit on the mass of the lightest graviton is between 560 and 1050 GeV. See their Fig. 3 for more details.

[18] AALTONEN 08S use $p\overline{p}$ collisions at $\sqrt{s}$ = 1.96 TeV to search for KK gravitons in warped extra dimensions. They search for graviton resonances decaying to four electrons via two Z bosons using 1.1 fb^{-1} of data. See their Fig. 8 for limits on $\sigma \cdot B(G \rightarrow ZZ)$ versus the graviton mass.

[19] ABAZOV 08J use $p\overline{p}$ collisions at $\sqrt{s}$ = 1.96 TeV to search for KK gravitons in warped extra dimensions. They search for graviton resonances decaying to electrons and photons using 1 fb^{-1} of data. For warp parameter values of $k/\overline{M}_P$ between 0.01 and 0.1 the lower limit on the mass of the lightest excitation is between 300 and 900 GeV. See their Fig. 4 for more details.

[20] AALTONEN 07G use $p\overline{p}$ collisions at $\sqrt{s}$ = 1.96 TeV to search for KK gravitons in warped extra dimensions. They search for graviton resonances decaying to photons using 1.2 fb^{-1} of data. For warp parameter values of $k/\overline{M}_P$ = 0.1, 0.05, and 0.01 the bounds on the graviton mass are 850, 694, and 230 GeV, respectively. See their Fig. 3 for more details. See also AALTONEN 07H.

[21] AALTONEN 07H use $p\overline{p}$ collisions at $\sqrt{s}$ = 1.96 TeV to search for KK gravitons in warped extra dimensions. They search for graviton resonances decaying to electrons using 1.3 fb^{-1} of data. For a warp parameter value of $k/\overline{M}_P$ = 0.1 the bound on the graviton mass is 807 GeV. See their Fig. 4 for more details. A combined analysis with the diphoton data of AALTONEN 07G yields for $k/\overline{M}_P$ = 0.1 a graviton mass lower bound of 889 GeV.

[22] ABAZOV 05N use $p\overline{p}$ collisions at $\sqrt{s}$ = 1.96 TeV to search for KK gravitons in warped extra dimensions. They search for graviton resonances decaying to muons, electrons or photons, using 260 pb^{-1} of data. For warp parameter values of $k/\overline{M}_P$ = 0.1, 0.05, and 0.01, the bounds on the graviton mass are 785, 650 and 250 GeV respectively. See their Fig. 3 for more details.

[23] ABULENCIA 05A use $p\overline{p}$ collisions at $\sqrt{s}$ = 1.96 TeV to search for KK gravitons in warped extra dimensions. They search for graviton resonances decaying to muons or electrons, using 200 pb^{-1} of data. For warp parameter values of $k/\overline{M}_P$ = 0.1, 0.05, and 0.01, the bounds on the graviton mass are 710, 510 and 170 GeV respectively.

Limits on Kaluza-Klein Gluons in Warped Extra Dimensions

This section places limits on the mass of the first Kaluza-Klein (KK) excitation of the gluon in warped extra dimension models with Standard Model fields propagating in the bulk. Bounds are given for a specific benchmark model with Γ/m = 15.3% where Γ is the width and m the mass of the KK gluon. See the "Extra Dimensions" review for more discussion.

VALUE (TeV)	CL%	DOCUMENT ID		TECN	COMMENT
• • • We do not use the following data for averages, fits, limits, etc. • • •					
>2.07	95	[1] AAD	13AQ	ATLS	$g_{KK} \rightarrow t\overline{t} \rightarrow \ell j$
>2.5	95	[2] CHATRCHYAN	13BM	CMS	$g_{KK} \rightarrow t\overline{t}$
		[3] CHEN	13A		$\overline{B} \rightarrow X_s\gamma$
>1.5	95	[4] AAD	12BV	ATLS	$g_{KK} \rightarrow t\overline{t} \rightarrow \ell j$

[1] AAD 13AQ use 4.7 fb^{-1} of data from pp collisions at $\sqrt{s}$ = 7 TeV.

[2] CHATRCHYAN 13BM use 19.7 fb^{-1} of data from pp collisions at $\sqrt{s}$ = 8 TeV. Bound is for a width of approximately 15–20% of the KK gluon mass.

[3] CHEN 13A place limits on the KK mass scale for a specific warped model with custodial symmetry and bulk fermions. See their Figures 4 and 5.

[4] AAD 12BV use 2.05 fb^{-1} of data from pp collisions at $\sqrt{s}$ = 7 TeV.

REFERENCES FOR Extra Dimensions

AAD	13A	PL B718 860	G. Aad *et al.*	(ATLAS Collab.)
AAD	13AD	JHEP 1304 075	G. Aad *et al.*	(ATLAS Collab.)
AAD	13AQ	PR D88 012004	G. Aad *et al.*	(ATLAS Collab.)
AAD	13AS	NJP 15 043007	G. Aad *et al.*	(ATLAS Collab.)
AAD	13C	PRL 110 011802	G. Aad *et al.*	(ATLAS Collab.)
AAD	13D	JHEP 1301 029	G. Aad *et al.*	(ATLAS Collab.)
AAD	13E	PR D87 015010	G. Aad *et al.*	(ATLAS Collab.)
CHATRCHYAN	13AF	PL B720 63	S. Chatrchyan *et al.*	(CMS Collab.)
CHATRCHYAN	13AQ	PR D87 072005	S. Chatrchyan *et al.*	(CMS Collab.)
CHATRCHYAN	13BM	PRL 111 211804	S. Chatrchyan *et al.*	(CMS Collab.)
CHATRCHYAN	13U	JHEP 1302 036	S. Chatrchyan *et al.*	(CMS Collab.)
CHATRCHYAN	13W	JHEP 1303 111	S. Chatrchyan *et al.*	(CMS Collab.)
CHEN	13A	CP C37 063102	J-B. Chen *et al.*	(DALI)
EDELHAUSER	13	JHEP 1308 091	L. Edelhauser, T. Flacke, M. Kramer	(AACH, KAIST)
XU	13	JP G40 035107	J. Xu *et al.*	
AAD	12AD	PL B712 331	G. Aad *et al.*	(ATLAS Collab.)
AAD	12BV	JHEP 1209 041	G. Aad *et al.*	(ATLAS Collab.)
AAD	12CC	JHEP 1211 138	G. Aad *et al.*	(ATLAS Collab.)
AAD	12CP	PL B718 411	G. Aad *et al.*	(ATLAS Collab.)
AAD	12X	PL B710 519	G. Aad *et al.*	(ATLAS Collab.)
AAD	12Y	PL B710 538	G. Aad *et al.*	(ATLAS Collab.)
AALTONEN	12V	PR D85 012008	T. Aaltonen *et al.*	(CDF Collab.)
ABAZOV	12M	PRL 108 131802	V.M. Abazov *et al.*	(D0 Collab.)
AJELLO	12	JCAP 1202 012	M. Ajello *et al.*	(Fermi-LAT Collab.)
BAAK	12	EPJ C72 2003	M. Baak *et al.*	(Gfitter Group)
CHATRCHYAN	12AP	JHEP 1209 094	S. Chatrchyan *et al.*	(CMS Collab.)
CHATRCHYAN	12J	PL B711 15	S. Chatrchyan *et al.*	(CMS Collab.)
CHATRCHYAN	12R	PRL 108 111801	S. Chatrchyan *et al.*	(CMS Collab.)
FLACKE	12	PR D85 126007	T. Flacke, C. Pasold	(WURZ)
NISHIWAKI	12	PL B707 506	K. Nishiwaki *et al.*	(KOBE, OSAK)
AAD	11AD	PRL 107 272002	G. Aad *et al.*	(ATLAS Collab.)
AAD	11F	PRL 106 121803	G. Aad *et al.*	(ATLAS Collab.)
AAD	11S	PL B705 294	G. Aad *et al.*	(ATLAS Collab.)
AAD	11X	EPJ C71 1744	G. Aad *et al.*	(ATLAS Collab.)
AALTONEN	11G	PR D83 112008	T. Aaltonen *et al.*	(CDF Collab.)
AALTONEN	11R	PRL 107 051801	T. Aaltonen *et al.*	(CDF Collab.)
AALTONEN	11U	PR D83 011102	T. Aaltonen *et al.*	(CDF Collab.)
AARON	11C	PL B705 52	F. D. Aaron *et al.*	(H1 Collab.)
ABAZOV	11H	PRL 107 011801	V. M. Abazov *et al.*	(D0 Collab.)
BEZERRA	11	PR D83 075004	V.B. Bezerra *et al.*	
CHATRCHYAN	11	JHEP 1105 093	S. Chatrchyan *et al.*	(CMS Collab.)
CHATRCHYAN	11A	JHEP 1105 085	S. Chatrchyan *et al.*	(CMS Collab.)
CHATRCHYAN	11U	PRL 107 201804	S. Chatychyan *et al.*	(CMS Collab.)
SUSHKOV	11	PRL 107 171101	A.O. Sushkov *et al.*	
AALTONEN	10N	PRL 104 241801	T. Aaltonen *et al.*	(CDF Collab.)
ABAZOV	10F	PRL 104 241802	V.M. Abazov *et al.*	(D0 Collab.)
ABAZOV	10P	PRL 105 221802	V.M. Abazov *et al.*	(D0 Collab.)
BEZERRA	10	PR D81 055003	V.B. Bezerra *et al.*	
ABAZOV	09AE	PRL 103 191803	V.M. Abazov *et al.*	(D0 Collab.)
ABAZOV	09D	PRL 102 051601	V.M. Abazov *et al.*	(D0 Collab.)
MASUDA	09	PRL 102 171101	M. Masuda, M. Sasaki	(ICRR)
AALTONEN	08AC	PRL 101 181602	T. Aaltonen *et al.*	(CDF Collab.)
AALTONEN	08S	PR D78 012008	T. Aaltonen *et al.*	(CDF Collab.)
ABAZOV	08J	PRL 100 091802	V.M. Abazov *et al.*	(D0 Collab.)
ABAZOV	08S	PRL 101 011601	V.M. Abazov *et al.*	(D0 Collab.)
DAS	08	PR D78 063011	P.K. Das, V.H.S. Kumar, P.K. Suresh	
GERACI	08	PR D78 022002	A.A. Geraci *et al.*	(STAN)
TRENKEL	08	PR D77 122001	C. Trenkel	
AALTONEN	07G	PRL 99 171801	T. Aaltonen *et al.*	(CDF Collab.)
AALTONEN	07H	PRL 99 171802	T. Aaltonen *et al.*	(CDF Collab.)
DECCA	07A	EPJ C51 963	R.S. Decca *et al.*	
HAISCH	07	PR D76 034014	U. Haisch, A. Weiler	
KAPNER	07	PRL 98 021101	D.J. Kapner *et al.*	
SCHAEL	07A	EPJ C49 411	S. Schael *et al.*	(ALEPH Collab.)
TU	07	PRL 98 201101	L.-C. Tu *et al.*	
ABDALLAH	06C	EPJ C45 589	J. Abdallah *et al.*	(DELPHI Collab.)
ABULENCIA,A	06	PRL 97 171802	A. Abulencia *et al.*	(CDF Collab.)
GERDES	06	PR D73 112008	D. Gerdes *et al.*	
GOGOLADZE	06	PR D74 093012	I. Gogoladze, C. Macesanu	
ABAZOV	05N	PRL 95 091801	V.M. Abazov *et al.*	(D0 Collab.)
ABAZOV	05V	PRL 95 161602	V.M. Abazov *et al.*	(D0 Collab.)
ABDALLAH	05B	EPJ C38 395	J. Abdallah *et al.*	(DELPHI Collab.)
ABULENCIA	05A	PRL 95 252001	A. Abulencia *et al.*	(CDF Collab.)
SMULLIN	05	PR D72 122001	S.J. Smullin *et al.*	
ACHARD	04E	PL B587 16	P. Achard *et al.*	(L3 Collab.)
ACOSTA	04C	PRL 92 121802	D. Acosta *et al.*	(CDF Collab.)
BARBIERI	04	NP B703 127	R. Barbieri *et al.*	
CASSE	04	PRL 92 111102	M. Casse *et al.*	
CHEKANOV	04B	PL B591 23	S. Chekanov *et al.*	(ZEUS Collab.)
HOYLE	04	PR D70 042004	C.D. Hoyle *et al.*	(WASH)
ABAZOV	03	PRL 90 251802	V.M. Abazov *et al.*	(D0 Collab.)
ABBIENDI	03D	EPJ C26 331	G. Abbiendi *et al.*	(OPAL Collab.)
ACHARD	03D	PL B572 133	P. Achard *et al.*	(L3 Collab.)
ADLOFF	03	PL B568 35	C. Adloff *et al.*	(H1 Collab.)
CHIAVERINI	03	PRL 90 151101	J. Chiaverini *et al.*	
GIUDICE	03	NP B663 377	G.F. Giudice, A. Strumia	
HANNESTAD	03	PR D67 125008	S. Hannestad, G.G. Raffelt	
Also		PR D69 029901(errat)	S. Hannestad, G.G. Raffelt	
HEISTER	03C	EPJ C28 1	A. Heister *et al.*	(ALEPH Collab.)
LONG	03	Nature 421 922	J.C. Long *et al.*	
ACHARD	02	PL B524 65	P. Achard *et al.*	(L3 Collab.)

ACHARD	02D	PL B531 28	P. Achard *et al.*	(L3 Collab.)
HANNESTAD	02	PRL 88 071301	S. Hannestad, G. Raffelt	
ABBOTT	01	PRL 86 1156	B. Abbott *et al.*	(D0 Collab.)
FAIRBAIRN	01	PL B508 335	M. Fairbairn	
HANHART	01	PL B509 1	C. Hanhart *et al.*	
HOYLE	01	PRL 86 1418	C.D. Hoyle *et al.*	
ABBIENDI	00R	EPJ C13 553	G. Abbiendi *et al.*	(OPAL Collab.)
ABREU	00A	PL B491 67	P. Abreu *et al.*	(DELPHI Collab.)
ABREU	00S	PL B485 45	P. Abreu *et al.*	(DELPHI Collab.)
ABREU	00Z	EPJ C17 53	P. Abreu *et al.*	(DELPHI Collab.)
CASSISI	00	PL B481 323	S. Cassisi *et al.*	
CHANG	00B	PRL 85 3765	L.N. Chang *et al.*	
CHEUNG	00	PR D61 015005	K. Cheung	
CORNET	00	PR D61 037701	F. Cornet, M. Relano, J. Rico	
GRAESSER	00	PR D61 074019	M.L. Graesser	
HAN	00	PR D62 125018	T. Han, D. Marfatia, R.-J. Zhang	
MATHEWS	00	JHEP 0007 008	P. Mathews, S. Raychaudhuri, K. Sridhar	
MELE	00	PR D61 117901	S. Mele, E. Sanchez	
RIZZO	00	PR D61 016007	T.G. Rizzo, J.D. Wells	
ABBIENDI	99P	PL B465 303	G. Abbiendi *et al.*	(OPAL Collab.)
ACCIARRI	99M	PL B464 135	M. Acciarri *et al.*	(L3 Collab.)
ACCIARRI	99R	PL B470 268	M. Acciarri *et al.*	(L3 Collab.)
ACCIARRI	99S	PL B470 281	M. Acciarri *et al.*	(L3 Collab.)
BOURILKOV	99	JHEP 9908 006	D. Bourilkov	
HOSKINS	85	PR D32 3084	J.K. Hoskins *et al.*	

WIMPs and Other Particles Searches for

OMITTED FROM SUMMARY TABLE

WIMPS AND OTHER PARTICLE SEARCHES

Revised August 2013 by K. Hikasa (Tohoku University).

We collect here those searches which do not appear in any of the above search categories. These are listed in the following order:

1. Galactic WIMP (weakly-interacting massive particle) searches
2. Concentration of stable particles in matter
3. General new physics searches
4. Limits on jet-jet resonance in hadron collisions
5. Limits on neutral particle production at accelerators
6. Limits on charged particles in e^+e^- collisions
7. Limits on charged particles in hadron reactions
8. Limits on charged particles in cosmic rays
9. Searches for quantum black hole production

Note that searches appear in separate sections elsewhere for Higgs bosons (and technipions), other heavy bosons (including W_R, W', Z', leptoquarks, axigluons), axions (including pseudo-Goldstone bosons, Majorons, familons), heavy leptons, heavy neutrinos, free quarks, monopoles, supersymmetric particles, and compositeness. We include specific WIMP searches in the appropriate sections when they yield limits on hypothetical particles such as supersymmetric particles, axions, massive neutrinos, monopoles, *etc.*

We omit papers on CHAMP's, millicharged particles, and other exotic particles. We no longer list for limits on tachyons and centauros. See our 1994 edition for these limits.

GALACTIC WIMP SEARCHES

These limits are for weakly-interacting stable particles that may constitute the invisible mass in the galaxy. Unless otherwise noted, a local mass density of 0.3 GeV/cm^3 is assumed; see each paper for velocity distribution assumptions. In the papers the limit is given as a function of the X^0 mass. Here we list limits only for typical mass values of 20 GeV, 100 GeV, and 1 TeV. Specific limits on supersymmetric dark matter particles may be found in the Supersymmetry section.

Limits for Spin-Independent Cross Section of Dark Matter Particle (X^0) on Nucleon

Isoscalar coupling is assumed to extract the limits from those on X^0–nuclei cross section.

For m_{X^0} = 20 GeV

VALUE (pb)	CL%	DOCUMENT ID		TECN	COMMENT
• • • We do not use the following data for averages, fits, limits, etc. • • •					
$<1.08\times10^{-4}$	90	[1] AARTSEN	13	ICCB	H, solar ν
$<1.5\times10^{-5}$	90	[2] ABE	13B	XMAS	Xe
$<3\times10^{-6}$	90	[3] AGNESE	13	CDM2	Si
$<3.5\times10^{-6}$	90	[4] AGNESE	13A	CDM2	Si
$<2.5\times10^{-6}$	90	[5] AGNESE	13A	CDM2	Si
$<5\times10^{-5}$	90	[6] LI	13B	TEXO	Ge
		[7] ZHAO	13	CDEX	Ge
$<1.2\times10^{-7}$	90	AKIMOV	12	ZEP3	Xe
		[8] ANGLOHER	12	CRES	$CaWO_4$
$<8\times10^{-6}$	90	[9] ANGLOHER	12	CRES	$CaWO_4$
$<7\times10^{-9}$	90	APRILE	12	X100	Xe
		[10] ARCHAMBAU..	12	PICA	F (C_4F_{10})
$<7\times10^{-7}$	90	[11] ARMENGAUD	12	EDE2	Ge
		[12] BARRETO	12	DMIC	CCD
$<1\times10^{-6}$	90	BEHNKE	12	COUP	CF_3I
$<7\times10^{-6}$		[13] FELIZARDO	12	SMPL	C_2ClF_5
$<1.5\times10^{-6}$	90	KIM	12	KIMS	CsI
$<5\times10^{-5}$	90	[14] AALSETH	11	CGNT	Ge
		[15] AALSETH	11A	CGNT	Ge
		[16] AHMED	11	CDM2	Ge, inelastic
$<2.7\times10^{-7}$	90	[17] AHMED	11A	RVUE	Ge
		[18] AHMED	11B	CDM2	Ge, low threshold
$<3\times10^{-6}$	90	[19] ANGLE	11	XE10	Xe
$<7\times10^{-8}$	90	[20] APRILE	11	X100	Xe
		[21] APRILE	11A	X100	Xe, inelastic
$<2\times10^{-8}$	90	APRILE	11B	X100	Xe
		[22] HORN	11	ZEP3	Xe
$<2\times10^{-7}$	90	AHMED	10	CDM2	Ge
$<1\times10^{-5}$	90	[23] AKERIB	10	CDM2	Si, Ge, low threshold
$<1\times10^{-7}$	90	APRILE	10	X100	Xe
$<2\times10^{-6}$	90	ARMENGAUD	10	EDE2	Ge
$<4\times10^{-5}$	90	FELIZARDO	10	SMPL	C_2ClF_3
$<1.5\times10^{-7}$	90	[24] AHMED	09	CDM2	Ge
$<2\times10^{-4}$	90	[25] LIN	09	TEXO	Ge
		[26] AALSETH	08	CGNT	Ge

[1] AARTSEN 13 search for neutrinos from the Sun arising from the pair annihilation of X^0 trapped by the sun in data taken between June 2010 and May 2011. The annihilation channel $X^0X^0 \to \tau^+\tau^-$ is assumed.

[2] See their Fig. 8 for limits extending down to m_{X^0} = 7 GeV.

[3] AGNESE 13 use data taken between Oct. 2006 and July 2007. See their Fig. 4 for limits extending down to m_{X^0} = 7 GeV.

[4] AGNESE 13A use data taken between July 2007 and Sep. 2008. Three candidate events are seen. Assuming these events are real, the best fit parameters are m_{X^0} = 8.6 GeV and $\sigma = 1.9\times10^{-5}$ pb.

[5] Limit from combined data of AGNESE 13 and AGNESE 13A. See their Fig. 4 for limits extending down to m_{X^0} = 5.5 GeV.

[6] See their Fig. 4 for limits extending down to m_{X^0} = 4 GeV.

[7] See their Fig. 5 for limits for m_{X^0} = 4–12 GeV.

[8] ANGLOHER 12 observe excess events above the expected background which are consistent with X^0 with mass $\sim$ 25 GeV (or 12 GeV) and spin-independent X^0-nucleon cross section of 2×10^{-6} pb (or 4×10^{-5} pb).

[9] Reanalysis of ANGLOHER 09 data with all three nuclides. See also BROWN 12.

[10] See their Fig. 7 for cross section limits for m_{X^0} between 4 and 12 GeV.

[11] See their Fig. 4 for limits extending down to m_{X^0} = 7 GeV.

[12] See their Fig. 13 for cross section limits for m_{X^0} between 1.2 and 10 GeV.

[13] See also DAHL 12 for a criticism.

[14] See their Fig. 4 for limits extending to m_{X^0} = 3.5 GeV.

[15] AALSETH 11A find indications of annual modulation of the data, the energy spectrum being compatible with X^0 mass around 8 GeV. See also AALSETH 13.

[16] AHMED 11 search for X^0 inelastic scattering. See their Fig. 8–10 for limits.

[17] AHMED 11A combine CDMS and EDELWEISS data.

[18] AHMED 11B give limits on spin-independent X^0-nucleon cross section for m_{X^0} = 4–12 GeV in the range 10^{-3}–10^{-5} pb. See their Fig. 3.

[19] See their Fig. 3 for limits down to m_{X^0} = 4 GeV.

[20] APRILE 11 reanalyze APRILE 10 data.

[21] APRILE 11A search for X^0 inelastic scattering. See their Fig. 2 and 3 for limits.

[22] HORN 11 perform detector calibration by neutrons. Earlier results are only marginally affected.

[23] See their Fig. 10 and 12 for limits extending to X^0 mass of 1 GeV.

[24] Superseded by AHMED 10.

[25] See their Fig. 6(a) for cross section limits for m_{X^0} extending down to 2 GeV.

[26] See their Fig. 2 for cross section limits for m_{X^0} between 4 and 10 GeV.

For m_{X^0} = 100 GeV

VALUE (pb)	CL%	DOCUMENT ID		TECN	COMMENT
• • • We do not use the following data for averages, fits, limits, etc. • • •					
$<6.01 \times 10^{-7}$	90	[1,2] AARTSEN	13	ICCB	H, solar ν
$<3.30 \times 10^{-5}$	90	[2,3] AARTSEN	13	ICCB	H, solar ν
$<1.9 \times 10^{-6}$	90	[1,4] ADRIAN-MAR.	13	ANTR	H, solar ν
$<1.2 \times 10^{-4}$	90	[3,4] ADRIAN-MAR.	13	ANTR	H, solar ν
$<7.6 \times 10^{-7}$	90	[4,5] ADRIAN-MAR.	13	ANTR	H, solar ν
$<2 \times 10^{-6}$	90	[6] AGNESE	13	CDM2	Si
$<1.6 \times 10^{-6}$	90	[1,7] BOLIEV	13	BAKS	H, solar ν
$<1.9 \times 10^{-5}$	90	[3,7] BOLIEV	13	BAKS	H, solar ν
$<7.1 \times 10^{-7}$	90	[5,7] BOLIEV	13	BAKS	H, solar ν
$<1.67 \times 10^{-6}$	90	[1,8] ABBASI	12	ICCB	H, solar ν
$<1.07 \times 10^{-4}$	90	[3,8] ABBASI	12	ICCB	H, solar ν
$<4 \times 10^{-8}$	90	AKIMOV	12	ZEP3	Xe
$<1.4 \times 10^{-6}$	90	[9] ANGLOHER	12	CRES	$CaWO_4$
$<3 \times 10^{-9}$	90	APRILE	12	X100	Xe
$<1.6 \times 10^{-7}$	90	BEHNKE	12	COUP	CF_3I
$<7 \times 10^{-6}$		FELIZARDO	12	SMPL	C_2ClF_5
$<2.5 \times 10^{-7}$	90	[10] KIM	12	KIMS	CsI
$<2 \times 10^{-4}$	90	AALSETH	11	CGNT	Ge
		[11] AHMED	11	CDM2	Ge, inelastic
$<3.3 \times 10^{-8}$	90	[12] AHMED	11A	RVUE	Ge
		[13] AJELLO	11	FLAT	
$<3 \times 10^{-8}$	90	[14] APRILE	11	X100	Xe
		[15] APRILE	11A	X100	Xe, inelastic
$<1 \times 10^{-8}$	90	APRILE	11B	X100	Xe
$<5 \times 10^{-8}$	90	[16] ARMENGAUD	11	EDE2	Ge
		[17] HORN	11	ZEP3	Xe
$<4 \times 10^{-8}$	90	AHMED	10	CDM2	Ge
$<9 \times 10^{-6}$	90	AKERIB	10	CDM2	Si, Ge, low threshold
		[18] AKIMOV	10	ZEP3	Xe, inelastic
$<5 \times 10^{-8}$	90	APRILE	10	X100	Xe
$<1 \times 10^{-7}$	90	ARMENGAUD	10	EDE2	Ge
$<3 \times 10^{-5}$	90	FELIZARDO	10	SMPL	C_2ClF_3
$<5 \times 10^{-8}$	90	[19] AHMED	09	CDM2	Ge
		[20] ANGLE	09	XE10	Xe, inelastic
$<3 \times 10^{-4}$	90	LIN	09	TEXO	Ge
		[21] GIULIANI	05	RVUE	

[1] The annihilation channel $X^0\overline{X}^0 \rightarrow W^+W^-$ is assumed.
[2] AARTSEN 13 search for neutrinos from the Sun arising from the pair annihilation of X^0 trapped by the sun in data taken between June 2010 and May 2011.
[3] The annihilation channel $X^0\overline{X}^0 \rightarrow b\overline{b}$ is assumed.
[4] ADRIAN-MARTINEZ 13 search for neutrinos from the Sun arising from the pair annihilation of X^0 trapped by the sun in data taken between Jan. 2007 and Dec. 2008.
[5] The annihilation channel $X^0X^0 \rightarrow \tau^+\tau^-$ is assumed.
[6] AGNESE 13 use data taken between Oct. 2006 and July 2007.
[7] BOLIEV 13 search for neutrinos from the Sun arising from the pair annihilation of X^0 trapped by the sun in data taken from 1978 to 2009. See also SUVOROVA 13 for an older analysis of the same data.
[8] ABBASI 12 search for neutrinos from the Sun arising from the pair annihilation of X^0 trapped by the Sun. The amount of X^0 depends on the X^0-proton cross section.
[9] Reanalysis of ANGLOHER 09 data with all three nuclides. See also BROWN 12.
[10] See their Fig. 6 for a limit on inelastically scattering X^0 for m_{X^0} = 70 GeV.
[11] AHMED 11 search for X^0 inelastic scattering. See their Fig. 8–10 for limits.
[12] AHMED 11A combine CDMS and EDELWEISS data.
[13] AJELLO 11 search for $e^{\pm}$ flux from X^0 annihilations in the Sun. Models in which X^0 annihilates into an intermediate long-lived weakly interacting particles or X^0 scatters inelastically are constrained. See their Fig. 6–8 for limits.
[14] APRILE 11 reanalyze APRILE 10 data.
[15] APRILE 11A search for X^0 inelastic scattering. See their Fig. 2 and 3 for limits.
[16] Supersedes ARMENGAUD 10. A limit on inelastic cross section is also given.
[17] HORN 11 perform detector calibration by neutrons. Earlier results are only marginally affected.
[18] AKIMOV 10 give cross section limits for inelastically scattering dark matter. See their Fig. 4.
[19] Superseded by AHMED 10.
[20] ANGLE 09 search for X^0 inelastic scattering. See their Fig. 4 for limits.
[21] GIULIANI 05 analyzes the spin-independent X^0-nucleon cross section limits with both isoscalar and isovector couplings. See their Fig. 3 and 4 for limits on the couplings.

For m_{X^0} = 1 TeV

VALUE (pb)	CL%	DOCUMENT ID		TECN	COMMENT
• • • We do not use the following data for averages, fits, limits, etc. • • •					
$<3.46 \times 10^{-7}$	90	[1,2] AARTSEN	13	ICCB	H, solar ν
$<7.75 \times 10^{-6}$	90	[1,3] AARTSEN	13	ICCB	H, solar ν
$<6.9 \times 10^{-7}$	90	[2,4] ADRIAN-MAR.	13	ANTR	H, solar ν
$<1.5 \times 10^{-5}$	90	[3,4] ADRIAN-MAR.	13	ANTR	H, solar ν
$<1.8 \times 10^{-7}$	90	[4,5] ADRIAN-MAR.	13	ANTR	H, solar ν
$<4.3 \times 10^{-6}$	90	[2,6] BOLIEV	13	BAKS	H, solar ν
$<3.4 \times 10^{-5}$	90	[3,6] BOLIEV	13	BAKS	H, solar ν
$<1.2 \times 10^{-6}$	90	[5,6] BOLIEV	13	BAKS	H, solar ν
$<2.12 \times 10^{-7}$	90	[2,7] ABBASI	12	ICCB	H, solar ν
$<6.56 \times 10^{-6}$	90	[3,7] ABBASI	12	ICCB	H, solar ν
$<4 \times 10^{-7}$	90	AKIMOV	12	ZEP3	Xe
$<1.1 \times 10^{-5}$	90	[8] ANGLOHER	12	CRES	$CaWO_4$
$<2 \times 10^{-8}$	90	APRILE	12	X100	Xe
$<1.2 \times 10^{-6}$	90	BEHNKE	12	COUP	CF_3I
$<4 \times 10^{-6}$		FELIZARDO	12	SMPL	C_2ClF_5
$<1.5 \times 10^{-6}$	90	KIM	12	KIMS	CsI
		[9] AHMED	11	CDM2	Ge, inelastic
$<1.5 \times 10^{-7}$	90	[10] AHMED	11A	RVUE	Ge
$<2 \times 10^{-7}$	90	[11] APRILE	11	X100	Xe
$<8 \times 10^{-8}$	90	APRILE	11B	X100	Xe
$<2 \times 10^{-7}$	90	[12] ARMENGAUD	11	EDE2	Ge
		[13] HORN	11	ZEP3	Xe
$<2 \times 10^{-7}$	90	AHMED	10	CDM2	Ge
$<4 \times 10^{-7}$	90	APRILE	10	X100	Xe
$<6 \times 10^{-7}$	90	ARMENGAUD	10	EDE2	Ge
$<3.5 \times 10^{-7}$	90	[14] AHMED	09	CDM2	Ge

[1] AARTSEN 13 search for neutrinos from the Sun arising from the pair annihilation of X^0 trapped by the sun in data taken between June 2010 and May 2011.
[2] The annihilation channel $X^0\overline{X}^0 \rightarrow W^+W^-$ is assumed.
[3] The annihilation channel $X^0\overline{X}^0 \rightarrow b\overline{b}$ is assumed.
[4] ADRIAN-MARTINEZ 13 search for neutrinos from the Sun arising from the pair annihilation of X^0 trapped by the sun in data taken between Jan. 2007 and Dec. 2008.
[5] The annihilation channel $X^0X^0 \rightarrow \tau^+\tau^-$ is assumed.
[6] BOLIEV 13 search for neutrinos from the Sun arising from the pair annihilation of X^0 trapped by the sun in data taken from 1978 to 2009. See also SUVOROVA 13 for an older analysis of the same data.
[7] ABBASI 12 search for neutrinos from the Sun arising from the pair annihilation of X^0 trapped by the Sun. The amount of X^0 depends on the X^0-proton cross section.
[8] Reanalysis of ANGLOHER 09 data with all three nuclides. See also BROWN 12.
[9] AHMED 11 search for X^0 inelastic scattering. See their Fig. 8–10 for limits.
[10] AHMED 11A combine CDMS and EDELWEISS data.
[11] APRILE 11 reanalyze APRILE 10 data.
[12] Supersedes ARMENGAUD 10. A limit on inelastic cross section is also given.
[13] HORN 11 perform detector calibration by neutrons. Earlier results are only marginally affected.
[14] Superseded by AHMED 10.

Limits for Spin-Dependent Cross Section of Dark Matter Particle (X^0) on Proton

For m_{X^0} = 20 GeV

VALUE (pb)	CL%	DOCUMENT ID		TECN	COMMENT
• • • We do not use the following data for averages, fits, limits, etc. • • •					
$< 1.29 \times 10^{-2}$	90	[1] AARTSEN	13	ICCB	H, solar ν
$< 3.17 \times 10^{-2}$	90	[2] APRILE	13	X100	Xe
$< 3 \times 10^{-2}$	90	ARCHAMBAU.	12	PICA	F (C_4F_{10})
$< 2 \times 10^{-2}$	90	BEHNKE	12	COUP	CF_3I
< 20	90	DAW	12	DRFT	F (CF_4)
$< 7 \times 10^{-3}$		FELIZARDO	12	SMPL	C_2ClF_5
< 0.15	90	KIM	12	KIMS	CsI
$< 1 \times 10^5$	90	[3] AHLEN	11	DMTP	F (CF_4)
< 0.1	90	[3] BEHNKE	11	COUP	CF_3I
$< 1.5 \times 10^{-2}$	90	[4,5] TANAKA	11	SKAM	H, solar ν
< 0.2	90	ARCHAMBAU.	09	PICA	F
< 4	90	LEBEDENKO	09A	ZEP3	Xe
< 0.6	90	ANGLE	08A	XE10	Xe
<100	90	ALNER	07	ZEP2	Xe
< 1	90	LEE	07A	KIMS	CsI
< 20	90	[6] AKERIB	06	CDMS	^{73}Ge, ^{29}Si
< 2	90	SHIMIZU	06A	CNTR	F (CaF_2)
< 0.5	90	ALNER	05	NAIA	NaI
< 1.5	90	BARNABE-HE.	05	PICA	F (C_4F_{10})
< 1.5	90	GIRARD	05	SMPL	F (C_2ClF_5)
< 35	90	MIUCHI	03	BOLO	LiF
< 30	90	TAKEDA	03	BOLO	NaF

[1] AARTSEN 13 search for neutrinos from the Sun arising from the pair annihilation of X^0 trapped by the sun in data taken between June 2010 and May 2011. The annihilation channel $X^0X^0 \rightarrow \tau^+\tau^-$ is assumed.
[2] The value has been provided by the authors. APRILE 13 note that the proton limits on Xe are highly sensitive to the theoretical model used.
[3] Use a direction-sensitive detector.
[4] The annihilation channel $X^0\overline{X}^0 \rightarrow b\overline{b}$ is assumed.
[5] TANAKA 11 search for neutrinos from the Sun arising from the pair annihilation of X^0 trapped by the Sun. The amount of X^0 depends on the X^0-proton cross section.
[6] See also AKERIB 05.

For m_{X^0} = 100 GeV

VALUE (pb)	CL%	DOCUMENT ID		TECN	COMMENT
• • • We do not use the following data for averages, fits, limits, etc. • • •					
$< 2.68 \times 10^{-4}$	90	[1,2] AARTSEN	13	ICCB	H, solar ν
$< 1.47 \times 10^{-2}$	90	[2,3] AARTSEN	13	ICCB	H, solar ν
$< 8.5 \times 10^{-4}$	90	[1,4] ADRIAN-MAR.	13	ANTR	H, solar ν
$< 5.5 \times 10^{-2}$	90	[3,4] ADRIAN-MAR.	13	ANTR	H, solar ν
$< 3.4 \times 10^{-4}$	90	[4,5] ADRIAN-MAR.	13	ANTR	H, solar ν
$< 1.00 \times 10^{-2}$	90	[6] APRILE	13	X100	Xe
$< 7.1 \times 10^{-4}$	90	[1,7] BOLIEV	13	BAKS	H, solar ν
$< 8.4 \times 10^{-3}$	90	[3,7] BOLIEV	13	BAKS	H, solar ν
$< 3.1 \times 10^{-4}$	90	[5,7] BOLIEV	13	BAKS	H, solar ν
$< 7.07 \times 10^{-4}$	90	[1,8] ABBASI	12	ICCB	H, solar ν
$< 4.53 \times 10^{-2}$	90	[3,8] ABBASI	12	ICCB	H, solar ν

<	7	$\times 10^{-2}$	90		ARCHAMBAU..12	PICA	F (C_4F_{10})
<	7	$\times 10^{-3}$	90		BEHNKE 12	COUP	CF_3I
<	1.8		90		DAW 12	DRFT	F (CF_4)
<	9	$\times 10^{-3}$			FELIZARDO 12	SMPL	C_2ClF_5
<	2	$\times 10^{-2}$	90		KIM 12	KIMS	CsI
<	2	$\times 10^{3}$	90	[9]	AHLEN 11	DMTP	F (CF_4)
<	7	$\times 10^{-2}$	90		BEHNKE 11	COUP	CF_3I
<	2.7	$\times 10^{-4}$	90	[1,10]	TANAKA 11	SKAM	H, solar ν
<	4.5	$\times 10^{-3}$	90	[3,10]	TANAKA 11	SKAM	H, solar ν
				[11]	FELIZARDO 10	SMPL	C_2ClF_3
<	6	$\times 10^{3}$	90	[9]	MIUCHI 10	NAGE	CF_4
<	0.4		90		ARCHAMBAU..09	PICA	F
<	0.8		90		LEBEDENKO 09A	ZEP3	Xe
<	1.0		90		ANGLE 08A	XE10	Xe
<	15		90		ALNER 07	ZEP2	Xe
<	0.2		90		LEE 07A	KIMS	CsI
<	1	$\times 10^{4}$	90	[9]	MIUCHI 07	NAGE	F (CF_4)
<	5		90	[12]	AKERIB 06	CDMS	^{73}Ge, ^{29}Si
<	2		90		SHIMIZU 06A	CNTR	F (CaF_2)
<	0.3		90		ALNER 05	NAIA	NaI
<	2		90		BARNABE-HE..05	PICA	F (C_4F_{10})
<100			90		BENOIT 05	EDEL	^{73}Ge
<	1.5		90		GIRARD 05	SMPL	F (C_2ClF_5)
<	0.7			[13]	GIULIANI 05A	RVUE	
				[14]	GIULIANI 04	RVUE	
				[15]	GIULIANI 04A	RVUE	
<	35		90		MIUCHI 03	BOLO	LiF
<	40		90		TAKEDA 03	BOLO	NaF

[1] The annihilation channel $X^0\overline{X}^0 \rightarrow W^+W^-$ is assumed.
[2] AARTSEN 13 search for neutrinos from the Sun arising from the pair annihilation of X^0 trapped by the sun in data taken between June 2010 and May 2011.
[3] The annihilation channel $X^0\overline{X}^0 \rightarrow b\overline{b}$ is assumed.
[4] ADRIAN-MARTINEZ 13 search for neutrinos from the Sun arising from the pair annihilation of X^0 trapped by the sun in data taken between Jan. 2007 and Dec. 2008.
[5] The annihilation channel $X^0X^0 \rightarrow \tau^+\tau^-$ is assumed.
[6] The value has been provided by the authors. APRILE 13 note that the proton limits on Xe are highly sensitive to the theoretical model used.
[7] BOLIEV 13 search for neutrinos from the Sun arising from the pair annihilation of X^0 trapped by the sun in data taken from 1978 to 2009. See also SUVOROVA 13 for an older analysis of the same data.
[8] ABBASI 12 search for neutrinos from the Sun arising from the pair annihilation of X^0 trapped by the Sun. The amount of X^0 depends on the X^0-proton cross section.
[9] Use a direction-sensitive detector.
[10] TANAKA 11 search for neutrinos from the Sun arising from the pair annihilation of X^0 trapped by the Sun. The amount of X^0 depends on the X^0-proton cross section.
[11] See their Fig. 3 for limits on spin-dependent proton couplings for X^0 mass of 50 GeV.
[12] See also AKERIB 05.
[13] GIULIANI 05A analyze available data and give combined limits.
[14] GIULIANI 04 reanalyze COLLAR 00 data and give limits for spin-dependent X^0-proton coupling.
[15] GIULIANI 04A give limits for spin-dependent X^0-proton couplings from existing data.

For m_{X^0} = 1 TeV

VALUE (pb)		CL%		DOCUMENT ID		TECN	COMMENT
• • • We do not use the following data for averages, fits, limits, etc. • • •							
<	4.48×10^{-4}	90	[1,2]	AARTSEN 13		ICCB	H, solar ν
<	1.00×10^{-2}	90	[2,3]	AARTSEN 13		ICCB	H, solar ν
<	8.9×10^{-4}	90	[1,4]	ADRIAN-MAR..13		ANTR	H, solar ν
<	2.0×10^{-2}	90	[3,4]	ADRIAN-MAR..13		ANTR	H, solar ν
<	2.3×10^{-4}	90	[4,5]	ADRIAN-MAR..13		ANTR	H, solar ν
<	7.57×10^{-2}	90	[6]	APRILE 13		X100	Xe
<	5.4×10^{-3}	90	[1,7]	BOLIEV 13		BAKS	H, solar ν
<	4.2×10^{-2}	90	[3,7]	BOLIEV 13		BAKS	H, solar ν
<	1.5×10^{-3}	90	[5,7]	BOLIEV 13		BAKS	H, solar ν
<	2.50×10^{-4}	90	[1,8]	ABBASI 12		ICCB	H, solar ν
<	7.86×10^{-3}	90	[3,8]	ABBASI 12		ICCB	H, solar ν
<	4 $\times 10^{-2}$	90		BEHNKE 12		COUP	CF_3I
<	8	90		DAW 12		DRFT	F (CF_4)
<	6 $\times 10^{-2}$			FELIZARDO 12		SMPL	C_2ClF_5
<	8 $\times 10^{-2}$	90		KIM 12		KIMS	CsI
<	8 $\times 10^{3}$	90	[9]	AHLEN 11		DMTP	F (CF_4)
<	0.4	90		BEHNKE 11		COUP	CF_3I
<	2 $\times 10^{-3}$	90	[3,10]	TANAKA 11		SKAM	H, solar ν
<	2 $\times 10^{-2}$	90	[1,10]	TANAKA 11		SKAM	H, solar ν
<	1 $\times 10^{-3}$	90	[11]	ABBASI 10		ICCB	KK dark matter
<	2 $\times 10^{4}$	90	[9]	MIUCHI 10		NAGE	CF_4
<	8.7 $\times 10^{-4}$	90	[1]	ABBASI 09B		ICCB	H, solar ν
<	2.2 $\times 10^{-2}$	90	[3]	ABBASI 09B		ICCB	H, solar ν
<	3	90		ARCHAMBAU..09		PICA	F
<	6	90		LEBEDENKO 09A		ZEP3	Xe
<	9	90		ANGLE 08A		XE10	Xe
<100		90		ALNER 07		ZEP2	Xe
<	0.8	90		LEE 07A		KIMS	CsI
<	4 $\times 10^{4}$	90	[9]	MIUCHI 07		NAGE	F (CF_4)
<	30	90	[12]	AKERIB 06		CDMS	^{73}Ge, ^{29}Si
<	1.5	90		ALNER 05		NAIA	NaI
<	15	90		BARNABE-HE..05		PICA	F (C_4F_{10})
<600		90		BENOIT 05		EDEL	^{73}Ge
<	10	90		GIRARD 05		SMPL	F (C_2ClF_5)
<260		90		MIUCHI 03		BOLO	LiF
<150		90		TAKEDA 03		BOLO	NaF

[1] The annihilation channel $X^0\overline{X}^0 \rightarrow W^+W^-$ is assumed.
[2] AARTSEN 13 search for neutrinos from the Sun arising from the pair annihilation of X^0 trapped by the sun in data taken between June 2010 and May 2011.
[3] The annihilation channel $X^0\overline{X}^0 \rightarrow b\overline{b}$ is assumed.
[4] ADRIAN-MARTINEZ 13 search for neutrinos from the Sun arising from the pair annihilation of X^0 trapped by the sun in data taken between Jan. 2007 and Dec. 2008.
[5] The annihilation channel $X^0X^0 \rightarrow \tau^+\tau^-$ is assumed.
[6] The value has been provided by the authors. APRILE 13 note that the proton limits on Xe are highly sensitive to the theoretical model used.
[7] BOLIEV 13 search for neutrinos from the Sun arising from the pair annihilation of X^0 trapped by the sun in data taken from 1978 to 2009. See also SUVOROVA 13 for an older analysis of the same data.
[8] ABBASI 12 search for neutrinos from the Sun arising from the pair annihilation of X^0 trapped by the Sun. The amount of X^0 depends on the X^0-proton cross section.
[9] Use a direction-sensitive detector.
[10] TANAKA 11 search for neutrinos from the Sun arising from the pair annihilation of X^0 trapped by the Sun. The amount of X^0 depends on the X^0-proton cross section.
[11] ABBASI 10 search for ν_μ from annihilations of Kaluza-Klein photon dark matter in the Sun.
[12] See also AKERIB 05.

Limits for Spin-Dependent Cross Section of Dark Matter Particle (X^0) on Neutron

For m_{X^0} = 20 GeV

VALUE (pb)		CL%		DOCUMENT ID		TECN	COMMENT
• • • We do not use the following data for averages, fits, limits, etc. • • •							
<	1.13×10^{-3}	90	[1]	APRILE 13		X100	Xe
<	0.02	90		AKIMOV 12		ZEP3	Xe
			[2]	AHMED 11B		CDM2	Ge, low threshold
<	0.06	90		AHMED 09		CDM2	Ge
<	0.04	90		LEBEDENKO 09A		ZEP3	Xe
<	50		[3]	LIN 09		TEXO	Ge
<	6 $\times 10^{-3}$	90		ANGLE 08A		XE10	Xe
<	0.5	90		ALNER 07		ZEP2	Xe
<	25	90		LEE 07A		KIMS	CsI
<	0.3	90	[4]	AKERIB 06		CDMS	^{73}Ge, ^{29}Si
<	30	90		SHIMIZU 06A		CNTR	F (CaF_2)
<	60	90		ALNER 05		NAIA	NaI
<	20	90		BARNABE-HE..05		PICA	F (C_4F_{10})
<	10	90		BENOIT 05		EDEL	^{73}Ge
<	4	90		KLAPDOR-K... 05		HDMS	^{73}Ge (enriched)
<600		90		TAKEDA 03		BOLO	NaF

[1] The value has been provided by the authors.
[2] AHMED 11B give limits on spin-dependent X^0-neutron cross section for m_{X^0} = 4–12 GeV in the range 10^{-3}–10 pb. See their Fig. 3.
[3] See their Fig. 6(b) for cross section limits for m_{X^0} extending down to 2 GeV.
[4] See also AKERIB 05.

For m_{X^0} = 100 GeV

VALUE (pb)		CL%		DOCUMENT ID		TECN	COMMENT
• • • We do not use the following data for averages, fits, limits, etc. • • •							
<	4.68×10^{-4}	90	[1]	APRILE 13		X100	Xe
<	0.01	90		AKIMOV 12		ZEP3	Xe
			[2]	FELIZARDO 10		SMPL	C_2ClF_3
<	0.02	90		AHMED 09		CDM2	Ge
<	0.01	90		LEBEDENKO 09A		ZEP3	Xe
<100		90		LIN 09		TEXO	Ge
<	0.01	90		ANGLE 08A		XE10	Xe
<	0.05	90	[3]	BEDNYAKOV 08		RVUE	Ge
<	0.08	90		ALNER 07		ZEP2	Xe
<	6	90		LEE 07A		KIMS	CsI
<	0.07	90	[4]	AKERIB 06		CDMS	^{73}Ge, ^{29}Si
<	30	90		SHIMIZU 06A		CNTR	F (CaF_2)
<	10	90		ALNER 05		NAIA	NaI
<	30	90		BARNABE-HE..05		PICA	F (C_4F_{10})
<	0.7	90		BENOIT 05		EDEL	^{73}Ge
<	0.2		[5]	GIULIANI 05A		RVUE	
<	1.5	90		KLAPDOR-K... 05		HDMS	^{73}Ge (enriched)
			[6]	GIULIANI 04		RVUE	
			[7]	GIULIANI 04A		RVUE	
			[8]	MIUCHI 03		BOLO	LiF
<800		90		TAKEDA 03		BOLO	NaF

[1] The value has been provided by the authors.
[2] See their Fig. 3 for limits on spin-dependent neutron couplings for X^0 mass of 50 GeV.
[3] BEDNYAKOV 08 reanalyze KLAPDOR-KLEINGROTHAUS 05 and BAUDIS 01 data.
[4] See also AKERIB 05.
[5] GIULIANI 05A analyze available data and give combined limits.
[6] GIULIANI 04 reanalyze COLLAR 00 data and give limits for spin-dependent X^0-neutron coupling.
[7] GIULIANI 04A give limits for spin-dependent X^0-neutron couplings from existing data.
[8] MIUCHI 03 give model-independent limit for spin-dependent X^0-proton and neutron cross sections. See their Fig. 5.

For m_{X^0} = 1 TeV

VALUE (pb)	CL%	DOCUMENT ID		TECN	COMMENT
• • • We do not use the following data for averages, fits, limits, etc. • • •					
$< 3.64 \times 10^{-3}$	90	[1] APRILE	13	X100	Xe
$< 8 \times 10^{-2}$	90	AKIMOV	12	ZEP3	Xe
< 0.2	90	AHMED	09	CDM2	Ge
< 0.1	90	LEBEDENKO	09A	ZEP3	Xe
< 0.1	90	ANGLE	08A	XE10	Xe
< 0.25	90	[2] BEDNYAKOV	08	RVUE	Ge
< 0.6	90	ALNER	07	ZEP2	Xe
< 30	90	LEE	07A	KIMS	CsI
< 0.5	90	[3] AKERIB	06	CDMS	^{73}Ge, ^{29}Si
< 40	90	ALNER	05	NAIA	NaI
<200	90	BARNABE-HE...	05	PICA	F (C_4F_{10})
< 4	90	BENOIT	05	EDEL	^{73}Ge
< 10	90	KLAPDOR-K...	05	HDMS	^{73}Ge (enriched)
$< 4 \times 10^3$	90	TAKEDA	03	BOLO	NaF

[1] The value has been provided by the authors.
[2] BEDNYAKOV 08 reanalyze KLAPDOR-KLEINGROTHAUS 05 and BAUDIS 01 data.
[3] See also AKERIB 05.

Cross-Section Limits for Dark Matter Particles (X^0) on Nuclei

For m_{X^0} = 20 GeV

VALUE (nb)	CL%	DOCUMENT ID		TECN	COMMENT
• • • We do not use the following data for averages, fits, limits, etc. • • •					
< 0.08	90	[1] ANGLOHER	02	CRES	Al
		[2] BENOIT	00	EDEL	Ge
< 0.04	95	[3] KLIMENKO	98	CNTR	^{73}Ge, inel.
< 0.8		ALESSAND...	96	CNTR	O
< 6		ALESSAND...	96	CNTR	Te
< 0.02	90	[4] BELLI	96	CNTR	^{129}Xe, inel.
		[5] BELLI	96C	CNTR	^{129}Xe
$< 4 \times 10^{-3}$	90	[6] BERNABEI	96	CNTR	Na
< 0.3	90	[6] BERNABEI	96	CNTR	I
< 0.2	95	[7] SARSA	96	CNTR	Na
< 0.015	90	[8] SMITH	96	CNTR	Na
< 0.05	95	[9] GARCIA	95	CNTR	Natural Ge
< 0.1	95	QUENBY	95	CNTR	Na
<90	90	[10] SNOWDEN-...	95	MICA	^{16}O
$< 4 \times 10^3$	90	[10] SNOWDEN-...	95	MICA	^{39}K
< 0.7	90	BACCI	92	CNTR	Na
< 0.12	90	[11] REUSSER	91	CNTR	Natural Ge
< 0.06	95	CALDWELL	88	CNTR	Natural Ge

[1] ANGLOHER 02 limit is for spin-dependent WIMP-Aluminum cross section.
[2] BENOIT 00 find four event categories in Ge detectors and suggest that low-energy surface nuclear recoils can explain anomalous events reported by UKDMC and Saclay NaI experiments.
[3] KLIMENKO 98 limit is for inelastic scattering $X^0\,^{73}\mathrm{Ge} \rightarrow X^0\,^{73}\mathrm{Ge}^*$ (13.26 keV).
[4] BELLI 96 limit for inelastic scattering $X^0\,^{129}\mathrm{Xe} \rightarrow X^0\,^{129}\mathrm{Xe}^*$(39.58 keV).
[5] BELLI 96C use background subtraction and obtain $\sigma < 150$ pb (< 1.5 fb) (90% CL) for spin-dependent (independent) X^0-proton cross section. The confidence level is from R. Bernabei, private communication, May 20, 1999.
[6] BERNABEI 96 use pulse shape discrimination to enhance the possible signal. The limit here is from R. Bernabei, private communication, September 19, 1997.
[7] SARSA 96 search for annual modulation of WIMP signal. See SARSA 97 for details of the analysis. The limit here is from M.L. Sarsa, private communication, May 26, 1997.
[8] SMITH 96 use pulse shape discrimination to enhance the possible signal. A dark matter density of 0.4 GeV cm^{-3} is assumed.
[9] GARCIA 95 limit is from the event rate. A weaker limit is obtained from searches for diurnal and annual modulation.
[10] SNOWDEN-IFFT 95 look for recoil tracks in an ancient mica crystal. Similar limits are also given for ^{27}Al and ^{28}Si. See COLLAR 96 and SNOWDEN-IFFT 96 for discussion on potential backgrounds.
[11] REUSSER 91 limit here is changed from published (0.04) after reanalysis by authors. J.L. Vuilleumier, private communication, March 29, 1996.

For m_{X^0} = 100 GeV

VALUE (nb)	CL%	DOCUMENT ID		TECN	COMMENT
• • • We do not use the following data for averages, fits, limits, etc. • • •					
< 0.3	90	[1] ANGLOHER	02	CRES	Al
		[2] BELLI	02	RVUE	
		[3] BERNABEI	02C	DAMA	
		[4] GREEN	02	RVUE	
		[5] ULLIO	01	RVUE	
		[6] BENOIT	00	EDEL	Ge
$< 4 \times 10^{-3}$	90	[7] BERNABEI	00D		^{129}Xe, inel.
		[8] AMBROSIO	99	MCRO	
		[9] BRHLIK	99	RVUE	
$< 8 \times 10^{-3}$	95	[10] KLIMENKO	98	CNTR	^{73}Ge, inel.
< 0.08	95	[11] KLIMENKO	98	CNTR	^{73}Ge, inel.
< 4		ALESSAND...	96	CNTR	O
<25		ALESSAND...	96	CNTR	Te
$< 6 \times 10^{-3}$	90	[12] BELLI	96	CNTR	^{129}Xe, inel.
		[13] BELLI	96C	CNTR	^{129}Xe
$< 1 \times 10^{-3}$	90	[14] BERNABEI	96	CNTR	Na
< 0.3	90	[14] BERNABEI	96	CNTR	I
< 0.7	95	[15] SARSA	96	CNTR	Na
< 0.03	90	[16] SMITH	96	CNTR	Na
< 0.8	90	[16] SMITH	96	CNTR	I
< 0.35	95	[17] GARCIA	95	CNTR	Natural Ge
< 0.6	95	QUENBY	95	CNTR	Na
< 3	95	QUENBY	95	CNTR	I
$< 1.5 \times 10^2$	90	[18] SNOWDEN-...	95	MICA	^{16}O
$< 4 \times 10^2$	90	[18] SNOWDEN-...	95	MICA	^{39}K
< 0.08	90	[19] BECK	94	CNTR	^{76}Ge
< 2.5	90	BACCI	92	CNTR	Na
< 3	90	BACCI	92	CNTR	I
< 0.9	90	[20] REUSSER	91	CNTR	Natural Ge
< 0.7	95	CALDWELL	88	CNTR	Natural Ge

[1] ANGLOHER 02 limit is for spin-dependent WIMP-Aluminum cross section.
[2] BELLI 02 discuss dependence of the extracted WIMP cross section on the assumptions of the galactic halo structure.
[3] BERNABEI 02C analyze the DAMA data in the scenario in which X^0 scatters into a slightly heavier state as discussed by SMITH 01.
[4] GREEN 02 discusses dependence of extracted WIMP cross section limits on the assumptions of the galactic halo structure.
[5] ULLIO 01 disfavor the possibility that the BERNABEI 99 signal is due to spin-dependent WIMP coupling.
[6] BENOIT 00 find four event categories in Ge detectors and suggest that low-energy surface nuclear recoils can explain anomalous events reported by UKDMC and Saclay NaI experiments.
[7] BERNABEI 00D limit is for inelastic scattering $X^0\,^{129}\mathrm{Xe} \rightarrow X^0\,^{129}\mathrm{Xe}$ (39.58 keV).
[8] AMBROSIO 99 search for upgoing muon events induced by neutrinos originating from WIMP annihilations in the Sun and Earth.
[9] BRHLIK 99 discuss the effect of astrophysical uncertainties on the WIMP interpretation of the BERNABEI 99 signal.
[10] KLIMENKO 98 limit is for inelastic scattering $X^0\,^{73}\mathrm{Ge} \rightarrow X^0\,^{73}\mathrm{Ge}^*$ (13.26 keV).
[11] KLIMENKO 98 limit is for inelastic scattering $X^0\,^{73}\mathrm{Ge} \rightarrow X^0\,^{73}\mathrm{Ge}^*$ (66.73 keV).
[12] BELLI 96 limit for inelastic scattering $X^0\,^{129}\mathrm{Xe} \rightarrow X^0\,^{129}\mathrm{Xe}^*$(39.58 keV).
[13] BELLI 96C use background subtraction and obtain $\sigma < 0.35$ pb (< 0.15 fb) (90% CL) for spin-dependent (independent) X^0-proton cross section. The confidence level is from R. Bernabei, private communication, May 20, 1999.
[14] BERNABEI 96 use pulse shape discrimination to enhance the possible signal. The limit here is from R. Bernabei, private communication, September 19, 1997.
[15] SARSA 96 search for annual modulation of WIMP signal. See SARSA 97 for details of the analysis. The limit here is from M.L. Sarsa, private communication, May 26, 1997.
[16] SMITH 96 use pulse shape discrimination to enhance the possible signal. A dark matter density of 0.4 GeV cm^{-3} is assumed.
[17] GARCIA 95 limit is from the event rate. A weaker limit is obtained from searches for diurnal and annual modulation.
[18] SNOWDEN-IFFT 95 look for recoil tracks in an ancient mica crystal. Similar limits are also given for ^{27}Al and ^{28}Si. See COLLAR 96 and SNOWDEN-IFFT 96 for discussion on potential backgrounds.
[19] BECK 94 uses enriched ^{76}Ge (86% purity).
[20] REUSSER 91 limit here is changed from published (0.3) after reanalysis by authors. J.L. Vuilleumier, private communication, March 29, 1996.

For m_{X^0} = 1 TeV

VALUE (nb)	CL%	DOCUMENT ID		TECN	COMMENT
• • • We do not use the following data for averages, fits, limits, etc. • • •					
< 3	90	[1] ANGLOHER	02	CRES	Al
		[2] BENOIT	00	EDEL	Ge
		[3] BERNABEI	99D	CNTR	SIMP
		[4] DERBIN	99	CNTR	SIMP
< 0.06	95	[5] KLIMENKO	98	CNTR	^{73}Ge, inel.
< 0.4	95	[6] KLIMENKO	98	CNTR	^{73}Ge, inel.
< 40		ALESSAND...	96	CNTR	O
<700		ALESSAND...	96	CNTR	Te
< 0.05	90	[7] BELLI	96	CNTR	^{129}Xe, inel.
< 1.5	90	[8] BELLI	96	CNTR	^{129}Xe, inel.
		[9] BELLI	96C	CNTR	^{129}Xe
< 0.01	90	[10] BERNABEI	96	CNTR	Na
< 9	90	[10] BERNABEI	96	CNTR	I
< 7	95	[11] SARSA	96	CNTR	Na
< 0.3	90	[12] SMITH	96	CNTR	Na
< 6	90	[12] SMITH	96	CNTR	I
< 6	95	[13] GARCIA	95	CNTR	Natural Ge
< 8	95	QUENBY	95	CNTR	Na
< 50	95	QUENBY	95	CNTR	I
<700	90	[14] SNOWDEN-...	95	MICA	^{16}O
$< 1 \times 10^3$	90	[14] SNOWDEN-...	95	MICA	^{39}K
< 0.8	90	[15] BECK	94	CNTR	^{76}Ge
< 30	90	BACCI	92	CNTR	Na
< 30	90	BACCI	92	CNTR	I
< 15	90	[16] REUSSER	91	CNTR	Natural Ge
< 6	95	CALDWELL	88	CNTR	Natural Ge

[1] ANGLOHER 02 limit is for spin-dependent WIMP-Aluminum cross section.
[2] BENOIT 00 find four event categories in Ge detectors and suggest that low-energy surface nuclear recoils can explain anomalous events reported by UKDMC and Saclay NaI experiments.
[3] BERNABEI 99D search for SIMPs (Strongly Interacting Massive Particles) in the mass range 10^3–10^{16} GeV. See their Fig. 3 for cross-section limits.
[4] DERBIN 99 search for SIMPs (Strongly Interacting Massive Particles) in the mass range 10^2–10^{14} GeV. See their Fig. 3 for cross-section limits.
[5] KLIMENKO 98 limit is for inelastic scattering $X^0\ ^{73}\mathrm{Ge} \rightarrow X^0\ ^{73}\mathrm{Ge}^*$ (13.26 keV).
[6] KLIMENKO 98 limit is for inelastic scattering $X^0\ ^{73}\mathrm{Ge} \rightarrow X^0\ ^{73}\mathrm{Ge}^*$ (66.73 keV).
[7] BELLI 96 limit for inelastic scattering $X^0\ ^{129}\mathrm{Xe} \rightarrow X^0\ ^{129}\mathrm{Xe}^*$(39.58 keV).
[8] BELLI 96 limit for inelastic scattering $X^0\ ^{129}\mathrm{Xe} \rightarrow X^0\ ^{129}\mathrm{Xe}^*$(236.14 keV).
[9] BELLI 96C use background subtraction and obtain $\sigma < 0.7$ pb (< 0.7 fb) (90% CL) for spin-dependent (independent) X^0-proton cross section. The confidence level is from R. Bernabei, private communication, May 20, 1999.
[10] BERNABEI 96 use pulse shape discrimination to enhance the possible signal. The limit here is from R. Bernabei, private communication, September 19, 1997.
[11] SARSA 96 search for annual modulation of WIMP signal. See SARSA 97 for details of the analysis. The limit here is from M.L. Sarsa, private communication, May 26, 1997.
[12] SMITH 96 use pulse shape discrimination to enhance the possible signal. A dark matter density of 0.4 GeV cm^{-3} is assumed.
[13] GARCIA 95 limit is from the event rate. A weaker limit is obtained from searches for diurnal and annual modulation.
[14] SNOWDEN-IFFT 95 look for recoil tracks in an ancient mica crystal. Similar limits are also given for ^{27}Al and ^{28}Si. See COLLAR 96 and SNOWDEN-IFFT 96 for discussion on potential backgrounds.
[15] BECK 94 uses enriched ^{76}Ge (86% purity).
[16] REUSSER 91 limit here is changed from published (5) after reanalysis by authors. J.L. Vuilleumier, private communication, March 29, 1996.

X^0 Annihilation Cross Section

Limits are on σv for X^0 pair annihilation at threshold.

VALUE (cm^{3}s^{-1})	CL%	DOCUMENT ID		TECN	COMMENT
• • • We do not use the following data for averages, fits, limits, etc. • • •					
		[1] AARTSEN	13C	ICCB	Galaxies
		[2] ABRAMOWSKI	13	HESS	Central Galactic Halo
		[3] ACKERMANN	13A	FLAT	Galaxy
		[4] ABRAMOWSKI	12	HESS	Fornax Cluster
		[5] ACKERMANN	12	FLAT	Galaxy
		[6] ACKERMANN	12	FLAT	Galaxy
		[7] ALIU	12	VRTS	Segue 1
$<10^{-22}$	90	[8] ABBASI	11C	ICCB	Galactic halo, m=1 TeV
$<3\times10^{-25}$	95	[9] ABRAMOWSKI	11	HESS	Near Galactic center, m=1 TeV
$<10^{-26}$	95	[10] ACKERMANN	11	FLAT	Satellite galaxy, m=10 GeV
$<10^{-25}$	95	[10] ACKERMANN	11	FLAT	Satellite galaxy, m=100 GeV
$<10^{-24}$	95	[10] ACKERMANN	11	FLAT	Satellite galaxy, m=1 TeV

[1] AARTSEN 13C search for neutrinos from X^0 annihilation in nearby galaxies and galaxy clusters. See their Figs. 5–7 for limits on $\sigma\cdot v$ for $X^0X^0 \rightarrow \nu\overline{\nu}$, $\mu^+\mu^-$, $\tau^+\tau^-$, and W^+W^- for X^0 mass between 300 GeV and 100 TeV.
[2] ABRAMOWSKI 13 search for monochromatic γ from X^0 annihilation in the Milky Way halo in the central region. Limit on $\sigma\cdot v$ between 10^{-28} and 10^{-25} cm^3 s^{-1} (95% CL) is obtained for X^0 mass between 500 GeV and 20 TeV for $X^0X^0 \rightarrow \gamma\gamma$. X^0 density distribution in the Galaxy by Einasto is assumed. See their Fig. 4.
[3] ACKERMANN 13A search for monochromatic γ from X^0 annihilation in the Milky Way. Limit on $\sigma\cdot v$ for the process $X^0X^0 \rightarrow \gamma\gamma$ in the range 10^{-29}–10^{-27} cm^3 s^{-1} (95% CL) is obtained for X^0 mass between 5 and 300 GeV. The limit depends slightly on the assumed density profile of X^0 in the Galaxy. See their Tables VII–X and Fig.10. Supersedes ACKERMANN 12.
[4] ABRAMOWSKI 12 search for γ's from X^0 annihilation in the Fornax galaxy cluster. See their Fig. 7 for limits on $\sigma\cdot v$ for X^0 mass between 0.1 and 100 TeV for the annihilation channels $\tau^+\tau^-$, $b\overline{b}$, and W^+W^-.
[5] ACKERMANN 12 search for monochromatic γ from X^0 annihilation in the Milky Way. Limit on $\sigma\cdot v$ in the range 10^{-28}–10^{-26} cm^{3}s^{-1} (95% CL) is obtained for X^0 mass between 7 and 200 GeV if X^0 annihilates into $\gamma\gamma$. The limit depends slightly on the assumed density profile of X^0 in the Galaxy. See their Table III and Fig. 15.
[6] ACKERMANN 12 search for γ from X^0 annihilation in the Milky Way in the diffuse γ background. Limit on $\sigma\cdot v$ of 10^{-24} cm^{3}s^{-1} or larger is obtained for X^0 mass between 5 GeV and 10 TeV for various annihilation channels including W^+W^-, $b\overline{b}$, gg, e^+e^-, $\mu^+\mu^-$, $\tau^+\tau^-$. The limit depends slightly on the assumed density profile of X^0 in the Galaxy. See their Figs. 17–20.
[7] ALIU 12 search for γ's from X^0 annihilation in the dwarf spheroidal galaxy Segue 1. Limit on $\sigma\cdot v$ in the range 10^{-24}–10^{-20} cm^{3}s^{-1} (95% CL) is obtained for X^0 mass between 10 GeV and 2 TeV for annihilation channels e^+e^-, $\mu^+\mu^-$, $\tau^+\tau^-$, $b\overline{b}$, and W^+W^-. See their Fig. 3.
[8] ABBASI 11C search for ν_μ from X^0 annihilation in the outer halo of the Milky Way. The limit assumes annihilation into $\nu\nu$. See their Fig. 9 for limits with other annihilation channels.
[9] ABRAMOWSKI 11 search for γ from X^0 annihilation near the Galactic center. The limit assumes Einasto DM density profile.
[10] ACKERMANN 11 search for γ from X^0 annihilation in ten dwarf spheroidal satellite galaxies of the Milky Way. The limit for $m = 10$ GeV assumes annihilation into $b\overline{b}$, the others W^+W^-. See their Fig. 2 for limits with other final states. See also GERINGER-SAMETH 11 for a different analysis of the same data.

Dark Matter Particle (X^0) Production in Hadron Collisions

Searches for X^0 production in association with observable particles (γ, jets, ...) in high energy hadron collisions. If a specific form of effective interaction Lagrangian is assumed, the limits may be translated into limits on X^0-nucleon scattering cross section.

VALUE	DOCUMENT ID		TECN	COMMENT
• • • We do not use the following data for averages, fits, limits, etc. • • •				
	[1] AAD	13AD	ATLS	jet + $\not{E}_T$
	[2] AAD	13C	ATLS	γ + $\not{E}_T$
	[3] AALTONEN	12K	CDF	t + $\not{E}_T$
	[4] AALTONEN	12M	CDF	jet + $\not{E}_T$
	[5] CHATRCHYAN	12AP	CMS	jet + $\not{E}_T$
	[6] CHATRCHYAN	12T	CMS	γ + $\not{E}_T$

[1] AAD 13AD search for events with a jet and missing E_T in pp collisions at $E_{cm} = 7$ TeV with $L = 4.7$ fb^{-1}. See their Figs. 5 and 6 for translated limits on X^0-nucleon cross section for m = 1–1300 GeV.
[2] AAD 13C search for events with a photon and missing $\not{E}_T$ in pp collisions at E_{cm} = 7 TeV with $L = 4.6$ fb^{-1}. See their Fig. 3 for translated limits on X^0-nucleon cross section for m = 1–1000 GeV.
[3] AALTONEN 12K search for events with a top quark and missing $\not{E}_T$ in $p\overline{p}$ collisions at $E_{cm} = 1.96$ TeV with $L = 7.7$ fb^{-1}. Upper limits on $\sigma(tX^0)$ in the range 0.4–2 pb (95% CL) is given for m_{X^0} = 0–150 GeV.
[4] AALTONEN 12M search for events with a jet and missing E_T in $p\overline{p}$ collisions at E_{cm} = 1.96 TeV with $L = 6.7$ fb^{-1}. Upper limits on the cross section in the range 2–10 pb (90% CL) is given for m_{X^0} = 1–300 GeV. See their Fig. 2 for translated limits on X^0-nucleon cross section.
[5] CHATRCHYAN 12AP search for events with a jet and missing E_T in pp collisions at E_{cm} = 7 TeV with $L = 5.0$ fb^{-1}. See their Fig. 4 for translated limits on X^0-nucleon cross section for m_{X^0} = 0.1–1000 GeV.
[6] CHATRCHYAN 12T search for events with a photon and missing $\not{E}_T$ in pp collisions at E_{cm} = 7 TeV with $L = 5.0$ fb^{-1}. Upper limits on the cross section in the range 13–15 fb (90% CL) is given for m_{X^0} = 1–1000 GeV. See their Fig. 2 for translated limits on X^0-nucleon cross section.

CONCENTRATION OF STABLE PARTICLES IN MATTER

Concentration of Heavy (Charge +1) Stable Particles in Matter

VALUE	CL%	DOCUMENT ID		TECN	COMMENT
• • • We do not use the following data for averages, fits, limits, etc. • • •					
$<4\times10^{-17}$	95	[1] YAMAGATA	93	SPEC	Deep sea water, M=5–1600m_p
$<6\times10^{-15}$	95	[2] VERKERK	92	SPEC	Water, M= 10^5 to 3×10^7 GeV
$<7\times10^{-15}$	95	[2] VERKERK	92	SPEC	Water, M= 10^4, 6×10^7 GeV
$<9\times10^{-15}$	95	[2] VERKERK	92	SPEC	Water, M= 10^8 GeV
$<3\times10^{-23}$	90	[3] HEMMICK	90	SPEC	Water, $M = 1000m_p$
$<2\times10^{-21}$	90	[3] HEMMICK	90	SPEC	Water, $M = 5000m_p$
$<3\times10^{-20}$	90	[3] HEMMICK	90	SPEC	Water, $M = 10000m_p$
$<1.\times10^{-29}$		SMITH	82B	SPEC	Water, M=30–400m_p
$<2.\times10^{-28}$		SMITH	82B	SPEC	Water, M=12–1000m_p
$<1.\times10^{-14}$		SMITH	82B	SPEC	Water, M >1000 m_p
$<(0.2\text{–}1.)\times10^{-21}$		SMITH	79	SPEC	Water, M=6–350 m_p

[1] YAMAGATA 93 used deep sea water at 4000 m since the concentration is enhanced in deep sea due to gravity.
[2] VERKERK 92 looked for heavy isotopes in sea water and put a bound on concentration of stable charged massive particle in sea water. The above bound can be translated into into a bound on charged dark matter particle (5×10^6 GeV), assuming the local density, ρ=0.3 GeV/cm^3, and the mean velocity $\langle v\rangle$=300 km/s.
[3] See HEMMICK 90 Fig. 7 for other masses 100–10000 m_p.

Concentration of Heavy Stable Particles Bound to Nuclei

VALUE	CL%	DOCUMENT ID		TECN	COMMENT
• • • We do not use the following data for averages, fits, limits, etc. • • •					
$<1.2\times10^{-11}$	95	[1] JAVORSEK	01	SPEC	Au, M= 3 GeV
$<6.9\times10^{-10}$	95	[1] JAVORSEK	01	SPEC	Au, M= 144 GeV
$<1\ \times10^{-11}$	95	[2] JAVORSEK	01B	SPEC	Au, M= 188 GeV
$<1\ \times10^{-8}$	95	[2] JAVORSEK	01B	SPEC	Au, M= 1669 GeV
$<6\ \times10^{-9}$	95	[2] JAVORSEK	01B	SPEC	Fe, M= 188 GeV
$<1\ \times10^{-8}$	95	[2] JAVORSEK	01B	SPEC	Fe, M= 647 GeV
$<4\ \times10^{-20}$	90	[3] HEMMICK	90	SPEC	C, $M = 100m_p$
$<8\ \times10^{-20}$	90	[3] HEMMICK	90	SPEC	C, $M = 1000m_p$
$<2\ \times10^{-16}$	90	[3] HEMMICK	90	SPEC	C, $M = 10000m_p$
$<6\ \times10^{-13}$	90	[3] HEMMICK	90	SPEC	Li, $M = 1000m_p$
$<1\ \times10^{-11}$	90	[3] HEMMICK	90	SPEC	Be, $M = 1000m_p$
$<6\ \times10^{-14}$	90	[3] HEMMICK	90	SPEC	B, $M = 1000m_p$
$<4\ \times10^{-17}$	90	[3] HEMMICK	90	SPEC	O, $M = 1000m_p$
$<4\ \times10^{-15}$	90	[3] HEMMICK	90	SPEC	F, $M = 1000m_p$
$<1.5\times10^{-13}$/nucleon	68	[4] NORMAN	89	SPEC	^{206}PbX^-
$<1.2\times10^{-12}$/nucleon	68	[4] NORMAN	87	SPEC	^{56,58}FeX^-

Searches Particle Listings

WIMPs and Other Particle Searches

[1] JAVORSEK 01 search for (neutral) SIMPs (strongly interacting massive particles) bound to Au nuclei. Here M is the effective SIMP mass.
[2] JAVORSEK 01B search for (neutral) SIMPs (strongly interacting massive particles) bound to Au and Fe nuclei from various origins with exposures on the earth's surface, in a satellite, heavy ion collisions, etc. Here M is the mass of the anomalous nucleus. See also JAVORSEK 02.
[3] See HEMMICK 90 Fig. 7 for other masses 100–10000 m_p.
[4] Bound valid up to $m_{X^-} \sim 100$ TeV.

GENERAL NEW PHYSICS SEARCHES

This subsection lists some of the search experiments which look for general signatures characteristic of new physics, independent of the framework of a specific model.

The observed events are compatible with Standard Model expectation, unless noted otherwise.

VALUE	DOCUMENT ID		TECN	COMMENT
• • • We do not use the following data for averages, fits, limits, etc. • • •				
	[1] AAD	13A	ATLS	$WW \to \ell\nu\ell'\nu$
	[2] AAD	13C	ATLS	$\gamma + \not{E}_T$
	[3] AALTONEN	13I	CDF	Delayed $\gamma + \not{E}_T$
	[4] CHATRCHYAN	13	CMS	$\ell^+\ell^-$ + jets + $\not{E}_T$
	[5] AAD	12C	ATLS	$t\bar{t} + \not{E}_T$
	[6] AALTONEN	12M	CDF	jet + $\not{E}_T$
	[7] CHATRCHYAN	12AP	CMS	jet + $\not{E}_T$
	[8] CHATRCHYAN	12Q	CMS	Z + jets + $\not{E}_T$
	[9] CHATRCHYAN	12T	CMS	$\gamma + \not{E}_T$
	[10] AAD	11S	ATLS	jet + $\not{E}_T$
	[11] AALTONEN	11AF	CDF	$\ell^\pm\ell^\pm$
	[12] CHATRCHYAN	11C	CMS	$\ell^+\ell^-$ + jets + $\not{E}_T$
	[13] CHATRCHYAN	11U	CMS	jet + $\not{E}_T$
	[14] AALTONEN	10AF	CDF	$\gamma\gamma + \ell$, $\not{E}_T$
	[15] AALTONEN	09AF	CDF	$\ell\gamma b\not{E}_T$
	[16] AALTONEN	09G	CDF	$\ell\ell\ell\not{E}_T$

[1] AAD 13A search for resonant WW production in pp collisions at $E_{cm} = 7$ TeV with $L = 4.7$ fb^{-1}.
[2] AAD 13C search for events with a photon and missing $\not{E}_T$ in pp collisions at $E_{cm} = 7$ TeV with $L = 4.6$ fb^{-1}.
[3] AALTONEN 13I search for events with a photon and missing E_T, where the photon is detected after the expected timing, in $p\bar{p}$ collisions at $E_{cm} = 1.96$ TeV with $L = 6.3$ fb^{-1}. The data are consistent with the Standard Model expectation.
[4] CHATRCHYAN 13 search for events with an opposite-sign lepton pair, jets, and missing E_T in pp collisions at $E_{cm} = 7$ TeV with $L = 4.98$ fb^{-1}.
[5] AAD 12C search for events with a $t\bar{t}$ pair and missing $\not{E}_T$ in pp collisions at $E_{cm} = 7$ TeV with $L = 1.04$ fb^{-1}.
[6] AALTONEN 12M search for events with a jet and missing E_T in $p\bar{p}$ collisions at $E_{cm} = 1.96$ TeV with $L = 6.7$ fb^{-1}.
[7] CHATRCHYAN 12AP search for events with a jet and missing E_T in pp collisions at $E_{cm} = 7$ TeV with $L = 5.0$ fb^{-1}.
[8] CHATRCHYAN 12Q search for events with a Z, jets, and missing $\not{E}_T$ in pp collisions at $E_{cm} = 7$ TeV with $L = 4.98$ fb^{-1}.
[9] CHATRCHYAN 12T search for events with a photon and missing $\not{E}_T$ in pp collisions at $E_{cm} = 7$ TeV with $L = 5.0$ fb^{-1}.
[10] AAD 11S search for events with one jet and missing E_T in pp collisions at $E_{cm} = 7$ TeV with $L = 33$ pb^{-1}.
[11] AALTONEN 11AF search for high-p_T like-sign dileptons in $p\bar{p}$ collisions at $E_{cm} = 1.96$ TeV with $L = 6.1$ fb^{-1}.
[12] CHATRCHYAN 11C search for events with an opposite-sign lepton pair, jets, and missing E_T in pp collisions at $E_{cm} = 7$ TeV with $L = 34$ pb^{-1}.
[13] CHATRCHYAN 11U search for events with one jet and missing E_T in pp collisions at $E_{cm} = 7$ TeV with $L = 36$ pb^{-1}.
[14] AALTONEN 10AF search for $\gamma\gamma$ events with e, μ, τ, or missing E_T in $p\bar{p}$ collisions at $E_{cm} = 1.96$ TeV with $L = 1.1$–2.0 fb^{-1}.
[15] AALTONEN 09AF search for $\ell\gamma b$ events with missing E_T in $p\bar{p}$ collisions at $E_{cm} = 1.96$ TeV with $L = 1.9$ fb^{-1}. The observed events are compatible with Standard Model expectation including $t\bar{t}\gamma$ production.
[16] AALTONEN 09G search for $\mu\mu\mu$ and $\mu\mu e$ events with missing E_T in $p\bar{p}$ collisions at $E_{cm} = 1.96$ TeV with $L = 976$ pb^{-1}.

LIMITS ON JET-JET RESONANCES

Heavy Particle Production Cross Section

Limits are for a particle decaying to two hadronic jets.

Units(pb)	CL%	Mass(GeV)	DOCUMENT ID		TECN	COMMENT
• • • We do not use the following data for averages, fits, limits, etc. • • •						
			[1] AAD	13D	ATLS	7 TeV $pp \to 2$ jets
			[2] AALTONEN	13R	CDF	1.96 TeV $p\bar{p} \to 4$ jets
			[3] CHATRCHYAN	13A	CMS	7 TeV $pp \to 2$ jets
			[4] CHATRCHYAN	13A	CMS	7 TeV $pp \to b\bar{b}X$
			[5] AAD	12S	ATLS	7 TeV $pp \to 2$ jets
			[6] CHATRCHYAN	12BL	CMS	7 TeV $pp \to t\bar{t}X$
			[7] AAD	11AG	ATLS	7 TeV $pp \to 2$ jets
			[8] AALTONEN	11M	CDF	1.96 TeV $p\bar{p} \to W+$ 2 jets
			[9] ABAZOV	11I	D0	1.96 TeV $p\bar{p} \to W+$ 2 jets
			[10] AAD	10	ATLS	7 TeV $pp \to 2$ jets
			[11] KHACHATRY...10		CMS	7 TeV $pp \to 2$ jets
			[12] ABE	99F	CDF	1.8 TeV $p\bar{p} \to b\bar{b}+$ anything
			[13] ABE	97G	CDF	1.8 TeV $p\bar{p} \to 2$ jets
<2603	95	200	[14] ABE	93G	CDF	1.8 TeV $p\bar{p} \to 2$ jets
< 44	95	400	[14] ABE	93G	CDF	1.8 TeV $p\bar{p} \to 2$ jets
< 7	95	600	[14] ABE	93G	CDF	1.8 TeV $p\bar{p} \to 2$ jets

[1] AAD 13D search for dijet resonances in pp collisions at $E_{cm} = 7$ TeV with $L = 4.8$ fb^{-1}. The observed events are compatible with Standard Model expectation. See their Fig. 6 and Table 2 for limits on resonance cross section in the range $m = 1.0$–4.0 TeV.
[2] AALTONEN 13R search for production of a pair of jet-jet resonances in $p\bar{p}$ collisions at $E_{cm} = 1.96$ TeV with $L = 6.6$ fb^{-1}. See their Fig. 5 and Tables I, II for cross section limits.
[3] CHATRCHYAN 13A search for qq, qg, and gg resonances in pp collisions at $E_{cm} = 7$ TeV with $L = 4.8$ fb^{-1}. See their Fig. 3 and Table 1 for limits on resonance cross section in the range $m = 1.0$–4.3 TeV.
[4] CHATRCHYAN 13A search for $b\bar{b}$ resonances in pp collisions at $E_{cm} = 7$ TeV with $L = 4.8$ fb^{-1}. See their Fig. 8 and Table 4 for limits on resonance cross section in the range $m = 1.0$–4.0 TeV.
[5] AAD 12S search for dijet resonances in pp collisions at $E_{cm} = 7$ TeV with $L = 1.0$ fb^{-1}. See their Fig. 3 and Table 2 for limits on resonance cross section in the range $m = 0.9$–4.0 TeV.
[6] CHATRCHYAN 12BL search for $t\bar{t}$ resonances in pp collisions at $E_{cm} = 7$ TeV with $L = 4.4$ fb^{-1}. See their Fig. 4 for limits on resonance cross section in the range $m = 0.5$–3.0 TeV.
[7] AAD 11AG search for dijet resonances in pp collisions at $E_{cm} = 7$ TeV with L = 36 pb^{-1}. Limits on number of events for $m = 0.6$–4 TeV are given in their Table 3.
[8] AALTONEN 11M find a peak in two jet invariant mass distribution around 140 GeV in $W + 2$ jet events in $p\bar{p}$ collisions at $E_{cm} = 1.96$ TeV with L = 4.3 fb^{-1}.
[9] ABAZOV 11I search for two-jet resonances in $W + 2$ jet events in $p\bar{p}$ collisions at $E_{cm} = 1.96$ TeV with L = 4.3 fb^{-1} and give limits $\sigma <$ (2.6–1.3) pb (95% CL) for $m =$ 110–170 GeV. The result is incompatible with AALTONEN 11M.
[10] AAD 10 search for narrow dijet resonances in pp collisions at $E_{cm} = 7$ TeV with L = 315 nb^{-1}. Limits on the cross section in the range 10–10^3 pb is given for $m =$ 0.3–1.7 TeV.
[11] KHACHATRYAN 10 search for narrow dijet resonances in pp collisions at $E_{cm} = 7$ TeV with L = 2.9 pb^{-1}. Limits on the cross section in the range 1–300 pb is given for $m =$ 0.5–2.6 TeV separately in the final states qq, qg, and gg.
[12] ABE 99F search for narrow $b\bar{b}$ resonances in $p\bar{p}$ collisions at E_{cm}=1.8 TeV. Limits on $\sigma(p\bar{p} \to X+$ anything)×B($X \to b\bar{b}$) in the range 3–10^3 pb (95%CL) are given for m_X=200–750 GeV. See their Table I.
[13] ABE 97G search for narrow dijet resonances in $p\bar{p}$ collisions with 106 pb^{-1} of data at $E_{cm} = 1.8$ TeV. Limits on $\sigma(p\bar{p} \to X +$ anything)·B($X \to jj$) in the range 10^4–10^{-1} pb (95%CL) are given for dijet mass m=200–1150 GeV with both jets having $|\eta| < 2.0$ and the dijet system having $|\cos\theta^*| < 0.67$. See their Table I for the list of limits. Supersedes ABE 93G.
[14] ABE 93G give cross section times branching ratio into light (d, u, s, c, b) quarks for $\Gamma = 0.02\,M$. Their Table II gives limits for $M =$ 200–900 GeV and $\Gamma = (0.02$–$0.2)\,M$.

LIMITS ON NEUTRAL PARTICLE PRODUCTION

Production Cross Section of Radiatively-Decaying Neutral Particle

VALUE (pb)	CL%	DOCUMENT ID		TECN	COMMENT
• • • We do not use the following data for averages, fits, limits, etc. • • •					
<(0.043–0.17)	95	[1] ABBIENDI	00D	OPAL	$e^+e^- \to X^0Y^0$, $X^0 \to Y^0\gamma$
<(0.05–0.8)	95	[2] ABBIENDI	00D	OPAL	$e^+e^- \to X^0X^0$, $X^0 \to Y^0\gamma$
<(2.5–0.5)	95	[3] ACKERSTAFF	97B	OPAL	$e^+e^- \to X^0Y^0$, $X^0 \to Y^0\gamma$
<(1.6–0.9)	95	[4] ACKERSTAFF	97B	OPAL	$e^+e^- \to X^0X^0$, $X^0 \to Y^0\gamma$

[1] ABBIENDI 00D associated production limit is for m_{X^0}= 90–188 GeV, m_{Y^0}=0 at E_{cm}=189 GeV. See also their Fig. 9.
[2] ABBIENDI 00D pair production limit is for m_{X^0} = 45–94 GeV, m_{Y^0}=0 at E_{cm}=189 GeV. See also their Fig. 12.
[3] ACKERSTAFF 97B associated production limit is for m_{X^0} = 80–160 GeV, m_{Y^0}=0 from 10.0 pb^{-1} at $E_{cm} = 161$ GeV. See their Fig. 3(a).
[4] ACKERSTAFF 97B pair production limit is for m_{X^0} = 40–80 GeV, m_{Y^0}=0 from 10.0 pb^{-1} at $E_{cm} = 161$ GeV. See their Fig. 3(b).

Heavy Particle Production Cross Section

VALUE (cm^2/N)	CL%	EVTS	DOCUMENT ID		TECN	COMMENT
• • • We do not use the following data for averages, fits, limits, etc. • • •						
			[1] ADAMS	97B	KTEV	m= 1.2–5 GeV
$< 10^{-36}$–10^{-33}	90		[2] GALLAS	95	TOF	m= 0.5–20 GeV
$<(4$–$0.3)\times10^{-31}$	95		[3] AKESSON	91	CNTR	m = 0–5 GeV
$<2 \times 10^{-36}$	90	0	[4] BADIER	86	BDMP	$\tau = (0.05$–$1.)\times10^{-8}$ s
$<2.5 \times 10^{-35}$		0	[5] GUSTAFSON	76	CNTR	$\tau > 10^{-7}$ s

[1] ADAMS 97B search for a hadron-like neutral particle produced in pN interactions, which decays into a ρ^0 and a weakly interacting massive particle. Upper limits are given for the ratio to K_L production for the mass range 1.2–5 GeV and lifetime 10^{-9}–10^{-4} s. See also our Light Gluino Section.

[2] GALLAS 95 limit is for a weakly interacting neutral particle produced in 800 GeV/c pN interactions decaying with a lifetime of 10^{-4}–10^{-8} s. See their Figs. 8 and 9. Similar limits are obtained for a stable particle with interaction cross section 10^{-29}–10^{-33} cm^2. See Fig. 10.

[3] AKESSON 91 limit is from weakly interacting neutral long-lived particles produced in pN reaction at 450 GeV/c performed at CERN SPS. Bourquin-Gaillard formula is used as the production model. The above limit is for $\tau > 10^{-7}$ s. For $\tau > 10^{-9}$ s, $\sigma < 10^{-30}$ cm^{-2}/nucleon is obtained.

[4] BADIER 86 looked for long-lived particles at 300 GeV π^- beam dump. The limit applies for nonstrongly interacting neutral or charged particles with mass >2 GeV. The limit applies for particle modes, $\mu^+\pi^-$, $\mu^+\mu^-$, $\pi^+\pi^-$X, $\pi^+\pi^-\pi^\pm$ etc. See their figure 5 for the contours of limits in the mass-τ plane for each mode.

[5] GUSTAFSON 76 is a 300 GeV FNAL experiment looking for heavy (m >2 GeV) long-lived neutral hadrons in the M4 neutral beam. The above typical value is for $m = 3$ GeV and assumes an interaction cross section of 1 mb. Values as a function of mass and interaction cross section are given in figure 2.

Production of New Penetrating Non-ν Like States in Beam Dump

VALUE	DOCUMENT ID		TECN	COMMENT
• • • We do not use the following data for averages, fits, limits, etc. • • •				
	[1] LOSECCO	81	CALO	28 GeV protons

[1] No excess neutral-current events leads to σ(production) $\times$ σ(interaction)$\times$acceptance $< 2.26 \times 10^{-71}$ cm^4/nucleon^2 (CL = 90%) for light neutrals. Acceptance depends on models (0.1 to 4. $\times 10^{-4}$).

LIMITS ON CHARGED PARTICLES IN e^+e^-

Heavy Particle Production Cross Section in e^+e^-

Ratio to $\sigma(e^+e^- \to \mu^+\mu^-)$ unless noted. See also entries in Free Quark Search and Magnetic Monopole Searches.

VALUE	CL%	EVTS	DOCUMENT ID		TECN	COMMENT
• • • We do not use the following data for averages, fits, limits, etc. • • •						
			[1] ACKERSTAFF	98P	OPAL	Q=1,2/3, m=45–89.5 GeV
			[2] ABREU	97D	DLPH	Q=1,2/3, m=45–84 GeV
			[3] BARATE	97K	ALEP	Q=1, m=45–85 GeV
$<2 \times 10^{-5}$	95		[4] AKERS	95R	OPAL	Q=1, m= 5–45 GeV
$<1 \times 10^{-5}$	95		[4] AKERS	95R	OPAL	Q=2, m= 5–45 GeV
$<2 \times 10^{-3}$	90		[5] BUSKULIC	93C	ALEP	Q=1, m=32–72 GeV
$<(10^{-2}$–1)	95		[6] ADACHI	90C	TOPZ	Q = 1, m = 1–16, 18–27 GeV
$<7 \times 10^{-2}$	90		[7] ADACHI	90E	TOPZ	Q = 1, m = 5–25 GeV
$<1.6 \times 10^{-2}$	95	0	[8] KINOSHITA	82	PLAS	Q=3–180, m <14.5 GeV
$<5.0 \times 10^{-2}$	90	0	[9] BARTEL	80	JADE	Q=(3,4,5)/3 2–12 GeV

[1] ACKERSTAFF 98P search for pair production of long-lived charged particles at E_{cm} between 130 and 183 GeV and give limits $\sigma <$(0.05–0.2) pb (95%CL) for spin-0 and spin-1/2 particles with m=45–89.5 GeV, charge 1 and 2/3. The limit is translated to the cross section at E_{cm}=183 GeV with the s dependence described in the paper. See their Figs. 2–4.

[2] ABREU 97D search for pair production of long-lived particles and give limits $\sigma <$(0.4–2.3) pb (95%CL) for various center-of-mass energies E_{cm}=130–136, 161, and 172 GeV, assuming an almost flat production distribution in cosθ.

[3] BARATE 97K search for pair production of long-lived charged particles at E_{cm} = 130, 136, 161, and 172 GeV and give limits $\sigma <$(0.2–0.4) pb (95%CL) for spin-0 and spin-1/2 particles with m=45–85 GeV. The limit is translated to the cross section at E_{cm}=172 GeV with the E_{cm} dependence described in the paper. See their Figs. 2 and 3 for limits on $J = 1/2$ and $J = 0$ cases.

[4] AKERS 95R is a CERN-LEP experiment with $W_{cm} \sim m_Z$. The limit is for the production of a stable particle in multihadron events normalized to $\sigma(e^+e^- \to$ hadrons). Constant phase space distribution is assumed. See their Fig. 3 for bounds for $Q = \pm 2/3$, $\pm 4/3$.

[5] BUSKULIC 93C is a CERN-LEP experiment with $W_{cm} = m_Z$. The limit is for a pair or single production of heavy particles with unusual ionization loss in TPC. See their Fig. 5 and Table 1.

[6] ADACHI 90C is a KEK-TRISTAN experiment with W_{cm} = 52–60 GeV. The limit is for pair production of a scalar or spin-1/2 particle. See Figs. 3 and 4.

[7] ADACHI 90E is KEK-TRISTAN experiment with W_{cm} = 52–61.4 GeV. The above limit is for inclusive production cross section normalized to $\sigma(e^+e^- \to \mu^+\mu^-)\cdot\beta(3-\beta^2)/2$, where $\beta = (1 - 4m^2/W_{cm}^2)^{1/2}$. See the paper for the assumption about the production mechanism.

[8] KINOSHITA 82 is SLAC PEP experiment at W_{cm} = 29 GeV using lexan and ^{39}Cr plastic sheets sensitive to highly ionizing particles.

[9] BARTEL 80 is DESY-PETRA experiment with W_{cm} = 27–35 GeV. Above limit is for inclusive pair production and ranges between 1. $\times 10^{-1}$ and 1. $\times 10^{-2}$ depending on mass and production momentum distributions. (See their figures 9, 10, 11).

Branching Fraction of Z^0 to a Pair of Stable Charged Heavy Fermions

VALUE	CL%	DOCUMENT ID		TECN	COMMENT
• • • We do not use the following data for averages, fits, limits, etc. • • •					
$<5 \times 10^{-6}$	95	[1] AKERS	95R	OPAL	m= 40.4–45.6 GeV
$<1 \times 10^{-3}$	95	AKRAWY	90O	OPAL	m = 29–40 GeV

[1] AKERS 95R give the 95% CL limit $\sigma(X\overline{X})/\sigma(\mu\mu) < 1.8\times10^{-4}$ for the pair production of singly- or doubly-charged stable particles. The limit applies for the mass range 40.4–45.6 GeV for $X^\pm$ and < 45.6 GeV for $X^{\pm\pm}$. See the paper for bounds for $Q = \pm 2/3$, $\pm 4/3$.

LIMITS ON CHARGED PARTICLES IN HADRONIC REACTIONS

MASS LIMITS for Long-Lived Charged Heavy Fermions

Limits are for spin 1/2 particles with no color and SU(2)$_L$ charge. The electric charge Q of the particle (in the unit of e) is therefore equal to its weak hypercharge. Pair production by Drell-Yan like γ and Z exchange is assumed to derive the limits.

VALUE (GeV)	CL%	DOCUMENT ID		TECN	COMMENT
• • • We do not use the following data for averages, fits, limits, etc. • • •					
>200	95	[1] CHATRCHYAN	13AB	CMS	$\|Q\| = 1/3$
>480	95	[1] CHATRCHYAN	13AB	CMS	$\|Q\| = 2/3$
>574	95	[1] CHATRCHYAN	13AB	CMS	$\|Q\| = 1$
>685	95	[1] CHATRCHYAN	13AB	CMS	$\|Q\| = 2$
>140	95	[2] CHATRCHYAN	13AR	CMS	$\|Q\| = 1/3$
>310	95	[2] CHATRCHYAN	13AR	CMS	$\|Q\| = 2/3$

[1] CHATRCHYAN 13AB use 5.0 fb^{-1} of pp collisions at E_{cm} = 7 TeV and 18.8 fb^{-1} at E_{cm} = 8 TeV. See paper for limits for $|Q| = 3, 4, \ldots, 8$.

[2] CHATRCHYAN 13AR use 5.0 fb^{-1} of pp collisions at E_{cm} = 7 TeV.

Heavy Particle Production Cross Section

VALUE (nb)	CL%	DOCUMENT ID		TECN	COMMENT
• • • We do not use the following data for averages, fits, limits, etc. • • •					
		[1] AAD	13AH	ATLS	|q|=(2–6)e, m=50–600 GeV
$<1.2 \times 10^{-3}$	95	[2] AAD	11I	ATLS	|q|=10e, m=0.2–1 TeV
$<1.0 \times 10^{-5}$	95	[3,4] AALTONEN	09Z	CDF	m>100 GeV, noncolored
$<4.8 \times 10^{-5}$	95	[3,5] AALTONEN	09Z	CDF	m>100 GeV, colored
$<$ 0.31–0.04 $\times 10^{-3}$	95	[6] ABAZOV	09M	D0	pair production
<0.19	95	[7] AKTAS	04C	H1	m=3–10 GeV
<0.05	95	[8] ABE	92J	CDF	m=50–200 GeV
<30–130		[9] CARROLL	78	SPEC	m=2–2.5 GeV
<100		[10] LEIPUNER	73	CNTR	m=3–11 GeV

[1] AAD 13AH search for production of long-lived particles with $|q|$=(2–6)e in pp collisions at E_{cm} = 7 TeV with 4.4 fb^{-1}. See their Fig. 8 for cross section limits.

[2] AAD 11I search for production of highly ionizing massive particles in pp collisions at E_{cm} = 7 TeV with L = 3.1 pb^{-1}. See their Table 5 for similar limits for $|q| = 6e$ and $17e$, Table 6 for limits on pair production cross section.

[3] AALTONEN 09Z search for long-lived charged particles in $p\overline{p}$ collisions at E_{cm} = 1.96 TeV with L = 1.0 fb^{-1}. The limits are on production cross section for a particle of mass above 100 GeV in the region $|\eta| \lesssim 0.7$, $p_T > 40$ GeV, and $0.4 < \beta < 1.0$.

[4] Limit for weakly interacting charge-1 particle.

[5] Limit for up-quark like particle.

[6] ABAZOV 09M search for pair production of long-lived charged particles in $p\overline{p}$ collisions at E_{cm} = 1.96 TeV with L = 1.1 fb^{-1}. Limit on the cross section of (0.31–0.04) pb (95% CL) is given for the mass range of 60–300 GeV, assuming the kinematics of stau pair production.

[7] AKTAS 04C look for charged particle photoproduction at HERA with mean c.m. energy of 200 GeV.

[8] ABE 92J look for pair production of unit-charged particles which leave detector before decaying. Limit shown here is for m=50 GeV. See their Fig. 5 for different charges and stronger limits for higher mass.

[9] CARROLL 78 look for neutral, $S = -2$ dihyperon resonance in $pp \to 2K^+$X. Cross section varies within above limits over mass range and p_{lab} = 5.1–5.9 GeV/c.

[10] LEIPUNER 73 is an NAL 300 GeV p experiment. Would have detected particles with lifetime greater than 200 ns.

Heavy Particle Production Differential Cross Section

VALUE (cm^{2}sr^{-1}GeV^{-1})	CL%	DOCUMENT ID		TECN	CHG	COMMENT
• • • We do not use the following data for averages, fits, limits, etc. • • •						
$<2.6 \times 10^{-36}$	90	[1] BALDIN	76	CNTR	–	Q= 1, m=2.1–9.4 GeV
$<2.2 \times 10^{-33}$	90	[2] ALBROW	75	SPEC	±	Q= ±1, m=4–15 GeV
$<1.1 \times 10^{-33}$	90	[2] ALBROW	75	SPEC	±	Q= ±2, m=6–27 GeV
$<8. \times 10^{-35}$	90	[3] JOVANOV...	75	CNTR	±	m=15–26 GeV
$<1.5 \times 10^{-34}$	90	[3] JOVANOV...	75	CNTR	±	Q= ±2, m=3–10 GeV
$<6. \times 10^{-35}$	90	[3] JOVANOV...	75	CNTR	±	Q= ±2, m=10–26 GeV
$<1. \times 10^{-31}$	90	[4] APPEL	74	CNTR	±	m=3.2–7.2 GeV
$<5.8 \times 10^{-34}$	90	[5] ALPER	73	SPEC	±	m=1.5–24 GeV
$<1.2 \times 10^{-35}$	90	[6] ANTIPOV	71B	CNTR	–	Q=–, m=2.2–2.8
$<2.4 \times 10^{-35}$	90	[7] ANTIPOV	71C	CNTR	–	Q=–, m=1.2–1.7, 2.1–4
$<2.4 \times 10^{-35}$	90	BINON	69	CNTR	–	Q=–, m=1–1.8 GeV
$<1.5 \times 10^{-36}$		[8] DORFAN	65	CNTR		Be target m=3–7 GeV
$<3.0 \times 10^{-36}$		[8] DORFAN	65	CNTR		Fe target m=3–7 GeV

[1] BALDIN 76 is a 70 GeV Serpukhov experiment. Value is per Al nucleus at $\theta = 0$. For other charges in range -0.5 to -3.0, CL = 90% limit is $(2.6 \times 10^{-36})/|(\text{charge})|$ for mass range (2.1–9.4 GeV) $\times$ $|(\text{charge})|$. Assumes stable particle interacting with matter as do antiprotons.

[2] ALBROW 75 is a CERN ISR experiment with E_{cm} = 53 GeV. θ = 40 mr. See figure 5 for mass ranges up to 35 GeV.

[3] JOVANOVICH 75 is a CERN ISR 26+26 and 15+15 GeV pp experiment. Figure 4 covers ranges $Q = 1/3$ to 2 and m = 3 to 26 GeV. Value is per GeV momentum.

[4] APPEL 74 is NAL 300 GeV pW experiment. Studies forward production of heavy (up to 24 GeV) charged particles with momenta 24–200 GeV (−charge) and 40–150 GeV (+charge). Above typical value is for 75 GeV and is per GeV momentum per nucleon.

[5] ALPER 73 is CERN ISR 26+26 GeV pp experiment. p >0.9 GeV, $0.2 < \beta < 0.65$.

[6] ANTIPOV 71B is from same 70 GeV p experiment as ANTIPOV 71C and BINON 69.

[7] ANTIPOV 71C limit inferred from flux ratio. 70 GeV p experiment.

[8] DORFAN 65 is a 30 GeV/c p experiment at BNL. Units are per GeV momentum per nucleus.

Long-Lived Heavy Particle Invariant Cross Section

VALUE ($cm^2/GeV^2/N$)	CL%	DOCUMENT ID		TECN	CHG	COMMENT
• • • We do not use the following data for averages, fits, limits, etc. • • •						
<5–700×10^{-35}	90	[1] BERNSTEIN	88	CNTR		
<5–700×10^{-37}	90	[1] BERNSTEIN	88	CNTR		
$<2.5\times10^{-36}$	90	[2] THRON	85	CNTR	−	Q= 1, m=4–12 GeV
$<1.\times10^{-35}$	90	[2] THRON	85	CNTR	+	Q= 1, m=4–12 GeV
$<6.\times10^{-33}$	90	[3] ARMITAGE	79	SPEC		m=1.87 GeV
$<1.5\times10^{-33}$	90	[3] ARMITAGE	79	SPEC		m=1.5–3.0 GeV
		[4] BOZZOLI	79	CNTR	±	Q = (2/3, 1, 4/3, 2)
$<1.1\times10^{-37}$	90	[5] CUTTS	78	CNTR		m=4–10 GeV
$<3.0\times10^{-37}$	90	[6] VIDAL	78	CNTR		m=4.5–6 GeV

[1] BERNSTEIN 88 limits apply at $x = 0.2$ and $p_T = 0$. Mass and lifetime dependence of limits are shown in the regions: m = 1.5–7.5 GeV and $\tau = 10^{-8}$–2×10^{-6} s. First number is for hadrons; second is for weakly interacting particles.
[2] THRON 85 is FNAL 400 GeV proton experiment. Mass determined from measured velocity and momentum. Limits are for $\tau > 3\times10^{-9}$ s.
[3] ARMITAGE 79 is CERN-ISR experiment at $E_{cm} = 53$ GeV. Value is for $x = 0.1$ and $p_T = 0.15$. Observed particles at $m = 1.87$ GeV are found all consistent with being antideuterons.
[4] BOZZOLI 79 is CERN-SPS 200 GeV pN experiment. Looks for particle with τ larger than 10^{-8} s. See their figure 11–18 for production cross-section upper limits vs mass.
[5] CUTTS 78 is pBe experiment at FNAL sensitive to particles of $\tau > 5\times10^{-8}$ s. Value is for $-0.3 < x < 0$ and $p_T = 0.175$.
[6] VIDAL 78 is FNAL 400 GeV proton experiment. Value is for $x = 0$ and $p_T = 0$. Puts lifetime limit of $< 5\times10^{-8}$ s on particle in this mass range.

Long-Lived Heavy Particle Production (σ(Heavy Particle) / $\sigma(\pi)$)

VALUE	EVTS	DOCUMENT ID		TECN	CHG	COMMENT
• • • We do not use the following data for averages, fits, limits, etc. • • •						
$<10^{-8}$		[1] NAKAMURA	89	SPEC	±	Q= (−5/3,±2)
	0	[2] BUSSIERE	80	CNTR	±	Q= (2/3,1,4/3,2)

[1] NAKAMURA 89 is KEK experiment with 12 GeV protons on Pt target. The limit applies for mass $\lesssim$ 1.6 GeV and lifetime $\gtrsim 10^{-7}$ s.
[2] BUSSIERE 80 is CERN-SPS experiment with 200–240 GeV protons on Be and Al target. See their figures 6 and 7 for cross-section ratio vs mass.

Production and Capture of Long-Lived Massive Particles

VALUE (10^{-36} cm^2)	EVTS	DOCUMENT ID		TECN	COMMENT
• • • We do not use the following data for averages, fits, limits, etc. • • •					
<20 to 800	0	[1] ALEKSEEV	76	ELEC	τ=5 ms to 1 day
<200 to 2000	0	[1] ALEKSEEV	76B	ELEC	τ=100 ms to 1 day
<1.4 to 9	0	[2] FRANKEL	75	CNTR	τ=50 ms to 10 hours
<0.1 to 9	0	[3] FRANKEL	74	CNTR	τ=1 to 1000 hours

[1] ALEKSEEV 76 and ALEKSEEV 76B are 61–70 GeV p Serpukhov experiment. Cross section is per Pb nucleus.
[2] FRANKEL 75 is extension of FRANKEL 74.
[3] FRANKEL 74 looks for particles produced in thick Al targets by 300–400 GeV/c protons.

Long-Lived Particle Search at Hadron Collisions

Limits are for cross section times branching ratio.

VALUE (pb/nucleon)	CL%	EVTS	DOCUMENT ID		TECN	COMMENT
• • • We do not use the following data for averages, fits, limits, etc. • • •						
<2	90	0	[1] BADIER	86	BDMP	$\tau = (0.05$–$1.)\times10^{-8}$s

[1] BADIER 86 looked for long-lived particles at 300 GeV π^- beam dump. The limit applies for nonstrongly interacting neutral or charged particles with mass >2 GeV. The limit applies for particle modes, $\mu^+\pi^-$, $\mu^+\mu^-$, $\pi^+\pi^-$X, $\pi^+\pi^-\pi^\pm$ etc. See their figure 5 for the contours of limits in the mass-τ plane for each mode.

Long-Lived Heavy Particle Cross Section

VALUE (pb/sr)	CL%	DOCUMENT ID		TECN	COMMENT
• • • We do not use the following data for averages, fits, limits, etc. • • •					
<34	95	[1] RAM	94	SPEC	$1015 < m_{X^{++}} < 1085$ MeV
<75	95	[1] RAM	94	SPEC	$920 < m_{X^{++}} < 1025$ MeV

[1] RAM 94 search for a long-lived doubly-charged fermion X^{++} with mass between m_N and m_N+m_π and baryon number +1 in the reaction $pp \to X^{++}n$. No candidate is found. The limit is for the cross section at 15° scattering angle at 460 MeV incident energy and applies for $\tau(X^{++}) \gg 0.1$ μs.

LIMITS ON CHARGED PARTICLES IN COSMIC RAYS

Heavy Particle Flux in Cosmic Rays

VALUE ($cm^{-2}sr^{-1}s^{-1}$)	CL%	EVTS	DOCUMENT ID		TECN	CHG	COMMENT
• • • We do not use the following data for averages, fits, limits, etc. • • •							
$\sim 6\times10^{-9}$		2	[1] SAITO	90			$Q \simeq 14$, $m \simeq 370m_p$
$<1.4\times10^{-12}$	90	0	[2] MINCER	85	CALO		$m \geq 1$ TeV
			[3] SAKUYAMA	83B	PLAS		$m \sim 1$ TeV
$<1.7\times10^{-11}$	99	0	[4] BHAT	82	CC		
$<1.\times10^{-9}$	90	0	[5] MARINI	82	CNTR	±	Q= 1, $m \sim 4.5m_p$
$2.\times10^{-9}$		3	[6] YOCK	81	SPRK	±	Q= 1, $m \sim 4.5m_p$
		3	[6] YOCK	81	SPRK		Fractionally charged
3.0×10^{-9}		3	[7] YOCK	80	SPRK		$m \sim 4.5$ m_p
$(4\ \pm1)\times10^{-11}$		3	GOODMAN	79	ELEC		$m \geq 5$ GeV
$<1.3\times10^{-9}$	90		[8] BHAT	78	CNTR	±	m >1 GeV
$<1.0\times10^{-9}$		0	BRIATORE	76	ELEC		
$<7.\times10^{-10}$	90	0	YOCK	75	ELEC	±	Q >7e or $<-7e$
$>6.\times10^{-9}$		5	[9] YOCK	74	CNTR		m >6 GeV
$<3.0\times10^{-8}$		0	DARDO	72	CNTR		
$<1.5\times10^{-9}$		0	TONWAR	72	CNTR		m >10 GeV
$<3.0\times10^{-10}$		0	BJORNBOE	68	CNTR		m >5 GeV
$<5.0\times10^{-11}$	90	0	JONES	67	ELEC		m=5–15 GeV

[1] SAITO 90 candidates carry about 450 MeV/nucleon. Cannot be accounted for by conventional backgrounds. Consistent with strange quark matter hypothesis.
[2] MINCER 85 is high statistics study of calorimeter signals delayed by 20–200 ns. Calibration with AGS beam shows they can be accounted for by rare fluctuations in signals from low-energy hadrons in the shower. Claim that previous delayed signals including BJORNBOE 68, DARDO 72, BHAT 82, SAKUYAMA 83B below may be due to this fake effect.
[3] SAKUYAMA 83B analyzed 6000 extended air shower events. Increase of delayed particles and change of lateral distribution above 10^{17} eV may indicate production of very heavy parent at top of atmosphere.
[4] BHAT 82 observed 12 events with delay $> 2.\times10^{-8}$ s and with more than 40 particles. 1 eV has good hadron shower. However all events are delayed in only one of two detectors in cloud chamber, and could not be due to strongly interacting massive particle.
[5] MARINI 82 applied PEP-counter for TOF. Above limit is for velocity = 0.54 of light. Limit is inconsistent with YOCK 80 YOCK 81 events if isotropic dependence on zenith angle is assumed.
[6] YOCK 81 saw another 3 events with $Q = \pm1$ and m about $4.5m_p$ as well as 2 events with $m > 5.3m_p$, $Q = \pm0.75 \pm 0.05$ and $m > 2.8m_p$, $Q = \pm0.70 \pm 0.05$ and 1 event with $m = (9.3 \pm 3.)m_p$, $Q = \pm0.89 \pm 0.06$ as possible heavy candidates.
[7] YOCK 80 events are with charge exactly or approximately equal to unity.
[8] BHAT 78 is at Kolar gold fields. Limit is for $\tau > 10^{-6}$ s.
[9] YOCK 74 events could be tritons.

Superheavy Particle (Quark Matter) Flux in Cosmic Rays

VALUE ($cm^{-2}sr^{-1}s^{-1}$)	CL%	EVTS	DOCUMENT ID		TECN	COMMENT
• • • We do not use the following data for averages, fits, limits, etc. • • •						
$<5\ \times10^{-16}$	90		[1] AMBROSIO	00B	MCRO	$m > 5\times10^{14}$ GeV
$<1.8\times10^{-12}$	90		[2] ASTONE	93	CNTR	$m \geq 1.5\times10^{-13}$gram
$<1.1\times10^{-14}$	90		[3] AHLEN	92	MCRO	$10^{-10} < m < 0.1$ gram
$<2.2\times10^{-14}$	90	0	[4] NAKAMURA	91	PLAS	$m > 10^{11}$ GeV
$<6.4\times10^{-16}$	90	0	[5] ORITO	91	PLAS	$m > 10^{12}$ GeV
$<2.0\times10^{-11}$	90		[6] LIU	88	BOLO	$m > 1.5\times10^{-13}$ gram
$<4.7\times10^{-12}$	90		[7] BARISH	87	CNTR	$1.4\times10^{8} < m < 10^{12}$ GeV
$<3.2\times10^{-11}$	90	0	[8] NAKAMURA	85	CNTR	$m > 1.5\times10^{-13}$gram
$<3.5\times10^{-11}$	90	0	[9] ULLMAN	81	CNTR	Planck-mass 10^{19}GeV
$<7.\times10^{-11}$	90	0	[9] ULLMAN	81	CNTR	$m \leq 10^{16}$ GeV

[1] AMBROSIO 00B searched for quark matter ("nuclearites") in the velocity range $(10^{-5}$–$1)$ c. The listed limit is for 2×10^{-3} c.
[2] ASTONE 93 searched for quark matter ("nuclearites") in the velocity range $(10^{-3}$–$1)$ c. Their Table 1 gives a compilation of searches for nuclearites.
[3] AHLEN 92 searched for quark matter ("nuclearites"). The bound applies to velocity $< 2.5\times10^{-3}$ c. See their Fig. 3 for other velocity/c and heavier mass range.
[4] NAKAMURA 91 searched for quark matter in the velocity range $(4\times10^{-5}$–$1)$ c.
[5] ORITO 91 searched for quark matter. The limit is for the velocity range $(10^{-4}$–$10^{-3})$ c.
[6] LIU 88 searched for quark matter ("nuclearites") in the velocity range $(2.5\times10^{-3}$–$1)c$. A less stringent limit of 5.8×10^{-11} applies for $(1$–$2.5)\times10^{-3}c$.
[7] BARISH 87 searched for quark matter ("nuclearites") in the velocity range $(2.7\times10^{-4}$–$5\times10^{-3})c$.
[8] NAKAMURA 85 at KEK searched for quark-matter. These might be lumps of strange quark matter with roughly equal numbers of u, d, s quarks. These lumps or nuclearites were assumed to have velocity of $(10^{-4}$–$10^{-3})$ c.
[9] ULLMAN 81 is sensitive for heavy slow singly charge particle reaching earth with vertical velocity 100–350 km/s.

Highly Ionizing Particle Flux

VALUE ($m^{-2}yr^{-1}$)	CL%	EVTS	DOCUMENT ID		TECN	COMMENT
• • • We do not use the following data for averages, fits, limits, etc. • • •						
<0.4	95	0	KINOSHITA	81B	PLAS	Z/β 30–100

SEARCHES FOR QUANTUM BLACK HOLE PRODUCTION

VALUE	DOCUMENT ID		TECN	COMMENT
• • • We do not use the following data for averages, fits, limits, etc. • • •				
	[1] AAD	14A	ATLS	8 TeV $pp \to \gamma +$ jet
	[2] AAD	13D	ATLS	7 TeV $pp \to$ 2 jets
	[3] CHATRCHYAN	13A	CMS	7 TeV $pp \to$ 2 jets
	[4] CHATRCHYAN	13AD	CMS	8 TeV $pp \to$ multijets
	[5] CHATRCHYAN	12W	CMS	7 TeV $pp \to$ multijets
	[6] AAD	11AG	ATLS	7 TeV $pp \to$ 2 jets

[1] AAD 14A search for quantum black hole formation followed by its decay to a γ and a jet, in pp collisions at $E_{cm} = 8$ TeV with $L = 20$ fb^{-1}. See their Fig. 3 for limits.

[2] AAD 13D search for quantum black hole formation followed by its decay to two jets, in pp collisions at $E_{cm} = 7$ TeV with $L = 4.8$ fb^{-1}. See their Fig. 8 and Table 3 for limits.

[3] CHATRCHYAN 13A search for quantum black hole formation followed by its decay to two jets, in pp collisions at $E_{cm} = 7$ TeV with $L = 5$ fb^{-1}. See their Figs. 5 and 6 for limits.

[4] CHATRCHYAN 13AJ search for quantum black hole formation followed by its evapolation to multiparticle final states, in multijet (including γ, ℓ) events in pp collisions at $E_{cm} = 8$ TeV with $L = 12$ fb^{-1}. See their Figs. 5–7 for limits.

[5] CHATRCHYAN 12W search for quantum black hole formation followed by its evapolation to multiparticle final states, in multijet (including γ, ℓ) events in pp collisions at $E_{cm} = 7$ TeV with $L = 4.7$ fb^{-1}. See their Figs. 5–8 for limits.

[6] AAD 11AG search for quantum black hole formation followed by its decay to two jets, in pp collisions at $E_{cm} = 7$ TeV with L = 36 pb^{-1}. See their Fig. 11 and Table 4 for limits.

REFERENCES FOR Searches for WIMPs and Other Particles

AAD	14A	PL B728 562	G. Aad *et al.*	(ATLAS Collab.)
AAD	13A	PL B718 860	G. Aad *et al.*	(ATLAS Collab.)
AAD	13AD	JHEP 1304 075	G. Aad *et al.*	(ATLAS Collab.)
AAD	13AH	PL B722 305	G. Aad *et al.*	(ATLAS Collab.)
AAD	13C	PRL 110 011802	G. Aad *et al.*	(ATLAS Collab.)
AAD	13D	JHEP 1301 029	G. Aad *et al.*	(ATLAS Collab.)
AALSETH	13	PR D88 012002	C.E. Aalseth *et al.*	(CoGeNT Collab.)
AALTONEN	13I	PR D88 031103	T. Aaltonen *et al.*	(CDF Collab.)
AALTONEN	13R	PRL 111 031802	T. Aaltonen *et al.*	(CDF Collab.)
AARTSEN	13	PRL 110 131302	M.G. Aartsen *et al.*	(IceCube Collab.)
AARTSEN	13C	PR D88 122001	M.G. Aartsen *et al.*	(IceCube Collab.)
ABE	13B	PL B719 78	K. Abe *et al.*	(XMASS Collab.)
ABRAMOWSKI	13	PRL 110 041301	A. Abramowski *et al.*	(H.E.S.S. Collab.)
ACKERMANN	13A	PR D88 082002	M. Ackermann *et al.*	(Fermi-LAT Collab.)
ADRIAN-MAR...	13	JCAP 1311 032	S. Adrian-Martinez *et al.*	(ANTARES Collab.)
AGNESE	13	PR D88 031104	R. Agnese *et al.*	(CDMS Collab.)
AGNESE	13A	PRL 111 251301	R. Agnese *et al.*	(CDMS Collab.)
APRILE	13	PRL 111 021301	E. Aprile *et al.*	(XENON100 Collab.)
BOLIEV	13	JCAP 1309 019	M. Boliev *et al.*	
CHATRCHYAN	13	PL B718 815	S. Chatrchyan *et al.*	(CMS Collab.)
CHATRCHYAN	13A	JHEP 1301 013	S. Chatrchyan *et al.*	(CMS Collab.)
CHATRCHYAN	13AB	JHEP 1307 122	S. Chatrchyan *et al.*	(CMS Collab.)
CHATRCHYAN	13AD	JHEP 1307 178	S. Chatrchyan *et al.*	(CMS Collab.)
CHATRCHYAN	13AJ	PL B723 280	S. Chatrchyan *et al.*	(CMS Collab.)
CHATRCHYAN	13AR	PR D87 092008	S. Chatrchyan *et al.*	(CMS Collab.)
LI	13B	PRL 110 261301	H.B. Li *et al.*	(TEXONO Collab.)
SUVOROVA	13	PAN 76 1367	O.V. Suvorova *et al.*	(INRM)
		Translated from YAF 76 1433.		
ZHAO	13	PR D88 052004	W. Zhao *et al.*	(CDEX Collab.)
AAD	12C	PRL 108 041805	G. Aad *et al.*	(ATLAS Collab.)
AAD	12S	PL B708 37	G. Aad *et al.*	(ATLAS Collab.)
AALTONEN	12K	PRL 108 201802	T. Aaltonen *et al.*	(CDF Collab.)
AALTONEN	12M	PRL 108 211804	T. Aaltonen *et al.*	(CDF Collab.)
ABBASI	12	PR D85 042002	R. Abbasi *et al.*	(IceCube Collab.)
ABRAMOWSKI	12	APJ 750 123	A. Abramowski *et al.*	(H.E.S.S. Collab.)
ACKERMANN	12	PR D86 022002	M. Ackermann *et al.*	(Fermi-LAT Collab.)
AKIMOV	12	PL B709 14	D.Yu. Akimov *et al.*	(ZEPLIN-III Collab.)
ALIU	12	PR D85 062001	E. Aliu *et al.*	(VERITAS Collab.)
ANGLOHER	12	EPJ C72 1971	G. Angloher *et al.*	(CRESST-II Collab.)
APRILE	12	PRL 109 181301	E. Aprile *et al.*	(XENON100 Collab.)
ARCHAMBAU...	12	PL B711 153	S. Archambault *et al.*	(PICASSO Collab.)
ARMENGAUD	12	PR D86 051701	E. Armengaud *et al.*	(EDELWEISS Collab.)
BARRETO	12	PL B711 264	J. Barreto *et al.*	(DAMIC Collab.)
BEHNKE	12	PR D86 052001	E. Behnke *et al.*	(COUPP Collab.)
BROWN	12	PR D85 021301	A. Brown *et al.*	(OXF)
CHATRCHYAN	12AP	JHEP 1209 094	S. Chatrchyan *et al.*	(CMS Collab.)
CHATRCHYAN	12BL	JHEP 1212 015	S. Chatrchyan *et al.*	(CMS Collab.)
CHATRCHYAN	12Q	PL B716 260	S. Chatrchyan *et al.*	(CMS Collab.)
CHATRCHYAN	12T	PRL 108 261803	S. Chatrchyan *et al.*	(CMS Collab.)
CHATRCHYAN	12W	JHEP 1204 061	S. Chatrchyan *et al.*	(CMS Collab.)
DAHL	12	PRL 108 259001	C.E. Dahl, J. Hall, W.H. Lippincott	(CHIC, FNAL)
DAW	12	ASP 35 397	E. Daw *et al.*	(DRIFT-IId Collab)
FELIZARDO	12	PRL 108 201302	M. Felizardo *et al.*	(SIMPLE Collab.)
KIM	12	PRL 108 181301	S.C. Kim *et al.*	(KIMS Collab.)
AAD	11AG	NJP 13 053044	G. Aad *et al.*	(ATLAS Collab.)
AAD	11I	PL B698 353	G. Aad *et al.*	(ATLAS Collab.)
AAD	11S	PL B705 294	G. Aad *et al.*	(ATLAS Collab.)
AALSETH	11	PRL 106 131301	C.E. Aalseth *et al.*	(CoGeNT Collab.)
AALSETH	11A	PRL 107 141301	C.E. Aalseth *et al.*	(CoGeNT Collab.)
AALTONEN	11AF	PRL 107 181801	T. Aaltonen *et al.*	(CDF Collab.)
AALTONEN	11M	PRL 106 171801	T. Aaltonen *et al.*	(CDF Collab.)
ABAZOV	11I	PRL 107 011804	V. M. Abazov *et al.*	(D0 Collab.)
ABBASI	11C	PR D84 022004	R. Abbasi *et al.*	(IceCube Collab.)
ABRAMOWSKI	11	PRL 106 161301	A. Abramowski *et al.*	(H.E.S.S. Collab.)
ACKERMANN	11	PRL 107 241302	M. Ackermann *et al.*	(Fermi-LAT Collab.)
AHLEN	11	PL B695 124	S. Ahlen *et al.*	(DMTPC Collab.)
AHMED	11	PR D83 112002	Z. Ahmed *et al.*	(CDMS Collab.)
AHMED	11A	PR D84 011102	Z. Ahmed *et al.*	(CDMS and EDELWEISS Collabs.)
AHMED	11B	PRL 106 131302	Z. Ahmed *et al.*	(CDMS Collab.)
AJELLO	11	PR D84 032007	M. Ajello *et al.*	(Fermi-LAT)
ANGLE	11	PRL 107 051301	J. Angle *et al.*	(XENON10 Collab.)
Also		PRL 110 249901 (errat)	J. Angle *et al.*	(XENON10 Collab.)
APRILE	11	PR D84 052003	E. Aprile *et al.*	(XENON100 Collab.)
APRILE	11A	PR D84 061101	E. Aprile *et al.*	(XENON100 Collab.)
APRILE	11B	PRL 107 131302	E. Aprile *et al.*	(XENON100 Collab.)
ARMENGAUD	11	PL B702 329	E. Armengaud *et al.*	(EDELWEISS II Collab.)
BEHNKE	11	PRL 106 021303	E. Behnke *et al.*	(COUPP Collab.)
CHATRCHYAN	11C	JHEP 1106 026	S. Chatychyan *et al.*	(CMS Collab.)
CHATRCHYAN	11U	PRL 107 201804	S. Chatychyan *et al.*	(CMS Collab.)
GERINGER-SA...	11	PRL 107 241303	A. Geringer-Sameth, S.M. Koushiappas	
HORN	11	PL B705 471	M. Horn *et al.*	(ZEPLIN-III Collab.)
TANAKA	11	APJ 742 78	T. Tanaka *et al.*	(Super-Kamiokande Collab.)
AAD	10	PRL 105 161801	G. Aad *et al.*	(ATLAS Collab.)
AALTONEN	10AF	PR D82 052005	T. Aaltonen *et al.*	(CDF Collab.)
ABBASI	10	PR D81 057101	R. Abbasi *et al.*	(IceCube Collab.)
AHMED	10	SCI 327 1619	Z. Ahmed *et al.*	(CDMS II Collab.)
AKERIB	10	PR D82 122004	D.S. Akerib *et al.*	(CDMS-II Collab.)
AKIMOV	10	PL B692 180	D.Yu. Akimov *et al.*	(ZEPLIN-III Collab.)
APRILE	10	PRL 105 131302	E. Aprile *et al.*	(XENON100 Collab.)
ARMENGAUD	10	PL B687 294	E. Armengaud *et al.*	(EDELWEISS II Collab.)
FELIZARDO	10	PRL 105 211301	M. Felizardo *et al.*	(The SIMPLE Collab.)
KHACHATRY...	10	PRL 105 211801	V. Khachatryan *et al.*	(CMS Collab.)
Also		PRL 106 029902	V. Khachatryan *et al.*	(CMS Collab.)
MIUCHI	10	PL B686 11	K. Miuchi *et al.*	(NEWAGE Collab.)
AALTONEN	09AF	PR D80 011102	T. Aaltonen *et al.*	(CDF Collab.)
AALTONEN	09G	PR D79 052004	T. Aaltonen *et al.*	(CDF Collab.)
AALTONEN	09Z	PRL 103 021802	T. Aaltonen *et al.*	(CDF Collab.)
ABAZOV	09M	PRL 102 161802	V.M. Abazov *et al.*	(D0 Collab.)
ABBASI	09B	PRL 102 201302	R. Abbasi *et al.*	(IceCube Collab.)
AHMED	09	PRL 102 011301	Z. Ahmed *et al.*	(CDMS Collab.)
ANGLE	09	PR D80 115005	J. Angle *et al.*	(XENON10 Collab.)
ANGLOHER	09	ASP 31 270	G. Angloher *et al.*	(CRESST Collab.)
ARCHAMBAU...	09	PL B682 185	S. Archambault *et al.*	(PICASSO Collab.)
LEBEDENKO	09A	PRL 103 151302	V.N. Lebedenko *et al.*	(ZEPLIN-III Collab.)
LIN	09	PR D79 061101	S.T. Lin *et al.*	(TEXONO Collab.)
AALSETH	08	PRL 101 251301	C.E. Aalseth *et al.*	(CoGeNT Collab.)
Also		PRL 102 109903 (errat)	C.E. Aalseth *et al.*	(CoGeNT Collab.)
ANGLE	08A	PRL 101 091301	J. Angle *et al.*	(XENON10 Collab.)
BEDNYAKOV	08	PAN 71 111	V.A. Bednyakov, H.P. Klapdor-Kleingrothaus, I.V. Krivosheina	
		Translated from YAF 71 112.		
ALNER	07	PL B653 161	G.J. Alner *et al.*	(ZEPLIN-II Collab.)
LEE	07A	PRL 99 091301	H.S. Lee *et al.*	(KIMS Collab.)
MIUCHI	07	PL B654 58	K. Miuchi *et al.*	
AKERIB	06	PR D73 011102	D.S. Akerib *et al.*	(CDMS Collab.)
SHIMIZU	06A	PL B633 195	Y. Shimizu *et al.*	
AKERIB	05	PR D72 052009	D.S. Akerib *et al.*	(CDMS Collab.)
ALNER	05	PL B616 17	G.J. Alner *et al.*	(UK Dark Matter Collab.)
BARNABE-HE...	05	PL B624 186	M. Barnabe-Heider *et al.*	(PICASSO Collab.)
BENOIT	05	PL B616 25	A. Benoit *et al.*	(EDELWEISS Collab.)
GIRARD	05	PL B621 233	T.A. Girard *et al.*	(SIMPLE Collab.)
GIULIANI	05	PRL 95 101301	F. Giuliani	
GIULIANI	05A	PR D71 123503	F. Giuliani, T.A. Girard	
KLAPDOR-K...	05	PL B609 226	H.V. Klapdor-Kleingrothaus, I.V. Krivosheina, C. Tomei	
AKTAS	04C	EPJ C36 413	A. Atkas *et al.*	(H1 Collab.)
GIULIANI	04	PL B588 151	F. Giuliani, T.A. Girard	
GIULIANI	04A	PRL 93 161301	F. Giuliani	
MIUCHI	03	ASP 19 135	K. Miuchi *et al.*	
TAKEDA	03	PL B572 145	A. Takeda *et al.*	
ANGLOHER	02	ASP 18 43	G. Angloher *et al.*	(CRESST Collab.)
BELLI	02	PR D66 043503	P. Belli *et al.*	
BERNABEI	02C	EPJ C23 61	R. Bernabei *et al.*	(DAMA Collab.)
GREEN	02	PR D66 083003	A.M. Green	
JAVORSEK	02	PR D65 072003	D. Javorsek II *et al.*	
BAUDIS	01	PR D63 022001	L. Baudis *et al.*	(Heidelberg-Moscow Collab.)
JAVORSEK	01	PR D64 012005	D. Javorsek II *et al.*	
JAVORSEK	01B	PRL 87 231804	D. Javorsek II *et al.*	
SMITH	01	PR D64 043502	D. Smith, N. Weiner	
ULLIO	01	JHEP 0107 044	P. Ullio, M. Kamionkowski, P. Vogel	
ABBIENDI	00D	EPJ C13 197	G. Abbiendi *et al.*	(OPAL Collab.)
AMBROSIO	00B	EPJ C13 453	M. Ambrosio *et al.*	(MACRO Collab.)
BENOIT	00	PL B479 8	A. Benoit *et al.*	(EDELWEISS Collab.)
BERNABEI	00D	NJP 2 15	R. Bernabei *et al.*	(DAMA Collab.)
COLLAR	00	PRL 85 3083	J.I. Collar *et al.*	(SIMPLE Collab.)
ABE	99F	PRL 82 2038	F. Abe *et al.*	(CDF Collab.)
AMBROSIO	99	PR D60 082002	M. Ambrosio *et al.*	(Macro Collab.)
BERNABEI	99	PL B450 448	R. Bernabei *et al.*	(DAMA Collab.)
BERNABEI	99D	PRL 83 4918	R. Bernabei *et al.*	(DAMA Collab.)
BRHLIK	99	PL B464 303	M. Brhlik, L. Roszkowski	
DERBIN	99	PAN 62 1886	A.V. Derbin *et al.*	
		Translated from YAF 62 2034.		
ACKERSTAFF	98P	PL B433 195	K. Ackerstaff *et al.*	(OPAL Collab.)
KLIMENKO	98	JETPL 67 875	A.A. Klimenko *et al.*	
		Translated from ZETFP 67 835.		
ABE	97G	PR D55 R5263	F. Abe *et al.*	(CDF Collab.)
ABREU	97D	PL B396 315	P. Abreu *et al.*	(DELPHI Collab.)
ACKERSTAFF	97B	PL B391 210	K. Ackerstaff *et al.*	(OPAL Collab.)
ADAMS	97B	PRL 79 4083	J. Adams *et al.*	(FNAL KTeV Collab.)
BARATE	97K	PL B405 379	R. Barate *et al.*	(ALEPH Collab.)
SARSA	97	PR D56 1856	M.L. Sarsa *et al.*	(ZARA)
ALESSAND...	96	PL B384 316	A. Alessandrello *et al.*	(MILA, MILAI, SASSO)
BELLI	96	PL B387 222	P. Belli *et al.*	(DAMA Collab.)
Also		PL B389 783 (erratum)	P. Belli *et al.*	(DAMA Collab.)
BELLI	96C	NC 19C 537	P. Belli *et al.*	(DAMA Collab.)
BERNABEI	96	PL B389 757	R. Bernabei *et al.*	(DAMA Collab.)
COLLAR	96	PRL 76 331	J.I. Collar	(SCUC)
SARSA	96	PL B386 458	M.L. Sarsa *et al.*	(ZARA)
Also		PR D56 1856	M.L. Sarsa *et al.*	(ZARA)
SMITH	96	PL B379 299	P.F. Smith *et al.*	(RAL, SHEF, LOIC+)
SNOWDEN-...	96	PRL 76 332	D.P. Snowden-Ifft, E.S. Freeman, P.B. Price	(UCB)
AKERS	95R	ZPHY C67 203	R. Akers *et al.*	(OPAL Collab.)
GALLAS	95	PR D52 6	E. Gallas *et al.*	(MSU, FNAL, MIT, FLOR)
GARCIA	95	PR D51 1458	E. Garcia *et al.*	(ZARA, SCUC, PNL)
QUENBY	95	PL B351 70	J.J. Quenby *et al.*	(LOIC, RAL, SHEF+)
SNOWDEN-...	95	PRL 74 4133	D.P. Snowden-Ifft, E.S. Freeman, P.B. Price	(UCB)
Also		PRL 76 331	J.I. Collar	(SCUC)
Also		PRL 76 332	D.P. Snowden-Ifft, E.S. Freeman, P.B. Price	(UCB)
BECK	94	PL B336 141	M. Beck *et al.*	(MPIH, KIAE, SASSO)
RAM	94	PR D49 3120	S. Ram *et al.*	(TELA, TRIU)
ABE	93G	PRL 71 2542	F. Abe *et al.*	(CDF Collab.)
ASTONE	93	PR D47 4770	P. Astone *et al.*	(ROMA, ROMAI, CATA, FRAS)
BUSKULIC	93C	PL B303 198	D. Buskulic *et al.*	(ALEPH Collab.)
YAMAGATA	93	PR D47 1231	T. Yamagata, Y. Takamori, H. Utsunomiya	(KONAN)
ABE	92J	PR D46 R1889	F. Abe *et al.*	(CDF Collab.)
AHLEN	92	PRL 69 1860	S.P. Ahlen *et al.*	(MACRO Collab.)
BACCI	92	PL B293 460	C. Bacci *et al.*	(Beijing-Roma-Saclay Collab.)
VERKERK	92	PRL 68 1116	P. Verkerk *et al.*	(ENSP, SACL, PAST)
AKESSON	91	ZPHY C52 219	T. Akesson *et al.*	(HELIOS Collab.)
NAKAMURA	91	PL B263 529	S. Nakamura *et al.*	
ORITO	91	PRL 66 1951	S. Orito *et al.*	(ICEPP, WASCR, NIHO, ICRR)
REUSSER	91	PL B255 143	D. Reusser *et al.*	(NEUC, CIT, PSI)
ADACHI	90C	PL B244 352	I. Adachi *et al.*	(TOPAZ Collab.)
ADACHI	90E	PL B249 336	I. Adachi *et al.*	(TOPAZ Collab.)
AKRAWY	90O	PR B252 290	M.Z. Akrawy *et al.*	(OPAL Collab.)
HEMMICK	90	PR D41 2074	T.K. Hemmick *et al.*	(ROCH, MICH, OHIO+)

Searches Particle Listings

WIMPs and Other Particle Searches

SAITO	90	PRL 65 2094	T. Saito *et al.*	(ICRR, KOBE)
NAKAMURA	89	PR D39 1261	T.T. Nakamura *et al.*	(KYOT, TMTC)
NORMAN	89	PR D39 2499	E.B. Norman *et al.*	(LBL)
BERNSTEIN	88	PR D37 3103	R.M. Bernstein *et al.*	(STAN, WISC)
CALDWELL	88	PRL 61 510	D.O. Caldwell *et al.*	(UCSB, UCB, LBL)
LIU	88	PRL 61 271	G. Liu, B. Barish	
BARISH	87	PR D36 2641	B.C. Barish, G. Liu, C. Lane	(CIT)
NORMAN	87	PRL 58 1403	E.B. Norman, S.B. Gazes, D.A. Bennett	(LBL)
BADIER	86	ZPHY C31 21	J. Badier *et al.*	(NA3 Collab.)
MINCER	85	PR D32 541	A. Mincer *et al.*	(UMD, GMAS, NSF)
NAKAMURA	85	PL 161B 417	K. Nakamura *et al.*	(KEK, INUS)
THRON	85	PR D31 451	J.L. Thron *et al.*	(YALE, FNAL, IOWA)
SAKUYAMA	83B	LNC 37 17	H. Sakuyama, N. Suzuki	(MEIS)
Also		LNC 36 389	H. Sakuyama, K. Watanabe	(MEIS)
Also		NC 78A 147	H. Sakuyama, K. Watanabe	(MEIS)
Also		NC 6C 371	H. Sakuyama, K. Watanabe	(MEIS)
BHAT	82	PR D25 2820	P.N. Bhat *et al.*	(TATA)
KINOSHITA	82	PRL 48 77	K. Kinoshita, P.B. Price, D. Fryberger	(UCB+)
MARINI	82	PR D26 1777	A. Marini *et al.*	(FRAS, LBL, NWES, STAN+)
SMITH	82B	NP B206 333	P.F. Smith *et al.*	(RAL)
KINOSHITA	81B	PR D24 1707	K. Kinoshita, P.B. Price	(UCB)
LOSECCO	81	PL 102B 209	J.M. LoSecco *et al.*	(MICH, PENN, BNL)
ULLMAN	81	PRL 47 289	J.D. Ullman	(LEHM, BNL)
YOCK	81	PR D23 1207	P.C.M. Yock	(AUCK)
BARTEL	80	ZPHY C6 295	W. Bartel *et al.*	(JADE Collab.)
BUSSIERE	80	NP B174 1	A. Bussiere *et al.*	(BGNA, SACL, LAPP)
YOCK	80	PR D22 61	P.C.M. Yock	(AUCK)
ARMITAGE	79	NP B150 87	J.C.M. Armitage *et al.*	(CERN, DARE, FOM+)
BOZZOLI	79	NP B159 363	W. Bozzoli *et al.*	(BGNA, LAPP, SACL+)
GOODMAN	79	PR D19 2572	J.A. Goodman *et al.*	(UMD)
SMITH	79	NP B149 525	P.F. Smith, J.R.J. Bennett	(RHEL)
BHAT	78	PRAM 10 115	P.N. Bhat, P.V. Ramana Murthy	(TATA)
CARROLL	78	PRL 41 777	A.S. Carroll *et al.*	(BNL, PRIN)
CUTTS	78	PRL 41 363	D. Cutts *et al.*	(BROW, FNAL, ILL, BARI+)
VIDAL	78	PL 77B 344	R.A. Vidal *et al.*	(COLU, FNAL, STON+)
ALEKSEEV	76	SJNP 22 531 Translated from YAF 22 1021.	G.D. Alekseev *et al.*	(JINR)
ALEKSEEV	76B	SJNP 23 633 Translated from YAF 23 1190.	G.D. Alekseev *et al.*	(JINR)
BALDIN	76	SJNP 22 264 Translated from YAF 22 512.	B.Y. Baldin *et al.*	(JINR)
BRIATORE	76	NC 31A 553	L. Briatore *et al.*	(LCGT, FRAS, FREIB)
GUSTAFSON	76	PRL 37 474	H.R. Gustafson *et al.*	(MICH)
ALBROW	75	NP B97 189	M.G. Albrow *et al.*	(CERN, DARE, FOM+)
FRANKEL	75	PR D12 2561	S. Frankel *et al.*	(PENN, FNAL)
JOVANOV...	75	PL 56B 105	J.V. Jovanovich *et al.*	(MANI, AACH, CERN+)
YOCK	75	NP B86 216	P.C.M. Yock	(AUCK, SLAC)
APPEL	74	PRL 32 428	J.A. Appel *et al.*	(COLU, FNAL)
FRANKEL	74	PR D9 1932	S. Frankel *et al.*	(PENN, FNAL)
YOCK	74	NP B76 175	P.C.M. Yock	(AUCK)
ALPER	73	PL 46B 265	B. Alper *et al.*	(CERN, LIVP, LUND, BOHR+)
LEIPUNER	73	PRL 31 1226	L.B. Leipuner *et al.*	(BNL, YALE)
DARDO	72	NC 9A 319	M. Dardo *et al.*	(TORI)
TONWAR	72	JP A5 569	S.C. Tonwar, S. Naranan, B.V. Sreekantan	(TATA)
ANTIPOV	71B	NP B31 235	Y.M. Antipov *et al.*	(SERP)
ANTIPOV	71C	PL 34B 164	Y.M. Antipov *et al.*	(SERP)
BINON	69	PL 30B 510	F.G. Binon *et al.*	(SERP)
BJORNBOE	68	NC B53 241	J. Bjornboe *et al.*	(BOHR, TATA, BERN+)
JONES	67	PR 164 1584	L.W. Jones	(MICH, WISC, LBL, UCLA, MINN+)
DORFAN	65	PRL 14 999	D.E. Dorfan *et al.*	(COLU)

INDEX

Greek letters are alphabetized by their English-language spelling. Bold page numbers signify entries in the Particle Properties Summary Tables.

Greek letters are alphabetized by their English-language spelling. Bold page numbers signify entries in the Particle Properties Summary Tables.

Greek letters are alphabetized by their English-language spelling. Bold page numbers signify entries in the Particle Properties Summary Tables.

Greek letters are alphabetized by their English-language spelling. Bold page numbers signify entries in the Particle Properties Summary Tables.

Greek letters are alphabetized by their English-language spelling. Bold page numbers signify entries in the Particle Properties Summary Tables.

Greek letters are alphabetized by their English-language spelling. Bold page numbers signify entries in the Particle Properties Summary Tables.

Greek letters are alphabetized by their English-language spelling. Bold page numbers signify entries in the Particle Properties Summary Tables.

Greek letters are alphabetized by their English-language spelling. Bold page numbers signify entries in the Particle Properties Summary Tables.

Greek letters are alphabetized by their English-language spelling. Bold page numbers signify entries in the Particle Properties Summary Tables.

Greek letters are alphabetized by their English-language spelling. Bold page numbers signify entries in the Particle Properties Summary Tables.

Greek letters are alphabetized by their English-language spelling. Bold page numbers signify entries in the Particle Properties Summary Tables.

Greek letters are alphabetized by their English-language spelling. Bold page numbers signify entries in the Particle Properties Summary Tables.

Greek letters are alphabetized by their English-language spelling. Bold page numbers signify entries in the Particle Properties Summary Tables.

Greek letters are alphabetized by their English-language spelling. Bold page numbers signify entries in the Particle Properties Summary Tables.